DNA EM-1
PART I

DEFENSE NUCLEAR AGENCY EFFECTS MANUAL NUMBER 1

CAPABILITIES OF NUCLEAR WEAPONS

1 JULY 1972

HEADQUARTERS
Defense Nuclear Agency
Washington, D.C. 20305

DNA EM-1
PART I
1 JULY 1972

DEFENSE NUCLEAR AGENCY EFFECTS MANUAL NUMBER 1

CAPABILITIES OF NUCLEAR WEAPONS

PART I
PHENOMENOLOGY

HEADQUARTERS
Defense Nuclear Agency
Washington, D.C. 20305

EDITOR
PHILIP J. DOLAN
STANFORD RESEARCH INSTITUTE

UNANNOUNCED

Accession For
NTIS GRA&I ☒
DDC TAB ☐
Unannounced ☐
Justification per ltr
By
Distribution/
Availability Codes
Dist | Avail and/or Special
A-1

[redacted]

TABLE OF CONTENTS

PART I PHENOMENOLOGY

CHAPTER 1 INTRODUCTION [redacted]

	Page
PURPOSE	1-1
CHARACTERISTICS OF NUCLEAR EXPLOSIONS	1-1
1-1 Fission Energy and the Chain Reaction	1-2
1-2 Fusion (Thermonuclear) Reactions	1-4
1-3 Weapon Yield Ratings	1-5
1-4 Effects of Environment and Time	1-6
1-5 Early Time History	1-6
AIR BURST	1-7
1-6 Development	1-7
1-7 Thermal Radiation	1-9
1-8 The Blast Wave	1-9
1-9 Nuclear Radiation	1-11
1-10 Electromagnetic Pulse	1-11
1-11 Electromagnetic Wave Propagation	1-11
1-12 The Cloud	1-12
THE SURFACE BURST	1-12
1-13 Ground Shock	1-12
1-14 The Crater	1-12
1-15 Thermal Radiation	1-12
1-16 Initial Nuclear Radiation	1-12
1-17 Residual Nuclear Radiation	1-14
1-18 Electromagnetic Pulse (EMP) Radiation	1-14
1-19 Electromagnetic Wave Propagation	1-14
1-20 The Cloud	1-14
1-21 Water Surface Bursts	1-14
THE TRANSITION ZONE BETWEEN AN AIR BURST AND A SURFACE BURST	1-14
THE HIGH-ALTITUDE BURST	1-15
1-22 Description	1-15
1-23 Development	1-15
1-24 The Blast Wave	1-17
1-25 Thermal Radiation	1-19
1-26 Nuclear Radiation	1-19
1-27 Electromagnetic Pulse	1-19
1-28 Electromagnetic-Wave Propagation	1-19

ERRATA extend. [illegible] 5/23/88

[redacted]

[redacted]

TABLE OF CONTENTS (Continued)

CHAPTER 1 INTRODUCTION [redacted] (Continued)

	Page
THE UNDERGROUND BURST	1-20
1-29 Development	1-20
1-30 Air Blast	1-20
1-31 Column, Cloud, and Base Surge	1-20
1-32 Ground Shock	1-20
1-33 Crater	1-20
1-34 Thermal and Nuclear Radiation	1-23
1-35 Electromagnetic Pulse	1-23
THE UNDERWATER BURST	1-23
1-36 Development	1-23
1-37 Water Shock Waves and Other Pressure Pulses	1-27
1-38 Air Blast	1-27
1-39 Surface Effects	1-27
1-40 Thermal and Nuclear Radiation	1-29
1-41 Electromagnetic Pulse	1-29
BIBLIOGRAPHY	1-30

CHAPTER 2 BLAST AND SHOCK PHENOMENA [redacted]

INTRODUCTION	2-1
SECTION I AIR BLAST PHENOMENA	2-1
RELIABILITY	2-2
2-1 Interpretation of Reliability Statements	2-3
2-2 Errors Due to Yield Scaling	2-3
2-3 Errors Due to Altitude Scaling	2-3
2-4 Errors at Long Ranges	2-3
2-5 Effects of the Earth's Surface	2-3
2-6 Effect of Weapon Characteristics	2-3
BLAST WAVE CALCULATIONS IN FREE AIR	2-4
2-7 Peak Overpressure	2-4
2-8 Peak Dynamic Pressure	2-4
2-9 Time of Arrival	2-5
2-10 Duration of the Positive Phases of Overpressure and Dynamic Pressure	2-5
2-11 Impulse	2-5
2-12 Waveforms	2-17

[redacted]

[redacted]

TABLE OF CONTENTS (Continued)

CHAPTER 2 BLAST AND SHOCK PHENOMENA [redacted] (Continued)

	Page
2-69 Bottom Reflection	2-~~198~~ 226
2-70 Secondary Shocks and Pressure Waves	2-~~198~~ 226
2-71 Refraction of Shock Waves	2-~~200~~ 228
2-72 Air Blast	2-~~203~~ 231
SURFACE EFFECTS OTHER THAN WAVES	2-~~203~~ 231
2-73 Spray Dome	2-~~214~~ 242
2-74 Plumes, Column, Cauliflower Cloud	2-~~214~~ 242
2-75 Base Surge	2-~~214~~ 242
2-76 Foam Patch and Ring	2-~~215~~ 243
WATER SURFACE WAVES	2-~~216~~ 244
2-77 Generation and Propagation of Water Surface Waves	2-~~216~~ 244
2-78 Refraction and Shoaling	2-~~223~~ 251
UNDERWATER CRATERING	2-~~223~~ 251
BIBLIOGRAPHY	2-~~270~~ 298

CHAPTER 3 THERMAL RADIATION PHENOMENA [redacted]

RADIANT EXPOSURE	3-1
3-1 Thermal Partition	3-2
3-2 Range Effects	3-5
TRANSMITTANCE	3-5
3-3 Specification of Transmittance	3-5
3-4 Model Atmospheres	3-6
3-5 Effects of Clouds and Reflecting Surfaces	3-27
3-6 Transmittance to Targets Above the Surface	3-30
3-7 Visual Range	3-33
3-8 Nighttime Visual Range	3-36
APPROXIMATE CALCULATIONS OF RADIANT EXPOSURE	3-37
SURFACE AND SUBSURFACE BURSTS	3-42
3-9 Surface Bursts	3-42
3-10 Subsurface Bursts	3-42
THE THERMAL PULSE	3-46
3-11 Thermal Power-Time Curve	3-46
3-12 Energy-Time Curve	3-46

[redacted]

[redacted]

TABLE OF CONTENTS (Continued)

CHAPTER 3 THERMAL RADIATION PHENOMENA [redacted] (Continued)

	Page
3-13 The Standard Thermal Pulse	3-46
3-14 Effect of Thermal Pulse Duration	3-52
3-15 Effect of Altitude on Pulse Shape	3-52
3-16 The Effects of Thermal Pulse Specifications on Thermal Partition	3-52
FIREBALL BRIGHTNESS	3-55
THE THERMAL PULSE FROM SPECIAL WEAPONS	3-56
3-17 Effective Thermal Yield of Special Weapons	3-57
3-18 Thermal Pulse Shape from Special Weapons	3-59
HIGH ALTITUDE THERMAL PHENOMENA	3-63
3-19 Thermal Partition	3-63
3-20 High Altitude Thermal Pulse Duration	3-64
3-21 Bursts Above 250 Kilofeet	3-70
RELIABILITY OF THERMAL SOURCE DATA	3-72
RELATION OF RADIANT EXPOSURE TO PEAK OVERPRESSURE	3-74
PHYSICS OF FIREBALL DEVELOPMENT	3-104
3-22 Black Body Radiation	3-104
3-23 Opacity	3-104
3-24 The Fireball Before Final Maximum	3-105
3-25 History of Fireball Evolution	3-107
3-26 Comparison with Recent Analysis of Experiments	3-109
BIBLIOGRAPHY	3-113

CHAPTER 4 X-RAY RADIATION PHENOMENA [redacted]

INTRODUCTION	4-1
4-1 Production of X-Rays	4-1
4-2 Black Body Radiation	4-3
4-3 Interactions of X-Rays with Matter	4-8
SECTION I NUCLEAR WEAPONS AS X-RAY SOURCES	4-9
4-4 X-Ray Production in Nuclear Weapons	4-9
4-5 X-Ray Energy Emitted	4-11
4-6 Rate of X-Ray Emission	4-11
4-7 Spectral Distribution of X-Rays	4-12
4-8 Real Nuclear Weapons as X-Ray Sources	4-12

[redacted]

[redacted]

TABLE OF CONTENTS (Continued)

CHAPTER 4 X-RAY RADIATION PHENOMENA [redacted] (Continued)

Page

SECTION II X-RAY ENVIRONMENTS PRODUCED BY NUCLEAR WEAPONS ... 4-25

4-9 Exoatmospheric (Vacuum) Detonations ... 4-25
4-10 Endoatmospheric Detonations ... 4-25
4-11 The Standard Atmosphere ... 4-25
4-12 Direct X-Ray Fluence in the Atmosphere ... 4-27
4-13 Scattered X-Ray Fluence ... 4-30
4-14 Low Altitude Endoatmospheric Detonations ... 4-30
4-15 High Altitude Endoatmospheric Detonations ... 4-39

BIBLIOGRAPHY ... 4-48

CHAPTER 5 NUCLEAR RADIATION PHENOMENA [redacted]

INTRODUCTION ... 5-1

SECTION I INITIAL NUCLEAR RADIATION ... 5-1

NEUTRONS ... 5-2
5-1 Neutron Source ... 5-2
5-2 Exoatmospheric (Vacuum) Transport ... 5-5
5-3 Neutron Transport Through Materials ... 5-5

GAMMA RAYS ... 5-17
5-4 Gamma Ray Sources ... 5-17
5-5 Prompt Gamma Rays ... 5-18
5-6 Air-Ground Secondary Gamma Rays ... 5-22
5-7 Fission Product Gamma Rays ... 5-23

INITIAL RADIATION DOSE TO PERSONNEL ... 5-24
5-8 Initial Neutron Dose ... 5-24
5-9 Air-Ground Secondary Gamma Ray Dose ... 5-25
5-10 Fission Product Gamma Ray Dose ... 5-25
5-11 Total Dose ... 5-25

SECTION II NEUTRON-INDUCED ACTIVITY IN SOILS ... 5-52
5-12 Height of Burst ... 5-52
5-13 Soil Types ... 5-52
5-14 Dose Rate and Dose Predictions ... 5-55

SECTION III RESIDUAL RADIATION ... 5-65

[redacted]

[redacted]

TABLE OF CONTENTS (Continued)

CHAPTER 5 NUCLEAR RADIATION PHENOMENA [redacted] (Continued)

	Page
FALLOUT	5-65
5-15 Early Fallout	5-65
5-16 Air Bursts	5-66
5-17 Land Surface Bursts	5-66
5-18 Deposition Patterns	5-67
5-19 Idealized Contours	5-67
5-20 Dose Rate Contour Dimensions	5-70
5-21 Decay of Early Fallout	5-72
5-22 Bursts in the Transition Zone	5-75
5-23 Underground Bursts	5-76
5-24 Beta Radiation	5-76
RESIDUAL RADIATION FROM WATER SURFACE AND UNDERWATER BURSTS	5-104
5-25 Water Surface Bursts	5-104
5-26 Underwater Bursts	5-106
DOSE RECEIVED WHILE FLYING THROUGH A NUCLEAR CLOUD	5-139
PRECIPITATION EFFECTS	5-145
5-27 Precipitation Scavenging	5-145
5-28 Prediction of Ground Contamination from Precipitation Effects	5-146
5-29 Some Specific Examples of Possible Contamination Resulting from Precipitation	5-148
BIBLIOGRAPHY	5-154

CHAPTER 6 TRANSIENT-RADIATION EFFECTS ON ELECTRONICS (TREE) PHENOMENA [redacted]

INTRODUCTION	6-1
ENVIRONMENT	6-3
6-1 Weapon Output	6-3
6-2 Time Considerations	6-4
6-3 Description of Radiation Fields	6-4
INTERACTIONS BASIC TO TREE	6-6
6-4 Ionization	6-6
6-5 Displacement	6-8
6-6 Heating	6-10

[redacted]

[redacted]

TABLE OF CONTENTS (Continued)

CHAPTER 6 TRANSIENT RADIATION EFFECTS ON ELECTRONICS (TREE) PHENOMENA [redacted] (Continued)

	Page
MANIFESTATIONS OF TREE IN MATERIALS	6-10
6-7 Ionization Effects	6-10
6-8 Displacement Effects	6-13
6-9 Heating Effects	6-14
BIBLIOGRAPHY	6-16

CHAPTER 7 ELECTROMAGNETIC PULSE (EMP) PHENOMENA [redacted]

ENVIRONMENT – GENERAL DESCRIPTION	7-1
7-1 Weapon Gamma Radiation	7-1
7-2 Compton Current	7-2
7-3 Air Conductivity	7-2
7-4 Radial Electric Field	7-2
ELECTROMAGNETIC FIELD GENERATION	7-5
7-5 Medium Altitude Air Burst	7-5
7-6 Surface Burst	7-9
7-7 High Altitude Burst	7-11
INTERNAL EMP	7-15
7-8 General Description	7-15
7-9 IEMP Generation	7-15
7-10 Problem Definition	7-17
COMPUTER CODE DESCRIPTIONS	7-17
7-11 Code Utility	7-17
7-12 Code Classes	7-18
SYSTEMS EFFECTS	7-18
7-13 System Definitions	7-18
7-14 Threat Definition	7-19
7-15 Effects Comparisons	7-20
BIBLIOGRAPHY	7-32

CHAPTER 8 PHENOMENA AFFECTING ELECTROMAGNETIC WAVE PROPAGATION [redacted]

INTRODUCTION	8-1

[redacted]

[redacted]

TABLE OF CONTENTS (Continued)

CHAPTER 8 PHENOMENA AFFECTING ELECTROMAGNETIC WAVE PROPAGATION [redacted] (Continued)

		Page
SECTION I	PHENOMENA AFFECTING RADIO FREQUENCIES	8-2
IONIZATION AND DEIONIZATION		8-2
8-1	Electron Density Within the Fireball	8-4
8-2	Electron Density Caused by Prompt Radiation Outside the Fireball	8-9
8-3	Electron Density Caused by Delayed Gamma Radiation Outside the Fireball	8-11
8-4	Electron Density Caused by Beta Particles Outside the Fireball	8-13
8-5	Electromagnetic Propagation in Ionized Regions	8-14
TRAVELING DISTURBANCES IN E AND F REGIONS OF IONOSPHERE		8-15
ELECTROMAGNETIC RADIATIONS		8-16
ABSORPTION		8-16
8-6	Absorption Within the Fireball	8-19
8-7	Absorption Caused by Prompt Radiation Outside the Fireball	8-20
8-8	Absorption Caused by Delayed Radiation Outside the Fireball	8-20
PHASE CHANGES		8-20
8-9	Velocity of Propagation	8-20
8-10	Frequency of Propagation	8-21
8-11	Direction of Propagation	8-21
8-12	Scatter and Scintillation	8-21
SECTION II	METHODS FOR CALCULATING ABSORPTION OF RADIO FREQUENCIES	8-23
8-13	Size and Location of Fireball and Debris Regions for Detonations Below 85 kilometers	8-25
8-14	Size and Location of Fireball and Debris Regions for Detonations Between 85 and 120 kilometers	8-25
8-15	Size and Location of Fireball and Debris Regions for Detonations Above 120 kilometers	8-25
BIBLIOGRAPHY		8-93

PART II DAMAGE CRITERIA

CHAPTER 9 INTRODUCTION TO DAMAGE CRITERIA [redacted]

SECTION I	CONTENT AND LIMITATIONS OF PART II	9-1

[redacted]

DNA EM-1
PART II
1 JULY 1972

DEFENSE NUCLEAR AGENCY EFFECTS MANUAL NUMBER 1

CAPABILITIES OF NUCLEAR WEAPONS

PART II
DAMAGE CRITERIA

HEADQUARTERS
Defense Nuclear Agency
Washington, D.C. 20305

EDITOR
PHILIP J. DOLAN
STANFORD RESEARCH INSTITUTE

QUALITY INSPECTED 4

UNANNOUNCED

Accession For
NTIS GRA&I ☒
DTIC TAB ☐
Unannounced ☐
Justification
By
Distribution/
Availability Codes
Dist | Avail and/or Special
A-1

[redacted]

FOREWORD

This edition of the *Capabilities of Nuclear Weapons* represents the continuing efforts by the Defense Nuclear Agency to correlate and make available nuclear weapons effects information obtained from nuclear weapons testing, small-scale experiments, laboratory effort and theoretical analysis. This document presents the phenomena and effects of a nuclear detonation and relates weapons effects manifestations in terms of damage to targets of military interest. It provides the source material and references needed for the preparation of operational and employment manuals by the Military Services.

The *Capabilities of Nuclear Weapons* is not intended to be used as an employment or design manual by itself, since more complete descriptions of phenomenological details should be obtained from the noted references. Every effort has been made to include the most current reliable data available on 31 December 1971 in order to assist the Armed Forces in meeting their particular requirements for operational and target analysis purposes.

Comments concerning this manual are invited and should be addressed:

Director
Defense Nuclear Agency
ATTN: STAP
Washington, D. C. 20305

C. H. DUNN
Lt General, USA
Director

[redacted]

[redacted]

TABLE OF CONTENTS (Continued)

CHAPTER 8 PHENOMENA AFFECTING ELECTROMAGNETIC WAVE PROPAGATION [redacted] (Continued)

		Page
SECTION I	PHENOMENA AFFECTING RADIO FREQUENCIES	8-2
	IONIZATION AND DEIONIZATION	8-2
	TRAVELING DISTURBANCES IN E AND F REGIONS OF IONOSPHERE	8-15
	ELECTROMAGNETIC RADIATIONS	8-16
	ABSORPTION	8-16
	PHASE CHANGES	8-20
SECTION II	METHODS FOR CALCULATING ABSORPTION OF RADIO FREQUENCIES	8-23

PART II DAMAGE CRITERIA

CHAPTER 9 INTRODUCTION TO DAMAGE CRITERIA [redacted]

SECTION I	CONTENT AND LIMITATIONS OF PART II	9-1
9-1	Introduction to Chapter 9	9-1
9-2	Organization of Part II	9-1
9-3	Limitations in Part II	9-2
SECTION II	BLAST AND SHOCK DAMAGE	9-2
	LOADING	9-3
9-4	Air Blast Loading in the Mach Reflection Region	9-3
9-5	Qualitative Examples of Net Loading	9-4
9-6	Regular and Mach Reflection	9-10
9-7	Target Motion	9-10
9-8	Nonideal Waveforms	9-10
9-9	Underwater Shock Wave Loading	9-10
9-10	Ground Shock Loading	9-11
	RESPONSE AND DAMAGE	9-11
9-11	Surface Structures	9-11
9-12	Shielded Structures	9-13
9-13	Aircraft	9-13
SECTION III	THERMAL RADIATION DAMAGE	9-13
	INTRODUCTION	9-13
9-14	Radiant Exposure	9-14
9-15	Thermal Pulse Duration	9-14

[redacted]

[redacted]

TABLE OF CONTENTS (Continued)

CHAPTER 9 INTRODUCTION TO DAMAGE CRITERIA [redacted] (Continued)

	Page
9-16 Target Response	9-14
9-17 Target Orientation	9-15
9-18 Shielding	9-15
THERMAL RESPONSE OF MATERIALS	9-15
9-19 Thickness Effects	9-16
9-20 Color	9-22
9-21 Transparency	9-23
9-22 Effect of Humidity	9-23
9-23 Response of Metal Sheets	9-25
9-24 Thermal Damage to Various Materials	9-25
SURVIVAL IN FIRE AREAS	9-28
9-25 Causes of Death	9-28
9-26 Shelters	9-29
9-27 Escape from the Fire Areas	9-30
9-28 Safe Areas Within the Fire	9-31
SECTION IV THERMAL RADIATION DEGRADATION OF STRUCTURAL RESISTANCE TO AIR BLAST	9-31
THERMAL ENERGY ABSORBED	9-32
9-29 Absorption	9-32
9-30 Energy Losses	9-35
CHANGES IN MATERIAL STATE AND MATERIALS PROPERTIES	9-38
9-31 Changes in Material State	9-38
9-32 Change in Materials Properties	9-46
RESISTANCE TO LOAD	9-63
SECTION V X-RAY DAMAGE EFFECTS	9-67
INTRODUCTION	9-67
X-RAY ENERGY DEPOSITION CALCULATIONS	9-68
9-33 X-ray Cross Sections	9-68
9-34 X-ray Energy Deposition and Shine Through Fluences	9-69
9-35 X-ray Energy Deposition Summary	9-93
INITIAL PRESSURIZATION OF MATERIALS DUE TO X-RAY DEPOSITION	9-93
9-36 Phase Changes Induced by X-ray Heating	9-93
9-37 The Gruneisen Parameter and the Equation of State	9-101
SHOCK WAVE PROPAGATION AND DAMAGE PREDICTIONS	9-103
9-38 Through-the-Thickness Elastic-Plastic Shock Propagation	9-105

[redacted]

[redacted]

TABLE OF CONTENTS (Continued)

CHAPTER 9 INTRODUCTION TO DAMAGE CRITERIA [redacted] (Continued)

	Page
9-39 Through-the-Thickness Material Response	9-107
IMPULSE AND STRUCTURAL RESPONSE ANALYSIS	9-107
9-40 Impulse Calculations	9-107
9-41 Structural Response Analysis	9-115
REENTRY VEHICLE HARDENING	9-115
9-42 Balanced Hardening with Respect to Neutrons and X-rays	9-116
9-43 X-ray Hardening Concepts	9-116
SECTION VI NUCLEAR RADIATION SHIELDING	9-118
SECTION VII TREE - COMPONENT PART AND CIRCUIT RESPONSE	9-121
SEMICONDUCTOR COMPONENT PARTS	9-122
9-44 Transient Effects	9-122
9-45 Permanent Effects	9-132
9-46 Heating and Thermomechanical Damage	9-140
OTHER ELECTRONIC COMPONENT PARTS	9-147
9-47 Electron Tubes	9-147
9-48 Capacitors	9-149
9-49 Resistors	9-151
9-50 Batteries and Cables	9-151
9-51 Quartz Crystals	9-153
9-52 Solder Joints	9-154
9-53 Infrared Detectors	9-154
ELECTRONIC CIRCUITS	9-155
9-54 Radiation Response of Discrete-Component-Part Circuits	9-155
9-55 Radiation Response of Integrated Circuits	9-158
SECTION VIII ELECTROMAGNETIC PULSE (EMP) DAMAGE MECHANISMS	9-170
ENERGY COUPLING	9-170
9-56 Basic Coupling Modes	9-170
9-57 Resonant Configurations	9-171
COMPONENT DAMAGE	9-172
9-58 Types of Damage	9-172
9-59 Damage Levels	9-173
EMP HARDENING	9-175
9-60 System Analysis	9-175
9-61 Recommended Practices	9-176
TESTING	9-178

[redacted]

[redacted]

TABLE OF CONTENTS (Continued)

CHAPTER 9 INTRODUCTION TO DAMAGE CRITERIA [redacted] (Continued)

Page

9-62 Importance of Testing 9-178
9-63 Simulation Facilities 9-179

BIBLIOGRAPHY 9-183

CHAPTER 10 PERSONNEL CASUALTIES [redacted]

INTRODUCTION 10-1

SECTION I AIR BLAST 10-1

MECHANISMS AND CRITERIA FOR INJURY 10-1
10-1 Direct Overpressure Effects 10-1
10-2 Translational Forces and Impact 10-2
10-3 Blast-Energized Debris 10-3
10-4 Miscellaneous Effects 10-3

CASUALTY PREDICTION 10-4
10-5 Personnel in the Open 10-4
10-6 Personnel in a Forest 10-4
10-7 Personnel in Structures 10-5
10-8 Personnel in Vehicles 10-5

SECTION II THERMAL RADIATION 10-10

SKIN BURNS 10-10

CLASSIFICATION OF BURNS 10-10
10-9 First Degree Burns 10-10
10-10 Second Degree Burns 10-10
10-11 Third Degree Burns 10-10
10-12 Reduction in Effectiveness by Burns 10-11

BURN INJURY ENERGIES AND RANGES 10-11
10-13 Personnel Parameters 10-11
10-14 Burn Exposures for Unprotected Skin 10-12
10-15 Burns Under Clothing 10-12
10-16 Body Areas Involved 10-12
10-17 Incapacitation from Burns 10-15
10-18 Modification of Injury 10-15

EFFECTS OF THERMAL RADIATION ON THE EYES 10-15
10-19 Flashblindness 10-15
10-20 Retinal Burns 10-15

[redacted]

[redacted]

TABLE OF CONTENTS (Continued)

CHAPTER 10 PERSONNEL CASUALTIES [redacted] (Continued)

Page

10-21 Modification of Thermal Effects on the Eye 10-17
10-22 Safe Separation Distance Curves 10-17

SECTION III NUCLEAR RADIATION 10-23

INITIAL RADIATION 10-23
10-23 Radiation Sickness 10-23
10-24 Incapacitation 10-24
10-25 Modification of Injury 10-25
10-26 Military Assumptions 10-25

RESIDUAL RADIATION 10-25
10-27 External Hazards 10-25
10-28 Internal Hazards 10-31
10-29 Modification of Injury 10-31

SECTION IV COMBINED INJURY 10-31

10-30 Radiation and Thermal Injuries 10-32
10-31 Mechanical and Radiation Injuries 10-33
10-32 Thermal and Mechanical Injuries 10-33

CASUALTY CRITERIA 10-33
PERSONNEL IN THE OPEN 10-33
PERSONNEL IN STRUCTURES 10-35
TREATMENT 10-35
BIBLIOGRAPHY 10-36

CHAPTER 11 DAMAGE TO STRUCTURES [redacted]

INTRODUCTION 11-1

SECTION I DAMAGE TO ABOVEGROUND STRUCTURES 11-1

AIR BLAST EFFECTS 11-2
11-1 Nature of Loading 11-2
11-2 Nature of Damage 11-3
11-3 Structural Characteristics 11-3
11-4 Isodamage Curves 11-9

[redacted]

[redacted]

TABLE OF CONTENTS (Continued)

CHAPTER 11 DAMAGE TO STRUCTURES [redacted] (Continued)

Page

11-5 Shallow Underground Bursts 11-12
11-6 Ground Shock and Cratering 11-12

SECTION II DAMAGE TO BELOWGROUND STRUCTURES 11-40

STRUCTURES BURIED IN SOIL 11-40
11-7 Definition of Burial Conditions 11-40
11-8 Deeply Buried Structures 11-41
11-9 Structures Buried at Shallow Depths 11-48
11-10 Intermediate Depths of Burial 11-49

LINED AND UNLINED OPENINGS IN ROCK 11-49
11-11 Definition of Damage to Openings in Rock 11-50
11-12 Types of Tunnel Linings 11-51
11-13 Procedures for Tunnel Vulnerability Evaluation 11-52
11-14 Vulnerability Evaluation of Surface Silos in Rock 11-55

SECTION III SHOCK VULNERABILITY OF EQUIPMENT AND PERSONNEL 11-97

11-15 Shock Mounting 11-97
11-16 Nature of Elastic Systems Comprised of Mounted Equipment 11-99
11-17 Design of Mounted Equipment to Resist Shock 11-99
11-18 Vulnerability Analysis 11-100

SECTION IV DAMS AND HARBOR INSTALLATIONS 11-109

AIR BLAST 11-109
11-19 Concrete Gravity Dams 11-109
11-20 Harbor Installations 11-109

WATER SHOCK 11-109
11-21 Concrete Dams and Water Locks 11-109

CRATERING 11-109
11-22 Cratering Earth Dams and Causeways 11-109

WATER WAVES 11-110
11-23 Impact and Hydrostatic Pressure 11-110
11-24 Drag Forces 11-110
11-25 Inundation 11-110

THERMAL-RADIATION DAMAGE 11-110

SECTION V PETROLEUM, OIL, AND LUBRICANT (POL) STORAGE TANKS 11-110

11-26 Damage Criteria 11-110
11-27 Loading and Response 11-111
11-28 Damage 11-111

[redacted]

[redacted]

TABLE OF CONTENTS (Continued)

CHAPTER 11 DAMAGE TO STRUCTURES [redacted] (Continued)

Page

SECTION VI FIELD FORTIFICATIONS 11-118

11-29 Air Blast Damage 11-118
11-30 Protection of Fortifications from Air Blast Damage 11-118
11-31 Thermal Radiation Damage 11-121

SECTION VII FIRE IN URBAN AREAS 11-127

INTRODUCTION 11-127

EVOLUTION OF MASS FIRES 11-127
11-32 Ignition Points 11-127
11-33 Room Flashover 11-128
11-34 Active Burning of a Structure 11-128
11-35 Fire Spread Between Structures 11-128
11-36 Mass Fires 11-129

ESTIMATION AND CONTROL OF THERMAL DAMAGE 11-130
11-37 Radiant Exposure Thresholds 11-130
11-38 Fire Radii 11-134
11-39 The San Jose Study 11-134
11-40 The New Orleans Study 11-136
11-41 Effects of Clouds 11-138
11-42 Firestorm Criteria 11-143
11-43 Conflagrations 11-144
11-44 Fire Control 11-144

BIBLIOGRAPHY 11-146

CHAPTER 12 MECHANICAL DAMAGE DISTANCES FOR SURFACE SHIPS AND SUBMARINES SUBJECTED TO NUCLEAR EXPLOSIONS [redacted]

INTRODUCTION 12-1
12-1 Damage Mechanisms 12-1
12-2 Damage Classification 12-1
12-3 Seaworthiness Impairment 12-1
12-4 Mobility Impairment 12-2
12-5 Weapon Delivery Impairment 12-2

SECTION I DAMAGE TO SURFACE SHIPS FROM AIR BURSTS 12-2

BLAST DAMAGE 12-2
12-6 General 12-2

[redacted]

[redacted]

TABLE OF CONTENTS (Continued)

CHAPTER 12 MECHANICAL DAMAGE DISTANCES FOR SURFACE SHIPS AND SUBMARINES SUBJECTED TO NUCLEAR EXPLOSIONS [redacted] (Continued)

Page

12-7 Damage Criteria 12-3
12-8 Damage Distances 12-3
12-9 Capsizing from Blast 12-6

DAMAGE FROM OTHER AIR BURST PHENOMENA 12-6
12-10 Thermal Radiation 12-6
12-11 Damage from Nuclear Radiation and Electromagnetic Pulse 12-8
12-12 (Omitted)

SECTION II SURFACE SHIP DAMAGE FROM UNDERWATER BURSTS 12-8

DAMAGE FROM THE SHOCK WAVE IN THE WATER 12-8
12-13 Damage Criteria 12-8
12-14 Damage Distances 12-9
12-15 Effect of Ocean Environment on Damage Ranges 12-9

DAMAGE FROM OTHER UNDERWATER BURST PHENOMENA 12-17

SECTION III SUBMARINE DAMAGE FROM UNDERWATER BURSTS 12-17

DAMAGE FROM THE SHOCK WAVE IN THE WATER 12-17
12-16 Damage Criteria 12-17
12-17 Damage Distances 12-18
12-18 Effect of Ocean Environment on Damage Ranges 12-18

DAMAGE FROM OTHER UNDERWATER BURST PHENOMENA 12-19

BIBLIOGRAPHY 12-30

CHAPTER 13 DAMAGE TO AIRCRAFT [redacted]

INTRODUCTION 13-1

SECTION I BLAST AND THERMAL EFFECTS ON AIRCRAFT 13-1

13-1 Sure-Safe and Sure-Kill Envelopes 13-2

NUCLEAR WEAPON EFFECTS ANALYSIS 13-4
13-2 Gust Effects 13-4
13-3 Overpressure Effects 13-7
13-4 Thermal Radiation Effects 13-7
13-5 Combined Effects 13-9

SECTION II AIRCRAFT RESPONSE TO BLAST AND THERMAL EFFECTS 13-10

AIRCRAFT RESPONSE TO GUST EFFECTS 13-10
13-6 Aerodynamic Coefficients for Aircraft 13-10

[redacted]

[redacted]

TABLE OF CONTENTS (Continued)

CHAPTER 13 DAMAGE TO AIRCRAFT [redacted] (Continued)

Page

13–7 Gust Effects on In-Flight Aircraft 13–27
13–8 Gust Effects on Parked Aircraft 13–27

AIRCRAFT RESPONSE TO OVERPRESSURE EFFECTS 13–50
13–9 Overpressure Effects on In-Flight and Parked Aircraft 13–50

AIRCRAFT RESPONSE TO THERMAL RADIATION EFFECTS 13–59
13–10 Thermal Effects on In-Flight and Parked Aircraft 13–59

BURST-TIME ENVELOPES 13–67
13–11 Requirement for Burst-Time Envelopes 13–67

BIBLIOGRAPHY 13–86

CHAPTER 14 DAMAGE TO MILITARY FIELD EQUIPMENT [redacted]

INTRODUCTION 14–1

SECTION I AIR BLAST DAMAGE 14–1
14–1 Damage Mechanisms 14–1
14–2 Air Blast Environment 14–2
14–3 Target Characteristics 14–4
14–4 Target Exposure 14–6
14–5 Effects of Ground Surface Conditions 14–12
14–6 Vehicle Status 14–14

SECTION II DAMAGE PREDICTIONS 14–17
14–7 Definitions of Damage Categories 14–17
14–8 Prediction Techniques 14–18
14–9 Untested Equipment 14–52

SECTION III DAMAGE FROM CAUSES OTHER THAN BLAST AND NUCLEAR RADIATION 14–57
14–10 Fire Damage 14–57
14–11 Obscuration of Optical Devices 14–58
14–12 Damage by Missiles 14–58
14–13 The Effects of Time 14–59

SECTION IV TREE DAMAGE CRITERIA 14–59

SYSTEMS ANALYSIS 14–60
14–14 Types of Systems Analysis Used in TREE 14–60

[redacted]

[redacted]

TABLE OF CONTENTS (Continued)

CHAPTER 14 DAMAGE TO MILITARY FIELD EQUIPMENT [redacted] (Continued)

Page

14–15 The Complexity of Performing System Analysis for TREE 14–60
14–16 Characteristics of the Analysis Used in This Section 14–61

REVIEW OF ELECTRONIC SUSCEPTIBILITY TO NUCLEAR RADIATION 14–62
14–17 Component Part Vulnerability 14–62
14–18 Subsystem Vulnerability 14–64

TREE-DAMAGE ESTIMATES 14–64
14–19 Ground Equipment 14–65
14–20 An Example of Ground Equipment Survivability Estimation 14–65
14–21 Aircraft Systems 14–67
14–22 An Example of Aircraft Survivability Estimation 14–67
14–23 Missile Systems 14–70

BIBLIOGRAPHY 14–72

CHAPTER 15 DAMAGE TO FOREST STANDS [redacted]

INTRODUCTION 15–1

SECTION I AIR BLAST 15–1
15–1 Forest Stand Types 15–1
15–2 Damage-Distance Relations 15–3

SECTION II TROOP AND VEHICLE MOVEMENT 15–41
15–3 Blowdown Debris Characteristics 15–42
15–4 Vehicle Movement 15–44
15–5 Troop Movement 15–46
15–6 Predicting Effects on Movement 15–49

SECTION III THERMAL RADIATION 15–52
15–7 Ignitions 15–52
15–8 Kindling Fuels 15–52
15–9 Thermal Radiation on Forests 15–56
15–10 Forest Fire Ignition and Spread 15–58

BIBLIOGRAPHY 15–64

CHAPTER 16 DAMAGE TO MISSILES [redacted]

SECTION I BLAST DAMAGE TO TACTICAL MISSILE SYSTEMS 16–1

[redacted]

[redacted]

TABLE OF CONTENTS (Continued)

CHAPTER 16 DAMAGE TO MISSILES [redacted] (Continued)

Page

SERGEANT WEAPON SYSTEM 16-3
16-1 Description of the SERGEANT Weapon System 16-3
16-2 Vulnerability Levels of the SERGEANT Missile System 16-7
16-3 Reliability of SERGEANT Vulnerability Estimates 16-10

LANCE WEAPON SYSTEM 16-12
16-4 Description of the LANCE Weapon System 16-12
16-5 Vulnerability Levels for the LANCE Missile System 16-12
16-6 Reliability of LANCE Vulnerability Estimates 16-17

HAWK WEAPON SYSTEM 16-19
16-7 Description of the HAWK Weapon System 16-19
16-8 Vulnerability Levels for the HAWK Missile System 16-23
16-9 Reliability of HAWK Vulnerability Estimates 16-24

SAMPLE PROBLEM: AIR BLAST DAMAGE TO A TACTICAL MISSILE SYSTEM 16-26
16-10 Description of the HONEST JOHN System 16-26
16-11 Vulnerability Levels for HONEST JOHN Missile System 16-31

SECTION II BLAST AND THERMAL VULNERABILITY OF IN-FLIGHT STRATEGIC SYSTEMS 16-34

INTRODUCTION 16-34
16-12 Sources of Data 16-38
16-13 Limitations in Application of the Data 16-38

BLAST LOADING ON REENTRY (RV) SYSTEMS 16-39
16-14 Environment Scaling 16-39
16-15 General Intercept Loads and Load Duration 16-47
16-16 Intercept Load Duration 16-51
16-17 Fireball Traversal Time 16-51
16-18 Total Traversal Time 16-52
16-19 Exit Loads 16-57
16-20 Blast Data Generalization 16-57
16-21 Typical RV Aerodynamics 16-57
16-22 Initial Interaction of Vehicle Flow-Field and Blast Wave (Shock-Shock) 16-58
16-23 Damage Envelopes 16-58

RESULTS OF SOME RV BLAST AND THERMAL LOAD AND VULNERABILITY CALCULATIONS 16-66
16-24 Blast Loads on the RV 16-66
16-25 Thermal Radiation Loads on the RV 16-70

[redacted]

[redacted]

TABLE OF CONTENTS (Continued)

CHAPTER 16 DAMAGE TO MISSILES [redacted] (Continued)

Page

16–26 Description of a Blast/Thermal Vulnerability Determination 16–75
16–27 Results of the RV Vulnerability Determination 16–77
16–28 Summary and Conclusions Concerning RV Vulnerability Calculations 16–81

ANTIMISSILE (ABM) SYSTEMS 16–81
16–29 Shell Breathing Response 16–86
16–30 Vehicle Bending Response 16–87
16–31 Thermal Radiation Effects 16–87
16–32 ABM Blast/Thermal Vulnerability Envelopes 16–90
16–33 Conclusions 16–91

BLAST AND THERMAL LETHALITY 16–96
16–34 Blast and Thermal Free Field Environments 16–96
16–35 ABM Blast Loads on Threat Vehicles (Point Mass) 16–96
16–36 Blast Loads on the RV Threat Vehicle 16–101
16–37 ABM Blast Kill Radii 16–106
16–38 Fireball Thermal Effects on Threat RV's 16–109

BIBLIOGRAPHY 16–116

CHAPTER 17 RADIO FREQUENCY SIGNAL DEGRADATION RELEVANT TO COMMUNICATIONS AND RADAR SYSTEMS [redacted]

INTRODUCTION 17–1

SECTION I DEGRADATION MECHANISMS 17–2

ATTENUATION 17–2
17–1 Fireball Absorption 17–2
17–2 Absorption in the Region Around the Fireball 17–2
17–3 D–Region Absorption 17–4
17–4 Absorption of Noise 17–4
17–5 Attenuation by Scattering and Beam Spreading 17–4
17–6 Effects of Reflection 17–6

INTERFERENCE 17–6
17–7 Noise 17–6
17–8 Reflection, Refraction, and Scatter 17–6

SIGNAL DISTORTION 17–6

SECTION II SYSTEM CHARACTERISTICS AND EFFECTS 17–7

VLF AND LF SYSTEMS 17–7

[redacted]

[redacted]

TABLE OF CONTENTS (Continued)

CHAPTER 17 RADIO FREQUENCY SIGNAL DEGRADATION RELEVANT TO COMMUNICATIONS AND RADAR SYSTEMS [redacted] (Continued)

Page

17-9 VLF and LF Propagation 17-7
17-10 Effects of Nuclear Bursts on VLF and LF Systems 17-7
17-11 Spread-Debris Environment 17-9
17-12 Effect of a [redacted] 6300-km Burst 17-9
17-13 Effect of Detonations Below About 300 km 17-13

HF SYSTEMS 17-13
17-14 HF Propagation 17-13
17-15 Effect of Nuclear Bursts on HF Systems 17-13
17-16 Effect of Surface or Near-Surface Bursts 17-16
17-17 Effect of a [redacted] 30-km Burst 17-16
17-18 Effects of a [redacted] 50-km Burst 17-17
17-19 Effect of Multiple Multimegaton 150-km Bursts 17-17
17-20 Effect of a 1-Mt, 250-km Burst 17-18
17-21 Effect of a [redacted] 1000-km Burst 17-19

SATELLITE COMMUNICATION SYSTEMS 17-19
17-22 Effects of Nuclear Bursts on Satellite Systems 17-19
17-23 Nuclear Effects on Two Typical Satellite Systems 17-20

TROPOSCATTER COMMUNICATION SYSTEMS 17-22
17-24 Effects of Nuclear Bursts on Troposcatter Systems 17-22
17-25 Nuclear Effects on Three Typical Troposcatter Systems 17-26

IONOSCATTER COMMUNICATION SYSTEMS 17-26
17-26 Effects of Nuclear Bursts on Ionoscatter Systems 17-27
17-27 Nuclear Effects on Typical Ionoscatter Systems 17-28

RADAR SYSTEMS 17-30
17-28 Ballistic Missile Defense Systems 17-32
17-29 Nuclear Effects on Area Defense Systems 17-32
17-30 Nuclear Effects on Hardsite Defense Systems 17-36

BIBLIOGRAPHY 17-40

APPENDIX A SUPPLEMENTARY BLAST DATA [redacted]

SECTION I MATHEMATICAL DESCRIPTION OF THE SHOCK FRONT A-1

A-1 The Rankine-Hugoniot Equations A-1
A-2 Equation of State of an Ideal Gas A-3
A-3 Shock Wave Equations for an Ideal Gas A-3
A-4 Units, Constants, and Conversion Factors A-5

[redacted]

[redacted]

TABLE OF CONTENTS (Continued)

APPENDIX A SUPPLEMENTARY BLAST DATA [redacted] (Continued) *Page*

A-5 Equation of State of Air A-5
A-6 Equations for Strong Shock Waves in Air A-5
SECTION II PHYSICAL DESCRIPTION OF SHOCK WAVE BEHAVIOR A-8
A-7 Step Function Shock Wave A-8
A-8 Shock-Front Formation A-9
A-9 Pressure-Momentum Interaction at a Shock Front A-9
A-10 Normal Reflection at a Solid Barrier A-10
A-11 Pressures on Simple Shapes A-12
A-12 The Rankine-Hugoniot Equations (Alternate Analysis) A-14
A-13 Dynamic Pressure A-16

APPENDIX B USEFUL RELATIONSHIPS [redacted]

B-1 General Equivalents B-1
B-2 Constants B-1
B-3 Standard Sea Level Atmosphere B-1
B-4 Conversions B-2
B-5 Fractional Power and Dimension Scaling B-4

APPENDIX C PROBABILITY CONSIDERATIONS [redacted]

C-1 Protective Design and Weapon Selection C-1
SECTION I DAMAGE PROBABILITIES C-2
DAMAGE CAUSED BY MOTION INPUT C-2
C-2 Description of Charts for Damage Caused by Motion Input C-2
C-3 Instructions for Motion Input Analyses C-3
C-4 Illustrative Examples for Motion Inputs C-3
DAMAGE CAUSED BY PRESSURE C-7
C-5 Description of Charts for Damage to Surface Structures Caused by Pressure Input C-7
C-6 Description of Charts for Damage to Underground Structures Caused by Pressure Input C-8
C-7 Instructions for Pressure Input Analyses C-8
C-8 Illustrative Examples for Pressure Inputs C-8
C-9 System Consideration C-9
SECTION II DERIVATION OF EQUATIONS USED IN SECTION I C-14
C-10 Properties of Lognormal Variates C-14
C-11 Probability of Failure or Survival C-14

[redacted]

[redacted]

LIST OF ILLUSTRATIONS (Continued)

Figure	*Title*	*Page*
10-5	[redacted] Distance Thresholds for Second Degree Burns for Various Evasion Times [redacted]	10-16
10-6	[redacted] Safe Separation Distances, for an Observer on the Ground, from Bursts at 10 kft and 50 kft During the Day [redacted]	10-18
10-7	[redacted] Safe Separation Distance, for an Observer at 50 kft, from Bursts at 10 kft and 50 kft During the Day [redacted]	10-19
10-8	[redacted] Safe Separation Distance, for an Observer on the Ground, from Bursts at 10 kft and 50 kft, During the Night [redacted]	10-20
10-9	[redacted] Safe Separation Distance, for an Observer at 50 kft, from Bursts at 10 kft and 50 kft, During the Night [redacted]	10-21
10-10	[redacted] Safe Separation Distance, for an Observer on the Ground, from Low Yield Weapons Exploded at 1,000 ft Height of Burst [redacted]	10-22
10-11	[redacted] Personnel Effectiveness After Exposure to 1,400 rads [redacted]	10-26
10-12	[redacted] Personnel Effectiveness After Exposure to 2,800 rads [redacted]	10-27
10-13	[redacted] Personnel Effectiveness After Exposure to 7,000 rads [redacted]	10-28
10-14	[redacted] Personnel Effectiveness After Exposure to 13,000 rads [redacted]	10-29
10-15	[redacted] Personnel Effectiveness After Exposure to 22,000 rads [redacted]	10-30
10-16	[redacted] Comparison of Effects from Low Altitude Bursts [redacted]	10-34
11-1	[redacted] Idealized Loading Functions [redacted]	11-4
11-2	[redacted] Isodamage Curves for Fifty Percent Probability of Severe Damage to Multistory Blast-Resistant Reinforced Concrete Buildings [redacted]	11-16
11-3	[redacted] Isodamage Curves for Fifty Percent Probability of Severe Damage to Multistory Reinforced Concrete Buildings with Concrete Walls, Small Window Area, Three to Eight Stories [redacted]	11-17
11-4	[redacted] Isodamage Curves for Fifty Percent Probability of Severe Damage to Multistory Wall Bearing Buildings, Brick Apartment House Type, up to Three Stories [redacted]	11-18
11-5	[redacted] Isodamage Curves for Fifty Percent Probability of Severe Damage to Multistory Wall Bearing Building, Monumental Type, up to Four Stories [redacted]	11-19
11-6	[redacted] Isodamage Curves for Fifty Percent Probability of Severe Damage to Wood Frame Buildings, House Type, One or Two Stories [redacted]	11-20
11-7	[redacted] Isodamage Curves for Fifty Percent Probability of Severe Damage to Light Steel Frame Industrial Buildings, Single Story, Frangible Walls, up to 5 Ton Crane Capacity [redacted]	11-21
11-8	[redacted] Isodamage Curves for Fifty Percent Probability of Severe Damage to Heavy Steel Frame Industrial Buildings, Single Story, Frangible Walls, 25 to 50 Ton Crane Capacity [redacted]	11-22

[redacted]

[redacted]

LIST OF ILLUSTRATIONS (Continued)

Figure	*Title*	*Page*
11-9	[redacted] Isodamage Curves for Fifty Percent Probability of Severe Damage to Heavy Steel Frame Industrial Buildings, Single Story, Frangible Walls, 60 to 100 Ton Crane Capacity [redacted]	11-23
11-10	[redacted] Isodamage Curves for Fifty Percent Probability of Severe Damage to Multistory Steel Frame Office Type Buildings, 3- to 10-Stories, Frangible Walls, Earthquake Resistant Construction [redacted]	11-24
11-11	[redacted] Isodamage Curves for Fifty Percent Probability of Severe Damage to Multistory Steel Frame Office Type Buildings, 3- to 10-Stories, Frangible Walls, Non-Earthquake Resistant Construction [redacted]	11-25
11-12	[redacted] Isodamage Curves for Fifty Percent Probability of Severe Damage to Multistory Reinforced Concrete Frame Office Type Buildings, 3- to 10-Stories, Frangible Walls, Earthquake Resistant Construction [redacted]	11-26
11-13	[redacted] Isodamage Curves for Fifty Percent Probability of Severe Damage to Multistory Reinforced Concrete Frame Office Type Buildings, 3- to 10-Stories, Frangible Walls, Non-Earthquake Resistant Construction [redacted]	11-27
11-14	[redacted] Isodamage Curves for Fifty Percent Probability of Severe Damage to Four-Lane Highway Truss Bridges and Double Track Ballast Floor Railroad Truss Bridges, Span 200 ft to 400 ft [redacted]	11-28
11-15	[redacted] Isodamage Curves for Fifty Percent Probability of Severe Damage to Two-Lane Highway Truss Bridges, Spans 200 ft to 400 ft; Single Track Ballast Floors and Double Track Open Floor Railroad Truss Bridges, Spans 200 ft to 400 ft; and Single Track Open Floor Railroad Truss Bridges, Span 400 ft [redacted]	11-29
11-16	[redacted] Isodamage Curves for Fifty Percent Probability of Severe Damage to Single Track Open Floor Railroad Truss Bridges, Span 200 ft [redacted]	11-30
11-17	[redacted] Isodamage Curves for Fifty Percent Probability of Severe Damage to Four-Lane Through Highway Girder Bridges, Spans 75 ft [redacted]	11-31
11-18	[redacted] Isodamage Curves for Fifty Percent Probability of Severe Damage to Two-Lane Deck, Two-Lane Through, and Four-Lane Deck Highway Bridges, Spans 75 ft; Double Track Deck, Open or Ballast Floor Railroad Girder Bridges, Span 75 ft; Single or Double Track Through, Ballast Floor Railroad Girder Bridges, Spans 75 ft [redacted]	11-32
11-19	[redacted] Isodamage Curves for Fifty Percent Probability of Severe Damage to Single Track Deck, Open or Ballast Floor, and Single or Double Track Through, Open Floor Railroad Girder Bridges, Spans 75 ft [redacted]	11-33
11-20	[redacted] Isodamage Curves for Fifty Percent Probability of Severe Damage to Two-Lane Through and Four-Lane Deck or Through Highway Girder	

[redacted]

[redacted]

LIST OF ILLUSTRATIONS (Continued)

Figure	*Title*	*Page*
	Bridges, Spans 200 ft; Double Track Deck or Through, Ballast Floor Railroad Girder Bridges, Spans 200 ft [redacted]	11-34
11-21	[redacted] Isodamage Curves for Fifty Percent Probability of Severe Damage to Two-Lane Deck Highway Girder Bridges, Spans 200 ft; Single Track Deck or Through, Ballast Floor, and Double Track Deck or Through, Open Floor Railroad Girder Bridges, Spans 200 ft [redacted]	11-35
11-22	[redacted] Isodamage Curves for Fifty Percent Probability of Severe Damage to Single Track Deck or Through, Open Floor, Railroad Girder Bridges, Spans 200 ft [redacted]	11-36
11-23	[redacted] Isodamage Curves for Fifty Percent Probability of Severe Damage to Floating Bridges, U.S. Army Standard M-2 and M-4, Random Orientation [redacted]	11-37
11-24	[redacted] Damage-Distance Reduction for Surface Structures from 1 kt Bursts in Soil [redacted]	11-39
11-25	[redacted] Depth of Cover Classification for Arches [redacted]	11-42
11-26	[redacted] Buried Arches, Average Depth of Earth Cover [redacted]	11-43
11-27	[redacted] Average Depth of Earth Cover for Buried Domes [redacted]	11-44
11-28	[redacted] Configuration of Mounded Arches [redacted]	11-45
11-29	[redacted] Correction for Attenuation with Depth [redacted]	11-71
11-30	[redacted] Damage Pressure Level [redacted]	11-72
11-31	[redacted] Correction for Arching [redacted]	11-73
11-32	[redacted] Definition of Effective Pulse Duration [redacted]	11-74
11-33	[redacted] Approximate Values of J and r_g for Common Shapes [redacted]	11-77
11-34a	[redacted] Conditions for Moderate Damage by Impulsive Loading [redacted]	11-78
11-34b	[redacted] Conditions for Heavy Damage by Impulsive Loading [redacted]	11-79
11-35	[redacted] Resistance of Deeply Buried Horizontal Reinforced Concrete Arches [redacted]	11-80
11-35a	[redacted] Arch Radius Versus Rise-Span Ratio [redacted]	11-81
11-35b	[redacted] Correction Factor for Material Properties for Deeply Buried Horizontal Reinforced Concrete Arches [redacted]	11-82
11-36	[redacted] Resistance of Deeply Buried Horizontal Steel Arches [redacted]	11-83
11-37	[redacted] Resistance of Deeply Buried Reinforced Concrete Domes [redacted]	11-84
11-37a	[redacted] Dome Radius Versus Rise-Span Ratio [redacted]	11-85
11-37b	[redacted] Correction Factor for Material Properties for Deeply Buried Reinforced Concrete Domes [redacted]	11-86
11-38	[redacted] Resistance of Horizontal One-Way Slabs [redacted]	11-87
11-39	[redacted] Resistance of Horizontal Square Two-Way Slabs – Restrained Edges [redacted]	11-88

[redacted]

[redacted]

LIST OF ILLUSTRATIONS (Continued)

Figure	*Title*	*Page*
11–40	[redacted] Resistance of Horizontal Square Two-Way Slabs – Two Adjacent Edges Supported [redacted]	11–89
11–41	[redacted] Aspect Ratio Correction Factor for Strength of Two-Way Slabs [redacted]	11–90
11–42	[redacted] Resistance of Horizontal Square Flat Slabs [redacted]	11–91
11–42a	[redacted] Aspect Ratio Correction Factor for Strength of Rectangular Flat Slabs [redacted]	11–92
11–43	[redacted] Radial Dead Load Soil Pressure on Vertical Cylinder [redacted]	11–93
11–44	[redacted] Interaction Diagram for Reinforced Concrete Beam – Columns [redacted]	11–94
11–45	[redacted] Basic Chart for Vulnerability of Tunnels in Rock [redacted]	11–96
11–46	[redacted] Vulnerability Criteria – Class A Equipment [redacted]	11–101
11–47	[redacted] Vulnerability Criteria for Personnel [redacted]	11–102
11–48	[redacted] Vulnerability Plot for Seismic Velocity (c_p) of 1500 fps – Vertical Motion [redacted]	11–105
11–49	[redacted] Vulnerability Plot for Seismic Velocity (c_p) of 5000 fps – Vertical Motion [redacted]	11–106
11–50	[redacted] Vulnerability Plot for Seismic Velocity (c_p) of 15,000 fps – Vertical Motion [redacted]	11–107
11–51	[redacted] Shock Response Spectra and Vulnerability Calculation [redacted]	11–108
11–52	[redacted] Blast Resistance of Unprotected Floating and Conical-roof Tanks for 20 kt [redacted]	11–114
11–53	[redacted] Blast Resistance of Protected Floating and Conical-roof Tanks for 20 kt [redacted]	11–115
11–54	[redacted] Blast Resistance of Unprotected Floating and Conical-roof Tanks for 500 kt [redacted]	11–116
11–55	[redacted] Blast Resistance of Protected Floating and Conical-roof Tanks for 500 kt [redacted]	11–117
11–5~~5~~7	[redacted] Command Posts and Personnel Shelters (reference Table 11–13) – Damage by 1 kt as Function of Height of Burst and Ground Distance [redacted]	11–12~~5~~6
11–5~~6~~	[redacted] Machine-gun Emplacements – Damage by 1 kt as a Function of Height of Burst and Ground Distance (reference Table 11–13) [redacted]	11–12~~4~~
11–58	[redacted] Damage Levels to Foxholes and Trenches in Selected Soils Versus Overpressure Impulse [redacted]	11–126
11–59	[redacted] Ignition Thresholds for Newspaper [redacted]	11–133
11–60	[redacted] Graphical Summary of San Jose Study [redacted]	11–135
11–61	[redacted] Graphical Summary of New Orleans Study [redacted]	11–137
11–62	[redacted] Graphical Analysis of the Thermal and Blast Effects of Two Nuclear Bursts [redacted]	11–142

[redacted]

[redacted]

LIST OF ILLUSTRATIONS (Continued)

Figure	*Title*	*Page*
14–2	[redacted] Target Response Modes [redacted]	14–5
14–3	[redacted] Illustration of the Damage vs Distance Curve [redacted]	14–7
14–4	[redacted] Damage to 1/4 Ton and 2-1/2 Ton Trucks, Side–On Orientation, as a Function of Ground Distance from a 1 kt Surface Burst [redacted]	14–8
14–5	[redacted] Damage to U.S. 57-mm and U.K. 25–Pounder, Side–On Orientation, as a Function of Ground Distance from a 1 kt Surface Burst [redacted]	14–9
14–6	[redacted] Damage to World War II and M38 1/4–Ton Trucks as a Function of Distance from a 1 kt Surface Burst [redacted]	14–10
14–7	[redacted] Illustration of the Effect of Target Orientation: Damage to World War II 1/4–Ton Trucks Oriented Side–On and End–On as a Function of Distance from a 1 kt Surface Burst [redacted]	14–11
14–8	[redacted] The Effect of Shielding [redacted]	14–12
14–9	[redacted] Effect of Weapon Yield on World War II 1/4–Ton Trucks Exposed Side–On in Shielded and Unshielded Conditions to Surface Explosions [redacted]	14–13
14–10	[redacted] Effect of Surface Condition on Damage Category Illustrated by Damage to 1/4–Ton Trucks Oriented Side–On to the Blast Wave from a 1 kt Surface Burst on Two Surfaces [redacted]	14–15
14–11	[redacted] Effect of Vehicle Status on the Distance for a Specified Damage Level from a 1 kt Surface Burst to U.S. 1/4–Ton Trucks (Brakes On, In Gear) and U.K. 1/4–Ton Trucks (Brakes Off, Out–of–Gear) Exposed in an End–On Orientation [redacted]	14–16
14–12	[redacted] Peak Dynamic Pressure as a Function of Peak Overpressure [redacted]	14–26
14–13	[redacted] Damage to *Wheeled Vehicles* as a Function of Height of Burst (HOB) and Ground Distance (GD) for a 1 kt Explosion Over Nonideal and Near–Ideal Surfaces. The curves show HOB and GD at which there is a 50 percent probability that the item of equipment will experience at least the level of damage shown. NOTE: HOB scales as $W^{1/3}$; GD scales as $W^{0.4}$ [redacted]	14–37
14–14	[redacted] Damage to *Artillery* as a Function of Height of Burst (HOB) and Ground Distance (GD) for a 1 kt Explosion Over Nonideal and Near–Ideal Surfaces. The curves show HOB and GD at which there is a 50 percent probability that the item of equipment will experience at least the level of damage shown. NOTE: HOB scales as $W^{1/3}$; GD scales as $W^{0.4}$ [redacted]	14–38
14–15	[redacted] Damage to *Tracked Vehicles (Except Tanks) and Engineer Heavy Equipment* as a Function of Height of Burst (HOB) and Ground Distance	

[redacted]

[redacted]

LIST OF ILLUSTRATIONS (Continued)

Figure	*Title*	*Page*
	(GD) for a 1 kt Explosion Over Nonideal and Near-Ideal Surfaces. The curves show HOB and GD at which there is a 50 percent probability that the item of equipment will experience at least the level of damage shown. NOTE: HOB scales as $W^{1/3}$; GD scales as $W^{0.4}$ [redacted]	14–39
14–16	[redacted] Damage to *Tanks (Light and Heavy)* as a Function of Height of Burst (HOB) and Ground Distance (GD) for a 1 kt Explosion Over Nonideal and Near-Ideal Surfaces. The curves show HOB and GD at which there is a 50 percent probability that the item of equipment will experience at least the level of damage shown. NOTE: HOB scales as $W^{1/3}$; GD scales as $W^{0.4}$ [redacted]	14–40
14–17	[redacted] Damage to *Small Arms* as a Function of Height of Burst (HOB) and Ground Distance (GD) for a 1 kt Explosion Over Nonideal and Near-Ideal Surfaces. The curves show HOB and GD at which there is a 50 percent probability that the item of equipment will experience at least the level of damage shown. NOTE: HOB scales as $W^{1/3}$; GD scales as $W^{0.4}$ [redacted]	14–41
14–18	[redacted] Damage to *Generators* as a Function of Height of Burst (HOB) and Ground Distance (GD) for a 1 kt Explosion Over Nonideal and Near-Ideal Surfaces. The curves show HOB and GD at which there is a 50 percent probability that the item of equipment will experience at least the level of damage shown. NOTE: HOB scales as $W^{1/3}$; GD scales as $W^{0.4}$ [redacted]	14–42
14–19	[redacted] Damage to *Locomotives* as a Function of Height of Burst (HOB) and Ground Distance (GD) for a 1 kt Explosion Over both Nonideal and Near-Ideal Surfaces. The curves show HOB and GD at which there is a 50 percent probability that the item of equipment will experience at least the level of damage shown. NOTE: HOB scales as $W^{1/3}$; GD scales as $W^{0.4}$ [redacted]	14–43
14–20	[redacted] Damage to *Box Cars* as a Function of Height of Burst (HOB) and Ground Distance (GD) for a 1 kt Explosion Over both Nonideal and Near-Ideal Surfaces. The curves show HOB and GD at which there is a 50 percent probability that the item of equipment will experience at least the level of damage shown. NOTE: HOB scales as $W^{1/3}$; GD scales as $W^{0.4}$ [redacted]	14–44
14–21	[redacted] Damage to *Supply Dumps* as a Function of Height of Burst (HOB) and Ground Distance (GD) for a 1 kt Explosion Over both Nonideal and Near-Ideal Surfaces. The curves show HOB and GD at which there is the indicated probability that the dump will experience at least the level of damage shown. NOTE: HOB scales as $W^{1/3}$; GD scales as $W^{0.4}$ [redacted]	14–45
14–22	[redacted] Damage to *Telephone Poles* as a Function of Height of Burst (HOB) and Ground Distance (GD) for a 1 kt Explosion Over both Nonideal and	

[redacted]

[redacted]

LIST OF ILLUSTRATIONS (Continued)

Figure	*Title*	*Page*
	Near-Ideal Surfaces. The curves show HOB and GD at which there is a 50 percent probability that the item of equipment will experience at least the level of damage shown. NOTE: HOB scales as $W^{1/3}$; GD scales as $W^{1/3}$ [redacted]	14–46
14–23	[redacted] Damage to *Water Storage Equipment* as a Function of Height of Burst (HOB) and Ground Distance (GD) for a 1 kt Explosion Over Nonideal and Near-Ideal Surfaces. The curves show HOB and GD at which there is a 50 percent probability that the item of equipment will experience at least the level of damage shown. NOTE: HOB scales as $W^{1/3}$; GD scales as $W^{1/3}$ [redacted]	14–47
14–24	[redacted] Damage to *Shielded Wheeled Vehicles* as a Function of Height of Burst (HOB) and Ground Distance (GD) for a 1 kt Explosion Over both Nonideal and Near-Ideal Surfaces. The curves show HOB and GD at which there is a 50 percent probability that the item of equipment will experience at least the level of damage shown. NOTE: HOB scales as $W^{1/3}$; GD scales as $W^{1/3}$ [redacted]	14–48
14–25	[redacted] Damage to *Shielded Engineer Heavy Equipment* as a Function of Height of Burst (HOB) and Ground Distance (GD) for a 1 kt Explosion Over both Nonideal and Near-Ideal Surfaces. The curves show HOB and GD at which there is a 50 percent probability that the item of equipment will experience at least the level of damage shown. NOTE: HOB scales as $W^{1/3}$; GD scales as $W^{1/3}$ [redacted]	14–49
14–26	[redacted] Damage to *Signal, Electronic Fire Control Equipment, Antennas and Rigid Radomes* as a Function of Height of Burst (HOB) and Ground Distance (GD) for a 1 kt Explosion Over Nonideal and Near-Ideal Surfaces. The curves show HOB and GD at which there is the indicated probability that the item of equipment will experience at least the level of damage shown. NOTE: HOB scales as $W^{1/3}$; GD scales as $W^{0.4}$ except for Radomes. For Radomes use $W^{1/3}$ [redacted]	14–50
14–27	[redacted] Damage to *Wire Entanglements* as a Function of Height of Burst (HOB) and Ground Distance (GD) for a 1 kt Explosion Over Nonideal and Near-Ideal Surfaces. The curves show HOB and GD at which there is a 50 percent probability that the item of equipment will experience at least the level of damage shown. NOTE: HOB scales as $W^{1/3}$ for yields < 1 kt, $W^{0.4}$ for yields > 1 kt [redacted]	14–51
15–1	[redacted] Light Damage to Various Broadleaf Forest Types [redacted]	15–7
15–2	[redacted] Moderate Damage to a Type I Forest [redacted]	15–8
15–3	[redacted] Severe Damage to a Type I Forest [redacted]	15–9
15–4	[redacted] Total Damage to a Type I Forest [redacted]	15–10
15–5	[redacted] Moderate Damage to a Type II Forest [redacted]	15–11

[redacted]

[redacted]

LIST OF ILLUSTRATIONS (Continued)

Figure	Title	Page
15-6	[redacted] Severe Damage to a Type II Forest [redacted]	15-12
15-7	Total Damage to a Type II Forest [redacted]	15-13
15-8	Moderate Damage to a Type III Forest [redacted]	15-14
15-9	Severe Damage to a Type III Forest [redacted]	15-15
15-10	Total Damage to a Type III Forest [redacted]	15-16
15-11	Moderate Damage to a Type IVa-1(f) Forest [redacted]	15-17
15-12	Severe Damage to a Type IVa-1(f) Forest [redacted]	15-18
15-13	Total Damage to a Type IVa-1(f) Forest [redacted]	15-19
15-14	Moderate Damage to a Type IVa-1(d) Forest [redacted]	15-20
15-15	Severe Damage to a Type IVa-1(d) Forest [redacted]	15-21
15-16	Total Damage to a Type IVa-1(d) Forest [redacted]	15-22
15-17	Moderate Damage to a Type IVa-2(f) Forest [redacted]	15-23
15-18	Severe Damage to a Type IVa-2(f) Forest [redacted]	15-24
15-19	Total Damage to a Type IVa-2(f) Forest [redacted]	15-25
15-20	Moderate Damage to a Type IVa-2(d) Forest [redacted]	15-26
15-21	Severe Damage to a Type IVa-2(d) Forest [redacted]	15-27
15-22	Total Damage to a Type IVa-2(d) Forest [redacted]	15-28
15-23	Moderate Damage to a Type IVb(f) Forest [redacted]	15-29
15-24	Severe Damage to a Type IVb(f) Forest [redacted]	15-30
15-25	Total Damage to a Type IVb(f) Forest [redacted]	15-31
15-26	Moderate Damage to a Type IVb(d) Forest [redacted]	15-32
15-27	Severe Damage to a Type IVb(d) Forest [redacted]	15-33
15-28	Total Damage to a Type IVb(d) Forest [redacted]	15-34
15-29	Moderate Damage to a Type IVc(f) Forest [redacted]	15-35
15-30	Total Damage to a Type IVc(f) Forest [redacted]	15-36
15-31	Moderate Damage to a Type IVc(d) Forest [redacted]	15-37
15-32	Total Damage to a Type IVc(d) Forest [redacted]	15-38
15-33	Moderate Damage to a Type IVd Forest [redacted]	15-39
15-34	Total Damage to a Type IVd Forest [redacted]	15-40
15-35	[redacted] Stem-ft per Acre Comparison Between a Rain Forest and a Coniferous Forest [redacted]	15-43
15-36	[redacted] Average Diameter of Stems Down, Comparison Between a Rain Forest and a Coniferous Forest, 1 kt [redacted]	15-44
15-37	[redacted] Debris Characteristics Preventing Radial Movement of Vehicles [redacted]	15-45
15-38	[redacted] Debris Characteristics Preventing Circumferential Movement of Vehicles [redacted]	15-46
15-39	[redacted] Minimum Radiant Exposures of Wildland Kindling Fuels by a 1 Kiloton Explosion [redacted]	15-55

[redacted]

[redacted]

LIST OF ILLUSTRATIONS (Continued)

Figure	*Title*	*Page*
15–40	[redacted] Probability of Exposure of the Forest Floor ("Standard Northern European Forest") as a Function of Elevation Angle: Examples of a Point Source and a Spherical Source Subtending an Angle of 10 Degrees [redacted]	15–57
15–41	[redacted] Probability of Exposure of Forest Floor for Different Levels of Tree Density [redacted]	15–59
16–1	[redacted] Missile Configurations, SERGEANT, LANCE, and HAWK [redacted]	16–2
16–2	[redacted] SERGEANT System, Semitrailer Transporter with Missile Section Containers [redacted]	16–4
16–3	[redacted] SERGEANT System, Launching Station with Missile in Firing Position [redacted]	16–5
16–4	[redacted] SERGEANT System, Launching Station Firing Set [redacted]	16–6
16–5	[redacted] SERGEANT System, Organizational Maintenance Test Station (OMTS) [redacted]	16–8
16–6	[redacted] SERGEANT, Major Item Blast Vulnerability [redacted]	16–11
16–7	[redacted] LANCE System, Primary Units of the Missile System [redacted]	16–13
16–8	[redacted] LANCE System, Prefire Tester and Fire Pack [redacted]	16–14
16–9	[redacted] LANCE, Major Item Blast Vulnerability [redacted]	16–18
16–10	[redacted] HAWK System, Basic Assault Firing Unit [redacted]	16–20
16–11	[redacted] HAWK System, Auxiliary Components [redacted]	16–21
16–12	[redacted] HAWK, Major Item Blast Vulnerability [redacted]	16–25
16–13	[redacted] HONEST JOHN, Major Components of Rocket [redacted]	16–26
16–14	[redacted] HONEST JOHN, Truck-Mounted Rocket Launcher in Traveling Position [redacted]	16–27
16–15	[redacted] HONEST JOHN Rocket Launcher in Firing Position [redacted]	16–28
16–16	[redacted] HONEST JOHN, Auxiliary Equipment [redacted]	16–29
16–17	[redacted] HONEST JOHN, Major Item Blast Vulnerability [redacted]	16–33
16–18	[redacted] ABM and RV Configuration Comparison [redacted]	16–35
16–19	[redacted] ABM and RV Operating Envelope Comparison [redacted]	16–35
16–20	[redacted] Response Regimes for Interceptor Missile [redacted]	16–36
16–21	[redacted] Nuclear Encounter and Event Sequence for RV and ABM [redacted]	16–37
16–22	[redacted] HARTS Configuration [redacted]	16–40
16–23	[redacted] Blast Intercept Conditions Nomenclature [redacted]	16–41
16–24	[redacted] Scaled Blast Wave Radius for Constant Hardness Level for Configuration A, 5,500 nm Range [redacted]	16–44
16–25	[redacted] Scaled Time of Blast Intercept for Constant Hardness Level for Configuration A, 5,500 nm Range [redacted]	16–45

[redacted]

[redacted]

LIST OF ILLUSTRATIONS (Continued)

Figure	Title	Page
16–26	[redacted] Variation of Hardness Level with Altitude and Slant Range for [redacted] Configuration A [redacted]	16–46
16–27	[redacted] Normal Reentry Trajectory; Initial Altitude = 400,000 ft, Initial Velocity (V_i) = 23,900 ft/sec, Initial Flight-Path Angle = 20°, Ballistic Coefficient $\beta = W/C_dA$ lb/ft^2 [redacted]	16–48
16–28	[redacted] Normal Reentry Trajectory; Initial Altitude = 400,000 ft, Initial Velocity (V_i) = 24,000 ft/sec, Initial Flight-Path Angle = 30°, Ballistic Coefficient $\beta = W/C_dA$ lb/ft^2 [redacted]	16–49
16–29	[redacted] Normal Reentry Trajectory; Initial Altitude = 400,000 ft, Initial Velocity (V_i) = 24,000 ft/sec, Initial Flight-Path Angle = 30°, Ballistic Coefficient $\beta = W/C_dA$ lb/ft^2 [redacted]	16–50
16–30	[redacted] Scaled Intercept Load Duration Time, 500 g Hardness, Configuration A [redacted]	16–54
16–31	[redacted] Scaled Fireball Traversal Time, 500 g Hardness, Configuration A [redacted]	16–55
16–32	[redacted] Scaled Total Blast Traversal Time, 500 g Hardness, Configuration A [redacted]	16–56
16–33	[redacted] Flow Pattern Around an Axisymmetric Blunt-Nosed Body [redacted]	16–57
16–34	[redacted] Steady State Flow Field Surface Pressures, Sphere-Cone-Flare Body [redacted]	16–59
16–35	[redacted] Steady State Flow Field Surface Pressures, Cone Sphere Body [redacted]	16–60
16–36	[redacted] Maximum Overpressure and Overpressure Duration for Typical Shock-Shock Interactions [redacted]	16–61
16–37	[redacted] Determination of Locus of Escape [redacted]	16–63
16–38	[redacted] Qualitative Iso-g Contours [redacted]	16–64
16–39	[redacted] In-Flight Intercept [redacted]	16–65
16–40	[redacted]	16–67
16–41	[redacted]	16–68
16–42	[redacted]	16–69
16–43	[redacted]	16–71

[redacted]

[redacted]

[redacted]

LIST OF TABLES (Continued)

Table	Title	Page
9-30	[redacted] Comparison of Guided Wave and Radiating Simulators [redacted]	9-181
10-1	[redacted] Estimated Casualty Production in Buildings for Three Degrees of Structural Damage [redacted]	10-6
10-2	[redacted] Response to Single Whole-Body Exposures [redacted]	10-24
11-1	[redacted] Damage to Types of Structures Primarily Affected by Blast Wave Overpressure During the Diffraction Phase [redacted]	11-5
11-2	[redacted] Damage to Types of Structures Primarily Affected by Dynamic Pressure During the Drag Phase [redacted]	11-6
11-3	[redacted] Building Parameter Values [redacted]	11-10
11-4	[redacted] Reference List of Isodamage Curves for Various Types of Bridges [redacted]	11-11
11-5	[redacted] Factors for Obtaining Distances Corresponding to 50 Percent Probability of Moderate Damage to the Indicated Structure Type [redacted]	11-13
11-6	[redacted] Ratio of Horizontal to Vertical Soil Pressures, K_o [redacted]	11-56
11-7	[redacted] Equivalent Friction Angles for Noncohesive Cohesive Soils [redacted]	11-57
11-8	[redacted] Typical Tunnel Design Concepts [redacted]	11-58
11-9	[redacted] Limits of Vulnerability in Terms of Overpressure for Surface Silos—1 Mt [redacted]	11-59
11-10	[redacted] Definition of γ and δ for Figures 11-32 and 11-34 [redacted]	11-75
11-11	[redacted] Estimates of Frequency and Vulnerability of Typical Items of Equipment [redacted]	11-98
11-12	[redacted] Light Damage to POL Tanks [redacted]	11-112
11-13	[redacted] Damage Criteria for Field Fortifications [redacted]	11-119
11-14	[redacted] Unified Soil Classification [redacted]	11-120
12-1	[redacted]	12-3
NAVY (b)(1) 12-2	[redacted]	12-8
12-3	[redacted]	12-10
12-4	[redacted]	12-18
13-1	[redacted] Selected Data Based on U.S. Standard Atmosphere, 1962 English Units [redacted]	13-15
13-2	[redacted] Overpressure Criteria [redacted]	13-51
13-3	[redacted] Average Properties of Selected Engineering Materials [redacted]	13-63
13-4	[redacted] Average Values of Absorptivities, α [redacted]	13-64
14-1	[redacted] Definitions of Damage Categories [redacted]	14-18
14-2	[redacted] Wheeled Vehicle Subsystems [redacted]	14-18

[redacted]

[redacted]

LIST OF TABLES (Continued)

Table	Title	Page
14–3	[redacted] Typical Subsystem Damage for Various Damage Categories [redacted]	14–19
14–4	[redacted] List of Equipment and Corresponding Prediction Tables [redacted]	14–22
14–5	[redacted] Equipment Sensitive to Total Impulse [redacted]	14–23
14–6	[redacted] Equipment Sensitive to Overpressure [redacted]	14–24
14–7	[redacted] Equipment Sensitive to Dynamic Pressure [redacted]	14–25
14–8	[redacted] Untested Equipment [redacted]	14–53
14–9	[redacted] Ambient Radiation Levels for "Sure Safe" and "Sure Kill" in Selected Ground Systems [redacted]	14–66
14–10	[redacted] Ambient Radiation Levels for "Sure Safe" and "Sure Kill" for General Aircraft Subsystems [redacted]	14–68
14–11	[redacted] Ambient Radiation Levels for "Sure Safe" and "Sure Kill" for Missile Systems [redacted]	14–71
15–1	[redacted] Average Height of Trees, Diameter, Tree Density, and Length of Tree Stem [redacted]	15–2
15–2	[redacted] Index of Isodamage Curves Showing Forest Stand Type and Applicable Figure Number for Indicated Degree of Damage [redacted]	15–3
15–3	[redacted] Effects of a 1 kt Weapon Burst at a Height of 270 Feet Over a Rain Forest [redacted]	15–41
15–4	[redacted] Effects of a 1 kt Surface Burst on a Coniferous Forest [redacted]	15–42
15–5	[redacted] Comparison of Radial and Circumferential Movement Rates for Troops in a Rain Forest Blowdown Area, Scaled to a 1 kt Nuclear Explosion [redacted]	15–48
15–6	[redacted] Comparison of Circumferential Movement Rates for Troops in a Coniferous Forest Blowdown Area, Scaled to a 1 kt Nuclear Explosion [redacted]	15–48
15–7	[redacted] Influence of Forest Damage on the Movement of Troops and Vehicles [redacted]	15–49
15–8	[redacted] Classes of Thin Wildland Kindling Fuels (Arranged in Order of Decreasing Flammability) [redacted]	15–52
15–9	[redacted] "Standard Northern European Forest" Data [redacted]	15–57
15–10	[redacted] Condition of Wildland Fuels During Fire Season [redacted]	15–60
15–11	[redacted] Criteria of "No-Spread" of Fires [redacted]	15–61
15–12	[redacted] Fire-Out Criteria [redacted]	15–62
15–13	[redacted] Burning Durations by Fuel Type [redacted]	15–63
16–1	[redacted] SERGEANT, Characteristics and Damage Levels for System Components [redacted]	16–9
16–2	[redacted] Blast Vulnerability Summary, SERGEANT Missile System [redacted]	16–10
16–3	[redacted] LANCE, Characteristics and Damage Levels for System Components [redacted]	16–15
16–4	[redacted] Blast Vulnerability Summary, LANCE Missile System [redacted]	16–19

[redacted]

[redacted]

LIST OF TABLES (Continued)

Table	Title	Page
16-5	[redacted] HAWK, Characteristics and Damage Levels for System Components [redacted]	16-22
16-6	[redacted] Blast Vulnerability Summary, HAWK Missile System [redacted]	16-24
16-7	[redacted] Missile System Components – HONEST JOHN [redacted]	16-30
16-8	[redacted] Summary – HONEST JOHN [redacted]	16-31
16-9	[redacted] Range of Basic Parameters for HARTS II [redacted]	16-39
17-1	[redacted] Satellite Communications Link Description, System A [redacted]	17-21
17-2	[redacted] Satellite Communications Link Description, System B [redacted]	17-21
17-3	[redacted] Estimated Outage Times for Fireball Intersection of the Propagation Path [redacted]	17-22
17-4	[redacted] Troposcatter Communication Link Description [redacted]	17-27
17-5	[redacted] Approximate Extent and Duration of Effects on Troposcatter Communications, Assuming Proper Burst Placement [redacted]	17-28
17-6	[redacted] Ionoscatter Communications Link Description [redacted]	17-30
17-7	[redacted] Approximate Outage Times 1000-, 1500-, and 2000-km Ionoscatter Links, Assuming Proper Burst Placement [redacted]	17-31
A-1	[redacted] Shock Wave Equations for an Ideal Gas [redacted]	A-4
A-2	[redacted] English and Metric Systems of Units [redacted]	A-5
A-3	[redacted] Equations for Strong Shock Waves [redacted]	A-7
C-1	[redacted] Standard Deviations for Use in Probability Analyses [redacted]	C-4
C-2	[redacted] Median Vulnerability to Overpressures Corresponding to Severe Damage of Diffraction Sensitive Structures [redacted]	C-10
C-3	[redacted] Median Vulnerability to Dynamic Pressures Corresponding to Severe Damage of Drag Sensitive Structures [redacted]	C-11
C-4	[redacted] Median Vulnerability to Overpressures Corresponding to Moderate Damage of Diffraction Sensitive Structures [redacted]	C-12
C-5	[redacted] Median Vulnerability to Dynamic Pressures Corresponding to Moderate Damage of Drag Sensitive Structures [redacted]	C-13

[redacted]

[redacted]

LIST OF PROBLEMS (Continued)

Problem	*Title*	*Page*
13–3	Calculation of Intercept-Time Envelopes that Determine Sure-Safe and Sure-Kill Regions with Respect to Material Velocity on Airplanes in Flight	13–29
13–4	Calculation of Intercept-Time Envelopes Determining Sure-Safe and Sure-Kill Regions with Respect to Gust Effects of the Material Velocity Behind the Blast Wave on Helicopters in Flight	13–39
13–5	Calculation of the Boundaries in Space that Define the Sure-Safe and Sure-Kill Regions with Respect to the Effects of Overpressure Behind the Blast Wave on Aircraft In-Flight or Parked	13–51
13–6	Calculation of Boundaries in Space (Envelopes) that Define the Sure-Safe and Sure-Kill Regions with Respect to Thermal Radiation on Aircraft In-Flight or Parked	13–60
13–7	Calculation of Burst-Time Envelopes for Gust or Overpressure Effects from Intercept-Time Envelopes	13–68
14–1	Calculation of Damage to Wheeled Vehicles	14–27
14–2	Calculation of Damage to Shielded Wheeled Vehicles	14–29
14–3	Calculation of Damage to Wire Entanglement	14–31
14–4	Calculation of Damage to Artillery	14–33
14–5	Calculation of the Advantage in Shielding Engineer Heavy Equipment	14–35
15–1	Calculation of Air Blast Damage to Forest Stands	15–5
15–2	Calculation of the Distance at Which Movement Will Be Impaired	15–50
15–3	Estimation of Movement Difficulty	15–51
15–4	Calculation of the Requirements for Wildland Kindling Fuel Ignition	15–54
16–1	Calculation of Hardness Level	16–43
16–2	Calculation of Load Characteristics, Fireball Traversal Time and Total Traversal Time	16–53
B–1	Use of Fractional Power Curves and Dimension Scaling Nomogram	B–5

[redacted]

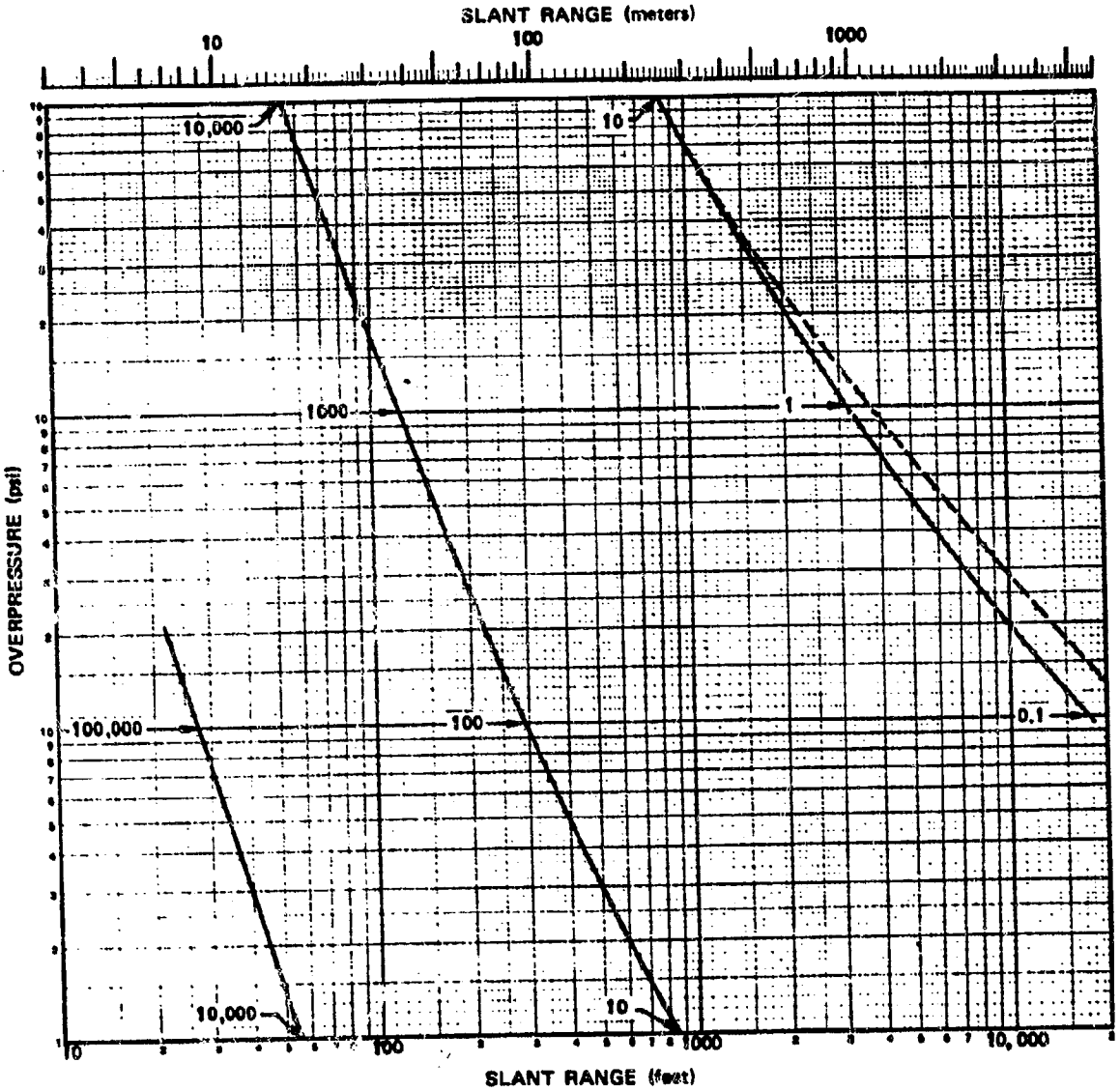

Figure 2-2. [redacted] Peak Overpressure from a 1 kt Free Air Burst in a Standard Sea Level Atmosphere [redacted]

[redacted]

[redacted]

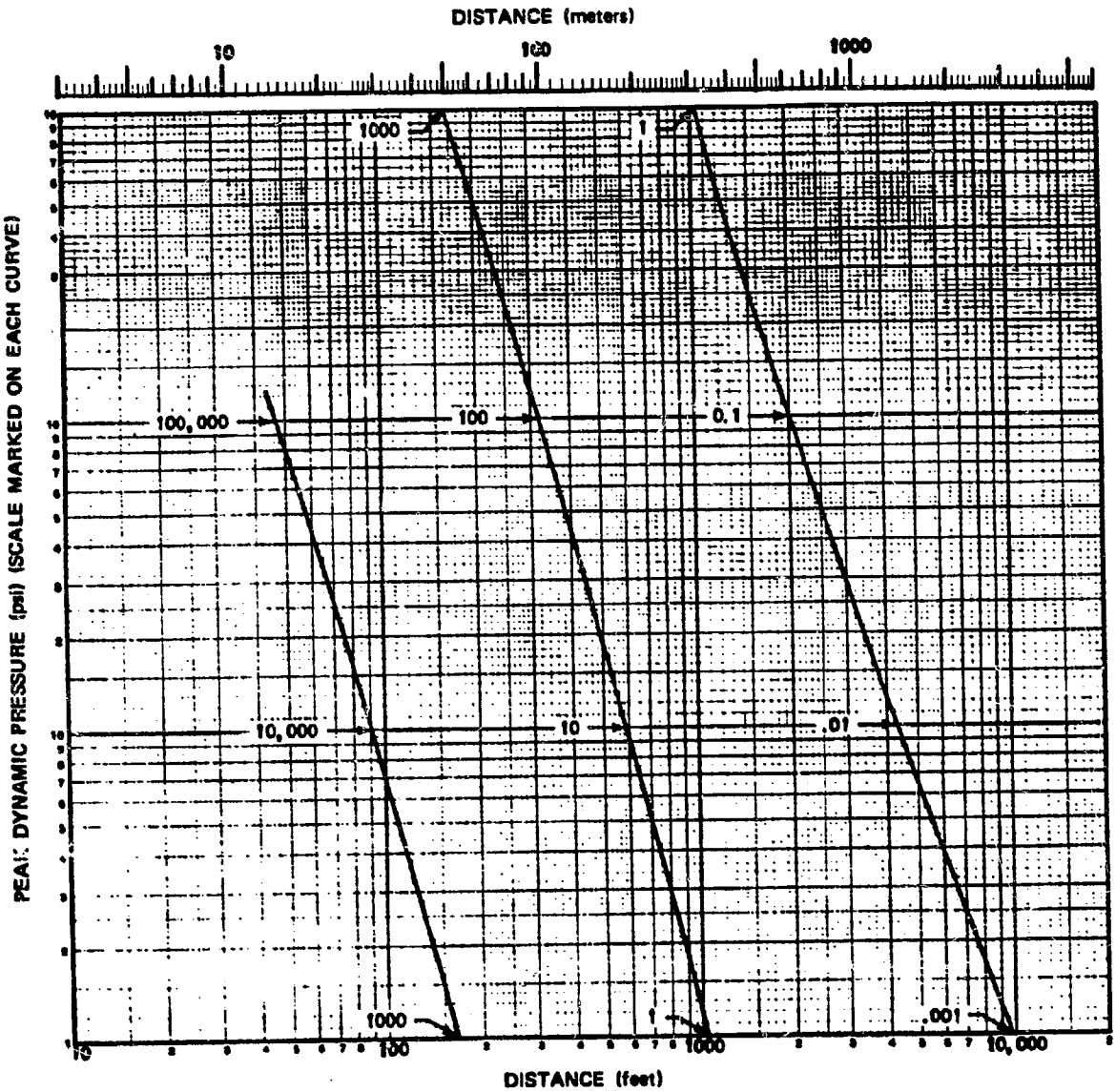

Figure 2-4. [redacted] Peak Dynamic Pressure from a 1 kt Free Air Burst in a Standard Sea Level Atmosphere [redacted]

[redacted]

[redacted]

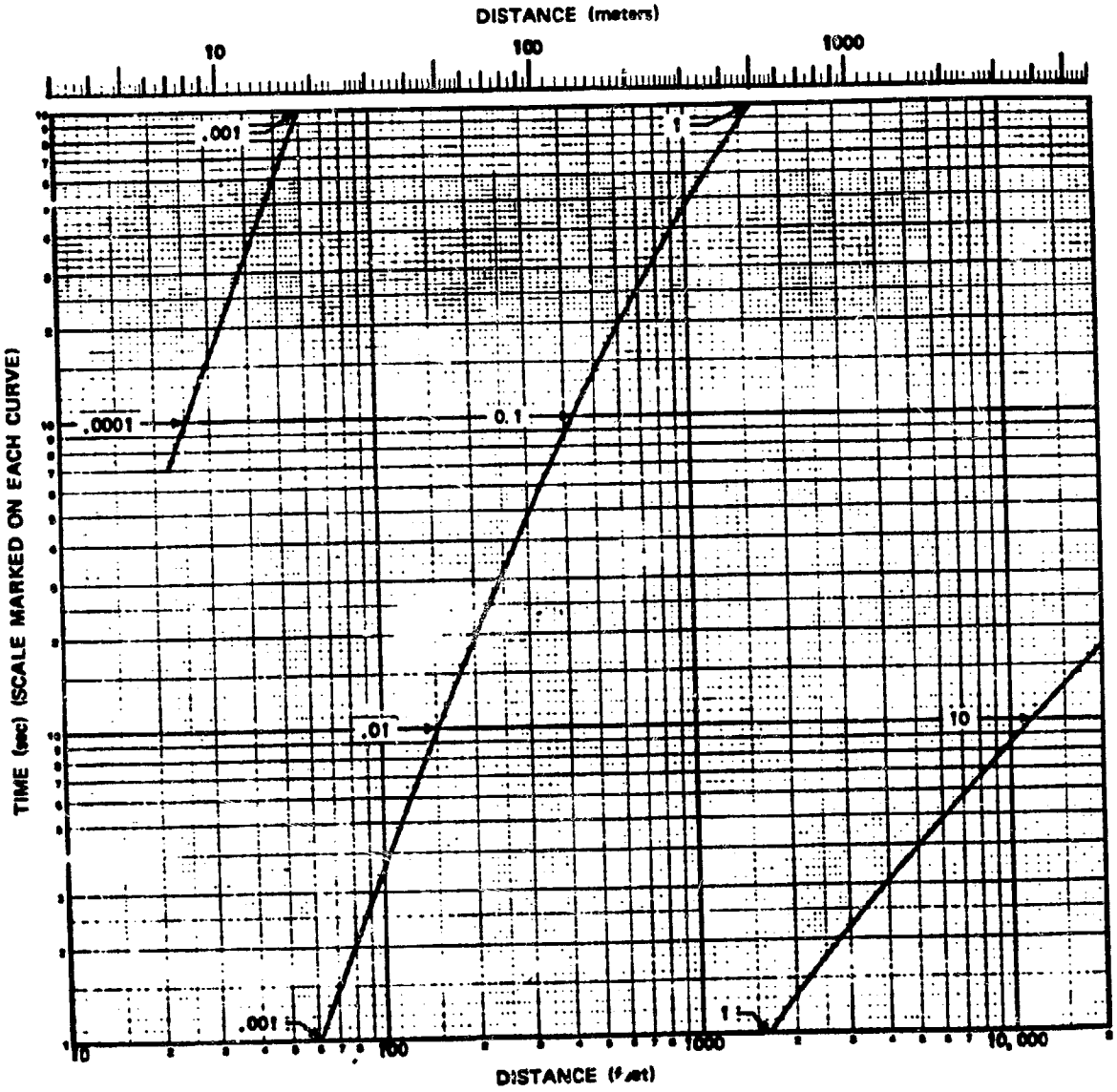

Figure 2-5. [redacted] Time of Arrival of the Shock Front from a 1 kt Free Air Burst in a Standard Sea Level Atmosphere [redacted]

[redacted]

[redacted]

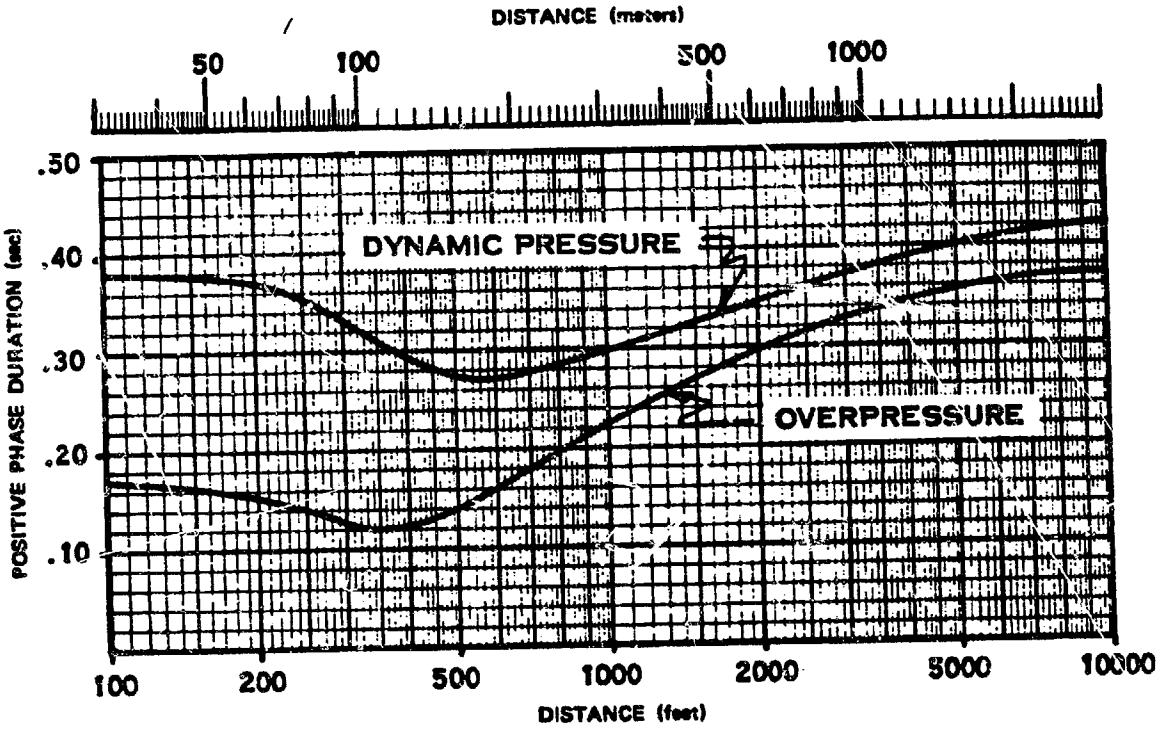

Figure 2-6. [redacted] Duration of Positive Overpressure and Dynamic Pressure Phases for a 1 kt Free Air Burst in a Standard Sea Level Atmosphere [redacted]

[redacted]

[redacted]

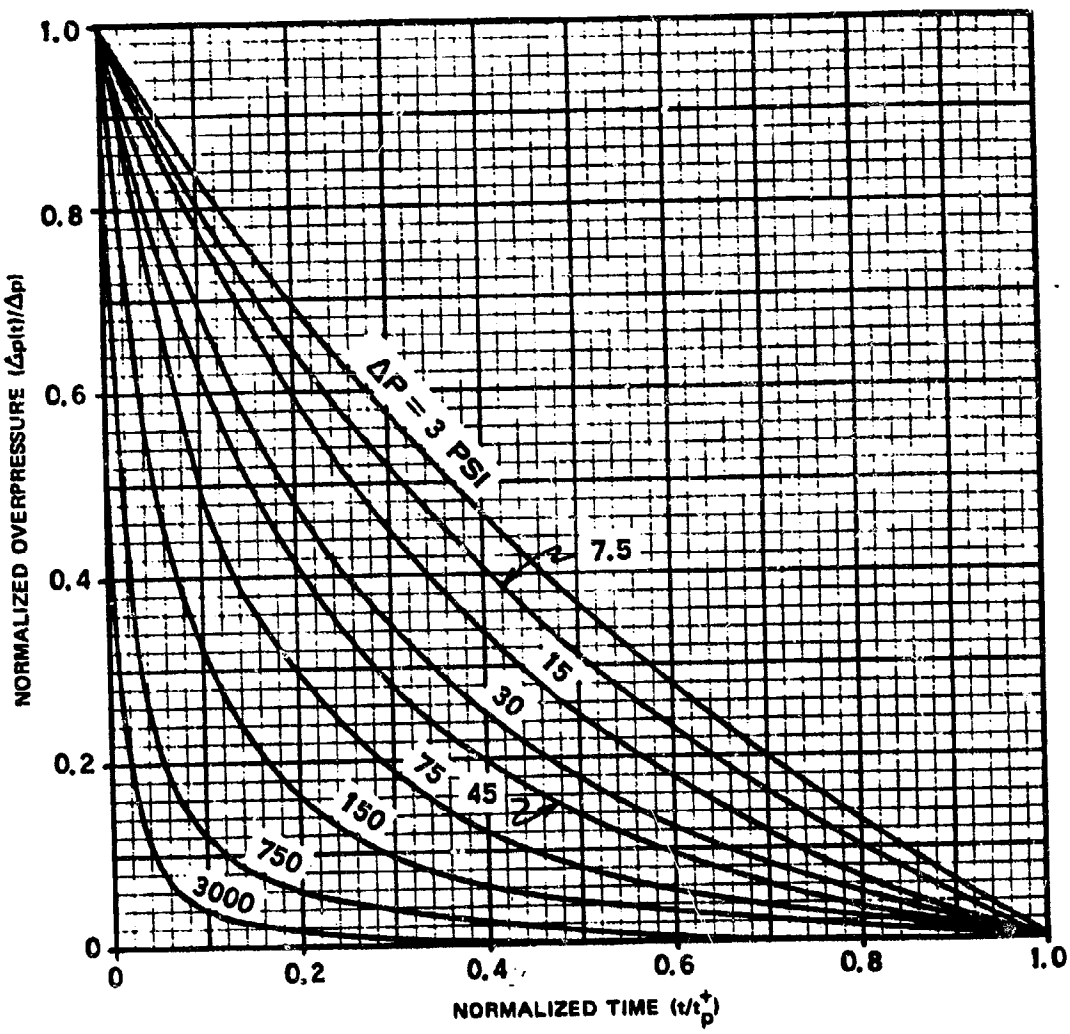

Figure 2-8. [redacted] Positive Overpressure Waveforms for an Ideal Shock Wave in a Standard Sea Level Atmosphere [redacted]

[redacted]

[redacted]

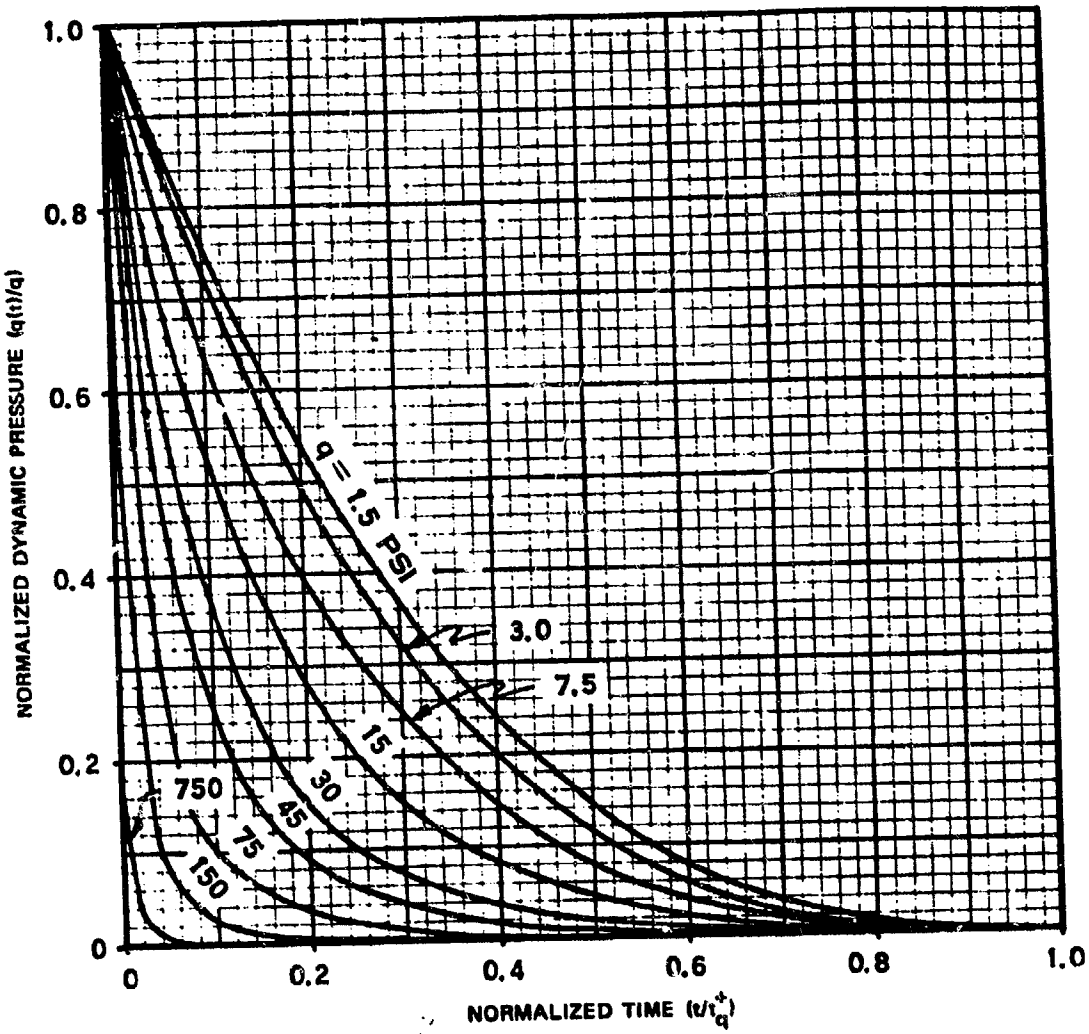

Figure 2-9. [redacted] Positive Dynamic Pressure Waveforms for an Ideal Shock Wave in a Standard Sea Level Atmosphere [redacted]

[redacted]

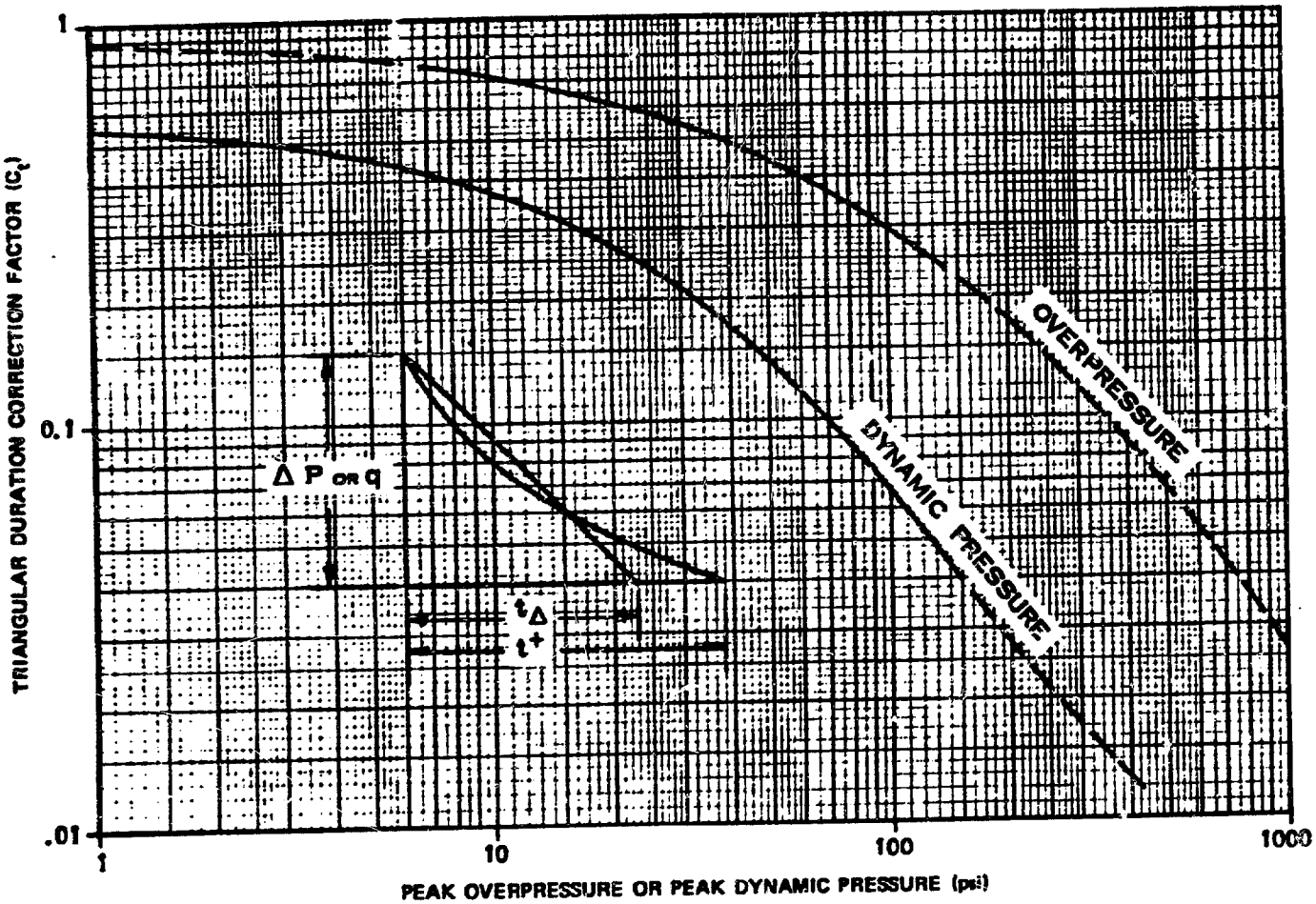

Figure 2-10. Effective Triangular Duration Correction Factors ($t\Delta = C_t t_p^+$ or $t\Delta = C_t t_q^+$)

2-16 Meteorological Phenomena

Nonuniformities in the atmosphere can produce mild focusing and dispersing effects that strengthen some portions of the blast wave and weaken others. Although these effects frequently occur near the surface, they are possible at any altitude and they may affect the blast wave in free air.

The manner in which these meteorological phenomena modify the blast wave may be illustrated by considering a layer of warm air, centered at burst altitude, as shown in Figure 2-14. Since the shock front velocity is greater in the warmer air, the shock front deviates from a perfect sphere. The modified shape causes the portion of the shock front that propagates through the warmer air to diverge and become weaker than the shock front as a whole.

At high shock strengths, the velocity of the shock front is much greater than sonic velocity, and it is a strong function of shock strength. This property tends to maintain a spherical shock front in spite of perturbations such as shown in Figure 2-14. Weakening the shock front reduces its speed, and the advance of the bulge becomes slower relative to the remainder of the shock front. This limits the distortion of the sphere and the divergence and weakening of the shock wave within the heated layer.

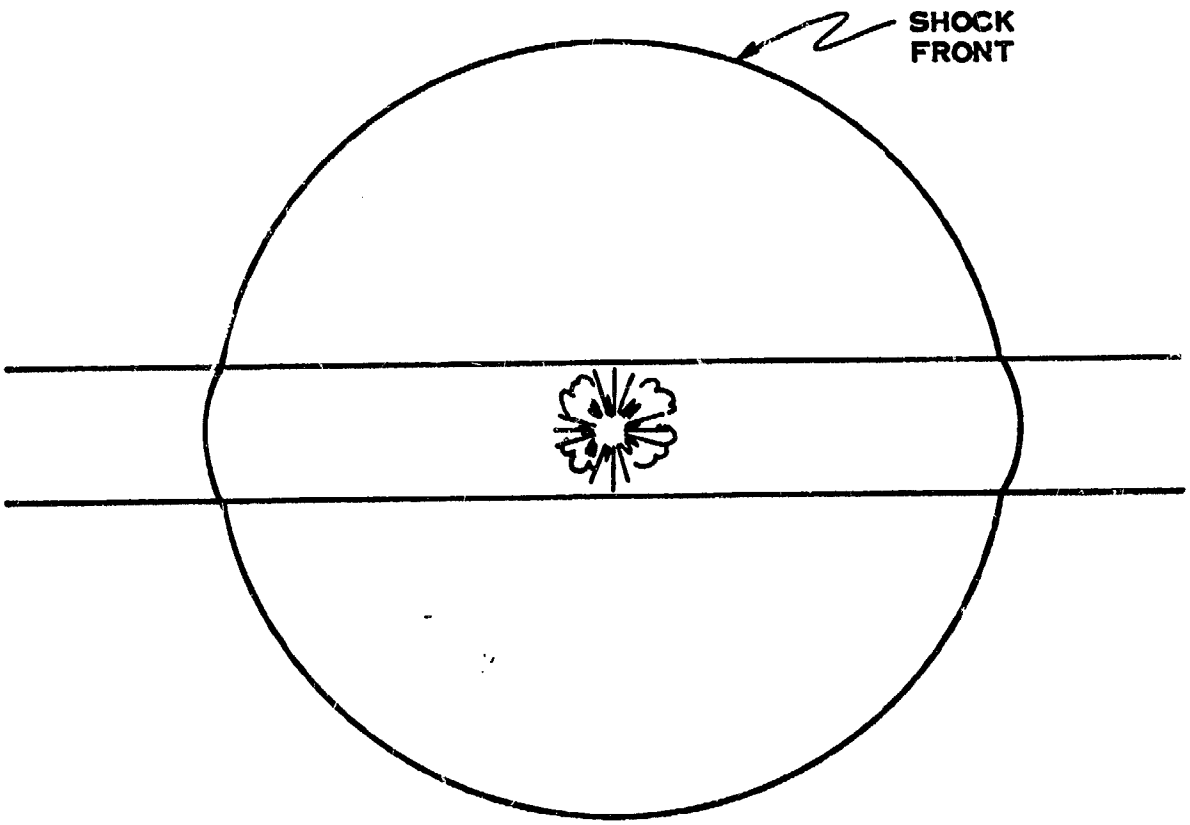

Figure 2-14. Distortion of Blast Wave by a Stratum of Warm Air

At low shock strengths, the reaction is different. The shock front velocity is only slightly greater than sound velocity and it is relatively insensitive to changes in shock strength. Development of a bulge and local weakening of the shock front can proceed much farther before changes in shock strength produce velocity changes that oppose further distortion.

For these reasons, a high overpressure blast wave is relatively insensitive to atmospheric disturbances, but a low pressure blast wave may be strongly affected. The factors that cause the disturbance can be any atmospheric nonuniformities that tend to distort the spherical shape of the shock front. Examples include shear winds and temperature gradients.

Shear winds are winds that change in velocity with changes in altitude. The velocity change may be in direction, in magnitude, or in both. Below 60,000 feet, the normal temperature gradient of the atmosphere produces lower temperatures at higher altitudes. This pattern tends to deflect blast energy upward. A temperature inversion is an increase in temperature with increasing altitude. This occurs normally at high altitudes. Above about 60,000 feet, temperature normally rises gradually with increasing altitude. The relatively sharp inversions that occur when a mass of warm air covers a mass of cold air are of more concern in blast calculations. Such an inversion can act as a mild reflecting surface, and downward deflection of the blast wave is intensified when the burst point is below the inversion.

These atmospheric effects normally produce only small deviations from predicted overpressure except for overpressures that are a small fraction of a psi. Larger deviations normally occur only when the blast wave is exposed to inhomogeneities in the atmosphere over an extended path. For example, when the burst and the target are at low altitudes and over 10 miles apart, observed overpressures have exceeded ten times the predicted values. Such strong focusing effects are possible only when sound travels faster aloft than it does on the ground. Incidents of this type have often been associated with the high winds in the jet stream; in these instances, abnormally high overpressures are observed only in the general direction of the wind motion. Prediction of the magnitude of the deviations that inhomogeneities in the atmosphere introduce into the values of the blast wave parameters is complex, and presentation of numerical methods to estimate the magnitude of these effects is beyond the scope of this manual.

BLAST-WAVE PHENOMENA AT THE SURFACE

When an air blast wave strikes a denser medium such as the earth's surface, it is reflected. If the surface is hard and flat, and if the incident blast wave has a very low peak overpressure, reflection follows simple laws, much like the reflection of light. If overpressures are moderate or high, or if the surface acts as a nonideal reflector, interactions between the blast wave and the surface can be complex. Study of the blast wave at the surface is largely concerned with these complex aspects of surface interactions.

2-17 Reflection at Normal Incidence

The peak reflected overpressure, Δp_r, produced by a normally incident* blast wave

*Although the various ways of describing the angle at which a blast wave strikes a surface are quite specific, they are not all consistent. A blast wave that strikes a surface head-on is said to be *normally incident*, because the direction of propagation makes an angle of 90° with the surface plane. However, the *angle of incidence* is defined as the angle between the shock front and the reflecting surface; its value is 0° for a head-on interaction. Reflection of a blast wave propagating along the surface as it strikes a rising slope is described in terms of slope angle, and slope angle is large for a steep slope. The head-on interaction that could occur at the face of a cliff occurs at a *slope angle* of 90°.

[redacted]

[redacted] depends on the peak overpressure, Δp, and the peak dynamic pressure, q, of the incident blast wave. An approximate equation for peak reflected overpressure (valid for shock strengths up to 6 or 7, i.e., or overpressures of about 75 to 90 at sea level) is

$$\Delta p_r = 2\Delta p + (\gamma + 1)q,$$

where Δp_r is the peak reflected overpressure, and the other quantities have been defined. If γ is taken to be 1.4 (see paragraph 2-15),

$$\Delta p_r = 2\Delta p + 2.4\ q.$$

Using the defined value of q,

$$q = \frac{1}{2}\rho_s u^2,$$

and the Rankine-Hugoniot equations introduced in paragraph 2-15 leads to the relation

$$q = \frac{\Delta p^2}{2\gamma P + (\gamma + 1)\Delta p},$$

and, if $\gamma = 1.4$, this becomes

$$q = \frac{5}{2} \cdot \frac{\Delta p^2}{7P + \Delta p}.*$$

Inserting this value of q into the equation for the reflected overpressure gives

$$\Delta p_r = 2\Delta p \left(\frac{1 + 4\Delta p/P}{1 + \Delta p/P}\right)$$

[redacted] This equation shows that, in the limiting case of low overpressures (at overpressures sufficiently low that dynamic pressure is negligible), the peak reflected overpressure is simply twice the peak overpressure of the reflected wave. This relation is a general one that is valid for any angle of incidence. It is valid because at low overpressures the reflected shock wave has the same strength as the incident shock wave, and the peak reflected overpressure is the sum of the overpressures of the incident and reflected waves.

[redacted] As Δp becomes very large the equation given above indicates that the peak reflected overpressure rises to eight times the incident

---

* [redacted] No derivation of this expression for q will be provided, but one numerical example will be shown below to establish its validity. The values for ρ_s and u shown in paragraph 2-15 for $\gamma = 1.4$ are

$$\rho_s = \rho\left(\frac{7P + 6\Delta p}{7P + \Delta p}\right)$$

$$u = \frac{5\Delta p}{7P} \cdot \frac{c}{\sqrt{\dfrac{7P + 6\Delta p}{7P}}}$$

$$u^2 = \frac{25\Delta p^2}{7P} \cdot \frac{c^2}{7P + 6\Delta p}$$

$$q = \frac{1}{2}\left[\rho\left(\frac{7P + 6\Delta p}{7P + \Delta p}\right)\right]\left[\frac{25\Delta p^2}{7P} \cdot \frac{c^2}{7P + 6\Delta p}\right]$$

Rearranging terms in this expression leads to

$$q = \left[\frac{5}{2} \cdot \frac{\Delta p^2}{7P + \Delta p}\right]\left[\frac{5}{7} \cdot \frac{\rho c^2}{P}\right].$$

It will be noted that the first term in brackets corresponds to the expression previously given for q. It should also be noted that the second term in brackets is dimensionless since both the numerator and denominator are in units of force per unit area. The sea level values of the parameters in the second term are

$$\rho = 2.38 \times 10^{-3}\ \text{slugs/ft}^3$$

$$c = 1{,}116\ \text{ft/sec}$$

$$P = 2{,}117\ \text{pounds/ft}^2$$

Inserting these values into the second term gives

$$\left(\frac{5}{7}\right)\frac{(2.38 \times 10^{-3})(1{,}116)^2}{2{,}117} = 1.$$

[redacted]

[redacted]

[redacted] overpressure. However, this equation fails at these high overpressures. It is based on the assumption that γ has a constant value, but γ drops to values below 1.4 in strongly shocked air. More accurate calculations for the high shock strengths show higher reflected overpressures than this equation predicts.

[redacted] Users of this manual will not use the equation for reflected overpressure very frequently; they will use it principally as an aid in understanding the reflection process. The numerical results that ordinarily are needed already have been calculated and have been incorporated in the various figures in this chapter.

2-18 Regular and Mach Reflection [redacted]

[redacted] The interaction between a blast wave and the surface of the earth is shown schematically in Figure 2-15. The reflected wave near the surface travels through a region that is heated and made denser than the ambient atmosphere by the incident shock front as it passes. Since shock front velocity is greater in heated air, a portion of the reflected shock can, under appropriate conditions, overtake and merge with the incident shock. This forms a single shock front, called the Mach stem, which produces higher peak overpressures and peak dynamic pressures at or near the surface than would be produced at the same distance in free air. The characteristics of the blast wave at or near the surface depend on yield, height of burst, and properties of the reflecting surface. The region where the incident and reflected shocks have not merged to form a Mach stem is referred to as the region of regular reflection; the region where they have merged is referred to as the region of Mach reflection. As the Mach stem travels along the surface, the triple point (the point of intersection of the incident wave, the reflected wave, and the Mach stem) rises.

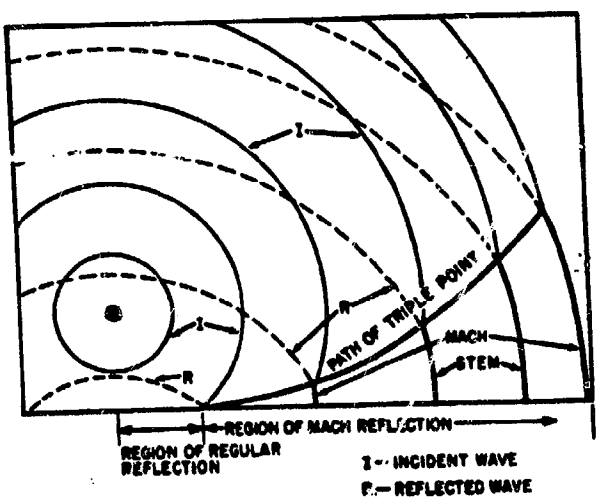

Figure 2-15. [redacted] Growth of the Mach Stem (Idealized) [redacted]

2-19 Blast Phenomena for Bursts in the Transition Zone [redacted]

[redacted] When the height of a burst is less than about $160W^{1/3}$ feet, additional phenomena affect the blast wave. If the burst is very close to the surface, within about $5W^{0.3}$ feet, fusion of the incident and reflected waves is complete, and the blast wave has a single, approximately hemispherical shock front. A burst this close to the surface is called a contact surface burst. The single shock front of a contact surface burst may be considered a special case of Mach stem formation in which the stem extends over the entire shock front.

[redacted] If a warhead is detonated above $5W^{0.3}$ feet but below about $160W^{1/3}$ feet, the portion of the reflected shock front that passes through the central region of the fireball moves fast enough to overtake the incident wave and fuse with it. The blast wave thus forms a single shock front above the fireball, a double shock front between this area of fusion and the triple point (or the ground if the Mach stem is absent), and a single shock front below the triple point. The strength of the fused wave above the fireball

[redacted]

varies with burst height. Unless the burst is considerably closer to the surface than $160W^{1/3}$, the reflected wave only makes a weak contribution to this portion of the blast wave. One reason for this weak contribution is that the reflected shock front is strongly attenuated by spherical divergence (produced by the lens-like action of the fireball). Another factor may be the attenuation resulting from the dissipation of energy when the shock front passes through heated air. The region between about $5W^{0.3}$ feet and $160W^{1/3}$ feet is called the transition zone, and a burst within this region is a surface burst for purposes of air blast phenomena.

If a burst is above the transition zone, fusion of the incident and reflected shock fronts is confined to the Mach stem region, and the burst is called an air burst. An air burst that only produces weak reflection effects at the surface is called a free air burst. The properties of such explosions were discussed in paragraphs 2-7 through 2-12. A low air burst is sometimes called a near surface burst. As described in Chapter 1, the limits of the scaled heights of burst as well as the scaling laws for defining the various zones are different for the various phenomena. The definitions given above for the heights of a contact surface burst, a surface burst, the transition zone, and a free air burst only apply to air blast phenomena.

2-20 Near-Ideal and Nonideal Surface Conditions

An ideal surface is defined as a perfectly flat surface that reflects all of the energy, both thermal and blast, that strikes it. No part of the surface of the earth is ideal in this sense, but a few surfaces act essentially as ideal. These surfaces are classified as near-ideal. A near-ideal surface is one that provides blast wave phenomena that are essentially free of the mechanical and thermal effects that are described in succeeding paragraphs. Some of the surfaces considered most nearly ideal are reasonably flat and consist of ice, hard-packed snow, frozen tundra, and water.

The phenomena that are characteristic of a mechanically nonideal surface are illustrated best by examples. When a blast wave that is traveling along a flat plain suddenly encounters a rising slope, a stronger overpressure impulse is produced than if the surface had remained flat. Buildings can decrease overpressure in certain areas by providing shielding from the blast; they also can increase overpressure in other areas by reflecting the blast wave. A very thick layer of snow will absorb a large amount of the blast energy that strikes it, which will produce a lower reflected overpressure than a near-ideal reflecting surface.

In most cases, blast wave calculations over mechanically nonideal surfaces are performed by first finding the desired blast parameters over a near-ideal surface. The results thus obtained then are corrected to account for the changes in blast wave properties produced by the mechanically nonideal features of the surface.

The phenomena produced by a thermally nonideal surface can distort overpressure and dynamic pressure waveforms of the blast wave at the surface. Whether or not the distortions are significant depends on height of burst and yield as well as the properties of the surface. Severe thermal effects are accompanied by the formation of a precursor, which alters several blast parameters severely. Precursors are described in the following paragraph.

Thermally nonideal surfaces may be defined loosely as those that absorb heat; thermally near-ideal surfaces reflect thermal energy incident upon them. Radiation from the fireball incident on thermally nonideal surfaces produces a layer of heated air that interacts with the blast wave, and which may form a precursor. This type of surface is sufficiently common that nearly all blast wave data at the surface are pre-

[redacted]

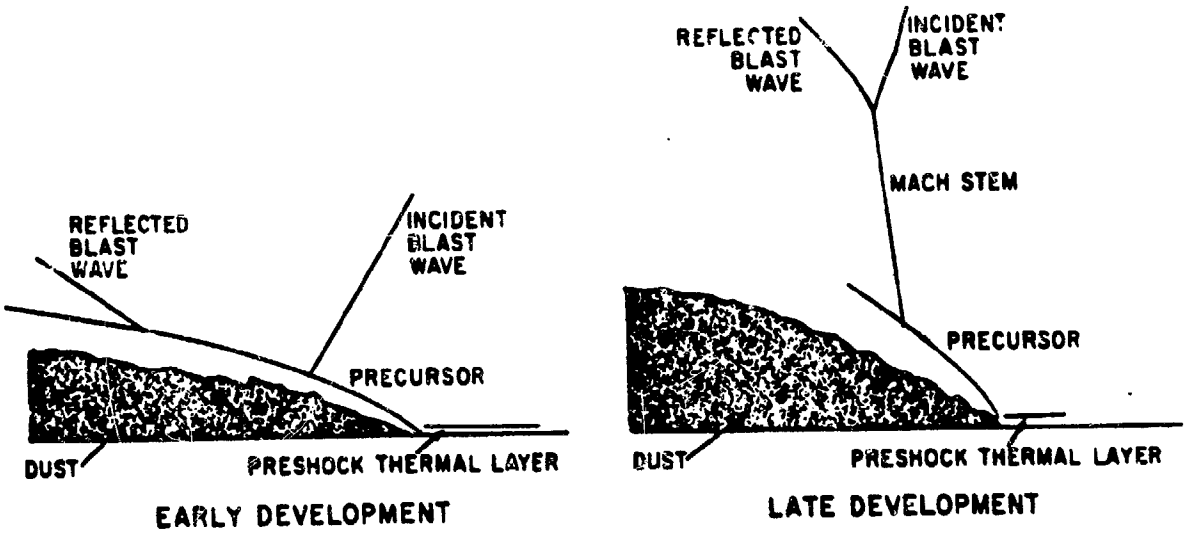

Figure 2-16. [redacted] Precursor Characteristics [redacted]

[redacted] sented as two sets of charts: one set for near-ideal surfaces, and one set for thermally non-ideal surfaces. Methods of classifying surfaces with respect to thermal properties are discussed in paragraph 2-22.

2-21 Precursor Formation [redacted]

[redacted] Thermal radiation from the fireball of a surface or near-surface burst can cause the surface of the earth in the vicinity of ground zero to reach a temperature of several thousand degrees in a short time. "Popcorning" may then occur, wherein volatile substances vaporize explosively, throwing hot particles into the air. This (or similar heat transfer processes) produces a layer of heated air just above the surface almost instantly. When the height of burst is less than $650W^{1/3}$ feet, and when the earth is dusty and dark in color, the thermal layer usually is intense enough to disturb the blast wave near the ground surface seriously.

[redacted] Under ideal conditions, none of the energy in a blast wave can propagate faster than the shock front itself; thus, the shock front forms an envelope within which the blast energy is confined. The thermal layer, however, provides a way for this energy to penetrate the confining surface. The energy in a blast wave propagates faster through hotter air, and the thermal layer allows energy to move ahead of the main shock front, which produces shock wave patterns such as those shown in Figure 2-16. The auxiliary blast wave that moves ahead of the main shock wave is called a precursor.

[redacted] Although the details of precursor formation are not well understood, its general patterns of pressure and flow have been observed and can be described. After the precursor forms, the main shock front no longer extends to the ground; if it does, the lower portion is so weakened and distorted that it is not easily recognized. Between the ground and the bottom edge of the main shock wave is a gap, probably not sharply defined, through which the energy that feeds the precursor may flow. Wind speed in this gap is higher than the wind speed behind the

[redacted]

[redacted]

[redacted] main shock front.* Overpressure in the gap is lower than that behind the main shock front, and it is this overpressure difference which produces the higher than ideal wind velocities in the gap.

[redacted] Ahead of the main shock front, the blast energy in the precursor is free not only to follow the rapidly moving shock front in the thermal layer, but also to propagate upward into the undisturbed air ahead of the main shock front. A near-equilibrium condition exists, because the energy continually fed into the precursor from the main blast wave tends to strengthen the precursor shock front, and the diverging flow pattern within the precursor itself tends to weaken it.

[redacted] This description of what happens within a precursor explains some of the precursor characteristics shown in Figure 2-16. Only that portion of the precursor shock front remaining in the thermal layer travels faster than the main shock front; the energy diverging upward, out of this layer loses some of its forward speed, and the intersection of the precursor and main shock fronts indicates that the main shock is continually overtaking this upward-traveling energy. Dust, typically billowing to heights of more than 100 feet, shows the upward flow of air in the precursor. At later times, the lower edge of the main shock front is distorted by the action of the precursor.

[redacted] Overpressure and dynamic pressure waveforms add information to that supplied by blast wave photographs. Typically, the waveform of a fully developed precursor shows a rounded leading edge and a slow rise to its peak amplitude. In severely disturbed waveforms, the pressure jump at the leading edge may be completely absent. These characteristics indicate that the precursor shock front is strongly attenuated and that, at least close to the ground, the precursor does not always have a true shock front of significant amplitude. These results are consistent with the diverging flow pattern described above. Dynamic pressure waveforms often have high frequency oscillations that indicate severe turbulence. The long time durations seen in both overpressure and dynamic pressure waveforms indicate two effects: the early arrival of the initial pressure disturbance, and the sustaining effects of the strong winds developed within the precursor.

[redacted] Peak amplitudes of the precursor waveforms show that overpressure has a lower peak value and dynamic pressure has a higher peak value than would appear over a surface that did not permit a precursor to form.† The drop in peak overpressure indicates the energy expended in producing the higher than ideal wind velocities. The higher dynamic pressure is partly due to the higher wind speeds, but dust loading, the increase in effective air density resulting from particulate matter carried by the wind, is believed to be a more important factor.

[redacted] Additional information on precursors, particularly a description of typical precursor overpressure and dynamic pressure waveforms, is given in paragraphs 2-31 and 2-32.

---

* [redacted] It is tempting to think of the wind in the gap as moving faster than the main shock front. However, two velocities characterize a shock wave: wind velocity and shock front velocity. The velocity of the main shock front is the velocity of propagation of the energy in the main shock. It should be compared not to the wind speed in the gap but to the velocity with which hydrodynamic energy propagates through the gap.

† [redacted] In an ideal blast wave, this relative variation of peak values would be impossible. Peak overpressure and peak dynamic pressure have a fixed relation to one another, specified by the Rankine-Hugoniot equations (paragraph 2-17 and Appendix A). However, these equations only hold at the shock front. In an ideal blast wave, shock-front amplitudes are also peak amplitudes, but in a precursor the peak values do not occur at the shock front. Thus the relation between them is not limited by these equations.

[redacted]

2-22 Identification of Thermally Near-Ideal and Nonideal Surfaces

To predict blast-wave parameters accurately, the reaction of the surface to thermal radiation from the fireball should be known. Nuclear tests have shown that a few specific types of surface act essentially as thermally ideal surfaces and a few others tend to produce a significant thermal layer. Unfortunately, a theoretical model that quantitatively explains the phenomena of surface reaction and precursor formation has not yet been developed. Without such a model, the response of untested surfaces cannot be predicted with assurance.

Despite this uncertainty, predictions have been made. Surfaces are classified as either thermally near-ideal (unlikely to produce significant precursor effects) or thermally nonideal (expected to produce a precursor for suitable combinations of burst height and ground distance). No other categories are used, i.e., no attempt is made to subdivide surface classifications according to the strength of the precursor that can form.

Examples of surfaces that are considered thermally near-ideal and thermally nonideal are shown in Table 2-3. Items in the table that are confirmed by experiment are marked with an asterisk.

Dark surfaces tend to be thermally nonideal, because they absorb thermal radiation from the fireball. Light (reflecting) surfaces tend to be near-ideal. Asphalt is the strongest precursor-forming surface for which test results are known.

The effect of moisture has not been established definitely. Since any specified amount of absorbed energy can raise the temperature of a dry surface more than the same absorbed energy would raise the temperature of a wet surface, moisture is expected to inhibit the formation of a thermal layer. This should be particularly true when the moisture is in the form of ice. Nuclear tests show that the dry, sandy

Table 2-3. Examples of Thermally Near-Ideal and Thermally Nonideal Surfaces

Thermally Near-Ideal (precursor unlikely)	Thermally Nonideal (precursor may occur for low air bursts)
*Water	*Desert sand
*Ground covered by white smoke layer	*Coral
Heat reflecting concrete	*Asphalt
Frozen tundra	*Surfaces with low, thick vegetation
Ice	*Surfaces covered by a dark smoke layer
Packed snow	Dark colored rock
Moist soil with sparse vegetation	Most agricultural areas; Residential areas in cities
Commercial and industrial areas	Dry soil with sparse vegetation

soil of the Nevada Test Site is thermally nonideal, and that water is a near-ideal surface (however, a blast wave over rough seas may fill the air with spray and produce a dynamic pressure effect similar to the dust loading encountered over desert surfaces). Untested surfaces classed as thermally near-ideal are listed in Table 2-3 in the order of increasing uncertainty.

Sparse vegetation probably should be ignored. Leaves or thick vegetation shield the ground, prevent popcorning, and minimize dust loading, but they also generate a heat-absorbing cloud of dark smoke when they absorb radiation from the fireball. The gases driven from the leaves have high sonic velocities. As a result, they create a thicker, and probably cooler, thermal layer than that formed over desert sand or asphalt. Taller vegetation is expected to produce a thicker thermal layer and a stronger precursor. The REDWING-Inca shot, over a surface covered by low grass and vines dominated by broad-leafed shrubs about 10 feet high, produced a precursor, but the characteristic precursor waveforms were apparently suppressed to some extent because higher-than-ideal blast-wave velocities near the surface were eliminated by the vegetation.

Tests at the Nevada Test Site show weakened precursor action over areas covered by dark smoke (the surface was desert sand which forms a strong precursor). Presumably the smoke absorbs enough heat to form a thermal layer, but it shields the ground to prevent popcorning and dust loading of the air.

Variable conditions occur in cities. Commercial and crowded industrial areas are expected to act as thermally near-ideal surfaces. Although these areas contain many surfaces that are favorable to precursor formation (e.g., asphalt-coated roofs), a continuous thermal layer would not be expected. The tendency to form a precursor would be offset by its difficulty in propagating through a heavily built up area. In typical residential areas, where the buildings are neither as close nor as tall as those in commercial areas, the surface is considered thermally nonideal.

The preceding descriptive information does not always provide clear guidelines for classifying surfaces. For example, the rules that might be applied to black, moist soil are conflicting. In such cases, blast-wave properties should be calculated for both near-ideal and thermally nonideal surface conditions in order to bracket the blast effects that can actually be expected.

BLAST-WAVE CALCULATIONS AT THE SURFACE

Height of burst (HOB) curves provide most of the data required to calculate blast-wave properties at the surface. The HOB charts in this subsection each show the distance from ground zero as a function of height of burst for several values of the various air blast parameters that would be expected to occur *along the surface* as a result of a 1 kt explosion.* For instance, any point on a curve for specified overpressure (see for instance Figure 2-17) shows a combination of burst height and ground distance at which a 1 kt explosion will produce that overpressure at the surface of the earth. Alternately, if a 1 kt burst occurs at a location corresponding to some point on a given overpressure curve, a target at the origin will receive that overpressure.

Separate families of curves are provided for near-ideal and thermally nonideal surface

---

*As described in paragraph 2-13, the heights of burst and distances from ground zero could be expressed in terms of scaled distances, e.g., $kt/W^{1/3}$, with W being the yield in kt. However, since other scaling laws apply to other phenomena, the convention of expressing absolute distances from a 1 kt explosion will be maintained throughout the remainder of this chapter and throughout the manual. When "scaled distances" are employed, e.g., Section I, Chapter 11, the exceptions will be indicated clearly.

conditions. Guidelines for classifying surfaces with respect to thermal properties are provided in paragraph 2-22. The effects of mechanically nonideal surfaces (paragraph 2-20) are discussed in paragraphs 2-37 through 2-41.

Many of the HOB curves show whether a given point on the surface is in the region of regular reflection or the Mach stem region (paragraph 2-18). This information is helpful if the target is some distance above the surface, because it indicates how closely blast-wave data at the surface correspond to blast-wave data at the target. The effect of target height on blast-wave parameters is discussed in paragraph 2-29.

The data for overpressure and dynamic pressure are peak values, regardless of where these peaks occur in the blast waveform. In an undisturbed blast waveform, these peak values occur at the shock front. If a precursor is present, they usually occur later in the waveform. Precursor overpressure and dynamic pressure waveforms are described in paragraphs 2-31 and 2-32.

Whenever ambient atmospheric conditions are different from standard sea level conditions (14.7 psi, 59°F), calculations of blast-wave parameters at the surface are more accurate if the altitude scaling factors described in paragraph 2-14 are applied. These factors may be used even if the departure from standard conditions is not caused by an altitude change.

2-23 Reliability

Blast-wave data at the surface are subject to the uncertainties described in paragraphs 2-1 through 2-6. As mentioned in paragraph 2-5, additional uncertainties arise because the earth is not a perfect reflector. Consequently, the blast wave at the surface is inherently less predictable than the blast wave in free air. Added to this problem is the difficulty of obtaining sufficient experimental data to cover all combinations of conditions. A blast parameter in free air may be represented by a single curve; at the surface, the available data must be scattered to cover a family of curves. Moreover, variable surface conditions require that more than one family be plotted. Consequently, a limited number of nuclear tests cannot document blast-wave data at the surface as completely as in free air. The usual reliability statements are supplemented in this section by showing portions of the curves as dashed lines. The solid lines are based upon experimental data from full-scale nuclear tests; the dashed portions are based upon theory and high-explosive experiments. In some cases, data for the dashed portions of curves are based on the assumption that for certain combinations of ground range and burst height the data for thermally nonideal surfaces should agree with data taken over near-ideal surfaces. In general, the reliability statements apply to the dotted as well as the solid portion of the HOB curves; however, the reliability of the dotted portions is purely an estimate, while the reliability stated for the solid portions is based on experimental data.

Uncertainties in the data presented in the HOB charts usually are expressed in terms of ground distance rather than in terms of blast parameters. This is an important distinction. For example, a ±10 percent uncertainty in ground distance corresponds to an uncertainty in peak overpressure that may be as high as ±30 percent. The curves become nearly horizontal close to ground zero, and a variation in ground distance produces very little change in blast parameters. For these portions of the HOB charts, the uncertainty should be applied to burst height rather than to ground distance. When a precursor forms, the air blast waveforms are distorted severely, and prediction of blast parameters becomes highly uncertain. As mentioned in paragraph 2-2, the scaling of most blast-wave parameters is reasonably dependable in the yield range of 1 kt to 20 Mt; however, scaling becomes questionable for yields over 50 kt at thermally non-

[redacted]

[redacted] ideal surfaces as a result of the difficulty in predicting the criteria for precursor formation.

[redacted] The scaling of subkiloton explosions at scaled heights of burst between 150 and 1,000 feet have shown large errors that correspond to discrepancies as high as factors of 2 or 3 in effective yield.

[redacted] Additional uncertainties appear in the measured data for contact surface bursts as a result of less dependable experimental determination of yield. This is caused in part by the difficulties added to radiochemical yield determination as a result of the large amount of crater material in the cloud and to the uncertainty introduced into yield determination by fireball size that result from uncertainties in the amount of energy absorbed by the earth.

2-24 Peak Overpressure [redacted]

[redacted] Figures 2-17 through 2-22 show the peak overpressure at the surface of the earth as a function of height of burst and distance from ground zero from a 1 kt explosion. Figure 2-23 shows peak overpressure as a function of distance from ground zero from a 1 kt contact surface burst. The same data could be obtained in less convenient form along the abscissas of Figures 2-17 through 2-20.

[redacted] These figures show that the same ground range for a given peak overpressure is produced by a burst either at the surface or some short distance above the surface. At low overpressures, the greatest distance from ground zero occurs for an explosion at some higher distance above the surface. This effect is prominent at overpressures of 15 psi and less, and contours for these overpressures show a pronounced "knee" (the knee is defined as the extreme right projection of a contour line).

[redacted] Figures 2-17 through 2-20 apply to near-ideal surface conditions; Figures 2-21 and 2-22 apply to thermally nonideal surfaces (suggestions for classifying various types of surfaces are given in paragraph 2-22). Figure 2-23 applies to near-ideal surfaces, but since the 1 kt reference burst detonated in contact with the surface is not expected to form a precursor, the curve also applies approximately to thermally nonideal surfaces.

[redacted] The shaded areas in Figure 2-20 reflect the uncertainty in the prediction of very low overpressures. The shaded areas in Figures 2-21 and 2-22 correspond to the ground distances at which precursor cleanup occurs. In this phenomenon, the hydrodynamic energy of the blast wave collects behind a single, well-defined shock front, forming a nearly ideal blast wave. As this occurs, the peak overpressure usually rises instead of undergoing the normal amount of attenuation with increasing ground range. Uncertainty in the ground range at which cleanup occurs is reflected in the HOB curves as additional uncertainty in peak overpressure data at this range. This is indicated by shading of the 10 psi contour and a portion of the 15 psi contour.

2-25 Peak Dynamic Pressure [redacted]

[redacted] Figures 2-24 through 2-26 show peak dynamic pressure at the surface as a function of scaled height of burst and ground distance from a 1 kt explosion. These curves show conditions after the blast wave has been reflected from the surface; therefore, these charts do not represent the dynamic pressure of the incident wave. At ground zero the wind in the incident blast wave is completely stopped by the ground surface, and all of the incident dynamic pressure is transformed to static overpressure. Therefore, the height of burst curves show that the peak dynamic pressure is zero at ground zero. At other locations, reflection of the incident blast wave produces winds that, at the surface, must

[redacted]

blow parallel to the surface.* The dynamic pressures associated with these winds tend to produce horizontal forces; however, the direction of wind forces on a target surface depend not only on wind direction but also on surface orientation.

The thermal properties of the surface are less significant for prediction of dynamic pressure than for most blast parameters. Dynamic pressure only appears to be strongly enhanced by dust loading (or, in the case of a water surface, spray loading) of the air, whether or not a precursor is formed. The dynamic pressure height of burst curves are therefore classed as ideal, "light dust," and "heavy dust" surface conditions. Light dust conditions usually may be taken to be equivalent to near-ideal surfaces, and heavy dust equivalent to thermally nonideal, but there are exceptions. For example, a surface covered by thick vegetation is expected to produce a precursor but little dust. Conversely, the interaction of a blast wave with very rough seas is expected to produce heavy spray loading but no precursor.

Figure 2-24 shows peak dynamic pressure at an ideal surface in the very high pressure region. It is based almost entirely on theory, and does not include dust loading effects (it should be noted that the 200 psi contour of Figure 2-23 does not agree with that in either Figure 2-25 or 2-26). Figure 2-25 shows peak dynamic pressure for light dust conditions, and Figure 2-26 shows peak dynamic pressure for heavy dust conditions. Since the latter is based on limited data, height of burst curves can be drawn only for scaled burst heights up to 300 feet. As a guide to the way in which the heavy dust curves might be extrapolated, portions of the light dust curves are shown for 1 kt burst heights between 330 feet and 600 feet. These latter curves do not represent heavy dust conditions. They should be used only as a guide to obtain rough estimates.

Figure 2-27 is presented to aid in the explanation of the effects of dust on peak dynamic pressure. The curves are drawn from data from Figures 2-25 and 2-26, and theoretical data for an ideal reflector. At a scaled distance of about 400 feet, the contribution of light dust to dynamic pressure is about twice that of heavy dust. This suggests that the inertia of heavy dust limits its velocity initially and probably also limits the velocity of the air in the blast wave by the drag force it exerts. After these inertial forces are overcome, heavy dust contributes strongly to dynamic pressure. At a scaled range of 900 feet, heavy dust exhibits its maximum effect, but the effect of light dust has diminished considerably. This also suggests an inertial effect acting to sustain the momentum of the air in the blast wave.

The explanation that has been given is only one of several possible explanations of Figure 2-27 and represents an oversimplification. For example, the explanation does not include the varying amount of dust that a given surface adds to the blast wave as a function of range. More detail may be found in DASA 1200 (see bibliography).

A large scatter exists in dynamic pressure data under heavy dust conditions. This is due to the nature and the varying amounts of particulate matter in the air. Fine grains of sand are readily carried by the air stream, flow with it as a part of a continuous fluid, and present a relatively small measurement problem. Larger

*This statement ignores the turbulence that is often associated with dynamic pressure. It is uncertain whether or not vertical components of air velocity contribute to dynamic pressure significantly. Gages used to measure dynamic pressure are usually mounted so as to be sensitive only to the horizontal force produced by dynamic pressure. For this reason curves such as those in Figures 2-24 through 2-26 are often labeled "horizontal component of dynamic pressure." It is desirable to avoid this phrase, because it tends to imply, incorrectly, that the forces produced by dynamic pressure may be resolved into components that can be treated by the ordinary rules of vector algebra.

[redacted]

[redacted] particles tend to plug gage openings, and their effect is difficult to measure. Large objects picked up by the blast wave and thrown through the air can be very destructive, but they cannot be measured as part of a continuous pressure record. Arbitrarily, dynamic pressure has been defined as representing the effects of only those particles that are small enough to behave essentially as air particles. Dynamic pressure as thus idealized cannot fully account for the destructive effects of blast momentum.

2-26 Time of Arrival [redacted]

[redacted] Figures 2-28 through 2-32 show the time of arrival of the blast wave from a 1 kt explosion in a standard, homogeneous, sea level atmosphere as a function of height of burst and distance from ground zero.

2-27 Duration of the Positive Phase of Overpressure and Dynamic Pressure [redacted]

[redacted] Figures 2-33 and 2-34 present families of curves that show values of the positive phase overpressure duration (t_p^+) at points along the surface as a function of height of burst and ground distance from a 1 kt explosion in a sea level atmosphere.

[redacted] Because of limited data, similar curves cannot be drawn for dynamic pressure; however, the data suggest that, as in the case of free air (paragraph 2-10 and Problem 2-4), the ratio of these two durations is a function of pressure level. Duration of dynamic pressure t_q^+ may be estimated by using the curves for positive overpressure duration and the relations shown in Table 2-4. If surface conditions are such that heavy dust (or spray) loading is predicted, the longer times found in Figure 2-34 probably provide a better basis for determining t_q^+ even if the surface is considered thermally near-ideal and Figure 2-33 is used to determine t_p^+.

Table 2-4. [redacted] Relations Between the Positive Duration of the Overpressure Blast Wave (t_p^+) and the Positive Duration of the Dynamic Pressure (t_q^+) for a 1 kt Explosion [redacted]

t_p^+ (sec)	t_q^+ (sec)
0.1	0.25
.15	.33
.2	.34
.25	.35
.3	.39
.35	.43
.4	.49

2-28 Overpressure Impulse [redacted]

[redacted] Figures 2-35 and 2-36 show the positive overpressure impulse (paragraph 2-11) at the surface as a function of height of burst and ground distance from a 1 kt explosion in a sea level atmosphere.

[redacted] Formation of a Mach stem changes the shape of the overpressure waveform by increasing the amplitude of the shock front without changing the area under the waveform appreciably. Consequently, the HOB curves for overpressure impulse differ from the HOB curves for peak overpressure in that the impulse curves do not show a characteristic change where they cross the boundary separating the region of regular reflection from the region of Mach reflection. Overpressure impulse at the surface appears to be primarily a function of slant range; it only fluctuates strongly as a function of reflecting angle for low heights of burst.

[redacted] Dynamic pressure impulse is another important blast-wave parameter, particularly under thermally nonideal conditions. Unfortun-

[redacted]

[redacted]

[redacted]

ately, it is a difficult parameter to measure, and there are not enough dependable data to allow HOB curves to be constructed.

2-29 Mach Stem Heights [redacted]

[redacted] The changes that occur in a blast wave as the incident and reflected waves fuse to form a Mach stem are among the changes associated with reflection from a surface. A target above the triple point, the top of the Mach stem (see paragraph 2-18), receives two shocks that correspond to the arrival of the incident and the reflected waves. A target at or below the triple point receives a single shock. As mentioned in paragraph 2-25, the reflection process transforms part of the incident dynamic pressure into overpressure. Thus, a target below the triple point is subjected to a higher overpressure impulse and a lower dynamic pressure impulse than a target above the triple point. Since a typical airborne target is more sensitive to dynamic pressure than to overpressure, such a target is usually safer below the triple point.

[redacted] The height of the Mach stem heigh affects tall structures on the ground. The nature of the response depends on whether the structure is more sensitive to overpressure or to dynamic pressure. The relative effects of a two shock front waveform and a single, nearly vertical shock wave also depend on the mechanical response properties of the target.

[redacted] Above the triple point, the strength of the first (or incident) shock wave may be found from free air data, and the time interval between the two shocks depends on the height of the target above the triple point. Below the triple point, shock parameters may be approximated best by data from the HOB charts, i.e., from data which, strictly speaking, apply only to targets at the surface. When the scaled height (that corresponding to a 1 kt burst) of the Mach stem is 50 feet or less, blast-wave properties anywhere on the stem are essentially the same as those at the surface. For taller Mach stems, the shock-front becomes curved. This modifies blast-wave properties along the stem. Pressure values decrease and arrival times increase with height above the surface. These variations have not been studied as thoroughly as blast-wave conditions at the surface have been, and data to describe them quantitatively are not presented here.

[redacted] The guidelines presented above must be applied with caution if a precursor is present. The two disturbing influences, dust and the thermal layer, are confined to a layer that is close to the ground. Above the region that is affected by the precursor, the near-ideal HOB curves are a better representation of the blast wave. The height above which the near-ideal curves apply is not known, but it is estimated to be between 50 and 300 feet (physical, not scaled height) under typical conditions.

[redacted] Although there are indications that the height of the Mach stem is affected by thermal effects and by surface hardness, these effects are not large, and the curves may be applied to both near-ideal and thermally nonideal surfaces. Both thermal effects and surface roughness will, however, make the position of the triple point less predictable.

[redacted] Figures 2-37 and 2-38 show the height of the Mach stem as a function of height of burst and ground distance from a 1 kt explosion in a sea level atmosphere.

[redacted]

[redacted]

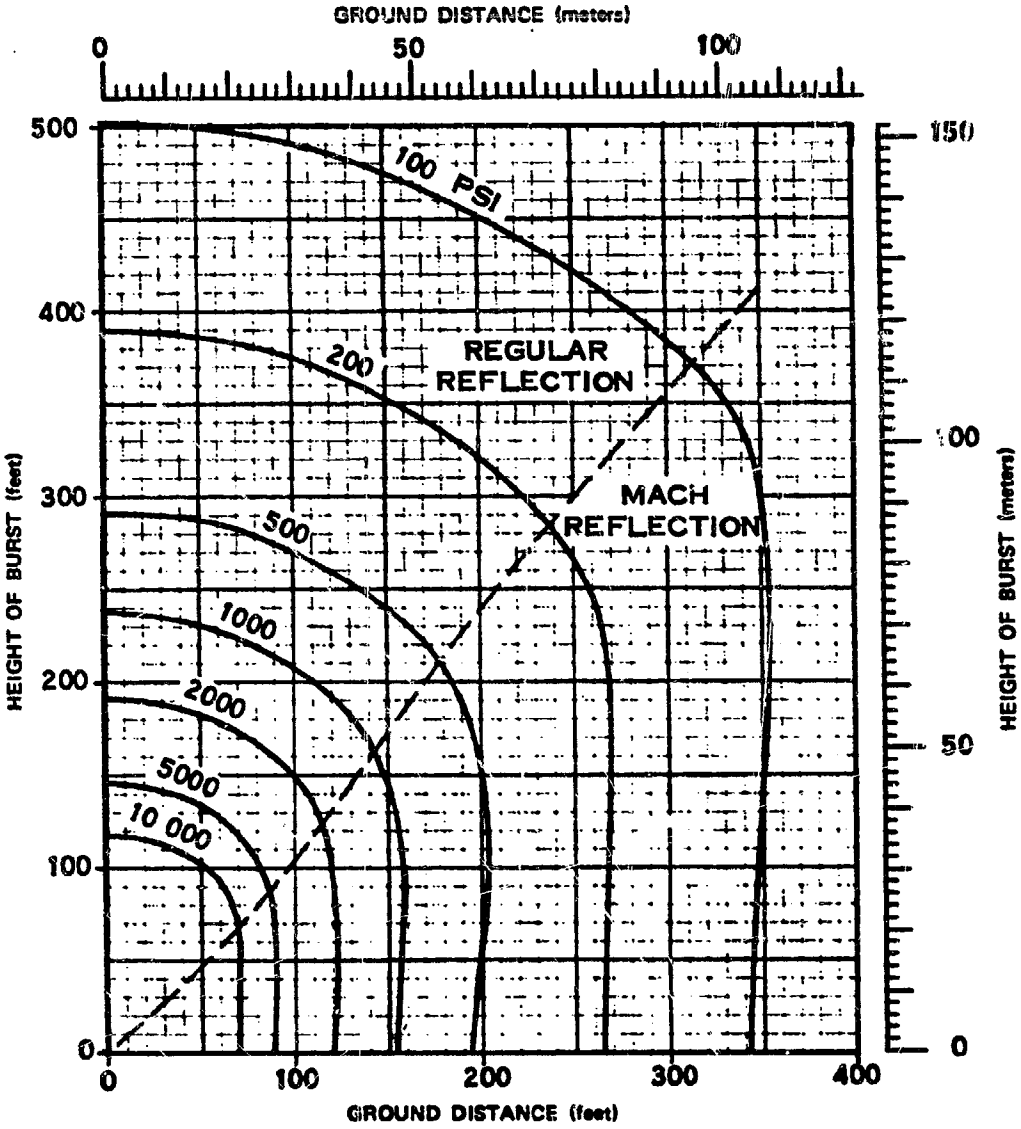

Figure 2-17. [redacted] Peak Overpressures at the Surface for a 1 kt Burst Over a Near-Ideal Surface, Very High Overpressure Region [redacted]

[redacted]

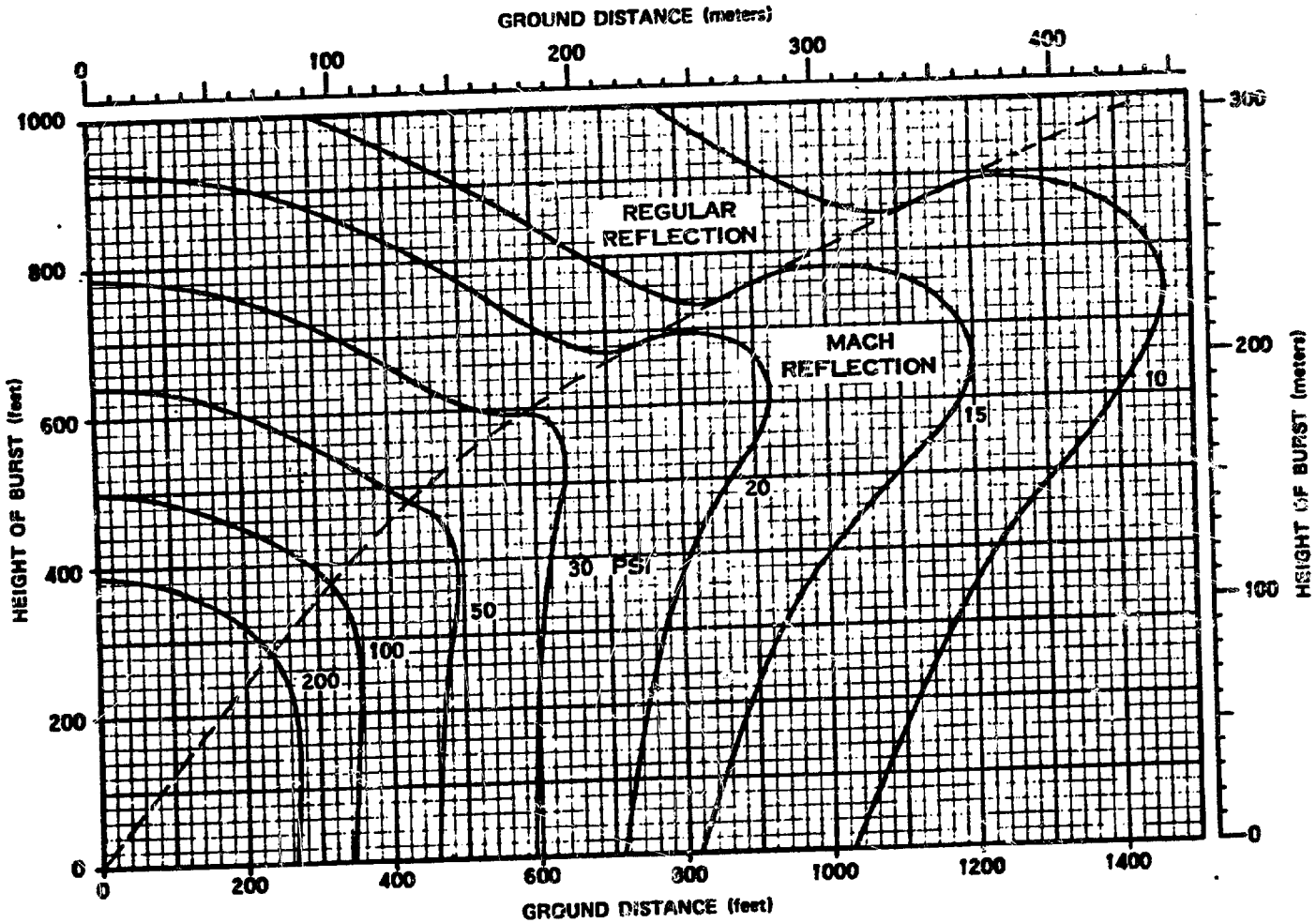

Figure 2-18. [redacted] Peak Overpressures at the Surface for a 1 kt Burst Over a Near-Ideal Surface, High Overpressure Region [redacted]

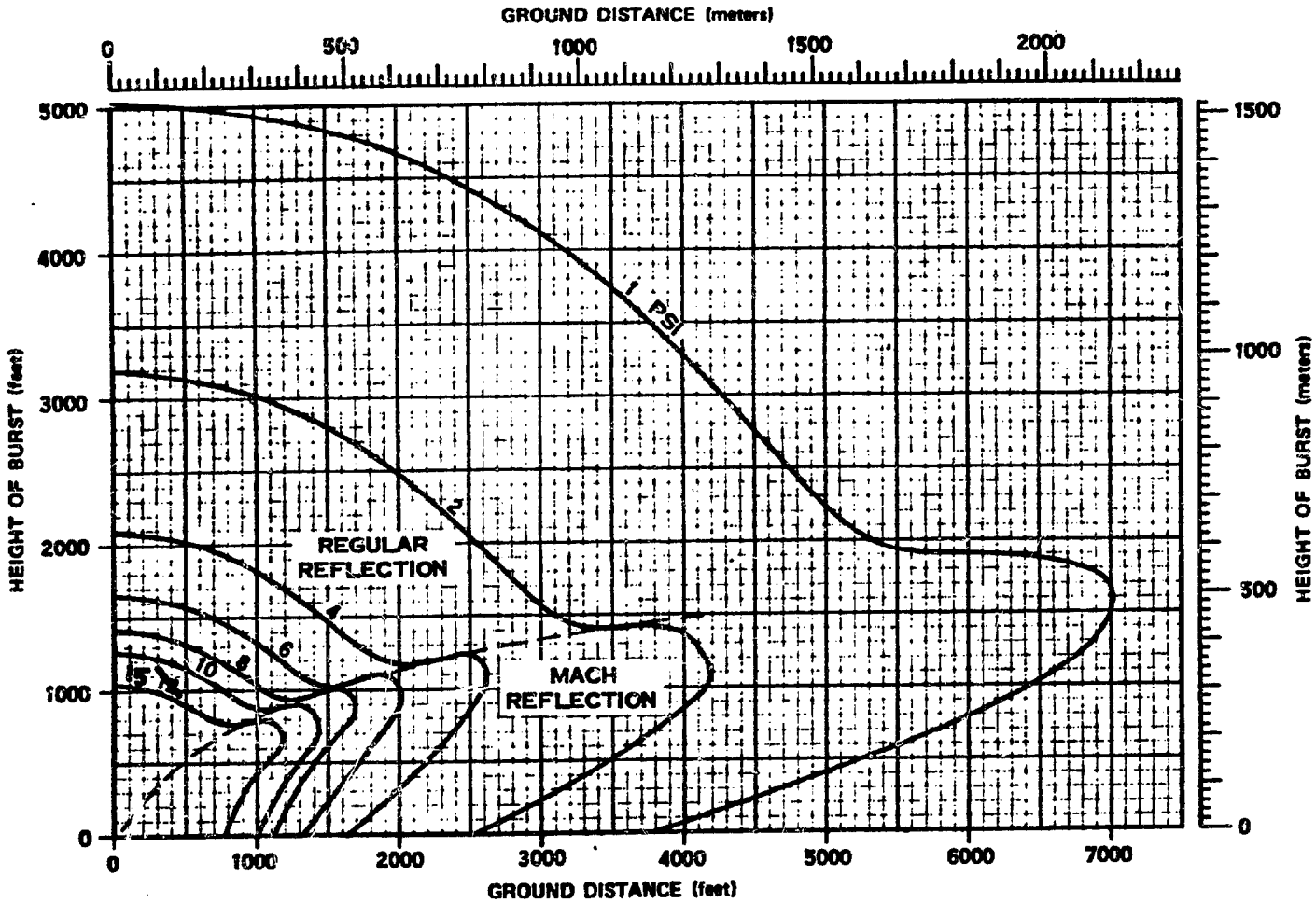

Figure 2-19. [redacted] Peak Overpressures at the Surface for a 1 kt Burst Over a Near-Ideal Surface, Low Overpressure Region [redacted]

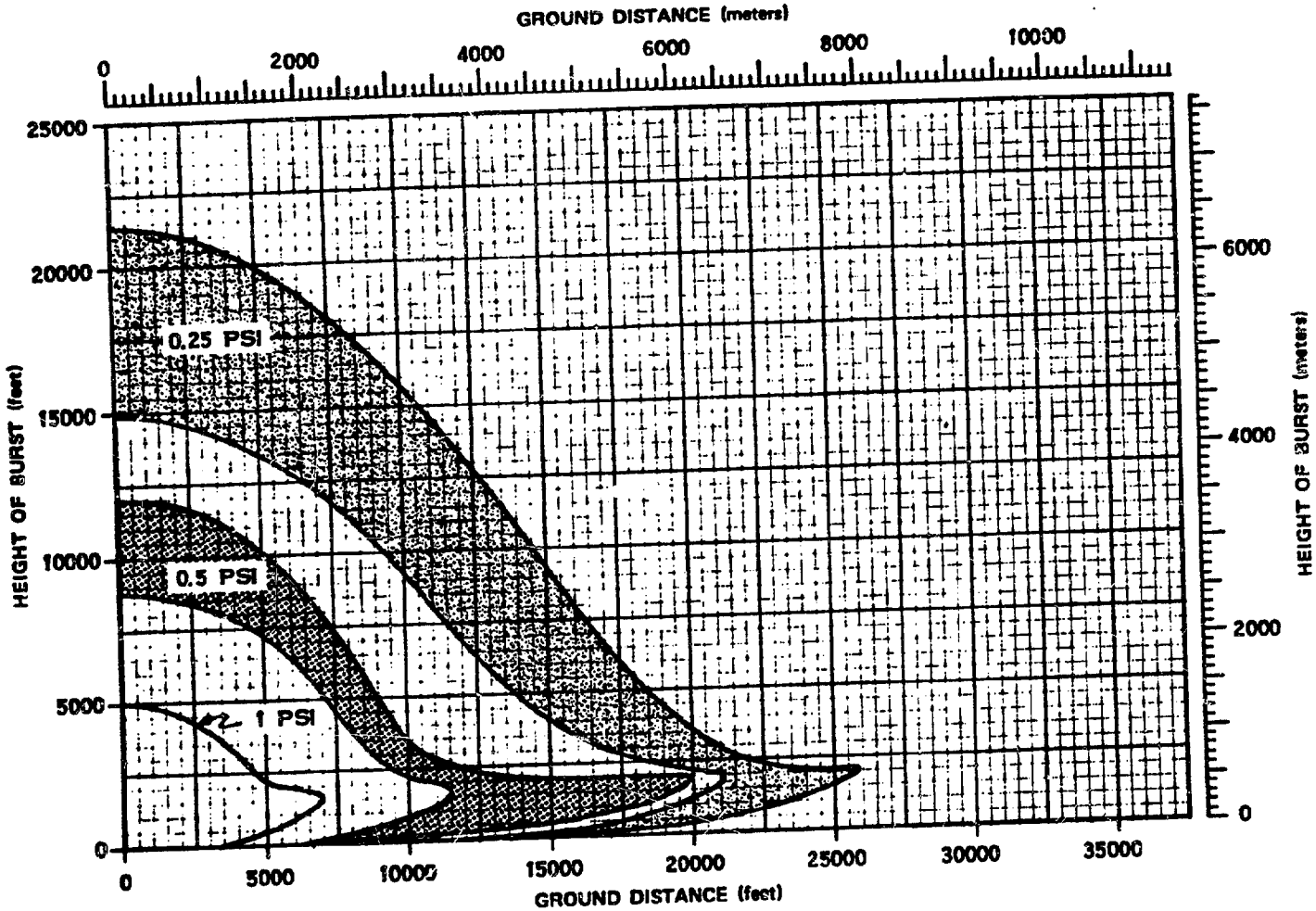

Figure 2-20. [redacted] Peak Overpressures at the Surface for a 1 kt Burst Over a Near-Ideal or Thermally Nonideal Surface, Very Low Overpressure Region [redacted]

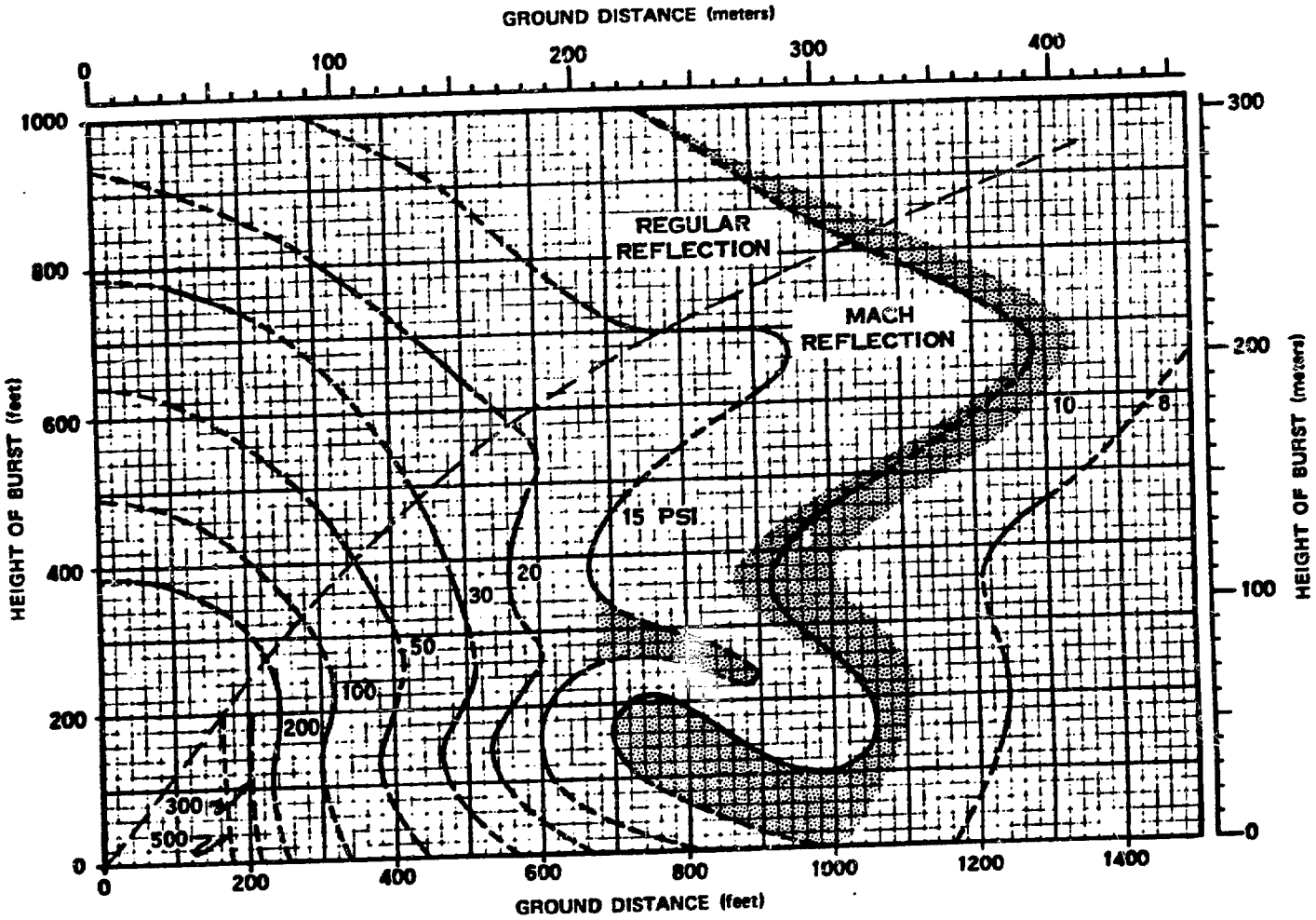

Figure 2-21. Peak Overpressures at the Surface for a 1 kt Burst Over a Thermally Nonideal Surface, High Overpressure Region

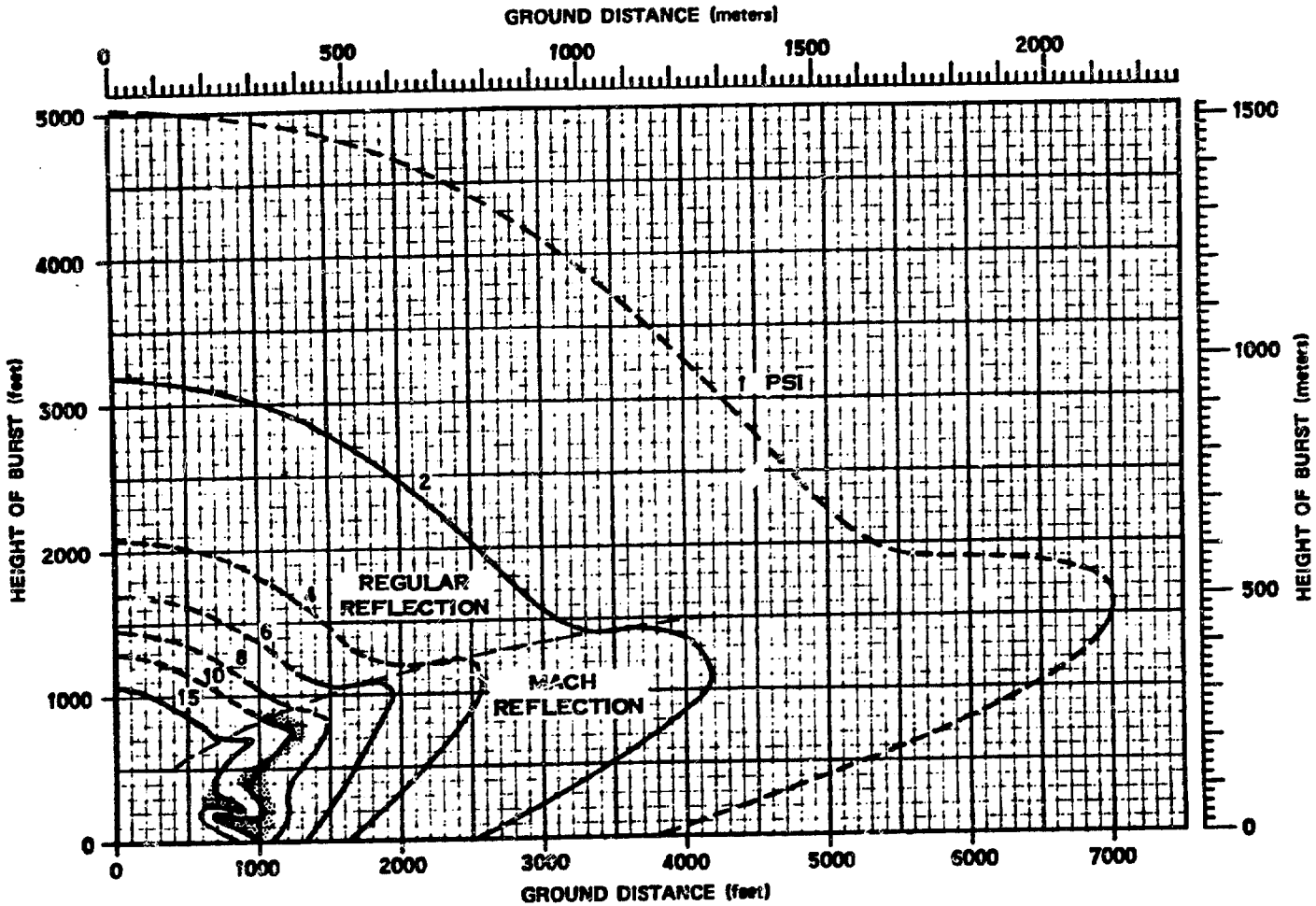

Figure 2-22. [redacted] Peak Overpressures at the Surface for a 1 kt Burst Over a Thermally Nonideal Surface, Low Overpressure Region [redacted]

[redacted]

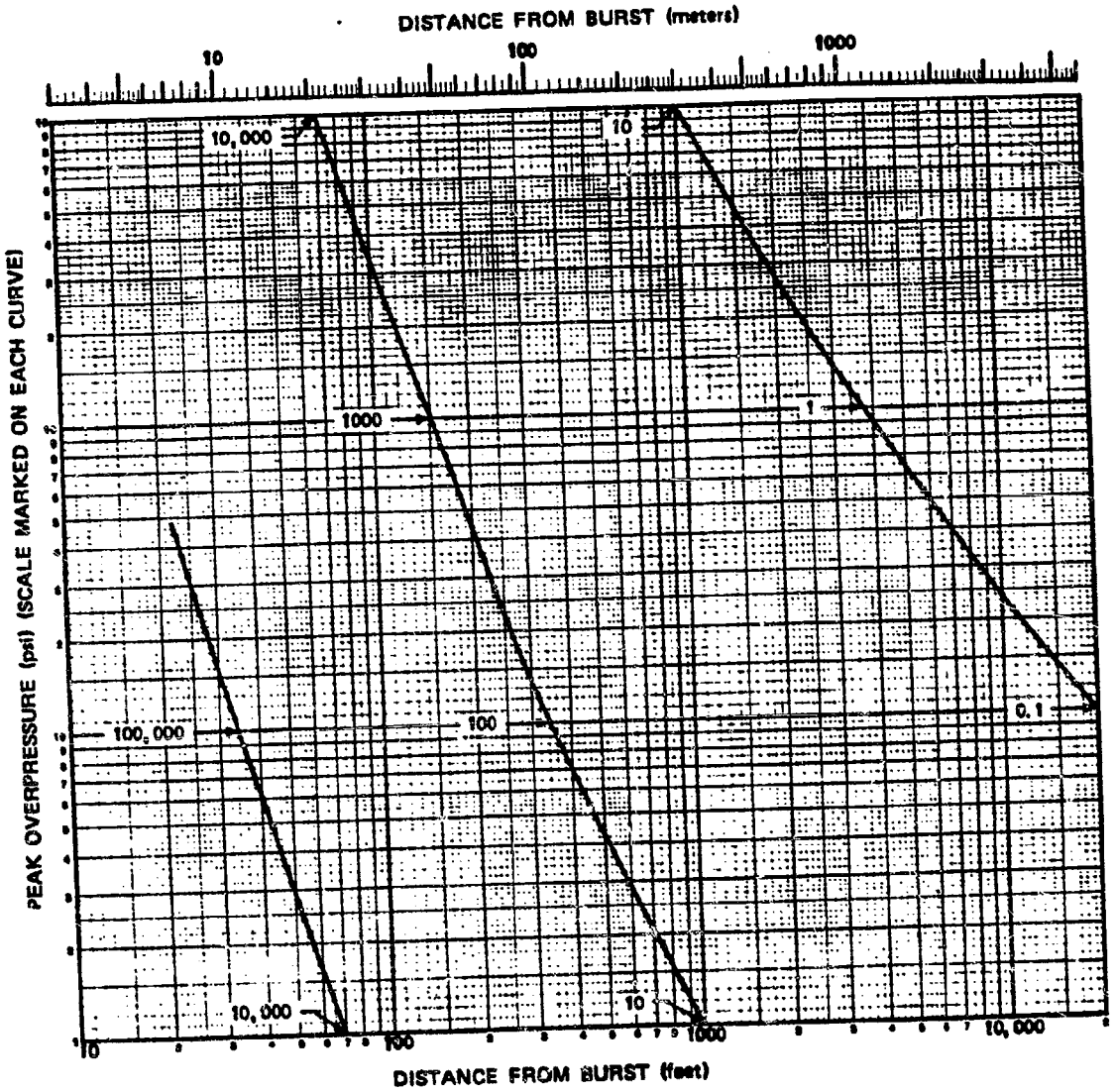

Figure 2-23. [redacted] Peak Overpressure from a Contact Surface Burst [redacted]

[redacted]

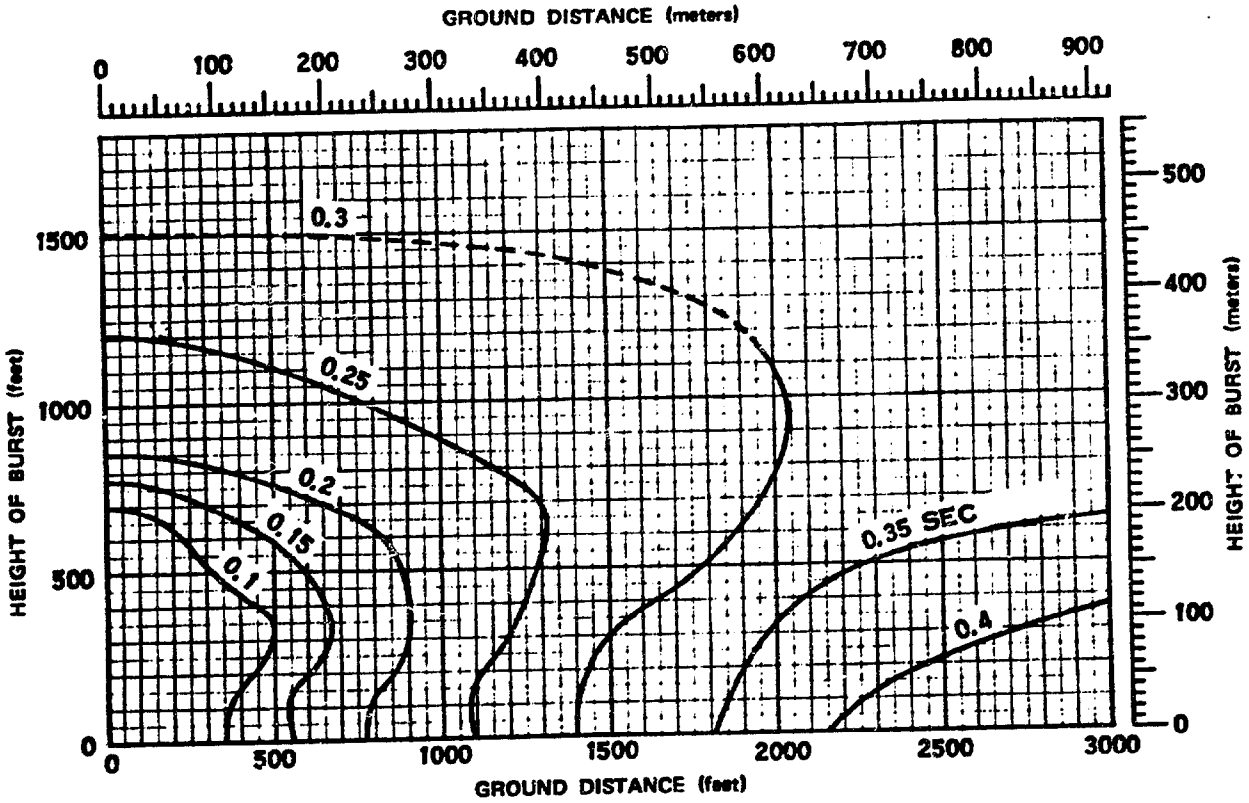

Figure 2-33. [redacted] Duration of Positive Overpressure at the Surface from a 1 kt Explosion Over a Near-Ideal Surface [redacted]

[redacted]

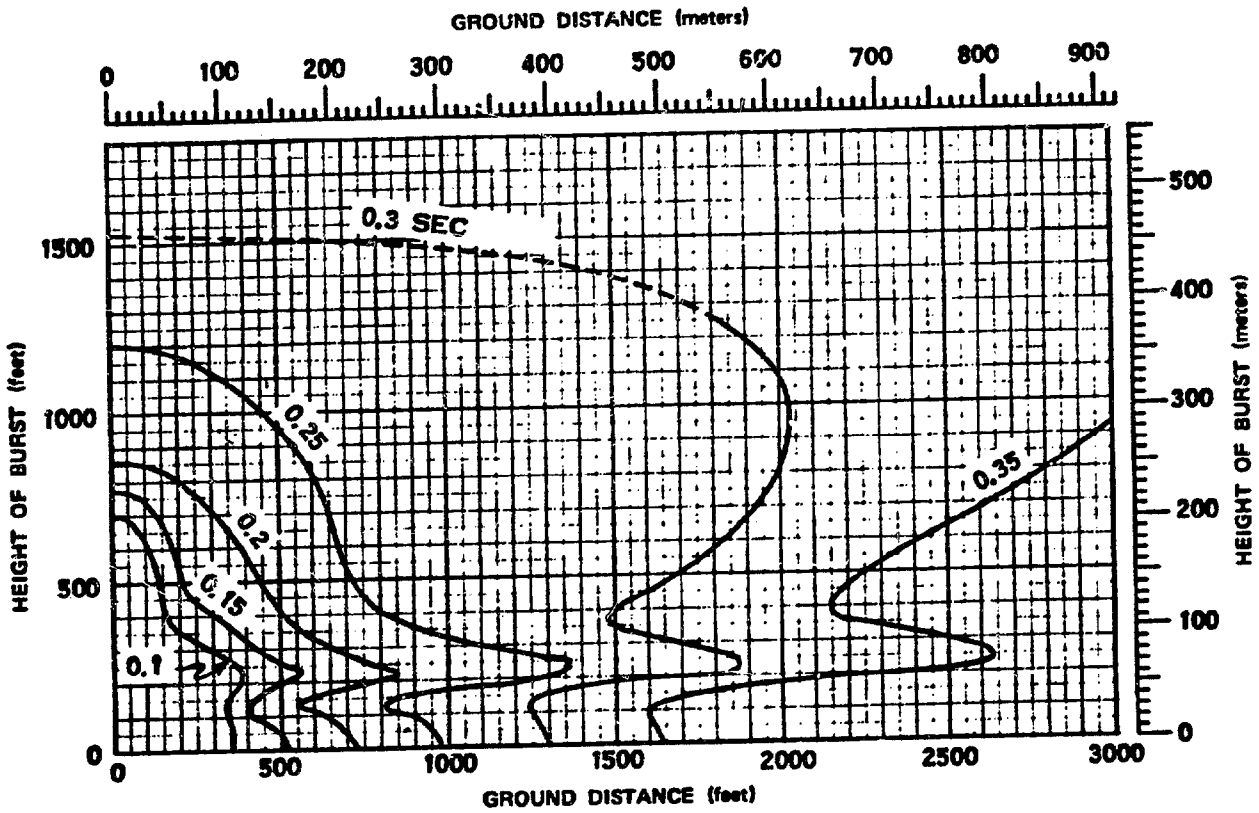

Figure 2-34. [redacted] Duration of Positive Overpressure at the Surface from a 1 kt Explosion Over a Thermally Nonideal Surface [redacted]

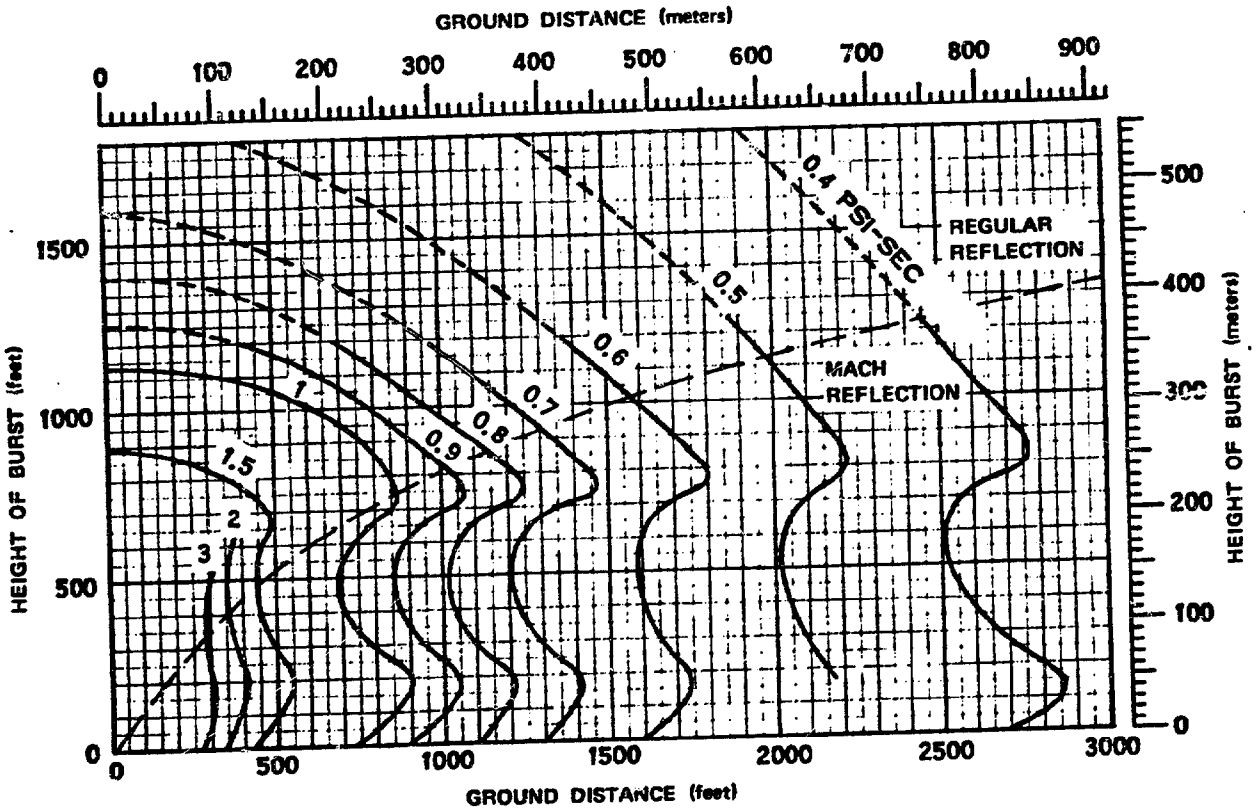

Figure 2-35. Positive Overpressure Impulse at the Surface from a 1 kt Explosion Over a Near-Ideal Surface

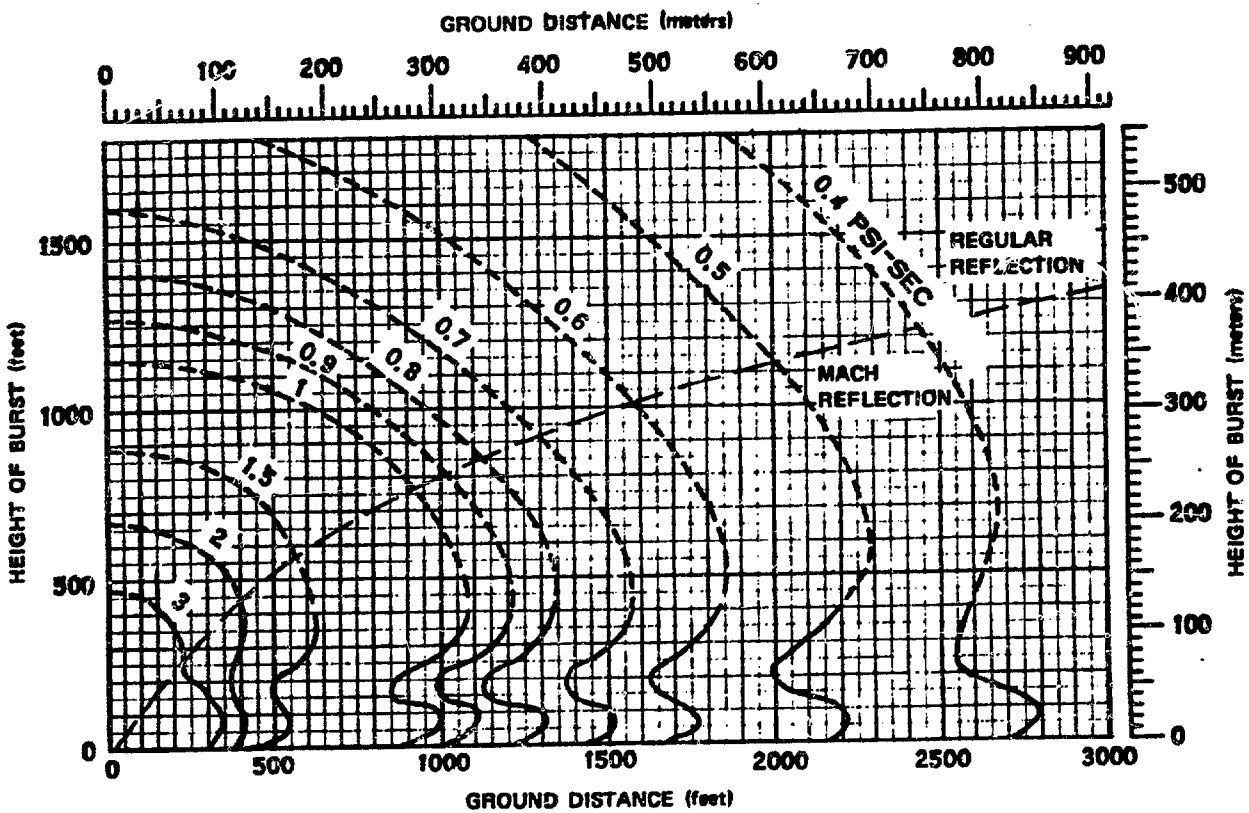

Figure 2-36. [redacted] Positive Overpressure Impulse at the Surface from a 1 kt Explosion Over a Thermally Nonideal Surface [redacted]

[redacted]

[redacted]

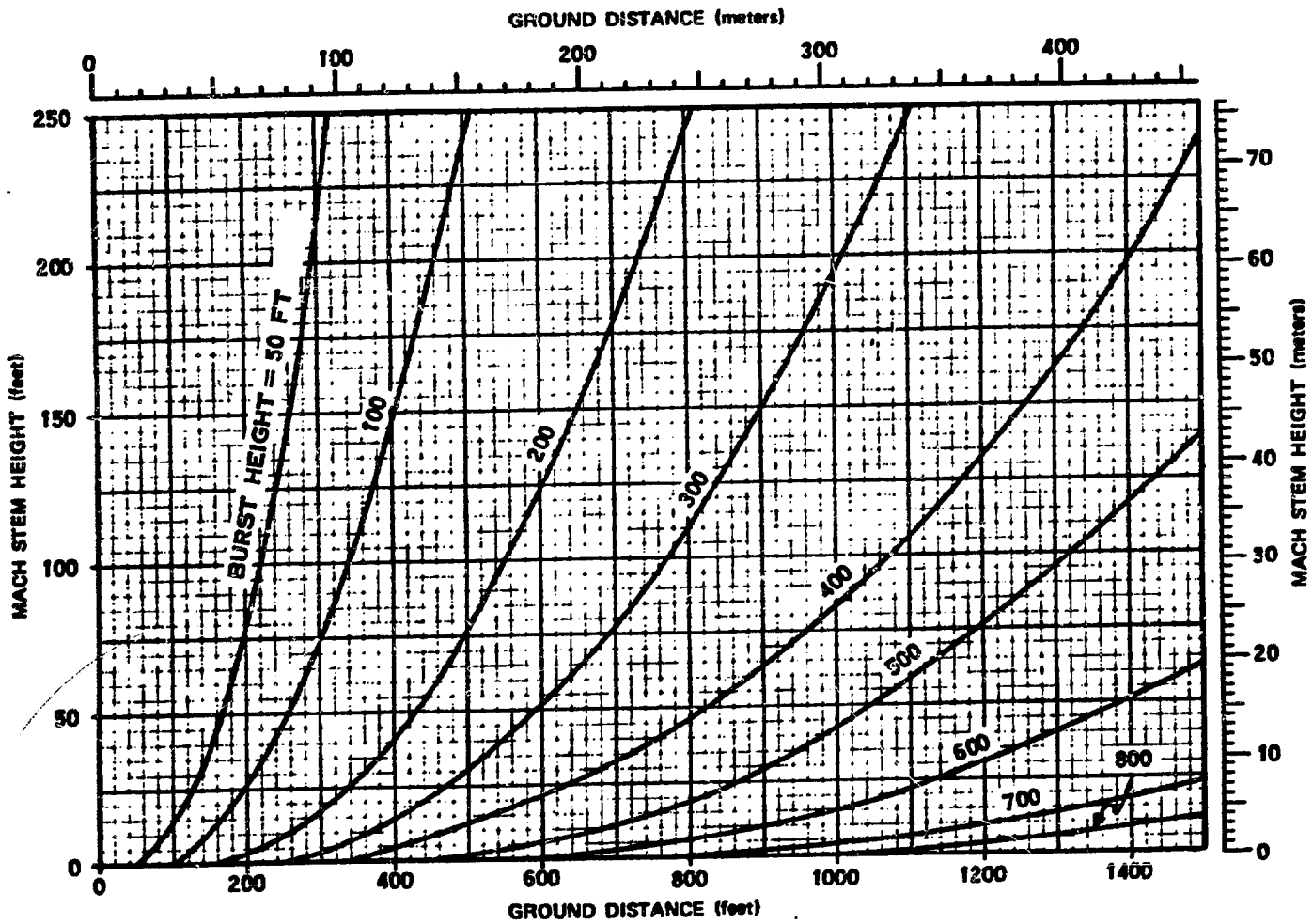

Figure 2-37. [redacted] Mach Stem Height for a 1 kt Explosion, High Overpressure Region [redacted]

[redacted]

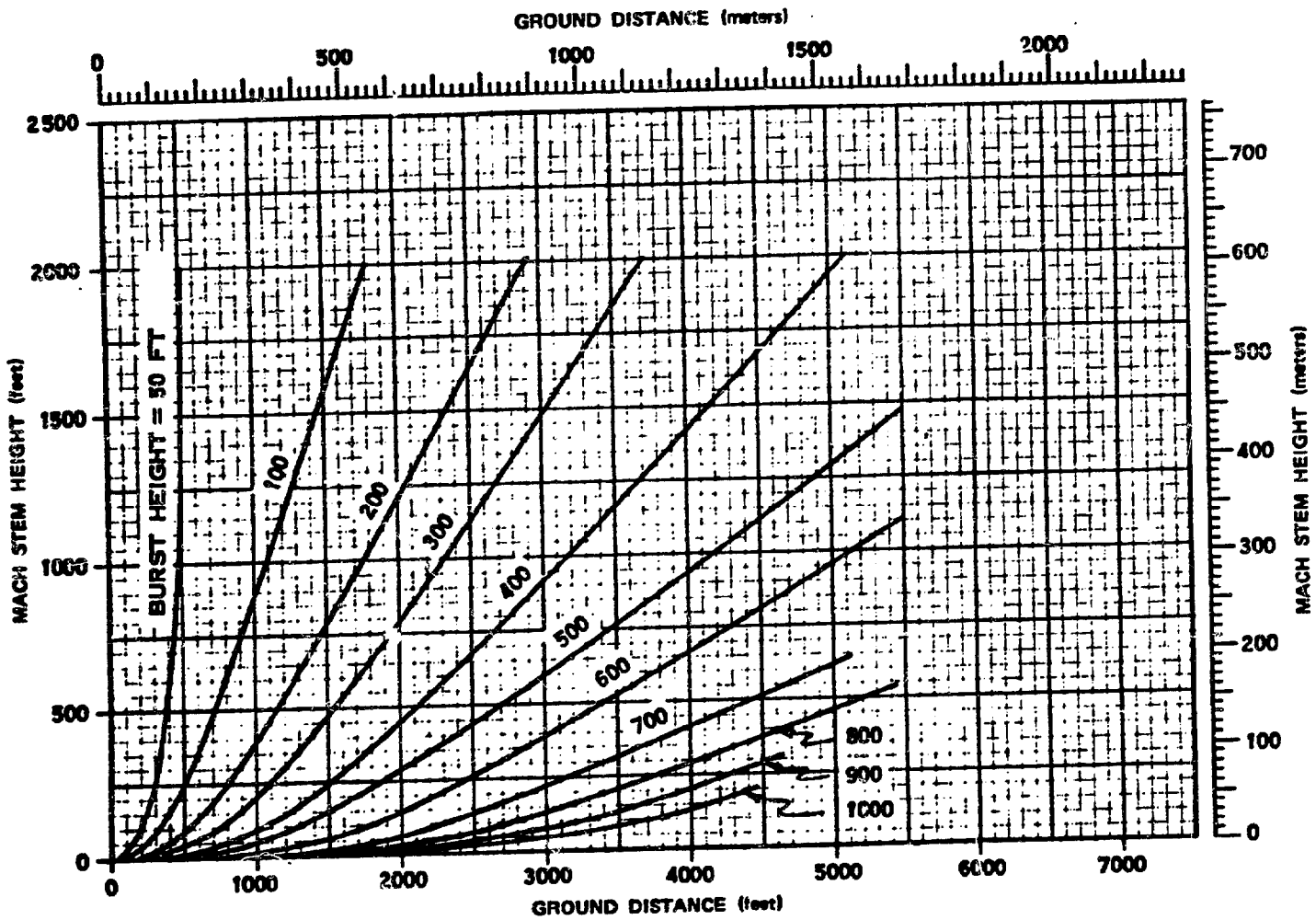

[redacted]

Figure 2-38. [redacted] Mach Stem Height for a 1 kt Explosion, Low Overpressure Region [redacted].

2-30 Criteria for Precursor Formation

Figure 2-39 shows heights of burst at which an explosion over a thermally nonideal surface is likely to produce a precursor. As indicated in Figure 2-39, bursts higher than 800 $W^{1/3}$ feet are not expected to form a precursor. This is the maximum height that will produce a precursor over asphalt, a surface that produces a precursor more readily than any other that has been tested. A burst below 650 $W^{1/3}$ feet will produce a precursor over desert sand. Since desert sand is considered a more typical nonideal surface than asphalt, it provides the basis for predicting precursors over most thermally nonideal surfaces.

Figure 2-39 also shows that a burst may be too low to produce a precursor as well as too high. At the ranges where a precursor might form, a contact surface burst of less than 30 kt is not expected to heat the surface sufficiently to produce a strong thermal layer; higher yields may create precursors over thermally nonideal surfaces.

Theories suggest that precursor formation depends not only on the amount of thermal energy absorbed by the surface, but also upon the time that is available for the thermal layer to form before the blast wave arrives. When time as well as thermal energy density is considered, theory indicates that the thermal layer and its influence on the blast wave might scale approximately as $W^{1/3}$, as indicated in Figure 2-39; however, no theory has yet been developed that explains the criteria for precursor formation in a completely satisfactory manner. For this reason, these criteria must be based on experimental data. Precursors have been observed from yields as high as 15 Mt; however, the yields that have been detonated between about 650 $W^{1/3}$ and 800 $W^{1/3}$ feet above the surface, and therefore the yields that are of value in confirming these criteria for precursor formation, are limited to the range of about 1 to 50 kt. Over this range of yields, the precursor seems to follow the cube root scaling; however, this may only result from the range of yields for which data are available being inadequate to reveal deviations. No reliability tolerances can be assigned to Figure 2-30, but if the surface is similar to desert sand, precursors may be predicted with reasonable accuracy for yields between 1 and 50 kt.

2-31 Overpressure Waveforms

The classical free air overpressure waveform (paragraph 2-12) is seldom found along the surface at overpressure levels above 6 psi. At higher overpressures, such waveforms approach the ideal for special surface conditions such as snow, ice, and water (where thermal effects are normally at a minimum). Even for these surfaces, minor mechanical effects may be present. For example, the rise time over water may not be instantaneous, and there may be a slight rounding of the peak of the overpressure waveform. When these near-ideal conditions exist, overpressure waveforms may be approximated by those for free air, shown in Figure 2-8.

In the simple case of ideal waveforms in free air, all of the properties of the blast wave, and therefore its damage potential, may be determined by specifying the ambient atmospheric conditions plus two blast parameters (for example, peak overpressure and positive overpressure impulse). When the blast wave loses its ideal characteristics, two other properties of the overpressure waveform become important: (1) for most overpressure-sensitive targets, a gradual rise to a given overpressure is less destructive than the abrupt rise of an ideal pulse; (2) as a result of the sustained overpressures often found in nonideal waveforms, a given peak overpressure may be associated with a much larger positive impulse than if overpressure pulse shape were ideal. Additional effects caused by changes in the dynamic pressure waveform are discussed in succeeding paragraphs.

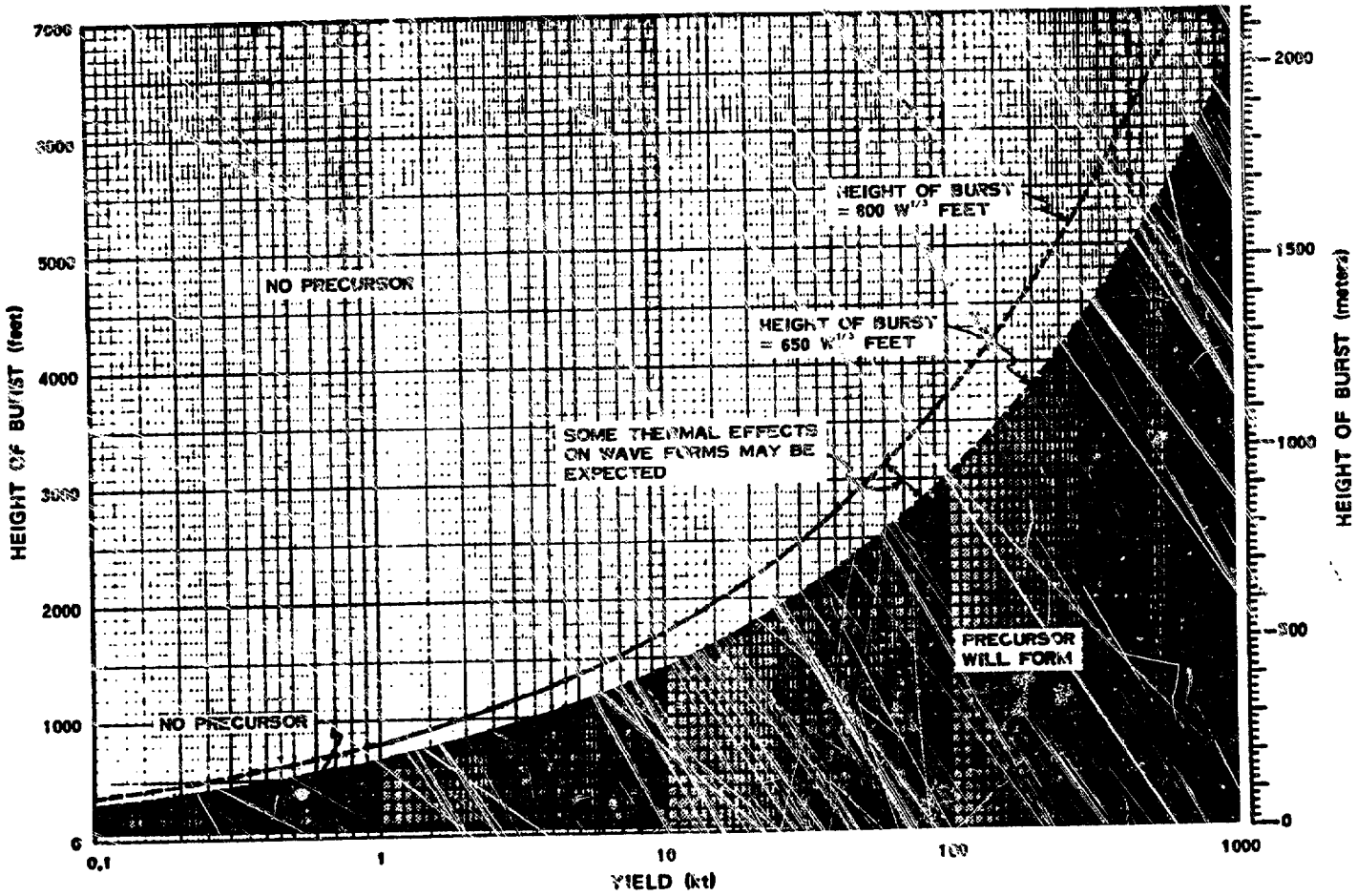

Figure 2-39. Criteria for Precursor Formation

[redacted]

[redacted] A series of eleven waveforms characteristic of the blast wave over a thermally nonideal surface is shown in time sequence in Figure 2-40. Although the evolution of a precursor is a continuous process, the waveforms may be classified loosely into five types, according to the state of development of the precursor:

Type I: Waveform before precursor forms (a)
Type II: Development of the precursor (b, c, d)
Type III: Evolution of fully developed precursor (e, f, g)
Type IV: Decline of precursor (h, i, j)
Type V: Return to nearly ideal waveform (k)

[redacted] The overpressure waveforms generated under any particular set of conditions depend strongly on the degree to which nonideal surface effects interact with the blast wave. In general, the more nonideal the surface conditions, the more nonideal will be waveforms near the surface. The waveforms shown in Figure 2-40 are typical for scaled heights of burst between 100 and 400 feet over flat desert surfaces. Characteristics of these waveforms are discussed below.

- Type I – Just before the precursor forms, the waveform *a* is relatively ideal.
- Type II – As the precursor starts to develop, a separate shock front forms in the thermal layer and moves out ahead of the main shock. In waveform *b* these two shock fronts are nearly ideal but, as the precursor develops, its diverging flow pattern weakens its own shock front. At the same time, the growing precursor interferes more strongly with the main blast wave, which apparently loses any semblance of a true shock front at the surface. Separation of the two peaks indicates the forward growth of the precursor; however, the second peak in waveforms *c* and *d* no longer marks the exact position of the main blast wave. Typical changes in Type II waveforms at early times are a rapid attenuation of the first peak and a rounding of the second peak. At later times, the second peak is attenuated more rapidly than the first, and the first loses its shock-like rise. The slow decay after the first peak in waveforms *c* and *d* is sometimes replaced by a plateau.
- Type III – As the distance from ground zero increases, the peaks and valleys become poorly defined. At close distances, the waveform *e* has a large rounded maximum followed by a slow decay, and a later and smaller second peak. At longer distances, the first peak is attenuated more rapidly than the second, and the two peaks become comparable in magnitude (f). The rise times also become longer. The second peak disappears at longer distances, leaving a low, rounded, flat-topped waveform *g* with a long initial rise and slow decay, during which there is considerable turbulence. This waveform is typical of strong precursor action.
- Type IV – Farther from ground zero, the thermal layer becomes less intense, and the precursor begins to weaken and lose forward speed. The second peak reappears, and both peaks become sharper. The rounded plateau in waveform *h* and the step-like appearance of *i* are typical. As the main shock overtakes the precursor, the waveform assumes an almost classical form *j* with a sharp rise to a more or less level plateau, followed by an essentially regular decay. This waveform is typical of the "clean-up" portion of the precursor cycle.
- Type V – After the precursor has disappeared, the pressure pulse again approaches a classical waveform *k*. This waveform is longer than it would be if a precursor had never formed.

[redacted] Methods for determining ground dis-

[redacted]

[redacted]

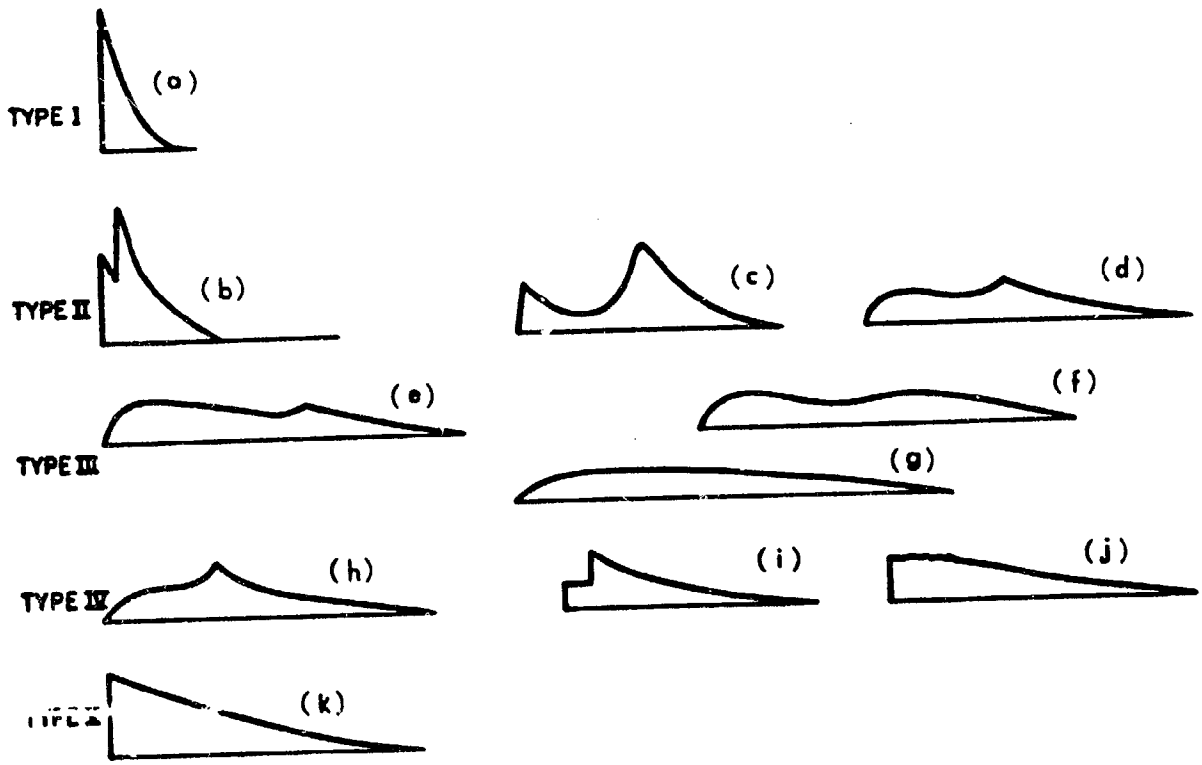

Figure 2-40. [redacted] Typical Sequence of Overpressure Waveforms Over Thermally Nonideal Surfaces [redacted]

[redacted]

[redacted]

tances at which the waveforms described above will occur are described in Problem 2-15.

2-32 Dynamic Pressure Waveforms [redacted]

[redacted] Dynamic pressure waveforms at the surface approach the classical shape shown in Figure 2-9 when the surface conditions are near-ideal. The conditions under which this occurs are more restricted than those for overpressure waveform. Differences result from surface conditions that do not lead to precursor formation but do lead to dust or spray loading of the air. Such surfaces are expected to modify the dynamic pressure waveform without changing the overpressure waveform to any great extent.

[redacted] Dynamic pressure waveforms that appear over thermally nonideal surfaces are more difficult to measure than overpressure waveforms, and the measurements are subject to wider variations. For these reasons it is not possible at this time to provide a figure that shows zones in which various waveforms can be expected. However, representative waveforms have been constructed (Figure 2-41), and tentatively have been classified into five categories: A, B, C, D, and E (letters rather than Roman numerals are used with dynamic pressure waveforms to emphasize that the various types cannot be directly correlated with the waveform types used to classify overpressure waveforms). These waveforms are discussed below.

- Type A – Before the precursor forms, the waveform is relatively ideal (1).
- Type B – As the precursor starts to develop, the waveform shows two distinct peaks. The first, corresponding to the precursor, has a shock type rise in most cases. The second is larger than the first at close distances (waveforms 2 and 3), but at longer distances (waveform 4) it becomes comparable in magnitude to the first.
- Type C – As the precursor becomes fully developed, the waveform retains its double peak but loses its rapid initial rise time. Actual record traces have a very turbulent appearance. The second peak is smaller than the first (5) and tends to become indefinite with increasing distance (6).
- Type D – As the precursor becomes weaker, the waveform assumes an essentially single peaked form, characterized at close distances (waveform 7) by a low-amplitude plateau with a slow rise. Actual traces have a very turbulent appearance. As the distance from ground zero increases (waveform 8), the turbulence lessens, and the plateau develops a shock rise with either a flat top or a slow steady increase to a second shock rise, followed by a smooth decay. The second shock eventually overtakes the first (waveform 9), leaving a smooth, clean trace with a slight rounding after the initial shock type rise.
- Type E – After precursor cleanup, the waveform (10) resumes its approximately classical shape. Positive phase duration is longer than it would be at this distance if a precursor had not formed. This longer duration is more marked for dynamic pressure than for overpressure.

[redacted]

[redacted]

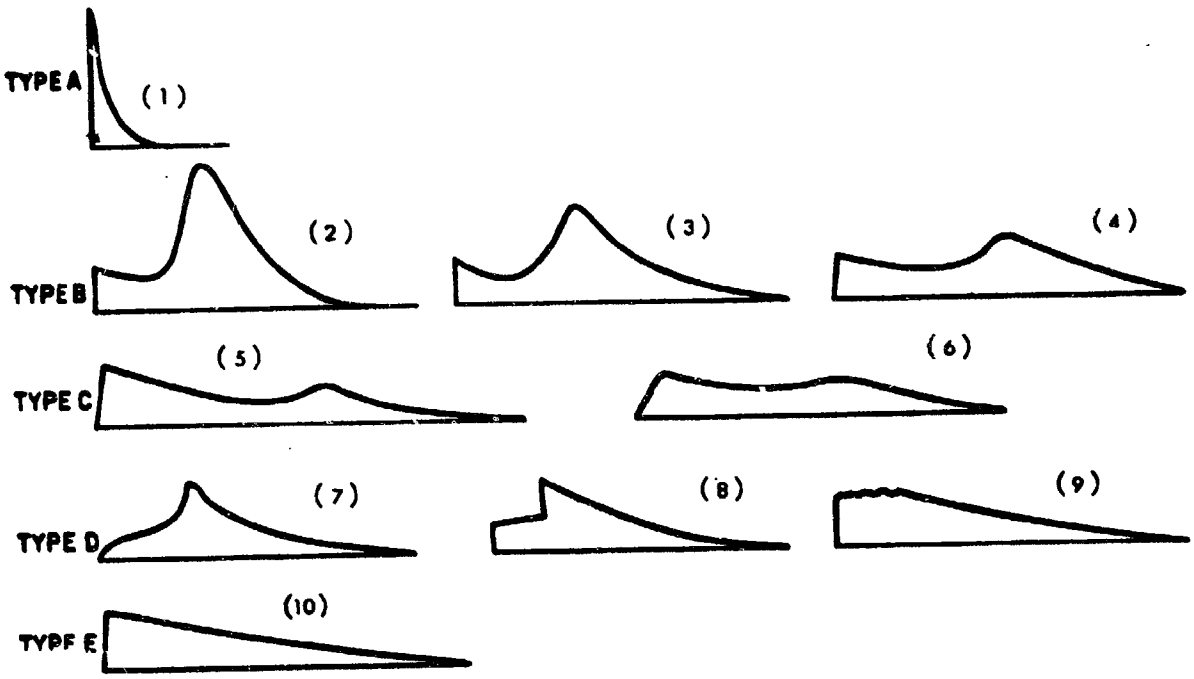

Figure 2-41. [redacted] Typical Sequence of Dynamic Pressure Waveforms Over Thermally Nonideal Surfaces [redacted]

[redacted]

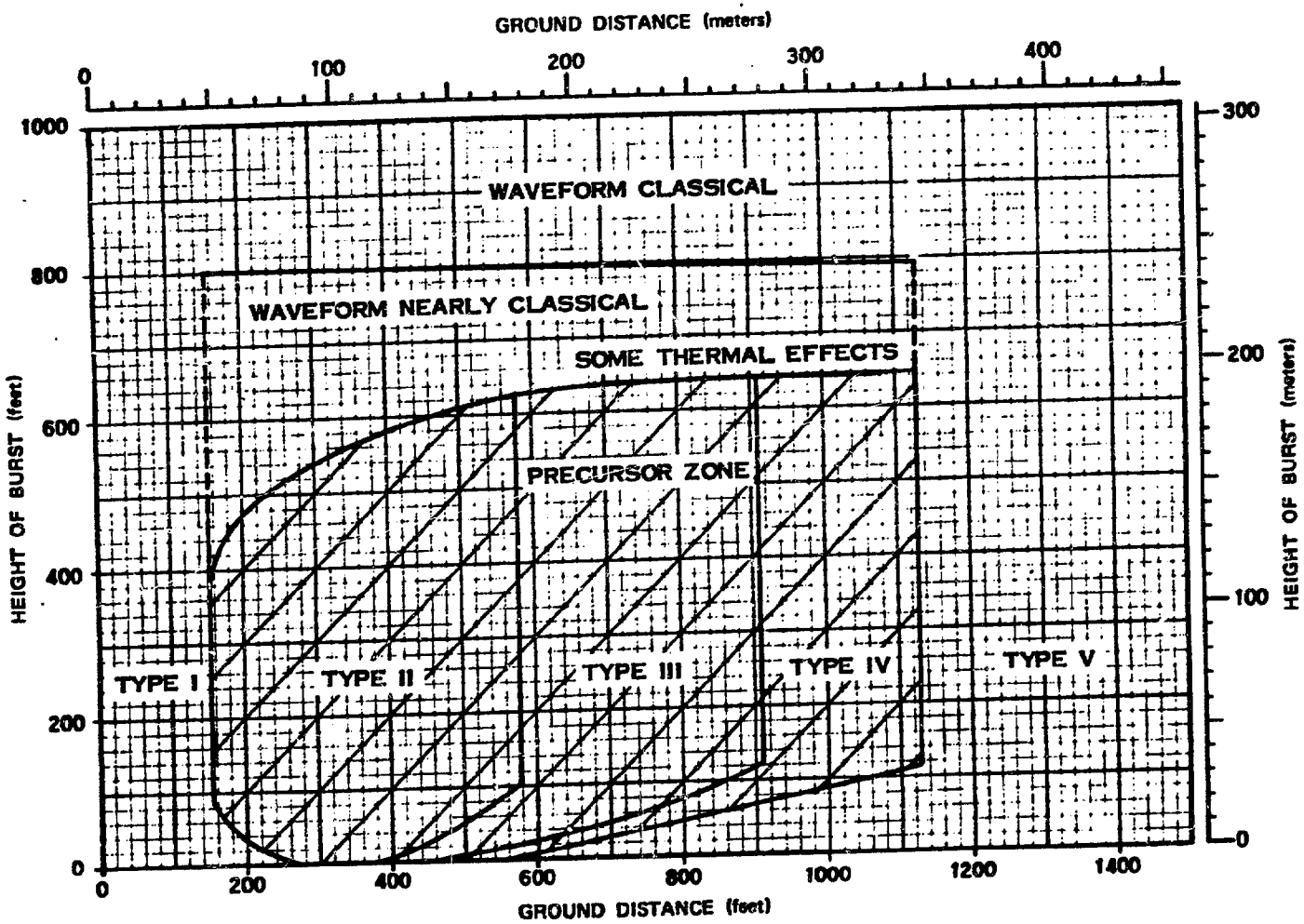

Figure 2-42. [redacted] Variation of Overpressure Waveform from a 1 kt Explosion Over a Thermally Nonideal Surface [redacted]

[redacted]

2-33 Effect of Rain and Fog on Overpressure [redacted]

[redacted] The effects of atmospheric moisture on blast propagation are not well known; however, theoretical studies agree qualitatively with the small amount of experimental data. As a strong blast wave propagates through air containing water droplets it vaporizes some or all of the water. Vaporization of the water absorbs energy that otherwise would be available for the blast wave to propagate through the air.* As a result, the blast wave is attenuated more rapidly in air that contains water droplets than in air that does not.

[redacted] The effect of water droplets on peak overpressure may be calculated in terms of effective yield. This procedure is used to obtain lower calculated overpressures at some distance from the burst. Rain or fog has a negligible effect on the amount of available energy close to the nuclear source. The energy density within the fireball is orders of magnitude higher than the energy required to vaporize whatever water may be present, and the amount by which the suspended liquid increases effective air density, even under the extreme conditions within clouds producing severe thunderstorms, is not likely to exceed 2 percent.

[redacted] Figure 2-43 shows the effective yield for three yields and two conditions of moisture content. Examination of these curves reveals several trends:

- The attenuation produced by heavy rain is greater than the attenuation produced by light rain or fog.
- Effective yield decreases as overpressure decreases, i.e., it decreases as distance (and, therefore, the amount of rain through which the blast wave must propagate) increases.
- At any overpressure level, the blast wave from a 1 kt burst is attenuated less than the blast wave from the two other yields. This difference results from the shorter distances for the 1 kt blast wave. Light rain or fog attenuates the blast wave from a 1 kt explosion to such a small extent that the curve is not included in Figure 2-43.
- At a given overpressure level, the blast wave from a 1 Mt burst is attenuated less than the blast wave from a 125 kt burst. This effect, opposite to that described above, probably results from the relatively large amount of hydrodynamic energy carried by the long-duration blast wave from a 1 Mt source.

[redacted] The curves shown in Figure 2-43 are based on the assumption of uniform water content between the source and the target. In an actual rainstorm, this assumption is artificial. Typically, water content is several times as high within a rain cloud as it is below the cloud, but without such an assumption the analysis of rain effects would be unduly complex. Actual water distribution patterns are complex, different for different rainstorms, and generally unpredictable. The water densities used in the calculations correspond roughly to precipitation rates of 0.1 and 0.5 inches per hour.

---

*[redacted] As a blast wave propagates through air, it continuously expends hydrodynamic energy at the shock front to compress and accelerate the air entering the blast wave. At the same time, the air behind the front expands and decelerates, thereby returning energy to the blast wave. The flow of energy in a weak shock wave resembles that in a sound wave. The expanding air returns nearly all of the energy that it received when it entered the shock front. Consequently, the attenuation of weak blast waves is due principally to spherical divergence. On the other hand, strong shock waves lose appreciable energy, because the sudden compression at the shock front is partially irreversible. Thus, the expanding air beyond the strong shock front returns less energy than was required to compress it, and the corresponding energy loss contributes to the attenuation of the blast wave. If the air contains water droplets, the energy extracted from the blast wave when the water evaporates is returned to the surrounding air when the water condenses; however, condensation occurs too slowly to contribute appreciable energy to the blast wave.

[redacted]

[redacted]

[redacted] Rain or fog effects should be evaluated only when the optimization of blast against soft targets is important, and then only if the rain or fog extends throughout a volume that includes both the target and the burst. HOB curves for thermally near-ideal surface conditions should be used with Figure 2-43 since thermal energy is attenuated by rain or fog and a wet surface is not expected to form a strong thermal layer.

[redacted] The effects of atmospheric moisture on other blast parameters, such as time of arrival, positive-phase duration, and dynamic pressure are not well known; however, theoretical considerations indicate that arrival times will remain essentially unchanged, positive-phase durations will be slightly reduced, and dynamic pressures will be slightly increased. Calculations for these other parameters should be made in the normal manner, without applying the yield correction factor obtained from Figure 2-43.

[redacted]

[redacted]

Problem 2-16. Calculation of Overpressure During a Rainstorm

[redacted] Figure 2-43 shows the reduced yield in percentage of actual yield, that should be used for overpressure calculations under conditions of rain and fog. This figure should be used together with Figures 2-17 through 2-19 to obtain overpressure values under conditions of rain or fog.

[redacted] *Scaling.* Interpolation between the curves of Figure 2-43 provides the only yield scaling available. After obtaining an effective yield from Figure 2-43, the scaling procedures described in Problem 2-9 are applicable.

[redacted] *Example* [redacted]

Given: A 50 [redacted] explosion at a height of burst of 3,000 feet during a heavy rainstorm.

Find: The peak overpressure 4,000 feet from ground zero.

Solution: The corresponding height of burst and ground distance for a 1 kt explosion yield are

$$h_1 = \frac{h}{W^{1/3}} = \frac{3{,}000}{(50)^{1/3}} = 815 \text{ feet,}$$

$$d_1 = \frac{d}{W^{1/3}} = \frac{4{,}000}{(50)^{1/3}} = 1{,}090 \text{ feet.}$$

From Figure 2-18, the peak overpressure expected in clear air is about 13 psi. At this peak overpressure, Figure 2-43 indicates that the effective yield during heavy rain is about 84 percent for 1 kt, 73 percent for a 125 kt burst. A probable effective yield for 50 kt should be between these values and may be about 77 percent. Uncertainty in the degree of attenuation produced by a rainstorm would cause the effective yield to vary according to the reliability estimates given below. This calculation will determine the most probable value of the peak overpressure rather than the upper and lower limits. The effective yield for further calculations is

$$50 \times 0.77 = 39 \text{ kt.}$$

The corresponding height of burst and ground distance for a 1 kt explosion are

$$h_1 = \frac{h}{W^{1/3}} = \frac{3{,}000}{(39)^{1/3}} = 885 \text{ feet,}$$

$$d_1 = \frac{d}{W^{1/3}} = \frac{4{,}000}{(39)^{1/3}} = 1{,}180 \text{ feet.}$$

Answer: From Figure 2-18, the most probable peak overpressure is 10 psi.

[redacted] *Reliability:* Figure 2-43 is based on theoretical calculations and a limited amount of data from small scale field tests and laboratory experiments. Thus, a high reliability cannot be assigned to the curves of Figure 2-43. The upper limit of the effective yield is 100 percent of the actual yield, while the lower limit is estimated to be 60 percent of the value obtained from Figure 2-43. If the burst is below or close to the cloud base in fairly uniform rainfall, somewhat greater reliability might be expected.

[redacted] *Related Material:* See paragraphs 2-24 and 2-33. See also Problem 2-9.

[redacted]

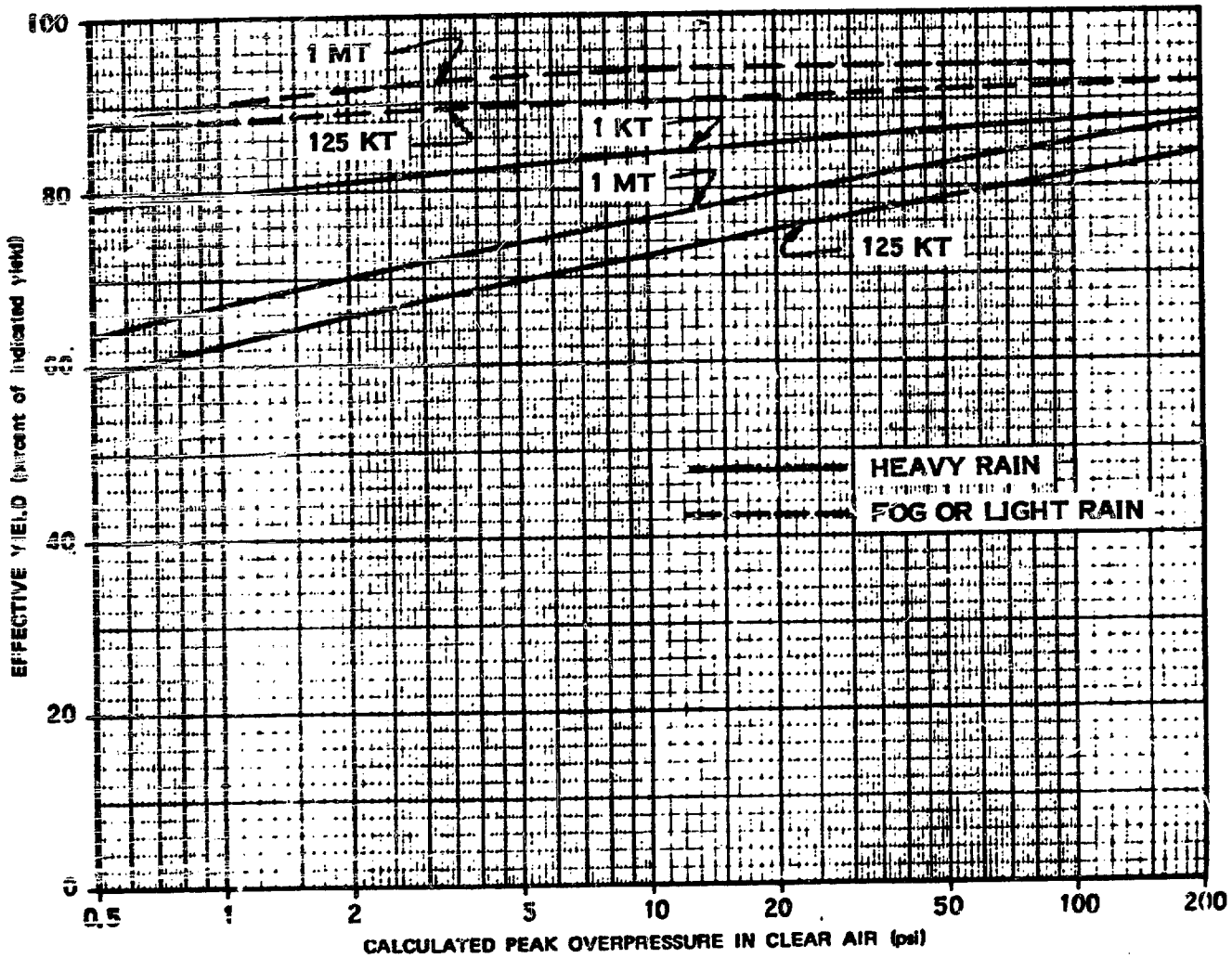

Figure 2-43. Reduction of Peak Overpressure at the Surface by Rain or Fog—Near-Ideal Surface Conditions

[redacted]

2-34 Peak Overpressure at the Surface of Deep Snow [redacted]

[redacted] When a shock front enters a layer of snow it is attenuated strongly. Drag forces on the snow crystals dissipate energy contained in the wind behind the shock front. The energy transmitted to the snow crystals is then consumed in compacting the snow layer.

[redacted] Reflection occurs at the top surface of a deep snow layer just as it does at a ground surface. Momentum is conserved in the interaction, and, in the case of a ground surface, the process is analogous to a light, elastic object striking a heavy one. The light object bounces away, retaining most of the energy that it had before the collision. The heavy object receives a small amount of energy. A blast wave striking the earth transmits only a small fraction of its energy as ground shock; consequently, the earth's surface approximates an ideal reflector. A blast wave striking a snow surface is analogous to a ball bouncing from a heavy rug. The reflecting surface has a cushioning effect that makes it a poorer reflector.

[redacted] In the case of a thin layer of snow, the cushioning effect ceases when the pressure wave penetrates the snow layer, reflects from the ground surface, and propagates back to the snow surface. At this time, the snow layer is supported by an internal pressure as high as the pressure produced by the blast wave reflecting from the surface; the reflecting qualities of the snow layer then approach the near-ideal reflecting qualities of the underlying surface.

[redacted] Neither theoretical nor experimental data are available on the effects of thin snow layers on a blast wave, however, a rough calculation is enlightening. If a shock front in snow moves with a speed comparable to that of sound in air, a layer of snow one foot thick, struck by a normally incident blast wave, will absorb energy from the blast wave for about 2 milliseconds and will have the properties of a near-ideal reflecting surface after that time. This 2-millisecond interval is appreciably long only when compared with relatively sharp blast waves. For example, it might alter a 750 psi blast wave from a 1 kt source significantly. The overpressure pulse of this blast wave has an effective triangular duration (see Figure 2-10) of about 20 milliseconds. At lower overpressures, the pulse becomes broader. For a given overpressure, larger yields than 1 kt also produce broader pulses. This comparison indicates the following:

- If a blast wave with a very narrow pressure pulse strikes a thin layer of snow, the snow may alter the leading edge of the pressure pulse enough to reduce peak reflected overpressure.
- In a more typical situation, i.e., one for lower overpressures and yields greater than 1 kt, a thin snow cover affects such a small portion of the overpressure pulse that peak reflected overpressure is essentially the same as at a near-ideal surface.

[redacted] Presently available experimental data on the properties of blast waves over deep snow surfaces are based on high-explosive (HE) experiments. In all of the tests, the snow layers were sufficiently thick to react as though they were infinitely thick. The thinnest snow layers tested (7 inches) correspond to snow layers about 60 $W^{1/3}$ feet thick (W in kt). For an 8 kt burst, this thickness is about 120 feet. Since snow layers thicker than about 120 feet compress to form glacial ice, the 7 inch snow layers have no real scaled counterpart for nuclear bursts larger than about 8 kt.

[redacted] The available data for the effects of snow on the blast wave, when scaled for calculations of the blast wave from bursts larger than 1 kt may be applied with confidence only to regions such as the arctic, where large areas are covered by very thick snow layers.

[redacted]

Scaling HE data over snow to the blast wave from a nuclear burst involves considerable uncertainty. Predictions of peak overpressure over a deep snow surface, are based on the following reasoning: (1) the HE studies show that snow reduces the ground distance to which a given peak overpressure extends by about 10 percent (this figure is never smaller than 0 percent or greater than 20 percent); (2) HE data over snow are not available at points near ground zero, and thus, the experimental data fail to show how much burst height should be changed for a given peak overpressure.

Figures 2-18 and 2-19 may be used to predict peak overpressures over deep snow by reducing all ground distances by 10 percent.

One significant effect of snow cover is that it forms a thermally near-ideal surface. Clean snow reflects most of the thermal radiation that strikes it. Dirty snow absorbs more energy than clean snow but it absorbs it in a way that is unlikely to produce a thermal layer. An experimental study indicates that thermal radiation from a nuclear burst will melt a negligible amount of a clean snow surface and that the water formed will be absorbed quickly by the remaining snow.

An important unknown is the degree to which propagation through snow lengthens the rise time of the overpressure pulse. Even when snow cover is not thick enough to reduce peak reflected overpressure significantly, a layer of snow covering overpressure-sensitive targets may offer protection by reducing the sharpness of the overpressure pulse. This effect may be particularly important in evaluation of ground-shock damage to buried targets.

In the absence of confirming data from nuclear tests over snow, use of the curves in Figures 2-18 and 2-19 must be regarded as tentative. Ground distances obtained from the curves are estimated to be reliable within ±25 percent for yields between 1 kt and 10 kt when used to predict peak overpressures over snow. Outside this range of yields, the curves may be used with somewhat less confidence.

2-35 Peak Overpressure at an Infinite Reflecting Surface

Curves showing peak reflected overpressure may apply to finite surfaces, such as the side of a building, or they may apply to the earth's surface, which is effectively infinite in extent. The two types of curves resemble one another except at angles of incidence close to 90°, i.e., at grazing incidence (see footnote to paragraph 2-17 for a summary of the conventions used in specifying the angular orientation of reflecting surfaces). At this grazing angle of incidence, a finite area produces no enhancement of the incident overpressure, the incident overpressure is sometimes called the "side-on" overpressure.

A reflecting surface that is infinite in extent affects the blast wave differently. Figure 2-44 shows that the reflection coefficient $\Delta p_r/\Delta p$ of such a surface at grazing incidence is greater than 1. A blast wave having an angle of incidence of exactly 90° with a flat, infinite surface is, by definition, a contact surface burst. The surface of the earth confines the blast wave from a contact surface burst to half of the volume it would occupy in free air. As a result, peak overpressure is higher than it would be in free air; this fact is indicated by a reflection coefficient greater than 1.

Figure 2-44 has two parts, corresponding to the regions of regular reflection and of Mach reflection. A peak occurs near the boundary between the two regions; at the lower incident overpressures, this peak shows a higher reflected overpressure than that produced by a blast wave striking a surface head-on. The same phenomenon appears in the height-of-burst charts as the knee of an overpressure curve.

At incident overpressures greater than

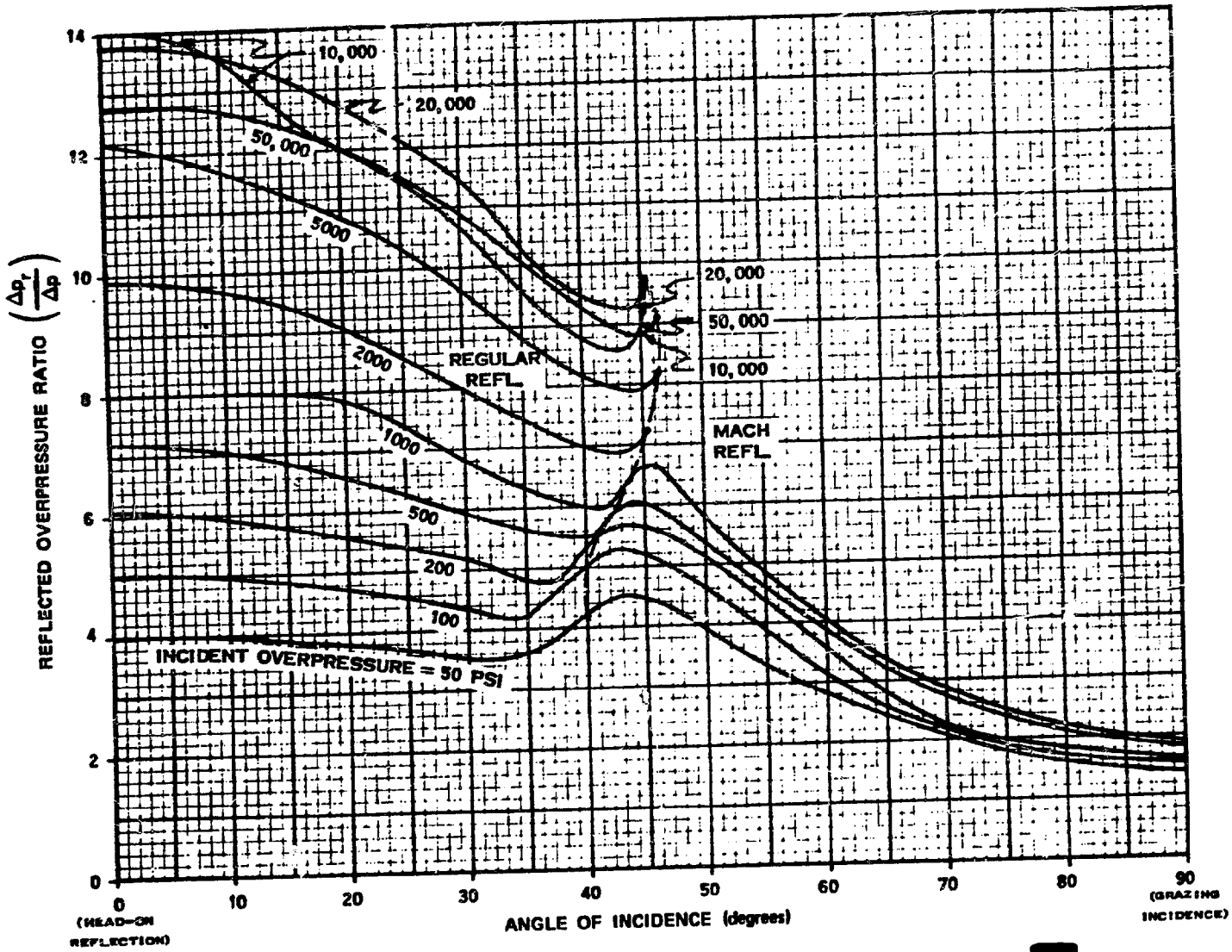

Figure 2-44. [redacted] Reflection Properties of Strong Shock Waves at an Infinite Surface [redacted]

5,000 psi, the curves in Figure 2-44 deviate from the regular pattern seen at lower incident overpressures. These deviations result from the high temperatures produced at the shock front, which cause dissociation and ionization of the air atoms to absorb energy that would otherwise increase the pressure of the gas.

The data in Figure 2-44 may be replotted to prepare a height of burst graph. An intermediate plot, consisting of a family of curves, each for a given angle of incidence should be plotted first. Figure 2-45 shows, as an example, the curve for an angle of incidence of 30°. Slant ranges for this intermediate plot are found as a function of incident overpressure from Figure 2-2, the overpressure-distance curve for free air. The data from the intermediate plot may be transferred to the HOB chart by plotting slant range and angle of incidence as shown in the inset of Figure 2-45.

Such a transformation should lead to the HOB chart shown in Figure 2-17; however, certain discrepancies exist between that HOB chart and the data in Figure 2-44. The principal difference is that the peaks shown at angles near 45° in Figure 2-44 have been rounded off in the HOB chart since it is uncertain how well the data in Figure 2-44 describe the actual reflecting properties of the surface of the earth for reasons described below. Although the peaks shown in Figure 2-44 probably occur, the angle at which they occur may be different from that indicated. Therefore, a transformation of every detail of the curves in Figure 2-44 to the HOB chart implies a more detailed knowledge of the shapes of the HOB curves than actually exists.

Uncertainty of the data in Figure 2-44 arises from the way in which these data had to be obtained. The Mach reflection portions of the curves in Figure 2-44 were obtained theoretically, using the shock-wave equations and the air equation of state given in Appendix A. The calculation is complex, involving successive approximations that are most appropriately handled on a computer.

A large portion of the regular reflection regions of the curves were obtained experimentally. Many data points from nuclear tests document the low pressure curves at angles close to 90°, and theory plus a few data points were used to extrapolate the data to smaller angles and to the highest overpressures shown.

Accuracy of the Mach reflection data is limited because the calculations for these data were based on an ideal reflecting surface. When the burst height is low, errors may result from the resiliency of the earth's surface (or, in the extreme case, cratering), and from thermal energy extracted from the fireball by absorption at the surface. Dirt thrown into the air may alter blast wave properties. Accuracy of the regular reflection data is limited by the difficulty of obtaining a large number of accurate blast wave data points at very high overpressures. These uncertainties are the reasons for smoothing the overpressure contours in Figure 2-17. They are also the reasons for omitting, as unrealistic, curves for peak reflected overpressures higher than 10,000 psi.

2-36 Peak Overpressure at a Finite Reflecting Surface

Since a finite surface may cause either regular or Mach reflection, the curves showing reflected overpressure at a finite surface resemble those showing reflected overpressure at an infinite surface.

Figure 2-46 shows curves of reflected overpressure as a function of peak incident overpressure. These curves apply directly to the reflection that occurs at flat surfaces (e.g., sides of buildings) when they are struck by the nearly vertical shock front which characterizes the Mach stem. Although the curves also may be used to determine peak reflected overpressure from the incident free air blast wave when regu-

[redacted]

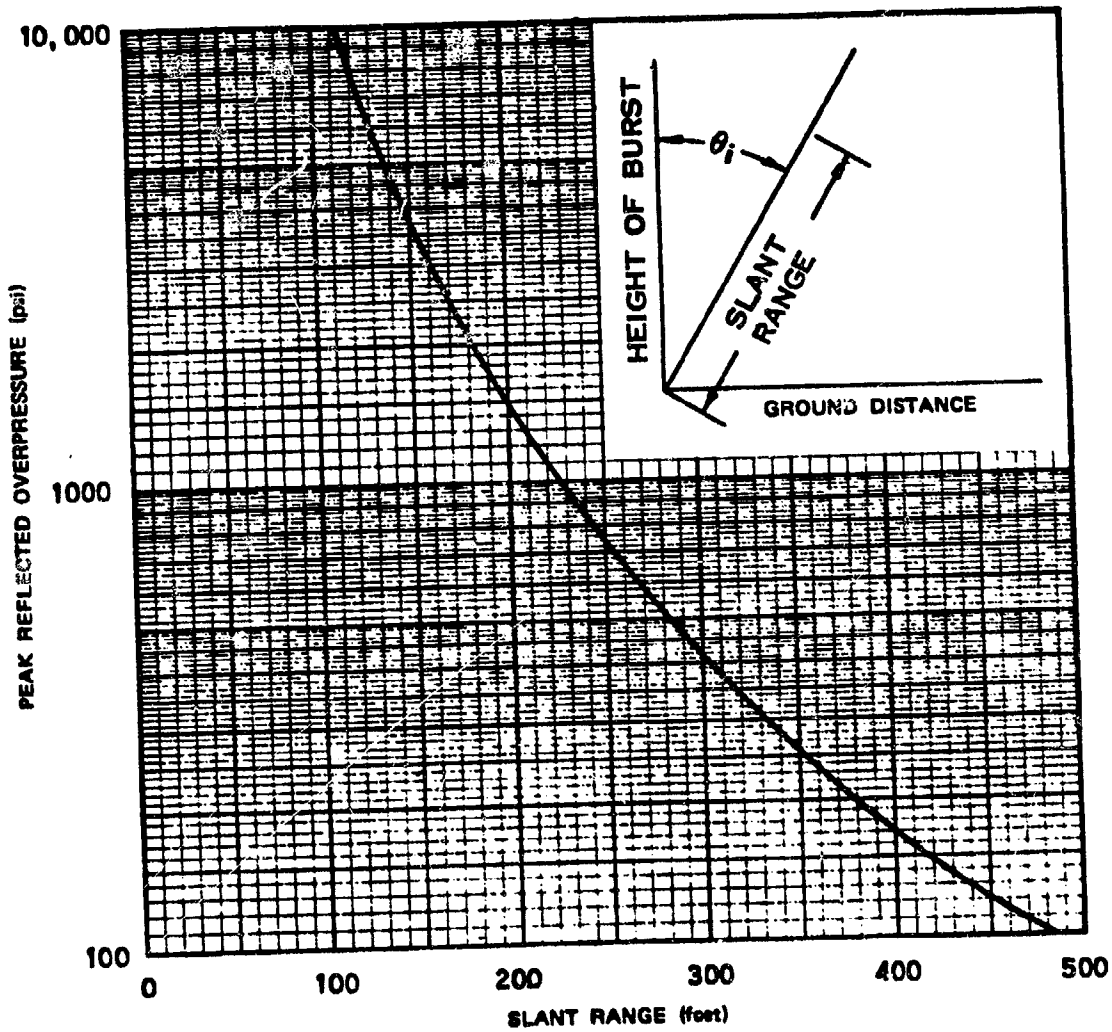

Figure 2-45. [redacted] Peak Reflected Overpressure Versus Slant Range for an Angle of Incidence θ_i of 30° [redacted]

[redacted]

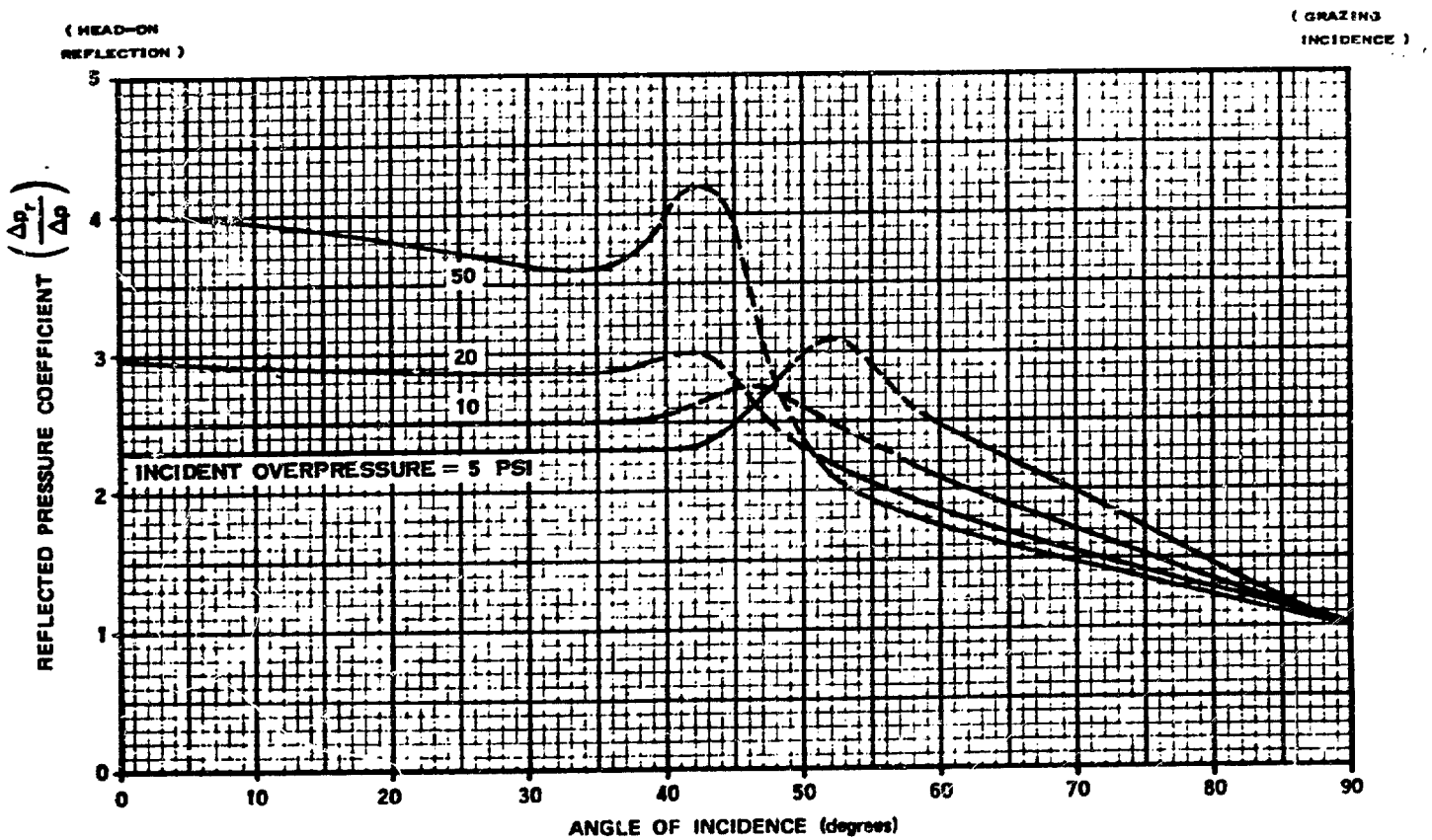

Figure 2-46. [redacted] Reflection Properties of Shock Waves at a Finite Surface [redacted]

[redacted]

[redacted] lar reflection is occurring at the surface of the earth, they do not represent the total effect of multiple reflections that occur when this direct wave strikes the angle formed by the earth and a vertical surface.

[redacted] These curves only predict the peak overpressure produced when the shock front arrives. In many problems, the total waveform produced by the blast-target interaction also is important; however, the latter is a function of target dimensions as well as blast wave properties as discussed in Section II of Chapter 9 and Section I of Chapter 11.

2-37 Peak Overpressure at Rising and Falling Slopes (U)

[redacted] If a shock wave that is travelling along the ground surface encounters a change in slope, the characteristics of the shock wave will change. If the terrain is characterized by large changes of slope, the changes in the blast wave can be significant. They can result in an overpressure increase by more than a factor of two or a decrease by more than a factor of three.

[redacted] Interactions with real topography can be exceedingly complex. Therefore both experimental and theoretical studies have, for the most part, dealt with idealized, simplified terrain features. Techniques have been devised for predicting the characteristics of the shock waves that encounter changes in terrain, and methods for applying these techniques to real terrain have been devised.

[redacted] If the level terrain in front of a slope is in the region of Mach reflection, the blast-wave incident on the slope will have a nearly vertical shock front, the Mach stem. (The nearly hemispherical shock front produced by a contact surface burst is considered a special case of an incident Mach stem.) If the level terrain in front of the slope is in the region of regular reflection, the first shock front striking the slope is the free air blast wave from the nuclear source. This shock front is not vertical, but forms an angle of less than 90° with the level ground in front of the slope.

[redacted] When the nearly vertical Mach stem strikes a rising slope, the incident wave undergoes either regular (two-shock) or Mach (three-shock) reflection, depending on the angle that the slope makes with the surface over which the shock wave has been moving and on the strength of the incident shock. For a falling slope, diffraction always occurs; the shock wave curves to orient itself normal to the slope. Differences between regular and Mach reflection on a rising slope are illustrated in Figure 2-47. Diffraction on a falling slope is illustrated in Figure 2-48 (in these figures, the shock wave direction of propagation is assumed to be normal to the slope contours).

[redacted] Similar interactions occur when the direction of shock wave motion makes an angle Φ with the line of steepest ascent or descent. The geometry of such an interaction is shown in Figures 2-49 and 2-50. In these figures, the angle that is important is θ, the effective slope angle. Its relationship to θ_s, the slope angle is

$$\sin \theta = \sin \theta_s \cos \Phi$$

This relationship is plotted in Figure 2-51. The relationship holds for both rising and falling slopes.

[redacted] When a Mach stem encounters a rising slope, the incident overpressure and the effective slope angle determine whether regular or Mach reflection will occur. The conditions under which regular or Mach reflection occurs are shown in Figure 2-52.

[redacted] Figure 2-53 shows how effective slope angle affects the peak overpressure produced by a 10-psi incident Mach stem. Similar data may be obtained from Figure 2-46 for other overpressures by noting that the angle of incidence to use with Figure 2-46 is equal to 90° minus the effective slope angle. The left-hand side of Fig-

[redacted]

[redacted]

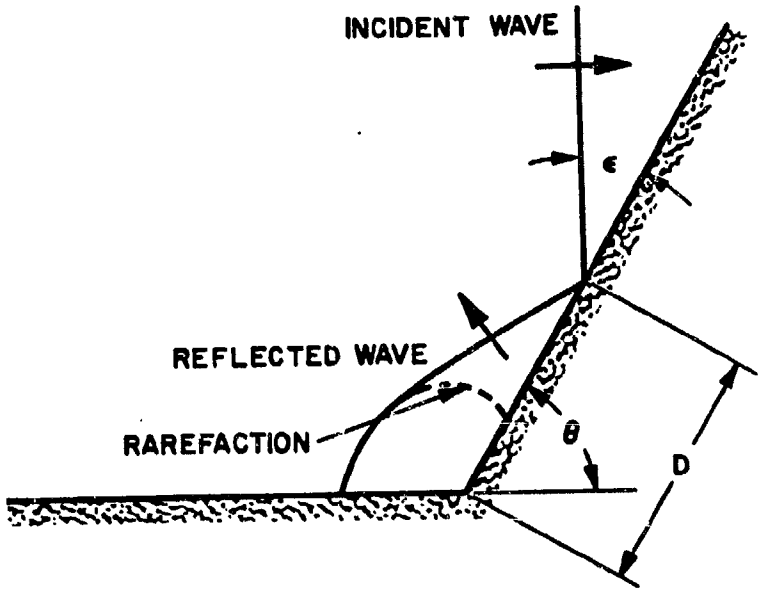

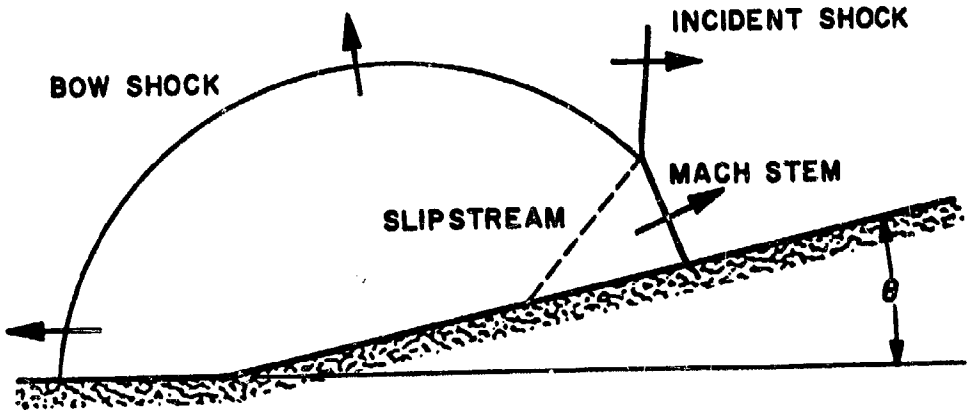

Figure 2-47. [redacted] Regular and Mach Reflection Patterns Formed by a Mach Stem Striking a Rising Slope [redacted]

[redacted]

[redacted]

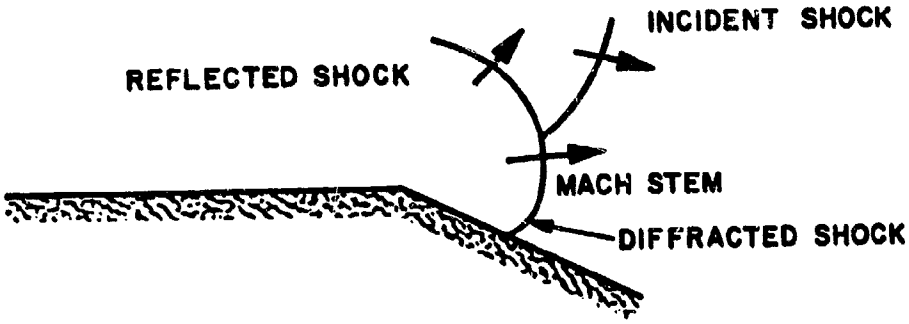

Figure 2-48. [redacted] Diffraction Shock Front Pattern Formed by a Mach Stem at a Falling Slope [redacted]

[redacted]

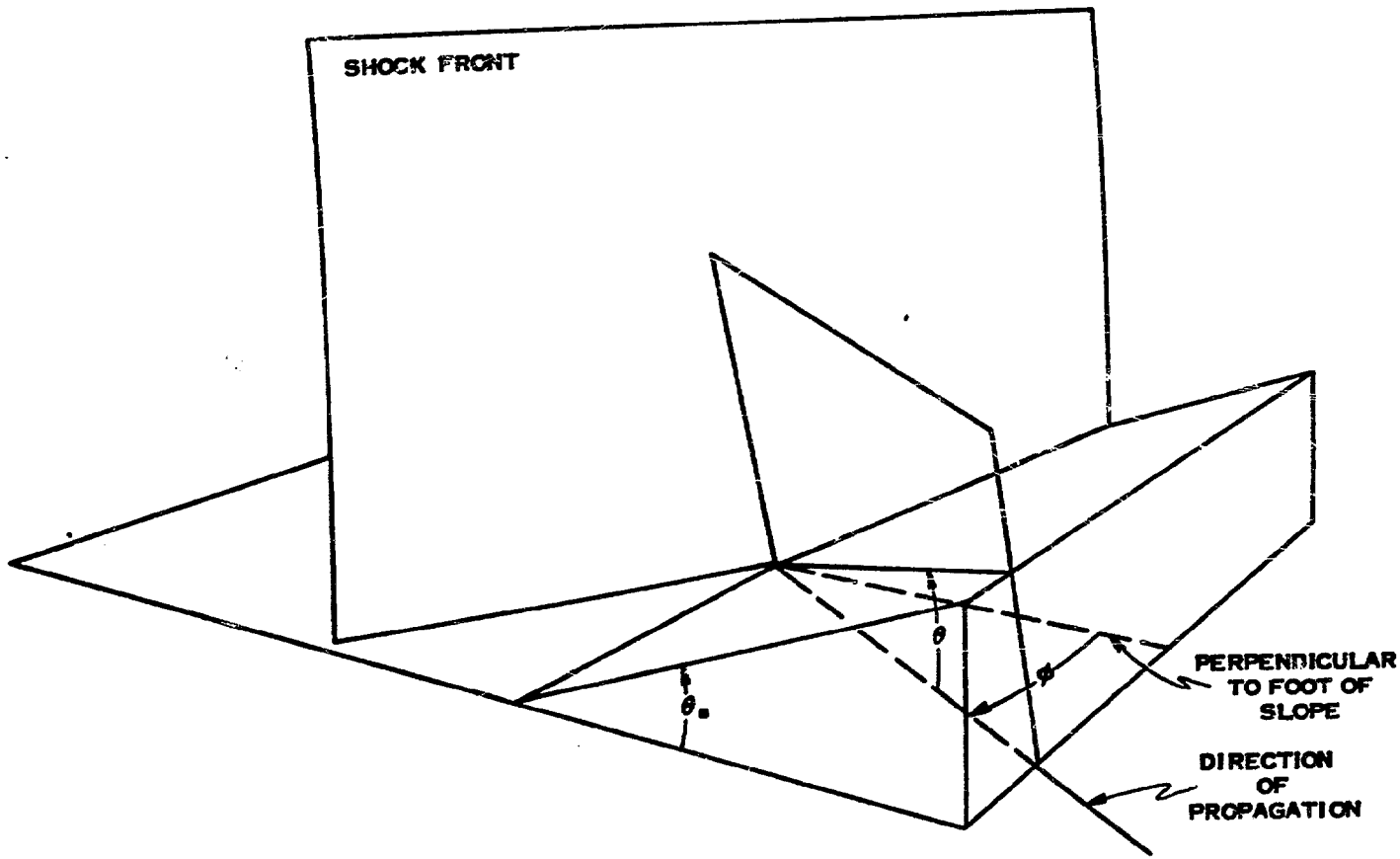

Figure 2-49. Mach Stem at a Rising Slope

[redacted]

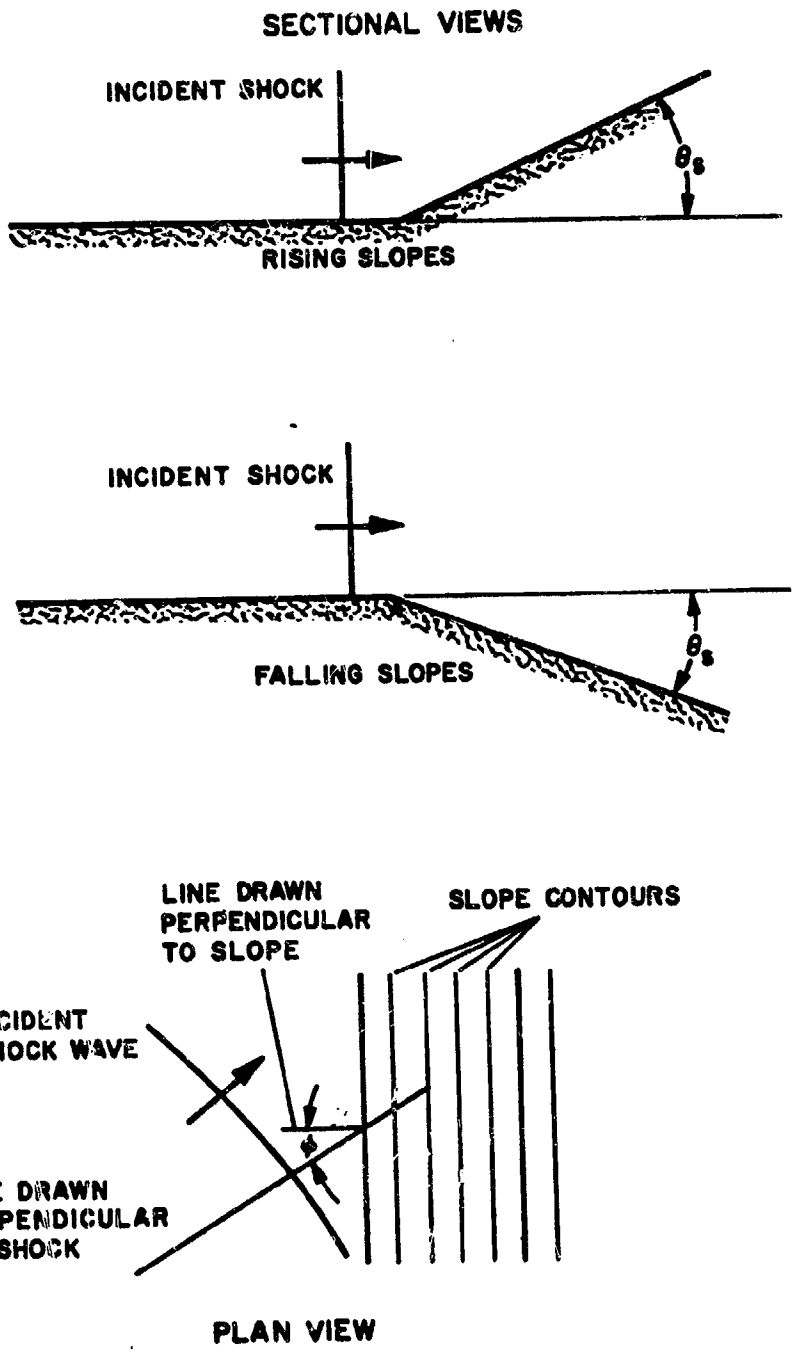

Figure 2-50. [redacted] Sectional and Plan Views of a Shock Front Approaching a Slope [redacted]

[redacted]

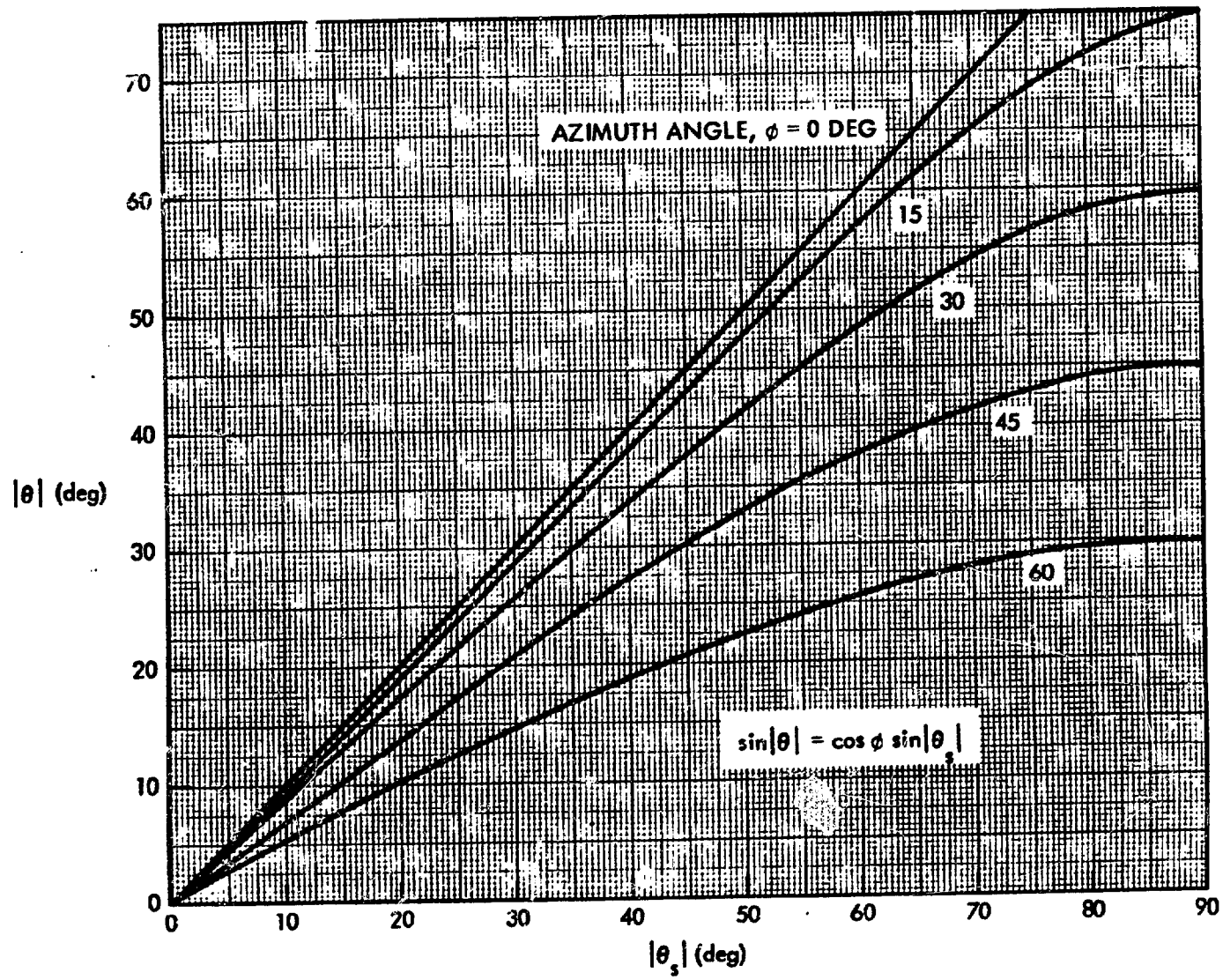

Figure 2-51. Effective Slope Angle θ as a Function of Slope Angle θ_s for Various Angles of Azimuth

[redacted]

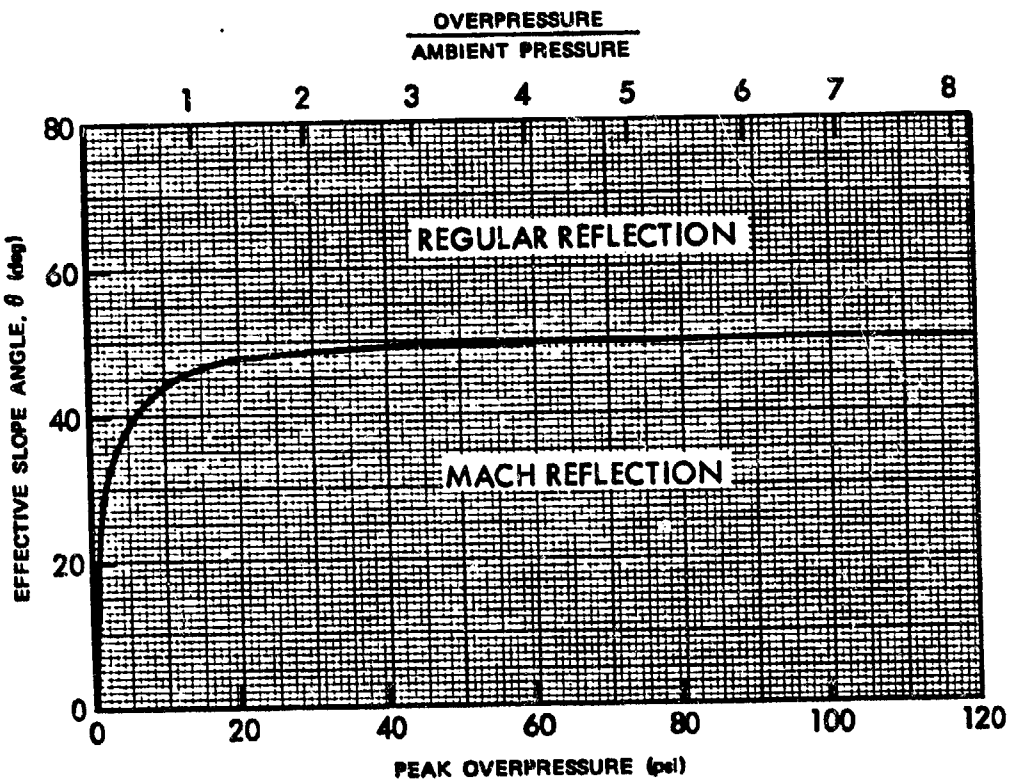

Figure 2-52. [redacted] Conditions for Regular or Mach Reflection of Incident Mach Stem [redacted]

[redacted]

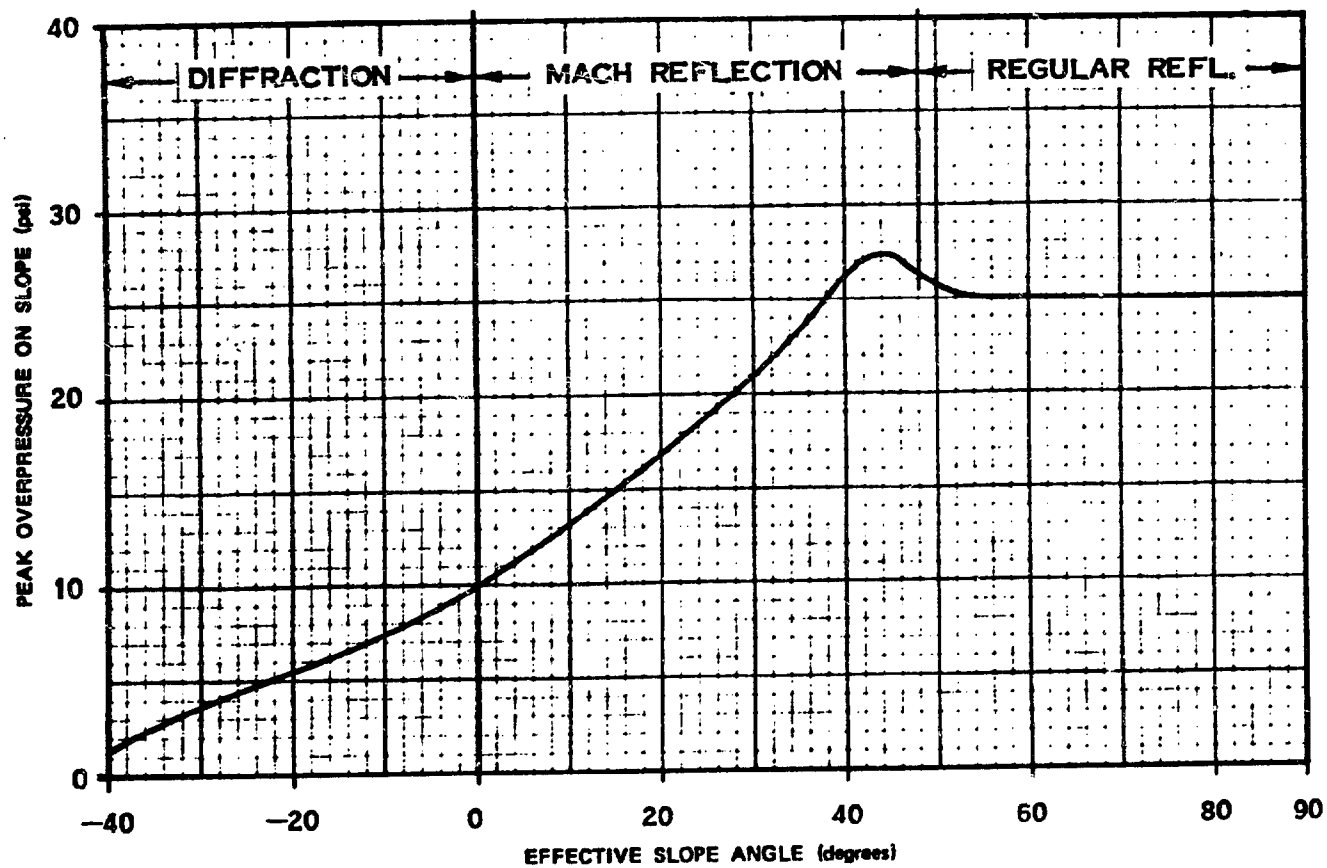

Figure 2-53. [redacted] Peak Overpressure Produced on a Slope by a 10-psi Incident Mach Stem as a Function of a Slope Angle [redacted]

[redacted]

[redacted]

ure 2-53 shows the effect of diffraction at a falling slope.

[redacted] Figures 2-54, 2-55, and 2-56 show similar data in a more convenient form. The overpressure scales only apply to reflection of shock waves in a sea level atmosphere. At other ambient pressures, the scales marked "overpressure/ambient pressure" should be used. Note that Figure 2-54 is plotted for various values of the angle of incidence while Figures 2-55 and 2-56 are plotted for various values of the effective slope angle.

[redacted] If the incident blast wave has been undergoing regular reflection before it encounters the rising or falling slope, approximate blast wave characteristics at the target can be determined by (1) constructing a sectional plot showing both the target area and the burst point, (2) drawing a "reference-plane line" through the target area showing the general plane in the vicinity of the target, and (3) drawing a line from the burst point perpendicular to the reference-plane line.

[redacted] As Figure 2-57 shows, the length of the perpendicular is the effective height of burst; the length along the reference plane line between this perpendicular and the target area is the effective ground range or distance from ground zero, and shock-wave characteristics may be determined from height of burst charts. Although this technique does not take into account the effect of azimuth angle Φ (where the shock wave moves at an angle to the line of steepest ascent or descent), further refinement is rarely justified.

[redacted]

[redacted]

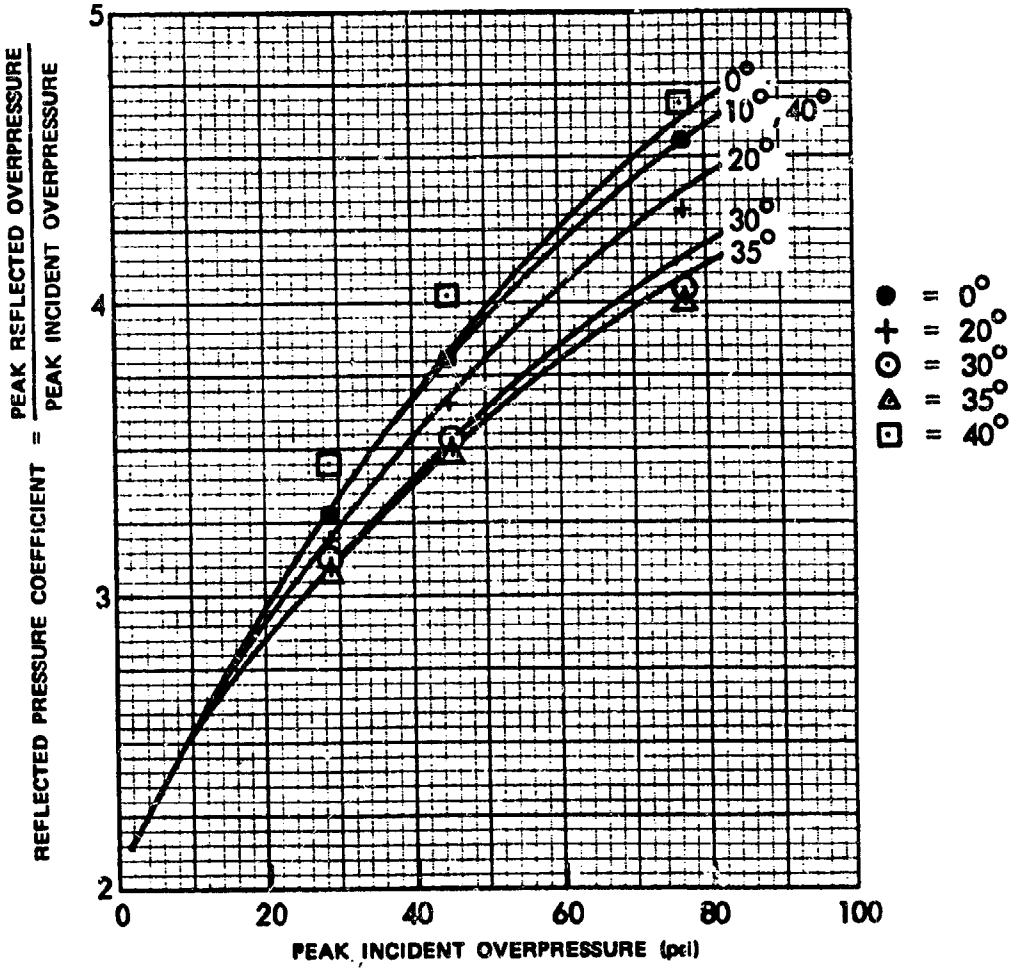

Figure 2-54. [redacted] Reflected Overpressure Coefficients for Regular Reflection as a Function Incident Overpressure for Various Angles of Incidence [redacted]

[redacted]

[redacted]

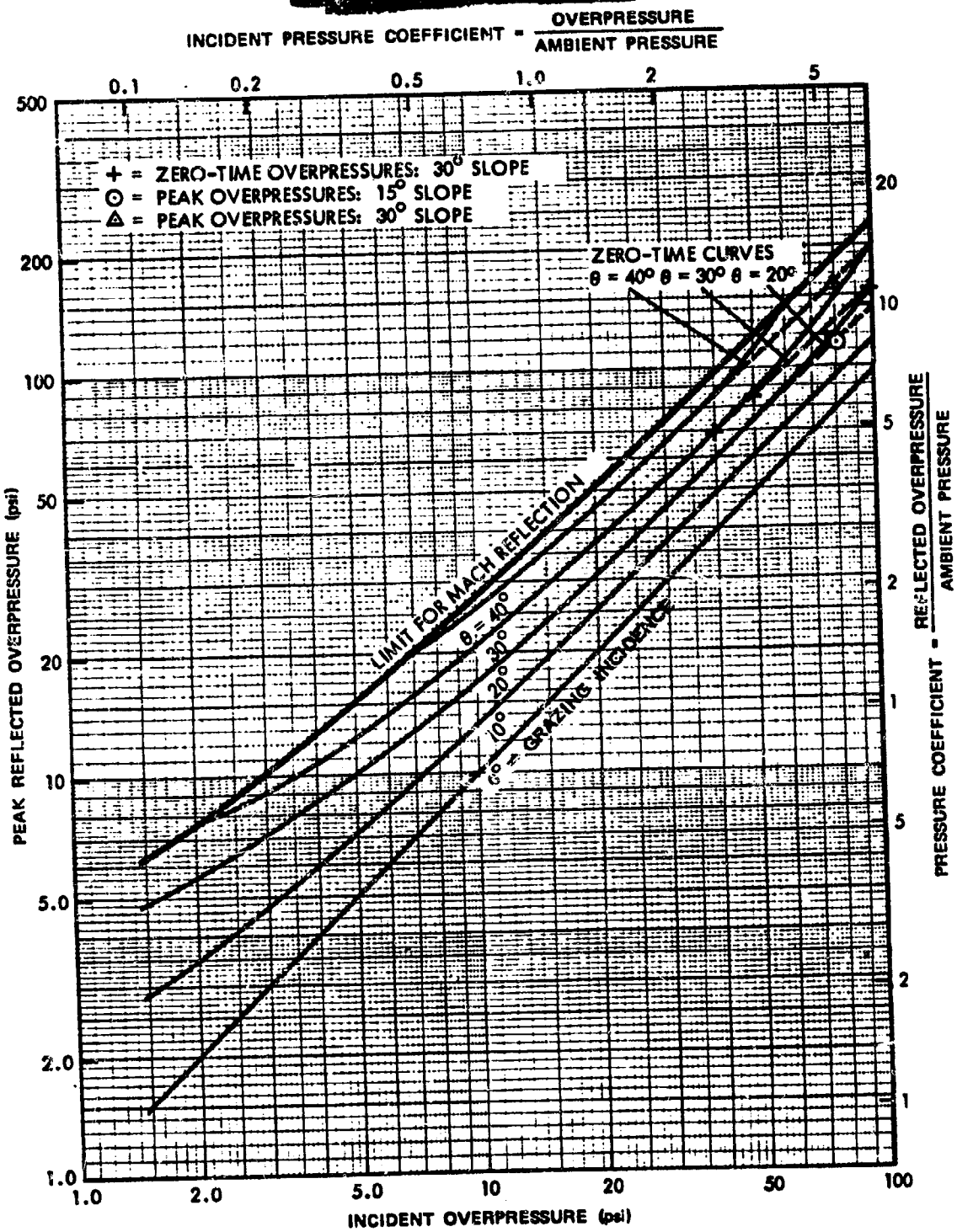

Figure 2-55. [redacted] Reflected Overpressure as a Function of Incident Mach-Stem Overpressure for Mach Reflection for Various Slope Angles [redacted]

[redacted]

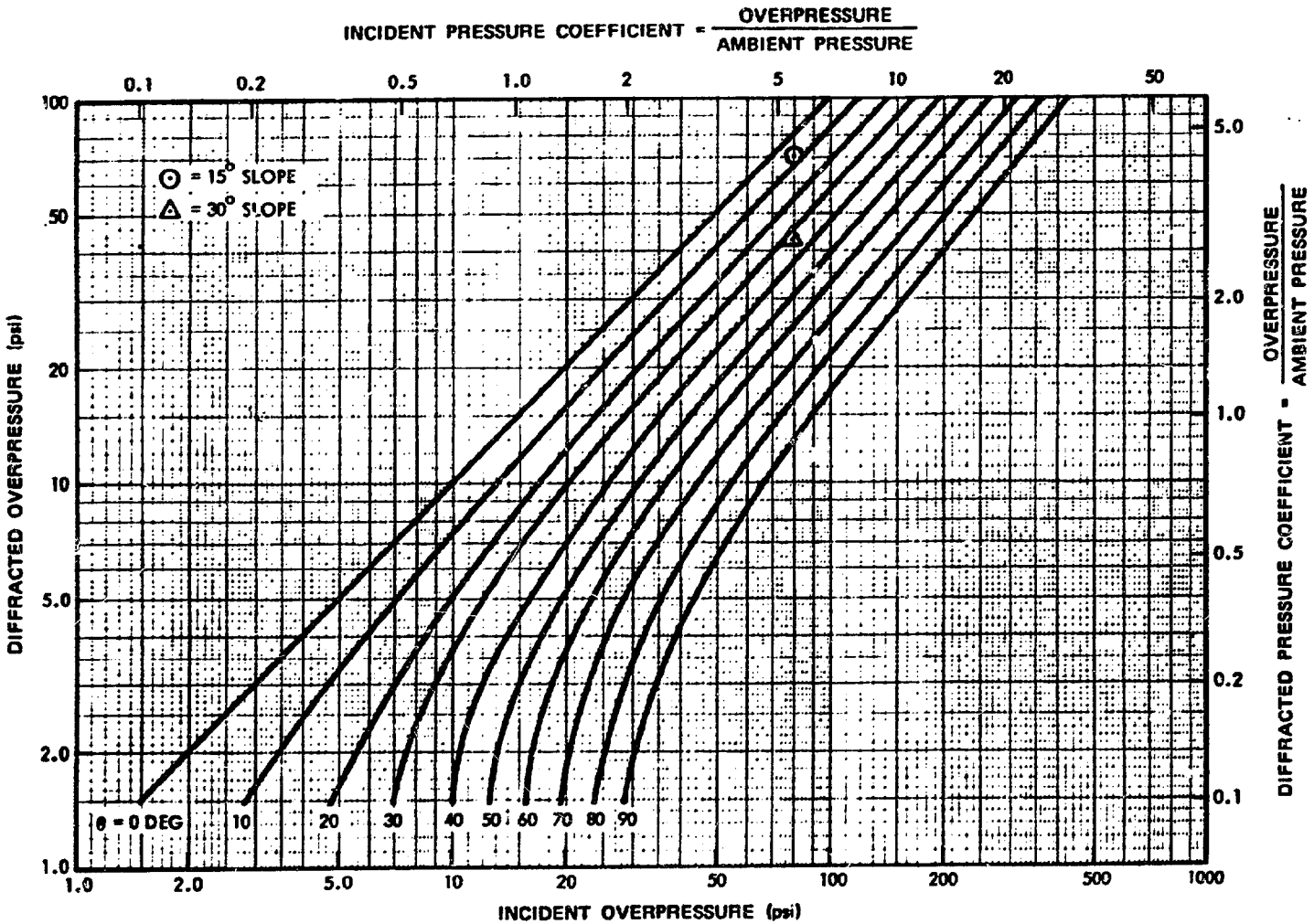

Figure 2-56. [redacted] Diffracted Overpressure as a Function of Incident Mach-Stem Overpressure for Various Slope Angles [redacted]

[redacted]

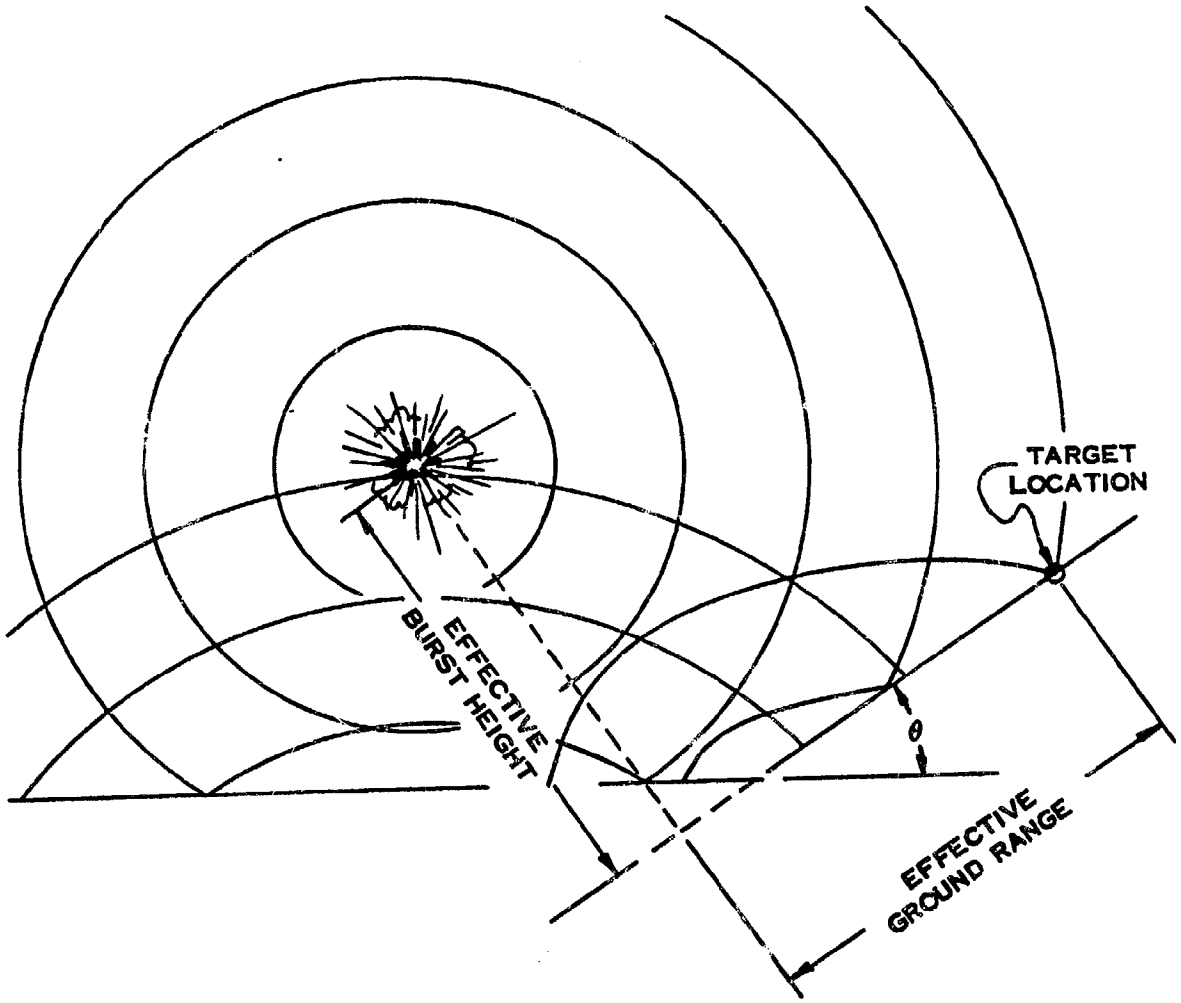

Figure 2-57. [redacted] Construction Procedure Recommended When the Blast Wave Incident on a Slope Has Been Undergoing Regular Reflection on Level Ground [redacted]

[redacted]

Problem 2-17. Calculation of Overpressure on a Slope

The information provided in paragraph 2-37 and in Figures 2-47 through 2-57 provides the data to calculate peak reflected overpressures when a blast wave encounters a rising or falling slope. The data are given relative to the incident overpressures that would be expected over flat terrain in a standard sea level atmosphere. These latter values may be obtained from Figures 2-17 through 2-22.

Scaling. For target altitudes above 5,000 feet, both the incident and the reflected overpressures scale according to the altitude scaling procedures described in paragraph 2-14, i.e.,

$$\frac{\Delta p_r}{\Delta p_{ro}} = \frac{\Delta p}{\Delta p_o} = S_p,$$

where Δp_{ro} and Δp_o are the reflected and incident peak overpressures, respectively, in a standard sea level atmosphere, Δp_r and Δp are the corresponding pressures at the desired altitude, and S_p is the pressure scaling factor described in paragraph 2-14 and tabulated in Tables 2-1 and 2-2.

Example

Given: A ridge with a slope angle of 27° on otherwise flat terrain at an altitude of 7,500 feet. For a particular set of burst conditions, the predicted blast wave in the absence of the ridge (but including altitude corrections) is a Mach stem with a peak overpressure between 10 and 15 psi. The direction of propagation of the blast wave makes an angle of 20° with the line of steepest ascent.

Find: The range of peak overpressures that may be expected on the side of the ridge facing the explosion.

Solution: From the equation given in paragraph 2-37 (or by interpolation in Figure 2-51), the effective slope angle is found as follows:

$$\sin\theta = \sin\theta_s \cos\Phi$$

$$= (\sin 27°)(\cos 20°)$$

$$= 0.427,$$

$$\theta = 25°.$$

From Table 2-1, the altitude scaling factor for pressure at 7,500 feet is

$$S_p = 0.76.$$

Under sea level conditions, the predicted value of the incident Mach stem overpressure would lie between

$$\Delta p_o = \frac{\Delta p}{S_p} = \frac{10}{0.76} = 13.2 \text{ psi, and}$$

$$\Delta p_o = \frac{15}{0.76} = 19.7 \text{ psi.}$$

Figure 2-55 shows that a rising slope will increase these sea level values to

$$\Delta p_{ro} = 19 \text{ psi, and}$$

$$\Delta p_{ro} = 28 \text{ psi, respectively.}$$

An uncertainty of about 20 percent exists in these values (see "Reliability" below). In order to bracket the range of expected values, the lower will be decreased by 20 percent, and the upper will be increased by 20 percent. The resulting sea level reflected overpressures are

[redacted]

[redacted]

Δp_{ro} = 15.2 psi, and

Δp_{ro} = 33.6 psi, respectively.

Answer: The corresponding values of reflected overpressure at an altitude of 7,500 feet are

$\Delta p_r = \Delta p_{ro} S_p = (15.2)(0.76) = 11.5$ psi, and

$\Delta p_r = (33.6)(0.76) = 25.5$ psi, respectively.

[redacted] *Reliability:* Full scale nuclear tests indicate that the increase or decrease in peak overpressure at a rising or falling slope is generally within 10 or 20 percent of the predicted value. In the presence of a precursor, less accuracy may be expected. Accuracy also decreases if the slope angle is close to the critical angle that separates the regions of regular and Mach reflection.

[redacted] *Related Material:* See paragraphs 2-14, 2-17 through 2-20, 2-22 through 2-24, and 2-37. See also Tables 2-1 and 2-2.

[redacted]

[redacted]

2-38 Effects of Slopes on Other Blast Wave Parameters [redacted]

[redacted] Methods for determining peak overpressures at rising and falling slopes are described in paragraph 2-37. This paragraph relates the peak dynamic pressure and the duration of the positive phases of the overpressure and the dynamic pressure to the expected overpressures that are determined by the methods described in paragraph 2-37. The relations of the dynamic pressure and positive phase durations to the overpressure will be discussed for three types of interactions of the blast wave with slopes: regular reflection of an incident Mach stem; Mach reflection of an incident Mach stem; and diffraction of an incident Mach stem.

[redacted] Figure 2-58 shows the reflected dynamic pressure as a function of incident Mach stem overpressure in the regular reflection region for various effective slope angles. The duration of the positive phase overpressure after regular reflection can be considered to be the same as that of the incident pulse. The dynamic pressure pulse, on the other hand, changes as the shock wave proceeds up the slope as a result of the presence and growth of a rarefaction wave from the slope corner (see Figure 2-47). The dynamic pressure pulse effectively terminates where the rarefaction wave intersects the reflected wave. The effect depends on the distance up the slope that the shock wave has moved, the slope angle, and the overpressure coefficient in the manner shown in Figure 2-59. In this figure, the number 1116 is the velocity of sound (in feet/sec) for standard sea level conditions (15°C or 59°F). For different ambient temperatures, the appropriate sound speed should be used (see Tables 2-1 and 2-2).

[redacted] In the case of Mach reflection of the incident Mach stem, the peak dynamic pressure at the shock front may be determined from Figure 2-13 once the reflected overpressure is determined as described in paragraph 2-37. Figure 2-13 is only valid when a single shock front is involved. If the rising slope is sufficiently steep to cause regular reflection (Figure 2-52), the peak dynamic pressure should be determined from Figure 2-58. The duration of the positive phase overpressure pulse in the Mach stem after Mach reflection can be assumed to be the same as that of the incident wave, while the positive phase dynamic pressure pulse is shorter than that of the incident wave. Over a range of overpressure coefficients from 2 to 11, and slope angles from 11.8 to 38 degrees, the reflected pulse after Mach reflection may be assumed to be 0.55 times as long as that of the incident blast wave.

[redacted] Figure 2-13 also may be used to determine the peak dynamic pressure from the peak overpressure in a diffracted wave. Although the positive phase duration of both the overpressure and dynamic pressure pulses are known to decrease as a result of the formation of low pressure vortices at the slope change point, neither experiment nor theory is sufficiently extensive to provide a satisfactory prediction technique. As an approximation, the positive phase duration of the diffracted overpressure pulse may be taken to be the same as that of the incident pulse, and the duration of the diffracted dynamic pressure pulse may be shortened by the ratio of diffracted peak dynamic pressure to incident peak dynamic pressure.

2-39 Channeling of an Incident Mach Stem Along the Axis of a Valley [redacted]

[redacted] Figure 2-60 illustrates a third type of idealized topographic feature: an elongated valley. Shock waves reflecting from the walls of such a valley tend to enhance each other in the vicinity of the axis of the valley. The simple relations shown in Figure 2-61 have been shown to hold for a wide range of valley forms and for incident overpressures below about 60 psi. The relation for "flat-bottomed valleys" holds for

[redacted]

[redacted]

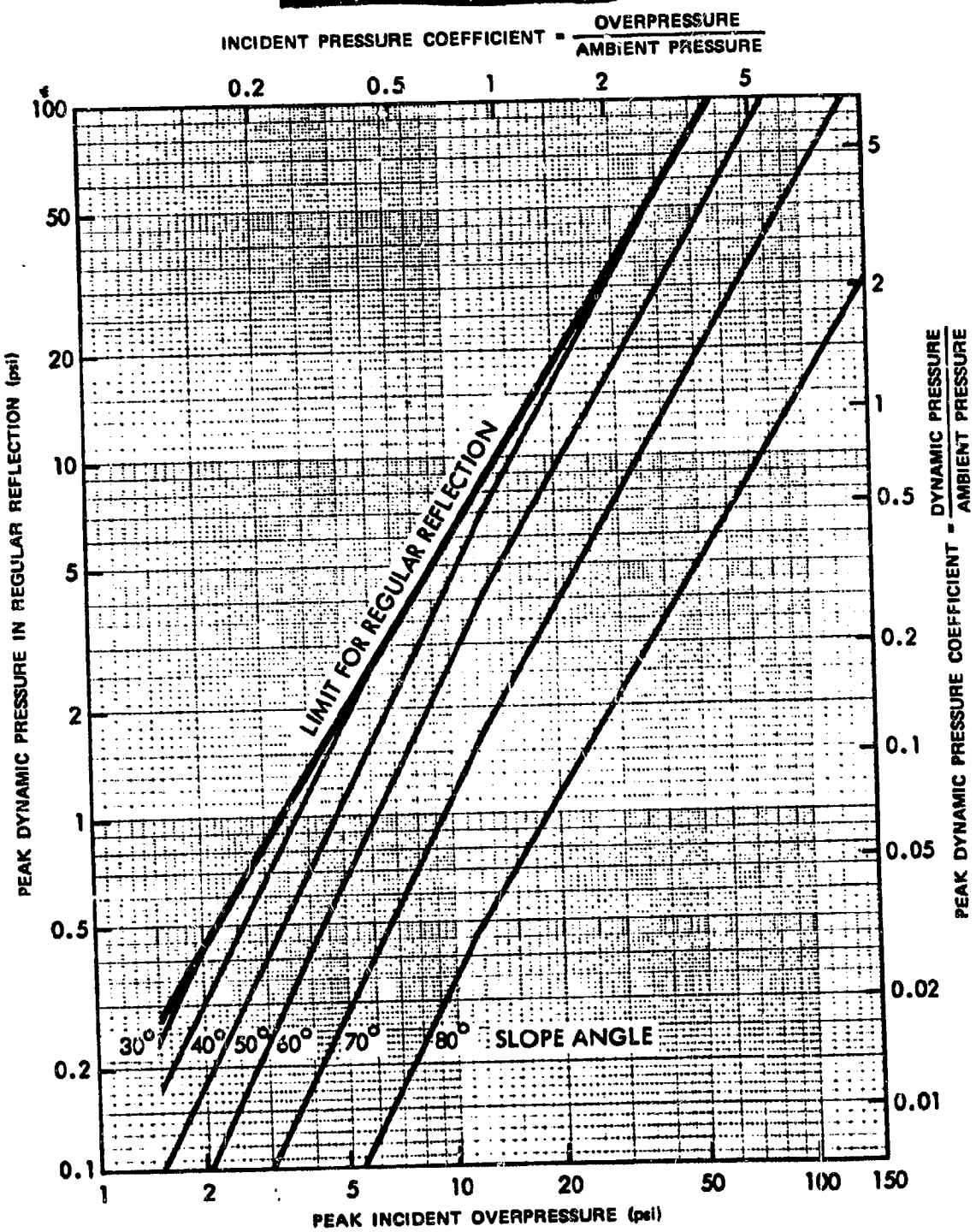

Figure 2-58. [redacted] Reflected Dynamic Pressure as a Function of Incident Mach Stem Overpressure for Regular Reflections for Various Effective Slope Angles [redacted]

[redacted]

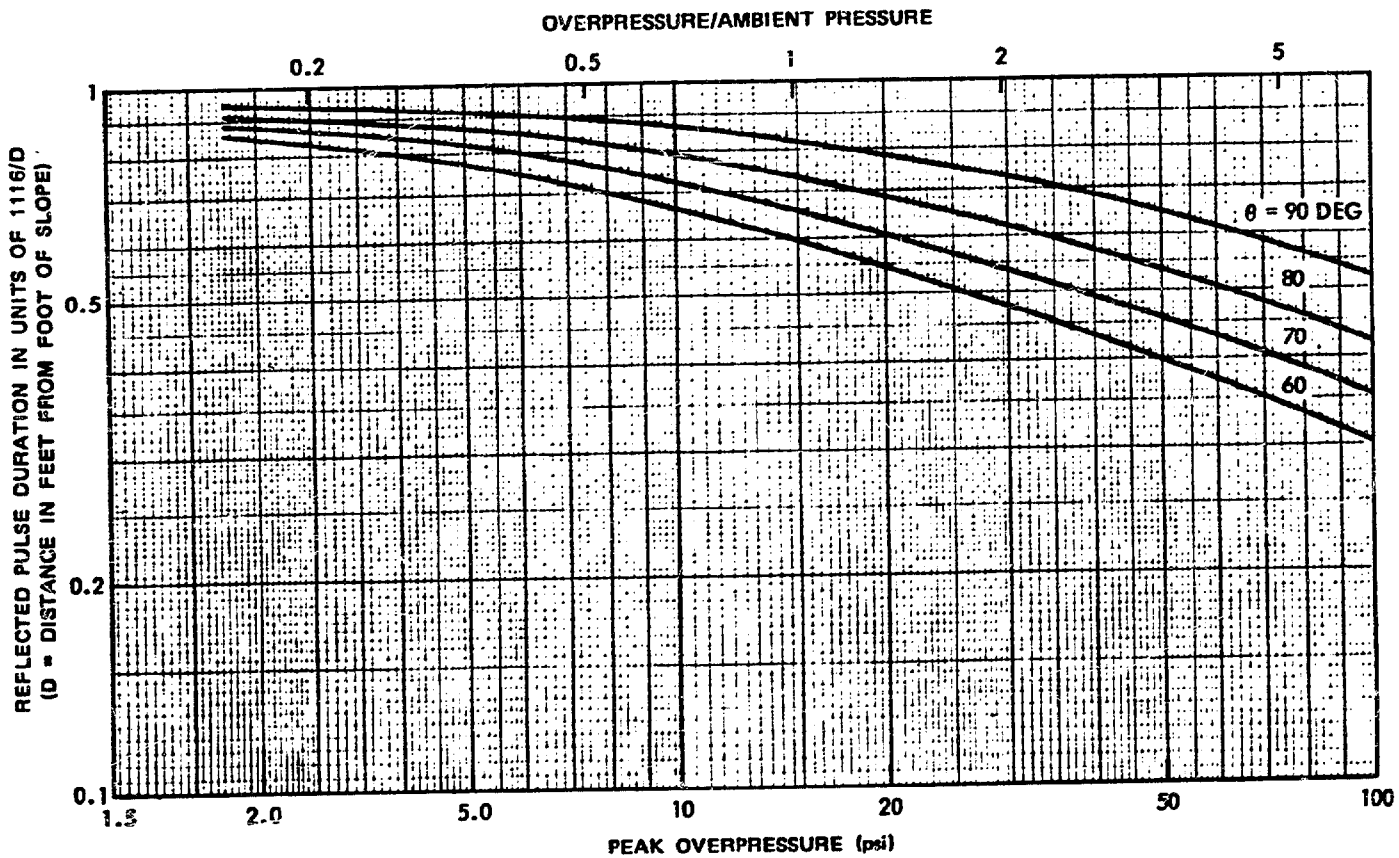

Figure 2-59. [redacted] Duration of the Reflected Dynamic Pressure Pulse for Regular Reflection [redacted]

[redacted]

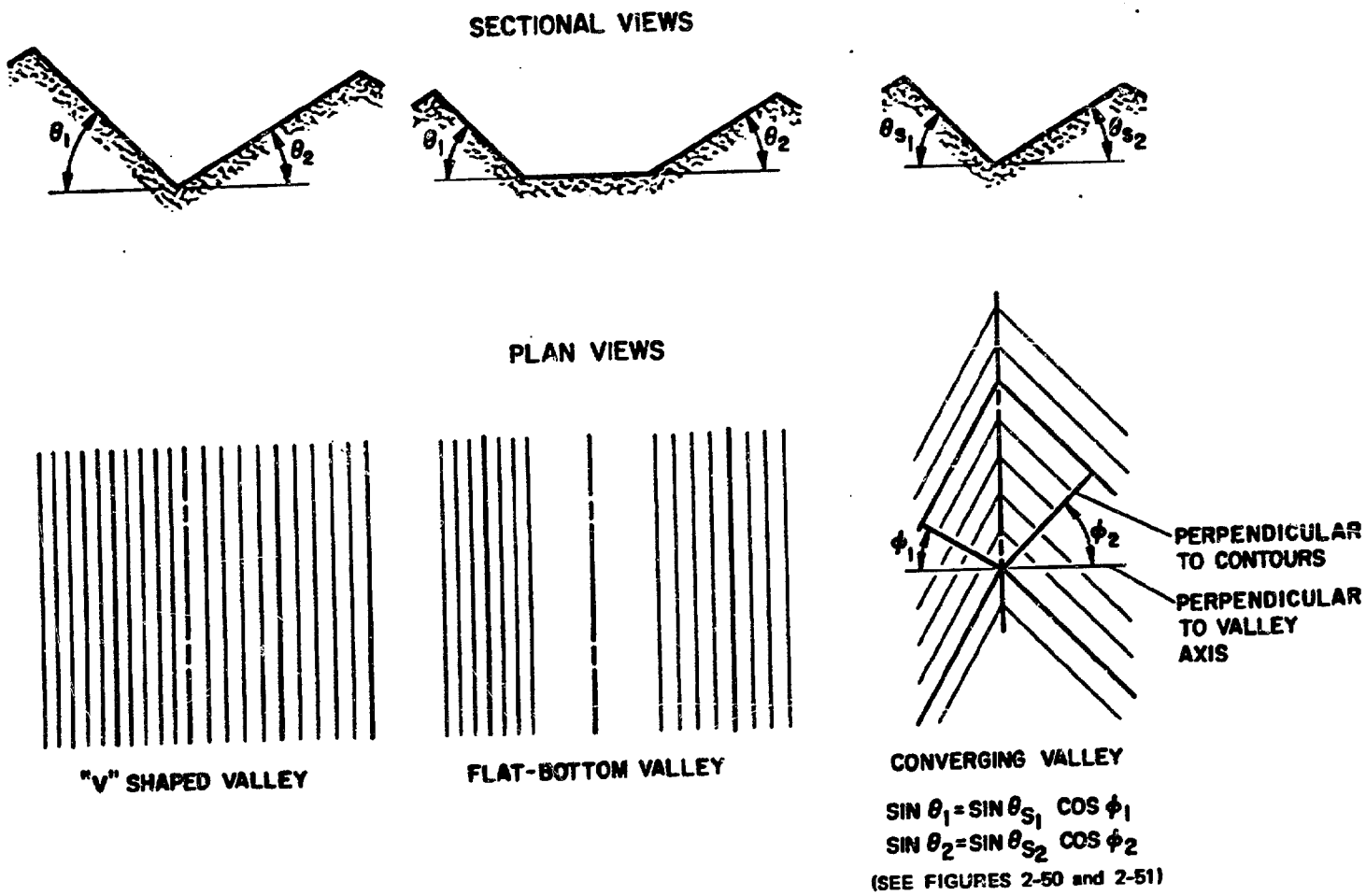

Figure 2-60. Sectional and Plan Views of Idealized Valley Shapes

[redacted]

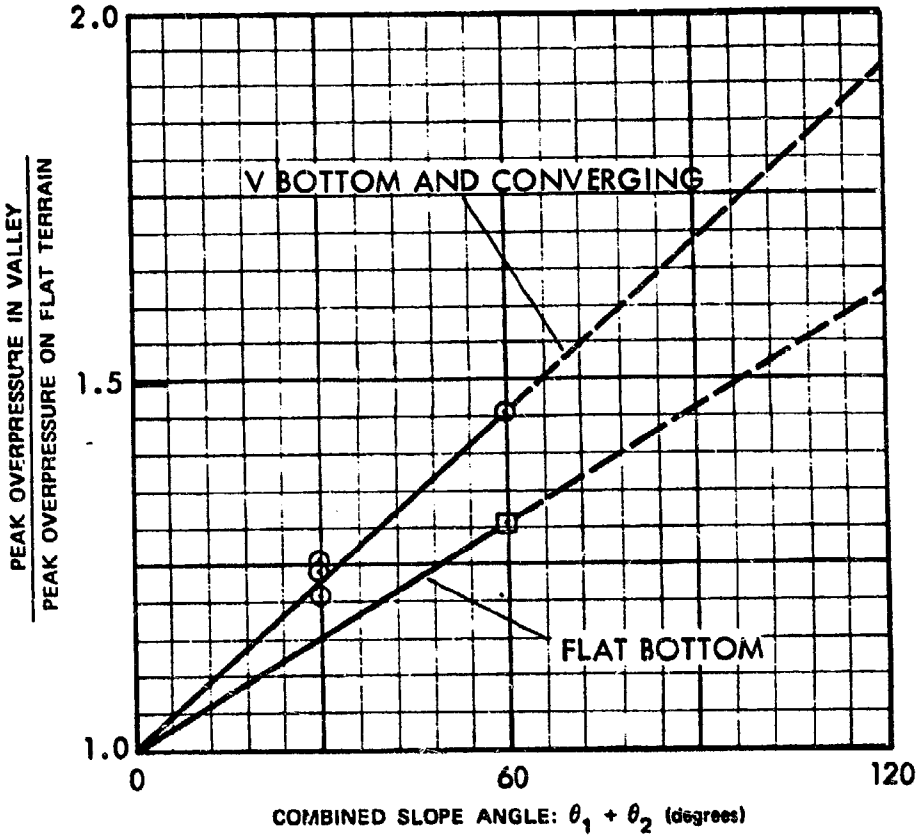

(SEE FIGURE 2-60)

Figure 2-61. [redacted] Average Peak Overpressure Amplification Factors at the Bottom of Valleys as a Function of Combined Slope Angle [redacted]

[redacted]

valleys whose floor widths (measured perpendicular to the valley axis) are of the same order as, or shorter than, the slope heights of the valley walls (also measured perpendicular to the valley axis). For wider flat-bottomed valleys, each side of the valley and a portion of the adjacent valley floor may be considered independently as a V-shaped valley.

2-40 General Application of Prediction Techniques to Actual Topographical Features

Paragraphs 2-37 and 2-38 provide data for only the most significant shock wave characteristics – peak pressures and positive phase durations. More detailed information, e.g., data on pressure waveforms, may be obtained from DASA 1200, "Nuclear Weapons Blast Phenomena" (see bibliography).

Applicability of the curves that have been presented depends largely on the size of a terrain feature relative to the size of the incident shock wave. If the incident shock is very much longer than a terrain feature of interest, the predicted changes in peak values of overpressure and dynamic pressure will occur on the slope; but the duration will not be affected greatly. The incident pulse length in feet is slightly more than 1116 times the incident pulse duration in seconds, and if this pulse length is more than about three times as long as the slope being considered, no changes in pulse duration can be expected.

Much of the complexity of actual terrain may be eliminated from blast wave calculations by application of the *local-slope* concept. This concept is based on the observation that, in many situations, a shock wave that has passed over a succession of terrain features (hills, valleys, etc.) before encountering a feature of interest interacts with that feature as if the shock wave had previously passed over flat terrain.

This trend was noted during testing programs and has been supported by theoretical inference. The Ranier nuclear test over fairly complex terrain, provided additional checks. Although much of the area around this explosion was subject to precursor type waves, sharp fronted waves traversed many regions that were protected from direct thermal radiation. Predictions of peak overpressures generally were within 10 to 20 percent of observed values.

Determining whether the local slope approximation will give reasonably accurate results requires application of judgment in an examination of the region between the target area and the presumed burst point to determine whether there are significant terrain features between the two, especially in the vicinity of the target. This examination is often based on a sectional plot of the terrain, made along a line between ground zero and the target. Although it is sometimes difficult to draw conclusions from this examination, the following criteria are helpful:

- Features that show slope angles of less than 10 degrees on a sectional plot of the terrain, i.e., about a 20 percent grade, will not create significant effects.
- Symmetrical features at an appreciable distance from the target generally can be ignored. Effects that occur on the front slope of such features compensate for effects that occur on the back slope.
- Terrain features near ground zero have a small effect on the blast wave at large ground distances.
- If the average slope of the terrain tends to follow a straight line, particularly if the deviations from this straight line are small or random, the local slope approximation is justified. However, if the average slope of the sectional plot clearly follows two straight lines, and the angle between these

lines exceeds 10 degrees, and if the break occurs in the region of Mach reflection, the blast wave calculations may have to treat the effects of two slopes in sequence.

Unless the average slope between ground zero and the target is essentially horizontal, use of the local slope concept requires establishment of the primary reference plane (PRP). Over complex terrain, the PRP often follows the average slope of the terrain between ground zero and the foot of the feature upon which the target lies. If the PRP does not seem clearly defined by this criterion, it is better to allow the terrain within the region of Mach reflection suggest the slope of the PRP. If the target is in the region of regular reflection, the average slope of the terrain near the target should be given more weight than the average slope of terrain closer to ground zero.

After the PRP has been established, effective burst height and ground distance *with respect to this plane* may be determined by means of a geometrical construction similar to that suggested by Figure 2-57. Properties of the blast wave incident on the terrain feature of interest may be read directly from height of burst curves in terms of these effective values of distance and height.

Although there are many cases in which the local slope concept will fail in detail if applied to features that are regular and uniform, ordinary terrain is so complex that the uncertainties engendered by terrain irregularities generally will exceed errors resulting from application of the local slope concept. Furthermore, the process of determining *approximate* terrain effects with the local slope concept is generally far simpler than that of obtaining more refined, *but still approximate*, effects with more rigorous techniques.

Once the blast wave properties are determined from height of burst curves, appropriate sectional plots should be made of the target area slope. Azimuth angle and valley slopes must be determined where appropriate.

2-41 Application of Prediction Techniques to Specific Topography

Figure 2-62 is a topographical map with a target area (designated by T) to be investigated. It is desired to determine the locus of ground zeros that would subject the target to an overpressure of 10 psi from a 1 Mt weapon burst at a height of 5,000 feet above the terrain.

Examination of Figure 2-62 shows that the highest point on the terrain around the target area is just over 4,000 feet (note that the grid lines and elevations are given in meters in Figure 2-62, and the highest point in the vicinity of the target is at an elevation of 1,243 meters), so altitude corrections are not required.

In accordance with the instructions in paragraph 2-20, the blast-wave parameters for explosions over mechanically nonideal surfaces are performed by first finding the desired blast parameters over a near-ideal surface. The results then are corrected for the change in the blast wave properties introduced by the mechanically nonideal features. The corresponding height of burst for a 1 kt explosion is

$$h_1 = \frac{h}{W^{1/3}} = \frac{5{,}000}{(1{,}000)^{1/3}} = 500 \text{ feet.}$$

From Figure 2-18, a 1 kt explosion at a height of burst of 500 feet will produce an overpressure of 10 psi at a ground distance of 1,315 feet (about 400 meters). The corresponding ground distance for a 1 Mt explosion is

$$d = d_1 W^{1/3} = (1{,}315)(1{,}000)^{1/3}$$

$$= 13{,}150 \text{ feet (or about 4,000 m).}$$

A circle, centered on the target, with this radius is shown in Figure 2-62. A 1 Mt explosion at a

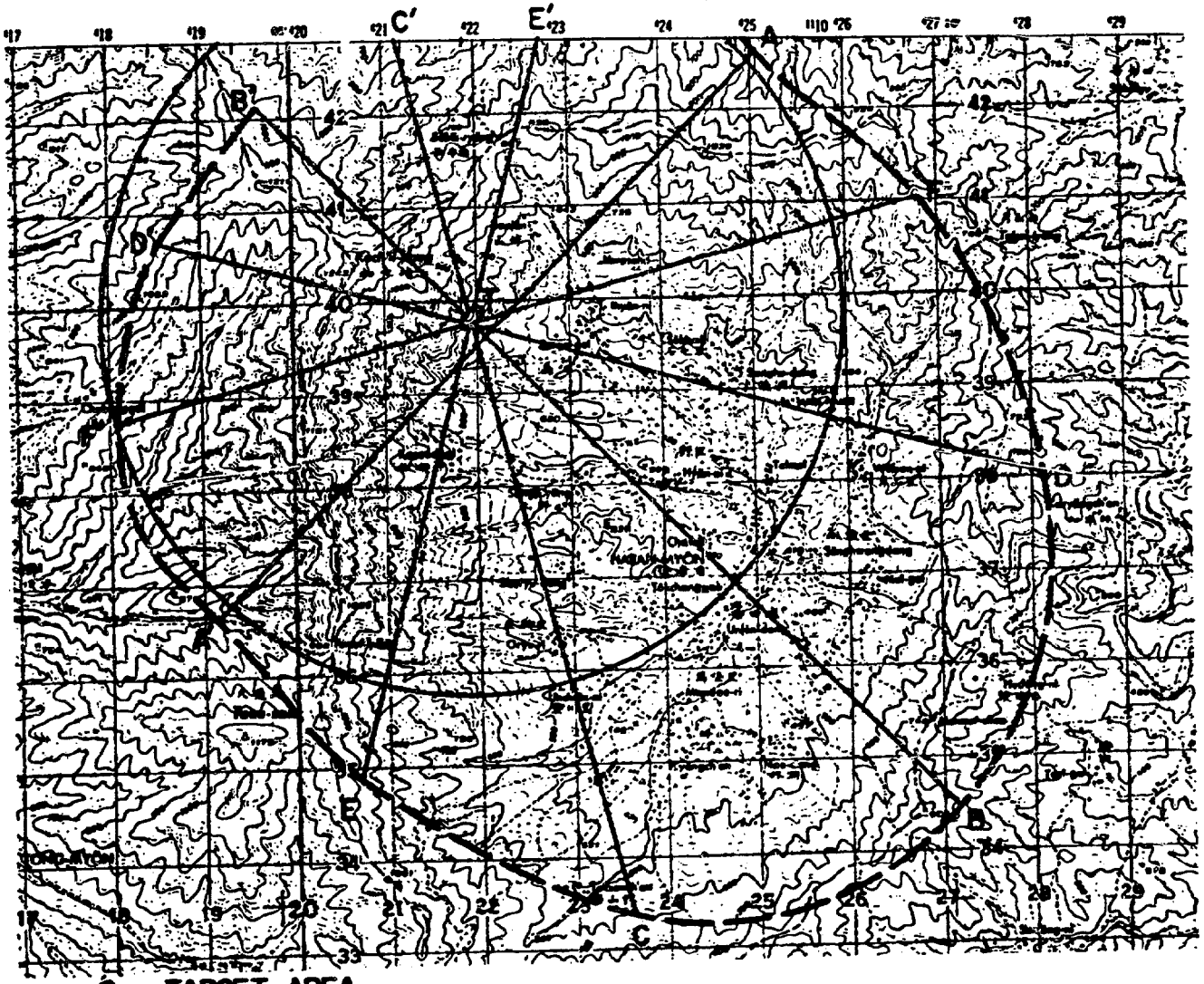

Figure 2-62. Terrain Map Used in Example

[redacted]

[redacted] height of burst of 5,000 feet over any point on the circle would produce an overpressure of 10 psi at the target area (burst over points within the circle would produce overpressures in excess of 10 psi at the target).

[redacted] The target area includes two small converging valleys that are relatively shallow and have relatively flat slopes normal to their axes. Figure 2-61 shows that relatively steep slopes are required to produce large effects in converging valleys, so these minor terrain irregularities may be ignored.

[redacted] The general direction of the contours in the target area is established as being parallel to line AA'; and a sectional plot along line BB', perpendicular to AA' and through the target area, is constructed (this sectional plot is shown in Figure 2-63 with the distance scales in meters for ease in comparison with the map). The plot in Figure 2-63 is not extended to the ground-zero circle (though it could easily be), since inspection of the area between the target and this circle, and reference to Figure 2-15 shows that Mach reflection would take place long before the shock would arrive at the target area. Furthermore, inspection of the area within the ground zero line indicates that an assumption of a horizontal datum for the slope of the primary reference plane is fairly good.

[redacted] From Figure 2-63, it can be determined that the tangent of the slope angle (vertical rise/horizontal distances) is 0.57. Thus, the slope angle is

$$\theta_s = 30°.$$

It is therefore necessary to determine the incident overpressure that will produce an overpressure of 10 psi when the shock wave encounters a 30 degree rising slope (along the line BT) or a 30 degree falling slope (along the line B'T). Figure 2-55 (Mach Reflection) gives an incident overpressure of 3.5 psi for the rising-slope condition, and Figure 2-56 (diffraction) shows an incident overpressure of 20 psi for the falling-slope condition. Figure 2-19 shows that 3.5 psi would occur at a ground distance of about 2,450 feet from a 1 kt burst or 24,500 feet (about 7,500 m) from a 1 Mt burst at heights of burst of 500 feet and 5,000 feet, respectively. Figure 2-18 shows that, for the same heights of burst, 20 psi occurs at a ground distance of 870 feet from a 1 kt burst or 8,700 feet (about 2,650 meters) from a 1 Mt burst.

[redacted] Lines CC' and DD' are drawn at 30° to line BB'. For these lines, the angle between the direction of shock wave propagation and the angle of steepest ascent or descent is

$$\Phi = 30°,$$

and the effective slope angle is determined by

$$\sin \theta = \sin \Phi_s \cos \Phi$$

$$= \sin 30° \cos 30° = 0.43$$

which yields

$$\theta = 26°.$$

The angle Φ for lines EE' and FF' is 60°, from which $\theta = 14.5°$. Using these two values of θ with Figures 2-55, 2-56, 2-18, and 2-19 provides the results shown in Table 2-5.

[redacted] Along line AA' the hill on which the target lies is, for all intents, a V-shaped valley with combined slope angle (see Figure 2-62) of 30°. Figure 2-60 indicates that an amplification factor of about 1.25 holds for such a valley, so an 8 psi incident overpressure (10/1.25) will yield 10 psi at the target area. Figure 2-19 shows that 8 psi would occur at a distance of approximately 1,375 feet for 1 kt or 13,750 feet for 1 Mt (about 4,200 meters for 1 Mt).

[redacted] When the various distances given above

[redacted]

[redacted]

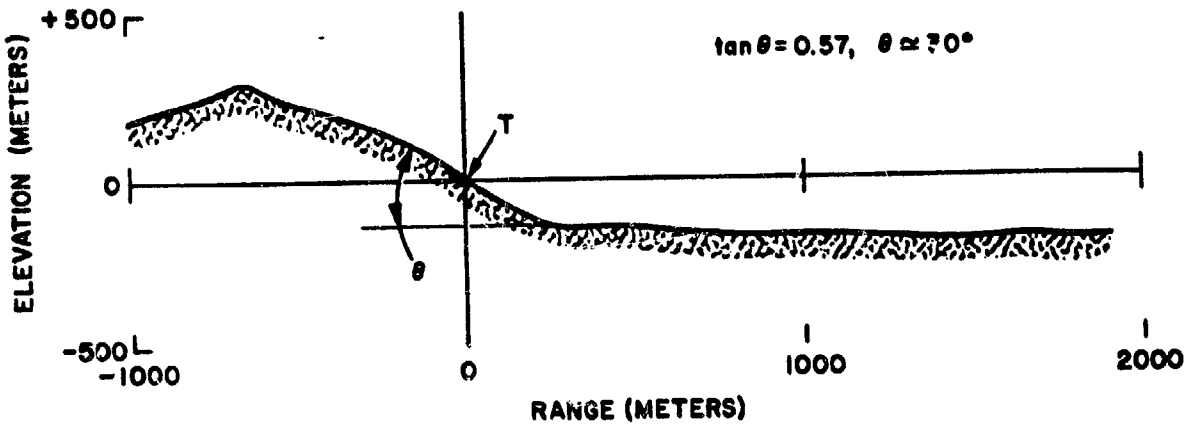

Figure 2-63. [redacted] Sectional Plot of the Terrain Along BB' in Figure 2-62 [redacted]

[redacted]

[redacted]

Table 2-5. [redacted] Incident Overpressure and Ranges [redacted]

Line	Φ	θ	Rising Slope Incident Overpressure (psi)	Approximate Distance Feet	Approximate Distance Meters
BT	0°	30°	3.5	24,500	7,500
CT, DT	30°	26°	4.1	21,500	6,600
ET, FT	60°	15°	6.0	17,000	5,000
			Falling Slope		
B'T	0°	30°	20.0	8,700	2,650
C'T, D'T	30°	26°	18.5	9,500	2,900
E'T, F'T	60°	15°	15.0	10,900	3,300

[redacted] are measured from the target area T along the appropriate lines, the points are connected, the dashed line shown in Figure 2-62 is the result. This line is the approximate locus of ground zeroes that will subject the target area to a peak overpressure of 10 psi.

[redacted] THE BLAST WAVE AT HIGH ALTITUDES [redacted]

[redacted] Nearly all of the energy from a nuclear burst detonated within the atmosphere is absorbed by air molecules. Within a few seconds, most of this energy evolves to three forms: blast energy, radiated thermal energy, and thermal energy retained in a large volume of air. The first two components of energy are useful nuclear effects; the third is harmlessly dissipated over a relatively long period of time. Deviations from Sachs' scaling laws (paragraphs 2-13 and 2-14) above 40,000 feet are caused principally by differences in the partitioning of these three energy components. Between sea level and 130,000 feet, blast energy decreases and radiated thermal energy increases with yield.

[redacted] These changes are, to a large degree, caused by changes in characteristic times. The blast wave develops more slowly at higher altitudes, and the thermal pulse radiates more rapidly. Thus, energy is radiated at high altitudes that would, at lower altitudes, have contributed to the blast wave. At altitudes higher than 130,000 feet, both blast and thermal* efficiencies drop.

2-42 Effective Blast Yield at High Altitudes [redacted]

[redacted] To account for the smaller fraction of the yield that appears as blast energy at higher altitudes, the actual yield is multiplied by the blast efficiency factor shown in Figure 2-64 to obtain the effective blast yield. Effective blast yield is that value of yield which, when used in Sachs' scaling laws, predicts the correct value of peak overpressure.

[redacted] Figure 2-64 shows approximate upper and lower limits rather than a single value for

*[redacted] Thermal radiation as used here includes ultraviolet through infrared, but excludes higher frequency radiations, e.g., X-rays. See Chapters 3 and 4.

[redacted]

the blast efficiency factor. At high altitudes, overpressure varies with distance in such a way that effective blast yield is different at different distances. For example, a 100 kt burst at 100,000 feet has an effective blast yield that varies from about 50 kt to 85 kt. It appears impossible to formulate simple rules that state where these numbers apply. It is preferable to consider the upper and lower effective blast yields as defining a range of uncertainty. Methods for making more detailed and complex calculations are suggested in DASA-1200 "Nuclear Weapons Blast Phenomena" (see bibliography).

Although blast efficiency is a correction factor established to determine peak overpressure, it also may be used to calculate other blast-wave parameters. However, because of the nonlinear properties of air, blast waves with high shock strengths cannot be scaled exactly, and shock-front parameters other than peak overpressure are defined less accurately by effective blast yield. The waveform behind the shock front is subject to additional variations, and the blast efficiency is least dependable when applied to parameters such as impulse and positive phase duration.

Problem 2-18. *Calculation of Peak Overpressure at High Altitudes

Figure 2-64 shows the blast efficiency factor as a function of height of burst. This efficiency factor when multiplied by the weapon yield provides the effective blast yield. The effective blast yield may then be used to obtain peak overpressure as a function of distance by the methods described in paragraph 2-7 and Problem 2-1 as modified by the altitude correction procedures described in paragraph 2-14. Other blast parameters may be obtained by using the effective blast yield in the manner described for total yield in paragraphs 2-8 through 2-11, as modified by the altitude scaling described in paragraph 2-14.

Scaling. After obtaining the effective blast yield, the various blast parameters are scaled according to the procedures described in Problems 2-1 through 2-5, as modified by the altitude scaling described in paragraph 2-14 and Problem 2-6.

Example

Given: A 200 kt explosion at an altitude of 100,000 feet.

Find: The highest value of peak overpressure that might be expected 5,000 feet below the explosion.

Solution: Since Figure 2-64 shows that the highest value of blast efficiency factor for a burst at 100,000 feet is 85 percent, the calculation is based on an effective yield, W_{eff}, of

$$W_{eff} = (0.85)(200) = 170 \text{ kt.}$$

While the blast efficiency factor is based on burst altitude, the altitude scaling factors are based on target altitude (paragraph 2-14). From Table 2-1, the distance and pressure scaling factors at 95,000 feet are

$$S_d \approx 4.2$$

$$S_p \approx 0.014.$$

The distance from a 1 kt explosion that corresponds to a distance of 5,000 feet from a 170 kt explosion is

$$d_1 = \frac{d}{S_d W^{1/3}} = \frac{5{,}000}{(4.2)(170)^{1/3}} = 215 \text{ feet.}$$

From Figure 2-2, the peak overpressure at this distance at sea level is 210 psi.

Answer: The corresponding peak overpressure at 95,000 feet is

$$\Delta p = \Delta p_o S_p = (210)(0.014) = 2.9 \text{ psi.}$$

The reliability statement of Problem 2-1 indicates that for scaled distances (distances from a 1 kt explosion) less than 1,000 feet the values of peak overpressure obtained from Figure 2-2 are accurate to within ±15 percent. The probable upper limit of the required overpressure is

$$\Delta p = 2.9 + (0.15)(2.9) = 3.3 \text{ psi.}$$

Reliability: The data curves in Figure 2-64 are based on computer calculations supported by limited data from full-scale nuclear tests. As a result of the experimental checks, the computed data are believed to be accurate at high overpressures; however, this accuracy is not considered confirmed. At low overpressures (scaled radii under 300 feet, shock strengths less than 7), some of the numerical methods used by the computer introduce errors, and reliable esti-

[redacted]

[redacted]

mates of effective blast yield are not available; however, even at low shock strengths, the blast efficiency factor is believed to be approximately within the limits shown in Figure 2-64. Yield scaling appears to be relatively accurate, introducing errors of only a few percent. Uncertainties in the overpressure values obtained from Figure 2-2 are described in Problem 2-1.

[redacted] *Related Material:* See paragraph 2-41. See also paragraphs 2-7 through 2-11 and 2-14. See also Problems 2-1 through 2-6.

[redacted]

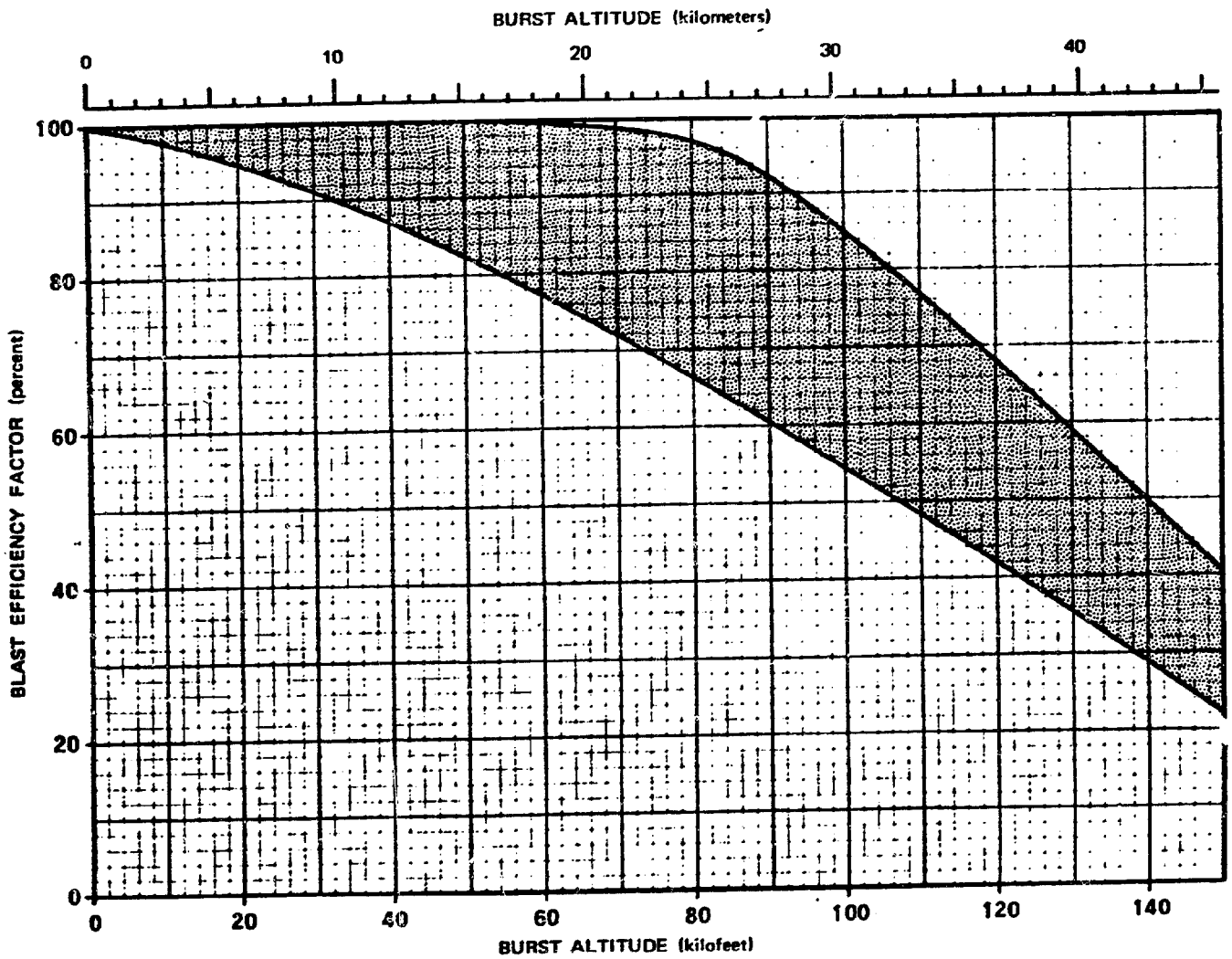

Figure 2-64. [redacted] Blast Efficiency Factor for High-Altitude Bursts [redacted]

[redacted]

2-43 Peak Overpressure on the Ground from High-Altitude Bursts [redacted]

[redacted] The conventional procedure for finding blast-wave parameters at one altitude produced by a burst at another altitude is modified Sachs' scaling (paragraph 2-14). Figure 2-65 uses this principle for the prediction of peak reflected overpressure at ground zero as a function of yield and burst altitude. The curves are based on computer calculations and are compatible with the curves in Figure 2-3, which show peak overpressure in free air.

[redacted] The curves are drawn as though effective blast yield (paragraph 2-41) were always equal to actual weapon yield. If the burst is above 40,000 feet, a correction for effective blast yield is appropriate, and this reduced yield (rather than actual weapon yield) should be used to enter Figure 2-65.

[redacted] Since the abscissa is slant range, Figure 2-65 may be used to predict peak reflected overpressure at locations other than at ground zero, provided the locations are within the region of regular reflection and are not too close to the range at which Mach reflection begins. Figure 2-46 may be used to determine the range over which the reflection coefficient has essentially the same value that it has at ground zero.

[redacted] Since modified Sachs' scaling is an empirical method, there may be doubt as to its application over a wide altitude range. However, comparisons of reflected overpressures at ground zero from Figure 2-65 with calculations performed in a way that is independent of the technique of modified Sachs' scaling show substantial agreement up to burst altitudes of about 150,000 feet, the limit of the latter calculations.

2-44 Effects of Early Blast Phenomena [redacted]

[redacted] At the overpressures that are ordinarily of interest in blast calculations, the blast wave from a sea level burst has propagated well away from the region in which it originated. At high altitudes, however, the blast wave forms at relatively low overpressures and at long ranges. In making a blast calculation at these altitudes, a possibility exists that the range of interest is closer than that at which a scalable shock front forms.

[redacted] The first stage of blast-wave formation occurs when the air around the burst, under high pressure because of its suddenly increased temperature, starts to move. In the analysis of computer runs, a convenient criterion for shock front formation is that the ratio of air density behind the shock to ambient air density (ρ_s/ρ) rises at some point to a value exceeding 1.5. This criterion indicates that the pressure waves originating in the air near the burst are starting to merge to form a shock front. Formation of the hydrodynamic shock front then proceeds rapidly, and the actual time and radius of shock formation are close to the values based on the $\rho_s/\rho = 1.5$ criterion.

[redacted]

[redacted]

Problem 2-19. Calculation of Peak Reflected Overpressure at Ground Zero from a High Altitude Explosion

[redacted] Figure 2-65 shows the peak reflected overpressure at the ground as a function of slant range for a selected family of weapon yields. The curves in Figure 2-65 are applicable at ground zero and at locations away from ground zero that are in the regular reflection region.

[redacted] *Scaling.* No scaling is required with Figure 2-65; however, for explosions above 40,000 feet, the effective yield obtained by use of Figure 2-64 should be used to enter Figure 2-65.

[redacted] *Example* [redacted]

Given: A 100 Mt explosion at an altitude of 120,000 feet.

Find: The maximum peak reflected overpressure expected at ground zero.

Solution: From Figure 2-64, the maximum blast efficiency factor for bursts at 120,000 feet is 68 percent. The effective yield is

$$W_{eff} = (0.68)(100) = 68 \text{ Mt}.$$

Answer: Interpolation in Figure 2-65 indicates that peak reflected overpressure at ground zero is about 2.5 psi.

[redacted] *Reliability* [redacted]

[redacted] The few available experimental data points tend to substantiate the curves in Figure 2-65. A certain amount of uncertainty occurs at low overpressures because the overpressure distance curves in Figure 2-65 are not identical to the results of the calculations independent of Sachs' scaling that were mentioned in paragraph 2-42.

[redacted] No reliability estimate has been made for these curves; however, it should be observed that, for the extreme range of atmospheric conditions found along the path of the blast wave, overpressure values that are within a factor of 2 often represent satisfactory agreement.

[redacted] *Related Material:* See paragraphs 2-7, 2-13, 2-14, and 2-42. See also Tables 2-1 and 2-2.

[redacted]

[redacted]

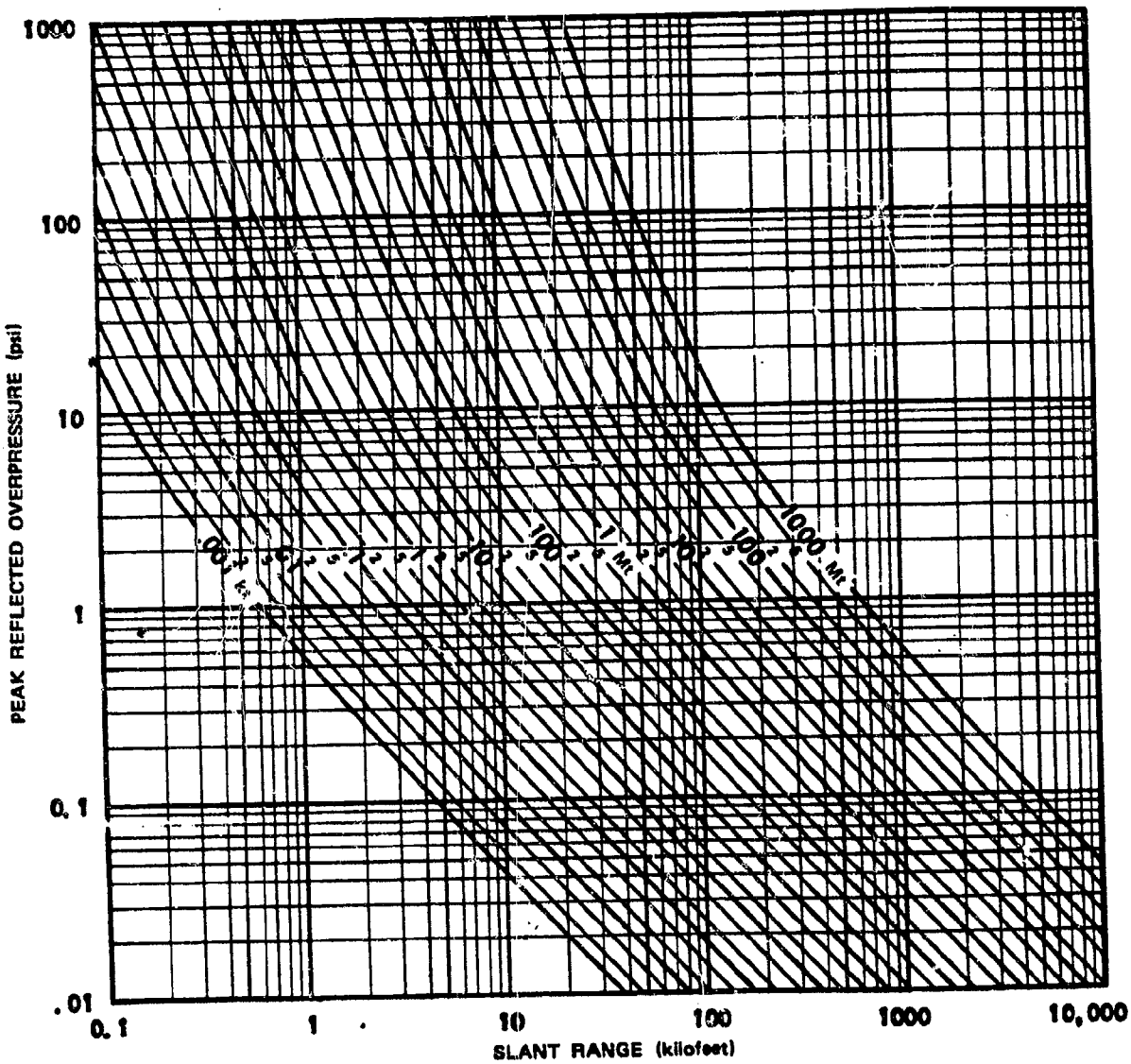

Figure 2-65. [redacted] Peak Reflected Overpressure at Ground Zero as a Function of Yield and Slant Range [redacted]

[redacted]

[redacted]

[redacted] The kinetic energy of the bomb debris, which is typically about 25 percent of the total yield, makes an important contribution to the strength of the blast wave. These high velocity debris atoms, pushing away the air surrounding the burst point, create a shock wave that is known as the nuclear shock or case shock. Until this shock front overtakes and merges with the hydrodynamic shock front, the blast wave will not have acquired its full energy. The fraction of the total energy carried by the debris is a function of weapon design. Therefore the arrival of the case shock at the hydrodynamic shock front, which marks the beginning of a scalable shock wave, also is a function of weapon design.

[redacted] Figure 2-66 shows the approximate ranges of shock-front formation and case-shock arrival as a function of burst altitude for a 1 kt explosion. These ranges were calculated for conventional nuclear devices. Different curves would be required to show these ranges accurately for weapons with enhanced radiation outputs (paragraph 2-45[redacted]

DNA (4)(3)

[redacted] Figure 2-66 also shows curves of blast-wave overpressure levels as a function of range and altitude. Since peak overpressure cannot be scaled accurately until the case-shock front joins the hydrodynamic shock front, the overpressure curves terminate on the curve for case-shock arrival. To emphasize the increasing uncertainty of peak overpressure data with increasing altitude, the overpressure contour lines are dashed above 100 kft.*

[redacted] These overpressure curves were obtained directly from Figure 2-2 and Sachs' scaling laws, including altitude corrections described in paragraph 2-14. However, correction for effective blast yield at high altitudes must be made, as illustrated in Problem 2-20.

[redacted] This procedure will give a reasonably accurate answer only if the range that is used exceeds the range for case-shock arrival. The latter range is obtained by multiplying range obtained from Figure 2-66 for case-shock arrival by $W'^{1/3}$ (note that actual yield W', not effective yield W'_{eff}, is required in this calculation). Similarly, the approximate range for shock front formation is obtained by multiplying the scaled range by $W'^{1/3}$.

[redacted] If a blast-wave calculation closer to the burst than the range of case-shock arrival is required, data from Figure 2-2 may be scaled to obtain a rough estimate of peak overpressure. If the calculation is for a range closer than the range for $\rho_s/\rho = 1.5$, the discrepancy between the actual overpressure and the calculated overpressure will probably be excessive. Requirement for a calculation of this type generally is a sign that other nuclear effects should be considered. Blast damage at ranges closer than shock-front formation usually is less serious than damage caused by neutrons, X-rays, gamma rays, and thermal energy.

[redacted] The stages of development of a nuclear blast wave are most accurately known in terms of time, because accurate comparisons can be made between experimental data and points in computer calculations. Approximate equations for determining three times of interest are given below.

[redacted]

DNA (4)(1)

[redacted] See NOTE in Reliability paragraph of Problem 2-20.

[redacted]

[redacted]

Problem 2-20. Calculation of Case-Shock Arrival and Peak Overpressure at High Altitudes

[redacted] Figure 2-66 shows the approximate ranges of shock-front formation and case-shock arrival as a function of burst altitude and distance from a 1 kt explosion.

[redacted] *Scaling.* For yields other than 1 kt, the range for case-shock arrival scales as follows:

$$\frac{d}{d_1} = W^{1/3},$$

where d_1 is the range for case-shock arrival for 1 kt (obtained from Figure 2-66), and d is the corresponding range for a yield of W kt. For heights of burst above 40,000 feet the range for a given *overpressure* scales as follows:

$$\frac{d}{d_1} = (W_{eff})^{1/3},$$

where d_1 is the range for the desired overpressure for a 1 kt explosion and d is the corresponding range for a yield of W_{eff} kt (W_{eff} is the effective yield for a high altitude burst obtained from Figure 2-64 as illustrated in Problem 2-18).

[redacted] *Example* [redacted]

Given: A 100 kt explosion at an altitude of 110 kilofeet above sea level.

Find: The peak overpressure at a range of 1,000 feet.

Solution: From Figure 2-66, the range for case shock arrival from a 1 kt burst at 110 kft is about 180 feet. The corresponding range for 100 kt is

$$d = d_1 W^{1/3} = (180)(100)^{1/3} = 835 \text{ feet.}$$

Since this is less than 1,000 feet, peak overpressure is scalable at the range of interest. From Figure 2-64, the blast efficiency for a burst at 110 kft is expected to be between 48 percent and 77 percent. The effective blast yield is therefore between 48 and 77 kt. The corresponding distances for a 1 kt explosion are

$$d_1 = \frac{d}{(W_{eff})^{1/3}} = \frac{1{,}000}{(48)^{1/3}} = 275 \text{ feet,}$$

and

$$d_1 = \frac{d}{(W_{eff})^{1/3}} = \frac{1{,}000}{(77)^{1/3}} = 235 \text{ feet.}$$

Answer: From Figure 2-66, the overpressures are 90 and 150 psi at these ranges from a 1 kt explosion at 110 kft. The 15 percent uncertainty in overpressure data (see "Reliability") extends the range of 1 kt overpressure values to between 75 and 170 psi.

[redacted] *Reliability* [redacted]

[redacted] Ranges for shock formation and case-shock arrival were obtained from computer calculations. Case-shock arrival has been observed in nuclear tests, and the experimentally determined ranges substantiate the computer data. For conventional weapons (unconventional weapons are discussed in the following subsection), the range for case-shock arrival is believed correct within a few percent. Yield scaling appears to be fairly accurate for these phenomena.

[redacted] Below 40,000 feet peak overpressure data are considered reliable within 15 percent for shock strengths greater than 1.5 (7 psi at sea level), within 20 percent for shock strengths between 1.5 and 1.03, and within 30 percent for shock strengths below 1.03 (~1/2 psi at sea

[redacted]

[redacted]

[redacted]

level). Above 40,000 feet, the additional uncertainty implied by Figure 2-64 should be considered.

[redacted] Note: Although Figure 2-66 was used in this example to calculate peak overpressure, it is not the preferred source of overpressure data. More accurate values may be obtained by scaling data from Figure 2-2 and, at high altitudes, following the method of Problem 2-18. Figure 2-66 is convenient for rough calculations, because it eliminates the requirement for altitude scaling. However, the important information in this figure is given by the curves that show the approximate ranges of shock-front formation (ρ_s/ρ = 1.5) and the beginning of a scalable shock wave (case-shock arrival).

[redacted] *Related Material:* See paragraphs 2-7, 2-41, and 2-43. See also Problem 2-18.

[redacted]

[redacted]

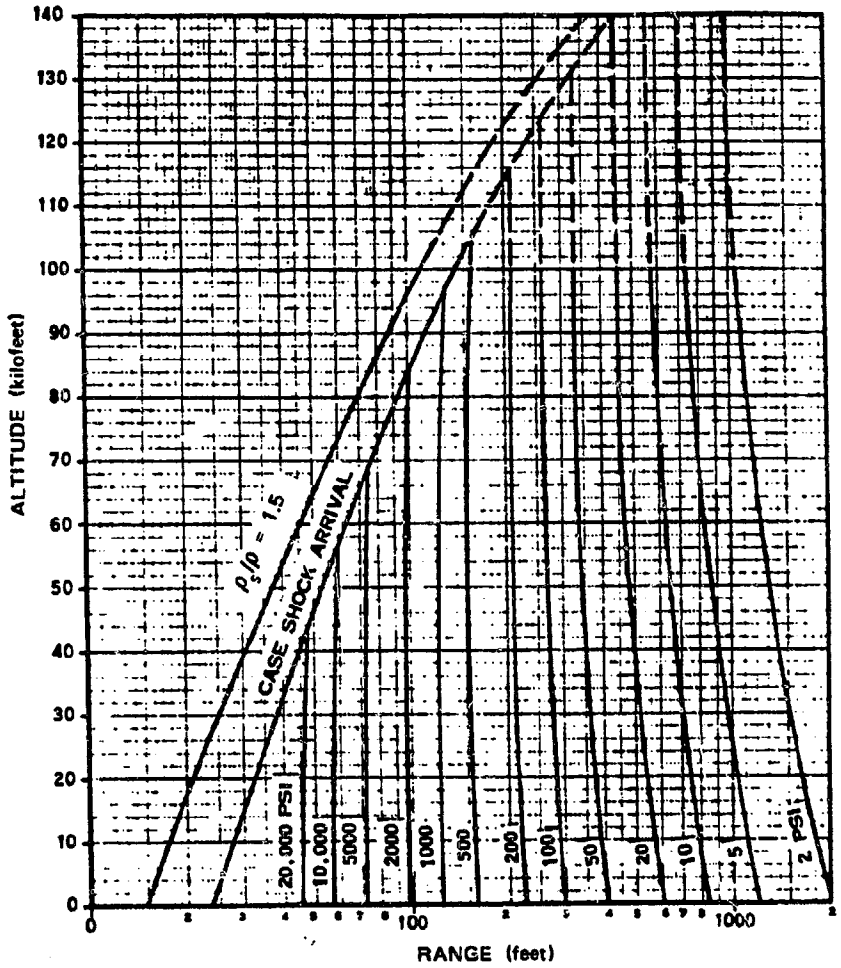

Figure 2-66. [redacted] Limits of Scalable Shock Wave and Calculated Peak Overpressure as a Function of Altitude as a Function of Distance from a 1 kt Explosion [redacted]

[redacted]

[redacted]

[redacted] WEAPONS WITH ENHANCED OUTPUTS [redacted]

[redacted] The initial output energy of a conventional nuclear weapon consists mainly of black body radiation [redacted] and kinetic energy of bomb debris as shown in Table 2-6. Table 2-7 shows the mean free path of various forms of energy that can be generated by a nuclear device. Most of the output of a conventional nuclear weapon interacts with air atoms near the burst.

DNA (b)(3)

[redacted]

DNA (b)(3)

[redacted]

DNA (b)(3)

[redacted]

2-45 Air Blast from Weapons with Enhanced Radiation Outputs [redacted]

[redacted] The strength of the blast wave from enhanced radiation weapons is a complex function of the radiant energy distribution. Accurate blast wave calculations require detailed energy transport calculations, followed by hydrodynamic calculations to account for the motion of the heated air and the bomb debris. Frequently, the variation of ambient air density with altitude is sufficiently important to be included in the calculations. A large digital computer is required to account for all of these factors.

---

*[redacted] The unit keV is commonly used in two senses. Strictly speaking, it is a unit of energy (1 keV = 1,000 electron volts = 1.602×10^{-9} erg) which has a magnitude that is convenient for specifying the energies of X-ray photons. However, by extension of its original meaning, the unit is used to define temperature (1 keV ≈ 11,600,000°K).

[redacted] The term *1 keV spectrum* means the spectrum of thermal radiation from a black body, i.e., a perfect radiator of thermal energy, that has a temperature of 1 keV. Note, however, that an energy of 1 keV is not representative of the energy of the photons constituting such a spectrum: about 15 percent of the photons have energies of 1 keV or less, and these photons represent less than 3.5 percent of the total spectral energy. Half of the energy is carried by photons with energies greater than 3.5 keV. The spectrum extends roughly to 10 keV; photons with energies higher than this constitute only 1 percent of the spectral energy. See Chapter 4 for further discussion of black body radiators.

[redacted]

[redacted]

Table 2-7[redacted] Representative Mean Free Paths of Nuclear Weapon Radiation [redacted]*

Source	Energy	Mean Free Path	
		Sea Level	80,000 ft
[redacted]			

*[redacted] The mean free paths shown in this table are for individual particles in ambient air. Collectively, the particles may travel farther. Debris atoms, for example, assist one another in pushing the air atoms away from the burst point. X-ray photons completely ionize a small region of air near the burst, thus creating a nearly transparent region through which other X-ray photons can travel freely.

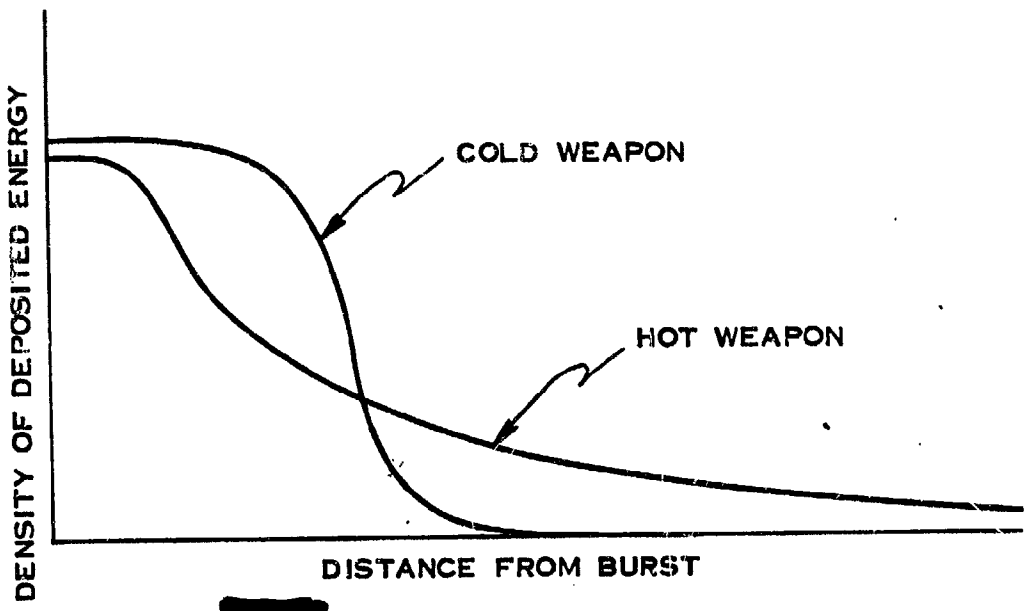

Figure 2-6[redacted] Energy Deposition in Air as a Function of Nuclear Source Characteristics (Not to Scale) [redacted]

[redacted]

[redacted]

[redacted] Rough calculation may be made, however, by applying the following rule of thumb to weapons with enhanced outputs: blast calculations for a given radius may be based on a weapon yield that is equal to the amount of energy contained in the sphere defined by that radius. As this rule implies, the blast wave, as it propagates outward, picks up hydrodynamic energy from the heated air through which it passes.

DNA (b)(3)

[redacted]

DNA (b)(3)

[redacted]

[redacted]

[redacted]

Deleted

Figure 2-68. [redacted] Distribution of Deposited X-ray Energy in a Sea Level Atmosphere as a Function of Source Spectrum [redacted]

[redacted]

DNA
(G)(3)

Deleted

Figure 2-69. [redacted] Density of Deposited Energy in Sea Level Air from Various Energy Sources [redacted]

[redacted]

[redacted]

[redacted]

[redacted] Many problems that require blast yield correction because of output spectrum will also require a blast yield correction because of altitude (paragraph 2-41). One correction factor does not replace the other, as illustrated in Problem 2-21.

[redacted] Effective blast yield, in percent, tends to increase with (1) increased range, (2) decreased radiating temperature, (3) increased yield, and (4) decreased altitude. [redacted]

DNA (b)(3)

[redacted] As yield increases, the range for a given overpressure increases, but the distance that a given form of prompt energy can travel remains essentially the same; therefore, at a given overpressure level the blast wave from a higher yield encloses a greater fraction of the weapon output [redacted]

DNA (b)(

[redacted] As altitude decreases, the denser air confines the radiated energy to a smaller volume. Since the range for a given peak overpressure is relatively insensitive to altitude (Figure 2-66), the sphere defined by this range encloses an increasing fraction of the source energy as altitude decreases.

[redacted]

[redacted]

[redacted]

Problem 2-21. Calculation of Peak Overpressure from a Hot X-ray Warhead [redacted]

[redacted] Paragraph 2-44 describes the differences between the characteristics of blast waves from enhanced radiation weapons and the blast waves from conventional weapons. The following example will illustrate the use of the information discussed in paragraph 2-44.

[redacted] *Scaling.* Range is scaled in such a way that at a given scaled range the X-ray energy has passed through a given amount of air.

$$\frac{R_o}{R} = \frac{\rho}{\rho_o},$$

where R_o and ρ_o are range and ambient air density at sea level and R is range in air with an ambient density of ρ. The ordinate of Figure 2-68 (percent of radiated energy deposited) does not require scaling. Energy density added to the air is scaled in a way that accounts for spherical divergence and for yield.

$$\frac{\Delta E}{\Delta E_1} = \left(\frac{R_o}{R}\right)^2 W.$$

This equation is equivalent to:

$$\frac{\Delta E}{\Delta E_1} = \left(\frac{\rho}{\rho_o}\right)^2 W,$$

where ΔE_1 is the energy deposited by 1 kt, ΔE is the corresponding energy deposited by W kt, and the other terms are as previously defined. In addition to the scaling described above, Sachs' altitude scaling (paragraph 2-14) probably will be required [redacted]

DNA (b)(3)

DNA (b)(3)

Page 2-145 Deleted.

[redacted]

[redacted]

[redacted]

[redacted] *Reliability:* The procedures described above have been substantiated by analysis of a limited number of computer calculations, and specific reliability estimates have not been made. The amount of error introduced by the procedures is expected to increase as the effective blast yield (in percent) decreases. In typical problems, the change in effective yield that the procedures predict is probably correct within about 25 percent.

[redacted] *Related Material:* See paragraphs 2-7, 2-14, 2-41, and 2-44. See also Tables 2-1 and 2-2.

[redacted]

[redacted]

[redacted]

SECTION II
CRATERING PHENOMENA

[redacted]

A crater is formed when an explosion occurs at or near the ground surface. Figure 2-70a shows an idealized cross section of a crater formed by such an explosion. The diagram illustrates the dimensions that are commonly used to describe the crater, and the zones of subsurface deformation that typically surround a crater. The apparent crater is defined as the crater that is visible on the surface, the dimensions being measured between fallback and the original ground surface elevation. Fallback is material that was lifted or thrown out by the explosion and has fallen back within the true crater. The true crater is delineated by the approximate boundary between the fallback material and the rupture zone. The shape of the true crater is disguised by the fallback.*

The primary variables that affect the size and shape of the crater are the weapon yield and output characteristics, the height or depth of burst (HOB or DOB), the properties of the earth medium, and the geologic structure. As these variables change, the shape, characteristics, and actual dimensions of the crater change. Figure 2-70b illustrates the general cross sectional shapes of craters formed as a result of various burst positions.

*It is hypothesized by some that in certain geologies (notably those that are highly porous and water filled) the shock waves from the excavated crater may fracture the geological matrix. This could lead to late-time reconsolidation and liquefaction that could cause the apparent crater and the true crater to coincide and to be larger than the crater in a more competent geology. This theory is one that has been proposed to explain the large shallow craters produced at the Pacific Proving Ground.

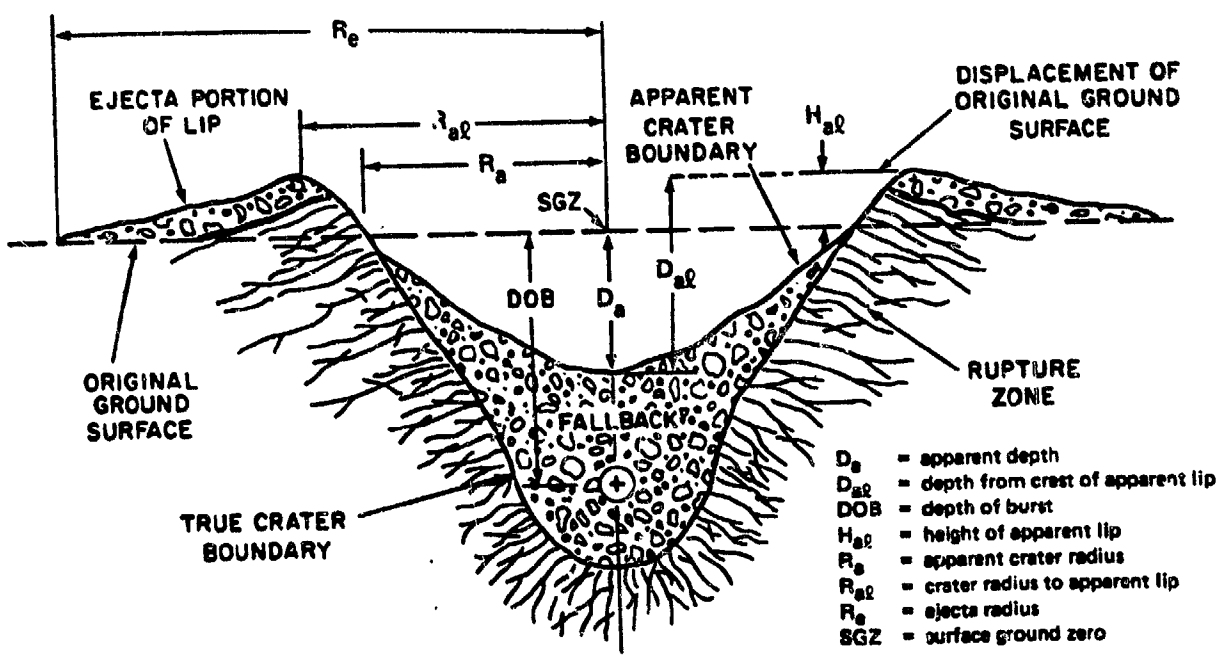

Figure 2-70a. Cross Section of a Crater from a Subsurface Nuclear Detonation

[redacted]

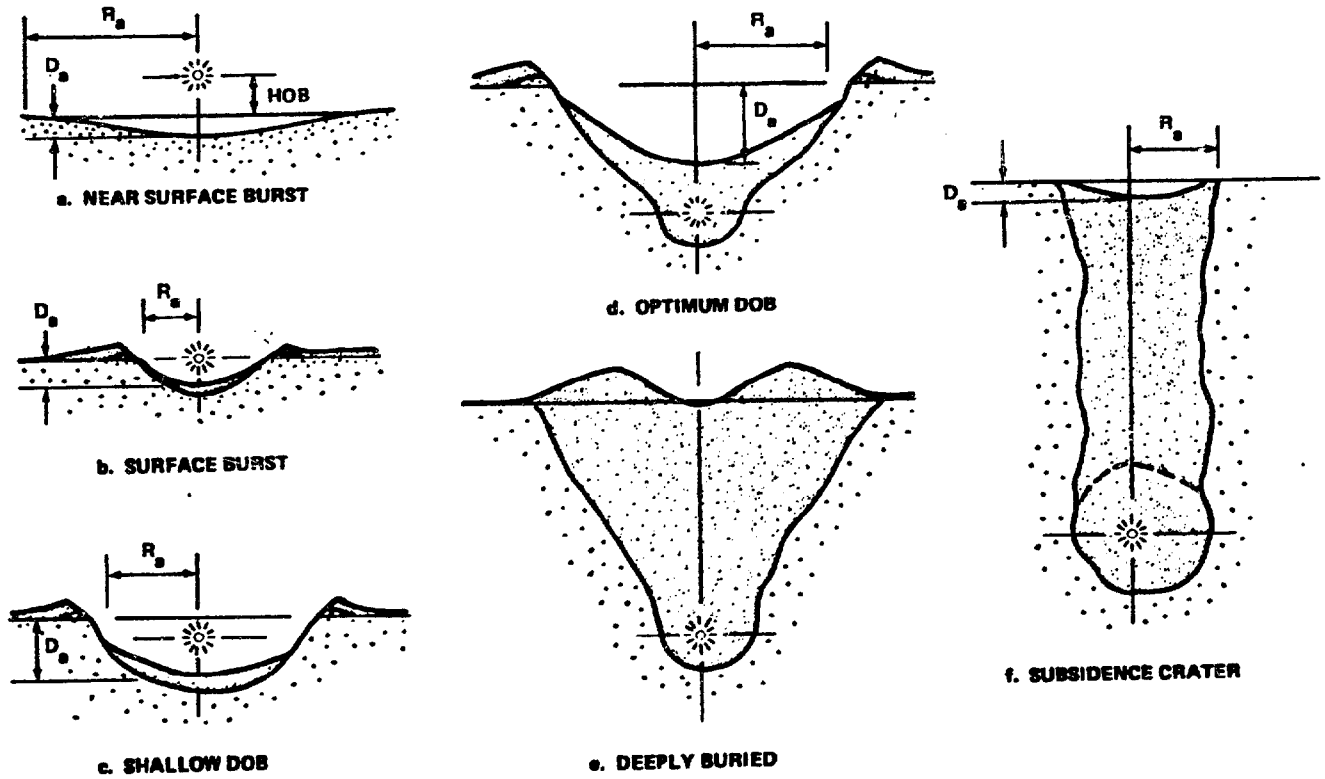

Figure 2-70b. Relative Crater Sizes and Shapes Resulting from Various Burst Positions

When a nuclear explosion occurs well above the surface, but low enough that the fireball still intersects the ground surface, a shallow crater is formed by compression of the earth beneath the explosion and no ejecta is produced. As the HOB decreases, the crater volume increases and the proportion of the crater volume that results from excavation and ejection also increases. This holds true in a continuum that includes surface bursts (HOB = 0) and buried bursts from the most shallow to the optimum DOB for the weapon being considered. If the burst takes place at the optimum depth of burial, i.e., at the depth that results in maximum apparent crater dimensions for the weapon being considered, the acceleration of the earth medium upward by the expanding explosion gases is the dominant feature of the cratering process. Figures 2.71a and 2.71b are photographs of apparent craters that occurred from nuclear explosions buried in soil and rock at depths near optimum for crater formation.

Finally, deeply buried explosions may lead to a subsidence crater, to a raised mound above the detonation point, or to no permanent displacement of the surface at all.

2-46 Energy coupling

When a nuclear weapon explodes at or above the surface of the earth, there are two phases in the process of energy flow into the ground. The initial phase is referred to as "radiation deposition." Part of the prompt radiation output from the weapon (x-rays; see Chapter 4) reaches the ground and is absorbed in a time that is so short (a fraction of a microsecond) that hydrodynamic motion in the ground will be negligible. The ground is heated rapidly, and most of the absorbed energy is reradiated back into the air above the surface.

In addition to the energy deposited directly in the ground, the atmosphere around the source is heated by radiation diffusion, producing a fireball that radiates energy into the ground. This creates a thin layer of very hot plasma. At this stage, before any significant mass motions have occurred, the plasma, a layer of very hot, high energy-density material, extends along the surface to a radius that depends on weapon yield (about 30 meters for a 1 Mt surface burst).

The radiative coupling is completed in approximately one to three tenths of a microsecond. The net energy permanently absorbed by the ground represents about 6 percent of the total explosive yield.

The second phase of the process of energy flow into the ground is the "debris impact" phase. Vaporized debris from the nuclear device and its associated material impact the ground surface and add more energy to the earth. This debris slap may last for 3 or 4 microseconds, depending on the height of burst, and may inhibit some reradiation out of the ground. The energy from the debris impact represents only about 2 percent of the nuclear warhead yield for a contact surface burst.

The radiation from the air in the fireball continues to add energy to the soil over a period of time that is much longer (up to several hundred microseconds) than the duration of the prompt-radiation deposition and debris impact phases. The amount of energy coupled by this process is very uncertain.

The height of burst has an important effect on the radiative coupling. The air acts as an energy sink for some of the downward directed x-rays, converting them into thermal energy. The radiative coupling of a 1 Mt burst at a height of burst of 5 meters could be a factor of two less than from a contact surface burst (HOB = 0 meters) of the same yield. Because of practical considerations, such as the location of the center of energy release in a reentry vehicle whose nose is just in contact with the ground, it is more likely that the HOB will be greater than zero.

[redacted]

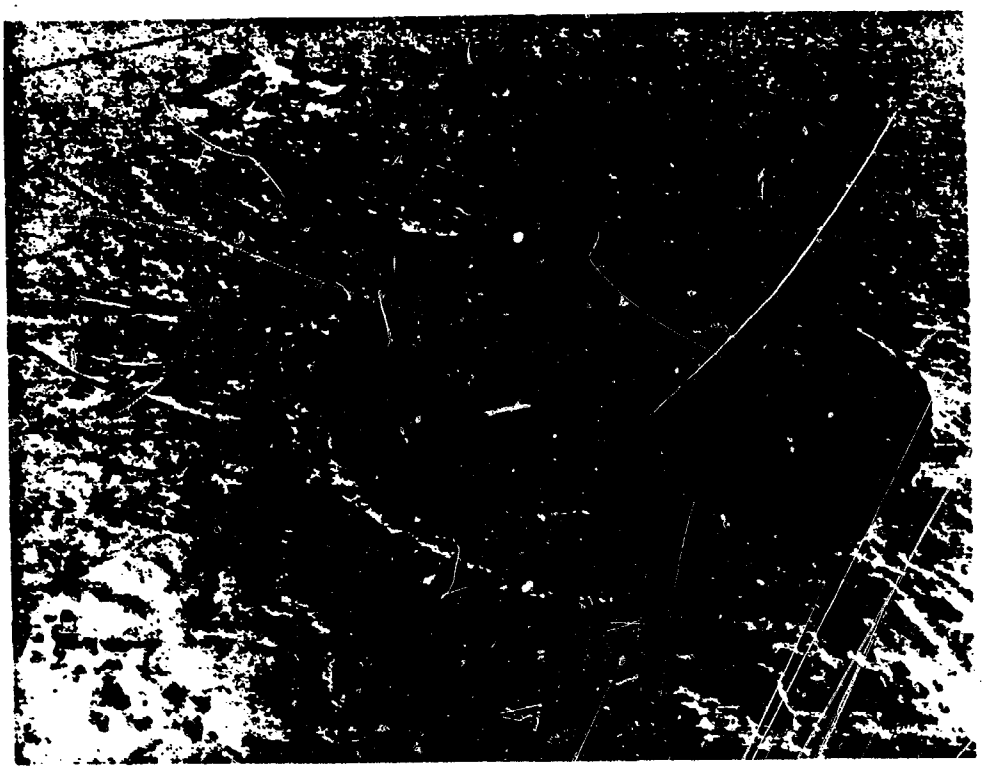

Figure 2-71a. SEDAN Event; Typical Crater Formed by a 100 kt Detonation in a Soil Medium at Optimum DOB: R_a = 186 m (611 ft.); D_a = 98.5 m (323 ft.); DOB = 194 m (635 ft.)

Figure 2-71b. DANNY BOY Event; Typical Crater Formed by a 0.43 kt Detonation in a Hard Rock Medium (Basalt) at Optimum DOB: R_a = 33.5 m (110 ft.); D_a = 18.9 m (62 ft.); DOB = 33.5 m (110 ft.)

[redacted]

[redacted]

On the other hand, the radiative coupling may be increased by as much as a factor of 5 compared to surface bursts if there is a slight penetration of the weapon into the surface of the ground (3 to 5 meters for a 1 Mt burst). This greater coupling is in addition to the well known increase in mechanical coupling, which is discussed in paragraph 2-47.

2-47 Mechanical Coupling

The preceding discussion outlined the flow of energy into the ground for cratering events that result from bursts at or above the surface. These processes take place during the first several milliseconds of actual crater formation. The hydrodynamic portion of crater formation may last for several seconds.

If the explosion occurs at a height-of-burst greater than 4 to 5 $m/kt^{1/3}$, the crater will be formed almost exclusively by compaction. Scouring, which results from airblast and airblast associated winds, contributes a small fraction of the crater volume. Since there is little fallback in such a crater, the true and apparent craters are essentially identical. As the height of burst is decreased, an increasing fraction of the crater is formed by excavation and ejection of ground material. In addition, compaction, plastic deformation and flow of the material in the rupture zone are principal mechanisms for crater formation of very near-surface bursts. These mechanisms produce a slight increase in material density as well as considerable brittle and plastic failure of the ground material. The mechanisms also cause a radial displacement with an overturning of crater material around the edge of the crater. The top of this mound is termed the crater lip. After detonation, the crater may be partially refilled by material falling back into the crater (fallback), by slumping, and by late-time rebound. The material thrown out beyond the crater lip (ejecta) forms a layer whose thickness diminishes with radial distance from the burst point.

The first diagram in Figure 2-70b illustrates the general crater shape that is expected from an above-surface burst. Despite many explosive cratering experiments with nuclear and high-explosive (HE) devices, the complex interrelationships that exist among the various mechanisms that could cause craters preclude the *quantitative* dynamics of crater formation by near-surface bursts from being well understood.

The size and shape of craters from subsurface detonations are affected significantly by the depth of burial. The dominant cratering mechanisms, which are discussed in succeeding paragraphs, will be related to the depths of burial shown in Figure 2-70b.

- *Crushing, Compaction, Plastic Deformation.* As the high pressure explosion gases expand against the surrounding medium, a spherical shock wave is generated. The initial shock pressures are as large as 10 to 100 million atmospheres. The medium surrounding a nuclear explosion is initially melted and vaporized as the shock passes through it. As the shock front moves outward in a spherically diverging shell, the medium behind the shock front is put into radial compression and tangential tension. The peak pressure in the shock front attenuates by spherical divergence and dissipative mechanisms in the medium. The material around the explosive charge (nuclear or HE) is crushed, heated, and physically displaced outward, forming a cavity. In regions outside this cavity, the shock wave will produce permanent deformation by plastic flow. This mechanism of crater formation is a significant contributor to crater size for bursts at or just below the ground surface (Figure 2-70b,(b)), and at depths of burial that result in subsidence craters (Figure 2-70b,(f)).

[redacted]

[redacted]

- *Spalling.* When an upward moving shock (compressive) front encounters the air-ground interface, the large mismatch of material properties results in the generation of a negative stress (rarefaction) wave. The refraction wave propagates back into the medium in which the burst occurred, and puts the medium (originally under high compression) into tension (or less compression). This phenomenon causes the medium to break up and move upward with a velocity characteristic of the total momentum imparted to it. In a loose soil material, this spalling ejects individual particles of similar size into the air. In a rock medium, however, the thickness and size of the spalled material generally is determined by the presence of pre-existing fracture patterns and zones of weakness. The velocity of the spalled material decreases in proportion to the decrease in peak compressive stress. The spall mechanism produces an extended rupture and plastic zone near the ground surface and contributes significantly to the true lip height of the crater. This mechanism appears to be dominant in determining crater size at shallow depths of burial (Figure 2-70b,(c)).
- *Gas Acceleration.* Gases are produced in the material surrounding the explosion by vaporization and chemical changes induced by heat and pressure. The near-adiabatic expansion of the gases imparts motion to the medium. At depths of burial at which crater dimensions are maximized (optimum DOB), the cavity gases produce appreciable acceleration in overlaying material before they escape (vent) through cracks extending from the cavity to the surface. Gas acceleration is the dominant crater producing mechanism at optimum DOB (Figure 2-70b,(d)). At shallow depths of burial the gases cannot exert significant pressure before venting occurs. In the case of very deep explosions, the weight of the overburden precludes any significant gas induced acceleration of the overlying material.
- *Overburden Collapse.* At depths of burial that are large (two or more times) compared to the optimum, the mechanism of overburden collapse (subsidence) becomes dominant. This effect is closely linked to the crushing, compaction and plastic deformation mechanism that produces an underground cavity. At these large depths of burial, spall and gas acceleration will not impart sufficient velocity to the overlying material to eject it physically from the crater. It would be expected that the crater volume would be determined largely by the underground cavity formed by the detonation. In a rock medium, however, material that is fractured and displaced from its original position tends to take up more space than it occupied in its natural state. This bulking action could result in no crater or, indeed, even a mound above the ground. A mound was produced after the SULKY detonation, as shown in Figure 2-72a.

In certain geologic materials yet another type of subsidence occurs. When the pressure in the cavity decreases below overburden pressure, the roof of the cavity begins to collapse. In most media, this collapse will continue upward and will form a "chimney" of collapsed material. In a soil medium, where the density of the material will not change significantly after it has fallen, the volume of the cavity will be transmitted to the surface, forming a "subsidence crater" on the surface (Figure 2-70b,(f)). This phenomenon is illustrated in Figure 2-72b.

[redacted]

Figure 2-72a. SULKY Event; Mound Created by the Bulking of Rock Material in a Deeply Buried 0.087 kt Nuclear Detonation:
Mound Diameter = 48.8 m (160 ft.); Mound Height = 7.6 m (25 ft.); DOB = 27 m (90 ft.)

Reproduced from best available copy.

[redacted]

Reproduced from best available copy.

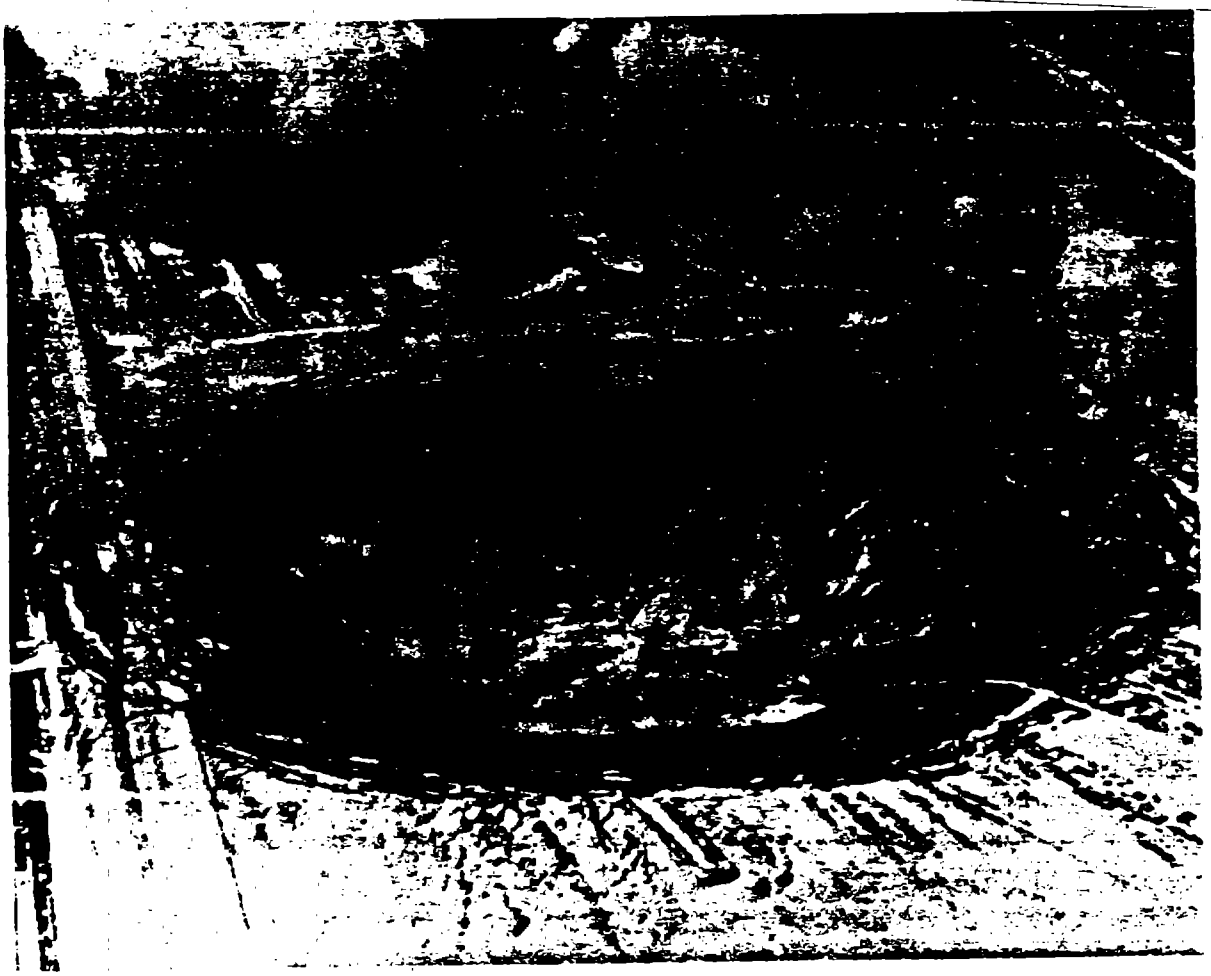

Figure 2-72b. PASSAIC Event; Subsidence Crater Produced by a Deeply Buried Nuclear Detonation in a Soil Medium

[redacted]

[redacted]

PREDICTION OF CRATER DIMENSIONS

The present prediction of crater dimensions for above-surface, surface, and shallow-buried bursts is based on the nuclear tests conducted in dry alluvial soil at the Nevada Test Site and the saturated coral at the Pacific Proving Ground. Extrapolation to other geologies is made on the basis of HE spherical-charge events. There have been no high-yield near-surface nuclear experiments in dry soil or rock. It is assumed that the influence of geology can be separated from that of the energy source. However, the nuclear tests conducted at the Pacific Proving Ground (saturated coral) and HE tests conducted at the Suffield Experiment Station (wet soil) suggest that the influence of geology is not *entirely* independent of the source. This fact is illustrated in Figure 2-73.

The dimensions of the crater vary in a complex manner as the HOB approaches the ground surface; but with lower HOBs the apparent depth of the crater generally increases and the ratio of the apparent radius to depth decreases. When crater dimensions for surface, above-surface, and shallow-buried bursts are scaled to yields much greater than 1 kt (for example, 1 Mt), the calculated change in the shape of the apparent crater as the yield increases is also an important consideration. This phenomenon, unfortunately, has not been observed in dry media.

2-48 Crater Dimension Scaling

The results of cratering explosions of various yields and burst geometries have been correlated by empirical scaling laws that express crater dimensions in terms of a standard yield of one kiloton. Crater dimensions for any other yield can be predicted by application of an empirical yield scaling exponent, as will be described in the succeeding paragraphs. The dimensions for which curves and scaling procedures will be presented are the radius of the apparent crater, R_a, the depth of the apparent crater, D_a, and the apparent volume V_a. Other pertinent crater dimensions such as the radius to the crest of the apparent lip and the height of the apparent lip, may be related to the above dimensions by scaling laws that will be described.

Several burst geometries will be considered: above-surface (near and contact), surface, shallow-buried, and deep-buried bursts. The actual height of burst (HOB) or depth of burst (DOB) is measured from the original ground surface to the *center of energy* of the weapon. The scaled HOB or DOB is the actual dimension divided by the scaled yield (described below). Of the *above-surface* bursts ($HOB/W^{1/3} > 0$), the lower bursts are of most significance to cratering, i.e., $HOB/W^{1/3} \leq 3$ m/kt$^{1/3}$. A *contact* burst is considered to be one wherein the weapon is in contact with the ground surface, and therefore has an actual HOB of approximately 0.5 m. A *surface* burst is one in which the HOB as defined above, is exactly zero. A *shallow-buried* burst has a $DOB/W^{1/3} \leq 5$m/kt$^{1/3}$ and the *deep-buried* burst has a $DOB/W^{1/3} > 5$ m/kt$^{1/3}$.

No single yield scaling exponent has been found to be valid for scaling apparent crater dimensions over a wide range of yield, geology, and HOB or DOB. However, the following yield scaling exponents, a, (yield, W (kt), to the a power) have been found to be approximately correct for scaling the apparent crater dimensions for surface/above-surface bursts and for deep-buried bursts:

$$a = 1/3 \text{ for } 0 < \frac{HOB}{W^{1/3}} \leq 3 \text{ m/kt}^{1/3},$$

$$a = 1/3.4 \text{ for } \frac{DOB}{W^{1/3}} > 5 \text{ m/kt}^{1/3}.$$

[redacted]

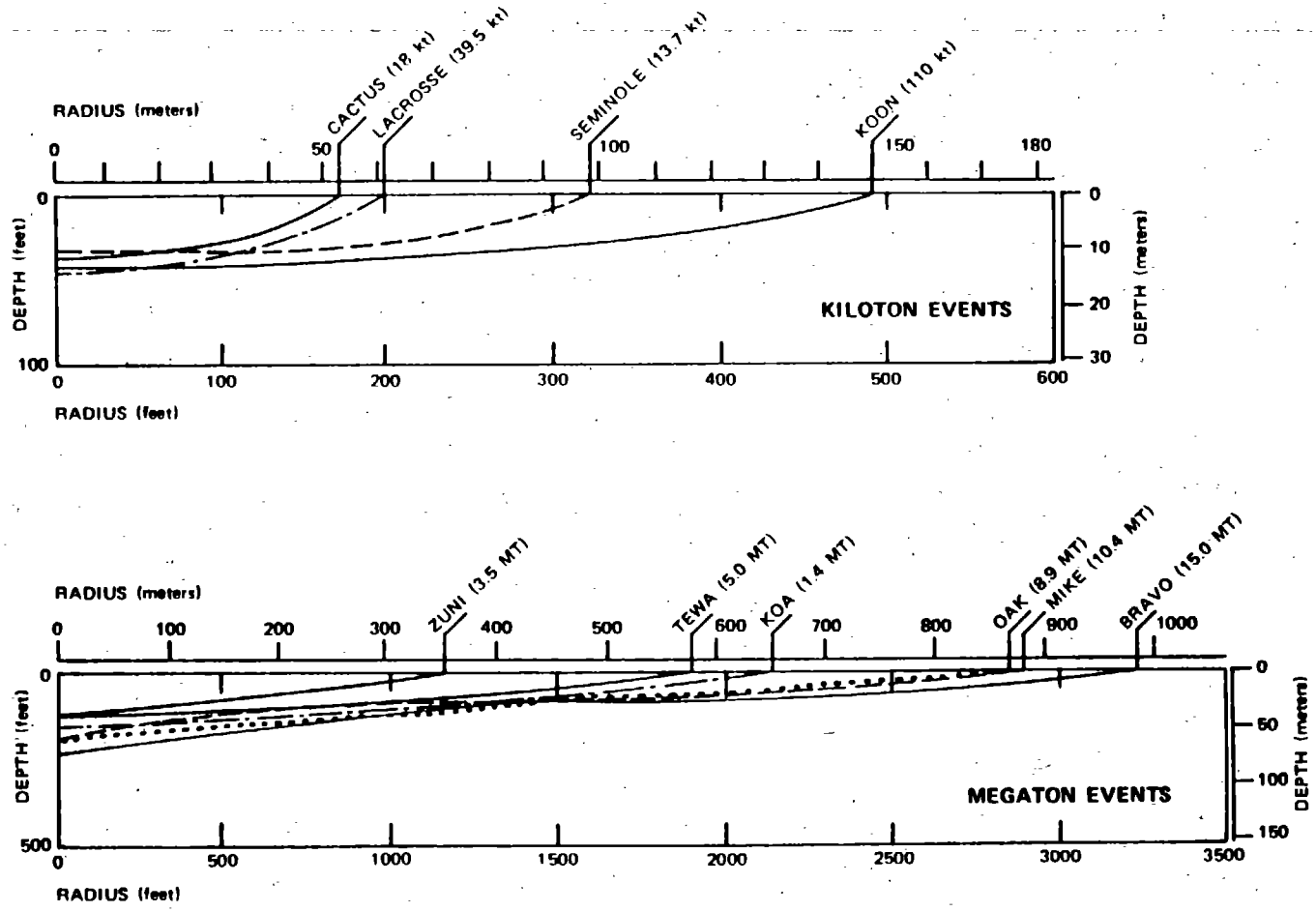

Figure 2-73. Typical Pacific Proving Ground Crater Profiles

[redacted]

In the shallow-buried region where the $DOB/W^{1/3}$ is less than 5 $m/kt^{1/3}$, the yield scaling exponent, a, is a function of depth of burial.* It is in this region that an interpolation procedure is required to determine a, as will be discussed in paragraph 2-49.

The near-surface region ($HOB/W^{1/3} \leq 3$ $m/kt^{1/3}$ to $DOB/W^{1/3} \leq 5$ $m/kt^{1/3}$) and the buried burst ($DOB/W^{1/3} > 5$ $m/kt^{1/3}$) region will be examined separately in the succeeding paragraphs. Five generic geologies have been chosen to describe the effect of various homogeneous media on cratering efficiency.

2-49 Volume of Craters from Surface and Near-Surface Bursts ($HOB/W^{1/3} \leq 3$ $m/kt^{1/3}$ to $DOB/W^{1/3} \leq 5$ $m/kt^{1/3}$)

Figures 2-74a through 2-75e show the apparent crater volume, as a function of height of burst,† for a near-surface 1 kt explosion in various homogeneous generic geologies. Figures 2-74a through 2-74e are valid for yields less than or equal to 1 kt and Figures 2-75a through 2-75e are valid for yields greater than 10 kt.

For yields between 1 and 10 kt, the crater volume may be estimated by using the best estimate curve of the appropriate geology for either 1 kt or 10 kt or a weighted average, depending upon the output characteristics of the warhead. The higher the radiative fraction, the closer the crater volume will be to the $W > 10$ kt curve. If, for example, it is known that a 3 kt weapon of interest has a high radiative output, the $W > 10$ kt curve should be used to determine the apparent crater volume. If, however, no information is available concerning the radiative output, the crater volume should be determined by interpolation, assigning a 60 percent weight to the $W \leq 1$ kt curve and 40 percent weight to the $W > 10$ kt curve, i.e., for a 3 kt weapon with no further information

$$V_a(3) = 0.6V_a(W \leq 1) + 0.4\ V_a(W > 10).$$

The yield scaling parameter, a, for near-surface bursts is determined as follows:

$$\frac{HOB}{W^{1/3}} \geq 0;\ a = 0.333$$

$$-5 \leq \frac{HOB}{W^{1/3}} < 0\ (m/kt^{1/3});\ a = \text{(see Figure 2-76a)}.$$

Once the value of a is known, the apparent scaled crater volume can be obtained from Figures 2-74a through 2-75e for a specified yield (W) and HOB/W^a in the appropriate geology. The value obtained by this procedure is the "best estimate" of the apparent crater volume for a 1 kt explosion (V_{a1}).

The crater volume for yields other than 1 kt may be obtained by the following scaling relation:

$$\frac{V_a}{V_{a1}} = W^{3a},$$

where V_{a1} is the apparent crater volume for a 1 kt explosion, and V_a is the corresponding volume for a yield of W kt. The height of burst scaling relation is

$$\frac{HOB}{HOB_1} = W^a,$$

where HOB_1 is the height of burst for a 1 kt explosion, and HOB is the corresponding height of burst for a yield of W kt.

*Craters from detonations on the islands of the Pacific Proving Ground (Eniwetok and Bikini atolls) indicate that, for a saturated coral medium, the scaling exponent for the apparent crater radius may be greater than 1/3 and for the crater depth, smaller than 1/3. Until the reason that it is necessary to depart from cube-root scaling in saturated coral is understood, it will not be possible to determine similar departures in other media.

†In this group of figures, HOB is used to indicate both HOB and DOB, i.e., buried bursts are shown with a negative HOB.

[redacted]

[redacted]

The uncertainty in the crater volume for $W \leq 1$ kt is based on HE cratering results. It is assumed that the uncertainty is independent of geology and yield. The bounds shown in Figures 2-74a through 2-74e are not the results of a detailed statistical analysis. These bounds contain 95 percent of the experimental data, but statistical implications should not be drawn from this fact.

The best estimate for the $W > 10$ kt curve was determined by nuclear data from the Pacific Proving Ground. The lower bound was suggested by calculations. and was influenced by the fact that all the nuclear data were obtained from devices that were *very* dissimilar to modern weapons.

2-50 Crater Shapes and Dimensions for Surface and near-Surface Bursts

The shape of the crater from a near-surface burst must be known to determine the radius and depth from the crater volume and the explosive yield. The shape depends mainly on the yield, the scaled height of burst, and the geology. Table 2-8 shows the shape to be expected as a function of these three variables. The succeeding discussion provides the necessary scaling relationships to determine the dimensions for the various shapes. Separate procedures are provided for each of the yield/HOB combinations shown in Table 2-8.

Table 2-8. Classification of Crater Shapes from Near Surface Bursts as a Function of Yield, Height of Burst, and Geology

Yield	Scaled HOB ($m/kt^{1/3}$)	Geology	Crater Shape
$W \leq 1$ kt	All	All	Bowl
$W > 1$ kt	$HOB/W^{1/3} \geq 0$	All	Dish
$W > 1$ kt	$-5 \leq HOB/W^{1/3} < 0$	Unsaturated	Dish/Bowl
		Saturated	Dish

a. $W \leq 1$ kt

The crater shape for near-surface bursts (-5 $m/kt^{1/3} \leq HOB/W^{1/3} \leq 3$ $m/kt^{1/3}$) in *all* geologies for $W \leq 1$ kt is best described as bowl-shaped. The dimensions of the apparent crater radius, R_a, and apparent crater depth (D_a) for these bursts are given by the following expressions:

$$1.1\ V_a^{1/3} \leq R_a \leq 1.4\ V_a^{1/3},$$
$$0.35\ V_a^{1/3} \leq D_a \leq 0.7\ V_a^{1/3}.$$

The best estimates for R_a and D_a are

$$R_a = 1.2\ V_a^{1/3},$$
$$D_a = 0.5\ V_a^{1/3},$$

where V_a = the best estimate apparent volume.

b. $W > 1$ kt

The crater shape for near-surface bursts in which $W > 1$ kt depends on the yield and HOB.

(1) $HOB/W^{1/3} \geq 0$.

For above-surface bursts ($HOB/W^{1/3} \geq 0$), in which $W > 1$ kt, the crater shape is best described as dish-shaped and the crater dimensions are determined by the expressions

$$1.1\ W^{0.08} \leq \frac{R_a}{V_a^{1/3}} \leq 1.4\ W^{0.08},$$

$$0.35\ W^{-0.12} \leq \frac{D_a}{V_a^{1/3}} \leq 0.7\ W^{-0.12}.$$

The best estimates for R_a and D_a are

$$\frac{R_a}{V_a^{1/3}} = 1.2\ W^{0.08},$$

$$\frac{D_a}{V_a^{1/3}} = 0.5\ W^{-0.12}.$$

where V_a = the best estimate apparent volume.

[redacted]

[redacted]

(2) $HOB/W^{1/3} < 0$

For near-surface buried events

$$\left(0 < \frac{DOB}{Wa} \leq 5 \text{ m/kt}^{a}\right),$$

in which $W' >$ kt, the shape of the crater may be either "bowl" or "dish" in nature or some combination of the two extremes. Mechanisms such as compaction, rebound, bulking, slumping and layering effects play a significant role in the final crater shape. Cratering experience to date is not sufficient to make quantitative judgments regarding the impact of each mechanism.

The apparent crater dimensions for near-surface buried events are determined by the expressions

$$\frac{R_a}{V_a^{1/3}} = 1.2\ W'^{b} \text{ meters},$$

$$\frac{D_a}{V_a^{1/3}} = 0.5\ W'^{-c} \text{ meters}.$$

The values of the exponents (b, c), as a function of DOB, are found in Figures 2-76b and 2-76c. These exponents are necessary to ensure a smooth continuous curve for the radii of large yield (1 Mt) bursts as the depth of burial increases. Existing data indicate that above-surface bursts of high yield nuclear explosions produce dish-shaped craters and buried nuclear explosions produce bowl-shaped craters. However, since no data exist in the region

$$0 < \frac{DOB}{Wa} \leq 5 \text{ (m/kt}^{a}\text{)},$$

it is necessary to provide a transition region in which the crater produced is neither dish-shaped nor bowl-shaped, but some intermediate of the two extremes. The above equations produce this smooth transition region for the crater dimensions.

It has been noted, however, that in highly saturated media slope failure and/or liquefaction can produce a shallow crater for buried events. High explosive tests conducted at Fort Polk, Louisiana are good examples of these phenomena.

Other pertinent crater dimensions may be related to the above dimensions as follows:

- The radius to the crater lip crest is

$$R_{a\ell} = 1.25R_a.$$

- The height of the apparent lip is

$$.25D_a \leq H_{a\ell} \leq .33D_a$$

(near-surface bursts).

A summary of the procedures for calculating craters from near-surface bursts is given on page 2-161, immediately preceding the applicable figures.

2-51 Dimensions of Craters from Deep-Buried Explosions

Cratering experiments with chemical explosives (HE) and nuclear explosions (NE) suggest that linear dimensions of craters from buried explosions scale according to a modified overburden rule. This scaling rule is somewhat cumbersome to use for the computation of crater dimensions, and the available data do not conclusively prove the validity of any single scaling rule. Therefore, a simplified yield scaling exponent, yield (kt) to the 1/3.4 power, has been chosen for scaling apparent crater dimensions for scaled DOBs greater than 5 m/kt$^{1/3}$. Figures 2-77 through 2-81 may be used to obtain apparent crater volumes for buried bursts in each of the soil types indicated. The curves in these figures are valid for *all* yields. The uncertainty in crater volume is independent of geology and yield, and is based on HE cratering results.

Crater radius and depth are given by the following expressions

$$1.1\ V_a^{1/3} \leq R_a \leq 1.4\ V_a^{1/3},$$

$$0.35\ V_a^{1/3} \leq D_a \leq 0.7\ V_a^{1/3}.$$

[redacted]

[redacted]

These expressions are valid for deep-buried bursts in *all* geologies for *all* yields. The best estimates for the crater dimensions are

$$R_a = 1.2\ V_a^{1/3},$$

$$D_a = 0.5\ V_a^{1/3},$$

where V_a is the best estimate of the apparent volume.

It is possible that slumping of the walls will produce a wide, shallow crater for some yield-DOB combinations in a saturated geology. The resulting crater shape is neither "bowl" nor "dish" in nature; it is some combination of the two. The only explosions to date that resulted in such occurrences in the craters have been in a very wet clay soil with the explosive charge at or near the optimum depth of burial.

The uncertainty in crater dimensions obtained from the expressions given above is, however, approximately correct for any specified crater volume. If the crater volume is chosen as the lower or upper uncertainty band from Figures 2-77 through 2-81, then the expressions for the radius and depth are still valid. A new range of crater dimensions is determined by using the equations and the chosen volume.

Figure 2-82 contains the best estimate prediction for high-explosive detonations in the five generic homogeneous geologies. These curves show the relative crater volumes for the geologies. The curves can be used as a guide as to the proper nuclear curve to use for a new or unknown geology. If some HE cratering data are available, the curves of Figure 2-82 can be used to determine which homogeneous geology is best for the problem. This figure should not be used to calculate crater volume for nuclear explosions.

Other pertinent crater dimensions may be related to the above dimensions as follows:

- The radius to the crater lip crest is

$$R_{a\ell} = 1.25R_a.$$

- The height of the apparent lip is

$$.20D_a \leq H_{a\ell} \leq .25D_a$$
(deep-buried bursts).

A summary of the procedures for calculating craters from deep-buried bursts is given on page 2-179, immediately preceding the applicable figures.

[redacted]

[redacted]

SUMMARY OF PROCEDURES FOR CALCULATING CRATERS FROM NEAR-SURFACE BURSTS ($-5\ m/kt^{1/3} \leq HOB/W^{1/3} \leq 3\ m/kt^{1/3}$)

Figures 2-74a through 2-75e and 2-76a, b and c, together with appropriate scaling laws, may be used to obtain crater volumes and dimensions from near-surface bursts in a variety of situations. The following summary provides a step-by-step procedure for obtaining such information. Example problems are provided on the pages immediately following the figures.

Required (either given or estimated)

Yield (W) in kt

Actual HOB or DOB (may be zero if required)

Soil type (one of the five generic types or a combination; see Figure 2-86b).

1. Determine yield scaling parameter, a, for burst position:
   a. $HOB/W^{1/3} \geq 0 \rightarrow a = 1/3 \equiv 0.333$,
   b. $0 < DOB/W^{1/3} \leq 5\ m/kt^{1/3} \rightarrow a$ from Figure 2-76a.

2. Compute HOB_1 (HOB for 1 kt) $= \dfrac{\text{Actual HOB}}{W^a}$

   or DOB_1 (DOB for 1 kt) $= \dfrac{\text{Actual DOB}}{W^a}$

3. Determine V_{a1} (apparent-crater volume for 1 kt):
   a. If $W \leq 1$ kt, use curve for given soil type from Figures 2-74a through 2-74e.
   b. If $W > 10$ kt, use curve for given soil type from Figures 2-75a through 2-75e.
   c. If 1 kt $< W \leq 10$ kt, with *low or unknown* radiative output, interpolate using $V_{a1} = 0.6\ V_{a1}$ (from $W \leq 1$ kt curve) $+ 0.4\ V_{a1}$ (from $W > 10$ kt curve).
   d. If 1 kt $< W \leq 10$ kt with *known high* radiative output, use curve for given soil type from Figures 2-75a to 2-75e.

4. Compute V_a (actual crater volume for yield other than 1 kt):

   $$V_a \text{ (actual volume)} = V_{a1}\ (W^{3a}).$$

   These curves are provided for each soil type: best estimate, upper bound, and lower bound. Using the following guidelines, select the curve most appropriate to the problem.
   a. Use *best estimate* V_{a1} if no specific geologic data are given. If actual HE tests are available for a specific site, compare them with the HE curves in Figure 2-82, and move toward the upper or lower bound NE curve to adjust for these data, depending on where the data are grouped.
   b. Use *lower bound* V_{a1} (if desirable) for target-oriented calculations (offensive-conservative) to calculate R_a or D_a. Consider lower-bound V_{a1} for targeting when calculating crater volume-related phenomena, such as ejecta, transient velocity or displacement.*
   c. Use *upper-bound* V_{a1} (if desirable) for design-oriented calculations (defense-conservative) to calculate R_a or D_a. Consider upper bound V_{a1} for design when calculating crater-related phenomena affected by volume.
   d. For $W > 10$ kt, the discrepancy between the theoretical calculations and the empirical data in our understanding of the energy coupling produced by modern weapons detonated at low HOBs or in contact with the earth (HOB = 0.5 m)

*In all instances it is recommended that upper and lower bound values be calculated in order to gain an appreciation of the effects of uncertainties on the particular problem under consideration.

[redacted]

[redacted]

must be considered. (See paragraph 2-49.) Since this discrepancy only occurs in the lower-bound V_a values, it principally influences targeting, or offensive-conservative, problems.

It is recommended that the lower-bound V_a values be considered in calculating kill probabilities (P_k) due to the crater, but that high credence in cratering P_k not be used in assessing overall system P_k.

Note: This cratering discrepancy is a systematic uncertainty and should not be treated as a random uncertainty.

5. Calculate R_a and D_a using the expression from the following table that fits the yield and HOB and inserting the appropriate V_a:

Yield	Near-Surface Bursts: Above Surface ($\frac{HOB}{W^{1/3}} \geq 0$)	Near-Surface Bursts: Below Surface ($\frac{DOB}{W^{1/3}} \leq 5\ m/kt^{1/3}$)
$W' \leq kt$	$R_a = 1.2\ V_a^{1/3}$	same
	$D_a = 0.5\ V_a^{1/3}$	same
$W' > 1$ kt*	$R_a = 1.2\ W^{0.08}\ V_a^{1/3}$	$R_a = 1.2\ W^{b}\ V_a^{1/3}$
	$D_a = 0.5 W'^{-0.12} V_a^{1/3}$	$D_a = 0.5\ W'^{-c}\ V_a^{1/3}$

*See Figures 2-76b and 2-76c for determining b and c.

The dimensions R_a, D_a, and V_a can be related to other pertinent crater dimensions as follows:

- The radius to the crest of the apparent-crater lip is

$$R_{a\ell} = 1.25\ R_a.$$

- The height of the apparent lip is

$$0.25\ D_a \leq H_{a\ell} \leq 0.33\ D_a$$

for near-surface bursts.†

Variations in the thickness of the ejecta as a function of range from the surface ground zero (SGZ) are discussed in paragraphs 2-52 and 2-53.

†An exception to this is a similar crater formed by an explosion at the Pacific Proving Ground. The crater had no lip and greatly reduced ejecta. It is thought that such a crater shape may have been the result of a late-time reconsolidation/liquefaction process, which caused the crater lip to be below the water surface.

[redacted]

[redacted]

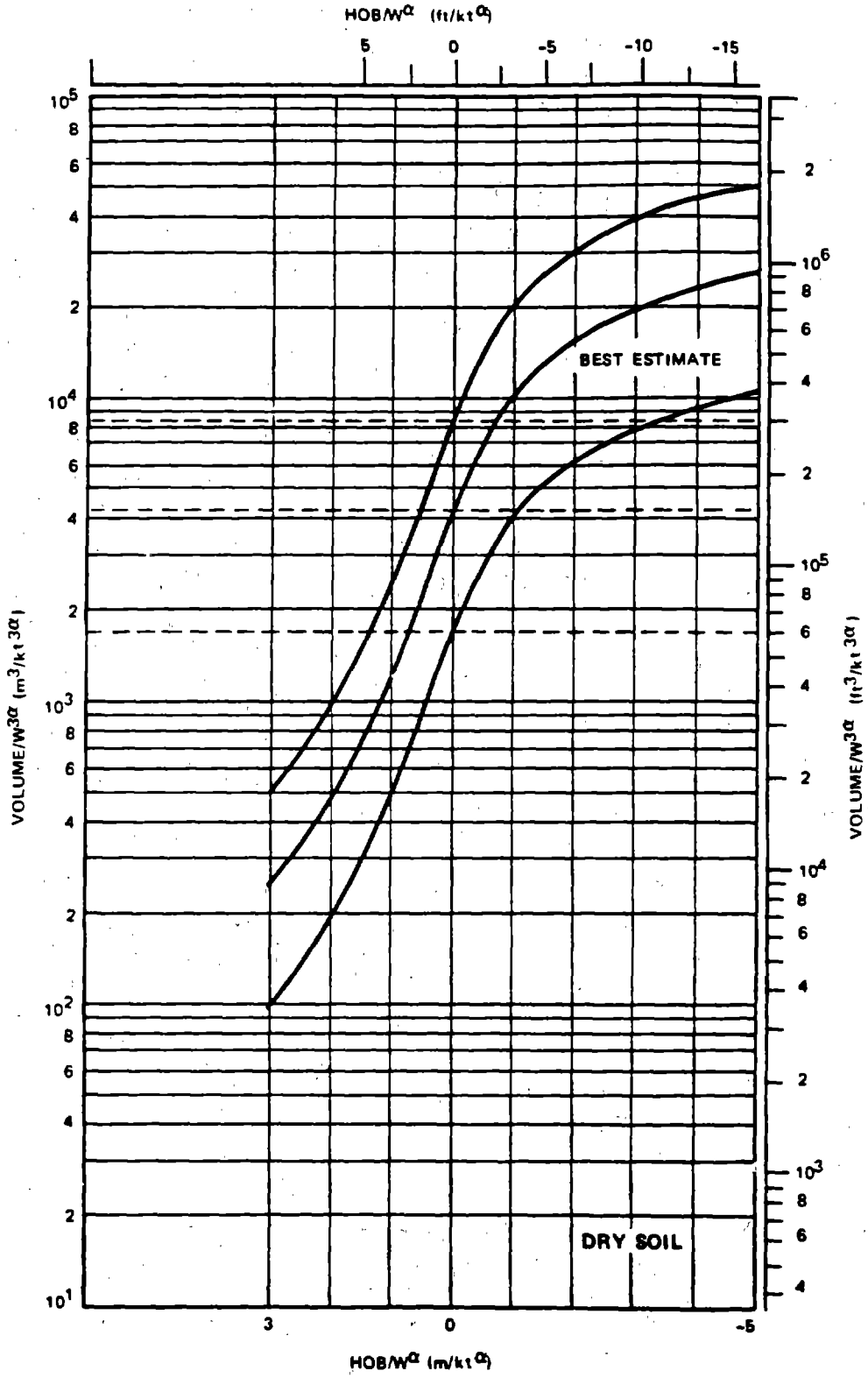

Figure 2-74a. Apparent Crater Volume for a 1-Kiloton Near-Surface Explosion in Dry Soil; Applicable for W ≤ 1 kt

[redacted]

[redacted]

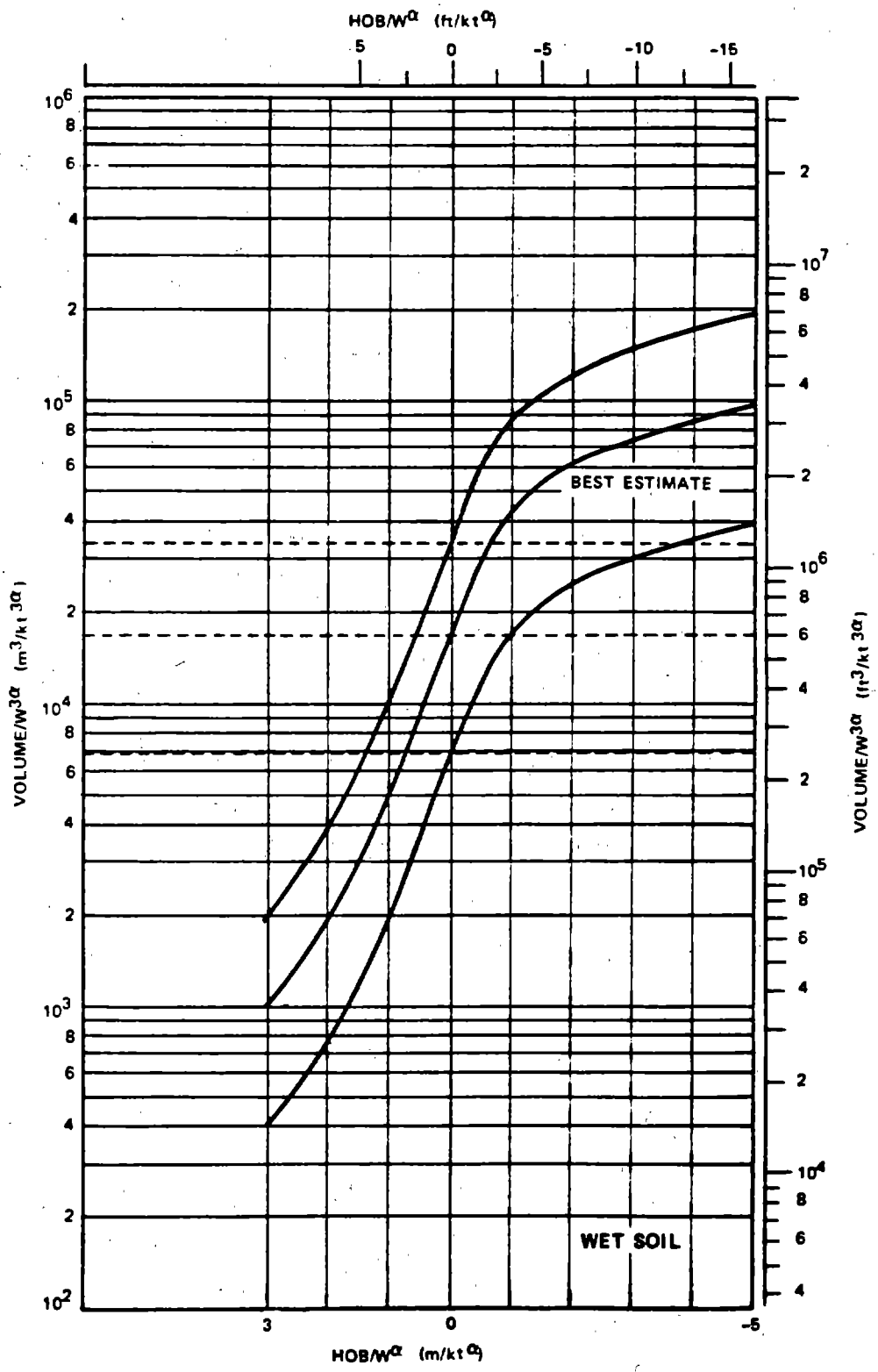

Figure 2-74b. Apparent Crater Volume for a 1-Kiloton Near-Surface Explosion in Wet Soil; Applicable for W ≤ 1 kt

[redacted]

[redacted]

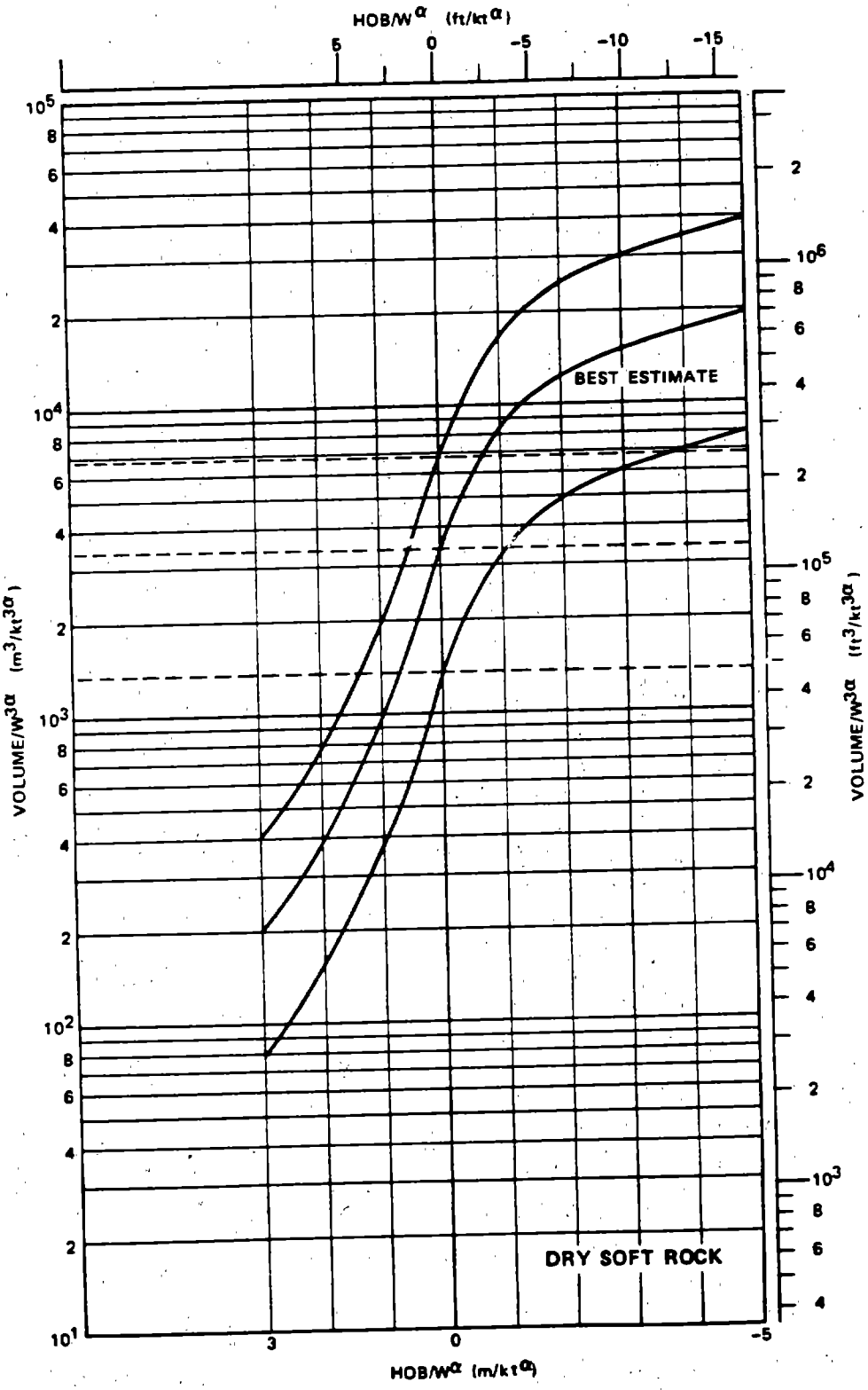

Figure 2-74c. Apparent Crater Volume for a 1 Kiloton Near-Surface Explosion in Dry Soft Rock; Applicable for W ≤ 1 kt

[redacted]

[redacted]

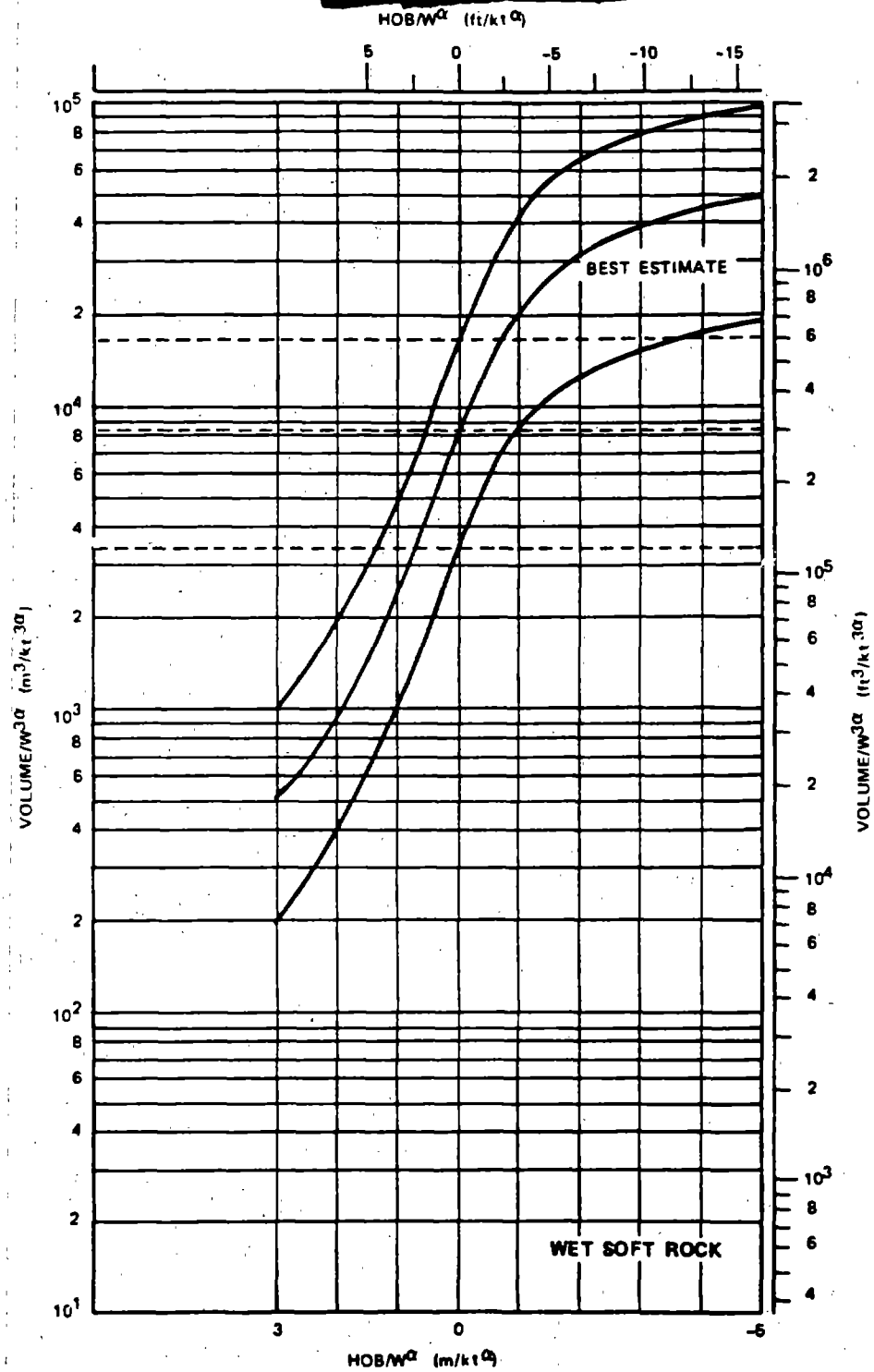

Figure 2-74d. Apparent Crater Volume for a 1-Kiloton Near-Surface Explosion in Wet Soft Rock; Applicable for W ≤ 1 kt

[redacted]

[redacted]

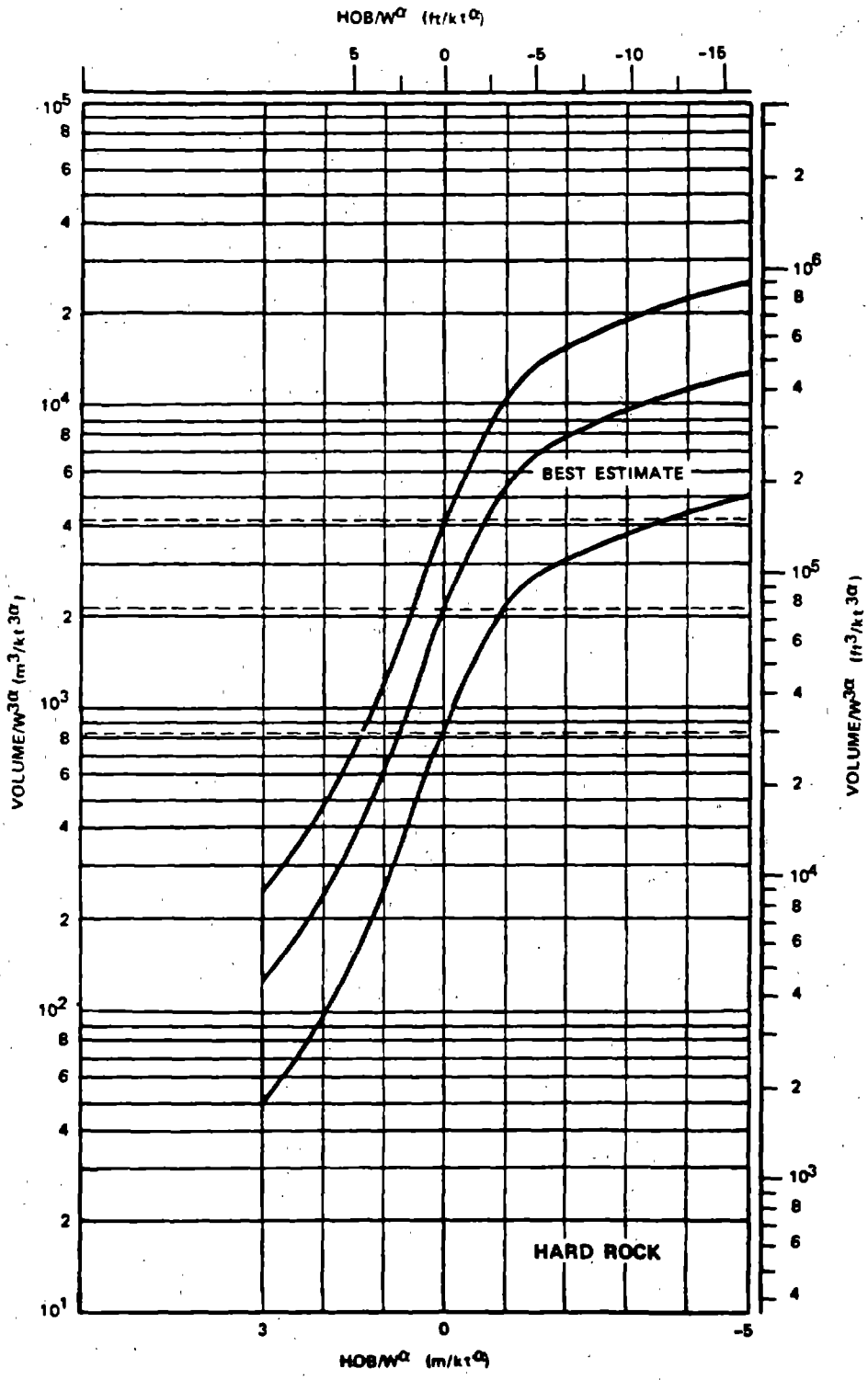

Figure 2-74e. Apparent Crater Volume for a 1 Kiloton Near-Surface Explosion in Hard Rock; Applicable for W ≤ 1 kt

[redacted]

[redacted]

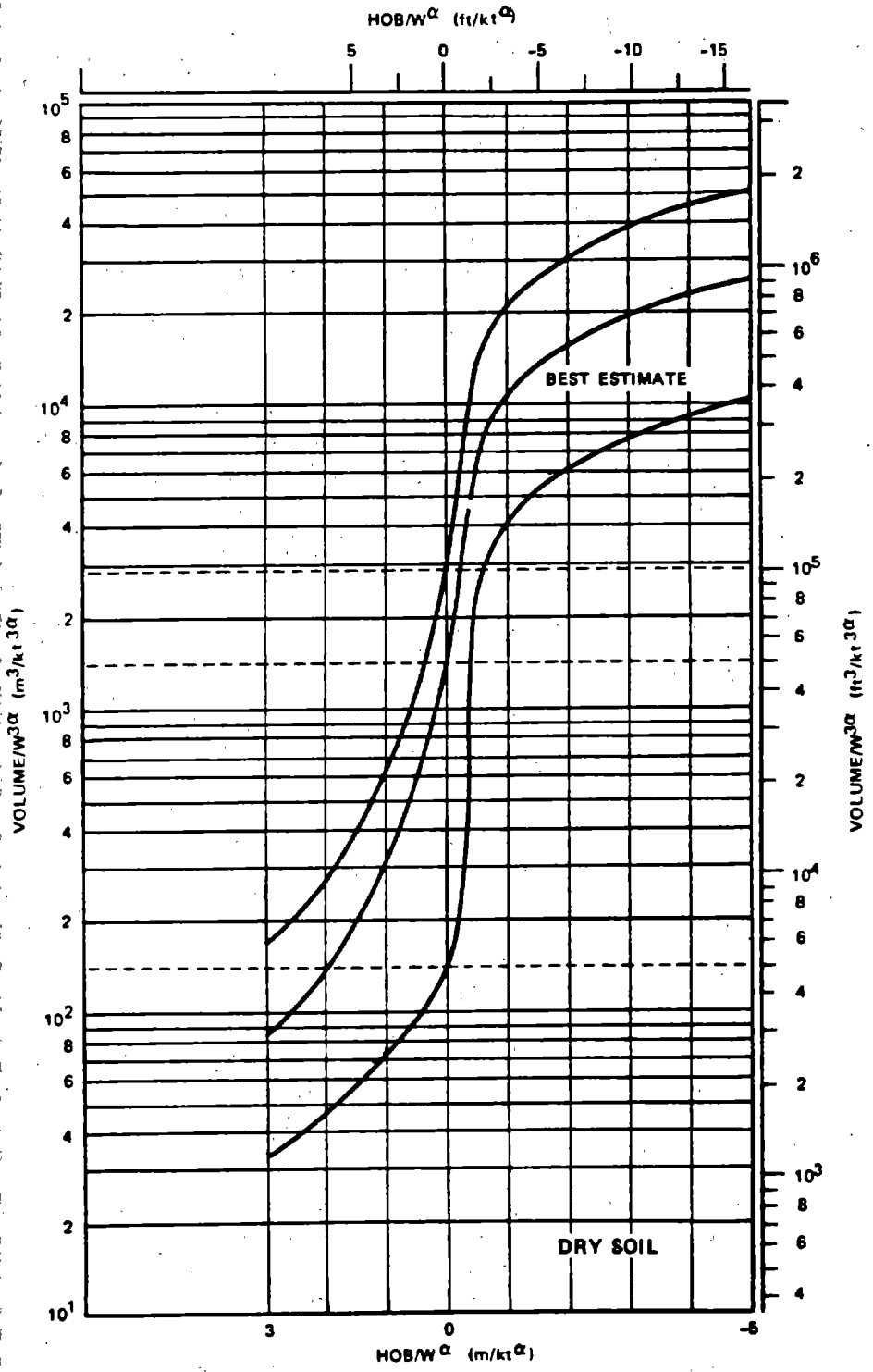

Figure 2-75a. Apparent Crater Volume for a 1 Kiloton Near-Surface Explosion in Dry Soil; Applicable for W > 10 kt

[redacted]

[redacted]

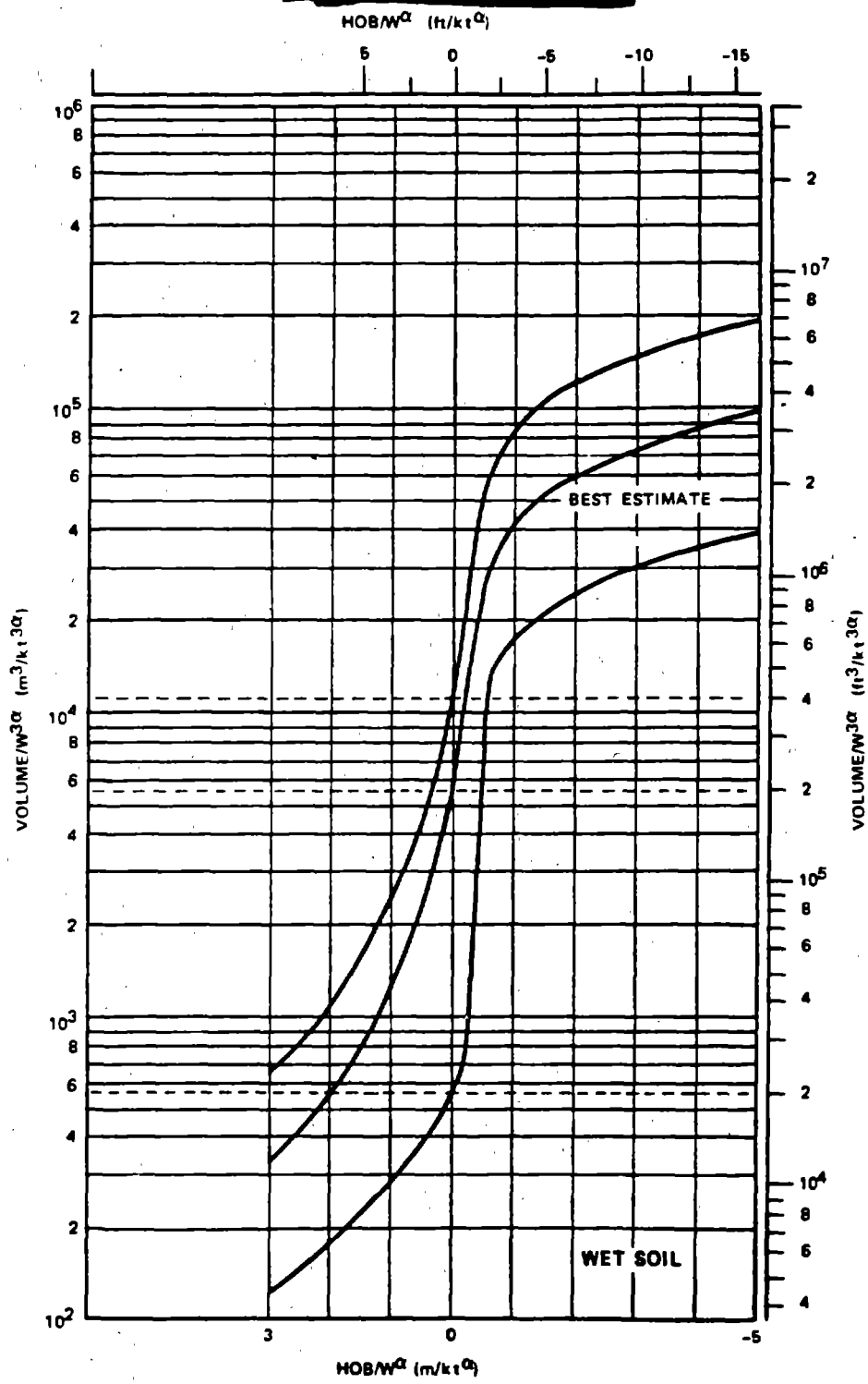

Figure 2-75b. Apparent Crater Volume for a 1 Kiloton Near-Surface Explosion in Wet Soil; Applicable for W > 10 kt

[redacted]

[redacted]

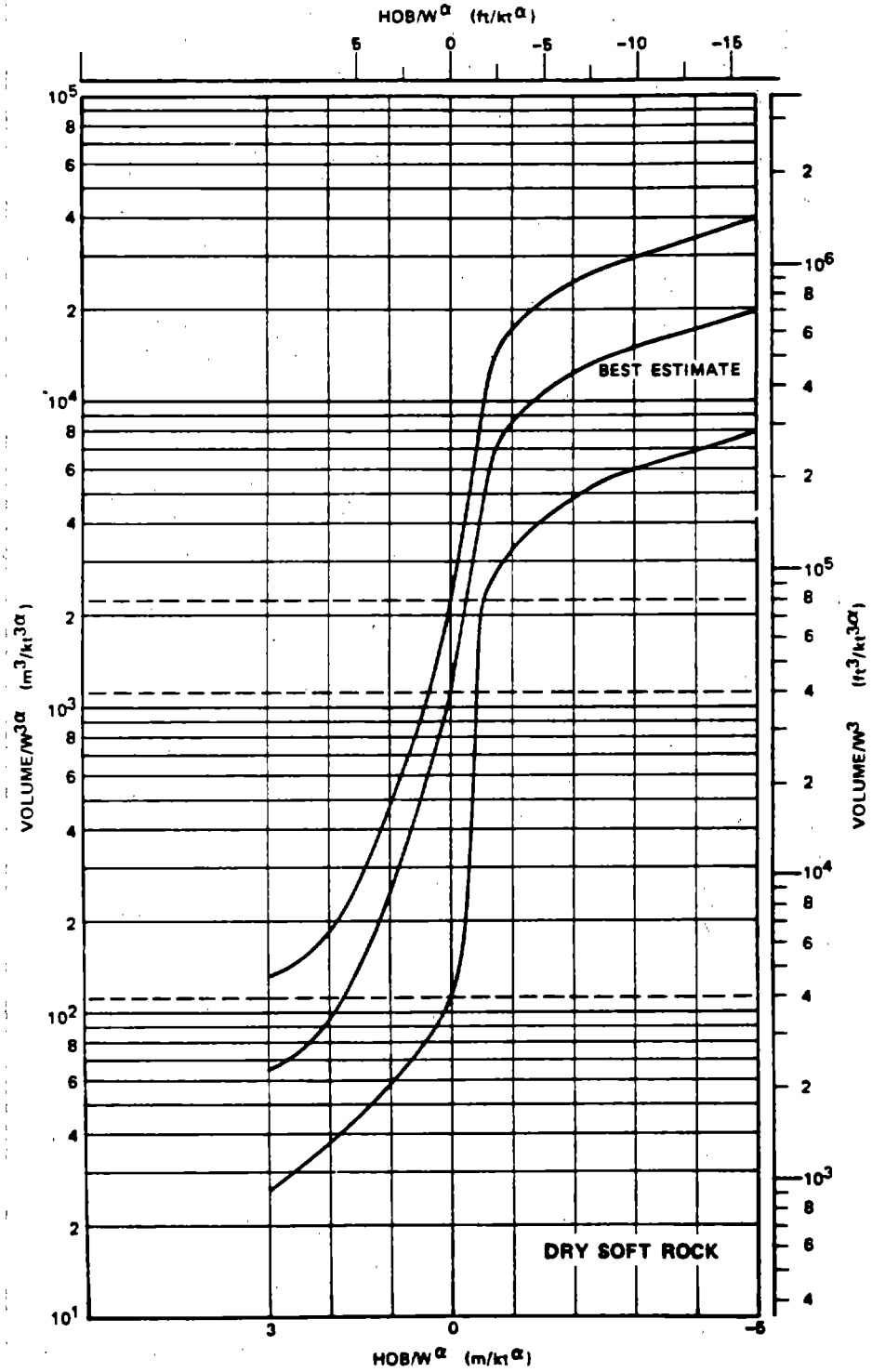

Figure 2-75c. Apparent Crater Volume for a 1 Kiloton Near-Surface Explosion in Dry Soft Rock; Applicable for W > 10 kt

[redacted]

[redacted]

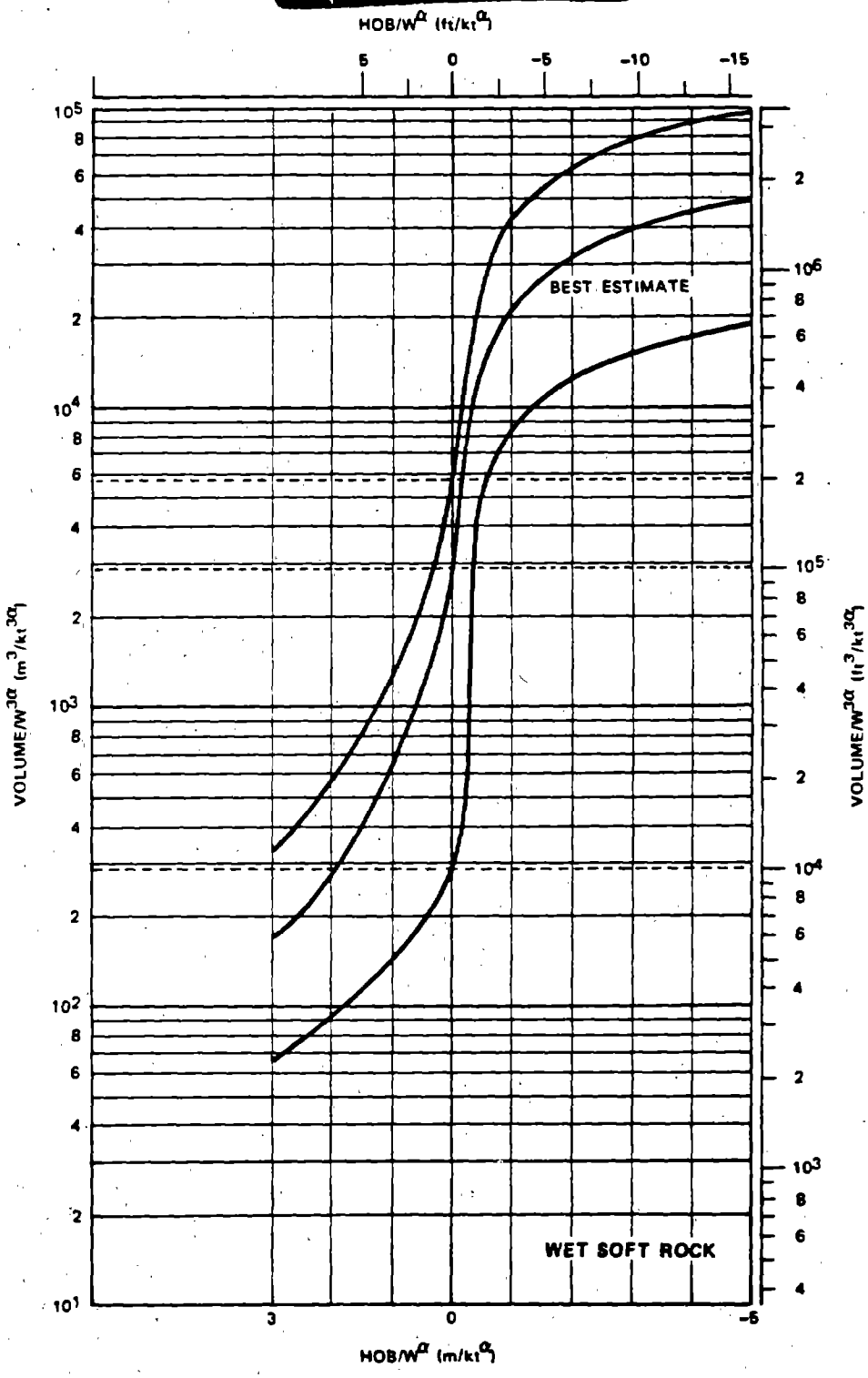

Figure 2-75d. Apparent Crater Volume for a 1-Kiloton Near-Surface Explosion in Wet Soft Rock; Applicable for W > 10 kt

[redacted]

[redacted]

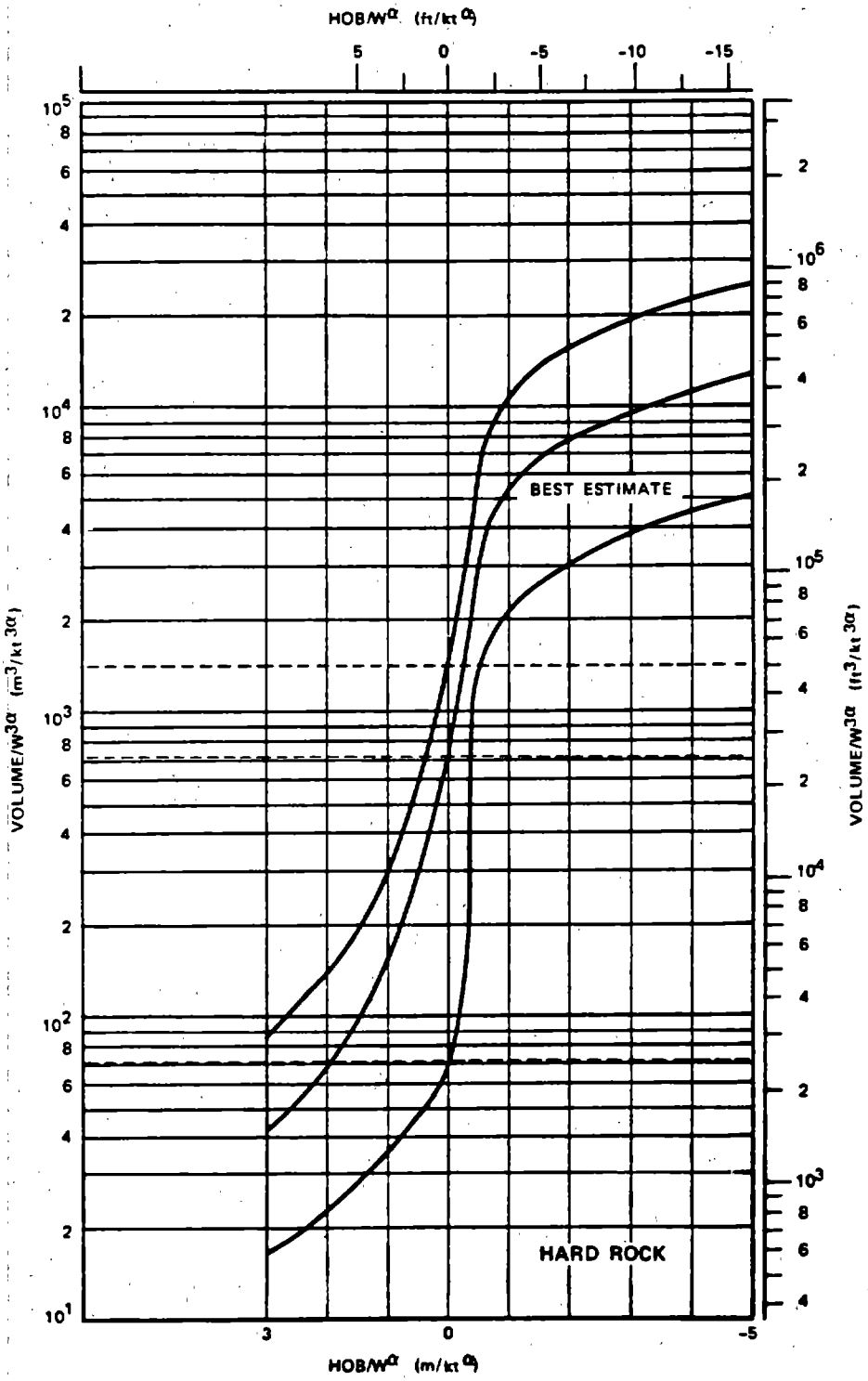

Figure 2-75e. Apparent Crater Volume for a 1 Kiloton Near-Surface Explosion in Hard Rock; Applicable for W > 10 kt

[redacted]

[redacted]

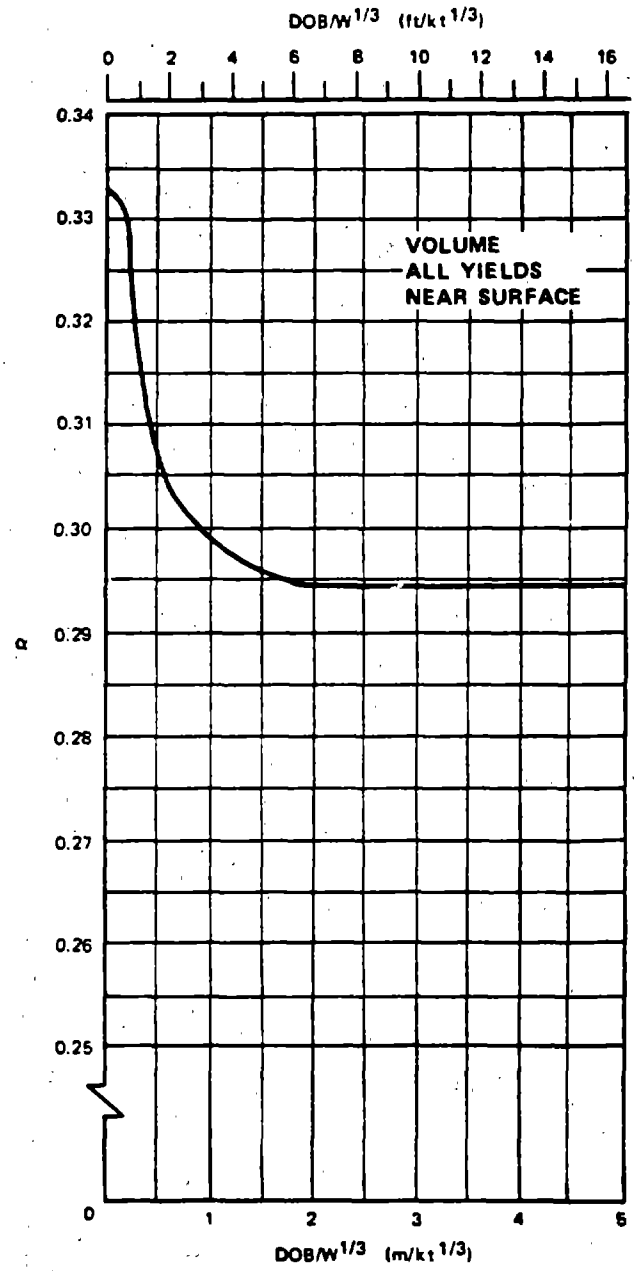

Figure 2-76a. Volume Scaling Exponent, α, as a Function of Scaled DOB for Near-Surface Explosions, All Yields

[redacted]

[redacted]

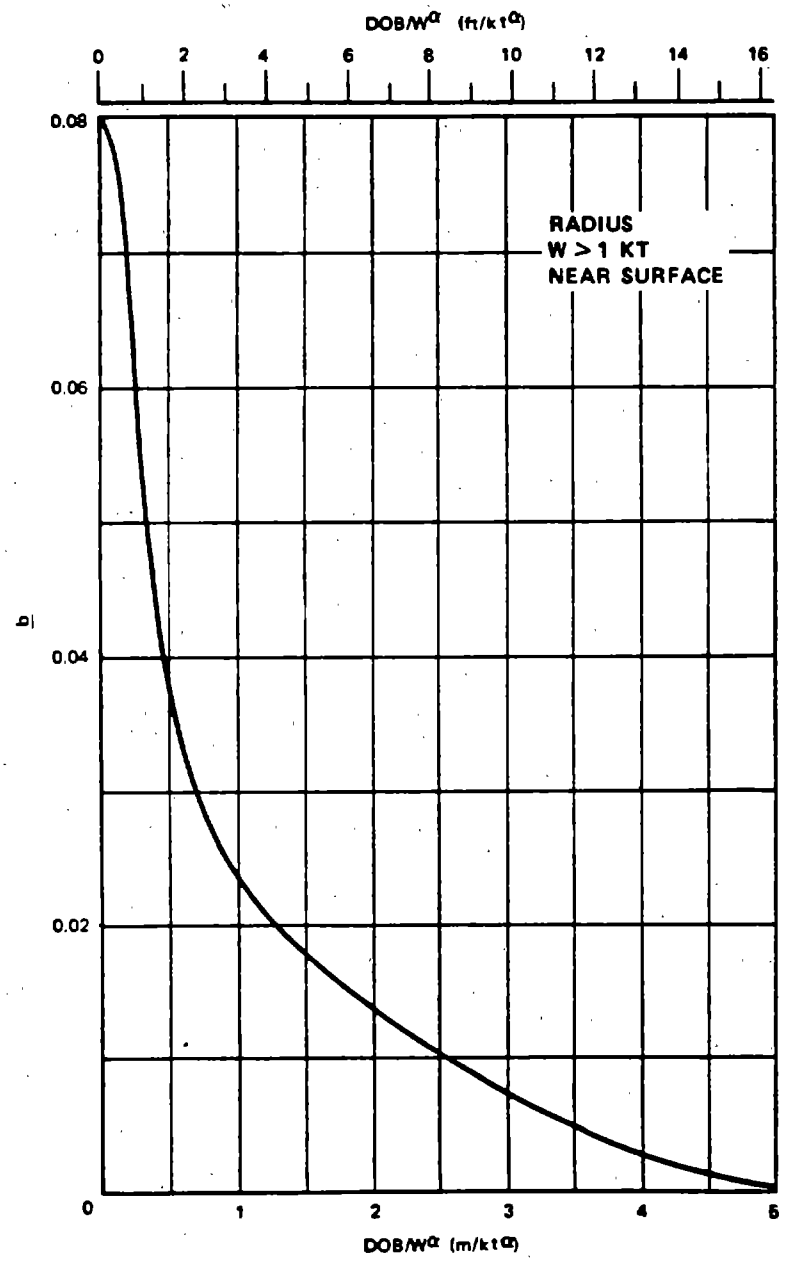

Figure 2-76b. Yield Transition Exponent, b, for Calculation of the Radius of Near-Surface, Buried Explosions W > 1 kt

[redacted]

[redacted]

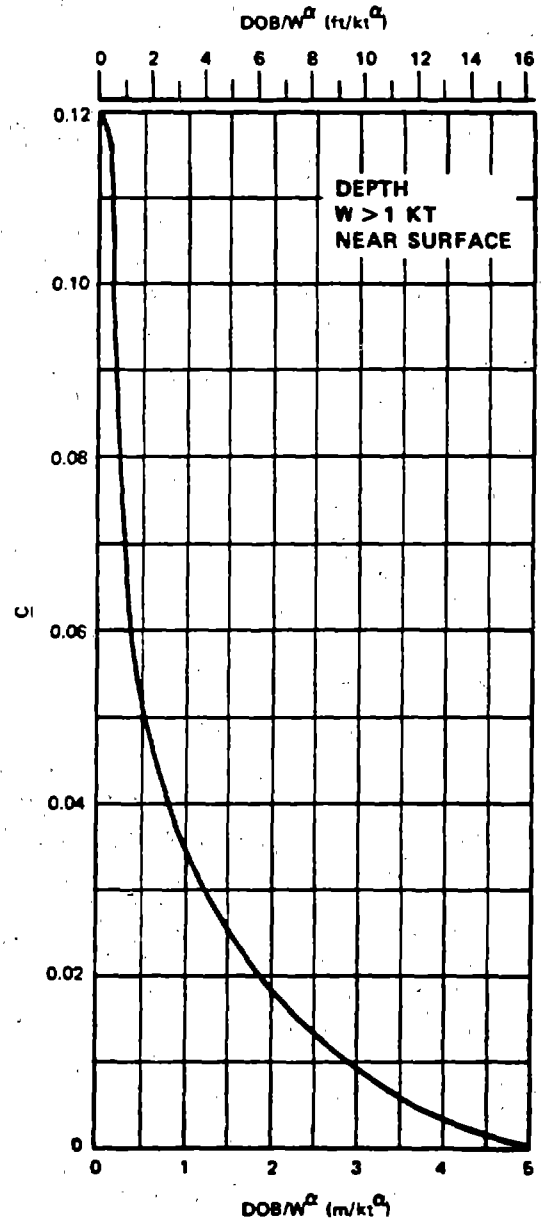

Figure 2-76c. Yield Transition Exponent, c, for Calculation of the Depth of Near-Surface, Buried Explosions, W > 1 kt

[redacted]

[redacted]

Problem 2-22. Crater Dimensions for Above-Surface Bursts (HOB > 0)

Figures 2-74a through 2-75e include curves that indicate the apparent crater volume as a function of HOB for a 1 kt explosion in various homogeneous media.

Scaling. For yields other than 1 kt, the crater volume scales as follows:

$$V_{a1} = W^{3a},$$

where V_{a1} is the apparent crater volume for a 1 kt explosion, and V_a is the corresponding volume for a yield of W kt. The height of burst scales as

$$\frac{\text{HOB}}{\text{HOB}_1} = W^a$$

Example:

Given: A hypothetical 300 kt contact burst on dry soil.

Find: The apparent crater radius and depth.

Solution: The HOB for a contact nuclear explosion is 0.5 meters. From paragraph 2-49,

$$a = 0.3333$$

for HOB $\geqslant$ 0. Therefore,

$$\text{HOB}_1 = \frac{\text{HOB}}{W^a} = \frac{0.5}{(300)^{1/3}} = 0.075 \text{ m/kt}^{1/3}.$$

From Figure 2-75a, the apparent crater volume for a 1 kt explosion at a scaled HOB of 0.075 m/kt$^{1/3}$ in dry soil is

$$V_{a1} = 1.25 \times 10^3 \text{ m}^3/\text{kt}^{3a}$$

$$V_a = V_{a1} (W)^{3a} = 1.25 \times 10^3 (300)^{1.0}$$
$$= 3.75 \times 10^5 \text{ m}^3.$$

Answer: The dimensions of the crater for a 300 kt contact burst are

$$\frac{R_a}{V_a^{1/3}} = 1.2\, W^{0.08} = 1.2\,(300)^{0.08} = 1.89,$$

$$R_a = 1.89\,(V_a)^{1/3} = 1.89\,(3.75 \times 10^5)^{1/3}$$
$$= 137 \text{ meters},$$

and

$$\frac{D_a}{V_a^{1/3}} = 0.5\, W^{-0.12} = 0.5\,(300)^{-0.12} = 0.252,$$

$$D_a = 0.252\,(V_a)^{1/3} = 0.252\,(3.75 \times 10^5)^{1/3}$$
$$= 18.2 \text{ meters}.$$

Uncertainty. The dimensions of the apparent crater obtained for the above problem have a range of uncertainties that are defined by the following:

$$1.1\, W^{0.08} \leqslant \frac{R_a}{V_a^{1/3}} \leqslant 1.4\, W^{0.08}$$

$$125 \leqslant R_a \leqslant 159 \text{ meters},$$

and

$$0.35\, W^{-0.12} \leqslant \frac{D_a}{V_a^{1/3}} \leqslant 0.7\, W^{-0.12}$$

$$13 \leqslant \frac{D_a}{V_a^{1/3}} \leqslant 25 \text{ meters}.$$

The characteristics of the medium represent a major uncertainty in the crater data presented in Figure 2-74a through 2-75e. Details concerning material properties and geologic structure are not usually known about any particular site, but, in many cases small changes in these media characteristics can cause large changes in crater dimensions. The largest changes usually occur in the presence of an intersecting water table or a layered medium. Therefore, the range of uncertainty for a generic geology such as "wet soil" can be quite large, especially in the prediction of the apparent crater depth.

Related Material: See paragraphs 2-46 through 2-50; see also paragraphs 1-14 and 1-33.

[redacted]

[redacted]

Problem 2-23. Crater Dimensions for a Shallow Buried Burst

Figures 2-74a through 2-75e include curves that indicate the apparent crater volume as a function of HOB for 1 kt explosion in various homogeneous media.

Scaling. For yields other than 1 kt, the crater volume scales as follows:

$$\frac{V_a}{V_{a1}} = W^{3a}.$$

where V_{a1} is the apparent crater volume for a 1 kt explosion, and V_a is the corresponding volume for a yield of W kt. The height of burst scales as

$$\frac{\text{HOB}}{\text{HOB}_1} = W^a.$$

Example:

Given. A hypothetical 30 kt burst in wet soft rock at a depth of burial of 3 meters.

Find. The apparent crater radius and depth.

Solution: The value of a is obtained from Figure 2-76a, which must be entered with the scaled DOB.

The scaled DOB is

$$\frac{\text{DOB}}{W^{1/3}} = \frac{3}{(30)^{1/3}} = 0.965 \text{ m/kt}^{1/3}.$$

From Figure 2-76a,

$$a = 0.299.$$

The scaled HOB is

$$\text{HOB}_1 = \frac{\text{HOB}}{W^a} = \frac{-3}{(30)^{0.299}} = -1.09 \text{ m/kt}^a.*$$

From Figure 2-75d,, the apparent crater volume for a 1 kt explosion, at HOB = −1.09 m/kt^a in wet soft rock, is,

$$V_{a1} = 2.20 \times 10^4 \text{ m}^3/\text{kt}^{3a},$$

and

$$V_a = V_{a1}\,(W)^{3a} = 2.20 \times 10^4\,(30)^{0.897}$$
$$= 4.65 \times 10^5 \text{ m}^3.$$

The dimensions for the 30 kt explosion are determined from the following expressions:

$$\frac{R_a}{V_a^{1/3}} = 1.2\,W^b,$$

$$\frac{D_a}{V_a^{1/3}} = 0.5\,W^{-c}.$$

From Figures 2-76b and 2-76c the values of the yield transition exponents, b and c, at a scaled DOB of 1.09 m/kt^a (HOB = −1.09 m/kt^a) are:

$$b = 0.023,$$
$$c = 0.033.$$

Answer: The dimensions of the crater for a 30 kt explosion at a DOB of 3 meters are:

$$\frac{R_a}{V_a^{1/3}} = 1.2\,W^{0.023} = 1.2\,(30)^{0.023} = 1.30,$$

$$R_a = 1.30\,(4.65 \times 10^5)^{1/3} = 101 \text{ meters},$$

and

$$\frac{D_a}{V_a^{1/3}} = 0.5\,W^{-0.033} = 0.5\,(30)^{-0.033} = 0.447,$$

$$D_a = 0.447\,(4.65 \times 10^5)^{1/3} = 34.6 \text{ meters}.$$

Uncertainty. The ranges of uncertainty for the radius and the depth are

$$1.1\,W^{0.023} \leq \frac{R_a}{V_a^{1/3}} \leq 1.4\,W^{0.023},$$

$$92 \leq R_a \leq 117 \text{ meters},$$

and

$$0.35\,W^{-0.033} \leq \frac{D_a}{V_a^{1/3}} \leq 0.7\,W^{-0.033},$$

$$24 \leq D_a \leq 49 \text{ meters}.$$

Related Material: See paragraphs 2-46 through 2-50; see also paragraphs 1-14 and 1-33.

*This could be written $\text{DOB}_1 = \frac{\text{DOB}}{W^a} = \frac{3}{(30)^{0.299}} = 1.09$ m/kt^a, i.e., HOB = −1.09 is equivalent to DOB = 1.09.

[redacted]

[redacted]

Problem 2-24. Crater Dimensions for a Low Yield Near-Surface Explosion

Figures 2-74a through 2-75e include curves that indicate the apparent crater volume as a function of HOB for 1 kt explosion in various homogeneous media.

Scaling. For yields other than 1 kt, the crater volume scales as follows

$$\frac{V_a}{V_{a1}} = W^{3\alpha},$$

where V_{a1} is the apparent crater volume for a 1 kt explosion, and V_a is the corresponding volume for a yield of W kt. The height of burst scales as

$$\frac{\text{HOB}}{\text{HOB}_1} = W^{\alpha}.$$

Example:

Given: A hypothetical 3 kt burst over wet soil at a height of burst of 1 meter.

Find: The apparent crater radius and depth.

Solution: From paragraph 2-49,

$$\text{HOB}_1 = \frac{\text{HOB}}{W^{\alpha}} = \frac{1.0}{(3)^{1/3}} = 0.693 \text{ m/kt}^{1/3}.$$

The apparent crater volume for a 3 kt burst will be determined by interpolating between the best estimate values from Figures 2-74b and 2-75b.

$$V_a(3) = 0.6\, V_a(W \leq 1) + 0.4\, V_a(W > 10).$$

From Figure 2-74b, the apparent crater volume for a 1 kt explosion (for $W \leq 1$), at a scaled HOB = 0.693 m/kt$^{1/3}$, in wet soil is

$$V_{a1} = 7.00 \times 10^3 \text{ m}^3/\text{kt}^{3\alpha},$$

and

$$V_a(W \leq 1) = V_{a1}(W)^{3\alpha} = 7.00 \times 10^3 (3)^{1.0} = 2.10 \times 10^4 \text{ m}^3.$$

From Figure 2-75b, the apparent crater volume for a 1 kt explosion ($W > 10$), at a scaled HOB = 0.693 m/kt$^{1/3}$, in wet soil is

$$V_{a1} = 1.80 \times 10^3 \text{ m}^3/\text{kt}^{3\alpha},$$

and

$$V_a(W > 10) = V_{a1}(W)^{3\alpha} = 1.80 \times 10^3 (3)^{1.0} = 5.40 \times 10^3 \text{ m}^3.$$

Therefore, for a 3 kt burst

$$V_a = 0.6\,(2.10 \times 10^4) + 0.4\,(5.40 \times 10^3) = 1.48 \times 10^4 \text{ m}^3.$$

Answer: The apparent crater dimensions for a 3 kt explosion with HOB of 1 meter are:

$$\frac{R_a}{V_a^{1/3}} = 1.2\, W^{0.08} = 1.2\,(3)^{0.08} = 1.31,$$

$$R_a = 1.31\,(V_a)^{1/3} = 32.2 \text{ meters},$$

and

$$\frac{D_a}{V_a^{1/3}} = 0.5\, W^{-0.12} = 0.5\,(3)^{-0.12} = 0.438,$$

$$D_a = 0.438\,(V_a)^{1/3} = 10.8 \text{ meters}.$$

Uncertainty. The dimensions of the apparent crater obtained for the above problem have a range of uncertainty that is defined by the following:

$$1.1\, W^{0.08} \leq \frac{R_a}{V_a^{1/3}} \leq 1.4\, W^{0.08}$$

$$29 \leq R_a \leq 38 \text{ meters}$$

and

$$0.35\, W^{-0.12} \leq \frac{D_a}{V_a^{1/3}} \leq 0.7\, W^{-0.12}$$

$$8 \leq D_a \leq 15 \text{ meters}.$$

If the 3 kt weapon in the preceding example were known to have a high radiative output, similar to weapons of larger yield (10 kt), then the best estimate for the apparent crater volume would be found using only Figure 2-75b. Therefore, V_a would be given by

$$V_a = 5.40 \times 10^3 \text{ m}^3,$$

and

$$R_a = 1.31\,(V_a)^{1/3} = 23.0 \text{ meters},$$

$$D_a = 0.438\,(V_a)^{1/3} = 7.7 \text{ meters}$$

Related Material: See paragraphs 2-46 through 2-50; see also paragraphs 1-14 and 1-33.

[redacted]

[redacted]

SUMMARY OF PROCEDURES FOR CALCULATING CRATERS FROM DEEP-BURIED BURSTS (DOB/$W^{1/3}$ > 5 m/kt $^{1/3}$)

Figures 2-77 through 2-81, together with appropriate scaling laws may be used to obtain crater volumes from deep-buried bursts in a variety of situations. The following summary provides a step-by-step procedure for obtaining such information. An example problem is provided immediately following the figures.

Required (either given or estimated):
Yield (W) in kt
Actual DOB
Soil Type (one of the five generic types or a combination; (see Figures 2-82 and 2-86b).
Yield-scaling parameters, α, for burst position:
DOB/$W^{1/3}$ > 5 m/kt$^{1/3}$ → α = 1/3.4

1. Compute DOB_1

$$(\text{DOB for 1 kt}) = \frac{\text{Actual DOB}}{W^{\alpha}}$$

2. Determine V_{a1} (apparent-crater volume for 1 kt), using curve for given soil type from Figures 2-77 to 2-81.
3. Compute V_a (actual crater volume for yield other than 1 kt):

$$V_a \text{ (actual volume)} = V_{a1}\ (W^{3\alpha}).$$

Three curves are provided for each soil type: best estimate, upper bound, and lower bound. Using the following guidelines, select the curve most appropriate to the problem.

a. Use *best estimate* V_{a1} if no specific geologic data are given. If actual HE test are available for specific site, compare them with the HE curves in Figure 2-82, and move toward the upper or lower bound NE curve to adjust for these data, depending on where the data are grouped.

b. Use *lower-bound* V_{a1} (if desirable) for target-oriented calculations (offensive-conservative) and to calculate R_a or D_a. Consider *lower-bound* V_{a1} for targeting when calculating crater-volume-related phenomena such as ejecta, transient velocity, or displacement.*

c. Use *upper-bound* V_{a1} (if desirable) for design-oriented calculations (defense-conservative) and to calculate R_a or D_a. Consider *upper-bound* V_{a1} for design when calculating crater-related phenomena affected by volume.

4. Calculate R_a and D_a using the following expressions:

$$R_a = 1.2\ V_a^{1/3}$$

$$D_a = 0.5\ V_a^{1/3}$$

The dimensions R_a, D_a, and V_a can be related to other pertinent crater dimensions as follows:

- The radius to the crest of the apparent-crater lip is

$$R_{a\ell} = 1.25\ R_a.$$

- The height of the apparent lip is

$$0.20 D_a < H_{a\ell} < 0.25\ D_a$$

for deep-buried bursts.

Variations in the thickness of the ejecta as a function of range from the surface ground zero (SGZ) are discussed in paragraphs 2-52 and 2-53.

*In all instances it is recommended that upper and lower bound values be calculated in order to gain an appreciation of the effects of uncertainties on the particular problem under consideration.

[redacted]

[redacted]

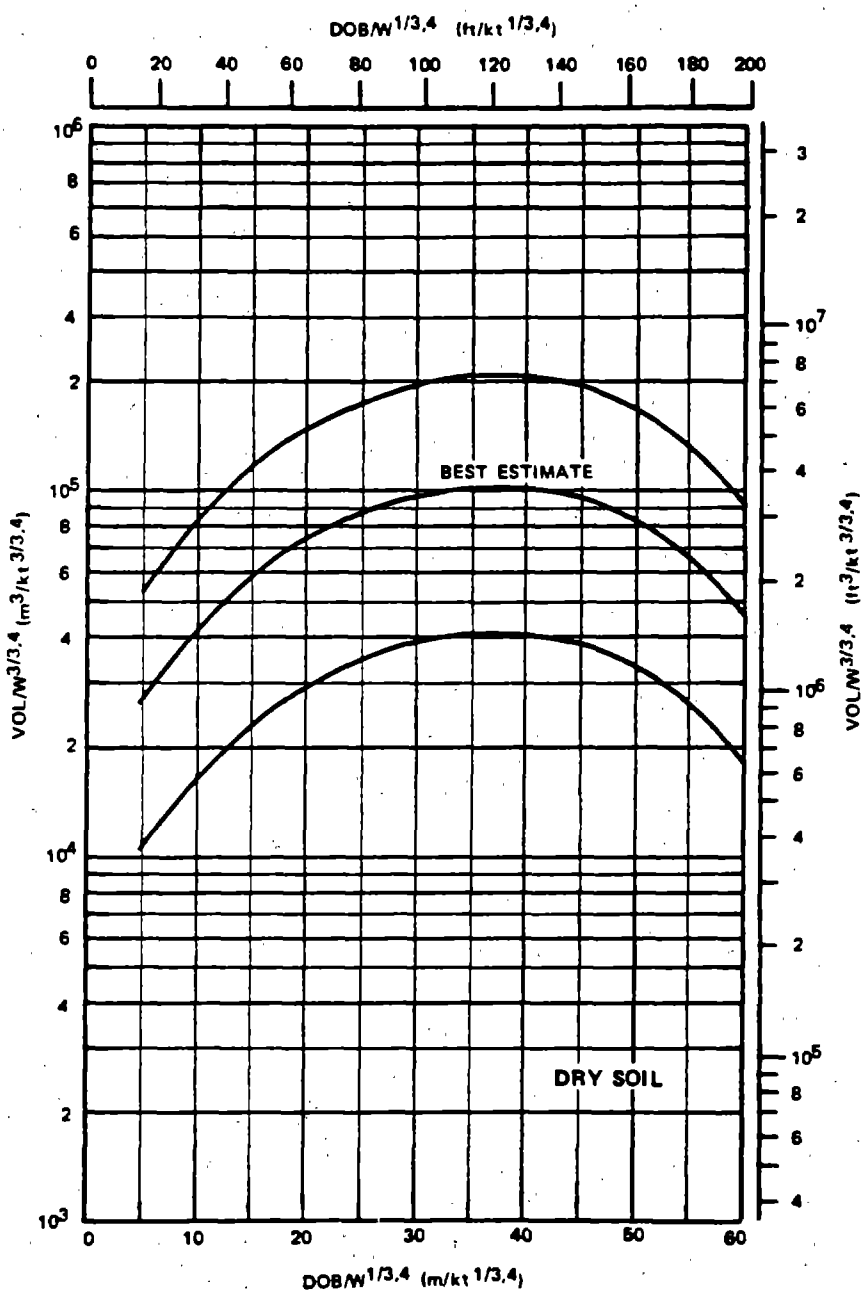

Figure 2-77. Crater Volume as a Function of Depth of Burial for a 1 Kiloton Explosion Buried in Dry Soil

[redacted]

[redacted]

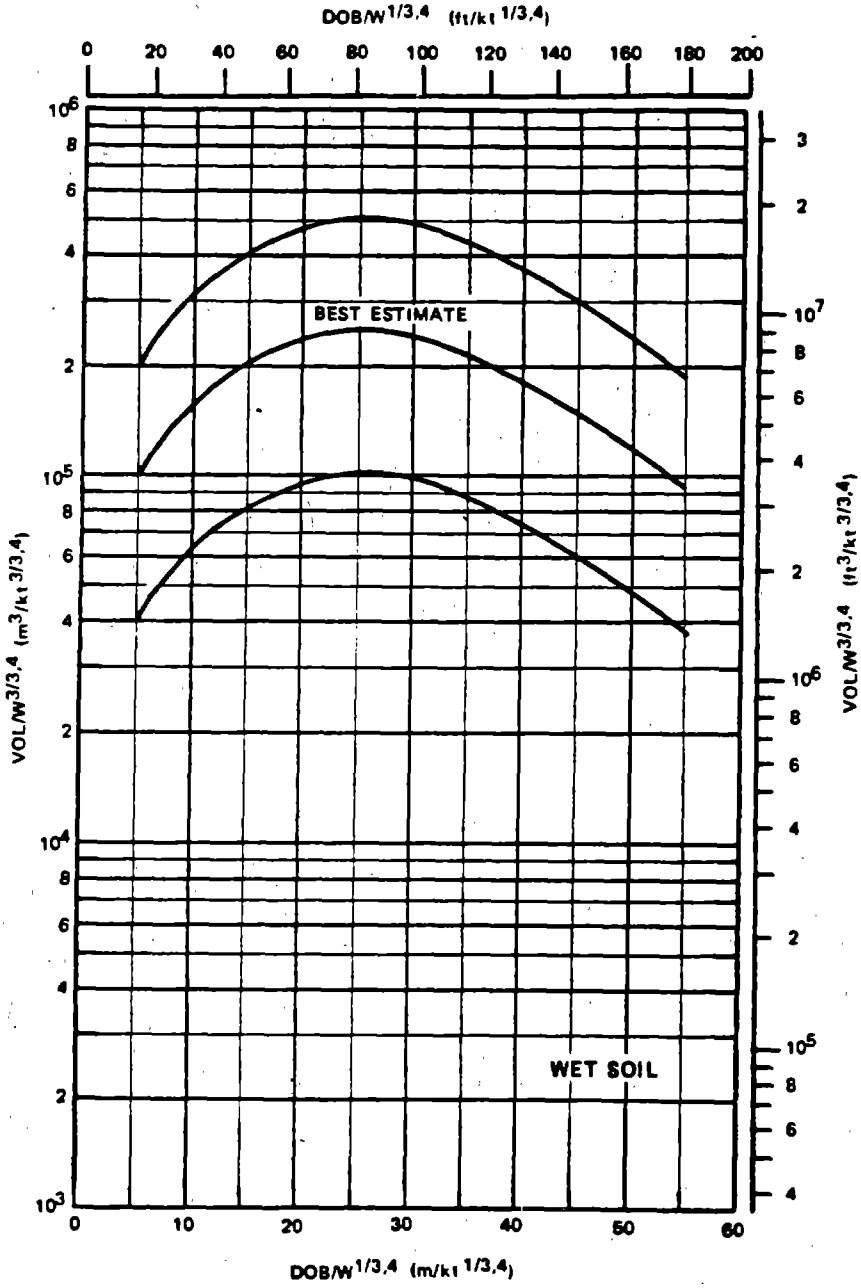

Figure 2-78. Crater Volume as a Function of Depth of Burial for a 1 Kiloton Explosion Buried in Wet Soil

[redacted]

[redacted]

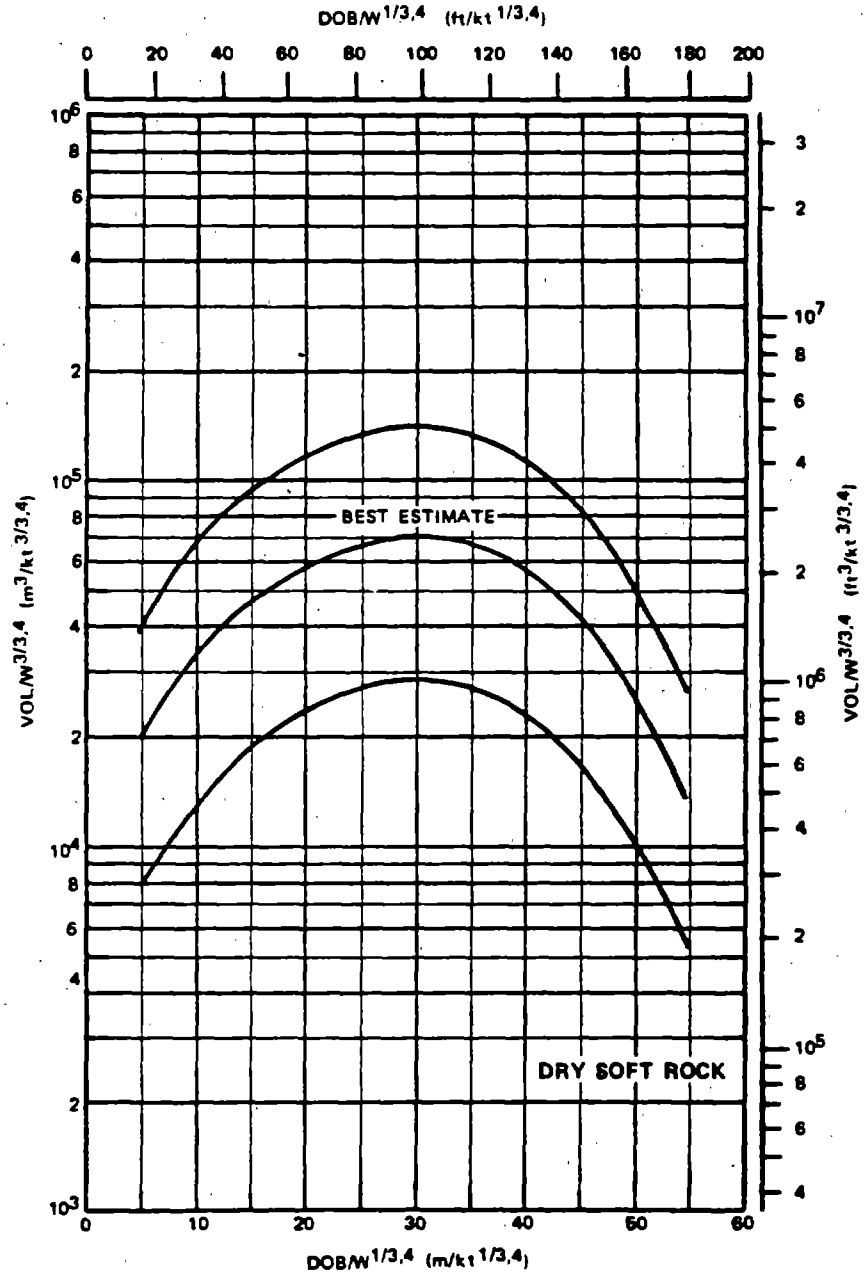

Figure 2-79. Crater Volume as a Function of Depth of Burial for a 1 Kiloton Explosion Buried in Dry Soft Rock

[redacted]

[redacted]

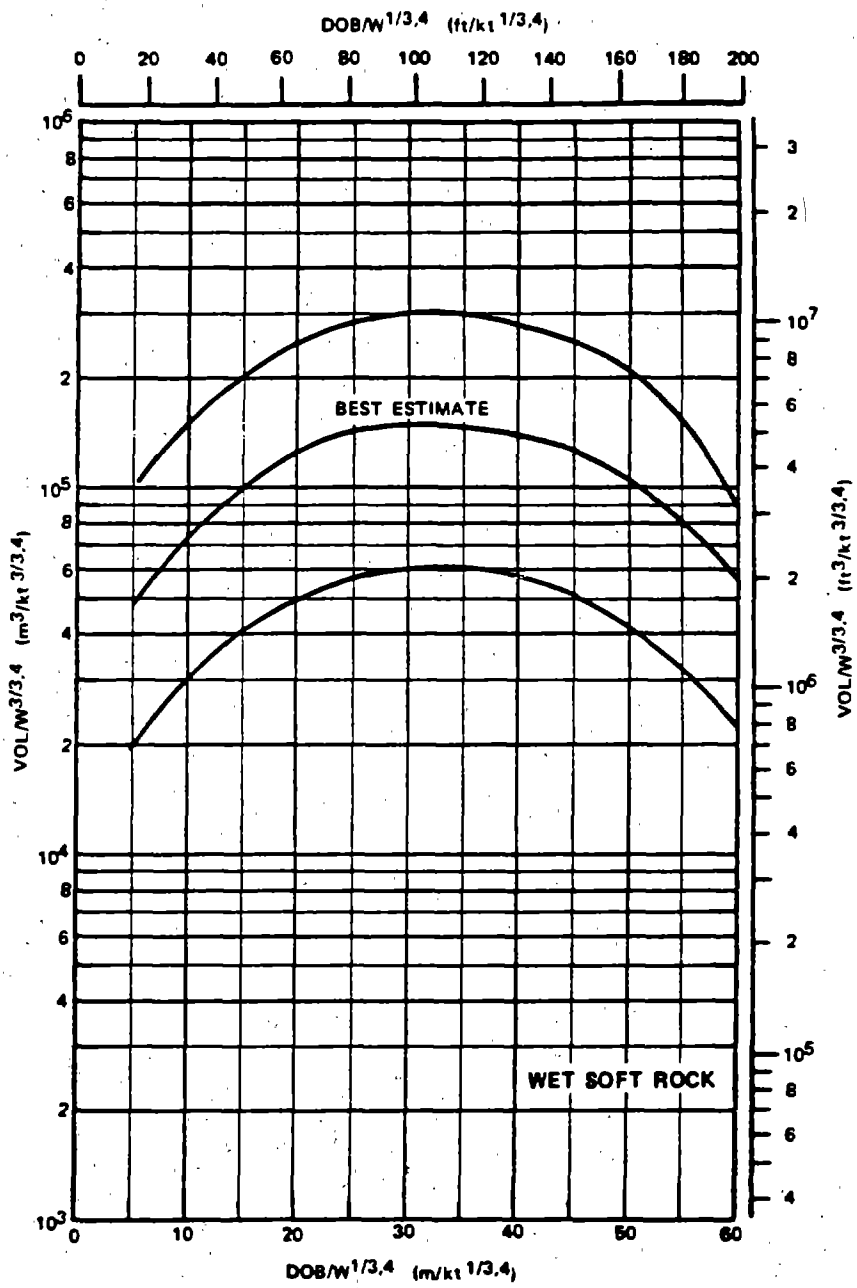

Figure 2-80. Crater Volume as a Function of Depth of Burial for a 1 Kiloton Explosion Buried in Wet Soft Rock

[redacted]

[redacted]

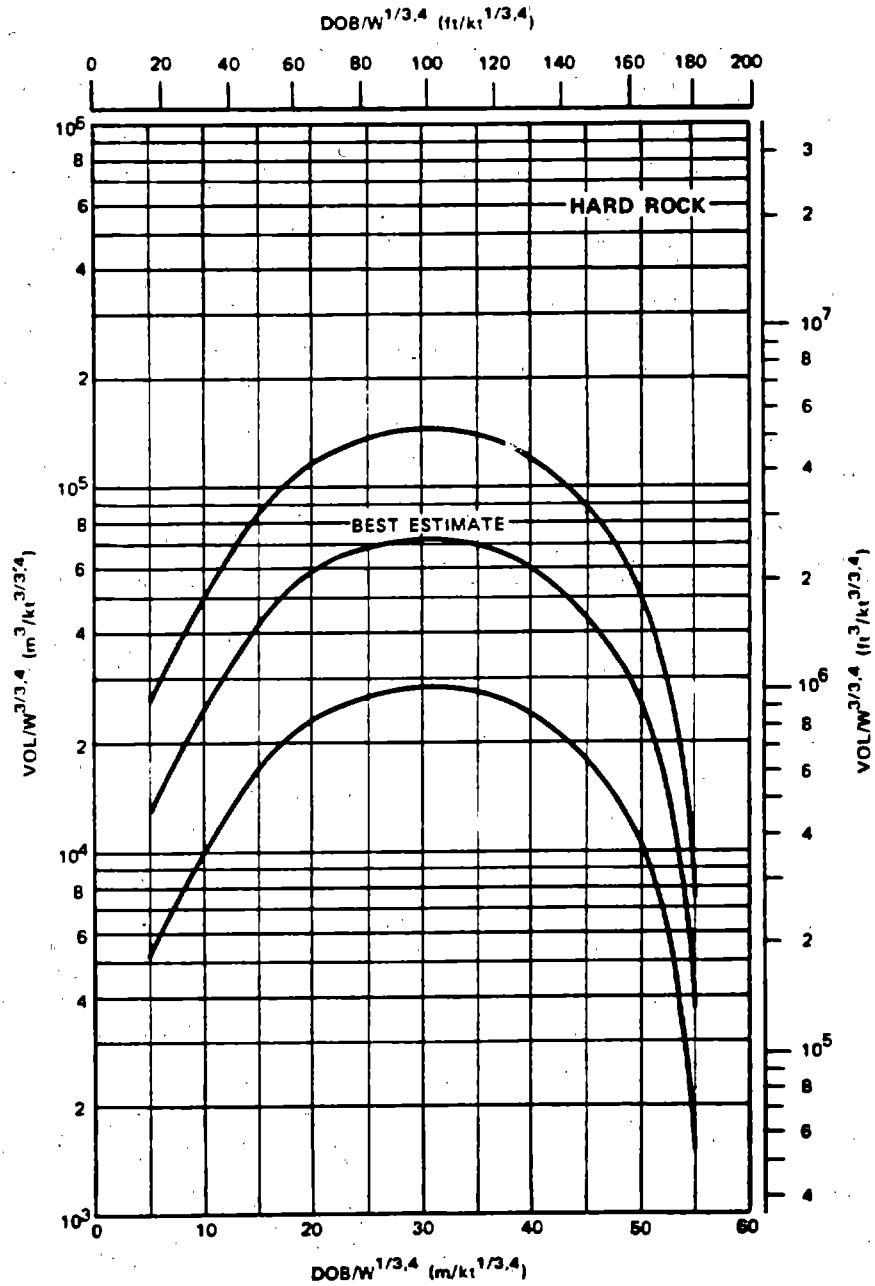

Figure 2-81. Crater Volume as a Function of Depth of Burial for a 1 Kiloton Explosion Buried in Hard Rock

[redacted]

[redacted]

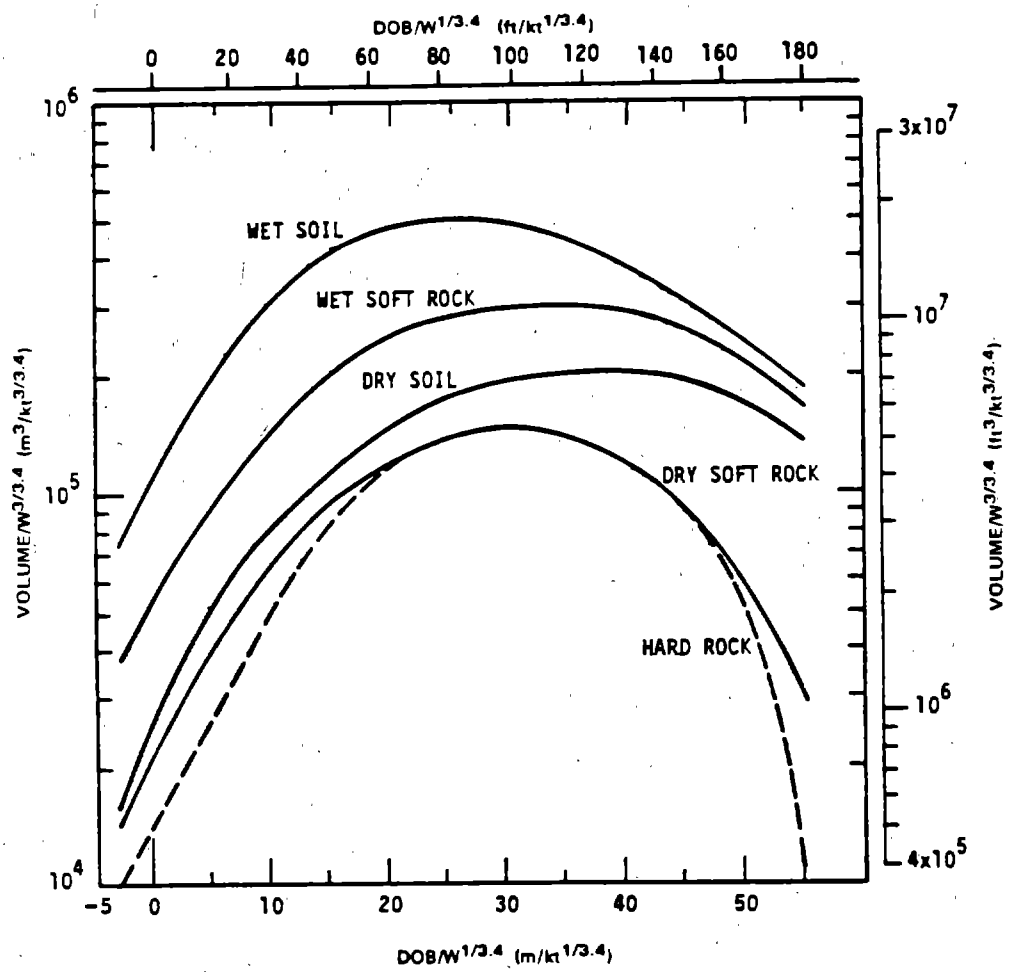

Figure 2-82. Crater Volume as a Function of Depth of Burst for HE Explosions in Five Homogenous Geologies

[redacted]

[redacted]

(This page is intentionally blank)

[redacted]

[redacted]

Problem 2-25. Calculation of Depth of Burial for Optimum Crater

Figures 2-77 through 2-81 show curves that indicate the apparent crater volume as a function of DOB for a 1 kt explosion in various media which are indicated in each figure.

Scaling. For yields other than 1 kt the crater volume and depth of burial scale as

$$\frac{\text{DOB}}{\text{DOB}_1} = W^{1/3.4},$$

$$\frac{V_a}{V_{a1}} = W^{3/3.4},$$

where DOB_1 and V_{a1} are the depth of burst and apparent crater volume for a 1 kt explosion, and DOB and V_a are the corresponding quantities for a yield of W kt.

Example:

Given: A hypothetical 3 kt explosion in hard rock.

Find: The depth of burst at which the maximum apparent crater will occur, and the dimensions of the apparent crater at this depth of burst.

Solution: From Figure 2-81, the maximum crater volume from a 1 kt explosion in hard rock occurs at a DOB_1 of 30.5 meters (note that the curve is flat in this region, and a variation of a few meters in DOB will have a small effect on V). The apparent volume of the crater from such a burst is

$$V_1 = 7.20 \times 10^4 \text{ m}^3.$$

Answer: The corresponding depth of burst and crater volume for a 3 kt explosion are

$$\text{DOB} = (\text{DOB}_1)(W)^{1/3.4} = 30.5\,(3)^{1/3.4}$$
$$= 42.1 \text{ meters},$$
$$V_a = (V_{a1})(W)^{3/3.4} = 7.20 \times 10^4\,(3)^{3/3.4}$$
$$= 1.90 \times 10^5 \text{ m}^3.$$

The apparent crater dimensions are defined by the expressions

$$R_a = 1.2\,V_a^{1/3} = 1.2\,(1.90 \times 10^5)^{1/3}$$
$$= 69.0 \text{ meters},$$
$$D_a = 0.5\,V_a^{1/3} = 0.5\,(1.90 \times 10^5)^{1/3}$$
$$= 28.7 \text{ meters}.$$

Uncertainty: The dimensions of the apparent crater have a range of uncertainty that is defined by the expressions

$$1.1\,V_a^{1/3} \leq R_a \leq 1.4\,V_a^{1/3},$$
$$63 \leq R_a \leq 80 \text{ meters},$$
$$0.35\,V_a^{1/3} \leq D_a \leq 0.70\,V_a^{1/3},$$
$$20 \leq D_a \leq 40 \text{ meters}.$$

In addition, the uncertainty in crater volume is given by

$$V_a\,(\text{min}) = V_{a1}\,(\text{min})\,W^{3/3.4},$$
$$V_a\,(\text{min}) = 2.80 \times 10^4\,(3)^{3/3.4},$$
$$= 7.38 \times 10^4 \text{ m}^3,$$
$$V_a\,(\text{max}) = V_{a1}\,(\text{max})\,W^{3/3.4},$$
$$V_a\,(\text{max}) = 1.45 \times 10^5\,(3)^{3/3.4},$$
$$= 3.82 \times 10^5 \text{ m}^3.$$

Related Material: See paragraph 2-51; see also paragraph 1-14 and 1-33.

[redacted]

[redacted]

EJECTA

Crater ejecta consists of soil or rock debris that is thrown beyond the boundaries of the apparent crater by an explosion. Together with the fallback, which lies between the true and apparent crater boundaries, ejecta comprises all material that is completely dissociated from the parent medium by the explosion. The ejecta field is divided into two zones:

- The crater lip, including the continuous ejecta surrounding the apparent crater.
- The discontinuous ejecta, comprised of the discrete natural missiles that fall beyond the limit of continuous ejecta.

The principal parameters used to describe the ejecta are:

- The average lip crest height.
- The radius to the crest of the crater lip from surface ground zero (SGZ).
- The depth of deposition.
- The ejecta mass density.
- The missile size distribution, which is a function of the azimuthal and radial distance from SGZ, the radius to the outer boundary of continuous ejecta, and the maximum missile range.

The principal variables that control the ejecta parameters are the yield and geometry, and the physical characteristics of the earth medium. Figure 2-83a shows the throwout of ejecta from the SEDAN Event, a 100 kt explosion at a depth of 635 feet.

2-52 Ejecta Thickness

The amount and linear extent of the continuously deposited ejecta in the crater lip are determined primarily by the yield. The radial limit of continuous ejecta, which is the outer edge of the lip, will usually vary between 2 and 3 times the apparent crater radius. The lip crest height above the original surface is estimated to be one-fourth of the apparent crater depth ($H_{a\ell} = 0.25\ D_a$, paragraphs 2-50 and 2-51). The depth of ejecta decreases rapidly in an exponential fashion as the distance from SGZ increases. About 80 to 90 percent of the entire ejecta volume generally is deposited within the area of continuous ejecta. Analysis of data for craters formed by near-surface bursts over soil indicates that ejecta mass represents approximately 55 percent of the apparent crater mass (the remainder being found in fallback, compaction, and the dust cloud, which is blown away). When the same yields explode at successively greater depths, ejecta mass increases significantly until the optimum DOB is reached. Ejecta thickness can be estimated for soil as follows (all dimensions are in feet):

$$t_e = 0.9V_a^{1.6}\ R^{-3.86},\ \text{for } R > 2.2V_a^{1/3}$$

where t_e is the ejecta thickness, V_a is the apparent crater volume, and R is the distance from SGZ to the point of interest. This formula for ejecta thickness assumes that the ejecta mass density will be approximately equal to the original in-situ density of the medium. The equation may be considered valid for a soil medium; however, the bulking, which is inherent in a disturbed rock medium would result in greater ejecta thicknesses than predicted by the formula. Therefore, in a rock medium, the ejecta thickness should be increased by 30 percent to account for the bulking, i.e., the formula for a rock medium is

$$t_e = 1.17V_a^{1.6}R^{-3.86},\ \text{for } R > 2.2V_a^{1/3}$$

2-53 Maximum Missile Range

Figure 2-83b shows the maximum missile range as a function of depth of burst for a 1 kt explosion in two soil types. These data are based on empirical results from several nuclear explosions.

[redacted]

[redacted]

Figure 2-83a. Throwout of Ejecta from the 100-kt SEDAN Event

Reproduced from best available copy.

[redacted]

Problem 2-26a. Calculation of Ejecta Thickness

Paragraph 2-52 provides formulas for the prediction of ejecta thickness as a function of distance from surface ground zero and the apparent crater volume (V_a). V_a may be obtained from Figures 2-74a through 2-76c for near surface bursts and 2-77 through 2-81 for deep-buried bursts by the methods described in paragraphs 2-49 through 2-51.

Example:

Given: A hypothetical 300 kt contact surface burst (center of gravity of the weapon 0.5 meters above the surface) will produce a crater predicted to have an apparent radius of 137 meters, an apparent depth of 18.2 meters and an apparent volume of 3.75×10^5 cubic meters in dry soil. (See problem 2-22).

Find: The thickness of the ejecta at a distance of 300 meters from SGZ.

Solution:

$R = 300$ meters,

$2.2V_a^{1/3} = 2.2(3.75\times10^5)^{1/3} = 159$ meters

$R > 2.2V_a^{1/3}$

Therefore the equation for soil given in paragraph 2-52 applies.

Answer: The ejecta thickness is

$$t_e = 0.9V_a^{1.6}\ R^{-3.86}$$

$$t_e = 0.9\,(3.75\times10^5)^{1.6}\,(300)^{-3.86} = 0.20 \text{ meters}$$

Reliability: Based on empirical formulas derived from high explosive and nuclear burst. Specific reliability has not been estimated.

Related Material: See paragraph 2-49 through 2-52. See also Problem 2-22.

[redacted]

[redacted]

Problem 2-26b. Calculation of Maximum Missile Range

Figure 2-83b shows the maximum range to which missiles might be expected from a 1 kt explosion as a function of depth of burial in two soil types.

Scaling. For yields other than 1 kt, the maximum missile range and depth of burst scale as follows:

$$\frac{R_m}{R_{m1}} = \frac{\text{DOB}}{\text{DOB}_1} = W^{0.3}$$

where R_{m1} is the maximum missile range for 1 kt, DOB_1 is the depth of burst for 1 kt, and R_m and DOB are the corresponding range and burial depth for W kt.

Example:

Given: A hypothetical 3 kt explosion at a depth of 85 meters in hard rock.

Find: The maximum missile range for the explosion.

Solution: The corresponding depth of burst for a 1 kt explosion is

$$\text{DOB}_1 = \frac{\text{DOB}}{W^{0.3}} = \frac{85}{(3)^{0.3}} = 61 \text{ meters.}$$

From Figure 2-83b, the maximum missile range for a 1 kt explosion at a depth of 61 meters in hard rock is 440 meters.

Answer: The corresponding maximum missile range for a 3 kt explosion at a depth of 85 meters in hard rock is

$$R_m = R_{m1}\, W^{0.3} = (440)\,(3)^{0.3} = 612 \text{ meters.}$$

Reliability: Based on empirical results from several nuclear explosions, but no specific reliability has been estimated.

Related Material: See paragraphs 2-46 through 2-52.

[redacted]

[redacted]

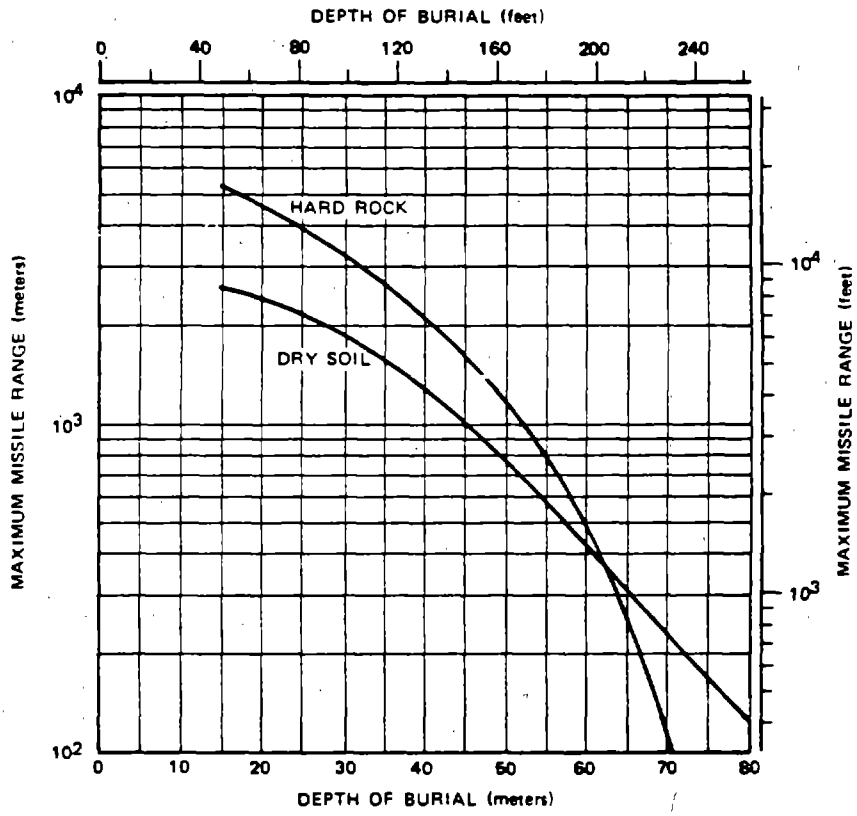

Figure 2-83b. Maximum Missile Range as a Function of Depth of Burial for a 1 kt Explosion

[redacted]

[redacted]

CHARGE STEMMING

The term charge stemming refers to the backfilling of material in the charge-emplacement hole. Ideally, charges should be completely stemmed and tamped to contain the explosive energy temporarily, which increases its coupling with the medium. Typical stemming materials are concrete, gravel, sand and water. The cratering curves shown in preceding paragraphs provide predictions for fully stemmed charges. There are, however, operational considerations that may require reduced stemming or the capability to emplace or remove the stemming material in a short period of time. Therefore, modified stemming geometries, including various degrees of stemming or no stemming at all, are important considerations in the evaluation of nuclear cratering phenomena.

The following changes in cratering phenomena generally may be expected when less than full stemming is used:

- Air blast and the fraction of radioactive materials that vents will be increased.
- Energy loss out of the emplacement hole will reduce the coupling effectiveness of the explosion. This will result in crater dimensions that are smaller than those from fully stemmed explosions.
- Energy deposited in the emplacement hole will cause a modification to the energy deposition pattern in the medium. The source will appear to be a distorted cylindrical source rather than a concentrated spherical source. Lip height, ejecta distribution, and maximum missile range will vary from those of a fully stemmed explosion.

2-54 Guidelines for Assessing the Effect of Stemming

The crater dimensions from a partially stemmed or an unstemmed emplacement hole will be affected primarily by the amount of stemming, the diameter of the emplacement hole, and the depth of burial. The following are some general conclusions concerning stemming that are based largely on HE experiments.

- The crater radius, which is the dimension of greatest military importance, does not increase significantly with increased stemming.
- Stemming about one-half of the emplacement hole (50% stemming) provides most of the crater depth that would be expected from a fully stemmed charge.
- Water appears to be a very efficient stemming material.

Figures 2-84a, b, and c illustrate the HE experimental results concerning the effect of stemming on crater volume, diameter, and depth, respectively.

EFFECTS OF GEOLOGICAL FACTORS

In most situations a weapon will *not* be burst in a homogeneous medium such as dry soil or wet soft rock. Instead, typical geologies may contain a water table at a shallow depth, a layering of one type of media over another (e.g., soil over rock), parallel planes of distant jointing in rock, or a steeply sloping ground surface. All of these factors can influence the formation of a crater and, in some cases, can change the size or characteristics of the crater significantly. The following paragraphs describe the general effects of geologic variations on cratering phenomena.

2-55 Sloping Topography

Terrain slopes of about five degrees or more will affect the geometry of a crater formed by either a surface or buried explosion. The ejecta distribution will also be affected. If the slope is gentle, the crater volume will be comparable

[redacted]

[redacted]

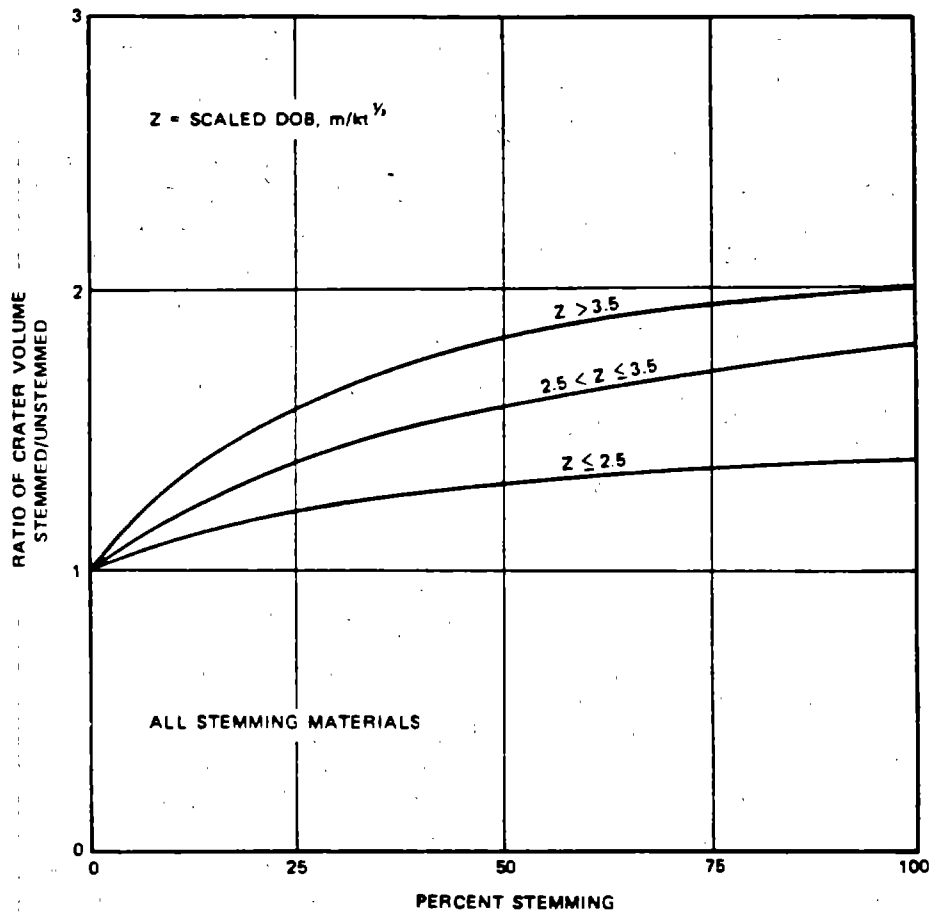

Figure 2-84a. Increase in HE Crater Volume as a Function of Stemming for Various DOBs

[redacted]

[redacted]

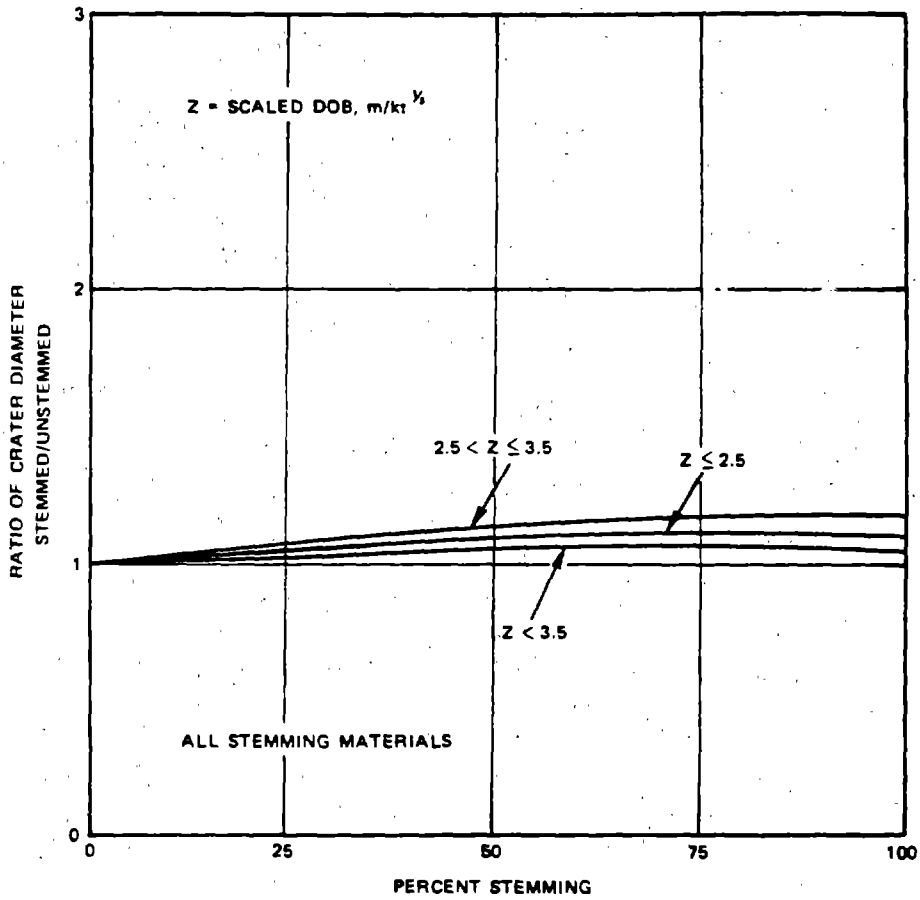

Figure 2-84b. Increase in HE Crater Diameter as a function of Stemming for Various DOBs

[redacted]

[redacted]

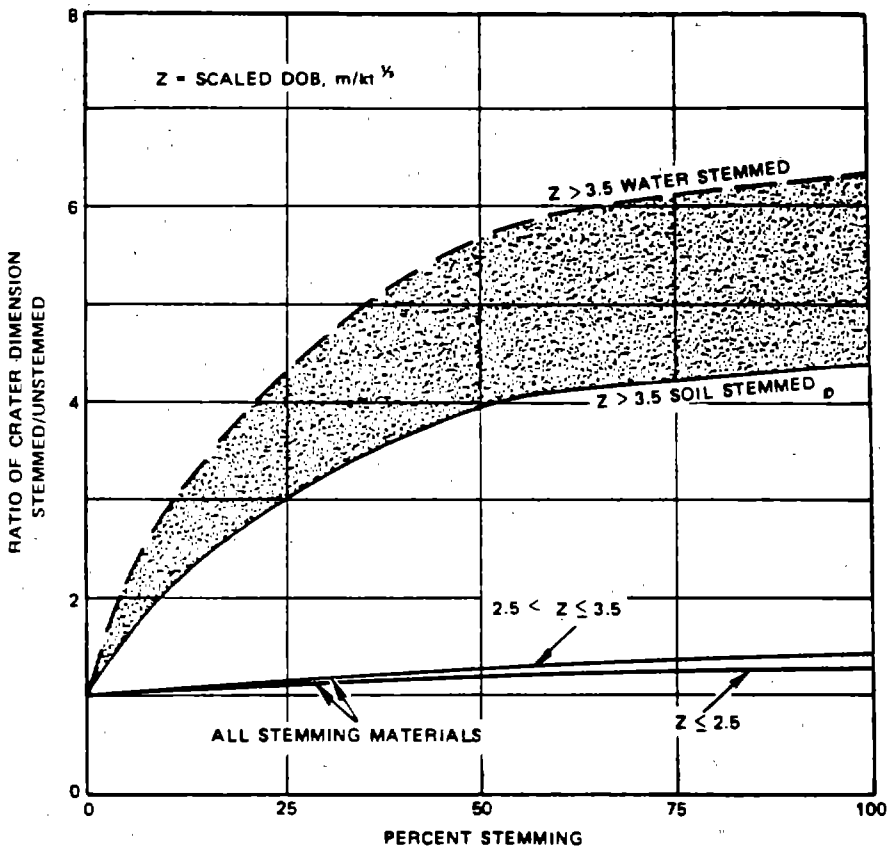

Figure 2-84c. Increase in HE Crater Depth as a Function of Stemming for Various DOBs

[redacted]

[redacted]

with that of craters on level ground, but the resulting crater will be asymmetrical; it will be wider up-slope and will have a larger lip down-slope. Figures 2-85a and b show a photograph and a schematic drawing, respectively, of the crater from a nuclear event buried 30 meters below a 30 degree slope in tuff. The shape of the crater formed by this explosion was influenced by the slope of the surface because almost all the debris formed a rock slide originating at the lower edge of the crater and terminating about 240 meters down the slope.

Limited small-scale cratering experiments have been conducted in moist, sandy soil and in desert alluvium on slopes ranging from 40 degrees to vertical wedges. For charges buried on severe but nonvertical slopes, with DOB measured normal to the sloping surface and with the vertical depth of overburden being greater than containment depth, crater dimensions decrease with increasing slope. Optimum vertical DOB appears larger by about one-third than optimum DOB on level terrain.

2-56 Water Tables

A subsurface ground water table in a soil medium will begin to influence the size and shape of the crater when its depth below the surface is equal to or less than three-fourths the predicted apparent crater depth. Its effect is to flatten and widen the crater. Figure 2-86a illustrates the effect of a shallow water table on the shape of the crater. As the water table depth decreases, its effect becomes more evident. Based upon HE experiments, it can be concluded that for a surface detonation, the influence of the water table is not significant for scaled water table depths greater than about 3.5 $m/kt^{1/3}$, and the apparent radius, volume and lip height increase exponentially as the water table approaches the ground surface. For shallow buried bursts ($DOB/W^{1/3} < 3\ m/kt^{1/3}$) the final crater radius may be as much as 50 percent greater than the predicted value and the depth as little as one-third that of the predicted value.

Figure 2-86b shows a normalization technique that has been developed for plotting crater volume for surface and shallow buried explosions in a layered geology. A shallow water table effectively causes a homogeneous medium to act as a two layered medium

d = depth to water table (thickness of upper layer)

V_a = apparent crater volume

V_u = apparent crater volume predicted in the upper layer alone (usually dry soil)

V_L = apparent crater volume predicted in the lower layer alone (usually wet soil).

The curve fitted to the water table crater volume data in Figure 2-86b is given by the expression

$$\frac{V_a - V_L}{V_u - V_L} = 1 - \exp(-5.4\, d/V_a^{1/3}).$$

Iteration is required to solve this expression for V_a; however, the technique converges very rapidly. It is recommended that the curve in Figure 2-86b be used to predict crater volume for sites having a shallow water table.

2-57 Bedrock

The influence of a bedrock layer below a soil medium is similar to that of a water table, though somewhat less pronounced. For surface explosions it appears that a hard layer may limit the crater depth while causing the crater shape to be more nearly trapezoidal than parabolic or conical (see Figure 2-86c). The bedrock layer may increase the crater radius slightly (5 to 10

[redacted]

[redacted]

Figure 2-85a. NEPTUNE Crater and its Position on Slope of Mesa

Reproduced from best available copy.

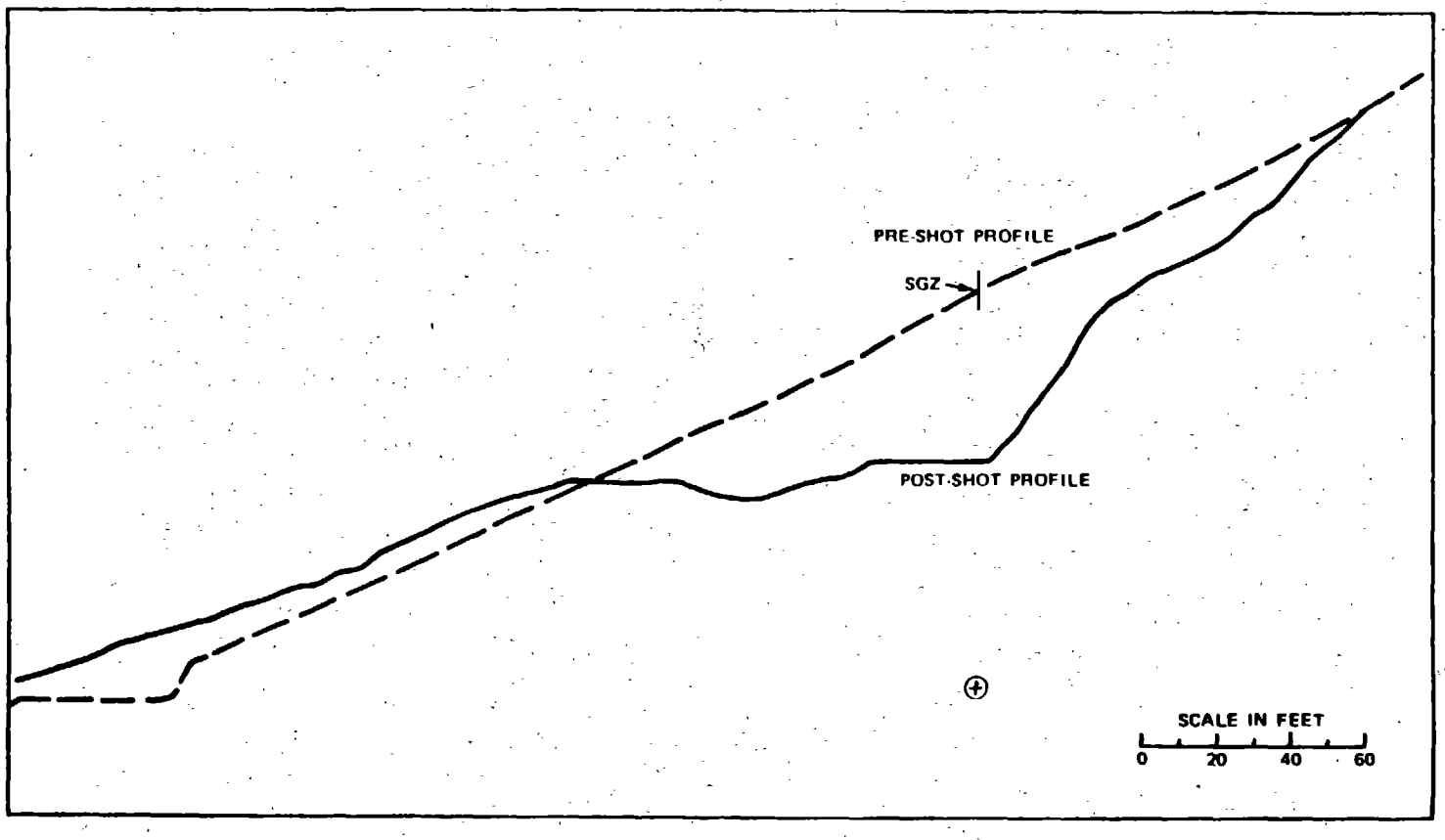

Figure 2-85b. Section of NEPTUNE Crater Normal to Slope Contours

Figure 2-88a. Crater Formed by a Surface Detonation of a 0.5 kt High Explosive Charge in a Wet Soil Medium with a Shallow Water Table (DIAL PACK Event); a 8.2 m (27 ft.) Diameter Sphere with the Bottom Tangent to the Ground:
R_a = 30.48 m (100 ft.); D_a = 4.6 m (15 ft.)

Reproduced from best available copy.

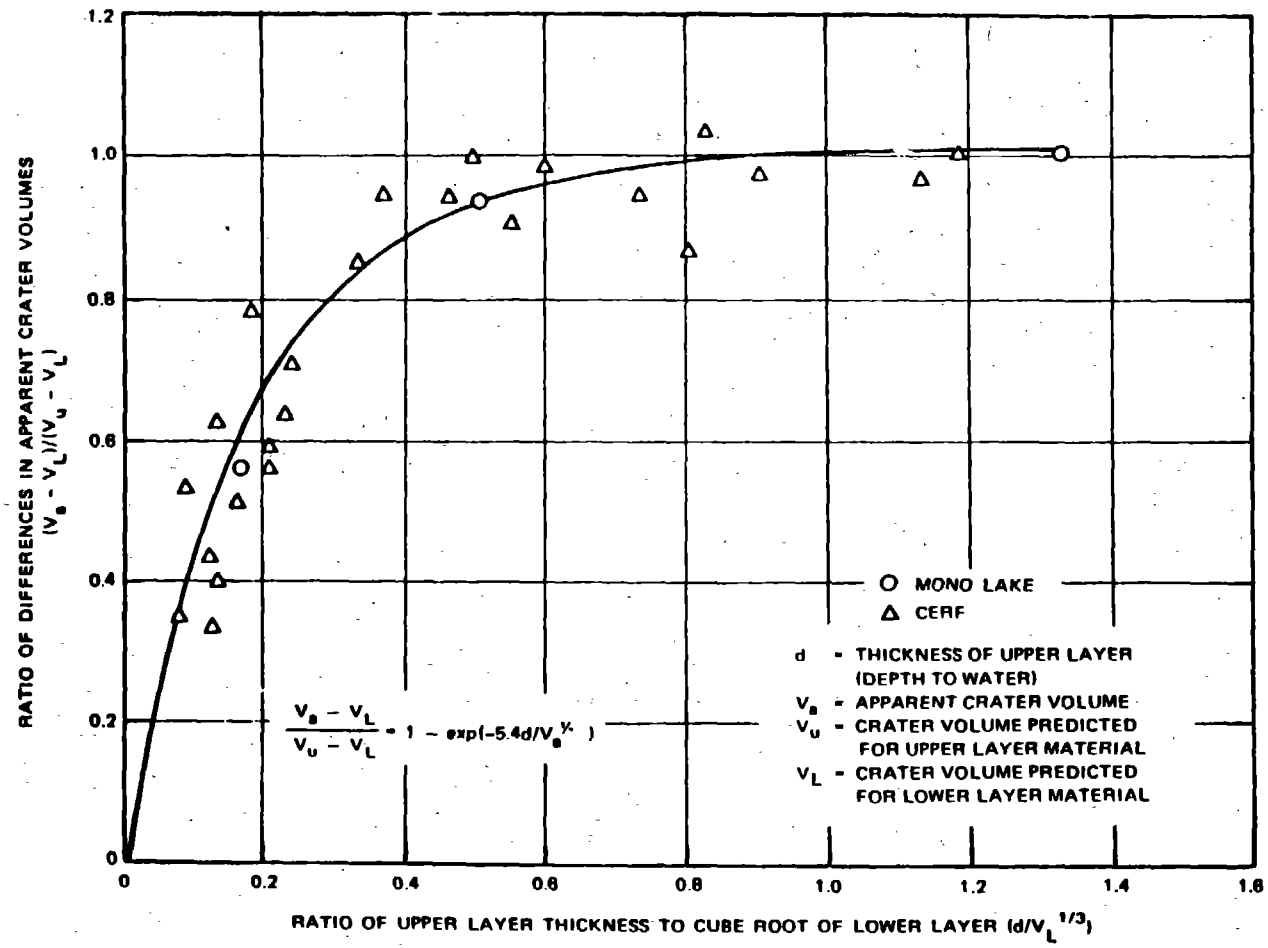

Figure 2-86b. Cratering Data for Dry Soil over Wet Soil

[redacted]

percent). The layer may decrease the final crater depth by as much as one-third when the overburden layer is as shallow as one-fourth the predicted apparent crater depth.

Although the effect of a water table and the effect of a hard layer are different, the water table curve is a good approximation for predicting the crater volume in a layered geology involving a gradual transition to rock. The water table curve should *not* be used for geologies involving a sharp transition to rock.

The two-layer problem can be generalized to three layers. Let V_1, V_2, and V_3 be the crater volume associated with the top, middle, and bottom materials considered separately. Then, V_{23} is the crater volume associated with the middle layer and bottom layer, and V is the crater volume in the total layered medium.

V_{23} is calculated by neglecting the top layer and then solving a two-layer problem with V_2 as the upper layer and V_3 as the lower layer. The thickness of the middle layer d_2 is used as the depth to the lower layer. This gives

$$\frac{V_{23} - V_3}{V_2 - V_3} = 1 - \exp\left(-5.4\, d_2 / V_{23}^{1/3}\right)$$

V is then calculated by solving another two-layer problem with V_1 as the upper layer and V_{23} as the lower layer. The thickness of the upper layer d_1 is used as the depth of the lower layer. This gives

$$\frac{V - V_{23}}{V_1 - V_{23}} = 1 - \exp\left(-5.4\, d_1 / V^{1/3}\right).$$

2-58 Rock Bedding/Jointing

If a low-yield explosion occurs at or very near the surface, the bedding or jointing planes in rock can influence the shape of the crater produced. The direction of the ejection process will also be affected. The formation of the crater will tend to follow the direction of the predominant joints, and the crater radius will be increased by as much as one-third in the direction parallel to the joints and decreased by as much as one-third in the direction normal to the joints. The magnitude of the crater depth is usually not affected significantly, but the deepest point may be shifted to one side of the crater. As the yield or the DOB is increased, the influence of rock jointing is reduced.

The dip of bedding planes will influence energy propagation, and this will cause the maximum crater depth to be offset in the down-dip direction. Little overall effect is noted on the size of the crater radius, but differences in ejection angles cause the maximum lip height and ejecta radius to occur down-dip.

2-59 Snow and Ice

Measured craters in snow or ice are a rarity; however, data for a few craters have been recorded for surface HE explosions. In general, these craters are larger than would be predicted in soil and they are characteristically wide and flat. The trends in crater size and shape for a surface explosion in a snow/ice medium are given by the expressions

$$R_a = 38.8\, W^{0.26} \text{ meters}$$

$$D_a = 5.75\, W^{0.15} \text{ meters}$$

where W is the yield in kilotons.

MULTIPLE BURST GEOMETRIES

Nuclear weapons may be detonated in close proximity to each other to create a linear crater or a series of interconnected craters. When simultaneous explosions are sufficiently close to cause interactions, the shot geometry is termed "multiple burst." A linear array of this nature is referred to as a row crater, as illustrated in Figure 2-87.

[redacted]

[redacted]

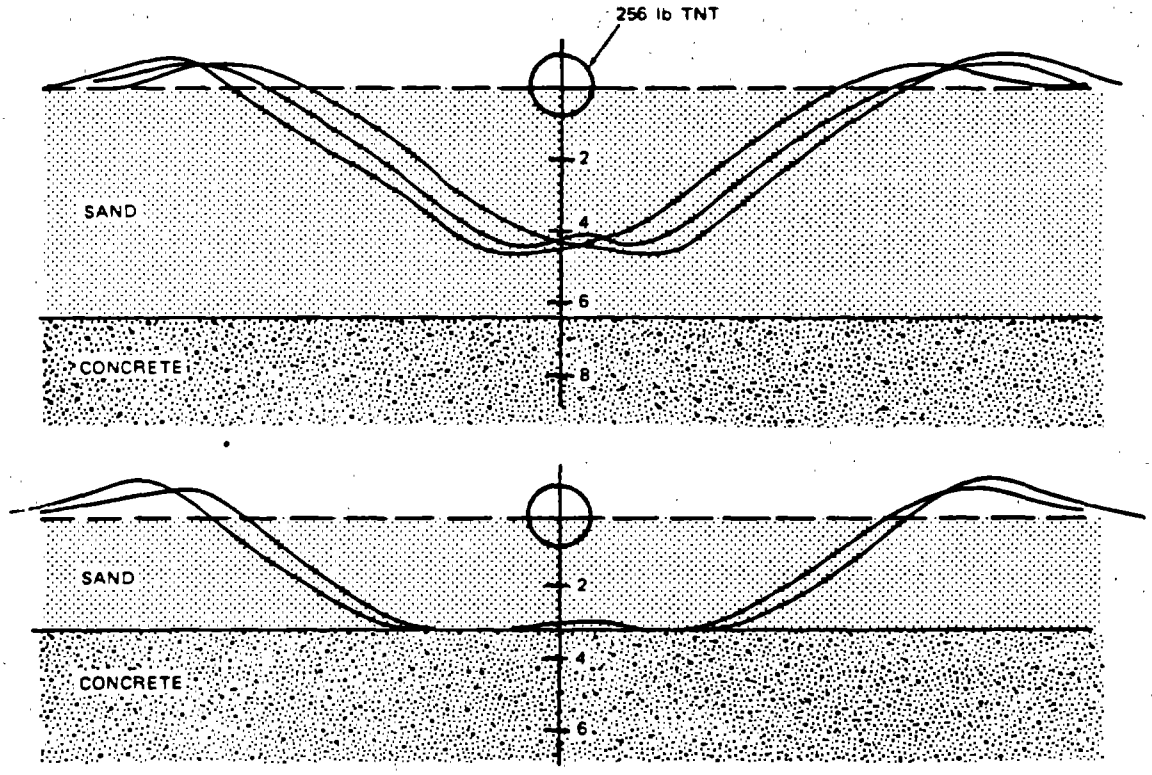

Figure 2-86c. Effects of a Hard Near-Surface Layer on Cratering

[redacted]

[redacted]

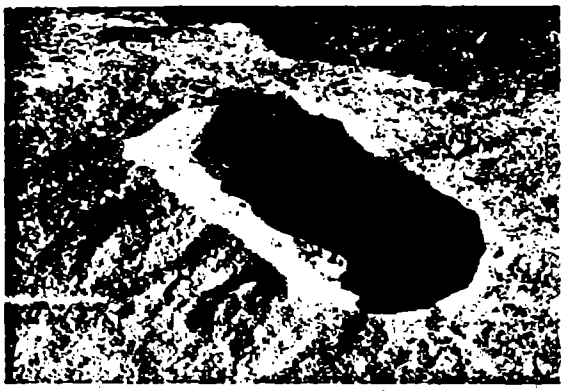

Figure 2-87. A Row Crater Produced by Simultaneous Explosions of Five 1.1 kt Nuclear Devices at Optimum DOB (BUGGY Event) in Basalt: DOB = 41 m (135 ft.); Spacing = 45.7 m (150 ft.); Width = 76.2 m (250 ft.); Depth = 19.8 m (65 ft.); Length = 262 m (860 ft.)

In addition to the parameters normally associated with an underground explosion, the results of a row charge also depend upon the spacing between charges (s) and the degree of simultaneity of the explosions. Differences of only a few milliseconds in the times of explosion of adjacent charges can result in significantly degraded row charge crater dimensions. Close spacing of weapons (less than 1.4 times a single weapon crater radius) increases both the crater radius and depth compared to single weapon craters at the same scaled DOB. Experience has shown that a spacing of 1.0 R_a (for explosions at optimum DOB) results in a smooth channel with crater depth and radius approximately 20 percent greater than those of single explosions. A spacing of 1.25 R_a will still form a smooth channel, but with less enhancement of crater dimensions, while spacing of 1.5 R_a will provide an adequate linear obstacle. The length of a row crater L can be found in the equation:

$$L = s(n - 1) + 2R_a,$$

where n is the number of charges in the row, and s is the spacing between charges.

SECTION III

[redacted] GROUND SHOCK PHENOMENA [redacted]

2-60 General Nature of Free-Field Effects [redacted]

[redacted] The position of the weapon at the time of detonation has a marked influence on the amount and nature of the energy transfer into the ground. The effects at depths below the surface from a high air burst will be primarily of the air-induced type. For surface or near surface bursts, both air-induced and direct-transmitted ground shock effects are produced, and both may be of importance. Deep underground bursts cause direct-transmitted effects almost exclusively.

[redacted] The nuclear field tests of the past several decades involving air, surface, and fully contained bursts have provided the data that permit development of the expressions for predicting the peak values of air-induced and direct-transmitted acceleration, velocity, and displacement. Field observations for regions where the air blast overpressures are less than 1,000 psi generally indicate that, within about 50 to 100 feet of the surface, ground motions are predominantly air-induced. The relatively few measurements of acceleration and displacement that have been made at significant distances below the ground surface show the effects of attenuation and dispersion as the air-induced pulse travels through the ground.

[redacted] A typical acceleration-time record from a gage mounted near the surface of the ground

[redacted]

Reproduced from best available copy.

[redacted]

[redacted] exhibits a systematic pulse shape corresponding to the passage of the shock wave, with a random type disturbance often superimposed on this systematic pulse. In the superseismic case, when the air blast propagation velocity is greater than the ground seismic velocity, the downward acceleration is large compared with the following upward acceleration. The velocity-time record is similar in shape to the overpressure-time pulse, at least in the early stages. In cases in which the ground motion outruns the air blast, there is a slower rise in the acceleration; it may even be reversed in direction initially, i.e., upward rather than downward. In such cases, the signals may last for a longer time than the positive phase overpressure duration. The associated velocity wave form usually exhibits a velocity jump as the air-shock wave passes over the position, but the overall record is characterized by a considerable degree of oscillation. When precursors are present, the acceleration and velocity records may exhibit higher frequency components and more random type of oscillation. Wave front diagrams for the superseismic and outrunning cases are shown in Figure 2-88.

[redacted] Most values of velocity have been obtained by integrating acceleration records. In general, velocities appear to be more predictable quantities than accelerations or displacements. Displacement data are even scarcer than velocity data, and only a few direct measurements have been made. For the most part, displacement data consist of integrated acceleration records or extrapolation of displacement spectra to zero frequency.

[redacted] Knowledge of direct-transmitted ground shock effects is limited. Those data that exist were obtained from buried high explosive shots, from several surface and near surface nuclear detonations, and from a number of fully contained bursts. For a completely buried shot, measurements indicate that at any particular range R, the strain or velocity pulse rises in a parabolic manner to a peak value in a time roughly corresponding to $T_r = R/6c_p$ to $R/12c_p$, where R is the range from the explosion, and c_p

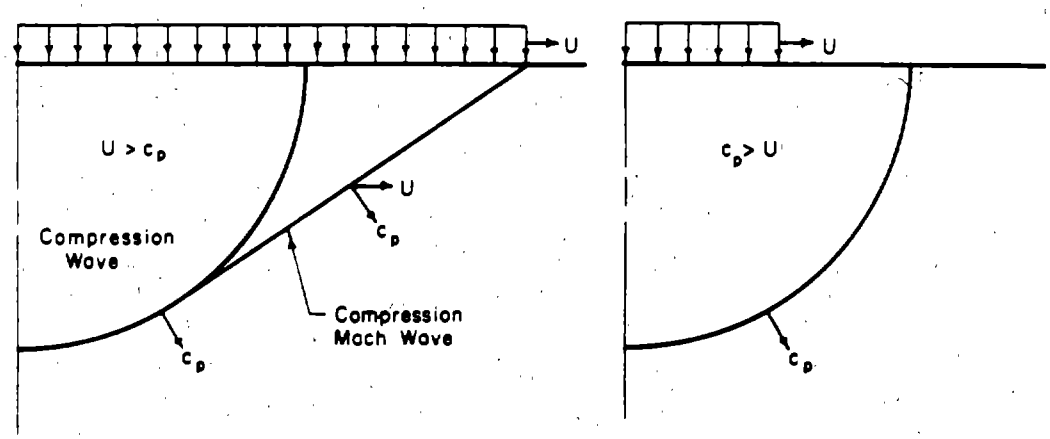

(A) Superseismic Blast Wave (B) Outrunning Ground Wave

Figure 2-88. [redacted] Wave Front Diagram for Superseismic Air Blast and Outrunning Ground Wave [redacted]

[redacted]

[redacted]

[redacted] is the effective seismic velocity of the medium. The signal then drops slowly with a total positive phase duration corresponding approximately to $T_o = R/2c_p$ to R/c_p. The effects of layering, reflection, and refraction, tend to introduce high frequency and random components of motion.

2-61 Types of Effects [redacted]

[redacted] It is convenient to consider the earth shock resulting from a nuclear explosion as producing both systematic and random effects. Systematic effects can be divided further into two major types:

- Air-induced shock associated with the passage of an air shock wave over the surface of the ground, and the overpressure at the surface above the structure transmitted downward with such attenuation and dispersion as may be consistent with the physical conditions at the site.
- Direct-transmitted ground shock that arises from direct energy transfer from surface, near surface, or underground bursts.

[redacted] Random effects include high frequency ground-transmitted shock, surface-wave effects, reflections, refractions, etc. The dominant effect depends on such factors as weapon yield, point of detonation with respect to the ground surface, range from ground zero, depth of the measurement, and, in particular, the geologic conditions.

[redacted] Reasonable estimates can be made of the maximum values of displacement, velocity, and acceleration associated with the air-induced shock and in more restricted cases for the direct-transmitted ground shock under more or less uniform geologic conditions.

2-62 Air-Induced Effects [redacted]

[redacted] At the surface in a homogeneous medium the maximum transient elastic vertical displacement may be expressed as

$$d_{se} = \frac{Hp_{so}}{2\bar{E}},$$

where H is the depth to which the air-induced shock wave extends during the effective duration of the shock, t_i, p_{so} is the side-on overpressure at the surface, and $\bar{E}$ is the restrained modulus. The duration of the shock may be approximated by

$$t_i \approx 0.37 \left(\frac{100}{p_{so}}\right)^{1/2} \left(W(\mathrm{Mt})\right)^{1/3}$$

for

$$2 \leq p_{so} \leq 10{,}000 \text{ psi.}$$

Thus

$$H = c_p t_i = 0.37 \left(\frac{100}{p_{so}}\right)^{1/2} \left(W(\mathrm{Mt})\right)^{1/3} c_p.$$

The restrained modulus is related to the effective seismic velocity, the mass density, and Young's modulus of elasticity of the medium as follows:

$$\frac{\bar{E}}{\rho} = c_p^2 = \left(\frac{E}{\rho}\right)\left(\frac{1-\nu}{(1+\nu)(1-2\nu)}\right),$$

where E is the Young's modulus of elasticity (psi), ρ is the mass density of the medium ($\rho = \gamma/g$ lb sec^2/ft^4, where γ is the unit weight of the medium in pounds per cubic foot and g is the gravitational acceleration constant), and ν is Poisson's ratio. For values of ν of 0.25 or less, the relation may be approximated by:

$$\bar{E} = \rho c_p^2 \approx E.$$

If the unit weight of the soil is about 115 lb/ft^3,

[redacted]

[redacted]

[redacted] an approximate value of $\bar{E}$ is

$$\bar{E} = 25{,}000 \left(\frac{c_p}{1{,}000}\right)^2, \text{ psi.*}$$

Substituting the values for H and $\bar{E}$ gives

$$d_{se} = 9 \left(\frac{p_{so}}{100}\right)^{0.5} \left(\frac{1{,}000}{c_p}\right)\left(W(\text{Mt})\right)^{1/3} \text{ inches.}$$

[redacted] The permanent vertical displacement is not so easily estimated; at present the best estimates can be made by considering the static stress-strain properties of the soil. In the absence of better information, it is suggested that the permanent displacement at the surface be taken to be the following for overpressures greater than 40 psi:

$$d_{sp} = \frac{p_{so} - 40}{30} \left(\frac{1{,}000}{c_p}\right)^2 \text{ inches,}$$

where c_p is the seismic velocity of the material *near the surface.*

[redacted] From wave propagation theory it may be demonstrated that the following relationship exists for particle velocities in terms of the dimensional units defined above.

$$v = c_p \frac{p_{so}}{\bar{E}} = c_p \epsilon,$$

where ϵ is the strain. Upon substitution this gives the maximum velocity

$$v_s = 50 \left(\frac{p_{so}}{100}\right)\left(\frac{1{,}000}{c_p}\right) \text{ in./sec.}$$

[redacted] For a rise time of velocity of about 0.002 seconds, and considering a parabolic rise with a 20 percent increase for nonlinearity, the maximum acceleration at the surface, computed as a rate of change of velocity, may be expressed by

$$a_s \approx 150 \left(\frac{p_{so}}{100}\right)\left(\frac{1{,}000}{c_p}\right), g.$$

[redacted] Since the surface acceleration is not related solely to the maximum velocity, but is partially dependent on the weapon yield and other factors, it is recommended that a value of c_p no greater than 2,000 fps be used in this expression, regardless of the actual surface seismic velocity.

[redacted] Horizontal effects data are lacking for the surface. At present, it is recommended that the maximum horizontal deflection be taken as one-third the vertical, the maximum horizontal velocity as two-thirds the vertical, and the maximum horizontal acceleration as equal to the vertical.

[redacted] The same type of reasoning can be followed in arriving at maximum values of acceleration, velocity, and displacement at depths below the surface. The difference in deflection between the surface and some point at a depth y beneath the surface cannot exceed the surface stress divided by the lower restrained modulus of deformation, $\bar{E}$, in the interval y, and multiplied by the depth y. Thus between the surface and a depth y, not greater than 100 ft, assuming no attenuation of pressure with depth, an upper limit of the elastic component of differential displacement is given by

$$d_s - d_y \approx \frac{p_{so}}{\bar{E}} y.$$

[redacted] The actual difference in deflection i more likely to be one-half this value, and may be

[redacted] If the unit weight of the medium differs significantly from 115 lb/ft^3, a representative value of $\bar{E}$ should be used rather than the approximation given here.

[redacted]

[redacted]

considered to vary linearly to a depth of 100 ft, which results in the following expression

$$d_{se} - d_{ye} = 2.4\left(\frac{p_{so}}{100}\right)\left(\frac{1{,}000}{c_p}\right)^2\left(\frac{y^*}{100\text{ ft}}\right)\text{inches}$$

where $y^* = y$ for depths of 0 to 100 ft, and $y^* =$ 100 ft for depths greater than 100 ft.

It is not generally considered desirable to assume any attenuation of displacement, except for very soft soils. Since total impulse must be preserved, the wavelength of the strain pulse probably increases with depth, and, therefore, it does not seem reasonable that there should be a reduction in elastic component of displacement consistent with the reduction in peak stress, as given by the attenuation relationships for stress or velocity with depth.

It is recommended that the permanent displacement of soils at depths below the surface be determined by multiplying the permanent displacement at the surface by $(100 - y^*)/100$, i.e.,

$$d_{yp} = d_{sp}\left(\frac{100 - y^*}{100}\right)$$

$$= \frac{p_{so} - 40}{30}\left(\frac{1{,}000}{c_p}\right)^2\left(\frac{100 - y^*}{100}\right)\text{inches.}$$

Thus, permanent displacements below 100 feet would be taken to be zero. At depths less than 100 feet, the total displacement should be taken as the sum of the elastic displacement at the surface, d_{se}, shown previously, and the permanent displacement, d_{yp}, given above.

The value of maximum stress below the surface is given approximately, for any yield or overpressure, by the following expression

$$p_y = \alpha p_{so}$$

where

$$\alpha = \frac{1}{1 + \frac{y}{H}},$$

and for depths that are not near the surface

$$H = 230\left(\frac{100}{p_{so}}\right)^{0.5}\left(W(\text{Mt})\right)^{1/3}.$$

Note: The attenuation factor, α, that is used in this section is different than the corresponding attenuation factor $1/\beta$ that is used in Section II, "Damage to Belowground Structures," of Chapter 11, "Damage to Structures." The attenuation factor given in Figure 11-29, Section II of Chapter 11 is the result of more recent studies. It reflects the influence of soil type (as represented by its seismic velocity) on peak pressure or soil particle velocity attenuation. The disparity between the two factors increases as the peak overpressure and/or the soil seismic velocity increase, but the disparity is relatively insensitive to variations in weapon yield. As a result of the influence of seismic velocity, the difference between the two factors also increases as the depth below ground surface increases. The factor given in Figure 11-29 gives substantially smaller attenuation rates under high overpressures and high seismic velocities than does the factor used in this section. Consequently, from the "vulnerability analysis" point of view, the factor of Figure 11-29 is more conservative, and its use in shock analysis studies is generally recommended. The attenuation factor obtained from Figure 11-29 may be introduced into the equations of this section by simply replacing "α" of this section with "$1/\beta$," where "β" is obtained from Figure 11-29. As mentioned previously, it is recommended that this replacement be made, in general; however, there is

[redacted]

one important exception. The factor $1/\beta$ is not compatible with the shortcut vulnerability curves shown in Figures 11-48 through 11-50, and calculations of similar curves that are compatible with the $1/\beta$ attenuation factor have not been performed at this time. It is for this reason that the α attenuation factor is introduced here, and its use will be illustrated in Problem 2-27. The use of the $1/\beta$ attenuation factor is illustrated in Problems 11-3 and 11-4.

At depths below the surface, it is recommended that velocities be attenuated in about the same manner as the maximum stress. Thus, the vertical velocity at any depth y is given by

$$v_y = \alpha v_s.$$

The peak downward acceleration attenuates sharply with depth, especially near the surface. The sharp attenuation is caused primarily by the increase of rise time in the stress or velocity with depth.

The time of rise of the maximum velocity from an initial zero value can be taken as one-half the transit time of the shock wave from the surface to depth considered. For a parabolic rise in velocity the acceleration can be considered to be twice the value for a linear rise, which leads to the expression

$$a_y = 2\frac{v_y}{t_r} = 5\left(\frac{p_{so}}{100}\right)\frac{100}{y}\alpha\ g,$$

where t_r is the effective velocity pulse rise time. This expression gives values which appear to agree well with test data for depths greater than 10 ft.

In the absence of better information at depths below the surface, it is recommended that the ratios of horizontal to vertical effects be taken equal to those previously specified for the surface, i.e., horizontal deflection is one-third the vertical, the maximum horizontal velocity is two-thirds the vertical, and the maximum horizontal acceleration is equal to the vertical.

Layered media pose a complicated situation, but with care and judgment, reasonable estimates of acceleration, velocity, and displacement can be made. A convenient method is to use the stepwise passage of a stress wave downward through the medium. In general, the basic concepts governing the computation of displacement, velocity, and acceleration are the same as those described for a uniform medium. The displacements at any particular time may be computed by dividing the average pressure in an interval by the modulus of elasticity to obtain the strain and then multiplying by the length of the interval to obtain the displacement; the total displacement occurring over the length of the pulse is the sum of the incremental displacements.

Complications arise at the interface of two media because of stress transmission and reflection. For soil and rock, the interface may not be sharply defined and the reflected and transmitted stresses probably do not follow the laws governing purely elastic media. If it is known that the interface is fairly sharp, an estimate of the reflected and transmitted stresses can be made from the following relationships:

$$p_r = \frac{1-\psi}{1+\psi}p_i$$

$$p_t = \frac{2}{1+\psi}p_i$$

where ψ is the ratio of the impedances of the two media. The stresses at the interface must be taken as equal, and, from considerations of continuity, the displacements also are equal.

2-63 Outrunning Ground Motion

Outrunning ground motion occurs when the air-shock velocity U decays below the seis-

[redacted]

[redacted]

mic wave velocity c of the medium. In the most general sense, outrunning ground motions and direct-transmitted ground shock are different phenomena. Direct-transmitted ground shock is ground motion propagated through the ground media from the region of the crater (this is often denoted outrunning when it clearly arrives, as reflected or refracted waves from deep-seated layers, ahead of the blast front). Outrunning ground motion occurs when the air-induced ground motion begins to propagate more rapidly than the air blast shock front, as illustrated in Figure 2-88. In actual fact, the motion-time history at a point in the medium can be quite complicated, even random in nature, when air-induced, outrunning, and direct-transmitted effects all arrive at about the same time.

[redacted] Some information on outrunning motions observed in field tests can be found in "Nuclear Geoplosics" (see bibliography). Computer codes that are presently being developed should provide guides to even better estimates or outrunning motions.

2-64 Direct-Transmitted Ground Shock [redacted]

[redacted] The energy transmitted directly to the earth from a surface or near-surface burst can be propagated effectively through competent material for long distances. Experimental data that demonstrate this are available from buried high explosive shots and from surface and contained nuclear weapon tests.

[redacted] For a completely buried shot, the first portion of the strain or velocity record at a distance R from the point of burst has the form described in paragraph 2-60, i.e.,

$$T_R = \frac{R}{6c_p} \text{ to } \frac{R}{12c_p} \quad \text{and} \quad T_o = \frac{R}{2c_p} \text{ to } \frac{R}{c_p}.$$

[redacted] Without serious error, the relation between peak strain ϵ and peak particle velocity v is given by the equation previously shown in paragraph 2-62, i.e.,

$$v = c_p \frac{p_{so}}{E} = c_p \epsilon.$$

Assuming that the steepest part of the velocity-time curve has a slope that is twice the average slope during the rise phase leads to the following relationship between the range of peak acceleration, peak velocity, and strain, all in the radial direction.

$$a_r = \frac{2v_r}{T_r} \approx \frac{12c_p^2}{R}\epsilon \text{ to } \frac{24c_p^2}{R}\epsilon.$$

[redacted] An estimate of the maximum displacement d_r in the radial direction may be obtained by integrating the area under the positive phase of the velocity curve. If the velocity waveform is parabolic, then

$$d_r = \frac{2}{3} v_r T_o \approx \frac{1}{3} R\epsilon \text{ to } \frac{2}{3} R\epsilon.$$

[redacted] If data for strain, acceleration, or displacement are available, approximate relations for the other quantities may be obtained. In general, the seismic velocity enters into the relationships as indicated in equations shown above.

[redacted] Most of the available test data from which direct-transmitted shock effects may be estimated were obtained from buried nuclear and high explosive detonations. To extrapolate from the test data to estimate shock effects produced by surface nuclear detonations requires establishment of the equivalence factor relating buried HE to buried nuclear yield, and also establishment of the equivalence of fully buried detonations to surface detonations of the same type of explosive.

[redacted] A yield effectiveness factor of 0.2 to 0.5 has been used to relate fully contained nuclear

[redacted]

[redacted]

[redacted] explosions to fully contained HE explosions. To relate a surface nuclear burst to a fully contained nuclear burst, factors of 0.02 for a burst slightly above the surface to 0.05 for a burst slightly below the surface are recommended. Significant uncertainties exist regarding these equivalence factors.

[redacted] Expressions for acceleration, velocity, and displacement have been derived on the basis of test data available for accelerations from shot RAINIER in Operation HARDTACK in volcanic tuff with a seismic velocity of 6,000 fps. For scaled ranges of 2,500 ft/Mt$^{1/3}$ and closer, and an equivalence factor of 0.05 as just discussed, the acceleration may be expressed as follows:

$$a_r = 0.4 \left(W(\mathrm{Mt})\right)^{5/6} \left(\frac{1{,}000}{R}\right)^{3.5} \left(\frac{c_p}{1{,}000}\right)^{2}, \ g.$$

[redacted] Using the relations between acceleration, velocity, and displacement, and choosing the equations with coefficients of 12 and 1/3, respectively, this equation for acceleration may be used to arrive at the following equations for radial velocity and displacement for materials with seismic velocities less than 10,000 feet per second:

$$v_r = 12 \left(W(\mathrm{Mt})\right)^{5/6} \left(\frac{1{,}000}{R}\right)^{2.5} \left(\frac{c_p}{1{,}000}\right) \text{in./sec}$$

$$d_r = 4 \left(W(\mathrm{Mt})\right)^{5/6} \left(\frac{1{,}000}{R}\right)^{1.5} \text{inches.}$$

[redacted] There is little or no information on tangential motions, and until additional information becomes available, it is recommended that maximum values of tangential acceleration, velocity, and displacement be taken as 1, 2/3, and 1/3 times the corresponding radial values.

[redacted] It is desirable to consider the direct-transmitted effects as being applicable only at some distance below ground surface, except possibly at close in ranges. At scaled distances greater than 2,500 ft/Mt$^{1/3}$, the limited available data suggest a decrease in the rate of decay of motion with distance. Approximate expressions for radial acceleration, velocity, and displacement for materials with an average seismic velocity less than 10,000 fps are as follows:

$$a_r = 0.081 \left(W(\mathrm{Mt})\right)^{0.25} \left(\frac{1{,}000}{R}\right)^{1.75} \left(\frac{c_p}{1{,}000}\right)^{2}, \ g.$$

$$v_r = 4.8 \left(W(\mathrm{Mt})\right)^{0.5} \left(\frac{1{,}000}{R}\right)^{1.5} \left(\frac{c_p}{1{,}000}\right) \text{in./sec}$$

$$d_r = 3.19 \left(W(\mathrm{Mt})\right)^{0.75} \left(\frac{1{,}000}{R}\right)^{1.25} \text{inches.}$$

These expressions give only very approximate values. Geologic conditions can produce large and random variations in the motions at large distances. For materials with seismic velocities greater than 10,000 fps, e.g., granite rock materials, the field test data suggest the following relationships as being applicable at scaled ranges of about 2,700 ft/Mt$^{1/3}$ and closer.

$$a_r = 180 \left(W(\mathrm{Mt})\right)^{5/6} \left(\frac{1{,}000}{R}\right)^{7/2} \left(\frac{165}{\gamma}\right)^{5/6} \left(\frac{c_p}{18{,}000}\right)^{1/3}, \ g,$$

$$v_r = 30 \left(W(\mathrm{Mt})\right)^{5/6} \left(\frac{1{,}000}{R}\right)^{5/2} \left(\frac{165}{\gamma}\right)^{5/6} \left(\frac{18{,}000}{c_p}\right)^{2/3}, \ \text{ft/sec,}$$

[redacted]

[redacted]

(U)

$$d_r = 12 \left(W(\mathrm{Mt})\right)^{5/6} \left(\frac{1{,}000}{R}\right)^{3/2} \left(\frac{165}{\gamma}\right)^{5/6} \left(\frac{18{,}000}{c_p}\right)^{5/3}, \text{ inches.}$$

[redacted] As would be expected from the different scaling relationships, the expression for materials with seismic velocities less than 10,000 feet per second and those for materials with seismic velocities greater than 10,000 feet per second show lack of agreement at a seismic velocity of 10,000 feet per second, which divides the areas of applicability. This matter is currently receiving further attention, but in the interim it is believed that the expressions provide the best estimates of such motions.

[redacted] No expressions exist for motions at large distances in hard materials that are comparable to the expressions presented above for soft materials. It was necessary to make approximate estimates to develop the relationships presented in Section III, Chapter 11.

2-65 Spectrum Concepts – Simple Systems [redacted]

[redacted] When structural systems or equipment are subject to a base disturbance, such as that arising from the ground motion associated with a nuclear explosion, the response of the system is governed by the distribution and magnitudes of the masses and resistance elements. A knowledge of the response of systems subjected to such loadings is extremely important from the standpoint of design in order to proportion the structure so that it will not undergo complete collapse, and to protect the structure, equipment, and personnel from shock damage. One of the simplest interpretations of ground motion data involves the concept of the response spectrum, which is a plot of the maximum response of a simple linear oscillator subjected to a given input motion as a function of frequency.

[redacted] The time history of the actual motions of the earth caused by the passage of a shock wave over the surface is complex and is subject to considerable uncertainty. However, the principal effects on equipment and structural components can be described by use of the concept of the shock-response spectrum.

[redacted] Consider a piece of equipment or an internal element of a structure supported at a point on an underground structure that is subjected to motion from blast. The equipment or element can be represented as a simple oscillator, consisting of a mass m attached by a linear spring of spring constant k to the base as shown in Figure 2-89(a). The natural frequency f of the oscillator is

$$f = \omega/2\pi = \frac{1}{2\pi}\sqrt{\frac{k}{m}}.$$

[redacted] For a given transient ground motion x, the mass m will be set into motion. If the motion of the mass m is designated by the coordinate y and the motion of the base by the coordinate x, the deformation in the spring u is $(y\text{-}x)$ and is positive when y exceeds x. For such a system the most useful spectra are found to be the following: the maximum relative displacement u of the system; the maximum relative velocity $\dot{u}$; the maximum pseudo relative velocity or the quantity ωu, the circular frequency ω times the displacement u, which is not quite the same as $\dot{u}$ and differs considerably from $\dot{u}$ at low frequencies; and the absolute acceleration of the mass, $\omega^2 u$, which is nearly the same as $\ddot{y}$. A plot of the maximum values (denoted D, $\bar{V}$, V, and Ag, respectively) as a function of the frequency of the system for a given type of input constitutes a response spectrum for the particular function. These quantities are defined as follows:

$$Ag = \left|\omega^2 D\right| = (2\pi f)^2 D$$

$$V = \left|\omega D\right| = 2\pi f D$$

[redacted]

[redacted]

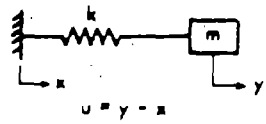

(a) SINGLE-DEGREE-OF-FREEDOM SYSTEM

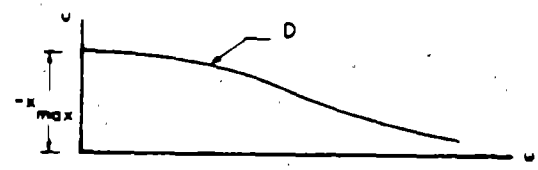

Displacement Spectrum

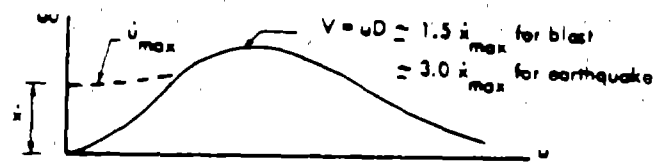

Velocity Spectrum

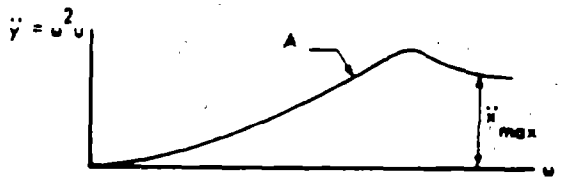

Acceleration Spectrum

(b) TYPICAL SPECTRA

Figure 2-89. [redacted] Single-Degree-of-Freedom System and Typical Response Spectra [redacted]

[redacted]

The maximum energy absorbed in the spring is associated with V. The quantity $\bar{V}$ is not particularly useful.

For inputs of the type associated with air-induced or direct-transmitted ground shock, the spectra for a simple system will have the characteristic appearances shown in Figure 2-89(b). The limiting conditions that apply to the spectra illustrated in Figure 2-89(b) are of particular interest. For example, as the frequency of the system approaches zero, the mass m does not move when the base of the system has a given motion applied. Then the relative displacement u is equal to the negative value of x, and the relative velocity $\dot{u}$ is equal to minus the maximum base velocity $\dot{x}$. The dotted line in Figure 2-89(b) indicates the difference between $\dot{u}_{max}$ and V that may be observed in the region of low frequencies; likewise, there is some difference between $\dot{u}_{max}$ and V at the high frequency end, but these differences are of a smaller order of magnitude. Typical values of V that might be expected for blast conditions are shown in Figure 2-89(b). An additional control is that as the frequency of the system becomes large, the displacement y approaches the displacement x, i.e., u approaches zero, and the acceleration $\ddot{y}_{max}$ approaches $\ddot{x}_{max}$. These controls are of special importance in arriving at design shock spectra.

Ordinarily, the input for ground motion consists of two parts, a systematic portion on which is superimposed a series of random oscillations. The magnitude of the peaks of the random components may be either small or large compared to the systematic portion. The random part may exist over the entire range of the systematic portion, over only part of the range, or even may be prior to the systematic portion.

For a random series of pulses, the relative velocity peak of the spectrum compared with the maximum input velocity can be high, but it is not likely to be much higher than about 3, unless an almost resonant condition is obtained with several pulses of alternate positive and negative signs of exactly the same shape and duration. Such a resonant condition for velocity is extremely unlikely from blast loading, although it has been observed in long duration earthquake phenomena. Even if, for some reason, partial resonance is achieved, the dampening in the system being excited will reduce the peaks considerably.

In general, the combined effect of the two input motions, systematic and random, depends on their individual effects. It can be shown that the combined spectrum will be either equal to or less than the sum of the absolute values of the spectra corresponding to the individual inputs. It also appears reasonable that the combined spectrum can be expected to be approximately equal to the square root of the sum of the squares of the individual spectra, point by point. In most practical cases of the type under consideration, the frequencies for which the spectrum values are important differ by a considerable amount, and the sums of the spectra or the square root of the sums of the squares are nearly the same as the maximum individual modal value.

2-66 Shock Spectra for Free Field Ground Motion

Using the concepts discussed above, it is possible to derive shock spectra that can be used in design to assess the relative effects in a structure (above or below ground) or the effects on equipment within a structure. Such spectra can be described best by the use of a logarithmic plot that permits values of displacement, pseudo-velocity, and acceleration to be read versus frequency in accordance with the relations given by the equations in paragraph 2-65.

In accordance with the limiting conditions discussed for Figure 2-89, the response spectrum can be represented by three regions, each region defined by a straight line constituting an envelope to the actual spectrum. An

example of such a spectrum for air-induced shock for conditions of 100 psi surface pressure, 5 Mt yield, and an acoustic velocity of 2,500 ft/sec is shown in Figure 2-90 for situations at the surface and at a depth of 100 ft. The left hand region, at the low frequency side, is influenced primarily by the maximum elastic transient displacement. The intermediate part of the spectrum (horizontal line) is a function of the maximum velocity reached in the free field. The right hand side depends on the maximum acceleration. In brief, the approximate response spectrum "envelope" is described by three straight lines (actually there are discrepancies that may be as high as a factor of 2 in some areas, but the actual ground motions are now known even this accurately, and the simplification of the spectrum in this way is permissible).

- A line D = constant, parallel to the displacement scales, drawn with a magnitude equal to the maximum ground displacement.
- A line V = constant, drawn with a magnitude of 1.5 times the maximum ground velocity.
- A line A = constant, parallel to the acceleration scales, drawn with a magnitude equal to twice the maximum ground acceleration.

Spectra may be sketched for horizontal and vertical motions at various depths and employed as appropriate. Detailed procedures for constructing more accurate spectra may be found in "Effect of Inelastic Behavior on the Response of Simple Systems to Earthquake Motions," A. S. Veletsos and N. M. Newmark, and "Response Spectra Approach to Behavior of Shock Isolation Systems," A. S. Veletsos and N. M. Newmark (see bibliography). In general, the air-induced and direct-transmitted ground motions, as well as the out-running ground motions, if applicable, are computed. The spectra of each are plotted, and the design is made according to the envelop of the spectra. If it is known that the motions will arrive at significantly different times, the design or analysis is only made for the worst case.

The response spectrum, such as that shown in Figure 2-90, may be used directly for elastic systems. If the frequency of equipment within a structure and its type and mode of support are known, it is possible to ascertain certain results in terms of the response of the system. For example, for a single-degree-of-freedom system, the number of gravities of acceleration corresponding to the natural frequencies may be considered as applied to the body to ascertain the dynamic stresses. For more complex systems, the analysis is more difficult, although consideration of the most significant mode will lead to useful estimates of dynamic loadings in many cases.

For purposes of comparison and interest, three shock spectra determined from reed gages or ground motion records in atomic field tests are shown in Figure 2-91. The Operation HARDTACK spectra exhibit high accelerations; this is likely to be the result of the high water table that tends to emphasize the high frequency end of the spectrum. The maximum velocity is much higher than would be expected in a typical soil site. The Operation PLUMBBOB data approximate the type of response that would be expected for more normal soil conditions.

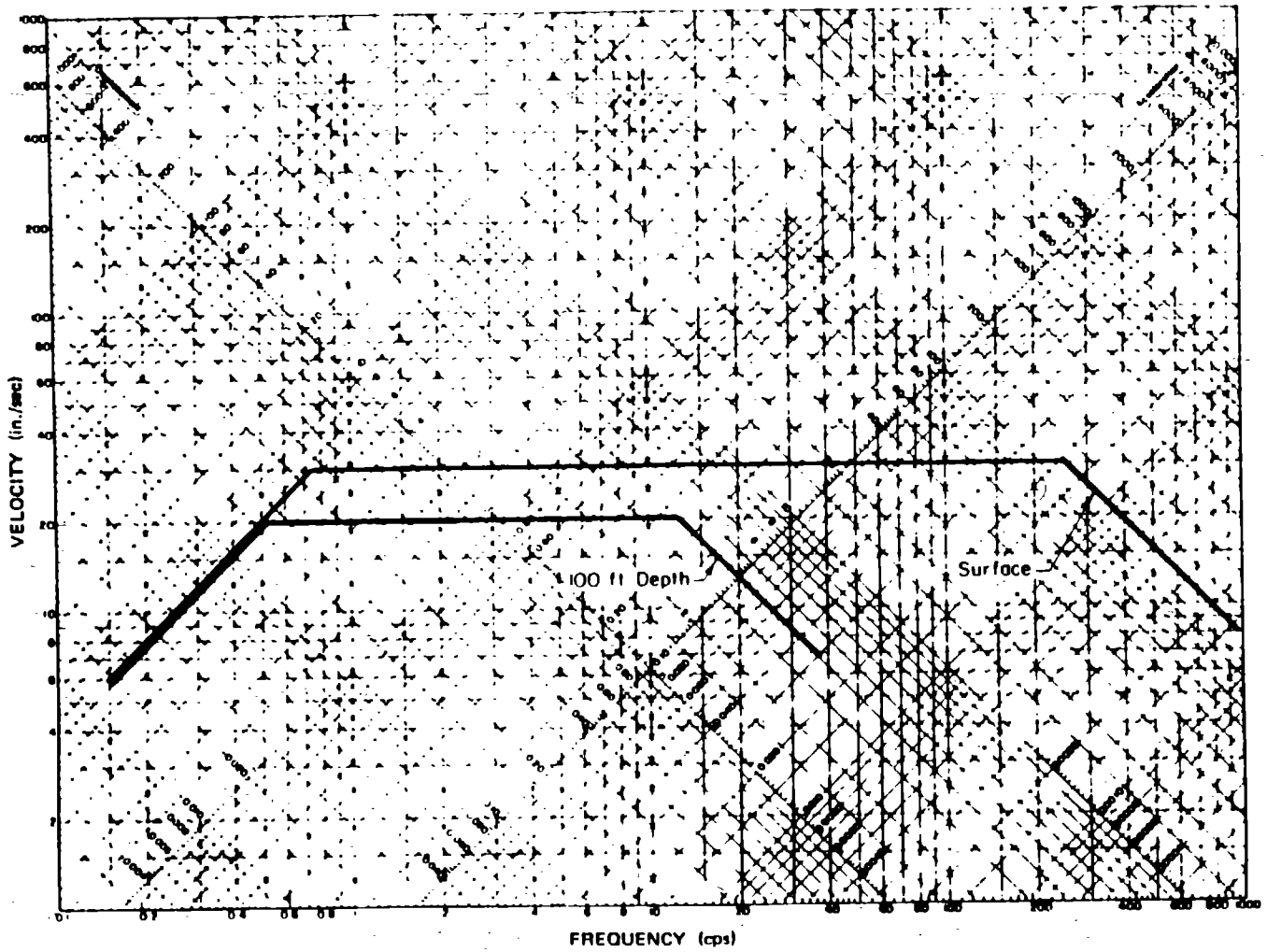

Figure 2-90. [redacted] Response Shock Spectra, 100 psi Overpressure, 5 Mt Yield, c = 2,500 fps (Vertical Motion – Air-Induced Effects) [redacted]

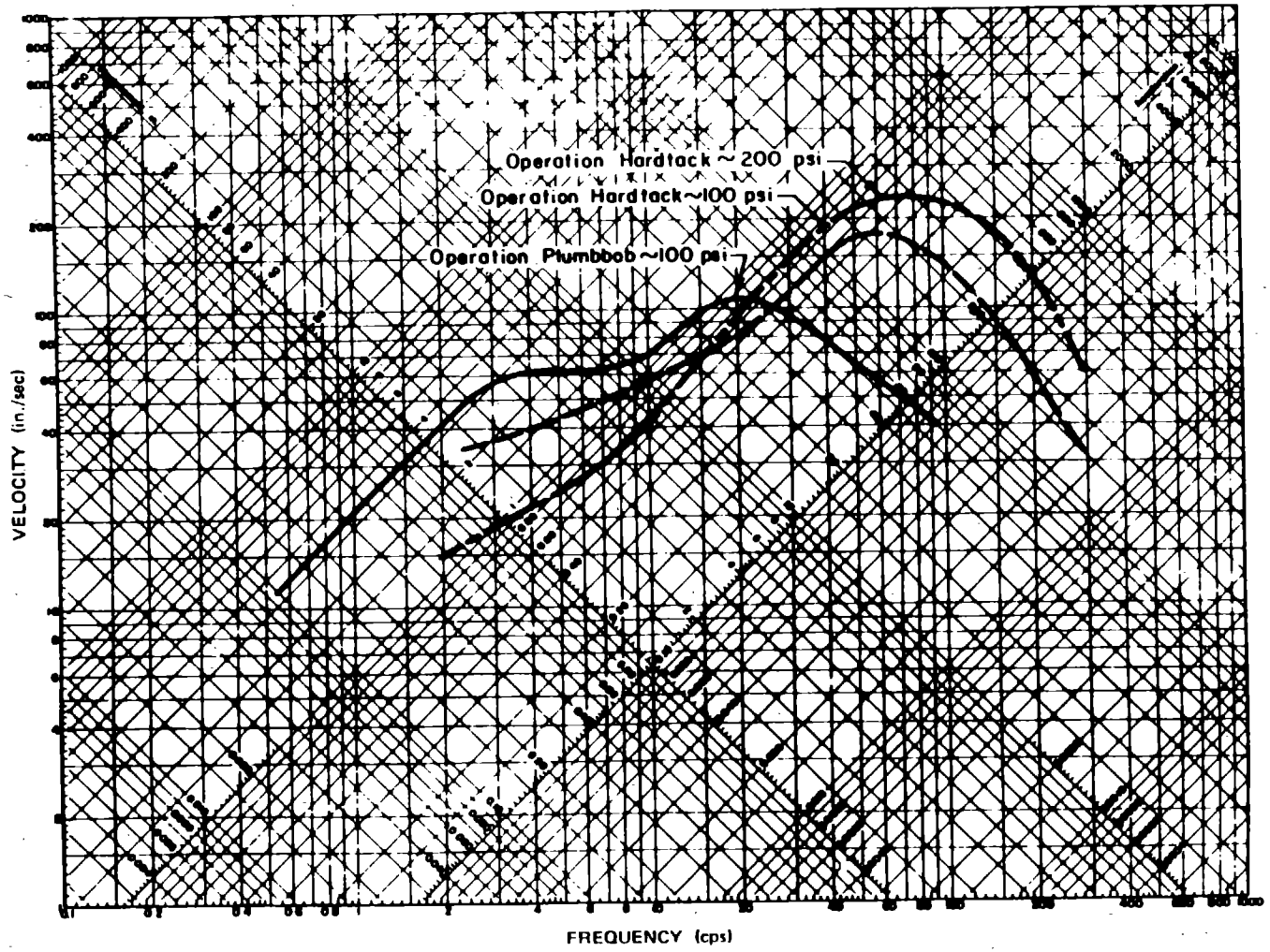

Figure 2-91. [redacted] Typical Shock Spectra from Field Tests – Surface Data [redacted]

[redacted]

Problem 2-27. Calculation of the Ground Motions from a Nuclear Explosion at the Surface

[redacted] The nature of the free field effects of ground motion are described in paragraphs 2-60 through 2-66. The attenuation factor α that is defined in paragraph 2-62 is used in the example presented below. As noted in paragraph 2-62, it generally is preferable to use the factor $1/\beta$ for attenuation, where β is described in Section II of Chapter 11, and more specifically in Figure 11-29. However, $1/\beta$ attenuation is not compatible with the equipment vulnerability curves in Figures 11-48 through 11-50. Therefore, the following example illustrates the use of the attenuation factor described in paragraph 2-62; use of the $1/\beta$ attenuation is illustrated in Problems 11-3 and 11-4.

[redacted] *Example* [redacted]

Given: A 1 Mt weapon burst on the surface of a medium that has a seismic velocity of 5,000 ft/sec.

Find: The vertical and horizontal displacement, velocity, and acceleration at a point 50 feet below the surface and at a ground distance of 1,500 feet from the explosion.

Solution: The equivalent distance for 1 kt is

$$d_1 = \frac{d}{\left(W(\text{kt})\right)^{1/3}} = \frac{1{,}500}{(1{,}000)^{1/3}} = 150 \text{ feet.}$$

From Figure 2-17, the overpressure at the surface is about 1,000 psi.

a. *Air Induced Motions:* The maximum elastic vertical displacement at the ground surface is given by the equation shown in paragraph 2-62:

$$d_{se} = 9\left(\frac{p_{so}}{100}\right)^{0.5}\left(\frac{1{,}000}{c_p}\right)\left(W(\text{Mt})\right)^{1/3}$$

$$= 9\left(\frac{1{,}000}{100}\right)^{0.5}\left(\frac{1{,}000}{5{,}000}\right)(1)^{1/3} = 5.7 \text{ inches.}$$

It is reasonable to assume that impulse is preserved in the stiff medium described in this case. Therefore, the vertical elastic displacement at a depth of 50 feet will be the same as that at the surface, i.e., 5.7 inches. As described in paragraph 2-62, the permanent displacement at a depth of 50 feet is

$$d_{yp} = \frac{p_{so} - 40}{30}\left(\frac{1{,}000}{c_p}\right)^2\left(\frac{100 - y^*}{100}\right)$$

$$= \left(\frac{1{,}000 - 40}{30}\right)\left(\frac{1{,}000}{5{,}000}\right)^2\left(\frac{100 - 50}{100}\right)$$

$$= 0.6 \text{ inches.}$$

Thus, from paragraph 2-62 the total vertical displacement is

$$d_y = d_{se} + d_{yp} = 5.7 + 0.6 = 6.3 \text{ inches.}$$

The peak vertical velocity given in paragraph 2-62 is:

$$v_y = \alpha v_s,$$

where

$$v_s = 50\left(\frac{p_{so}}{100}\right)\left(\frac{1{,}000}{c_p}\right),$$

$$\alpha = \frac{1}{1 + \frac{y}{H}},$$

[redacted]

[redacted]

[redacted]

and

$$H = 230 \left(\frac{100}{p_{so}}\right)^{0.5} \left(W(\mathrm{Mt})\right)^{1/3}.$$

This gives

$$H = (230) \left(\frac{100}{1{,}000}\right)^{0.5} (1)^{1/3} = 73$$

$$\alpha = \frac{1}{1 + \frac{50}{73}} = 0.59$$

$$v_s = 50 \left(\frac{1{,}000}{100}\right) \left(\frac{1{,}000}{5{,}000}\right) = 100 \text{ in./sec,}$$

$$v_y = (0.59)(100) = 59 \text{ in./sec.}$$

The vertical acceleration is given by the equation in paragraph 2-62 as:

$$a_y = 5 \left(\frac{p_{so}}{100}\right)\left(\frac{100}{y}\right) \alpha$$

$$= (5) \left(\frac{1{,}000}{100}\right) \left(\frac{100}{50}\right) (0.59) = 59 \text{ g.}$$

As described in paragraph 2-62, the horizontal values of the motions are taken to be 1/3, 2/3, and 1 times the vertical displacement, velocity and acceleration, respectively, i.e.,

$$d_x = 1/3\ d_y = \left(\frac{1}{3}\right) (6.3) = 2.1 \text{ inches,}$$

$$v_x = \frac{2}{3} v_y = \left(\frac{2}{3}\right) (59) = 39 \text{ in./sec,}$$

$$a_x = a_y = 59 \text{ g.}$$

b. *Direct Transmitted Motions:* The expressions given in paragraph 2-64 are applicable for direct transmitted motions. The radial motions are essentially horizontal for the distance and depth of this example. These are (note the distance is less than 2,500 ft/Mt$^{1/3}$):

$$d_r = 4 \left(W(\mathrm{Mt})\right)^{5/6} \left(\frac{1{,}000}{R}\right)^{1.5}$$

$$= (4)\ (1)^{5/6} \left(\frac{1{,}000}{1{,}500}\right)^{1.5} = 2.2 \text{ inches.}$$

$$v_r = 12 \left(W(\mathrm{Mt})\right)^{5/6} \left(\frac{1{,}000}{R}\right)^{2.5} \left(\frac{c_p}{1{,}000}\right)$$

$$= 12\ (1)^{5/6} \left(\frac{1{,}000}{1{,}500}\right)^{2.5} \left(\frac{5{,}000}{1{,}000}\right)$$

$$= 22 \text{ in./sec,}$$

$$a_r = 0.4 \left(W(\mathrm{Mt})\right)^{5/6} \left(\frac{1{,}000}{R}\right)^{3.5} \left(\frac{c_p}{1{,}000}\right)^2$$

$$= (0.4)\ (1)^{5/6} \left(\frac{1{,}000}{1{,}500}\right)^{3.5} \left(\frac{5{,}000}{1{,}000}\right)^2$$

$$= 2.4 \text{ g.}$$

In this case, the motions normal to the radial motions may be taken to be vertical. These are 1/3, 2/3, and 1 times the corresponding radial values of displacement, velocity and acceleration, i.e.,

$$d_y = \frac{1}{3} d_r = \left(\frac{1}{3}\right) (2.2) = 0.7 \text{ inches,}$$

$$v_y = \frac{2}{3} v_r = \left(\frac{2}{3}\right) (22) = 15 \text{ in./sec,}$$

$$a_y = a_r = 2.4 \text{ g.}$$

[redacted]

[redacted]

Answer: The peak values of both horizontal and vertical motions, for air-induced and direct-transmitted shocks are:

	d(in.)	v(in./sec)	a(g)
Vertical			
Air-induced	6.3	59	59
Direct-transmitted	0.7	15	2.4
Horizontal			
Air-induced	2.1	39	59
Direct-transmitted	2.2	22	2.4

In this particular example the air-induced motions, with the exception of the horizontal displacement, are the largest values for both the vertical and horizontal directions. In the horizontal direction, the direct-transmitted value of displacement is nearly equal to that of the air-induced value. In many cases, especially at short range and for stiff media, it will be found that the direct-transmitted motions will be the largest, and will control the analysis. From paragraph 2-66, the bounds for the shock response spectra are obtained by multiplying the controlling displacement, velocity, and acceleration values by 1, 1.5, and 2.0, respectively.

Vertical Response Spectrum Bounds:

$D = 1.0d = 6.3$ in.

$V = 1.5v = 89$ in./sec

$A = 2.0a = 118g$

Horizontal Response Spectrum Bounds:

$D = 1.0d = 2.2$ in.

$V = 1.5v = 59$ in./sec

$A = 2.0a = 118g$

These spectra bounds are shown in Figure 11-51. They show the response spectra for a single-degree-of-freedom system. These bounds are used in the analysis of the vulnerability of equipment mounted in an underground structure in Problem 11-8.

[redacted] *Related Material:* See paragraphs 2-24, 2-60 through 2-66, and Sections II and III of Chapter 11.

[redacted]

[redacted]

SECTION IV

[redacted] UNDERWATER EXPLOSION PHENOMENA [redacted]

[redacted] An underwater nuclear explosion is characterized initially by the formation and propagation of an underwater shock wave. The dissipation of heat at the shock front causes the water to vaporize in the vicinity of the explosion and results in the formation of a large bubble of steam. The interaction of the bubble and the shock wave with the air-water interface produces various surface phenomena, including spray domes, columns, plumes, base surges, radioactive pools and surface waves. If the explosion is on or near the bottom, a crater is formed.

[redacted] An underwater nuclear explosion also can result in thermal, nuclear, and electromagnetic radiation above the surface, but these phenomena are insignificant, except in the case of a shallow burst. These phenomena, when caused by a shallow burst, should approximate those from a shallow underground explosion.

2-67 Underwater Bubble [redacted]

[redacted] An underwater nuclear explosion releases large amounts of thermal and nuclear radiation, essentially all of which is absorbed by the surrounding water within several feet of the explosion (some radiation in the visible spectrum can be radiated to greater distances, depending on the transparency of the water).

[redacted] During the early stages of the explosion, the warhead materials attain a very high temperature (tens of millions of degrees) and a very high pressure (on the order of millions of atmospheres). Energy acquired by these materials is transferred to the layer of water nearest the bomb, which is heated and compressed and which, then, heats and compresses the next outward layer. A compression wave (or hydrodynamic shock front) is formed by this mechanism, and this wave moves outward from the explosion at a speed greater than that of sound. This shock front expands faster than the material that it engulfs, which also moves outward, but at a slower rate.

[redacted] As the shock front moves away from the point of explosion, energy is dissipated as heat, which raises the temperature of the water engulfed by the shock front. The largest temperature increase occurs near the center of the explosion, where the water is not only vaporized but dissociated as well. At greater distances, the water is vaporized and turned to steam at the shock front. At still greater distances, the water is not heated by the shock front sufficiently to boil. The bubble that is formed does not have a clearly defined "surface." Figure 2-92 shows this progression in a highly stylized form.

[redacted] Thus, shortly after an underwater burst an expanding bubble is formed, which is composed largely of vaporized water with radioactive bomb debris at its center, surrounded by heated water. Large quantities of neutron-activated elements in the sea water are also present in the steam and layer of surrounding water; however, the total induced radioactivity is relatively small compared to the fission product radioactivity. Continued expansion of this bubble reduces the pressure within it. As the bubble pressure falls below the vapor pressure of the heated water, additional water flashes to steam at the interface of the bubble and the water.

[redacted] If the explosion is deep underwater, the bubble continues to expand at a decreasing rate until a maximum size is reached. If it is not too near the surface or the bottom, the bubble remains nearly spherical to this point. As a result of the inertia of the water surrounding the expanding bubble, the bubble actually overexpands, i.e., when it attains its maximum size, its pressure is below the ambient water pressure. The high pressure around the bubble then causes it to contract with an increase in its pressure and

[redacted]

[redacted]

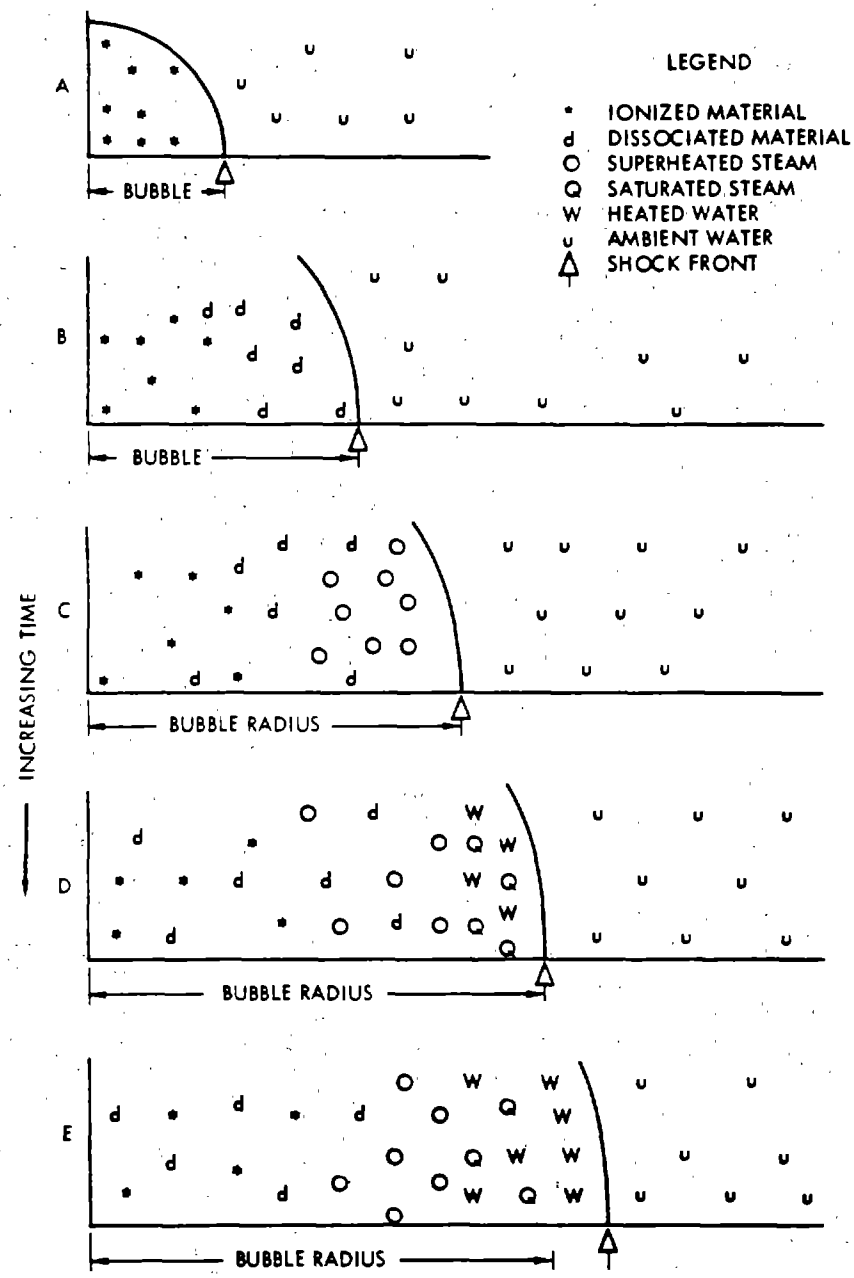

Figure 2-92. [redacted] Representation of Bubble Development [redacted]

[redacted]

[redacted]

[redacted] condensation of some of its steam. Since the hydrostatic pressure is larger at the bottom of the bubble than at the top, the bubble does not remain spherical during the contracting phase. The bottom moves upward faster than the top (which may even remain stationary) and contacts the top to form a toroidal, or doughnut-shaped, bubble as viewed from above. This causes turbulence and mixing of the bubble contents with the surrounding water.

[redacted] The inertia of the water set in motion by the bubble contraction causes it to overcontract, and its internal pressure becomes very much higher than the ambient water pressure. A second compression wave (the first bubble pulse) commences when the bubble reaches its minimum volume. This wave has a lower peak pressure, but a longer duration, than the initial shock. A second cycle of bubble expansion and contraction begins.

[redacted] When the bubble pulse is emitted, the bubble surface becomes exceedingly unstable; a multitude of water spray jets shoot inward, thereby condensing much of the steam and degrading the bubble energy. Figure 2-93 shows the relative partitioning of the energy of the explosion with time qualitatively.

[redacted] The bubble is relatively stationary during the initial expansion cycle, but upon contracting, it begins to migrate upward under the action of buoyant forces. The rate of upward migration is greatest when it is contracted and nearly zero when it is expanded.

[redacted] If the bubble is far enough below the surface, it continues to pulsate and rise, though after three complete cycles enough steam will have condensed to make additional pulsations unlikely. During the pulsation and upward motion of the bubble, the water surrounding the bubble acquires considerable upward momentum and eventually breaks through the surface with a high velocity (about 200 mph for Wigwam, a deep underwater shot) thereby creating a large plume.

[redacted] If the explosion is at a shallow depth, the bubble may break through the surface during one of the early pulsations, or even during the first pulsation cycle. If such a breakthrough occurs when the bubble pressure is higher than ambient (as with a very shallow explosion), a phenomenon known as a "blowout" occurs. If a breakthrough occurs when bubble pressure is below ambient, "blowin" occurs. The surface effects differ markedly for the two phenomena (see Figures 2-100 and 2-101 and accompanying text). A migrating bubble will not produce a bubble pulse if the bubble minimum occurs at or above the original water surface.

[redacted] A strongly migrating bubble might continue to expand and not pass through a maximum size, somewhat like a balloon rising through the atmosphere. This is the balloon effect. A bubble migrating in this manner will not emit any bubble pulses. The conditions that cause a nuclear bubble to balloon rather than to pulsate are still subject to speculation; however, the absence of an expected bubble pulse might be explained by the balloon effect.

[redacted] The maximum bubble radius and the first bubble period (time between burst and first minimum) are related to yield and depth of burst, as illustrated by the following two equations, which pertain to submerged bursts, i.e., the depth of burst, d_b is greater than A_{max}:

$$A_{max} = J' \frac{W^{1/3}}{Z^{1/3}},$$

$$T_1 = K' \frac{W^{1/3}}{Z^{5/6}},$$

where

A_{max} = Maximum bubble radius (ft),

[redacted]

[redacted]

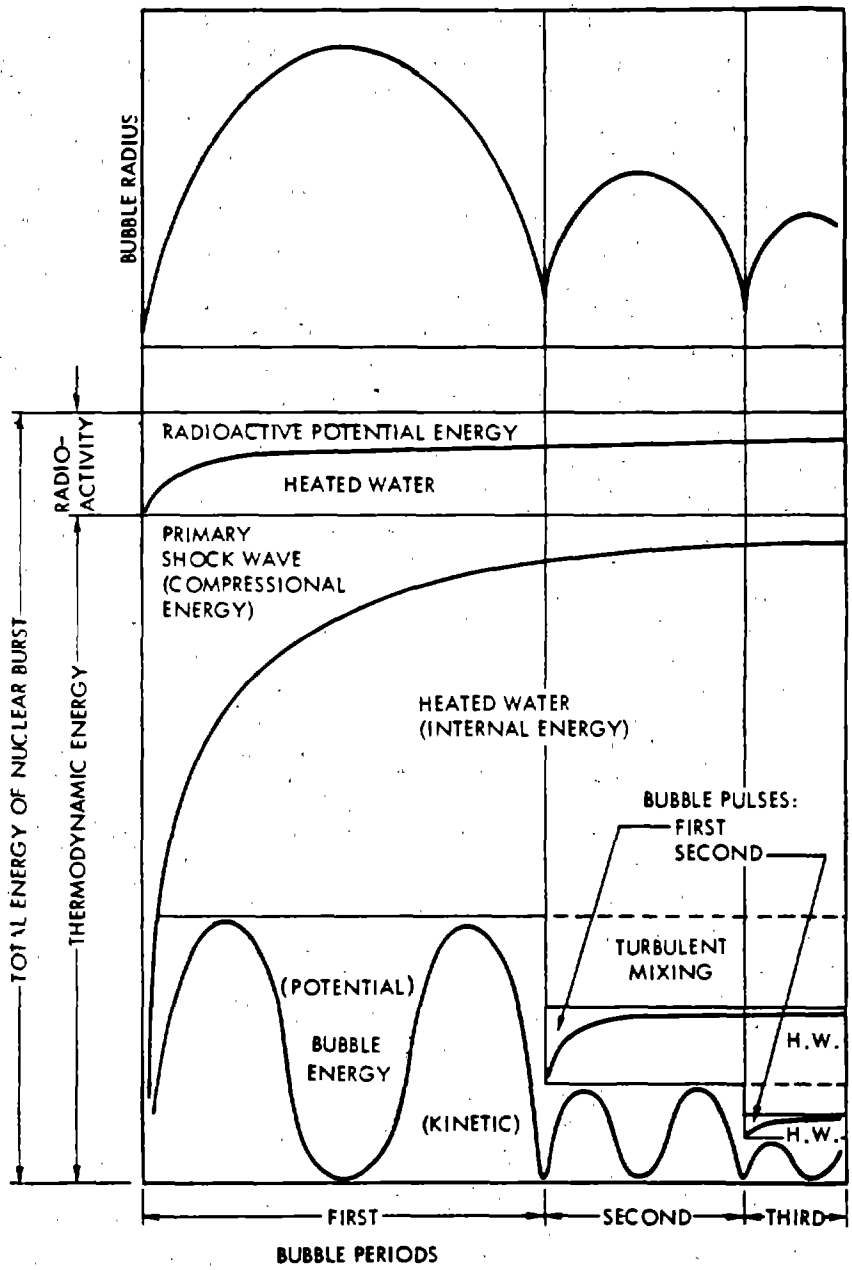

Figure 2-93. [redacted] Energy Distribution Following an Underwater Nuclear Burst [redacted]

[redacted]

[redacted]

[redacted]

J' = Empirical constant, 1500,

K' = Empirical constant, 515,

T_1 = First bubble period (sec),

W = Yield (kt),

Z = Hydrostatic head (d_b + 33) (ft).

The form of the equations is the same as those given by Cole for high explosives. The constants, J' and K', are slightly different because an underwater nuclear burst forms a steam bubble rather than gas bubble (as do high explosives) and because of other differences, mainly the distribution of total energy between bubble energy, shock wave energy, and residual radioactive energy.

[redacted] It is likely that the constants J' and K' are actually somewhat dependent on depth. This can be understood qualitatively as follows: J' and K' implicitly include the fraction of explosion energy included in the bubble. As the depth of burst is increased, a smaller fraction of explosion energy is converted to steam by the expanding shock wave (and more energy goes into heating water) because of the greater hydrostatic pressure that must be overcome to boil water.

[redacted] The second and third bubble maximum radii, the periods between minima, and the migration between periods, depend on the fraction of bubble energy that remains following succeeding bubble minima. The energy loss that occurs is due primarily to steam condensation at bubble minima as previously described, but the amount of energy loss is influenced by the depth at which the minimum occurs. An analytical representation of the energy as a function of bubble migration, which is best solved by use of a high-speed computer, has been developed,* however, satisfactory solutions to bubble problems can be obtained by use of curves derived from the representation, as illustrated in Problem 2-28.

[redacted] WATER SHOCK WAVE AND OTHER PRESSURE PULSES [redacted]

[redacted] The initial shock wave from an underwater explosion propagates radially from the source. This shock wave is characterized by an abrupt, virtually instantaneous, increase in pressure followed by a decrease that is approximately exponential. Near the explosion, the peak shock wave pressure is extremely high, but energy losses to the water cause the pressure to decrease somewhat faster than inversely with radius. Similarly, early shock wave propagation velocities are high, but by the time the peak pressure falls to about 3,000 psi, the propagation velocity becomes nearly equal to the acoustic speed in water (about 5,000 ft/sec), and the energy losses become small.

[redacted] If an explosion takes place far from either the surface or the bottom, the shock wave remains spherical as long as it propagates into water having constant acoustic velocity. This velocity depends on temperature, hydrostatic pressure, and salinity, however, and in regions of the ocean in which significant sound velocity gradients exist, the shock wave can be bent or refracted. Refraction can either increase or decrease the shock wave pressures locally, depending on ambient water conditions. No general prediction techniques can be given, but the subject is discussed further in paragraph 2-71.

[redacted] When a shock wave moving in water encounters another medium, it may be reflected as a tensile or rarefaction wave, as in the case of a water-air boundary; a compression or shock wave, as in the case of a water-bottom interface if the angle of incidence is not too far from the normal; or a distorted pulse having in general

* [redacted] This expression is described in "The Parameters of Underwater Nuclear Explosion Bubbles" (see bibliography).

[redacted]

[redacted]

both a positive and a negative phase, as in the case of more glancing incidence at the bottom. These are discussed separately in the following paragraphs.

2-68 Surface Reflection [redacted]

[redacted] The rarefaction wave, generated by the reflection of the primary shock wave from the surface, propagates downward and relieves the pressure behind the primary shock wave. If the shock wave is treated as a weak (acoustic) wave, this interaction instantaneously decreases the pressure in the primary shock wave to a value that might be well below the vapor pressure of the water, as shown by the broken line in Figure 2-94, Point A. Cavitation occurs in seawater when its pressure decreases to a value somewhat below its vapor pressure. The pressure of the primary shock wave is, therefore, reduced to a value which, when compared with the peak pressure, is usually so close to ambient water pressure that the shock wave pulse appears to have been truncated, i.e., reduced to ambient pressure.

[redacted] For a strong primary shock wave, the reflected rarefaction wave propagates into water that has already been set in motion by the shock wave. Therefore, the rarefaction wave arrives earlier than predicted from the acoustic approximation, and the pressure cutoff is not instantaneous. This effect typically gives a pulse shape shown by the solid line for Point A of Figure 2-94. The shallower the point at which pressure measurements are made, the sooner the primary shock pulse is "cut off" and, hence, the shorter its duration (see Figure 2-94, Point B). At sufficiently shallow locations, the rarefaction wave interacts with the shock front and reduces the peak pressure (see Figure 2-94, Points C and D). The region in which peak pressure is reduced is known as the "anomalous region."

[redacted] The effects of surface reflection decrease rapidly with increased depth of either the explosion or the point of measurement. Conversely, as the depth of burst is decreased (or the yield increased for a given depth of burst), the effects increase. The size of the anomalous region increases with decreased depth of burst until, for a surface burst, the anomalous region ~~increases~~ includes all points beneath the water surface except those close to the explosion and directly under it.

[redacted] A limited amount of data are available concerning the reflection of shock waves from an ice layer. To date all tests have been with relatively small explosive charges (a majority of the test shots have been in the 1- to 40-lb range, with one shot of 630 lb). The situation is complicated by reflection and refractions at both the water-ice boundary and the ice-air boundary.

2-69 Bottom Reflection [redacted]

[redacted] Under certain circumstances, the shock wave from the bottom can be more damaging to surface ships and shallow submarines than the primary shock. Although the peak pressure of the reflected wave is usually smaller, the wave arrives at a steeper angle, and therefore may induce more damaging shock motion to a target at or near the surface.

2-70 Secondary Shocks and Pressure Waves [redacted]

[redacted] An underwater burst can cause compression waves in addition to those described above, but these effects are usually negligible. These waves include retransmitted pulses, cavitation pulses, bubble pulses, and others that are described briefly below.

- *Retransmitted Pulses.* Upon reflecting from the surface and bottom, some primary shock energy is transmitted into the air or bottom material, and some of this energy can be retransmitted back into the water.
- *Cavitation Effects.* As noted earlier, the reflection of the shock wave from the sur-

[redacted]

[redacted]

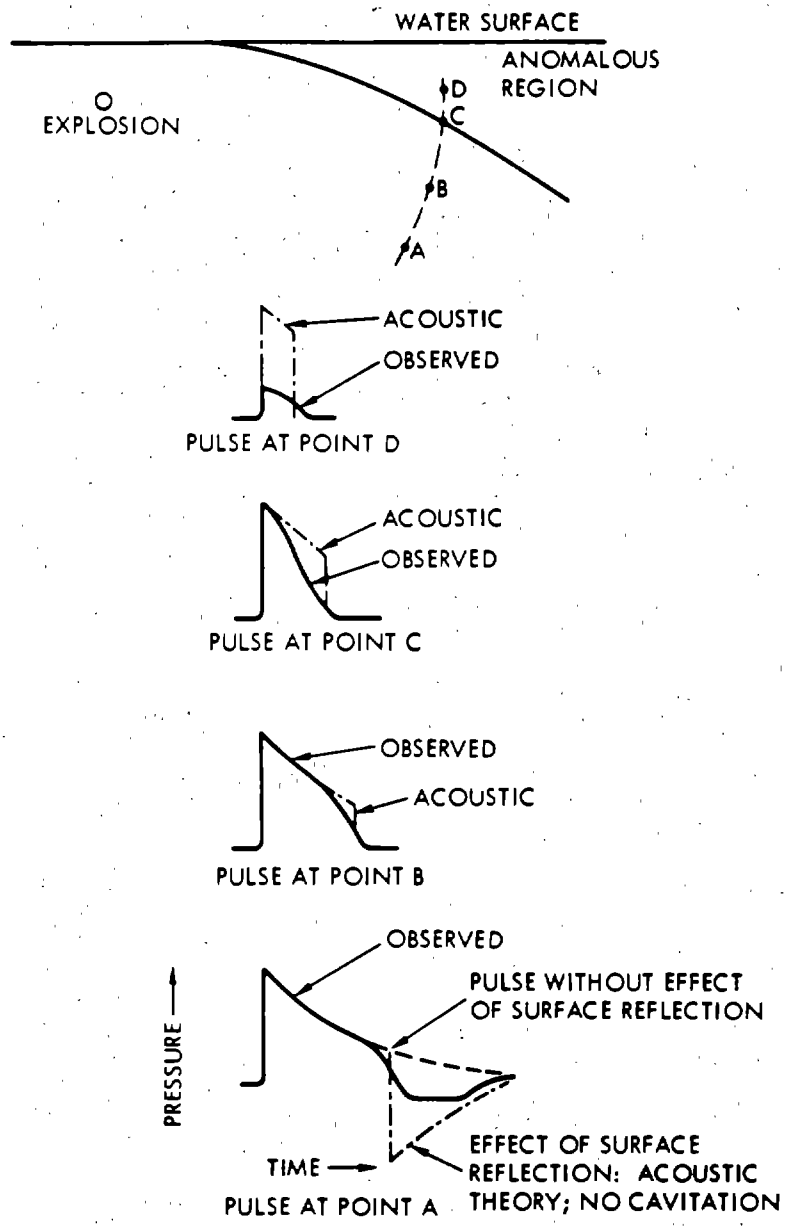

Figure 2-94. [redacted] Typical Pressure Pulses Affected by Surface Reflection [redacted]

[redacted]

[redacted]

face can lead to bulk cavitation below the surface. During the period of cavitation, the cavitated region can absorb further shock waves impinging on it. In the formation of the cavitation region, the rupture of the water by the shock wave causes a liquid surface layer (sometimes called "spall") to project upward in almost a ballistic trajectory. The impact of this spall when it returns to the surface can lead to further secondary shock waves. These shock waves account for the occasional larger damage to ships at intermediate ranges compared with the damage at shorter or longer ranges.

- *Bubble Pulses.* If an explosion is deep enough for one or more bubble pulsations to occur, compression waves are generated at the time of each bubble minimum.
- *Other Pulses.* All pressure waves are subject to multiple reflection from the surface and bottom. Also, in areas of irregular bottom topography, more than one reflected pulse can be generated.

Figure 2-95 shows typical shock wave and pressure pulse patterns for various burst and measurement conditions.

2-71 Refraction of Shock Waves

The shock front from an explosion far from a boundary (surface, bottom, etc.) remains spherical provided that it expands into water having constant acoustic velocity (isovelocity). However, the acoustic velocity in water depends on the temperature, salinity, and hydrostatic pressure, and these properties are not necessarily constant throughout a large body of water. As a result of variations in these properties, generally in horizontal layers, a region of water can have a characteristic acoustic velocity profile (sound velocity vs depth). Under such conditions, the shock wave is bent (refracted) because one part of the wave moves faster than another.

Refraction of the shock wave can result in convergence and reinforcement of the shock wave. This reinforcement commonly occurs along a surface called a "caustic." This effect may be illustrated by the use of a ray diagram* (Figure 2-96). The acoustic velocity profile that corresponds to the ray diagram is also shown in the figure. The formation of several caustics for one burst is observed frequently. Regions of relatively low pressure also occur, such as the "shadow zone" above the caustic in the figure.

The caustic can reinforce the peak pressure by a factor of five or more over the isovelocity value, while the pressure observed deep in the shadow zone can be essentially negligible. Shock wave impulse amplification factors do not go through a maximum at the caustic position. They remain much closer to unity than do peak pressure and energy factors.

As a result of ocean currents and underwater swells, the acoustic velocity profile in the ocean is rarely stable. Thus, the location of the caustics can shift rather quickly and unpredictably (similar to optic mirages).

Common types of sound velocity profiles can give rise to caustics at various distances greater than about one mile. In particular, in about half of the areas of the oceans, a caustic occurs at what is known as the convergence zone, typically 30 (10 to 40) miles from an underwater burst. Therefore, it is conceivable that a submarine might suffer damage from its own multi-kiloton weapon detonated at a distance of about 30 miles if it happened to lie on the caustic of its shot.

In Figure 2-96, sound speed is considered to vary with depth only. Actually this would rarely happen. The velocity can vary considerably across the ocean within the range of interest. Generally, the region of focusing is sharper

* A ray is generated by a curve that is always perpendicular to the expanding shock front.

[redacted]

[redacted]

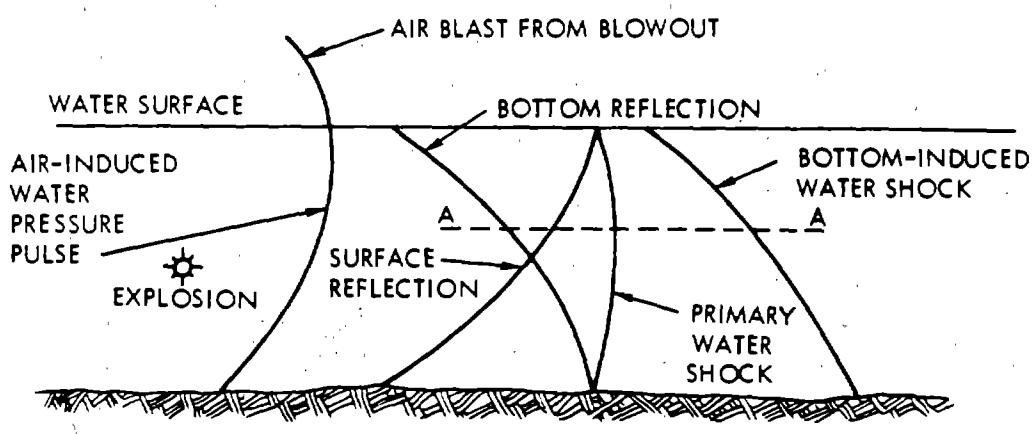

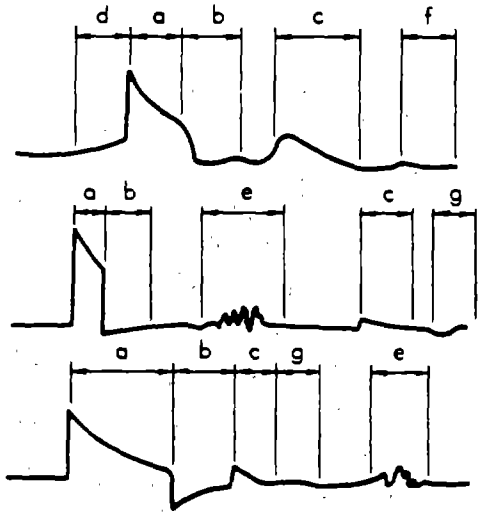

1. SHALLOW EXPLOSION IN SHALLOW WATER MEASUREMENT IN SHALLOW WATER
2. DEEP EXPLOSION IN MUCH DEEPER WATER MEASUREMENT AT SHALLOW DEPTH
3. DEEP EXPLOSION IN MUCH DEEPER WATER MEASUREMENT AT DEEP DEPTH

a. PRIMARY SHOCK WAVE
b. SURFACE REFLECTION
c. BOTTOM REFLECTION
d. BOTTOM-INDUCED PRESSURE PULSE
e. SHOCK FROM CAVITATION COLLAPSE
f. AIR-INDUCED WATER SHOCK
g. OTHER

Figure 2-95. [redacted] Typical Shock Wave Patterns Along Line A-A [redacted]

[redacted]

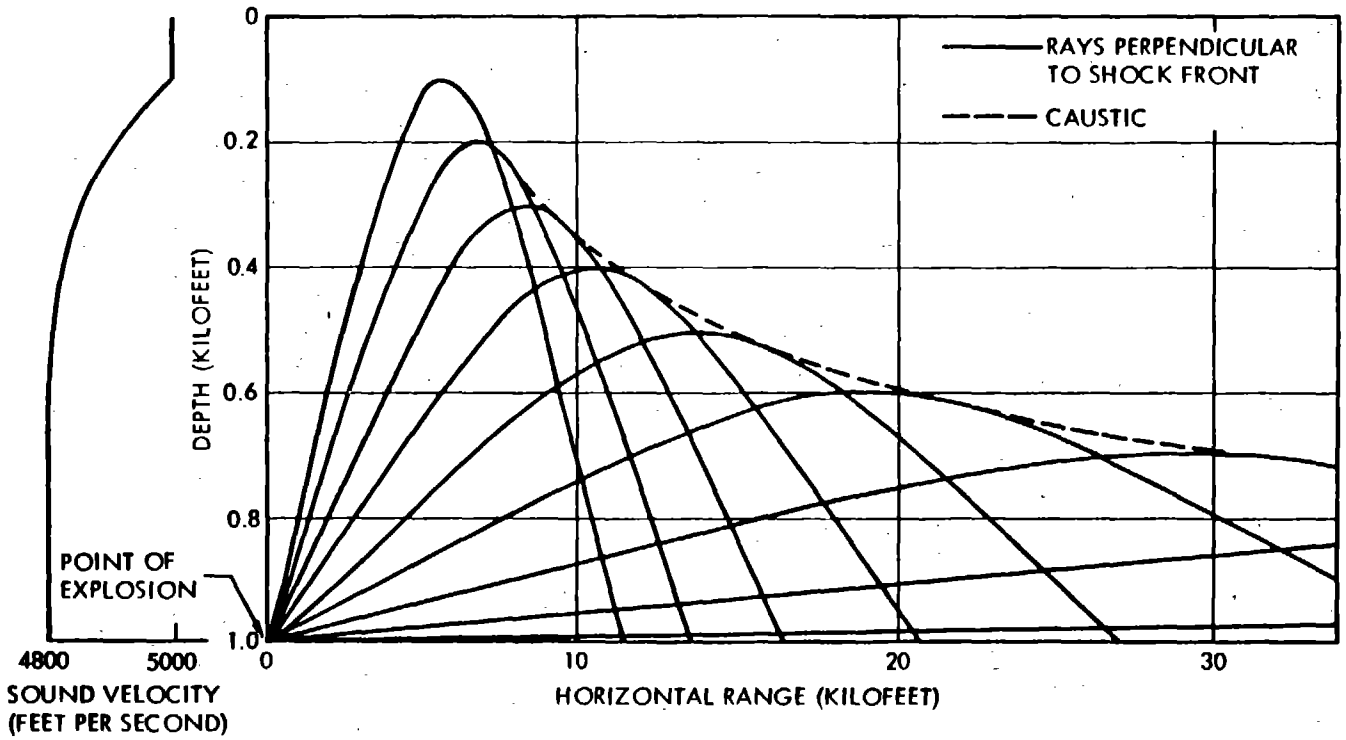

Figure 2-96. Ray Diagram for an Idealized Velocity Profile

[redacted]

and the maximum value of the amplification is greater for smaller yields.

2-72 Air Blast [redacted]

[redacted] The air blast wave has one to three pulses of various amplitudes, depending on the burst depth and the location of the observation point with reference to surface zero. These pulses are generated by two underwater explosion mechanisms. One is the underwater shock wave that transmits a portion of its energy across the water-air interface. The other is the underwater explosion bubble, which manifests itself in two ways: for burst depths shallower than about $35W^{1/3}$ feet, the bubble vents, causing an air pressure pulse; for burst depths deeper than $35W^{1/3}$ feet, a spray dome is pushed up by the expanding bubble, causing a bow wave.

[redacted] For burst depths shallower than about $50W^{1/3}$ feet the transmitted pulse and the bubble generated pulse are formed almost simultaneously, resulting in a single intense pressure pulse over surface zero. For burst depths between $50W^{1/3}$ feet and about $150W^{1/3}$ feet, up to three pulses can be seen. The transmitted shock in air bifurcates near surface zero to form two air pulses, and the bow shock causes the third air pulse. For burst depths deeper than about $150W^{1/3}$ feet, the spray dome rises so slowly that no bow shock is formed and only the air pulse from the transmitted shock is important.

[redacted] This discussion of the generation of air blast from underwater bursts is a simplified discussion of a complex subject. Much analytical, theoretical, and experimental work has been done to understand the physics of air blast generation. More complete discussions of the subject are given in Malme, Carbonell and Dyer (1966); Peckham and Pittman (1968); Pittman (1968); and Rudlin and Silva (1960) (see bibliography). Only a limited number of air blast measurements are available from nuclear weapon tests. The data are not sufficient to form a basis for predicting air blast for a spectrum of burst depths and pressure levels. The available predictive measures are based mainly on high explosive tests as described in Problem 2-31.

[redacted] SURFACE EFFECTS OTHER THAN WAVES [redacted]

[redacted] The first surface effect of an underwater burst is caused by the intersection of the primary shock wave and the surface. Viewed from above, the effect frequently appears to be a rapidly expanding ring of darkened water, often called the "slick" (Figure 2-97). A white circular patch (the "crack") follows closely behind the darkened region. The crack probably is caused by underwater cavitation produced by the reflected rarefaction wave. Shortly after appearance of the crack, the water above the explosion rises vertically and forms a white mound of spray, called the "spray dome" (Figure 2-98). This dome is caused by the velocity imparted to the water near the surface by the reflection of the shock wave and the subsequent breakup of the surface layer into drops of spray. Additional slick, crack, and spray dome phenomena may result if the bottom-reflected shock waves and bubble-pulse compression waves reach the surface with sufficient intensity (Figure 2-99).

[redacted] The spray dome from a shallow burst changes rapidly to a shallow column formed by the upward and outward motion of the water surrounding the explosion bubble. If blowout occurs, the upper part of the column is likely to resemble a crown, which contains explosion products blown out of the column (Figure 2-100). If blowin occurs, the crown is likely to be absent (Figure 2-101a). In its later stages, the column may break up into column jets (relatively broad spouts of water that disintegrate into spray as they travel through the air) (Figure 2-101b).

[redacted] If the burst is sufficiently deep to prevent blowout, but shallow enough for the bubble to continue to oscillate as it approaches the

[redacted]

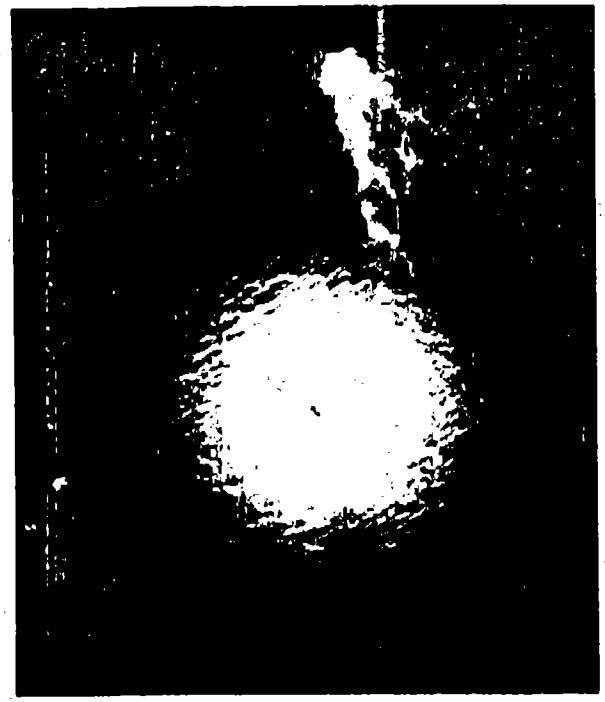

(a) PRIMARY SHOCK WAVE
Slick and Spray Dome
(0.28 sec after burst)

(b) CAVITATION PULSE
Slick and Spray Ring
(0.73 sec after burst)

Figure 2-97. [redacted] Slick Spray Dome and Cavitation Pulse Spray Ring (aerial view) [redacted]

Reproduced from best available copy.

[redacted]

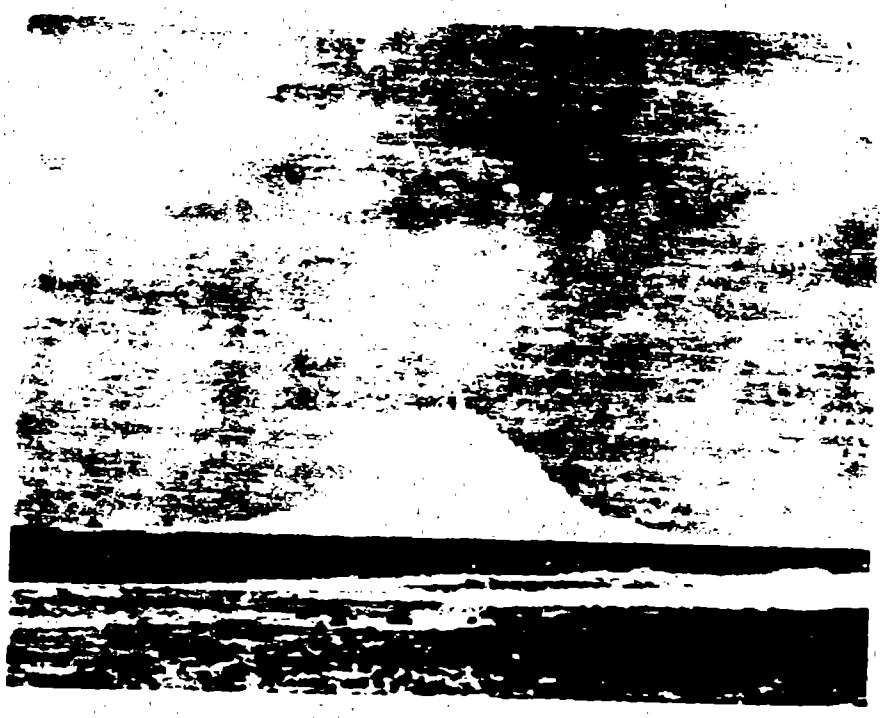

Figure 2-98. [redacted] Spray Dome (3.3 sec after burst) [redacted]

[redacted]

Reproduced from best available copy.

[redacted]

Figure 2-99. [redacted] Bottom-Reflected Shock Wave Slick
(aerial view 1.38 sec after burst) [redacted]

[redacted]

Reproduced from
best available copy.

[redacted]

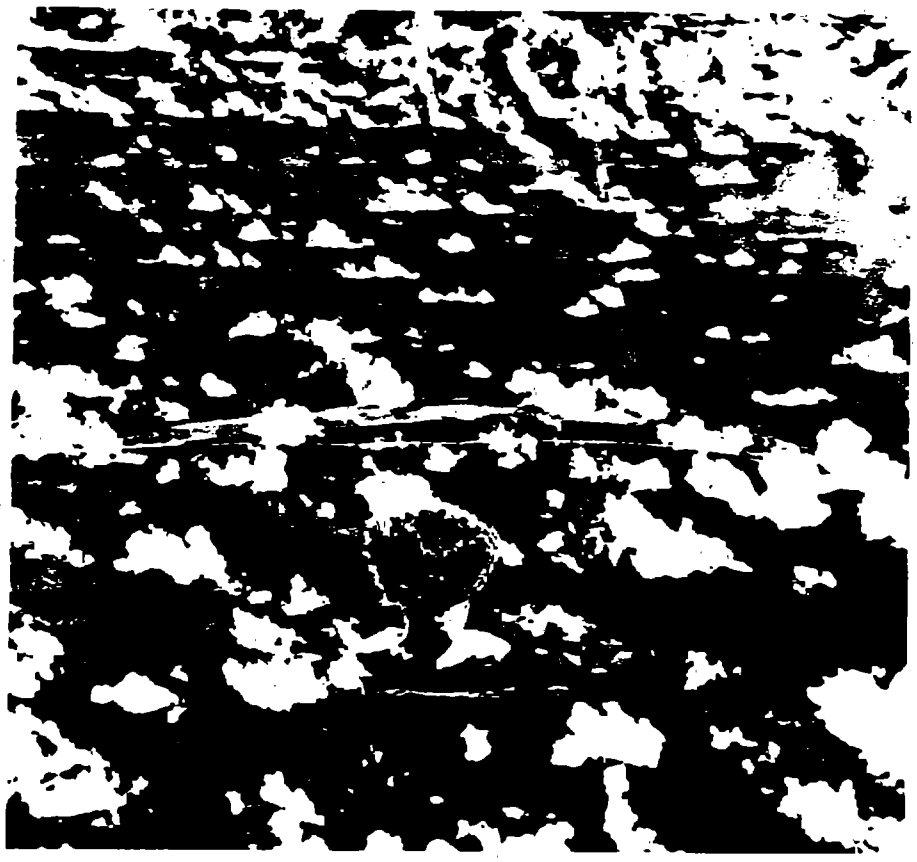

Figure 2-100. [redacted] Very Shallow Burst Showing Crown of Explosion Products on Column (oblique aerial view 0.7 sec after burst) [redacted]

[redacted]

Reproduced from best available copy.

Reproduced from best available copy.

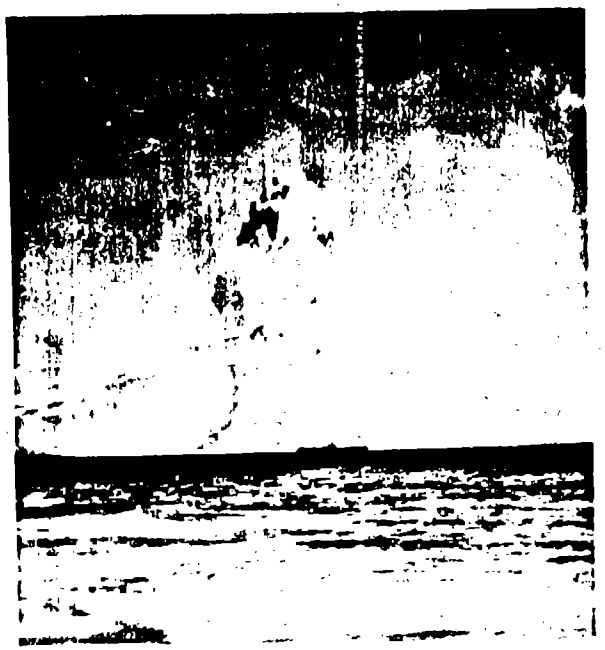

(a) EARLY STAGE
(2.5 sec after burst)

(b) LATER STAGE SHOWING COLUMN JETS
(8.2 sec after burst)

Figure 2-101. [redacted] Column from Shallow Underwater Burst (no blowout) [redacted]

[redacted]

surface, plumes of upwelled water and steam can occur (Figure 2-102).

[redacted] Upon subsidence of the column and plumes from an underwater explosion, a "doughnut-shaped ring" of mist is formed, which is called the base surge and which is highly radioactive (Figure 2-103). This ring, or series of rings, expands radially in the absence of wind, but in the presence of wind, it elongates and drifts with the wind until it dissipates. A train of surface waves also expands radially from the explosion.

[redacted] After dissipation of the base surge, the water surface around the explosion appears white (Figure 2-104). This "foam-patch" results from the upward motion of water and gaseous explosion products in the vicinity of the bubble, their spreading over the surface of the patch, and their downward motion at the edge of the patch. During its later stages, the foam-patch appears as a ring of foam and debris that is left floating where the water circulates downward.

[redacted] As previously noted, the surface phenomena described above vary with the weapon yield and the depth of burst. Although clear-cut distinctions cannot be made in all cases, six explosion categories have been established to aid in establishing safe weapon delivery criteria. These categories are defined in Table 2-8. The classifications have been tested at yields as large as 30 kt, but they probably are valid for yields up to about 100 kt.

[redacted] The limits of the relations given in Table 2-8 are plotted in Figure 2-105, and the phenomena that establish the categories are described below.

- *Near-surface bursts.* The layer of water above the burst is vaporized by the explosion. The surface phenomena for this type of burst and the associated hazards are unknown. The radiological hazard of the base surge is considered to be unimportant compared with air blast and fallout hazards.
- *Very shallow bursts.* The bubble vents early during the first expansion cycle, i.e., when the bubble pressure is greater than ambient, and fission products are blown out at that time.
- *Shallow bursts.* The bubble vents late during the first cycle, after the bubble pressure has dropped below ambient, and fission products are blown in.
- *Deep bursts.* The depth of burst is equal to or greater than the radius of the fully expanded bubble, but not as deep as the very deep burst described below.
- *Very deep burst.* The explosion is at sufficient depth that the bubble breaks up, becomes a vortex ring, or loses its identity before reaching the surface.

[redacted] The surface radioactivity from a very deep burst is operationally insignificant within about an hour and may be faint enough to escape detection.

Table 2-8. [redacted] Classification of Burst Depth Categories [redacted]

Classification	Definition
Near surface	$0 < d_b < 21W^{1/3}$
Very shallow	$21W^{1/3} < d_b < 75W^{1/3}$
Shallow	$75W^{1/3} < d_b < 240W^{1/4}$
Deep	$240W^{1/4} < d_b < 700W^{1/4}$
Very deep	$700W^{1/4} < d_b$
Contained*	$1550W^{1/4} < d_b$
No spray dome*	$2500W^{1/3} < d_b$

*[redacted] These values are derived from H.E. tests. They have not been confirmed by nuclear tests; therefore, they are to be interpreted as "containment *possible*" and "*possible* limiting depth for spray dome formation."

[redacted]

[redacted]

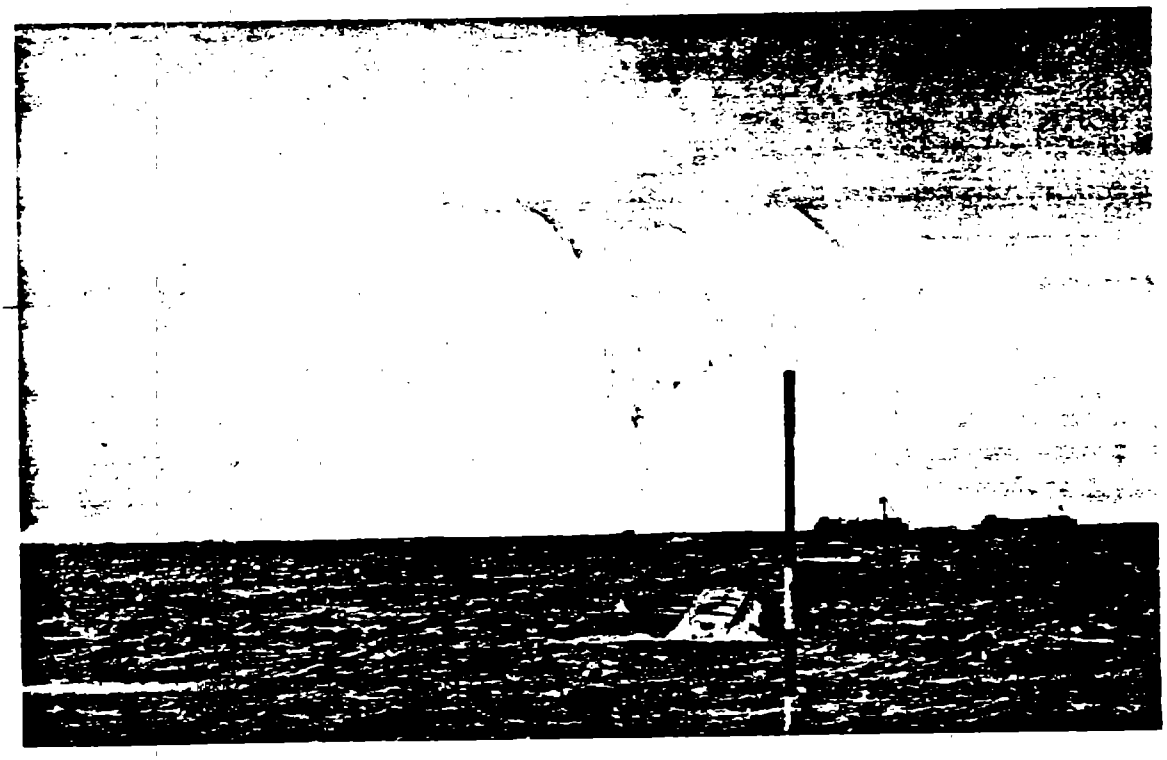

Figure 2-102. [redacted] Plume from Upwelling of Water from Very Deep Burst (24 sec after burst) [redacted]

[redacted]

Reproduced from best available copy.

Figure 2-103. [redacted] Base Surge "Doughnut-Shaped" Ring (oblique aerial view 100 sec after burst) [redacted]

Reproduced from best available copy.

[redacted]

Figure 2-104. [redacted] Foam Patch (oblique aerial view 6.3 min after burst) [redacted]

[redacted]

Reproduced from best available copy.

[redacted]

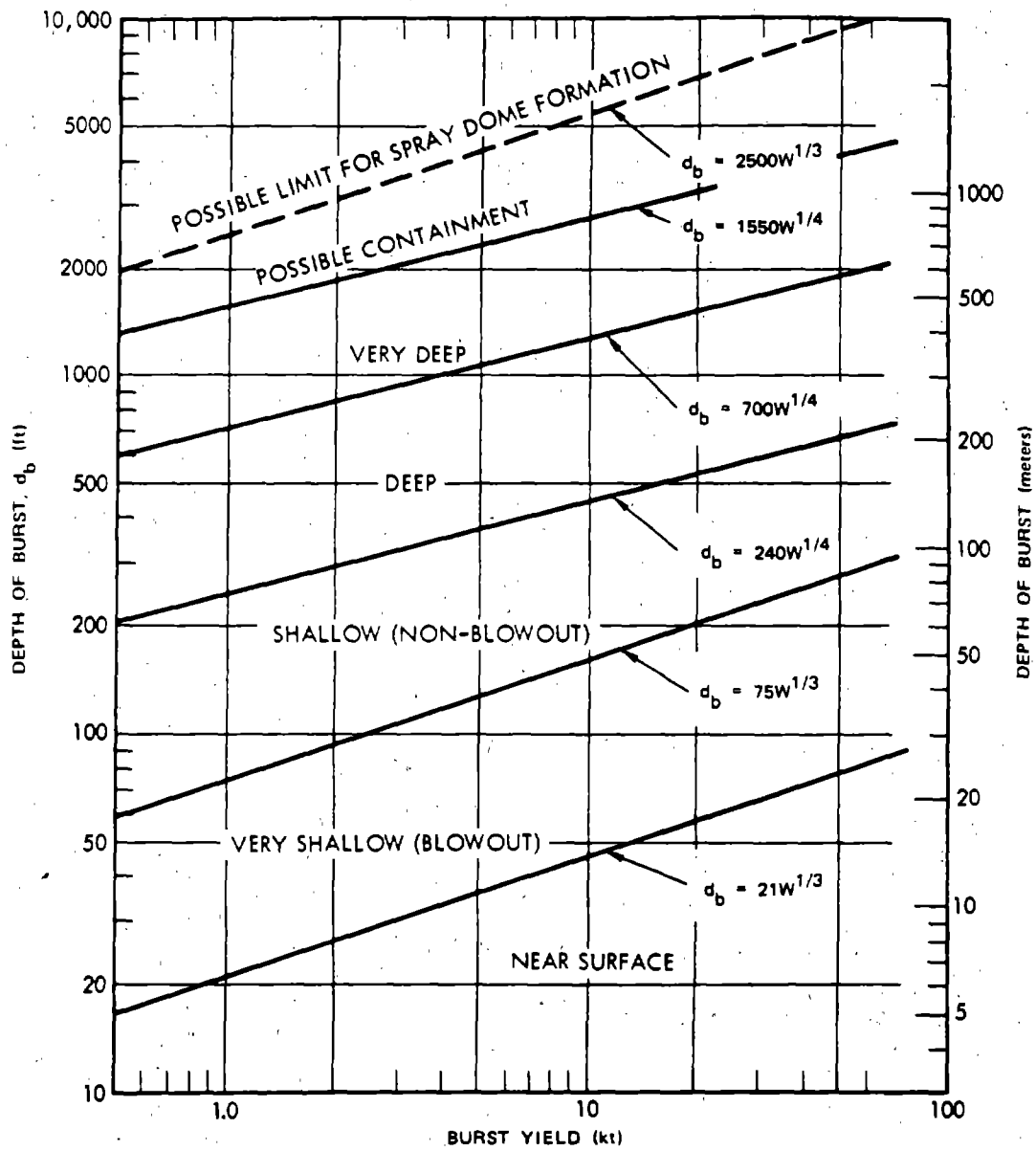

Figure 2-105. [redacted] Classification of Underwater Nuclear Bursts [redacted]

[redacted]

[redacted]

[redacted] No radioactive debris would be observed on the surface from contained bursts. The probability of containment of the radioactive debris is a function of the oceanic density profile. The relation in Figure 2-105 probably is valid in certain tropical waters, but bursts at these same depths in northerly latitudes probably would not be contained.

[redacted] No surface effects due to bubble pulsation or migration occur as a result of bursts that do not produce a spray dome.

[redacted] Although water depths may also influence surface phenomena, and consequently burst classification, the mathematical definitions in Table 2-8 do not include this influence.

[redacted] The various surface phenomena can be divided into two categories according to their origin, i.e., those produced by shock waves and those produced by the water motion accompanying bubble pulsation and rise. In the former category, the slick, crack, and spray dome are of operational importance. In the latter category, columns, plumes, base surge, and the long-lasting foam patch can be significant. More detailed descriptions of the surface phenomena are given in the following paragraphs.

2-73 Spray Dome [redacted]

[redacted] The spray dome (or spall), is formed by the acceleration and breakup of the surface water layer. The initial surface velocity directly above the burst is the sum of the water particle velocities imparted by the incident and reflected waves; elsewhere, the initial velocity is approximately the sum of the vertical components of these velocities (some initial surface velocities have been observed to be higher than so calculated). The height of the spray dome is limited by deceleration of gravity and air drag.

[redacted] If the depth of burst is sufficiently deep for one or more bubble oscillations to occur before venting, there may be secondary spray domes from reflection of compression waves emitted by the later bubble expansions. These can be several times higher than the primary dome from very deep bursts.

[redacted] The calculations of spray dome extent, vertical water velocity, and spray height are described in Problem 2-32. Plumes appear over the central portion of the spray dome from shallow bursts; therefore, a calculation of spray dome height may have little value.

2-74 Plumes, Column, Cauliflower Cloud [redacted]

[redacted] If the burst is deep enough to prevent blowout (shallow to very deep bursts), expansion, pulsation, and rise of the bubble produce a violent upheaval and expansion of water above the surface to form plumes. In those deep explosions where the bubble collapses just beneath the surface, the rising bottom of the bubble jets through the layer of water above the bubble and probably will form a plume. In deep and very deep explosions, the upward motion of the water about the rising bubble also forms a plume.

[redacted] The water displaced by the expanding bubble from very shallow bursts forms a dome-shaped shell of water over the bubble. Later, this shell ruptures and blows out the bubble constituents. For a very shallow nuclear explosion, blowout is accompanied by the formation of a "cauliflower cloud" at the top of the plume.

[redacted] Since there are insufficient data for a comprehensive prediction technique, predictions of plumes, columns, and clouds are based on direct scaling from four nuclear bursts. Predictive relationships and examples of their use are given in Problem 2-33.

2-75 Base Surge [redacted]

[redacted] As the plume from a deep burst or the column from a shallow burst falls back to the surface, it generates a cloud of fine spray, or aerosol, called "base surge," which usually is a

[redacted]

[redacted]

[redacted] radiation hazard. The base surge expands and circulates as a toroidal cloud under the influence of the collapsing water plume. The expansion is rapid at first (exceeding 100 ft/sec); however, it decelerates upon mixing with the ambient air. During this period, part of the cloud evaporates and cools the air. As its kinetic energy dissipates and the cloud reaches its maximum diameter, it tends to thin out, and it may even become invisible as a consequence of diffusion and continued evaporation. In a sense, the base surge still exists, because some ocean salts and detonation products remain airborne.

[redacted] Two types of base surge have been encountered during weapon tests:

- "Doughnut-shaped" clouds from very shallow and shallow detonations
- "Disc-shaped" clouds or, more properly, a series of concentric "doughnut-shaped" clouds from deep and very deep detonations.

[redacted] Although visible configurations are actually quite irregular, the base surge configuration for very shallow and shallow detonations can be represented as a hollow cylinder or a hollow truncated cone for radiation exposure estimates. The inner diameter of the cylinder is approximately two-thirds the outer diameter. For very deep and deep bursts, a cylinder or truncated cone are adequate model configurations. The height of the visible base surge clouds at various weapon tests have varied between about 1,000 and 2,000 ft, probably as a result of turbulence and meteorological conditions.

[redacted] A base surge is transported by the wind during its formation and growth. As a general rule, the transport should depend upon the wind speeds at altitudes between the surface and the maximum surge height. The downwind growth curve may be predicted by adding the highest wind speed reported between these levels to the average growth curves. The upwind growth should lie between a predicted curve based on subtracting half the surface wind speed (a rule-of-thumb to account for friction with the surface) and a curve obtained by subtracting the wind speed used for the downwind curve. At early times the former would be more accurate while at later times the latter would be more correct. Base surge prediction relationships and an example of their use are given in Problem 2-34.

2-76 Foam Patch and Ring [redacted]

[redacted] After subsidence of the plume, column, and base surge, a roughly circular area of disturbed water is still visible. This area is primarily defined by its white color and indications of turbulence at the perimeter. In the case of deep explosions, the patch can result from an upsurge of water caused by bubble migration. This water spreads out and then sinks, the overall motion being somewhat toroidal. Foam and flotsam tend to collect at the edge of the patch.

[redacted] The whiteness from deep shots is believed to be caused by foam generated by the agitation of the water, particularly as the plumes fall back. Similar foam patches occur from shallow detonations, but their whiteness is caused partly by suspended bottom material. The foam patch contains appreciable quantities of weapon debris and presents a potential radiation hazard to personnel in small boats or ships.

[redacted] The foam patches developing from test explosion have been on the order of 1.5 to 2.5 miles in diameter about 15 min after detonation, but they continued to expand slowly and irregularly with water currents and diffusion into the water, until the last visible manifestation was a ring of foam and debris. Their radioactivity could be traced for many days, although they had been invisible for quite some time.

[redacted]

[redacted]

[redacted] WATER SURFACE WAVES [redacted]

2-77 Generation and Propagation of Water Surface Waves [redacted]

[redacted] A submerged nuclear explosion, like any other physical event that produces a localized disturbance on the water surface, generates a group of surface waves that expand radially. The characteristics of explosively generated waves depend upon the yield, the depth of burst, and the range to the point of observation. If the water is sufficiently shallow, the bottom contour also can affect the generation and propagation of the waves.

[redacted] The following physical description of the wave generation process and the succeeding prediction technique are based on:

- Laboratory experiments with small H.E. charges
- Wave data for the nine nuclear shots that have been fired on or in the lagoons at Eniwetok and Bikini, as listed in Table 2-9.
- Wave data for all the known tests in water with H.E. charges larger than 10 lb, as listed and referenced in Table 2-10.

Surface waves produced by an underwater explosion are generated by pulsations of the cavity formed at the surface when the oscillating bubble breaks through the surface (vents).

[redacted] At a short range, within a few cavity radii, the first wave crest is so high and steep that it is unstable, and it spills forward turbulently and dissipates much of its energy. However, as the wave train expands and attenuates, the waves become shallow and smooth, their number increases, their energy remains nearly constant, and the highest wave appears successively later in the train. A wave gage record for such an expanded wave train is shown in Figure 2-106. The height H of the highest wave (trough-to-crest) decreases nearly inversely with range R; but the length, speed, and period all remain nearly constant for this peak wave, which is the one temporarily located at the first anti-node of the wave envelope as the waves move back in the envelope.

[redacted] An approximate mathematical theory has been developed for shallow waves propagating from a shallow disturbance on the surface of water with constant depth. The results of this theory compare well with measured wave trains when a motionless "pseudo-cavity" is selected to approximate the wave generator or initial conditions. The "pseudo-cavity" is a shallow motionless depression of the water surface near the explosion. Its shape is derived empirically to correspond with the waves measured far from an explosion, but it does not necessarily correspond accurately with the actual shape of the water surface at any time.

[redacted] All of the known measurements of peak wave height over deep water for charges greater than 10 lb are plotted in Figure 2-107. The vertical bars indicate the variation of HR for repeated shots and/or various gage ranges R. There is little discernible effect of depth of burst except near the "upper critical depth," where the H.E. charges were only partially submerged and where the peak wave height nearly doubled. Although current studies indicate that the upper critical depth effect may exist for nuclear as well as for H.E. charges, there is no firm evidence to support the inference as yet.

[redacted] A plot comparable with Figure 2-107 of the data for H.E. charges smaller than 10 lb exhibits a pronounced upward hump in wave height versus depth of burst at $d_b \approx 3W_{HE}^{0.3}$ (and possibly also at $d_b \approx 8W_{HE}^{0.3}$). This increase in wave generation efficiency at the "lower critical depth" occurs when the expanding underwater cavity ruptures the layer of water above it (or vents) just before it becomes fully expanded. For large submerged explosions, the expanded bubble becomes tangent to the surface when the

[redacted]

[redacted]

Table 2-9. [redacted] Measured Wave Data from Nuclear Tests [redacted]

DNA (b)(3)

NUMBER SERIES SHOT	YIELD	WATER DEPTH AT CHARGE	DEPTH OF BURST	PEAK WAVE* HEIGHT x RANGE	CAVITY RADIUS	$d_w/100(W)^{1/4}$	$HR/2 \times 10^4 \sqrt{W}$
	W (kt) $100(W)^{1/4}$	d_w (ft)	d_b (ft)	HR/2,000 (ft)† min - max	R_c (ft)		min - max
1 HARDTACK UMBRELLA	[redacted]	140	140	[redacted]	[redacted]	[redacted]	[redacted]
2 HARDTACK WAHOO	[redacted]	3,000	500	[redacted]	[redacted]	[redacted]	[redacted]
3 CROSSROADS BAKER	23.5 220	180	90	36 - 60	1,000‡	0.82 Shallow	0.74 - 1.24
4 WIGWAM	32 238	15,000	2,000	118	490†	63 Very Deep	2.08
5 REDWING FLATHEAD	[redacted]	120	0	[redacted]	[redacted]	[redacted]	[redacted]
6 REDWING DAKOTA	[redacted]	140	0	[redacted]	[redacted]	[redacted]	[redacted]
7 REDWING NAVAHO	[redacted]	230	0	[redacted]	[redacted]	[redacted]	[redacted]
8 CASTLE UNION	7,000 916	145	7	232 - 312	1,000†	0.16 Shallow	0.16 - 0.28
9 CASTLE YANKEE	13,500 1,080	220	7	426 - 438	1,000†	0.20 Shallow	0.37 - 0.38

*H is twice the measured height of the peak crest except for shots 8 and 9 where H is the measured height of the first crest from the following trough. H is corrected for uniform water depth = d_b by Green's law.

†Value deduced from measured surface wave train (Kaplan and Wallace, see bibliography) is a lower limit considerably smaller than actual values, which are unknown.

‡Measured values of the column radius (Young, DASA 1240–1(9)), see bibliography.

[redacted]

[redacted]

[redacted]

Table 2-10. [redacted] Measured Wave Data from Large H.E. Tests [redacted]

SHOT	YIELD	WATER DEPTH	DEPTH OF BURST	PEAK WAVE HEIGHT	CAVITY RADIUS	$d_w/100(W)^{1/4}$	$HR/2 \times 10^4\sqrt{W}$
	W (kt)	d_w (ft)	d_b (ft)	HR/2 $(ft)^2$	R_C (ft)		min - max
WES Test Series at Lake Ouachita (from Pinkston and from Whalin)							
125 lb	0.625×10^{-4}	100	0 - 25	80 - 110		22.5	.90 - 1.24
385 lb	1.97×10^{-4}	100	0 - 36	147 - 225		17.0	1.25 - 1.91
WES Test Series at Mono Lake (1965 - 1966) (Preliminary data by private communication with R. Whalin and M. Pinkston and from Walter)							
1965 - 6	0.46×10^{-2} (9,200 lb)	130	0	1650 - 1900	68	5.2	2.4 - 2.8
- 2	↓	↓	.67	2100 - 3900	69	↓	3.1 - 5.7
- 4	↓	↓	1.04	2100 - 2850	71	↓	3.1 - 4.2
- 3	↓	↓	1.40	1750 - 3000	74	↓	2.6 - 4.4
-5, 7, 8, 9	↓	↓	9 - 51		61 - 80	↓	
1966 - 3	↓	≈130	5.2	1150 - 1250		↓	1.7 - 1.8
- 2	↓	↓	23	850 - 1200		↓	1.2 - 1.8
- 1	↓	↓	60	1300 - 1400		↓	1.9 - 2.1
HYDRA 11a (Van Dorn) W = 10^4 lb HBX							
- 7	0.723×10^{-2} (14,450 lb)	300	140	1650 - 1970		10.3	1.94 - 2.31
- 8	↓	↓	80	975 - 1340		↓	1.15 - 1.55
- 9	↓	↓	35.5	1260 - 1590		↓	1.48 - 1.87
- 10	↓	↓	7.1	1610		↓	1.88
- 11	↓	↓	15.9	1510 - 1840		↓	1.77 - 2.16
- 12	↓	↓	15.9	1490		↓	1.75
- 13	↓	↓	17.7	1450		↓	1.71

[redacted]

[redacted]

[redacted]

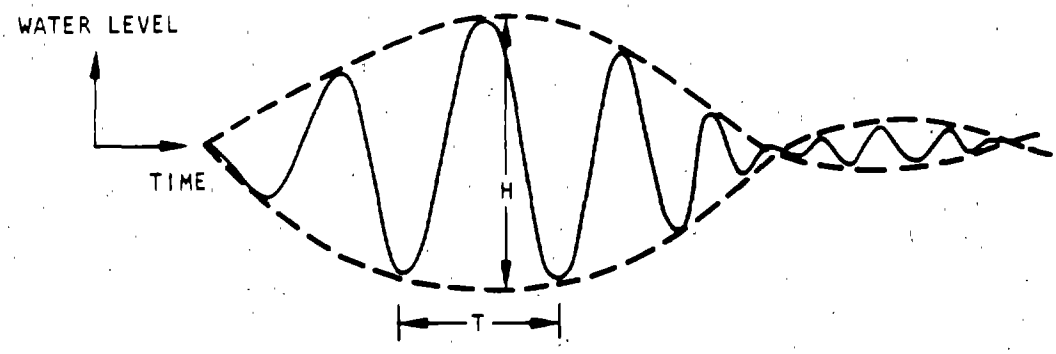

Figure 2-106. [redacted] Wave Gage Record for an Explosion-Generated Wave Train [redacted]

[redacted]

[redacted]

burst depth d_b equals $240W^{1/4}$. The lower critical depth is somewhat smaller at about $d_b = 170W^{1/4}$. However, the effect on wave generation is much smaller for the larger charges in Figure 2-107, and the height of the peak wave generated by large explosions in "deep" water can be approximated simply by

$$HR/W_{HE}^{0.54} = 16 \pm 4,$$

where H is the amplitude of the maximum of the first envelope trough-to-crest in feet, R is the radial distance from the explosion in feet, and W_{HE} is the charge weight in equivalent pounds of TNT. An equivalent approximation is

$$HR = 40{,}500\ (W)^{0.54} \pm 25 \text{ percent},$$

where W is the yield in kilotons and the other symbols are as defined above. Similarly, the length and period of the peak wave can be approximated by

$$L = 15.5\ \left(W_{HE}\right)^{0.288} \text{ ft},$$

$$T = 1.74\ \left(W_{HE}\right)^{0.144} \text{ sec}.$$

These three relationships were derived empirically from test data for 125- and 385-lb H.E. charges and the two nuclear explosions shown in Figure 2-107. For a pseudo-cavity of a given shape, which has a potential (gravitational) energy comprising a fixed fraction of the explosive yield, all the dimensions of the cavity and the wave train are proportional to $W_{HE}^{1/4}$ or $W^{1/4}$ (Froude scaling), and the exponents in the three equations given above are 1/2, 1/4, and 1/8, respectively. Since the empirical exponent in the first equation was found to be 0.62 for small H.E. charges, it seems reasonable to suppose that the "theoretical" value of 1/2 may be the best value to use for extrapolation to large yields (the high kiloton and megaton range). With this exponent, the data in Figure 2-107 have been replotted as a function of reduced water depth (rather than charge depth) for use in Problem 2-35 (Figure 2-128).

[redacted] The horizontal line in Figure 2-128 can be used to predict the peak wave height in deep water. However, it can be derived by the following simple procedure to illustrate qualitatively the physical process of wave generation in "deep" water to define "deep." The approximation is made that an explosion in deep water at any depth of burst above the lower critical depth generates a parabolic (nearly hemispherical) cavity upon venting, and that the potential energy of this cavity E_c is equal to 5 percent of the explosive yield E_o. That is:

$$E_c = \frac{\pi}{6}\rho_w g R_c^4 = 0.05E_o$$

$$= 0.05 \times 2.86 \times 10^{12}\ W \text{ ft-lb}.$$

[redacted] This gives the following cavity radius, which is taken equal to the cavity depth and the radius of the plume (or column) of water projected upward:

$$R_c = 256\ (W)^{1/4} \text{ ft}.$$

$$\text{if } d_w > R_c,$$

and if the density of seawater and the hydrodynamic yield of the explosion are taken as

$$\rho_w g = 65\ \frac{\text{lb}}{\text{ft}^3}, \text{ and } e_o = 1{,}025\ \frac{\text{cal}}{\text{gm}}.$$

This cavity radius is not much larger than the bubble radius and depth of burst corresponding to the lower critical depth. The restriction on

[redacted]

[redacted]

[redacted]

[redacted] water depth d_w in the equation for R_c is taken as the minimum water depth that can be considered "deep" i.e., the depth for which the assumed cavity shape touches bottom as it vents.

[redacted] The dissipative effects close to the cavity are approximated by the assumption that the leading peak wave crest spills forward and breaks turbulently at $R = 2R_c$ to the limiting height of a wave that can propagate in a stable manner over deep water (the Michell limit, or $H_{max} = 0.14L$). Finally it is assumed that the amplitude of the wave envelope H is attenuated inversely with range R as it continues to expand without dissipation. This gives the "predicted" peak wave height when the water depth at the charge location is "deep" ($d_w \geq 256W^{1/4}$) as

$$HR = 49{,}000 \sqrt{W},$$

which corresponds to the horizontal line in Figure 2-128. This "predicted" value can be used for depths of burst ranging from zero to at least five times the lower critical depth (at $d \doteq 170W^{1/4}$) judging by the comparison with WIGWAM data, even though the cavity radius becomes too large for depths of burst much below the lower critical depth.

[redacted] The line in Figure 2-128 can be extended into "shallow" water by a comparable simple procedure. In shallow water the cavity both touches bottom and vents to the atmosphere early during its expansion. Hence, much less work is done on the water by the expanding gaseous bubble, and much less energy is propagated as water surface waves over shallow water. Experimental data indicate that explosions in shallow water generate a dry cavity surrounded by a nearly vertical wall of water which extends upward as a thin lip to form the "column." A lower limit for the maximum radius of this cavity (or column) is given by the following relationship, which was derived from the energy calculated from measured wave trains over *shallow* water (Table 2-9) and which will be discussed in succeeding paragraphs.

$$R_c = 100\ (W)^{1/4} \text{ if } d_w < R_c$$

Once again, the dissipative effects close to the cavity are approximated by the assumption that the leading peak wave breaks down to the limiting height of a stable progressive wave, but, for shallow water, the approximation is that $H_{max} = (3/4)\, d_w$ = Miche limit at $R = 2R_c$. If this peak wave height is then attenuated inversely with range R, the "predicted" peak wave height when the water depth at the charge location is "shallow," ($d_w < 100W^{1/4}$), becomes

$$HR = 150\ d_w W^{1/4},$$

which gives the line with the 45 degree slope in Figure 2-128. This "prediction" can be used for any depth of burst ($0 < d_b < d_w$) as shown by measured data for H.E. charges in shallow water. As shown in Figure 2-128, there is much scatter in the nuclear wave data in shallow water and some of the measured peak wave heights are more than twice as large as "predicted" by the foregoing equation, which should be regarded only as a rough rule-of-thumb for correlating the measured data in Figure 2-128.

[redacted] The only actual measured data for the radii of the water columns (or cavities) for nuclear bursts near the surface of water are for shots BAKER and UMBRELLA (Table 2-9). These values of R_c and those measured for submerged H.E. explosives are roughly equal to the value given by the equation for maximum bubble radius in paragraph 2-67, which gives a burst estimate for R_c [redacted]

DNA (b)(3)

[redacted]

[redacted]

[redacted]

DNA (b)(3)

[redacted] In soil, TNT charges detonated at the surface generate crater radii approximately twice as large as nuclear explosions of the same yield, so the nuclear-TNT equivalence is only about 10 percent. The *column* radii observed for TNT detonations near the surface of the water are roughly equal to $470W^{1/3}$, which is the bubble radius given by the equation in paragraph 2-67 for a surface burst. This occurs even when the bubble radii exceed the water depth by a factor of 5. Therefore, it might be expected that a nuclear burst at the surface of water would produce a column radius about half as large as the H.E. value, or $240W^{1/3}$. This latter value is much larger than the lower limit estimated above ($R_c = 100W^{1/4}$). This lower limit is also exceeded by the crater radii measured in the bottom after explosions in shallow water, and the water column radii probably exceed the crater radii. Although there are no substantiating data, nuclear explosions at the surface of water of any depth probably generate water columns with radii between $100W^{1/4}$ and $240W^{1/3}$ feet.

2-78 Refraction and Shoaling [redacted]

[redacted] Explosion-generated waves, in common with wind waves and tsunami (earthquake-generated) waves, are affected by changes in the depth over which they propagate. As the waves move into water shallower than about one-third their length (or shoal), their period remains fixed, but both their speed and their length decrease (between successive crests) and their height first decreases about 10 percent and then begins to increase. Because of the change in speed, a wave bends or refracts if it moves into shallow water at an angle to the bottom contours. Refraction can increase or decrease the localized wave height, depending on the hydrography over which the wave moves. No general methods for determining refraction effects are given here; however, such techniques for calculating these effects are available ("Oceanographical Engineering," R. L. Wiegel, see bibliography).

[redacted] The increase in height of a wave relative to its length (steepening) continues until the wave becomes unstable and breaks, unless the bottom slope is so shallow that bottom friction dissipates the wave before it breaks. In shallow water without dissipation, steepening increases the wave height as the inverse fourth root of the water depth. Many types of waves become unstable and break (or spill) when their height exceeds either 75 percent of the water depth (the Miche limit) or 14 percent of the wave length over deep water (the Michell limit) as described by Weigel (see bibliography).

[redacted] UNDERWATER CRATERING [redacted]

[redacted] If an explosion occurs in or even close to a layer of water overlaying bottom material, a significant crater forms in the bottom material whenever the gaseous bubble or water cavity formed by the explosion contacts the bottom. An underwater crater is similar to an onshore crater formed by an explosion near the ground since both are characterized by a dish-shaped depression, wider than it is deep, and surrounded by a lip raised above the undisturbed surface. In the case of most underwater craters, however, the observed ratio of crater radius to depth is larger and the lip height is smaller than for craters from comparable bursts in similar bottom materials onshore. These differences are caused by water displaced by the explosion washing back over the crater. This flow increases the crater radius by as much as 10 percent and decreases the crater depth by as much as 30 percent. An exception to this general rule occurs when the water layer is so shallow that the lip formed by the initial cratering extends above the surface of the water. Such craters (termed "un-

[redacted]

[redacted]

[redacted]

washed craters") approach onshore craters in appearance, with higher lips and larger depth-to-radius ratios than washed craters. This section describes only the crater characteristics directly related to the explosion. The effects of tidal currents and the collapse of unwashed crater lips by hydrostatic forces are not considered.

[redacted] The characteristics of underwater craters can be predicted at least qualitatively from the depth of burst, water depth, bottom composition, and weapon yield. The use of empirical curves relating the depth and radius of the crater for surface and bottom bursts over a clayey-sand bottom is described in Problem 2-36. Predictions for other bottom materials can be made by applying tabulated factors to the values predicted for clayey sand, as described in Problem 2-36. It is evident that larger craters are produced by moving the charge toward the bottom; increasing the water depth above a bottom burst (up to a point); or decreasing the water depth beneath a surface burst.

[redacted] A very large yield is required to form an unwashed crater in water having a depth that is common to most harbors. For example, with 30 ft of water over clayey-sand, 4 Mt would be required on the bottom to produce a dry crater lip. It is quite unlikely that materials that tend to flow, such as oceanic ooze or fine-grained silt, could support the hydrostatic pressure exerted on a dry crater lip.

[redacted]

[redacted]

[redacted]

Problem 2-28. Calculations of Underwater Explosion Phenomena

[redacted] Calculations can be performed to determine bubble characteristics described in paragraph 2-67. The characteristics include the maximum radii, bubble periods, and migration between maxima for events to the end of the second bubble period. The calculation methods do not apply to cases where the bubble touches the bottom, and the methods contain uncertainties not yet fully resolved when the bubble center is very close to or above the surface. Furthermore, predictions that are made for events increasingly removed in time from the first maximum have increasing uncertainty. Two methods for calculating these bubble characteristics are demonstrated in the example. The first method uses the equations given in paragraph 2-67 and Figures 2-108 through 2-110. The second method uses equations introduced in the example and Figure 2-111. The first method is graphical and is less accurate than the second, but it provides a quick estimate.

[redacted] *Example* [redacted]

Given: 32 kt fired at a depth of 2,000 ft in very deep water.

Find:

a. The initial bubble period and radius,

b. The depth of the second maximum radius,

c. The second bubble period,

d. The radius at second maximum,

e. The depth of third maximum radius,

f. The third bubble period and radius at third maximum.

Solution (Method 1):

a. Calculate the initial radius A_1 and the period T_1, by using equations given in paragraph 2-67:

$$A_1 = J' \frac{W^{1/3}}{Z^{1/3}},$$

$$A_1 = (1{,}500)\left(\frac{(32)^{1/3}}{(2{,}000 + 33)^{1/3}}\right) = 376 \text{ ft.}$$

$$T_1 = K' \frac{W^{1/3}}{Z^{5/6}},$$

$$T_1 = (515)\left(\frac{(32)^{1/3}}{(2{,}033)^{5/6}}\right) = 2.86 \text{ sec.}$$

b. Find the reduced hydrostatic head:

$$\frac{Z_1}{A_1} = \frac{2{,}033}{376} = 5.41.$$

From Figure 2-108, for $n = 1$,

$$\frac{\Delta Z_1}{Z_1} = 0.28,$$

$$\Delta Z_1 = (0.28)(2{,}033) = 569 \text{ ft}$$
(migration during first period),

$$d_2 = d_b - \Delta Z_1,$$

$$d_2 = 2{,}000 - 569 = 1{,}431 \text{ ft.*}$$

---

*[redacted] Note that results are sensitive to graph readings.

[redacted]

[redacted]

c. From Figure 2-109, for $n = 2$,

$$T_2 = 0.90\ T_1,$$

$$T_2 = (0.90)(2.86) = 2.57 \text{ sec.}$$

d. From Figure 2-110, for $n = 2$,

$$A_2 = 0.77\ A_1 = (0.77)(376) = 290 \text{ ft.}$$

e. From Figure 2-108, using $Z_1/A_1 = 5.41$ and $n = 2$,

$$\frac{\Delta Z_2}{Z_1} = 0.23,$$

$$\Delta Z_2 = 0.23\ Z_1 = (0.23)(2{,}033) = 468 \text{ ft,}$$

$$d_3 = d_2 - \Delta Z_2,$$

$$d_3 = 1{,}431 - 468 = 963 \text{ ft.}$$

f. From Figure 2-109, for $n = 3$,

$$T_3 = 0.66\ T_1,$$

$$T_3 = (0.66)(2.86) = 1.89 \text{ sec.}$$

From Figure 2-110, for $n = 3$,

$$\frac{A_3}{A_1} = 0.47,$$

$$A_3 = 0.47\ A_1 = (0.47)(376) = 177 \text{ ft.}$$

Solution (Method 2): This method uses Figure 2-111 to obtain values for bubble energy ratio, r_n/r_{n-1}, and the following reduced equations:

$$\left(\frac{\Delta Z_n}{Z_n}\right) = 3.5\left(\frac{A_1}{Z_1}\right)^{3/2}\left(\frac{r_n}{r_1}\right)^{1/2}\left(\frac{Z_1}{Z_n}\right)^2,$$

$$\left(\frac{A_n}{A_1}\right) = \left(\frac{Z_1}{Z_n}\right)^{1/3}\left(\frac{r_n}{r_1}\right)^{1/3},$$

$$\left(\frac{T_n}{T_1}\right) = \left(\frac{Z_1}{Z_n}\right)^{5/6}\left(\frac{r_n}{r_1}\right)^{1/3}.$$

a. By the same procedures used in Method 1,

$$A_1 = 376 \text{ ft,}$$

$$T_1 = 2.86 \text{ sec.}$$

b. Using the first reduced equation given above,

$$\left(\frac{\Delta Z_1}{Z_1}\right) = 3.5\left(\frac{A_1}{Z_1}\right)^{3/2}\left(\frac{r_1}{r_1}\right)^{1/2}\left(\frac{Z_1}{Z_1}\right)^2,$$

$$\left(\frac{\Delta Z_1}{Z_1}\right) = 3.5\left(\frac{375}{2{,}033}\right)^{3/2}(1)^{1/2}(1)^2 = 0.277,$$

$$\Delta Z_1 = 0.277\ Z_1,$$

$$\Delta Z_1 = (0.277)(2{,}033) = 564,$$

$$d_2 = d_b - \Delta Z_1,$$

$$d_2 = 2{,}000 - 564 = 1{,}436 \text{ ft.}$$

c. The second bubble period T_2 can be obtained from the third reduced equation given above, and T_1 from (a) after finding the energy

[redacted]

[redacted]

ratio between the first and second bubbles. Using the reduced migration $\Delta Z_1/Z_1 = 0.277$ to enter Figure 2-111, the energy ratio is $r_2/r_1 = 0.324$. Thus,

$$\left(\frac{T_2}{T_1}\right) = \left(\frac{Z_1}{Z_2}\right)^{5/6} \left(\frac{r_2}{r_1}\right)^{1/3},$$

$$\left(\frac{T_2}{T_1}\right) = \left(\frac{2{,}033}{1{,}469}\right)^{5/6} (0.324)^{1/3},$$

$$\frac{T_2}{T_1} = 0.90,$$

$$T_2 = (0.90)(2.86) = 2.57 \text{ sec.}$$

d. The radius of the second maximum is obtained from the second reduced equation given above.

$$\left(\frac{A_2}{A_1}\right) = \left(\frac{Z_1}{Z_2}\right)^{1/3} \left(\frac{r_2}{r_1}\right)^{1/3},$$

$$\left(\frac{A_2}{A_1}\right) = \left(\frac{2{,}033}{1{,}469}\right)^{1/3} (0.324)^{1/3},$$

$$\left(\frac{A_2}{A_1}\right) = 0.765,$$

$$A_2 = 0.765\ A_1 = (0.765)(376) = 288 \text{ ft.}$$

e. To calculate the depth of the third maximum, it is first necessary to find the reduced migration $\Delta Z_2/Z_2$. From the first reduced equation,

$$\left(\frac{\Delta Z_2}{Z_2}\right) = 3.5 \left(\frac{A_1}{Z_1}\right)^{3/2} \left(\frac{r_2}{r_1}\right)^{1/2} \left(\frac{Z_1}{Z_2}\right)^2,$$

$$\left(\frac{\Delta Z_2}{Z_2}\right) = 3.5 \left(\frac{376}{2{,}033}\right)^{3/2} (0.324)^{1/2} \left(\frac{2{,}033}{1{,}469}\right)^2,$$

$$\left(\frac{\Delta Z_2}{Z_2}\right) = 0.303,$$

$$\Delta Z_2 = 0.303\ Z_2 = (0.303)(1{,}469) = 445 \text{ ft,}$$

$$d_3 = d_2 - \Delta Z_2,$$

$$d_3 = 1{,}436 - 445 = 991 \text{ ft.}$$

f. From c., $r_2/r_1 = 0.324$. Using the reduced migration $\Delta Z_2/Z_2 = 0.303$ to enter Figure 2-111, the energy ratio $r_3/r_2 = 0.158$.

$$\left(\frac{r_3}{r_1}\right) = \left(\frac{r_2}{r_1}\right)\left(\frac{r_3}{r_2}\right)$$

$$\left(\frac{r_3}{r_1}\right) = (0.324)(0.158) = 0.0512.$$

From the third reduced equation

$$\left(\frac{T_3}{T_1}\right) = \left(\frac{Z_1}{Z_3}\right)^{5/6} \left(\frac{r_3}{r_1}\right)^{1/3},$$

$$\left(\frac{T_3}{T_1}\right) = \left(\frac{2{,}033}{1{,}024}\right)^{5/6} (0.0512)^{1/3} = 0.658,$$

$$T_3 = 0.658\ T_1$$

$$T_3 = (0.658)(2.86) = 1.88 \text{ sec.}$$

[redacted]

[redacted]

[redacted]

From the second reduced equation,

$$\left(\frac{A_3}{A_1}\right) = \left(\frac{Z_1}{Z_3}\right)^{1/3}\left(\frac{r_3}{r_1}\right)^{1/3}$$

$$\left(\frac{A_3}{A_1}\right) = \left(\frac{2{,}033}{1{,}024}\right)^{1/3} (0.0512)^{1/3} = 0.467$$

$$A_3 = 0.467\ A_1$$

$$A_3 = (0.467)(376) = 176 \text{ ft.}$$

Answer:	*Method 1*	*Method 2*
a. The initial bubble period and radius	A_1 = 376 ft T_1 = 2.86 sec	376 ft 2.86 sec
b. The depth of the second maximum radius	d_2 = 1,431 ft	1,436 ft
c. The second bubble period	T_2 = 2.57 sec	2.57 sec
d. The radius at second maximum	A_2 = 290 ft	288 ft
e. The depth of third maximum radius	d_3 = 963 ft	991 ft
f. The third bubble period and radius at third maximum	T_3 = 1.89 sec A_3 = 177 ft	1.88 sec 176 ft

[redacted] *Reliability:* The uncertainty in the values for maximum radii calculated by the methods described above are about +20 percent and -35 percent, based on very limited information.

[redacted] *Related Material:* See paragraph 2-67.

[redacted]

[redacted]

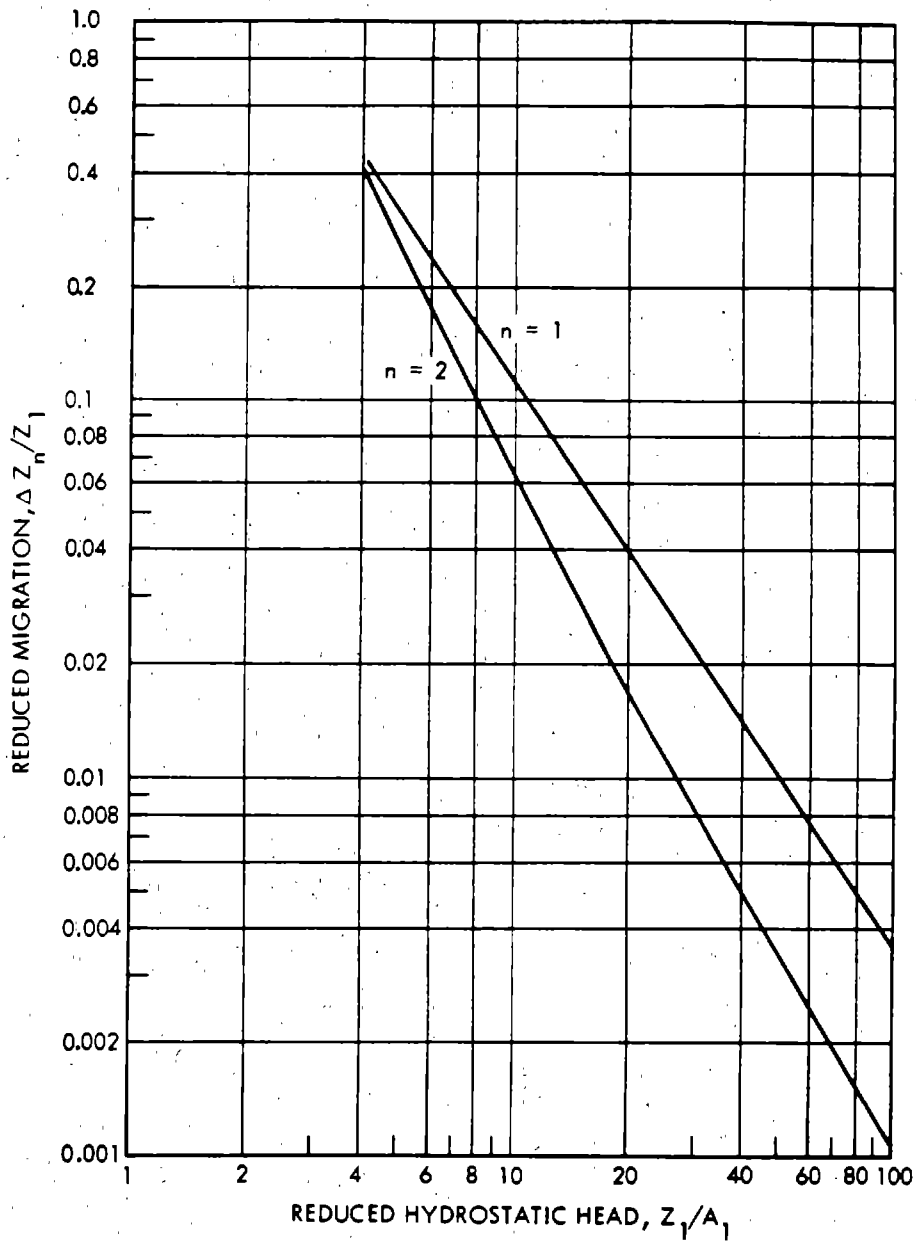

Figure 2-108. [redacted] Reduced Nuclear Bubble Migration [redacted]

[redacted]

[redacted]

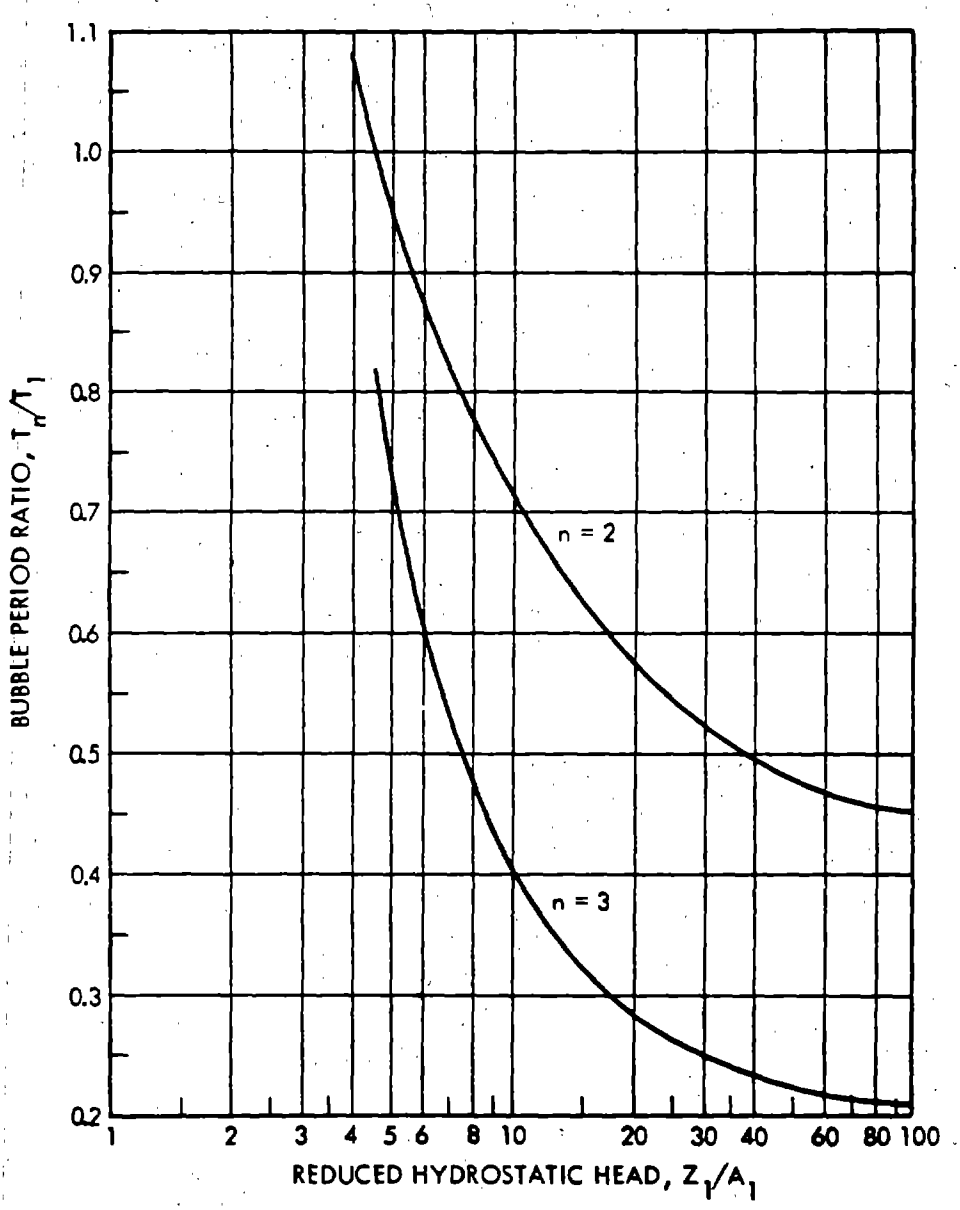

Figure 2-109. [redacted] Successive Nuclear Bubble Period Ratios [redacted]

[redacted]

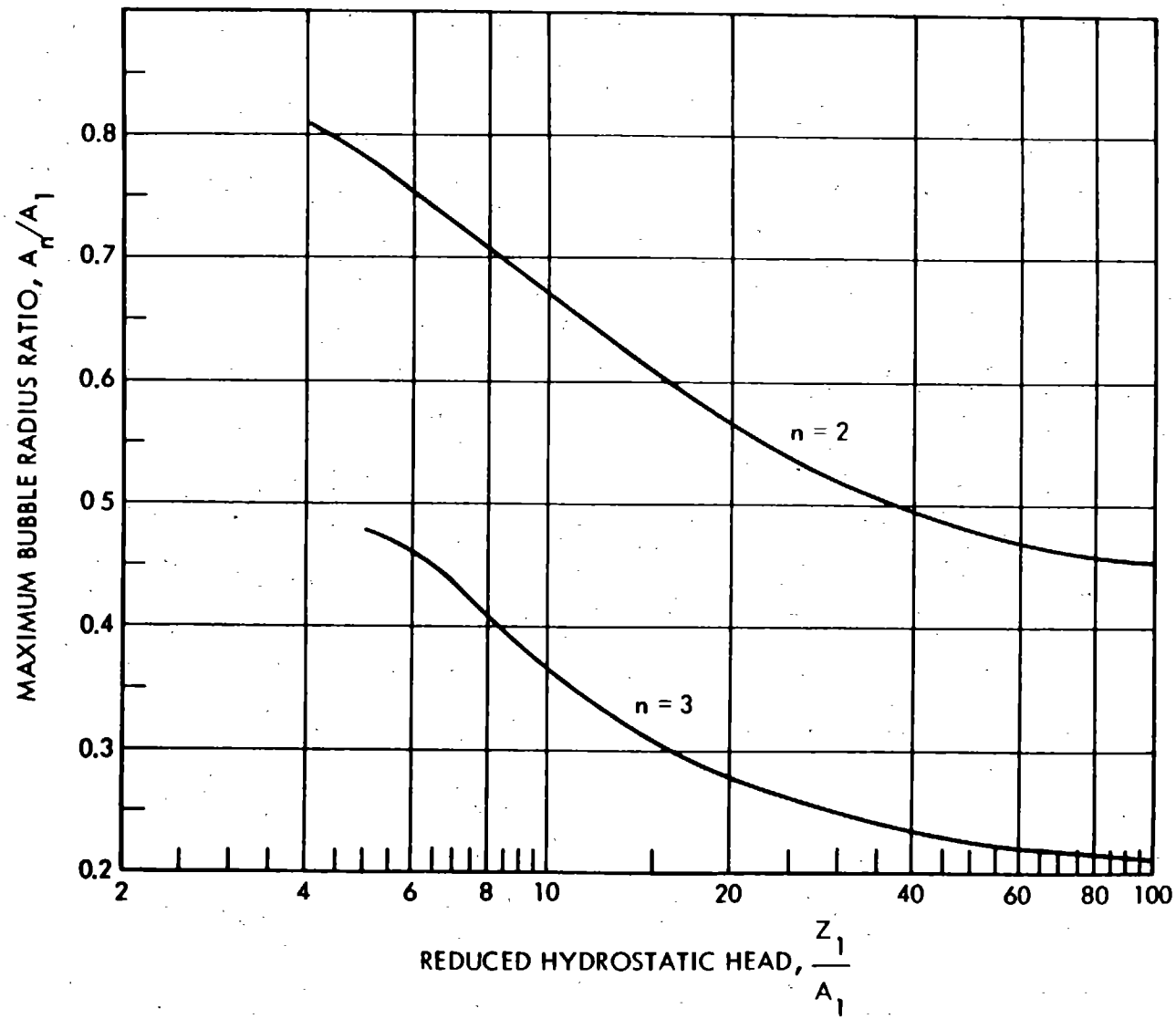

Figure 2-110. [redacted] Successive Nuclear Maximum Bubble Radius Ratios [redacted]

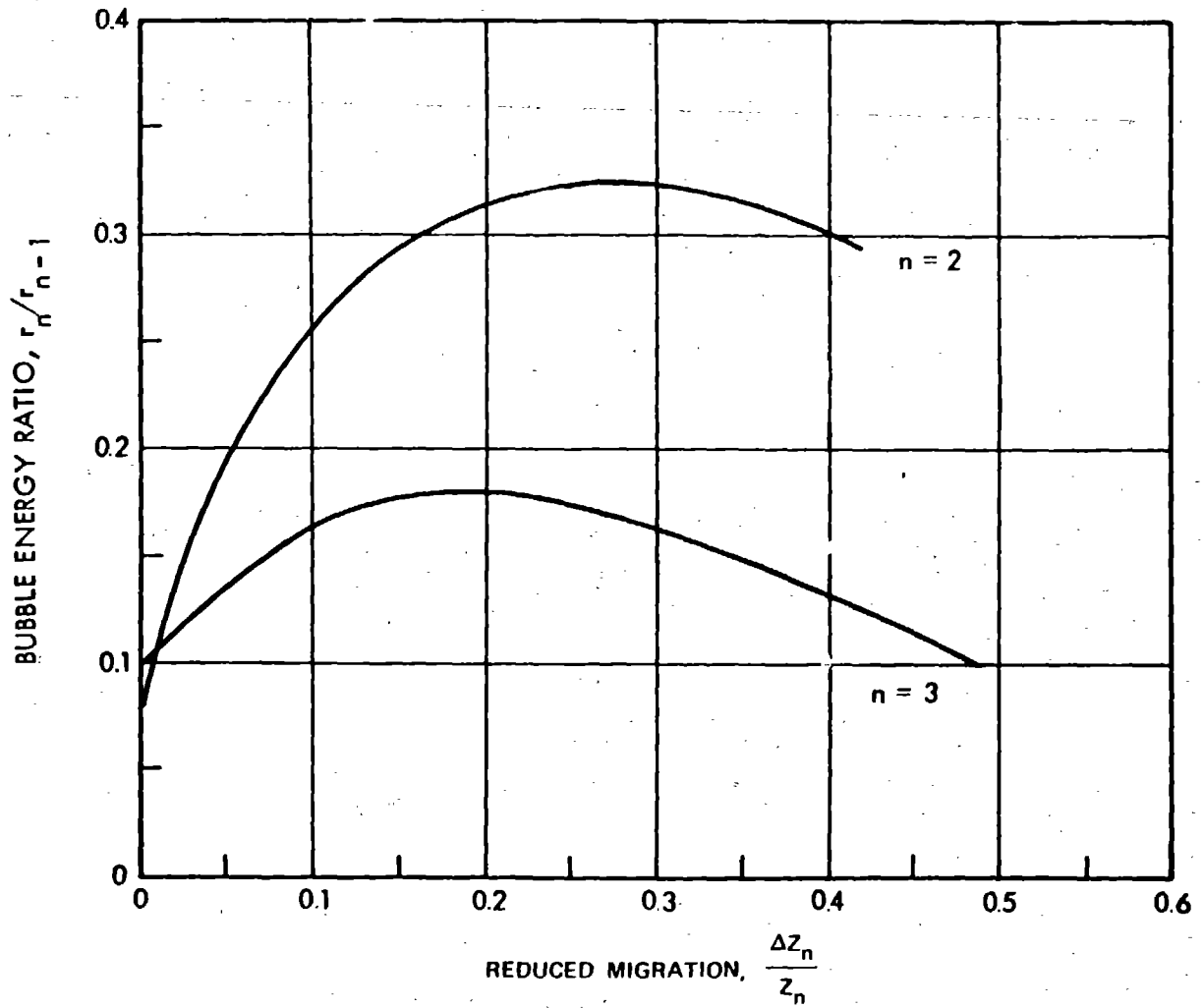

Figure 2-111. [redacted] Nuclear Bubble Energy Ratios [redacted]

[redacted]

Problem 2-29. Calculation of Shock Wave Parameters for Free Water (Deep Bursts)

[redacted] Figures 2-112 through 2-116 show the parameters for the primary shock wave from an underwater explosion in free, isovelocity water (no reflections, no refractions). Figure 2-112 shows the peak pressure as a function of slant range for various yields, where the peak pressure is lower than 3,000 psi, and as a function of reduced slant range ($R/W^{1/3}$) for peak pressures above 3,000 psi. Figure 2-113 shows the shock wave impulse as a function of slant range for various yields, while Figure 2-114 shows the shock wave energy flux as a function of slant range for the same yields. These latter two families of curves show values of impulse and energy flux integrated to a time of 6.7θ, where θ is the time constant for the shock wave, which is defined as the time for the shock wave pressure to fall to approximately 37 percent of its peak value.

[redacted] The time constant θ is shown in Figure 2-115 as a function of slant range for the same family of yields shown in Figures 2-113 and 2-114. Figure 2-116 shows a dimensionless pressure-time curve. Using values of θ from Figure 2-115 and values of p_m from Figure 2-112, Figure 2-116 may be used to construct the pressure-time shape of the shock wave in free water at various ranges from underwater explosions of various yields.

[redacted] *Scaling.* For yields other than those shown in Figure 2-112 through 2-115, use linear interpolation between appropriate curves.

[redacted] *Example* [redacted]

Given: A 50 kt burst at a depth of 1,000 ft in deep water.

Find: The peak shock pressure p_m, the shock wave impulse I, energy flux E, and time constant θ at a 1,000 ft depth, 4,000 yd from the burst.

Solution: The desired shock wave parameters can be read directly from Figures 2-112 through 2-115.

Answer:

$$p_m \approx 470 \text{ psi},$$

$$I \approx 28 \text{ psi-sec},$$

$$E \approx 10^3 \text{ in.-lb/in.}^2,$$

$$\theta \approx 50 \text{ msec}.$$

[redacted] *Reliability:* Values shown in Figures 2-112 through 2-115 are estimated to be accurate within ±10 percent for shock pressure, and ±20 percent for the other parameters for yields between 1 kt and 1 Mt. For yields below 1 kt or above 1 Mt, the values are more uncertain. The assumption of isovelocity water becomes increasingly uncertain for ranges beyond a few kiloyards in the ocean.

[redacted] *Related Material:*

See paragraphs 2-68 through 2-72.

Figures 2-112 through 2-115 are based on the following equations:

$$p_m = 4.38 \times 10^6 \left(\frac{W^{1/3}}{R}\right)^{1.13} \text{ psi}$$

$$I \text{ (to } 6.7\theta) = 1.176 \times 10^4 \; W^{1/3} \left(\frac{W^{1/3}}{R}\right)^{0.91} \text{ psi-sec}$$

$$E \text{ (to } 6.7\theta) = 3.976 \times 10^9 \; W^{1/3} \left(\frac{W^{1/3}}{R}\right)^{2.04} \frac{\text{in.-lb}}{\text{in.}^2}$$

[redacted]

[redacted]

[redacted]

$$\theta = 2.274\, W^{1/3} \left(\frac{W^{1/3}}{R}\right)^{-0.22} \text{ msec.}$$

The values of these parameters are related to those for TNT (Cole, 1948) by an approximate equivalence factor. Snay and Butler (1957) (see bibliography) report that an underwater nuclear burst with a radiochemical yield of 1 kt gives approximately the same shock wave parameters at the same distance as a TNT charge weighing 0.67 kiloton (where 1 ton = 2,000 lbs).

[redacted]

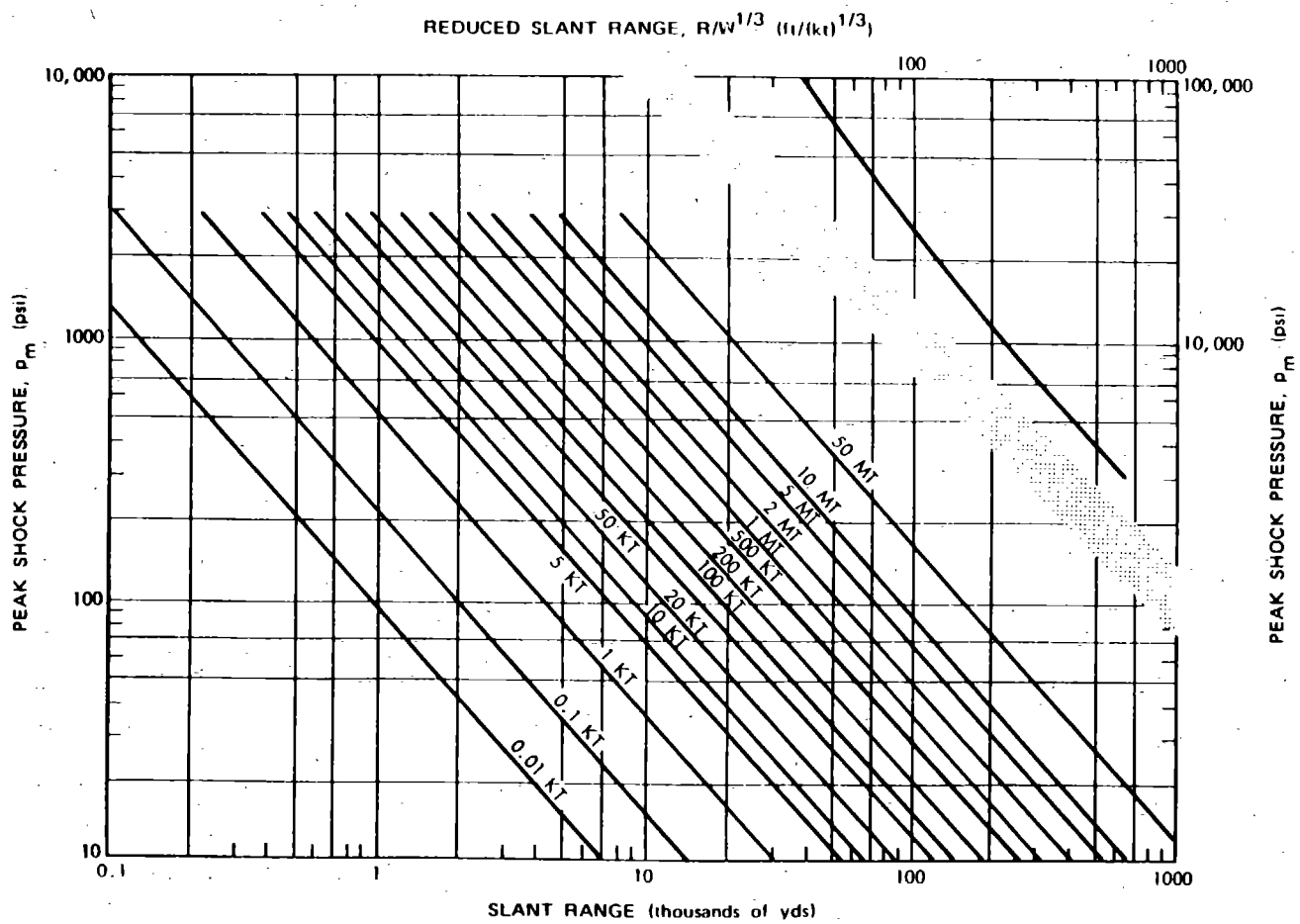

Figure 2-112. [redacted] Shock Wave Peak Pressure in Free Isovelocity Water [redacted]

[redacted]

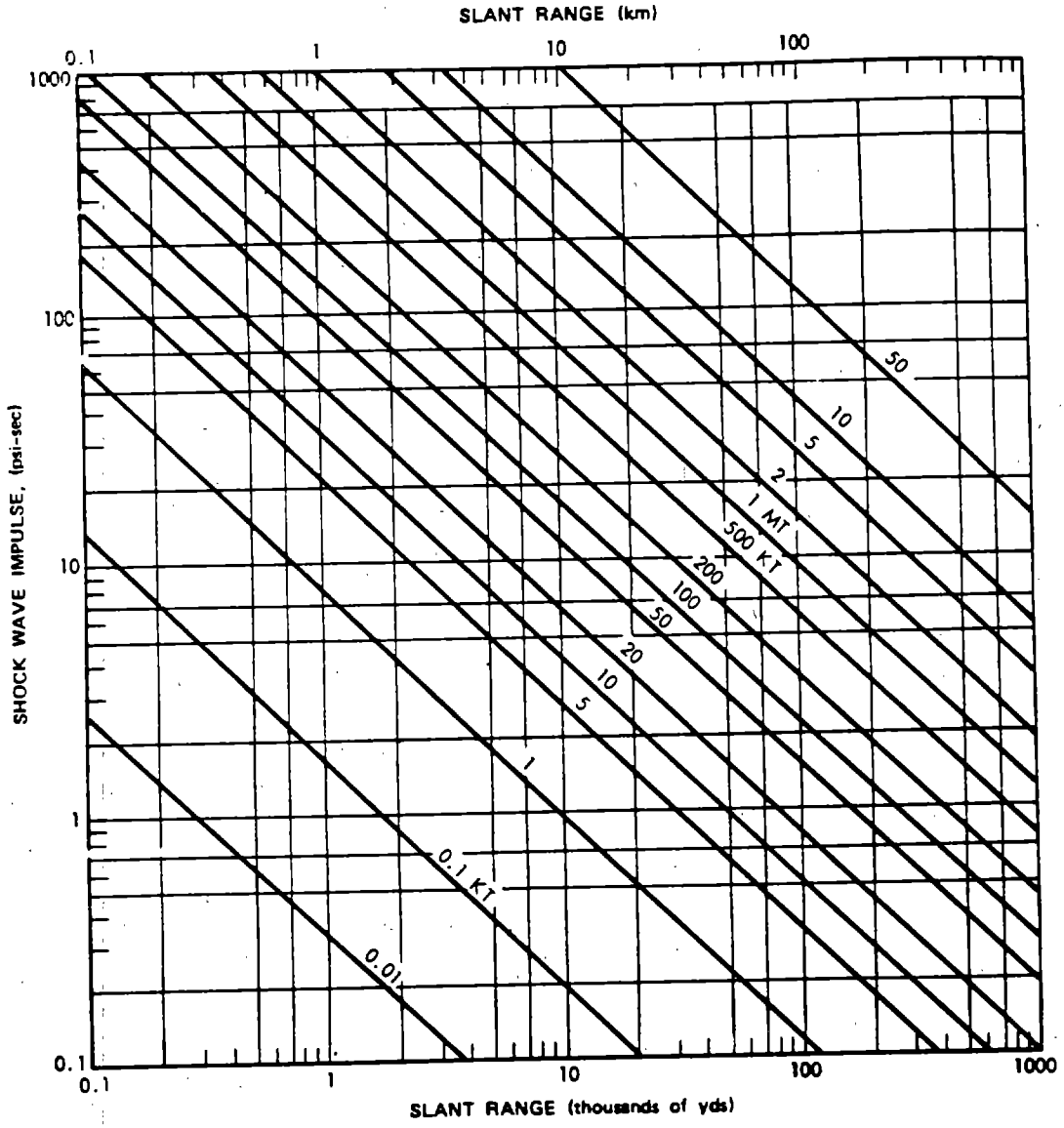

Figure 2-113. [redacted] Shock Wave Impulse vs Slant Range in Free Isovelocity Water [redacted]

[redacted]

[redacted]

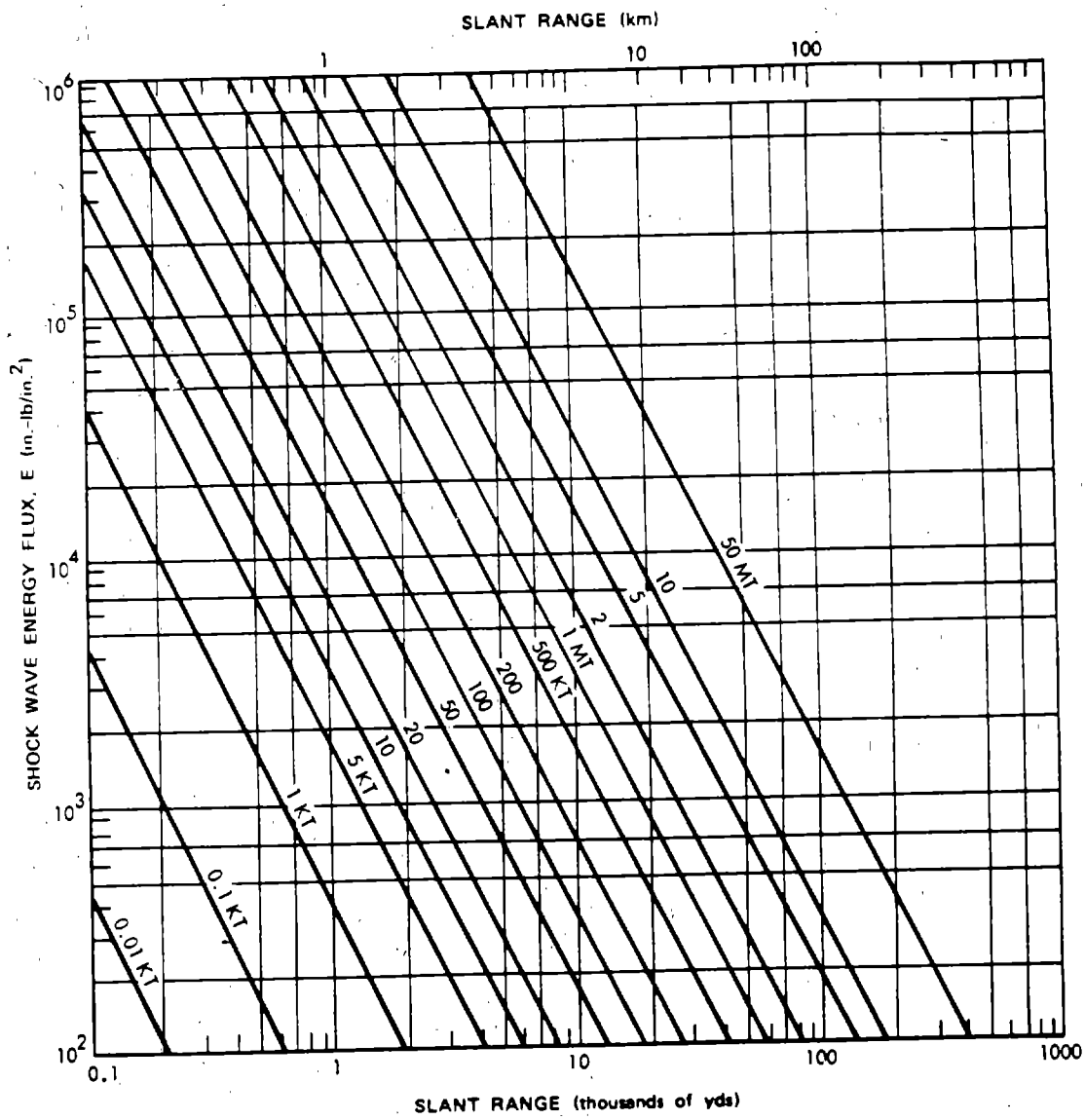

Figure 2-114. [redacted] Shock Wave Energy Flux vs Slant Range in Free Isovelocity Water [redacted]

[redacted]

[redacted]

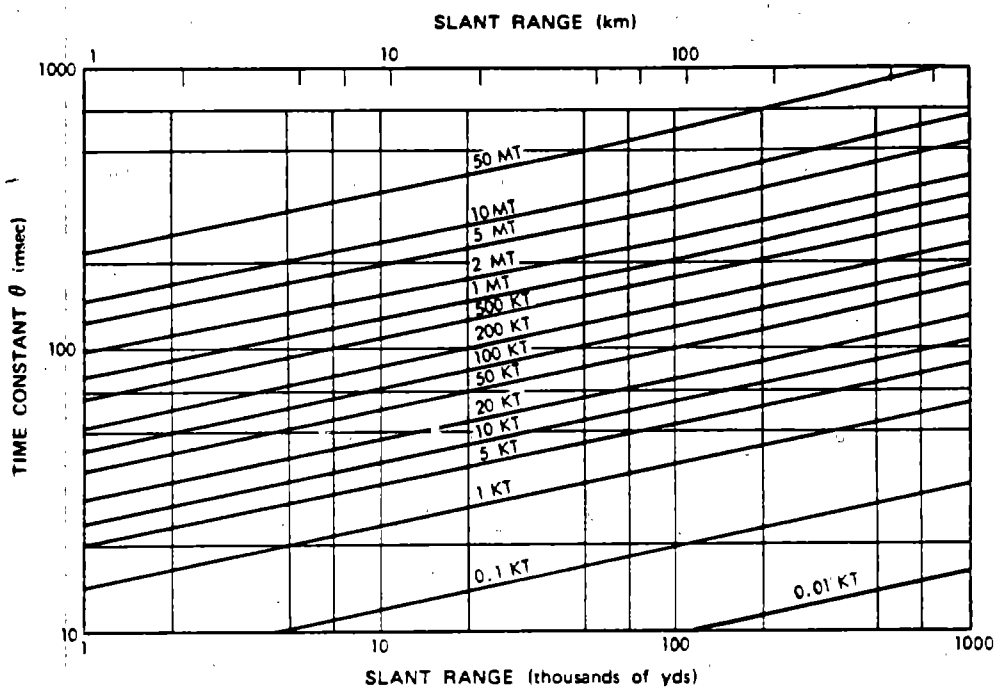

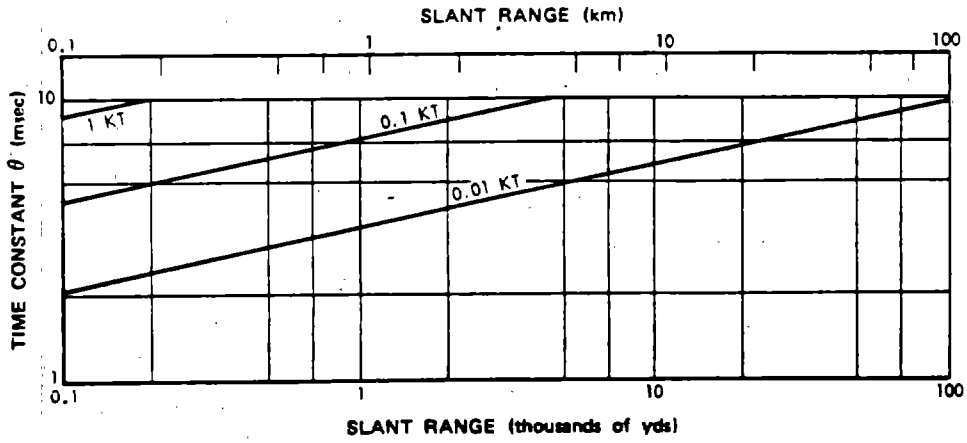

Figure 2-115. [redacted] Shock Wave Time Constant in Free Isovelocity Water vs Slant Range [redacted]

[redacted]

[redacted]

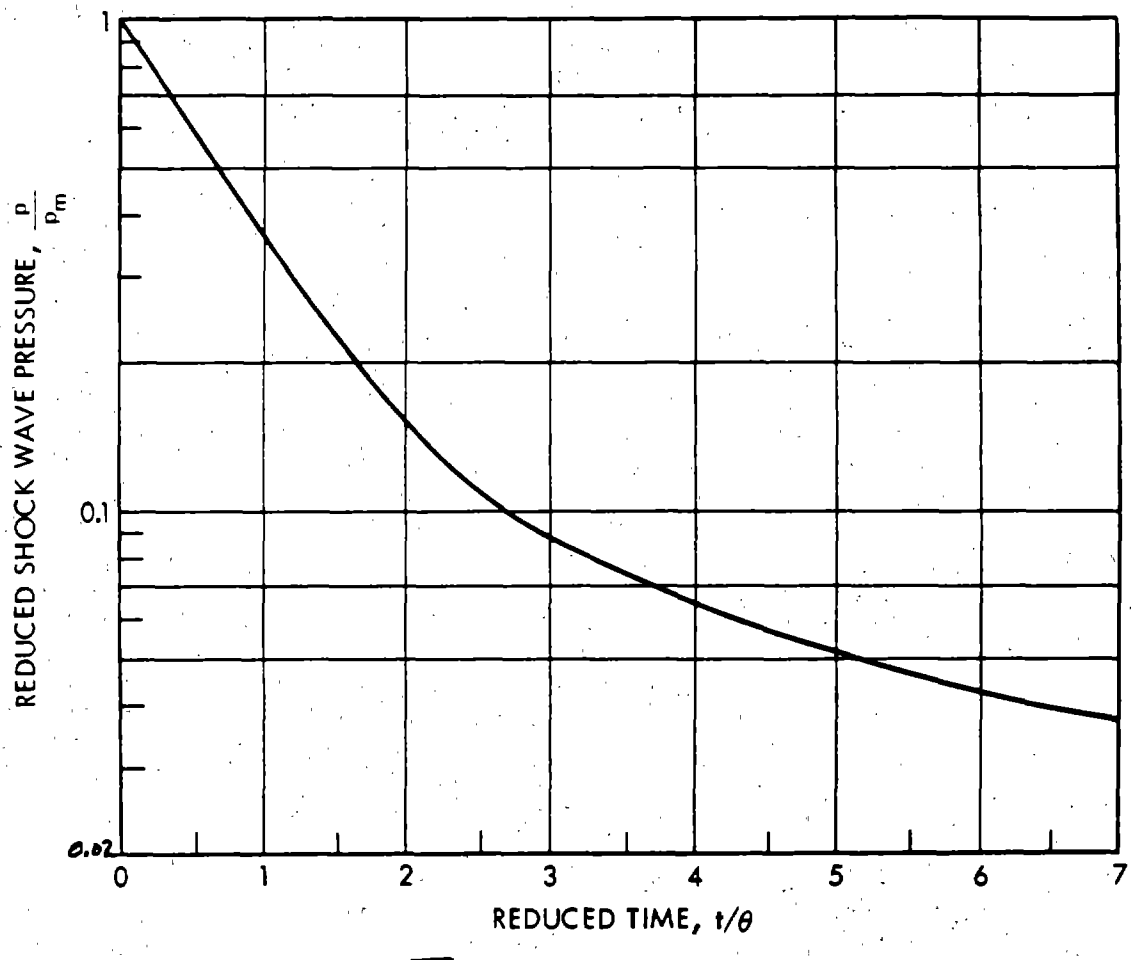

Figure 2-116. [redacted] Pressure-Time for Free Isovelocity Water Shock Waves from Nuclear Explosion [redacted]

[redacted]

[redacted]

Problem 2-30. Calculation of Shock Wave Parameters for Reduced Water Depths, $d_w/W^{1/3} \leq 2{,}000$ ft/kt$^{1/3}$

[redacted] Figures 2-117 through 2-120 show the influence of surface and bottom reflection on the primary shock wave. The curves are drawn through values of peak pressure and impulse at mid-depth both for explosions at mid-depth (Figures 2-117 and 2-118) and at the bottom (Figures 2-119 and 2-120). The solid curves indicate the approximate coverage of the data. As the water depth approaches zero the dashed curves approach the values for air blast at ground level. Transition to the free-water shock parameters (Figures 2-112 through 2-116) occurs as the water depth increases. In the anomalous region near the water surface, the reflected tension waves lead to a sharp reduction of pressure and impulse (Figure 2-94).

[redacted] The curves in Figures 2-117 through 2-120 were derived mainly from H.E. data; however, they were shifted to agree with nuclear data for the limit of free isovelocity water. In most instances, the shift (or conversion factor) was in agreement with the factors determined separately for converting from H.E. to nuclear data in deep water. Most of the data were obtained for the mid-depth location of both the charge and the pressure gauges. All of the curves pertain to either a coral sand or an ordinary sand bottom material. [redacted]

DNA (b)(3)

[redacted] Detailed shock wave measurements have been made over concrete, sand, and clayey-silt bottoms to assess the effects of shock reflection from various bottom materials. Measurements were made within 48 ft from 10-lb TNT charges in 20 ft of water. Both the charge and gauges were placed deeper than mid-depth to minimize the effects of surface reflection.

[redacted] Briefly, the following effects were observed for the shock strength, impulse, and energy flux as compared with values at the same range in free water. Near the bottom and away from the charge, the pressure fronts of the incident and reflected shocks were nearly equal. Near the charge and away from the bottom, the reflected shock was about one-fifth as strong as the incident shock. The impulse of the shock wave increased as much as 100 percent near the charge over concrete, but there was little change at the greatest range from the charge. The impulse increased near the charge but decreased further away from it over clayey-silt and sand. The increase was as much as 40 percent over silt and 20 percent over sand. The decrease was as much as 50 percent over silt and 30 percent over sand. The observed changes in energy flux were roughly comparable with those for impulse, although the energy decreased as much as 30 percent away from the charge over concrete.

[redacted] The shock wave duration T in milliseconds can be approximated with

$$T = \frac{KI}{p_m}$$

$$K \approx 1.8 + 0.0021 \left(d_w/W^{1/3}\right)$$

$$\text{for } 2{,}000 > \left(d_w/W^{1/3}\right) > 100$$

$$K \approx 3.0 - 0.01 \left(d_w/W^{1/3}\right)$$

[redacted]

[redacted]

[redacted]

[redacted]

$$\text{for } \left(d_w/W^{1/3}\right) < 100$$

where

d_w = water depth (ft)

I = shock wave impulse (psi-msec)

p_m = peak shock pressure (psi).

[redacted] The shock wave energy flux for an explosion at a reduced depth of approximately 250 ft/(kt)$^{1/3}$ is related to the shock wave impulse I, and peak pressure by

$$E_{250} \approx 1.2 \times 10^{-4} p_m I \text{ in.-lb/in.}^2,$$

and at reduced depths equal to or greater than 2,000 ft/(kt)$^{1/3}$ by

$$E_{2,000} \approx 9.0 \times 10^{-5} p_m I \text{ in.-lb/in.}^2.$$

For intermediate depths, a linear interpolation between the two values can be adopted.

[redacted] The following approximations can be used to estimate the shock parameters at various gauge depths when the charge is at mid-depth, when $250 < R/W^{1/3} < 2{,}500$ and when $70 < d_w/W^{1/3} < 200$.

Gauge Depth / Water Depth	*Fraction of Value at Mid-Depth*
3/4 to 1	0.9 for peak pressure 0.8 for impulse 0.7 for energy impulse
1/4	0.8 for peak pressure 0.7 for impulse 0.6 for energy flux
0	Use air blast loading

[redacted] *Example* [redacted]

Given: A 1 Mt explosion at a depth 2,500 ft in water having a depth of 5,000 ft.

Find: The peak pressure, the impulse, shock wave duration, and the energy flux depth of 2,500 ft and a horizontal range 20,000 ft.

Solution: The reduced water depth is

$$\frac{d_w}{W^{1/3}} = \frac{5{,}000}{(1{,}000)^{1/3}} = 500 \text{ ft.}$$

The reduced burst depth is

$$\frac{d_b}{W^{1/3}} = \frac{2{,}500}{(1{,}000)^{1/3}} = 250 \text{ ft.}$$

The reduced range is

$$\frac{R}{W^{1/3}} = \frac{20{,}000}{(1{,}000)^{1/3}} = 2{,}000 \text{ ft.}$$

Since the explosion is at mid-depth, Fig 2-117 and 2-118 apply. From Figure 2-117, peak pressure is

$$p_m = 700 \text{ psi.}$$

From Figure 2-118, the reduced positive imp is

$$\frac{I}{W^{1/3}} = 9{,}000 \text{ psi-msec/(kt)}^{1/3}.$$

Since $2{,}000 > \left(d_w/W^{1/3}\right) > 100$, the shock v duration equations give

$$K = 1.8 + 0.0021 \left(d_w/W^{1/3}\right)$$

[redacted]

[redacted]

[redacted]

[redacted]

$$K = 1.8 + (0.0021)(500) = 2.85$$

Answer: The peak pressure is

$$p_m = 700 \text{ psi.}$$

The positive impulse is

$$I = (9{,}000)(W^{1/3}) = 90{,}000 \text{ psi-msec}$$

The shock wave duration is

$$T = \frac{KI}{p_m} = \frac{(2.85)(9 \times 10^4)}{700} = 366 \text{ msec.}$$

The shock wave energy flux is

$$E_{250} = 1.2 \times 10^{-4} p_m I$$

$$E_{250} = (1.2 \times 10^{-4})(700)(9 \times 10^4)$$
$$= 7.6 \times 10^3 \text{ in. lb/in.}^2.$$

[redacted] *Reliability:* Peak pressures obtained from Figures 2-117 and 2-119 are estimated to be reliable within about ±30 percent. Impulses obtained from Figures 2-118 and 2-120, and energy fluxes are estimated to be reliable to within about ±50 percent.

[redacted] *Related Material:* See paragraphs 2-68 through 2-72.

[redacted]

[redacted]

[redacted]

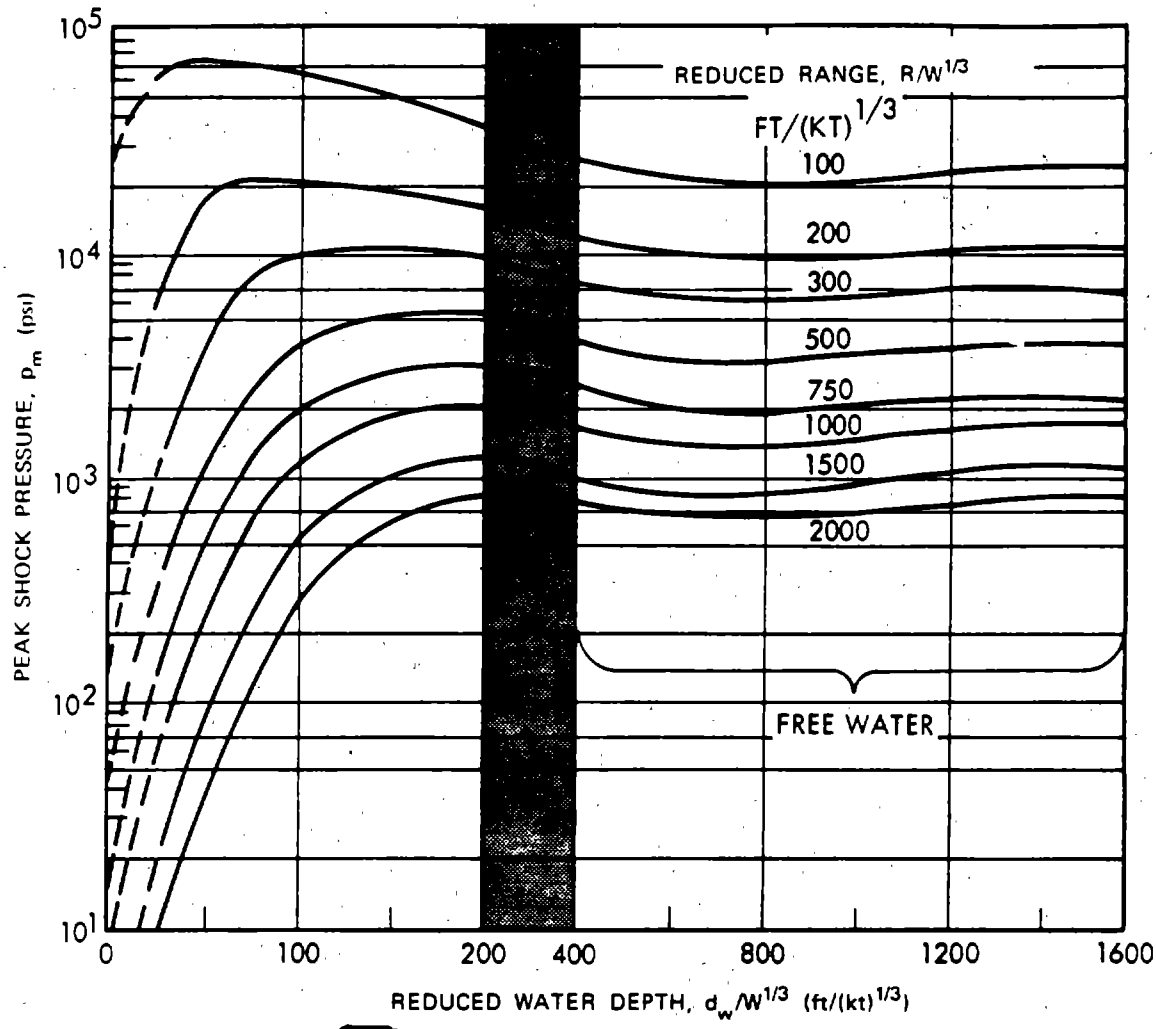

Figure 2-117. [redacted] Peak Shock Pressure vs Reduced Water Depth. Explosion and Gauges at Mid-Depth. [redacted]

[redacted]

[redacted]

[redacted]

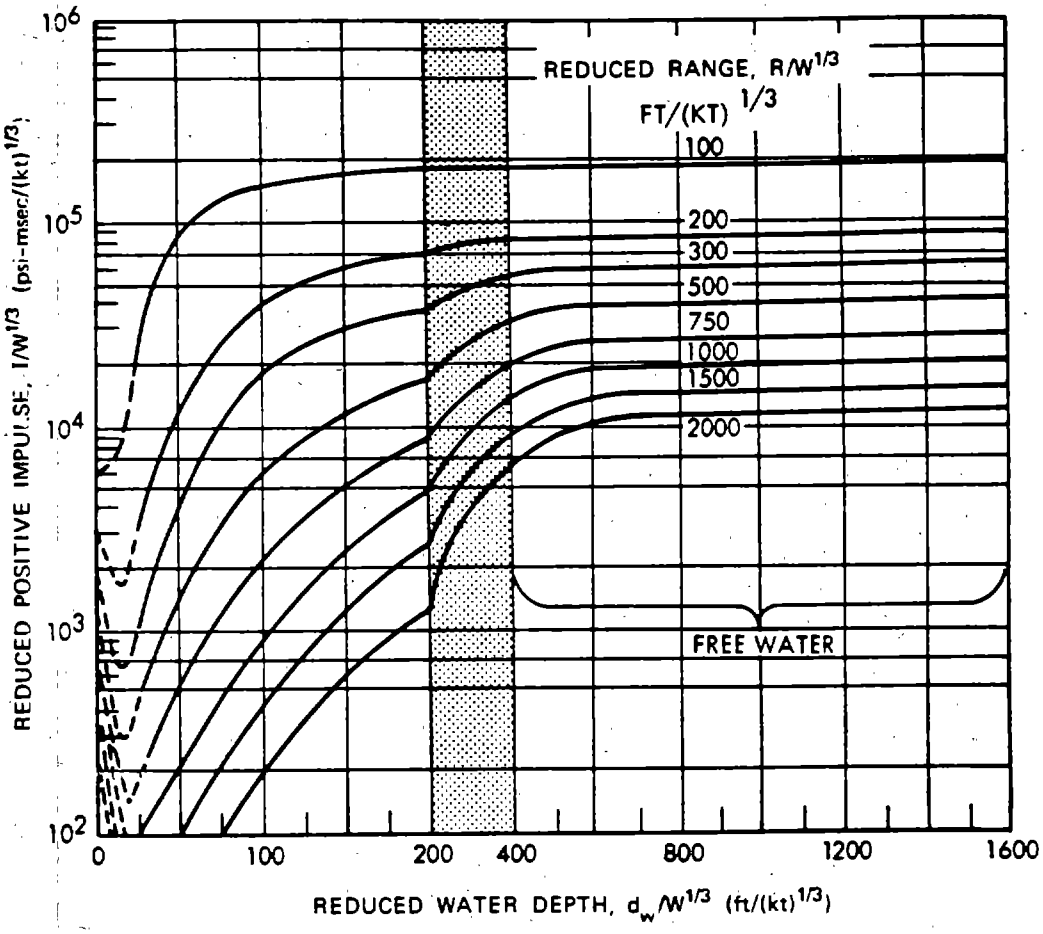

Figure 2-118. [redacted] Reduced Positive Impulse of Shock Wave vs Reduced Water Depth. Explosion and Gauges at Mid-Depth. [redacted]

[redacted]

[redacted]

[redacted]

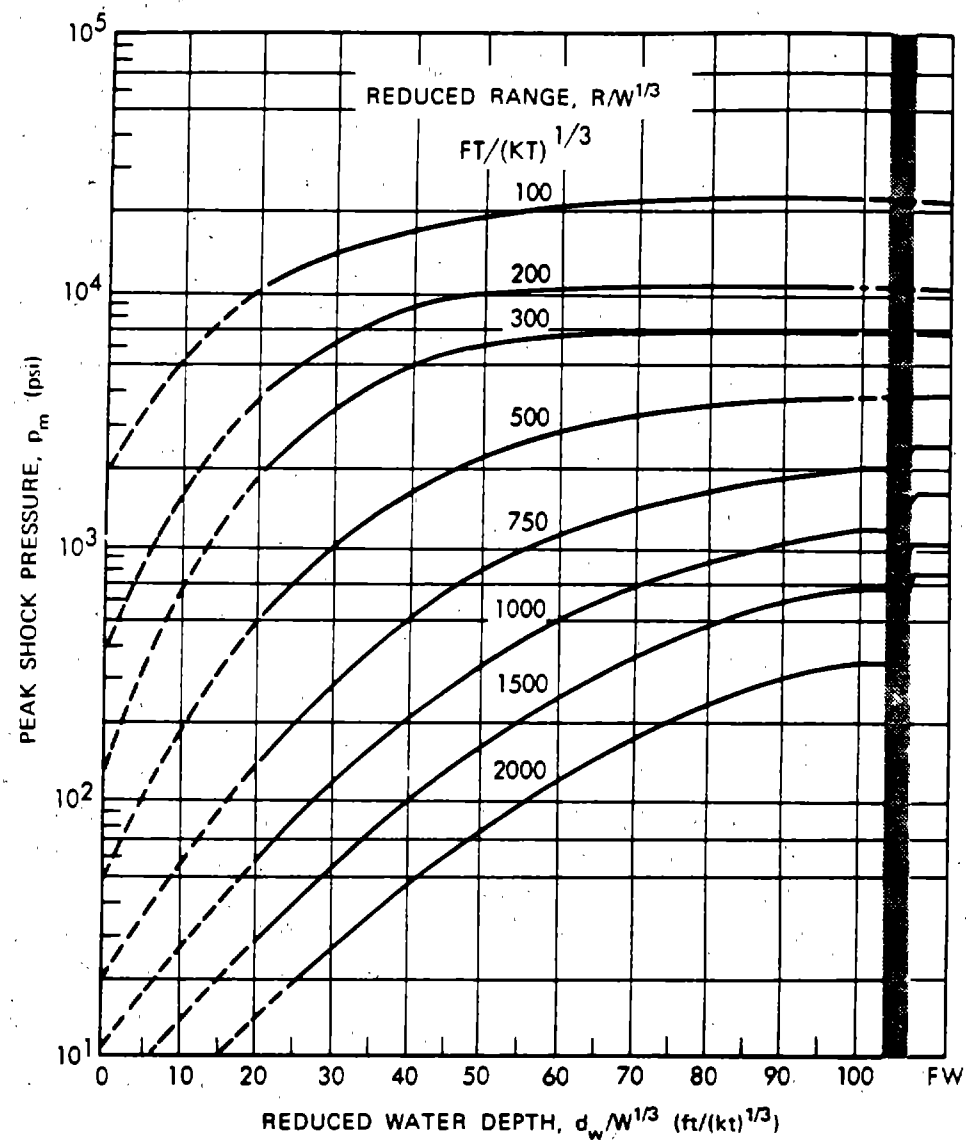

Figure 2-119. [redacted] Peak Shock Pressure vs Reduced Water Depth. Explosion on Bottom, Gauges at Mid-Depth. [redacted]

[redacted]

[redacted]

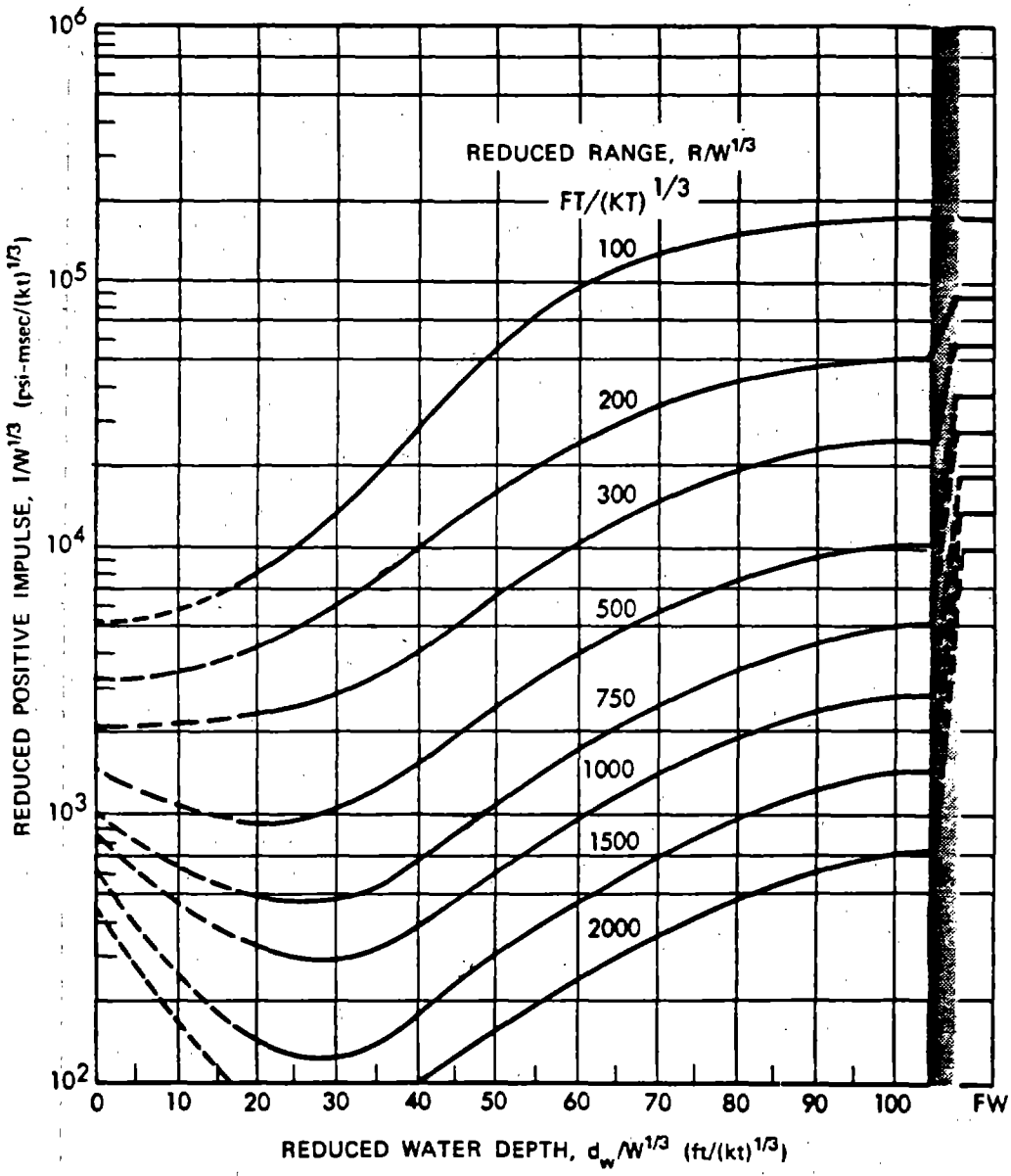

Figure 2-120. [redacted] Reduced Positive Impulse vs Reduced Water Depth. Explosion on Bottom, Gauges at Mid-Depth. [redacted]

[redacted]

[redacted]

Problem 2-31. Calculation of Peak Overpressure Along the Water Surface as a Function of Underwater Burst Depth

[redacted] Figure 2-121 shows the relations to obtain the maximum air blast overpressure from a scaled underwater explosion as a function of depth of burst and horizontal distance. The air blast is for an altitude just above the surface of the water. To determine the air blast at other altitudes, see the references listed in paragraph 2-72.

[redacted] *Example* [redacted]

Given: A 10 kt explosion at a depth of 500 ft in deep water.

Find:

a. The horizontal distance at which a 0.5 psi peak air blast overpressure would be predicted.

b. The upper and lower limits of the range for item a. that would cover the estimated accuracy.

Solution: The reduced depth of burst is

$$\frac{d_b}{W^{1/3}} = \frac{500}{(10)^{1/3}} = 232 \text{ ft/(kt)}^{1/3}.$$

From Figure 2-121, the intersection of the 0.5 psi curve with a reduced depth of 232 ft/(kt)$^{1/3}$ occurs at a reduced horizontal distance of 0.7 kft/(kt)$^{1/3}$.

Answer:

a. The predicted horizontal distance at which 0.5 psi will occur is

$$d = 0.7\ W^{1/3} = (0.9)(10)^{1/3}$$

$$d = 1.50 \text{ kilofeet} = 1{,}500 \text{ feet}.$$

b. The estimated accuracy in predicting the distance for a given overpressure is ±30 percent (see "Reliability" below). Thus, the limits are

$$d = 1{,}500 \times 1.3 = 1{,}950 \text{ ft (upper limit)}.$$

$$d = 1{,}500 \times 0.7 = 1{,}050 \text{ ft (lower limit)}.$$

[redacted] *Reliability:* The accuracy of the relation in Figure 2-121 has not been tested rigorously. The relations provide an approximation based on high-explosive underwater tests and confirmed by a few measurements made at nuclear underwater tests. However, it is felt that ±30 percent in predicting the distances for maximum overpressure is a realistic accuracy estimate.

[redacted] *Related Material:* See paragraph 2-72.

[redacted]

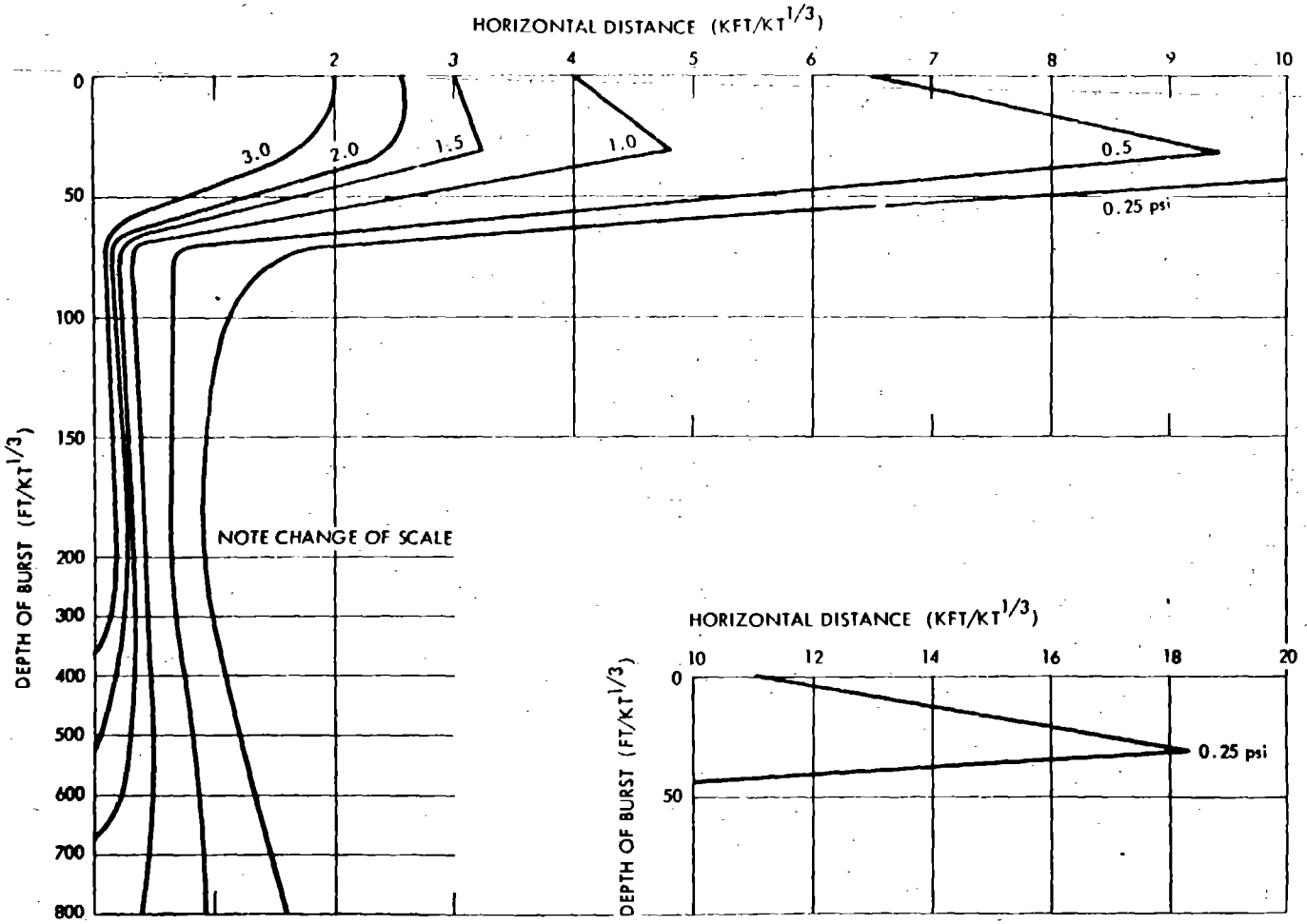

Figure 2-121. [redacted] Peak Air Blast Overpressure Along the Water Surface from Underwater Nuclear Explosions [redacted]

[redacted]

Problem 2-32. Calculation of the Extent, Initial Vertical Velocity, and Approximate Height of the Spray Dome

[redacted] The maximum extent of the spray dome can be estimated with the following relations, which are valid for reduced depths of burst as large as:

$$d_b/W^{1/3} \leqslant 1{,}260 \text{ ft/(kt)}^{1/3}$$

$$r_{sd} = d_b \tan \delta_{max}$$

$$\delta_{max} = 85.3 - 0.021\ (d_b/W^{1/3})$$

where (as shown in the following sketch)

r_{sd} = the horizontal extent of the spray dome (ft).

δ = the spray dome angle, the angle between a vertical line passing through the center of the burst and a line passing through the point of interest on the surface and the center of the burst (degrees).

d_b = the burst depth (ft).

W = the weapon yield (kt).

h = maximum spray dome height (ft).

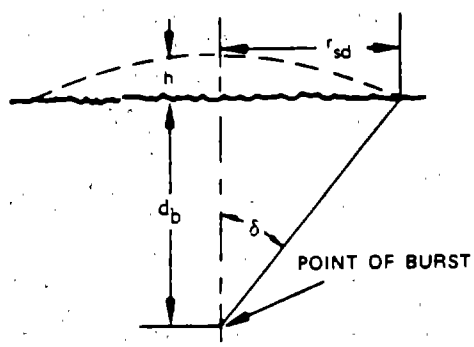

[redacted] Initial spray velocities can be calculated from:

$$V_o = (144 \cos \delta) \frac{p_m}{U}$$

where at a point on the surface,

p_m = peak shock pressure (psi).

U = shock front propagation velocity (ft/sec).

V_o = initial spray velocity (ft/sec.)

[redacted] Values of p_m are given in Figure 2-112. Values of U are given in Figure 2-122 as a function of p_m. In practice, the presence of the bottom does not appear to have an influence upon the value for the spray velocity. However, for bursts on the bottom, the yield should be doubled (as an upper limit estimate) when calculating spray velocities.

[redacted] Higher velocities than given by the above equation have been observed for deep bursts,* therefore a 50 percent safety factor should be added to calculate values of initial dome velocity.

[redacted] An upper limit of dome height h can be derived from:

$$h = V_o t - (f)t^2$$

where

t = time (sec),

f = retardation factor (ft/sec^2),

[redacted] Choppy sea, together with "Taylor instability" appear to account qualitatively for this observation.

[redacted]

[redacted]

[redacted]

by assuming that gravity is the only retarding force and, therefore, that f = 16 ft/sec^2. The time that the upper limit height is reached can be determined that the first derivative of h with respect to time (that is, dome velocity) = zero at that time. Therefore,

$$\frac{dh}{dt} = 0 = V_o - 2(f)t$$

[redacted] *Example* [redacted]

DNA (b)(3)

Given: [redacted]

[redacted]

DNA (b)(3)

[redacted] *Reliability:* Spray dome angles are estimated to be reliable to within ±10 percent for $d_b/W^{1/3} < 1{,}260$ ft/(kt)$^{1/3}$. Initial vertical velocities that are calculated by the equations given above might be low by as much as 50 percent, therefore, a safety factor is included in the method. The retardation factor f is taken to be 16 ft/sec^2 to obtain an upper limit for dome height. Actual retardation factors as large as 30 ft/sec^2 have been observed during nuclear tests. [redacted] *Related Material:* See paragraph 2-73.

[redacted]

[redacted]

[redacted]

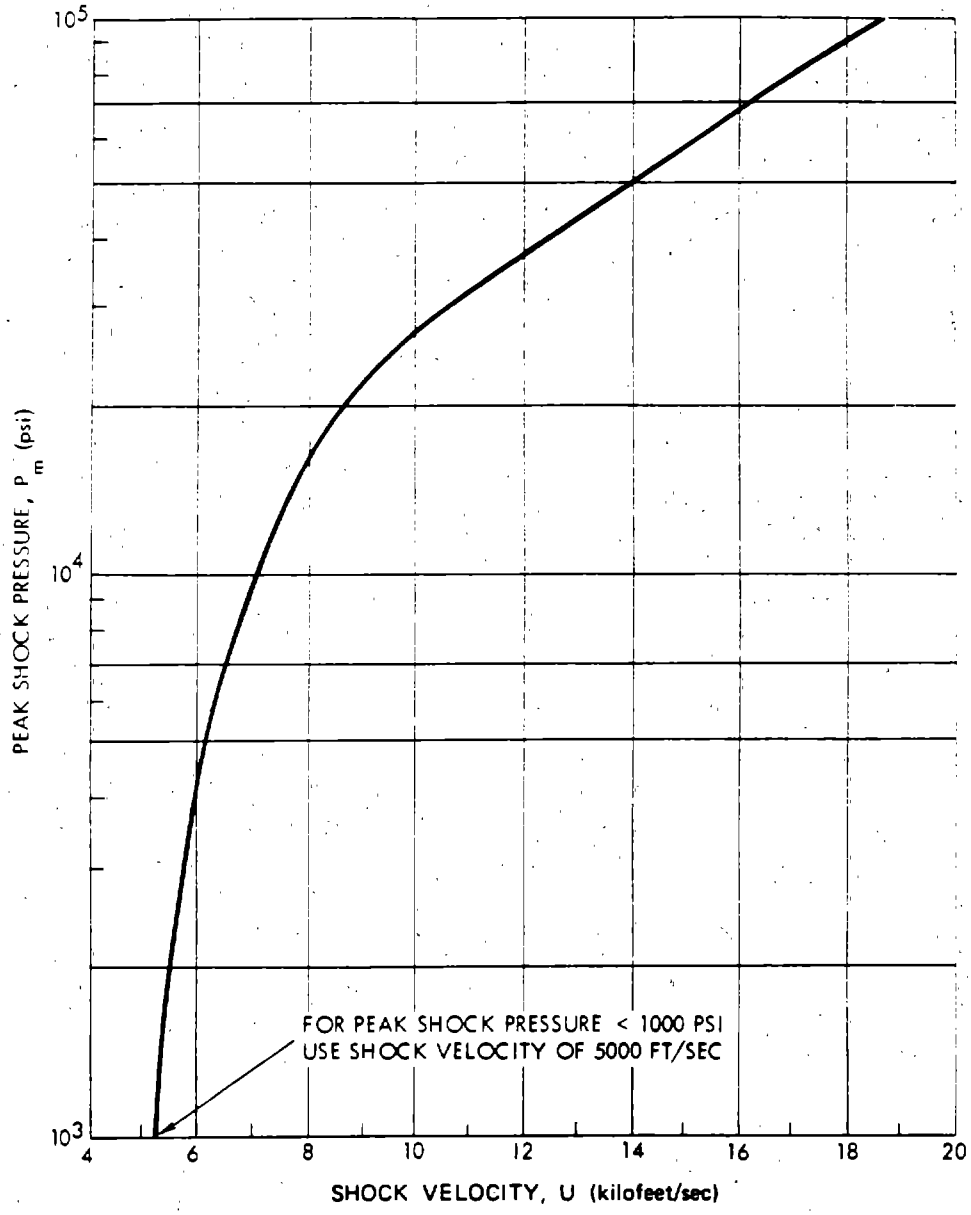

Figure 2-122. [redacted] Velocity of Shock Wave in Free Water vs Peak Shock Pressure [redacted]

[redacted]

[redacted]

Problem 2-33. Calculation of Plume, Column, and Cauliflower Formation

[redacted] Figure 2-123 shows reduced plume dimensions as a function of reduced time for very deep and deep explosions. Figure 2-124 shows reduced plume dimensions for shallow bursts and cloud dimensions. The criteria for determining the explosion categories as a function of depth of burst and weapon yield are given in Figure 2-105 and Table 2-8. The accuracy of the predictions obtained from Figures 2-123 and 2-124 has not been established firmly because of the limited number of nuclear tests upon which they are based.

[redacted] *Example* [redacted]

Given: A 10 kt explosion at a depth of 500 ft in deep water.

Find: The plume radius and plume height 15 seconds after the explosion.

Solution:

$$240\ W^{1/4} = 427\ \text{ft}$$

$$700\ W^{1/4} = 1{,}245\ \text{ft}.$$

Since $240\ W^{1/4} < d_b < 700\ W^{1/4}$, this is a deep burst. The reduced time is

$$\frac{t}{W^{1/3}} = \frac{15}{(10)^{1/3}} \approx 7\ \text{sec/(kt)}^{1/3}.$$

From Figure 2-123, the reduced plume height is about 800 ft/(kt)$^{1/3}$, and the reduced plume radius is about 700 ft/(kt)$^{1/3}$.

Answer:

$$\text{Plume height} \approx 800\ W^{1/3} \approx (800)(10)^{1/3} \approx 1{,}700\ \text{ft},$$

$$\text{Plume radius} \approx 700\ W^{1/3} \approx (700)(10)^{1/3} \approx 1{,}500\ \text{ft}.$$

[redacted] *Reliability:* The curves in Figures 2-123 and 2-124 are estimated to be reliable to within ±30 percent. For safety considerations, multiply the radius and the height by 1.3. For assurance of damage, multiply the values obtained from the figures by 0.7.

[redacted] *Related Material:* See "SURFACE EFFECTS OTHER THAN WAVES," in particular paragraph 2-74. See also Table 2-8 and Figure 2-105.

[redacted]

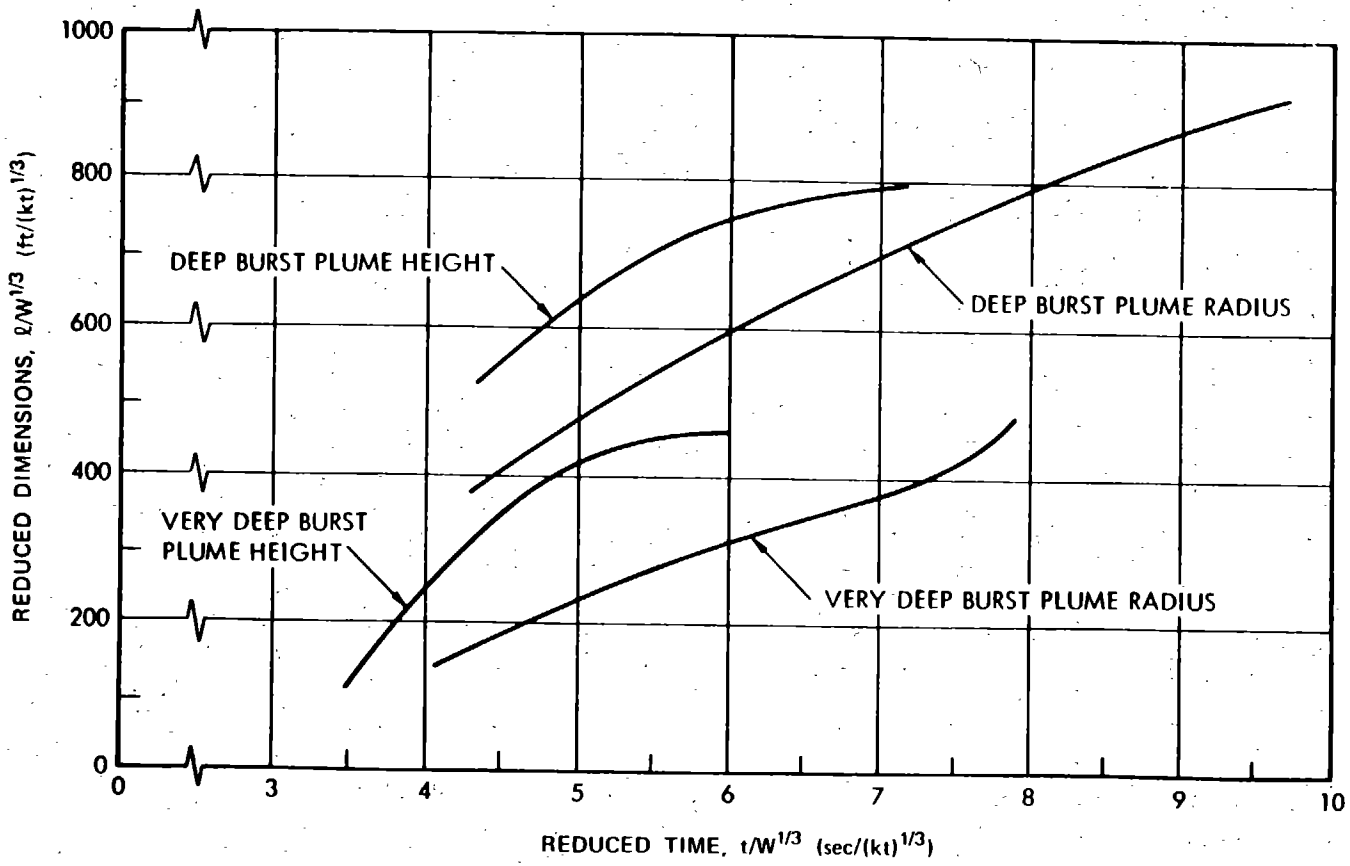

Figure 2-123. [redacted] Plume Dimensions for Deep and Very Deep Underwater Bursts [redacted]

[redacted]

[redacted]

[redacted]

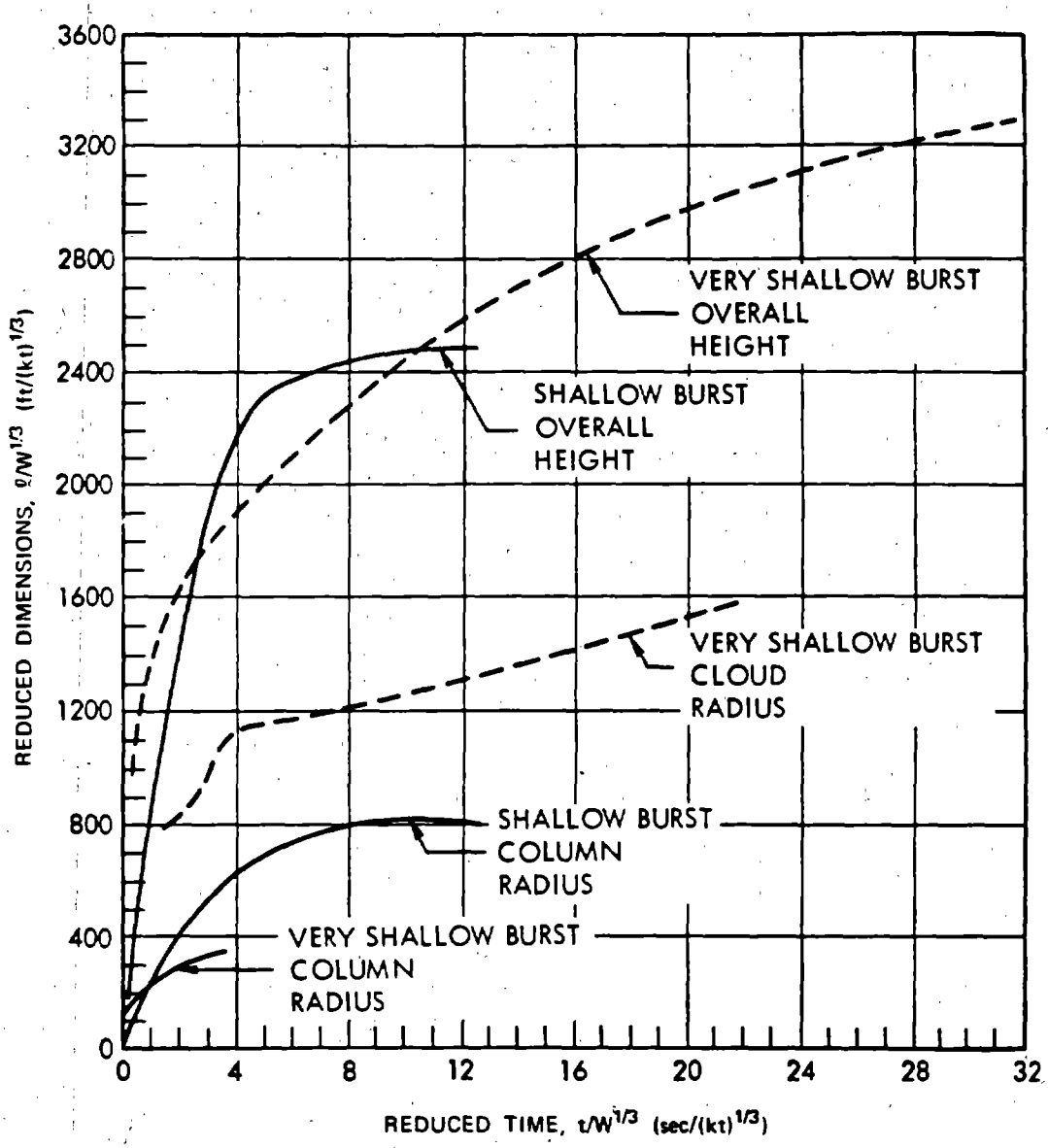

Figure 2-124. [redacted] Column and Cloud Dimensions for Shallow and Very Shallow Bursts [redacted]

[redacted]

[redacted]

Problem 2-34. Calculation of Base Surge Growth and Cloud Height

[redacted] The reduced outside radius of various base surge clouds is shown in Figures 2-126 and 2-127 as a function of reduced time after burst. Figure 2-126 shows a curve that is applicable to shallow and very shallow bursts, while Figure 2-127 shows separate curves for deep and very deep bursts (see Table 2-8 and Figure 2-105 for burst depth categories). Equations that relate the reduced radii and times to actual radii and times for various explosion conditions are shown below:

Burst Classification	Reduced Radius, R_{sr} (Dimensionless)	Reduced Time, t_{sr} (sec/ft$^{1/2}$)	Equation for Estimated* D_{max} (ft) or A_{max}	Applicable Figure
Very shallow	R_s/D_{max}	$t_s(D_{max})^{1/2}$	$D_{max} = 710\ W^{1/3}$*	2-125
Shallow	R_s/D_{max}	$t_s(D_{max})^{1/2}$	$D_{max} = 377\ W^{1/3}\ (d_b/W^{1/3})^{1/6}$	2-125
Deep and very deep	R_s/A_{max}	$t_s(A_{max})^{1/2}$	$A_{max} = 1{,}500\ (W/Z)^{1/3}$	2-126

[redacted] [redacted] The equation $D_{max} = 710\ W^{1/3}$ is valid for very shallow explosions off the bottom. The equation $D_{max} = 377\ W^{1/3}\ (d_b/W^{1/3})^{1/6}$ is valid for very shallow and shallow explosions on a bottom.

[redacted]

[redacted]

[redacted]

[redacted]

where

W = yield of the weapon (kt)

R_s = radius of the base surge (ft)

t_s = time after explosion (sec)

d_b = depth of the explosion (ft)

Z = $d_b + 33$ = total hydrostatic pressure at d_b (ft of water)

D_{max} = estimated maximum column radius (ft)

A_{max} = estimated maximum bubble radius (ft).

[redacted] Figure 2-125 was developed to approximate the height of the visible base surge for use with radiation exposure calculations. The curve in Figure 2-125 was drawn under the assumption that the height is not a function of yield or depth of burst. This assumption probably is not correct, but there is not sufficient information to incorporate these parameters.

[redacted] *Example (U):*

Given: A 40 kt explosion at a depth of 200 feet.

Find:

a. The base surge radius R_s.

b. The height of the visible cloud h_c 10 minutes after burst.

Solution: Refer to Table 2-8:

$$21\ W^{1/3} = (21)(40)^{1/3} = 72 \text{ ft},$$

$$75\ W^{1/3} = (75)(40)^{1/3} = 256 \text{ ft},$$

therefore, a 40 kt explosion at a depth of 200 feet is a very shallow explosion. From the relations given above (since the burst was not described as being on the bottom)

$$D_{max} = 710\ W^{1/3} = (710)(40)^{1/3} = 2{,}430 \text{ ft},$$

and

$$t_{sr} = \frac{t_s}{(D_{max})^{1/2}} = \frac{600}{(2{,}430)^{1/2}} = 12.2 \text{ sec.}$$

From Figure 2-126, the reduced base surge radius is about 7.

Answer:

a. $R_s \approx R_{sr} \times D_{max} = (7)(2{,}430)$

$$R_s \approx 17{,}000 \text{ ft.}$$

b. From Figure 2-125, the height of the base surge cloud is

$$h_c \approx 2{,}000 \text{ ft.}$$

[redacted] *Reliability:* Base surge radii obtained from Figures 2-125 and 2-126 are estimated to be reliable to within ±20 percent. No estimate can be made of the reliability of the height of the base surge cloud obtained from Figure 2-127.

[redacted] *Related Material:* See paragraph 2-75. See also Table 2-8 and Figure 2-105.

[redacted]

[redacted]

[redacted]

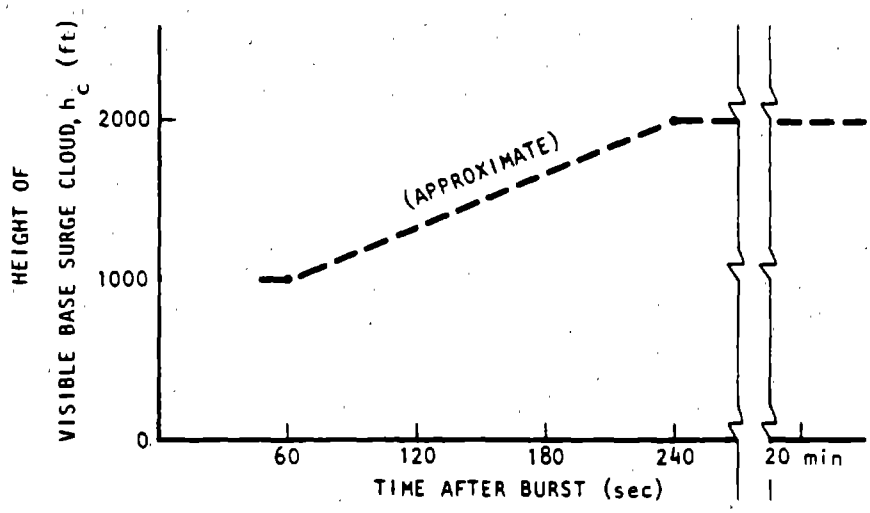

Figure 2-125. [redacted] Height of Visible Base Surge Cloud as a Function of Time After Burst [redacted]

[redacted]

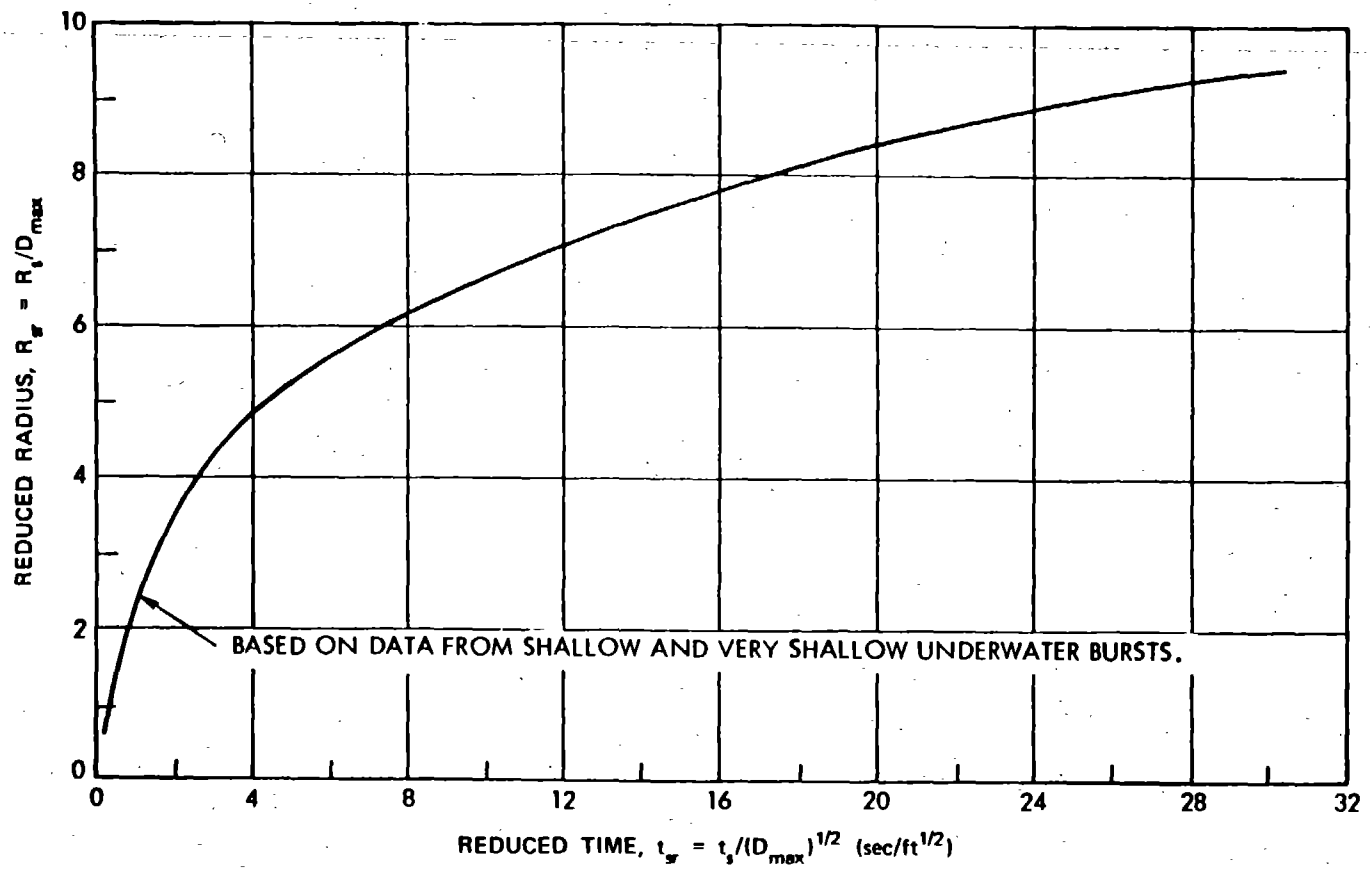

Figure 2-126. Reduced Base Surge Radius vs Reduced Time for Shallow and Very Shallow Bursts

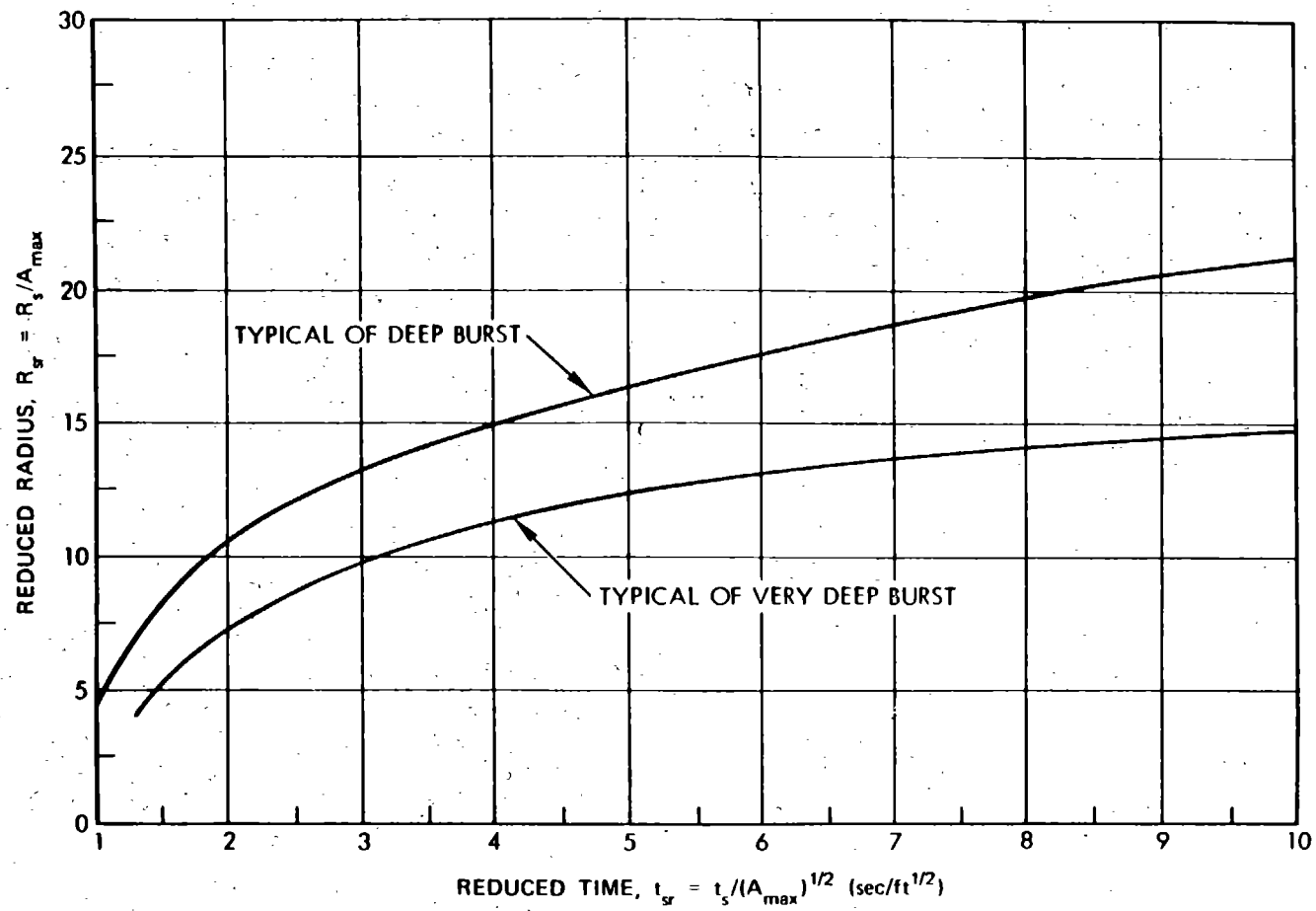

Figure 2-127. [redacted] Reduced Base Surge Radius vs Reduced Time for Deep and Very Deep Bursts [redacted]

[redacted]

[redacted]

Problem 2-35. Calculation of the Properties of Water Surface Waves

[redacted] Figure 2-128 shows the peak wave height (crest to trough) for any depth of burst in shallow water (for waves, shallow water is $0 \leq d_w \leq 100\ W^{1/4}$, see paragraph 2-77), and for any depth of burst not greater than five times the lower critical depth ($0 \leq d_b/5 \leq 170\ W^{1/4}$, see paragraph 2-77) in deep water (for waves $d_w \geq 256\ W^{1/4}$). The dashed transitional curve in Figure 2-128 can be used for intermediate depths. For any depth of burst in shallow water, and for bursts as low as the lower critical depth ($d_b = 170\ W^{1/4}$) in deep water, the foregoing limits on water depth are also the estimated cavity radii as shown in Figure 2-128. For nuclear explosions in deep water at shallow depths of burst near the upper critical depth ($d_b \approx 8.6\ W^{1/3}$), the peak wave height may be nearly twice as large as predicted in Figure 2-128 (see Figure 2-107).

[redacted] *Example*

DNA (b)(3)

[redacted]

[redacted] ***Reliability*** [redacted]

1. Deep water.
   a. The cavity radius given by the equation

DNA (b)(3)

[redacted]

[redacted]

[redacted]

in paragraph 2-77 agrees within [redacted] percent with the measured values shown in Table 2-10 for the H.E. tests at Mono Lake (for which the predicted value is 66.5 ft). [redacted]

DNA (b)(3)

b. The peak wave height given in Figure 2-128 and the equation in paragraph 2-77 agrees with the measured H.E. data within a factor of two, and within [redacted] percent of the measured data of the two nuclear explosions. [redacted]

DNA (b)(3)

2. Shallow water.

a. The cavity radius given by the equation in paragraph 2-77 (and Figure 2-128) provides a lower limit for explosions in shallow water. An upper limit is probably half the maximum bubble radius given by the equation in paragraph 2-67.

b. The peak wave height given by the equation in paragraph 2-77 (and in Figure 2-128) agrees with the measured values within about a factor of 2, which is roughly the uncertainty of the data. [redacted]

Related Material: See paragraphs 2-67 and 2-77. See also Tables 2-9 and 2-10.

[redacted]

[redacted]

[redacted]

Problem 2-36. Calculation of Underwater Crater Dimensions

[redacted] Figures 2-129 through 2-131 show the apparent crater radius, the apparent crater depth, and the average height of the crater lip, respectively, as a function of weapon yield. Figures 2-129a, 2-130a, and 2-131a are for surface bursts. Figures 2-129b, 2-130b, and 2-131b are for bursts near a clayey sand bottom. Linear interpolation between the curves may be used for bursts between the surface and the bottom. [redacted] The curves in Figures 2-129 through 2-131 were developed from nuclear cratering data; however, H.E. data were used to obtain scaling laws and the shape of the curves for bottom placement. Data from about 600 H.E. and [redacted] nuclear explosions were used in the preparation of the curves. The nuclear data are shown in Table 2-11, [redacted]

DNA (b)(3)

[redacted] The critical water depth dividing washed and unwashed craters can be found from Figure 2-132 for a clayey-sand bottom. An unwashed crater results when the water depth is less than the minimum height of the irregular cavity lip and when the lip does not fail. For other bottom materials, the critical water depth can be found by multiplying the value of d_c by the appropriate soil factor for crater lip height in Table 2-12. [redacted]

Example [redacted]

Given: A 40 kt explosion on the bottom, which consists of oceanic ooze, in 60 feet of water.

Find: The radius, depth, and lip height of the apparent crater.

Solution: From Figures 2-129, 2-130, and 2-131, the crater dimensions in clayey sand are

[redacted]

[redacted]

Table 2-12. [redacted] Soil Factors for Cratering in Various Materials as Compared with Clayey Sand [redacted]

Material	Soil Factors		
	Crater Radius	Crater Depth	Crater Lip Height
Clayey sand	1.0	1.0	1.0
Sand	1.1	0.8	0.7
Loess	0.9	1.3	1.2
Muck*	1.5	0.5	0.4
Clayey silt	1.1	1.1	1.0
Coral sand	0.9	0.8	0.7
Clay	0.9	1.4	1.3
Soft rock	0.8	0.6	0.6
Hard rock*	0.6	0.4	0.4
Oceanic ooze*	1.7	0.2	0.1

*([redacted] Soil Factors estimated or interpolated from the others based on experimental data.

[redacted]

radius, r_{ac} $\approx$ 750 ft,

depth, d_{ac} $\approx$ 42 ft,

lip height, h_ℓ $\approx$ 1.7 ft.

Answer: The corresponding dimensions for oceanic ooze are (Table 2-12)

$$r_{ac} \approx (1.7)(750) \approx 1{,}275 \text{ ft},$$

$$d_{ac} \approx (0.2)(42) \approx 8 \text{ ft},$$

$$h_\ell \approx (0.1)(1.7) \approx 0.2 \text{ ft}.$$

[redacted] *Reliability* [redacted]

[redacted]

[redacted] Dimensions from these curves are considered to have the following reliabilities:

radius	+150%–50%
depth	+150%–50%
lip height	+160%–60%

The accuracy of the soil factors shown in Table 2-12 is unknown.

[redacted] *Related Material:* See "UNDERWATER CRATERING," page 2-223.

[redacted]

[redacted]

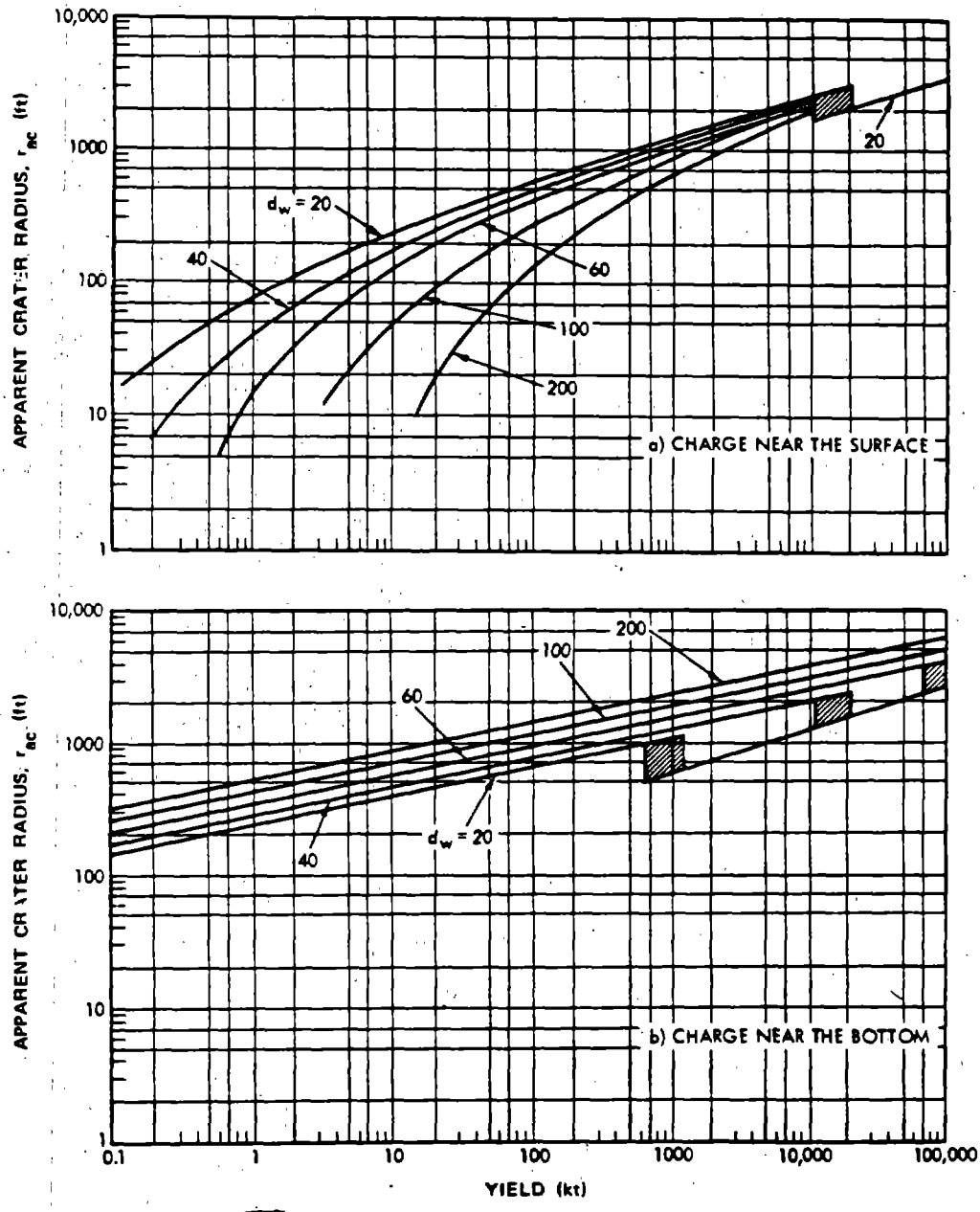

Figure 2-129. [redacted] Apparent Crater Radius as a Function of Yield for Various Water Depths Over a Clayey Sand Bottom, where d_w = Water Depth in Feet. Shaded Areas Denote Possible Transition Regions from a Washed to an Unwashed Crater for d_w = 20, 40, and 60. [redacted]

[redacted]

[redacted]

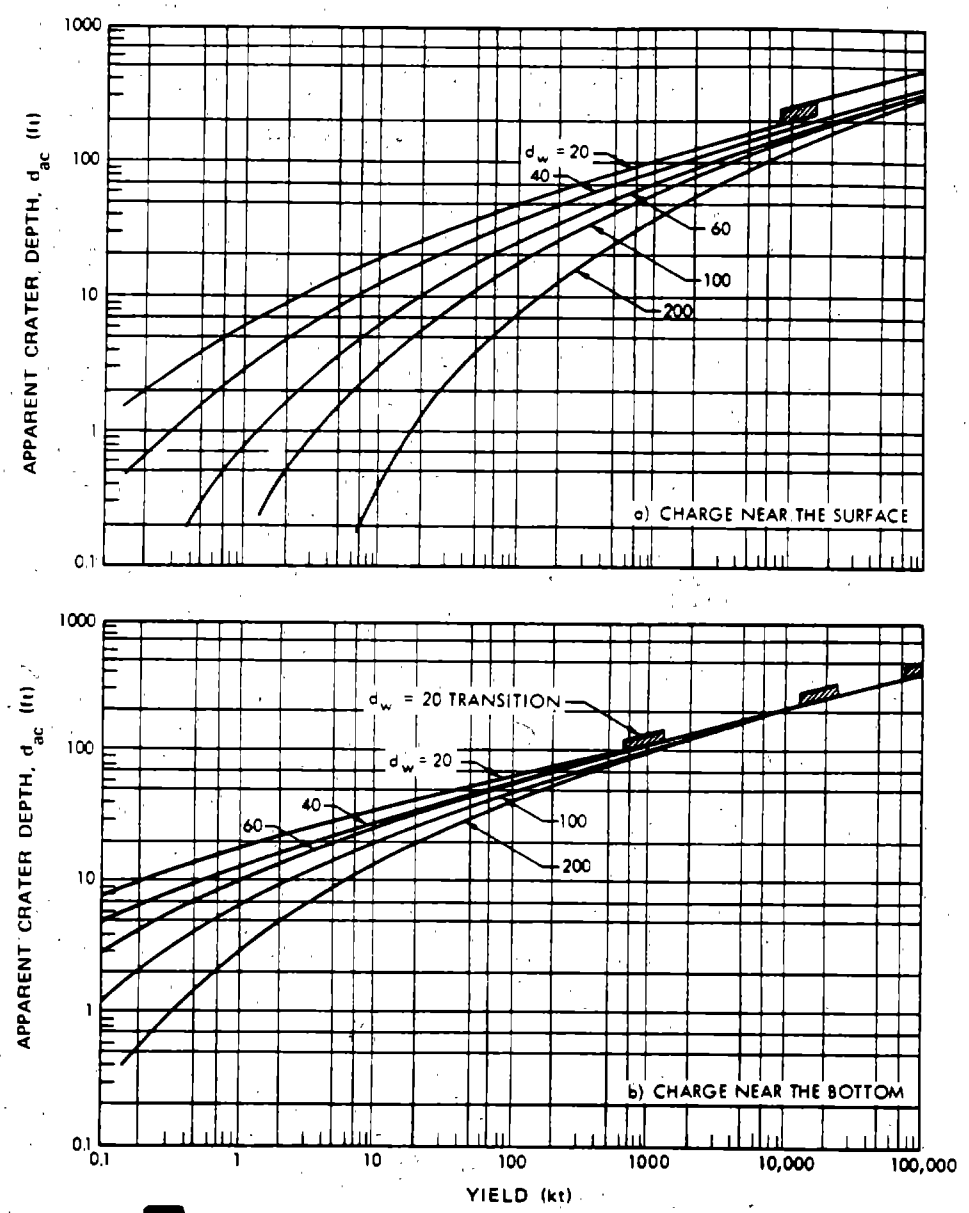

Figure 2-130. [redacted] Apparent Crater Depth as a Function of Yield for Various Water Depths Over a Clayey Sand Bottom, where d_w = Water Depth in Feet. Shaded Areas Denote Possible Transition Regions from a Washed to an Unwashed Crater for d_w = 20, 40, and 60. [redacted]

[redacted]

[redacted]

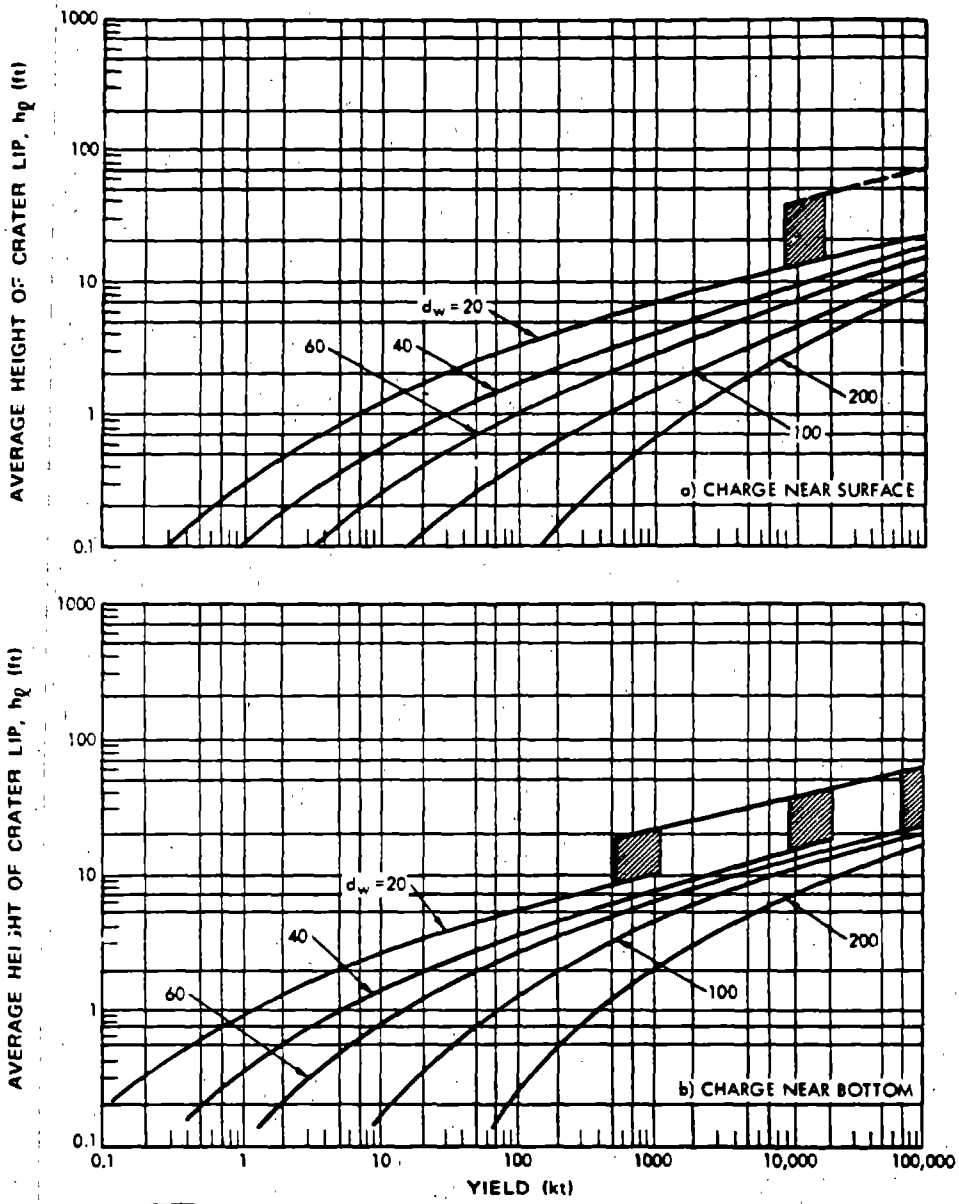

Figure 2-131. [redacted] Average Height of Crater Lip as a Function of Yield for Various Water Depths with the Charge Near a Clayey Sand Bottom, where d_w = Water Depth in Feet. Shaded Areas Denote Possible Transition Regions from Crater for d_w = 20, 40, and 60. [redacted]

[redacted]

[redacted]

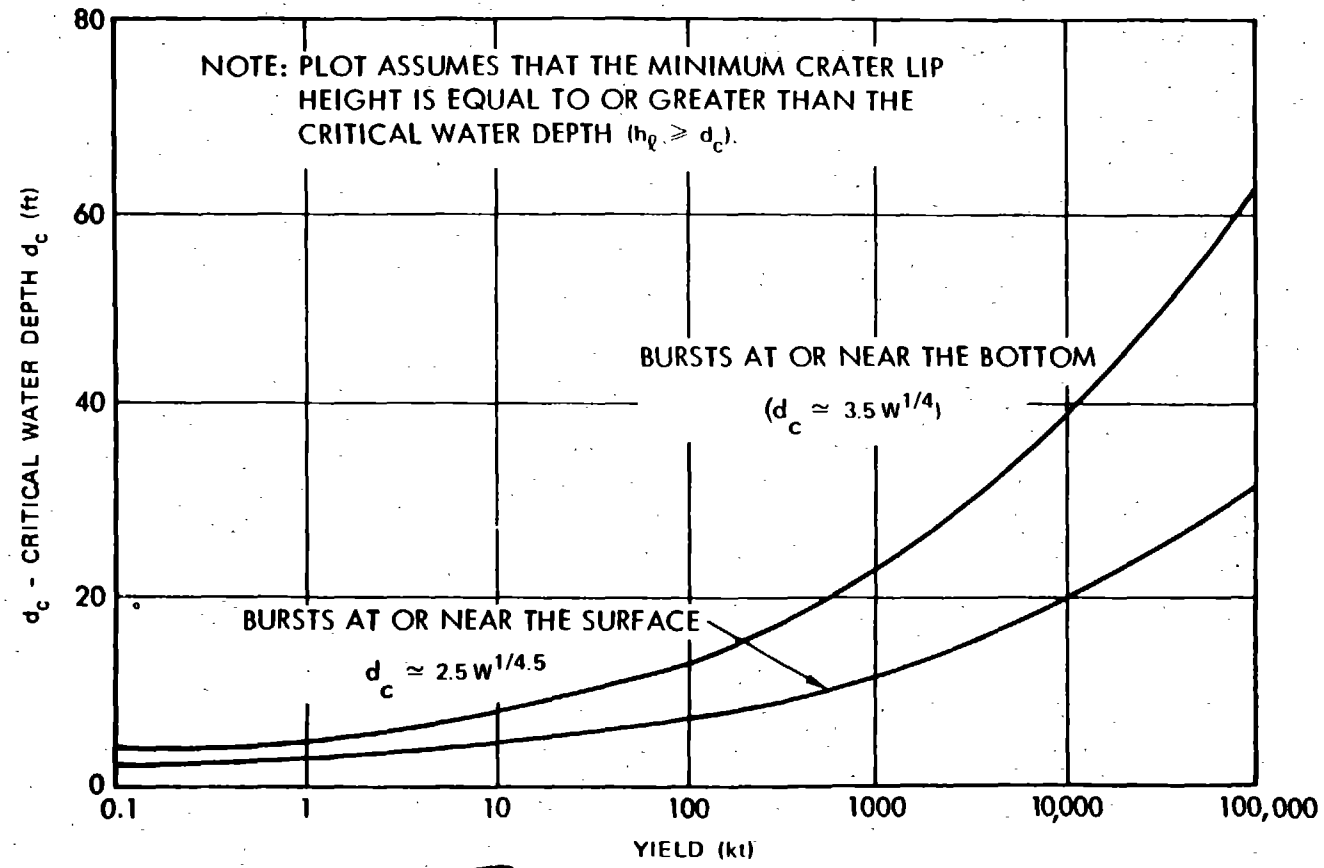

[redacted]

Figure 2-132. [redacted] Estimated Critical Water Depth as a Function of Yield for a Clayey Sand Bottom [redacted]

[redacted]

3-2 Range Effects [redacted]

[redacted] As the thermal energy propagates away from the fireball, the divergence that results from the increasing area through which it passes causes the radiant exposure to decrease as the inverse square of the slant range. At a slant range R centimeters from the source, the thermal energy is distributed over a spherical area of $4\pi R^2$. Since the thermal yield in calories is 10^{12} Wf*, where W is the yield in kilotons, the radiant exposure at a distance R cm in a clear atmosphere is

$$Q = \frac{10^{12} Wf}{4\pi R^2} \text{ cal/cm}^2.$$

[redacted] Kilofeet and kilometers are more convenient units than centimeters for measuring the range from a nuclear burst. Appropriate conversion factors change the form of the equation to

$$Q = \frac{100\ Wf}{4\pi R_{km}^2} = 7.96\ Wf/R_{km}^2 \text{ cal/cm}^2,$$

and

$$Q = 85.7\ Wf/R_{kft}^2 \text{ cal/cm}^2,$$

where R_{km} and R_{kft} are slant ranges in kilometers and kilofeet, respectively.

[redacted] TRANSMITTANCE [redacted]

[redacted] The equations presented above ignored the attenuation by the atmosphere that would affect the thermal energy received by a target. In many cases, particularly when the air is clear and the range is short, atmospheric attenuation is not important. In other situations, scattering and absorption of thermal energy by the atmosphere can reduce the amount of thermal energy reaching the target significantly.

[redacted] In addition to atmospheric attenuation, other effects also must be considered. A cloud layer above a fireball can scatter radiation downward and can increase the thermal energy that reaches the ground. If the ground also is highly reflecting, e.g., if the ground is covered by a layer of snow, further enhancement of the thermal radiation may result.

[redacted] All of these effects are approximated by one factor, the transmittance T. Transmittance is the ratio of the radiant exposure at a target facing the fireball to the radiant exposure that the target would receive if the intervening atmosphere were perfectly transparent.

[redacted] Adding the transmittance factor to the equations given in paragraph 3-2 gives

$$Q = \frac{7.96\ WfT}{R_{km}^2} \text{ cal/cm}^2,$$

and

$$Q = \frac{85.7\ WfT}{R_{kft}^2} \text{ cal/cm}^2.$$

The corresponding expressions for slant range in terms of yield and transmittance are†

$$R_{km} = 2.82\ \sqrt{WfT/Q}$$

$$R_{kft} = 9.26\ \sqrt{WfT/Q}$$

3-3 Specification of Transmittance [redacted]

[redacted] A difficult task in applying transmittance data to a thermal problem is deciding which model atmosphere to use. Various model

---

* [redacted] One kiloton equals 10^{12} calories (see Table 1-2).

† [redacted] A relationship that is easy to remember and that is reasonably correct if it is assumed that the thermal partition, $f = 1/3$, and the transmittance, $T = 1.0$, is that the radiant exposure at one statute mile is about $Q = 1$ cal/cm^2 per kt.

[redacted]

[redacted]

[redacted] atmospheres are identified in terms of parameters that can be measured without special instruments. The first of these is visual range, a parameter that indicates the light transmission properties of the layer of air near the surface. A second is the appearance of the sky, which can be used to indicate the amount of haze or fog that thermal radiation from a high altitude burst must penetrate to reach a target at the surface.

[redacted] Although transmittance can be calculated between any two points in space, a large number of thermal problems involve ground targets. The material presented in this paragraph has been developed primarily to calculate transmittance between the point of burst and a target on the ground. These methods may be extended to calculate transmittance to airborne targets, but the validity of such calculations has not been checked as carefully as has the validity of transmittance calculations for ground targets.

[redacted] Whether or not a particular transmittance calculation is useful depends on the nature of the problem. If the burst is a specific test, the weather at the particular time can be determined, and appropriate transmittances can be assigned. If the burst involves a hypothetical attack at some unknown date, a reliable prediction of the transmittance, and, as a result, the extent of the thermal damage from a particular explosion, is impossible. The atmosphere could be clear or foggy; light combustibles such as leaves or paper could be wet or dry. Yield and position of the weapon are unknown and can only be estimated.

[redacted] Two types of problems provide answers that are sufficiently reliable to be useful. A calculation intended to be conservative from the point of view of the defense indicates the level of damage that an explosion could inflict on a day when the air is clear and the ground is dry. This type of calculation is useful for designating safe areas or designing defense systems. Useful answers also can be obtained in tactical situations. The minimum intercept altitude of a defensive missile might be lowered on a foggy day, and an attacking force might use current weather conditions to determine whether their weapon would produce significant thermal damage or whether they must rely primarily on other effects.

3-4 Model Atmospheres [redacted]

[redacted] The typical cloudless atmosphere has a haze layer near the surface. Often this haze layer is relatively uniform, with a sharply defined upper boundary; when cumulus clouds are present, the bases of these clouds may mark the top of the haze layer.

[redacted] At higher altitudes, the air usually is clearer, and, in the absence of clouds, about 80 percent of the attenuation of radiation from a high altitude source occurs at altitudes below 3 miles. The low density air several miles above the surface offers almost no interference to radiation in the visible and infrared regions of the spectrum.

[redacted] A set of cloudless model atmospheres provides an approximate representation of the optical properties of real atmospheres. These models only represent the atmosphere in a general way, but they form a basis for transmittance calculations. They have the advantage that selection of the appropriate model is based on the simple criterion of daytime visual range. The model atmospheres are cloudless; correction factors introduced into the transmittance calculations account for the effects of clouds. These model atmospheres and the empirical equations that are used with them give reasonably accurate estimates of transmittance if the transmittance is above about 0.1.

[redacted] Current reports consistently use visibility, which is called "visual range" in this chapter, as one means for classifying model atmospheres; however, no standard definition of visibility is adopted consistently. The atmo-

[redacted]

[redacted]

[redacted] sphere described in this chapter as having a visual range of 16 miles would be assigned a visibility of 12 miles by at least one author and a visibility of 24 miles by some others.

[redacted] The extent to which the atmosphere impedes the flow of thermal energy and limits visibility depends largely on the amount of scattering of radiant energy by atmospheric particles. Absorption of energy also affects radiative transport, but absorption usually is less important than scattering. A description of these phenomena is the first step in explaining visual range and transmittance.

[redacted] The thermal radiation of concern in this chapter consists of electromagnetic radiations from the ultraviolet to the infrared. The photons that make up electromagnetic radiations can react with matter in many complex ways, but the photons that constitute the thermal radiation spectrum of a nuclear fireball interact almost exclusively by being absorbed or elastically scattered. If the photon is absorbed, it gives up its energy to the absorbing particle, and this energy ultimately appears as heat. Scattering may be thought of as reflection from a small particle. Its effect is to change the direction in which the photon is traveling. The term "elastic" means that the photon does not lose energy during the scattering process. Other interactions of electromagnetic radiations with matter that are more probable for higher frequency (shorter wavelength) radiations than those of the thermal radiation are described in paragraph 4-3, Chapter 4.

[redacted] The scattering and absorption properties of the atmosphere depend partly on the wavelength of the radiant energy. Wavelength is often measured in microns (1 micron = 10^{-6} meter), for which the symbol is μ. Wavelengths in the visible spectrum may be identified by the relation between wavelength and color: light with a wavelength of 0.7 μ is red; 0.58 μ light is yellow; and 0.48 μ light is blue. White light is a mixture containing all wavelengths in the visible spectrum, which extends from 0.38 to 0.78 μ. The infrared spectrum consists of radiant energy at wavelengths longer than 0.78 μ, and the ultraviolet spectrum consists of radiant energy at wavelengths shorter than 0.38 μ.

[redacted] The energy transport properties of atmospheric particles may be expressed in terms of scattering and absorption cross sections, which are fictitious areas that are a measure of the probability that scattering or absorption will occur. Particles that are small compared to the wavelength of light have scattering cross sections that are inversely proportional to the fourth power of the wavelength. Therefore, air molecules scatter light from the extreme blue end of the visible spectrum (wavelength = 0.38 μ) about 16 times as effectively as they scatter light from the red end of the spectrum (wavelength = 0.78 μ). Blue smoke, which consists of very small particles, has similar scattering properties. Particles that are large compared to the wavelength of light (e.g., haze or fog particles) have scattering cross sections that are much less dependent on wavelength. Individual particles have a scattering cross section that varies somewhat with wavelength, but the mixture of particle sizes found in a haze or fog usually results in an average cross section that is nearly independent of wavelength.

[redacted] The sky is blue because most of the scattering at high altitudes is by air molecules, which scatter blue light more efficiently than they scatter other colors of the visible spectrum. A distant mountain appears blue on a clear day for the same reason.

[redacted] The scattering properties of larger airborne particles may be observed on days when a very light haze reduces visibility to about 10 miles or less. Near the surface, scattering by haze particles contributes more to the light in the air than does scattering by air molecules. The sky still appears blue, but the color is not as deep as

[redacted]

[redacted]

it would be on a clearer day. Distant hills and the sky near the horizon appear to be more gray than blue, which indicates that the lower atmosphere is scattering all wavelengths of light about equally.

Water droplets cause nearly all of the scattering that occurs in a fog or a thick cloud. Consequently, clouds are white and fogs tend to wash out all impressions of color.

Absorption usually has little effect on visible light, but it can affect the infrared and ultraviolet portions of the spectrum significantly. The principal absorber of thermal energy usually is water vapor, which has strong absorption bands in the infrared spectrum. Dry air transmits infrared energy more efficiently than humid air. Carbon dioxide and other gases present in the atmosphere in small amounts also absorb infrared energy.

Ultraviolet energy is absorbed most strongly at the shorter wavelengths: the limiting wavelength that air in the lower atmosphere will transmit is about 0.2 micron. Ozone, appreciable quantities of which are found between roughly 60,000 and 80,000 feet, absorbs ultraviolet radiation with wavelengths shorter than 0.29 micron. As a result of these absorption bands ultraviolet energy that reaches the earth from the sun is almost entirely limited to the spectral band between 0.38 micron (the violet edge of the visible spectrum) and 0.29 micron.

Dark colored particles absorb appreciable energy in all regions of the thermal spectrum. Dust, smoke, and the smoky haze from large cities fall into this category.

Detailed calculations of the complex scattering and absorption processes that can occur between a nuclear explosion and a target require computer codes that are capable of considering detailed changes in the atmosphere and the effect that these changes can have on the entire spectrum of frequencies emitted by the fireball. Monte Carlo calculations have been performed for several model atmospheres and for several discrete wavelengths; however, as of this time, these calculations have not been generalized into a form that is suitable for inclusion in this manual. Therefore, the formulas and curves for atmospheric transmittance that are given below are based on a simplified model based on the concept of effective optical height for single wavelengths.

One way to specify the attenuating properties of the atmosphere as a function of altitude is to assume that the transmittance between the point of burst and ground zero follows an equation of the form

$$T = e^{-\tau(h)},$$

where T is transmittance and $\tau(h)$ is the *effective optical height* of the burst height h. This concept was applied in 1966 to specify one particular model atmosphere for which the visual range is 16 miles.* The attenuation for light of 0.65 micron wavelength was used to specify $\tau(h)$. This choice was a purely empirical one, used because it brought the calculated values of transmittance into general agreement with experimentally determined values. The wavelength that was selected is attenuated less than is the thermal radiation spectrum as a whole;

*[redacted] "Transmissivity of the Atmosphere for Thermal Radiation from Nuclear Weapons" (see bibliography). A 12 mile visual range was assigned to this model atmosphere. This choice was based on a comparison between a large number of visual range estimates at an airport weather station and simultaneous measurements with instruments designed to measure meteorological range. The 16 mile figure is used here because it is consistent with the definition of visual range given in this chapter. Qualitatively, this range is defined as the distance at which a dark object silhouetted against the sky is visible and recognizable. This range is more specifically defined in paragraph 3-7.

[redacted] Although the specification for this model atmosphere has been changed, the reason for having assigned the 12 mile figure carries a useful warning. There is no assurance that even trained meteorologists will make estimates that are consistent with a precise mathematical definition of visual range.

[redacted]

[redacted]

[redacted]

therefore, this choice makes allowance for additional energy that reaches the target by scattering. For bursts below one-quarter mile and surface targets, a wavelength of 0.55 microns was used together with a buildup factor, as described below.

[redacted] Figure 3-2 shows $\tau(h)$ as a function of altitude for this particular model atmosphere. This model shows no attempt to represent an abrupt increase in transparency at the top of the haze layer; optical height is a smoothly varying function of altitude. This approximation to the actual atmosphere does not appear to introduce serious error into the calculations, and it is more convenient than a model atmosphere that requires an estimate of the height of the haze layer as well as an estimate of visual range.

[redacted] When visual range is different from 16 miles, the model atmosphere is specified by multiplying the values of effective optical height in Figure 3-2 by $16/V$, where V is visual range in miles. For example, if the visibility is 8 miles, all values of optical height are doubled, indicating that transparency at all altitudes is reduced by a factor of 2. This transformation may be stated mathematically as

$$\tau(h)_V = \tau(h)_{16} \frac{16}{V}$$

where $\tau(h)_V$ is the effective optical height at a given altitude for the model atmosphere for which visual range is V and $\tau(h)_{16}$ is the effective optical height of the 16 mile model atmosphere at the same altitude.

[redacted] Visual range, a surface measurement, is a poor criterion for predicting the clarity of the air a few miles up. Although there is some correlation between these two quantities, the main justification for this somewhat arbitrary procedure is that the optical thickness assigned to the upper atmosphere, since it is a small fraction of the total optical thickness, has little influence on the calculated transmittance to targets on the ground.

[redacted] If the burst height is less than about one-quarter mile, the line-of-sight path from the burst to the target passes through air which, in most cases, has optical properties that are fairly uniform. In a uniform atmosphere, the attenuation of a direct beam of thermal energy may be related to the visibility of distant objects by the equation.

$$T_d = e^{-2.9\ R/V},$$

where T_d is the transmission coefficient for *direct* flux over a path of slant range R, and V is visual range. As mentioned above, scattered as well as direct flux must be considered. Consequently, transmittance is larger than the transmission coefficient for direct flux and is given approximately by the following empirical equation:

$$T = e^{-2.9\ R/V}\ (1 + 1.9\ R/V).$$

[redacted] The exponential factor in this equation accounts for energy loss from the direct beam by scattering. The expression in brackets is a buildup factor that accounts for energy scattered toward the target. This equation does not specifically involve any property of the model atmosphere other than visual range; however, the properties of the model atmosphere are involved implicitly, because the rate at which transparency changes with altitude helps determine the magnitude of the coefficient 1.9 in the buildup factor. Figure 3-3 shows this relation in graphical form.

[redacted] When the burst height h is greater than about one-quarter mile, transmittance may be calculated from

$$T = e^{-\tau(h)\ \frac{16}{V}\ \frac{R}{h}}$$

[redacted]

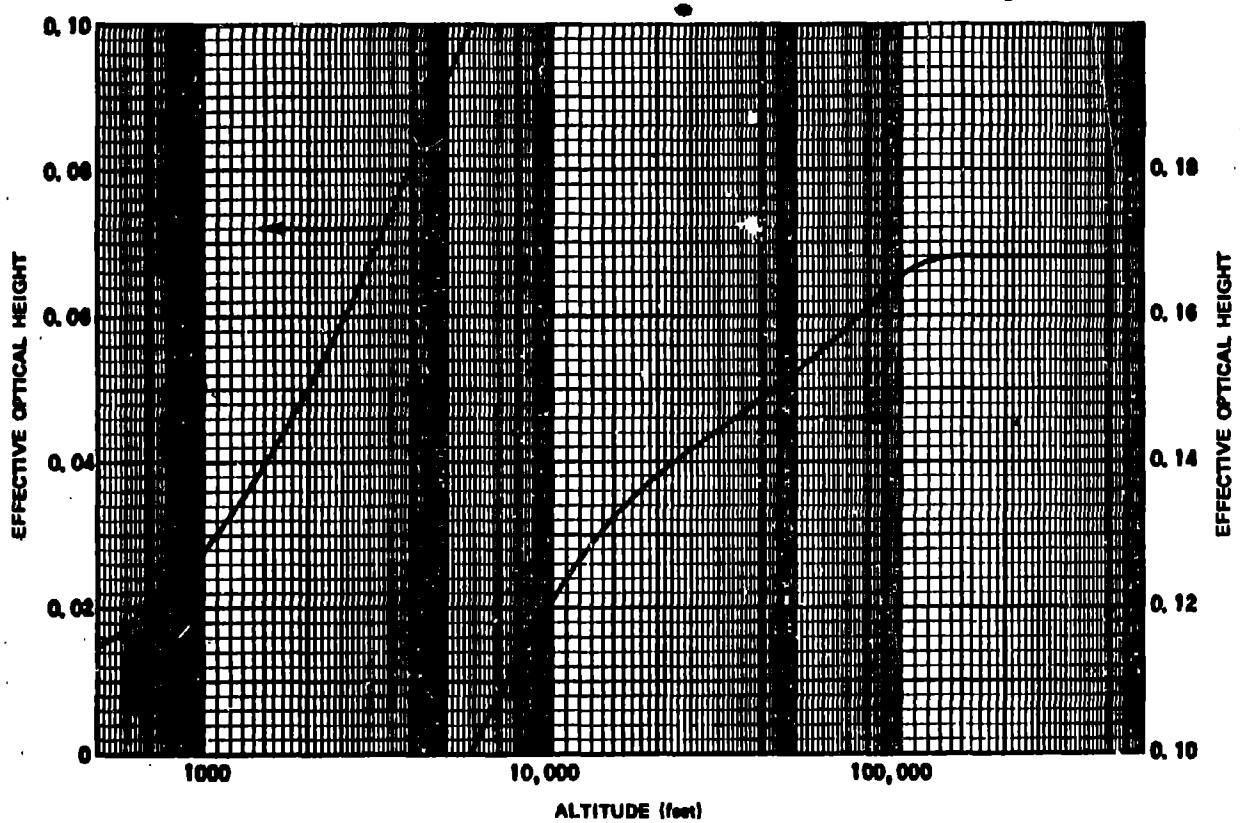

Figure 3-2. Effective Height of Model Atmosphere (Visual Range = 16 Miles)

[redacted]

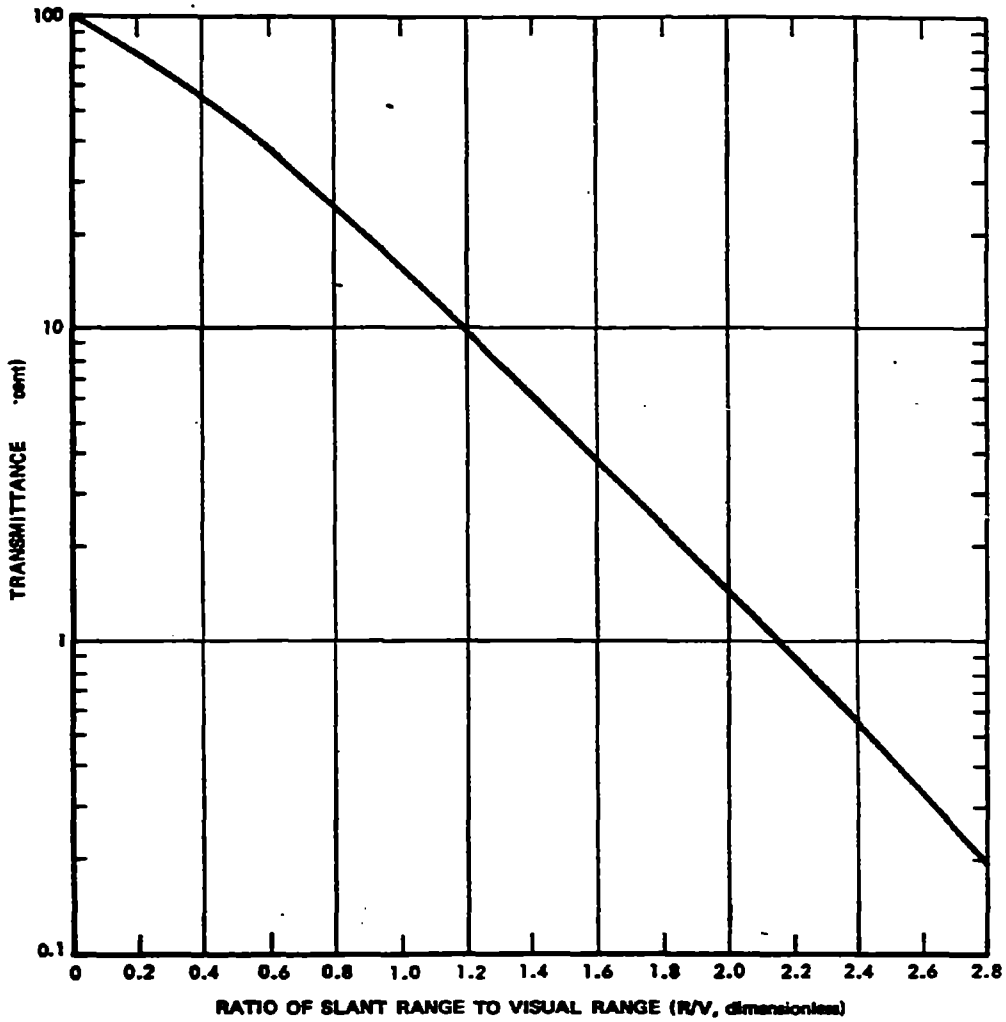

Figure 3-3. [redacted] Transmittance Between a Burst Within 1/4 Mile of the Surface and a Target on the Ground [redacted]

[redacted]

[redacted]

[redacted] where $\tau(h)$ (from Figure 3-2) is the effective optical height of the model atmosphere with 16 mile visual range, and $\tau(h)\ 16/V$ is the effective optical height in the model atmosphere for which visual range is V. The factor R/h converts effective optical height to the effective optical distance measured along the slant path of length R, where h is the height of burst.

[redacted] The two equations just given are for cloudless (but not necessarily clear) atmospheres. The effects of cloud layers are considered later in this subsection.

[redacted] Height-of-burst curves provide a convenient means for applying these transmittance equations to thermal effects calculations. Figures 3-4 through 3-14 are a series of such curves.

[redacted] The height-of-burst curves do not show transmittance data for bursts above 100,000 feet (with the exception of Figure 3-13a). Transmittance above this altitude depends only on elevation angle. If the burst is above 130 kilofeet, the transmittance is independent of altitude, and the contours become straight lines. This is illustrated for a 16 mile visual range in Figure 3-13a, in which the height of burst is extended to 250,000 feet. As mentioned above, these curves are based on two empirical equations, one of which applies when the burst height exceeds one-quarter mile (1.32 kilofeet) and the other of which applies to lower bursts. The discontinuities that occur where these two families of curves meet has no particular significance other than to suggest the degree of uncertainty inherent in any transmittance data. The discontinuities have been allowed to remain; joining the contour lines would produce shapes that may have no physical basis (for example, the curves should not be interpreted to imply that for short ground ranges the optimum burst height for thermal effects on the ground is necessarily below 1/4 mile).

[redacted]

[redacted]

Problem 3-2. Calculation of Radiant Exposure

[redacted] Figures 3-4 through 3-14 show atmospheric transmittance as a function of height of burst and ground distance for various visual ranges. These curves, together with the equations given in paragraph 3-2 allow the calculation of radiant exposure for a variety of circumstances.

[redacted] For bursts above one-fourth mile height of burst, interpolation between the figures (to obtain data for visual ranges other than those for which curves are provided) may be accomplished as follows:

$$T_2 = T_1^{\,V_1/V_2}$$

where T_1 is the label of a given contour line on a figure for a visual range of V_1 and T_2 is the label that this same curve would have if the figure were for a visual range of V_2. If the height of burst is below one-fourth mile, the transmittance may be obtained from Figure 3-3 for any combination of slant range and visual range.

[redacted] *Example 1* [redacted]:

Given: A 5 kt nuclear warhead is being considered for a defensive missile warhead.

Find: The minimum burst altitude such that the radiant exposure on the ground will not exceed 1 cal/cm^2.

DNA (b)(3)

[redacted]

[redacted]

DNA (b)(3)

[redacted] *Example 2* [redacted]

Given: A 100 kt explosion at an altitude of 10,000 feet at a location where the visual range is 16 miles.

Find: The thermal radiant energy incident on a target at a ground distance of 9,000 feet from ground zero.

[redacted]

DNA (b)(3)

[redacted]

[redacted]

Reliability: The calculated transmittances exceeding 0.1 are believed to be correct to ±30 percent; however, this tolerance is seldom required in practical problems. When transmittance exceeds 0.1, the product fT is believed to be within the range obtained by setting upper and lower limits on f as specified in "Reliability" in Problem 3-1. The reliability of transmittance calculations decreases as transmittance decreases. Transmittances below 0.1 are very uncertain, and errors that amount to a factor of 2 to 10 are not unusual. When correction factors for reflecting surfaces are required, an additional tolerance of ±30 percent should be applied to the fT product.

Related Material: See paragraphs 3-2 through 3-6.

[redacted]

[redacted]

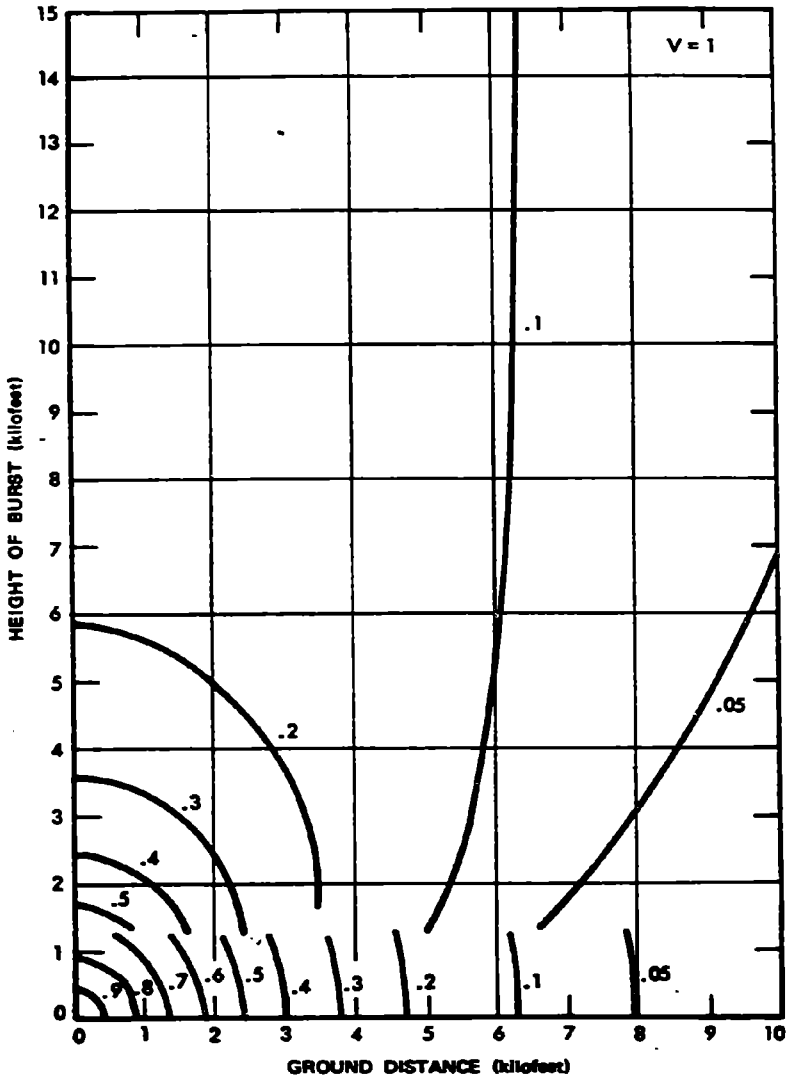

Figure 3-4. [redacted] Transmittance to a Target on the Ground on a Clear Day (Visual Range = 1 Mile) [redacted]

[redacted]

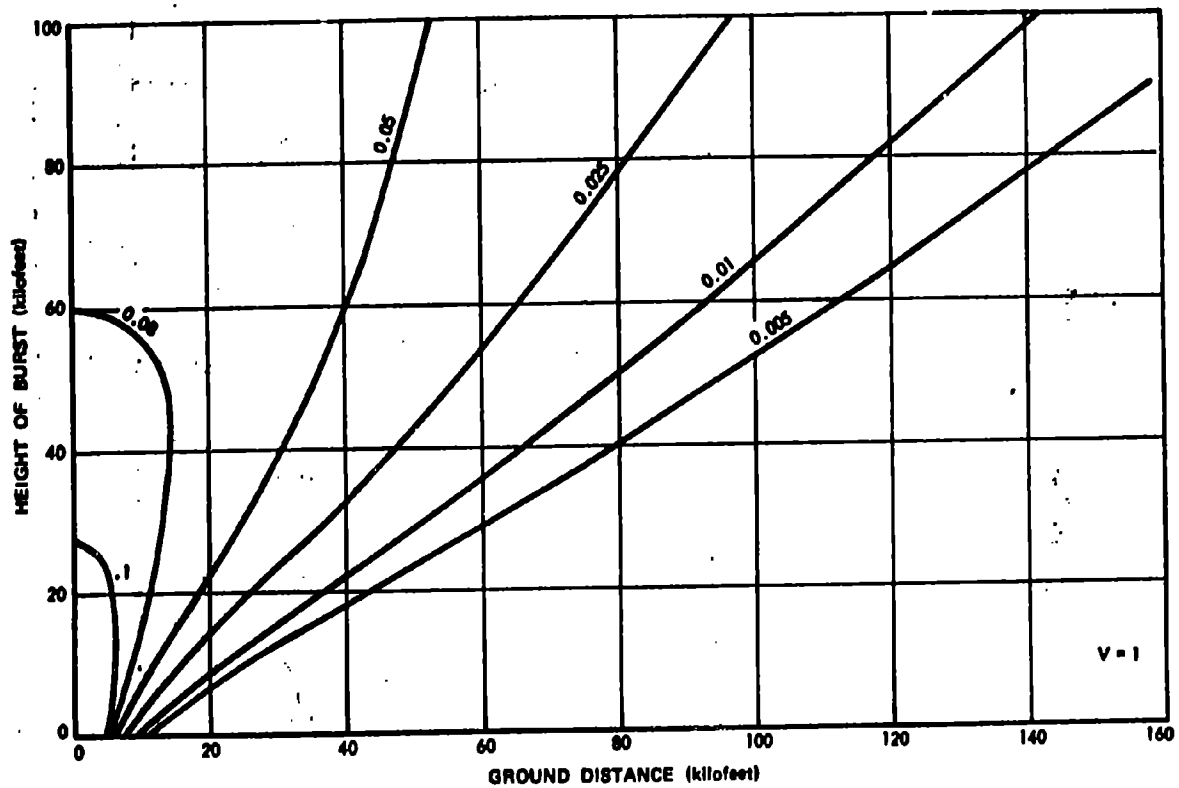

Figure 3-5. [redacted] Transmittance to a Target on the Ground on a Clear Day (Visual Range = 1 Mile) [redacted]

[redacted]

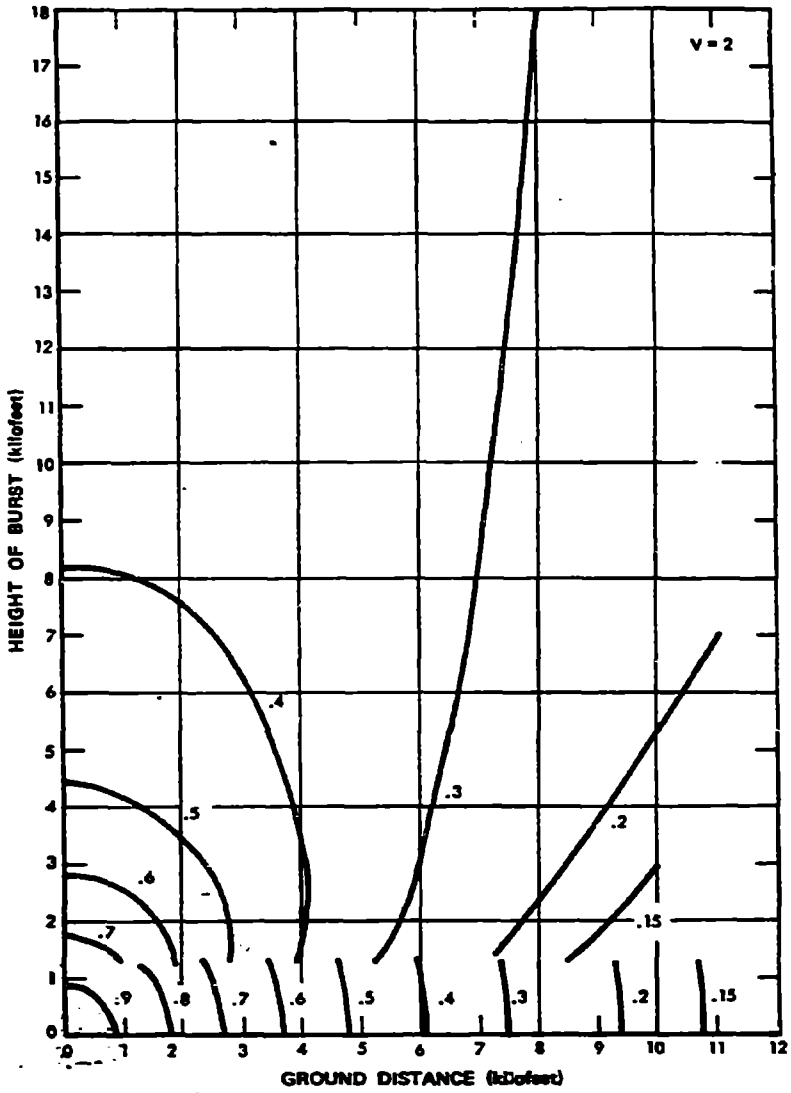

Figure 3-6. [redacted] Transmittance to a Target on the Ground on a Clear Day (Visual Range = 2 Miles) [redacted]

[redacted]

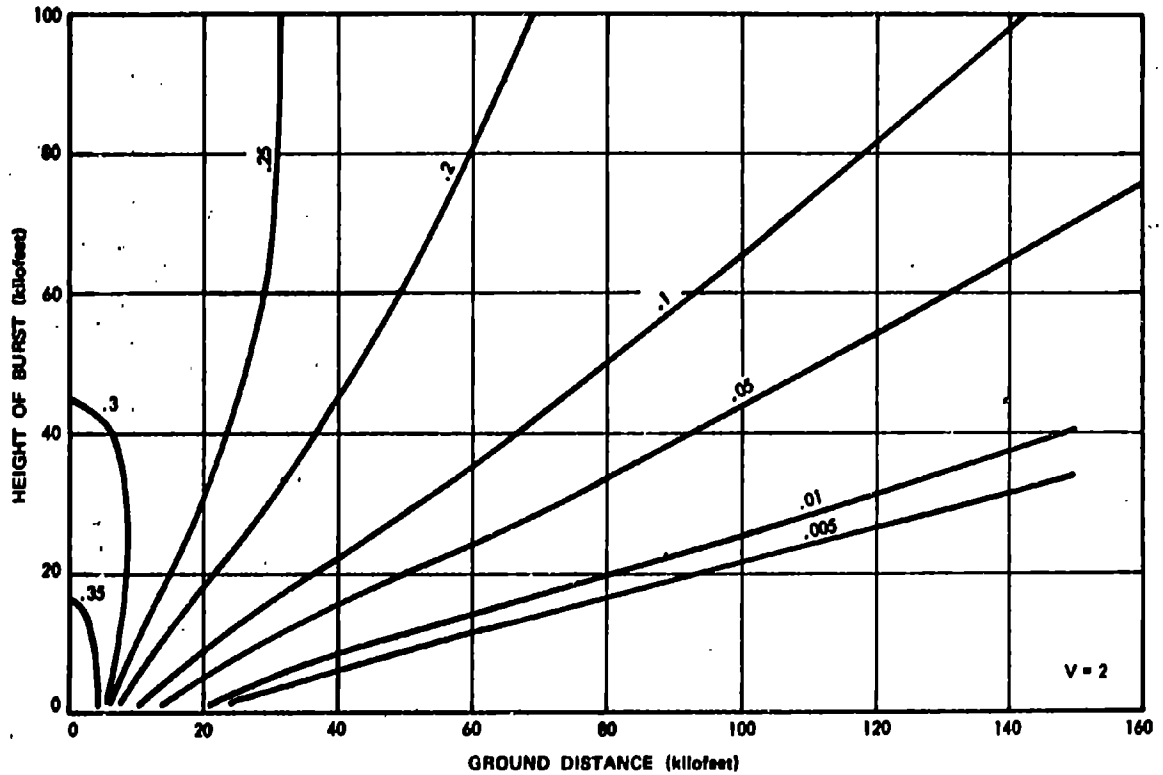

Figure 3-7. [redacted] Transmittance to a Target on the Ground on a Clear Day (Visual Range = 2 Miles) [redacted]

[redacted]

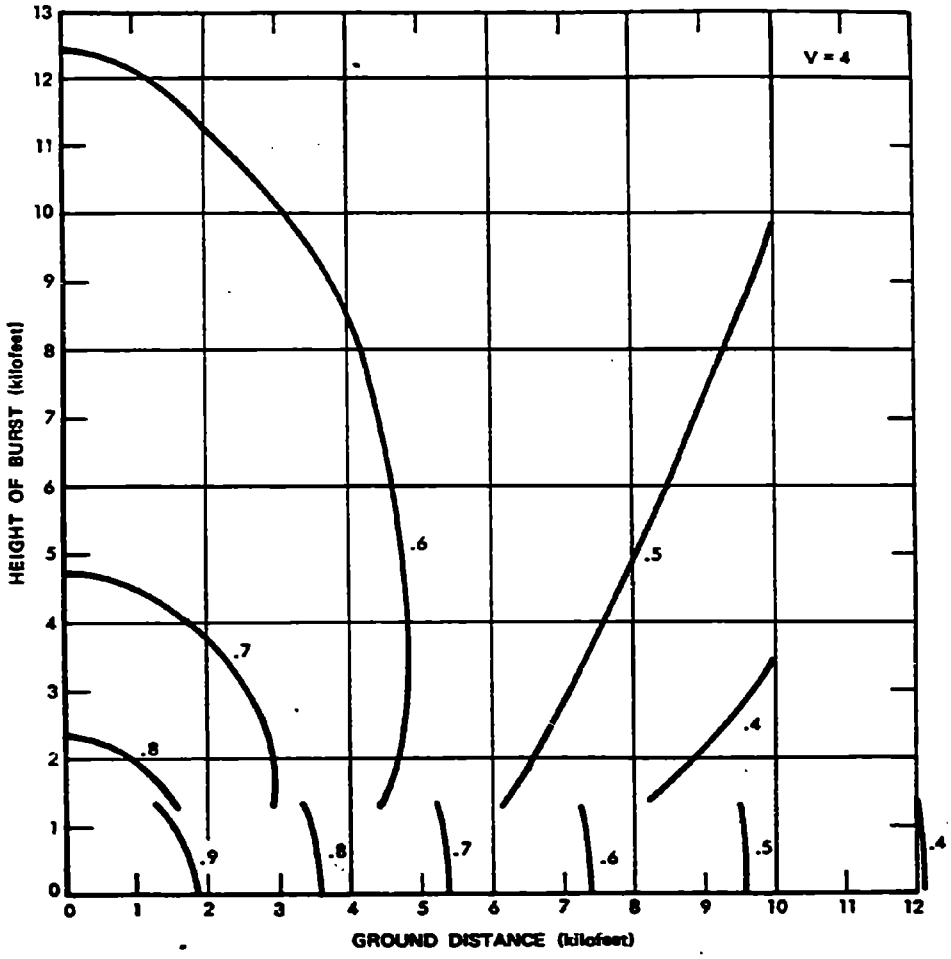

Figure 3-8. [redacted] Transmittance to a Target on the Ground on a Clear Day (Visual Range = 4 Miles) [redacted]

[redacted]

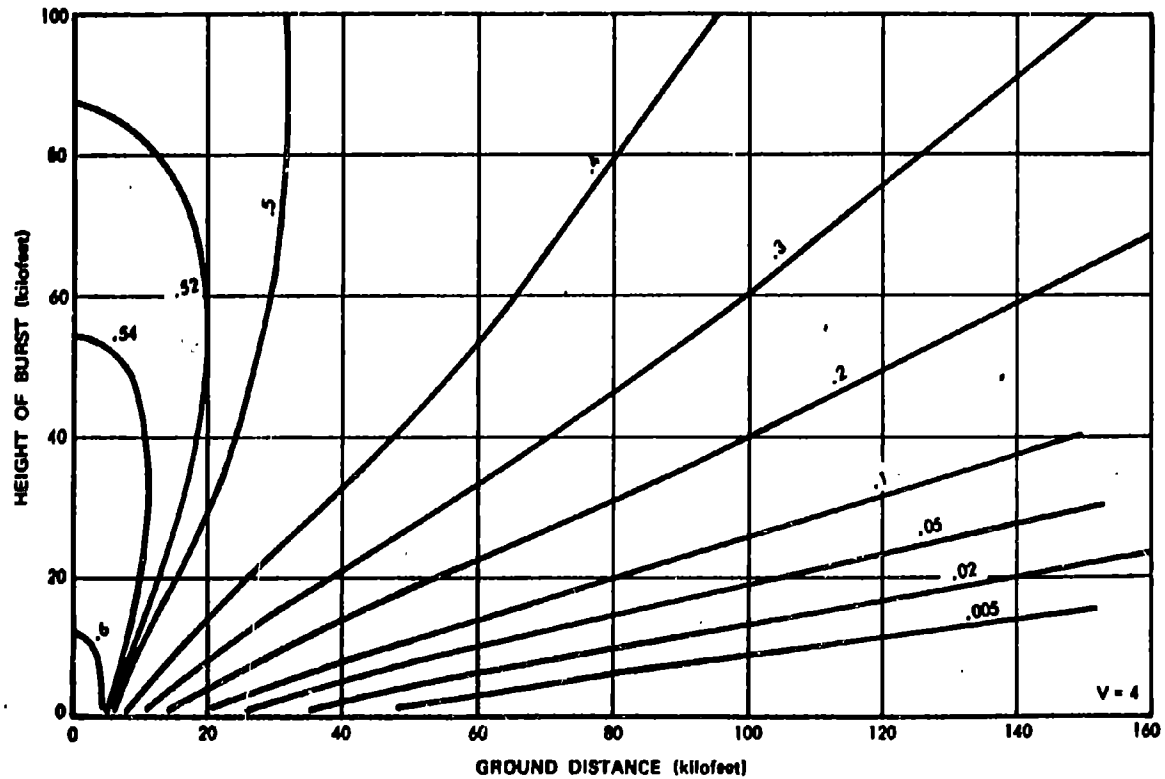

Figure 3-9. [redacted] Transmittance to a Target on the Ground on a Clear Day (Visual Range = 4 Miles) [redacted]

[redacted]

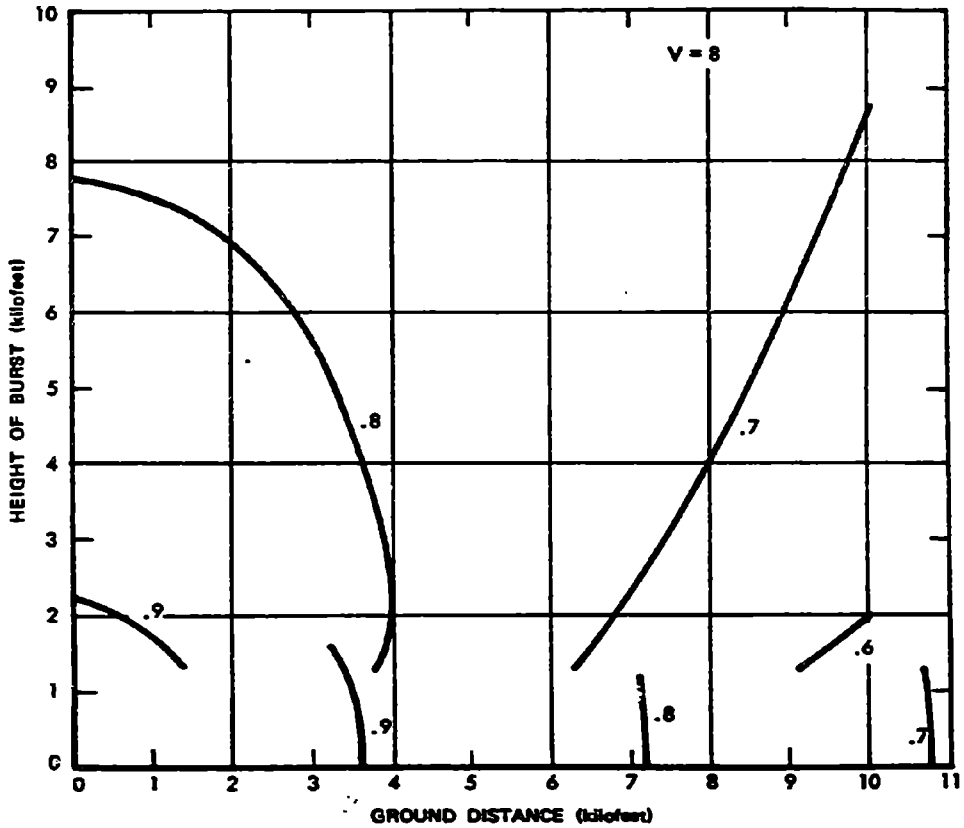

Figure 3-10. [redacted] Transmittance to a Target on the Ground on a Clear Day (Visual Range = 8 Miles) [redacted]

[redacted]

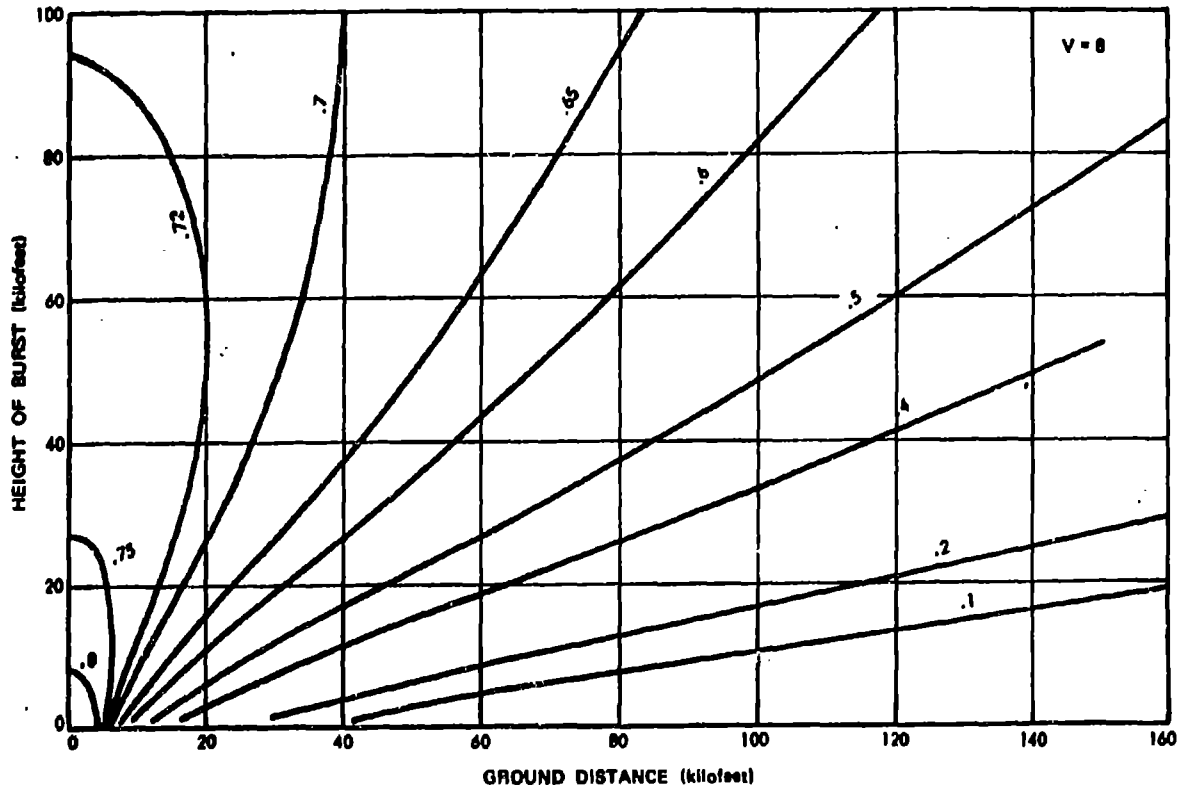

Figure 3-11. [redacted] Transmittance to a Target on the Ground on a Clear Day (Visual Range = 8 Miles) [redacted]

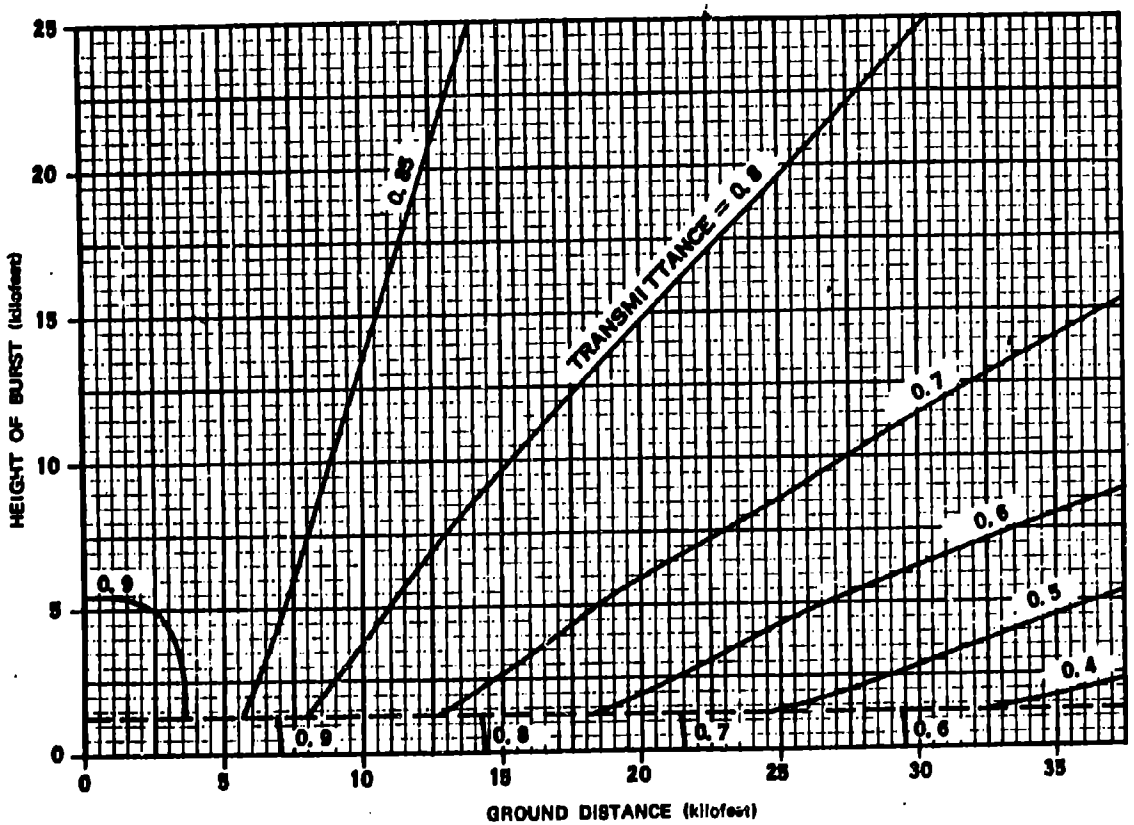

Figure 3-12. [redacted] Transmittance to a Target on the Ground on a Clear Day (Visual Range = 16 Miles) [redacted]

[redacted]

[redacted]

[redacted]

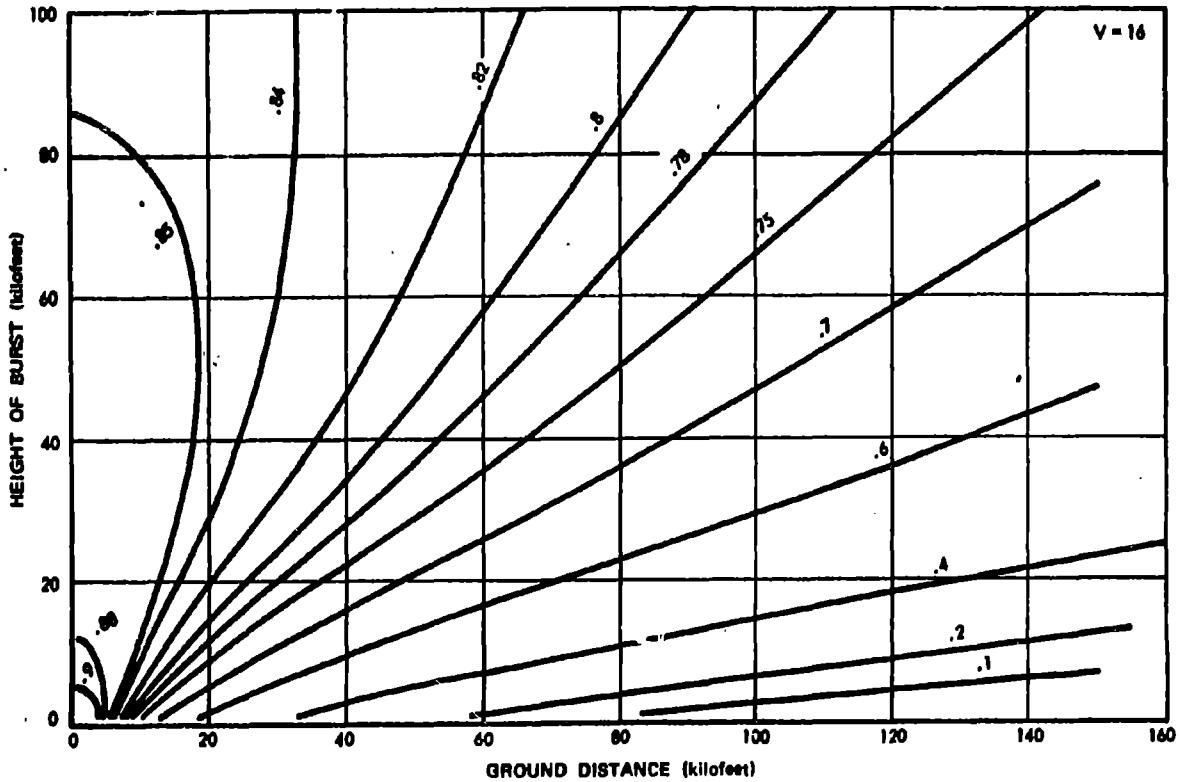

Figure 3-13. [redacted] Transmittance to a Target on the Ground on a Clear Day (Visual Range = 16 Miles) [redacted]

[redacted]

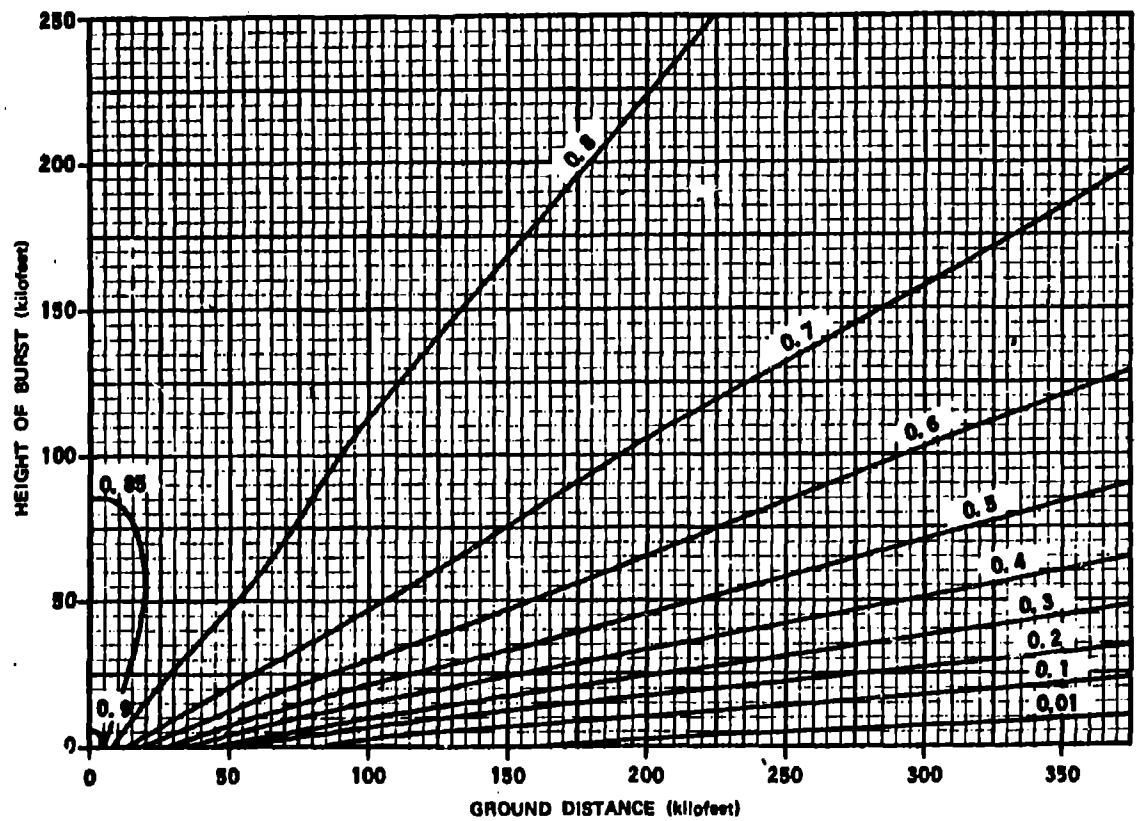

Figure 3-13a. [redacted] Transmittance to a Target on the Ground on a Clear Day (Visual Range = 16 Miles) [redacted]

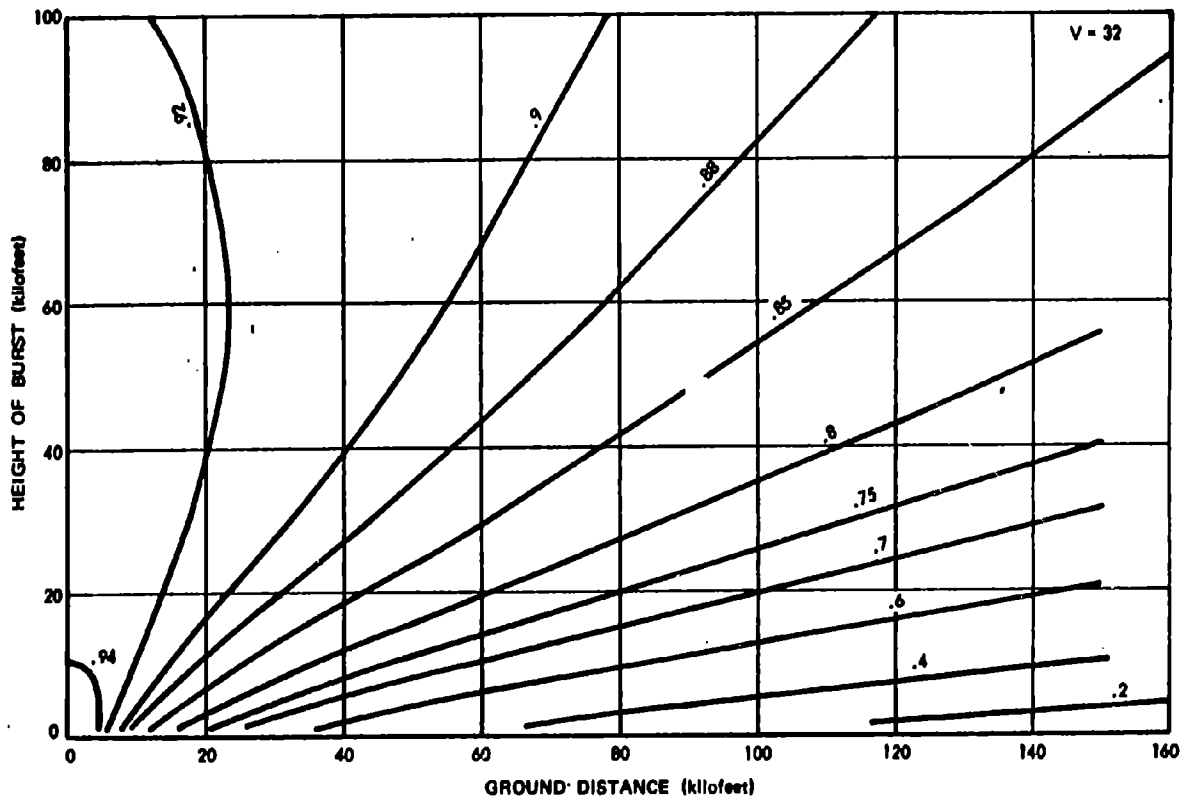

Figure 3-14. [redacted] Transmittance to a Target on the Ground on a Clear Day (Visual Range = 32 Miles) [redacted]

[redacted]

[redacted] Figure 3-15 shows transmittance data for bursts above 100,000 feet. As mentioned above, transmittance above this altitude depends only on the elevation angle. For convenience, Figure 3-15 shows the transmittance as a function of the ratio of slant range to height of burst as well as the elevation angle.

3-5 Effects of Clouds and Reflecting Surfaces [redacted]

[redacted] The model atmospheres are cloudless, and all have the same basic pattern of transparency as a function of altitude. When the actual atmosphere does not conform to these limitations, the calculation procedure must be modified.

[redacted] If a cloud layer is present and the burst is above the clouds, a transmission modifying factor is used to account for the attenuation produced by the cloud layer. Table 3-1 provides a list of transmission correction factors in terms of the appearance of the daytime sky. Transmittance is calculated as though the air were clear and no cloud layer were present, and the result is multiplied by the correction factor obtained from the table.*

[redacted] Table 3-1 suggests two ways to calculate the transmittance for a high-altitude burst (high enough to be in clear air, above the haze and clouds) when the haze (or fog) extends to the ground. For example, if a medium haze exists, a 4 mile visual range could be assumed, and from Figure 3-9 the transmittance of a high altitude overhead burst would be 0.51. Alternatively, the transmittance of a typical clear day (visual range = 16 miles), 0.85, could be used as a starting point. This with the modifying factor for medium haze, 0.5, gives a transmittance value of about 0.43. The discrepancy is within the uncertainty of the calculation.

[redacted] Judgment must be used to determine whether a transmittance calculation should be based on visual range or on sky appearance. If the burst is directly over the target and high enough to be above cloudy or hazy air, sky conditions provide the better basis for the calculation. If the burst is at a low height and the target is at a long ground distance, visual range is preferred. When the situation is less clear, looking through the atmosphere may suggest which criterion is the more representative of conditions along the path from the burst to the target.

[redacted] The transmission modifying factors ordinarily should be used with the HOB curves for 16 mile visual range, otherwise the attenuation of the atmosphere is counted twice.

[redacted] Since a cloud layer appears thicker when the sun is low in the sky, cloud cover estimates made under this condition should be modified by taking the type listed just above the cloud description that fits the observed conditions best. Similarly, when the elevation angle of the burst is below 30°, the effect of a given cloud cover will be greater than if the burst were more nearly above the target area. In this case it is appropriate to take the transmission modifying factor just below the one that would ordinarily be selected.

[redacted] This procedure is based on the similarity between the solar spectrum and the spectrum of thermal radiation from a fireball. Although the spectra are by no means identical, the ability of the atmosphere to transmit solar radiation often is the best available indication of its ability to transmit thermal energy. The appearance of the sky is, of course, an indication of its effect on light from the sun.

---

*[redacted] It might appear that thermal radiation that passes through a cloud at an angle with the vertical would be attenuated more than the same radiation would be if it passed through the cloud vertically; however, the radiation does not follow a line-of-sight path but follows randomly directed paths characteristic of diffusion. The attenuation depends on the angle of the line-of-sight path to some extent, but the dependence is not strong, and radiation will penetrate a thick cloud about equally well regardless of the angle at which it enters.

[redacted]

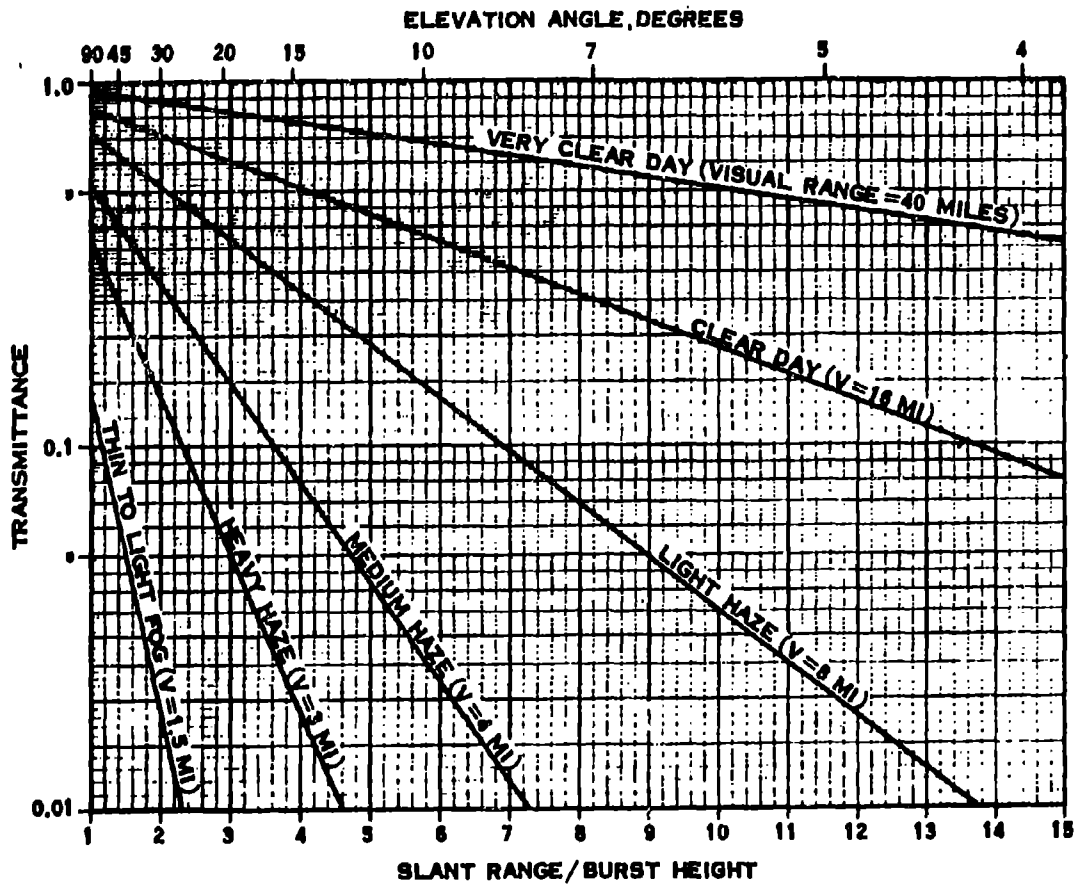

Figure 3-15. [redacted] Atmospheric Transmittance for Thermal Radiation from High Altitude Nuclear Bursts (Height of Burst > 100 kft) [redacted]

[redacted]

Table 3-1. [redacted] Modifying Factors for Transmission Under Various Atmospheric Conditions [redacted]

If Haze or Fog Layer Extends to the Surface		If Haze or Cloud Layer is Overhead		
Type	Probable Visual Range (miles)	Type	Description	Transmission Modifying Factor
Very clear	32.0	Very clear	This condition rare except at high-altitude locations.	1.1–1.0
Clear	16.0	Clear	Sky deep blue. Shadows distinct, dark.	1.0–0.9
Light haze	8.0	Light haze	Sky white; dazzling near sun. Shadows visible, gray.	0.9–0.6
Medium haze	4.0	Medium haze	Sky bright grayish-white. View sun without serious discomfort. Shadows visible but faint.	0.6–0.4
Heavy haze	3.0	Heavy haze	Sky dull gray-white. Sun's disc just visible. Shadows barely discernible.	0.5–0.3
Thin fog	1.5	Light cloud	Sky light gray with maximum luminance around sun. Sun's disc not visible, no shadows.	0.4–0.2
Light fog	0.8	Medium cloud	Sky dull gray with maximum luminance at zenith.	0.3–0.1
–	–	Heavy cloud	Sky dark gray; brightness pattern gives no indication of sun's position.	0.2–0.06
–	–	Dense cloud	The low luminance level suggests the approach of nightfall. Gloomy.	0.1–0.02

[redacted]

[redacted]

[redacted] If a cloud layer lies above the burst, it will scatter thermal energy toward the ground. The calculated value of transmittance should be multiplied by the modifying factor 1.5 when a cloud layer is above the explosion.

[redacted] If the burst is between cloud layers, the upper layer will act as a reflector and the lower layer as an attenuator. If the two layers are equally thick, as much thermal energy will emerge from the bottom of the lower cloud layer as will emerge from the top of the upper layer. In most situations of this type, the cloud structure cannot be determined well enough to make detailed transport calculations meaningful; consequently, systematic calculation procedures for this case have not been developed. However, the procedures already described may be used to set approximate limits on the values of transmittance that may apply.

[redacted] Similar problems arise when a broken cloud cover lies between the burst and the target. Whether the target will be in the shadow of a cloud at the time of burst is, in most practical situations, impossible to determine, and the results of transmittance calculation become much more uncertain. If the individual clouds are sufficiently thick that they do not reveal the location of the sun by a local bright area, and if they are spaced sufficiently close that they shade each other (i.e., so that some of the cloud areas appear dark gray), transmittance to targets shaded from direct radiation from the fireball will be roughly 20 percent of the transmittance calculated for a cloudless atmosphere.

[redacted] When any cloud or haze layer listed in Table 3-1 is in contact with the surface, that layer has a most probable value of visual range associated with it. Under these conditions, the appearance of the sky may be used, in the absence of more direct measurements, to estimate visual range. Table 3-1 includes a rough assignment of visual range values in terms of the appearance of the sky.

[redacted] An additional modifying factor relates to surface albedo, which is the reflection coefficient of the surface of the earth. Most surfaces, including water and desert areas, have low albedos (usually 25 percent or less). Only surfaces such as snow and white sand are in the high albedo class. These latter surfaces enhance thermal radiation because they can reflect energy directly toward the target and also because they reflect energy into the atmosphere, where some of it is scattered back toward the target. When such a surface is present, the calculated transmittance is multiplied by 1.5. If the burst is between a cloud layer and a high albedo surface, the enhancement factor is applied twice, giving a factor of 2.25.

3-6 Transmittance to Targets Above the Surface [redacted]

[redacted] Transmittance to targets above the surface (e.g., aircraft in flight) may be calculated by using an equation similar to that given in paragraph 3-4 for the model atmosphere above one-quarter mile,

$$T = e^{-\Delta\tau(h)\,\frac{16}{V}\,\frac{R}{\Delta h}}$$

where $\Delta\tau(h)$ is the absolute value of the difference between $\tau(h)$ at burst altitude and $\tau(h)$ at target altitude (values of $\tau(h)$ can be obtained from Figure 3-2), Δh is the absolute value of the altitude difference between the burst and the target, V is visual range at the surface, and R is slant range between burst and target.

[redacted] If the burst and target altitudes are equal, the exponent in the equation becomes indeterminate. An estimate may be obtained in this case by increasing burst altitude a small amount, decreasing target altitude the same amount, and holding slant range constant. Estimates obtained from this equation must be regarded as very rough approximations to actual transmittance.

[redacted]

[redacted]

Problem 3-3. Calculation of Transmittance

[redacted] Table 3-1 provides descriptions of various atmospheric conditions from which visual range may be estimated. The table also provides transmission modifying factors to be applied to the transmittance values for a 16 mile visual range when appropriate. Conditions under which the appearance of the sky should be used rather than the measured or estimated ground level visual range to determine transmittance are described in paragraph 3-5.

[redacted] *Example 1* [redacted]

Given: A nuclear explosion at an altitude of 5,000 feet. The appearance of the sky suggests a light haze atmosphere.

Find: The transmittance to a target on the surface 50,000 feet from ground zero.

Solution: Since the line of sight from the burst to the target is low and nearly horizontal, visual range rather than sky appearance would provide a better criterion for selecting a model atmosphere. Nevertheless, this problem must be solved on the basis of sky appearance, because a direct visual range measurement is not available. From Table 3-1, a light haze condition corresponds to a visual range of 8 miles.

Answer: From Figure 3-11, the transmittance is 0.15. No definite tolerance can be placed on this value of transmittance, and it must be regarded as a rough estimate.

[redacted] *Example 2* [redacted]

Given: A nuclear explosion at an altitude of 30,000 feet. The visual range is 6 miles, and the sky appearance fits the medium cloud condition. The time is one hour before sunset, and the ground is covered with snow.

Find: The transmittance to a target on the surface 10,000 feet from ground zero.

Solution: Since the burst is nearly over the target and is sufficiently high that it probably is above most of the haze and clouds, the sky conditions provide the best indication of transmittance. Therefore, the visual range will be ignored in the solution. As a result of the low elevation angle of the sun, the cloud layer appears to be thicker than it actually is. Therefore, the transmission modifying factor for light cloud conditions should be used rather than medium cloud conditions.

Answer: From Figure 3-13, transmittance on a clear day (16 mile visual range) would be 0.86. From Table 3-1, the transmission modifying factor for light cloud conditions is between 0.2 and 0.4. Reflection from the snow covered surface requires an additional correction factor of 1.5. The calculated transmittance therefore lies between

$$(0.2)(1.5)(0.86) = 0.26,$$

and

$$(0.4)(1.5)(0.86) = 0.52.$$

[redacted] *Reliability* [redacted]

[redacted] In general, transmittance calculations are most reliable when transmittance is high and when the atmosphere is relatively clear. A tolerance of ±30 percent is assigned when transmittance exceeds 0.1 and when visual range is 5 miles or greater. This tolerance is based on comparisons between transmittance calculations made by the methods of several different investigators. When reflection from snow cover or an overhead cloud cover must be considered, the uncertainty rises to ±60 percent.

[redacted] Comparisons of calculated values with data from full scale nuclear tests show uncertainty that basically relates to the product fT, since thermal partition and transmittance cannot be measured independently. When transmittance

[redacted]

[redacted]

exceeds 0.1 and visual range exceeds 5 miles, the tolerance on thermal partition f accounts for all of the uncertainty in the fT product. No additional tolerance on T is required. When reflecting surfaces are present or when visual range drops below 5 miles, an additional ±30 percent tolerance should be applied.

No reliability estimate is assigned to calculated transmittances below 0.1. At these low values, transmittance estimates become increasingly uncertain, and errors may rise to factors of 2-10.

Errors in the estimation of visual range also can affect the error in the calculation of transmittance. If a visual range of 3 miles is estimated as 2 miles, which is not an unreasonable error, the percent error in transmittance rises rapidly as the transmittance drops to low values.

Additional errors are produced by approximations in the calculation procedure. These errors tend to be small when transmittance is high and large when transmittance is low. Three approximations are made in transmittance calculations.

First, a single parameter, visual range, serves as the basis for transmittance calculations in cloudless atmospheres. Although visual range at the surface is only one of the parameters required to specify the transmitting properties of the region between the burst and the target, it is one of the very few parameters that can be observed directly from the ground. Other parameters necessary to define the atmosphere completely are supplied by a set of model atmospheres that include the measured visual range at the surface and an increasing transparency with increasing altitude. This change in transparency with altitude is chosen to match the changes that occur in real atmospheres under typical conditions; however, there is no assurance that the model atmosphere is a particularly good match to any single real atmosphere.

Second, the transport of thermal energy through these model atmospheres is calculated from empirical equations confirmed by experimental data. The results of more accurate computational procedures are expected at some future date.

Third, the model atmospheres are cloudless. Cloud effects are accounted for by correction factors that modify the transmittance calculated for a cloudless atmosphere. An empirical treatment of some kind is unavoidable; cloud effects are too complex to be treated rigorously.

Any of these sources of error can, under certain conditions, cause the calculated transmittance to be wrong by a factor of 10 or more, but these extremely high errors appear when the atmosphere attenuates thermal energy from the fireball strongly and therefore when thermal effects are unlikely to be as important as other effects such as blast.

[redacted]

[redacted]

3-7 Visual Range [redacted]

[redacted] Ordinarily, the purpose of visibility measurements is to determine the ability of an observer to see through the atmosphere; such a measurement may determine the approximate distance at which a pilot can recognize a runway. In the study of thermal effects, visibility measurements are useful because they indicate the transparency of the atmosphere and its ability to transmit thermal radiation. The model atmosphere that should be used in a particular transmittance calculation is selected on the basis of daytime visual range.

[redacted] The term *visual range* as used in this chapter is synonymous with *daytime visibility* as commonly measured at weather stations. Although "visibility" is a more widely used term than "visual range," the latter is used in this chapter because it indicates that the quantity being discussed is a distance and not a measure of the clarity with which a particular object can be seen. Visual range is defined as the distance at which a dark object silhouetted against the sky is visible and recognizable. It is commonly measured in statute miles.

[redacted] Two factors make it advisable for the person who must develop the ability to make weapon effects calculations in tactical situations to understand the procedures for measuring visual range. First, he will not always have access to weather station information. Second, he may wish to question the information he obtains from weather stations. For the usual purposes of visual range measurements, underestimates of this range are less serious errors than are overestimates. For troop safety calculations, the opposite is true. Some meteorologists, not in the habit of thinking in terms of weapons effects, may shade their estimates incorrectly.

[redacted] At the visual range, all objects appear so nearly alike in both brightness and color that a dark object silhouetted against the sky is barely recognizable. This reduction in contrast may be described quantitatively in terms of the brightness B of an object and the brightness of B' of the background. Contrast is defined as the ratio

$$C = \frac{B - B'}{B'}$$

If the object is darker than its background, the contrast is negative, reaching -1 for a perfectly black object. On the other hand, lights have very large positive values of contrast at night.

[redacted] A hypothetical example illustrates the problems of estimating visual range and the accuracy that may be expected from such estimates. Table 3-2 shows a series of values calculated for the condition that the fifth pole of a row of telephone poles closely spaced in a uniform fog is at the visual range as it would be

Table 3-2. [redacted] Contrast Ratio for a Series of Black Telephone Poles in a Fog: Visual Range = 500 Feet [redacted]

Pole Number	Distance (feet)	Contrast Ratio
1	100	0.56
2	200	0.31
3	300	0.18
4	400	0.098
5	500	0.055
6	600	0.031
7	700	0.017
8	800	0.010

[redacted]

[redacted]

measured by a transmissometer.* If the poles have a dark color, the inherent contrast of each pole with its background may be assumed to be nearly 100 percent. The contrast, as seen by the observer is given in the last column, and is, by definition, 0.055 at the visual range.†

What an observer sees may be affected by factors such as the uniformity of the fog layer. The first three or four poles are distinct, the fog has changed the apparent color of even the first pole to gray. The fourth pole is sufficiently distinct that if the cross arms are of lighter wood than the pole itself the difference in color is discernible. The fifth pole, at the visual range, is little more than a shadow, but it would be visible instantly and would be recognized as a telephone pole even if it were standing alone.

An observer looking at the sixth pole standing alone probably would see it if he knew where to look, but he might question its identity. Although the line separating the image of the pole from its background is sharp, the faintness of the contrast makes the outline appear slightly blurred.

The seventh pole is at approximately the distance known as the *meteorological range*, which is the range that gives a contrast of 0.02 between a black object and the sky. If the pole were standing alone and the observer did not know where to look for it, he very likely would miss it. Meteorological range has often been used as a measure of visual range; it corresponds more closely to the threshold of detection than to the implications of the presently used standard of "visible and recognizable."

The eighth pole probably is not visible because of its size. A car parked beside it might be visible, but only if the observer, looking down the row of poles, knows exactly where to look for it. Detection at this contrast level requires a background uniformity that is rare except under laboratory conditions.

Many observers would estimate visual range as the distance to the fourth or sixth pole; a few might select the seventh; still fewer, the third. As Table 3-2 shows, the error in range that this uncertainty produces is not excessive.

The factors that would lead some observers to select the fourth pole may include more than overly conscientious application of the "visible and recognizable" rule. The fifth pole is only about 1/4 as wide as the ideal distance marker (which should subtend an angle of

---

*A transmissometer is an instrument designed to measure light transmission characteristics of the atmosphere. It consists of a light and a detector separated by a baseline of either 500 or 750 feet. The transmissometer reading is called transmissivity. It is the ratio of the light received at the detector to the light that would be received if the air were perfectly transparent. The transmissivity defines the ability of a direct beam of light to penetrate a specified distance (the transmissometer baseline) through the atmosphere. The transmittance, as used in this chapter, defines the ability of radiant energy to pass through the atmosphere between a nuclear explosion and a target either directly or by scattering.

†The visual range may be defined as the range at which the apparent contrast between a black object and its sky background is reduced to 5-1/2 percent or as the range at which a beam of light is reduced to 5-1/2 percent of the intensity it would have in a transparent atmosphere. Light from the sky generally appears to come from the region behind objects on the horizon, but air light originating beyond an object at the visual range actually contributes little to the sky brightness that the observer sees. All but 5-1/2 percent of this distant light is scattered out of the line of sight before it reaches the observer. The air between the object and the observer contributes as much to the apparent brightness of the object as it does to the brightness of the sky, but, if the object is black, it fails to contribute the 5-1/2 percent of total sky brightness that reaches the observer from the air beyond the object. The contrast to the observer is reduced from 100 percent to 5-1/2 percent. These conclusions are strictly correct: if the brightness and color of the sky as seen at the object is the same as the brightness and color of the sky as the observer sees it; if the atmosphere is not hazy, i.e., if the atmosphere is clear enough that the scattering cross section varies appreciably with wavelength and contrast is reduced to 5-1/2 percent for all colors; absorption of light is assumed negligible.

In practice, these three restrictions usually may be ignored. The errors they introduce are in most cases no more serious than other problems (such as nonuniformities in the atmosphere) that limit the precision of visual range measurements.

[redacted]

[redacted]

at least 1/2°), and for this reason it may not appear to be as distinct as a larger object would.

[redacted] Additional factors that could cause an observer to underestimate visual range can occur when the seeing conditions are different from those assumed in this example. For example, the fog was assumed to be perfectly uniform. Actually, the atmosphere near the surface over land is rarely uniform, and patches of haze that can be misjudged for distant objects are common. Shimmer, an optical effect similar to the heat waves observed over a metal object on a sunny summer day, can distort images of distant objects and can reduce the apparent visual range even though the air is clear.

[redacted] An observer who uses a distant hill for a range marker may be inclined to overestimate visual range. This is particularly true if he knows, perhaps from the pattern formed by closer hills, exactly where to look. Aided by such landmarks, he may detect so many details of the familiar outline that, to him, the hill is definitely "visible and recognizable." The observer, if he is unsure of the mark, should ask himself whether he sees the hill clearly enough that *conspicuous* surface features (e.g., patches of trees separated by large areas of light-colored, vegetation-free rock) would be faintly discernible, even though such features may not actually be present. He should also ask whether an observer unfamiliar with the terrain would be reasonably sure that he was looking at a hill instead of cloud structure near the horizon. If the answers to these questions are "yes," he should judge the hill within the visual range.

[redacted] Distance markers that are appreciably easier or harder to see than the standard dark-colored marker should be avoided if possible, since they lead to inaccurate measurements of visual range. A snow-covered mountain is likely to be an unreliable marker for two reasons: If the peak is at a high altitude, the observer sees it through air that is usually clearer than the air along a line of sight closer to the surface. Also, under strong illumination the snow is visible from a greater distance than darker portions of the mountain would be. Either effect can cause an artificially high measured value of visual range, implying a clearer atmosphere than actually exists. On the other hand, the tree-covered base of a mountain is an excellent marker for long visual ranges.

[redacted] Surfaces with high reflection coefficients are not always more easily seen than dark objects. An observer looking in the general direction of the sun may see a white object as darker than the horizon sky, because the side of the object facing the observer is not illuminated strongly. If the angle of the sun is just right, there may be virtually no brightness contrast between a white object and its sky background. On the other hand, the inherent contrast between a very dark object and the sky never varies greatly from 100 percent; therefore, the use of dark objects as distance markers results in reasonably consistent visual range measurements.

[redacted] The observer should be aware of phenomena related to lighting effects. If he is looking at a distance marker that is in the general direction of the sun, the strong forward scattering property of haze particles will make the air light between him and the marker will appear to be particularly bright. This does not affect the distance at which a dark marker can be seen. The sky behind the marker is similarly bright, and the apparent contrast between the marker and its background is no different than if, for example, the sun were overhead.

[redacted] The preceding discussion provides the user with information that will help him to make accurate estimates of visual range. Much of this information can be condensed to a set of rules.

- Range markers should be as dark as possible. If the reflection coefficient of the

[redacted]

[redacted]

marker is more than 30 percent and the sun is behind the plane of the observer, the marker should be avoided.*

- The range marker should be silhouetted against the sky, or its background should be at least half again as far from the observer as is the marker itself. When such a marker is at the visual range, the background will be so nearly obscured that it is indistinguishable from the sky.
- The distance marker should be sufficiently large that increasing its size would not increase the range at which it can be recognized. This requirement is met if the angular size of the marker (vertically and horizontally) is 1/2°, which is the diameter of the full moon. A distance of 5/16 inch on a ruler held at arm's length is an approximate measure of this angle. If shimmer is not a serious problem (if the image is steady), binoculars may make a smaller distance marker usable.
- Distance markers should be available in several directions so that nonuniformities in the atmosphere can be detected.
- When a requirement for visual range measurements in a given area can be anticipated, a map showing usable distance markers should be prepared. It should indicate the range, direction, and identification of each marker. (Heights of hills or tall buildings should also be recorded, because such objects sometimes provide useful indications of cloud height.)
- The altitude of distance markers should be such as to place the line of sight as close as possible to the average ground level.

[redacted] Usually it is necessary to use some markers that fall short of these standards. The markers may be too small or the wrong color, and often no marker will exist at the visual range. In this case the observer must use judgment to decide the visual range that ideal markers would indicate. One important clue is the apparent color of markers that are within the visual range. Clear, undistorted colors indicate that the amount of air light from the intervening air is small, and that objects at considerably greater ranges would be clearly visible.

3-8 Nighttime Visual Range [redacted]

[redacted] The distance at which a person can see a light depends partly on the transparency of the atmosphere. However, it also depends on the state of dark adaptation of the observer, the brightness of the light, and the amount of background produced by whatever other lights may be illuminating the air. Only the first of these four factors concerns the ability of the atmosphere to transmit thermal energy. In general, the variations caused by the last three factors make measurements of nighttime visual range a poorer indication of the transport properties of the atmosphere than measurements of daytime visual range.

[redacted] In the absence of definite changes in the weather, the transparency of the air usually does not change much from day to night. Daytime visual range, which usually can be measured more readily than nighttime visual range, is often the most satisfactory means for estimating the transport properties of the atmosphere the following night.

[redacted] Exceptions occur in regions where the relative humidity exceeds 90 percent in polar regions, and in areas subject to air pollution. In the latter case, the source of pollution (e.g., domestic heating or cooking and industrial exhausts) are likely to vary from day to night. Polluted atmospheres also often produce a haze

*[redacted] The reflection coefficient is about 4 percent for a pine woods and about twice that amount for a deciduous woods. A grassy field, for which the reflection coefficient may exceed 20 percent, is a much less reliable mark.

[redacted]

[redacted]

[redacted] layer near dawn, particularly when a steep temperature inversion forms near the surface. Such a haze layer may be dense enough to offer some protection from thermal radiation.

[redacted] If nighttime visual ranges must be measured, these ranges should be converted to the equivalent daytime visual ranges. This is necessary because daytime visual range is the parameter on which transmittance calculations are based. Figure 3-16 may be used to convert nighttime ranges to equivalent daytime ranges.

[redacted] Figure 3-16 is based on a large number of observations to determine the distance that a 25 candlepower light (25 candlepower is approximately the output of a 25 watt incandescent lamp) can be seen through various atmospheres. The data were originally taken to correlate transmissometer data with visual range measurements; therefore the seeing conditions would be similar to those existing at airport weather stations.

[redacted] In practice, the 25 candlepower source can be replaced by any light of moderate intensity. In a transparent atmosphere, a 100 watt lamp could be seen about twice as far as a 25 watt lamp, but in an attenuating atmosphere the difference is less. When nighttime visual range is 50,000 feet, the 100 watt lamp could be seen from about 65,000 feet. When nighttime visual range is 5,000 feet, the 100 watt lamp can be seen from about 6,000 feet.

[redacted] APPROXIMATE CALCULATIONS OF RADIANT EXPOSURE [redacted]

[redacted] The procedures described in the preceding subsections permit the calculation of radiant exposure by methods that are as accurate as present knowledge of thermal partition and transmittance allows the information to be presented in a manner suitable for this manual. In many cases, a quicker but less accurate estimation of radiant exposure is desirable. Such an estimate may indicate whether more time consuming calculations are necessary. Figures 3-17a and b are intended for use in such cases.

[redacted] These figures are based on transmittance values for a moderately clear, cloudless atmosphere (visual range = 16 miles) and on thermal partition values for an intermediate value of yield, 200 kt. Transmittances were calculated using the high altitude equation only, and some loss in accuracy is expected for burst heights below 1/4 mile.

[redacted]

[redacted]

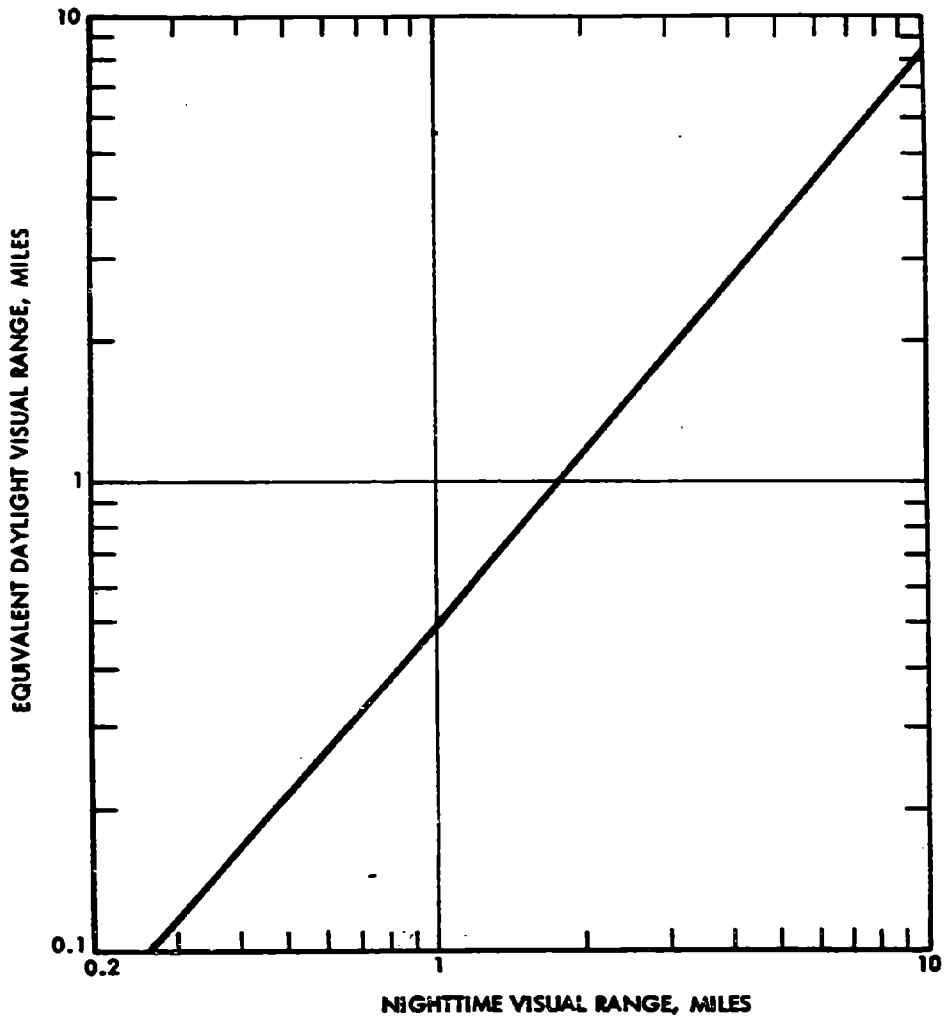

Figure 3-16. [redacted] Equivalent Daytime Visual Range as a Function of Nighttime Visual Range [redacted]

[redacted]

[redacted]

Problem 3-4. Approximate Calculation of Radiant Exposure

[redacted] Figures 3-17a and b show approximate radiant exposure to targets on the surface from a 1 kt explosion as a function of distance from ground zero and height of burst. These curves are based on calculations for a 200 kt explosion under the assumption that the radiant exposure could be scaled to 1 kt directly with yield. Visual range was assumed to be 16 miles.

[redacted] *Scaling.* For yields other than 1 kt, the radiant exposure is

$$Q = Q_1 W,$$

where Q_1 is the radiant exposure for 1 kt obtained from Figure 3-17a or b for the height of burst and ground distance of interest, and Q is the corresponding exposure for W kt.

[redacted] *Example* [redacted]

Given: A 500 kt explosion at an altitude of 30,000 feet.

Find: The radiant exposure on the surface 150,000 feet from ground zero.

Solution: From Figure 3-17b, a 1 kt explosion at an altitude of 30,000 feet will produce a radiant exposure 150,000 feet from ground zero

$$Q_1 = 0.0007 \text{ cal/cm}^2.$$

Answer: The radiant exposure from a 500 kt explosion is

$$Q = Q_1 W = (0.0007)(500) = 0.35 \text{ cal/cm}^2.$$

[redacted] *Reliability:* Radiant exposures from Figures 3-17a and b are approximations. For the assumed atmospheric conditions and burst altitudes below 100 kilofeet, values of radiant exposure obtained from Figures 3-17a and b are estimated to be reliable within ±40 percent. Additional loss of accuracy is expected for bursts below one-quarter mile altitude since the transmittances were calculated with the high altitude equations. The reliability also drops for bursts above 100,000 feet as a result of the uncertainty in the values assumed for thermal partition.

[redacted] *Related Material:* See paragraphs 3-1 through 3-8.

[redacted]

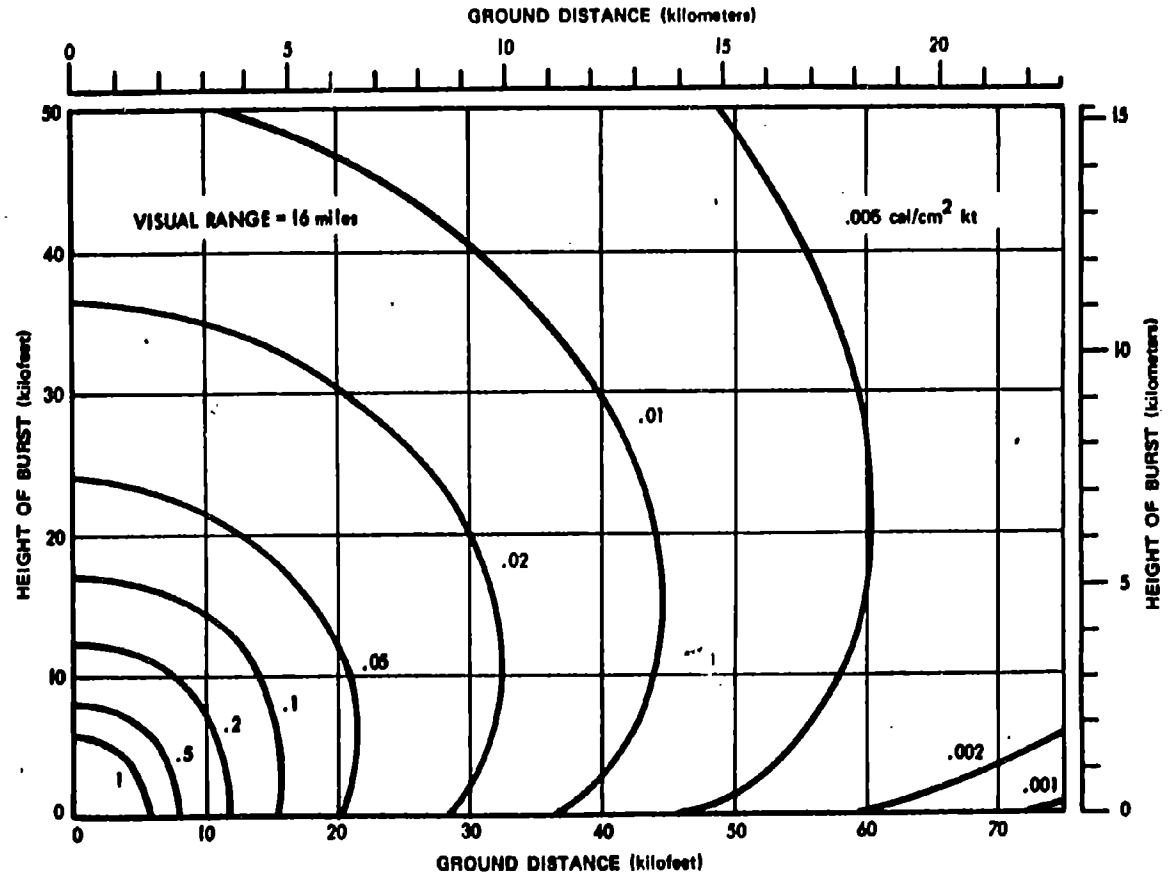

Figure 3-17a. [redacted] Approximate Values of Radiant Exposure Through a Clear Atmosphere [redacted]

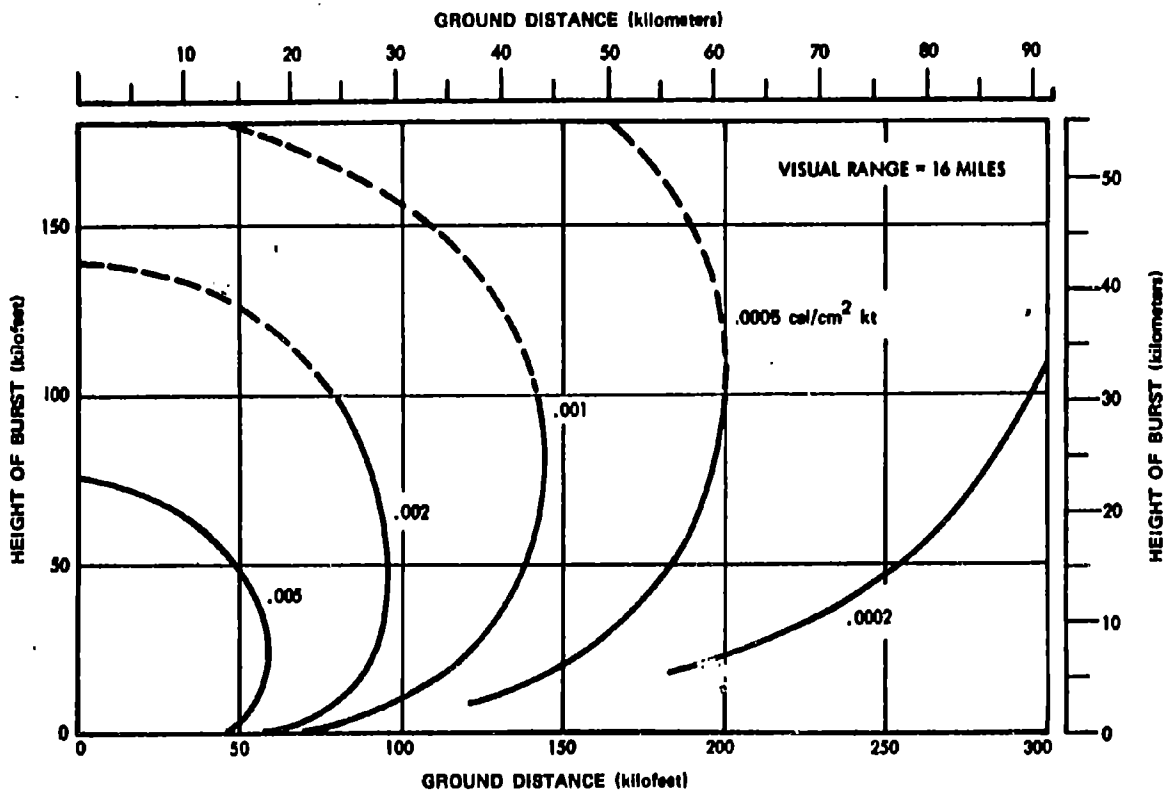

Figure 3-17b. [redacted] Approximate Values of Radiant Exposure Through a Clear Atmosphere [redacted]

[redacted]

[redacted] SURFACE AND SUBSURFACE BURSTS [redacted]

[redacted] Clouds of dust (or spray) partly obscure the fireball of surface bursts and reduce the thermal radiation received by targets on the ground. Even less thermal radiation escapes from underground and underwater bursts. If the burst is deep enough, the earth or water absorbs almost all of the thermal energy; the amount of radiated thermal energy is insignificant.

3-9 Surface Bursts [redacted]

[redacted] The terms contact surface burst, surface burst, and air burst, when used in connection with thermal effects, have meanings similar to those assigned to the same terms in Chapter 2 (see paragraph 2-19). A contact surface burst is one that is no more than 5 $W^{0.3}$ feet above or below the surface. The region between 5 $W^{0.3}$ and 180 $W^{0.4}$ feet (±20 percent for yields between 10 and 100 kt, and ±30 percent for other yields) is called the transition zone, and a burst within this region is a surface burst for purposes of thermal radiation phenomena. Since the fireball is approximately 180 $W^{0.4}$ feet in radius for explosions in the lower atmosphere, a surface burst is any burst above 5 $W^{0.3}$ feet but low enough that the fireball will interact strongly with the surface of the earth. As mentioned in paragraph 3-1, an air burst occurs above 180 $W^{0.4}$ feet.

[redacted] Experimental data indicate that the thermal partition of contact surface bursts is about 0.21. Figure 3-18 assumes a thermal partition of 0.21 for a contact surface burst, assigns the air burst partition (Figure 3-1) to a burst at 180 $W^{0.4}$ feet, and provides intermediate values by linear interpolation. This procedure is arbitrary and is only supported in a general way by experimental data. Points above the dashed line in Figure 3-18 represent air bursts; points below the dashed line are surface bursts. The radiant exposure from surface bursts may be calculated by the formulas given in paragraph 3-2 with the values of thermal partition, f, taken from Figure 3-18.

[redacted] Figure 3-18 describes the fireball as it would be seen by targets on the surface. Clouds of dust would not obscure the fireball from above; consequently, radiant exposure of airborne targets should be calculated on the basis of the thermal partition of free air bursts given in Figure 3-1.

[redacted] Since confinement of the fireball by the surface is roughly equivalent to reflection, the fireball radius for a contact surface burst is larger than that for the same burst in free air. Blast wave theory suggests that the fireball of a contact surface burst as viewed from above might resemble that of a free air burst with a yield of 2.0 W. In fact, determination of fireball yield by hydrodynamic scaling uses the 2.0 W assumption.

3-10 Subsurface Bursts [redacted]

[redacted] Two effects reduce the amount of thermal energy radiated by the nuclear explosions below the surface of the earth: a large amount of thermal energy is absorbed in fusing and vaporizing the earth; and the fireball that does develop above the surface is obscured to a great extent by earth that is thrown from the crater. Even relatively shallow underground bursts throw dirt up as a cone shaped cloud that screens surface targets from thermal radiation effectively.

[redacted] Since surface reactions are complex and different types of surfaces react in different ways, the effects of underground bursts are extremely variable. As a result of these complexities as well as the fact that thermal effects from underground bursts usually are unimportant compared to other effects, methods for predicting thermal partition have not been developed for underground bursts.

[redacted]

[redacted]

[redacted] Underwater bursts are similar to underground bursts in that thermal radiation is greatly reduced by the heat absorbed by the water and by the screening effect of water thrown from the crater. Thermal effects usually are insignificant. For example, a 20 kt burst in 90 feet of water produced negligible thermal radiation.

[redacted]

[redacted]

Problem 3-5. Calculation of Thermal Partition for a Surface Burst

[redacted] Figure 3-18 contains a family of curves that provide an effective thermal partition for surface targets from nuclear explosions that occur at heights of burst greater than 5 $W^{0.3}$ feet and less than 180 $W^{0.4}$ feet. A thermal partition of 0.21 should be used for surface targets for bursts 5 $W^{0.3}$ feet above or below the surface. Thermal partition for targets directly above the burst should be obtained from Figure 3-1 or from the upper portion (above the dashed line) of Figure 3-18.

[redacted] *Example* [redacted]:

Given: A 500 kt explosion at a height of burst of 300 feet.

Find: The effective thermal partition.

Solution: From Figure 3-18, the effective thermal partition is 0.24.

Answer: The effective thermal partition for a surface target is 0.24. The effective thermal partition for a target directly above the burst is 0.45 (from Figure 3-1, or from the intersection of the dashed line in Figure 3-18 with a yield of 500 kt). The thermal partition for targets at intermediate altitudes would fall between these values. As a result of the uncertainties (see Reliability), the thermal partition for surface targets could fall between 0.44 and 0.1, and the thermal partition for targets directly over the burst could fall between 0.65 and 0.25.

[redacted] *Reliability:* Interaction of the fireball with the surface produces complex effects, and thermal radiation from surface bursts cannot be predicted as reliably as thermal radiation from air bursts. Values of effective thermal partition obtained from Figure 3-18 are estimated to be reliable within ±0.20 if the value is greater than 0.33. If the value that is read is less than 0.33, the lower limit of the expected range of values is 40 percent of the value that is read. The same tolerance is estimated for the effective thermal partition of the fireball as seen from above.

[redacted] *Related Material:* See paragraphs 3-1 through 3-3. See also Figure 3-1.

[redacted]

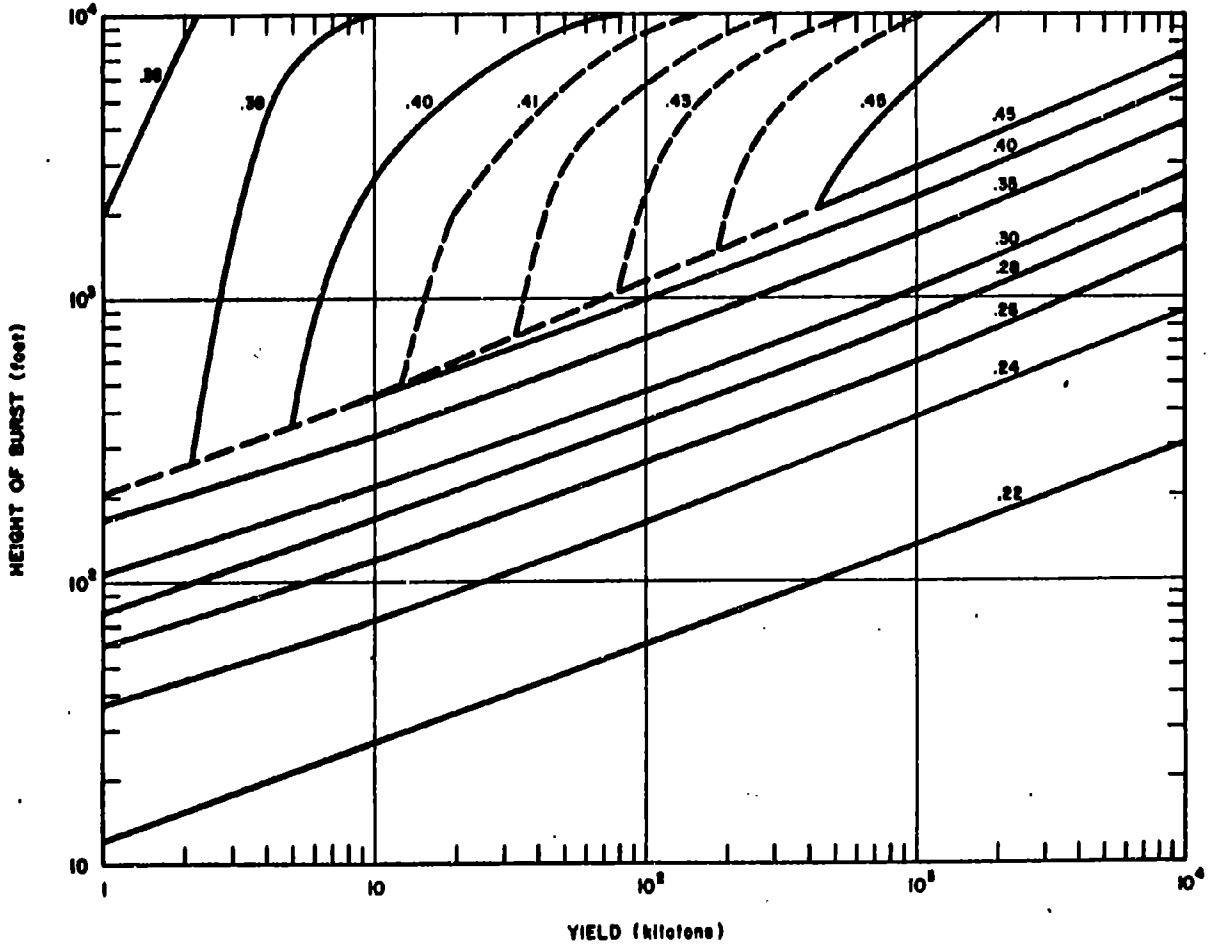

Figure 3-18. [redacted] Thermal Partition for Surface Bursts [redacted]

[redacted]

[redacted] THE THERMAL PULSE [redacted]

[redacted] Next in importance to the radiant energy incident on a target is the rate at which the energy is delivered. Dry leaves that receive a radiant exposure of 5 cal/cm^2 within a fraction of a second would ignite, but bright sunshine produces the same radiant exposure within about 3 minutes without producing ignition.

3-11 Thermal Power-Time Curve [redacted]

[redacted] Figure 3-19 shows the power-time curve for a 200 kt burst at an altitude of 5,000 feet. The shape is complex, with three peaks showing the results of competing processes (largely associated with the changing optical effects produced by the shock front) that alter the level of thermal radiation as the fireball evolves. Changes in burst altitude and weapon design can change the number and sizes of the peaks, therefore a complete, general description of thermal pulses is complex.

[redacted] If the curve of Figure 3-19 is normalized and plotted on linear graph paper it becomes much simpler, as shown in Figure 3-20. Also, since equal areas on the linear graph represent equal amounts of energy, the curve in Figure 3-20 is a more realistic indication of the amount of thermal damage that each portion of the pulse can produce. The first peak, which lasts only a fraction of a millisecond and which contains slightly over 0.1 percent of the energy of the pulse, cannot be seen. Even the second peak is so compressed by the linear time scale that most of it shows up as only a vertical line.

[redacted] When the features of the thermal pulse were first named, little more was known about the pulse than is shown in Figure 3-20; consequently, these two peaks and the valley were called *first maximum, light minimum,* and *second maximum.* Since the earlier features of the pulse produce negligible damage, many discussions ignore them; consequently, the names originally assigned to the later features still tend to be used even though these names are not strictly appropriate. In most of this chapter, the features shown in Figure 3-20 are called first maximum, principal minimum, and final maximum (i.e., the first maximum and first minimum shown in Figure 3-19 are ignored). The first maximum of low altitude bursts is sometimes called the shock exposure maximum, a name that suggests its physical origin. However, this name does not apply at all altitudes: above about 60,000 feet, the mechanism responsible for the first maximum changes.

3-12 Energy-Time Curve [redacted]

[redacted] The energy curve in Figure 3-20 shows the fraction of the thermal pulse energy that is radiated by a given normalized time. For example, it shows that 0.5 percent of the energy is radiated prior to principal minimum, that about 28 percent has been radiated by the time of final maximum, and that 15 percent is radiated at times later than are shown on the graph.

3-13 The Standard Thermal Pulse [redacted]

[redacted] Analysis of thermal radiation phenomena may be simplified by selecting the curves in Figure 3-20 as being representative of thermal pulses in general. Since changes in yield, altitude, and weapon design affect the shape of the pulse, use of such a standard is an approximation. Fortunately, this approximation is reasonably accurate for most bursts below 100,000 feet. The 200 kt burst at 5,000 feet was chosen as the basis for the standard thermal pulse for this manual because both yield and altitude have midrange values for typical thermal problems.

[redacted] Both of the curves in Figure 3-20 appear in dimensionless form. The normalizing parameters are t_{max}, the time of final maximum, and P_{max}, the radiated power at final maximum. Of these parameters, the more frequently calculated is t_{max}, which specifies the time scale of the entire thermal pulse. Values of t_{max} may be

[redacted]

Deleted

Figure 3-19. [redacted] Calculated Power-Time Curve for a 200 kiloton Burst at 5,000 feet [redacted].

DNA (b)(3)

[redacted]

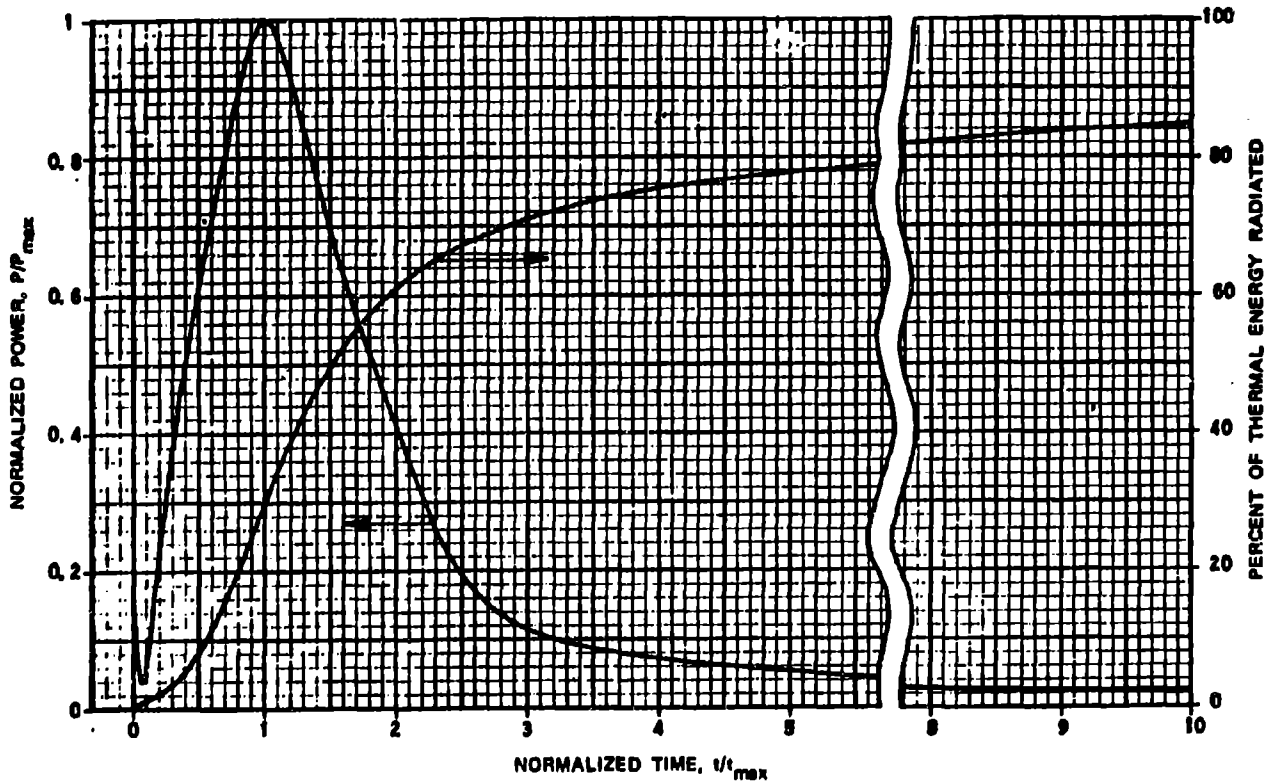

[redacted]

Figure 3-20. [redacted] Power-Time and Energy-Time Curves for a 200 kiloton Burst at 5,000 feet [redacted]

[redacted]

[redacted]

obtained from Figure 3-21. Data for altitudes above 100,000 feet should not be used without consulting paragraph 3-19. Values of t_{max} also may be obtained from the equation

$$t_{max} = 0.043\ W^{0.43}\ (\rho/\rho_o)^{0.42}\ \text{sec},$$

where W is the yield in kilotons and ρ/ρ_o is the ratio of the air density at the altitude of interest to the air density at sea level. Equations for various thermal phenomena (including P_{max}) are summarized in paragraph 3-25. Table 3-4 shows values of ρ/ρ_o as a function of altitude.

[redacted]

[redacted]

Problem 3-6. Calculation of Time to Final Maximum

[redacted] Figure 3-21 shows the time to final maximum as a function of weapon yield and burst altitude. Values of t_{max} obtained from Figure 3-21 can be used to convert the normalized time scale in Figure 3-20 to actual time after burst.

[redacted] *Example* [redacted]

Given: A 25 kiloton explosion at an altitude of 50,000 feet.

Find: The time of the final maximum.

Solution: The value of t_{max} may be obtained directly by interpolation in Figure 3-21, or it may be calculated from the equation given in paragraph 3-13.

Answer: From Figure 3-21,

$$t_{max} \approx 0.078 \text{ sec.}$$

From the equation

$$t_{max} = 0.043\ (W)^{0.43}\ (\rho/\rho_o)^{0.42}.$$

From Table 3-4, $\rho/\rho_o = 0.153$ at an altitude of 50,000 feet in a standard atmosphere. Therefore,

$$t_{max} = (0.043)(25)^{0.43}\ (0.153)^{0.42}$$

$$= 0.078 \text{ sec.}$$

[redacted] *Reliability:* Figure 3-21 was obtained from a combination of theoretical and experimental data. A description of the manner by which these numbers were derived is given in paragraph 3-25. Additional comments on the reliability are given in the subsection RELIABILITY OF THERMAL SOURCE DATA. Times given by this figure are estimated to be reliable within ±25 percent.

[redacted] *Related Material:* See paragraphs 3-11 through 3-13. See also paragraphs 3-24 and 3-25 and Table 3-4.

[redacted]

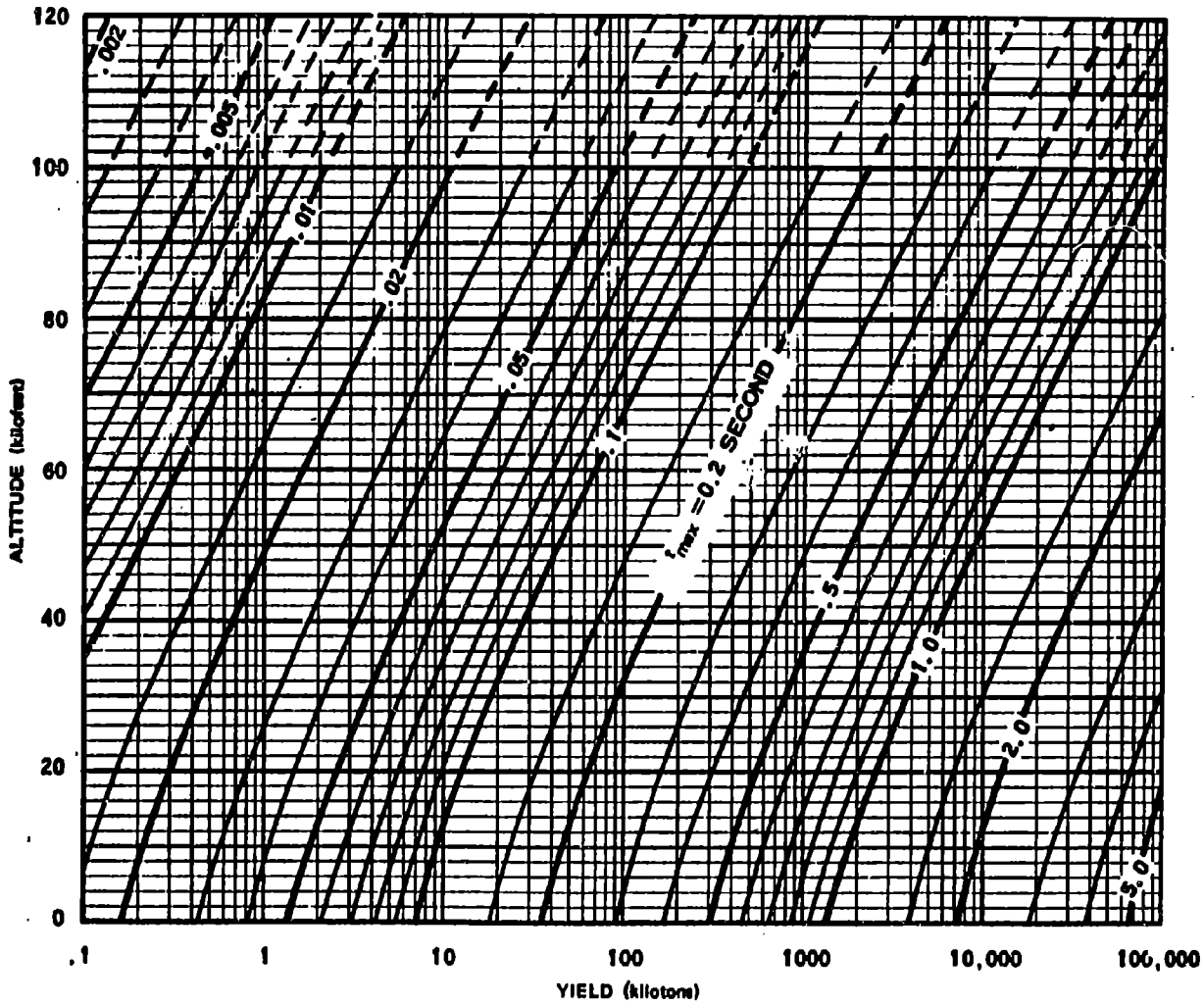

Figure 3-21. [redacted] Time of Final Maximum as a Function of Yield and Altitude [redacted]

[redacted]

3-14 Effect of Thermal Pulse Duration [redacted]

[redacted] For most target materials and a particular level of radiant exposure, there is a value of thermal pulse length that will produce maximum damage. If the pulse is too short, there will be too little time for the energy to penetrate the material of an opaque target. Consequently, the heat is confined to a thin surface layer. This layer will vaporize rapidly, and will carry the deposited energy away with it. Often, this vapor will be in the form of smoke, which will shield the target from later portions of the thermal pulse. If the pulse is too long, a thin target (e.g., paper) will dissipate the heat as it is received or a thick target will absorb the energy harmlessly in a thick layer of material.

[redacted] For the types of damage that receive the most attention – ignition of waste materials and skin burns – most nuclear bursts produce thermal pulses that are longer than the pulse that would produce maximum damage. Consequently, in almost every situation a short thermal pulse is more damaging than a long one. Short thermal pulses are produced by low yields and high burst altitudes.

[redacted] The reasoning that has been applied to different thermal pulses also can be applied to different portions of the same pulse. The first pulse is unimportant because of the small total energy that it contains. The final pulse radiates about 70 percent of the total pulse energy by 3 t_{max}, and this portion of the pulse produces most of the thermal damage. Another 15 percent of the pulse energy is radiated between 3 t_{max} and 10 t_{max}. This also contributes to thermal damage, but with reduced effectiveness because of the lower power level. The remaining 15 percent of the pulse is released after 10 t_{max} so slowly that it fails to add significantly to the total thermal damage.

3-15 Effect of Altitude on Pulse Shape [redacted]

[redacted] Although both yield and altitude affect the shape of the thermal pulse, the effect of altitude is the more severe. Below 100,000 feet, the changes are relatively minor. As illustrated in Figure 3-22, higher altitudes increase the relative width of the "first" pulse, which now contains sufficient energy to produce significant damage in some situations. The higher altitudes also decrease the depth of the principal minimum. The width of the final pulse on the dimensionless plot remains about the same, and the standard pulse shape is still a fair representation of the ability of the thermal pulse from a burst at 100,000 feet to produce damage. Thermal radiation damage to materials is discussed in Section III, Chapter 9, and thermal injuries are discussed in Section II, Chapter 10.

[redacted] Figure 3-23 shows a thermal pulse that was calculated for a 200 kt burst at an altitude of 40 km (131,000 feet). Between 100,000 feet and 131,000 feet, the pulse shape changes drastically. The principal minimum has disappeared, and even a logarithmic plot of this power-time curve would show only a single maximum. These differences in shape are caused by low air density (about 0.33 percent of sea level density) and the resulting weakness of shock wave effects. (As discussed in paragraph 3-25, the oscillations in the power-time curves of low altitude bursts depend strongly on the optical properties of the shock wave.)

3-16 The Effects of Thermal Pulse Specifications on Thermal Partition [redacted]

[redacted] The time at which the prompt thermal pulse ends must be specified in order to define the total energy of the thermal pulse. Among the logical choices are the following:

[redacted]

Deleted

Figure 3-22. [redacted] Power-Time Curve for a 200 kiloton Burst at 100,000 feet [redacted]

DNA 4111(3)

Deleted

Figure 3-23. [redacted] Power-Time Curve for a 200 kiloton Burst at 40 kilometers [redacted]

[redacted]

- Since the energy radiated after about 10 t_{max} produces little damage, 10 t_{max} is a logical cutoff time. This choice would have the effect of increasing the height of the energy curve so that it reaches 100 percent at 10 t_{max} in Figure 3-20.
- At times on the order of 20 or 30 t_{max}, fireball radiation becomes difficult to measure; therefore, the experimentally measured thermal pulse typically ends in this time range.

[redacted] Precedent may be found for either alternative. The definition selected in this chapter is approximately equivalent to the second choice listed above: the portion of the pulse after 10 t_{max} is assigned a value of 15 percent of the total pulse energy. This definition of the prompt thermal pulse agrees within a few percent with the thermal pulse as described in most reports on thermal pulse measurements and on thermal damage effects.

[redacted] Reports of theoretical calculations of the thermal pulse usually define the pulse energy in a way that corresponds roughly to the first alternative. The reason is a purely practical one: since calculation of the pulse beyond 10 t_{max} is neither accurate nor economical, the calculations usually are terminated at about 10 t_{max}. The reported energy content of the pulse is the energy contained in that portion of the pulse covered by the calculation. In reports describing these calculated results, a radiant exposure of 8.5 cal/cm^2 may imply the identical thermal pulse that is implied in this chapter by a radiant exposure of 10 cal/cm^2. Similarly, a thermal partition of 0.34 as reported, for example, in DASA 1589 (see bibliography) is reported in this chapter as approximately 0.40.

[redacted] The use of a standard thermal pulse introduces another problem. Since different thermal pulses have different shapes, the convenience of a standard pulse requires some sacrifice in accuracy. To minimize the effects of this loss in accuracy, the most damaging portion of the pulse is matched carefully but substantial errors are tolerated where power levels are low. Comparison of the pulse for 200 kt at 100,000 feet (Figure 3-22) with the standard pulse (Figure 3-20) shows that the two pulses are nearly equivalent near the time of final maximum but quite different at late times.

[redacted] To achieve this match, all parameters, including thermal partition, are chosen to give the correct power level and time scale at the time of final maximum. For the burst at 100,000 feet, the value of thermal partition so chosen is a few percent higher than a value based solely on total thermal energy. The standard pulse shape implies a level of late time radiation that the calculated thermal pulse for 100,000 feet fails to maintain. To match the high power portions of the calculated pulse to the standard pulse shape, thermal partition must be made artificially high.

[redacted] These matters of definition present no particular problem within this manual. Thermal pulses below 100,000 feet are specified so that the standard pulse shape, the assigned value of thermal energy, and the time of final maximum imply a pulse that provides a close match to the actual pulse in its ability to produce thermal damage. On the other hand, the user must keep these details in mind if he wishes to compare thermal data as given in this chapter with similar data from other sources.

[redacted] FIREBALL BRIGHTNESS [redacted]

[redacted] The surface of a nuclear fireball is many times brighter than the surface of the sun. The image of the fireball, brought to a focus on the retina of the eye, can produce burns and permanently damage the area covered by that image (see paragraph 10-20, Chapter 10). Fireball brightness is therefore one of the important parameters of the thermal source.

[redacted] A detailed study of eye damage also re-

[redacted]

[redacted]

quires knowledge of the spectral distribution of thermal radiation and the transport properties of the air as a function of wavelength; however, the present discussion is limited to the most important and most easily used parameter, surface brightness. This quantity may be measured in terms of the total power per unit area radiated by the fireball. Convenient units are watts/cm^2. Brightness of the sun provides a useful standard for comparison. As viewed from outside of the atmosphere, the surface brightness of the sun is 6,350 watts/cm^2.

[redacted] For bursts below 100,000 feet, the approximate brightness of the fireball at final maximum is

$$B = \frac{2.7 \times 10^4}{W^{0.14}(\rho/\rho_o)^{0.42}} \text{ watts/cm}^2,$$

where W is yield in kilotons and ρ/ρ_o is the ratio of ambient air density at burst altitude to ambient air density at sea level. This equation gives a rough approximation of fireball brightness: more complete and accurate data for a particular yield and altitude may be found from the equation.

$$B = \frac{P}{4 \times 10^4 \pi R_f^2}$$

where P is power in watts radiated by the fireball and R_f is fireball radius in meters. Values of P and R_f as functions of time may be found for a wide range of yields and altitudes in "Theoretical Models for Nuclear Fireballs," DASA 1589 (see bibliography).

[redacted] Scattered light from a nuclear fireball can contribute to temporary flashblindness, but it is too diffuse to produce retinal burns. Consequently, the direct flux from the nuclear fireball is the only parameter of interest in the study of eye damage. Transmittance calculations are not appropriate, because they include scattered as well as direct flux.

[redacted] The direct flux received from a low altitude burst (burst height about 1/4 mile or less) is attenuated by the factor

$$T_d = e^{-2.9R/V}$$

where T_d is the transmission coefficient of the atmosphere for direct flux, R is the slant range, and V is visual range. For higher altitude bursts, the transmission coefficient is

$$T_d = e^{-\tau(h)\frac{R}{h}\frac{16}{V}}$$

where $\tau(h)$ is optical thickness of the model atmosphere with 16-mile visual range (Figure 3-2), and h is the height of burst.

[redacted] These equations give average attenuation for the entire fireball spectrum and underestimate the amount of infrared energy that the atmosphere can transmit. Since infrared contributes substantially to eye damage, exposure to fireball radiation may be somewhat more serious than the equations given above would indicate. Figures 10-6 through 10-10 provide estimates of safe separation distances for eye damage for various observer and burst altitudes.

[redacted] Cloud layers attenuate direct flux more than they attenuate radiant exposure. A cloud layer between the burst and the ground will produce the approximate attenuations shown in Table 3-3. The transmission coefficients shown in Table 3-3 are based on visible light, but they are expected to apply to the entire fireball spectrum within the limits to which a transmission coefficient can be matched to a particular sky condition.

[redacted] THE THERMAL PULSE FROM SPECIAL WEAPONS [redacted]

[redacted] As stated in paragraph 2-45, Chapter 2, weapons that have enhanced radiation out-

[redacted]

[redacted]

Table 3-3. [redacted] Attenuation of Direct Thermal Radiation by a Cloud or Haze Layer [redacted]

Type of Atmosphere	Description of Sky	Transmission Coefficient for Direct Flux
Very clear	Visual range is 25 miles or more. This condition is rare except at high altitude locations.	90.0%
Clear	Sky deep blue. Shadows are distinct and dark.	80.0%
Light haze	Sky white; dazzling near the sun. Shadows visible, gray.	3.0%
Medium haze	Sky bright grayish white. Can view sun without discomfort. Shadows are visible but faint.	0.1%
Heavy haze	Sky dull gray-white. The sun's disk is just visible. Shadows are barely discernible.	0.003%

[redacted]

DNA (b)(3)

puts, i.e., weapons that produce a large fraction of their output in the form of neutrons, gamma rays, or X-rays [redacted] will, in most cases, generate a weaker blast wave than a nominal weapon of the same yield. Similarly, the thermal pulse from such special weapons may be weaker than that from a nominal weapon. The explanation for the reduced thermal output is the same as the explanation for a weaker blast wave: neutrons, gamma rays, and high energy X-rays travel much farther through the atmosphere than the energy from a conventional weapon; therefore, a large portion of the weapon energy may be absorbed by air far from the burst. This air will not become sufficiently hot to contribute effectively to either the blast wave or to the thermal pulse.

[redacted] The terms "nominal weapon" and "conventional weapon" used in the preceding paragraph refer to a nuclear weapon that radiates 70 to 80 percent of its energy as X-rays [redacted] and retains nearly all of the remaining energy as thermal and kinetic energy of the weapon debris (see paragraph 4-4, Chapter 4). Such a source serves as a convenient starting point for calculations involving weapons with other characteristics. The procedures described in this subsection apply to burst altitudes of 100,000 feet and lower.

3-17 Effective Thermal Yield of Special Weapons [redacted]

[redacted] The modified thermal effects produced by weapons with enhanced outputs may be calculated in terms of an effective thermal yield. This is defined as the yield that a nominal warhead would have in order to radiate the same thermal energy as the special weapon. Effective thermal yield should not be interpreted to mean

[redacted]

[redacted]

[redacted] thermal energy radiated (a quantity sometimes assigned to the term "thermal yield"). Effective thermal yield means *the effective value of total yield to be used in thermal calculations.*

[redacted] The concept of effective thermal yield is an oversimplification, and it cannot describe the performance of special weapons precisely. For example, the effective thermal yield calculated on the basis of time of final maximum will, in general, be slightly different from the effective thermal yield that gives the correct value of total thermal energy radiated. A still different effective thermal yield would predict the correct power at final maximum.

[redacted] In this subsection, effective thermal yield is the value that gives the correct value for thermal energy radiated, because, in most applications, this is the most important of the thermal parameters. Other parameters may be calculated by using this same value of effective thermal yield, but the calculation will be somewhat less accurate than if the procedure had been designed to calculate those parameters.

[redacted] Effective thermal yield is roughly the amount of energy that the nuclear source deposits within a sphere the size of the fireball at the time of the principal minimum. This radius is

$$R_{min} = \frac{95\ W^{0.36}}{(\rho/\rho_o)^{0.22}} \text{ feet}$$

$$= \frac{29\ W^{0.36}}{(\rho/\rho_o)^{0.22}} \text{ meters,}$$

where W is the weapon yield in kilotons, ρ is the ambient air density at the burst altitude, and ρ_o is the ambient density at sea level. Table 3-4 shows the ratio ρ/ρ_o as a function of altitude. Energy that is deposited beyond the radius R_{min} is assumed to make a negligible contribution to the energy radiated by the fireball.

Table 3-4. [redacted] Relative Air Density as a Function of Altitude [redacted]

Altitude (feet)	Relative Density,* ρ/ρ_o	Altitude (feet)	Relative Density,* ρ/ρ_o
0	1.000	80,000	0.0361
1,000	0.971	85,000	0.0284
2,000	0.943	90,000	0.0224
3,000	0.915	95,000	0.0176
4,000	0.888	100,000	0.0140
5,000	0.862	110,000	8.69-3†
10,000	0.739	120,000	5.43
15,000	0.629	130,000	3.45
20,000	0.533	140,000	2.22
25,000	0.449	150,000	1.45
30,000	0.375	160,000	9.77-4
35,000	0.311	170,000	6.69
40,000	0.247	180,000	4.65
45,000	0.194	190,000	3.22
50,000	0.153	200,000	2.22
55,000	0.121	210,000	1.54
60,000	0.0949	220,000	1.05
65,000	0.0747	230,000	7.05-5
70,000	0.0586	240,000	4.62
75,000	0.0459	250,000	2.60

* [redacted] $\rho_o = 2.38 \times 10^{-3}$ slugs/ft^3 = 1.225 gm/cm^3.
† [redacted] 8.69-3 means 8.69×10^{-3}.

[redacted] Since the size of the fireball is determined by the thermal energy it contains, it would be logical to let W represent effective thermal yield rather than total weapon yield. To do this requires a trial-and-error approach. Effective yield is unknown until the equation given above has been solved and the energy deposited within R_{min} has been determined. In practice, the accuracy of this method for calculating effective thermal yield is sufficiently uncertain that this refinement is seldom justified. Unless

[redacted]

[redacted]

[redacted] the effective thermal yield is less than half of the total yield, it is recommended that W be equated to total yield in the equation.

[redacted] To determine the amount of energy deposited within a radius R_{min} of the burst, the form of the energy emitted by the weapon must be determined. [redacted]

DNA (b)(3)

[redacted] The steps in calculating the energy contained within R_{min} are:

1. Find the scaled radius

$$(\rho/\rho_o)\ R_{min} = 95\ W^{0.36}\ (\rho/\rho_o)^{0.78} \text{ feet}$$

$$= 29\ W^{0.36}\ (\rho/\rho_o)^{0.78} \text{ meters.}$$

This is the path length at sea level that passes through the same amount of air that a path of length R_{min} passes through at the burst altitude. Use of this scaled radius makes further scaling unnecessary.

2. Assume that 100 percent of the debris is contained within the radius.

3. [redacted]

DNA (b)(3)

4. In a similar manner, find the amount of gamma ray energy that is deposited within R_{min} of the burst. The 1 MeV gamma photon curve in Figure 3-24 is approximately representative of the energy deposition properties of the gamma spectrum of a nuclear weapon.

5. [redacted]

DNA (b)

6. The components of energy deposited within R_{min} of the burst are added together to obtain the effective thermal yield [redacted]

The calculation is then repeated on the basis of this new value of scaled radius.

[redacted] The effective thermal yield calculated by the procedures described above may be used to calculate other thermal parameters by the methods described in preceding paragraphs. For example, the effective thermal yield may be used as the weapon yield to calculate thermal partition as described in paragraph 3-1.

3-18 Thermal Pulse Shape from Special Weapons [redacted]

[redacted] The two properties that characterize special weapons (in the sense that the term is used in this chapter) are that the initial deposition of energy fills a large volume and that the density of the deposited energy drops gradually with distance from the point of burst when compared to nominal weapons. The early fireball of a conventional weapon rapidly develops a sharply defined edge, formed by the shock front. The sharply defined edge results in a very bright fireball; the diffuse fireball from an enhanced weapon is relatively dim, becoming bright only when the shock wave propagates through the incandescent region of the initial fireball and reaches cooler air.

[redacted]

[redacted]

[redacted]

DNA (b)(3)

[redacted] The thermal pulse assumes its conventional appearance at a time that depends on yield, altitude, and output properties of the nuclear device. [redacted]

DNA (b)(3)

[redacted]

[redacted]

DNA (b)(3)

[redacted]

[redacted]

Problem 3-7. Calculation of the Effective Thermal Yield of a Hot X-ray Warhead [redacted]

[redacted] Paragraph 3-17 outlines six steps to be used together with Figure 3-24 to determine the effective thermal yield of weapons with enhanced radiation outputs. The effective thermal yield thus obtained is used in place of the weapon yield to calculate the various thermal parameters as described in preceding paragraphs of this chapter.

[redacted] *Example* [redacted]

DNA (b)(3)

[redacted]

DNA (b)(3)

[redacted] *Related Material:* See paragraphs 3-1 through 3-6, 3-17 and 3-18. See also paragraphs 4-4 through 4-8, Chapter 4.

[redacted]

[redacted]

[redacted]

Deleted

[redacted]

Figure 3-24. [redacted] Distribution of Deposited X-ray Energy in a Sea Level Atmosphere as a Function of Source Spectrum [redacted]

[redacted]

[redacted] HIGH ALTITUDE THERMAL PHENOMENA [redacted]

DNA (b)(3)

[redacted] Both experimental and theoretical data are very limited, so the methods described are based on information that is sketchy at b[illegible]. An additional problem affects theoretical data: the approximations necessary to limit computer programs to a usable size become poorer at higher altitudes. Although many points of agreement exist between experimental data and the corresponding computer calculations, the confidence that can be placed on theoretical results is less at high altitudes than at low altitudes.

3-19 Thermal Partition [redacted]

[redacted] Two factors affect thermal partition at high altitudes. First, shock waves form much less readily in the thinner air; consequently the fireball is able to radiate thermal energy that would have been transformed to hydrodynamic energy of the blast wave at lower altitudes. Second, the thinner air allows energy from the nuclear source to travel much farther than is possible at sea level. Some of this energy travels so far from the source that it makes no contribution to the energy contained in the fireball.

[redacted] In general, the first of these factors becomes effective between about 100,000 and 140,000 feet, and, as a result, thermal efficiency rises. Above 140,000 feet, the second factor becomes the more important and efficiency drops.

DNA (b)(3)

[redacted] As in the previous subsection on special weapons, this method requires that the X-ray output of the weapon be represented by the sum of several black body spectra. The energy density deposited at a given range may then be obtained from Figure 3-25a or 3-25b. Briefly, the scaling procedure is the following: the energy ΔE_2 = 2,500 cal/gm is scaled by the equation

$$\frac{\Delta E_2}{\Delta E_1} = \left(\frac{\rho}{\rho_o}\right)^2 \frac{W_2}{W_1}.$$

This equation is solved for ΔE_1, the value of energy to be read directly from Figure 3-25a or 3-25b. In this equation, ρ/ρ_o is the ratio of ambient air density at burst altitude to ambient

[redacted]

[redacted]

[redacted] density at sea level (Table 3-4), W_1 is a reference yield of 1 kt and W_2 is the energy, in kilotons, contained in a particular black body temperature component of the nuclear source.

[redacted] The scaled radius R_1 is read directly from the horizontal axis of Figure 3-25a or 3-25b. This radius is related to the actual radius R_2 by the scaling equation

$$\frac{R_1}{R_2} = \frac{\rho}{\rho_o}.$$

However, the rest of the problem does not require that R_2 be known; the calculation is based only on the scaled radius R_1. In general, R_1 is determined by more than a single spectral component; the way in which this calculation is performed is made clear in Problem 3-7.

[redacted] The method of treating debris, gamma, and neutron energy is identical to that described in paragraph 3-17.

DNA (6)(3)

[redacted]

[redacted] The procedures described above apply to burst altitudes up to about 250,000 feet.

3-20 High Altitude Thermal Pulse Duration [redacted]

[redacted] Since the thermal pulse from a high altitude explosion rises to its maximum in an extremely short time and declines from that time (see Figure 3-23), pulse duration no longer can be specified in terms of the time to final maximum. A number that is useful in many applications is t_{70}, the time required for a pulse to deliver 70 percent of the total energy. At low altitudes,

$$t_{70} \approx 2.9\ t_{max}$$

and it follows that at high altitudes it might be possible to assign an effective time of final maximum such that

$$t_{max}\ (\text{effective}) = t_{70}/2.9.$$

[redacted]

DNA (6)(3)

[redacted] Analyses of a limited number of computer calculations of high altitude burst phenomena show the following trends: below 80,000 feet, the equation holds within the scatter of the data; above 80,000 feet, the thermal pulse is delivered more rapidly than this equation predicts, until at 160,000 feet the pulse is only about a third as long as predicted by the equation, above 200,000 feet, the pulse approaches and, in one case, exceeds the predicted value. This behavior is shown in Figure 3-26.

[redacted]

[redacted]

[redacted]

Problem 3-8. Calculation of Thermal Energy Radiated from a High Altitude Explosion

[redacted] Figures 3-25a and 3-25b show the density of deposited energy from various energy sources as a function of range from a 1 kiloton explosion at sea level. These figures, together with the equations given in paragraph 3-19 provide the means to determine the thermal energy radiated by various yields at burst altitudes between about 120,000 feet and 250,000 feet. If the burst altitude is between 100 kft and 120 kft, thermal partition should be obtained by interpolation between the thermal partition obtained for 100 kft by the methods described in paragraph 3-1 and the thermal part' 'on determined by the methods illustrated b..ow. If the burst altitude is above 250,000 feet, refer to paragraph 3-21.

[redacted]

DNA (b)(

Example 1 [redacted]

[redacted]

DNA (b)(3)

Example 2 [redacted]

[redacted]

DNA (b)(3)

[redacted]

[redacted]

[redacted]

DNA (b)(3)

[redacted]

[redacted] *Related Material:* See paragraphs 3-1 through 3-6 and 3-19 through 3-21. See also Table 3-4.

[redacted]

[redacted]

[redacted]

DNA
(b)(3)

Deleted

Figure 3-25a. [redacted] Density of Deposited Energy from Various Energy Sources [redacted]

[redacted]

[redacted]

[redacted]

DNA
(b)(3)

Deleted

Figure 3-25b. [redacted] Density of Deposited Energy from Various Energy Sources [redacted]

[redacted]

Deleted

Figure 3-28. [redacted] A Comparison of Calculated Effective Times of Final Maximum with Predictions from the Simplified Equation [redacted]

DNA (A)(3)

[redacted]

3-21 Bursts Above 250 Kilofeet [redacted]

[redacted] The calculations indicate that at heights of burst at or above about 290,000 feet the incandescent air heated by absorption of X-rays from the explosion is approximately at the same altitude, regardless of the actual height of burst. The heated region then reradiates at the longer wavelengths which could reach the ground. The reradiating region is in the form of a frustum of a cone, pointing upward, with a vertical thickness of approximately 45,000 feet and a mean altitude of 270,000. At this altitude, the radius of the frustum is roughly equal to the difference between the height of burst h and 270,000 feet, i.e., h - 270,000 feet. Consequently, as the burst altitude increases, the radius of the radiating region becomes greater but its thickness and altitude remain roughly constant. The shape of the region thus approaches a thick disk centered at about 270,000 feet altitude. The debris energy still is contained fairly locally until the height of burst reaches the debris stopping altitude of about 380,000 feet (see Table 8-1, Chapter 8), but the main effects of thermal energy delivered as a result of debris deposition at these altitudes are flashblindness or retinal burns (see Section II, Chapter 10). The total thermal energy emitted as a result of the debris deposition is masked by that energy emitted at lower altitudes as a result of X-ray deposition insofar as total energy that reaches the earth is concerned.

[redacted] About one-fourth of the X-ray energy from the explosion is absorbed in the low density air of the reradiating region, and only a small fraction, which decreases with the height of burst, is reradiated as secondary radiation. Consequently, only a few percent of the weapon energy is emitted as radiation capable of causing damage at the earth's surface. In fact, for bursts at altitudes exceeding about 330,000 feet the thermal radiation from a nuclear explosion even in the megaton range is essentially ineffective on the ground.

[redacted] If the horizontal distance d from ground zero, i.e., from the point on the ground immediately below the center of the disk-like region, to the position where the incident thermal energy is to be calculated is less than the height of burst, h, the source may be regarded as being located at the median radius of the disk in an altitude of 270,000 feet; this is indicated by the point S in Figure 3-27. Hence, for the target point X, the appropriate slant range is given by

$$R \text{ (kilofeet)} = \left\{(270)^2 + [1/2\,(h - 270) - d]^2\right\}^{1/2},$$

with d and h in kilofeet. This expression holds even when d is greater than 1/2 (h - 270); although the quantity in the square brackets is then negative, the square is positive. The slant range, R_o, for ground zero is obtained by setting d equal to zero; thus,

$$R_o \text{ (kilofeet)} = [(270)^2 + 1/2\,(h - 270)^2]^{1/2}.$$

If the distance d is greater than the height of burst, and equivalent point source is located at

[redacted]

[redacted]

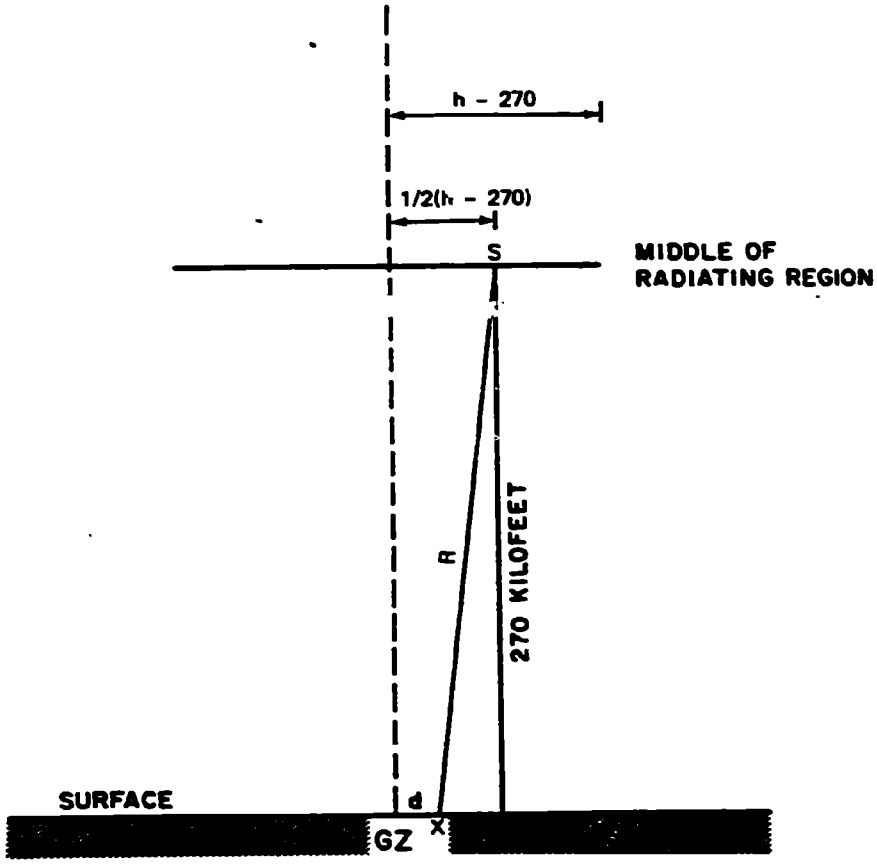

Figure 3-27. [redacted] Equivalent Point Source at Median Radius When Height of Burst Exceeds Distance of Target, X, from Ground Zero [redacted]

[redacted]

the center of the radiating disk at 270,000 feet altitude; then

$$R \text{ (kilofeet)} = [(270)^2 + d^2]^{1/2}.$$

The calculations assumed that 80 percent of the total yield is emitted as X-ray energy and that 25 percent of this energy is absorbed in the radiating disk region. Hence, 0.8 x 0.25 = 0.2 of the total yield is absorbed. For calculating the radiant exposure, the total yield W in the equations in paragraph 3-2 is consequently replaced by 0.2 W. Furthermore, the equivalent of the thermal partition is called the "thermal efficiency," ϵ, defined as the effective fraction of the absorbed energy that is reradiated. Hence, if R is in kilofeet, the equation for radiant exposure given in paragraph 3-2 becomes

$$Q = \frac{17.1\epsilon\, WT}{R^2} \text{ cal/cm}^2.$$

The values of ϵ given in Figure 3-28 as a function of height of burst and yield were obtained by the theoretical calculations mentioned previously. The transmittance may be estimated from Figure 3-15, but no serious error would be involved by setting it equal to unity for the large burst heights involved. No attempt should be made to interpolate between values of radiant exposure obtained for a burst height of 250,000 feet by the method described in paragraph 3-19 and the values obtained for 290,000 feet by the method described in this paragraph. If values of radiant exposure from bursts between these altitudes are desired, it is recommended that the radiant exposure be calculated for each altitude (250,000 feet and 290,000 feet) and that the higher or lower value be taken as an estimate, depending on the direction of conservatism that is desired.

RELIABILITY OF THERMAL SOURCE DATA

Most of the thermal radiation source data presented in this chapter were obtained from the series of computer runs reported in DASA 1589, "Theoretical Models for Nuclear Fireballs" (see bibliography). These data are not purely theoretical: development of the computer code included comparisons of calculated results with experimental data, and adjustments in the assumed weapon characteristics were made as a result of these comparisons.

The advantages of computer data (provided that this choice can be justified) are:

(1) This method eliminates many random errors that are inherent in experimental data. These random errors include uncertainty in the exact value of nuclear yield, instrument errors, uncertainty in atmospheric transmittances, blurring of some results as a result of finite time resolution of certain instruments, and uncertainty in the methods for transforming measured data to the parameters required for thermal calculations.

(2) Computer calculations can generate a large amount of data for a wide range of yields and altitudes that are not available from experiments.

(3) Errors that appear in the code results are likely to be consistent; therefore, the code probably predicts the trends produced by changes in yield or altitude more accurately than it predicts the results of any individual burst.

The disadvantage of using the code is that at best it gives only an approximation of the many processes that determine, directly or indirectly, the amount of thermal energy radiated. The method of accounting for spectral absorption lines is an example of the approximations that are required. A subroutine stores data for 151,528 different spectral lines, yet this is a small fraction of the number of lines that affect

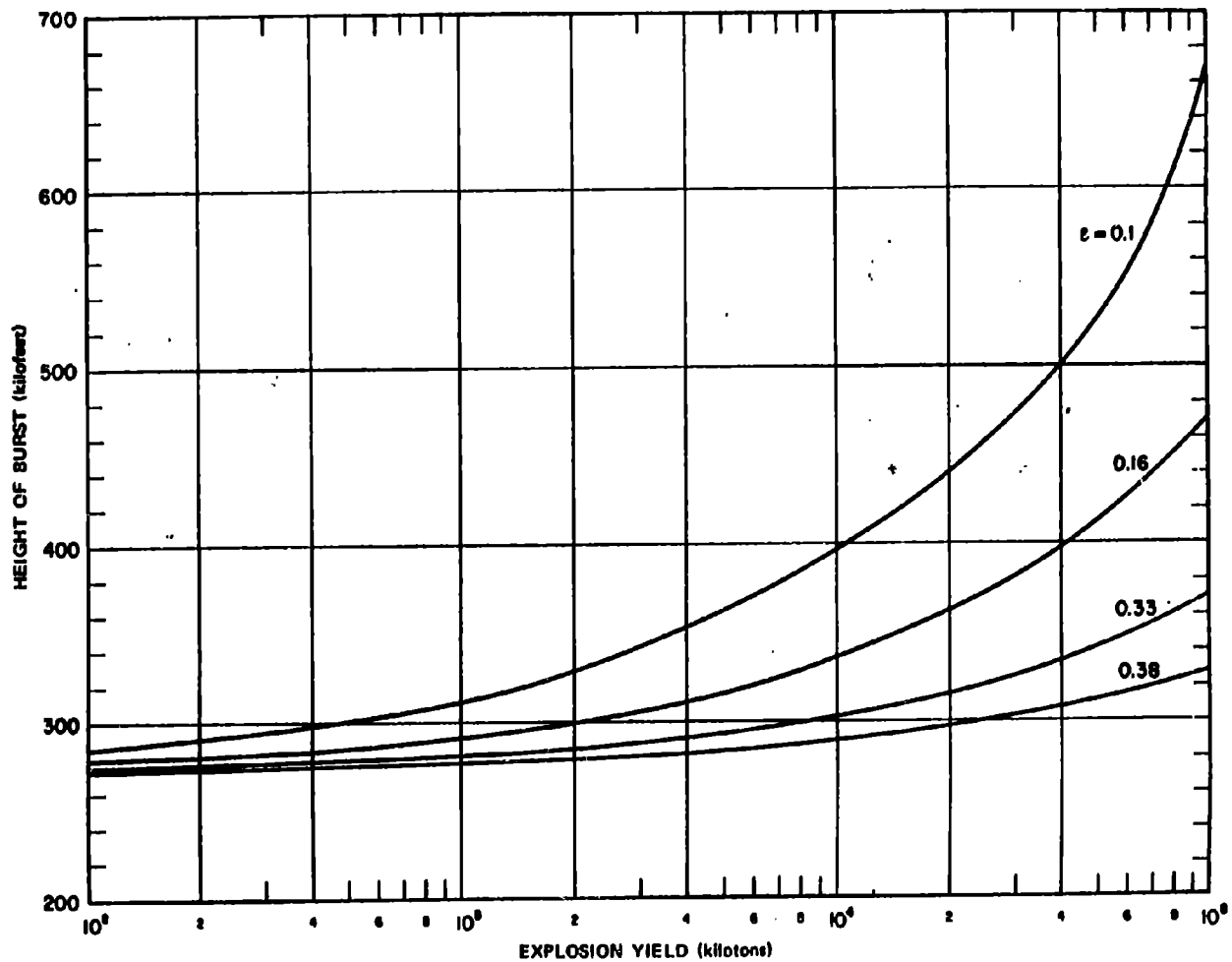

Figure 3-28. [redacted] Fraction of Absorbed X-ray Energy Reradiated [redacted]

radiative transport within the fireball.

Justification for using the code is the agreement between code results and measured data. The most striking areas of agreement are: (1) radius-time data, which are the most accurate experimental data, and (2) the ability of the code to reproduce intricate details of fireball evolution such as the fluctuations of the power-time curve (Figure 3-19) and the complex structure observed in high altitude fireballs.

Unfortunately, the code-calculated parameters that are of more direct interest in this chapter (e.g., thermal partition) cannot be confirmed as accurately by experimental data. Since uncertainty in the experimental data generally is as great as the discrepancy between theory and experiment, the experimental data provide no clear indication of the reliability of the code results, e.g., the code reproduces observed fireball phenomena within the accuracy of most test measurements.

This agreement has been obtained by comparisons of early code results with experimental data; however, changes in the code have never taken the form of arbitrary correction factors. Two examples illustrate the procedure used to correct the code.

The code, as originally written, did not predict the correct level of radiation during the first maximum. Analysis of the radiative properties of the shock front revealed that a shock precursor (discussed in paragraph 3-25), a very thin layer of heated air ahead of the shock front, determines the radiative properties of the fireball during this interval. The fine structure of this precursor was lost by the approximate methods that were required to represent the shock front on the computer. A possible solution, much finer zoning in the region of the shock front, was rejected as uneconomical; however, a separate program to calculate shock-wave properties gave results that agree with the observed first maximum. This separate program was used to correct the radiation level that was calculated by the main computer program.

DNA (6X3)

These illustrations show that the computed results are based on physical data. In a sense, experimental data are represented indirectly because they indicated the parts of the computer program that should be examined more closely. Nevertheless, agreement between code results and observations indicate that the physics of radiative transport and hydrodynamic motion is understood well enough that the computer program is an adequate representation of the fireball itself. Therefore, in this chapter these code results are tentatively accepted as the preferred source of data concerning the source of thermal radiation from nuclear fireballs.

RELATION OF RADIANT EXPOSURE TO PEAK OVERPRESSURE

In many weapons effects problems, the first step is to determine which nuclear effect establishes the damage radius for a given burst. The series of figures in this subsection (Figure 3-29 through 3-56) show radiant exposure and peak overpressure as a function of height of burst and ground distance for 7 yields. The curves in these figures provide an aid in the determination of whether blast or thermal effects will be more important for specific situations. Four families of curves are presented for each yield. In each case the first two families of

[redacted]

[redacted]

curves are for no atmospheric attenuation of the thermal radiation, i.e., the worst case thermal exposure, and the second two families of curves are for a visual range of 16 miles (a clear day). Table 3-5 shows a summary of the data presented in the figures.

[redacted] These curves reflect the data presented in preceding paragraphs of this chapter and the free field air blast data from Chapter 2 accurately for the yields and conditions shown on each figure; however, they do not provide the answers to all potential problems, e.g., only 7 yields are included, and no data are presented for visual ranges less than 16 miles. The curves are intended to be used as an aid in determining the relative importance of blast and thermal radiation. Their use can be extended beyond the particular values that are plotted. For instance, the value of radiant exposure obtained from the curves for no atmospheric attenuation may be converted to the value for any visual range by multiplying by the transmittance appropriate to the given conditions. Interpolation between yields will provide a first order, and frequently sufficient, estimate of the more important effect.

Table 3-5. [redacted] Summary of Blast-Thermal Curves [redacted]

Figure Number	Yield (kt)	Atmospheric Attenuation	Blast Values (psi)
3-29	0.01	None	10-50
3-30	0.01	None	1- 4
3-31	0.01	16 Mile Visual Range	10-50
3-32	0.01	16 Mile Visual Range	1- 4
3-33	0.1	None	10-50
3-34	0.1	None	1- 4
3-35	0.1	16 Mile Visual Range	10-50
3-36	0.1	16 Mile Visual Range	1- 4
3-37	1.0	None	10-50
3-38	1.0	None	1- 4
3-39	1.0	16 Mile Visual Range	10-50
3-40	1.0	16 Mile Visual Range	1- 4
3-41	10	None	10-50
3-42	10	None	1- 4
3-43	10	16 Mile Visual Range	10-50
3-44	10	16 Mile Visual Range	1- 4
3-45	100	None	10-50
3-46	100	None	1- 4
3-47	100	16 Mile Visual Range	10-50
3-48	100	16 Mile Visual Range	1- 4
3-49	1,000	None	10-50
3-50	1,000	None	1- 4
3-51	1,000	16 Mile Visual Range	10-50
3-52	1,000	16 Mile Visual Range	1- 4
3-53	10,000	None	10-50
3-54	10,000	None	1- 4
3-55	10,000	16 Mile Visual Range	10-50
3-56	10,000	16 Mile Visual Range	1- 4

[redacted]

[redacted]

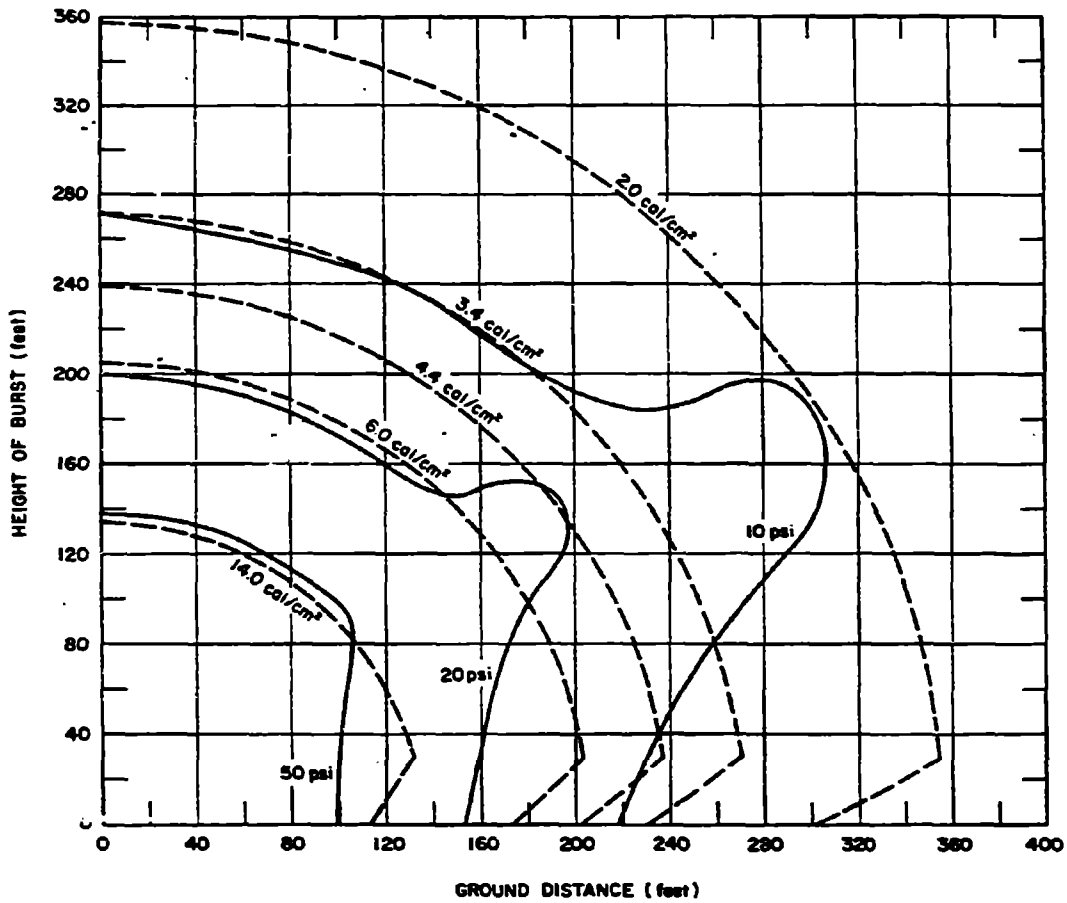

Figure 3-29. [redacted] Free Field Radiant Exposure and Air Blast Overpressure at the Surface, as a Function of Height of Burst and Ground Distance, for 0.01 kilotons, No Atmospheric Attenuation, High Overpressure Region [redacted]

[redacted]

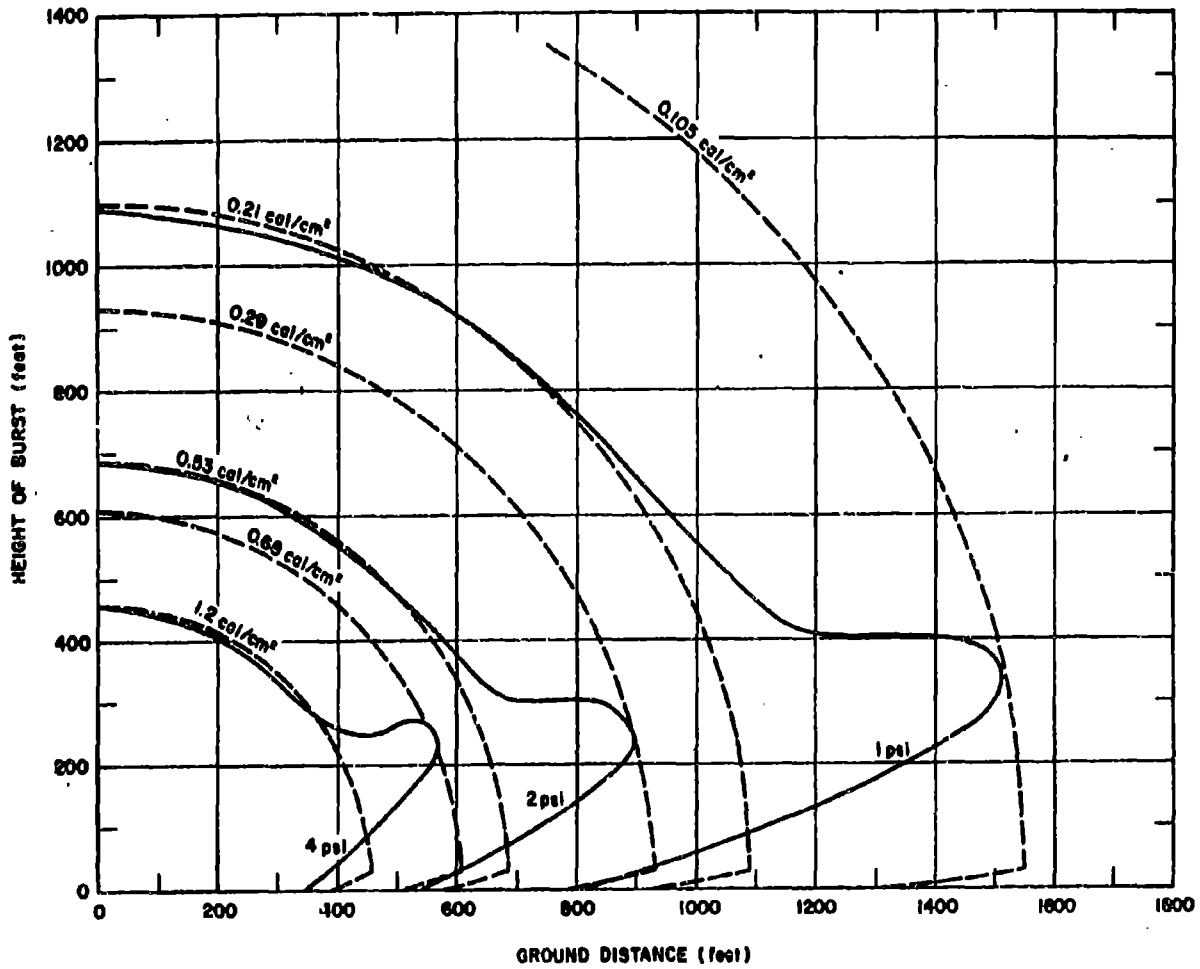

Figure 3-30. [redacted] Free Field Radiant Exposure and Air Blast Overpressure at the Surface, as a Function of Height of Burst and Ground Distance, for 0.01 kilotons, No Atmospheric Attenuation, Low Overpressure Region [redacted]

[redacted]

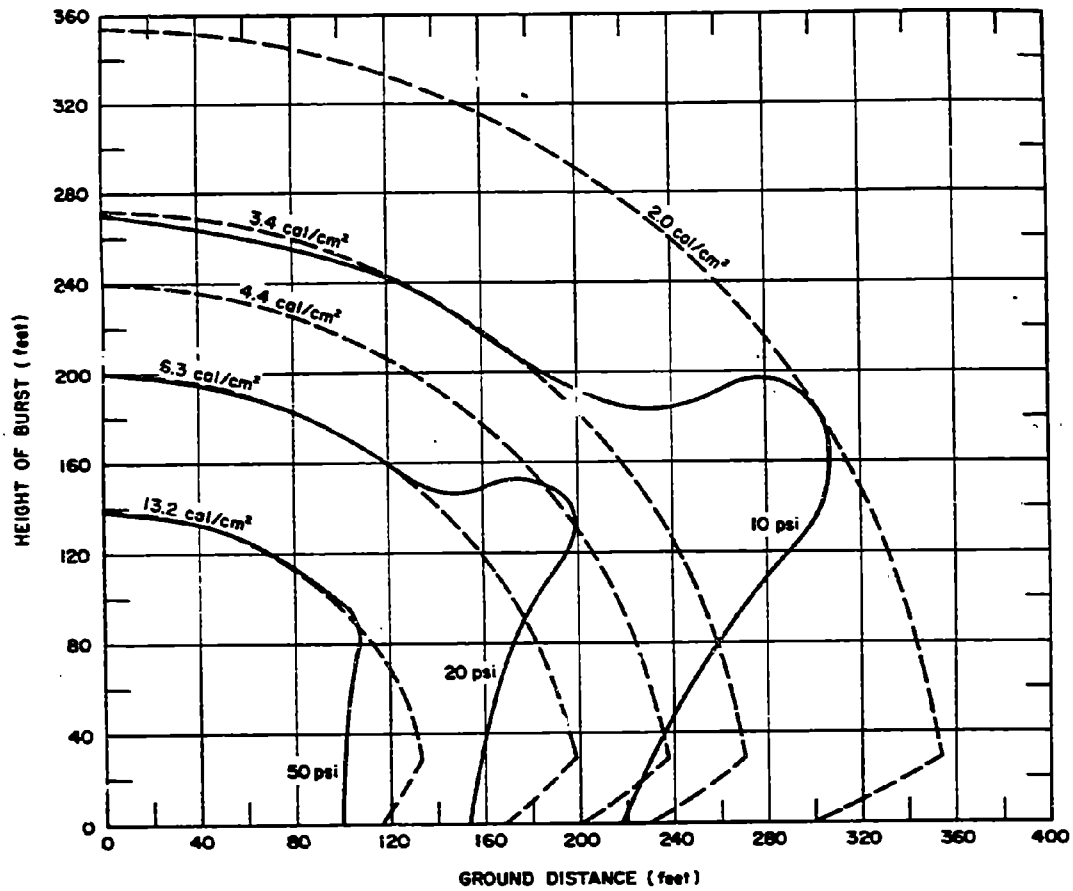

Figure 3-31. [redacted] Free Field Radiant Exposure and Air Blast Overpressure at the Surface, as a Function of Height of Burst and Ground Distance, for 0.01 kilotons, 16 Mile Visual Range, High Overpressure Region: [redacted]

[redacted]

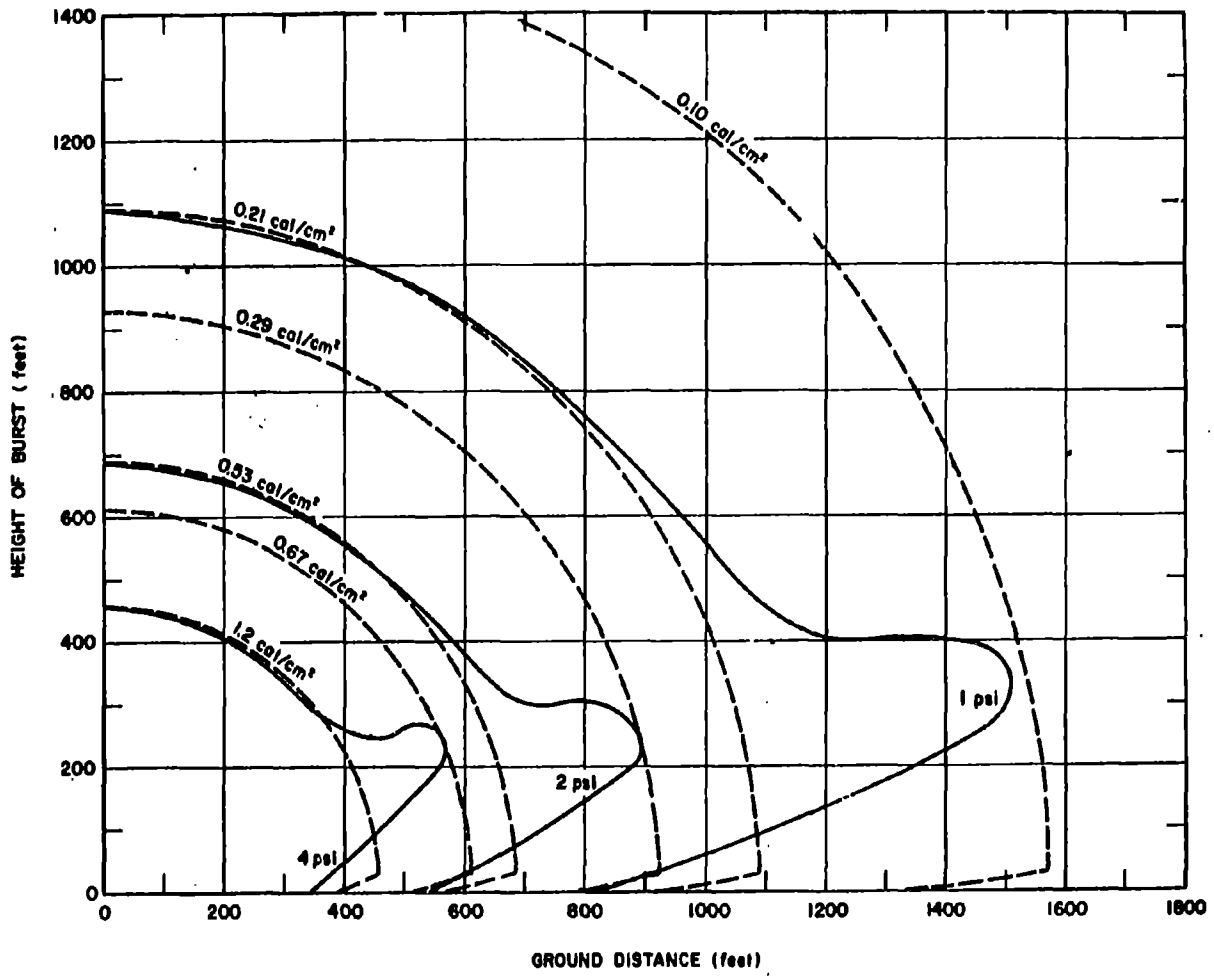

Figure 3-32. [redacted] Free Field Radiant Exposure and Air Blast Overpressure at the Surface, as a Function of Height of Burst and Ground Distance, 0.01 kilotons, 16 Mile Visual Range, Low Overpressure Region [redacted]

[redacted]

[redacted]

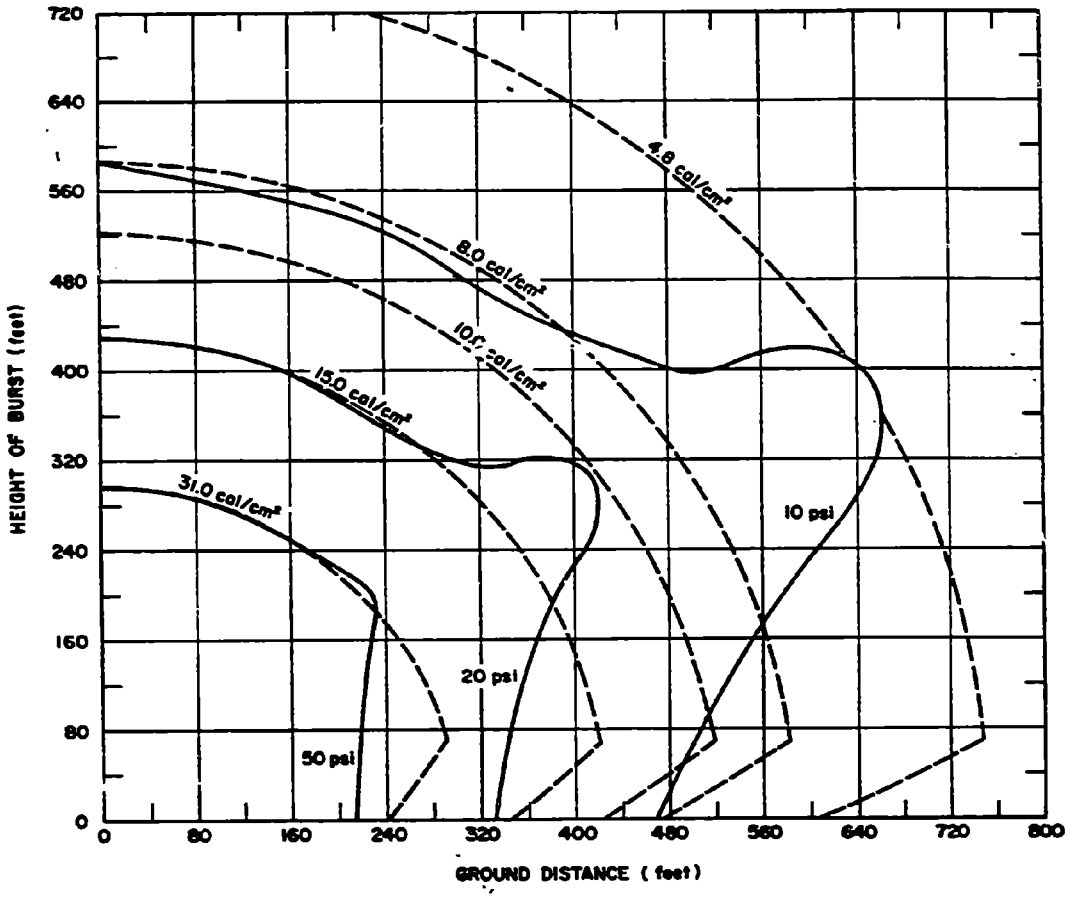

Figure 3-33. [redacted] Free Field Radiant Exposure and Air Blast Overpressure at the Surface, as a Function of Height of Burst and Ground Distance, for 0.1 kilotons, No Atmospheric Attenuation, High Overpressure Region [redacted]

[redacted]

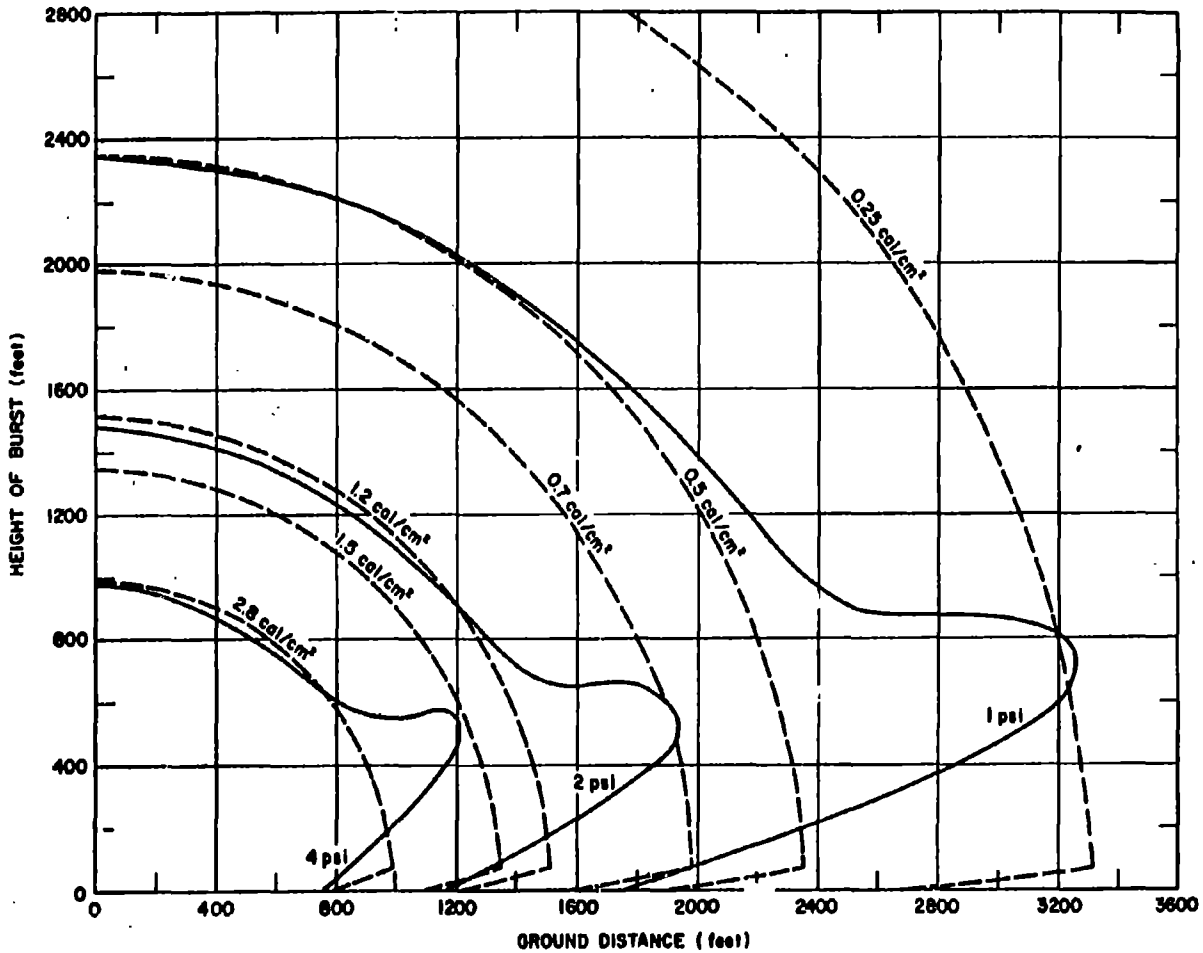

Figure 3-34. [redacted] Free Field Radiant Exposure and Air Blast Overpressure at the Surface, as a Function of Height of Burst and Ground Distance, for 0.1 kilotons, No Atmospheric Attenuation, Low Overpressure Region [redacted]

[redacted]

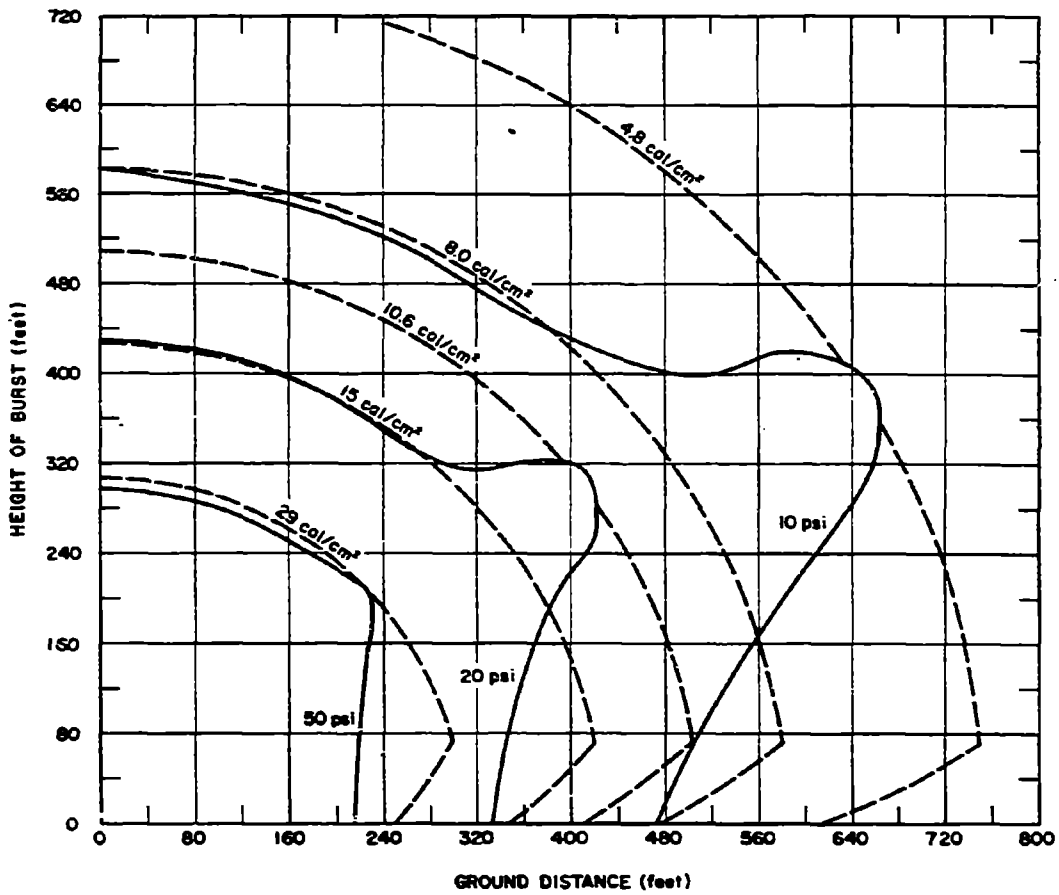

Figure 3-35. [redacted] Free Field Radiant Exposure and Air Blast Overpressure at the Surface, as a Function of Height of Burst and Ground Distance, for 0.1 kilotons, 16 Mile Visual Range, High Overpressure Region [redacted]

[redacted]

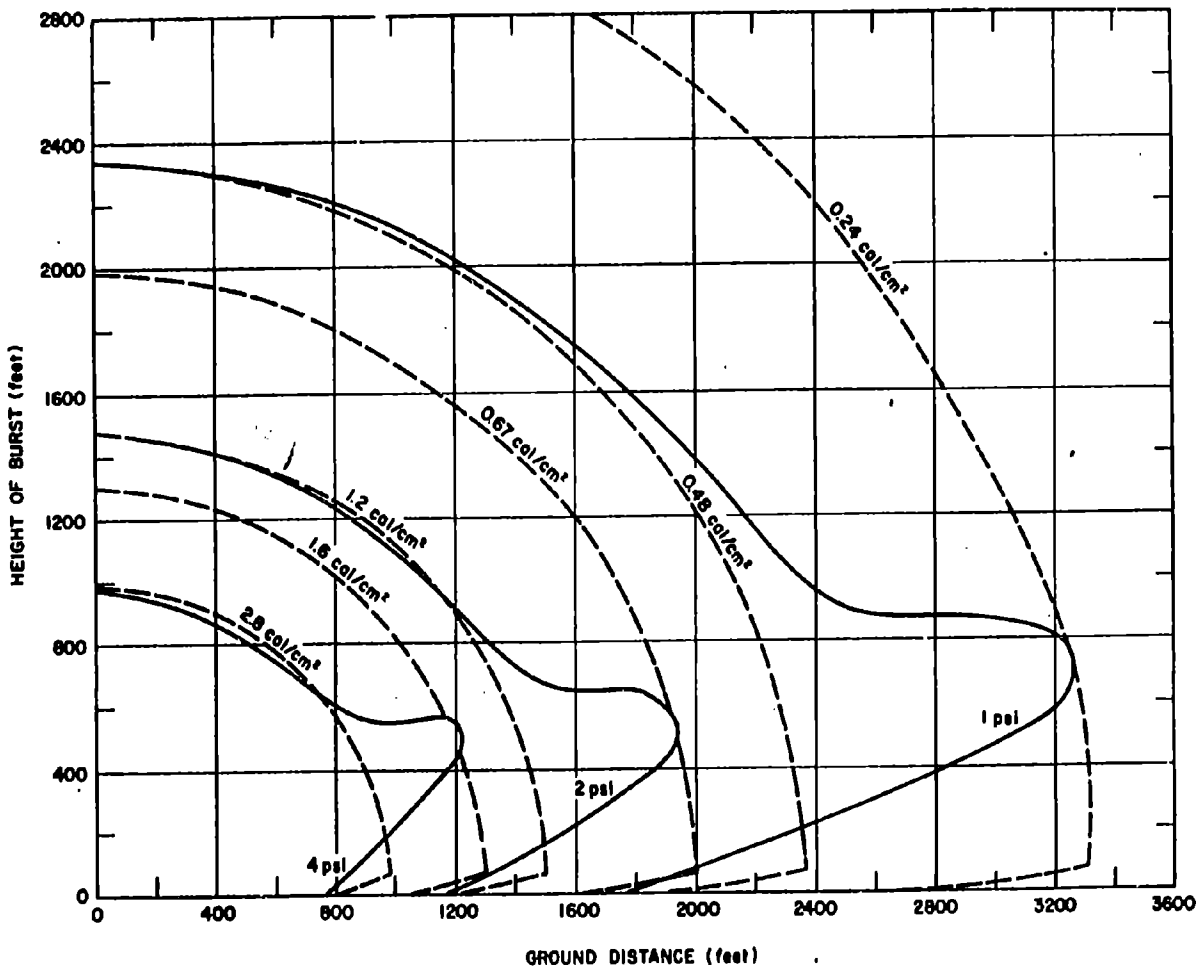

Figure 3-36. [redacted] Free Field Radiant Exposure and Air Blast Overpressure at the Surface, as a Function of Height of Burst and Ground Distance, for 0.1 kilotons, 16 Mile Visual Range, Low Overpressure Region [redacted]

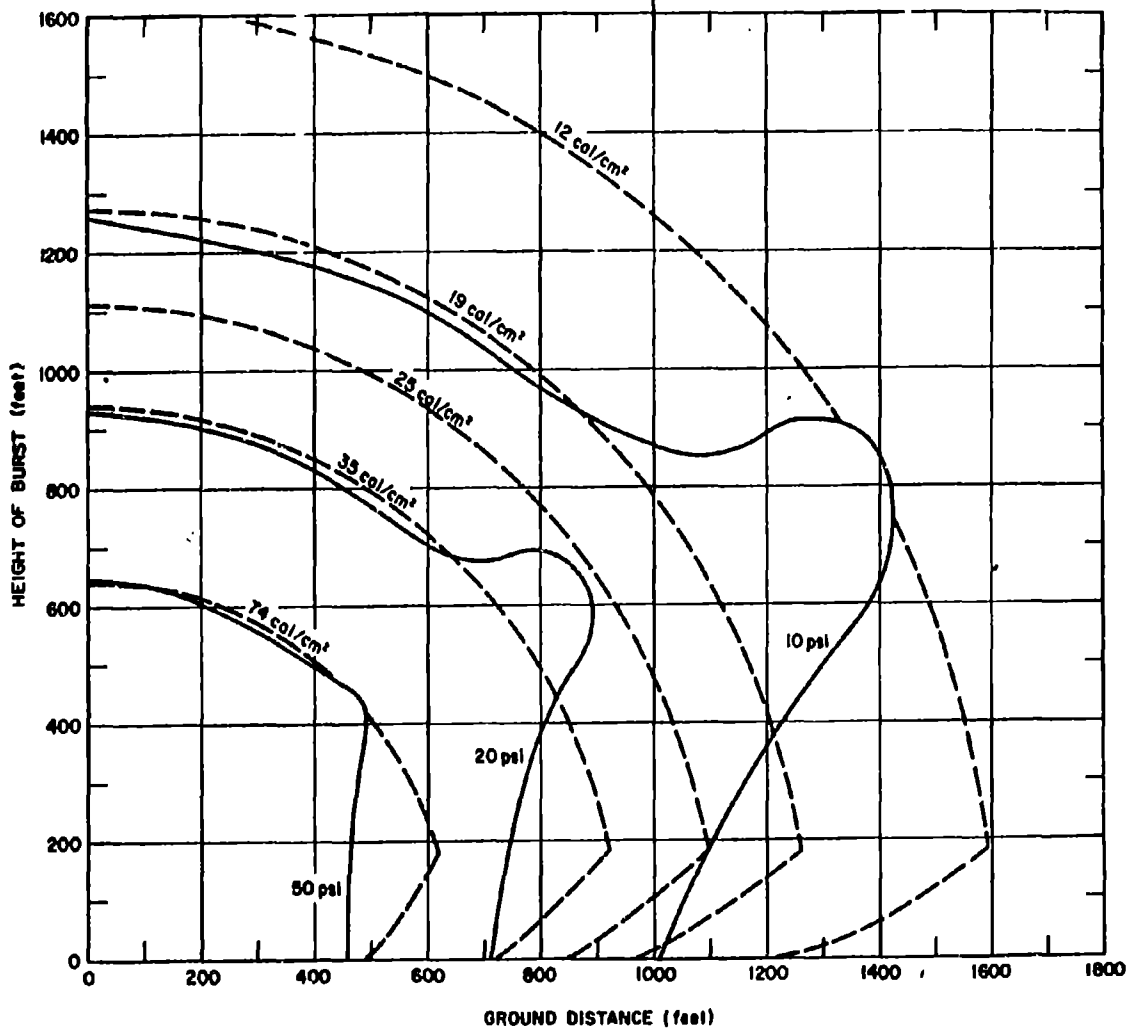

Figure 3-37. [redacted] Free Field Radiant Exposure and Air Blast Overpressure at the Surface, as a Function of Height of Burst and Ground Distance, for 1 kiloton, No Atmospheric Attenuation, High Overpressure Region [redacted]

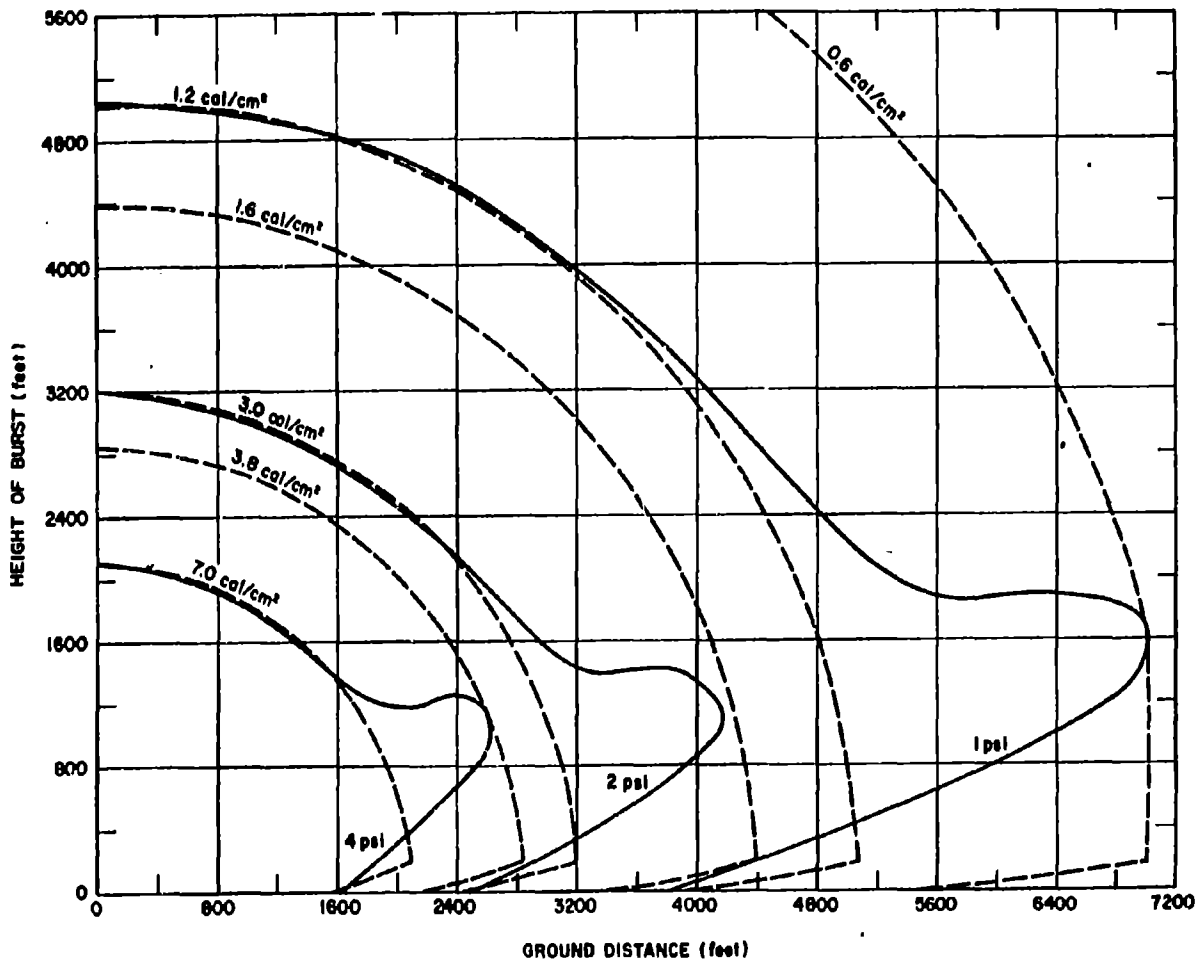

Figure 3-38. [redacted] Free Field Radiant Exposure and Air Blast Overpressure at the Surface, as a Function of Height of Burst and Ground Distance, for 1 kiloton, No Atmospheric Attenuation, Low Overpressure Region [redacted]

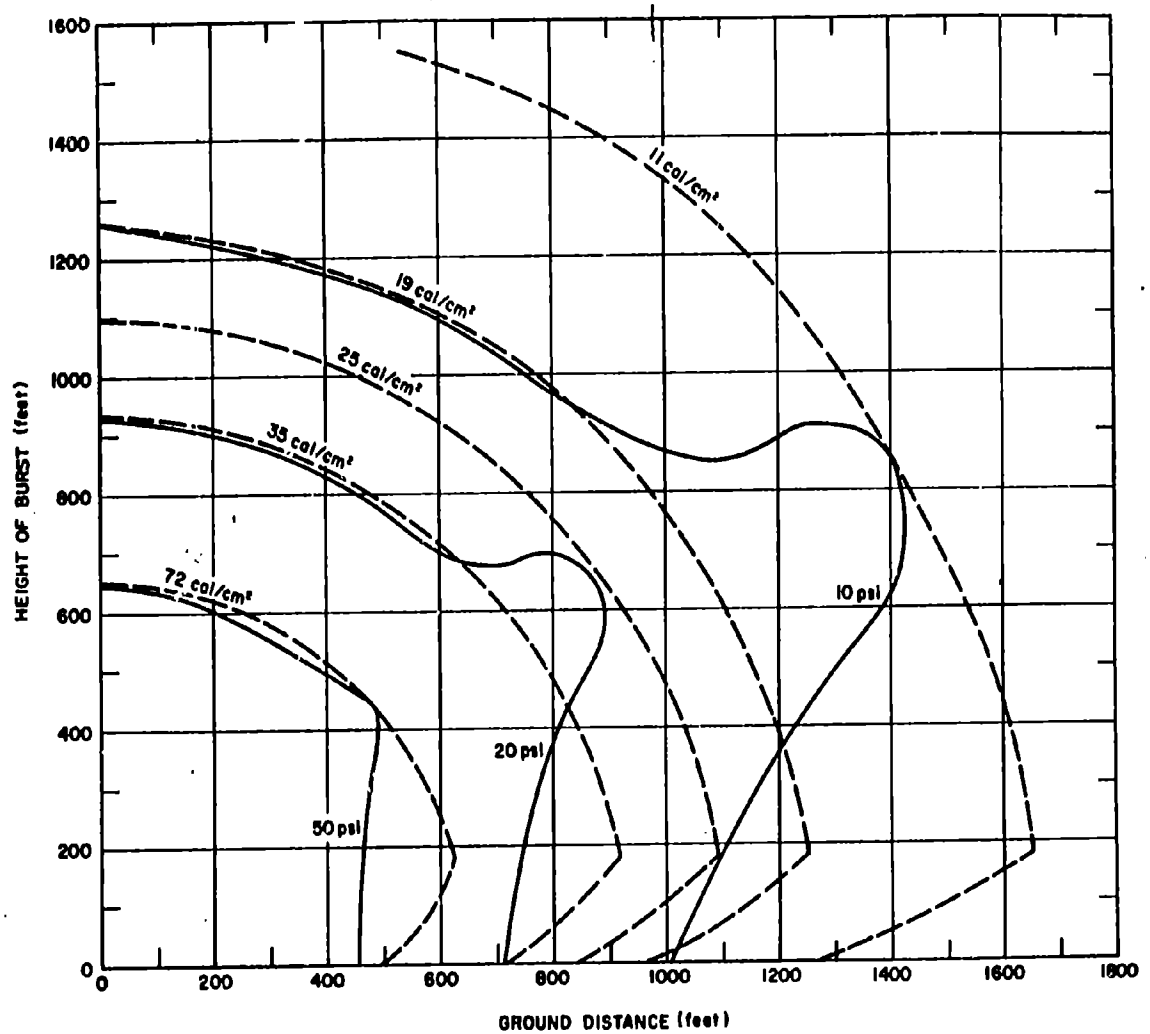

Figure 3-39. [redacted] Free Field Radiant Exposure and Air Blast Overpressure at the Surface, as a Function of Height of Burst and Ground Distance, for 1 kiloton, 16 Mile Visual Range, High Overpressure Region [redacted]

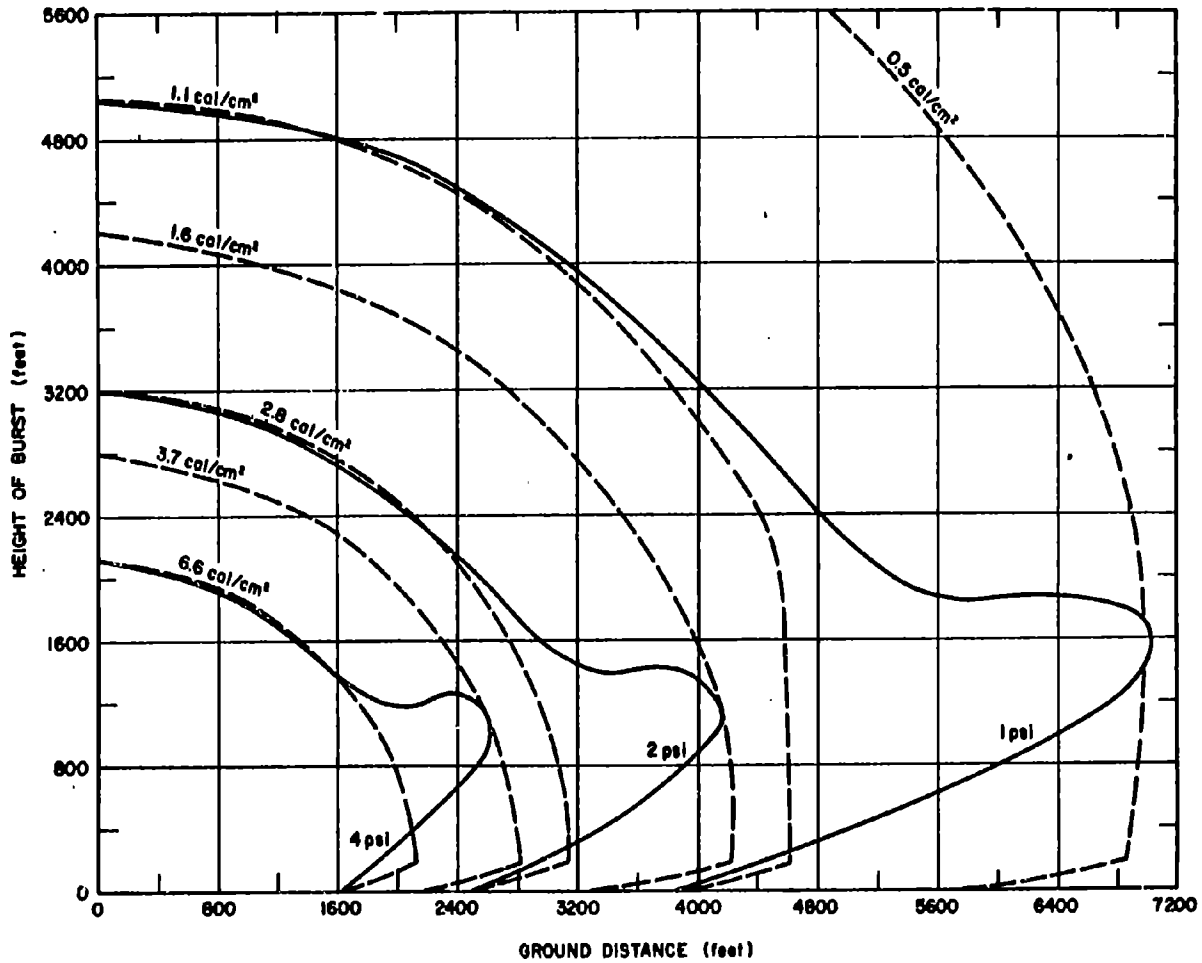

Figure 3-40. [redacted] Free Field Radiant Exposure and Air Blast Overpressure at the Surface, as a Function of Height of Burst and Ground Distance, for 1 kiloton, 16 Mile Visual Range, Low Overpressure Region [redacted]

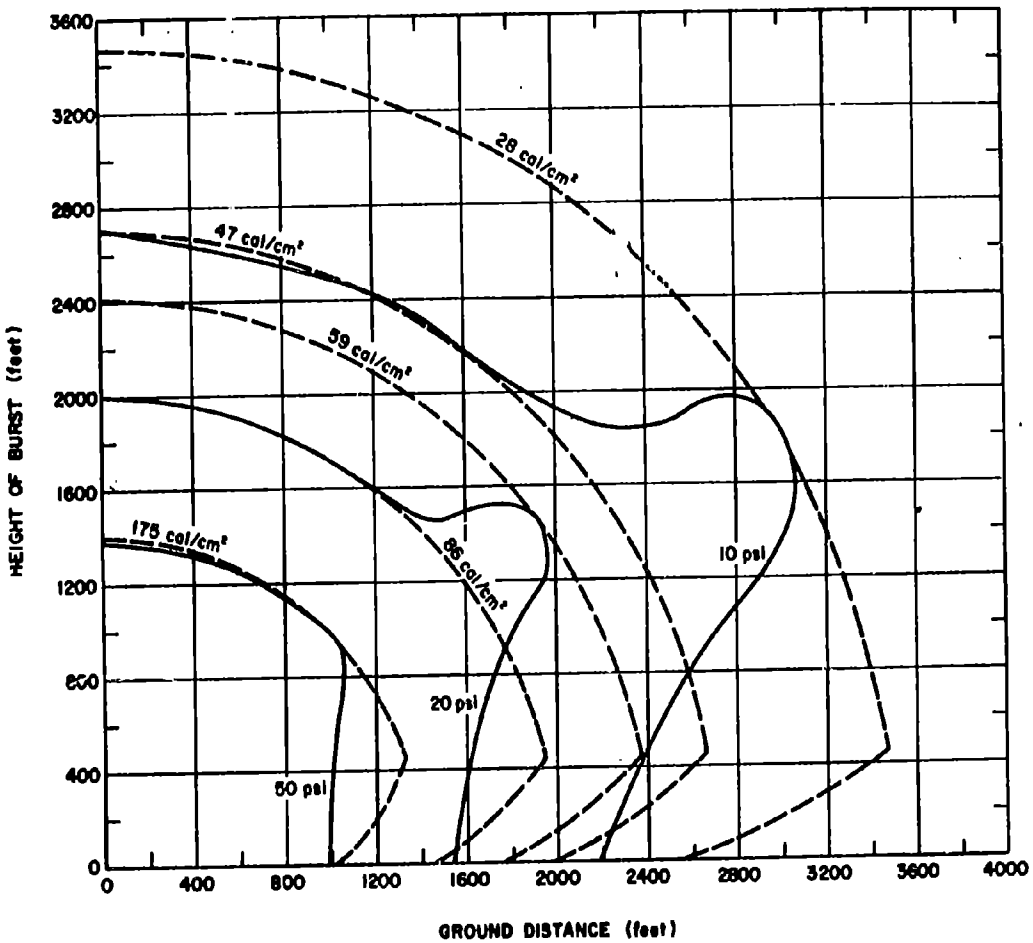

Figure 3-41. [redacted] Free Field Radiant Exposure and Air Blast Overpressure at the Surface, as a Function of Height of Burst and Ground Distance, for 10 kilotons, No Atmospheric Attenuation, High Overpressure Region [redacted]

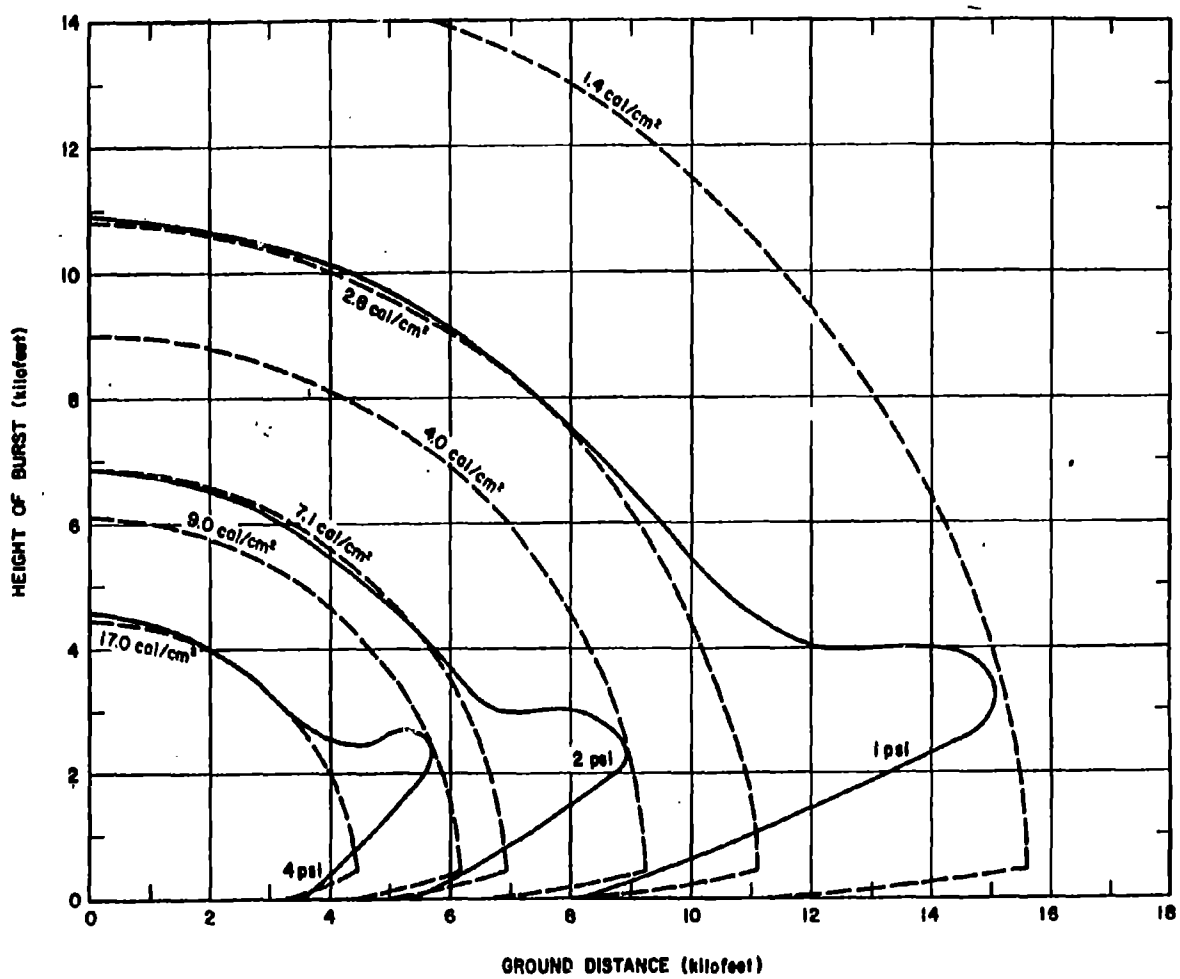

Figure 3-42. [redacted] Free Field Radiant Exposure and Air Blast Overpressure at the Surface, as a Function of Height of Burst and Ground Distance, for 10 kilotons, No Atmospheric Attenuation, Low Overpressure Region [redacted]

[redacted]

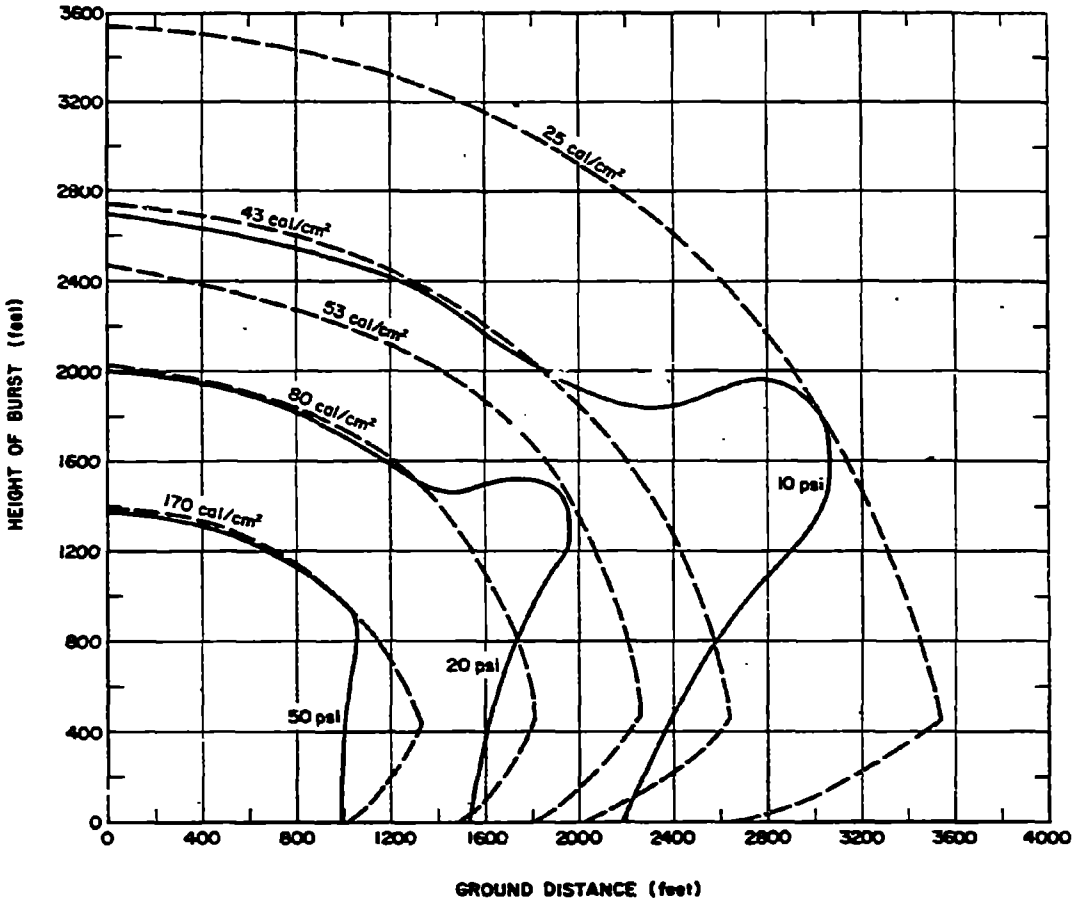

Figure 3-43. [redacted] Free Field Radiant Exposure and Air Blast Overpressure at the Surface, as a Function of Height of Burst and Ground Distance, for 10 kilotons, 16 Mile Visual Range, High Overpressure Region [redacted]

[redacted]

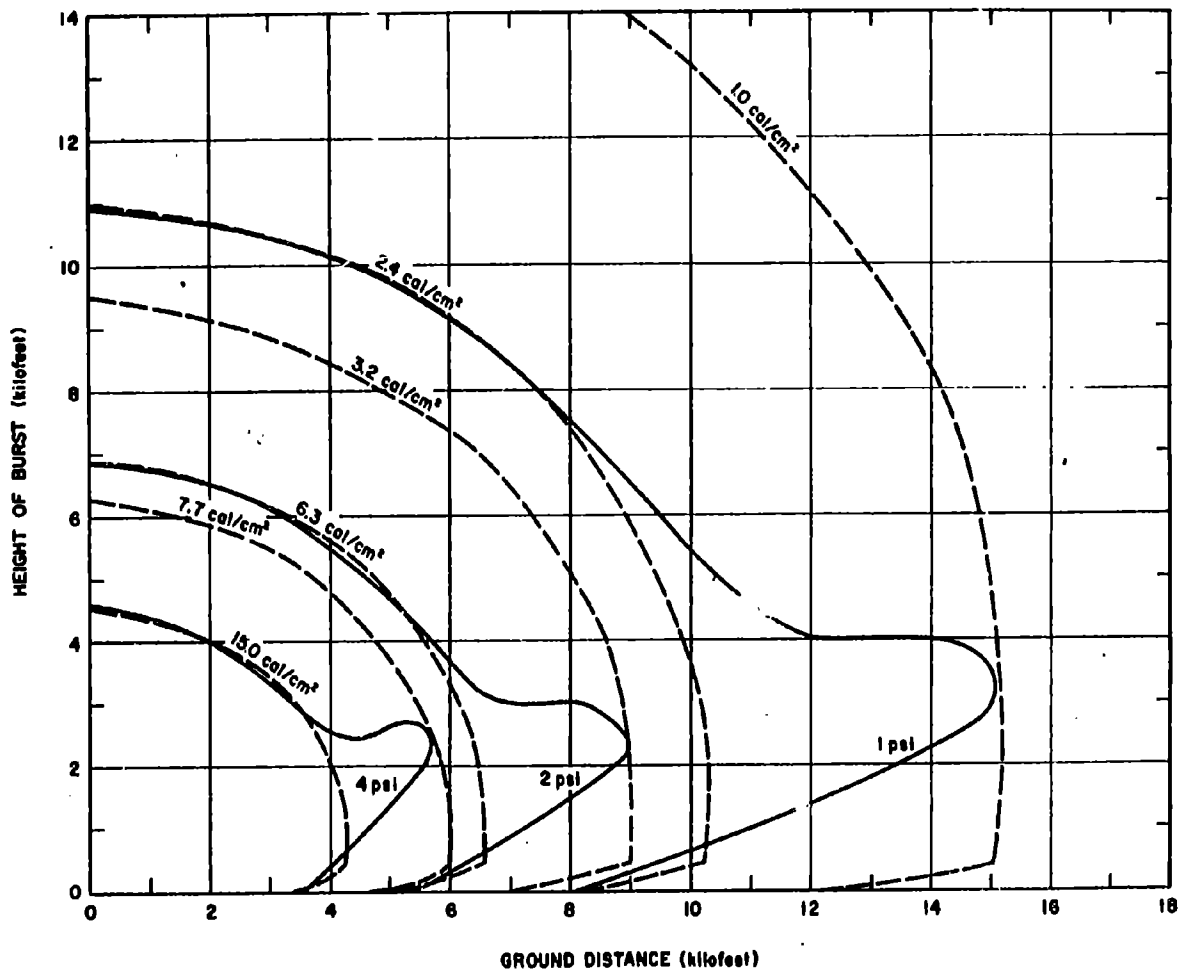

Figure 3-44. [redacted] Free Field Radiant Exposure and Air Blast Overpressure at the Surface, as a Function of Height of Burst and Ground Distance, for 10 kilotons, 16 Mile Visual Range, Low Overpressure Region [redacted]

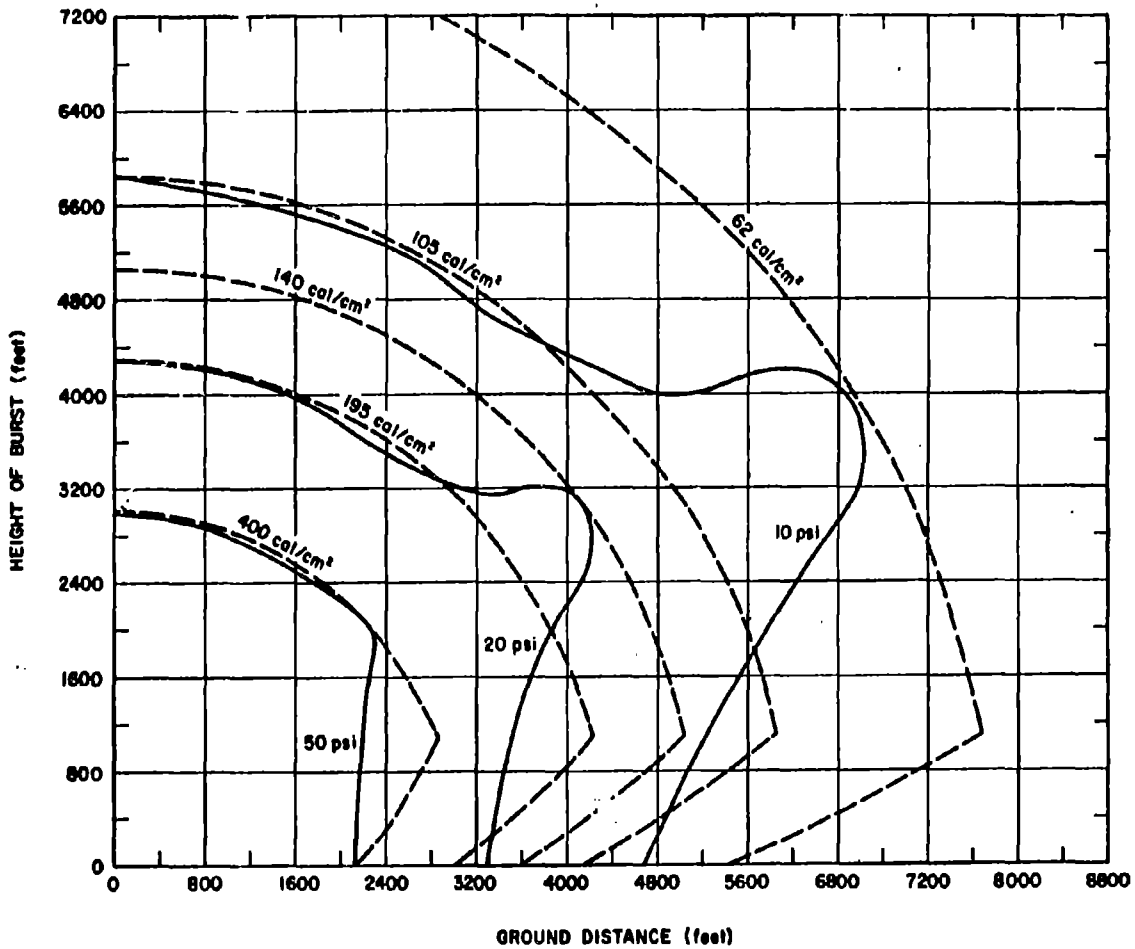

Figure 3-45. [redacted] Free Field Radiant Exposure and Air Blast Overpressure at the Surface, as a Function of Height of Burst and Ground Distance, for 100 kilotons, No Atmospher's Attenuation, High Overpressure Region [redacted]

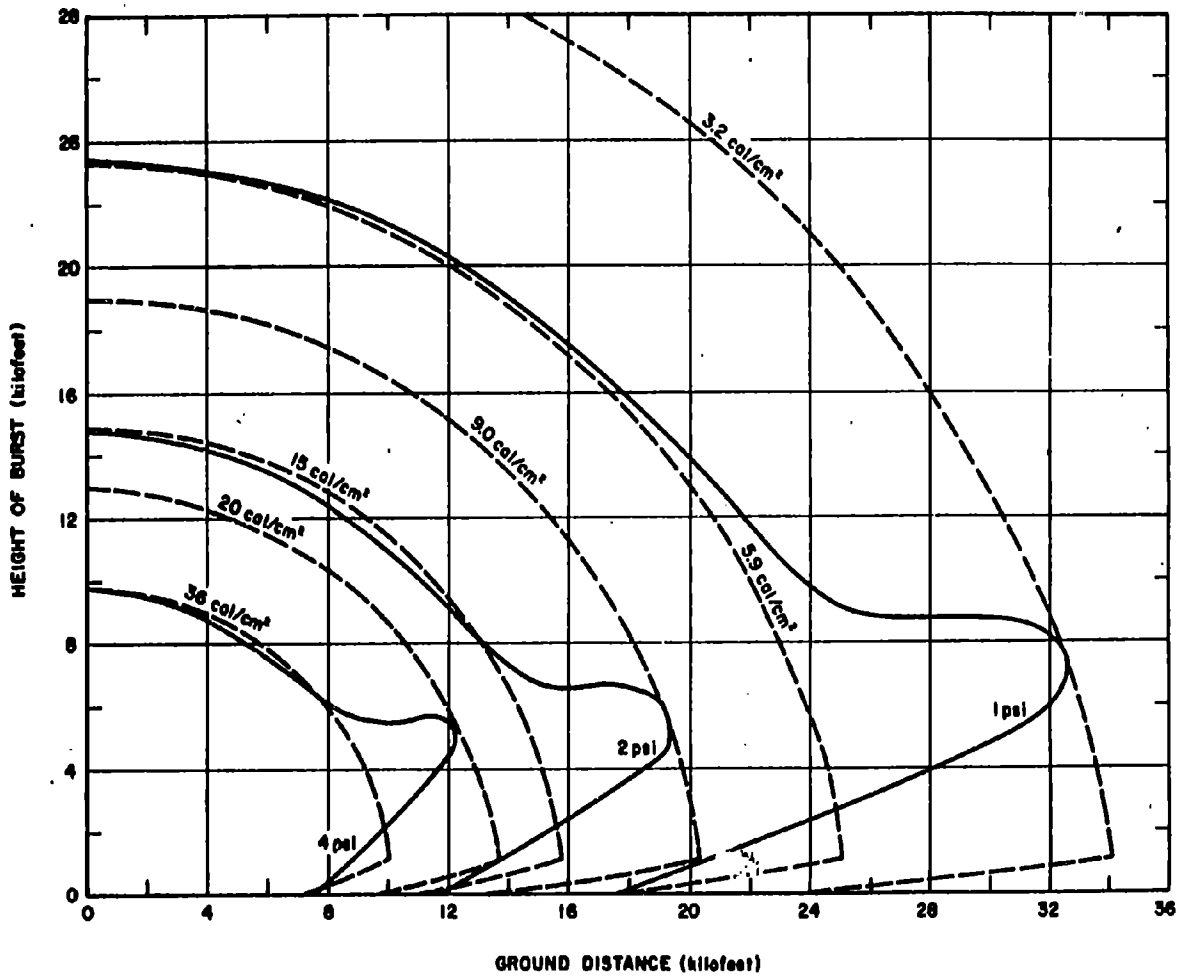

Figure 3-46. [redacted] Free Field Radiant Exposure and Air Blast Overpressure at the Surface, as a Function of Height of Burst and Ground Distance, for 100 kilotons, No Atmospheric Attenuation, Low Overpressure Region [redacted]

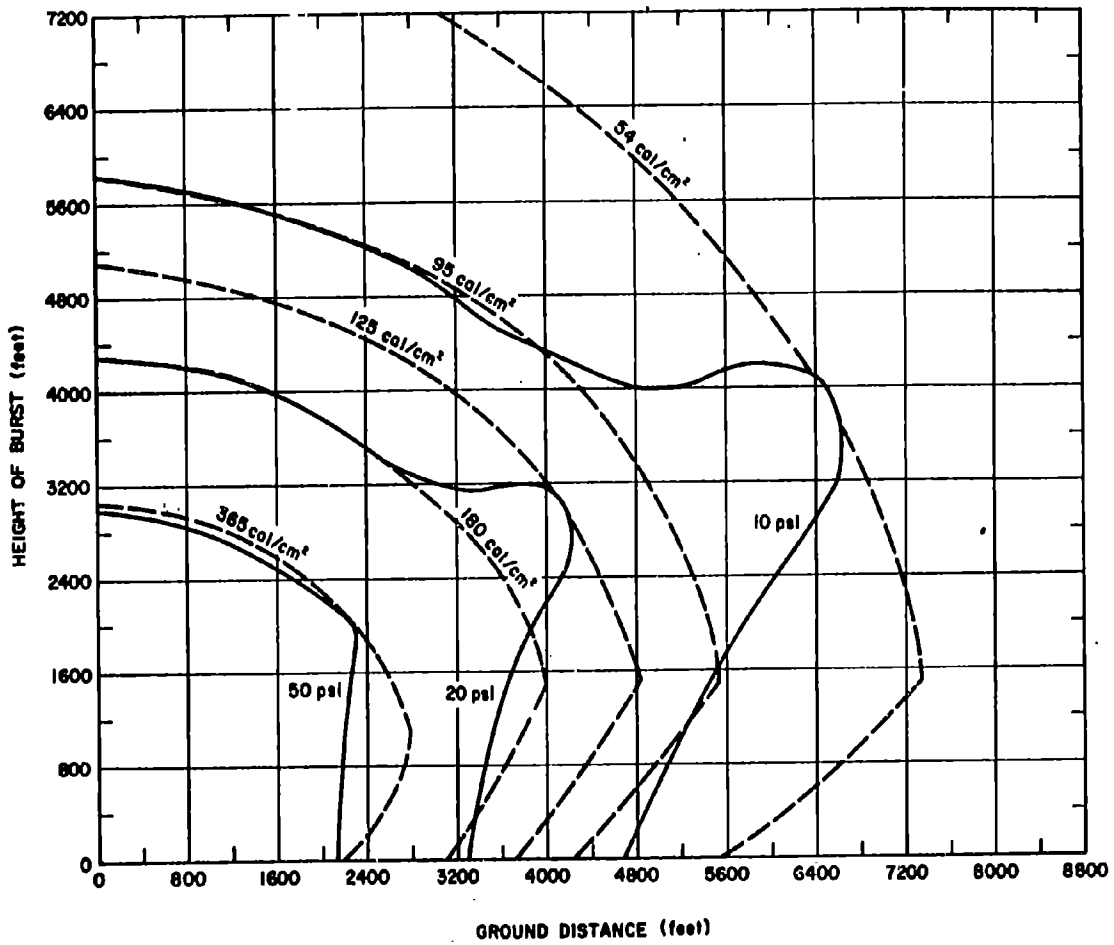

Figure 3-47. [redacted] Free Field Radiant Exposure and Air Blast Overpressure at the Surface, as a Function of Height of Burst and Ground Distance, for 100 kilotons, 16 Mile Visual Range, High Overpressure Region [redacted]

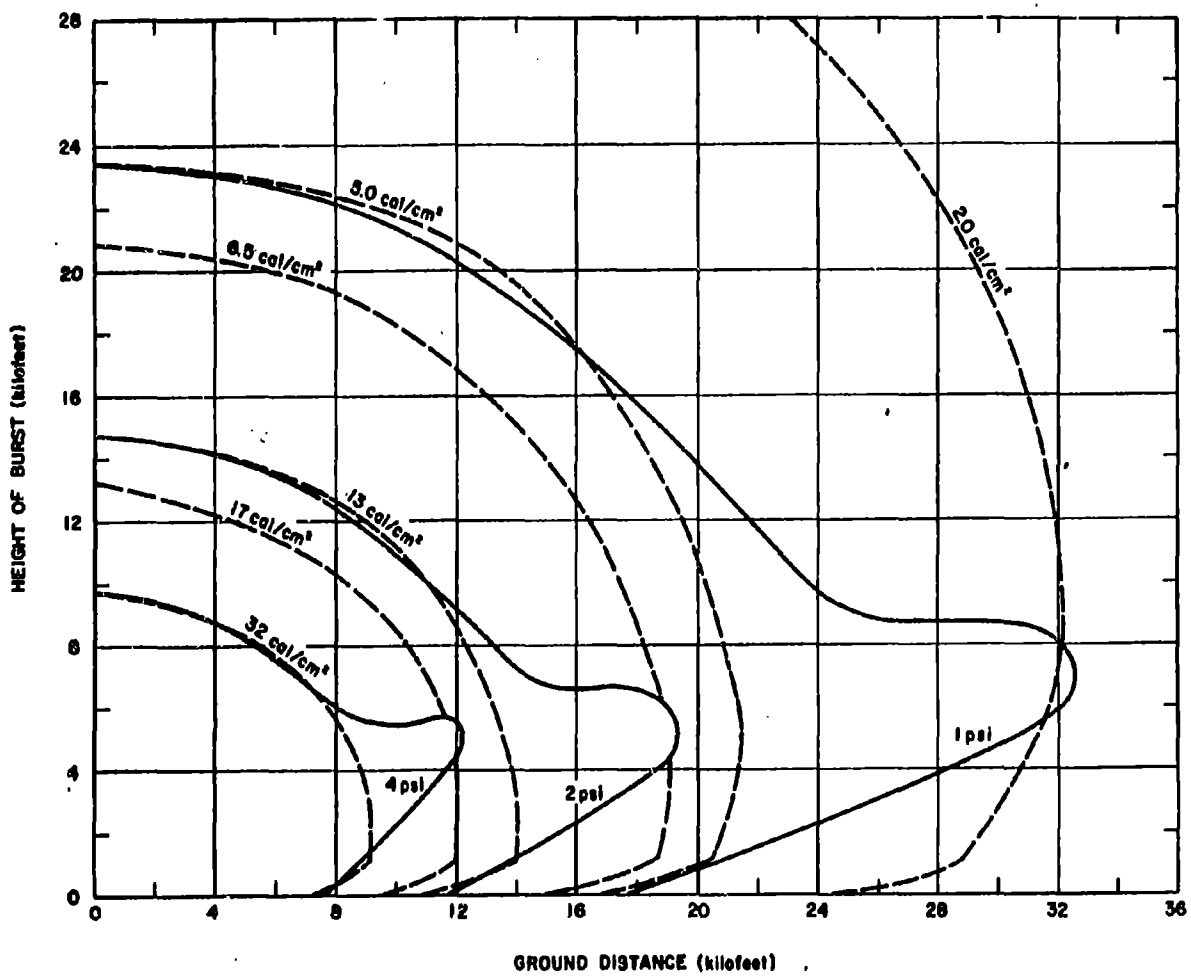

Figure 3-48. [redacted] Free Field Radiant Exposure and Air Blast Overpressure at the Surface, as a Function of Height of Burst and Ground Distance, for 100 kilotons, 16 Mile Visual Range, Low Overpressure Region [redacted]

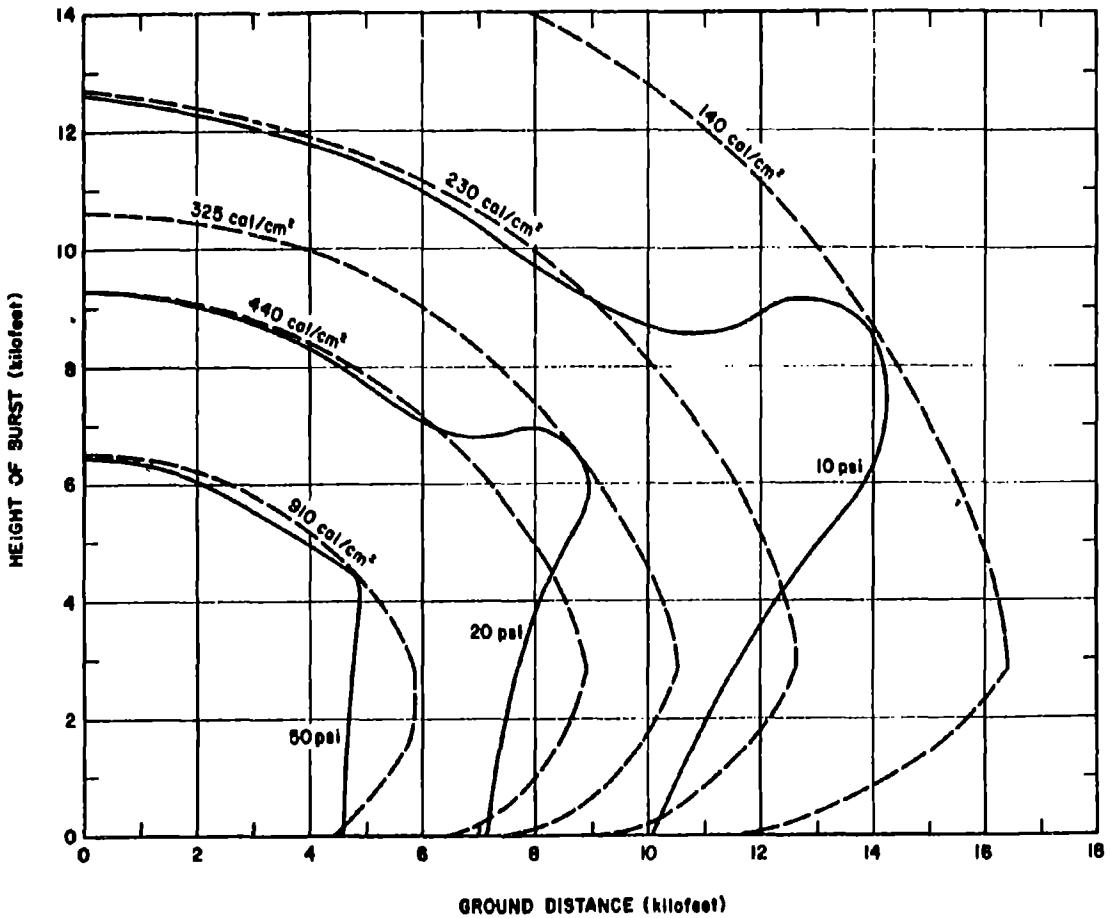

Figure 3-49. [redacted] Free Field Radiant Exposure and Air Blast Overpressure at the Surface, as a Function of Height of Burst and Ground Distance, for 1 megaton, No Atmospheric Attenuation, High Overpressure Region [redacted]

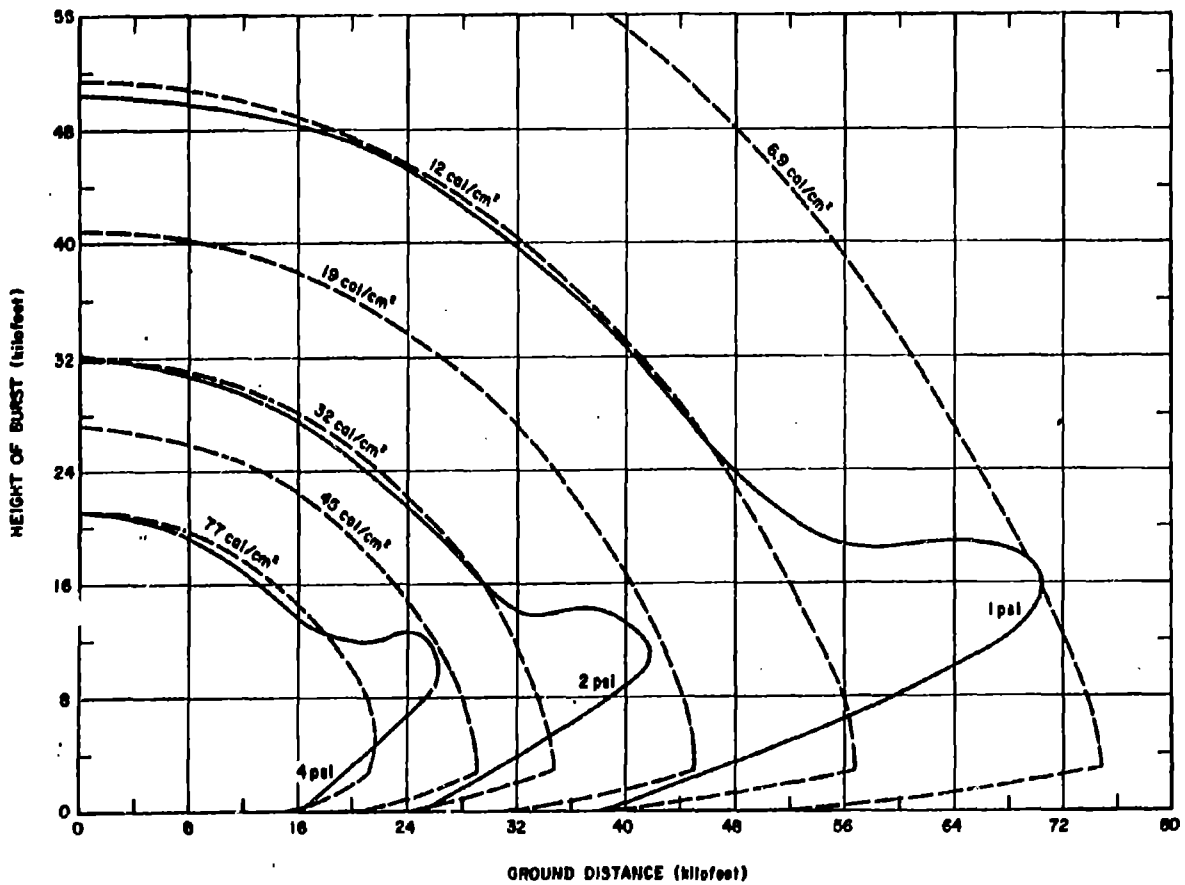

Figure 3-60. [redacted] Free Field Radiant Exposure and Air Blast Overpressure at the Surface, as a Function of Height of Burst and Ground Distance, for 1 megaton, No Atmospheric Attenuation, Low Overpressure Region [redacted]

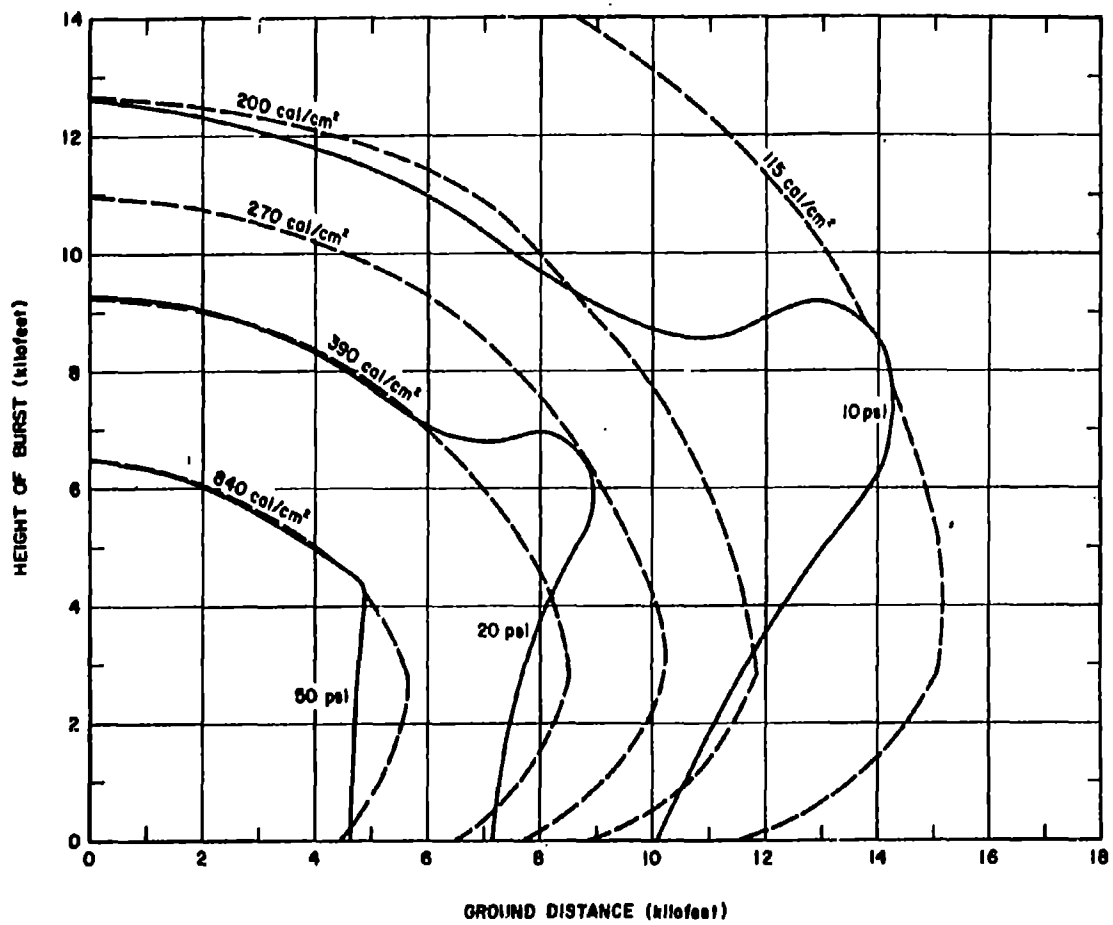

Figure 3-51. [redacted] Free Field Radiant Exposure and Air Blast Overpressure at the Surface, a Function of Height of Burst and Ground Distance, for 1 megaton, 16 Mile Visual Range, High Overpressure Region [redacted]

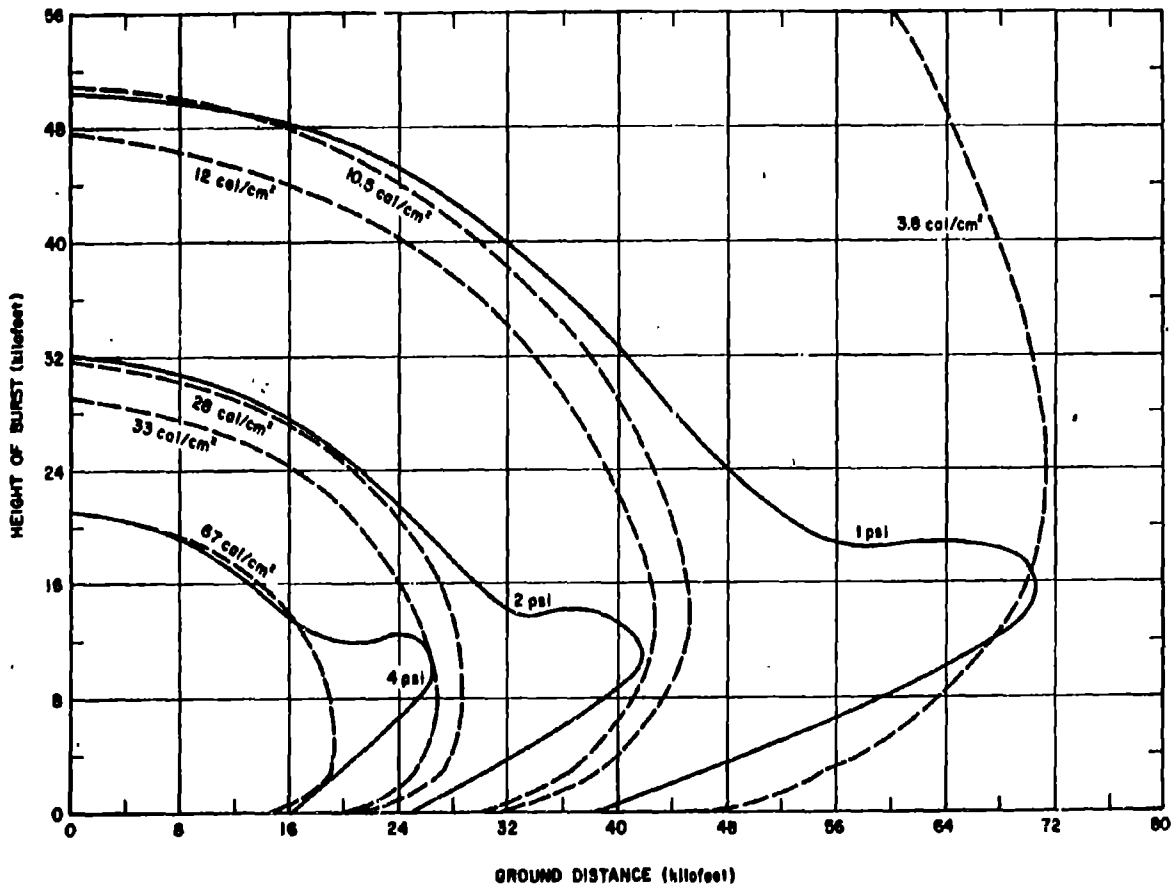

Figure 3-52. [redacted] Free Field Radiant Exposure and Air Blast Overpressure at the Surface, as a Function of Height of Burst and Ground Distance, for 1 megaton, 16 Mile Visual Range, Low Overpressure Region [redacted]

[redacted]

[redacted]

[redacted]

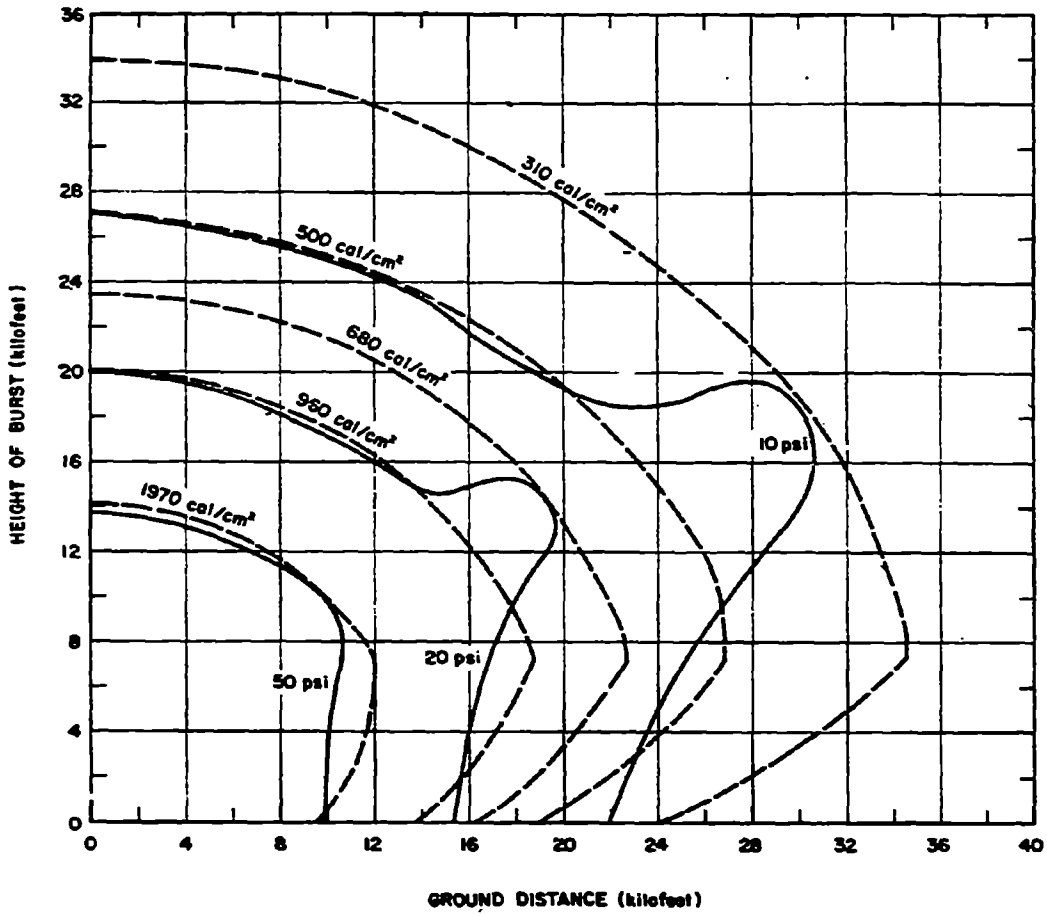

Figure 3-53. [redacted] Free Field Radiant Exposure and Air Blast Overpressure at the Surface, as a Function of Height of Burst and Ground Distance, for 10 megatons, No Atmospheric Attenuation, High Overpressure Region [redacted]

[redacted]

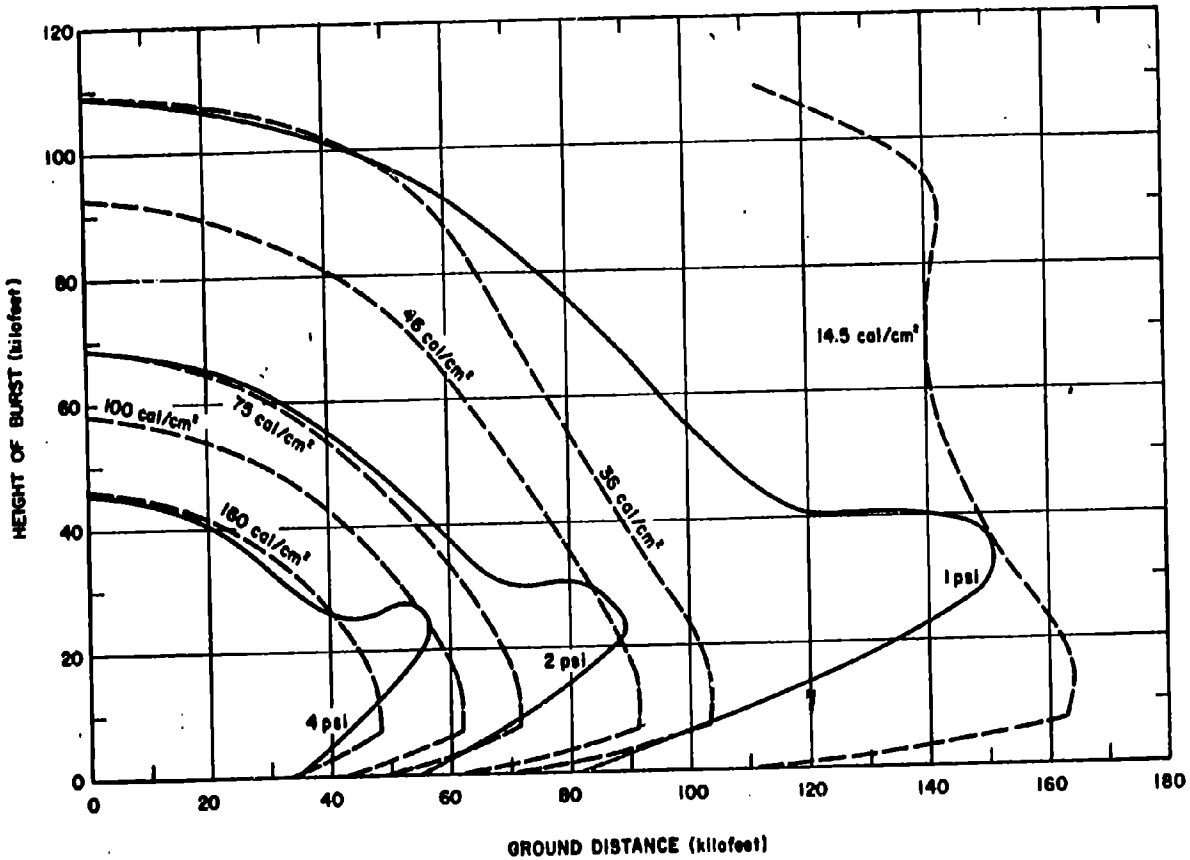

Figure 3-54. [redacted] Free Field Radiant Exposure and Air Blast Overpressure at the Surface, as a Function of Height of Burst and Ground Distance, for 10 megatons, No Atmospheric Attenuation, Low Overpressure Region [redacted].

[redacted]

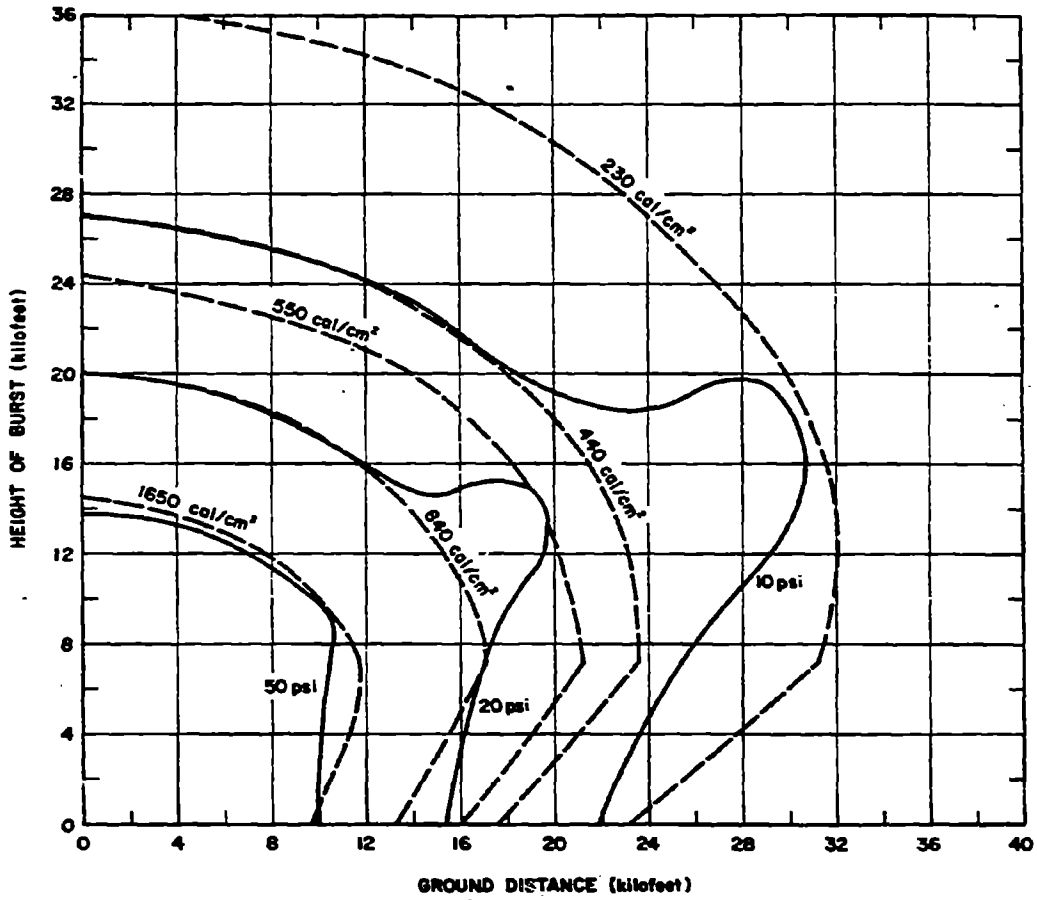

Figure 3-55. [redacted] Free Field Radiant Exposure and Air Blast Overpressure at the Surface, as a Function of Height of Burst and Ground Distance, for 10 megatons, 16 Mile Visual Range, High Overpressure Region [redacted]

[redacted]

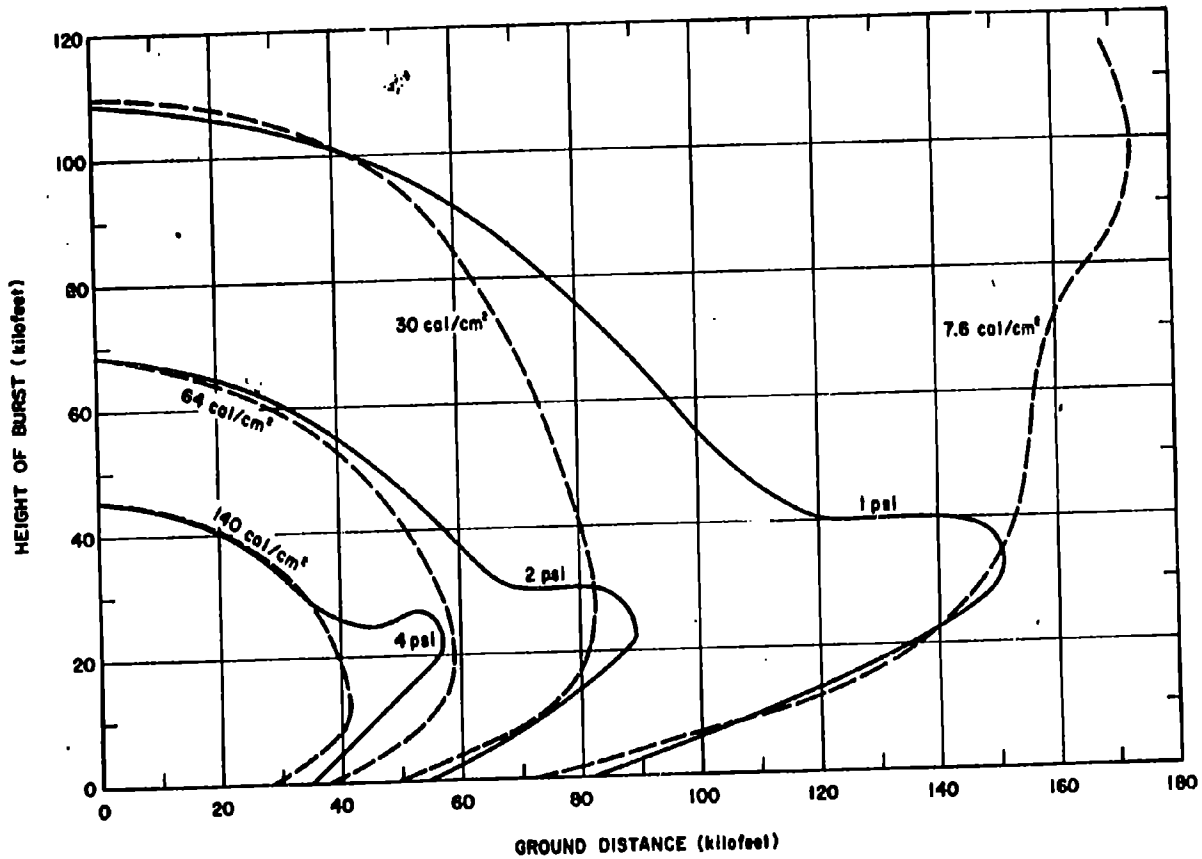

Figure 3-56. [redacted] Free Field Radiant Exposure and Air Blast Overpressure at the Surface, as a Function of Height of Burst and Ground Distance, for 10 megatons, 16 Mile Visual Range, Low Overpressure Region [redacted]

[redacted]

[redacted]

[redacted]

[redacted] PHYSICS OF FIREBALL DEVELOPMENT [redacted]

[redacted] It is not necessary to understand the physics that govern fireball evolution to perform the calculations of the thermal environment that are described in the preceding paragraphs. The following discussion is an introduction to the subject of fireball physics that is intended to introduce certain additional fireball phenomena and to serve as a bridge to more advanced discussions found in the references.

3-22 Black Body Radiation [redacted]

[redacted] A basic principal of physics is that a good radiator is also a good absorber of radiation. Thus, a perfectly black object, i.e., one that absorbs all of the radiation that is incident on it, is an ideal radiator of thermal radiation. Consequently, black body radiation is a convenient standard to which thermal radiation from actual sources can be compared.

[redacted] The radiation properties of nuclear weapons frequently may be described as a black body source of a given temperature or as a combination of several such sources. Paragraph 4-2, Chapter 4, describes the properties of an ideal black body source. Paragraphs 4-4 through 4-7, Chapter 4, describe the spectral characteristics of nuclear weapons in terms of black body sources.

3-23 Opacity [redacted]

[redacted] The flow of energy through a nuclear fireball is strongly affected by the opacity of heated air. The term opacity correctly suggests impedance to the flow of radiation, i.e., energy flows more slowly through those parts of the fireball in which the opacity of the air is high. A less obvious but equally important effect of opacity arises from the physical principle described in paragraph 3-22: in order to be a good radiator of thermal energy a material must also be a good absorber. For this reason the late time fireball cannot radiate effectively. The gas becomes relatively transparent and, as a result, radiates its energy so slowly that it produces negligible thermal damage.

[redacted] In radiation transport theory, the term opacity is assigned a more specific meaning than it has as a nontechnical world. In a medium that absorbs much more radiation than it scatters (this is generally true of the hot gases that constitute the fireball), opacity is the reciprocal of the mean free path, the average distance that a photon travels before it is absorbed. Thus, the units of opacity are reciprocal distance, and values given in the following discussion are in $meters^{-1}$.

[redacted] The terms "opaque" and "transparent" are used in a less specific sense. A zone of air is opaque if it is thick compared to the mean free path of the radiation passing through it. For example, if a region 1 meter thick has an opacity of 10 $meter^{-1}$ (mean free path = 1/10 meter), it is definitely opaque; if its opacity is 0.01 $meter^{-1}$ (mean free path = 100 meters), it is quite transparent.

[redacted] The opacity of a gas is different for photons of different energy; therefore, the radiation to which the value of opacity applies must be specified. Normally, opacity is given as an average value that represents the transport properties of that black body spectrum which corresponds to the temperature of the gas.

[redacted] There is an optimum value of opacity that allows the fireball to radiate at the highest possible rate. This value is low enough to permit rapid flow of thermal energy from the hot interior of the fireball to the cooler surface layers, but it is high enough that all regions of the fireball are able to radiate the thermal energy that they contain.

[redacted] The physical processes that determine opacity over the range of temperature and photon energies that are of interest are changes in the energy levels of atoms or molecules. At

[redacted]

[redacted]

[redacted] photon energies of a few eV* or higher, these processes involve absorption of the photon energy by the electrons of the atom or molecule. At the lower photon energies characteristic of infrared photons, the interactions may involve changes in the vibrational states of atoms. All of these interactions involve changes between two allowable energy states of the atom or molecule. In many cases the photon encounters an atom that has no allowable energy level that exceeds its present energy level by exactly the photon energy. In these cases, absorption of the photon is impossible. Photons of visible light propagating through air illustrate this condition. The photon energy is too high to excite the small changes in molecular energy that certain infrared photons can produce, and it is too low to produce the electronic excitation or ionization that certain photons in the ultraviolet region can produce. Consequently, pure air is transparent to these photons, affecting them only by infrequent scattering interactions.

[redacted] The radiating properties of the fireball and the surrounding air are strongly affected by a particular absorption band of the oxygen molecule, the Schumann-Runge band. Although several mechanisms render air opaque to photons with energies of the order of 10 eV, the Schumann-Runge band is particularly important because it is effective at lower values of photon energy than other strong absorption bands. For this reason, it determines the cutoff energy of the spectrum of transmitted photon energies.

[redacted] The Schumann-Runge band normally absorbs only those photons with energies greater than about 6.7 eV. However, when air is heated to temperatures of a few thousand degrees, oxygen molecules are excited to high vibrational energy levels, with reduces the energy gap between the equilibrium molecular states and the Schumann-Runge continuum. This smaller energy gap reduces the energy that a photon must have in order to induce a transition, and air at 4,000°K absorbs photons with energies as low as 3 eV strongly. This is the photon energy that is associated with violet lights. Thus, the hot layer of air surrounding the luminous region of the fireball removes most ultraviolet energy from thermal radiation, causing fireball radiation to contain a much lower fraction of ultraviolet energy than does sunlight.

3-24 The Fireball Before Final Maximum [redacted]

[redacted] A discussion of a low altitude fireball close to the final maximum is valuable for two reasons: this stage of development is of practical interest because the bulk of the thermal pulse is emitted during this final pulse; it is of theoretical interest because most of the physical phenomena affecting all stages of fireball development are active at the time of final maximum. Figure 3-57 shows the opacity properties of a particular fireball in terms of four zones.

- *Zone I:* The hot core of the fireball has a relatively uniform temperature. For this reason, it is called the "isothermal sphere." Since this zone is fairly transparent at most stages of fireball development, thermal energy flows rapidly from hotter regions to cooler ones, and large temperature differences cannot form. At the time shown in Figure 3-57, the opacity is about 1 meter.
- *Zone II:* At the edge of the isothermal sphere, opacity rises rapidly because of increasing air density. Air in this zone not only is more opaque to its own radiation (the mean free path drops to about 12 cm); it has much higher opacity to the higher temperature radiation from the isothermal sphere. Zone I is expanding by heating the air in Zone II; as a result, Zone II has a high temperature gradient. The outer edge of

---

*[redacted] 1 eV = 1.6×10^{-12} erg.

[redacted]

[redacted]

DNA
(b)(3)

Deleted

Figure 3-57. [redacted] Fireball Properties after Breakaway [redacted]

[redacted]

[redacted]

[redacted] Zone II forms the radiating surface of the visible fireball.

- *Zone III:* Between the fireball and the shock front, air is too cool to radiate energy efficiently. The low opacity of this region to its own radiation reflects this property. This region is, however, opaque to portions of the radiation from Zone II. It absorbs the blue and ultraviolet regions of the spectrum. As a result, it intercepts part of the energy radiated by the fireball and changes the spectral distribution of fireball radiation as seen from a distance.
- *Zone IV:* Ambient air is relatively transparent to infrared, visible, and near-ultraviolet radiation, and will transmit that portion of the fireball radiation that is emitted in this spectral region.

3-25 History of Fireball Evolution [redacted]

[redacted] Most of the stages of fireball development are of little interest in connection with thermal damage, but, for some purposes, the entire sequence of observable phenomena provides useful information. The most obvious application is the comparison of computer calculations with experimental data. This comparison is an excellent indication of the degree to which the computer program simulates actual fireball phenomena.

[redacted] It is not the purpose of this discussion to consider phenomena that contribute only minutely to the total thermal output in detail. The user who desires such detail should consult "Theoretical Models for Nuclear Fireballs [redacted]" DASA 1589, or "Thermal Radiation Phenomena," DASA 1917 (see bibliography).

[redacted] Figure 3-58 shows a calculated power-time curve for a 200 kt burst at 5,000 feet (this curve was presented previously in Figure 3-19 and forms the basis for the standard therm pulse in Figure 3-20). The labeled points correspond to the following events:

1. Deposition of the X-ray energy from the nuclear source produces an extremely hot zone of completely ionized air surrounded by a transition region in which the temperature drops to the ambient value. This transition region is produced by the higher energy X-ray photons radiated by the source. It is hot (and therefore

DNA
(b)(3

Deleted

Figure 3-58. [redacted] Calculated Power-Time Curves for a 200 kiloton Burst at 5,000 feet [redacted]

[redacted]

[redacted]

[redacted]

opaque) enough to obscure visible radiation from the central zone. The radiation that is seen is produced by this so-called X-ray veil.

2. The isothermal sphere continually expands as radiation from the hot plasma is absorbed by the cooler, opaque gases at the edge of the sphere. The jump in radiated power at point 2 occurs as this hot sphere breaks through the X-ray veil and the brightness suddenly increases.

3. As the fireball continues to grow by radiative expansion, it engulfs more and more of the partially opaque air surrounding the veil itself.

4. Hydrodynamic motion, delayed by the inertia of the strongly heated air, has developed to the point that a shock front has formed at the surface of the fireball. The abrupt temperature rise created by the shock front produces a sudden brightening of the fireball surface. This event is partially obscured by the shock precursor, a thin zone of air ahead of the shock front that has been heated by radiation from the shock front. It is similar to the X-ray veil formed at earlier times. The peak at 4 is called the shock formation maximum.

5. As the shock front is attenuated by its expansion, both the shock temperature and the shock precursor temperature fall, and radiated power declines. At 5, the shock precursor is becoming transparent; power starts to increase as radiation from the shock front penetrates beyond the edge of the fireball. This point is called the shock precursor minimum.

6. At some altitudes, a peak known as the debris shock maximum occurs as the shock wave produced by bomb debris overtakes and intensifies the main shock wave. In this case, this event happens to coincide with the shock precursor minimum; therefore, it is not evident on the power-time curve.

7. As the shock precursor continues to cool, radiation from the shock front is transmitted increasingly well, and the traditional first maximum occurs. Power then falls as the shock front drops in temperature. Point 7 is more descriptively termed the shock exposure maximum.

8. The air heated by the shock front, screening the hot regions deeper in the fireball, produces essentially the same phenomenon that was produced at point 5 by the shock precursor. As the air behind the front cools and starts to become transparent, the radiated power first drops and then levels off at the principal minimum as radiation from the hotter inner regions of the fireball begins to penetrate to the outside.

9. During the final maximum (traditionally, the second maximum), the fireball radiates the bulk of the thermal energy. The air behind the shock front continues to become more transparent, and the radiated power comes from the large volume of hot air that constitutes the fireball. As each zone of air radiates its energy and cools below about 6,000°K, it becomes transparent and transmits radiation from a zone closer to the center. Power output drops as the so-called radiative cooling wave propagates inward and the area of the radiating surface decreases.

10. The fireball becomes largely transparent, but is still capable of radiating energy as spectral lines. This final phase of fireball evolution is called the late time radiative phase.

[redacted]

DNA
b(3)

[redacted]

[redacted]

DNA (b)(3)

DNA (b)(3)

[redacted] Figure 3-59 shows the way in which the relative timing of some of these events changes with altitude for a 200 kt burst. The numbers in circles are the same numbers that appear in Figure 3-58 to label various events.

[redacted] From the point of view of thermal damage, the most important change that Figure 3-59 shows is that the principal minimum weakens and finally disappears as it merges with the debris-air shock catch-up and the final maximum at high altitudes. This effect changes the shape of the main thermal pulse and is the reason that the standard thermal pulse is roughly representative of thermal pulses only at altitudes below about 100,000 feet.

3-26 Comparison with Recent Analysis of Experiments [redacted]

[redacted] Although, as mentioned previously, the computer calculations agreed well with the experimental data with which they were compared, and the calculations form the basis for a complete set of data that is compatible and can be put into a form that is suitable for this manual, they do not necessarily represent the ultimate answers. A set of semi-empirical equations has recently been developed that give t_{max} and t_{min} of the thermal pulses produced by bursts up to 100 kilometers. These equations are

$$t_{max} = 0.042\ (\rho W)^{0.44}\ (\rho_s/\rho)^{-\rho_s/\rho}\ \text{sec},$$

[redacted]

Deleted

Figure 3-59. [redacted] Altitude Variation of Phenomena for a 200 kiloton Burst [redacted]

DNA (E)

[redacted]

where ρ is the atmospheric density at burst altitude, and ρ_s is the density at the "singular" altitude for the yield being considered, which is the altitude at which the thermal pulse changes from a two peaked pulse to a single peaked pulse, and which is given by

$$\rho_s = 0.033\ W^{-1/2},$$

and

$$t_{min} = 0.00365\ (\rho W)^{0.44}\ \text{sec.}$$

For comparative purposes, these values are plotted together with the equations given previously for t_{max} and t_{min} as a function of yield for scaled burst heights of 180 $W^{0.4}$ feet, i.e., low air bursts, in Figure 3-60. This one comparison is presented only to show some of the uncertainty associated with the prediction of the thermal radiation environment. As pointed out previously, the computer calculations were used as the basis for the prediction of the thermal environment in this manual for several reasons, one being that they provide a complete description of all of the various phenomena in a compatible format. Further investigations may reveal that changes in the presentation of the data are required.

[redacted]

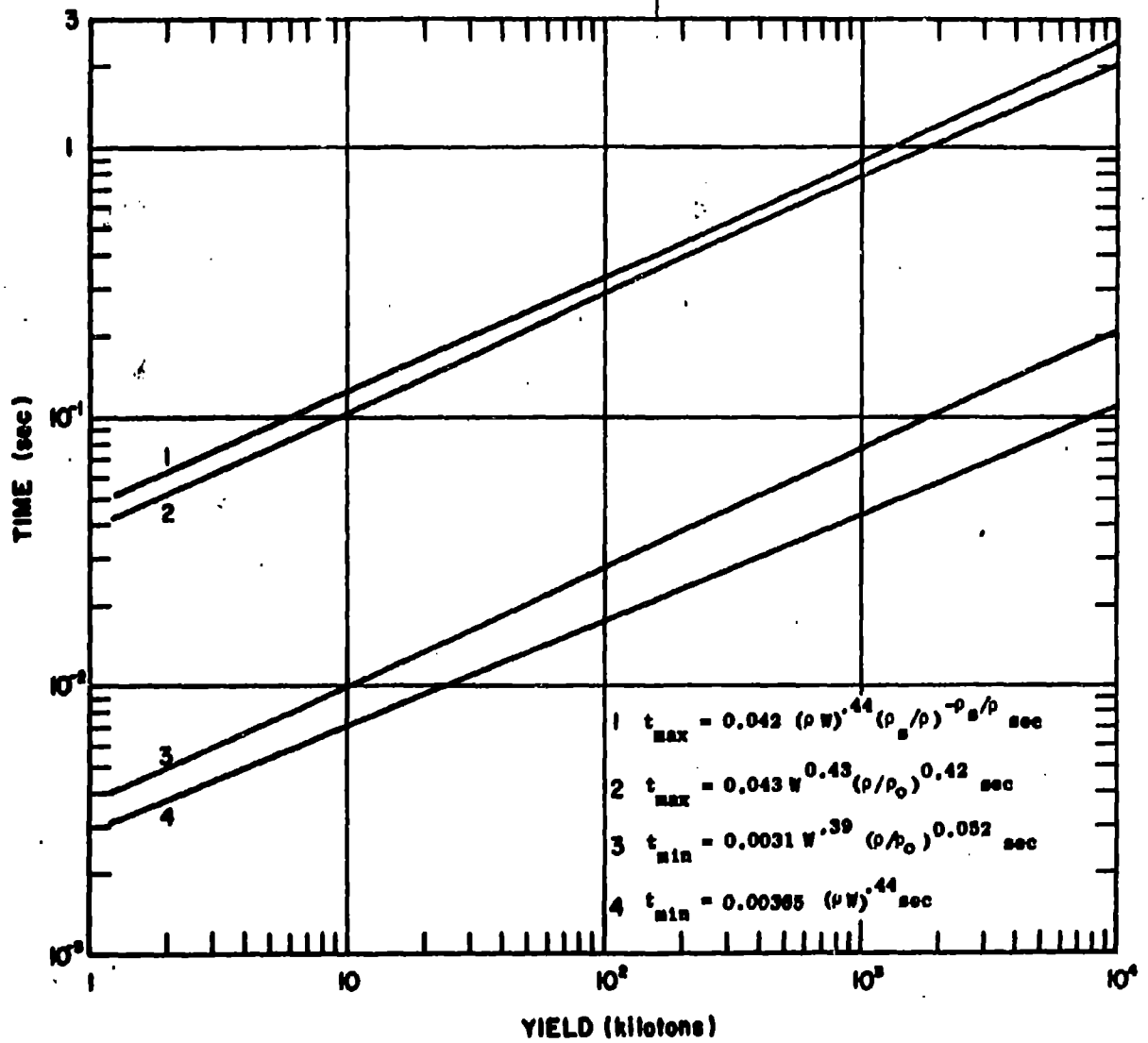

Figure 3-60. Comparison of Equations for t_{min} and t_{max}, $HOB = 180\ W^{0.4}$ feet

[redacted]

[redacted] BIBLIOGRAPHY [redacted]

Duntley, S. O., *The Visibility of Distant Objects*, Journal of the Optical Society of America, 38, 237-249, 1948 [redacted]

Ellis, P. A., *A Note on the Prediction of Thermal Pulse from Special Nuclear Weapons* [redacted] DASA 2097, KN-717-68-3, Kaman Nuclear, Colorado Springs, Colorado, 20 March 1968 [redacted]

Gibbons, M. G., *Transmissivity of the Atmosphere for Thermal Radiation from Nuclear Weapons*, USNRDL-TR-1060, U.S. Naval Radiological Defense Laboratory, San Francisco, California, 12 August 1966 [redacted]

Hillendahl, R. W., *Theoretical Models for Nuclear Fireballs* [redacted] (41 Volumes) DASA 1589, Lockheed Missiles and Space Company, Sunnyvale, California, 1965-1968 (Part A, [redacted] Part B, [redacted] Volumes 1-39, [redacted]

Landshoff, R. M., *Thermal Radiation Phenomena* [redacted] (6 Volumes), DASA 1917, Lockheed Missiles and Space Company, Palo Alto, California, 1967 (Volumes 1-5, [redacted] Volume 6, [redacted].

Manual of Surface Observations (WBAN), 7th Edition, Circular N., U.S. Government Printing Office, Washington, D.C., 1966 [redacted].

Middleton, W. E. Knowles, *Vision Through the Atmosphere*, University of Toronto Press, 1958 [redacted]

Passell, T. O., and R. I. Miller, *Radiative Transfer from Nuclear Detonations Above 50-km Altitude*, Fire Research Abstracts and Reviews, Vol. 6, No. 2, 1964 [redacted]

Shnider, R. W., *A Compilation and Semi-Emperical Analysis of Thermal Pulse Times* [redacted] URS 7007, DASA 2677, URS Research Company, San Mateo, California, September 1970 [redacted]

Wells, P. B., J. R. Keith, R. E. Wellick, and D. C. Sachs, *Air Blast from Special Weapons* [redacted] (3 Volumes) KN-68-168(R), Kaman Nuclear, Colorado Springs, Colorado, October 1968 (Volume 1, [redacted] Volume 2, [redacted] Volume 3, [redacted]

[redacted]

[redacted]

4-3 Interactions of X-Rays with Matter [redacted]

[redacted] Just as X-rays are produced principally by phenomena involving electrons, the principal interactions of X-rays with matter also depend on atomic electrons.

[redacted] In the photoelectric effect, an X-ray is totally absorbed; its energy is partly used in overcoming the binding energy of an atomic electron, and the remainder is imparted as kinetic energy to the electron and (to a much lesser extent) to the recoiling ion. No scattered X-ray is observed; however, the deexcitation of the ionized atom can result in secondary X-ray, ultraviolet, or optical radiation. This phenomenon is known as fluorescence. Photoelectric absorption is most probable when the X-ray energy just exceeds the binding energy of a particular electron. Thus, as the wavelength of the incident X-ray increases (the energy decreases), the probability of absorption gradually rises until the binding energy of the K-shell electron is reached. It then abruptly drops (the "K-absorption edge"), and then begins rising again until the next absorption edge is reached, and so on.

[redacted] Another effect is Compton (inelastic) scattering. When an X-ray collides with an electron, it is possible that, not only a resultant energetic electron, but also a scattered X-ray photon of lower frequency (longer wavelength) will be observed. This usually happens when the target electron is free or very loosely bound. If it is assumed that the electron is free, the interaction can be analyzed as collision between two particles. Conservation of momentum and energy then yield the relation

$$\lambda' - \lambda = \frac{h}{m_o c}(1 - \cos\theta)$$

where λ is the wavelength of the incident photon, λ' that of the scattered photon, θ the angle of scattering, and m_o the mass of the electron (9.1×10^{-28} g).

[redacted] A third effect is elastic scattering. If an electron is excited by an electromagnetic wave, it will gain energy and oscillate. As a moving charge, it will then reradiate the energy as electromagnetic radiation of the same frequency, which appear as scattered photons. The scattered photons may be coherent (in phase) or incoherent (random phases).

[redacted] The probability that any of the above scattering or photoelectric processes will take place is given in terms of a cross-section σ (so called because it has units of area), which is the probability of a given interaction taking place under the condition that one interaction per unit area is possible.

[redacted] If the medium with which the X-rays interact is characterized by an electron density ρ_e, then for every centimeter an X-ray traverses, there are ρ_e electrons within a cross-sectional area of one cm^2 with which it can interact. The probability of interaction per centimeter is therefore $\mu = \rho_e \sigma$. Since this is also the probability that an X-ray disappears from the incident beam, the beam intensity falls by a factor $e^{-\mu x}$ after having penetrated a distance x into the material. It is often convenient to express the penetration in terms of the total amount of material "seen" by the beam, ρx, where ρ is the mass density of the material. In this case, the mass attenuation coefficient $\kappa = \mu/\rho$ is used. The mass attenuation coefficients for air are shown as a function of X-ray photon energy in Table 4-2 and in Figure 4-4.

[redacted] If the X-rays radiate isotropically from a point source rather than in a narrow beam, the flux, Φ, of X-rays (photons per unit area per unit time) at any point depends not only on the exponential attenuation described above but also on the spherical attenuation, so that

$$\Phi = Ne^{-\kappa(\rho R)}/4\pi R^2$$

where R is the radial distance from the source

[redacted]

[redacted]

Table 4-2. [redacted] Mass Attenuation Coefficients for Air [redacted]

Photon Energy (keV)	Total Scatter (cm^2/g)	Photoelectric (cm^2/g)	Total Attenuation (cm^2/g)
2	9.791×10^{-1}	4.95×10^{2}	4.960×10^{2}
3.2*	7.754×10^{-1}	1.34×10^{2}	1.348×10^{2}
3.2*	7.754×10^{-1}	1.56×10^{2}	1.568×10^{2}
4	6.707×10^{-1}	8.27×10^{1}	8.337×10^{1}
6	5.070×10^{-1}	2.30×10^{1}	2.351×10^{1}
8	4.126×10^{-1}	9.54×10^{0}	9.953×10^{0}
10	3.529×10^{-1}	4.57×10^{0}	4.923×10^{0}
20	2.409×10^{-1}	4.96×10^{-1}	7.369×10^{-1}
40	1.885×10^{-1}	5.07×10^{-2}	2.393×10^{-1}
60	1.690×10^{-1}	1.33×10^{-2}	1.823×10^{-1}
80	1.569×10^{-1}	5.29×10^{-3}	1.622×10^{-1}
100	1.480×10^{-1}	2.61×10^{-3}	1.506×10^{-1}
200	1.210×10^{-1}	1.68×10^{-4}	1.212×10^{-1}
400	9.468×10^{-2}	9.80×10^{-6}	9.469×10^{-2}
600	8.014×10^{-2}	3.92×10^{-6}	8.014×10^{-2}

*Argon K-Absorption Edge.

[redacted]

and N is the total number of photons emitted by the source per unit time. This, however, is only the component that reaches the point directly from the source. Scattered photons (coherent, incoherent, and Compton) originating at other points also reach the point. The result is that the flux of that point is larger by a buildup factor B. The magnitude of B depends on the distance from the source, the energy spectrum of the X-rays, and properties of the scattering material in complex ways. It is ordinarily calculated by computer codes. The integral of the flux over [redacted] time, or the total number of X-ray photons per unit area reaching a point, is known as the fluence. *Flux and fluence are also commonly described in terms of the energy carried by the photons instead of their number.*

SECTION I

[redacted] NUCLEAR WEAPONS AS X-RAY SOURCES [redacted]

4-4 X-Ray Production in Nuclear Weapons [redacted]

[redacted] The multitude of processes that occur very early in the detonation of a nuclear weapon are described in Chapter 1. The result,

[redacted]

[redacted]

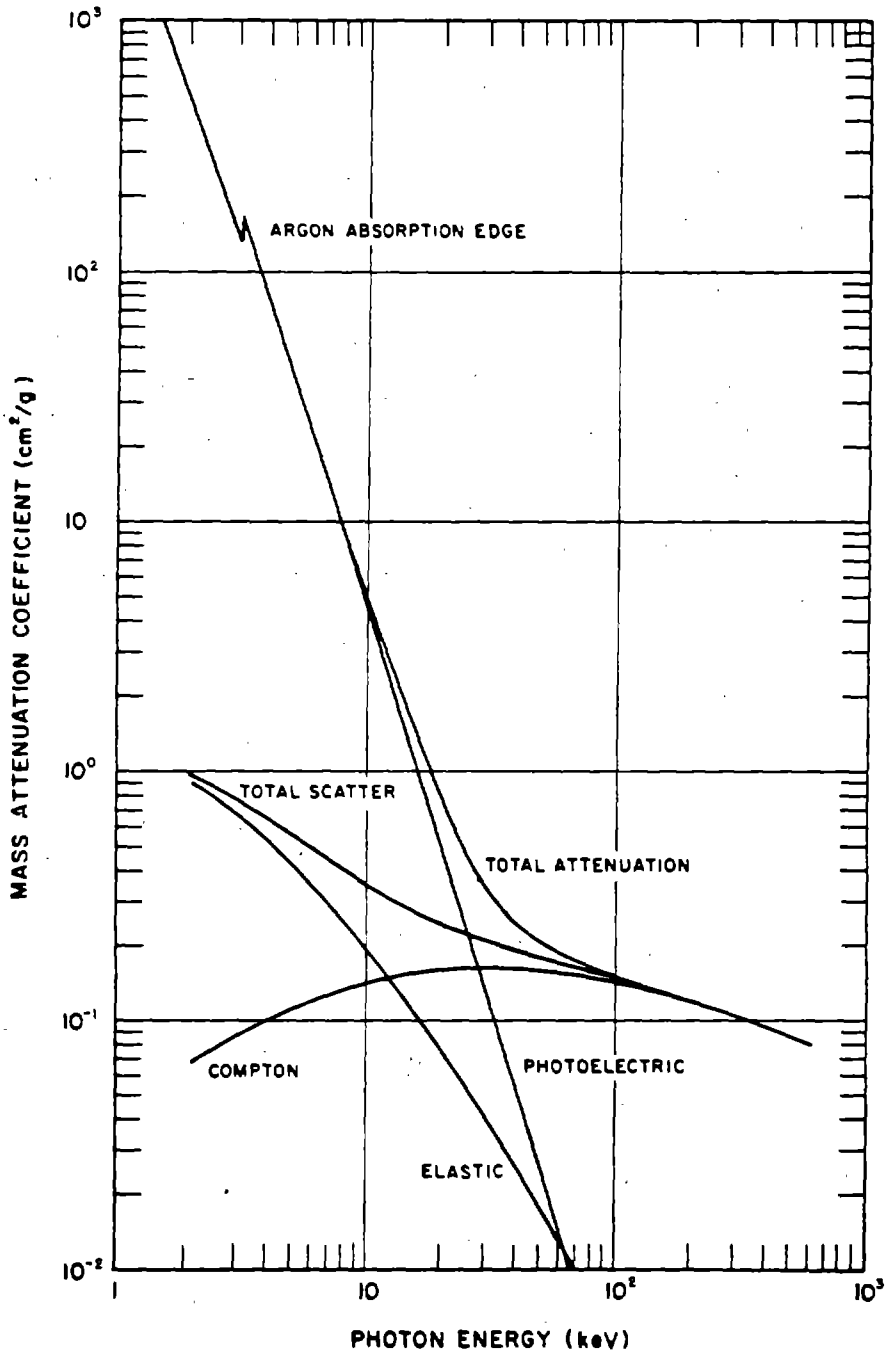

Figure 4-4. [redacted] Mass Attenuation Coefficients for Air [redacted]

[redacted]

[redacted]

[redacted]

as far as X-ray production is concerned, is that a very hot (tens of millions of degrees Kelvin) plasma is formed, consisting of electrons and the stripped nuclei of the fission and fusion products, of the elements in the casing materials, and of any other elements in the immediate vicinity of the detonation, such as nitrogen and oxygen in the air. Although the spectrum of emissions from this plasma is not that of a black body, particularly because the temperature is by no means uniform, it often approximates a black body spectrum, or a combination of two or more such spectra. The disposition of X-rays is further complicated by interactions with the atmosphere.

[redacted] Approximately 70 to 80 percent of the total prompt yield of many nuclear weapons is radiated in the form of X-rays. [redacted] In recent years, considerable attention has been devoted to designing "hot" nuclear weapons with effective radiation temperatures greater than [redacted]

DNA (b)(3)

DNA (b)(3)

4-5 X-Ray Energy Emitted [redacted]

[redacted] A temperature gradient, decreasing outward, exists between the enormously hot interior nuclear materials and the somewhat cooler exterior bomb casing materials of the nuclear weapon. The X-rays, of course, are continuously being absorbed and reradiated, but with a temperature gradient, the conditions for an ideal black body with isotropic radiation at every point do not exist, and there is a net flow of energy outward from the point of detonation. The outward flux at the surface is, in fact, about twice what would be implied by black body radiation at the temperature of the surface because of X-rays from the interior escaping without interaction at the surface. If the actual surface temperature is T_s, then the surface energy flux is given by

$$\Phi_s = \sigma T_e^4$$

where

$$T_e = 2^{1/4} T_s = 1.19\ T_s .$$

The effective temperature, T_e, will be used in the succeeding discussions.

4-6 Rate of X-Ray Emission [redacted]

[redacted]

DNA (b)(3)

[redacted]

[redacted]

DNA (b)(3)

[redacted] Actually, radiation cannot continue at the peak emission rate because the loss of energy cools the plasma and it radiates correspondingly less rapidly as time goes on. The time necessary to radiate a given fraction (about 90 percent) of the weapon energy increases with the size of the emitting sphere *(r)*, and of course is larger than the time calculated from the peak emission rate; however, it is still generally measured in shakes or tenths of a shake for most weapons.

4-7 Spectral Distribution of X-Rays [redacted]

[redacted] An approximation of the X-ray spectra from nuclear weapons can be obtained from the normalized Planck distribution by applying the appropriate multiplicative factors to the independent *(u)* and dependent *(F* and *G)* variables for the black body temperature indicated (see paragraph 4-2). [redacted]

DNA (b)(3)

[redacted] Similarly, the effective X-ray temperature and equivalent black body fluence may be obtained from experimental measurements [redacted]

DNA (b)(3)

[redacted] This example is given in more detail in Problem 4-3. The equivalent black body spectrum can now be constructed and compared with the rest of the measured spectrum. Some examples of such comparisons will be shown in subsequent paragraphs.

[redacted] For the purpose of calculating X-ray effects, the spectrum is most useful if tabulated by intervals in *u* enclosing approximately equal energy increments of the cumulative distribution function. In such computations, each increment is treated as being composed of monoenergetic photons of the central energy. Table 4-3 shows the boundaries of the energy intervals for approximately five percent increments of the normalized cumulative distribution function and the corresponding boundaries of photon energies for several source temperatures. Five percent increments may be too coarse for estimating effects both at the very low and very high ends of the spectrum. For these regions, the one percent increments shown in Table 4-4 may be useful.

4-8 Real Nuclear Weapons as X-Ray Sources [redacted]

[redacted] Since X-rays are attenuated rapidly by air, very little can be ascertained about the initial properties of nuclear weapons as X-ray sources from atmospheric weapons tests. However, X-ray effects may constitute the principal kill mechanism for high altitude interception of ballistic missiles [redacted]

DNA (b)(3)

[redacted]

Page 4-13 is deleted.

[redacted]

[redacted]

Table 4-3. [redacted] Five Percent Energy Intervals for a Planck Spectrum [redacted]

Cumulative Distribution Function	Photon Energy in keV for Various Black Body Temperatures			
	1 keV	2 keV	8 keV	10 keV
0	0	0	0	0
0.0506	1.16	2.32	9.28	11.60
0.1008	1.54	3.08	12.32	15.40
0.1511	1.84	3.68	14.72	18.40
0.2007	2.10	4.20	16.80	21.00
0.2500	2.34	4.68	18.72	23.40
0.3013	2.58	5.16	20.64	25.80
0.3493	2.80	5.60	22.40	28.00
0.4017	3.04	6.08	24.32	30.40
0.4491	3.26	6.52	26.08	32.60
0.4994	3.50	7.00	28.00	35.00
0.5515	3.76	7.52	30.08	37.60
0.6007	4.02	8.04	32.16	40.20
0.6499	4.30	8.60	34.40	43.00
0.7010	4.62	9.24	36.96	46.20
0.7519	4.98	9.96	39.84	49.80
0.8004	5.34	10.68	42.62	53.80
0.8499	5.88	11.76	47.04	58.80
0.9003	6.56	13.12	52.48	65.60
0.9502	7.64	15.28	61.12	76.40

DNA (b)(3)

[redacted]

Figures 4-6 through 4-11 show some X-ray spectra from real nuclear weapons, both observed and predicted. Figure 4-6 shows the observed spectrum of a warm X-ray weapon.

DNA (b)(3)

[redacted]

DNA (b)(3)

[redacted]

[redacted]

[redacted]

SECTION II

[redacted] X-RAY ENVIRONMENTS PRODUCED BY NUCLEAR WEAPONS [redacted]

4-9 Exoatmospheric (Vacuum) Detonations [redacted]

[redacted] X-ray environments from nuclear detonations are completely specified by the magnitude of the source and the distance from the source to the point of interest if the detonation occurs in a vacuum. If the detonation occurs at an altitude sufficiently high that essentially vacuum conditions prevail, it is designated an exoatmospheric detonation. Since, in any case, the vacuum will be less than perfect, the distinction between exoatmospheric and endoatmospheric detonations will depend on the degree to which effects vary from those predicted for a vacuum. This will depend on weapon design features, particularly whether the X-ray spectrum is hot or cold.

[redacted] For perfect vacuum conditions, the X-ray energy fluence at a range R from the point of detonation is

$$\varphi = \frac{E_o}{4\pi R^2} \text{ cal/cm}^2$$

where E_o is the X-ray yield of the weapon in calories and R is the distance in centimeters. If E_o is not known, it may be estimated as 75 percent of the total yield of the weapon. Using the relationship that 1 kt = 10^{12} calories, the vacuum fluence is shown as a function of distance from detonations of various x-ray yields in Figure 4-12. The fluence may also be calculated from the equation

$$\varphi = \frac{85.7\ W'_x}{R_f^2}$$

where W'_x is the X-ray yield in kilotons and R_f is the range in kilofeet.

[redacted] Since no interactions can take place in an empty medium, no changes in the spectral distribution of X-rays occurs in exoatmospheric detonations. For the same reason, the time dependence of X-ray energy flux is unchanged, and the time of arrival of the pulse at range R is R/c, where c is the velocity of light. Since, for the calculation of effects, only times relative to the arrival time are important, the only variation of effects with range is due to the variation in total fluence.

4-10 Endoatmospheric Detonations [redacted]

[redacted] The X-ray environment produced by nuclear detonations within the atmosphere are much more complicated because of the many interactions that can take place between the X-rays and the atmospheric constituents. Photoelectric absorption, elastic scattering, and inelastic (Compton) scattering all play a part in altering the total X-ray fluence that reaches a given range, the spectral distribution at that point, and the time rate of energy delivery. Density gradients and other inhomogeneities in the atmosphere cause the X-ray environment to deviate from the spherical symmetry exhibited in vacuum detonations. Because of scattering, the X-ray photons arriving at a given point do not all arrive from the direction of the detonation; in fact, some may arrive from precisely the opposite direction.

4-11 The Standard Atmosphere [redacted]

[redacted] The estimation of X-ray environments around an endoatmospheric nuclear detonation requires a knowledge of the atmospheric properties along any path that an X-ray photon might traverse from the weapon to the point of interest. Although atmospheric properties can change somewhat from day to day and place to place, most calculations are based on a standard atmosphere such as the one described by the National Bureau of Standards in 1962. The im-

[redacted]

[redacted]

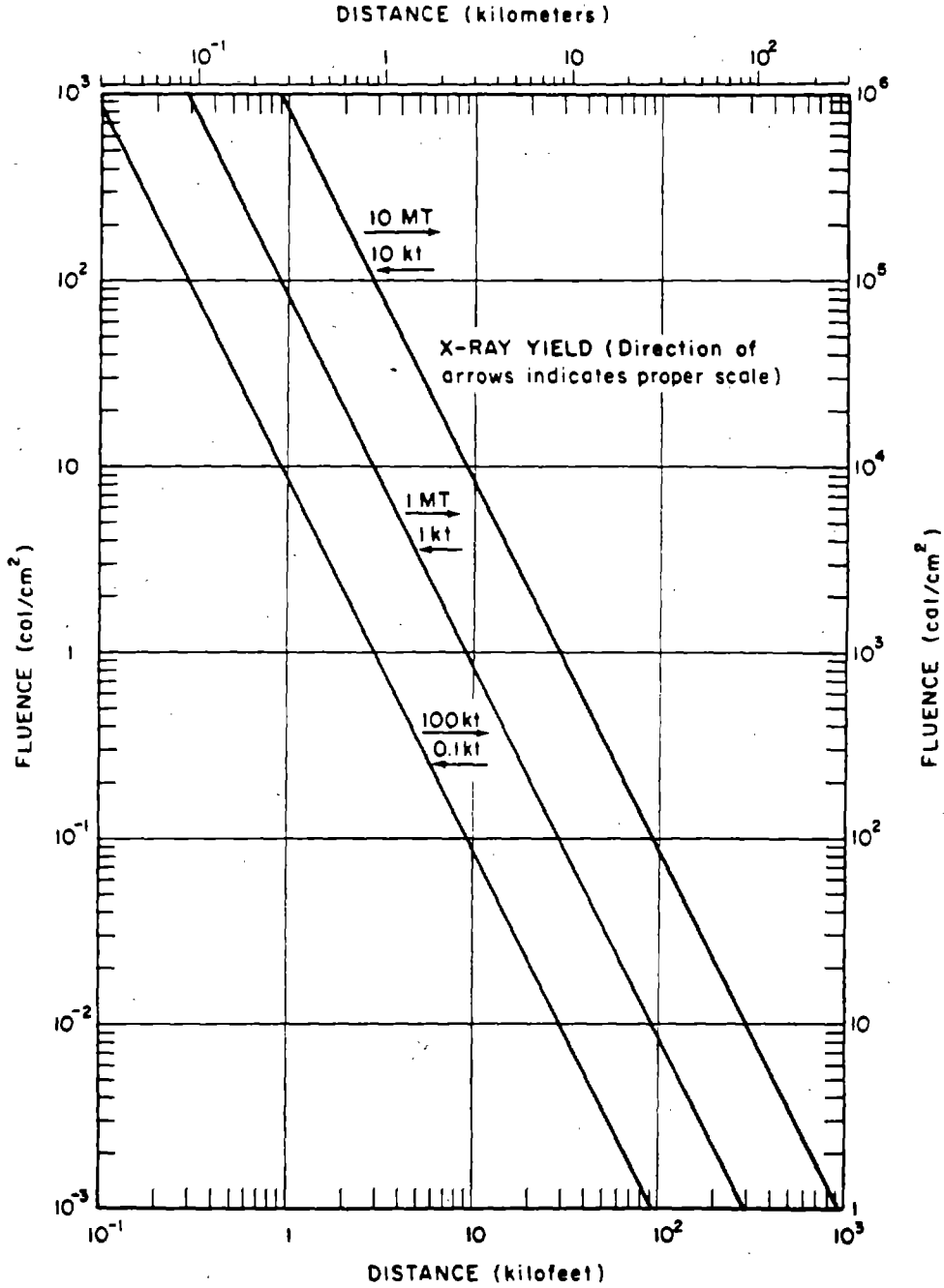

Figure 4-12. [redacted] X-Ray Fluence in a Vacuum [redacted]

[redacted]

[redacted]

[redacted]

portant atmospheric constituents are

	Fraction by Weight
Nitrogen	0.7553
Oxygen	0.2318
Argon	0.0129

Argon is included because its photoelectric absorption cross section for X-rays is large and serious errors can be made if it is neglected. The other minor components of the atmosphere, however, can be neglected without serious loss of accuracy.

[redacted] The other principal feature of the standard atmosphere is its variation in density with altitude. The density, ρ, falls approximately exponentially with increasing altitude, as is shown in Table 4-5 and Figure 4-13. Also shown is the quantity of air above a given altitude, h, which is given by the mass integral

$$q(h) = \int_h^\infty \rho(h')dh'$$

Table 4-5 also shows the density normalized to the sea level density, ρ_o.

[redacted] If two points are at altitudes h_1 and h_2 and are separated by a horizontal distance, d, then the slant range R is given by

$$R = \sqrt{d^2 + (h_2 - h_1)^2}$$

and the mass integral between them is given by

$$q(R) = \int_o^R \rho(h')ds' = R\,\frac{q(h_2) - q(h_1)}{h_2 - h_1}$$

[redacted] This expression reduces to

$$q(R) = q(h_2) - q(h_1)$$

when $d = 0$ and (in the limit) to

$$q(R) = \rho(h)R$$

when $h_1 = h_2$ (the coaltitude case).

[redacted] These values for the mass integral between the source of X-rays and the point of observation are to be used for the quantity ρR in the flux or fluence attenuation equations as described in paragraph 4-3. When the mass integral is used instead of the absolute range, the X-ray environment is substantially independent of other parameters; this property is known as mass integral scaling.

4-12 Direct X-Ray Fluence in the Atmosphere [redacted]

[redacted] If the attenuation equations are combined with the results for vacuum fluence, the direct fluence from a weapon with W_x kilotons of X-ray yield is

$$\varphi_{dir} = \frac{85.7\ W_x}{R_f^2}\, e^{-\kappa q(R)}$$

at a range R, where q is the mass integral calculated along R and κ is the mass attenuation coefficient. Notice that q will not be the same for different directions of R unless the atmosphere is essentially uniform, so that contours of constant fluence usually are not spherically symmetric about the burst point, although they usually are cylindrically symmetric about a vertical axis.

[redacted] Moreover, the value of the mass attenuation coefficient κ varies with X-ray photon energy according to the curve shown in Figure 4-4, so that the direct fluence must be calculated by weighting monoenergetic calculations by the spectral distribution. For a given penetration of the atmosphere, $q(R)$, this weighting process can be replaced by using an effective κ, but the value of this effective κ will change with $q(R)$. Similar-

[redacted]

[redacted]

Table 4-5. [redacted] The Standard Atmosphere [redacted]

Altitude (kft)	Air Density (g/cm^3)	Mass Integral Above Altitude (g/cm^2)	Density Normalized to Sea Level
0	1.2250×10^{-3}	1.0331×10^{3}	1.0000×10^{0}
5	1.0556×10^{-3}	8.5967×10^{2}	8.6170×10^{-1}
10	9.0477×10^{-4}	7.1059×10^{2}	7.3859×10^{-1}
20	6.5312×10^{-4}	4.7525×10^{2}	5.3316×10^{-1}
30	4.5904×10^{-4}	3.0749×10^{2}	3.7473×10^{-1}
40	3.0267×10^{-4}	1.9305×10^{2}	2.4708×10^{-1}
50	1.8756×10^{-4}	1.1973×10^{2}	1.5311×10^{-1}
60	1.1628×10^{-4}	7.4292×10^{1}	9.4919×10^{-2}
70	7.1742×10^{-5}	4.6182×10^{1}	5.8565×10^{-2}
80	4.4174×10^{-5}	2.8855×10^{1}	3.6060×10^{-2}
90	2.7391×10^{-5}	1.8151×10^{1}	2.2360×10^{-2}
100	1.7101×10^{-5}	1.1493×10^{1}	1.3960×10^{-2}
110	1.0647×10^{-5}	7.3417×10^{0}	8.6918×10^{-3}
120	6.6487×10^{-6}	4.7534×10^{0}	5.4275×10^{-3}
130	4.2214×10^{-6}	3.1247×10^{0}	3.4460×10^{-3}
140	2.7222×10^{-6}	2.0831×10^{0}	2.2222×10^{-3}
150	1.7810×10^{-6}	1.4070×10^{0}	1.4539×10^{-3}
160	1.1968×10^{-6}	9.5903×10^{-1}	9.7697×10^{-4}
180	5.6991×10^{-7}	4.4396×10^{-1}	4.6523×10^{-4}
200	2.7163×10^{-7}	1.9859×10^{-1}	2.2174×10^{-4}
250	3.6248×10^{-8}	2.0476×10^{-2}	2.9590×10^{-5}
300	2.3839×10^{-9}	1.5137×10^{-3}	1.9460×10^{-6}
400	1.8645×10^{-11}	2.7532×10^{-5}	1.5220×10^{-8}
500	1.6329×10^{-12}	6.2391×10^{-6}	1.3330×10^{-9}
1,000	3.2769×10^{-14}	0	2.6750×10^{-11}

[redacted]

ly, the spectrum changes as matter is traversed because of the varying proportions of photons absorbed or scattered out of the flux at varying photon energies.

[redacted] In practice, the most accurate method for calculating fluences uses Monte Carlo computer codes with accurate photon cross sections for each energy group and each scattering or absorbing process. This technique is also essential for following those X-ray photons scattered out of the direct fluence, as will be discussed subsequently.

[redacted]

[redacted]

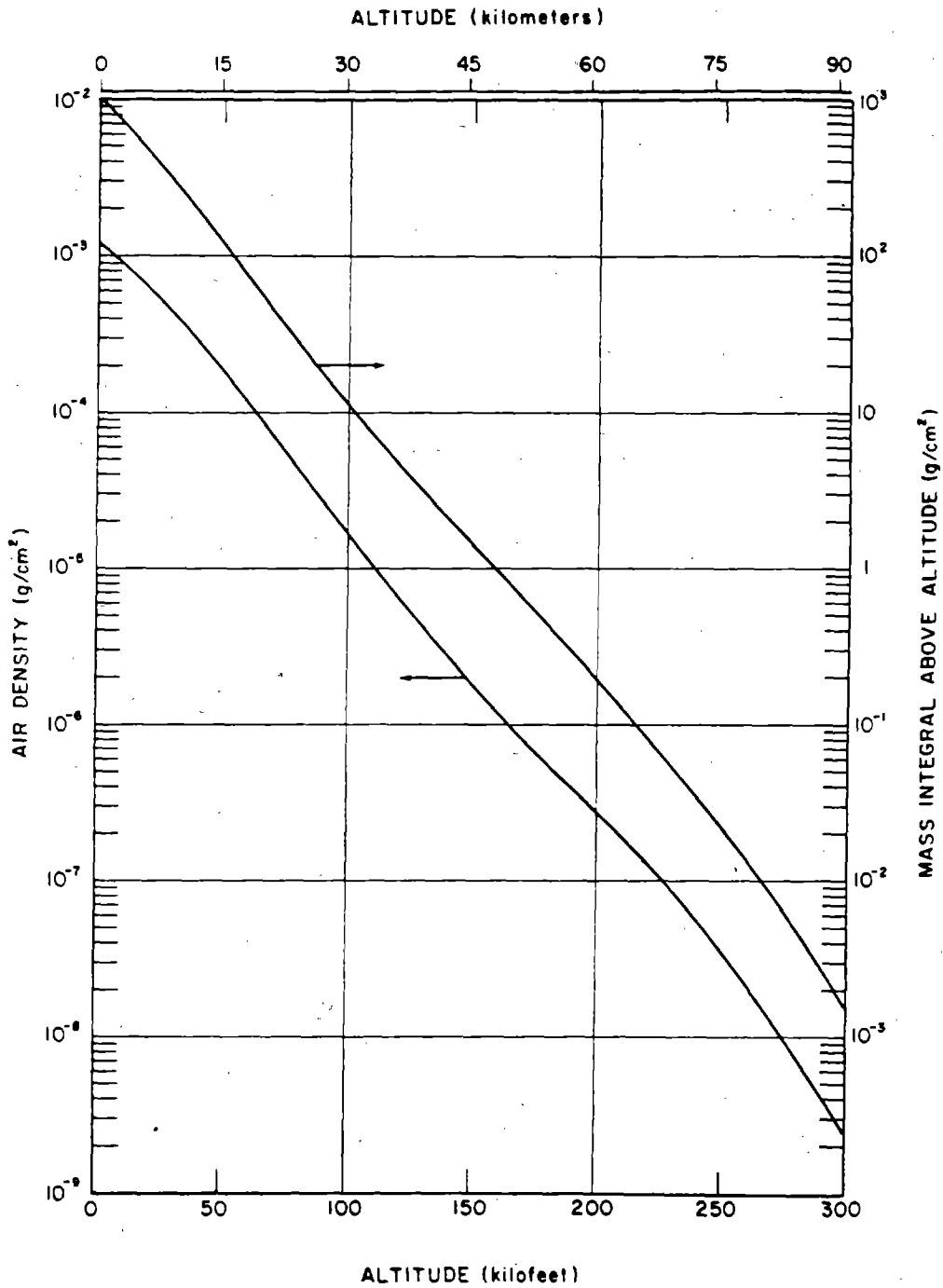

Figure 4-13. [redacted] The Standard Atmosphere [redacted]

[redacted]

[redacted]

DNA (b)(3)

[redacted]

4-13 Scattered X-Ray Fluence [redacted]

[redacted] The X-rays arriving at a given point come not only directly from the source but also indirectly (and usually from other directions) after one or more scattering events. The probabilities of scattered photons contributing to the flux depends on the total cross sections for scattering and the differential cross sections for scattering at specific angles. The flux of scattered photons is usually computed by a Monte Carlo simulation of the paths taken by a representative sample of photons, taking into account also the possibility of degradation of energy in Compton scattering. The resultant flux adds to that penetrating directly from the source, and the ratio of the total fluence to the direct fluence is known as the build-up factor. The build-up factor increases from unity very near the source to more than one hundred for longer ranges.

[redacted] No simple analytic expression gives the build-up factor, but Figures 4-14 through 4-16 give direct and total fluences and the build-up factor for three representative X-ray sources. In the monoenergetic source case (Figure 4-14), the direct fluence is attenuated exponentially (in addition to the spherical divergence, which is not included since the fraction of vacuum fluence is the quantity shown). The build-up factor, which includes photons of degraded energy, rises so rapidly that the total fluence for short ranges actually exceeds that expected for the vacuum case, in which only spherical divergence would be operating. Figure 4-15 and 4-16 show results for black body source spectra, also normalized to the vacuum fluence. Notice that the direct fluences are no longer exponential, although in the latter case a mass attenuation coefficient corresponding to about five times the black body temperature gives reasonable results. The normalized fluences for the latter two cases are also tabulated in Table 4-6.

[redacted] The cold X-rays are attenuated much more quickly in air, because the mass attenuation coefficient is so much larger for lower energies. [redacted]

DNA (b)(3)

DNA (b)(3)

4-14 Low Altitude Endoatmospheric Detonations [redacted]

[redacted] Low altitude (deep) endoatmospheric detonations are the next simplest case – after vacuum detonations – because the air density is sufficiently high that most of the attenuation occurs close to the burst point. Therefore, there are no large variations in density to affect critically the computation of fluences. In particular, the density of air through which the scattered X-rays reach a given point does not differ greatly from that through which the direct X-rays penetrate. Although whether or not altitudes are low (detonations are deep) depends on the energy

[redacted] [redacted]

[redacted]

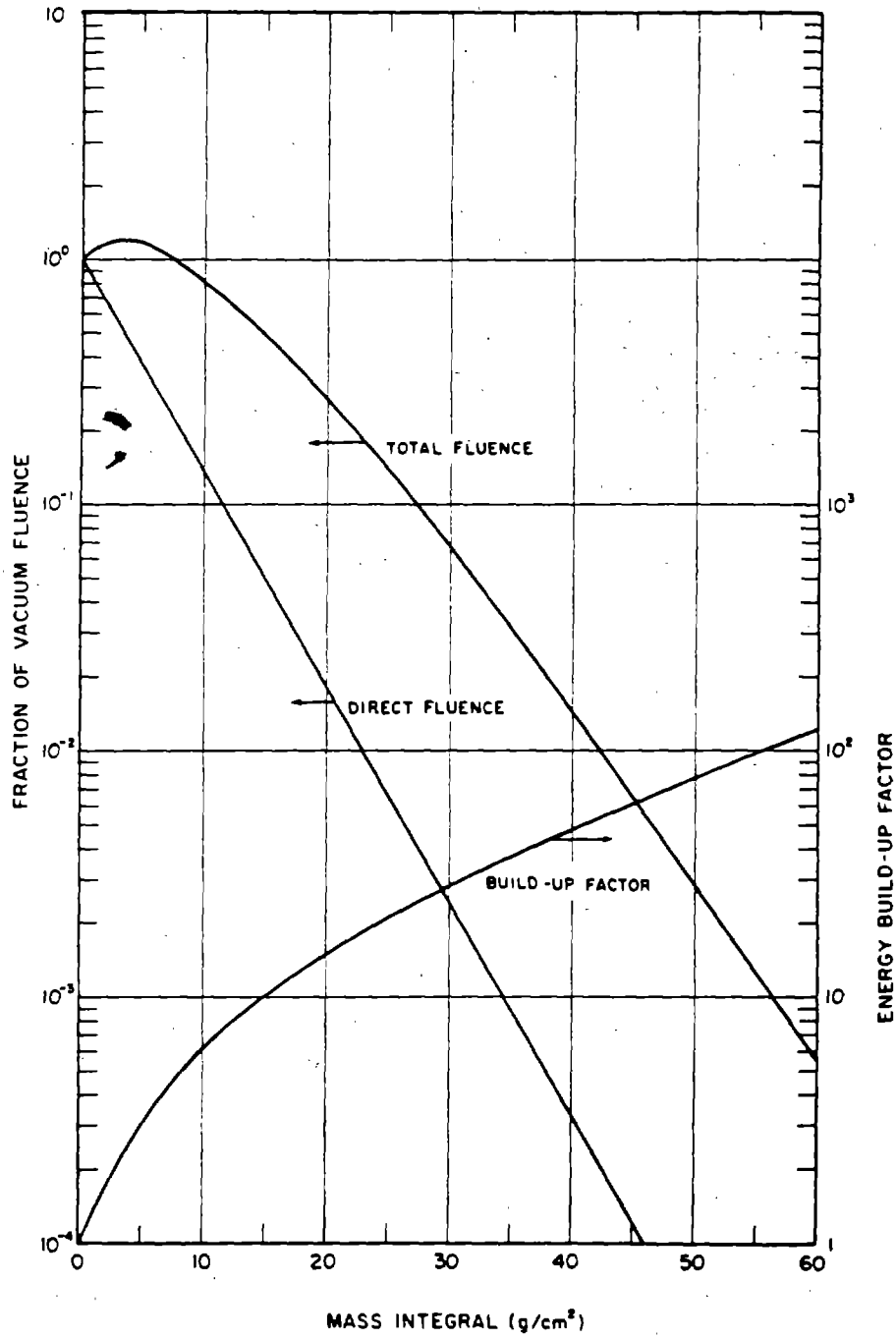

Figure 4-14. [redacted] Energy Fluence and Build-up Factor for a 50 keV Monoenergetic Source in Homogeneous Air [redacted]

Pages 4-32 + 4-33 are deleted.

[redacted] [redacted]

[redacted]

[redacted] high energy X-rays increases – as the mass of air penetrated increases. This phenomenon occurs because the higher cross sections, particularly for photoelectric absorption, occur at lower energies and preferentially remove low energy X-rays from the direct fluence. However, every Compton scattering process degrades the energy of the scattered photon, and the scattered component of the fluence tends to become increasingly soft as the penetration increases. These two effects partially compensate for one another, and the typical black body spectrum is little affected by passage through air.

[redacted] The rate of X-ray production from nuclear weapons as sources has already been discussed in paragraph 4-6. [redacted] Because the scattered component is softer than the direct component and arrives later, the spectrum of X-rays incident also varies with time in a complex fashion, and the dependence varies with the quantity of air traversed. Similarly, the direct fluence is all moving radially outward from the source, whereas the scattered photons can be incident from all directions, even from directly opposite the source. Thus the fraction of the energy flux moving outward (angles less than 90° from the radial vector) varies with time and location. In general, the fraction decreases from unity as time increases. However, when all times are considered, about 80 percent of the total fluence is outward for most ranges, and the fact that a portion of the fluence is backscattered can be neglected for most applications.

DNA (b)(3)

4-15 High Altitude Endoatmospheric Detonations [redacted]

[redacted] When nuclear detonations are so high that mass integral scaling is not correct, but yet sufficiently endoatmospheric that vacuum conditions are not satisfied, special and detailed calculations must be made for each case of interest. Although mass integral scaling is applicable for the direct fluence, the scattered component traverses paths of varying composition, and detailed Monte Carlo computer codes are necessary to describe the interactions.

[redacted] The spectrum of Figure 4-10 was used. In computing horizontal ranges, the curvature of the earth was considered. The resulting total fluence contours are shown in Figure 4-21. Contours for the mass integral are also shown. Vacuum fluences and attenuation factors can be computed and direct fluences predicted from these contours.

DNA (b)(3)

Pages 4-40 through 4-44 are deleted.

[redacted] [redacted]

[redacted]

[redacted] BIBLIOGRAPHY [redacted]

Christian, R. H., and P. G. Fischer, *Phenomenology Estimates and a Proposed Experimental Program for Sentinel Environment Tests* [redacted] DASA 2116, 68TMP-30, General Electric Company, TEMPO, Santa Barbara, California, 29 February 1968 [redacted]

Evans, B. S. and F. H. Shelton, *A Table of the Planck Radiation Function and Its Integral*, KN-770-70-36, Kaman Nuclear, Colorado Springs, Colorado, 2 February 1970 [redacted]

Gilmore, F. R., *A Table of the Planck Radiation Function and Its Integral*, RM-1743, RAND Corporation, Santa Monica, California, 2 July 1956 [redacted]

Latter, A. L., *Another Vulnerability* [redacted] RM-3981-PR, RAND Corporation, January 1964 [redacted]

Latter, A. L., *A High Temperature Nuclear Weapon* [redacted] RM-3978-AEC, RAND Corporation, Santa Monica, California, 23 December 1963 [redacted]

LRL Warheads for Advanced Spartan [redacted] LRL-CMA 68-154, Lawrence Radiation Laboratory, Livermore, California, 31 October 1968 [redacted]

Shelton, F. H., *Some Notes on the Spectral Distribution of Blackbody Sources* [redacted] KN-655-65-12, Kaman Nuclear, Colorado Springs, Colorado, 31 March 1965 [redacted]

Shelton, F. H., and J. R. Keith, *X-Ray Air Transport* [redacted] DASA 1981, KN-717-67-1, Kaman Nuclear, Colorado Springs, Colorado, 1 July 1967 [redacted]

Shelton, F. H., and J. R. Keith, *Time Dependent X-Ray Air Transport* [redacted] DASA 2138, KN-717-68-4, Kaman Nuclear, Colorado Springs, Colorado, 31 May 1968 [redacted]

Shelton, F. H., and J. R. Keith, *Initial Radiation Environments Produced by SPARTAN Events and Some of Their Aerospace Systems Effects* [redacted] DASA 2371, KN-774-69-4, Kaman Nuclear, Colorado Springs, Colorado, 24 July 1969 [redacted]

Shelton, F. H., *Nuclear Weapons as X-Ray Sources, the Environments They Produce, and Some Effects on Aerospace Systems* [redacted] *Volume I – X-Ray Sources and the Environments They Produce* [redacted] DASA 2397-1, KN-770-69-30, Kaman Nuclear, Colorado Springs, Colorado, September 1969 [redacted]

[redacted] [redacted]

[redacted]

[redacted] NEUTRONS [redacted]

5-1 Neutron Source [redacted]

[redacted] As mentioned previously, the neutrons of interest originate during the fission and fusion processes. The neutron source of interest is that which exists at the weapon case, i.e., the source of interest consists of those neutrons that escape from the exploding weapon. Both the number of neutrons and their spectrum are altered during transit through the weapon materials. Thus, the source of interest may be quite different from the source of origin (fission or fusion). The neutron source can be defined properly only by considering the actual design of a specific weapon. No average source can be defined that will represent most weapons with any degree of accuracy. It is beyond the scope of this manual to describe the output of a sufficient number of weapon types to present the user with adequate information concerning the neutron output for any possible specific situation. The examples that are presented in succeeding paragraphs are truly examples and should not be taken to be representative for purposes of generalization. Further information concerning nuclear weapons as neutron sources may be obtained from "Status of Neutron and Gamma Output from Nuclear Weapons," DASA 2567 (see bibliography). On the other hand, the curves shown in Figures 5-9 through 5-13 that provide the total dose to personnel on or near the surface of the earth were calculated for eight specific sources. It is believed that, with the descriptions of the eight sources provided in Table 5-3, one of the eight sources may be selected that will represent a reasonable estimate of the total dose to personnel on or near the surface of the earth for most situations.

[redacted] Table 5-1 shows the spectra for two weapons, one pure fission and one thermonuclear, for which calculations are available.* These spectra are also shown in Figure 5-1 and 5-2.

[redacted] As mentioned before, the spectra shown in Table 5-1 should not be construed as

*[redacted] These spectra are those that were used in the calculation of dose to personnel from weapon types II and VIII, respectively, as shown in Figures 5-9 through 5-13.

Table 5-1. [redacted] Weapon Neutron Output Spectra [redacted]

Neutron Energy (MeV)	Fission Weapon (neutrons/kt)	Thermonuclear Weapon (neutrons/kt)
12.2 -15.0		1.62×10^{22}
10.0 -12.2		8.53×10^{21}
8.18 -10.0	7.32×10^{20}	6.08×10^{21}
6.36 - 8.18	1.27×10^{21}	5.46×10^{21}
4.06 - 6.36	3.00×10^{21}	6.41×10^{21}
2.35 - 4.06	8.90×10^{21}	1.22×10^{22}
1.11 - 2.35	2.52×10^{22}	2.84×10^{22}
0.111 - 1.11	3.84×10^{22}	6.18×10^{22}
0.0033- 0.111	2.22×10^{22}	1.71×10^{23}
Total	9.97×10^{22}	3.16×10^{23}

[redacted]

[redacted]

C [redacted]

DNA (b)(1)

being representative. They are merely examples. [redacted] The spectral characteristics, however, will vary with weapon design even for weapons with the same total neutron output per kiloton.

5-2 Exoatmospheric (Vacuum) Transport [redacted]

[redacted] Neutron environments are completely specified by the description of the source and the distance from the source to the point of interest if the explosion occurs in a vacuum. If an explosion occurs sufficiently high that essentially vacuum conditions prevail, it is designated an exoatmospheric explosion. Since in any case, the vacuum will be less than perfect, the distinction between exoatmospheric and endoatmospheric explosions will depend on the degree to which effects vary from those predicted for a vacuum.

[redacted] For perfect vacuum conditions, the neutron fluence is given by

$$\varphi = \frac{N_o}{4\pi R^2} \text{ n/cm}^2$$

where N_o is the total number of neutrons emitted by the weapon and R is the distance in centimeters. Under these conditions the spectrum will remain constant, since no interactions can take place in a vacuum. However, as a result of the energy differences the flux (neutrons cm^{-2} sec^{-1}) will be a function of the distance from the source, i.e., the more energetic neutrons will arrive ahead of the less energetic ones. The energies associated with neutrons produced by nuclear explosions are sufficiently low compared to their rest mass energy that their velocities may be determined from their kinetic energy by non-relativistic mechanics, i.e.,

$$\frac{1}{2}Mv^2 = \text{K.E.},$$

where M is the neutron mass, 1.67×10^{-24} gm, v is the velocity, cm/sec, and K.E. is the kinetic energy in ergs. Using the relationship

$$1 \text{ MeV} = 1.6 \times 10^{-6} \text{ ergs},$$

the velocity is related to the kinetic energy in MeV as follows

$$v = 1.38 \times 10^9 \sqrt{\text{K.E. (MeV)}} \text{ cm/sec},$$

or

$$v = 1.38 \times 10^4 \sqrt{\text{K.E. (MeV)}} \text{ km/sec}.$$

Thus the velocities of 14 MeV, 4 MeV, and 1 MeV neutrons are

$$v_{14} = 1.38 \times 10^4 \sqrt{14} = 5.16 \times 10^4 \text{ km/sec},$$

$$v_4 = 1.38 \times 10^4 \sqrt{4} = 2.76 \times 10^4 \text{ km/sec},$$

$$v_1 = 1.38 \times 10^4 \sqrt{1} = 1.38 \times 10^4 \text{ km/sec}.$$

Expressed in a different manner, the times of flight will be 19.3, 36.2, and 72.4 μ sec/km for the 14 MeV, 4 MeV, and 1 MeV neutrons, respectively. Thus, although the spectrum will remain unchanged, the neutrons will arrive at points several kilometers from the explosion over periods of tens of microseconds.

5-3 Neutron Transport Through Materials [redacted]

[redacted] Neutrons undergo three main types of reactions when traversing matter: elastic scatter-

C [redacted]

[redacted]

[redacted]

ing; inelastic scattering; and capture. In the elastic scattering process, the neutron interacts with the nucleus of an atom and is scattered away from its original line of flight. If the nucleus is light (e.g., the proton that constitutes a hydrogen nucleus), the neutron may transmit a significant amount of its energy to the nucleus, and the scattered neutron will be less energetic than the incident neutron. If the nucleus is heavy, however, the energy transmitted to the nucleus will be insignificant, and the neutron will continue in a new direction with essentially the same energy as before the collision. In the inelastic scattering process, the neutron interacts with the nucleus with the subsequent emission of a gamma ray and a neutron with degraded energy. There are a variety of capture reactions, most of which result in the subsequent emission of a charged particle (generally a proton or alpha particle) and/or a gamma ray. When the reaction results solely in the emission of a gamma ray, it is generally referred to as a radiative capture reaction. As a rule, the probability for capture reactions is small compared to elastic and inelastic scattering when the neutron energy exceeds a few keV. The nuclei remaining after neutron capture are frequently radioactive. The fission process described in paragraph 1-1 is a special case of neutron-induced reactions. Neutrons that do not undergo any of the reactions described above will decay into a proton and an electron with a half life of about 12.8 minutes. The same is true of neutrons that undergo scattering, if they do not undergo some other reaction prior to decaying. The probabilities of the various reactions are such that the decay process is most important for neutrons traveling upwards from a relatively high altitude burst.

[redacted] The primary reactions that occur during neutron transport through air are elastic scattering, inelastic scattering, and capture by nitrogen nuclei. These latter two reactions provide a source of secondary gamma rays that can be important in some cases, as will be discussed in subsequent paragraphs.

[redacted] The neutron environment produced by nuclear explosions within the atmosphere are much more complicated than those described in paragraph 5-2 for exoatmospheric cases because of the interactions that take place with the atmospheric constituents. Even for a monoenergetic source the interactions described above alter the total neutron fluence that reaches a given range, result in a spectral distribution at that point, and change the time rate and direction of arrival at the point. As a result of scattering, the neutrons may arrive at a given point from any direction. If the source consists of a spectrum such as those shown in Figures 5-1 and 5-2, the situation is even more complex. In practice, the calculation of neutron fluences, fluxes, and spectra at some point distant from an endoatmospheric nuclear explosion, or for the interior of a system that is operating exoatmospherically, is performed by complex computer codes. It is beyond the scope of this manual to provide the means for calculating all of these quantities or even to provide a description of the methodology. The latter is contained in Volume III of the "Weapons Radiation Shielding Handbook," DASA 1892-3 (see bibliography). Selected examples of the change in fluence and spectrum will be provided in succeeding paragraphs and figures.

[redacted] An extensive set of tabulated results of computer calculations of neutron fluxes and doses is contained in "Time-Dependent Neutron and Secondary Gamma-Ray Transport in an Air-Over-Ground Geometry," ORNL-4289, Vol. II, (see bibliography). These data were used to obtain the spectra that would result from the source spectra shown in Figures 5-1 and 5-2 at slant ranges of 390, 1,050, and 1,500 meters. The resulting spectra are shown in Figures 5-3 and 5-4, respectively. Note that the spectra in Figures 5-3 and 5-4 show 4π (slant range)^2 x

[redacted]

[redacted]

[redacted]

[redacted] fluence. This does not mean that the spectra will be the same in all directions. The spectra shown in Figures 5-3 and 5-4 only apply to low air bursts and to *targets located on or near the surface of the earth.* The units for the ordinates in Figures 5-3 and 5-4 were chosen to allow a convenient visual comparison with Figures 5-1 and 5-2, respectively. Inspection of Figures 5-1 through 5-4 indicates that the shape of the fission source spectrum is not changed appreciably during transit through 1,500 meters of air (the relative abundance of extremely low energy neutrons, much lower energies than shown in Figures 5-1 through 5-4, will increase, however). The shape of the thermonuclear spectrum, on the other hand, does change as the neutrons penetrate air. The peak that exists at 14 MeV at the source becomes lower relative to the total, and the valley between about 8 and 12 MeV at the source becomes filled in as the higher energy neutrons are degraded to the 8 to 12 MeV range.

[redacted] Figures 5-5 and 5-6 show the neutron fluence for a receiver located on or near the surface of the earth as a function of slant range for the source spectra shown in Table 5-1. The fluence is shown for each of the energy intervals in Table 5-1. The total number fluence for neutron energies above 3.3 keV is also shown for each source. Once again the user is cautioned that these fluences should not be considered representative. They are presented as illustrative examples. Changes in weapon design will change the source spectrum, and this will modify the spectrum as well as the total number fluence at some distance from the explosion. Figures 5-5 and 5-6 also illustrate the large change in the spectral characteristics of the thermonuclear spectrum when compared to the variations in the fission spectrum with slant range.

[redacted] The preceding paragraphs have provided estimates of neutron fluences and spectra from low air bursts for detectors on or near the surface of the ground. The presence of an air-ground interface can increase or decrease the neutron intensities by as much as an order of magnitude compared to intensities at corresponding distances in an infinite air medium as a result of reflections and absorption by the ground. For source detector separation distances less than a mean-free path,* localized reflection from the ground generally tends to increase the intensity of high energy neutrons; however, initial nuclear radiation is only of interest in very low yields at such short distances since other weapon effects normally will be dominant. At longer distances, the high energy neutron intensity may be reduced by a factor of five or more compared to infinite air when both the source and the detector are at the ground surface. These effects have been included in the calculations from which the preceding figures were derived.

[redacted] The estimation of neutron environments around an endoatmospheric nuclear explosion for receivers away from the surface of the earth requires a knowledge of the atmospheric properties along any path that a neutron might traverse from the weapon to the point of interest. Although atmospheric properties can change from day to day and from place to place, most calculations are based on a standard atmosphere such as the one described by the National Bureau of Standards in 1962. The important atmospheric constituents that affect neutron transport are

	Fraction by Weight
Nitrogen	0.7553,
Oxygen	0.2318.

*[redacted] A mean-free path is the distance in which the radiation intensity is decreased by a factor of e, where e is the base of the natural logarithms (about 2.718). The length of a mean-free path depends on the neutron energy and on whether only the direct fluence or the total (direct plus scattered) fluence is being considered.

[redacted]

[redacted]

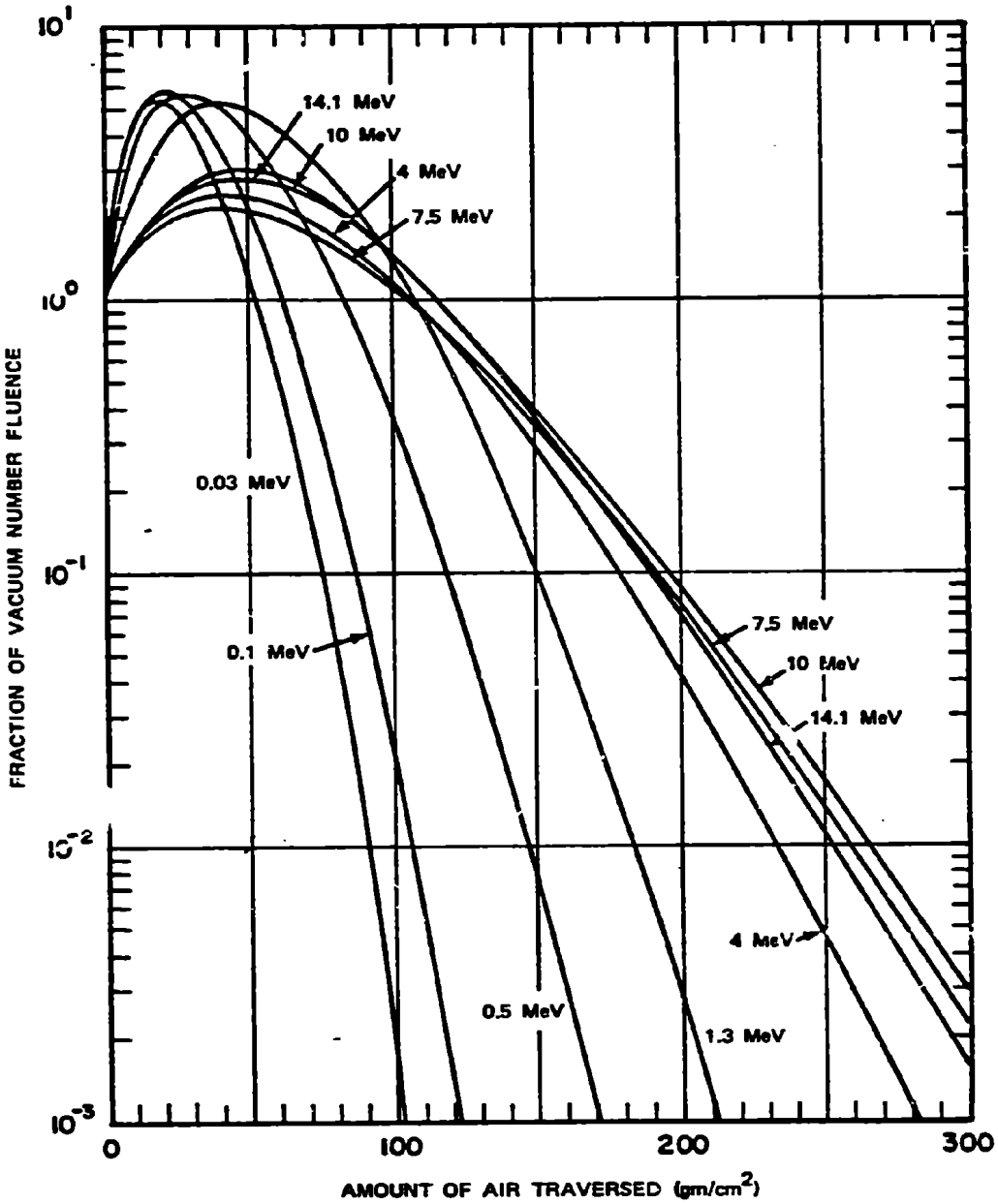

Figure 5-7. [redacted] Neutron Energy Build-Up Factors for Various Monoenergetic Sources in Homogeneous Air [redacted]

[redacted]

[redacted]

[redacted] per kt from a large yield weapon. The dotted curves in Figure 5-8 show the source as it would exist in a vacuum, i.e., the gammas resulting from inelastic scattering and neutron capture in the air would not be present under vacuum conditions. Not shown in Figure 5-8, but of potential importance for receivers near the surface of the earth in the vicinity of a low air burst are gammas that result from neutron interactions with the ground. It is convenient to divide the initial gamma radiation into two components: prompt gamma rays that result from the fission process and some neutron interactions with weapon materials, and are generally emitted within 1 to 2 shakes;* and delayed gamma radiation which originates from the sources described above subsequent to the prompt gamma ray emission and up to 1 minute after burst.

5-5 Prompt Gamma Rays [redacted]

[redacted] Prompt fission gamma rays are released essentially simultaneously with the fission process and thus their source rate behavior is determined by the rate profile of fission events in the weapon. These gamma rays escape before the detonation has appreciably deformed the weapon case or perturbed the atmosphere. The energy distribution of the fission gamma rays has been investigated using small samples of fissionable material; however, extrapolation of the small sample information to a weapon source involves considerable uncertainty because of the requirements to define the fission rate profile and to evaluate the attenuation provided by weapon materials as a function of time.

[redacted] Another source of very early gamma rays that contributes to the prompt pulse results from the non-fission interaction of neutrons with weapon materials.† These two sources combine to form a pulse of extremely short duration. Although the total amount of radiation given off during this period is small relative to the total, the peak rate of the pulse is extremely high. In some cases, such as for high altitude systems, the high ionization rate produced by this pulse may be the damage mechanism extending to the greatest range from the explosion. At low altitudes, the peak rate is attenuated rapidly, as a result of gamma ray absorption and scattering out of the time region of the peak rate.

[redacted] The prompt gamma environment is very sensitive to weapon design and to weapon yield. Moreover, comparison of theory and experiment for specific weapons is poor. Most calculations and experiments agree that the prompt gamma yield ranges between 0.1 and 0.3 percent of the total yield. The prompt gamma energy output rate may be expressed as

$$\Phi_{\gamma p} = \frac{2.6 \times 10^{25}\ fW}{\tau}\ \text{MeV/sec},$$

where f is the fraction of the weapon energy emitted as prompt gamma, W is the weapon yield in kt, and τ is the emission time (2.6×10^{25} is the energy equivalent of 1 kt in MeV; see paragraph 1-1). Using the limits quoted above for f and τ would lead to

$$\frac{(2.6 \times 10^{25})(10^{-3})}{2 \times 10^{-8}} < \Phi_{\gamma p}\ (\text{MeV/sec/kt}) < \frac{(2.6 \times 10^{25})(3 \times 10^{-3})}{10^{-8}}$$

$$1.3 \times 10^{30} < \Phi_{\gamma p}\ (\text{MeV/sec/kt}) < 7.8 \times 10^{30}.$$

[redacted] A shake is 10^{-8} seconds.

† [redacted] Gamma rays from these interactions may continue to times on the order of 10 microseconds, but their contribution is generally small compared to other sources after one or two shakes beyond the time of peak gamma emission.

[redacted]

[redacted]

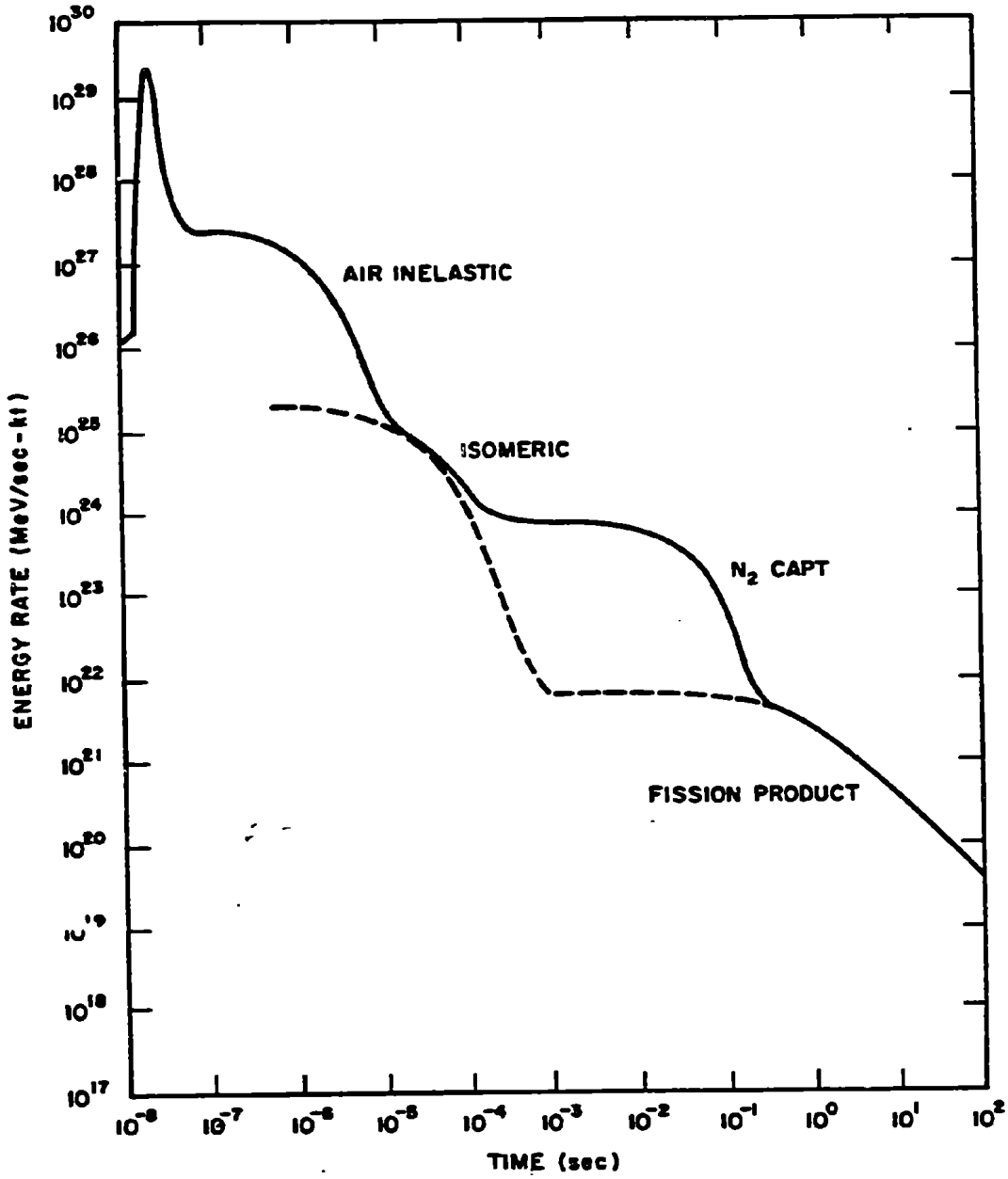

Figure 5-8. [redacted] Calculated Time Dependence of the Gamma Ray Output from a Large Yield Explosion, Normalized to 1 kt [redacted]

[redacted]

[redacted]

However, results of calculations and experiments indicate that the peak gamma energy output rate is more likely to lie between 5×10^{29} MeV/sec/kt and 1×10^{31} MeV/sec/kt. As mentioned previously, the peak gamma energy output rate depends on yield and on weapon design. The yield dependence shows a rough correlation as follows

$$\Phi_{\gamma P} = (W)^{-0.29} \times 10^{31} \text{ MeV/sec/kt},$$

at least between about 2 kt and 10 Mt. However, this does not account for the variation with weapon design, which might introduce differences on the order of plus or minus a factor of 3. Therefore, rather than use the yield dependent expression given above, it is recommended that the upper and lower limits given above be used for defensive and offensive estimates of the peak gamma energy output rate, respectively. Since no interactions take place in a vacuum, the peak prompt gamma exposure for exoatmospheric conditions should lie between

$$\Phi_{\gamma P} = \frac{10^{31} W}{4\pi R^2} \text{ MeV/cm}^2\text{/sec, and}$$

$$\Phi_{\gamma P} = \frac{3 \times 10^{30} W}{4\pi R^2} \text{ MeV/cm}^2\text{/sec},$$

where W is the yield in kilotons, and R is the slant range in centimeters. These expressions are equivalent to

$$\Phi_{\gamma P} = \frac{8.57 \times 10^{20} W}{R_f^2} \text{ MeV/cm}^2\text{/sec, and}$$

$$\Phi_{\gamma P} = \frac{4.28 \times 10^{19} W}{R_f^2} \text{ MeV/cm}^2\text{/sec},$$

where R_f is the slant range in kilofeet.

[redacted] Gamma rays interact with matter in three ways. The first is called the Compton effect. In this type of interaction, a gamma ray (primary photon) collides with an electron, and its energy is transferred to the electron. A secondary photon, with less energy, is created and departs in a direction at an angle to the direction of motion of the primary photon. The second type of interaction of gamma rays with matter is the photoelectric effect. A gamma ray with energy somewhat greater than the binding energy of an electron in an atom, transfers all its energy to the electron, which is consequently ejected from the atom. Since the photon involved in the photoelectric effect transfers all of its energy, it ceases to exist and is said to be absorbed. The third type of interaction is pair production. When a gamma ray photon with energy in excess of 1.02 MeV passes near the nucleus of an atom, the photon may be converted into matter with the formation of a pair of electrons, equally but oppositely charged. The positive electron soon annihilates with a negative electron to form two photons, each having an energy of at least 0.51 MeV. In some cases, if the interaction takes place near the nucleus of a heavy atom, only one photon of about 1.02 MeV energy may be created. Figure 6-1, Chapter 6, illustrates the three processes qualitatively.

[redacted] Any photon (e.g., an X-ray or a gamma ray) can produce ionization in a material by these processes of creating secondary electrons that deposit their kinetic energy by ionizing the medium in which they are created. The relative importance or frequency with which each process occurs depends upon the photon energy and the characteristics of the material. The Compton process is the dominant ionization mechanism for most gamma rays of interest, particularly in electronic materials such as silicon, of which many solid-state devices are fabricated.

[redacted] The spectra of the prompt gamma rays are sensitive to weapon design and yield, just as

[redacted]

[redacted]

[redacted] the gamma energy output rate is. It is beyond the scope of this manual to provide spectral information concerning sufficient samples of weapons spectra to be of general use (some such samples are provided in "Status of Neutron and Gamma Output from Nuclear Weapons (U)," DASA 2567 (see bibliography)). Moreover, with the wide range of prompt gamma output energy rates provided above, precise spectral data would be of little use. However, most of the prompt gamma rays lie in the energy range between 0.2 and 2 MeV, and in this energy range the Compton fractional energy loss is relatively constant. As mentioned above, the Compton process is the dominant energy transfer process for most electronic materials of interest (atomic number less than 20). These facts lead to a simplification in the relations between the incident prompt gamma energy fluence or energy flux and the energy absorbed by the material.

[redacted] The unit of the absorbed energy, or dose, is the rad. One rad is the absorption of 100 ergs per gram of material being irradiated. Thus, the rad is independent of the type of radiation (e.g., gamma rays, neutrons, X-rays), but the material absorbing the radiation must be specified (e.g., rad (Si), rad (Ge), rad (tissue)). However, in view of the simplification mentioned above, in the case of *prompt gamma rays* and *materials with atomic numbers less than 20*, a simple conversion is possible, i.e.,

$$1 \text{ rad} = 2 \times 10^9 \text{ MeV/cm}^2, \text{ or}$$

$$1 \text{ rad/sec} = 2 \times 10^9 \text{ MeV/cm}^2\text{/sec}.$$

These are, of course, approximations. However, in view of the approximate nature of the prompt gamma energy flux that has been provided, and in view of the fact that effects of the prompt gamma dose rates on electronics given in Section VII of Chapter 9 and Section 4 of Chapter 14 are not provided for system design or for specific system vulnerability analyses but only as a general guide to vulnerability, the approximation is considered to be adequate.

[redacted] As an example of the use of the dose conversion, consider a system with essentially no shielding for gamma rays that is operating exoatmospherically and that is 2,000 feet from a 100 kt explosion. It is desired to determine the peak gamma dose rate to a silicon transistor within the system. From the equations given previously, the maximum peak gamma energy flux incident on the system is expected to be

$$\Phi_{\gamma p} = \frac{8.57 \times 10^{20} W}{R_f^2},$$

$$\Phi_{\gamma p} = \frac{(8.57 \times 10^{20})(100)}{(2)^2}$$

$$\approx 2 \times 10^{22} \text{ MeV/cm}^2\text{/sec},$$

and the minimum energy flux is expected to be

$$\Phi_{\gamma p} = \frac{4.28 \times 10^{19} W}{R_f^2},$$

$$\Phi_{\gamma p} = \frac{(4.28 \times 10^{19})(100)}{(2)^2}$$

$$\approx 1 \times 10^{21} \text{ MeV/cm}^2\text{/sec}.$$

Thus the peak dose rate is expected to lie between

$$\dot{D}_{\gamma p} = \frac{2 \times 10^{22}}{2 \times 10^9} = 10^{13} \text{ rads (Si)/sec, and}$$

$$\dot{D}_{\gamma p} = \frac{10^{21}}{2 \times 10^9} = 5 \times 10^{11} \text{ rads (Si)/sec.}$$

[redacted] In view of the lack of spectral data that has been provided, the prompt gamma ener-

[redacted]

[redacted]

[redacted]

gy flux for endoatmospheric can only be determined by use of an effective mass attenuation coefficient (see the discussion of neutron transport in paragraph 5-3). A reasonable effective mass attenuation coefficient for prompt gammas is about 2.8 x 10^{-2} cm^2/gm. Combining this with the exoatmospheric equations given previously, the direct peak prompt gamma ray energy flux may be *estimated* to lie between

$$\Phi_{\gamma p} = \frac{10^{31} W}{4\pi R^2} e^{-(2.8 \times 10^{-2})\rho R} \text{ MeV/cm}^2\text{/sec, and}$$

$$\Phi_{\gamma p} = \frac{5 \times 10^{29} W}{4\pi R^2} e^{-(2.8 \times 10^{-2})\rho R} \text{ MeV/cm}^2\text{/sec,}$$

where W is the yield in kt, ρ is the density in gm/cm^3, and R is the range in centimeters. As in the case for neutrons, the quantity ρR may be replaced by the mass integral $q(R)$. The mass integral may be determined from the equations given in paragraph 5-3 and the data tabulated in Table 5-2.

[redacted] The prompt gamma dose may be bounded by multiplying the minimum and maximum dose rates by 1 and 2 shakes, respectively.

5-6 Air-Ground Secondary Gamma Rays [redacted]

[redacted] Potentially important sources of secondary gamma rays result from the inelastic scattering of high-energy neutrons by the nuclei of the air and ground, and the capture of thermal neutrons by the nitrogen-14 in the air and by various elements in the ground. The relative importance of the inelastic and capture gamma rays depends strongly upon the neutron spectrum of the source.

[redacted] Most of these gamma rays are produced near the neutron source where the neutron fluence is highest. The short neutron flight time to the regions of most intense interaction, and the practically instantaneous character of the nuclear interaction accounts for the early ($10^{-7} < t < 10^{-5}$ sec) appearance of the secondary gamma components. The number of inelastic-scattering gamma rays relative to the total depends directly on the relative abundance of high-energy neutrons. The fraction of the total may be negligible in fission warheads or in large thermonuclear warheads. As the fusion yield fraction is increased the importance of the inelastic component will increase.

[redacted] Any determination of the intensity of inelastic-scattering gamma rays must rely primarily upon analysis because of the difficulty in distinguishing the source of the different gamma rays measured in field tests. The first step in the analysis is that of neutron transport calculations. The local source strength of inelastic gamma rays is an energy dependent response to the local fluence of neutrons. Once the source intensity resulting from neutron interactions in air and ground is known, a gamma ray transport calculation must be performed to obtain the intensity at points of interest.

[redacted] The energy spectrum of the gamma rays evolved in elastic scattering depends on the energy of the neutrons and the energy level structure of the nuclei with which the neutrons interact. However, the inelastic gamma rays are generally high in energy and, consequently, take on added significance when the target is behind a shield such as in a hardened military installation. Even though only a few percent of the gamma radiation incident on the shield results from inelastic scattering, it may be the source that is responsible for the maximum rate experienced by equipment inside the shielded installation since prompt gamma rays are attenuated more rapidly by shielding materials than the inelastic scattered gamma rays. Thus, where hardened installations are concerned, the inelastic gamma rays should be evaluated even in cases where they do not constitute a large fraction of the total free-field exposure. Methods for calculating the

[redacted]

[redacted]

[redacted]

[redacted]

tissue dose from secondary gamma rays are provided in the following subsection.

5-7 Fission Product Gamma Rays [redacted]

[redacted] Gamma rays produced by the decay of fission products following a fission detonation are an important source of radiation during the initial radiation time regime (the first minute following the explosion). The intensity of fission product gamma rays reaching a location of interest is affected by the complex source and media dynamics consisting of the formation and evolution of the fireball, the cloud expansion and rise, and the decay of the fission products with time. The fission products disperse throughout the cloud with the passage of time and the shape of the cloud may vary from spherical to toroidal as the materials forming the cloud rise through the atmosphere.

[redacted] The formation of the fireball and the expansion and rise of the cloud depends upon weapon yield, weapon design, atmospheric conditions, and other parameters. The distribution of fission products in the cloud as a function of time is not well known, and, consequently, the attenuation of fission-product gamma rays within the cloud can only be approximated.

[redacted] Atmospheric perturbation caused by the passage of the shock front also has a pronounced effect on the transport of fission-product gamma rays. The distribution of energy from a low altitude conventional fission weapon is such that roughly 50 percent of the energy is released in the form of blast and shock. The actual percentage depends on the weapon design and yield and on the nature of the surrounding environment (see Section I, Chapter 2). The percentage decreases for neutron enhanced weapons.

[redacted] The sudden release of energy in the form of blast and shock produces an immediate increase in temperature and pressure thus producing hot, compressed gases from the weapon material. A pressure wave is initiated in the surrounding medium (paragraphs 1-4 through 1-6, 1-8, and Section I, Chapter 2). The characteristics of a shock wave is that there is a sudden increase of pressure at the front with a gradual decrease behind it. A severe change in the density of the heated air behind the shock front is associated with the pressure change. The large reduction in the air density, or optical depth, between the rising source and the receiver produces an enhancement of gamma ray intensities from hydrodynamic effects that is known as "hydrodynamic enhancement." These effects may last for several minutes and may extend to large distances from the explosion. The intensity and duration of hydrodynamic effects are yield dependent.

[redacted] At early times when the shock front is located between the cloud and the receiver, the gamma ray intensity may increase because of the geometric displacement of the air. After the blast wave has passed the receiver, the gamma ray intensity is enhanced as a result of the reduced air density. This hydrodynamic enhancement becomes increasingly more important with higher weapon yields. For high yield weapons (in the megaton range), hydrodynamic enhancement can increase the fission-product gamma ray intensity by several orders of magnitude, with the result that fission product gamma rays can become the most important of all initial radiation sources.

[redacted] With minimal hydrodynamic enhancement, as in the case of very low-yield weapons, the intensity of fission product gamma rays reaching a given point may be of approximately the same magnitude as that resulting from the secondary gamma ray sources. However, the average energy of the fission product gamma rays is considerably less than that of the secondary gamma rays, and the angle distribution of the fission product gamma rays is diffused by

[redacted]

[redacted]

the rise of the cloud. Each of these factors tends to reduce the penetrating power of fission product gamma rays relative to secondary gamma rays.

A reasonably accurate calculation of the transport of fission product gamma rays must consider such time-dependent parameters as cloud rise, source decay, and hydrodynamic enhancement. The curves presented in the following subsection that show tissue dose from fission product gamma rays were constructed by the use of such a model.*

INITIAL RADIATION DOSE TO PERSONNEL

The preceding paragraphs have described the complexity of the calculations of the source and environments produced by the initial nuclear radiations. Simplified, but reasonably accurate, methods have been developed to predict the dose to personnel located on or near the surface of the earth. These methods are described in the succeeding paragraphs and figures, and illustrations of their use are provided in four problems.†

Various units have been used to describe the radiation dose to personnel. One of the earliest, originally used to describe X-ray environments, is the roentgen, which is defined in terms of ionization produced in air. In view of the long history of the roentgen, various attempts have been made to develop units that described the response of living creatures or physical objects in terms of "roentgen equivalent" units. None of these was completely satisfactory since they depended strongly on the type and energy of the radiation, and their relationship to an exposure measured in roentgens was not always descriptive of the response of the target. Since the response of a target to radiation generally can be related to the energy absorbed, the rad has come into general use for the description of dose to any target. As previously defined in paragraph 5-5, one rad is the absorption of 100 ergs per gram of material being irradiated. Thus, the rad is independent of the type of radiation, but the material absorbing the radiation must be specified. The curves provided in this subsection provide a methodology for determining the dose in rads (tissue) for the various components of the initial nuclear radiation. The response of personnel, as a function of absorbed dose, is given in Section III of Chapter 10.

In view of the strong dependence of the neutron and secondary gamma ray environments on weapon design, no one representative weapon could be chosen to provide a basis for calculating dose to humans. The fission product dose is relatively independent of design specifics, but it is strongly dependent on total yield and the ratio of fission yield to total yield. Consequently, eight different weapons, for which case output data were available, were selected to perform the basic calculations from which the curves presented below were developed. It is believed that these eight weapons provide a sufficiently wide spectrum of designs that one of the eight will represent a given weapon of interest in a reasonable manner. The eight weapons are described in Table 5-3.

5-8 Initial Neutron Dose

Figures 5-9 through 5-11 provide all of the information necessary to calculate the contribution of neutrons to the initial nuclear radiation dose from each of the weapon types listed

* The development of this model is explained in "Improved Models for Predicting Nuclear Weapon Initial Radiation Environments (U)," DASA 2615 (see bibliography).

† ATR, which stands for Atmospheric Radiation Transport library, may be used to obtain exact answers to problems involving radiation transport in the atmosphere without the necessity of making specific transport calculations. ATR is documented in DNA 28031, "Models of Radiation Transport in Air – the ATR Code" (see bibliography). The Code itself may be obtained from the Radiation Shielding Information Center (RSIC), Oak Ridge, Tennessee.

[redacted]

Table 5-3. [redacted] Representative Types of Nuclear Weapons [redacted]

Type	Description	Representative Yield Range
I	Subkiloton Fission	[redacted]
II	Pure Fission Implosion	
III	Large (physically) Boosted Fission	
IV	Small (physically) Boosted Fission	
V	Enhanced Neutron Weapon	
VI	Gun-Assembly Fission Weapon	
VII	Thermonuclear Weapon	
VIII	Thermonuclear Weapon	

DNA (b)(3)

[redacted]

in Table 5-3. Problem 5-1 describes the use of these figures to obtain the neutron dose.

5-9 Air-Ground Secondary Gamma Ray Dose [redacted]

[redacted] Figures 5-11 through 5-13 provide all of the information necessary to calculate the contribution of air-ground secondary gamma rays to the initial nuclear radiation dose from each of the weapon types listed in Table 5-3. Problem 5-2 describes the use of these figures to obtain the air-ground secondary gamma ray dose.

5-10 Fission Product Gamma Ray Dose [redacted]

[redacted] Figures 5-14 through 5-17 provide all of the information necessary to calculate the contribution of fission product gamma rays to the initial nuclear radiation dose. Problem 5-3 describes the procedures for obtaining the fission product dose from these figures. Note the caution given in Problem 5-3 concerning interpolation between the hydrodynamic enhancement curves.

5-11 Total Dose [redacted]

[redacted] The total initial radiation dose is simply the sum of the contributions of the neutrons, the secondary gamma rays, and the fission product gamma rays. Problem 5-4 illustrates the calculation of total initial radiation dose.

[redacted]

[redacted]

Problem 5-1. Calculation of Neutron Radiation Dose

[redacted] The spectrum and intensity of neutron radiation depends strongly upon the details of design of a nuclear weapon; however, it is possible to obtain neutron dose to personnel from a weapon of interest with reasonable accuracy if it is "similar" to one for which detailed calculations have been made. Eight "representative" types of weapons, listed in Table 5-3, provide the basis for such calculations within the following constraints:

- The weapon of interest must be similar to one of the representative types,
- The range of interest must lie between 400 and 5,000 yards,
- The detonation takes place in the "lower atmosphere," and
- The target is located on or near the surface of the earth.

[redacted] Within the constraints listed above, Figures 5-9 through 5-11 provide the information necessary to obtain the dose to personnel located on or near the surface of the earth. If the air density is $\rho_o = 1.225 \times 10^{-3}$ gm/cm^3, the neutron dose is

$$D_N = \frac{W F_N H_1}{R^2}$$

where

D_N	is the total neutron dose (rads (tissue)),
R	is the slant range (yards)
F_N	is the value taken from Figure 5-9a or b or from Figure 5-10a or b for the most representative weapon type (yards^2 rads/kt).
W	is the weapon yield (kt), and
H_1	is the detonation height correction factor from Figure 5-11 (dimensionless).

[redacted] If the air density differs from ρ_o, Figures 5-9 or 5-10 are entered with a scaled range R_ρ which is given by

$$R_\rho = \frac{\rho}{\rho_o} R = \bar{\rho} R,$$

where $\bar{\rho}$ is the relative air density. Values of ρ/ρ_o are given in Table 5-2, and with smaller altitude increments in Table 2-1, Chapter 2. If the values of ρ/ρ_o are different at the burst and the receiver, the average value should be used for $\bar{\rho}$. Note that R, not R_ρ, is still used in the denominator of the equation given above for D_N.

[redacted] *Example 1* [redacted]:

Given: A 30 kt surface burst of a weapon similar to type IV in air of average relative density $\bar{\rho} = 1.0$.

Find: The neutron dose delivered to a surface target 1,500 yards from the burst.

Solution: From Figure 5-9a, $F_N = 8.5 \times 10^6$ yards^2 rad (tissue)/kt for a type IV weapon at 1,500 yards.

Answer: The neutron dose delivered to a surface target 1,500 yards from a 30 kt surface burst of a type IV weapon is:

$$D_N = \frac{(30)(8.5 \times 10^6)(1.0)}{(1{,}500)^2},$$

$$D_N = 113 \text{ rads (tissue)},$$

[redacted] *Example 2* [redacted]

Given: A 500 kt burst at a [illegible]ht of 100 yards of a weapon similar to type [illegible] in air of average relative density $\bar{\rho} = 0.9$.

Find: The neutron dose delivered to a target near the surface 2,000 yards from the burst.

[redacted]

[redacted]

[redacted]

Solution: The scaled range R_ρ = (0.9)(2,000) = 1,800 yards. From Figure 5-10a, $F_N = 1.6 \times 10^6$ yards^2 rads (tissue)/kt for a type VII weapon at 1,800 yards. From Figure 5-11, $H_1 = 2.07$ for type VII at 100 yards *HOB*.

Answer: The neutron dose delivered to a target near the surface 2,000 yards from a type VII weapon at 100 yards *HOB* is:

$$D_N = \frac{(500)(1.6 \times 10^6)(2.07)}{(2{,}000)^2}$$

$$D_N = 414 \text{ rads (tissue)}.$$

[redacted] *Reliability.* For weapons closely similar to one of the eight representative types, the predicted neutron dose is estimated to be correct within ±25 percent.

[redacted] *Related Material.* See paragraphs 5-1 through 5-3. See also Tables 5-2 and 5-3.

[redacted]

[redacted]

Problem 5-2. Calculation of Secondary Gamma Ray Dose

[redacted] Secondary gamma rays are those that result from neutron interactions, primarily with nitrogen in the air, as described in paragraph 5-6. Since the neutron output is strongly dependent upon details of weapon design, the secondary gamma ray output also depends upon weapon design; however, it is possible to obtain the secondary gamma ray dose to personnel from a weapon of interest if it is "similar" to one for which detailed calculations have been made. Eight "representative" types of weapons, listed in Table 5-3, provide the basis for such calculations within the following constraints:

- The weapon of interest must be similar to one of the representative types,
- The range of interest must lie between 400 and 5,000 yards,
- The detonation takes place in the "lower atmosphere," and
- The target is located on or near the surface of the earth.

[redacted] Within the constraints listed above, Figures 5-11 through 5-13 provide the information necessary to obtain the secondary gamma dose to personnel located on or near the surface of the earth. If the air density is $\rho_o = 1.225 \times 10^{-3}$ gm/cm^3, the secondary gamma dose is

$$D_{\gamma s} = \frac{W\ F_{\gamma s}\ H_1}{R^2}$$

where

$D_{\gamma s}$ is the secondary gamma ray dose (rads (tissue)),

R is the slant range (yards),

$F_{\gamma s}$ is the value taken from Figure 5-12a or b or from Figure 5-13a or b for the most representative weapon type (yards^2 rads/kt),

W is the weapon yield (kt), and

H_1 is the detonation height correction factor from Figure 5-11 (dimensionless).

[redacted] If the air density differs from ρ_o, Figures 5-12 or 5-13 are entered with a scaled range R_ρ.

$$R_\rho = \frac{\rho}{\rho_o} R = \bar{\rho} R,$$

where $\bar{\rho}$ is the relative air density. Values of ρ/ρ_o are given in Table 5-2, and with smaller altitude increments in Table 2-1, Chapter 2. If the values of ρ/ρ_o are different at the burst and the receiver, the average value should be used for $\bar{\rho}$. Note that R, not R_ρ, *is still used in the denominator of the equation given above for* $D_{\gamma s}$.

[redacted] *Example 1* [redacted]

Given: A 15 kt explosion at a height of 150 yards of a weapon similar to weapon type VI, in air of average relative density $\bar{\rho} = 1.0$.

Find: The secondary gamma ray dose delivered to personnel on the surface 1,500 yards from the burst.

Solution: From Figure 5-13a, $F_{\gamma s} = 3.7 \times 10^6$ yards^2 rads (tissue)/kt for a type VI weapon at 1,500 yards. From Figure 5-11, $H_1 = 2.03$ for a type VI weapon burst at 150 yards.

Answer: The secondary gamma ray dose delivered to a surface target 1,500 yards from a 15 kt burst of weapon type VI at 150 yards *HOB* is:

$$D_{\gamma s} = \frac{(15)(3.7 \times 10^6)(2.03)}{(1{,}500)^2}$$

$$D_{\gamma s} = 50 \text{ rads (tissue)}$$

[redacted] *Example 2* [redacted]

Given: A 0.08 kt burst at a height of 20

[redacted]

[redacted]

[redacted] yards of a weapon similar to type I in average air density of $\bar{\rho} = 0.9$.

Find: The secondary gamma ray dose delivered to personnel on the surface 500 yards from the burst.

Solution: From Figure 5-12a, $F_{\gamma s} = 1.6 \times 10^8$ yards^2 rads/kt for a type I weapon at 500 yards. From Figure 5-11, $H_1 = 1.52$ for a type I weapon burst at 20 yards.

Answer: The secondary gamma ray dose delivered to a target near the surface 500 yards from a 0.08 kt burst of a type I weapon at 20 yards *HOB* is

$$D_{\gamma s} = \frac{(0.08)(1.6 \times 10^8)(1.52)}{(500)^2}$$

$$D_{\gamma s} = 78 \text{ rads (tissue).}$$

[redacted] *Reliability.* For weapons closely similar to one of the eight representative types, the predicted secondary gamma ray dose is estimated to be correct to within ±25 percent for slant ranges up to 1,500 yards. At longer ranges, the predicted values might be high although a precise estimate cannot be made.

[redacted] *Related Material.* See paragraph 5-6. See also Tables 5-2 and 5-3.

[redacted]

[redacted]

Problem 5-3. Calculation of Fission Product Gamma Ray Dose

[redacted] Figures 5-14 through 5-17 provide the information necessary to calculate the fission product contribution to the initial nuclear radiation dose to personnel on or near the surface of the earth. Figures 5-14a through c provide the nominal dose per kt fission yield as a function of slant range for several relative air densities. The gamma dose as a function of slant range depends on cloud rise, which depends on weapon yield. The effects of cloud rise on exposure for a given yield depends on the burst height, and, to a slight extent, on the ambient air density. Analysis of the interdependence of these parameters has shown that reasonable accuracy can be retained by the use of two independent burst height adjustment factors, one associated with slant range, as shown in Figure 5-15, and the other associated with weapon yield, as shown in Figure 5-16. Figures 5-17a through e show hydrodynamic enhancement factors as a function of slant range for selected yields and several air densities. In using Figures 5-17a through e, no attempt should be made to perform a visual interpolation of the hydrodynamic enhancement factor between yields that are shown. Rather, a plot of the hydrodynamic enhancement factor as a function of yield should be made at the slant range and relative air density of interest, and the hydrodynamic enhancement factor should be obtained from this plot for the desired yield.

[redacted] The tissue dose from fission product gamma rays is obtained as follows:

$$D_{\gamma f} = W_f F_{\gamma f} H_R H_W E$$

where

$D_{\gamma f}$ is the fission product gamma ray dose at slant range R (rads (tissue)),

W_f is the fission yield (kt),

$F_{\gamma f}$ is the value taken from Figures 5-14a through c (rads (tissue)/kt),

H_R is the range dependent burst height adjustment factor from Figure 5-15 (dimensionless),

H_W is the yield dependent burst height adjustment factor from Figure 5-16 (dimensionless), and

E is the hydrodynamic enhancement factor from Figures 5-17a through e (dimensionless).

[redacted] Note that *fission* yield is used in the equation given above for fission product gamma ray dose; however, *total* yield is used to enter Figure 5-16 and Figures 5-17a through e.

[redacted] *Example 1* [redacted]

Given: A 50 kt pure fission weapon burst at a height of 100 yards in air of relative air density $\bar{\rho} = 0.8$.

Find: The fission product gamma ray dose to personnel on the ground at a slant range of 2,000 yards from the burst.

Solution: From Figure 5-14a, $F_{\gamma f} = 1.5$ rads (tissue)/kt for $\bar{\rho} = 0.8$ at 2,000 yards. From Figure 5-15, $H_R = 0.94$ for a height of burst of 100 yards and a slant range of 2,000 yards. From Figure 5-16, $H_W = 0.71$ for 50 kt total yield at a height of burst of 100 yards. From Figure 5-17d ($\bar{\rho} = 0.8$), $E = 6$ for a 50 kt total yield at 2,000 yards.

Answer:

$$D_{\gamma f} = (50)(1.5)(0.94)(0.71)(6),$$

$$D_{\gamma f} = 300 \text{ rads (tissue)}.$$

[redacted] *Example 2* [redacted]

Given: A 200 kt, 1:1 fission/fusion ratio

[redacted]

[redacted]

(i.e., 1/2 fission, 1/2 fusion) surface burst in air of average relative density $\bar{\rho} = 1.1$.

Find: The fission product gamma ray dose delivered to a target near the ground 1,000 yards from the burst.

Solution: The fission yield $W_f = (1/2)(200) = 100$ kt for a 1:1 fission/fusion ratio. From Figure 5-14a, $F_{\gamma f} = 17$ rads (tissue)/kt for $\bar{\rho} = 1.1$ at 1,000 yards. From Figure 5-15, $H_R = 0.94$ for a surface burst at 1,000 yards range. From Figure 5-16, $H_W = 0.63$ for a surface burst at 200 kt total yield. From Figure 5-17a, $E \simeq 24$ for 200 kt total yield at 1,000 yards (the best interpolation scheme for this figure is to make a plot on linear paper of E vs W at a constant R, and draw a smooth curve through the points).

Answer: The fission product gamma ray dose delivered to a target near the ground 1,000 yards from a 200 kt (1:1 fission/fusion) surface burst in air of average relative density 1.1 is:

$$D_{\gamma f} = (100)(17)(0.94)(0.63)(24)$$

$$D_{\gamma f} = 2.4 \times 10^4 \text{ rads (tissue).}$$

[redacted] *Reliability.* For submegaton yields the radiation dose predicted by equation 5.4 will be within 15 percent of the values calculated by the most sophisticated methods. The variations may approach 40 percent for megaton yields at ranges less than 1,000 yards; however, these are generally not interesting combinations. The total gamma ray dose predicted by the methods illustrated in Problems 5-2 and 5-3 when added together generally agrees with weapons test data within 50 percent and seldom disagrees by more than a factor of 2.

[redacted] *Related Material.* See paragraph 5-7. See also Table 5-2.

[redacted]

[redacted]

Problem 5-4. Calculation of Total Initial Radiation Dose

[redacted] The total initial radiation dose may be determined by calculating the neutron dose, the secondary gamma ray dose, and the fission product gamma ray dose separately, as described in Problems 5-1, 5-2, and 5-3 and summing the individual results.

[redacted] *Example* [redacted]

Given: A 10 Mt burst, 2:3 fission/fusion ratio (i.e., 2/5 fission, 3/5 fusion), of a weapon similar to type VIII at a height of 2,000 yards in air of average relative density $\bar{\rho} = 0.8$.

Find: The total radiation dose delivered to a target near the surface at a slant range of 4,000 yards from the burst.

Solution: For the neutron dose, the scaled range is $R_\rho = (0.8)(4{,}000) = 3{,}200$ yards. From Figure 5-10b, $F_N = 5 \times 10^3$ yards^2 rads (tissue)/kt for type VIII at 3,200 yards. From Figure 5-11, $H_1 = 2.16$ for type VIII over 200 yards *HOB*. For the secondary gamma ray dose, the same scaled range and height correction factors apply. From Figure 5-13b, $F_{\gamma s} = 5 \times 10^4$ yards^2 rads (tissue)/kt for type VIII at 3,200 yards. For the fission product gamma ray dose, the fission yield is $W_f = (2/5)(10{,}000) = 4{,}000$ kt for a 2:3 fission/fusion ratio. From Figure 5-14b, $F_{\gamma f} = 1.3 \times 10^{-3}$ rads (tissue)/kt for $\bar{\rho} = 0.8$ at 4,000 yards. From Figure 5-15, $H_R = 0.62$ for a 2,000 yard *HOB* and a slant range of 4,000 yards. From Figure 5-16, $H_W = 0.24$ for a 2,000 yard *HOB* and a total yield of 10 Mt. From Figure 5-17d, $E = 4.1 \times 10^3$ for 10-Mt total yield at 4,000 yards.

Answer:

$$D_N = \frac{WF_N H_1}{R^2}$$

$$D_N = \frac{(10{,}000)(5 \times 10^3)(2.16)}{(4{,}000)^2}$$

$$D_N = 6.8 \text{ rads (tissue)}$$

$$D_{\gamma s} = \frac{WF_{\gamma s} H_1}{R^2}$$

$$D_{\gamma s} = \frac{(10{,}000)(5 \times 10^4)(2.16)}{(4{,}000)^2}$$

$$D_{\gamma s} = 68 \text{ rads (tissue)}$$

$$D_{\gamma f} = W_f F_{\gamma f} H_R H_W E$$

$$D_{\gamma f} = (4{,}000)(1.3 \times 10^{-3})(0.62)(0.24)(4.1 \times 10^3)$$

$$D_{\gamma f} = 3{,}170 \text{ rads (tissue)}$$

$$\text{Total Dose} = D_N + D_{\gamma s} + D_{\gamma p}$$

$$\text{Total Dose} = 6.8 + 68 + 3{,}170 = 3{,}245 \text{ rads (tissue).}$$

[redacted] *Reliability.* See problems 5-1, 5-2, and 5-3 for reliability statements for the individual components of the total dose. There are no corroborating data; however, it is estimated that the total dose prediction would fall within ±25 percent of the true value, except for megaton yield weapons at slant ranges less than 1,000 yards, where the error is likely to be ±50 percent.

[redacted] *Related Material.* See paragraphs 5-5 through 5-7. See also Tables 5-2 and 5-3.

[redacted]

[redacted]

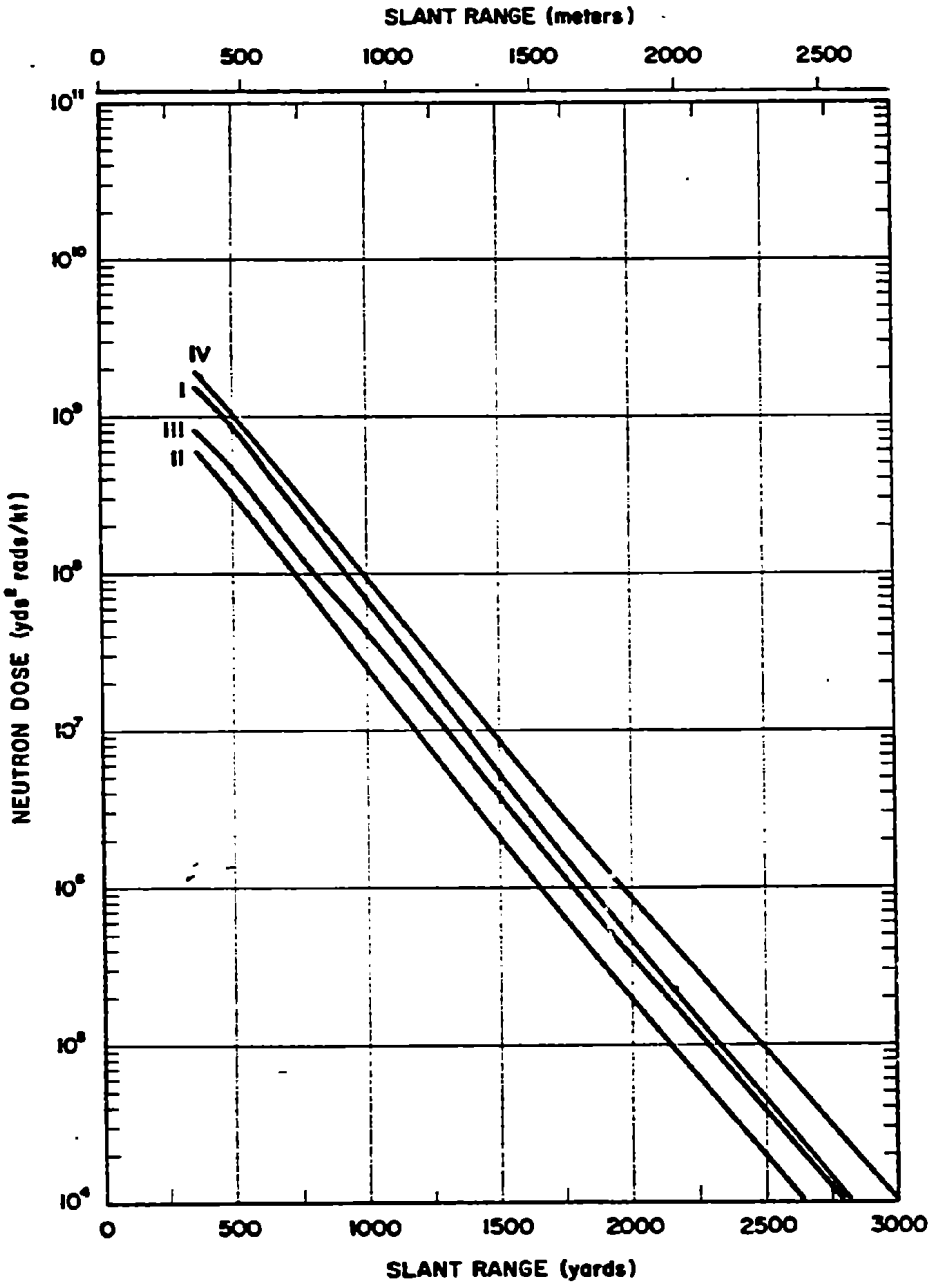

Figure 5-9a. [redacted] Neutron Dose as a Function of Slant Range from a 1 kt Surface Burst, Weapon Types I through IV, Short Ranges [redacted]

[redacted]

[redacted]

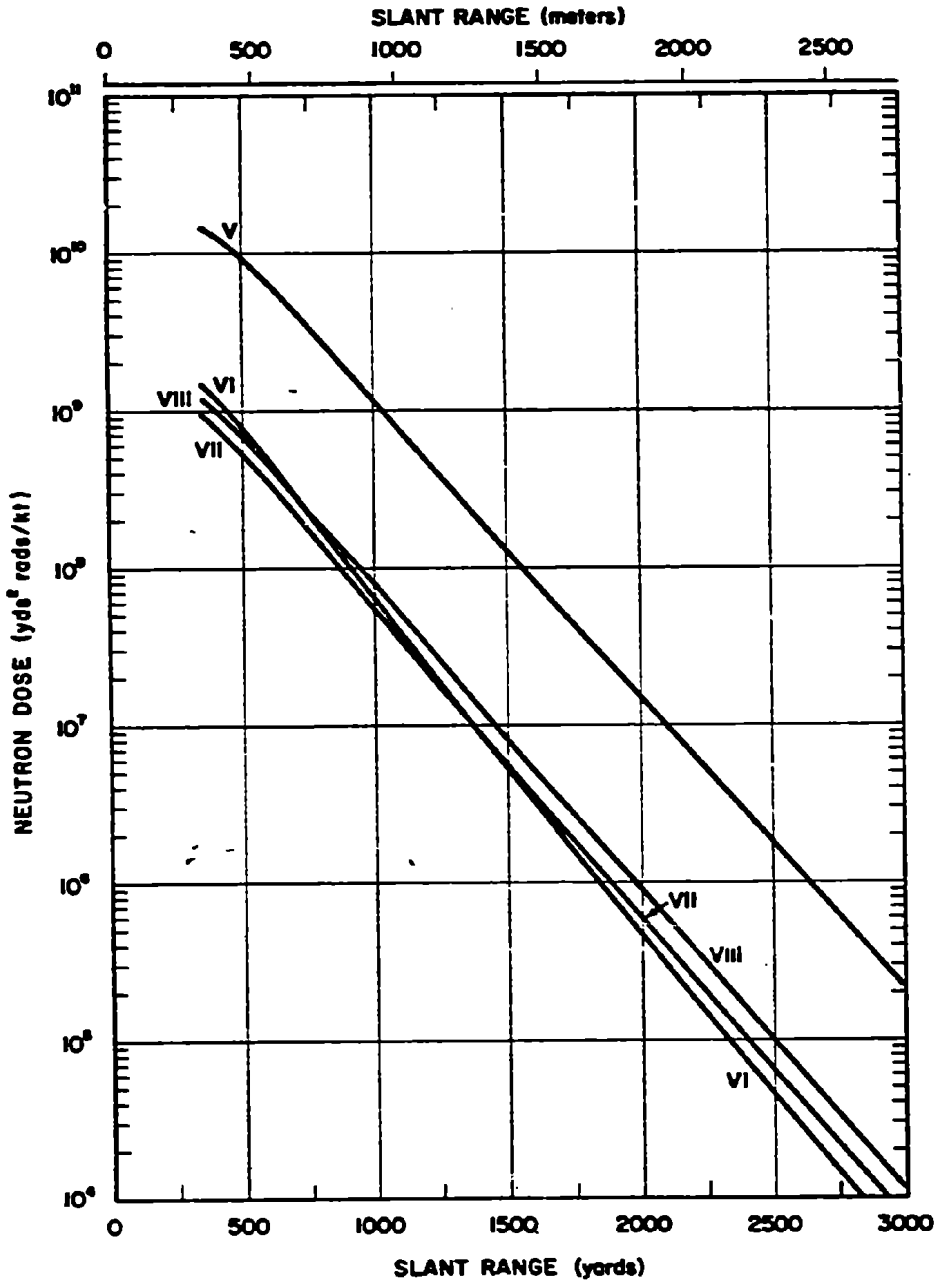

Figure 5-10a. [redacted] Neutron Dose as a Function of Slant Range from a 1 kt Surface Burst, Weapon Types V through VIII, Short Ranges [redacted]

[redacted]

[redacted]

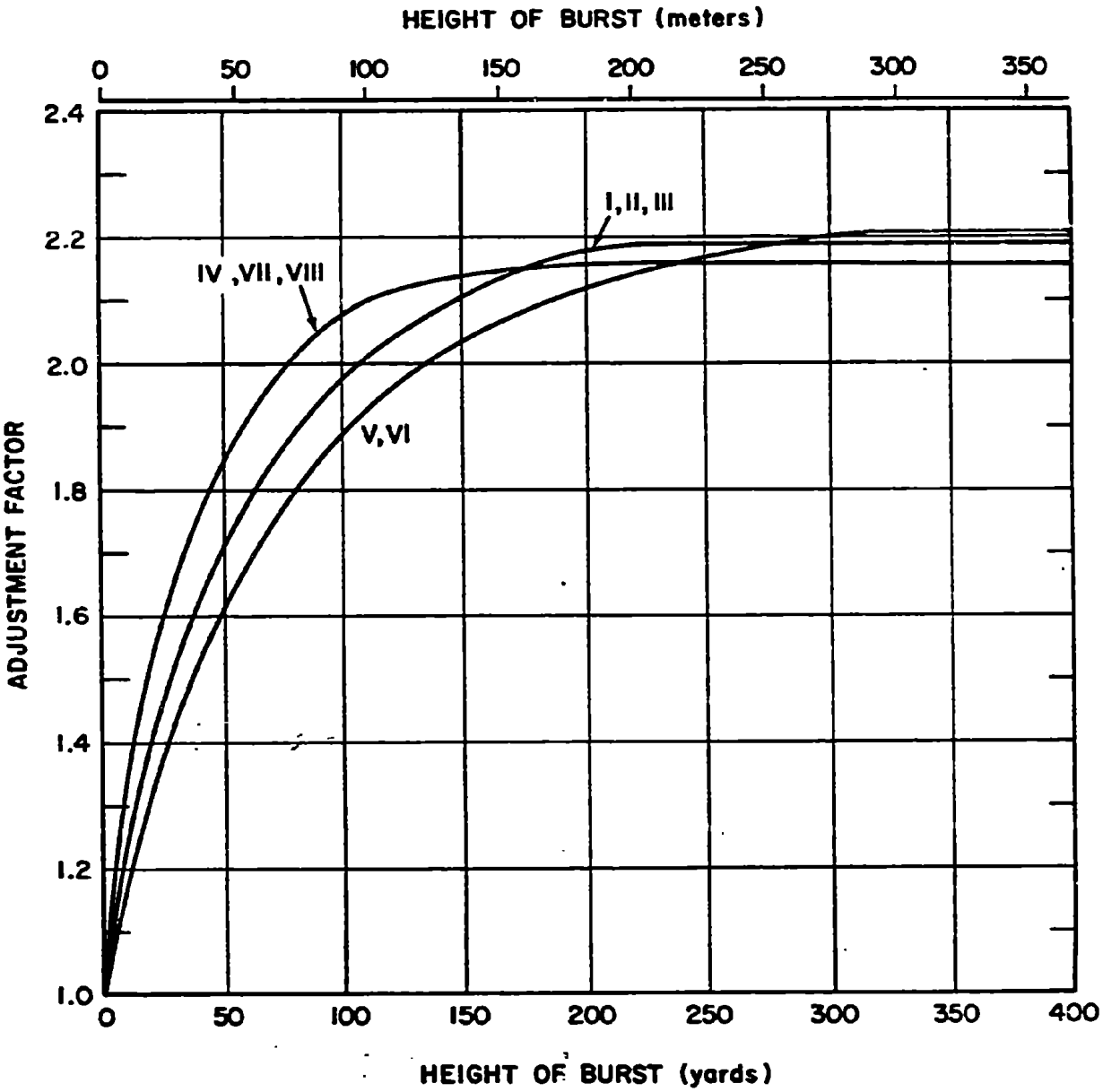

Figure 5-11. [redacted] Burst Height Adjustment Factors for Neutrons and Secondary Gamma Rays [redacted]

[redacted]

[redacted]

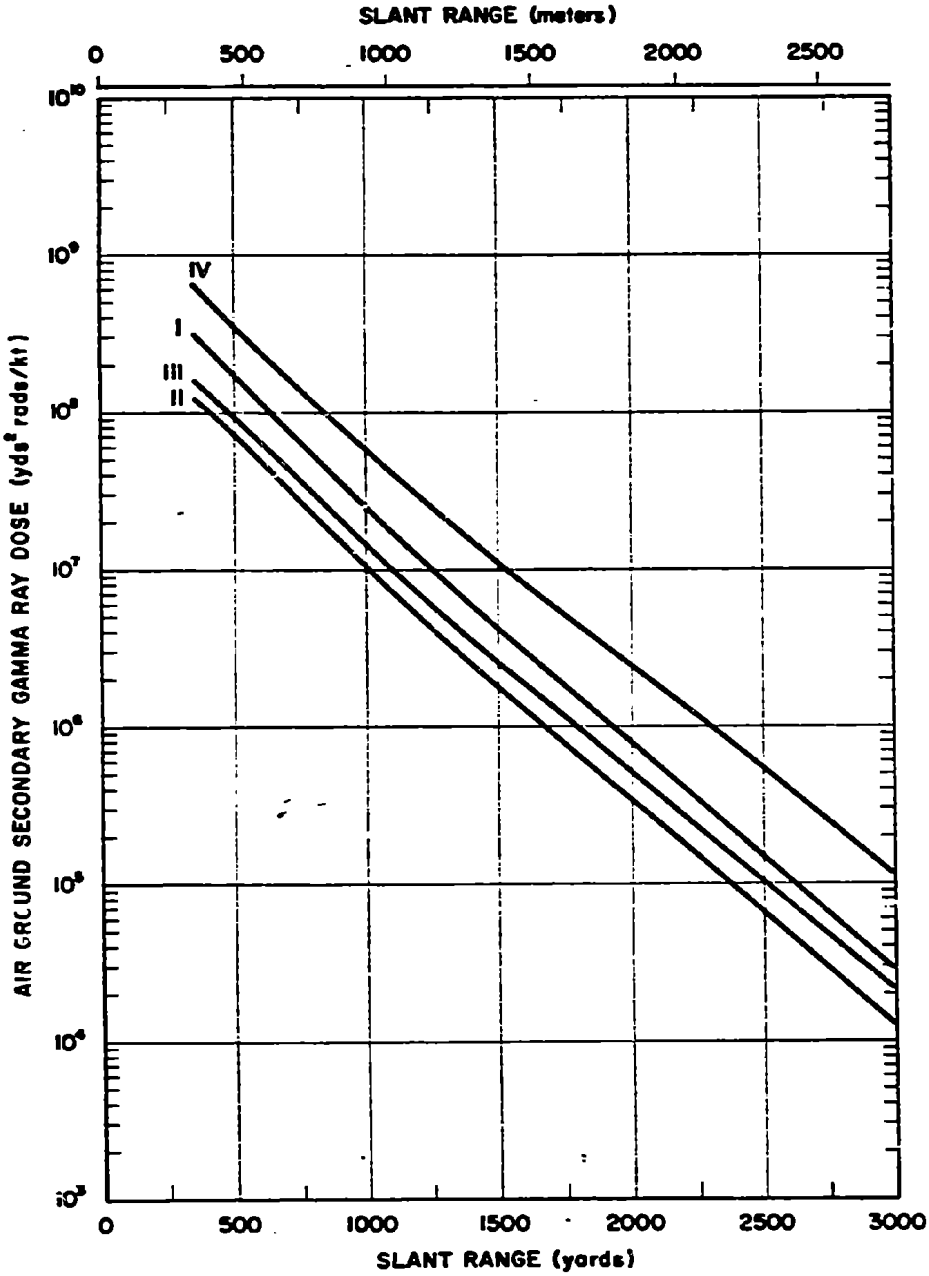

Figure 5-12a. [redacted] Secondary Gamma Ray Dose as a Function of Slant Range from a 1 kt Surface Burst, Weapon Types I through IV, Short Ranges [redacted]

[redacted]

[redacted]

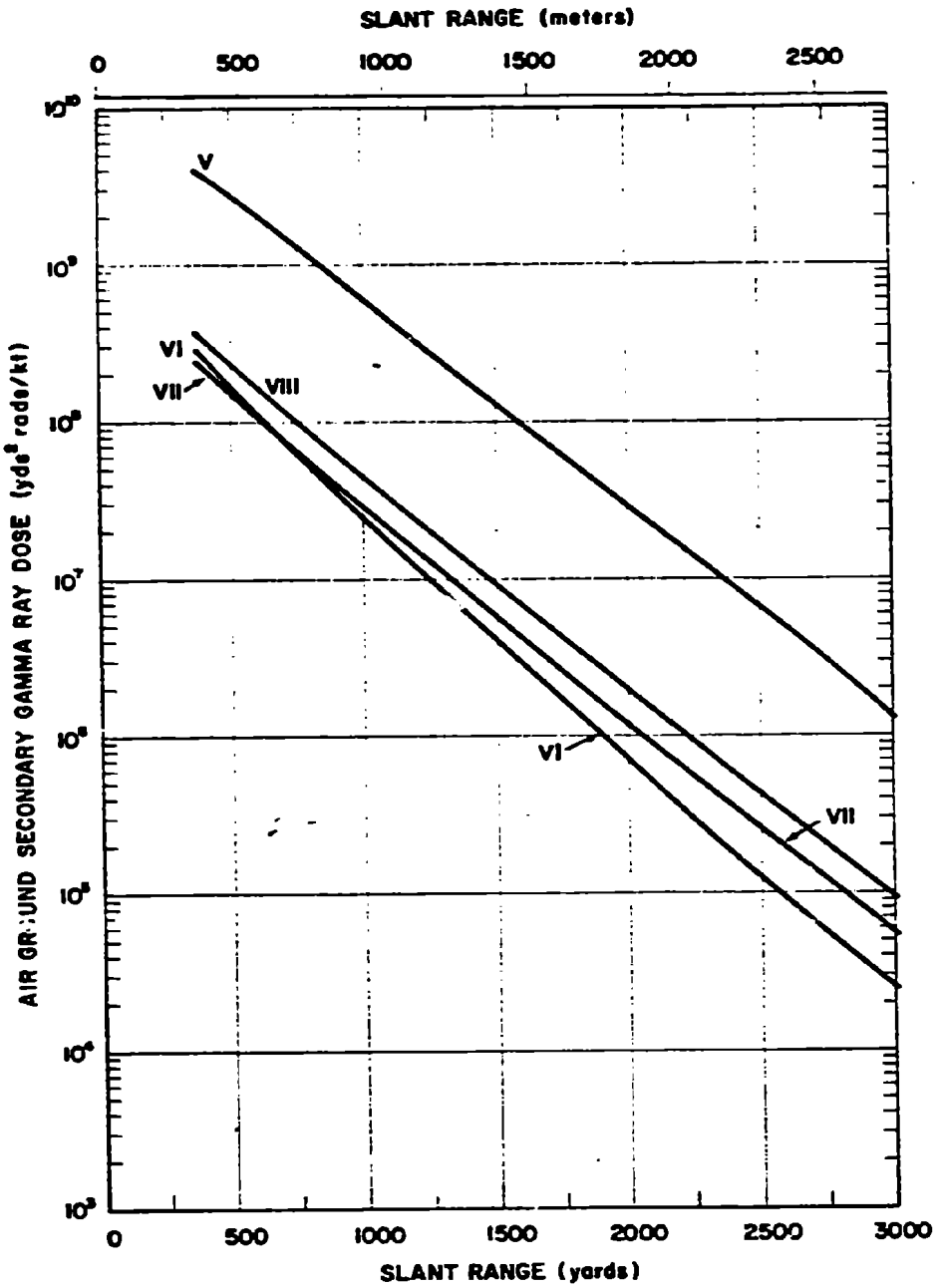

Figure 5-13a. [redacted] Secondary Gamma Ray Dose as a Function of Slant Range from a 1 kt Surface Burst, Weapon Types V through VIII, Short Ranges [redacted]

[redacted]

[redacted]

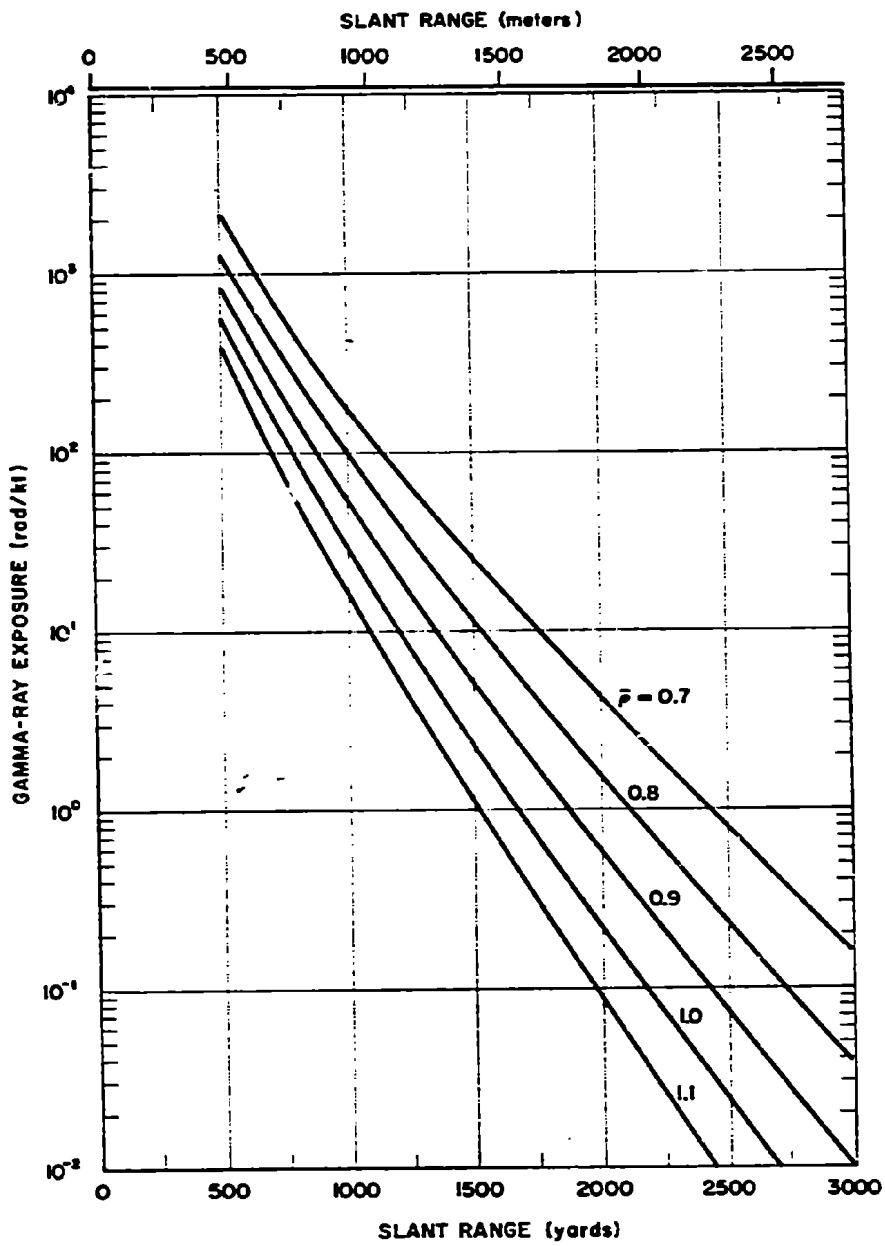

Figure 5-14a. [redacted] Fission Product Gamma Ray Dose as a Function of Slant Range from a 1 kt (Fission Yield) Surface Burst, Short Ranges [redacted]

[redacted]

[redacted]

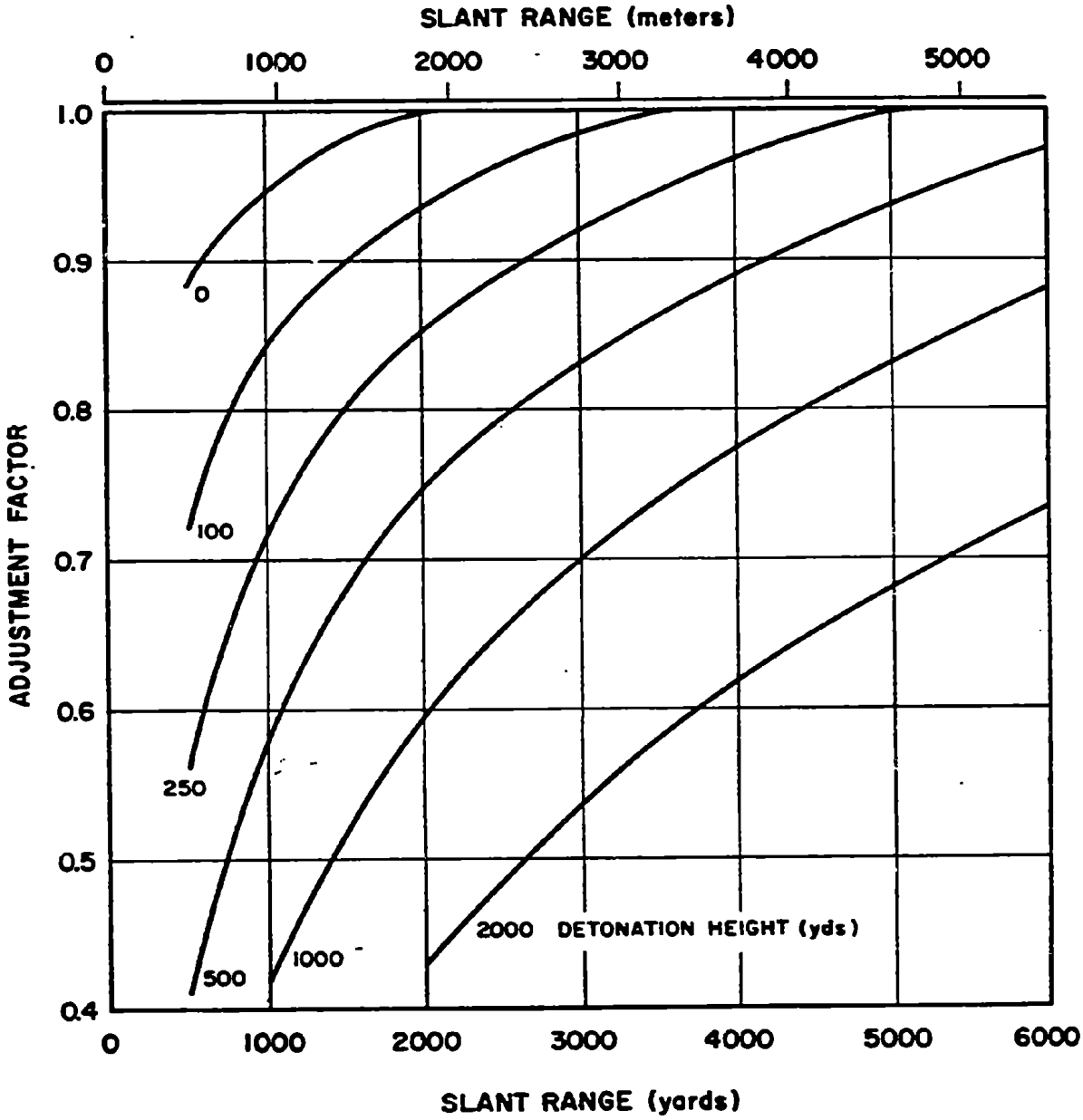

Figure 5-15. [redacted] Range Dependent Burst Height Adjustment Factors for Fission Product Gamma Rays [redacted]

[redacted]

[redacted]

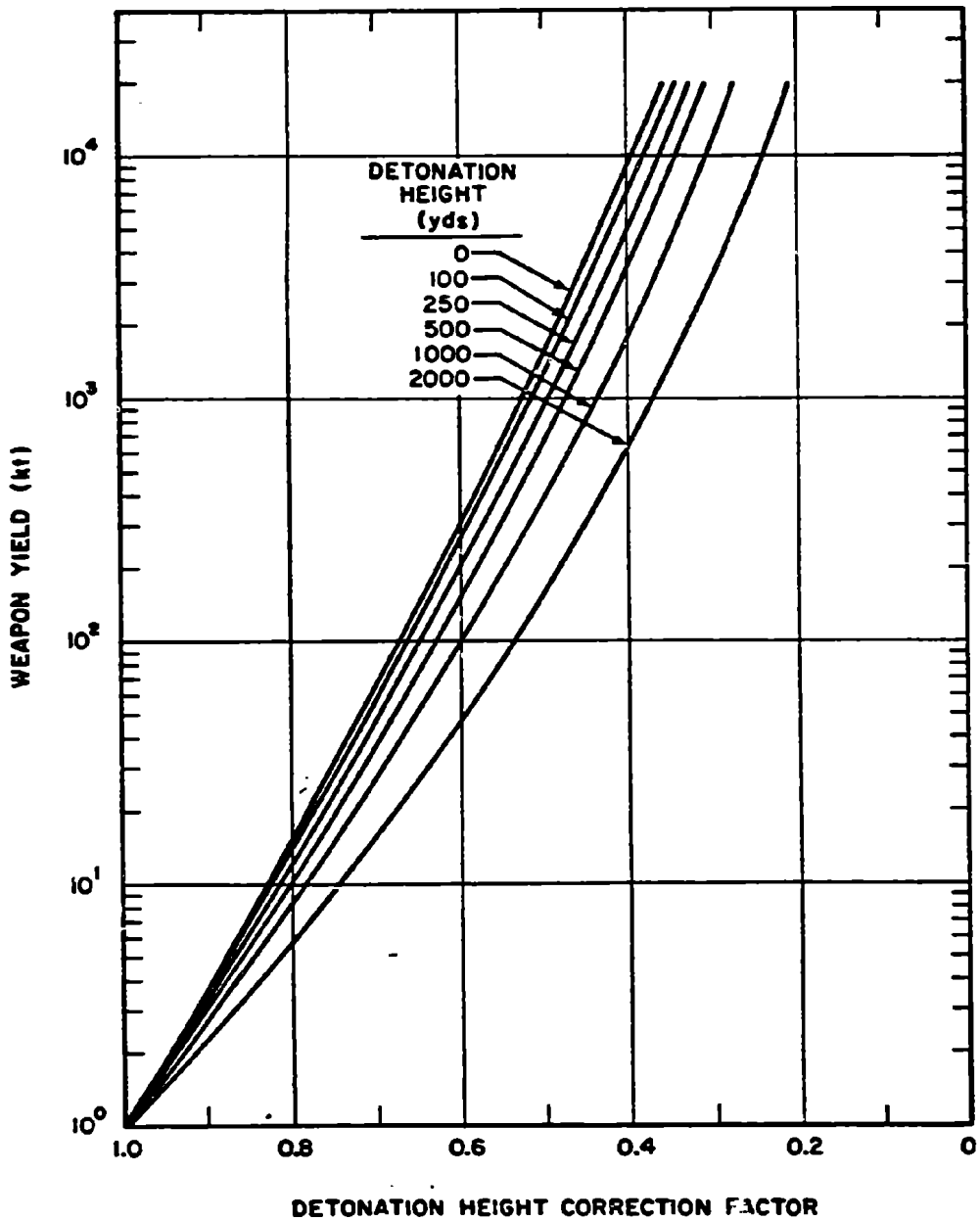

Figure 5-16. [redacted] Yield Dependent Burst Height Adjustment Factors for Fission Product Gamma Rays [redacted]

[redacted]

[redacted]

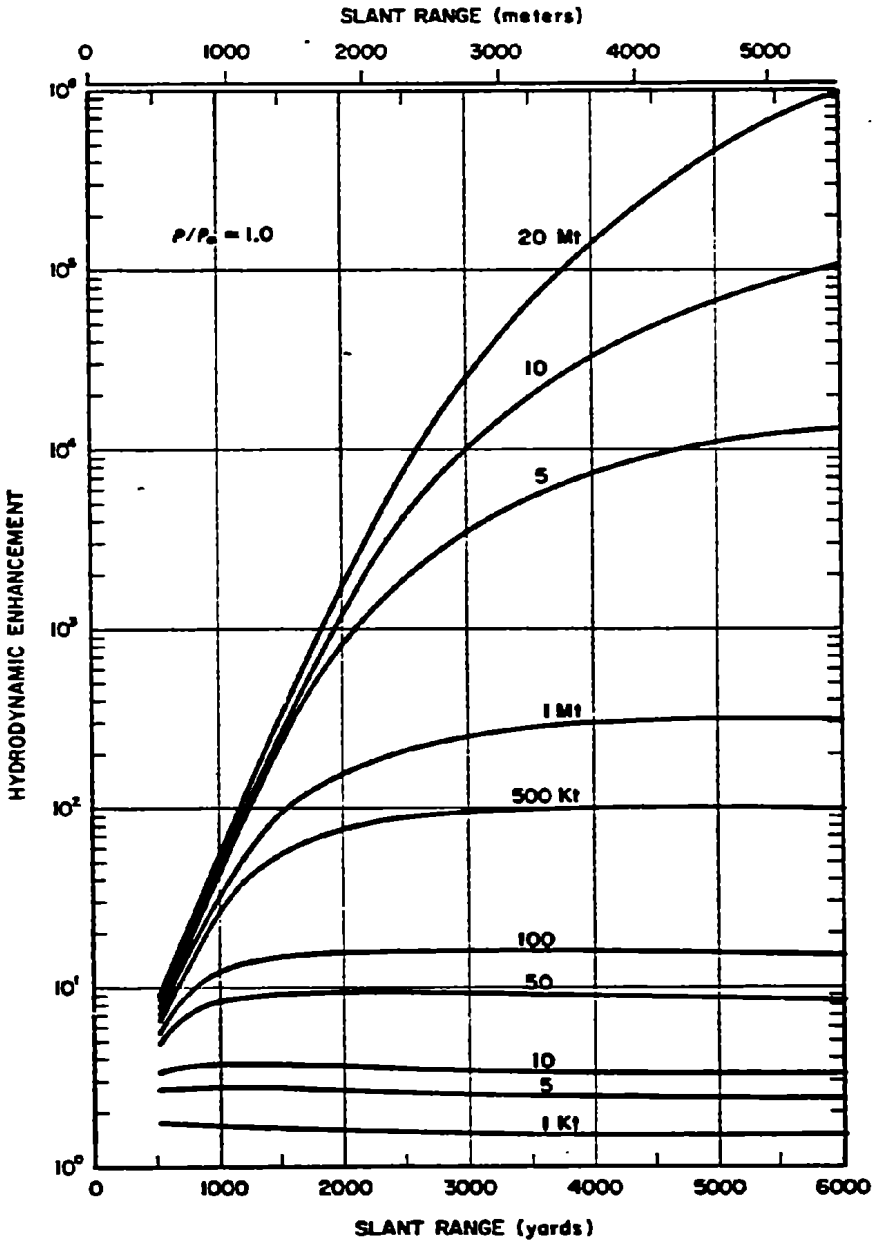

Figure 5-17b. [redacted] Fission Product Gamma Ray Hydrodynamic Enhancement Factors as a Function of Slant Range for Relative Air Density of 1.0 [redacted]

[redacted]

[redacted]

[redacted]

tion of the soil. Induced contamination contours are independent of wind, except for some wind redistribution of the surface contaminant. The contours can be expected to be roughly circular.

[redacted] Examination of several thousand analyses of the chemical composition of soils and the relative probabilities of neutron capture by the various elements present in the various samples has indicated that sodium, manganese, and aluminum generally will contribute most of the induced radioactivity. Small changes in the quantities of these materials can change the activity significantly. Other elements can also influence the radioactivity. Some elements have a relatively high probability for capturing neutrons (cross section), but the isotope that is formed after the capture either is not radioactive, does not emit gamma rays, or has such a long half life that the low activity does not produce a hazardous dose rate. The presence of such elements in the soil will tend to lower the hazard from neutron-induced activity.

[redacted] As described in paragraph 5-3, scattering of neutrons from light elements may cause the neutron to transmit a significant amount of its energy to the nucleus, and the scattered neutron will be less energetic than the incident neutron. Since the probability of neutron capture generally increases as the neutron energy decreases (in particular, this is true for sodium, manganese, and aluminum), the presence of light elements in the soil will tend to cause a larger number of neutrons to be captured near the surface rather than at some depth (the peak intensity from neutron activated radionuclides generally is two to three inches below the surface). Thus, it might be expected that the presence of light elements might increase the hazard from neutron-induced activity by raising the primary gamma ray source to a level nearer the surface, where attenuation of the earth above the source would be less. A study of many soil samples indicates that the light element that is most likely to cause such an effect is hydrogen that might be present in moisture (water) in the soil.* Thus, it might be expected that soil saturated with water might be more hazardous from neutron-induced activity than the same soil when dry. However, competing effects occur because the hydrogen absorbs neutrons to form nonradioactive deuterium. These neutrons otherwise could produce gamma ray emitters. Experiments have confirmed that moisture content does increase the hazard from neutron-induced activity; however, this effect does not appear to be of major importance in view of the uncertainties in soil composition and variations in possible weapon neutron outputs.

[redacted] Four soils have been chosen to illustrate the extent of the hazard that may be expected from induced activity. These soils were selected to show wide variations in predicted dose rates; the activity from most other soils should fall within the range of activities presented for these soils. Table 5-4 shows the chemical composition of the selected soils. The elements listed in Table 5-4 are in the order of probable importance so far as induced activity is concerned.

[redacted] When applying the data presented in this section to soils other than the four types shown, the activity should be estimated by using the data for the type that most closely resembles the soil in question in chemical composition. If none of the four types resembles the soil in question very closely, the following points should be kept in mind. For times less than $H + 1/2$ hour, aluminum is the most important contributor. Between $H + 1/2$ hour and $H + 5$ hours, manganese is generally the most important element. In the

[redacted] Hydrogen, being the lightest element, will have many more atoms per unit volume for the same percentage concentration by weight. It is also the most effective element in reducing the energy of the neutron, since its nucleus (a proton) has essentially the same mass as a neutron and energy transfer by elastic collision is very effective.

[redacted]

[redacted]

Table 5-4. [redacted] Chemical Composition of Illustrative Soils [redacted]

Element	Percentage of Soil Type (by weight)			
	Type I (Liberia, Africa)	Type II (Nevada desert)	Type III (lava, clay, Hawaii)	Type IV (beach, sand, Pensacola, Florida)
Sodium	–	1.30	0.16	0.001
Manganese	0.008	0.04	2.94	–
Aluminum	7.89	6.90	18.79	0.006
Iron	3.75	2.20	10.64	0.005
Silicon	33.10	32.00	10.23	46.65
Titanium	0.39	0.27	1.26	0.004
Calcium	0.08	2.40	0.45	–
Potassium	–	2.70	0.88	–
Hydrogen	0.39	0.70	0.94	0.001
Boron	–	–	–	0.001
Nitrogen	0.065	–	0.26	–
Sulfur	0.07	0.03	0.26	–
Magnesium	0.05	0.60	0.34	–
Chromium	–	–	0.04	–
Phosphorous	0.008	0.04	0.13	–
Carbon	3.87	–	9.36	–
Oxygen	50.33	50.82	43.32	53.332

[redacted]

absence of manganese, the sodium content will probably govern the activity for this period. Between H +5 hours and H + 10 hours, sodium and manganese content are both important. After H + 10 hours, sodium will generally be the only large contributor. If the sodium, manganese, and aluminum contents are low, the neutron-induced activity generally will be low. Soil type IV is an example of such a soil. Using these guidelines, it may be possible to obtain better data for a given soil by using data for a different illustrative soil at each of several times of interest. A word of caution is in order, however. While the content of sodium and aluminum will generally be relatively constant over fairly large areas, manganese generally is a trace element and the content may vary by an order of magnitude over a few hundred yards. Between H + 1/2 hour and H + 5 hours, the dose rate will vary almost directly in proportion to the magnitude of the variation in manganese content. In view of the uncertainty in the soil composition at any location under

[redacted]

[redacted]

[redacted] operational conditions, and the possibility of variations in composition over short distances, the data presented herein should only be used for rough estimates and should not be used as the basis for operational planning.

5-14 Dose Rate and Dose Predictions [redacted]

[redacted] As described in paragraph 5-1, both the spectrum and the total number of neutrons emitted during a nuclear explosion are sensitive functions of weapon design. Thus, no "representative" weapon was used for the prediction of neutron-induced activity, and, in view of the other uncertainties discussed above, presentation of prediction techniques for several weapon designs is not warranted. Figure 5-18 shows a broad band that indicates the variation of neutron-induced gamma activity as a function of slant range from the explosion. It is believed that the activity produced by most weapons will fall within the band.* Dose rates at $H + 1$ hour after burst may be obtained by multiplying the dose rates from Figure 5-18 by the multiplying factors given in Problem 5-5.

[redacted] Figure 5-19 represents the radioactive decay characteristics of the four soil types shown in Table 5-4. The decay factors taken from Figure 5-19 are multiplied by the $H + 1$ hour dose rate for a particular soil to give the dose rate for that soil at any other time.

[redacted] Figures 5-20 through 5-23 are presented to facilitate the computation of total dose. Multiplying factors may be obtained from these figures, which, when applied to the $H + 1$ hour dose rate for the particular soil, will give the dose accumulated over any of several periods of time for various times of entry into the contaminated area.

---

*[redacted] This band considers the representative types of nuclear weapons shown in Table 5-3 with the exception of Type V.

[redacted]

[redacted]

Problem 5-5. Calculation of Neutron-Induced Activity at 1 Hour After Explosion

[redacted] Figure 5-18 shows a range of normalized neutron-induced dose rates as a function of slant range from a 1 kt explosion. To estimate the H +1 hour dose rate, enter the slant range axis with the slant range in yards and read the range of normalized dose rates. Multiply these dose rates by the appropriate factor for the soil type of interest from the following list.

Soil Type	Multiplying Factor
I	1.0
II	9.1
III	109.0
IV	0.024

[redacted] *Scaling.* For yields other than 1 kt, multiply the dose rates obtained from Figure 5-19 by the weapon yield in kt.

[redacted] *Example* [redacted]

Given: A 50 kt explosion at a height of burst of 900 feet above soil type III.

Find: The range of H + 1 hour dose rates that might be expected: at ground zero and at a ground distance of 950 yards from ground zero.

Solution: The corresponding slant ranges are 300 yards to ground zero and 996 yards to a point at a ground distance of 950 yards from ground zero. From Figure 5-18, the normalized H + 1 hour dose rate at a slant range of 300 yards from ground zero are expected to be between 0.8 rad/hr/kt and 1.8 rads/hr/kt. The corresponding dose rates at a slant range of 996 yards are 1.6×10^{-2} rad/hr/kt and 5×10^{-2} rad/hr/kt. The multiplying factor for soil type III is 109.

Answer: The H + 1 hour dose rates at ground zero should be between

$$50 \times 109 \times 0.8 = 4{,}360 \text{ rads/hr},$$

and

$$50 \times 109 \times 1.8 = 9{,}800 \text{ rads/hr}.$$

The H + 1 hour dose rates at a ground distance of 950 yards from ground zero should be between

$$50 \times 109 \times 1.6 \times 10^{-2} = 87 \text{ rads/hr},$$

and

$$50 \times 109 \times 5 \times 10^{-2} = 272 \text{ rads/hr}.$$

[redacted] *Reliability.* H + 1 hour dose rates are expected to fall within the limits of the band shown in Figure 5-19 for the specific soils shown. For other soils, even with small variations in the content of sodium and manganese, the data merely will furnish an estimate of the magnitude of the hazard.

[redacted] *Related Material.* See paragraphs 5-1 through 5-3, and paragraphs 5-12 through 5-14.

[redacted]

[redacted]

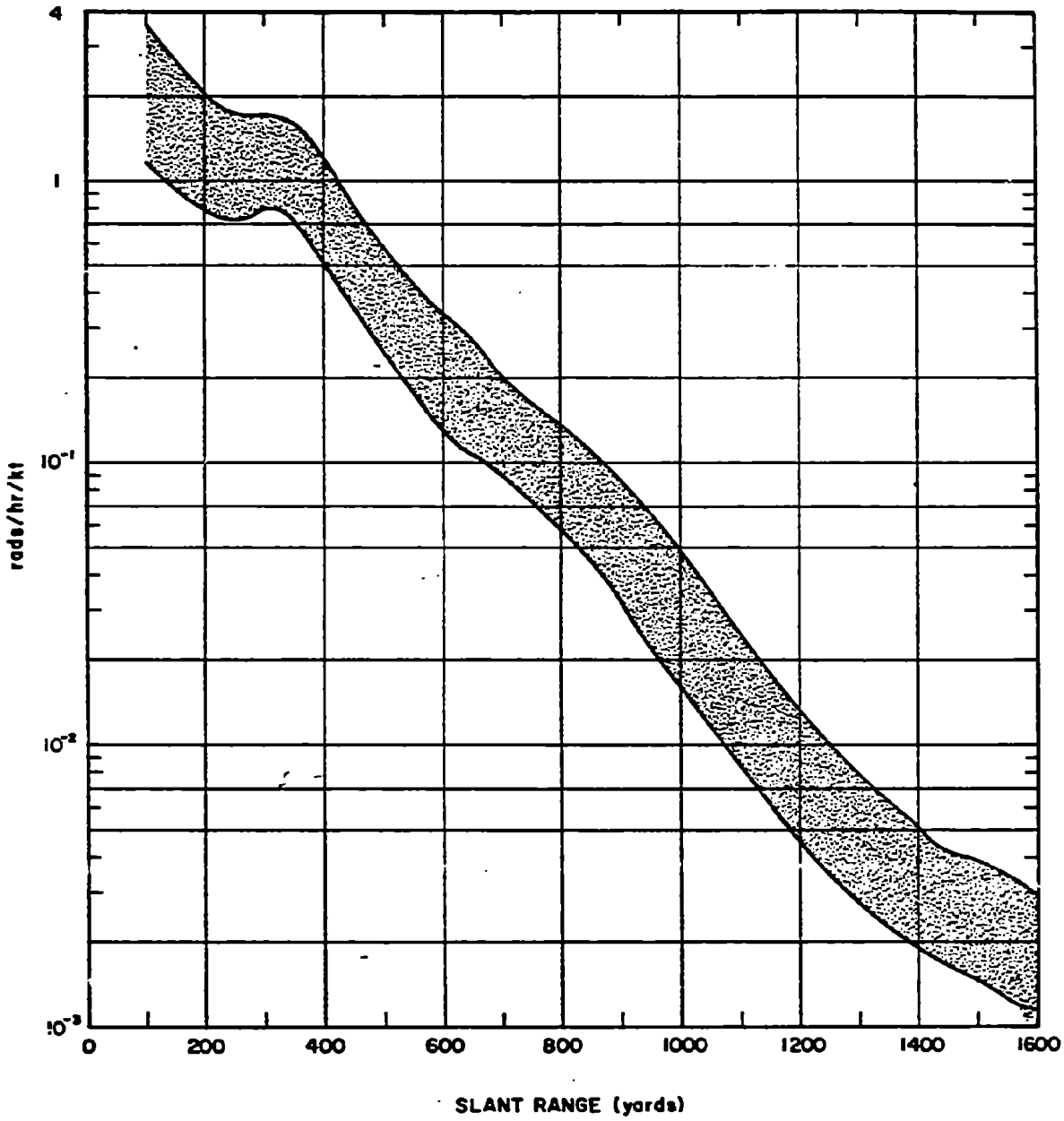

Figure 5-18. [redacted] Neutron-Induced Gamma Dose Rate as a Function of Slant Range at a Reference Time of 1 Hour After Burst [redacted]

[redacted]

[redacted]

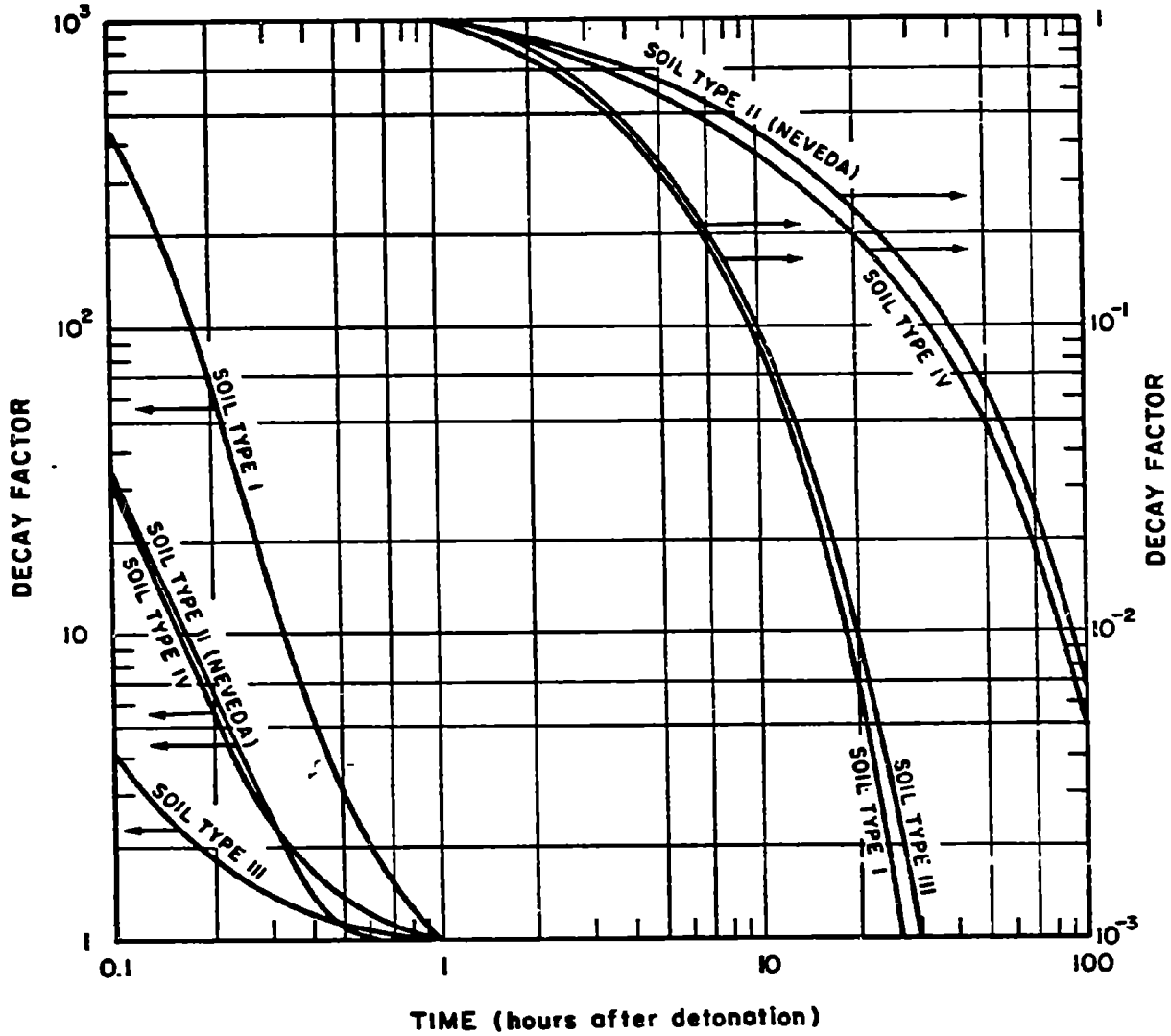

Figure 5-19. [redacted] Decay Factors for Neutron-Induced Gamma Activity [redacted]

[redacted]

[redacted]

Problem 5-7. Calculation of Total Dose from Neutron-Induced Activity

[redacted] Figures 5-20 through 5-23 provide the means to obtain the total dose received when entering an area contaminated with neutron-induced activity and remaining for a specified interval of time. The various curves represent times that an individual remains in the contaminated area. To determine the dose, obtain the multiplying factor from the vertical axis that corresponds to the time of entry on the horizontal axis and the stay time from the appropriate curve (or by interpolation between curves).

[redacted] *Example* [redacted]

Given: A dose rate of 105 rads/hr was measured on entering a contaminated area of soil type III 5 hours after an air burst nuclear explosion.

Find: The total dose that would be received by an individual who remained in that area for 1 hour.

Solution: From Figure 5-19, the decay factor for soil type III at $H + 5$ hours is 0.35. The 1 hour dose rate is therefore

$$\frac{105}{0.35} = 300 \text{ rads/hr.}$$

Figure 5-22 is the appropriate figure from which the dose multiplying factor should be obtained for soil type III. From this figure, the intersection of the line for a time of entry of 5 hours after burst with the 1 hour stay time curve gives a factor of 0.32.

Answer: If the individual remains in the area for 1 hour, the accumulated dose will be

$$(0.32)(300) = 96 \text{ rads.}$$

[redacted] *Reliability.* Figures 5-20 through 5-23 are integrals of the curves in Figure 5–19. The same reliability statement given in Problem 5-6 applies.

[redacted] *Related Material.* See paragraphs 5-13 and 5-14. See also Problems 5-5 and 5-6.

[redacted]

[redacted]

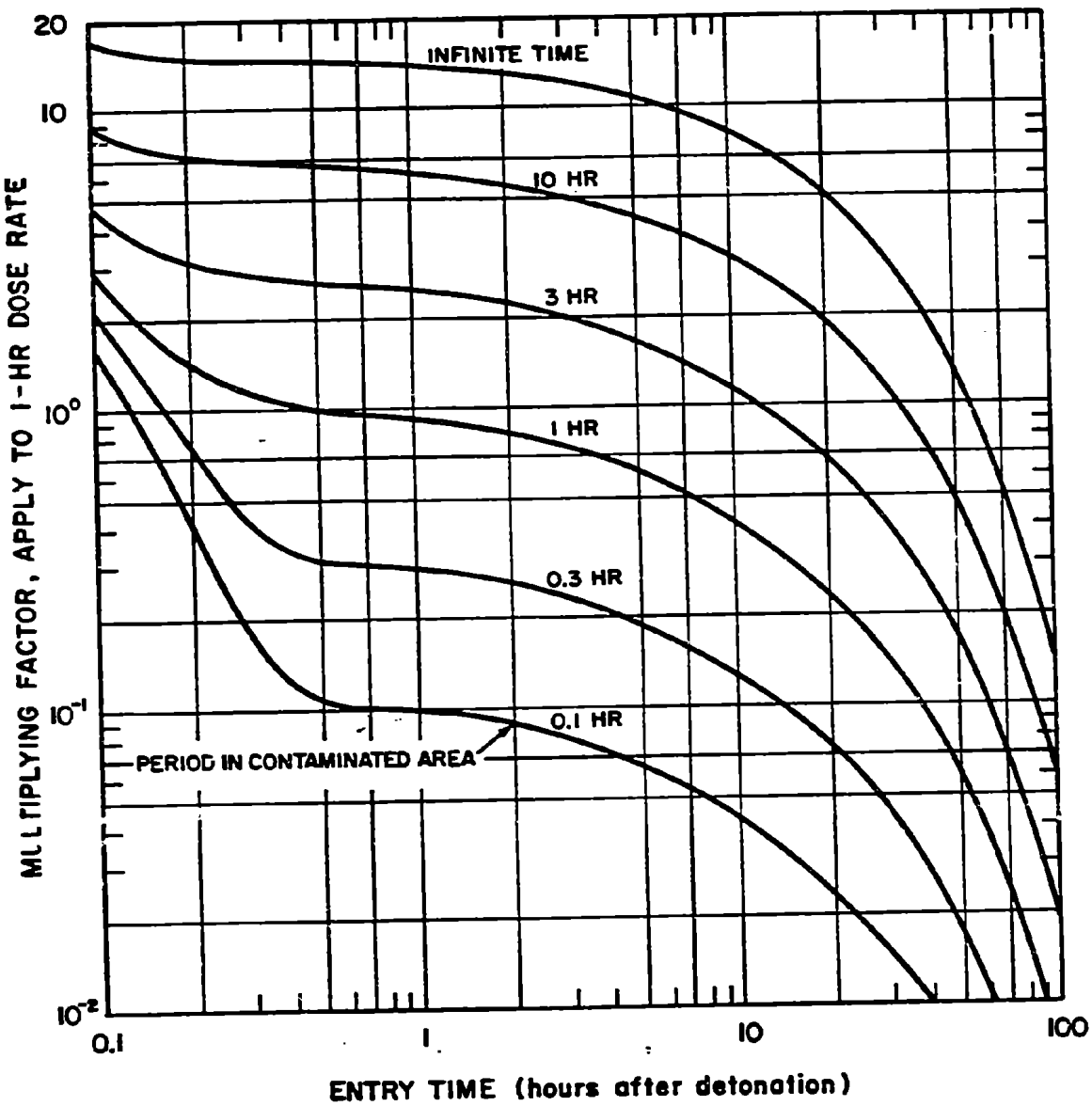

Figure 5-21. [redacted] Total Radiation Dose Received in an Area Contaminated by Neutron-Induced Gamma Activity, Soil Type II [redacted]

[redacted]

[redacted]

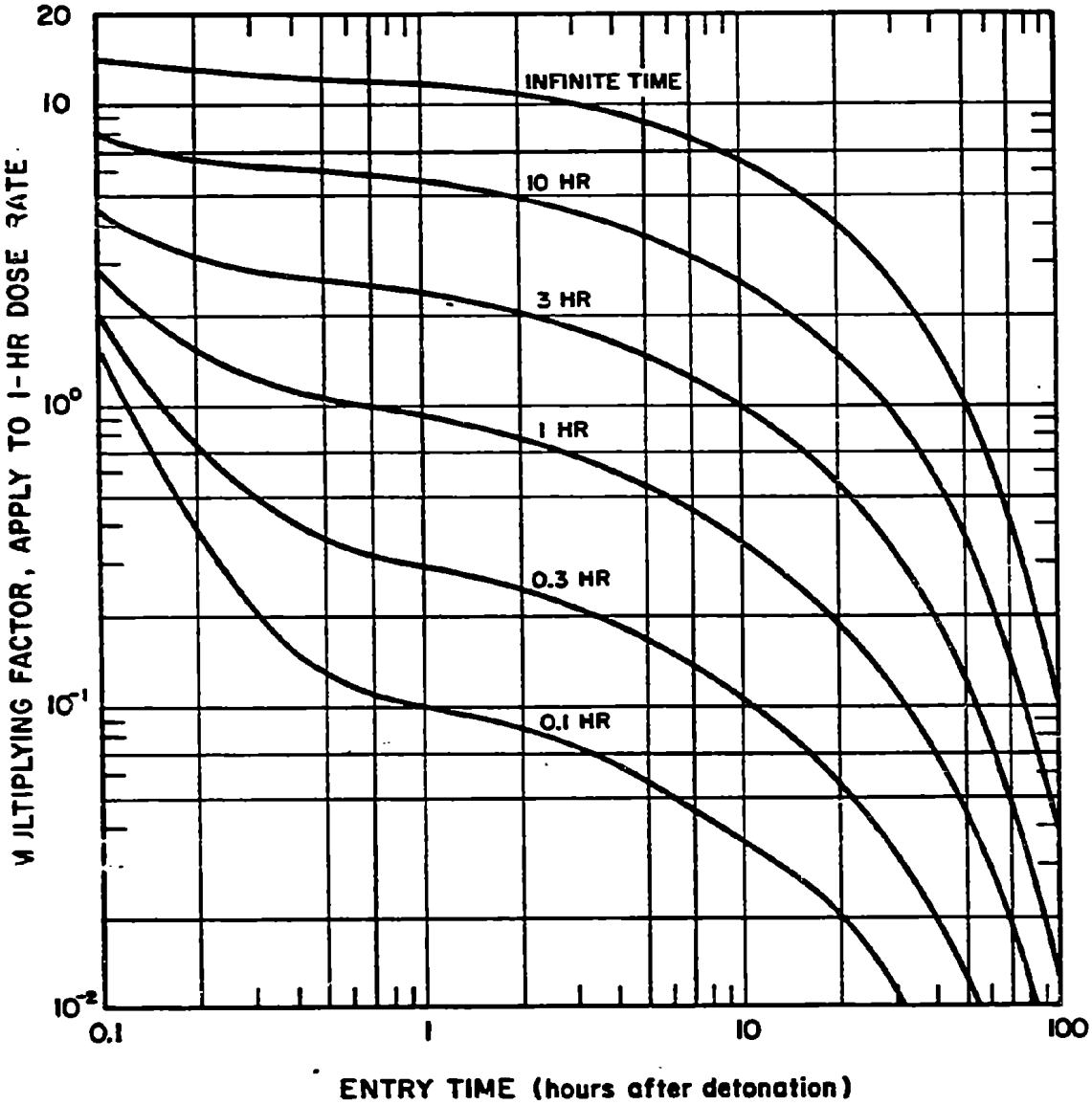

Figure 5-23. [redacted] Total Radiation Dose Received in an Area Contaminated by Neutron-Induced Gamma Activity, Soil Type IV [redacted]

[redacted]

[redacted]

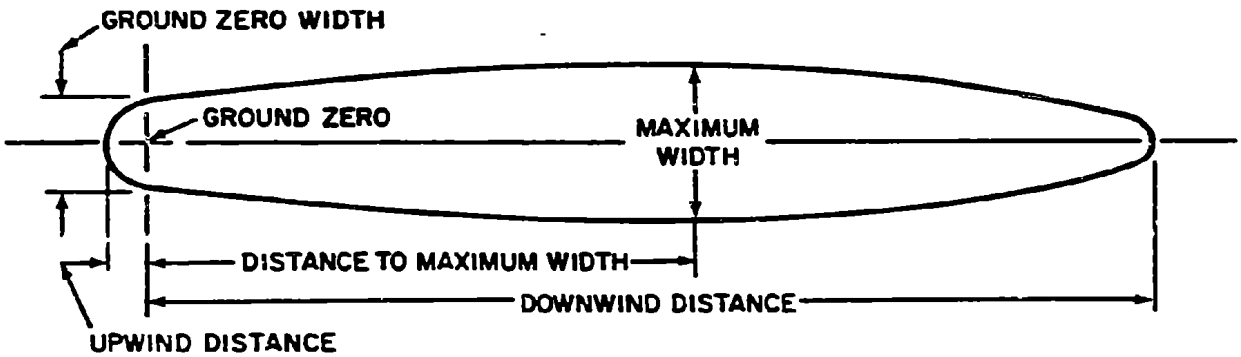

Figure 5-24. (U) Idealized Early Fallout Dose Rate Contour (U)

[redacted]

called effective wind, as described in paragraph 5-20. Usually wide discrepancy from the idealized pattern will result if there are large directional shears in the winds from the surface up to the altitudes of the stabilized cloud. Such shears can distort the idealized pattern seriously, so that, in practice, radical departures from the idealized patterns can be expected. Figure 5-25 compares the idealized dose rate contour pattern to the observed pattern normalized to 1 hour after shot SMALL BOY, a low yield shot in Nevada during which the wind shear was not [illegible] The actual winds had an effective velocity of about 8 knots and an effective shear of about 30 degrees (effective velocity and effective shear are defined in paragraph 5-20). The idealized pattern is shown for an effective velocity of 10 knots and an effective shear of 15 degrees, for the reasons explained in paragraph 5-20. The downwind distance is expected to increase and the crosswind distance to decrease both with an increase in velocity and with a decrease in shear. These tendencies are noticeable in Figure 5-25; however, for this case of low yield and minimal shear, the idealized contours represent a reasonable approximation of the observed contours.

[redacted] Figure 5-26 shows a hodograph of a typical summer wind structure over Fort Worth, Texas. This is an example of a severely sheared wind structure. The average wind speed to altitudes of the stabilized cloud from a 2 Mt burst is about 10 knots, but, as a result of directional changes, the effective velocity is only 2.5 knots. The direction of this effective wind is 43.5 degrees east of north.

[redacted] Figure 5-27 shows a comparison of the idealized dose rate contours for a 2 Mt explosion on the surface and the contours computed by the "Defense Land Fallout Interpretive Code (DELFIC)" (see bibliography) for the wind hodograph shown in Figure 5-26 assuming that the winds stayed constant in time and distance. While this comparison is not a comparison with actual data, it is a comparison with the results of a complex computer code that was developed independent of empirical data and which has demonstrated a very good agreement with available data. The general direction as well as the areas of the two patterns are quite divergent. This comparison is intended to illustrate the lack of confidence that can be placed in the idealized contours for prediction of a fallout pattern for a particular explosion, even if meteorological data

[redacted]

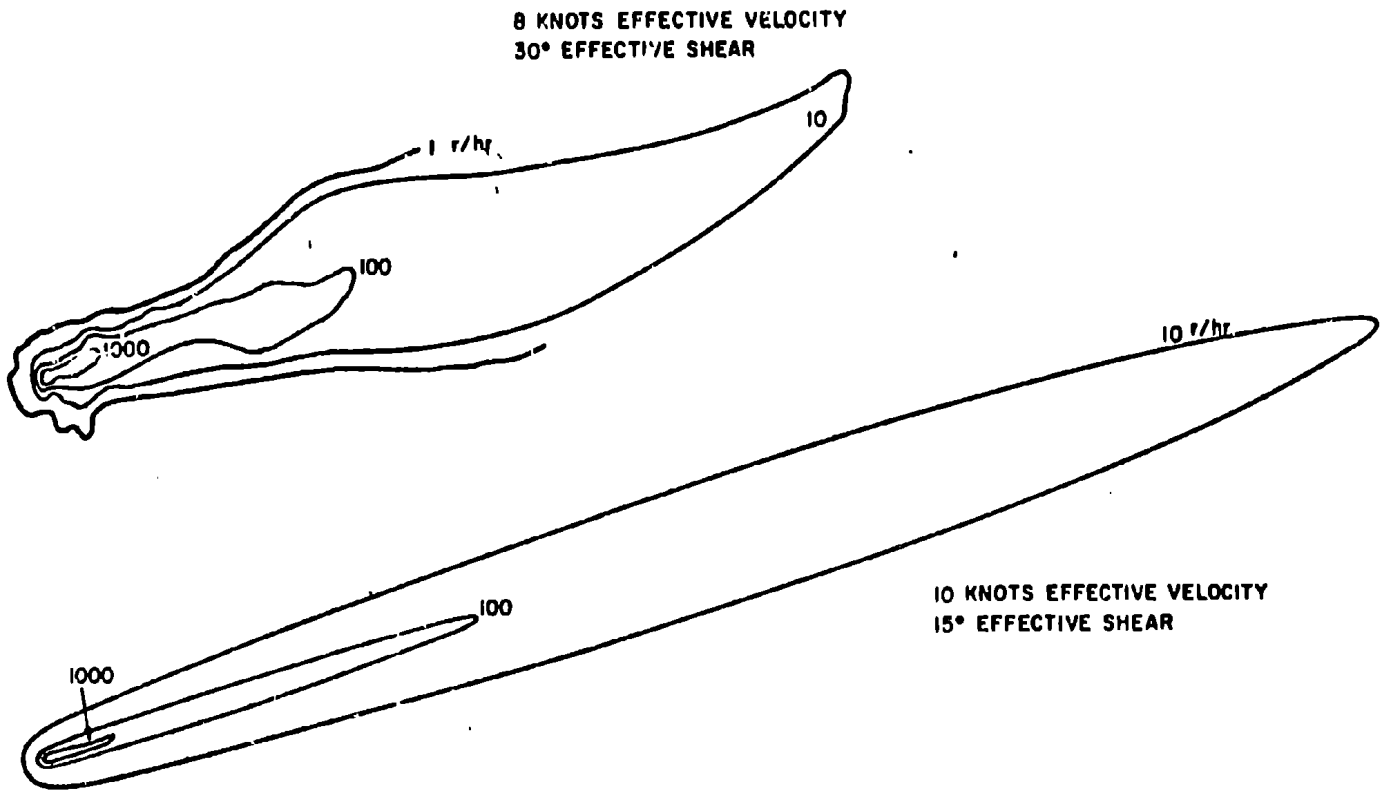

Figure 5-25. [redacted] Comparison of Idealized Dose Rate Contours with Observed Contours from a Low Yield Explosion [redacted]

[redacted]

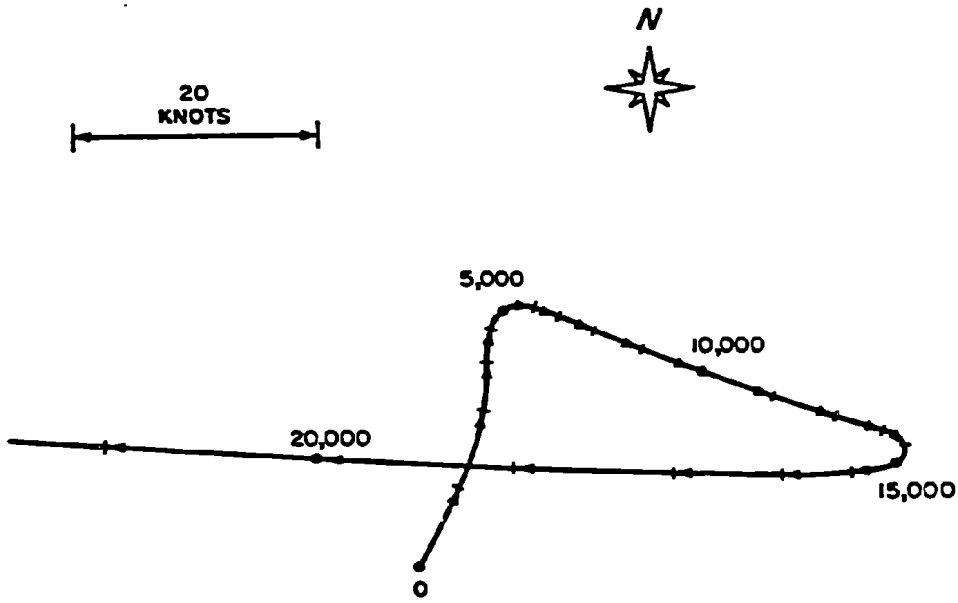

NOTE: NUMBERS ARE METERS OF ALTITUDE.

Figure 5-26. [redacted] Hodograph of a Typical Summer Wind Structure Over Fort Worth, Texas [redacted]

[redacted]

at the burst point are known. The contours for the idealized curves were extrapolated to a speed of 2.5 knots even though extrapolation below 10 knots is not recommended. On the other hand, for small yields, or for the case of many weapons, the total dose predicted by the idealized contours over large areas probably would provide a reasonable basis upon which to base casualty predictions.

5-20 Dose Rate Contour Dimensions [redacted]

[redacted] Figures 5-28 through 5-37 may be used to draw idealized dose rate contours for land surface explosions with yields between 0.01 kt and 30 Mt. Separate sets of curves are provided for downwind distance, maximum width, and downwind distance to maximum width for effective wind speeds of 10, 20, and 40 knots. Since actual winds are seldom unidirectional and since the radioactive particles that cover the area around ground zero include many that were not carried to high altitudes, the ground zero width is presented independent of wind velocity in Figure 5-37. The upwind distance is estimated to be one-half the ground zero contour widths, i.e., they may be represented by a semi-circle, centered at ground zero, with a radius equal to one-half the ground zero width. The dose rate values obtained from the curves correspond to the values existing at a reference time of 1 hour after burst, 3 feet above a hypothetical smooth, infinite plane; therefore, they must be reduced to account for ground roughness. A reduction

[redacted]

[redacted]

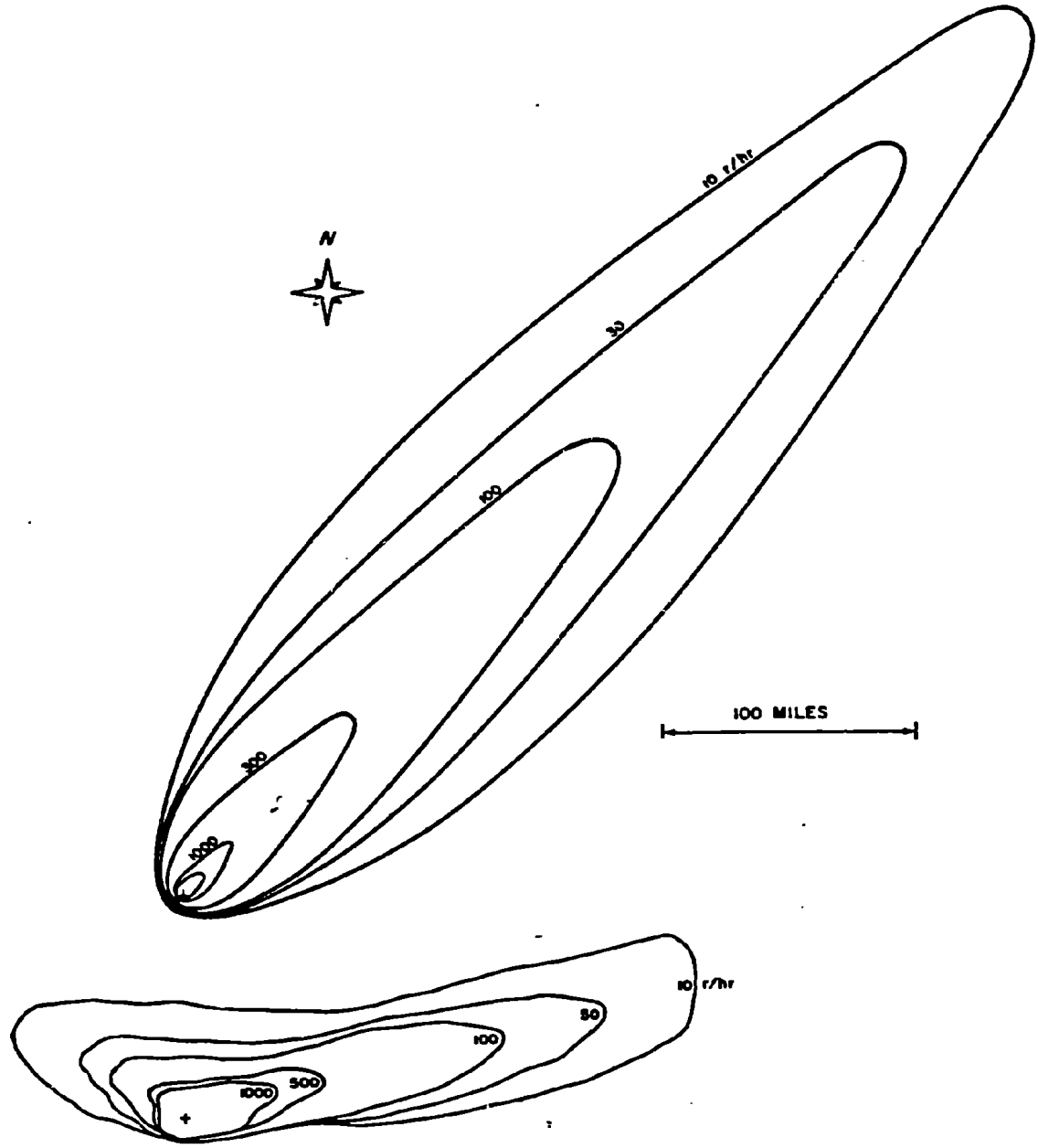

Figure 5-27. [redacted] Comparison of Idealized Dose Rate Contours with Those Calculated by a Complex Computer Code for a 2 Mt Explosion and the Winds of Figure 5-25 [redacted]

[redacted]

[redacted]

[redacted]

factor of 0.7 is appropriate for reasonably level terrain. A factor of 0.5 to 0.6 would be more appropriate for rough and hilly terrain. If additional shielding exists (e.g., foxholes, buildings, tanks), additional shielding factors should be obtained from Section VI, Chapter 9.

[redacted] To obtain the effective wind for use with Figures 5-28 through 5-36, a wind hodograph similar to that shown in Figure 5-26 should be prepared. The vector averages of the winds from ground zero to the base of the stabilized cloud and to the top of the stabilized cloud should then be obtained. The average of these two average vectors is the effective wind for use with Figures 5-28 through 5-36. The heights of the bottom and top of the stabilized cloud are shown as a function of yield in Figures 5-38 and 5-39, respectively. For wind speeds between the values of 10, 20, and 40 knots that are shown in Figures 5-28 through 5-36, contour values may be obtained by linear interpolation. Extrapolation to values below 10 knots or above 40 knots is not recommended.

[redacted] As used herein the term "effective shear" refers to the angle between the average vectors to the bottom and top of the stabilized cloud. In the absence of a sufficient quantity of test data with which empirical curves for determining the idealized contours could be con- [illegible] were generated by use of the Defense Land Fallout Interpretive Code (DELFIC) (see bibliography). An effective shear of 15 degrees was used in the computer calculations from which the curves of Figures 5-28 through 5-36 were derived. In general, increased wind velocity tends to lengthen and narrow the pattern, while increased directional shear tends to shorten and widen the pattern. An effective velocity and an effective directional shear do not define a unique wind structure, i.e., different wind structures could have the same effective velocity and directional shear. It is not recommended that any attempt be made to change the contour values for effective directional shears different from 15 degrees; however, the user should be aware that differences from this value are more likely to result in idealized contours that are farther from reality than if the shear is nearly equal to 15 degrees.

5-21 Decay of Early Fallout [redacted]

[redacted] Fission products are composed of a complex mixture of over 200 different forms (isotopes) of 36 elements. Most of these isotopes are radioactive, decaying by the emission of beta particles, frequently accompanied by gamma radiation. About 2 ounces of fission products are formed for each kiloton (or 125 lb/Mt) of fission energy yield. The total radioactivity of the fission products initially is extremely large but it falls off rapidly as the result of radioactive decay.

[redacted] At 1 minute after a nuclear explosion, when the residual nuclear radiation is postulated to begin, the gamma ray activity of the 2 ounces of fission products from a 1 kt fission yield explosion is comparable with that of about 30,000 tons of radium. For explosions in the megaton-energy range the amount of radioactivity produced is enormous. Although there is a decrease from the 1 minute value by a factor of over 6,000 by the end of a day, the radiation intensity still will be large.

[redacted] Early fallout consists mainly, but not entirely, of fission products. The following rule indicates how the dose rate of the actual mixture decreases with time: for every seven-fold increase in time after the explosion, the dose rate decreases by a factor of 10. For example, if the radiation dose rate at 1 hour after the explosion is taken as a reference point, then at 7 hours after the explosion the dose rate will have decreased to 1/10; at 7 x 7 = 49 hours (or roughly 2 days) it will be 1/100; and at 7 x 49 = 343 hr (or roughly 2 weeks) the dose rate will be 1/1,000 of that at 1 hour after the burst.

[redacted]

[redacted]

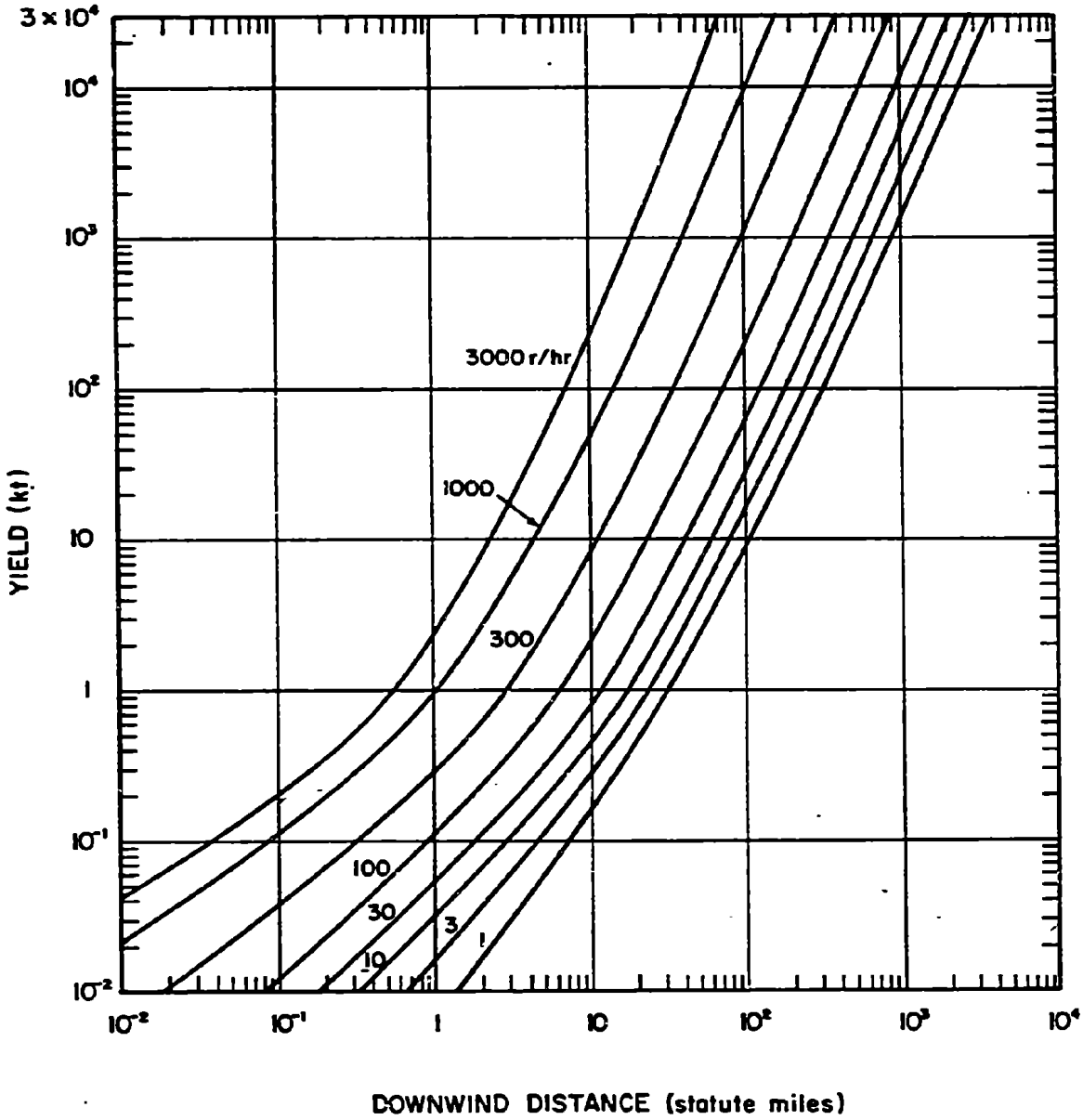

Figure 5-28. [redacted] Downwind Distance as a Function of Yield, .10 Knot Effective Wind [redacted]

[redacted]

[redacted]

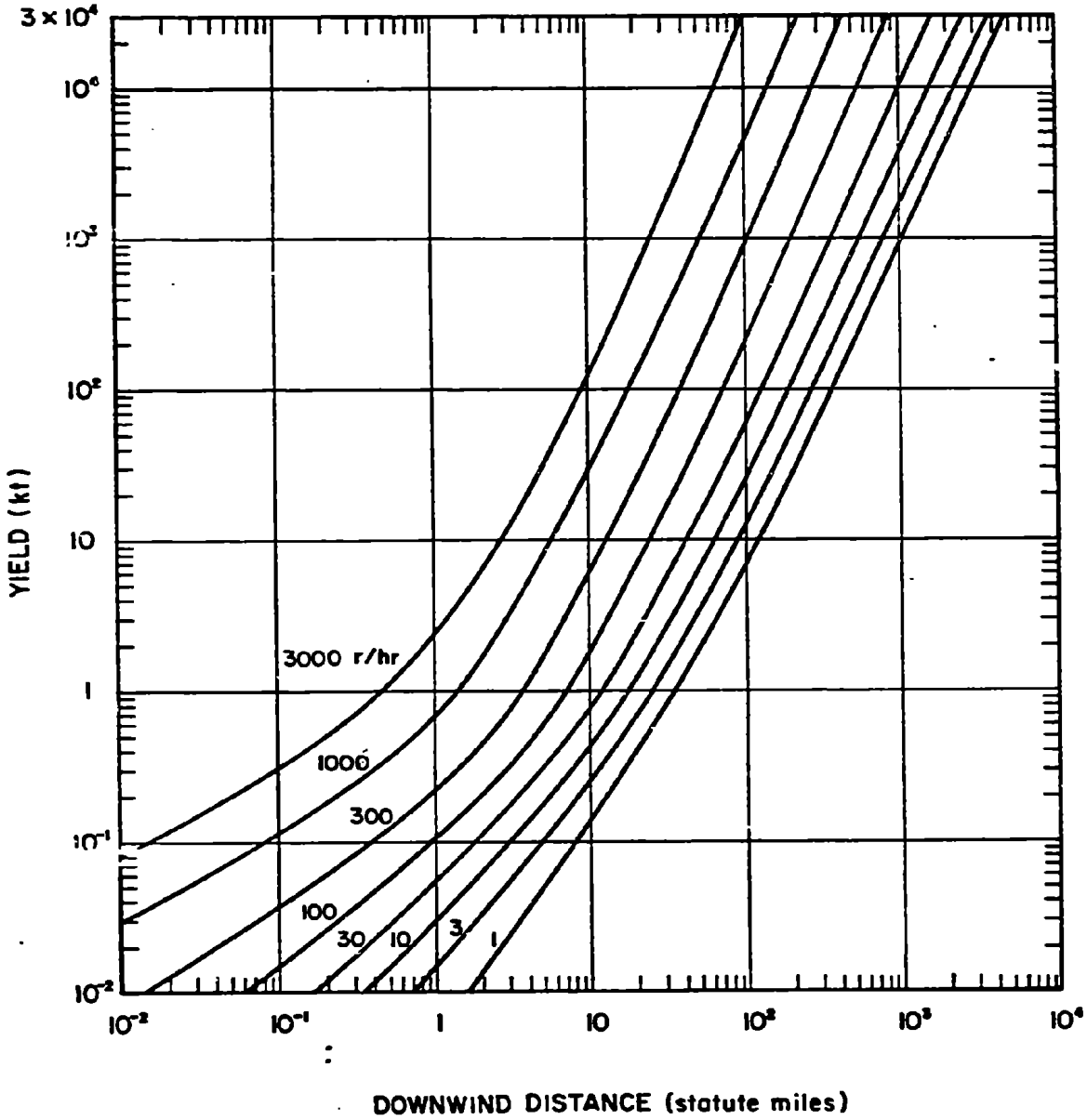

Figure 5-29. [redacted] Downwind Distance as a Function of Yield, 20 Knot Effective Wind [redacted]

[redacted]

[redacted]

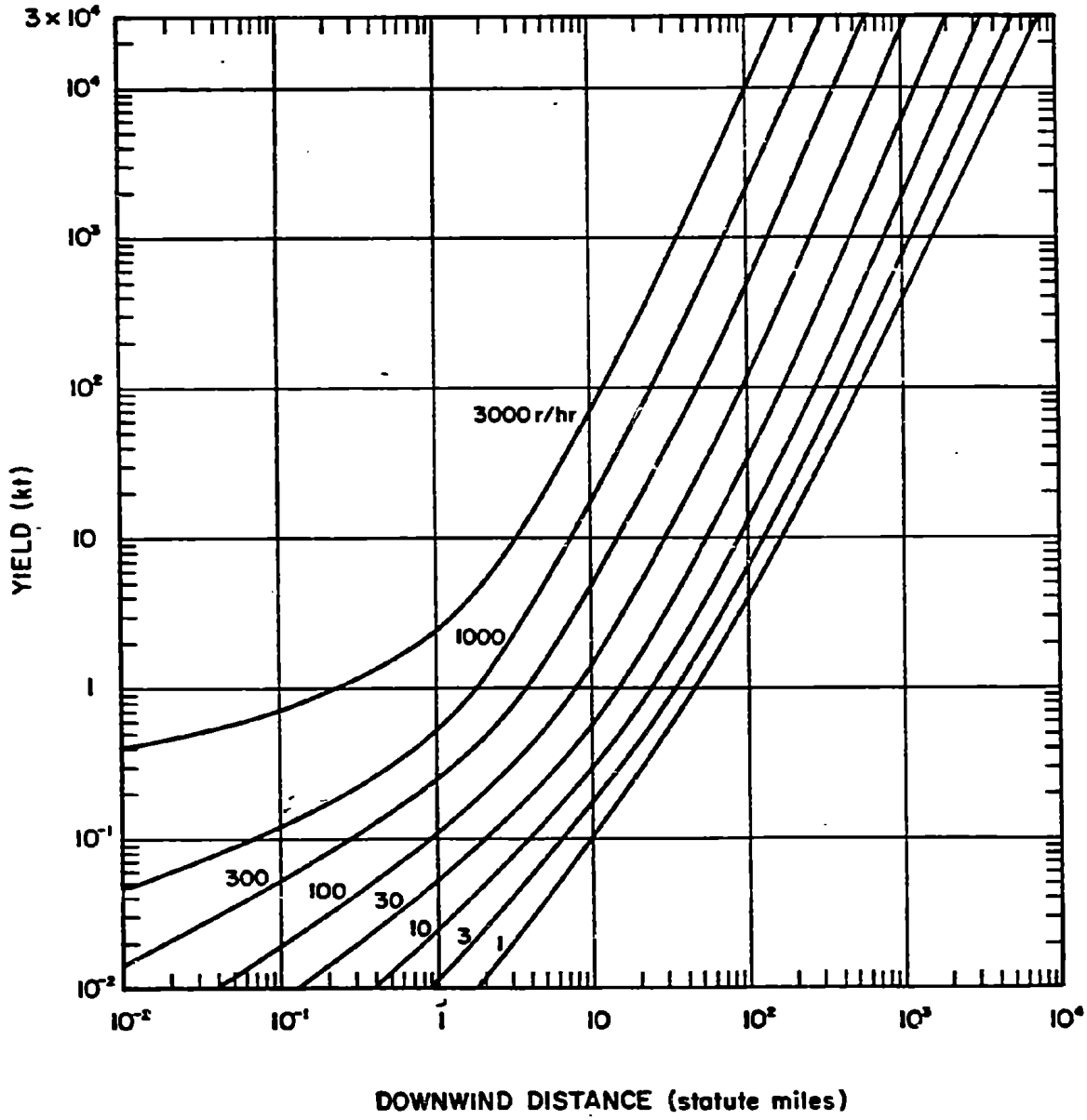

Figure 5-30. [redacted] Downwind Distance as a Function of Yield, 40 Knot Effective Wind [redacted]

[redacted]

[redacted]

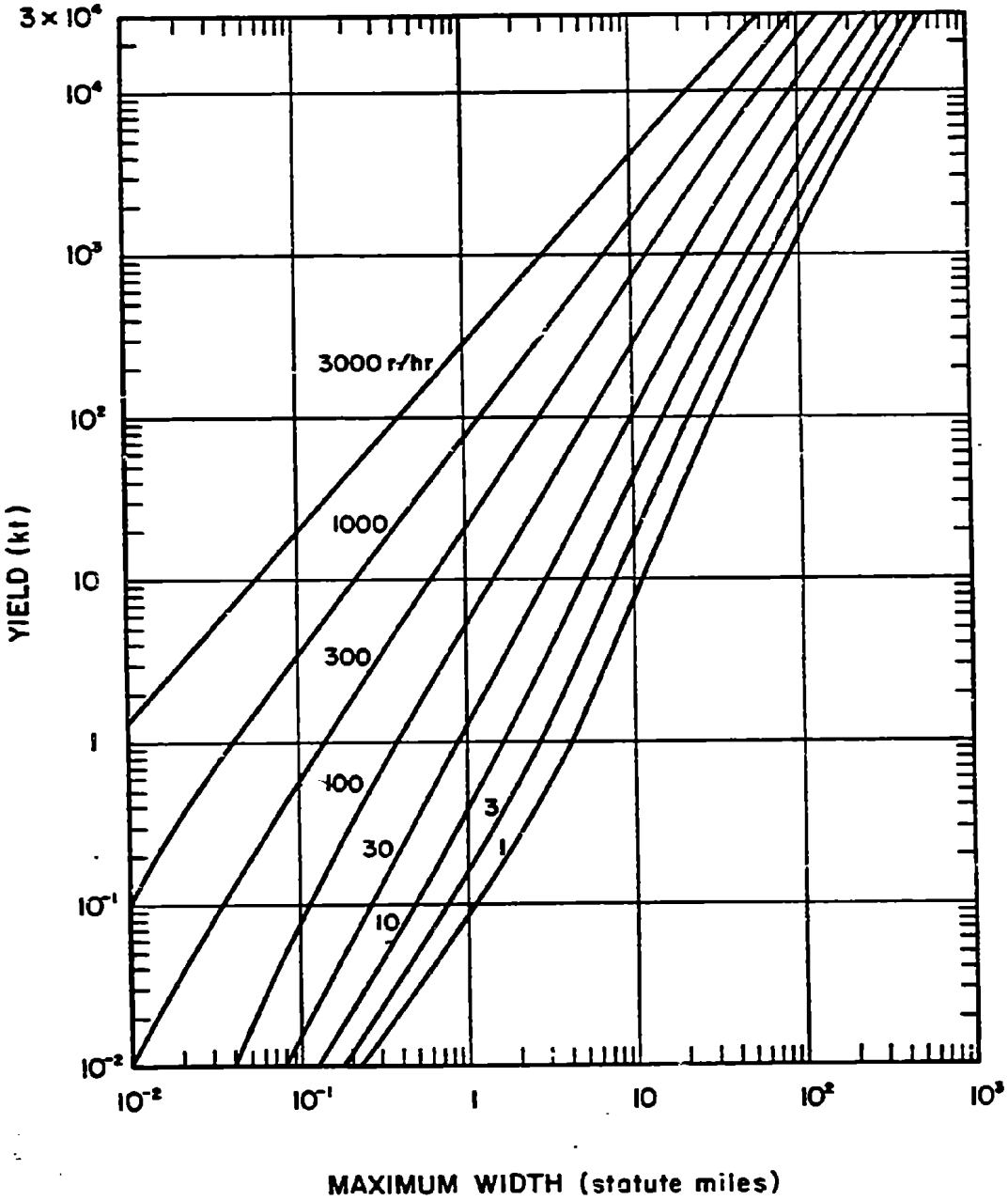

Figure 5-31. [redacted] Maximum Width as a Function of Yield, 10 Knot Effective Wind [redacted]

[redacted]

[redacted]

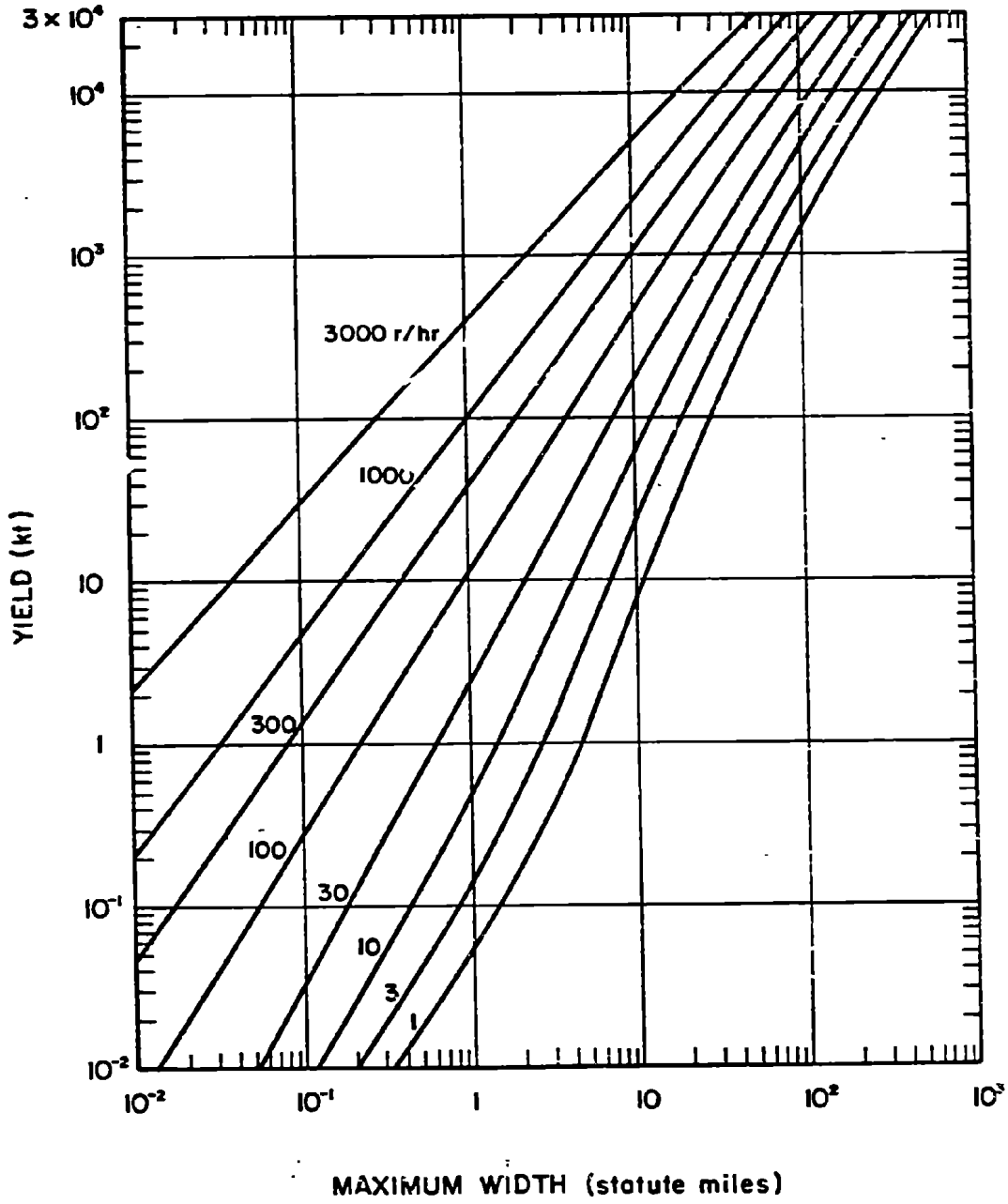

Figure 5-32. [redacted] Maximum Width as a Function of Yield, 20 Knot Effective Wind [redacted]

[redacted]

[redacted]

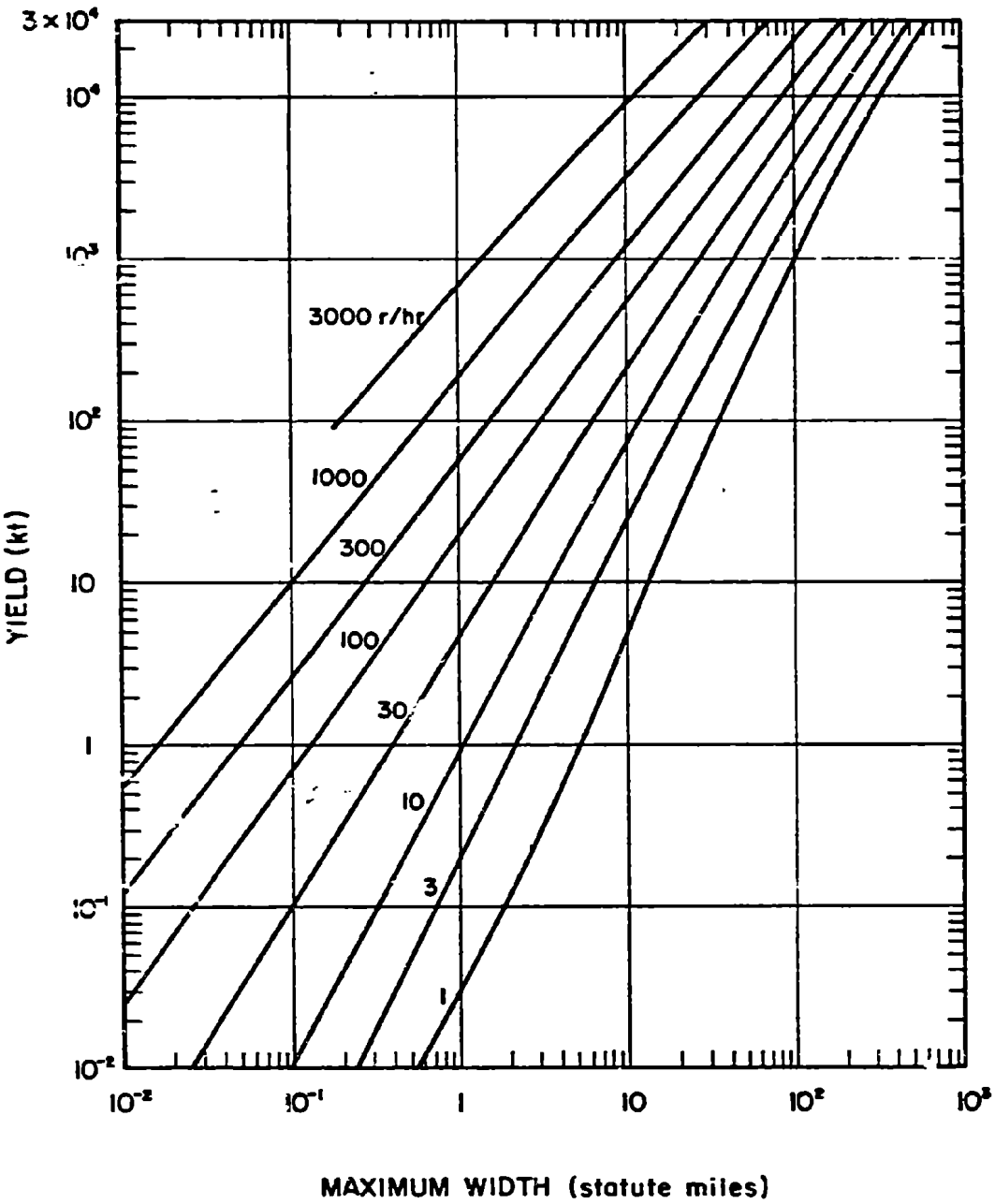

Figure 5-33. [redacted] Maximum Width as a Function of Yield, 40 Knot Effective Wind [redacted]

[redacted]

[redacted]

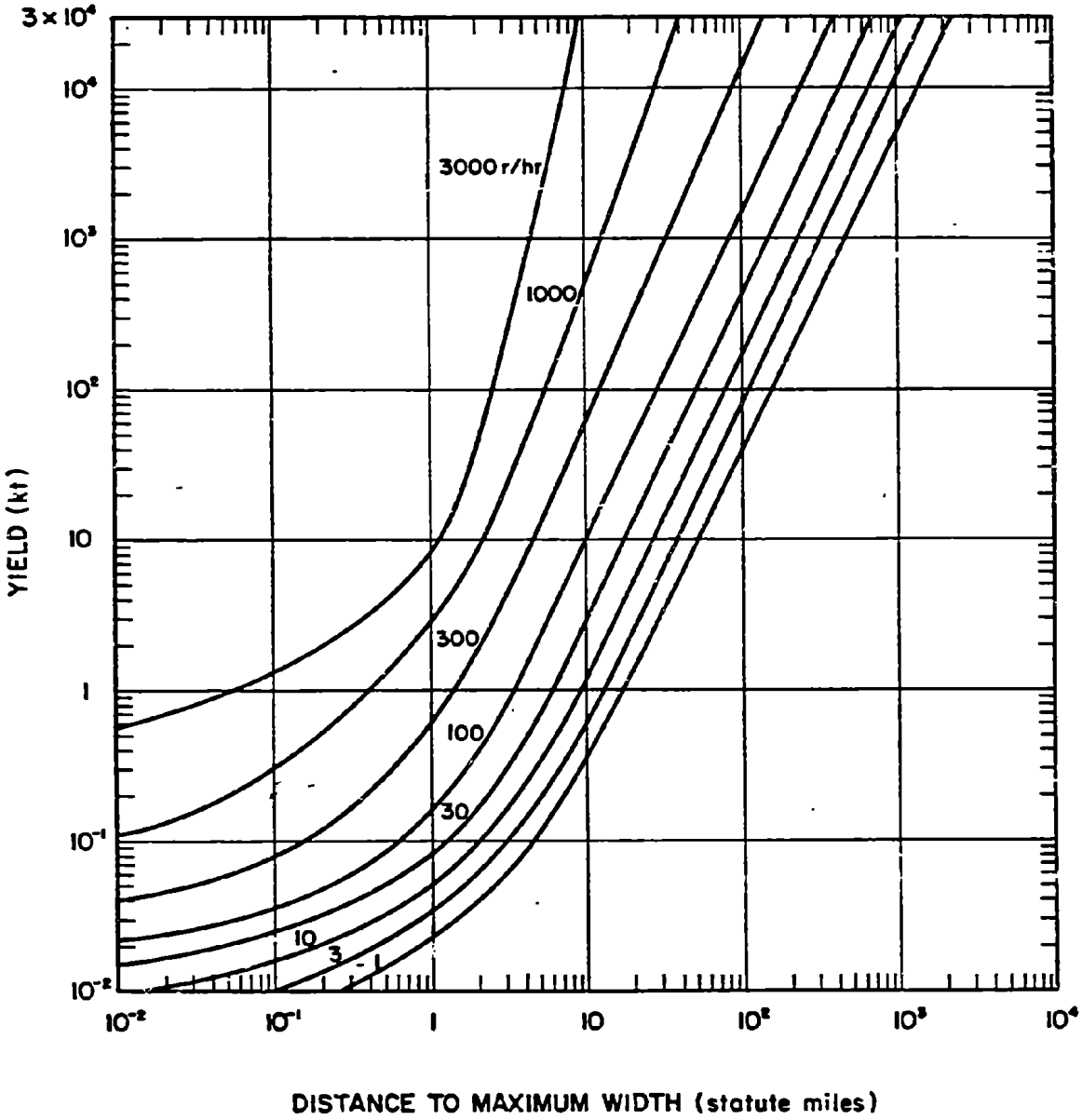

Figure 5-34. [redacted] Distance to Maximum Width as a Function of Yield, 10 Knot Effective Wind [redacted]

[redacted]

[redacted]

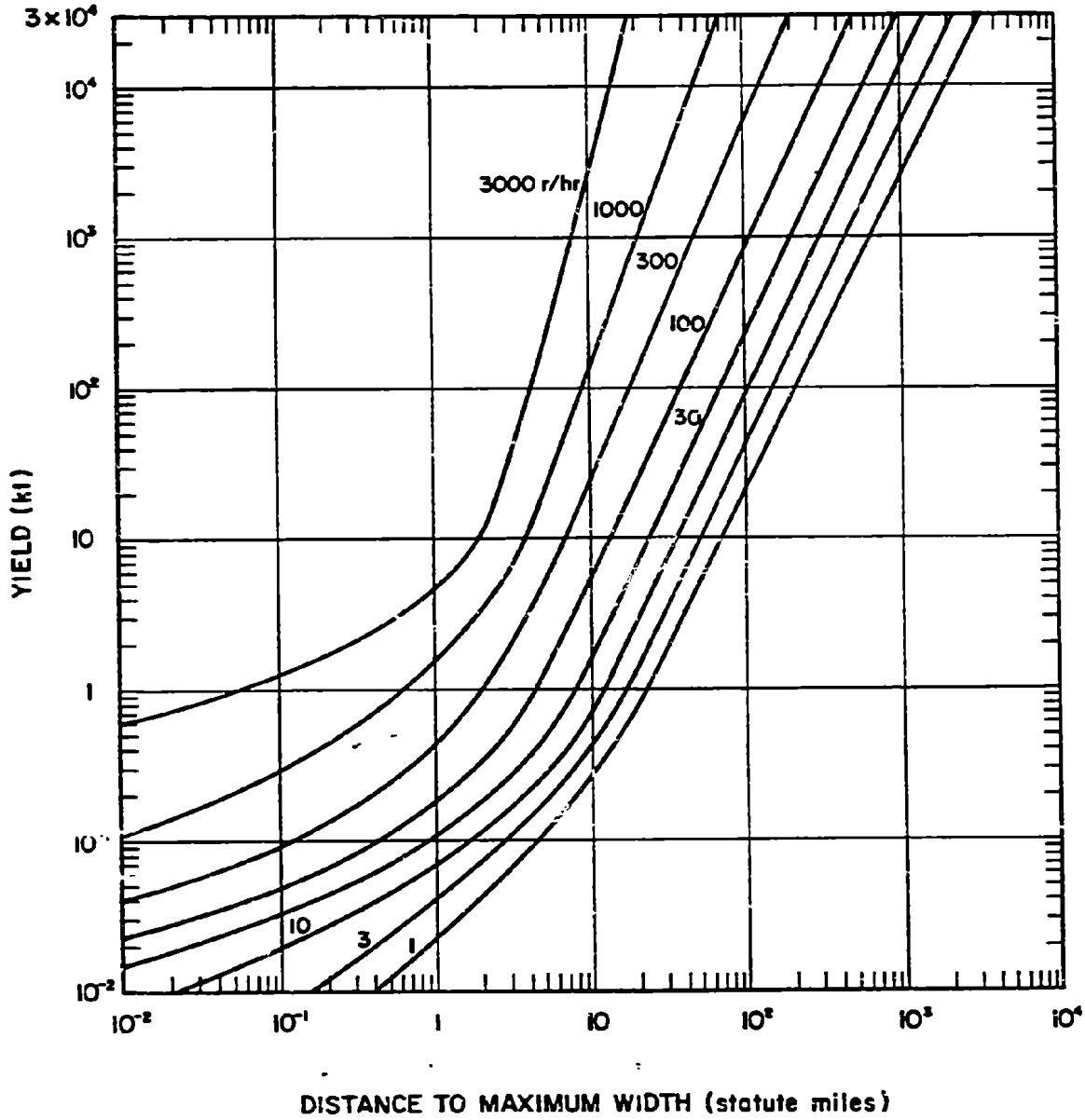

Figure 5-35. [redacted] Distance to Maximum Width as a Function of Yield, 20 Knot Effective Wind [redacted]

[redacted]

[redacted]

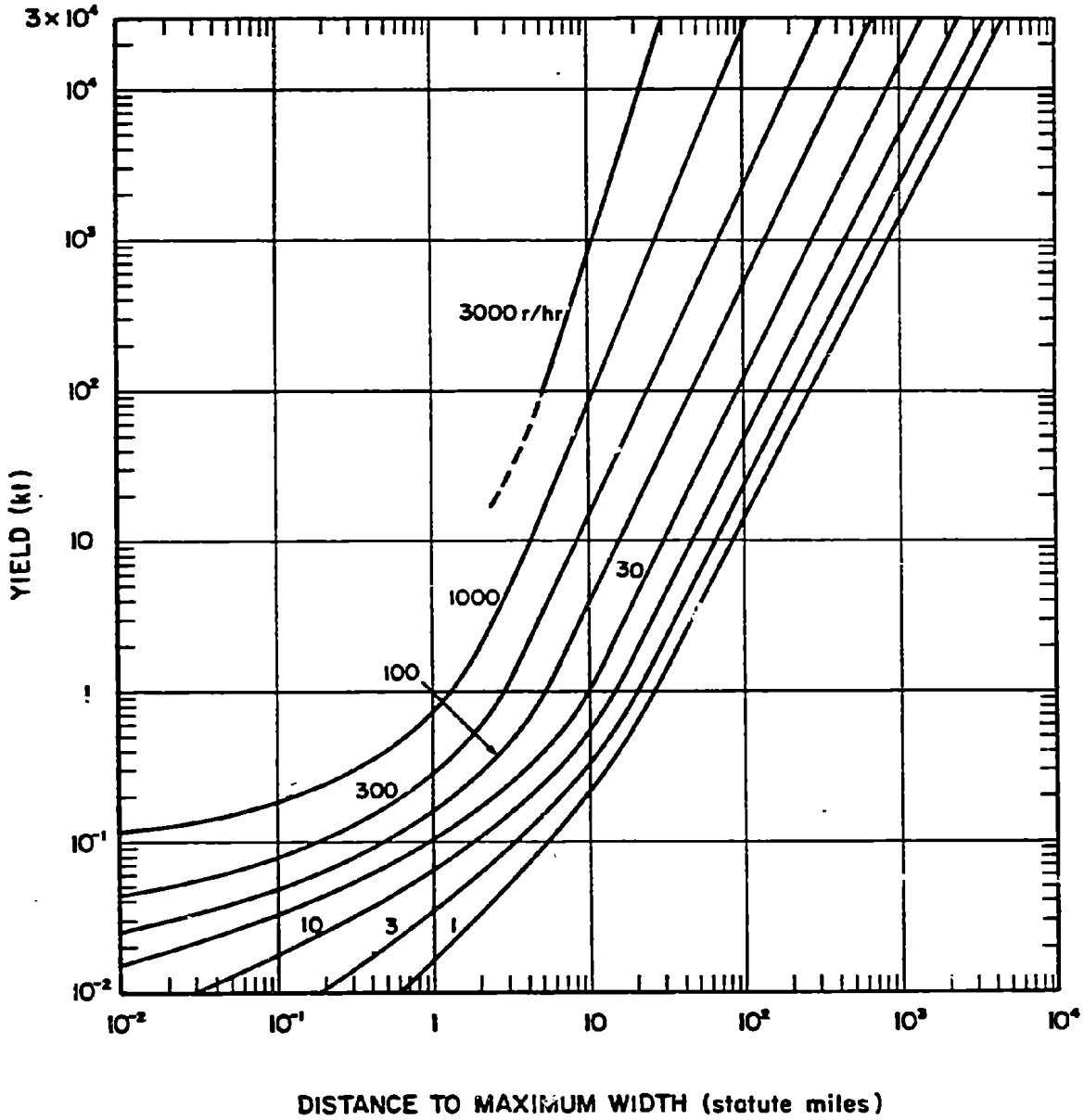

Figure 5-36. [redacted] Distance to Maximum Width as a Function of Yield, 40 Knot Effective Wind [redacted]

[redacted]

[redacted]

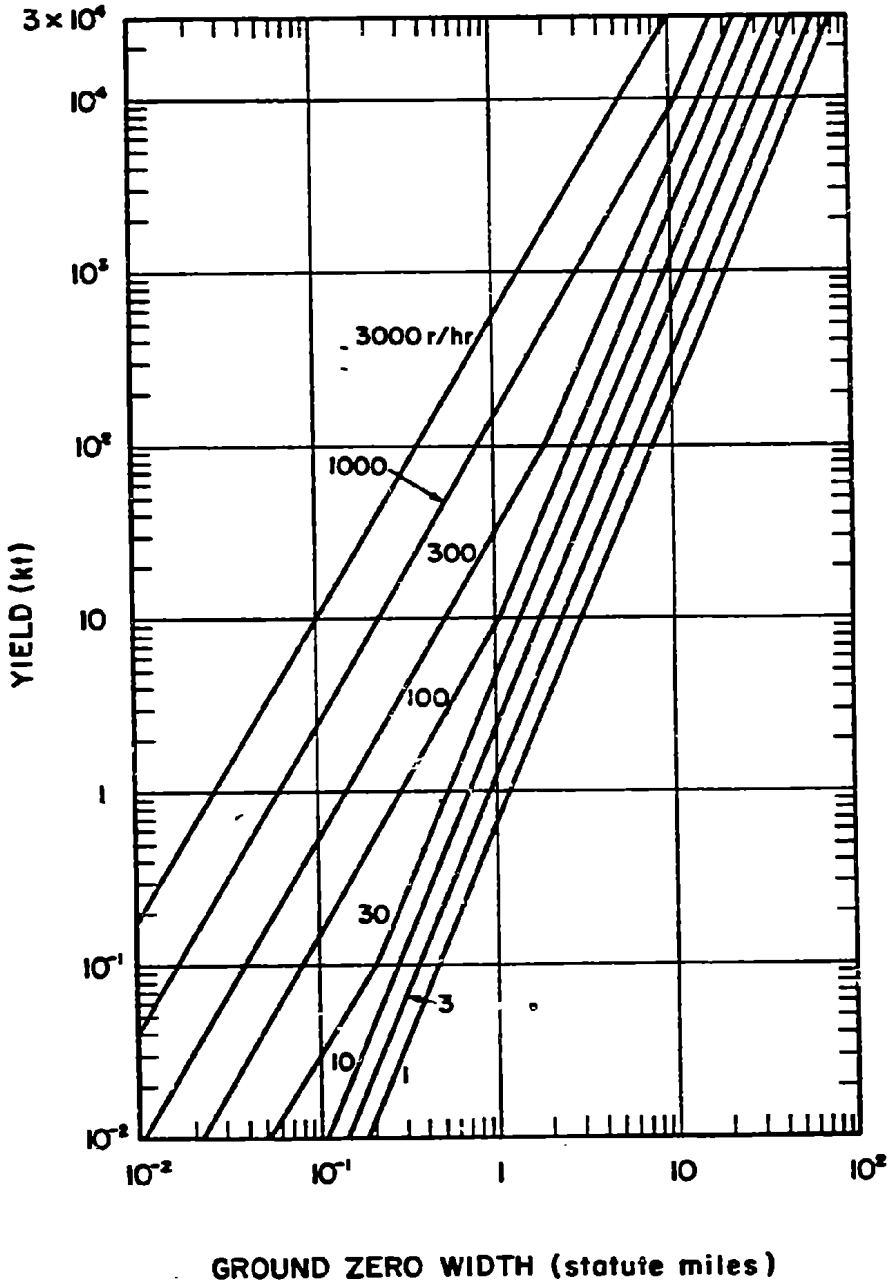

Figure 5-37. [redacted] Ground Zero Width as a Function of Yield [redacted]

[redacted]

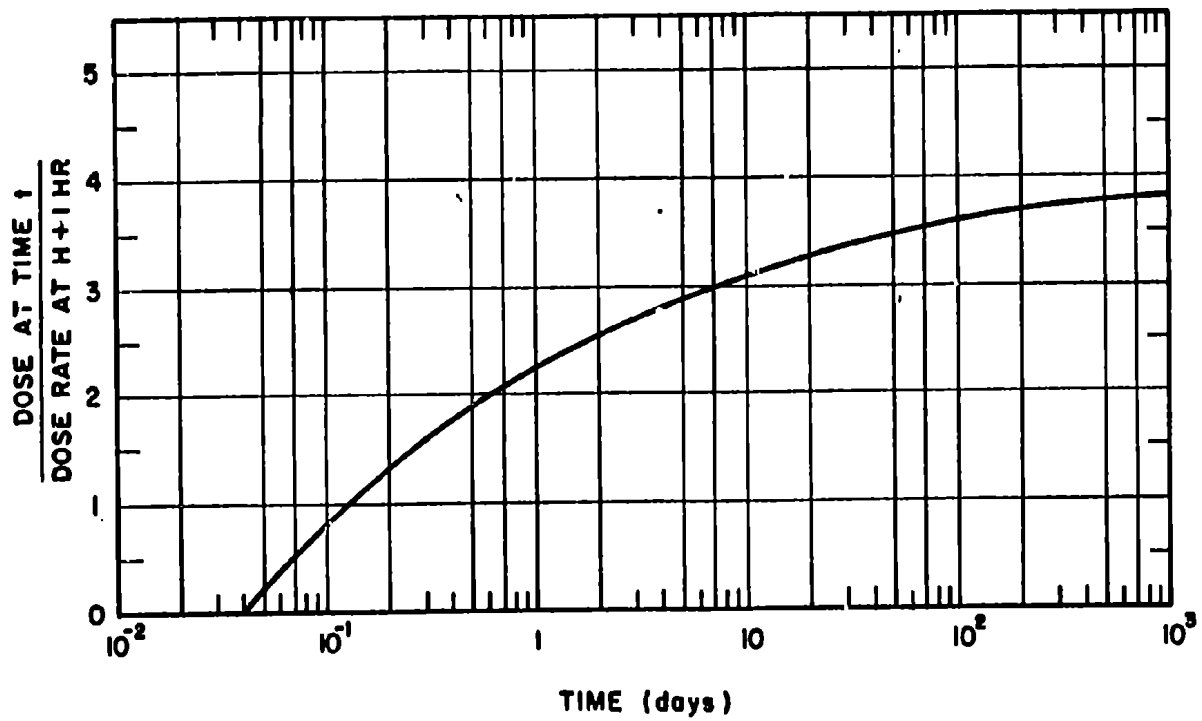

Figure 5-41. Normalized Dose Accumulated in a Fallout Contaminated Area from *H* + 1 Hour to *H* + 1,000 Days

[redacted]

Problem 5-12. Calculation of Fallout Gamma Radiation Dose Rate Contours for Bursts in the Transition Zone

[redacted] Figure 5-43 may be used to determine whether or not a burst is in the transition zone, i.e., below a height of burst of $100W^{0.35}$ feet. Burst heights below the curve in Figure 5-43 are in the transition zone. Burst heights above the curve are air bursts. In some situations, it may be desirable to consider bursts below $180W^{0.4}$ feet to be in the transition zone for conservative estimates. The means for doing this are discussed below. When a burst occurs in the transition zone, an approximation of the resulting fallout contamination patterns may be obtained by multiplying the dose rate contour values for a contact surface burst weapon of the same yield by an adjustment factor from Figure 5-44. The curves of Figure 5-44 were constructed under the assumption that the ratio of the dose rate values from a burst in the transition zone to the dose rate values for the same contour from a surface burst are proportional to the ratio of the volume of a segment of a sphere intercepted by the ground surface to the volume of the hemisphere, where the radius of the sphere is $100W^{0.35}$ feet, i.e.,

$$\text{Adjustment Factor} = \frac{\left(100 - \frac{h}{W^{0.35}}\right)^2 \left(200 + \frac{h}{W^{0.35}}\right)}{2 \times 10^6},$$

where h is the actual height of burst in feet, and W is the total weapon yield in kilotons.

[redacted] In view of the lack of data from bursts in the transition zone over a land surface, a more conservative estimate may be desired. In this case, the height of burst for the upper limit of the transition zone is taken to be $180W^{0.4}$ feet. The adjustment factor to be applied to dose rate values for the same contours from a surface burst of the same yield can be calculated from:

$$\text{Adjustment Factor} = \frac{\left(180 - \frac{h}{W^{0.4}}\right)^2 \left(360 + \frac{h}{W^{0.4}}\right)}{1.17 \times 10^7}.$$

[redacted] *Example* [redacted]

Given: A hypothetical weapon with a total yield of 600 kt, of which 200 kt results from fission, is burst 560 feet over a land surface with 10 knot effective wind conditions.

Find: The contour parameters for a dose rate of 15 rads/hr at $H + 1$ hour reference time over smooth terrain.

Solution: From Figure 5-43, a 600 kt weapon burst below about 940 feet would be in the transition zone. A height of burst of 560 feet is less than three quarters of the limiting altitude of the transition, so fallout is the only residual radiation to be considered. The 15 rads/hr contour for a fission yield to total yield ratio of 200/600 = 1/3 corresponds to the contour for 15 ÷ 1/3 = 45 rads/hr for a weapon of 600 kt fission yield. The dose rate over reasonably level terrain is about 70 percent of that over an ideal smooth plane. Thus, the ideal smooth plane contour parameters for this weapon burst on the surface would correspond to

$$\frac{45}{0.7} = 64 \text{ rads/hr}.$$

From Figure 5-44 (or from the normal adjustment factor equation given above) the height of burst adjustment factor for a 600 kt weapon burst at 560 feet is 0.21. Therefore, the desired contour parameters can be obtained by entering Figures 5-28, 5-31, 5-34, and 5-37 with a yield of 600 kt and reading the parameter values corresponding to an $H + 1$ hour dose rate of

$$\frac{64}{0.21} = 300 \text{ rads/hr}.$$

[redacted]

[redacted]

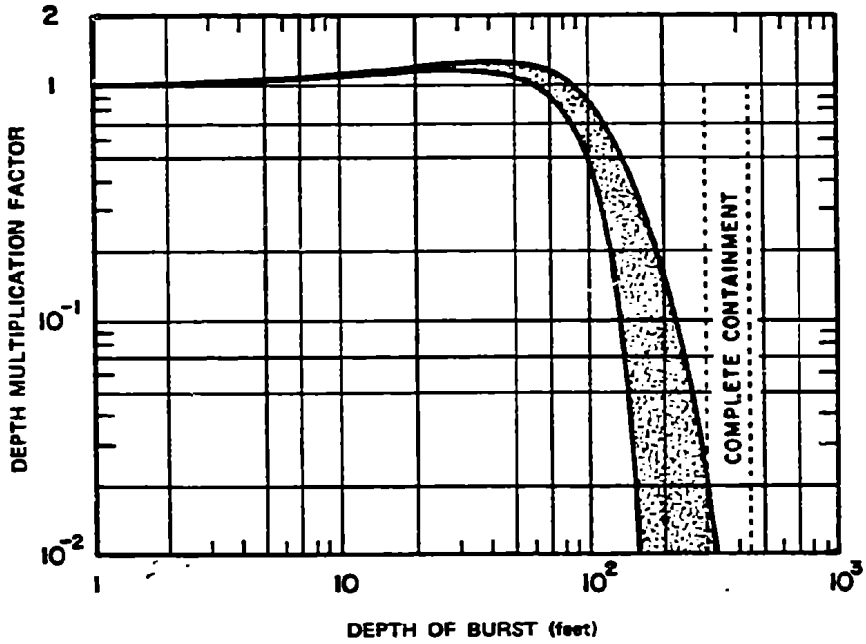

Figure 5–45. [redacted] Depth Multiplication Factor for Linear Dimensions of the Fallout Pattern from a 1 kt Explosion as a Function of Depth of Burst [redacted]

[redacted]

[redacted]

[redacted] RESIDUAL RADIATION FROM WATER SURFACE AND UNDERWATER BURSTS [redacted]

[redacted] The distinction between initial and residual radiation from underwater bursts is much less distinct than it is for air bursts or land surface or subsurface bursts. The radiation accompanying the base surge expands sufficiently rapidly as to become merged with what is normally considered initial radiation. In the case of water surface bursts, the distinction between initial and residual radiation is somewhat more clear cut, but in most cases the residual radiation will not be of great significance.

5-25 Water Surface Bursts [redacted]

[redacted] A base surge (paragraph 2-75, Chapter 2) is not expected to form as a result of a water surface burst, consequently a separation between initial and residual nuclear radiation can be made as in the case of a land surface explosion. An approximation of the initial nuclear radiation dose may be obtained from Figures 5-9 through 5-17 in Section I of this chapter. It must be emphasized, however, that the dose so obtained will be an approximation. The curves of Figures 5-9 through 5-17 are based on extensive computer calculations for a receiver on or near a *land* surface. These calculations included the effect of the ground-air interface, and a number of comparisons with measured data have substantiated the validity of the calculations. A limited number of comparisons of the same computer calculations have also indicated good agreement with initial gamma ray dose measurements made near a water surface after high yield explosions; however, these were not true water surface explosions, and no comparisons with neutron dose are available. Thus, in the absence of data and in the absence of comprehensive computer calculations, the curves of Figures 5-9 through 5-17 provide the best available data for simplified calculations of initial nuclear radiation dose from water surface bursts.

[redacted] For yields of more than a few kilotons, the cloud from a sea water surface burst is similar to that from a land surface or low air burst of the same yield. The cloud height and horizontal extent are determined primarily by the yield and by atmospheric conditions. For megaton yields, the maximum cloud height may be somewhat greater than that for a land surface burst, as a result of the release of latent heat from condensation of vaporized sea water. For very low yields, it is possible that the maximum cloud height may be less than for a land or low air burst, as a result of interference from the disturbed water. It is also possible, under certain atmospheric conditions, that the sea salt raised and dispersed in the atmosphere by low yield explosions may have a cloud-seeding effect. In this event, the water burst could produce a larger, higher cloud than a land burst, and the dispersion of salt would trigger a rainout of radioactivity.

[redacted] The possible cloud seeding described above is only one example of the extreme sensitivity of fallout from water surface bursts to atmospheric conditions, especially relative humidity. This sensitivity results from the hygroscopic (water-absorbing) nature of the fallout particles. These particles consist mainly of sea salt and water. When dry, they are generally much smaller and lighter than fallout particles from land surface bursts. Because water burst particles are smaller than those from land bursts, water bursts produce less close-in fallout than land bursts. In particular, water bursts, unlike land bursts, generally will not produce a region of intense fallout (several thousand r/hr) near surface zero. The one possible exception is a water burst in an extremely humid atmosphere.

[redacted] Water surface bursts are even less likely to produce regular cigar-shaped fallout patterns than land surface bursts. The effect of atmo-

[redacted]

[redacted]

[redacted] spheric humidity introduces further irregularities in fallout patterns. Also, because water surface burst particles take longer to fall than particles from land surface bursts, wind and weather conditions are more likely to change during the time of fallout transport and deposition. It is often difficult to define a downwind direction in the fallout pattern. The apparent downwind direction may vary with yield and with time after burst at which the pattern is observed or calculated.

[redacted] In almost all cases, the region of maximum deposit intensity is not around surface zero but considerably downwind. Thus, for a 10 Mt burst, the calculated region of a normalized dose rate of at least 300 r/hr at 1 hour extends from about 125 to 300 miles from surface zero. The dose rate would, of course, be much lower at the time of arrival and would vary throughout the area as a result of varying arrival times.

[redacted] As material in the cloud rises, it cools by entraining ambient air, and by expanding with increasing altitude. Fallout particles form by condensation of vapor and grow by coagulation; that is, by collision and adhesion of smaller particles to form larger particles. The vapor condensation may be considered a 3-stage process.

[redacted] In the first stage, calcium and magnesium from the sea water and iron, and other metals from the weapon condense as oxides. In the second stage sodium chloride, which is about 90 percent of dried sea salt, condenses on the nuclei provided by the stage 1 particles. In the third stage, water vapor condenses to liquid water or to ice, on the stage 2 particles.

[redacted] The median diameter of the stage 1 particles is about 1 micron contrasted to a few hundred microns for a land surface burst. The size is expected to increase slightly with yield, because the particles are formed by diffusion onto nuclei while the fireball is cooling by thermal radiation. The larger the fireball, the slower the cooling rate. The slower the cooling rate, the more time is available for diffusive growth.

[redacted] During and after the three condensation stages, coagulation causes particle growth. Particles of sub-micron size coagulate as a result of Brownian motion. Somewhat larger particles coagulate due to turbulent accelerations in the cloud. Turbulent coagulation only appears to be of importance in clouds from megaton bursts. Even larger particles grow by gravitational coagulation; that is, as they fall through the cloud they overtake and capture smaller particles. Gravitational coagulation is particularly important for low-yield bursts in humid atmospheres. The process is similar to one of the mechanisms for growth of ordinary raindrops. The largest particles formed, i.e., those from low yield bursts in a humid atmosphere, may have actual diameters of 2,000 microns. Particles of this size fall out of the cloud rapidly. Thus, there is a practical limit on the growth of particles in the cloud.

[redacted] Moisture effects play a dominant part in water surface burst fallout. In general, the more humid the atmosphere, the more radioactivity is deposited as close-in fallout. Most of the moisture contained in the clouds of low yield bursts comes from entrained air. Consequently, the higher the humidity, the greater the cloud moisture content. In turn, the salt particles absorb more water, and, as they get larger, gravitational coagulation proceeds faster.

[redacted] Moisture not only has a direct effect on particle formation, but also has an indirect effect on cloud height. The top of the cloud from a 20 kt water surface burst in a very humid tropical atmosphere may reach the tropopause at about 55,000 feet. In a less humid atmosphere, the cloud from a burst of the same yield may rise less than half as high (see Figure 5-39). Salt particles absorb moisture from humid air; the moisture evaporates when the particles are exposed to relatively dry air. Consequently the

[redacted]

[redacted]

[redacted] size, falling rate, and time and place of deposit of water surface burst fallout particles vary with the atmospheric humidity the particles encounter during their trajectories. As the particles fall, they usually shrink by evaporation and may become completely dry, with a diameter of at most 100 to 200 microns. They then fall very slowly, and move large horizontal distances as a result of the forces exerted by the wind. Finally, the particles reach the more humid air near sea level, begin to grow by absorbing moisture, and fall faster. Thus, although particles from a megaton burst may leave the cloud with a water content almost entirely derived from sea water, this water may evaporate completely during fall, and the water content of the particles that reach the surface is entirely atmospheric moisture. An exception to this situation could occur for a burst in an arctic atmosphere. The cold air retards evaporation, even if humidity is low, and some of the original sea water could remain on the particles.

[redacted] Maximum fallout intensity, as well as the area covered by fallout from a water surface burst increases with weapon yield. For yields between 1 kt and 100 kt, the normalized $H + 1$ hour exposure rates are expected to be negligible. The highest normalized intensities from a 100 kt explosion are expected to be more than 50 roentgens per hour (r/hr), but less than 100 r/hr. The highest intensities from a 1 Mt burst are expected to be over 100 r/hr but less than 300 r/hr. Finally, a 10 Mt burst is expected to produce intensities over 300 r/hr, but less than 1,000 r/hr. Since all of these exposure intensities are normalized to $H + 1$ hour, and the fallout will arrive at significantly longer times after burst for the larger yields (depending upon the wind), the radioactivity will have decayed to much smaller levels prior to the time of arrival and fallout generally is not expected to be a governing effect from water surface bursts.

5-26 Underwater Bursts [redacted]

[redacted] An underwater burst creates a highly energetic bubble, whose history determines the major above-surface effects. For very shallow explosions, the bubble expands through the water surface with a high internal pressure, and develops a hollow column through which the bubble blows out into the atmosphere in the form of a cloud at the column top. For a somewhat greater depth, the bubble expands through the water surface at lower internal pressure and a column again forms, but no blowout occurs. Transition from columnar formations to plume-like eruptions, hemispherical in shape, takes place as the depth increases. The migration of the underwater bubble through the surface near its minimal phase at or shortly after its maximum-expansion phase creates the plumes. For deep explosions, the bubble may experience several oscillations as it migrates upwards. If the explosion is very deep, the bubble will degenerate and break up before reaching the surface. It is possible that an explosion may take place at such a great depth that little, if any, disturbance will be noted on the surface.

[redacted] The ejected water, whether a column or a plume, will fall back to the surface rapidly. This massive subsidence creates a radially expanding aerosol cloud, or base surge, at the water surface. The base surge expands as a ring or disk until it dissipates energy received from the subsidiary plumes or columns. After expanding, it drifts with the surface winds. Some evidence suggests the base surge has the same initial bulk density as that of the plumes or columns from which it is formed, being several times the density of air. As it travels downwind, it will react to the existing atmospheric conditions; e.g., evaporating or developing into low-cloud formations. These physical phenomena are described in more detail in Section IV, Chapter 2.

[redacted] Three sources of radioactivity are the

[redacted]

[redacted]

[redacted] major contributors to the radiation above the surface subsequent to an underwater explosion: initial, above surface nuclear radiation; base surge; and residual radioactivity deposited in the mixed layer of the ocean. These sources are very time dependent, and they are affected by atmospheric and oceanic variables.

[redacted] Even for a shallow underwater explosion the neutron and secondary gamma portions of the initial nuclear radiation are essentially negligible. The initial above-surface source includes the fission product activity contained in the visible column and crown, or plume. This source contains radioactivity ejected into the atmosphere as a result of underwater hydrodynamic phenomena. The scaled depth of burst is a major factor in determining the extent to which this initial radiation contributes to the total above surface exposure. The rapid development and spread of the base surge (paragraph 2-75, Chapter 2) causes the initial and residual radioactivity from an underwater burst to merge into one more or less continuous source.

[redacted] The base surge develops as a result of both underwater flow phenomena and the collapse of the water masses associated with the initial source. This radially expanding surge grows to large dimensions as a dense, fog-like aerosol carrying with it a substantial fraction of suspended fission products. This source is either annular or disk-shaped in geometry and extends from the ocean surface to a height of several thousand feet. The base surge is influenced strongly by the wind, moving as an entity at the existing wind speed and direction. Initially it is highly radioactive; however, as it expands and dilutes, the concentration of the fission products decreases. This dispersion, coupled with rapid radioactivity decay, results in comparatively low exposure rates by the first half-hour after burst.

[redacted] The residual radioactivity in the surface layer of the ocean is the third, and final, major source of radiation. This radioactive pool is moved by the local currents, which depend on the existing oceanographic conditions. The pool is initially a disk which upon expansion approximates an annulus, although at times significantly later than a half-hour, it reverts to an irregular disk shape. Eventual mixing down to the top of the thermocline and the action of horizontal turbulent diffusion result in rapid dilution of the pool, reducing its hazard as time progresses.

[redacted] The gamma radiation hazard created by the initial source, base surge, and pool resulting from an underwater nuclear explosion varies significantly with weapon yield and burst depth, proximity of the ocean bottom to the point of detonation, wind velocity and current velocity. Consequently, a description of the radiation fields (exposure rate and total exposure) associated with an underwater burst is complex, and no simplified prediction system suitable for general application has been developed.

[redacted] A prediction system, DAEDALUS, has been developed to compute the radiological effects of underwater nuclear bursts. In this system, all above-surface sources, as well as the radioactive pool, are approximated by cylinders homogeneously contaminated with mixed fission products. The dimensions, water concentrations, and fission product contents of these cylindrical sources are estimated from empirical and theoretical considerations. Having defined the radioactive sources, DAEDALUS calculates, for each time of interest, exposure rates from these sources at specified detector locations. At each location the exposure rates are summed over time and the total exposure is thus cumulated. In the absence of a simple prediction system suitable for inclusion in this manual, examples of the results of DAEDALUS calculations are presented to provide an appreciation of the potential magnitude of the problems associated with radioactivity from underwater nuclear bursts.

[redacted]

[redacted]

Table 5-7. [redacted] Examples Selected for Base Surge and Pool Exposure Rates [redacted]

Yield (kt)	Explosion Depth (ft)	Depth of Water (ft)	Base Surge Figure Number	Pool Figure Number
10	65	5,000	5-46	5-52
10	65	65	5-47	5-53
10	150	5,000	5-48	5-54
10	500	5,000	5-49	5-55
10	1,000	5,000	5-50	5-56
10	1,500	5,000	5-51	5-57

[redacted] A yield of 10 kt was selected to illustrate the effects of depth of burst and water depth on the time dependence of the gamma ray exposure rates from the base surge and the pool. Table 5-7 shows combinations of depth of burst and water depth that were selected. Table 5-7 also indicates the corresponding figures that show exposure rates as a function of time and radial distance from the source for the base surge and the pool respectively. A no-wind environment was chosen for these examples, and, in the case of the pools, a no-current environment was assumed.

[redacted] Figures 5-58 through 5-75 show the accumulated exposures for two scaled depths ($d_b \approx 30W^{1/3}$ and $d_b \approx 280W^{1/4}$), corresponding to very shallow and deep explosions, respectively (Figure 2-105, Chapter 2). The doses are shown for 1, 10, and 100 kt explosions at each scaled depth. Two minute, 10 minute, and 30 minute exposures are shown for each yield at each scaled depth. In all cases it was assumed that the depth of the water was 5,000 feet, the effective wind was 15 knots, and a no-current condition existed. Table 5-8 identifies the figure for each combination of yield, burst depth, and exposure time.

Table 5-8. [redacted] Examples Selected for Total Exposure [redacted]

Yield (kt)	Explosion Depth (ft)	Exposure Time		
		2 Minutes	10 Minutes	30 Minutes
1	30	Fig. 5-58	Fig. 5-59	Fig. 5-60
10	65	Fig. 5-61	Fig. 5-62	Fig. 5-63
100	140	Fig. 5-64	Fig. 5-65	Fig. 5-66
1	280	Fig. 5-67	Fig. 5-68	Fig. 5-69
10	500	Fig. 5-70	Fig. 5-71	Fig. 5-72
100	890	Fig. 5-73	Fig. 5-74	Fig. 5-75

[redacted]

[redacted]

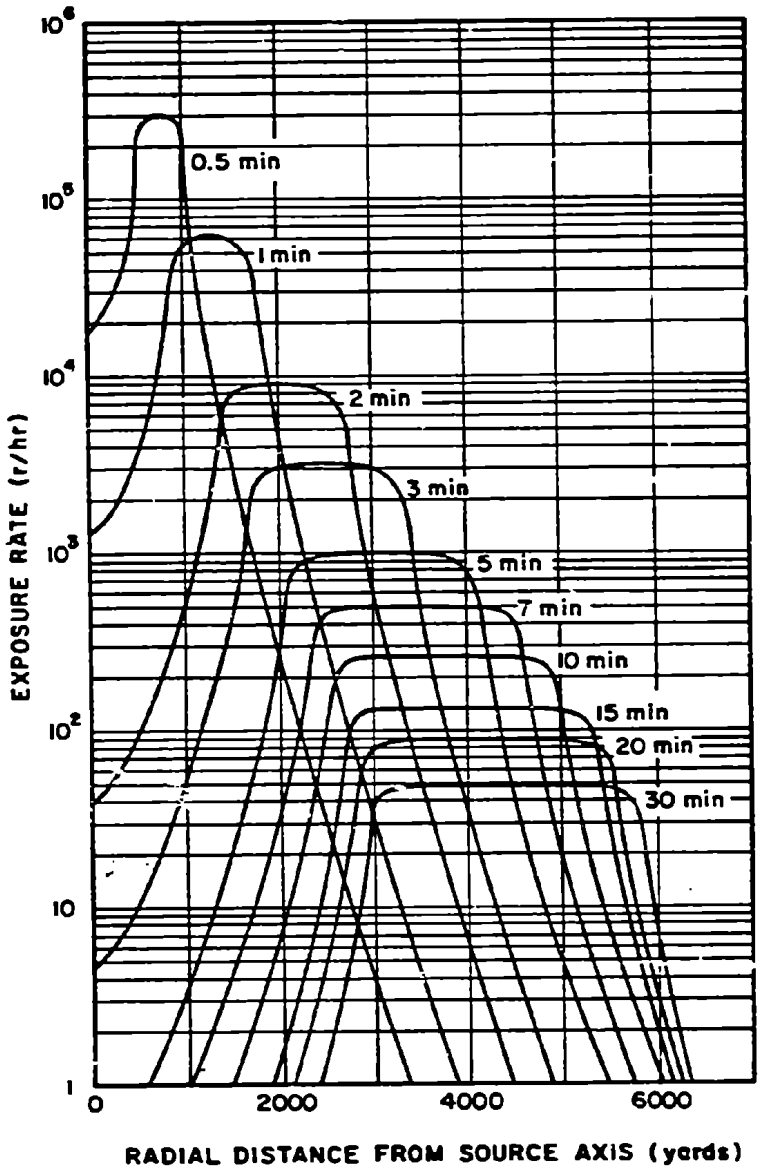

Figure 5-46. [redacted] Base Surge Radiation Exposure Rate 15 Feet Above the Water Surface from a 10 kt Explosion at a Depth of 65 Feet in 5,000 Feet of Water, No-Wind Environment [redacted]

[redacted]

[redacted]

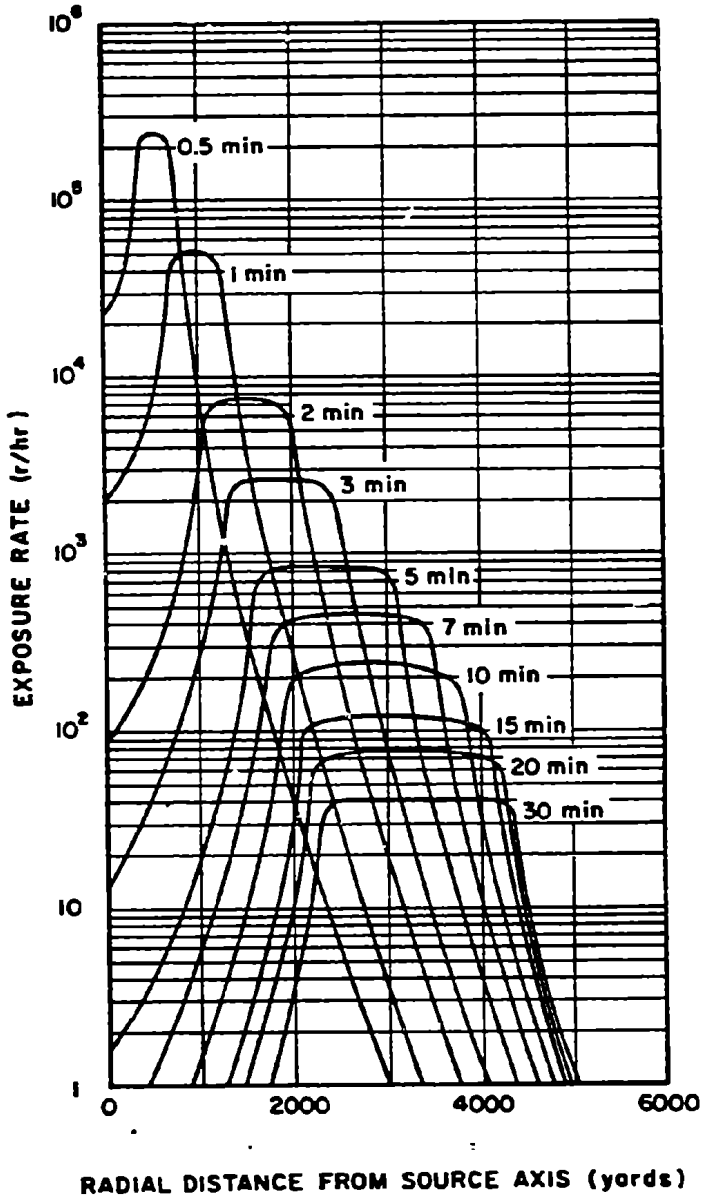

Figure 5-47. [redacted] Base Surge Radiation Exposure Rate 15 Feet Above the Water Surface from a 10 kt Explosion on the Bottom in 65 Feet of Water, No-Wind Environment [redacted]

[redacted]

[redacted]

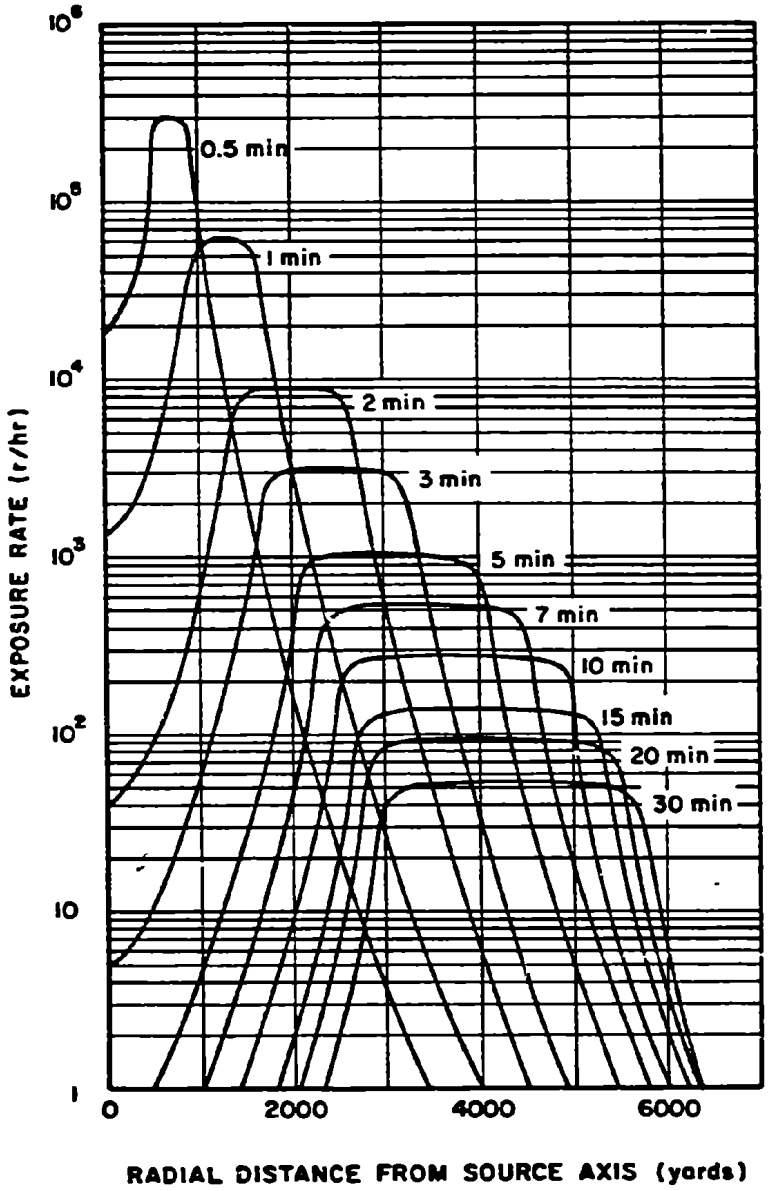

Figure 5-48. [redacted] Base Surge Radiation Exposure Rate 15 Feet Above the Water Surface from a 10 kt Explosion at a Depth of 150 Feet in 5,000 Feet of Water, No-Wind Environment [redacted]

[redacted]

[redacted]

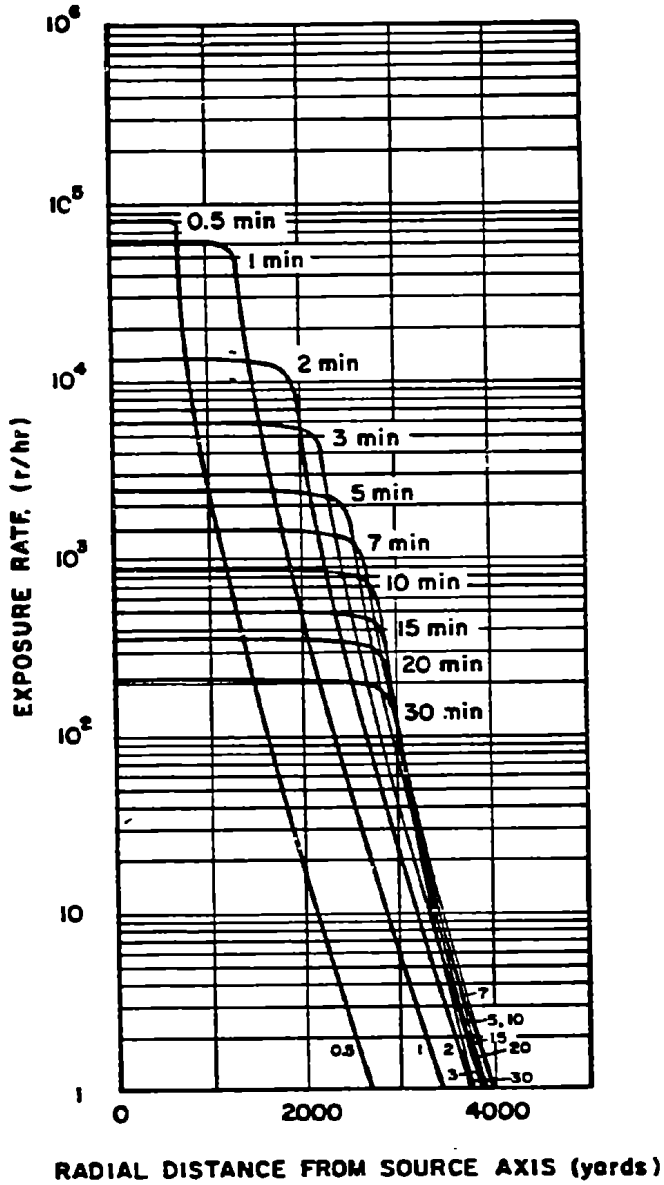

Figure 5-49. [redacted] Base Surge Radiation Exposure Rate 15 Feet Above the Water Surface from a 10 kt Explosion at a Depth of 500 Feet in 5,000 Feet of Water, No-Wind Environment [redacted]

[redacted]

[redacted]

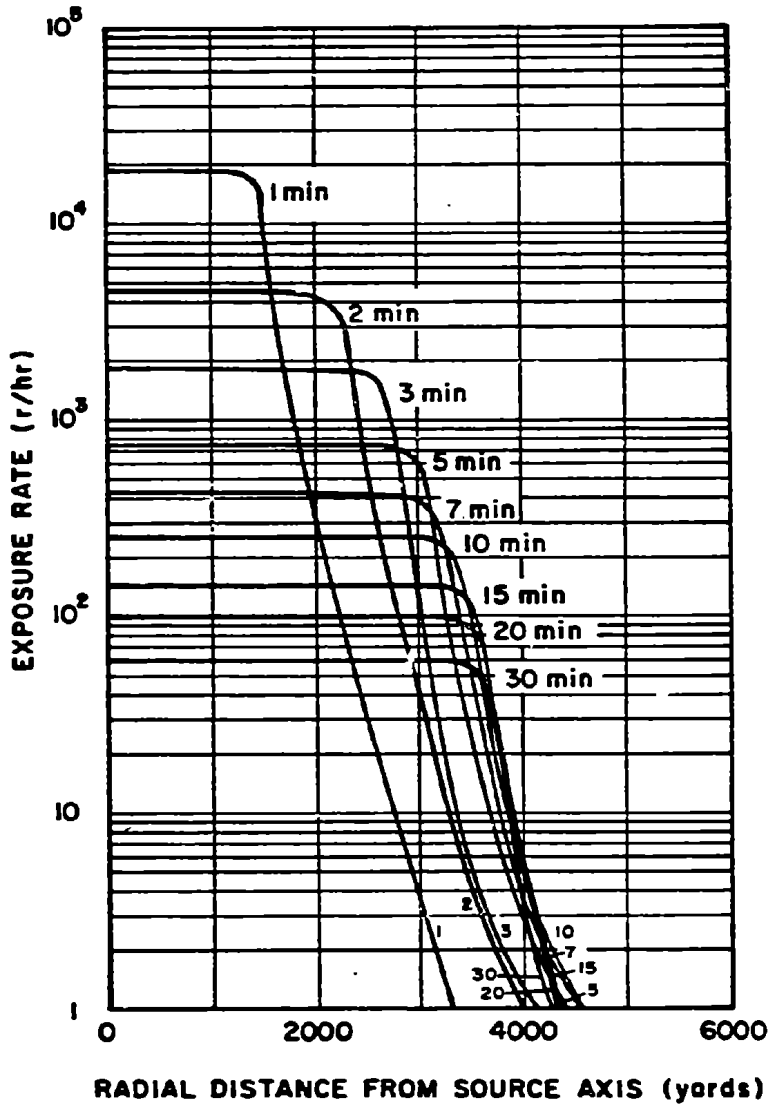

Figure 5-50. [redacted] Base Surge Radiation Exposure Rate 15 Feet Above the Water Surface from a 10 kt Explosion at a Depth of 1,000 Feet in 5,000 Feet of Water, No-Wind Environment [redacted]

[redacted]

[redacted]

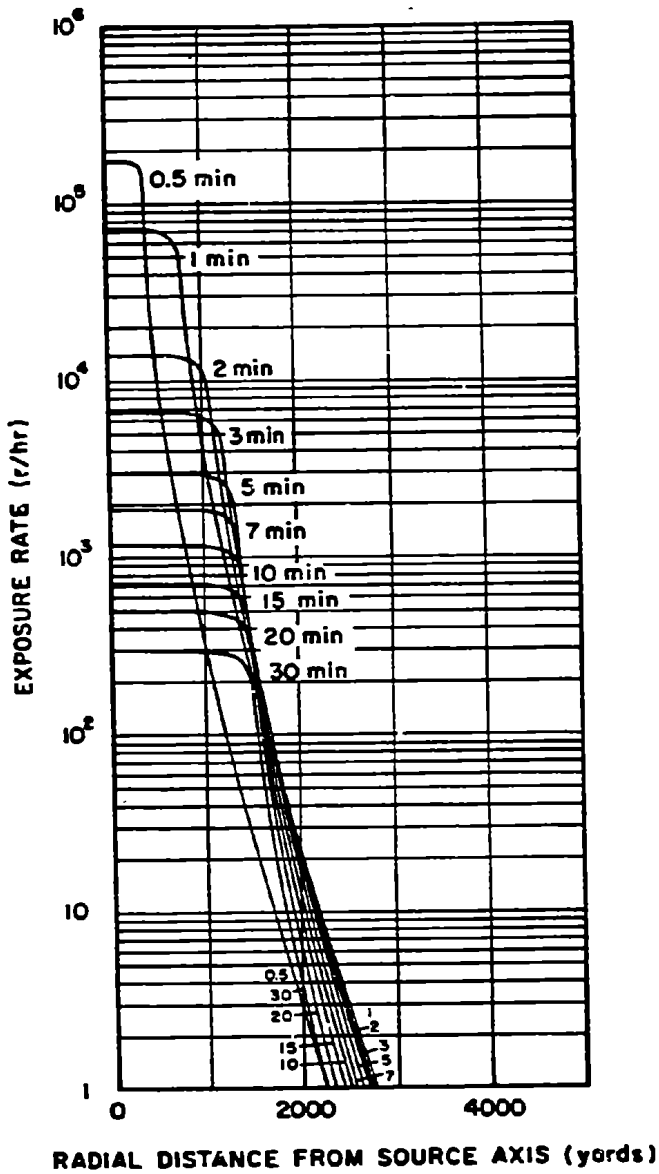

Figure 5-51. [redacted] Base Surge Radiation Exposure Rate 15 Feet Above the Water Surface from a 10 kt Explosion at a Depth of 1,500 Feet in 5,000 Feet of Water, No-Wind Environment [redacted]

[redacted]

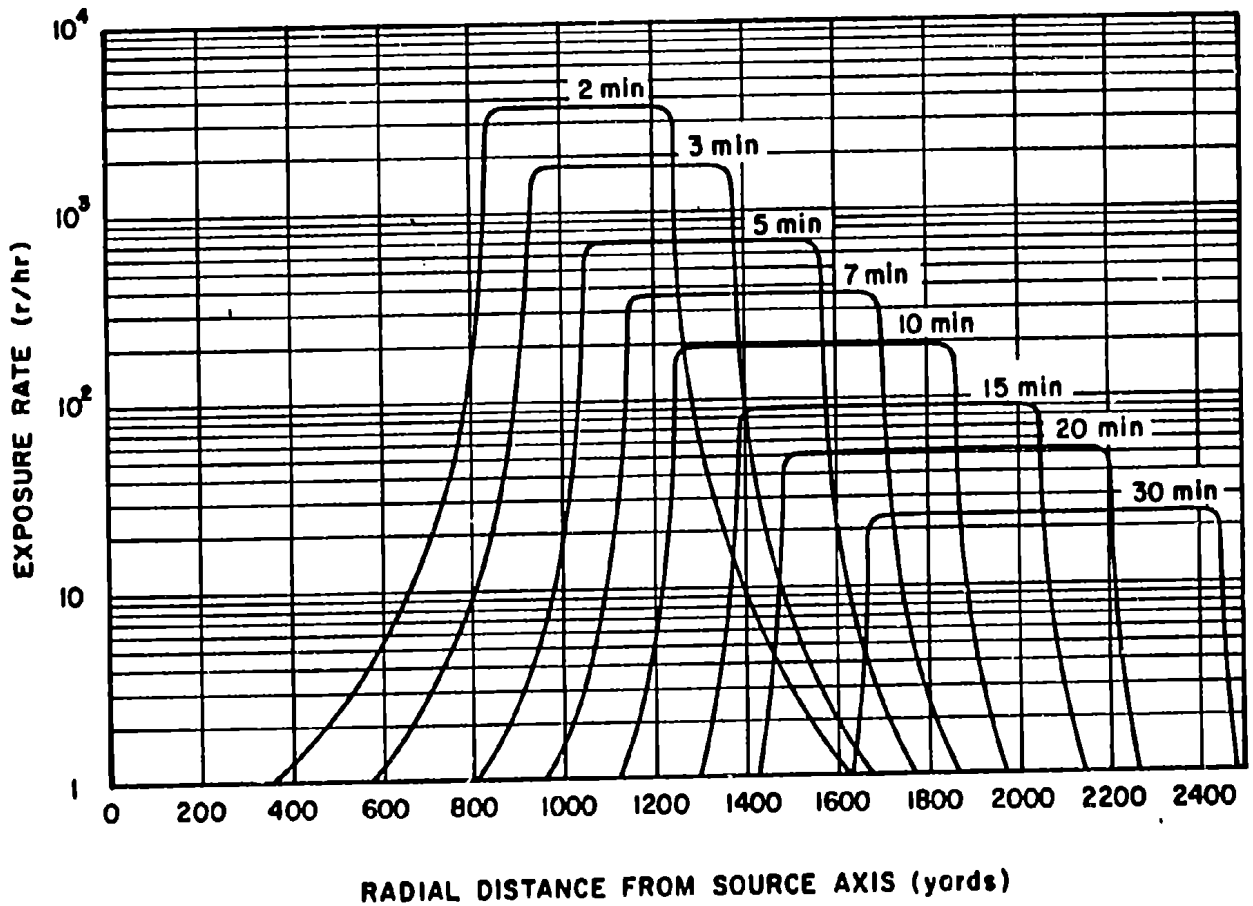

Figure 5-52. [redacted] Pool Radiation Exposure Rate 15 Feet Above the Water Surface from a 10 kt Explosion at a Depth of 65 Feet in 5,000 Feet of Water, No-Current Environment [redacted]

[redacted]

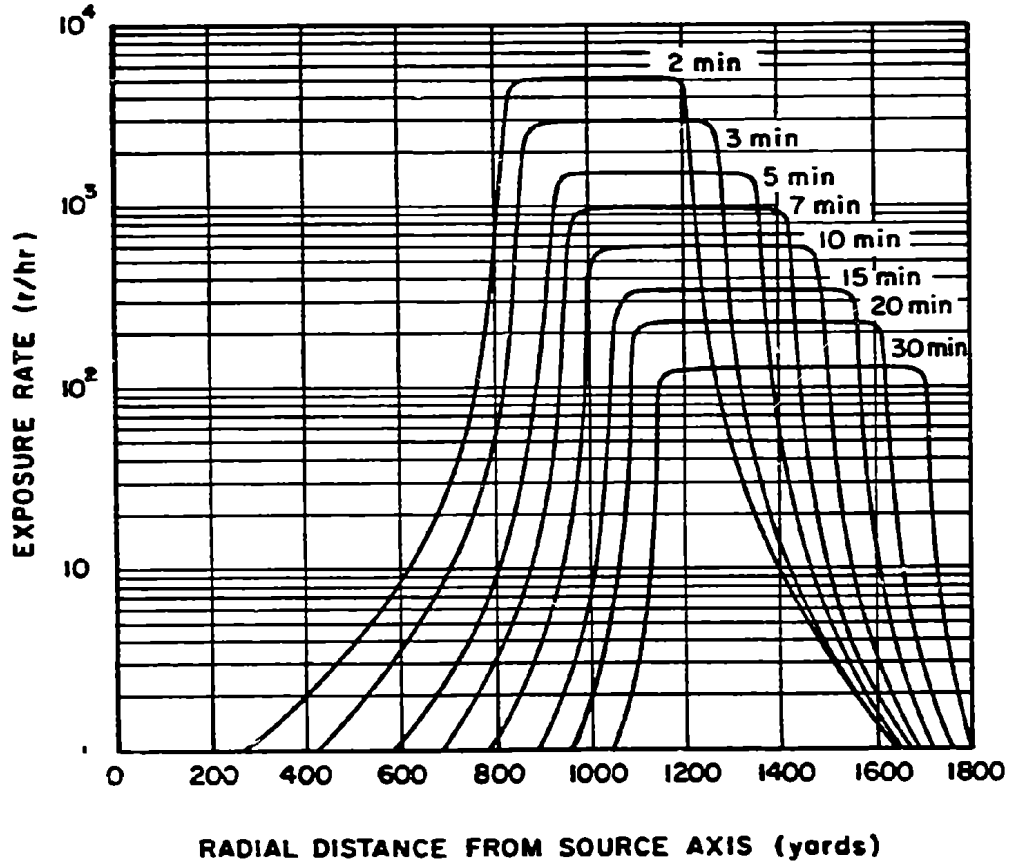

Figure 5-53. [redacted] Pool Radiation Exposure Rate 15 Feet Above the Water Surface from a 10 kt Explosion on the Bottom in 65 Feet of Water, No-Current Environment [redacted]

[redacted]

[redacted]

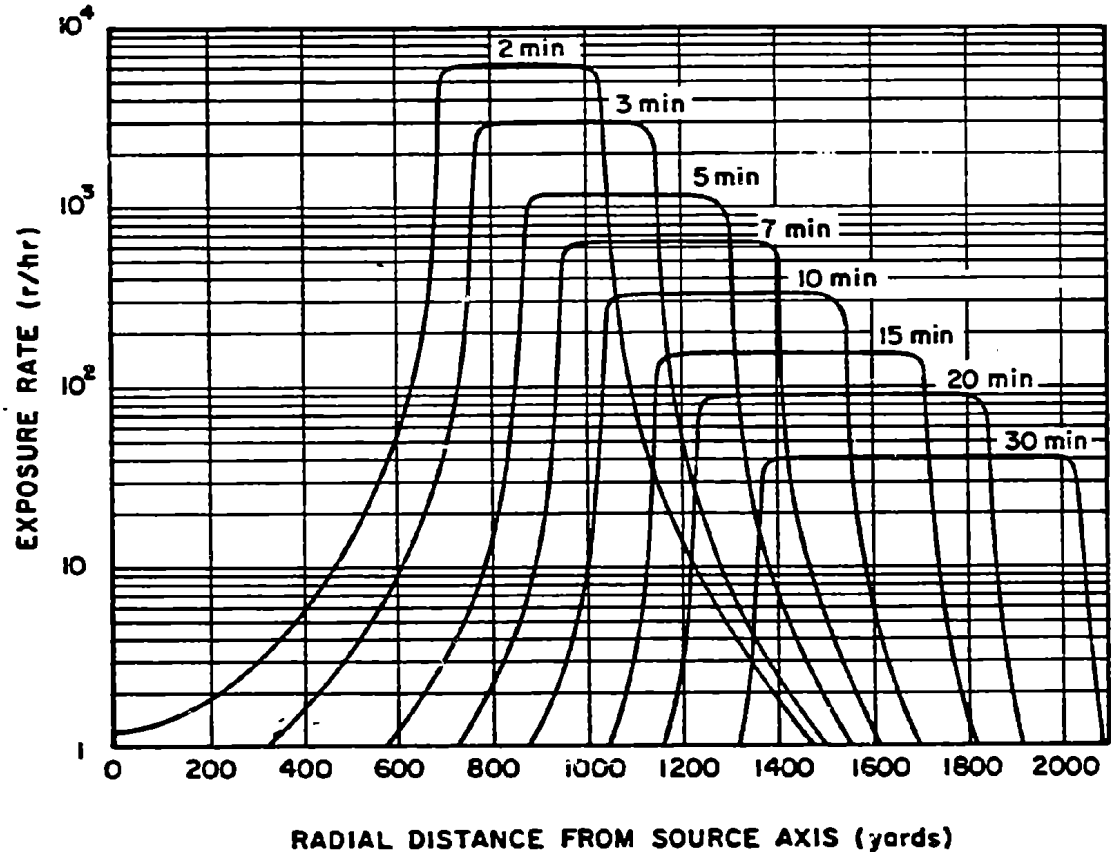

Figure 5-54. [redacted] Pool Radiation Exposure Rate 15 Feet Above the Water Surface from a 10 kt Explosion at a Depth of 150 Feet in 5,000 Feet of Water, No-Current Environment [redacted]

[redacted]

[redacted]

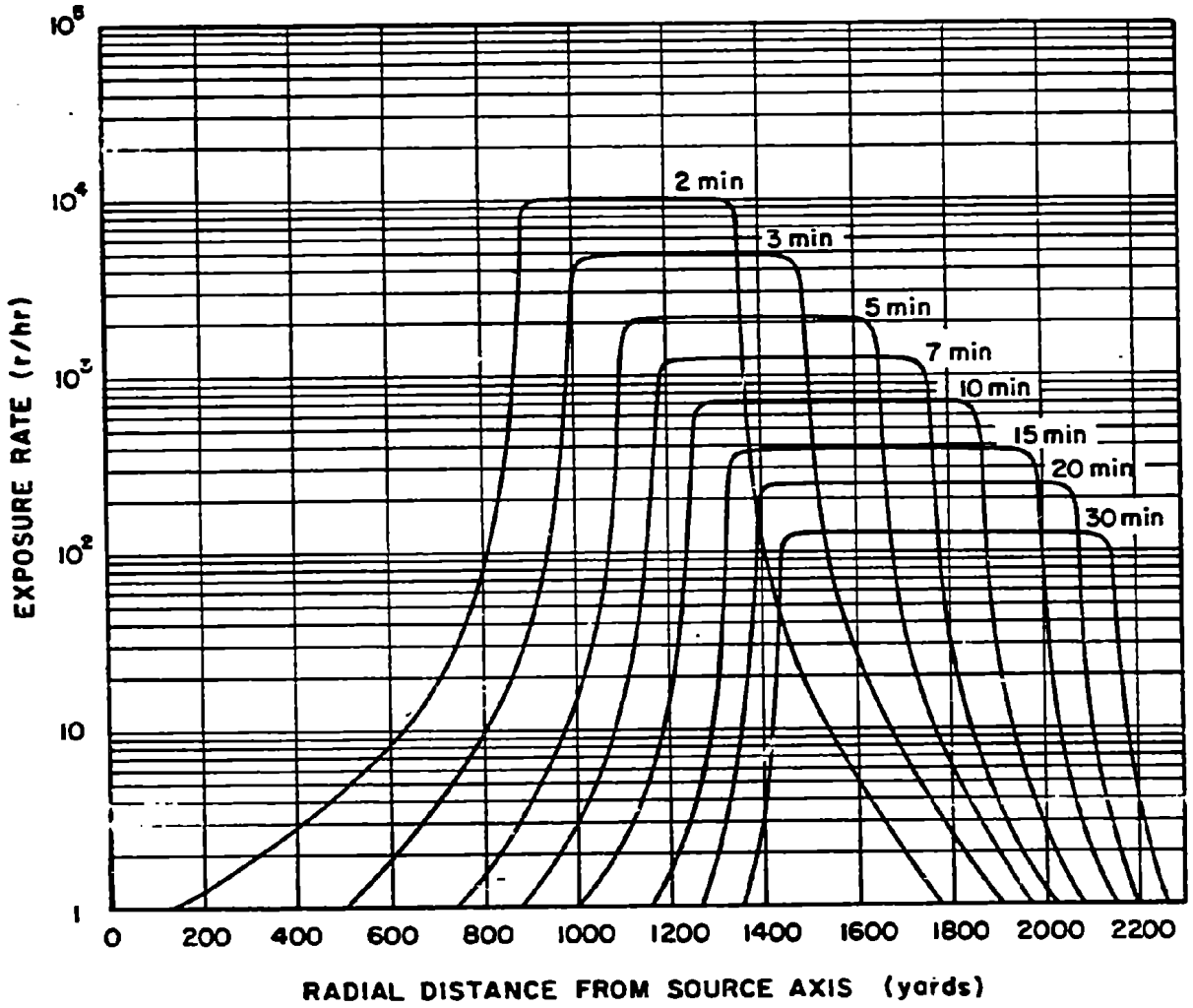

Figure 5-55. [redacted] Pool Radiation Exposure Rate 15 Feet Above the Water Surface from a 10 kt Explosion at a Depth of 500 Feet in 5,000 Feet of Water, No-Current Environment [redacted]

[redacted]

[redacted]

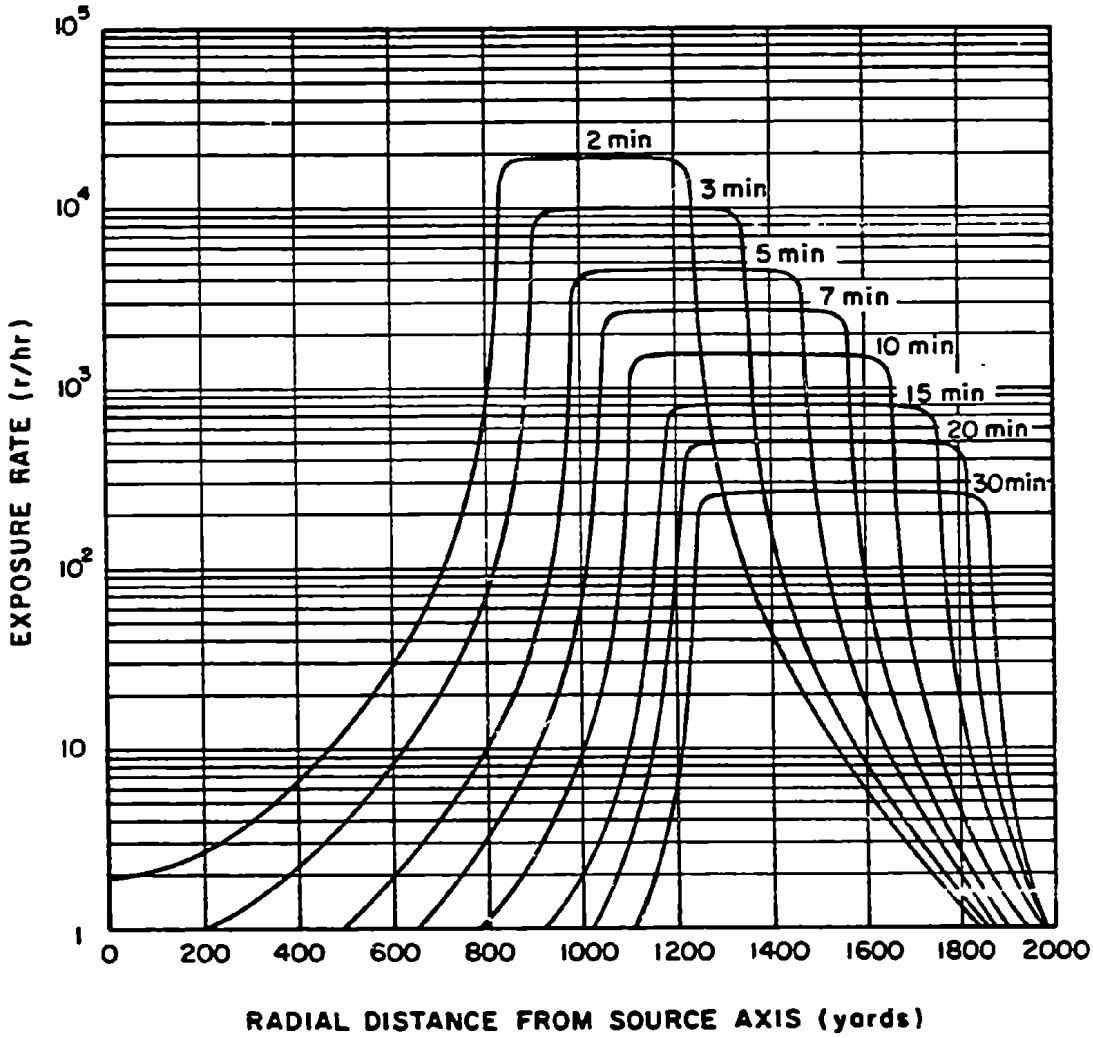

Figure 5-56. [redacted] Pool Radiation Exposure Rate 15 Feet Above the Water Surface from a 10 kt Explosion at a Depth of: 1,000 Feet in 5,000 Feet of Water, No-Current Environment [redacted]

[redacted]

[redacted]

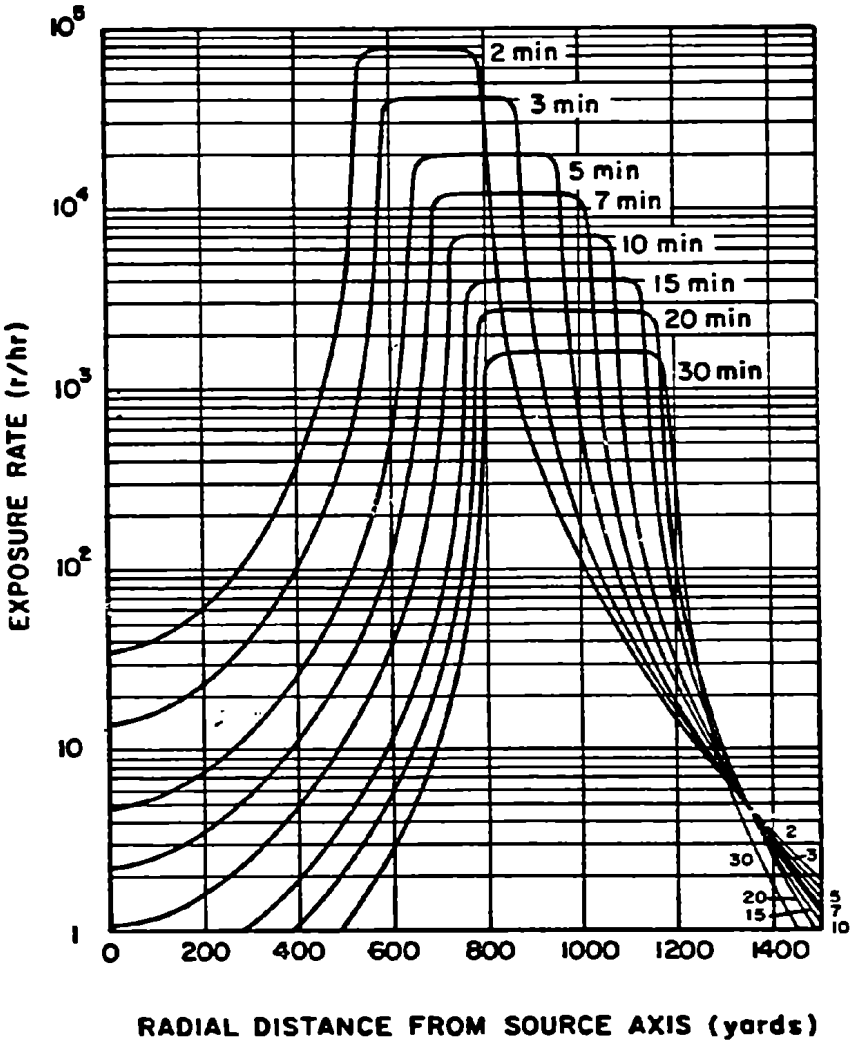

Figure 5-57. [redacted] Pool Radiation Exposure Rate 15 Feet Above the Water Surface from a 10 kt Explosion at a Depth of 1,500 Feet in 5,000 Feet of Water, No-Current Environment [redacted]

[redacted]

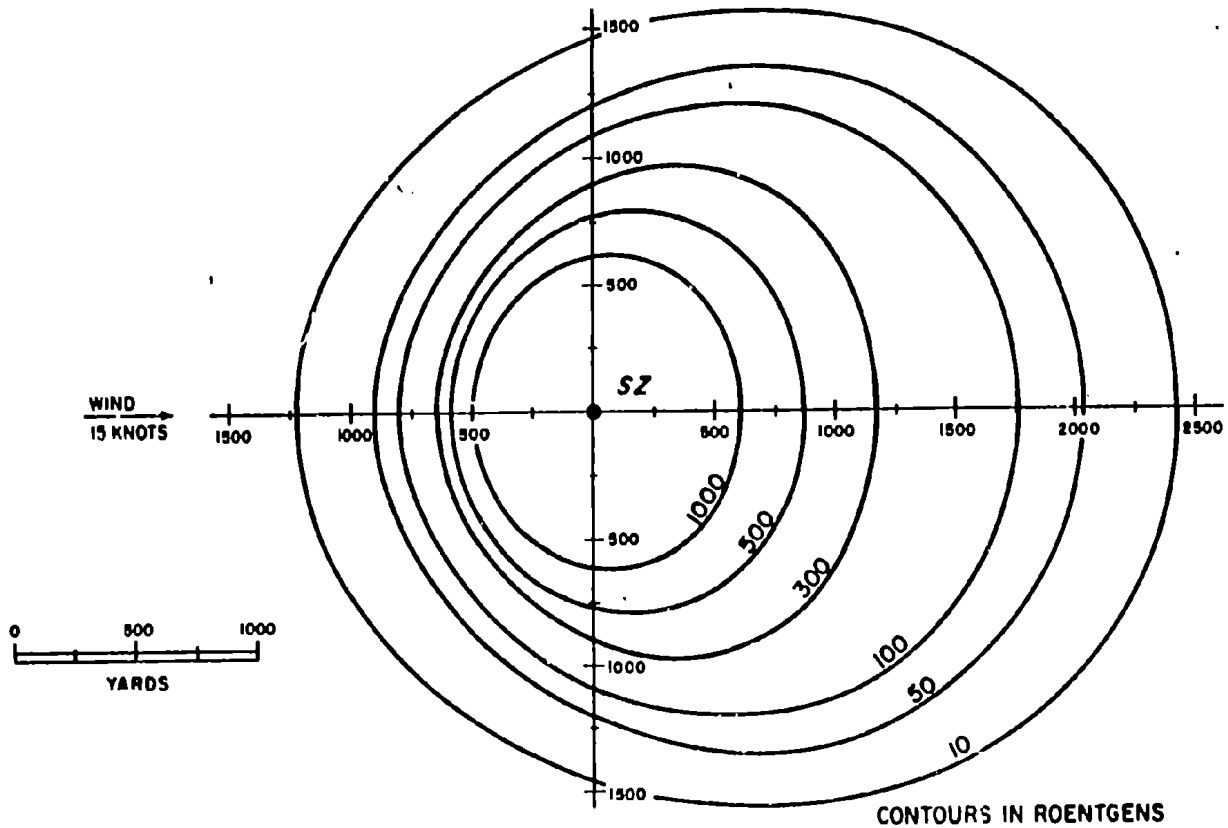

Figure 5-58. [redacted] Two-Minute Total Exposure 15 Feet Above the Water Surface from a 1 kt Explosion at a Depth of 30 Feet in 5,000 Feet of Water, 15 Knot Wind, No-Current Environment [redacted]

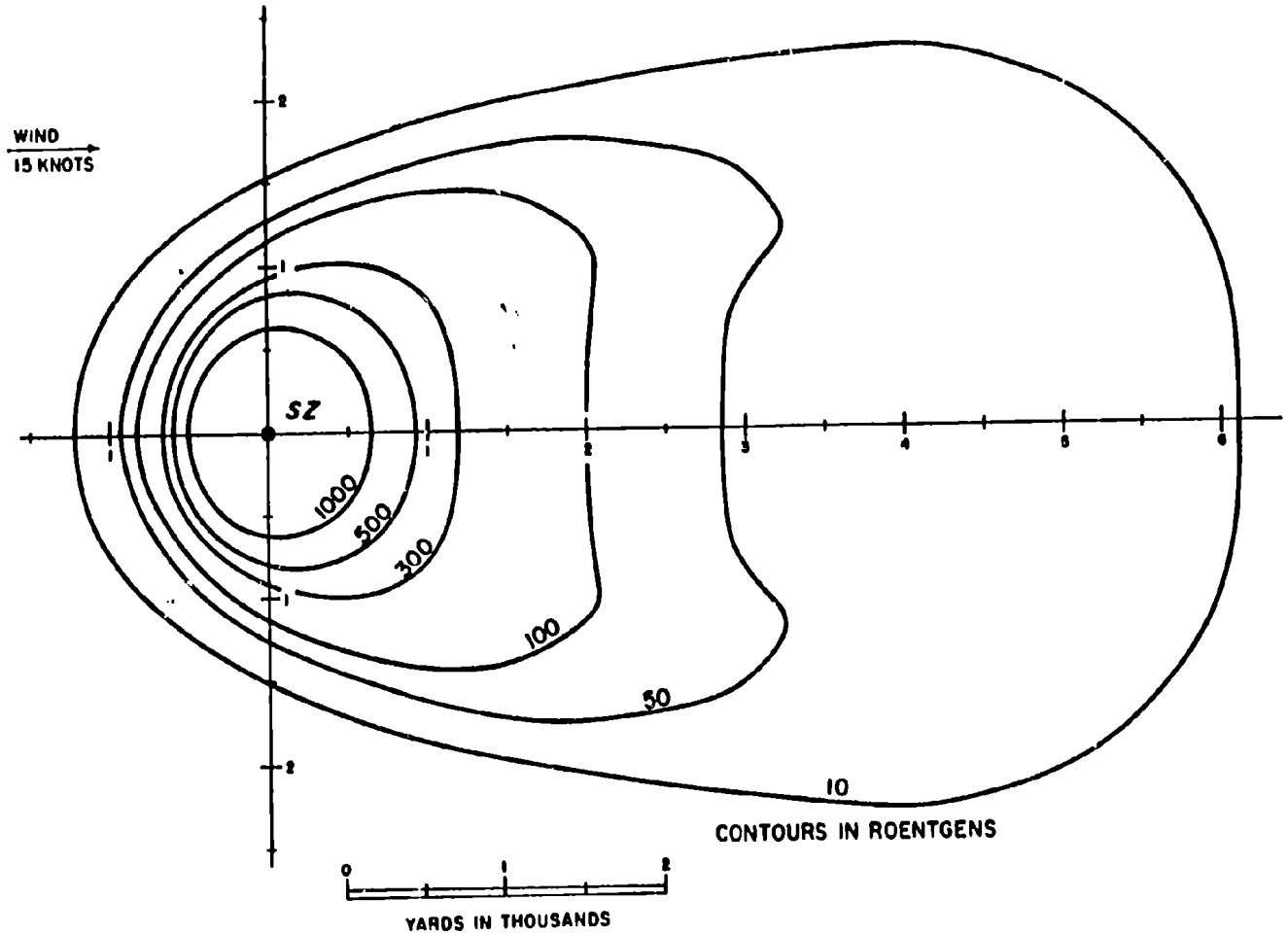

Figure 5-59. [redacted] Ten-Minute Total Exposure 15 Feet Above the Water Surface from a 1 kt Explosion at a Depth of 30 Feet In 5,000 Feet of Water, 15 Knot Wind, No-Current Environment [redacted]

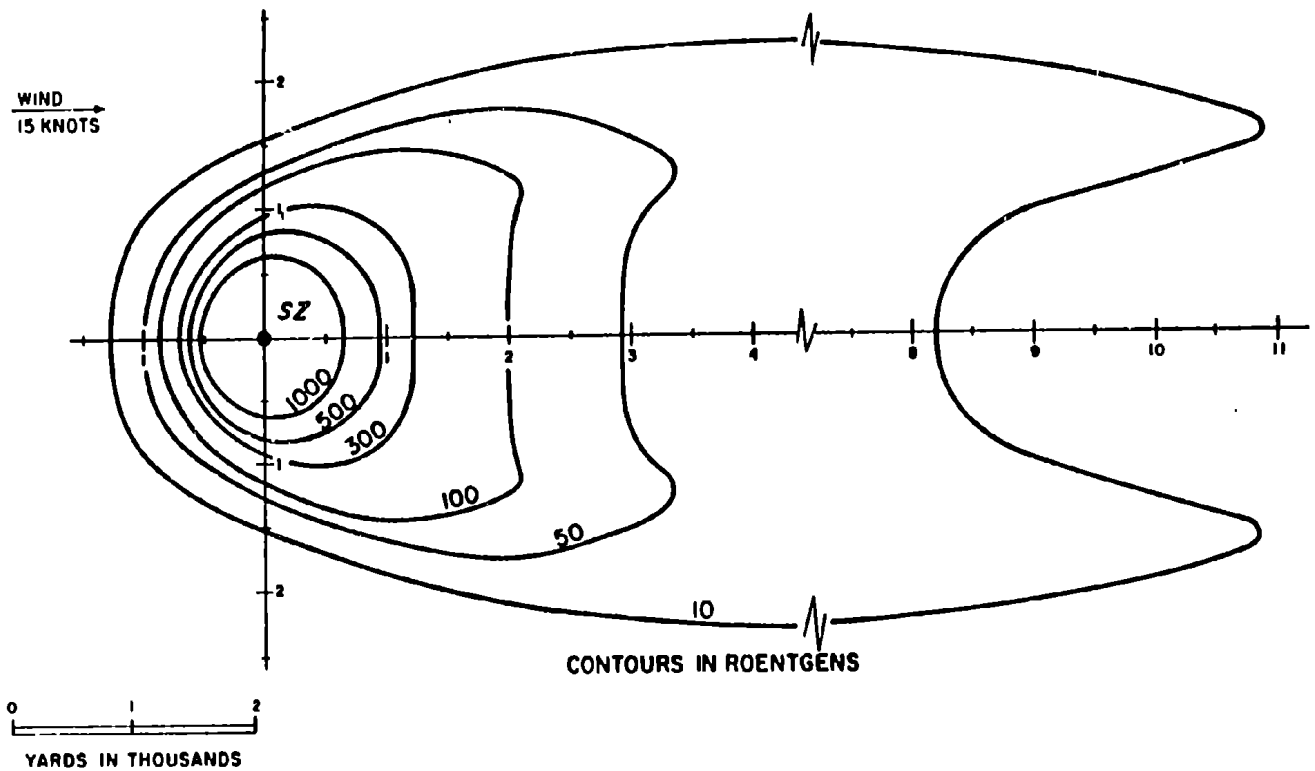

Figure 5-60. [redacted] Thirty-Minute Total Exposure 15 Feet Above the Water Surface from a 1 kt Explosion at a Depth of 30 Feet in 5,000 Feet of Water, 15 Knot Wind, No-Current Environment [redacted]

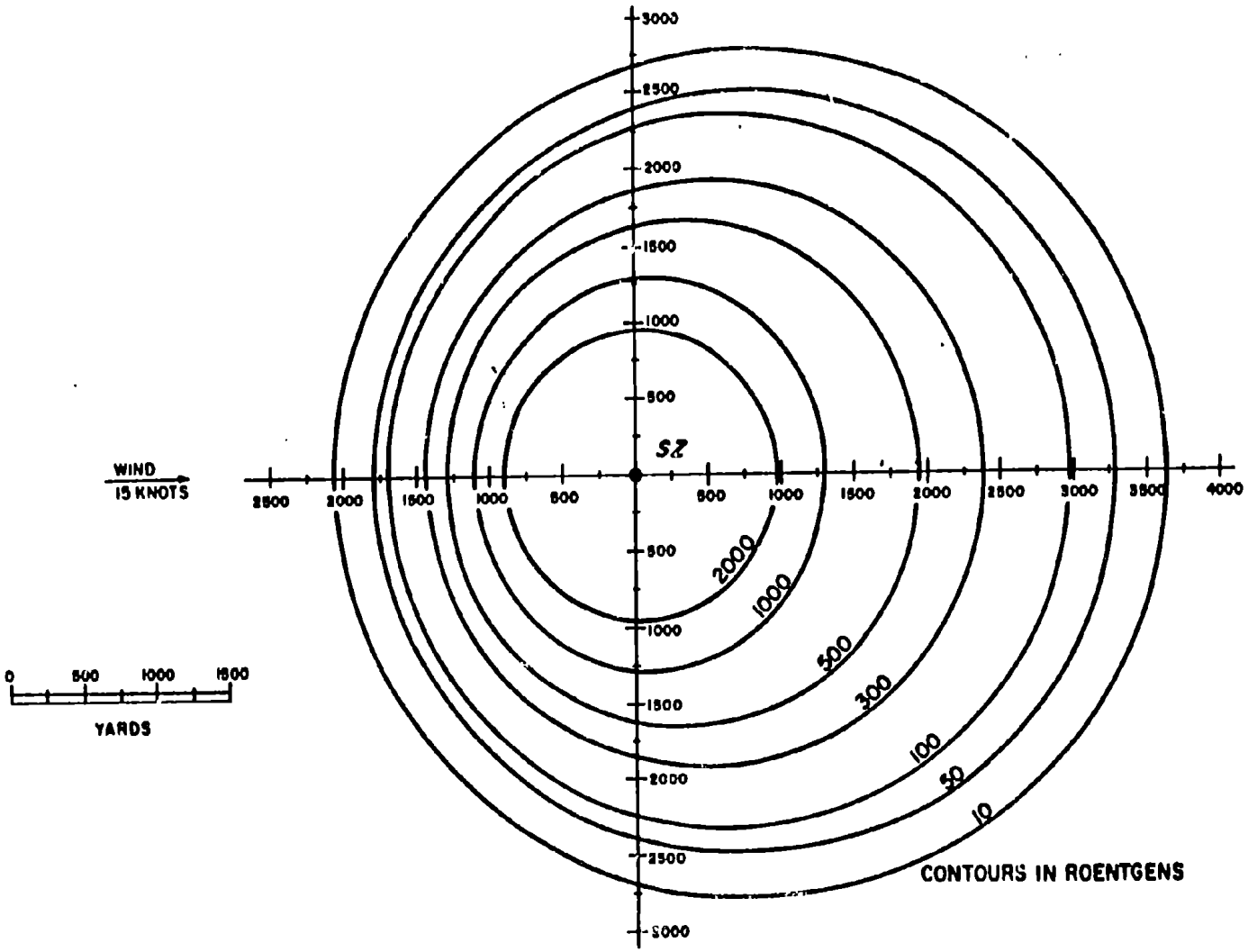

Figure 5-61. [redacted] Two-Minute Total Exposure 15 Feet Above the Water Surface from a 10 kt Explosion at a Depth of 65 Feet in 5,000 Feet of Water, 15 Knot Wind, No-Current Environment [redacted]

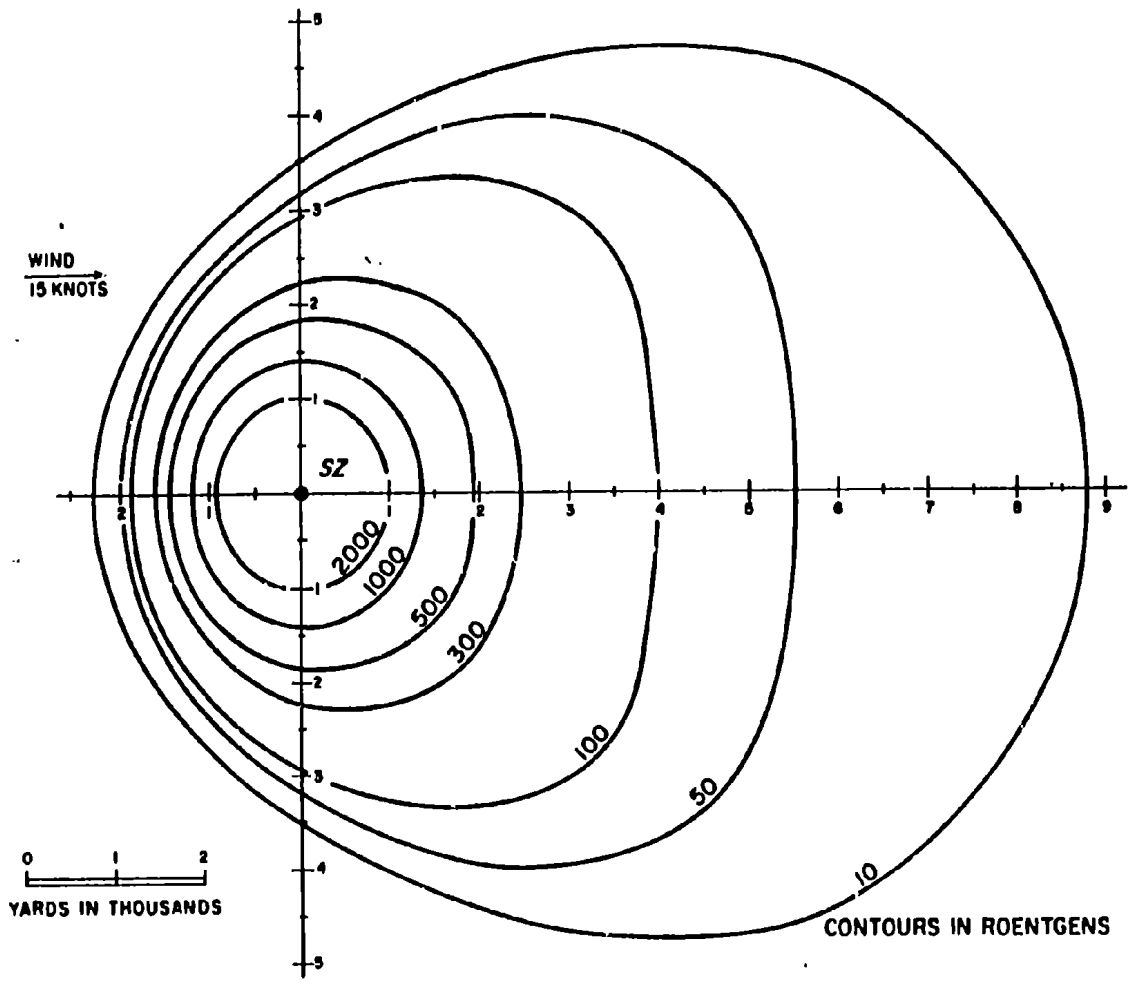

Figure 5-62. [redacted] Ten-Minute Total Exposure 15 Feet Above the Water Surface from a 10 kt Explosion at a Depth of 65 Feet in 5,000 Feet of Water, 15 Knot Wind, No-Current Environment [redacted]

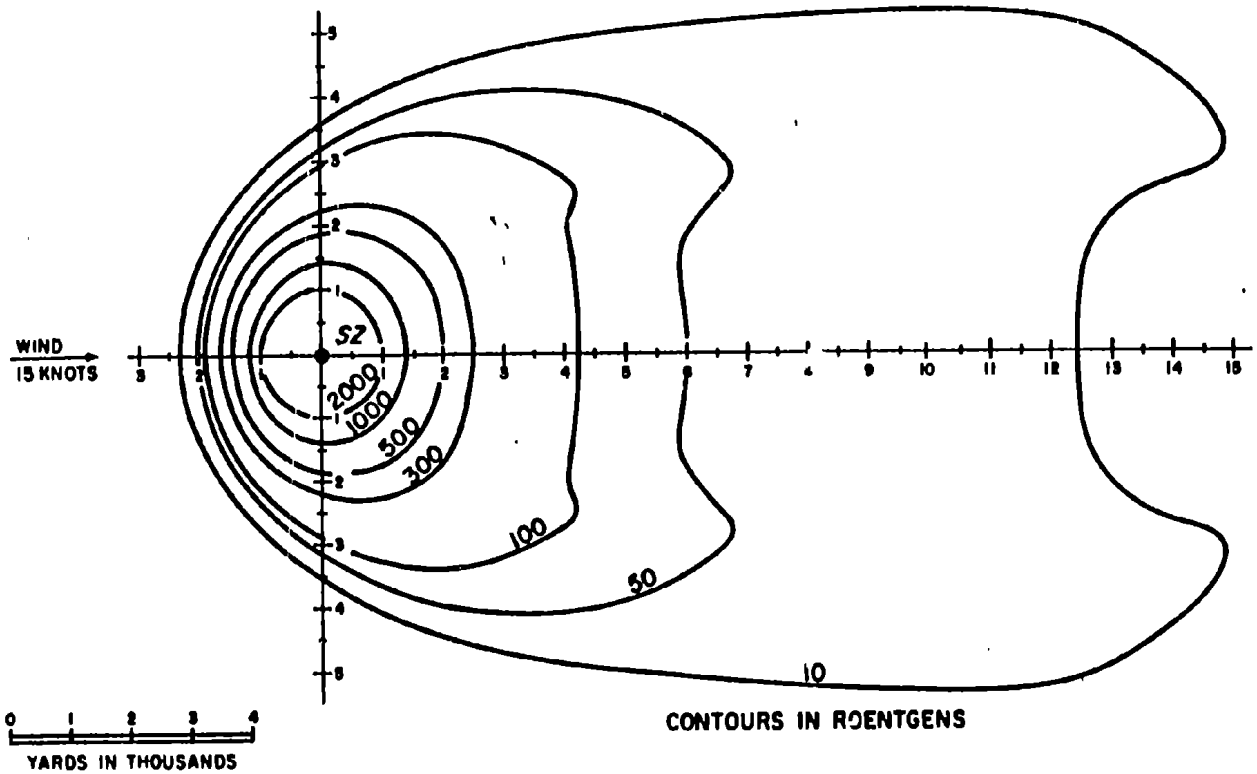

Figure 5-63. [redacted] Thirty-Minute Total Exposure 15 Feet Above the Water Surface from a 10 kt Explosion at a Depth of 65 Feet in 5,000 Feet of Water, 15 Knot Wind, No-Current Environment [redacted]

[redacted]

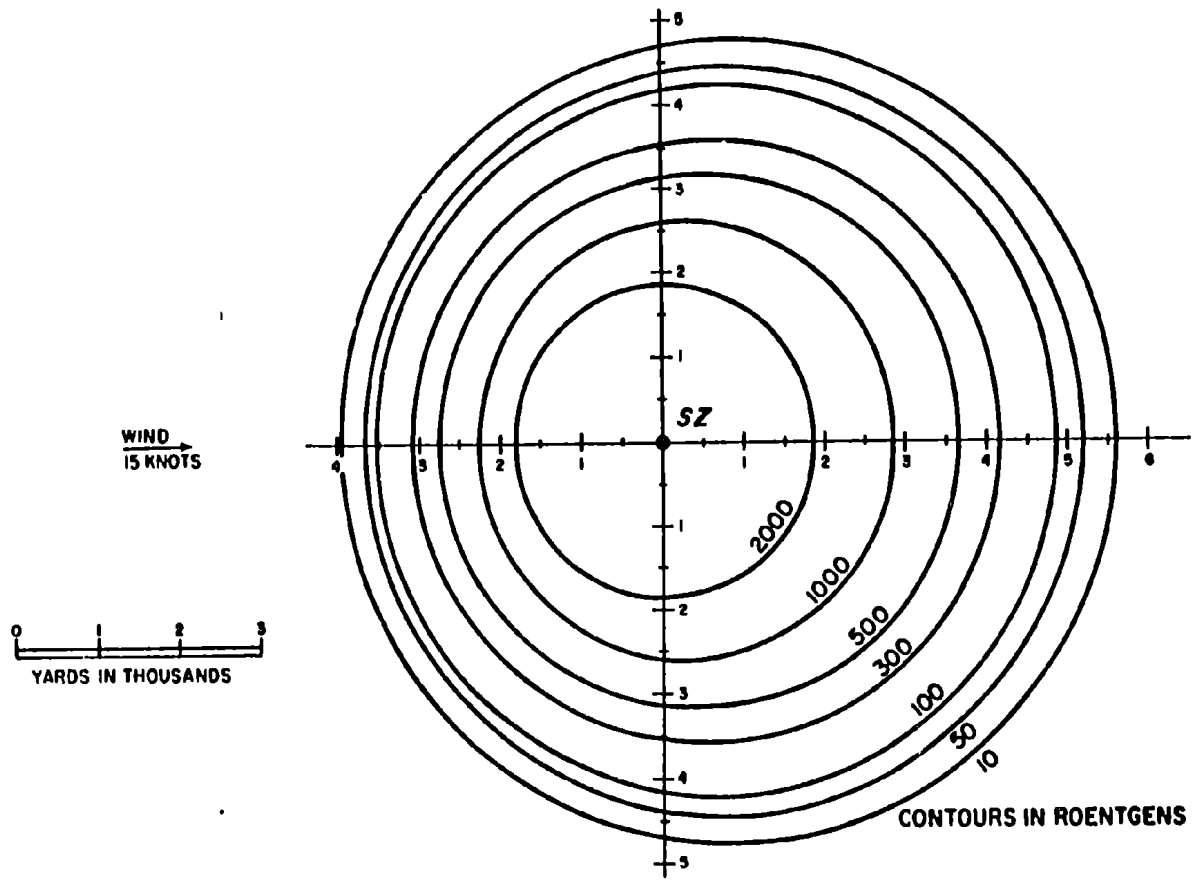

Figure 5-64. [redacted] Two-Minute Total Exposure 15 Feet Above the Water Surface from a 100 kt Explosion at a Depth of 140 Feet in 5,000 Feet of Water, 15 Knot Wind, No-Current Environment [redacted]

[redacted]

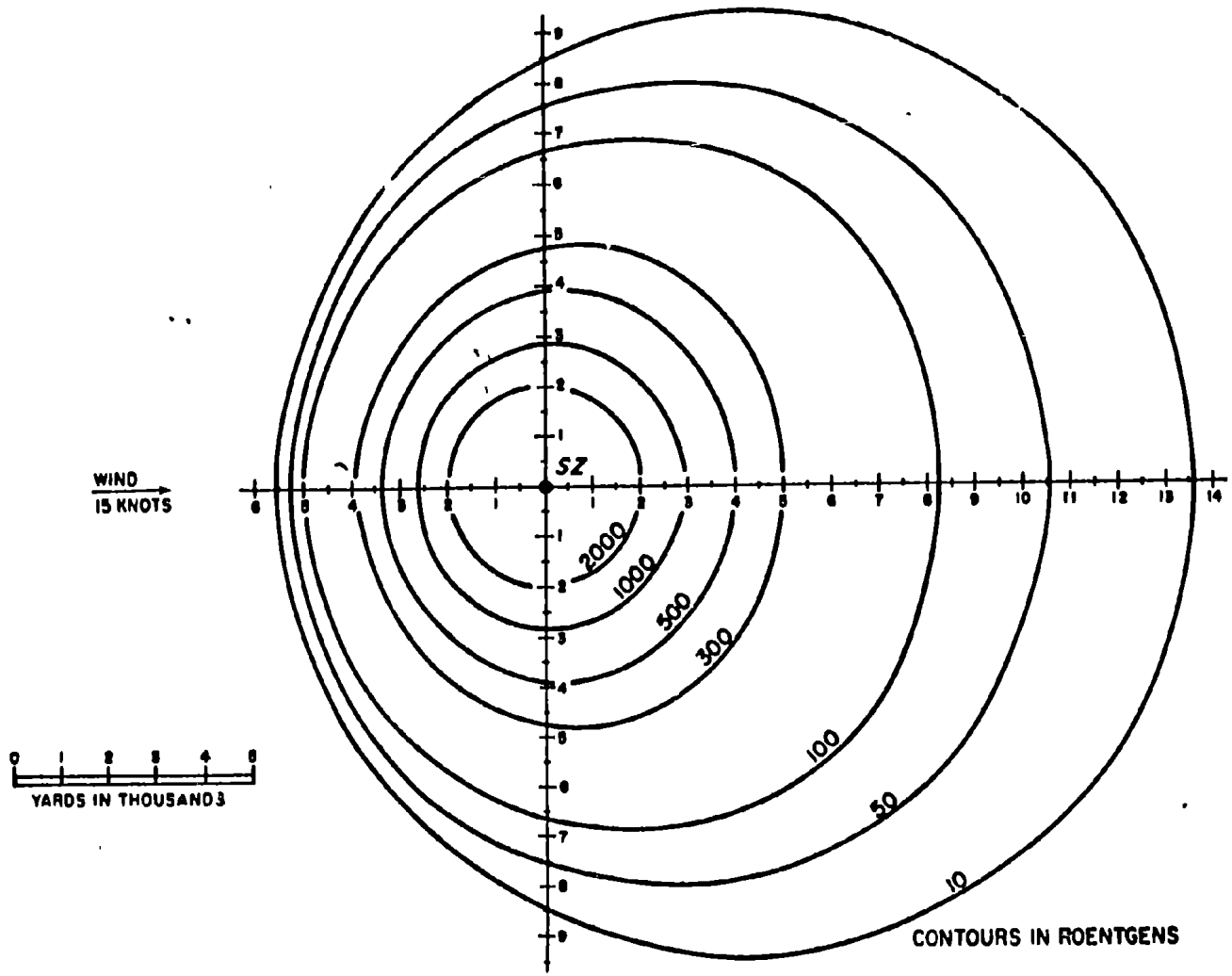

Figure 5-65. [redacted] Ten-Minute Total Exposure 15 Feet Above the Water Surface from a 100 kt Explosion at a Depth of 140 Feet in 5,000 Feet of Water, 15 Knot Wind, No-Current Environment [redacted]

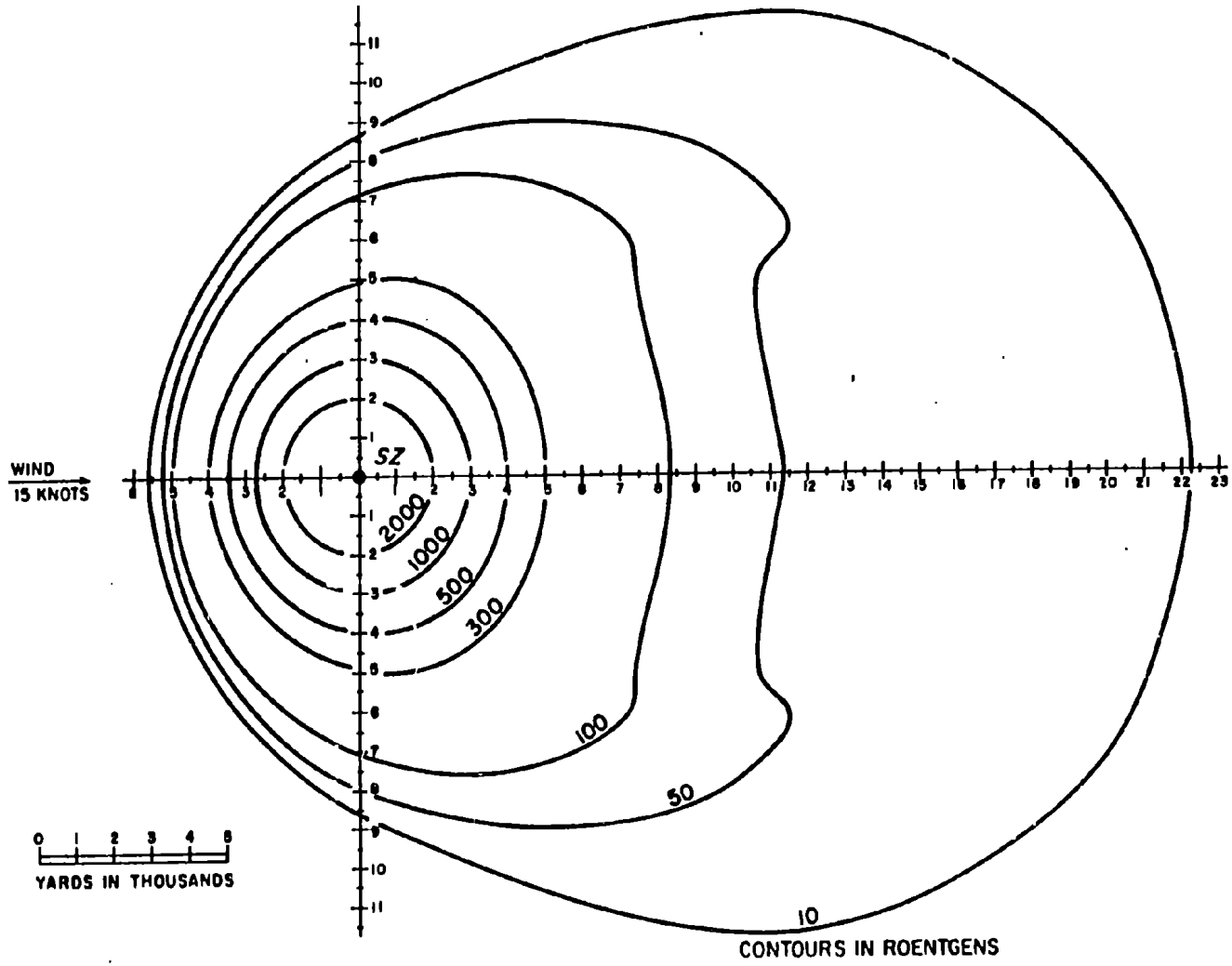

Figure 5-66. [redacted] Thirty-Minute Total Exposure 15 Feet Above the Water Surface from a 100 kt Explosion at a Depth of 140 Feet in 5,000 Feet of Water, 15 Knot Wind, No-Current Environment [redacted]

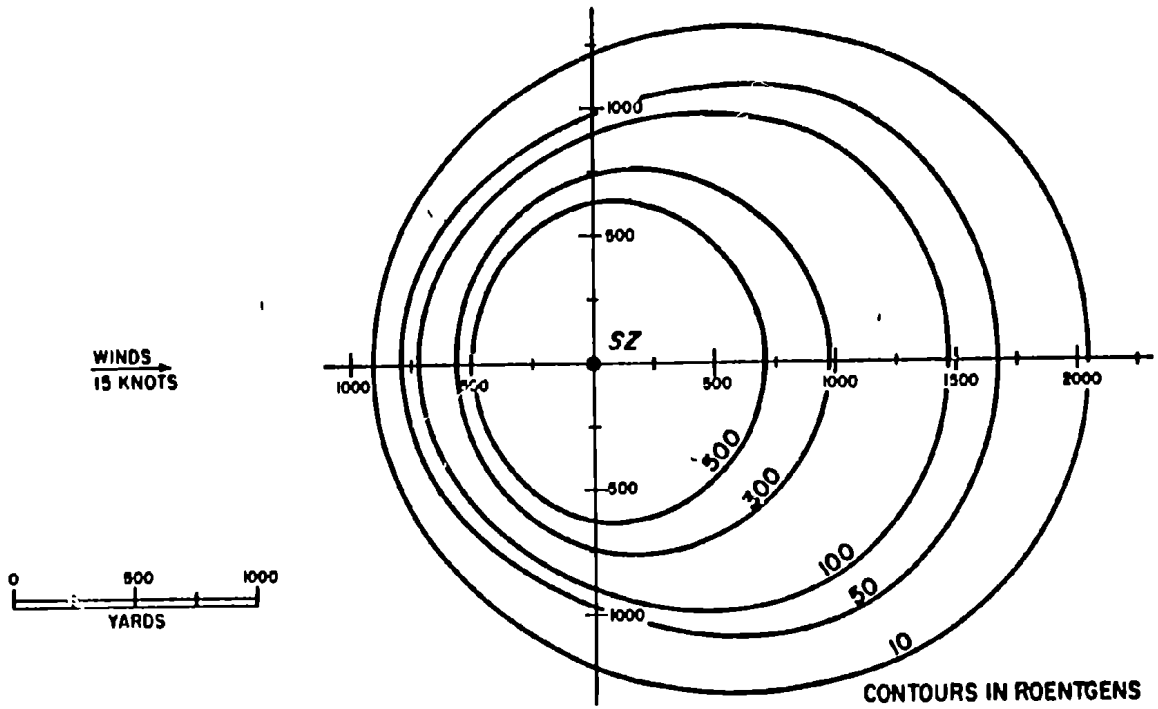

Figure 5-67. [redacted] Two-Minute Total Exposure 15 Feet Above the Water Surface from a 1 kt Explosion at a Depth of 280 Feet In 5,000 Feet of Water, 15 Knot Wind, No-Current Environment [redacted]

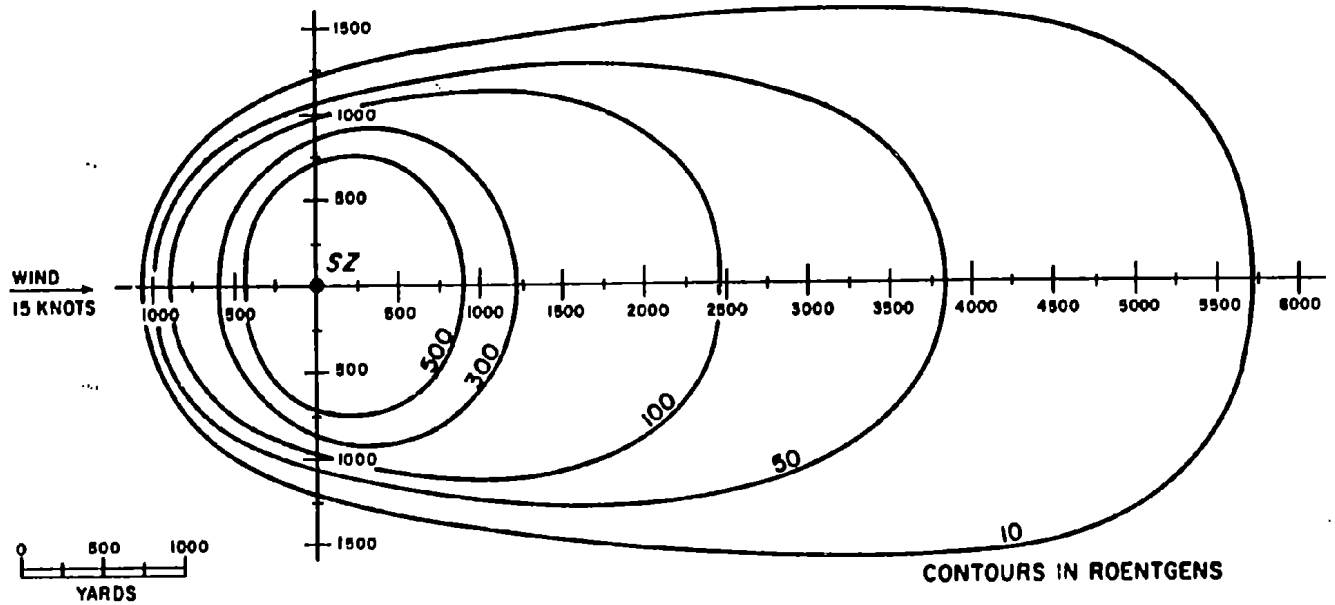

Figure 5-68. [redacted] Ten-Minute Total Exposure 15 Feet Above the Water Surface from a 1 kt Explosion at a Depth of 280 Feet in 5,000 Feet of Water, 15 Knot Wind, No-Current Environment [redacted]

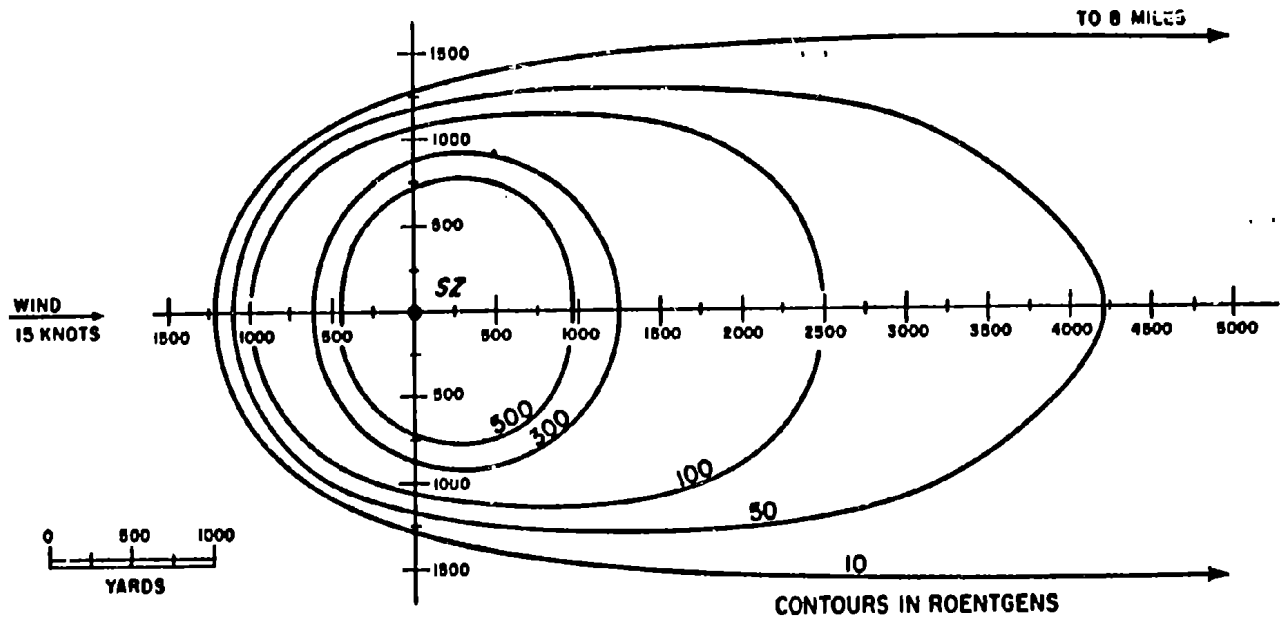

Figure 5-69. [redacted] Thirty-Minute Total Exposure 15 Feet Above the Water Surface from a 1 kt Explosion at a Depth of 280 Feet in 5,000 Feet of Water, 15 Knot Wind, No-Current Environment [redacted]

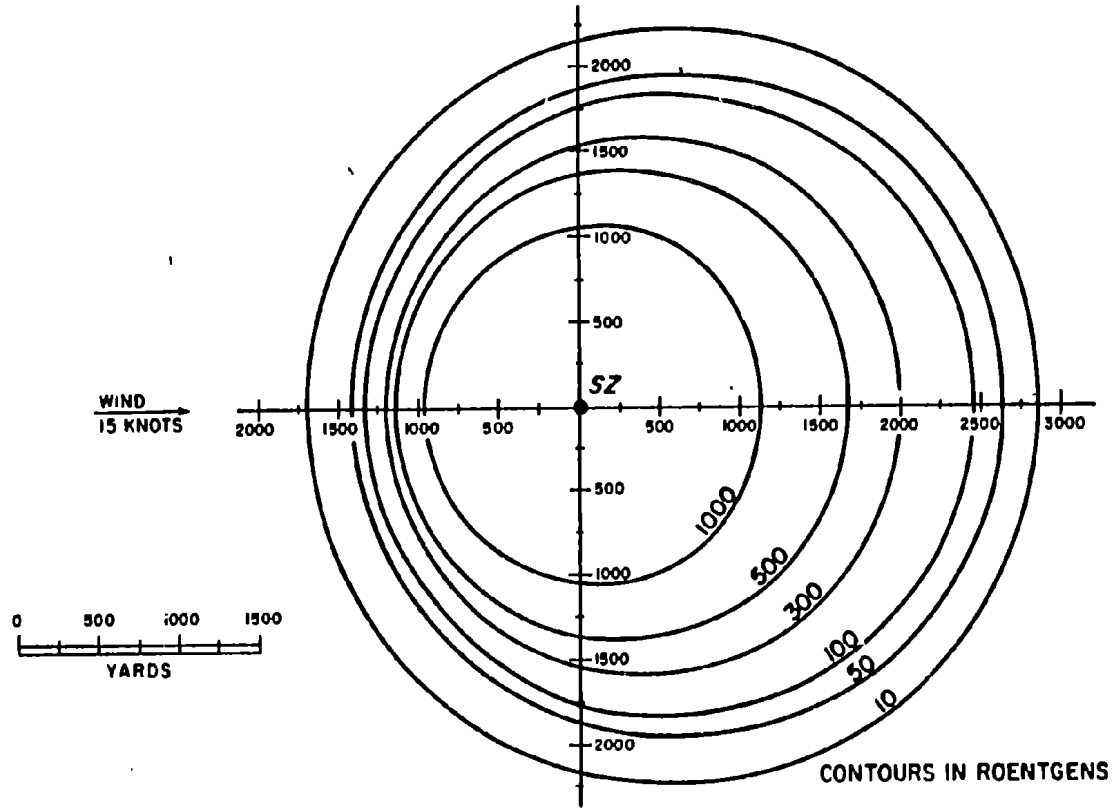

Figure 5-70. [redacted] Two-Minute Total Exposure 15 Feet Above the Water Surface from 10 kt Explosion at a Depth of 500 Feet in 5,000 Feet of Water, 15 Knot Wind, No-Current Environment [redacted]

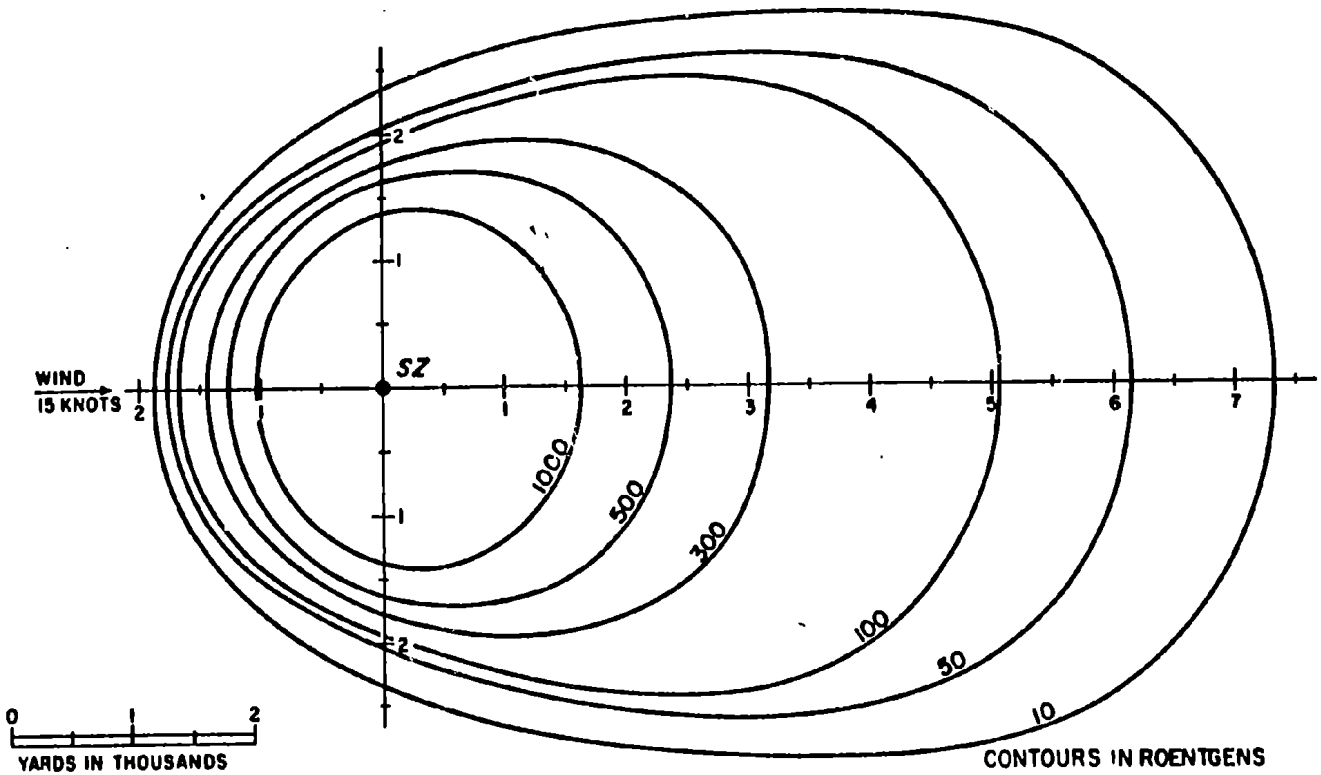

Figure 5-71. [redacted] Ten-Minute Total Exposure 15 Feet Above the Water Surface from a 10 kt Explosion at a Depth of 500 Feet in 5,000 Feet of Water, 15 Knot Wind, No-Current Environment [redacted]

[redacted]

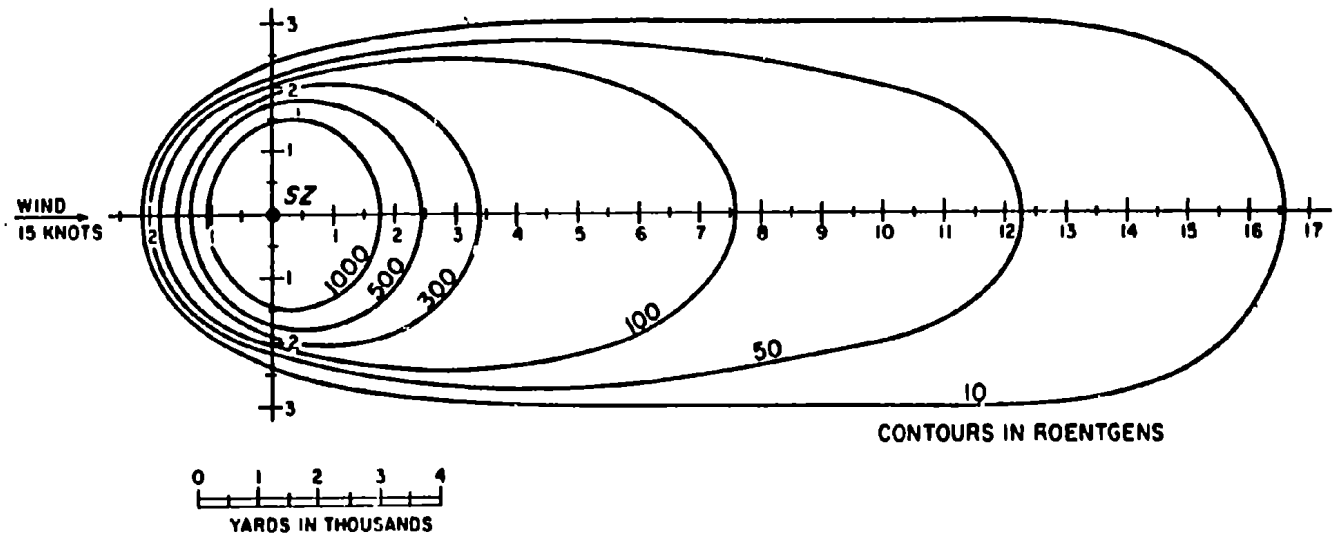

Figure 5-72. [redacted] Thirty-Minute Total Exposure 15 Feet Above the Water Surface from a 10 kt Explosion at a Depth of 500 Feet in 5,000 Feet of Water, 15 Knot Wind, No-Current Environment [redacted]

[redacted]

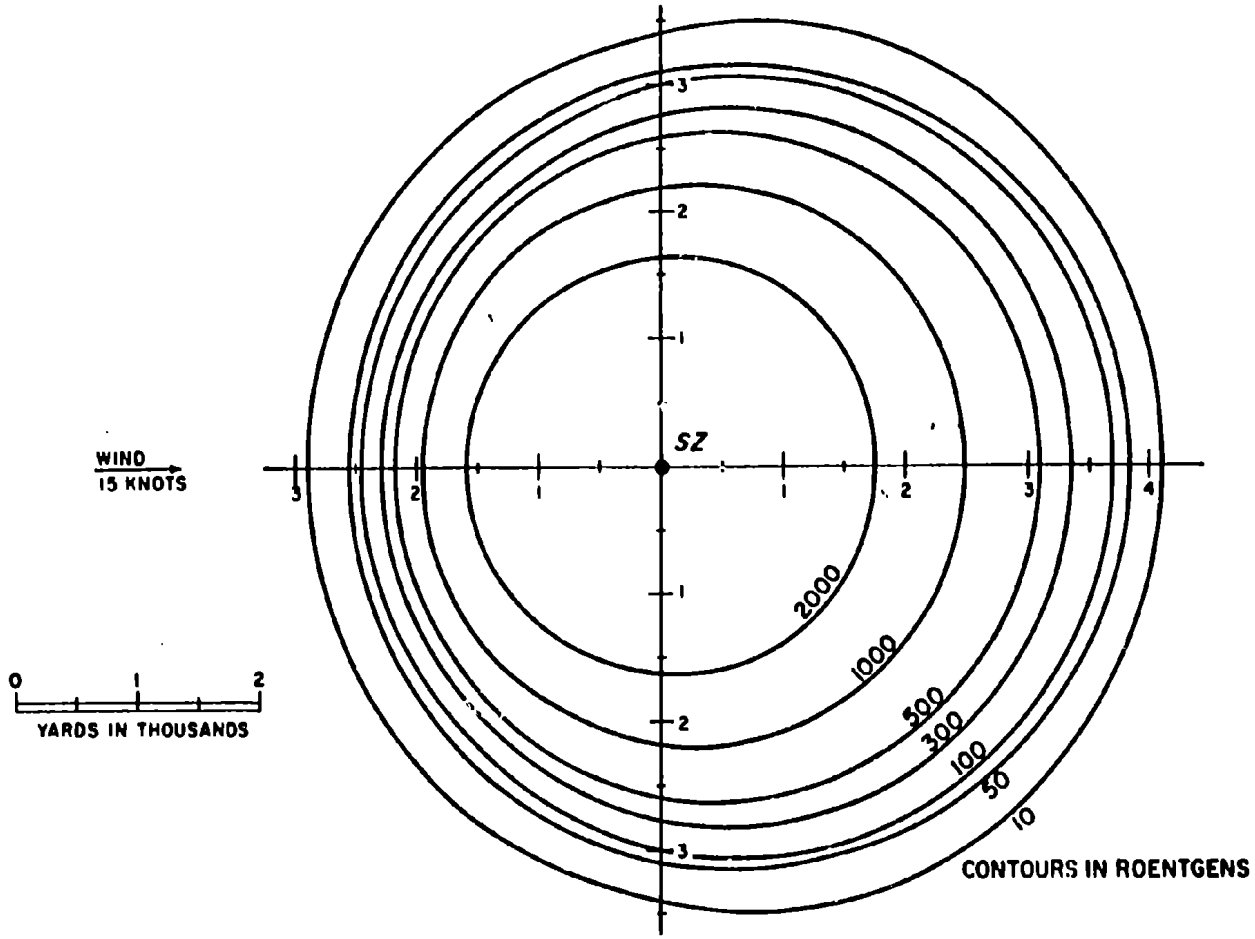

Figure 5-73. Two-Minute Total Exposure 15 Feet Above the Water Surface from a 100 kt Explosion at a Depth of 890 Feet in 5,000 Feet of Water, 15 Knot Wind, No-Current Environment

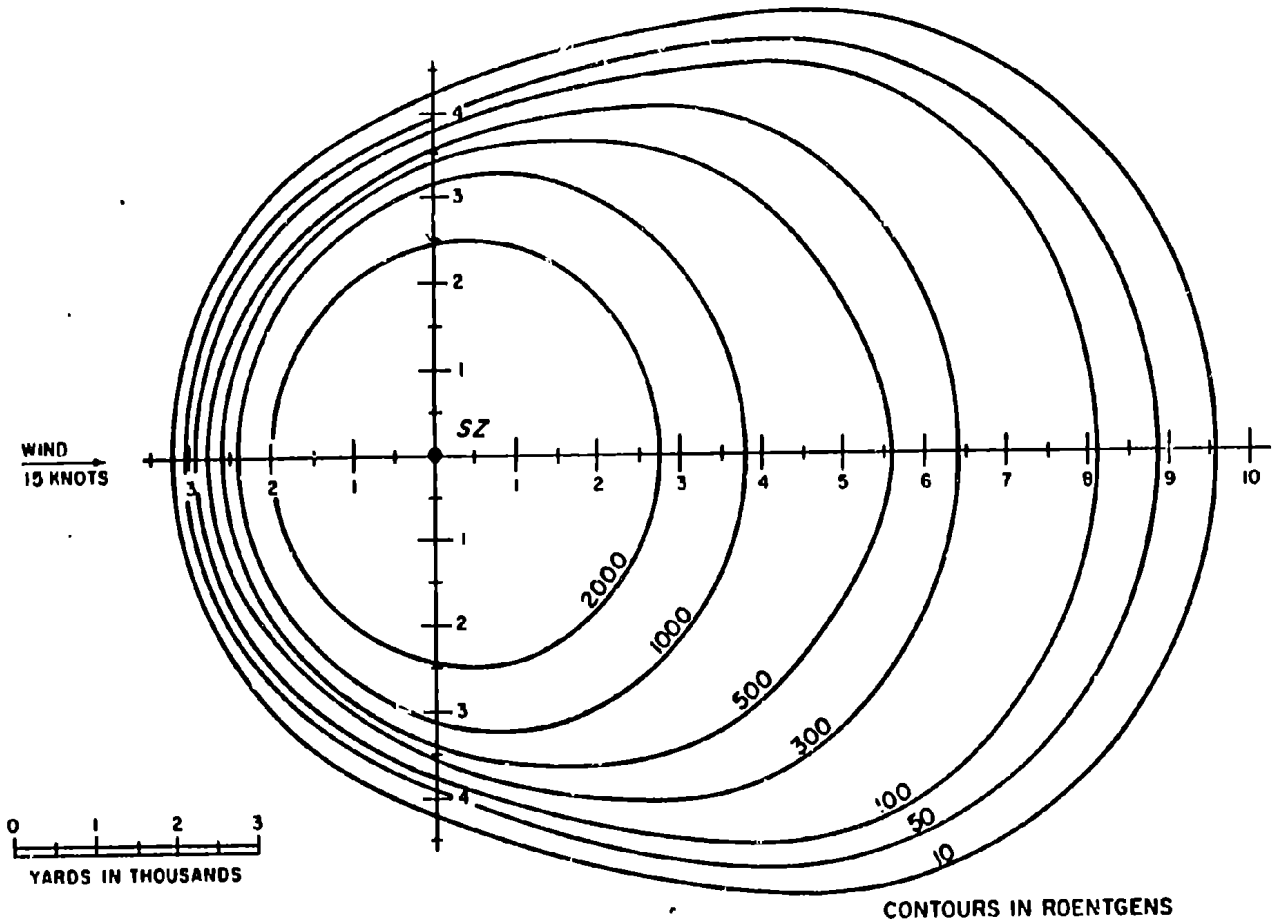

Figure 5-74. [redacted] Ten-Minute Total Exposure 15 Feet Above the Water Surface from a 100 kt Explosion at a Depth of 890 Feet In 5,000 Feet of Water, 15 Knot Wind, No-Current Environment [redacted]

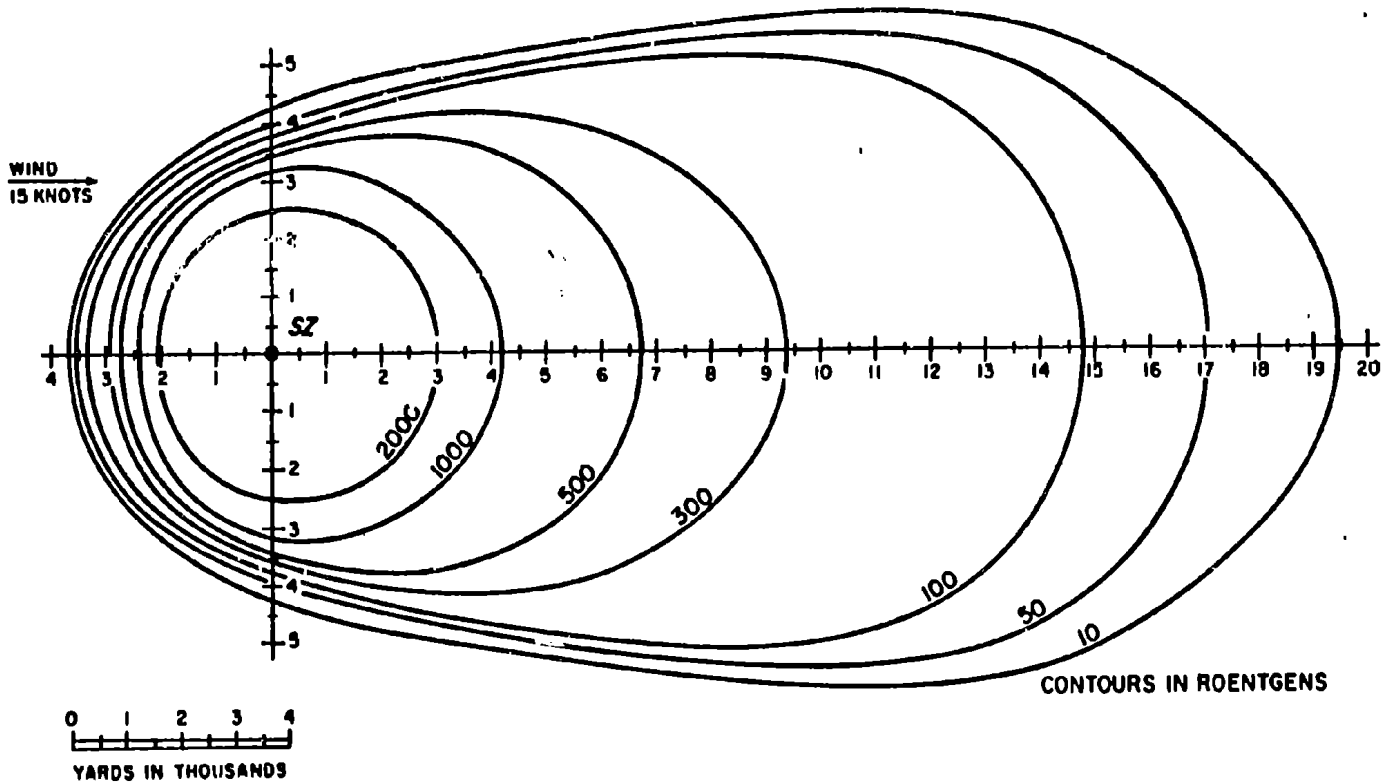

Figure 5-75. [redacted] Thirty-Minute Total Exposure 15 Feet Above the Water Surface from a 100 kt Explosion at a Depth of 890 Feet in 5,000 Feet of Water, 15 Knot Wind, No-Current Environment [redacted]

[redacted]

[redacted] DOSE RECEIVED WHILE FLYING THROUGH A NUCLEAR CLOUD [redacted]

[redacted] The radioactive nuclear cloud represents a potential hazard to crews of aircraft that fly through the cloud. The dose that a crew might receive will depend upon many variables including the time after burst (which determines the intensity of the radiation as well as the size of the cloud), the portion of the cloud traversed, and the length of transit time through the cloud. [redacted] After stabilization, the particles that make up the radioactive cloud will travel with the winds as they fall, and, since the wind speed and direction are both likely to vary with altitude and time, the size and shape of the cloud can only be described by complex computer codes that can accept temporal and spatial variations in weather data. No simple idealized shape can describe the cloud adequately. Even during the time of cloud rise, the winds will act on the particles, and the cloud probably will not stabilize directly above ground zero; however, the shape can be approximated roughly by a right circular cylinder, with a stem of smaller diameter below it, at the time of stabilization. Figures 5-76 through 5-78 show the cloud diameter, the height of the cloud bottom, and the height of the cloud top, respectively, as functions of time after burst for various yields. These figures allow approximations of the cloud dimensions during the first few minutes after an explosion. [redacted] Even if the cloud geometry were known, no satisfactory model exists from which simple scaling procedures could be developed to predict the dose received while flying through the cloud. Figure 5-79 shows estimates of the transit dose as a function of transit time for several entry times. These estimates were extrapolated from a limited amount of test data. The relative hazard for flight through the stem is even less certain, but it is believed to be less than that from flight through the center of the cloud.

[redacted]

[redacted]

Problem 5-14. Calculation of Dose Received While Flying Through a Nuclear Cloud

[redacted] The curves in Figure 5-79 show the total dose received while passing through nuclear clouds at various times after burst. Figures 5-76 through 5-78 provide the dimensions of the cloud as a function of time after burst.

[redacted] *Example* [redacted]

Given: An aircraft flying at 235 knots at an altitude of 23,000 feet passes through a nuclear cloud from a 50 kt weapon 5 minutes after the explosion.

Find: The probable maximum exposure of the crew, assuming that the shielding of the aircraft structure is negligible.

Solution: From Figure 5-77, the height of the cloud bottom will be about 16,000 feet 5 minutes after a 50 kt explosion, and from Figure 5-78, the corresponding height of the cloud top is 30,000 feet. Thus, the aircraft is flying at an altitude corresponding to the vertical center of the cloud. The maximum dose (corresponding to maximum transit time) will occur if the aircraft flies through the horizontal center of the cloud, i.e., if the aircraft traverses the entire diameter. From Figure 5-76, the diameter of a cloud from a 50 kt explosion will be 2.7 miles at 5 minutes after the burst. The aircraft speed is

$$235 \times 1.15 = 270 \text{ mph.}$$

The transit time is

$$\frac{2.7}{270} = 0.01 \text{ hr}$$

$$= 0.6 \text{ min.}$$

Answer: From Figure 5-79, with an entry time of 5 minutes and a transit time of 0.6 minutes, the expected dose is 37 rads. The maximum dose might be twice this value (see Reliability below), or

$$2 \times 37 = 74 \text{ rads.}$$

[redacted] *Reliability.* The doses obtained from Figure 5-79 are estimated to be accurate within a factor of 2 for flight paths that pass near the cloud center. If the path is near the cloud boundary, the predicted dose probably will be higher than the actual dose, although the magnitude of the error is unknown. Additional uncertainties of unknown magnitude are introduced by the prediction of the cloud size, but these uncertainties are not believed to be large for times of entry soon after burst and for short transit times.

[redacted] *Related Material:* See paragraphs 5-15 through 5-19.

[redacted]

[redacted]

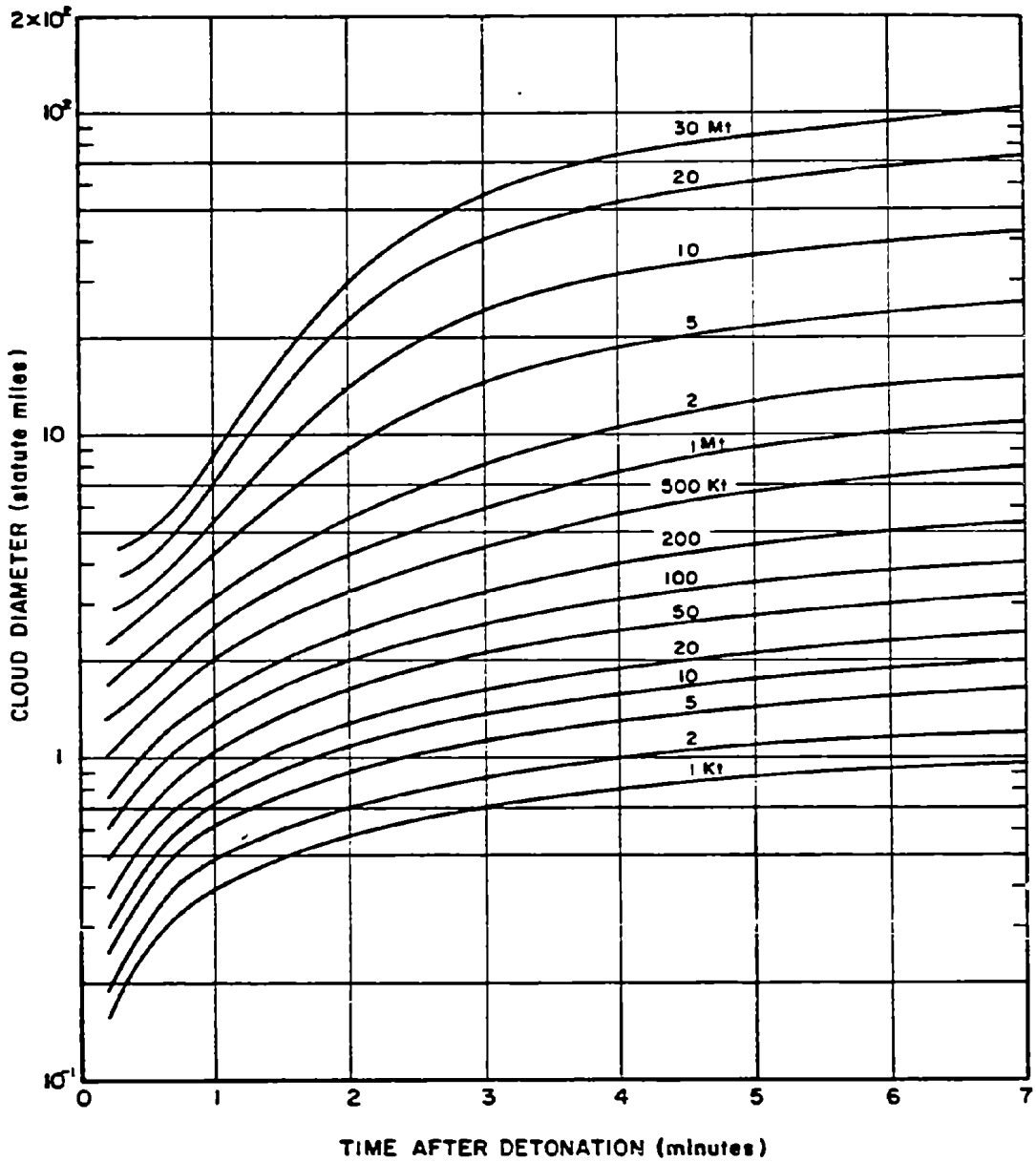

Figure 5-76. [redacted] Cloud Diameter as a Function of Time After Burst for Various Weapon Yields [redacted]

[redacted]

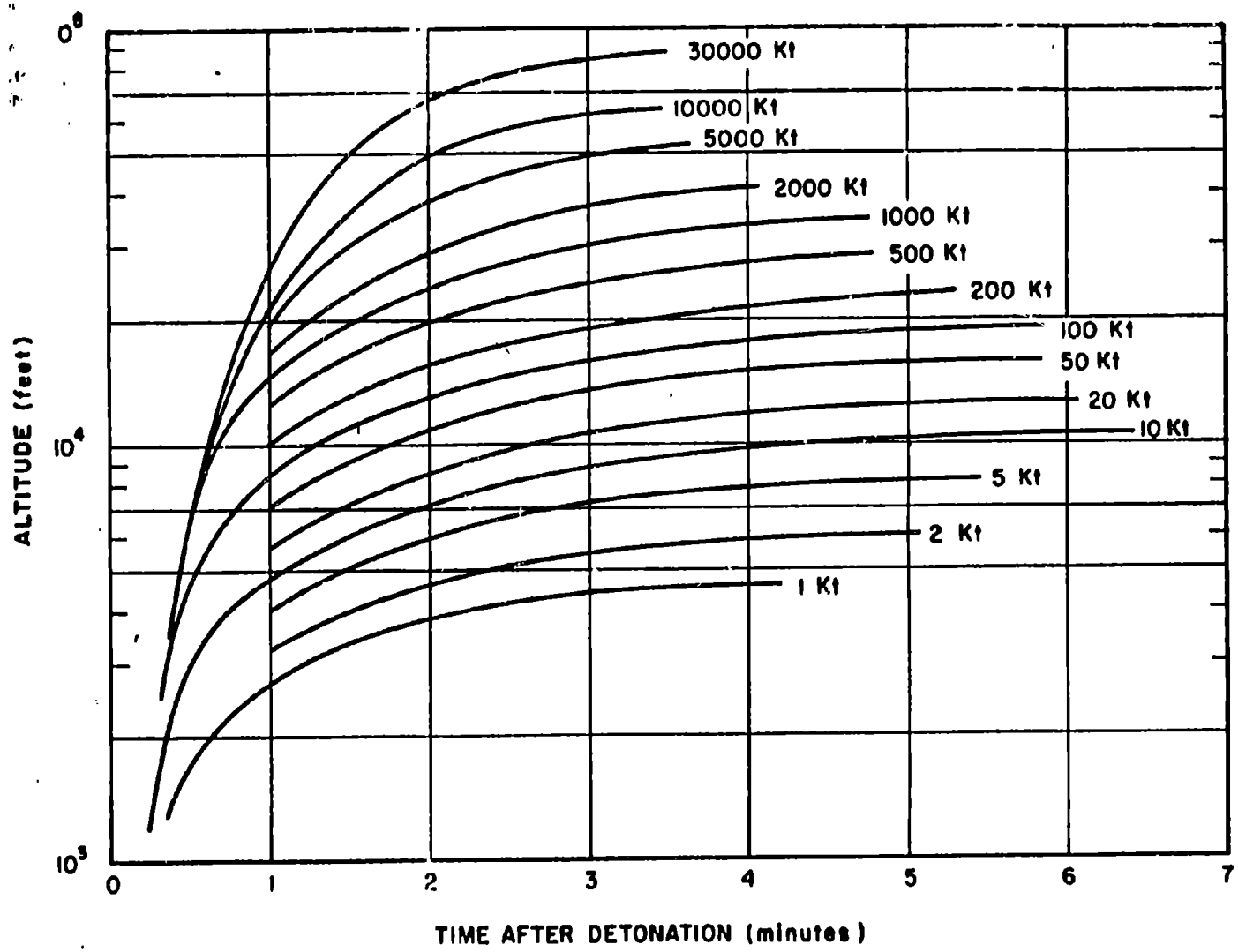

Figure 5-77. [redacted] Height of Cloud Bottom as a Function of Time for Various Weapon Yields [redacted]

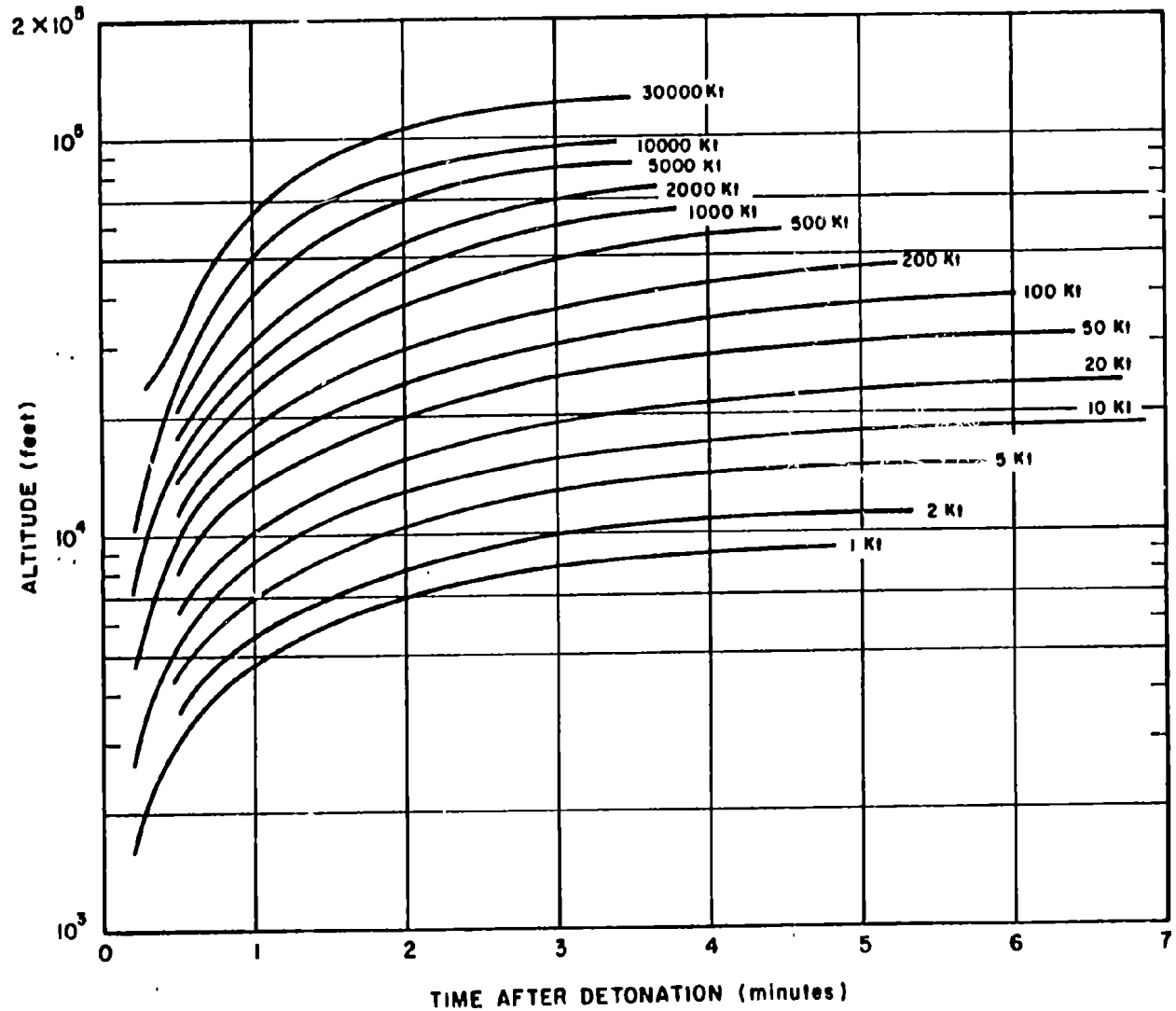

Figure 5-78. [redacted] Height of Cloud Top as a Function of Time for Various Weapon Yields [redacted]

[redacted]

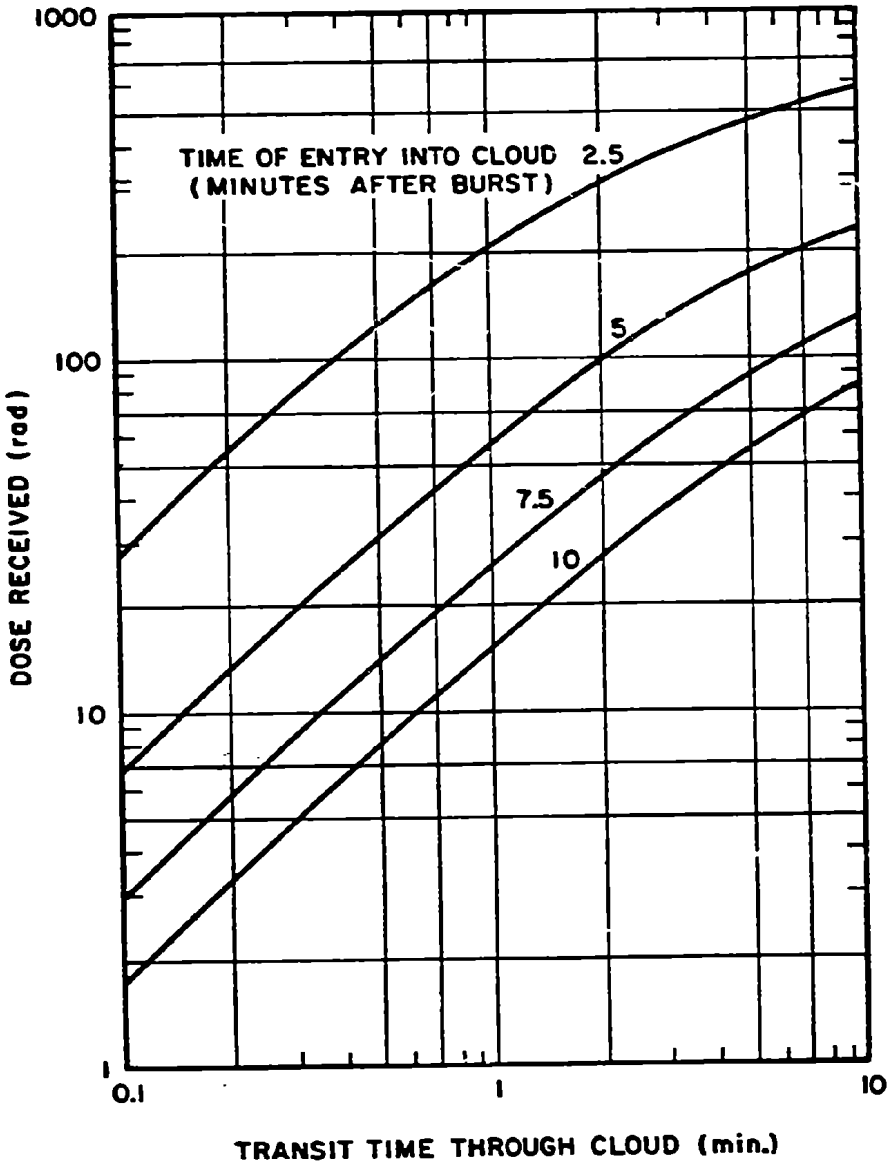

Figure 5-79. [redacted] Dose Received While Flying Through a Nuclear Cloud as a Function of Transit Time Through the Cloud [redacted]

[redacted]

[redacted] PRECIPITATION EFFECTS [redacted]

[redacted] As mentioned in paragraph 5-16, the surface contamination from an air burst weapon will be militarily insignificant in most cases. The radioactive particles remaining from the weapon debris are extremely small, having diameters that range roughly between 0.01 and 20 micrometers. The weapon cloud carries these particles to high altitudes, with the exact altitude being dependent on the weapon yield and atmospheric conditions. These particles are too small to fall, but they can diffuse downward and can be deposited by atmospheric turbulence processes. In the absence of precipitation, the deposition process takes place over sufficiently long periods of time that the cloud will have spread over a large volume as a result of diffusion and the action of winds at different levels, thereby reducing the particle concentration. Over this same period of time the radioactive decay decreases the activity levels. The net result is that dry deposition of particles from air burst weapons will not be militarily significant although there may be some long-term effects, e.g., thyroid exposures from radioactive iodine. If precipitation occurs in or above the nuclear cloud, however, there is a possibility that contamination that could be considered militarily significant may be deposited on the ground as a result of scavenging of the radioactive particles by the rain or snow. Precipitation also can affect the fallout from a surface or subsurface burst, but contamination is expected from these bursts with or without precipitation. The primary effect of precipitation on the contamination resulting from surface or subsurface bursts would be to change the location and shape of the militarily significant fallout contours. If precipitation scavenges and deposits that portion of the radioactive debris from surface or subsurface bursts that would have been delayed fallout rather than early fallout (see Section III, "RESIDUAL RADIATION," "FALLOUT"), the resulting contamination on the ground is not expected to be militarily significant.

5-27 Precipitation Scavenging [redacted]

[redacted] Precipitation scavenging may be divided into two types: scavenging when the nuclear cloud is within the rain cloud, usually called rainout or snowout; and scavenging when the nuclear cloud is below the rain (snow) cloud, usually called washout. Rainout is generally considered to be a much more efficient form of scavenging than washout, but there are many factors that affect precipitation scavenging and the ground contamination resulting therefrom. These factors are discussed in the succeeding paragraph.

5-28 Factors Affecting the Prediction of Ground Contamination from Precipitation Effects [redacted]

[redacted] The prediction of the contamination patterns that may result from precipitation scavenging of air burst nuclear weapons is complicated by many factors. Some of the important factors are discussed below.

- *The burst occurs during precipitation.* If the burst occurs during heavy precipitation, or if heavy precipitation begins at the burst location during stabilization time, the pattern will be roughly circular around ground zero, and will be roughly the size of the nuclear cloud (if the rain cloud extends to distances beyond the nuclear cloud radius).

- *The weapon yield.* The cloud from low yield weapons will be completely contained beneath the rain layers; as the yield is increased, the percentage of the nuclear cloud beneath the rain layer decreases; at a sufficiently high

yield, the entire stabilized cloud will be above the rain layers. Specific yields will, of course, depend upon the height of the rain layer.

- *The size and shape of the nuclear cloud.* If no precipitation occurs during or very soon after burst, the nuclear cloud will reach its stabilized altitude. The size and shape of the radioactive cloud will depend upon the meteorological conditions after the stabilization time (the stabilization altitudes of both the top and bottom of the cloud will depend on the atmosphere within which the explosion occurs, and the position of the stabilized cloud will depend upon the winds that act on it during its rise, but these effects are generally small compared to the changes in cloud shape and size after stabilization). In the absence of precipitation or velocity shear in the wind, the dominant physical phenomena responsible for reducing the activity concentration in a nuclear cloud is diffusion produced by turbulent eddies in the atmosphere. Reasonable estimates of the diffusion in a horizontal plane exist. Less is known about vertical diffusion; however, unless the vertical diffusion causes the particles to enter a zone where the wind speed or direction changes, it will not affect the horizontal concentration. Changes in wind speed and direction can have a significant effect on the size and shape of the nuclear cloud. Since the particles from an air burst are so small that they will not actually "fall," they will be acted on by winds within a specific altitude layer. Frequently, several such layers will exist within the thickness of the cloud at stabilization, each having a different speed and/or direction. Changes in both speed and direction of the wind are likely to occur as a function of time and space. Since most of the particles within any one altitude layer will remain in that layer for long periods of time, differences in wind velocity (speed and direction) between layers, as well as changes within a layer, generally will tend to decrease the horizontal concentration as viewed from above (exceptions may occur, of course, e.g., changes in direction may cause two layer that have separated to overlap after some time). The net result of all of the factors acting on the nuclear cloud from a low altitude air burst is that it generally will tend to increase in size horizontally without drastic changes in the vertical dimension for relatively long periods of time, unless precipitation scavenging occurs. This increase in horizontal dimensions will decrease the concentration of radioactive particles available for scavenging.

- *Radioactive decay.* While the nuclear cloud is drifting, the radioactive isotopes decay continuously. Thus, the longer the time between the explosion and the time that the nuclear cloud encounters precipitation, the smaller the total intensity of radiation that will be available (see Problem 5-9 and Figure 5-40). This, together with the general decrease in horizontal concentration described above, reduces the potential hazard with increasing time.

- *The rain cloud size, and the type and during of the precipitation.* If the rain cloud is smaller than the nuclear cloud, only that portion of the nuclear cloud that is in or below the rain cloud will be available for scavenging (any part of the nuclear cloud that is above the rain cloud is not available, as discussed under the effects of yield above). If the rain cloud is larger than the nuclear cloud in horizontal dimensions, any portion of the nuclear cloud that is in or below the rain cloud will be available for scavenging. The length of time during which the nuclear cloud is available for scavenging will depend on the relative directions and speed of travel of the nuclear and

rain clouds. The efficiency of the scavenging process will depend on the debris characteristics, scavenging mechanisms, and the type of rain. Heavy precipitation generally is considered to be more efficient in the scavenging process than light rainfall. Finally, strong updrafts and downdrafts of wind are frequently found around and within a rain cloud. These vertical air motions could prevent the intersection of the nuclear cloud and the rain cloud, but under some circumstances the air motions could enchance the mixing of the two clouds.

- *The effects of precipitation on the contamination once it reaches the ground.* After radioactive particles are brought to the ground by precipitation, they may or may not stay in place. There is a possibility that water run-off will create hot spots in some areas while decreasing the activity in other areas. Some of the radioactive particles may be leached into the ground and, as a result of the attenuation by the ground between the particle and the ground-air surface, the dose rate above the ground will be reduced.

[redacted] There are no data concerning precipitation effects where the resulting contamination was militarily significant. Also, no computer model has been developed that can include all of the factors described above either on a deterministic or a statistical basis. The results of theoretical studies, field simulations, and laboratory experiments have, however, provided some general conclusions concerning the importance of precipitation effects. First, contamination resulting from precipitation scavenging is *not* considered to be a major problem from the standpoint of effects on military operations. Second, weapons may be separated into three groups according to their relative importance with regard to precipitation effects: 1. weapons in the yield range from 1 to 10 kt are most likely to have an effect on military operations, if any such effect occurs; 2. weapons with yields greater than 10 kt and less than about 60 kt may have some effect on military operations, with the probability of such an effect decreasing with increasing yield; 3. weapons with yields greater than 60 kt or less than 1 kt are not expected to have any effect on military operations. The potential hazard may be reduced by making use of available shelter.

[redacted]

[redacted] BIBLIOGRAPHY [redacted]

Baum, S., P. W. Wong, and P. J. Dolan, *NUCROM: A Model of Rainout from Nuclear Clouds*, DNA 3389F, Stanford Research Institute, Menlo Park, California, August 1974 [redacted]

Biggers, W. A., and K. C. Kohr, *Neutron Outputs from Selected LASL Nuclear Devices* [redacted] LA 3688, Los Alamos Scientific Laboratory, Los Alamos, New Mexico, April 1967 [redacted]

Beyster, J. R., et al., *Status of Neutron and Gamma Output from Nuclear Weapons* [redacted] SAI 70-205, DASA 2567, Science Applications Incorporated, La Jolla, California, May 1971 [redacted]

Bunney, L. R., and D. Sam, *Gamma-Ray Spectra of Fractionated Fission Products*, NOLTR 71-103, Naval Ordnance Laboratory, White Oak, Silver Spring, Maryland, 18 June 1971 [redacted]

Canu, J. F., and P. J. Dolan, *Prediction of Neutron Induced Activity in Soils* [redacted] Technical Analysis Report AFSWP 518, Headquarters, Armed Forces Special Weapons Project, Washington, D.C., 4 June 1957 [redacted]

Crawford, T. V., and K. R. Peterson, *BANEBERRY – Discussion of Diffusion Calculations Including Potential Exposure to Child's Thyroid from I-131 Via the Forage-Cow-Milk Pathway* [redacted] COPK 71-20, Lawrence Radiation Laboratory, Livermore, California, 3 March 1971 [redacted]

Crawford, T. V., *Precipitation Scavenging and 2BPUFF*, UOPKA 71-14, Lawrence Livermore Laboratory, Livermore, California, 6 December 1971 [redacted]

Crocker, G. R., *Fission Product Decay Chains: Schematics with Branching Fractions, Half-Lives, and Literature References*, USNRDL-TR-67-111, U.S. Naval Radiological Defense Laboratory, San Francisco, California, 24 June 1967 [redacted]

Crocker, G. R., and T. Turner, *Calculated Activities, Exposure Rates, and Gamma Spectra for Unfractionated Fission Products*, USNRDL-TR-1009, U.S. Naval Radiological Defense Laboratory, San Francisco, California, 28 December 1965 [redacted]

Crocker, G. R., and M. A. Connors, *Gamma-Emission Data for the Calculation of Exposure Rates from Nuclear Debris, Volume I, Fission Products*, USNRDL-TR-876, U.S. Naval Radiological Defense Laboratory, San Francisco, California, 10 June 1965 [redacted]

Crocker, G. R., J. D. O'Connor, and E. C. Freiling, *Physical and Radiochemical Properties of Fallout Particles*, NRDL-TR-899, Naval Radiological Defense Laboratory, San Francisco, California, 15 June 1965 [redacted]

Department of Defense Land Fallout Prediction System, DASA 1800-I through 1800-VII, Defense Atomic Support Agency, Washington, D.C.; U.S. Army Nuclear Defense Laboratory, Edgewood Arsenal, Maryland; U.S. Naval Radiological Defense Laboratory, San Francisco, California; Technical Operations Research, Burlington, Massachusetts; 1966 [redacted]

[redacted]

[redacted]

Dolan, P. J., *Gamma Spectra of Uranium-235 Fission Products at Various Times After Fission*, AFSWP 524, Headquarters, Armed Forces Special Weapons Project, Washington, D.C., March 1959 [redacted]

Dolan, P. J., *Gamma Spectra of Uranium-238 Fission Products at Various Times After Fission*, DASA 526, Headquarters, Defense Atomic Support Agency, Washington, D.C., May 1959 [redacted]

Dolan, P. J., *Theoretical Dose Rate Decay Curves for Contamination Resulting from Land Surface Burst Nuclear Weapons* [redacted] DASA 528, Defense Atomic Support Agency, Washington, D.C., 6 August 1959 [redacted]

Englemann, R. J., and W. G. N. Slinn, *Precipitation Scavenging (1970)*, AEC Symposium Series, U.S. Atomic Energy Commission, Washington, D.C., 22 December 1970 [redacted]

Englemann, R. J., *Priorities in Scavenging Research*, AEC Symposium Series U.S. Atomic Energy Commission, Washington, D.C., 22 December 1970 [redacted]

French, R. L., *A First-Last Collision Model of the Air/Ground Interface Effects on Fast-Neutron Distributions*, *Nucl. Sci. Engr.*, *19*, 151-157, 1964 [redacted]

Freiling, E. C., and N. E. Ballou, *Nature of Nuclear Debris in Sea Water*, *Nature 195*, No. 4848, pp. 1283-1287, 29 September 1962 [redacted]

Fritzsche, A. E., N. E. Lorimier, and Z. G. Burson, *Measured Low-Altitude Neutron and Gamma Dose Distributions Due to a 14-MeV Neutron Source*, *EGG 1183-1449*, *E. G., and G., Inc.*, *1969* [redacted]

Fritzsche, A. E., N. E. Lorimier, and Z. G. Burson, *Measured High-Altitude Neutron and Gamma Dose Distributions Due to a 14-MeV Neutron Source*, EGG 1183-1438, E. G., and G., Inc., 1969 [redacted]

Harris, R. J., Jr., et al., *Models of Radiation in Air – The ATR Code*, DNA 28031, SAI-71-557.LV, Science Applications Incorporated, La Jolla, California, May 1972 [redacted]

Huebsch, I. O., *Fallout Predictions for Water-Surface Nuclear Bursts*, USNRDL-TR-67-147, U.S. Naval Radiological Defense Laboratory, San Francisco, California, 28 November 1967 [redacted]

Heubsch, I. O., *Development of a Water-Surface-Burst Fallout Model: The Formation, Dispersion and Deposition of Fallout Particles*, USNRDL Technical Report, U.S. Naval Radiological Defense Laboratory, San Francisco, California [redacted]

Keith, J. R., and F. H. Shelton, *Neutron Transport in Non-Uniform Air by Monte Carlo Calculation, Volume I*, DASA 2236-I KN-774-69-1, Kaman Nuclear, Colorado Springs, Colorado, 15 January 1969 [redacted]

[redacted]

[redacted]

Keith, J. R., and F. H. Shelton, *Neutron Transport in Non-Uniform Air by Monte Carlo Calculation* [redacted] Volume II, KN-774-69-1, DASA 2236-II, Kaman Nuclear, Colorado Springs, Colorado, 15 January 1969 [redacted]

Knox, J. G., and A. L. Williams, *Rainout Studies at Lawrence Livermore Laboratory*, UCRL 51530, Lawrence Livermore Laboratory, University of California/Livermore, Livermore, California, 11 February 1974 [redacted]

Krey, P. W., et al., *Soil Activation by Neutrons* [redacted] Project 2.1, WT-1410, U.S. Army Chemical Warfare Laboratories, Army Chemical Center, Maryland, 16 May 1960 [redacted]

Lee, H., P. W. Wong, and S. L. Brown, SEER II: *A New Damage Assessment Fallout Model*, DNA 3008F, Stanford Research Institute, Menlo Park, California, May 1972 [redacted]

Marshall, J. D., and M. B. Wells, *The Effects of Cut-Off Energy on Monte Carlo Calculated Gamma-Ray Dose Rates in Air*, RRA-M67, Radiation Research Associates, Fort Worth, Texas, 1966 [redacted]

Mooney, L. G., and R. L. French, *Improved Models for Predicting Nuclear Weapon Initial Radiation Environments* [redacted]. RRA-T93, DASA 2615, Radiation Research Associates, Fort Worth, Texas, 31 December 1969 [redacted]

Norment, H. G., and E. J. Tichovolsky, *A New Fallout Transport Code for the DELFIC System: The Diffusive Transport Module*, DASA 2669, Arcon Corporation, Wakefield, Massachusetts, 1 March 1971 [redacted]

Norment, H. G., *A Precipitation Scavenging Model for Studies of Tactical Nuclear Operations, Volume I – Theory and Preliminary Results, Volume II – The DELFIC-PSM Code*, DNA 3661F-1, -2, Mt. Auburn Research Associates, Inc., Newton, Massachusetts, 18 June 1975 [redacted]

Read, P. A., *Neutron Induced Activity on a Beach: A Method for Calculating the Dose Rate*, USNRDL-TR-67-133, U.S. Naval Radiological Defense Laboratory, San Francisco, California, 27 October 1967 [redacted]

Ritchie, R. H., and V. E. Anderson, *Some Monte Carlo Results on the Penetration of Neutrons from Weapons in an Air-Over-Ground Geometry* [redacted] ORNL-3116, Oak Ridge National Laboratory, Oak Ridge, Tennessee, 26 July 1962 [redacted]

Schuert, E. A., *Distribution of the Radioactive Debris and Associated Nuclear Radiation from Underwater Nuclear Explosions* [redacted] USNRDL-TR-67-28, DASA 1240, Part I, Chapter 11, U.S. Naval Radiological Defense Laboratory, San Francisco, California, 15 December 1966 [redacted]

[redacted]

Selph, W. E., and M. B. Wells, *Weapons Radiation Shielding Handbook, Chapter 6, Methods for Predicting Radiation Fields Produced by Nuclear Weapons*, DASA-1892-4, Oak Ridge National Laboratory, Oak Ridge, Tennessee, December 1969

Shelton, F. H., *Nuclear Weapons as Neutron Sources, The Neutron Environments They Produce, and Some Neutron Effects on Aerospace Systems*, DASA-2383-1, Volume I, Neutron Sources, KN 774-69-6, Kaman Nuclear, Colorado Springs, Colorado, October 1969

Shelton, F. H., and J. R. Keith, *Nuclear Weapons as Neutron Sources, The Neutron Environments They Produce, and Some Neutron Effects on Aerospace Systems, Volume II, Neutron Environments and Some Effects*, DASA 2383-2, KN 774-69-6, October 1969

Slade, D. H. (Ed.), *Meteorology and Atomic Energy – 1968*, USAEC Report TID-24190, Environmental Science Services Administration, Washington, D.C., July 1968

Smith, R. J., R. F. Benck, and E. E. Lissak, *Initial Gamma Data from Nuclear Weapon Tests, 1948 Through 1962*, NDL-TR-53, U.S. Army Nuclear Defense Laboratory, Edgewood Arsenal, Maryland, July 1965

Snay, H. G., *The Hydrodynamic Background of the Radiological Effects of Underwater Nuclear Explosions*, Proceedings of the Tripartite Symposium on the Technical Status of Radiological Defense in the Fleets, U.S. Naval Radiological Defense Laboratory, San Francisco, California, 16-20 May 1960, Vol. II, USNRDL Reviews and Lectures, No. 103

Stensland, G. J., *Further Numerical Model Studies of the Washout of Hygroscopic Particles in the Atmosphere*, UCRL-51614, Lawrence Radiation Laboratory, University of California/Livermore, Livermore, California, 2 July 1974

Straker, E. A., *Time-Dependent Neutron and Secondary Gamma-Ray Transport in an Air-Over-Ground Geometry, Volume II, Tabulated Data*, ORNL 4289, Vol. II, Oak Ridge National Laboratory, Oak Ridge, Tennessee, September 1968

Williams, A. L., *Rain Scavenging of Radioactive Particles*, UCRL-517765, Lawrence Radiation Laboratory, University of California/Livermore, Livermore, California, 28 February 1975

Wong, P. W., and H. Lee, *Utilization of the SEER Fallout Model in a Damage Assessment Computer Program (DACOMP)*, DNA 3608F, Stanford Research Institute, Menlo Park, California, 27 February 1975

Young, F. H., et al., *The Radiological Effects from Underwater Nuclear Explosions*, USNRDL-TR-68-1, U.S. Naval Radiological Defense Laboratory, San Francisco, California, 17 October 1967

[redacted]

Chapter 6

TRANSIENT-RADIATION EFFECTS ON ELECTRONICS (TREE) PHENOMENA [redacted]

AD-A955 390

[redacted] INTRODUCTION [redacted]

[redacted] This chapter introduces the subject of transient-radiation effects on electronics and provides a basic description of the interaction of nuclear radiation with matter as it applies to electronic components. The response of electronics to the radiation from a nuclear weapon burst depends not only on the radiation present at the electronics but also depends on the specific operating state of the electronics at the time of the radiation exposure and on the specific electronics in the system. A knowledge of the individual characteristics of the circuits contained in an electronics package, of the exact electronic components used in the circuits, and of the specific construction techniques and materials used in making the electronic components constitutes the necessary background for determining the radiation response of the electronic system. This chapter explains how the radiation interacts with different materials to produce a wide variety of effects. These material effects are used in the discussions of the component-part responses in Section VII of Chapter 9. Section IV of Chapter 14 contains a brief discussion of circuit and electronic-system response supplemented with discussions of general electrical responses of classes of systems (radios, radar, etc.).

[redacted] The cumbersome name applied to the class of effects that are the subject of this chapter, transient-radiation effects on electronics, is generally abbreviated to the acronym TREE. In general, TREE means those effects occurring in electronics as a result of the transient radiation from a nuclear weapon explosion or as a result of an environment designed to simulate that radiation. It should be understood that the transient-radiation from a nuclear explosion can be and is simulated by the use of controlled sources of steady-state and transient radiation since the environment produced can be correlated to the actual environment of interest, and thereby the effects on electronics can be studied.

[redacted] Although the weapons radiation environment lasts for a very short time, its effect on electronics can be both short or long term. For emphasis, it must be stated that the word transient in TREE modifies the word radiation and does not modify the word effects: the effects may be transient, semipermanent, or permanent.

[redacted] The term electronics means any one or all of the following: electronic component parts, electronic component parts assembled into a circuit, and circuits assembled into a system. TREE studies also may include the response of electromechanical components connected to the electronics, e.g., gyros, inertial instruments, etc. TREE does, however, specifically exclude other types of component parts or systems such as hydraulic cylinders and hydraulic systems, fuel lines and fuel systems, etc. This exclusion is made since electronics as a group or as part of a hybrid system are one of the most radiation-sensitive portions of a system.

[redacted] There are several points to be emphasized about TREE. The TREE interest is in the environment at the electronics produced by the

[redacted]

This document has been approved for public release and sale; its distribution is unlimited.

89 3 02 043

[redacted]

[redacted] ENVIRONMENT [redacted]

[redacted] In order to specify the hardness required of an electronic system, or to formulate an analysis or test program on which its hardness level will be established, it is necessary to describe the radiation environment to which the electronic systems may be exposed. Since the multitude of components of this environment leads to confusion in understanding the variety of mechanisms whereby a nuclear explosion can affect the operation of electronic systems, the primary outputs of a nuclear weapon and the mechanisms whereby secondary radiation are generated will be reviewed. In quantifying the environment to which the electronics are exposed, it is first necessary to treat the primary output of the nuclear explosion, then transport this radiation through the atmosphere and generate secondary radiations by interaction with the atmosphere. At this point, the radiation incident at the system of interest can be quantified. Since most of the electronics are enclosed by some structural material, there is the additional effect of transport through such shields, and it becomes necessary to describe the radiation field as it interacts with the affected part.

[redacted] This step-wise description of the radiation explains the variety of methods and units by which the radiation field is described. The weapon designer usually describes the output from the nuclear explosion-total energy output, total number of neutrons emitted, total gamma-ray energy, and reaction pulse shape. The person who formulates specifications for system design usually describes the radiation field as it impinges on the system, e.g., energy per unit area, neutron fluence, gamma exposure, pulse shape as affected by radiation transport through intervening material. Finally, the designer of the individual electronic piece-part or circuit is concerned with describing the radiation in units that are convenient for quantifying the radiation effect that he has to take into account, e.g., energy deposition per unit mass or volume, 1-MeV equivalent neutron fluence, gamma dose, radiation pulse shape at the device.

6-1 Weapon Output [redacted]

[redacted] The weapon radiation output and its interaction with the atmosphere will be summarized in succeeding paragraphs, together with the units in which these radiations are usually described. Following this summary, the individual radiation effects of concern will be discussed, and the appropriate methods of describing the radiation at the affected parts or circuits will be described for each type of effect.

[redacted] The majority of the energy released in a nuclear explosion heats the material of which the nuclear device was composed, to temperatures of tens and hundreds of millions of degrees. A smaller fraction (0.1 to 10%) escapes promptly in the form of fast neutrons and prompt gamma rays (see Chapters 4 and 5). The intense thermal source radiates most of its energy in the form of X-rays. If the explosion occurs in a vacuum, or, if the weapon is a "hot" X-ray device (see Section II, Chapter 4) that explodes in relatively thin atmosphere, these X-rays can produce important TREE effects. Depending upon the specific temperature of the source, the X-rays have energies varying from a few to a few hundred kilovolts. One method by which the energy spectrum from such a source is frequently described is by specifying the temperature of a black body which would emit a spectrum that approximates the observed X-ray spectrum (Chapter 4). It should be noted that even though the temperature is usually specified as a number in units of keV (kilo-electron-Volts), this unit describes a spectrum of photon energies extending significantly below and above the quoted number [redacted] DNA (6)(3

[redacted]

[redacted]

[redacted]

initial nuclear radiation (i.e., that radiation emitted within 1 minute following the burst) which, in turn, consists of both prompt and delayed radiation. The weapon-burst radiations of interest are neutrons, gamma rays, X-rays, and to a much less extent, electrons. The effects of interest are both temporary and permanent even though the radiation persists only for a short time. [redacted] Examples of system responses to TREE and their consequences are given below. These examples represent only a small sample and are not necessarily representative of present day problems.

Effect in System Due to Temporary Disturbances of the Electronics	Typical Consequence
Change in logic state in missile-borne guidance computer	Program jump or disturbance of key data causing mission failure
Spurious (ill-timed) fuzing signal	Warhead dudding or premature detonation
Excess currents in transistors and capacitors in servo control loop	Excessive steering maneuvers causing structural instability
Excess currents in memory write circuits	Writing erroneous data in memory, usually causing mission failure
Microcircuit latchup following ionization pulse	Functional disabling of microcircuit until power is cycled off and on

Effect in System Due to Permanent Degradation of the Electronics	Typical Consequence
Neutron-induced loss of gain in lower-frequency transistors	Loss of power supply regulation; decreased servo-loop gain
Delamination of semiconductor wire bonds due to thermomechanical shock	Functional failure of the affected device, usually leading to mission failure
Neutron-induced loss of gain in higher-frequency transistor structures	Decreased fan-out capability in computer logic
Metallization burnout due to excess ionization-induced currents	Functional failure of affected device, usually causing mission failure

[redacted]

[redacted]

[redacted] After the prompt radiations have been emitted from the nuclear explosion, a residue of hot and radioactive debris remains. Some of its energy continues to be irradiated as thermal energy in the ultra violet and visual regions of the spectrum. Subsequent radioactive decay of the debris produces lower intensity gamma rays as well as emitting high energy electrons. These electrons are particularly important for high altitude nuclear detonations, which may inject the electrons into orbits trapped by the earth's magnetic field. These electrons are of particular concern to space vehicles whose orbits intercept the earth's radiation belts, because continued exposure to the electrons can cause significant permanent degradation.

[redacted] If the explosion occurs within or near the atmosphere, the prompt radiations interact with the constituents of the atmosphere, producing secondary effects. The X-rays are absorbed most strongly and, depending upon altitude, the air is heated by the interaction to produce an intense thermal source and a blast wave in the air (Chapters 1 through 4). The gamma rays interact to produce secondary electrons. In concert with the earth's magnetic field and/or inhomogeneities, such as the surface of the earth, these electrons create a radiating electromagnetic pulse (EMP) (Chapter 7). The neutrons interact with the atmosphere to produce secondary gamma rays (Chapter 5).

6-2 Time Considerations [redacted]

[redacted] The general time frame for the arrival of the various radiation components at the electronics package is sometimes important. In general, for the purposes of electronic vulnerability, the prompt gamma radiation can be considered as a single pulse. Since the flight time for X-rays and gamma rays of all energies equals the speed of light, *unscattered* photons arrive at the equipment with the same time distribution they had at the source, with a time delay of 3.33 μsec/km from the weapon burst. The arrival of the gamma pulse approximately coincides with the unscattered prompt X-rays.

[redacted] The neutrons arrive after the initiation of the gamma- and X-radiation. Their arrival time depends on the neutron energy and the range to the receiver. The first neutrons to arrive will be the unscattered 14-MeV neutrons. Their time of flight is 19.3 μsec/km, therefore, they will arrive 16 μsec/km after photon arrival. The photons resulting from neutron inelastic-scattering (Chapter 5) will also begin to arrive at about this time. Within 32.8 μsec/km (the arrival time after photon arrival for 4-MeV neutrons), the photons resulting from neutron inelastic-scattering will be completed, since the inelastic-scatter contribution is negligible for lower energy neutrons. Within 69.0 μsec/km, the bulk of the unscattered 1-MeV neutrons will have been deposited. The photons resulting from neutron capture (or thermalization) typically will peak shortly after the arrival of the 1-MeV neutrons depending on the system configuration being studied. Both the thermalization time and the capture time following thermalization depend strongly on the interacting materials and the system configuration. The radiation of interest to TREE is complete in less than 1 minute.

6-3 Description of Radiation Fields [redacted]

[redacted] A complete description of the radiation field produced at the system should include the time dependence, angular distribution, and energy spectrum of each of the components. Of course, this should be done for a wide variety of conditions to cover all possible interaction scenarios. In practice, it is not necessary to be so thorough, and the following approximations are usually made:

- A worst case radiation environment is spe-

[redacted]

[redacted]

[redacted] cified and the objective is to have the system tolerate all combinations of environments that are less stringent than the specification.

- The incident radiation is assumed to be unidirectional. This is usually the worst case angular distribution, and it represents a reasonable approximation to reality.
- Where possible, the individual radiation fields are specified in units that facilitate conversion to those units that are convenient for describing the effect.

[redacted] For example, it is possible to specify the time dependent neutron energy spectrum incident on the system. Since the time dependence of arrival of unscattered neutrons is correlated with neutron energy, as discussed above, specifying the neutron energy spectrum, and the range of distances between nuclear explosion and the irradiated system, also is equivalent to specifying the time dependence. Finally, if the only effect of interest is permanent neutron-induced displacement effects, the spectrum can be replaced by a single quantity such as the 1-MeV damage equivalent neutron fluence. The meaning of these units and the method of calculating them will be discussed in following paragraphs. It must be emphasized, however, that such convenient units are intended for simplification only. They are useful only if the assumptions underlying their use are valid. In the foregoing example, specifying only the 1-MeV damage equivalent neutron fluence is useless for determining the magnitude of neutron-induced ionization effects quantitatively.

[redacted] The degree to which such simplifications can be used depends in large measure upon the simplicity of the interaction of the incident radiation with the target materials. A particularly simple case is the description of the gamma-ray environment. High energy gamma rays suffer negligible attenuation in passing through significant quantities of material, and they interact with matter to produce approximately the same energy deposition, independent of atomic composition of the target. Therefore, it has been possible to describe the gamma ray environment fairly simply and this has frequently led to carelessness. A more complicated situation, in which carelessness cannot be tolerated, is represented by the X-ray interactions. X-rays of energies of tens to a few hundred kilovolts are attenuated significantly even by thin missile skins and electronic subsystem boxes, and the energy deposition produced by such X-rays is a strong function of the atomic number of the target material. For this reason, it is invariably necessary to specify not only the total X-ray energy fluence incident on the system (usually given in calories/cm^2), its pulse width (usually given in nanoseconds), but also a range of possible energy spectra (sometimes given as explicit spectra, and at other times specified by a range of characteristic black body temperatures). The relating of such an exposure to the intensity of the radiation present at the affected area, such as the junction region of a transistor, requires detailed and specific calculations of the transport of the spectrum through the intervening material and the resultant energy deposition in the affected volume.

[redacted] The transport of the various radiation components to the site of the equipment of interest is discussed in Chapters 4 and 5. It is of value, however, to note that typical electronic packaging materials will not produce significant attenuation of the neutron and gamma ray components of the environment. They do represent significant shields of X-rays, particularly if high-Z materials are used for electronic envelopes. Only the higher energy photons penetrate to the electronics of interest. Since the lower energy photons produce the highest energy deposition per unit volume when they interact, such shielding is especially useful because it removes preferentially that portion of the photon energy spectrum that would be most damaging if it were

[redacted]

[redacted]

allowed to penetrate to the sensitive devices. This fact reinforces the observation that is necessary to specify both the X-ray energy fluence and its spectrum outside and inside the shield. Indicating only the energy-fluence attenuation factor of a shield would ignore the fact that remaining photons are less effective in producing damage.

[redacted] INTERACTIONS BASIC TO TREE [redacted]

6-4 Ionization [redacted]

[redacted] Ionization is that process by which electrons are freed from their parent atoms in a material. A free electron carries a negative charge. After losing an electron, the atom (then called an ion) carries a net positive charge. Thus, the process of ionization results in the formation of electron-ion pairs in a material. If none of the electrons or ions leave the material, the material remains electrically neutral, since the positive and negative charges balance one another. Nevertheless, characteristics of the material may be altered considerably by ionization. The number of electron-ion pairs formed and their subsequent behavior are of prime interest in determining the effects of ionization.

[redacted] Gamma rays interact with matter in three ways. The first is called the Compton effect. In this type of interaction, a gamma ray (primary photon) collides with an electron, and some of its energy is transferred to the electron (see Figure 6-1a). A secondary photon, with less energy, is created and departs in a direction at an angle to the direction of motion of the primary photon. The second type of interaction of gamma rays with matter is the photoelectric effect (see Figure 6-1b). A gamma ray, with energy somewhat greater than the binding energy of an electron in an atom, transfers all its energy to the electron, which is consequently ejected from the atom. Since the photon involved in the photoelectric effect transfers all of its energy, it ceases to exist and is said to be absorbed. The third type of interaction is pair production (see Figure 6-1c). When a gamma ray photon with energy in excess of 1.02 MeV passes near the nucleus of an atom, the photon may be converted into matter with the formation of a pair of electrons, equally but oppositely charged. The positive electron soon annihilates with a negative electron to form two photons, each having an energy of at least 0.51 MeV. In some cases, if the interaction takes place near the nucleus of a heavy atom, only one photon of about 1.02 MeV energy may be created.

[redacted] Any photon (e.g., an X-ray or a gamma ray) can produce ionization in a material by these processes of creating secondary electrons that deposit their kinetic energy by ionizing the medium in which they are created. The relative importance or frequency with which each process occurs depends upon the photon energy and the characteristics of the material. The Compton process is the dominant ionization mechanism for most gamma rays of interest, particularly in electronic materials such as silicon, of which many solid-state devices are fabricated.

[redacted] Fast neutrons can produce ionization indirectly. As neutrons undergo inelastic scattering and capture in a material (see Section I, Chapter 5), gamma rays that are emitted can cause ionization. In addition, collision of a neutron with an atom may impart sufficient energy to the atom for it to cause ionization. Only high-energy neutrons ($E > 1$ MeV) contribute significantly to ionization. The 14-MeV neutrons arising from fusion reactions in a weapon are particularly important.

[redacted] The types of radiation that cause ionization in materials – namely, gamma rays, electrons, X-rays, and, to a lesser extent, fast neutrons – are known collectively as ionizing radiation.

[redacted] Once created by the ionization processes (either primary or secondary), the charged par-

[redacted]

[redacted]

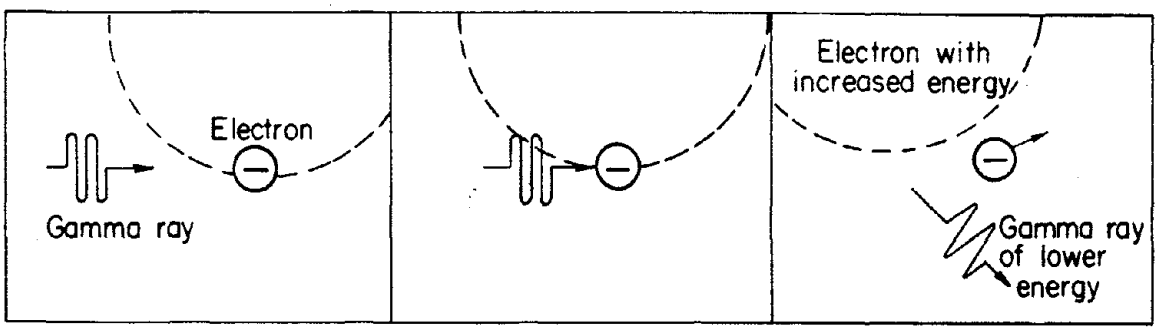

a. Compton Effect

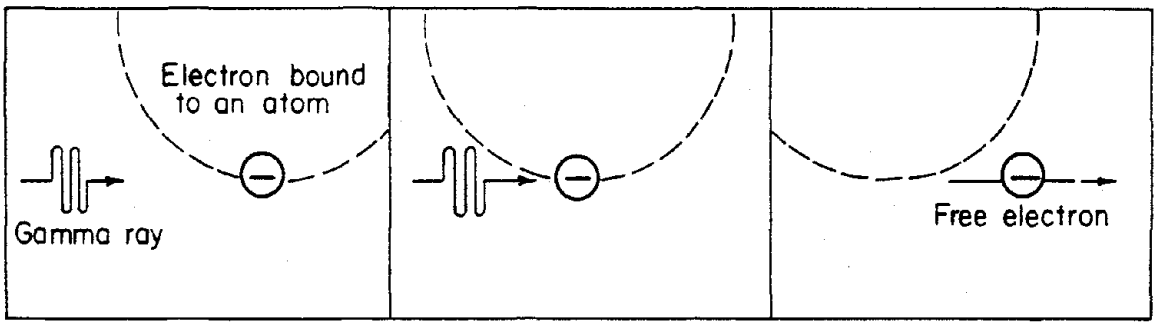

b. Photoelectric Effect

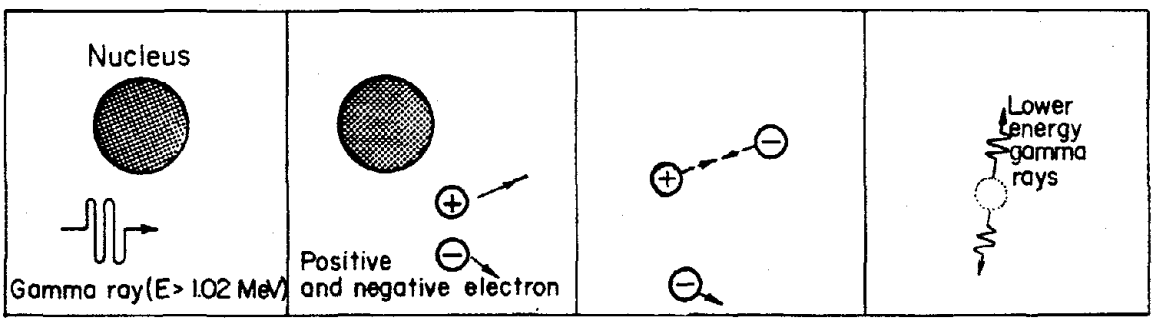

c. Pair Production

Figure 6-1. [redacted] Gamma Ray Interaction with Matter [redacted]

[redacted]

[redacted]

[redacted] ticles (electrons or ions) are free to move in a material, scattering frequently and following a random-walk pattern. If the concentration of electric charge carriers throughout the material is not uniform, and if no externally applied electric field is present, the carriers will move from regions of high concentration to regions of low concentration. This movement is known as diffusion and it would be superimposed on the normal random-movement. If an electric field is present (e.g., as a result of an intentionally applied voltage), the carriers drift in the electric field while they undergo a predominantly random scattering. If impurities are present in the material (as they always are in solid-state devices, such as transistors and diodes), carriers may be captured (trapped) and immobilized by impurity atoms (traps). Eventually, the trapped carriers will be annihilated by their mates (oppositely-charged carriers) in a process called recombination. The net result of these processes is that the carriers diffuse and/or drift until they are trapped and usually recombined.

6-5 Displacement [redacted]

[redacted] As described above, ionization involves the movement of electrically charged electrons and ions in a material. Displacement involves the movement of atoms (which are electrically neutral).

[redacted] Any material may be described as being either crystalline or amorphous. The atoms of a crystalline material (a crystal) are arranged in a definite, repeated, three-dimensional pattern called a lattice; the atoms of an amorphous material have no definite arrangement. Displacement is an important phenomenon in crystalline materials, and it is a very important phenomenon in TREE because many electronic devices (e.g., transistors, diodes, integrated circuits) are constructed from crystalline semiconductors – primarily silicon and germanium. Lattice defects result from the displacement of atoms from their usual sites in crystal lattices. The simplest lattice defects are extra atoms inserted between lattice positions (interstitials) and unoccupied lattice positions (vacancies). At least part of the resultant damage to the material is stable and accounts for permanent property changes of irradiated crystalline materials.

[redacted] The production of displacement damage in a crystalline solid is a complex process. An abbreviated history of this process follows.

(1) Radiation of an appropriate form enters the material, interacts with a lattice atom, and imparts to it a certain energy.

(2) The target (recoil) atom leaves its lattice site, thus creating a vacancy, and collides with other lattice atoms (see Figure 6-2).

(3) Other atoms are displaced from their sites, creating more vacancies.

(4) Eventually, most recoil atoms come to rest in interstitial positions, while a few fall into vacancies. Some of the interstitials and vacancies may be isolated, but most of them will be associated with other defects in cluster formations.

(5) The simple defects and defect clusters migrate through the crystal.

(6) Eventually, the mobile defects are annihilated by recombination of vacancy-interstitial pairs, are immobilized by the formation of stable defect clusters with other impurities of lattice defects (either present in the original material or created by the irradiation), or escape to a free surface.

(7) Meanwhile, the physical properties of the material are changed by the presence of the defects.

[redacted] Fast neutrons are very effective in producing displacement damage. Energetic electrons can also produce displacement damage; however, their displacement effects are negligible compared to those of fast neutrons.

[redacted]

[redacted]

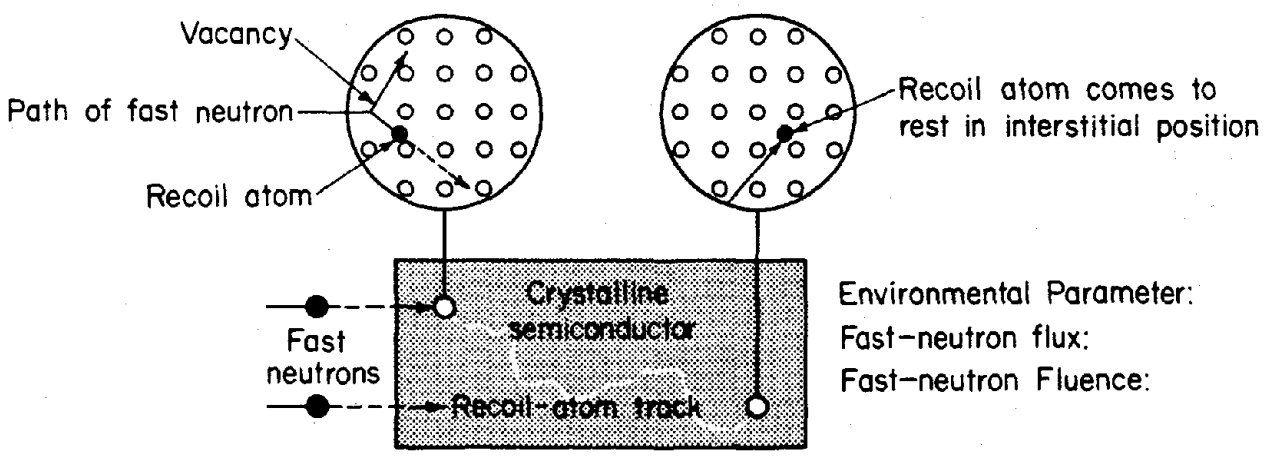

Figure 6-2. [redacted] Displacement Damage in a Crystalline Solid [redacted]

[redacted] The absolute magnitude of damage in a material caused by neutrons is difficult to predict because some of the defects that are produced will effectively disappear at room temperature, that is, anneal. However, much useful information can be gained from the relative value of the concentration of defects produced before annealing. Assuming the same fraction anneals, the relative concentration of stable defects would be in the same ratio. It has been found that the number of unannealed defects that are generated depends on the energy of the impinging neutron. The number of unannealed defects generated by a 14-MeV neutron (one from a fusion weapon) is about 2.5 times the number of unannealed defects generated by a 1-MeV neutron (roughly the average energy for a neutron from a fission weapon). As will be discussed below, the number of defects generated in semiconductor materials is directly related to the change in semiconductor device parameters.

[redacted] Not all of the defects produced in the displacement process are stable. Some defects are annihilated by recombination of vacancy-interstitial pairs, some combine with pre-existing lattice defects, and some eventually escape to a free surface of the material. The stable defects contribute to the permanent damage of the material. The unstable defects are said to disappear, or anneal, with time. In practice, this means that the degree of displacement damage in a crystalline semiconductor varies with time, reaching a peak rapidly and then partially annealing with time. The temperature of the material exerts a considerable influence on the amount of annealing that takes place. More annealing is observed at elevated temperatures.

[redacted] Annealing may be divided roughly into two time frames. Rapid, or short term, annealing occurs in times of the order of hundredths of a second. Long term annealing continues at a slower rate for times of the order of tens of seconds (see Figure 6-3). If the temperature remains constant, annealing will be essentially complete after one-half hour. The ratio of the damage observed at early times (number of defects present) to the damage after a very long time is called the annealing factor, which is a function of the time of measurement and other parameters. The maximum damage created at short times following the fast-neutron burst frequently is important to electron-system perfor-

[redacted]

[redacted]

[redacted]

mance. Therefore, the maximum annealing factor is an important quantity, because it indicates the peak damage that must be tolerated above the permanent damage in the steady state. Values of the annealing factor depend on the temperature and on the electrical condition of the material. An annealing factor of three is commonly used for room temperature at ~10 msec. Larger factors have been observed at shorter times, or low injection conditions (e.g., cut-off transistors).

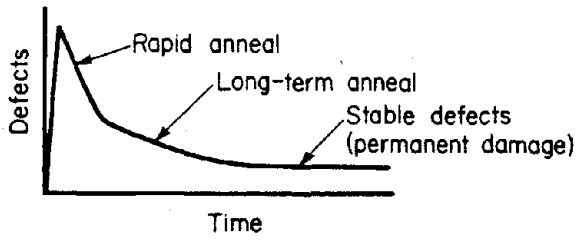

Environmental Parameters:
Fast-neutron flux:
Fast-neutron Fluence:

Figure 6-3. [redacted] Annealing Due to Vacancy-Interstitial Recombination and Escape of Defects from Semiconductor [redacted]

6-6 Heating [redacted]

[redacted] Whenever a material absorbs energy from its surroundings and cannot instantaneously dissipate that energy, the temperature of the material will rise, i.e., the material will be heated. The temperature will return to ambient at a rate determined by the efficiency with which the material can dissipate heat to its surroundings. If the energy deposition is great, and the mechanisms for heat dissipation are inadequate, the temperature rise will be significant and will persist for a considerable time (see Figure 6-4).

[redacted] X-rays are the primary contributors to heating. Therefore, the relevant environmental parameters are the X-ray dose rate, and the X-ray dose. Predictions of the X-ray environment from nuclear weapon bursts and the X-ray absorption mechanisms are discussed in Chapter 4. Responses of electronic components to heating are discussed in Section VII, Chapter 9.

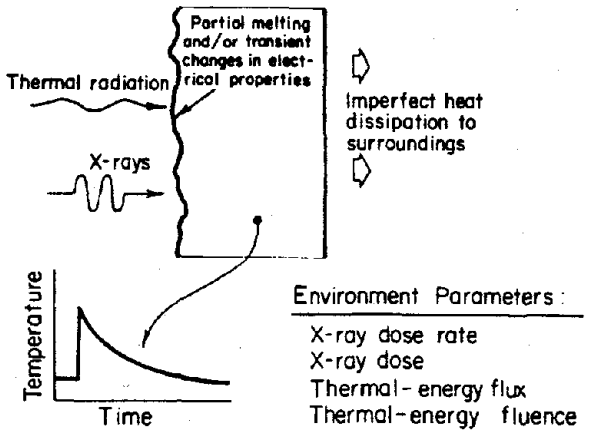

Figure 6-4. [redacted] Heating [redacted]

[redacted] MANIFESTATIONS OF TREE IN MATERIALS [redacted]

6-7 Ionization Effects [redacted]

[redacted] The important manifestations of ionization include (1) charge transfers, (2) bulk-conductivity increases, (3) excess minority-carrier generation, (4) charge trapping, and (5) chemical effects.

[redacted] Charge transfer results from the escape of some electrons produced during ionization from the surface of the material being ionized. If the net flow of electrons is out of the material, the material will be left with a net positive charge. If these electrons are stopped in an adjacent material, a transfer of charge will have occurred from one material to the other, and a difference of potential (or voltage) will exist between the two materials.

[redacted]

[redacted] The transfer of charge from one material to another can have a number of effects. The most obvious one is that a current will flow through any electrical circuit connecting the two materials to restore charge neutrality. The charge will produce electric and magnetic fields during transit. If there is matter in the gap between the materials, the charge transfer also will produce ionization and conduction in response to local electrical fields. Finally, if the charge either originates or embeds itself in an insulator, a long-lived local space charge may result. Charge transfer, therefore, may result in either a temporary or a semipermanent effect.

[redacted] The free carriers produced during ionization respond to an applied electric field by producing a net drift current. This is precisely the mechanism by which a material conducts electricity. Therefore, ionization induces a transient increase in conductivity. An example of a detrimental effect to the operation of electronic equipment resulting from an increase in bulk conductivity occurs in a capacitor exposed to a weapon burst environment. The ability of a capacitor to retain, or restore, electrical charge is dependent upon the low conductivity of the dielectric, or insulating material, that is contained within the capacitor. In an ionizing environment the increase in bulk conductivity results in a decrease of stored charge in the capacitor.

[redacted] The ionization effect of excess minority carriers is a prime concern in many semiconductors and is usually the most important manifestation of TREE. Semiconductor devices, such as transistors and diodes, employ both positive and negative charge carriers, either of which may be in the minority with respect to concentration. The characteristics of many such devices depend strongly upon the instantaneous concentration of minority carriers in various regions of the device. Since ionizing radiation creates large (and equal) numbers of positive and negative charge carriers, the concentration of minority carriers in the device is temporarily enhanced by a large percentage, and the electrical operation of the device may be affected adversely. The most familiar example of this effect is the current flow across a reverse-biased PN junction, such as those that are found in a diode or the base-collector junction of a transistor (see Section VII, Chapter 9).

[redacted] When free carriers are created in insulating materials, and are trapped at impurity sites, many may not undergo recombination with their mates, which may be trapped elsewhere. In these cases, the material properties may be altered semipermanently, even though there is no net charge in the material. This ionization effect is known as charge trapping.

[redacted] Trapped charge can change the optical properties of materials (e.g., F centers in alkali halides, coloration of glasses). The trapped carriers may be released thermally, either at the irradiation temperature or by elevating the temperature. In either case the resultant creation of some free carriers is manifested by an increase in conductivity and sometimes by the emission of light.

[redacted] The chemical effects of ionization occur during the processes of trapping and recombination when sufficient energy is available to disrupt chemical bonds. At the completion of the ionization cycle (i.e., after recombination is complete), the material may return to electrical inactivity, but its chemical composition may be altered permanently. The resulting chemical changes may be manifested as permanent changes in physical and/or electrical properties of the material. The radiation dose required to cause such effects is larger than normally will be encountered; therefore, the effect will not be discussed further.

[redacted] Since ionization effects do not occur and/or recover in the same time period, the time domain for their occurrence and recovery must be considered. There are three categories of time

[redacted]

[redacted] dependence – prompt, delayed, and long term.

[redacted] Prompt effects are those in which the width of the ionization pulse is longer than the times required for atoms or electrons within the material being exposed to make a specified amount of recovery. The magnitude of the effect is a function of the density of the positive and negative particles created during the ionization, which in turn is a function of the dose rate. Examples of prompt effects are charge transfer and prompt bulk-conductivity increases in insulating and semiconductor materials.

[redacted] Delayed effects are those in which the width of the ionization pulse is shorter than the times required for atoms or electrons within the material being exposed to make a specified amount of recovery. The initial response of the material or device is a function of dose, and its persistence is determined by the length of the specified recovery time. An example of this effect is delayed bulk conductivity of insulator materials. In this particular example the recovery times for the prompt and delayed effects are based on different mechanisms of carrier generation (ionization induced or thermal trapping) and, hence, they have very different time periods.

[redacted] Long-term effects are those which persist for periods longer than minutes. These effects can be, but are not necessarily, permanent. Recovery may be so slow that it takes days, months, or years for apparent complete recovery. Examples of long-term effects are some cases of trapped charge and chemical effects.

[redacted] An important point, emphasized here, is that a general class of materials or devices (plastics, transistors, etc.) could be both dose and dose-rate sensitive with respect to the ionization effects observed.

[redacted] It has been established that, with the exception of charge transfer, the magnitude of the ionization effects is primarily a function of the total concentration of thermalized charge carriers (electrons and holes). These carriers are generated at a rate proportional to the instantaneous ionization energy deposition and independent of the nature of the radiation producing that energy deposition. Therefore, it is appropriate to use units that quantify the energy deposition in the material of interest when describing the radiation field at the responding device. Such units include ergs/gram (material), rads (material), and calories/gram (material). Since these are descriptions of energy deposition in a given material, they are called units of dose. The time dependence of energy deposition can be specified by these same units per second, and are called dose rate.

[redacted] Unfortunately, the magnitude of charge transfer depends not only on the energy deposition but the spectrum of the secondary electrons. Therefore, quantitative evaluations of systems in which charge transfer represents a significant vulnerability mode must use a more complex characterization of the spectrum of the incident photons, together with a calculation of the photon interactions, to produce the spectrum of secondary electrons.

[redacted] In some materials, particularly insulators, the ionization effects are also a weak function of the microscopic concentration of the ionization around individual particle tracks. For example, neutron-induced ionization created by intensively ionizing recoil atom may be less effective in producing conductivity in an insulator than the same dose or dose rate imparted by lightly ionizing gamma rays. Units for describing this process include specific ionization (ratios of ionization to the minimum level of ionization at high velocities of a singly charged particle), and linear energy transfer (MeV/cm or MeV cm^2/gram). Fortunately, these effects are of second order importance for most TREE applications. A specification of dose rate and dose is adequate in the majority of applications.

[redacted] The gamma-ray field incident on a

[redacted]

[redacted]

[redacted]

system is frequently described by its exposure measure in roentgens. The roentgen is determined by specifying the energy deposition in a standard material (dry air under standard temperature and pressure conditions). For high energy gamma rays that interact primarily via the Compton process, exposure of almost any material to one roentgen of gamma rays produce (within 20%) approximately one rad of energy deposition in any material. This factor has enabled the users of these units to become somewhat careless, without serious consequence, so long as only high-energy photons are of interest. However, these relations do not carry over into photons of lower energies (200 kilovolts or less in medium atomic-number materials) and careful treatment of the units is required. One way of minimizing the chances of misinterpretation is to use units of calories/cm^2 with a defined spectrum for external exposure and units of cal/gram (material) for dose.

6-8 Displacement Effects [redacted]

[redacted] The displacement effects of prime concern to TREE are those generated in semiconductor materials. The lattice damage resulting from displacement degrades the electrical characteristics of semiconductor devices by increasing the number of trapping, scattering, and recombination centers. The effect of displacement in semiconductors is, therefore, threefold: (1) the trapping centers remove charge carriers from the electrical conduction process (reduces electrical current flow), (2) the additional scattering centers reduce the capability of the charge carriers to move through the semiconductor material (reduces charge-carrier mobility), and (3) the recombination centers reduce the time that the minority charge carriers are available for electrical conduction (reduces the lifetime of the minority-charge carriers). This last effect is most important for prediction of semiconductor device performance in radiation environments that cause displacement. The decrease in minority-carrier lifetime (τ) is predicted according to the relationship

$$\frac{1}{\tau_\varphi} = \frac{1}{\tau_0} + K\varphi ,$$

where

τ_φ = minority-carrier lifetime at fluence φ in seconds,

τ_0 = initial minority-carrier lifetime in seconds

K = lifetime damage constant, cm^2/(neutron · second)

φ = total fast-neutron fluence, neutrons/cm^2.

[redacted] Typical values for τ_φ in device materials of interest are 10^{-8} to 10^{-4} seconds. The value of the lifetime damage constant, K, is dependent on the type of material, the type and amount of impurities in the material, the operating voltage applied to the material, the temperature, the energy spectrum of incident neutrons, and, because of defect annealing, the time after the nuclear radiation is incident on the material. A general value for silicon, the prime material used in transistors, diodes, and integrated circuits, is $K \approx 1 \times 10^{-6}$ cm^2/(n · sec).

[redacted] To illustrate the magnitude of displacement effects that occur in semiconductors compared to those that occur in other materials, a comparison of neutron fluences that will cause significant effects is made in the following paragraph. Interest is focused only on those property changes that affect the normal use of the materials being compared.

[redacted] Semiconductor lifetime can begin to show significant effects in devices at a fluence of 10^{11} n/cm^2 (Pu, fission)* and by 10^{16} n/cm^2

*Accurate neutron dosimetry requires that the foil used for making the neutron measurement and the energy spectrum of the neutrons be specified with the value measured. Therefore, in the example presented here, 10^{11} neutrons per square centimeter were detected with a plutonium foil and the energy spectrum of the neutrons was a nominal fission spectrum.

[redacted]

[redacted]

[redacted]

(Pu, fission) the lifetime in most semiconductor devices is so short that the device is no longer useful. Metals such as nickel and copper start to show effects in material strength at a fluence of 10^{18} n/cm^2 (Pu, fission). As a general rule, the electrical properties will not start to change in structural materials until the material properties change. Glasses and ceramics are much less susceptible to neutron damage than semiconductors, but they are more susceptible than metals. The point that is emphasized is that semiconductors are among the devices that are most susceptible to displacement effects.

[redacted] It is frequently desirable to express neutron effects data observed by different experimenters using different neutron-energy spectra in terms of an equivalence fluence unit in addition to the measured flux and fluence units. This permits easy comparison of damage levels obtained from different neutron test facilities. Since silicon is the material of most interest to displacement effects, the equivalence is usually based upon damage in silicon. The energy spectrum typically used as a standard for comparison is a hypothetical 1-MeV monoenergetic neutron source. The damage caused by the neutrons (of some known spectrum) is compared to the damage done by the neutron spectrum which is used as a standard. The neutron fluence of the standard which would cause the same damage in the given material as observed for the known spectrum is then specified as the damage equivalent fluence for that material. An example of this equivalence unit for 1-MeV neutrons standard spectrum and silicon material is: 10^{13} n/cm^2 (1-MeV damage equivalence in silicon). The procedures for obtaining a 1-MeV equivalent fluence for any known neutron spectrum are specified in the TREE Handbook (see bibliography).

6-9 Heating Effects [redacted]

[redacted] The radiation environment, especially the X-rays, produced by nuclear weapons can deposit considerable energy in electronic materials. The energy deposited is sufficient to heat some materials to such an extent as to cause partial melting, and it is sufficient to change electrical properties in other materials. These temperature transients may last from fractions of a second to minutes. If the energy is deposited in the material in a very short time (deposition time is typically 10^{-8} seconds for a nuclear weapon) an additional effect is observed; the material is heated very rapidly but does not have time to expand. The result is the instantaneous creation of a shock wave, or pressure pulse, which tends to compress the material. This compression wave starts at the point of energy absorption, typically close to the material's front surface upon which the incident energy impinges, and quickly propagates to the back surface. When it reaches the back surface, it is reflected, becomes a tension wave, and propagates toward the front surface. For energy deposition of sufficient magnitude delivered in a sufficiently short interval, the tension wave can be intense enough to exceed the strength of the material. Several consequences are possible.

(1) Portions of the material may be removed from the back surface – spallation (see Figure 6-5).

(2) Fragments of the material may separate from the front surface – blowoff.

(3) The material may separate between front and back surfaces – delamination.

(4) Agglomerates or layers of dissimilar materials bonded together will tend to separate at the interfaces – also called delamination.

(5) In brittle crystalline materials (e.g., Si or Ge), crystal fracture can occur.

Generally, effects of this nature are referred to as thermo~~chemical~~ mechanical shock effects. Obviously, the consequences of these effects can be catastrophic. An example important to transistors and inte-

[redacted]

[redacted]

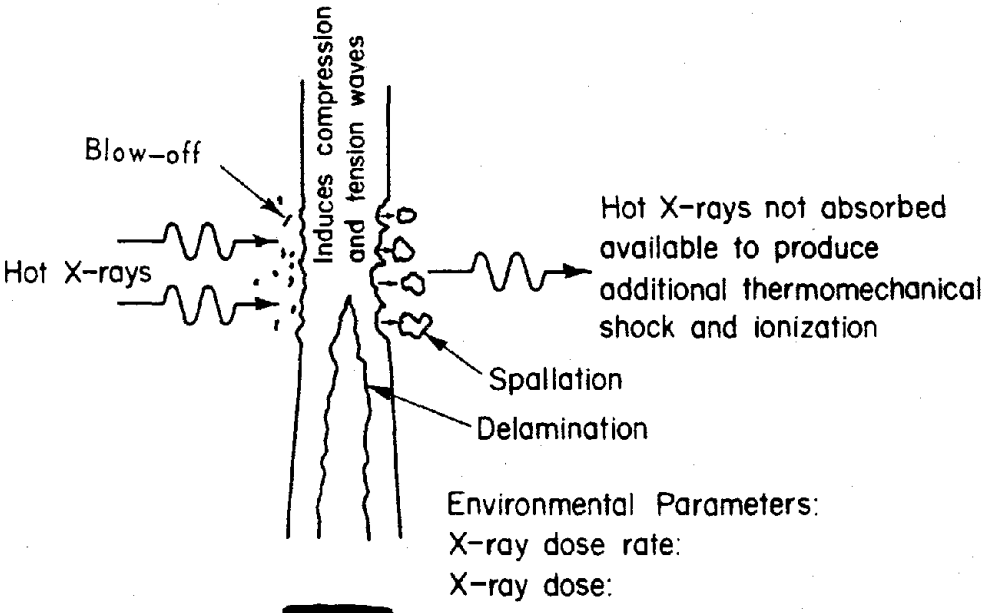

Figure 6-5. [redacted] Thermomechanical Shock Effects [redacted]

[redacted]

grated circuits is the delamination of the electrical contacts to the semiconductor chip, resulting in complete loss of the device function. The thermomechanical-effect damage threshold is difficult to determine. It depends not only on the energy deposition and energy spectrum but also on the thickness of the materials, the compressibility, the expansion coefficient, and the dynamic strength of the materials. Thermomechanical effects on materials are discussed in more detail in Section VII of Chapter 9.

[redacted]

[redacted]

[redacted] BIBLIOGRAPHY [redacted]

DASA EMP (Electromagnetic Pulse) Handbook, DASA 2114-1, DASIAC, Santa Barbara, California, September 1968, [redacted] (to be replaced by DNA 2114H-1 during calendar year 1972).

DASA EMP (Electromagnetic Pulse) Handbook, Classified Supplement [redacted] DASA 2114-2, DASIAC, Santa Barbara, California, September 1968, [redacted] (to be replaced by DNA 2114H-2, 2114H-3, and DNA 2114H-4 during calendar year 1972).

Gwyn, C. W., D. L. Scharfetter, and J. L. Wirth, *The Analysis of Radiation Effects in Semiconductor Junction Devices,* SC-R-67-1158, Sandia Corporation, Albuquerque, New Mexico, July 1967 [redacted]

Kalinowski, J. J., *A Management Guide to Transient-Radiation Effects on Electronics (TREE)* [redacted] DNA 2051H, Battelle Memorial Institute, Columbus, Ohio, February 1972 [redacted]

Larin, F., *Radiation Effects in Semiconductor Devices,* John Wiley and Sons, Inc., New York, 1968 [redacted]

TREE (Transient-Radiation Effects on Electronics) Handbook [redacted] Vol. 1 Edition No. 3, DNA 1420H-1, Battelle Memorial Institute, Columbus, Ohio, December 1971 [redacted]

TREE (Transient-Radiation Effects on Electronics) Handbook [redacted] *(Classified Supplement),* Edition 2, Revision 2, DASA 1420-1, Battelle Memorial Institute, Columbus, Ohio, September 1970, [redacted] (to be replaced by DNA 1420H-2 during calendar year 1972).

TREE Preferred Procedures (Selected Electronic Parts), DASA 2028, Defense Atomic Support Agency, Washington, D.C., May 1968, [redacted] (to be replaced by DNA 2028H during calendar year 1972).

Vook, F. L., Editor, *Radiation Effects in Semiconductors,* Proceedings of the Santa Fe Conference on Radiation Effects in Semiconductors, Plenum Press, New York, 1968 [redacted]

[redacted]

[redacted]

Chapter 7

ELECTROMAGNETIC PULSE (EMP) PHENOMENA [redacted]

AD-A955 391

[redacted] The nuclear electromagnetic pulse (EMP) is the time-varying electromagnetic radiation resulting from a nuclear burst. It has a very broad frequency spectrum, ranging from near dc to several hundred MHz.

[redacted] The generation of EMP from a nuclear detonation was predicted even before the initial test, but the extent and potentially serious degree of EMP effects were not realized for many years. Attention slowly began to focus on EMP as a probable cause of malfunction of electronic equipment during the early 1950s. Induced currents and voltages caused unexpected equipment failures during nuclear tests, and subsequent analysis disclosed the role of EMP in such failures. Finally in 1960 the possible vulnerability of hardened weapon systems to EMP was officially recognized. Increased knowledge of the electric and magnetic fields became desirable for both weapons diagnostics and long-range detection of nuclear detonations. For all these reasons a more thorough investigation of EMP was undertaken.

[redacted] Theoretical and experimental efforts were expanded to study and observe EMP phenomenology and to develop appropriate descriptive models. A limited amount of data had been gathered on the phenomenon and its threat to military systems when all aboveground testing was halted in 1962. From this time reliance has been placed on underground testing, analysis of existing atmospheric test data, and nonnuclear simulation for experimental knowledge. Extended efforts have been made to improve theoretical models and to develop associated computer codes for predictive studies. At the same time, efforts to develop simulators capable of producing threat-level pulses for system coupling and response studies have been expanded.

[redacted] This chapter describes the EMP generation mechanism and the resulting environment for various burst regimes. The description is largely qualitative, since the complexity of the calculations requires that heavy reliance be placed on computer code calculations for specific problems. Some results of computer code calculations are presented, but generalization of these results is beyond the scope of this chapter. More complete treatments of the EMP phenomena may be found in the "DNA EMP (Electromagnetic Pulse) Handbook (U)" (see bibliography).

[redacted] ENVIRONMENT – GENERAL DESCRIPTION [redacted]

7-1 Weapon Gamma Radiation [redacted]

[redacted] The gamma radiation output from a nuclear burst initiates the processes that shape the development of an electromagnetic pulse. The gamma radiation components important in EMP generation are the prompt, air inelastic, and isomeric gammas (see Chapter 5). Briefly, the prompt gammas arise from the fission or fusion reactions taking place in the bomb and from the inelastic collisions of neutrons with the weapon materials. The fraction of the total weapon energy that may be contained in the prompt gammas will vary nominally from about 0.1% for high yield weapons to about 0.5% for low yield weapons, depending on weapon design and size. Special designs might increase the gamma fraction, whereas massive, inefficient designs would decrease it. This component is generated within

[redacted]

This document has been approved for public release and sale; its distribution is unlimited.

[redacted]

[redacted]

less than a microsecond of detonation time. High energy neutrons, which result from the fusion process, emerge from the bomb debris with energies on the order of four to fourteen MeV. For a surface or air burst, these neutrons lose their energies primarily through a large number of inelastic collisions with the surrounding air molecules over a time period of many microseconds. This gives rise to a source of gammas over the same time span. Isomeric gammas are given off by nuclei of certain fission products in decaying from excited states to the ground state. They are important at times after the peaks in prompt and air inelastic contributions (see Section 1, Chapter 5).

7-2 Compton Current [redacted]

[redacted] When gamma radiation from any of the sources mentioned in the preceding paragraph impinges upon air molecules, high energy electrons are created by the Compton effect. In this effect, illustrated in Figure 7-1, the incident gamma ray interacts with an electron in the shell of an atom, imparting to it a large amount of energy. Both the electron and a less energetic

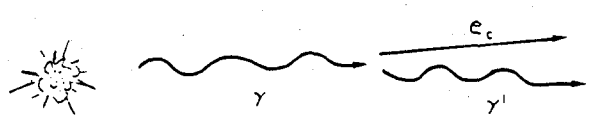

Figure 7-1. (U) The Compton Effect (U)

gamma ray scatter, primarily in the forward direction, and the scattered gamma rays frequently retain sufficient energy to repeat the process. In addition to the generation of Compton electrons, over ten percent of the gamma rays with energy above 5 MeV may generate electron-positron pairs (pair production). The positrons will cause ionization by inelastic collisions and eventually will be annihilated on collision with an electron, resulting in two 0.511 MeV gamma rays. The radial beams of scattered high energy electrons comprise a current termed the Compton current. If certain spatial and time conditions are met by a current, an electromagnetic field is generated. Since the prompt gamma ray pulse increases rapidly to a peak value and then decays (Section 1, Chapter 5), and since the Compton electrons lose energy as described in the following paragraph, the Compton current rises to a peak value rapidly and then decays as illustrated in Figure 7-2.

7-3 Air Conductivity [redacted]

[redacted] The high energy electrons in the Compton current lose some energy to the surrounding air molecules through inelastic collisions. The energy lost in these collisions goes into the freeing of additional electrons from the air molecules, i.e., further ionization. A drastic change in the conductivity of air takes place as it is ionized to become a plasma consisting of molecules, atoms, ions, electrons and accompanying electromagnetic radiation (see paragraph 4-2, Chapter 4). The conductivity will vary in space and time with the density and mobility of the ions and electrons, and the mobility depends on the electric field strength. Under certain conditions of air density and distance the x-rays from the bomb may contribute significantly to the air conductivity. Further complications are introduced by the recombination of ions and electrons. Initially the dominant process is the attachment of electrons to neutral oxygen molecules, reducing their mobility. Later the negative ions and electrons recombine with positive ions, reducing the charge density. Both processes, which are strongly dependent on air density, water content of the air, and the electric field, tend to reduce the conductivity of this partially ionized plasma. Figure 7-3 shows an example of air conductivity. The sudden rise at 8 microseconds

[redacted]

QUALITY INSPECTED 4
UNANNOUNCED

Deleted

DNA
(b)(1)

Figure 7-2 [redacted] Compton Current at 500 Meters from a 4200 TJ (1 Mt) Ground Burst [redacted]

[redacted]

Deleted

DNA
(b)(1)

[redacted]

Figure 7-3[redacted] Conductivity at 500 Meters from a 4200 TJ (1 Mt) Low-Altitude Burst[redacted]

[redacted]

[redacted]

is due to the local arrival of the neutron flux that produces ionization by nuclear reactions other than inelastic collision, namely (n,p) and (n,γ) reactions; however, earlier times are of greatest interest for the generation of EMP.

7-4 Radical Electric Field [redacted]

[redacted] If a nuclear burst occurs in homogeneous (constant density) atmosphere, with no geomagnetic fields present, a charge-separation model may be used to describe the resulting electric fields. Positive and negative charges are separated as the Compton electrons sweep off in a radial direction from the explosion, while the heavier ions tend to remain behind. Thus, two shells of charge are created, an inner positive ion shell and an outer shell of electrons. This separation produces a large local electric field in the radial direction shown as E_r in Figure 7-4. The magnitude of the field is limited as the air conductivity rises to permit return currents. Conductivity is higher closer to the burst where the current are more dense, so this region is the first to saturate and to limit the radial field although the radial electric field is higher when saturation occurs. These effects are depicted schematically in Figure 7-5.

[redacted] It is to be noted, however, that the total current distribution and the resulting radial electric field are perfectly spherically symmetric in this hypothetical illustration. It is a fundamental property of such a current distribution that no magnetic field is generated and no electromagnetic field is radiated away. The various asymmetries that occur in practice, and the resulting fields that are generated in the source region or radiated away are discussed in the following paragraphs.

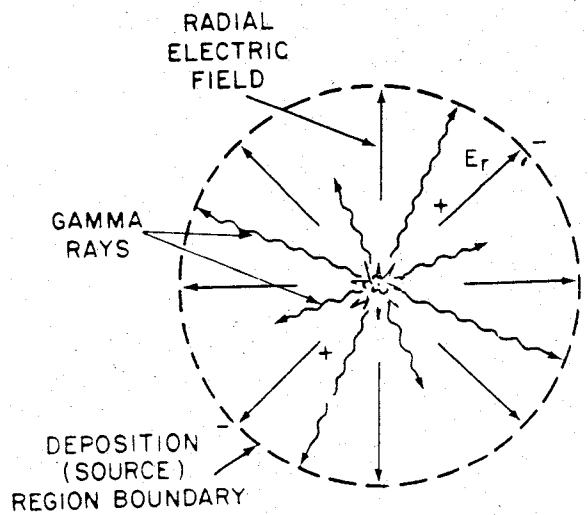

Figure 7-4. [redacted] Charge Separation Model [redacted]

[redacted] ELECTROMAGNETIC FIELD GENERATION [redacted]

7-5 Medium Altitude Air Burst [redacted]

[redacted] This category of nuclear explosions is defined to include weapon bursts under about 30 kilometers (19 miles) altitude, but sufficiently high that the deposition region containing the source currents does not touch the earth. In this case there are three principal factors tending to destroy the spherical symmetry of the current distribution discussed in the preceding paragraph: the atmospheric density gradient, the earth's magnetic field, and the configuration of the weapon itself. Since the earth's magnetic field is a much more important influence in less dense atmosphere, it will be discussed in succeeding paragraphs in connection with high-altitude bursts.

[redacted]

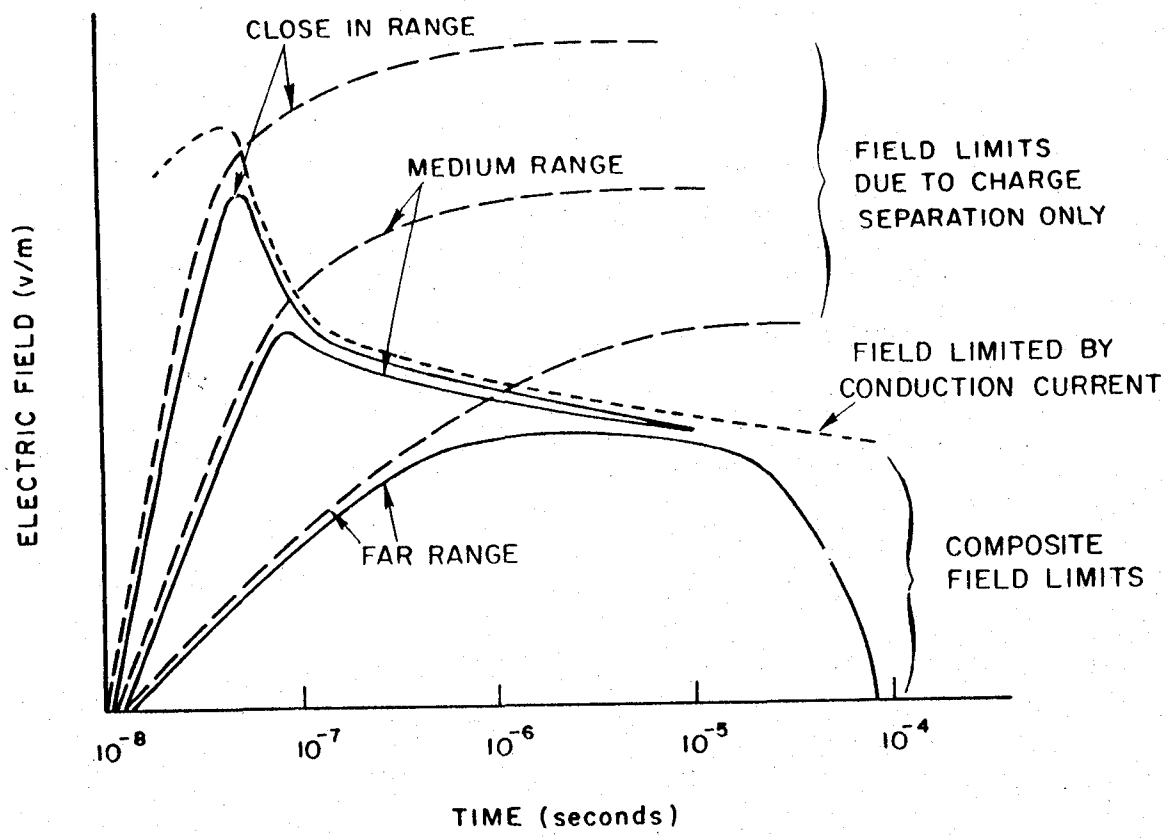

Figure 7-5. [redacted] Limits on Electric Field Waveforms [redacted]

[redacted]

[redacted] The density gradient in the lower atmosphere leaves the current distribution in the deposition region symmetric in azimuth only, since the strength of all the deposition region interactions depends on the density of its constituents. Thus there is a net vertical current component, the strength of which is expresed in terms of a dipole moment. This quantity is responsible for the generation of a magnetic field in the deposition region and the radiation of an electromagnetic wave from this region. These effects are shown in Figure 7-6, assuming no weapon asymmetry. The radiation, which is in the form of a simple vertical electric dipole, is a high intensity brief pulse that includes a broad spectrum of frequencies up to many MHz. Figure 7-7 demonstrates the relationship of energy per unit frequency as a function of frequency. The electric field as a function of range, R, and azimuth, θ, follows the form

$$E(t) = \frac{R_o}{R} E_o(t) \sin\theta \quad .$$

where R_o is the radius of the deposition region and E_o is the time dependent electric field at R_o. The angular dependence of radiated electromagnetic radiation is such that maximum intensity is radiated horizontally from the burst and is minimum directly above or below the burst. Simplified general waveforms of the quantities discussed here are presented in Figure 7-8.

DNA (b)(1)

[redacted]

[redacted]

DNA (b)(1)

7-6 Surface Burst [redacted]

[redacted] The presence of the ground introduces a strong asymmetry in addition to the ones described above. The ground is a very good absorber of neutrons and gamma rays and a good conductor of electricity compared with air. Therefore, the deposition region consists approximately of a hemisphere, resulting in a very large dipole moment and consequently large radiated fields. Further, the conducting ground allows an effective return path for the electron shell near the surface with the result that current loops are formed. That is, electrons travel outward from the burst in the air, then return through the higher conductivity ground toward the burst point. These current loops form a toroidal shaped solenoid resulting in very large azimuthal magnetic fields in the deposition region, especially close to the ground. These effects are shown in Figure 7-9. Figure 7-10 shows a typical toroidal magnetic field waveform in the deposition region near the surface.

[redacted] There can be extremely large electric and magnetic fields as well as the presence of a highly conducting plasma within the deposition region. As a result of the number of variables that can affect the magnitude and shape of the fields, it is not possible to provide a simple description of the fields.

[redacted] The peak radiated electric fields are ten to a hundred times stronger than for a similar air burst. The range, R_o, at which the radiation region begins is a function of weapon yield as shown in Table 7-1.

[redacted] The magnitude of the peak value of the radiated electric waveform for a surface burst is a weak function of yield, varying from about 1,300 volts per meter at R_o for a 4.2 TJ (1KT)

[redacted]

[redacted]

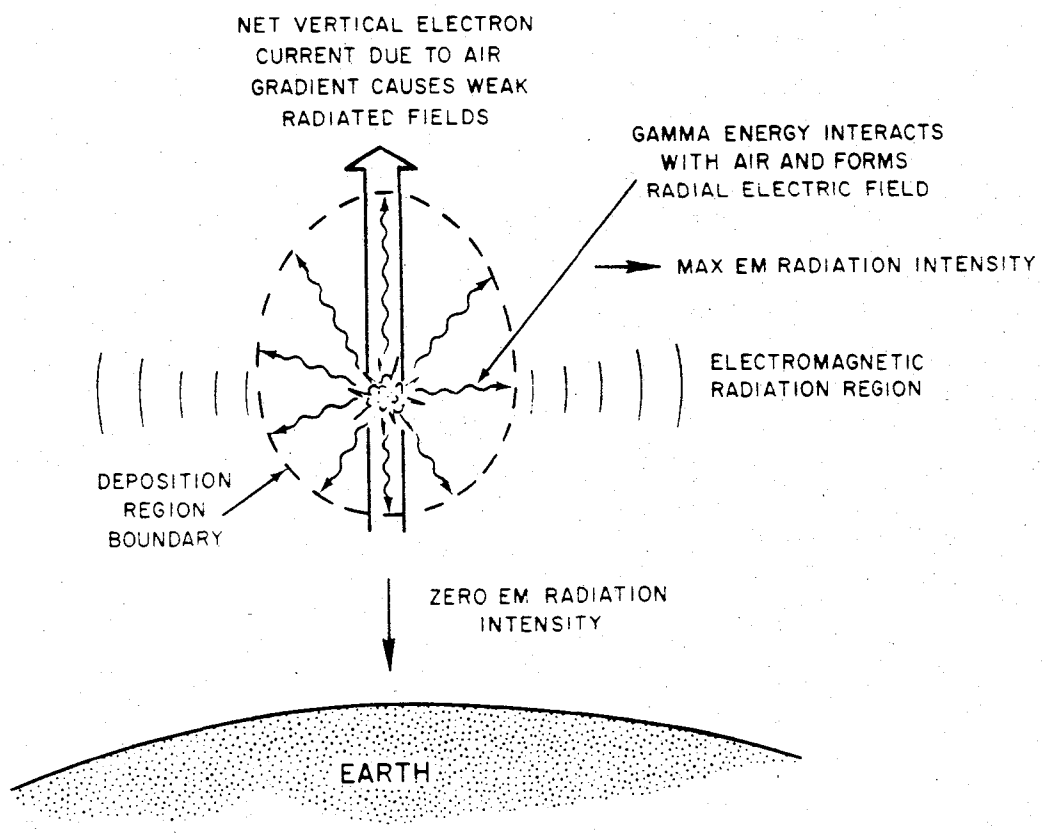

Figure 7-6. [redacted] Simple Illustration of Air-Burst EMP [redacted]

[redacted]

[redacted]

Deleted

DNA
(b)(1)

Figure 7-7 [redacted] Normalized Frequency Spectrum of the Electric-Dipole Radiated EMP for Air Bursts [redacted]

[redacted]

[redacted]

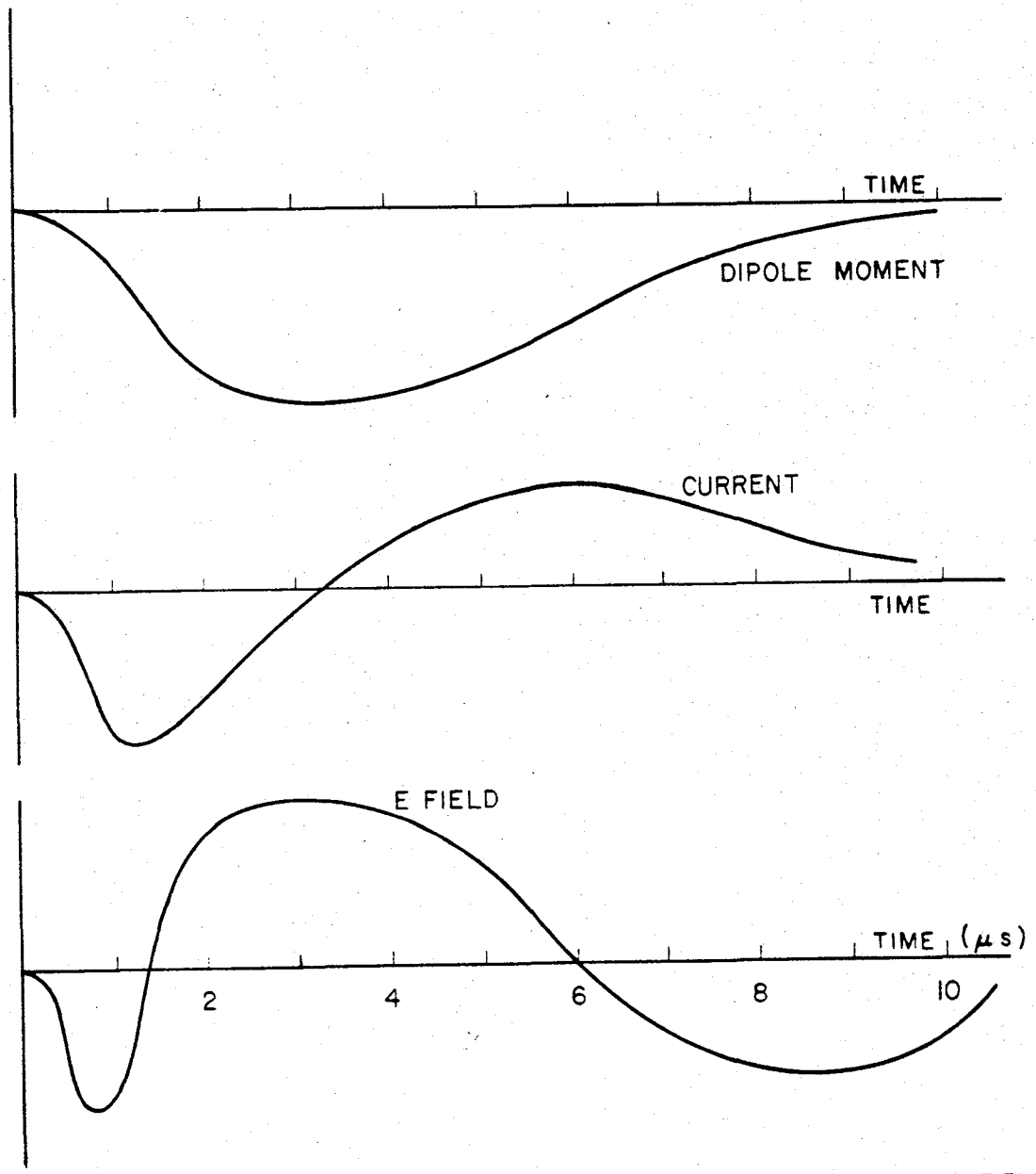

Figure 7-8 [redacted] Comparison of General Waveforms for the Dipole Moment, the Current, and the E-Field for and Air Burst [redacted]

[redacted]

[redacted]

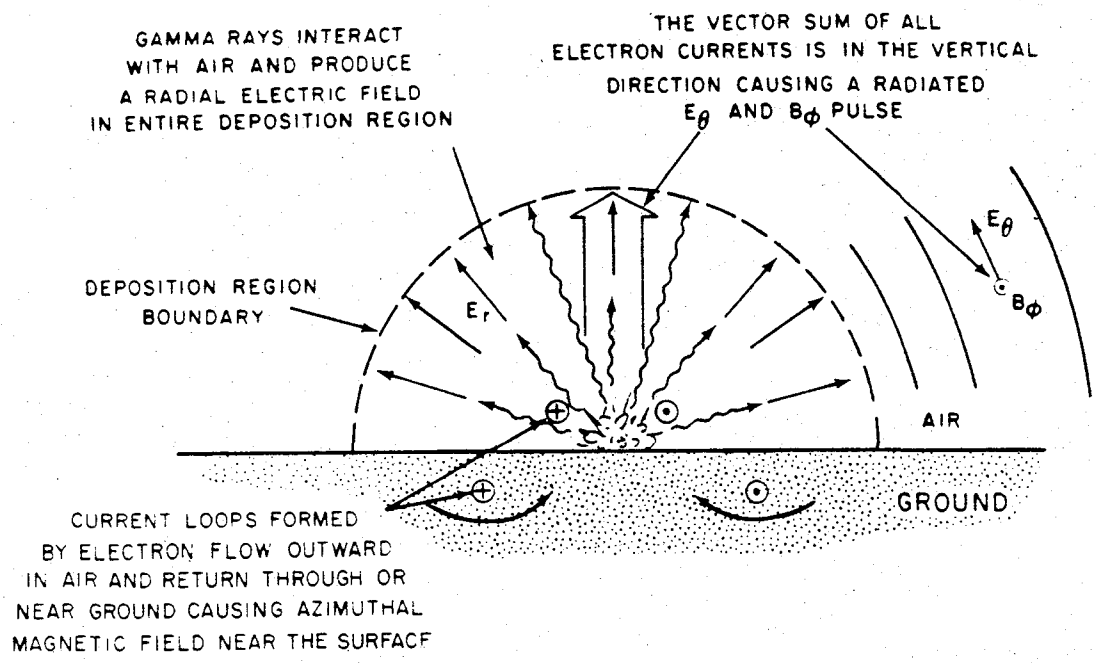

Figure 7-9 [redacted] Simple Illustration of Surface Burst EMP [redacted]

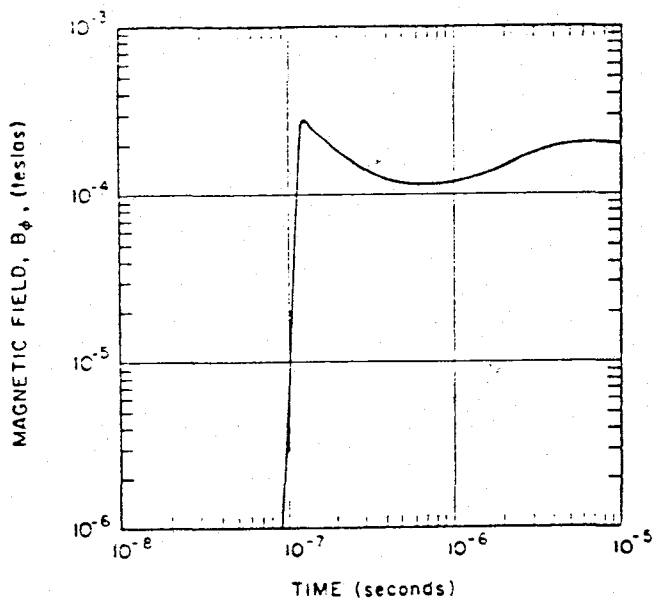

Figure 7-10 [redacted] Shape of Magnetic Field for Toroid Model [redacted]

[redacted]

explosion to about 1,670 volts per meter for a 4.2×10^4 TJ (10 MT) explosion. For most cases, a value of 1,650 volts per meter may be assumed. At ranges along the surface beyond R_o, the peak radiated electric field varies inversely with the distance from the burst. Thus, the magnitude of the peak radiated electric field along the surface may be estimated from the equation

$$E = \frac{R_o}{R} E_o ,$$

where R_o is the range to the beginning of the radiation region, R is the distance along the surface to the point of interest, E_o is the peak value of the radiated field at R_o (assumed to be about

[redacted]

[redacted]

[redacted]

Table 7-1. [redacted] Variation of Range, R_o' at which the Radiation Region Begins, with Yield [redacted]

DNA (b)(3)

[redacted]

1,650 volts per meter), and E is peak value of the radiated field at R. For example, the peak electric field 10 kilometers from a 4200 TJ (1 MT) surface burst would be

$$E = \left(\frac{7.2}{10}\right)(1{,}650) \approx 1{,}200 \text{ v/m}.$$

The peak electric field at the same distance from a 420 TJ (100 KT) surface burst would be

$$E = \left(\frac{5.8}{10}\right)(1{,}650) \approx 950 \text{ v/m}.$$

The spatial distribution of the radiated signal involves not only the inverse range attenuation discussed above, but also the polar angle. The magnitude of the $R \cdot E_\theta$ product follows a complicated function of the polar angle, θ. Figure 7-11 shows the computed variation of the radiated EMP signals as a function of θ. The variation in the waveform shape, as well as in the peak amplitude, as a function of angle should be noted. Because of the greater rise time of the waveforms as the vertical is approached, it is apparent that the high frequency content of the signals decreases. The frequency spectrum is an important parameter for coupling analysis. Figure 7-12 shows the normalized frequency spectrum of the horizontally radiated EMP from a surface burst. Comparing this spectrum with that shown in Figure 7-7 shows significantly greater high frequency content for the surface burst.

[redacted] The preceding discussion was intended to illustrate the general characteristics of the EMP fields generated by surface bursts and the variation of the peak radiated electric fields in space. In addition to the behavior of the electric and magnetic fields, the air conductivity is important for more accurate coupling analysis. A few selected examples of these quantities are presented in later sections of this chapter; however, it is beyond the scope of this manual to provide complete EMP environmental data upon which vulnerability analyses may be based.

7-7 High Altitude Burst [redacted]

[redacted] This burst regime is defined to include any nuclear burst at an altitude above about 30 kilometers (19 miles). In this regime the atmosphere is so sparse above the burst that relatively little Compton current is generated there. The deposition region, departing far from spherical symmetry, consists principally of a pancake shaped volume extending from about 20 to 50 kilometers (12 to 30 miles) in altitude and to the horizon as viewed from the burst. Thus, very high altitude bursts may cover vast geographical areas. A further asymmetry, the earth's magnetic field, is responsible for the form of the radiation. The Compton electrons, which result from collisions of the prompt gammas and x-rays with the air molecules in the deposition regions, are deflected by the earth's field to follow helical paths significantly long

[redacted]

[redacted]

[redacted]

Deleted

DNA
(b)(1)

Figure 7-11 [redacted] Variation of the Radiated EMP for a Surface Burst with Angle θ Measured from the Vertical in Radians [redacted]

[redacted]

[redacted]

DNA
(b)(1)

Deleted

Figure 7-12 [redacted] Normalized Frequency Spectrum of the Horizontally Radiated EMP for a Surface Burst [redacted]

[redacted]

[redacted]

[redacted]

during the time between collisions in the rarefield medium. The accelerated electrons produce the characteristic synchrotron radiation with a large high-frequency content. The peak amplitude of the electric field near the surface may be quite large, a few tens of thousands of volts/meter for high bursts. Figure 7-13 illustrates the basic geometry of this burst.

[redacted]

DNA (b)(1)

[redacted]

DNA (b)

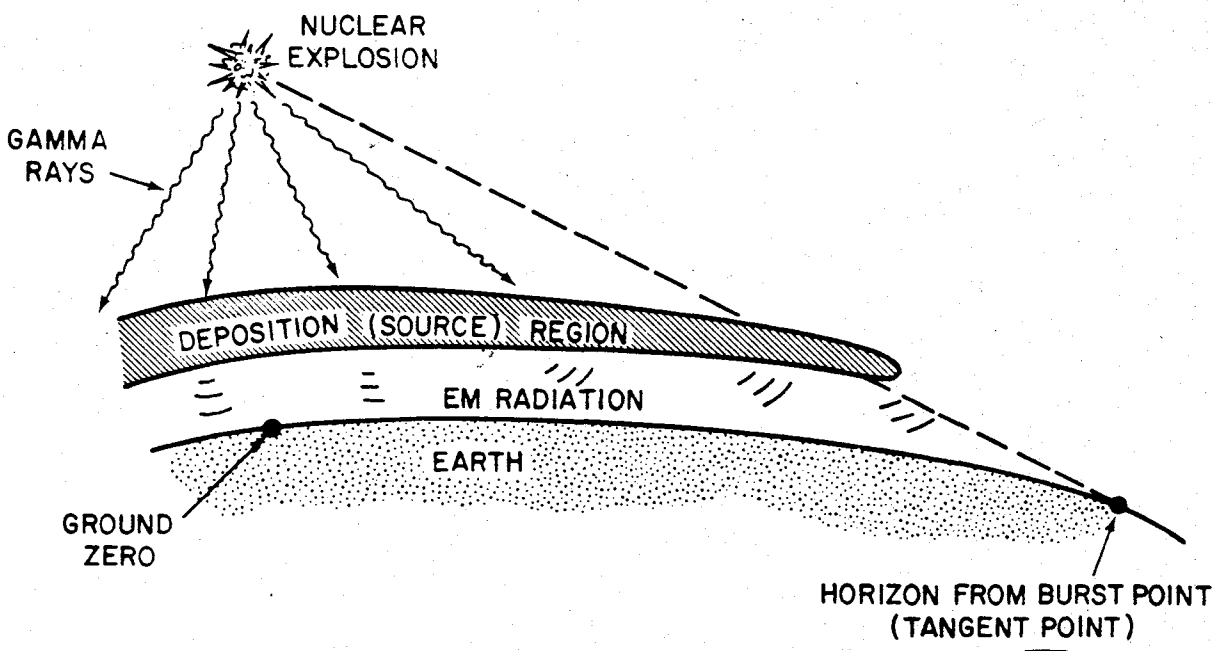

Figure 7-13 [redacted] Illustration of the Basic Geometry of the High-Altitude Burst [redacted]

[redacted]

[redacted]

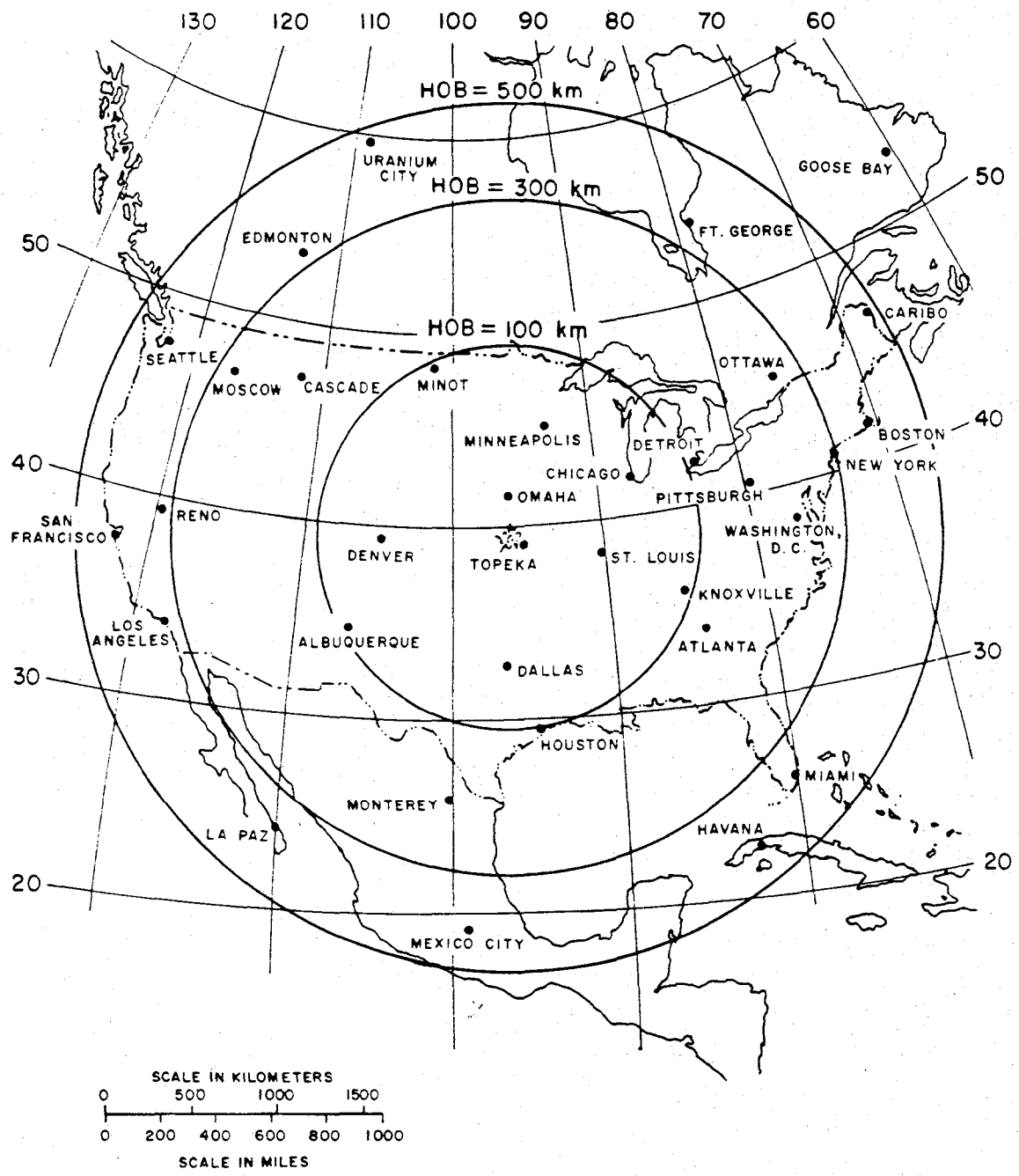

Figure 7-14 [redacted] Ground Coverage for Bursts of 100, 300, and 500 km (about 62, 186, and 310 miles) for a Large Yield Burst Above the Geographical Center of the (counterminous) United States [redacted]

[redacted]

[redacted]

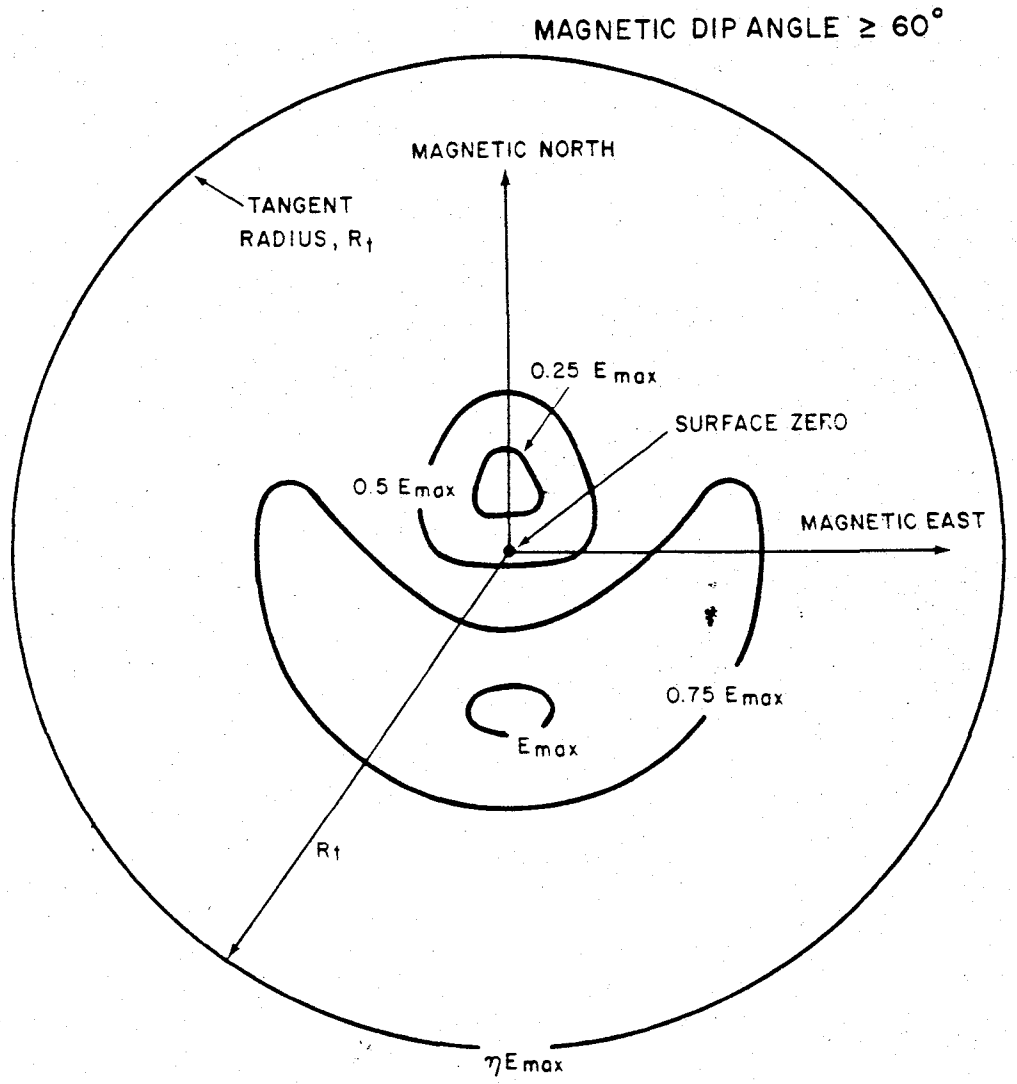

Figure 7-15 [redacted] Basic Variations in Incident Peak Electric Field for Locations on the Earth's Surface for HOB above 500 km [redacted]

[redacted]

[redacted]

[redacted]

DNA (G)(3)

DNA (G)(1)

[redacted]

DNA (G)(3)

Deleted

Figure 7-16 [redacted] Maximum Peak Electric Field as a Function of Gamma Ray Yield for Selected Burst Heights [redacted]

[redacted]

[redacted]

[redacted]

[redacted]

DNA (b)(1)

[redacted] The radiated EMP from a high altitude burst rises to a peak value much more rapidly than that from a surface or low air burst. Figure 7-17 illustrates the time waveform of the radiated signal from a high altitude burst. The analytic expression

$$E(t) = 5.3 \times 10^4 \left(e^{-4t} - e^{-476t}\right) \text{ v/m} ,$$

where t is in microseconds, describes the waveform in Figure 7-17. The frequency spectrum of this pulse is illustrated in Figure 7-18. As the gamma yield of the weapon decreases, the pulse width tends to increase, decreasing the relative high frequency content of the signal. Similarly, increasing the angle between the line-of-sight and the vertical through the burst point increases the pulse width.

[redacted] The high altitude burst is the dominant threat to exoatmospheric systems. The most severe EMP environment for such a system comes from a line-of-sight path that passes

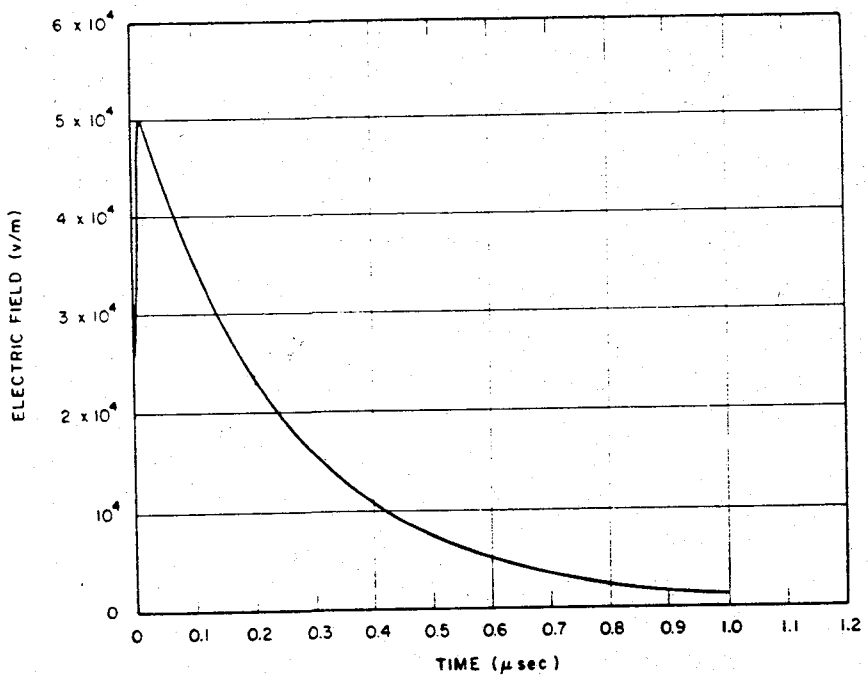

Figure 7-17 [redacted] Time Waveform of High-Altitude Radiated [redacted]

[redacted]

[redacted]

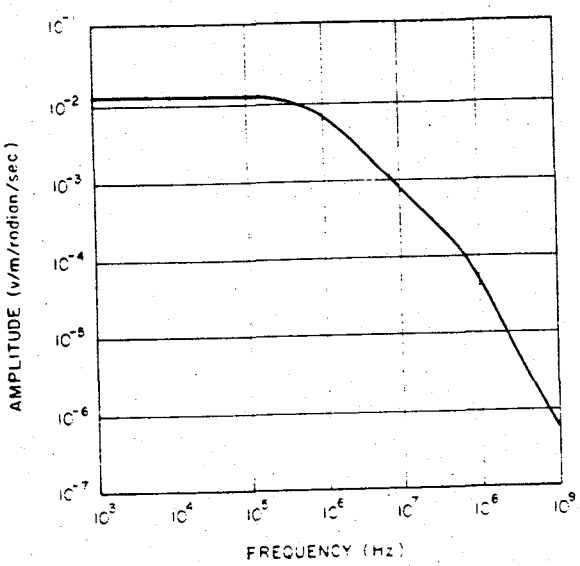

Figure 7-18 [redacted] Amplitude of High-Altitude Radiated Signal [redacted]

[redacted]

through the deposition region but misses the earth and is propagated through the ionosphere (see Figure 7-19). The ionosphere acts as a high pass filter, and only frequencies above a given cutoff are observed. The cutoff frequency depends on the altitude, time of day and sunspot activity, and, for example, varies between about 3 and 14 MHz at night, depending on the altitude of the observer. Daytime cutoff frequencies of 30 MHz may be encountered for a 1000 km high observer. In addition, the effective index of refraction, and therefore the group velocity of the EMP signal also varies, with the higher frequencies traveling fastest. Also, the transmission for frequencies near the cutoff is very large, rising to near unity for higher frequencies. Although the amplitude of the dispersed pulse will be much smaller than that of the undispersed pulse, the signal will be stretched out greatly in time. For frequencies above the cutoff there will be little energy loss. Figure 7-20 shows a predicted dispersed EMP (DEMP) signal from a high altitude burst as viewed by an observer at 100 km altitude. This is based on a nighttime ionosphere at sunspot minimum.

[redacted] SYSTEM GENERATED EMP [redacted]

7-8 General Description [redacted]

[redacted] The term System Generated Electromagnetic Pulse (SGEMP) refers to the fields and currents generated by the interaction of weapons-produced radiation (principally X-rays and gamma rays) with a system or portion of a system. The system generated electromagnetic pulse is produced inside or in the vicinity of a system when an incident photon pulse interacts with the material of the system. Photoelectric and Compton electrons are created, and the resulting emission current produces electric and magnetic fields. Internal EMP, or IEMP, which refers to the electromagnetic fields interior to systems and containers, and which is generally generated by gamma rays, or high energy X-rays, is included in the general category of SGEMP. SGEMP specifically excludes the internal effects associated with transient radiation effects on electronics (TREE).

[redacted] The system-generated EMP is most important for electronic components in satellites and ballistic systems above the deposition region that would be exposed directly to the nuclear radiations from a high-altitude burst. The system-generated EMP can also be significant for surface and moderate-altitude bursts if the system is within the deposition region but is not subject to damage by other weapons effects. This could possibly occur for surface systems exposed to a burst of relatively low yield or for airborne (aircraft) systems and burst of higher yield.

[redacted]

[redacted]

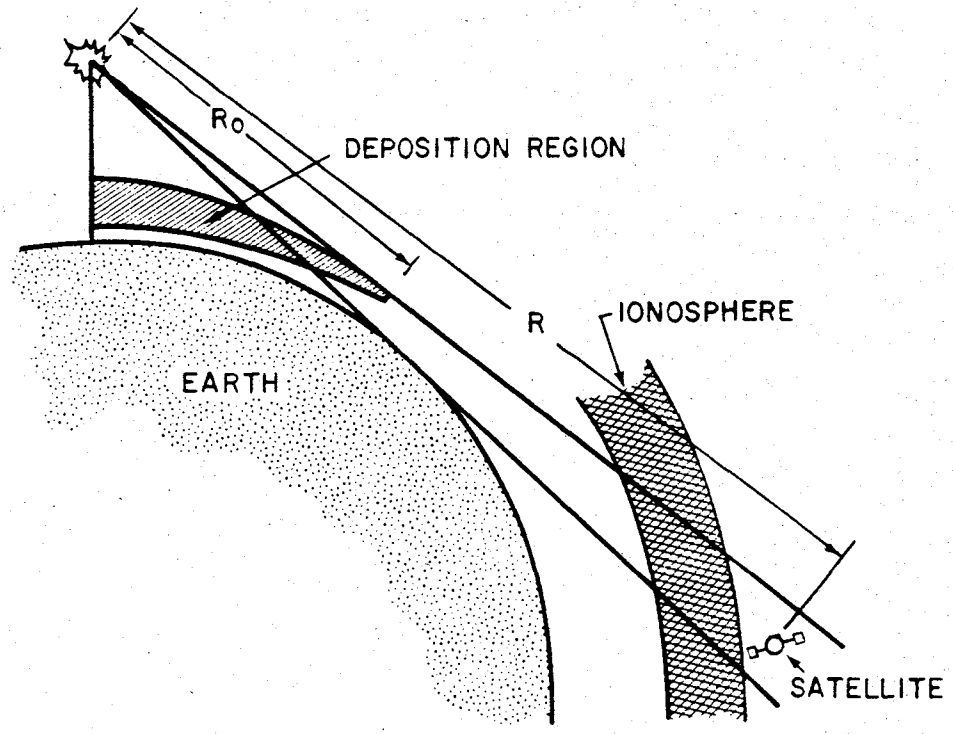

Figure 7-19 [redacted] The Geometry for Producing Dispersed EMP for Exoatmospheric Systems [redacted]

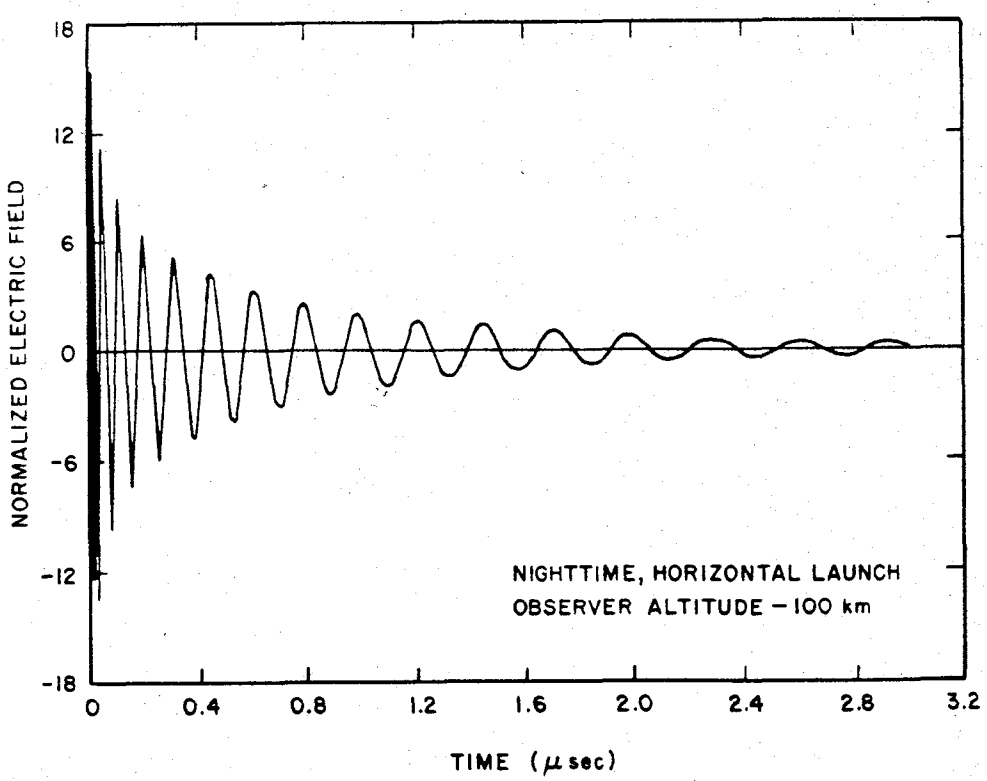

Figure 7-20 [redacted] Electric Field Time Waveform of High-Altitude EMP after Dispersion by Nighttime Ionosphere [redacted]

[redacted]

[redacted]

7-9 SGEMP Generation [redacted]

[redacted] The generation of SGEMP is a complex function of many physical phenomena. The complexity of the problem precludes quantifying SGEMP generation for any broad class of systems. This section, therefore, will attempt to describe some of the generation phenomena for one simple problem. The "DNA EMP (Electromagnetic Pulse) Handbook," DNA 2114H-3, Volume 3, should be consulted for an in-depth treatment of the subject (see bibliography).

[redacted] Figure 7-21 illustrates SGEMP generation in a cavity. The incident X-rays and gamma rays create photo- and Compton electrons, respectively, within the cavity walls. The generation is, of course, dependent on the energy flux of the incoming photons and the properties of the wall material. The photo- and Compton electrons subsequently interact with the atoms of the wall material to produce secondary electrons. Those electrons created near the surface (within an electron mean-free-path) with velocity vectors toward the surface generally will be emitted. The net electron currents, both within and without the cavity, gives rise to a magnetic field which will induce currents in circuit loops via magnetic coupling.

[redacted] For this discussion, it is assumed that the electron emission and subsequent field generation are separable problems. Further, the electron emission from the external wall surfaces will be ignored. The problem under consideration is thus one in which electrons are emitted from two internal surfaces of the cavity in the forward and reverse directions, the emission being described as a time and energy dependent electron flux.

[redacted] As the emitted electrons traverse the cavity, a net forward current will be observed within the cavity while a space charge is established concurrently. If the cavity is at vacuum or near-vacuum conditions (0.13 pascal - 10^{-3} Torr or less) and of appropriate size, space charge limitation will occur. This will result in the creation of high electric fields (10^5 - 10^6 volts/meter) near the walls.

[redacted] If the cavity pressure is above 0.13 pascal, another phenomenon will occur in sufficient intensity to alter the SGEMP. The emission electrons will interact with the gas molecules to produce additional secondary electrons (hereafter called gas electrons) and positive ions. The gas electrons will tend to "stream" to the cavity walls in comparison to the heavier and slower gas ions that are created concurrently. The gas ions will neutralize the space charge, thereby allowing more electrons to traverse the cavity. Thus the E-field intensity near the walls will decrease while the current in the cavity, and concurrently the magnetic field, will increase. It should be noted that quantitative analysis of the electron emission and subsequent SGEMP generation for even this simple problem requires the use of complex computer codes on large computers.

7-10 Problem Definition [redacted]

[redacted] It is emphasized that the above discussion dwells on only *one* small aspect of the SGEMP problem: the generation of an idealized SGEMP in a simplified geometry. A complete treatment of the SGEMP for a given system must start with the threat definition and the incoming photon flux. This must then be translated into electron emission from all surfaces, cables, components, etc., of the system. From the emission, fields and currents throughout and external to the system must be determined in a self-consistent manner. Next, coupling of the fields and currents to the system electronics must be established. Finally, the reaction of the electronics to the coupled energy must be determined and evaluated.

[redacted]

[redacted]

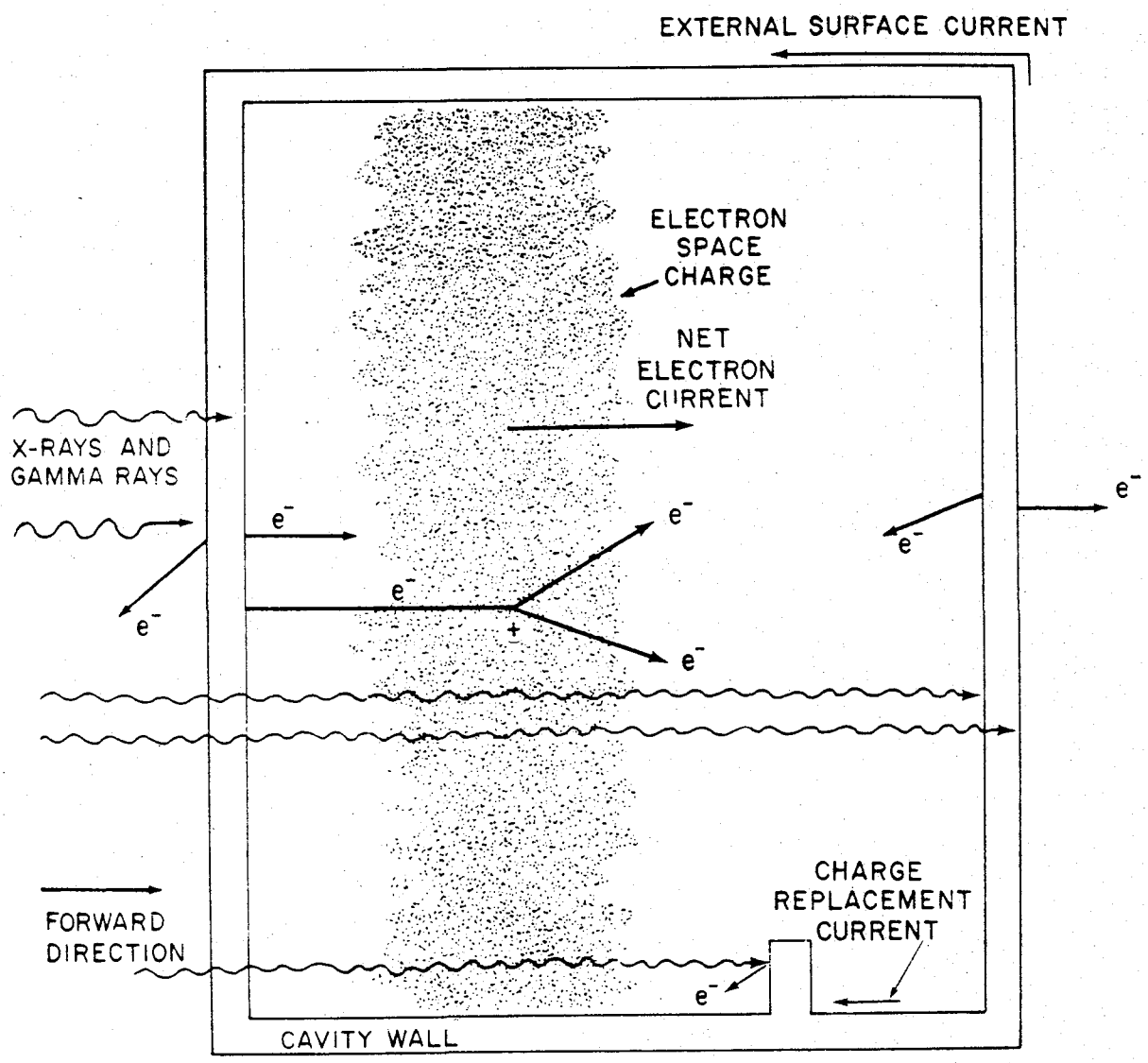

Figure 7-21 [redacted] SGEMP Generation [redacted]

[redacted]

[redacted]

[redacted] It is possible that this evaluation procedure may be terminated after any given step. For example, consider an electronically very "hard" system for which the "threat" is specified as 4.2×10^4 joules/meter^2 (1 cal/cm^2) received uniformly over a period of a year. By inspection, SGEMP is not a problem. At the other extreme, consider a system that is easily upset by small (milliamp), short duration (30 nsec) electrical pulses. If the threat for this system is 4.2×10^5 joules/meter^2 (10 cal/cm^2) in a period of 100 nanoseconds, SGEMP *may* be a significant problem. An in-depth analytical/experimental program must be undertaken to make an evaluation of SGEMP effects.

[redacted] Clearly, the above examples are extremes. They only serve to illustrate that an all encompassing definition of SGEMP problems is impossible because of the highly complex, system-specific nature of this phenomenon. Likewise, it is not possible to formulate a specific solution to the SGEMP threat for general application. Thus, the susceptibility and vulnerability of each system to SGEMP effects must be considered separately.

[redacted] COMPUTER CODE DESCRIPTIONS [redacted]

7-11 Code Utility [redacted]

[redacted] From the physical descriptions provided in the preceding paragraphs, it is apparent from the large number of variables involved that even approximate solutions to practical problems of interest demand a large investment in electronic computation. The complete problem of the coupling of the EMP from a specific detonation into the components of a specific system is an extremely complex problem. There are no computer codes which even remotely approach a treatment of the complex problem. As a consequence, various aspects of the EMP problem are studied individually with the aid of existing codes, and good engineering judgment must be used to couple these various parts of the solution into a quantitative estimate of the effects of EMP upon a given system.

7-12 Code Classes [redacted]

[redacted] There are three general classes of computer codes in use: environment codes, system generated EMP codes, and circuit-analysis codes. The codes that are currently in use are described in the "DNA EMP (Electromagnetic Pulse) Handbook," Volume 4 (see bibliography).

[redacted] SYSTEMS EFFECTS [redacted]

7-13 System Definitions [redacted]

[redacted] Many systems that are physically different can be grouped together in terms of the EMP environments they will encounter. For this purpose it is useful to consider classification of systems in terms of operating altitude and nuclear hardness.

[redacted] From the previous description of the EMP environment, the altitude categories suggested in Figure 7-22 are evident. It should be noted that certain systems may operate successively in more than one category.

[redacted] For the purposes of this manual it is adequate to consider system hardness in only two categories. A hard system is one that has been designed to operate in some nuclear environment. A soft system is not so designed, and its hardness is due solely to its inherent design. For a ground system, the blast usually is considered to be the indicator of the nuclear hardness of the system. The dominant effect will change from blast to nuclear radiation, defined here in terms of the total dose in rad (Si), as the system altitude increases. A system is considered to be

[redacted]

[redacted]

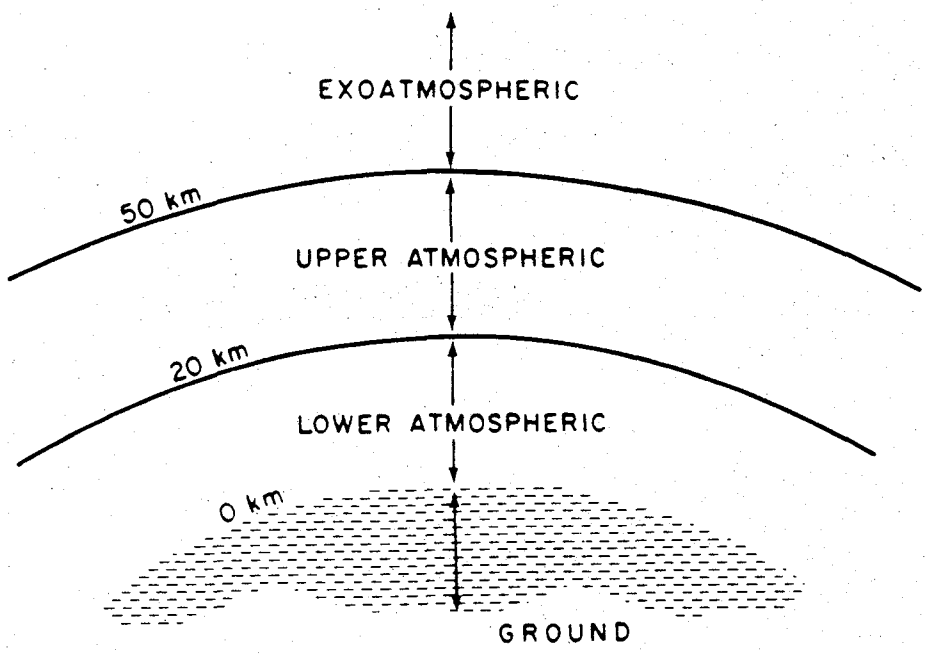

Figure 7-22 [redacted] Categories of System Operation Regions [redacted]

[redacted]

hard if it is built to withstand blast overpressures of about 70 kilopascals (10 psi) or more or a radiation dose of 1 rad (Si) or more. Corresponding figures for a soft system are 7 kilopascals (1 psi) or less and 0.1 rad (Si) or less. Systems marginal with respect to either criterion should be reviewed in both categories.

[redacted]

DNA (b)(1)

7-14 Threat Definition [redacted]

DNA (b)(1)

[redacted]

[redacted]

[redacted]

MISSION		EMP ENVIRONMENT								
		DEPOSITION			RADIATION			PROPAGATION		
		SURFACE	AIR	HIGH ALTITUDE	SURFACE	AIR	HIGH ALTITUDE	SURFACE	AIR	HIGH ALTITUDE
HARD	GROUND	X					X			
HARD	LOWER ATMOSPHERIC		X				X			
HARD	UPPER ATMOSPHERIC			X			X			
HARD	EXO ATMOSPHERIC									X
SOFT	GROUND				X		X			
SOFT	LOWER ATMOSPHERIC				X	X	X			
SOFT	UPPER ATMOSPHERIC						X			
SOFT	EXO ATMOSPHERIC									X

Figure 7-23 [redacted] Mission/Environment Matrix [redacted]

[redacted]

[redacted]

DNA (b)(1)

[redacted] Blocks are shaded in on the diagram on the basis of dominant environments for a given mission, not on the basis of whether EMP exists at all for that situation. Thus, based on the definitions given, Figure 7-23 may be used as a guide for which environments constitute a dominant threat for given situations of interest.

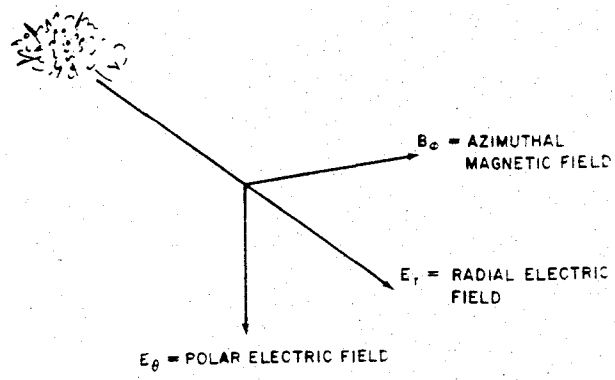

Figure 7-24 [redacted] Field Directions of Ground-Burst EMP [redacted]

7-15 Effects Comparisons [redacted]

[redacted] It is well beyond the scope of this chapter to attempt meaningful effects comparisons for every system altitude, burst altitude, and environment combination for which EMP may be the dominant threat. However, it is instructive to consider one such combination in order to gain some impression of how the magnitude of the threat might be compared to other effects. Accordingly, the deposition region environment created by a surface burst will be examined with regard to the effects on hardened ground systems, a category in which the EMP threat may dominate according to Figure 7-23. As mentioned previously, the nuclear hardness of such a system is generally described in terms of its over-pressure level. Using this quantity as an indicator of hardness, the EMP field waveforms, peak values and frequency content for the principal field components $B\varphi$, E_r, and E_θ, as defined in Figure 7-24 and the associated air conductivity waveforms and peak values will be examined.

[redacted] The peak values as a function of overpressure are considered first. Figures 7-25, 7-26, and 7-27 show these values for the three field components for two yields and two values of ground conductivity (σ_g). It should be kept in mind that a large shift in frequencies present can occur between 70 and 7,000 kilopascals (10 and 100 psi). The coupling of systems to the fields in this intense region is complicated by the high air conductivity. Figure 7-28 shows how peak air conductivity varies with overpressure. It should be noted that the lower yield weapon produces higher conductivity for a given overpressure level.

[redacted] The variation of these same quantities in time for the 4,200 terajoules (1 MT) yield and a ground conductivity of 10^{-2} mho/m is illustrated next. The waveform for the $B\varphi$ component is shown for various overpressure levels in Figure 7-29, and the frequency spectrum is illustrated in Figure 7-30. Corresponding waveforms and spectra for E_r and E_θ components are shown in Figures 7-31, 7-32, 7-33, and 7-34. Finally, the corresponding air conductivity waveforms are presented in Figure 7-35.

[redacted] It is apparent from these figures that meaningful effects comparisons can be made and presented to the systems designer for a given set of physical conditions. However, it is also clear that the results vary drastically with changes in

[redacted]

[redacted]

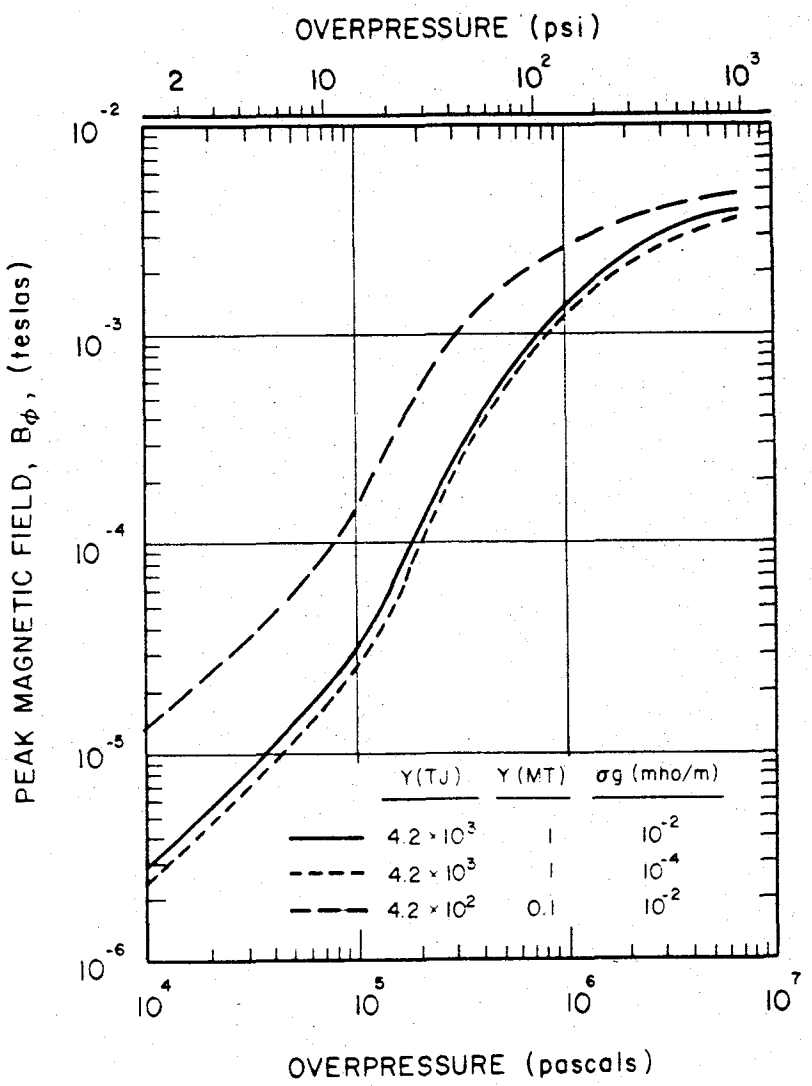

Figure 7-25 [redacted] Peak Magnetic Field B_ϕ Versus Overpressure for Varying Ground Conductivities and Yields [redacted]

[redacted]

[redacted]

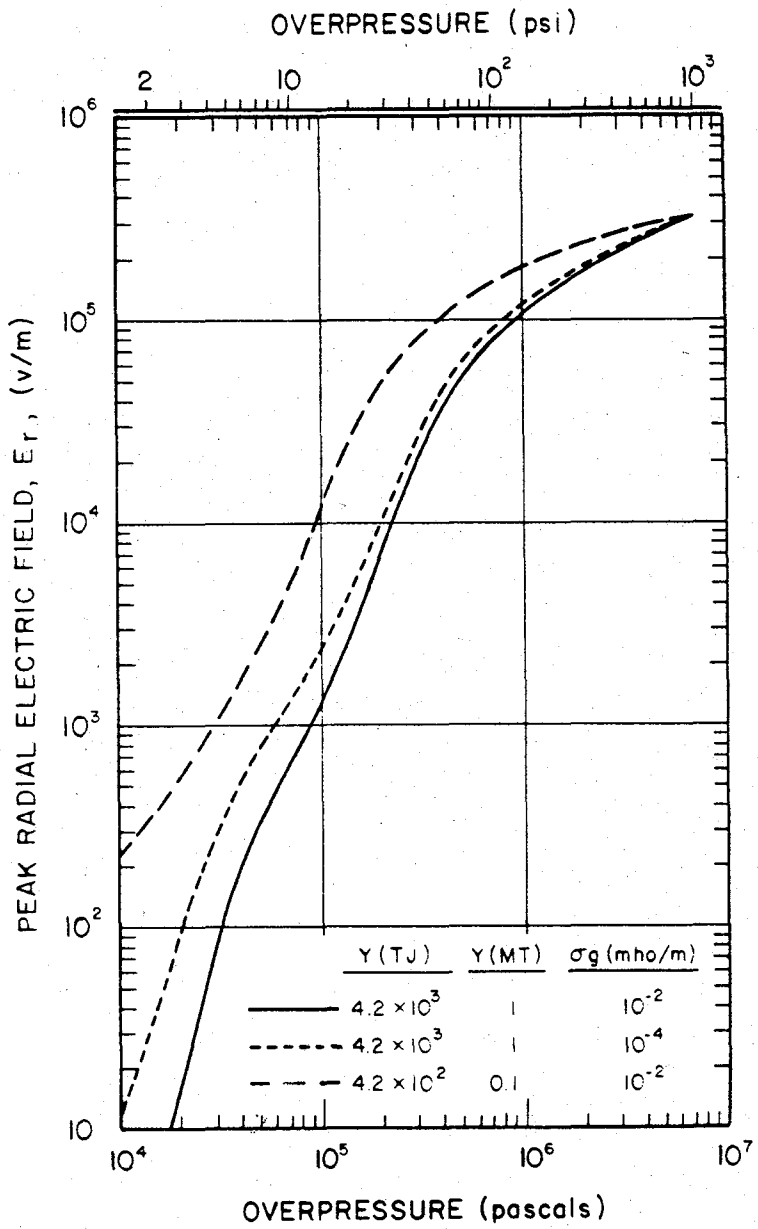

Figure 7-26 [redacted] Peak Radial Electric Field E_r Versus Overpressure for Varying Ground Conductivities and Yields [redacted]

[redacted]

[redacted]

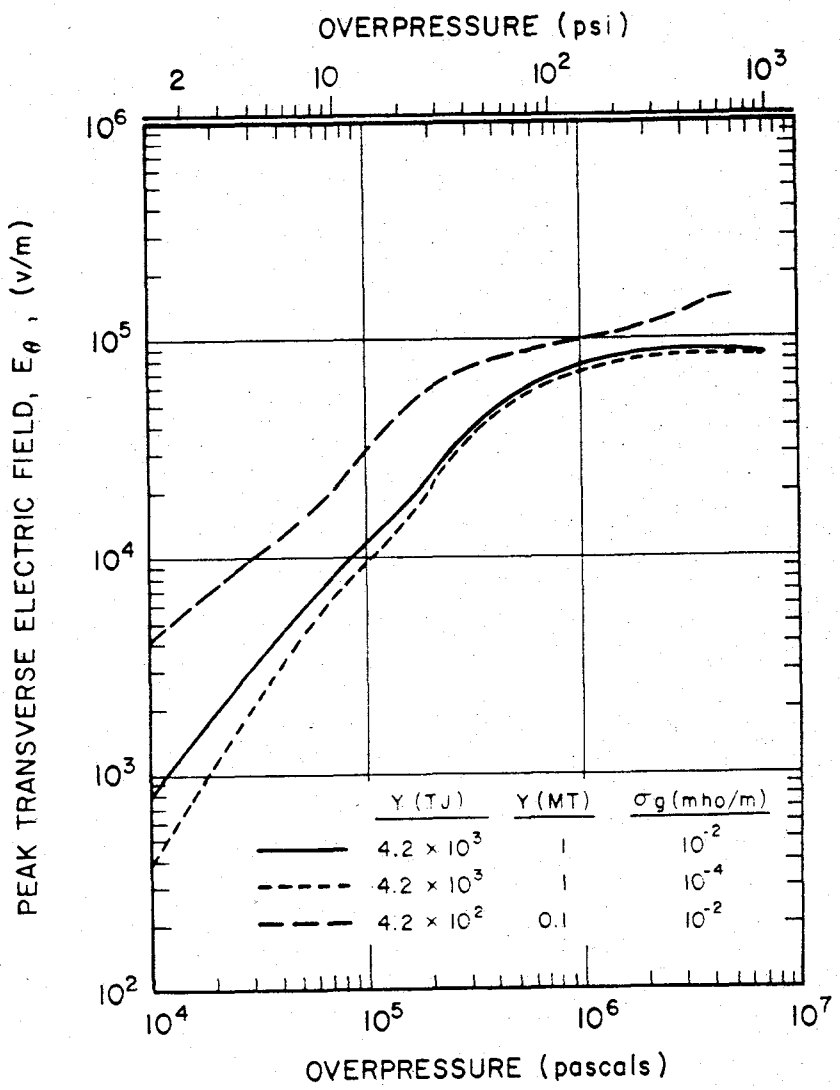

Figure 7-27[redacted] Peak Transverse Electric Field E_θ Versus Overpressure for Varying Ground Conductivities and Yields[redacted]

[redacted]

[redacted]

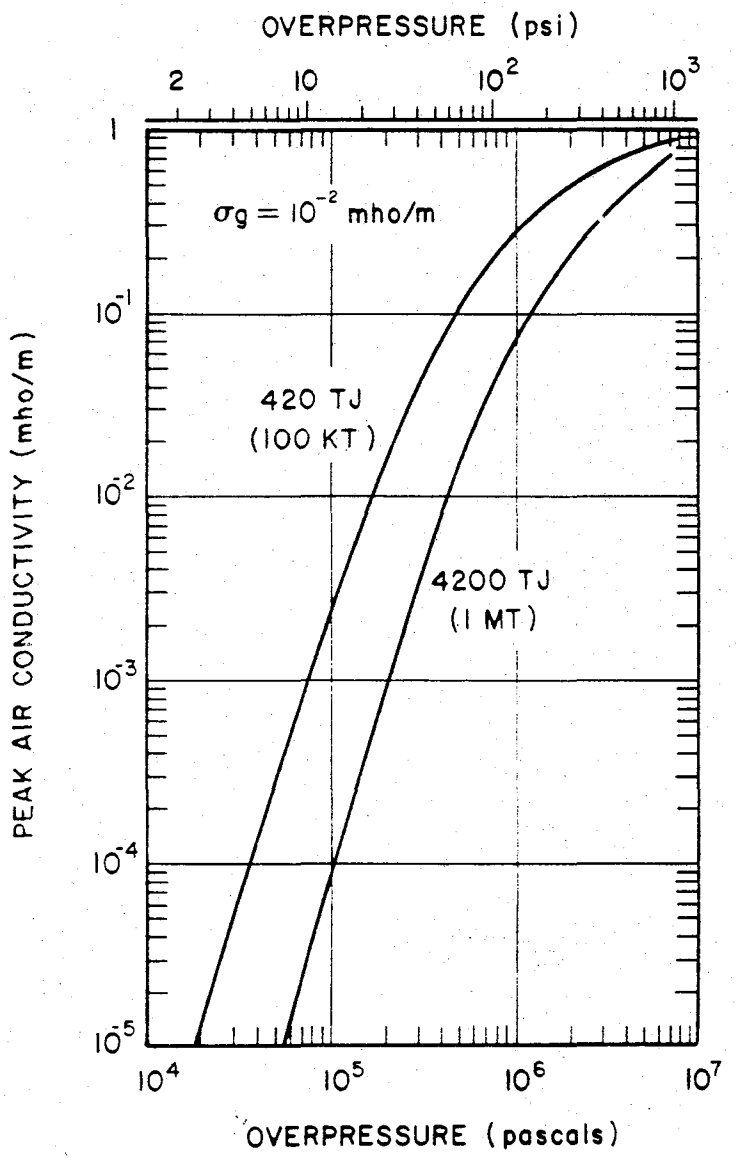

Figure 7-28 [redacted] Peak Air Conductivity Versus Overpressure for Yields of 420 TJ (100 kt) and 4.2 x 10^3 TJ (1 Mt) [redacted]

[redacted]

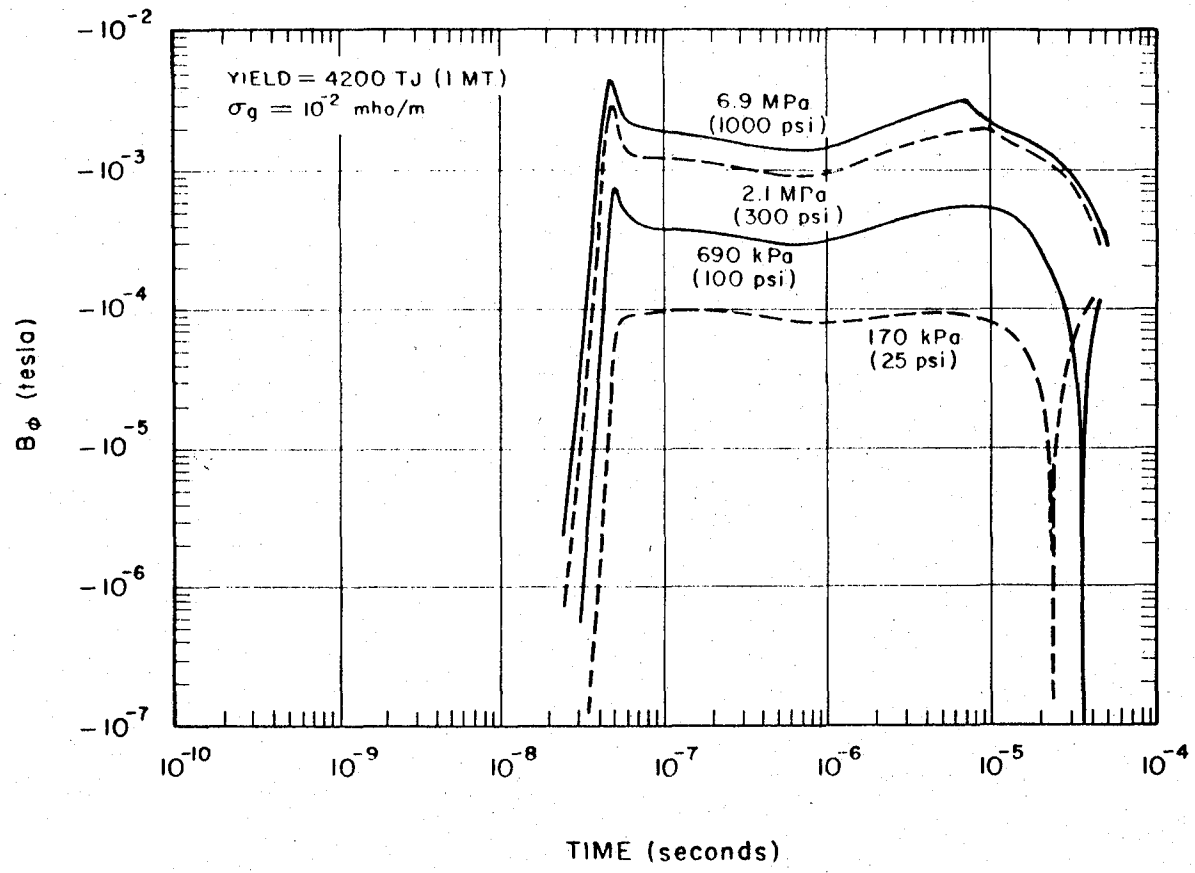

Figure 7-29 $B\varphi$ Time Waveform at the Air-Ground Interface for Several Pressure Levels

[redacted]

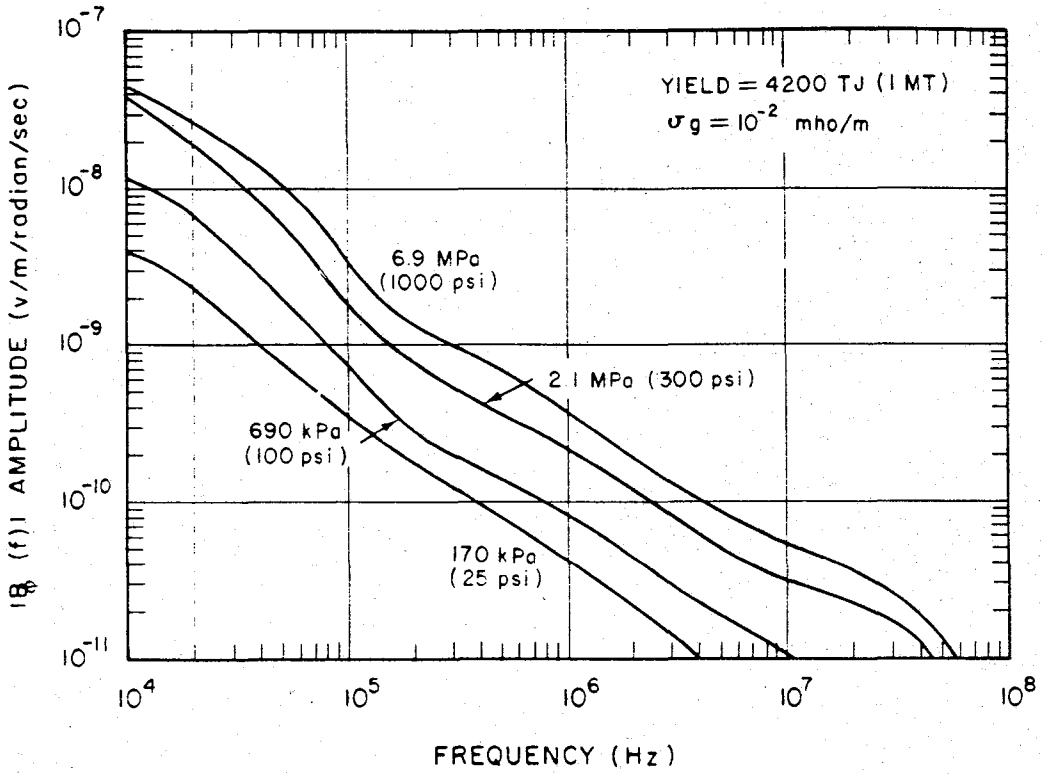

Figure 7-30 [redacted] Fourier Amplitude of B_φ Waveform of Figure 7-29 [redacted]

[redacted]

[redacted]

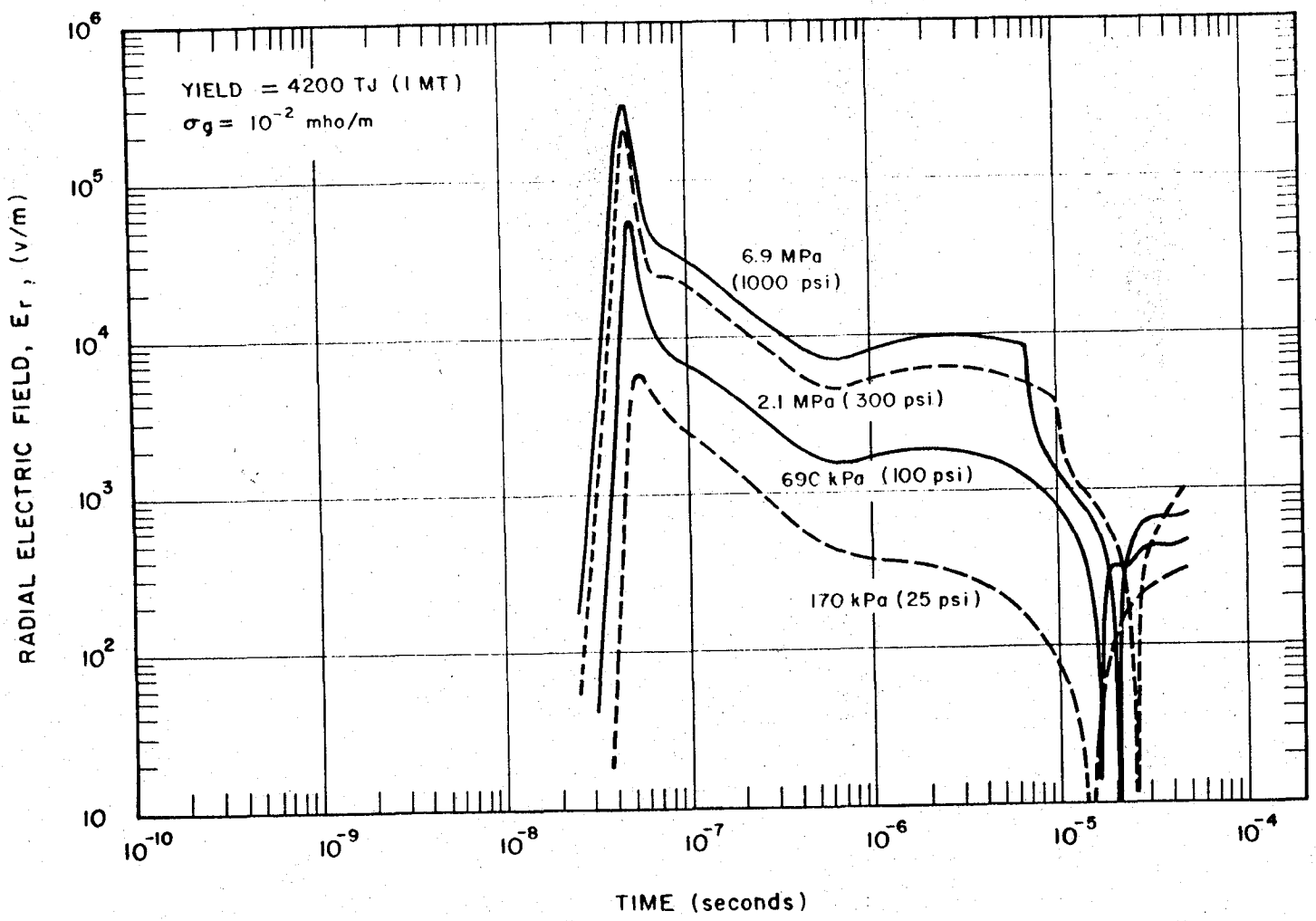

[redacted]

Figure 7-31 [redacted] E_r Time Waveform at the Air-Ground Interface for Several Pressure Levels, $\sigma_g = 10^{-2}$ mho/m [redacted]

[redacted]

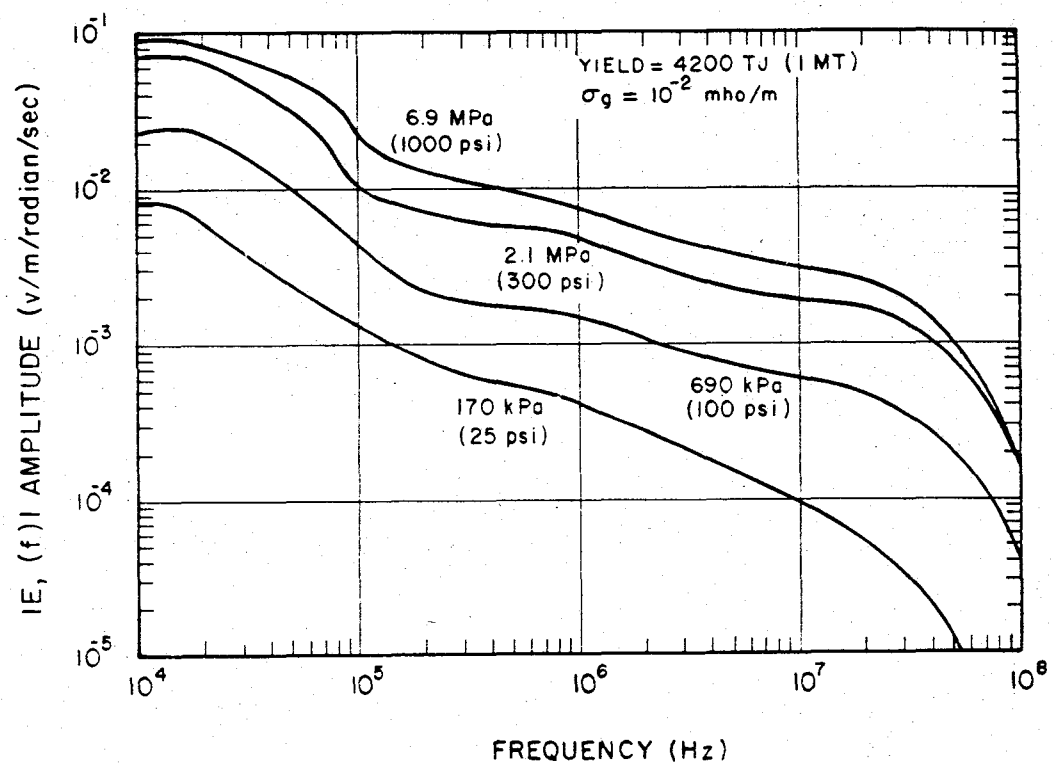

Figure 7-32 [redacted] Fourier Amplitude of E_r Waveform of Figure 7-31 [redacted]

[redacted]

[redacted]

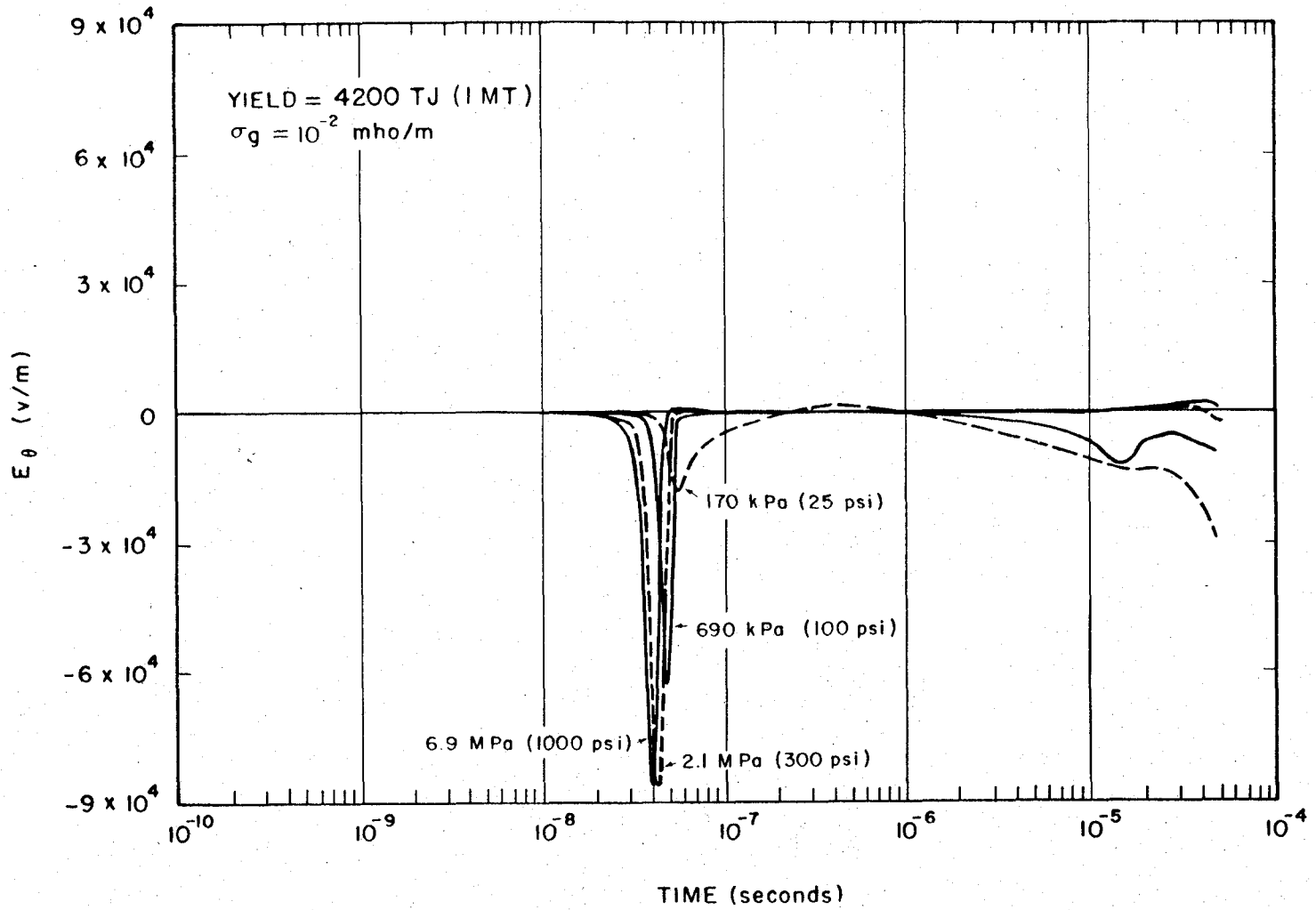

Figure 7-33 [redacted] E_θ Time Waveform at the Air-Ground Interface for Several Pressure Levels, $\sigma_g = 10^{-2}$ mho/m [redacted]

[redacted]

[redacted]

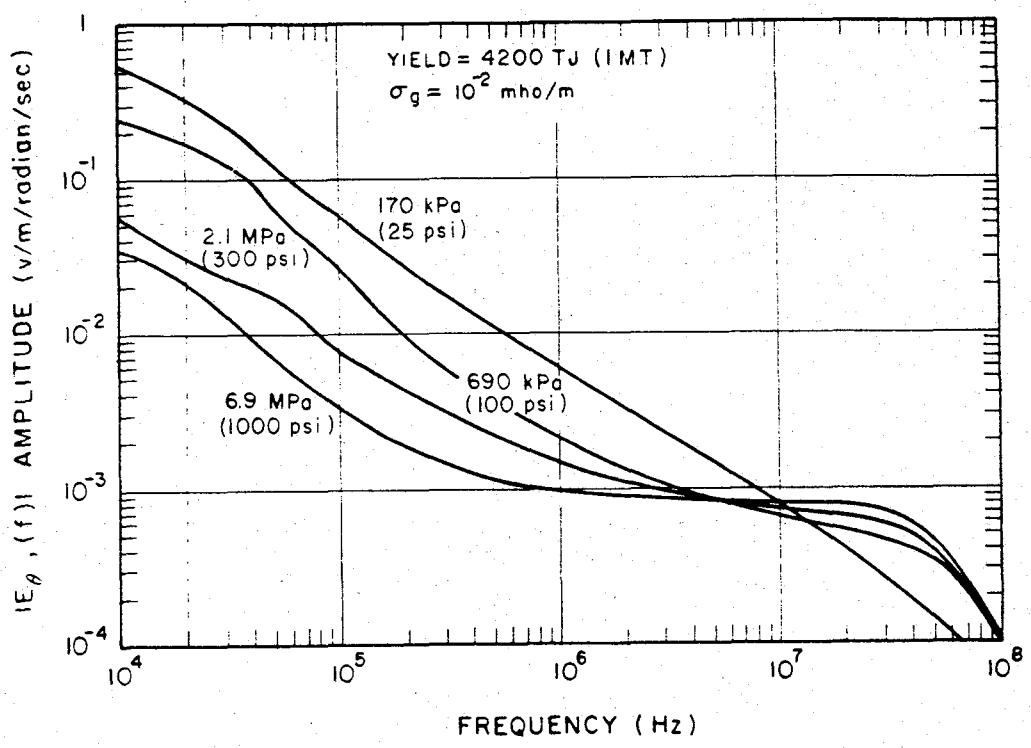

Figure 7-34 [redacted] Fourier Amplitude of E_θ Waveform of Figure 7-33 [redacted]

[redacted]

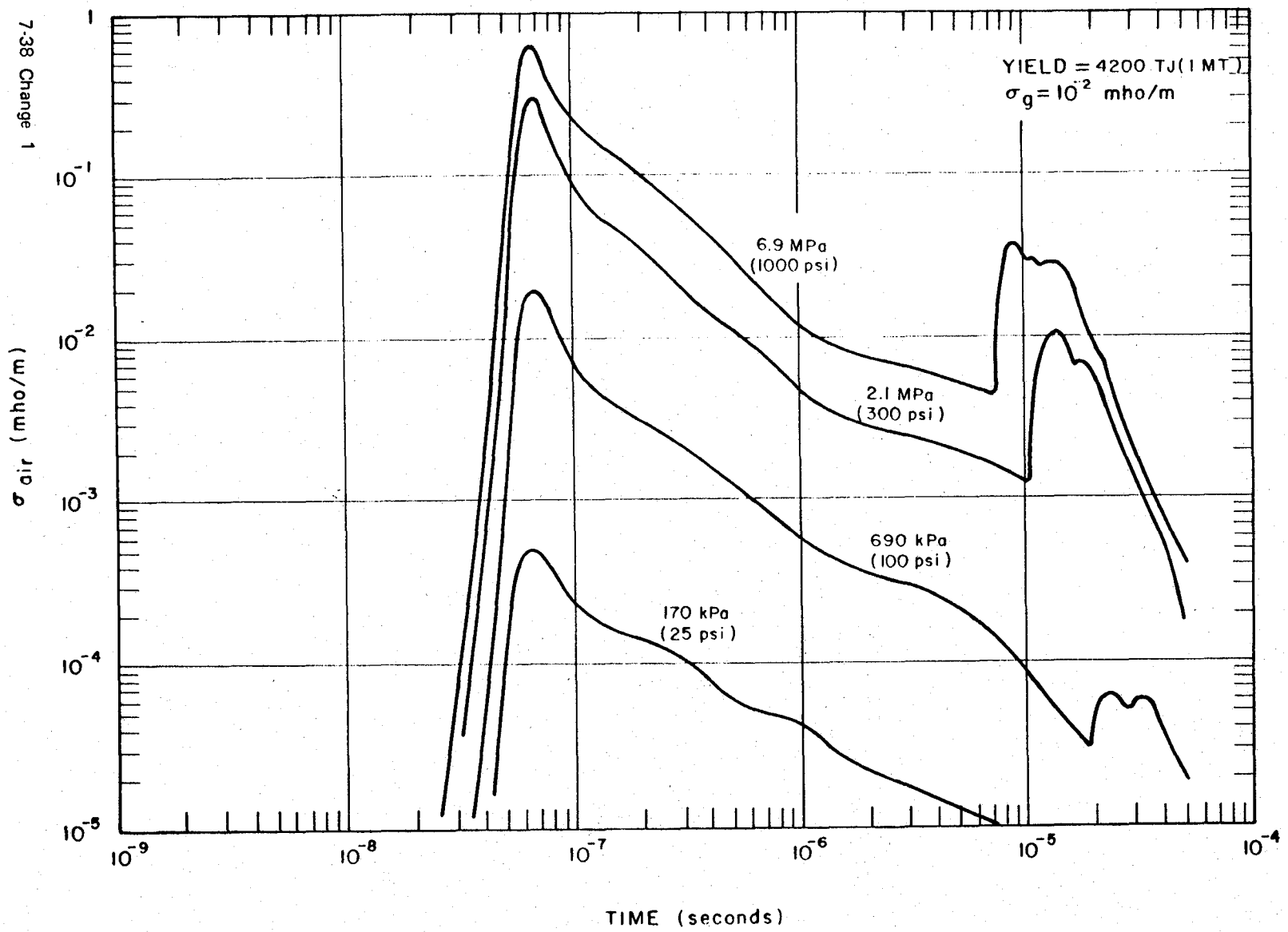

Figure 7-35 [redacted] Air Conductivity Time Waveforms at the Air-Ground Interface for Several Pressure Levels, $\sigma_g = 10^{-2}$ mho/m [redacted]

the conditions, and that the very many combinations possible in the conditions preclude concise generalizations to cover every situation. Strictly speaking, a system imbedded in the deposition region must be included as part of the environment itself in formulating the problem. This limitation should be kept in mind while examining the figures described.

[redacted]

[redacted] BIBLIOGRAPHY [redacted]

DNA EMP (Electromagnetic Pulse) Handbook [redacted] DNA 2114H-1, DNA 2114H-2, DNA 2114H-3, DNA 2114H-4, Defense Nuclear Agency, Washington, D.C., August 1976. (I, II, IV – [redacted] III – [redacted]

EMP Simulator Study [redacted] DASA 2049, DASIAC SR-92, DASIAC, Santa Barbara, California, May 1968 [redacted]

Glasstone, S. and P. J. Dolan, eds., *The Effects of Nuclear Weapons*, Third Edition, U.S. Department of Defense and U.S. Department of Energy, December 1977 [redacted]

Jordan, T. M., et al., *Prediction of Internal Electromagnetic Pulse* [redacted] DNA 2966D, Defense Nuclear Agency, Washington, D.C., August 1972 [redacted]

Longmire, C. L., *Ground Fields and Cable Currents Produced by Electromagnetic Pulse from a Surface Nuclear Burst* [redacted] DASA 1913, DASIAC SR-54, DASIAC, Santa Barbara, California, March 1968 [redacted]

Proceedings: DASA EMP Technical Conference – 1969 [redacted] DASA 2280, DASIAC SR-91, DASIAC, Santa Barbara, California, March 1969 [redacted]

Schlegel, G. K., M. A. Messier and W. A. Radasky, (edited by W. C. Hart), *Electromagnetic Pulse Environment Handbook* [redacted] AFWL EMP PHENOMENOLOGY 1-1, Air Force Weapons Laboratory, Albuquerque, N.M., January 1972 [redacted]

Tompkins, J. E., and J. A. Rosado, *Internal Electromagnetic Pulse: Electric and Magnetic Fields in Complex Enclosures* [redacted] HDL-TR-1500, Harry Diamond Laboratories, Washington, D.C., June 1970 [redacted]

[redacted]

DTIC FILE COPY

DTIC
ELECTE
2 MAR 1989
S D
E

[redacted]

Chapter 8

PHENOMENA AFFECTING ELECTROMAGNETIC PROPAGATION[1] [redacted]

AD-A955 392

[redacted] INTRODUCTION [redacted]

[redacted] The two principal phenomena caused by a nuclear detonation that affect electromagnetic propagation are electromagnetic emissions and ionization of the atmosphere. The short duration electromagnetic pulse described in Chapter 7 is in the first category. Also included in this first category are continuing thermal radiation and emissions from various chemical reactions within the atmosphere. These radiations and emissions produce noise throughout the radio and optical spectra. The second phenomenon, atmospheric ionization, involves alterations of the electrical properties of the atmosphere that can affect the propagation of electromagnetic waves. Both types of effects are caused by energy radiated from the nuclear explosion, from the subsequent fireball, and from the radioactive debris. The severity of the effects on the propagation of electromagnetic waves may vary from being completely negligible to intolerable degradation of system performance.

[redacted] For the purpose of discussing the effects on propagation, the electromagnetic spectrum is divided into two frequency bands: the radio band, which includes radar applications, and the optical band, as shown in Figure 8-1. The most important effects in the radio band usually are those that affect the propagation of the desired electromagnetic signal (effects that change the amplitude, phase, direction, etc.). Electromagnetic radiations from the fireball and other regions can interfere with desired signals, and in some cases, interference from other sources (e.g., atmospheric noise) will be enhanced or diminished. The most important effect in the optical band is radiation from the fireball and other regions that interferes with desired signals. The source of this radiation is described in Chapter 3.

[redacted] The current state of knowledge concerning the effects of nuclear detonations on electromagnetic wave propagation stems from full scale tests, laboratory experiments, theoretical studies, and simulation with certain atmospheric phenomena. Meaningful testing of high-altitude nuclear weapon effects requires a sophisticated space capability (e.g., instrumented rocket probes), and only a relatively few high-altitudes tests were performed prior to the test moratorium in 1962.

[redacted] While those tests provided information to develop models to calculate the various phenomena, considerable uncertainty exists in scaling to burst or atmospheric conditions that are much different from those of the tests. All of the high-altitude tests have been single bursts. Significant differences are expected when two or more nuclear detonations occur near one another in time and space.

[redacted] Detailed theoretical descriptions for most burst phenomena are highly complex and require specification of poorly known parameters for quantitative results. Laboratory measurements have been used to obtain estimates of some parameters, but usually the results have to be scaled to conditions much different than those

---

[redacted] Although the English system of units for measuring distance is given priority throughout most chapters of this manual, wavelengths and other dimensions dealing with electromagnetic wave propagation usually are given in the metric system. Therefore, in this chapter and in Chapter 17, the metric system is used for distance dimensions. Conversion factors from the metric system to the English system are provided in Appendix B.

[redacted]

This document has been approved for public release and sale; its distribution is unlimited.

89 3 02 041

[redacted]

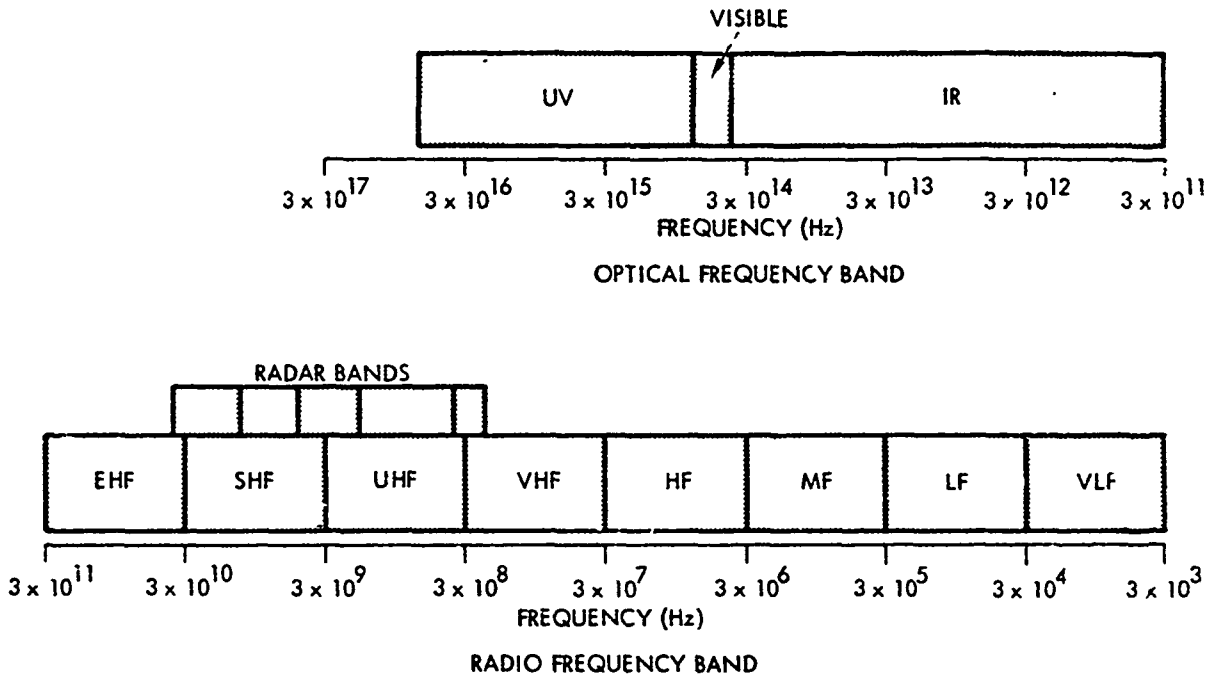

Figure 8-1. [redacted] Optical and Radio Frequency Bands [redacted]

[redacted]

used in the measurements. Some understanding of electromagnetic p.opagation in disturbed environments has been obtained from propagation measurements during eclipses, solar flares, and auroral disturbances. However, natural phenomena often involve the superposition of different phenomena than those brought about by nuclear bursts, and extrapolation to burst conditions can be misleading.

SECTION I

[redacted] PHENOMENA AFFECTING RADIO FREQUENCIES [redacted]

[redacted] The number of free electrons in the atmosphere is increased greatly by weapon radiations from high altitude bursts. These free electrons can absorb energy from electromagnetic waves and can change the phase velocity of the waves (changing the direction of propagation and signal characteristics). Electromagnetic radiations from heated regions and from trapped electrons are a source of noise.

[redacted] IONIZATION AND DEIONIZATION [redacted]

[redacted] Most of the energy of a nuclear detonation is emitted in forms that can produce ionization.[2] Some of this energy is in particulate matter (neutrons, beta particles, and high-speed debris that originally constituted the warhead and adjacent structure), and some is in photons (thermal radiation from the weapon case and gamma rays). Between 90 and 95 percent of the energy is emitted promptly (within a microsecond); about 5 to 10 percent is delayed radiation from the radioactive decay of fission debris.

[2]The ionization process is described in paragraph 6-4, Chapter 6.

[redacted]

QUALITY INSPECTED 4

UNANNOUNCED

By
Distribution/
Availability Codes
Dist | Avail and/or Special

[redacted]

[redacted] If a nuclear explosion occurred in a vacuum with no magnetic field, the flux of radiated energy would decrease as the square of the distance traveled. In the atmosphere, collisions and scattering processes absorb energy and produce ionization and excitation. (See Chapters 3, 4, and 5 for discussion of atmospheric absorption of photons, neutrons, and beta particles.)

[redacted] Radiation entering the atmosphere from above is absorbed rapidly when it reaches the altitude, termed the stopping altitude, where the mean-free path equals one scale height (an altitude region over which the atmospheric density changes by a factor of e (approximately 2.7). Stopping altitudes for the principal radiations from a nuclear weapon are shown in Table 8-1.

Table 8-1 [redacted] Approximate Stopping Altitudes for Principal Weapon Outputs Causing Ionization [redacted]

Weapon Output	Stopping Altitude (km)
Prompt Radiation	
x-rays (1 kev radiator)	80
Neutrons	25
Gamma rays	25
Debris (kinetic energy)	115
Delayed Radiation	
Gamma rays	25
Beta particles (1 Mev)	60

[redacted] For detonations below the stopping altitude of a particular radiation, most of that radiation will be contained locally. When detonations occur above the stopping altitude of a particular radiation, that radiation can spread large distances before being deposited and causing ionization. About 3×10^4 ion pairs are produced for each 1 Mev of energy deposited in the atmosphere. Since about 3×10^{28} Mev are released per megaton of weapon yield, even a small fraction of the weapon output can cause large electron densities. The lifetime for many of the electrons produced is short, however, and it depends critically on the altitude at which they are produced.

[redacted] Electrons and ions produced by the ionization sources undergo various atmospheric reactions that change their number density. Four principal reactions must be considered:

1. Attachment. Electrons can attach to neutral air particles (primarily to oxygen molecules and/or atoms) to form negative ions.
2. Detachment. Once attached, electrons can be detached from negative ions by collisions, solar radiation, or radiation from the fireball.
3. Recombination. Electrons and positive ions can recombine to form neutral particles.
4. Mutual Neutralization. Positive ions can combine with negative ions formed by attachment, to produce neutral particles.

[redacted] The rate at which these reactions proceed is a strong function of altitude. Thus, the altitude distribution of electron density after a period of time generally will not coincide with the altitude distribution immediately after the deposition of weapon energy. Detailed solutions of the time history of electron density require consideration of a large number of atmospheric species. Many reaction-rate coefficients are not well known, even for the natural atmosphere. The uncertainties in these coefficients provide a significant source of uncertainty in the prediction of electron density time history. In the natural atmosphere above about 70 km, where neutral particle density is low, recombination accounts for the major electron loss. At lower altitudes, attachment becomes increasingly important in the removal of free electrons, particularly at night

[redacted]

[redacted]

[redacted] when there is no photodetachment of electrons from negative ions by sunlight.

[redacted] In heated or highly ionized regions, the air chemistry (interaction between species) is modified, and electron loss processes are changed. The expansion of heated regions also reduces the electron density.

[redacted] In discussing electron density caused by nuclear weapons, it is convenient and useful to consider the electron density resulting from prompt radiation and delayed radiation separately. Also, since ionization and deionization processes are significantly different inside and outside the fireball, these regions will be discussed separately. Although electrons are the principal cause of effects on electromagnetic propagation, ions can affect propagation in the VLF and LF bands (frequencies below a few hundred kilohertz).

8-1 Electron Density Within the Fireball [redacted]

[redacted] Initially the incandescent region termed the fireball is highly ionized. For detonations below about 60 km, thermal ionization of air and debris from the weapon and carrier maintains high electron densities until the fireball cools below about 2500°K. For cooler fireballs, beta particles deposited within the fireball may be a significant ionization source. Predictions of electron density within the fireball require knowledge of the distribution of temperature and debris within the fireball, the shape of the fireball as a function of time, and the detailed chemistry of heated regions.

[redacted] Detailed calculations, which have been performed for a few burst conditions, are imprecise, particularly with regard to inhomogeneities and gradients in fireball properties. However, for many cases, relatively simple fireball models in which the mass density and temperature are assumed uniform within the fireball can be used. Figures 8-2 and 8-3 show calculated values of average fireball electron density and temperature following 1-Mt detonations at altitudes of 25 and 50 km, respectively. The calculations contained the assumption that the fireball gas was in thermal equilibrium, as well as being homogeneous.

[redacted] When detonations occur above about 60 km, losses of free electrons within the fireball are slower and the electron density does not decay rapidly enough to remain in equilibrium with the cooling fireball. Volume expansion controls the decline of electron density during the first few tens of seconds following detonation. Later, recombination of electrons with positive atomic ions predominates.

[redacted] For detonations at altitudes above about 80 km, the geomagnetic field influences the fireball expansion and location. After a few tens of seconds, magnetic forces cause the expansion across the magnetic field to become slower, while expansion along the magnetic field continues. Thus, the fireball becomes elongated along the magnetic field in a roughly cylindrical or tube shape. Figures 8-4 and 8-5 show calculations of average fireball electron density and temperature following 1-Mt detonations at altitudes of 75 and 150 km, respectively.

[redacted] Photographs of fireballs affected by the magnetic field show many field-aligned striations within the fireball (see Figure 1-4C). The optical striations also indicate large variations of electron density within the fireball. The size of the striations and the variation of electron density from the average value cannot be scaled accurately with burst parameters at present.

[redacted] For detonations at altitudes above about 300 km, the mean-free path of both X-rays and debris particles is large, and localized fireball may not form around the detonation point. However, debris particles initially directed downward may heat and ionize a region below the detonation point. This region, if sufficiently disturbed, is termed a fireball region. The formation of a fireball region depends on the detonation altitude, the weapon yield, and the atmospheric density

[redacted]

[redacted]

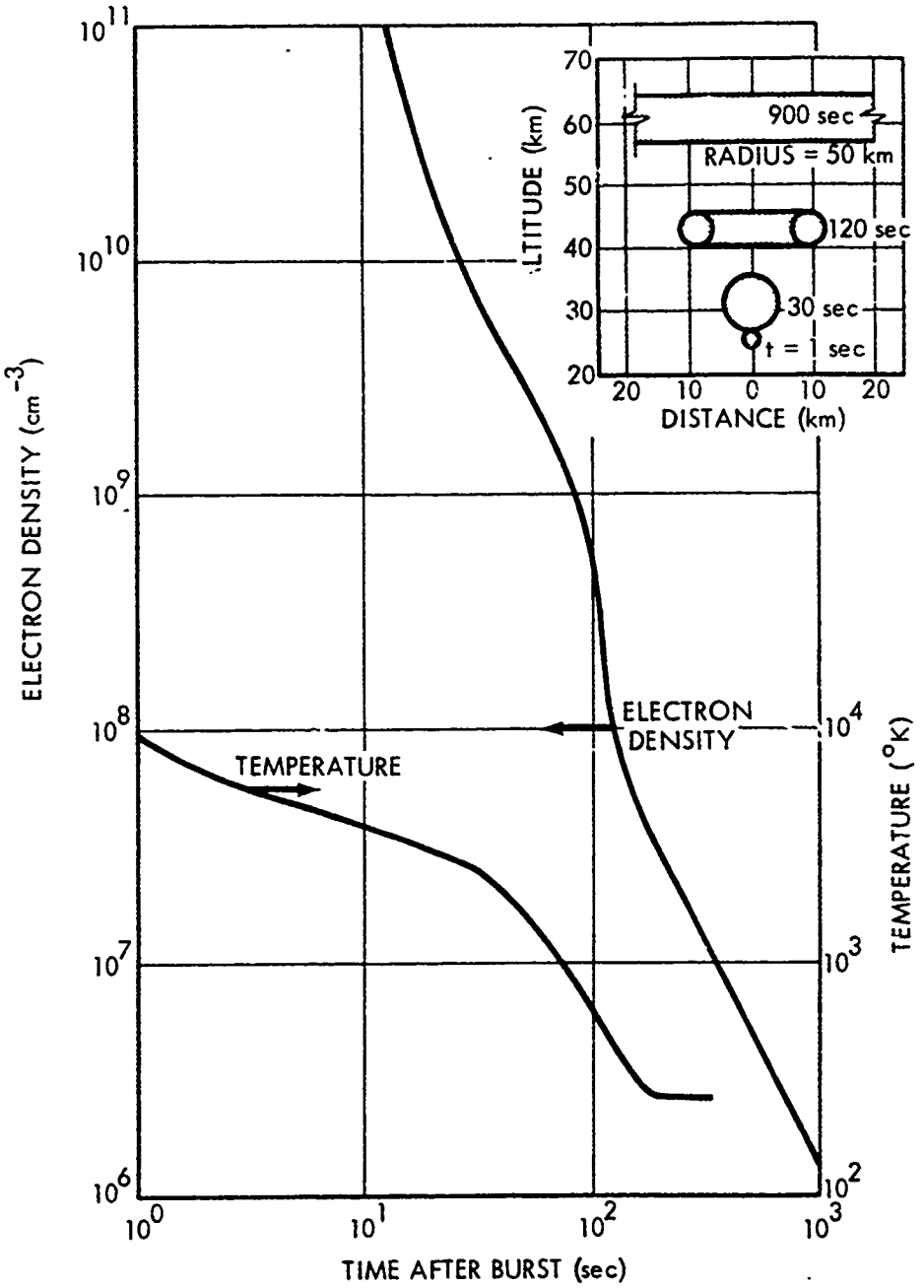

Figure 8-2. [redacted] Fireball Electron Density and Temperature, 1-Mt at 25 km [redacted]

[redacted]

[redacted]

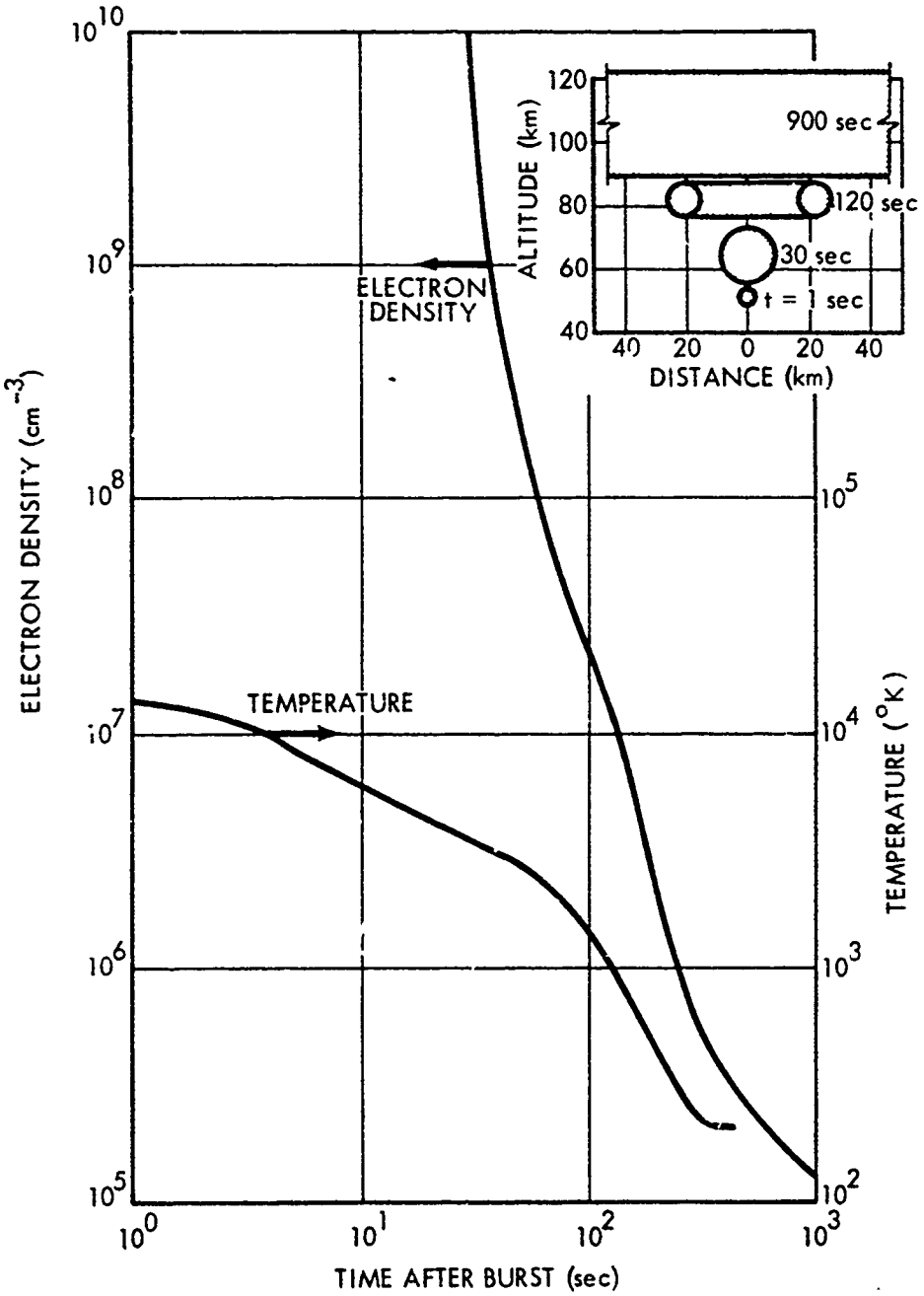

Figure 8-3. [redacted] Fireball Electron Density and Temperature, 1-Mt at 50 km [redacted]

[redacted]

[redacted]

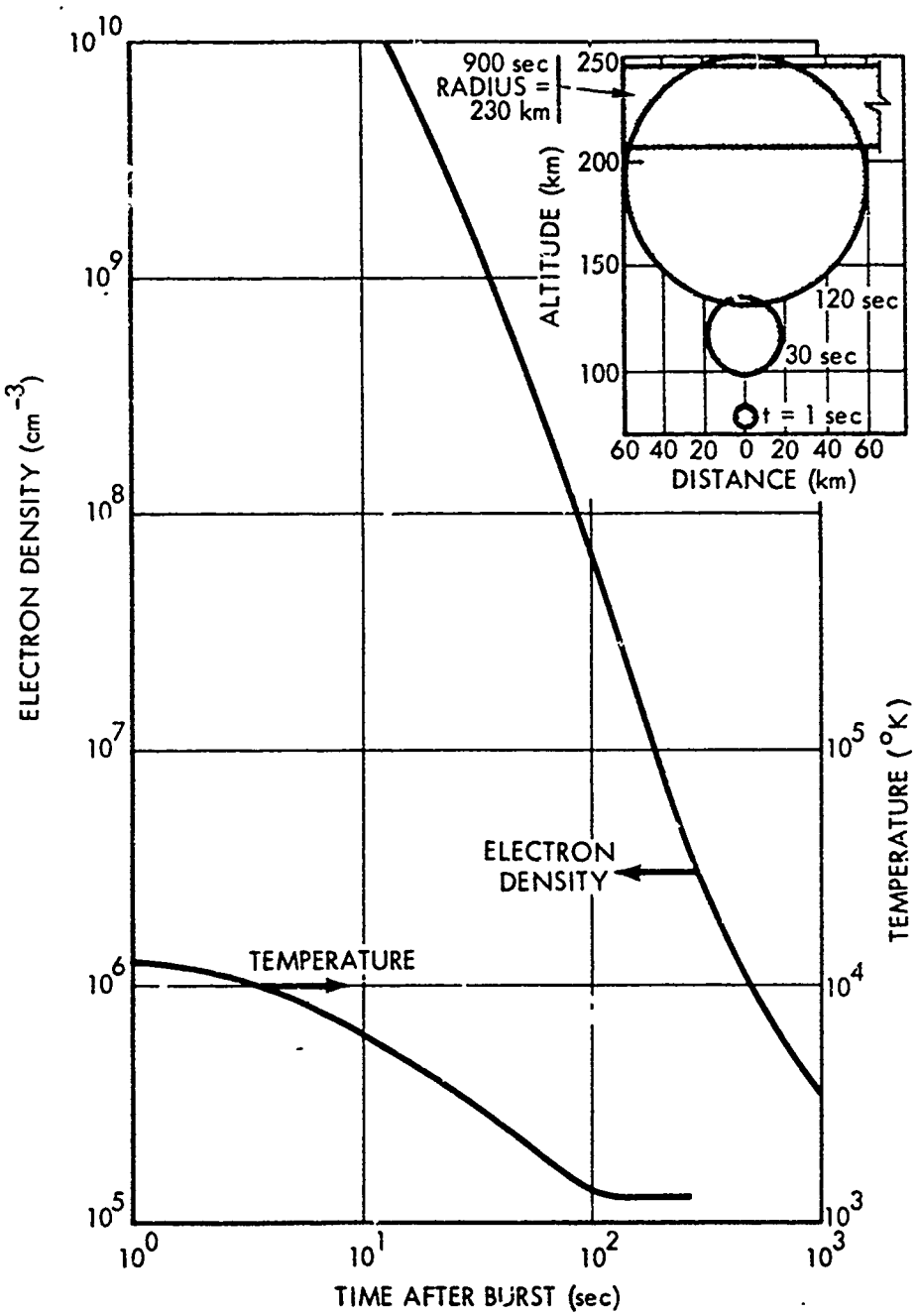

Figure 8-4. [redacted] Fireball Electron Density and Temperature, 1-Mt at 75 km [redacted]

[redacted]

[redacted]

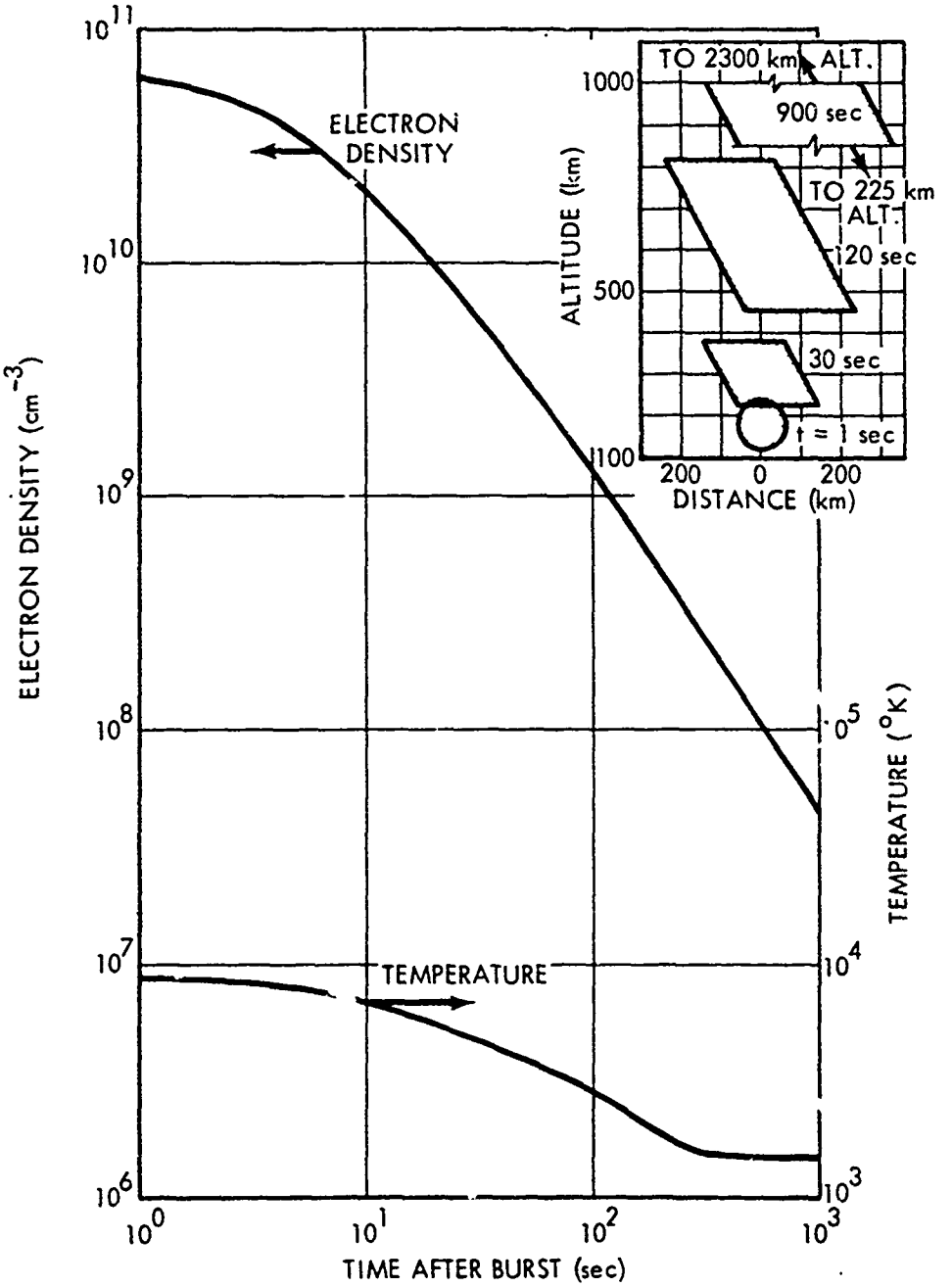

Figure 8-5. [redacted] Fireball Electron Density and Temperature, 1-Mt at 150 km [redacted]

[redacted]

[redacted]

at burst time. Figure 8–6 shows calculated values of electron density and temperature within the fireball following a 1-Mt detonation at an altitude of 400 km.

[redacted] Only a few nuclear tests have been carried out by the U.S. at detonation altitudes above 80 km; therefore, theoretical calculations of fireball formation, size, location, and properties are dependent on parameters that are poorly known. Calculations of fireball properties for detonations at altitudes above 80 km should be considered illustrative of the general order of magnitude rather than as detailed quantitative results.

8-2 Electron Density Caused by Prompt Radiation Outside the Fireball [redacted]

[redacted] Ionization produced outside the fireball by prompt gamma rays can be neglected insofar as effects on radio propagation are concerned. For detonations at altitudes below about 25 km, both neutrons and X-rays are deposited within or close to the fireball, and the effects of prompt radiation outside the fireball are minimal. For detonation altitudes between 25 and about 80 km, X-rays are largely confined, but neutrons produce ionization over distances of several hundred kilometers. For higher altitude detonations, both X-rays and neutrons cause widespread ionization. Figure 8–7 shows the initial ionization caused by prompt radiation from a nominal megaton weapon detonated at 120 km. Because of earth's curvature, radiation reaching a given altitude at large horizontal distances from the source must pass through lower altitudes where it is strongly attenuated by the denser air.

[redacted] The decay of electron and ion densities following the ionization impulse depends on electron and ion loss rates, which are functions of altitude and time of day. Below about 100 km, the electron and ion density after 1 second will be essentially independent of the initial ionization if the initial ion pair density is greater than 10^7 ion pairs cm^{-3}. This condition is termed saturation; larger initial ionization will not increase the electron or ion density remaining after 1 second. Figure 8–7 shows that the initial ion-pair density below 100 km exceeds 10^7 ion pairs cm^{-3} out to about 500 km from the burst.

[redacted] Figure 8–8 shows the altitude dependence of the electron density for several times after a saturation impulse. At night the electron concentration decays rapidly, particularly at low altitudes where attachment of electrons to neutral particles is the predominant reaction. During the day, electron densities greater than normal can persist for tens of minutes. The insert in Figure 8–8 illustrates the horizontal extent of the region that can be saturated by prompt radiation as a function of detonation altitude. The decay of electron and ion densities above 100 km depends on processes that may be affected by atmospheric chemistry changes caused by the deposition of prompt radiation. Because of the additional complications introduced at those altitudes, a simple representation of the decay is not possible.

[redacted] Many of the neutrons produced by the explosion will travel upward and will escape the atmosphere. Since neutrons are not affected by the geomagnetic field, they will spread isotropically over a large area. Each neutron eventually disintegrates spontaneously into a proton, a neutrino, and a beta particle (half-life for disintegration is about 12 minutes). Since the beta particle (a high-energy electron) is charged, it can move only in the direction of the geomagnetic field (motion normal to the magnetic field direction causes the beta particle to spiral around the magnetic field lines). The beta particles are guided by the geomagnetic field until reaching altitudes near the beta-particle stopping altitude (see paragraph 8–4 and Figure 8–10), where they deposit their energy to produce ionization. The amount of ionization caused by neutron-decay beta particles is small, but it has been noted at distances of many thousands of kilometers from the burst point.

[redacted]

[redacted]

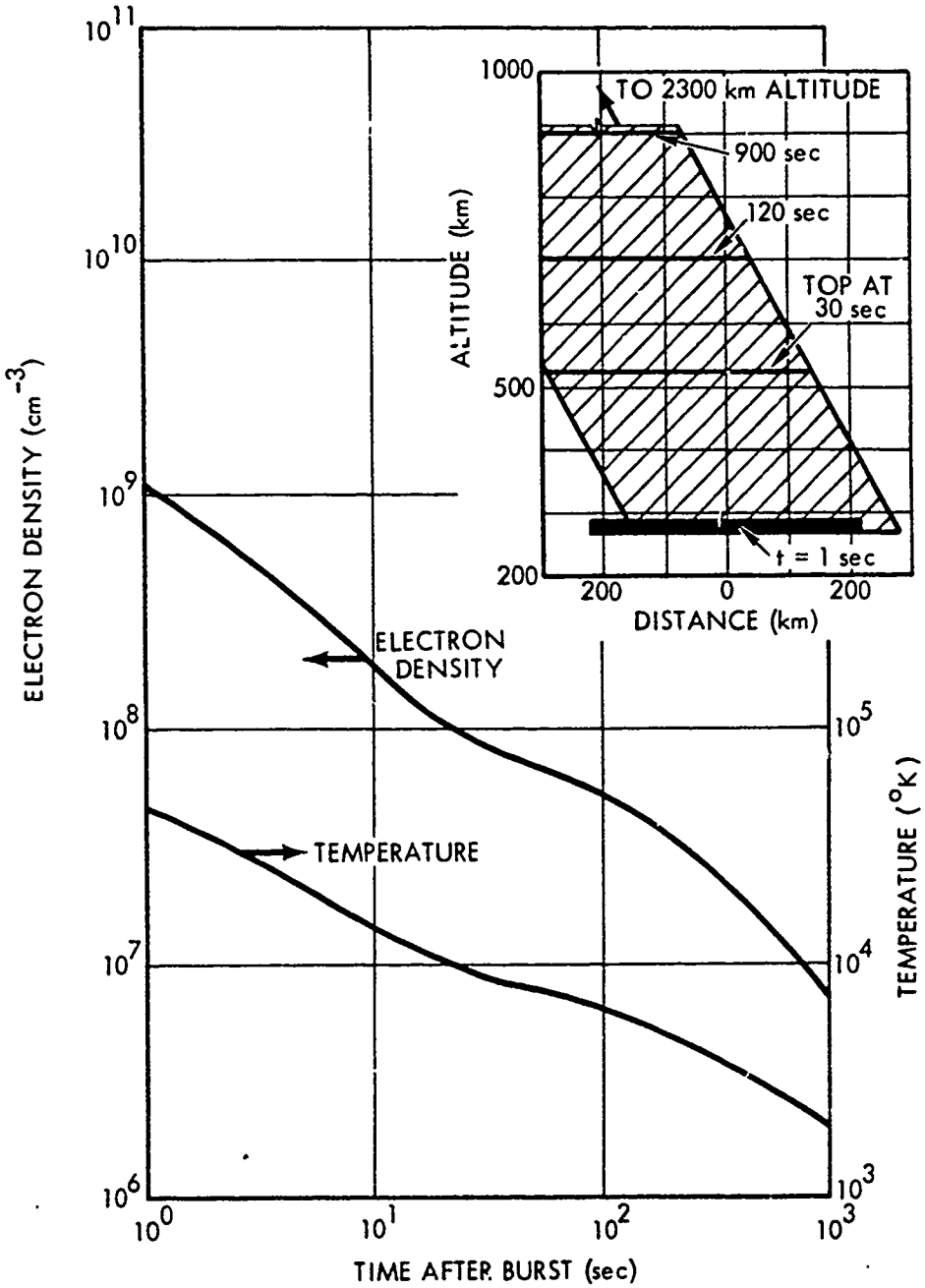

Figure 8-6. [redacted] Fireball Electron Density and Temperature, 1-Mt at 400 km [redacted]

[redacted]

[redacted]

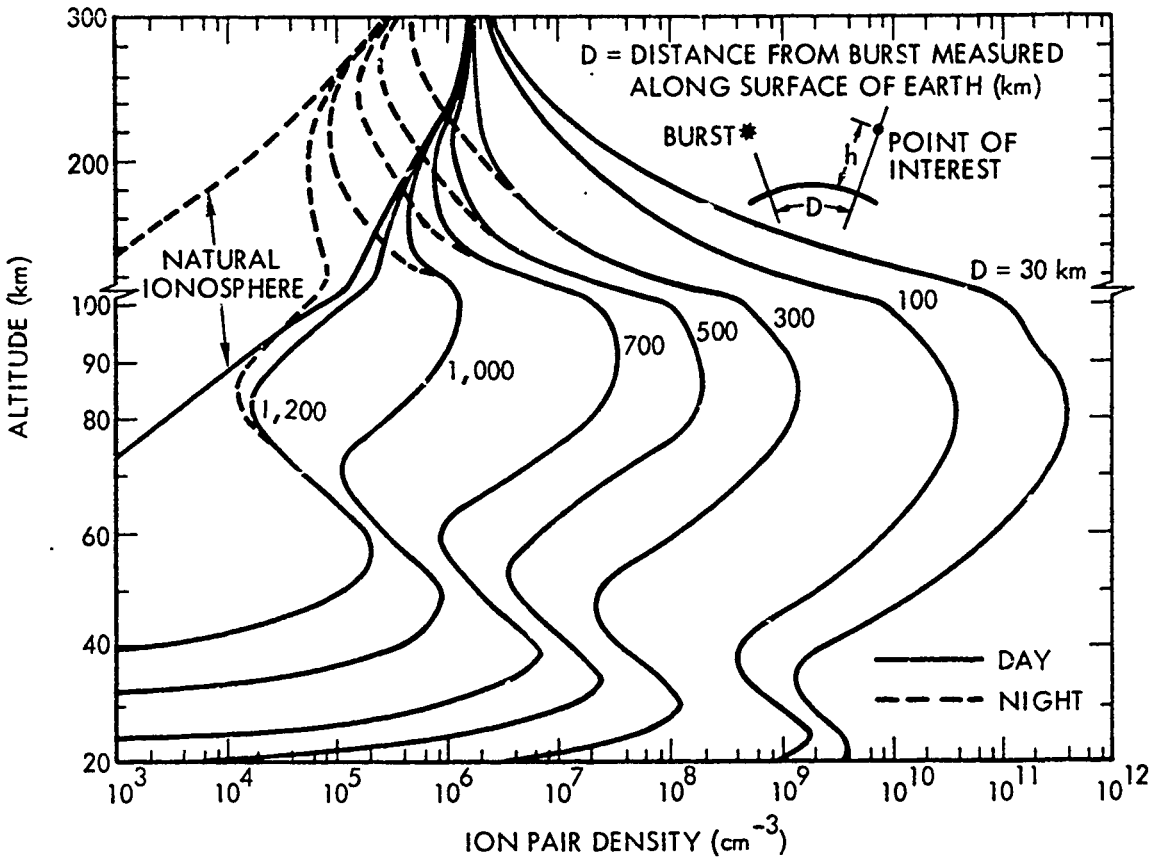

Figure 8-7. [redacted] Ion-Pair Density Due to Prompt Radiation from a 1-Mt Burst Detonated at 120 km, t = 0 [redacted]

8-3 Electron Density Caused by Delayed Gamma Radiation Outside the Fireball [redacted]

[redacted] In addition to prompt radiation, delayed gamma rays and beta particles (discussed in Section III, Chapter 5) are produced during the radioactive decay of the fission debris. This continuing radiation produces ionization characterized by a production rate of ion pairs per unit volume per unit time. For detonations below several hundred kilometers, the fission debris (assumed to be mixed with the total weapon debris) is initially within the fireball and is carried upward as the fireball rises and expands.

[redacted] When the debris is below the gamma-ray stopping altitude, gamma rays can only penetrate a short distance, and the ionized region that they produce around the fireball is small. If the debris rises above the gamma-ray stopping altitude, gamma rays produce ionization over larger distances. The resulting electron and ion densities are a function of both the ion-pair production rate and the electron and ion loss processes. Most of the gamma-ray energy is deposited near the stopping altitude, but the electrons produced below about 40 km are lost quickly by attachment. Maximum electron density usually occurs at higher altitudes where the electron lifetimes

[redacted]

[redacted]

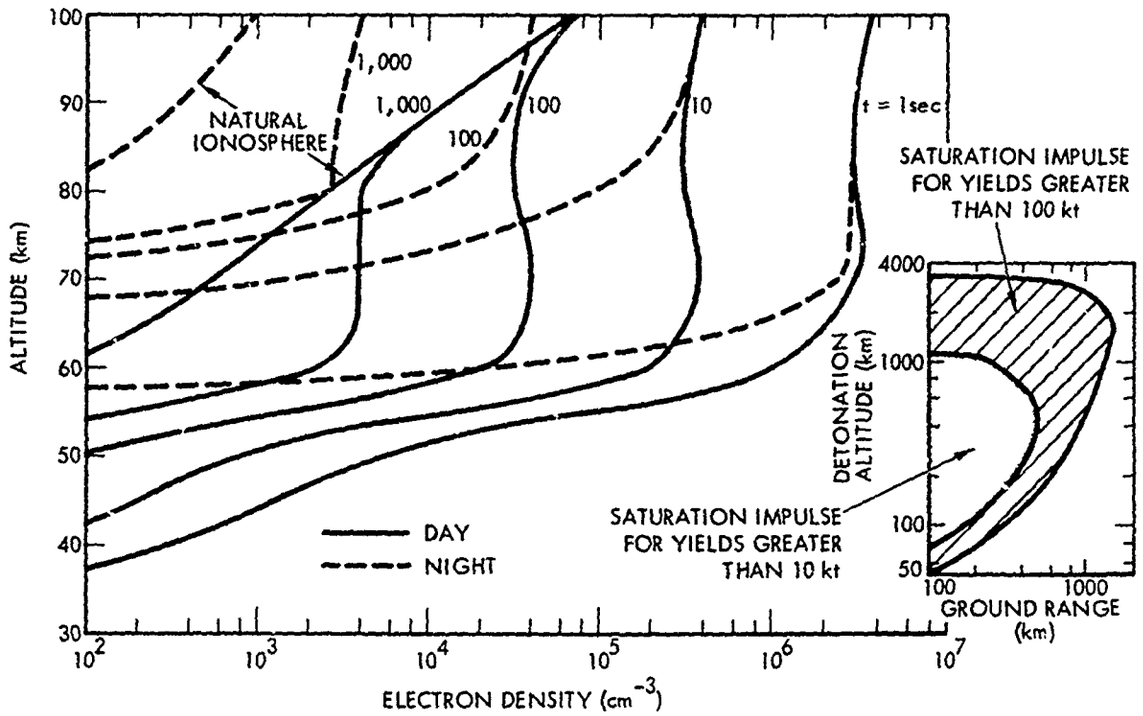

Figure 8-8. [redacted] D-Region Electron Density Caused by Prompt Radiation (Saturation) [redacted]

[redacted] are longer. Near the debris region, where the gamma ray flux is large, substantial electron densities can be maintained even though the debris is at an altitude where free electrons are lost by attachment rapidly.

[redacted] When the fission debris and the point of interest are both well above the gamma-ray stopping altitude, the ion-pair production rate and electron and ion densities caused by gamma rays can be expressed conveniently in terms of a radiation intensity parameter, I_γ, defined by

$$I_\gamma = \frac{4 \times 10^{-7} W_F}{4\pi R^2 (1+t)^{1.2}} \text{ watts } m^{-2},$$

where

W_F = fission yield in megatons,

R = radial distance from debris center to point of interest in km,

t = time after detonation in seconds.

Figure 8-9 shows quasi-equilibrium electron densities for particular values of I_γ. The values are called quasi-equilibrium because they are the values that would be reached if the production rate remained constant and if sufficient time were allowed for equilibrium conditions to be reached. In an actual situation, the production rate changes with time because of the radioactive decay of the fission debris and the changing geometry as the debris moves. However, for most cases, the time to reach equilibrium is short, and the quasi-equilibrium values are close approximations to the electron densities. The insert in Figure 8-9 illustrates the horizontal extent as a function of

[redacted]

[redacted]

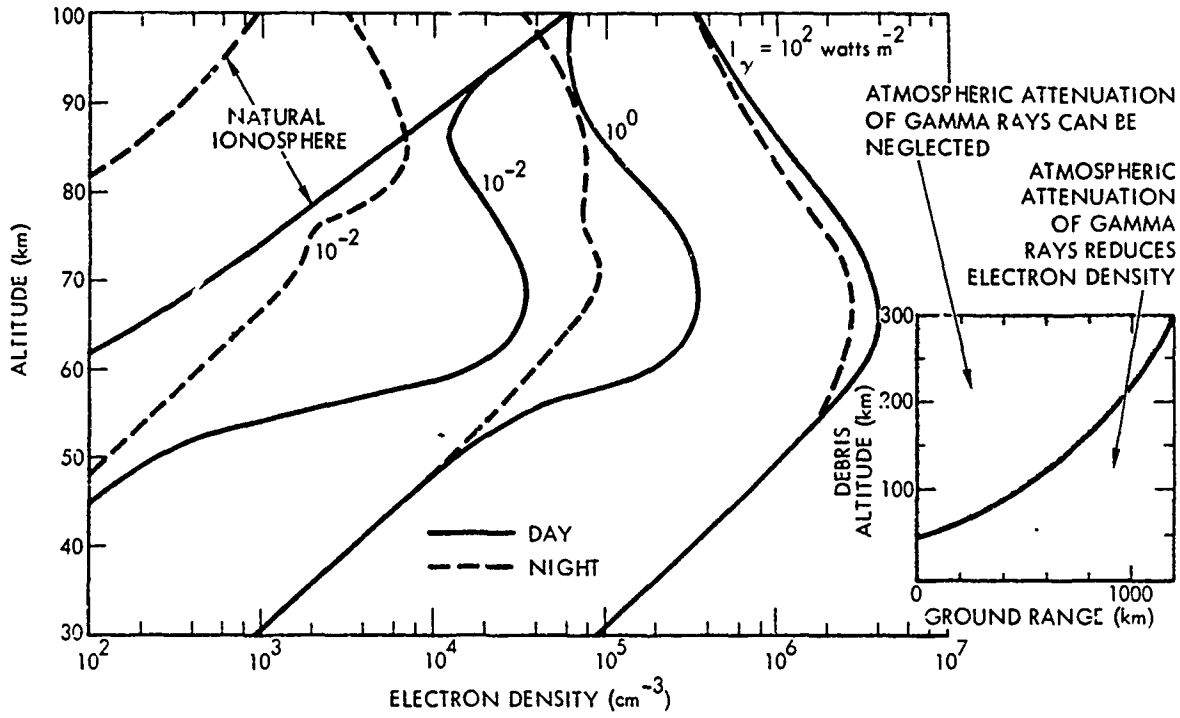

Figure 8-9. [redacted] Quasi-Equilibrium Electron Density Due to Gamma Rays [redacted]

debris altitude for which the electron densities are applicable.

[redacted] Most delayed gamma rays deposit their energy in the atmosphere by first producing high-energy electrons (Compton electrons). Compton electrons travel very short distances in the lower atmosphere; however, some Compton electrons produced above about 60 km can escape to the conjugate region, as described for beta particles in paragraph 8-4. Ionization in the conjugate region caused by Compton electrons is of interest primarily for studies of propagation in and below the HF band (frequencies below 30 megahertz).

8-4 Electron Density Caused by Beta Particles Outside the Fireball [redacted]

[redacted] Since beta particles are electrically charged, their motion in the atmosphere is affected by the geomagnetic field. When the fission debris is above the beta-particle stopping altitude, about half of the betas will travel down the geomagnetic field lines, producing ionization (similar to auroral ionization at high latitudes) until they are deposited near the stopping altitude. The other half of the betas (those emitted upward) will follow the geomagnetic field lines across the geomagnetic equator and will produce ionization at the geomagnetic conjugate.[3]

[redacted] Figure 8-10 illustrates the location of the beta-particle ionization regions. Because of the slope (dip angle) of the magnetic field lines, the beta-particle ionization region is offset from the debris. When the geomagnetic field is undisturbed by the detonation, the location of the

[3] As used herein, geomagnetic conjugate points are points at the north and south ends of a geomagnetic field line that are at corresponding altitudes.

[redacted]

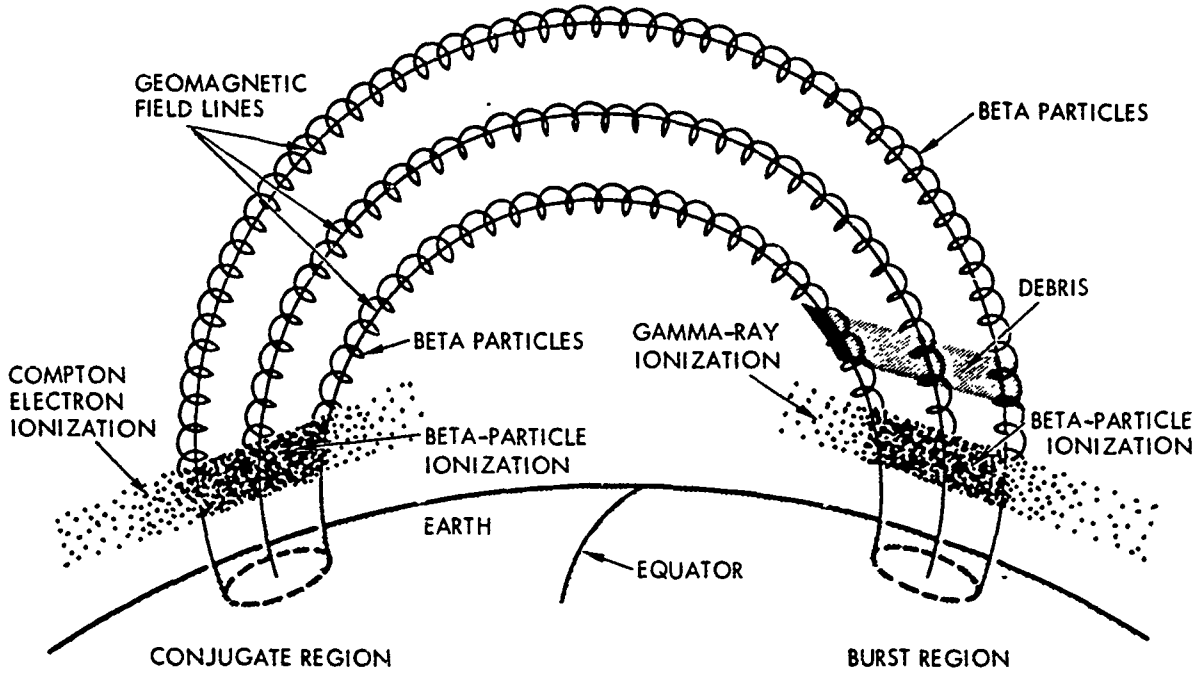

Figure 8-10. Location of Delayed Ionization Regions

beta-particle ionization region can be determined from a knowledge of the size and location of the debris region and the geomagnetic field lines. However, the geomagnetic field can be severely distorted for tens of seconds after a nuclear detonation. Determination of the magnetic dip angle and location of the conjugate point for undisturbed magnetic-field conditions are discussed in Problems 8-8 and 8-9.

The location of the gamma-ray ionization region and the region ionized by Compton electrons escaping to the conjugate region are also illustrated in Figure 8-10.

The ion-pair production rate and electron density caused by beta particles can be expressed conveniently in terms of a radiation intensity parameter, N_β, defined by:

$$N_\beta = \frac{8.8 \times 10^{15} W_F}{A(1+t)^{1.2}} \text{ betas cm}^{-2}\text{sec}^{-1}, \quad (8.1)$$

where

A = area covered by fission debris in square kilometers.

Figure 8-11 shows the quasi-equilibrium electron density caused by beta particles for particular values of N_β. These curves apply if the fission debris is well above the beta stopping altitude and if the debris is uniformly distributed over the area A.

8-5 Electromagnetic Propagation in Ionized Regions

An electromagnetic wave propagating through an ionized region does work on charged particles in the region and transfers a portion of the wave energy to charged-particle kinetic energy. The electric field exerts a force on all charged particles; however ions, because of their larger mass, absorb less energy than electrons and can usually be neglected (an exception is wave

[redacted]

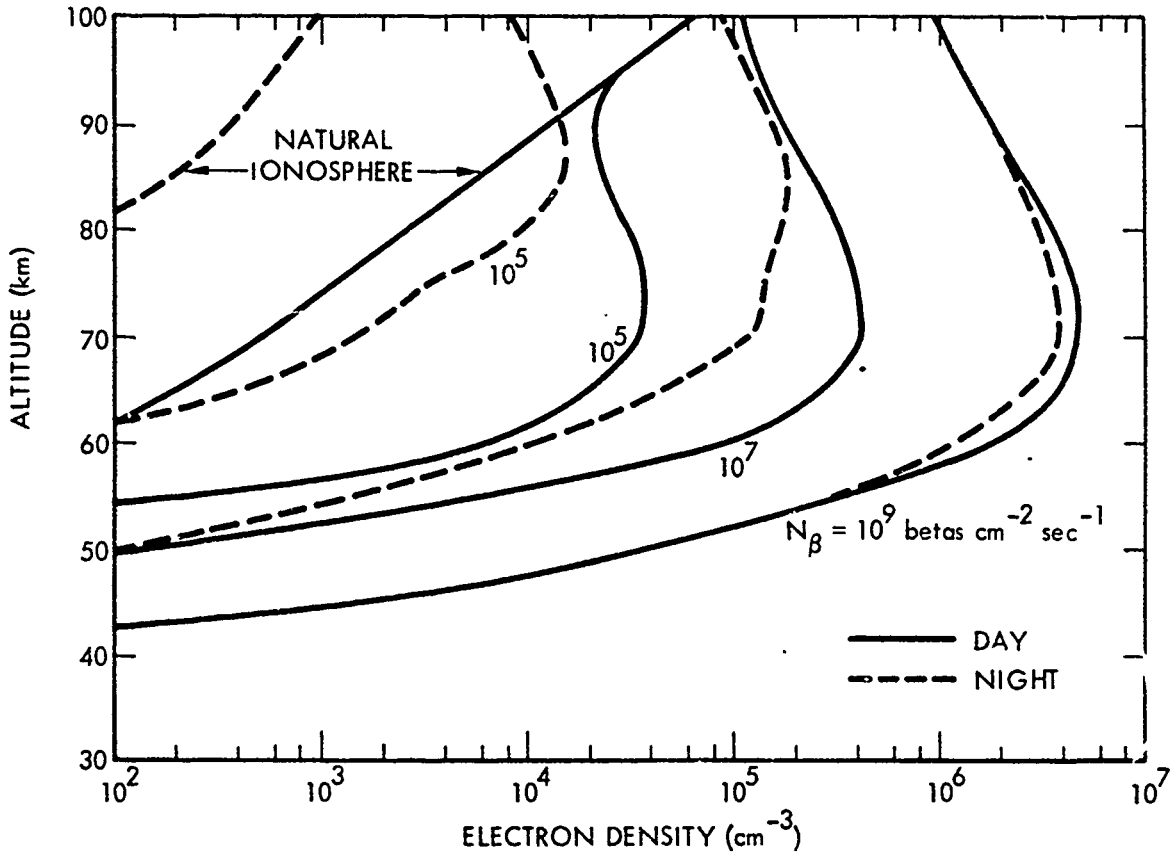

Figure 8-11. [redacted] Quasi-Equilibrium Electron Density Due to Beta Particles, Debris Altitude Greater than 60 km [redacted]

[redacted]

propagation at frequencies below a few hundred kilohertz). If the electrons do not collide with other particles, the energy is returned to the propagating wave without loss, but the phase of the wave is modified. Unless the geomagnetic field is parallel to the electric field of the propagating wave, some of the energy returned to the wave will have an electric field that is perpendic[redacted]ular to the incident electric field. The propagation wave then can be described as the sum of two plane waves termed the ordinary and the extra[redacted]ordinary waves—which have different phase velocities. One effect is to change the polarization of the propagation wave as it travels through the ionized medium. Electron collisions with other particles change the ordered motion of electrons into random motion (heat), and energy is absorbed from the wave. For many cases of interest, detonation-produced absorption is the overriding effect on electromagnetic propagation and it is the effect that is understood best.

[redacted] **TRAVELING DISTURBANCES IN E AND F REGIONS OF IONOSPHERE** [redacted] The preceding paragraphs discuss ionization sources from a nuclear explosion that add to the free electron content of the atmosphere. Following Teak and Orange (megaton

[redacted]

[redacted]

[redacted]

detonations at altitudes of 76 and 43 kilometers, respectively: 1958 test series) and again during Operation Fish Bowl (1962 test series), the normal E-region and F-region electron content appeared to be disturbed by hydrodynamic or hydromagnetic waves created by the detonation (the E-region includes the volume from 90 to 160 kilometers altitude, and the F-region begins at about 160 kilometers). [redacted]

DHA (b)(3)

DHA (b)(3)

[redacted] ELECTROMAGNETIC RADIATIONS [redacted]

[redacted] A heated region emits thermal radiation according to its temperature and emissivity. The emissivity at a given frequency approaches unity as the absorption becomes large (10 decibels or more). The fireball may remain hotter than several thousand degrees Kelvin for about a hundred seconds. It may be sufficiently emissive for frequencies less than a few gigahertz that systems with antennas pointing at the fireball would register antenna temperatures equal to the fireball temperature if there were no intervening absorption outside the fireball. Generally, absorption caused by prompt and delayed radiation outside the fireball will reduce the escaping thermal radiation. The effective antenna noise temperature will depend on the size of the fireball relative to the antenna beam width, the location of the fireball relative to the antenna beam, and the absorption outside the fireball, as well as the temperature and emissivity of the fireball.

[redacted] A second source of electromagnetic radiation in the radio band is synchrotron radiation, which is caused by beta particles spiraling along geomagnetic field lines. A spiraling beta particle continually accelerates, and, therefore, it radiates electromagnetic energy. The radiation is maximum in the HF band, and it is approximately inversely proportional to frequency cubed for higher frequencies. The radiation is concentrated in the direction of the vector of electron motion. Because of its directivity, low intensity, and frequency dependence, synchrotron radiation does not appear to degrade present military systems seriously.

[redacted] ABSORPTION [redacted]

[redacted] Exact expressions for the absorption or energy loss involve components of the earth's magnetic field as well as electron density, collision frequency (number of collisions an electron makes per second), and wave frequency. For frequencies above about 10 megahertz and when bending of the wave is negligible, the incremental path absorption can be found from the following equation.

$$a = 4.6 \times 10^4 \frac{N_e \nu}{\omega^2 + \nu^2} \; dB/km, \qquad (8.2)$$

where

N_e = electron density (electrons/cm^3)

ν = collision frequency (collisions/sec)

ω = wave frequency (radians/sec).

[redacted]

[redacted]

[redacted]

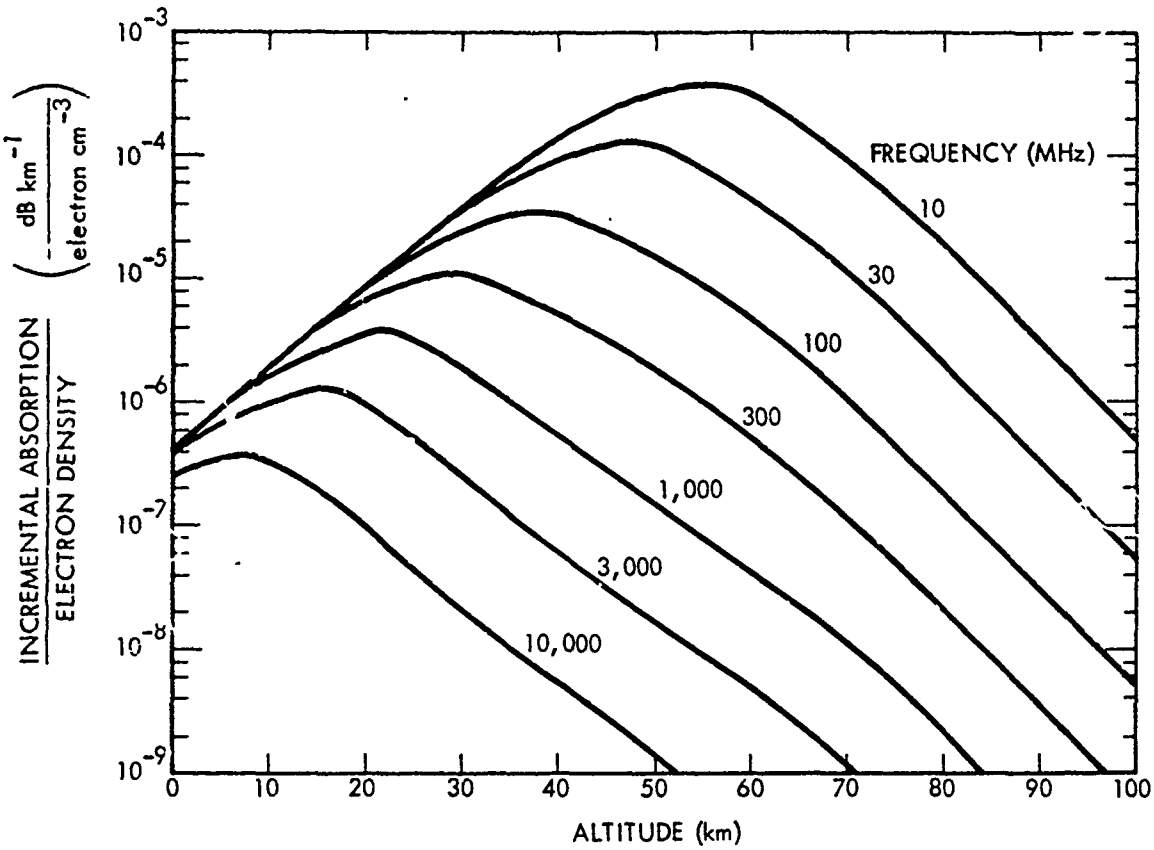

Figure 8-12. [redacted] Incremental Absorption Due to Electron-Neutral Collisions [redacted]

[redacted] Figure 8-12 shows incremental path absorption per electron per cubic centimeter as a function of altitude due to electron-neutral collisions. Above about 100 km, where the neutral particle density is low, absorption due to electron-neutral collisions is small; however, absorption due to electron-ion collisions may be important. Figure 8-13 shows incremental absorption due to electron-ion collisions for a temperature of 1000°K (approximate value of the atmospheric temperature above 200 km). The incremental absorption is proportional to $(1000/T)^{3/2}$ for other temperatures. The dotted portion of the curves indicates the volume where the electron density causes considerable bending of the wave, and a more detailed solution is required to obtain better values for the absorption. Figures 8-12 and 8-13 can be used with estimates of electron density (obtained from Figures 8-2 through 8-9 and 8-11) to determine incremental path absorption. The integral of the incremental path absorption along the propagation path gives the total path loss. Equation 8.1 and Figures 8-12 and 8-13 neglect ion-neutral collisions, which are important at low frequencies (VLF and LF bands). Problems 8-4 through 8-7 provide methods for estimating total one-way path absorption for various propagation paths.

[redacted] As was the case for electron density, it is convenient and useful to present absorption in-

[redacted]

[redacted]

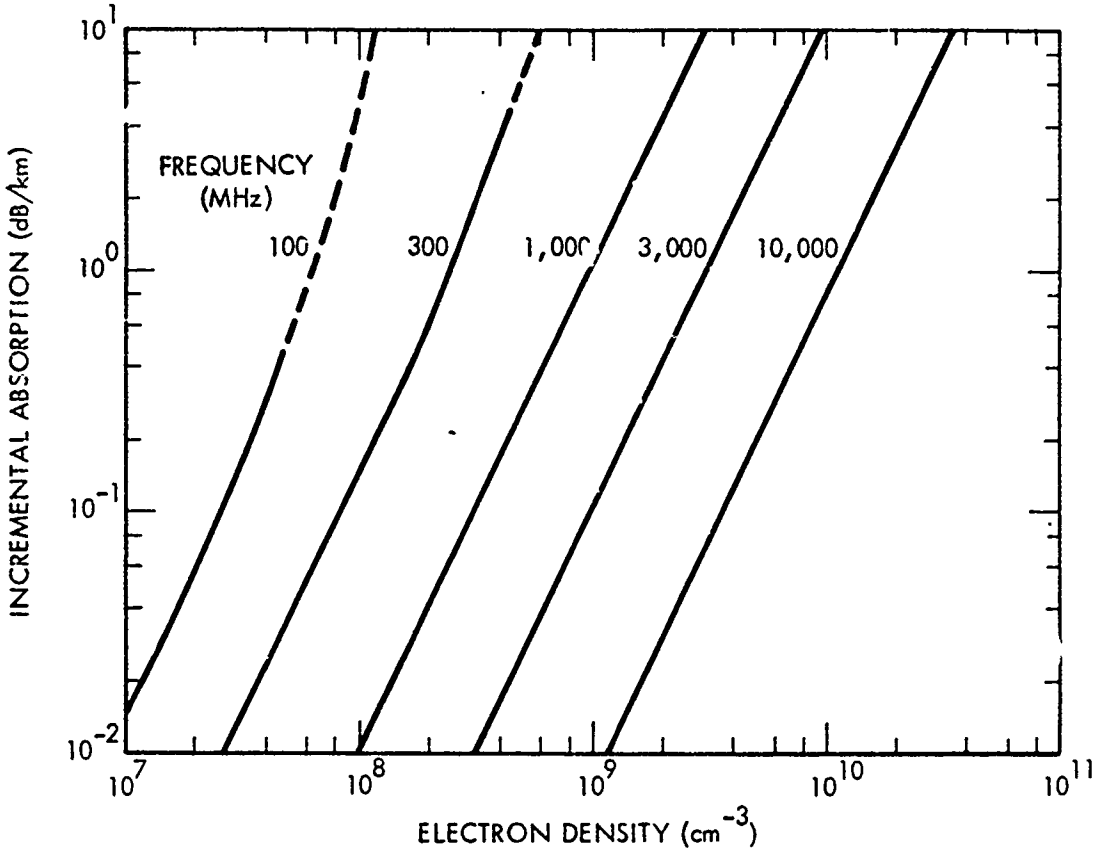

Figure 8-13. [redacted] Incremental Absorption Due to Electron-Ion Collisions, Electron Temperature = 1,000°K [redacted]

[redacted] side the fireball and absorption caused by prompt and delayed radiation outside the fireball separately. With the exception of propagation paths that pass close to the fireball, absorption outside the fireball is maximum in the D-region (40 to 90 km). Generally it is sufficiently accurate to consider the largest of the separate absorptions as the total absorption along a particular propagation path.

[redacted] Scaling relations for the attenuation of low frequencies (VLF and LF bands) are difficult to present, because the amount of absorption for a particular propagation path depends in detail on the penetration of the wave into the atmosphere. A description of low-frequency propagation in nuclear environments is given in Chapter 17. Scaling relations for absorption of propagation at frequencies greater than a few megahertz are given in succeeding paragraphs; however detailed solutions of absorption for propagation paths associated with communication and radar systems usually require numerous calculations that cannot be obtained readily from simple hand-computation procedures. Figure 8-14 shows the burst conditions (detonation altitudes and yield) for which prompt and delayed radiation can cause absorption outside the fireball. The figure can be used in conjunction with the discussion in para-

[redacted]

[redacted]

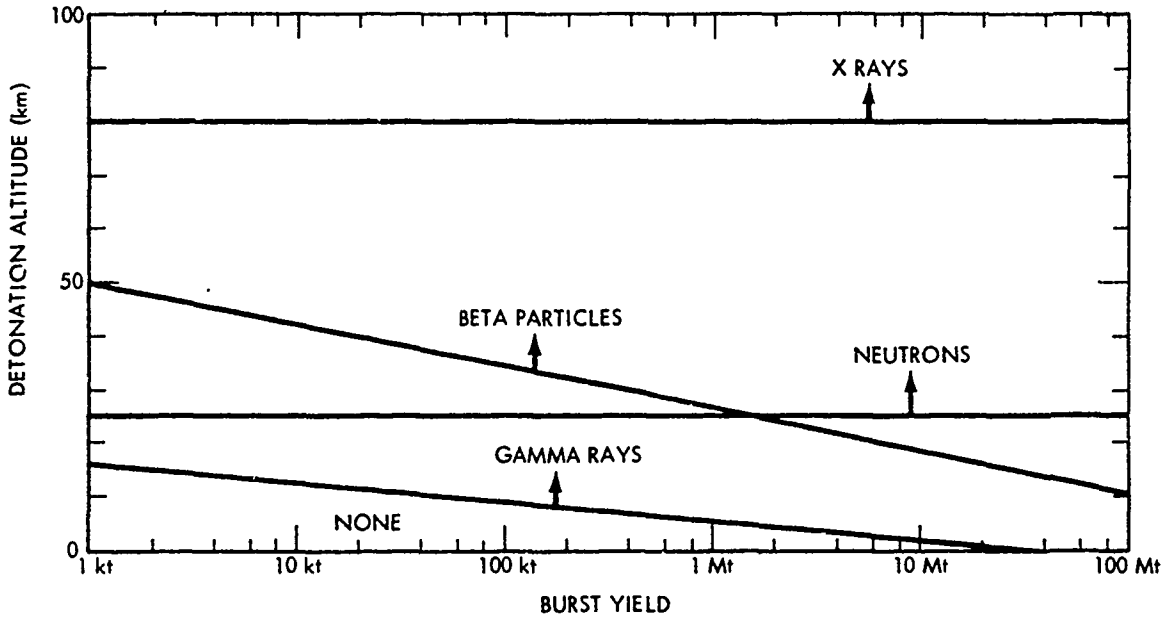

Figure 8-14. [redacted] Radiation Sources Causing Absorption Outside the Fireball [redacted]

[redacted]

graphs 8-7 and 8-8 to determine whether absorption outside the fireball need be considered and which radiation sources are important.

8-6 Absorption Within the Fireball [redacted]

[redacted] Fireball ionization is localized and very intense: for most purposes, the fireball may be considered opaque at all radio frequencies for at least a few seconds. Calculations of the magnitude of absorption at a given time, or the duration of a given magnitude of absorption, are subject to considerable error because of uncertainties in predictions of the electron density within the fireball (see paragraph 8-1) and the fireball geometry. Methods for estimating fireball size and absorption through the fireball are given in Problems 8-1 through 8-4.

[redacted] For detonations below about 80 km and weapon yields greater than 100 kt, absorption through the fireball is expected to exceed 25 decibels for about 50 seconds at 10 gigahertz and for longer than 100 seconds at 1 gigahertz. Because the fireball rises a significant distance during these time periods, the duration of degradation due to absorption will generally be determined by the relative motion of fireball and propagation path.

[redacted]

[redacted]

[redacted]

[redacted]

[redacted]

DNA (b)(3)

8-7 Absorption Caused by Prompt Radiation Outside the Fireball [redacted]

[redacted] Absorption outside the fireball caused by prompt radiation may last from tens of seconds in the VHF band to tens of minutes in the HF band for daytime conditions. At night the absorption decreases more rapidly. For bursts below about 100 kilometers, the horizontal radius of the prompt absorption region only extends a few hundred kilometers from the burst point; for higher detonations the extent can be much longer.

8-8 Absorption Caused by Delayed Radiation Outside the Fireball [redacted]

[redacted] Absorption caused by delayed radiation (gamma rays and beta particles) is a function of the location and distribution of the fission debris. Estimates of debris rise and expansion for use in computing delayed-radiation effects are given in Problems 8-1 through 8-3.

[redacted] Delayed gamma rays can produce significant absorption when the debris is at altitudes above about 25 kilometers. Problem 8-6 describes methods that can be used to estimate one-way path absorption. The horizontal extent of the absorption region caused by gamma rays depends on weapon fission yield, debris altitude, time after burst, and wave frequency. The insert in Figure 8-9 shows the maximum possible extent of ionization and, thus the maximum extent of absorption; for most cases the region of significant absorption will be smaller.

[redacted] When the debris is above about 60 kilometers, beta particles produce D-region absorption at the burst locale and on the opposite side of the magnetic equator. Figures 8-49 through 8-51 can be used to obtain estimates of absorption caused by beta particles in terms of the beta-radiation intensity parameter that was defined in paragraph 8-4 for debris above the beta-particle stopping altitude (60 km). The location of the absorption region is offset from the debris region because of the effect of the geomagnetic field on the motion of beta particles, as illustrated in Figure 8-10. The horizontal radius of the absorption region is approximately equal to the debris radius. This radius can vary from a few kilometers to a few thousand kilometers depending on weapon yield, detonation altitude, and time after burst.

[redacted] PHASE CHANGES [redacted]

[redacted] Phase changes resulting from propagation through a region of uniform electron density affect propagation velocity and signal characteristics. Relative phase changes due to gradients in electron density change the direction of propagation and scatter energy from the propagating wave. Some phase effects become important only for electron densities that cause significant absorption. Evaluation of direction changes and scattering requires detailed information concerning the spatial distribution of electron density, which is difficult to predict theoretically and for which there is only limited experimental data.

8-9 Velocity of Propagation [redacted]

[redacted] Within an ionized region the phase velocity is increased over that in vacuum, but the group velocity, associated with the transmission of energy, is reduced. The increased time required to propagate energy through the region is proportional to the integral of electron density along the propagation path. Typical values of time delays associated with ionization caused by nuclear bursts range from a few nanoseconds to a few tens of microseconds. The larger time delays usually are accompanied by significant absorption when the ionized region occurs below 100 km.

[redacted] The phase velocity in an ionized region depends on the frequency. Therefore, the region

[redacted]

[redacted]

separates waves of different frequencies, i.e., the region is dispersive. The significance of dispersion depends critically on the type of signal being propagated and the type of signal processing being employed. For frequency-modulated signals, dispersion causes intermodulation and harmonic distortion. For digital systems, dispersion causes pulse-envelope distortion. Dispersion effects caused by electrons below 100 kilometers appear to be negligible when compared to absorption. At higher altitudes, electrons can only cause important dispersion effects for wide-band signals (bandwidths of the order of 1 percent or more of the carrier frequency), and these effects will probably only occur for propagation paths through fireball regions after the electron density has decreased sufficiently that absorption is not overriding.

8-10 Frequency of Propagation

A time-dependent phase change is equivalent to a frequency shift. The frequency shift is proportional to the time rate of change of the electron density integral along the propagation path. Frequency changes may be caused by changes in electron density with time along a fixed propagation path or by motion of the propagation path in a region of inhomogeneous electron density. For a fixed propagation path, frequency changes caused by nuclear-weapon-produced ionization are small (a few hertz for a 10 megahertz signal) by a few seconds after burst. Larger frequency changes may occur when the propagation path moves through regions of high electron density, such as the fireball; however, in those cases absorption generally will be overriding.

8-11 Direction of Propagation

Spatial gradients in electron-density can change the direction of propagation. When the electron density gradient is steep, part of the energy can be reflected. Reflection is important in the propagation of low frequencies (tens of kilohertz) over paths that are remote from the fireball. It also may be important in the propagation of much higher frequencies for paths that pass near the fireball, where high electron density gradients can exist.

Smaller electron-density gradients cause ray bending (refraction). Refraction in the ambient ionosphere (E- and F-region) is important for beyond-the-horizon propagation in the HF band. For radar systems, refraction in the D-region caused by nuclear-burst-produced ionization normally is accompanied by significant absorption. Possible exceptions may occur if the propagation path passes close to the fireball or close to regions ionized by beta particles (particularly when the propagation path is nearly parallel to the geomagnetic field lines). Changes in the E- and F-region electron density caused by the fireball or by traveling disturbances may modify HF and VHF propagation significantly. E- and F-region electron densities sufficient to change the direction of propagation at higher frequencies by a few degrees can occur without causing significant absorption.

8-12 Scatter and Scintillation

Inhomogeneities in the propagation medium (variations in the dielectric constant of the medium) cause a small amount of incident energy to be scattered away from the original propagation direction. The direction of scatter depends on the shape of the inhomogeneities and their orientation relative to that of the incident beam. Energy that is forward scattered as the wave traverses inhomogeneous regions can cause fluctuations in the amplitude and the phase of the wave, called scintillation. The phase fluctuations are equivalent to fluctuations in the direction of propagation that result in random variations in the angle of arrival of received signals. Small amounts of backscattered energy can produce interference to radar systems called clutter.

The analysis and quantitative description

[redacted]

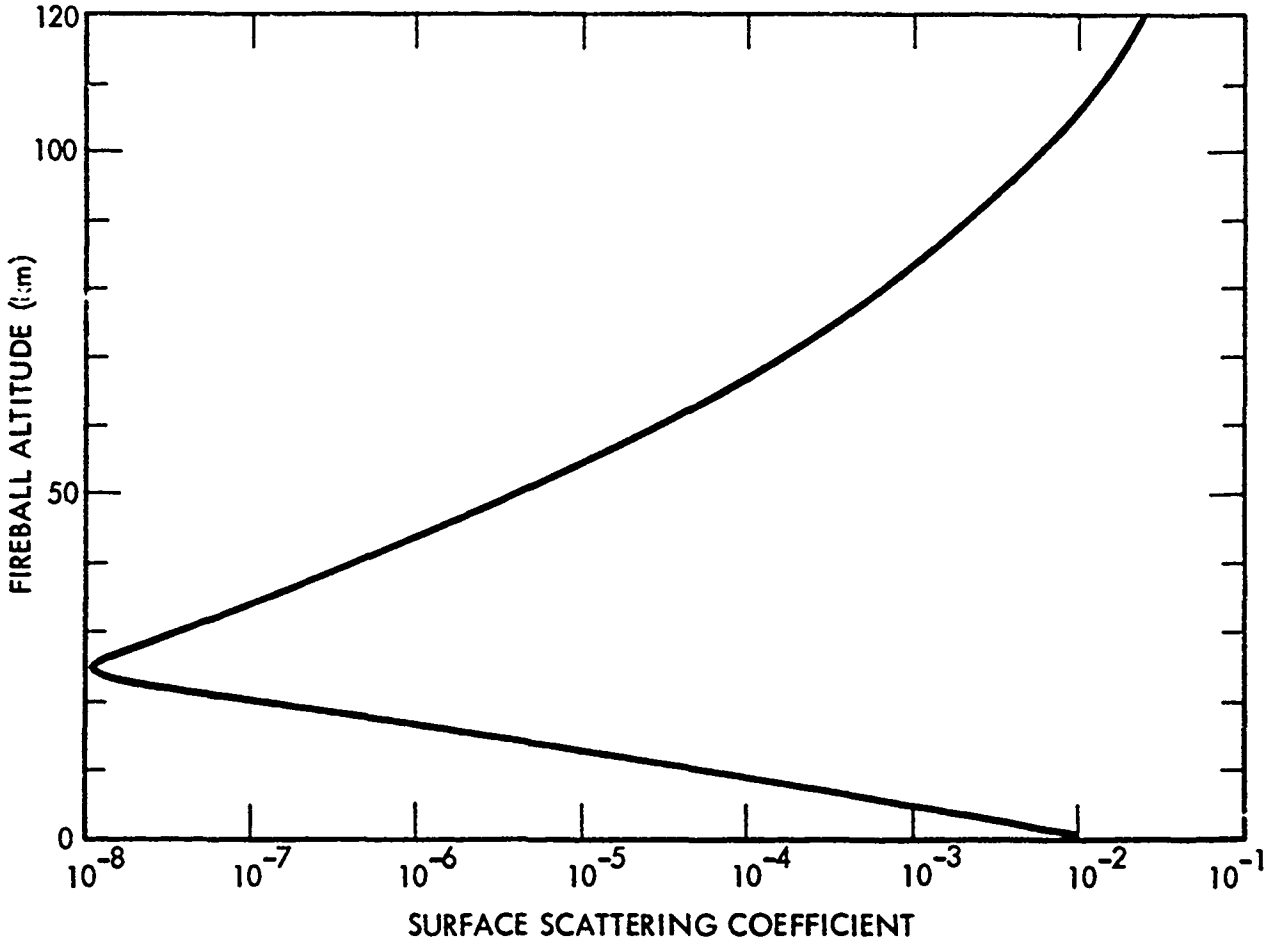

Figure 8-15. [redacted] Apparent Fireball Surface Scattering Coefficient at 400 MHz [redacted]

[redacted] of scatter requires a statistical model of the spatial distribution of inhomogeneities in the propagating medium. Sufficient information from which such models could be constructed for nuclear-weapon-produced ionization is not available. There are limited experimental data from nuclear weapon tests concerning backscatter; however, interpretation of these data is difficult, and sufficient information for the construction of a complete empirical model is not available.

[redacted] Significant backscatter has been observed from fireball regions from a few tens of seconds to a few minutes after burst. Figure 8-15 shows the general order of magnitude of the surface scattering coefficient (multiply by the area of the scattering surface to obtain radar cross section) derived from experimental data. Below about 20 km, scattering is apparently due to variations in air density across fireball boundaries and across shock waves. For surface bursts, dust, dirt, and water vapor appear to cause backscatter

[redacted]

[redacted]

[redacted]

from the stem of the rising cloud. Backscatter from fireballs above 20 km can be explained in terms of partial reflection, or scatter from inhomogeneities in electron density in the fireball or in the shock fronts. The cross section appears to decrease with increasing frequency. The minimum in the apparent cross section near 20 km is due to several mechanisms, the prime of which is the absorption sheath caused by beta particles escaping from the fireball. The scattering coefficients shown in Figure 8-15 are only illustrative; observed values vary over an order of magnitude, depending on the relative geometry of propagation path and fireball, the characteristics of radars used in obtaining the data, and the time after burst.

[redacted] Backscatter is also observed from regions of field-aligned ionization (ionized regions that are elongated along the geomagnetic field, often referred to as auroral ionization) which can be produced above about 80 km by beta particles. Field-aligned ionization can also occur within the fireball after a few tens of seconds for detonations above about 80 kilometers. The magnitude of backscatter is aspect sensitive; maximum backscatter occurs when the propagation path is normal to geomagnetic field lines. Backscatter from field-aligned ionization is thought to be a volume effect; volume scattering coefficients of about 10^{-13} m^2/m^3 at 400 MHz have been observed from beta-particle ionization regions. Significantly larger coefficients may occur from field-aligned ionization caused by the fireball. The cross section scales inversely as about the 4.5 power of frequency. Returns have been recorded for several hours after burst.

[redacted] SECTION II METHODS FOR CALCULATING ABSORPTION OF RADIO FREQUENCIES [redacted]

[redacted] As discussed previously, absorption frequently is the most important phenomena affecting propagation of radio frequencies; however, detailed solutions of absorption for propagation paths associated with communication and radar systems usually require numerous computations that cannot be obtained readily by hand calculations. The procedure for calculating absorption that are described below offer a means for obtaining reasonable estimates of radio frequency absorption for many situations of interest, however, the user should maintain awareness of the limitations defined for each of the calculations.

[redacted] The calculation of the absorption of radio frequencies will be described separately for three conditions: absorption of propagation paths going through the fireball, absorption caused by prompt radiation outside of the fireball, and absorption caused by delayed radiation outside of the fireball (this last condition is divided further into absorption caused by delayed gamma rays and absorption caused by delayed beta particles).

[redacted] Prior to the determination of the absorption along any of the paths discussed above, the size and location of the fireball region and/or the debris region must be determined. The spatial and temporal characteristics of the fireball and the debris regions created by nuclear bursts are complex. Idealized geometric models have been adopted for the purpose of analysis. The dimensions of three scaling models, based largely on interpolations of data from high-altitude nuclear tests, are used to represent detonations in three burst altitude regimes; below 80 kilometers, between 85 and 120 kilometers, and above 120 kilometers. The characteristics of the fireball and the debris are discussed separately for these three burst altitude regimes in succeeding paragraphs. Figure 8-16 illustrates the idealized geometric models referred to in the discussions. Dimensions shown in Figure 8-16 are defined in the discussions or in the illustrative problems that follow.

[redacted]

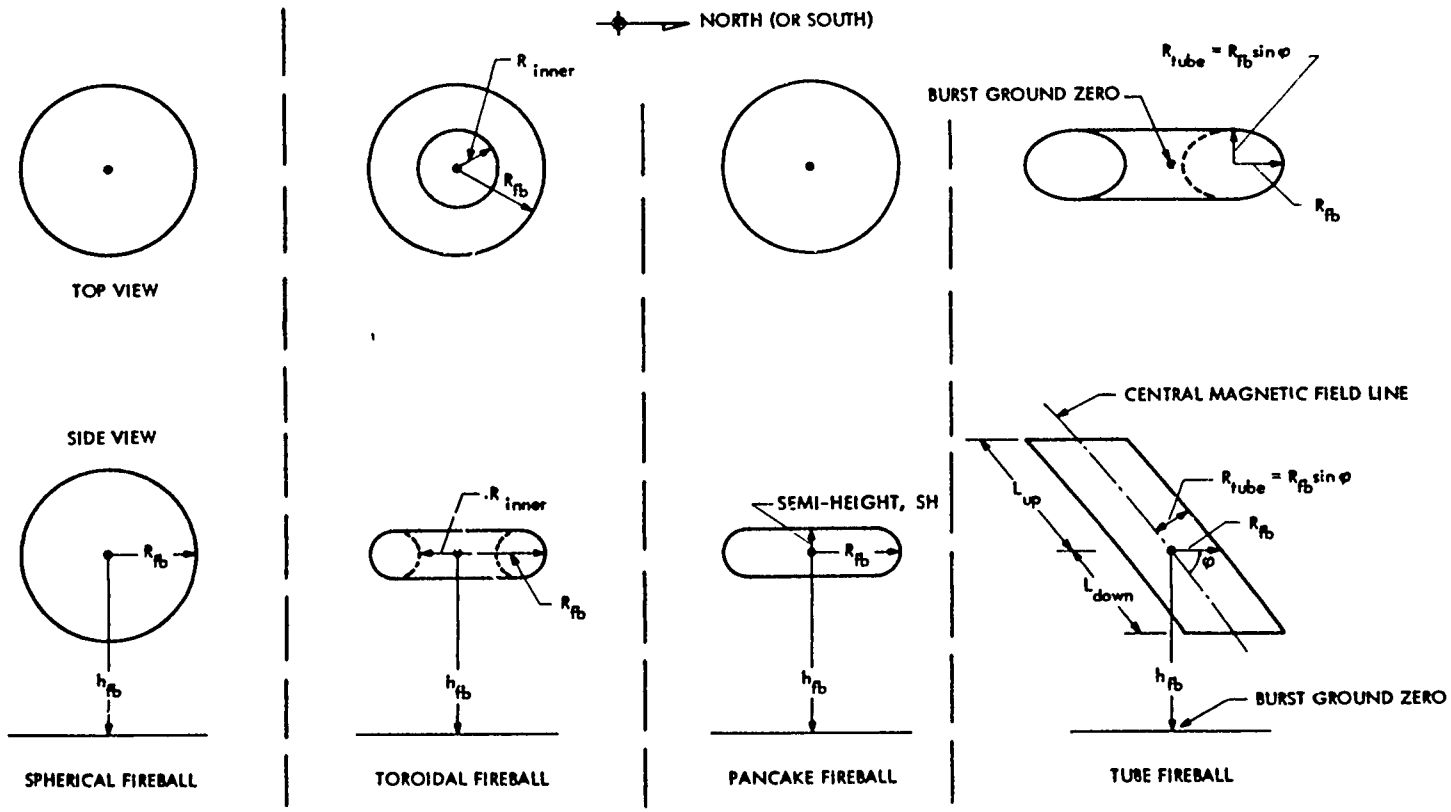

Figure 8-16. Examples of Fireball Geometry

[redacted]

8-13 Size and Location of Fireball and Debris Regions for Detonations Below 85 Kilometers [redacted]

[redacted] When a nuclear weapon is detonated at an altitude below about 85 kilometers, the fireball initially is a reasonably well defined and relatively small spherical region (see Chapter 1). After the fireball is formed, it expands and rises above the detonation point, carrying the fission debris with it. Depending on the weapon yield and the detonation altitude, the fireball may become toroidal in shape as it rises. After rising, the fireball will become stabilized in altitude and will diffuse into a pancake shape.

[redacted] If the fireball rises above 200 kilometers, it is assumed to fall back to 200 kilometers. If the peak altitude of the fireball is less than 200 kilometers, it is assumed to stabilize at its peak altitude.

[redacted] The initial fireball radius is the parameter used to determine whether the fireball will form a toroid. The toroid is assumed to transform into a pancake at 7 minutes after burst, with a vertical thickness equal to the vertical dimension of the toroid at 7 minutes. If the fireball does not form a toroid, the fireball is assumed to transform from a sphere to a pancake when the radius becomes 100 kilometers. The vertical thickness of the pancake is assumed to be 100 kilometers.

[redacted] The model provided for determining the location of the debris is intended for calculation of delayed-radiation (gamma rays and beta particles) effects. For times later than a few tens of minutes after burst, the size and location of the debris region will depend on atmospheric winds and diffusion, and the model may be considerably in error.

[redacted] Figures 8-19 through 8-25 are used to determine the spatial and temporal history of the fireball (and the debris), for bursts that occur below 85 kilometers.

8-14 Size and Location of Fireball and Debris Regions for Detonations Between 85 and 120 Kilometers [redacted]

[redacted] When a nuclear detonation occurs between 85 and 120 kilometers, the fireball transforms from a sphere to a cylinder or tube aligned along the geomagnetic field. The model used for the calculations described herein assumes that the fireball stabilizes at its maximum altitude above ground zero. The fireball radial dimension also is assumed to remain constant after 7 minutes. A fireball region is not defined for times longer than 2 hours after burst.

[redacted] Delayed radiation (gamma rays and beta particles) is assumed to be emitted from a single debris pancake, which is assumed to rise with the fireball and then to settle slowly along the geomagnetic field until it reaches 200 kilometers altitude at approximately 2 hours after burst. As the debris settles, the center is offset from ground zero toward the nearest magnetic pole, as illustrated in Figure 8-17. Figures 8-19 through 8-29 are used to determine the spatial and temporal history of the fireball (and the debris) for bursts that occur at altitudes between 85 and 120 kilometers.

8-15 Size and Location of Fireball and Debris Regions for Detonations Above 120 Kilometers [redacted]

[redacted] Theoretical and experimental data are incomplete for this altitude region; therefore, scaling relations are given only for a few parametric yields and detonation altitudes. Three shapes are used to model the fireball region: a sphere, a pancake, and a cylinder or tube aligned along the geomagnetic field. Figure 8-16 illustrates the fireball geometry.

[redacted] As the detonation altitude is increased above 120 kilometers, the debris is distributed over a larger region. Some debris can be transported across the magnetic equator. The single-pancake debris region used at lower altitudes to

[redacted]

[redacted]

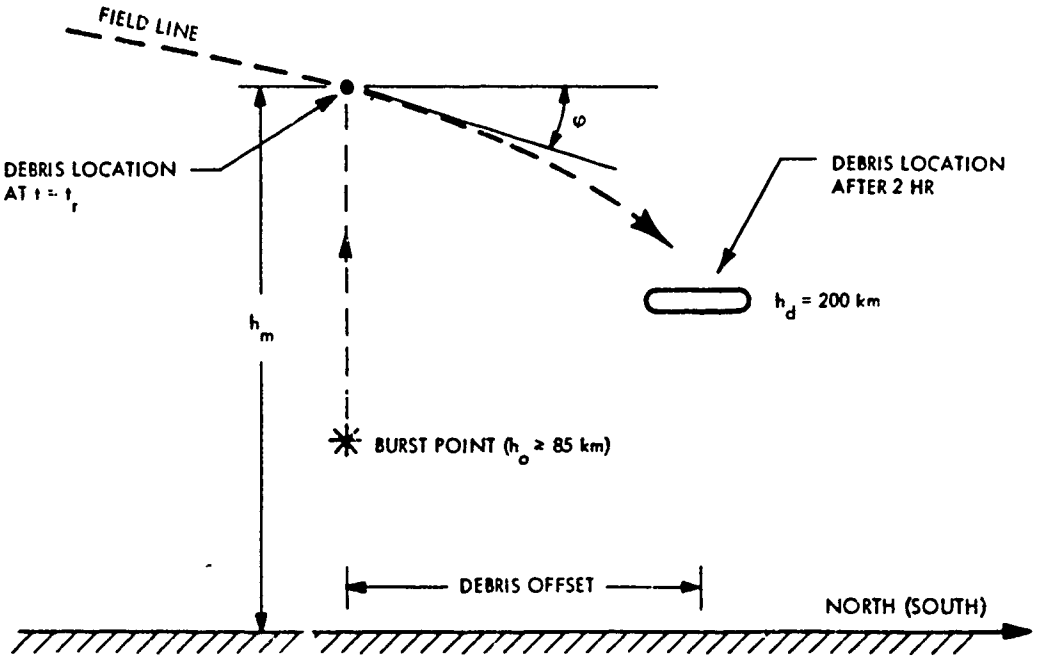

Figure 8-17. [redacted] Debris Behavior for Detonation Altitudes Greater Than 85 km [redacted]

[redacted]

model delayed radiation effects is not adequate, so multiple regions are used.

[redacted] Up to three debris regions are used to determine the delayed radiation resulting from detonations above 120 kilometers. Figure 8-18 illustrates the geometry. Two of these regions (Regions 1 and 2) model debris in the burst region, and the third (Region 3) models debris transported across the magnetic equator to the conjugate region. For convenience and because little is known about the debris location in the conjugate region, the beta-particle ionization in the burst and conjugate regions associated with Debris Region 3 is assumed to coincide with that associated with Debris Region 1. Debris Region 3 is used to compute gamma-ray ionization in the conjugate region. For weapons detonated above 250 kilometers, Region 2 is used to determine both gamma-ray and beta-particle ionization.

[redacted] in the model used herein, the fraction of debris transported across the magnetic equator is assumed to be independent of geomagnetic dip angle for detonations above 250 kilometers. A small amount of debris can reach the conjugate region for detonations below 250 kilometers and low dip angles. The time required for the debris to reach the conjugate region depends on detonation altitude and geomagnetic dip angle; however, for purposes of calculating delayed gamma radiation, the debris can be assumed to reach the conjugate region immediately after burst.

[redacted] About 20 percent of the debris for detonations above 120 kilometers is not accounted for in the model. This debris is assumed to escape to large distances; some may be carried into space and some may be spread world-wide. At least part of this debris will be trapped on the magnetic field lines above the burst. While this debris probably is not important for single bursts, it could cause significant delayed radiation after

[redacted]

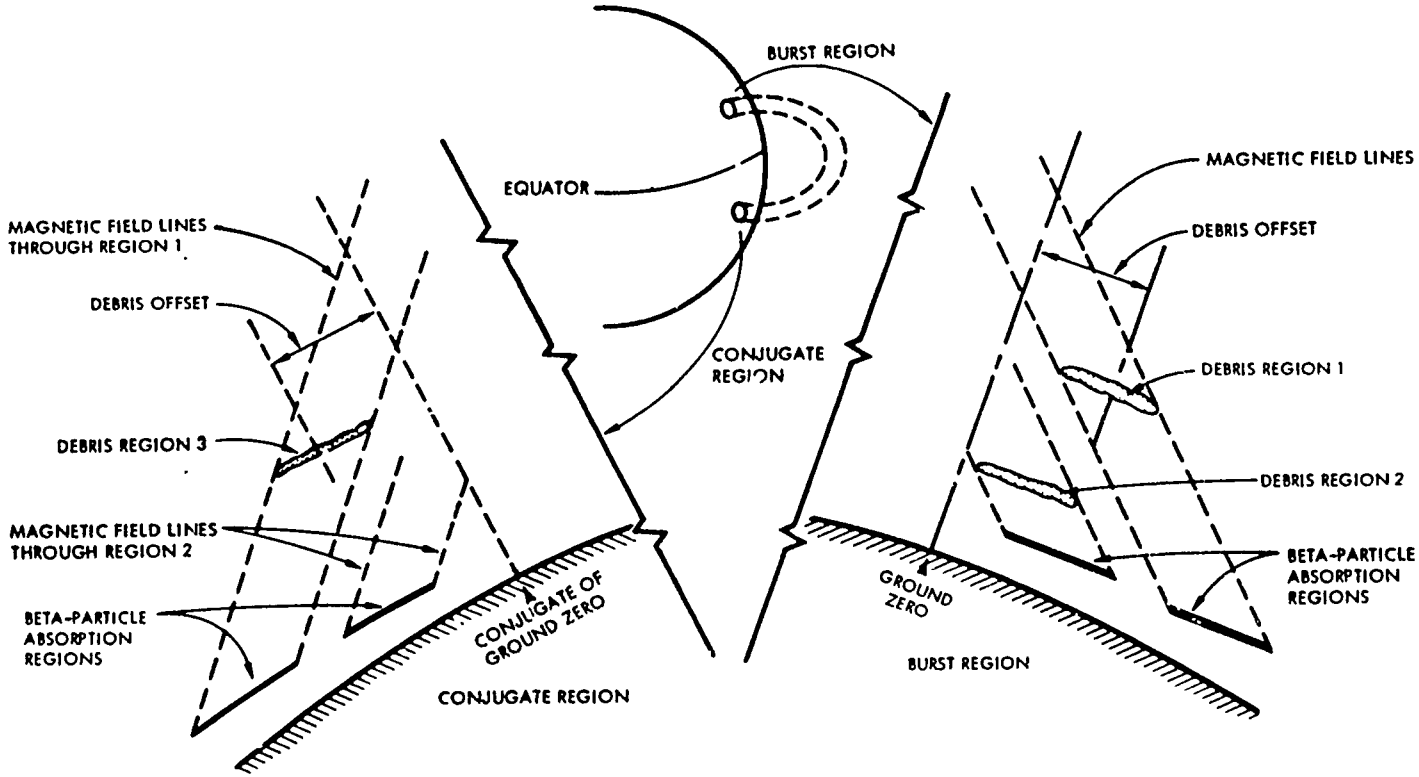

Figure 8-18. [redacted] Illustration of Debris and Beta-Particle Absorption Regions for Times Later Than 10 Minutes After Burst, H_0 Above 120 km [redacted]

[redacted]

[redacted]

multiple weapon detonations.

[redacted] After rising to peak altitude, the three debris regions are assumed to settle along the geomagnetic field lines until they reach 200 kilometers altitude at about 2 hours after burst. The debris regions are offset from ground zero or the conjugate of ground zero toward the magnetic pole.

[redacted]

[redacted]

Problem 8-1 Calculation of Fireball Size, Shape, and Location for a Burst Below 85 Kilometers

[redacted] Figures 8-19 through 8-25 contain families of curves with which the size, shape, and location of the fireball resulting from a nuclear detonation below 85 kilometers may be estimated. For bursts in this altitude regime, the debris altitude h_d is assumed to be the same as the fireball altitude h_{fb}. The debris is distributed non-uniformly within the fireball region. However, for simplified calculations of delayed radiation effects, the debris region can be assumed to be a thin pancake region with radius R_d equal to the fireball radius R_{fb}.

[redacted] The altitude of the fireball at a time t after burst is obtained from Figures 8-19 through 8-22 by a series of steps, as follows:

1. Enter Figure 8-19 with the weapon yield and detonation altitude h_o to obtain h_r, the distance the fireball will rise above the detonation point. The maximum fireball altitude, h_m, is

$$h_m = h_o + h_r \text{ km.}$$

Enter Figure 8-20 with h_r to obtain the time required to reach maximum altitude t_r. If $t \geqslant t_r$ and $h_m \leqslant 200$ km, go to 3; otherwise go to 2.

2. If $t < t_r$, enter Figure 8-21 with time after burst and h_r to obtain h_N, an altitude normalizing factor. If $h_m > 200$ km, enter Figure 8-22 with $\tau = t/t_r$ to obtain f_h, the fireball height factor.

3. Compute h_{fb}, the fireball altitude at time t:

$$h_{fb} = \begin{cases} (h_o + h_N h_r) \text{ km} & \text{when } t < t_r \\ h_m \text{ km} & \text{when } t \geqslant t_r,\ h_m < 200 \\ [200 + f_h\,(h_m - 200)] \text{ km} & \text{when } t > t_r,\ h_m > 200 \end{cases}$$

[redacted] The radius and shape of the fireball at a time t after burst are obtained from Figures 8-23 through 8-25, as follows:

1. Enter Figure 8-23 with weapon yield and detonation altitude h_o to obtain the initial fireball radius R_o. If $R_o < 4$ km, go to 2; otherwise go to 3 when $t < 7$ minutes or go to 4 when $\geqslant 7$ minutes.

2. Determine t_{toroid}, the time of toroid formation, from Figure 8-24 by selecting the fireball radius curve for the value of R_o determined above, by locating the intercept of this curve with the toroid formation time curve, and by reading t_{toroid} on the abscissa.

3. Enter Figure 8-24 with the time of interest t and the initial fireball radius R_o. Determine R_{fb}, the fireball radius at time t, then go to 5.

4. Enter Figure 8-24 with $t = 7$ minutes and the initial fireball radius R_o; obtain the fireball radius at 7 minutes after burst, $R_{fb}(7)$. Enter Figure 8-25 with t and h_m to obtain ΔR. Compute R_{fb}, as follows:

$$R_{fb} = R_{fb}(7) + \Delta R.$$

5. The fireball will be a

sphere if $R_o \leqslant 4$ km and $t < t_{toroid}$, or if

$$R_o > 4 \text{ km and } R_{fb} < 100 \text{ km;}$$

toroid if $R_o < 4$ km and $t_{toroid} \leqslant t < 7$ minutes;

pancake if $R_o \leqslant 4$ km and $t \geqslant 7$ minutes, or if

$$R_o > 4 \text{ km and } R_{fb} \leqslant 100 \text{ km.}$$

If the fireball shape is a toroid, compute the inner toroid radius:

$$R_{inner} = \frac{R_{fb}}{2}$$

[redacted]

[redacted]

[redacted]

If the fireball shape is a pancake, compute the pancake semithickness:

$$SH = \begin{cases} \frac{1}{4} R_{fb}(7) & R_o \leqslant 4 \text{ km} \\ 50 & R_o > 4 \text{ km.} \end{cases}$$

[redacted] *Example* [redacted]

Given: A 1 Mt weapon burst at an altitude of 50 km.

Find: The size, shape, and location of the fireball and debris region 2 minutes after the burst.

Solution:

a. From Figure 8-19 $h_r \approx 50$ km for a 1 Mt weapon burst at 50 km.

b. $h_m = h_o + h_r = 50 + 50 = 100$ km.

c. From Figure 8-20, $t_r = 10$ min for $h_r = 50$ km.

d. From Figure 8-21, $h_N = 0.6$ for $t = 2$ min and $h_r = 50$ km.

e. Since $t < t_r$,

$$h_{fb} = h_o + h_N h_r = 50 + (0.6)(50) = 80 \text{ km}$$

f. From Figure 8-23, $R_o = 2$ km for a 1 Mt weapon detonation at 50 km.

g. From Figure 8-24, $t_{toroid} = 1.7$ min for $R_o = 2$ km.

h. From Figure 8-24, $R_{fb} = 30$ km 2 min after a burst with $R_o = 2$ km.

i. Since $t_{toroid} < t < 7$ minutes, the fireball shape is a toroid, and

$$R_{inner} = \frac{R_{fb}}{2} = \frac{30}{2} = 15 \text{ km.}$$

Answer: The fireball is a toroid centered at 80 kilometers altitude. The outer radius is 30 kilometers and the inner radius is 15 kilometers (see Figure 8-16). The altitude and radius of the debris pancake are 80 kilometers and 30 kilometers, respectively.

[redacted] *Reliability* [redacted] The size and location of the debris region depend on atmospheric winds and diffusion. Since these effects are neglected in the model described herein, the results predicted by the model may be considerably in error.

[redacted] *Related Material* [redacted] See paragraph 8-13.

[redacted]

[redacted]

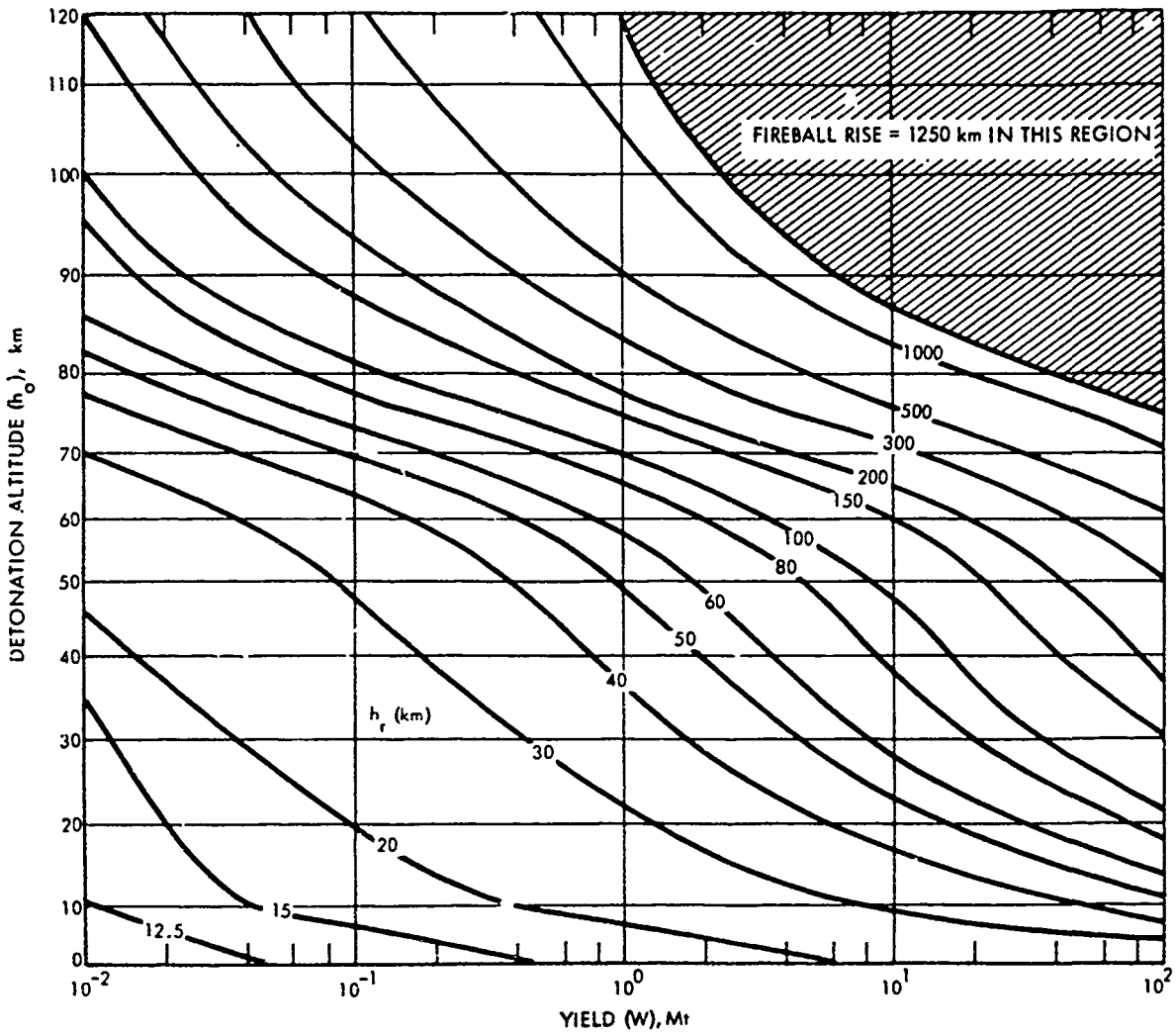

Figure 8-19. [redacted] Maximum Fireball Rise [redacted]

[redacted]

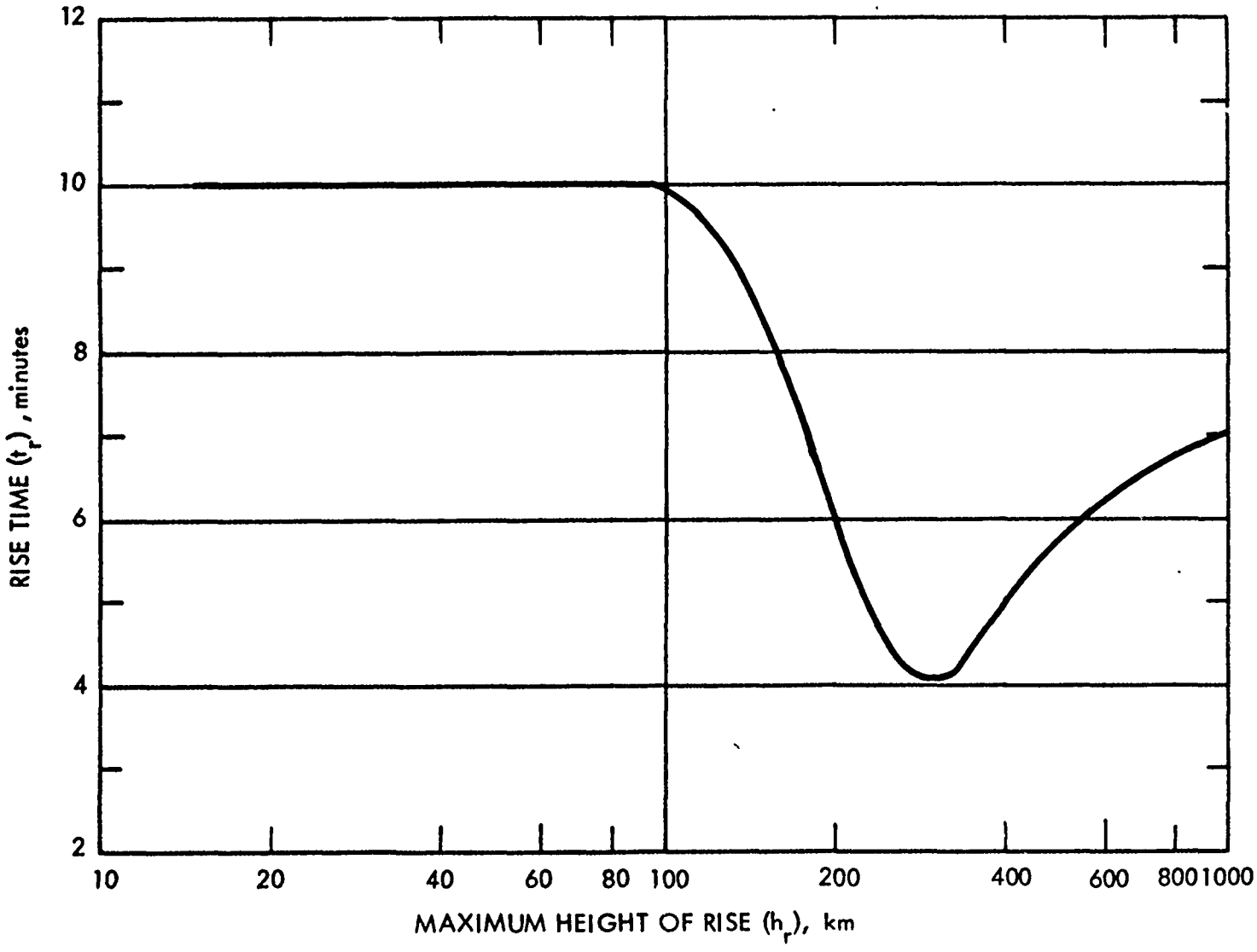

Figure 8-20. [redacted] Time for Fireball to Reach Its Maximum Altitude [redacted]

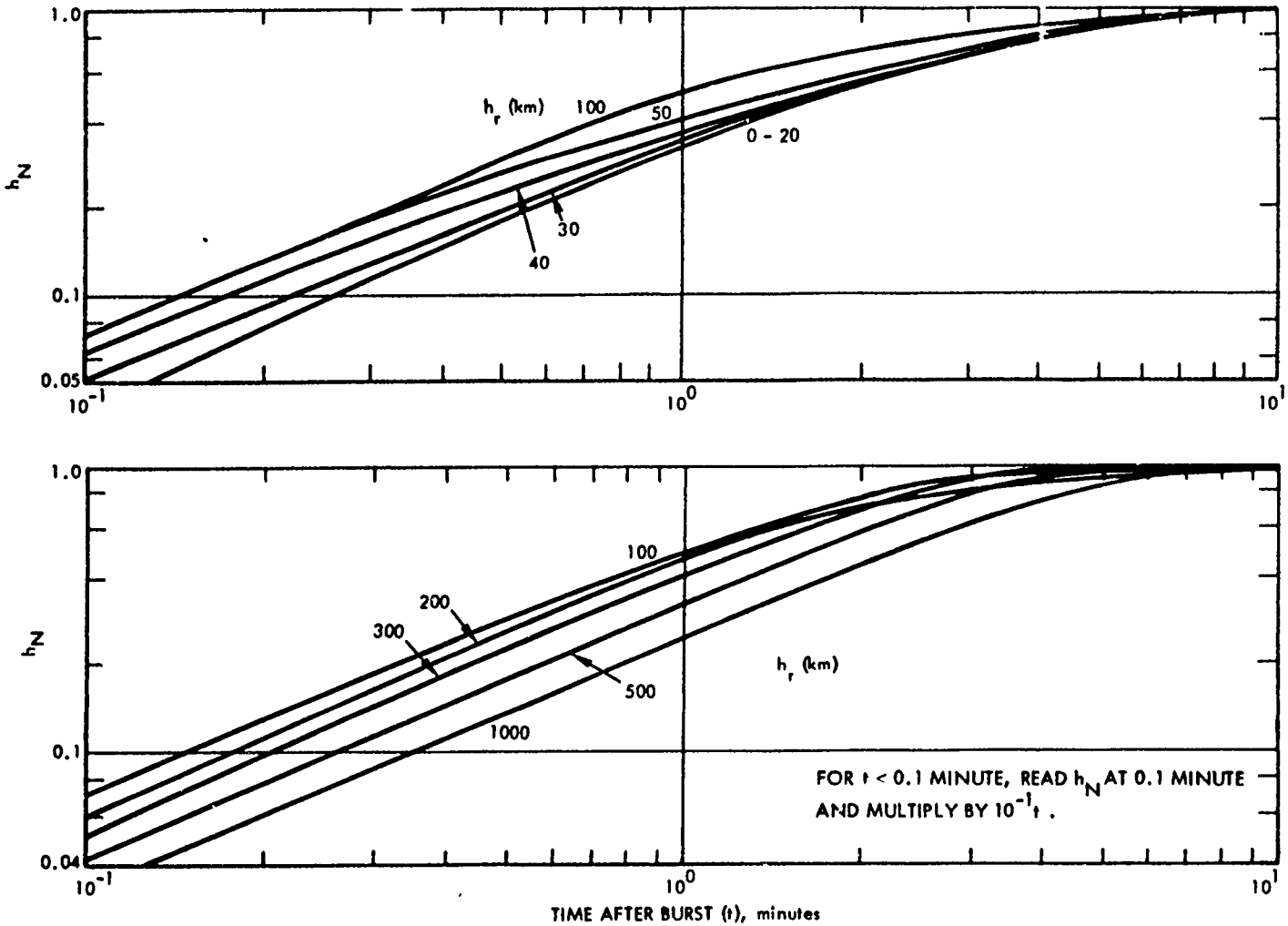

Figure 8-21. [redacted] Altitude Normalizing Factor h_N [redacted]

[redacted]

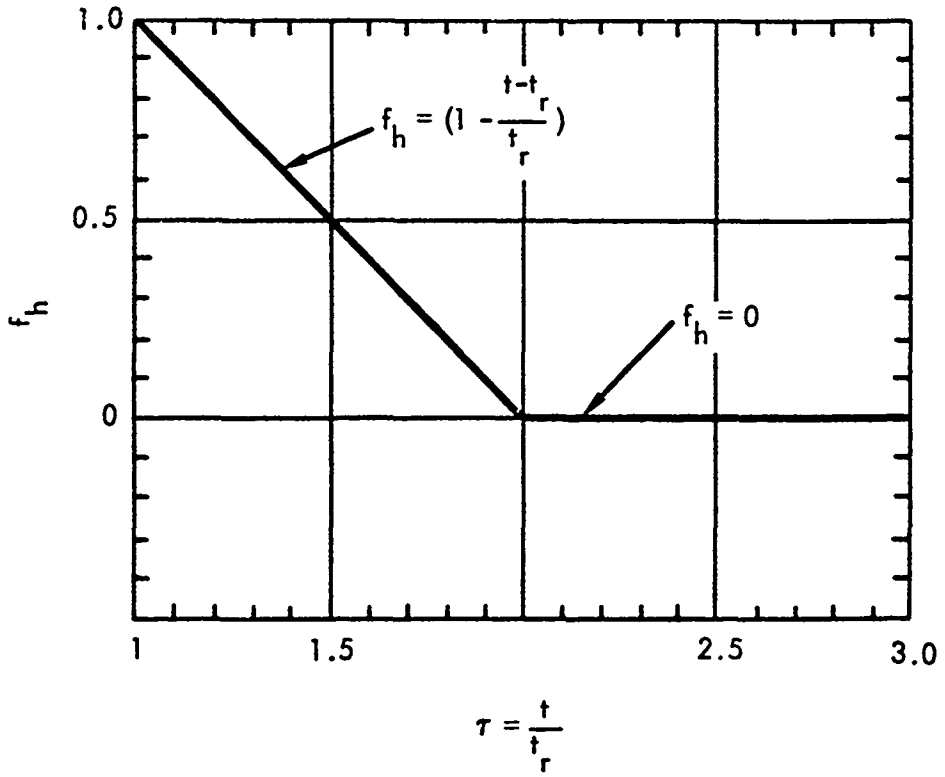

Figure 8-22. [redacted] Fireball Height Factor [redacted]

[redacted]

[redacted]

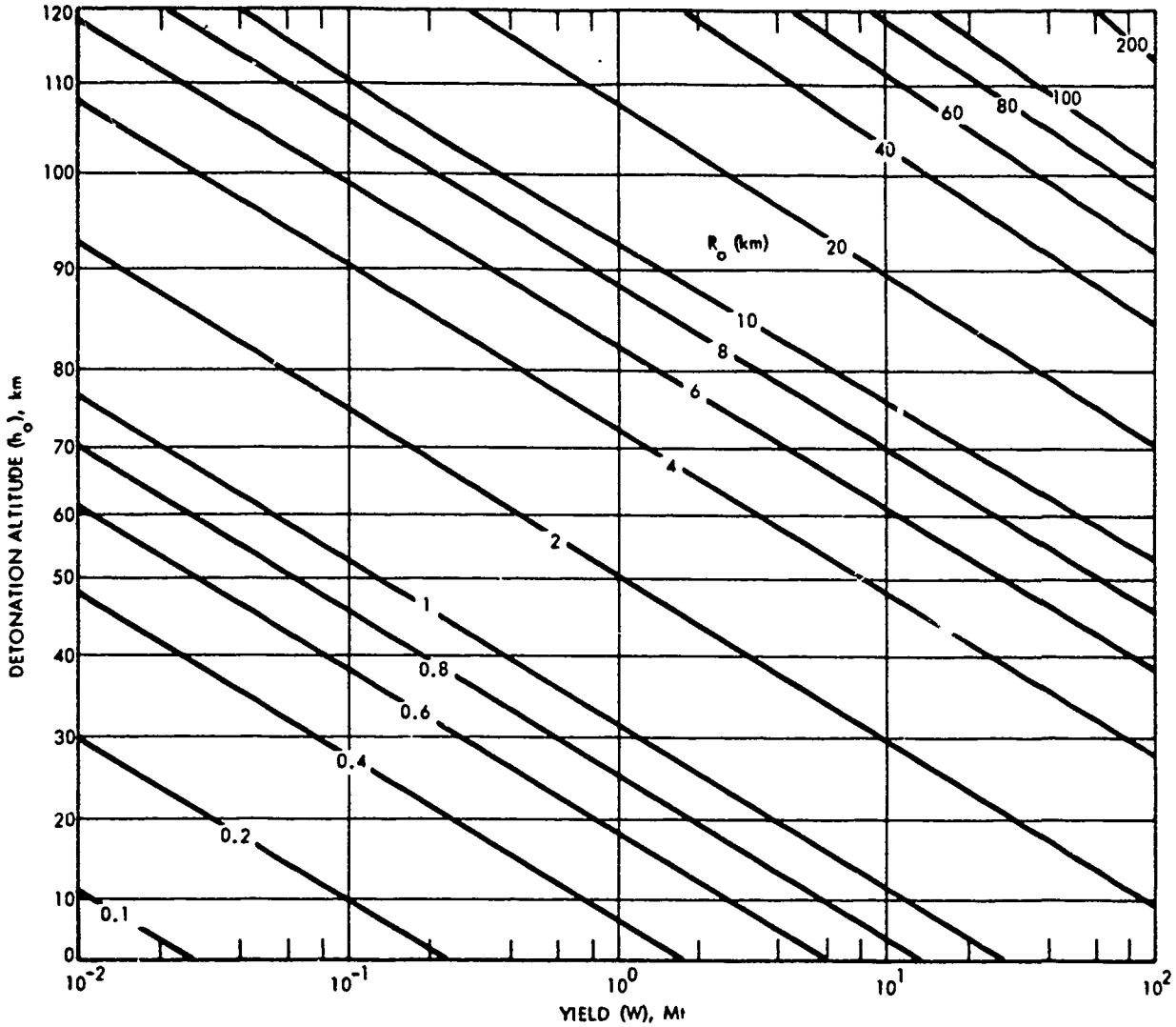

Figure 8-23. [redacted] Initial Fireball Radius [redacted]

[redacted]

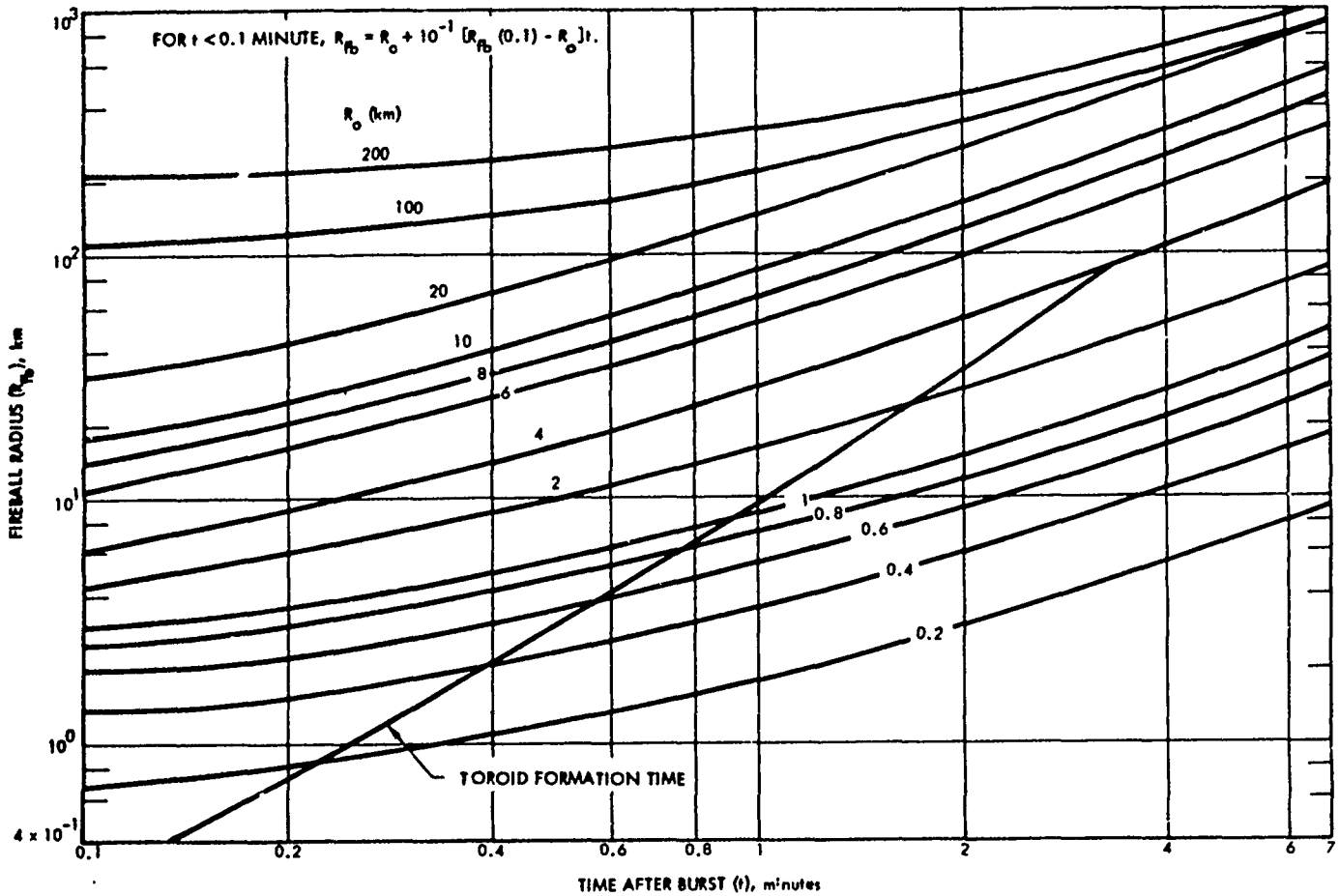

Figure 8-24. [redacted] Fireball Radius [redacted]

[redacted]

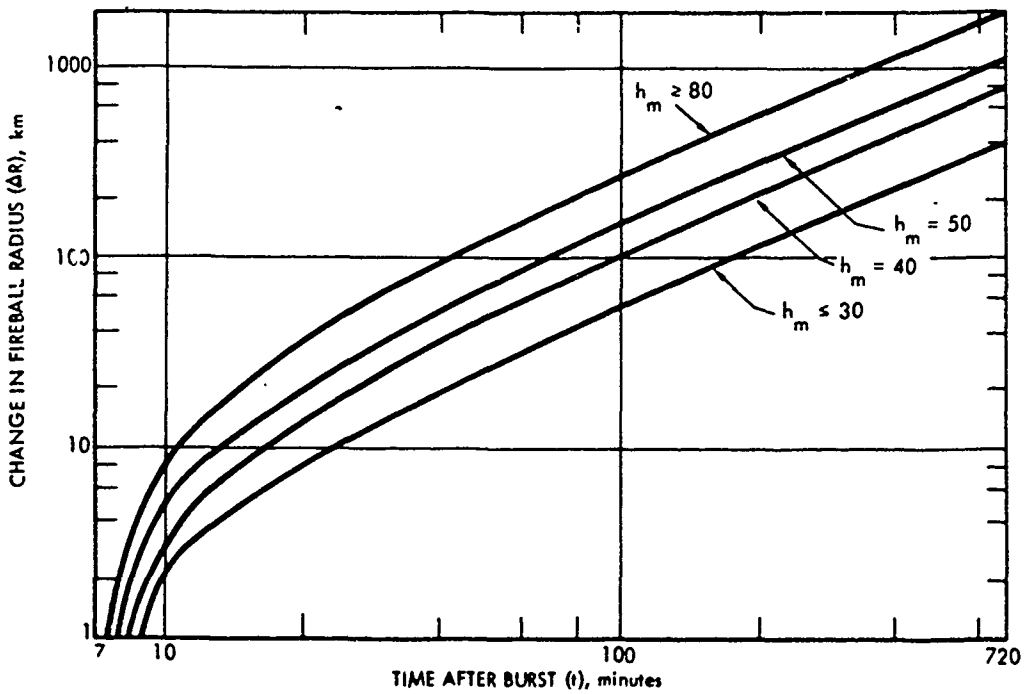

Figure 8-25. [redacted] Change in Fireball/Debris-Region Radius After Sever Minutes [redacted]

[redacted]

[redacted]

Problem 8-2 Calculation of Fireball Size, Shape, and Location for a Burst Between 85 and 120 kilometers

[redacted] Figures 8-19 through 8-29 contain families of curves with which the size, shape, and location of the fireball resulting from a nuclear detonation between 85 and 120 kilometers may be estimated. For bursts in this altitude regime, the fireball transforms from a sphere to a cylinder or tube aligned along the geomagnetic field line. A fireball region is not defined for times after burst greater than 2 hours.

[redacted] The altitude of the fireball at a time t after burst is obtained from Figures 8-19 through 8-21 by a series of steps, as follows:

1. Enter Figure 8-19 with weapon yield W and detonation altitude h_o to obtain h_r, the distance the fireball will rise above the detonation point. The maximum fireball altitude, h_m, is

$$h_m = h_r + h_o \quad km.$$

Enter Figure 8-20 with h_r to obtain the time to reach maximum altitude t_r. If $t \geqslant t_r$ go to 3; otherwise go to 2.

2. If $t < t_r$, enter Figure 8-21 with time after burst and h_r to obtain h_N, and altitude normalizing factor.

3. Compute h_{fb}, the fireball altitude at time t:

$$h_{fb} = \begin{cases} (h_o + h_N h_r) \quad km \\ \qquad t < t_r \text{ minutes} \\ h_m \quad km \\ \qquad t_r < t < 120 \text{ minutes} \end{cases}$$

[redacted] The radius and shape of the fireball at a time t after burst are obtained from Figures 8-23, 8-24, and 8-26, as follows:

1. Enter Figure 8-23 with weapon yield and detonation altitude h_o to obtain fireball radius R_o. Enter Figure 8-26 with weapon yield to obtain the magnetic equilibrium radius R_{eq}. Determine the time to reach R_{eq}, t', from Figure 8-24 by selecting the fireball radius curve for the value of R_o obtained from Figure 8-23 and by determining the time when the fireball radius (R_{fb}) is equal to R_{eq}. If $t > t'$, go to 3; otherwise go to 2.

2. Enter Figure 8-24 with t and R_o to obtain R_{fb}, the fireball radius at time t. Go to Step 4.

3. Compute R_{fb}:

$$R_{fb} = \begin{cases} (R_{eq} + (t - t')\, R_o \quad km \\ \qquad t < 7 \text{ minutes,} \\ (R_{eq} + (7 - t')\, R_o) \quad km \\ \qquad t \geqslant 7 \text{ minutes.} \end{cases}$$

4. The fireball shape will be a

sphere if $t < t'$

tube if $t \geqslant t'$.

[redacted] If the time of interest t is greater than t', the time to reach the magnetic equilibrium radius, the tube fireball dimensions are obtained as follows:

1. If $t' > t_r$ (obtained from Figure 8-20 above), go to 2; otherwise enter Figure 8-21 with $t = t'$ and h_r (from Figure 8-19) and obtain $h_N(t')$.

2. Compute $h_{fb}(t')$:

$$h_{fb}(t') = \begin{cases} (h_o + h_N(t')h_r) \quad km \\ \qquad t' \leqslant t_r \text{ minutes,} \\ h_m \quad km \\ \qquad t' > t_r \text{ minutes.} \end{cases}$$

Compute the altitude of the base of the

[redacted]

[redacted]

[redacted]

tube h_b (h_b is taken as the altitude of the base if $h_b > 200$ km):

$$h_b = h_{fb}(t') - R_{eq} \quad km.$$

Compute the length of the fireball up the tube in the direction of the magnetic field line, L_{up}:

$$L_{up} = 6\ (t - t')\ R_o + R_{fb} \quad km.$$

Compute the quantity L':

$$L' = \begin{cases} \dfrac{h_{fb} - h_b}{\sin \varphi}\ km & h_b \leqslant 200 \text{ km} \\[2ex] \dfrac{h_{fb} - 200}{\sin \varphi}\ km & h_b > 200 \text{ km,} \end{cases}$$

where φ is the magnetic dig angle at the burst location. If the magnetic dip angle is not known for the burst location, it can be determined from Figure 8-54. The length of the fireball down the tube will be the smaller of L_{up} and L'.

[redacted] If the time of interest t is equal to or less than t_r, the time to reach maximum altitude, or if the maximum fireball altitude, h_m, is less than 200 kilometers, the debris altitude, h_d, is determined from the fireball altitude as described below. If the time of interest is equal to or greater than the time to reach maximum altitude ($t \geqslant t_r$), and the maximum fireball altitude is greater than 200 kilometers ($h_m > 200$), Figure 8-27 is entered with the quantity $(t - t_r)$ to obtain the debris height factor f_h. The debris altitude is then determined as follows:

$$h_d = \begin{cases} h_{fb} \quad km \\ \qquad t \leqslant t_r \text{ min} \\[2ex] h_m \quad km \\ \qquad t \geqslant t_r \text{ min, } h_m \leqslant 200 \text{ km} \\[2ex] [200 + f_h(h_m - 200)] \quad km \\ \qquad t \geqslant t_r \text{ min, } h_m \geqslant 200 \text{ km} \end{cases}$$

[redacted] If the maximum fireball altitude, h_m, is equal to or less than 200 kilometers, the debris offset is zero (see Figure 8-17). If h_m is greater than 200 kilometers, enter Figure 8-28 with h_m and the magnetic dip angle, φ, to obtain the maximum debris offset D_d. Then enter Figure 8-29 with the quantity $(t - t_r)$ to obtain a value of the debris offset correction factor f_o. The debris offset, Δd, is:

$$\Delta d = f_o D_d \quad (h_m > 200 \text{ km}).$$

[redacted] The radius of the debris is obtained from previously determined dimensions, as follows:

$$R_d = \begin{cases} R_{fb} \quad km \\ \qquad t \leqslant 120 \text{ minutes} \\[2ex] [R_{eq} + (7 - t')\ R_o \\ \qquad + 3\ (t - 120)] \quad km \\ \qquad t > 120 \text{ minutes} \end{cases}$$

[redacted] *Example* [redacted]

Given: A 1 Mt weapon burst at an altitude of 100 km, at a location where the magnetic dip angle, φ, is 60°.

Find: The shape, size, and location of the fireball, and the altitude, radius, and offset of the debris region 20 minutes after the burst.

Solution:

a. From Figure 8-19, h_r = 800 km for a 1 Mt weapon burst at 100 km.

b. $h_m = h_r + h_o = 800 + 100 = 900$ km.

c. From Figure 8-20, t_r = 7 minutes for h_r = 800 km.

d. Since $t_r < t$,

$$h_{fb} = h_m = 900 \text{ km}$$

e. From Figure 8-23, R_o = 15 km for a 1 Mt burst at 100 km altitude.

[redacted]

[redacted]

[redacted]

f. From Figure 8-26, R_{eq} = 100 km for a 1 Mt weapon.

g. From Figure 8-24, t' = 0.9 min for R_o = 15 km and $R_{fb} = R_{eq}$ = 100 km.

h. Since $t > 7$ min, the fireball shape is a tube, and

$$R_{fb} = R_{eq} + (7 - t')\,R_o$$
$$= 100 + (6.1)(15) = 192 \text{ km}$$

i. From Figure 8-21, $h_N(t)$ = 0.25 for $t = t'$ = 0.9 min and h_r = 800 km.

j. Since $t' < t_r$,

$$h_{fb}(t') = h_o + h_N(t')\,h_r$$
$$= 100 + (0.25)(800) = 300 \text{ km.}$$

k. The height of the fireball base is

$$h_b = h_{fb}(t') - R_{eq} = 300 - 100 = 200 \text{ km}$$

l. The length up the fireball tube is

$$L_{up} = 6(t - t')\,R_o + R_{fb}$$
$$= (6)(19.1)(15) + 192 = 1911 \text{ km}$$

m. Since h_b = 200 km, the quantity L' is

$$L' = \frac{h_{fb} - h_b}{\sin\varphi} = \frac{900 - 200}{0.87} = 810 \text{ km}$$

n. Since $L' < L_{up}$

$$L_{down} = L' = 810 \text{ km.}$$

o. Since $t > t_r$ and $h_m > 200$ km, the quantity f_h must be determined from Figure 8-27. Entering Figure 8-27 with $t - t_r$ = 13, the quantity is determined to be

$$f_h = 0.9.$$

The altitude of the debris is, therefore,

$$h_d = 200 + f_h(h_m - 200)$$
$$= 200 + (0.9)(900 - 200) = 830 \text{ km.}$$

p. From Figure 8-28, the maximum debris offset D_d = 350 km for $\varphi = 60°$ and h_m = 900 km. From Figure 8-29, the debris offset correction factor is f_o = 0.1 for $(t - t_r)$ = 13 min. Therefore, the debris offset is

$$\Delta d = f_o D_d = (0.1)(350) = 35 \text{ km.}$$

q. Since $t < 120$ minutes,

$$R_d = R_{fb} = 192 \text{ km.}$$

Answer:

a. The fireball is a tube with dimensions as follows (refer to Figure 8-16):

$$h_{fb} = 900 \text{ km,}$$
$$R_{fb} = 192 \text{ km,}$$
$$L_{up} = 1911 \text{ km,}$$
$$L_{down} = 810 \text{ km.}$$

b. The debris region is a pancake with a radius of 192 km centered at an altitude of 830 km. It is offset 35 km towards the north pole from the burst point (refer to Figure 8-17).

[redacted] *Reliability* [redacted] The size and location of the fireball and debris, particularly late time debris expansion, are affected by atmospheric winds and diffusion. Since these effects are neglected in the model described herein, the results predicted by the model may be considerably in error.

[redacted] *Related Material* [redacted] See paragraph 8-14.

[redacted]

[redacted]

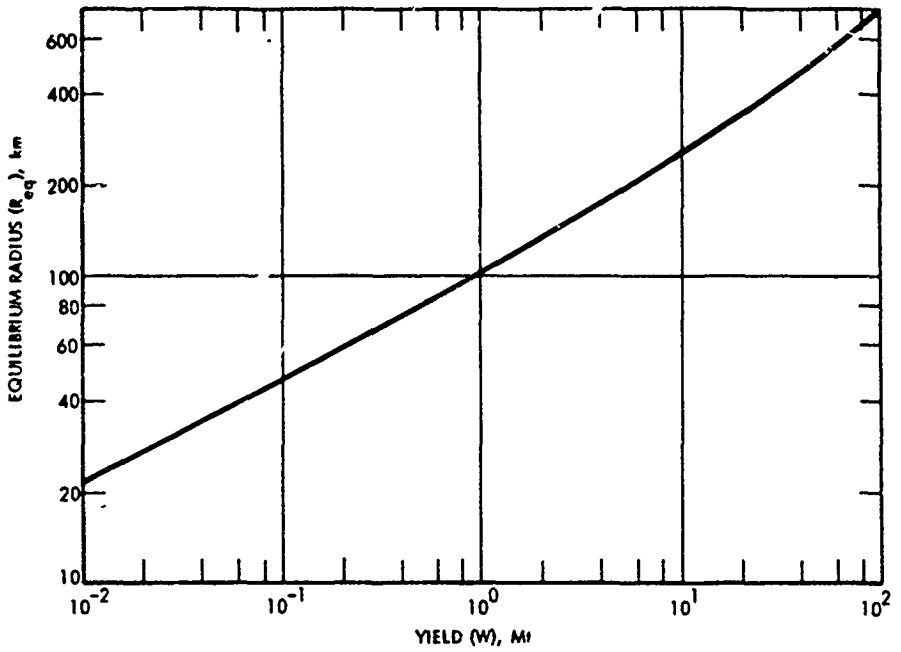

Figure 8-26. [redacted] Magnetic Equilibrium Radius [redacted]

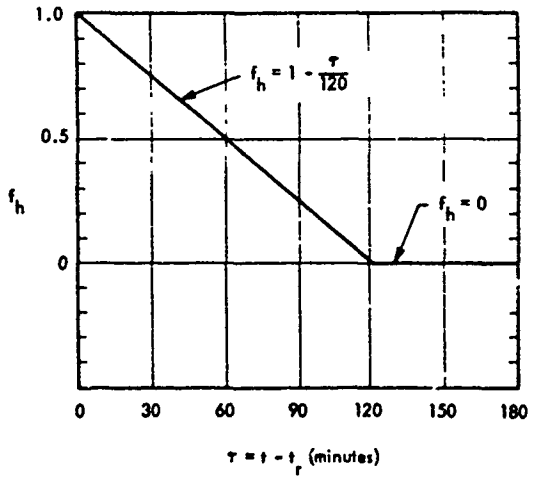

Figure 8-27. [redacted] Debris Height Factor [redacted]

[redacted]

[redacted]

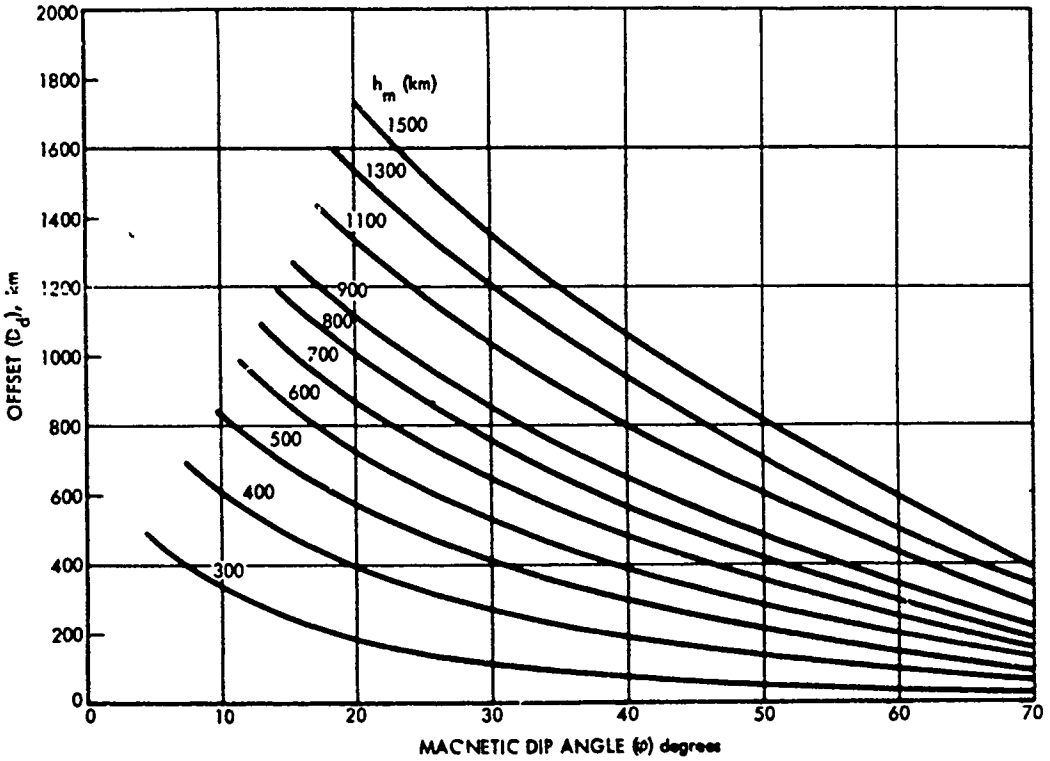

Figure 8-28. [redacted] Maximum Debris Offset [redacted]

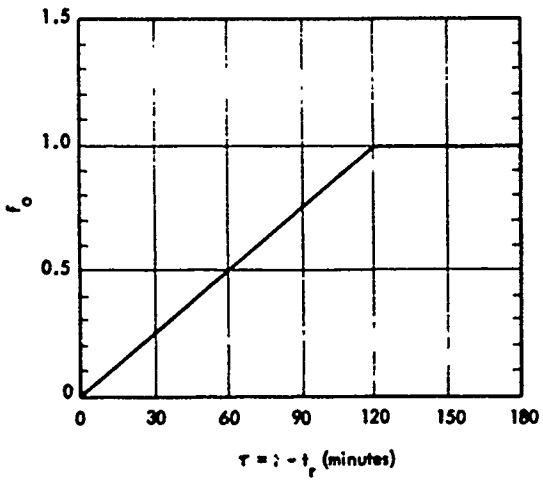

Figure 8-29. [redacted] Debris Offset Correction Factor [redacted]

[redacted]

[redacted]

Problem 8-3 Calculation of Size, Shape, and Location of Fireball and Debris Regions for a Burst Above 120 kilometers

[redacted] Table 8-2 and Figures 8-27 through 8-38 contain data with which estimates may be made of the size, shape, and location of the fireball and the debris regions for nuclear detonations above 120 kilometers. As discussed in paragraph 8-15 and shown in Figure 8-18, three separate debris regions are considered. Three shapes are used to model the fireball region: a sphere, a pancake, and a tube (cylinder) along the geomagnetic field. The shapes are illustrated in Figure 8-16.

[redacted] Table 8-2 is used to determine the fireball size, shape, and location (note that time after burst is given in *seconds* in Table 8-2). The table provides relations for a few parametric yields and detonation altitudes. In view of the uncertainties in both theoretical and experimental data in this burst altitude regime, interpolation between sections of Table 8-2 is not warranted. Data provided in the table for the yield and altitude combination nearest to those desired should be used. If either the desired yield or the desired detonation altitude is midway between values given in the table, values for the next higher yield and/or detonation altitude should be used. The phenomenology is very uncertain for yields greater than 10 Mt. If estimates are required for yields greater than 10 Mt, the dimensions and location given for a 10 Mt burst should be used. Table 8-2 indicates the shape of the fireball for the various yields and burst altitudes as a function of time (in seconds) after burst. The size and location of the fireball are determined as described below.

1. If the fireball is a sphere, the fireball altitude, h_{fb}, and fireball radius, R_{fb}, are read directly from Table 8-2 for the time of interest.

2. If the fireball is a pancake, the fireball altitude, h_{fb}, and the fireball radius, R_{fb}, are read directly from Table 8-2 for the time of interest. The semithickness of the pancake in kilometers (see Figure 8-16) is equal to the value shown in the column headed "x" in Table 8-2. Together, these values provide the size and location of the fireball at the desired time.

3. If the fireball is a tube, the fireball altitude, h_{fb}, and fireball radius, R_{fb}, are once again read directly from Table 8-2. The fireball lengths up and down the tube (see Figure 8-16) are determined from the values in the columns headed "x" and "y" in Table 8-2, as follows:

$$L_{down} = \frac{h_{fb} - 200}{|\sin \varphi|} \text{ km, or}$$

$$L_{down} = \frac{x}{2|\sin \varphi|} \quad \text{whichever is smaller,}$$

$$L_{up} = \frac{y}{2|\sin \varphi|} \text{ km,}$$

where φ is the magnetic dip angle at the burst point. If the magnetic dip angle is not known, it can be obtained from Figure 8-54. A negative value for y in Table 8-2 means that both x and y are dimensions down the geomagnetic field and the fireball is below h_{fb}.

[redacted] Figures 8-30 through 8-38 contain families of curves with which the size and location of the three debris regions may be estimated. Once again, the uncertainties in the data are such that interpolation between figures is not warranted. Data on the figure for the yield nearest to that desired should be used. If the desired yield is midway between values provided, data for the next higher value should be used.

[redacted] The fraction of the total weapon debris in each of the debris regions is obtained by use of Figure 8-30 and the calculations described below. Enter Figure 8-30 with the magnetic dip angle φ and the altitude of detonation h_o to obtain the fraction of debris going to debris region

[redacted]

[redacted]

[redacted]

3, X (see Figure 8-18). Compute the fraction of the debris in each of the three regions as follows:

$$FF1 = \begin{cases} 0.8 - X & h_o \leqslant 250 \text{ km}, \\ 0.6 - X & h_o > 250 \text{ km}, \end{cases}$$

$$FF2 = \begin{cases} 0 & h_o \leqslant 250 \text{ km}, \\ 0.2 & h_o > 250 \text{ km}, \end{cases}$$

$$FF3 = X,$$

where FF1, FF2, and FF3 are the fractions of total weapon debris in regions 1, 2, and 3, respectively. The sum of the three fractions is always less than 1.0, since some debris is assumed to escape to long distances (see paragraph 8-15).

[redacted] The altitude, h_d, for debris region 1 is obtained from Figures 8-31 through 8-34 by selecting the figure with the yield closest to that desired, and by determining h_{d1} for the time and burst altitude of interest. The maximum altitude to which the debris rises in region 1, h_{m1} should also be obtained for use in determining the debris offset as described later.

[redacted] The debris radius, R_{d1}, for debris region 1 is obtained from Figures 8-35 through 8-38 by selecting the figure with the yield closest to that desired, and by determining R_{d1} for the time and burst altitude of interest.

[redacted] If $t \leqslant 10$ minutes, the offset for debris region 1, Δd, is zero. If $t > 10$ minutes, the offset of debris region 1 is determined as follows.

1. Obtain the maximum debris offset D_d from Figure 8-28 for $h_m = h_{m1}$, as determined above, and the magnetic dip angle, φ, of interest.
2. Calculate τ:

$$\tau = t - 10 \text{ min.}$$

Enter Figure 8-29 with τ to obtain the debris offset correction factor f_o.

3. The offset of debris region 1 is

$$\Delta d_1 = f_o D_d \quad \text{km.}$$

[redacted] Debris region 2 is only defined for bursts above 250 km. The size and location are determined by a series of steps, as follows. If $t \leqslant 10$ minutes, go to 2; otherwise go to 1.

1. Enter Figure 8-27 with $\tau = t - 10$ min to obtain the debris height correction factor f_h.
2. Compute the maximum altitude, h_{m2}, for debris region 2:

$$h_{m2} = h_o + 500\ W^{1/3} \text{ km}$$

Compute the altitude for debris region 2 at time t:

$$h_{d2} = \begin{cases} h_{m2} \text{ km} & t \leqslant 10 \text{ min}, \\ 200 + f_h(h_o + 500\ W^{1/3} - 200) \text{ km} & t > 10 \text{ min}, \end{cases}$$

where W is the weapon yield in megatons.

3. Compute the radius for debris region 2, R_{d2}:

$$R_{d2} = \begin{cases} 500\ W^{1/3} \text{ km} & t \leqslant 120 \text{ min}, \\ 500\ W^{1/3} + 3\ (t - 120) \text{ km} & t > 120 \text{ min}, \end{cases}$$

4. If $t \leqslant 10$ minutes, the debris offset, Δd_2, equals zero. If $t > 10$ minutes, Δd_2 is determined from Figures 8-28 and 8-29. Enter Figure 8-28 with magnetic dip angle, φ, and $h_m = h_{m2}$ to obtain D_d. Calculate τ:

$$\tau = t - 10 \text{ min.}$$

Enter Figure 8-29 to obtain the debris offset

[redacted]

[redacted]

[redacted]

correction factor, f_o. Calculate Δd_2, the debris offset for region 2:

$$\Delta d_2 = D_d f_o.$$

[redacted] The debris altitude, radius, and offset for debris region 3 are assumed to be the same as those determined for debris region 1, but they are located in the magnetic conjugate area (see Figure 8-18).

[redacted] *Example* [redacted]

Given: A 1 Mt weapon detonated at 250 km altitude at a location where the magnetic dip angle is 60°.

Find: The shape, size, and location of the fireball, and the altitude, radius, and offset of the debris regions 2 minutes after the burst.

Solution:

a. Since the altitude of interest is midway between the altitudes provided in Table 8-2, the larger (300 km) is used. From the data provided in Table 8-2 for 1 Mt at a burst altitude of 300 km, the following values are obtained for t = 120 sec:

Fireball shape is a tube.

$$h_{fb} = 290 \text{ km}$$

$$R_{fb} = 150 \text{ km}$$

$$x = 160$$

$$y = 300$$

b.

$$(1) \quad \frac{h_{fb} - 200}{|\sin \varphi|} = \frac{290 - 200}{0.87} = 103 \text{ km.}$$

$$(2) \quad \frac{x}{2|\sin \varphi|} = \frac{160}{(2)(0.87)} = 92 \text{ km.}$$

Since the result obtained in (2) is less than that obtained in (1),

$$L_{down} = 92 \text{ km.}$$

$$L_{up} = \frac{y}{2|\sin \varphi|} = \frac{300}{(2)(0.87)} = 172 \text{ km.}$$

c. From Figure 8-30, the fraction of debris transported to debris region 3, X, is 0.2 for a burst altitude of 250 km. Therefore,

$$FF1 = 0.6$$

$$FF2 = 0$$

$$FF3 = 0.2$$

d. From Figure 8-33,

$$h_{d1} = 625 \text{ km, and}$$

$$h_{m1} = 800 \text{ km.}$$

e. From Figure 8-37,

$$R_{d1} = 150 \text{ km.}$$

f. Since $t < 10$ min, $\Delta d_1 = 0$.

g. Since the burst altitude is not greater than 250 km, no debris region 2 is defined.

h. The size and altitude of debris region 3 are the same as those of debris region 1, but debris region 3 is centered over the magnetic conjugate of the burst point.

Answer:

a. The fireball is a tube with the following dimensions (see Figure 8-16 for illustration of the meaning of the dimensions):

$$h_{fb} = 290 \text{ km}$$

$$R_{fb} = 150 \text{ km}$$

$$L_{down} = 92 \text{ km}$$

$$L_{up} = 172 \text{ km}$$

b. There are two debris pancake regions for use in determining delayed radiation effects. Debris region 1 is a pancake centered over the burst point with an altitude and radius of 625 km and 150 km, respectively. Debris region 3 is a pancake directly over the conjugate of the burst

[redacted]

[redacted]

[redacted]

point, and it has the same altitude and radius as debris region 1. Sixty percent of the fission debris is in debris region 1, and twenty percent is in debris region 3. (Twenty percent is assumed to escape to large distances.)

[redacted] *Reliabilit*[redacted] Because of the theoretical and experimental uncertainties concerning bursts above 120 km, together with the uncertainties introduced by using fixed parametric yield/detonation altitude combinations, results predicted by the model described above may be considerably in error.

[redacted] *Related Material*[redacted] See paragraph 8-15.

[redacted]

Table 8-2 [redacted] Fireball Location and Dimensions for Detonations Above 80 km [redacted]

Time is in seconds, distances are in kilometers. E refers to the power of 10, e.g., 1.5E4 = 1.5×10^4.

10 kt, 150 km

t	Shape	h_{fb}	R_{fb}	x	y
1	Sphere	1.5E2	1.2E1		
3	"	1.6E2	1.3E1		
10	"	1.6E2	1.7E1		
30	Tube	1.9E2	2.2E1	3.0E1	3.0E1
60	"	2.1E2	2.6E1	6.0E1	6.0E1
120	"	2.4E2	3.2E1	1.0E2	1.0E2
300	"	2.6E2	5.1E1	1.4E2	2.2E2
600	"	2.7E2	6.3E1	1.6E2	4.4E2
900	"	"	"		6.4E2
1800	"	"	"		1.4E3

10 kt, 200 km

t	Shape	h_{fb}	R_{fb}	x	y
1	Sphere	2.0E2	1.8E1		
3	"	2.1E2	1.9E1		
10	Tube	"	2.2E1	4.0E1	4.0E1
30	"	2.3E2	2.3E2	5.0E1	5.0E1
60	"	2.6E	2.6E1	6.0E1	6.0E1
120	"	2.8E2	3.2E1	1.0E2	1.0E2
300	"	3.0E2	4.9E1	1.4E2	2.0E2
600	"	"	6.1E1	"	4.2E2
900	"	"	"	"	6.0E2
1800	"	"	"	"	1.3E3

10 kt, 300 km

t	Shape	h_{fb}	R_{fb}	x	y
1	Tube	3.1E2	3.2E1	4.0E1	4.0E1
3	"	"	"	"	"
10	"	3.2E2	3.3E1	5.0E1	5.0E1
30	"	3.4E2	3.5E1	6.0E1	6.0E1
60	"	3.7E2	3.8E1	8.0E1	8.0E1
120	"	4.0E2	4.5E1	1.4E2	1.4E2
300	"	4.2E2	6.5E1	2.6E2	2.6E2
600	"	4.3E2	7.8E1	4.0E2	4.8E2
900	"	"	"	"	7.0E2
1800	"	"	"	"	1.5E3

10 kt, 400 km

t	Shape	h_{fb}	R_{fb}	x	y
1	Tube	4.1E2	4.7E1	6.0E1	6.0E1
3	"	"	4.8E1	"	"
10	"	4.2E2	4.9E1	8.0E1	8.0E1
30	"	4.[illegible]2	5.1E1	1.0E2	1.0E2
60	"	[illegible]2	5.5E1	1.2E2	1.2E2
120	"	5.2E2	6.3E1	1.6E2	1.6E2
300	"	5.4E2	8.4E1	3.0E2	3.0E2
600	"	5.5E2	1.0E2	5.6E2	5.6E2
900	"	"	"	"	8.0E2
1800	"	"	"	"	1.9E3

Table 8-2 Fireball Location and Dimensions for Detonations Above 80 km (Continued)

Time is in seconds, distances are in kilometers. E refers to the power of 10, e.g., 1.5E4 = 1.5×10^4.

10 kt, 500 km

t	Shape	h_{fb}	R_{fb}	x	y
1	Tube	5.1E2	6.5E1	8.0E1	8.0E1
3	"	5.2E2	6.5E1	"	"
10	"	"	6.6E1	1.0E2	1.0E2
30	"	5.6E2	6.9E1	1.2E2	1.2E2
60	"	5.9E2	7.3E1	1.4E2	1.4E2
120	"	6.4E2	8.2E1	2.0E2	2.0E2
300	"	6.6E2	1.0E2	3.4E2	3.4E2
600	"	6.7E2	1.2E2	6.2E2	6.2E2
900	"	"	"	8.8E2	8.6E2
1800	"	"	"	"	1.9E3

100 kt, 150 km

t	Shape	h_{fb}	R_{fb}	x	y
1	Sphere	1.6E2	2.7E1		
3	"	"	2.9E1		
10	"	1.8E2	3.6E1		
30	Tube	2.3E2	4.8E1	8.0E1	8.0E1
60	"	2.9E2	5.5E1	1.2E2	1.2E2
120	"	3.9E2	6.8E1	2.0E2	2.0E2
300	"	4.8E2	1.0E2	4.4E2	4.4E2
600	"	"	1.3E2	5.2E2	8.4E2
900	"	"	"	"	1.2E3
1800	"	"	"	"	2.6E3

100 kt, 200 km

t	Shape	h_{fb}	R_{fb}	x	y
1	Sphere	2.1E2	4.0E1		
3	"	2.2E2	4.2E1		
10	Tube	2.3E2	4.7E1	6.0E1	6.0E1
30	"	2.7E2	5.1E1	8.0E1	8.0E1
60	"	3.3E2	5.6E1	1.2E2	1.2E2
120	"	4.2E2	6.8E1	2.0E2	2.0E2
300	"	4.8E2	1.0E2	4.2E2	4.2E2
600	"	"	1.2E2	5.2E2	7.8E2
900	"	"	"	"	1.2E3
1800	"	"	"	"	2.4E3

100 kt, 300 km

t	Shape	h_{fb}	R_{fb}	x	y
1	Tube	3.2E2	7.0E1	1.0E2	1.0E2
3	"	3.3E2	7.1E1	8.0E1	8.0E1
10	"	3.4E2	7.2E1	1.2E2	1.2E2
30	"	3.9E2	7.6E1	1.4E2	1.4E2
60	"	4.6E2	8.3E1	1.8E2	1.8E2
120	"	5.7E2	9.6E1	2.6E2	2.6E2
300	"	6.7E2	1.3E2	5.2E2	5.2E2
600	"	"	1.6E2	9.0E2	8.6E2
900	"	"	"	"	1.3E3
1800	"	"	"	"	2.9E3

Table 8-2 [redacted] Fireball Location and Dimensions for Detonations Above 80 km (Continued) [redacted]

Time is in seconds, distances are in kilometers. E refers to the power of 10, e.g., 1.5E4 = 1.5 x 10^4.

100 kt, 400 km

t	Shape	h_{fb}	R_{fb}	x	y
1	Tube	4.3E2	1.1E2	1.4E2	1.4E2
3	"	4.4E2	"	"	"
10	"	4.6E2	"	1.6E2	1.6E2
30	"	5.1E2	"	1.8E2	1.8E2
60	"	5.8E2	1.2E2	2.2E2	2.2E2
120	"	7.1E2	1.3E2	3.4E2	3.4E2
300	"	8.5E2	1.7E2	7.0E2	7.0E2
600	"	"	2.0E2	1.1E3	1.1E3
900	"	"	"	1.3E3	1.5E3
1800	"	"	"	"	3.3E3

100 kt, 500 km

t	Shape	h_{fb}	R_{fb}	x	y
1	Tube	5.5E2	1.4E2	2.0E2	2.0E2
3	"	"	1.5E2	"	"
10	"	5.7E2	"	"	2.2E2
30	"	6.3E2	"	2.4E2	2.4E2
60	"	7.1E2	1.6E2	3.0E2	3.0E2
120	"	8.5E2	1.8E2	5.0E2	5.0E2
300	"	1.0E3	2.2E2	6.4E2	8.0E2
600	"	"	2.5E2	1.1E2	1.2E3
900	"	"	"	1.6E2	1.8E3
1800	"	"	"	"	3.6E3

1 Mt, 150 km

t	Shape	h_{fb}	R_{fb}	x	y
1	Sphere	1.8E2	6.1E1		
3	"	1.9E2	6.4E1		
10	"	2.2E2	7.7E1		
.0	Tube	3.0E2	1.1E2	1.4E2	1.4E2
60	"	4.2E2	1.2E2	2.2E2	2.2E2
120	"	6.5E2	1.4E2	3.6E2	3.6E2
300	"	1.1E3	2.0E2	8.0E2	8.0E2
600	"	1.2E3	2.5E2	1.4E3	1.4E3
900	"	"	"	2.0E3	2.0E3
1800	"	"	"	"	4.8E3

1 Mt, 200 km

t	Shape	h_{fb}	R_{fb}	x	y
1	Sphere	2.4E2	9.1E1		
3	"	2.5E2	9.5E1		
10	Tube	2.8E2	1.1E2	1.4E2	1.4E2
30	"	3.5E2	1.1E2	2.0E2	2.0E2
60	"	4.6E2	1.2E2	2.4E2	2.4E2
120	"	6.7E2	1.4E2	4.0E2	4.0E2
300	"	1.0E3	2.0E2	8.0E2	8.0E2
600	"	1.1E3	2.4E2	1.4E3	1.4E3
900	"	"	"	1.8E3	2.0E3
1800	"	"	"	"	4.6E3

Table 8-2 [redacted] Fireball Location and Dimensions for Detonations Above 80 km (Continued) [redacted]

Time is in seconds, distances are in kilometers. E refers to the power of 10, e.g., 1.5E4 = 1.5×10^4.

1 Mt, 300 km

t	Shape	h_{fb}	R_{fb}	x	y
1	Pancake	2.2E2	1.5E2	9.1E0	
3	"	"	"	1.7E1	
10	"	2.5E2	"	4.6E1	
30	Tube	2.9E2	"	1.1E2	1.1E2
60	"	"	"	1.6E2	1.6E2
120	"	"	"	"	3.0E2
300	"	"	"	"	6.5E2
600	"	"	"	"	2.4E3
900	"	"	"	"	3.6E3
1800	"	"	"	"	8.0E3

Mt, 400 km

t	Shape	h_{fb}	R_{fb}	x	y
1	Pancake	2.8E2	2.2E2	1.1E1	
3	"	2.9E2	"	2.2E2	
10	"	3.3E2	"	6.2E2	
30	Tube	3.9E2	"	2. E2	2.8E2
60	"	"	"	"	4.0E2
120	"	"	"	"	6.6E2
300	"	"	"	"	1.4E3
600	"	"	"	"	2.6E3
900	"	"	"	"	3.8E3
1800	"	"	"	"	8.2E3

1 Mt, 500 km

t	Shape	h_{fb}	R_{fb}	x	y
1	Pancake	3.4E2	3.0E2	1.2E1	
3	"	3.5E2	"	2.7E1	
10	"	4.0E2	"	8.0E1	
30	Tube	4.8E2	"	3.2E2	3.4E2
60	"	"	"	"	4.6E2
120	"	"	"	"	7.2E2
300	"	"	"	"	1.4E3
600	"	"	"	"	2.6E3
900	"	"	"	"	3.8E2
1800	"	"	"	"	8.2E3

10 Mt, 150 km

t	Shape	h_{fb}	R_{fb}	x	y
1	Sphere	2.5E2	1.5E2		
3	"	2.6E2	1.5E2		
10	"	2.9E2	1.7E2		
30	"	3.9E2	2.1E2		
60	"	5.2E2	2.7E2		
120	Tube	7.9E2	3.0E2	5.2E2	5.2E2
300	"	1.3E3	3.7E2	1.0E3	1.0E3
600	"	1.5E3	4.1E2	1.8E3	1.8E3
900	"	"	"	2.6E3	2.6E3
1800	"	"	"	"	5.6E3

Table 8-2 [redacted] Fireball Location and Dimensions for Detonations Above 80 km (Concluded) [redacted]

Time is in seconds, distances are in kilometers. E refers to the power of 10, e.g., 1.5E4 = 1.5×10^4.

10 Mt, 200 km

t	Shape	h_{fb}	R_{fb}	x	y
1	Sphere	3.4E2	2.2E2		
3	"	3.5E2	2.3E2		
10	"	3.8E2	2.4E2		
30	Tube	4.8E2	2.7E2	3.8E2	3.8E2
60	"	6.1E2	2.8E2	4.4E2	4.4E2
120	"	8.8E2	3.0E2	5.2E2	6.2E2
300	"	1.4E3	3.7E2	1.0E3	1.0E3
600	"	1.6E3	4.2E2	2.0E3	2.0E3
900	"	"	"	2.8E3	2.8E3
1800	"	"	"	"	5.6E3

10 Mt, 300 km

t	Shape	h_{fb}	R_{fb}	x	y
1	Pancake	1.6E2	3.1E2	7.6E0	
3	"	1.7E2	"	1.3E1	
10	"	1.8E2	"	3.1E1	
30	Tube	2.1E2	"	1.2E2	1.6E2
60	"	"	"	"	2.8E2
120	"	"	"	"	5.4E2
300	"	"	"	"	1.2E3
600	"	"	"	"	2.4E3
900	"	"	"	"	3.6E3
1800	"	"	"	"	8.0E3

10 Mt, 400 km

t	Shape	h_{fb}	R_{fb}	x	y
1	Pancake	2.0E2	4.7E2	8.6E0	
3	"	2.1E2	"	1.6E1	
10	"	2.3E2	"	4.1E1	
30	Tube	2.7E2	"	1.6E2	2.0E2
60	"	"	"	"	3.2E2
120	"	"	"	"	5.8E2
300	"	"	"	"	1.3E3
600	"	"	"	"	2.5E3
900	"	"	"	"	3.7E3
1800	"	"	"	"	8.1E3

10 Mt, 500 km

t	Shape	h_{fb}	R_{fb}	x	y
1	Pancake	2.4E2	6.4E2	9.6E0	
3	"	2.5E2	"	1.9E1	
10	"	2.8E2	"	5.1E1	
30	Tube	3.2E2	"	1.8E2	2.4E2
60	"	"	"	"	3.6E2
120	"	"	"	"	6.2E2
300	"	"	"	"	1.3E3
600	"	"	"	"	2.6E3
900	"	"	"	"	3.8E3
1800	"	"	"	"	8.2E3

[redacted]

[redacted]

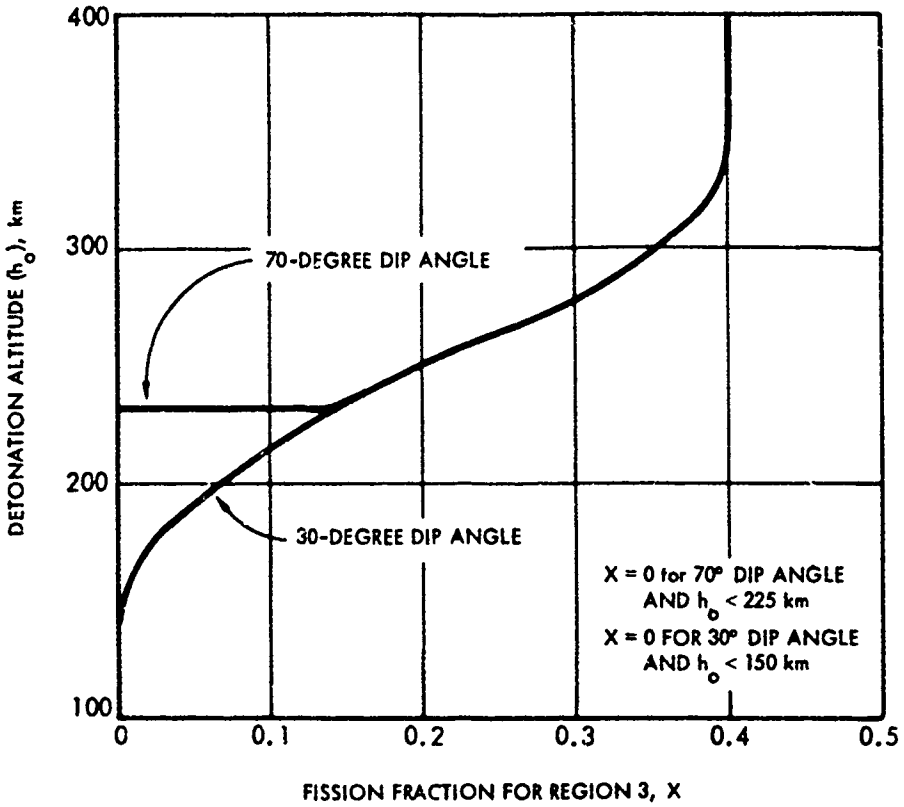

Figure 8-30. [redacted] Fraction of Total Debris Transported to Conjugate Region (Region 3) [redacted]

[redacted]

[redacted]

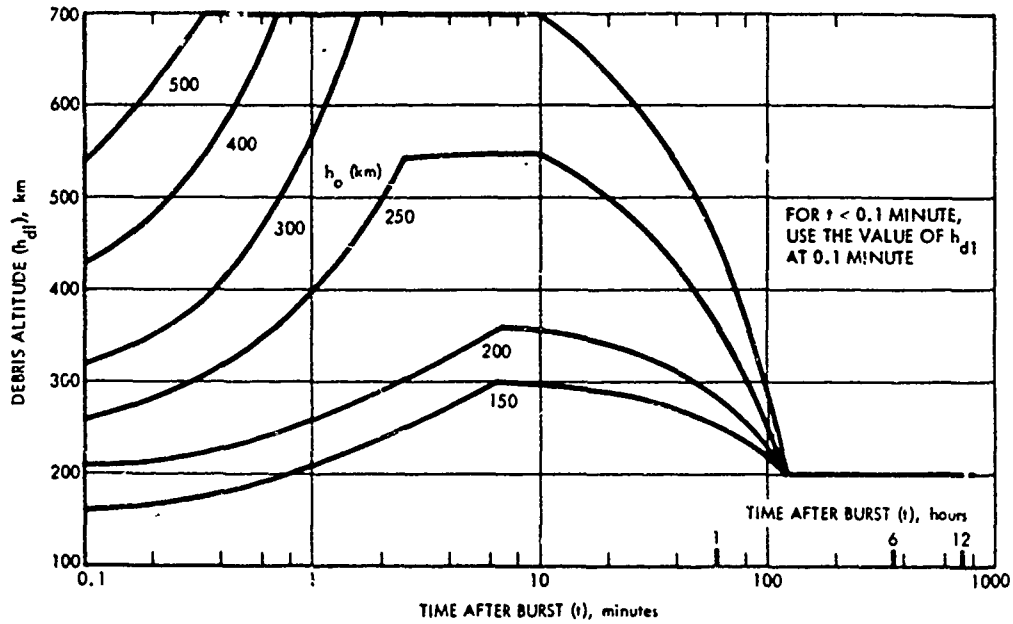

Figure 8-31. [redacted] Altitude of Debris Region 1, 10-kt Burst [redacted]

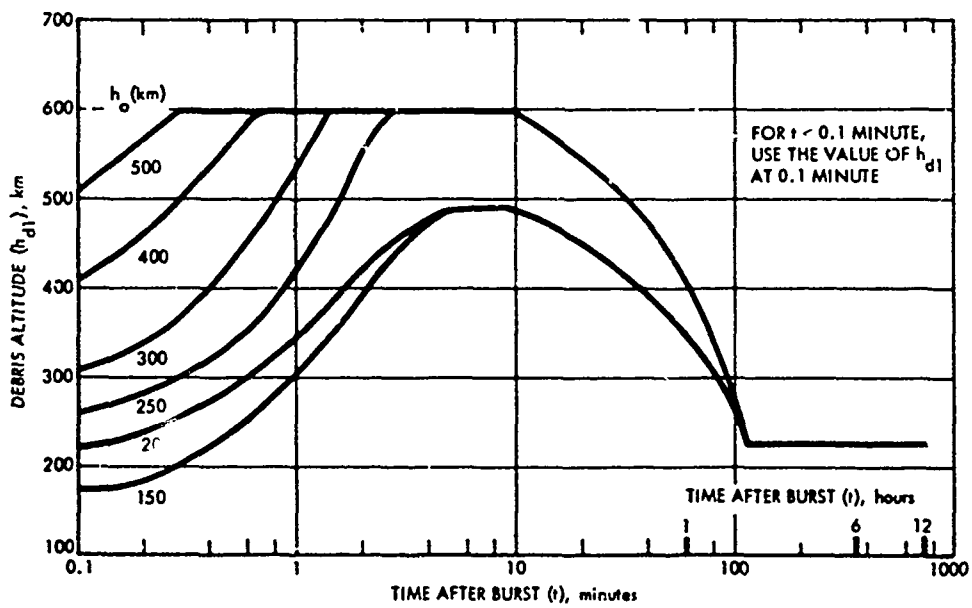

Figure 8-32. [redacted] Altitude of Debris Region 1, 100-kt Burst [redacted]

[redacted]

[redacted]

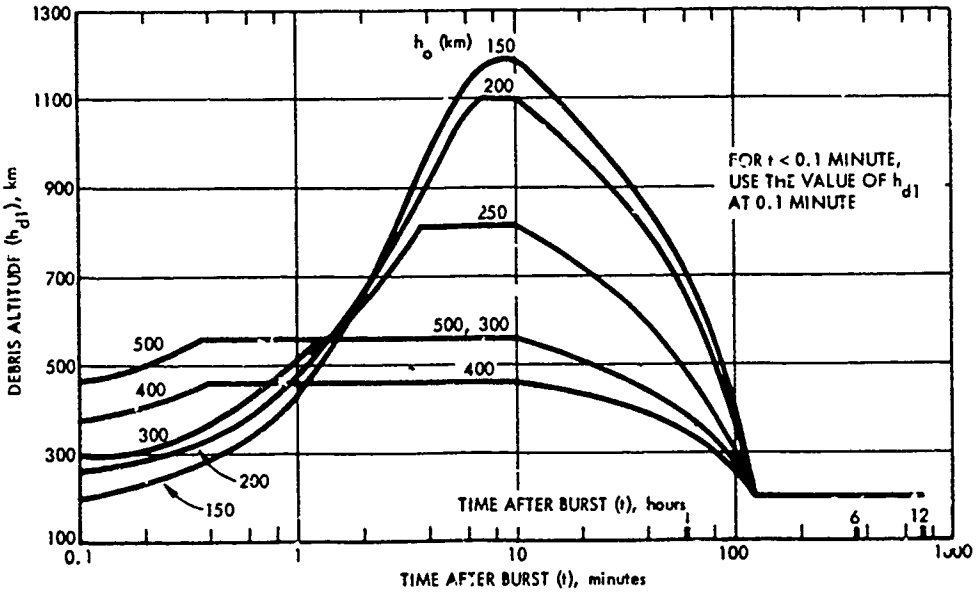

Figure 8-33. [redacted] Altitude of Debris Region 1, 1-Mt Burst [redacted]

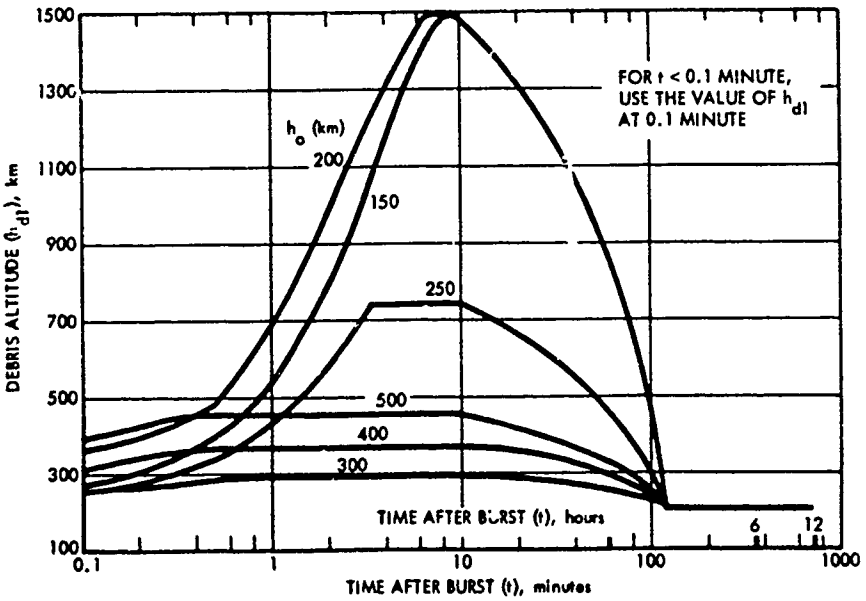

Figure 8-34. [redacted] Altitude of Debris Region 1, 10-Mt Burst [redacted]

[redacted]

[redacted]

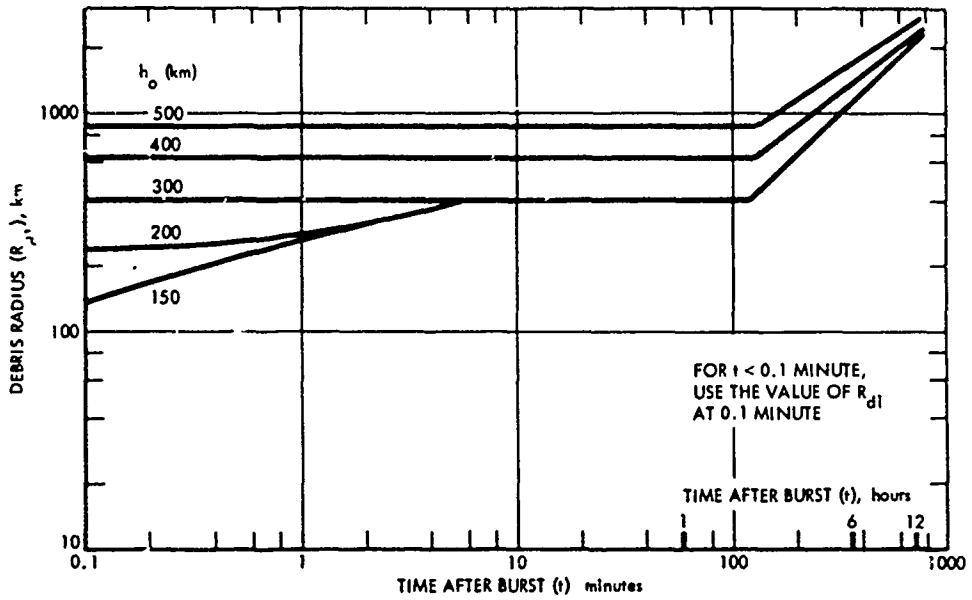

Figure 8-35. [redacted] Radius of Debris Region 1, 10-kt Burst [redacted]

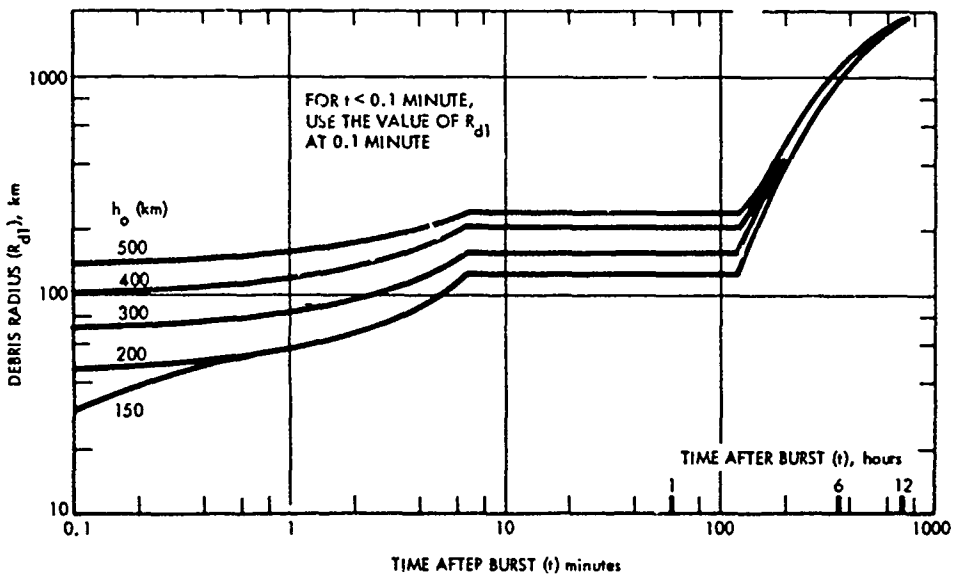

Figure 8-36. [redacted] Radius of Debris Region 1, 100-kt Burst [redacted]

[redacted]

[redacted]

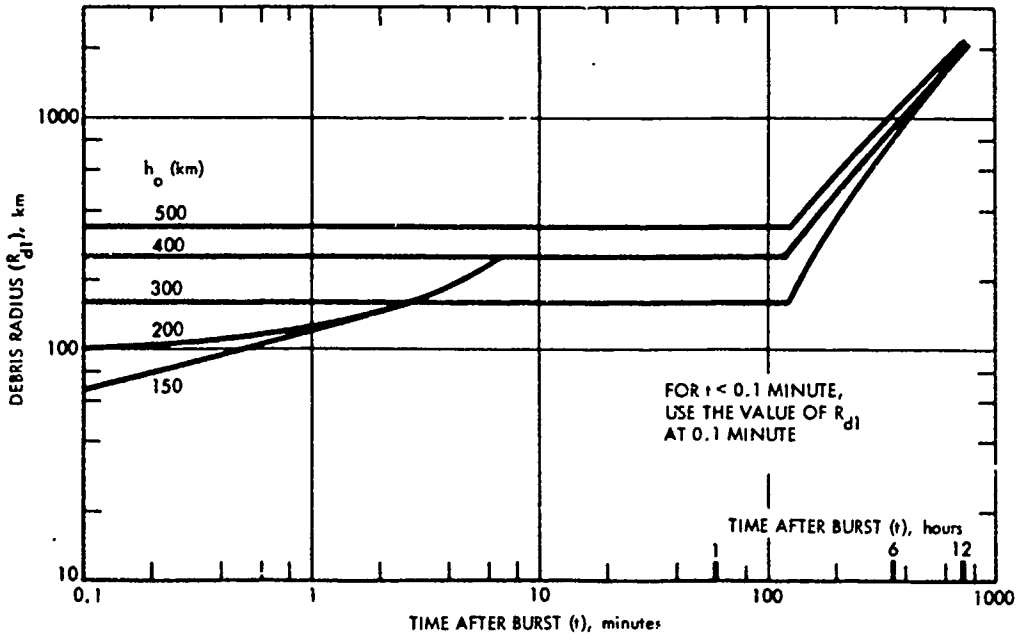

Figure 8-37. [redacted] Radius of Debris Region 1, 1-Mt Burst [redacted]

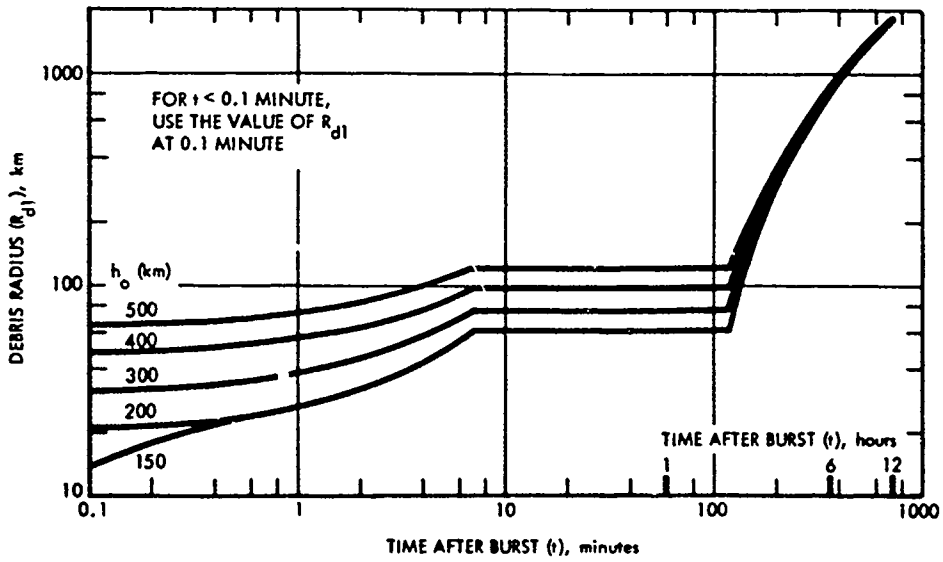

Figure 8-38. [redacted] Radius of Debris Region 1, 10-Mt Burst [redacted]

[redacted]

[redacted]

Problem 8-4 Absorption through the Fireball [redacted]

[redacted] Tables 8-3 through 8-7 and Figure 8-39 are used to obtain estimates of the absorption of signals propagating through the fireball for parametric burst yields and detonation altitudes. The temperature and electron density within the fireball are assumed to be uniformly distributed; thus, the absorption through the fireball is linearly dependent upon the distance the propagation path travels through the fireball. The fireball location and size can be determined from Table 8-2 and Figures 8-16 through 8-38, as described in Problems 8-1 through 8-3.

[redacted] The absorption data are given for a path length through the fireball equal to the fireball diameter if the fireball is a sphere, equal to the diameter of the toroid arm if the fireball is a toroid, equal to the vertical thickness of a pancake if the fireball is a pancake, or equal to the diameter of the tube if the fireball is a tube. For detonations that occur above about 50 km, the fireball absorption scales inversely with the square of the frequency.

[redacted] When the fireball is below an altitude of about 60 km, beta particles deposit their energy within the fireball, and they are the major source of ionization and absorption after the fireball has cooled to the atmospheric temperature. When the altitude of the fireball is greater than 60 km, absorption caused by beta-particle ionization should be determined by the methods described in Problem 8-7.

[redacted] Tables 8-3 through 8-6 provide data to determine absorption of signals propagating through the fireball of bursts that occur below 80 km at times after burst less than 300 seconds and fireball altitudes greater than 60 km (the fireball altitude at the time of interest may be obtained by the methods described in Problem 8-1). If the detonation altitude is below 50 km, the absorption A_{fb} is read directly from the table with the weapon yield closest to the desired yield at the closest detonation altitude, time after burst, and frequency given in the table. If the detonation altitude is 50 km or greater (but not greater than 80 km), the absorption for 1000 MHz, A'_{fb} is read from the appropriate table at the closest detonation altitude and time after burst. The absorption is then calculated as follows:

$$A_{fb} = A'_{fb} \frac{10^6}{f^2} ,$$

where f is the desired frequency in MHz.

[redacted] If the time after burst is greater than 300 seconds and the fireball altitude is less than 60 kilometers, the absorption of signals propagating through the fireball may be estimated from Figure 8-39. The quantity L'_a is obtained from Figure 8-39 for the appropriate fireball altitude and frequency. The absorption is then calculated as follows:

$$A_{fb} = L'_a \frac{N_\beta}{10^9} ,$$

where N_β is the beta particle radiation intensity parameter defined by equation 8.1 in paragraph 8-4.

[redacted] Table 8-7 provides data to determine absorption of signals propagating through the fireball of bursts that occur at altitudes above 80 km. The absorption of a 1000 MHz signal (A'_{fb}) is read from Table 8-7 for the weapon yield and altitude closest to those desired. The absorption at the desired frequency (A_{fb}) is then calculated as follows:

$$A_{fb} = A'_{fb} \frac{10^6}{f^2} ,$$

where f is the frequency in MHz.

[redacted]

[redacted]

[redacted] *Example 1* [redacted]

Given: A 1 Mt weapon burst at an altitude 50 km.

Find: The absorption of a 400 MHz signal propagating through the fireball 2 min after burst.

Solution: From Table 8-5, the absorption of a 1000 MHz signal 2 min after a burst at 50 km is

$$A'_{fb} = 0.2 \text{ dB};$$

therefore,

$$A_{fb} = (0.2)\frac{10^6}{(400)^2} = 1.25 \text{ dB}.$$

Answer: The absorption of a 400 MHz signal propagating through the fireball of a 1 Mt weapon 2 min after the weapon was detonated at an altitude of 50 km is 1.25 dB.

[redacted] *Example 2* [redacted]

Given: A 4 Mt weapon burst at an altitude of 150 km.

Find: The absorption of a 400 MHz signal propagating through the fireball 15 min after burst.

Solution: The yield and time nearest to those desired that are tabulated in Table 8-7 are 1 Mt and 10 min (600 sec). The absorption for a 1000 MHz signal 10 min after a 1 Mt burst at 150 km is

$$A'_{fb} = 3.2 \text{ dB};$$

therefore,

$$A_{fb} = (3.2)\frac{10^6}{(400)^2} = 20 \text{ dB}.$$

Answer: The absorption of a 400 MHz signal propagating through the fireball of a 4 Mt weapon 15 min after the weapon was detonated at an altitude of 150 km is approximately 20 dB.

[redacted] *Reliability* [redacted] The uncertainties in predicting fireball dimensions and electron density are such that estimates of the duration of a given level of absorption are uncertain by at least a factor of two. In general, the duration of absorption caused by the rising fireball will be determined by how long the fireball interdicts the propagation path, rather than the time period that the fireball remains absorbing at a given frequency.

[redacted] *Related Material* [redacted] See paragraph 8-6 and Problems 8-1 through 8-3.

[redacted]

[redacted]

Table 8-3 [redacted] Absorption (dB) Through Fireball for Detonations Below 80 km, W = 10 kt [redacted]

Time (sec)	Freq. (MHz)	Detonation Altitude (km)								
		0	10	20	30	40	50	60	70	80
10	100	8.5E3	2.0E4	2.7E5	9.1E6	1.7E7				
	400	8.5E3	1.9E4	2.4E5	2.5E6	1.4E6				
	1,000	8.5E3	1.9E4	1.4E5	5.0E5	2.2E5	1.4E5	1.1E3	3.8E2	1.7E2
	4,000	8.2E3	1.2E4	1.7E4	3.3E4	1.4E4				
	10,000	6.7E3	3.7E3	2.8E3	5.3E3	2.2E3				
20	100	3.1E3	1.2E4	2.9E4	5.2E4	3.0E5				
	400	3.2E3	1.2E4	2.4E4	1.2E4	2.2E4				
	1,000	3.1E3	1.2E4	1.3E4	2.3E3	3.6E3	1.3E4	3.7E2	1.0E2	2.7E1
	4,000	3.0E3	6.7E3	1.4E3	1.5E2	2.3E2				
	10,000	2.4E3	2.0E3	2.3E2	2.3E1	3.6E1				
30	100	7.4E2	8.5E3	2.2E4	3.8E4	1.5E4				
	400	7.4E2	8.4E3	1.8E4	7.5E3	1.1E3				
	1,000	7.3E2	8.0E3	8.7E3	1.4E3	[illegible]	[illegible]	[illegible]	4.2E2	8.8E0
	4,000	7.0E2	4.1E3	8.5E2	8.7E1	[illegible]				
	10,000	5.4E2	1.1E3	1.4E2	1.4E1	1.7E0				
40	100	7.3E1	3.2E3	1.7E4	2.9E4	9.9E3				
	400	7.3E1	3.1E3	1.4E4	5.0E3	6.9E2				
	1,000	7.3E1	3.0E3	6.0E3	8.9E2	[illegible]	1.7E1	1.8E1	2.0E1	3.8E0
	4,000	6.9E1	1.4E3	5.5E2	5.7E1	7.0E0				
	10,000	5.2E1	3.5E2	9.0E1	9.1E0	1.1E0				
50	100	4.6E0	4.7E2	1.2E4	2.3E4	7.0E3				
	400	4.6E0	4.7E2	8.6E3	3.5E3	4.8E2				
	1,000	4.6E0	4.3E2	3.5E3	6.1E2	7.6E1	1.1E1	1.1E1	2.2E0	1.9E0
	4,000	4.3E0	1.8E2	3.0E2	3.9E1	4.9E0				
	10,000	3.2E0	4.4E1	4.9E1	6.2E0	7.7E-1				
60	100	2.6E-1	3.9E1	3.8E3	1.8E4	5.1E3				
	400	2.6E-1	3.9E1	2.7E3	2.4E3	3.4E2				
	1,000	2.6E-1	3.5E1	1.0E3	4.1E2	5.5E1	8.0E0	6.6E0	1.3E0	1.1E0
	4,000	2.3E-1	1.4E1	8.3E1	2.6E1	3.4E0				
	10,000	1.7E-1	3.1E0	1.4E1	4.2E0	5.5E-1				
90	100	5.6E-3	4.8E-1	3.3E1	6.5E2	1.5E3				
	400	5.6E-3	4.6E-1	2.0E1	6.9E1	9.9E1				
	1,000	5.6E-3	4.0E-1	6.1E0	1.2E1	1.6E1	3.3E0	2.1E0	3.4E-1	7.7E-2
	4,000	5.0E-3	1.2E-1	4.5E-1	7.2E-1	9.9E-1				
	10,000	3.2E-3	2.4E-2	7.3E-2	1.2E-1	1.6E-1				
120	100		3.1E-1	1.7E1	2.2E-2					
	400		2.9E-1	8.4E0	1.9E-1					
	1,000		2.3E-1	2.2E0	3.2E0	1.7E0	9.0E-1	7.8E-1	1.1E-1	3.5E-2
	4,000		5.8E-2	1.7E-1	2.1E-1					
	10,000		1.0E-2	2.4E-2	3.2E-2					
150	100		2.7E-1	1.5E1	1.7E2					
	400		2.6E-1	6.4E0	1.4E1					
	1,000		2.0E-1	1.5E0	2.3E0	1.2E0	5.5E-1	4.3E-1	6.0E-2	2.3E-2
	4,000		3.8E-2	1.0E-1	1.4E-1					
	10,000		6.9E-3	1.7E-2	2.3E-2					
180	100		2.4E-1	1.3E1	1.3E2					
	400		2.2E-1	4.9E0	1.0E1					
	1,000		1.6E-1	1.1E0	1.7E0	8.8E-1	4.0E-1	2.6E-1	3.6E-2	1.6E-2
	4,000		2.6E-2	6.9E-2	1.0E-1					
	10,000		4.9E-3	1.2E-2	1.7E-2					
300	100		1.3E-1	5.7E0	5.0E1					
	400		1.2E-1	1.7E0	3.5E0					
	1,000		6.9E-2	3.2E-1	5.6E-1	3.4E-1	1.7E-1	4.4E-2	4.9E-3	1.2E-3
	4,000		8.2E-3	2.1E-2	3.5E-2					
	10,000		1.4E-3	3.3E-3	5.6E-3					

Notes: E refers to the power of 10, e.g., 1.5E4 = 1.5×10^4. If f^{-2} scaling applies, only 1,000 MHz values are given.

[redacted]

[redacted]

Table 8-4 [redacted] Absorption (dB) Through Fireball for Detonations Below 80 km, W = 100 kt [redacted]

Time (sec)	Freq. (MHz)	Detonation Altitude (km)								
		0	10	20	30	40	50	60	70	80
10	100	1.3E5	6.5E5	4.3E6	2.5E7	4.8E7				
	400	1.3E5	6.4E5	3.7E6	6.5E6	3.8E6				
	1,000	1.3E5	6.2E5	2.1E6	1.3E6	6.1E5	4.8E5	2.1E3	9.5E2	9.2E2
	4,000	1.2E5	3.7E5	2.3E5	8.2E4	3.8E4				
	10,000	1.0E5	1.1E5	3.9E4	1.3E4	6.1E3				
20	100	9.0E3	4.3E4	1.0E5	3.5E6	4.7E6				
	400	9.0E3	4.3E4	8.3E4	6.9E5	3.3E5				
	1,000	3.3E3	2.4E4	2.5E4	3.4E3	3.7E3	4.0E3	2.3E2	3.1E1	2.5E1
	4,000	8.6E3	2.2E4	3.9E3	8.0E3	3.4E3				
	10,000	6.8E3	6.0E3	6.5E2	1.2E3	5.4E2				
30	100	3.3E3	2.6E4	8.1E4	1.3E5	3.3E5				
	400	3.3E3	2.6E4	6.1E4	2.0E4	2.3E4				
	1,000	5.8E2	1.4E4	1.7E4	2.1E3	2.5E2	1.[illegible]E2	1.1E2	1.2E1	[illegible].1E0
	4,000	3.1E3	1.1E4	2.2E3	2.2E2	2.3E2				
	10,000	2.3E3	2.8E3	3.7E2	3.5E1	3.7E1				
40	100	5.8E2	1.5E4	6.7E4	9.4E4	2.3E4				
	400	5.8E2	1.5E4	4.7E4	1.2E4	1.6E3				
	1,000	5.8E2	1.4E4	1.7E4	2.1E3	2.5E2	1.7E2	1.1E2	1.2E1	9.1E0
	4,000	5.4E2	5.5E3	1.4E3	1.3E2	1.6E1				
	10,000	4.0E2	1.3E3	2.3E2	2.1E1	2.5E0				
50	100	5.5E1	5.5E3	5.7E4	7.1E4					
	400	5.5E1	5.4E3	3.6E4	8.0E3					
	1,000	5.5E1	4.8E3	1.2E4	1.3E3	1.6E2	9.2E1	6.0E1	5.7E0	4.2E0
	4,000	5.0E1	1.7E3	8.8E2	8.5E1					
	10,000	3.5E1	3.6E2	1.4E2	1.4E1					
60	100	4.0E0	8.9E2	4.2E4	5.5E4					
	400	4.0E0	8.7E2	2.4E4	5.5E3					
	1,000	4.0E0	7.5E2	6.9E3	9.[illegible]E2	1.1E2	1.4E1	3.3E1	3.0E0	2.2E0
	4,000	3.6E0	2.2E2	5.0E2	5.7E1					
	10,000	2.4E0	4.5E1	8.1E1	9.1E0					
90	100	2.3E-2	3.6E0	7.0E2	1.5E4					
	400	2.3E-2	3.5E0	2.8E2	1.2E3					
	1,000	2.2E-2	2.7E0	6.3E1	2.0E2	3.9E1	4.5E0	1.7E0	1.3E-1	5.4E-1
	4,000	2.0E-2	5.4E-1	4.3E0	1.2E1					
	10,000	1.1E-2	1.0E-1	6.9E-1	2.0E0					
120	100	1.4E-2	2.2E0	1.7E2	1.1E3					
	400	1.4E-2	2.0E0	4.7E1	8.0E1					
	1,000	1.4E-2	1.3E0	9.2E0	1.3E1	7.7E0	1.6E0	4.6E-1	4.8E-2	3.5E-2
	4,000	1.2E-2	2.1E-1	6.7E-1	9.1E-1					
	10,000	5.4E-3	3.3E-2	9.6E-2	1.3E-1					
150	100	1.2E-2	2.2E0	1.6E2	8.2E2					
	400	1.2E-2	2.0E0	3.4E1	5.6E1					
	1,000	1.2E-2	1.1E0	6.2E0	9.1E0	3.6E0	7.8E-1	2.2E-1	2.9E-2	1.7E-2
	4,000	9.0E-3	1.4E-1	4.0E-1	5.7E-1					
	10,000	4.0E-3	2.4E-2	6.4E-2	9.1E-2					
180	100	1.0E-2	2.2E0	1.5E2	6.1E2					
	400	1.0E-2	1.8E0	2.6E1	4.1E1					
	1,000	1.0E-2	9.8E-1	4.7E0	6.6E0	2.5E0	4.5E-1	1.2E-1	1.9E-2	7.9E-3
	4,000	7.2E-3	1.0E-1	2.9E-1	3.9E-1					
	10,000	3.0E-2	1.7E-2	4.8E-2	6.6E-2					
300	100	6.1E-3	1.7E0	8.5E1						
	400	6.1E-3	1.2E0	9.3E0						
	1,000	5.8E-3	4.2E-1	1.6E0	2.2E0	9.3E-1	8.6E-2	1.5E-2	2.6E-3	5.7E-4
	4,000	3.4E-3	3.4E-2	9.8E-2						
	10,000	1.0E-3	5.5E-3	1.6E-2						

Notes: E refers to the power of 10, e.g., 1.5E4 = 10^4. If f^{-2} scaling applies, only 1,000 MHz values are given.

[redacted]

[redacted]

Table 8-5 [redacted] Absorption (dB) Through Fireball for Detonations Below 80 km, W = 1 Mt [redacted]

Time (sec)	Freq. (MHz)	Detonation Altitude (km)								
		0	10	20	30	40	50	60	70	80
10	100	3.4E5	1.8E6	1.4E7	9.7E7	1.8E8				
	400	3.4E5	1.8E6	1.2E7	1.9E7	1.3E7				
	1,000	3.4E5	1.8E6	3.4E7	2.2E6	7.5E6	7.5E6	1.6E4	1.4E4	3.2E3
	4,000	3.3E5	1.0E6	6.2E5	2.2E5	1.4E5				
	10,000	2.7E5	3.0E5	1.0E5	3.5E4	2.2E4				
20	100	5.2E4	2.4E5	1.5E6	1.1E7	9.2E6				
	400	5.2E4	2.3E5	1.1E6	1.4E6	6.0E5				
	1,000	5.2E4	2.2E5	4.5E5	2.4E5	9.7E4	6.8E4	1.2E3	9.2E2	2.3E2
	4,000	5.0E4	1.0E5	3.8E4	1.5E4	6.0E3				
	10,000	3.8E4	2.6E4	6.3E3	2.4E3	1.0E3				
30	100	1.4E4	8.8E4	9.0E5	1.4E6	9.5E5				
	400	1.4E4	8.6E4	5.7E5	1.5E5	6.1E4				
	1,000	1.4E4	7.8E4	1.9E5	2.4E4	9.7E3	4.2E3	2.4E2	1.7E2	4.7E1
	4,000	1.3E4	3.0E4	1.4E4	1.5E3	6.0E2				
	10,000	1.0E4	6.8E3	2.3E3	2.5E2	9.7E1				
40	100	5.8E3	6.3E4	2.7E5	1.0E6	1.1E5				
	400	5.8E3	6.1E4	1.4E5	8.4E4	6.7E3				
	1,000	5.7E3	5.4E4	4.0E4	1.4E4	1.1E3	4.0E2	7.0E1	4.6E1	1.6E1
	4,000	5.3E3	1.7E4	2.9E3	8.6E2	1.7E1				
	10,000	3.7E3	3.4E3	4.6E2	1.4E2	1.1E1				
50	100	1.3E3	4.5E4	2.4E5	6.5E5	6.2E4				
	400	1.3E3	4.3E4	1.0E5	5.1E4	3.9E3				
	1,000	1.3E3	3.6E3	2.5E4	8.3E3	6.2E2	4.0E1	2.6E1	1.7E1	6.8E0
	4,000	1.1E3	8.9E3	1.7E3	5.2E2					
	10,000	7.4E2	1.7E3	2.7E2	8.3E1					
60	100	1.6E2	2.5E4	2.2E5	1.0E5					
	400	1.6E2	2.4E4	7.4E4	7.4E3					
	1,000	1.6E3	1.9E4	1.6E4	1.2E3	3.8E2	2.2E1	1.1E1	7.4E0	3.5E0
	4,000	1.4E2	3.8E3	1.1E3	7.5E1					
	10,000	8.7E1	6.9E2	1.7E2	1.2E1					
90	100	2.4E-1	2.2E2	7.8E4	3.4E4					
	400	2.4E-1	1.9E2	1.5E4	2.3E3					
	1,000	2.4E-1	1.2E2	2.6E3	3.6E2	2.4E1	4.5E0	1.6E0	1.3E0	6.4E-1
	4,000	1.9E-1	1.5E1	1.7E2	2.3E1					
	10,000	9.4E-2	2.6E0	2.7E1	3.6E0					
120	100	7.0E-2	2.7E1	3.1E3	7.6E3					
	400	7.0E-2	2.1E1	3.6E2	4.8E2					
	1,000	6.9E-2	9.3E0	6.1E1	7.8E1	6.8E0	2.0E-1	3.5E-1	3.2E-1	1.3E-1
	4,000	5.2E-2	9.6E-1	4.9E0	6.6E0					
	10,000	1.9E-2	1.4E-1	6.2E-1	7.8E-1					
150	100	6.9E-2	2.8E1	2.1E3						
	400	6.8E-2	1.9E1	2.0E2						
	1,000	6.6E-2	7.1E0	3.3E1	2.5E1	3.1E0	7.5E-2	3.2E-2	1.6E-1	9.5E-3
	4,000	4.3E-2	5.8E-1	2.1E0						
	10,000	1.4E-2	9.4E-2	3.4E-1						
180	100	6.8E-2	3.2E1	1.8E3						
	400	6.7E-2	1.9E1	1.5E2						
	1,000	6.5E-2	6.0E0	2.5E1	1.6E1	1.5E0	3.2E-2	1.8E-2	7.4E-2	3.9E-3
	4,000	3.6E-2	4.3E-1	1.5E0						
	10,000	1.1E-2	7.3E-2	2.5E-1						
300	100	5.2E-2	3.6E1	8.5E2						
	400	5.1E-2	1.2E1	5.8E1						
	1,000	4.6E-2	2.5E0	9.3E0	4.7E0	4.7E0	2.4E-3	3.3E-3	1.0E-3	1.8E-4
	4,000	1.7E-2	1.7E-1	5.8E-1						
	10,000	3.8E-3	2.7E-2	9.3E-2						

Notes: E refers to the power of 10, e.g., 1.5E4 = 1.5×10^4. If f^{-2} scaling applies, only 1,000 MHz values are given.

[redacted]

[redacted]

Table 8-6 [redacted] Absorption (dB) Through Fireball for Detonations Below 80 km, W = 10 Mt [redacted]

Time (sec)	Freq. (MHz)	Detonation Altitude (km)								
		0	10	20	30	40	50	60	70	80
10	100	1.2E6	7.4E6	8.4E7	8.8E8	1.0E10				
	400	1.1E6	7.4E6	6.2E7	2.9E8	5.2E9				
	1,000	1.1E6	7.0E6	2.5E7	6.0E7	1.4E9	1.2E10	7.8E4	2.5E4	8.2E3
	4,000	1.1E6	3.7E6	2.1E6	4.0E6	1.0E8				
	10,000	8.8E5	1.0E6	3.4E5	6.4E5	1.6E7				
20	100	1.3E5	6.6E5	1.2E7	5.0E7	1.8E8				
	400	1.3E5	6.4E5	4.9E6	4.5E6	1.2E7				
	1,000	1.3E5	5.9E5	1.1E6	7.3E5	2.0E6	8.8E6	4.8E3	1.6E3	5.9E2
	4,000	1.2E5	2.3E5	7.8E4	4.6E4	1.2E5				
	10,000	9.1E4	5.3E4	1.3E4	7.4E3	2.0E4				
30	100	9.0E4	5.3E5	4.3E6	2.4E6					
	400	8.9E4	5.1E5	1.1E6	1.6E5					
	1,000	8.9E4	4.4E5	2.2E5	2.6E4	4.5E4	7.1E4	7.4E2	2.5E2	1.2E2
	4,000	8.2E4	1.3E5	1.4E4	1.6E3					
	10,000	5.7E4	2.5E4	2.3E3	2.6E2					
40	100	6.8E4	4.7E5	3.4E6						
	400	6.8E4	4.4E5	6.1E5						
	1,000	6.7E4	3.5E5	1.1E5	4.0E3	1.8E3	2.3E3	1.8E2	6.7E1	3.9E1
	4,000	6.1E4	7.4E4	6.9E3						
	10,000	3.9E4	1.4E4	1.1E3						
50	100	2.1E4	4.3E5	2.7E6						
	400	2.1E4	4.0E5	3.4E5						
	1,000	2.1E4	2.8E5	5.9E4	1.4E3	2.5E2	5.9E1	6.0E1	2.4E1	1.7E1
	4,000	1.8E4	4.5E4	3.7E3						
	10,000	1.1E4	7.9E3	5.9E2						
60	100	9.2E3	2.0E5	2.0E6						
	400	9.2E3	1.7E5	2.1E5						
	1,000	9.1E3	1.1E5	3.4E4	6.9E2	9.2E1	1.6E1	2.4E1	1.1E1	1.7E0
	4,000	7.6E3	1.3E4	2.2E3						
	10,000	4.0E3	2.3E3	3.4E2						
90	100	7.4E1	7.7E4	2.3E5						
	400	7.3E1	5.4E4	1.7E4						
	1,000	7.2E1	2.1E4	2.7E3	1.4E2	8.9E2	1.3E0	3.1E0	1.8E0	2.0E-1
	4,000	5.1E1	1.7E3	1.7E2						
	10,000	2.0E1	2.8E2	2.7E1						
120	100	6.6E-1	1.3E3	6.2E4						
	400	6.5E-1	6.3E2	4.1E3						
	1,000	6.2E-1	1.6E2	6.5E2	6.8E0	1.2E0	1.7E-1	6.4E-1	6.1E-2	3.1E-2
	4,000	4.3E-1	2.0E1	5.2E1						
	10,000	1.0E-1	1.8E0	6.5E0						
150	100	5.5E-1	7.6E2							
	400	5.4E-1	2.5E2							
	1,000	5.1E-1	5.3E1	1.8E2	2.5E0	9.1E-2	5.3E-2	2.2E-2	1.1E-2	1.4E-2
	4,000	2.3E-1	3.5E0							
	10,000	5.6E-2	5.6E-1							
180	100	5.9E-1	8.2E2							
	400	5.7E-1	2.0E2							
	1,000	5.2E-1	3.8E1	9.6E1	1.0E0	2.7E-2	2.0E-2	2.2E-2	8.9E-3	4.5E-3
	4,000	1.9E-1	2.3E0							
	10,000	4.3E-2	3.9E-1							
300	100	6.5E-1	9.3E2							
	400	6.1E-1	9.8E1							
	1,000	4.6E-1	1.6E1	2.1E1	5.3E-2	5.8E-4	9.8E-4	4.0E-4	2.0E-4	2.7E-4
	4,000	8.7E-2	1.0E0							
	10,000	1.6E-2	1.6E-1							

Notes: E refers to the power of 10, e.g., 1.5E4 = 1.5×10^4. If f^{-2} scaling applies, only 1,000 MHz values are given.

[redacted]

[redacted]

Table 8-7 [redacted] Absorption (dB) Through Fireball at 1000 MHz for Detonations Above 80 km [redacted]

Time (sec)	Yield (Mt)	Detonation Altitude (km)								
		100	150	200	250	300	350	400	450	500
10	0.01	5.2E2	7.9E2	1.7E2	1.4E1	6.1E0	2.1E0	6.1E-1	2.0E-1	7.3E-2
	0.1	1.1E3	2.0E3	3.8E2	3.1E1	1.4E1	4.8E0	1.4E0	4.5E-1	1.6E-1
	1	3.2E3	5.4E3	9.0E2	5.0E1	5.5E0	7.9E-1	1.5E-1	3.3E-2	8.7E-3
	10	1.4E4	2.0E4	3.3E3	2.6E3	3.5E2	6.9E1	1.7E1	4.9E0	1.6E0
20	0.01	7.2E1	2.1E2	1.2E2	1.2E1	5.4E0	1.9E0	5.5E-1	1.8E-1	6.8E-2
	0.1	1.4E2	5.8E2	2.8E2	2.6E1	1.2E1	4.3E0	1.3E0	4.2E-1	1.5E-1
	1	4.1E2	1.8E3	6.7E2	4.3E1	5.1E0	7.6E-1	1.4E-1	3.2E-2	8.4E-3
	10	2.2E3	8.0E3	1.9E3	1.4E3	2.7E2	5.9E1	1.5E1	4.5E0	1.5E0
30	0.01	2.2E1	1.3E2	9.6E1	1.0E1	4.8E0	1.7E1	5.1E-1	1.7E-1	6.4E-2
	0.1	3.8E1	3.0E2	2.2E1	2.3E1	1.1E1	4.0E0	1.2E0	3.9E-1	1.5E-1
	1	1.2E2	7.2E2	5.3E2	4.6E1	6.2E0	1.0E0	2.0E-1	4.8E-2	1.30-2
	10	6.6E2	4.0E3	1.5E3	3.2E3	8.4E2	2.2E2	6.5E1	2.1E1	7.4E0
40	0.01	9.2E0	8.8E1	7.7E0	9.1E0	4.4E0	1.6E0	4.7E-1	1.6E-1	6.0E-2
	0.1	1.5E1	2.0E2	1.8E2	2.1E1	1.0E1	3.7E0	1.1E0	3.7E-1	1.4E-1
	1	4.6E1	4.9E2	4.3E2	3.6E1	5.3E0	9.1E-1	1.8E-1	4.4E-2	1.2E-2
	10	2.7E2	2.3E3	1.2E3	1.0E3	5.9E2	1.7E2	5.4E1	1.8E1	6.5E0
50	0.01	4.6E0	6.4E1	6.4E1	8.2E0	4.0E0	1.5E0	4.4E-0	1.5E-1	5.7E-0
	0.1	7.1E0	1.5E2	1.5E2	1.9E1	9.2E0	3.4E0	1.0E0	3.5E-1	1.3E-1
	1	2.2E1	3.6E2	3.5E2	3.0E1	4.6E0	8.2E-1	1.7E-1	4.1E-2	1.1E-2
	10	1.4E2	1.4E3	1.0E3	1.3E3	4.4E2	1.4E2	4.5E1	1.6E1	5.8E0
60	0.01	2.3E0	4.9E1	5.4E1	7.5E0	3.7E0	1.4E0	4.2E-1	1.4E-1	5.4E-2
	0.1	4.8E0	1.1E2	1.2E2	1.7E1	8.6E0	3.2E0	9.7E-1	3.3E-1	1.3E-1
	1	1.1E1	2.7E2	3.0E2	2.4E1	4.1E0	7.4E-1	1.6E-1	3.9E-2	1.1E-2
	10	7.5E1	9.3E2	8.7E2	9.3E2	3.4E2	1.1E2	3.9E1	1.4E1	5.2E0
90	0.01	9.9E-1	2.7E1	3.6E1	6.0E0	3.1E0	1.8E0	3.6E-1	1.2E-1	4.7E-2
	0.1	1.5E0	6.0E1	8.2E1	1.4E1	7.1E0	2.7E0	8.4E-1	2.9E-1	1.1E-1
	1	3.7E0	1.4E2	2.0E2	1.5E1	2.9E0	5.7E-1	1.3E-1	3.2E-2	9.2E-3
	10	2.0E1	4.1E2	5.8E2	4.2E2	1.8E2	6.8E1	2.5E1	9.9E0	3.9E0
125	0.01	4.7E-1	1.6E-1	2.5E1	5.0E1	2.6E0	1.0E0	3.1E-1	1.1E-1	4.2E-2
	0.1	5.5E-1	3.5E1	5.7E1	1.1E1	6.0E0	2.4E0	7.4E-1	2.6E-1	9.9E-2
	1	1.5E0	8.3E1	1.4E2	9.7E0	2.1E0	4.4E-1	1.0E-1	2.7E-2	7.8E-3
	10	6.8E0	2.3E2	3.9E2	1.8E2	1.0E2	4.2E1	1.8E1	7.1E0	3.0E0
180	0.01	2.8E1	9.9E0	1.8E1	4.0E0	2.1E0	8.6E-1	2.7E-1	9.4E-2	3.7E-2
	0.1	2.1E-1	2.1E1	3.8E1	9.2E0	5.0E0	2.0E0	6.4E1	2.2E1	8.7E0
	1	5.6E-1	4.8E1	9.0E1	5.9E0	1.4E0	3.3E-1	8.0E-2	2.1E-2	6.4E-3
	10	2.6E1	1.3E2	2.5E2	6.8E1	5.0E1	2.5E1	1.1E1	4.9E0	2.1E0
300	0.01	4.5E-2	4.6E0	1.0E1	2.8E0	1.6E0	6.5E-1	2.1E-1	7.5E-2	2.9E-2
	0.1	5.9E-2	7.7E0	2.0E1	6.4E0	3.6E0	1.5E0	4.9E-1	1.8E-1	6.9E-2
	1	1.3E-1	2.0E1	4.5E1	2.4E0	7.0E-1	1.8E-1	4.9E-2	1.4E-2	4.4E-3
	10	5.6E-1	4.9E1	1.2E2	1.4E1	1.2E1	9.1E0	5.0E0	2.4E0	1.2E0
600	0.01	7.3E-3	9.3E-1	3.3E0	1.3E0	7.1E-1	3.1E-1	1.2E-1	4.6E-2	1.8E-2
	0.1	1.1E-2	1.6E0	5.8E0	2.6E0	1.6E0	8.1E-1	3.0E-1	1.1E-1	4.4E-2
	1	1.7E-2	3.2E0	1.2E1	4.1E-1	2.4E-1	7.6E-2	2.3E-2	7.2E-3	2.4E-3
	10	7.0E-2	1.2E1	3.6E1	1.6E0	1.5E0	1.4E0	1.1E0	8.5E-1	4.5E-1
2000	0.01	2.2E-4	2.7E-2	1.2E-1	1.1E-1	8.5E-2	5.1E-2	2.2E-2	9.1E-3	4.0E-3
	0.1	2.8E-4	5.3E-2	2.5E-1	2.4E-1	2.1E-1	1.3E-1	5.9E-2	2.6E-2	1.2E-2
	1	5.7E-4	1.2E-1	5.7E-1	1.2E-2	10.0E-3	7.0E-3	4.1E-3	1.7E-3	6.4E-4
	10	2.2E-3	5.2E-1	2.3E0	3.5E-2	3.7E-2	3.9E-2	3.8E-2	3.5E-2	3.0E-2

Note: E refers to the power of 10, e.g., 1.5E4 = 1.5×10^4.

[redacted]

[redacted]

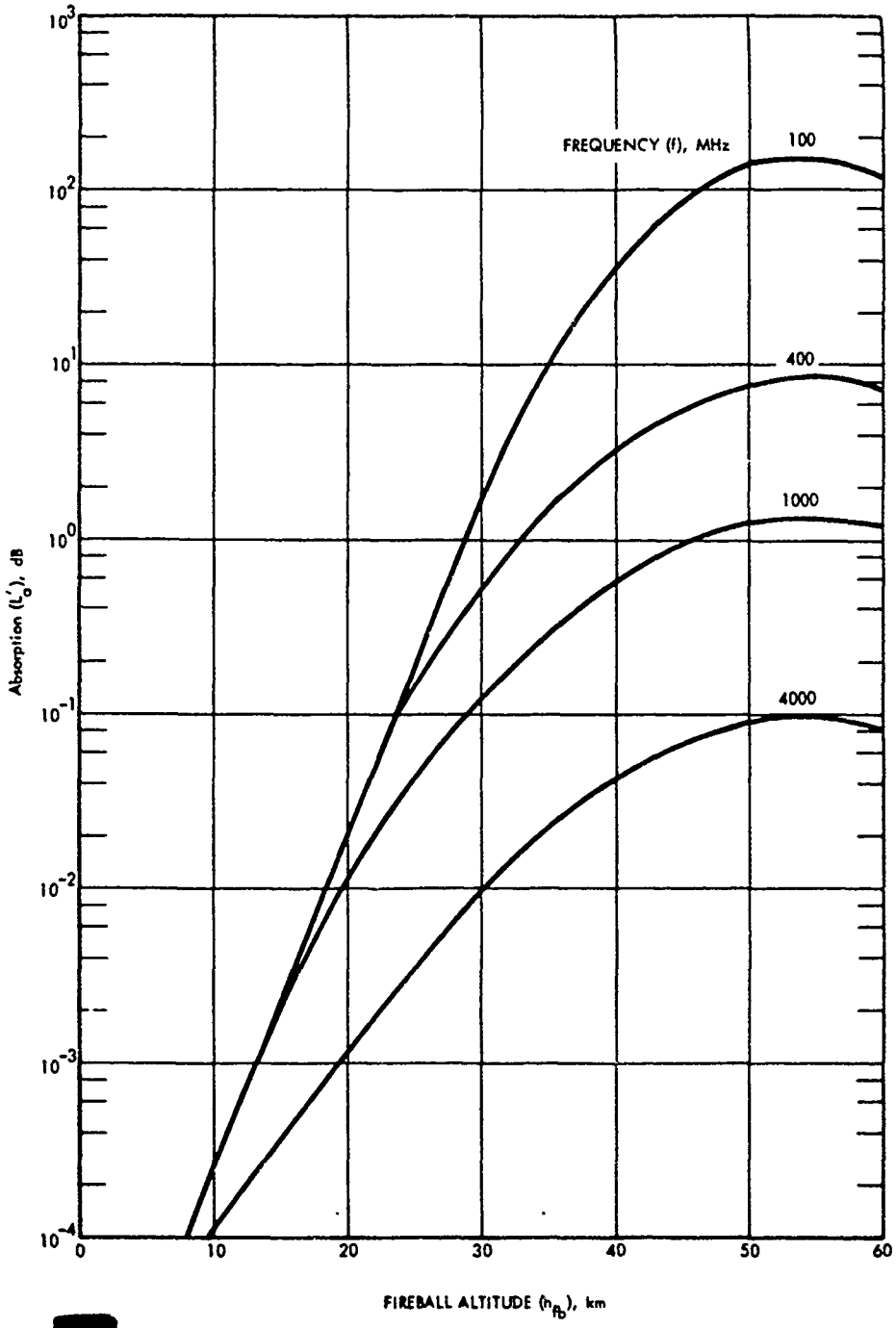

Figure 8-39. [redacted] One-Way Absorption Through Debris Region Due to Beta-Particle Ionization [redacted]

[redacted]

[redacted]

Problem 8-5 Absorption Due to Prompt Radiation Outside the Fireball [redacted]

[redacted] Figures 8-40 and 8-41 are used to obtain the one-way absorption along a propagation path caused by prompt radiation in terms of the one-way vertical absorption (the absorption for a single vertical traversal of the atmosphere) at a time t after burst. The absorption for the vertical path may be converted to that for an oblique path by using the secant of the angle of incidence at the altitude of peak absorption (approximately 65 km, see Problem 8-10).

[redacted] Using the detonation altitude and the ground range between the burst and the point where the propagation path intersects 65 km altitude, a reference yield W_r is obtained from Figure 8-40 (note that W_r differs for night and day). The location of the 65-km intersect point with respect to the propagation-path ground location can be determined from Figure 8-55 as described in Problem 8-10. If the actual weapon yield, W, is less than W_r, go to 2; otherwise go to 1.

1. Enter Figure 8-41 with time after burst in seconds and the radio frequency to obtain A_p', the one-way vertical absorption (note that the absorption differs for night and day). Go to 3.

2. Compute t_r:

$$t_r = \frac{W_r}{W} \text{ sec},$$

where W_r and W are both in Mt or kt. If $t > t_r$, go to 4; otherwise go to 3.

3. Enter Figure 8-41 with time after burst equal to t_r and the frequency to obtain $A_p'(t_r)$. Compute A_p':

$$A_p' = \frac{t_r A_p'(t_r)}{0.5t_r + 1.5t}.$$

Go to 5.

4. Enter Figure 8-41 with time after burst, t, and the frequency to obtain $A_p'(t)$. Compute A_p':

$$A_p' = \frac{tA_p'(t)}{t + t_r}.$$

5. Compute A_p, the one-way path absorption along the oblique path:

$$A_p = A_p' \sec\theta,$$

where $\sec\theta$ is the secant of the angle of incidence at 65 km determined from Figure 8-55.

[redacted] *Example 1* [redacted]

Given: A 1 Mt weapon detonated at an altitude of 300 km. The ground range between the burst and the propagation path is 800 km; the secant of the angle of incidence ($\sec\theta$) at 65 km is 3 for the propagation path.

Find: The one-way path absorption due to prompt radiation for a 100 MHz signal 10 seconds after the burst during the daytime.

Solution:

a. From Figure 8-40, W_r = 100 kt for a detonation altitude of 300 km and a ground range of 800 km.

b. Since $W_r < W$, A_p' is determined to be 12 dB from Figure 8-41.

c. $A_p = A_p' \sec\theta = (12)(3) = 36$ dB.

Answer: The one-way path absorption for a 100 MHz signal having a propagation path with an angle of incidence at 65 km whose secant is 3, resulting from prompt radiation from a 1 Mt weapon detonated at an altitude of 300 km, is 36 dB 10 seconds after burst at a ground range of 800 km from the burst point.

[redacted] *Example 2* [redacted]

Given: A 1 Mt weapon detonated at an

[redacted]

[redacted]

[redacted]

altitude of 200 km. The ground range between the burst and the propagation path is 1000 km; the secant of the angle of incidence (sec θ) at 65 km is 3 for the propagation path.

Find: The one-way path absorption due to prompt radiation for a 100 MHz signal 10 seconds after the burst during the daytime.

Solution:

a. From Figure 8-40, W_r = 5 Mt for a detonation altitude of 200 km and a ground range of 1000 km.

b. $t_r = \frac{W_r}{W} = 5.$

c. $t > t_r$; therefore, from Figure 8-41 $A_p'(t)$ = 12 dB, and

$$A_p' = \frac{tA_p'(t)}{t + t_r} = \frac{(10)(12)}{10 + 5} = 8 \text{ dB}.$$

d. $A_p = A_p' \sec\theta = (8)(3) = 24$ dB.

Answer: The one-way path absorption for a 100 MHz signal having a propagation path with an angle of incidence at 65 km whose secant is 3, resulting from prompt radiation from a 1 Mt weapon detonated at an altitude of 200 km, is 24 dB 10 seconds after burst at a ground range of 1000 km from the burst point.

[redacted] *Reliability* [redacted] The procedures given for computing absorption due to prompt radiation outside the fireball are based on simplified weapon design, atmospheric chemistry, and geometry models. More detailed models are required for specific communications and radar system problems.

[redacted] *Related Material* [redacted] See paragraph 8-2 and Problem 8-10.

[redacted]

[redacted]

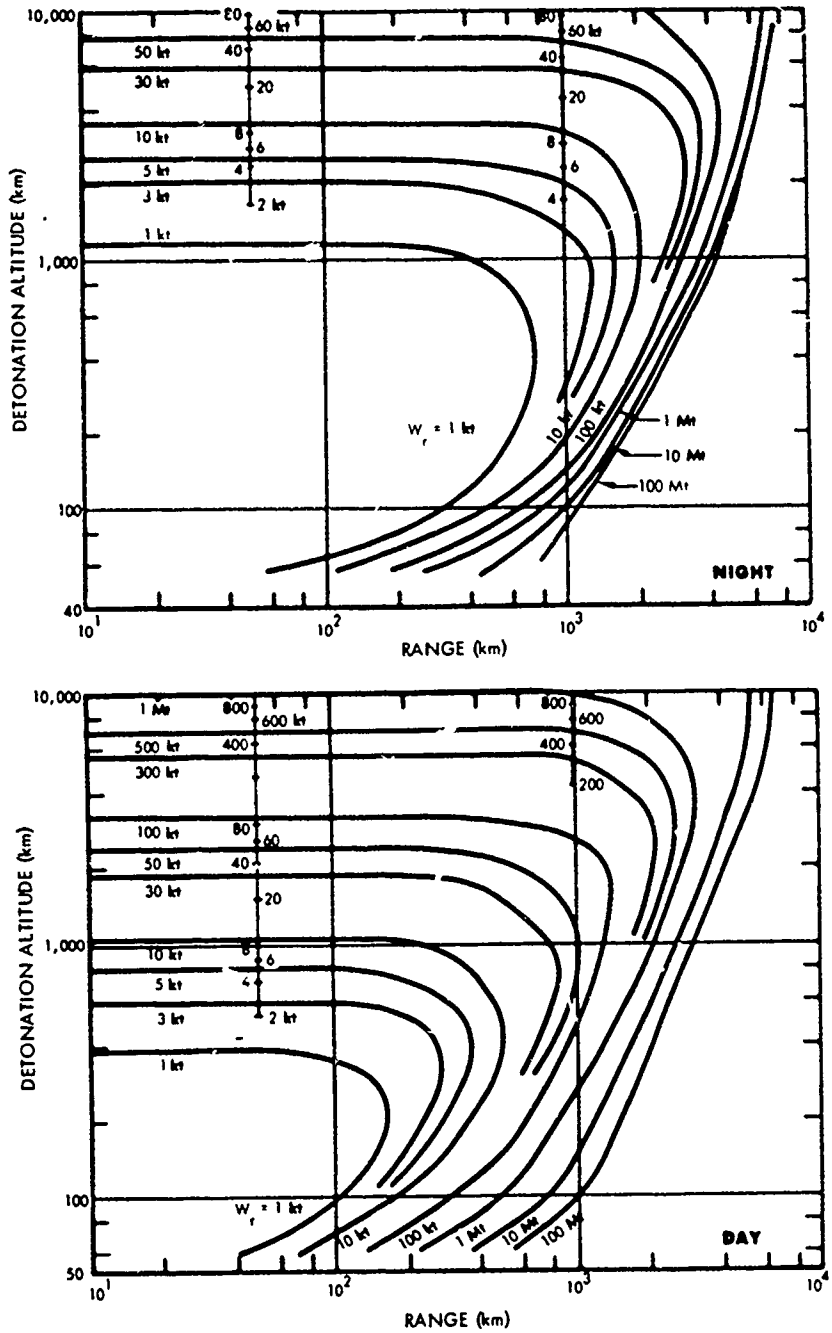

Figure 8-40. [redacted] Reference Weapon Yield W_r [redacted]

[redacted]

[redacted]

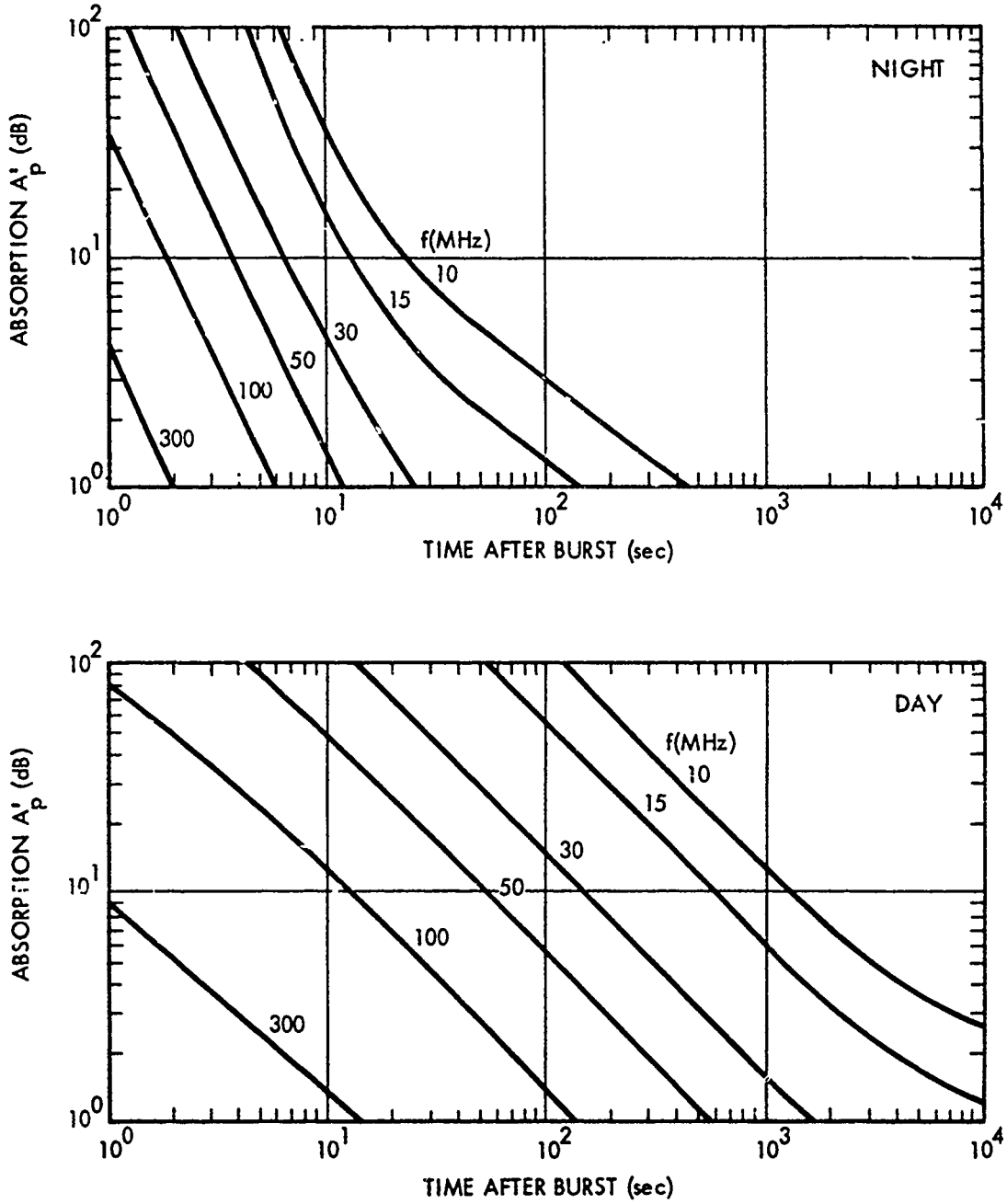

Figure 8-41. [redacted] One-Way Vertical Absorption Due to Prompt Radiation [redacted]

[redacted]

[redacted]

Problem 8-6 Absorption Outside the Fireball Due to Delayed Gamma Rays [redacted]

[redacted] Figures 8-42 through 8-48 are used to estimate the absorption caused by gamma rays emitted by the radioactive decay of fission debris. When the propagation path is within 100 km of the debris region and the debris region is below 120 km, the absorption depends on the orientation of the propagation path with respect to the debris region. Data are provided for three cases: a vertical path, a path passing above the debris region, and a path passing below the debris region. The geometry is illustrated in Figure 8-42.

[redacted] If the debris is at an altitude greater than 120 km or if the propagation path passes farther than 100 km from the debris region, absorption caused by gamma rays is given in terms of the gamma ray intensity parameter, I_γ. In determining I_γ, the debris region is modeled as a thin pancake region. Methods to determine the altitude and radius of the pancake debris region as a function of the burst parameters are described in Problems 8-1 through 8-3. If the altitude of detonation is below 85 km, the debris region is centered over the burst point (see Problem 8-1). For higher detonation altitudes, the center of the debris region is offset horizontally from the burst point toward the nearest magnetic pole after reaching maximum altitude (see Problem 8-2 and Figure 8-17). If the detonation altitude is greater than 120 km, up to three debris regions are defined (see Problem 8-3 and Figure 8-18).

[redacted] Figures 8-42 through 8-45 are used to obtain the one-way path absorption for bursts below 120 km and ground ranges from the debris less than 100 km. Choose the figure with the angle θ_d (see Figure 8-42) closest to the case of interest. Enter the figure with debris altitude, h_d, closest point of approach, X_d (see Figure 8-42), and time of day (day or night); obtain A'_γ, the one-way path absorption for a 1000 MHz signal 10 seconds after a 1 Mt fission yield detonation. Compute A_γ, the one-way path absorption:

$$A_\gamma = A'_\gamma W_F \frac{18}{(1 + t)^{1.2}} \frac{10^6}{f^2}$$

where W_F is the fission yield in Mt, t is the time in sec, and f is the propagation frequency in MHz.

[redacted] Figures 8-46 through 8-48 are used to obtain the one-way path absorption for bursts above 120 km or for cases where the ground range from the debris to the point where the propagation path intersects the altitude of 65 km is greater than 100 km. The following series of steps describe the procedure for obtaining the absorption.

1. Compute the quantity R', as follows:

$$R' = \begin{cases} \left[D^2 + (h_d - 60)^2\right]^{1/2} & D > R_d/2 \\ \left[\left(\frac{R_d}{2}\right)^2 + (h_d - 60)^2\right]^{1/2} & D \leq R_d/2 \end{cases}$$

where D is the ground range between the debris center and the point where the propagation path intersects 65 km altitude (see Figures 8-42 and 8-55 and Problem 8-10), and h_d and R_d are the debris altitude and radius, respectively (see Problems 8-1, 8-2, and 8-3).

2. Determine the debris-region fission yield W'_F:

$$W'_F = W_F \qquad h_o \leq 120 \text{ km}$$

$$W'_F = FF\ W_F \qquad h_o > 120 \text{ km}$$

where FF is the fraction of the total weapon fission yield in the debris region (see Problem 8-3).

[redacted]

[redacted]

[redacted]

3. Enter Figure 8-46 with debris-region fission yield (W_F'), time after burst t, and R' to obtain I_γ'.

4. Enter Figure 8-47 with debris altitude h_d, debris radius R_d, and the ground range where the propagation path intersects 65 km altitude D, to obtain C_γ. Compute I_γ:

$$I_\gamma = C_\gamma I_\gamma'.$$

If there is more than one debris region (if the detonation is above 120 km or if there are multiple bursts), the radiation intensity parametric I_γ should be found for each debris region and the sum of the radiation intensity parameters used to obtain the absorption.

5. Enter Figure 8-48 with I_γ, time of day (day or night), and frequency to obtain A_γ', the one-way vertical absorption. Compute A_γ, the one-way path absorption:

$$A_\gamma = A_\gamma' \sec \theta$$

where $\sec \theta$ is the secant of the angle of incidence at 65 km (see Problem 8-10).

[redacted] *Example 1* [redacted]

Given: A 1 Mt weapon, 50% fission $(W_F = 0.5$ Mt$)$, detonated at an altitude of 30 km during the daytime.

Find: The one-way absorption resulting from gamma ray ionization for a 1000 MHz signal 2 min after burst if the ground range between debris center and the propagation path is less than 100 km, the closest point of approach of the propagation path to the debris center, X_d, is 20 km, and θ_d is 60° (see Figure 8-42).

Solution: By the methods described in Problem 8-1, the debris altitude is determined to be:

$$h_d = 49 \text{ km}.$$

From Figure 8-43, $A_\gamma' = 14$ dB for $h_d = 49$ km and $X_d = 20$ km. Therefore,

$$A_\gamma = A_\gamma' W_F \frac{18}{(1+t)^{1.2}} \frac{10^6}{f^2},$$

$$A_\gamma = (14)(0.5) \frac{18}{(121)^{1.2}} \frac{10^6}{10^6} = 0.4 \text{ dB}$$

Answer: The one-way path absorption for a 1000 MHz signal propagating on a path as described above 2 min after a daytime 1 Mt burst $(W_F = 0.5$ Mt$)$ is 0.4 dB.

[redacted] *Example 2* [redacted]:

Given: A 1 Mt weapon, 50% fission, detonated at an altitude of 30 km during the nighttime.

Find: The one-way path absorption resulting from gamma ray ionization for a 100 MHz signal 2 min after burst if the ground range between the debris center and the point where the propagation path intersects 65 km is 200 km and $\sec \theta = 3$.

Solution:

a. By the methods described in Problem 8-1, the debris height, h_d, and radius, R_d, are determined to be:

$$h_d = 49 \text{ km},$$

$$R_d = 15 \text{ km}.$$

b. Since $D > R_d/2$,

$$R' = \left[D^2 + (h_d - 60)^2\right]^{1/2}$$

$$R' = \left[(200)^2 + (49 - 60)^2\right]^{1/2} \approx 200 \text{ km}$$

c. From Figure 8-46, $I_\gamma' = 0.15$ watts m^{-2}, for $W_F = 0.5$ Mt, $(1 + t) = 121$ sec, and $R' = 200$ km.

d. From Figure 8-47, $C_\gamma = 0.8$ for $(D - R_d) = 185$ km and $h_d = 49$ km. Therefore,

$$I_\gamma = C_\gamma' I_\gamma' = (0.8)(0.15) = 0.12 \text{ watts m}^{-2}$$

[redacted]

[redacted]

[redacted]

e. From Figure 8-48, A'_γ = 1.0 dB for I_γ = 0.12 watts m^{-2} and f = 100 MHz during the night. Therefore,

$$A_\gamma = A'_\gamma \sec\theta = 3.0 \text{ dB}.$$

Answer: The one-way path absorption for a 100 MHz signal propagating on a path as described above 2 min after a nighttime 1 Mt burst (W_F = 0.5 Mt) is 3.0 dB.

[redacted] *Example 3* [redacted]

Given: A 1 Mt weapon, 50% fission, detonated at an altitude of 300 km during the day at a location where the magnetic dip angle θ is 60°:

Find: The one-way path absorption resulting from gamma ray ionization for a 30 MHz signal 60 min after burst if the ground range between the point where the propagation path intersects 65 km is 1000 km due magnetic north of the burst point and sec θ = 3.

Solution:

a. By the methods described in Problem 8-3, the height, h_d, radius, R_d, offset, Δd, and fraction of the debris, FF for the three debris regions (see Figure 8-18), are found to be:

Debris Region	h_d (km)	R_d (km)	Δ_d (km)	FF
1	390	170	75	0.25
2	550	500	125	0.2
3	390	170	75	0.35

Debris region 1 is centered 75 km magnetic north of the burst point. The ground range, D, between the debris center and the point where the propagation path intersects 65 km is 1000 − 75 = 925 km. The ground range between the center of debris region 2 and the propagation path is 875 km. Debris region 3 is offset 75 km south of the conjugate of the burst point and is too far from the propagation path to produce gamma ray ionization.

b. The quantity R' for debris region 1 is:

$$R'_1 = \left[D^2 + (h_d - 60)^2\right]^{1/2}$$
$$= \left[(925)^2 + (330)^2\right]^{1/2} = 980 \text{ km}.$$

c. The debris region 1 fission yield is:

$$W'_{F1} = FF_1 \; W_F = 0.125 \text{ Mt}.$$

d. From Figure 8-46, $I'_{\gamma 1}$ is 2 x 10^{-5} watts m^{-2} for W'_{F1} = 0.125 Mt, t = 3600 sec, and R'_1 = 980 km.

e. From Figure 8-47, $C_{\gamma 1}$ is 1 for $(D - R_d)$ = 775 km and h_d = 390 km.

f. $I_{\gamma 1} = C_{\gamma 1} I'_{\gamma 1}$ = 2 x 10^{-5} watts m^{-2}.

g. The quantity R' for debris region 2 is:

$$R'_2 = \left[(875)^2 + (490)^2\right]^{1/2} = 1000 \text{ km}$$

h. The debris region 2 fission yield is:

$$W'_{F2} = FF_2 \; W_F = 0.1 \text{ Mt}$$

i. From Figure 8-46, $I'_{\gamma 2}$ is 1.5 x 10^{-5} watts m^{-2} for W'_{F2} = 0.1 Mt, t = 3600 sec, and R'_2 = 1000 km.

j. From Figure 8-47, $C_{\gamma 2}$ is 1 for $(D - R_d)$ = 375 km and h_d = 550 km.

k. $I_{\gamma 2} = C_{\gamma 2} I'_{\gamma 2}$ = 1.5 x 10^{-5} watts m^{-2}.

l. $I_\gamma = I_{\gamma 1} + I_{\gamma 2}$ = 3.5 x 10^{-5} watts m^{-2}.

m. From Figure 8-48, A'_γ = 1 dB for I_γ = 3.5 x 10^{-5} watts m^{-2} and f = 30 MHz.

n. $A_\gamma = A'_\gamma \sec\theta$ = 3 dB.

Answer: The one-way path absorption for a 30 MHz signal propagating on a path as described above 60 min after a daytime burst (W_F = 0.5 Mt) is 3 dB. If the propagation path had been located near the conjugate of the burst point, gamma rays from debris regions 1 and 2 would not reach the path, and only debris region 3 would have been considered.

[redacted]

[redacted]

[redacted] *Reliability* [redacted] The procedures given for computing absorption due to gamma ray ionization are based on simplified-debris, atmospheric-chemistry, and geometry models. More detailed models are required for most radar and communication system problems.

[redacted] *Related Material* [redacted] See paragraphs 8-3, 8-8, 8-13, 8-14, and 8-15, and Problems 8-1, 3-2, and 8-3.

[redacted]

[redacted]

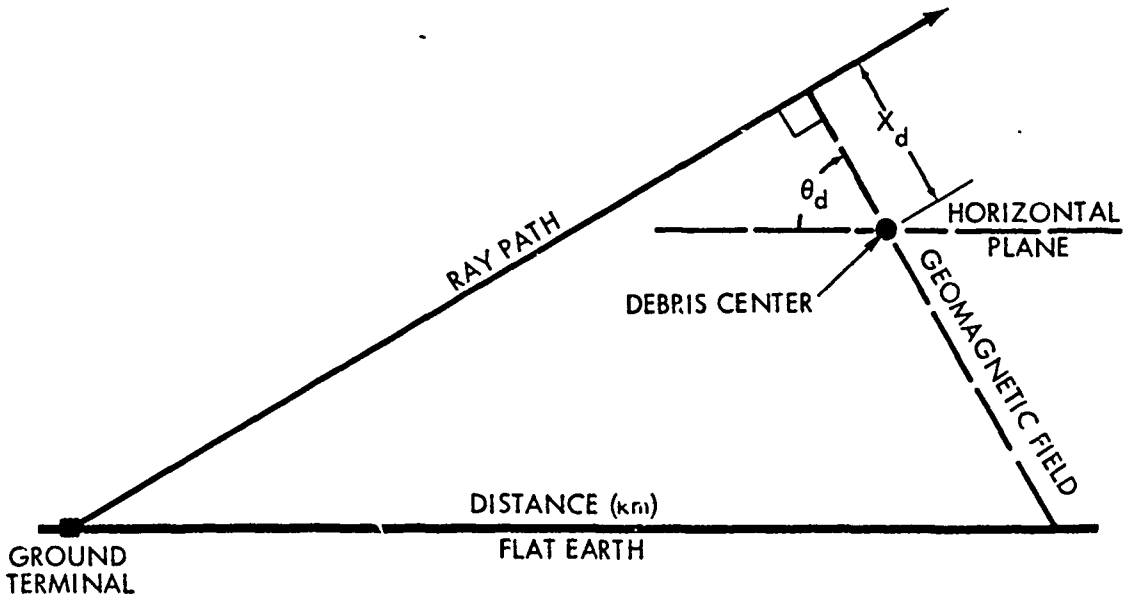

Figure 8-42. [redacted] Geometry for Gamma Ray Absorption [redacted]

[redacted]

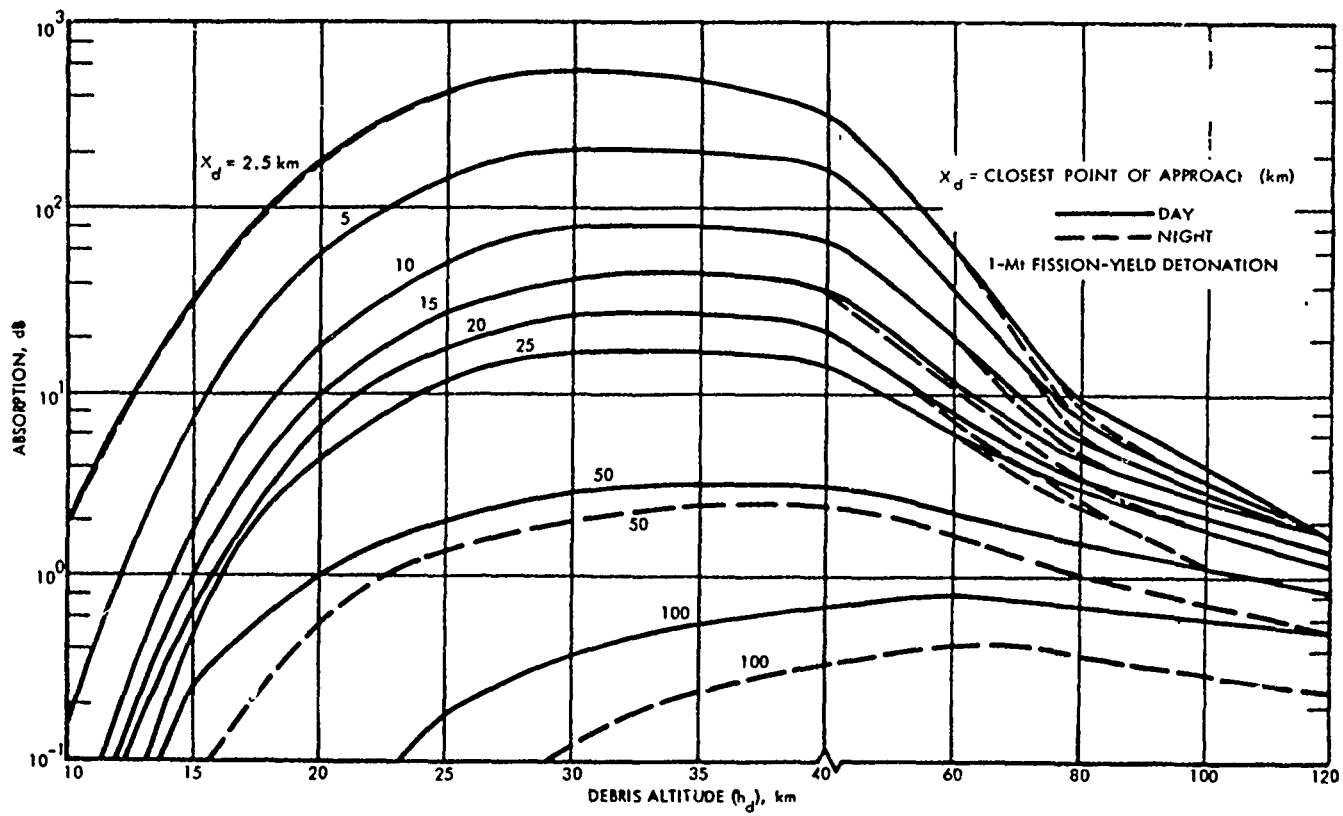

Figure 8-43. One-Way Absorption Due to Gamma Rays, f = 1000 MHz, θ_d = +60 Degrees

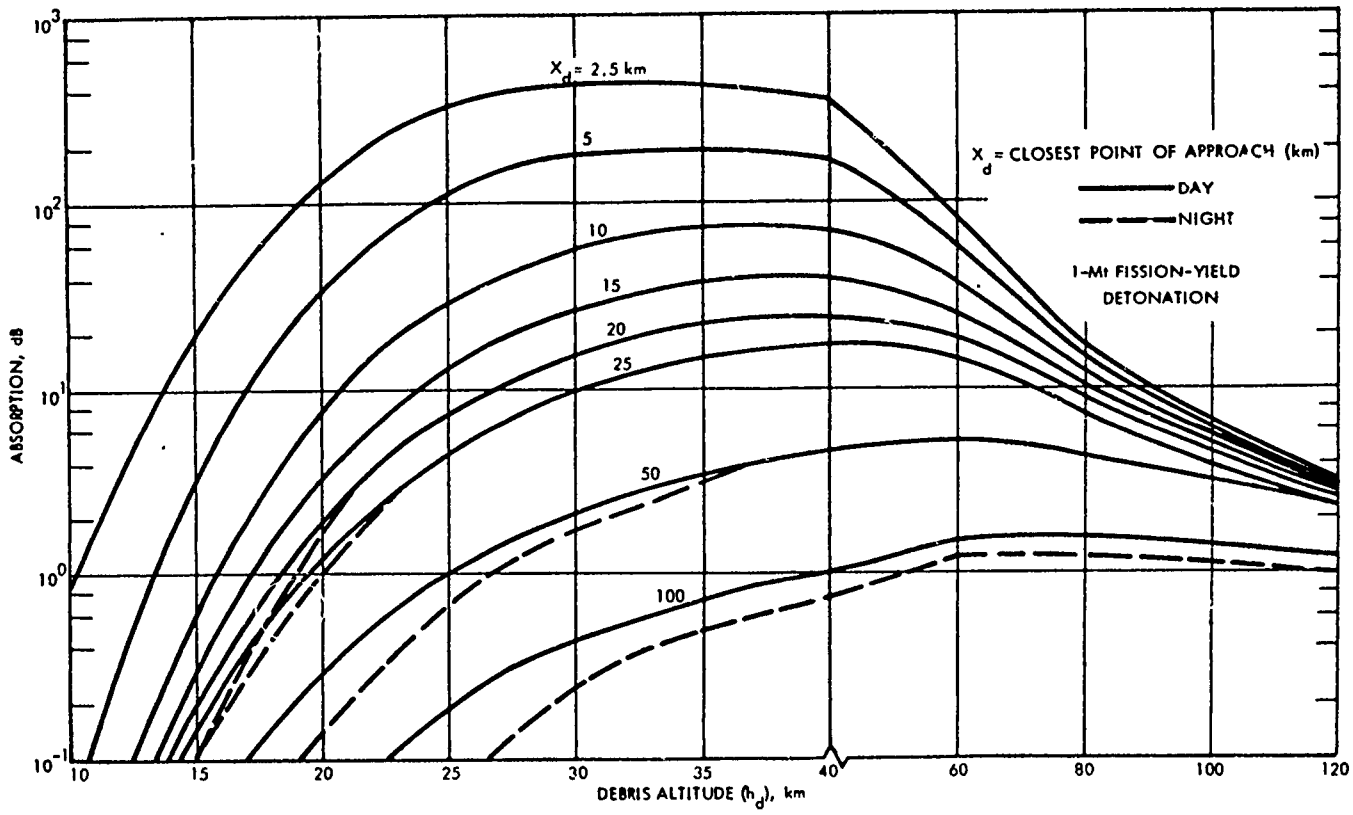

Figure 8-44. [redacted] One-Way Absorption Due to Gamma Rays, f = 1000 MHz, θ_d = 0 Degrees [redacted]

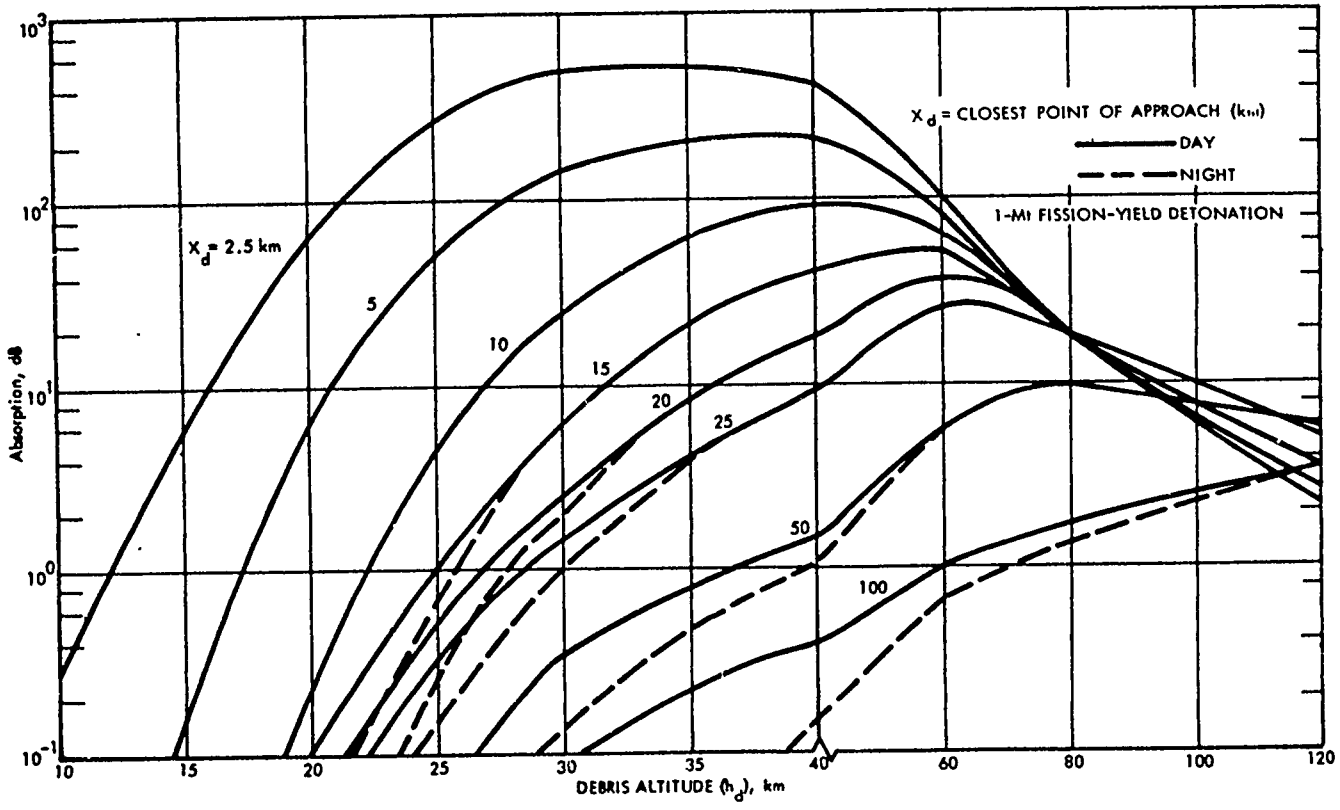

Figure 8-45. [redacted] One-Way Absorption Due to Gamma Rays, f = 1000 MHz, θ_d = -60 Degrees [redacted]

[redacted]

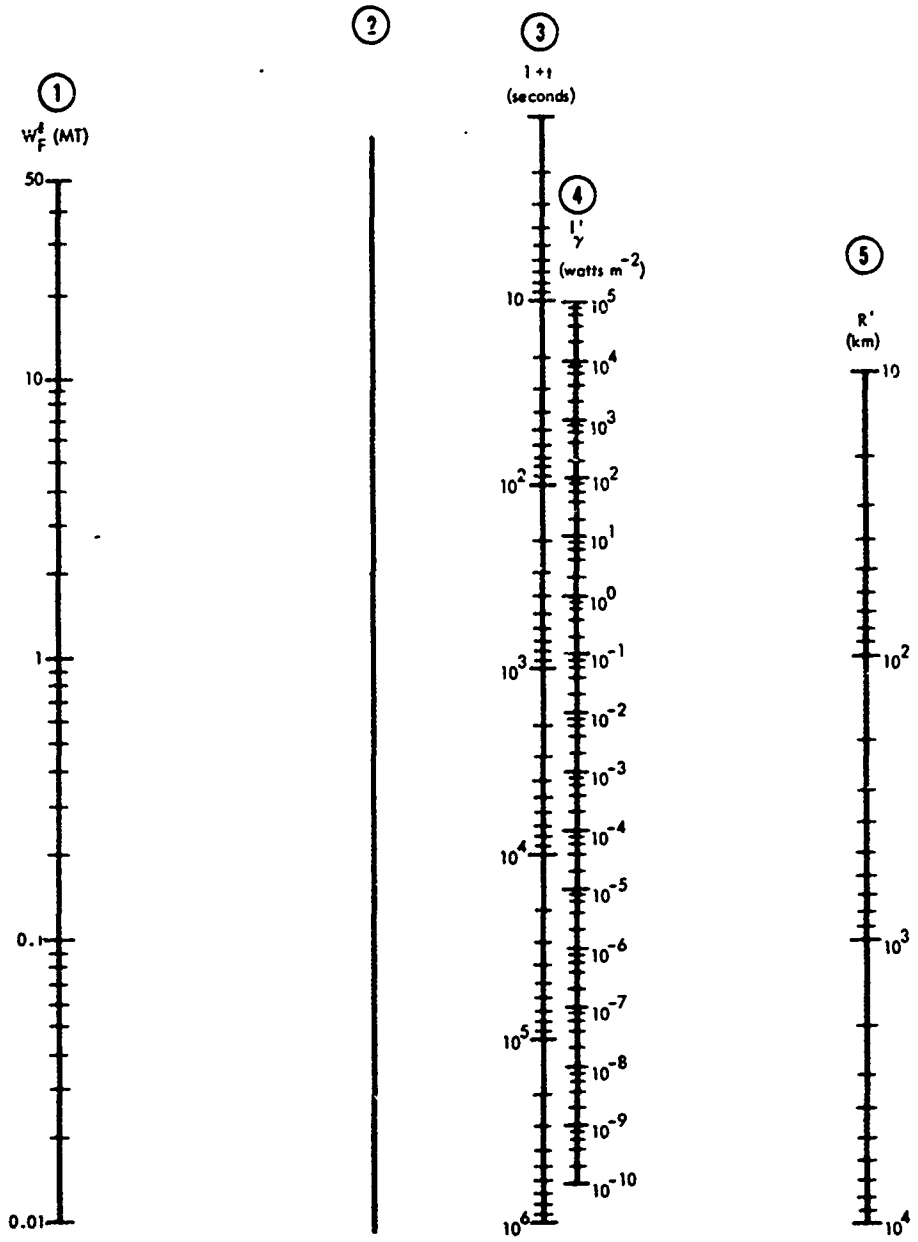

INSTRUCTIONS: To find I'_γ connect a straight line from fission yield (Scale 1) to time after detonation on Scale 3 (note this is a 1+t scale). Mark the intersection on Scale 2. Connect a straight line from the point determined on Scale 2 to the appropriate distance, R', on Scale 5. The intersection with Scale 4 is I'_γ.

Figure 8-46. [redacted] Gamma Radiation Intensity Nomogram [redacted]

[redacted]

[redacted]

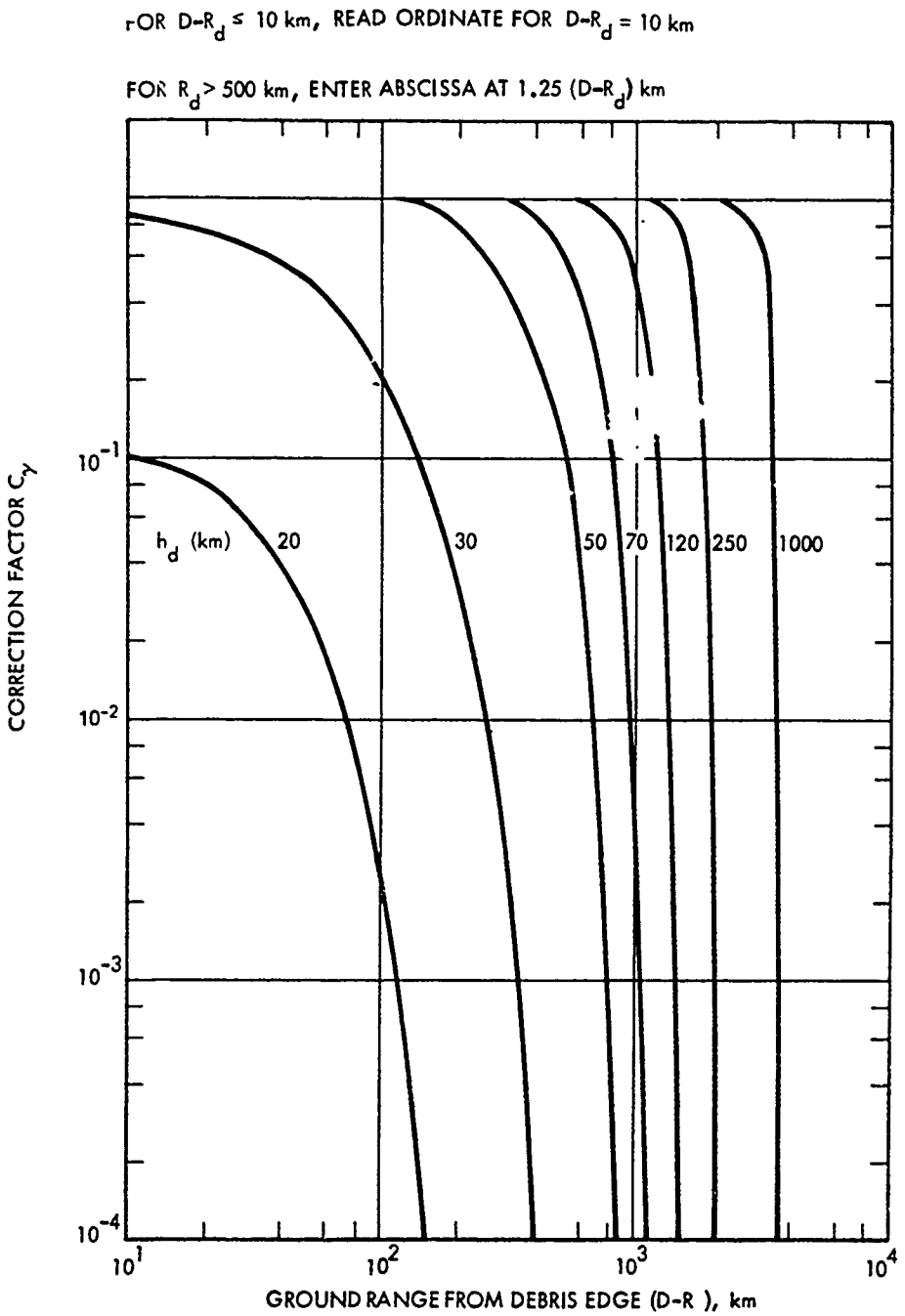

Figure 8-47. [redacted] Correction Factor for Gamma Ray Flux [redacted]

[redacted]

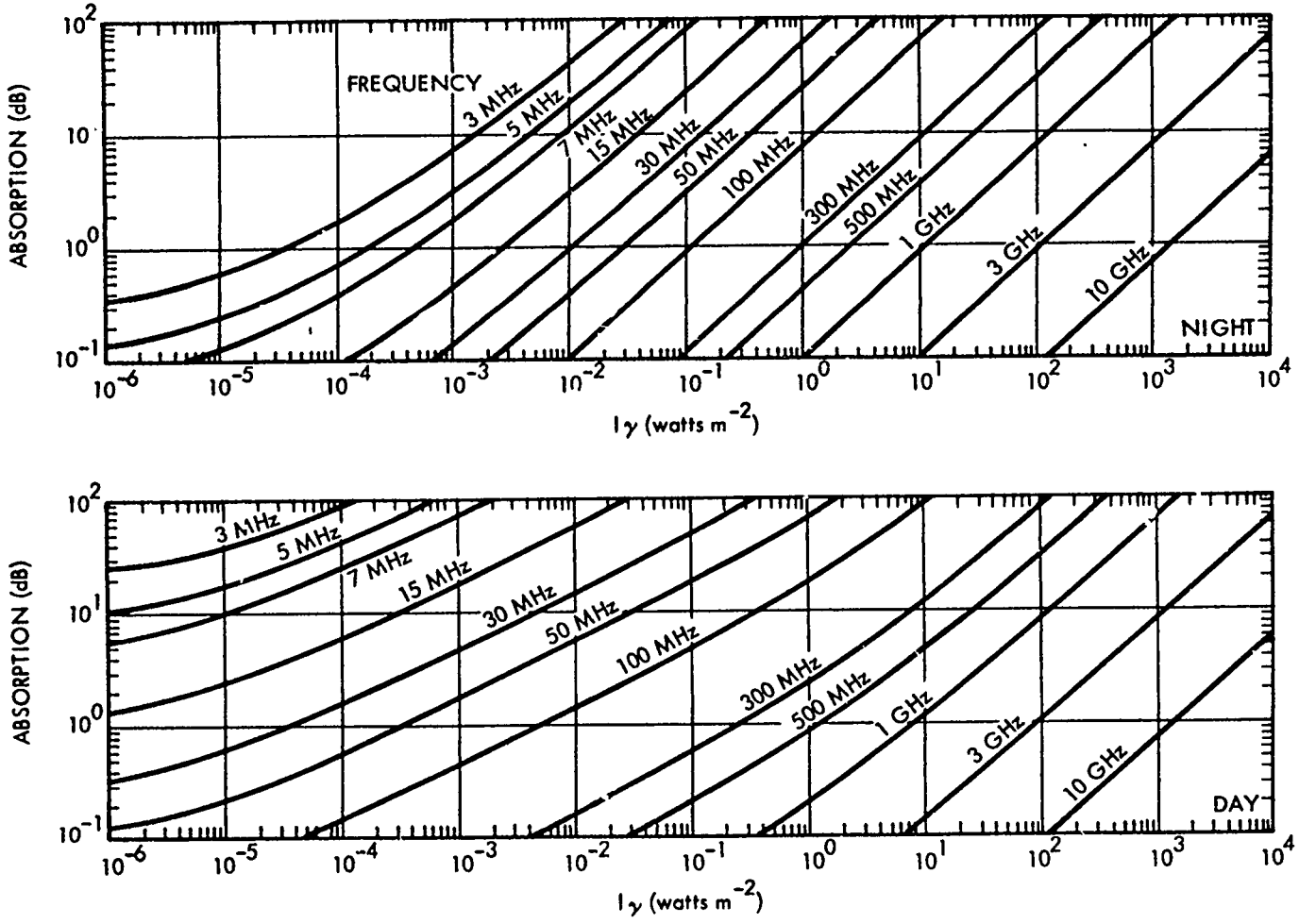

Figure 8-48. [redacted] One-Way Vertical Absorption Due to Gamma Rays [redacted]

[redacted]

Problem 8-7 Calculation of Absorption Outside the Fireball Due to Beta Particles [redacted]

[redacted] Figures 8-49 through 8-51 are used to estimate the absorption outside the fireball region caused by beta particle ionization when the fission debris is above 60 km. If the debris is below 60 km, the absorption caused by beta particle ionization can be computed by the methods described in Problem 8-4.

[redacted] When the fission debris is above 60 km, the location of the beta particle absorption region with respect to the debris region is determined by the geomagnetic field (see paragraph 8-4). Most of the absorption occurs between the altitudes of 60 and 80 km. The predictions of absorption apply to beta particle radiation from fission debris that is uniformly distributed in a thin pancake-shaped region.

[redacted] Obtain the debris altitude, h_d, and debris radius, R_d, by the methods described in Problems 8-1, 8-2, or 8-3. If the detonation altitude, h_o, is greater than 85 km and the time after burst is greater than 10 minutes, determine the maximum debris altitude, h_m (km). Compute h:

$$h = h_d \quad \begin{cases} h_o < 85 \text{ or if} \\ h_o \geqslant 85 \text{ and } t < 10 \text{ minutes.} \end{cases}$$

$$h = h_m \qquad h_o \geqslant 85 \text{ and } t > 10 \text{ minutes.}$$

Enter Figure 8-49 with h and φ, the magnetic dip angle at the burst point to obtain Δ_β, the offset of the beta particle absorption region. If the magnetic dip angle at the burst point is not known, it can be obtained from Figure 8-54 as described in Problem 8-9.

[redacted] There are two beta particle absorption regions for each debris region; one is in the burst region and is offset a distance Δ_β from ground zero toward the nearest magnetic pole (see Figure 8-49), and the other is in the conjugate region and is offset from the conjugate of ground zero toward the nearest magnetic pole. Location of the conjugate of ground zero can be estimated from Figure 8-53 as described in Problem 8-8. The horizontal extent of the beta particle absorption region is approximately the same as that of the debris region (this neglects convergence of the magnetic field).

[redacted] If the propagation path passes through a beta particle absorption region, the one-way absorption can be found by the following procedure:

1. Determine the debris region fission yield, W_F':

$$W_F' = W_F \qquad h_o \leqslant 120 \text{ km}$$

$$W_F' = FF\ W_F \qquad h_o > 120 \text{ km}$$

where FF is the fraction of the total weapon fission yield in the debris region (see Problem 8-3).

2. Enter Figure 8-50 with debris region fission yield, W_F', time after burst, t, and debris radius, R_d, to obtain N_β. If the propagation path passes through more than one beta particle absorption region, compute the value of N_β for each region and use the sum to compute the one-way vertical absorption.

3. Enter Figure 8-51 with N_β, the frequency, f, and the time of day (day or night) to obtain A_β', the one-way vertical absorption. Compute A_β, the one-way absorption:

$$A_\beta = A_\beta' \sec \theta,$$

where $\sec \theta$ is the secant of the angle of incidence of the propagation path at 65 km which may be determined by the methods described in Problem 8-10.

[redacted]

[redacted]

[redacted] *Example 1* [redacted]

Given: A 1 Mt weapon, 50% fission, detonated at an altitude of 80 km at a location where the magnetic dip angle is 60° during daytime.

Find: The one-way absorption resulting from beta particle ionization for a 400 MHz signal 5 min after burst if sec $\theta = 3$.

Solution:

a. By the methods described in Problem 8-1, the debris height and radius are determined to be:

$$h_d = 305 \text{ km},$$

$$R_d = 200 \text{ km}.$$

b. Since $h_o < 85$ km,

$$h = h_d = 305 \text{ km}.$$

c. From Figure 8-49, $\Delta_\beta = 150$ km for $h = 305$ km, and $\theta = 60°$.

d. Since $h_o < 120$ km,

$$W_F' = W_F = 0.5 \text{ Mt}.$$

e. From Figure 8-50, $N_\beta = 4 \times 10^7$ betas cm^{-2} sec^{-1} for $W_F' = 0.5$ Mt, $t = 300$ sec, and $R_d = 200$ km.

f. From Figure 8-51, $A_\beta' = 2$ dB; therefore,

$$A_\beta = A_\beta' \sec \theta = 6 \text{ dB}.$$

Answer: There are two absorption regions caused by beta particle ionization. One is in the burst locale and is centered 150 km towards the nearest magnetic pole. The other is on the opposite side of the magnetic equator and is centered 150 km towards the nearest magnetic pole from the conjugate of the burst point. The horizontal radius of each absorption region is 200 km. The one-way path absorption for a 400 MHz signal passing through either absorption region is 6 dB.

[redacted] *Example 2* [redacted]

Given: A 1 Mt weapon, 50% fission, detonated at an altitude of 300 km at a location where the magnetic dip angle is 60° during daytime.

Find: The one-way absorption resulting from beta particle ionization for a 40 MHz signal 60 min after burst if the ground terminal is at burst ground zero, the propagation path is at an elevation of 15° along a zero degree magnetic azimuth, and sec $\theta = 3.4$.

Solution:

a. By the methods described in Problem 8-3, the height, h_d, radius, R_d, maximum altitude of rise, and fraction of the debris, FF, for the three debris regions (see Figure 8-18) are found to be:

Debris Region	h_d (km)	R_d (km)	h_m (km)	FF
1	390	170	550	0.25
2	550	500	800	0.2
3	390	170	550	0.35

b. Since $h_o > 85$ km and $t > 10$ min:

$$h_1 = h_{m1} = 550 \text{ km},$$

$$h_2 = h_{m2} = 800 \text{ km},$$

$$h_3 = h_{m3} = 550 \text{ km}.$$

c. From Figure 8-49, the beta particle absorption region offsets are:

$$\Delta_{\beta 1} = 300 \text{ km},$$

$$\Delta_{\beta 2} = 450 \text{ km},$$

$$\Delta_{\beta 3} = 300 \text{ km}.$$

d. Since $W_F = 0.5$ Mt, the fission yields contained in the debris regions are:

$$W_{F1}' = 0.125 \text{ Mt},$$

$$W_{F2}' = 0.1 \text{ Mt},$$

$$W_{F3}' = 0.175 \text{ Mt}.$$

[redacted]

[redacted]

[redacted]

e. Entering Figure 8-50 with the debris radii from "a," the fission yields from "d," and a time t = 3600 sec, the following values of N_β are obtained:

$$N_{\beta 1} = 10^6 \text{ betas cm}^{-2} \text{ sec}^{-1},$$

$$N_{\beta 2} = 8 \times 10^4 \text{ betas cm}^{-2} \text{ sec}^{-1},$$

$$N_{\beta 3} = 1.75 \times 10^6 \text{ betas cm}^{-2} \text{ sec}^{-1},$$

f. A sketch of the location of the absorption regions in the burst locale caused by beta particle ionization is shown in Figure 8-52. The propagation path chosen for this example traverses the absorption regions caused by all three debris regions. Thus, the values of N_β for each debris region are added together before finding the absorption.

$$N_\beta = N_{\beta 1} + N_{\beta 2} + N_{\beta 3}$$
$$= 2.8 \times 10^6 \text{ betas cm}^{-2} \text{ sec}^{-1}$$

g. From Figure 8-51, the one-way vertical absorption for a 40 MHz signal is

$$A'_\beta = 40 \text{ dB}$$

and

$$A_\beta = A_\beta \sec \theta = 136 \text{ dB}.$$

Answer: The one-way path absorption for a 40 MHz signal propagating on the path as described above 60 min after a 1 Mt (W_F = 0.5 Mt) daytime burst at 300 km is the sum of the absorptions caused by all three debris regions and is 136 dB.

[redacted] *Reliability* [redacted]: The procedures given for computing absorption due to beta particle ionization are based on simplified debris, atmospheric chemistry, and geometry models. More detailed models are required for most radar and communication system problems.

[redacted] *Related Material* [redacted] See paragraphs 8-4, 8-5, 8-8, 8-13, 8-14, and 8-15, and Problems 8-1, 8-2, and 8-3.

[redacted]

[redacted]

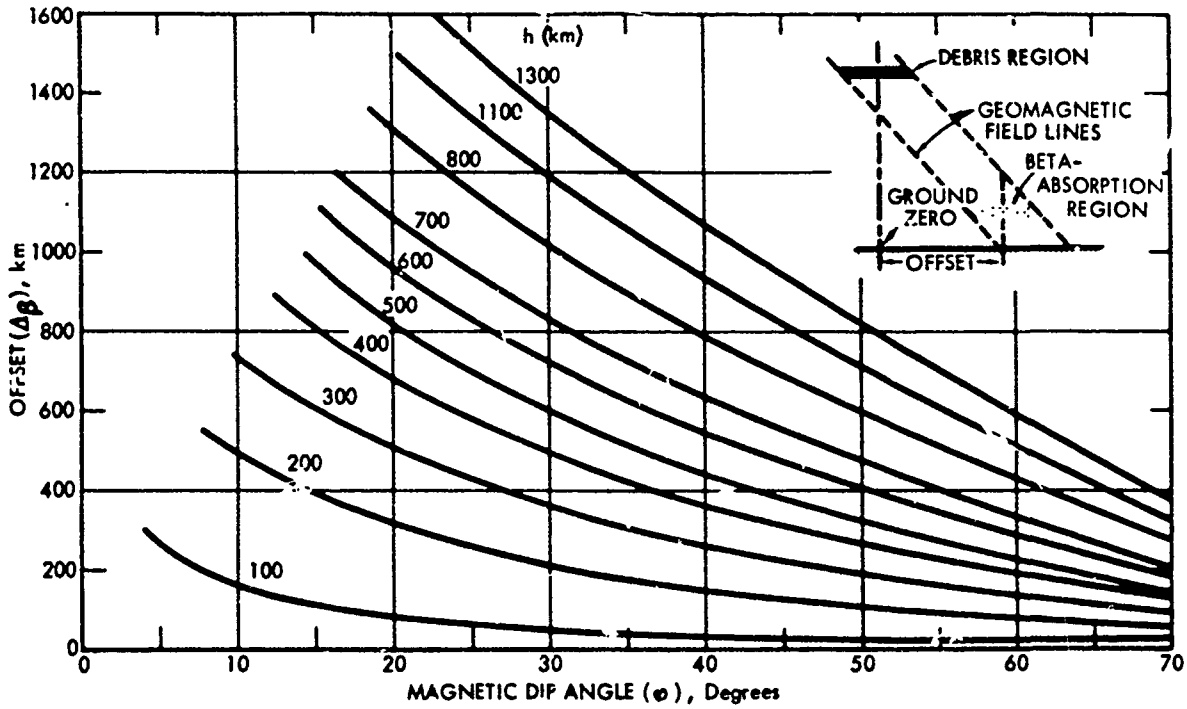

Figure 8-49. [redacted] Offset of Beta-Absorption Region [redacted]

[redacted]

[redacted]

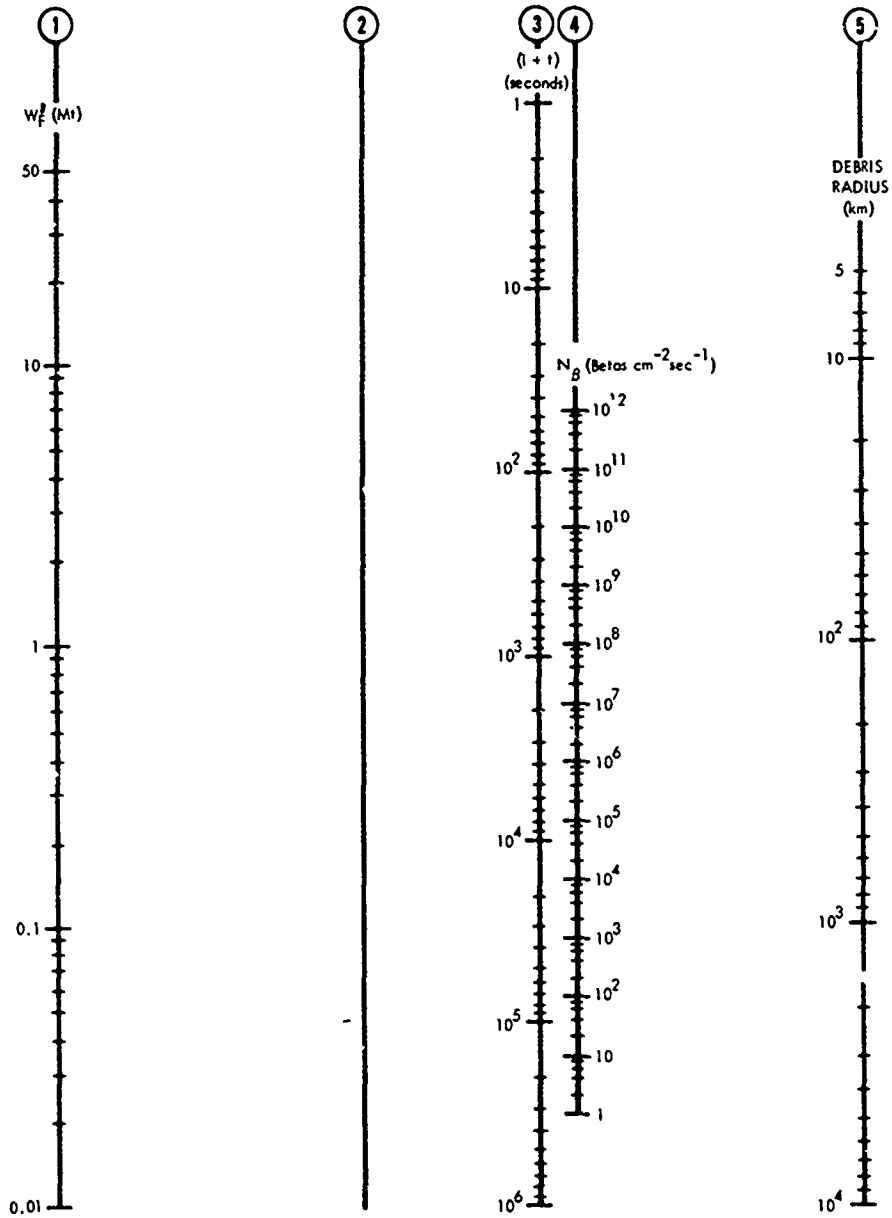

INSTRUCTIONS: To find N_β connect a straight line from fission yield (Scale 1) to time after detonation (Scale 3- this is a 1 + t scale). Mark the point of intersection of this line with Scale 2. Then draw a straight line from this point to the appropriate debris radius on Scale 5. The intersection of the latter line with Scale 4 is N_β.

Figure 8-50. [redacted] Beta Radiation Intensity Nomogram [redacted]

[redacted]

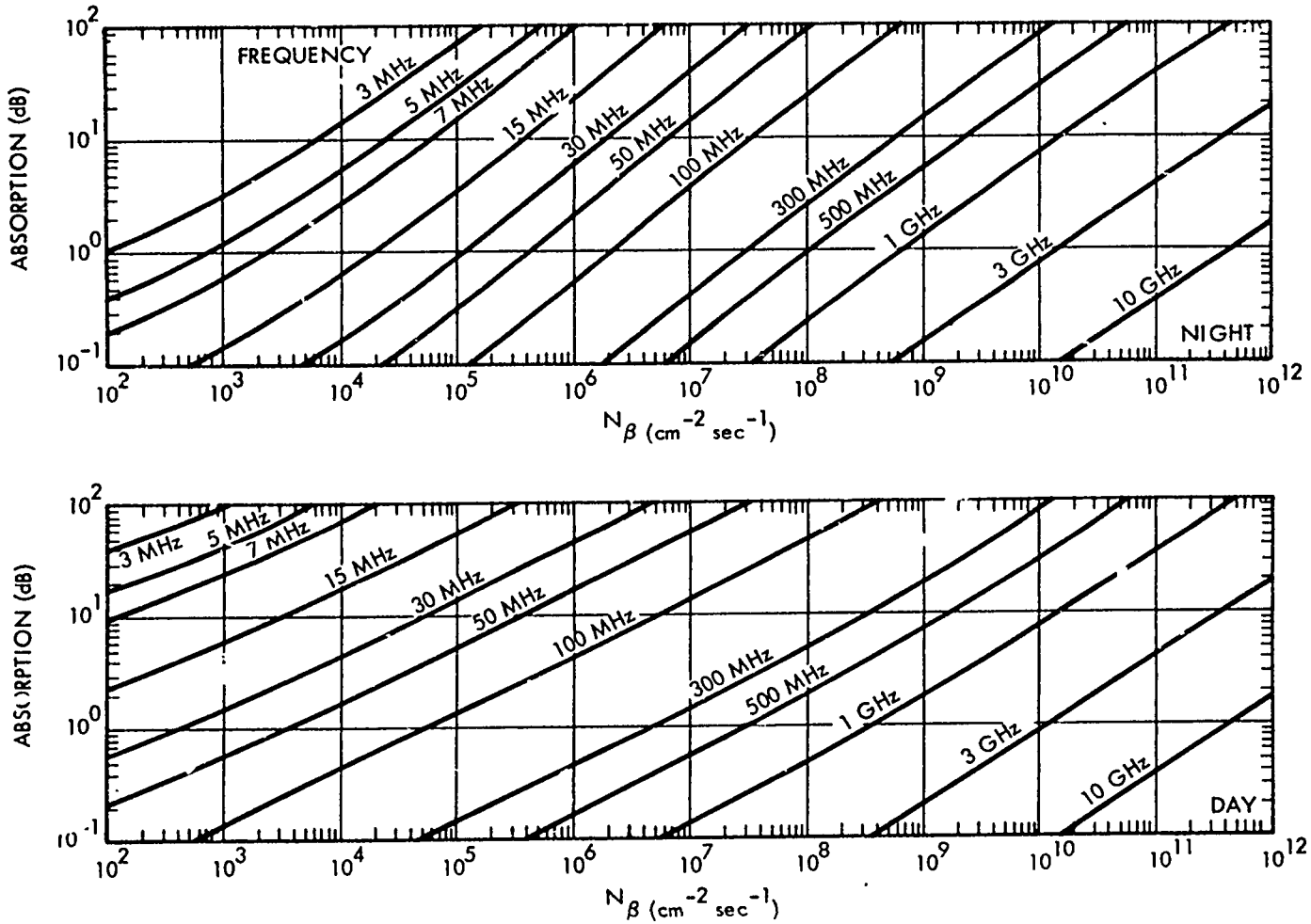

Figure 8-51. [redacted] One-Way Vertical Absorption Due to Beta Particles, Debris Altitude Above 60 km [redacted]

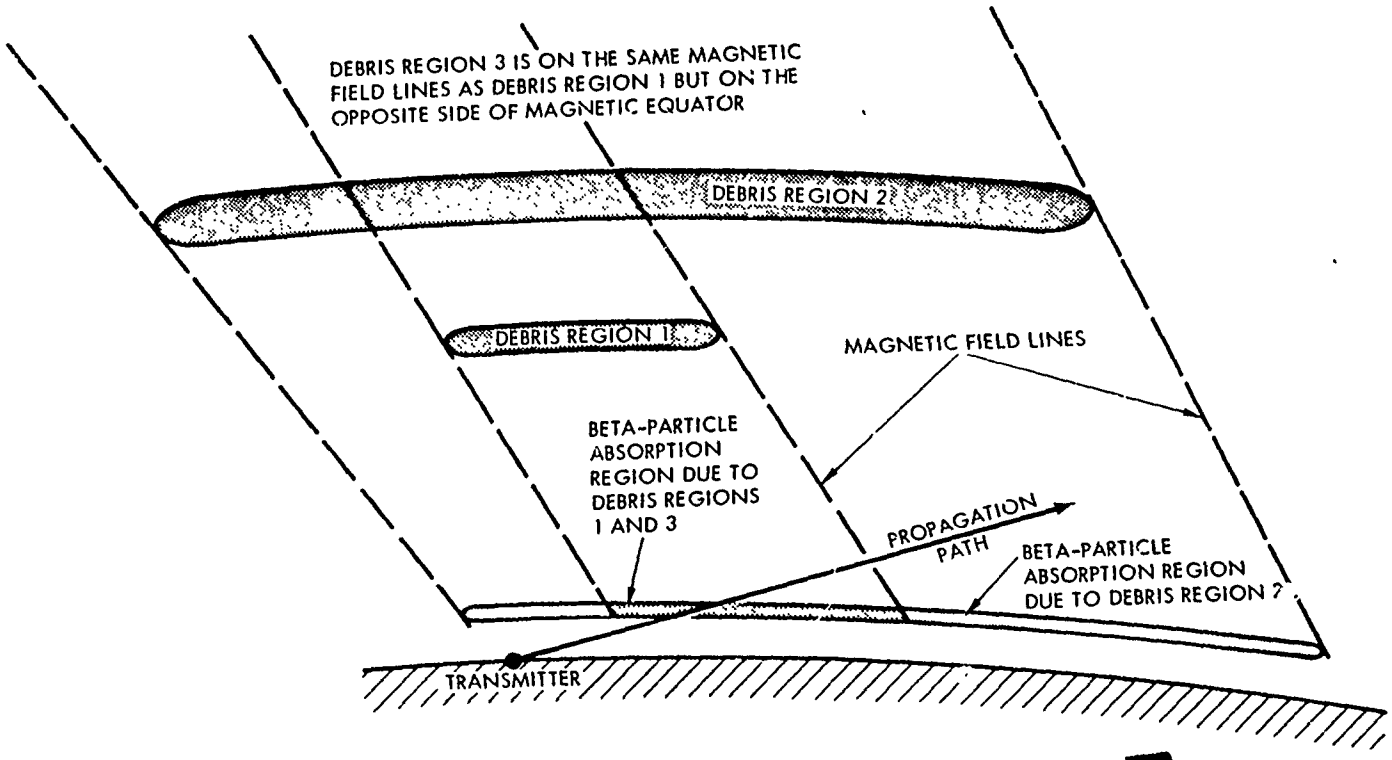

Figure 8-52. Sketch of Absorption-Region Geometry for Example 2

[redacted]

Problem 8-8 Magnetic Conjugate Map [redacted]

[redacted] Figure 8-53 presents the location of geomagnetic conjugate points on the earth's surface. Using the geographic coordinates of a given point, enter Figure 8-53 on the straight-line rectangular grid, and read the geographic coordinates of the magnetic conjugate point on the heavy curved grid.

[redacted] In reading Figure 8-53, note that the east-west curved dashed lines indicate conjugate latitude, plus for degrees north latitude and minus for degrees south latitude. Similarly, the north-south curved solid lines indicate conjugate longitude, plus for degrees east longitude and minus for degrees west longitude:

[redacted] *Example* [redacted]

Given: Geographic coordinates 45°N, 77°W (point near Ottawa, Canada).

Find: The coordinate of the conjugate point.

Solution: The given coordinates occur at the intersection of the -71° and -93° heavy grid lines.

Answer: The approximate geographic coordinates of the conjugate point are 71°S and 93°W.

[redacted] *Reliability* [redacted] In addition to uncertainties in the geomagnetic field, distortions of the geomagnetic field caused by the burst may persist for tens of seconds. Thus, the locations of conjugate debris and beta particle ionization regions may be significantly different than predicted by Figure 8-53.

[redacted] *Related Material* [redacted] See paragraph 8-4.

[redacted]

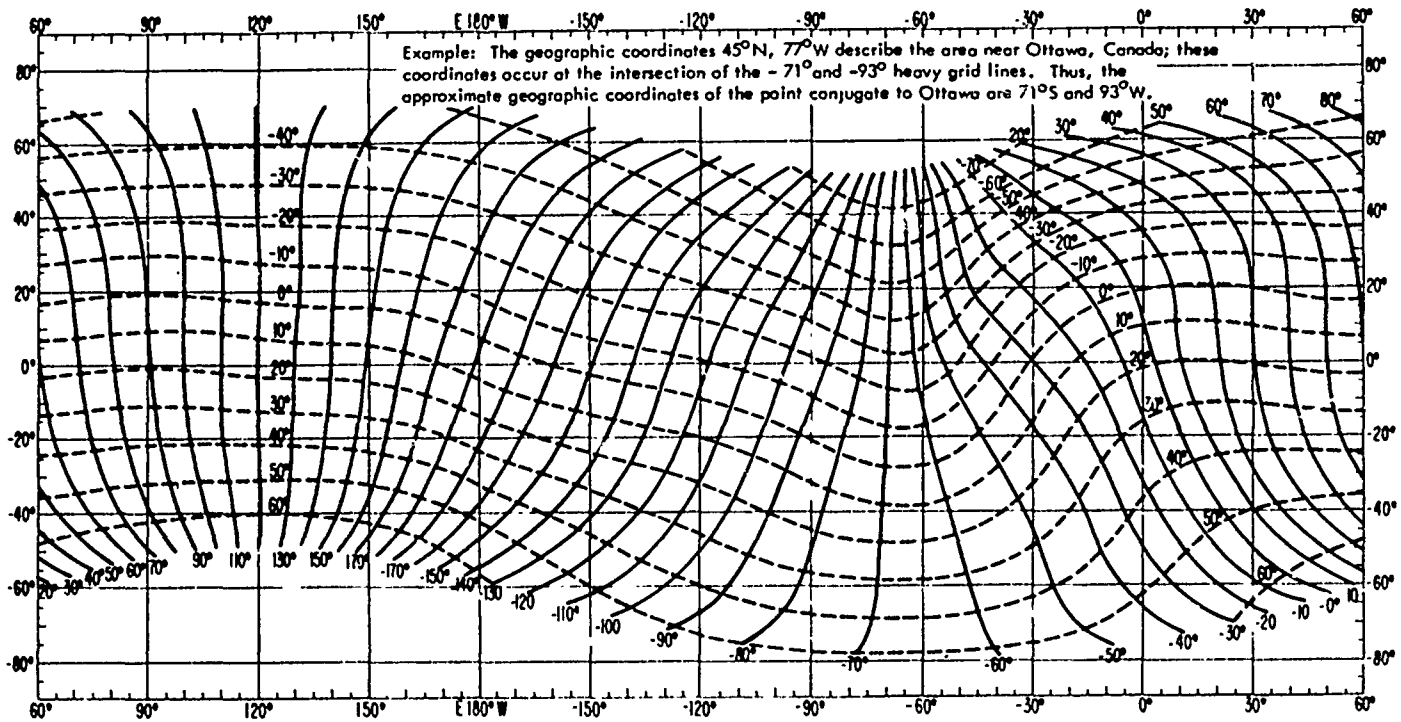

Figure 8-53. Magnetic Conjugate Map

[redacted]

Problem 8-9 Geomagnetic Dip Angle Map [redacted]

[redacted] Figure 8-54 presents the geomagnetic dip angle (declination) as a function of the geographic coordinates of a position on the earth's surface.

[redacted] *Example* [redacted]

Given: A point with geographic coordinates 40°N latitude, 100°W longitude.

Find: The geomagnetic dip angle.

Answer: From Figure 8-54 the magnetic dip angle is 70°.

[redacted] *Reliability* [redacted] Figure 8-54 shows the geomagnetic dip angle for undisturbed magnetic field conditions. The geomagnetic field may be distorted for tens of seconds after a nuclear detonation. Therefore, the locations of the debris and beta particle ionization regions may differ significantly from those predicted by Figure 8-54.

[redacted] *Related Material* [redacted] See paragraph 8-4.

[redacted]

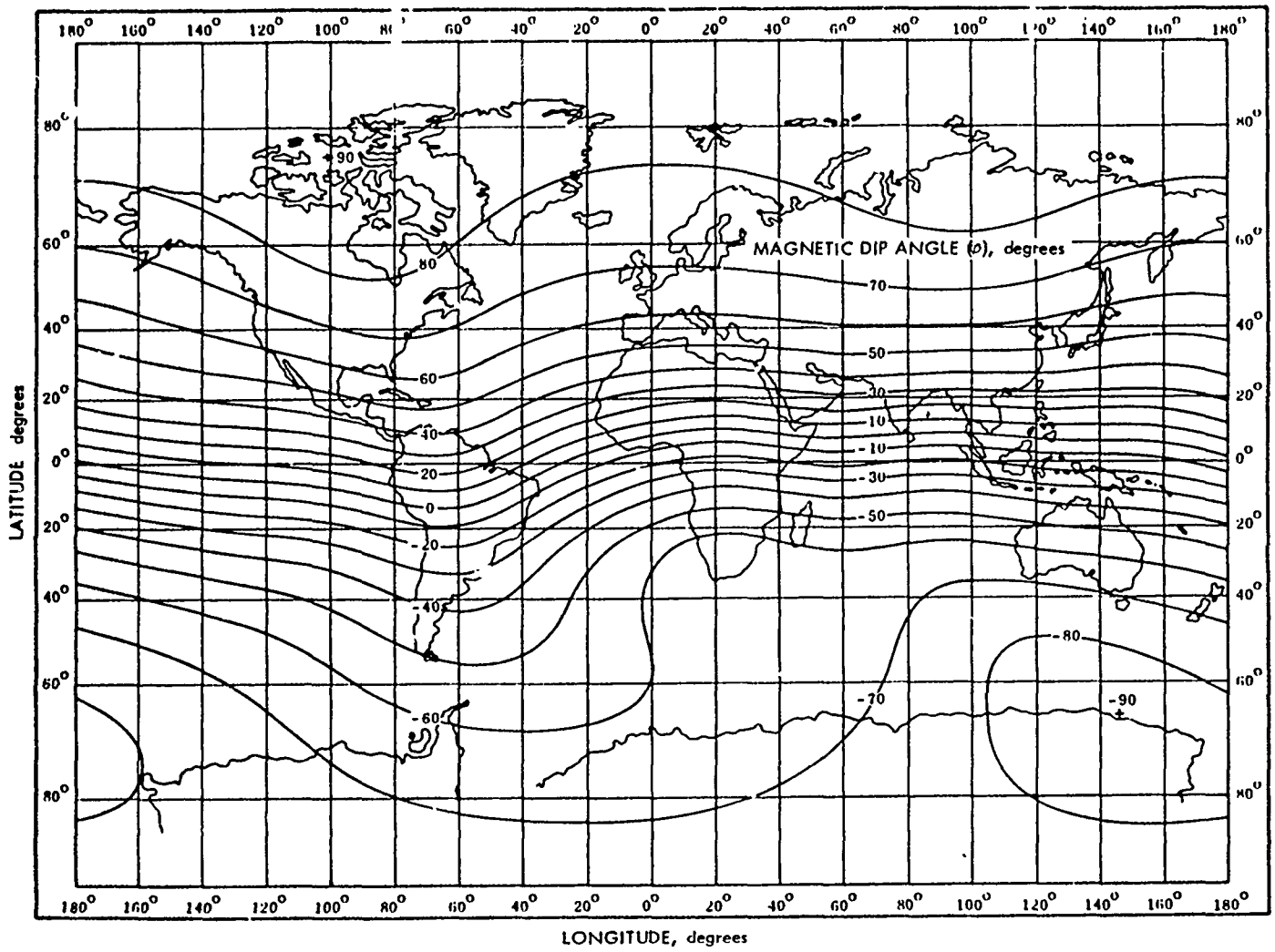

Figure 8-54. [redacted] World Map of Magnetic Dip [redacted]

[redacted]

Problem 8-10 Secant θ Chart [redacted]

[redacted] Figure 8-55 presents the secant of the angle of incidence of a ray path at 65 km altitude as a function of elevation angle or distance from the ground terminal to E- and F-region reflection points. The angle of incidence, θ, is illustrated in the sketch in Figure 8-55.

[redacted] *Example 1* [redacted]

Given: A propagation path with a 10-degree elevation angle (β).

Find: The horizontal distance from the ground terminal to the point where the propagation path intersects 65 km altitude, and the secant of the angle of incidence θ at the intersection.

Solution: Enter Figure 8-55 on the line sloping downward to the right labeled 10 degrees. Locate the intersection of this line with the line sloping upward to the right labeled h = 65 km. The abscissa of this intersection is the horizontal distance, and the ordinate is secant θ.

Answer: The horizontal distance from the ground terminal to the point where the propagation path intersects 65 km altitude is 320 km. The secant of the angle of incidence at the intersection is 4.6.

[redacted] *Example 2* [redacted]

Given: A HF propagation path that reflects from the F-region (300 km), 1500 km from the ground terminal.

Find: The horizontal distance from the ground terminal to the point where the propagation path intersects 65 km altitude, and secant θ at the intersection.

Solution: Enter the abscissa of Figure 8-55 at 1500 km. Proceed upward to the line labeled F-region Reflection Altitude (300 km). Note the elevation angle (β) corresponding to this point. Find the intersection of the elevation angle line with the line labeled D-region Absorption Altitude (65 km). The abscissa of this intersection is the desired horizontal distance, and the ordinate is secant θ.

Answer: The horizontal distance from the ground terminal to the point where the propagation path intersects 65 km altitude is 500 km. The secant of the angle of incidence at the intersection is 6.

[redacted] *Reliability* [redacted] The curves of Figure 8-55 are accurate for the simplified geometry assumed; however, the D, E, and F absorption and reflection altitudes are not single lines but occupy a volume of space which changes in ltitude with time of day and which may be affected by solar activity. Therefore, more detailed models are generally required for radar and communication system problems.

[redacted] *Related Material* [redacted] See paragraphs 8-1, 8-3, 8-4, 8-6, 8-7, 8-8, and Problems 8-1 through 8-6.

[redacted]

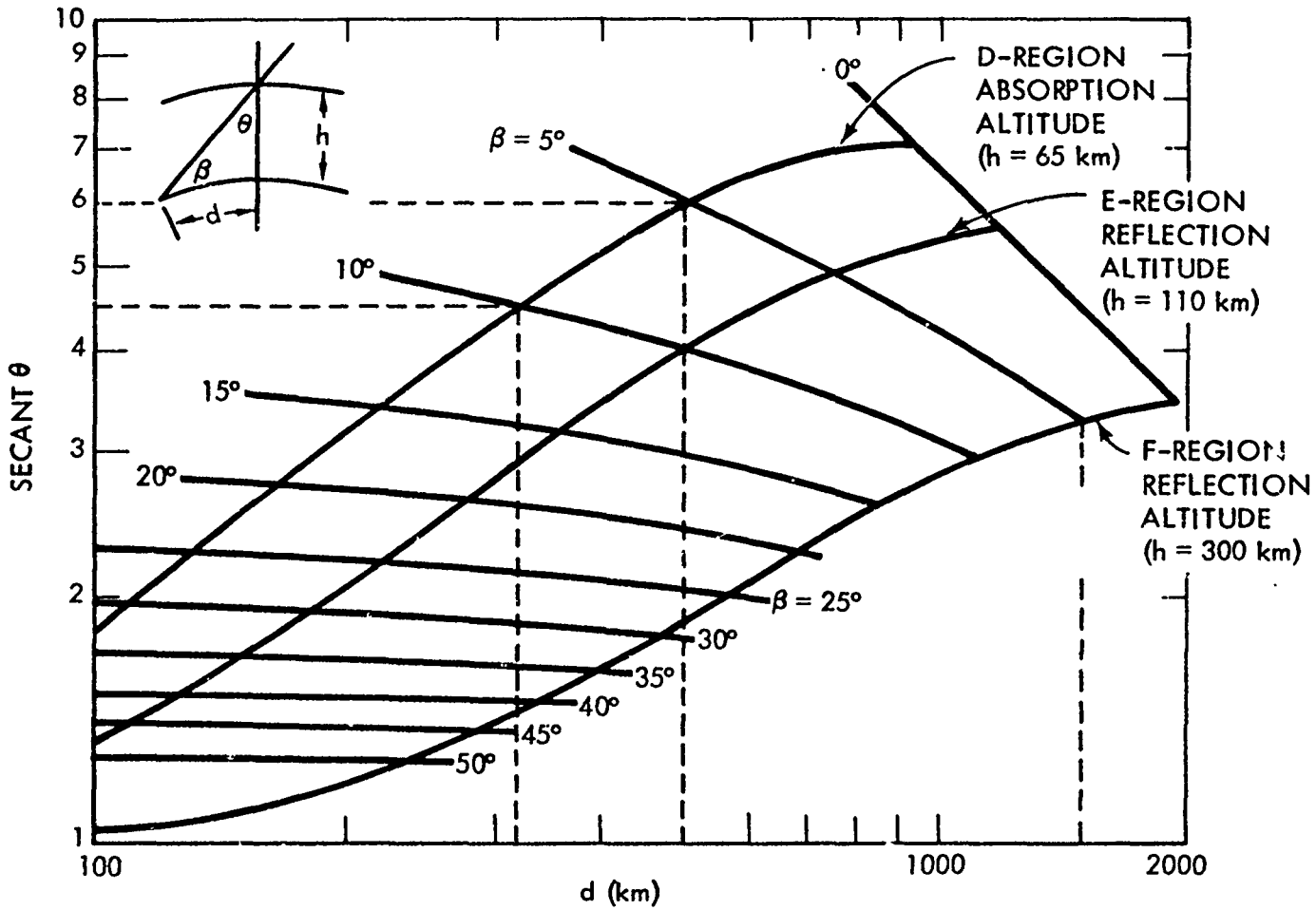

Figure 8-55. [redacted] Secant θ Chart [redacted]

[redacted]

[redacted] BIBLIOGRAPHY [redacted]

Atmospheric Ionization and Effects on Radar and Communications, A Bibliography, DASA 2069, Defense Atomic Support Agency, Washington, D.C., January 1968 [redacted]

Bibliography of Open and Unclassified Literature Pertaining to the Effects of High Altitude Nuclear Explosions, Parts I and II, Final Report, DASA 1795, Defense Atomic Support Agency, Washington, D.C., May 1966 [redacted]

DASA Reaction Rate Handbook, DASA 1948, Defense Atomic Support Agency, Washington, D.C., October 1967 [redacted] (will be revised as DNA 1948H during calendar year 1972).

Electromagnetic Blackout Handbook [redacted] Second Edition, Volume I: *Guide to Systems Effects* [redacted] DASA 1580, Defense Atomic Support Agency, Washington, D.C., December 1964 [redacted]

Electromagnetic Blackout Handbook [redacted] Second Edition, Volume II: *Nuclear Weapons Effects* [redacted] DASA 1580-1, Defense Atomic Support Agency, Washington, D.C., February 1965 [redacted]

High Altitude Tests Measurement Summary [redacted] DASA 1970, Defense Atomic Support Agency, Washington, D.C., September 1967 [redacted]

Knapp, W. S., and P. G. Fischer, *Aids for the Study of Electromagnetic Blackout*, DASA 2499, General Electric, TEMPO, Santa Barbara, Calif., July 1970 [redacted]

RANC IV, Computer Simulation of Radar Propagation in a Nuclear Environment, Volume I: *Computational Models*, DASA 2497-1, Defense Atomic Support Agency, Washington, D.C., July 1970 [redacted]

Weapon Effects Computer Code Directory, DASA 1727, Special Report 43, Defense Atomic Support Agency, Washington, D.C., April 1969 [redacted]

[redacted]

[redacted]

PART II

DAMAGE CRITERIA [redacted]

Chapter 9

INTRODUCTION TO DAMAGE CRITERIA [redacted]

AD-A955 393

[redacted] Part I of this manual describes the basic phenomena associated with a nuclear explosion for various burst conditions. These phenomena include: blast and shock, thermal radiation, X-ray radiation, nuclear radiation, transient radiation effects on electronics (TREE), electromagnetic pulse (EMP) phenomena, and phenomena affecting electromagnetic wave propagation. Part II treats the mechanisms of casualty production and damage to military targets, and describes the response of these targets by correlating the basic physical phenomena with various defined degrees of damage.

SECTION I

[redacted] CONTENT AND LIMITATIONS OF PART II [redacted]

9-1 Introduction to Chapter 9 [redacted]

[redacted] The information in Part I is divided according to the phenomenology, with one chapter being devoted to each of the seven phenomena listed above. This chapter provides a general discussion of the physical damage mechanisms associated with each of the first six phenomena listed above (the last phenomenon does not produce physical damage; the degradation of signals from radio and radar systems is discussed in Chapter 17). Separate sections describe the damage mechanisms associated with each of the six phenomena. In addition, Section IV of this chapter discusses the degradation of equipment by thermal radiation that might affect its response to the blast wave.

9-2 Organization of Part II [redacted]

[redacted] Part II of this manual is divided into chapters according to types of targets that exhibit similar response characteristics. Further subdivisions within the chapters separate the types of targets into subtypes, and for each subtype there are frequently further subdivisions according to the phenomena that cause the damage.

[redacted] The data presented here are interpretations of complex results of the nuclear weapons effects research and test programs of the Department of Defense. A constant effort is made to deduce theoretical models and scaling laws for the various weapons effects that permit a quantitative prediction of the extent of a given effect from a weapon of one yield related to weapons of other yields. Since the initiation of the limited nuclear test ban treaty, a large amount of effort has been devoted to the development of complex computer codes to predict the environments created by the various phenomena resulting from nuclear explosions and the interactions of these environments with personnel and military systems. A large number of scaling laws presented in Part I that are useful in predicting the environment from a given explosion were derived from the calculations performed with these codes. Many additional scaling laws,

[redacted]

89 3 02 032

[redacted]

[redacted]

derived from field and laboratory experiments, and theoretical studies, as well as the codes, are presented in the chapters of Part II to aid in the predictions of the response of personnel and systems to the environment. Graphical presentation is used in preference to tabular or purely computational presentations wherever possible. The damage curves are drawn for a probability of 50 percent of producing the indicated damage. Curves of 90 and 10 percent probability are included when the quantity and quality of the data permit. In addition, Appendix C provides the methodology for estimating any probability of damage, provided that the median values of the response of a given system are known. Estimates of such median values for the equipment discussed in Sections I through III of Chapter 11 are provided in Appendix C. Effort has been made to provide a comprehensive set of data in a readily usable form; however, certain categories of damage are not amenable to generalization. Some limitations in the content of Part II are discussed in paragraph 9-3.

[redacted] An estimate of the degree of reliability accompanies most of the data presented herein. Statements of the reliability of damage data only pertain to the basic response data, which, for the target analyst represent the "radius of effect." They should not be confused with the terms variability and probability of damage, which pertain to target response; nor do these estimates include operational considerations such as linear, circular, or spherical aiming and fuzing errors, yield variations, and target intelligence.

9-3 Limitations in Part II [redacted]

[redacted] As mentioned in paragraph 9-2, the remaining chapters of Part II each contain descriptions of damage to a category of targets that exhibit similar response characteristics. Unfortunately, the response to certain of the phenomena depends so strongly on a specific system design that it is impossible to present response data for a "category" of targets (e.g., communications equipment, aircraft, missiles). These phenomena include X-ray radiation and EMP. Therefore, general discussions of the types of systems that are likely to be affected by these phenomena and the general nature of the responses are given in Sections V and VIII of this chapter. No response criteria are provided in subsequent chapters; however, the potential importance of these phenomena are mentioned where appropriate. TREE response is also very dependent on specific system design. The response of electronic components and circuits is described in Section VII of this chapter. Section IV of Chapter 14 contains a brief review of component and circuit response supplemented with discussions of general electrical responses of classes of systems. This latter discussion is intended to include a cross section of systems that should provide some basis for estimating the radiation damage threshold of other similar equipment.

SECTION II

[redacted] BLAST AND SHOCK DAMAGE [redacted]

[redacted] When a blast or shock wave strikes a target, the target may be damaged (distorted sufficiently to impair usefulness) by the blast or shock wave itself, by being translated by the blast wave and striking another object or the ground, or by being struck by another object translated by the blast wave. For example, the air blast wave can shatter windows, dish in walls, collapse roofs, deflect structural frames of buildings, and bend or rupture aircraft panels and frames. Vehicles, tanks, artillery pieces, and personnel can strike other objects on the ground while being hurled through the air or tumbled along the ground by the blast wave. Ship hulls may be split or crushed by the water shock wave. Buried structures or structural founda-

ssion For
GRA&I
TAB
ounced
ication
By
Distribution/
Availability Co
Dist | Avail and/
Special
A-1 | 23

QUALITY INSPECTED 4

[redacted]

UNANNOUNCED

tions can be displaced, collapsed, or ruptured by the ground shock wave. Usually, the degree of damage sustained by a particular target cannot be correlated specifically to a single blast or shock parameter. The total damage received by the target may depend on a combination of air blast and ground or water shock parameters. The orientation of the target with respect to the blast wave, and the type of surface (the topography or the type of soil) associated with the target also determine damage.

LOADING

The blast loading on an object is a function not only of the blast characteristics of the incident wave (rise time, peak overpressure, peak dynamic pressure, decay, and duration), but also of the size, shape, orientation, and response of the object. The influence of the target characteristics on the loading is discussed below, with emphasis on air blast loading.

9-4 Air Blast Loading in the Mach Reflection Region

The loading on an object exposed to air blast is a combination of the forces exerted by the overpressure and the dynamic pressure of the incident blast wave. The loading at any point on a surface of an object can be described as the sum of the dynamic pressure, multiplied by a local drag coefficient, and the overpressure after any initial reflections have cleared the structure. Since the loading changes rapidly while the blast wave is reflecting from the front surfaces and diffracting around the object, loading generally comprises two distinct phases: the initial diffraction phase; and the phase following diffraction when the object is completely engulfed by the blast wave. This latter phase approaches a steady state and usually is referred to as the drag phase, because during this phase the drag forces (i.e., the forces resulting from the dynamic pressures) are the predominant factors in the production of a net translational force on the object. The following discussion of the loading process is based on an ideal blast wave as described in Section I (Figure 2-1), Chapter 2. Where nonideal blast waves, with slow rise time, irregular shapes, and high dynamic pressures (paragraphs 2-21 through 2-31, Chapter 2) introduce complications into the loading process, further explanation is provided. The loading on an object can be described conveniently in three parts: diffraction loading, drag loading, and net loading. These are discussed separately below.

Diffraction Loading. The side of an object facing the shock front of an air blast wave bears overpressures several times that of the incident overpressure because it both receives and reflects the shock. In the Mach reflection region the overpressure incident on the object is actually that of the original free air blast wave which has been reflected from the ground surface to a higher value. The reflection off the object therefore constitutes a second reflection process. In the regular reflection region, the incident overpressure is that of the free air blast wave (see paragraph 9-6). The magnitude of the reflected overpressure depends on the angle between the shock front and the face of the object, the rise time of the incident blast wave, and the initial incident shock strength. The greatest reflected overpressures occur when the direction of propagation of the shock front is normal to the face of the object, when the rise to the peak overpressure is essentially instantaneous, and when the incident shock strength is high. As the blast wave progresses it bends or diffracts around the object, eventually exerting overpressures on all sides. Before the object is entirely engulfed in the pressure region, however, overpressure is exerted on the front side of the object, whereas only ambient air pressure exists on the back side. During the diffraction phase this pressure differential produces a translational force on the object in the direction of blast wave propaga-

[redacted]

[redacted]

tion. When the blast wave has completely surrounded a small object, the translational force that results from diffraction loading is reduced essentially to zero, because the pressures on the front and on the back are almost equal. In the cases of long objects or short duration blast waves, the net force may actually reverse, because the overpressure on the front face may decay to a value lower than that on the rear face. The importance of this translational loading in the production of damage to the target depends on the duration of the loading or on the time required for the shock front to traverse the target and, therefore, on the size of the target. The effects of the translational load decrease as the duration of the load is decreased until, in some instances, translational load effects can be ignored. The overpressures continue on all sides of the object until the positive phase of the blast wave has passed. These pressures may be sufficient to crush an object (a 55-gallon drum may be damaged in this manner in addition to damage that might be incurred by translation). Thus, the diffraction phase translational loading depends primarily on the object size, pressure pulse duration, and on increases in differential overpressures resulting from reflection on the front face.

[redacted] *Drag Loading.* During the time of diffraction and until the blast wave has passed, the wind behind the shock front causes dynamic pressures to be exerted on the object as drag loading. Except in the case where shock strengths are high, these pressures are much lower than the reflected overpressures; however, they produce a translational force that the target component receives for the entire positive phase duration of the blast wave. For a given blast wave, the loading that results from dynamic pressure depends principally on the shape and orientation of the object, ranging from less than four-tenths of the dynamic pressures in the case of a cylinder (when normal to the cylindrical axis), to over twice the dynamic pressures for an irregular, sharp-edged object.

[redacted] *Net Loading.* Net loading is the combined load on the element that tends to translate it in the direction of propagation of the blast wave. Thus, it is the difference between the load on the front face and the load on the back face; the loads on the sides are of no effect in producing translation.

9-5 Qualitative Examples of Net Loading [redacted]

[redacted] The net load on a target can be developed most simply by considering the idealized case shown in Figure 9-1, in which a classical, sharp fronted blast wave moving along the surface of the ground encounters a simple, rigid, fixed cube. When the blast wave arrives at the front face of the target, this face experiences a sudden rise in overpressure to a value p_r that is greater than the peak overpressure Δp of the incident blast wave (also frequently called "side on" overpressure). As the shock wave moves over the cube, subjecting its top and side faces to side on overpressure, the pressure on the front face of the cube begins to drop as the result of rarefaction waves that are generated at the edges of the front face, and which move across that face. When the wave encounters the back face of the cube, that face experiences a gradual pressure increase. The air behind the front of the incident shock wave is in motion, and as the wave envelopes the cube this air motion also affects the pressures experienced by the various faces of the cube.

[redacted] After a time that is related to the cube dimensions and to the velocity of the incident shock wave, the pressure on the front face becomes

$$p_f = \Delta p(t) + C_{df} q(t)$$

where

$\Delta p(t)$ = the overpressure in the incident shock wave as a function of time, t,

[redacted]

[redacted]

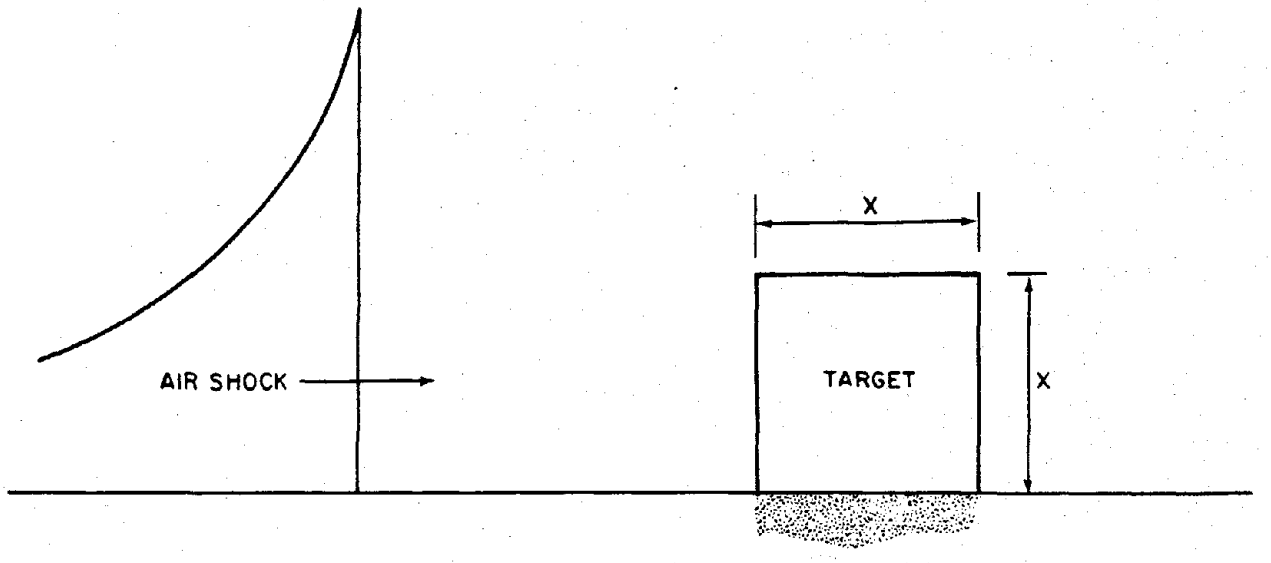

Figure 9-1. [redacted] Initial Conditions for Loading of a Rigid, Fixed Cube [redacted]

[redacted]

C_{df} = the drag coefficient of the front face of the cube,

$q(t)$ = the dynamic pressure in the incident shock wave as a function of time, t.

After the shock wave has passed over the cube and has reached the back face, the pressure on that face begins to rise and, at a later time also related to the cube dimensions and the velocity of the incident shock wave, the pressure becomes

$$p_b = \Delta p(t) - C_{db} q(t)$$

where

C_{db} = the drag coefficient of the back face of the cube.

Note that both expressions contain overpressure and dynamic pressure components. As far as the *net* horizontal (translational) loading on the cube is concerned (i.e., the pressures tending to move the cube to the right in Figure 9-1), the overpressure contributions must be subtracted from one another (pressure on the back face tends to move the cube to the left) while the dynamic pressure contributions must be added to each other.

[redacted] It is convenient to consider the two contributions separately. Figure 9-2 illustrates the overpressure loadings only (dynamic pressure contributions are not included) experienced by the front and back faces of the cube both during the early (diffraction) phases – up to time t_1 on the front face and time t_3 on the back face of the cube – and after the times that the equations given above apply.

[redacted] The incident shock wave is of the classical (peaked) form with peak overpressure and overpressure duration of Δp and t_p^+ respectively; t_1 is the time after which the total front face loading is represented by the equation for p_f

[redacted]

[redacted]

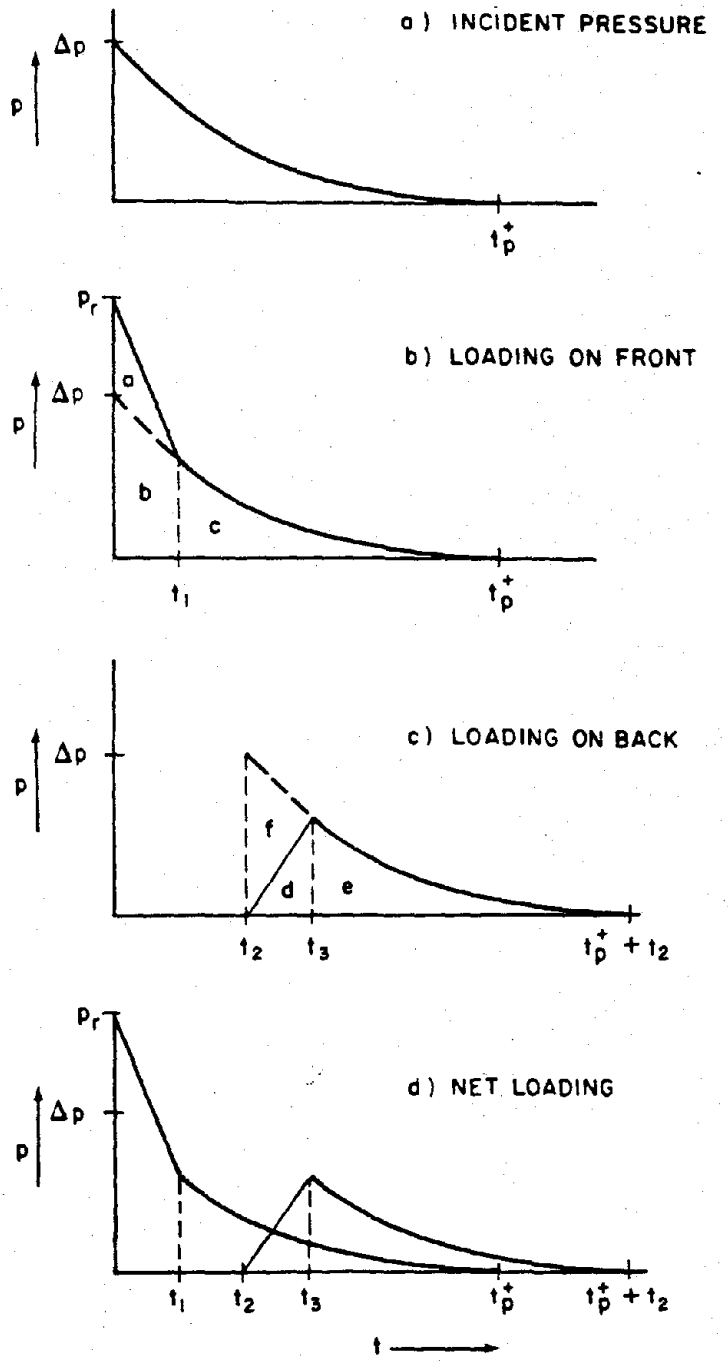

Figure 9-2. [redacted] Target Loading by Overpressure [redacted]

[redacted]

[redacted]

[redacted]

above: t_2 is the time for the shock wave to reach the back face, and t_3 is the time after which the total back face loading is represented by the equation for p_b above.

[redacted] From Figure 9-2b, the total impulse on the front face, I_F (i.e., the area under the curve multiplied by the area of the cube face, A) is equal to the sum of the areas a, b, and c.

$$I_F = (a + b + c)A$$

The total impulse on the back face, I_B, is (Figure 9-2c)

$$I_B = (d + e)A$$

The net overpressure impulse is $I_F - I_B$. If the cube is not too large compared to the duration of the blast wave, the following approximations hold among the areas:

$$b = d + f,$$

$$c = e.$$

Thus, the net overpressure impulse is

$$I_N = (a + f)A.$$

If the initial drop of pressure on the front face and the build up of pressure on the rear face are assumed to be linear, the net impulse is

$$I_N = A\left[1/2\left(p_r - \Delta p\right)t_1 + 1/2\,\Delta p\left(t_3 - t_2\right)\right]$$

in which the term containing t_1 is area "a," and the term containing t_2 and t_3 is area "f" of Figure 9-2. Note in particular that the only times are t_1, t_2, and t_3, i.e., those times related to the initial envelopment of the cube by the blast wave. I_N does not, in this simple analysis, depend on overpressure duration t_p^+.

[redacted] Substitution of commonly accepted values of t_1, t_2, and t_3 for a curve leads to the following expression for the net impulse from *overpressure* diffraction around the target:

$$I_N = A\left[\frac{X}{2U}\left(3p_r + \Delta p\right)\right]$$

where

X = one-half the width or the height, whichever is smaller,

U = velocity of the shock wave.

These values of t_1, t_2 and t_3 originally were derived from early shock tube experiments and full scale nuclear tests on structures at low pressure levels. Consequently, they are used for illustrative purposes only in this simple analysis. More recent work with two and three dimensional models in the shock tube has shown that the exact values for these times depend strongly on model shape and pressure level as well as sound velocity in the reflected pressure region on the face of the model rather than shock front velocity.

[redacted] The impulse on the cube due to dynamic pressure I_q is

$$I_q = A\int_0^{t+} q(t)C_d\,dt$$

where

I_q = drag impulse,

q = dynamic pressure,

C_d = drag coefficient of the entire object, a combination of C_{df} and C_{db}.

[redacted] By expressing p_r in terms of Δp and shock strength ξ, and U in terms of the sound velocity, c and the shock strength ξ, the drag impulse equation may be solved in terms of Δp,

[redacted]

[redacted]

[redacted] ξ, C_d, and shock wave duration* t^+. The combined impulse is

$$I_T = \left\{ \left[\frac{X\Delta p}{2c} \left(\frac{42 + 24\xi}{\xi + 7} + 1 \right) \left(1 + \frac{6\xi}{7} \right)^{-1/2} \right] + \left[\frac{0.54 \Delta p C_d t^+ \xi}{\xi + 7} \right] \right\}.$$

The first expression in brackets, which is independent of duration, is the overpressure contribution. The second expression is the contribution of dynamic pressure.

[redacted] If height of burst and ground distance are scaled as the cube root of the yield W for weapons of different yields, Δp remains constant, but the shock wave duration t^+ varies as the cube root of the yield. Thus, the yield dependence is

$$I_T = A \left[B + C \left(W^{1/3} \right) \right]$$

where B, the overpressure contribution (I_N for a 1 kt yield), and C, the dynamic pressure contribution (I_q for a 1 kt yield), are both constants. Thus, the contribution to total impulse from overpressure remains constant, while that from dynamic pressure increases as the cube root of the yield. For very low fractional kiloton yields, the loading is highly impulsive with most of the load coming from the overpressure contribution. As the yield increases, at a constant scaled height of burst and ground distance, the total impulse also increases, with an increasing fraction resulting from dynamic pressure.

[redacted] Figures 9-3a and b show representative net loadings for two classes of weapon yield and two classes of structures, one small and one large. A small element would be about the size of a telephone pole or a jeep; a large element would be the size of a house or larger. Since the reflected overpressure is more than twice the incident pressure on the front face of the element, the loading displays an initial peak value. The reflected pressure decays or clears the front face at a time that depends on the size of the element. The rapid decay for the small element may make the reflected pressure spike of no significance, whereas the slow decay for the large element creates a load that may govern the response of the target entirely. For the representative cases shown, the diffraction phase terminates at time t_{diff}, the time at which the reflected pressure has decayed to the incident pressure. At this time the drag phase begins. It continues until the end of the positive phase of the incident blast wave. The load during the drag phase is shown to be equal to the dynamic pressure, i.e., the drag coefficients of the elements are equal to 1.0. The characteristics of the target element determine whether the response of the element is governed primarily by the diffraction phase or the drag phase. Figures 9-3a and b show that for medium and high yield weapons and small elements, a much greater impulse (the area under the loading curve) occurs during the drag phase than during the diffraction phase. As the yield increases the drag phase impulse increases in importance. For large elements and large yield weapons, the diffraction phase and drag phase impulses are about equal. In this latter case the drag phase impulse may still be of no importance, because the significant target response may occur during the diffraction phase. The diffraction phase impulses are not changed by the yield of the weapon (this is true for all but very large structures exposed to low yield weapons), whereas the drag phase impulses are directly related to the weapon yield (for the same peak dynamic pressures).

[redacted] In this solution it is assumed that the difference between t_p^+ and t_q^+ may be neglected, and $t_p^+ = t_q^+ = t^+$.

[redacted]

[redacted]

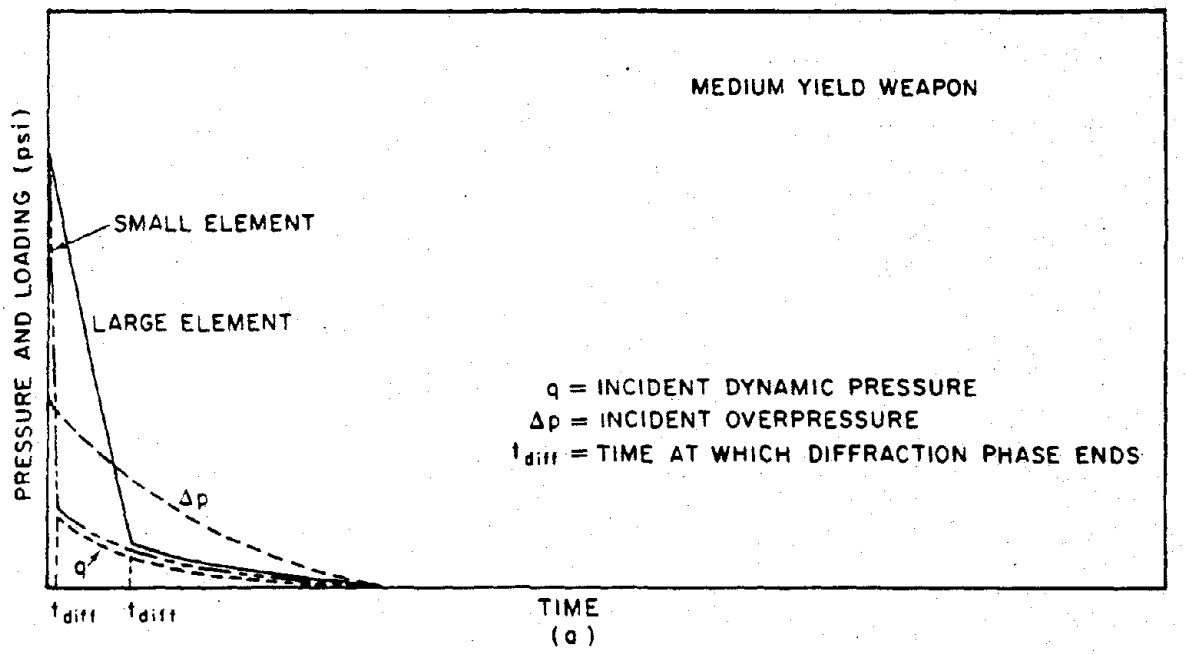

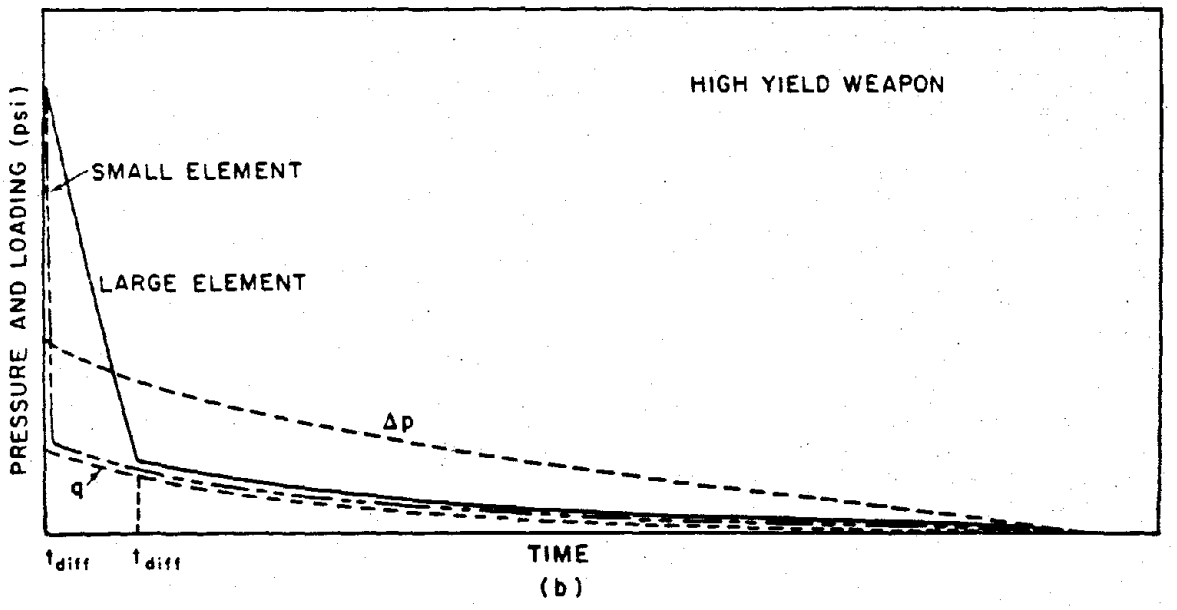

Figure 9-3. [redacted] Net Blast Loading on Representative Structures [redacted]

[redacted]

9-6 Regular and Mach Reflection [redacted]

[redacted] Specific aspects of the blast wave propagation must be considered when computing the load on a target. The loading of a surface target in the regular reflection region (pargraph 2-18, Chapter 2) is complicated by the vertical component of the incident blast wave, which causes multiple reflections between the ground and the target and additional reflected pressures on horizontal surfaces. In the Mach reflection region (paragraph 2-18), the loading is simplified because the blast wave propagation is horizontal. Near the surface of the ground, the vertical component of the drag forces in the regular reflection region is cancelled by the reflected wave rapidly; therefore, the brief vertical drag loading is ignored, except when the target is near the ground zero of an air burst. For aircraft in flight, the loading may be a single horizontal shock from a Mach stem or two separate shocks; the first from the free air wave and the second from the ground reflected wave. In establishing the damage curves for surface targets, the loadings on targets in the regular reflection region during the diffraction phase are considered separately from the loadings on similar targets in the Mach reflection region. The surface conditions are assumed to be average unless otherwise indicated in the figures that provide the damage curves. Objects that are primarily susceptible to horizontal drag loading in the Mach reflection region may become primarily susceptible to crushing action if they are in the early regular reflection region.

9-7 Target Motion [redacted]

[redacted] When air blast loading is considered, the movement of the target component during loading is assumed to have negligible effect on the loading itself. Aircraft and missiles in flight are exceptions. Their speed, orientation, and movement during loading assume increased importance (see Chapters 13 and 16).

9-8 Nonideal Waveforms [redacted]

[redacted] As discussed in paragraphs 2-31 and 2-32, ideal waveforms are seldom found along the surface for overpressure levels above 6 psi. The description of the diffraction and drag phases given in preceding paragraphs is not true in regions of nonideal waveforms. If the overpressure wave has a long rise time (30 to 40 msec) to a peak value, full reflection of the wave from the surface of a structure will not occur. At the same time, the relationship between dynamic pressure and overpressure is different from that described for the ideal blast wave. During the diffraction phase, the drag forces caused by high dynamic pressures may be the predominant damage-producing criteria. Since many conventional surface structures sustain severe damage at low peak overpressure levels, and nonideal waveforms occur only in the higher overpressure regions, such waveforms were not considered in determining damage criteria for such structures. Careful consideration must be given to nonideal waveforms when assessing the vulnerability of protective structures that were designed to withstand high overpressures. The dynamic pressures for such waveforms generally will be higher than would be expected if the blast wave were ideal. There are few data on blast loading in the high pressure regions.

9-9 Underwater Shock Wave Loading [redacted]

[redacted] The air blast wave operates in a compressible fluid, while the water shock wave operates in a noncompressible fluid. This difference in medium accounts for the differences in detail betweeen air blast and water shock loading. The peak values in water are higher than they would be at the same distance from an explosion of the same yield in air. However, the duration of the shock wave in water is shorter than in air. When the shock wave strikes a rigid, submerged surface, such as the sea bottom, it is reflected.

[redacted]

When the shock wave reaches the air-water surface (a less rigid medium), however, a refraction (or negative pressure) wave occurs. The combination of the surface reflected shock wave and the direct shock wave produces a sharp decrease or "cutoff" in the water shock overpressure, as shown in Figure 9-4. Incidence of a shock wave on a ship or structure produces damage through the direct mechanism of overpressure (or excess impulse) and by imparting a transitional velocity to the target structure.

9-10 Ground Shock Loading

The loading of buried structures by ground shock is connected intimately to the response of the structures. For certain underground structures, serious damage will only occur if the ground shock is so intense that the damage area for those structures is confined closely to the crater area of a surface or underground explosion. For structures near the surface, air blast induced ground shock may cause significant damage. The damage to these structures is more closely related to air blast pressures than it is to crater dimensions. Loading pressures are numerically equal to the ground stress normal to the structure. Such pressures do not produce detectable reflected pressures. Internal equipment of a structure may be subjected to ground shock accelerations that will severely damage the equipment without damaging the structure. For a discussion of accelerations resulting from ground shock see Section III, Chapter 2, and Sections II and III, Chapter 11.

RESPONSE AND DAMAGE

Damage to a target is closely related to, and is a direct derivative of, its response. For targets anchored to the ground, damage is usually the result of displacement of one part of the target with respect to another part, resulting in permanent distortion, collapse, or toppling. For movable targets, however, the target may be moved by the loading with or without a resulting damage. In the latter case, the damage to the target is governed primarily by the manner in which the moving target comes to rest. Whether drag phase loading or diffraction phase loading causes the greater damage will depend upon the weapon yield, target characteristics, and the damage level considered.

9-11 Surface Structures

The predominant cause of failure to large targets, such as buildings that have small window areas compared to wall areas that either support the structure or are as strong as the structural frames, is the pressure differential between the front and rear faces that exists for a relatively long period of time. If the window area is large, the pressure on each wall is equalized quickly by the entry of the blast wave through the windows. The pressures exerted on the inside of the wall reduce the translational force on the wall. This translational force also is reduced because of a smaller wall area on which the pressures can act; however, the force exerted on interior partitions and rear walls tends to offset the reduction in front face loading in the production of total damage. When the overpressures causing translational force on the structural component are equalized quickly as a result of the geometry or construction of the building, the primary damaging forces are those that are significant in damaging structural components that have fairly small cross sections, such as columns and beams. Structures that are normally damaged by drag forces include smoke stacks, telephone poles, truss bridges, and steel or reinforced concrete frame buildings with light walls. These buildings are drag sensitive, because the light walls of corrugated steel, asbestos, or cinder block fail at low reflected pressures, and they do not transmit a significant load to the structure frame. Only the frame is exposed to the blast, and, being composed of small cross

[redacted]

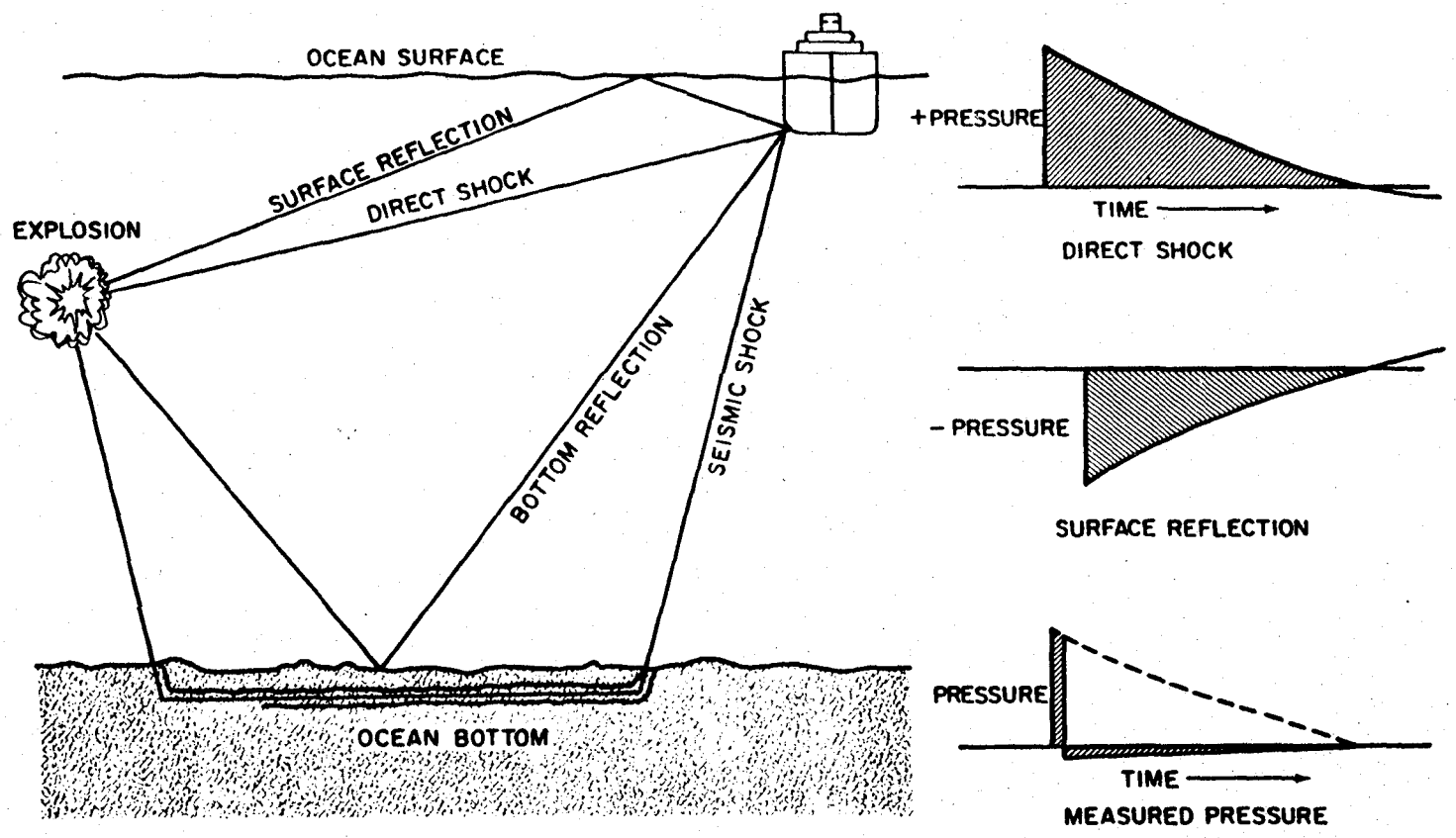

Figure 9-4. Direct and Reflected Shock Waves from an Underwater Burst

section structural elements, it is distorted primarily by drag forces. These buildings are not considered severely damaged unless the structural frame has collapsed or is near the point of collapse. A tree is a good example of a drag sensitive target, because the duration of the diffraction phase is extremely short and there is considerable force applied by the high wind velocity drag loading. Most military field equipment is drag sensitive, because damage generally results from the tumbling or overturning caused by the drag forces.

9-12 Shielded Structures

If the target is shielded from the drag forces, or if it lies within the early regular reflection region, high overpressures may become the damage producing criteria. For blast resistant aboveground structures designed to resist more than 5 to 10 psi overpressure, the distinction between diffraction and drag sensitivity cannot be defined well, because full reflection from the surface of the structure does not occur, and dynamic pressures exceed those expected in the case of the incident waveform. As a result, drag forces may be predominant in producing damage, even during the diffraction phase.

9-13 Aircraft

Aircraft may be damaged by the forces developed in the diffraction phase, in the drag loading phase, or in both. Parked aircraft can receive light, crushing forces corresponding to low overpressures. For example, light skins and frames are easily dished and buckled at relatively low overpressures. At higher overpressure levels, drag loading (referred to as "gust loading" with respect to aircraft) adds to the damage. At these levels, much of the damage may result from translation and overturning of the aircraft. For aircraft in flight, the diffraction and drag forces combine with the existing aerodynamic forces to develop destructive loads on airfoils at low overpressure levels. The diffraction or crushing overpressure effects on the fuselage and other thin skinned components, however, are usually of secondary importance for most in-flight aircraft. Responses of aircraft are discussed in more detail in Chapter 13.

SECTION III
THERMAL RADIATION DAMAGE

INTRODUCTION

Two important effects of thermal radiation are injuries to personnel (burns) and fires that might be ignited in the target area. Burns to personnel are treated in Section II of Chapter 10. Section VII of Chapter 11 discusses fires in urban areas. Section III of Chapter 15 discusses fires in forest stands. The effects of thermal radiation on various classes of equipment are described in other chapters of Part II. This section contains a description of the properties of materials that might result in ignition or degradation of their physical properties. A brief discussion of survival in fire areas is also provided. Section IV describes the degradation of structural resistance to air blast of materials, primarily metals, as a result of thermal radiation.

Chapter 3 provides the data necessary to estimate the thermal environment. In general, thermal damage is likely to be more important than blast damage for surface targets for high yield weapons that are air bursts rather than surface bursts. As discussed in Chapter 3, the influence of weather makes thermal effects much less predictable than blast effects. Clouds or haze can provide a protective screen, and moisture from an earlier rain can reduce the number of fires in outdoor targets. In some cases, cloud cover can enhance thermal effects on the ground. The criteria for thermal damage given in succeeding paragraphs are representative values

[redacted]

for dry materials directly exposed to the thermal source. These values should be applied with the understanding that they can be modified by a variety of factors discussed briefly in the following paragraphs.

9-14 Radiant Exposure [redacted]

[redacted] The thermal damage inflicted on a target depends upon the incident energy per unit area. This quantity is called radiant exposure and, as described in Chapter 3, it usually is expressed in calories per square centimeter (cal/cm^2). Radiant exposures below 2 cal/cm^2 will produce little damage other than possible eye injury (Section II, Chapter 10). Radiant exposures above 10 cal/cm^2 usually produce significant damage in unprotected target areas.

9-15 Thermal Pulse Duration [redacted]

[redacted] The radiant exposure required to damage a particular target varies with the duration of the thermal pulse. The reason is readily seen from the following example: about 3 to 5 cal/cm^2 from a short thermal pulse, e.g., from a 1 kt detonation, will produce a second degree burn on bare skin, but direct sunlight delivers the same radiant exposure in a little over 2 minutes with no serious effects.

[redacted] The time scale of the thermal pulse from low altitude nuclear weapon bursts may be characterized by the parameter t_{max}, the time during the final pulse at which the fireball is radiating maximum power. This time increases with increasing yield and decreases with increasing altitude. The relation of t_{max} to pulse duration and the method for calculating t_{max} are given in Chapter 3. As described in Chapter 3, the time scale of the thermal pulse may be specified indirectly in terms of yield for low altitude bursts. The thermal pulse for high altitude bursts (up to about 100,000 feet) may be described in terms of an equivalent sea level burst. Specifying the thermal pulse duration in terms of yield is convenient since it eliminates the necessity to calculate t_{max}; therefore, many damage criteria are given in terms of radiant exposure and yield rather than radiant exposure and time to final maximum.

9-16 Target Response [redacted]

[redacted] For most materials, the heat absorbed from the thermal pulse initially is confined to a thin surface layer. Damage usually results from high surface temperatures. The nature and the degree of the damage depend not only on the intensity and duration of the thermal pulse, but also on several properties of the material that are described below.

[redacted] *Thickness.* Thick organic materials such as wood, plastics, and heavy fabrics char and may burst into flame while exposed to the thermal pulse; however, this flaming is only a transient effect. As the radiant pulse decays, the absorbed thermal energy continues to penetrate the material. This flow of heat allows the surface to cool to a temperature too low to support combustion.

[redacted] Thin materials, such as light fabrics, newspaper, dry leaves, and dry grass tend to become hotter than the surfaces of thicker materials since the absorbed thermal energy is confined to a relatively small volume of material. Also, since these materials are heated throughout, they usually continue to burn once they are ignited. Moreover, subsequent arrival of the blast wave frequently will fail to extinguish the fire.

[redacted] *Thermal Conductivity.* Most metals allow rapid penetration of thermal energy to depths below the surface as a result of their high values of thermal conductivity. Consequently, the peak surface temperatures induced in thick pieces of metal are considerably less than the peak surface temperatures induced in most nonmetallic materials. Thin pieces of metal may fail as a result of the combined effects of the thermal pulse, which reduces the strength of the metal by heating it, and the blast wave, which causes it to bend or collapse. This effect is dis-

[redacted]

[redacted]

[redacted] cussed in more detail in Section IV. Dry rotted wood (or punk) has a lower thermal conductivity than sound wood as a result of its porous structure. When the surface of punk is ignited by a thermal pulse, conduction of heat to the interior is too slow to allow significant cooling of the surface, and burning continues.

[redacted] *Color.* Light colored objects of a given thickness are more resistant to thermal radiation than dark colored objects, because they reflect more of the incident energy. Color has little effect on the response of materials that blacken (char) early in the thermal pulse, because the energy delivered during the remainder of the pulse is absorbed efficiently by the charred surface.

[redacted] *Transparency.* Transparent materials are relatively resistant to thermal damage (even though transparency in the visible region does not assure that the material is transparent to infrared) because the radiant energy that passes through them usually does not contribute to heating. Partially transparent materials are thermally resistant because the incident thermal energy is deposited over a range of depths rather than being confined to a thin surface layer. Peak temperatures induced in partially transparent materials therefore are likely to be lower than the peak temperatures produced at the surfaces of opaque materials.

[redacted] *Moisture Content.* Thermal damage to materials that absorb moisture depends on the percentage of water in such materials. Usually, the moisture content varies with the prevailing relative humidity. Exposure to recent rain, however, may alter the moisture content significantly. Scorching or charring of an organic surface by radiant energy is preceded by vaporization of the water. Consequently, more energy is required to produce a given damage effect on wet surfaces or on targets in highly humid atmospheres. Materials located indoors and exposed to thermal radiation through windows are damaged more readily during the latter part of the heating season (late winter and early spring), largely because of decreased interior humidities.

9-17 Target Orientation [redacted]

[redacted] In clear atmospheres and in the absence of reflecting surfaces, the amount of energy incident on a unit area of a target surface is greatest when the surface is directly facing the burst. If the target surface is not facing the burst, the energy per unit area depends on the angle between the perpendicular to the surface and the direction of the incoming radiation.

[redacted] When the atmosphere is hazy, much of the energy received at the target is scattered by atmospheric particles, arrives from all directions, and reaches portions of the target that are not exposed to direct radiation. Scattered energy is likely to be a large fraction of the total energy received when the slant range from the burst to the target exceeds about half the visual range. Reflection from clouds and from the ground can produce similar effects.

9-18 Shielding [redacted]

[redacted] Any object that casts a shadow is capable of shielding objects behind it from the direct component of thermal radiation. Trees, buildings, foxholes, hills, etc. offer effective protection except when the scattered component of thermal radiation is large. After leaves have been stripped by the dynamic pressure (wind) of a nuclear burst, the trees offer little shielding from the thermal radiation produced by a second burst. Reflection of thermal radiation from exposed walls of foxholes is about 5 percent.

[redacted] THERMAL RESPONSE OF MATERIALS [redacted]

[redacted] The amount of thermal radiation that a material will absorb depends on the properties of the material discussed in paragraph 9-16. The amount of energy absorbed usually is determined by multiplying the incident energy by an

[redacted]

[redacted]

[redacted]

absorption coefficient. The absorption coefficient cannot be measured directly, but a good estimate can be made by performing spectral measurements of reflectance (the fraction of incident energy reflected from the surface) over the range of wave lengths of the nuclear spectral distribution and by finding an average value of reflectance. The coefficient of absorptance is equal to one minus the average value of the reflectance. The absorptance determined in this manner is valid only as long as the surface does not change as a result of the absorbed thermal energy. Another approach is to divide the quantity of energy absorbed by the incident energy. The absorbed energy is determined from experimentally determined temperature vs time relationships and appropriate theoretical energy balance relationships. Absorptance is a function of time and temperature although an average value is usually employed. This function when known may be found as an input specification for certain computer programs. In the absence of more definitive data for a specific systems, an absorption coefficient of 0.5 is a reasonable value to assume for many materials, particularly metals. For a conservative defensive assumption, the absorption coefficient may be taken to be 1.0 (i.e., total absorption), particularly for dark porous materials.

[redacted] In many cases, it is appropriate to consider only one or two fuel types, assuming that these fuels are the critical items that will determine whether fires are started in a particular area. In other cases, more detail is required. For example, an estimate of the thermal energy that will ignite a particular type of material used in military uniforms may be desired. The data contained in the succeeding paragraphs is intended as a guide in the solution of more specific problems.

9-19 Thickness Effects [redacted]

[redacted] The time required for thermal energy to penetrate very thin materials is short compared to the duration of the thermal pulse. At the end of the pulse, the absorbed thermal energy is distributed more or less uniformly throughout the material. In very thick materials, the end of the pulse finds most of the absorbed thermal energy in a surface layer, with the bulk of the material almost unaffected.

[redacted] If the terms thermally "thin" and thermally "thick" are used to distinguish between materials that are heated throughout from those that are initially heated only at the surface, it is apparent that physical thickness is not the only parameter involved. For example, as a result of the rapid penetration of heat into metals, a sheet of metal is more likely to be thermally thin than is a sheet of insulating material of the same physical thickness.

[redacted] The ability of a short pulse of energy to penetrate a target material is most readily measured in the laboratory and most readily treated analytically if the thermal pulse is given a rectangular waveform rather than the more complex waveform produced by a nuclear weapon. A parameter that is useful for calculating thermal response of materials is the characteristic thermal response time τ_o, given by the equation

$$\tau_o = \rho C_p L^2/k \text{ sec},$$

where k is thermal conductivity (cal-sec^{-1} cm^{-1} °C^{-1}), ρC_p is heat capacity per unit volume (ρ = density in g-cm^{-3} and C_p = specific heat at constant pressure in cal-g^{-1} °C^{-1}), and L is the thickness, in centimeters, of the layer of material.

[redacted] The quantity

$$\alpha = \frac{k}{\rho C_p}$$

is called thermal diffusivity (cm^2/sec). Use of this quantity simplies the previous equation to

[redacted]

[redacted]

[redacted]

$$\tau_o = \frac{L^2}{\alpha} \text{ sec.*}$$

Thermal diffusivity and other properties of a number of materials are shown in Table 9-1.

[redacted] Characteristic time may be related in several ways to the thermal response of a target. Most important is that the ignition of thin fuels by a rectangular thermal pulse requires the least radiant exposure when pulse duration is about equal to τ_o.

[redacted] Two other relations apply to a thick slab of material. For any particular material exposed to a rectangular pulse of length τ, the previous equation can be transformed to give a characteristic thickness

$$\delta = \sqrt{\alpha\tau} \text{ cm},$$

for which the characteristic time is equal to the pulse duration. If a thick slab of this material is exposed to a pulse of length τ, the temperature rise at the surface is the same as would be produced by uniformly distributing the absorbed thermal energy in a slab of thickness δ, and the peak temperature rise at depth δ in the thick slab is about half as great as the peak temperature rise at the surface.

[redacted] For example, consider a block of red pine that is exposed to 15 cal/cm^2 from a rectangular pulse of 3 seconds duration. From Table 9-1, the properties of red pine are

$$\rho = 0.51 \text{ g/cm}^3,$$

$$C_p = 0.4 \text{ cal/g} \cdot {}^\circ C,$$

$$\alpha = 24 \times 10^{-4} \text{ cm}^2/\text{sec}.$$

The characteristic depth is

$$\delta = \sqrt{\alpha\tau} = \sqrt{(24 \times 10^{-3})(3)} = 0.085 \text{ cm}.$$

The mass of wood per unit area in a slab of this thickness is

$$\rho\delta = (0.51)(0.085) = 0.043 \text{ g/cm}^2.$$

The heat absorbed by the wood before it begins to scorch is equal to the product of the incident radiant energy, Q, and the absorption coefficient, A. If the absorption coefficient is assumed to be 0.5,

$$QA = (15)(0.5) = 7.5 \text{ cal/cm}^2.$$

Absorption of this amount of energy in a layer of thickness δ would result in an energy density of

$$\frac{QA}{\rho\delta} = \frac{7.5}{0.043} = 174 \text{ cal/g}.$$

If the energy were evenly distributed through this layer, the resulting temperature rise would be

$$\frac{QA}{\rho\delta C_p} = \frac{174}{0.4} = 435^\circ\text{C},$$

and the peak temperature rise at the surface of the wood would be about the same.

[redacted] The result obtained above may be generalized as follows:

$$\Delta T_s = \frac{QA}{\rho\delta C_p} = \frac{QA}{\rho C_p \sqrt{\alpha\tau}} = \frac{QA}{\rho C_p \sqrt{\tau k/\rho C_p}}.$$

---

*[redacted] This equation is useful, but it is by no means exact. The simplified heat-flow analysis from which this equation is derived neglects the effects of radiation and convection heat losses from the surfaces of the exposed sample. It also assumes an isotropic medium, i.e., a medium whose structure and properties in the neighborhood of any point are the same relative to all directions through the point. It also neglects the changes in thermal properties that occur as the exposed material heats, volatilizes, chars, and bursts into flame.

[redacted]

[redacted]

Table 9-1. [redacted] Thermal Properties of Materials [redacted]

Materials	Density, ρ (gm/cm^3)	Specific Heat, C_p (cal/gm · °C)	Conductivity, k (cal/sec · cm · °C)	Diffusivity, α (cm^2/sec)
Insulating Materials				
Air	9.46×10^{-4}	0.24	0.55×10^{-4}	0.22
Asbestos	0.58	0.20	4.6×10^{-4}	$40. \times 10^{-4}$
Balsa	0.12	0.4	1.2×10^{-4}	$25. \times 10^{-4}$
Brick (common red)	1.8	0.2	$16. \times 10^{-4}$	$18. \times 10^{-4}$
Celluloid	1.4	0.35	5.0×10^{-4}	$10. \times 10^{-4}$
Cotton, sateen, green	0.70	0.35	1.5×10^{-4}	2.5×10^{-4}
Fir, Douglas-				
spring growth	0.29	0.4	$2. \times 10^{-4}$	$17. \times 10^{-4}$
summer growth	1.00	0.4	$5. \times 10^{-4}$	$12. \times 10^{-4}$
Fir, white	0.45	0.4	2.6×10^{-4}	$14. \times 10^{-4}$
Glass, window	2.2	0.2	$19. \times 10^{-4}$	$43. \times 10^{-4}$
Granite	2.5	0.19	$66. \times 10^{-4}$	$140. \times 10^{-4}$
Leather sole	1.0	0.36	3.8×10^{-4}	$11. \times 10^{-4}$
Mahogany	0.53	0.36	3.1×10^{-4}	$16. \times 10^{-4}$
Maple	0.72	0.4	4.5×10^{-4}	$16. \times 10^{-4}$
Oak	0.82	0.4	5.0×10^{-4}	$15. \times 10^{-4}$
Pine, white	0.54	0.33	3.6×10^{-4}	$18. \times 10^{-4}$
Pine, red	0.51	0.4	$5. \times 10^{-4}$	$24. \times 10^{-4}$
Rubber, hard	1.2	0.5	3.6×10^{-4}	$60. \times 10^{-4}$
Teak	0.64	0.4	4.1×10^{-4}	$16. \times 10^{-4}$
Metals (100°C)				
Aluminum	2.7	0.22	0.49	1.0
Cadmium	8.65	0.057	0.20	0.45
Copper	8.92	0.094	0.92	1.1
Gold	19.3	0.031	0.75	1.2
Lead	11.34	0.031	0.081	0.23
Magnesium	1.74	0.25	0.38	0.87
Platinum	21.45	0.027	0.17	0.29
Silver	10.5	0.056	0.96	1.6
Steel, mild	7.8	0.11	0.107	1.2
Tin	6.55	0.056	0.14	0.38
Miscellaneous Materials				
Ice (0°C)	0.92	0.492	$54. \times 10^{-4}$	$120. \times 10^{-4}$
Water	1.00	1.00	$14. \times 10^{-4}$	$14. \times 10^{-4}$
Skin (porcine, dermis, dead)	1.06	0.77	$9. \times 10^{-4}$	$11. \times 10^{-4}$
Skin (human, living, averaged for upper 0.1 cm)	1.06	0.75	$8. \times 10^{-4}$	$30. \times 10^{-4}$
Polyethylene (black)	0.92	0.55	$8. \times 10^{-4}$	$17. \times 10^{-4}$

[redacted]

[redacted]

where ΔT_s is the peak temperature rise at the surface. The parameters that define the thermal pulse may be separated from those that define the material properties, and

$$\Delta T_s = \left(\frac{Q}{\sqrt{\tau}}\right)\left(\frac{A}{\sqrt{k\rho C_p}}\right).$$

For a fixed rectangular pulse, $Q/\sqrt{\tau}$ is a constant, and the equation may be written

$$\Delta T_s = (K)\left(\frac{A}{\sqrt{k\rho C_p}}\right).$$

[redacted] In practice, the surface temperature rise produced in a thick material is approximately proportional to $A/\sqrt{k\rho C_p}$ over a wide range of pulse shapes and pulse times. Thus, this parameter may be used as a measure of the relative susceptibility of various materials to surface heating.

[redacted] Direct measurements of the ignition properties of a representative cellulosic fuel have been reported. The material is α-cellulose, blackened by the addition of carbon, and made into sheets of various thicknesses. This material has the uniformity required to obtain repeatable test results, and its thermal properties are similar to those of common cellulosic fuels, such as paper and dry leaves.

[redacted] Figure 9-5 shows the results of exposing this material to the idealized rectangular thermal pulse. Figure 9-6 shows the results obtained in the more practical case of a simulated weapon pulse. These curves show data for black α-cellulose sheets of a variety of thicknesses by using normalized coordinates. The ordinate is normalized radiant exposure. One unit on this scale corresponds to the energy per unit area that will raise the temperature of the entire sheet 1°C. Thus, a given value of the ordinate represents a higher radiant exposure for a thicker sheet of cellulose. The abscissa of Figure 9-5 is normalized pulse duration, the duration of the rectangular pulse divided by τ_o, the characteristic thermal response time of the sheet of material. The abscissa of Figure 9-6 is a similar normalized time, t_{max}/τ_o. Normalization fails in the case of long pulses, and the curves break into families of curves for different thicknesses of material.

[redacted] If the pulse has such a short duration that the exposed surface reaches the ignition temperature while the back surface remains cool, two distinct ignition thresholds appear. Low values of radiant exposure produce high surface temperatures and flames, but the flames do not persist after the end of the thermal pulse. This region is labeled transient ignition in Figures 9-5 and 9-6. Sustained ignition only occurs when higher radiant exposures raise the temperature throughout the thickness of the cellulose to a level that is sufficiently high to sustain the flow of combustible gases from breakdown of the fuel. It is difficult to supply sufficient energy with short pulses, since a large amount of the energy that is deposited is carried away by the rapid ablation of the thin surface layer. This transient flaming phenomenon is typical of the response of sound wooden boards to a thermal pulse.

[redacted] If the pulse is of long duration, the ignition threshold rises because the exposed material can dissipate an appreciable fraction of the energy while it is being received. For very long rectangular pulses an irradiance of about 0.5 cal · $cm^{-2} sec^{-1}$ is required to ignite the cellulose. Heat supplied to the material at a slow rate is just sufficient to offset radiative and convective heat losses, while maintaining the cellulose at the ignition temperature of about 300°C.

[redacted] Materials respond to the thermal pulse from a nuclear weapon in much the same way that they respond to a rectangular thermal pulse; however, a number of practical effects make a thorough analysis of ordinary fuels ignited by

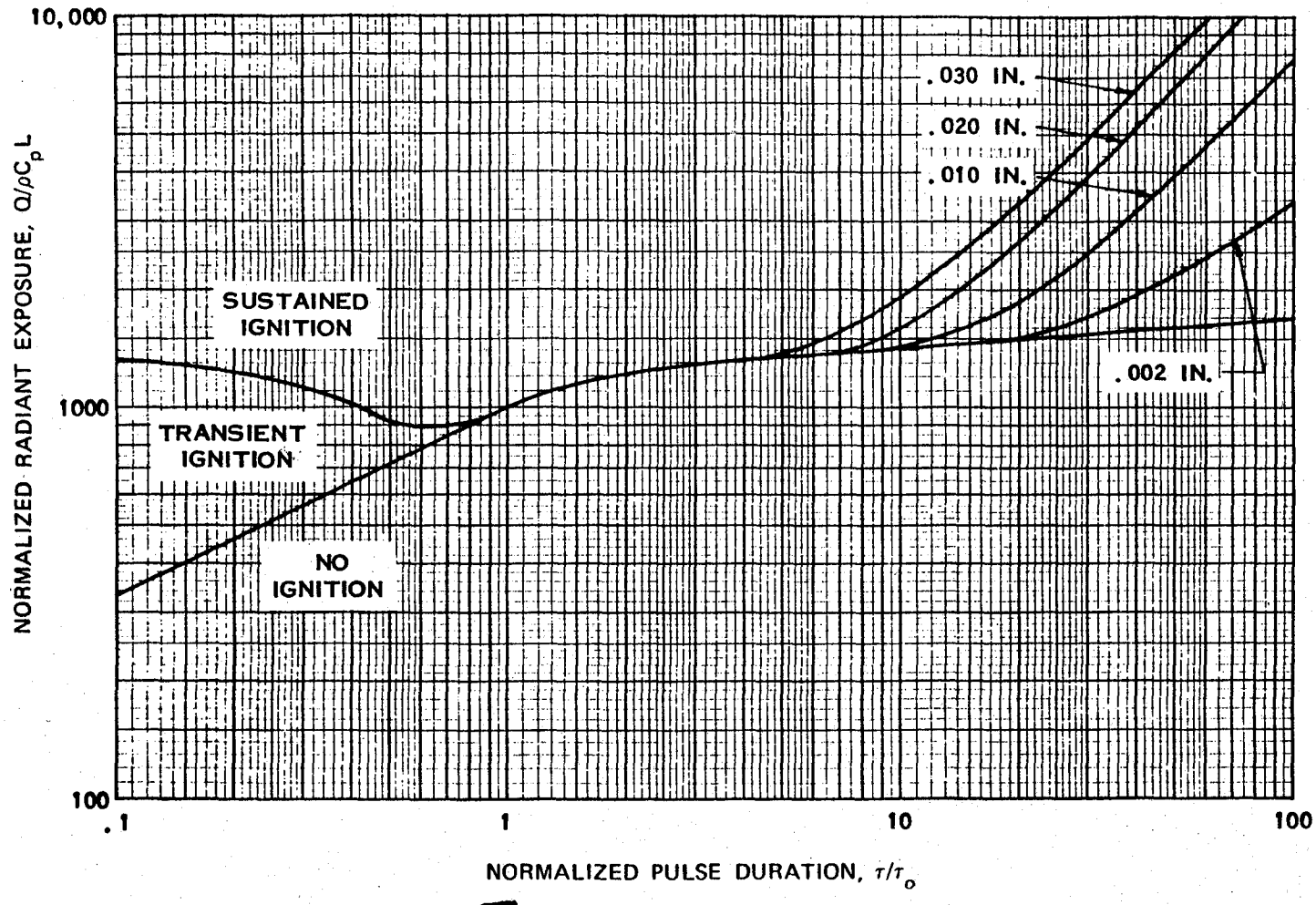

Figure 9-5. [redacted] Ignition Thresholds for Black α-Cellulose Exposed to a Rectangular Thermal Pulse [redacted]

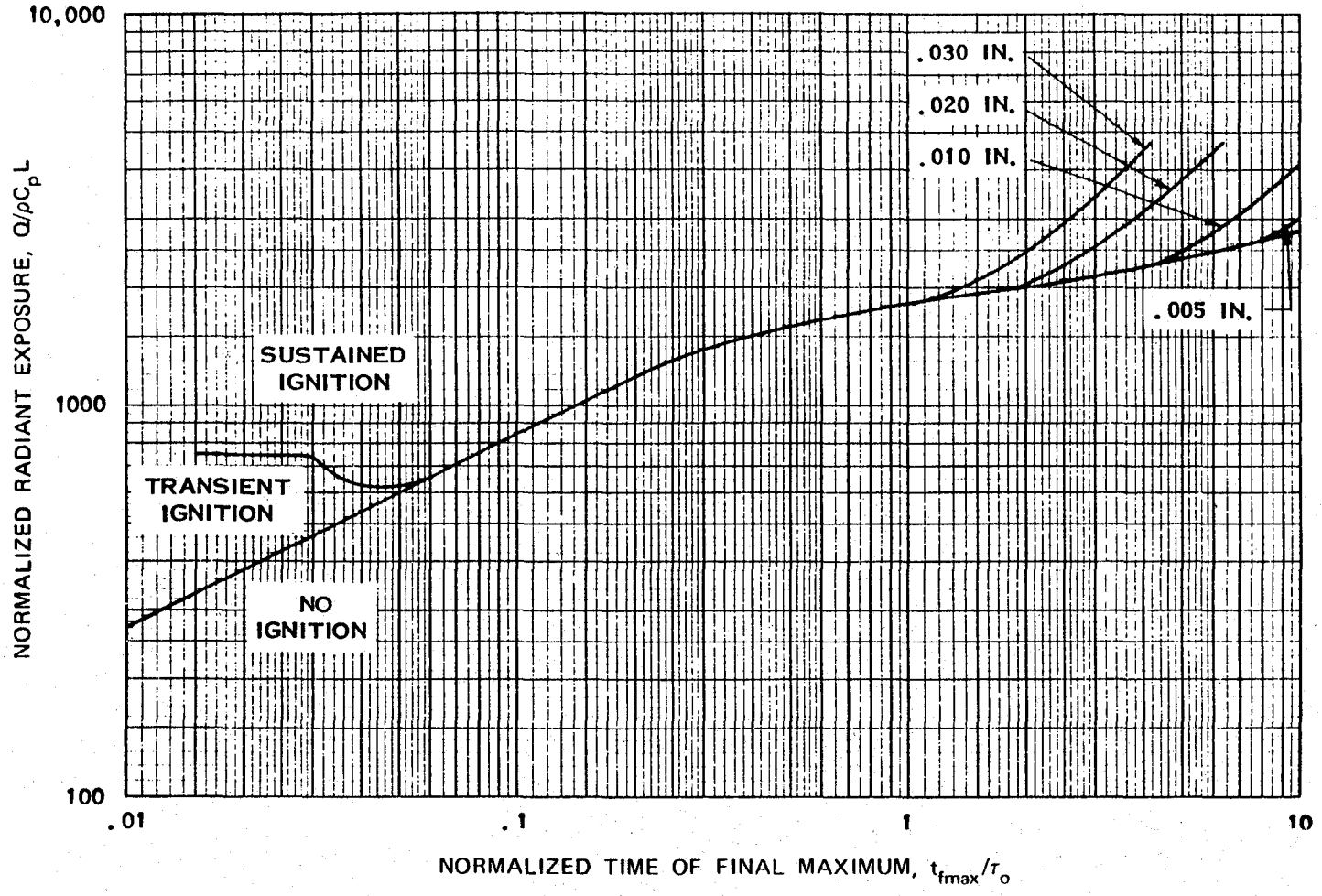

Figure 9-6. [redacted] Ignition Thresholds for Black α-Cellulose Exposed to a Simulated Weapon Pulse [redacted]

[redacted]

weapon pulses difficult. While the fuel absorbs heat and its surface chars, its absorption coefficient changes. As a result, the shape of the energy pulse actually absorbed by the material differs from that of the incident energy pulse (this effect is avoided in the α-cellulose by making the material black initially). A weapon pulse has no single rectangular wave equivalent, since the nature of material response to a thermal pulse varies with pulse shape as well as pulse length. However, for many calculations a rough equivalence may be obtained by assigning between 2.5 and 3 times the irradiance of the rectangular pulse to the weapon pulse.

[redacted] Both rectangular and weapon pulse data show an optimum pulse length for igniting materials. For the rectangular pulse, this optimum occurs with a pulse length slightly shorter than the characteristic thermal response time of the material. A pulse of this optimum duration lasts long enough to allow an appreciable amount of heat to penetrate to the back face, but it is short enough that only a small heat loss occurs during the pulse.

[redacted] For example, consider newsprint that is 0.008 cm thick, which has a thermal diffusivity, α, of 10^{-3} cm^2/sec. From the equation given previously

$$\tau_o = \frac{L^2}{\alpha}.$$

From Figure 9-6, the threshold for sustained ignition of black α-cellulose is a minimum when

$$\frac{t_{max}}{\tau_o} = \frac{t_{max}\alpha}{L^2} = 0.045.$$

The properties of newspaper are similar to those of α-cellulose, so the same relation may be assumed to hold for the newsprint. Thus,

$$t_{max} = 0.045\,\frac{L^2}{\alpha} = \frac{(0.045)(0.008)^2}{0.001}$$

$$t_{max} = 2.9 \times 10^{-3} \text{ sec.}$$

From the equation given in Chapter 3

$$t_{max} = 0.043\ W^{0.43}\ (\rho/\rho_o)^{0.42} \text{ sec.}$$

At sea level $\rho = \rho_o$, and

$$W = (t_{max}/0.043)^{2.3}$$

$$W = \left(\frac{2.9 \times 10^{-3}}{4.3 \times 10^{-2}}\right)^{2.3} = 0.002 \text{ kt.}$$

This yield is so small that little confidence may be placed in the result; however, this example demonstrates the general rule that short thermal pulses are more likely to ignite newsprint than long pulses over the range of yields that probably will be of practical importance.

9-20 Color [redacted]

[redacted] Although thermal damage depends on the radiant exposure to which a target is subjected, it depends in a much more direct manner on the amount of thermal energy absorbed. Thus color, which indicates the amount and spectral distribution of the visible energy reflected, is one indication of the resistance of a material to thermal damage.

[redacted] White materials reflect most of the energy in the visible portion of the spectrum that is incident on them, but all cellulosic fuels (which constitute the commonest potential ignition sites) absorb energy in the near infrared region. Cellulosic materials also char in response to high radiant exposures, and once the surface begins to blacken they absorb strongly. The total amount of energy absorbed depends on the absorption coefficient averaged not only over the spectrum of energies contained in the thermal pulse, but also over the interval of time during which the pulse is received. For a thin cellulosic material exposed to a moderately high level of radiant energy (just enough to ignite the ma-

[redacted]

[redacted]

[redacted] terial) blackening will not occur immediately, and the following rules give an effective average for the absorption coefficient that is roughly correct.

- If the material is white or nearly white, the effective absorption coefficient for the thermal pulse is about the square root of the absorption coefficient for visible light. *Example:* If the visible absorption coefficient is 0.1, the effective absorption coefficient for the thermal pulse is about 0.3.
- If the material has a color that is as dark as or darker than dove gray (a fairly light shade of gray), the effective absorption coefficient for thermal radiation is about equal to the visible absorption coefficient.
- The response of most of the nonwhite materials that provide potential ignition sites may be approximated by assigning an effective absorption coefficient of 0.5.

9-21 Transparency [redacted]

[redacted] The energy that passes through a partially transparent material cannot heat it. Thus, the energy deposited in the material is the incident energy minus the reflected energy minus the transmitted energy.

[redacted] The depth of penetration of thermal energy into a partially transparent material is determined by two mechanisms: heat absorbed at or near the surface penetrates by diffusion; and heat penetrates as radiant energy before it is absorbed. As shown in paragraph 9-19, the diffusion of heat may be associated with a transient thickness δ. Similarly, the penetration of thermal energy due to diathermancy (partial transparency) may be associated with a characteristic depth of $1/\beta$, where β is the extinction coefficient. In a practical situation, both of these mechanisms work simultaneously, and the heat penetrates deeper than it would if only one mechanism were effective.

[redacted] Usually, one or the other of the two mechanisms is dominant. If the product $\beta\delta$ exceeds 3 or 4, penetration will occur principally by diffusion. If the product is less than about 1/4, penetration will be principally by transmission of radiant energy. Temperature profiles in a semi-infinite solid are shown in Figure 9-7 in terms of dimensionless parameters, where ΔT is temperature rise, k is thermal conductivity, ρ is density, C_p is specific heat, H is energy absorbed (not the incident energy) per unit area, τ is rectangular pulse duration, and δ is characteristic depth defined in paragraph 9-19.

9-22 Effect of Humidity [redacted]

[redacted] The water content of thin fuels responds rapidly to changes in humidity. The radiant exposure that is required to ignite a thin cellulosic fuel is approximately

$$Q = Q_0 \ (1 + h/2),$$

where h is relative humidity and Q_0 is the radiant exposure that will ignite the fuel when it is completely dry.

[redacted] In general, ignition data give radiant exposure thresholds for average rather than extremely dry conditions. If the tabulated value of radiant exposure Q_1 applies to a relative humidity of h_1, the equation given above becomes

$$Q = Q_1 \ \frac{1 + h/2}{1 + h_1/2}.$$

[redacted] For example, if the radiant exposure from a 1 Mt explosion that is required to ignite new white bond paper is 30 cal/cm^2 when the relative humidity is 65 percent, the ignition threshold for the same explosion when the relative humidity is 15 percent is

$$Q = (30) \left(\frac{1 + 0.15/2}{1 + 0.65/2}\right) = 24 \ \text{cal/cm}^2.$$

[redacted]

[redacted]

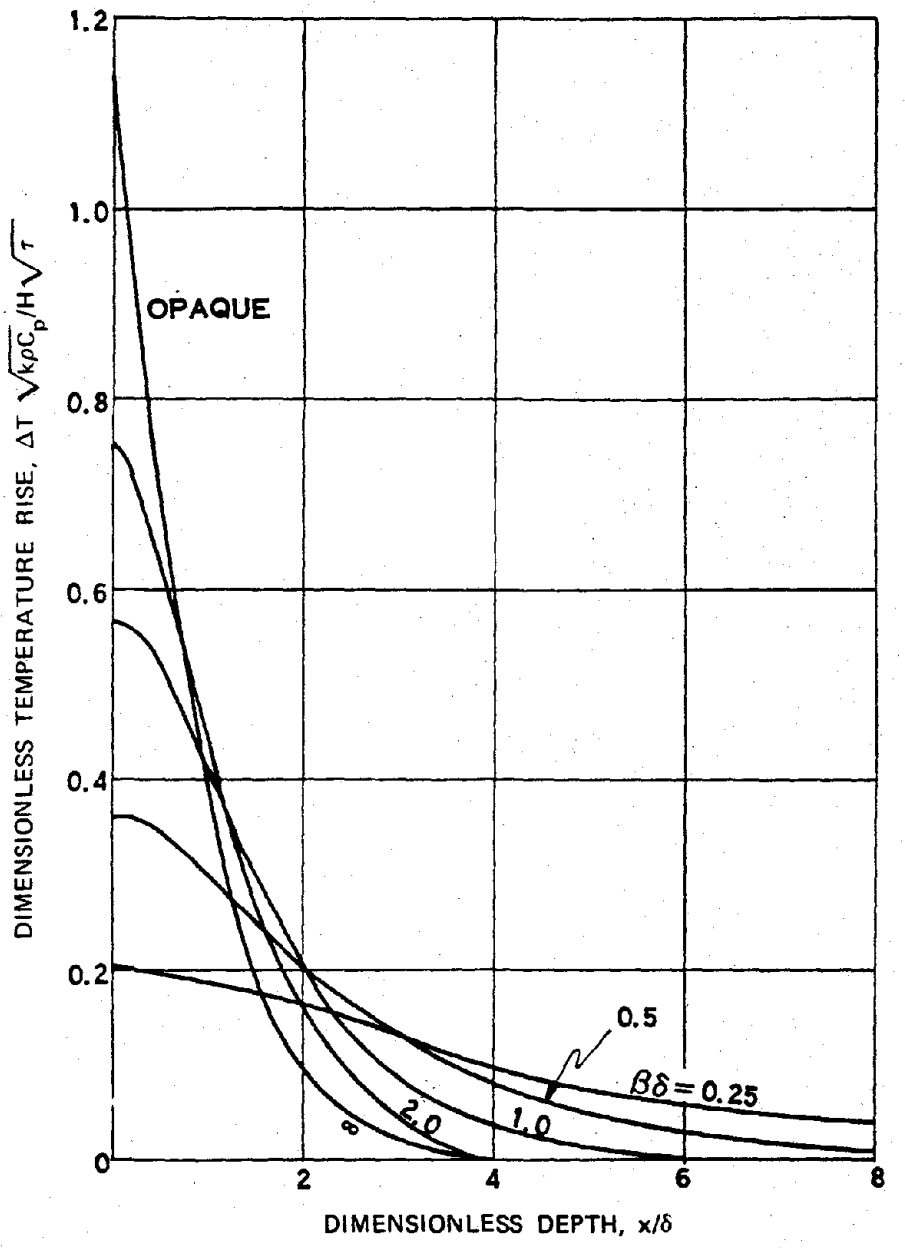

Figure 9-7. [redacted] Dimensionless Temperature Profiles in Opaque and Diathermanous Semi-Infinite Solids Exposed to a Rectangular Thermal Pulse [redacted]

[redacted]

[redacted]

9-23 Response of Metal Sheets [redacted]

[redacted] Both the tensile strength and the elastic modulus of metals tend to decrease with increasing temperature. Thus, thermal energy has the potential to weaken metallic structural members. If exposed metal parts are essential to the strength of a structure or a piece of equipment, weakening the metal by heating it may make the unit more susceptible to damage by the blast wave.

[redacted] Most structural metal is relatively immune to this form of damage in the loading levels of interest. If a heavy part such as a steel I-beam is subjected to a thermal pulse that is sufficiently intense to weaken it appreciably, it is probably so close to the burst that the blast wave could demolish the structure without assistance from the thermal pulse. Walls or roofs usually shield heavy structural members from the thermal pulse.

[redacted] Light weight units are more likely to be vulnerable to this synergistic damage. The outer covering and the materials that give these units mechanical strength are frequently one and the same. The material is likely to be an aluminum alloy, which loses strength at a much lower temperature than steel.

(U) The degradation of the response of metals to the blast wave as a result of thermal exposure is discussed in more detail in Section IV of this chapter.

9-24 Thermal Damage to Various Materials [redacted]

[redacted] The general trends discussed in the preceding paragraphs are illustrated by a number of specific examples in Tables 9-2 and 9-3. These tables show the critical radiant exposures for specified damage to fabrics and to various other materials, respectively. The radiant exposures are shown for three weapon pulse durations. The corresponding yields are shown in the footnote for low air bursts (note that altitude scaling is required for a 24 Mt burst to be considered an air burst (see Chapter 3)). Various yield/altitude combinations that will give the same values of t_{max} may be obtained by the methods described in Chapter 3.

[redacted] The values presented in Table 9-2 for fabrics apply for an ambient relative humidity of 65 percent and an ambient temperature of 20°C. For extremely dry conditions, the values shown for fabrics should be reduced by 25 percent. For extremely high relative humidities, near 100 percent (at 20°C), the values for fabrics should be increased by 25 percent. If the fabrics are water-soaked, the critical radiant exposures should be increased by 300 percent. The values for uniforms in Table 9-2 refer to damage to the material itself. They are not applicable for predicting skin burns under uniforms. However, when the outer garment ignites, the probability of skin burns should be considered.

[redacted] The effect, "tears on flexing," indicates the radiant exposure level at which the outer garment ceases to serve as a reliable barrier to the environment. Under certain environmental conditions the garment would require immediate replacement.

[redacted] Cotton or rayon fabrics generally can be ignited by exposure to thermal radiation. Nylons, dacrons, and similar synthetics generally are not ignited but melt at relatively low radiant exposures. Woolens do not ignite, but the fibers scorch and coalesce. When a sufficient thickness of the woolen fabric is scorched it becomes brittle and can be torn or crumbled readily.

[redacted] Most thick, dense materials that ordinarily are considered inflammable do not ignite to persistent flaming ignition when exposed to transient thermal radiation pulses. Wood, in the form of siding or beams, may flame during the exposure but the flame is extinguished when the exposure ceases.

[redacted]

[redacted]

Table 9-2. [redacted] Approximate Radiant Exposures for Ignition of Fabrics [redacted]

Material	Weight (oz/yd^2)	Color	Effect on Material	Radiant Exposure* (cal/cm^2) t_{max} 0.2 sec	t_{max} 1.0 sec	t_{max} 3.2 sec
Clothing Fabrics						
Cotton	8	White	Ignites	32	48	85
		Khaki	Tears on flexing	17	27	34
		Khaki	Ignites	20	30	39
		Olive	Tears on flexing	9	14	21
		Olive	Ignites	14	19	21
		Dark blue	Tears on flexing	11	14	17
		Dark blue	Ignites	14	19	21
Cotton corduroy	8	Brown	Ignites	11	16	22
Cotton denim, new	10	Blue	Ignites	12	27	44
Cotton shirting	3	Khaki	Ignites	14	21	28
Cotton-nylon mixture	5	Olive	Tears on flexing	8	15	17
	5	Olive	Ignites	12	28	53
Wool	8	White	Tears on flexing	14	25	38
		Khaki	Tears on flexing	14	24	34
		Olive	Tears on flexing	9	13	19
		Dark blue	Tears on flexing	8	12	18
	20	Dark blue	Tears on flexing	14	20	26
Rainwear (double-neoprene-coated nylon twill)	9	Olive	Begins to melt	5	9	13
	9	Olive	Tears on flexing	8	14	22
Drapery Fabrics						
Rayon gabardine	6	Black	Ignites	9	20	26
Rayon-acetate drapery	5	Wine	Ignites	9	22	28
Rayon gabardine	7	Gold	Ignites	**	24†	28†
Rayon twill lining	3	Black	Ignites	7	17	25
Rayon twill lining	3	Biege	Ignites	13	20	28
Acetate-shantung	3	Black	Ignites	10†	22†	35†
Cotton heavy draperies	13	Dark colors	Ignites	15	18	34
Tent Fabrics						
Canvas (cotton)	12	White	Ignites	13	28	51
Canvas	12	Olive drab	Ignites	12	18	28
Other Fabrics						
Cotton chenille bedspread		Light blue	Ignites	**	11†	15†
Cotton venetian blind tape, dirty		White	Ignites	10	18	22
Cotton venetian blind tape		White	Ignites	13†	27†	31†
Cotton muslin window shade	8	Green	Ignites	7	13	19

*[redacted] Radiant exposures for the indicated responses (except where marked †) are estimated to be valid to ±25% under [redacted]ndard laboratory conditions. Under typical field conditions the values are estimated to be valid within ±50% with a greater likelihood of higher rather than lower values. For materials marked †, ignition levels are estimated to be valid within ±50% under laboratory conditions and within ±100% under field conditions. For low air bursts, values of t_{max} of 0.2, 1.0, and 3.2 sec correspond roughly to yields of 40 kt, 2 Mt, and 24 Mt, respectively.

**[redacted] Data are not available or appropriate scaling not known.

[redacted]

[redacted]

Table 9-3. [redacted] Approximate Radiant Exposures for Ignition of Various Materials [redacted]

Material	Weight (oz yd^{-2})	Color	Effect of Material	Radiant Exposure* (cal/cm^2) t_{max} 0.2 sec	t_{max} 1.0 sec	t_{max} 3.2 sec
Household Tinder Materials						
Newspaper, shredded	2		Ignites	4	6	11
Newspaper, dark picture area	2		Ignites	5	7	12
Newspaper, printed text area	2		Ignites	6	8	15
Crepe paper	1	Green	Ignites	6	9	16
Kraft paper	3	Tan	Ignites	10	13	20
Bristol board, 3 ply	10	Dark	Ignites	16	20	40
Kraft paper carton, used (flat side)	16	Brown	Ignites	16	20	40
New bond typing paper	2	White	Ignites	24†	30†	50†
Cotton rags		Black	Ignites	10	15	20
Rayon rags		Black	Ignites	9	14	21
Cotton string scrubbing mop (used)		Gray	Ignites	10†	15†	21†
Cotton string scrubbing mop (weathered)		Cream	Ignites	10†	19†	26†
Paper book matches, blue head exposed			Ignites	11†	14†	20†
Excelsior, ponderosa pine	2 lb ft^{-3}	Light yellow	Ignites		23†	23†
Outdoor Tinder Materials***						
Dry rotted wood punk (fir)			Ignites	4†	6†	8†
Deciduous leaves (beech)			Ignites	4	6	8
Fine grass (cheat)			Ignites	5	8	10
Coarse grass (sedge)			Ignites	6	9	11
Pine needles, brown (ponderosa)			Ignites	10	16	21
Construction Materials						
Roll roofing, mineral surface			Ignites	**	>34	>116
Roll roofing, smooth surface			Ignites	**	30	77
Plywood, douglas fir			Flaming during exposure	9	16	20
Rubber, pale latex			Ignites	50	80	110
Rubber, black			Ignites	10	20	25
Other Materials						
Aluminum aircraft skin (0.020 in. thick) coated with 0.002 in. of standard white aircraft paint			Blisters	15	30	40
Cotton canvas sandbags, dry filled			Failure	10	18	32
Coral sand			Explodes (popcorning)	15	27	47
Siliceous sand			Explodes (popcorning)	11	19	35

[redacted] Radiant exposures for the indicated responses (except where marked †) are estimated to be valid to ±25% under standard laboratory conditions. Under typical field conditions the values are estimated to be valid within ±50% with a greater likelihood of higher rather than lower values. For materials marked †, ignition levels are estimated to be valid within ±50% under laboratory conditions and within ±100% under field conditions. For low air burst, values of t_{max} of 0.2, 1.0, and 3.2 sec correspond roughly to yields of 40 kt, 2 Mt, and 24 Mt, respectively.

** [redacted] Data are not available or appropriate scaling not known.

*** [redacted] Radiant exposures for ignition of these substances are highly dependent on the moisture content.

[redacted]

SURVIVAL IN FIRE AREAS

The best documented fire storm in history (but not the one causing the greatest loss of life) occurred in Hamburg, Germany during the night of July 27-28, 1943, as a result of an incendiary raid by Allied forces. Factors that contributed to the fire included the high fuel loading of the area and the large number of buildings ignited within a short period of time.

The main raid lasted about 30 minutes. Since the air raid warning and the first high explosive bombs caused most people to seek shelter, few fires were extinguished during the attack. By the time the raid ended, roughly half the buildings in the 5 square-mile fire storm area were burning, many of them intensely. The fire storm developed rapidly and reached its peak in two or three hours.

Many people were driven from their shelters and then found that nearly everything was burning. Some people escaped through the streets; others died in the attempt; others returned to their shelters and succumbed to carbon monoxide poisoning.

Estimates of the number that were killed range from about 40,000 to 55,000. Most of the deaths resulted from the fire storm. Two equally heavy raids on the same city (one occurred two nights earlier; the other, one night later) did not produce fire storms, and they resulted in death rates that have been estimated to be nearly an order of magnitude lower.

More surprising than the number killed is the number of survivors. The population of the fire storm area was roughly 280,000. Estimates have been made that about 45,000 were rescued, 53,000 survived in non-basement shelters, and 140,000 either survived in basement shelters or escaped by their own initiative.

9-25 Causes of Death

The evidence that can be reconstructed from such catastrophes as the Hamburg fire storm indicates that carbon monoxide and excessive heat are the most frequent causes of death in mass fires. Since the conditions that offer protection from these two hazards generally provide protection from other hazards as well, the following discussion is limited to these two causes of death.

Carbon Monoxide. Burning consists of a series of physical and chemical reactions. For most common fuels, one of the last of the reactions is the burning of carbon monoxide to form carbon dioxide near the tips of the flames. If the supply of air is limited, as it is likely to be if the fire is in a closed room or at the bottom of a pile of debris from a collapsed building, the carbon monoxide will not burn completely. Fumes from the fire will contain a large amount of this tasteless, odorless, toxic gas.

During the Hamburg fire, many basement shelters were exposed to fumes. Imperfectly fitting doors and cracks produced by exploding bombs allowed carbon monoxide to penetrate these shelters. The natural positions of many of the bodies recovered after the raid indicated that death had often come without warning, as is frequently the case for carbon monoxide poisoning.

Carbon monoxide kills by forming a more stable compound with hemoglobin than either oxygen or carbon dioxide will form. These latter are the two substances that hemoglobin ordinarily carries through the blood stream. Carbon monoxide that is absorbed by the blood reduces the oxygen carrying capacity of the blood, and the victim dies from oxygen deficiency.

As a result of the manner that carbon monoxide acts, it can contribute to the death of a person who leaves a contaminated shelter to attempt escape through the streets of a burning city. A person recovering from a moderate case of carbon monoxide poisoning may feel well while he is resting, but his blood may be unable

[redacted]

[redacted] to supply the oxygen his body needs when he exerts himself. After the air raid at Hamburg, victims of carbon monoxide poisoning, apparently in good health, collapsed and died from the strain of walking away from a shelter. It is suspected that many of the people who died in the streets of Hamburg were suffering from incipient carbon monoxide poisoning.

[redacted] *Heat.* The body cools itself by perspiration. When the environment is so hot that this method fails, body temperature rises. Shortly thereafter, the rate of perspiration decreases rapidly, and, unless the victim finds immediate relief from the heat, he dies of heat exhaustion. Death from excessive heat may occur in an inadequately insulated shelter; it also may occur in the streets if a safe area cannot be located in a short time.

9-26 Shelters [redacted]

[redacted] The results of the Hamburg fire storm illustrate the value of shelters during an intense mass fire. The public air raid shelters in Hamburg had very heavy walls to resist large bombs. Reinforced concrete three feet thick represented typical walls. Some of these shelters were fitted with gas proof doors to provide protection from poison gas. These two features offered good protection from the heat and toxic gases generated by the fire storm.

[redacted] The public shelters were of three types:

- *Bunkers.* These were large buildings of several shapes and sizes, designed to withstand direct hits by large bombs. The fire storm area included 19 bunkers designed to hold a total of about 15,000 people. Probably twice this number occupied the bunkers during the fire storm, and all of these people survived.
- *Splinterproof Shelters.* These were long single story shelters standing free of other buildings and protected by walls of reinforced concrete at least 2-1/2 feet thick. No deaths resulting from the fire storm were reported among occupants of these shelters. These structures were not gas-proof. Distance from burning structures and low height of the shelters probably provided protection from carbon monoxide.
- *Basement Shelters.* The public shelters that were constructed in large basements had ceilings of reinforced concrete 2 to 5 feet thick. Although reports indicate that some of the occupants of these shelters survived and some did not, statistics to indicate the chance of survival in such structures are not available.
- *Private Basement Shelters.* Private basements were constructed solidly, but most of them lacked the insulating value of very thick walls and the protection of gas-tight construction. Emergency exits (usually leading to another shelter in an adjacent building) could be broken if collapse of the building caused the normal exit to be blocked. As a result of the total destruction in the fire storm area, this precaution was of limited value. Many deaths occurred in these shelters as a result of carbon monoxide poisoning, and the condition of the bodies indicated that intolerable heat followed the carbon monoxide frequently. In some cases, the heat preceded the poisonous gas and was the cause of death. Generally, these shelters offered such a small amount of protection that the occupants were forced out within 10 to 30 minutes. Most of these people were able to move through the streets and escape. Others were forced out later when the fire storm was nearer its peak intensity, and few of these escaped. A few people survived in private basement shelters.

[redacted] Experience in Hamburg and other mass fire areas suggests the following requirements for

[redacted]

shelters for fire protection:

- *Location.* Shelters should be located as far away from combustible structures as possible. The bottom of a mass of burning debris is very hot and can remain so for days. An open area also may be exposed to considerable heat, but not so much as the basement of a burned-out building. Three feet of earth will provide sufficient insulation for a shelter if no heavy fuels are nearby. However, material scattered by the blast wave could fall on a shelter and render it less safe. The choice of a suitable location for a shelter is most difficult in heavily built-up areas, where mass fires are most likely to occur. Shelters in such areas would have to be designed to withstand the severe environment to which they would be subjected in case of a mass fire. When the shelters in Hamburg were built, the problems of mass fires were not anticipated.
- *Ventilation.* Any shelter that is large enough to house its occupants in reasonable comfort contains sufficient air to sustain life for the duration of a mass fire. The shelter should be constructed so that it can be sealed from the entry of gases from the outside during the period of active burning. After the fire subsides, air will be available inside the shelter if burning debris has not fallen on or near the air intake.
- *Provisions.* If escape from a shelter is necessary, wet coats or blankets would improve the chance of survival in the open. Since any shelter built for protection against a mass fire would logically serve also as a fallout shelter, such items as blankets and water normally would be available.

9-27 Escape from the Fire Areas

A large number of people, chiefly the occupants of basement shelters, escaped from the Hamburg fire simply by leaving while the streets were still passable. In areas where damage is sufficiently light that people can attempt escape, the rate at which the fire builds up is expected to be slow enough to allow 30 minutes or more before movement through the streets will become dangerous.

Escape from the Hamburg fire storm area was simplified by the limited size of the fire. In the event of a mass fire caused by a nuclear attack, the fire area probably will be much larger. Although escape to the edge of the fire may be impossible, parks, bodies of water, or even areas that are not heavily built up may offer relative safety from the fire.

As the fire grows in intensity, selection of a suitable escape route becomes important. Moving through a narrow street, with tall buildings burning intensely on both sides, will subject people to an excessive amount of heat.

Preplanned escape routes are desirable. The safest routes are those that minimize exposure to thermal radiation from burning structures. A safe street would be wide compared to the heights of the buildings facing it. Masonry buildings with few windows would be a lesser threat than buildings with many windows. The solid wall blocks radiant exposure from fires burning inside the building, and it also protects the contents of the building from direct ignition by the thermal pulse from the nuclear weapon.

Simple rules for distinguishing safe from unsafe streets are not available; however, calculations of the street width for which the thermal radiation would be intense enough to ignite clothing in a short time have been made, assuming that buildings on both sides of the street were burning. The results of these calculations are shown in Table 9-4.

Whether or not such streets are safe will depend on many factors, such as fire intensity, percentage of the building fronts occupied by windows, wind speed and direction, protective

[redacted]

clothing, and exposure time. In general, the streets of Hamburg were 45 to 60 feet wide, and the buildings were 3 to 5 stories high. Table 9-4 predicts that such streets would be dangerous, and experience shows that they were. However, even these streets provided escape for some.

Table 9-4. [redacted] Minimum Structure Separation for Escape Route [redacted]

Building Height (feet)	Distance Between Buildings (feet)
20	40
30	57
40	67
50	83
60	96

9-28 Safe Areas Within the Fire [redacted]

[redacted] Experience indicates that large open areas within a fire storm area probably are safe. A park 1,000 feet in diameter provided adequate protection from the Hamburg fire storm; a similar area of 400 x 400 feet did not.

[redacted] In Tokyo, during the Kanto earthquake and fire of 1923, fire whirlwinds sweeping across some large open areas killed many who would otherwise have survived. Thus, safety in a particular location depends to some extent on unpredictable aspects of the fire.

SECTION IV

[redacted] THERMAL RADIATION DEGRADATION OF STRUCTURAL RESISTANCE TO AIR BLAST [redacted]

[redacted] Section III of this chapter contains a description of the properties of materials that might result in ignition or degradation of their physical properties. The emphasis of the discussion in Section III concerns the ignition of combustible materials. This section provides a somewhat expanded treatment of the degradation of structural resistance to air blast that is brought about by exposure to thermal radiation.

[redacted] The problem of integrated thermal/blast effects can be divided into several elements. One element is the free field thermal and air blast environments to which a system element is exposed. Methods of predicting these environments are presented in Chapters 2 and 3. As pointed out in Chapter 3, prediction of the thermal environment is difficult because of the importance of climatic conditions. A statistical or probabilistic description of weather conditions frequently will have to be used to form some estimate of the validity of the results.

[redacted] The first element of the overall problem treated in this section is the coupling of thermal energy into the structure or system element of interest. The condition of the target surface, its orientation to the detonation, and coatings employed all can affect the amount of thermal energy that is absorbed by the target.

[redacted] The second element is the mechanisms for the loss of energy from the structure through convective heat losses or reradiation. The third element is the effect of absorbed energy on the state of the target material. The primary effect of this change of state is the fourth element, which is the change in material properties.

[redacted] The final and fifth element of the problem is the effect of changes in material properties on the structural resistance to air blast loading.

[redacted] Insufficient data are available concerning the thermophysical properties of nonmetallic materials to provide a realistic discussion of the combined blast/thermal effects on such materials. Any current prediction would be highly uncertain, both with regard to the occurrence of any specific physical phenomena and to the quantitative evaluation of the phenomena. Con-

[redacted]

sequently the discussion in this section will be limited to metallic materials.

THERMAL ENERGY ABSORBED

9-29 Absorption

The amount of thermal radiation that a metallic element will absorb depends on the properties of the metal, color, surface condition, orientation to the burst, the absence or presence of some type of coating (either accidental such as dirt or grease or intentional such as a paint system).* The amount of thermal energy absorbed by a target usually is determined by multiplying the incident energy by an absorption coefficient. The absorption coefficient cannot be directly measured; however, a good estimate can be made by performing spectral measurements of reflectance over the range of wavelengths representative of the nuclear radiation spectral distribution, and finding an average value of reflectance. The coefficient of absorptance then equals one minus this average value of reflectance. The absorptance determined in this manner is valid only as long as the surface does not change as a result of the absorbed thermal energy. Another approach is to divide the quantity of energy absorbed by the incident energy. The absorbed energy is determined from experimentally determined temperature vs time relationships and appropriate theoretical energy balance relationships.† Some typical values for absorption coefficients for bare metals are shown in Table 9-5. A value of 0.5 would be a good value to assume for the absorption coefficient in the absence of more definitive data for a specific system under investigation.

A coating or surface treatment on a metal substrate can alter the effective absorption coefficient significantly, and thereby can alter the amount of energy absorbed by the metal structure. The amount of energy absorbed depends on color, thickness, adhesiveness, and heat transfer characteristics of the coating. The most common type of coating is, of course, paint. The importance of paint in altering the amount of thermal radiation absorbed was noted in early investigations where it was found that the thin aircraft skin under painted insignia had melted, whereas the skin of adjacent areas was not affected. It should not be assumed, however, that paint or other coating is necessarily a detriment. In some instances the smoke that results from the breakdown of the paint can reduce the amount of energy absorbed and thereby reduce the maximum temperature reached by the substrate. Figure 9-8 illustrates this factor. The only true general statement that can be made about coatings is that they can alter the amount of thermal energy absorbed by the substrate. In fact some coatings, even paint systems, can be designed to reduce the amount of energy absorbed. As a general rule, however, most coating systems on present tactical military equipment

Table 9-5. Absorption Coefficients for Bare Metals

Material	Absorption Coefficient
Polished metals	0.25–0.5
Especially clean aluminum	0.2–0.4
Clean aluminum	0.5
Unpolished metals	0.45–0.55
Average over aircraft	0.5

*Implicit in this statement and throughout this discussion is the fact that energy coupling depends on the wavelength of the incident radiation.

†Absorptance is a function of time and temperature, although an average value usually is employed. This function when known may be found as an input specification for certain computer programs.

[redacted]

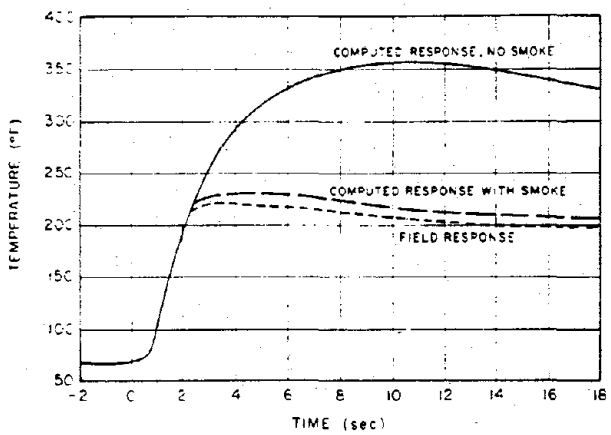

Figure 9-8. [redacted] Exposed Facing Temperature-Time Histories of Aluminum Honeycomb. Facing, 0.016-in. Gray Painted Skin; Core 1/8-in., Cell Size 1/2-in. Thick. 21-24.2 cal/cm^2, 3.8 Mt [redacted]

will cause an increase in the amount of energy absorbed. The mechanisms of the response of coatings and the transfer of energy to the substrate are so complex that theoretical descriptions have not been successful. The response of coatings depends upon both the rate at which thermal radiation is received and the total incident energy. A given amount of radiation received at a slow rate may only cause discoloration or slight scorching, whereas if it were received at a very rapid rate it would cause charring or blistering. The latter response is more typical in a nuclear environment. The change in state of the coating reduces the amount of energy available to be transferred to the substrate, because these processes are irreversible. However, the change in state usually increases the absorption coefficient of the coating, and the net result usually is an increase on the amount of energy absorbed by the substrate. An exception occurs if the absorption coefficient was initially high, and energy was absorbed by the smoke layer generated by the decomposing paint. Coatings that respond by physically separating from the surface, i.e., blister, potentially can reduce the amounts of energy transferred to the substrate. Since the response of the coating-substrate system to nuclear weapon thermal radiation is so complex, effective absorption coefficients usually are determined experimentally.

[redacted] The average value of the absorption coefficient, A, depends on the properties of the substrate as the flow of thermal energy from the coating influences the response of the coating. A series of experiments with laser heating provides data to illustrate this point. Various metallic samples were prepared with a Silicon-carbide-synar binder coating (spectrophotometric measurements gave an average absorption coefficient of 0.85 for the coated aluminum sample for equilibrium temperatures of 70 and 600°F for a 10.6 micron wavelength). The average values of the absorption coefficients for a range of irradiances based on temperature vs time data are shown in Table 9-6. The effect of substrate properties is significant.

[redacted] Values of absorption coefficients are shown in Table 9-7. Generally, values range from 0.3 to 0.6 for light or reflective paints, and from

Table 9-6. [redacted] Average Absorption Coefficients for Laser Heated Coated Substrates [redacted]

Substrate	Average Absorption Coefficient
2024-T81 clad aluminum alloy	0.7 ± 0.1
6AL-4V annealed titanium	0.35 ± 0.1*
301 full hard stainless steel	0.80 ± 0.05

[redacted] Evaluation of titanium specimens showed considerable scatter. Erratic behavior probably resulted from improper bonding of the coating and cracking or flaking of the coating during straining.

[redacted]

[redacted]

Table 9-7. [redacted] Representative Values of Absorption Coefficients for Metals with Various Coatings or Surface Treatments [redacted]

Substrate	Coating or Surface Treatment	Absorption Coefficient
Metallic skins	Aluminum paint	0.5
Painted metals (aircraft skins)	White paint	0.3 - 0.5
	White paint (clean)	0.25
	White paint w/oil film	0.30
	Yellow paint	0.4 - 0.55
	Olive paint	0.6 - 0.7
	Gray paint (clean)	0.6
	Black paint	0.65 - 0.95
	Insignia blue	0.9
5032-H32AL	Black paint	0.7 - 1.0
Aluminums	Reflecting white paint	0.32
	Camouflage paint	1.00
6061 Al-Mg alloy	Haze gray Navy paint	0.78 ± 0.04
	Volcanol	0.99 ± 0.05
2024-T3	Anodized black	0.67

[redacted]

0.6 to 1.0 for dark paints or treated surfaces.

[redacted] It is apparent that the selection of an absorption coefficient based on the information in Table 9-7 for use in analyzing the response of a military system could be in error by as much as ±50 percent. Currently, the best solution is to perform upper and lower bound calculations. The upper and lower bound calculations should be based on the best estimate of the condition of the surface at the time of exposure, i.e., dirty, corroded, prior exposures, etc.

[redacted] One additional factor affects the amount of energy absorbed. This factor is the orientation of the surface to the thermal pulse. Ideally, if incident parallel rays are assumed, with no scattering, reflection or refraction, the target surface receives all of the radiation if it is oriented normal to the rays. If the surface is rotated about an axis normal to the rays, it cuts fewer of the rays, and the amount of thermal energy received is reduced. The energy received by a differential area on a curved surface also can be treated in this manner. With such assumptions, the absorbed energy function takes the following form:

$$Q_a = QA_e \cos \theta$$

where

Q = incident energy, usually expressed in cal/cm^2

Q_a = absorbed energy, usually expressed in cal/cm^2

[redacted]

[redacted]

[redacted]

A_e = effective absorption coefficient

θ = incident angle, angle between a line from the source to the surface and a line normal to the plane of the surface.

Under those ideal conditions, the amount of absorbed energy follows the cosine law; however, there will be conditions where scattering, reflection, and refraction, will invalidate the parallel ray assumption in addition to altering Q. This would principally occur at large angles of incidence such as shown schematically in Figure 9-9. A computer program called TRAP has recently been developed to handle these conditions.

[redacted] Figure 9-9 also illustrates the amount of energy received by the surface of a cylinder with its axis oriented normal to the ray paths. The quantity θ then becomes the distance, in radians, along the circumference, from the point nearest the source.

[redacted] Both the absorption coefficient and orientation are important in determining the amount of energy absorbed into the target. Errors in orientation are of greater significance at large angles on incidence; however, orientation usually can be inferred, at least for worst cases, whereas the absorption coefficient usually is not well known unless it has been determined experimentally.

9-30 Energy Losses [redacted]

[redacted] The absorption of thermal radiation energy into a material has been discussed in the previous paragraph. Before discussing the effect of this absorbed energy on material properties or change in structural resistance, the form and significance of energy losses from the material

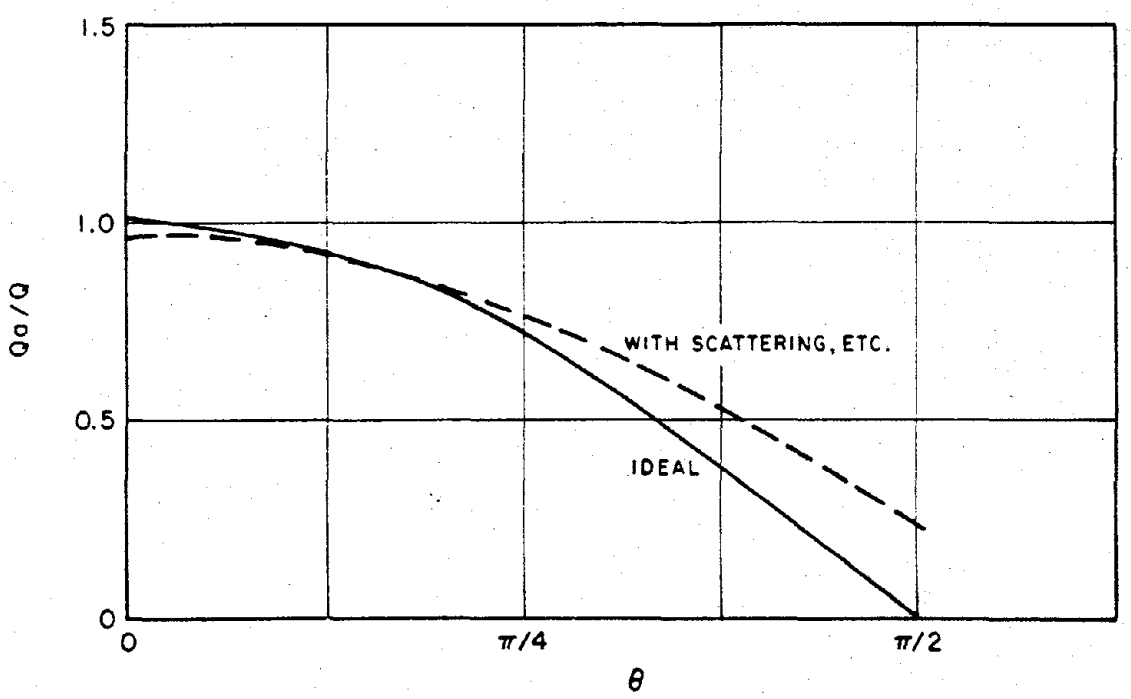

Figure 9-9. [redacted] Schematic Comparison of Ideal Cosine Law with Function Including Scattering, Reflection, and Refraction [redacted]

[redacted]

[redacted]

[redacted] must be discussed. The three ways in which thermal energy can be dissipated are conduction, radiation, and convection. For purposes of this discussion, conductive dissipation is not really a loss, in that energy is redistributed throughout the material system rather than lost from the system. This form of heat dissipation is considered in more detail in the following subsection that discusses the change in material state, and the discussion of temperature profiles.

[redacted] Radiation losses normally are considered negligible, because the temperature rises in a material are relatively small, even though the radiation heat loss is a function of the fourth power of absolute temperatures. The heat loss through radiation is expressed by:

$$Q_r = \sigma\epsilon(T^4 - T_0^4)$$

where

Q_r = radiative heat loss, cal/cm^2-sec,

σ = Stephan Bolzman Coefficient = 1.36 x 10^{-12} cal/cm^2 sec °K^{-4},

ϵ = emissivity, nondimensional,

T = absolute temperature, °K, of radiator (may be time dependent),

T_0 = absolute temperature, °K, of surrounding air.

If a 200°C temperature difference is assumed, and an emissivity of 0.2 (for oxidized aluminum at temperatures of a few hundred °C), and the ambient air temperature is 300°K, the radiative heat loss becomes:

$$Q_r = (1.36 \times 10^{-12})(0.2)(500^4 - 300^4)$$

$$= 1.48 \times 10^{-2} \text{ cal/cm}^2 \cdot \text{sec}$$

If the temperature rise is 400°C then Q_r becomes equal to 6.3 x 10^{-2} cal/cm^2 sec. Thus, it can be seen that even at high elevated temperatures, the heat loss through radiative processes is small.

[redacted] Convective heat losses occur when there is a flow of air over the heated surface. This type of heat loss is most important for aircraft in flight and is a weak function of position on the airfoil, and the speed and altitude of the aircraft. The rate of convective heat loss also depends on whether the boundary layer flow is laminar or turbulent. These processes are generally understood, and a number of formulas that are available are given below:

$$h_{cv} = 0.67(10)^{-4} T^{0.3} \frac{(V\rho)^{0.8}}{x^{0.2}}$$

where

h_{cv} = convective heat loss coefficient for turbulent flow,

T = air temperature, °R,

V = flight speed, ft/sec,

ρ = density of air, lb/ft^3,

x = distance from leading edge of airfoil, ft.

$$h_{cv} = 0.176\ \rho V C_p (\log_{10} Re)^{-2.45},$$

$$h_{cv} = 0.01445\ k/x\ (Re)^{0.8}\ (Pr)^{0.33},$$

$$h_{cv} = 0.0282\ k/x\ (Re)^{0.8}\ (Pr)^{0.33},$$

$$h'_{cv} = 0.318\ k/x\ (Pr)^{1/3}\ (Re)^{1/2},$$

$$h'_{cv} = 0.332\ \rho V C_p (Pr)^{-2/3}\ (Re)^{-1/2},$$

where

h_{cv} = convective heat loss coefficient for turbulent flow, cal/cm^2 · sec · °C

[redacted]

[redacted]

[redacted]

h'_{cv} = convective heat loss coefficient for laminar flow, cal/cm^2 · sec · °C

ρ = density of air, gm/cm^3

V = flight speed, cm/sec

C_p = specific heat of air, cal/gm · °C

Re = Reynolds number, $\rho Vx/\mu$, dimensionless

k = thermal conductivity of air, cal/cm · sec · °C

x = distance from leading edge of airfoil, cm

Pr = Prandtl number, $C_p\mu/k$, dimensionless

μ = viscosity of air, gm/sec · cm

These formulas are based on the assumption that a reasonable approximation may be obtained by analysis of airflow over a heated flat plate. Experimental data indicate that the average error in using this approximation may be as much as 30 percent with a mean error of from 10 to 15 percent. The value for h_{cv} ranges from zero to 0.03 cal/cm^2 · sec · °C for a range of reasonable air properties and velocities. Generally, convective heat losses are marginally important for relatively low yield weapons; however, for long duration thermal pulses and under conditions when the temperature difference between the aircraft skin and the air boundary layer is large, the convective heat loss can be significant for high speed aircraft.

[redacted] Values of h_{cv} have been calculated (see Table 9-8) for purposes of comparing the results of the equations given above, under the following assumed conditions.

Aircraft type = fixed wing

Aircraft speed = 100 mph (4.47 x 10^3 cm/sec)

Aircraft altitude = 1,000 ft

Air temperature = 70°F, 20°C

x = 4 ft, 121.92 cm

ρ = 7.5(10)$^{-2}$ lb/ft^3

Table 9-8. [redacted] Values of h_{cv} Obtained from Various Functions in the Order in Which the Equations are Given Above [redacted]

Flow Condition	h_{cv} $\left(\frac{\text{cal}}{\text{cm}^2 \cdot \text{sec} \cdot {}^\circ\text{C}}\right)$
Turbulent	2.27(10)$^{-3}$
	2.27(10)$^{-3}$
	1.14(10)$^{-3}$
	2.23(10)$^{-3}$
Laminar	2.15(10)$^{-4}$
	2.82(10)$^{-4}$

= 1.2(10)$^{-3}$ gm/cm^3

k = 6.0874(10)$^{-5}$ cal/cm · sec · °C

C_p = 0.2404 cal/gm · °C

μ = 1.798(10)$^{-4}$ gm/cm · cm

[redacted] The use of the convective heat loss coefficient, h_{cv}, is shown below:

$$Q_{cv} = h_{cv}\ (T_s - T)$$

where

Q_{cv} = convective heat loss, cal/cm^2 · sec

T_s = surface temperature, °C (may be time dependent)

T = surrounding air temperature, °C

For high speed aircraft, it may not be appropriate to assume that the temperature of the surrounding air is the temperature of the air boundary layer next to the heated surface. This

[redacted]

[redacted]

[redacted]

is particularly true if aerodynamic heating occurs. For this situation, the recovery temperature T_r should replace T in the equation given above.

[redacted] For tactical systems of interest to this section, radiative and convective heat losses generally can be neglected. However, these are and normally should be included in detailed analyses and computer calculations for completeness, particularly for high speed aircraft and large yield weapons.

[redacted] CHANGES IN MATERIAL STATE AND MATERIALS PROPERTIES [redacted]

9-31 Changes in Material State [redacted]

[redacted] The change in material state of primary interest is the change in temperature caused by absorbed thermal radiation. The temperature changes are controlled by the energy absorbed in the material as a function of time and position and by the geometry of the member being analyzed. Geometry can have a significant impact on heat flow through the member as well as heat absorption and losses. There are a number of techniques available for determining temperature changes. These techniques vary from simple formulas to large computer programs depending on the simplifying assumptions that are made and the complexity of the system geometry. The greatest amount of effort has been devoted to the study of temperature changes in flat plates, primarily because of the interest in aircraft safety/survivability problems. Therefore, the following discussion is dominated by analysis of flat plates, although most of what can be learned about the processes affecting plate temperature applies to other geometries because the basic equations describing the processes are the same.

[redacted] Plates can be divided into several types according to the temperature profile through the plate. A thermally "thin" plate usually is defined as a plate where the temperature gradient between the front and back of the plate is small. Thermally thin plates simplify the analysis problem, because, if a significant thermal gradient exists, the thermal stresses become more complex. Plates usually are assumed to be one dimensional, with no heat flow to a supporting structure, so heat sink effects can be neglected, unless the plate is part of a fuel tank.

[redacted] Whether a plate is thermally thin depends not only on the thermophysical properties of the material, but also on the thermal pulse characteristics and the time during the pulse that the criterion is applied. Some materials conduct heat more quickly than others, and the temperature on the back face of these materials will not lag behind the temperature on the front as much as for materials with lower conductivities. For example, the thermal conductivity of aluminum is about 0.4 cal/sec · cm · °C, and that of titanium is about 0.04 cal/sec · cm · °C. Therefore, aluminum conducts 10 times as much heat as titanium in a given amount of time. Other material factors that control the ratio of front to back temperature are specific heat, density, and thickness.

[redacted] The temperature difference also depends on pulse characteristics. For a pulse that is delivered slowly, there may be sufficient time for energy to be conducted to the back face, so the thermal gradient at the time of interest is minimized. Conversely, a pulse that is delivered rapidly may cause a steep thermal gradient. For a given pulse, material, and thickness, the time at which the temperature response is of interest determines whether the thermal gradient is small.

[redacted] A number of techniques have been developed to determine whether a plate can be considered to be thermally thin. One technique that gives a good approximation is illustrated in Figure 9-10. The values of $\eta = t/t_{max}$ and $\alpha t_{max}/b^2$ must be evaluated to use the curves in Figure 9-10. From Chapter 3

[redacted]

[redacted]

[redacted]

$$t_{max} = 0.043\ W^{0.43}\ (\rho/\rho_o)^{0.42}\ \text{sec},^*$$

where t_{max} is the time to the principle thermal maximum, W is the weapon yield in kilotons, and ρ/ρ_o is the ratio of the air density at the burst altitude to the air density at sea level. The parameter α is defined as

$$\alpha = k/\rho_m C_p\ \text{cm}^2/\text{sec}$$

where

k = thermal conductivity of air, cal/cm · sec · °C,

ρ_m = material density, gm/cm^3,

C_p = specific heat of air, cal/gm · °C

and b is the thickness of the plate in centimeters. The point where the values of η and $\alpha t_{max}/b^2$ meet determines whether the plate is thin, finite, or thick. A thin plate is one in which the difference between back and front temperatures is less than 10 percent. A thick plate is one in which there is no temperature rise on the back face. A finite plate falls between the other two criteria.

[redacted] A technique for predicting the temperatures of thermally thin plates uses the relationships shown in Figure 9-11. This technique is believed to provide good results over a fairly wide range of problems of interest. The technique assumes that thermophysical properties and the rate of convective heat loss are constant, that radiation losses are negligible, and that there is no heat loss from the back of the plate.

---

* [redacted] The examples provided in this section will all be concerned with air bursts that are sufficiently low that the term $(\rho/\rho_o)^{0.42}$ is near enough to 1.0 to be neglected (e.g., at 4,000 feet $(\rho/\rho_o)^{0.42} \approx 0.99$). Therefore, the approximation $t_{max} \approx 0.043\ W^{0.43}$ will be used throughout the remainder of this section.

[redacted]

[redacted]

Problem 9-1. Calculation of Thermal Thickness of a Metal Plate

[redacted] Figure 9-10 contains curves that define regions where metal plates may be considered thermally thin, finite, and thick, respectively. The curves are plotted as a function of the parameters η and $\alpha t_{max}/b^2$, which are defined in paragraph 9-31. Their use is demonstrated in the following example.

[redacted] *Example* [redacted]

Given: A 5086 Aluminum alloy plate is an important part of a structure under analysis. The plate is 0.875 cm thick and the range of air blast exposures for the system of which it is a part are expected to be from 8 to 15 psi from a 100 kt explosion at a height of burst of 1,000 feet.

Find: Whether the plate can be considered thermally thin.

Solution: The corresponding height of burst for a 1 kt explosion is

$$h_1 = \frac{h}{(W^{1/3})} = \frac{1{,}000}{(100)^{1/3}} = 215 \text{ feet.}$$

From Figures 2-18 and 2-19, Chapter 2, the ground distances from a 1 kt explosion at a height of burst of 215 feet that correspond to 15 and 8 psi overpressure are 895 and 1,250 feet respectively. From Figure 2-28, Chapter 2, the times of arrival of the blast wave from a 1 kt explosion to these distances are 0.37 seconds and 0.61 seconds, respectively. The corresponding times for a 100 kt explosion are

$$t = t_1 W^{1/3}$$

$$t = (0.37)(100)^{1/3} = 1.72 \text{ sec for 15 psi,}$$

and

$$t = (0.61)(100)^{1/3} = 2.83 \text{ sec for 8 psi.}$$

The time to final maximum for a 100 kt low air burst is

$$t_{max} \approx 0.043\ W^{0.43}$$

$$= (0.043)(100)^{0.43} = 0.31 \text{ sec.}$$

Therefore,

$$\eta = t/t_{max}$$

$$\eta = \frac{1.72}{0.31} = 5.5 \text{ for 15 psi,}$$

and

$$\eta = \frac{2.83}{0.31} = 9.1 \text{ for 8 psi.}$$

The properties of the alloy are

$$k = 0.28 \text{ cal/sec} \cdot {}^\circ\text{C},$$

$$C_p = 0.22 \text{ cal/gm} \cdot {}^\circ\text{C},$$

$$\rho = 2.66 \text{ gram/cm}^3.$$

Since

$$\alpha = \frac{k}{\rho C_p},$$

$$\frac{\alpha t_{max}}{b^2} = \frac{k t_{max}}{\rho C_p b^2}$$

$$= \frac{(0.28)(0.31)}{(2.66)(0.22)(0.875)^2}$$

$$= 0.19.$$

Answer: From Figure 9-10, at the 15 psi overpressure level where $\eta = 5.5$, the plate should be considered finite; at the 8 psi overpressure level, where $\eta = 9.1$, the plate can be considered thermally thin.

[redacted] *Related Material:* See paragraph 9-31.

[redacted]

[redacted]

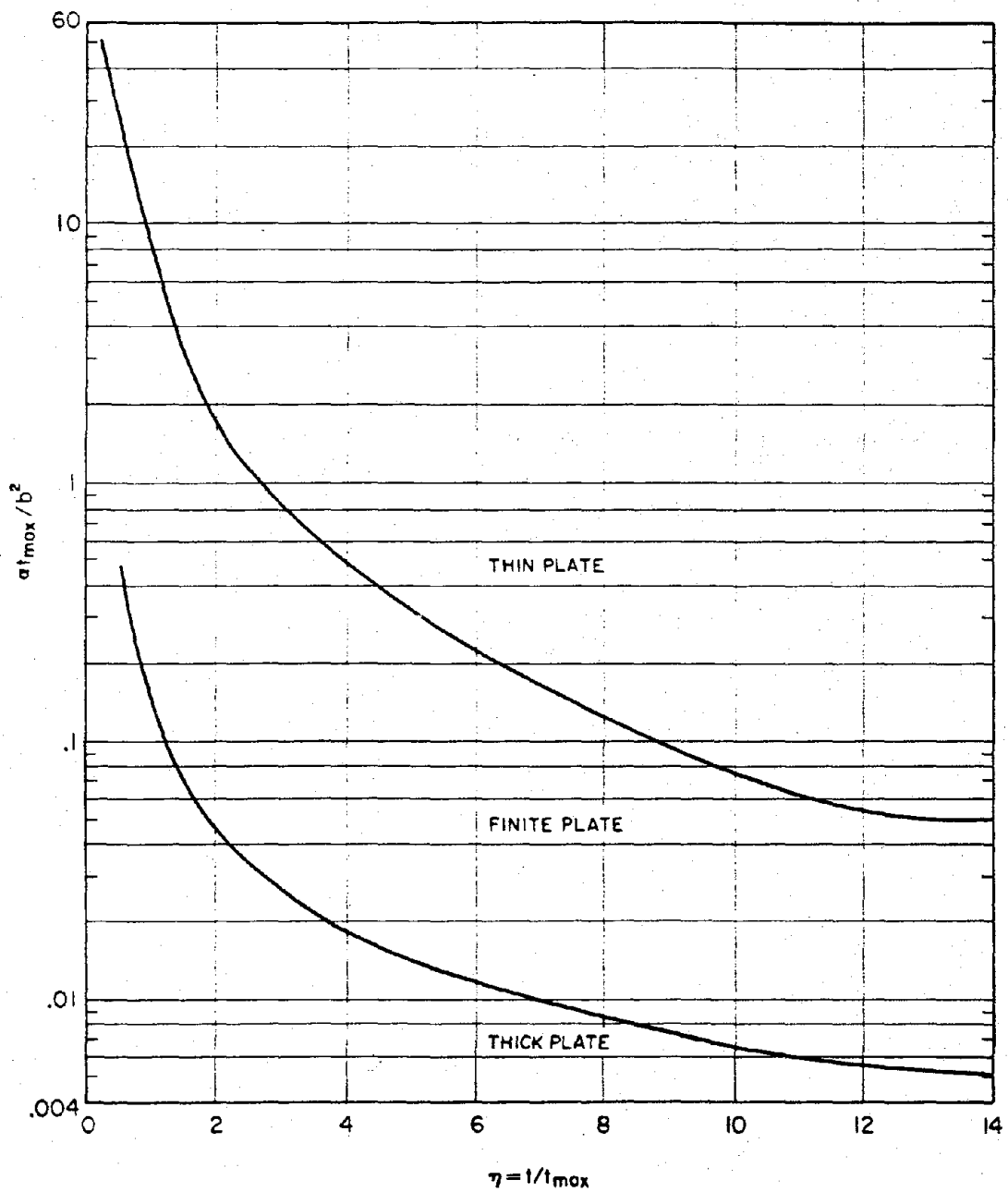

Figure 9-10. [redacted] Thin Plate, Thick Plate, and Finite Plate Regions for Exposure to Nuclear Weapons Thermal Radiation [redacted]

[redacted]

[redacted]

[redacted] The variables used in this technique have units in the cgs system and have been defined previously; however, they are listed below for convenience.

T_o = temperature of the plate prior to exposure,

ΔT = temperature rise, °C,

A = absorption coefficient

Q = thermal exposure, cal/cm^2 (effective thermal exposure may be used where $Q = Q \cos \theta$),

ρ_m = specific gravity of material, gm/cm^3,

C_p = specific heat, cal/gm · °C,

b = plate thickness, cm,

h_{cv} = convective heat loss, cal/cm^2 · sec · °C,

η = t/t_{max}.

Use of the technique is illustrated in Problem 9-2.

[redacted]

[redacted]

Problem 9-2. Calculation of Temperature Rise in a Thermally Thin Plate

[redacted] Figure 9-11 contains a family of curves that relate thermophysical properties of a thin metal plate to thermal pulse parameters in a manner that allows calculation of the temperature rise in the plate. The procedures for the calculation are made clear in the following examples. Symbols for the various parameters are listed in paragraph 9-31.

[redacted] *Example 1* [redacted]

Given: A 6061-16 Aluminum alloy plate is exposed to the thermal pulse from a 100 kt low air burst at a location where the incident radiant energy is 76 cal/cm^2 and arrives at an angle of incidence of 30°. Properties of the plate are

$$T_o = 30°C,$$

$$A = 0.8,$$

$$\rho_m = 2.7 \text{ gm/cm}^3,$$

$$C_p = 0.216 \text{ cal/gm} \cdot °C,$$

$$b = 0.15875 \text{ cm},$$

$$h_{cv} = 0.$$

Find: The temperature of the plate when $\eta = 2, 4,$ and 6.

Solution: The effective radiant exposure is

$$Q_e = Q \cos\theta = 76 \cos 30° = 65.8 \text{ cal/cm}^2.$$

From Figure 9-11, with

$$\frac{h_{cv} t_{max}}{\rho C_p b} = 0,$$

when

$$\eta = 2, \frac{\Delta T}{AQ/\rho C_p b} = 0.47,$$

when

$$\eta = 4, \frac{\Delta T}{AQ/\rho C_p b} = 0.67,$$

and when

$$\eta = 6, \frac{\Delta T}{AQ/\rho C_p b} = 0.74.$$

The value of $AQ/\rho C_p b$ is

$$\frac{AQ_e}{\rho C_p b} = \frac{(0.8)(65.8)}{(2.7)(0.216)(0.15875)} = 569°C.$$

The temperature rises are

$$\Delta T = (0.47)(569) = 267°C \text{ for } \eta = 2,$$

$$\Delta T = (0.67)(569) = 381°C \text{ for } \eta = 4,$$

and

$$\Delta T = (0.74)(569) = 421°C \text{ for } \eta = 6.$$

Answer: The plate temperatures are

$$T = T_o + \Delta T.$$

Therefore,

$$T_{\eta=2} = 30 + 267 = 297°C$$

$$T_{\eta=4} = 30 + 381 = 411°C$$

$$T_{\eta=6} = 30 + 421 = 451°C.$$

[redacted] *Example 2* [redacted]

Given: The same conditions as Example 1,

[redacted]

[redacted]

[redacted] except that $h_{cv} = 3.0 \times 10^{-2}$ cal/cm^2 · °C.*

Find: The temperature of the plate when $\eta = 2, 4$, and 6.

Solution:

$$t_{max} = 0.043\ W^{0.43} = (0.043)(100)^{0.43}$$

$$= 0.31 \text{ sec.}$$

$$\frac{h_{cv} t_{max}}{\rho C_p b} = \frac{(3.0 \times 10^{-2})(0.31)}{(2.7)(0.216)(0.15875)} = 0.1.$$

From Figure 9-11, when

$$\eta = 2, \frac{\Delta T}{AQ/\rho C_p b} = 0.44,$$

when

$$\eta = 4, \frac{\Delta T}{AQ/\rho C_p b} = 0.53,$$

and when

$$\eta = 6, \frac{\Delta T}{AQ/\rho C_p b} = 0.51.$$

From Example 1,

$$\frac{AQ}{\rho C_p b} = 569°\text{C}.$$

The temperature rises are

$$\Delta T = (0.44)(569) = 250°\text{C for } \eta = 2,$$

$$\Delta T = (0.53)(569) = 302°\text{C for } \eta = 4,$$

and

$$\Delta T = (0.51)(569) = 290°\text{C for } \eta = 6.$$

Answer: The plate temperatures are

$$T = T_o + \Delta T.$$

Therefore,

$$T_{\eta=2} = 30 + 250 = 280°\text{C},$$

$$T_{\eta=4} = 30 + 302 = 332°\text{C},$$

and

$$T_{\eta=6} = 30 + 290 = 320°\text{C}.$$

[redacted] *Related Material:* See paragraph 9-31.

---

*[redacted] This value corresponds roughly to an airplane speed of 200 mi/hr.

[redacted]

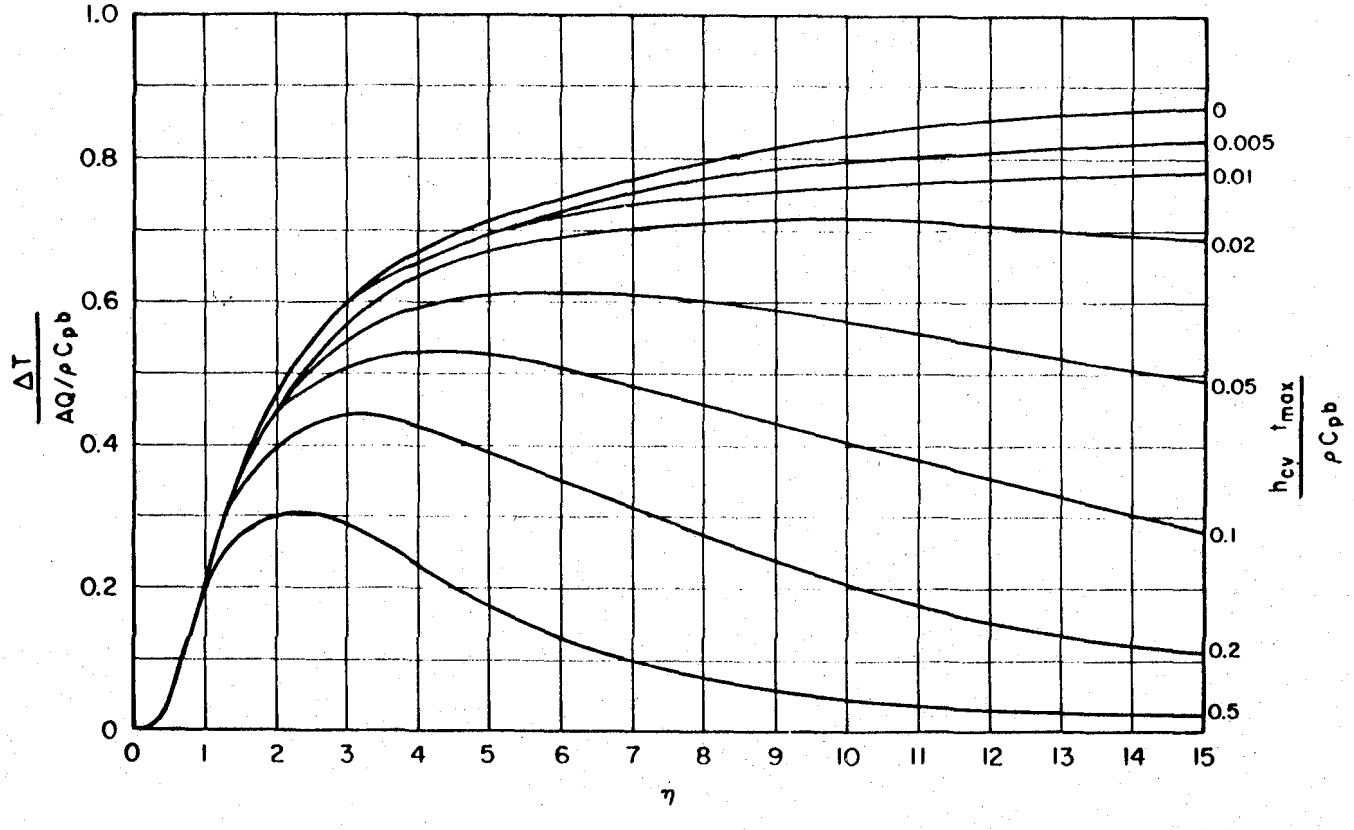

Figure 9-11. [redacted] Thermal Response of a Thin Plate to Nuclear Weapons Thermal Radiation Pulse [redacted]

[redacted]

[redacted] Thermally thick plates are those that do not have a temperature rise on the back surface at the time of interest. Finite plates have a temperature gradient between the front and back surfaces and a temperature rise at both surfaces.

[redacted] Computer codes generally are required to calculate the temperature history of thermally thick and thermally finite plates. Simple graphical techniques have been developed to determine the temperature rise on the front face of a thermally thick plate and on the front face, mid place, and back face of thermally finite plates. These are not included herein because the techniques depend upon thermal source characteristics that are very different from the source characteristics described in Chapter 3.* If graphical techniques that are compatible with the thermal source data of Chapter 3 become available, they will be included in revisions to this manual. In the meantime, users who are interested in the techniques should consult "Thermal Degradation of Structural Resistance to Air Blast" (see bibliography).

[redacted] Requirements to analyze geometries that are more complex than single layer plates (even if they are layered thin plates) or to examine plates with temperature dependent thermophysical properties or heat losses require the use of a computer code. Codes for more complex geometries, such as cylinders and tee beams, have been developed specifically for the types of analysis of concern to this section. As noted previously, the TRAP computer program can calculate temperatures and stresses for two dimensional structures.

[redacted] Honeycomb structures or sandwich construction must be considered as a multi-layered system. A five layer system was used to examine thin sandwich construction. The five layers consisted of the core, the two skins, and the two bonding layers between the skins and core. Most sandwich construction has been found to fail at the bonding layer. Consequently, the temperature of the bond and the thermal stresses in the face sheets (or skins) can be of equal importance. Studies and experiments show that a calculational procedure that includes five layers was required to duplicate experimental results accurately. A code developed for dual layer plates has been used to calculate thick single layer plates by considering both layers to be the same material.

9-32 Change in Materials Properties [redacted]

[redacted] The rise in temperature that occurs when thermal radiation is absorbed can be expected to cause changes in materials prop-

---

* [redacted] The important differences in source characteristics are the time to final maximum, where

$$t_{max} = 0.032\ W^{1/2}\ \text{sec}$$

was used in developing the graphical techniques, while a more recent value

$$t_{max} = 0.043\ W^{0.43}\ (\rho/\rho_o)^{0.42}\ \text{sec}$$

is given in Chapter 3, and the power at thermal maximum, where

$$P_{max} = 4\ W^{1/2}\ \text{kt/sec}$$

was used in developing the graphical techniques while a more recent value of

$$P_{max} = \frac{4.3\ W^{0.6}}{(\rho/\rho_o)^{0.44}}\ \text{kt/sec}$$

is given in Chapter 3. The latter determines the maximum irradiance (thermal energy per unit area per unit time) incident on the target. Actually, the procedures described in Problems 9-1 and 9-2 were developed for use with the older expression for t_{max}; however, since the two expressions agree within a few percent for low air bursts and for yields from a few kt to a few Mt, the use of the techniques with the value of t_{max} from Chapter 3 was illustrated. The values of P_{max}, on the other hand, differ widely at all yields. Since the temperature histories presented in the graphical techniques for finite and thick plates depend strongly on irradiance, it is not possible to use the thermal source data with the curves derived for use with the older expression for P_{max}.

[redacted]

erties. Properties of mechanical strength are of greatest concern, since these properties influence structural resistance.

Thermal stresses may be present in either unrestrained or restrained structures or elements thereof if thermal gradients, which usually are caused by increased temperatures, are present. The magnitude of the stresses depends upon the amount of expansion the structure experiences, which depends on the value of the coefficient of thermal expansion, α_e, for the material. The dimensions of this coefficient are length per length per temperature unit, often expressed as in./in.°F or cm/cm/°C. The value of α_e depends on the temperature, as shown in Figures 9-12 through 9-15 for a number of materials. Use of an improper value of α_e can cause serious errors in the estimation of the thermal stress level in some materials. For example, the use of the room temperature value of α_e for AISI 301 stainless steel when the value of 1200°F (~650°C) should have been used, would result in a value of thermal stress that is 20 percent too low. For 2024 Aluminum Alloy, the error would be about 18 percent, whereas for Ti-8Mn Titanium Alloy, the error would be 45 percent. Thus, for large temperature rises, the assumption of a constant value for the coefficient of thermal expansion could lead to significant errors. However, for small temperature rises, on the order of 200°F (110°C), the error would not be significant. For most metallic materials, the error in thermal stress is about 2 percent per 100°F or 3 percent per 100°C temperature rise above room temperature values of α_e. Additional data may be obtained from "Metallic Materials and Elements for Aerospace Vehicle Structures" (see bibliography).

Changes in mechanical strength are the prime reason for concern about the effects of absorbed thermal radiation. Data from several sources are incorporated into Figures 9-16 through 9-18 to provide some indication of the effects of elevated temperature on the tensile strength properties of 2014-T6 Aluminum Alloy, Titanium Alloy 6AL-4V, and 301 full, hard stainless steel. The various curves in these figures provide some indication of the effect of elevated temperature and also the effects of the speed at which the sample was heated and the time it remained at a given temperature.

The data that will be discussed comes from several sources. Since the techniques for testing that were used in these sources differ considerably, it will be of value to discuss the various techniques employed.

The four basic types of loading tests that have been used to determine mechanical properties at elevated temperatures are illustrated in Figure 9-19 and 9-20. Figures 9-19a and b illustrate an adaptation of the conventional tensile test for elevated temperature. The sample is heated rapidly to an equilibrium temperature. At some finite time after thermal equilibrium, called the soak time, a conventional tensile loading test is conducted with a constant strain rate loading mechanism. Two loading rates are shown in Figure 9-19a. Figure 9-19b illustrates the type of results that are obtained from the type of test illustrated in Figure 9-19a.

Figures 9-19c and d illustrate another type of tensile test where the sample is loaded with a constant load, then heated at some rate until rupture occurs. Figure 9-19d illustrates the type of results that are obtained from the type of test illustrated in Figure 9-19c. Figure 9-20 illustrates two types of short time creep tests and their results.

Results from these types of tests are shown for three aluminum alloys in Figures 9-21 through 9-23. Some data shown in Figure 9-21 were obtained by the type of the test illustrated in Figure 9-19a. The soak time of the sample was one-half hour before a standard constant strain rate of 0.00033 in./in./sec tensile test was performed. Other data in Figure 9-21 also were

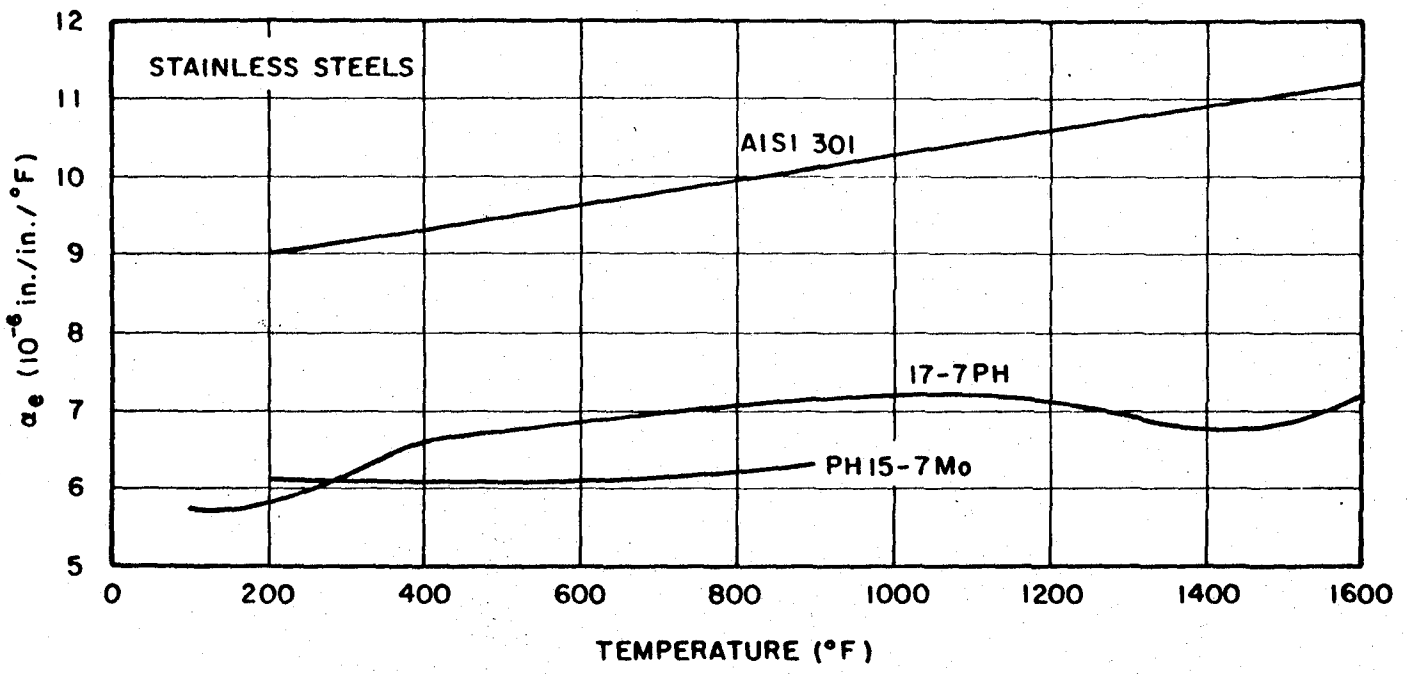

Figure 9-12. [redacted] Coefficient of Linear Expansion as a Function of Temperature for Stainless Steels [redacted]

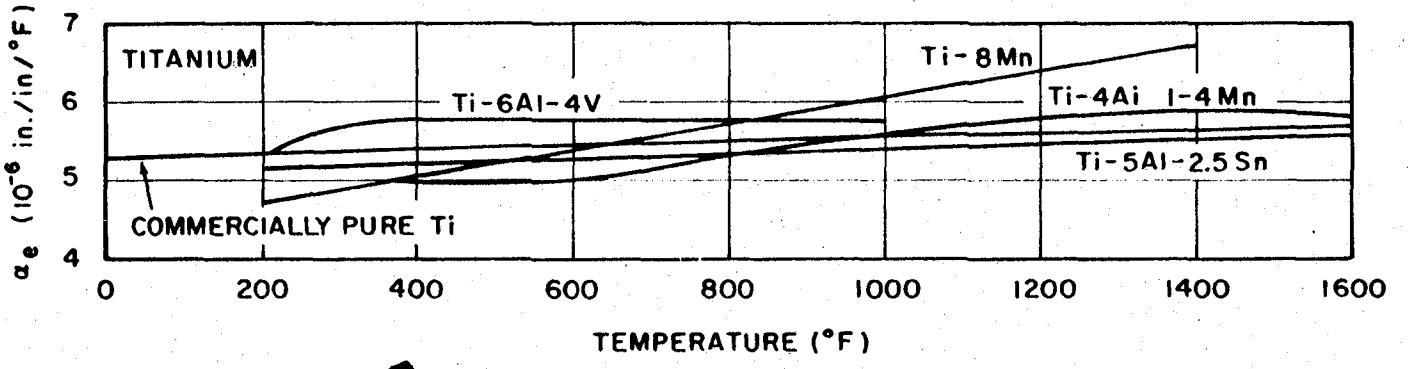

Figure 9-13. Coefficient of Linear Expansion as a Function of Temperature for Titanium Alloys

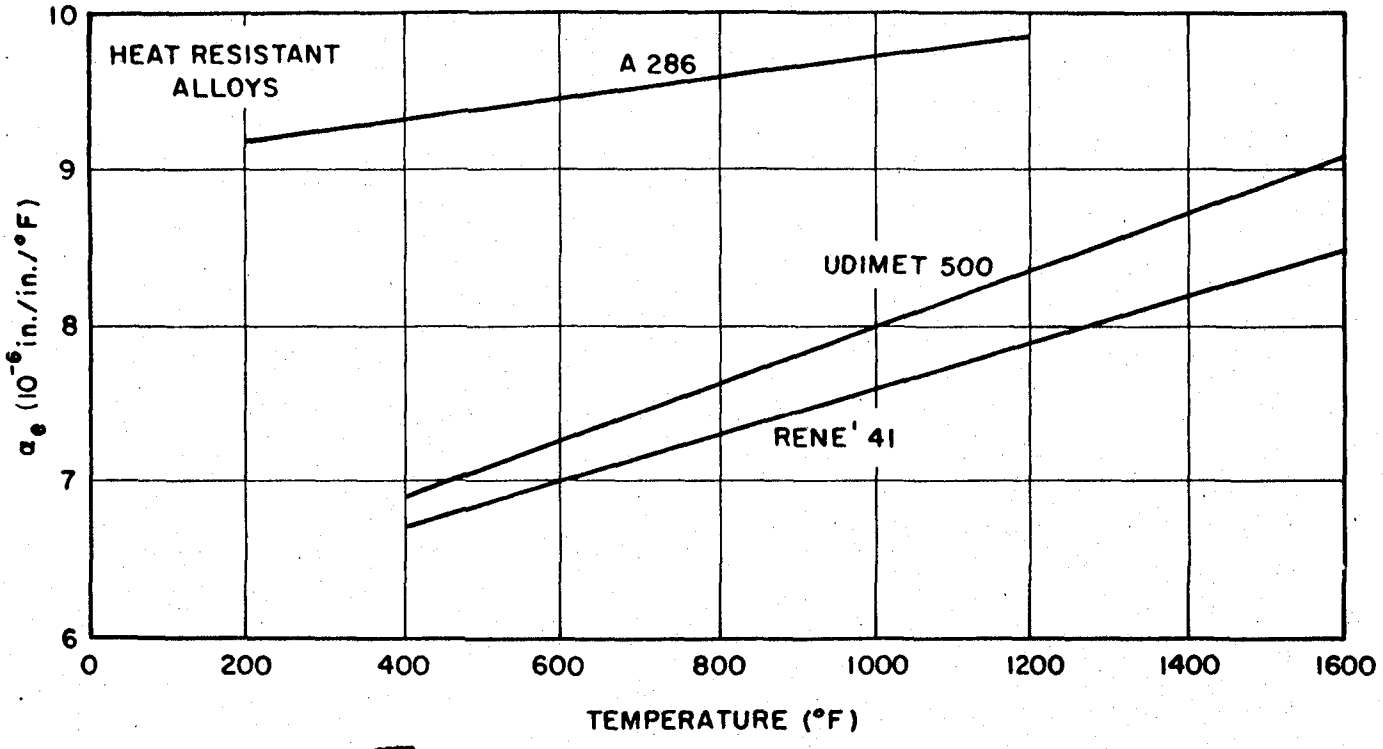

Figure 9-14. [redacted] Coefficient of Linear Expansion as a Function of Temperature for Heat Resistant Alloys [redacted]

[redacted]

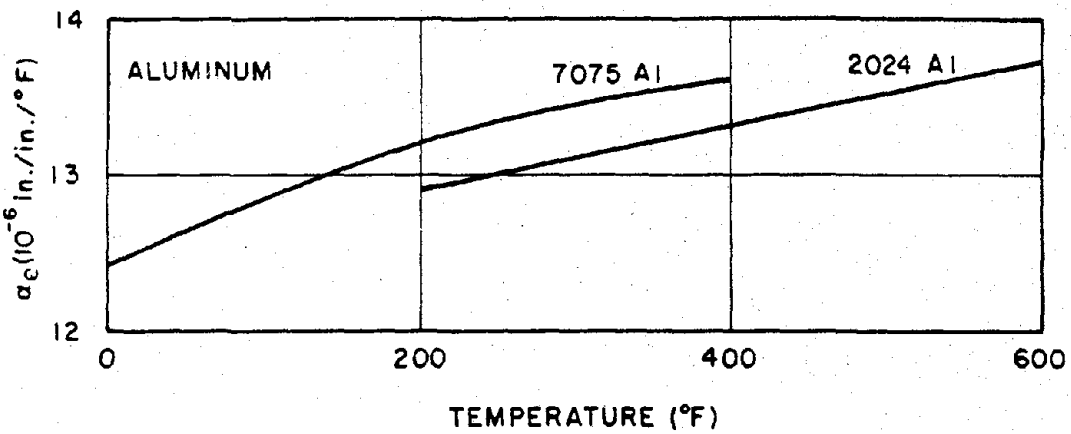

Figure 9-15. [redacted] Coefficient of Linear Expansion as a Function of Temperature for Aluminum Alloys [redacted]

[redacted]

[redacted]

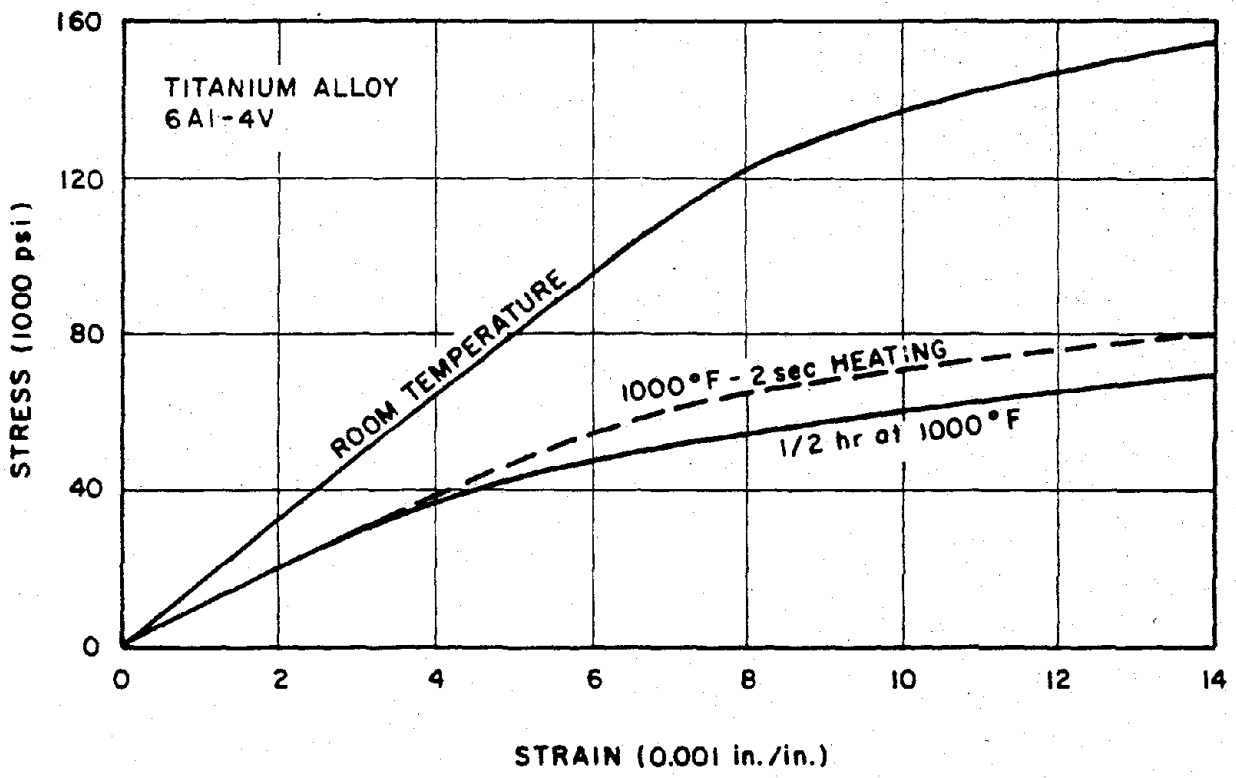

Figure 9-16. [redacted] Typical Stress-Strain Curves for Titanium 6Al-4V Alloy at Room and Elevated Temperatures [redacted]

[redacted]

[redacted]

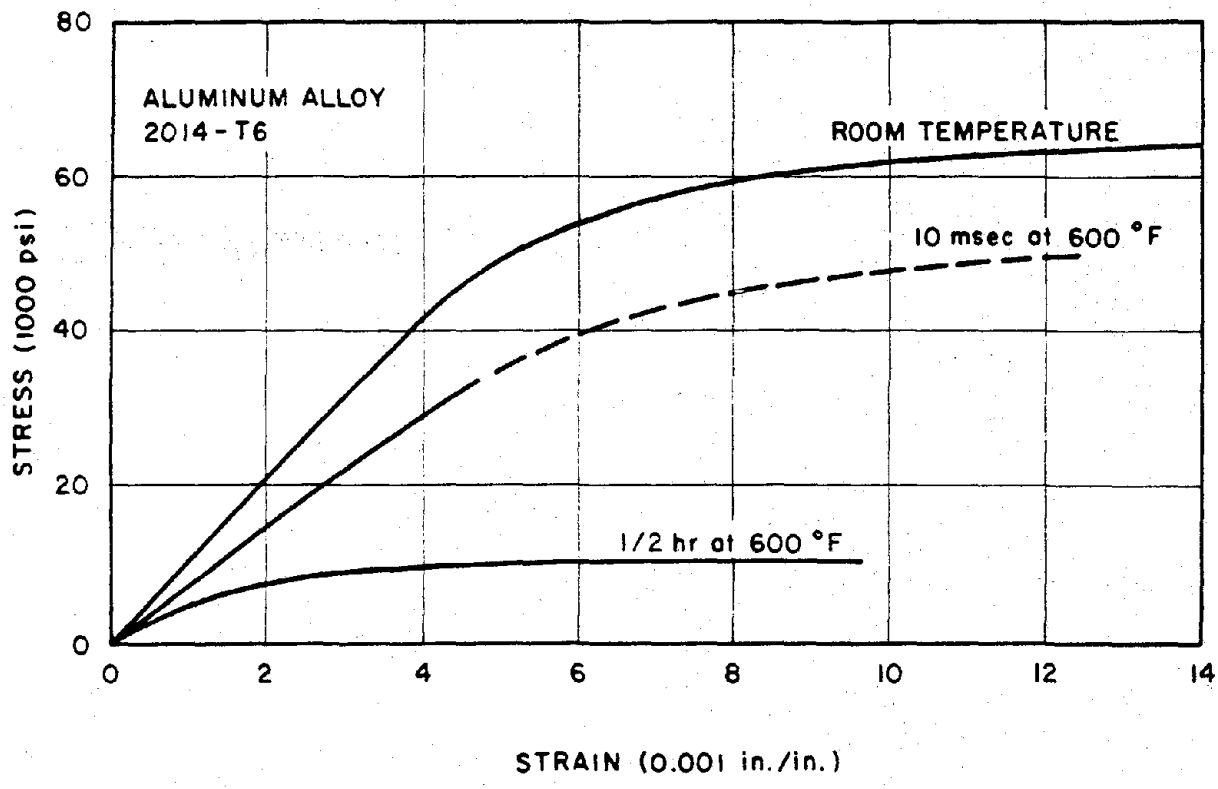

Figure 9-17. [redacted] Typical Stress-Strain Curves for 2014-T6 Aluminum Alloy at Room and Elevated Temperatures [redacted]

[redacted]

[redacted]

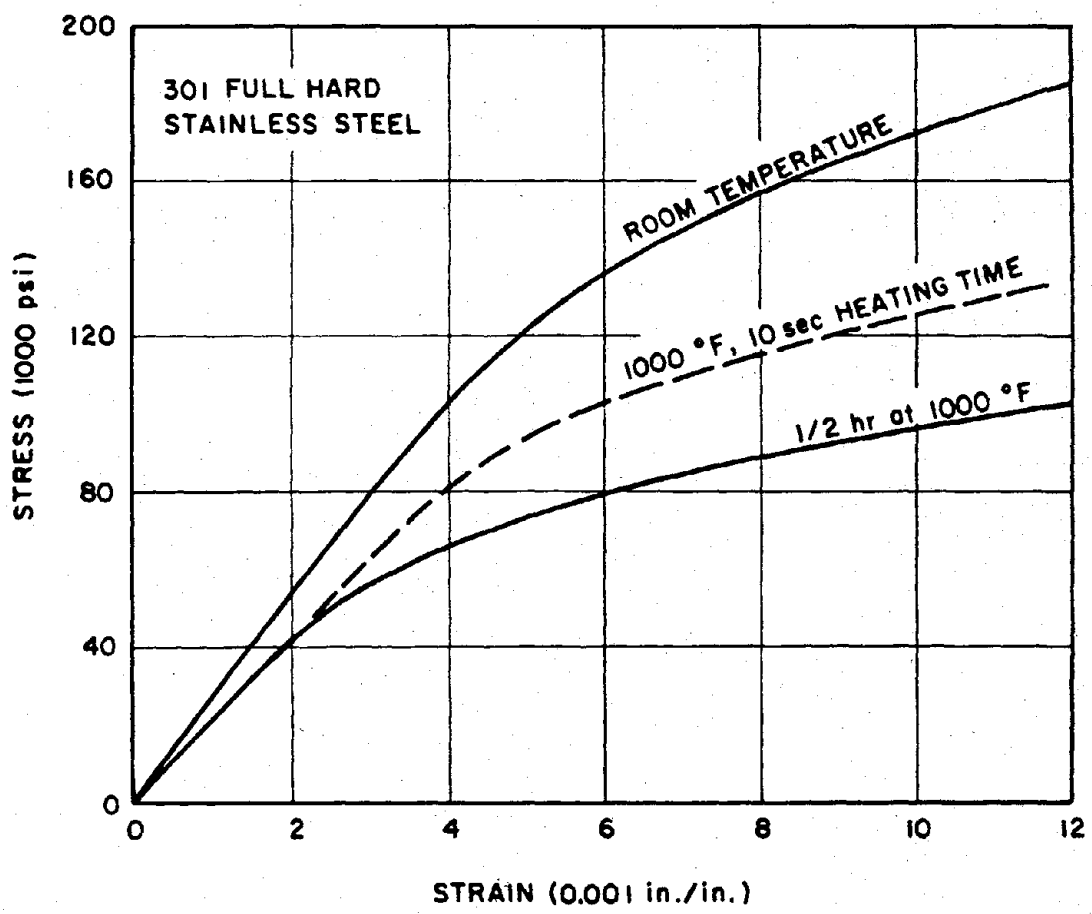

Figure 9-18. [redacted] Typical Stress-Strain Curves for 301 Stainless Steel at Room and Elevated Temperatures [redacted]

[redacted]

[redacted]

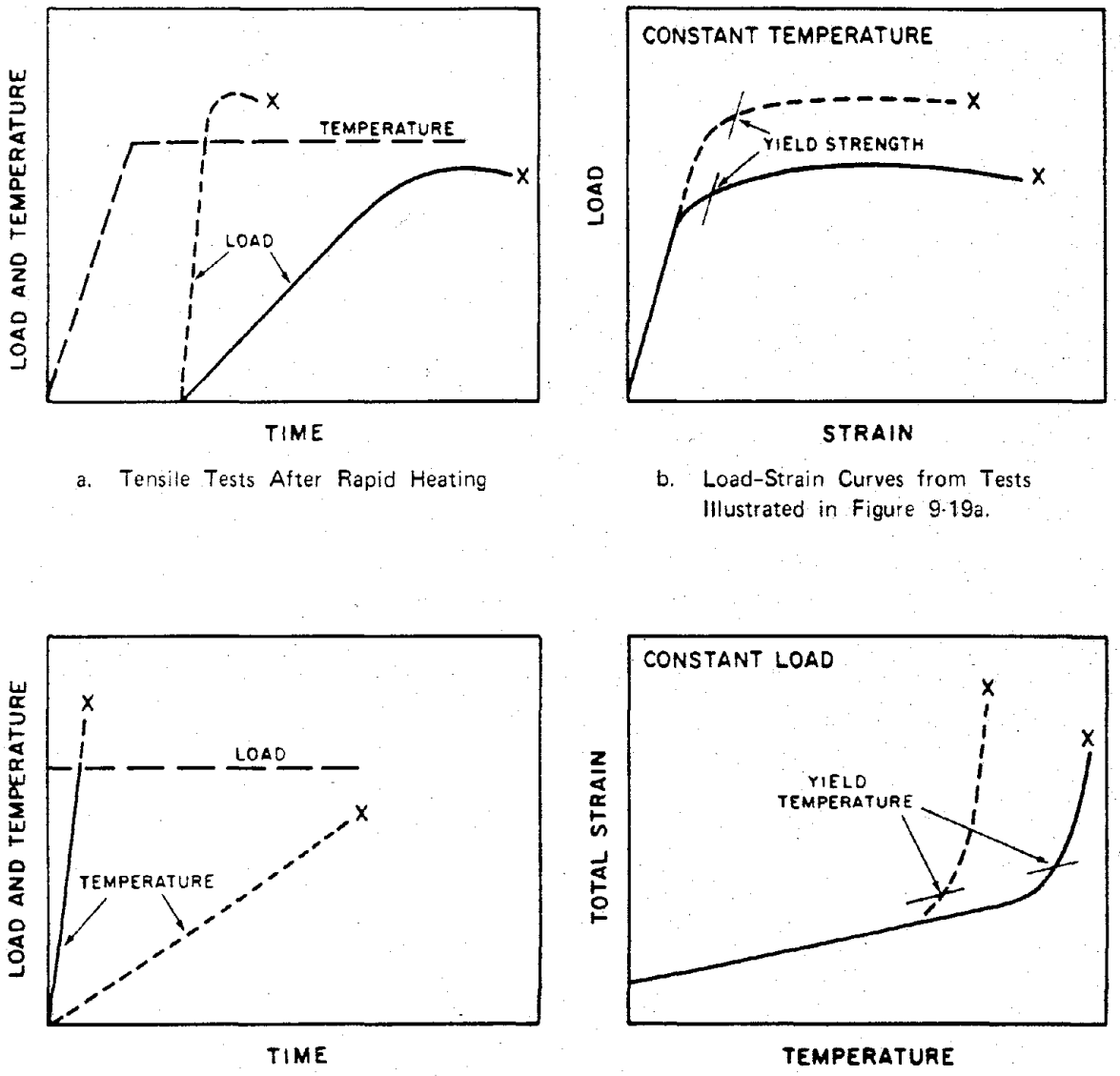

a. Tensile Tests After Rapid Heating

b. Load-Strain Curves from Tests Illustrated in Figure 9-19a.

c. Rapid-Heating Constant-Load Tensile Tests

d. Strain-Temperature Curves from Tests Illustrated in Figure 9-19c.

Figure 9-19. [redacted] Types of Rapid Heating Tensile Tests [redacted]

[redacted]

[redacted]

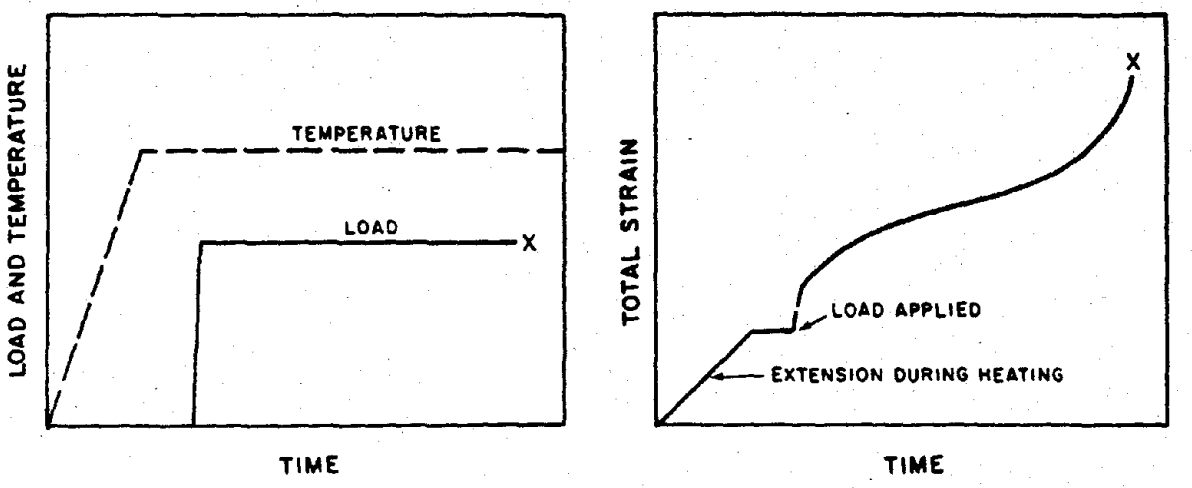

a. Very Short-Time Creep Tests After Rapid Heating

b. Time-Strain Curve

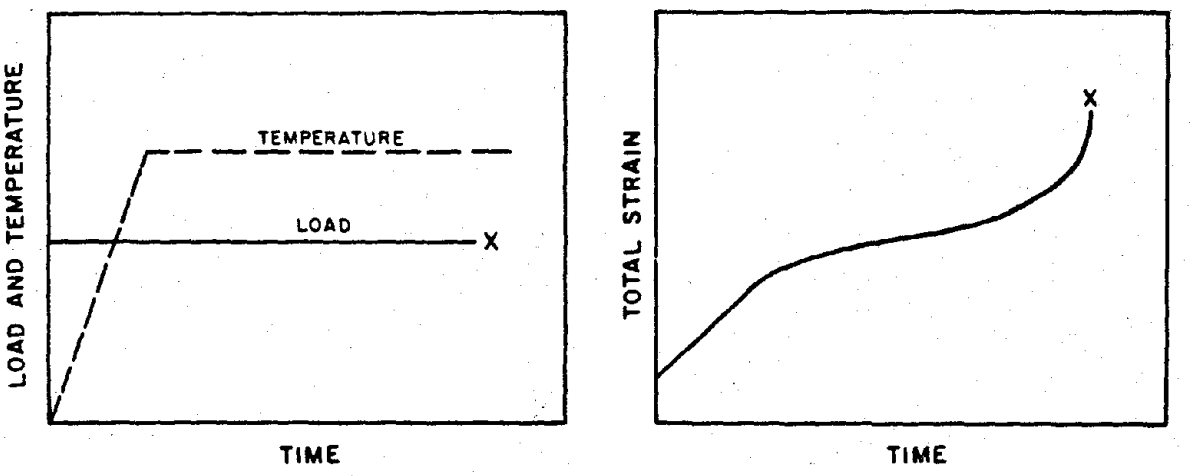

c. Very Short-Time Rapid-Heating Creep Tests

d. Time-Strain Curve

Figure 9-20. [redacted] Types of Short Time Creep Tests [redacted]

[redacted]

[redacted]

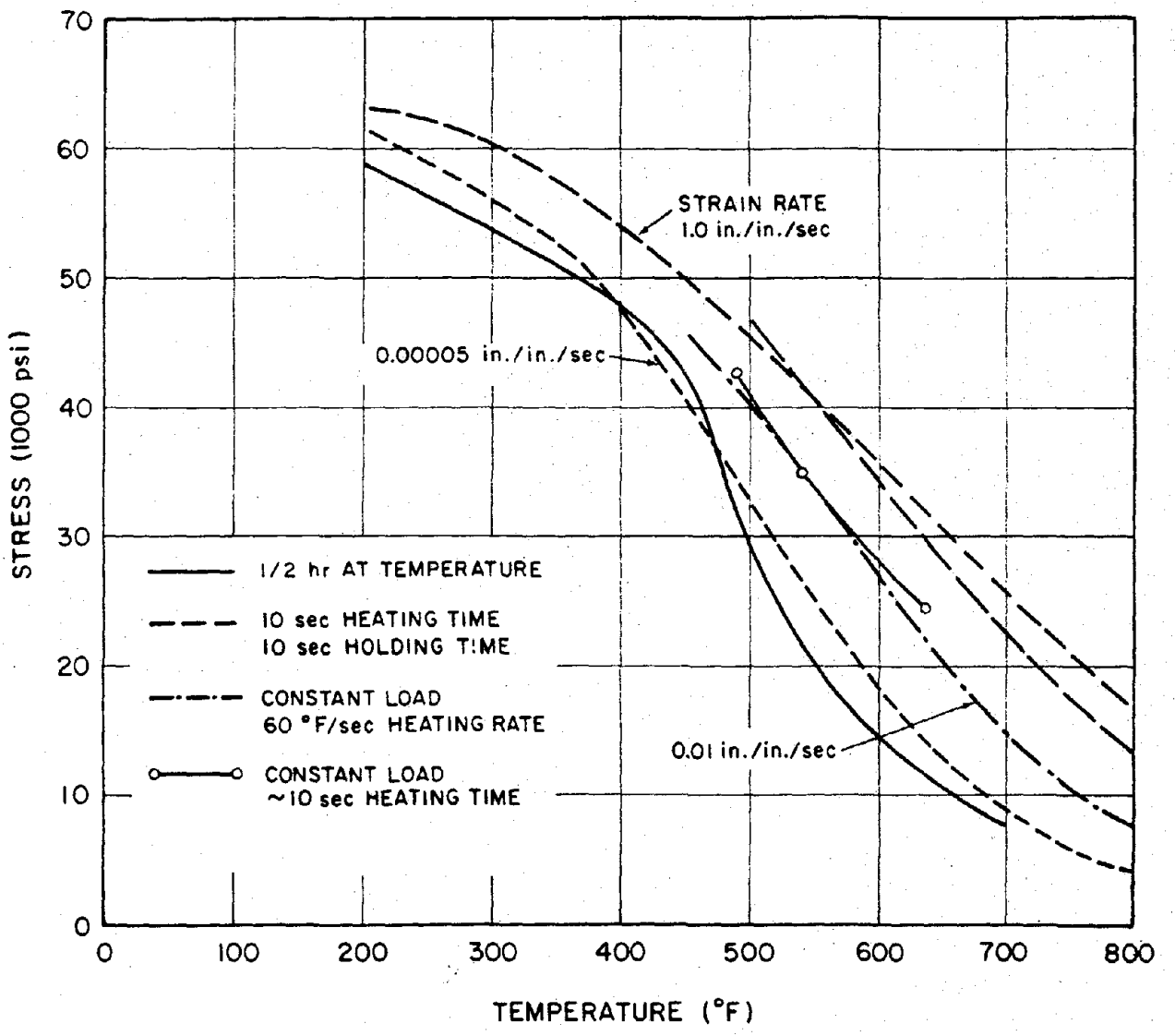

Figure 9-21. [redacted] 2024-T3 Aluminum Alloy Ultimate Strength at Elevated Temperature [redacted]

[redacted]

[redacted]

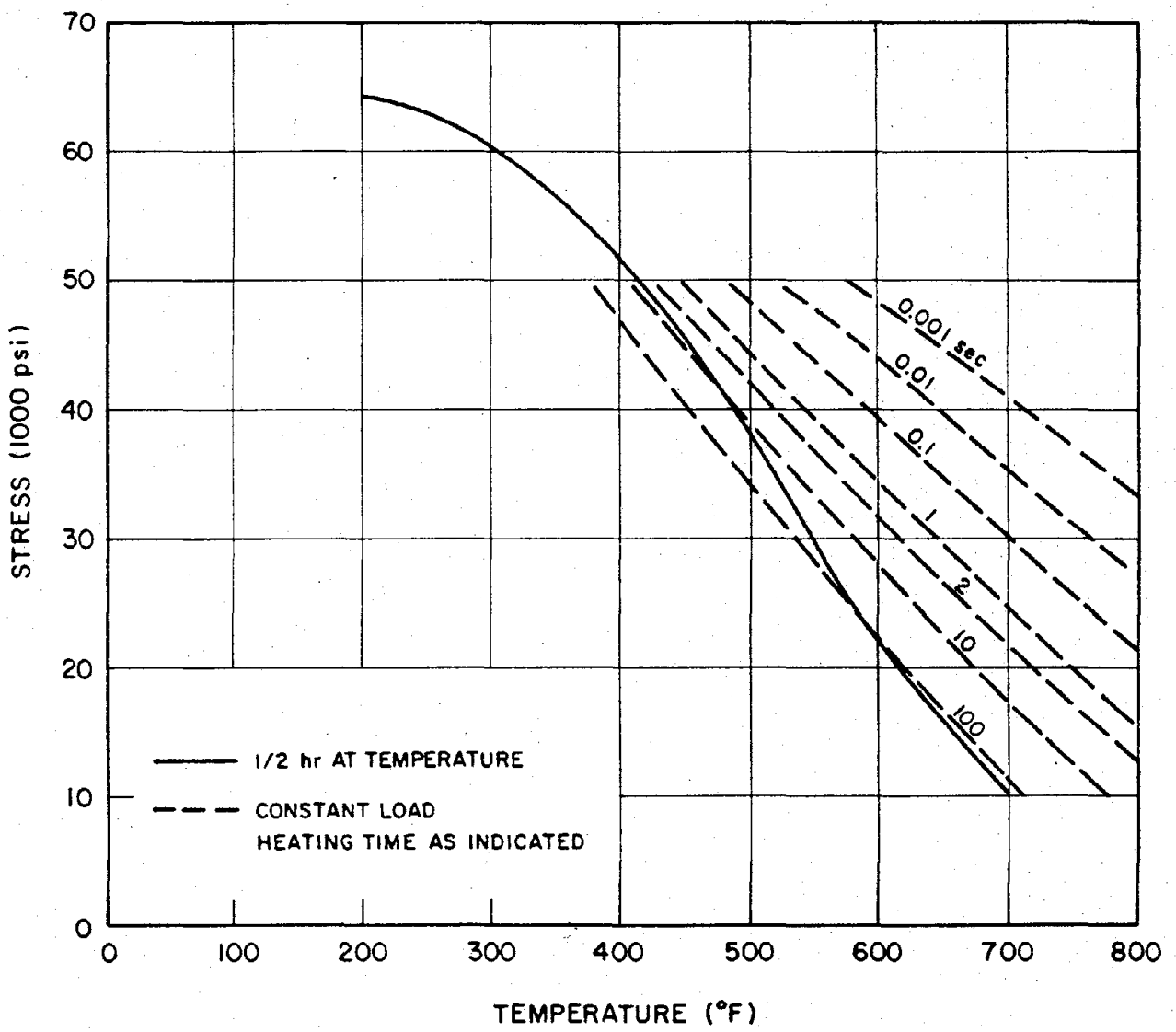

Figure 9-22. [redacted] 2024-T81 Aluminum Alloy Ultimate Strength at Elevated Temperature [redacted]

[redacted]

[redacted]

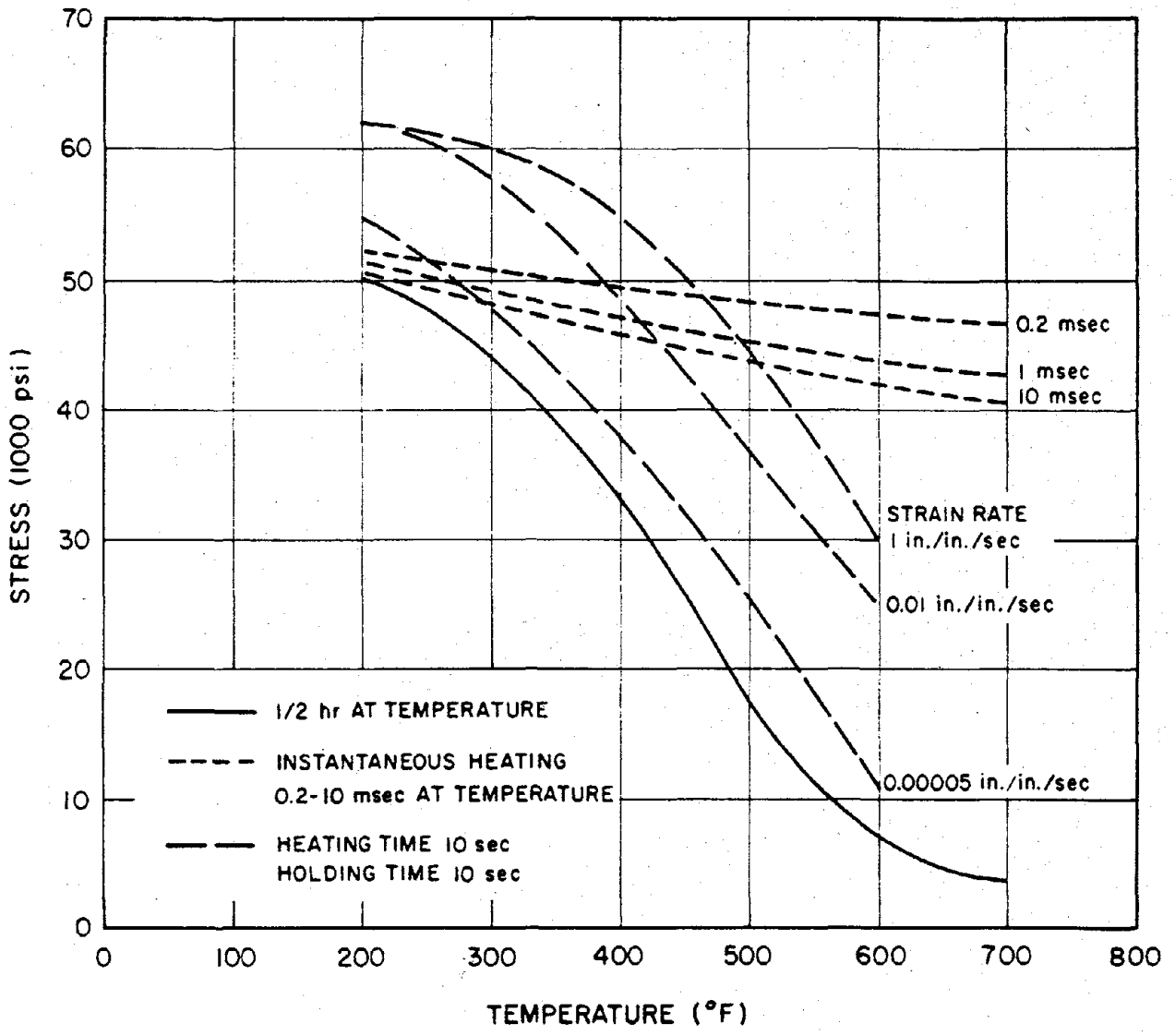

Figure 9-23. [redacted] 2014-T6 Aluminum Alloy Yield Strength at Elevated Temperature [redacted]

[redacted]

[redacted]

[redacted] obtained in the manner illustrated in Figure 9-19a, but with the equilibrium temperature being reached in 10 sec and with a 10 sec soak time, and with three different strain rates used in the tensile tests. Other data were obtained in the manner illustrated in Figure 9-19c with a heating rate of 60°F/sec. The final data in Figure 9-21 also were obtained in a manner similar to that illustrated in Figure 9-19c with a heating time and time of rupture each approximately 10 sec.

[redacted] The ultimate strength data in Figure 9-21 tend to show the importance of temperature and strain rate, but the data from the different sources are not consistent and are, therefore, difficult to evaluate. For example, the 0.00005 in./in./sec strain rate curve for 10 sec soak times from one source lies close to the 0.00033 in./in./sec strain rate curve for one-half hour soak times from a different source. Interpolation between the strain rate data for 10 sec soak times would indicate that a 0.00033 in./in./sec strain rate curve for a 10 sec soak time would lie slightly to the right of the 0.00005 in./in./sec curve and, therefore, slightly to the right of the one-half hour soak time curve. However, there are ample data, as shown in Figures 9-16 through 9-18, to justify the expectation that the 10 second curve should fall significantly to the right of the one-half hour curve; that is, for a given temperature and strain rate, the shorter the soak time, the smaller the decrease in tensile strength. It should also be noted that constant load curves should agree more closely.

[redacted] The ultimate strength data in Figure 9-22 suggest a similar inconsistency although the data were taken from two different types of loading tests. The one-half hour data is from loading tests similar to that shown in Figure 9-19a, and "constant load, heating time as indicated" data is from loading tests similar to that shown in Figure 9-19c. The latter data clearly shows the influence of heating times or heating rates on rapid heating, constant load tensile test results.

[redacted] The yield strength data shown in Figure 9-23 for 2014-T6 Aluminum Alloy is somewhat more consistent. The instantaneous heating data were obtained in a manner similar to that illustrated in Figure 9-19a, although times are very short. Specimens were heated instantaneously by an electron beam, then a stress wave was sent up the specimen. An analysis of the stress wave characteristics on either side of the heated region provided yield and ultimate strength data as well as elastic modulus data. The times indicated for these data are the delay times between time of heating and the arrival of the stress wave. Thus, the data are for instantaneous heating, very short soak times, and extremely high strain rates ($\sim 10^{-9}\,sec^{-1}$). The comparable strain rate data for 1/2 hour and 10 sec soak times are in the relative positions that would be expected. The one factor that may explain why the comparable strain rate data of Figures 9-21 and 9-23 are relatively close together despite the different soak times is the heating rate.

[redacted] Similar data from a single source are shown in Figures 9-24 and 9-25 for 6AL-4V Titanium Alloy and full, hard 301 stainless steel. The data in these figures also illustrates the inconsistencies in data discussed for Figures 9-21 through 9-23.

[redacted] One other mechanical strength property of interest is the elastic or Young's modulus of the material. One source indicates that for soak times of from 1/2 to 10,000 hours, the elastic modulus depends only on temperature and not on soak time for a number of different materials. A separate source indicates that this is true for 6061-T6 and 2014-T6 Aluminum Alloys with soak times of 0.2, 1, and 10 msec. Although this conclusion has not been validated for other materials at small soak times, it appears reasonable to assume that the elastic

[redacted]

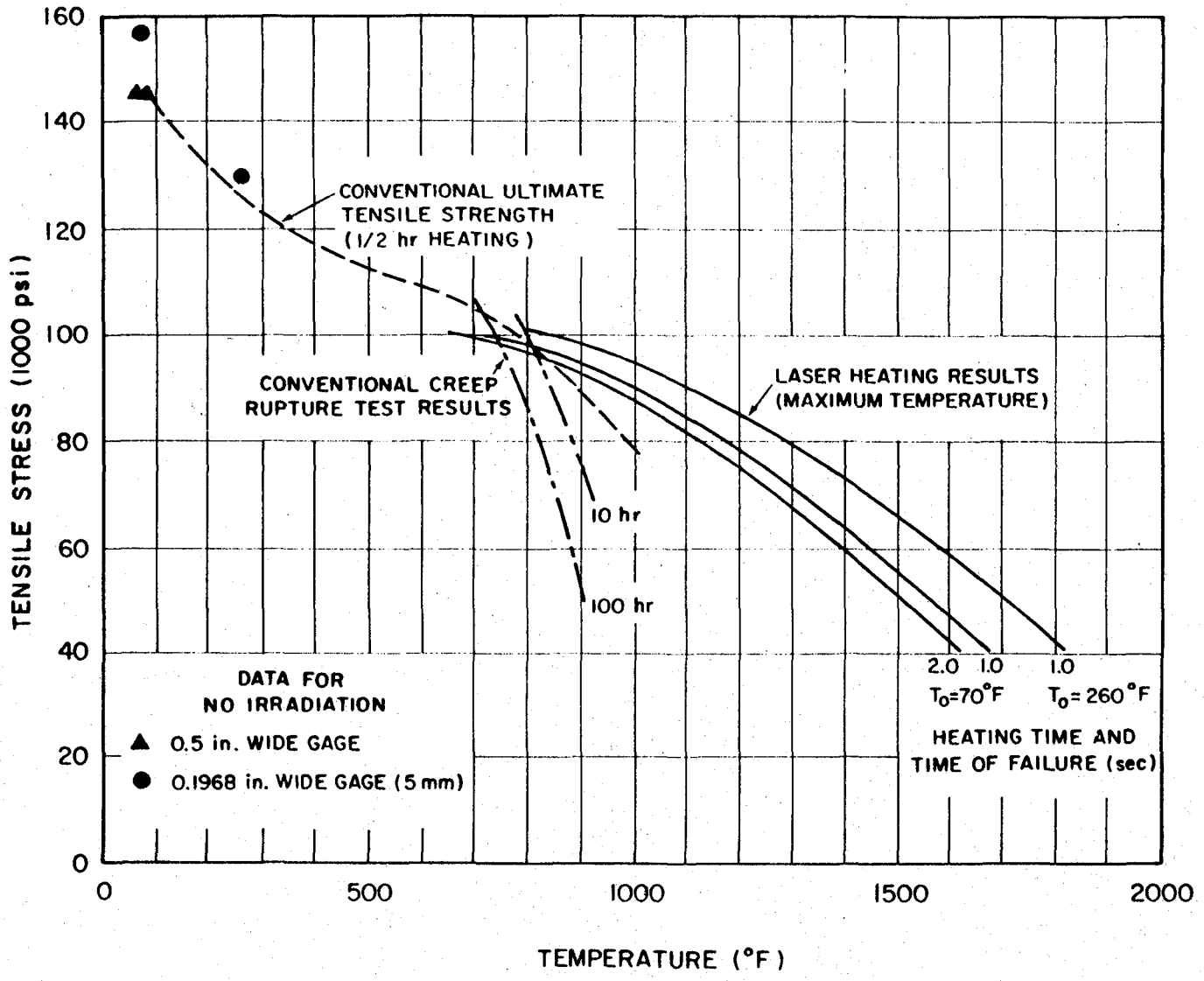

Figure 9-24. [redacted] Ultimate Strength Test Results for 6Al-4V Titanium Alloy at Elevated Temperatures [redacted]

[redacted]

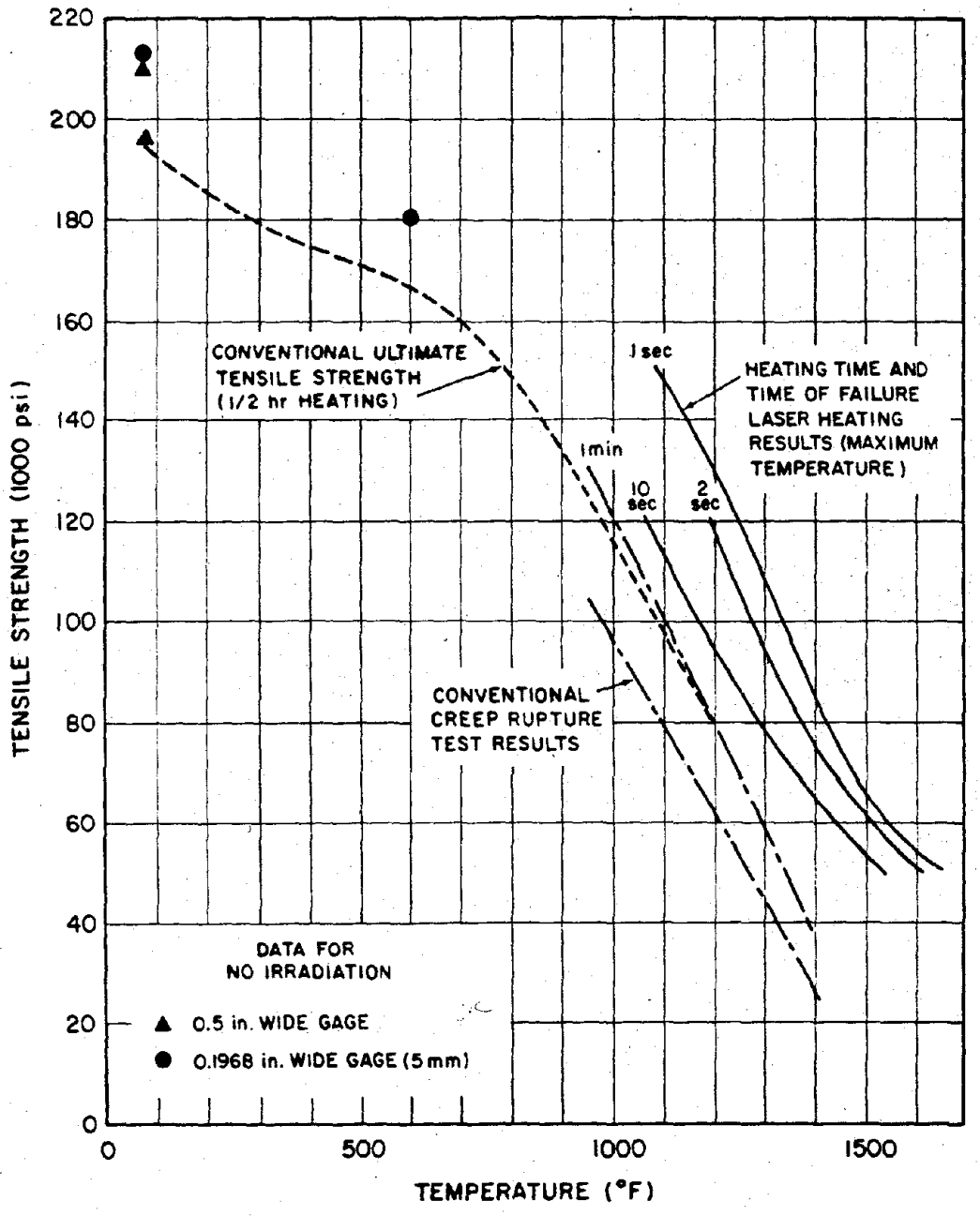

Figure 9-25. [redacted] Ultimate Strength Test Results for Full Hard Stainless Steel at Elevated Temperature [redacted]

[redacted]

[redacted]

[redacted] modulus only depends on temperature for metallic materials.

[redacted] In evaluating the information available on changes in mechanical strength properties of materials, it should be reemphasized that a variety of testing techniques have been used to obtain the data presented in this section. Constant strain rate and constant load techniques have both been used. A variety of heating techniques have been used, including ovens, resistance heating, inductive heating, hot-fluid bath heating, radiant heating, lasers, and electron beams. A considerable amount of data have been obtained on a number of different materials.

[redacted] The data indicate that there are five basic variables that influence the degradation of mechanical strength properties at elevated temperature for particular materials: initial temperature, heating rate, final temperature, soak time, and strain rate. Not much is known about the effect of initial temperature since most data report "room temperature" as the reference temperature. Increases in heating rate, final temperature, or soak times cause a decrease in ultimate and yield strengths. An increase in strain rate at a particular final temperature apparently increases the strength. Because of the different testing techniques employed, the relative importance of these variables in determining material strengths is difficult to determine; however, it appears that soak time and final temperature are most important, followed closely by strain rate, and finally heating rate as long as final temperature is reached in less than one minute.

[redacted] Although there are considerable data available on rapid heating effects, it is difficult to extrapolate to other than test conditions with any confidence. In any event, in estimating strength, data available on rapid heating and short times appear to be more appropriate than those for slow heating, long soak times for the general class of problems of interest in this manual.

[redacted] RESISTANCE TO LOAD [redacted]

[redacted] The ultimate concern of combined thermal/blast effects is the change, if any, in the vulnerability/survivability of tactical systems compared to vulnerability/survivability to thermal or blast effects separately.

[redacted] Figure 9-26 illustrates typical experimental stress-strain curves for 2014-T6 Aluminum Alloy with two approximations to this curve: the more or less classical straight line; and the so-called Bell's stress-strain law for dynamic deformation:

$$\sigma = \beta \left(1 - \frac{T}{T_m}\right) \epsilon^{1/2}$$

where

σ = stress, psi,

ϵ = strain, in./in.,

T = temperature of interest, °K,

T_m = melting temperature, °K,

β = parabolic coefficient.

The area under each of these curves is equal to the strain energy absorbed by the material. For the straight line approximation the area under the room temperature curve equals about 433 in. · lb/in.^{3} to a strain (ϵ) of 0.01 in./in. This compares well with the area of 432 in. · lb/in. under the typical curve to the same ϵ. The Bell stress-strain law gives an area of 441 in. · lb/in.^{3}.

[redacted] The change in allowable uniform equivalent static load that will give the same maximum deflection as a uniform dynamic load has been determined for degraded 2014-T6 Aluminum alloy properties using elastic theory for large deflections of simply supported square plates.* The allowable load was defined as the maximum

[redacted] An air blast loading of long duration, or a flat top wave, was assumed.

[redacted]

[redacted]

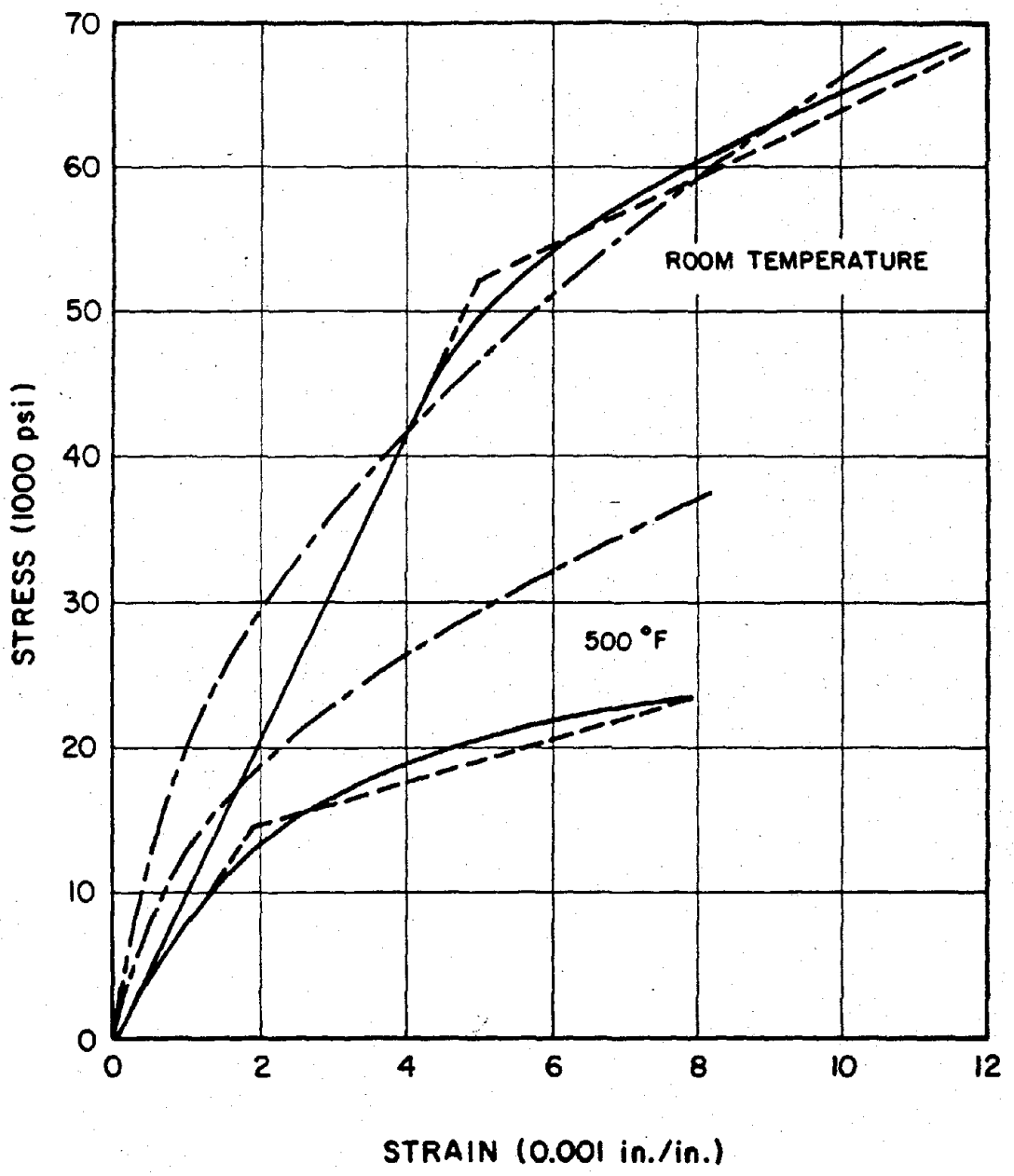

Figure 9-26. [redacted] Stress-Strain Approximation for 2014-T6 Aluminum Alloy [redacted]

[redacted]

[redacted]

[redacted] static load the plate could carry without exceeding the yield stress. One-half hour soak time data were used to determine the strength properties, and a 20-in. square plate, 1/4-in. thick was assumed. The results are shown in Table 9-9. As can be seen, the maximum allowable load is almost a linear function of allowable stress. The explanation of this can be seen in the following equation, which is the elastic stress equation for the plate under study.

$$\sigma = 7{,}356.8p + 4.632E^{1/3}p^{2/3}.$$

The second term of the equation is for membrane stresses and is the only term that contains the temperature dependent Young's modulus. As the temperature increases, the value of E decreases, so the contribution from the second term is further decreased, and a fairly linear dependence on the pressure, p, remains.

[redacted] The allowable stress in the above example was taken from 1/2 hour soak time data. This provides a lower bound for the allowable load. Examination of Figure 9-21 through 9-25 indicates that the rapid heating, short soak time data generally fall above the 1/2 hour soak time curves. More reliable estimation of allowable loads will depend on the availability and appropriateness of the material data that is required for the type of analysis and calculation techniques being employed by an investigator. [redacted] The truly dynamic case may be analyzed similarly. In both cases, however, the basic factor that influences structural degradation is allowable stress as long as the elastic analysis approach is used.

[redacted] Where deformation or plastic response is responsible for failure, allowable stress no longer can be used to determine allowable load; either total deformation or total energy absorbed must be used.

[redacted] The energy approach consists of stating that the energy absorbed by a structure as it deforms is proportional to the product of the overpressure and the impulse values, ΔpI, of the blast wave that causes the deformation. Thus, for a constant value of absorbed energy used as a measure of damage, any combination of overpressure and impulse that yields the same product will cause the same amount of "damage."

[redacted] The effect of elevated temperature on the damage values has been investigated. One source indicates that for face-centered cubic materials, such as aluminum, the value of the parabolic coefficient of Bell's stress-strain law varies linearly with the temperature. For 2014-T6 Aluminum, the equation would be

$$\sigma = 9.65 \times 10^5 \epsilon^{1/2}$$

Table 9-9. [redacted] Allowable Uniform Static Load for Aluminum Plate at Three Temperatures [redacted]

Temperature (°F)	σy (10^3 psi)	Young's Modulus, E (10^6 psi)	Deflection (in.)	Allowable Load (psi)
70	57	10.5	0.323	7.25
350	43	9.77	0.261	5.45
500	17	8.4	0.117	2.10

[redacted]

[redacted]

[redacted] where the value of β was obtained by fitting the curve to pass through the room temperature yield stress for the material. The Bell's law equation indicates that the energy under the stress-strain curve is a linear function of temperature by varying values of β linearly. This infers that the damage value, ΔpI, should depend on a linear function of temperature, i.e.,

$$(\Delta pI)_{T_2} = (\Delta pI)_{T_1} \left[\frac{1 - \frac{T_2}{T_m}}{1 - \frac{T_1}{T_m}} \right]$$

where

$(\Delta pI)_{T_1}$ = damage value at temperature T_1

and

$(\Delta pI)_{T_2}$ = damage value at temperature T_2.

If this relation were true, it would be a simple matter to evaluate the vulnerability of a structure. Once the value of ΔpI had been determined for ambient temperatures, the ΔpI value at elevated temperatures could be determined easily.

[redacted] The Bell's law equation also indicates that yield strength, ultimate strength, and Young's modulus are linear functions of temperature for dynamic deformation. The data that were used to develop the equation were obtained from impact tests of oven heated samples. No information was provided as to what the heating rates or soak times were. The only other comparable data, at least in the dynamic sense, were shown in Figure 9-24, which indicate that data from dynamic tests do seem to approximate a straight line to some degree. Thus, with further testing and research, it may be that a relatively simple approach to assessing structural vulnerability to combined thermal/blast effects will be possible for dynamic deformation damage criteria.

[redacted] The previous discussion has been concerned primarily with unstressed, unrestrained structural elements. There are three main structural conditions that are encountered in the analysis of structural response to combined thermal/blast effects. These are: unstressed members with no edge or end restraints; unstressed members with restraints; and prestressed members with restraints. These conditions refer to the status of a structure before either thermal or blast loading. The first condition is the easiest to analyze since there are no restraints to dimensional changes during or after heating so the thermal degradation of mechanical strength properties is the main concern. The second condition is more complex since dimension changes are prevented in varying degrees and appreciable thermal stresses may exist at the time of blast loading. The inclusion of these thermal stresses is not uncommon in structural elastic analysis. Thermal stresses caused by thermal gradients in the structural member also are included under this condition. The inclusion of stresses induced by the thermal gradient in an elastic structural analysis generally will require the use of a finite element structural analysis computer code. Unfortunately, it cannot be assumed that either form of thermal stress will be inconsequential, and they should both be addressed specifically in the solution of a particular problem. The final condition is the most difficult to analyze because a member may be stressed prior to thermal or blast loading.

[redacted] The final factor to consider in determining structural response is the possibility of changes in failure modes, particularly materials rupture. Visual examination of a 1/4-in. by 0.040-in. 2024-T3 Aluminum specimen that fail-

[redacted]

[redacted]

[redacted] ed indicated little necking down at the failure point. This may be due to the small area (about 17 mm diameter) exposed to thermal radiation. Failure occurred on a 45° plane, with no cupping. Postshot photos of cylindrical/aluminum shells, exposed to HE air blast after rapid heating, indicated an almost brittle-like fracture mode of failure. Failure of similar shells at normal temperature under the same type of loading was of a ductile deformation type. The possibility of a change in failure mode under dynamic loading at elevated temperatures has not been investigated, but is of concern since residual load carrying capabilities of deformed structures are sometimes used in determining vulnerability.

[redacted] In summary, if elastic criteria are used to determine survivability/vulnerability, and if the necessary materials strength properties are known, a fairly straight forward but not necessarily simple stress analysis may be performed. If dynamic or deformation criteria are necessary, the problem becomes very difficult, if not impossible, because of the lack of validated analysis techniques. A third criterion, material melting, may be used to bound the problem. A temperature criterion may be chosen that is or nearly equal to the melting point of the materia[redacted] with the inference that, at that temperature, the material has no strength, and therefore, no resistance to load. This latter criterion has been used, for example, to establish kill criteria for Army aircraft.

SECTION V

[redacted] X-RAY DAMAGE EFFECTS [redacted]

[redacted] INTRODUCTION [redacted]

[redacted] Nuclear weapons as X-ray sources and the environments they produce are described in Chapter 4. This section discusses the interaction of the X-ray environment with aerospace systems and some typical damage mechanisms that result from the interaction. The damage mechanisms depend on the fluence and energy, or temperature, of the X-rays and on the protective and structural materials involved in the interaction. For purposes of discussion the damage mechanisms can be divided conveniently into the effects caused by hot X-rays and those caused by cold X-rays. Some familiarity with the material discussed in Chapter 4 is assumed in the following discussion.

[redacted] Cold X-rays (typically 1 to 3 keV black body temperatures) are absorbed in a thin surface layer. At sufficiently high fluence, a short pulse of X-rays can heat the surface rapidly and may cause it to vaporize and blow off. This results in: (1) an impulse imparted to the total structure; and (2) generation of a strong shock wave that propagates into the structure, and which may cause spallation of material at free boundaries and internal fracture of materials and bonds. These latter effects are produced by shock wave propagation through the thickness of a surface structure such as the thermal protection shell of a reentry vehicle. The former effects may produce damage by whole vehicle modes of response to the net impulse.

[redacted] The hot X-rays are more penetrating. They can cause: (1) thermally generated shock waves in the vehicle structural materials and internal components; (2) melting and vaporization of the substructure; (3) internal deposition of energy in electronic components producing transient or permanent damage (see Chapter 6 and Section 7 of this chapter); or (4) produce internal EMP signals (see Chapter 7).

[redacted] While some nuclear weapons emit only cold X-rays, all hot X-ray weapons have a cold component. Hence, for exoatmospheric events the hot X-ray effects are accompanied by cold X-ray effects. On the other hand, for endoatmospheric explosions, the cold X-rays have short mean free paths, and the X-ray effects beyond distances of a few tens of meters are produced by hot X-rays alone.

[redacted]

[redacted]

[redacted] Damage to a particular system depends on the structural details of the system as well as the X-ray spectrum. Accurate damage prediction even for the simplest geometries, generally require elaborate computer programs to calculate the energy deposition and the response of the system. All vulnerability analyses follow similar computational steps:

1. The X-ray energy deposition is computed using known processes for the materials and structure. This energy is assumed most often to be deposited instantaneously.

2. From the calculated energy deposition and the equation of state for the materials in the structure (if known) for the liquid, solid, and vapor phases of the material, a stress wave, which propagates through the surface structure, is calculated.

3. Damage to the surface structure that results from the stress wave (spallation, internal fracturing, delamination and debonding), is determined. These calculations generally are based on experimentally derived damage response curves. A good deal of progress has been made in the last few years in understanding and predicting fractures in most homogeneous and some composite materials. Even a small amount of fracturing may cause a significant loss in strength of material. One of the most complicating factors involved in making reliable damage predictions is that of in-depth heating prior to stress wave propagation through the material.

4. The response of the whole structure that results from the impulse imparted to it is determined. This response also is generally based on experimentally determined damage or properties degradation measurements. In these computations, the effects of the loss of strength of the structural material as a result of fracturing caused by the immediately preceding stress wave or by in-depth heating must be included. The structure may be broken by the impulse loading, or it may be weakened (buckled) so that it will fail under subsequent stresses, for example, reentry into the atmosphere.

[redacted] X-RAY ENERGY DEPOSITION CALCULATIONS [redacted]

[redacted] The starting point of all X-ray vulnerability analysis is a calculation of the X-ray energy deposition. The determination of the transmitted X-ray fluence, or shine through, into the interior of the aerospace system, is implicit in these calculations. Calculation of X-ray energy deposition involves the use of energy dependent photon absorption cross sections and energy and angle dependent scattering cross sections. Corrections for fluorescence, i.e., reradiation of X-rays, may be significant for high energy photons in certain materials. Sophisticated energy deposition and transport calculations, using detailed energy dependent cross sections and their angular dependence can be made by computers using Monte Carlo techniques. The results serve as an accuracy check and provide "effective" cross section data for simpler techniques. Approximation techniques greatly reduce the amount of effort and time involved in system analysis. Fairly accurate approximate values sometimes can be obtained even by hand calculations, as will be shown with examples.

9-33 X-ray Cross Sections [redacted]

[redacted] The probability of a photon of energy $h\nu$ traversing a distance of absorbing material x is $e^{-\mu x}$, where μ is the linear attenuation coefficient. This probability also can be written as $e^{-(\mu/\rho)\rho x}$, where μ/ρ is the mass attenuation coefficient for the material (see paragraph 4-3). In this representation, μ/ρ is in cm^2/gm and ρx is the thickness in gm/cm^2, i.e., the mass of material in the column of 1 square centimeter cross section and x centimeters long.

[redacted] If the monoenergic X-ray fluence incident normal (perpendicular) to the material sur-

[redacted]

[redacted]

[redacted]

[redacted] face is φ_o, the direct fluence after traversing a thickness ρx of absorbing material is

$$\varphi_{dir} = \varphi_o e^{-(\mu/\rho)\rho x} \text{ cal/cm}^2.$$

[redacted] The total mass attenuation coefficient μ/ρ is the sum of several components that represent the various mechanisms that can remove a primary photon from the direct flux, while it traverses a material. These mechanisms are described in paragraph 4-3, Chapter 4, and are: the photoelectric process, Compton inelastic scattering, Compton elastic scattering (incoherent elastic scattering) and Rayleigh elastic scattering (coherent elastic scattering). The first two processes result in photon energy being absorbed and the production of secondary electrons, the photoelectrons and Compton recoil electrons, respectively. The kinetic energy of these electrons is dissipated in the material and heats it. Energy deposition usually is calculated to have occurred at the depth at which the electrons are produced. However, in the case of very thin samples, the range of the freed electrons can exceed the material thickness, and energy deposition cannot be considered to be local. The energy removed from the primary photon beam in the Compton elastic process or the Rayleigh elastic process is not locally absorbed. A clear distinction must be made between attenuation of the primary flux and absorption of energy from the primary flux. For this reason the total linear attenuation coefficient usually is written as $\mu = \mu_a + \mu_s$. Here, μ_a is an absorption coefficient. It represents the first two processes mentioned above, which result in energy absorption. The second term, μ_s, is an elastic scattering coefficient, which contributes to the attenuation of the primary flux but not to local energy absorption. It is sometimes convenient to ignore the Rayleigh coherent scattering coefficient in the total attenuation coefficient. The coherent radiation has the same energy, and nearly the same direction, as the primary photon and cannot be distinguished from it in the "bad" geometry situations that usually occur in nuclear effects applications.*

[redacted] Mass attenuation coefficients for the elements beryllium, aluminum, iron, copper, tungsten, and uranium are given in Tables 9-10 through 9-15, and Figures 9-27 through 9-32, respectively. These are representative of metallic materials used in aerospace systems. Mass attenuation coefficients for ablator materials, carbon phenolic and tape-wound silicon phenolic are shown in Figures 9-33 and 9-34, respectively. In these tables and figures, Z is the atomic number, μ_{ce}/ρ is the coherent elastic scattering coefficient, μ_{ie}/ρ is the incoherent Compton elastic coefficient, μ_{is}/ρ is the inelastic Compton coefficient, and μ_p/ρ is the photoelectric coefficient. As designated previously, μ_a/ρ and μ/ρ are the energy absorption coefficient and the total attenuation coefficient.†

9-34 X-ray Energy Deposition and Shine Through Fluences [redacted]

[redacted] X-ray energy deposition in a thickness δ at a depth x due to direct fluence photons is given by

$$A'_{dir} = \varphi_o \left[1 - e^{-\left(\frac{\mu_a}{\rho}\right)\rho\delta}\right] e^{-\left(\frac{\mu}{\rho}\right)\rho x}.$$

If $\mu_a\delta << 1$, and if φ_o is in cal/cm^2, this expression can be written as

$$A'_{dir} = \varphi_o \left(\frac{\mu_a}{\rho}\right) \rho\delta \; e^{-\left(\frac{\mu}{\rho}\right)\rho x} \text{ cal/cm}^2.$$

[redacted] A "good" geometry is one in which the distinction between primary and scattered photons can be made accurately.

[redacted] The symbols K, L_1, L_2, etc., in the tables and figures indicate the binding energies of the various electron shells (see paragraph 4-3, Chapter 4).

[redacted]

[redacted]

[redacted] Frequently, the absorption is written in terms of cal/gm by dividing out the thickness $\rho\delta$,

$$A_{dir} = \varphi_o \left(\frac{\mu_a}{\rho}\right) e^{-\left(\frac{\mu}{\rho}\right) \rho x} \text{ cal/gm.}$$

This expression for the absorption is in terms of a dose; however, this assumes that very little of the flux is absorbed in the deposition region at depth x, i.e., the deposition region considered is very thin. Clearly, more energy than is in the incident flux cannot be absorbed.

[redacted] The equation for direct fluence (φ_{dir}) given in paragraph 9-32 can be used to represent a small energy band of photons in X-ray energy spectra such as those tabulated in Table 4-3, Chapter 4, for various black body spectra. The total energy in the direct X-ray fluence after traversing thickness x is obtained by summing over the energy bands.

$$\varphi = \sum_i \varphi_{oi} \, e^{-\left(\frac{\mu}{\rho}\right)_i \rho x} \text{ cal/cm}^2.$$

In a like manner, the total direct fluence X-ray energy absorption at depth ρx is obtained by summing for each energy band.

$$A = \sum_i \left(\frac{\mu_a}{\rho}\right)_i \varphi_{oi} \, e^{-\left(\frac{\mu}{\rho}\right)_i \rho x} \text{ cal/cm}^2.$$

[redacted] Problems 9-3 and 9-4 illustrate how these equations can be used to calculate approximate values for energy deposition and shine through.

[redacted]

[redacted]

Problem 9-3. Calculation of X-ray Energy Deposition at the Surface

[redacted] The information contained in Tables 9-10 through 9-15 and Figures 9-27 through 9-34 together with the equation for energy absorption given in paragraph 9-34 provide the means to obtain the approximate X-ray energy absorbed for various spectra and several materials. If the energy deposition at the surface on which the X-rays are incident is desired, the thickness, x, reduces to zero, and the energy deposition equation becomes

$$A = \sum_i (\mu_a/\rho)_i \, \varphi_{oi} \text{ cal/gm.}$$

[redacted]

[redacted]

Page 9-72 deleted.

[redacted]

Related Material: See paragraphs 9-33 and 9-34. See also Tables 9-10 through 9-15 and Figures 9-27 through 9-34. See also paragraphs 4-1 through 4-3 and Tables 4-3 and 4-4, Chapter 4.

[redacted]

[redacted]

Problem 9-4. Calculation of X-ray Energy Deposition at a Depth in a Material and the Shine Through Fluence

DNA (b)(3)

[redacted] The information contained in Tables 9-10 through 9-15 and Figures 9-27 through 9-34 together with the equation for energy absorption given in paragraph 9-34 provide the means to obtain the approximate X-ray energy absorbed for various spectra and several materials at a depth x in the materials, as well as the fluence at that depth or the fluence emerging from the back face of the material (shine through).

[redacted]

[redacted] Problem 4-1, Chapter 4, describes the method to obtain energy distributions for various source temperatures from the normalized Planck distributions given in Table 4-1, Chapter 4.

Page 9-75 deleted.

[redacted]

DNA
(b)(3)

Reliability: The reliability of the procedures described above depends on the X-ray spectrum and the absorbing material. The accuracy depends primarily on the relative importance of the scattering cross sections, and, for some materials, fluorescence. No definite reliability estimate can be made.

Related Material: See paragraphs 9-33 and 9-34. See also Tables 9-10 through 9-15 and Figures 9-27 through 9-34. See also paragraphs 4-1 through 4-3 and Tables 4-3 and 4-4, Chapter 4.

[redacted]

Table 9-10. [redacted] X-ray Cross Sections, Beryllium Z = 4 (cm^2/gm) [redacted]

Photon Energy keV	μ_{ce}/ρ	μ_{ie}/ρ	μ_{is}/ρ	μ_p/ρ	μ_a/ρ	μ/ρ
0.1	7.097-1*	1.154-3	2.770-7	1.507+4	1.507+4†	1.507+4
0.111K	7.094-1	1.331-3	3.560-7	1.109+4	1.109+4	1.109+4
0.111	7.094-1	1.331-3	3.560-7	2.323+5	2.323+5	2.323+5
0.15	7.079-1	2.007-3	7.257-7	1.105+5	1.105+5	1.105+5
0.2	7.054-1	2.972-3	1.421-6	5.302+4	5.302+4	5.302+4
0.3	6.984-1	5.171-3	3.685-6	1.816+4	1.816+4	1.817+4
0.4	6.889-1	7.660-3	7.223-6	8.292+3	8.292+3	8.292+3
0.5	6.770-1	1.039-2	1.218-5	4.456+3	4.456+3	4.456+3
0.6	6.631-1	1.332-2	1.866-5	2.662+3	2.662+3	2.662+3
0.8	6.306-1	1.972-2	3.650-5	1.165+3	1.165+3	1.165+3
1.0	5.939-1	2.674-2	6.137-5	6.072+2	6.072+2	6.078+2
1.5	4.986-1	4.648-2	1.591-4	1.820+2	1.820+2	1.825+2
2.0	4.153-1	6.151-2	2.771-4	7.626+1	7.626+1	7.674+1
3.0	3.019-1	7.946-2	5.309-4	2.199+1	2.199+1	2.237+1
4.0	2.371-1	9.009-2	7.911-4	9.004	9.004	9.332
5.0	1.968-1	9.831-2	1.066-3	4.481	4.482	4.778
6.0	1.685-1	1.053-1	1.356-3	2.527	2.528	2.802
8.0	1.285-1	1.170-1	1.971-3	1.019	1.021	1.267
10.0	1.003-1	1.261-1	2.613-3	5.024-1	5.050-1	7.314-1
15.0	5.780-2	1.386-1	4.173-3	1.384-1	1.426-1	3.390-1
20.0	3.677-2	1.432-1	5.589-3	5.539-2	6.098-2	2.410-1
30.0	1.844-2	1.433-1	8.064-3	1.525-2	2.331-2	1.851-1
40.0	1.098-2	1.395-1	1.017-2	6.126-3	1.630-2	1.668-1
50.0	7.251-2	1.348-1	1.199-2	3.027-3	1.502-2	1.570-1
60.0	5.132-2	1.299-1	1.357-2	1.705-3	1.528-2	1.503-1
80.0	2.947-3	1.207-1	1.617-2	6.930-4	1.686-2	1.406-1
100.0	1.898-3	1.126-1	1.819-2	3.464-4	1.854-2	1.331-1
150.0	8.554-4	9.646-2	2.164-2	9.953-5	2.174-2	1.191-1
200.0	4.811-4	8.476-2	2.364-2	4.159-5	2.368-2	1.089-1
300.0	2.138-4	6.877-2	2.559-2	1.241-5	2.560-2	9.458-2
400.0	1.203-4	5.830-2	2.630-2	5.346-6	2.631-2	8.473-2
500.0	8.019-5	5.080-2	2.645-2	2.811-6	2.645-2	7.733-2
600.0	5.346-5	4.516-2	2.634-2	1.675-6	2.634-2	7.156-2
800.0	2.807-5	3.708-2	2.571-2	7.501-7	2.571-2	6.282-2
1000.0	1.737-5	3.157-2	2.487-2	4.074-7	2.487-2	5.646-2

[redacted] $7.097 - 1 = 7.097 \times 10^{-1}$.
† [redacted] $1.507 + 4 = 1.507 \times 10^{4}$.

[redacted]

[redacted]

Table 9-11. [redacted] X-ray Cross Sections, Aluminum Z = 13 (cm^2/gm) [redacted]

Photon Energy keV	μ_{ce}/ρ	μ_{ie}/ρ	μ_{is}/ρ	μ_p/ρ	μ_a/ρ	μ/ρ
0.1	2.504	5.614-4*	1.348-7	4.462+5†	4.462+5	4.462+5
$0.118L_1$	2.503	7.044-4	1.998-7	2.849+5	2.849+5	2.849+5
0.118	2.503	7.044-4	1.998-7	4.273+5	4.273+5	4.273+5
0.15	2.501	9.872-4	3.568-7	2.192+5	2.192+5	2.192+5
0.2	2.496	1.473-3	7.102-7	9.926+4	9.926+4	9.926+4
0.3	2.482	2.591-3	1.874-6	3.250+4	3.250+4	3.250+4
0.4	2.463	3.867-3	3.706-6	1.472+4	1.472+4	1.472+4
0.5	2.439	5.276-3	6.286-6	7.962+3	7.962+3	7.964+3
0.6	2.411	6.799-3	9.696-6	4.819+3	4.819+3	4.822+3
0.8	2.345	1.015-2	1.917-5	2.183+3	2.183+3	2.185+3
1.0	2.269	1.384-2	3.251-5	1.181+3	1.181+3	1.183+3
1.5	2.063	2.431-2	8.474-5	3.866+2	3.866+2	3.887+2
5.560K	2.036	2.533-2	9.169-5	3.473+2	3.473+2	3.493+2
1.560	2.036	2.533-2	9.169-5	4.403+3	4.403+3	4.405+3
2.0	1.869	3.295-2	1.514-4	2.352+3	2.352+3	2.354+3
3.0	1.557	4.629-2	3.164-4	8.087+2	8.087+2	8.103+2
4.0	1.326	5.732-2	5.166-4	3.674+2	3.674+2	3.688+2
5.0	1.143	6.618-2	7.381-4	1.960+2	1.960+2	1.972+2
6.0	9.910-1	7.543-2	1.004-3	1.162+2	1.162+2	1.172+2
8.0	7.482-1	9.132-2	1.598-3	5.004+1	5.004+1	5.088+1
10.0	5.730-1	1.045-1	2.258-3	2.571+1	2.571+1	2.639+1
15.0	3.272-1	1.228-1	3.861-3	7.471	7.475	7.925
20.0	2.133-1	1.319-1	5.390-3	3.057	3.062	3.407
30.0	1.148-1	1.388-1	8.161-3	8.505-1	8.587-1	1.112
40.0	7.319-2	1.394-1	1.052-2	3.394-1	3.499-1	5.625-1
50.0	5.116-2	1.374-1	1.256-2	1.657-1	1.783-1	3.668-1
60.0	3.792-2	1.343-1	1.432-2	9.199-2	1.063-1	2.785-1
80.0	2.209-2	1.268-1	1.719-2	3.625-2	5.344-2	2.024-1
100.0	1.466-2	1.194-1	1.943-2	1.759-2	3.702-2	1.711-1
150.0	6.855-3	1.035-1	2.324-2	4.728-3	2.797-2	1.383-1
200.0	3.935-2	9.131-2	2.549-2	1.868-3	2.736-2	1.226-1
300.0	1.775-3	7.425-2	2.775-2	5.092-4	2.826-2	1.043-1
400.0	1.000-3	6.297-2	2.861-2	2.044-4	2.881-2	9.279-2
500.0	6.384-4	5.490-2	2.880-2	1.014-4	2.890-2	8.444-2
600.0	4.397-4	4.880-2	2.868-2	5.749-5	2.874-2	7.797-2
800.0	2.455-4	4.012-2	2.798-2	2.374-5	2.800-2	6.837-2
1000.0	1.540-4	3.417-2	2.706-2	1.208-5	2.707-2	6.139-2

* [redacted] $5.614 - 4 = 5.614 \times 10^{-4}$.
† [redacted] $4.462 + 5 = 4.462 \times 10^{5}$.

[redacted]

[redacted]

Table 9-12. [redacted] X-ray Cross Sections, Iron Z = 26 (cm^2/gm) [redacted]

Photon Energy keV	μ_{ce}/ρ	μ_{ie}/ρ	μ_{is}/ρ	μ_p/ρ	μ_a/ρ	μ/ρ
0.1	4.842	2.910-4*	6.986-6	1.036+6†	1.036+6	1.036+6
0.15	4.838	5.217-4	1.879-7	3.413+5	3.413+5	3.413+5
0.2	4.833	7.893-4	3.798-7	1.552+5	1.552+5	1.553+5
0.3	4.817	1.415-3	1.023-6	5.115+4	5.114+4	5.115+4
0.4	4.796	2.140-3	2.063-6	2.327+4	2.327+4	2.327+4
0.5	4.769	2.950-3	3.557-6	1.263+4	1.263+4	1.263+4
0.6	4.737	3.835-3	5.522-6	7.665+3	7.665+3	7.670+3
$0.708L_3$	4.696	4.867-3	8.224-6	4.870+3	4.870+3	4.874+3
0.708	4.696	4.867-3	8.224-6	1.741+4	1.741+4	1.742+4
$0.721L_2$	4.691	4.995-3	8.597-6	1.652+4	1.652+4	1.653+4
0.721	4.691	4.995-3	8.597-6	2.479+4	2.479+4	2.479+4
0.8	4.658	5.800-3	1.105-5	1.838+4	1.838+4	1.838+4
$0.846L_1$	4.638	6.280-3	1.265-5	1.564+4	1.564+4	1.564+4
0.846	4.638	6.280-3	1.265-5	2.346+4	2.346+4	2.346+4
1.0	4.564	7.993-3	1.897-5	1.449+4	1.449+4	1.450+4
1.5	4.288	1.431-2	5.045-5	4.505+3	4.505+3	4.509+3
2.0	3.989	2.022-2	9.432-5	1.966+3	1.966+3	1.970+3
3.0	3.419	3.115-2	2.148-4	6.112+2	6.112+2	6.146+2
4.0	2.917	4.126-2	3.757-4	2.668+2	2.668+2	2.697+2
5.0	2.487	5.035-2	5.713-4	1.402+2	1.402+2	1.428+2
6.0	2.128	5.855-2	7.910-4	8.293+1	8.293+2	8.511+1
$6.404L_3K$	1.994	6.147-2	8.830-4	6.873+1	6.873+1	7.079+1
$7.112K$	1.796	6.649-2	1.055-3	5.081+1	5.081+1	5.267+1
7.112	1.796	6.649-2	1.055-3	4.197+2	4.197+2	4.215+2
8.0	1.594	7.257-2	1.288-3	3.095+2	3.095+2	3.112+2
10.0	1.241	8.321-2	1.832-3	1.714+2	1.714+2	1.727+2
15.0	7.684-1	1.013-1	3.263-3	5.622+1	5.622+1	5.709+1
20.0	5.320-1	1.118-1	4.688-3	2.483+1	2.483+1	2.548+1
30.0	2.931-1	1.211-1	7.311-3	7.632	7.639	8.054
40.0	1.828-1	1.242-1	9.651-3	3.258	3.268	3.575
50.0	1.242-1	1.240-1	1.168-2	1.675	1.687	1.935
60.0	8.974-2	1.223-1	1.341-2	9.709-1	9.843-1	1.196
80.0	5.290-2	1.172-1	1.623-2	4.104-1	4.266-1	5.967-1
100.0	3.479-2	1.114-1	1.843-2	2.108-1	2.292-1	3.754-1
150.0	1.593-2	9.800-2	2.220-2	6.353-2	8.573-2	1.997-1
200.0	9.058-3	8.699-2	2.441-2	2.751-2	5.192-2	1.480-1
300.0	4.053-3	7.124-2	2.665-2	8.699-3	3.535-2	1.106-1
400.0	2.281-3	6.057-2	2.752-2	3.945-3	3.146-2	9.432-2
500.0	1.457-3	5.284-2	2.778-2	2.175-3	2.996-2	8.425-2
600.0	1.008-3	4.698-2	2.770-2	1.354-3	2.905-2	7.704-2
800.0	5.618-4	3.863-2	2.707-2	6.590-4	2.773-2	6.692-2
1000.0	3.548-4	3.291-2	2.619-2	3.863-4	2.658-2	5.984-2

* [redacted] 2.910 - 4 = 2.910×10^{-4}.
† [redacted] 1.036 + 6 = 1.036×10^{6}.

[redacted]

[redacted]

Table 9-13. [redacted] X-ray Cross Sections, Copper Z = 29 (cm^2/gm) [redacted]

Photon Energy keV	μ_{ce}/ρ	μ_{ie}/ρ	μ_{is}/ρ	μ_p/ρ	μ_a/ρ	μ/ρ
0.1	5.295	1.655-4*	3.975-8	3.001+5†	3.001+5	3.001+5
$0.120M_1$	5.294	2.185-4	6.291-8	1.976+5	1.976+5	1.976+5
0.120	5.294	2.185-4	6.291-8	2.174+5	2.174+5	2.174+5
0.15	5.292	3.090-4	1.112-7	1.293+5	1.293+5	1.293+5
0.2	5.288	4.814-4	2.315-7	6.645+4	6.645+4	6.646+4
0.3	5.276	8.992-4	6.502-7	2.602+4	2.602+4	2.602+4
0.4	5.259	1.401-3	1.350-6	1.338+4	1.338+4	1.338+4
0.5	5.238	1.975-3	2.380-6	7.984+3	7.984+3	7.990+3
0.6	5.213	2.615-3	3.774-6	5.238+3	5.238+3	5.243+3
0.8	5.151	4.072-3	7.768-6	2.693+3	2.693+3	2.698+3
$0.931L_3$	5.102	5.145-3	1.138-5	1.896+3	1.896+3	1.901+3
0.931	5.102	5.145-3	1.138-5	8.043+3	8.043+3	8.048+3
$0.951L_2$	5.094	5.314-3	1.201-5	7.593+3	7.593+3	7.598+3
0.951	5.094	5.314-3	1.201-5	1.139+4	1.139+4	1.139+4
1.0	5.074	5.741-3	1.364-5	9.932+3	9.932+3	9.937+3
$1.097L_1$	5.020	6.617-3	1.722-5	7.725+3	7.725+3	7.730+3
1.097	5.020	6.617-3	1.722-5	1.159+4	1.159+4	1.159+4
1.5	4.840	1.071-2	3.782-5	4.935+3	4.935+3	4.940+3
2.0	4.569	1.578-2	7.372-5	2.254+3	2.254+3	2.258+3
3.0	4.006	2.566-2	1.775-4	7.465+2	7.465+2	7.505+2
4.0	3.470	3.499-2	3.191-4	3.409+2	3.409+2	3.444+2
5.0	2.987	4.352-2	4.938-4	1.856+2	1.856+2	1.886+2
6.0	2.571	5.130-2	6.952-4	1.129+2	1.129+2	1.155+2
8.0	1.934	6.489-2	1.155-3	5.156+1	5.156+1	5.356+1
$8.048L_3K$	1.921	6.517-2	1.166-3	5.073+1	5.073+1	5.272+1
$8.979K$	1.697	7.046-2	1.399-3	3.765+1	3.765+1	3.941+1
8.979	1.697	7.046-2	1.399-3	2.978+2	2.978+2	2.995+2
10.0	1.499	7.607-2	1.676-3	2.234+2	2.234+2	2.250+2
15.0	9.085-1	9.494-2	3.065-3	7.373+1	7.373+1	7.473+1
20.0	6.245-1	1.059-1	4.458-3	3.285+1	3.285+1	3.358+1
30.0	3.479-1	1.166-1	7.071-3	1.026+1	1.026+1	1.073+1
40.0	2.195-1	1.201-1	9.378-3	4.434	4.443	4.783
50.0	1.502-1	1.203-1	1.137-2	2.301	2.312	2.583
60.0	1.090-1	1.187-1	1.309-2	1.344	1.357	1.585
80.0	6.473-2	1.140-1	1.587-2	5.736-1	5.895-1	7.678-1
100.0	4.256-2	1.085-1	1.803-2	2.963-1	3.143-1	4.654-1
150.0	1.958-2	9.568-2	2.172-2	8.966-2	1.114-1	2.267-1
200.0	1.117-2	8.510-2	2.390-2	3.869-2	6.259-2	1.589-1
300.0	5.014-3	6.974-2	2.609-2	1.204-2	2.813-2	1.129-1
400.0	2.821-3	5.933-2	2.696-2	5.346-2	3.231-2	9.466-2
500.0	1.804-3	5.177-2	2.721-2	2.882-3	3.009-2	8.367-2
600.0	1.249-3	4.603-2	2.715-2	1.754-3	2.890-2	7.619-2
800.0	6.967-4	3.785-2	2.654-2	8.161-4	2.736-2	6.590-2
1000.0	4.407-4	3.224-2	2.568-2	4.584-4	2.614-2	5.882-2

* [redacted] $1.655 - 4 = 1.655 \times 10^{-4}$.
† [redacted] $3.001 + 5 = 3.001 \times 10^{5}$.

[redacted]

[redacted]

Table 9-14. [redacted] X-ray Cross Sections, Tungsten Z = 74 (cm^2/gm) [redacted]

Photon Energy keV	μ_{ce}/ρ	μ_{ie}/ρ	μ_{is}/ρ	μ_p/ρ	μ_a/ρ	μ/ρ
0.1	1.191+1*	1.678-4*	4.091-8	3.230+6	3.230+6	3.230+6
0.15	1.191+1	2.957-4	1.070-7	1.089+6	1.089+6	1.089+6
0.2	1.190+1	4.421-4	2.123-7	5.037+5	5.037+5	5.037+5
0.3	1.188+1	7.791-4	5.609-7	1.699+5	1.699+5	1.699+5
0.4	1.184+1	1.165-3	1.120-6	7.857+4	7.857+4	7.858+4
$0.492N_2$	1.181+1	1.553-3	1.841-6	4.520+4	4.520+4	4.522+4
0.492	1.181+1	1.553-3	1.841-6	4.972+4	4.972+4	4.974+4
0.5	1.180+1	1.590-3	1.915-6	4.752+4	4.752+4	4.753+4
$0.595N_1$	1.176+1	2.028-3	2.906-6	2.981+4	2.981+4	2.982+4
0.595	1.176+1	2.028-3	2.906-6	3.279+4	3.279+4	3.280+4
0.6	1.175+1	2.052-3	2.965-6	3.206+4	3.206+4	3.207+4
0.8	1.163+1	3.066-3	5.907-6	1.483+4	1.483+4	1.484+4
1.0	1.149+1	4.186-3	1.008-5	8.152+3	8.152+3	8.164+3
1.5	1.104+1	7.370-3	2.633-5	2.749+3	2.749+3	2.760+3
$1.809M_5$	1.070+1	9.219-3	3.957-5	1.664+3	1.664+3	1.674+3
1.809	1.070+1	9.219-3	3.957-5	4.159+3	4.159+3	4.170+3
$1.872M_4$	1.063+1	9.599-3	4.262-5	3.798+3	3.798+3	3.808+3
1.872	1.063+1	9.599-3	4.262-5	5.696+3	5.696+3	5.707+3
2.0	1.052+1	1.039-2	4.926-5	4.768+3	4.768+3	4.779+3
$2.281M_3$	1.016+1	1.198-2	6.459-5	3.352+3	3.352+3	3.362+3
2.281	1.016+1	1.198-2	6.459-5	4.022+3	4.022+3	4.033+3
$2.575M_2$	9.844	1.368-2	8.289-5	2.907+3	2.907+3	2.916+3
2.575	9.844	1.368-2	8.289-5	3.197+3	3.197+3	3.207+3
$2.820M_1$	9.613	1.510-2	9.999-5	2.507+3	2.507+3	2.516+3
2.820	9.613	1.510-2	9.999-5	2.757+3	2.757+3	2.767+3
3.0	9.457	1.616-2	1.136-4	2.335+3	2.335+3	2.344+3
4.0	8.471	2.164-2	2.013-4	1.080+3	1.080+3	1.088+3
5.0	7.580	2.681-2	3.092-4	5.937+2	5.937+2	6.013+2
6.0	6.791	3.164-2	4.342-4	3.642+2	3.642+2	3.710+2
8.0	5.500	4.012-2	7.259-4	1.684+2	1.684+2	1.740+2
10.0	4.521	4.786-2	1.078-3	9.260+1	1.260+1	9.717+1
$10.207L_3$	4.424	4.849-2	1.114-3	8.766+1	8.766+1	9.213+1
10.207	4.424	4.849-2	1.114-3	1.824+2	1.824+2	1.869+2
$11.544L_2$	3.884	5.238-2	1.351-3	1.300+2	1.300+2	1.339+2
11.544	3.884	5.238-2	1.351-3	1.950+2	1.950+2	1.989+2
$12.100L_1$	3.694	5.392-2	1.453-3	1.713+2	1.713+2	1.751+2
12.100	3.694	5.392-2	1.453-3	2.570+2	2.570+2	2.608+2
15.0	2.936	1.162-2	2.030-3	1.423+2	1.423+2	1.453+2
20.0	2.071	7.112-2	3.079-3	6.448+1	6.448+1	6.663+1
30.0	1.227	8.246-2	5.173-3	2.113+1	2.113+1	2.245+1
40.0	8.196-1	8.822-2	7.145-3	9.575	9.582	1.049+1
50.0	5.854-1	9.076-2	8.918-3	5.182	5.191	5.867

[redacted]

[redacted]

Table 9-14. (Concluded)

Photon Energy keV	μ_{ce}/ρ	μ_{ie}/ρ	μ_{is}/ρ	μ_p/ρ	μ_a/ρ	μ/ρ
59.318L_3K	4.454-1	9.151-2	1.039-2	3.238	3.248	3.785
60.0	4.373-1	9.150-2	1.050-2	3.138	3.148	3.677
69.525K	3.377-1	9.100-2	1.180-2	2.092	2.104	2.533
69.525	3.377-1	9.100-2	1.180-2	1.020+1	1.021+1	1.064+1
80.0	2.597-1	9.037-2	1.313-2	7.367	7.380	7.730
100.0	1.741-1	8.768-2	1.522-2	4.265	4.280	4.542
150.0	8.216-2	8.022-2	1.884-2	1.471	1.490	1.652
200.0	4.733-2	7.237-2	2.086-2	6.666-1	6.875-1	8.071-1
300.0	2.141-2	6.024-2	2.287-2	2.144-1	2.373-1	3.189-1
400.0	1.209-2	5.160-2	2.365-2	9.661-2	1.203-1	1.839-1
500.0	7.750-3	4.522-2	2.387-2	5.287-2	7.674-2	1.297-1
600.0	5.366-3	4.031-2	2.383-2	3.281-2	5.664-2	1.023-1
800.0	3.014-3	3.323-2	2.334-2	1.606-2	3.940-2	7.565-2
1000.0	1.916-3	2.831-2	2.263-2	9.610-3	3.224-2	6.246-2

[redacted] 1.191 + 1 = 11.91.

[redacted] 1.684 - 4 = 1.684×10^{-4}.

[redacted]

[redacted]

Table 9-15. [redacted] X-ray Cross Sections, Uranium Z = 92 (cm^2/gm) [redacted]

Photon Energy keV	μ_{ce}/ρ	μ_{ie}/ρ	μ_{ζ}/ρ	μ_p/ρ	μ_a/ρ	μ/ρ
0.1	1.423+1*	3.177-5	7.748-9	1.180+6	1.180+6	1.180+6
0.15	1.422+1	6.810-5	2.473-8	4.701+5	4.701+5	4.701+5
0.2	1.421+1	1.169-4	5.624-8	2.446+5	2.446+5	2.446+5
0.3	1.417+1	2.507-4	1.804-7	9.744+4	9.744+4	9.745+4
0.4	1.413+1	4.307-4	4.138-7	5.071+4	5.071+4	5.072+4
0.5	1.407+1	6.551-4	7.884-7	3.055+4	3.055+4	3.057+4
0.6	1.400+1	9.230-4	1.334-6	2.020+4	2.020+4	2.021+4
0.8	1.383+1	1.585-3	3.054-6	1.051+4	1.051+4	1.052+4
1.0	1.362+1	2.410-3	5.803-6	6.333+3	6.333+3	6.347+3
$1.273M_5$	1.327+1	3.791-3	1.160-5	3.664+3	3.664+3	3.677+3
1.273	1.327+1	3.791-3	1.160-5	4.030+3	4.030+3	4.043+3
$1.4215M_4$	1.306+1	4.785-3	1.650-5	3.040+3	3.040+3	3.053+3
1.421	1.306+1	4.785-3	1.650-5	3.344+3	3.344+3	3.358+3
1.5	1.303+1	5.160-3	1.850-5	3.052+3	3.052+3	3.065+3
2.0	1.239+1	8.109-3	3.849-5	1.588+3	1.588+3	1.601+3
3.0	1.113+1	1.464-2	1.035-4	6.327+2	6.327+2	6.438+2
$3.552M_3$	1.043+1	1.819-2	1.513-4	4.313+2	4.313+2	4.417+2
3.552	1.043+1	1.819-2	1.513-4	9.717+2	9.717+2	9.822+2
$3.728M_2$	1.024+1	1.935-2	1.687-4	8.640+2	8.640+2	8.742+2
3.728	1.024+1	1.935-2	1.687-4	1.296+3	1.296+3	1.306+3
4.0	9.966	2.118-2	1.977-4	1.092+3	1.092+3	1.102+3
$4.303M_1$	9.619	2.277-2	2.281-4	9.140+2	9.140+2	9.236+2
4.303	9.619	2.277-2	2.281-4	1.097+3	1.097+3	1.106+3
5.0	8.944	2.642-2	3.059-4	7.616+2	7.616+2	7.705+2
$5.182N_5$	8.763	2.721-2	3.262-4	6.981+2	6.981+2	7.069+2
5.182	8.763	2.721-2	3.262-4	7.679+2	7.679+2	7.767+2
$5.548N_4$	8.430	2.883-2	3.691-4	6.506+2	6.506+2	6.590+2
5.548	8.430	2.883-2	3.691-4	7.156+2	7.156+2	7.241+2
6.0	8.004	3.078-2	4.249-4	5.916+2	5.916+2	5.997+2
8.0	6.649	3.780-2	6.857-4	2.939+2	2.939+2	3.000+2
10.0	5.504	4.232-2	9.528-4	1.709+2	1.709+2	1.765+2
15.0	3.753	5.184-2	1.718-3	6.377+1	6.377+1	6.769+1
$17.166L_3$	3.246	5.562-2	2.090-3	4.594+1	4.594+1	4.924+1
17.166	3.246	5.562-2	2.090-3	9.787+1	9.787+1	1.012+2
20.0	2.725	6.021-2	2.611-3	6.586+1	6.586+1	6.865+1
$20.948L_2$	2.568	6.145-2	2.785-3	5.841+1	5.841+1	6.104+1
20.948	2.568	6.145-2	2.785-3	6.663+1	6.663+1	6.926+1
$21.757L_1$	2.443	6.247-2	2.935-3	6.030+1	6.030+1	6.281+1
21.757	2.443	6.247-2	2.935-3	9.045+1	9.045+1	9.296+1
30.0	1.601	7.173-2	4.528-3	3.883+1	3.883+1	4.050+1
40.0	1.043	7.894-2	6.444-3	1.821+1	1.821+1	1.933+1
50.0	7.277-1	8.241-2	8.168-3	1.012+1	1.012+1	1.094+1

[redacted]

[redacted]

Table 9-15. (Concluded)

Photon Energy keV	μ_{ce}/ρ	μ_{te}/ρ	μ_{rs}/ρ	μ_p/ρ	μ_a/ρ	μ/ρ
60.0	5.339-1	8.375-2	9.690-3	6.261	6.271	6.888
80.0	3.178-1	8.353-2	1.226-2	2.936	2.948	3.349
98.440L_3K	2.176-1	8.189-2	1.416-2	1.700	1.714	2.014
100.0	2.114-1	8.166-2	1.431-2	1.632	1.646	1.939
115.606K	1.646-1	7.956-2	1.560-2	1.114	1.130	1.374
115.606	1.646-1	7.956-2	1.560-2	5.035	5.046	5.295
150.0	9.832-2	7.573-2	1.799-2	2.166	2.184	2.358
200.0	5.627-2	6.872-2	1.999-2	9.940-1	1.013	1.139
300.0	2.533-2	5.625-2	2.150-2	3.873-1	4.088-1	4.904-1
400.0	1.429-2	4.935-2	2.273-2	2.034-1	2.261	2.898-1
500.0	9.149-3	4.340-2	2.299-2	1.196-1	1.426	1.952-1
600.0	6.343-3	3.869-2	2.292-2	7.428-2	9.720-2	1.422-1
800.0	3.557-3	3.128-2	2.200-2	3.107-2	5.307-2	8.792-2
1000.0	2.264-2	2.725-2	2.178-2	1.381-2	3.559-2	6.511-2

[redacted] 1.423 + 1 = 14.23.
† [redacted] 3.177 − 5 = 3.177 x 10^{-5}.

[redacted]

[redacted]

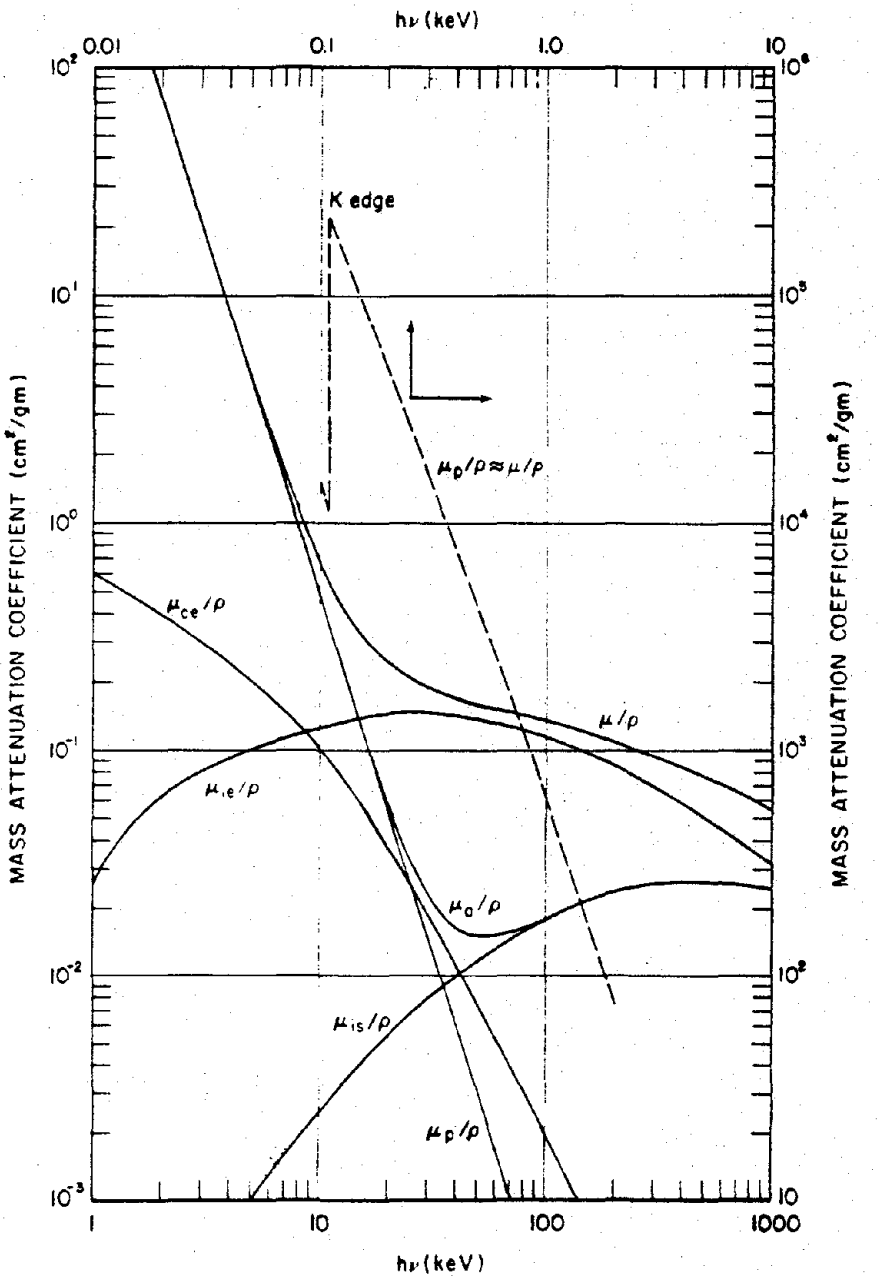

Figure 9-27. [redacted] Photon Cross Sections in Beryllium [redacted]

[redacted]

[redacted]

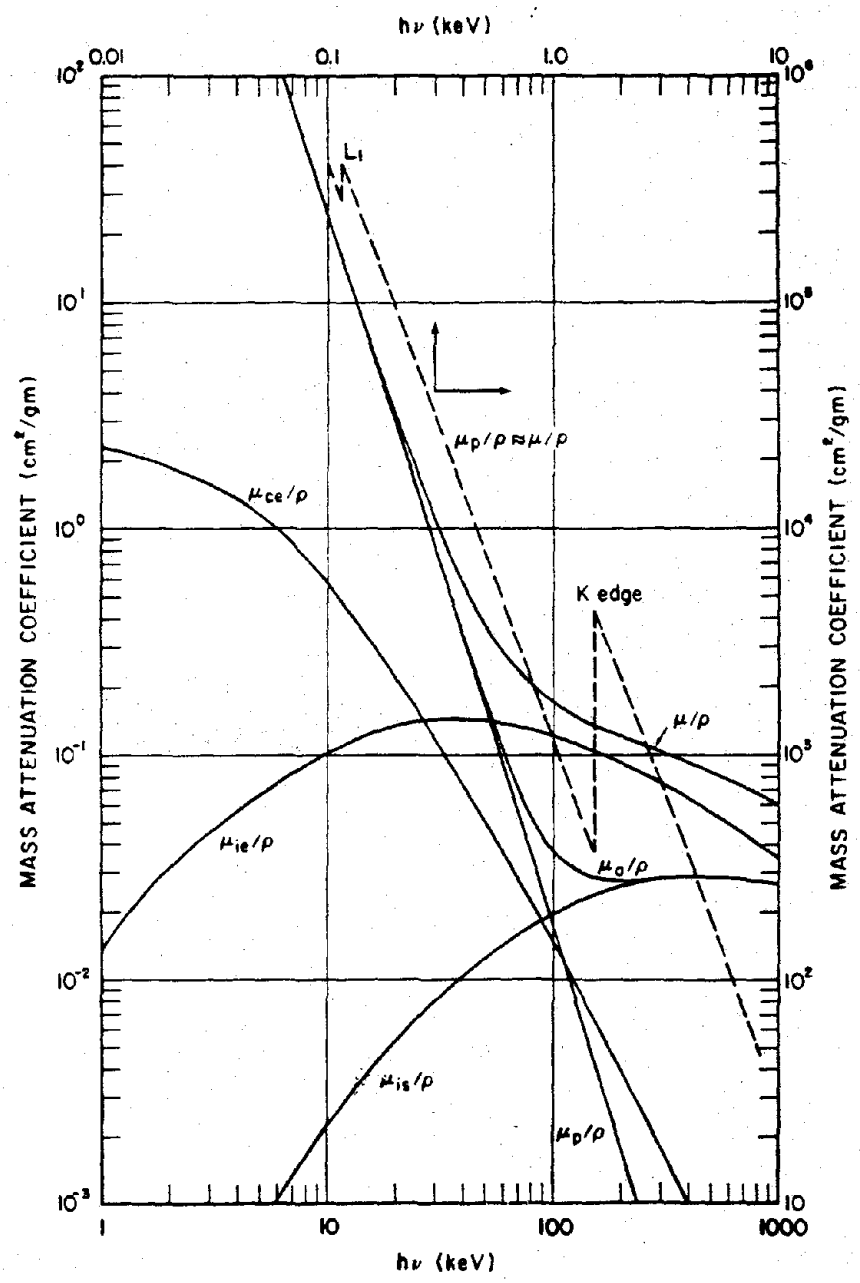

Figure 9-28. [redacted] Photon Cross Sections in Aluminum [redacted]

[redacted]

[redacted]

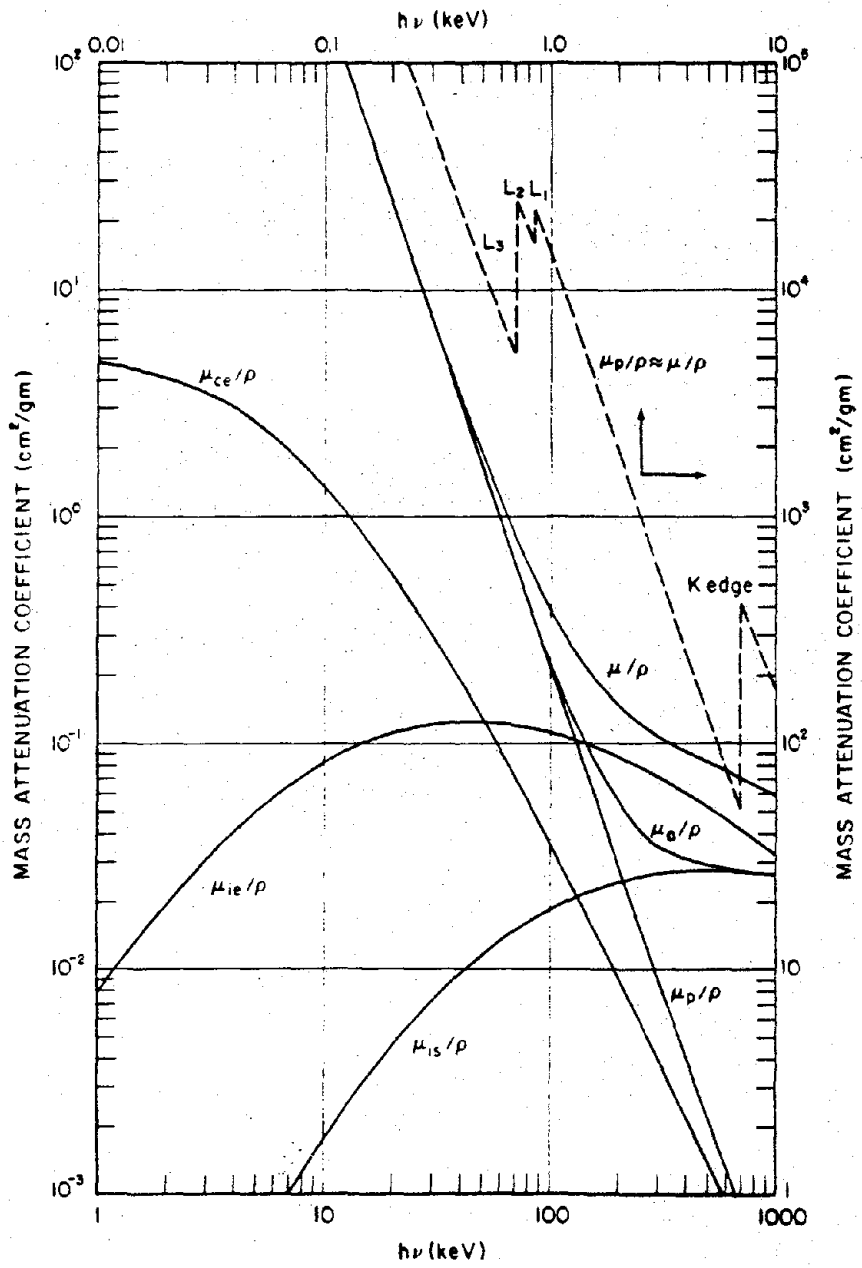

Figure 9-29. [redacted] Photon Cross Sections in Iron [redacted]

[redacted]

[redacted]

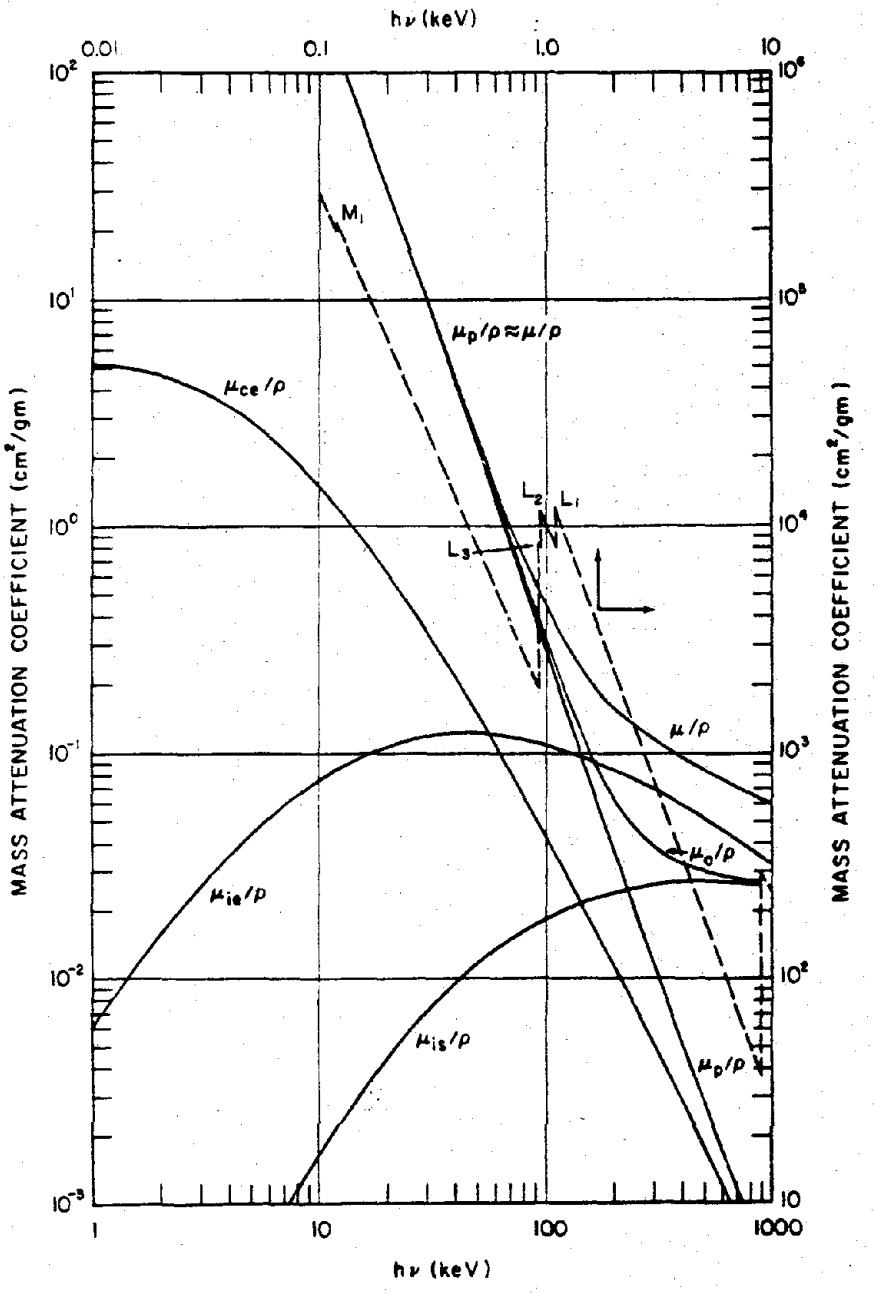

Figure 9-30. [redacted] Photon Cross Sections in Copper [redacted]

[redacted]

[redacted]

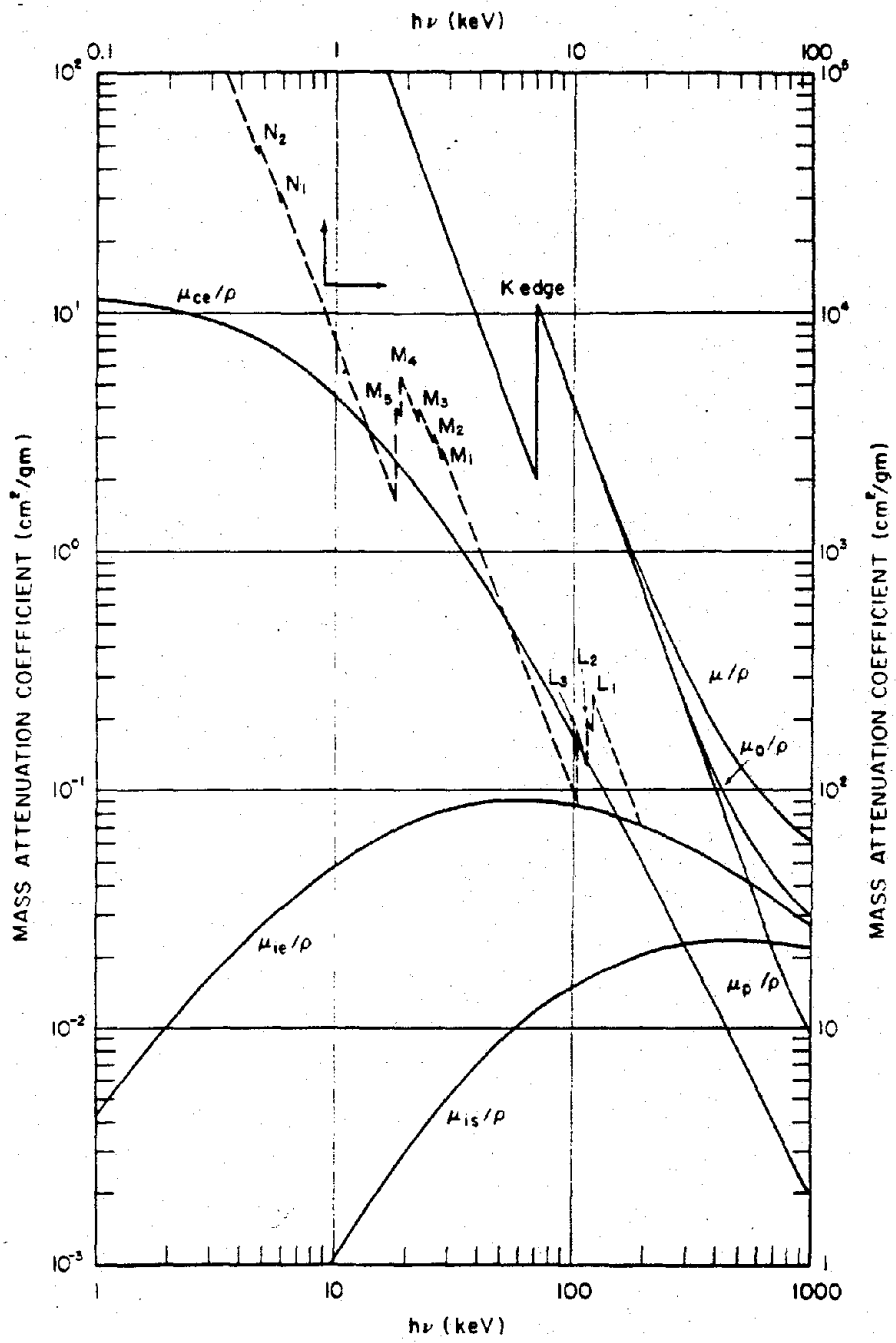

Figure 9-31. [redacted] Photon Cross Sections in Tungsten [redacted]

[redacted]

[redacted]

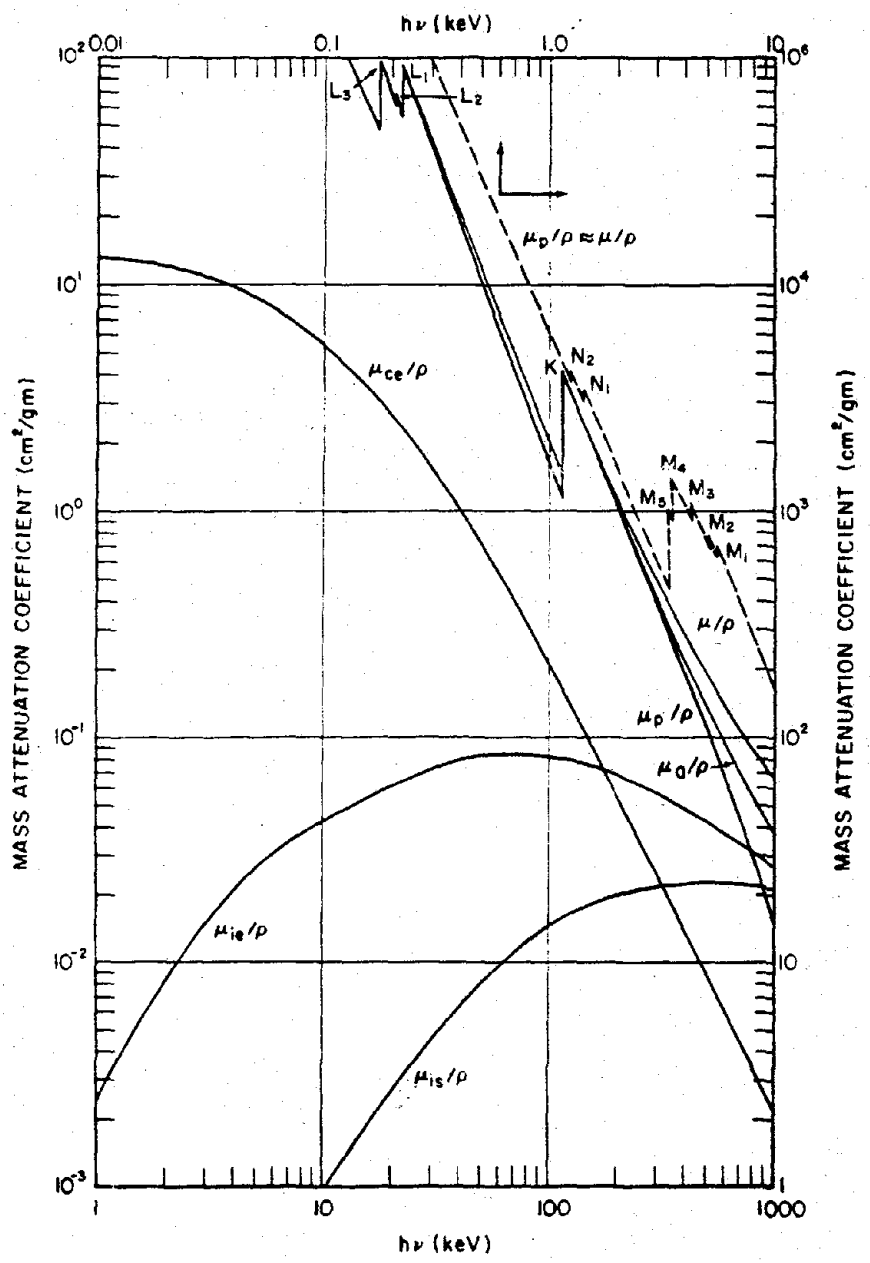

Figure 9-32. [redacted] Photon Cross Sections in Uranium [redacted]

[redacted]

[redacted]

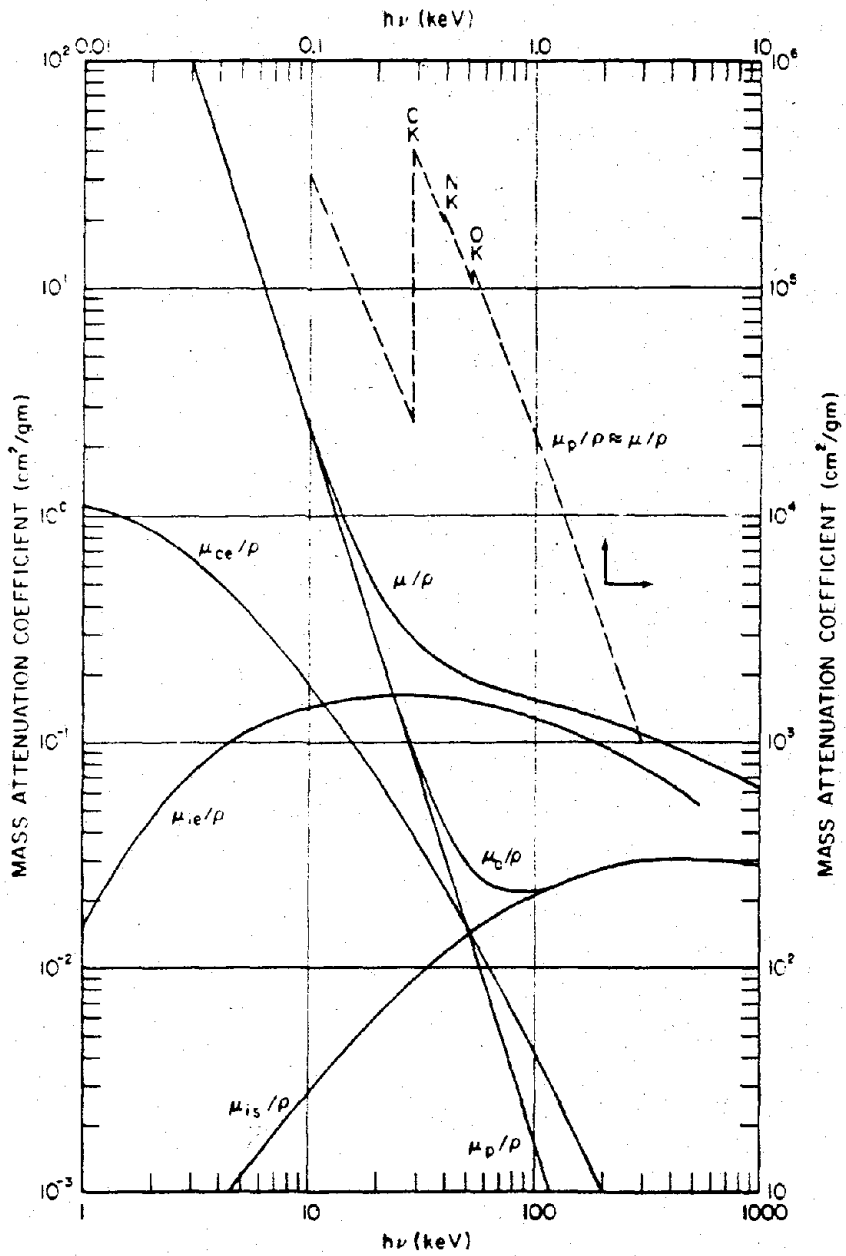

Figure 9-33. [redacted] Photon Cross Sections in Carbon Phenolic (CP), $\bar{Z}$ = 6.08 [redacted]

[redacted]

7

[redacted]

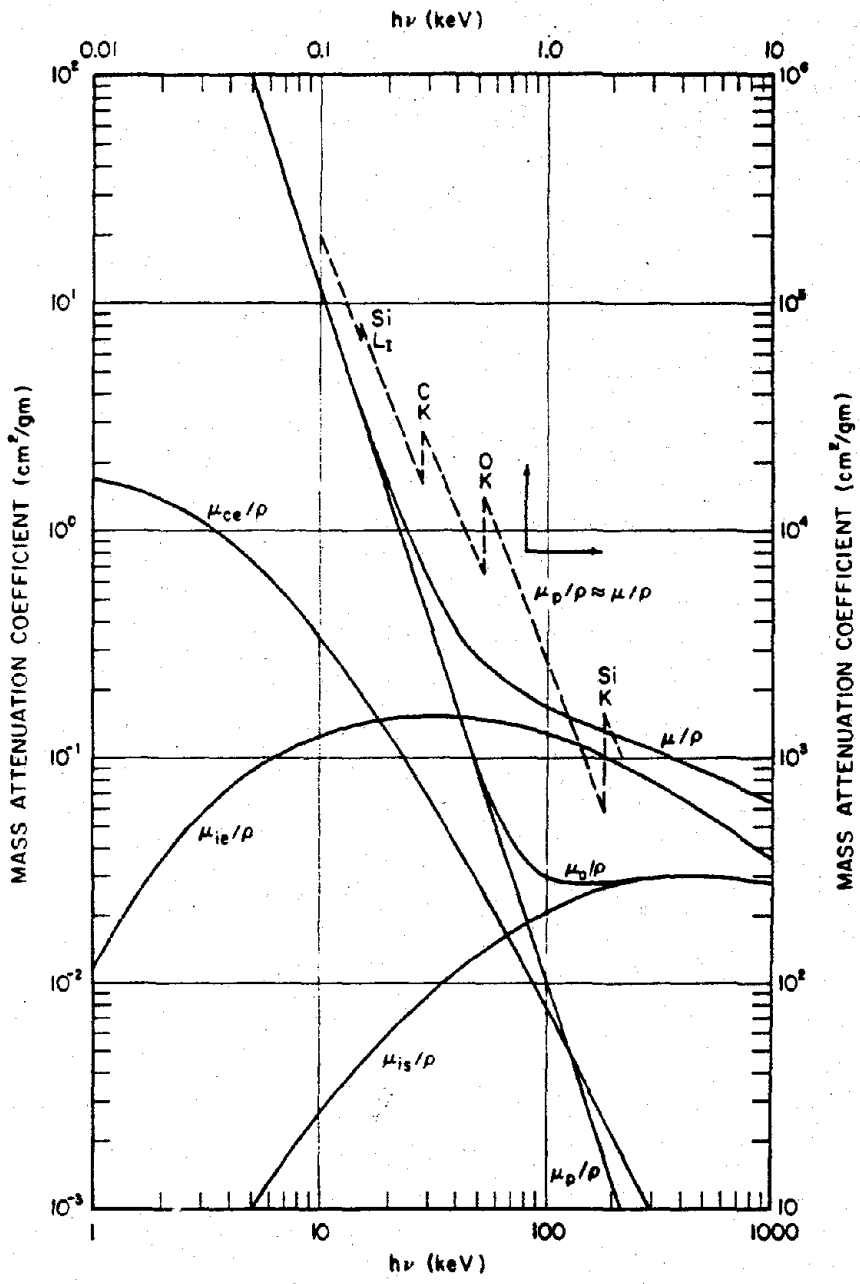

Figure 9-34. [redacted] Photon Cross Sections in Tape Wound Silicon Phenolic (TWSP), $\bar{Z}$ = 9.01 [redacted]

[redacted]

[redacted]

9-35 X-ray Energy Deposition Summary [redacted]

[redacted] The methods described in paragraphs 9-33 and 9-34 and illustrated in Problems 9-3 and 9-4 allow the calculation of curves that show approximations of energy deposition as a function of depth for black body spectra incident on any material, if the cross sections are known for the material [redacted]

INITIAL PRESSURIZATION OF MATERIALS DUE TO X-RAY DEPOSITION [redacted]

[redacted] An immediate consequence of the deposition of X-ray energy is the rapid heating of the material. This heating causes an initial pressure distribution as a function of depth in the structure. The initial pressurization generates shock waves that propagate through the thickness of the shell of the structure. The heating can result in a solid material changing phase, that is, melting or vaporizing. The melting and vaporization cause blowoff, which imparts an impulse to the structure and excites whole structure modes of response.

9-36 Phase Changes Induced by X-ray Heating [redacted]

[redacted] In most nuclear weapon X-ray environments, the X-ray energy is deposited in a very short time, a few nanoseconds to a few hundred nanoseconds. The material cannot expand appreciably during this time, so the energy deposition process can be considered to occur at a constant volume or at normal material density, ρ_0. Rapid melting and vaporization are accompanied by enormous pressure increases. Values

[redacted]

[redacted]

DNA
(b)(3)

Deleted

Figure 9-35. [redacted] Energy Deposited in Aluminum by Black Body Spectra [redacted]

[redacted] [redacted]

[redacted]

Deleted

Figure 9-36. [redacted] Energy Deposited in Copper by Black Body Spectra [redacted]

[redacted]

[redacted]

DNA
(b)(3)

Deleted

Figure 9-37. [redacted] Energy Deposited by Black Body X-ray Spectra in Carbon Phenolic (CP) [redacted]

[redacted] [redacted]

[redacted]

Deleted

Figure 9-38. [redacted] Energy Deposited by Black Body X-ray Spectra in Tape Wound Silica Phenolic (TWSP) [redacted]

[redacted] [redacted]

[redacted]

[redacted]

for enthalpy changes for melting and vaporization for the metals discussed in the previous subsection are given in Table 9-17. These values are for one atmosphere pressure. In most X-ray problems of interest the material is initially at very high pressure, so these values can be considered to be only approximate. This approach is not correct for ablators as a class although it might apply to carbon phenolic in a cold environment. Confining the discussion to metals will not restrict the transfer of principles.*

[redacted] The rising pressure that results from heating at constant density is illustrated in Figures 9-39 and 9-40 where isoenergy lines of aluminum are shown in pressure-density plots. If the internal energy is above the critical energy, 3,016 cal/gm for aluminum, the material can be considered as a vapor. Figure 9-40 shows the high pressure, high energy intercepts with the normal density abscissa (ρ_0 = 2.7 gm/cm^3). The release adiabats for expansion from density ρ_0 to low density and pressure also are shown in this figure. Expansion along the adiabat results in decreasing internal or potential energy as the material develops kinetic energy during "blowoff." For example, a 6,000 cal/gm energy deposition in aluminum at ρ_0 = 2.7 gm/cm^3 results in a pressure of about 1.5 megabars (Mb). The aluminum would expand from that state to low pressure and density, with final internal energy of about 3,000 cal/gm and about 3,000 cal/gm of kinetic energy. The 3,000 cal/gm of internal or potential energy is used to overcome the physical and chemical forces that bind the atoms together in the solid. This leads to the concept of heat of sublimation. The heat of sublimation at absolute zero, E_{so}, is the energy required to form the saturated vapor from the solid at a temperature of absolute zero. Thus, E_{so} does not include any energy of kinetic motion. The energy of sublimation generally is a function of temperature becoming larger for larger deposition energies (temperatures).

* [redacted] The problem of phase changes in a composite heat shield ablator is more complicated since different deposition profiles, material enthalpy, and thermal conductivities are involved in the calculations. While some materials, e.g., tape-wrapped carbon phenolic, may behave like metals in a cold environment, the techniques described here generally are not applicable to the description of the blowoff process in the broad category of composite materials that use three dimension (3-D) weaves for heat shields or for X-ray shields that use dispersed high Z materials for loading.

Table 9-17. [redacted] Enthalpy Change for Selected Metals [redacted] (cal/gm)

Metal-Atomic Weight	To Melt	Through Melt	To Vapor	Through Vapor	Sublimation Energy
Be 9.013	876.0	1,187.0	2,147.0	10,040.0	8,682.0
Al 26.98	160.4	255.3	771.1	3,347.0	2,891.0
Fe 55.85	250.8	315.8	573.0	2,071.0	1,782.0
Cu 63.54	110.0	160.0	336.0	1,481.0	1,275.0
W 183.85	153.9	200.0	304.0	1,353.0	1,110.0
U 238.00	49.0	64.5	171.9	596.1	492.1

[redacted] [redacted]

[redacted]

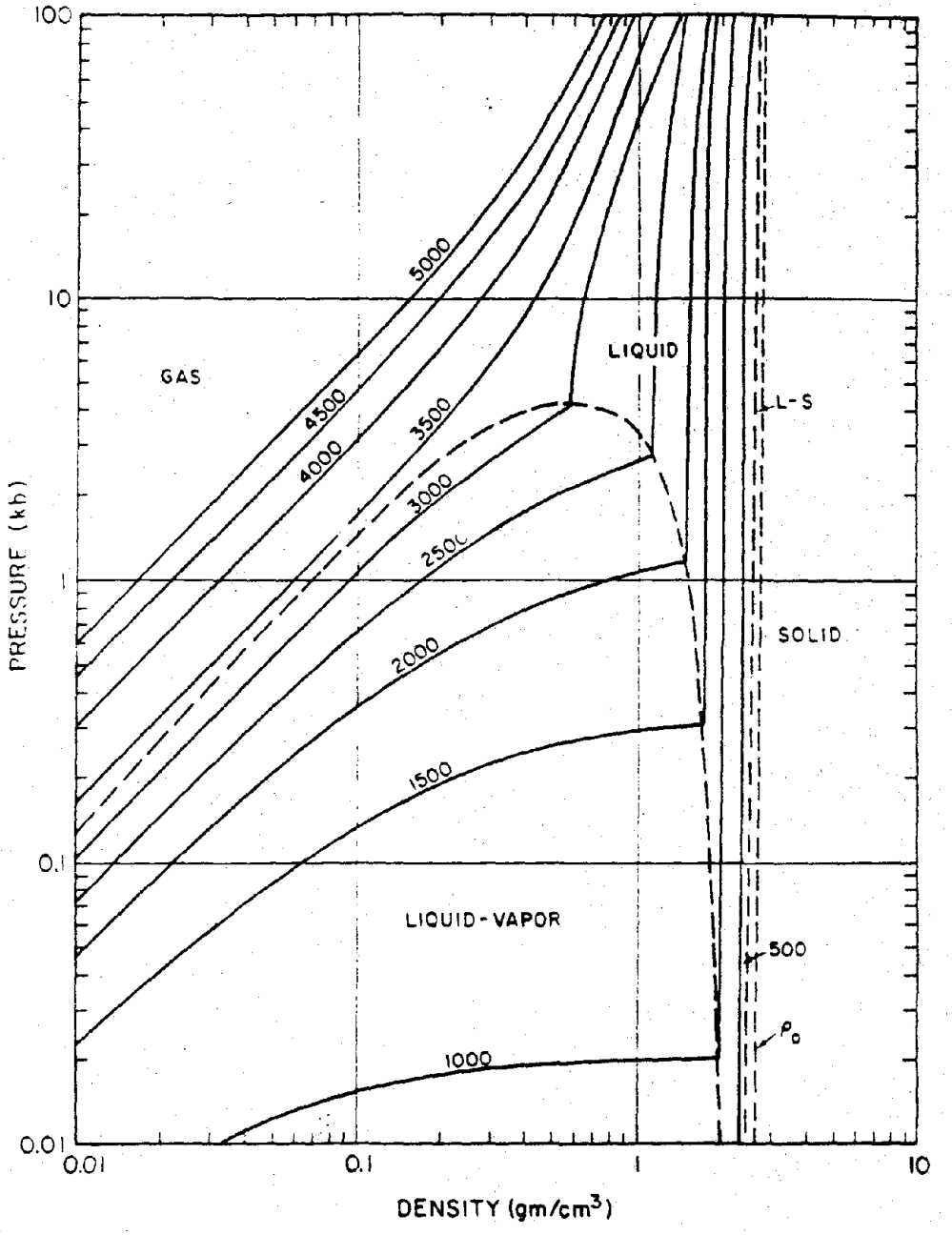

Figure 9-39. [redacted] Aluminum Isoenergy Lines.
Parameter is Energy in cal/gm [redacted]

[redacted]

[redacted]

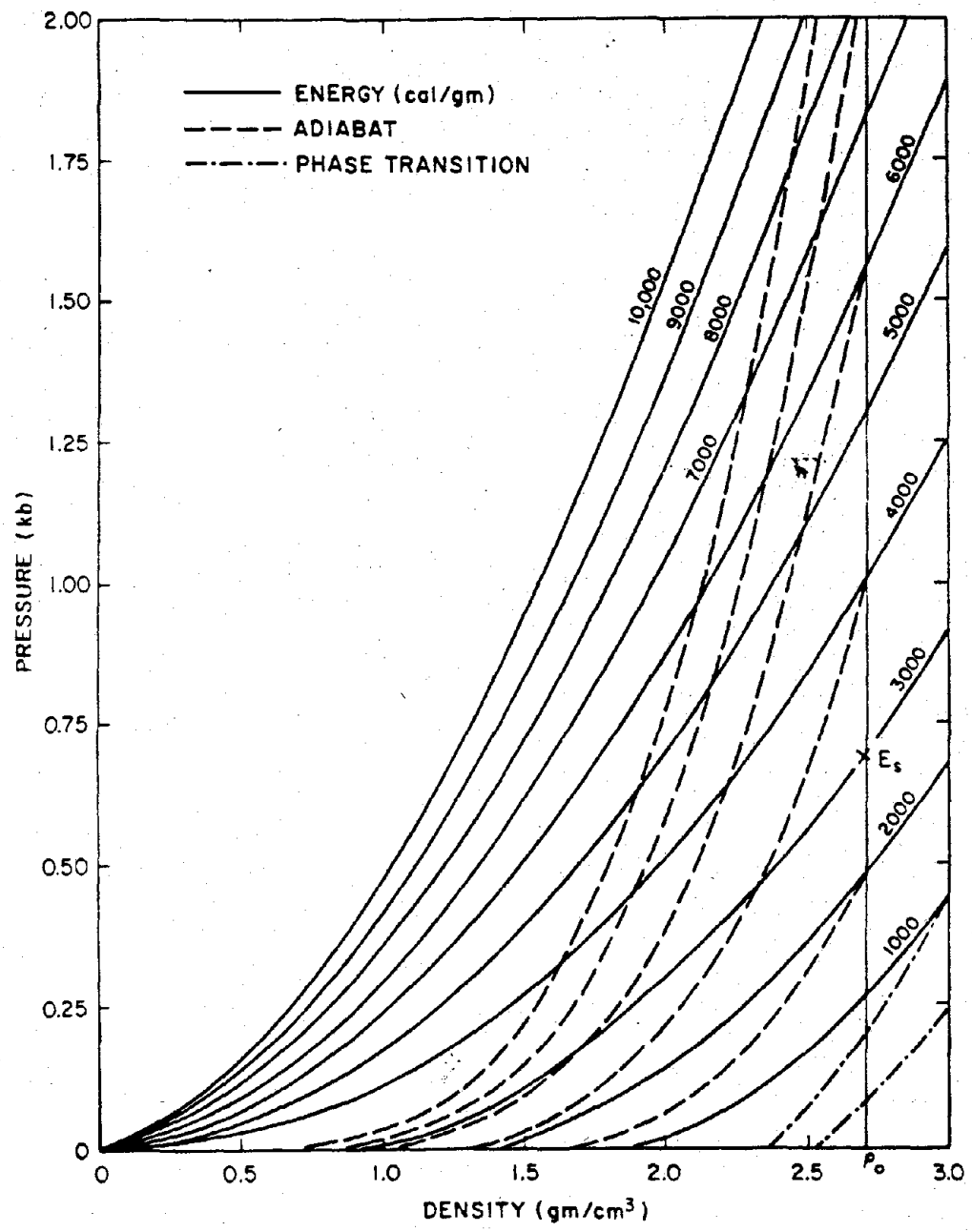

Figure 9-40. [redacted] Aluminum Isoenergy Lines and Adiabats [redacted]

[redacted]

[redacted]

9-37 The Grüneisen Parameter and the Equation of State [redacted]

[redacted] As a first approximation to the equation of state of material, it is assumed that the pressure in the material increases linearly with the deposited internal energy per unit volume,

$$P = G\eta\epsilon,$$

where G is the Grüneisen ratio for the material, ϵ is the internal energy per unit volume, and $\eta =$

[redacted]

[redacted]

ρ/ρ_o, the ratio of the density to a normalized density of the material, usually the ambient density. In codes used to calculate shock wave propagation, for example the PUFF type codes, more elaborate equations of state are used to fit the experimentally determined behavior of the solid and vapor phases. The equations used in the PUFF codes reduce to the equation given above when $\eta = 1$, and generally only one value of G is used to specify a material.

[redacted] Although there may be small errors in calculating the X-ray energy deposition as a function of depth, the significant sources of errors in pressure predictions are the accuracy and validity of the Grüneisen parameter for solid and vapor equations of state. Experimental values of G obtained by different methods result in factors of about two uncertainty even for some of the common materials such as aluminum, beryllium, and tungsten. Even though indications are that G is not well known as a function of deposited energy, some very good correlations have been obtained for computed and measured values of pressure waves in X-ray tests, when careful calculations are made employing elastic plastic properties of the materials.

[redacted] Initial pressurization in distended materials such as porous metals and foams present a particularly difficult and uncertain condition for current analytical techniques.

[redacted] The units for ϵ in the equation given above are energy per unit volume, which have the same dimensions as pressure. Therefore, the energy required in cal/gm for a phase change can be expressed in units of pressure, if the density of the material is specified. If the internal energy, E, is given per unit mass, the relation to ϵ is

$$\epsilon\ (\text{cal/cm}^3) = E\ (\text{cal/gm})\ \rho_o(\text{gm/cm}^3).$$

The value of ϵ in megabars may then be obtained by the relation

$$\epsilon\ (\text{Mb}) = \epsilon\ (\text{cal/cm}^3) \times 4.18 \times 10^7 \left(\frac{\text{erg}}{\text{cal}}\right) \times 1 \left(\frac{\text{dyne} \cdot \text{cm}}{\text{erg}}\right) \times 1 \left(\frac{\text{Mb}}{10^{12}\ \text{dyne/cm}^2}\right)$$

$$\epsilon\ (\text{Mb}) = 4.8 \times 10^{-5}\ \epsilon \left(\frac{\text{cal}}{\text{cm}^3}\right)$$

$$= 4.18 \times 10^{-5}\ \rho_o E \left(\frac{\text{cal}}{\text{gm}}\right).$$

Thus, the previous equation for pressure may be written

$$P\ (\text{Mb}) = G\ \frac{\rho}{\rho_o}\ \epsilon\ (\text{Mb}),$$

or

$$P\ (\text{Mb}) = 4.18 \times 10^{-5}\ G\rho\ E\ (\text{cal/gm}).$$

The enthalpy changes of the metals shown in Table 9-17 in cal/gm are given in Table 9-19.

Table 9-19. [redacted] Enthalpy Changes ϵ (Mb) [redacted]

Metal	ρ_o (gm/cm^3)	To Melt	Through Melt	To Vapor	Through Vapor	Sublimation Energy, E_s
Be	1.85	0.068	0.0918	0.166	0.776	0.671
Al	2.70	0.0181	0.0288	0.087	0.378	0.326
Fe	7.86	0.0824	0.1036	0.188	0.680	0.585
Cu	8.92	0.0410	0.0596	0.125	0.552	0.475
W	19.3	0.124	0.161	0.245	1.092	0.895
U	18.7	0.0383	0.0504	0.134	0.466	0.385

[redacted]

[redacted]

Table 9-20. [redacted] Pressure Change, P (Mb) [redacted]
($\rho = \rho_o$, $\eta = 1$)

Metal	G	To Melt	Through Melt	To Vapor	Through Vapor	Sublimation Energy, E_s
Be	1.45	0.099	0.133	0.241	0.12	0.973
Al	2.13	0.0386	0.0613	0.185	0.805	0.694
Fe	1.69	0.139	0.175	0.318	1.15	0.989
Cu	2.00	0.082	0.119	0.250	1.10	0.950
W	1.43	0.177	0.230	0.350	1.56	1.28
U	2.03	0.078	0.102	0.273	0.946	0.782

[redacted]

The pressures associated with these changes at ambient density, i.e., when $\rho = \rho_o$, and P (Mb) = $G\epsilon$ (Mb), are shown in Table 9-20.

[redacted] From Table 9-20, aluminum has a sub[redacted]mation pressure of about 0.7 Mb at ambient density, corresponding to sublimation energy of about 2,900 cal gm (Table 9-17). This point is shown in Figure 9-40, labeled E_s at about 3,000 cal gm. Table 9-20 indicates that the pressures associated with vaporization of metals at ambient density are with some exceptions about 1 Mb. A survey of more than 30 common metal elements indicates that an average of 1 Mb for vaporization is a good approximation, especially if the Grüneisen value for the material is uncertain. Since a bar corresponds to 14.7 psi a Mb is the enormous pressure of about 1.45×10^7 psi. Thus, tremendous forces are involved in the pressure gradients associated with metal vaporization at ambient density. Table 9-17 shows that vaporization usually involves several thousand calories per gram of energy. High explosive materials (TNT, etc.) release about 1,000 cal/gm. Therefore, on a mass basis there is more energy associated with metal vaporization than with high explosives. Generally, the thicknesses of material evaporated by X-ray absorption is small, and, the total mass of material that is vaporized generally is small.

[redacted] SHOCK WAVE PROPAGATION AND DAMAGE PREDICTIONS [redacted]

[redacted] The sequence of events for the generation and propagation of a stress wave through the thickness of an aerospace shell and the damage produced is illustrated in Figure 9-41. Cold X-rays are deposited primarily in a relatively thin sheet of material at the front surface (Figure 9-41a). After the energy is deposited a compression wave propagates inward from the front surface, followed by a rarefaction that causes the vapor and liquid to blow off (Figure 9-41b). This rarefaction also may cause a spall of solid material from the front surface (Figure 9-41c). Later the compression wave reflects from the back surface and returns as a rarefaction wave. This rarefaction wave, or the coincidence of this wave with the rearward moving rarefaction may cause the rear surface to spall (Figure 9-41d), or may cause fracturing or debonding. This process occurs within the order of a microsecond and generally is complete before the overall structural motion occurs. The shock effects are

[redacted]

[redacted]

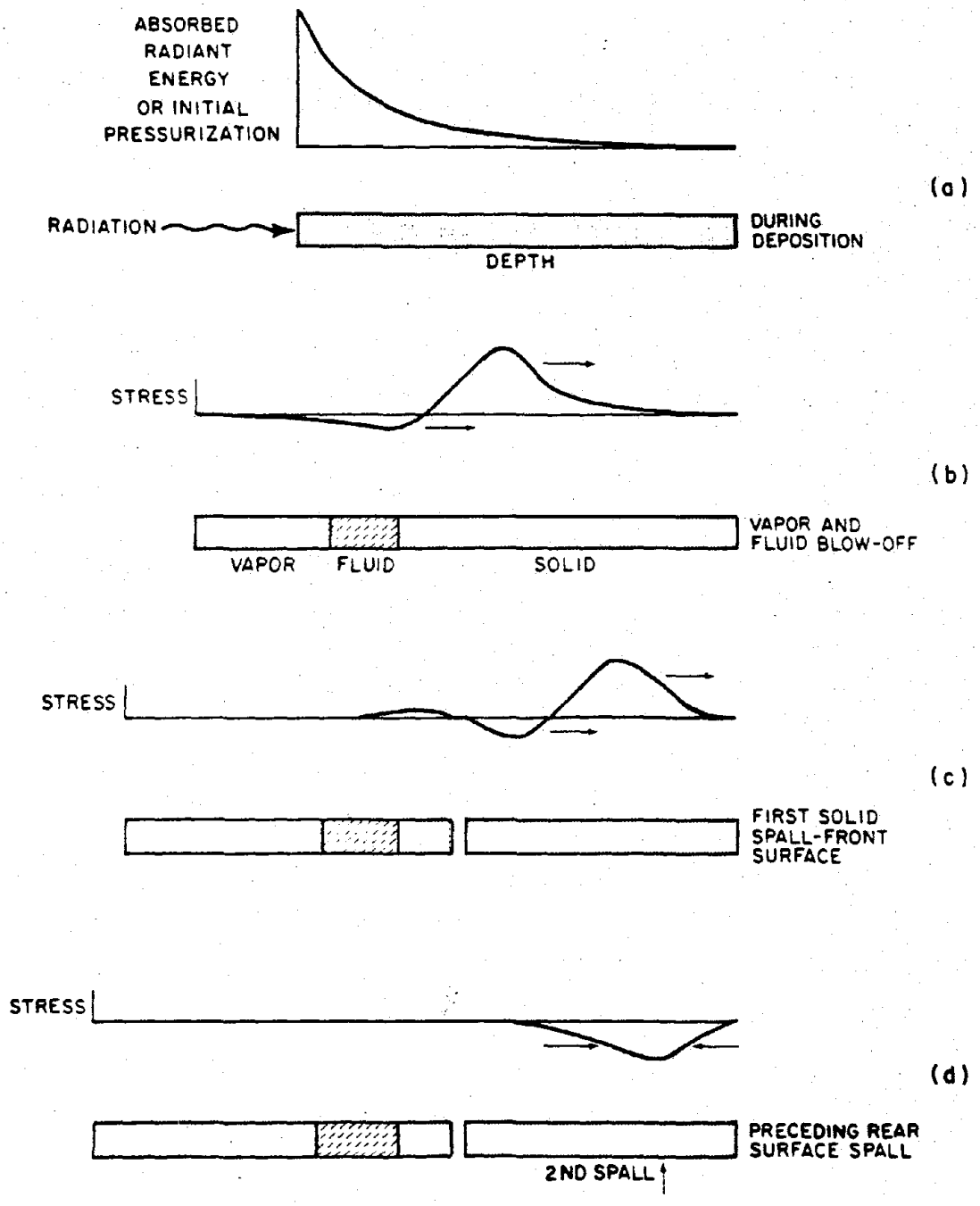

Figure 9-41. [redacted] Sequence of Spallation Following Radiation Deposition [redacted]

[redacted]

[redacted]

[redacted]

extremely local, depending on the sheet thickness and not on the overall geometry of the structure, so spall damage, including fracturing and debonding, usually cannot be scaled according to the laws that govern structural behavior. Since the spall damage occurs early, possibly weakening the structure, it can have a strong effect on the subsequent response to the structure to the impulse that has been imparted.

[redacted] Propagation of stress waves and the damage predictions are not amenable to hand calculations. Most stress wave propagation calculations are performed on computers using one dimensional (1-D) models to represent a cross section of an aerospace vehicle shell. These stress wave propagation calculations are used routinely in design analysis and are the direct outputs of PUFF-like codes or their variations. The stress wave propagation predictions are used to:

1. Obtain a calculated pressure time history at the rear surface of a 1-D sample for direct comparison to experimental values that are obtained by laboratory simulation or by underground nuclear tests. The agreement or lack of correlation serve as an important criteria for judging the adequacy of analytical techniques. The conclusions are almost universal that the largest sources of error in stress wave propagation codes are associated with the mechanical aspects of the material behavior, such as failure criteria, and the elastic-plastic models, which should include strain rate and temperature dependence.

2. Obtain maximum tension as a function of depth in the materials to indicate regions of potential material failure, debonding, and spalling. Definitions that are required for the materials failure level under these dynamic tensile loads are obtained experimentally.

3. Obtain input data for structural response analysis.

[redacted] There also are some 2-D shock propagation codes being used for specific calculations involving cylinders, nose tips, etc. Peak pressure predictions using pure hydrodynamic representations of the material in code calculations are generally high by a factor of 2 to 4. If a dynamic elastic-plastic constitutive relationship is included, the predictions are improved significantly.

9-38 Through-the-Thickness Elastic-Plastic Shock Propagation [redacted]

[redacted] Considerable progress has been made in correlating measured and calculated through-the-thickness shock propagation in one dimension by using the elastic-plastic materials description in PUFF-type codes. The stress strain diagram shown in Figure 9-42 illustrates a two-wave nature of the elastic-plastic shock wave propagation. The total stress, σ, is the sum of the hydrostatic pressure, P, and an elastic stress offset of $2/3\ Y_o$, where Y_o is the yield strength of the material (its compressive yield strength if that is different from its yield strength in simple tension). The effect of the yield stress path OAB is to propagate two stress waves having different velocities into the undisturbed material. The slope of the elastic portion, OA, is larger than the plastic portion, AB. The propagation speed is larger if the slope of the stress strain curve is larger. Hence, an elastic precursor shock traveling with the elastic velocity, c_E, runs in front of the slower total stress wave which propagates with a bulk sound speed, c_o

$$c_E = \sqrt{\frac{K}{\rho_o} + \frac{4/3S^*}{\rho_o}}$$

$$c_o = \sqrt{\frac{K}{\rho_o}}$$

where K is the bulk modulus and S^* is the shear modulus.

[redacted] An elastic rarefaction stress ($4/3\ Y_o$ or twice the stress offset) propagates from the rear of the shock wave at velocity c_E and overtakes

[redacted]

[redacted]

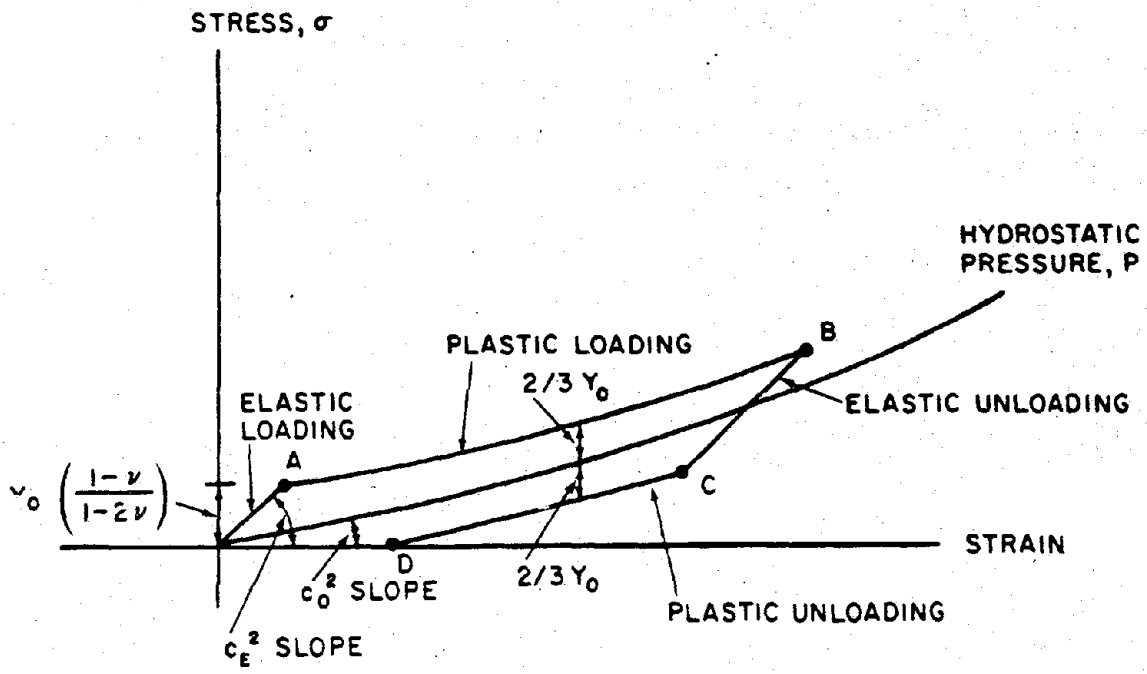

Figure 9-42. [redacted] Equation of State for Elastic-Plastic Material Description [redacted]

[redacted]

the slower plastic wave (path BC). This rarefaction wave causes a greater attenuation of the main stress pressure wave than is obtained in pure hydrodynamic calculations (up and down the Hugoniot). This greater attenuation of the elastic plastic wave propagation compared to purely hydrodynamic calculations results in better correlation with measured values of stress. The plastic unloading to a stress-free condition, path CD in Figure 9-42, also propagates with velocity c_0 and completes the cycle.

[redacted] Although the elastic-plastic code calculations improved the correlation of measured and computed through-the-thickness stresses for some materials, if a material has strong strain rate or temperature dependence these features also must be incorporated into the calculations. Stress wave propagation through materials such as foams require an entirely different constitutive expression, and anisotropic materials such as three-dimensional quartz phenolic, can have quite different material properties in different directions. Similarly, propagation characteristics of inhomogeneous materials or materials that contain small radiation absorbers lead to complicated propagation analysis. Propagation in these materials has not been treated in an analytically satisfactory manner. Most of the current analytical techniques used in the solution of stress wave propagation in the materials are deficient in varying degrees in the following ways.

1. There is incomplete understanding of the material behavior under the types of conditions that result from X-ray energy deposition, so the material representations are inadequate in most cases.

2. Experimental data for verification and modification of the equations of state and con-

[redacted]

[redacted]

[redacted]

[redacted] stitutive relations in the analytical techniques have been limited and of poor quality.

9-39 Through-the-Thickness Material Response [redacted]

[redacted] Simulation tests and underground nuclear weapons tests can identify failure and damage modes that result from shock wave propagation and through-the-thickness material response on samples that are meaningful in terms of the expected response of reentry vehicles or aerospace shells. The experimental results are most meaningful when appropriate analytical techniques are used to correlate the experimental results with the stress wave characteristics producing the response modes. Hundreds of complex aerospace structure composites as well as samples of metals and plastics have been exposed during underground nuclear weapons tests at various X-ray fluence levels with different X-ray spectra and deposition times.

[redacted]

DNA (b)(1)

[redacted] DNA (b)

[redacted] IMPULSE AND STRUCTURAL RESPONSE ANALYSIS [redacted]

[redacted] The vapor and/or liquid blowoff following X-ray deposition imparts a reactive impulse to the aerospace structure. The structural response takes place for the most part after the shock wave discussed in the last section has dissipated. This shock wave may have damaged or weakened the structure by spallation, debonding, or fracture. The damage to the structure should be considered in the structural response analysis if an accurate prediction is to be made. Obviously, this is a complicated problem and is not amenable to hand calculation. However, some rough estimates of impulse can be made and serve to illuminate the processes that take place.

[redacted]

DNA (b)(1)

9-40 Impulse Calculations [redacted]

[redacted]

DNA (b)(1)

[redacted]

Page 9-108 deleted.

[redacted]

DNP
(1-13)

Deleted

Figure 9-43. [redacted] Normalized Vapor Impulses Produced in Aluminum by Various Black Body X-ray Spectra [redacted]

[redacted] [redacted]

[redacted]

DNA
(1-)(3)

Figure 9-44. [redacted] Normalized Vapor Impulses Produced in Copper by Various Black Body X-ray Spectra [redacted]

Deleted

[redacted] [redacted]

Pages 9-111 and 9-112 are deleted.

[redacted]

Problem 9-5. Calculation of Vapor Blowoff Impulse

[redacted] The information presented in the preceding paragraphs provides a means to obtain an approximation of blowoff impulse for certain materials. The following example is presented to illustrate the procedures. In practice, these calculations are performed with computer codes.

DNA (1)(3)

[redacted]

Related Material: See paragraphs 9-34 through 9-37, and 9-40. See also Figures 9-35 through 9-38, 9-43 and 9-44, and Table 9-17.

[redacted] [redacted]

[redacted]

Problem 9-6. Calculation of the Location of Phase Change Boundaries

[redacted] The preceding paragraphs provide the information necessary to calculate the location of the various phase change boundary layers. The procedure is illustrated in the following example.

DNA (b)(3)

[redacted]

Related Material: See paragraphs 9-34 through 9-37, and 9-40. See also Table 9-17 and Figure 9-35.

[redacted] [redacted]

[redacted]

9-41 Structural Response Analysis

[redacted]

Most of the structure response analyses of reentry vehicles have been developed for survivability. Since low level failure criteria responses have been selected, only elastic deformation has been considered. Such survivability analyses are probably inadequate for the determination of inelastic deformation failure modes and the levels required to define lethality. Essentially all structural response calculations require data on: (1) structural material properties such as stress and strain relations as a function of strain rate and temperature, for yield, stress and strain, fracture points, elastic moduli, and so forth; (2) structural response forcing functions, including asymmetric impulse loads, and in-depth heating and thermal loads applied as distributed and point loads; and (3) structural variation in shell wall thickness and material densities in various layers.

[redacted]

[redacted] REENTRY VEHICLE HARDENING [redacted]

[redacted] X-ray hardening refers to techniques

[redacted]

[redacted]

that reduce the susceptibility of reentry vehicles to damage from X-rays. [redacted] It is beyond the scope of this manual to provide a complete discussion of reentry vehicle hardening techniques. Therefore, a brief general discussion of the techniques, with a few specific examples, is presented in the following paragraphs.

DNA (b)(3)

[redacted]

DNA (b)(3)

9-42 Balanced Hardening with Respect to Neutrons and X-rays [redacted]

[redacted]

[redacted]

Page 9-117 deleted.

[redacted]

[redacted]

DNA (b)(3)

SECTION VI

[redacted] NUCLEAR RADIATION SHIELDING [redacted]

[redacted] Any mass of material between a nuclear radiation source and personnel or sensitive equipment will reduce the dose to the personnel or equipment compared to the free field dose at the same location relative to the source. The dose received by a person behind a building, in a building, in a field fortification, in a tank, or in a

[redacted]

[redacted]

[redacted]

ship will be less than that which would be received in an exposed free field position.

[redacted] In principle, it would be possible to calculate the dose behind a shield by using simplified neutron and gamma ray transport equations similar to those given in Chapter 5; however, several considerations make hand calculations impractical.

- The neutrons and gamma rays will arrive at the shield from many directions after having been scattered during their transport through the atmosphere.
- Calculation of radiation transport from a point source through single geometries can be done with reasonable accuracy by using an exponential factor and a buildup factor similar to those described in Section I, Chapter 5 for transport through homogeneous air, but the geometries of shielding enclosures are seldom simple, and, as mentioned above, the radiation incident on the shield is not unidirectional. This has the effect of making the problem similar to a multi-source problem.
- The attenuation of neutrons by inelastic scatter or radiative capture results in the emission of one or more gamma rays, which can contribute to the dose within the shielded area even though the neutrons are removed from the penetrating radiation beam.
- The specific location of the burst and the receiver can affect the degree of attenuation, e.g., different members of a tank crew will have different degrees of protection from the same explosion, and any particular member of the crew will have a different degree of protection from initial radiation from bursts at different locations relative to the tank. In other words, each location within each shielded structure must be evaluated separately, or at least a sufficient number of locations must be evaluated to determine the overall shielding efficiency of the structure or piece of equipment.

These complexities, and others, make it necessary to use computer codes to determine the shielding efficiency of any structure or piece of equipment. Even when using the codes, some simplification in the description of the shield geometry usually is necessary. However, satisfactory methods for treating fairly complex geometries have been developed. These are described in DASA 1892, "Weapons Radiation Shielding Handbook" (see bibliography). Results of some sample calculations are also provided. Unfortunately, sufficient calculations have not been performed to permit the development of a generalized simple method for shielding calculations that would be suitable for inclusion in this manual.

[redacted] Table 9-22 provides some estimates of the shielding afforded by various structures and types of military material. These estimates are given in terms of a "dose transmission factor," which is defined as the ratio of the dose measured behind the shield to the dose that would be measured in the absence of the shield. Some of the transmission factors shown in Table 9-22 were obtained by measurements at weapon tests or are extrapolations from such measurements. Other transmission factors were obtained by relatively detailed calculations, while still others are mere estimates. Ranges of values are given for the dose transmission factors for most structures. These ranges result from two causes: uncertainty in the estimates themselves, and variations in the degree of shielding that may be obtained at different locations within a structure. Separate transmission factors are given for initial gamma rays and residual (fallout) gamma rays for two reasons: the average energy of the initial gamma rays is higher than the average energy of the residual gamma rays, and there are different source geometries.

[redacted]

[redacted]

Table 9-22. [redacted] Estimated Dose Transmission Factors (Interior Dose/Exterior Dose) [redacted]

DNA
(b)(1)

Deleted

[redacted]

[redacted]

[redacted] No specific reliability can be attached to the dose transmission factors shown in Table 9-22. They are felt to be reasonable values for generalized applications; however, specific shielding problems should be addressed by methods such as those described in DASA 1892.

SECTION VII

[redacted] TREE – COMPONENT PART AND CIRCUIT RESPONSE [redacted]

[redacted] This section contains a discussion of the effects of nuclear radiation on electronic component parts and circuits. The intent is to provide an introduction to the failure modes and responses that result from ionization, displacement, and thermomechanical shock. A more detailed description of the effects is contained in the TREE Handbook (see bibliography).

[redacted] Since semiconductor devices generally are considered to be the most sensitive devices in an electronic circuit, emphasis is placed on them. However, the discussion does include other electronic component parts.

[redacted] Within the scope of this manual, this section can only aid in establishing levels where electronic equipment might experience failures as a result of the radiation environment and indicate the extent of the problems. The numbers presented are only estimates for a generic grouping or subgrouping. It must be understood that it is very difficult to give accurate radiation effects data for generic types of electronics. For example, transistors can show sufficient amplification loss to be useless after receiving 10^{10} to 10^{15} n/cm^2 ($E > 10$ keV, fission). That is 5 orders of magnitude difference and is relatively useless information. Fortunately, transistors can be subgrouped to improve their characterization. The problem of accurate prediction, however, is not completely solved. Even if one particular type of transistor is considered, the neutron fluence required to reduce the amplification to a particular value can vary more than an order of magnitude. Additionally, the failure threshold for a transistor in one circuit may be greatly different from the failure threshold for that same transistor in a different circuit, i.e., the response of each component part and the circuit configuration must be known to make a reasonable estimate of circuit response.

[redacted] The transient radiation effects are classified into three groups: transient, permanent, and thermomechanical. The transient effects result from nonequilibrium free-charge conditions introduced through the ionization phenomena (see Chapter 6). The permanent effects are attributed to physical property changes of the irradiated materials caused by energetic particles (neutrons and secondary electrons). The thermomechanical effects result primarily from the absorption of low energy photons.

[redacted] The class of effect is defined by the primary effect induced by the radiation. For example, the short term currents that result from ionization may trigger a digital state change or may permanently damage a device in some other manner. This phenomenon is treated as a transient effect, because the permanent consequences result from circuit action and/or device construction rather than from direct radiation induced material property change.

[redacted] The terms "radiation hardened" or "radiation resistance" frequently are connotated incorrectly. These terms mean that someone or some group has examined the component part, circuit, or system, made some modification and/or used part selection criteria and has determined that the electronics will withstand certain levels of certain types of radiation. The experience of the person making the examination as well as the resulting modifications can both vary widely. Consequently, when these terms are used they should be accompanied by the answers to the following questions.

- Hardened to what type of radiation?

[redacted]

[redacted]

[redacted]

- Hardened to what levels of radiation?
- What procedure was used for hardening?
- How has the hardening been verified?

Based on the answers to these questions, the applicability of that "hardened" component part, circuit, or system for his intended use can be judged.

[redacted] SEMICONDUCTOR COMPONENT PARTS [redacted]

9-44 Transient Effects [redacted]

[redacted] The transient effects observed in semiconductor devices exposed to nuclear radiation result from the creation of excess charge carriers (ionization) that cause current and voltage changes. These changes do not cause permanent damage directly to the semiconductor material. However, their presence may produce permanent changes as a result of current overloads to some components, loss of information stored in memory units, or by the creation of premature signals. Furthermore, such transients can cause saturation of some circuits for times that are long compared to the duration of the ionizing radiation pulse, and may thus cause system failure during a significant and possibly critical period.

[redacted] Most of the ionization produced in a nuclear weapon environment is due to the photons and 14-MeV-neutrons, although all nuclear radiation can contribute. Because of this predominance of photon excitation of carriers, the observed currents and voltages are often referred to as photocurrents and photovoltages, even though the prefix may not always be proper. The mechanisms whereby this ionization occurs are described in Chapter 6.

[redacted] Before discussing the transient effects in particular semiconductor devices, it is desirable to review briefly the important basic physical processes responsible for device behavior. These processes are common to all semiconductor devices and must be reasonably well understood before the description of the device response can be followed intelligently.

[redacted] Current is the manifestation of charge carrier movement within a material. As described in paragraph 6-4, the movement may be random, random with a diffusion from regions of high concentration to regions of low concentration, or, if an electric field is present, the movement may be a drift in the field superimposed on the normal random scattering. Carriers may be trapped by impurities, which are always present in solid state devices. Eventually, the trapped carriers may be annihilated by their mates (oppositely charged carriers) in a process called recombination. The net result of these processes is that the free carriers diffuse and/or drift until they are trapped and are then promptly recombined. Therefore, any electrical currents in the materials are considered to have two components – the drift component and the diffusion component. The time during which a charge carrier is free to move by drift and/or diffusion is called the lifetime of the charge carrier.

[redacted] The simplest semiconductor device is the diode. The diode is made up of pure semiconductor material doped with impurities so as to be considered to have two regions. Using pure silicon as the example, its atomic structure is considered to have four electrons in the outer orbit. In its crystal form, these outer orbiting electrons are considered to be shared with neighboring silicon atoms (see Figure 9-45). When the pure silicon is doped with an impurity, the impurity atom replaces one of the silicon atoms in the crystal lattice. The impurities are selected to have either three or five outer orbiting electrons. Silicon doped with an impurity having five outer orbiting electrons will have extra electrons that are more or less free to move around, and hence are available for conduction. Silicon doped with impurities with only

[redacted]

[redacted]

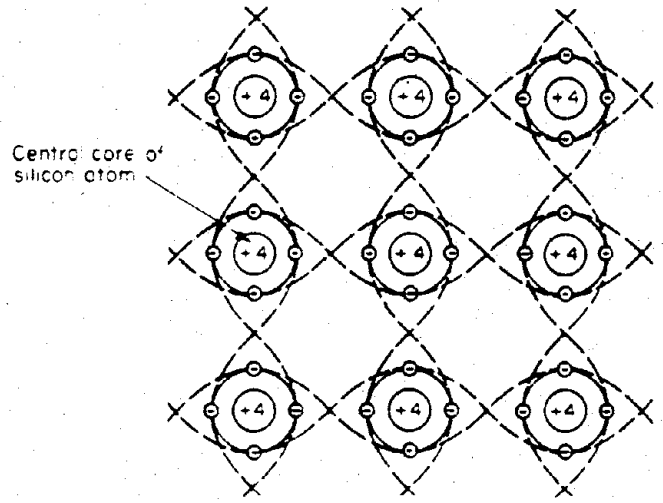

a. Pure Silicon

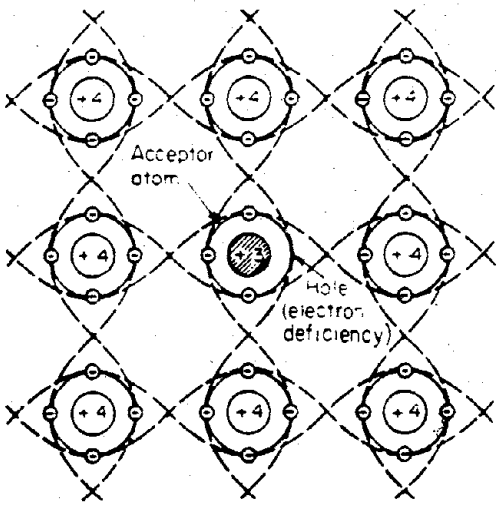

b. Silicon with Acceptor Impurity Atom

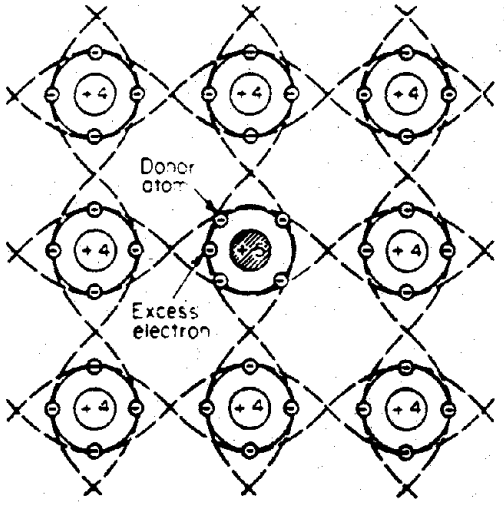

c. Silicon with Donor Impurity Atom

Figure 9-45. [redacted] Two-Dimensional Lattice Structure of Silicon [redacted]

[redacted]

three orbiting electrons does not have sufficient electrons to share with its neighboring silicon atoms. This lack of an electron is called a hole. For conceptual purposes, the hole can be treated like an electron with a positive charge. Consequently, in semiconductor discussion the term charge carriers refers to the electrons and holes made available for the conduction process by the impurity doping.

Figure 9-46 illustrates a semiconductor junction (diode), with the two impurity regions shown separated by a solid line. This represents what conceptually would be the junction of the two materials. However, in reality the silicon is all one crystal, and there is really no physical junction. There are, as illustrated, regions at both ends of the crystal which are predominantly either P type (excess of free holes) or N type (excess of free electrons). A transition region, called the depletion region, exists in the center. Within this region, holes from the P region combine with equal numbers of electrons from the N region. As a result, only a few free charge carriers remain in the region when equilibrium has been reached. Depending on the number of charges removed from each region, a voltage (electric field) will be developed across the depletion region. The voltage across the depletion region under equilibrium is such that any holes (positive charge carriers) introduced into the region would migrate by the drift process to the P region, and a negative charge carrier (electron) introduced into the depletion region would migrate by the drift process to the N region. Under normal conditions conventional current flow* would allow current to flow for ideal diodes only from the P side to the N side. If, however, free carriers were generated in the depletion region, conventional current flow would dictate that a current, proportional to the number of free charge carriers generated, would flow from the N region to the P region. This is in the reverse direction from the normal conventional current flow through an ideal diode. This reverse current, if generated in the depletion region by ionizing radiation, is called the drift component of the photocurrent in a PN junction. The diffusion component of the photocurrent is the result of free carrier generation by the ionizing radiation in the P and N regions near the depletion region. Those hole-electron pairs generated far from the depletion region will be trapped and recombined before they can become effective. The effect of the radiation is to

* In this chapter, normal current flow is considered to be conventional current flow. This is opposite to actual electron flow.

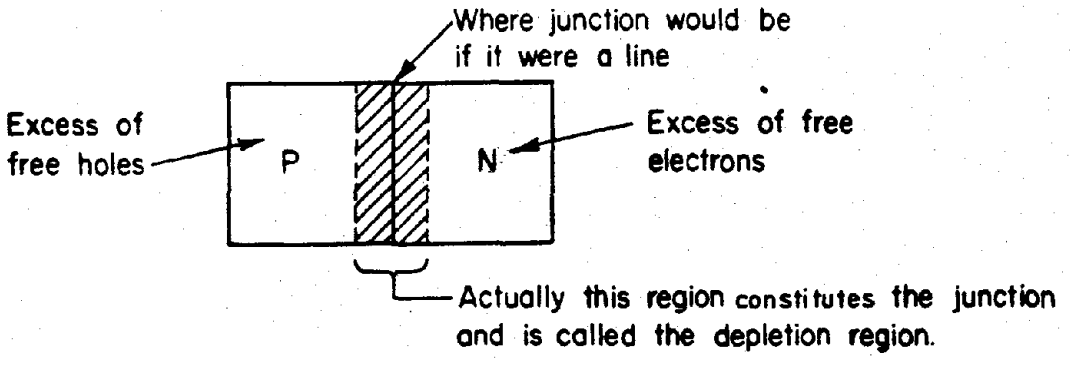

Figure 9-46. Illustration of a Semiconductor Junction

[redacted]

[redacted] generate a current in the reverse direction through the diode junction, which tends to forward bias the diode. An expression that generally will predict the photocurrent for many cases of interest is:

$$I_{pp\ max} = qK_g\dot{D}A\ (w + L).$$

where

$I_{pp\ max}$ = the maximum* primary photocurrent for a PN junction

q = electronic charge 1.60 x 10^{-19} coulombs

K_g = the energy-dependent free-charge-carrier-generation constant (electron-hole pairs/ cm^3 · roentgen)

K_g (for silicon) = 4.2 x 10^{13} electron-hole pairs/cm^3 · R

K_g (for germanium) = 1 x 10^{14} electron-hole pairs/cm^3 · R

$\dot{D}$ = the gamma exposure rate, R/sec (The gamma ray photons have energies which would give best results with the K_g constants given above.)

A = junction area in cm^2 (A can typically vary from 0.3 x 10^{-4} to 0.2 x 10^{-1} cm^2)

w = depletion layer width in cm (w varies with applied voltage and is best expressed as $w = w_1\ (V_o - V_j)^{-b}$ where V_o is the built-in junction potential (~0.35 volts for germanium and ~0.72 volts for silicon) w_1 typically varies from 0.5 x 10^{-4} cm to 1 x 10^{-3} cm, V_j is the junction voltage, and b typically varies from 0.05 to 0.5.

L = diffusion length for minority carriers on the side of the junction with the longer diffusion length in cm (L can vary typically from 0.15 x 10^{-1} cm to 0.2 x 10^{-4} cm).

[redacted] The duration of the photocurrent depends on the time required for free holes and free electrons to be trapped and to recombine. Since these times are short, the photocurrent is a pulse of current of relatively short duration. Typical pulse shapes are shown in Figure 9-47.

[redacted] Tunnel diodes are at least an order of magnitude more radiation resistant than diodes in general, since they are characterized by small geometry, heavily doped PN regions, and narrow junctions. The short-circuit photocurrent can be estimated from the equations applicable to general diodes. Since the lifetime of minority carriers in tunnel diodes is very short, the response of a tunnel diode to a pulse of radiation is expected to follow the radiation pulse. Normally, the width of the depletion region for tunnel diodes is so narrow that the photocurrent will consist primarily of the diffusion component. The maximum photocurrent under short

---

*[redacted] For those more theoretically inclined this equation applies in the case where $\tau < t_p/4$ and is the steady-state value. A more detailed equation and development is the *TREE Handbook*.

[redacted]

[redacted]

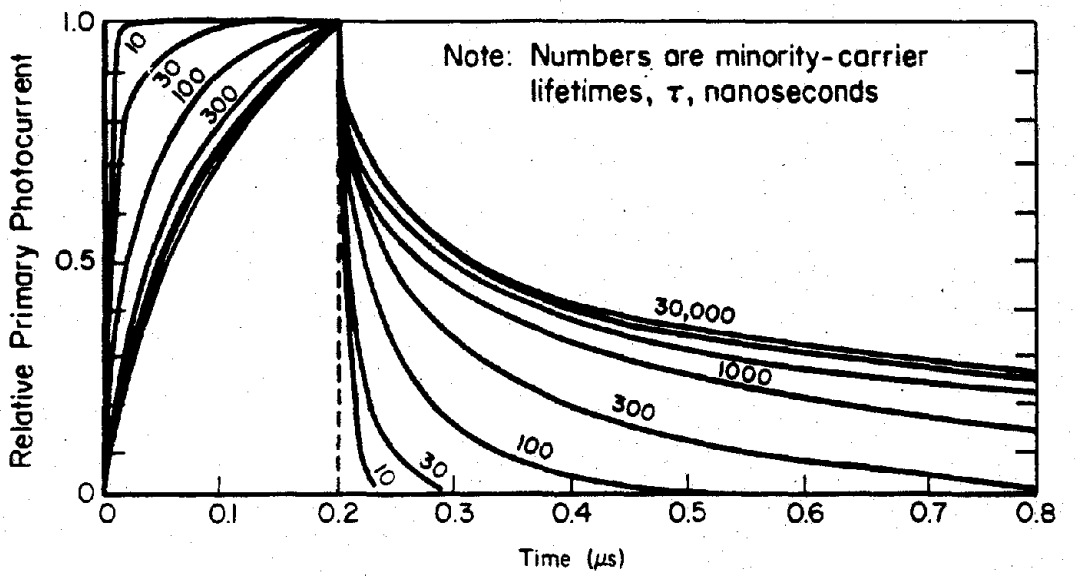

Figure 9-47. [redacted] Relative Shapes of Diffusion Component of Primary Photocurrent [redacted]

[redacted]

circuit conditions can thus be estimated as follows:

$$I_{pp\ max} = qK_g\dot{D}A\ (L_n + L_p)$$

where

q, K_g, $\dot{D}$ and A are defined as in the diode expression, and L_n and L_p are the diffusion lengths in the N and P regions, respectively. Diffusion lengths are comparable on each side of the junction.

[redacted] The radiation induced offset voltage in an open circuited tunnel diode is influenced by the tunneling current at low dose rates, but at higher dose rates a tunnel diode behaves like a conventional diode. This behavior occurs because very little induced voltage is required to set up a tunneling current equal to the diffusion current of excess carriers. When the tunneling current reaches a maximum, the induced voltage rises sharply to the value for a conventional diode.

[redacted] A transistor is a more complicated device than a diode, both structurally and functionally. The main functional advantage of the transistor is the fact the transistor has the ability to amplify its input signal. The transistor has three impurity regions that alternate, i.e., NPN or PNP. When an operating transistor* is exposed to transient ionizing radiation, a current pulse is observed in the external circuit. This current pulse, which may be orders of magnitude larger than that of a diode with comparable dimensions, can reach a peak value at a time later than the radiation peak, and can, in some cases, continue for milliseconds.

* [redacted] The following paragraphs are concerned with bipolar transistors; not to MOS, junction field-effect transistors, or thin-film transistors.

[redacted]

[redacted]

[redacted] This characteristic behavior of transistors is the result of the amplifying properties acting on the primary radiation induced photocurrents. The electrical action of the transistor creates a secondary photocurrent that is typically greater than the primary photocurrent by a factor equal to the gain (a measure of ability of the transistor to amplify) of the transistor. Analysis of the radiation response of a transistor involves the determination of the primary photocurrent, followed by a calculation of the magnitude and duration of secondary photocurrents under the given circuit conditions.

[redacted] In transistors, the primary photocurrent is generated in five regions: in the collector- and emitter-junction depletion regions, in the base, and in the emitter and collector bodies lying within a diffusion length of the junctions. In most cases, the generation of primary photocurrent in the emitter body and within the junctions can be neglected since the emitter body and the junction volumes are a relatively small part of the total generating volume (see Figure 9-48).

[redacted] The secondary photocurrent is produced by the accumulation of excess majority carriers in the base region as a result of the flow of primary photocurrents across the PN junctions of the device. This excess charge, which is confined in the base by the built-in junction fields, is the correct polarity to forward bias the emitter base junction and to cause normal current to flow. The collector current that is produced is called secondary photocurrent. This collector

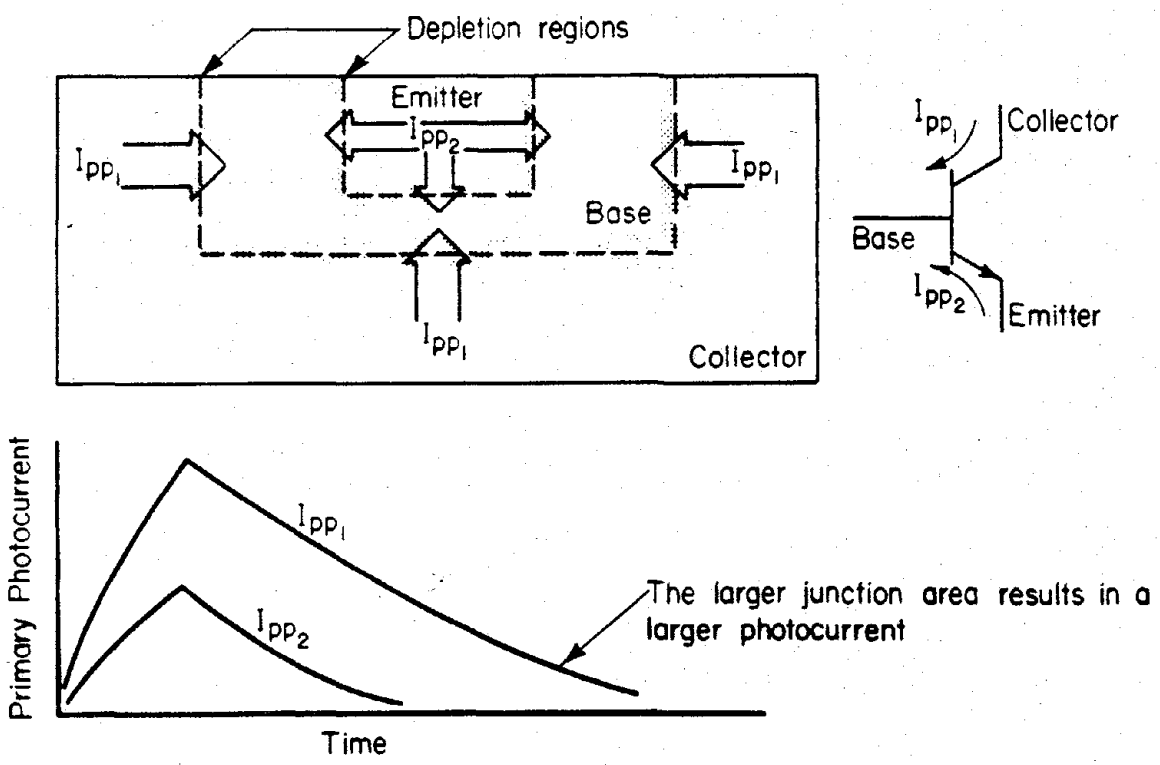

Figure 9-48. [redacted] NPN Transistor Illustrating the Primary Photocurrent [redacted]

[redacted]

[redacted]

[redacted] current continues to flow until the excess charge stored in the base can either recombine with minority carriers or flow out through the external base lead.

[redacted] The magnitude of the collector current pulse will depend on the dose rate if the radiation pulse is long compared to the lifetimes of the transistor base and collector, but it will depend on the total dose if the pulse is shorter than those lifetimes. This results from the charge transferred from the collector by the primary photocurrent being stored in the base region. Since many transistors have lifetimes that are as long as or longer than typical nuclear weapon radiation pulses, the prompt dose is quite often the most important factor.

[redacted] A simplified linear approximation of the primary photocurrent in a transistor can be estimated with the following equation:

$$I_{PP} = \frac{\dot{D}}{CONST.} [t_s + 0.03],$$

where

D = the gamma ray exposure rate, R/s

$CONST.$ = 0.83×10^8 for NPN devices and 0.42×10^8 for PNP devices*

t_s = charge storage time (in μs) for the device of interest (t_s typically can vary from a few nanoseconds to hundreds of microseconds).

[redacted] The duration of the photocurrent response depends on the radiation pulse width, the radiation storage time (which is different than the charge storage time (t_s)), and the time for holes and electrons to recombine. The radiation pulse width is determined by the weapon. The time for holes and electrons to recombine is illustrated for a diode in Figure 9-47, which applies generally for transistors. The radiation storage time, t_{sr}, is defined by Figure 9-49a. The radiation storage times for several dose rates are shown in Figure 9-49b. These latter curves are

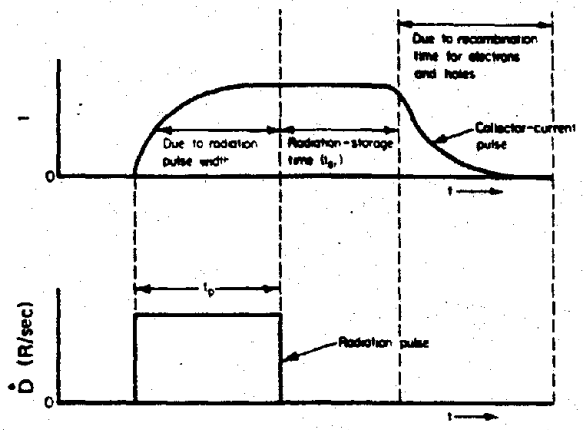

a. Definition of the Device Radiation-Response Times

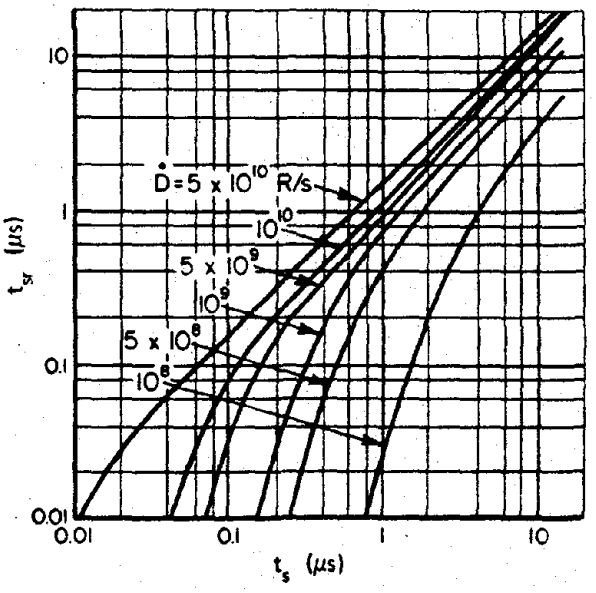

b. t_{sr} vs t_s Curves

Figure 9-49. [redacted] Radiation Storage Time [redacted]

[redacted] These equations only apply for the steady-state estimate of the primary photocurrent for silicon planar and mesa transistors with rated maximum continuous collector dissipation below 0.8 watt at 250C. More detailed information about prediction is available in the TREE Handbook (see bibliography).

[redacted]

[redacted]

[redacted] for a particular bias and radiation condition during storage. They are presented as being illustrative, and no attempt should be made to generalize from the curves. It is necessary to analyze a transistor or diode in the particular circuit configuration in which it is used to determine the threshold for circuit malfunction. As a result of the many different circuit configurations and bias conditions that can occur for transistors and diodes, failure thresholds that would be of value can not be specified generally for the TREE environment.

[redacted] A silicon controlled rectifier (SCR) is a solid state semiconductor device composed of four layers of alternate-impurity semiconductor material containing three PN junctions. The SCR is an active switching element that will remain in a nonconducting or "off" state until turned on or "fired" by a low-level control signal on the gate. It will then remain "on" without need for a sustaining control signal. The SCR is turned "off" by reducing its output (anode) current below the "dropout" level. Radiation induced currents, like those discussed for diodes and transistors, are a direct function of the junction areas, diffusion lengths, etc., and thus are difficult to predict since values for the parameters usually are not available. Since these currents, above a threshold, can induce changes in the state of an SCR, some method is required to predict the magnitude of the radiation induced currents, or, more specifically, the radiation threshold above which switching occurs.

[redacted] It has been found that the transient radiation switching thresholds (critical radiation exposure rate) for SCR's are functions of the radiation pulse width. The exposure rate required to trigger an SCR becomes constant for pulse widths longer than a critical value. This critical value is a function of the device minority carrier lifetime and the device delay "turn on" time. For pulse widths less than the critical value, the exposure rate required to trigger an SCR increases rapidly as the pulse width approaches zero. The dependence of the switching threshold of a 3A60A SCR on pulse widths and gamma ray exposure rate is shown in Figure 9-50. The critical pulse width for this device is approximately 2 microseconds.

[redacted] Typically the SCR type of device would not be expected to fire below 10^6 rads (Si)/sec. For most cases, however, the pulse width is sufficiently short that the devices are dose dependent. Failures occur typically at prompt doses between 0.1 and 1 rad (Si).

[redacted] Field-effect transistors (FET) are a family of unipolar devices that have pentode-like characteristics. The three major categories within this family are the junction FET, the metal-oxide insulated-gate FET (MOSFET), and the thin-film insulated-gate FET (TFT). The geometry and construction features of typical field-effect transistors are shown in Figure 9-51. The basic structure of the FET devices involves a source, a gate, and a drain in rough functional correspondence to the familiar cathode, grid, and plate of vacuum tube technology.

[redacted] The mechanisms by which radiation generates photocurrents in an FET are not substantially different from those for bipolar transistors and diodes. The important radiation parameters in an FET are the transient gate and drain-to-source currents. Possible sources of transient currents in FET's can be grouped into the following categories:

- Leakage currents across PN junctions that behave like PN junction photocurrents discussed previously.
- Direct modulation of the channel conductivity and mobility (usually applicable at high ($>10^8$ rads (Si)/s) dose rates).
- Leakage currents through the gate oxide layer (applicable to the metal oxide and thin-film FET's).
- Secondary emission (see Chapter 6) and atmosphere ionization currents.

[redacted]

[redacted]

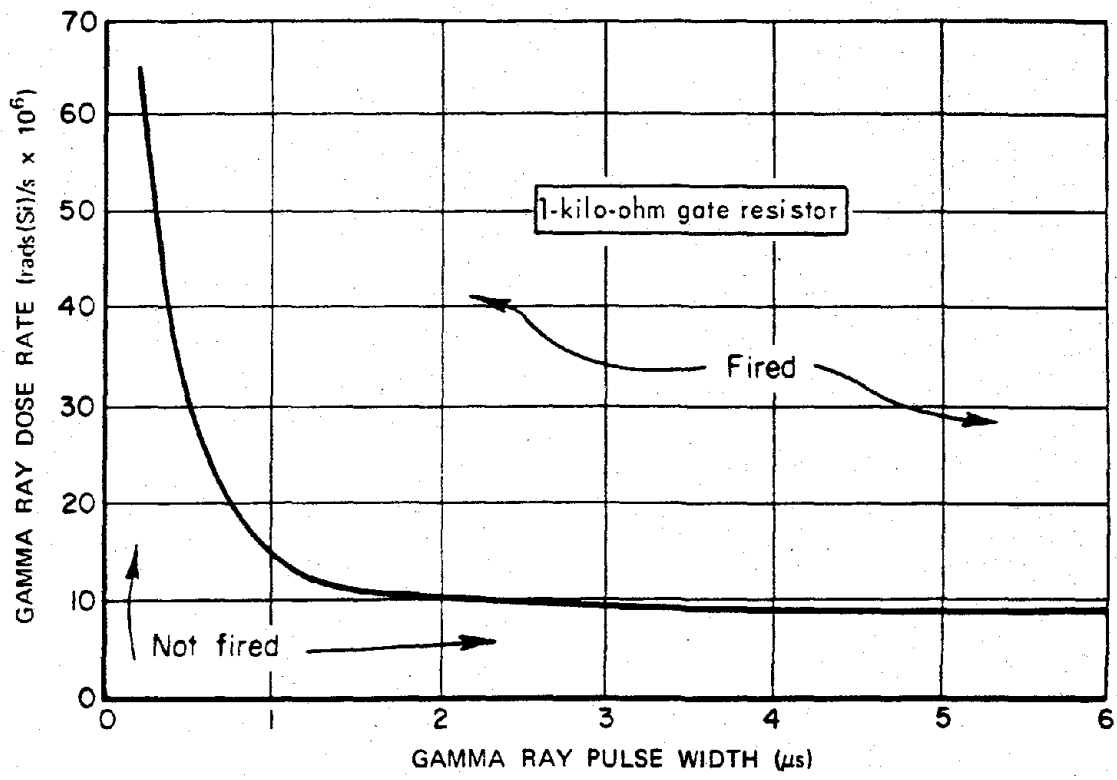

Figure 9-50. [redacted] Gamma Ray Exposure Rate as a Function of Pulse Width Switching Thresholds for a 3A60A SCR [redacted]

[redacted]

[redacted]

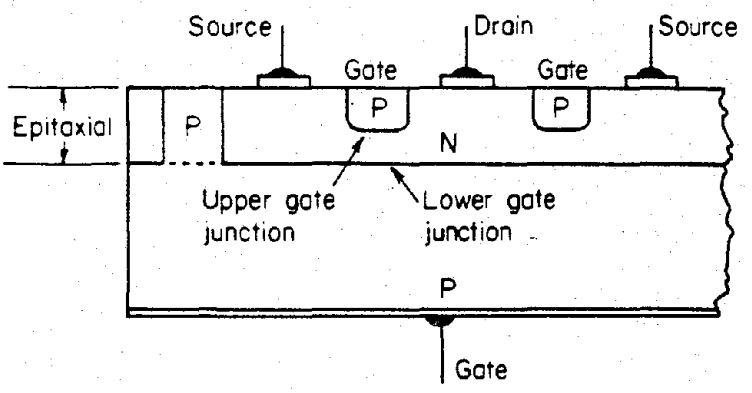

a. Junction Field-Effect Transistor

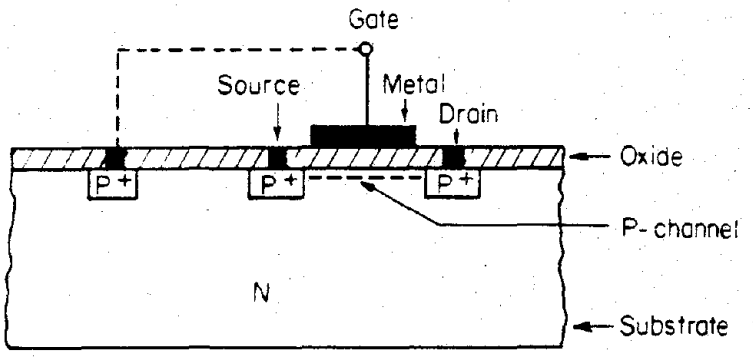

b. MOS Field-Effect Transistor

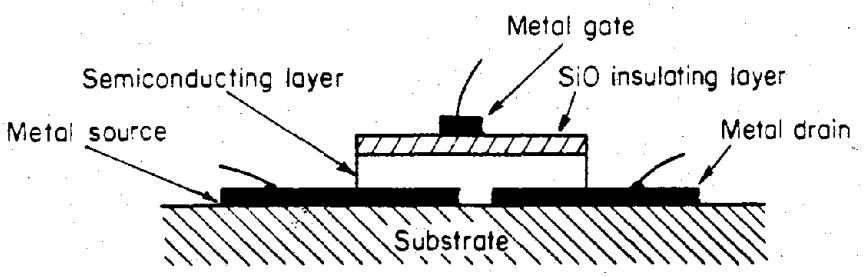

c. Thin-Film Field-Effect Transistor

Figure 9-51. [redacted] Construction of Typical Junction, MOS, and Thin-Film Field-Effect Transistors [redacted]

[redacted]

[redacted]

[redacted] Significant problems generally are not caused in field-effect transistors at dose rates below 10^6 rads (Si)/sec.

9-45 Permanent Effects [redacted]

[redacted] Permanent effects in semiconductor devices are those that can be attributed to physical property changes that result from the direct interaction of the radiation with the material of interest. These property changes typically last for periods that are long with respect to the recovery times of the components. These property changes occur in a very short time period and result in a rapid change in the operating characteristics of the device. A closely related effect is called rapid annealing, which is the process by which an initially large change in device parameters recovers very rapidly, approaching the smaller change observed several minutes after the radiation exposure.

[redacted] Most permanent effects in semiconductor devices subjected to a nuclear radiation pulse result from damage to the semiconductor material by energetic neutrons ($E > 10$ keV); however, the effects of gamma rays and secondary electrons must not be underestimated. In certain devices such as MOS field-effect transistors the effects of ionizing radiation can be the principal causes of permanent failure.

[redacted] Permanent effects can be grouped into two categories – bulk, and surface effects. Bulk effects are changes in the device characteristics that can result from damage to the bulk material. Surface effects are changes that are generally caused by radiation induced ionization near the surface of the device. Bulk damage effects from neutron radiation usually can be predicted within a factor of 2, while surface effects are generally unpredictable.

[redacted] Bulk effects result from electron, gamma ray, and neutron induced lattice displacements in the bulk of the material (see Chapter 6). Fast neutrons lose energy primarily by elastic collisions with the semiconductor atoms and cause large disordered clusters to be formed within the material. Gamma radiation loses energy by creating Compton electrons (see Section I, Chapter 5), which may cause lattice displacements. Since electrons have such a small mass, they primarily cause vacancy-interstitial pairs rather than clusters of defects that are typical of neutron damage. Lattice damage that results from gamma radiation usually is of secondary importance, unless a large gamma dose ($>10^5$ rads) is absorbed by the material.

[redacted] Lattice damage degrades the electrical characteristics of semiconductor devices by increasing the number of trapping, scattering, and recombination centers.

- The trapping centers remove carriers from the conduction process.
- The additional scattering centers reduce the mean free path of the free carriers. Since the mobility is directly proportional to the mean free path, radiation exposure reduces the mobility of charge carriers.
- The recombination centers decrease the minority carrier lifetime according to the relationship (see Chapter 6).

$$\frac{1}{\tau_\varphi} = \frac{1}{\tau_0} + K\varphi,$$

where

τ_φ = minority-carrier lifetime at fluence φ in seconds,

τ_0 = initial minority-carrier lifetime (bulk lifetime), in seconds,

K = lifetime damage constant, cm^2/(neutron-seconds),

φ = fast neutron fluence, neutrons/cm^2.

[redacted] Permanent effects also can be caused by radiation induced changes in the semiconductor surface. The changes in the surface conditions

[redacted]

[redacted]

[redacted]

attributed to radiation that can cause permanent effects are surface charging mechanisms and changes in the surface recombination velocity. The most likely charging mechanisms are the collection of ions from a gas in the atmosphere surrounding the semiconductor device and the ejection of electrons from dielectric materials which are either deposited on the semiconductor surface or in which the device is encapsulated. These ions migrate under the influence of electric fields. As a result of the collection of these charges, inversion layers can form near the surface, causing large increases in leakage currents. In silicon devices these leakage currents result from recombination-generation in the enlarged depletion region.

[redacted] Ionizing radiation can cause changes in recombination velocity, which has deleterious effects on the effective lifetime according to the relation

$$\frac{1}{\tau_{eff}} = \frac{1}{\tau_{\varphi}} + \frac{1}{\tau_{surf}},$$

where

τ_{eff} = effective lifetime,

τ_{φ} = bulk lifetime,

τ_{surf} = surface lifetime (an inverse function of recombination velocity).

Surface effects usually are negligible compared to bulk lifetime damage for most conventional devices in a transient radiation environment. Field-effect devices, where radiation induced surface changes are the primary damage mechanisms, represent an important exception. [redacted] The general effects of nuclear radiation on semiconductor diodes are summarized below and are illustrated in Figure 9-52 and 9-53.

- The forward voltage of the diode at constant current normally will increase as a

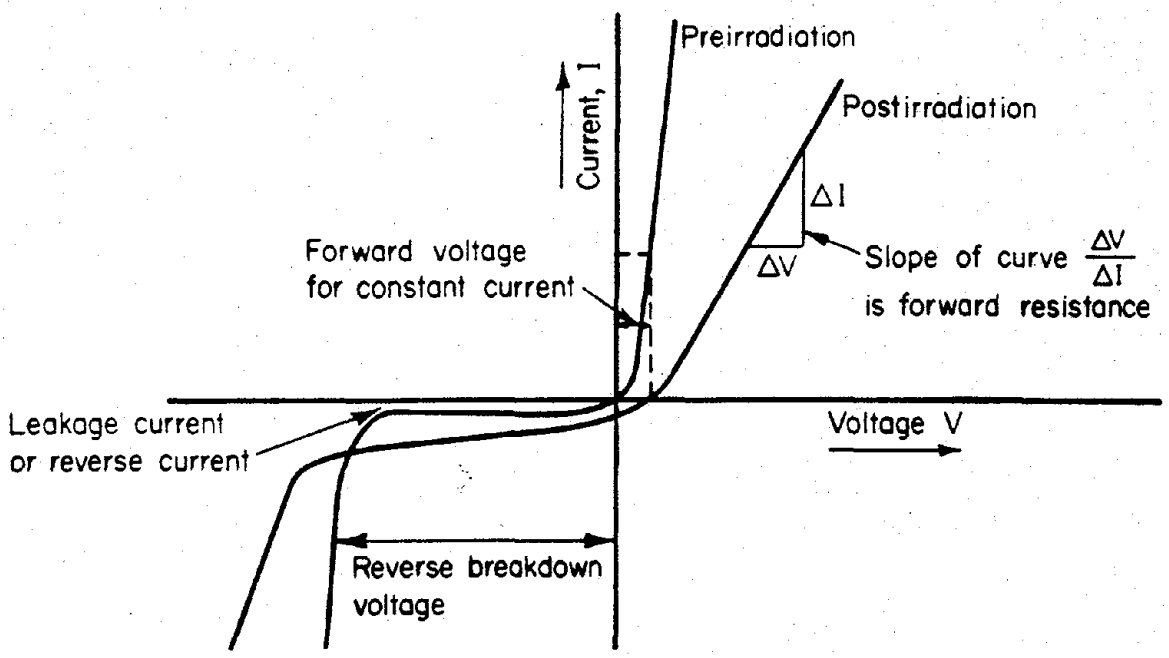

Figure 9-52. [redacted] An Illustrative Diode Characteristic for Pre- and Post-irradiation by Neutrons [redacted]

[redacted]

[redacted]

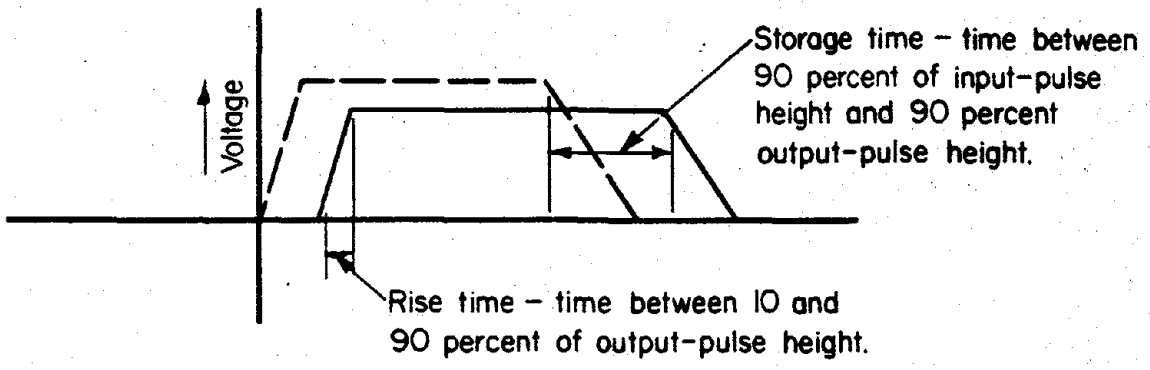

Figure 9-53. [redacted] An Illustration of Rise Time and Storage Time [redacted]

[redacted]

result of changes in resistivity and mobility in the bulk material.

- The dynamic forward resistance will increase as a result of changes in resistivity and conductivity modulation.
- The surface effects and increases in carrier generation in the space-charge region will cause the reverse current to increase.
- The reverse breakdown voltage normally will increase because of an increase in resistivity.
- The switching characteristic of the diode generally will be changed. The rise time will increase, and the storage time will decrease as a result of lifetime damage.

[redacted] Diodes generally are an order of magnitude more resistant to radiation than transistors of similar type. For this reason, theoretical and experimental studies have concentrated on transistors rather than diodes. Prediction techniques for diodes are complicated by the fact that the various bulk and surface damage mechanisms interact in an intricate manner. The wide variety of diode types, i.e., material, doping level and profile, geometry, etc., all tend to make comprehensive prediction schemes difficult and inaccurate. However, some quantitative trends in the changes in diode parameters can be given. The more important changes in diode characteristics, from a circuits point of view, are the increase in forward voltage at constant current and the increase of reverse leakage current. Changes in the dynamic forward resistance, breakdown voltage, and switching characteristics usually are of secondary importance.

[redacted] The forward voltage at constant current generally starts to increase at a fluence of 10^{13} to 10^{14} n/cm^2 ($E > 10$ keV, fission), though some diodes exhibit changes at fluences as low as 10^{12} n/cm^2 ($E > 10$ keV, fission) while others show no change up to fluences as large as 10^{15} n/cm^2 ($E > 10$ keV, fission). Usually, fluences of about an order of magnitude greater than the fluences required to cause the initial change will double the forward voltage.

[redacted] The reverse leakage current usually increases with exposure, but decreases also have been observed. Nominally, changes begin at fluences from 10^{13} to 10^{14} n/cm^2 ($E > 10$ keV, fission). Gamma ray doses as low as 5×10^4 rads (Si) have caused significant leakage currents. Germanium devices generally have larger changes in leakage current than silicon devices.

[redacted] The changes in breakdown voltage are typically the largest for diodes with high breakdown voltage. Reference voltage diodes (zener

[redacted]

[redacted]

[redacted]

diodes) are relatively resistant to radiation with reference voltage changes less than 5 percent at 10^{15} n/cm^2 ($E > 10$ keV, fission).

[redacted] The storage time is directly proportional to lifetime. Hence, the fluence at which the storage time will be reduced to one-half the preirradiation value will be

$$\varphi = \frac{1}{\tau_o K},$$

where

τ_o is the minority carrier lifetime,

K is the damage constant (see Chapter 6).

[redacted] Other diode types are specifically designed for rectifier application where high breakdown voltage and a low voltage drop are required even at high current. These diodes usually are designed with a PIN junction, which results in a device that is less sensitive to radiation than the standard type diodes.

[redacted] Selenium rectifiers and hot carrier diodes (metal semiconductor junction) appear to be more radiation resistant than either germanium or silicon diodes because of their material and structural differences. Reactor tests conducted on the HPA-2300 series hot carrier diodes confirm the relative radiation hardness of these devices. Most units tested remained within manufacturer's specifications at fluences of 3×10^{15} n/cm^2 ($E > 0.1$ MeV, fission) and 9×10^5 rads (Si).

[redacted] Diodes classified as "tunnel diodes" are easily recognized by their forward current characteristic, which shows a region of negative resistance. The effect of radiation on tunnel diodes is observable on the current-voltage (I-V) characteristic at fluences between 10^{15} and 10^{16} n/cm^2 ($E > 10$ keV, fission), and can be summarized as follows:

- The slope of the primary tunneling current is not changed; however, the peak current is slightly reduced as a result of the redistribution of the electrons in the defect states.
- The valley current at a given voltage increases due to the additional tunneling via defect states.
- For voltages larger than valley voltage, there is an increased current for a given voltage due to the excess current, which predominates over the diminishing normal diode current.

[redacted] Figures 9-54 and 9-55 show representative germanium and silicon tunnel diodes under neutron irradiation. The figures show that tunnel diodes are still operational at 5×10^{15} n/cm^2 ($E > 10$ keV, fission), which indicates the relative radiation hardness of these devices.

[redacted] The general effects of nuclear radiation on bipolar transistors can be summarized as follows:

- The current gain (amplification) of the transistor will be degraded as a result of lifetime damage to the bulk material. Degradation of gain will be greatest immed-

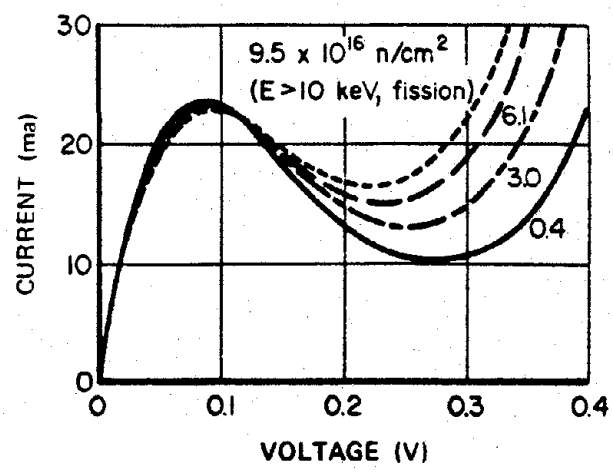

Figure 9-54. [redacted] Fast Neutron Bombardment Effect on Voltage-Current Characteristic of a Germanium Tunnel Diode [redacted]

[redacted]

[redacted]

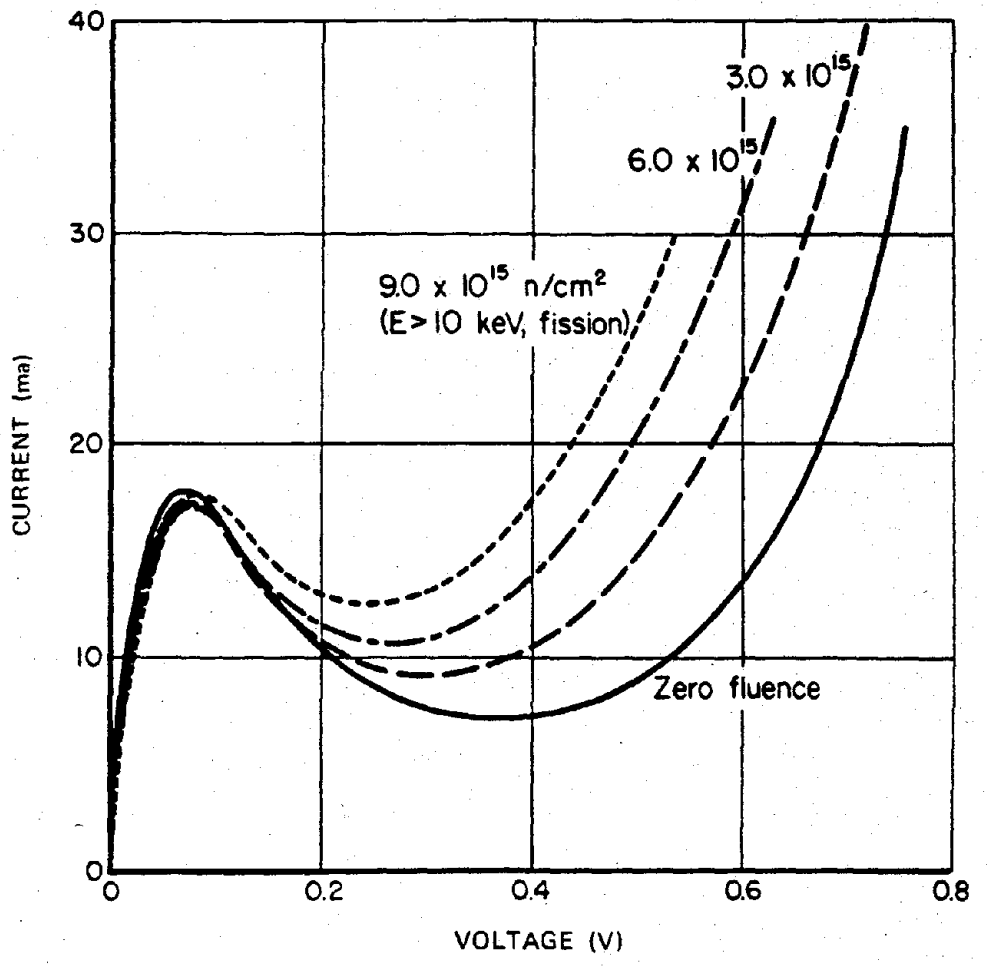

Figure 9-55. [redacted] Fast Neutron Bombardment Effect on Voltage-Current Characteristic of a Silicon Tunnel Diode [redacted]

[redacted]

[redacted]

[redacted] iately following a burst of nuclear radiation, and the gain will recover rapidly to a quasi steady-state value. The annealing can go on for weeks, but usually the current gain recovery is small or negligible after the initial recovery.

- The reverse leakage current will increase as a result of surface effects and carrier generation in the space-charge region.
- Changes occur in the punch-through voltage, and the base-to-emitter and collector-to-base breakdown voltage as a result of changes in resistivity.
- Increases in base-spreading resistance, collector body resistance, and saturation voltage result from changes in resistivity and conductivity modulation.
- The switching characteristics also are changed slightly – exemplified by decreased storage time and increased turn-on time as a result of changes in lifetime and resistivity.

[redacted] Since transistors usually are the most vulnerable devices used in conventional circuits, predictions of circuit response under radiation conditions will be limited by the accuracy with which transistor behavior can be predicted. The reduction of current gain generally will limit the usefulness of the component before the other factors listed above become a serious problem. Therefore, emphasis is placed on the prediction of current gain degradation. However, in some applications saturation voltages and/or leakage currents across reverse biased junctions may be the limiting factors.

[redacted] The structure of a device is an important factor in determining its radiation resistance. A general rule is that the thinner base, higher frequency, and smaller junction area devices usually have better radiation resistance. For example, the diffused-junction devices usually offer a resistance to radiation about one order of magnitude better than that offered by the alloy-junction devices.

[redacted] Experimental data for conventional transistors in the form of generalized gain degradation curves are shown in Figure 9-56 for some common transistor types. The ratio β_φ/β_o represents the ratio of gain at some fast neutron fluence to the gain prior to irradiation. Figure 9-56 is representative of preliminary data from steady-state reactor experiments. The transistor types have been placed in their respective regions on the basis of where a majority of samples of a given type fell on the graph. Caution should be exercised in using and interpreting the information in the figure, since irradiation temperature, irradiation source, measurement conditions, etc. are not specified.

[redacted] A further word of caution should be injected concerning the interpretation of gain degradation data. A sharp decrease in β occurs during exposure and then rapidly anneals to a final value that is commonly measured. The time dependence of gain degradation can best be interpreted with the use of the annealing factor, F, defined as follows:

$$F(t) = \frac{\dfrac{1}{\beta_\varphi(t)} - \dfrac{1}{\beta_o}}{\dfrac{1}{\beta_\varphi(\infty)} - \dfrac{1}{\beta_o}} = \frac{K(t)}{K(\infty)} ,$$

where

$\beta_\varphi(t)$, $K(t)$ are gain and damage constants as a function of time after a fast burst of nuclear radiation.

$\beta_\varphi(\infty)$, $K(\infty)$ are the steady-state values of gain and damage constants.

[redacted] The magnitude and form of F varies with temperature, injection level, doping level, and impurity content. Typical values for the annealing factor at 1 msec range from approximately two to three for NPN transistors and

[redacted]

[redacted]

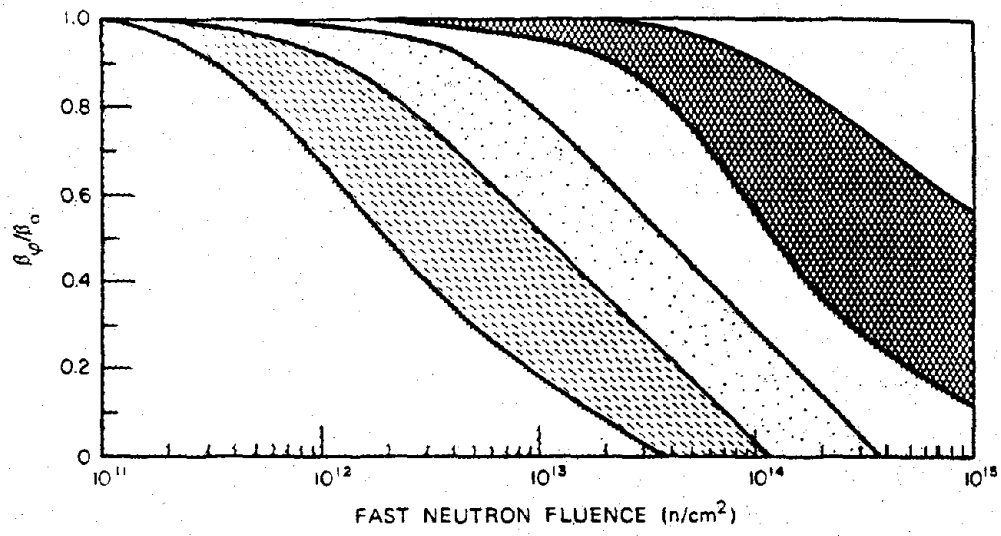

I	II	III		IV			V
2N329A	2N336	2N697	2N3244	2N404	2N2708	S-7241	2N700
2N1016E	2N699	2N708	2N3251	2N585	2N2784	S-7242	2N706B
2N1486	2N861	2N718	2N3252	2N705	2N2808	PT 2600	2N709
2N1653	2N917	2N720A	2N3300	2N706	2N2845	XF 805	2N797
2N1722	2N1016	2N722	2N3444	2N707A	2N2857	4907974	2N918
2N2187	2N1132	2N869	2N3486	2N708	2N2894		2N955A
2N2484	2N1184	2N910	2N3497	2N743	2N3013		2N964
	2N1613	2N1306	2N3499	2N744	2N3017		2N1195
	2N1711	2N1342	2N3509	2N834	2N3119		2N1709
	2N1900	2N1506	3TE240	2N835	2N3209		2N2537
	2N1936	2N1717	BR100A	2N914	2N3227		2N2616
	2N2187	2N1893	7900302	2N915	2N3252		2N2808
	2N2219	2N2192A	7900329	2N916	2N3287		2N3014
	2N2223	2N2193A		2N917	2N3303		2N3283
	2N2243A	2N2217		2N1306	2N3309		2N3287
	2N2297	2N2222		2N1307	2N3327		2N3309
	2N2411	2N2223		2N1506	2N3375		S-6781
	2N2878	2N2368		2N1709	2N3546		
	2N3072	2N2481		2N2218	2N3570		
	2N3439	2N2699		2N2369	2N3633		
	2N3499	2N2801		2N2538	2N3723		
	2N3501	2N2887		2N2540	FT 0040		
	2N3502	2N2907		2N2656			
	2N3637						

Figure 9-56. [redacted] Current Gain Degradation Characteristics for Some Common Transistor Types [redacted]

[redacted]

[redacted]

[redacted] slightly smaller for PNP transistors. The annealing factor can be as high as 7 for low injection situations and immediately after turning on a device that was off during the neutron pulse.

[redacted] Other transistor parameters also can be degraded. Permanent increases occur in leakage currents across reverse-biased junctions. In general, the discussion of diode leakage is applicable to transistor leakage.

[redacted] Changes in breakdown voltages, punch-through voltage, and collector and emitter body resistances are negligible at fluences where the gain is still usable. The effects of nuclear radiation on these parameters can be analyzed from comments made about diodes.

[redacted] The changes in saturation voltage and in the switching time as a result of nuclear radiation are of interest for switching applications. In many cases the saturation voltage may appear to increase at relatively low levels of radiation, but actually the transistor is losing base drive and is coming out of saturation. The only significant increases in saturation voltage are seen at high collector currents. These increases, however, occur at high neutron fluences.

[redacted] The switching time of a transistor is referred to as the turn-on time and the turn-off time, which consist of the delay time, t_d, the rise time, t_r, the storage time, t_s, and the fall time, t_f. First-order theory indicates that, with the exception of the rise time, these parameters either remain relatively constant or decrease with radiation. Normally, the decreases are larger than the increases in these parameters; thus a net reduction of transistor switching time occurs with radiation, which usually is desirable. The largest changes occur in the storage time, which is proportional to the lifetime. Thus,

$$\varphi = \frac{1}{K\tau_0}$$

is the fluence at which the storage time is reduced by one half.

[redacted] The general effects of nuclear radiation on field-effect transistors can be summarized as follows:

- Changes occur in the threshold voltage, V_T. These changes in threshold voltage affect most of the field-effect transistor parameters.
- Increases in leakage current occur.
- Changes in channel resistivity and carrier mobility occur.

[redacted] Damage in MOS field-effect transistors is due primarily to ionizing radiation. For this reason damage is reported in terms of dose (in rads) or exposure (in Roentgens) rather than fluence (in n/cm^2). The most sensitive parameter to radiation in field-effect transistors is the threshold voltage, V_T. In general, degradation in V_T proceeds rapidly in the range of 10^3 and 10^4 rads (Si), but becomes more gradual above this dose. Complete failures, i.e., complete degradation in transconductance, have been observed at doses of 10^6 to 10^7 rads (Si).

[redacted] Considerable interest has been shown in the use of junction field-effect transistors (JFETS) in a radiation environment, since these are unipolar devices and do not depend on minority-carrier lifetime for operation. The primary effect of radiation on JFET's is the removal of carriers in the channel region. Radiation induced carrier removal is a strong function of resistivity. Thus, increased radiation tolerances is expected from JFET's with a high initial carrier concentration. The planar process has allowed heavily doped JFET's to be manufactured with the necessary control to make them commercially available. These heavily doped JFET's have demonstrated a very significant improvement in radiation hardness, e.g., approximately 15 percent degradation in transconductance after a neutron fluence of 7×10^{14} n/cm^2 ($E > 10$ keV, fission).

[redacted] Thin-film field-effect transistor (TFT) devices have been found to be more radiation

[redacted]

[redacted]

[redacted] resistant than conventional field-effect transistors. Tests indicate that both the cadmium selenide and the silicon on sapphire type TFT's are operational at 10^6 rads (Si) or 10^{15} n/cm^2 ($E >$ 10 keV, fission).

[redacted] The negative resistance characteristic of the unijunction transistor depends upon the conductivity modulation of a moderately high resistivity silicon bar by means of injected minority carriers from the rectifying emitter contact. This transistor is highly sensitive to radiation induced changes in minority-carrier lifetime and resistivity. Typical failure thresholds for unijunction transistors are of the order of 5×10^{11} to 5×10^{12} n/cm^2 ($E > 10$ keV, fission). The degradation is manifested by an increase in valley voltage, a decrease in valley current, and increases in the interbase and emitter-base resistances.

[redacted] The three basic types of silicon PNPN devices are: the silicon-controlled rectifier, SCR; the silicon-controlled switch, SCS, and the Shockley diode. All of these devices may be considered to consist of overlapping NPN and PNP transistors, the primary difference being the external accessibility of the various layers; that is, the Shockley diode provides external access to only the outer P- and N-layers, the SCR has leads to all but the central N-region, and the SCS has leads to all four regions. The "two transistors" of the PNPN structure operate in a positive-feedback configuration, and the current-transfer ratios of the two sections add together for the composite device.

[redacted] As previously discussed for transistors, radiation induced defects reduce the current gain for both "transistors" so that the required gate current, holding current, and breakover voltage should increase with radiation at fluences comparable to the bulk damage fluence levels in silicon transistors. Theoretical considerations of the mechanisms of PNPN device operation also indicate that excessive leakage currents will cause premature triggering of the devices. Hence, increases in surface and bulk leakage currents induced by radiation may cause the device to conduct continuously. This effect will depend upon the bias level applied in the application.

[redacted] Since PNPN devices are used in medium- to high-power applications, they cannot be compared to high-frequency transistors in radiation resistance. Typical failure thresholds for PNPN devices range between 10^{12} and 5×10^{14} n/cm^2 ($E > 10$ keV, fission). Some narrow base PNPN devices have performed well at 10^{15} n/cm^2 ($E >$ 10 keV, fission).

9-46 Heating and Thermomechanical Damage [redacted]

[redacted] Any electronic component parts in which sufficient energy has been deposited by the electronic system environment will experience a transient rise in its temperature. The performance characteristics of most component parts are sensitive to temperature. Therefore, a temporary perturbation in the response of electronic component parts can be expected. The severity of the perturbation is a function of the deposited energy and the manner in which components are interconnected and mounted. Semiconductor devices are particularly vulnerable to temperature transients.

[redacted] Fortunately, most of the common circuit design techniques for compensation for temperature rises are directly applicable to the circumvention of heating effects caused by the TREE environment. Consequently, heating effects seldom are emphasized, and other effects predominate. However, in some particularly sensitive components such as inertial-guidance devices, heating effects remain a serious problem.

[redacted] The thermomechanical-shock effects arise from the deposition of short pulses of high intensity X-ray energy. The component part response differs from the effects discussed so far in that the primary manifestation is the loss of

[redacted]

[redacted]

[redacted] mechanical integrity. The processes of spallation, blowoff, and delamination combine to produce mechanical damage. In most cases, this mechanical damage results in a permanent, catastrophic electrical failure of the component parts.

[redacted] All electronic components are potentially vulnerable to thermomechanical shock, but semiconductor devices are among the most vulnerable components. The failure modes for transistors exposed to X-rays depend on the materials and geometries employed in their construction. It is, therefore, worthwhile to consider device fabrication in some detail.

[redacted] Transistors are composed of a combination of materials, and the relationship of these materials to each is best illustrated in terms of the processes by which these devices are fabricated. Transistors are produced from single crystal semiconducting material, which is processed into regions of desired type and resistivity to form the junctions necessary for transistor action. The many techniques employed to achieve the required junction configurations include growing the desired material from suitably doped melts and alloying-in the dopant impurities from appropriately metallized surfaces. However, the most prevalent technology being used to fabricate silicon transistors is the so-called "planar" process in which the required dopants are allowed to diffuse through area-defining masks formed on the surface of the silicon. These masks are made of silicon dioxide, which (1) is thermally grown on the surface of the silicon, (2) may be etched to form windows for diffusion, and (3) is a natural barrier to the diffusion of phosphorous and boron (the most commonly employed dopants for producing N- and P-type silicon, respectively). The windows in the silicon dioxide are defined by photoetching techniques initially developed and employed in the fabrication of etched wiring boards and subsequently refined in resolution to permit application in the fabrication of semiconductor devices.

[redacted] Figure 9-57 shows the steps employed in the fabrication of a typical transistor by the planar process. The oxide layer grown in Step (a) is removed in a selected area by photoetching (Step b), and a P-type dopant is allowed to diffuse into the starting N-type silicon to form what will be the base region of the transistor (Step c). A new oxide is grown next (Step d) and is photoetched to form a window over a smaller area, and an N-type dopant in high concentration is allowed to diffuse into this portion of the P-type region (Step e), converting it to (N^+)-type silicon. This forms the emitter region of the transistor. Depth of penetration of the dopant materials is controlled by the times and temperatures at which the diffusion operations are conducted. A final oxide growth (Step f) and selective photoetching (Step g) expose the emitter and base contact points. The whole surface is subsequently coated with aluminum (Step h) and selectively etched to produce the desired current paths and land areas (tabs) for connection (Step i).

[redacted] Since transistors fabricated in the above manner usually are prepared in multiple arrays containing hundreds of identical devices, the next steps are the separation of the individual devices by some technique such as diamond scribing and the mounting of each of the resultant chips (or dice) into a separate package. Typical chips for high-frequency transistors are less than 0.025 x 0.025 in. in area.

[redacted] The transistor package can take many forms (see Figure 9-58a), but in each form there is usually a section of the package that contains the lead wires to which the emitter, base, and collector portions of the device must be connected. This section is called the header. In a typical package this is the bottom section of the can, which contains the three lead wires. A cap is attached to complete the package. The header usually is made of Kovar, a nickel-iron alloy frequently used for glass-to-metal seals because of their comparable thermal-expansion coefficients.

[redacted]

[redacted]

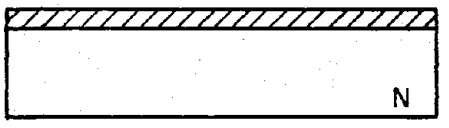

a. Growth of the SiO_2 Layer

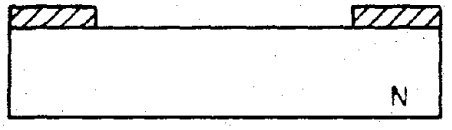

b. Removal of SiO_2 by Photoetching

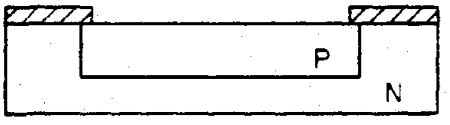

c. Diffusion of P-Type Dopant

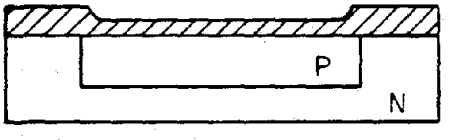

d. Regrowth of the SiO_2 Layer

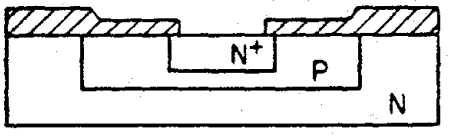

e. Photoetch Followed by Diffusion of N Type Dopant to form N+Emitter Region

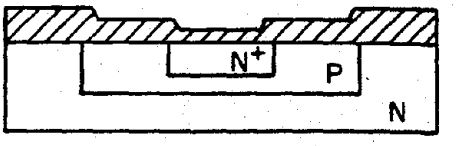

f. Regrowth of the SiO_2 Layer

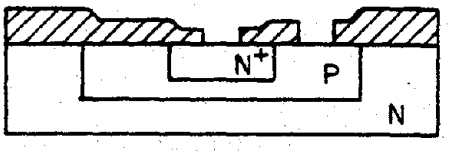

g. ~~Potoetch~~ Photoetch of Emitter and Base Contacts

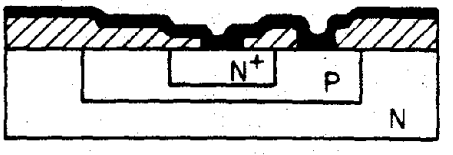

h. Vapor Deposition of Al

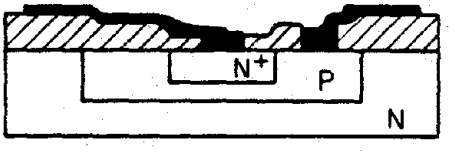

i. Selective Etch of Al to Produce Desired Current Paths

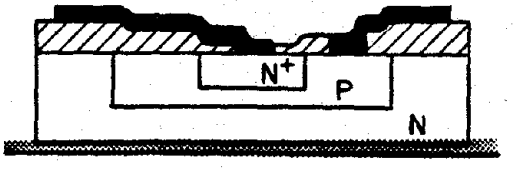

j. Mounting of the Die or Die Bonding

Figure 9-57. [redacted] Steps in the Fabrication of an NPN Silicon Planar Transistor [redacted]

[redacted]

[redacted]

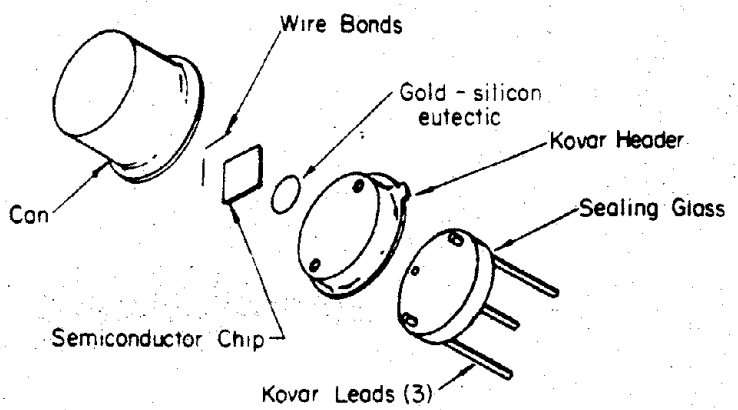

a) Transistor Package [redacted]

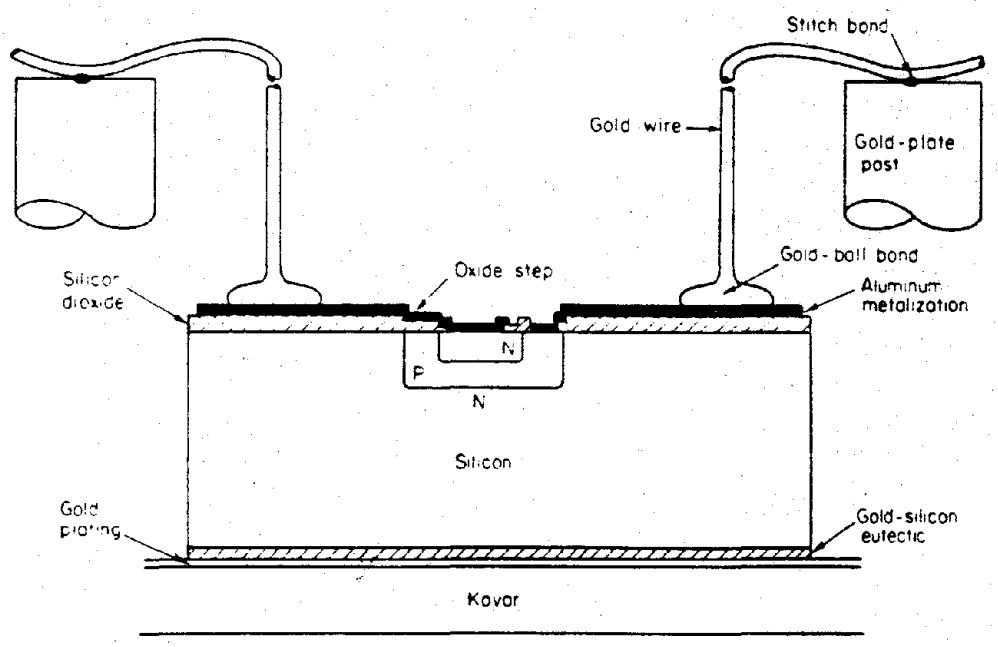

b) Cross-Sectional View of NPN Silicon Planar Transistor [redacted]

Figure 9-58. [redacted] Transistor Cross Section and Package [redacted]

[redacted]

[redacted]

[redacted] The three Kovar leadout wires are electrically insulated from each other by glass feed-throughs in the Kovar header. Since Kovar oxidizes easily, the external leads, and often the internal leads, on the transistor usually are plated to facilitate subsequent soldering or welding.

[redacted] The processed semiconductor chip is attached to the header by a fabrication step known as die bonding. Die bonding involves soldering, brazing, or glazing the die to the header. This attachment serves as a mechanical contact, a thermal path, and in some cases (such as the example being employed) an electrical contact. When the connection is to a metal portion of the header, the attachment usually is accomplished by brazing using a eutectic brazing alloy (generally containing gold). This is superior to a soft solder because the high melting point of the eutectic permits use of higher temperatures in sealing the top on the header and in preconditioning the devices if desired. Some disadvantages in the use of eutectic alloys for die bonding are that they generally are expensive, quite brittle, difficult to form into unusual shapes, and they cannot be vacuum evaporated to form thin films. A preform of the eutectic alloy is placed on the header on a platform directly connected to the collector leadout wire. In many applications, a simple gold plating on the Kovar platform suffices as the preform, since on heating in contact with the silicon chip, a gold-silicon eutectic will form. Heat is applied (390°-400°C), the transistor chip is placed on the preform, and the eutectic is chilled with a jet of nitrogen. This operation attaches the chip to header and forms the chip-to-header bond (Step j, Figure 9-57).

[redacted] Wire bonding makes electrical contact to the emitter and base regions. In some devices this connection is made by attaching the bridging wires directly to suitably metallized etched-open areas on the silicon chip. In many devices, however, these areas are much too small to permit forming quality connections, so the connections are made to extended tabs formed in the aluminum metallization on top of the silicon oxide. This latter configuration is illustrated in Figure 9-58b. The bridging wires, 1/2 to 3 mils in diameter, may be composed of any of a number of materials, but generally they are either gold or aluminum. Gold is used because it forms ohmic contact when alloyed with silicon, is available as extremely fine wire with reasonable strength, and may be bonded by thermocompression. Aluminum wire is used because it provides a one metal system when aluminum metallization is employed for extended tabs and avoids the formation of gold/aluminum alloys ("purple" and "white" plagues), it is available as fine wire, and it makes ohmic contact to both P-type and (N^+)-type silicon.

[redacted] In thermocompression bonding, the two metals (such as the wire and the bonding pad) are made to seize without a third intermediate phase (such as solder) and without melting. This is accomplished with high pressures and temperatures. The high temperature keeps the metals in the annealing range as they flow into atomic intimacy under the bond. One form of thermocompression bonding (called ball bonding or nail-head bonding) employs gold wire that is heated at the tip with a hydrogen flame to form a ball, which is subsequently driven against the heated chip under pressure to form the bond and concurrently is flattened into a nailhead configuration. In stitch bonding (another form of thermocompression bonding), the wire is bent under pressure from the tool head and forced into the heated pad in such a way that the wire is wedged flat at the point of contact. Either gold or aluminum may be employed in stitch bonding. In ultrasonic bonding, ultrasonic energy is employed to force the two metals into atomic intimacy. The resultant bond resembles a stitch bond. These three bonding techniques are illustrated in Figures 9-59a, b, and c, respectively.

[redacted]

[redacted]

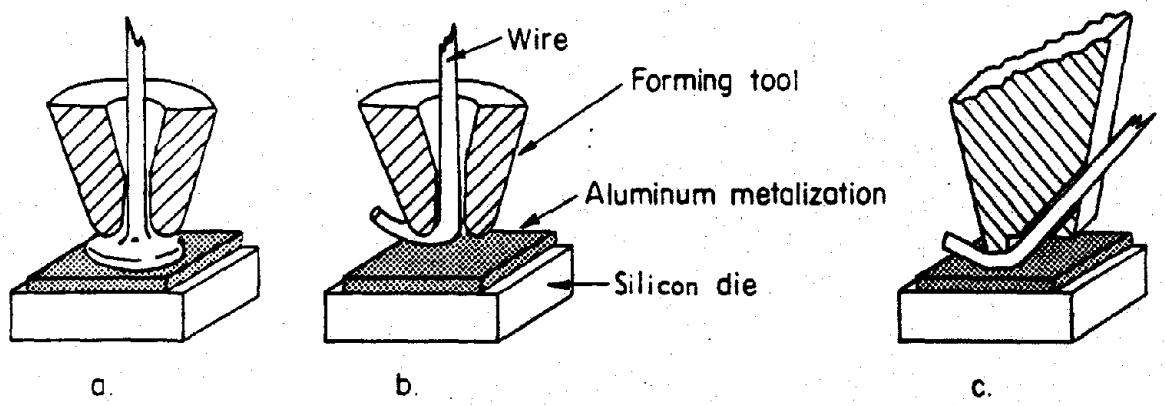

Figure 9-59. [redacted] Ball Stitch and Ultrasonic Bonding [redacted]

DNA (1)(3)

[redacted] Several general modes of failure (see Figure 9-60) are apparent: (a) the wires may break; (b) the emitter or base bonds may separate from the chip; (c) the silicon chip might fracture; (d) the chip may separate from the header; (e) the aluminum metallization constituting the extended tabs might become discontinuous; and (f) the wire bonds at the post may separate. [redacted]

DNA (1)(3)

[redacted]

[redacted] [redacted]

[redacted]

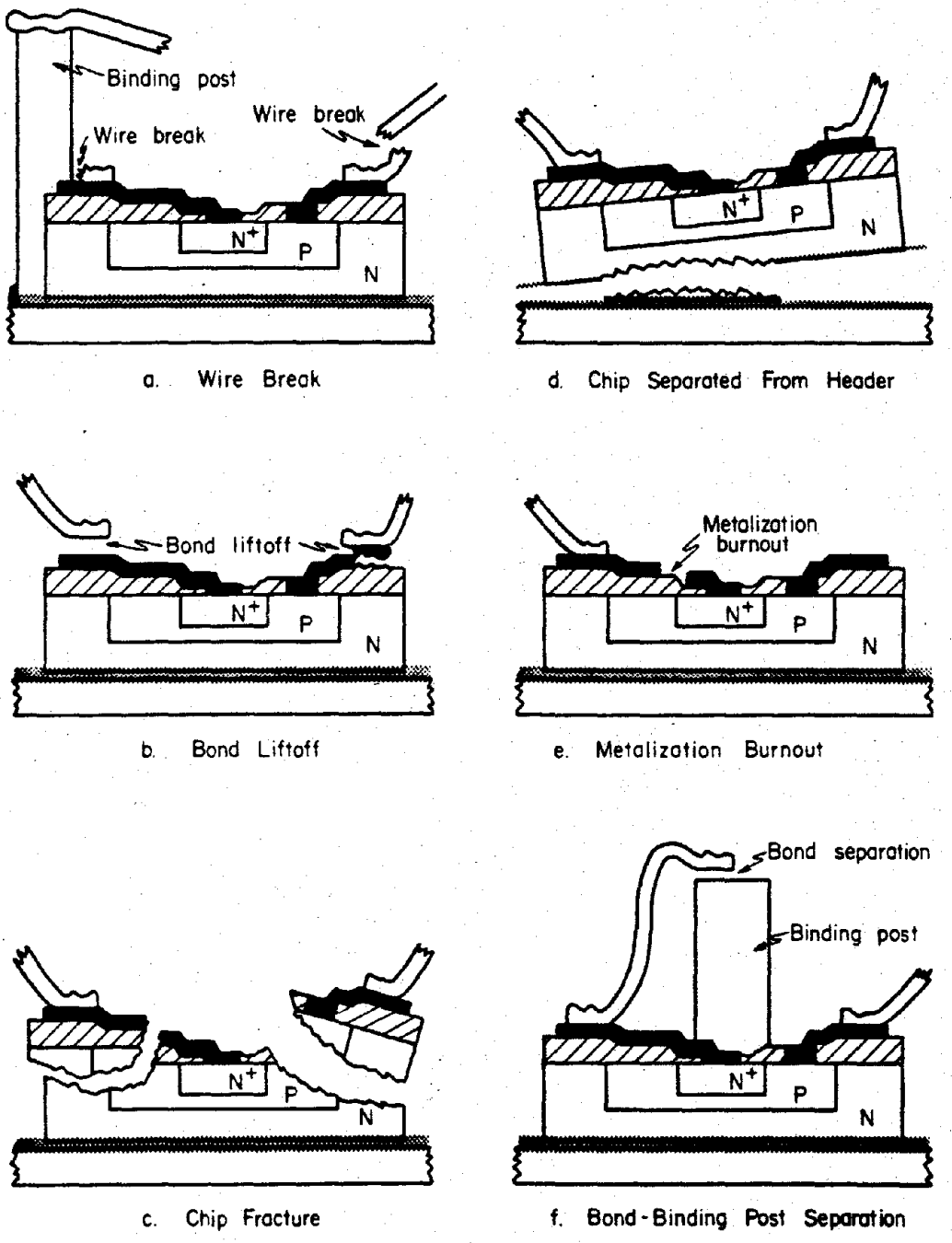

Figure 9-60. [redacted] Semiconductor Failure Modes [redacted]

[redacted]

[redacted]

DNA
(1)(3)

[redacted]

[redacted] OTHER ELECTRONIC COMPONENT PARTS [redacted]

9-47 Electron Tubes [redacted]

[redacted] The electron tubes discussed in this subsection are divided into three categories: vacuum tubes, gas-filled tubes, and phototubes. These categories include nearly all types of conventional electron tubes with the exception of microwave tubes. Because of the known differences in interaction of nuclear radiation with metals, gases, and photoemissive materials, as well as with glasses and other ceramics, the observable effects of these interactions might be expected to differ for each category of tube.

[redacted] Permanent damage to vacuum tubes is associated with thermal and fast neutron exposure. No significant permanent damage has been observed in conventional vacuum tubes or Nuvistors exposed to test radiation pulses or to a thermal neutron fluence of less than 10^{13} n/cm^2 (fission). Moderate damage may occur in standard size glass or metal tubes at thermal neutron fluences from 10^{13} to 10^{16} n/cm^2 (fission), and severe damage may occur at fluences greater than 10^{16} n/cm^2 (fission). "Severe damage" is often the failure of the glass envelope, usually at a glass-to-metal seal; "moderate damage" is generally a permanent change in tube operating characteristics. Miniature, subminiature, and ceramic-type tubes are less subject to both moderate and permanent damage than standard size tubes, largely because of the smaller area and mass of the tube parts. However, thermal-neutron fluences sufficient to cause permanent damage to high-vacuum tubes are greater than neutron fluences expected to be encountered in the nuclear weapon environment, e.g., $>10^{16}$ n/cm^2 (fission).

[redacted] The principal transient effect that results from exposure of vacuum tubes, including the Nuvistor, to nuclear radiation is produced by Compton scattering of electrons from structural members by gamma rays. Leakage currents caused by ionization of air between external electrodes, or reduction of resistance of insulating materials such as glass, ceramics, and mica, caused by electron excitation within the material, may have minor effects on tube performance. There is no appreciable radiation induced liberation of gas from tube parts, or ionization of residual gases within the tube.

[redacted] Most of the Compton electrons produced in the structural parts of the tube and ejected into the evacuated region are too energetic to be influenced significantly by the electronic fields in the tube. However, the impact of

[redacted] [redacted]

[redacted]

[redacted] high energy electrons on the interior surfaces of the tube assembly produces low energy secondary electrons that can be influenced by the existing electric fields, and thus can alter the normal operating characteristics of the tube. The ejected electrons can be collected by one or more electrodes, depending upon the electrode potential and position. The magnitudes of the resulting transient voltages that appear at the respective electrodes depend on the magnitudes of the transient current and the circuit resistance. The grid circuit is particularly affected by this phenomenon, since it usually suffers a net loss of electrons and therefore may assume a positive charge. The resulting increase in plate current is determined largely by the grid resistance and the gain of the tube.

[redacted] Gas filled tubes (thyratrons), under extensive neutron bombardment, most likely will fail by breaking of the glass envelope or glass-to-metal seals. Such damage occurs at thermal neutron fluences exceeding 10^{16} n/cm^2 (fission).

[redacted] The principal transient effect in a thyratron subjected to a nuclear radiation pulse is spurious firing caused by ionization of the filling gas. The filling gas, in these cases xenon, becomes partially ionized, primarily by gamma rays. Additional ions are created by ion-neutral molecule collisions in the electric field between the plate and the grid. A positive ion sheath can form around the negatively-biased control grid, which will neutralize the grid charge and will permit electrons to be accelerated from the cathode space charge toward the plate. As ion density increases, a sustaining discharge ensues, which can be shut off only by removing the plate voltage.

[redacted] Phototubes are designed to exhibit peak sensitivities to electromagnetic radiation in the visible and near-infrared regions by choosing photosensitive cathodes with low work functions. The presence of photosensitive material in a vacuum tube introduces effects other than those found in receiving type electron tubes in a radiation field.

[redacted] Severe permanent damage to phototubes, as with other vacuum tubes, is attributable to large thermal neutron fluences. Severe damage starts in phototubes at about 10^{15} n/cm^2 (fission). However, moderate permanent damage may occur at thermal neutron fluences two orders of magnitude lower. Moderate damage in some cases is an increase in dark current, or a decrease in anode luminous sensitivity, but in most cases it is a darkening of the glass envelope. This darkening effectively reduces tube sensitivity. The glass discoloration has been observed at fast neutron fluences of 5.5×10^{12} ($E > 10$ keV, fission), and gamma ray doses of 6.3×10^6 rads (C). Thus, both gamma and neutron components of mixed radiation contribute to permanent damage.

[redacted] The principal transient effect in photomultiplier exposed to pulsed X-ray radiation (and presumably to gamma radiation) is an increase in anode current. The increase can be as much as the space-charge-limiting value for a given tube. Furthermore, the duration of the current increase is much greater than that of the radiation pulse. At first, the current increases as a result of currents initiated by luminescence of those areas of the glass envelope that are optically coupled to the cathode of the photomultiplier. This current increase also has been demonstrated in steady-state gamma fields. Glass luminesces at wavelengths and intensities determined by the glass composition and by the dose rate. Since a great deal of the radiant energy is in the visible portion of the light spectrum, where common photomultipliers are sensitive, it would be expected that the degree of photomultiplier response to X-ray and gamma radiation would depend upon both the type of glass used for the envelope and the spectral sensitivity of the cathode material.

[redacted] [redacted]

[redacted]

[redacted] A second mechanism is required to explain the relatively slow decay of anode current after the radiation field is removed, since glass luminescence decays rapidly. It is believed that decay of anode current may be retarded by electric-field changes in the tube when electrical insulators become charged as a result of large initial current pulses.

DNA (C)(1)

[redacted]

9-48 Capacitors [redacted]

[redacted] Nuclear radiation affects most of the electronic properties of capacitors to some extent. Changes in the capacitance value, dissipation factor, and leakage resistance have been observed during steady-state reactor experiments. These effects generally are not considered severe for fast neutron fluences less than 10^{15} n/cm^2 ($E > 10$ keV, fission), and for most capacitors this limit is about 10^{17} n/cm^2 ($E >$ 10 keV, fission).

[redacted] During a high-intensity pulse of nuclear radiation, the most pronounced effect in a capacitor is a transient change in the conductivity of the dielectric material with a corresponding increase in the leakage currents through the capacitor. The most recent concept of ionization effects in insulating and dielectric materials indicates that the ionizing particles create ionizing tracks in the irradiated material. This means that, microscopically, the material is not uniformly ionized (an exception to this occurs at very high dose rates, $\approx 10^{12}$ rads (Si)/sec, where there should be sufficient overlap of the ionized tracks for the material to be considered uniformly ionized).

[redacted] The excess conductivity induced in a material irradiated with a short pulse of ionizing radiation is generally classified in two components: the prompt component, and the delayed component. The prompt component is primarily the result of excess carrier concentration from direct ionization by the radiation and the concurrent recombination and trapping of these carriers. The delayed component is that component of conductivity that remains after the termination of the ionizing pulse. This does not mean to imply that it does not make a small contribution during the radiation pulse. The delayed component is the result of thermal generation of excess carriers from shallow traps, in which they are caught during the prompt pulse, and their concurrent loss to recombination and retrapping. The rate at which these carriers are thermally regenerated depends on the energy level of the trap site, the concentration of filled traps, and the temperature. As there is usually more than one energy level trap in a material, more than one regeneration rate usually is observed in the delayed component.

[redacted] The excess conductivity is proportional to the number of carriers available to drift under the influence of the applied electric field. However, the microscopic nonuniformity of the carrier concentration must be considered for the pulsed irradiation case. For irradiation with ionizing particles with a low specific ionization (the ratio of the number of ion pairs produced per unit path length to the number produced per unit path length by a minimum ionizing particle), the excess prompt conductivity will be the same as if these carriers were generated uniformly throughout the material. However, if the specific ionization is increased (by bombardment with more heavily ionizing particles), a point will be approached where the separation of ionization sites is less than the distance traveled by the electron before it has become thermalized and is able to drift under the influence of

[redacted] [redacted]

[redacted]

the applied electric field. As this point is approached, the probability that the electron will be captured in the field of a neighboring ion increases, and the contribution to excess conductivity will be reduced. Thus, a plot of prompt conductivity as a function of specific ionization would show the prompt conductivity constant at low specific ionization and decreasing slowly after some threshold values of specific ionization is reached.

[redacted] The rate at which carriers are lost concurrent with their generation by the ionizing radiation is proportional to the concentration of recombination centers and unfilled trapping centers. While an insignificant number of the total traps in the material might be filled at low doses, the concentration of filled traps within a track depends only on the specific ionization. Thus, the trapping rate is affected by the specific ionization. The result of this effect is to cause an increase in prompt conductivity with specific ionization, which would serve in part to compensate for the decreasing effect mentioned above. However, this effect on the carrier loss rate should be slight, since most of the carriers are lost to recombination rather than trapping.

[redacted] When the radiation is delivered in a time short compared with the regeneration time of carriers from the traps, and the dose delivered in the pulse is large enough that significant numbers of tracks near the end of the pulse overlap tracks generated earlier, the concentration of filled traps in a track late in the pulse is different from that in a track created earlier in the pulse. When this occurs, the observed prompt conductivity becomes a function of the total dose delivered in the pulse, as well as of the specific ionization of the irradiating particle. It should be noted that a sufficient fraction of traps in a track must be filled to significantly affect the response. Hence, it is quite possible that trap densities in many insulators are high enough so that this condition is not realized in most pulse experiments.

[redacted] The delayed conductivity component depends on the rates of carrier regeneration and retrapping from trap sites, which depend on the concentration of filled traps and the energy levels of the traps. The concentration of filled traps is a function of the specific ionization of the irradiating particle and, in the case of overlapping tracks, the total dose. As the initial concentration of filled traps within a track is usually a significant fraction of the total concentration of traps, the retrapping probability changes during the time the traps are emptying, thus altering the characteristic time for emptying the remainder of the filled traps. As a result, the decay of the delayed component does not usually follow a simple law. Only in certain cases, where the trapping probability is negligibly perturbed by the radiation, will simple exponential decays be observed.

[redacted] Neutrons produce ionization by a number of collision processes that give rise to ionizing secondary particles. These processes include:

- Elastic scattering when the recoil atom receives sufficient energy to produce ionization.
- Inelastic scattering, producing a recoil atom that may or may not ionize but that emits a gamma photon that can produce a secondary ionization.
- Capture, resulting in the emission of a photon and/or an ionizing secondary particle (primarily thermal neutrons).
- Reactions resulting in an ionizing particle, e.g., (n,p), or (n,α) reactions (high-energy neutrons).

There are, therefore, many possible different specific ionizations associated with ionized tracks in neutron bombarded materials.

[redacted] In hydrogenous materials, the principal ionization is caused by recoil protons, which have a high specific ionization. For this reason, neutron induced conductivity in hydrogenous dielectrics has been found to be approximately

[redacted]

[redacted]

one-fifth to one-half that of gamma ray induced conductivity for equal ionization energy deposition rates. For nonhydrogenous dielectrics, the most important contribution to neutron induced ionization is by the interactions of very high-energy neutrons ($E > 2$ MeV).

[redacted] A "polarization effect" that is attributed to space charge buildup within the dielectric material due to nonuniform trapping has been observed with some capacitors, particularly with Mylar, mica, polycarbonate, tantalum oxide and Vitamin Q devices. This effect is manifested in several ways. One is an apparent decrease in the induced conductance with sequential radiation pulsing. Charge transfer across the dielectric during a radiation pulse builds up a space charge field opposing the applied electric field. If the applied electric field is then removed, subsequent radiation pulses result in a current in the external circuit opposite in direction to that observed with the field applied. This is caused by the discharge of the space charge field. Similarly, if the electric field is reversed rather than removed after the space charge has been built up, the space charge field enhances the applied field, and a larger current results than would be observed normally.

[redacted] Saturation of the polarization effect, where no further decrease in the charge transfer is observed with subsequent radiation pulses, occurs after one or more pulses, depending on the capacitor and on the dose delivered in each pulse. Decreases of 50 to 70 percent for mica, 10 to 20 percent for tantalum oxide, and 30 percent for Mylar have been observed due to this space charge buildup during radiation pulsing.

DNA (b)(1)

[redacted]

9-49 Resistors [redacted]

[redacted] Radiation effects in resistors are generally small compared with effects in semiconductors and capacitors and are usually neglected. However, in circuits requiring high precision resistors transient effects may be significant at dose rates of as low as 10^7 rads (C)/sec and at neutron fluences of 10^{14} n/cm^2 ($E > 10$ keV, fission).

[redacted] The transient effects are generally attributed to gamma rays that interact with materials to produce electrons, primarily by the Compton process; however, energetic neutrons can also produce significant ionization. Transient effects include (1) a change in the effective resistance due to radiation induced leakage in the insulating material and the surrounding medium, (2) induced current that is the result of the difference between the emission and absorption of secondary electrons by the resistor materials, and (3) change in the conductivity in the bulk material of the resistor. There is no substantial evidence, however, that the third effect is a first-order transient effect.

[redacted] The permanent effects are generally caused by the displacement of atoms by neutrons, causing a change in the resistivity of the material.

[redacted]

DNA (b)(1)

9-50 Batteries and Cables [redacted]

[redacted] Batteries are affected much less by radiation than other component parts. The effects of radiation on nickel-cadmium batteries appear to be insignificant at dose rates up to 10^7 rads (air)/sec. No radiation damage was apparent in a number of batteries and standard cells that were subjected to 10^{13} n/cm^2 ($E > 10$ keV, fission). Transient radiation effects on an ammonia fuze indicated that pulsed gamma ray irradiation of 10^8 rads (air)/sec had no effect on the operation of the battery.

[redacted]

[redacted]

[redacted] It has been recognized for some time that intense pulses of radiation produce significant perturbations in electrical cables and wiring, including coaxial and triaxial signal cables. Even with no voltage applied to a cable, a signal is seen when the cable is exposed to a pulsed radiation environment. The current associated with this signal is defined as a replacement current, since it is most likely a current in an external circuit that is necessary to replace electrons or other charged particles that are knocked out of their usual positions by the radiation. The replacement current definition also applies to the effect of charged carriers associated with the incident radiation embedded in a test sample.

[redacted] The magnitude of the radiation induced signal varies with the voltage applied to the cable. This voltage-dependent portion of the signal, i.e., the total signal exclusive of the replacement current, is called conduction current, thus it is ascribed to the conductivity induced in the insulating dielectric by the radiation. However, it may also contain major contributions from polarization or depolarization processes in the dielectric. These can usually be identified by their gradual disappearance (saturation) after repetitive exposures and by their reappearance in additional "shots" in which the applied voltage is changed greatly, e.g., removed or reversed.

[redacted] Ionizing radiation of any type produces free electrons that contribute to the conductivity of the material. Hence, insulators are expected to have a transient enhanced conductivity in an ionizing radiation environment. Conduction in the insulator is frequently characterized by two components: for very short radiation pulses, a prompt component whose magnitude is a function of only the instantaneous exposure rate, and frequently at the end of the short radiation exposure, a delayed component having approximately exponential decay.

[redacted] Although the replacement, conduction, and polarization currents are fairly well understood in terms of the interactions between the ionizing radiation and the metal-dielectric target system, it is not yet possible to predict quantitatively the response for a given cable in a specified environment. In a mixed neutron-gamma environment, the induced replacement current usually contains positive and negative components, and may therefore assume either polarity. The conduction current sometimes exhibits a rather complicated time dependence consisting of prompt- and delayed-conductivity contributions. The polarization current appears to be greatly affected by the properties of the metal-dielectric interface.

[redacted] Permanent damage effects in cables and wiring are manifested as changes in the physical and electrical properties of the insulating materials. When such damage becomes appreciable, e.g., when the insulation resistance is reduced severely, electrical characteristics may be affected. The extent of the damage to insulating materials is an increasing function of neutron fluence, exposure or dose, humidity, and irradiation temperature. Certain types of wire insulation are quite susceptible to permanent damage. For example, silicon rubber becomes severely cracked and powdered after approximately 2×10^{15} n/cm^2 ($E > 10$ keV, fission). The approximate damage thresholds for three common types of cable insulation are: polyethylene, 1×10^7 rads (C); Teflon TFE, 1×10^4 rads (C); and Teflon FEP, 2×10^6 rads (C). On the other hand, some irradiated polyolefins are capable of withstanding up to 5×10^9 rads (C). A considerable degree of annealing has been observed with respect to insulation resistance, which implies the possibility of adequate electrical serviceability after moderate physical damage.

[redacted] It is not expected that radiation effects on wiring with thin insulation will exhibit the strange behavior observed in coaxial cables. In particular, the very limited measurements that have been performed indicate that the replace-

[redacted]

[redacted]

[redacted]

[redacted]

ment current is primarily a function of the gamma environment. To a good approximation, it can be assumed that the replacement current for a wire or most other objects placed in the radiation environment will amount to the emission of a number of electrons between 1 and 5 x 10^{-3} times the number of gamma photons traversing the object.

[redacted] The conduction current is a very sensitive function of the amount of insulation around the wire and its immediate environment. For a bare wire in air with a ground plane nearby, conduction is due predominantly to the ionization produced in the air. Placing insulation around the wire reduces this conduction, but at the price of increasing the area of the wire and hence the effective replacement current.

9-51 Quartz Crystals [redacted]

[redacted] The radiation response of a quartz crystal oscillator is primarily a function of radiation dose. The type of material from which the oscillator is fabricated, e.g., natural quartz, Z-growth synthetic, Z-growth swept synthetic, etc., and to a lesser extent the type of cut, e.g., AT, BT, etc., and the frequency and mode of operation determine the sensitivity of the oscillator to the radiation. The primary effect of the radiation is a shift in the frequency of the oscillator. Both transient and steady-state shifts have been observed.

[redacted] The steady-state frequency offsets are a result of changes in the elastic stiffness constants of the crystal. For example, perturbations in the crystal bonds due to charge trapping at defects or to formation of new defect complexes will result in steady-state frequency offsets. Of materials tested to date, Z-growth swept-synthetic quartz has been the most radiation tolerant to steady-state frequency offsets. Swept natural quartz is slightly more sensitive and unswept natural quartz and unswept synthetic quartz, respectively, are even more sensitive. The response of a particular crystal also varies with the manner in which the crystal is mounted, the material used for the electrodes, and to a lesser extent differs for each quartz bar grown, even among bars grown under similar conditions. Both swept synthetic and natural quartz crystals can recover 80 percent to 90 percent of their original frequency change after annealing at 500°C for times on the order of 100 to 160 hours.

[redacted] Transient shifts in the frequency of an oscillator and reduction or cessation of the output result from energy deposition and any subsequent temperature rise in the crystal. Temperature gradients in the crystal due to faster removal of heat near the support wires and due to the electrodes absorbing more energy than the crystal, can give rise to frequency shifts induced by the resulting strain.

[redacted] Irradiation of general purpose crystal units has shown that they do not suffer significant permanent effects, within the limits of their stability, at a neutron fluence of 10^{13} n/cm^2 ($E > 10$ keV, fission) and a gamma dose of 4.4 x 10^3 rads (air). Transient phase and amplitude changes resulting from this environment are not of sufficient magnitude to cause concern about their operation under such conditions.

[redacted] Moderate precision crystal units display negligible frequency and amplitude changes when subjected to a reactor pulse. Weapon tests as well as steady-state gamma source tests indicate that a gamma dose greater than 10^4 rads (air) is required to induce significant permanent frequency changes in these devices. Frequency changes up to almost one part in 10^5 were observed after exposure to 7.5 x 10^4 rads (air) and 10^{12} n/cm^2 at a weapon test. The possibility that causes other than radiation contributed to the changes observed at this test cannot be excluded.

[redacted] High precision natural quartz-crystal units either stop oscillating or exhibit appreci-

[redacted]

[redacted]

[redacted]

[redacted] able decreases in the amplitude of the output signal during nuclear pulses of approximately 10^{12} n/cm^2 ($E > 3$ MeV, fission), and 3×10^3 rads (H_2O). If oscillation stops, its cessation persists for minutes. The cessation of oscillation is apparently independent of the voltage, current, or power at which the units are being driven. Resumption of oscillation occurs at a reduced drive current and lower frequency. The drive current is tens of microamperes below the specified rated drive when oscillation resumes. Frequency changes as high as 1 part in 10^7 have been observed when this type of crystal was exposed to 7.9×10^{11} n/cm^2 ($E > 3$ MeV, fission), and 2.9×10^3 rads (H_2O).

DNA (b)(1) [redacted]

9-52 Solder Joints [redacted]

DNA (b)(1) [redacted]

9-53 Infrared Detectors [redacted]

[redacted] The infrared detectors that exhibit the greatest sensitivity to infrared radiation are also the most sensitive to nuclear radiation. For radiation pulses that are short compared to the relaxation time, the response of a photoconductive type of infrared detector cell is an excess conductance that is proportional to the radiation exposure. For long pulses the excess conductance is proportional to the radiation intensity and the carrier recombination time. Neutron bombardment causes permanent degradation of output-signal level and signal-to-noise ratio.

[redacted] Irradiation of a lead sulfide device to 1.3×10^{14} n/cm^2 ($E > 0.48$ eV, fission) at 134°F revealed a 67 percent reduction of output signal level and greater than 40 percent reduction in the signal-to-noise ratio. Damage was essentially catastrophic after 6.9×10^{15} n/cm^2 ($E > 0.48$ eV, fission).

[redacted] Lead selenide devices appear to be somewhat more tolerant to neutron irradiation than lead sulfide detectors. After a neutron fluence of 1.2×10^{14} n/cm^2 ($E > 0.48$ eV, fission) at 135°F, the output signal level of a lead selenide cell was reduced by 36 percent, and the signal-to-noise ratio was down more than 46 percent. The output level was down by 96 percent after 1.8×10^{16} n/cm^2 ($E > 0.48$ eV, fission). Lead selenide cells that are designed to operate at low temperatures are more sensitive to radiation than those that are not designed for low temperatures.

[redacted] Indium antimode photovoltaic cells that operate at liquid nitrogen temperature showed significant voltage signals at doses less than 0.88 rads (air). The cells exhibited radiation induced voltages roughly proportional to the logarithm of the dose when the radiation was delivered in short pulses. Recovery to within 2 percent of the maximum voltage occurred within 175 μsec after the highest intensity radiation pulses. A complete loss of output from these cells has been observed after a neutron fluence of 2×10^{16} n/cm^2 ($E > 0.48$ eV, fission).

[redacted] Thermistor-bolometer infrared detectors are the most neutron tolerant of the devices that have been tested. After 9.6×10^{13} n/cm^2 ($E >$

[redacted]

[redacted]

[redacted] 0.48 eV, fission), the output signal level was down by 28 percent, and the signal-to-noise ratio was down about 11 percent. After 1.6 x 10^{16} n/cm^2 ($E > 0.48$ eV, fission), the output level was down 57 percent, and the signal-to-noise ratio was down 66 percent. The detector may be usable for some applications under these conditions.

[redacted] Thermomechanical shock effects in infrared detectors will be similar to those discussed for semiconductor devices, and will occur at about the same levels.

[redacted] ELECTRONIC CIRCUITS [redacted]

9-54 Radiation Response of Discrete-Component-Part Circuits [redacted]

[redacted] Determination of the response of a circuit is complex because of the large variations in circuit configuration and in the component parts that can be used within a circuit configuration. Therefore, determining circuit response becomes a problem of detailed circuit analysis and/or testing. The radiation effects material necessary for this kind of analysis and testing are beyond the scope of this manual. Guidance may be obtained from the *TREE Handbook* and the *TREE Preferred Procedures* (see bibliography). General circuit effects and typical analysis techniques are discussed in this manual.

[redacted] The transient effects that can cause a system to malfunction can result in circuit responses that, like component-part responses, can be both dose and dose rate dependent. If the radiation pulses are short with respect to component-part recovery times the circuit time constants, the circuits will integrate the effects and will be sensitive to the total dose rather than the dose rate. However, when the pulse widths are wide, the circuits are dose rate sensitive. This can be illustrated by reference to Figure 9-61. Assume that for the circuit response plotted, the malfunction threshold is 1.5 volts. Therefore, a 0.15 μs pulse at 1 x 10^9 rad (Si)/sec will cause a malfunction. It is obvious from the curve that the malfunction dose rate is much lower for wider pulses.

[redacted] Discrete digital circuits and circuits that contain silicon controlled rectifiers (SCR's) have displayed failure at doses as low as 0.1 to 1.0 rad (Si) for short pulse widths. It is difficult to design a circuit specially that will not malfunction above a prompt dose of 100 rads (Si).

[redacted] Another effect that can result from the ionizing radiation is the initiation of a catastrophic action or catastrophic failure. An example would be the firing of a pyrotechnic device or the premature initiation of a firing signal. A second type of catastrophic action occurs if a circuit destroys itself as a result of the effects caused by ionization (burnout). Figure 9-62 shows an output stage of a power supply inverter. In normal operation, Q1 and Q2 are turned on alternately. The output at the transformer secondary is a square wave. Ionizing radiation may cause Q1 and Q2 to turn on simultaneously. After the radiation pulse, the transistors will recover to normal operation, and one of the transistors will attempt to turn off. At this time a large voltage will be induced across the transistor that is attempting to turn off. If this voltage exceeds the breakdown voltage, the transistor may be damaged.

[redacted] General statements applicable to both permanent and transient effects include:

- Circuits that use low frequency, thick base semiconductors usually are more susceptible to radiation effects than those circuits that contain high frequency, thin base devices
- Germanium devices generally will show larger photocurrents and leakage currents than comparable silicon devices
- High impedance circuitry generally will be more susceptible to radiation effects than low impedance circuitry

[redacted]

[redacted]

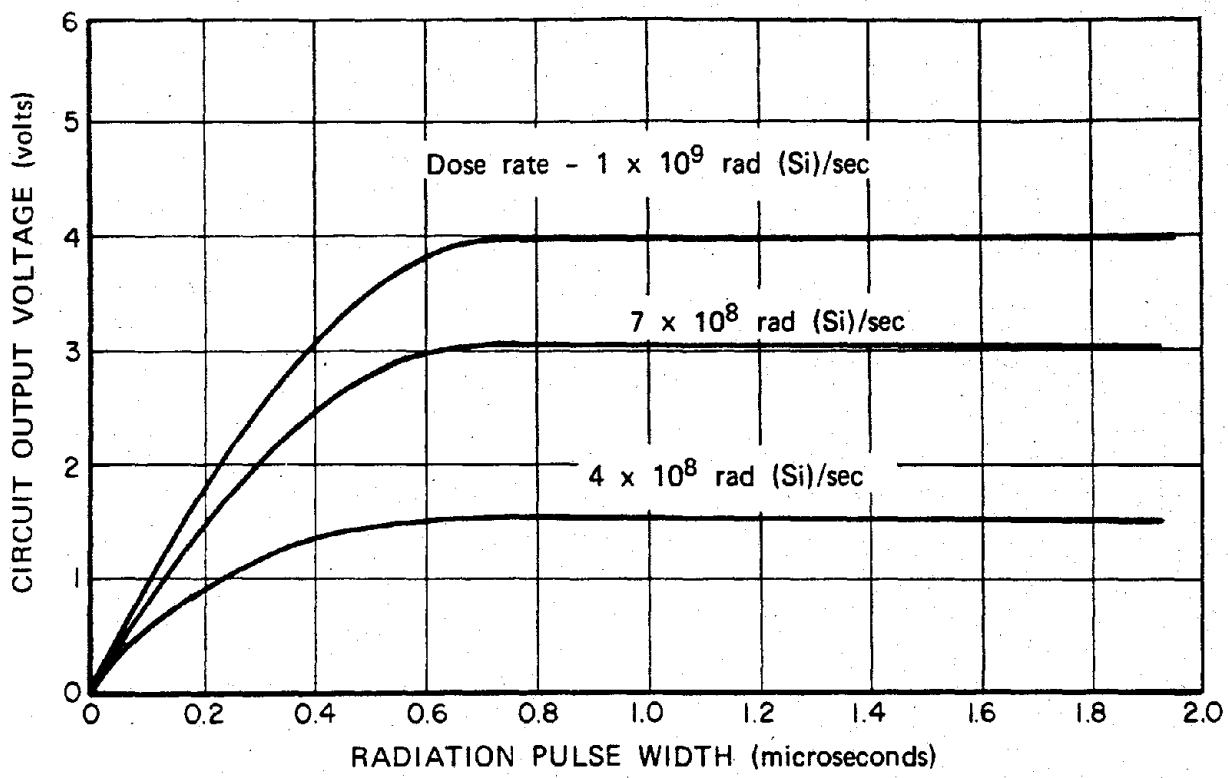

Figure 9-61. [redacted] Circuit Response as a Function of Radiation-Pulse Width [redacted]

[redacted]

- Magnetic memory devices will not be sensitive to the neutron and gamma environments typically specified as the environment in which an electronic system must survive.

[redacted] The primary permanent effects on circuits will be the degradation of semiconductor devices. The solid-state power supplies and regulators with their low frequency transistors will fail to perform their required function when exposed to fluence between 10^{11} and 10^{13} n/cm^2 ($E > 10$ keV, fission) depending on the circuit configuration, component parts, and design margins in the system. Circuits that use MOSFET can fail at gamma doses between 10^3 and 10^5 rads (Si).

[redacted] The failure threshold for thermomechanical shock will be established by the threshold of the component parts.

[redacted] It is desirable to have a method of analysis that can be used to predict the response of components, circuits, and systems. The analysis methods that are used consist of established techniques to calculate circuit and system responses by replacing radiation effects by their corresponding electrical effects. Thus, the problem that is solved eventually is wholly electrical in character. A major advantage of analysis as a simulation tool is that it is not necessary for a circuit or system to exist in a physical state before it can be analyzed. In addition, the analyst has control over the "environment," and it is theoretically possible to simulate the total

[redacted]

[redacted]

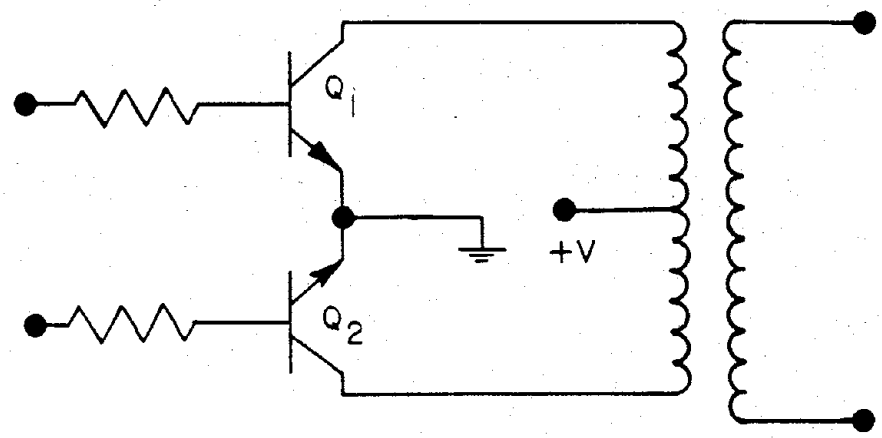

Figure 9-62. [redacted] Circuit in Which Burnout Could Occur [redacted]

[redacted]

environment during a single (but complicated) analysis. Perhaps the major disadvantage of analysis (for TREE) is the relatively low confidence in the results. This low confidence level usually arises from the simplifying assumptions that are often made to expedite the analysis and which, themselves, are subject to verification, typically by environmental testing.

[redacted] Certain requirements or inputs are needed for any circuit or system analysis. First, an accurate mathematical description of the electrical characteristics must be obtained. Such a description usually is checked by comparing the computed electrical response to the measured electrical response of a circuit or system. Second, the radiation effects on electronic materials and devices must be represented, or modeled, by electrical effects. For example, displacement effects may be modeled by making transistor current gain a function of time. This step generally requires environmental testing and/or sound analytical procedures to obtain the required radiation effects data. Third, an analysis method must be employed to make an accurate calculation of the steady-state and transient responses of the electronic network of interest. This may be done by hand or with the aid of a computer.*

[redacted] Hand analysis techniques are useful for a quick qualitative and, to a limited degree, quantitative appraisal of the sensitivity of linear circuits and logic circuits to radiation environments. Manual techniques are valuable in the prediction of permanent effects of transient radiation, particularly when the relevant electrical parameters assume constant, degraded values after irradiation. The hand analysis techniques are often quite adequate to establish the initial estimate of radiation induced voltage and current transients and of the steady-state performance degradation. This type of analysis is suitable for a rough estimate of the peak-amplitude radiation response. In practice, only small, simple circuits can be handled.

[redacted] In doing analysis, there is an inevitable choice between time (man-hours) and accuracy. If great confidence in the results is not required (e.g., when the analysis results are to be used to

* [redacted] A more detailed discussion of hand and computer analysis techniques is contained in the "TREE Handbook" (see bibliography).

[redacted]

[redacted]

[redacted] plan further environmental tests), a large number of simplifying assumptions can be made, and the analysis can be carried out quickly by hand.

[redacted] If the results of an analysis are to be used directly in a survivability assessment, high accuracy is desirable. This implies that few simplifying assumptions may be made. If a circuit contains more than one or two active devices (e.g., transistors), the circuit model will be complex, and the speed and accuracy of a digital computer should be used. Both hand analysis and computer aided analysis require an equivalent-circuit model that represents electrical and radiation induced phenomena. A notable difference is that the computer can handle an equivalent circuit model in its entirety and can generate the desired response function without making engineering approximations.

[redacted] Both analog and digital computers have been used for response predictions, and each has advantages and disadvantages; however, recently developed mathematical techniques and programming capabilities make the digital computer preferable for most problems. Several digital programs are available for circuit analysis. These are described in some detail in the "TREE Handbook" (see bibliography). These codes do not do the analysis. They do perform the tedious, error-prone calculations. The individual who uses them must provide the accurate description of the equivalent circuit model and must interpret the results.

[redacted] Two factors control the accuracy of the results of any TREE analysis method. The first factor is the accuracy and completeness of the description of the response of individual components to a particular radiation environment. This information is basic to the success of any analysis technique and frequently has been the major stumbling block for analysis attempts.

[redacted] The second factor that affects the accuracy of the analysis results is the assumptions that are made to simplify the analysis problem. Certain aspects of the radiation response of individual components generally are neglected by assuming that they will contribute only a small or negligible portion to the radiation response of the circuit. These assumptions are made on the basis of general experience with the radiation response of circuits and with knowledge of the limits over which they might be valid. Although these assumptions are generally correct, there are specific instances and specific circuit configurations for which they may not hold, and care must be taken in making such assumptions.

[redacted] In practice most of the analysis approaches result in a fairly reasonable correlation with experimental results. However, it is common knowledge that any experimental result can be explained by a theory, but the theory will not always predict the correct result in a new situation. Therefore, caution should be exercised when accepting a component representation or an analysis technique that predicts the results for a pulsed reactor environment reasonably accurately, if these results are to be applied to a nuclear weapon environment. It is also possible that techniques applicable to switching circuits or nonlinear circuits will not apply to all linear circuit analysis.

9-55 Radiation Response of Integrated Circuits [redacted]

[redacted] Integrated circuits include many circuit types differing in construction materials and methods. The four construction types are the monolithic semiconductor, thin film, multichip, and hybrid integrated circuits. The scope of this section will be limited to monolithic and thin film circuits since the radiation response of both multichip and hybrid circuits can be inferred from the discussion of monolithic and film circuits or discrete devices. The discussion includes junction isolated, dielectrically isolated, and air isolated integrated circuits.

[redacted]

[redacted]

[redacted] In junction isolated circuits, the components are defined within a single crystalline substrate by regions of alternate doping that are electrically isolated by reverse biased PN-junction boundaries. The doped regions are formed by the geometrically controlled diffusion of appropriate impurities into the substrate. One or more uniformly doped, epitaxial layers may be grown upon the substrate prior to diffusion (planar epitaxial). The dielectric-isolated circuit is distinguished by the use of a dielectric (silicon dioxide or ceramic) instead of a PN-junction isolation between critical components. A single component or a small number of components are formed within individual single crystalline islands (called tubs) that are imbedded in a polycrystalline substrate. The active elements in both the junction and dielectric isolated circuits can be bipolar transistors, junction FET's, or insulated gate (MOS) FET's. The air isolated circuit usually employs aggregates of unipolar (i.e., field effect) transistors of metal-oxide-silicon construction.* Since this type of transistor may be used as a bias-dependent resistor, complete designs usually are constructed without the use of other circuit elements. Air isolated MOS integrated circuits are fabricated by growing silicon on sapphire (SOS). Portions of the silicon are etched away, leaving isolated islands of silicon upon which transistors are fabricated.

[redacted] Thin-film integrated circuits employ geometrically controlled surface films of conductive and dielectric materials upon a glass or ceramic substrate to define passive circuit elements and interconnections. The active elements may be formed as an integral part of the process (thin film, insulated gate, field effect transistors) or welded to the circuit (conventional, discrete transistors). Circuits of the latter type are referred to as hybrid thin film circuits.

[redacted] The categorization of circuit types given above is somewhat arbitrary. It is based on the present developments in the integrated circuit industry, rather than on strict lines of variance between the types. The categorization is used for convenience of discussion with respect to the effects of transient radiation, where distinctly different effects may occur. For example, the PN junction used for isolation is a source of photocurrents during an ionizing radiation pulse, and may result in large substrate (and hence, power-supply) currents in junction isolated monolithic circuits. This effect is absent in either the air or dielectric-isolated monolithic circuit or the thin film, hybrid circuit.

[redacted] Transient radiation may cause both transient, permanent and thermomechanical shock effects. On a qualitative basis, the primary electrical effects introduced in integrated circuits by transient radiation are similar to the effects described for conventional solid-state circuitry. The magnitude, duration, and electrical consequences of these effects, however, do not follow directly from conventional circuit experience.

[redacted] The effects of radiation on an integrated circuit are more closely related to its geometrical and physical characteristics than to its electrical function or circuit configuration. The proximity of circuit elements within the device, and in some cases its integral structure, make several modes of secondary interaction possible. This is especially important in the case of junction isolated integrated circuits.

[redacted] The transient effects observed in integrated circuits result from the generation of excess charge carriers that cause photocurrents and voltage changes. As previously described for transistors, the motion of excess carriers is governed by the response of carriers to electric fields and concentration gradients. The charge carriers will cause currents to occur until they

---

* [redacted] Air-isolated bipolar integrated circuits have also been constructed.

[redacted]

[redacted]

[redacted] are swept out by external fields and electron-hole recombination. The peak photocurrents can be a function of either dose rate or dose depending on the duration of the radiation pulse. As a result, if the radiation pulse is long compared to the circuit radiation response time, the microcircuit response is dose rate dependent. However, for radiation pulses that are short compared to the circuit radiation response time, microcircuit response will be dose dependent. Thus, the width of the radiation pulse can be of considerable significance, since the peak photocurrent generated can be a function of the duration of the pulse as well as its amplitude.

[redacted] In a transient-radiation environment, the semiconductor integrated circuit reacts to several mechanisms that have been discussed in connection with conventional circuitry. One point of departure that is made necessary by the monolithic nature of the circuit, is the significant and often predominant interelement effects that occur in addition to the intraelement effects. It is important to consider current paths between as well as within component parts of the microcircuit.

[redacted] Quite generally, the transient effects in any integrated electronic device are a consequence of a sequence of events that may be described as follows:

- The radiation interacts with the circuit material and surrounding encapsulant to introduce charge carriers and to establish a nonequilibrium charge distribution.
- Acting under nonequilibrium electric fields and concentration gradients, mobile carriers flow in the direction that restores equilibrium and thereby produce primary electrical currents. These electrical currents may be semiconductor-junction photocurrents, replacement currents, dielectric-leakage currents, gas-ionization currents, etc.
- The nonequilibrium charge distribution and the primary electrical currents may interact with the electrical circuit to produce secondary effects, e.g., secondary photocurrents. Under certain circumstances, the secondary effects may be sufficiently regenerative to be self-sustaining, and a new stable circuit state will result. In addition, localized electrical stresses may introduce permanent damage.
- The cumulative effects of the radiation induced currents and circuit action are voltage, current, and impedance changes of variable duration at the terminals of the integrated circuit.

[redacted] In junction isolated circuits, the predominant effect is PN-junction photocurrents resulting from ionization in the semiconductor material. Important secondary effects include secondary photocurrents produced by transistor action in any three adjacent doped regions, potentially large substrate currents, and "latchup."

[redacted] The predominant effect in dielectric isolated circuits is also PN-junction photocurrents. The major difference from other monolithic structures is the absence of the extra PN-junction between the components and the substrate and its associated photocurrent. Also, current paths are more restrictive.

[redacted] In air isolated integrated circuits, the important primary transient effects are PN-junction photocurrents, replacement currents resulting from charge scattered from device lead wires and the case, and ionization currents through the surrounding encapsulant. The predominant secondary effect is a secondary photocurrent resulting from the radiation induced gate current and transistor action. In addition, photocurrent is generated in the Zener diode employed for protection in the gate lead of MOS circuits.

[redacted] In MOS integrated circuits, the important primary transient effects are drain-substrate and source-substrate PN-junction photocurrents,

[redacted]

[redacted]

[redacted] replacement currents resulting from charge scattered from device lead wires and the case, and ionization currents through the surrounding encapsulant. The predominant secondary effect is a secondary drain current resulting from the radiation induced gate current. In addition, photocurrent is generated in the Zener diode employed for protection in the gate load.

[redacted] For the most part, thin film circuits may be treated as conventional circuits with extremely small geometries. Ionization currents within and between elements have specific importance, especially in the high-impedance circuitry associated with thin film circuits that employ field effect transistors. Nevertheless, in most cases of interest, the transistor is the predominant element that determines the transient radiation response of the circuit.

[redacted] Semiconductor integrated circuits of the planar-diffused (or planar-epitaxial) type experience transient effects that may be attributed to the interaction of the circuit elements through the active substrate. Two predominant interelement effects that must be considered are the presence of large substrate currents and the occurrence of latchup.

[redacted] In practice, the high packing density of elements on a substrate chip results in the presence of isolation diodes over most of the area of the chip. Thus, a chip 40 x 40-mils may have 1,500 mils^2 of effective isolation-diode area. The total substrate photocurrent may be 100 times that of a typical diode in the circuit. Since the substrate is connected to the power supply system, the substrate currents will be reflected in large currents appearing in the power supply leads. Radiation induced power supply currents of the order of 1 ampere, with durations of a few microseconds have been observed at prompt doses of approximately 10 rads (Si). The potential hazards to the power supply system, which must supply many such circuits, are evident.

[redacted] Present evidence indicates that the very large power supply currents occur primarily in those circuits where transistor action through the substrate is possible. In circuits of this type, radiation thresholds above which the current increases suddenly have been observed. The thresholds have been attributed to the turning on of an equivalent four layer device. Other possibilities include second breakdown and sustaining voltage breakdown.

[redacted] Transients induced in integrated circuits by pulsed ionizing radiation last from less than a microsecond in high speed digital circuits to several tens of microseconds in slower circuits. Occasionally, pulsed-radiation effects with considerably longer recovery times can be explained by circuit time constants. In the extreme case, the abnormal state persists until the dc power is interrupted. When this occurs, normal circuit operation is inhibited and latchup has occurred. In some cases, which are referred to as incipient latchup, the condition lasts only for periods that are long with respect to normal recovery times of the circuits. Latchup can be induced in three ways: by exposure to ionizing radiation; by particular sequences of applying voltage to circuits employing more than one power supply; and other electrical stimulations such as high voltage pulses. Only radiation induced latchup is considered here. Radiation induced latchup has been observed in only a small percentage of the device types that have been irradiated with pulsed ionizing radiation, and of these device types usually only a small percentage of the samples exhibit latchup. In a few cases, a majority of the samples of a certain part from a manufacturer of integrated circuit part types have exhibited latchup.

[redacted] Integrated circuit latchup is always caused by one or more normally reverse biased PN junctions becoming conductive, either by the initiation of a breakdown mechanism or by becoming forward biased. In either case, a sustain-

[redacted]

[redacted]

[redacted] ing mechanism must act to maintain the breakdown or forward bias condition, once it has been initiated. Three latchup mechanisms have been postulated and observed in junction isolated integrated circuits. These are: PNPN action, second breakdown, and transistor sustaining voltage breakdown. No other mechanisms for sustaining latchup are known, although several others have been postulated.

[redacted] Latchup is normally associated with junction isolation since it usually involves some type of interaction with the silicon substrate through an isolating PN junction. Dielectric isolation is effective in isolating elements from one another and from the silicon substrate and, thus, is an important step in reducing the latchup vulnerability of integrated circuits. However, analyses of the structural characteristics of certain dielectric-isolated circuit types have indicated that the possibility of latchup cannot be ruled out in dielectric-isolated circuits. It is possible that some of the same mechanisms that are responsible for latchup in junction-isolated circuits also can exist in a dielectric-isolated circuit. These mechanisms include second breakdown, sustaining voltage breakdown of transistors and PNPN action if 4 layer structures are included within a dielectrically-isolated region.

[redacted] No latchup mechanisms have been found that are peculiar to dielectric isolation. While photocurrents can be generated in dielectric isolation, there are no sustaining mechanisms for these currents unless the isolation is defective or is subjected to destructively high voltages.

[redacted] Hybrid thin film circuits may be expected to be as tolerant of radiation as their conventional circuit counterparts. The radiation response is determined primarily by the active elements in the circuits.

[redacted] Undoubtedly, dielectric isolated circuits are much less vulnerable to latchup than are their junction isolated counterparts. However, dielectric isolated circuits probably are more latchup-prone than discrete component circuits because: dielectric isolated process limitations occasionally permit four layer structures; diffused resistors are present in some dielectric isolated circuits; and protective surface coatings occasionally are used in special purpose potting compounds or encapsulants, which might compromise the isolation. Component isolation in a dielectric isolated circuit, while much superior to that in a junction-isolated circuit, is still somewhat less complete than that in a discrete component circuit because of photocurrents through the dielectric.

[redacted] A large number of integrated circuits have been irradiated, but the testing has been concentrated on specific microcircuit types, and a broad base of experimental data on the response of microcircuits to radiation is not available. This lack of data is especially true for linear circuits. Representative radiation failure levels for some common digital junction-isolated types are shown in Table 9-23. The levels are listed either in terms of gamma dose or of dose rate, depending upon whether the circuit is normally dose or dose rate dependent. Design and production changes in integrated circuits are common in the industry. The broad ranges given reflect highly variable experimental results and indicate the necessity of considering each circuit as a separate problem.

[redacted] The proximity and intercoupling of elements do not assume importance in the production of permanent effects by nuclear radiation. Integrated circuits may be treated as conventional circuits of small dimensions. The primary factor that determines the tolerance of the circuits to radiation induced permanent effects is the degradation of the active elements with accumulated radiation exposure.

[redacted] Changes in the electrical parameters of diodes and transistors that result from radiation have been discussed. Experiments have shown that the circuits will experience failure when the

[redacted]

[redacted]

Table 9-23. [redacted] Representative Radiation-Failure Levels* for Digital Junction-Isolated Semiconductor Integrated Circuits [redacted]

Type†	Radiation-Failure Level
Large area, slow speed	5 -20 rads (Si)
Large area, moderate speed	10^6-10^7 rads (Si)/sec 20 -60 rads (Si)
Small area, moderate or high speed	10^7-10^9 rads (Si)/sec

[redacted] Here, the "failure" level corresponds to exceeding the circuit's noise margin.

† [redacted] Type designations defined as follows: Large area – chip area > 5,000 mil^2, Small area – chip area < 5,000 mil^2, Slow speed – propagation delay > 100 nsec, Moderate speed – propagation delay between 25 and 100 nsec, High speed – propagation delay < 25 nsec.

[redacted] gain of the transistors has dropped to the point that they will no longer support proper circuit action. The radiation resistance of the circuits is determined by the stability of the gain of the transistor elements with respect to radiation exposure and the tolerance of the circuit design with respect to gain degradation. Although no class of integrated circuits has been shown to be inherently superior to another, those circuits employing faster transistors usually can withstand a greater neutron fluence. Epitaxial transistors usually, but not exclusively, represent the faster transistor types. Radiation failure levels have been shown to vary from 10^{12} to 10^{15} n/cm^2 (E > 10 keV, fission), with the faster circuit types at the high end. The normally conservative design and digital function of most integrated circuits accounts for the circuit longevity beyond what would be considered the minimum useful transistor gain point.

[redacted] The radiation induced circuit response of microcircuits is manifested by changes in both the dc and switching characteristics. The effect on the integrated circuit parameters of changes in components after irradiation will, of course, depend on the specific circuit configuration involved. Frequently, the radiation sensitivity of the circuit is determined by the tolerance of the circuit design with respect to gain degradation.

[redacted] The most radiation sensitive circuit parameter of digital gates and flip-flop circuits is the output low voltage. Circuit failures result when normally ON transistors leave saturation. The amount of current that an output transistor can sink is directly proportional to the current gain. The changes in the output transistor current gain are reflected directly in the current-drive capability (fan-out) of both digital gates and flip-flops.

[redacted] Changes resulting from radiation are observed for other digital-circuit parameters. The saturation voltage of transistors, V_{SAT}, increases with neutron fluence, even though sufficient base drive is supplied to maintain the transistor in saturation, as a result of an increase in the saturation resistance. These changes in saturation resistance usually are negligible at threshold fluences applicable for maximum fan-out. The input threshold voltage of gate circuits normally will increase with radiation exposure as a result of changes in the base-emitter voltage of the output transistor and increased diode forward voltage. Changes in this parameter, however, are not considered significant. Increases in leakage currents also have been observed with radiation exposure, but the changes in this parameter usually will not affect circuit performance.

[redacted] The switching characteristics of typical digital circuits also are affected by radiation.

[redacted]

[redacted]

[redacted] The rise and fall times of the transistor elements of the microcircuit are increased and its storage time is decreased after neutron exposure. These effects combine, and usually a small net increase of switching time is observed.

[redacted] A good estimate of the radiation tolerance (at different fan-out conditions) of digital circuits can be made by measuring the output current-voltage characteristics. The gain degradation can be calculated, and the degraded characteristics can be plotted with the measured characteristic. An example prediction with experimental results is shown in Figure 9-63 for the RD 308 flip-flop.*

[redacted] Failure in MOS logic circuits results from changes in the threshold voltage of the transistors caused by ionizing radiation. Since a large, negative supply voltage permits greater degradation in threshold voltage before circuit failure occurs, the radiation failure threshold of MOS circuits depends on the maximum supply voltage rating. Experiments indicate that MOS digital microcircuits fail at radiation levels from 10^5 to 6×10^7 rads (Si) at manufacturer's rated supply voltages. Such an exposure can be associated with a neutron fluence of 1 to 2×10^{14} n/cm^2 ($E > 10$ keV, fission) for the mixed neutron-gamma flux of a typical fast-burst reactor. The characteristics of a particular MOS integrated circuit must be established with reasonable confidence before meaningful predictions can be made.

[redacted] As with digital circuits, the primary cause of linear-microcircuit failure is transistor gain degradation. The degradation of performance of a linear circuit is characterized by radiation induced changes in the transfer characteristics. In linear circuits, the functional dependence of the overall circuit performance on individual transistor elements can be determined only by a detailed circuit analysis. This analysis usually is frustrated by circuit complexity and the inability to measure individual microcircuit elements as a result of the lack of accessible terminals. Therefore, prediction of the performance of linear circuits under irradiation is difficult. The large variety of linear circuits precludes a discussion of each type; however, some general comments can be made concerning the performance of some devices.

[redacted] The radiation responses of both differential and operational amplifiers have been studied. A typical transfer characteristic of a differential amplifier is shown in Figure 9-64. The gain of the circuit began to decrease at a fluence of 3×10^{13} n/cm^2 ($E > 10$ keV, fission) and was degraded to roughly 50 percent of its initial value after an order-of-magnitude-larger fluence. These amplifiers were found to maintain their balance during irradiation significantly better than amplifiers made from discrete devices.

[redacted] The largest changes in operational amplifiers induced by radiation were observed in the open loop voltage gain and input bias current. The reduction in the open loop gain is a direct consequence of degradation of transistor gain. The use of lateral and substrate PNP transistors results in a relatively low radiation tolerance of these amplifiers compared to logic circuits. These PNP transistors are widebase units that are degraded at lower fluences than vertical NPN transistors. Changes in voltage gain begin to be observed (5 percent changes) at fluence levels near 10^3 n/cm^2 ($E > 0.1$ MeV, fission) for 709-type operational amplifiers. The neutron fluence where the voltage gain has decreased by 50 percent is about 8×10^{13} n/cm^2 ($E > 10$ keV, fission) for units with lateral and substrate transistors. Amplifiers that have eliminated lateral and substrate transistors show improved performance in the presence of radiation. The degradation in gain that is induced by radiation in operational amplifiers depends on the elec-

[redacted] * More details are given in the "TREE Handbook" (see bibliography).

[redacted]

[redacted]

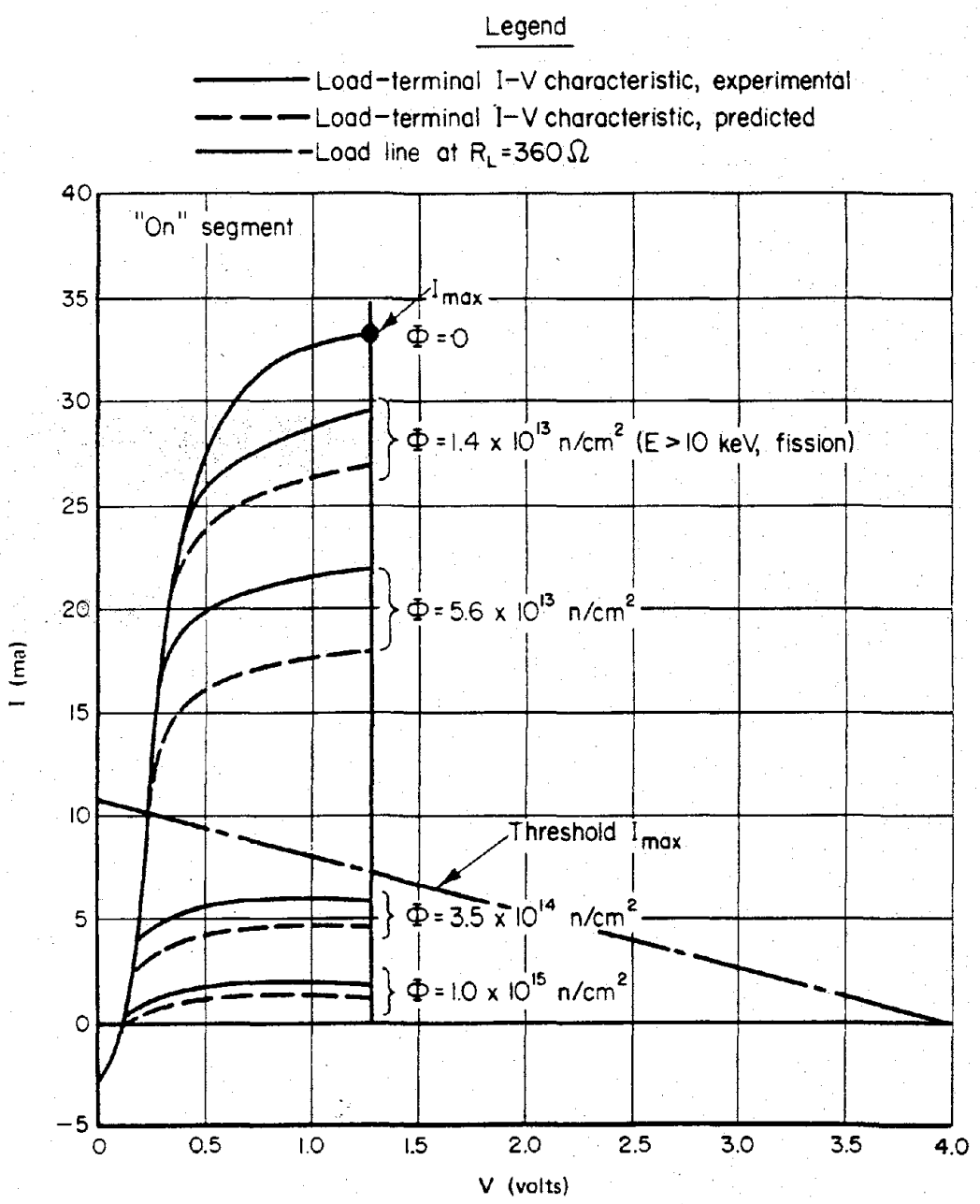

Figure 9-63. [redacted] Load-Terminal I-V Characteristic ("On" Segment) of RD 308 in Neutron Environment [redacted]

[redacted]

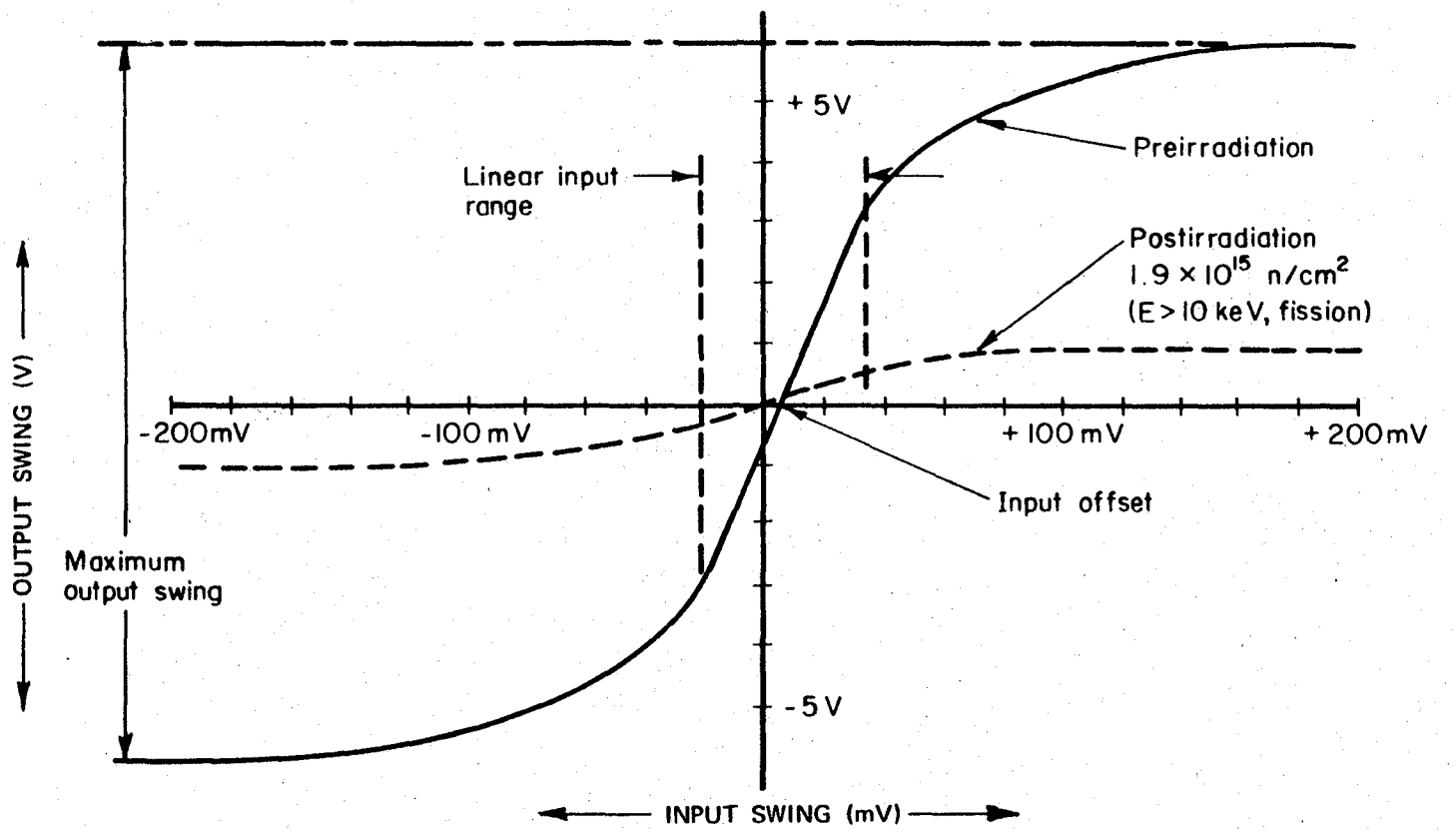

Figure 9-64. MC1525 Typical Transfer Characteristics

[redacted]

[redacted]trical design. For example, it is important to determine whether the open-loop gain is determined by resistor ratios or by transistor gains. The changes in the input bias current can be correlated directly with changes in the common base current gain of the input transistors. It should be noted that the input transistors of operational amplifiers operate at very low currents (high input impedance), thus degradation of the base-transport factor is accompanied by degradation of the emitter efficiency as well. Factor-of-two increases in bias current have been observed for 709 amplifiers after 3×10^{13} n/cm^2 ($E > 10$ keV, fission). Offset voltage and offset current were found to increase after irradiation. These changes result from emitter-base-voltage and current-gain mismatches after irradiation. The changes in both current and voltage offsets were small at fluences where the gain and the bias current were degraded appreciably, which indicates the uniformity of active elements on the same chip.

[redacted] Even though a large number of integrated microcircuits have been tested, data on the effects of neutron irradiation on microcircuits are still sparse. This is especially true for the linear types of integrated circuits. Radiation experiments indicate that the failure threshold of digital microcircuits is fairly independent of the construction technique. For buffered circuits the failure threshold, at unity fan-out, is near 10^{15} n/cm^2 ($E > 10$ keV, fission), while it is somewhat lower for the nonbuffered circuit types; however, the failure level at rated fan-out (~10) usually occurs over an order of magnitude lower in fluence than the failure level at unity fan-out. Representative radiation failure levels for some common digital microcircuits are shown in Table 9-24. The failure level is specified when the output voltage of the test circuit

Table 9-24. [redacted] Failure Thresholds for Typical Digital Microcircuits [redacted]

Designation	Function	Construction	Failure Level, (n/cm^2)	
MC 201	DTL Gate	Junction Isolation	1.5×10^{15}*	1.2×10^{14}†
DT μL 932	DTL Gate	Junction Isolation	3.0×10^{15}	1.5×10^{14}
RD 209	DTL Gate	Oxide Isolation	3.0×10^{15}	1.5×10^{14}
MC 507	TTL Gate	Junction Isolation	0.8×10^{15}	0.8×10^{14}
SN 54932	TTL Gate	Junction Isolation	1.5×10^{15}	1.2×10^{14}
DT μL 945	DTL Flip-Flop	Junction Isolation	1.5×10^{15}	1.2×10^{14}
SE 124	DTL Flip-Flop	Junction Isolation	0.85×10^{15}	0.8×10^{14}
RD 208	DTL Flip-Flop	Oxide Isolation	0.85×10^{15}	0.8×10^{14}

*[redacted] Failure level at fan-out of 1; neutron fluence specified as ($E > 10$ keV, fission).
†[redacted] Failure level at fan-out of 10; neutron fluence specified as ($E > 10$ keV, fission).

[redacted]

[redacted]

[redacted] exceeds the noise margin of the following circuit. Typical radiation failure levels for some linear circuits are shown in Table 9-25. Table 9-26 contains irradiation test results for some representative MOS integrated circuits. The failure level is specified as the point when the circuit would not operate or when the threshold voltage exceeded the supply voltage.

[redacted] The test results presented are only intended to provide a broad range of failure levels for order-of-magnitude reference purposes and should be treated with appropriate caution. It should be borne in mind that design and production changes in integrated circuits are common in industry. For this reason, each circuit should be considered a separate problem.

[redacted] The thermomechanical shock effects for all integrated circuit types are the same as those effects on discrete semiconductor parts. The only difference to consider is the increased number of bonds used in each device package, which increases the change of bond failure.

Table 9-25. [redacted] Failure Thresholds for Typical Linear Microcircuits [redacted]

Designation	Function	Construction	Failure Level* (n/cm^2)†
μA 709	Operational Amplifier	Junction Isolation	0.8×10^{14}
RA 909	Operational Amplifier	Oxide Isolation	0.8×10^{14}
Ph 709	Operational Amplifier	Oxide Isolation	3.0×10^{14}
MC 1709	Operational Amplifier	Oxide Isolation	3.0×10^{14}
MC 1525	Differential Amplifier	Junction Isolation	3.0×10^{14}
NM 1024	Differential Amplifier	Oxide Isolation	3.0×10^{14}
NM 1006	Differential Amplifier	Junction Isolation	4.0×10^{14}
RA 138	Amplifier	Oxide Isolation	1.5×10^{14}

[redacted] Failure level – gain degradation 50 percent.
† [redacted] Neutron fluence specified as ($E > 10$ keV, fission).

[redacted]

[redacted]

Table 9-26. [redacted] Failure Thresholds for Typical MOS Digital Microcircuits [redacted]

Designation	Function	Failure Level: Gamma, (rads (Si))	Failure Level: Neutron.* (n/cm^2)
SC 1171	NAND gate	2×10^5†	–
MEM 529	Binary element	1.4×10^5‡	–
SC 1171	Binary element	1. [illegible] 10^5‡	–
MEM 501	Shift register	1. [illegible] x 10^5§	–
MEM 590	Chopper	Not measured**	3×10^{14}
SC 1149	Flip-Flop	Not measured**	8×10^{14}
MC 1155	AND/OR gate	2×10^5 (Cobalt-60)††	
3300	25-bit static shift register	$>5 \times 10^3$ (FXR)‡‡ $>8 \times 10^4$ (TRIGA)‡‡	
3003	100-bit shift register	$>2 \times 10^4$ (FXR)‡‡ $>5 \times 10^4$ (TRIGA)‡‡	
1406	100-bit shift register	$>10^5$ (FXR)‡‡ $<2.5 \times 10^4$ (TRIGA)	
1101	256-random access memory	4×10^4 (FXR) 2×10^4 (TRIGA)	3×10^{11}

* [redacted] Neutron fluence specified as (E > 10 keV, fission).
† [redacted] Supply voltage - 20 volts.
‡ [redacted] Supply voltage - 15 volts.
§ [redacted] Clock voltage - 10 volts.
** [redacted] Supply voltage - 10 volts.
†† [redacted] Type of facility in which test was performed.
‡‡ [redacted] No failures at these levels.

[redacted]

[redacted]

SECTION VIII

[redacted] ELECTROMAGNETIC PULSE (EMP) DAMAGE MECHANISMS [redacted]

[redacted] As described in Chapter 7, the nuclear electromagnetic pulse (EMP) is part of a complex environment produced by a nuclear environment. The EMP contains only a very small part of the total energy produced by a nuclear explosion; however, under the proper circumstances, EMP is capable of causing severe disruption and sometimes damage to electrical and electronic systems at distances where all other effects are absent.

[redacted] As with the EMP generation described in Chapter 7, the complexity of the calculation of EMP damage mechanisms requires that heavy reliance be placed on computer code calculations for specific problems, and even these calculations must be supplemented by testing in most cases. Consequently, the information presented herein is largely qualitative and will only serve as an introduction to the subject. More complete treatments of EMP damage mechanisms may be found in the "DNA EMP (Electromagnetic Pulse) Handbook" (see bibliography).

[redacted] Figure 7-18, Chapter 7, provides a matrix that provides some indication of whether EMP constitutes a threat in a given situation relative to the hardness of a system to blast overpressure. This section provides a brief description of EMP energy coupling, component damage, EMP hardening, and testing.

[redacted] ENERGY COUPLING [redacted]

9-56 Basic Coupling Modes [redacted]

[redacted] There are three basic modes of coupling the energy contained in an electromagnetic wave into the conductors that make up an electric or electronic system: electric induction, magnetic induction, and resistive coupling.

[redacted] Electric induction arises as the charges in a conductor move under the influence of the tangential component of an impinging electric field. The overall result is that of a voltage source distribution along the conductor. One such point-voltage source is shown in Figure 9-65 for a simple conducting wire, where the current I is produced as a result of the tangential component $E_{i\ tan}$ of the incident electric field $\bar{E}_i$.

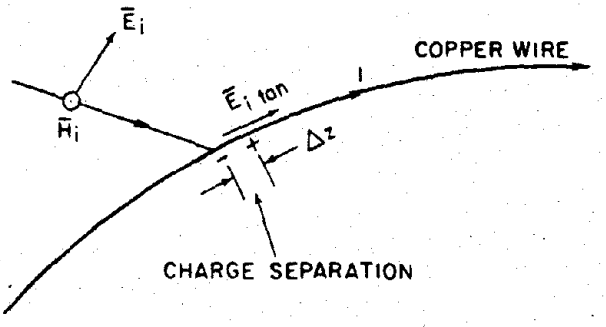

Figure 9-65. [redacted] Electric Induction in a Copper Wire [redacted]

[redacted] Magnetic induction occurs in conductors shaped to form a closed loop when the component of the impinging magnetic field perpendicular to the plane of the loop varies in time, causing charges to flow in the loop. This effect is illustrated in Figure 9-66 for a simple wire loop. Here the magnetic field is shown coming out of the plane of the loop. The loop need not be circular, and magnetic induction may occur with any set of conducting components assembled so as to form a loop.

[redacted] Resistive coupling comes about indirectly as a conductor that is immersed in a conducting medium, such as ionized air or the ground, is influenced by the currents induced in the medium by the other coupling modes. In effect the conductor shares part of the current as an alternate conducting path. This effect is illustrated in Figure 9-67 for the simple case of a

[redacted]

[redacted]

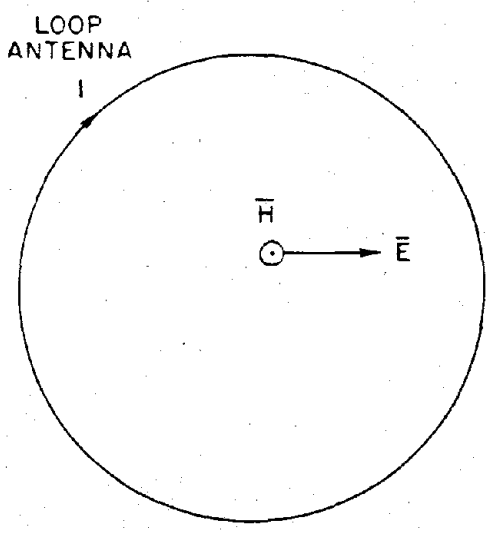

Figure 9-66. [redacted] Magnetic Induction in a Simple Loop [redacted]

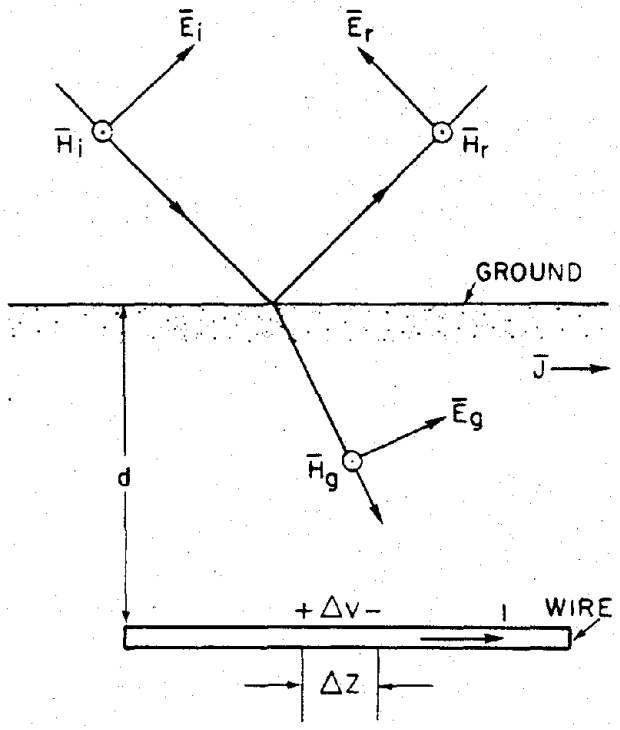

Figure 9-67. [redacted] Resistive Coupling as a Result of Currents in the Ground [redacted]

[redacted] conductor immersed in the ground. The tangential component of the incident electric field $\bar{E}_i$ induces a current density $\bar{J}$ in the ground. A distributed voltage drop appears along the wire as a result of the current flow in the ground, and this incremental voltage causes current flow I in the wire. Current also may be induced in the wire directly by the tangential component of the refracted electric field, shown as $\bar{E}_g$. The reflected EMP, $\bar{E}_r$, $\bar{H}_r$, is also shown in Figure 9-67. The potential importance of these reflected fields is discussed below.

9-57 Resonant Configurations [redacted]

[redacted] The coupling of energy to a conductor is particularly efficient when the maximum dimension of the conductor configuration is about the same size as the wavelength of the radiation. In this event the voltages that are induced along the conductor at various points are all approximately in phase, so the total voltage induced on the conductor is a maximum. The conductor is said to be resonant, or to behave as an antenna, for frequencies corresponding to near this wavelength. Since EMP has a broad spectrum of frequencies (see Chapter 7), only a portion of this spectrum will couple most efficiently into a specific conductor configuration. Thus, a particular system of interest must be examined with regard to its overall configuration as well as its component configuration. Eash aspect will have characteristic dimensions that determine what part of the pulse (strength and frequencies) constitutes the principal threat.

[redacted] Gross system features that are not normally considered antennas, such as structural features, beams, girders, buried cable, overhead conduit or ducting, wings, fuselage, missile skins, and any wall apertures, must be considered to be potential collectors and conductors of energy into the system. In particular, radiation that

[redacted]

[redacted]

[redacted] enters through an aperture is analogous to radiation that originates from a plate of the same size and shape as the aperture. Thus, it is resonant, and the aperture is resonant, and it admits a maximum of energy from the pulse for those frequencies near its resonance.

[redacted] When the EMP strikes the ground, a portion of the pulse will be transmitted through the interface, inducing currents in the ground or any system components buried there, and a portion normally will be reflected as shown in Figure 9-68. Thus, a system that is above the ground will receive the reflected pulse as well as the direct pulse. These may cancel one another partially, but in the worst case they may reinforce and may constitute a greater threat level.

[redacted] It can be seen that most practical systems in their operational environment present exceedingly complex coupling problems for an arbitrary explosion. The solution for any combination of system and environment is probably unique and will be very sensitive to even minor changes in the parameters. Two approximate approaches have been tried: computer studies as mentioned in Chapter 7, and threat simulation, which will be discussed in succeeding paragraphs.

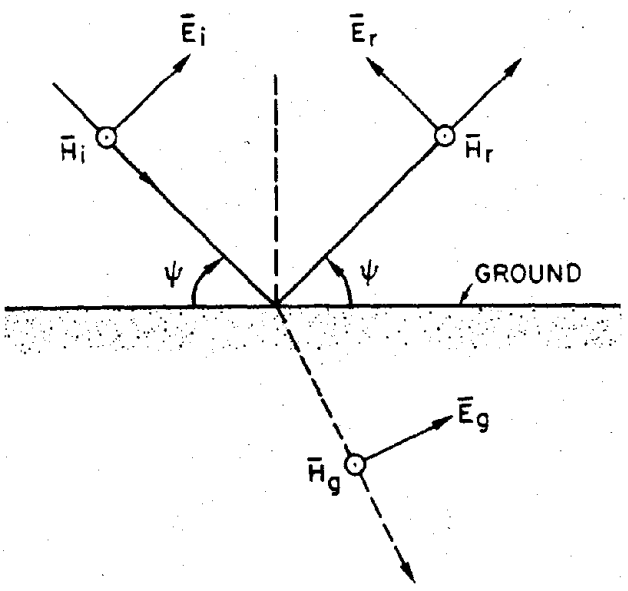

Figure 9-68. [redacted] Reflected and Refracted Waves at the Air-Ground Interface [redacted]

[redacted] COMPONENT DAMAGE [redacted]

9-58 Types of Damage [redacted]

[redacted] Degradation of system performance may occur as a result of functional damage or operational upset. A system will suffer damage if it is damaged permanently as a result of a large electrical transient. For example, a catastrophic failure of a device or component will render its operation unsatisfactory in any circuit. A parametric failure of a device occurs when degradation of some parameter has proceeded to a point where the circuit will continue to operate but at reduced efficiency. These latter failures are classed as functional damage. On the other hand, a system suffering operational upset is only impaired temporarily.

[redacted] Electronic components that are sensitive to functional damage or burnout are listed below in the order of decreasing sensitivity to damage effects:

microwave semiconductor diodes,
field-effect transistors,
radio-frequency transistors,
audio transistors,
silicon-controlled rectifiers,
power rectifier semiconductor diodes,
vacuum tubes.

Thus, on the basis of components alone, vacuum tubes are less susceptible to EMP damage effects than transistors.

[redacted] Electronic or electrical systems that are subject to malfunction include:

Most susceptible:

- Low power, high speed digital computer

[redacted]

[redacted]

[redacted] (upset) either transistorized or vacuum tube

- Systems employing transistors or semiconductor rectifiers (either silicon or selenium), such as

  computers

  computer power supplies

  transistorized components terminating long cable runs, especially between sites

  alarm systems

  intercom systems

  life-support system controls

  some telephone equipment which is partially transistorized

  transistorized receivers

  transistorized transmitters

  transistorized 60 to 400 cps converters

  transistorized process control systems

  power system controls; communication links

Less susceptible:

- Vacuum tube equipment (does not include high speed digital equipment and equipment with semiconductor or selenium rectifiers)

transmitters	intercoms
receivers	teletype-telephone
alarm systems	power supplies

- Equipment employing low current switches, relays, meters

alarms	panel indicators, status boards
life-support systems	process controls
power system control panels	

- Hazardous equipment containing

detonators	explosive mixtures
squibs	rocket fuels
pyrotechnical devices	

- Other

  Long power cable runs employing dielectric insulation, equipment associated with high energy storage capacitors or inductors

Least susceptible:

- High-voltage 60 cps equipment

transformers, motors	rotary converters
lamps, filament	heavy duty relays, circuit breakers
heaters	air-insulated power cable runs

[redacted] The less susceptible equipment or components would be made more susceptible if they are connected to long exposed cable runs, such as intersite wiring or overhead exposed power or telephone cables. The equipment can be made less vulnerable if it is protected.

9-59 Damage Levels [redacted]

[redacted] The nature of a circuit has a strong bearing on the transients that cause damage; however, in general pulse lengths of microsecond and submicrosecond duration are required to cause problems. Table 9-27 shows a list of common active devices and the approximate energy required to cause functional damage. The wide range of energies should be noted.

[redacted] The minimum energy required to damage meters or to ignite fuel vapors is about the same as that required to damage semiconductors as shown in Table 9-28. Good composition resistors can withstand pulse powers more than 10,000 times their power rating for micro-

[redacted]

[redacted]

Table 9-27. [redacted] Minimum Observed Joule Energy to Cause Burnout [redacted]

Type	Minimum Joule Energy	Material	Other Data
2N36	4.0×10^{-2}	Ge	PNP Audio Transistor
2N327A	1.6×10^{-2}	Si	PNP Audio Transistor
2N1041	2.0×10^{-2}	Ge	PNP Audio Transistor
2N1308	5.0×10^{-5}	Ge	NPN Switching Transistors
2N706	6.0×10^{-5}	Si	NPN Switching Transistors
2N594	6.0×10^{-3}	Ge	NPN Switching Transistors
2N398	8.0×10^{-4}	Ge	PNP Switching Transistors
2N240	1.0×10^{-2}	Ge	PNP Switching Transistors
MC715	8.0×10^{-5}	Si	Data Input Gate Integrated Circuit
2N4220	1.0×10^{-5}	Si	RF General Purpose FET
2N4224	3.0×10^{-5}	Si	VHF Amp and Mixer FET
1N3659	8.0×10^{-3}	Si	Automotive Rectifier Diode
1N277	2.0×10^{-5}	Ge	High Speed Switching Diode
1N3720	5.0×10^{-4}		Tunnel Diode
1N238	1.0×10^{-7}	Si	Microwave Diode
2N3528	3.0×10^{-3}	Si	Silicon Controlled Rectifier
67D-5010	1.0×10^{-4}		G.E. Varistar (30-joule Rating)
6AF4	1.0×10^{0}		UHF Oscillator Vacuum Tube
66N8	2.0×10^{0}		General Purpose Triode Vacuum Tube

[redacted]

[redacted]

Table 9-28. [redacted] Minimum Joule Energy to Cause Permanent Degradation Indicated [redacted]

Designation	Minimum Joule Energy	Malfunction	Other Data
Relay	2×10^{-3}	Welded Contact	Potter-Brumfield (539) low-current relay
Relay	1×10^{-1}	Welded Contact	Sigma (IIF) one-ampere relay
Microammeter	3×10^{-3}	Slammed Meter	Simpson Microammeter (Model 1212C)
Explosive Bolt	6×10^{-4}	Ignition	EBW 8 amp for 10 μsec detonator, MK1
Squib	2×10^{-5}	Ignition	Electric Squib, N8 3.5 watts for 5 μsec detonator
Fuel Vapors	3×10^{-3}	Ignition	Propane-air mixture 1.75 mm ignition gap

[redacted] second pulses. Capacitors are also fairly hard components. The approximate energies required for degradation of several common components are shown in Table 9-28.

[redacted] The minimum energy necessary for operational upset is a factor of 10 to 100 less than that which is required to damage the most sensitive semiconductor component. Table 9-29 shows the levels required to cause operational upset to some common components to illustrate this factor.

[redacted] A gross comparison of the energy required to damage several classes of electrical equipment is provided in Figure 9-69.

[redacted] The large range of damage levels emphasizes the fact that it is important to consider EMP damage criteria early during the design stage of any piece of equipment that might be susceptible. It is also important to realize that energy collected in one part of a system may be transmitted to other parts of the system as a result of the currents that are induced. Thus, it is not necessary that the EMP couple directly to a sensitive component; energy coupled to various parts of a system may ultimately reach a particular component in sufficient quantity to cause malfunction. With the current state of the art in EMP vulnerability evaluation, the design and hardening of complicated systems requires the joint efforts of systems engineers and professional EMP effects personnel.

[redacted] EMP HARDENING [redacted]

9-60 System Analysis [redacted]

[redacted] A general approach to the examination

[redacted]

[redacted]

Table 9-29. [redacted] Minimum Joule Energy to Cause Circuit Upset or Interference [redacted]

Designation	Minimum Joule Energy	Malfunction	Other Data
Logic Card	3×10^{-9}	Circuit Upset	Typical logic transistor inverter gate
Logic Card	1×10^{-9}	Circuit Upset	Typical flip-flop transistor assembly
Integrated Circuit	4×10^{-10}	Circuit Upset	Sylvania J-K flip-flop monolithic integrated circuit (SF50)
Memory Core	2×10^{-9}	Core Erasure Via Wiring	Burroughs fast computer core memory (FC2001)
Memory Core	5×10^{-8}	Core Erasure Via Wiring	Burroughs medium speed computer core memory (FC8001)
Memory Core	3×10^{-9}	Core Erasure Via Wiring	RCA medium speed, core memory (269M1)
Memory Core	2×10^{-8}		Minimum observable energy in a typical high-gain subsystem
Amplifier	4×10^{-21}	Interference	Minimum observable energy in a typical high-gain amplifier

[redacted]

of a system with regard to its EMP vulnerability could include the following steps. First information concerning the system components and devices is collected. The information is categorized methodically into physical zones based on the susceptibility and worst case exposure for these items. Using objective criteria, problem areas are identified, analyzed, and tested. Suitable changes are made as necessary to correct deficiencies, and the modified system is examined and tested. The approach may be followed on proposed systems or those already in place, although experience indicates that the cost of retrofitting EMP protection is usually overwhelming.

9-61 Recommended Practices [redacted]

[redacted] Within the scope of this manual it is only possible to mention a few of the practices that may be employed in hardening a system to EMP. The following discussion is intended to convey some impression of the extra effort involved in hardening a system to the EMP rather than to provide a comprehensive treat-

[redacted]

[redacted]

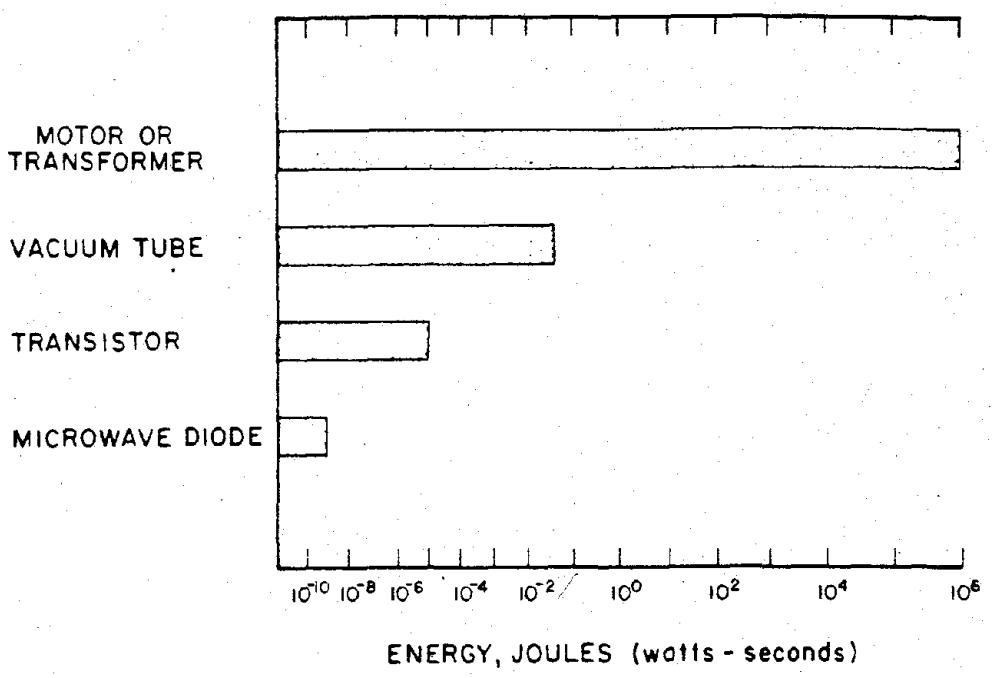

Figure 9-69. [redacted] Energy Required to Damage Various Classes of Equipment [redacted]

[redacted]

ment of what is a highly technical and specialized field.

[redacted] Some general methods for reduction of the EMP environment include geometric arrangement of the equipment, shielding, geographic relocation, and proper grounding.

[redacted] Circuit layout recommendations include the use of common ground points, twisted cable pairs, system and intrasystem wiring in "tree" format (radial spikes) avoiding loop layouts and circuit routes coupling to other circuits, use of conduit or cope trays, and shielded isolated transformers. Avoiding ground return in cable shields is also recommended. Many specific practices carry over from communications and power engineering while many do not. Each must be examined carefully.

[redacted] Good shielding practices include the use of independent zone shields, several thin shields to replace a thick one, continuous shield joints, and keeping sensitive equipment away from shield corners. Avoiding shield apertures, and avoiding the use of the shield as a ground or return conductor is also recommended. The shielding effectiveness of many enclosures frequently is defeated by energy carried by cables or pipes (including water pipes, sewage lines, etc.) into the enclosure.

[redacted] Cabling recommendations include the use of deeply buried intersystem cables (more than 3 feet), shield layer continuity at splices, and good junction box contact. Ordinary braid shielding should be avoided. Cable design represents an extension of shielding and circuit practices from the viewpoint of EMP protection. It is an area where compromises frequently are made in the interests of economy, and thus is an area where professional EMP effects personnel can be

[redacted]

[redacted]

[redacted] of considerable assistance.

[redacted] Good grounding practices must be employed. In general, a "ground" is thought of as a part of a circuit that has a relatively low impedance to the local earth surface. A particular ground arrangement that satisfies such a definition may not be optimum, and may be worse than no ground from the EMP viewpoint. A ground can be identified as: the chassis of an electronic circuit, the "low" side of an antenna system, a common bus, or a metal rod driven into the earth. The last depends critically on local soil conditions, and it may result in resistive induced currents in the ground circuit. A good starting point is to provide a single point ground for a circuit cluster, usually at the lowest impedance element – the biggest piece of the system that is electrically immersed in the earth, e.g., the water supply system. It is beyond the scope of this manual even to list all of the grounding recommendations. Once again, this is an area where professional EMP effects personnel can be of considerable assistance.

[redacted] Finally, various protective devices represent a means to counter other protective shortcomings indirectly. Filters, absorbers, limiters, decouplers, switching devices, arc arresters, fuses, etc., are part of this class of components. When other design practices cannot be used or are not adequate, such devices must be added. Typically they are found in an "EMP room" at the cable entrance to underground installations, in aircraft antenna feeds, in telephone lines, at power entry panels to shielded rooms, etc. On a smaller scale, diodes, nonlinear resistors, SCR clamps, and other such items are built into circuit boards or cabinet entry panels. Few of these devices by themselves are sufficient as a complete solution to a specific problem area, because each has some limitation in speed of response, voltage rating, power dissipation capacity or reset time. Thus, most protective devices are hybrids. A few prepackaged hybrids are available for the protection of audio and power lines from lightning strokes and power surges and, if modified, may be used for EMP protection. No such packages are readily available for high frequency lines, multiple wire cables, antennas, etc., and usually must be custom designed for each application.

[redacted] TESTING [redacted]

9-62 Importance of Testing [redacted]

[redacted] Even with present day sophistication in analytic techniques, it is clear from the complexities described above that sole reliance cannot be placed in analysis and prediction alone. Testing has a number of important functions.

[redacted] Testing is essential to verify prior analysis of devices, components, and complete systems early in the design stage. Testing also is the only known method that can be used to identify surprises. Surprises can be unexpected coupling or interaction modes or weaknesses that were overlooked during the design. Nonlinear effects in interaction are a form of surprise that only can be found by testing. After the test, many of the original approximations made in analysis can be refined and improved for future analysis, and the data can improve the analytic capability for more complex problems.

[redacted] Testing quickly locates weak or susceptible points in components or systems early enough for economic improvement. After the improvements, testing quickly verifies that the improvements bring the performance up to standards.

[redacted] Testing provides assurance and confidence that the complete system is actually hardened to EMP to the specified threat level. Actual certification can only be obtained by providing the actual nuclear threat environment. Further, periodic testing insures that system hardness is not degraded as a result of environmental or human factors.

[redacted]

[redacted]

9-63 Simulation Facilities [redacted]

[redacted] As a result of the limited test ban treaty, heavy reliance must be placed on simulation to test the EMP hardness of systems. A brief description of generic simulation techniques is given below. A more thorough description of these techniques is contained in the "DNA EMP (Electromagnetic Pulse) Handbook, Volume 2, Analysis and Testing" (see bibliography).

[redacted] The classes of EMP tests are:

- Low level current mapping,
- High level current mapping,
- High level fields.

Low level current mapping is a good test for the beginning of any program. With the system power turned off and a low-level field, the magnitudes and signatures on internal cables are determined. This provides an insight on the work that must follow. After this test and the indicated improvements are made, a high-level current can be injected directly into the system with the system power on to explore for nonlinearities, and to uncover initial indications of system effects. If subsystems malfunction, it may be desirable to conduct extensive subsystem tests in the laboratory. Finally, a high level field test is essential.

[redacted] The type of excitation must be defined in any type of test. The two principle choices are:

- Waveform simulations (time-domain data),
- Continuous wave signals (frequency-domain data).

If the intent is to match a system analysis in the frequency domain to measured system response, continuous wave (CW) signals may be more suitable. If the desire is to compare the test results to known electronic thresholds, it is frequently necessary to test in the time domain. For a complete analysis, it is advisable to consider both types of tests.

[redacted] Large-scale simulators are required for the final test of large systems. The two principal kinds of large simulators are:

- Metallic structures that guide an EM wave past a test object,
- Antennas that radiate an EM field to a test object.

Guided wave simulators use pulse generators that simulate EMP waveforms and operate in the time domain. Radiating antennas use either pulse generators (time domain) or continuous wave (CW) signal generators (frequency domain). Pulse generators themselves can be either high level single shot or low level repetitive.

(U) The essential elements of a guided wave or transmission line simulator include:

- Pulser
- Transition section
- Working volume
- Termination.

An electromagnetic wave of suitable amplitude and waveshape is generated by the pulser. This wave is guided by a tapered section of transmission line (the transition section) from the small cross sectional dimension of the pulser otuput to the working volume. The working volume, where the test object is located, should be large enough to provide a certain degree of field uniformity over the test object. A test object dimension one-fifth that of the working volume satisfies this condition. The termination region prevents the reflection of the guided wave back into the test volume, and consists of a transition section that guides the incident wave to a geometrically small resistive load whose impedance is equal to the characteristic impedance of the transmission line structure.

[redacted] The basic types of radiating simulators are:

- Long wire
- Biconic dipole or conical monopole.

The long wire is usually a long dipole oriented

[redacted]

[redacted]

[redacted] parallel to the earth's surface. It is supported above the ground by nonconducting poles with high-voltage insulators. The two arms of the dipole are symmetric about the center and constructed from sections of light weight cylindrical conductor, such as irrigation pipe. Pipe sections decrease in diameter with increasing distance from the center, and resistors are placed between the pipe sections to shape the current wave and reduce resonances. The two arms of the dipole are oppositely charged, and when the voltage across the spark gap at the dipole center reaches the breakdown voltage, the gap begins conducting and a current wave front propagates away from the gap.

[redacted] Conical and biconical antennas use pulsers, such as Marx generators, or CW transmitters instead of relying on the discharge of static surface charges. The antennas are fabricated out of lightweight conducting surfaces or wire grids.

[redacted] Differences between guided wave and radiating simulators are listed in Table 9-30.

[redacted] Electromagnetic scale modeling is an important alternative to full scale testing under the following conditions:

- Test facilities or available equipment are at a premium,
- The system to be tested is very large,
- The system dedication cost for full scale testing is high.

In addition to the advantages of modeling under these conditions, benefits can be derived as follows:

- Perhaps sensors can be placed better during full scale testing as a result of model experiments,
- Design modifications or cable reroutes can be made prior to full scale testing,
- EM angles-of-arrival can be determined for worst- and best-case conditions,
- Effects of changes in the conductivity of the surrounding media can be explored to an extent,
- Estimates can be made of some of the responses of a complex system prior to full scale testing,
- Design confirmation of costly systems can be made prior to system fabrication and costs can be reduced,
- Quantitative data can be obtained to validate analysis.

[redacted] It should be pointed out that because of the difficulty in introducing minute openings or poor bonds into models, and since these often control interior fields, the usefulness of modeling ordinarily is limited to the measurement of external fields, voltages, and currents. Once the exterior fields, voltages, and currents are known for a complex structure, perhaps having cable runs, analysis can often provide internal field quantities of interest.

[redacted] In actually setting up a scale model test, the following should be kept in mind:

- Broadband pulse response determination involves much more than a steady-state, single-frequency response test does.
- Special EM illumination sources that are coherent, have uniform time delay, and use antennas with constant effective height are required.
- Special modeling techniques are required to study exposed conductors that pass over or within a lossy dielectric, such as earth.

A pulse-type waveform theoretically can be replaced by a continuous wave (CW) source with a sensing system which references the sensed CW signal to a reference phase from the source. Complex Fourier transfer functions can be developed by processing the recorded data on a computer. However, long sweep times are required to ensure that all narrow band responses are explored adequately, and the actual physical implementation of such an approach in the

[redacted]

[redacted]

Table 9-30. [redacted] Comparison of Guided Wave and Radiating Simulators [redacted]

	Guided Wave	Radiating
Energy use	Efficient – mostly directed toward test object	Energy radiated symmetrically about axis – only fraction directed toward test object
Test volume	Limited by size of simulator – difficult to construct large enough for sizable test objects	Limited by desired field intensity
Polarization	Fixed (or bipolar, e.g., ARES)	Variable*
Angle of incidence	Fixed†	Variable*
Earth reflection effects	No	Yes
Geometric attenuation of EM wave amplitude	No – relatively uniform within test volume	Yes (1/R)
Planar wave capability	Yes	Only at distance
Interference with nearby electronics	Limited	Yes

*[redacted]These are, however, limited by the height of the antenna unless it is airborne.
†[redacted]Polarization is fixed relative to earth coordinates; however, a range of polarizations and angles of incidence can be provided in some facilities by changing the position and orientation of the object that is being tested. For example, a missile can be rotated on several axes in ARES to change these to items relative to the missile.

[redacted]

[redacted]

[redacted]

microwave band poses additional difficulties. On the other hand, the use of scaled real time waveforms allows quick development of actual responses, from which complex Fourier transfer functions also can be developed with the aid of computers.

[redacted] Several variations of each type of simulation technique described above are currently operational. Each has some advantages and disadvantages when compared to others. As mentioned previously, it is beyond the scope of this manual to describe individual facilities. The interested user should consult the "DNA EMP (Electromagnetic Pulse) Handbook, Volume 2, Analysis and Testing," (see bibliography), and the references listed therein.

[redacted]

[redacted]

[redacted] BIBLIOGRAPHY [redacted]

Abbott, L. S., H. C. Claiborne, and C. E. Clifford, Eds., *Weapons Radiation Shielding Handbook* [redacted] DASA 1892-1, through 1892-6, Oak Ridge National Laboratory, Oak Ridge, Tennessee, December 1966 through March 1972 (Vols. I, II, III, V, [redacted] Vol. VI, [redacted] Vol. IV [redacted]

Barash, R. M., and J. A. Goertner, *Refraction of Underwater Explosion Shock Waves: Pressure Histories Measured at Caustics in a Flooded Quarry*, NOLTR-67-9, U.S. Naval Ordnance Laboratory, White Oak, Silver Spring, Maryland, 19 April 1967 [redacted]

Batter, J. F., *Transient Effects of a Time Varying Thermal Pulse*, Part II, AFSWP1058, TOI Report No. 58-7, Technical Operations Incorporated, Burlington, Massachusetts, March 1958 [redacted]

Bell, J. F., *Single Temperature-Dependent Stress-Strain Law for Dynamic Plastic Deformation of Annealed Face-Centered Cubic Metals*, Journal of Applied Physics, Vol. 34, No. 1, January 1963 [redacted]

Bergman, P., and N. Griff, *A Method for Evaluation of the Response of Coatings to Thermal Radiation from a Nuclear Weapon*, Naval Applied Science Laboratory Project 940-105, Progress Report 9, November 12, 1968 [redacted]

Bergman, P., et al., *Temperature Response Charts for Opaque Plates Exposed to the Thermal Radiation Pulse from a Nuclear Detonation*, Naval Applied Science Laboratory Project 940-105, Progress Report 10, July 10, 1969 [redacted]

Bethe, H. A., and W. L. Bade, *Theory of X-Ray Effects of High Altitude Nuclear Bursts and Proposed Vehicle Hardening Method* [redacted] RAD-TR-9(7)-60-2, AVCO Corporation, Wilmington, Massachusetts, 8 April 1960 [redacted]

Bothell, L. E., *PUFF IV-EP Code Comparisons to Test Results* [redacted] KN-664-67-2, Kaman Nuclear, Colorado Springs, Colorado, 16 January 1967 [redacted]

Bothell, L. E., and C. E. Archuleta, *PUFF V-EP Code* [redacted] Parts I and II, KN-703-67-101(R), Kaman Nuclear, Colorado Springs, Colorado, December 1967 (Part I, [redacted] Part II [redacted]

Bridges, J. E., *DNA EMP Awareness Course Notes*, DNA 2772T, Illinois Institute of Technology Research Institute, Chicago, Illinois, August 1971 [redacted]

Chandler, C. C., et al., *Prediction of Fire Spread Following Nuclear Explosions*, U.S. Forest Service Research Paper PSW-5, Pacific Southwest Forest and Range Experiment Station, Berkeley, California, 1963 [redacted]

[redacted]

[redacted]

Clarke, T. C., *Interaction Study, Vol. IV, Structural Degradation by Short Time Heating,* AFWL TR-70-157, Boeing Company, Seattle, Washington, December 1970 [redacted]

Cohen, M. L., *A Numerical Technique to Determine the Thermal Histories of Two-Dimensional Solids in the Nuclear Environments,* Naval Applied Science Laboratory Project 940-105, Progress Report 5, June 1958 [redacted]

Cole, R. H., *Underwater Explosions,* Dover Publications, Inc., New York, N.Y., 1965 [redacted]

Davis, G. T., et al., *Project TROIKA, Re-Entry Vehicle Vulnerability Assessment for Advanced Planning for Underground Tests* [redacted] DASA 2230, AVCO Corporation, Wilmington, Massachusetts, January 1969 [redacted]

Derkesen, W. L., *Ship Vulnerability to Nuclear Attack-Thermal Radiation Effects,* Technical Briefing to the Chief of Naval Material, 2 March 1967.

DNA EMP (Electromagnetic Pulse) Handboo [redacted] DNA 2114H1-2114H4, DASIAC, General Electric TEMPO, Santa Barbara, California, Volume 1, Design Principles, November 1971, Volume 2, Analysis and Testing, November 1971, Volume 3, Environment and Applications, to be distributed during early calendar year 1973, Volume 4, Resources, November 1971 (Volumes 1, 2, and 4, [redacted] Volume 3, [redacted]

Electromagnetic Pulse Sensor and Simulation Notes, Volumes 1-10, AFWL EMP 1-1 through EMP 1-10, Air Force Weapons Laboratory, Kirtland Air Force Laboratory, New Mexico, April 1967 through 1972 [redacted]

Goodwin, L. K., et al., *An Equation of State for Metals,* DASA 2286, Aeroneutronics Division of Philco-Ford, Newport Beach, California, April 1969 [redacted]

Hall, W. J., and N. M. Newmark, *Interpretation of Event Pile Driver Tunnel Liner Results* [redacted] DASA 2374, University of Illinois, Urbana, Illinois, February 1970 [redacted]

Hall, W. J., and N. M. Newmark, *Supplemental Studies of Event Pile Driver Backpacked Tunnel Liner Results* [redacted] DASA 2374-1, University of Illinois, Urbana, Illinois, October 1970 [redacted]

Harrison, G., *A Plan for the Development and Evaluation of an Advanced Re-Entry Vehicle* [redacted] DASA 2208-I, General Electric Corporation, Philadelphia, Pennsylvania, June 1969 [redacted]

Hillendahl, R. W., *Theoretical Models for Nuclear Fireball* [redacted] DASA 1589-1 through 1589-39, Lockheed Missiles and Space Company, Sunnyvale, California, 1965-68 [redacted]

[redacted]

[redacted]

[redacted]

Julian, A., and C. E. Eves, *Thermal Effects on Strength of Aircraft Structural Sandwich-Type Panels,* WT 1341, Project 8.4, Operation REDWING, Cook Research Laboratories, Skokie, Illinois, 30 April 1958 [redacted]

Julian, A. N., *In-Flight Structural Response of FJ-4 Aircraft to Nuclear Detonations,* WT 1432, Project 5.3, Operation PLUMBBOB, Bureau of Aeronautics, Washington, D.C., 10 February 1960 [redacted]

Kalinowski, J. J., *A Management Guide to Transient-Radiation Effects on Electronics (TREE)* [redacted] DNA 2051H, Battelle's Columbus Laboratories, Columbus, Ohio, February 1972 [redacted]

Kaplan, K., and C. Wiehle, *Air Blast Loading in the High Shock Strength Region* [redacted] Part II, Prediction Methods and Examples, URS 633-3, DASA 1460-1, URS Corporation, Burlingame, California, February 1965 [redacted]

Kaufmann, R., and R. J. Heilferty, *Equations and Computer Program to Calculate the Temperature Distribution and History in a Cylinder Subject to Thermal Radiation from a Nuclear Weapon,* NASL Project 940-105, PR-8, U.S. Naval Applied Science Laboratory, Brooklyn, New York, 18 July 1968 [redacted]

Kaufmann, R., and R. J. Heilferty, *Equations and Computer Program to Calculate the Temperature Distribution and History in a Tee Beam Subject to Thermal Radiation from a Nuclear Weapon,* NASL Project 940-105, PR-6, U.S. Naval Applied Science Laboratory, Brooklyn, New York, 20 February 1968 [redacted]

Larin, F., *Radiation Effects in Semiconductor Devices,* John Wiley and Sons, Inc., New York, 1968 [redacted]

Martin, S. B., and S. Holton, *Preliminary Computer Program for Estimating Primary Ignition Ranges for Nuclear Weapons,* USNRDL-TR-866, U.S. Naval Radiological Defense Laboratory, San Francisco, California, 3 June 1965 [redacted]

Melin, J. W., and S. Sutcliff, *Development of Procedures for Rapid Computation of Dynamic Structural Response,* University of Illinois Final Report on Contract AF33(600)-24994 for Physical Vulnerability Division of Intelligence, USAF [redacted]

Moon, D. P., and W. F. Simmons, *Methods for Conducting Short-Time Tensile, Creep, and Creep-Rupture Tests under Conditions of Rapid Heating,* Defense Metals Information Center Report 121, December 28, 1959 [redacted]

Moon, D. P., and W. F. Simmons, *Selected Short-Time Tensile and Creep Data Obtained under Conditions of Rapid Heating,* Defense Metals Information Report 130, June 17, 1960 [redacted]

[redacted]

[redacted]

Morris, P. J., *Proposed Addition to Chapter 7, DASA EM-1, Section 7.6, Thermal Radiation Degradation of Structural Resistance to Air Blast* [redacted] URS 7029-6, URS Research Company, San Mateo, California, December 1971 [redacted]

Newmark, N. M., et al., *Analysis of Design of Flexible Underground Structures*, DA-22-079-eng-255, University of Illinois; Urbana, Illinois; 31 October 1962 [redacted]

Newmark, N. M., *An Engineering Approach to Blast Resistant Design*, Paper No. 2786, Transactions, ASCF, *121*, 45-64, 1956 [redacted]

Nuclear Weapons Blast Phenomena, DASA 1200-I, -II, -III, -IV, Defense Atomic Support Agency, Washington, D.C., Vol. I, March 1971, Vol. II, December 1970, Vol. III, March 1970, Vol. IV to be issued during calendar year 1972 (Vol. I, [redacted] Vol. II [redacted] Vol. III, [redacted]

Old, C. C., et al., *TROIKA Study Final Report* [redacted] DASA 2191-I, -II, -III, and -IV, Lockheed Missiles and Space Company, Sunnyvale, California, August 1968 (Vols. I and II, [redacted] Vols. III and IV, [redacted]

Reaugh, J., *Equation-of-State Evaluation Predix Topical Report* [redacted] PITR-239-1, DASA 2596, Physics International Co., San Leandro, California, April 1972 [redacted]

Seaman, L., et al., *Dynamic Fracture Criteria of Homogeneous Materials*, AFWL-TR-71-156, Stanford Research Institute, Menlo Park, California, February 1972 [redacted]

Seaman, L., *Spall and Fracture Phenomena in the Response of Materials to Nuclear Effects* [redacted] Third Annual Meeting of Nuclear Survivability Working Group on Propulsion and Ordnance, Stanford Research Institute, Menlo Park, California, 29-30 August 1971 [redacted]

Shelton, F., *Nuclear Weapons as X-Ray Sources, the Environments They Produce, and Some Effects on Aerospace Systems* [redacted] *Volume II, Some Effects on Aerospace Systems*, DASA 2397-2, KN-770-69-30, Kaman Nuclear, Colorado Springs, Colorado, September 1969 [redacted]

Snay, H. G., *Underwater Explosion Phenomena: The Parameters of Migrating Bubbles*, NAVORD Report 4185, U.S. Naval Ordnance Laboratory, White Oak, Silver Spring, Maryland, 12 October 1962 [redacted]

Snay, H. G., *Hydrodynamic Concepts Selected Topics for Underwater Nuclear Explosions*, NOLTR 65-52, DASA 1240-1(2), U.S. Naval Ordnance Laboratory, White Oak, Silver Spring, Maryland, 15 September 1966 [redacted]

[redacted]

[redacted]

Staff of Kaman Avidyne, *Handbook for Analysis of Nuclear Weapon Effects on Aircraft* [redacted] KA-TR-50A, DASA-2048, Kaman Avidyne, Burlington, Massachusetts, April 1970 [redacted]

Staff of Kaman Avidyne, *Handbook of Computer Programs for Analysis of Nuclear Weapon Effects on Aircraft* [redacted] KA-TR-50S, DASA-2048S, Kaman Avidyne, Burlington, Massachusetts, April 1970 [redacted]

Timoshenko, S., and S. Woinowsky-Krieger, *Theory of Plates and Shells*, McGraw-Hill Book Company, 1959 [redacted]

TREE (Transient-Radiation Effects on Electronics) Handbook [redacted] DNA 1420H-1, Vol. 1, Edition 3, Battelle's Columbus Laboratories, Columbus, Ohio, December 1971 [redacted]

TREE (Transient-Radiation Effects on Electronics) Handbook [redacted] DASA 1420-1, Edition 2, Revision 2, Battelle Memorial Institute, Columbus, Ohio, September 1970 [redacted] (to be replaced by DNA 1420H-2 during early calendar year 1973).

TREE Preferred Procedures (Selected Electronic Parts), DNA-2028H, Battelle's Columbus Laboratories, Columbus, Ohio, June 1972 [redacted]

TREE Simulation Facilities, DASA 2432, Edition 1, Battelle Memorial Institute, Columbus, Ohio, September 1970 [redacted]

Veigele, W. J., et al., *X-Ray Cross Section Compilation from 0.1 keV to 1 MeV*, DNA 2433F Vols. 1 and 2, Revision 1, KN-71-431(R), Kaman Nuclear, Colorado Springs, Colorado, 31 July 1971 [redacted].

Whitaker, W. A., and R. A. Deliberis, *Aircraft Thermal Vulnerability to Large High-Altitude Detonations* [redacted] AFWL-TR 67-85, Air Force Weapons Laboratory, Kirtland Air Force Base, New Mexico, August 1967 [redacted]

Whitener, J. E., *Deflection of Ballistic Missiles by Nuclear Weapons* [redacted] RM-2345, RAND Corporation, Santa Monica, California, April 1959 [redacted]

[redacted]

[redacted]

Chapter 10
PERSONNEL CASUALTIES

INTRODUCTION

The three principal phenomena associated with nuclear explosions that result in casualties to personnel are blast and shock, thermal radiation, and nuclear radiation. Blast injuries may be direct or indirect; the former are caused by the high air pressure (overpressure), while the latter may be caused by missiles or by displacement of the body.

The frequency of burn injuries resulting from a nuclear explosion is exceptionally high. Most of these are flash burns caused by direct exposure to the thermal radiation, although personnel trapped by spreading fires may be subjected to flame burns. In addition, personnel in buildings or tunnels close to ground zero may be burned by hot gases and dust entering the structure even though they are shielded adequately from direct or scattered radiation.

The harmful effects of the nuclear radiations appear to be caused by ionization and excitation (see paragraph 6-4, Chapter 6) produced in the cells composing living tissue. As a result of ionization, some of the constituents, which are essential to the normal functioning of the cells, are altered or destroyed. As described in Section III, these changes may result in sickness that may terminate with death in some cases.

The effects of these three phenomena on personnel are described in the succeeding three sections. A brief discussion of the effects of combinations of the phenomena is provided in Section IV.

SECTION I
AIR BLAST

MECHANISMS AND CRITERIA FOR INJURY

Injury that results from exposure of personnel to air blast may occur from sudden changes in environmental pressure acting directly on the exposed subject, from displacement of personnel involving decelerative tumbling or impact against a rigid object, from blast-energized debris striking the individual, and from a variety of miscellaneous changes in the immediate environment. Individuals who are injured to such an extent that they are unable to perform assigned tasks are designated casualties. Such a condition typically starts almost immediately following airblast trauma and it can be expected to last from hours to several days, depending on the nature and severity of the injury. The biological effects which may result from exposure to a blast wave are divided into four categories: (1) direct overpressure effects, (2) effects from translational forces and impact, (3) effects of blast energized debris, and (4) miscellaneous effects. These effects are discussed separately in the following paragraphs.

10-1 Direct Overpressure Effects

Casualties that result from direct overpressure effects are those that result from man's inability to withstand rapid changes in his environmental pressure. The body is relatively resistant to the crushing forces from air blast loading; however, large sudden pressure differences resulting from blast wave overpressure may cause serious injury. Anatomic localization of such injury occurs predominantly in air-bearing organ systems such as the lungs, gastroenteric tract, ears and perinasal sinuses. At high overpressures both early (less than 30 minutes) and delayed (30 minutes to several days) lethality will occur as a result of disruption of lung tissue. Early lethality is generally caused by interruption in the blood supply to the heart or brain as a result of air emboli entering the circulatory system

[redacted]

AD-A955 394

This document has been approved for public release and sale; its distribution is unlimited.

[redacted]

from the damaged lung. Delayed lethality occurs as a result of suffocation caused by continuing hemorrhage within the lung or the development of pulmonary edema. Delayed appearance of casualties also may occur at high overpressures as a result of internal hemorrhage from ruptured organs or as a result of infection due to perforation of the intestine.

Experiments conducted with animals indicate that direct overpressure effects depend upon the peak overpressure, duration and shape of the incident blast wave, and the orientation of the subject. Both the peak overpressure and the duration appear to be important for fast-rising blast waves that have durations less than 50 msec, whereas peak overpressure predominates for positive phase air-blast durations greater than 50 msec. If the time to peak overpressure is greater than a few milliseconds, there is a lower probability of injury because the anatomic structures will be subjected to pressure differences that occur less rapidly. This effect can take place in a structure where the pressure rises gradually due to a long fill time or it may occur near a reflecting surface where the pressure rises in "steps" as a result of a separation in the arrival times of the incident and reflected waves. In general, personnel who are oriented with the feet or head toward the oncoming blast wave will be injured less than those who are oriented with the long axis perpendicular to the blast wave. This is apparently caused by the action of the dynamic pressure to increase the load on the thorax in the latter case. A potentially more hazardous exposure condition occurs when personnel are situated against a flat surface, since normal reflection of a blast wave results in pressures two or more times the magnitude of the incident wave.

Current criteria for direct overpressure effects, based on extrapolations from animal data, predict 50-percent casualties and one percent mortality for randomly oriented, prone personnel exposed to a long-duration fast-rising blast wave of 41 psi and one percent casualties for those exposed to 12 psi. Animal experiments and human accident cases have shown that a 50-percent incidence of eardrum rupture may be expected to occur at 16 psi, whereas one percent might be anticipated at 3.4 psi. Although in certain situations auditory acuity is imperative, eardrum rupture currently is not considered to be a disabling injury in terms of overall effectiveness to individuals in military units.

10-2 Translational Forces and Impact

Injuries caused by translational impact occur as a result of whole body displacement of personnel by blast winds. Anatomic localization of such injuries is not as readily definable as the case for direct overpressure effects. In instances where head impact occurs, concussion, skull fractures, and intracranial hemorrhage may result in rapid loss of consciousness and, in many cases, early lethality. By contrast, impact in which the head is not involved results in a variety of traumatic injuries such as skeletal fractures, ruptured internal organs, blood loss and, in more serious cases, the development of shock. Recovery following such injuries may be more delayed than recovery from direct overpressure effects.

The translational and rotational velocities that are attained by personnel during the accelerative phase of blast-induced displacement depend upon the geometry of exposure and the shape and magnitude of the dynamic-pressure wave. In general, a longer duration of the positive phase of the blast wave will result in a lower peak overpressure being required to produce a given translational velocity. Therefore, larger yields will produce injuries at lower pressures (see Section I, Chapter 2). The severity of the injuries caused by displacement depends to a large extent on the nature of the decelerative phase of the motion. If deceleration occurs by an "impact" with a rigid object, resulting in a stopping distance of less than a few inches, the

QUALITY INSPECTED 4

[redacted]

UNANNOUNCED

[redacted]

[redacted] probability of a serious injury is much greater than if deceleration occurs by "tumbling" over open terrain, which will result in much longer stopping distances.

[redacted] Because of the limited data available, casualty criteria for translational impact are far less certain than those for direct overpressure effects. In addition, there are marked differences in impact velocities that are associated with serious injury following head trauma compared with those for noncranial impact. Human cadaver studies indicate that 50 percent mortality may occur following head impact at velocities of 18 ft/sec, whereas large animal studies and human free-fall experience suggest that 54 ft/sec is required for 50 percent mortality when head impact is minimized. Decelerative tumbling experiments involving a limited number of animals suggest that significant mortality does not occur at translational velocities below 88 ft/sec.

[redacted] Although tentative in nature, estimates based on human accidents and animal experiments predict that a peak translational velocity of 70 ft/sec will result in 50 percent casualties for personnel when deceleration occurs by tumbling over open terrain. If translation occurs where 50 percent of the personnel impact against structures (buildings, vehicles, trees or other rigid objects) the peak translational velocity for 50 percent casualties is expected to be near 35 ft/sec. Similar figures for one percent casualties are 13 ft/sec for decelerative tumbling and 8.5 ft/sec for translation near structures.

10-3 Blast-Energized Debris [redacted]

[redacted] The effects of blast-energized debris include injuries that result from the impact of penetrating or nonpenetrating missiles energized by winds, blast overpressures, ground shock, and, in some cases, gravity. The wounding potential of blast-energized debris depends upon the nature and velocity of the moving object and the portion of the body where impact occurs. The types of injuries range from simple contusions and lacerations to more serious penetrations, fractures, crushing injuries, and critical damage to vital organs. The physical factors that determine the velocity attained by debris and thereby determine the severity of potential injury, are similar to those described for translation of personnel. When small light objects are displaced by a blast wave, they reach their maximum velocity quite rapidly, often after only a small portion of the wave has passed; therefore, the maximum velocity is not as dependent on duration as it is for large heavy objects. There are too many variables to establish definitive criteria for injury from debris.

[redacted] In the specific instance of personnel in forests, tentative casualty criteria are available based on the probability of being struck by falling trees. These criteria are related to the amount of forest damage. Fifty percent casualties are predicted at ranges where the forest damage is moderate to severe, and one percent casualties are anticipated where the damage is light (see Forest Damage Data, Chapter 15).

10-4 Miscellaneous Effects [redacted]

[redacted] Miscellaneous blast injuries are those that result from non-line-of-sight thermal phenomena, ground shock, blast-induced fires and high concentrations of dust,

- Non-line-of-sight thermal burns have been observed on animals located in open underground shelters in close proximity to nuclear explosions. Although this phenomenon is not well understood, it has been suggested that the burns resulted from contact with hot dust-laden air that was carried into the structures by the blast wave.
- Ground shock may be a serious problem for personnel in blast-hardened underground structures at close ranges. The magnitude of this hazard may be estimated from the horizontal and vertical motions of the structure, which in turn may be estimated from

[redacted]

the predicted ground motions discussed in Chapter 2.

- Blast-induced fires are primarily a problem for urban areas. The likelihood of such fires depends on the amount of burning and combustible materials in the vicinity of an explosion.
- The evidence indicates that a high concentration of dust represents more of a discomfort than a serious hazard to personnel.

With the possible exception of ground shock, currently there is inadequate information to predict the hazards associated with these miscellaneous effects reliably.

CASUALTY PREDICTION

10-5 Personnel in the Open

For most burst conditions casualties from whole body translation of personnel in the open will extend farther than those from direct overpressure hazards, excluding eardrum rupture. This is especially true for larger yield weapons because of the increased duration of the blast wave. The translation hazard will be less for personnel located in relatively open terrain than for personnel located where they may be blown against buildings, vehicles, trees or other structures. Warned personnel can reduce the translation risks by assuming a prone position, and in the case of larger yields there will be sufficient time for the fireball flash to serve as a warning. It should be noted, however, that for overhead bursts, the direct overpressure effects would be less severe for a standing man than for a prone man because of the "step" loading of the thorax in the former case.

Unless the target area is cluttered with materials subject to fragmentation with displacement, blast-energized debris is not expected to be an overriding hazard for personnel in the open. For small yield surface bursts, however, crater ejecta may extend beyond the other blast effects, although nuclear or thermal radiation may produce casualties at greater distance. In general, the probability of being struck by flying missiles can be reduced by lying down; however crater ejecta, which is likely to be falling nearly vertically at the greater distances may strike more prone personnel than those who are standing. As in the case of blast-energized debris, the miscellaneous air blast effects are not generally expected to represent major hazards for personnel in the open.

If a precursor form of blast wave should develop, personnel located in its proximity would probably be subjected to greater translation and debris hazards than would be expected otherwise because of the increased dynamic pressures. Burst conditions associated with precursor development are discussed in Section I of Chapter 2.

Figures 10-1 and 10-2 show the ground distances for 50 percent and one percent casualties, respectively, from the indicated air blast effects as a function of height of burst for randomly oriented, prone personnel exposed in the open to a one kt burst. These figures were derived on the basis of the criteria and assumptions discussed earlier in this section, with the added conditions that crater ejecta was not present and no precursor formed. Since a man with a ruptured eardrum may or may not be considered a casualty depending on the tasks he is expected to perform, this effect has been removed from the other direct overpressure effects, and separate curves are provided. Two translation curves are shown in each figure and the one that is more appropriate to the existing conditions should be used. The figures show the effects for one kt, but they may be scaled to other yields by the scaling rules provided in Problem 10-1.

10-6 Personnel in a Forest

For personnel in a relatively dense forest, the hazard of being struck by falling and translating trees generally will override that resulting from any other air-blast effect. In addition, for

[redacted]

[redacted] most burst conditions a forest will provide significant protection from thermal radiation and will provide some shielding from nuclear radiation. Therefore, casualties resulting from forest blowdown generally will extend to greater ranges than those from any other weapon effect (direct overpressure, translation, thermal radiation, nuclear radiation, etc.). Exceptions to this general rule are casualties resulting from initial nuclear radiation associated with low yield weapons, and casualties resulting from forest fires ignited by the thermal radiation pulse.

[redacted] Casualty prediction curves for forest blowdown are given in Figures 10-1 and 10-2 as a function of height of burst and ground range for randomly oriented, prone personnel exposed to a one kt burst. These curves may be scaled to other yields by multiplying both the burst heights and the ground ranges by the four-tenths power of the yield. In general, a forest does not greatly reduce or otherwise modify a blast wave. For this reason the other curves in Figures 10-1 and 10-2, which were developed to predict air-blast casualties for personnel in the open, also may be used for personnel in a forest. A description of the particulars concerning these curves has been given in the above discussion for personnel in the open.

10-7 Personnel in Structures [redacted]

[redacted] In addition to providing shielding against thermal and nuclear radiations, blast-resistant structures such as bomb shelters, permanent gun emplacements and, to a certain extent, foxholes usually reduce the blast hazards unless personnel are located directly in the entryway of the structure. The design of these structures may, however, permit the buildup of blast overpressures to a value in excess of the overpressures outside the structure as a result of multiple reflections. Nevertheless, there is generally a lower probability of injury from direct overpressure effects inside a structure than at equivalent distances on the outside, particularly if personnel do not lean against the walls of the structure or sit or lie on the floor. This results from alterations in the pattern of the overpressure wave upon entering the structure.

[redacted] Structural collapse and damage are the major causes of casualties for personnel located in buildings subjected to air blast; for this reason, the number of such casualties can be estimated from the extent of the structural damage. Table 10-1 shows estimates of casualties in two types of buildings for three damage levels. Data from Chapter 11 may be used to predict the ground distances at which specified structural damage will occur for various yields. Collapse of a brick house is expected to result in approximately 25 percent mortality, 20 percent serious injury and 10 percent light injury to the occupants. Reinforced concrete structures, though much more resistant to blast forces, will produce almost 100 percent mortality on collapse. Casualty percentages in Table 10-1 for brick homes are based on data from British World War II experience. They may be assumed to be reasonably reliable for cases where the population expects bombing and most personnel have selected the safest places in the buildings. If there were no warning or preparation, the number of casualties would be expected to be considerably higher. To estimate casualties in structures other than those listed in Table 10-1, the type of structural damage that occurs, and the characteristics of the resultant flying objects must be considered. Broken glass may produce large numbers of casualties, particularly to an unwarned population, at overpressures where personnel would be relatively safe from other effects. Overpressures as low as one or two psi may result in penetrating wounds to bare skin.

10-8 Personnel in Vehicles [redacted]

[redacted] Personnel in vehicles may be injured as a result of the response of the vehicle to blast forces. Padding, where applicable, and the use of safety belts, helmets and harnesses can reduce

[redacted]

[redacted]

Table 10-1 [redacted] Estimated Casualty Production in Buildings for Three Degrees of Structural Damage [redacted]

Structural Damage	Percent of Personnel*		
	Killed Outright	Serious Injury (hospitalization)	Light Injury (no hospitalization)
1-2 story brick homes (high-explosive data from England):			
Severe damage	25	20	10
Moderate damage	<5	10	5
Light damage	–	<5	<5
Reinforced-concrete buildings (nuclear data from Japan):			
Severe damage	100	–	–
Moderate damage	10	15	20
Light damage	<5	<5	15

*These percentages do not include the casualties that may result from fires, asphyxiation, and other causes from failure to extricate trapped personnel. The numbers represent the estimated percentages of casualties expected at the maximum range where a specified structural damage occurs. See Chapter 11 for the distances at which these degrees of damage occur for various yields.

[redacted] this source of casualties significantly, at least within armored vehicles that are strong enough to resist collapse. Serious injury may result to personnel in ordinary wheeled vehicles from flying glass as well as from impact with the vehicle's interior. Comparative numbers of casualties are almost impossible to assess because of the many variables involved.

[redacted]

[redacted]

Problem 10-1 Calculation of Casualties for Personnel in the Open or in a Forest

[redacted] Figures 10-1 and 10-2 are families of curves that show 50 percent and 1 percent casualties, respectively, from the indicated air-blast effects, as a function of height of burst and distance from ground zero. The curves apply to randomly oriented, prone personnel exposed in the open to a 1 kt burst.

[redacted] *Scaling.* For yields other than 1 kt, scale as follows:

1. For the direct overpressure and eardrum rupture curves

$$\frac{d}{d_1} = \frac{h}{h_1} = W^{1/3}$$

where d_1 and h_1 are the distance from ground zero and height of burst respectively, for 1 kt; and d and h are the corresponding distance and height of burst for a yield of W kt.

2. For the translation and forest blowdown curves

$$\frac{d}{d_1} = \frac{h}{h_1} = W^{0.4}$$

where d_1 and h_1 are the distance from ground zero and height of burst, respectively, for 1 kt; and d and h are the corresponding distance and height of burst for a yield of W kt.

[redacted] *Example* [redacted]

Given: A 50 kt weapon burst at an altitude of 860 feet over open terrain.

Find: The distance from ground zero at which translational effects would produce 50 percent casualties among prone personnel.

Solution: The corresponding height of burst for 1 kt is

$$h_1 = \frac{h}{W^{0.4}} = \frac{860}{(50)^{0.4}} = 180 \text{ ft.}$$

From Figure 10-1, at a height of burst of 180 feet, the distance from ground zero at which 50 percent casualties among personnel in the open will occur for a 1 kt burst is 660 feet.

Answer: The corresponding distance for a 50 kt weapon is

$$d = d_1 \times W^{0.4} = 660 \times (50)^{0.4} = 3150 \text{ ft.}$$

Reliability: The distances obtained from Figures 10-1 and 10-2 are estimated to be reliable to within ±15 percent for the indicated effects; however, in view of the uncertainties discussed in paragraphs 10-5 and 10-6 (e.g., the presence of debris, crater ejecta, etc.) no precise estimate of the reliability can be made for a specific situation.

Related Material: See paragraphs 10-1 through 10-6.

[redacted]

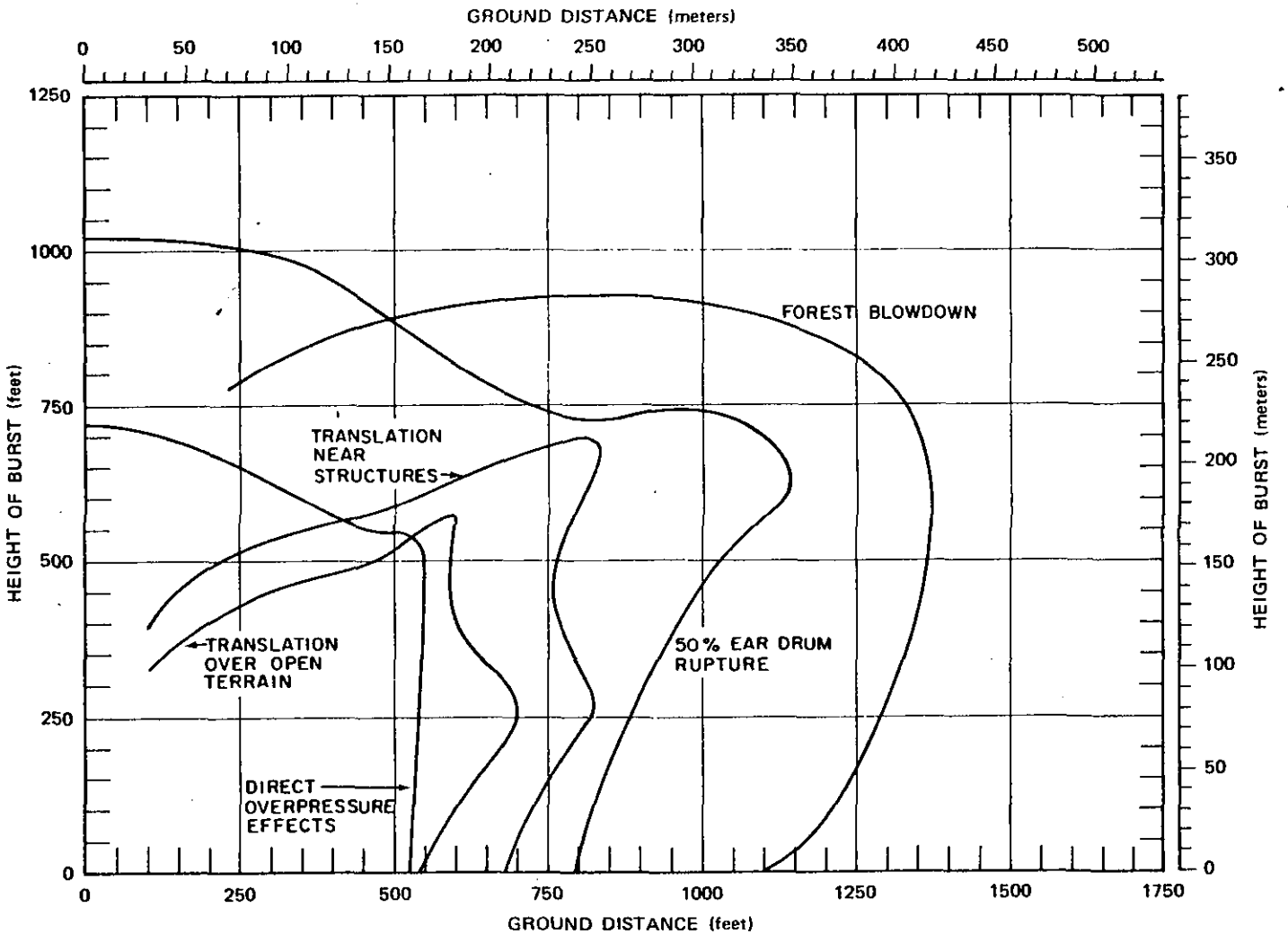

Figure 10-1. [redacted] Fifty Percent Casualties for the Indicated Blast Effects for Prone Personnel Exposed in the Open or in a Forest to a 1 kt Burst [redacted]

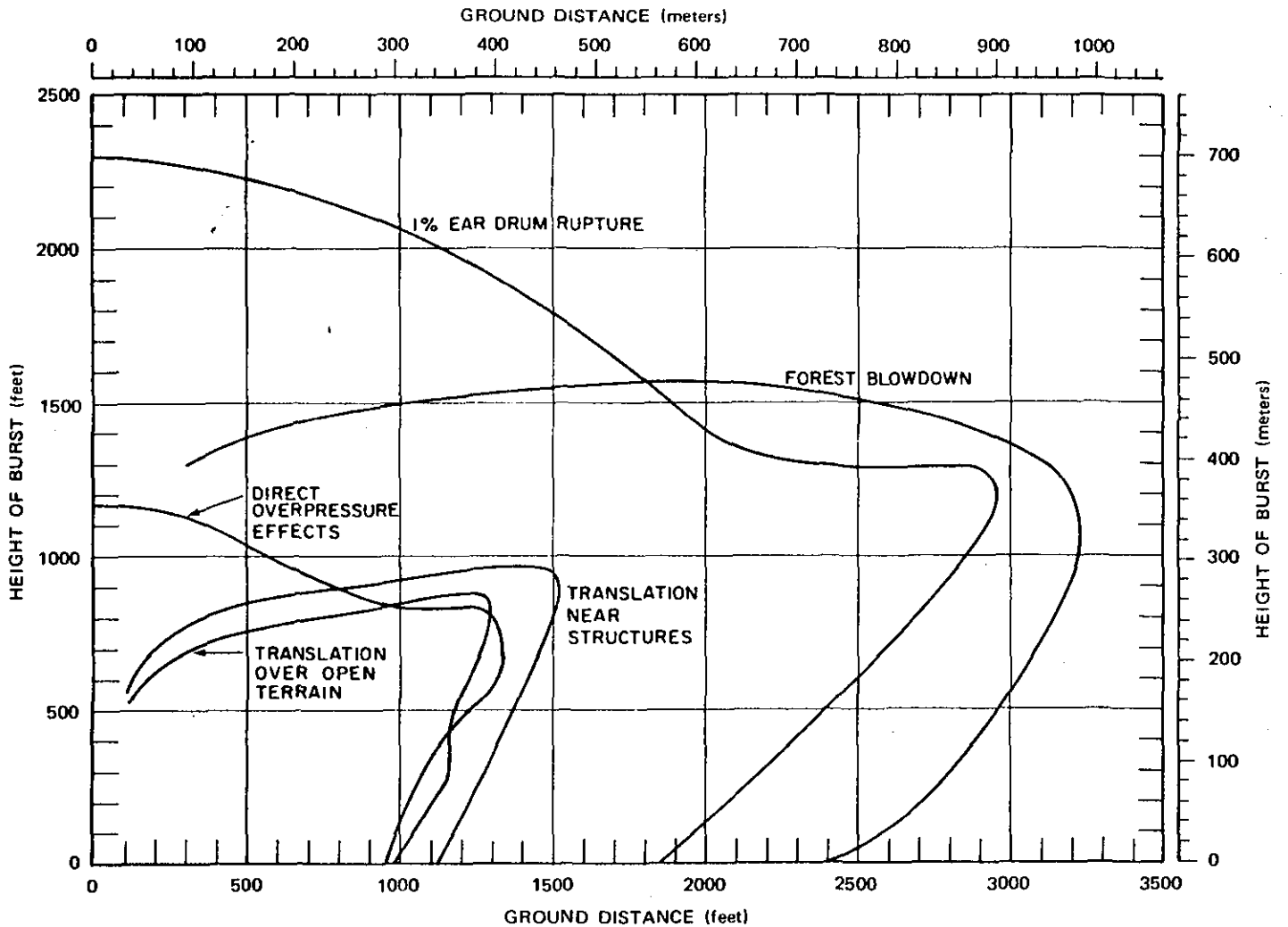

Figure 10-2. [redacted] One Percent Casualties for the Indicated Blast Effects for Prone Personnel Exposed in the Open or in a Forest to a 1 kt Burst [redacted]

[redacted]

SECTION II

[redacted] THERMAL RADIATION [redacted]

[redacted] SKIN BURNS [redacted]

[redacted] When a nuclear weapon detonates, personnel will sustain skin burns at distances that may be larger than those distances at which injury occurs as a result of blast or nuclear radiation. These burns may be produced directly by the absorption of radiant energy by the skin, or indirectly by heat transference through clothing or by ignition of the clothing. Thermal radiation is composed of light in the ultraviolet, visible and infrared regions of the spectrum and travels in a straight line at the speed of light. It is emitted within periods of a few milliseconds to several tens of seconds.

[redacted] If there is substantial material between the individual and the nuclear burst, the thermal radiation will be absorbed and no burns will be produced. Thus, persons in or behind buildings, vehicles, etc., will be shielded from the thermal pulse either partially or completely. In some instances, burns may be avoided or reduced if evasive action is taken during the delivery of the thermal pulse, since heating takes place only during direct exposure. These and other protective measures will be discussed later.

[redacted] CLASSIFICATION OF BURNS [redacted]

[redacted] Burn severity is related to the degree of elevation of skin temperature and the length of time of this elevation. Pain, a familiar warning sensation, occurs when the temperature of certain nerve cells near the surface of the skin is raised to 43°C (109°F) or more. If the temperature is not elevated to a high enough degree or for a sufficient period of time, pain will cease and no injury will occur. The amount of pain is not related to burn severity as is the classification of first degree (1°), second degree (2°) or third degree (3°) burns but it is a useful tool in warning an individual to evade the thermal pulse.

10-9 First Degree Burns [redacted]

[redacted] A skin burn is an injury to skin caused by temperature elevation following application of heat by absorption of direct thermal radiation or by transference through cloth. First degree burns are characterized by immediate pain which continues after exposure and by ensuing redness of the exposed area. The first degree burn is a reversible tissue injury; the classic example is sunburn.

10-10 Second Degree Burns [redacted]

[redacted] Second degree burns are caused by temperatures that are higher and/or of longer duration than those necessary for first degree skin burns. The injury is characterized by pain and may be accompanied by either no immediate visible effect or by a variety of skin changes including blanching, redness, loss of elasticity, swelling and blisters. After 6 to 24 hours, a scab will form over the injured area. The scab may be flexible, tan or brown, if the injury is moderate, or it may be thick, stiff and dark, if the injury is more severe. Second degree burn wounds will heal within one to two weeks unless they are complicated by infection. Second degree burns do not involve the full thickness of the skin, and the remaining uninjured cells may be able to regenerate normal skin without scar formation.

10-11 Third Degree Burns [redacted]

[redacted] Third degree burns are caused by temperatures of a higher magnitude and/or longer duration than second degree burns. The injury is characterized by pain at the peripheral, less injured areas only, since the nerve endings in the centrally burned areas are damaged to the extent that they are unable to transmit pain impulses. Immediately after exposure, the skin may appear normal, scalded, or charred, and it may lose its elasticity. The healing of third degree burns takes several weeks and always results in scar formation unless new skin is grafted over the

[redacted]

[redacted]

[redacted]

burned area. The scar results from the fact that the full thickness of the skin is injured, and the skin cells are unable to regenerate normal tissue.

10-12 Reduction in Effectiveness by Burns [redacted]

[redacted] The distribution of burns into three groups obviously has certain limitations since it is not possible to draw a sharp line of demarcation between first- and second-degree, or between second- and third-degree burns. Within each class the burn may be mild, moderate, or severe, so that upon preliminary examination it may be difficult to distinguish between a severe burn of the second degree and a mild third-degree burn. Subsequent pathology of the injury, however, will usually make a distinction possible. In the following discussion, reference to a particular degree of burn should be taken to imply a moderate burn of that type.

[redacted] The depth of the burn is not the only factor in determining its effect on the individual. The extent of the area of the skin which has been affected is also important. Thus, a first-degree burn over the entire body may be more serious than a third-degree burn at one spot. The larger the area burned, the more likely is the appearance of symptoms involving the whole body. Furthermore: there are certain critical, local regions, such as the hands, where almost any degree of burn will incapacitate the individual.

[redacted] Persons exposed to a low or intermediate yield nuclear weapon burst may sustain very severe burns on their faces and hands or other exposed areas of the body as a result of the short pulse of directly absorbed thermal radiation. These burns may cause severe superficial damage similar to a third degree burn, but the deeper layers of the skin may be uninjured. This would result in rapid healing similar to a mild second degree burn. Thermal radiation burns occurring under clothing or from ignited clothing or other tinder will be similar to those ordinarily seen in burn injuries of nonnuclear origin. Because of the longer duration of the thermal pulse, the differences between flash burns on exposed skin from air burst high yield weapons and burns of nonnuclear origin may be less apparent.

[redacted] BURN INJURY ENERGIES AND RANGES [redacted]

[redacted] The critical radiant exposure for a skin burn changes as the thermal radiation pulse duration and spectrum change; therefore, the critical distance cannot be determined simply from the calculated radiant exposure. The effective spectrum shifts with yield and altitude; the thermal radiation pulse is shorter for smaller yields or higher burst altitudes (see Chapter 3).

10-13 Personnel Parameters [redacted]

[redacted] The probability and severity of an individual being burned will depend upon many factors including: pigmentation, absorptive properties, thickness, conductivity and initial temperature of the skin; distance from the detonation and the amount of shielding; clothing, orientation with respect to the burst, and voluntary evasive action.

[redacted] Severity of the burn cannot be determined by temperature elevation and pulse duration alone. The energy absorbed by the skin in a normal population may vary by as much as 50 percent because of the variance in skin pigmentation. It is known that depths in skin of 0.001 to 0.002 centimeter are the sites of the initial damage that results in a burn from thermal radiation pulses and that skin temperatures of 70°C (158°F) for a fraction of a second or temperatures of 48°C (118°F) for minutes can result in burns. Skin temperatures for first degree and third degree burns are roughly 25 percent lower and higher, respectively, than those for second degree burns.

[redacted] For pulses of 0.5 second duration and longer, the amount of energy absorbed is an im-

[redacted]

portant factor. Figure 10-3 shows the effect of absorptive differences of human skin as calculated from measurements of the spectral absorptance and the spectral distribution of the peak power of nuclear weapons bursts in the lower atmosphere. As shown in Figure 10-3, very dark skinned people will receive burns from approximately two-thirds the energy required to produce the same degree of burns on very light skinned people.

10-14 Burn Exposures for Unprotected Skin

Figure 10-4 shows ranges of radiant exposures for the probabilities of burn occurrence. The solid lines represent 50 percent probability for an average population taking no evasive action to receive the indicated type of burns. The dotted lines divide the burn probability distributions into ranges for the three burn levels with average burn probabilities of 18 percent and 82 percent assigned within these exposure ranges.

For example, from Figure 10-4, it can be predicted that, if a normal population is exposed to the thermal pulse at distances producing between 4.5 and 6.0 calories per square centimeter from a 1 megaton weapon, 18 percent of the population will receive second degree burns and 82 percent will receive first degree burns.

A radius from ground zero that produces areas of equal burn probability may be obtained by employing the radiant exposures for skin burn probability from Figure 10-5 and the weapon yield-distance relationship for radiant exposures from Chapter 3.

10-15 Burns Under Clothing

Skin burns under clothing are produced several ways: by direct transmittance through the cloth if the cloth is thin and merely acts as an attenuating screen; by heating the cloth and causing steam or volatile products to impinge on the skin; by conduction from the hot fabric to the skin; or the fabric may ignite, and consequent volatiles and flames will cause burns where they impinge on the skin.

Heat transfer mechanisms cause burns beneath clothing as a result of heat transfer for some time after the thermal pulse ends. These burns generally involve deeper tissues than those that result from the direct thermal pulse on bare skin. Burns caused by ignited clothing also result from longer heat application, and thus will be more like burns occurring in nonnuclear weapon situations.

10-16 Body Areas Involved

The pattern of body area involved in thermal radiation burns from nuclear weapons will differ from the areas injured from conventional means. For weapons of 100 kt or less, where effective evasive action cannot be taken, burns would occur primarily on the directly exposed parts of the body unless the clothing ignites. First and second degree burns of the uncovered skin, and burns through thin clothing occur at lower radiant exposures than those which ignite clothing. Because of these factors, first and second degree burns for this low yield range would involve limited body area and would occur only on one side of the body. For closer distances where the direct thermal pulse produces burns and clothing ignition takes place, persons wearing thin clothing would have third degree burns over that area of the body facing the burst. This phenomenon is typically seen in persons whose clothing catches fire by conventional means.

For the yield range 100 kt and less, persons wearing heavy clothing (in the third degree bare skin burn and clothing ignition zone) will have third degree burns on one exposed body surface and third degree burns on other areas resulting from the burning clothes prior to its removal, or full body third degree burns if the clothing cannot be removed.

[redacted]

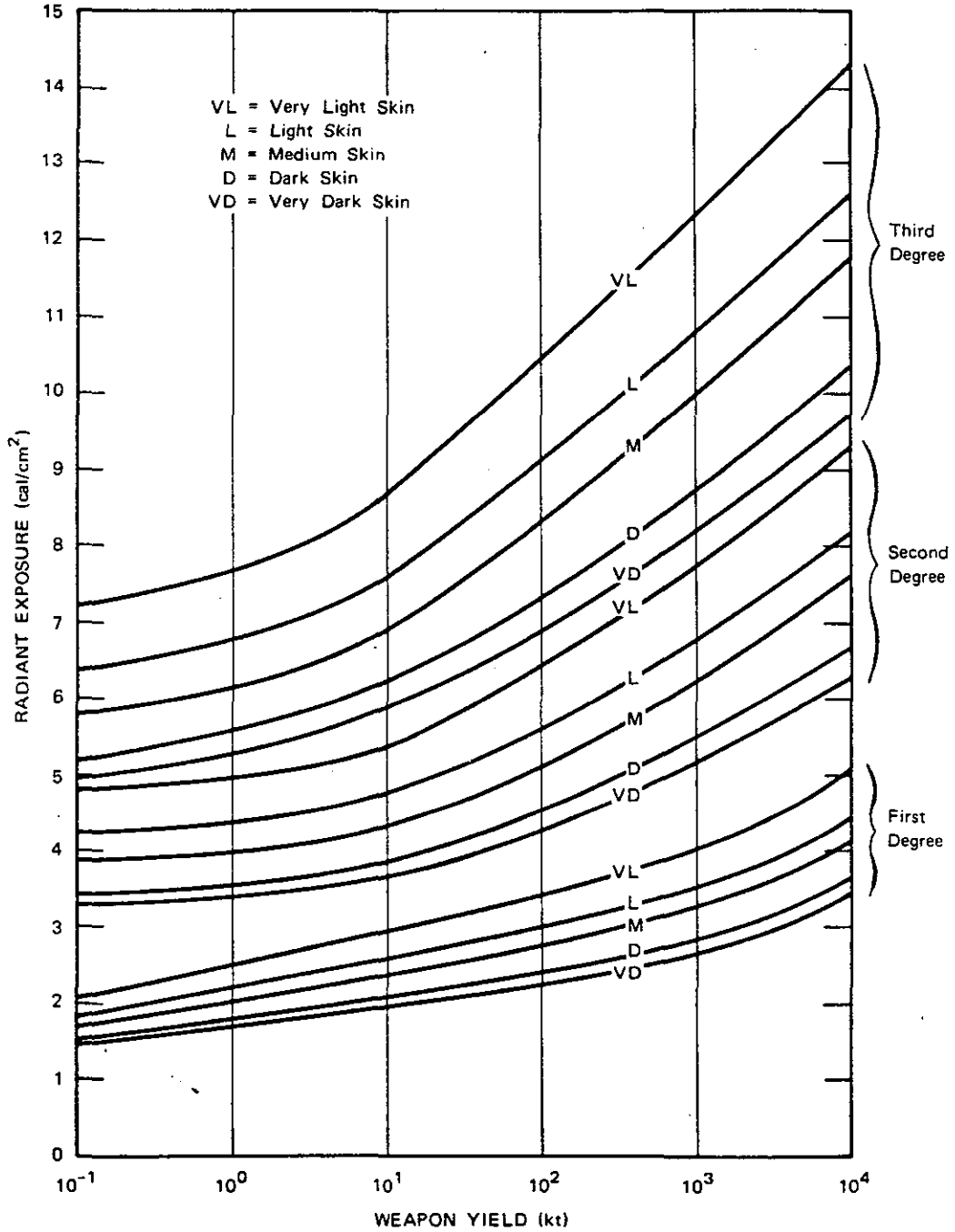

Figure 10-3. [redacted] Radiant Exposure Required to Produce Skin Burns for Different Skin Pigmentation [redacted]

[redacted]

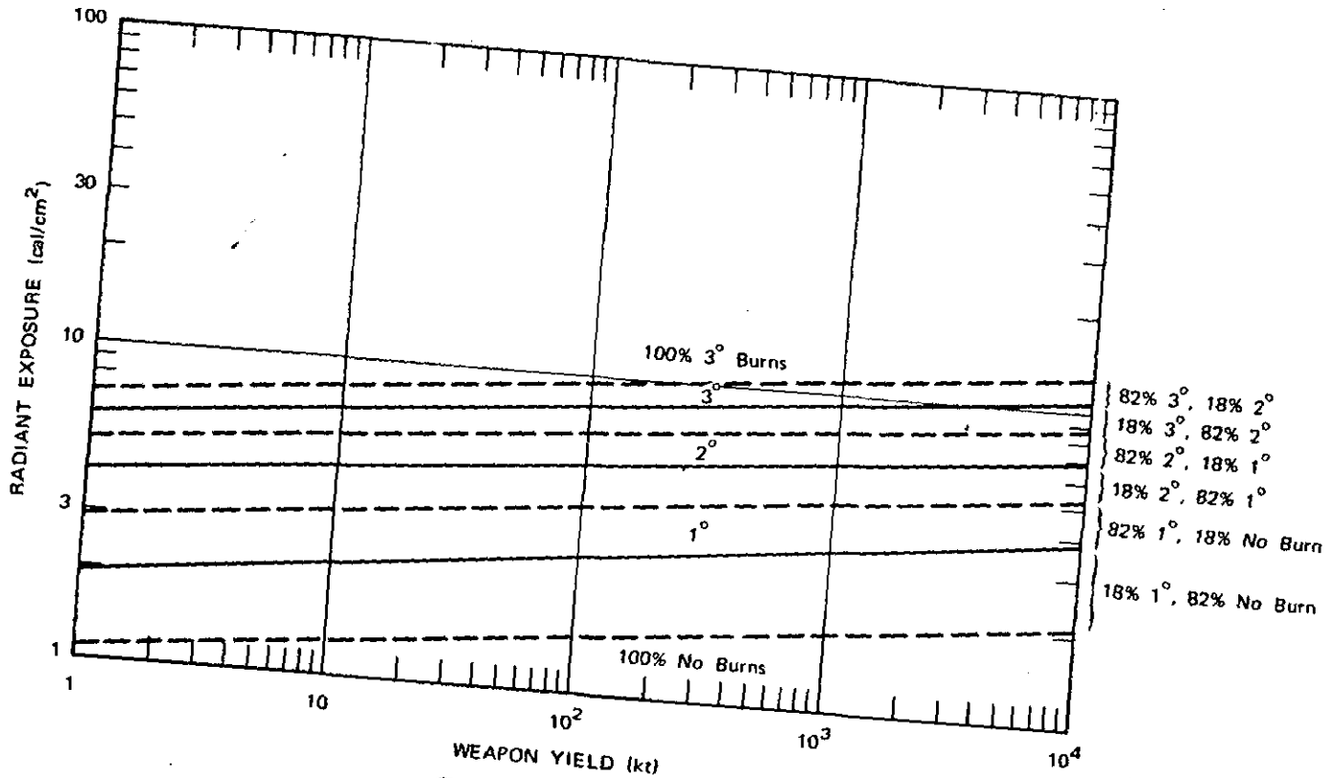

Figure 10-4. Skin Burn Probabilities for an Average Population Taking No Evasive Action

[redacted]

10-17 Incapacitation from Burns [redacted]

[redacted] Burns to certain anatomical sites of the body, even if only first degree, will frequently cause ineffectiveness because of their critical location. Any burn surrounding the eyes that causes occluded vision because of the resultant swelling of the eyelids, will be incapacitating. Burns of the elbows, knees, hands and feet produce immobility or limitation of motion as the result of swelling, pain or scab formation, and will cause ineffectiveness in most cases. Burns of the face and upper extremity areas are most likely to occur because these areas will more frequently be unprotected. Second or third degree burns in excess of 20 percent of the surface area of the body should be considered a major burn and will require special medical care in a hospital.

[redacted] Shock is a term denoting a generalized state of severe circulatory inadequacy. It will result in ineffectiveness and if untreated may cause death. Third degree burns of 25 percent of the body and second degree burns of 30 percent of the body will generally produce shock within 30 minutes to 12 hours and require prompt medical treatment. Such medical treatment is complicated and causes a heavy drain on medical personnel and supply resources.

10-18 Modification of Injur[redacted]

[redacted] Timely evasion can be effective in reducing burns with weapons yields of 100 kt and greater. The length of time between the burst and the point at which critical radiant exposure occurs increases with increasing yields, permitting personnel to react prior to receiving severe burns. With yields of less than about 100 kt, or for high altitude bursts of larger yields, the thermal pulse is too short for personnel to react and take cover. Since pain occurs at low radiant exposures and at lower temperatures than those that cause first degree burns, it is the initial sensation that occurs, and involuntary action due to pain can be expected instinctively. More effective action can be expected with proper training. Figure 10-5 illustrates the effect of evasion on the production of burns.

[redacted] Personnel in the shadow of buildings, vehicles, or other objects at the time of detonation will be shielded from the pulse and will not be burned.

[redacted] EFFECTS OF THERMAL RADIATION ON THE EYES [redacted]

[redacted] Exposure of the eye to a bright flash of a nuclear detonation produces two possible effects; flashblindness and/or retinal burns.

10-19 Flashblindness [redacted]

[redacted] Flashblindness (dazzle) is a temporary impairment of vision caused by the saturation of the light sensitive elements (rods and cones) in the retina of the eye. It is an entirely reversible phenomena which will normally blank out the entire visual field of view with a bright afterimage. Flashblindness normally will be brief, and recovery is complete.

[redacted] During the period of flashblindness (several seconds to minutes) useful vision is lost. This loss of vision may preclude effective performance of activities requiring constant, precise visual function. The severity and time required for recovery of vision are determined by the intensity and duration of the flash, the viewing angle from the burst, the pupil size, brightness necessary to perform a task and the background, and the visual complexity of the task. Flashblindness will be more severe at night since the pupil is larger and the object being viewed and the background are usually dimly illuminated.

[redacted] Flashblindness may be produced by scattered light and does not necessarily require eye focusing on the fireball.

10-20 Retinal Burns [redacted]

[redacted] A retinal burn is a permanent eye injury that occurs whenever the retinal tissue is heated.

[redacted]

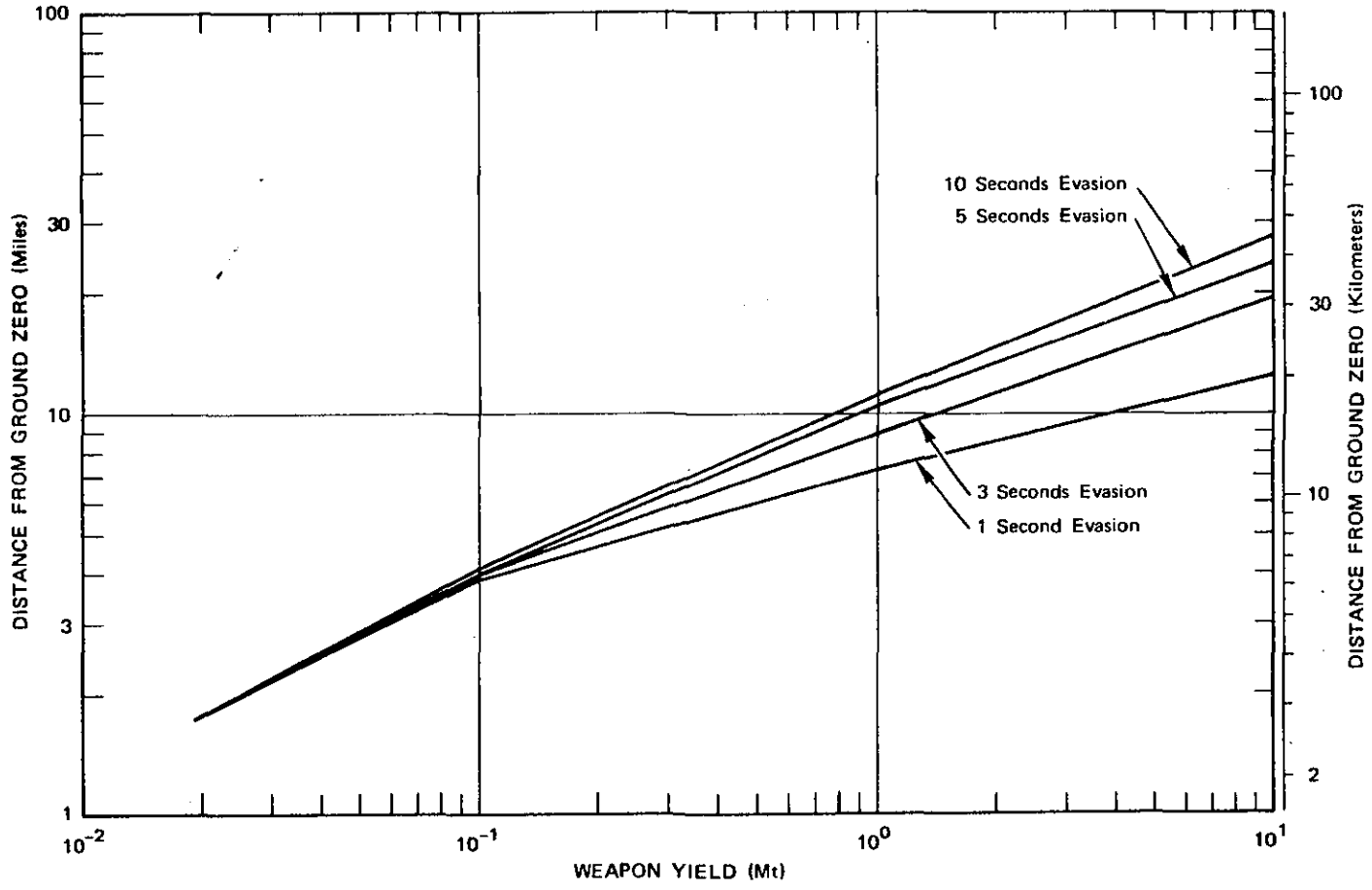

Figure 10-5. Distance Thresholds for Second Degree Burns for Various Evasion Times

[redacted]

[redacted] excessively by the focused image of the fireball within the eye. The underlying pigmented cells absorb much of the light and raise the temperature in that area. A temperature elevation of 12–20°C (22–36°F) in the eye produces a thermal injury which involves both the pigmented layer and the adjacent rods and cones, so the visual capacity is permanently lost in the burned area. The natural tendency of personnel to look directly at the fireball tends to increase the incidence of retinal burns.

[redacted] Retinal burns can be produced at great distances from nuclear detonations, because the probability of eye burns does not decrease as the square of the distance from the detonation as is true of many other nuclear weapons effects. Theoretically, the optical process of image formation within the eye negates the inverse square law and keeps the intensity per unit area on the retina a constant, regardless of the distance. However, meteorological conditions and the fact that the human eye is not a perfect lens, all contribute toward reducing the retinal burn hazard as the distance is increased between the observer and the detonation.

[redacted] Explosion yields greater than one megaton, and at heights of burst greater than about 130 kilofeet may produce retinal burns as far out as the horizon on clear nights. Bursts above 490 kilofeet probably will not produce any retinal burns in personnel on the ground unless the weapon yield is greater than 10 Mt.

(U) A retinal burn normally will not be noticed by the individual concerned if it is off the central axis of vision; however, very small burned areas may be noticeable if they are centrally located. Personnel generally will be able to compensate for a small retinal burn by learning to scan around the burned area.

10-21 Modification of Thermal Effects on the Eye [redacted]

[redacted] The thermal pulse from a nuclear weapon is emitted at such a rapid rate that any device designed to protect the eye must close extremely fast (<100 μsec) to afford a sure degree of protection for all situations. During the daytime, when the pupil is smaller and objects are illuminated brightly, the 2 percent transmission gold goggle/visor will reduce flashblindness recovery times to acceptable levels. At present, this goggle is unsatisfactory for use at night, and there is no protective device that is adequate for night use.

[redacted] The blink reflexes of the eye are sufficiently fast (~0.2 second) to provide some protection against weapons greater than 100 kt detonated below about 130 kilofeet. The blink time is too slow to provide any appreciable protection for smaller weapon yields or higher burst altitudes.

[redacted] When personnel have adequate warning of an impending nuclear burst, evasive action including closing or shielding the eyes will prevent flashblindness and retinal burns.

10-22 Safe Separation Distance Curves [redacted]

[redacted] Figures 10–6 through 10–10 present flashblindness and retinal burn curves for a number of burst heights as a function of weapon yields and safe separation distance, e.g., that distance where personnel will not receive incapacitating eye injuries. The retinal burn curves show distances that current data show to be safe. The curves for flashblindness were specifically designed for pilots of strategic bombers, where a pilot can effectively read his instruments and complete his mission after a temporary 10 second complete loss of vision. These curves are also applicable to any task where the same criteria of dim task lighting, visual demands, and the 10 second visual loss can be applied. Data are not available for specific distances at which flashblindness will not occur.

[redacted] It should be noted that the flashblindness and the retinal burn safe separation distances do not bear the same relationship to one another as the yield changes. In circumstances that require determination of complete eye safety (realizing

[redacted]

[redacted]

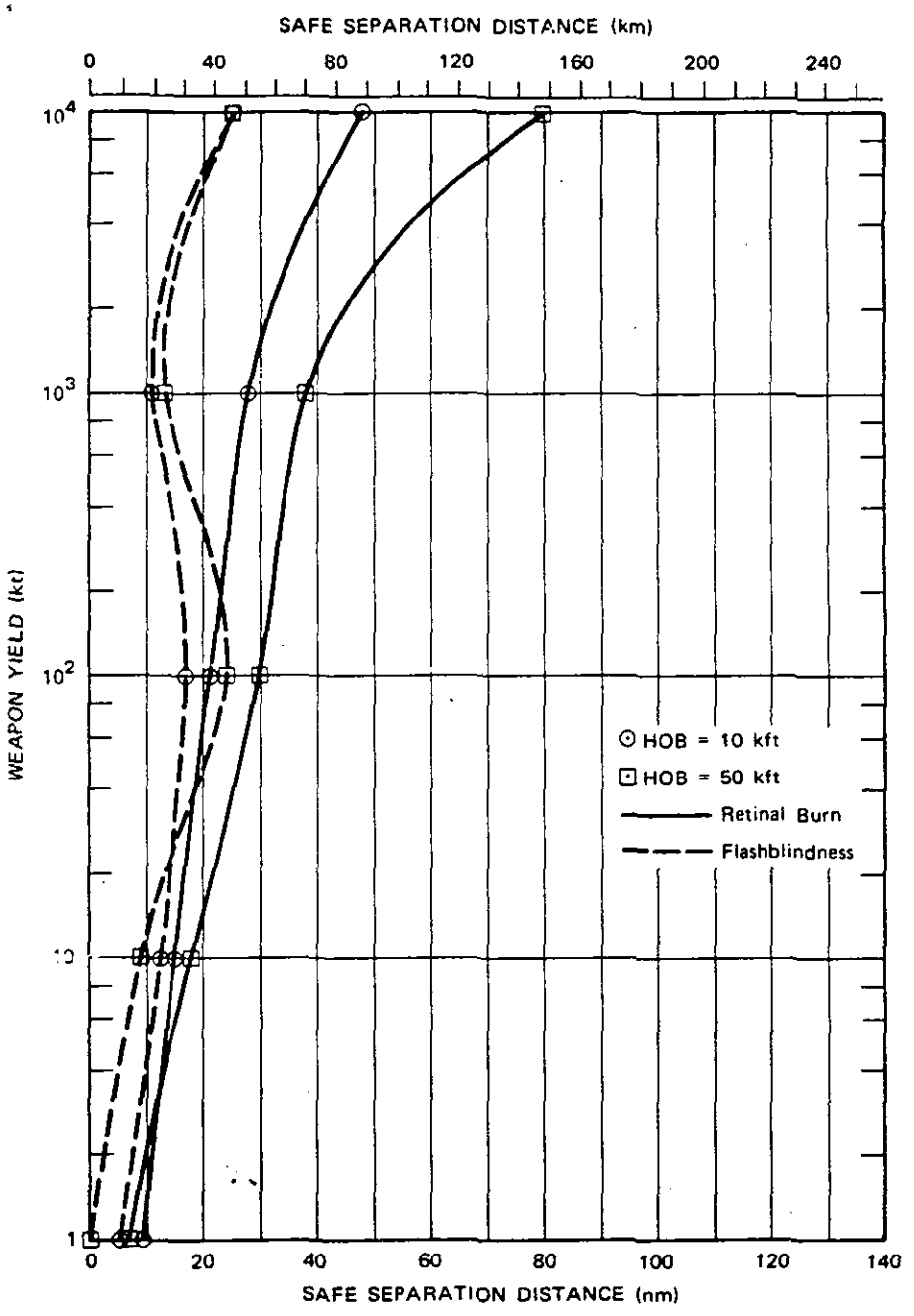

Figure 10-6. [redacted] Safe Separation Distances, for an Observer on the Ground, from Bursts at 10 kft and 50 kft During the Day [redacted]

[redacted]

[redacted]

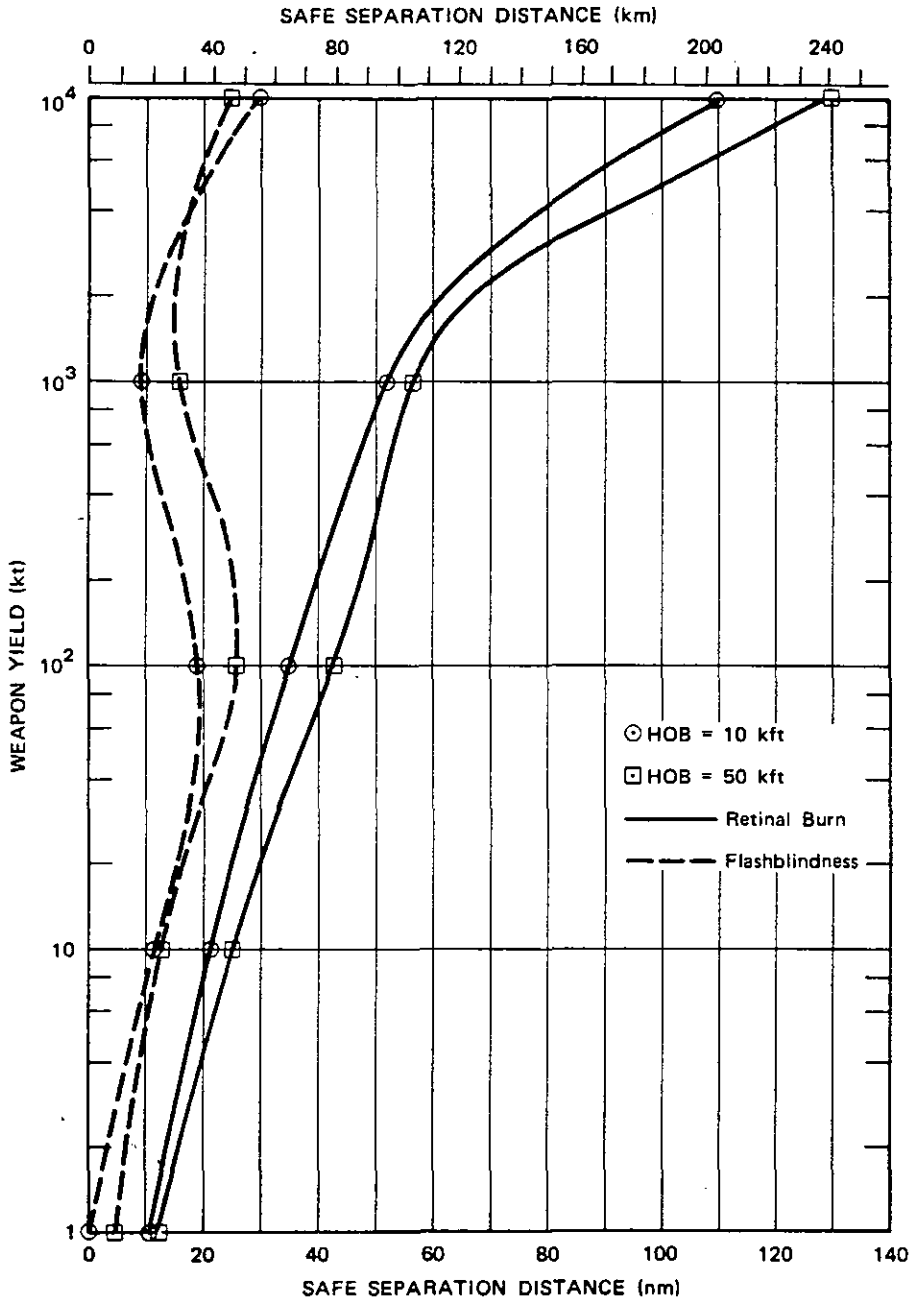

Figure 10-7. [redacted] Safe Separation Distance, for an Observer at 50 kft, from Bursts at 10 kft and 50 kft During the Day [redacted]

[redacted]

[redacted]

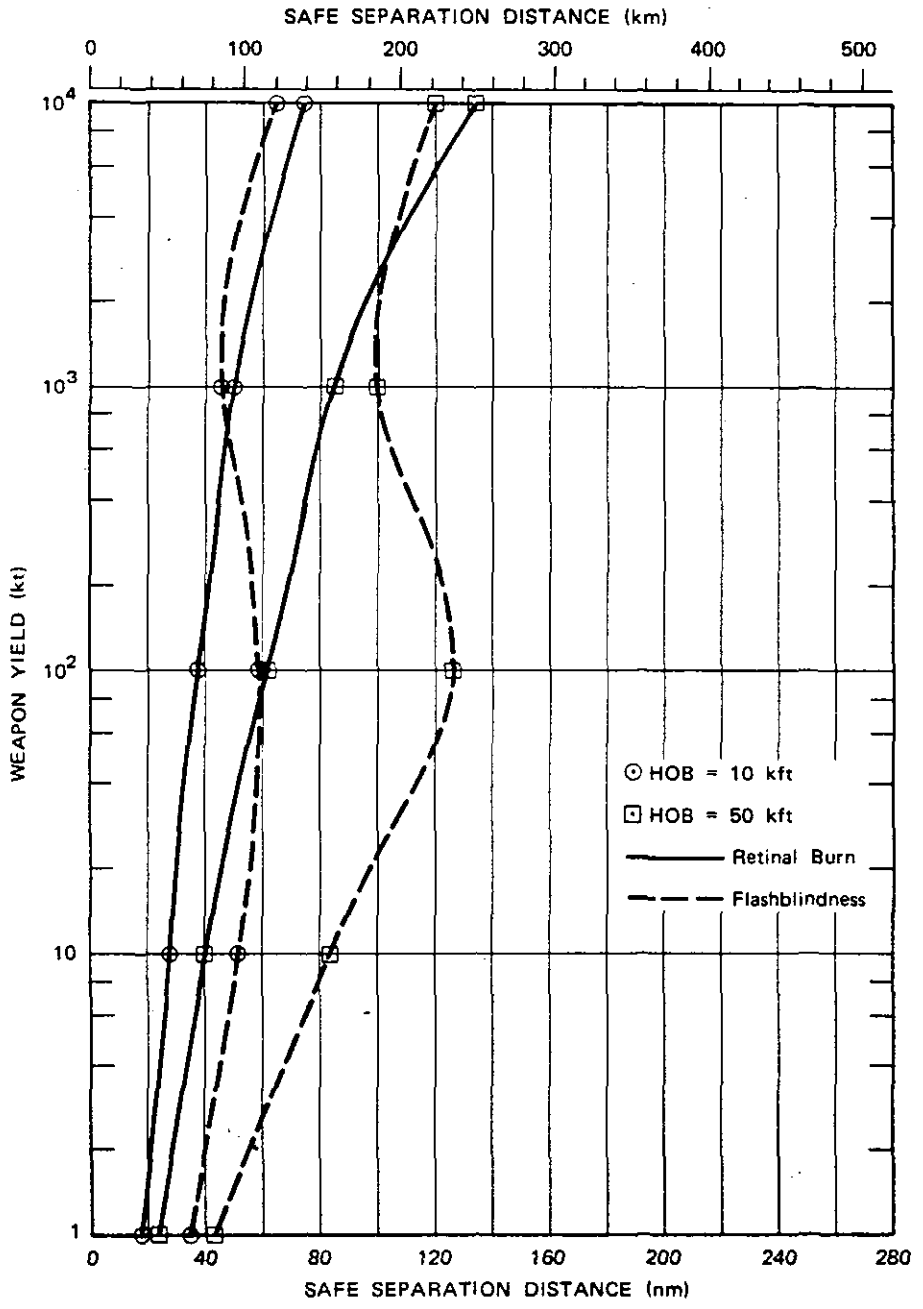

Figure 10-8. [redacted] Safe Separation Distance, for an Observer on the Ground, from Bursts at 10 kft and 50 kft, During the Night [redacted]

[redacted]

[redacted]

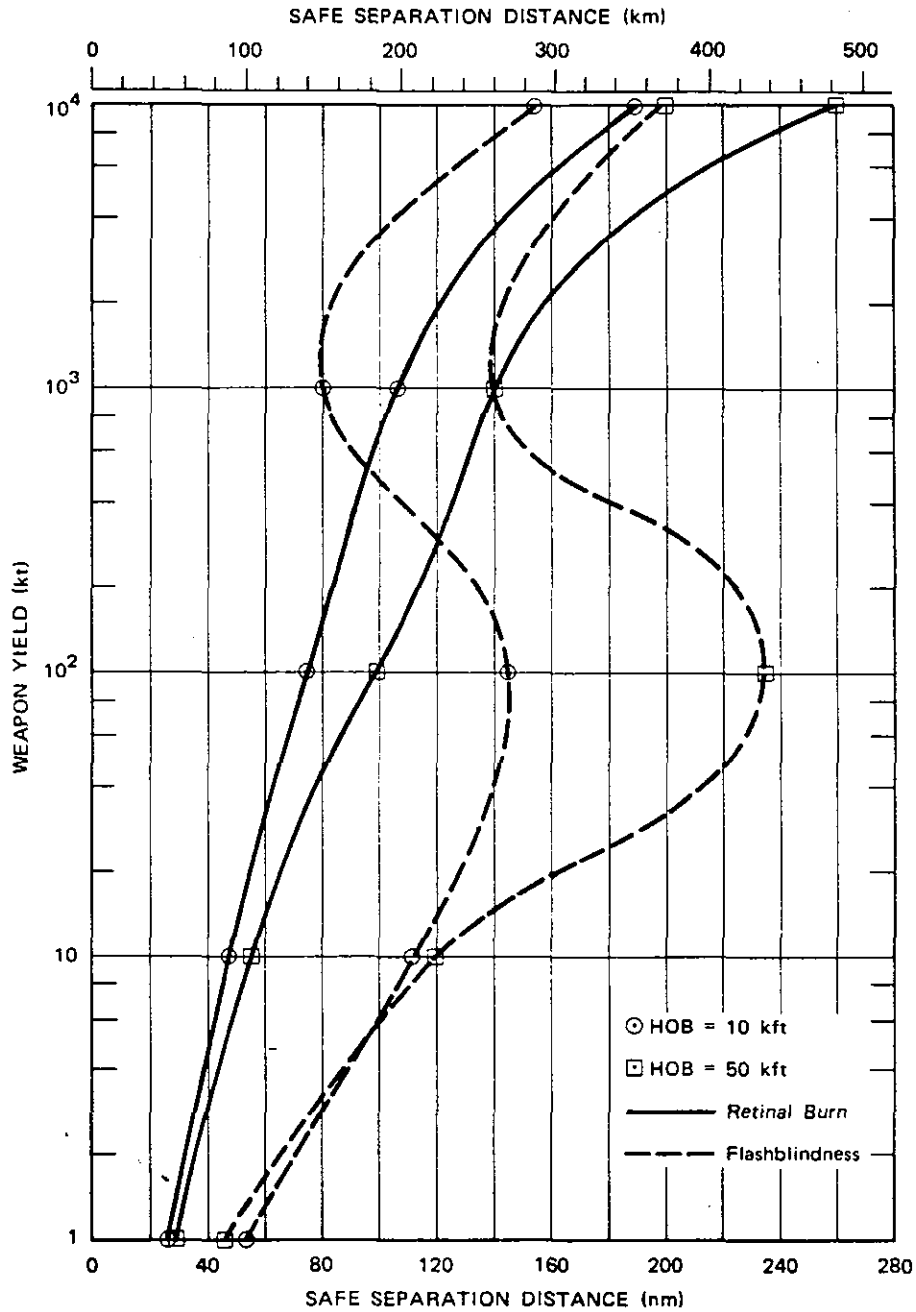

Figure 10-9. [redacted] Safe Separation Distance, for an Observer at 50 kft, from Bursts at 10 kft and 50 kft, During the Night [redacted]

[redacted]

[redacted]

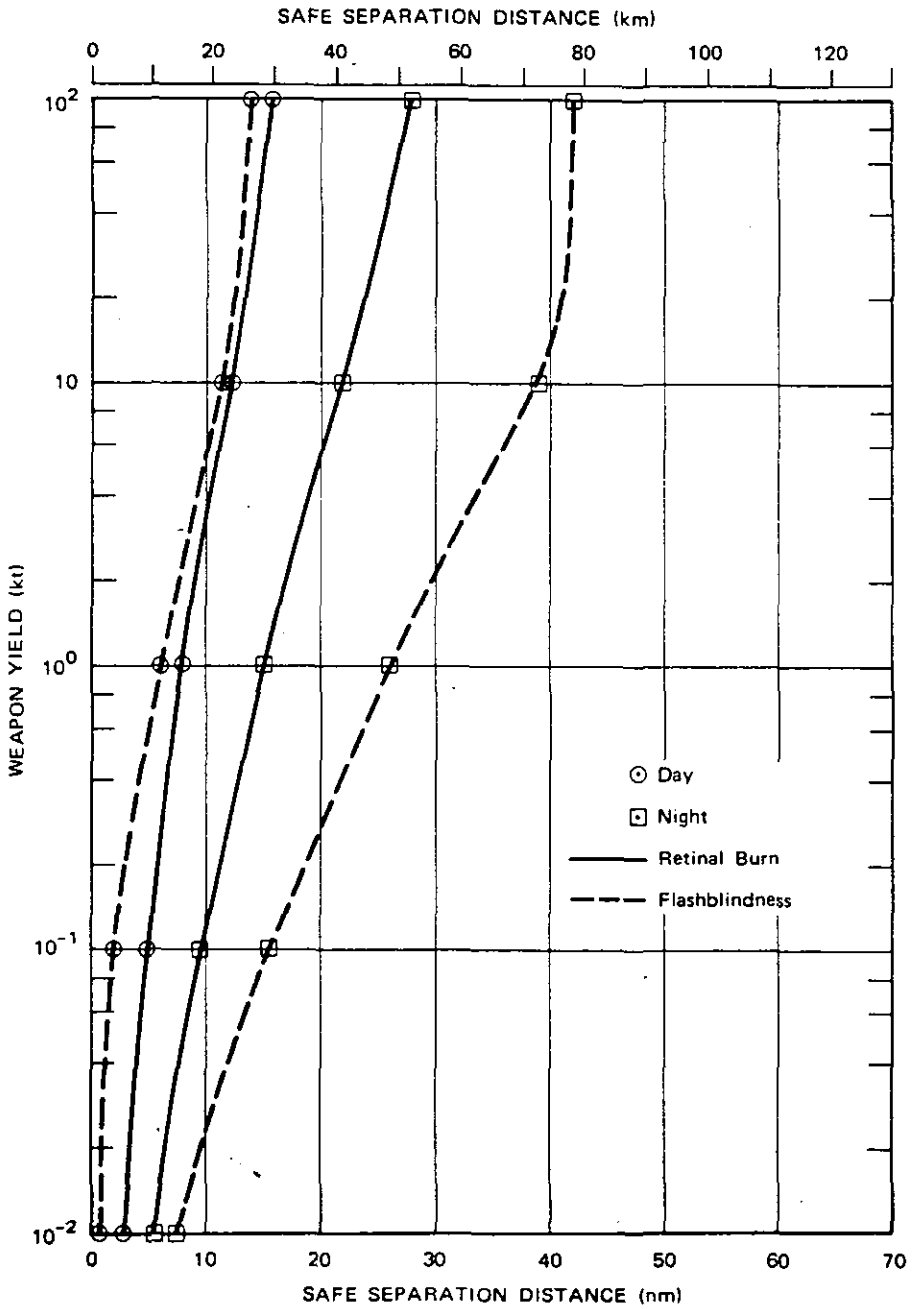

Figure 10-10. [redacted] Safe Separation Distance, for an Observer on the Ground, from Low Yield Weapons Exploded at 1,000 ft Height of Burst [redacted]

[redacted]

the 10 second loss of vision criterion in the flashblindness curves), the retinal burn or flashblindness curve that shows the effect that occurs at the greatest distance from the burst should be used. For example, using Figure 10–8 and a 50 kilofeet height of burst, to determine the distance from a nuclear detonation where there will be no incapacitating eye effects, the flashblindness curve is the limiting factor up to about 3 megatons, then the retinal burn curve becomes the limiting factor.

In instances where only permanent eye damage is of interest, and the temporary loss of vision from flashblindness is not of concern, only the retinal burn curves should be used.

The retinal burn curves show distances at which a nuclear burst will not produce retinal burns provided the eye can blink within 250 milliseconds. A faster blink time would not change the distances appreciably. The curves are based on a very clear day (60 mile visual range). For a cloudy day with a 5 mile visual range, the safe separation distances would be reduced by about 50 percent.

SECTION III
NUCLEAR RADIATION

The injurious effects of nuclear radiations (gamma rays, neutrons, beta particles and alpha particles) on the human target represent a phenomenon that is completely absent from conventional explosives. Since there has not been sufficient experience with humans in the exposure ranges of military interest, the material presented below is based largely on animal experimentation that has been extrapolated to the area of human response. Even if sufficient human data were available, they would be expected to show similar responses and the same wide range of biological variability within species as is seen in animals. Data are presented in terms of absorbed dose at or near the body surface in order to relate to source and transport factors given in Chapter 5. Current radiobiological research results are frequently reported as *midline tissue dose* in rad, a dose significantly lower than doses measured by radiac instruments and absorbed within those volumes near the surface of the body that faces toward the source. For nuclear weapon radiation, the midline tissue doses would be approximately 70 percent of the body surface doses presented in the following paragraphs.

INITIAL RADIATION

Neutrons and gamma rays in various proportions are responsible for biological injury from initial radiation. For military purposes, and until further animal experimentation provides evidence to the contrary, it must be assumed that damage to tissue is directly proportional to the absorbed dose regardless of whether it is delivered by neutrons or gamma rays. For effects of military interest, it is assumed that injury from a neutron rad is equal to that from a gamma rad, and that one rad absorbed dose results from exposure to one roentgen.

10-23 Radiation Sickness

Individuals exposed to whole body ionizing radiation may show certain signs and symptoms of illness. The time interval to onset of these symptoms, their severity, and their duration generally depend on the amount of radiation absorbed, although there will be significant variations among individuals. Within any given dose range, the effects that are manifested can be divided conveniently into three time phases: initial, latent, and final.

During the initial phase, individuals may experience nausea, vomiting, headache, dizziness and a generalized feeling of illness. The onset time decreases and the severity of these symptoms increases with increasing doses. During the latent phase, exposed individuals will experience few, if any, symptoms and most likely will be able to perform operational duties. The final phase is characterized by frank illness that re-

[redacted]

[redacted] quires hospitalization after exposure to the higher doses. In addition to the recurrence of the symptoms noted during the initial phase, skin hemorrhages, diarrhea and loss of hair may appear, and, at high doses, seizures and prostration may occur. The final phase is consummated by recovery or death. At doses above 1000 rad, death may be expected in all cases. Maximum recovery of survivors exposed to lower doses may require as much as three to six months time. With the foregoing in mind, Table 10-2 is presented as the best available summary of the effects of various whole-body dose ranges of ionizing radiation in human beings.

10-24 Incapacitation [redacted]

[redacted] Direct effects of high doses of external radiation administered over a short time period may result in loss of ability to perform purposeful actions. At doses greater than 2,000 rads, an acute collapse may occur in a short time. The collapse may persist from several minutes to a few hours. A period of relatively normal performance capability will then occur; however, after some time permanent incapacitation and death will result. This early incapacitation, followed by a temporary period of recovery, is defined as early transient incapacitation (ETI). Following this transient incapacitation, exposed personnel *may* be reasonably well oriented, lucid, and able to perform tasks requiring coordination of visual and auditory sensory input. The duration of early transient incapacitation is believed to be dose dependent, i.e., the greater the dose, the longer the transient incapacitation phase. The duration of the temporary period of effec-

Table 10-2 [redacted] Response to Single Whole-Body Exposures [redacted]

	100-200 Rad	200-400 Rad	400-600 Rad	600-1000 Rad	1000-2500 Rad
Initial Phase					
1. Onset of symptoms after irradiation	3-6 hrs	1-6 hrs	1/2 to 6 hrs	1/4 to 4 hrs	5-30 min
2. Duration of phase	≤1 day	1-2 days	1-2 days	≤2 days	≤1 day
Latent Phase					
1. Onset after irradiation	≤1 day	1-2 days	1-2 days	≤2 days	≤1 day
2. Duration of phase	≤2 weeks	2-4 weeks	1-2 weeks	5-10 days	0-7 days*
Final Phase					
1. Onset of symptoms after irradiation	10-14 days	2-4 weeks	7-14 days	5-10 days	4-8 days
2. Duration of phase	4 weeks	2-8 weeks	1-8 weeks	1-4 weeks	2-10 days
3. Time from irradiation to death	—	4-12 weeks	2-10 weeks	1-6 weeks	4-14 days
4. Deaths (% of those exposed)	No deaths	0-30%	30-90%	90-100%	100%

*At the higher doses within this range there may be no latent period.

[redacted]

[redacted]

[redacted] tiveness is inversely related to the dose. At doses in excess of 15,000 rads, most individuals will experience permanent complete incapacitation within a few minutes post-irradiation, followed by death within 2 to 24 hours.

[redacted] Figures 10-11 through 10-15 list estimated personnel effectiveness at various times following acute radiation doses of 1,400 rads and greater. It should be noted that incapacitation, or performance, decrement, and not death, is the endpoint of interest in these figures.

10-25 Modification of Injury [redacted]

[redacted] When only a portion of the body is exposed to radiation, the effects are significantly less than those described in the preceding two sections. The reduction of the effects depends on the magnitude of exposure and the particular portion of the body that is exposed. Thus, partial shielding afforded by natural or man-made structures can be expected to decrease the severity of radiation injury.

[redacted] Considerable effort has been expended in searching for compounds that will reduce the extent and seriousness of radiation injury when they are administered prior to exposure. At present, there is no satisfactory compound available for issue, although research continues in this area.

[redacted] Treatment of radiation injury is supportive in nature. The treatment is based primarily on symptomology rather than measured or estimated dose received by the individual.

10-26 Military Assumptions [redacted]

[redacted] In order to apply the material above to other than single exposures, it may be assumed that multiple exposures within any 24-hour period are arithmetically additive. This assumption is necessary because the information concerning the results of multiple exposures is limited.

[redacted] Although there is reason to believe that recovery from radiation exposure(s) is never really complete (i.e., some residual injury not necessarily affecting effectiveness remains), it may be assumed for military planning purposes that recovery is complete in approximately 30 days following a single sublethal exposure. Table 10-2 lists more specific information regarding durations of ineffectiveness under varying exposure conditions.

[redacted] RESIDUAL RADIATION [redacted]

[redacted] The importance of residual radiation as a source of injury to personnel depends upon the necessity for military operations in or near areas of local fallout. Time of arrival, weathering, and decay of the deposited fallout all result in a constantly changing rate of external protracted exposure to personnel in contrast to the almost instantaneous exposure to initial radiation. An added hazard results from the presence of small, finely divided, radioactive particulate sources that can contribute to injury by both external and internal irradiation.

10-27 External Hazards [redacted]

[redacted] Gamma rays present the major militarily significant external hazard from residual radiation. Effects on personnel will range from those described previously for initial radiation exposures (in new, high dose-rate, fallout fields) to lesser effects for the same total exposure in low dose-rate fields.

[redacted] Beta burns can occur if fallout particles remain on the skin for periods of hours or more. They will occur most frequently when the fallout particles are deposited on moist skin areas, body crevices, in the hair, or when the particles are held in contact by clothing. While minor skin symptoms may occur during the first 48 hours following exposure, the appearance of burns will be delayed two weeks or more after exposure. Severity of the burns is a function of the radioactivity of the fallout particles and the time period during which they adhere to the body. Personnel ineffectiveness will depend on the severity of the burn and its location on the body.

[redacted]

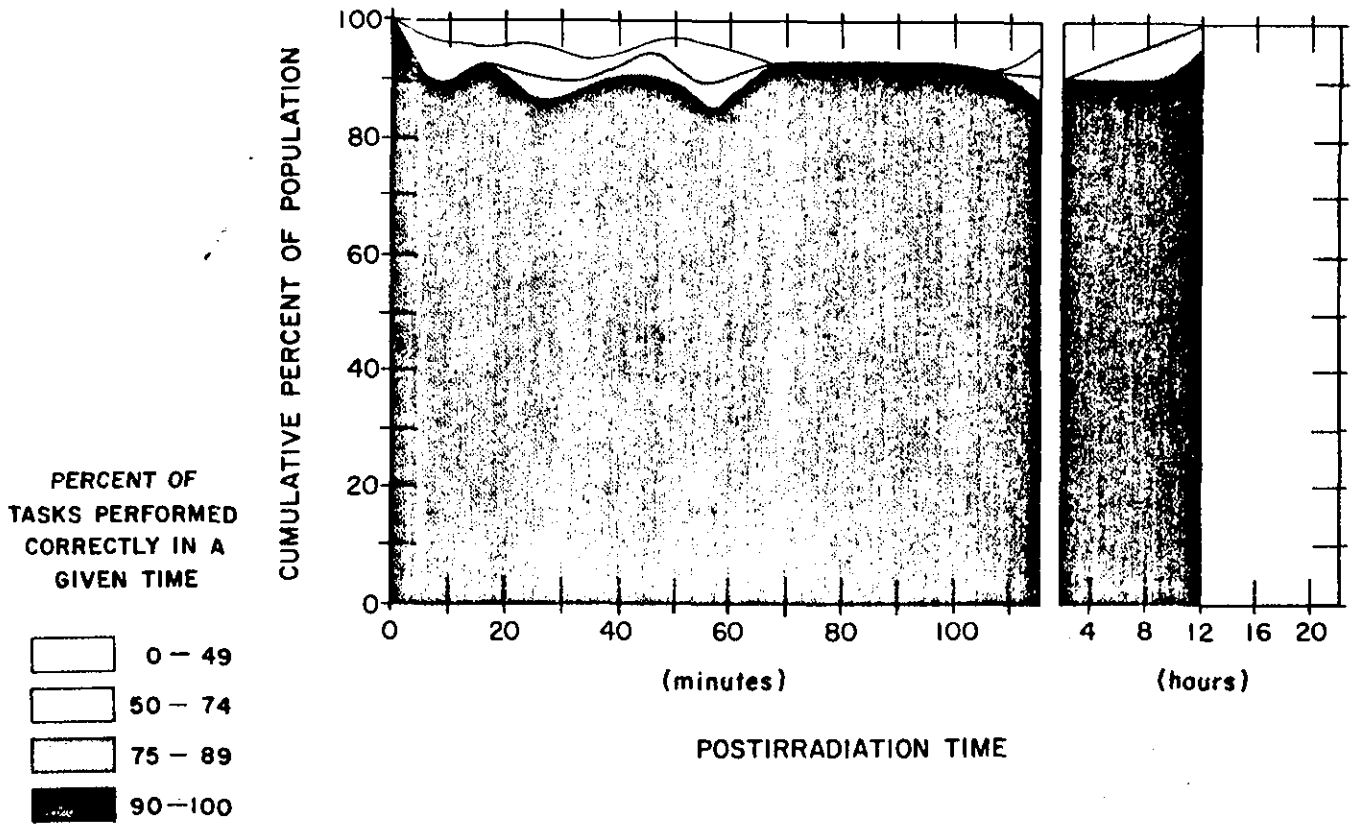

Figure 10-11. Personnel Effectiveness After Exposure to 1,400 rads

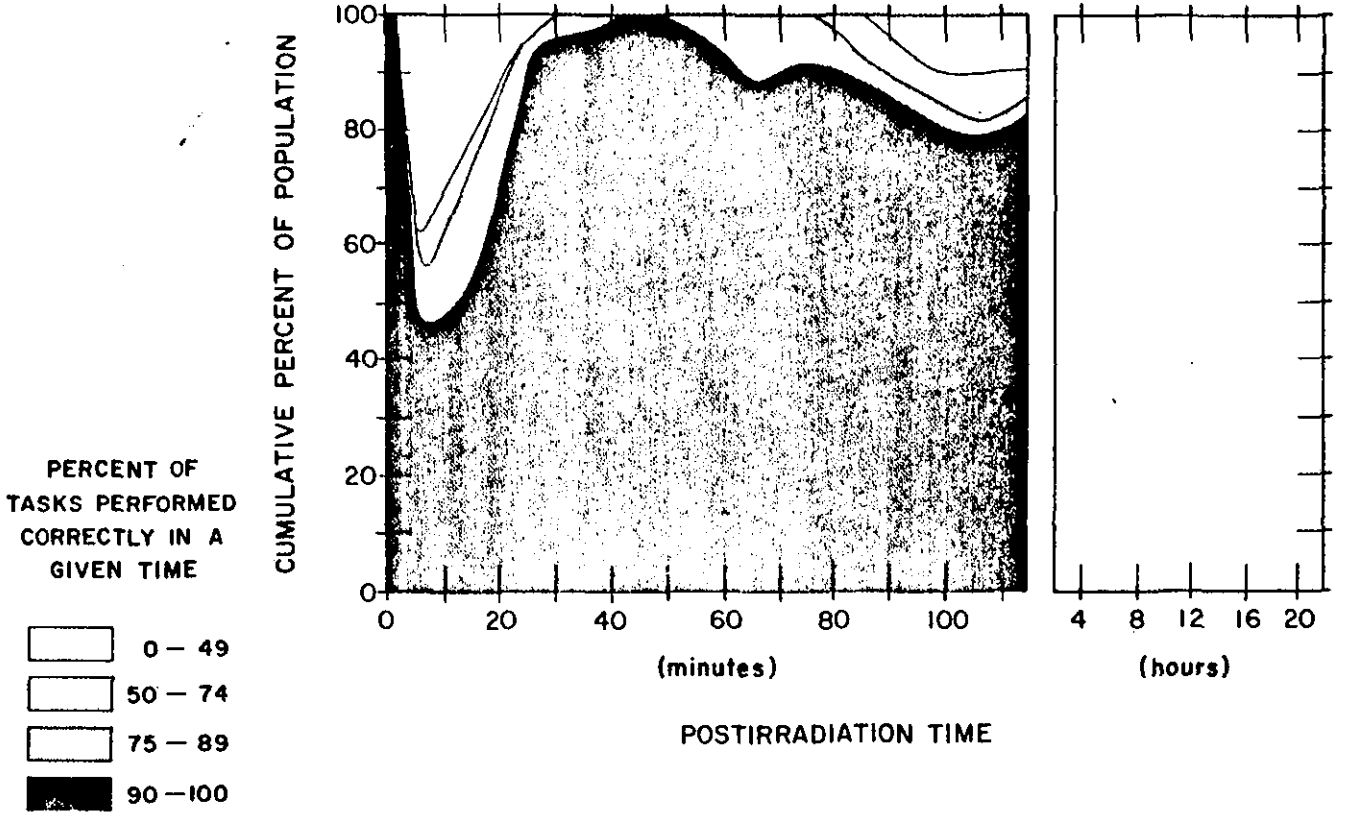

Figure 10-12. Personnel Effectiveness After Exposure to 2,800 rads

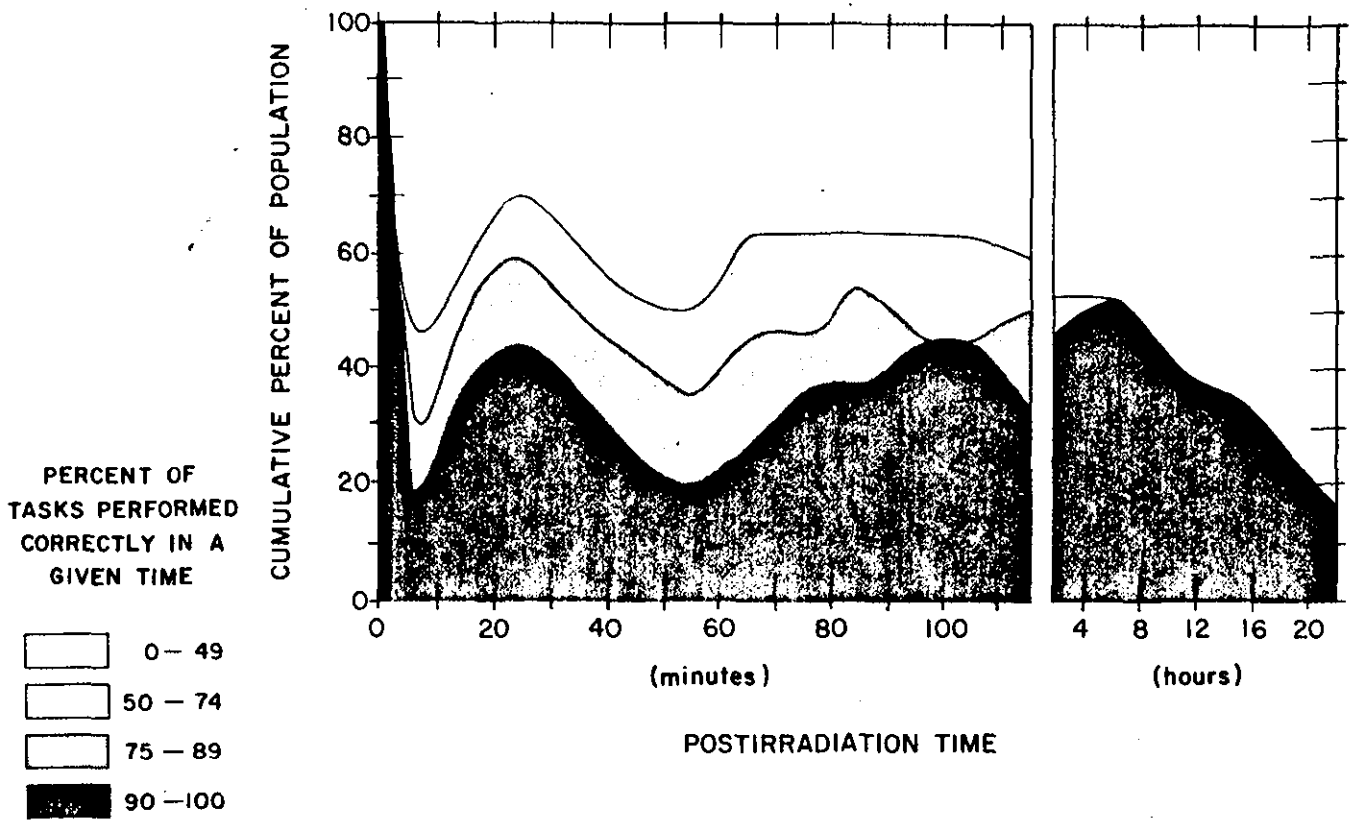

Figure 10-13. Personnel Effectiveness After Exposure to 7,000 rads

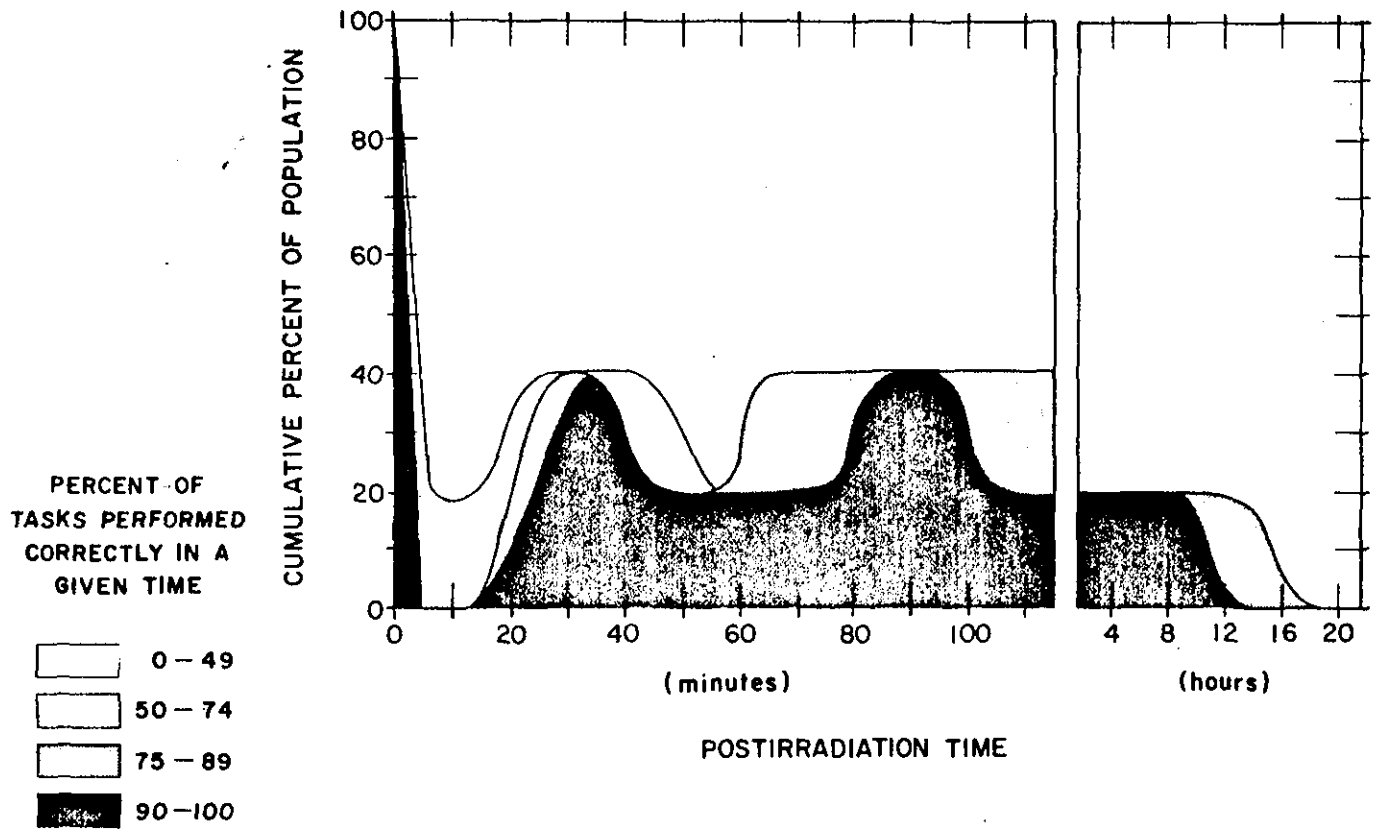

Figure 10-14. Personnel Effectiveness After Exposure to 13,000 rads

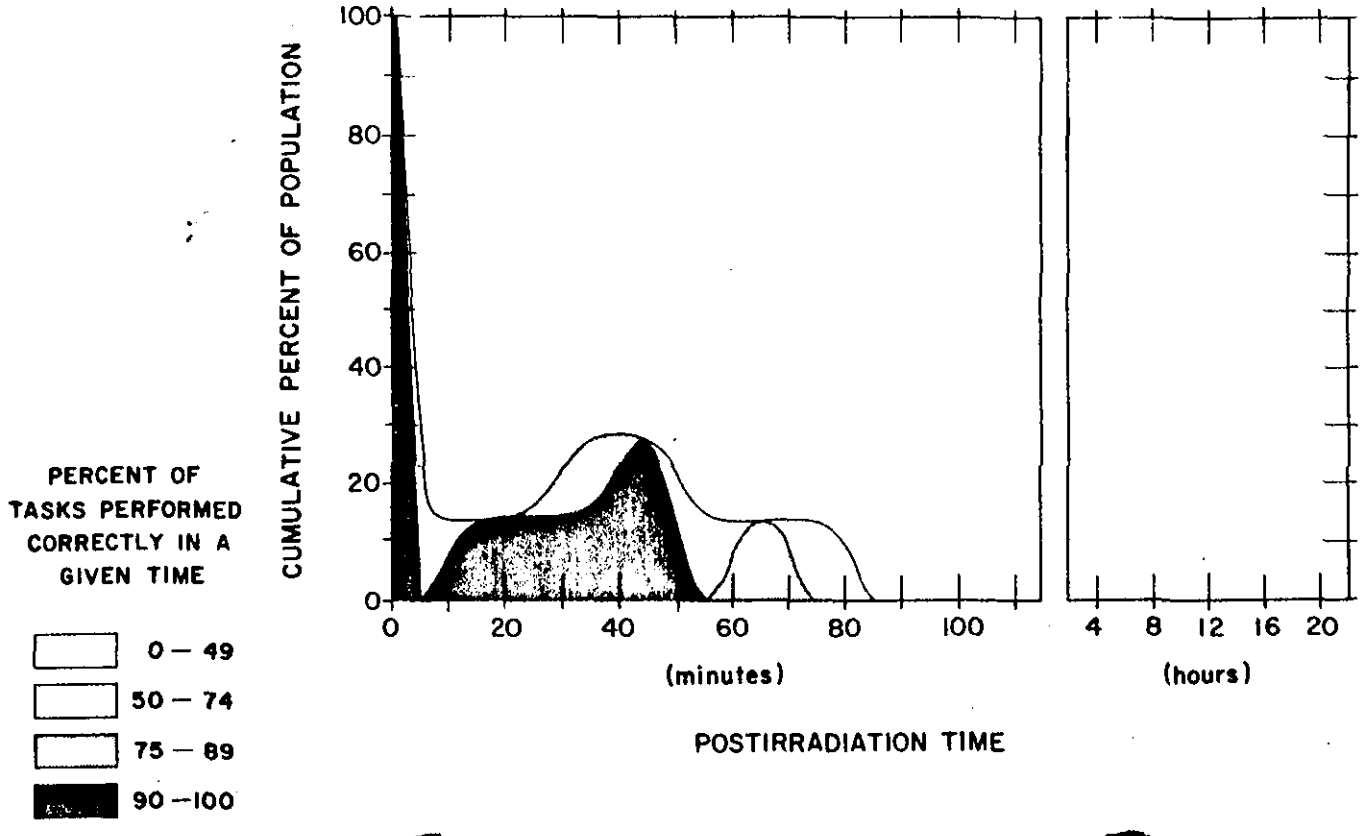

Figure 10-15. Personnel Effectiveness After Exposure to 22,000 rads

[redacted]

10-28 Internal Hazards [redacted]

[redacted] Radioactive materials entering the body by inhalation, eating, or through wounds or breaks in the skin may be deposited in the body where alpha particles, beta particles or gamma rays continue to bombard adjacent tissues. Once fixed within the body, removal is almost impossible, except through natural processes. Effects of internal emitters usually become apparent after a period of years, so, while of not immediate concern insofar as personnel effectiveness is concerned, this deposition may eventually be of great concern to the individual.

[redacted] Inhalation as a route of entry can be expected as the result of resuspension of radioactive materials from dust-producing activities, such as the operations of helicopter and fast-moving vehicles. Handling of contaminated equipment, supplies, and clothing may result in the hands becoming contaminated. The contamination then may enter the body while eating. Ingestion of contaminated foodstuffs and water supplies is another source of internal emitters.

10-29 Modification of Injury [redacted]

[redacted] External residual radiation can be reduced by shielding, i.e., interposition of dense material between personnel and the source of radiation, as described previously for initial radiation. Protection is afforded to varying degrees by armored vehicles, foxholes, buildings and underground shelters. However, in a residual radiation environment, it is probable that radioactive materials will be brought into the protected areas as a result of their adherence to clothing, skin, hair, and equipment. Thus, to reduce exposure, it is necessary to decontaminate both the individual and his equipment. Additionally, as much time as is militarily feasible should be spent in protected environments while the residual radiation is decaying to lower levels. Decontamination of the outer surfaces of structures also will reduce the total dose to personnel.

[redacted] If the outer packaging of foodstuffs is undamaged, they may be consumed without hazard, provided care is taken to insure that the food is not contaminated during removal of the protective covering. Cans should be washed before opening. Normal water filtration procedures will remove a majority of the fallout radioactive materials.

[redacted] Treatment of individuals showing radiation sickness symptoms from exposure to residual radiation is similar to the treatment of sickness caused by initial radiation. Burns caused by prolonged contact of beta emitters with the skin can be reduced in severity, or prevented, by early removal of the fallout material. Burns which do occur respond to conventional methods of treatment for similar burns resulting from other causes.

[redacted] Medical management of conditions arising at later times as a result of fixed internal emitters depends on the organ(s) in which the material is fixed, the number of demonstrated lesions, and the threat of this damage to life.

SECTION IV

[redacted] COMBINED INJURY [redacted]

[redacted] Thus far in this chapter little has been said about the possibility of personnel receiving multiple types of injury; however, such injuries probably would be a common occurrence in the advent of a nuclear war. Multiple injuries might be received nearly simultaneously (e.g., from exposure to a single detonation without fallout radiation) or separated in time by minutes to days (e.g., from exposure to a single detonation followed by fallout radiation, or exposure to multiple detonations). These injuries may consist of any combination of radiation, blast and thermal injuries from nuclear weapons as well as wounds from conventional weapons. Furthermore, such injuries may be influenced by other conditions that might be expected during or after a nuclear attack, such as malnutrition, poor

[redacted]

[redacted]

[redacted] sanitation, fatigue, and various other environmental factors. Since there are insufficient quantitative data to indicate the manner in which casualty production might be influenced by these latter factors, only combinations of pairs of the following three categories will be discussed in this section: (1) ionizing radiation injuries, (2) thermal injuries, and (3) mechanical injuries (e.g., injuries that result from blast effects).

[redacted] Most of our current knowledge concerning combined injuries is derived from studies of Japanese bomb victims in Hiroshima and Nagasaki and from laboratory and field test experiments involving a variety of animals. In Hiroshima and Nagasaki, 50 percent of the injured 20-day survivors within about 2,200 yards of ground zero received combined injuries whereas an incidence of 25 percent was observed in those located between 2,200 and 5,500 yards. The contribution of such injuries to overall mortality and morbidity has never been determined adequately, but two general impressions have emerged: the combination of mechanical and thermal injury was responsible for the majority of deaths that occurred within the first 48 hours; delayed mortality was higher and complications were more numerous among burned people who had received radiation than what would be anticipated in a burned population where no radiation exposure had occurred. It should be recognized that the stated incidences of combined injuries apply only to the conditions existing in the two Japanese cities at the time of attack and that the number and types of combined injuries are sensitive to yield, burst height, and conditions of exposure. Yields smaller than 10 kilotons probably would result in a significant number of casualties with combinations of prompt-radiation, thermal, and mechanical injuries. On the other hand, larger yields would be expected to result in a marked increase in the number of people with burns associated with mechanical injuries, and prompt-radiation injuries would be relatively insignificant in the surviving population. A weapon detonated at a burst height where fallout is minimized would result in a large number of thermal and mechanical injuries, and, depending upon yield, might also produce a significant number of prompt-radiation injuries. A weapon detonated near (above or below) the surface would maximize the number of injuries due to fallout and would produce a large number of casualties where such injuries would be combined with mechanical and thermal trauma. Personnel outside and unshielded would have a greater likelihood of sustaining prompt and/or fallout radiation in combination with thermal burns than would be the case for personnel inside of any form of structure. In the latter case, thermal burns would be minimized, whereas combinations of mechanical and radiation injury might dominate.

[redacted] Combined injuries may result in synergistic effects, additive effects, or antienergistic effects. That is, the resultant response, whether measured as percent combat ineffectiveness (CI) or mortality, may be greater than, equal to, or less than what would be predicted based on the assumption that the various injuries act independently of one another in producing casualties. Quantitative data from laboratory experiments suggests that, in situations where a combined effect has been observed, the interaction of the various forms of trauma has resulted in enhanced delayed mortality, with little apparent effect on early mortality.

10-30 Radiation and Thermal Injuries [redacted]

[redacted] Depending upon the radiation dose and the severity of burn, mortality has been found to increase by as much as a factor of six above that which might be expected from the two injuries administered singly. Thus, burns which serve as a portal of entry for infection may be considerably more hazardous to a person whose resistance to infection has been lowered by ioniz-

[redacted]

[redacted]

[redacted] ing radiation. However, enhanced mortality has not been observed when low radiation doses have been administered in combination with minimal burn injuries. Very little information is available on fallout radiation in combination with thermal or any other form of injury.

10-31 Mechanical and Radiation Injuries [redacted]

[redacted] Mechanical and radiation injuries can be expected to be frequent, particularly if fallout is present. Studies indicate that a delay in wound healing is observed with doses in excess of 300 rads, and that wounds in irradiated subjects are considerably more serious if treatment is delayed for more than 24 hours. In addition, missile and impact injuries that result in disruption of the skin and damage to the soft tissues would provide a portal of entry for infection, and thus may be extremely hazardous to irradiated people. Injuries that are associated with significant blood loss would be more serious in personnel who have received a radiation dose large enough to interfere with normal blood clotting mechanisms.

10-32 Thermal and Mechanical Injuries [redacted]

[redacted] Burns and mechanical injuries in combination are often encountered in victims of conventional explosions and increased delayed complications, shorter times-to-death and enhanced mortality are frequent occurrences. However, little quantitative data are available on this form of combined injury.

[redacted] CASUALTY CRITERIA [redacted]

[redacted] No reliable criteria for combat ineffectives are known for personnel receiving combined injuries. The available data do indicate, however, that individuals receiving combined injuries that occur nearly simultaneously are unlikely to become casualties within a few hours, provided the individual injuries would not produce casualties if administered separately. Consequently, it is not unreasonable to make early casualty predictions for a single nuclear detonation on the basis of the most far-reaching effect. In regard to troop-casualty predictions, combined effects can be considered as a bonus, helping to assure the attainment of predicted CI levels, especially since there is a reasonable amount of uncertainty in the predictions for individual effects. If exposure exceeds any "minimal" risk level, that effect could contribute to combined injury and could result in increased casualties at later times. This becomes an important factor in terms of troop safety.

[redacted] PERSONNEL IN THE OPEN [redacted]

[redacted] Figure 10-16 indicates expected burn levels, prompt ionizing-radiation doses, and peak translational velocities as functions of yield and ground distance for randomly-oriented, prone personnel exposed in the open. The curves were derived, assuming a visual range of 16 miles and a burst height such that the fireball would just touch the surface. This is the minimum height of burst which would result in negligible early, or local, fallout. The curves, which are presented for illustrative purposes only, form the limits of a band for each effect. These limits correspond to 50 percent early casualties and "minimal" early risk. The ionizing-radiation dose required to produce 50 percent CI within one hour, e.g., approximately 5,000 rads, is so large that it will result in 100 percent mortality within several days. For this reason, a 500-rad curve, which would correspond to approximately 50 percent mortality within 60 days, is included in Figure 10-16. Direct overpressure effects are not included in the figure since, except for eardrum rupture, which is not normally considered to produce CI, translational effects extend to greater ranges for all of the yields considered.

[redacted] In the case of troop-casualty predictions, prompt-radiation predominates for yields less

[redacted]

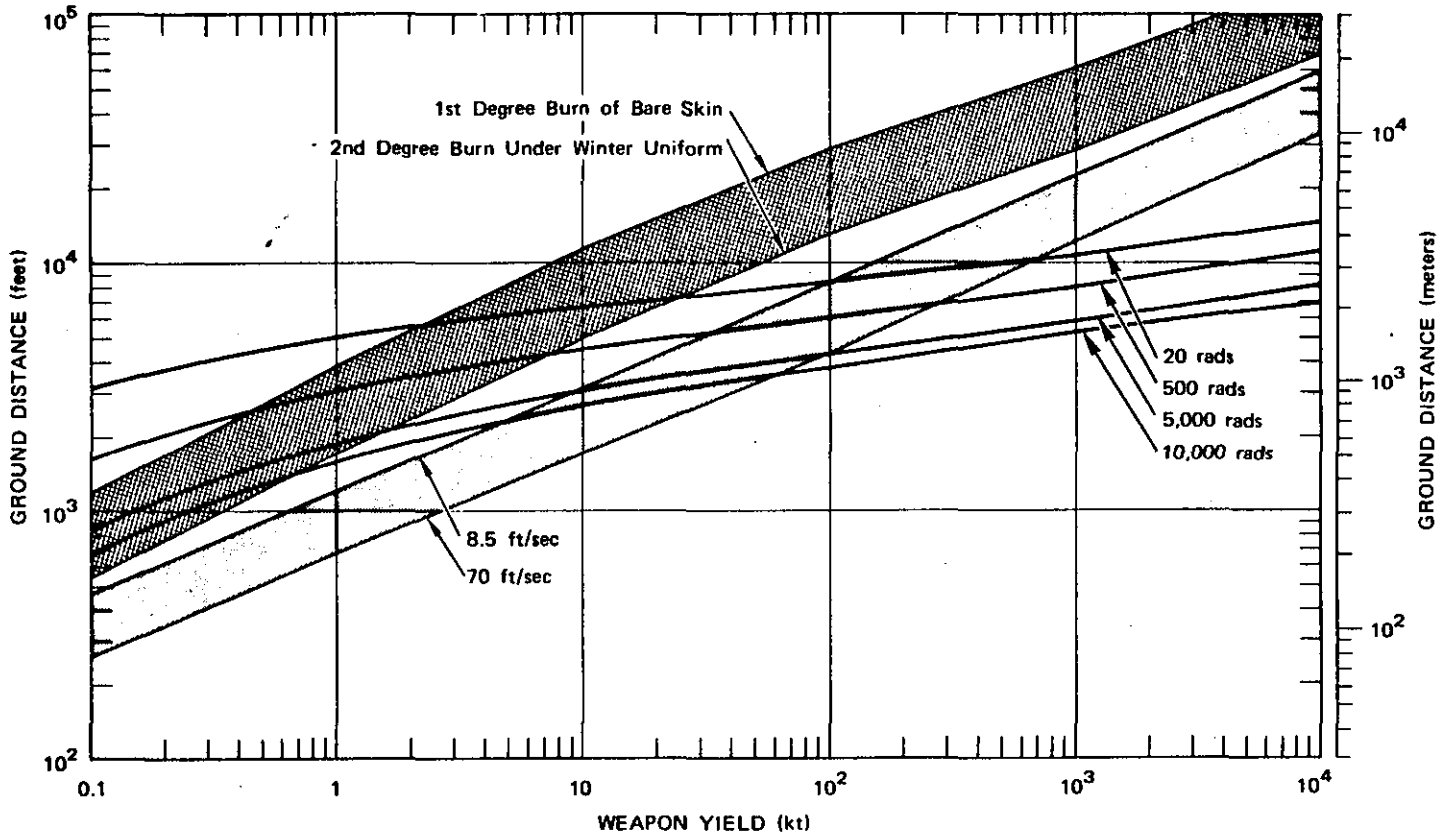

Figure 10-16. [redacted] Comparison of Effects from Low Altitude Bursts [redacted]

[redacted]

[redacted]

than 2 kt whereas thermal radiation is the most far-reaching hazard for yields greater than 2 kt. In situations where thermal exposure is neglected as a casualty-producing factor, ionizing radiation is the major effect in producing a 50 percent CI level for yields below 100 kt, while for larger yields, blast effects (translation) predominate.

[redacted] With regard to troop safety, ionizing radiation is the major hazard below 1 kt, while thermal radiation predominates for larger yields. If the troops can be shielded adequately from the thermal pulse, ionizing radiation is the major hazard for yields up to 100 kt, above which blast effects are the most far-reaching hazard.

[redacted] PERSONNEL IN STRUCTURES [redacted]

[redacted] In order to predict casualty levels for troops in situations other than open terrain, for example, inside armoured vehicles or field fortifications, the amount of nuclear radiation, thermal radiation, and blast shielding, as well as the degree of blast hardness of the surrounding materials must be taken into account for each geometry of exposure. As was the case for personnel in the open, casualty predictions must be made on the basis of the most far-reaching single effect rather than on the basis of combined effects. In general, for troops in structures, the major effect producing early casualties is likely to be ionizing radiation for small yields and blast effects for larger yields, with the cross-over point depending on the degree of hardness of the structure. While the hazards from thermal and ionizing radiation levels are reduced in a structure, the hazards from air blast may be magnified as a result of structural collapse, whole-body impact, and falling debris. This is particularly true for relatively soft structures at greater distances.

[redacted] In the case of personnel in field fortifications, severe damage to the structure (Section VI ~~IV~~, Chapter 11 ~~8~~) should be taken as representative of 50 percent early CI from blast. Shielding factors (Section VI ~~IV~~, Chapter 9) must be considered when estimating nuclear radiation responses of personnel in such structures.

[redacted] TREATMENT [redacted]

[redacted] The triage and treatment of combined injuries present special problems, particularly if significant radiation exposure has occurred. Certain modifications in accepted medical and surgical practices must be considered since radiation exposure, depending upon dose, is known to increase susceptibility to infection, to decrease the efficiency of wound and fracture healing, to increase the likelihood of hemorrhage, to decrease tolerance to anesthetic agents, and to decrease the immune response.

[redacted] It is imperative that primary closure of wounds be accomplished at the earliest possible time and that patients be treated with a broad spectrum antibiotic throughout the period of maximum bone marrow depression. Secondary closure of small soft-tissue wounds should be accomplished by the second or third day. Reparative surgery of an extensive nature should not be performed later than four to five days after injury since skin and soft-tissue healing should have occurred before the effects of ionizing radiation occur. If reparative surgery is not performed within this limited period of time, it must be postponed until the bone marrow has recovered (one to two months post-exposure). Wounds of injuries that require longer than three weeks for healing, such as severe burns and most fractures, should not be definitively treated until radiation recovery is evident. Although reconstructive surgery in the absence of radiation exposure might be performed within the second month or earlier after conventional trauma, it must be postponed for at least three months in instances where radiation exposure is a significant contributory factor. In all instances, extra precaution must be taken to avoid infection and blood loss.

[redacted]

[redacted]

[redacted] BIBLIOGRAPHY [redacted]

Allen, R. G., et al., *The Calculation of Retinal Burn and Flashblindness Safe Separation Distances,* U.S. Air Force School of Aerospace Medicine, Brooks Air Force Base, Texas, September 1968, SAM-TR-68-106 [redacted]

Anderson, R. S., F. W. Stemler, and E. B. Rogers, *Air Blast Studies with Animals,* Chemical Research and Development Laboratories, Army Chemical Center, Maryland, April 1961, DASA 1193 [redacted]

Behrens, C. F., *Atomic Medicine,* Williams & Wilkins, Baltimore, 1959. *Biological and Environmental Effects of Nuclear War,* Hearings before the Special Subcommittee on Radiation of the Joint Committee on Atomic Energy, Congress of the United States, June 1959. U.S. Government Printing Office, Washington, D.C [redacted]

Blatz, H., *Radiation Hygiene Handbook,* McGraw-Hill Book Co., Inc., New York, 1959 [redacted]

Bowen, I. G., A. F. Strehler, and M. B. Wetherbe, *Distribution of Missiles from Nuclear Explosions,* Lovelace Foundation for Medical Education and Research, Albuquerque, New Mexico, December 1956, WT-1168 [redacted]

Bowen, I. G., et al., *Biophysical Mechanisms and Scaling Procedures Applicable in Assessing Responses of the Thorax Energized by Air-Blast Overpressures or Non-Penetrating Missiles,* Lovelace Foundation for Medical Education and Research, Albuquerque, New Mexico, November 1966, DASA 1857 [redacted]

Bowen, I. G., F. R. Fletcher, and D. R. Richmond, *Estimate of Man's Tolerance to the Direct Effects of Air Blast,* Lovelace Foundation for Medical Education and Research, Albuquerque, New Mexico, October 1968, DASA 2113 [redacted]

Brucer, M., *The Acute Radiation Syndrome: Y-12 Accident,* Oak Ridge Institute of Nuclear Studies, April 1959, ORINS-25 [redacted]

Bryant, F. J., et al., U.K. Atomic Energy Authority Report AERE HP/R 2353 (1957); *Strontium in Diet,* Brit. Medical Journal, *1*, 1371 (1958) [redacted]

Claus, W. D. (Ed.), *Radiation Biology and Medicine,* Addison-Wesley Publishing Co. Inc., Reading, Mass., 1958 [redacted]

Conard, R. A., et al., *Medical Survey of Rongelap People Five and Six Years After Exposure to Fallout,* Brookhaven National Laboratory, September 1960, BNL-609 [redacted]

Fletcher, E. R., et al., *Determination of Aerodynamic-Drag Parameters of Small Irregular Objects by Means of Drop Tests,* Lovelace Foundation for Medical Education and Research, Albuquerque, New Mexico, October 1961, CEX-59.14 [redacted]

[redacted]

Fletcher, E. R., and I. G. Bowen, *Blast Induced Translational Effects*, Lovelace Foundation for Medical Education and Research, Albuquerque, New Mexico, November 1966, DASA 1859

Gerstner, H. B., *Acute Radiation Syndrome in Man*, U.S. Armed Forces Medical Journal, *9*, 313 (1958)

Hayes, D. F., *A Summary of Accidents and Incidents Involving Radiation in Atomic Energy Activities*, TID-5360, August 1956; Supplement No. 1, August 1957; Supplement No. 2, September 1959. U.S. Atomic Energy Commission, Washington, D.C.

Hirsch, F. G., *Effects of Overpressure on the Ear – A Review*, Lovelace Foundation for Medical Education and Research, Albuquerque, New Mexico, November 1966, DASA 1858

Kulp, J. L., A. R. Schulert, and E. J. Hodges, *Strontium-90 in Man IV*, Science, *132*, 448 (1960)

Lappin, P. W., and C. F. Adams, *Analysis of the First Thermal Pulse and Associated Eye Effects*, Aerospace Medical Research Laboratories, Wright Patterson Air Force Base, Ohio, December 1968, AM RL-TR-67-214

Loutit, J. F., and R. S. Russell, (Eds.), *The Entry of Fission Products into Food Chains*, Progress in Nuclear Energy, Series VI, Vol. 3, Pergamon Press, Inc., New York, 1961

Miller, R. W., *Delayed Radiation Effects in Atomic Bomb Survivors*, Science, *166*, 569 (1969)

National Academy of Sciences-National Research Council, *The Biological Effects of Atomic Radiation*, 1956; *Pathological Effects of Atomic Radiation*, Publication No. 452, 1961; *Long-Term Effects of Ionizing Radiations from External Sources*, Publication No. 849, 1961; *Effects of Ionizing Radiation on the Human Hematopoietic System*, Publication No. 875, 1961; *Effects of Inhaled Radioactive Particles*, Publication No. 848, 1961, Washington, D.C.

National Council on Radiation Protection and Measurements, *Basic Radiation Protection Criteria*, NCRP Report No. 39, 1971, Washington, D.C

Oughterson, A. W., and S. Warren, *Medical Effects of the Atomic Bomb in Japan*, National Nuclear Energy Series VIII, McGraw-Hill Book Co., Inc., New York, 1956

Proceedings of the International Conferences on the Peaceful Uses of Atomic Energy, Geneva, *Biological Effects of Radiation*, Volume 11, 1956; Vol. 22, 1958; United Nations, New York

[redacted]

Richmond, D. R., I. G. Bowen, and C. S. White, *Tertiary Blast Effects: The Effects of Impact on Mice, etc.* Aerospace Medicine, *32*, 789 (1961) [redacted]

Richmond, D. R., and C. S. White, *Biological Effects of Blast and Shock*, Lovelace Foundation and Research, Albuquerque, New Mexico, April 1966, DASA 1777 [redacted]

Richmond, D. R., et al., *The Relationship Between Selected Blast Wave Parameters and the Response of Mammals Exposed to Air Blast*, Lovelace Foundation for Medical Education and Research, Albuquerque, New Mexico, November 1966, DASA 1860 [redacted]

Symposium on Radioactive Fallout in Foods, *Agricultural and Food Chemistry*, *9*, 90 (1961) [redacted]

United Nations General Assembly, *Report of the United Nations Scientific Committee on the Effects of Atomic Radiation*, UN A/3838 Suppl. 17, (13th Sess.) w/Annexes A through I, 1958, United Nations, New York [redacted]

Wald, N., and G. E. Toma, Jr., *Radiation Accidents through December 1958*, Oak Ridge National Laboratory, March 1961, ORNL-2748, Part B [redacted]

White, C. S., et al., *Comparative Nuclear Effects of Biomedical Interest*, Civil Effects Study, January 1961, CEX-58.8 [redacted]

White, C. S., and D. R. Richmond, *Blast Biology*, Lovelace Foundation for Medical Education and Research, September 1959, TID-5764 [redacted]

White, C. S., I. G. Bowen, and D. R. Richmond, *A Comparative Analysis of Some of the Immediate Environmental Effects at Hiroshima and Nagasaki*, Health Physics, Pergamon Press, *10*, 89 (1964) [redacted]

White, C. S., *Tentative Biological Criteria for Assessing Potential Hazards from Nuclear Explosions*, Lovelace Foundation for Medical Education and Research, Albuquerque, New Mexico, December 1963, DASA 1462 [redacted]

White, C. S., *The Scope of Blast and Shock Biology and Problem Areas in Relating Physical and Biological Parameters*, Lovelace Foundation for Medical Education and Research, Albuquerque, New Mexico, November 1966, DASA 1856 [redacted]

White, C. S., *The Nature of Problems Involved in Estimating Immediate Casualties from Nuclear Explosions*, Lovelace Foundation for Medical Education and Research, Albuquerque, New Mexico, November 1968 [redacted]

White, C. S., I. G. Bowen, and D. R. Richmond, *The Environmental Medical Aspects of Nuclear Blast*, Lovelace Foundation for Medical Education and Research, Albuquerque, New Mexico, November 1962, DASA 1341 [redacted]

White, C. S., et al., *The Biodynamics of Air Blast*, Lovelace Foundation for Medical Education and Research, Albuquerque, New Mexico, July 1971, DNA 2738T [redacted]

[redacted]

11-2 Isodamage Curves for Fifty Percent Probability of Severe Damage to Multistory Blast-Resistant Reinforced Concrete Buildings

11-3 Isodamage Curves for Fifty Percent Probability of Severe Damage to Multistory Reinforced Concrete Buildings with Concrete Walls, Small Window Area, Three to Eight Stories

11-4 Isodamage Curves for Fifty Percent Probability of Severe Damage to Multistory Wall Bearing Buildings, Brick Apartment House Type, up to Three Stories

11-5 Isodamage Curves for Fifty Percent Probability of Severe Damage to Multistory Wall Bearing Building, Monumental Type, up to Four Stories

11-6 Isodamage Curves for Fifty Percent Probability of Severe Damage to Wood Frame Buildings, House Type, One or Two Stories

11-7 Isodamage Curves for Fifty Percent Probability of Severe Damage to Light Steel Frame Industrial Buildings, Single Story, Frangible Walls, up to 5 Ton Crane Capacity

11-8 Isodamage Curves for Fifty Percent Probability of Severe Damage to Heavy Steel Frame Industrial Buildings, Single Story, Frangible Walls, 25 to 50 Ton Crane Capacity

11-9 [redacted] Isodamage Curves for Fifty Percent Probability of Severe Damage to Heavy Steel Frame Industrial Buildings, Single Story, Frangible Walls, 60 to 100 Ton Crane Capacity [redacted] .....
11-10 [redacted] Isodamage Curves for Fifty Percent Probability of Severe Damage to Multistory Steel Frame Office Type Buildings, 3- to 10-Stories, Frangible Walls, Earthquake Resistant Construction [redacted] .....
11-11 [redacted] Isodamage Curves for Fifty Percent Probability of Severe Damage to Multistory Steel Frame Office Type Buildings, 3- to 10-Stories, Frangible Walls, Non-Earthquake Resistant Construction [redacted] .....
11-12 [redacted] Isodamage Curves for Fifty Percent Probability of Severe Damage to Multistory Reinforced Concrete Frame Office Type Buildings, 3- to 10-Stories, Frangible Walls, Earthquake Resistant Construction [redacted] ..
11-13 [redacted] Isodamage Curves for Fifty Percent Probability of Severe Damage to Multistory Reinforced Concrete Frame Office Type Buildings, 3- to 10-Stories, Frangible Walls, Non-Earthquake Resistant Construction [redacted] ...
11-14 [redacted] Isodamage Curves for Fifty Percent Probability of Severe Damage to Four-Lane Highway Truss Bridges and Double Track Ballast Floor Railroad Truss Bridges, Span 200 ft to 400 ft [redacted] .....
11-15 [redacted] Isodamage Curves for Fifty Percent Probability of Severe Damage to Two-Lane Highway Truss Bridges, Spans 200 ft to 400 ft; Single Track Ballast Floors and Double Track Open Floor Railroad Truss Bridges, Spans 200 ft to 400 ft; and Single Track Open Floor Railroad Truss Bridges, Span 400 ft [redacted] .....
11-16 [redacted] Isodamage Curves for Fifty Percent Probability of Severe Damage to Single Track Open Floor Railroad Truss Bridges, Span 200 ft [redacted] .....
11-17 [redacted] Isodamage Curves for Fifty Percent Probability of Severe Damage to Four-Lane Through Highway Girder Bridges, Spans 75 ft [redacted] .....
11-18 [redacted] Isodamage Curves for Fifty Percent Probability of Severe Damage to Two-Lane Deck, Two-Lane Through, and Four-Lane Deck Highway Bridges, Spans 75 ft; Double Track Deck, Open or Ballast Floor Railroad Girder Bridges, Span 75 ft; Single or Double Track Through, Ballast Floor Railroad Girder Bridges, Spans 75 ft [redacted] .....
11-19 [redacted] Isodamage Curves for Fifty Percent Probability of Severe Damage to Single Track Deck, Open or Ballast Floor, and Single or Double Track Through, Open Floor Railroad Girder Bridges, Spans 75 ft [redacted] ....
11-20 [redacted] Isodamage Curves for Fifty Percent Probability of Severe Damage to Two-Lane Through and Four-Lane Deck or Through Highway Girder

Bridges, Spans 200 ft; Double Track Deck or Through, Ballast Floor Railroad Girder Bridges, Spans 200 ft [redacted] .....

11-21 [redacted] Isodamage Curves for Fifty Percent Probability of Severe Damage to Two-Lane Deck Highway Girder Bridges, Spans 200 ft; Single Track Deck or Through, Ballast Floor, and Double Track Deck or Through, Open Floor Railroad Girder Bridges, Spans 200 ft [redacted] .....

11-22 [redacted] Isodamage Curves for Fifty Percent Probability of Severe Damage to Single Track Deck or Through, Open Floor, Railroad Girder Bridges, Spans 200 ft [redacted] .....

11-23 [redacted] Isodamage Curves for Fifty Percent Probability of Severe Damage to Floating Bridges, U.S. Army Standard M-2 and M-4, Random Orientation [redacted] .....

[redacted]

Table C-2. [redacted] Median Vulnerability to Overpressures Corresponding to Severe Damage of Diffraction Sensitive Structures [redacted]

Weapon Yield	Type of Structure				
	11-2	11-3	11-4	11-5	11-6
	(Median Vulnerability Overpressure, psi)				
30 mt	28	10	5.0	9.0	3.4
10 mt	29	10	5.0	9.0	3.4
3 mt	30	10	5.0	9.0	3.4
1 mt	30	11	5.0	9.0	3.5
300 kt	30	11	5.0	9.0	3.5
100 kt	32	11	5.0	9.5	3.5
30 kt	34	12	5.0	9.5	3.6
10 kt	34	13	5.5	10.0	3.6
3 kt	36	15	5.5	10.0	3.8
1 kt	48	17	5.5	11.0	4.0
[illegible] kt	–	20	6.0	12.0	4.4
0.1 kt	–	22	6.5	12.0	4.8
0.03 kt	–	24	7.0	13.0	5.2
0.01 kt	–	28	7.5	14.0	5.8

[redacted]

Table C-3. [redacted] Median Vulnerability to Dynamic Pressures Corresponding to Severe Damage of Drag Sensitive Structures [redacted]

Weapon Yield	Type of Structure																
	11-7	11-8	11-9	11-10	11-11	11-12	11-13	11-14	11-15	11-16	11-17	11-18	11-19	11-20	11-21	11-22	11-23
	(Median Vulnerability of Dynamic Pressure, psi)																
30 mt	0.8	1.6	2.6	5.0	2.4	5.0	2.6	2.4	2.0	2.0	9.6	5.0	2.8	3.3	2.0	1.4	0.6
10 mt	0.8	1.6	2.6	6.0	2.6	5.0	2.8	2.4	2.0	2.0	10.0	5.0	2.8	3.3	2.0	1.4	0.6
3 mt	0.9	1.8	2.8	7.0	3.0	6.0	3.0	2.6	2.0	2.0	13.0	5.2	2.8	3.3	2.0	1.4	1.0
1 mt	1.0	2.0	3.2	8.5	3.6	7.0	3.4	3.0	2.0	2.0	20.0	6.0	2.8	3.4	2.0	1.4	1.6
300 kt	1.2	2.2	3.6	12.0	4.8	9.0	4.2	3.8	2.5	2.0	48.0	8.0	3.0	4.0	2.0	1.4	2.8
100 kt	1.4	2.6	4.4	18.0	6.0	11.0	5.2	5.0	3.0	2.2		12.0	3.4	5.2	2.2	1.4	4.5
30 kt	2.0	3.6	5.8	34.0	10.0	16.0	7.0	10.0	4.0	2.6	–	20.0	4.0	10.0	2.6	1.4	7.5
10 kt	3.2	5.2	7.5	–	16.0	26.0	10.0	24.0	7.0	3.5	–	40.0	5.2	24.0	3.4	1.6	12.0
3 kt	5.4	7.5	12.0	–	36.0	–	18.0		15.0	5.0		–	7.0	–	4.6	2.0	20.0
1 kt	9.5	13.0	20.0	–	60.0	–	28.0	–	35.0	12.0	–	–	12.0	–	8.0	2.2	32.0
0.3 kt	18.0	26.0	38.0	–	–	–					–		22.0	–	18.0	3.0	55.0
0.1 kt	–	–	–	–	–	–	–	–	–		–	–	–	–		4.0	85.0
0.03 kt	–	–	–	–	–		–	–		–	–		–	–	–	6.0	
0.01 kt	–	–	–	–		–	–	–		–	–	–	–	–	–	9.0	–

[redacted]

Table C-4. [redacted] Median Vulnerability to Overpressures Corresponding to Moderate Damage of Diffraction Sensitive Structures [redacted]

Weapon Yield	Type of Structure				
	11-2	11-3	11-4	11-5	11-6
	(Median Vulnerability Overpressure, psi)				
30 mt	20	6.5	3.4	6.5	2.2
10 mt	20	6.5	3.4	6.5	2.2
3 mt	20	6.5	3.4	6.5	2.2
1 mt	20	6.5	3.4	6.5	2.2
300 kt	20	6.5	3.4	6.5	2.2
100 kt	20	7.0	3.4	6.5	2.2
30 kt	20	7.0	3.4	6.5	2.2
10 kt	20	7.0	3.6	6.5	2.2
3 kt	22	7.5	3.6	6.5	2.2
1 kt	24	8.0	3.6	6.5	2.2
0.3 kt	28	9.0	3.8	7.0	2.4
0.1 kt	–	10.0	4.0	7.5	2.6
0.03 kt	–	11.0	4.2	7.5	2.8
0.01 kt	–	12.0	4.4	8.0	3.0

[redacted]

Table C-5. [redacted] Median Vulnerability to Dynamic Pressures Corresponding to Moderate Damage of Drag Sensitive Structures [redacted]

Weapon Yield	Type of Structure																
	11-7	11-8	11-9	11-10	11-11	11-12	11-13	11-14	11-15	11-16	11-17	11-18	11-19	11-20	11-21	11-22	11-23
	(Median Vulnerability of Dynamic Pressure, psi)																
30 mt	0.6	1.2	2.0	3.4	1.6	3.6	2.0	2.4	2.0	2.0	9.6	5.0	2.8	3.2	2.0	1.4	0.2
10 mt	0.6	1.2	2.0	3.4	1.6	3.6	2.0	2.4	2.0	2.0	10.6	5.0	2.8	3.2	2.0	1.4	0.2
3 mt	0.6	1.2	2.0	3.4	1.6	3.6	2.0	2.4	2.0	2.0	12.0	5.2	2.8	3.2	2.0	1.4	0.4
1 mt	0.6	1.2	2.0	3.6	1.8	3.8	2.0	2.6	2.0	2.0	16.0	5.8	2.8	3.2	2.0	1.4	0.6
300 kt	0.6	1.2	2.0	4.0	2.0	4.0	2.2	2.8	2.0	2.0	26.0	7.4	2.8	3.4	2.0	1.4	1.0
100 kt	0.6	1.2	2.2	4.4	2.0	4.4	2.4	3.2	2.2	2.0	46.0	9.0	3.0	4.0	2.0	1.4	2.0
30 kt	0.6	1.4	2.4	5.4	2.4	5.2	2.6	4.0	2.8	2.2	88.0	14.0	3.4	5.0	2.2	1.4	3.0
10 kt	0.8	1.4	2.6	7.5	3.0	6.0	3.0	6.0	3.6	2.8	–	22.0	4.0	8.4	2.4	1.4	5.0
3 kt	0.8	1.6	3.2	12.0	4.4	9.0	3.6	12.0	6.4	4.2	–	40.0	5.4	18.0	3.4	1.6	8.0
1 kt	1.0	2.0	4.0	20.0	7.5	12.0	5.0	30.0	12.0	6.2	–	–	7.4	36.0	4.6	1.8	13.0
0.3 kt	1.2	3.0	6.0	40.0	13.0	22.0	9.0	–	–	16.0	–	–	10.0	–	6.4	2.2	22.0
0.1 kt	2.2	5.0	10.0	–	20.0	–	16.0	–	–	–	–	–	15.0	–	14.0	2.6	60.0
0.03 kt	–	–	–	–	–	–	–	–	–	–	–	–	–	–	–	3.4	100.0
0.01 kt	–	–	–	–	–	–	–	–	–	–	–	–	–	–	–	4.2	–

AD-A955 396

DTIC
ELECTE
2 MAR 1989
S D
E

Chapter 12

MECHANICAL DAMAGE DISTANCES FOR SURFACE SHIPS AND SUBMARINES SUBJECTED TO NUCLEAR EXPLOSIONS

INTRODUCTION

12-1 Damage Mechanisms

An air burst nuclear weapon may cause mechanical damage to surface ships by air burst, thermal radiation, ionizing radiation, and the electromagnetic pulse. Ship operations may also be affected by personnel casualties; however, only mechanical damage is considered in this chapter.

An underwater burst may cause damage to surface ships by the shock wave in the water, by the water column or plumes thrown up by the burst, by the surface gravity waves produced, or by the ionizing radiation from the base surge, fallout, or contaminated water pool. As for an air burst, the ship status may be affected by personnel casualties; however, only mechanical damage is considered in this chapter.

An underwater burst may cause damage to submerged submarines by the shock wave in the water, and, in special shallow water cases, by collision with the ocean bottom induced by the waves.

12-2 Damage Classification

Damage to surface ships and submarines is described by the degree of impairment of three major ship capabilities: seaworthiness, mobility, and weapon delivery. Complete loss of a capability is characterized as 100-percent impairment; no impairment is considered 0 percent. Levels of impairment of 90 percent and 10 percent are intended to signify nearly complete and slight impairment, respectively. These degrees of impairment should be interpreted as being the midpoints of a band of percent impairments.

The concept of degree of capability impairment is closely related to the fact that, for any given burst condition, a continuous spectrum of degrees of damage would be inflicted on ships of the same type located over a continuous spread of ranges from the burst. A ship is so complex a system that it is not possible to predict damage precisely for any given attack situation. Another consideration is that the crew of a damaged ship will attempt to repair damage; i.e., to decrease the degree of impairment of capability as quickly as possible. The time consumed by such repair is a vital aspect of the total damage assessment, but available knowledge does not justify an attempt to consider it in detail.

Damage ranges are given in this chapter in terms of zones within which varying degrees of impairment of each capability are to be expected. The outer boundary of a given zone corresponds to slight, and possibly temporary, impairment of the indicated capability; the inner boundary corresponds to nearly complete impairment that would require shipyard facilities for repair. The locations of the boundaries are determined by damage criteria derived from experimental data. There are, however, uncertainties involved as a result of a lack of sufficient experimental data. It is estimated that uncertainties concerning damage criteria cause uncertainties in the boundary locations on the order of 15 to 30 percent.

12-3 Seaworthiness Impairment

The degrees of seaworthiness impairment are defined as follows:

- 100 percent: The ship or submarine is sunk.
- 90 percent: The ship is in danger of sinking,

This document has been approved for public release and sale; its distribution is unlimited.

89 3 02 038

capsizing, or breaking up as a result of widespread, uncontrollable flooding or the loss of girder strength. Danger is present even in normal weather, but there is some chance of saving the ship. As a result of damage to its structure or to its buoyancy-control gear, a submarine will be in danger of settling to the bottom.

- 10 percent: Slight plastic deformation of the structure that may cause minor leakage. Hogging or sagging, or topside structural damage can occur, but not to an extent sufficient to endanger the ship in stormy weather. For submarines, this degree of impairment includes that damage that can at worst reduce the maximum safe diving depth slightly, but otherwise allows the submarine to submerge in a controlled manner.
- 0 percent: No plastic deformation of structure and no leakage.

12-4 Mobility Impairment

The degrees of mobility impairment are defined as follows:

- 100 percent: The ship or submarine lacks any ability to operate its propulsion devices.
- 90 percent: The ship can at best just barely maintain steerageway in a desired direction, either as a result of damage to main propulsion machinery and control gear, or as a result of personnel casualties.
- 10 percent: Slight loss of ability to achieve top speed and/or to maneuver normally, as a result of damage or personnel casualties.
- 0 percent: No impairment of mobility.

12-5 Weapon Delivery Impairment

The degrees of weapon delivery impairment are defined as follows:

- 100 percent: The ship or submarine cannot release its weapons.
- 90 percent: Weapons can be released, but it is almost impossible to deliver them effectively because the ship's target-acquisition and communication equipment are inoperative, either as a result of damage to equipment or to topside structure, or as a result of personnel casualties.
- 10 percent: Slight reduction in weapon-delivery efficiency as a result of damage to equipment or topside-structure or as a result of personnel casualties.
- 0 percent: No loss.

SECTION I

DAMAGE TO SURFACE SHIPS FROM AIR BURSTS

BLAST DAMAGE

12-6 General

Air blast damage may be significant for surface ships when the burst is at or above the water surface. The following general description of air blast effects on ships is applicable to existing Navy ships.

At close ranges, air blast can cause hull rupture that can result in flooding and sinking. Hull rupture appears likely to begin near the waterline on the side facing the blast. The main hull of existing Navy ships is, however, stronger than the superstructure and equipment. At ranges beyond those at which hull rupture is likely to occur the main effect of air blast is to distort, rupture, or carry away light structures and equipment vulnerably exposed above the waterline, and to cause casualties among topside personnel. Such damage can cause complete impairment of the weapon delivery capability. Blast pressures penetrating through weather openings of ventilation systems and stack-uptake systems can cause damage to interior equipment and compartments, and also to boilers; the latter may result in immobilization. The distortion of weather bulkheads may cause fracture or render interior equip-

[redacted]

12-9 Capsizing from Blast [redacted]

[redacted] Figure 12-2 shows estimates of ranges for capsizing various types of ships as a result of air blast from surface bursts. The distances are shown as functions of weapon yield, since cube-root scaling does not apply. The estimates are based on theoretical calculations alone, since experimental data are not available on capsizing. The width of the bands in Figure 12-2 corresponds to the difference between two sets of theoretical calculations. The ranges are valid for broadside attack only. Air blast will not capsize a ship in a fore-and-aft attack direction. For an attack direction of 45 degrees off the bow or stern, it is roughly estimated that capsizing ranges are 5 to 10 percent smaller. The capsizing distances from an air burst may be greater than those shown for a surface burst in Figure 12-2. For a given yield the increase in range can be determined approximately by assuming that the capsizing overpressure is independent of burst height (within the Mach region), and then by referring to curves of range versus height of burst for constant overpressures (see Section I, Chapter 2).

[redacted] DAMAGE FROM OTHER AIR BURST PHENOMENA [redacted]

12-10 Thermal Radiation [redacted]

[redacted] Material exposed to thermal radiation may be charred, scorched, ignited, melted, or otherwise changed. In addition, the heat may affect the mechanical properties of structural metals by annealing (reduction of strength). The rapid rate of delivery of thermal energy may induce large temperature gradients, and the resulting thermal stresses may produce effects such as surface spalling or cracking, and/or permanent distortions of structures or structural elements. Weakening of structural elements may cause weapon system and superstructure components to be more vulnerable to the air blast, which arrives after most of the thermal exposure has been received. Distortion of radar antennas and other superstructure components may cause functional impairment.

[redacted] Thermal radiation can affect only the exposed topside personnel and material of a surface ship. Any opaque object along the fireball-to-target line of sight will furnish protection from thermal radiation. Topside personnel or material in the shadow or the ship's structural or topside gear would be shielded from thermal radiation.

[redacted] Fires are not likely to originate except perhaps when severe, and probably overriding, blast damage is also sustained. Normally there is insufficient combustible material topside on combatant ships to sustain fire. Possible exceptions may be vessels carrying inflammable liquids, which may spill as a result of the blast (aircraft carriers), and vessels carrying combustible deck loads (cargo ships). Water washdown systems, installed primarily for protection against deposited radioactive debris, should reduce fire hazards and thermal radiation damage, provided they are turned on prior to the burst.

[redacted] The main steel hulls of naval ships are not likely to be weakened by thermal radiation, except when severe, and probably overriding, blast damage is also sustained. Of the metallic components in use on present ships, those made of aluminum may be most susceptible to thermal radiation effects (annealing, melting). The effect will be greatest on thin aluminum components. Aluminum plates of alloy 5456-H321 less than 5/16 inch in thicknesses may suffer more than 50-percent loss of strength prior to the arrival of the blast at the 10-psi range from a 1-Mt burst. Lightweight aluminum-alloy components, which have been used extensively in radar antennas as support members, reflector elements, and wave guides, appear to be susceptible to melting, sagging, and buckling when exposed to free-field thermal radiation at the 10 psi overpressure

PAGE 12-7 DELETED

[redacted]

[redacted]

[redacted] BIBLIOGRAPHY [redacted]

Hansen, I. S., *Handbook of Underwater Nuclear Explosions, Part II – Effects, Chapter 2 – Surface Ship Structural Response and Damage Development – Section 2.2 – The Effects of Air Blast* [redacted] DASA 1240 (2.2), David Taylor Model Basin Report C-2023, August 1965 [redacted]

Hansen, I. S., *Handbook of Underwater Nuclear Explosions, Part II – Effects, Chapter 3 – Surface Ship Equipment, Section 3.2 – The Effects of Air Blast on Surface Ship Equipment* [redacted] DASA 1240 II (3.2), David Taylor Model Basin Report C-2096, October 1965 [redacted]

Hansen, I. S., *Weapon Delivery Impairment Ranges for DLG-16 and DDG-2 Class Ships Subjected to Air Blast – Preliminary SAILOR HAT Results* [redacted] Proceedings, DASA Conference on SAILOR HAT, DASA 1775, p. 190, May 1966 [redacted]

Hirsch, A. E., *Handbook of Underwater Nuclear Explosions, Part II – Effects, Chapter 8 – Submarine Personnel Casualties, Section 8.1 – Underwater Shock Effects* [redacted] DASA-1240 II (8.1), David Taylor Model Basin Report C-2148, January 1966 [redacted]

Irick, J. T., S. Silverman, and W. E. Baker, *The Rigid-Body Response of Naval Surface Vessels to Air Blast* [redacted] Final Report, Southwest Research Institute, prepared for Naval Ship Research and Development Center, September 1967 [redacted]

Manny, P. A., *Damage Criteria for Naval Ships and Submarines Subjected to Nuclear Explosions* [redacted] Naval Ship Research and Development Center (in preparation) [redacted]

Murray, W. W., *Engineering Predictions of the Early Bodily Response of Submarines to Underwater Explosion Attacks*, Underwater Explosions Research Division, Norfolk Naval Shipyard, Portsmouth, Va., UERD Report 7-58, October 1958.

Murray, W. W., *Ship Damage Classification and Prediction Methods* [redacted] David Taylor Model Basin Report C-1230, September 1961 [redacted]

Murray, W. W., *Loading and Response of Surface-Ship Hull Structures from Underwater Bursts* [redacted] Project 3.4, Operation HARDTACK, WT-1628, December 1961 [redacted]

Murray, W. W., and R. M. Santamaria, *Handbook of Underwater Nuclear Explosions, Part II – Effects, Chapter 2 – Surface Ship Structural Response and Damage Development, Section 2.1 – The Effects of Underwater Phenomena* [redacted] DASA 1240-II (2.1), David Taylor Model Basin Report C-2261, December 1966 [redacted]

[redacted]

[redacted]

Parnell, U. C., and H. M. Schauer, *Handbook of Underwater Nuclear Explosions, Part II – Effects, Chapter 6 – Submarine Hull Response and Damage Development* [redacted] DASA 1240 II (6), David Taylor Model Basin Report C-2188, June 1966 [redacted]

Rich, H. L., et al., *Shock Loading in Ships from Underwater Bursts and Response of Shipboard Equipment*, Project 3.3, Operation HARDTACK, WT-1627, September 1959 [redacted]

Shrider, P. W., *The Interaction of Surface Ships with the Thermal and Radiological Environment* [redacted] Chapter IV of DASA Handbook of Underwater Nuclear Explosions, Part II, Effects, DASA 1240-II (4), U.S. Naval Radiological Defense Laboratory Report USNRDL-475, January 1964 [redacted]

Weinberger, F., and R. M. Santamaria, *Mechanical Damage Ranges for Surface Ships and Submarines Subjected to Nuclear Underwater and Air Bursts* [redacted] David Taylor Model Basin, Report C-1323, November 1961 [redacted]

Zagorites, H. A., and R. L. Hopton, *Survey of the EMP in Shipboard Systems* [redacted] U.S. Naval Radiological Defense Laboratory Report USNRDL-LR-190, July 1966 [redacted]

PAGE 12-32 INTENTIONALLY LEFT BLANK

[redacted]

[redacted]

Problem 13-1. Calculation of the Aerodynamic Coefficient for Wing and Horizontal Tail

[redacted] The transient airloads may be obtained on a quasi-steady basis using the instantaneous quantities (angle of attack, density, etc.) and steady-state coefficients. Typically, the theoretical methods predict a lift for a swept wing-body combination which is about 10 percent greater than for an isolated wing without a body, provided that the wing and body are at the same incidence. In wind tunnel tests, however, the lift on a swept wing-body combination was found to be the same as on an isolated wing. In these cases, the area of the isolated wing includes the area submerged within the body. Other methods indicate that the lift on a delta wing-body combination with a typical ratio of body diameter to wing span and traveling at supersonic speeds is within 2 percent of the lift for the same delta wing alone. In view of these results, the lift on the wing (tail)-body combinations is computed for an isolated wing (tail) having the same wing area, including the wing (tail) area submerged within the fuselage.

[redacted] The calculation of the aerodynamic coefficient for wings and/or horizontal tails, C_{L_α}, is presented in the following series of steps.

1. Using the silhouette profile of the aircraft (for example, see Figures 13-1 and 13-2), from which lengths and surfaces may be found, determine the following:

S = wing/horizontal tail area (sq ft), defined as the extension of the leading and trailing edges of both wings/horizontal tail to the aircraft centerline.

c_r = wing/horizontal tail root chord, i.e., the length along the fuselage centerline (ft) subtended by extensions of the leading and trailing edges.

c_t = wing/horizontal tail tip chord (ft), defined as the length along the fuselage centerline subtended by the wing tip.

b = wing/horizontal tail span, tip to tip (ft).

Λ_{LE} = sweepback angle at wing/horizontal tail leading edge, measured from a line perpendicular to the fuselage centerline (deg).

M = Mach Number = V/c, where V is the aircraft velocity and c is the ambient speed of sound.

2. Calculate the taper ratio λ:

$$\lambda = \frac{c_t}{c_r}$$

and the aspect ratio AR:

$$AR = \frac{b^2}{S}.$$

3. Calculation of the slope of the lift coefficient depends on the value of the Mach number, M. Three regions are defined as follows:

Region 1: $M \leqslant 0.85$,

Region 2: $M \geqslant 1.2$,

Region 3: $0.85 < M < 1.2$.

Region 1. Steps a through d present the calculation of the slope C_{L_α} for $M \leqslant 0.85$.

a. Calculate the value of β^2:

$$\beta^2 = 1 - M^2.$$

[redacted]

[redacted]

b. Determine the tangent of the sweep angle of the mid-chord line, $\tan \Lambda_{c/2}$:

$$\tan \Lambda_{c/2} = \tan \Lambda_{LE} - \frac{2}{AR}\left[\frac{1-\lambda}{1+\lambda}\right].$$

c. Compute the parameter,

$$AR\left[\beta^2 + \tan^2 \Lambda_{c/2}\right]^{1/2},$$

and enter Figure 13-3, with the value of the parameter to obtain the corresponding value of C_{L_α}/AR.

d. Calculate the slope of the lift coefficient curve as follows:

$$C_{L_\alpha} = \left[\frac{C_{L_\alpha}}{AR}\right] AR.$$

Region 2. Calculation of C_{L_α} for $M \geqslant 1.2$ is performed by the following steps.

a. Calculate the value of β:

$$\beta = (M^2 - 1)^{1/2}.$$

b. Calculate the values of the parameters:

$$\frac{\beta}{\tan \Lambda_{LE}},$$

and

$$(AR) \tan \Lambda_{LE}.$$

c. Enter Figure 13-4 and select the figure corresponding to the taper ratio λ. Select the curve corresponding to the value of the parameter $(AR) \tan \Lambda_{LE}$. If

$$\frac{\beta}{\tan \Lambda_{LE}} < 1,$$

use the left side of the figure to obtain the value of $\tan \Lambda_{LE} C_{N_\alpha}$. Calculate C_{L_α} as follows:

$$C_{L_\alpha} = \frac{\tan \Lambda_{LE} C_{N_\alpha}}{\tan \Lambda_{LE}},$$

where the normal force coefficient C_{N_α} and C_{L_α} are taken to be equal within the scope of this method.

If

$$\frac{\beta}{\tan \Lambda_{LE}} > 1,$$

determine its reciprocal,

$$\frac{\tan \Lambda_{LE}}{\beta},$$

and use the right side of the figure to obtain the value of βC_{N_α}.

The slope is calculated by:

$$C_{L_\alpha} = \frac{\beta C_{N_\alpha}}{\beta},$$

where C_N is represented as C_L within the scope of this method.

Region 3. The following steps a through c, are used to calculate C_{L_α} for $0.85 < M < 1.2$.

a. Calculate C_{L_α} at $M = 0.85$ following the method in Region 1.

b. Calculate C_{L_α} at $M = 1.2$ following the method in Region 2.

c. Interpolate linearly for the slope at the actual Mach number:

$$C_{L_\alpha} = C_{L_\alpha}(\text{at } M = 0.85) + \frac{M - 0.85}{0.35}\left[C_{L_\alpha}(\text{at } M = 1.2) - C_{L_\alpha}(\text{at } M = 0.85)\right].$$

[redacted]

[redacted]

Table 13-1. [redacted] Selected Data Based on U.S. Standard Atmosphere, 1962 English Units [redacted]

Altitude feet	Temperature °F	Pressure psi	Density Ratio* ρ/ρ_o	Temperature Ratio T/T_o	Sound Speed ft/sec
0	59.0	14.696	1.0000	1.000	1116
1 000	55.4	14.17	.9711	.993	1113
2 000	51.9	13.66	.9428	.986	1109
3 000	48.3	13.17	.9151	.979	1105
4 000	44.7	12.69	.8881	.973	1101
5 000	41.2	12.23	.8617	.966	1097
10 000	23.4	10.11	.7386	.931	1077
15 000	5.5	8.297	.6295	.897	1057
20 000	-12.3	6.759	.5332	.863	1037
25 000	-30.0	5.461	.4486	.828	1016
30 000	-47.8	4.373	.3747	.794	995
35 000	-65.6	3.468	.3106	.760	973
40 000	-69.7	2.730	.2471	.752	968
45 000	-69.7	2.149	.1945	.752	968
50 000	-69.7	1.692	.1531	.752	968
55 000	-69.7	1.332	.1206	.752	968
60 000	-69.7	1.049	.09492	.752	968
65 000	-69.7	.826	.07475	.752	968
70 000	-67.4	.651	.05857	.756	971
75 000	-64.7	.514	.04591	.762	974
80 000	-62.0	.406	.03606	.767	978
85 000	-59.3	.322	.02837	.772	981
90 000	-56.5	.255	.02236	.777	984
95 000	-53.8	.203	.01765	.782	988
100 000	-51.1	.162	.01396	.788	991
110 000	-41.3	.103	8.692-3	.807	1003
120 000	-26.1	.0667	5.428	.836	1021
130 000	-10.9	.0438	3.446	.865	1038
140 000	4.3	.0292	2.222	.894	1056
150 000	19.4	.0197	1.454	.924	1073
160 000	27.5	.0135	9.770-4	.939	1082
170 000	27.5	9.23-3	6.690	.939	1082
180 000	18.9	6.31	4.652	.923	1072
190 000	8.1	4.27	3.225	.902	1060
200 000	-2.7	2.87	2.217	.881	1048

NOTE: 7.011-3 means 7.011×10^{-3}

*$\rho_o = 2.38 \times 10^{-3}$ slugs/ft^3
$= 7.65 \times 10^{-2}$ lbs/ft^3

[redacted]

[redacted]

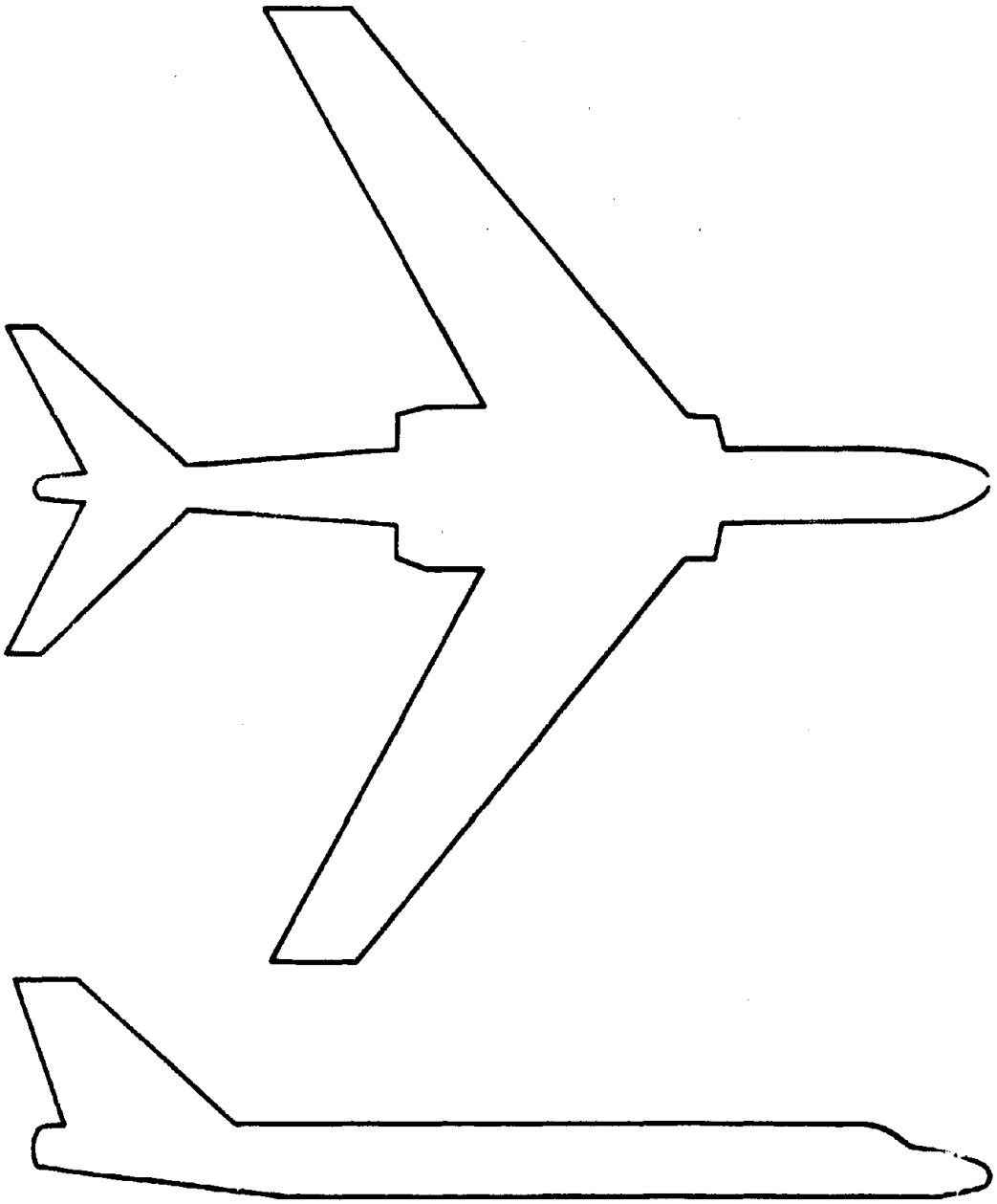

SCALE: 1" = 30'

Figure 13-1. [redacted] Example Airplane (American) [redacted]

[redacted]

[redacted]

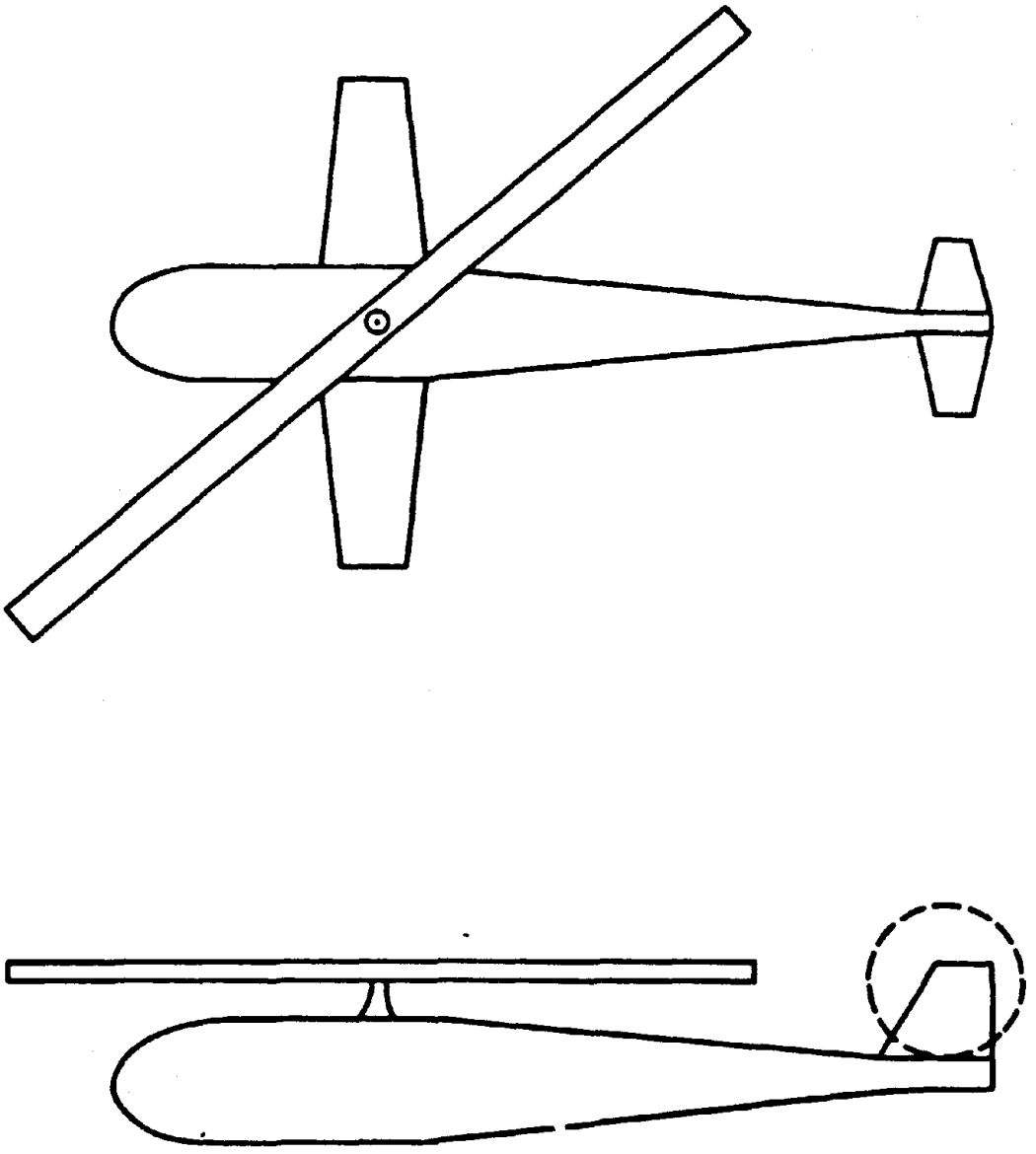

SCALE: 1" = 10'

Figure 13-2. [redacted] Example Helicopter [redacted]

[redacted]

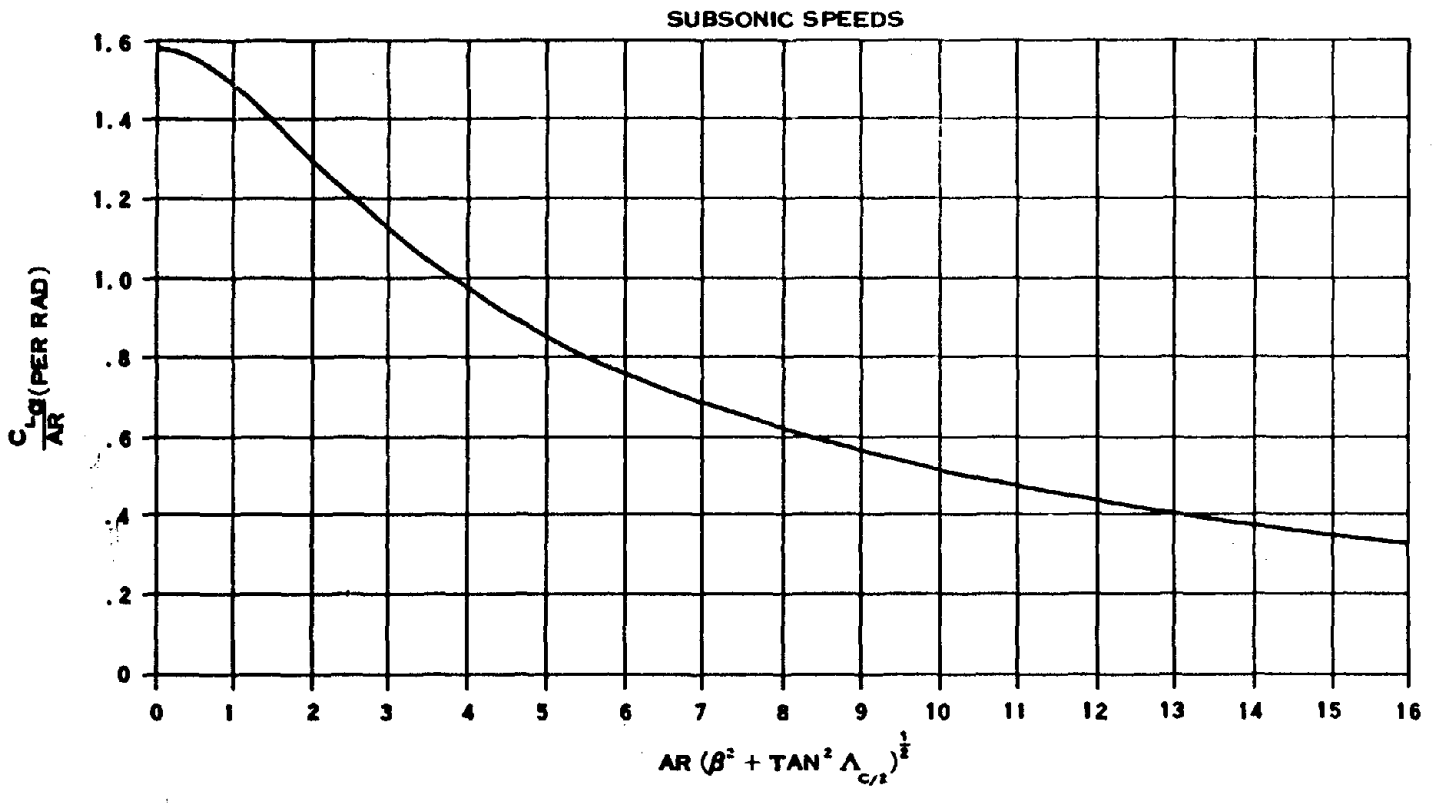

Figure 13-3. [redacted] Subsonic Wing Lift Curve Slope [redacted]

[redacted]

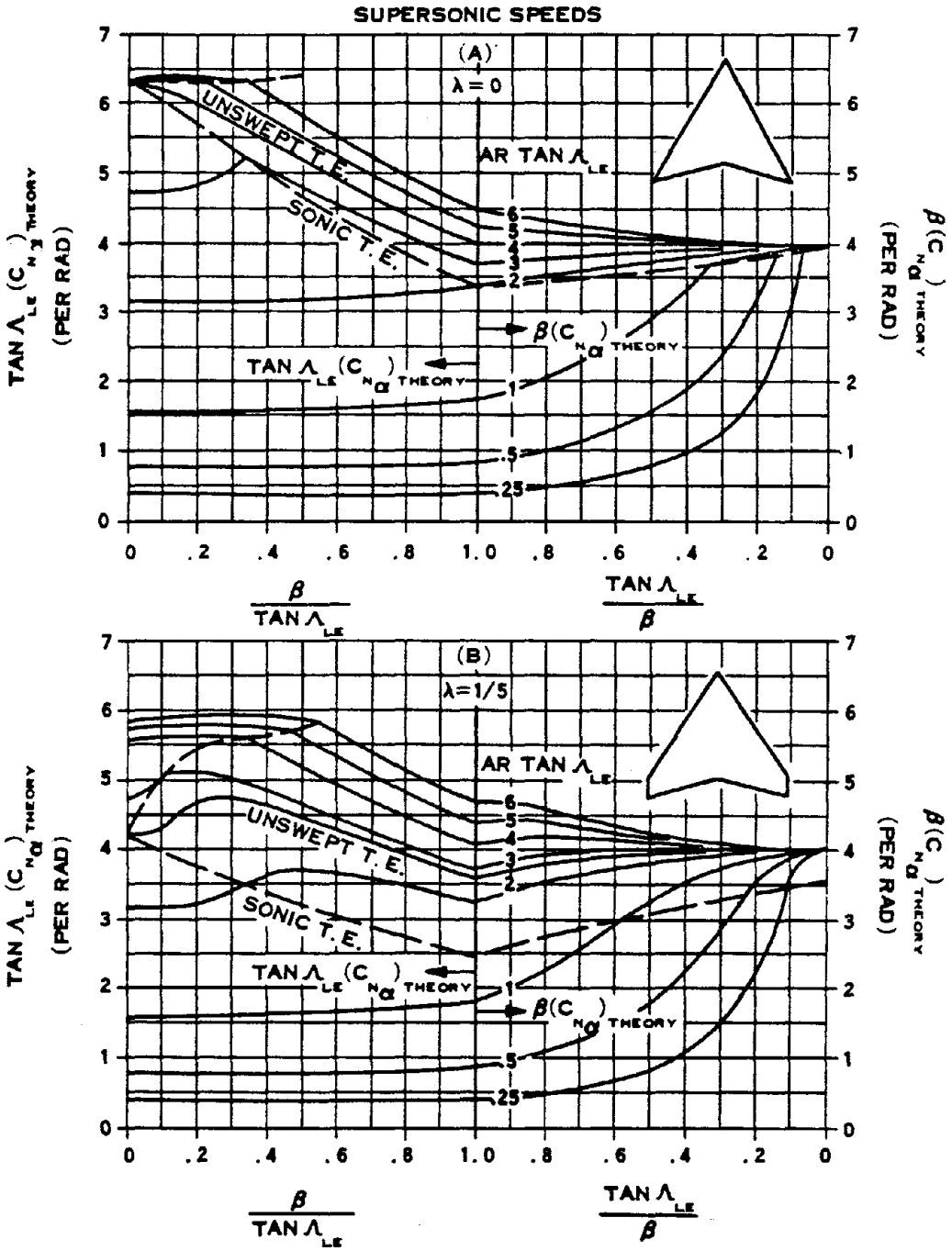

Figure 13-4a. [redacted] Wing Supersonic Normal Force Curve Slope [redacted]

[redacted]

[redacted]

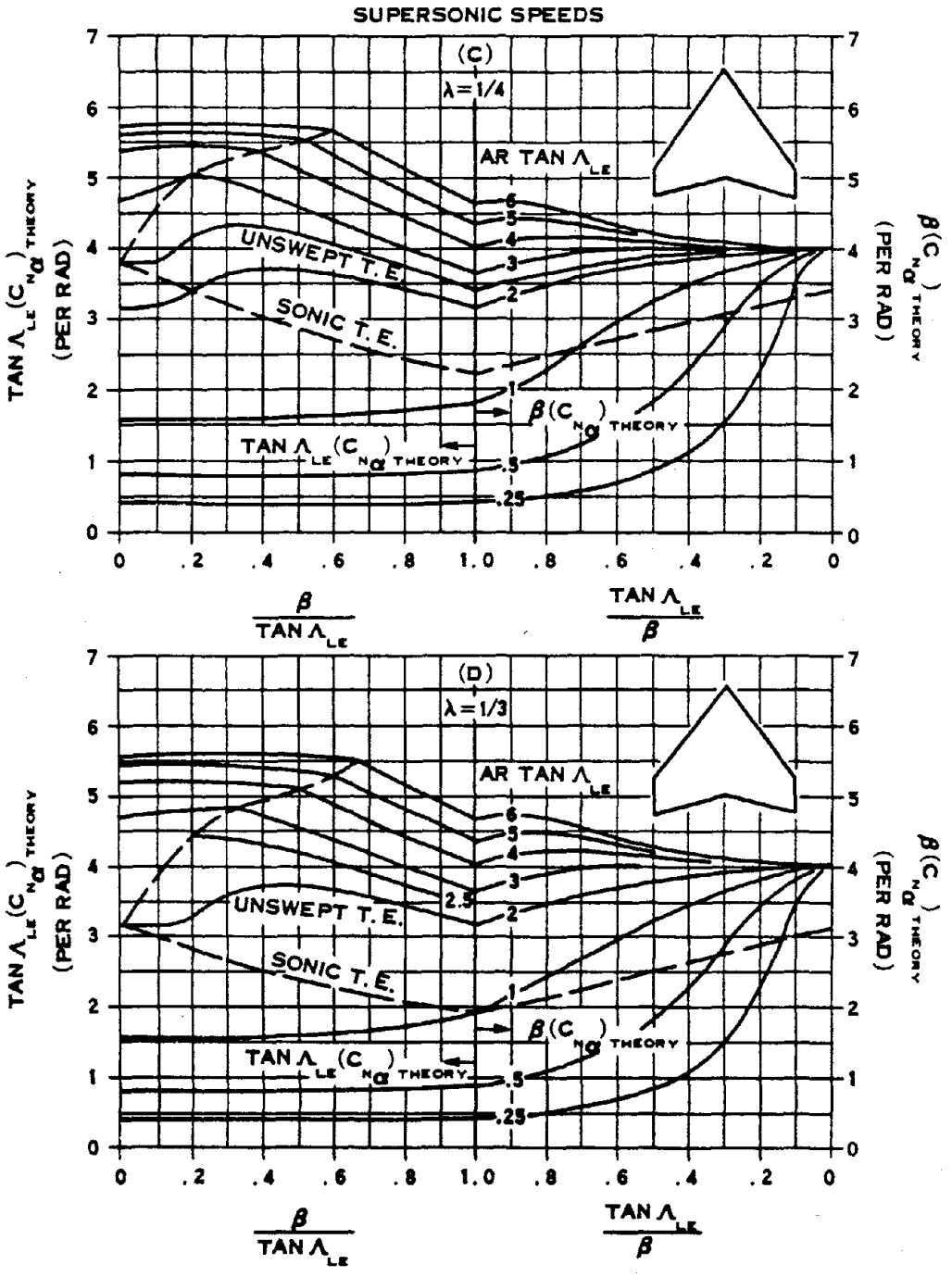

Figure 13-4b. [redacted] Wing Supersonic Normal Force Curve Slope [redacted]

[redacted]

[redacted]

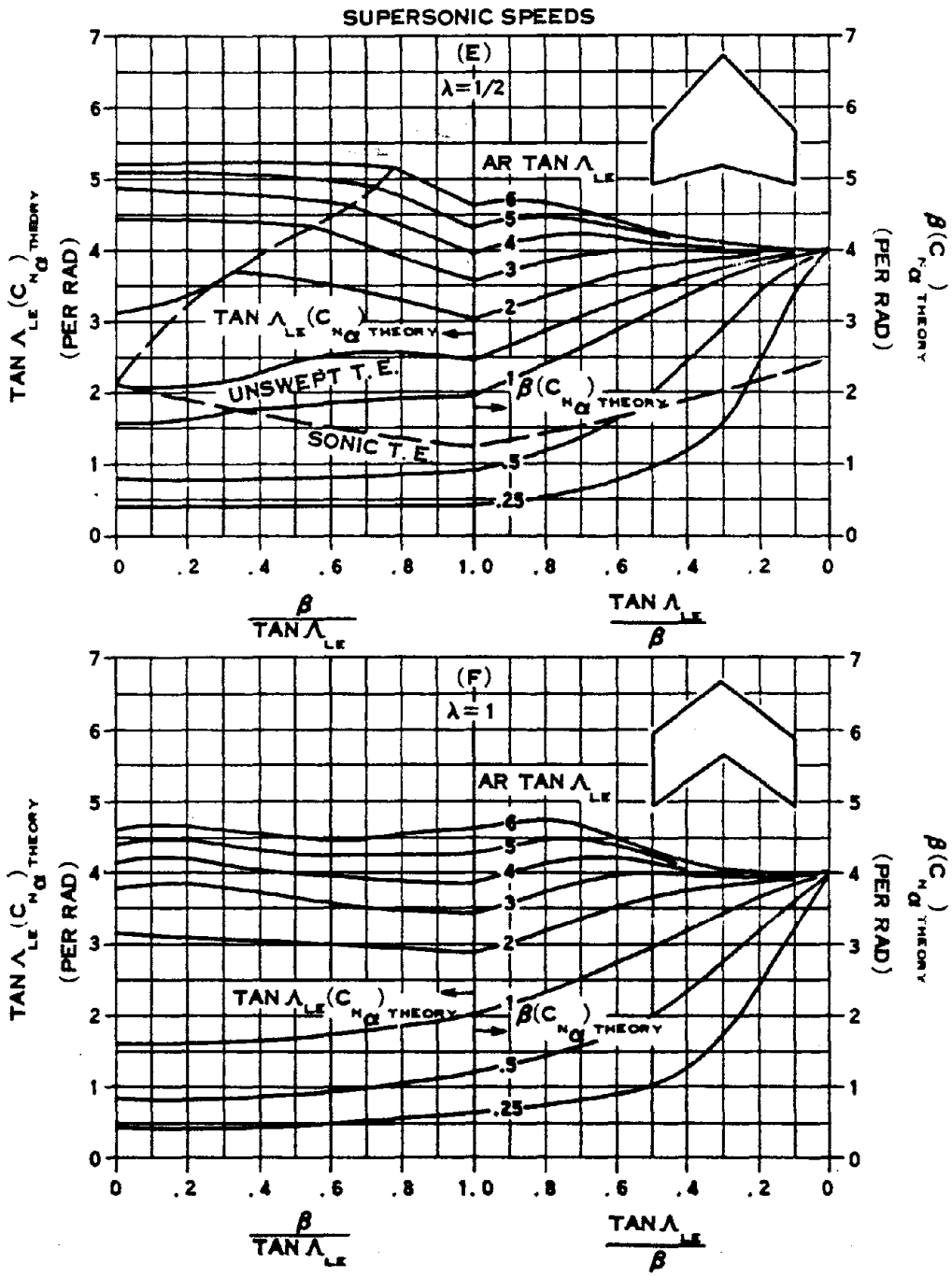

Figure 13-4c. [redacted] Wing Supersonic Normal Force Curve Slope [redacted]

[redacted]

[redacted]

Problem 13-2. Calculation of the Aerodynamic Coefficient for the Vertical Tail

[redacted] An effective aspect ratio is derived to account for interference effects from the body and the horizontal tail to predict the lateral force on the vertical tail at subsonic speed:

$$AR_{\text{eff}} = \left\{\frac{(AR)_B}{AR}\right\}\left\{1 + K_H\left[\frac{(AR)_{HB}}{(AR)_B} - 1\right]\right\}(AR),$$

where AR is the aspect ratio of the isolated vertical tail, with the span and area of the vertical tail measured to the fuselage centerline; the factor $(AR)_B/AR$ is the ratio of the aspect ratio of the vertical tail in the presence of the fuselage to the aspect ratio of the isolated tail (this ratio is shown in Figure 13-5); the factor K_H accounts for the relative size of the horizontal and vertical tails, and it varies from 0 to about 1.1; and the factor $(AR)_{HB}/(AR)_B$ is the ratio of the vertical tail aspect ratio in the presence of *both* the horizontal tail and body to that of the vertical tail in the presence of the body alone, which varies from 0.9 to 1.2 for typical configurations. Within the accuracy goals of the present calculations, it is reasonable to take this ratio as unity, which gives

$$(AR)_{\text{eff}} = \left(\frac{(AR)_B}{AR}\right) AR.$$

A first approximation for the lift coefficient for the vertical tail, $\overline{C}_{L_\alpha}$, is determined from the wing lift curve slopes shown in Figures 13-3 and 13-4, using the effective aspect ratio $(AR)_{\text{eff}}$. The value of C_{L_α} should be corrected by an empirical factor k, which is a function of the vertical tail span and the body diameter:

$$C_{L_\alpha} = k\ \overline{C}_{L_\alpha}.$$

The diameter k may be obtained from Figure 13-6. All coefficients are based on the dynamic pressure and the elevation area of the isolated vertical tail.

[redacted] For *direct* side-on blast orientation cases for parked aircraft, the normal force coefficient is obtained from drag data for flat plates in streams normal to the plates. Data indicate that a drag coefficient of 1.2 would apply to plates having an aspect ratio from unity to about 10, which essentially encompasses the range of aspect ratios for vertical tails of current aircraft. Therefore, for analysis of effects on side-on gusts on parked aircraft, a coefficient of 1.2 has been used.

[redacted] The drag force on the fuselage also becomes important for parked aircraft subjected to side-on gusts. Values of the steady-state drag coefficient vary from about 0.35 to 1.2, depending upon the Reynolds number, which dictates whether the flow is laminar or turbulent. In the case of unsteady drag, a drag coefficient slightly below the laminar value of 1.2 appears to be applicable at early times. Therefore, a drag coefficient of 1.2 has been used for the fuselage for the analysis of the effects of side-on gusts on parked aircrafts.

[redacted] For supersonic speeds, the slope of the lift coefficient curve C_{L_α} is estimated by the normal force slope for similar wings. In this calculation, C_{L_α} is computed for a wing having a planform of the isolated vertical tail plus its image about the fuselage centerline, using the method given in Problem 13-1, e.g., C_{L_α} is computed for the isolated vertical tail with its image as if it were a wing. The isolated vertical tail which extends from the tip to the fuselage centerline is considered; its area includes, in addition to the exposed part, that area within

[redacted]

[redacted]

the fuselage bounded by the extensions of the leading and trailing edges and the fuselage centerline.

[redacted] The calculation of the aerodynamic coefficient for vertical tails is presented in the following steps. Several of the lengths and areas that are required already will have been determined in the particular response method being followed, which requires the calculation of C_{L_α} (see Problem 13-1).

1. Using the silhouette profile of the aircraft (for example, see Figures 13-1 and 13-2), from which lengths and surfaces may be found, determine the following:

S = vertical tail area (sq ft), defined by the extensions of the leading and trailing edges to the fuselage centerline.

c_r = vertical tail root chord (ft), i.e., the length along the fuselage centerline subtended by the leading and trailing edges.

c_t = vertical tail tip chord (ft), defined as the length along the fuselage centerline subtended by the vertical tail tip.

b = vertical tail span, fuselage centerline to tip (ft).

Λ_{LE} = sweepback angle of vertical tail leading edge, measured from the vertical (deg).

d = fuselage depth at the intersection of the vertical tail leading edge and the fuselage (ft).

M = Mach Number = V/c, where V is the velocity of the aircraft, and c is the ambient speed of sound.

2. Calculate the taper ratio λ:

$$\lambda = \frac{c_t}{c_r}$$

and the aspect ratio AR:

$$AR = \frac{b^2}{S}.$$

3. Calculation of the aerodynamic coefficient for the vertical tail depends on the value of the Mach number, M. Three regions are defined as follows:

Region 1: $M \leqslant 0.85$,

Region 2: $M \geqslant 1.2$,

Region 3: $0.85 < M < 1.2$.

Region 1. Steps a through g present the calculation of the aerodynamic coefficient for the vertical tail C_{L_α} for $M \leqslant 0.85$.

a. Calculate the value of β^2:

$$\beta^2 = 1 - M^2.$$

b. Determine the tangent of the sweep angle of the mid-chord line, $\tan \Lambda_{c/2}$:

$$\tan \Lambda_{c/2} = \tan \Lambda_{LE} - \frac{2}{AR}\left[\frac{1-\lambda}{1+\lambda}\right].$$

c. Calculate the parameter b/d. With the value of this parameter and the value of λ from step 2, enter Figure 13-5 to obtain the value of AR_B/AR.

d. Calculate the effective aspect ratio

$$(AR)_{eff} = \left(\frac{(AR)_B}{AR}\right) AR.$$

e. Compute the parameter

$$(AR)_{eff}\left[\beta^2 + \tan^2 \Lambda_{c/2}\right]^{1/2},$$

[redacted]

[redacted]

[redacted]

and enter Figure 13-3 with this parameter to obtain the value of C_{L_α}/AR.

f. With the value of b/d from step c, enter Figure 13-6 to obtain the value of k, an empirical factor, which is a function of the vertical tail span and the body diameter.

g. Calculate the aerodynamic coefficient for the vertical tail C_{L_α}:

$$C_{L_\alpha} = k\left(\frac{C_{L_\alpha}}{AR}\right)(AR)_{\text{eff}}.$$

Region 2. The calculation of C_{L_α} is the same as that given for Region 2, in Problem 13-1, except that AR is twice that calculated in step two of Problem 13-1, i.e.,

$$AR = 2\left(\frac{b^2}{S}\right).$$

The remaining steps are described once again below.

a. Calculate the value of β:

$$\beta = (M^2 - 1)^{1/2}.$$

b. Calculate the values of the parameters:

$$\frac{\beta}{\tan \Lambda_{LE}}$$

$$(AR) \tan \Lambda_{LE}.$$

c. Enter Figure 13-4 and select the figure corresponding to the taper ratio λ. Select the curve corresponding to the value of the parameter $(AR) \tan \Lambda_{LE}$. If

$$\frac{\beta}{\tan \Lambda_{LE}} < 1,$$

use the left side of the figure to obtain the value of $\tan \Lambda_{LE} C_{N_\alpha}$. Calculate C_{L_α} as follows:

$$C_{L_\alpha} = \frac{\tan \Lambda_{LE} C_{N_\alpha}}{\tan \Lambda_{LE}},$$

where the normal force coefficient C_{N_α} and C_{L_α} are taken to be equal within the scope of this method.

If

$$\frac{\beta}{\tan \Lambda_{LE}} > 1,$$

determine its reciprocal,

$$\frac{\tan \Lambda_{LE}}{\beta},$$

and use the right side of the figure to obtain the value of βC_{N_α}. The slope is calculated by:

$$C_{L_\alpha} = \frac{\beta C_{N_\alpha}}{\beta},$$

where C_N is represented as C_L within the scope of this method.

Region 3. The following steps, a through c, are used to calculate C_{L_α} for $0.85 < M < 1.2$.

a. Calculate C_{L_α} at $M = 0.85$ following the method in Region 1.

b. Calculate C_{L_α} at $M = 1.2$ following the method in Region 2.

c. Interpolate linearly for the slope at the actual Mach number:

$$C_{L_\alpha} = C_{L_\alpha}\,(\text{at } M = 0.85) + \frac{M - 0.85}{0.35}\left[C_{L_\alpha}\,(\text{at } M = 1.2) - C_{L_\alpha}\,(\text{at } M = 0.85)\right].$$

[redacted] No numerical example is provided with this problem since the procedures are so similar to those of Problem 13-1, and since the calculation of the aerodynamic coefficient for the vertical tail is not required for the calculation of the simplified gust loading sure-safe and sure-kill envelopes described in succeeding problems.

[redacted]

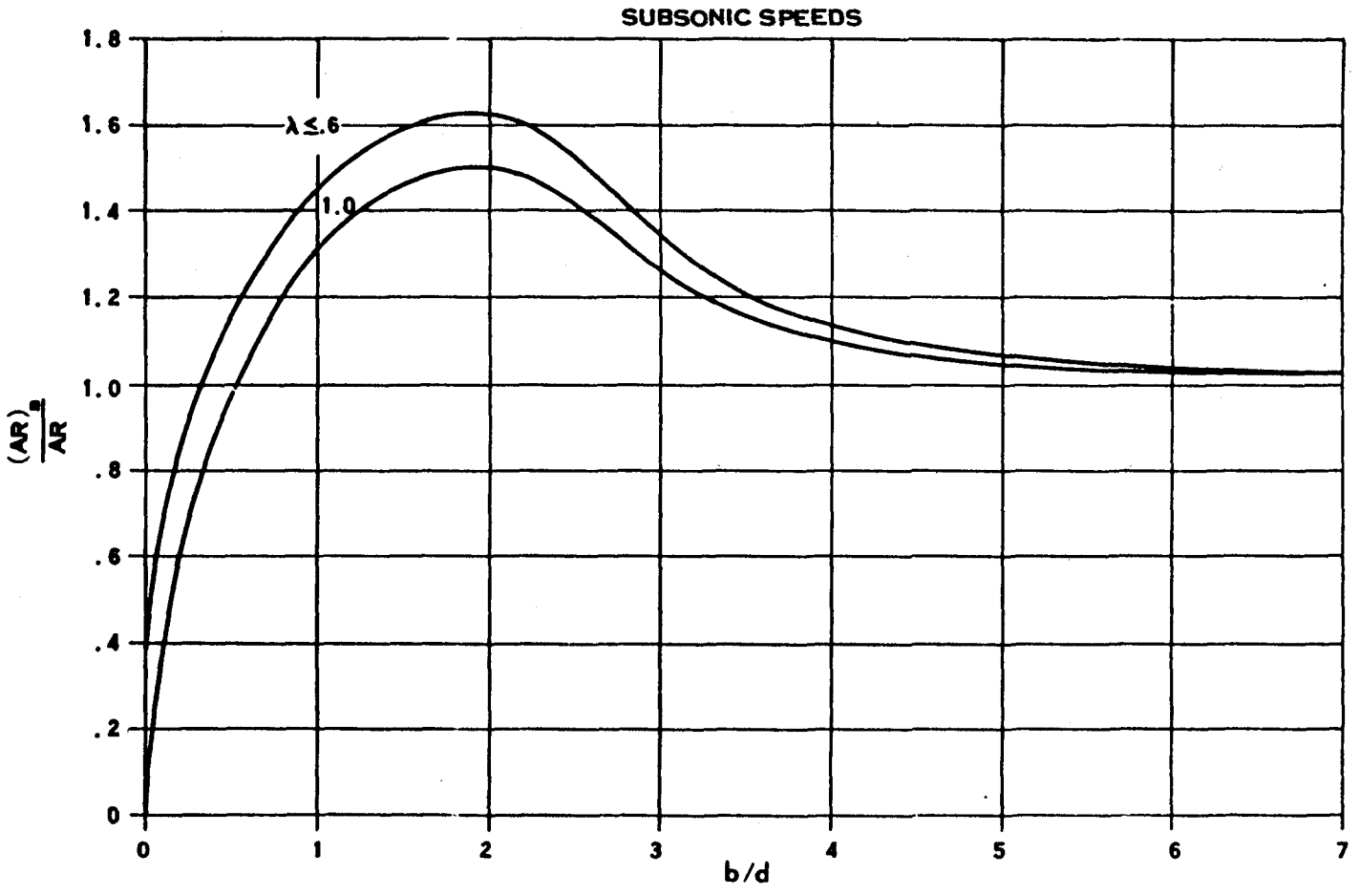

Figure 13-5. [redacted] Ratio of the Aspect Ratio of the Vertical Tail in the Presence of the Body to That of the Isolated Vertical Tail at Subsonic Speeds [redacted]

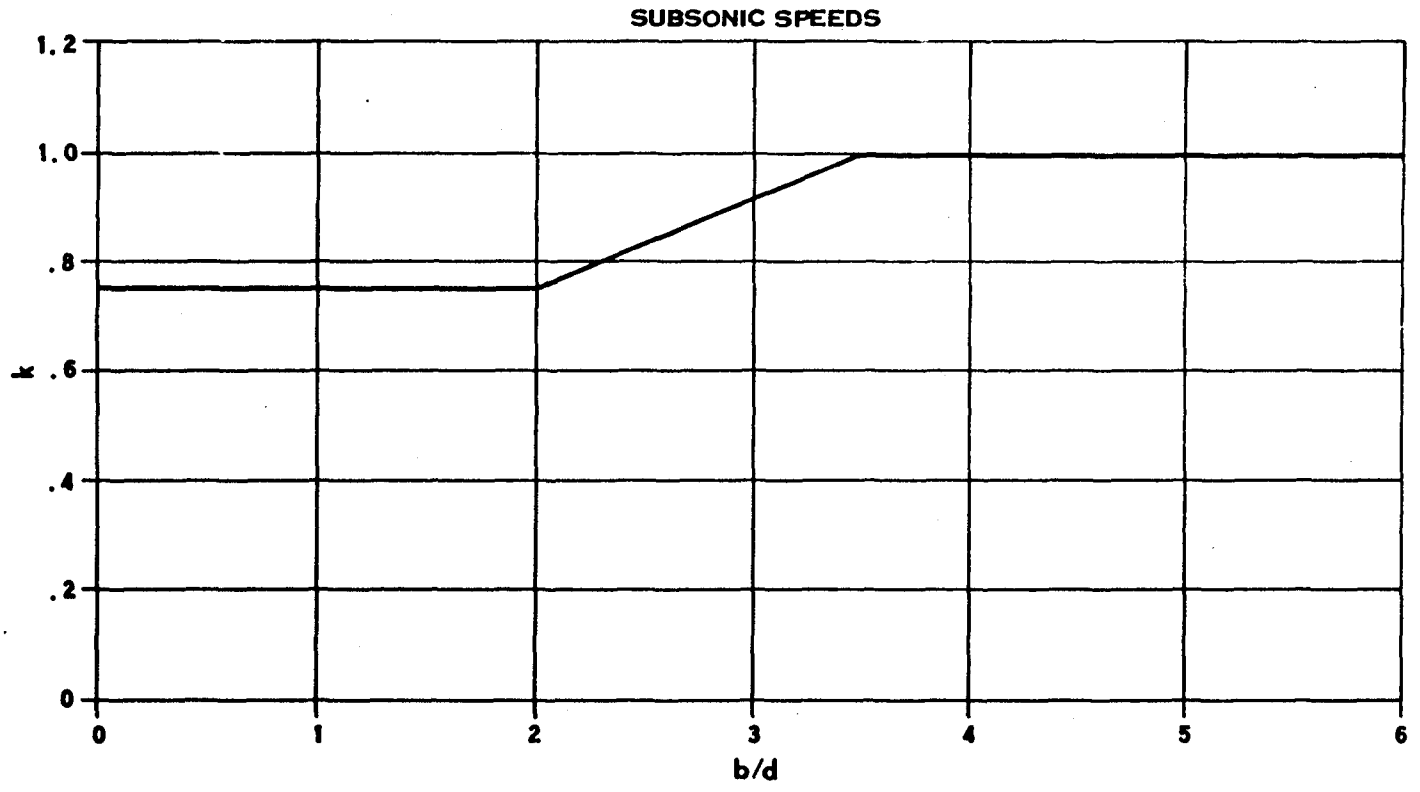

Figure 13-6. [redacted] Empirical Factor for Estimating C_{L_α} for Vertical Tails [redacted]

[redacted]

13-7 Gust Effects on In-Flight Aircraft [redacted]

[redacted] A nuclear explosion produces a blast wave that travels outward from the explosion, decaying in strength as it travels. The blast wave induces a flow velocity in the material (in this case, air), through which it passes. This material velocity, or gust, produces changes in the dynamic pressure and the angle of attack of an airplane that is intercepted by the blast wave. An increase in air density also is associated with the blast wave, and this increase in density also contributes to changing the dynamic pressure. The changes in angle of attack and dynamic pressure result in changes in the aerodynamic forces acting on the airplane. These changes in aerodynamic forces produce rigid-body and elastic motions of the airplane. In the sure-kill case, inelastic motions also are important. These motions produce additional aerodynamic forces. The aerodynamic forces and inertia forces may be summed to determine structural loads (such as bending moments) acting on the structure. Comparison of these structural loads with the allowable loads determines the safety of the airplane.

[redacted] Gust effects on helicopters must be considered in two categories; first, the effects on the main rotor blades, and second, the effects on major components other than the main rotor blades. The second category of effects is very similar to the gust effects on airplanes. The only difference lies in the introduction of rotors as lift-producing devices. Helicopters have fuselages, horizontal tails, vertical tails, and, in some cases, even wings. These components may be analyzed in substantially the same way that the corresponding airplane components are analyzed.

[redacted] The main rotor blades on the other hand, are unique to helicopters, and thus require special techniques. Three different types of blades must be considered: hinged, rigid (hingeless), and teetering. In the hinged version, a hinge somewhat offset from the center of rotation permits free rotation of the blade outboard of the hinge in an up-and-down, or flapping, direction. The rigid, or hingeless, blade does not use a flapping hinge. The teetering blade roughly combines the characteristics of the hinged and hingeless blades. A teetering blade is essentially a seesaw about a hinge at the center of rotation. The blades on each side of the hinge are rigidly connected.

[redacted] Problems 13-3 and 13-4 describe the calculation of intercept-time envelopes for sure-safe and sure-kill regions for airplanes and helicopters, respectively.

13-8 Gust Effects on Parked Aircraft [redacted]

[redacted] The material velocity and the increased density behind the blast wave give rise to a dynamic pressure that may be sufficiently high to impose large aerodynamic forces on a parked vehicle. For purposes of damage analysis, dynamic pressure effects are classified in two categories:

1. Direct damage to structural components that result from aerodynamic loading.
2. Gross aircraft motions that might produce indirect damage to structural components as a result of lifting the aircraft from the ground and the subsequent impact, or as a result of overturning the aircraft or crushing the landing gear.

[redacted] The possibility of lifting the aircraft exists whenever the vehicle is subjected to lift forces that are comparable to the vehicle weight, even if tie-downs are employed. An aircraft with a low wing loading (gross weight divided by the wing area, GW/S) is particularly susceptible to this type of damage since, in the parked position, the wing is set at a large angle of attack relative to the ground. Head-on encounter presents the most severe loading condition for this case.

[redacted]

[redacted]

[redacted] Skidding is possible whenever the drag, coupled with the lift, can overcome the frictional forces between the ground and the vehicle tires. With a large lift force, the normal force between ground and tire is reduced. The side force required to cause the vehicle to skid may thus be quite small compared with the weight of the vehicle. Vehicle orientations somewhere between head-on and side-on to the gust are expected to present the worst situation for this type of motion. No definitive criteria can be given for damage from skidding, because the damage criteria depend upon the distance of the aircraft from other objects.

[redacted] In some cases, the vehicle will overturn before skidding. Overturning will occur whenever the aerodynamic moments (about an axis joining appropriate wheel contact points) are of sufficient magnitude to overcome the stabilizing gravity moment and the frictional forces are sufficiently large to prevent skidding. A gust orientation somewhere between head-on and side-on is expected to provide the most severe condition. Other effects will almost always be predominant compared to overturning, and it is exceedingly difficult to devise a meaningful overturning solution that does not involve a substantial computer program.

[redacted] Negative lift results from tail-on encounters (blast approaching from the rear). The negative lift produces downward forces on the wheels, which, if sufficiently large, will damage the landing gear and perhaps the main supporting structure.

[redacted] Tie-downs would be expected to reduce the likelihood of lift-off, skidding, and overturning; however, tests have indicated that tie-downs are not very effective in reducing damage induced by motion when aircraft encounter high strength blast waves.

[redacted] Since helicopters do not have the large lifting surfaces that are present on airplanes, the problems of lift-off and crushing of the landing gear are much less severe for helicopters than for airplanes.

[redacted] Overpressure usually dictates the largest envelopes among all of the damage modes for parked aircraft. No calculation methodology is presented for gust effects on parked aircraft. The sure-safe and sure-kill overpressure envelopes may be accepted as the complete envelopes (see paragraph 13-9 and Problem 13-5).

[redacted]

[redacted]

Problem 13-3. Calculation of Intercept-Time Envelopes that Determine Sure-Safe and Sure-Kill Regions with Respect to Material Velocity on Airplanes in Flight

[redacted] The analysis of gust effects on airplanes in flight is based upon determining the load factor produced on the airplane during the blast encounter, accounting roughly for the fact that this load factor is dynamically applied, and comparing the resultant effective load factor with the critical load factor. For sure-safe conditions, the critical load factor is based upon design limit conditions. For sure-kill conditions, the critical load factor is based upon design ultimate conditions and a lethal ratio factor. The lethal ratio factor is determined from a simple representation of post-failure response by a single degree of freedom system.

[redacted] Standard shapes for the gust envelopes at intercept time are assumed applicable for all airplanes, weapon yields, and altitudes. Each point on the envelope shows the critical position of the airplane relative to the burst point at the time when the airplane is intercepted by the blast wave. The size of the envelopes is determined by evaluating the critical slant ranges, or distances from the burst point, associated with intercepts of the airplane from directly above, below and to the side.

[redacted] The three slant ranges R_a, R_b, and R_s that represent critical distances from above, below and to the side of the airplane, respectively, from which intercept-time envelopes are determined, must be calculated. The data required for the calculations include:

h = airplane altitude (ft),

W = weapon yield (kt),

GW = airplane gross weight at time of interest (lbs),

V = preblast airplane velocity (ft/sec),

n = airplane preblast load factor (for a level flight, $n = 1$) (dimensionless),

N^+ = up-loading airplane limit load factor corresponding to gross weight condition being considered (dimensionless),

N^- = down-loading airplane limit load factor corresponding to gross weight condition being considered (N^- should be used as a negative number) (dimensionless),

Wing planform (see Figure 13-1).

Calculation of the three slant ranges for sure-safe conditions is performed by the following series of steps.

1. Enter Table 13-1 with the airplane altitude, h, to obtain P, the ambient pressure (psi), ρ, the ambient density (slugs/ft^3), and c, the ambient speed of sound (ft/sec).

2. Calculate the Mach number, M:

$$M = \frac{V}{c}.$$

With M, and data defining wing planform, calculate the slope of the lift coefficient curve for the wing, C_{L_α}, using the method described in Problem 13-1.

3. Enter Figure 13-7 and select the curve corresponding to GW, airplane gross weight. Obtain the value of DF, the dynamic factor corresponding to the weapon yield, W.

4. To determine the slant range, R_a, for a burst from above

$$N = N^-,$$

where N is the critical load factor.

[redacted]

[redacted]

[redacted]

5. If

$$n < 0 \text{ and } N < 0,$$

or

$$n < 0 \text{ and } N > 0,$$

reverse the signs of both n and N. Otherwise, leave the signs as they were calculated. If

$$n < 0.01,$$

set

$$n = 0.01.$$

Thus, n will become positive in this step, regardless of its original sign.

6. Calculate $\Delta L/L$, ratio of the incremental lift due to blast to the preblast value of lift as follows:

$$\frac{\Delta L}{L} = \left[\frac{N}{n} - 1\right]\left[\frac{1}{(DF)}\right].$$

7. Calculate w/c, the ratio of the component of the airplane velocity normal to the wing (w) to the speed of sound:

$$\frac{w}{c} = \frac{2n\ (GW)}{\rho\ VSC_{L_\alpha}c},$$

where S is the airplane wing area, and the other symbols have been defined.

8. Calculate the product of $\Delta L/L$ and w/c.

9. Select the curve in Figure 13-8 corresponding to the value of w/c obtained in step 7. Enter the graph with the value of (w/c) $(\Delta L/L)$ obtained in step 8, and read the corresponding value of the range parameter $\bar{R}$. If N is positive, use Figure 13-8a. If N is negative, use Figure 13-8b.

10. Compute R_a, the range (ft), which defines the distance at which a nuclear explosion would produce critical effects, as follows:

$$R_a = \bar{R}\left[\frac{14.7\ W}{P}\right]^{1/3}.$$

11. Repeat steps 4 through 10 to calculate R_b. In step 4, set

$$N = N^+$$

for bursts from below, and replace R_a with R_b in the equation of step 10.

12. Set

$$N = N^+,$$

and $n = 1$ (corresponding to straight on level flight). Repeat steps 6 through 10 to calculate R_s (R_s replaces R_a in the equation of step 10). A burst from the side is taken to be equivalent to a burst from below with the airplane in straight and level flight.

13. The ranges R_a, R_b, and R_s define the size of the standard sure-safe envelopes as illustrated in Figure 13-9. R_a represents the diameter of a sphere above the airplane; R_b is the diameter of a sphere below; and R_s is the diameter of a sphere to the side of the airplane. The X-Y plane is the plane of symmetry of the airplane, with the preblast velocity vector pointing in the direction of the positive X-axis; the Y-axis points in the direction of the right wing; the Z-axis is directed upward, thus determining an orthogonal, left-handed system. The envelopes are symmetric with respect to the X-Z plane.

[redacted] Calculation of the slant ranges R_a, R_b, and R_s, that define the size of the standard envelopes at intercept time for sure-kill conditions is performed by the following series of steps.

1. Follow steps 1 through 3 in the calculation of the ranges for sure-safe conditions.

[redacted]

[redacted]

[redacted]

2. Enter Figure 13-10 and select the curve corresponding to GW, airplane gross weight. With weapon yield, W, obtain the value of LR, the lethal ratio.

3. To determine R_a, the slant range for burst from above, calculate N, the critical load factor:

$$N = (1.5)(N^-)(LR),$$

where the factor 1.5 is the usual factor between limit load and ultimate load. Follow steps 5 through 10 in the calculation for sure-safe conditions.

4. To determine R_b for burst from below, calculate N:

$$N = (1.5)(N^+)(LR),$$

and follow steps 5 through 10 in the calculation for sure-safe conditions.

5. To determine R_s, the slant range for burst from the side, calculate N:

$$N = (1.5)(N^+)(LR)$$

and let $n = 1$ since burst from the side is taken as burst from below corresponding to a straight and level flight. Repeat steps 6 through 10 in the calculation for sure-safe conditions.

6. Construct the sure-kill envelopes as described in step 13 in the calculation for sure-safe conditions.

[redacted]

DNA
(b)(1)

[redacted]

PAGE 13-32 DELETED

[redacted]

[redacted]

[redacted]

[redacted]

DNA
(b)(1)

The resulting intercept time envelopes are illustrated in Figure 13-9.

[redacted] *Reliability:* A typical airplane is used to represent each airplane class for purposes of defining a dynamic factor and a lethal ratio factor. The airplane is in a symmetric flight prior to blast intercept. This definition includes a straight and level flight. All degrees of freedom are ignored except for the two previously mentioned. The atmosphere is assumed homogeneous, having characteristics associated with the altitude at which the airplane is flying. The standard shapes for the gust envelopes at intercept time are assumed to be applicable for all airplanes, weapon yields, and altitudes. The maximum error in the calculation is estimated to be a factor of 2.

[redacted] *Related Material:* See paragraphs 13-1, 13-2, 13-6, and 13-7. See also Table 13-1.

[redacted]

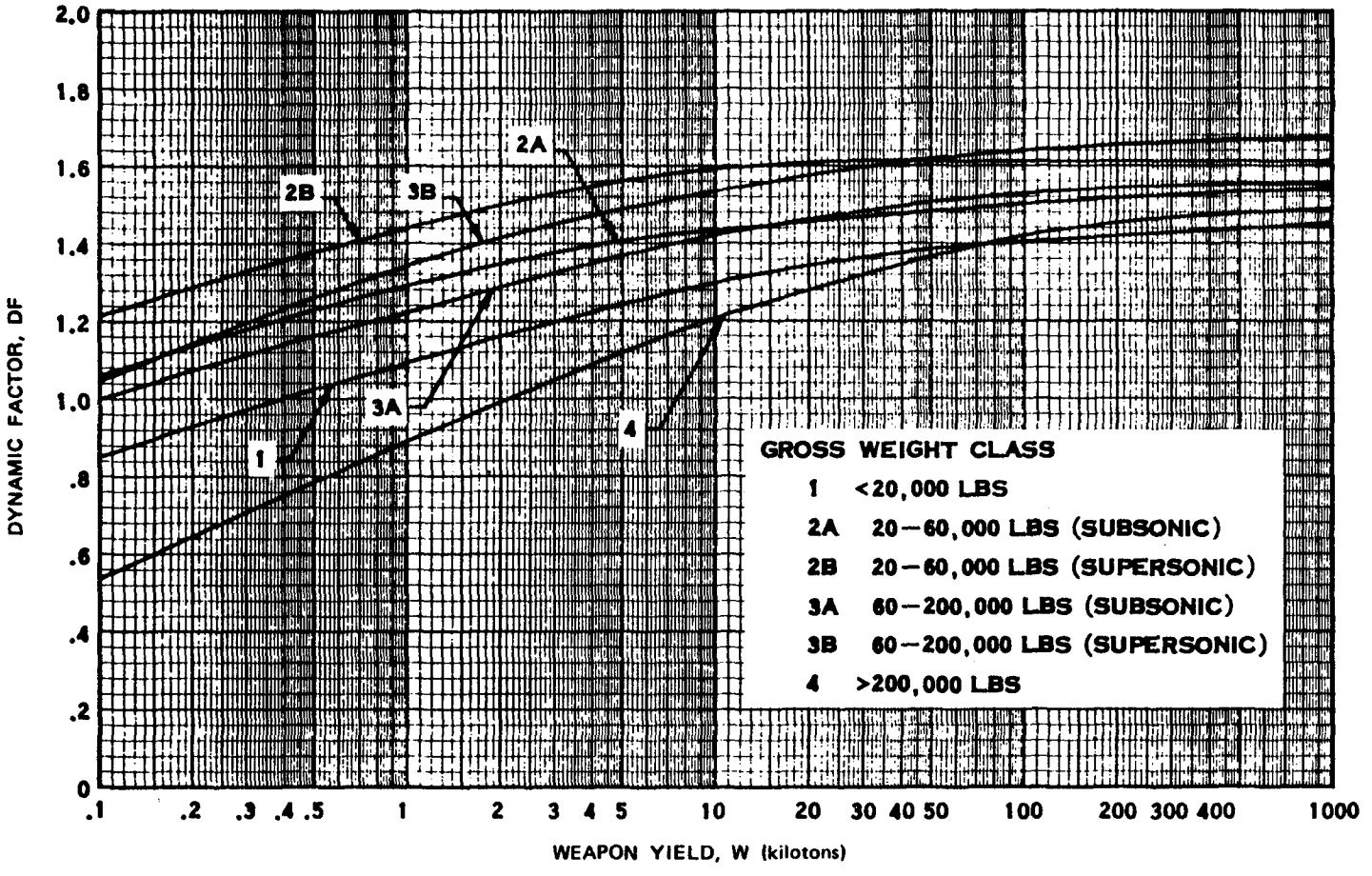

Figure 13-7. [redacted] Dynamic Factor vs Weapon Yield [redacted]

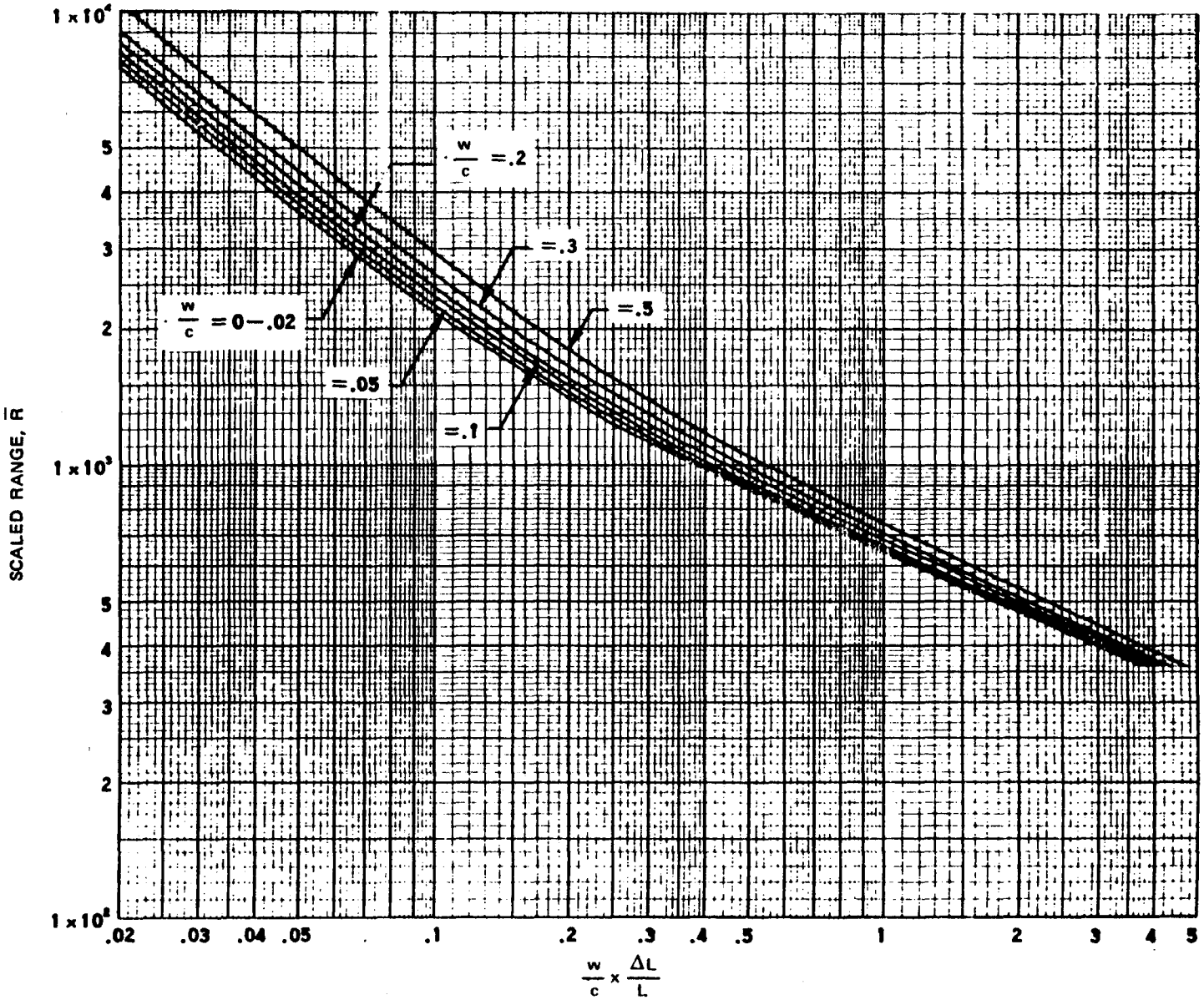

Figure 13-8a. [redacted] $\frac{w}{c} \times \frac{\Delta L}{L}$ as a Function of Scaled Range (N > 0) [redacted]

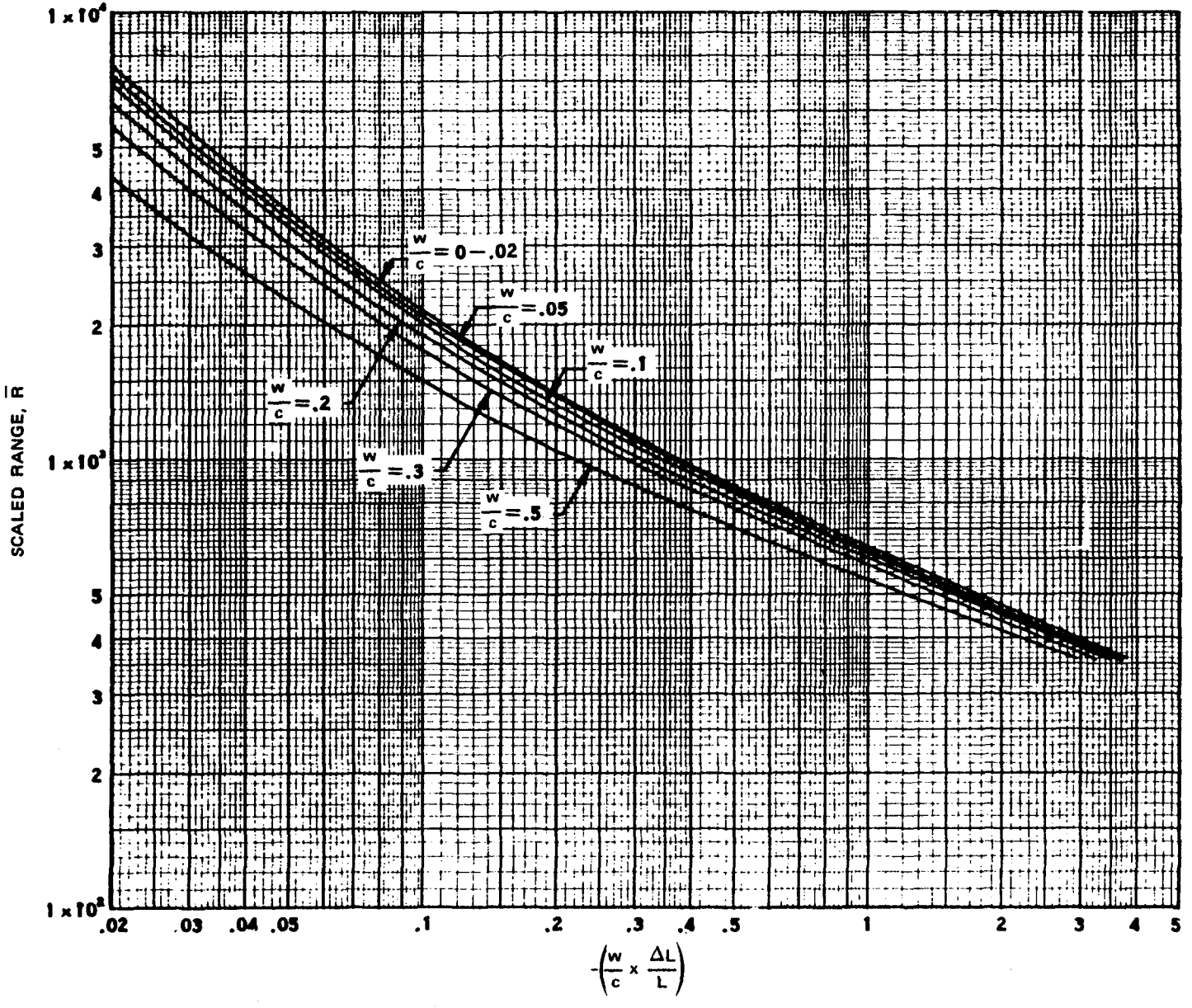

Figure 13-8b. $\frac{w}{c} \times \frac{\Delta L}{L}$ as a Function of Scale I Range (N < 0)

[redacted]

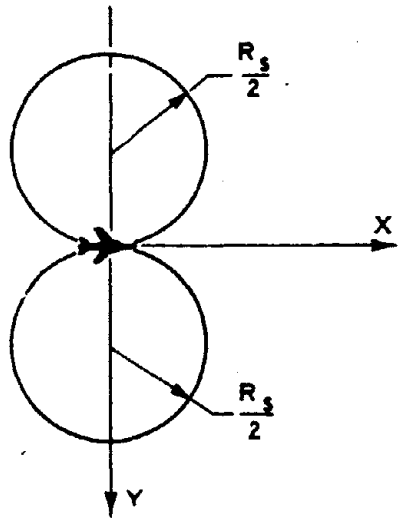

TOP VIEW (SECTION IN X–Y PLANE)

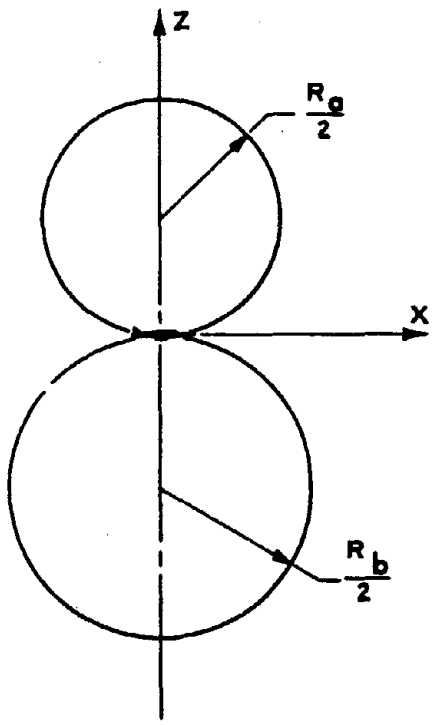

SIDE VIEW (SECTION IN X–Z PLANE)

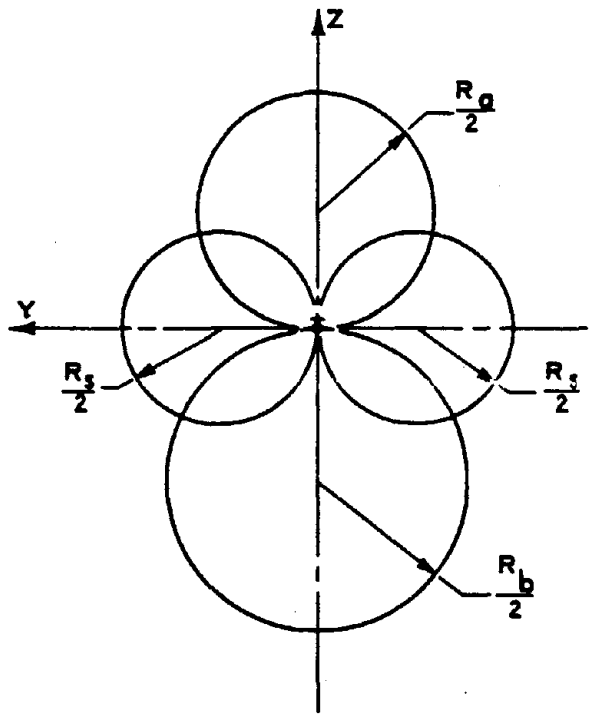

FRONT VIEW (SECTION IN Y–Z PLANE)

Figure 13-9. [redacted] Standard Shapes for Gust Envelopes at Intercept Time [redacted]

[redacted]

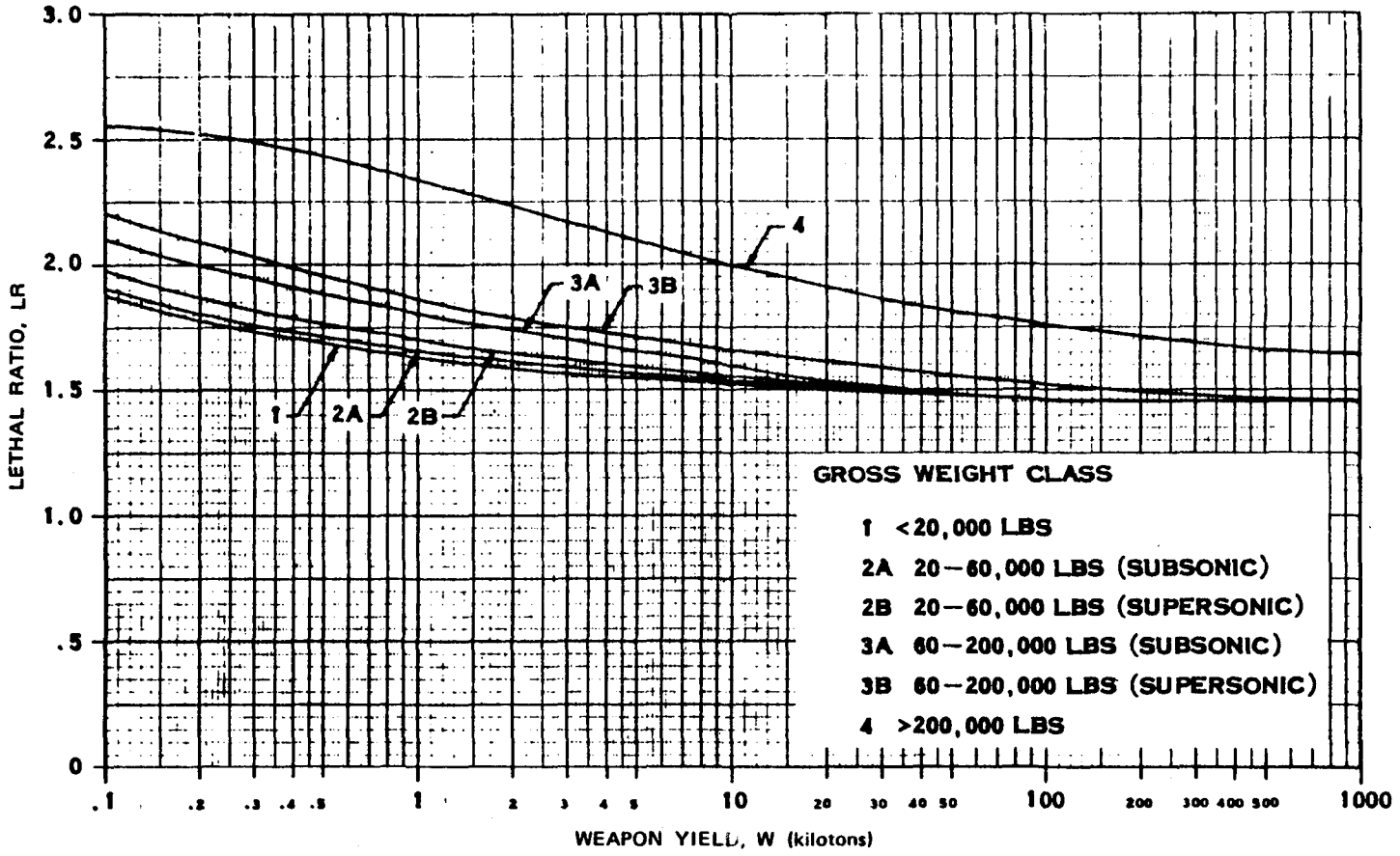

Figure 13-10. [redacted] Lethal Ratio vs Weapon Yield [redacted]

[redacted]

Problem 13-4. Calculation of Intercept-Time Envelopes Determining Sure-Safe and Sure-Kill Regions with Respect to Gust Effects of the Material Velocity Behind the Blast Wave on Helicopters in Flight

[redacted] The analysis of gust effects on helicopters is based upon determining the load factor produced during the blast encounter, accounting roughly the fact that this incremental load factor is dynamically applied, and comparing the resultant effective load factor with the critical load factor. For sure-safe conditions, the critical load factor is based upon design limit conditions. For sure-kill conditions, the critical load factor is based upon design ultimate conditions and a lethal ratio factor.

[redacted] Gust effects on helicopters must be considered in two categories: first, the effects on the main rotor blades (hinged, rigid and teetering); and second, the effects on major components other than the main rotor blades, which are very similar to the gust effects on airplanes.

[redacted] The constraints in the calculation are as follows:

- Representative values of helicopter parameters can be used in defining a dynamic factor and a lethal ratio factor. All other calculations involve the actual helicopter characteristics.
- The helicopter is in a symmetric maneuver prior to blast intercept. This definition includes straight and level forward or hovering flight.
- For a hinged blade, blade response to gust is not considered in this problem; the flapping of a teetering rotor is not considered in the calculation.
- The lift distribution along the blade is linear, starting at zero at the hub and fitted to the actual running lift at the 3/4 blade span position.
- Rigid-body motions of the helicopter are neglected, and the rotor tilt angle is ignored.
- Inflow resulting from the gust is considered to occur too late to influence the response. The effect of the preblast inflow on dynamic pressure is ignored.
- The preblast atmosphere is homogeneous, having characteristics associated with the altitude at which the helicopter is flying.
- Standard shapes for the gust envelopes at intercept time are applicable for all helicopters, weapon yields, and altitudes.

[redacted] The envelopes calculated in this problem are intercept-time envelopes. The size of the envelopes is determined by evaluating the critical slant ranges, or distances from the burst point, associated with intercepts of the helicopter from directly above, below and to the side.

[redacted] The three slant ranges R_a, R_b, and R_s representing the critical distances from above, below and to the side, respectively, are calculated first for sure-safe conditions in the following series of steps. The data that are required for the calculations include:

h = helicopter altitude (ft)

W = weapon yield (kt)

GW = helicopter gross weight at time of interest (lbs)

V = preblast helicopter velocity (ft/sec)

Ω_{MR} = main rotor angular velocity (rad/sec)

R_{MR} = main rotor blade radius (ft)

c_{MR} = main rotor blade chord (ft)

[redacted]

[redacted]

[redacted]

b_{MR} = number of blades in main rotor (dimensionless)

n = helicopter preblast load factor; for straight and level flight, $n = 1$ (dimensionless)

N^+ = up-loading helicopter limit load factor corresponding to gross weight condition being considered (dimensionless)

N^- = down-loading helicopter limit load factor corresponding to gross weight condition being considered. Note: N^- should be used as a negative number (dimensionless)

Wing planform (if helicopter has wings).

1. Determine the ambient atmospheric conditions at helicopter altitude h from Table 13-1; P, the ambient pressure (psi); ρ, the ambient density (slugs/ft^3); and c, ambient speed of sound (ft/sec).

2. If the helicopter has no wings, or if a helicopter having wings is hovering, i.e., $V = 0$, go to step 4. Otherwise, calculate the total wing area, S_W, which is defined as the extension of the leading and trailing edges of both wings to the helicopter centerline (ft^2).

3. Using the wing planform (Figure 13-2), with the Mach Number, M, equal to zero, calculate the slope of the lift coefficient curve for the wing, $C^W_{L\alpha}$, using the method described in Problem 13-1. Let $C^{MR}_{L\alpha} = 5.7$, where $C^{MR}_{L\alpha}$ is the lift curve slope for the main rotor.

4. Enter Figure 13-11 with the weapon yield, W, and obtain the corresponding value of DF, the dynamic coefficient.

5. To determine the slant range, R_a, for a burst from above

$$N = N^-,$$

where N is the critical load factor.

6. If

$$n < 0 \text{ and } N < 0,$$

or

$$n < 0 \text{ and } N > 0,$$

reverse the signs of both n and N. Otherwise, leave the signs as they were calculated. If

$$n < 0.01,$$

set

$$n = 0.01.$$

Thus, n will become positive in this step, regardless of its original sign.

7. Calculate $\Delta L/L$, the ratio of the incremental lift due to blast to the preblast value of lift as follows:

$$\frac{\Delta L}{L} = \left[\frac{N}{n} - 1\right]\left[\frac{1}{(DF)}\right].$$

8. Calculate the parameter η:

a. If the helicopter has wings,

$$\eta = \frac{2n\,(GW)}{\rho c\left[\frac{1}{2}C^{MR}_{L\alpha}\left(b_{MR}R_{MR}c_{MR}\right)\Omega_{MR}R_{MR} + C^W_{L\alpha}VS_W\right]}.$$

b. If the helicopter has no wings,

$$\eta = \frac{2nGW}{\rho c\left[\frac{1}{2}C^{MR}_{L\alpha}\left(b_{MR}R_{MR}c_{MR}\right)\Omega_{MR}R_{MR}\right]}$$

9. Obtain the product

$$\left[\frac{\Delta L}{L}\right]\eta.$$

10. Enter Figure 13-12a if $N > 0$ or 13-12b if $N < 0$, and select the curve corresponding to the value of η from step 8. With the value of

$$\left[\frac{\Delta L}{L}\right]\eta$$

from step 9, obtain the range parameter $\bar{R}$.

[redacted]

[redacted]

[redacted]

11. Compute R_a, the range (ft), which defines the distance at which a nuclear explosion would produce critical effects, as follows:

$$R_a = \bar{R} \left[\frac{14.7\ W}{P}\right]^{1/3}.$$

12. Repeat steps 5 through 11 to calculate R_b. In step 5, set

$$N = N^+$$

for bursts from below, and replace R_a with R_b in the equation of step 10.

13. Set

$$N = N^+,$$

and $n = 1$ (corresponding to straight on level flight). Repeat steps 7 through 11 to calculate R_s (R_s replaces R_a in the equation of step 10). A burst from the side is taken to be equivalent to a burst from below with the helicopter in straight and level flight.

14. The ranges R_a, R_b, and R_s define the size of the standard sure-safe envelopes as illustrated in Figure 13-13. R_a represents the diameter of a sphere above the helicopter; R_b is the diameter of a sphere below; and R_s is the diameter of a sphere to the side of the helicopter. The X-Y plane is the plane of symmetry of the helicopter with the preblast velocity vector pointing in the direction of the positive X-axis; the Y-axis points to the right side of the helicopter; the Z-axis is directed upward, thus determining an orthogonal, left-handed system. The envelopes are symmetric with respect to the X-Z plane.

(U) Calculation of the slant ranges R_a, R_b, and R_s, that define the size of the standard envelopes at intercept time for sure-kill conditions is performed by the following series of steps.

1. Follow steps 1 through 4 in the calculation of the ranges for sure-safe conditions.

2. Enter Figure 13-14 with weapon yield, W, and obtain the value of LR, the lethal ratio.

3. To determine R_a, the slant range for burst from above, calculate N, the critical load factor:

$$N = (1.5)(N^-)(LR),$$

where the factor 1.5 is the usual factor between limit load and ultimate load. Follow steps 6 through 11 in the calculation for sure-safe conditions.

4. To determine R_b for burst from below, calculate N:

$$N = (1.5)(N^+)(LR),$$

and follow steps 6 through 11 in the calculation for sure-safe conditions.

5. To determine R_s, the slant range for burst from the side, calculate N:

$$N = (1.5)(N^+)(LR)$$

and let $n = 1$ since burst from the side is taken as burst from below corresponding to a straight and level flight. Repeat steps 7 through 11 in the calculation for sure-safe conditions.

6. Construct the sure-kill envelopes as described in step 14 in the calculation for sure-safe conditions.

[redacted]

PAGES 13-42 THRU 13-43 DELETED

[redacted]

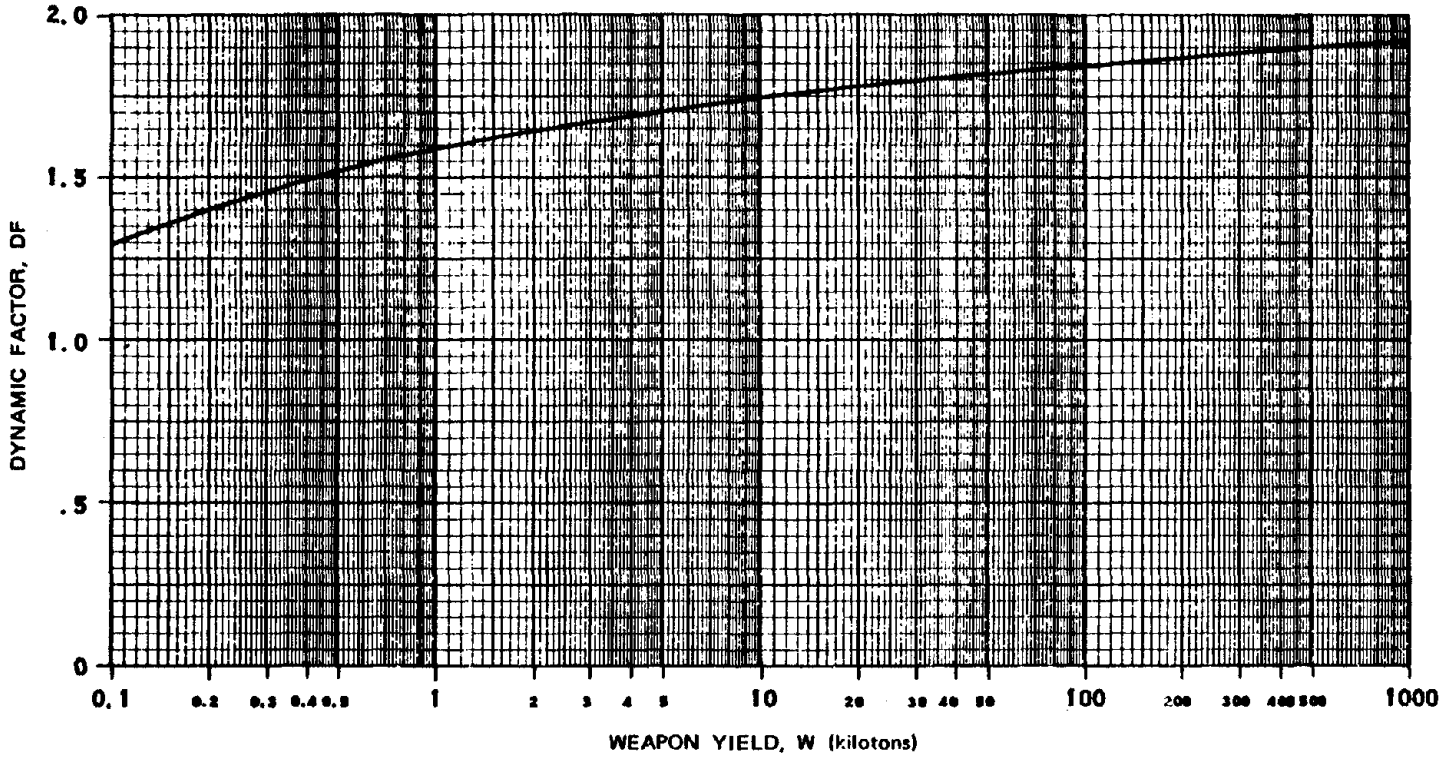

Figure 13-11. [redacted] Dynamic Factor vs Weapon Yield [redacted]

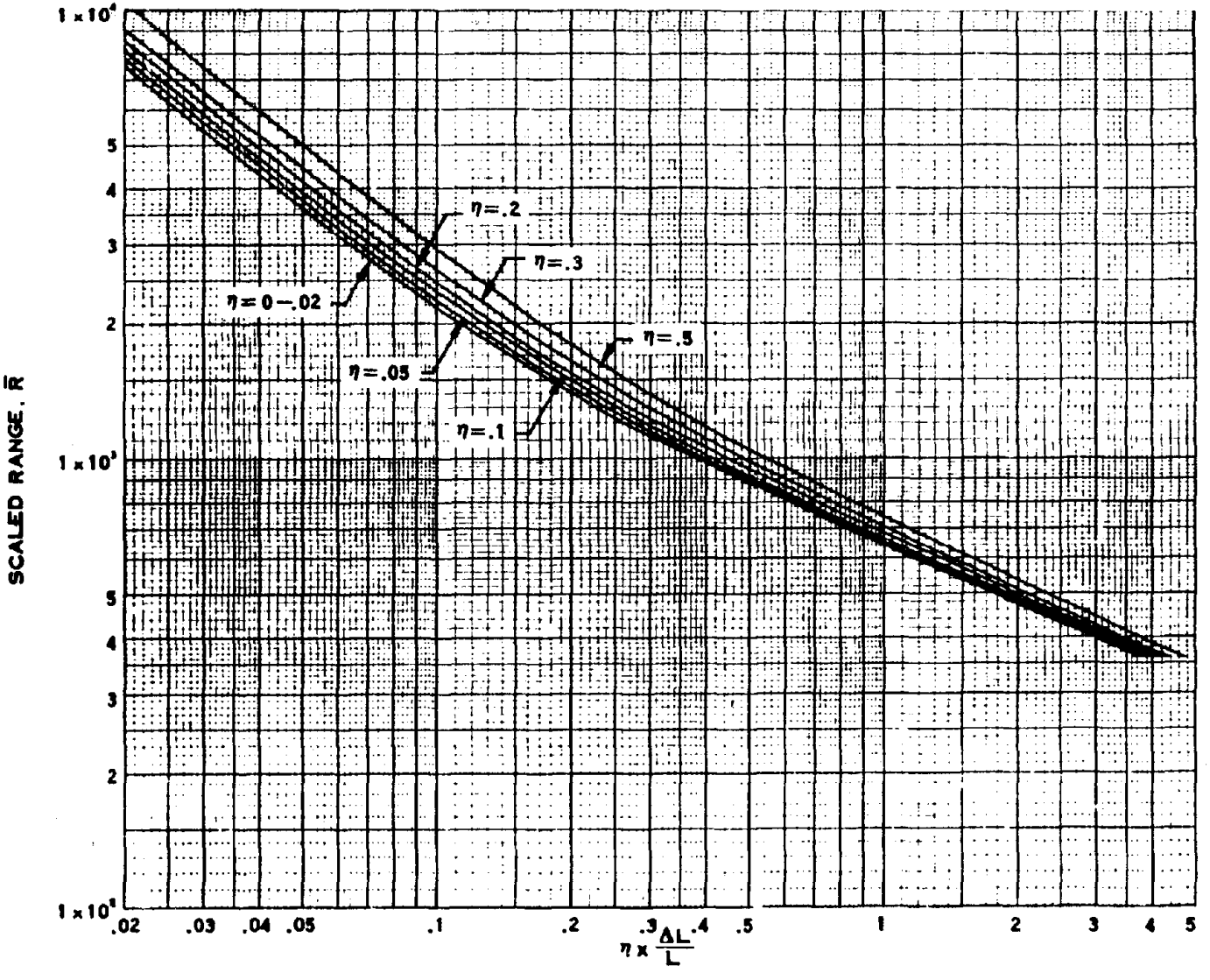

Figure 13-12a. $\eta \times \frac{\Delta L}{L}$ as a Function of Scaled Range (N > 0)

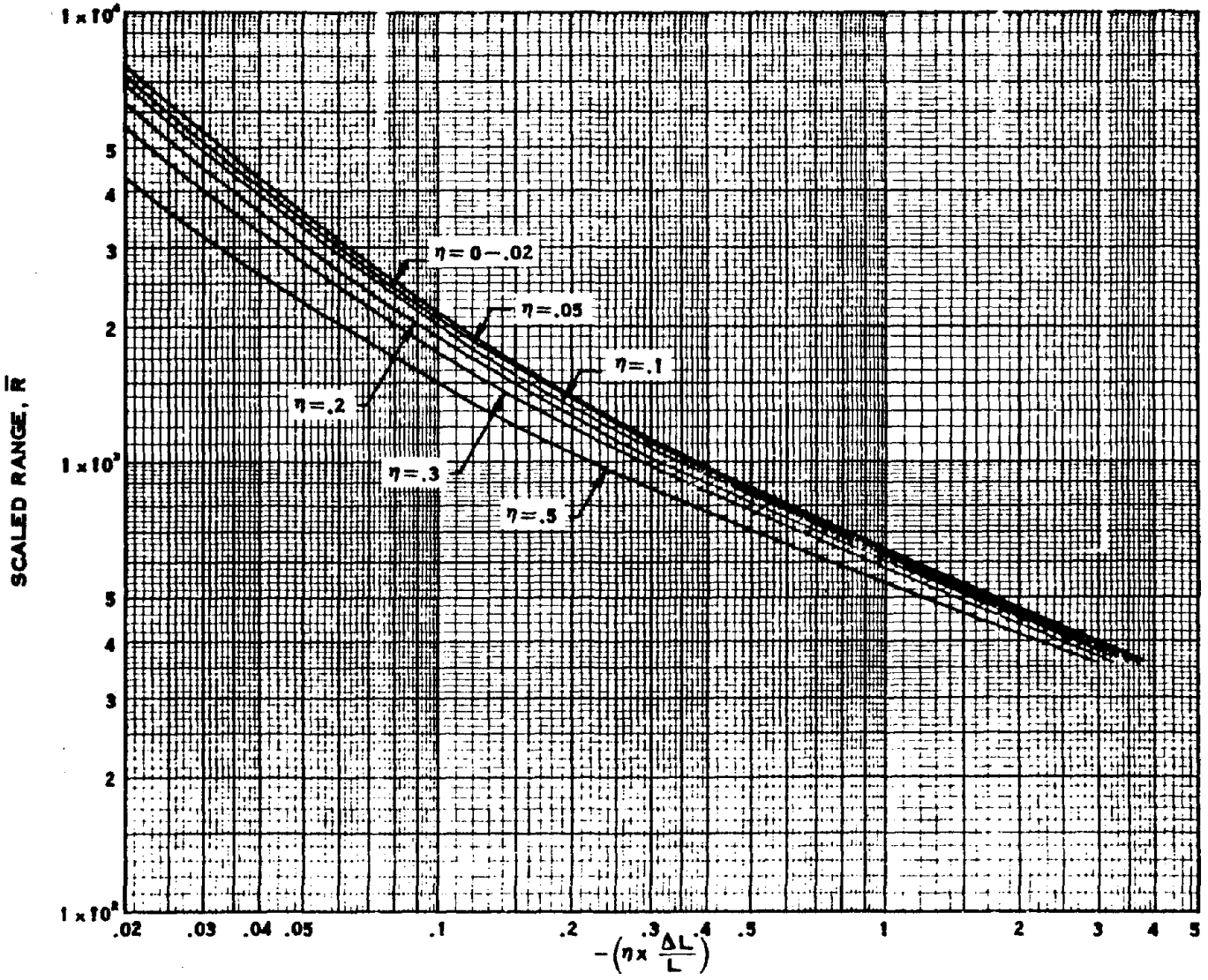

Figure 13-12b. [redacted] $\eta \times \frac{\Delta L}{L}$ as a Function of Scaled Range ($N < 0$) [redacted]

[redacted]

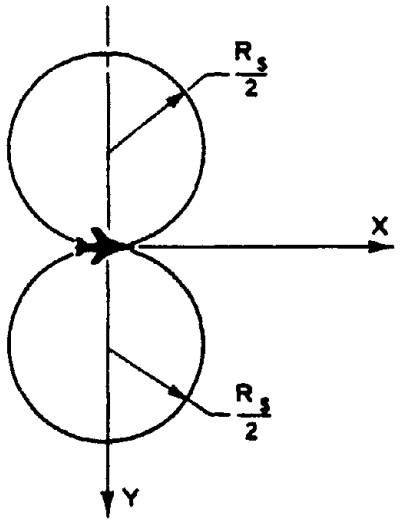

TOP VIEW (SECTION IN X–Y PLANE)

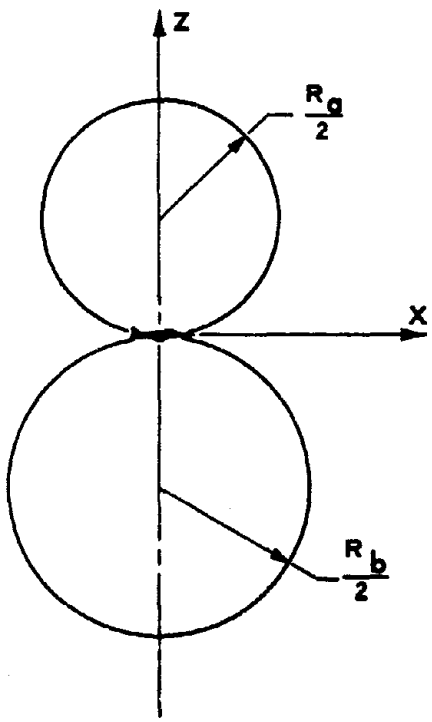

SIDE VIEW (SECTION IN X–Z PLANE)

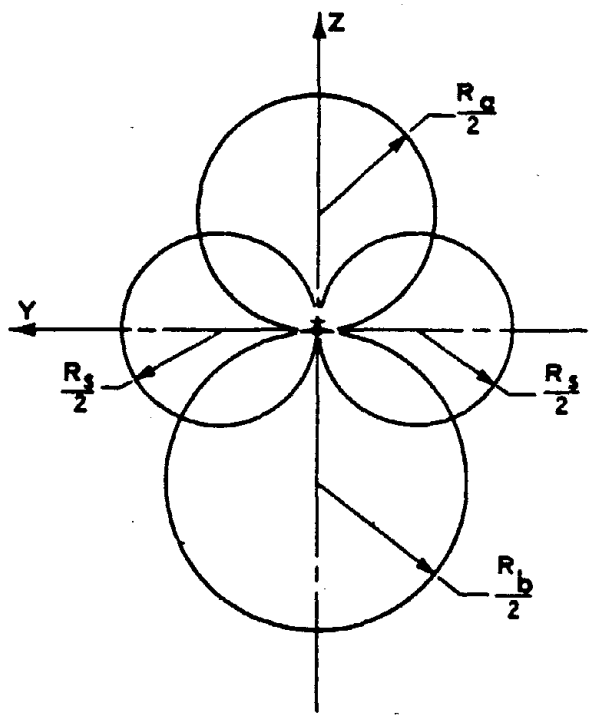

FRONT VIEW (SECTION IN Y–Z PLANE)

Figure 13-13. [redacted] Standard Shapes for Gust Envelopes at Intercept Time [redacted]

[redacted]

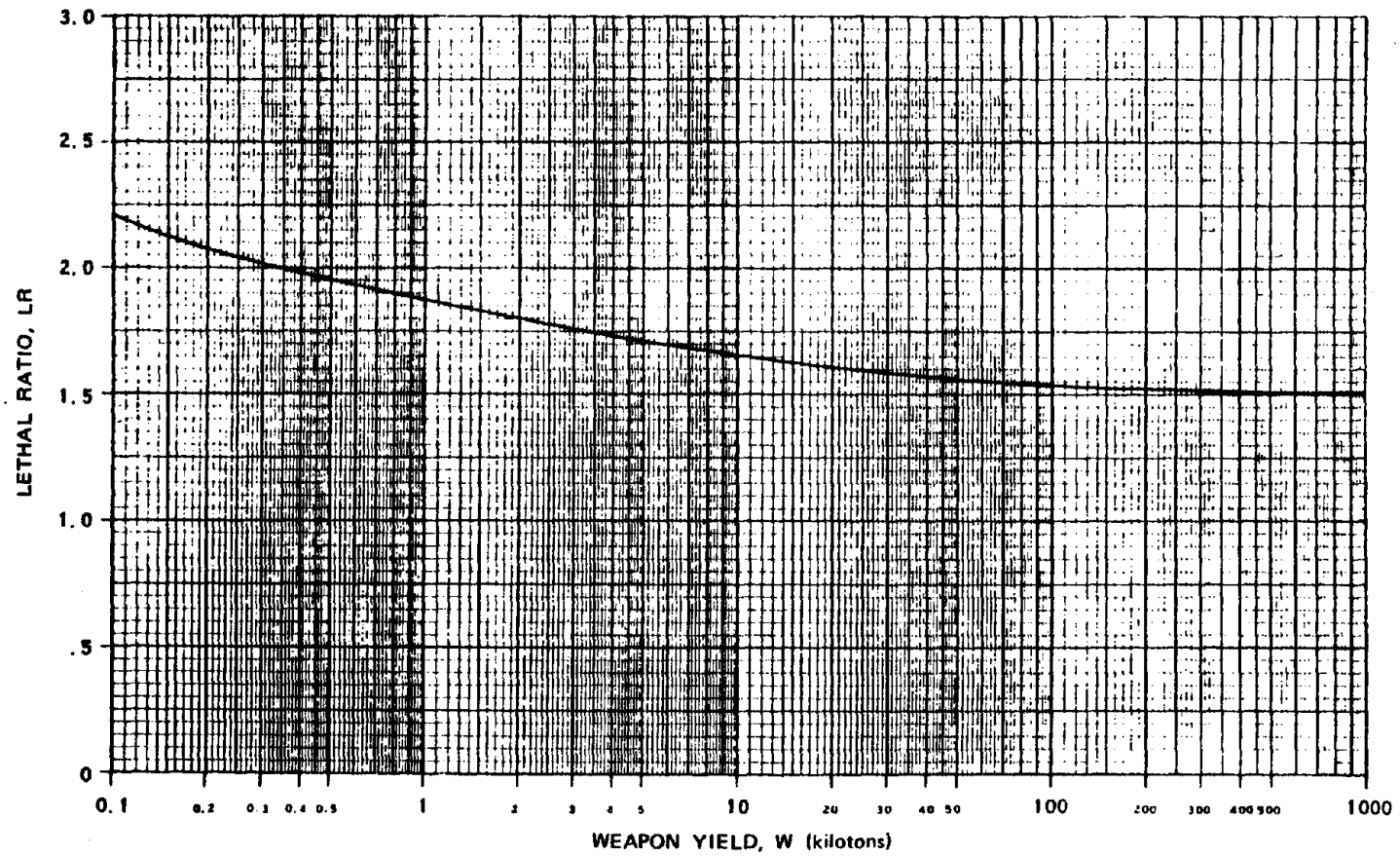

Figure 13-14. [redacted] Lethal Ratio vs Weapon Yield [redacted]

[redacted]

[redacted] AIRCRAFT RESPONSE TO OVERPRESSURE EFFECTS [redacted]

13-9 Overpressure Effects on In-Flight and Parked Aircraft [redacted]

[redacted] If an aircraft is located in the vicinity of the nuclear explosion, the expanding blast wave eventually engulfs the aircraft. Depending on the distance of the aircraft from the burst, the pressure rise, or overpressure, experienced by an aircraft can be of a sufficient magnitude to damage the structural components.

[redacted] An aircraft subjected to an overpressure loading can experience structural damage in several ways. Skin panels may yield or rupture; longerons, stringers, and frames may fail by compressive yielding or local buckling. The fuselage generally is the most susceptible to these types of damage; hence, *only the fuselage is examined for overpressure effects.* The method presented in this section for analyzing overpressure damage is applicable to all types of aircraft and helicopters both in-flight and parked. Methods for performing the analysis are given in Problem 13-5.

[redacted]

[redacted]

Problem 13-5. Calculation of the Boundaries in Space that Define the Sure-Safe and Sure-Kill Regions with Respect to the Effects of Overpressure Behind the Blast Wave on Aircraft In-Flight or Parked

[redacted] As discussed in paragraph 13-9, overpressure loading can produce structural damage in several ways; however, since the fuselage generally is the most susceptible item, only fuselage damage is considered in the following analysis. [redacted] The major constraints in the analysis are:

- Overpressure damage to an aircraft is the same for all aircraft in a given class.
- The preblast atmosphere is homogeneous, having characteristics associated with the aircraft altitude.

[redacted] The data required for the analysis are aircraft altitude (ft), weapon yield, and aircraft class. Table 13-2 lists various aircraft classes and corresponding overpressure limits for sure-safe and sure-kill conditions.

[redacted]

DNA (b)(1)

[redacted]

[redacted] The overpressure analysis is performed in a series of steps as described below.

1. Determine the ambient pressure P at the aircraft altitude, h, from Table 13-1.

2. Knowing the class of aircraft being considered, obtain the critical overpressure level, Δp, for either sure-safe or sure-kill conditions from Table 13-2.

3. Using the value of the critical overpressure, determine the corresponding value of sea level overpressure by the scaling law given in paragraph 2-14, i.e.,

$$\Delta p_o = \frac{P_o \Delta p}{P} = \frac{14.7\ \Delta p}{P},$$

where the subscript zero indicates sea level values of overpressure and ambient pressure, and the absence of a subscript indicates the corresponding values at altitude h.

4. Enter Figure 13-15* with Δp_o, and determine the corresponding slant range, R_1, from a 1 kt explosion in a sea level atmosphere.

5. Calculate the corresponding slant range, R, for a yield of W kt,

$$R = R_1 \left[\frac{14.7\ W}{P}\right]^{1/3}.$$

6. The critical volume is defined by a sphere of radius R centered on the aircraft. For in-flight aircraft, continue to step 7; for parked aircraft, go to step 8.

7. The volume defined in step 6 is an intercept-time volume; that is, each point on the surface shows the critical position of the aircraft relative to the burst point at the time when the aircraft is intercepted by the blast wave. Ordi-

*[redacted] Figure 13-15 is identical to Figure 2-2, Chapter 2. It is reproduced here for convenience of the user.

[redacted]

[redacted]

[redacted]

narily, burst-time volumes are desired for in-flight aircraft, rather than intercept-time volumes. A point on a burst-time volume defines the critical position of the aircraft relative to the burst point at the time of burst. Thus, a sure-kill burst-time volume shows the regions in space, relative to the airplane, in which the explosion of a given size nuclear weapon will result in the destruction of the aircraft. This is the information that ordinarily is desired. To obtain the burst-time volume, it is necessary to transform the intercept-time volume obtained in step 6 into a burst-time volume. This transformation is demonstrated in Problem 13-7. This concludes the analysis for in-flight aircraft.

8.* For parked aircraft only, the sphere found in step 6 (more properly, the hemisphere) must be modified for ground reflection effects. Enter Figure 13-16 with sea level overpressure determined in step 3, and read three horizontal range parameters, $\overline{HR}_i$ (i = 1, 2, 3).

9. Enter Figure 13-17 with $\overline{HR}_i$ and read three corresponding burst height parameters, $\overline{BH}_i$ (i = 1, 2, 3). (Note $\overline{BH}_1$ is always zero.)

10. Calculate the burst heights and horizontal ranges, in feet.

$$BH_i = \overline{BH}_i \left[\frac{14.7\ W}{P}\right]^{1/3}$$

$$HR_i = \overline{HR}_i \left[\frac{14.7\ W}{P}\right]^{1/3}.$$

11. Plot the burst height versus horizontal range, by connecting the three points determined in step 10. Draw a radial line from the origin to point 3. The volume defined by rotating this envelope about a vertical axis through the aircraft is the ground-effects volume, which is to be combined with the hemisphere already found. Ground reflection effects are seen to add a "collar" around the base of the hemisphere.

[redacted]

DNA (b)(1)

[redacted]

[redacted]

[redacted]

[redacted]

* [redacted] The envelope generated by following steps 8 through 11 could be obtained by using the air blast height of burst curves in Chapter 2; however, these steps (and the accompanying figures) present the information in a more convenient form that is suitable to the accuracy of this analysis.

[redacted]

[redacted]

DNA (b)(1)

Answer: The resulting envelope is shown in Figure 13-18.

[redacted] *Reliability:* Overpressure damage to an aircraft is assumed to be the same for all aircraft in a given class. The preblast atmosphere is assumed to be homogeneous, having characteristics associated with the aircraft altitude. The maximum error in the calculation is estimated to be a factor of 1.8.

[redacted] *Related Material:* See paragraph 13-9. See also Table 13-1, and paragraph 2-14, Chapter 2.

[redacted]

[redacted]

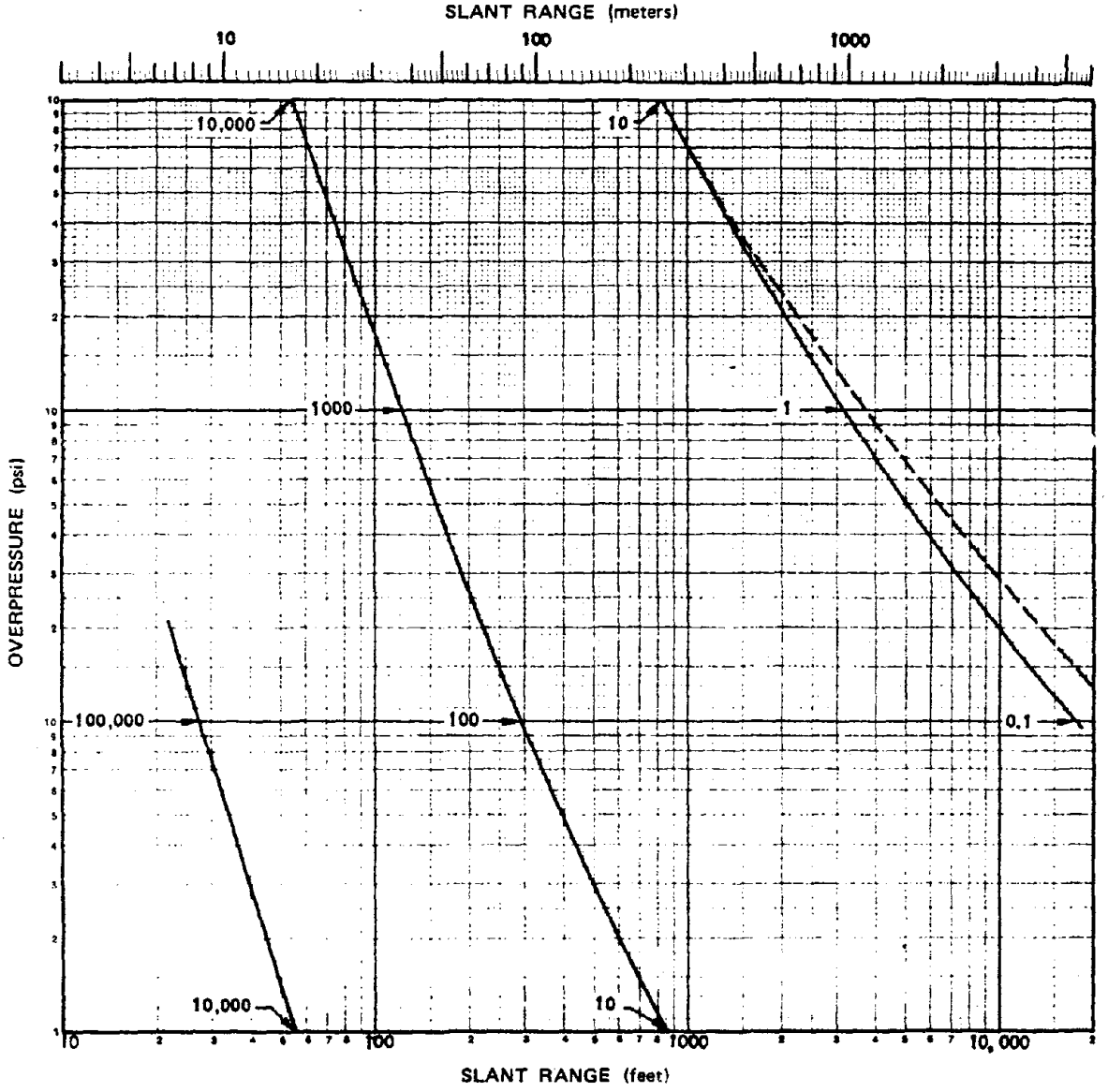

Figure 13-15. [redacted] Peak Overpressure from a 1 kt Free Air Burst in a Standard Sea Level Atmosphere [redacted]

[redacted]

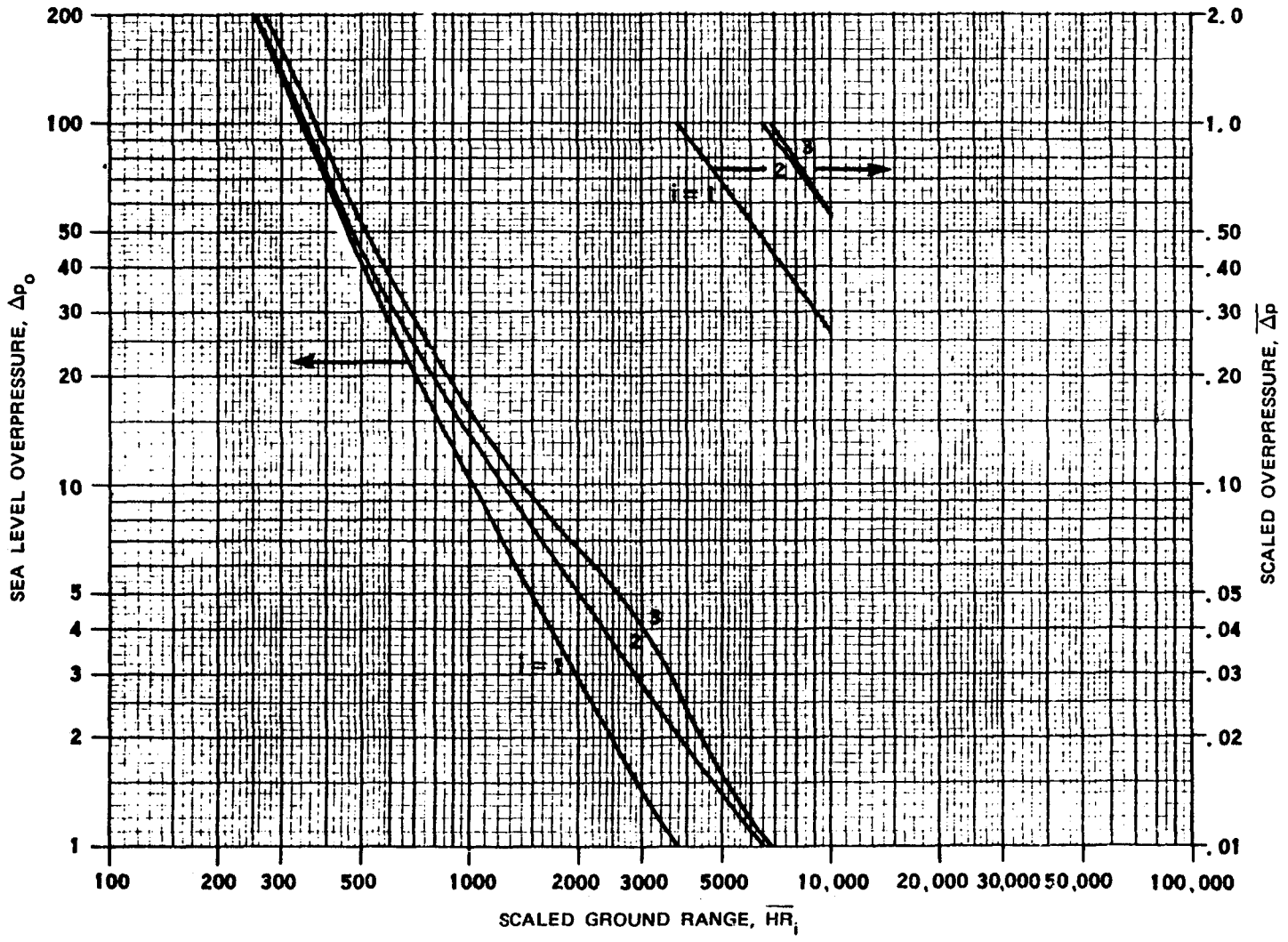

Figure 13-16. [redacted] The Range Parameter $\overline{HR}_i$ as a Function of Sea Level Overpressure [redacted]

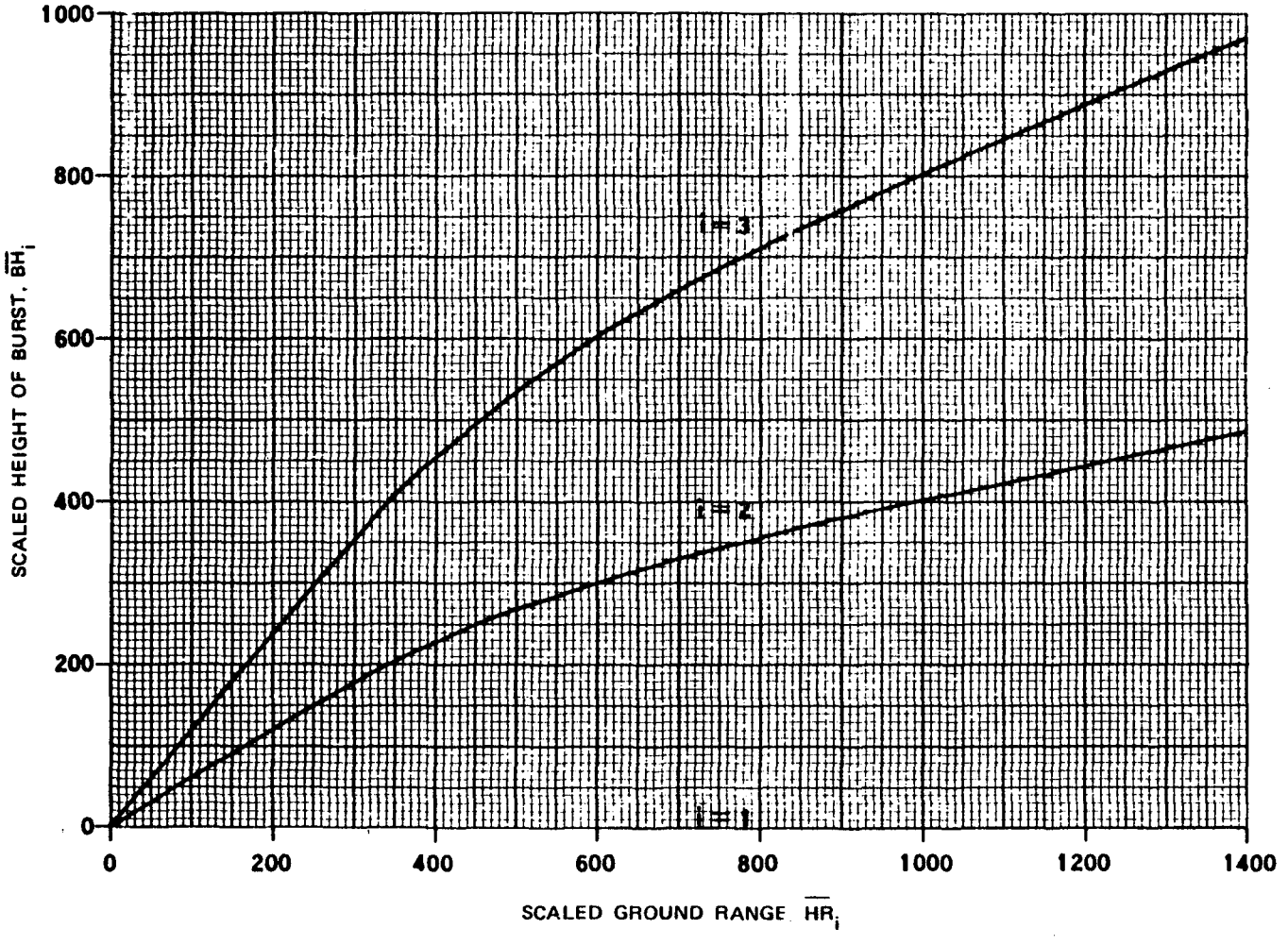

Figure 13-17a. [redacted] $\overline{BH}_i$ as a Function of $\overline{HF}_i$, Short Ranges [redacted]

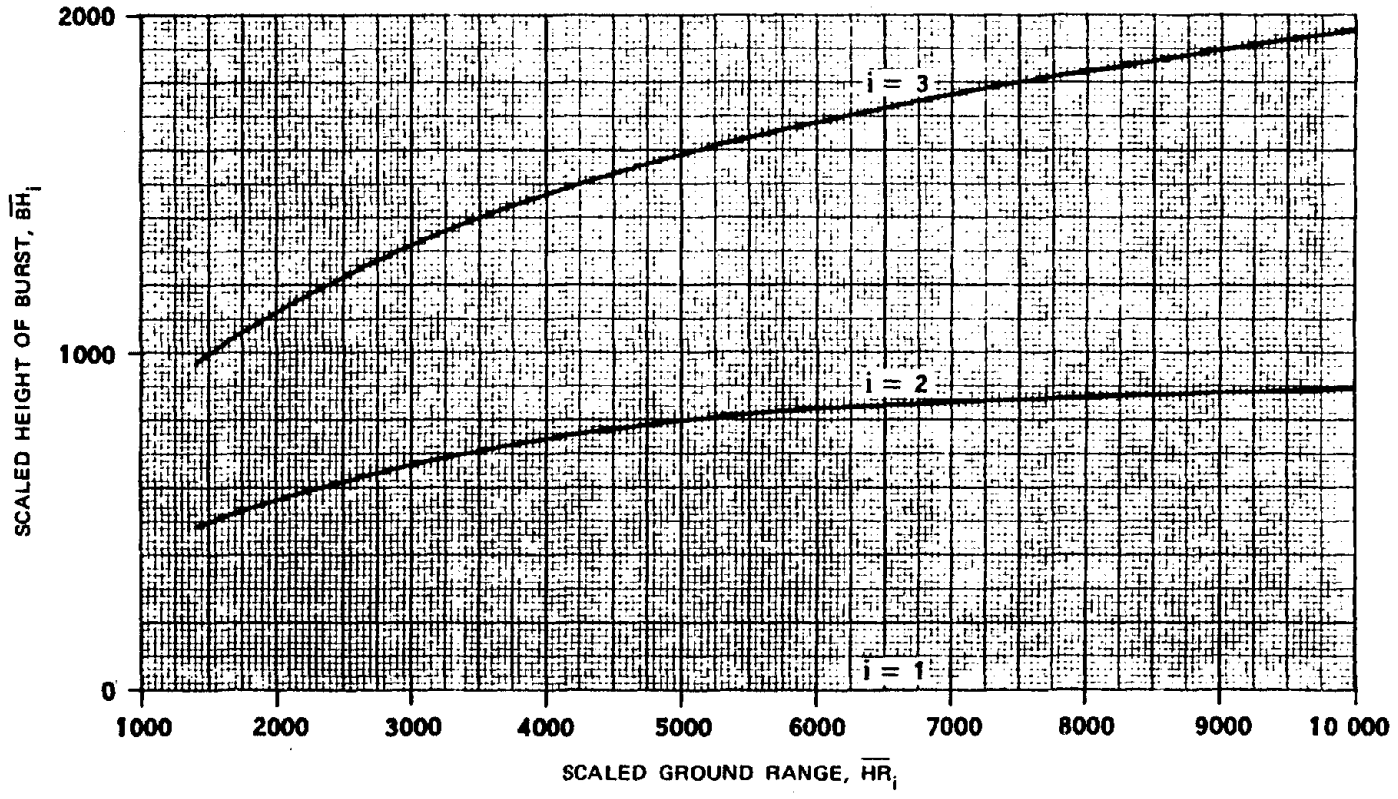

Figure 13-17b. [redacted] $\overline{BH}_i$ as a Function of $\overline{HR}_i$, Long Ranges [redacted]

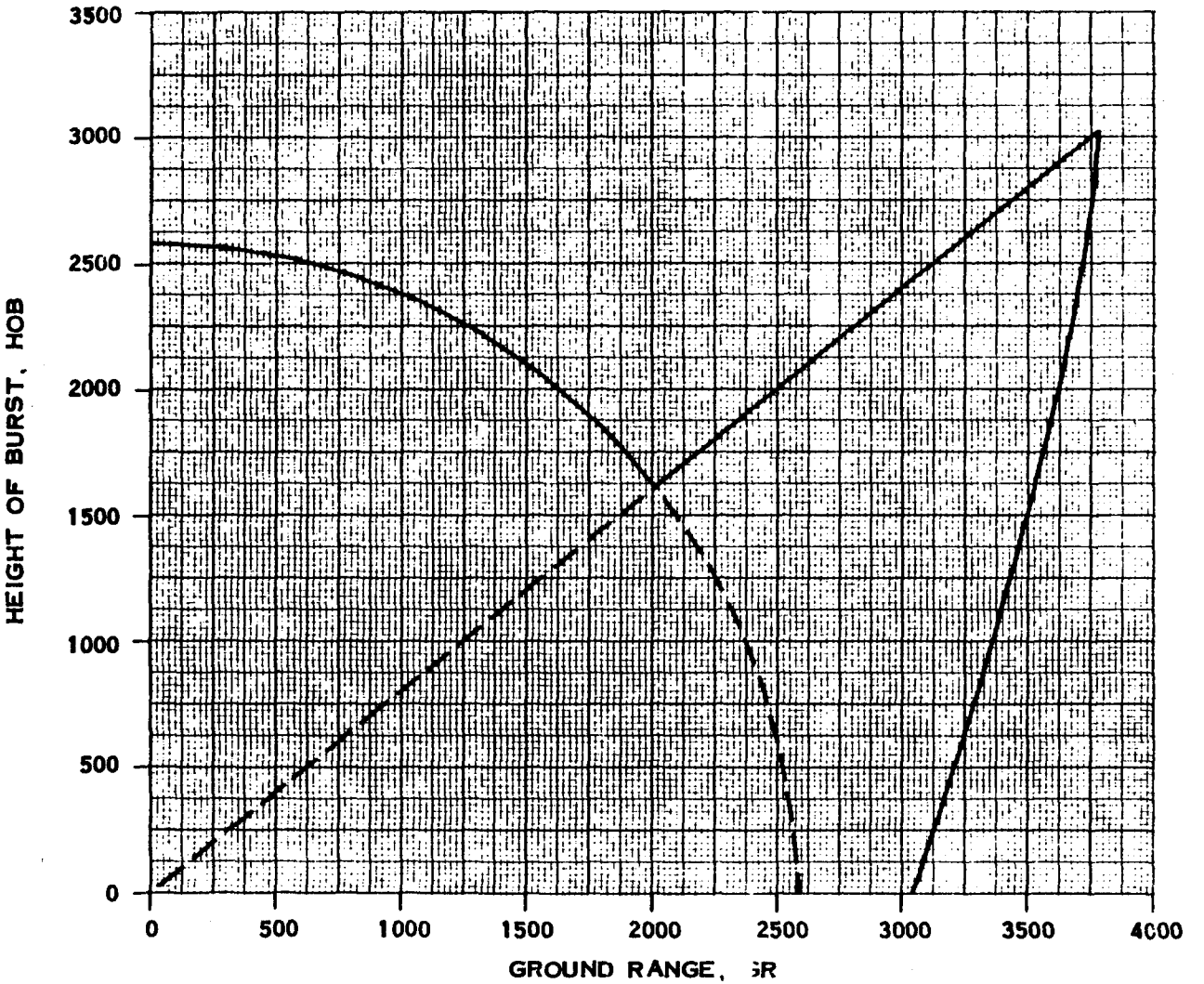

Figure 13-18. Overpressure Envelope for Parked Aircraft

[redacted]

[redacted] AIRCRAFT RESPONSE TO THERMAL RADIATION EFFECTS [redacted]

13-10 Thermal Effects on In-Flight and Parked Aircraft [redacted]

[redacted] The response of an aircraft to thermal energy is exhibited as a temperature rise in the aircraft skin. Several parameters influence the magnitude of the temperature rise. The most important parameters are skin thickness, skin material, surface condition, cooling effect of the air flowing over the outer surface of the aircraft, reradiation of thermal energy to the atmosphere, and conduction of the incident energy to the inner layers of the skin and substructure.

[redacted] Sure-safe conditions are based on an allowable temperature rise of the aircraft skin; however, melting of the skin is required for sure-kill. To produce kill, the temperature must increase to the melt temperature, and further heat must be applied to cause melting. The method for analysis of thermal effects on aircraft that is described in Problem 13-6 applies to both airplanes and helicopters.

[redacted]

[redacted]

Problem 13-6. Calculation of Boundaries in Space (Envelopes) that Define the Sure-Safe and Sure-Kill Regions with Respect to Thermal Radiation on Aircraft In-Flight or Parked

[redacted] The analysis is based on calculating the amount of heat required to produce some specified effect. For sure-safe, this effect is raising the temperature of a skin panel to a value which produces a 20 percent reduction in the modulus of elasticity. This criterion is applied to the thinnest structural skin on the fuselage. For sure-kill, the specified effect is melting of the thickest skin on the fuselage. The critical amount of heat, Q_c, which is the heat required to produce the specified effect is assumed to be equal to the thermal energy absorbed by the skin, Q_a. The critical heat, Q_c, is

$$Q_c = \rho_m C_p t \Delta T,$$

where ρ_m is the weight density of the material, C_p is the specific heat of the material, t is the skin thickness, and ΔT is the effective critical temperature rise.

(U) The constraints in the calculation are:

- The aircraft skin is thermally thin, i.e., the incident thermal energy heats the skin uniformly throughout its depth.
- The equilibrium temperature is based on an average set of conditions for turbulent flow.
- At the equilibrium temperature, all degradations of material properties from room temperature values are negligible.
- Cooling effects resulting from airflow over the aircraft are negligible.
- Reradiation is negligible.
- Aircraft motion is neglected.
- Attenuation of the thermal energy by the atmosphere is negligible.
- Reflected radiation from the ground is negligible.
- The fireball is a point source.

(U) Under the constraints

$$Q_a = \alpha Q,$$

where Q is the radiant exposure, i.e., the energy received per unit area (normal to the direction of propagation under the assumed constraints), and α is the absorptivity coefficient for the aircraft surface being considered.

(U) From Chapter 3,

$$Q = \frac{10^{12} Wf}{4\pi R^2} \text{ cal/cm}^2,$$

where

W = weapon yield (kt),

f = thermal partition of energy (dimensionless),

R = distance (cm),

Since 39 cal/cm^2 = 1 Btu/in.^{2}, and 929 cm^2 = 1 ft^2,

$$Q = \frac{10^{12} Wf}{4\pi R^2 (39)(929)} \text{ Btu/in.}^2$$

or

$$Q = \frac{2.19 \times 10^6 Wf}{R^2} \text{ Btu/in.}^2$$

where R is now expressed in feet. Since

[redacted]

[redacted]

[redacted]

$$Q_a = \alpha Q,$$

$$Q_a = \frac{2.19 \times 10^6 Wf\alpha}{R^2},$$

and

$$R = \left[\frac{2.19 \times 10^6 Wf\alpha}{Q_a}\right]^{1/2},$$

or

$$R = 1{,}480 \sqrt{\frac{Wf\alpha}{Q_a}},$$

which can be solved directly for the critical range R. If Q_c is taken to be equal to Q_a,

$$R = 1{,}480 \sqrt{\frac{Wf\alpha}{Q_c}}$$

$$= 1{,}480 \sqrt{\frac{Wf\alpha}{\rho_m C_p t \Delta T}}.$$

[redacted] The data required for solution include:

h = aircraft altitude (ft),

W = weapon yield (kt),

V = preblast aircraft velocity (ft/sec),

Detailed layout drawings of the fuselage, showing skin thickness,

Material of the skin, and

Surface condition of the skin.

[redacted] The analysis is performed in a series of steps.

1. Select the critical skin panels on the fuselage. Three panels should be selected, one each for bursts occurring directly below, directly above, and directly to the side of the aircraft. For each burst orientation, skin panels located in the following regions should be considered:

a. For a burst directly below the aircraft, the lower surface of the fuselage, within 45° of the normal to the bottom of the fuselage.

b. For a burst directly above the aircraft, the upper surface of the fuselage, within 45° of the normal to the top of the fuselage.

c. For a burst directly to the side of the aircraft, the side surface of the fuselage not covered by a and b above.

The selection of the critical skin panel from the locations defined above is based primarily on the thickness of the skin and depends upon whether sure-safe or sure-kill envelopes are sought.

- For sure-safe, select the *thinnest* structural skin. Nonstructural skin, such as access panels, should not be selected. If more than one material is used for the fuselage, investigate the thinnest skin for each material and base the envelopes on the *most* vulnerable.
- For sure-kill, select the *thickest* skin at a fuselage station near the forward end of the tail cone. If more than one material is used for the fuselage, investigate the thickest skin for each material and base the envelopes on the *least* vulnerable.

For a parked aircraft, skip steps 2 and 3 and proceed to step 4. For an in-flight aircraft, proceed to step 2.

2. Determine the ambient speed of sound c (ft/sec) at altitude h from Table 13-1.

3. Calculate the Mach Number,

$$M = \frac{V}{c}.$$

4. Determine the equilibrium temperature, T_e, of the skin.

a. For in-flight aircraft, enter Figure 13-19 with the Mach number, M, and the altitude, h, and read T_e.

b. For parked aircraft, use T_e = 60°F.

[redacted]

[redacted]

[redacted]

5. Determine the material properties for each of the skin panels selected from Table 13-3.

T_c = critical temperature (°F)

C_p = specific heat (Btu/lb°F)

ρ_m = weight density (lb/in.^{3})

For sure-kill only, determine

H = heat of fusion (Btu/lb)

6. Calculate the effective critical temperature rise, ΔT:

a. For sure-safe,

$$\Delta T = T_c - T_e.$$

b. For sure-kill,

$$\Delta T = T_c - T_e + \frac{H}{C_p}.$$

7. Determine the effective absorptivity coefficient, α, from Table 13-4.

8. Determine f from Figure 13-20*, and calculate the critical range in feet,

$$R = 1{,}480 \sqrt{\frac{Wf\alpha}{\rho_m C_p t \Delta T}}.$$

When steps 5 through 8 have been completed for a burst directly below the aircraft, they should be repeated for bursts directly above and directly to the side of the aircraft. Three ranges will have been determined, R_b, R_a, and R_s, where subscripts *"b," "a,"* and *"s"* designate below, above, and side, respectively. Note that, if the critical skin panels for R_a and R_s are of the same material and have the same surface conditions as the skin panel analyzed for R_b, only step 8 need be repeated, introducing the proper value of skin thickness, t.

9. Calculate the average of the three ranges, R_b, R_a, and R_s,

$$R_{av} = \frac{1}{3}\left(R_b + R_a + R_s\right).$$

10. The critical volume is defined by a sphere of radius R_{av} centered on the aircraft.

[redacted]

DNA (4)(1)

[redacted]

* [redacted] Note that Figure 13-20 is identical to Figure 3-1. It is reproduced here for convenience.

[redacted]

[redacted]

[redacted] *Reliability:* The constraints on this analysis are described in the introductory paragraphs of this problem. The maximum error is between a factor of 1.5 and 3.

[redacted] *Related Material:* See paragraphs 13-1, 13-4, and 13-10. See also Table 13-1.

Table 13-3. [redacted] Average Properties of Selected Engineering Materials [redacted]

Material	Critical Temperature, T_c (°F)		Specific Heat, C_p (Btu/lb°F)		Weight Density ρ_m (lb/in.^{3})	H (Btu/lb)
	Sure-Safe	Sure-Kill	Sure-Safe	Sure-Kill		
Steel	800	2,550	0.13	0.15	0.28	117
Inconel X	1,000	2,550	0.12	0.13	0.30	117
Aluminum	480	1,076	0.22	0.24	0.10	170
Magnesium	200	1,120	0.25	0.26	0.064	160
Titanium	500	2,850	0.13	0.24	0.17	187

[redacted]

[redacted]

Table 13-4. [redacted] Average Values of Absorptivities, α [redacted]

	Sure-Safe	Sure-Kill
Polished Metals	0.25	0.50
Unpolished metals	0.45	0.55
Painted metals		
Paint color		
White	0.30	0.50
Yellow	0.40	0.55
Olive	0.70	0.60
Black	0.90	0.65

[redacted]

[redacted]

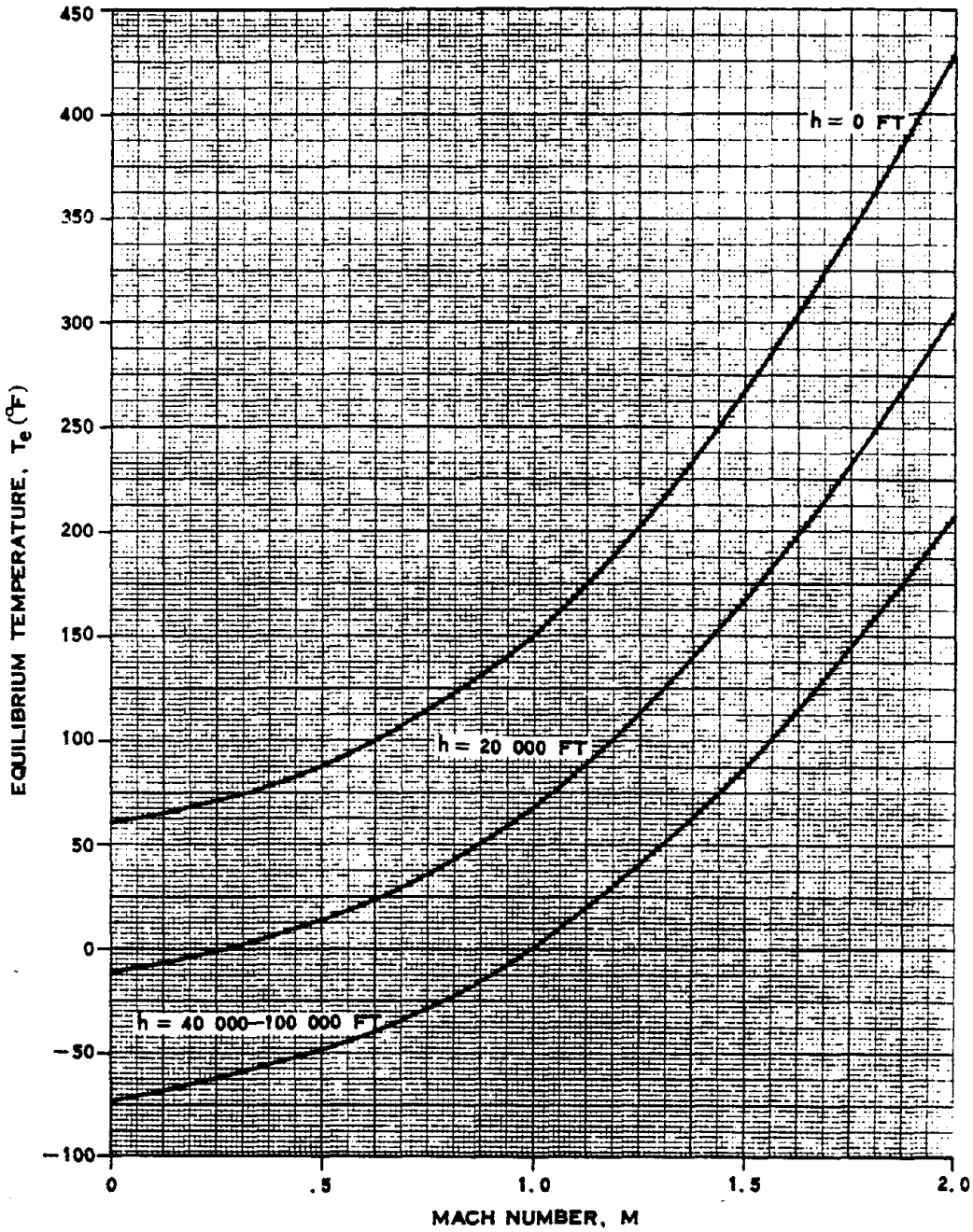

Figure 13-19. [redacted] Equilibrium Temperature as a Function of Mach Number [redacted]

PAGE 13-66 DELETED

[redacted]

[redacted]

[redacted] BURST-TIME ENVELOPES [redacted]

13-11 Requirement for Burst-Time Envelopes [redacted]

[redacted] The envelopes that are obtained by the methods described in Problems 13-3 through 13-6 define the locus of the center of burst relative to the *position of the aircraft at intercept,* for a specified criterion. It usually is preferable to define the corresponding envelope relative to the *position of the aircraft at burst time.* For parked aircraft and for those envelopes corresponding to thermal radiation, which reaches the aircraft almost instantaneously, the two envelopes are the same, i.e., the methodology presented in Problem 13-5 for overpressure effects on parked aircraft and that presented in Problem 13-6 for thermal effects on in-flight or parked aircraft apply equally well to intercept-time and to burst-time envelopes. When considering the response of in-flight aircraft to gust or overpressure, however, the relative positions of the aircraft and the burst center are different at the time of burst than at the time of intercept as a result of the distance traveled by the aircraft during the finite time required for the blast wave to propagate to the intercept point. Methods for transforming the intercept-time envelopes obtained by the methods described in Problems 13-3 through 13-5 for in-flight aircraft into burst-time envelopes for the same aircraft are described in Problem 13-7.

[redacted]

[redacted]

Problem 13-7. Calculation of Burst-Time Envelopes for Gust or Overpressure Effects from Intercept-Time Envelopes

[redacted] As discussed in paragraph 13-1, the assumption must be made that the aircraft is following an unaltered flight path when transforming intercept-time envelopes into burst-time envelopes. This assumption is necessary, since it would be impossible to guess the course changes. The assumption is valid for low yield weapons because of the small distances and times between burst and intercept. In the case of high yield weapons, the blast wave arrival time may be of the order of seconds, and the pilot may have time to change his course, so, for these weapons, the assumption must be considered as a source of error.

[redacted] Two major assumptions, arising from the limitations discussed above, are included in the simplified calculation method described below.

- The aircraft is represented by a point mass traveling at a constant velocity.
- The aircraft is performing a constant symmetric maneuver. As a result of this assumption, the flight path of the aircraft is circular (or straight, for the special case of no maneuver).

[redacted] Two left-handed, body-centered coordinate systems employed in the analysis are shown in Figure 13-21.

- The intercept reference frame (X_I, Y_I, Z_I), the origin of which is located at the aircraft's center of mass at intercept, with the X_I axis collinear with the velocity vector, positive forward, and the Z_I axis in the aircraft plane of symmetry, positive upward.
- The burst reference frame (X_B, Y_B, Z_B), the origin of which is located at the aircraft's center of mass at burst time, with the X_B axis collinear with the velocity vector, positive forward, and the Z_B axis in the aircraft plane of symmetry, positive upward.

[redacted] The X_I - Z_I and X_B - Z_B planes coincide, hence the Y_I and Y_B coordinates of any point are the same.

[redacted] If the center of burst has coordinates (X_I, Y_I, Z_I) in the intercept frame, its position in the burst frame is given by the coordinates (X_B, Y_B, Z_B), where

$$X_B = X_I \cos \Phi + (r - Z_I) \sin \Phi$$

$$Y_B = Y_I,$$

$$Z_B = X_I \sin \Phi - (r - Z_I) \cos \Phi + r,$$

and

r = radius of turn,

Φ = angular change in flight path between burst and intercept times.

The parameters r and Φ are obtained from the relations

$$r = \frac{V^2}{Ng},$$

$$\dot{\Phi} = \frac{V}{r},$$

where

V = preblast aircraft velocity,

N = maneuver normal load factor,

g = acceleration of gravity,

and a dot indicates differentiation with respect to time. It should be noted that N is the *maneuver* normal load, and not the load factor, n, used to calculate the intercept envelopes. N is related to the load factor n by

$$N = n - 1.$$

[redacted]

[redacted]

[redacted]

If the equation for $\dot{\Phi}$ is integrated from burst time to intercept time, the result is,

$$\Phi = \frac{Vt_a}{r}$$

where

t_a = time of arrival of the blast wave at the intercept point; i.e., the time required for the blast front to propagate to the intercept point.

For the special case when the aircraft is not performing a maneuver ($N = 0$), the equations for the position of the burst point in the burst frame simplify to

$$X_B = X_I + Vt_a$$

$$Y_B = Y_I$$

$$Z_B = Z_I.$$

By means of the above equations, the burst frame coordinates (X_B, Y_B, Z_B) may be found for any point on an intercept-time envelope (X_I, Y_I, Z_I). Unfortunately, a general planar burst-time envelope cannot be obtained by merely transforming an intercept envelope point by point. For maneuvering aircraft, only those envelopes in the X_I - Z_I plane (side view) or parallel to the X_I - Z_I plane, may be resolved directly into corresponding planar envelopes in the X_B - Z_B plane or parallel to it. All other intercept-time envelopes will transform into three-dimensional surfaces in the burst frame. In the case of no maneuver, any intercept-time envelope parallel to the X_I axis may be resolved directly into a burst-time envelope in the same plane. This includes envelopes in both the X_I - Z_I plane (side view), and the X_I - Y_I plane (top view). However, in neither case can the Y_B - Z_B plane (front view) envelope be obtained directly. In order to find the burst envelopes for side, front, and top views (or in any arbitrary plane), it is necessary to adopt an indirect procedure. Since the intercept-time envelopes define a volume in space, this entire volume may be transformed into an equivalent volume in the burst frame. The burst-time envelopes then may be determined as the intersection of this volume with the planes in which burst-time envelopes are desired.

[redacted] The most convenient way of performing this volume transformation is to take "slices" through the intercept-time volume parallel to the X_I - Z_I plane, for selected values of Y_I. Each of these slices may be resolved directly into a slice of the burst-time volume in a plane corresponding to the same value of Y_B. Definition of the burst-time envelopes in several Y_B planes is equivalent to defining the burst-time volume.

[redacted] The data required to perform the analysis include:

V = preblast aircraft velocity (ft/sec)

h = aircraft altitude (ft)

W = weapon yield (kt)

n = aircraft preblast load factor; for straight and level flight, $n = 1$ (dimensionless)

X_I, Y_I, Z_I = coordinates of points on intercept-time envelopes, as defined in Figure 13-21 (ft).

[redacted] The analysis is performed in a series of steps, as follows.

1. Determine the ambient atmospheric conditions at altitude h from Table 13-1.

2. Calculate the maneuver normal load factor, N,

$$N = n - 1.$$

3. Calculate the radius of turn, r (not required if $N = 0$.),

$$r = \frac{V^2}{32.2N}.$$

[redacted]

[redacted]

[redacted]

4.* Select a point on the X_I - Z_I plane (side view) intercept-time envelope. Its coordinates are (X_I, Y_I, Z_I), with $Y_I = 0$.

5. Determine the slant range, R, from the center of burst to the selected intercept point.

$$R = \left(X_I^2 + Y_I^2 + Z_I^2\right)^{1/2}.$$

6. Calculate the equivalent range for a 1 kt burst in a sea level atmosphere by the scaling procedures described in paragraph 2-14, Chapter 2,

$$R_1 = R\left(\frac{P}{P_o W}\right)^{1/3} = R\left(\frac{P}{14.7W}\right)^{1/3}.$$

7. Enter Figure 13-22 with R_1, and read the time of arrival, t_1, for a 1 kt burst in a sea level atmosphere.† Calculate the time of arrival of the blast wave at a range R from a yield W at altitude h by the scaling procedures given in paragraph 2-14,

$$t_a = t_1\left(\frac{WP_o}{P}\right)^{1/3}\left(\frac{T_o}{T}\right)^{1/2}.$$

A satisfactory expression for the time of arrival within the accuracy of the methodology presented herein is

$$t_a = t_1\left(\frac{WP_o}{P}\right)^{1/3}\left(\frac{c_o}{c}\right)$$

$$= t_1\left(\frac{14.7W}{P}\right)^{1/3}\left(\frac{1{,}116}{c}\right).$$

8. Calculate the turn angle, Φ, in degrees (not required if $N = 0$),

$$\Phi = 57.3\,\frac{Vt_a}{r}.$$

9. Calculate the coordinates of the point in the burst frame (X_B, Y_B, Z_B).

a. If $N = 0$,

$$X_B = X_I + Vt_a,$$

$$Y_B = Y_I,$$

$$Z_B = Z_I.$$

b. If $N \neq 0$,

$$X_B = X_I \cos\Phi + (r - Z_I)\sin\Phi,$$

$$Y_B = Y_I,$$

$$Z_B = Z_I \sin\Phi - (r - Z_I)\cos\Phi + r.$$

10. Repeat steps 5 through 9 for other points on the intercept-time envelope, until the burst-time envelope has been defined satisfactorily.

11. Determine the intercept-time envelope for a "slice" parallel to the X_I - Z_I plane, with $Y_I \neq 0$. Repeat steps 5 through 10 for points on this envelope.

12. Repeat step 11 for as many "slices" as necessary to define the burst-time volume adequately. Note that only positive values of Y_I need be used since the envelopes are symmetric about the X_I - Z_I or X_B - Z_B plane.

[redacted] At this point, the problem is essentially solved, since the burst-time volume effectively has been defined. The burst-time envelope in any desired plane may be determined from the burst-time volume. The calculation of the burst-

*[redacted] In certain special cases, simpler procedures may be used, although the procedures given above are general and will work in all cases. A description of the special cases is given at the end of the Stepwise Calculation Procedure.

†[redacted] Note that Figure 13-22 is identical to Figure 2-5, Chapter 2. It is reproduced here for convenience.

[redacted]

[redacted]

time envelopes in three planes, The X_B - Z_B plane (side view), the Y_B - Z_B plane (front view), and the X_B - Y_B plane (top view) is described for illustration.

13. The side-view burst-time envelope is the intersection of the X_B - Z_B plane with the burst-time volume. This is just the transformed side-view intercept-time envelope (Y_I = 0), which was the first burst-time envelope defined in the steps given above.

14. The front-view burst-time envelope is the intersection of the Y_B - Z_B plane with the burst-time volume. For each of the burst-time volume "slices," determine the values of Z_B corresponding to X_B = 0, and plot these using the value of Y_B for the slice being considered.

15. The top-view burst-time envelope is the intersection of the X_B - Y_B plane with the burst-time volume. For each of the burst-time volume "slices," determine the values of X_B corresponding to Z_B = 0, and plot these using the value of Y_B for the slice being considered.

16. *Special Cases.* In certain cases, simpler procedures may be used. The methodology of Problem 13-5 results in a spherical intercept-time volume for overpressure effects on in-flight aircraft. The sphere is centered at the origin of the intercept frame (X_I, Y_I, Z_I). Hence, R, R_1, r, and Φ (steps 5-8) are the same for *all* points on the intercept-time volume, and the sphere transforms into a sphere of the same radius in the burst frame. The coordinates of the center of the sphere are

a. If $N = 0$,

$$X_B = Vt_a,$$

$$Y_B = 0,$$

$$Z_B = 0.$$

b. If $N \neq 0$,

$$X_B = r \sin \Phi,$$

$$Y_B = 0,$$

$$Z_B = r(1 - \cos \Phi).$$

Another special case occurs for the gust effects on in-flight aircraft (see Problems 13-3 and 13-4). The complete intercept-time volumes are made up of four spheres. The intersection of any plane with a sphere is a circle. Consider the intersection of a plane parallel to the X_I - Z_I plane and defined by constant Y_I with the sphere at the side of the aircraft. The intersection is a circle on the Y_I axis. All points on this circle are equidistant from the origin; hence, the circle transforms into a circle of the same radius in the burst frame. The coordinates of the center of the circle are

a. If $N = 0$,

$$X_B = Vt_a,$$

$$Y_B = Y_I,$$

$$Z_B = 0.$$

b. If $N \neq 0$,

$$X_B = r \sin \Phi,$$

$$Y_B = Y_I,$$

$$Z_B = r(1 - \cos \Phi).$$

For the case of $N = 0$ only, the intersection of a plane parallel to the X_I - Y_I plane and defined by constant Z_I with the sphere above or below the aircraft transforms into a circle of the same radius in the burst frame. The coordinates of the center of the circle are

$$X_B = Vt_a$$

[redacted]

[redacted]

$$Y_B = 0$$

$$Z_B = Z_I.$$

In all of the above transformations, it should be emphasized that t_a corresponds to a point on the intercept-time envelope being considered, *not* to the center of the circle.

[redacted]

DNA (b)(1)

PAGES 13-73 THRU 13-74 DELETED

[redacted]

[redacted]

[redacted] *Reliability:* The aircraft is assumed to be represented by a point mass traveling at a constant velocity and performing a constant symmetric maneuver. As a result of this assumption, the flight path of the aircraft is circular (or straight for the special case of no maneuver). The maximum error is estimated to be a factor of 1.1.

[redacted] *Related Material:* See paragraphs 13-1, 13-2, 13-6, 13-7, and 13-11. See also Problems 13-3 and 13-4, and Table 13-1.

[redacted]

[redacted]

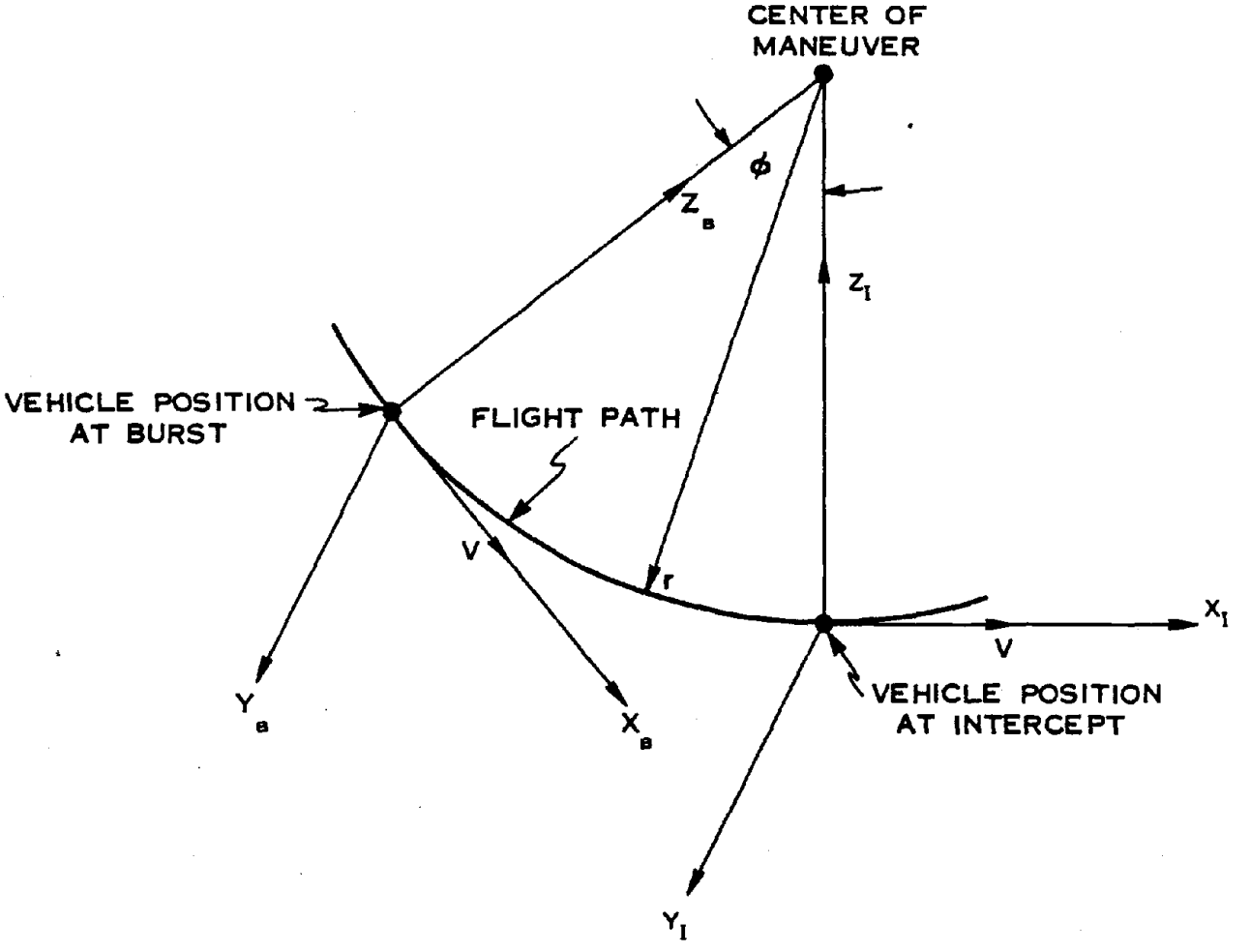

Figure 13-21. [redacted] Geometry of Burst and Intercept Reference Frames [redacted]

[redacted]

[redacted]

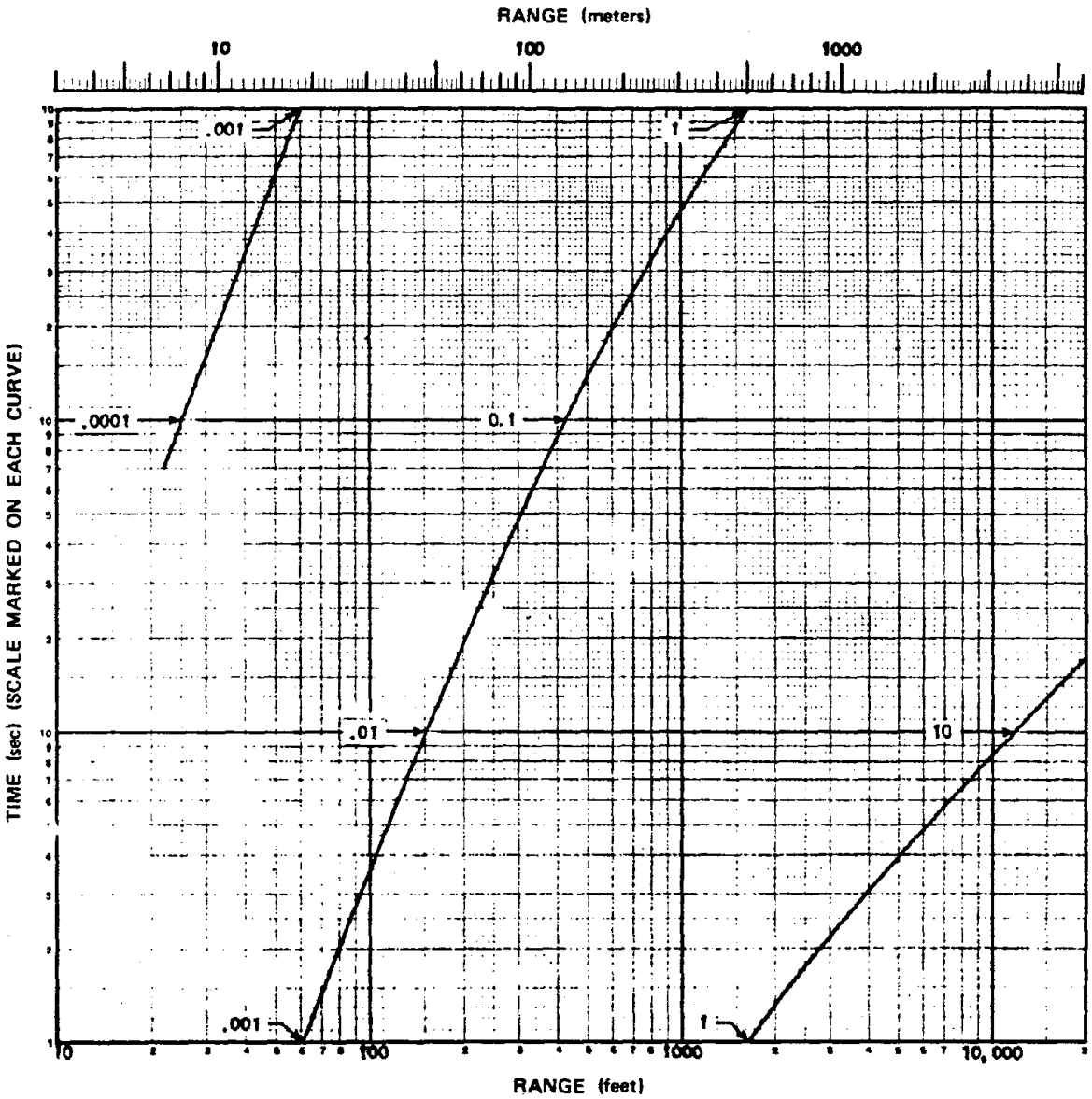

Figure 13-22. [redacted] Time of Arrival of the Shock Front from a 1 kt Free Air Burst in a Standard Sea Level Atmosphere [redacted]

[redacted]

[redacted]

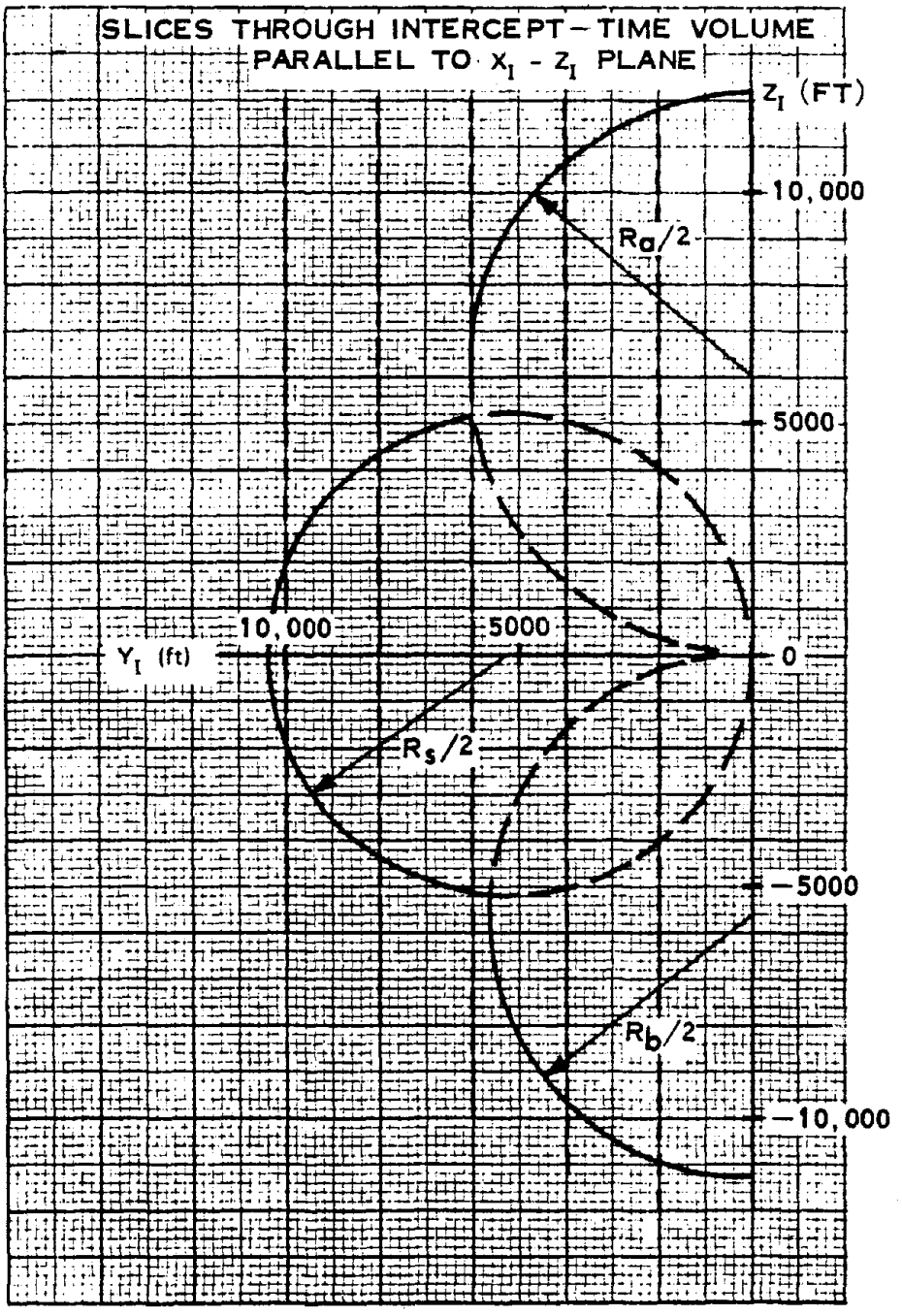

Figure 13-23. [redacted] Intercept-Time Envelope (Front View) [redacted]

[redacted]

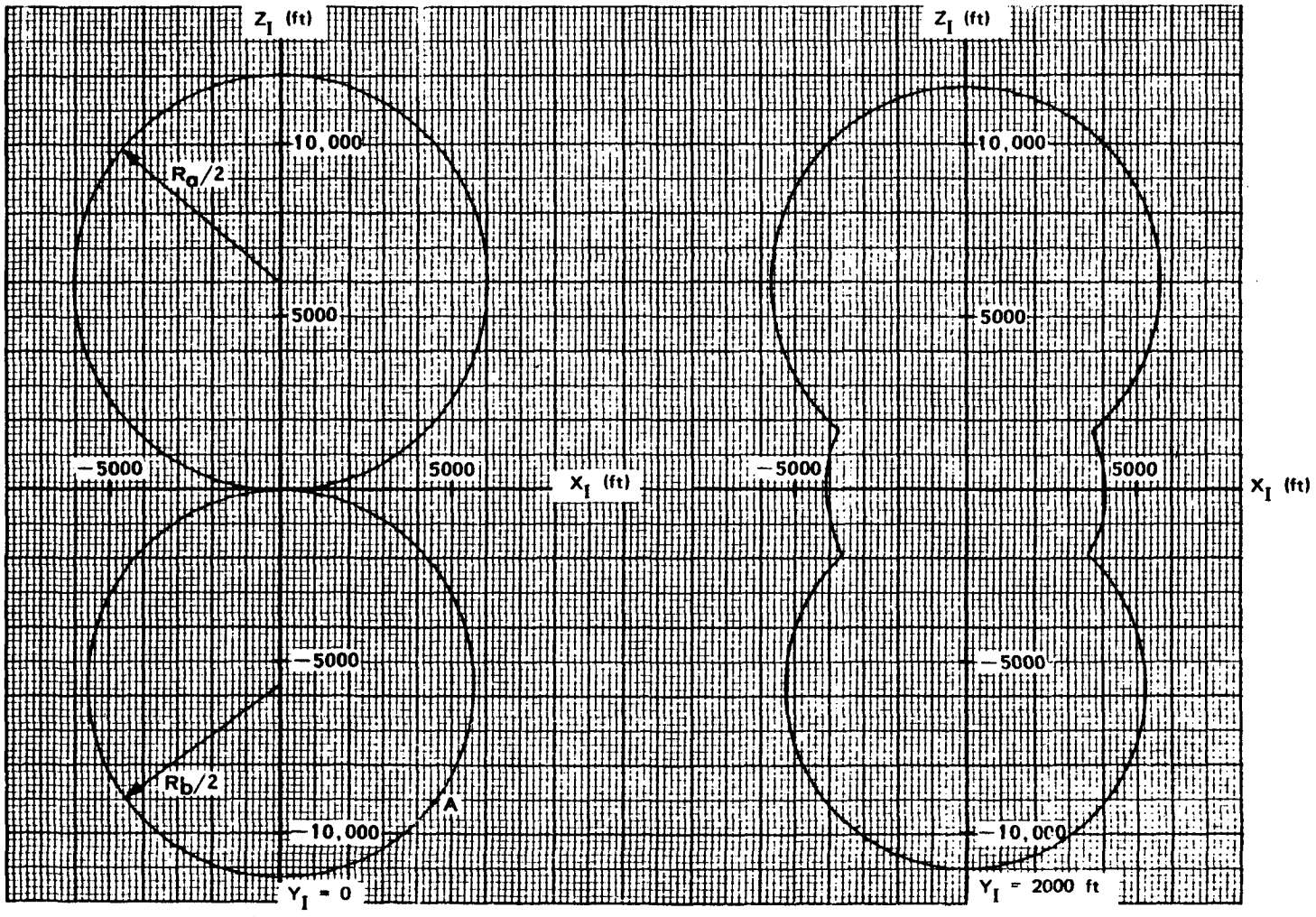

Figure 13-24a. [redacted] Intercept-Time Envelope (Side View) [redacted]

Figure 13-24b. [redacted] Slice Through Intercept-Time Volume at Y_I = 2,000 Feet [redacted]

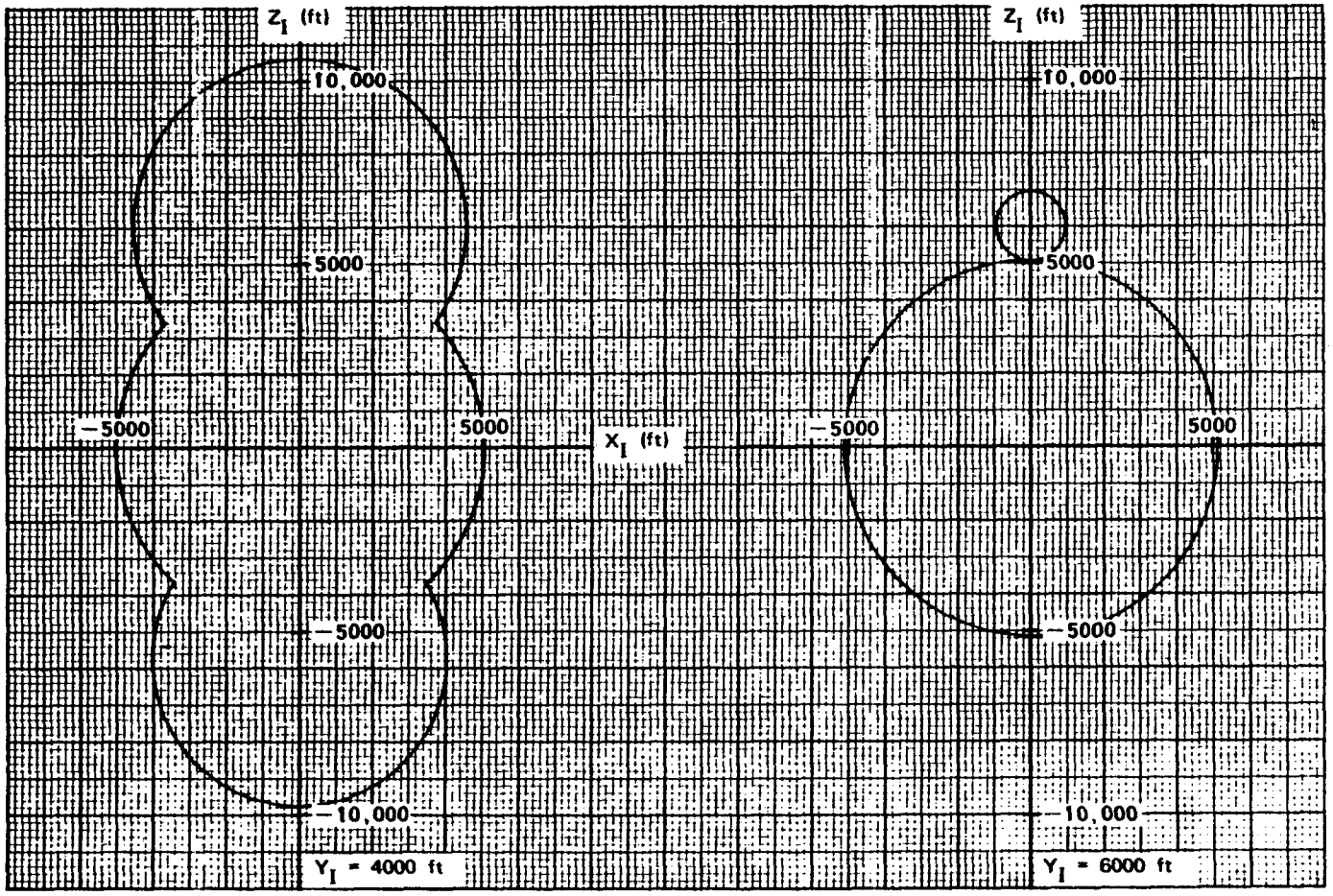

Figure 13-24c. [redacted] Slice Through Intercept-Time Volume at Y_I = 4,000 Feet [redacted]

Figure 13-24d. [redacted] Slice Through Intercept-Time Volume at Y_I = 6,000 Feet [redacted]

[redacted]

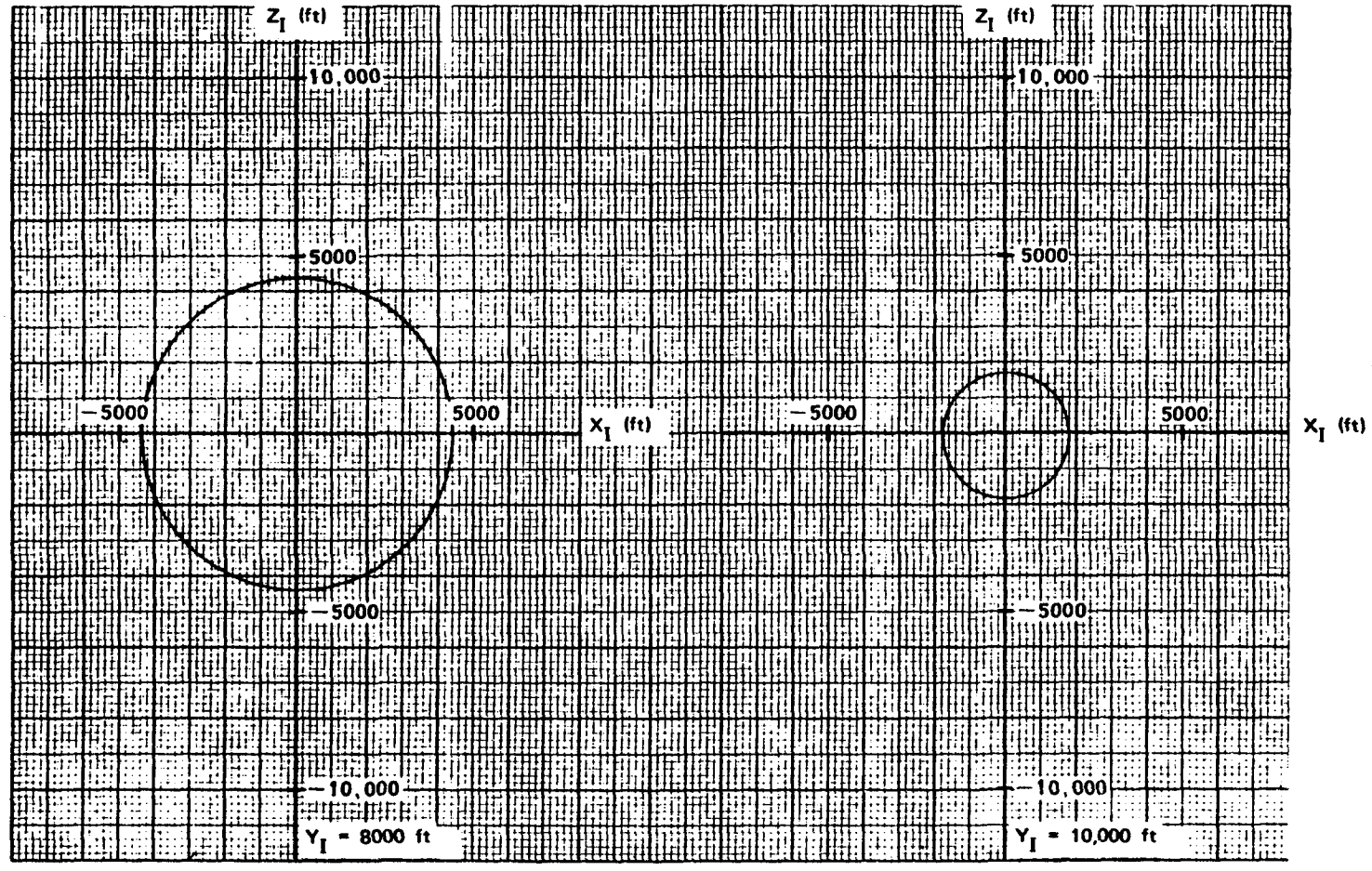

Figure 13-24e. [redacted] Slice Through Intercept-Time Volume at Y_I = 8,000 Feet [redacted]

Figure 13-24f. [redacted] Slice Through Intercept-Time Volume at Y_I = 10,000 Feet [redacted]

[redacted]

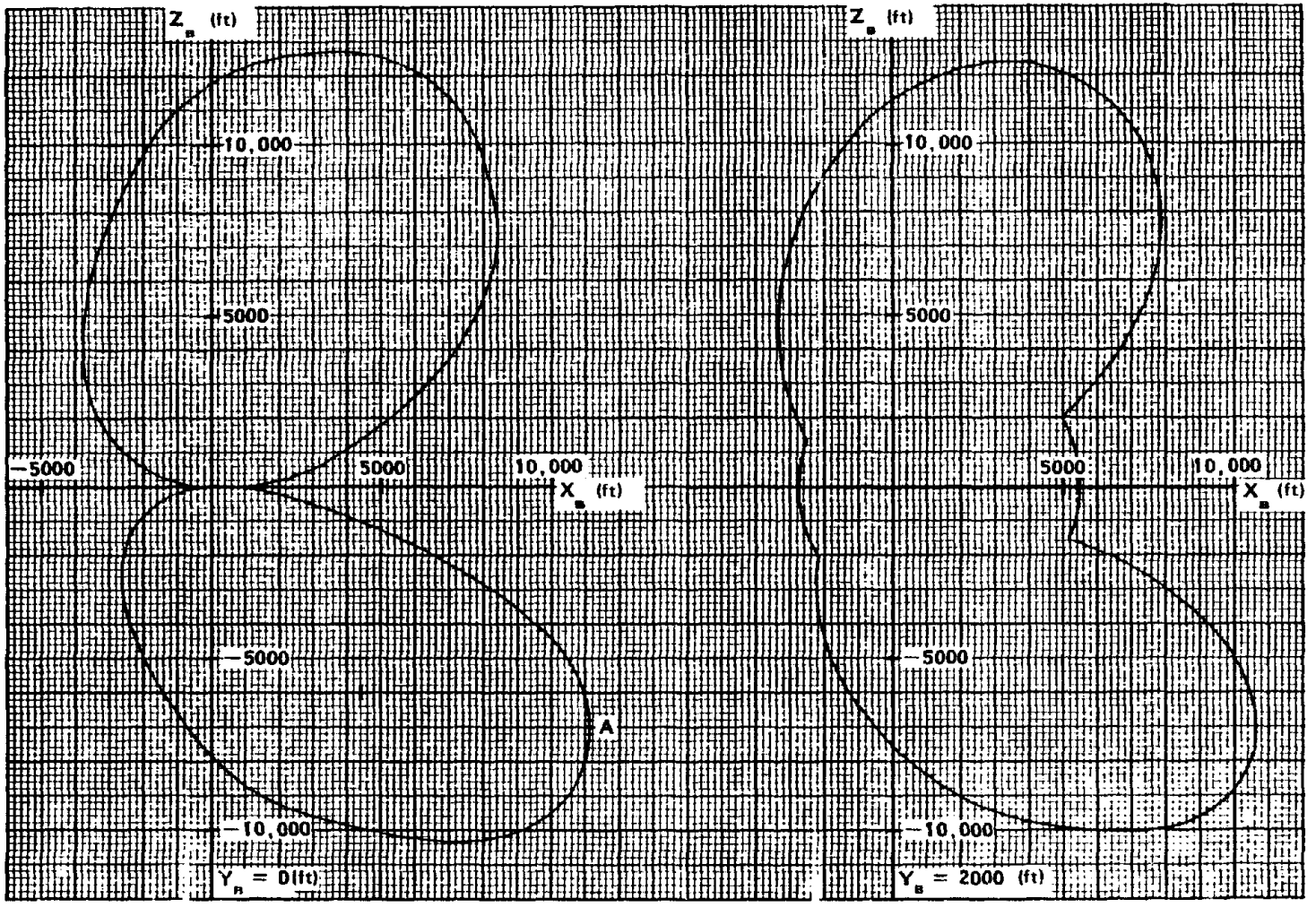

Figure 13-25a. Burst-Time Envelope (Side View)

Figure 13-25b. Slice Through Burst-Time Volume at Y_B = 2,000 Feet

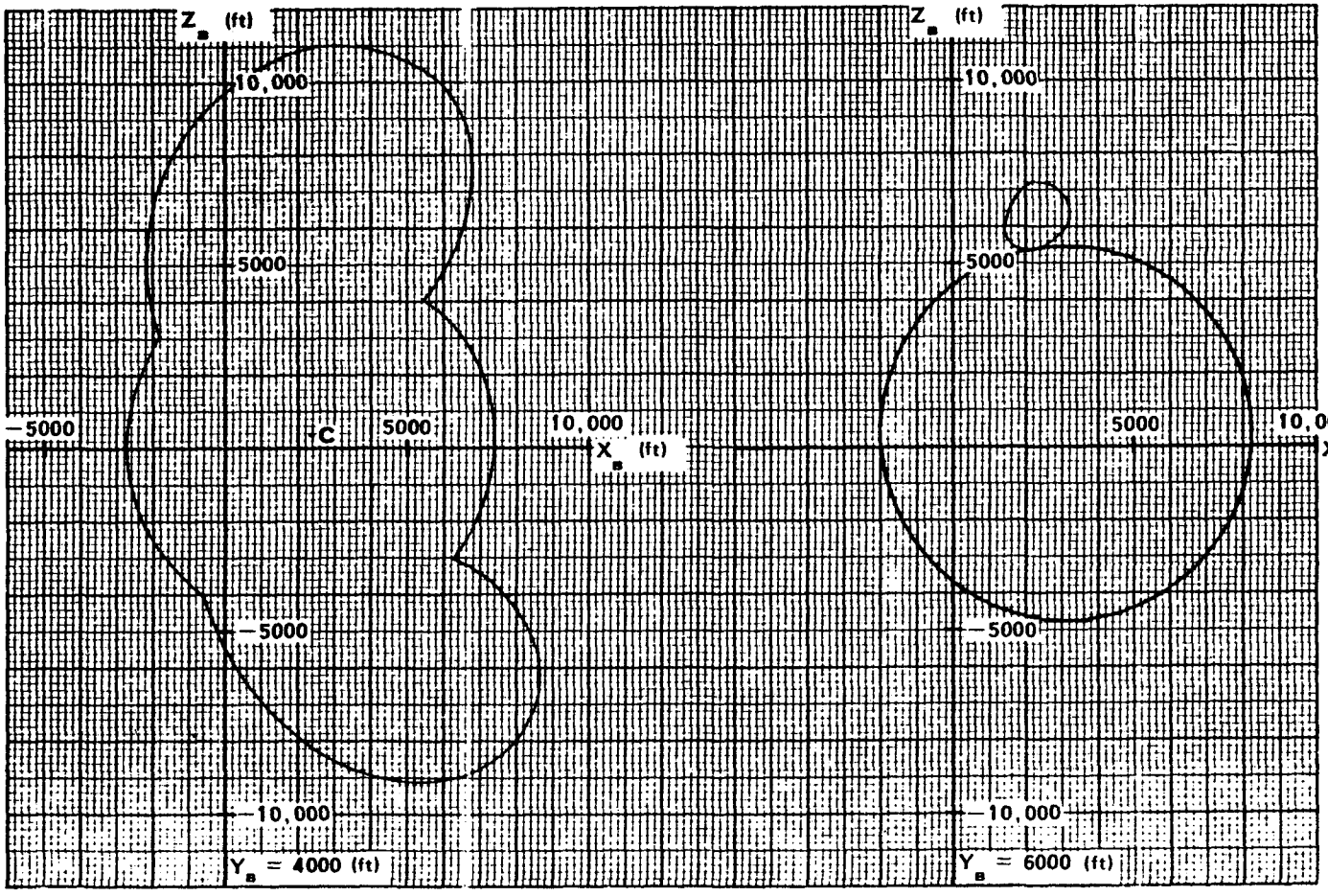

Figure 13-25c. [redacted] Slice Through Burst-Time Volume at Y_B = 4,000 Feet [redacted]

Figure 13-25d. [redacted] Slice Through Burst-Time Volume at Y_B = 6,000 Feet [redacted]

[redacted]

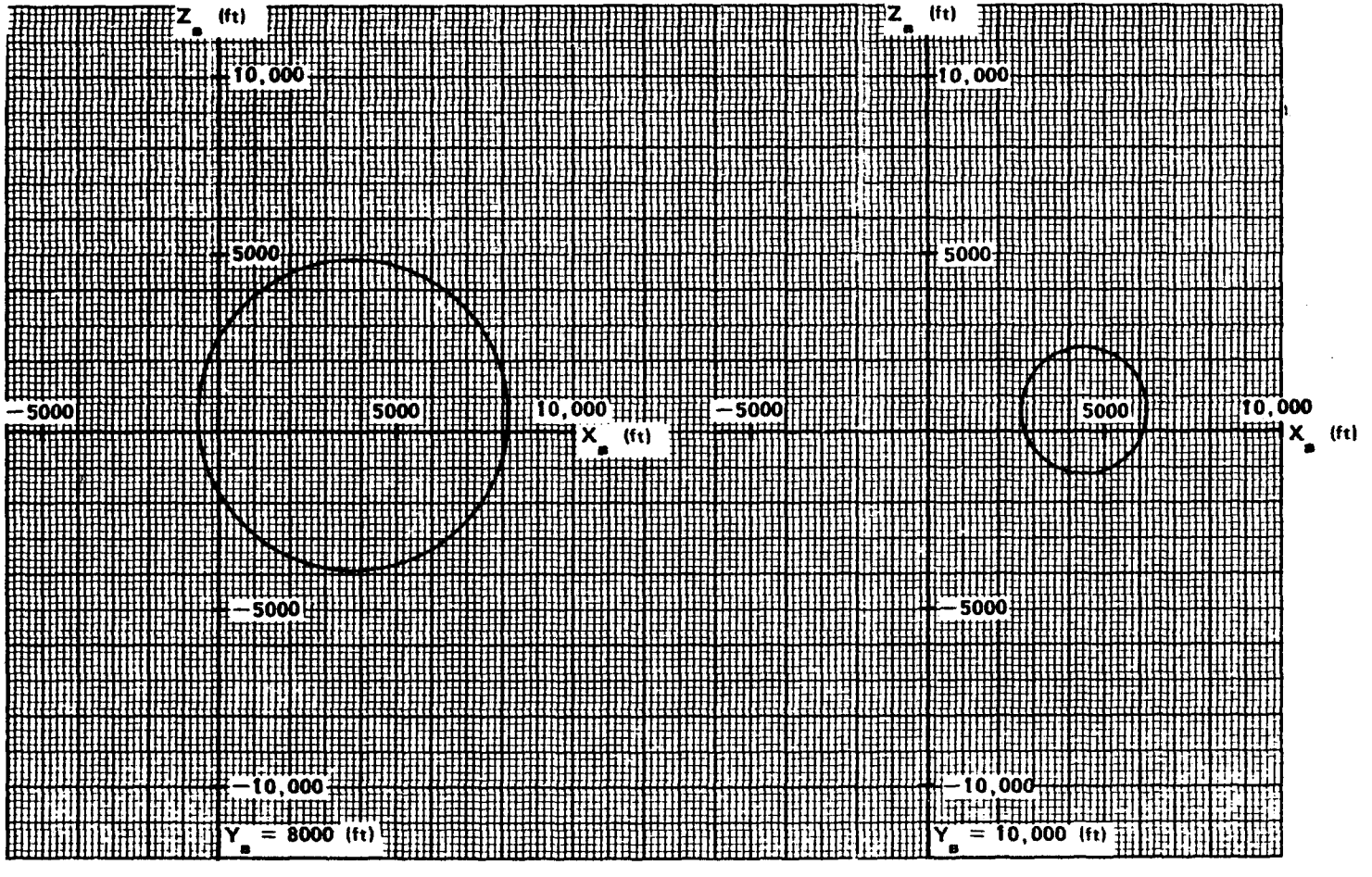

Figure 13-25e. [redacted] Slice Through Burst-Time Volume at Y_B = 8,000 Feet [redacted]

Figure 13-25f. [redacted] Slice Through Burst-Time Volume at Y_B = 10,000 Feet [redacted]

[redacted]

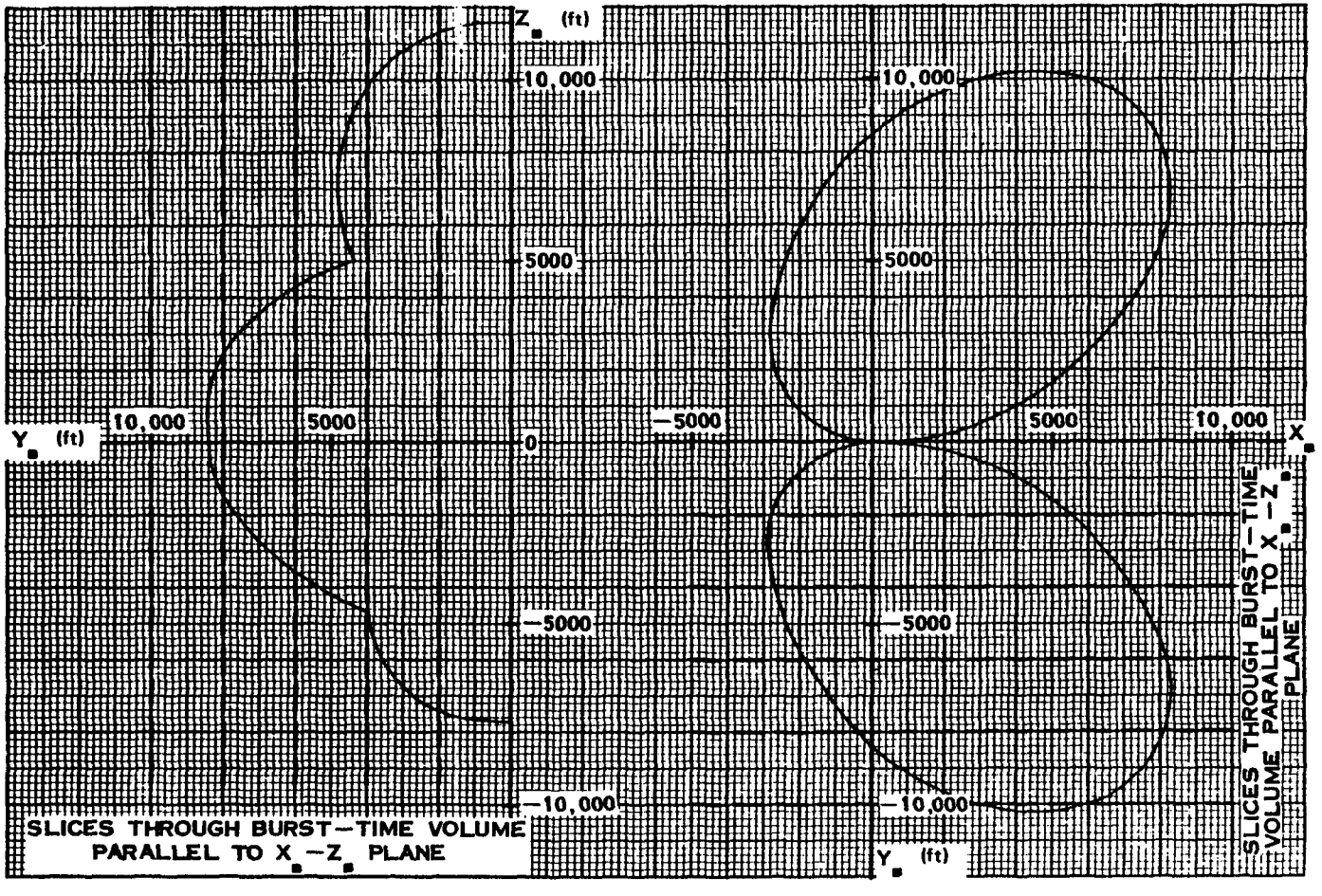

Figure 13-26a. [redacted] Burst-Time Envelope (Front View) [redacted]

Figure 13-26b. [redacted] Burst-Time Envelope (Top View) [redacted]

[redacted]

[redacted] BIBLIOGRAPHY [redacted]

Atkinson, G. W., and H. G. Laursen, *Nomographs for Determining the Relationships Between Pressure, Range, Altitude, and Yield in the Shock Front Resulting from a Nuclear Detonation* [redacted] NAVWEPS Report 8295, Naval Weapons Evaluation Facility, Albuquerque, New Mexico, 31 January 1965 [redacted]

Ayvazian, M., E. S. Criscione, and N. P. Hobbs, *Comparison Between Predicted and Measured Structural Responses of a Supersonic Delta Wing to Blast Loads,* AFFDL-TR-65-212, Kaman AviDyne, Burlington, Massachusetts, March 1966 [redacted]

Criscione, E., and J. Putukian, *Preliminary Estimates of the Effect of Blast-Thermal Interaction on the Vulnerability of High-Speed Aircraft in the Vicinity of a Nuclear Detonation* [redacted] ASD-TR-61-135, AviDyne Research Inc., Burlington, Massachusetts, January 1962 [redacted]

Davis, H. T., W. C. Kaufman, *An Experimental Determination of the Maximum Safe Thermal Radiation Loads for a Fighter-Bomber Cockpit,* ASRMDS-TM-63-4, Flight Dynamics Laboratory, Wright-Patterson, Ohio, January 1963 [redacted]

De Hart, R. C., N. L. Basdekas, *Response of Aircraft Fuselages and Missile Bodies to Blast Loading,* ASD TDR-62-458, Southwest Research Institute, San Antonio, Texas, January 1963 [redacted]

Donovan, A. F., and H. R. Lawrence, eds., *Aerodynamic Components of Aircraft at High Speeds, Volume VII of High Speed Aerodynamics and Jet Propulsion,* Princeton University Press [redacted]

Friedman, M. D., and J. R. Ruetenik, *An Analysis of Measured Blast Loads on Swept Wings at High Subsonic Speeds,* AFFDL-TR-65-170, MIT/ASRL TR-102-1, Massachusetts Institute of Technology, Cambridge, Massachusetts, March 1966 [redacted]

Handbook for Analysis of Nuclear Weapon Effects on Aircraft [redacted] DASA 2048, KA-TR-50A, Kaman AviDyne, Burlington, Massachusetts, April 1970 [redacted]

Hobbs, N. P., and K. R. Wetmore, *Lethality Criteria for Aircraft Exposed to Nuclear Blasts* [redacted] AFFDL-TR-66-221, Kaman AviDyne, Burlington, Massachusetts, April 1967 [redacted]

Hobbs, N. P., G. J. Frassinelli, and E. S. Criscione, *Effects of Variations in Aircraft Parameters on Blast Lethality Envelopes* [redacted] RTD-TDR-63-4087, AviDyne Research Inc., Burlington, Massachusetts, February 1964 [redacted]

Nuclear Weapons Blast Phenomena, Volume I, Source and Development of Blast Waves in Air [redacted] DASA 1200-I, DASIAC, Santa Barbara, California, 1 March 1971 [redacted]

Nuclear Weapons Blast Phenomena, Volume II, Blast Wave Interaction [redacted] DASA 1200-II, DASIAC, Santa Barbara, California, 1 December 1970 [redacted]

[redacted]

[redacted]

[redacted]

Nuclear Weapons Blast Phenomena, Volume III, Air and Subsurface Burst Explosions [redacted] DASA 1200-III, DASIAC, Santa Barbara, California, 1 March 1970 [redacted]

Pugh, E. J., and G. B. Bennett, *Vulnerability of Aeronautical Systems to Nuclear Effects, Volume I – Methods of Structural Analysis* [redacted] RTD-TDR-64-1, January 1965 [redacted]

Schlej, E. J., and D. H. Whitford, *The Vulnerability of Parked Army Aircraft to Nuclear Detonations* [redacted] WADC-TR-56-354, University of Dayton, Dayton, Ohio, June 1956 [redacted]

Sears, W. R., ed., *General Theory of High Speed Aerodynamics, Volume VI of High Speed Aerodynamics and Jet Propulsion,* Princeton University Press [redacted]

Witmer, E. A., J. F. Duvivier, and M. Ayvazian, *The Effects of Atomic Explosions on the Main Rotor of Helicopters in Flight* [redacted] WADC-TR-58-301, MIT/ASRL, November 1958 [redacted]

Whitaker, W. A., and R. A. Deliberis, Jr., *Aircraft Thermal Vulnerability to Large High-Altitude Detonations* [redacted], AFWL-TR-67-85, Air Force Weapons Laboratory, Kirtland Air Force Base, New Mexico, August 1967 [redacted]

PAGE 13-88 INTENTIONALLY LEFT BLANK

[redacted]

[redacted]

Chapter 14

DAMAGE TO MILITARY FIELD EQUIPMENT [redacted]

[redacted] INTRODUCTION [redacted]

[redacted] One of the primary uses of nuclear weapons would be for the destruction of military field equipment. This chapter describes how a nuclear explosion can damage military field equipment and provides techniques for estimating certain types and categories of damage. Section I provides a description of the mechanisms of air blast damage to military field equipment, and some examples of variations in damage with weapon yield and exposure conditions. Section II provides the techniques for estimating the various categories of air blast damage to military material. Section III provides a brief description of damage that might be caused by missile (objects translated by the blast wave), fire, and other secondary effects. Section IV discusses transient radiation effects on electronic systems (TREES).

SECTION I

[redacted] AIR BLAST DAMAGE [redacted]

[redacted] The military equipment that is included in this section generally can be described as that material that is used by ground forces in the field. The major types include vehicles (wheeled and tracked), artillery, small arms, communications, field radars, mines, railroad rolling stock, generators, and other miscellaneous items. Types of equipment that are specifically excluded are stationary structures, aircraft, and missile systems. The blast and thermal effects on these three types are discussed in Chapters 11, 13, and 16, respectively. This section discusses the causes and categories of blast-induced damage to the types of equipment listed above, while techniques for predicting the damage are given in Section II.

14-1 Damage Mechanisms [redacted]

[redacted] Most damage to military equipment is caused by the deforming action of blast overpressure or by target movement associated with the air in motion within a blast wave, i.e., the dynamic pressure. The sudden application of high pressure to the surface of a target as a blast wave envelops it can cause crushing, distortion, or buckling of components and subsystems. These may be either closed components and subsystems whose strengths are less than the forces imposed by the differential pressure between the outside and the inside of the element (e.g., fuel tanks), or open elements on which differential forces occurring during the time taken for the blast wave to envelop the element are large enough to cause failure. This type of damage predominates for very low yield weapons or for short duration pulses.

[redacted] If the weapon yield is greater than several hundred tons, however, the predominant type of damage to targets in the open results from the drag force caused by dynamic pressures. These drag forces may be large enough to move properly oriented, unshielded targets great distances. They may slide, roll, or bounce along the ground surface and may be damaged seriously by the violent motions. There have been instances in which heavy equipment has been picked up and thrown dozens of feet, and then has hit the ground with sufficient force to be dismembered. Stresses induced by dynamic pressure on other types of equipment, e.g., radar or

[redacted]

radio antennas, can be large enough to cause failure even though the target is not crushed and no gross movement occurs prior to failure.

The preceding discussion shows that the three most important parameters involved in damage to equipment from air blast are the air blast environment, the characteristics of the target, i.e., those factors that influence its reactions to blast loadings, and the target exposure, i.e., those factors, principally target orientation and shielding, that influence the target loading and the reaction of a target to a particular blast loading.

14-2 Air Blast Environment

The various means by which air blast can damage a target can be developed most simply by considering the idealized case in which a classical, sharp fronted blast wave moving over the ground encounters a rigid, fixed cube, as previously described in Section II of Chapter 9. If the height of burst (HOB) and ground distance are scaled as the cube root of the yield, the overpressure Δp remains constant, but the shock wave duration t^+ (as in Chapter 9, the positive phase overpressure duration t_p^+ and the positive phase dynamic pressure duration t_q^+ are assumed to be equal and are designated t^+) varies as the cube root of the yield. Thus, as shown in Chapter 9, the total impulse is represented by

$$I_T = A\left[B + C\,(W^{1/3})\right],$$

where A is the area of the face of the cube normal to the blast wave, B is the overpressure contribution to the impulse, and C is the dynamic pressure contribution to the impulse. Thus, the contribution to total impulse from overpressure remains constant, while that from dynamic pressure increases as the cube root of the yield. For very low fractional kiloton yields, the loading is highly impulsive with most of the load coming from the overpressure contribution. As the yield increases, at a constant scaled HOB and ground distance, the total impulse also increases, with an increasing portion resulting from the dynamic pressure contribution.

To maintain the *same* loading on a target as the yield increases (with a constant $W^{1/3}$ scaled HOB), the actual ground distance must increase at a faster rate than would be necessary to maintain peak overpressure constant, that is, faster than the cube root of the yield. In other words, if HOB is scaled as $W^{1/3}$, ground distance must be scaled as W^n, where $n > 1/3$, to maintain the same loading on the target.

This fact has been demonstrated by theoretical calculations of the relationships between yield and ground distance for a particular target, and a particular total impulse. Typical of such calculations is that performed for the blast wave from surface burst incident on a 20 foot fixed cube at distances such that the total impulse would be 0.5 psi-sec. The results of the calculation are shown in Figure 14-1.

An excellent fit to the curve shown in Figure 14-1 was achieved with an equation of the form

$$\text{Ground Distance} = (\text{constant})(\text{yield})^n,$$

where $n = 0.4138$.

For many years, it has been observed that experimental data concerning damage to military equipment required ground distance scaling of about $W^{0.4}$. The closeness of this exponent to that derived above suggests strongly that the reason for the observed scaling is that the damage was related closely to total impulse. This hypothesis was confirmed by curve-fitting analyses of the relationships between damage to various types of equipment and various air blast parameters. Typical of the results of these analyses is one for damage to 1/4-ton trucks whose sides were exposed to blast waves from weapons ranging in yield from 0.01 kt to 10 Mt. Damage

[redacted]

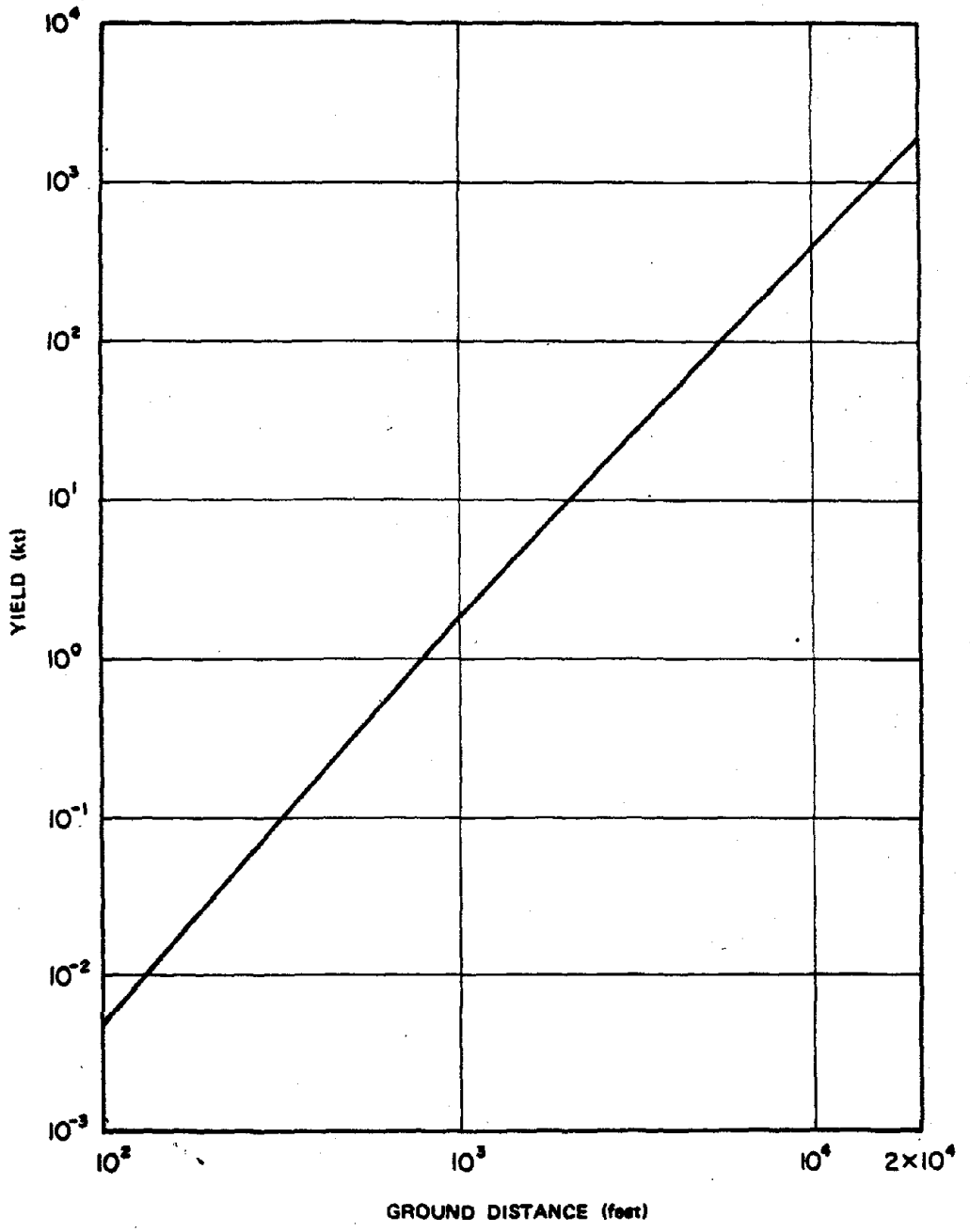

Figure 14-1. [redacted] Surface Burst Ground Range as a Function of Yield for Constant Total Impulse of 0.50 psi-sec [redacted]

[redacted]

correlation was best with total impulse (with an index of determination, I.D., of 0.77),* but the correlation was almost as good with dynamic pressure impulse (I.D. = 0.74). Much poorer correlation was achieved with dynamic pressure, diffraction impulse, and overpressure (with I.D.'s of 0.26, 0.24 and 0.22 respectively).

Most of the foregoing discussion is concerned with air blast phenomena in the Mach reflection region, where the majority of targets usually are found. In the regular reflection region, the overpressure portion of the total impulse usually dominates. This is because the target is exposed to both the incident and reflected air shock, and the horizontal components of dynamic pressure for the two shocks are small, largely because the horizontal component of dynamic pressure is proportional to the square of the sine of the angle θ that the shock front makes with the surface. For example, if θ is 45-deg, the horizontal component of dynamic pressure would be about one-half as much as the dynamic pressure for a shock making an angle of 90-deg with the surface (which is essentially the case in the Mach region). For 30-deg, the horizontal component would be only about one-fourth as much.

In this review of the discussion of the response of a simple cube to air blast a classical, sharp fronted shock wave was assumed to be incident on the cube. The influence of disturbed or non-classical wave shapes on the impulse delivered to a target can be extensive. If the wave form is not sharp-fronted, a considerable rise time may occur before the peak pressure is observed (see the wave shapes in Figures 2-40 and 2-41 of Chapter 2). If the peak overpressure is not at the front of the wave, the relationships between reflected pressure, shock velocity, sound speed, and overpressure are not valid. Furthermore, such nonideal shock waves usually are associated with precursors, within which peak dynamic pressure is not related to peak overpressure as it is with sharp fronted waves, and the dynamic pressure impulse contribution to total impulse given in Section II of Chapter 9 for a simple cube is not valid. Damage still can be related to observed air blast parameters (observed overpressures and dynamic pressures) for such wave shapes, but these parameters are not interrelated as they are for ideal waves.

14-3 Target Characteristics

Two types of target characteristics generally are of importance: the overall geometry of the target, on which blast loadings depend; and the distribution of mass in the target, which determines the kind of motions induced by the blast loading. (These can be interrelated in cases when the response of a target during loading changes its geometry and therefore its loading.)

The influence of geometry can be illustrated by considering two targets with the same cross-sectional area, one of which is composed of flat surfaces and sharp edges while the other has curved surfaces and a more streamlined shape. The target with flat surfaces and sharp edges will have a higher load because its shape will result in higher reflected pressures and drag coefficients than will occur on the smoother target. Consequently, the level of air blast required to induce motion in the non-streamlined target will be less than for the streamlined target.

The influence of mass distribution in a target can be seen by noting that for two targets of the same shape, mass, and area, but with different centers of gravity, the one with the higher center of gravity is more likely to sustain damaging motions than the one with the lower center of gravity. Furthermore, a target with a low mass will undergo greater motions than one with a high mass, if the two have the same area, shape, and location of the center of gravity. Figure 14-2 illustrates some of the types of blast-induced motion that may occur, depending

* The index of determination (ID) is used as a measure of goodness of fit of a curve. The closer the ID is to the number one, the better the fit of the curve.

[redacted]

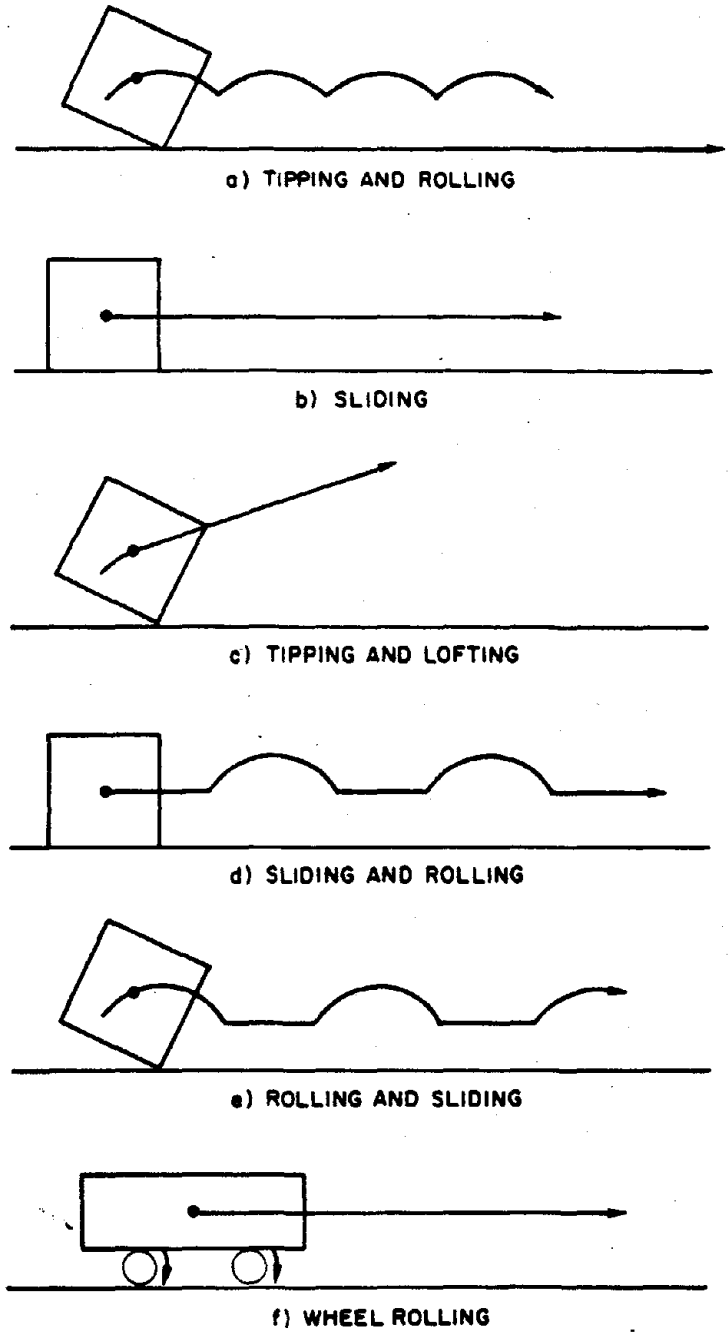

Figure 14-2. [redacted] Target Response Modes [redacted]

[redacted]

upon geometry and mass distribution.

A detailed assessment of the influences of geometry and mass distribution for each piece of equipment is not presented in this chapter. The damage assessment techniques that are presented in Section II for a variety of equipment types (e.g., wheeled vehicles, artillery pieces, tanks) and for a number of items of equipment within each type, are all based on experimental observations. One purpose of this paragraph is to emphasize the fact that different items of equipment within a single type, and even different production runs of the same item of equipment, can exhibit significant differences in damage from the same blast loadings, but they also can exhibit similarities. These differences and similarities are illustrated by several curves that show damage as a function of distance in a manner similar to Figure 14-3, in which damage on an increasing scale from none to severe is the vertical coordinate (the meanings of the damage categories shown in Figure 14-3 are described in Section II), and distance from a 1 kt surface burst at which the various categories of damage have been observed is the horizontal coordinate.* Increasing distance implies decreasing values of blast parameters, so the curve indicates that damage decreases with an increase in distance from the burst point. There are infrequent exceptions to this rule, which generally occur in the regular reflection region for large heights of burst.

Figure 14-4 shows a comparison of the damage-distance curves for two types of wheeled vehicles. Although the two vehicles differ markedly in their characteristics, the ground distances at which they sustain moderate and severe damage are not very different; however, the difference in the distances for light damage is large. Figure 14-5 shows larger differences in the damage-distance curves for the similar artillery pieces. Finally, Figure 14-6 shows fairly substantial differences in the distances at which severe and light damage occurs for two different production runs of the same vehicle.

These comparisons illustrate the difficulties that can be expected to be encountered in making damage predictions for new items of equipment for which little or no information is available.

14-4 Target Exposure

The orientation of the target with respect to the direction of travel of the blast wave, and shielding afforded by nearby terrain features can affect the response of the target significantly. The effects that differences in target exposure can have on damage may be illustrated by curves similar to the schematic presentation in Figure 14-3.

The terminology that is usually used when discussing target orientation describes which side faces the oncoming blast wave, i.e., side-on,† front-on, or rear-on to the blast. A flat surface oriented obliquely or normal to the blast will receive substantially different loads than it would if it were parallel to the blast wave. Little difference in damage is observed for front-on and rear-on orientations for many targets; in this chapter the two orientations are grouped into a single category, end-on orientation. Figure 14-7 illustrates the importance of target orientation to the extent of damage.

A target may be shielded from some of the air blast and thermal radiation effects when some substantial object or terrain feature (natural or man-made) is in the vicinity of the

---

* Curves were drawn by finding the horizontal scaled distances (d1, d2, etc.) at which changeover from each category of damage to the next higher category occurred. The points so derived were connected by smooth curves.

† The term "side-on" is also used in an alternate designation for incident pressure in a blast wave, i.e., "side-on overpressure" is the overpressure in an incident blast wave before it interacts with a target or object.

[redacted]

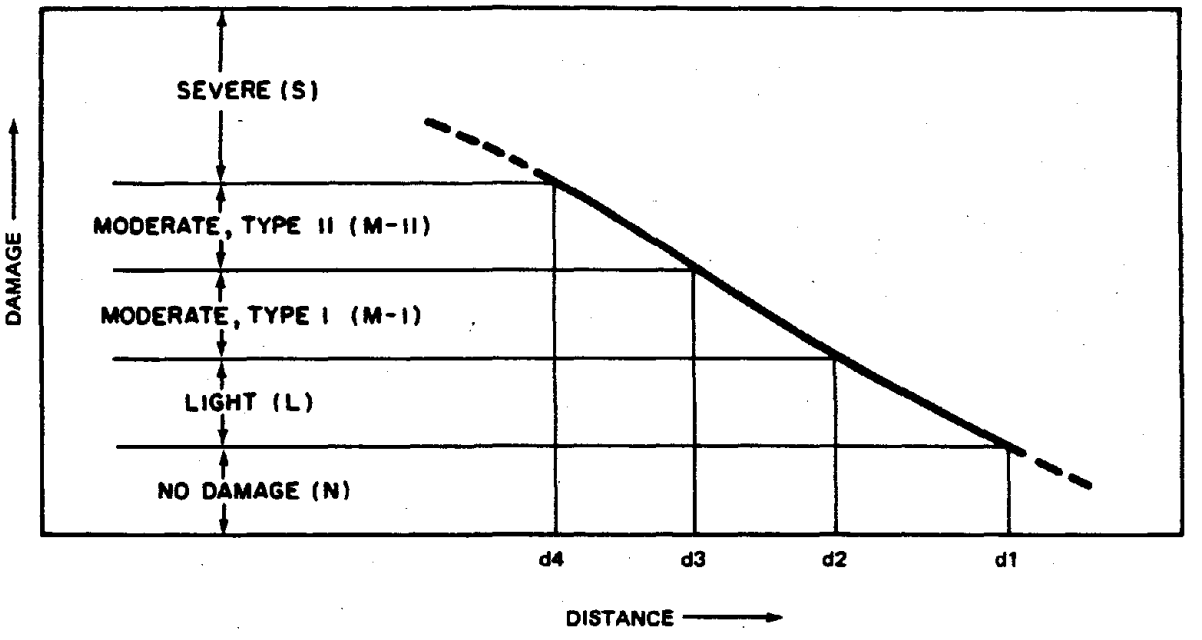

Figure 14-3. [redacted] Illustration of the Damage vs Distance Curve [redacted]

Figures 14-5 through 14-7
(Pages 14-8 through 14-11)
Deleted USANCA
(b)(1)

[redacted]

[redacted]

target. Shielding is most effective when the obstacle is between the target and ground zero.

[redacted] Obstacles that are considered in the assessment of the effects of shielding from air blast are local obstacles, such as ravines, constructed slots, or revetments (the effects of large terrain features on blast waves are discussed in paragraphs 2-38 through 2-41 of Chapter 2). The importance of shielding is well documented. Comparisons of damage between shielded and unshielded vehicles exposed to blast from both nuclear and chemical explosions are available. The effectiveness of an obstacle in shielding a target generally results as much from its capability to reduce the target movement as from its ability to modify the blast environment. Figure 14-8 illustrates this point. When the obstacle is between the blast wave and the target most of the impulse or translational force that induces motion (drag loading) does not act on the target. When the obstacle is "behind" the target, the translational force initially applied to the target is the same as it would have been without an obstacle, but the obstacle not only can modify later translational forces (as a result of shock wave reflection), but it can restrict movement, the major cause of damage. The overpressure effects of crushing and fracturing still occur in both cases, and these effects provide lower limits for damage ground distances.

[redacted] Most damage resulting from low yield weapons is caused by overpressure impulse rather than translation, even for unshielded targets, and, since overpressure impulse is not altered drastically by shielding, the effects of shielding are relatively minor for such weapons. However, most damage caused to non-shielded targets by higher yield weapons results from the translational effects of dynamic pressure. Since shielding can reduce translational effects substantially, it can be quite effective as a protection from large yield weapons. Damage to shielded targets results largely from overpressure effects, for which damage distances scale as the cube root of the yield ($W^{1/3}$), while damage to unshielded targets results largely from total impulse effects (including those of dynamic pressure), for which damage distances generally scale as $W^{0.4}$. The effects of shielding are illustrated in Figure 14-9, in which damage distances for shielded targets have been scaled as $W^{1/3}$, and those for unshielded targets by $W^{0.4}$.

14-5 Effects of Ground Surface Conditions [redacted]

[redacted] Ground surface conditions affect damage in two ways: by modification of the blast parameters; and by modification of target response. The former is discussed in paragraphs 2-20 through 2-22 and 2-37 through 2-41 of

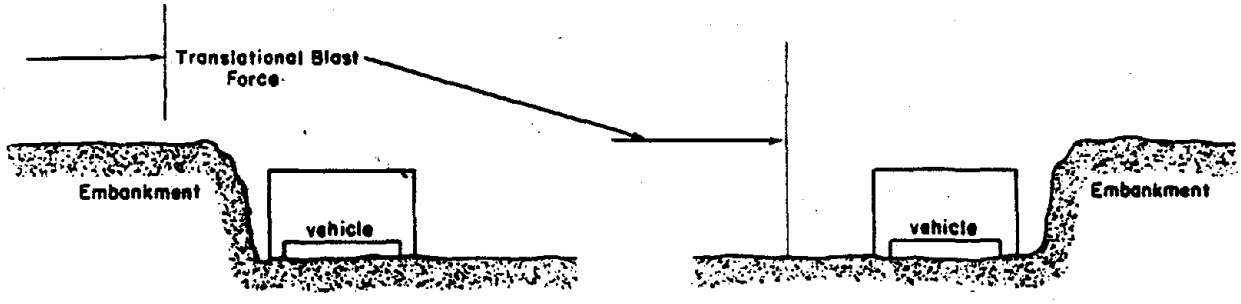

(a) No translation because Translational Force is not applied

(b) No or little translation because embankment restricts movement

Figure 14-8. [redacted] The Effect of Shielding [redacted]

Fig 14-9 Page 14-13 Deleted. USANCA (b)(1)

[redacted]

[redacted]

[redacted] Chapter 2. The latter is discussed here. Information on the effects of ground condition comes from available test data on vehicles exposed on test surfaces constructed to investigate precursor phenomena. These surfaces were desert, asphalt, and desert covered with water. An analysis of these data concluded that there was a significant difference in damage to vehicles on "hard" (non-yielding, non-deforming) and "soft" (yielding, deforming) surfaces. This is illustrated by the curves in Figure 14-10. Blast wave characteristics were different at comparable scaled distances over the two surfaces. Therefore, a scale showing comparable blast wave conditions, dynamic pressure impulse, was substituted for the distance scale shown in previous figures in order to remove the influence of surface conditions on the blast wave from the comparison.

[redacted] Figure 14-10 shows that surface conditions can influence damage substantially, particularly in the moderate-to-severe categories. This is believed to result from the difference in the target response caused by the difference between the two surfaces shown in Figure 14-10. A soft surface will yield and can be deformed. These surface reactions produce resistive forces against the wheels, which tend to cause the vehicle to tip over. The same vehicle would tend to slide on a hard surface and would not necessarily overturn. The response of a vehicle on a soft surface is likely to resemble the response modes illustrated in Figure 14-2a, c, or e, whereas the same vehicle exposed on a hard surface would be more likely to exhibit the response modes illustrated in Figure 14-2b and d.

[redacted] Data, such as shown in Figure 14-10, are insufficient to incorporate the effects of surface conditions in the damage prediction techniques given in Section II, except as a source of error that degrades the reliability.

14-6 Vehicle Status [redacted]

[redacted] The response of a vehicle to the air blast wave can be influenced by whether or not the brakes are on and/or the transmission is in gear at the time of exposure. Information concerning these influences is available [redacted] Differences in the resulting damage occur primarily for end-on orientation of vehicles. Figure 14-11 illustrates the differences between the damage categories for two comparable [redacted] vehicles. A similar comparison for side-on orientation showed very good agreement, thus the difference shown in Figure 14-11 can be attributed chiefly to differences in vehicle status and not to difference of configuration between [redacted] 1/4-ton trucks.

DNA (b)(1)

[redacted] When a vehicle is exposed end-on with the brakes off and the transmission out of gear, the primary response is rolling on its wheels rather than sliding or overturning. As shown in Figure 14-11, there appears to be an upper limit on the blast forcing function, above which the vehicle will overturn because the forces are too great to be absorbed by rolling or sliding, or because the probability of encountering an obstacle to substantial movement is high. The status of the vehicle at the time of exposure may be as significant in determining the resulting damage as the orientation or even shielding; however, there are insufficient data to include this factor in the damage prediction techniques with any degree of confidence.

Fig 14-10 + 14-11 on Pages 14-15 + 14-16 Deleted. HSANCA (b)(1)

[redacted]

SECTION II

DAMAGE PREDICTIONS

14-7 Definitions of Damage Categories

The causes of damage to military field equipment by the air blast wave were described in Section I. The description of the various levels of damage (ranging from none to total) must be defined before damage predictions can be made. Various descriptors have been employed over the years by informed and experienced appraisers of damage to describe what they considered to be the degradation of the military effectiveness of various items of equipment. These descriptors, while useful, tend to be somewhat subjective, and they could result in different appraisals of the importance of damage to various items of equipment by different people.

An attempt has been made throughout this manual to describe the damage categories in sufficient detail to indicate the specific damage that applies to a given descriptor (e.g., Tables 11-1 and 11-2, Chapter 11, and Table 12-1, Chapter 12). In this chapter, an attempt has also been made to make the definitions of the damage descriptors less subjective in terms of the availability of a target to perform its intended military functions than descriptor definitions that have been used previously. The definitions that will be presented below include descriptions of the type and level of effort that would be required to restore a target to a condition in which it could perform its intended function, i.e., the definitions provide some insight into the time that would be required to perform essential repairs, although they do not include a measure of any effects that might arise as a result of a time lag before repair (see paragraph 14-13).

To arrive at less subjective definitions, the various items of equipment, which have been examined subsequent to exposure to nuclear and H.E. tests, were divided into functional subsystems. This was done for two reasons: (1) more precise descriptions of damage could be obtained by considering subsystems than could be obtained by considering the item as a whole; (2) different subsystems can have different degrees of impact on the ability of a particular item of equipment to perform its basic function. Four damage levels were defined for each subsystem: no damage; damaged, but functional; damaged, nonfunctional, but repairable; damaged, nonfunctional, and not repairable.

Damage categories for the entire piece of equipment were then defined *in terms of damage sustained by the subsystem.* The damage categories that were adopted are defined in Table 14-1.

The subsystems that were identified for wheeled vehicles are shown in Table 14-2 to illustrate the type of system divisions that were employed.

Of the subsystems listed in Table 14-2, the engine, power train, wheels, and chassis were designated critical subsystems which, if they sustain any damage – even easily repairable damage – so as to render them nonfunctional, would render the entire piece of equipment nonfunctional. Operator appliances and parts of the body generally can sustain some degree of damage that might make the individual element nonfunctional (a windshield may be broken, for example, or the hood could be torn off) but would not prevent the vehicle from performing its basic function.

Although the system for identifying damage categories described above reduces the chances of differences in making damage appraisals, some subjectivity is unavoidable, especially in the determination of whether an element of a subsystem can be repaired. A bent steering column, for example, (part of a noncritical subsystem – operator appliances) is deemed to be non-repairable, i.e., normal prac-

[redacted]

Table 14-1. [redacted] Definitions of Damage Categories [redacted]

Damage Category	Explanation
Light	Damaged, functional (no critical subsystems – and less than half of all subsystems – are nonfunctional)
Moderate Type I	Damaged, nonfunctional, repairable with little or no special tools, parts or skills (at least one *critical* subsystem is nonfunctional, but repairable)
Moderate Type II	Damaged, nonfunctional, repairable with special tools, skills, and parts (at least half of all subsystems are nonfunctional but repairable)
Severe	Damaged, nonfunctional, very difficult to repair (at least one subsystem is nonfunctional and not repairable)*

* [redacted] An exception to this rule could occur if an otherwise not repairable subsystem could be made functional by replacing it with an immediately available spare.

[redacted]

tice would be to replace it although with difficulty, and with appropriate tools, it could be repaired.

[redacted] Some typical descriptions of damage to various subsystems of a variety of items of equipment that have been assigned to the four damage categories are shown in Table 14-3. For obvious reasons this table is by no means complete (many equipment items have five or more subsystems). It is included to make the meanings of the damage categories clearer.

14-8 Prediction Techniques [redacted]

[redacted] Two types of prediction techniques are presented in this section. For individual pieces of equipment, tables are used to relate (directly or indirectly) the damage categories described in the previous paragraphs to the air blast parameter that results in a particular level of damage.

[redacted] To determine ground distance for a particular level of damage, the tables are consulted first, then air blast height of burst curves in Chapter 2 are used to find the scaled (1 kt) ground distance associated with the particular air blast parameter. Finally, appropriate scaling

Table 14-2. [redacted] Wheeled Vehicle Subsystems [redacted]

Subsystem	Name and Description
A	Operator Appliances – such as instruments, driving controls, windshield
B	Body – sheet metal work such as fenders, hood, etc.
C	Engine – including fuel, electrical, and cooling systems
D	Power Train – transmission, drive shaft, axles
E	Wheels – tires, suspension, brakes
F	Chassis – basic frame of vehicle

[redacted]

[redacted]

Table 14-3. [redacted] Typical Subsystem Damage for Various Damage Categories [redacted]

Type of Equipment	Damage Category							
	Light		Moderate Type I		Moderate Type II		Severe	
	Subsystem	Damage Description	Subsystem	Damage Description	Subsystem	Damage Description	Subsystem	Damage Description
Wheeled vehicles	Body	Glass breakage, bent fenders.	Engine	Air cleaner blown off.	Power train	Transmission broken.	Chassis	Gross frame distortion.
Artillery	Sighting	Glass breakage in optics.	Aiming	Traversing mechanism jammed.	Tube	Recoil mechanism inoperable.	Aiming	Elevating mechanism destroyed.
Tanks	External fittings Gun tube	Bent fenders. Some dirt in tube.	Aiming	Elevating mechanism jammed.	Tracks	Idlers broken, tracks bent and twisted.	Hull	Turret torn off.
Small arms	Stock/Grip	Cracked stock.			Stock/Grip	Broken stock.	Receiver/-barrel	Dismembered.
Supply dumps*	Packaging	Packaging not ruptured, items may be scattered.					Packaging	Packaging ruptured.

*POL in 5 and 55 gal. drums; ammunition and rations in standard packages; other items in small containers.

[redacted]

factors are applied to the scaled ground distance to find the actual ground distance. For broader classes of equipment, "Damage-HOB" curves are presented. These are curves that give scaled distances for particular damage categories as a function of scaled height of burst.

[redacted] The first technique, though it incorporates one additional step to find damage ranges, provides the user with some knowledge of the air blast parameters that cause damage and, by inference for certain pieces of equipment, some insight into how the equipment is damaged. For shielded equipment, for example, where, as has been discussed, the principle agents of damage are overpressure effects, the tables show this dependence as well as the need for $W^{1/3}$ scaling. Similarly, some items of equipment (antenna masts, wire entanglements subjected to bursts from medium or large weapons) are particularly susceptible to wind loading (dynamic pressure) damage, with little or no damage due to overpressure effects. Again the tables show this as well as the required $W^{1/3}$ scaling which is appropriate for dynamic pressures.

[redacted] The largest variety of equipment should be sensitive (for reasons given in Section I) to total impulse delivered to the target. Unfortunately, actual total impulse is very difficult to determine. The overpressures portion of total impulse is sensitive to the particular geometry of

[redacted]

the item of equipment being examined. It was demonstrated in paragraph 14-2 that, at least for 1/4-ton trucks oriented side-on to the blast, dynamic pressure impulse ranked second only to total impulse as an air blast parameter to which damage could be related. Thus, with a relatively small loss in accuracy (which would be largest for low yield weapons, for which overpressure effects tend to dominate), dynamic pressure impulse could be employed as an air blast parameter to correlate damage levels.

Unfortunately, height of burst curves are not readily available for dynamic pressure impulse (which would be employed in the second step in the analysis). Therefore, the tables give values of "equivalent overpressure" (Δp_{eq}) or "equivalent dynamic pressure" (q_{eq}), defined as that overpressure under near-ideal conditions, or that dynamic pressure under nonideal conditions (see paragraph 2-20 for a discussion of near-ideal and nonideal surfaces) for a particular yield and height of burst at which the dynamic pressure impulse that would cause a particular level of damage would be experienced. Where Δp_{eq} or q_{eq} are listed as damage causing parameters, ground distance scaling of $W^{0.4}$ should be used.

The damage prediction technique for individual items of equipment uses three tables and a single graph. Table 14-4 lists the equipment and identifies the appropriate table (14-5, 14-6, or 14-7) from which damage information may be obtained. Table 14-5 is for equipment that is damaged principally by total impulse (as measured by Δp_{eq} or q_{eq}), with which $W^{0.4}$ scaling should be used; Table 14-6 is for equipment that is sensitive to overpressure (Δp), with which $W^{1/3}$ scaling should be used; and Table 14-7 is for equipment that is sensitive to dynamic pressure (q), with which $W^{1/3}$ scaling should be used. Tables 14-5 and 14-6 are for use in the Mach shock region only. Table 14-7 can be used in both the Mach and regular reflection region (see paragraph 2-18 for a discussion of Mach and regular reflection regions).

The graph used in the prediction technique, Figure 14-12, relates peak dynamic pressure q to peak overpressure Δp for sharp fronted shock waves. It is useful for determining ground distances for damage to equipment that is sensitive to either equivalent dynamic pressure (q_{eq}) or actual dynamic pressure (q) for values of q below those shown in the dynamic pressure height of burst curves in Chapter 2 (distances beyond about 1,200 to 1,400 feet for a 1 kt burst). Beyond these distances, the shock waves generally are of classical form, and dynamic pressure at the wave front can be related to peak overpressure (see paragraph 2-17). The peak overpressure height of burst curves of Chapter 2 extend to about 12,000 ft from a 1 kt surface burst, and to about 25,000 feet for a 1 kt air burst (where overpressure is as low as 0.25 psi and dynamic pressure as low as 0.0015 psi).

Tables 14-5 through 14-7 generally show the value of the air blast parameter at which there is a 50 percent probability that the item of equipment will experience the indicated damage or greater. In those cases where sufficient information is available to determine the effect of orientation, values are shown for side-on (SO), end-on (EO), and random orientation. If sufficient information is not available, values are only shown for random orientation.

Figures 14-13 through 14-27 show isodamage – height of burst curves for broad classes of equipment as listed below:

Figure	Equipment
14–13	Wheeled Vehicles,
14–14	Artillery,
14–15	Tracked Vehicles (Except Tanks and Engineer Heavy Equipment),
14–16	Tanks (Light and Heavy),
14–17	Small Arms,

[redacted]

[redacted]

14-18 Generators,
14-19 Locomotives,
14-20 Box Cars,
14-21 Supply Dumps,
14-22 Telephone Poles,
14-23 Water Storage Equipment,
14-24 Shielded Wheeled Vehicles,
14-25 Shielded Engineer Heavy Equipment,
14-26 Signal, Electronic Fire Control Equipment, Antennas, and Rigid Radomes
14-27 Wire Entanglements.

A discussion of damage to untested equipment that is not included in Tables 14-5 through 14-7 or in Figures 14-13 through 14-27 is provided in paragraph 14-9 together with estimates of some damage levels.

[redacted] Scaling procedures for use with Figures 14-13 through 14-27 are described in Problems 14-4 and 14-5 as well as on each figure. Strictly speaking, the damage-distance relationship does not scale as a simple power of yield for the classes of equipment included in this family of figures. The yield dependence of the scaling should be reflected by the curves in a manner similar to the presentations of damage to structures in Figures 11-2 through 11-23. Such a family of curves is in preparation; however, they are not available for inclusion in this manual. It is anticipated that such curves will be incorporated in a future change.

[redacted]

[redacted]

Table 14-4. [redacted] List of Equipment and Corresponding Prediction Tables [redacted]

Equipment Item	Air Blast Parameter: Near-Ideal	Air Blast Parameter: Nonideal	Table
	Unshielded Equipment		
Wheeled Vehicles			
U.S. WW II 1/4-ton truck	Δp_{eq}	q_{eq}	14-5
U.S. M-38 1/4-ton truck	"	"	"
U.S. 2-1/2-ton truck	"	"	"
U.K. scout car	"	"	"
U.K. 1/4-ton truck	"	"	"
Artillery			
Towed U.S. 57-mm anti-tank gun	"	"	"
Towed U.K. 25-pounder gun	"	"	"
Self-propelled guns	q	q	14-7
Landing Vehicle, Tracked	Δp_{eq}	q_{eq}	14-5
Armored Personnel Carrier, M-59	"	"	"
Construction Equipment			
Crawler tractor	"	"	"
Road grader	"	"	"
Tanks	Δp_{eq}	q_{eq}	14-5
Generators	"	"	"
Railroad Cars	"	"	"
Radio Sets	"	"	"
Radio Aerials			
Antenna masts	q	q	14-7
Whip antennas	"	"	"
Wire Entanglements			
Yields < 1 kt	Δp	Δp	14-6
Yields > 1 kt	q	q	14-7
Small Arms	Δp_{eq}	q_{eq}	14-5
Water Storage Equipment			
Lyster bag, 36 gal	Δp	Δp	14-6
Tank, cylindrical, open top	"	"	"
	Shielded Equipment		
1/4-ton Trucks	Δp	Δp	14-6
Crawler Tractors	"	"	"
Road Graders	"	"	"
Lightweight Radios	"	"	"

[redacted]

Tables 14-5 through 14-7
Pages 14-23 through 14-25
Deleted. USADCA (b)(1)

[redacted]

14-9 Untested Equipment [redacted]

[redacted] Although a wide variety of equipment is included in Tables 14-5 through 14-7, many items are not listed, principally because they were never subjected to the air blast environment of nuclear or large HE tests. In some cases it is possible to deduce an approximate set of damage criteria, either because the untested equipment is comparable in some degree to some item that was tested, or because subsystems of the new equipment are similar to subsystems on tested equipment. The principles and the damage agents described in paragraphs 14-1 through 14-6 should aid in predicting damage to untested equipment, although familiarity with subsystem response (a subject beyond the scope of this chapter) would be more satisfactory.*

[redacted] Table 14-8 lists a number of items of equipment for which approximate levels of damage were deduced from the principles outlined previously. The response information shown in Table 14-8 is generally considered to be accurate to within ±50 percent, unless otherwise stated. This is caused by the inherent inaccuracies associated with the use of the comparability principle, which is primarily useful for obtaining estimates. The remainder of this section describes how the damage levels were determined.

[redacted] *Bridges, Mobile Assault:* A specific example of this equipment is the "Bridge, Floating: Mobile Assault, 36-ft." This item should be examined for its response when on the road, and when in the water. Unfortunately no information about its response in the water exists.

[redacted] When on the road and side-on, the critical angle† for overturning is about 45 degrees, which is comparable with a 2-1/2-ton truck. The area of the side-on vehicle is at least twice that of a 2-1/2-ton truck, and the weight is about four times as much. Because the moment of inertia about an overturning axis would be large, the primary response mode is expected to be sliding. However, because of the box-like configuration and the large, flat-topped surface, a large lifting force is quite possible. In addition, the large weight force on each of four wheels is likely to cause a buildup of resistive force during sliding. It therefore appears reasonable to assume that overturning occurs shortly after sliding begins.

[redacted] In the end-on configuration, the sloping surface of the vehicle will cause a significant vertical force. However, the extremely large moment of inertia in this orientation should provide resistance to overturning. The construction of the item, in addition to the flotation gear, may make it vulnerable to low overpressures. A rupture of the hull or flotation gear would make the item useless until repairs are made. In this instance, whether the item was made of steel or aluminum, the thickness of hull, and whether of riveted or welded construction, would be significant. Thermal effects on flotation gear are not expected to cause rupture or burning except at high yields, although the flotation gear may be torn loose in the end-on configuration.

[redacted] Additional information concerning this item would increase the reliability of damage predictions. Until such time as more information becomes available, the following values are recommended.

[redacted]

USANCA (b)(1)

*[redacted] P. J. Morris, *Study of Military Field Equipment Response to Air Blast and Prediction of Damage (U)* describes predictions based on subsystem response (see bibliography).

†[redacted] Angle through which the item must rotate for the center of mass to be placed over the center of rotation.

‡[redacted] Use $W^{0.4}$ scaling for ground range.

Table 14-8 page 14-53 is deleted. USANCA (b)(1)

[redacted]

[redacted]

[redacted] *Camouflage Nets.* These items are rarely considered in damage predictions. They are included in Table 14-8 primarily as a possible source of fires. Very low dynamic pressures, on the order of 2 psi, are sufficient to destroy their effectiveness for concealment. Cloth netting generally is destroyed by a thermal exposure of 15 cal/cm^2. Cloth nets can be a considerable fire hazard if this amount of thermal energy is received prior to the arrival of a low overpressure blast of about 5 psi, which may be insufficient to extinguish pre-blast flames. Plastic netting is not as susceptible to burning, but it will melt and char at a thermal exposure of approximately 10 cal/cm^2.

[redacted] *Carriers, Full Tracked.* Some data are available on equipment that predates present equipment, e.g., the Armored Infantry Vehicle, M59. So few data are available on similar current equipment, however, that any attempt to apply M59 information to current equipment could be misleading. Present vehicles are significantly different from the M59 since they are constructed of aluminum, whereas the M59 was constructed of steel. The response of carriers is believed to be similar to that of wheeled vehicles in that a boxlike construction and large areas make it susceptible to overturning. It appears that the damage values for 1/4-ton trucks may be appropriate until actual response information becomes available.

[redacted] *Engineer Construction Equipment.* Tabulated values for road grader and tracked tractors are probably appropriate for the present equipment; however, these response tables are based on very few data points, which undoubtedly affects their reliability. The characteristics of the equipment exposed in nuclear tests are not known, and comparisons with present items cannot be made. It is believed, however, that differences will be relatively small.

[redacted] No test information is available for wheeled scoop loader type equipment. Since it is a four-wheeled, rubber-tired vehicle, comparison with other wheeled vehicles is inevitable. [redacted]

USAMC (b)(1)

[redacted] *Howitzers, Self-Propelled.* The M108 105-mm, M109 155-mm, and M110 8-in. self-propelled howitzers are examples of this equipment type. The M108 and M109 howitzers are more similar in mass distribution and geometry to tanks than to the howitzers exposed during nuclear tests. Their somewhat higher profile and more "bulky" construction of the turret indicate they would be more susceptible to overturning than tanks. Nevertheless, the damage values for tanks should provide a good estimate until a closer examination of these items is made. The 8-in. howitzer on the other hand has a configuration similar to howitzers that were exposed at tests; thus, the damage values for the T97 self-propelled howitzer should provide a good estimate.

[redacted] Damage values for self-propelled howitzers are based on very little data, and care should be exercised in using the tank damage values for the M108 and M109. One major consideration not previously mentioned with regard to these items is the lack of data or analysis for howitzers exposed with their gun tubes in a firing position. Such a configuration could change the response of these items materially as a result of a change in the dispositions of blast forces and resisting moments.

[redacted] *Howitzer, Towed.* Three examples of this category of equipment are the M101A1 105-mm light howitzer, M114A1 155-mm medium howitzer, and M115 8-in. heavy howitzer. Damage values are available for the 57-mm antitank gun and the U.K. 25 pounder. The damage values for the 57-mm AT gun probably can be used for the M101A1 105-mm light how-

[redacted]

[redacted]

[redacted] itzer, but insufficient information is available for the M114A1 155-mm medium howitzer, and M115 8-in. heavy howitzer.

[redacted] *Radar Sets.* The AN/MPQ-4A radar set is used primarily to locate hostile mortars and to adjust low-velocity artillery fire. When this equipment is in transit, the antenna group and power supply are each mounted on two-wheeled trailers. The antenna trailer has outriggers for stability. The control unit for the radar and power supply can be removed for remote operation from the power supply trailer, which contains a gasoline generator. When in remote operation the control unit is mounted on a tripod-type stand and weighs about 575 pounds. The only response tables which deal with items that resemble any of this equipment are the ones for skid- and trailer-mounted generating sets. The vulnerability of the power supply trailer might be correlated with a trailer-mounted generator, and the antenna group with a skid-mounted generator. The antenna group is difficult to analyze because of its uniqueness, plus the fact that the trailer outriggers should significantly reduce its vulnerability to overturning. The antenna reflector should be the most vulnerable subsystem of this group, and damage to it would probably determine the overall damage category of the radar system. Thus the damage values for generators may be used as an estimate if the antenna reflector is added as another subsystem, which results in the following approximate damage values for both near-ideal and non-ideal blast conditions.

USANCA (LX1)

[redacted]

[redacted] Another radar set that may be used as an example is the AN/TPS-25. This is a combat surveillance, night vision, target acquisition radar. There are three major groupings of components in the system. The antenna, antenna mast, radar modulator, and receiver-transmitter are grouped together and connected by cable to the shelter that contains the radar controls and plot board, and houses operating personnel. The system is powered by a remotely located gasoline generator. The shelter may be located either on the ground or on its transporting vehicle, a 2-1/2-ton cargo truck or 3/4-ton or 1-1/2-ton two-wheeled trailer. All components are packed in the shelter during transit or when not in use. The antenna mast comes in three 6-1/2 foot tubular sections, one, two, or three of which may be used. The antenna mounted on the mast weighs about 150 pounds. The modulator rests on the ground next to the antenna mast. [redacted]

USAN

[redacted] *Radio Sets and Terminal Telegraph.* The radio sets AN/GRC-26D, AN/GRC-50, AN/MRC-80, and terminal telegraph-telephone

* [redacted] Use $W^{0.4}$ scaling for ground range.

[redacted]

[redacted]

[redacted] AN/MCC-6 are normally located in electrical shelters mounted on a 2-1/2-ton cargo truck. These shelters have sheet metal walls, metal frames, and wooden interior walls, ceiling and floor. [redacted]

USAMCA (b)(1)

[redacted] The last example of radio sets is the AN/VRC-12. This is the basic means of communication for vehicles and crew-served weapons upon or within which it is mounted. Its power comes from the vehicle or weapon electrical system. These radios use a whip antenna; they are transistorized except for two tubes in the transmitter driver and power-output stages. The VRC-12 is constructed with printed circuit boards. Therefore, vulnerability should differ considerably from the damage values given for lightweight radios in Table 14-5. Printed circuit boards generally are more vulnerable to shock and vibration than wired circuits. Since these radios are located on or in vehicles and crew-served weapons, the response of the carrier controls the response of the radios to some degree. [redacted] For low yields and shielded vehicles, the following values apply for damage to radios from overpressure.

USAMCA (b)(1)

[redacted]

USAMCA (b)(1)

[redacted] *Wheeled Vehicles.* An example of how untested wheeled vehicles might be analyzed is given by this analysis of the M51A2 5-ton dump truck. Few data exist for a 5-ton dump truck (no vehicles exposed at nuclear tests were loaded). The response of a loaded vehicle could be significantly different because the overturning forces would have to be increased. In fact, the possibility of a sliding response would have to be closely examined. The gross unloaded weight of this vehicle is quite large, about 23,000 lb with a center of gravity that is undoubtedly below the center of pressure, so the vehicle probably would overturn were it not for the high overturning moment and angle required. It is not possible to state categorically how this vehicle will respond. Test data do indicate that when it does overturn, the dump body is separated from the chassis, resulting in serious damage. Therefore, the application of the Table 14-5 damage values for 2-1/2-ton trucks will quite likely result in an overestimation of the low-damage-category ground ranges and an underestimation of the high-damage-category ground ranges.

[redacted] A truck-mounted water purification set is an example of a special-purpose wheeled vehicle. This item is quite likely to have different responses, depending on whether the water purification set is in operation or the equipment is closed down for transport. In operation, side

* [redacted] Use $W^{1/3}$ scaling for ground range.

[redacted]

[redacted]

panels of the truck body are opened, exposing the purification equipment directly to blast. In addition, the open compartment would increase the clearing times for the reflected pressure and increase the drag coefficient for dynamic pressure. The weight of this item is not known, but it is obvious that the center of gravity would be relatively high. Coupled with the high surface areas, this virtually assures overturning at relatively low blast values. The response of the purification equipment mounted on the truck chassis cannot be estimated without detailed analysis. However, the response of the item as a whole is believed to be quite similar to a 1/4-ton truck.

Supply Dumps. Damage to supply dumps should be considered in a functional sense. The purpose of a supply dump is to serve as a collection, storage, and dispensing point for materiel. Available information indicates the effect of a blast wave is to scatter containers, at times rupturing the containers and spilling the contents. If the contents are not in bulk form, such as fuel, the contents generally are not damaged. Thus the collection and storage of materiel is not significantly affected. However, the scattering of supplies and blocking of access aisles can degrade the effectiveness of the dump in issuing supplies. The size of the stacks of supplies appears to influence the amount of scattering through some type of volume-vs-area ratio. The blast winds remove boxes, etc., from outer layers in an unravelling process. Since, for a given volume, the area exposed to blast winds depends upon the number of stacks, shielding of supply dumps, such as placing them below ground level, is quite effective in that dynamic pressures have much less area to act on. Overpressure then becomes the dominant factor causing damage. Since contents of supply dumps generally are resistant to crushing forces, an overpressure level of 30 psi is recommended for shielded supply dumps. A dynamic pressure of 5 psi is recommended for unshielded supply dumps. These values are expected to cause major disruption of the supply dump either through damage to or loss of contents or scattering and mixing of containers.

SECTION III

DAMAGE FROM CAUSES OTHER THAN BLAST AND NUCLEAR RADIATION

14-10 Fire Damage

Damage to equipment by fire is referred to in some damage reports. Although some 20 occurrences have been noted, they involved only a very small percentage of the equipment exposed. Most fires appeared to be secondary in nature, that is, they were not started by direct thermal radiation ignition. Two equipment items were burned during nuclear tests under exposure conditions in which they could have received virtually no thermal radiation. In addition, a 1/4-ton truck exposed at a 100-ton high explosive test (in which thermal radiation was negligible) also burned.

The damage to a 6-kVA generator exposed on a U.K. test is particularly interesting. In the damage report the notation is made, "Fire may have started from fuel from broken carburetor spilling on hot muffler." U.K. practice at nuclear tests was to expose running equipment, that is, the engines were running at the time of the explosion. The six recorded occurrences of fires on U.K. tests represents a considerably larger percentage (about 10 percent) of all U.K. equipment exposed than does the number of fires recorded on U.S. tests. Since this may be due to the U.K. practice of running engines during a test, the incidence of secondary fires in an operational situation may be higher than the U.S. test data indicate.

Although it is believed that most fires in the U.S. tests were from secondary rather than

[redacted]

[redacted]

[redacted] primary thermal ignitions, the source of some of these secondary ignitions is not clear. The two 1/4-ton trucks that burned on one U.S. test were believed to have been ignited by burning asphalt. In one case of a tank exposed to a very low yield burst, personnel reentered the area of the burst shortly after detonation, approaching within 2,000 ft of ground zero at $H + 1$ hour. No smoke or open flames were observed. However, approximately 1/2 hour later some smoke was observed, although its cause is not known.

[redacted] Shielding from direct thermal radiation occurs when the target is below a line from the burst point to the top of any obstacle, that is when the target is in the shadow cast by the obstacle. The obstacle blocks essentially all thermal radiation. Some thermal radiation will still reach the target via the scattering of radiation by the atmosphere. This scattered radiation can be substantial for large yields because the long distances traveled by the radiation increase the opportunities for scattering. Considerable radiation can also be backscattered from clouds. There is not, however, enough information on scattering to be able to predict damage resulting from thermal radiation to shielded targets.

[redacted] Because the incidence of fires was so low in the U.S. tests (though limited British experience suggests that fires could more frequently occur in operational situations), fire damage is not normally considered in assessing damage to military equipment.

14-11 Obscuration of Optical Devices [redacted]

[redacted] Obscuration of optical devices can be an important type of damage. Evidently, the thermal radiation impinging on coated or painted surfaces near an optical surface, together with blast winds, results in the deposit of sufficient sooty material that the optical surface would have to be cleaned prior to use. Most of the information on this phenomenon was obtained from U.S. and U.K. damage reports on exposed tanks, and some scattered data are available on the artillery optics. Although there is no physical damage to the optics, the obscuration is sufficient to preclude their use, and some remedial action must be taken to make them useful. [redacted] USAMCA (b)(1)

[redacted] Little is discernible in the data about the effect that orientation has on which surfaces become sooted, but it seems wise to develop criteria for sooting of all surfaces. Since most nuclear tests were conducted under nearly ideal atmospheric conditions, and there probably was little scattering of thermal radiation, sooting was probably limited to those surfaces more directly facing GZ. [redacted] USAMCA (b)(1)

[redacted] The data from the exposure of tanks at nuclear tests are sufficiently extensive that obscuration of optics is included in damage estimates for tanks; however, there is insufficient information to apply this process to other optical systems with any reliability.

14-12 Damage by Missiles [redacted]

[redacted] Missiles are objects that are picked up and translated by the blast wave with sufficient velocity that, upon impact with an item of equipment, the stem may be damaged. Examples of such objects are rocks, gravel, sticks, structural debris, battlefield debris, etc. Instances of missile damage are scattered throughout the damage reports of nuclear tests. Some examples are the puncturing of a tire, fuel tank, or radiator by a stick or stone.

[redacted] Missile damage usually has not been included in damage analysis and prediction tech-

[redacted]

[redacted]

[redacted] niques because its frequency of occurrence is quite low, and it is rarely possible to predict when an item of equipment would be damaged by a missile. Missile damage, therefore, generally is not considered in damage analysis. (An exception for sand and gravel missiles is the chipping and cracking of glass surfaces by blast-wind-transported material. This phenomenon is mentioned in damage reports with sufficient regularity to include it as a damage mechanism even though it rarely makes optical systems completely inoperable.)

[redacted] Another possible agent of damage that falls under the general category of missile damage is the deposit of dirt, sand, and gravel in gun tubes and in some cases machine-gun barrels. Although there are several specific references to this problem in the test reports, there are no references for dynamic pressures above 10 psi. The more spectacular physical damage that occurred at high dynamic pressures may have caused this effect to be neglected in the examination of the equipment. There are rare references to sand and dirt getting into the breech mechanism, making it difficult to operate.

[redacted] Deposition of foreign matter in gun tubes does not seem to depend upon orientation of the tubes, which may be explained by the fact that material is transported by both the positive and negative phase of dynamic pressure. In actual combat, there might not be as much sand and gravel as on the desert where nuclear tests were conducted, but there could be other sources of particulate matter available. A little dirt in a gun tube may only mean an increased rate of wear if the gun is fired before cleaning, but it could also lead to more catastrophic damage. Consequently, the possible effects of material deposition within gun tubes should be considered in assessing damage to equipment with such tubes.

14-13 The Effects of Time [redacted]

[redacted] Time itself is not a damage mechanism. However, the time lag between occurrence of damage and efforts to repair the damage may alter the damage level of one or more subsystems of military equipment significantly. For example, hydrostatic lock may develop in overturned engines; fuel, water, and oil may leak, and require replacement before the equipment is functional; the corrosive action of spilled battery acid or solvents can render subsystems inoperable; soft systems, such as electronics, may be exposed to weather, making them inoperable. Such events can not only increase damage levels but also can increase the amount and nature of effort necessary to repair the damage.

[redacted] The damage reported on nuclear tests frequently included some effects of time, although damage reports attempted to compensate for time delays. Test areas often were not reentered nor damage assessments made until many days after the explosion. In an operational situation, particularly if personnel are in a warned protected status at detonation time, recovery efforts would probably start in a matter of hours rather than days. Since the significance of time after damage is extremely difficult to assess quantitatively (because of unknowns in the disposition and capability of repair or recovery efforts soon after detonation) damage assessments included herein do not include the effects of time before repairs can be made.

SECTION IV

[redacted] TREE DAMAGE CRITERIA [redacted]

[redacted] The phenomena associated with transient radiation effects on electronics (TREE) are discussed in Chapter 6. Section VII of Chapter 9 discusses component part and circuit response to nuclear radiation. This section provides estimates of nuclear radiation levels sufficient to cause moderate to severe effects in military equipment. The discussion in this section is limited to electronics, without regard to the system structure or the operator.

[redacted]

[redacted]

[redacted] SYSTEMS ANALYSIS [redacted]

14-14 Types of Systems Analysis Used in TREE [redacted]

[redacted] Two approaches may be used in systems analysis with respect to TREE, and each leads to a different result. The first approach to survivability analysis addresses the question of whether the system will malfunction during or after exposure to a specifically defined threat or a given set of radiation hardness criteria. The end result is that a system can be classified as vulnerable, questionable, or hard to that specified radiation threat. The survivability of the system can then be improved by redesign of the more vulnerable circuits or subsystems. Although the system may be classified as hard to the specified radiation threat, there is no certainty that the vulnerability levels of the system will have been identified. This approach to survivability analysis may be adequate in some instances, but changes in threat environment, system mission or tactics will require another complete analysis.

[redacted] The second approach to survivability analysis differs from the analysis described above in two major respects. First, it includes a detailed vulnerability assessment which defines the susceptibility level of each circuit or subsystem to all types of radiation threats, not just a particular one. Second, it is concerned with the statistics of failure for any component or subsystem variations in failure level for all radiation threats. With these data, the system may be evaluated for a specifically defined threat and any variations in the threat resulting from changes in system employment or tactics. In this section interest centers on the expanded survivability analysis approach.

14-15 The Complexity of Performing System Analysis for TREE [redacted]

[redacted] The complexity of circuit and system analysis is increased when it becomes necessary to understand the system response during and after exposure to nuclear radiation. This environmental constraint can change or modify the characteristics of the electronics in a very time dependent manner. The level of understanding and the accuracy in prediction of individual component part response often is not sufficient to allow accurate analysis. Therefore testing (in many cases extensive testing) is necessary to establish component part response and to verify circuit analysis. This, however, is not the complete answer to the additional complexity. The radiation response of component parts can vary widely. For example, samples of a certain transistor type can sustain significant variations in percentage of gain degradation for a given neutron exposure. Component part response can also depend on the particular bias conditions under which the part is being operated. That is, the component part could be most vulnerable to a particular radiation component (e.g., gamma rays) in one bias condition while in another bias condition it may be most vulnerable to a different radiation component (e.g., neutrons). The degree of susceptibility can change with bias conditions. As stated in Section VII of Chapter 9, the response of component parts can depend on prompt dose or dose rate. In survivability analysis, both cases must be considered. This possibility of double dependence also applies at the circuit and subsystem levels of response.

[redacted] The circuit and subsystem design also are critical with respect to radiation susceptibility. The fact that a component has a significant response to a certain level of radiation does not mean that the circuit that uses that component will be susceptible to the same level of radiation. The radiation susceptibility level of the circuit could be higher or lower than the levels of any of the component parts used in the circuit. The tolerances within which each component part and circuit has to perform in order for the system to achieve its function is a factor

[redacted]

[redacted]

in establishing the susceptibility of the circuit. Information of this nature, however, usually is only available during the design phase and frequently must be obtained through a detailed circuit analysis. The tolerances of the critical component parts and circuits, once obtained, are typically so narrow that another complete analysis of the component response and circuit interactions is required to establish the survivability of the system.

[redacted] For similar reasons a problem occurs in the analysis of generic functions, such as an amplifier, flip-flop, or clock circuit. Circuit functions can be performed by a large number of circuit configurations using a very large variety of component part types. Thus, it would be necessary to review all pertinent configurations and component part types that would accomplish the desired function in order to determine the survivability of the generic function. Also, the level of confidence associated with a specific vulnerability level for a generic function would be much lower than that for a specific circuit with specific component parts.

[redacted] The last factor that affects the accuracy of the system analysis is the determination of the environment. That is, the environment that is used to generate the TREE response data (for use in the analysis) has to be correlated to the actual use environment. This correlation may be in error by as much as an order of magnitude unless care is taken to include all factors that may affect the correlation.

[redacted] All these influences are in addition to the normal circuit and systems analysis problems. The resultant analysis becomes a complex manipulation of many interactions. Hence this type of analysis requires skill and understanding in order to approach a reasonably good characterization of the system response to a nuclear-weapon threat.

14-16 Characteristics of the Analysis Used in This Section [redacted]

[redacted] A primary concern of this section is to provide an appreciation for the survivability levels of military electronic equipment exposed to radiation from nuclear weapons. For the purposes of this section, only two levels of survival are used – a "sure safe" level and a "sure kill" level. The term "sure safe" implies a zero percent probability of failure while the "sure kill" implies a 100 percent probability of failure. A great deal of generalizing has taken place in this section (i.e., the discussion is by generic term, and each generic term, such as radio, has hundreds of variations). As a result very low confidence levels are necessarily placed on the "sure safe" and "sure kill" terms. Even with a particular system it is difficult to establish a particular probability of failure with a high degree of confidence because of the problems involved in evaluation of circuit and system responses.

[redacted] These levels of "sure safe" and "sure kill" were established without regard as to whether the system was operating or not operating at the time of the explosion. The levels were established on the basis of system analyses that have been performed on systems in each of the categories. Where analysis information was lacking, estimates were made on the basis of the component parts typically used in that particular generic class and worst-case circuit conditions were assumed. No consideration was given to the aging of the equipment.

[redacted] Utilization of the estimates presented in the latter portion of this section requires that the system be considered to be divided into subsystems according to function. The relative vulnerability of each subsystem can then be estimated on the basis of the subsystem levels presented in the text of this section. If by chance a subsystem does not fit the generic functions listed, the best estimate would have to be based on

[redacted]

[redacted]

the susceptibility of the component parts used in that system. Component part susceptibility is reviewed in the following subsection and is discussed in more detail in Section VII of Chapter 9.

THE SURVIVABILITY LEVELS PROVIDED IN LATER PARTS OF THIS SECTION ARE MEANT TO BE USED ONLY AS GUIDES. THEY *SHOULD NOT* BE USED TO FULFILL A REQUIREMENT OR TO ESTABLISH THE VULNERABILITY OR SURVIVABILITY OF A PARTICULAR SYSTEM. More detailed information may be obtained from the TREE (Transient-Radiation Effects on Electronics) Handbook (see bibliography) as well as other references listed in the bibliography.

REVIEW OF ELECTRONIC SUSCEPTIBILITY TO NUCLEAR RADIATION

14-17 Component Part Vulnerability

Any discussion of vulnerability or survivability is ultimately based on some definition of failure. In keeping with the scope of this manual, two cases of failure are considered. First, any condition which renders the electronic equipment inoperable following exposure to a nuclear burst constitutes a system failure. The second definition of failure involves those cases where it is critical that the equipment function during the radiation exposure in order to complete a critical mission. In the latter case, a system malfunction initiated during the exposure that causes loss of the mission objective is classified as a failure.

Under the first definition of failure, consideration is given primarily to permanent damage in the electronics. The loss of one or more bits of information within a computer as a result of transient effects would not constitute a failure by this definition, if, after reinitialization, the computer functioned satisfactorily, and if the system operation was not critical during the time of the weapon burst.

Permanent damage to electronics can result from (see Section VII, Chapter 9):

USAWC (b)(1)

Collectively speaking, burnout problems from voltage and current transients normally are not a problem with

Infrequent exceptions may occur by gate breakdown in MOS transistors, or in poorly designed circuitry. Since gamma rays are not attenuated appreciably in their passage through the electronics package,

USAWC (b)(3)

The internal and external X-ray environments can differ considerably, depending on packaging, and other shielding, and the X-ray spectrum (hot or cold, see Chapter 4).

This assumes roughly 98 percent attenuation of X-rays in transit through packaging, which implies a relatively cold source or effective shielding.

Neutrons normally affect semiconductor component parts long before they affect other component parts such as capacitors, resistors, and transformers. Among the semiconductor types, unijunction transistors, silicon-controlled

[redacted]

[redacted]

rectifiers, low-frequency and power-type transistors are notably poor performers. The maximum tolerable neutron fluence (or range of fluences) for various semiconductor types are listed below.

[redacted]

USANCA (b)(1)

[redacted] Thus, in analyzing systems for hardness, the subsystems containing sensitive semiconductors are likely to be the most vulnerable.

[redacted] The third type of permanent damage, likely to occur during a nuclear burst is X-ray induced thermomechanical shock. Thermomechanical-shock effects are such that, for a specific device type, there is no unique radiation level that will cause a specific effect.

[redacted]

USANCA (b)(1)

These levels are the values *at* the component part. Because of the variation in X-ray spectra for various conditions, it is not possible to suggest general X-ray levels external to the systems that will result in these effects.

[redacted]

USANCA (b)(1)

[redacted] The second type of failures (failures during exposure) typically are caused by the ionization (gamma and X-ray) dose rate. In component parts, the typical effect is the introduction of potentially large photocurrents that result in a temporary malfunction of the component. This effect could result in a system malfunction if, for example, the extraneous current pulse fired a pyrotechnic device prematurely, or changed a bit of data in a logic circuit required for critical guidance functions. Devices particularly susceptible to large photocurrents are large-area, and/or high-gain devices. Typically the photocurrents generated below 10^6 rads (Si)/s are not sufficient to cause malfunction. Failures resulting from prompt dose effects are closely associated with the dose rate effects. Prompt dose is that dose accumulated during the initial gamma pulse (~0.1 microseconds, see Chapter 5) whereas the total dose is that accumulated over seconds or up to a minute (or longer, if the equipment is in a residual radiation field). Prompt doses as low as 0.1 rad (Si) can

---

*[redacted] To a first approximation, n/cm^2 ($E > 10$ keV, fission) $\simeq$ n/cm^2 (1 MeV silicon damage equivalent).

†[redacted] Some quartz resonator crystals and MOS field-effect transistors are very sensitive to gamma radiation.

[redacted]

[redacted]

[redacted] cause silicon control rectifiers to malfunction, and, normally, prompt doses over 100 rads (Si) will perturb most component parts sufficiently to cause all unhardened circuits to malfunction.

14-18 Subsystem Vulnerability [redacted]

[redacted] Generally it is those subsystems that use the more vulnerable semiconductor component parts that will limit the hardness of a system to radiation. The relative sensitivity of semiconductor devices to radiation was outlined in paragraph 14-3. Some of the more common circuits that are likely to use these component parts, and the attendant approximate hardness levels will now be described.*

[redacted] Unijunction transistors commonly are employed in time-delay circuits, pulse generators, clocks, pulse-shaping circuits, and as a trigger device driving SCR's. [redacted]

USANCA (L)(1)

[redacted] Power transistors generally are of two types: low-frequency types, such as those used in power supply dc-dc convertors or series regulators; and radio frequency (rf) power-amplifier types. [redacted]

USANCA (L)(1)

[redacted] Linear integrated circuits (amplifiers, etc.) are more susceptible to permanent damage than digital types, but the former are not used widely in military equipment. [redacted]

USANCA (L)(1)

[redacted] Possibly the most critical part of a system is its power source. Power supplied from a motor-generator, dynamotor or battery is least likely to fail in a radiation environment. [redacted] Failure levels are typical of those listed for power transistors.

USANCA (L)(1)

[redacted] Circuits that must retain information are susceptible to transient damage. That is, transient photocurrents can introduce erroneous information into the memory system or even change the information in the memory system.

[redacted] Integrated circuits can be triggered into a malfunction called "latchup" by the prompt ionizing dose at levels from 10 to 100 rads (Si). Latchup can be important because this particular condition may burn out the circuit or just simply not allow recovery to proper operation for periods long compared to the normal circuit-recovery times.

[redacted] Section VII, Chapter 9 provides more detailed information concerning circuit response to radiation.

[redacted] TREE-DAMAGE ESTIMATES [redacted]

[redacted] Estimates of system damage from nuclear-burst radiation are based on two factors. First is the likelihood that a given system type contains a susceptible circuit or subsystem as described in paragraph 14-18. Second is the probable environment in which the equipment will be used. Differences in shielding afforded by aircraft, missile, ship, or jeep installations could be significant for some components of nuclear burst radiations.

[redacted] The estimates that are given in succeeding paragraphs are not all inclusive in the types

---

* [redacted] Estimates are based on the assumption that the equipment was not designed with radiation hardness as a parameter, i.e., they are unhardened.

[redacted]

[redacted]

[redacted]

of systems or installations covered. The cross section of systems should provide some basis for estimating the radiation damage threshold of other similar equipment.

[redacted] Radiation levels given in the following paragraphs are considered to be external ambient levels. The gamma environment assumes monoenergetic photons having an energy of approximately 1 to 1.5 MeV. A slightly degraded fission spectrum is assumed for neutrons. The X-ray sources postulated for these estimates are blackbody spectra [redacted]

DNA (b)(3)

14-19 Ground Equipment [redacted]

[redacted] Estimates of radiation levels sufficient to cause failures as previously discussed are shown in Table 14-9 for typical ground installations or ground support equipment under the heading "sure kill." A lower threshold for failure, below which the equipment in question may be considered operable is referred to as "sure safe." All radiation levels are external ambient values that have meaning only for *unhardened* systems. For hardened systems, the hardening specifications should be consulted. It should be borne in mind that the fact that a system has been hardened does *not* mean that it will survive all radiation environments. It should, however, survive at least those to which it was hardened. It is further assumed that for most reasonable surface encounters, [redacted]

USANCA (b)(1)

[redacted] No ambient exposures are given for X-rays (cal/cm^2), since these depend strongly on the X-ray spectrum, which in turn, is extremely dependent on the weapon type and the degradation of the spectrum through the intervening space. [redacted] Except under unusual circumstances, X-rays probably do not pose a significant threat for ground equipment.

USANCA (b)(1)

14-20 An Example of Ground Equipment Survivability Estimation [redacted]

[redacted] The Lance support system provides an illustration of the use of Table 14-9. The missile itself is found under the heading "Ground and Sea Support Equipment"; however, the levels listed for the Lance are associated only with the missile and not with the launch support equipment or the communications equipment necessary to direct the launch. The associated critical electronic equipment for launch can be listed as follows:

1. Radio receiver and transmitter, or transceiver
2. Batteries to fire the missile and to operate the launch vehicle
3. Fire control system for the missile.

[redacted] The survivability levels for most of these subsystems can also be found in Table 14-9 and are listed on page 14–67. The firing system, not being listed in the table, must be estimated. A basic description of this system implies that it is a box of electrical toggle switches and lights; which apply power and indicate operation. These component parts are not particularly susceptible to radiation. Therefore, they should be at least as hard as the systems with semiconductor devices. Therefore, they will be considered as part of the communication electronics without affecting the analysis.

[redacted] With this summarized information any of three possible situations can be visualized for analysis:

[redacted]

USANCA (b)(1)

[redacted] The critical factors affecting mission completion in the first case are:

Page 14-66 with Table 14-9 Deleted. USANCA (b)(1)

[redacted]

[redacted]

USANCA (b)(1)

USANCA (b)(1)

For this case the gamma rate would not be critical, since the missile is not in operation and the other equipment does not have to function during the burst.

USANCA (b)(1)

Either the neutrons or gamma rays specified for the sure-kill level could cause significant problems, and both should be considered.

The second case.

USANCA (b)(1)

The sure-safe and sure-kill levels for this situation appear to be the same as the previous case. However, the gamma dose rate could cause problems and should be considered in the sure-safe level.

For the third case the missile is dependent solely on itself for control and the levels of survivability are the same as those shown for the missile alone.

14-21 Aircraft Systems

Estimates of sure safe and sure kill radiation levels in aircraft systems are shown in Table 14-10. These levels are considered to represent external ambient conditions. As was the case for ground equipment, the total dose is not considered to be a problem, and thermomechanical shock from X-rays is not considered important. However, the ionization rate includes both the X-ray and gamma-ray rates.

The functional breakdown for aircraft systems is more complex than that for ground systems, since many mission functions require several generic functions within the subsystems. As an example, penetration aids, such as terrain clearance radars, include power sources, radars, computers, flight control links and crew station data display consoles. A brief listing of subsystems that are considered to be part of a mission function are shown in the table. Depending on the type and mission of the aircraft of interest, some of these functions may not be critical or may not even be present in the system. For specific equipment it may be necessary to refer to the levels presented in the previous Table 14-9.

14-22 An Example of Aircraft Survivability Estimation

To clarify the process of analysis, two cases are considered. The first case is a single-engine spotter plane and the second is a jet fighter similar to the F-111A.

Considering first, the spotter aircraft, the generic functions are:

Pages 14-68 and 14-69 with Table 14-10 deleted. USANCA (b)(1)

[redacted]

[redacted]

1. Flight control
2. Crew station
3. Propulsion system
4. Mission and traffic control.

Of these, one function that might be critical to the mission is the Mission and Traffic Control. The crew may not be able to communicate their observations at a critical time, even though they may be able to escape if other generic functions failed. [redacted] If all functions except the crew station were considered, the survivability levels would still be the same. [redacted] Considering the modern fighter aircraft, it would appear that all generic functions listed in Table 14-10 might be associated with the aircraft. Depending on the mission of the plane, various combinations of these generic functions might be critical. For example, if the fighter was used for battlefield support, penetration aids would not be critical. The worst-case survivability levels would occur if both penetration aids and either the air-to-air or air-to-surface missiles were critical for mission completion. [redacted]

USANCA (b)(1)

USANCA (b)(1)

USANCA (b)(1)

14-23 Missile Systems [redacted]

[redacted] The missile systems included in Table 14-11 are categorized according to mission and guidance type. Thus, the damage criteria, in general, are not representative of a specific system, but reflect the mean susceptibility of systems within each category. Furthermore, unless otherwise specified, all systems are assumed to be unhardened. The categories are not all-encompassing. Where no information was available, estimates were made as noted. Sure-safe and sure-kill levels are given in terms of radiation levels external to the system. Although not a great problem for ground or aircraft systems, X-rays represent a much more formidable threat to missile systems operating at altitudes above 20 kilometers, hence, this information is included. The sources of X-rays postulated for these estimates are blackbody spectra [redacted] No problems are anticipated with the total gamma dose effects unless the dose exceeds 10^5 rads (Si). The prompt dose effects are taken into consideration in the dose rate terms. The dose rate estimates include both the X-ray and gamma ray rates. The dose-rate estimates are based on the damage caused by ionization effects, whereas the column head the "X-ray Exposure" includes estimates based on the damage caused by the thermomechanical effects. No example is provided since it is only necessary to select the correct classification for the missile to establish its survivability levels. There are basically three phases critical to the flight of missiles:

DNA (b)(3)

1. Storage
2. Powered flight
3. Reentry.

A prime factor that would influence the survivability of a missile in storage is not necessarily the electronics vulnerability associated with the missile but, rather, the shielding effectiveness provided by the storage area (e.g., missile silo). The activation and ground-control electronics would be evaluated by using Table 14-9. The powered flight would be concerned with both the missile and the reentry vehicle. And, last, the reentry would be concerned only with the reentry vehicles.

[redacted]

[redacted]

Page 14-71 with Table 14-11 deleted. USANCA (b)(1)

[redacted]

[redacted] BIBLIOGRAPHY [redacted]

Analysis of Atomic Weapons Effects Upon Army Ground Operations Equipment [redacted], Project Attack, Third Phase Report, ORO-S-200, Armour Research Foundation, Chicago, Illinois, 18 June 1951 [redacted]

Analysis of Atomic Weapons Effects Upon Army Ground Operations Equipment [redacted], Project Attack, Fourth Phase Report, Vol. I, ORO-S-208, Armour Research Foundation, Chicago, Illinois, 9 October 1951 [redacted]

Analysis of Atomic Weapons Effects Upon Army Ground Operations Equipment [redacted] Technical Memo ORO-T-223, Vol. I, Blast Effects, Armour Research Foundation, Chicago, Illinois, 16 March 1953 [redacted]

Berning, W. W., *Predicted Effects of Atomic Weapons Upon Ordnance Equipment* [redacted], BRL 847, U.S. Army Ballistic Research Laboratories, Aberdeen Proving Ground, Maryland, January 1953 [redacted].

Berning, W. W. and N. W. Arnold, *Combat Vehicle Exposure* [redacted] Operation Greenhouse, Annex 6.3, WT 90, U.S. Army Ballistic Research Laboratories, Aberdeen Proving Ground, Maryland, August 1952 [redacted]

Bowen, I. G., et al., *A Model Designed to Predict the Motion of Objects Translated by Classical Blast Waves* [redacted] Civil Effects Study CEX-58-9, Lovelace Foundation for Medical Research, Albuquerque, New Mexico, 29 June 1961 [redacted]

Brode, H. L., *Point Source Explosion in Air*, RM-1824-AEC, The RAND Corporation, Santa Monica, California, 3 December 1956 [redacted]

Bryant, E. J. and F. E. Grubbs, *Statistical Estimation of Damage to Ordnance Equipment Exposed to Nuclear Blast* [redacted], BRL 657-RD, U.S. Army Ballistic Research Laboratories, Aberdeen Proving Ground, Maryland, April 1953 [redacted]

Bryant, E. J., N. H. Ethridge, and J. L. McCoy, *Statistical Estimation of Damage to Ordnance Equipment Exposed to Nuclear Blasts* [redacted], Operation UPSHOT-KNOTHOLE, Project 3.21, WT-733, U.S. Army Ballistic Research Laboratories, Aberdeen Proving Ground, Maryland, February 1955 [redacted]

Bryant, E. J., and J. D. Day, *Effects of Rough Terrain on Drag-Sensitive Targets* [redacted] Operation PLUMBBOB, Project 1.8b Final Report, WT-1408, U.S. Army Ballistic Research Laboratories, Aberdeen Proving Ground, Maryland, 9 November 1959 [redacted]

Bryant, E. J., N. H. Ethridge, and M. R. Johnson, *Response of Drag-Type Equipment Targets in the Precursor Zone* [redacted] Operation TEAPOT, Project 3.1 Final Report, WT-1123, U.S. Army Ballistic Research Laboratories, Aberdeen Proving Ground, Maryland, 28 October 1959 [redacted]

[redacted] [redacted]

[redacted]

Burden, H. S. and J. D. Day, *Transient Drag Loading of Actual and Idealized Shapes from High-Yield Detonations* [redacted] Operation REDWING, Project 1.5, WT-1305, U.S. Army Ballistic Research Laboratories, Aberdeen Proving Ground, Maryland, 15 March 1960 [redacted]

Calvin, R. L. et al., *The Effects of Atomic Blast on Military Field Equipment* [redacted] Armour Research Foundation Report M041, Armour Research Foundation, Chicago, Illinois, 28 February 1955 [redacted]

Deeds, F. E., et al., *Mine Field Clearance by Nuclear Weapons* [redacted] Operation PLUMBBOB, Project 6.1 Final Report, WT-1435, Midwest Research Institute, Kansas City, Missouri, and U.S. Army Engineer Research and Development Laboratories, Fort Belvoir, Virginia, 16 August 1960 [redacted]

Effects of the Atomic Bomb on Nagasaki, Japan, U.S. Strategic Bombing Survey, Physical Damage Division, Vol. I, II, III, June 1947 [redacted]

Effects of the Atomic Bomb on Hiroshima, Japan, U.S. Strategic Bombing Survey, Physical Damage Division, Vol. I, II, III, May 1947 [redacted]

Ethridge, N. H., *Blast Effects on Simple Objects and Military Vehicles* [redacted] Operation SUN BEAM, Project 1.3, POR-2261, U.S. Army Ballistic Research Laboratories, Aberdeen Proving Ground, Maryland, 18 September 1964 [redacted]

Gwyn, C. W., D. L. Scharfetter, and J. L. Wirth, *The Analysis of Radiation Effects in Semiconductor Junction Devices*, SC-R-67-1158, Sandia Corporation, Albuquerque, New Mexico, July 1967 [redacted]

Hearn, J. N. W., Lt. Col., *Operation BUFFALO: Interim Report of the Target Response Ordnance Group* [redacted] FWE-142, AWRE Report T25/57, Atomic Weapons Research Establishment, Aldermaston, Berks, England, June 1957 [redacted]

Henderson, J. E., *Vulnerability of Radar to Nuclear Explosions* [redacted] AWEC/P(57)44, FWE-136, Air Ministry, Ministry of Defence, U.K., August 1957 [redacted]

Heyman, R. J. and H. G. Myer, *Transient Drag and Its Effects on Structures* [redacted] AFSWC-TR-56-46, American Machine and Foundry, Chicago, Illinois, November 1956 [redacted]

Kalionowski, J. I., *A Management Guide to Transient-Radiation Effects on Electronics (TREE)* [redacted] DNA 2051H, Battelle Columbus Laboratories, Columbus, Ohio, February 1972 [redacted]

Kaplan, K., and C. Wiehle, *Air Blast Loading in the High Shock Strength Region* [redacted] *Part I – Analysis and Correlation, Part II – Prediction Methods and Examples*, URS 633-3, DASA 1460, URS Corporation, Burlingame, California, February 1965, [redacted]

Larin, F., *Radiation Effects in Semiconductor Devices*, John Wiley and Sons, Inc., New York, 1968

Martin, A. R. F., *The Effects of Blast on Dummies and Scout Cars* Operation ANTLER, Target Response Group, AWRE Report T6/59, FWE 238, Atomic Weapons Research Establishment, Aldermaston, Berks, England, August 1959.

McCoy, J. L., *Damage Reports on Exposed Ordnance Equipment* Operation UPSHOT-KNOTHOLE, Supplement to Project 3.21, WT-821, U.S. Army Ballistic Research Laboratories, Aberdeen Proving Ground, Maryland, December 1954

Morris, P. J., *Study of Military Field Equipment Response to Air Blast and Prediction of Damage* DASA 2005-1 and 2005-2, URS 660-9, URS Research Company, San Mateo, California, 2005-1, October 1971 2005-2, January 1972

Morris, W. E., et al., *Air Blast Measurements* Operation UPSHOT-KNOTHOLE, Projects 1.1a and 1.2, WT-710, U.S. Naval Ordnance Laboratory, White Oak, Silver Spring, Maryland, August 1955

Nelson, R. C., Capt., *The Effects of Atomic Weapons on Engineer Heavy Equipment* ERDL Report 1443, U.S. Army Engineer Research and Development Laboratories, Fort Belvoir, Virginia, 25 April 1956

Nuclear Weapons Blast Phenomena: Volume I, Source and Development of Blast Waves in Air DASA 1200-I, Defense Atomic Support Agency, Washington, D.C., 1 March 1971

Nuclear Weapons Blast Phenomena: Volume II, Blast Wave Interaction, DASA 1200-II, Defense Atomic Support Agency, Washington, D.C., 1 December 1970

Nuclear Weapons Blast Phenomena: Volume III, Air and Subsurface Explosions DASA 1200-III, Defense Atomic Support Agency, Washington, D.C., 1 March 1970

Olesen, H. L., *Radiation Effects on Electronic Systems* General Electric Systems, General Electric Company, Missile and Space Division, Philadelphia, Pennsylvania, Plenum Press, New York, 1966

Operation CROSSROADS Atomic Bomb Tests Army Ground Group (Task Group 1.4), Report Number XRD-149, Volume I, 27 January 1946 to 27 September 1946

Operation CROSSROADS Atomic Bomb Tests Report of Commander, Task Unit 1.4.3 (Ordnance), Report Number XRD-152, Volume IV, Appendix VII, January 27 to September 30, 1946

[redacted]

Seager, E. R. Drake, R. F. C. Butler, *Operation TOTEM Group 12 Report: Effects on a Landrover (car, 5 CWT, 4x4) and Generating Sets* [redacted] AWRE Report T 79/54(x), FWE-131, Atomic Weapons Research Establishment, Aldermaston, Berks, England, September 1956 [redacted]

TREE (Transient-Radiation Effects on Electronics) Handbook [redacted] Volume 1, Edition Number 3, DNA 1420 H-1, Battelle Columbus Laboratories, Columbus, Ohio, December 1971 [redacted]

TREE (Transient-Radiation Effects on Electronics) Handbook [redacted] Edition 2, Revision 2, DASA 1420-1, Battelle Memorial Institute, Columbus, Ohio, September 1970 [redacted], (to be replaced by DNA 1420 H-2 during calendar year 1972).

TREE Preferred Procedures (Selected Electronic Parts), DASA 2028, Battelle Memorial Institute, Columbus, Ohio, May 1968 [redacted] (to be replaced by DNA 2028H during calendar year 1972).

Vook, F. L., Editor, *Radiation Effects in Semiconductors* [redacted] Proceedings of the Santa Fe Conference on Radiation Effects in Semiconductors, Plenum Press, New York, 1968 [redacted]

Willoughby, A. B., K. Kaplan, and R. I. Condit, *Effects of Topography on Shock Waves in Air* [redacted] AFSWC TR-57-9, Broadview Research and Development, Burlingame, California, March 1956 [redacted]

[redacted]

AD-A955 399

DTIC
ELECTE
2 MAR 1989
S D
E

Chapter 15
DAMAGE TO FOREST STANDS

INTRODUCTION

Forest stands may protect personnel from some effects of nuclear weapon explosions, for example, the direct effects of thermal radiation; however, the trees themselves are quite vulnerable to breaking, uprooting, and ignition. Falling limbs and trees may be a hazard, and the debris on the forest floor may impede troop and vehicle movement. In dry, windy weather a nuclear explosion may ignite forest fires, and the smoke and flame may extend the range of hazardous effects many times. The vulnerability of forests depends upon recent local weather history, and upon the type of tree stand involved.

This chapter is divided into three sections. Section I provides data concerning air blast damage to various types of forest stands. Section II contains a discussion of the effects of tree blowdown on troop and vehicle movement and provides methods to predict the degree to which movement might be impaired as a result of tree blowdown. Section III provides information concerning the effects of thermal radiation on forests and the fire hazards that might arise therefrom.

SECTION I
AIR BLAST

15-1 Forest Stand Types

Forest stands may be divided into four general types for the purpose of discussing air blast effects. Types I through IV as well as the subtypes of Type IV are described in the following discussion.

TYPE I: IMPROVED NATURAL OR PLANTED CONIFER FORESTS OF EUROPEAN TYPE. Stands of this type generally occur in Western Europe. They either have been planted or are natural stands that have been cultivated. Characteristics of this type of forest include uniform tree spacing, uniform height and diameter, and a dense crown canopy. Low stumps usually will be found within the stand as a result of thinning. Lower limbs will be clear as a result of pruning, and there will be little or no underbrush. All of these characteristics combine to provide good visibility and easy passage through the forest. Damage to these stands generally is caused by breaking the trunks rather than by uprooting.

TYPE II. UNIMPROVED NATURAL CONIFER FORESTS THAT HAVE DEVELOPED UNDER UNFAVORABLE GROWING CONDITIONS. This type of forest is found in Western Europe and Southeast Asia. Random tree spacing, height, and diameter together with irregular crown canopy characterize this type of stand. The forest floor is partially covered with dead fallen trees, and where clearings occur there is usually heavy underbrush. Visibility is generally poor and passage through the forest is difficult. Damage usually results from uprooting rather than breaking.

TYPE III. UNIMPROVED NATURAL CONIFER FORESTS THAT HAVE DEVELOPED UNDER FAVORABLE GROWING CONDITIONS. This type of forest occurs in Western Europe and Southeast Asia. These forests are characterized by random tree spacing and diameter, uneven crown canopy, and irregular clearings. Visibility and passage through these stands are difficult in Western Europe, although the underbrush generally is light, since dead fallen trees clutter the forest floor.

This document has been approved for public release and sale; its distribution is unlimited.

89 3 02 035

[redacted]

[redacted]

In Southeast Asia, dense shrub undergrowths usually cover the forest floor. Damage to this type of forest usually results from uprooting.

TYPE IV. ALL TYPES OF DECIDUOUS FORESTS. The trees in these stands are similar to the deciduous trees of Western Europe and Southeast Asia. Since damage to these trees depends on the condition of the foliage, two categories must be considered: IV (f) is category type IV with foliation, and IV (d) is type IV without foliation. In both cases extensive crown damage and breakage of limbs will occur. In most ground, trunk damage will be caused mainly by uprooting. This class of forests is broken down into four subtypes:

TYPE IVa. This subtype includes two further subtypes that have different characteristics but produce similar blowdown obstacles equidistant from a particular nuclear burst. Two categories are required as a result of the difference in time required to clear away blowdown obstacles.

TYPE IVa-1. This subtype occurs in Western Europe and Southeast Asia. It includes most temperate zone deciduous forests, such as the shorter, more open parts of the dry season deciduous forests of Northern Southeast Asia and the evergreen oak forests at elevations of 3,000 to 7,000 feet in Southeast Asia. The trees

Table 15-1 [redacted] Average Height of Trees, Diameter, Tree Density, and Length of Tree Stem [redacted]

Forest Stand Type	Tree Diameter	Average Height of Trees* (feet)	Average Tree Density per Acre*	Average Total Tree Stem-feet per Acre*
I	up to 24 in.	130	75	9,750
II	up to 20 in.	50	260	13,000
III	up to 40 in.	80	200	16,000
IVa†	up to 40 in.	80	200	16,000
IVa‡	24-in. average	100	140	14,000
IVb‡	40-in. average	100	850	85,000
IVc§	up to 18 in.	35	40	1,400
IVd	up to 18 in.	40	100	4,000

[redacted] Stem-feet per acre is determined by multiplying average tree height by tree density.

† [redacted] Considers only trees 6 in. or larger in diameter.

‡ [redacted] Height varies up to 200 ft in rain forest and up to 150 ft in dry season deciduous forest for about 10 percent of trees. Diameter varies up to 80 in. for 10 percent of rain forest trees and up to 60 in. for 10 percent of dry season deciduous forests.

§ [redacted] Height varies from 10–50 ft.

[redacted]

[redacted]

[redacted]

of this subtype are defoliated in the winter in the temperate zone with the exceptions of the evergreen oak (not defoliated) and the dry season forests of Northern Southeast Asia, which are defoliated in the summer.

TYPE IVa-2. Teak plantations and the denser, taller cloud forests that occur at lower elevations are included in this type. The teak plantation trees are planted 15 to 20 feet apart and produce a continuous canopy when foliated. No foliation is present during the dry season. The cloud forests start at an elevation of about 3,500 feet on the mountain slopes of Southeast Asia. The canopy of these forests gives a matted appearance from the air.

TYPE IVb. This subtype includes rain forests of Southeast Asia and the majority of the dry season deciduous forests of Northern Southeast Asia. Although no data are available concerning attenuation of the air blast wave, it is probable that these forests are sufficiently dense to decrease the radius of blast effect, thereby reducing the damage distance of a nuclear explosion.

TYPE IVc. This type includes cloud forests at high elevations, savannas, and low open forests that are made up of small scattered trees. This type of forest, when defoliated, is a good approximation for open deciduous wooded areas, such as orchards, in temperate zones.

TYPE IVd. This type consists of rubber plantation trees that occur mainly in Southeast Asia. The characteristics include little underbrush and dense, overlapping crowns.

[redacted] Table 15-1 shows the characteristic dimensions, tree densities, and tree stem-feet per acre for the forest stand types described above.

Table 15-2 [redacted] Index of Isodamage Curves Showing Forest Stand Type and Applicable Figure Number for Indicated Degree of Damage [redacted]

Forest Stand Type	Light Damage	Moderate Damage	Severe Damage	Total Damage
I	NA	15- 2	15- 3	15- 4
II	NA	15- 5	15- 6	15- 7
III	NA	15- 8	15- 9	15-10
IVa-1(f)	*	15-11	15-12	15-13
IVa-1(d)	15-1	15-14	15-15	15-16
IVa-2(f)	*	15-17	15-18	15-19
IVa-2(d)	15-1	15-20	15-21	15-22
IVb(f)	*	15-23	15-24	15-25
IVb(d)	*	15-26	15-27	15-28
IVc(f)	*	15-29	†	15-30
IVc(d)	15-1	15-31	†	15-32
IVd	*	15-33	†	15-34

* [redacted] The ground range for Light Damage, 50% branch breakage, is less than the ground range for Moderate Damage, 750 stem-feet down per acre.

† [redacted] Forest is of insufficient density and/or height to produce 7,500 stem-feet down per acre.

15-2 Damage-Distance Relations [redacted]

[redacted] Isodamage curves that are functions of weapon yield, distance, and height-of-burst are shown in Figures 15-1 through 15-34 for the forest stand types described in paragraph 15-1. Table 15-2 provides an index of the figures as a function of forest stand type and degree of damage. The degrees of damage shown in Table 15-2 are defined as follows:

TOTAL DAMAGE: 90 percent or more of trees are uprooted.

[redacted]

[redacted]

[redacted]

SEVERE DAMAGE: 9,000 feet of tree stem down per acre for coniferous forests and 7,000 feet of tree stem down per acre for deciduous forests.

MODERATE DAMAGE: 1,500 feet of tree stem down per acre for coniferous forests and 750 feet of tree stem down per acre for deciduous forests.

LIGHT DAMAGE: 50 percent breakage of crowns and branches for deciduous forests. Does not exist for coniferous forests.

Accession For
NTIS GRA&I ☒
DTIC TAB ☐
Unannounced ☐
Justification per basis doc
By
Distribution/
Availability Codes
Dist | Avail and/or Special
A-1

QUALITY INSPECTED 4

UNANNOUNCED

[redacted]

[redacted]

Problem 15-1 Calculation of Air Blast Damage to Forest Stands

[redacted] Figures 15-1 through 15-34 show total, severe, moderate, and light isodamage curves for different types of forest stands. Definitions of the degrees of damage are provided in paragraph 15-2. Decreases in the damage distances for shallow subsurface bursts may be estimated from Figure 11-24 by the methods described in Problem 11-2.

[redacted] *Scaling.* For yields between those for which isodamage curves are provided, scale as follows:

$$\frac{d}{d_i} = \frac{h}{h_i} = \left(\frac{W}{W_i}\right)^{1/3}$$

where d_i and h_i are the distance from ground zero and the height of burst, respectively, for yield W_i, which is the nearest yield to the desired yield for which a curve is provided; and d and h are the corresponding distance and height of burst for a (desired) yield of W kt or Mt (W and W_i must be in the same units).

For yields greater than 10 Mt this scaling becomes

$$\frac{d}{d_{10}} = \frac{h}{h_{10}} = \frac{[W(Mt)]^{1/3}}{(10)^{1/3}} = \frac{[W(Mt)]^{1/3}}{2.15}$$

where d_{10} and h_{10} are the distance from ground zero and height of burst, respectively, for 10 Mt; and d and h are the corresponding distance and height of burst for a yield of W Mt.

[redacted] *Example* [redacted]

Given:

a. A 5 kt weapon burst at a height of 400 feet above a Type IVa-1(f) forest stand.

b. A 20 Mt weapon burst at a height of 1,000 feet above a Type I forest stand.

Find:

a. The distance to which severe damage extends for the Type IVa-1(f) forest stand.

b. The distance to which moderate damage extends for the Type I forest stand.

Solution:

a. Table 15-2 shows that Figure 15-12 contains the isodamage curves appropriate for a Type IVa-1(f) forest stand. Examination of Figure 15-12 shows that the yield nearest 5 kt for which an isodamage curve is provided is 3 kt. The corresponding height of burst for a 3 kt weapon is

$$h_3 = h\left(\frac{3}{W}\right)^{1/3} = 400 \times \left(\frac{3}{5}\right)^{1/3} = 340 \text{ ft.}$$

From Figure 15-12, at a height of burst of 340 feet, the distance from ground zero to which severe damage will occur to a Type IVa-1(f) forest stand is 3,000 feet.

b. Table 15-2 shows that Figure 15-2 contains isodamage curves appropriate for moderate damage to a Type I forest stand. The corresponding height of burst for a 10 Mt weapon is

$$h_{10} = \frac{2.15\ h}{(W)^{1/3}} = \frac{2.15 \times 1{,}000}{(20)^{1/3}} = 790 \text{ ft.}$$

From Figure 15-2, at a height of burst of 790 feet, the distance from ground zero to which moderate damage to a Type I forest stand occurs from a 10 Mt weapon is 42,000 feet.

Answer:

a. The corresponding distance for severe damage to a Type IVa-1(f) forest stand from a 5 kt weapon burst at a height of 400 feet is

$$d = d_3\left(\frac{W}{3}\right)^{1/3} = 3{,}000 \times \left(\frac{5}{3}\right)^{1/3} = 3{,}560 \text{ ft.}$$

b. The corresponding distance for moderate damage to a Type I forest stand from a 20 Mt

[redacted]

[redacted]

weapon at a height of 1,000 feet is

$$d = \frac{d_{10}[W(Mt)]^{1/3}}{2.15} = \frac{42{,}000 \times (20)^{1/3}}{2.15}$$

$$= 53{,}000 \text{ ft.}$$

Reliability: The curves of Figures 15-1 through 15-34 are based on observed results of limited full scale tests, limited high explosive field tests, and extensive laboratory experiments. No definite estimate of the reliability of the scaling for yields above about 30 Mt can be made.

Related Material: See paragraphs 15-1 and 15-2. See also Figure 11-24 and Problem 11-2.

[redacted]

[redacted]

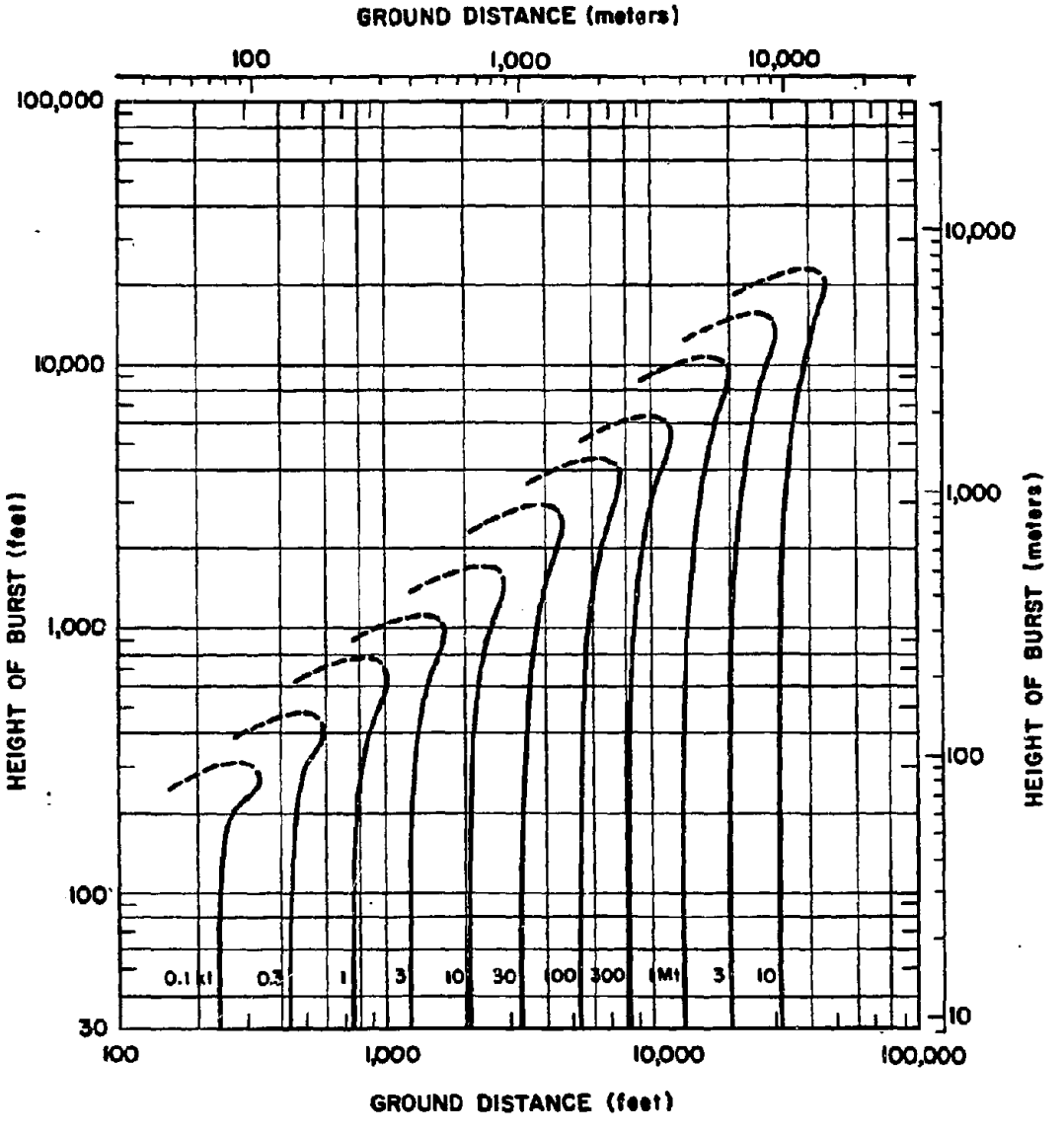

Figure 15-3. [redacted] Severe Damage to a Type I Forest [redacted]

[redacted]

[redacted]

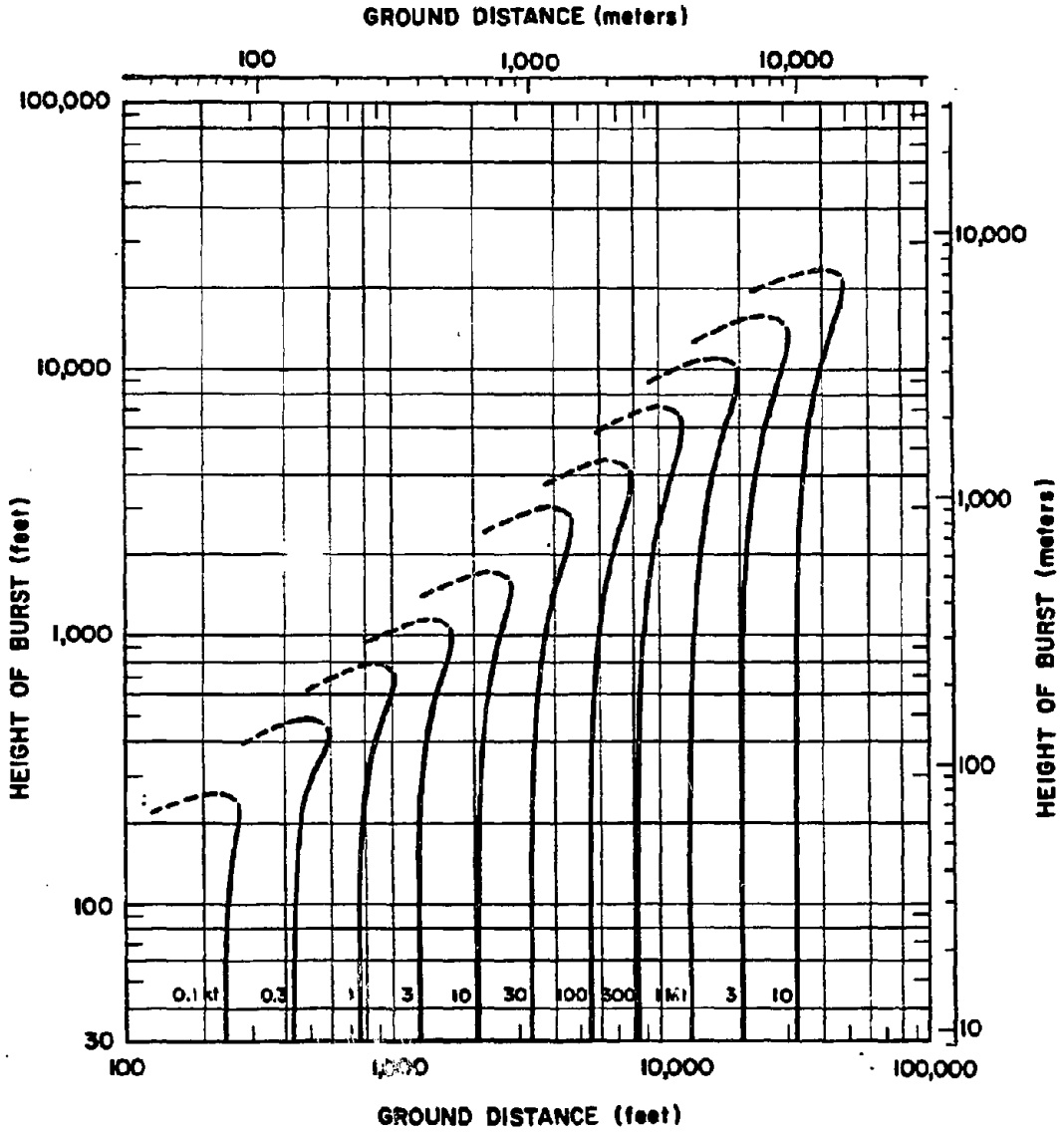

Figure 15-4. [redacted] Total Damage to a Type I Forest [redacted]

[redacted]

[redacted]

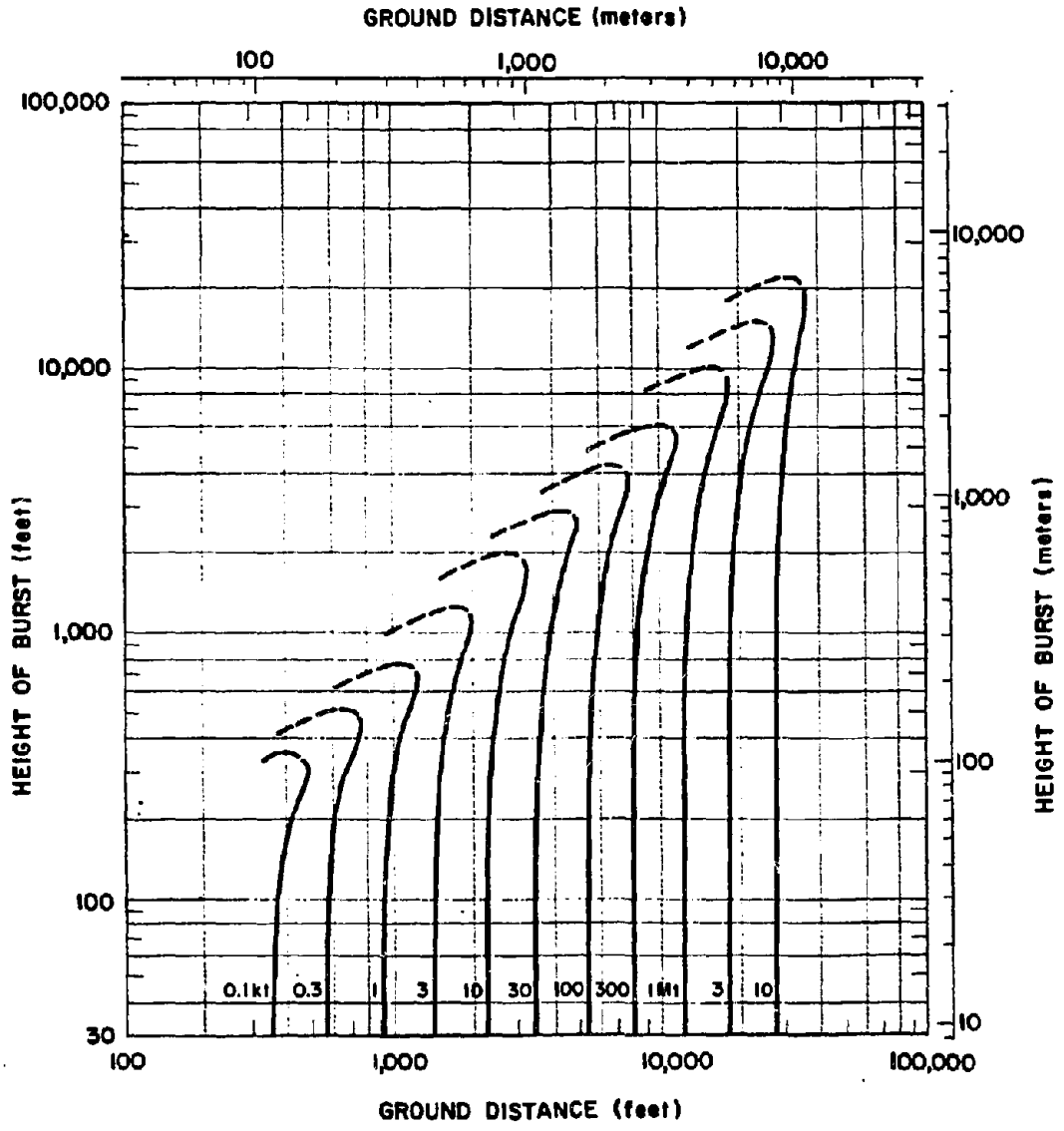

Figure 15-6. [redacted] Severe Damage to a Type II Forest [redacted]

[redacted]

[redacted]

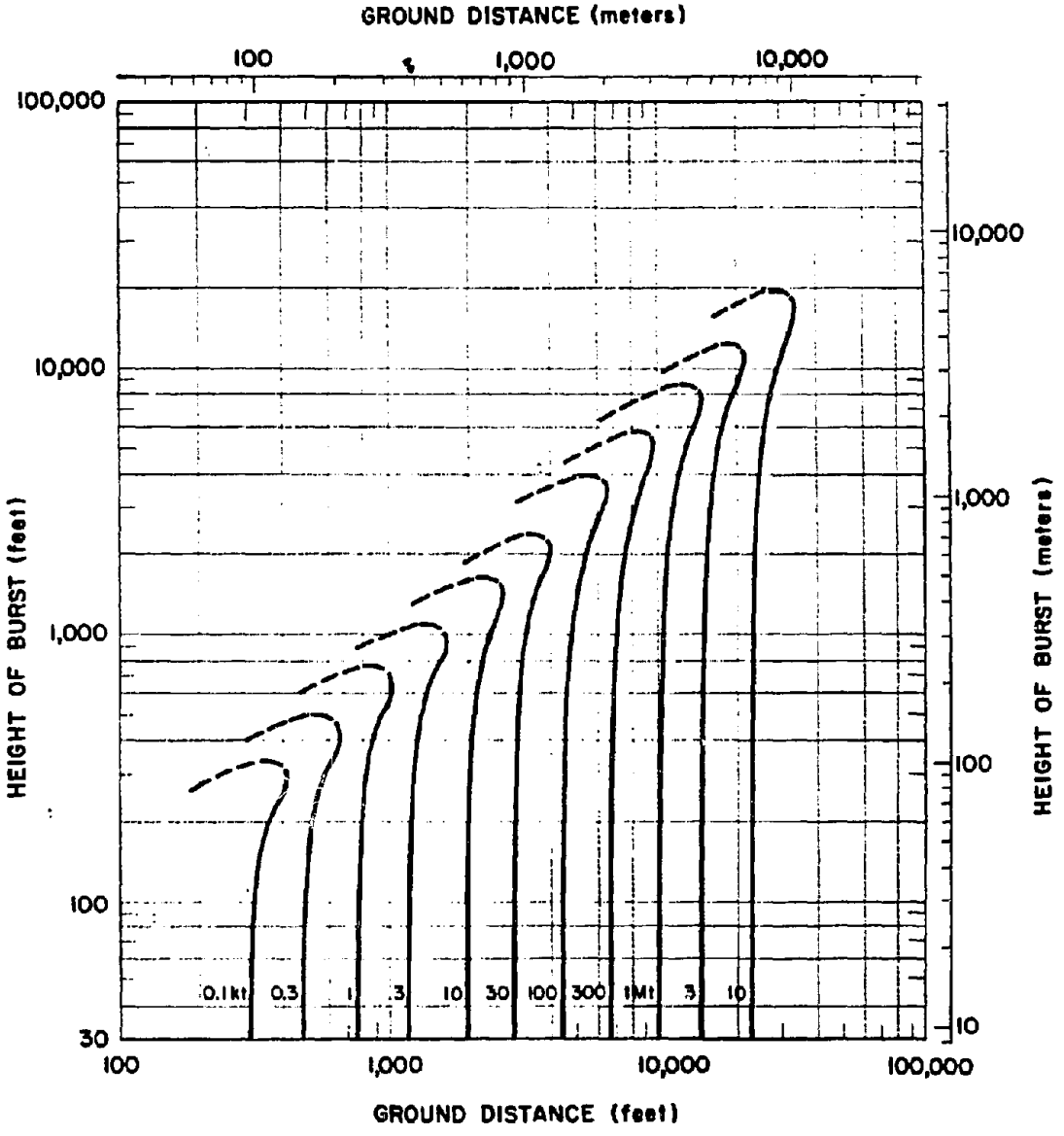

Figure 15-7. [redacted] Total Damage to a Type II Forest [redacted]

[redacted]

[redacted]

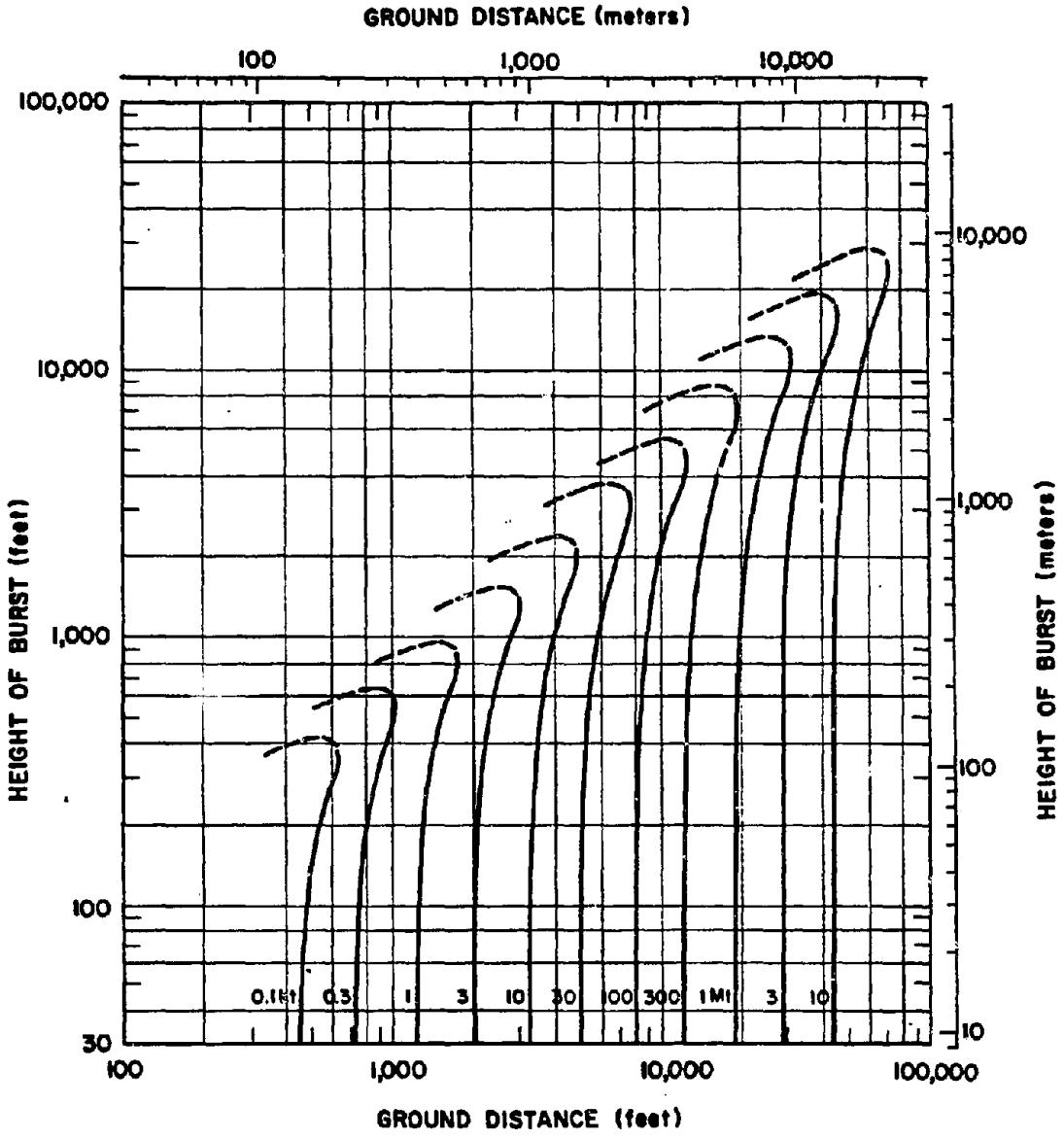

Figure 15-9. [redacted] Severe Damage to a Type III Forest [redacted]

[redacted]

[redacted]

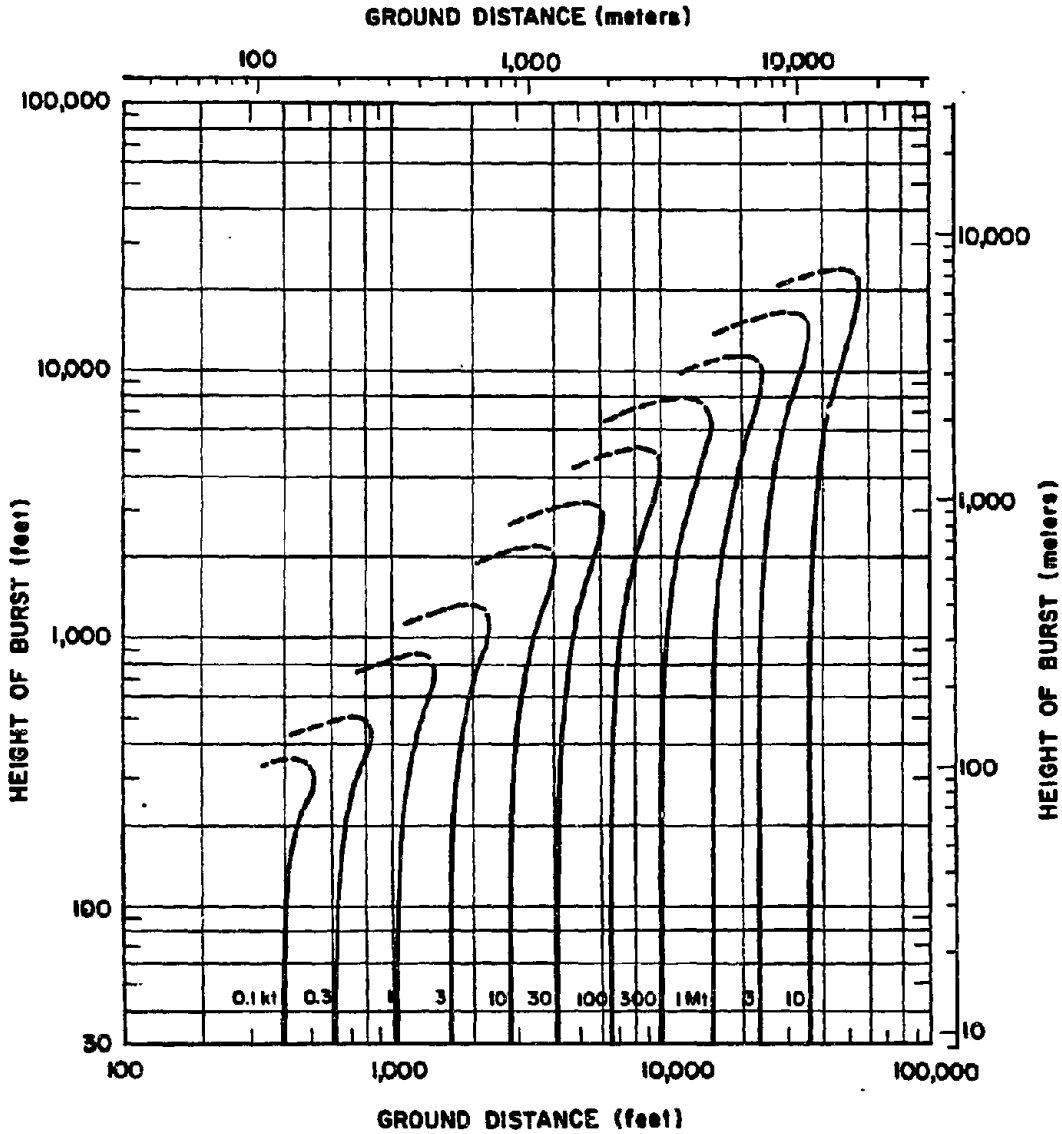

Figure 15-10. [redacted] Total Damage to a Type III Forest [redacted]

[redacted]

[redacted]

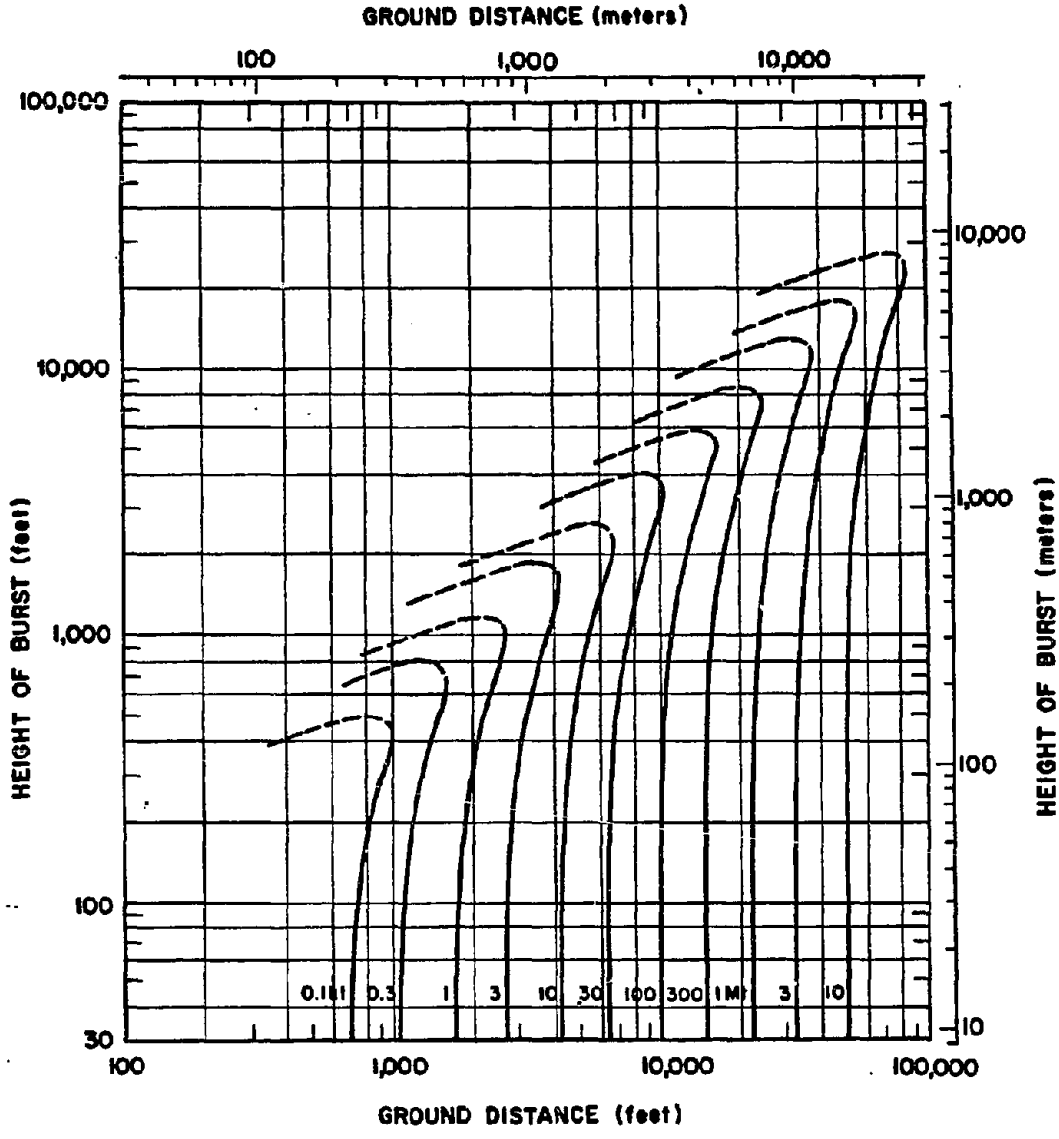

Figure 15-12. [redacted] Severe Damage to a Type IVa-1(f) Forest [redacted]

[redacted]

[redacted]

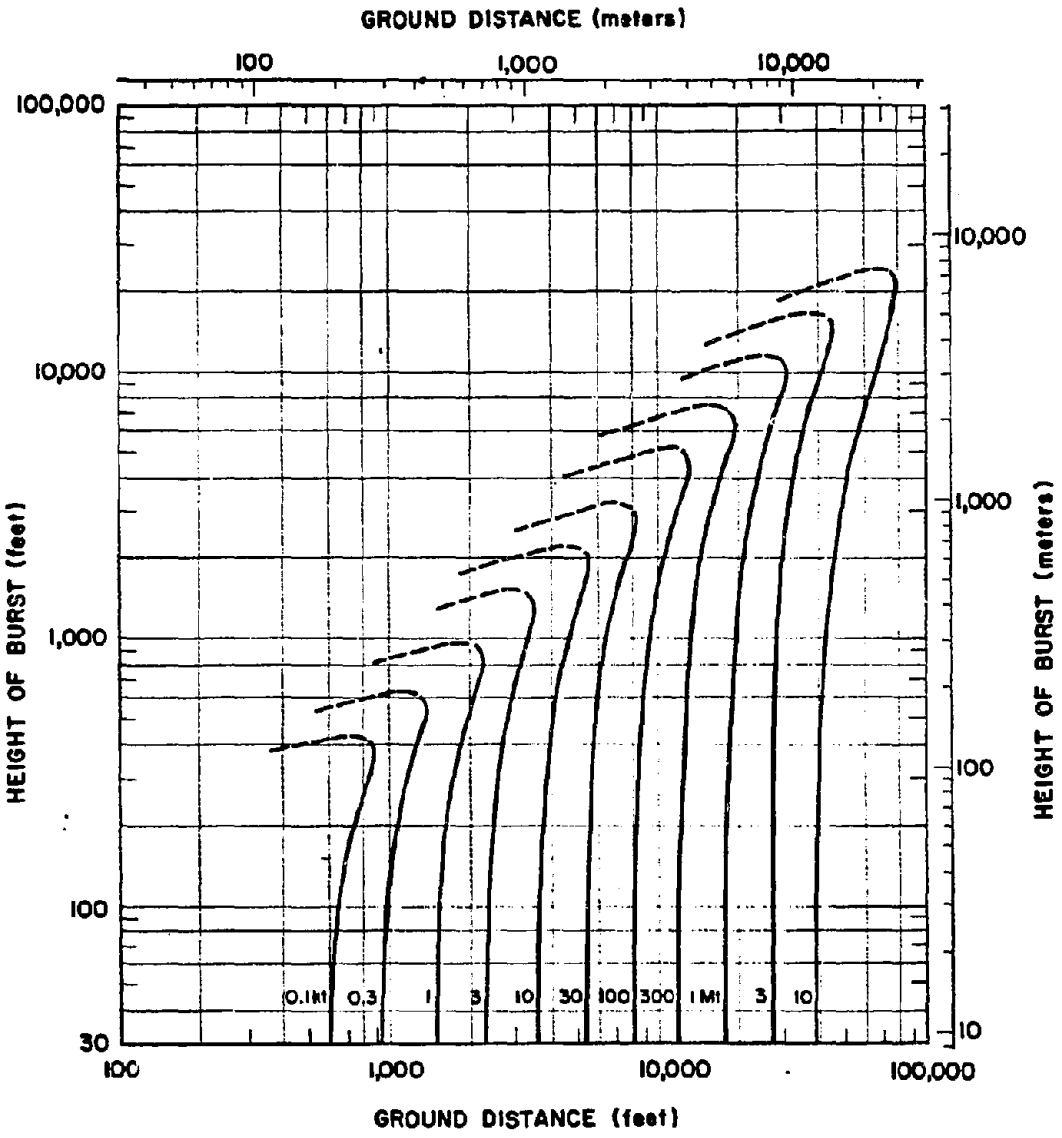

Figure 15-13. [redacted] Total Damage to a Type IVa-1(f) Forest [redacted]

[redacted]

[redacted]

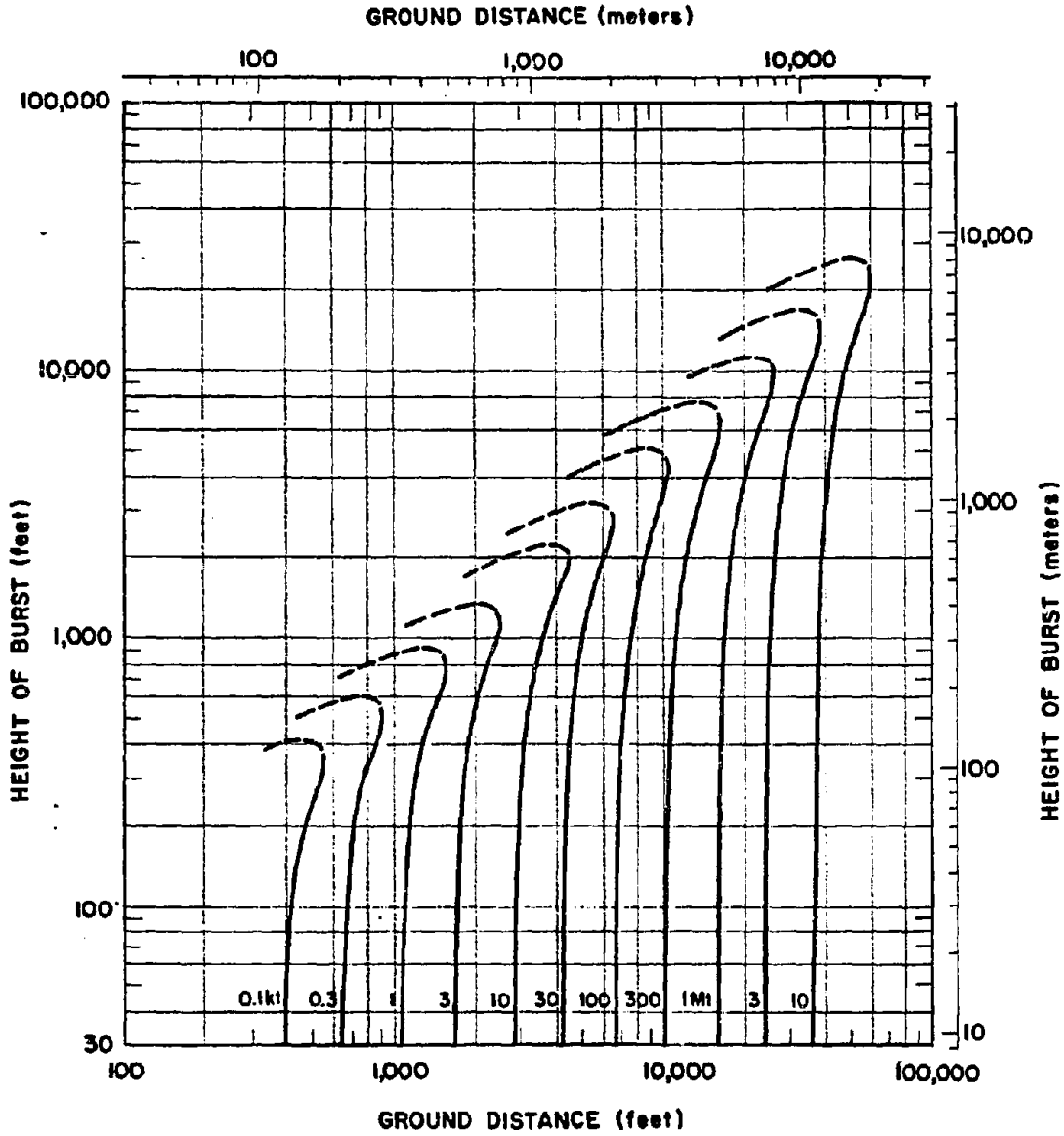

Figure 15-15. [redacted] Severe Damage to a Type IVa-1(d) Forest [redacted]

[redacted]

[redacted]

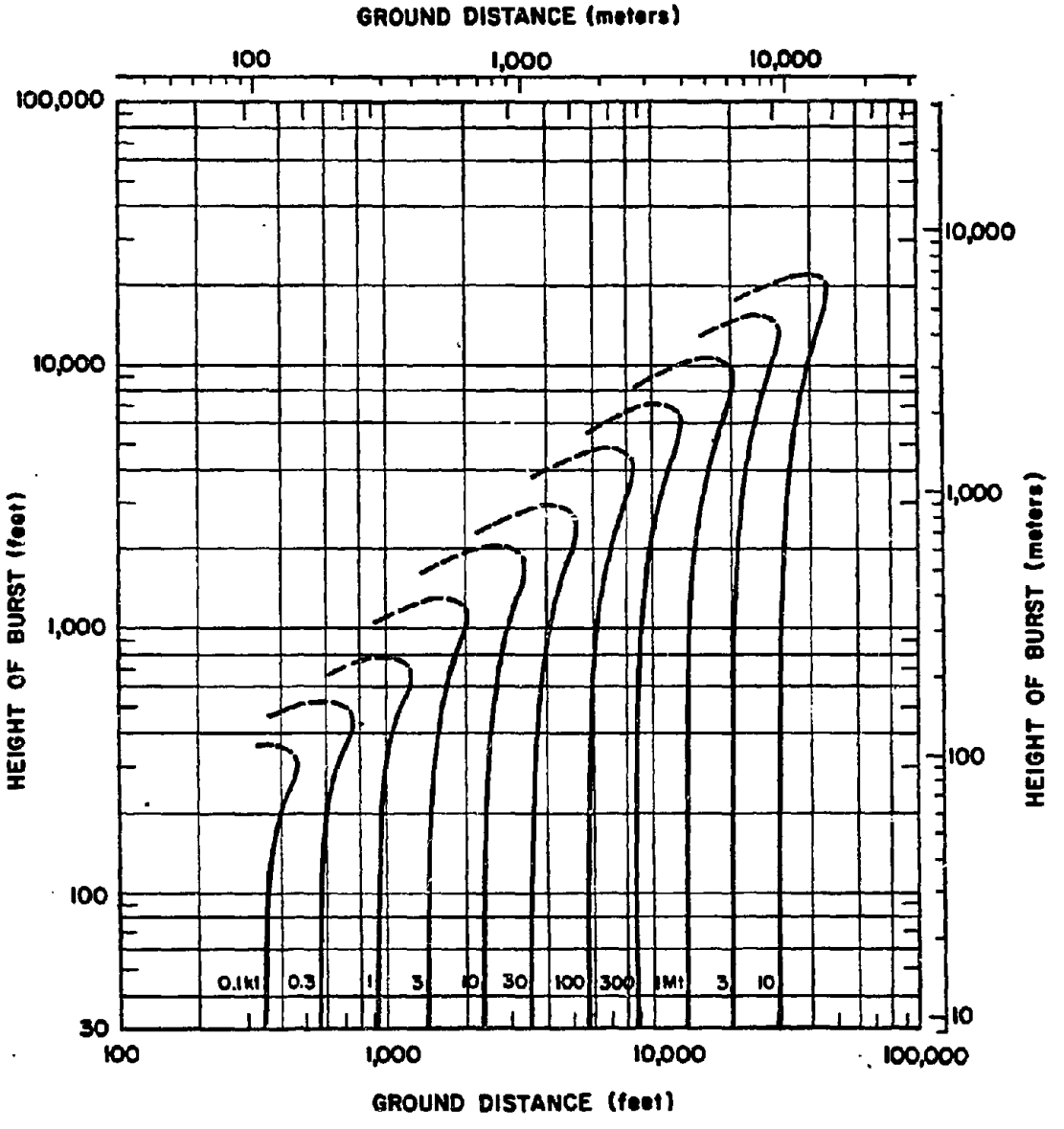

Figure 15-16. [redacted] Total Damage to a Type IVa-1(d) Forest [redacted]

[redacted]

[redacted]

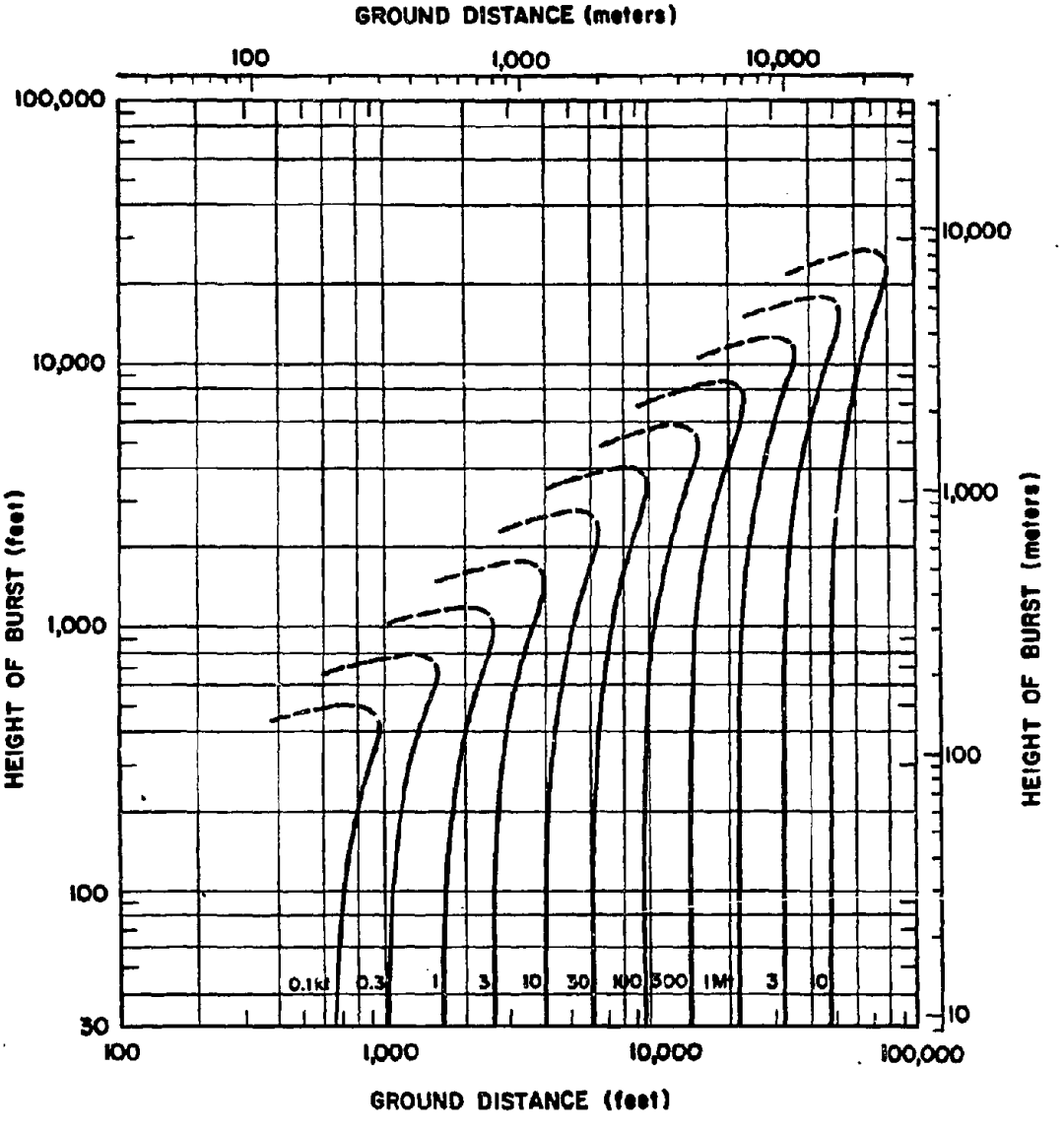

Figure 15-18. [redacted] Severe Damage to a Type IVa-2(f) Forest [redacted]

[redacted]

[redacted]

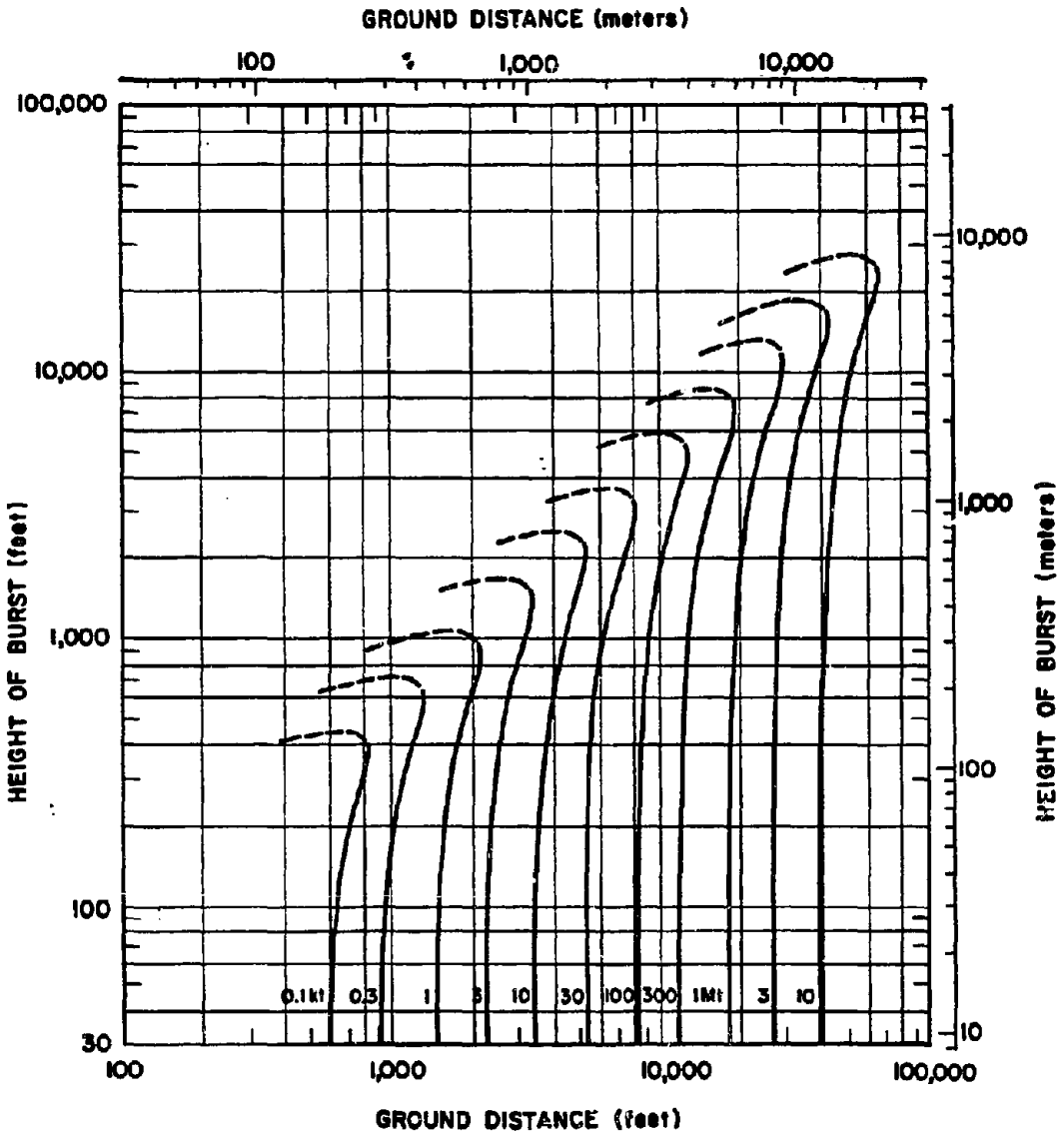

Figure 15-19. [redacted] Total Damage to a Type IVa-2(f) Forest [redacted]

[redacted]

[redacted]

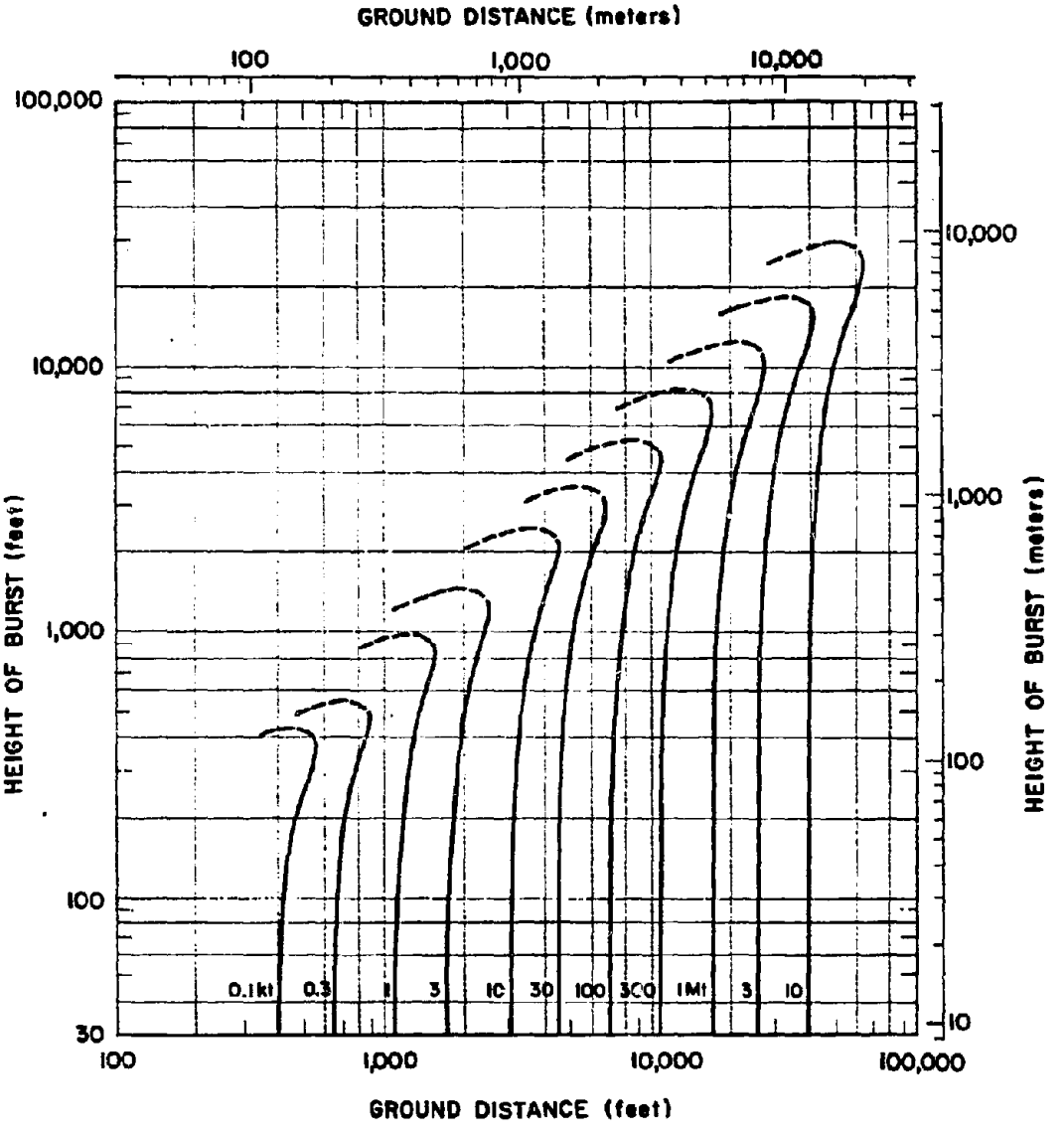

Figure 15-21. [redacted] Severe Damage to a Type IVa-2(d) Forest [redacted]

[redacted]

[redacted]

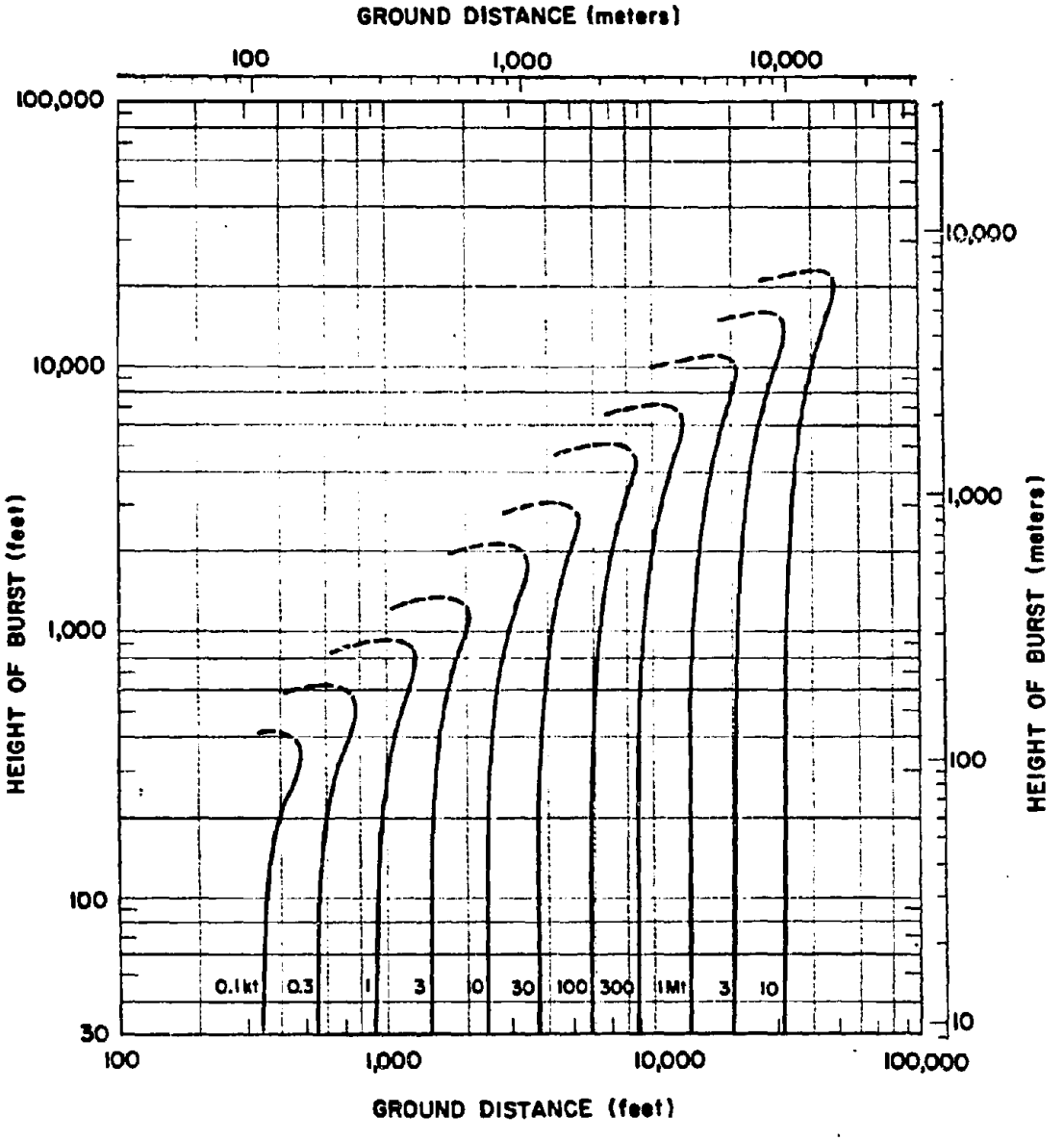

Figure 15-22. [redacted] Total Damage to a Type IVa-2(d) Forest [redacted]

[redacted]

[redacted]

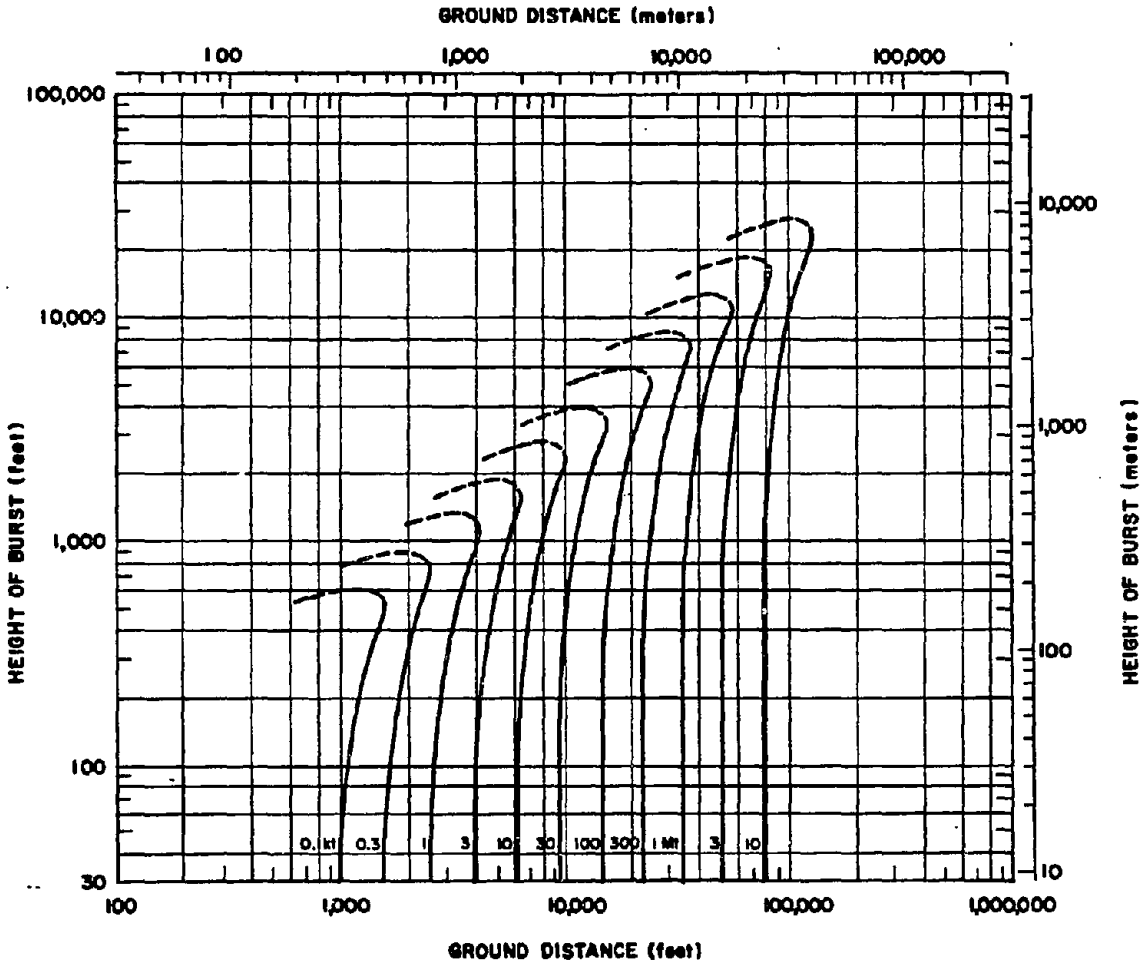

Figure 15-24. [redacted] Severe Damage to a Type IVb(f) Forest [redacted]

[redacted]

[redacted]

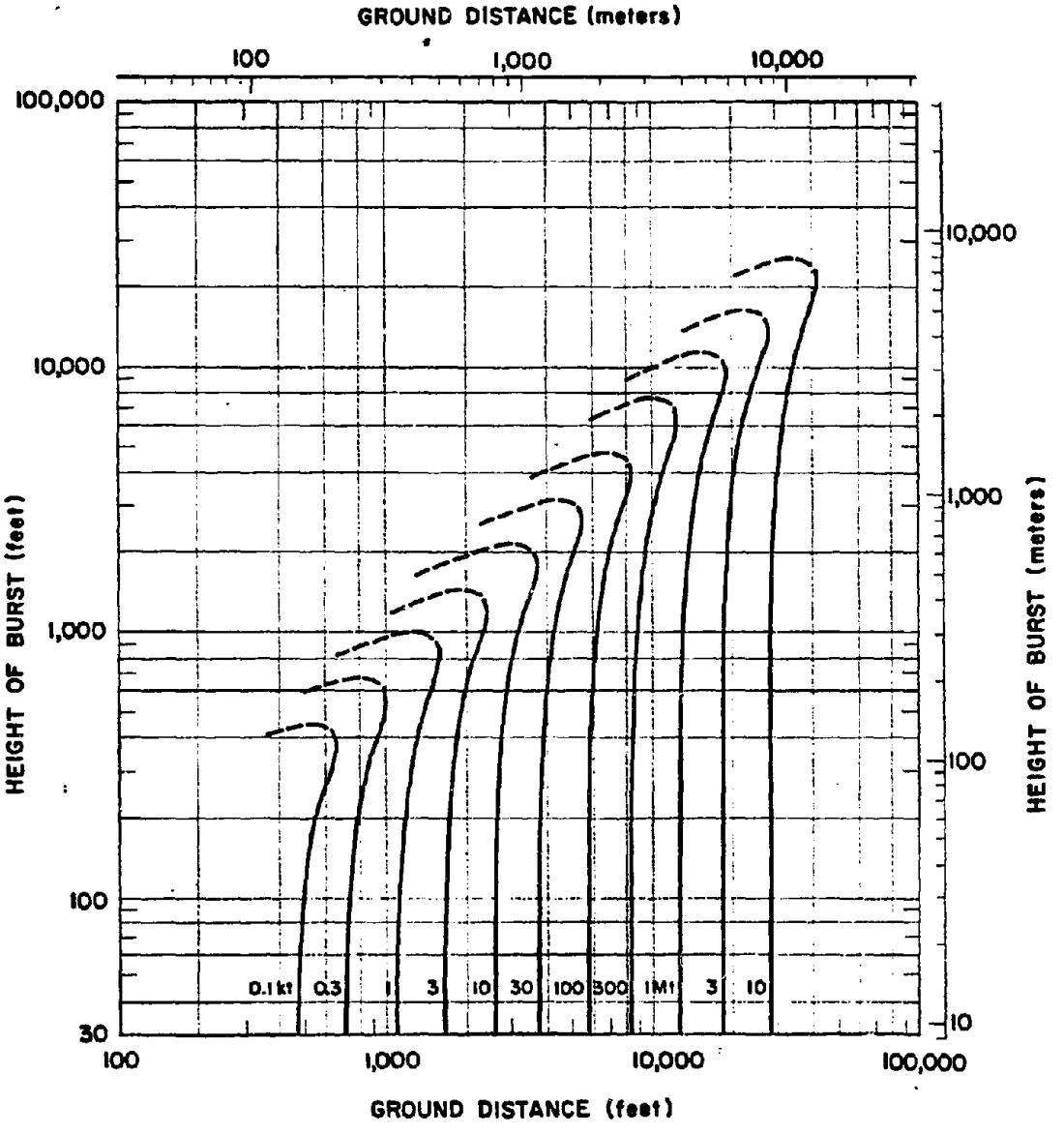

Figure 15-25. [redacted] Total Damage to a Type IVb(f) Forest [redacted]

[redacted]

[redacted]

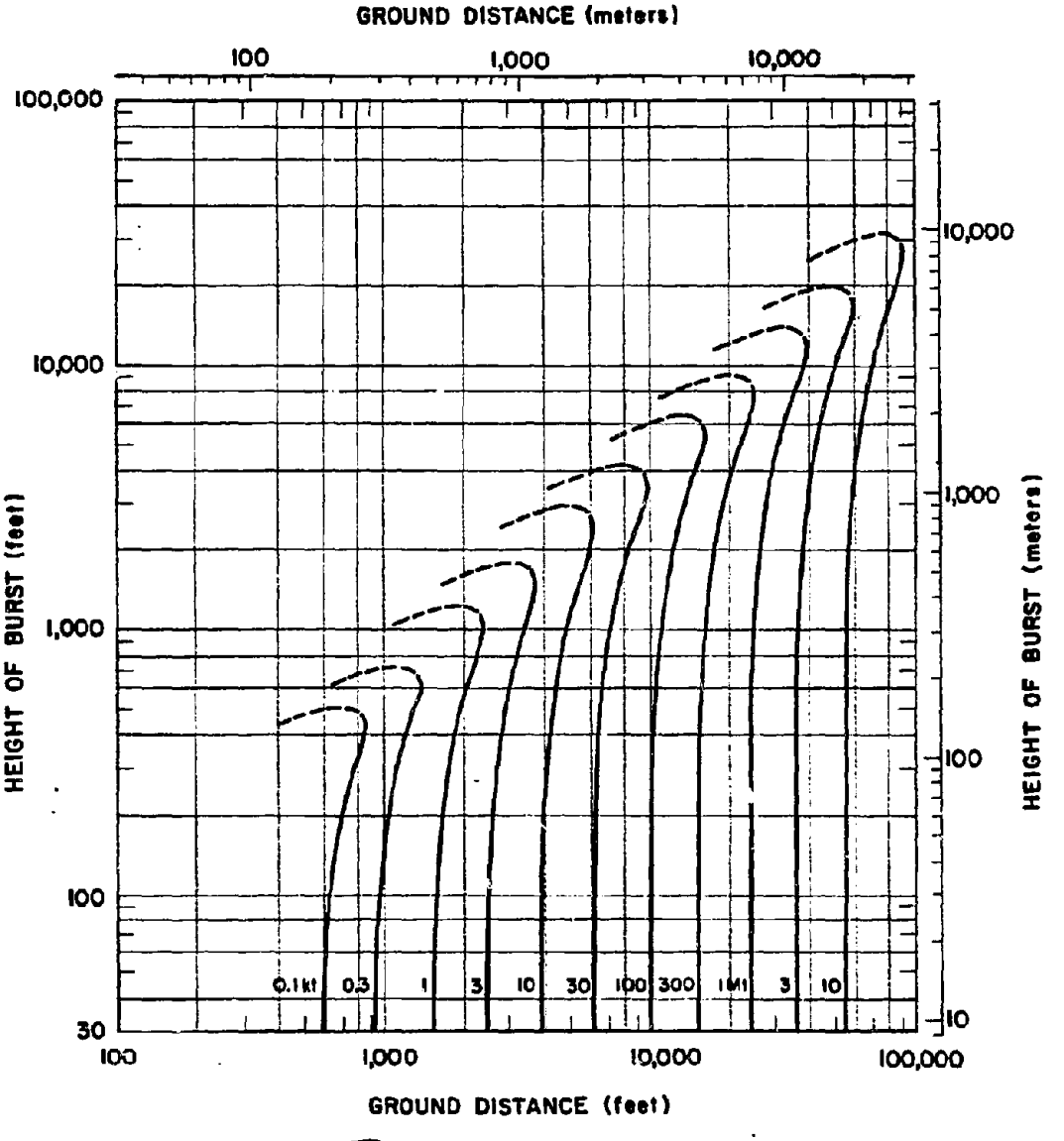

Figure 15-27. [redacted] Severe Damage to a Type IVb(d) Forest [redacted]

[redacted]

[redacted]

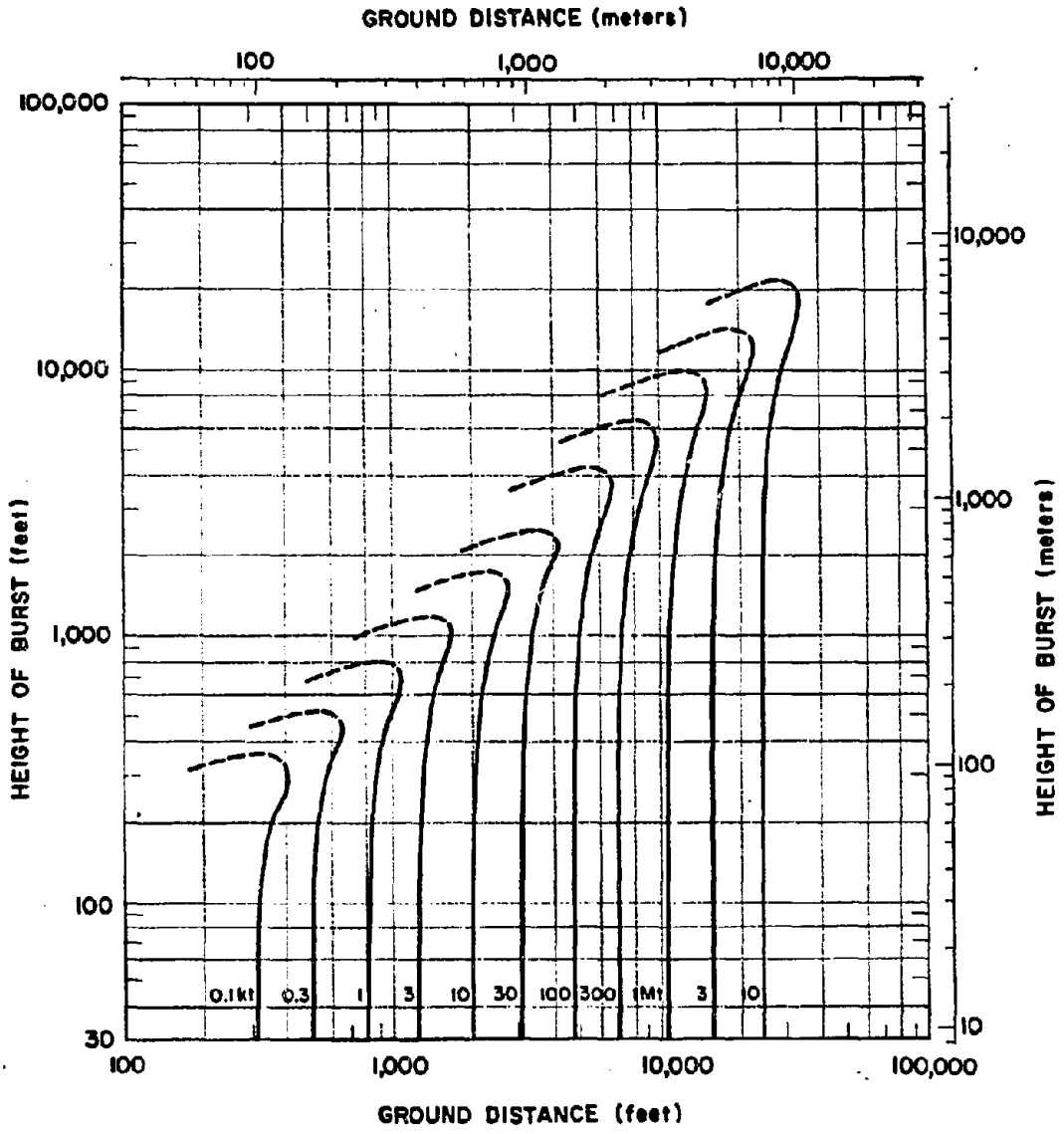

Figure 15-28. [redacted] Total Damage to a Type IVb(d) Forest [redacted]

[redacted]

[redacted]

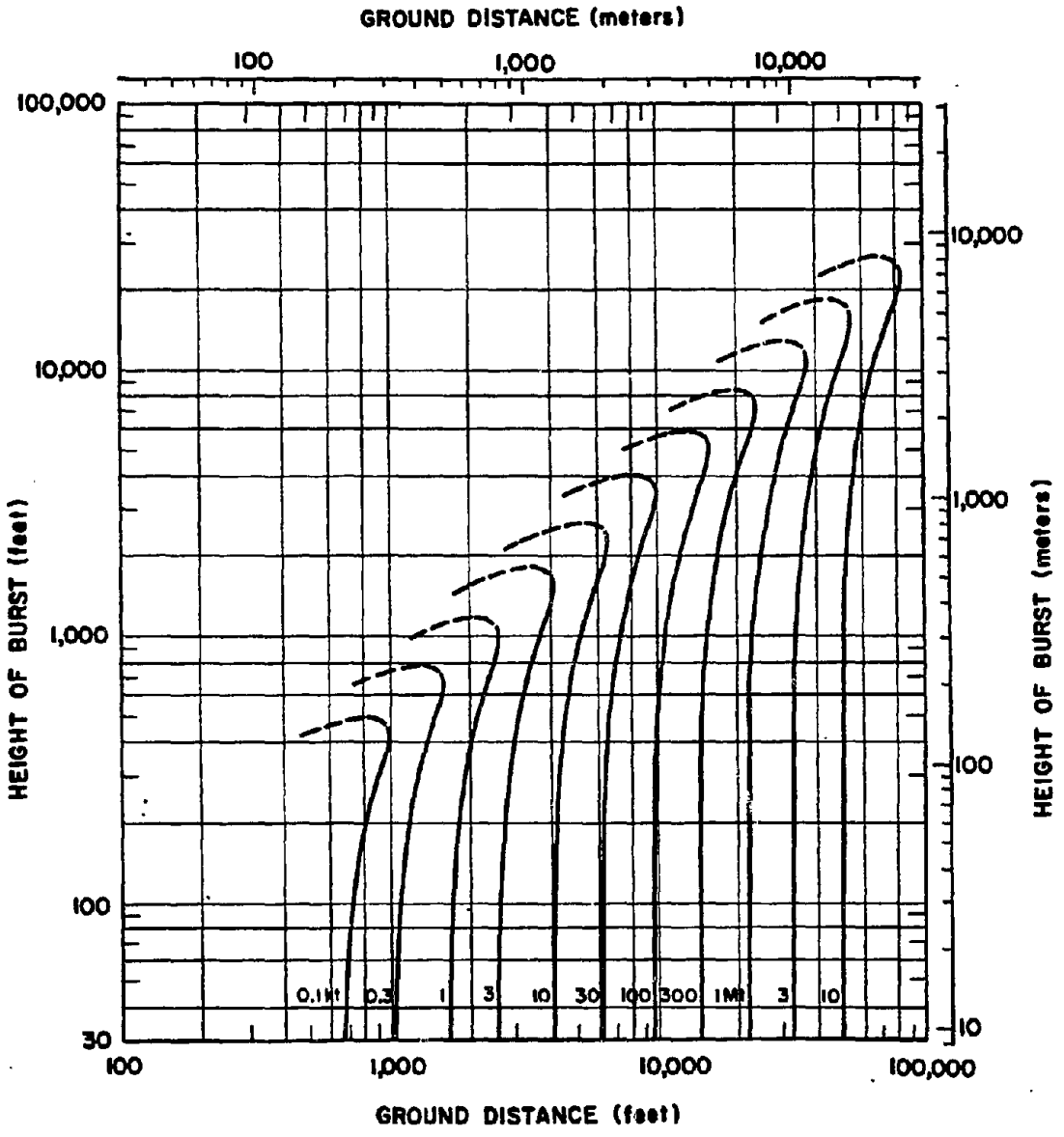

Figure 15-30. [redacted] Total Damage to a Type IVc(f) Forest [redacted]

[redacted]

[redacted]

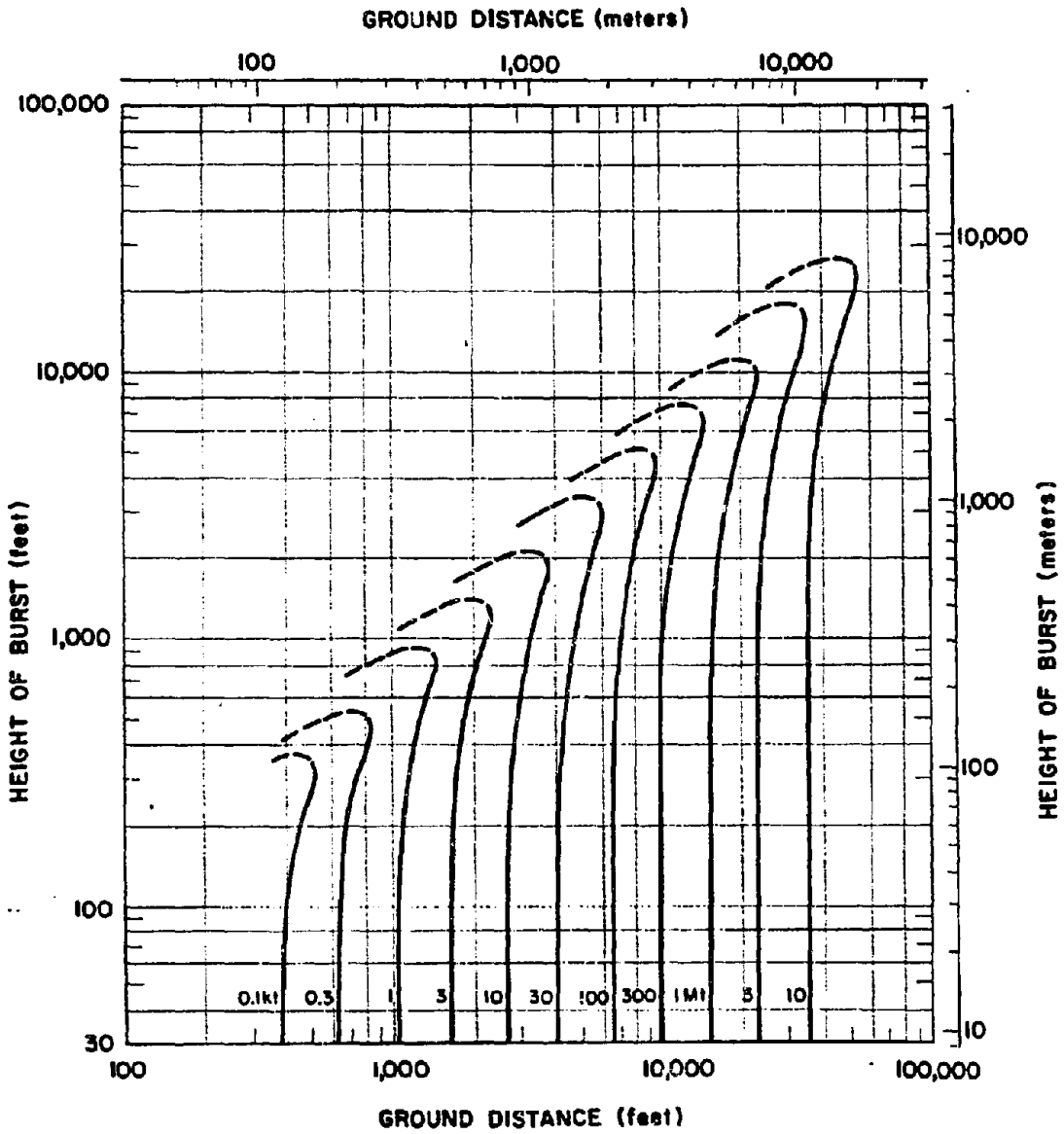

Figure 15-32. [redacted] Total Damage to a Type IVc(d) Forest [redacted]

[redacted]

[redacted]

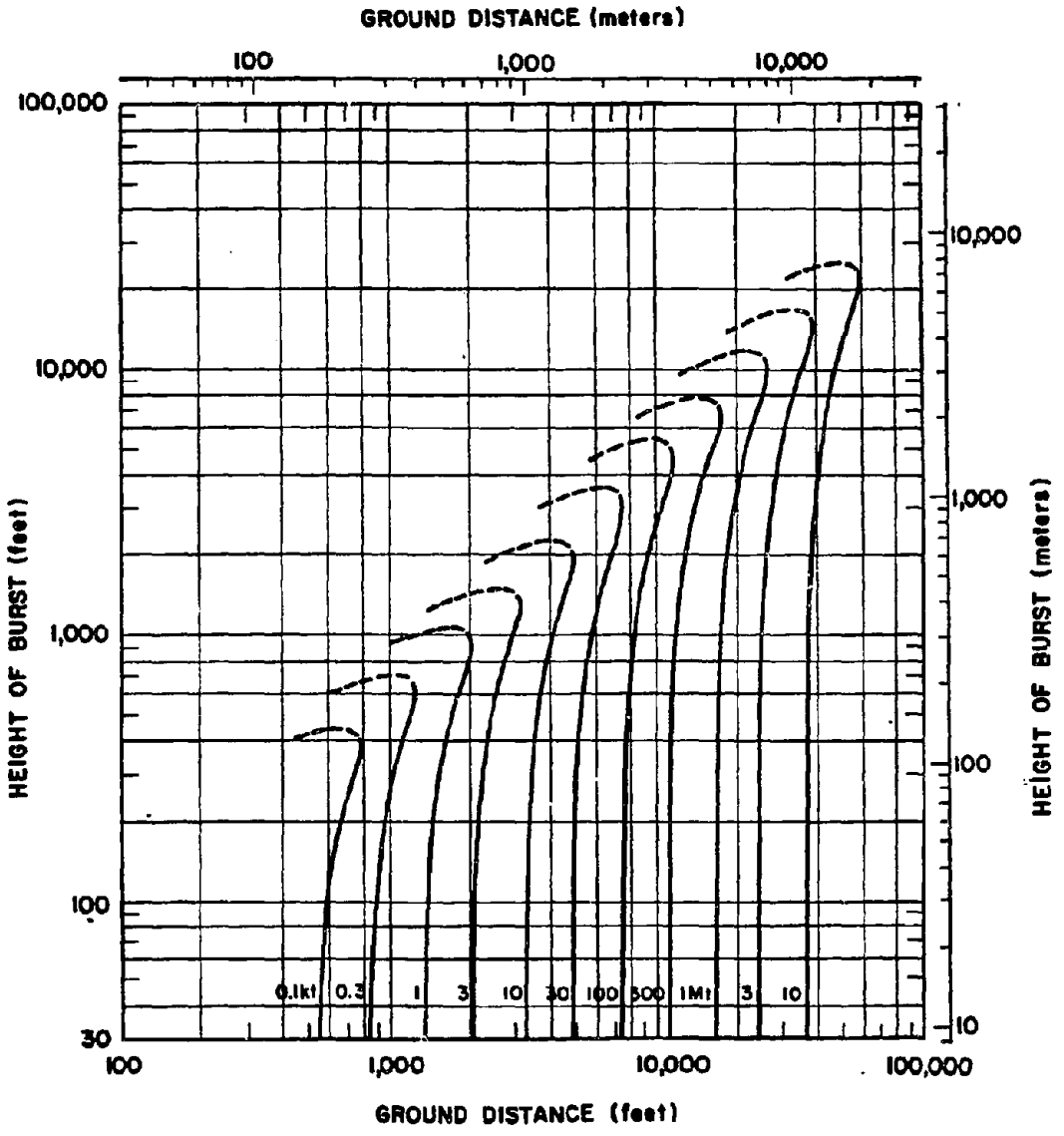

Figure 15-34. [redacted] Total Damage to a Type IVd Forest [redacted]

[redacted]

[redacted]

SECTION II

[redacted] TROOP AND VEHICLE MOVEMENT [redacted]

[redacted] The effects of a nuclear explosion on a forest may have a significant influence on military operations within the region of the forest that is affected by the burst.

[redacted] Two H.E. tests have provided information concerning the character of the region that is damaged and the effect on vehicular and troop movement that the damage will cause. [redacted]

DNA (b)(1)

[redacted] An important difference between the ef-

[redacted] The information in these tables may be used for yields ≤ 20 kt by determining the ground ranges for equivalent dynamic pressure impulses.

Table 15-3 [redacted] Effects of a 1 kt Weapon Burst at a Height of 270 Feet Over a Rain Forest [redacted]

DNA (b)(1)

[redacted]

[redacted]

[redacted]

[redacted] fects on broadleaf and coniferous forests is the nature of the debris. [redacted]

DNA (b)(1)

15-3 Blowdown Debris Characteristics

[redacted] The impact of the damaged region of a forest on movement is determined by the number and diameter of stems in the path of the vehicles or troops. The variation in these parameters throughout various regions of damage are discussed in the following paragraphs.

[redacted] Data from the two TNT detonations that were mentioned previously are presented in Figures 15-35 and 15-36. Figure 15-35 shows the relation between stem-feet per acre* and ground range for a rain forest and for a coniferous forest. [redacted] The difference in maximum stem-feet per acre between the two forests results from the difference in average tree density and tree height of the

DNA (b)(1)

*[redacted] See footnote to Table 15-1.

Table 15-4 [redacted] Effects of a 1 kt Surface Burst on a Coniferous Forest [redacted]

[redacted]

DNA (b)(1)

[redacted]

[redacted]

[redacted]

DNA (b)(1)

[redacted]

Figure 15-35. [redacted] Stem-ft per Acre Comparison Between a Rain Forest and a Coniferous Forest [redacted]

[redacted]

forests. The curve for the rain forest is based on data gathered by observation, while the curve for the coniferous forest is based on calculations, using preshot and postshot tree surveys. Figure 15-36 shows the relation between ground range and average diameter of the debris. [redacted]

DNA (b)(1)

DNA (b)

[redacted]

[redacted]

DNA (b)(1)

Figure 15-36. [redacted] Average Diameter of Stems Down, Comparison Between a Rain Forest and a Coniferous Forest, 1 kt [redacted]

DNA (b)(1) [redacted] This distance is determined easily from photo reconnaissance, as are the debris zones described in Tables 15-3 and 15-4.

15-4 Vehicle Movement [redacted]

[redacted] The movement rates of various wheeled and tracked vehicles have been measured for both radial and circumferential traverses of various debris zones. Although quantitative data were obtained and can be used, correlations between vehicle movement and debris characteristics are incomplete and are not refined to the point of high reliability. Nevertheless, curves have been constructed that indicate in terms of the debris parameters (number of stem-feet per acre and diameter of debris) when a vehicle will not be able to move. These curves are presented in Figure 15-37 and 15-38 for radial movement from ground zero and circumferential movement, respectively. The general radial orientation of tree stems is significant in terms of movement, because selection of easier routes between stems is possible in some cases of radial movement, while all stems must be crossed in circumferential movement. The shaded areas on the graphs indicate debris characteristics where movement is difficult. The solid line indicates that movement is not possible. For example, from Figure 15-37, for debris characteristics of 10,000 stem-feet per acre with average diameters of 4, 6, and 8 inches, radial movement of wheeled vehicles would be possible, difficult, and not possible, respectively. Curves for wheeled vehicles are fairly well documented with data; however, the curves for the M113 and tank are not, because

[redacted]

[redacted]

DNA (b)(1)

Deleted

Figure 15-37. [redacted] Debris Characteristics Preventing Radial Movement of Vehicles [redacted]

[redacted]

[redacted]

DNA (b)(1)

Deleted

Figure 15-38. [redacted] Debris Characteristics Preventing Circumferential Movement of Vehicles [redacted]

[redacted] these vehicles were slowed but not stopped by the debris zones in which they were tested. Tracked vehicles can climb onto the debris and mat it down after a number of passes, with the result that wheeled vehicles might pass, although this technique was not tested.

15-5 Troop Movement [redacted]

[redacted] The effect of blowdown debris on the movement of troops is difficult to present quantitatively. Many factors other than the physical obstacle itself, such as visibility, leadership, size of force, mission, and what the troops are carrying are also influenced by the debris and indirectly affect movement. Movement of troops through a debris zone can be compared with moving through a thick jungle, although radial movement is generally easier than circumferential movement. Branch debris in a broadleaf forest blowdown area adds difficulties, particularly in visibility, that are not as severe in coniferous forest debris. Troop trials were conducted on both TNT detonations previously described.

[redacted] The troop tests conducted in conjunction with the rain forest detonation involved comparisons between preshot and postshot tests of day and night patrols, platoon exercises with a mortar squad, and tests with stretcher parties.

DNA (b)(1)

Deleted

[redacted]

[redacted]

[redacted]

DNA (b)(1)

Deleted

[redacted] The night and day patrols were conducted over a route that was about 700 yards long, with one leg from virgin forest to the vicinity of ground zero, then back to the virgin forest on a different bearing.

DNA (b)(1)

Deleted

[redacted] In the platoon attack trials, control problems were considerably eased in the blowdown area compared to the virgin forest, as a result of increased visibility.

DNA (b)(1)

Deleted

Deleted

[redacted] Tests with a loaded two-man stretcher indicated that passage through blowdown debris was very difficult. The stretcher bearers' attention was diverted from the patient as a result of the need to concentrate on locating suitable footing. Consequently, the simulated casualty had a very rough trip and was frequently struck by debris. The conclusion drawn from this trial was that the probability for survival of a casualty with a severe wound would be significantly reduced by transit through blowdown debris. If the casualty survived the carriage, it is almost certain that he would experience a marked degree of secondary shock.

[redacted] Troop trials conducted in the coniferous forest blowdown consisted of radial and circumferential platoon exercises, including a mortar squad, and a simulated casualty-moving test. Some movement rate data that were obtained are shown in Table 15-6.

DNA (b)(1)

Deleted

[redacted]

Table 15-5 Comparison of Radial and Circumferential Movement Rates for Troops in a Rain Forest Blowdown Area, Scaled to a 1 kt Nuclear Explosion

DNA (b)(1)

Deleted

An administrative march also was conducted over a radial–circumferential–radial route. The circumferential portion was in the area of maximum blowdown debris.

A platoon night attack similar to the first circumferential trial described but in the opposite direction was performed. The platoon was organized as three attacking squad columns in line, except for the last 100 yards, where they deployed as a skirmish line. The 2-to-1 ratio in time was observed once again.

The moving of a simulated casualty by two- and four-man stretcher bearer teams trav-

Table 15-6 Comparison of Circumferential Movement Rates for Troops in a Coniferous Forest Blowdown Area, Scaled to a 1 kt Nuclear Explosion

Deleted

DNA (b)(1)

[redacted]

[redacted]

eling circumferentially also was tested. Results were essentially the same as those from the rain forest trials.

15-6 Predicting Effects on Movement [redacted]

[redacted] The results of the tests conducted after the two TNT detonations, together with the forest descriptions in Section I and Table 15-1, and the forest damage definitions in paragraph 15-2, have been combined in Table 15-7 for use with Table 15-2 and Figures 15-1 through 15-34 to predict the ground distances at which movement will be affected to various degrees. The forest damage levels in Table 15-7 are restricted to Severe and Total, because Light and Moderate damage to forests have little influence on movement, except as a result of changes in visibility. Example problems will illustrate the use of Table 15-7 and will outline the limitations of the information presented.

Table 15-7 [redacted] Influence of Forest Damage on the Movement of Troops and Vehicles [redacted]

Deleted

DNA (b)(1)

[redacted]

[redacted]

Problem 15–2 Calculation of the Distance at Which Movement Will Be Impaired

[redacted] Table 15–7 together with Table 15–2 and Figures 15–1 through 15–34 provide the information necessary to estimate the area within which movement will be affected to various degrees as a result of tree blowdown. The information contained in these tables and figures allows determination of the affected area for movement of troops or vehicles as a function of weapon yield and forest stand type.

[redacted] *Example* [redacted]

Given: A 2-Mt burst at 1,640 feet above a Type III forest stand.

Find: Will wheeled vehicles be stopped by the forest damage and at what maximum range?

[redacted]

DNA(b)(1)

[redacted]

[redacted]

Problem 15-3 Estimation of Movement Difficulty

DNA (b)(1)

[redacted] Therefore, it is possible to perform some evaluation of a forest using Figures 15-37 and 15-38 together with the forest characteristics. The forest characteristics required are tree density in trees per acre, average forest height in feet, average girth at breast height of the forest trees in either inches or centimeters, and tree type. The following parameters can then be determined:

Maximum Debris = (Forest density) (average height)

Average Debris Diameter in inches; girth, g, given in centimeters

DNA (b)(1)

[redacted]

Average Debris Diameter in inches; girth, g, in inches

DNA (b)(1)

[redacted]

With these two parameters, the potential obstacle of a forest can be estimated.

[redacted] *Example* [redacted]

Given: A coniferous forest with a density of 200 trees per acre and average height of 50 feet. Girth at breast height averages 33 inches.

Find: What obstacle could be formed if the forest were damaged by a nuclear burst.

[redacted]

DNA (b)(1)

[redacted]

[redacted]

15-9 Thermal Radiation on Forests [redacted]

[redacted] Probably the largest uncertainty associated with thermal radiation on forested areas arises from a lack of information about the transmission of the radiation through the foliage and other obscuring features of forest stands for high-yield air bursts.

[redacted] Methods for approximating the fraction of the free-field thermal radiation exposure that is transmitted by the forest environment will be considered here. The methods for calculating the free-field exposure are discussed in Chapter 3.

[redacted] Both from the point of view of causing injury to exposed personnel and of starting fires, the primary interest is in assessing the exposure of the forest floor to thermal radiation from the nuclear fireball. The foliage making up the crowns of the trees, while it has a high probability of being exposed to the full free-field radiation environment from air bursts and may be severely dessicated, thermally (even explosively) decomposed, and, at high enough flux levels, flash ignited, is not likely to contribute to subsequent sustained fires. It may, however, materially reduce the exposure of the forest floor by generating quantities of smoke and steam as well as by direct shading.

[redacted] Neglecting these thermally-induced, self-protective screening effects (noting that "scattering in" may effectively offset "scattering out"), an approximation to attenuation by trees and associated vegetation may be obtained by assuming that the attenuation is proportional to the extent of coverage of the field of view of the fireball by the elements of the forest canopy, i.e., that the exposure of any spot on the ground is roughly proportional to the apparent area of the fireball seen by that spot. Hence, height of burst and yield are important geometrical parameters that must be considered.* [redacted]

DNA (b)(1)

[redacted]

DNA (b)(1)

[redacted] Size of openings and tree height are other important determinants of the susceptibility of a forest to ignition from an air burst. This indicates the need for on-the-ground or from-the-air appraisal of forests and presumed explosion situations. This can be done with reasonable accuracy and much more rapidly from aerial observation or photographs than from surface measurements.

[redacted]

DNA (b)(1)

[redacted] Note that this assumes the source of thermal radiation to be above the tree tops. It will be seen in the subsequent discussion that thermal transmission is negligibly small for the low line-of-sight angles corresponding to burst heights less than tree heights, except perhaps for the short transmission paths that accompany bursts in the extreme low-end of the range of yields. Significant thermal exposures will never occur from these weapons, even in a sparsely vegetated forest environment, at distances corresponding to peak overpressures of 10 psi and less, because free-field exposure at these distances are only about 4 cal/cm^2 and less.

[redacted]

[redacted]

DNA (b)(1)

[redacted]

[redacted]

DNA (b)(1)

Table 15-9 [redacted] "Standard Northern European Forest" Data† [redacted]

[redacted]

[redacted] The "standard Northern European forest" represents a composite of the characteristics of the forests of northern Europe obtained by averaging the features of 10 different forest stands chosen as representative of type (pine woods, spruce and deciduous forests, and mixtures of these) and tree density (range of about 200 to 1,000 trees/acre).

[redacted] Sites were chosen on flat terrain in Northern Europe having uniform density distributions and generally uniform tree height (not more than 15% variation for not less than 90% of the trees in the stand). This uniformity is typical of the managed forests of Europe along with a general absence of undergrowth. These characteristics are not common to unmanaged (natural) forests. There is no reason to expect that information derived from these studies are in any way applicable to tropical hardwood forests.

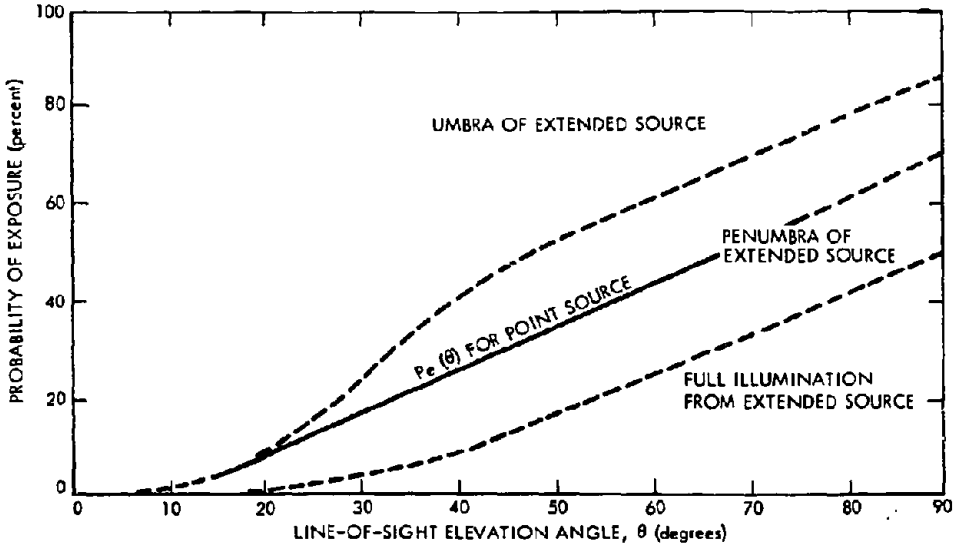

Figure 15-40. [redacted] Probability of Exposure of the Forest Floor ("Standard Northern European Forest") as a Function of Elevation Angle; Examples of a Point Source and a Spherical Source Subtending an Angle of 10 Degrees [redacted]

[redacted]

DNA (b)(1)

[redacted]

Obviously $Pe(\theta)$ functions, as illustrated by the "standard Northern European forest" in Figure 15–40, must depend on forest characteristics, notably tree density, with increased dispersion expected toward the larger angles of elevation. The data presently available do not reflect the degree of dispersion nor its dependence on forest characteristics adequately. Some idea of dispersion with tree density can be obtained from Figure 15–41, which displays the range of available results.

Although the current data base is quite poor, particularly as it applies to unmanaged forests and tropical or temperate-broad-leaf forests, it can be inferred that direct thermal effects in the forest environment do not contribute substantially to damage and casualties at distances where blast effects are not extreme, except, perhaps, in the least densely populated stands (less than 50 to 100 trees per acre). For most tactical situations where survival of blast effects can be expected, radiant exposures would be much less than half the free field over most of the floor of forests having densities of a few hundred or more trees per acre, and probabilities of exposure to the full free-field level would be negligibly small.

Deleted

15-10 Forest Fire Ignition and Spread

Under certain conditions, the explosion of a nuclear weapon over a forest or wildland area may cause fires. During the fire season, even when the burning potential is low, fires may spread. If fires are started in regions of high-fuel density when the fire potential is high, complete evacuation of personnel and equipment may be necessary. Organized control may be impossible until changes occur in the weather or the fire runs out of fuel.

An important exception to kindling fuel exposure to the full free-field radiant environment occurs in unmanaged forests of the temperate and cold regions. Many of these forests contain an abundance of dead and frequently punky

[redacted]

[redacted]

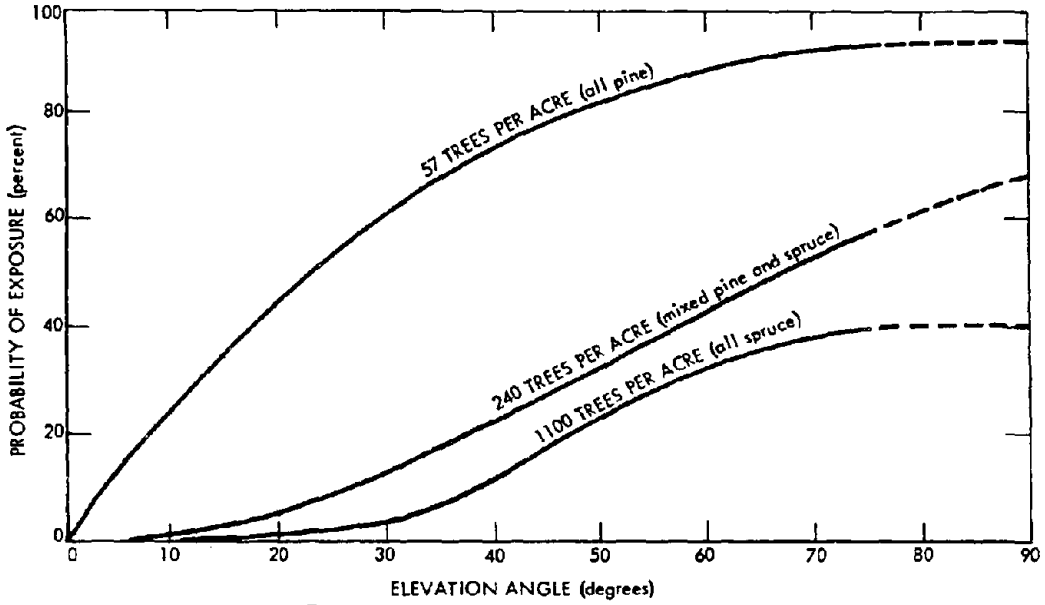

Figure 15-41. [redacted] Probability of Exposure of Forest Floor for Different Levels of Tree Density [redacted]

[redacted] wood exposed at or above the general canopy level. Of the common forest fuels, wood punk is probably the most susceptible to ignition by the thermal pulse. Moreover, since ignition is by charring or glowing combustion, these fuels are less susceptible to extinction by the blast wave than those that ignite with flame. These punky fuels, often easily detached from the parent tree, may be carried downwind for considerable distances and dropped to the forest floor as live embers. More rapid decomposition of dead wood makes this a less likely phenomenon in the moist tropics.

[redacted] As mentioned previously, the blast wave may extinguish fires at substantial overpressures, but the current state of the art does not permit quantitative evaluation of this phenomenon. On the other hand, at close-in distances where the blast wave arrives early during the thermal pulse (at times less than about 8 t_{max}) sufficient radiant exposure may follow the blast wave to re-ignite fuels and/or to ignite blast-created tinder.

[redacted] Current interpretations of the qualitative effects of blast on the persistence of incipient fires are based largely on experiments where kindling fuels were anchored in place. Had these fuels been free to move with the blast, many of them would have been translated for considerable distances as effective firebrands. Fire spread following ignitions by these brands would be influenced significantly by the return flow through the negative blast phase of the blast wave.

[redacted] The high degree of shading by tree crowns and stems for detonations at or below the canopy level often may be offset by scattering of burning debris ignited within the fireball. Many forest types contain large quantities of dead and rotten wood on and above the ground surface. If these materials are in flammable condition they may be expected to travel outward to the approximate limits of tree blowdown and provide plentiful ignition sources. Initial spread of fire from these

[redacted]

[redacted]

Table 15-10 [redacted] Condition of Wildland Fuels During Fire Season [redacted]

Fuel Type	Amount and Density of Fuel Required to Constitute a Fire Hazard	Condition During Fire Season
Grass or heath: Grassland; dry bracken ferns and other seasonal plants; dry regrowth in previously burned areas.	Uniform grass cover one-half ton or more per acre.	Vegetation nearly cured or dead.
Evergreen brush: Perennial evergreen shrubs and brush; chapparal; young evergreen growth.	75 percent or more covered.	15-25 percent by weight of leaves and associated twigs dead.
Deciduous broadleaf forest: Forest predominantly of trees such as oak, birch, maple, leaves of which die and fall every year.	Ground covered with more or less continuous layer of dead leaves.	Leaves off trees; ground vegetation dead or nonexistent.
Coniferous forest: Forest of evergreen pines, firs, spruces, etc.; generally the family of needle bearing trees.	Ground covered with more or less continuous layer of dead needles and twigs.	Needles and twigs dry enough to break easily when bent. Grass and other ground vegetation, if present, curing or dead.

[redacted]

sources would also respond to the inflow during the negative phase of the blast wave. Later behavior would depend on the degree of involvement of blowdown debris and the ambient weather.

[redacted] Times of the year during which the fire hazard is apt to be high are referred to as fire seasons. These are determined principally by the annual rainfall–temperature pattern and the amount and kinds of vegetation associated with it. Fire seasons vary widely from place to place throughout the world. Conditions associated with fire seasons in some typical wildland fuels are shown in Table 15-10. The more difficult problem is that of obtaining and systematically appraising local forest flammability data within a fire season on a day-to-day basis for fire spread predictions. No one formula will fit all situations.

[redacted] The main factors, aside from the fuels, that determine the fire hazard are: the nature of the terrain; the wind speed close to the ground; the relative humidity; and the precipitation history. Fuels seldom burn vigorously, regardless of wind conditions, when fuel moisture content exceeds about 16 percent. This corresponds to an equilibrium moisture content for a condition of 80 percent relative humidity. Rainfall of only a fraction of an inch will render most fuels temporarily nonflammable and may extinguish fires in thin fuels. The time required to restore the fire-danger condition may vary from hours to days depending on weather and soil conditions. Surface fuels in the interior of timber stands are exposed to reduced wind velocities; generally, these fuels retain their moisture as a result of

[redacted]

[redacted]

Table 15-11[redacted] Criteria of "No-Spread" of Fires [redacted]

Fuel Type	Criteria
All forest fuels	Over 1 inch of snow on the ground at the nearest weather stations.
Grass	Relative humidity above 80 percent.
Brush or hardwoods	0.1 inch of precipitation or more within the past 7 days and: Wind 0-3 mph; relative humidity 60 percent or higher, or Wind 4-10 mph; relative humidity 75 percent or higher, or Wind 11-25 mph; relative humidity 85 percent or higher.
Conifer timber	1. One day or less since at least 0.25 inch of precipitation and: Wind 0-3 mph; relative humidity 50 percent higher, or Wind 4-10 mph; relative humidity 75 percent higher, or Wind 11-25 mph; relative humidity 85 percent or higher. 2. Two to three days since at least 0.25 inch of precipitation and: Wind 0-3 mph; relative humidity 60 percent or higher, or Wind 4-10 mph; relative humidity 80 percent or higher, or Wind 11-25 mph; relative humidity 90 percent or higher. 3. Four to five days since at least 0.25 inch of precipitation and wind 0-3 mph; relative humidity 80 percent or higher. 4. Six to seven days since at least 0.25 inch of precipitation and wind 0-3 mph; relative humidity 90 percent or higher.

[redacted]

shielding from the wind and shading from sunlight by the canopy. The spread or no-spread criteria are summarized in Table 15-11. This table lists the conditions under which fire would not be expected to spread.

[redacted] The criteria of Table 15-11 have been compared to the records of 4,378 wildland fires. Of the fires for which "no spread" would be predicted, 97.8 percent did not spread; only 40 percent of the fires that were predicted to spread actually did spread (at a rate of 0.005 mph or faster). This failure to spread often may be attributable to lack of fuel continuity around the point of origin.

[redacted] The criteria of Table 15-11 are considered to be reliable for American forests and suitably conservative to assure a low level of hazard to friendly forces. On the other hand, the criteria are probably not overly conservative to predict conditions for which enemy forces may be denied forested areas because of fire whenever the local weather history and conditions at the time of

[redacted]

[redacted]

Table 15-12 [redacted] Fire-Out Criteria [redacted]

Fuel Type	Criteria
Grass	"No-spread" conditions, or measurable precipitation.
Brush or hardwoods	0.1 inch of precipitation or more, or "no-spread" conditions for the next 12-hour period.
Conifer timber	1. 0.5 inch of precipitation or more; 2. 0.25 to 0.5 inch of precipitation and "no-spread" conditions for the following two 12-hour periods; 3. "No-spread" conditions for eight consecutive 12-hour periods and measurable precipitation during any two 12-hour periods; 4. "No-spread" conditions for 14 consecutive 12-hour periods.

[redacted]

detonation are known reliably, or whenever the initial fire is expected to be of substantial size.

[redacted] Weather conditions are subject to change, sometimes unpredictably, and fires that have been spreading may stop or go out. Conversely, fires that have not been spreading (other than on the microscale necessary to keep them dormantly alive) may flare up quite suddenly and spread rapidly as a result of a change in the weather. Whenever this threat of weather change cannot be tolerated, it is necessary to choose conditions for the employment of nuclear weapons so that dormant fires will not persist for times that are long compared to reliable weather-forecast periods. The "fire-out" criteria in Table 15-12 provide guidelines for this purpose. These criteria are derived from opinions of experienced fire personnel and should not, therefore, be considered to be as reliable as the "no-spread" criteria.

[redacted] Under identical weather conditions, concentrations of heavy fuels are more hazardous than thin fuels, even though they tend to reduce wind speeds locally and do not respond as rapidly to changes in relative humidity. This results from the fact that trees and heavy limbs on the forest floor may be ignited by an otherwise nonhazardous surface fire, and when heavy fuels are present near the borders of standing timber, the fire may travel into the tree crowns and spread from top to top even though ground fuel concentrations are low. Coniferous trees are most susceptible to crown fires. Hardwoods (deciduous trees) rarely, if ever, exhibit a true crown fire.

[redacted] Considerable information exists concerning rates of fire spread in American forests from historical records of major forest fires. Rates of spread rarely exceed 1 mile per hour except for brief periods of time during extreme burning conditions. Crown fires are capable of spreading at rapid rates, exceeding the rates of progress by men on foot attempting to out-run them. The high rate of progress of fire through crowns of trees probably results from the unimpeded wind-flow velocities above the forest canopy.

[redacted] Because of their potentially rapid rates of spread, crown fires represent a much higher level of hazard to personnel in forests than surface fires. Accordingly, it is desirable to be able to predict the occurrence of crown fires. Unfortunately, only qualitative criteria are available.

[redacted]

[redacted]

Table 15-13 [redacted] Burning Durations by Fuel Type [redacted]

Fuel Type	Violent Burning Time (min)	Violent Burning Energy Release (percent)	Residual Burning Time (min)	Residual Burning Energy Release (percent)	Total Burning Time
Grass	1.5	90	0.5	10	30 min
Light Brush (12 tons/acre)	2.	60	6.	40	16 hr
Medium Brush (25 tons/acre)	6.	50	24.	50	36 hr
Heavy Brush (40 tons/acre)	10.	40	70.	60	72 hr
Timber	24.	17	157.	83	7 days

[redacted] Surface fires exhibit brief "runs" at high speeds (a few miles per hour for several minutes, and a large fraction of a mile per hour for up to an hour or more), but average speeds over long periods of time range generally from 0.01 mile per hour to 0.5 mile per hour, with the most frequently noted values in the range of 0.1 to 0.5 mile per hour for 6- to 11-hour periods and in the range of 0.01 to 0.1 mile per hour for durations of 12 hours and more. These values are for American forests and should not be expected for managed forests (such as those of Europe) or tropical hardwood forests (such as those of some areas of Southeast Asia).

[redacted] An additional factor that affects the hazard of fire to military personnel and equipment is the burning duration of forest fuels. Examples of burning durations for fuels that are typical of American wildlands are summarized in Table 15-13.

[redacted] Table 15-13 refers to natural fuels in their undisturbed states. Experience shows that the highest fire intensities and fuel consumptions occur in the areas of greatest fuel accumulation. This fact has two implications with respect to nuclear detonations: if burning conditions are favorable, incipient fires from the thermal pulse falling on areas covered with a large amount of blast debris may build up rapidly; the blast debris accumulation may subsequently desiccate sufficiently to be a prime target for ignition by any means, either friendly or enemy.

[redacted]

[redacted]

[redacted] BIBLIOGRAPHY [redacted]

Bowe, T. W., et al., *Operation Blowdown, Scientific Observations and Analysis*, Commonwealth of Australia, July 1964, Report No. DSL 273 (3 volumes).

Chandler, C. C., et al., *Prediction of Fire Spread Following Nuclear Explosions*, Pacific Southwest Forest and Range Experiment Station, Berkeley, California, 1963, U.S. Forest Service Research Paper PSW-5.

Fons, W. L., F. M. Sauer, and W. Y. Pong, *Blast Effects on Forest Stands by Nuclear Weapons*, U.S. Department of Agriculture Forest Services, December 1957, AFSWP 971.

Kerr, J. W., et al., *Nuclear Weapons Effects in a Forest Environment—Thermal and Fire* [redacted] Panel N-2, TTCP, N2:TR 2-70, DASIAC Special Report No. 112, March 1971 [redacted]

Martin, S. and S. Holton, *Preliminary Computer Program for Calculating Ignition Ranges*, U.S. Naval Radiological Defense Laboratory, San Francisco, California, June 1965, USNRDL TR 866.

Nuclear Weapons Effects in a Forest Environment—Blowdown, Panel N-2, TTCP, August 1969, N2:TR 1-69, DASIAC Special Report No. 73.

Sauer, F. M., *Forest Blowdown in Comparison of the Results of High Explosive Experiments and Prediction Experiments*, Poulter Laboratory, Stanford Research Institute, Menlo Park, California, July 1969, DASA 2300.

Zaccor, J., et al., *Prediction and Significance of Forest Damage from a 50-Ton HE Surface Burst*, Project 7.01 Operation Distant Plane, Event 4, URS Research Company, June 1967, DASA 2065.

[redacted]

July 1973
AD763750
AD763750

DNA 3054F
URS 7049-10, Rev. 1

FOREST BLOWDOWN FROM NUCLEAR AIRBLAST

by

Phillip J. Morris

for

Headquarters
DEFENSE NUCLEAR AGENCY
Washington, D.C. 20305

Contract No. DNA-001-72-C-0021

A sensitivity analysis is performed on a computer model of tree response to airblast loading. This effort was undertaken, with success, to reduce the number of input parameters required by the model to those available to the field commander. Based on the results of this analysis, a new prediction technique was developed which determines the extent of tree blowdown and the resultant effects on troop and vehicle movement. The technique was developed for inclusion in DNA Effects Manual Number 1.

A URS Systems Affiliate

URS RESEARCH COMPANY

Fig. 15-35 in DNA-EM-1 (1972)

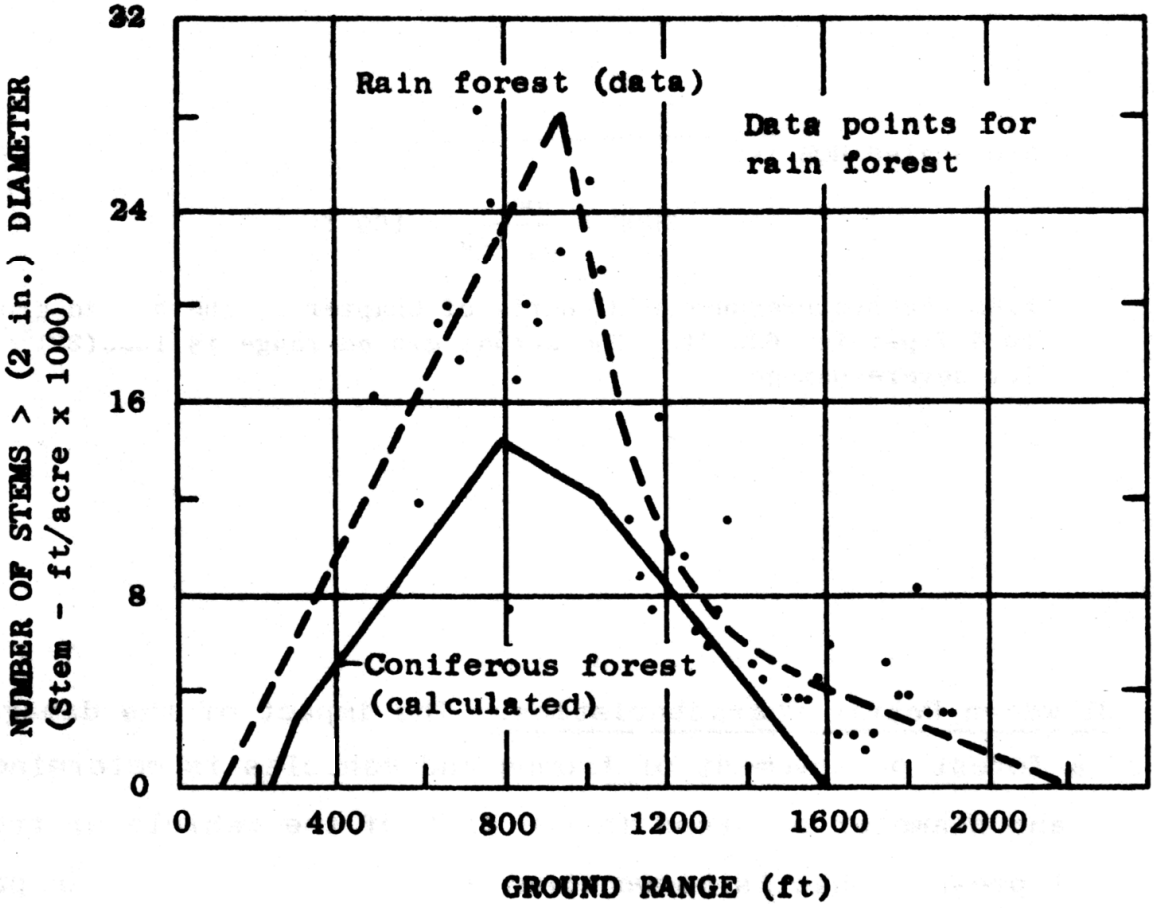

Fig. 15-8. Stem-ft per Acre Comparison Between a Rain Forest and a Coniferous Forest, 1 KT

Fig. 15-36 in DNA-EM-1 (1972)

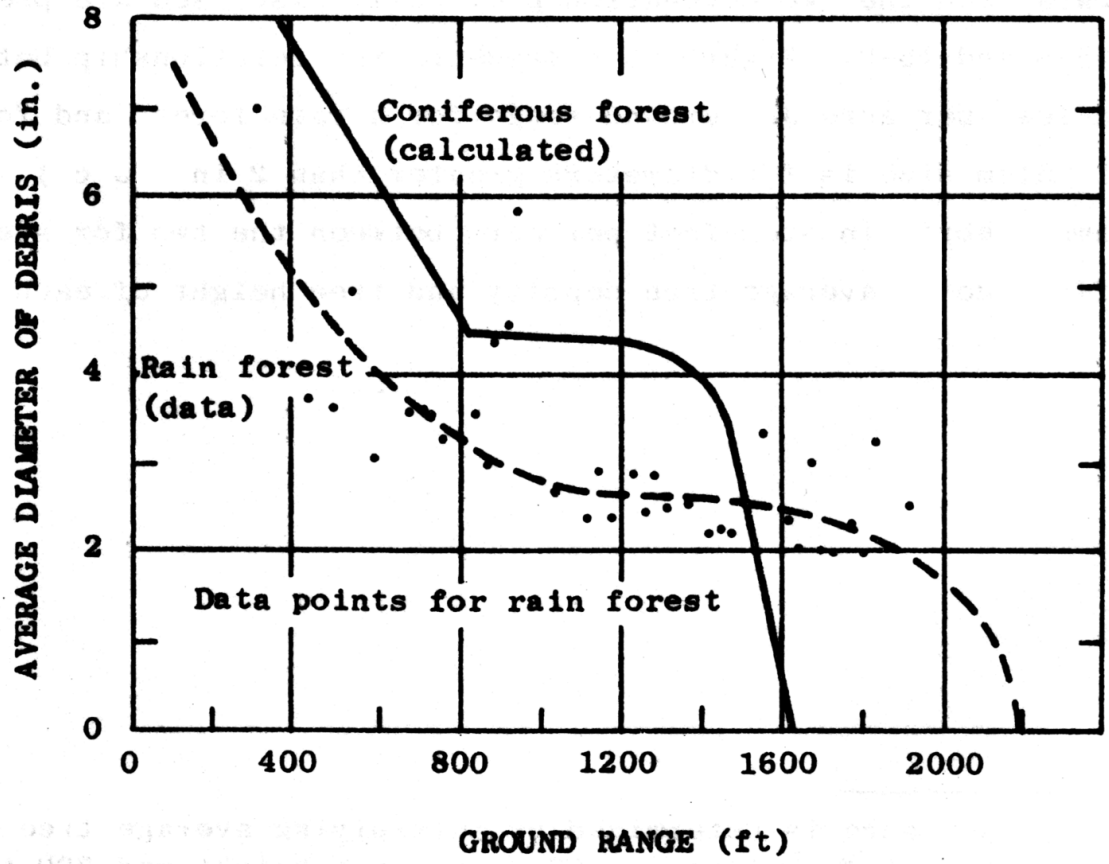

Fig. 15-9. Average Diameter of Stems Down, Comparison Between a Rain Forest and a Coniferous Forest, 1 KT

Fig. 15-46 in DNA-EM-1 (1972)

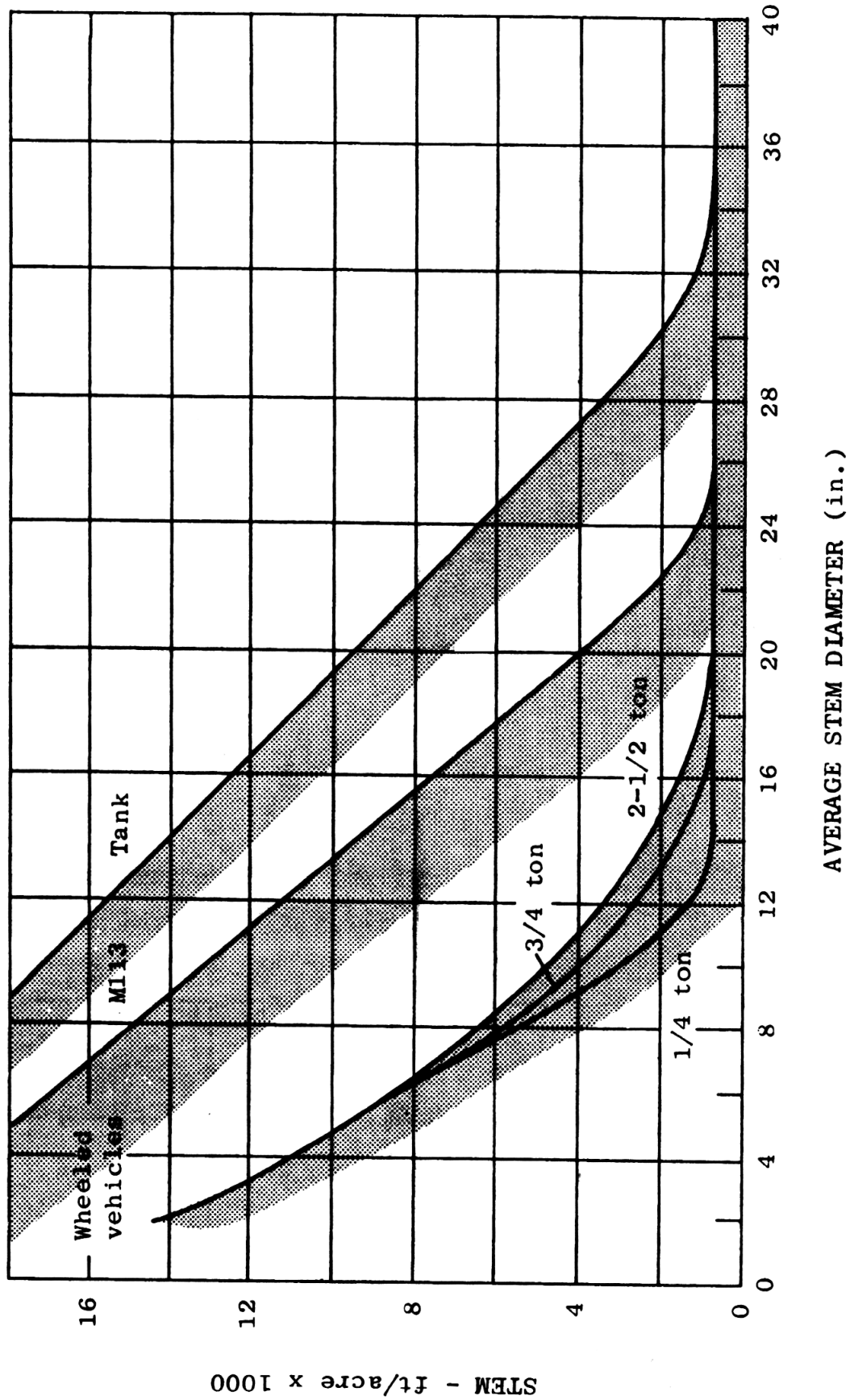

Fig. 15-10. Debris Characteristics Preventing Circumferential Movement of Vehicles

Fig. 15-37 in DNA-EM-1 (1972)

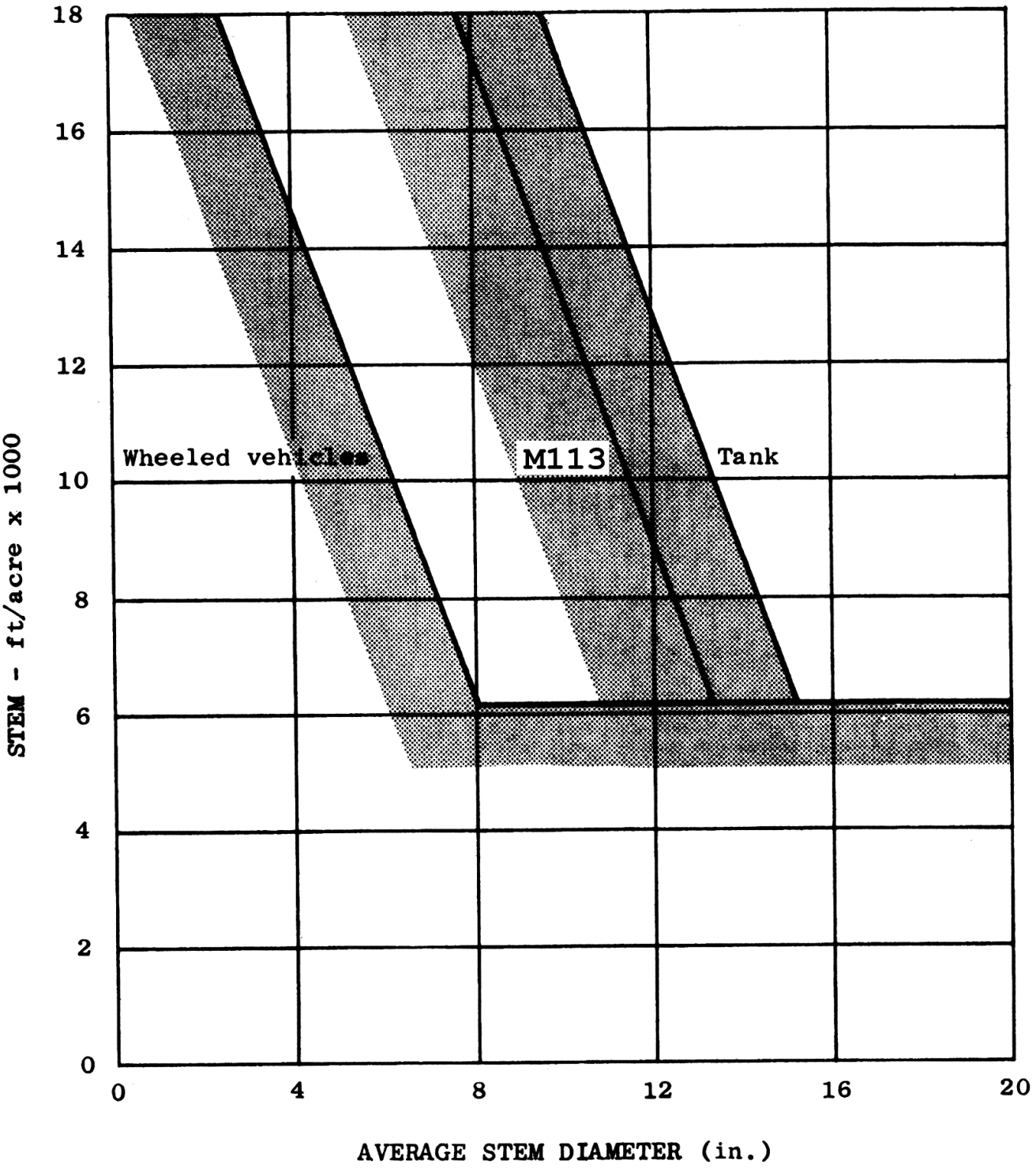

Fig. 15-11. Debris Characteristics Preventing Radial Movement of Vehicles

[redacted]

DTIC
ELECTE
12 MAR 1989
S D
E

Chapter 16

DAMAGE TO MISSILES [redacted]

AD-A955 400

[redacted] Missile systems are subject to damage by essentially all of the phenomena described separately in Chapters 2 through 8, Part I, of this manual, i.e., all or part of the system may be damaged by blast and shock (Chapter 2), by thermal radiation (Chapter 3), by X-ray radiation (Chapter 4), by nuclear radiation (Chapter 5) mainly in the form of transient radiation effects on electronics (TREE) phenomena (Chapter 6), or by the electromagnetic pulse (EMP (Chapter 7)). Communications and/or radar subsystems are also subject to degradation of their propagation characteristics as described in Chapter 8.

[redacted] The damage that might result from several of the phenomena listed above is so dependent on specific system design that general methods for predicting specific missile system response cannot be provided. These phenomena include X-ray radiation, TREE, and EMP. Consequently, general descriptions of the damage mechanisms associated with these phenomena, applicable to missiles as well as other systems, are provided in Sections V, VII, and VIII, respectively, of Chapter 9. Additionally, some ambient nuclear radiation levels for "sure safe" and "sure kill" of missiles are given in Table 14-11, Chapter 14. Chapter 17 discusses the signal degradation of communications and radar systems. No further discussion of the damage or degradation from these phenomena is included herein.

[redacted] This chapter is divided into two sections. Section I describes blast damage to tactical missiles. Section II describes the response of strategic systems to blast and thermal phenomena. Where appropriate, separate discussions are provided in Section II for antimissile systems (commonly called ABM) and reentry vehicles (*RV's*).

SECTION I

[redacted] BLAST DAMAGE TO TACTICAL MISSILE SYSTEMS [redacted]

[redacted] The effects of air blast on three specific sample systems, the SERGEANT, the LANCE, and the HAWK, are described in this section. The vulnerability analysis of these missiles and their support equipment is intended to provide information from which the probable effects of air blast on other tactical missile systems may be estimated. An example of such an estimation for the HONEST JOHN missile is also provided. Outline drawings of the sample systems are shown in Figure 16-1 for comparison purposes.

[redacted] In the case of each system, it is assumed that the system may be attacked from the time that the missiles are in stockpile until the missile warhead is detonated over the target. During any phase of this stockpile-to-target sequence, the system vulnerability is determined by the most susceptible component that is essential to completion of the mission. The vulnerability of all critical components is tabulated for each system. Vulnerability is expressed in terms of peak overpressure, assuming that the blast wave is from a contact surface burst with a yield between 1 kt and 300 kt. A range of values is given for the overpressure vulnerabilities, e.g., 12 to 19 psi. These numbers mean that either 12 psi from a 300 kt burst or 19 psi from a 1 kt burst is estimated to be sufficient to render the system component incapable of performing its necessary functions to complete the mission. Each vulnera-

DISTRIBUTION STATEMENT A
Approved for public release;
Distribution Unlimited

[redacted]

89 3 02 034

[redacted]

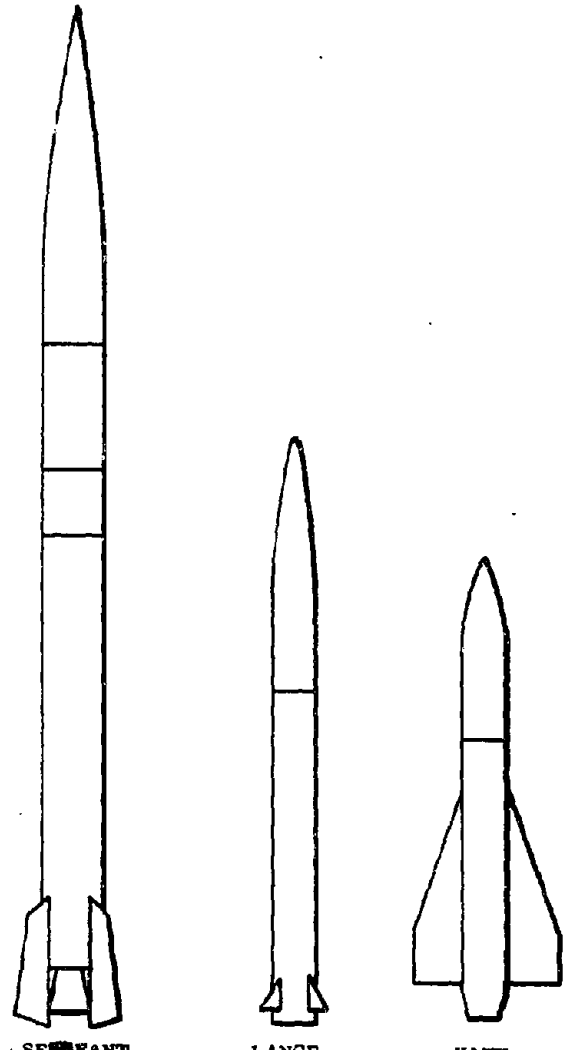

Missile	SERGEANT	LANCE	HAWK
Length ~ Ft.	34½	20	16
Diameter ~ In.	31	22	14
Weight ~ Lbs.	10,000	3100	1300
Application	Surface to Surface	Surface to Surface	Surface to Air
Range	46 to 137 NM.	5 to 75 NM.	to [redacted] Altitude with [redacted] Horizontal Range
Warhead Section	1500 Lbs Nuclear	1000 Lbs Nuclear	73 Lbs. H.E.

Figure 16-1. [redacted] Missile Configurations, SERGEANT, LANCE, and HAWK [redacted]

QUALITY INSPECTED 4

Accession For
NTIS GRA&I ☒
DTIC TAB ☐
Unannounced ☐
Justification
By
Distribution/
Availability Codes
Dist | Avail and/or Special
A-1

UNANNOUNCED

AFXC
(b)(1)
(b)(1)

[redacted]

[redacted]

[redacted] bility level is also shown in the form of a number curve, which allows critical values of range and overpressure to be determined as a function of weapon yield.

[redacted] Many circumstances alter the vulnerability threshold of specific system components. For example, a truck that is carrying a missile to the launch site is less likely to be overturned by a blast wave if it is facing the burst than if it is hit from the side (see Table 14-5, Chapter 14). The velocity and orientation of a missile in flight both are important. If the terrain is conducive to the formation of a precursor, the truck may be subjected to a greatly enhanced dynamic pressure impulse, capable of overturning it much more easily than if it were exposed to the same burst at the same range under near-ideal conditions (paragraph 14-2, Chapter 14). The overpressure and dynamic pressure at the target depend on height of burst as well as distance. In order to reduce vulnerability data to a manageable set of numbers, the following conditions are assumed for the analysis in this section.

- The orientation of the system component with respect to the blast wave is such that the probability of serious damage is a maximum.
- Near-ideal surface conditions exist (no precursor).
- The blast wave is produced by a contact surface burst.

If radically different conditions are expected, appropriate changes in vulnerability levels must be made. In the case of a burst that produces a precursor, the dynamic pressure would be enhanced, and drag sensitive targets, i.e., those susceptible to toppling or overturning, probably would be damaged at an overpressure *lower* than predicted. Also, an air burst could produce a double shock on a target located in the regular reflection region; again this could lead to significant target damage at an overpressure lower than predicted. Thus, the numbers given should only be used as guides to the assessment of system blast damage.

[redacted] Damage to targets that are primarily drag sensitive is determined by the dynamic pressure level. However, for near-ideal surface conditions, there is a known correspondence between peak overpressure and peak dynamic pressure (although the pulse durations can be somewhat different). Therefore, for the purpose of this chapter, all damage levels are expressed as overpressure levels, including the damage levels that apply to drag sensitive targets.

[redacted] SERGEANT WEAPON SYSTEM [redacted]

16-1 Description of the SERGEANT Weapon System [redacted]

[redacted] The SERGEANT weapon system is a second generation surface-to-surface missile system capable of being used under all terrain and weather conditions. Major items of the system are:

- *SERGEANT missile M15 and containers.* The SERGEANT missile body consists of four major assemblies:

  (1) rocket motor M53; (2) guidance section M38; (3) warhead section M65; and (4) control surface assemblies M58. Figure 16-1 shows a drawing of the missile. Figure 16-2 shows the missile parts in containers and ready for transport.
- *Four-wheel, semitrailer mounted guided missile launching station M504.* Figure 16-3 shows this unit in firing position. One component, the launching station firing set, is shown in more detail in Figure 16-4.
- *Four-wheel, 6 ton, low-bed semitrailer M527.*
- *Organizational Maintenance Test Station* (OMTS) *AN/MSM-35.* This trailer housed

[redacted]

[redacted]

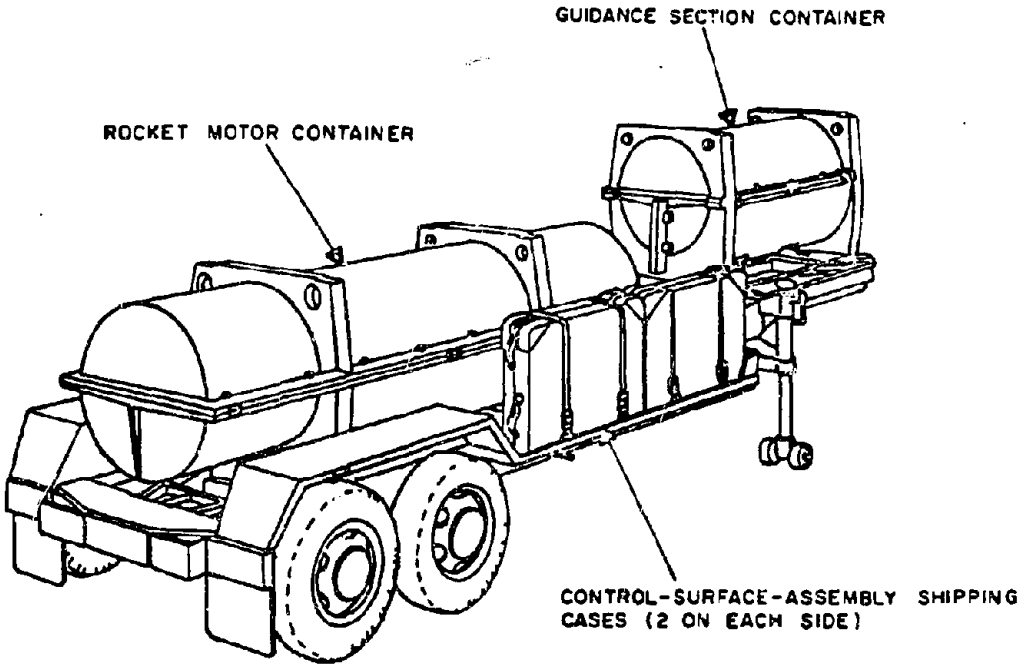

Figure 16-2. [redacted] SERGEANT System, Semitrailer Transporter with Missile Section Containers [redacted]

[redacted]

[redacted]

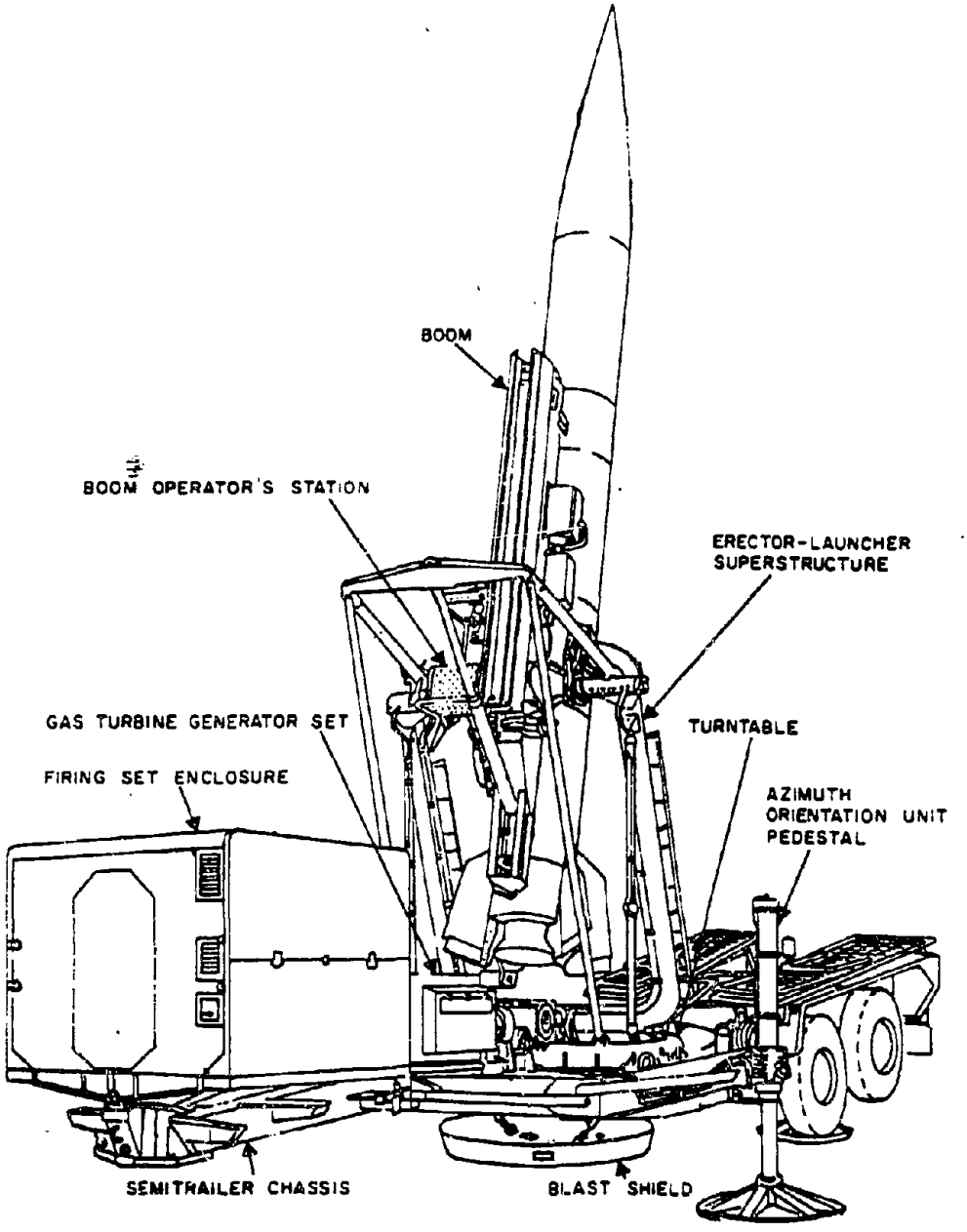

Figure 16-3. [redacted] SERGEANT System, Launching Station with Missile in Firing Position [redacted]

[redacted]

[redacted]

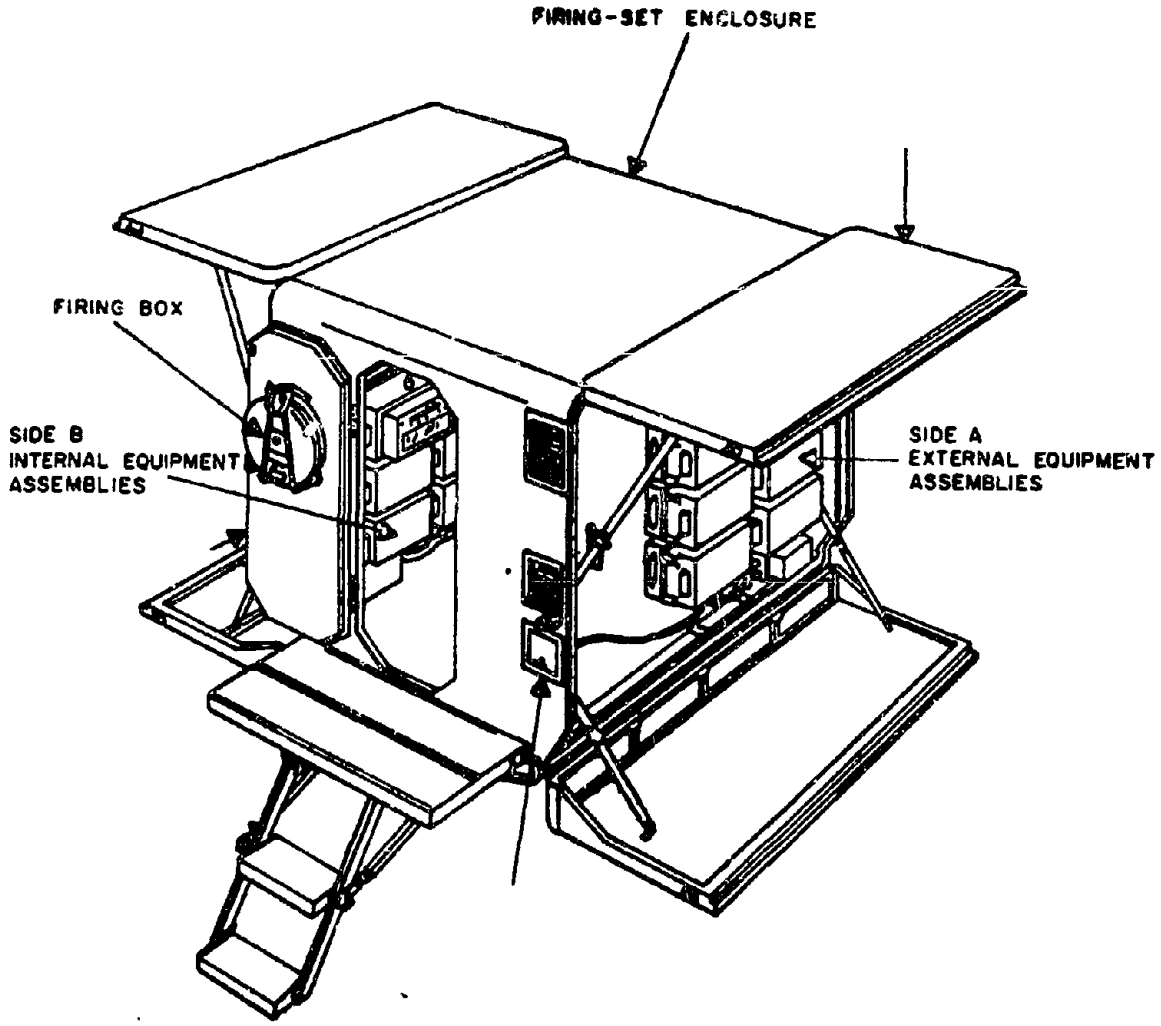

Figure 16-4. [redacted] SERGEANT System, Launching Station Firing Set [redacted]

[redacted]

[redacted]

[redacted] unit, shown in Figure 16-5, is used for prelaunch testing and replacement of defective assemblies.

- *Field Maintenance Test Station (FMTS) AN/MSM-36.* This unit is similar to the OMTS. It can be used to perform many of the functions of the OMTS, and it is also used in situations that require more extensive testing and repair work than normally is done by the OMTS.
- *Warhead Section Container*
- *Truck, M35*

In addition to the equipment listed above, an M55 cargo truck is used to transport the rocket motor when the M527 is not available.

16-2 Vulnerability Levels of the SERGEANT Missile System [redacted]

[redacted] The vulnerability levels of the various components of the SERGEANT missile system are shown in Table 16-1.

[redacted] The estimated vulnerability levels of the system in its various operational phases are described below. The most likely damage modes are also described.

- *Missiles in Containers at Storage Site (SERGEANT).* Figure 16-2 shows the type of containers used to store missile parts. The warhead section container, which is slightly longer than the guidance section container, is not shown. [redacted]

DNA (b)(1)

[redacted]

DNA (b)(1)

- *Missiles in Containers in Transit (SERGEANT).* Since the transport vehicles afford partial protection for the containers, the vulnerability estimates were based on the pressure levels required to overturn the more vulnerable vehicle, [redacted]

DNA (b)(1)

- *Equipment and Missile at the Firing Site (SERGEANT).* [redacted]

DNA (b)(1)

- *Missile in Flight (SERGEANT).* [redacted]

DNA (b)(1)

[redacted]

[redacted]

[redacted]

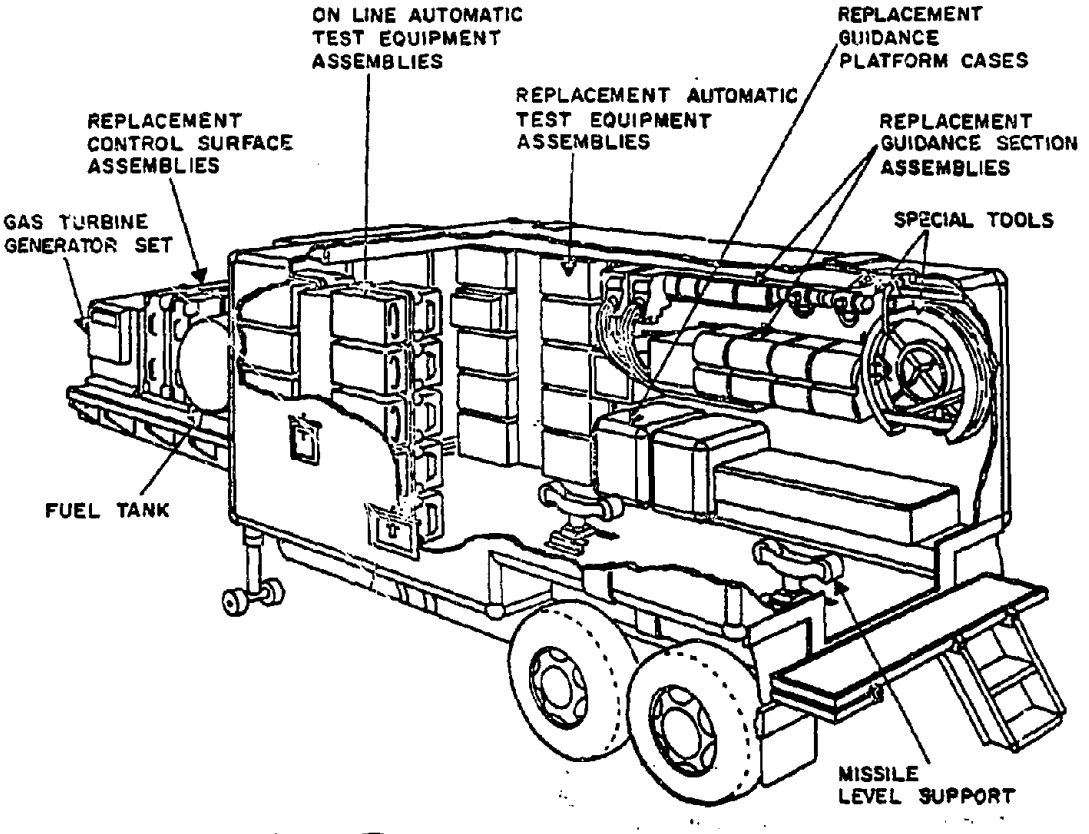

Figure 16-5. [redacted] SERGEANT System, Organizational Maintenance Test Station (OMTS) [redacted]

[redacted]

[redacted]

[redacted]

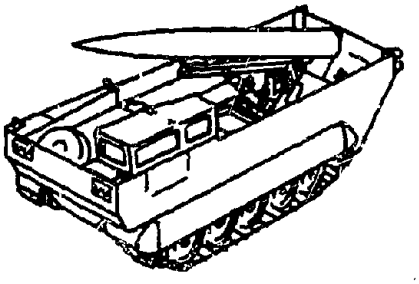

SELF-PROPELLED
LAUNCHER

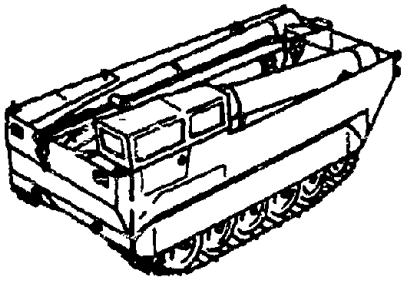

TRANSPORTER
LOADER

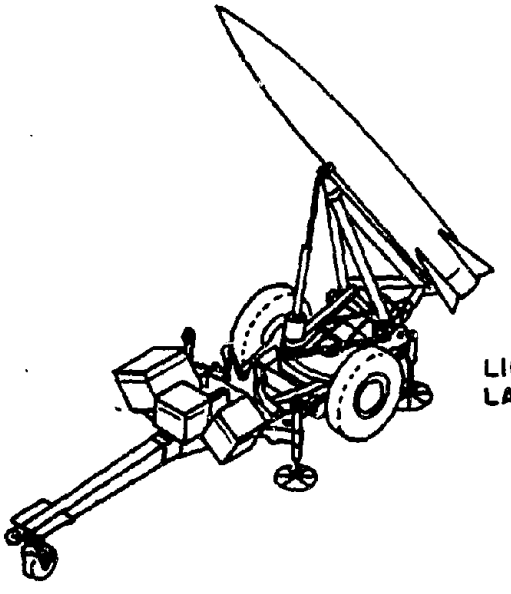

LIGHTWEIGHT
LAUNCHER

Figure 16-7. [redacted] LANCE System, Primary Units of the Missile System [redacted]

[redacted]

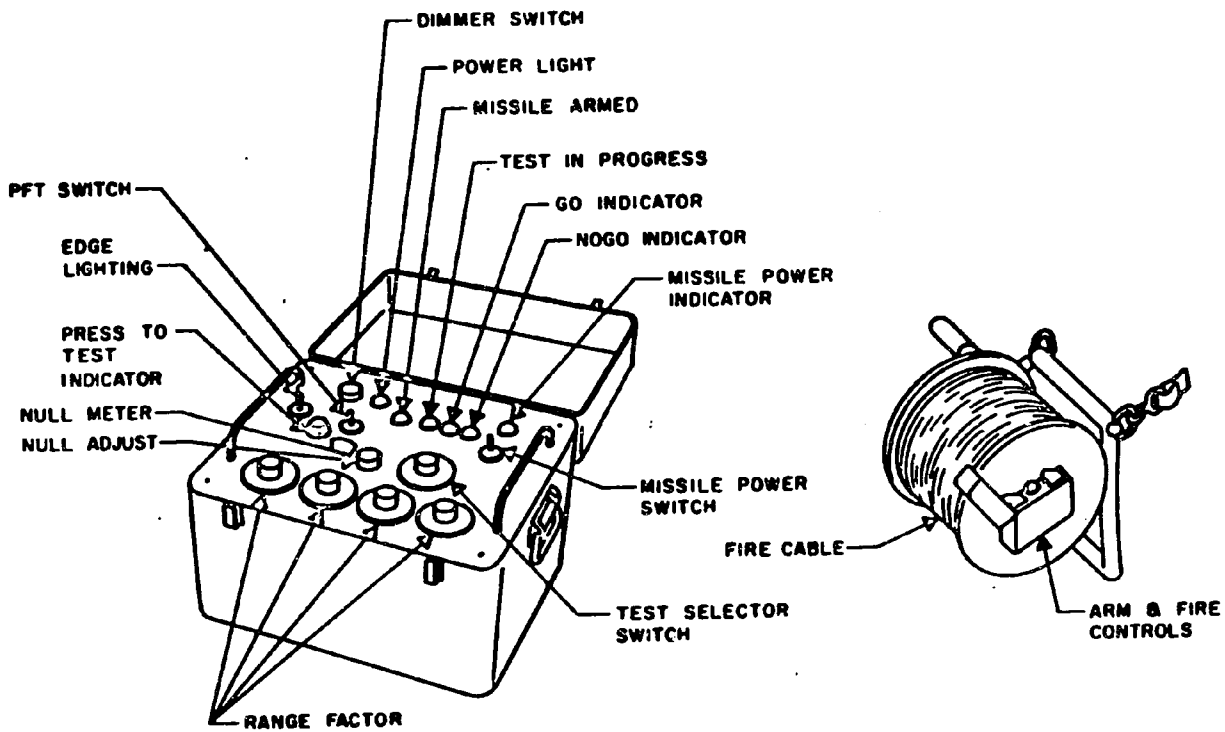

Missile Test Set (MTS) Firing Device (FD)

Figure 16-8. LANCE System, Prefire Tester and Fire Pack

[redacted]

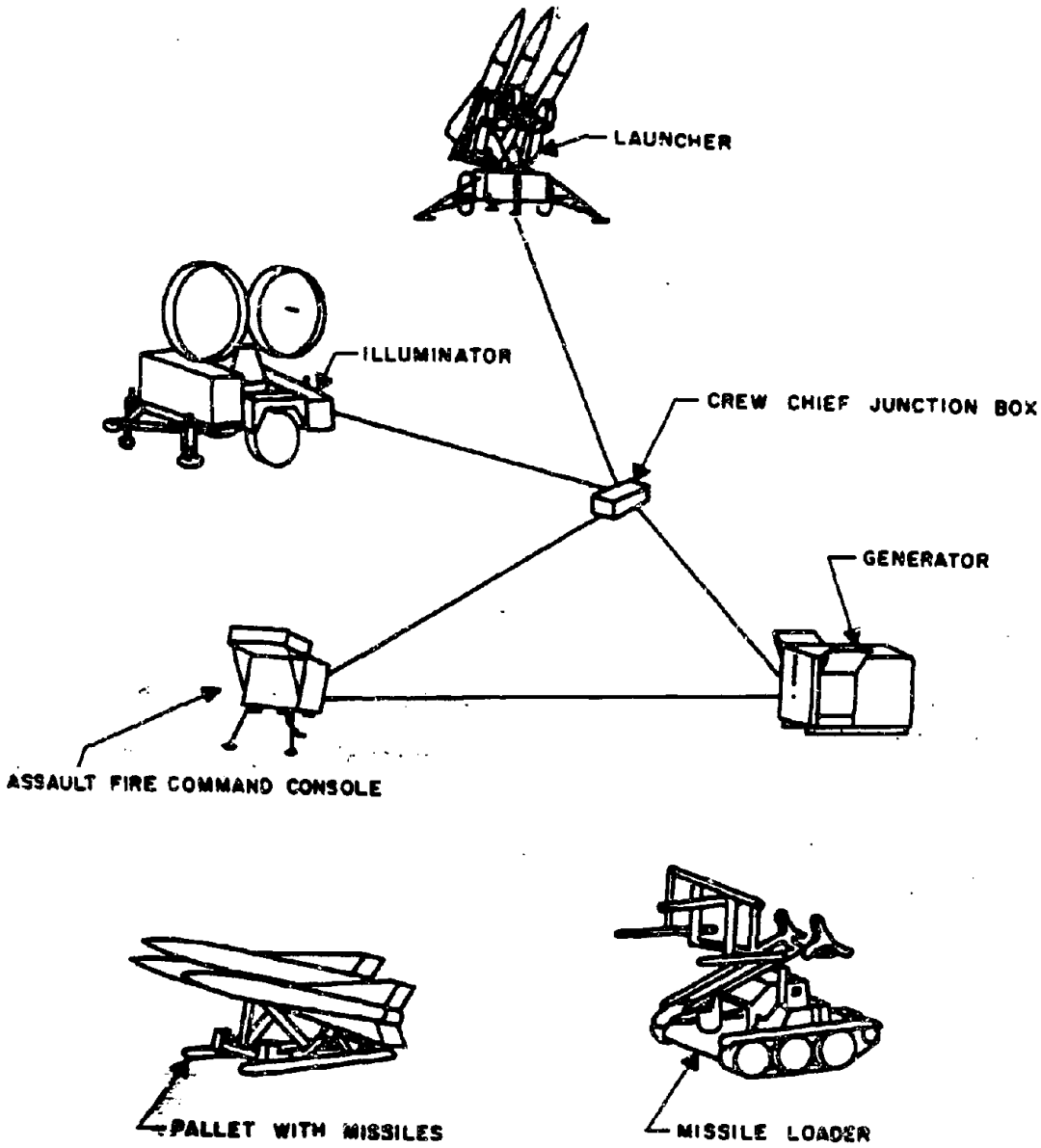

Figure 16-10. [redacted] HAWK System, Basic Assault Firing Unit [redacted]

[redacted]

[redacted]

DNA (6X1)

[redacted]

[redacted] SAMPLE PROBLEM: AIR BLAST DAMAGE TO A TACTICAL MISSILE SYSTEM [redacted]

[redacted] The material presented above concerning the SERGEANT, LANCE, and HAWK weapon systems is used to estimate the blast vulnerability of the HONEST JOHN weapon system as an illustration of the methods by which the vulnerability data may be applied.

16-10 Description of the HONEST JOHN System [redacted]

[redacted] The HONEST JOHN is a 762 nm, surface-to-surface, field artillery rocket designed to deliver warheads, weighing between 1,000 and 1,500 pounds, at horizontal ranges up to about 26 miles. It uses solid propellant, and it follows a ballistic trajectory after firing (no guidance).

[redacted] The HONEST JOHN system is mobile by both ground and air transport. The principal units of the system are the following:

- *Complete rocket.* The rocket includes a warhead section, motor assembly, and fins, for which containers are provided (see Figure 16-13).
- *Launcher, truck-or trailer-mounted.* The launcher includes the launching beam assembly, elevating and traverse mechanisms, and electrical controls (see Figures 16-14 and 16-15).
- *Other ground support equipment.* A wrecker, transporter trailer, generator, motor and warhead cradles, and handling beam make up the ground support equipment (see Figure 16-16).

[redacted] Table 16-7 lists the weight and size of the various HONEST JOHN components. The principal operational phases can be listed as follows:

- Storage at Storage Site,

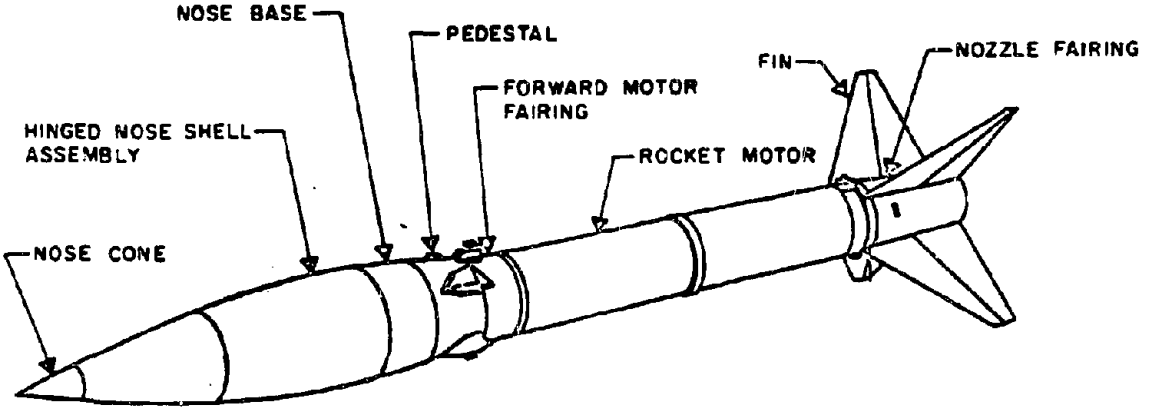

Figure 16-13. [redacted] HONEST JOHN, Major Components of Rocket [redacted]

[redacted]

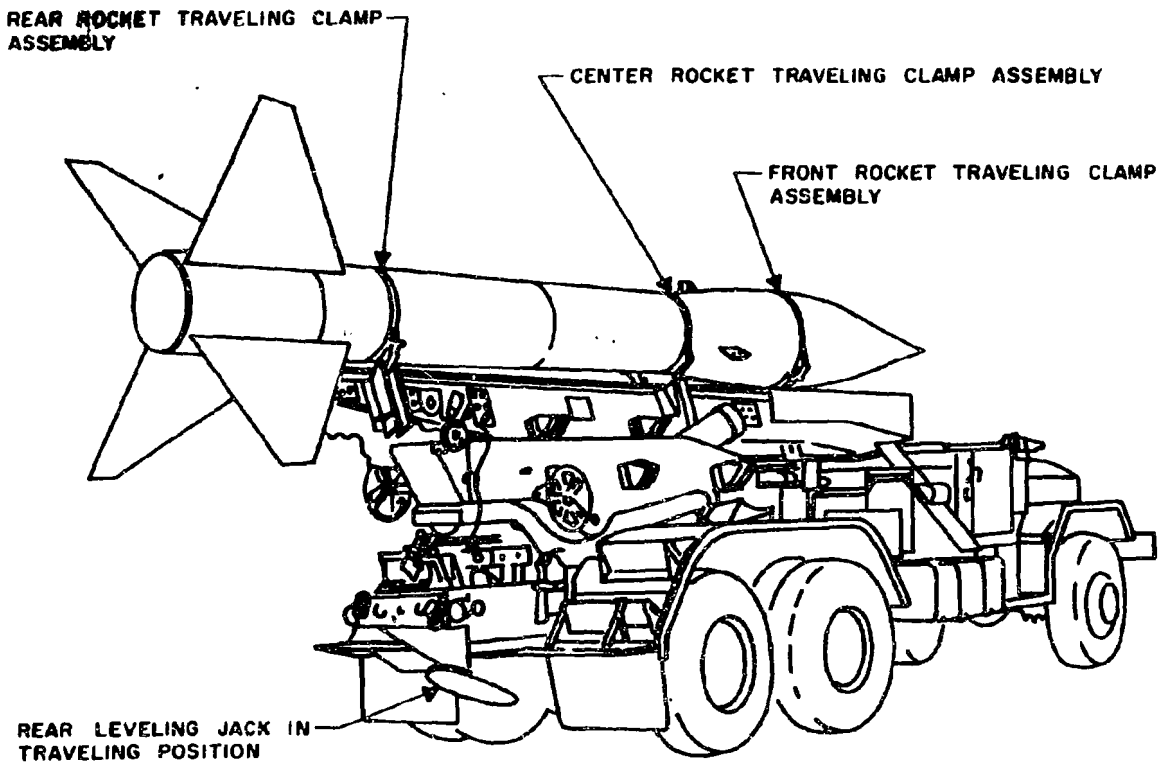

Figure 16-14. HONEST JOHN, Truck-Mounted Rocket Launcher in Traveling Position

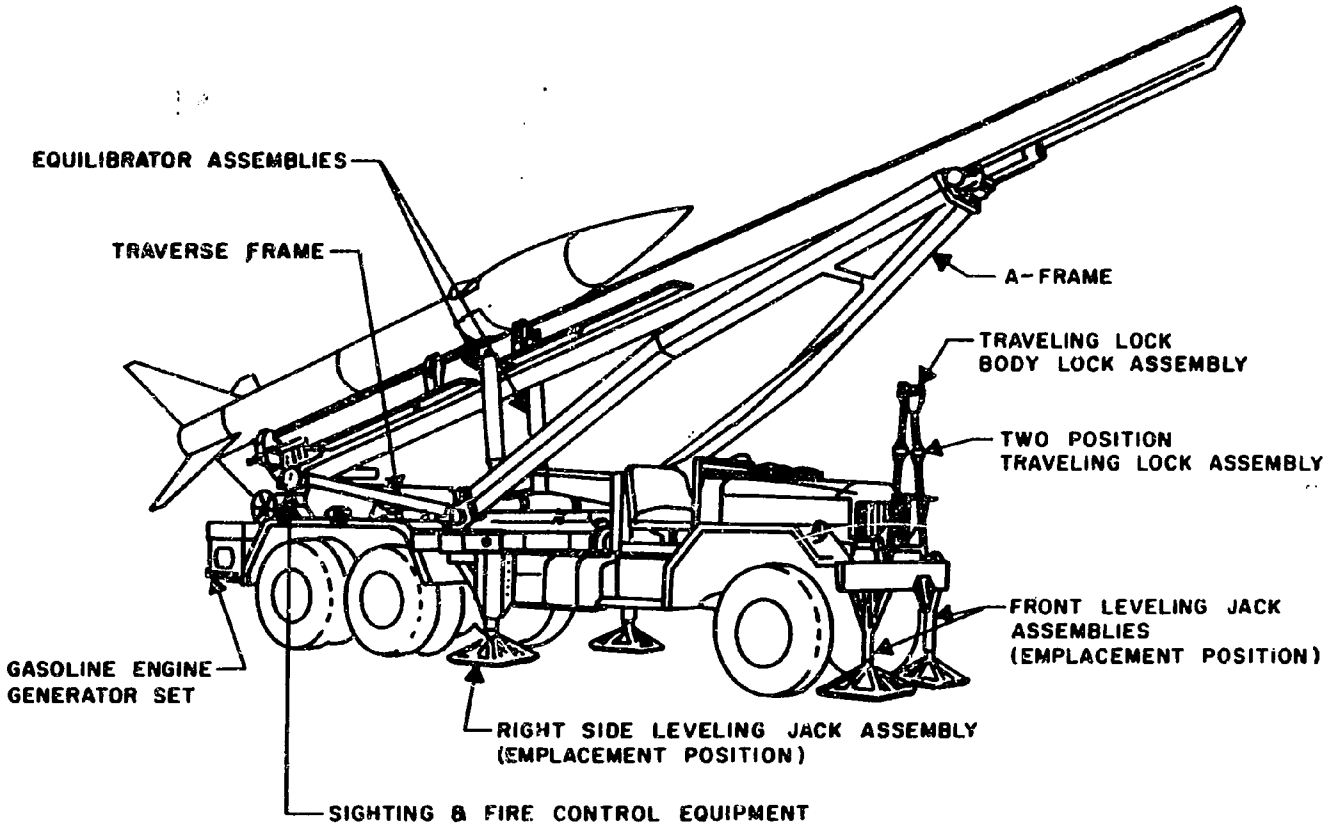

Figure 16-15. HONEST JOHN Rocket Launcher in Firing Position

[redacted]

Table 16-7. [redacted] Missile System Components – HONEST JOHN [redacted]

Item	Refer to Figure	Dimensions (in.) (Weight (lbs))	Remarks
1. Missile Components (in containers)			
(a) Warhead sections	–	144 x 50 x 45 (2,500)	Plywood containers
(b) Guidance sections	None	–	
(c) Rocket motor sections (d) Fins	–	235 x 44 x 38 (3,500)	Plywood containers
2. Missile Body (assembled)			
(a) Ready for launch	13	327 x 28 (3,750)	
(b) In-flight (near target)	13	327 x 28 (2,000)	Propellant burned
3. Transport Equipment			
(a) Semitrailers	16	315 x 97 x 48 (3,500)	w/o missile
(b) Trucks (M543 or M62)	16	310 x 97 x 103 (34,000)	
4. Launch Equipment			
(a) Lightweight launchers	–	346 x 83 x 61 (4,375)	w/o missile
(b) Self-propelled launchers	14, 15	508 x 121 x 151 (42,000)	w/o missile
(c) Loaders (handling unit on M62 truck)	16	310 x 97 x 210 (40,000)	w/o missile
5. Auxiliary Ground Equipment			
(a) Firing unit assembly	–	36 x 24 x 24 (300)	
(b) Sighting equipment	–	36 x 20 (175)	
(c) Generator set	16	60 x 30 x 30 (1,800)	On truck chassis

[redacted]

[redacted]

SECTION II

[redacted] BLAST AND THERMAL VULNERABILITY OF IN-FLIGHT STRATEGIC SYSTEMS [redacted]

[redacted] INTRODUCTION [redacted]

[redacted] The blast and thermal damage to strategic systems are considered together since blast and thermal effects are closely associated in the physics of a nuclear explosion and also because the damage mechanisms of these two effects tend to interact and, at times, complement each other. It should be noted that this section only treats damage to in-flight aerospace systems; blast and thermal damage to surface and underground installations characteristic of the ground support portions of a strategic system are treated separately in Chapter 11.

[redacted] Blast effects are important to in-flight strategic systems from sea level to altitudes of approximately 100,000 feet (about 30 kilometers). When a nuclear explosion occurs in this altitude region, the blast wave is formed by conventional hydrodynamic processes as the fireball expands. The details of these processes depend on the yield of the weapon, the altitude of burst, and the weapon design (see Chapter 2). The latter consideration (weapon design) is becoming increasingly important as warheads are tailored to [redacted] or to enhance specific elements of the output. The mechanisms of blast wave formation are reasonably well understood from a theoretical viewpoint for nuclear bursts up to altitudes as high as 50 kilometers but experimental verification is lacking (see paragraphs 2-42 through 2-44).

(U) Blast is important to in-flight strategic systems operating below about 100,000 feet, in terms of the following effects:

- Overpressure (static or dynamic) crushing or bending of the primary structure.
- Gust (or deceleration) loading on primary and/or secondary (internal) structures.
- Trajectory deviation (CEP degradation).
- Alteration of aerodynamic stability.

[redacted] The thermal radiation (excluding X-ray effects*) associated with a nuclear burst must be considered from two main aspects:

- "Early" time thermal radiation emitted from a distant source that is incident on the missile surface; this radiation comes from the fireball and from the high-pressure shock front.
- Missile "fly-through" of the fireball region at "later" times, with the associated thermal radiation imposed on the body surface while it is inside the fireball region.

[redacted] In addition to considering the effects of blast and thermal radiation on in-flight strategic systems separately, the possible coupling of these two effects in producing damage to the system should be considered. The magnitude of possible coupling effects probably will depend on the details of the system design; general statements are not valid.

[redacted] The two major strategic systems of concern are defensive antimissile missiles (AMM), more commonly known as ABM, and offensive reentry vehicles (RV). Both systems respond to exposures to the environment produced by nuclear explosions in similar manners, despite significant differences in their configurations (Figure 16-18). The degree to which any system will respond depends on the flight characteristics of the specific vehicle involved, but, in general, there is considerable overlap between RV's and ABM's with respect to their velocity at different altitudes within the atmosphere. A comparison of operational regimes is shown in Figure 16-19.

---

*[redacted] See Section V, Chapter 9 for a discussion of X-ray effects on aerospace vehicles.

[redacted] [redacted]

[redacted]

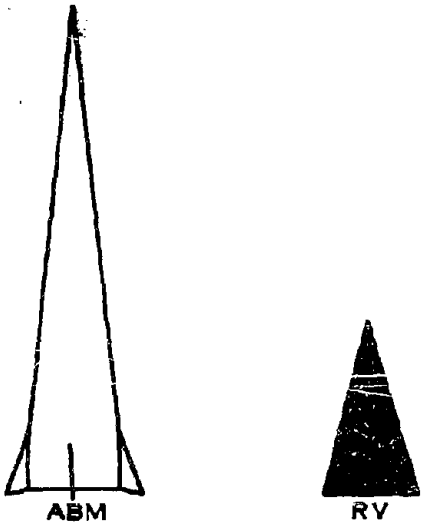

Figure 16-18. [redacted] ABM and RV Configuration Comparison [redacted]

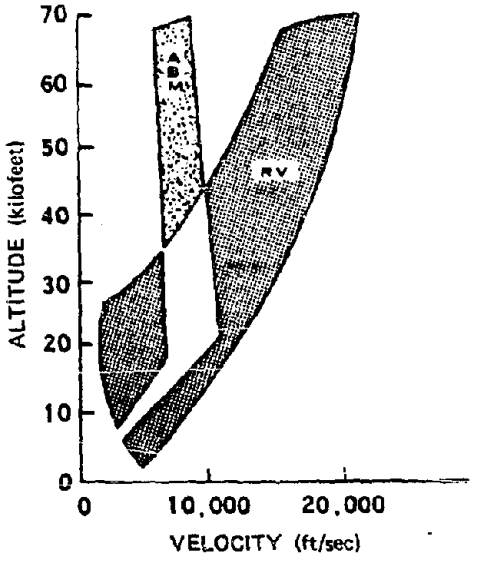

Figure 16-19. [redacted] ABM and RV Operating Envelope Comparison [redacted]

[redacted] The first two categories of blast effects listed above, static and dynamic overpressure crushing (or bending) and gust (acceleration) loading can damage the system physically, i.e., the blast wave from a nuclear explosion at altitudes up to 100,000 feet can cause permanent structural deformation to reentry vehicles, interceptor missiles, boosters, and aircraft. As the structure crosses the shock front, it is suddenly immersed in a "new," transient pressure field, hence, the term "pressure crushing." There is, of course, a complicated shock interaction when the bow shock surrounding a supersonic vehicle intersects the shock front of the blast wave. This interaction results in a high pressure transient ("shock-on-shock" load) that decays quickly to a quasi-steady loading behind the front. The duration of this transient or "spike" can be quite short (tens of microseconds) compared to the response time of the vehicle. At the same time, the vehicle structure is suddenly subjected to a gust loading or an additional aerodynamic loading that results from the particle velocity and the over-density behind the shock front that causes a jump in the dynamic pressure, which causes an abrupt deceleration of the whole vehicle body.

[redacted] The extent of physical damage or structural response from either pressure crushing or gust loading depends on the distance from the target to the burst point, the orientation of the target, the strength and duration of the blast wave, and the preblast flight loads imposed on the vehicle. These last loads depend on the speed, trajectory, and physical design characteristics of the vehicle. For an incoming reentry vehicle, the altitude of maximum deceleration from atmospheric drag depends on the ballistic coefficient, β. The ballistic coefficient is defined as $\beta = W/C_d A$, where W is the vehicle mass, C_d is the drag coefficient, and A is the body reference area. As the ballistic coefficient is increased, the

[redacted]

[redacted]

[redacted]

altitude at which the vehicle experiences maximum deceleration is decreased. The high performance, thin, cone-shaped vehicles have very high ballistic coefficients. Figure 16-20 shows the various response regimes for an interceptor missile including structural, e.g., shell buckling and beam bending, rigid body, and thermal response.

[redacted] Rigid body response describes the gross whole body motion of an in-flight strategic vehicle that results from passing through the blast sphere and the fireball interior. It includes trajectory deviation (CEP degradation), aerodynamic stability changes, and the drag forces exerted on the overall vehicle; it should be noted that the deceleration forces imposed on the whole body also are transmitted, in a complex manner, to the internal components of the missile system. Trajectory deviation occurs when the blast wave deflects or displaces an in-flight vehicle from its preassigned (or benign environment) trajectory. Since this trajectory alteration results from the direction of the blast winds behind the shock front, this type of rigid body response depends on the relative geometry of the target and the explosion. If the system misses the target by an unacceptably wide margin, it will not be effective.

[redacted] Passing through the hot fireball results in a thermal load on the system in addition to the thermal loads caused by the benign reentry heating or the supersonic flight of an ABM. Consequently, the impact of the *total* environment of a high altitude nuclear burst must be examined. Figure 16-21 shows the nuclear encounter sequence for RV and ABM systems. The loading and response of the vehicle at each point from 1 through 6 is a function of the local environment, the physical characteristics of the vehicle, and its flight profile.

[redacted] After the vehicle enters the blast sphere, it may traverse a region of density lower than

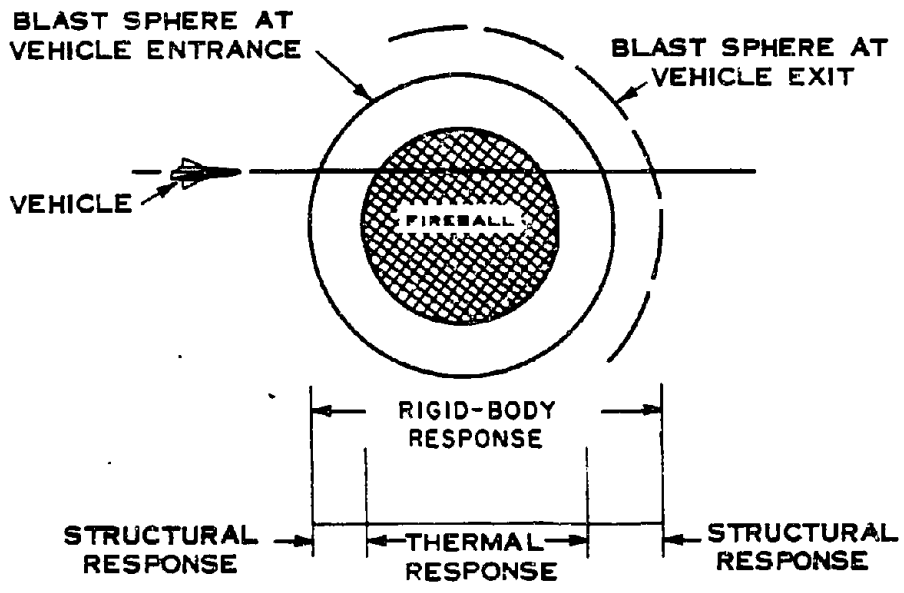

Figure 16-20. [redacted] Response Regimes for Interceptor Missile [redacted]

[redacted]

[redacted]

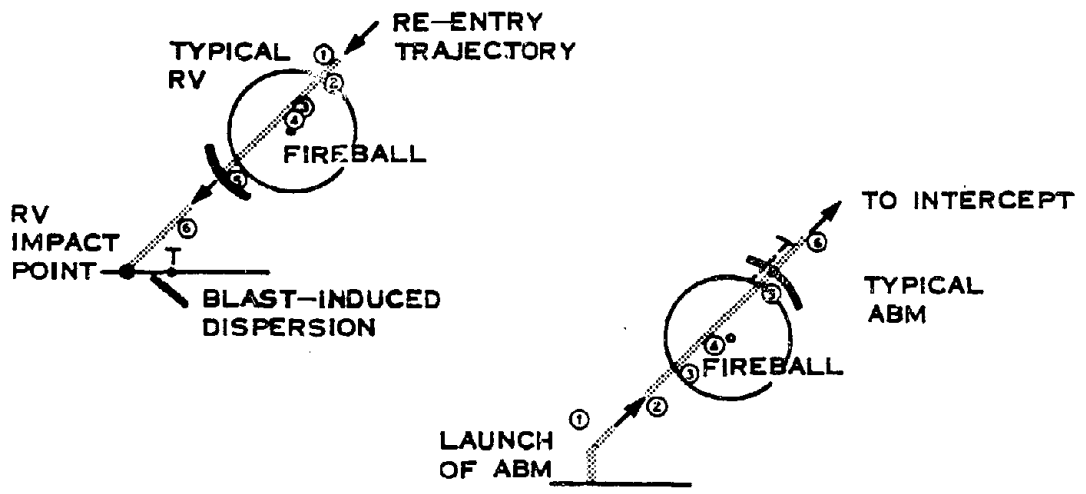

Figure 16-21. [redacted] Nuclear Encounter and Event Sequence for RV and ABM [redacted]

[redacted] ambient before it exits the blast sphere. This may affect its flight stability, depending on the design characteristics, i.e., static margin and rate of damping. Under some conditions, a reentry vehicle on a ballistic trajectory may tumble in this region and/or subsequently emerge from the blast sphere with a large flight angle of attack, which may cause severe structural loading and may result in serious damage. Even if tumbling does not occur, exit loads imposed on a vehicle at a large angle of attack sometimes could be greater than initial entrance loads. Also, since the RV may exit the blast sphere at a large angle of attack, loss of accuracy and increased dispersion are likely. This is particularly true for advanced systems that use slender body configurations whose drag coefficients are very sensitive to changes in angle of attack.

[redacted] Maneuvering reentry vehicles are being considered with a view toward avoiding a nuclear encounter or reducing the exposure time by altering the usual ballistic trajectory on reentry. However, while the maneuverability of the reentry vehicle could increase its survivability, it could, under some circumstances, also increase its vulnerability to blast. The maneuvering vehicle would experience more severe aerodynamic preloads, to which the air blast induced loads would be added.

[redacted] These maneuver load effects also can be important for ABM systems. Since ABM's are required to maneuver within the atmosphere, control surfaces, which also are susceptible to damage from gust loading, are involved. For many situations, assuming a range of yields and warhead designs, spacing between interceptors is governed by blast fratricide. In a saturation attack, the stepdown firing doctrine for defense tactics depends directly on the hardness of the interceptor to all nuclear effects. Consequently, a complete description of the nuclear environment is necessary to predict the effects of a nuclear burst on in-flight strategic systems. With respect to the blast wave, the parameters of interest include overpressure, particle velocity, density and temperature, as a function of both time and distance.

[redacted]

[redacted]

[redacted] The propagation of the blast wave from the point of burst downward through a non-homogeneous atmosphere must be considered. Atmospheric inhomogeneity is not a serious problem for small yields at moderate heights, although it does distort the blast sphere somewhat. Blast wave inhomogeneity becomes more severe as the altitude of burst is raised above about 100,000 feet; however, it is significant that at these higher altitudes, blast begins to be less severe as a damage mechanism than other competing effects.

16-12 Sources of Data [redacted]

[redacted] The blast effects on early RV's were expressed in terms of rigid body gust loading or "g" levels of deceleration. When these g loads were added to the normal "peaceful" reentry loads and then compared to design safety factors, it was found that the early RV designs were relatively soft and had large radii of blast vulnerability that outreached over nuclear effects. At these "vulnerable" ranges, overpressure levels were so low that local crushing or beam bending was not a problem.

[redacted] As better theoretical models of the nuclear environment have been developed, blast loading and structural response calculations have become more sophisticated. Progress has been made, from the early engineering analysis of simple spring-mass models subjected to idealized loading, to more complex computer codes that handle rings and shells subjected to loads more representative of the nuclear engagement, including local body pressures. Through the use of 6-degree-of-freedom trajectory codes, the trajectory dispersions induced by the blast wave can be computed and the tumbling within the blast sphere can be predicted using approximate values of environment levels. Theoretical analyses have been developed to treat the shock-on-shock interaction and these analyses have been confirmed at normal incidence by experiments. Test techniques have been developed to determine properties of materials at high strain rates.

[redacted] Early programs to determine blast and thermal vulnerability of in-flight strategic vehicles include HARTS, SPINE, and ABM Vulnerability and Hardening. These research programs were closely coordinated with the research requirements of systems designers. This coordination is shown by the following list of the various configurations of research vehicles that have been studied and their counterparts in terms of military systems.

Program	Research Vehicle	System Application
Air Force	HARTS A	Mark 12 (RV)
Air Force	HARTS B	Mark 11A (RV)
Army	AIRS I	SPRINT (ABM)
Army	AIRS II	SPARTAN (ABM)

This correlation permits use of physical data and the aerodynamic coefficients obtained during the development of the specific systems.

16-13 Limitations in Application of the Data [redacted]

[redacted] Since vulnerability (or damage) assessment of an in-flight strategic vehicle is such a strong function of the detailed characteristics of the specific vehicle, it is virtually impossible to devise a general method of vulnerability determination that could be applied to any vehicle. Some of the parameters that enter the problem are the details of the design of the primary structure of the vehicle (including all materials used, internal supports, field joint fixtures, etc.), the design features of the internal components and how they are supported on the primary structure, the detailed aerodynamic characteristics of the body and how it may fly (including the possible requirements for maneuvers). Therefore, it is obvious that an accurate definition of

[redacted]

[redacted]

[redacted] the blast and thermal vulnerability of a *particular* in-flight strategic vehicle requires a great deal of analysis and the use of specialized computational models as well as experiments. Such analyses are beyond the scope of this manual.

[redacted] The following discussion will attempt to explain, in general terms, the technical aspects of the problem that appear to have the most important influence on the determination of nuclear weapon blast and thermal damage to in-flight strategic vehicles. The technical discussion will be presented under two main sections, one devoted to RV bodies and the other to ABM vehicles; some of the material appearing under the RV section will be applicable to the ABM and, where this is the case, it will be noted.

[redacted] BLAST LOADING ON REENTRY (RV) SYSTEMS [redacted]

[redacted] The general approach used herein to describe the important factors related to the determination of blast and thermal vulnerability of reentry vehicles was generated primarily under the Hardening Technology Study (HARTS). The HARTS vehicles that were studied are shown in Figure 16-22. Configuration A is a blunted cone and Configuration B is a sphere-cone-cylinder-flare. The dimensions and the ballistic coefficients are shown in the figure. Table 16-9 lists the range of parameters that were used in the HARTS studies. The term "hardness level" will be explained below.

16-14 Environment Scaling [redacted]

[redacted] The nomenclature used to describe RV/blast intercept conditions is shown schematically in Figure 16-23. The conditions pictured correspond to those where the RV does not traverse the center of the burst fireball ($\varphi \neq 0°$). As described in Chapter 2, blast scaling has been used extensively to predict air blast environments. Since RV intercept loads and traversal phenomena depend on the blast parameters, it is possible to scale RV intercept loads and traversal phenomena in a manner similar to the blast parameters.

Table 16-9. [redacted] Range of Basic Parameters for HARTS II [redacted]

Blast yield	30, 200, and 440 kt – blast environment from Hillendahl FIREBALL code
Intercept altitude	30,000 to 100,000 ft
Intercept angle (φ)	0 to 90 deg
Trajectory	Minimum energy trajectories for 2,000, 5,500, and 7,000 nm ranges
Hardness levels (axial acceleration for head-on intercept)	200 to 1,000 g
Configurations (see Figure 16-22)	A: β = 2,150 lb/ft^2 B: β = 680 lb/ft^2

[redacted] Figure 16-23 indicates that there are two important radii. First, the distance between the burst center and the vehicle at the time of detonation, denoted by RD, is significant for the comparison of *prompt* effects (e.g., neutrons, X-rays, etc.) as well as blast effects. Consideration of these RD values for various vehicle paths and orientations results in vulnerability envelopes referred to as *burst time* envelopes. Second, the distance between the burst center and the vehicle when the blast wave intercepts the vehicle, denoted by RB, results in envelopes referred to as *intercept time* envelopes. The reference time for which the envelope is constructed must be specified for each envelope.

[redacted] "Hardness Level" is a useful parameter to hold constant when studying blast phenomena. Hardness level is defined as that *axial* load

[redacted]

[redacted]

NOTE: ALL DIMENSIONS IN INCHES

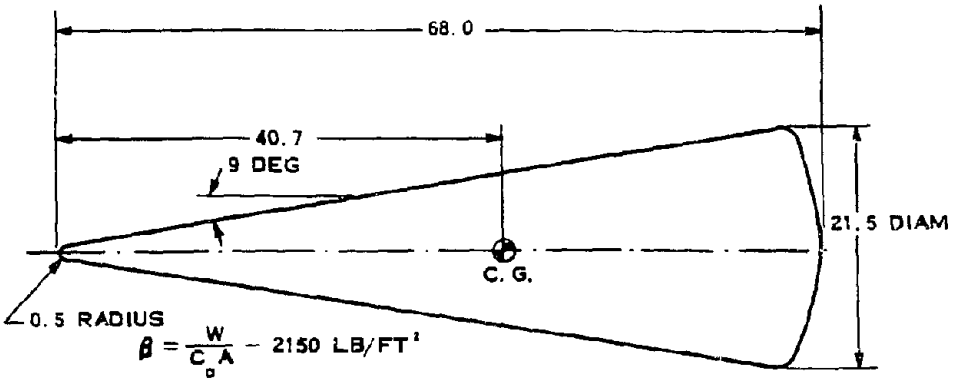

CONFIGURATION A

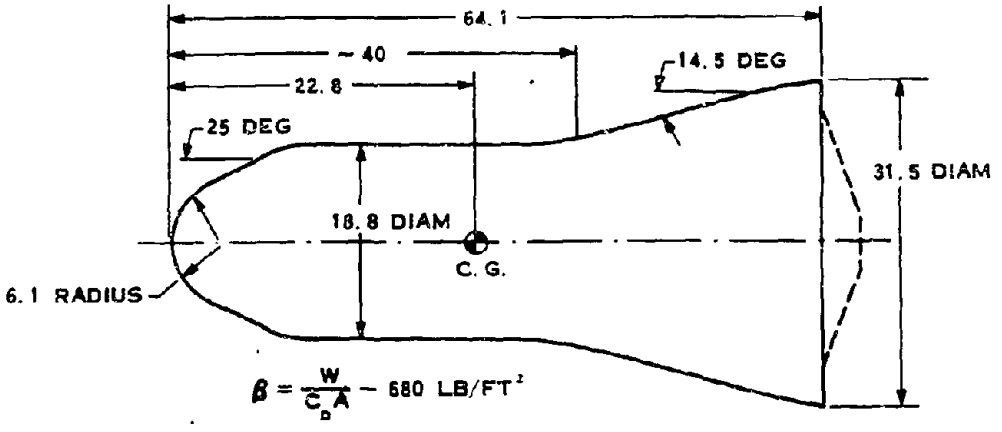

CONFIGURATION B

Figure 16-22. [redacted] HARTS Configuration [redacted]

[redacted]

[redacted]

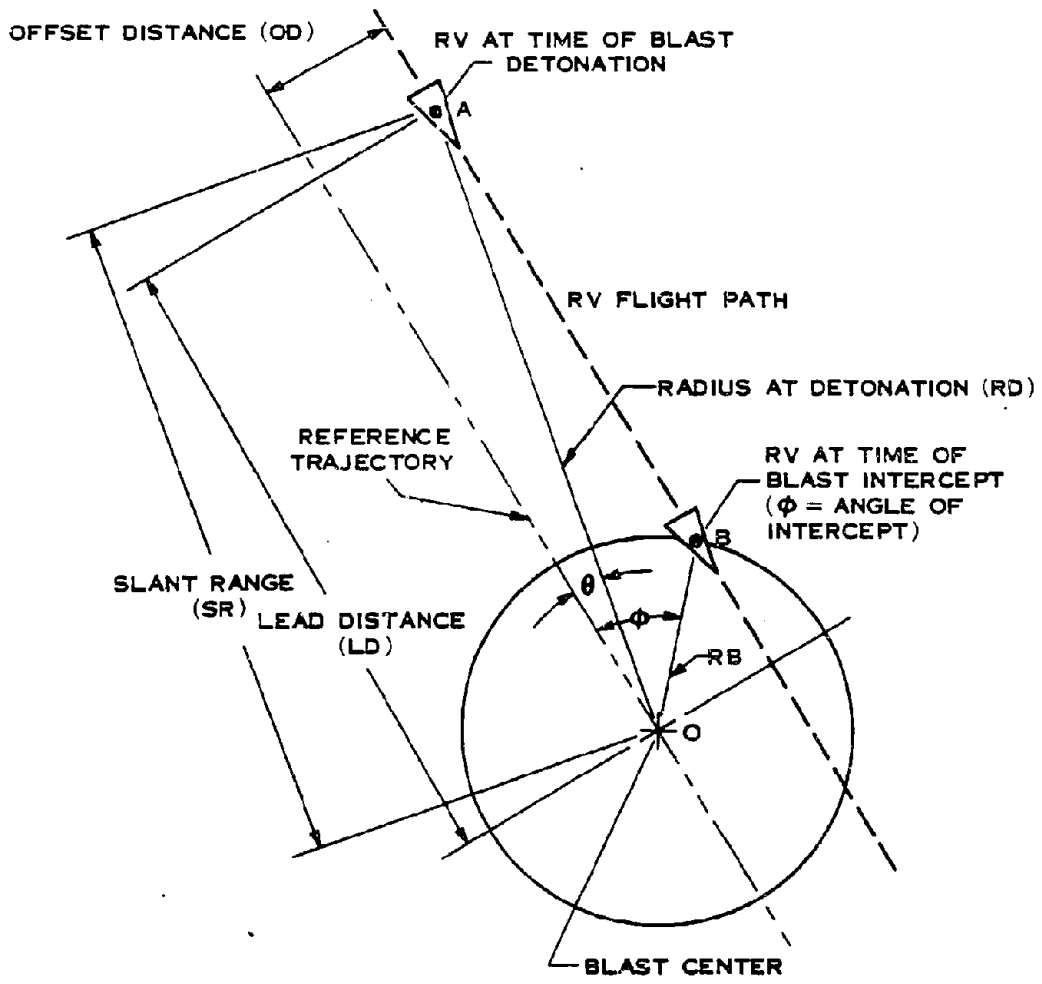

Figure 16-23. [redacted] Blast Intercept Conditions Nomenclature [redacted]

[redacted] [redacted]

[redacted]

[redacted]

acceleration experienced by a vehicle intercepting a blast wave head on ($\varphi = 0°$) at zero angle-of-attack ($\alpha = 0$). For a given yield, burst altitude, and configuration combination, the specification of a blast intercept hardness level *determines the blast wave radius.* This in turn determines the blast *front* environment. Blast scaling laws indicate that these blast front conditions are identical to those at a different yield and radius where the new radius is equal to the old radius multiplied by the cube root of the ratio of the yields. For example:

$$RB_2 = RB_1 (W_2/W_1)^{1/3} \quad \text{(ft)},$$

where RB_2 and RB_1 are the blast intercept radii for yields of W_2 and W_1, respectively, and in general,

$$RS = RB/W^{1/3} \quad (\text{ft/kt}^{1/3}),$$

where RS is known as the scaled intercept radius. Values of scale radius, RS, at constant hardness level for varying altitude are shown in Figure 16-24. A similar presentation of scale time of blast intercept can be made, since time and radius are proportional. Thus, in general,

$$\tau_I = t_I W^{1/3} \quad (\text{sec/kt}^{1/3}),$$

where t_I is the time after burst to intercept and τ_I is the scaled time. Values of scaled time, τ_I, for constant hardness levels for varying altitude are shown in Figure 16-25.

[redacted] The hardness level, position-time relationships are defined in a manner that data for any yield can be derived over the given range of hardness levels and burst altitudes. System analysis parameters such as slant range SR, lead distance LD, and offset distance OD, from the burst at time of explosion also can be derived simply. For a given hardness level and burst altitude one RS and τ_I combination exists. For specified yield,

$$RB = RS\ W^{1/3} \quad \text{(ft)}$$

$$t_I = \tau_I W^{1/3} \quad \text{(sec)}.$$

Referring to Figure 16-23, the following spacing relationships are apparent.

$$OD = RB \sin \varphi,$$

$$LD \approx RB \cos \varphi + Vt_I,$$

$$SR = (LD^2 + OD^2)^{1/2},$$

where V is the RV velocity, and the other symbols are defined in Figure 16-23.

[redacted] Determination of lead distance is illustrated in Problem 16-1. The variation of hardness level with altitude and slant range is shown in Figure 16-26[redacted]

DNA (4)(3)

[redacted]

[redacted]

[redacted]

Problem 16-1. Calculation of Hardness Level

[redacted] Figures 16-24 and 16-25 show the scaled blast radius and scaled time of blast intercept, respectively, for a Configuration A vehicle on a 5,500 nautical mile flight path as a function of burst altitude for various hardness levels. Various system parameters may be determined from Figures 16-24 and 16-25 as discussed in paragraph 16-14.

[redacted] *Example* [redacted]

Given: A HARTS Configuration A vehicle (Figure 16-22) is on a 5,500 nm trajectory. The RV hardness level is 500 g.

Find: The slant range at which the RV would experience a head on ($\varphi = 0°$) load equal to its hardness level if it were exposed to the blast wave [redacted]

DNA (b)(3)

[redacted]

Answer: If the *RV* is more than [redacted] away from the specified explosion at the time of burst, it will not be damaged by blast.

DNA (b)(3)

[redacted]

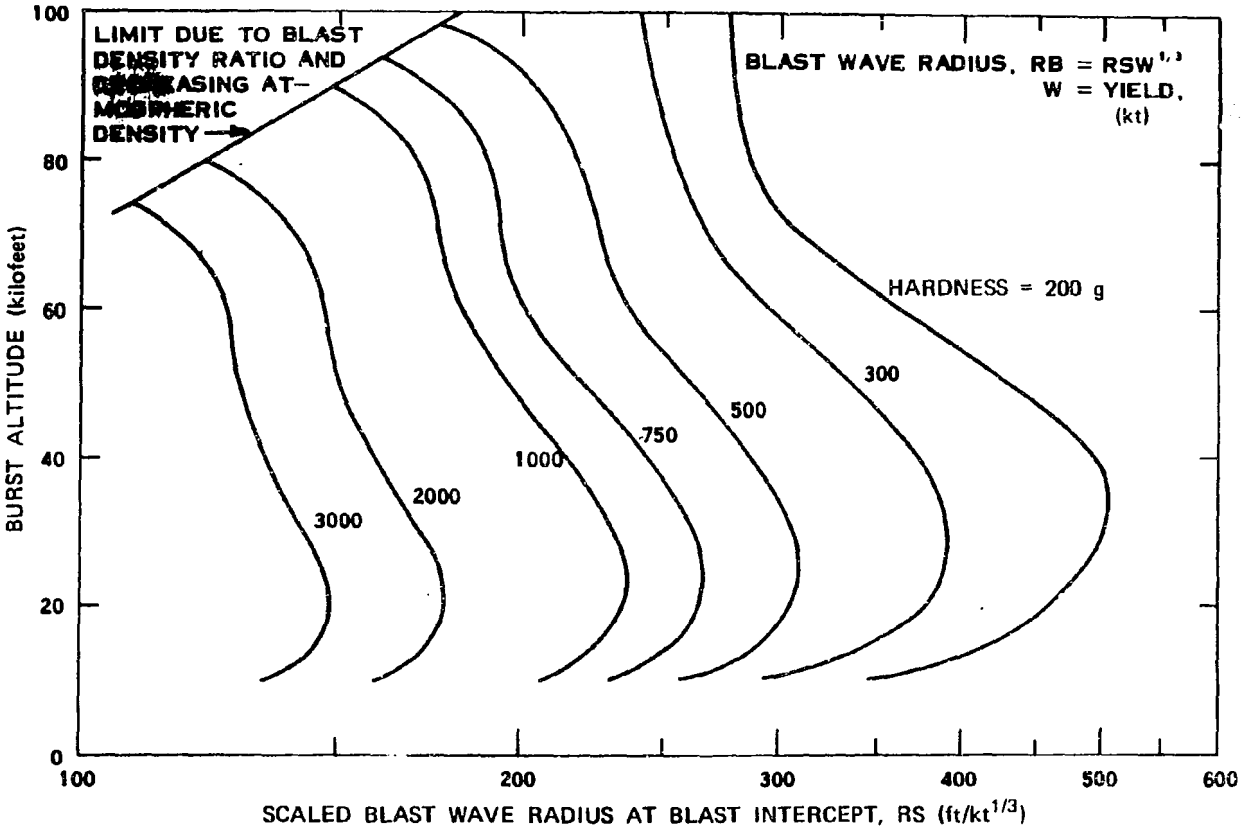

Figure 16-24. Scaled Blast Wave Radius for Constant Hardness Level for Configuration A, 5,500 nm Range

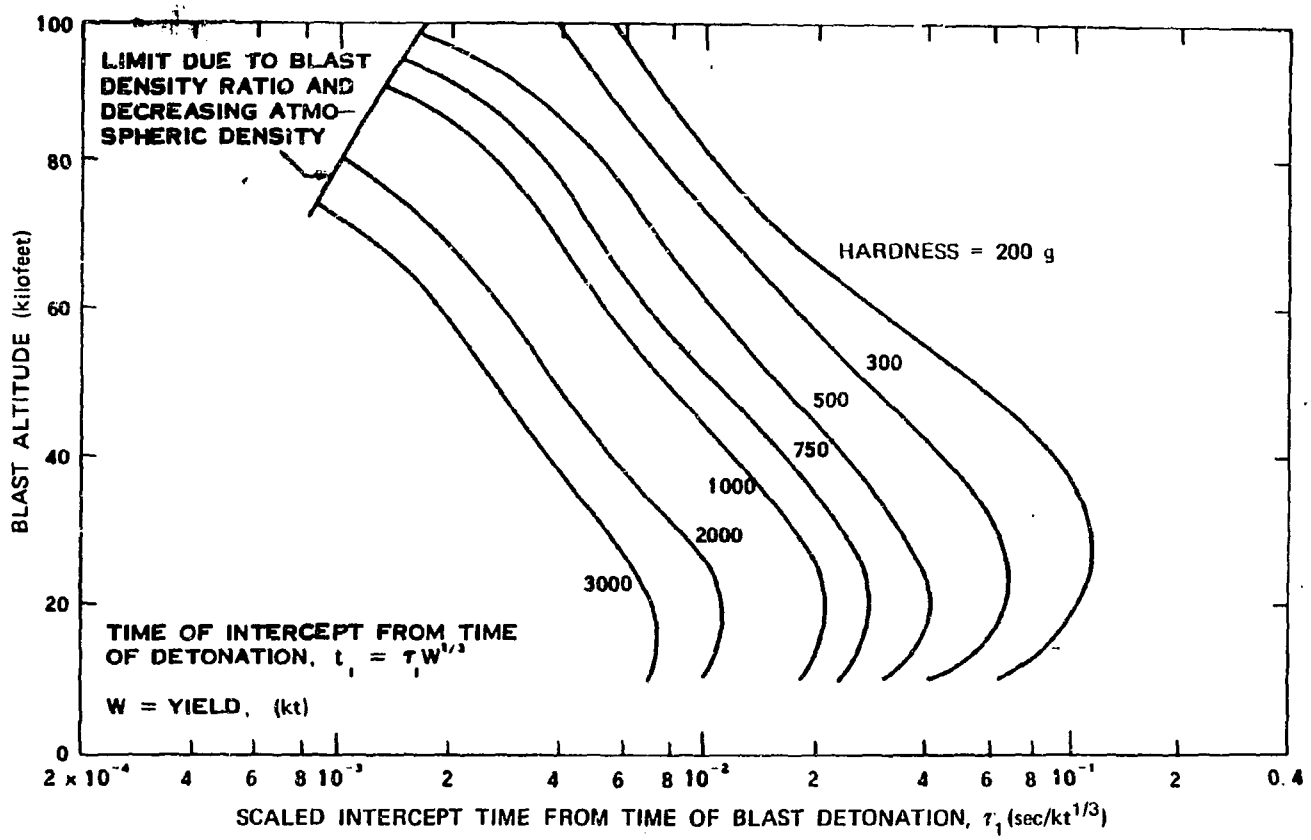

Figure 16-25. [redacted] Scaled Time of Blast Intercept for Constant Hardness Level for Configuration A, 5,500 nm Range [redacted]

[redacted]

16-15 General Intercept Loads and Load Duration [redacted]

[redacted] The aerodynamic loading on hypersonic reentry vehicles can be divided into two general categories: steady state loading and transient loading. Steady state loading occurs when the pressure, density, particle velocity, and temperature do not change with time. Transient loading occurs when there is a time change in the environment surrounding the reentry body.

[redacted] The vehicle experiences a continuing change in environment during normal reentry. However, since this change is relatively slow, steady state drag loading provides a good approximation for normal reentry conditions. For any type of flow over a body, the local pressure at any point on the surface can be found from the relation:

$$P_b = P_f + qc_p,$$

where

P_b = pressure at some point on the body surface,

P_f = free stream ambient pressure,

q = free stream dynamic pressure,

c_p = local pressure coefficient.

Classic Newtonian impact theory provides a simple closed-form solution for the local pressure coefficient, c_p. For steady state, hypersonic flow (above Mach 5) this theory provides adequate loading predictions. For any body of revolution the Newtonian theory predicts:

$$c_p = 2(\cos\alpha \sin\delta - \sin\alpha \cos\delta \sin\beta_r)^2,$$

where

α = angle between the vehicle longitudinal axis and the relative wind vector,

δ = vehicle semivertex angle,

β_r = rotational angle about axis of reentry vehicle.

[redacted] A vehicle experiences axial and lateral decelerations and local pressure loading during normal reentry. The amount of deceleration and local pressure depends on the vehicle reentry angle, velocity, shape, weight, and altitude. Figures 16-27 through 16-29 show some nominal reentry trajectories. These graphs only include the combinations of reentry velocity and reentry angle that correspond to a ballistic missile having a nominal range of 5,500 nm. The reentry vehicle is characterized by the ballistic coefficient, which is varied over a range of values typical for reentry vehicle designs. Calculations for the parameters (velocity, altitude, and time) of the reentry trajectories were begun at an altitude of 400,000 feet, since this altitude is well above that of appreciable aerodynamic forces for the reentry vehicles considered. The reentry angles measured from the local horizontal at 400,000 feet were chosen arbitrarily as 20 and 30 degrees. The corresponding reentry velocities at 400,000 feet were determined from the basic equation for vacuum ballistic trajectories. The ballistic coefficients vary from 800 to 2,500 lb/ft^2. Below 100,000 feet the angle of attack is largely damped out, and the lateral force is very small.

[redacted] The hardness level curves in Figure 16-24 represent one value on the intercept/load matrix of axial rigid body loads, G_A, for zero blast intercept angle ($\varphi = 0°$). It was determined that, at constant hardness level, the blast front environments for varying yields are essentially identical. The last variable to be accounted for in intercept loads is blast intercept angle. At constant hardness level and altitude, the intercept angle is the only factor that can affect intercept loads by changing the angle between the blast wind vector and the vehicle velocity vector, thereby causing a blast induced angle of attack at blast intercept.

(U) Blast yield scaling also can be applied to the scaling of intercept load duration, fireball

[redacted]

[redacted]

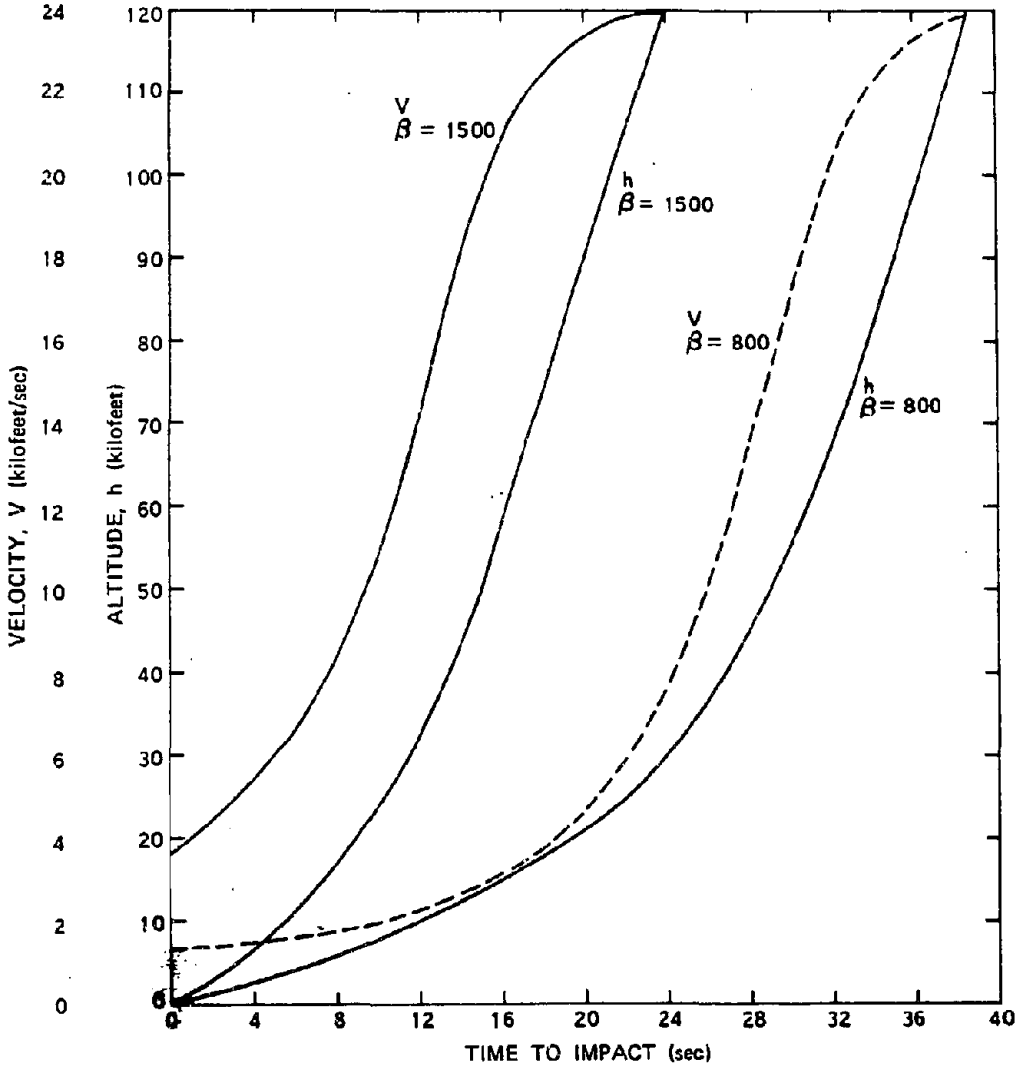

Figure 16-27. [redacted] Normal Reentry Trajectory; Initial Altitude = 400,000 ft, Initial Velocity (V_i) = 23,900 ft/sec, Initial Flight-Path Angle = 20°, Ballistic Coefficient $\beta = W/C_dA$ lb/ft^2 [redacted]

[redacted]

[redacted]

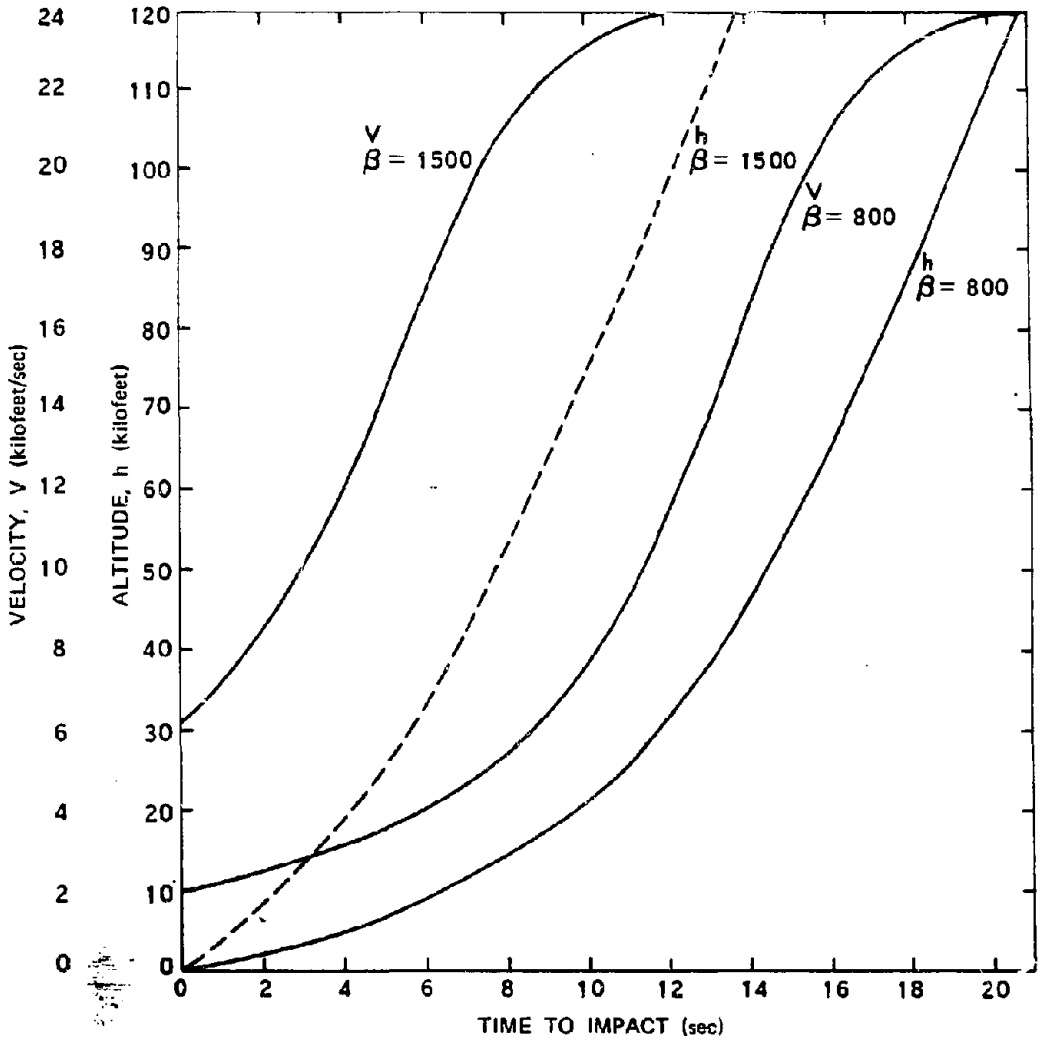

Figure 16-28. [redacted] Normal Reentry Trajectory; Initial Altitude = 400,000 ft, Initial Velocity (V_i) = 24,000 ft/sec, Initial Flight-Path Angle = 30°, Ballistic Coefficient $\beta = W/C_dA$ lb/ft^2 [redacted]

[redacted]

[redacted]

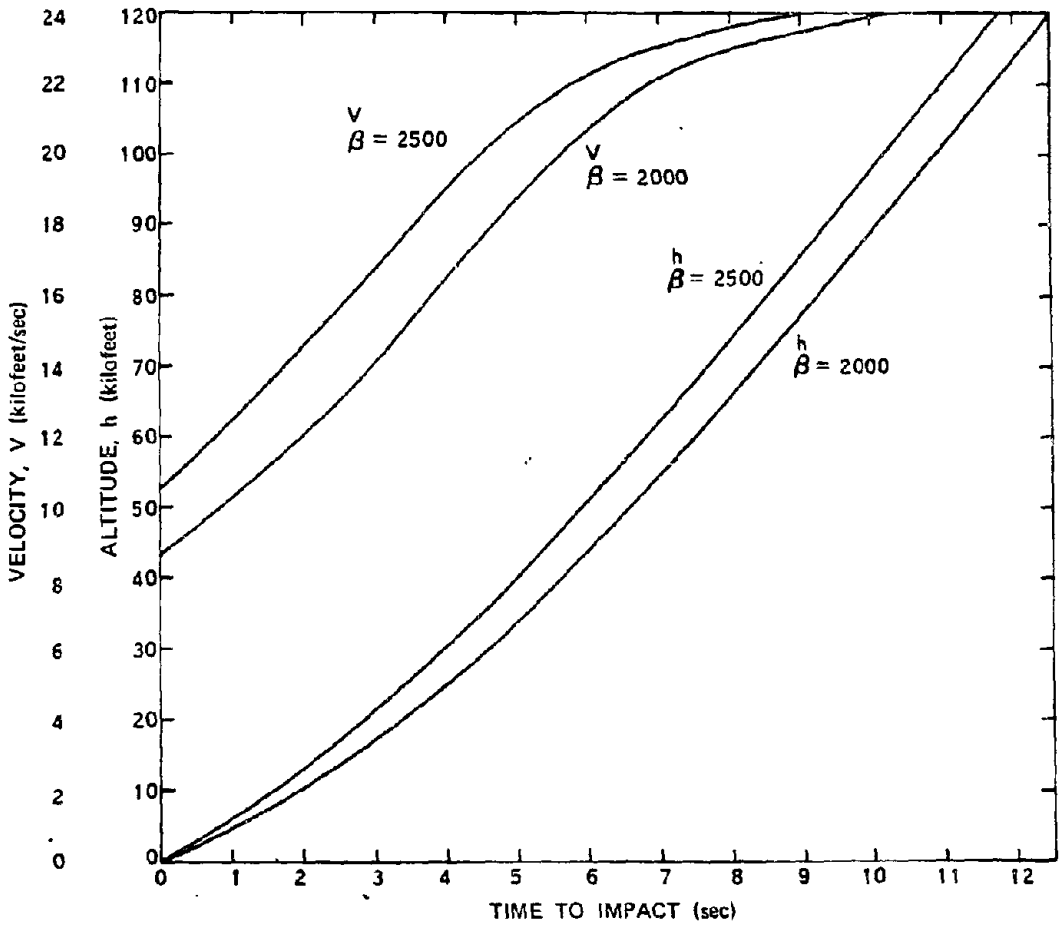

Figure 16-29. [redacted] Normal Reentry Trajectory; Initial Altitude = 400,000 ft, Initial Velocity (V_i) = 24,000 ft/sec, Initial Flight-Path Angle = 30°, Ballistic Coefficient $\beta = W/C_dA$ lb/ft^2 [redacted]

[redacted]

[redacted]

[redacted] traversal time, and total traversal time. Time and radial distance are scaled with the cube root of the yield. Interior blast phenomena can be assumed to scale with the cube root of the yield to obtain reduced radius or time. At any point in time the blast can be imagined to have a size of unity for 1 kt. The blast size for larger yields is unity times the cube root of yield in kilotons, on a relative basis. Since blast loading duration depends on the blast size, which can be scaled, the loading duration also can be scaled.

16-16 Intercept Load Duration [redacted]

[redacted] intercept loads are a function of hardness level, blast intercept angle, and blast altitude. The duration of the load is necessary to describe the intercept loading phase adequately. Under most conditions, the intercept loading history can be approximated by a triangular shaped pulse, i.e., intercept impulse is essentially one-half the maximum load multiplied by the duration time.

$$I_I = \frac{G_I \Delta t_{ILP}}{2} \text{ g-sec.}$$

The intercept load time constant, Δt_{ILP}, is

$$\Delta t_{ILP} = t_I - t_{10\%} \text{ sec,}$$

where $t_{10\%}$ is the point at which the intercept load decays to 10 percent of its maximum value. The scaled intercept load duration time, τ_{ILP}, is

$$\tau_{ILP} = \frac{\Delta t_{ILP}}{W^{1/3}} \text{ sec/kt}^{1/3}.$$

[redacted] Scaled intercept load duration times for a hardness level of 500 g are shown in Figure 16-30 for various intercept angles and altitudes. The intercept load duration times and intercept loads provide a usable set of data for estimating the intercept load impulse. The duration times apply to axial, normal, or total resultant loads. In general,

$$\Delta t_{ILP} = \tau_{ILP} W^{1/3} \text{ sec,}$$

and any load impulse is

$$I_I = \frac{1}{2} \Delta t_{ILP} G_I \text{ g-sec}$$

where I_I and G_I represent any intercept load impulse and maximum load, respectively.

16-17 Fireball Traversal Time [redacted]

[redacted] The time at which the intercept load has decayed to 10 percent of its maximum value (end of the intercept load pulse) corresponds approximately to the time when the vehicle enters the fireball (temperature ≈ 10,000 to 15,000° R). For practical considerations, the end of the intercept load pulse and initial fireball immersion can be considered as the same time. The time of fireball traversal is

$$\Delta t_{FB} = t_{EFB} - t_{10\%} \text{ sec.}$$

where t_{EFB} is the time of exiting the fireball, and the scaled time of fireball traversal is

$$\tau_{FB} = \Delta t_{FB} / W^{1/3} \text{ sec/kt}^{1/3}.$$

Scaled fireball traversal time for a hardness level of 500 g is shown in Figure 16-31 for various intercept angles and altitudes. The time of exiting the fireball, t_{EFB}, is that time during the exit phase when increasing dynamic pressure reaches the ambient level at the blast altitude. This time also is approximately when the temperature level drops below 10,000 to 15,000° R. It should be noted that the point during entry at which the decreasing dynamic pressure reaches

[redacted]

[redacted]

[redacted] ambient level is about the same as the point of 10 percent load.

16-18 Total Traversal Time [redacted]

[redacted] Total blast traversal time is

$$\Delta t_t = t_E - t_I \text{ sec},$$

where t_E is the time of exit from the blast wave shell, and as before, t_i is the time of intercept. The scaled time of blast traversal is

$$\tau_t = \Delta t_t / W^{1/3} \text{ sec/kt}^{1/3}.$$

Scaled total blast traversal time for a hardness level of 500 g is shown in Figure 16-32 for various intercept angles and altitudes.

[redacted]

[redacted]

Problem 16-2. Calculation of Load Characteristics, Fireball Traversal Time and Total Traversal Time

[redacted] Figures 16-30 through 16-32 provide the information necessary to calculate the load characteristics, the fireball traversal time, and the total blast traversal time for a vehicle similar to Configuration A with a hardness level of 500 g that enters the blast front at various intercept angles.

[redacted] *Example* [redacted]:

Given: An *RV* similar in design to HARTS Configuration A (see Figure 16-22) with a hardness level of 500 g that is traveling on a 5,500 nm trajectory.

Find: The intercept load characteristics, and traversal times if the *RV* is exposed [redacted]

DNA (1-)(3)

[redacted]

DNA (1-)(3)

[redacted]

[redacted]

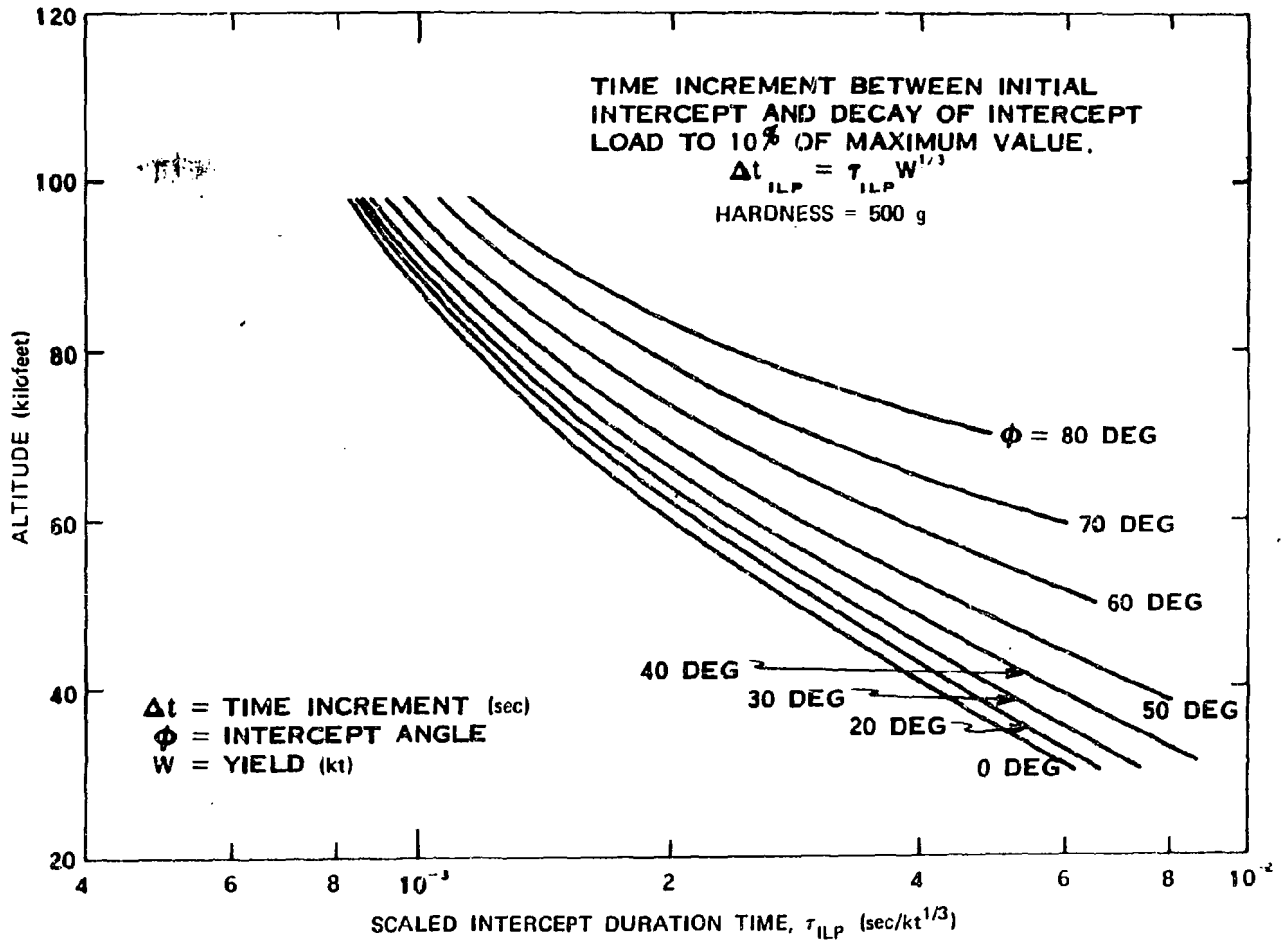

Figure 16-30 [redacted] Scaled Intercept Load Duration Time, 500 g Hardness, Configuration A [redacted]

[redacted]

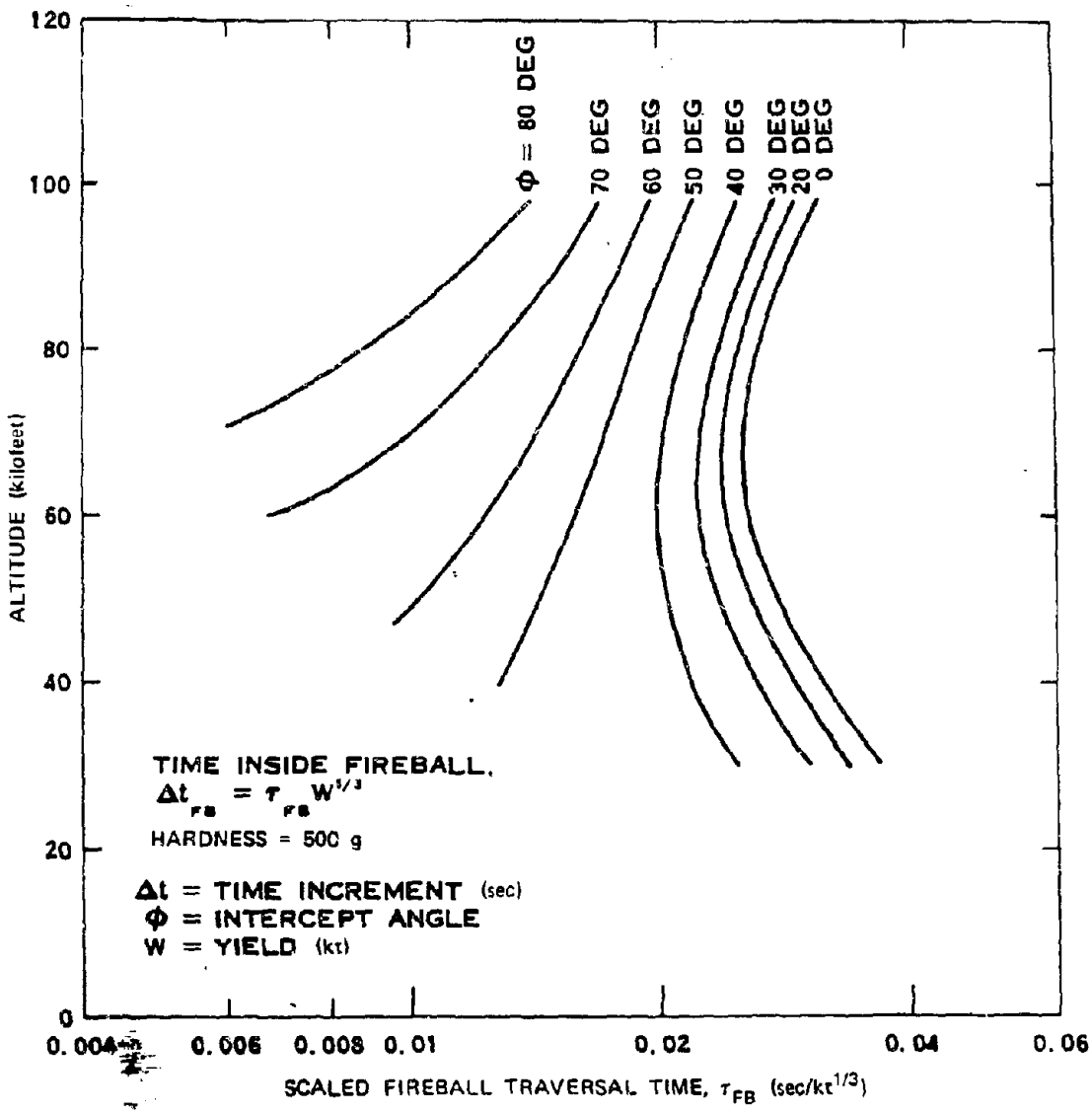

Figure 16-31. [redacted] Scaled Fireball Traversal Time, 500 g Hardness, Configuration A [redacted]

[redacted]

[redacted]

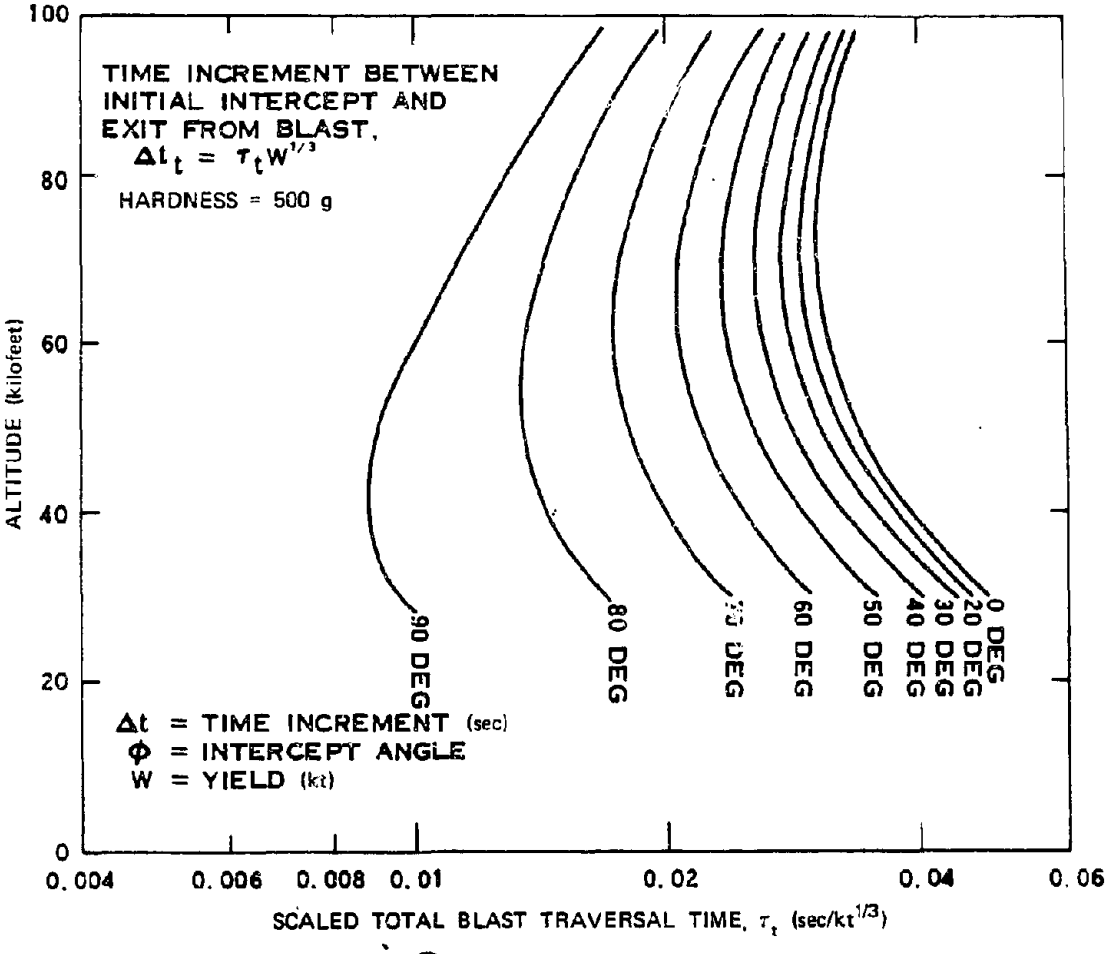

Figure 16-32. [redacted] Scaled Total Blast Traversal Time, 500 g Hardness, Configuration A [redacted]

[redacted]

[redacted]

16-19 Exit Loads [redacted]

[redacted] Intercept load, intercept load duration, fireball traversal time, and total traversal time are functions of hardness level, blast intercept angle, and blast altitude (on a scaled basis). Exit loads also depend on blast yield as well as the functions listed above. This precludes any universal scaling of exit loading: however, the following are generally true of exit loading conditions:

- The probability of obtaining higher exit than intercept loads is very low for vehicles similar to Configuration A.
- Exit loads decrease with decreasing intercept hardness level.

16-20 Blast Data Generalization [redacted]

[redacted] The data summarized in the preceding paragraphs were generated for Configuration A with a 5,500 nautical mile range minimum energy trajectory. Loading and duration scaling procedures applicable to the blast problem were demonstrated for this case. These specific data are *not* directly applicable to *any* configuration-range combination. However, by some simple relationships and approximations, the data can be applied to different configurations and ranges, or combinations of both, within limits. [redacted] *Configuration Variations.* For other configurations, *assume that the velocity, flight path angle, and intercept conditions at the same blast altitude are identical.* With these constraints, the intercept loads become a function of ballistic coefficient and lift characteristics. For axial loads,

$$\frac{G_{AI_1}}{G_{AI_2}} \approx \frac{\beta_2}{\beta_1}$$

and for normal loads,

$$\frac{G_{NI_1}}{G_{NI_2}} \approx \frac{\beta_{\alpha_2}}{\beta_{\alpha_1}}$$

where

$$\beta = \frac{W}{C_D A} \text{ lb/ft}^2$$

$$\beta_\alpha = \frac{W}{C_{N_\alpha} A} \frac{\text{lb-deg}}{\text{ft}^2}.$$

The term β_α is defined as the normal force ballistic coefficient.

16-21 Typical RV Aerodynamics [redacted]

[redacted] A body that is moving along a reentry trajectory at hypersonic velocities has a flow field associated with it. The flow field is composed of the following main regions or characteristics (see Figure 16-33): stagnation point,

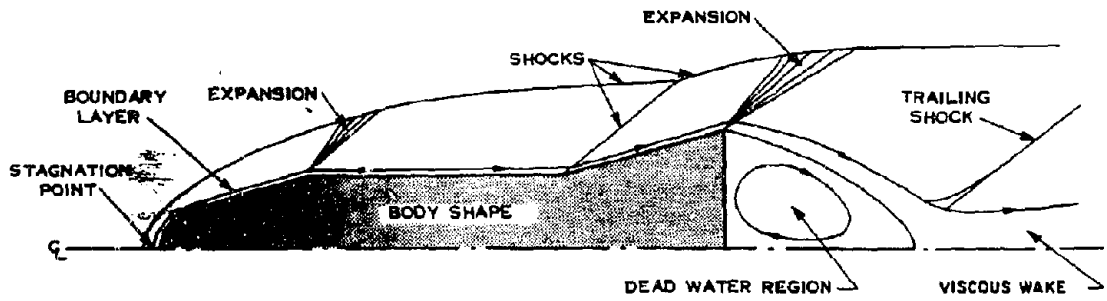

Figure 16-33. [redacted] Flow Pattern Around an Axisymmetric Blunt-Nosed Body [redacted]

[redacted]

[redacted]

[redacted] shock layer, boundary layer, expansion shocks, pressure and density contours, wake, etc. The details of these flow regions are a strong function of the body shape, its velocity, and the properties of the air (i.e., altitude) through which the body is moving. Consequently, the flow field associated with even a single body is constantly changing during the reentry process. [redacted] Figure 16-34 shows the pressure distribution (in terms of pressure ratio) over the surface of a body similar to a HARTS Configuration B vehicle as a function of vehicle velocity. The pressure ratio is $(P_b - P)/P$, where P_b is the local pressure at any point along the surface and P is the ambient pressure. The overpressure $(P_b - P_o)$ are shown for sea level conditions (P_o is the ambient pressure at sea level) to provide some idea of the overpressures involved. It is evident that the overpressures near the stagnation region exceed all other pressures by a wide margin for this blunt body. It should be pointed out that these pressures do not take account of boundary layer perturbations, but the calculated pressures are indicative of actual flow field conditions; the overpressures associated with the flow field shock *front* are slightly higher than pressures on the surface. The curves in Figure 16-34 may be used to interpret the flow fields at altitude. For instance, the ambient pressure at 50 kilofeet is about one-tenth that at sea level. Thus, a vehicle at 50 kilofeet traveling at Mach 10 would have an overpressure on the flare of about 12 psi (i.e., 120/10) and stagnation value in excess of 150 psi. If the vehicle were traveling at Mach 20, the flare overpressure would be about 41 psi (410/10).

[redacted] Another typical reentry flow field, which gives the pressure ratio distribution over a body similar to the HARTS Configuration A (i.e., cone-sphere shape), is shown in Figure 16-35. Figures 16-34 and 16-35 emphasize the differences caused by body shape. Depending on the bluntness of the nose section, there is a very small region over which high stagnation pressures exist. The pressures are virtually constant over the conical section. Figure 16-36 also shows sea level overpressure values for reference; the overpressures shown indicate that at altitudes near 50 kilofeet with the body traveling at Mach 20, the overpressure at the surface of the cone section is about 32 psi.

16-22 Initial Interaction of Vehicle Flow-Field and Blast Wave (Shock-Shock) [redacted]

[redacted] When the reentry vehicle bow wave and the blast wave contact each other a region of high pressure is generated. This region is characterized by a value of pressure that is larger than the value of pressure associated with either shock wave before the interaction. The HARTS results can be summarized by referring to a representative figure. Figure 16-36 shows the variation of maximum overpressure ratio (shock-shock maximum overpressure divided by quasi-steady maximum overpressure, *after interaction*) and duration with the nose surface angle for a hemispherical nose at typical intercept conditions (M_∞ = 15 to 22 and M_B = 5 to 8) assuming $\gamma = 1.4$. The general conclusion to be drawn from the upper curve of Figures 16-36 is that the shock-shock interaction peak overpressure will not exceed a factor of two larger than the quasi-steady overpressure (after interaction). Also, the lower curve on Figure 16-36 indicates that the duration of the shock-shock interaction is extremely short; as an example, if $\tau V_v/R$ is 0.2, then τ = 1 μsec (10^{-6} sec) for V_v = 20,000 ft/sec and R = 0.1 ft. However, it is evident that for the same nose radius (R), the value of τ increases as the vehicle speed (V_v) decreases.

16-23 Damage Envelopes [redacted]

[redacted] The culmination or end result of loading and response calculations is the damage envelope. The damage envelope defines a volume

[redacted]

[redacted]

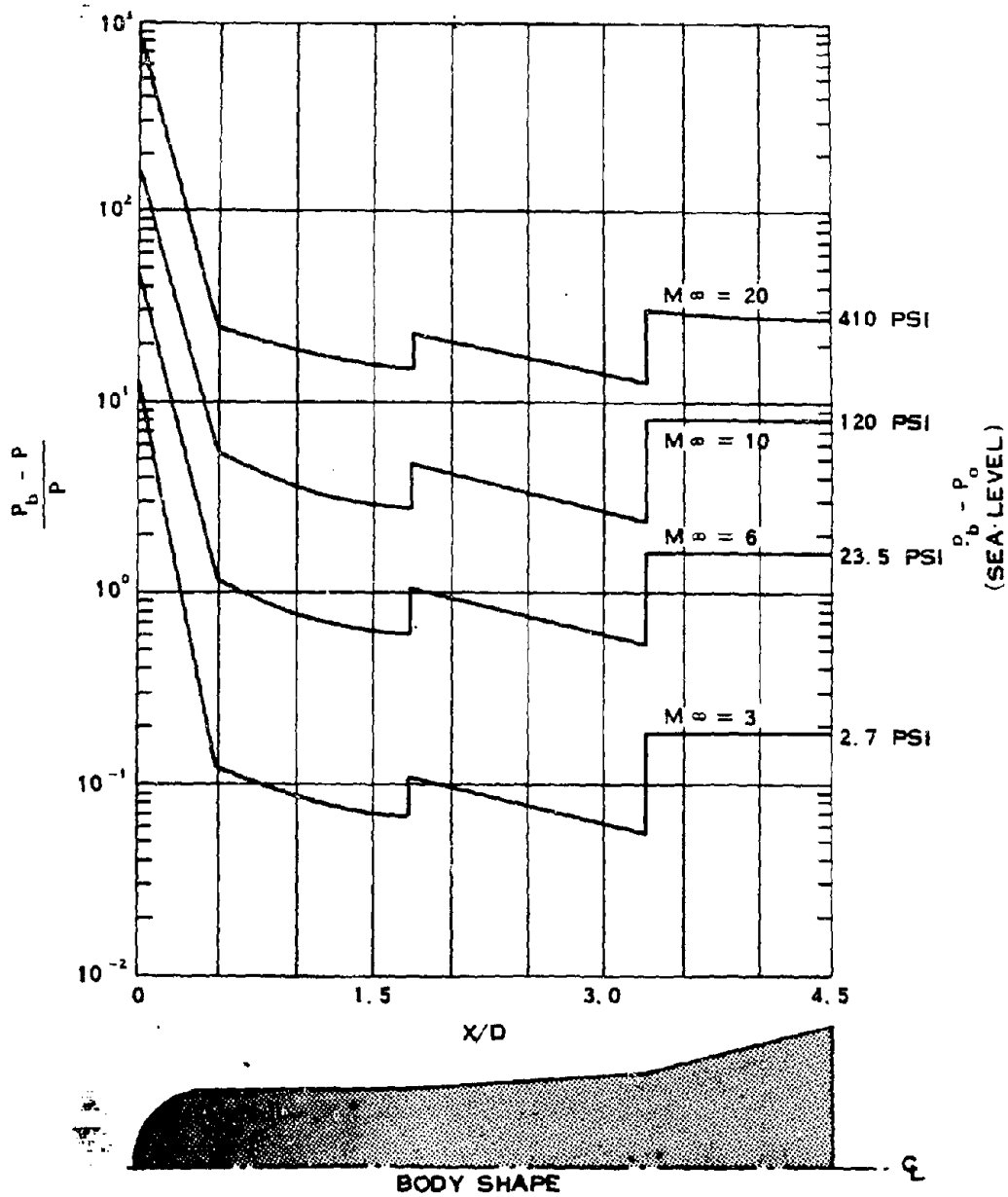

Figure 16-34. [redacted] Steady State Flow Field Surface Pressures, Sphere-Cone-Flare Body [redacted]

[redacted]

[redacted]

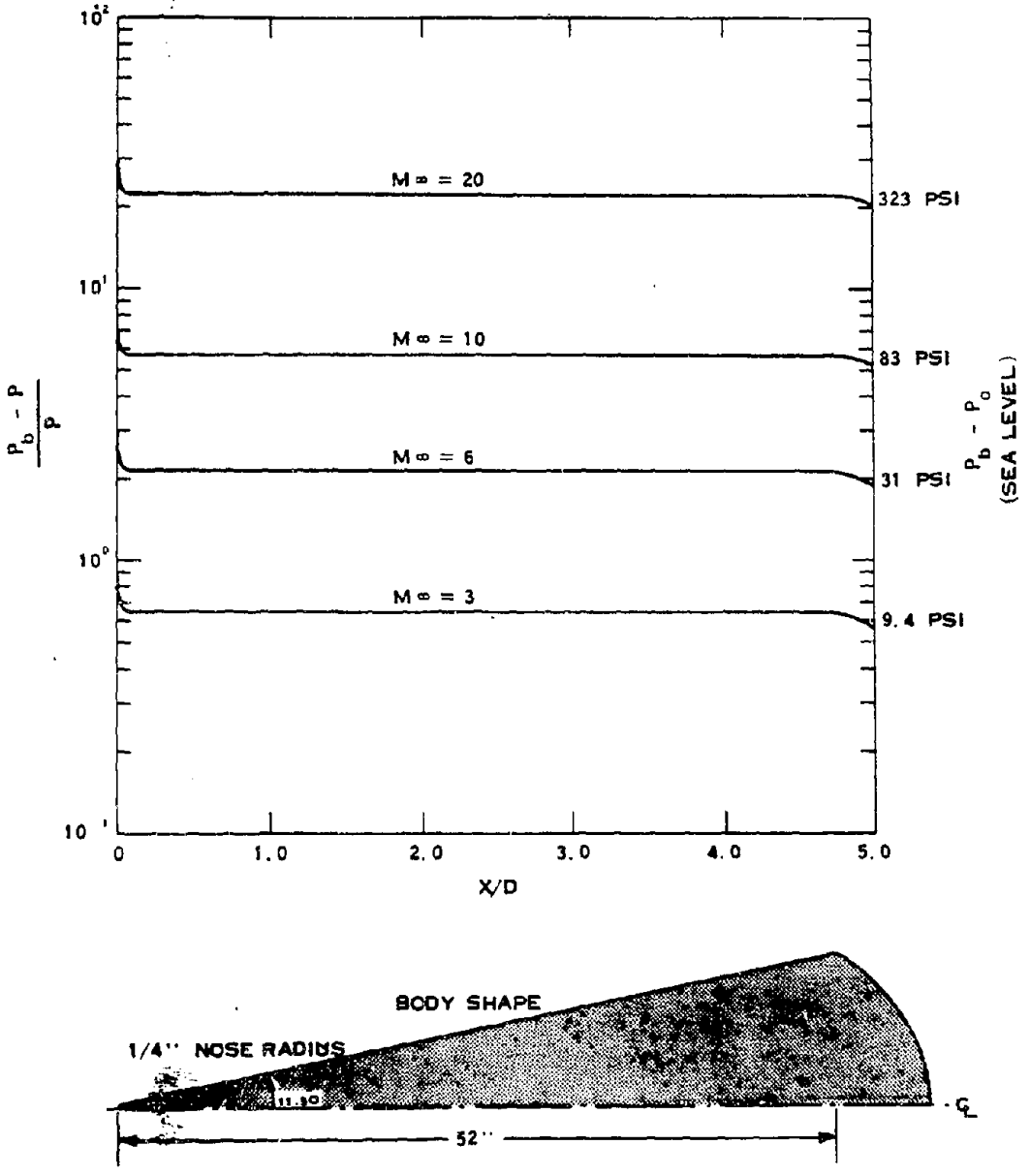

Figure 16-35. [redacted] Steady State Flow Field Surface Pressures, Cone Sphere Body [redacted]

[redacted]

[redacted]

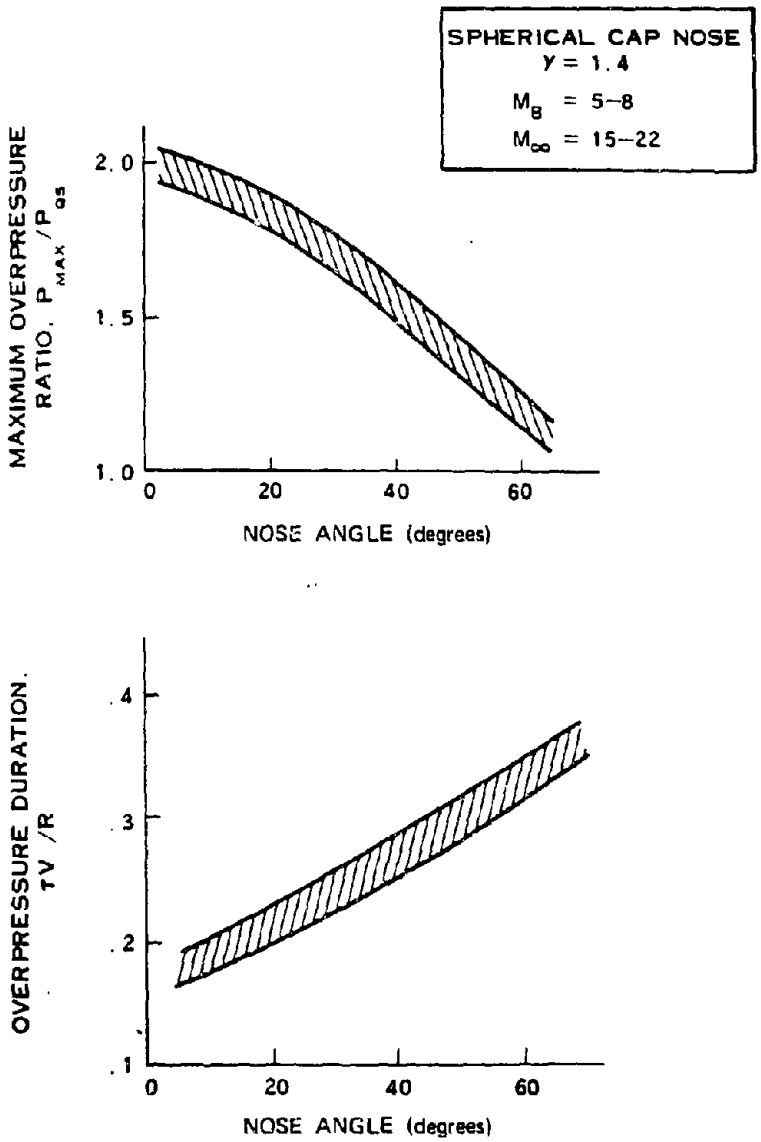

Figure 16-36. [redacted] Maximum Overpressure and Overpressure Duration for Typical Shock-Shock Interactions [redacted]

[redacted]

[redacted]

within which a burst of specific yield will cause axial or lateral forces greater than those for which the vehicle was designed. This envelope is required as part of the iterative processes in which tradeoffs involving weight penalties, yields, target damage criteria, defense capabilities, dispersion and booster capabilities must be considered. Two basic steps in determining the damage envelopes for an *RV* are: construction of the Locus of Escape (*LOE*); and location of points, relative to burst point, where the *RV* is subjected to forces equal to design loads.

[redacted] The nomenclature defined by Figure 16-23 will be used for simplicity and clarity. In this blast-intercept configuration, point A is the position of the *RV* at time of detonation; B is the point of intercept of the *RV* and the blast sphere; *OD* is the distance of closest approach of the *RV* to the burst center. The distance *LD* is called the lead distance, and *RB* is the radius of intercept.

[redacted] A reference trajectory is introduced to define a new coordinate system. This trajectory, which is one axis of the new coordinate system, is parallel to the *RV* trajectory and intersects the burst point (0) (see Figure 16-23). With the center of this coordinate system at 0, the other axis is perpendicular to the reference trajectory. This coordinate system locates the position of the vehicle at the time of detonation relative to the reference trajectory.

[redacted] The following procedure is used to construct the locus of escape (*LOE*). The *LOE* defines a volume, outside of which the reentry vehicle will not intercept the blast shock wave. Figure 16-37 illustrates a situation from which one point on the *LOE* is defined. During the time interval $(t_c - t_o)$ the shock front expands to point C. During the time interval $(t_c - t_x)$ the vehicle travels from point X to point C where it intersects the shock front. If $(t_c - t_x) = (t_c - t_o)$, X is a point on the *LOE*. The distance *XC* is the lead distance, while *OC* is the cross range. To determine another point on the *LOE*, pick another radius of intercept and find a distance *X'C'* such that $(t'_c - t'_x) = (t'_c - t_o)$. Determination of several points, both above and below the reference trajectory, will define the *LOE*.

[redacted] The next step in defining the damage envelope is to determine locations, with relation to the burst, at which the reentry vehicle would suffer lateral and axial forces equal to the design loads. Sufficient locations must be selected and g loads calculated for each point so that iso-g contours can be constructed. Correlation of design loads with these iso-g contours defines the damage envelope. In this case, a g level is specified as the damage criterion.

(U) Figure 16-38 is a qualitative example that shows the *LOE* and the lateral and axial iso-g contours. This figure is oriented with respect to a reference trajectory. Figure 16-39 shows the relation between Figure 16-38 and a real situation.

[redacted] It must be realized that the g loadings described in the above examples are those experienced by a rigid body vehicle. Since the forces are applied dynamically, dynamic amplification factors must be considered. Displacements that result from dynamic loading can be greater than those that result from static loading. Thus, the effective force experienced by the warhead or other internal components may be more than the rigid body g's.

[redacted] It should also be noted that the response of reentry vehicles depends not only on peak values of the force, but also on the rate of application and the rate of decay of the force. Having sustained the peak value of the force, which occurs at the shock front, the reentry vehicle suffers lesser forces and pressures as it penetrates the blast sphere. Complete and accurate definition of the damage envelope must include responses during the entire force-pressure time history. This will be discussed further in connection with the structural response analyses of

[redacted]

[redacted]

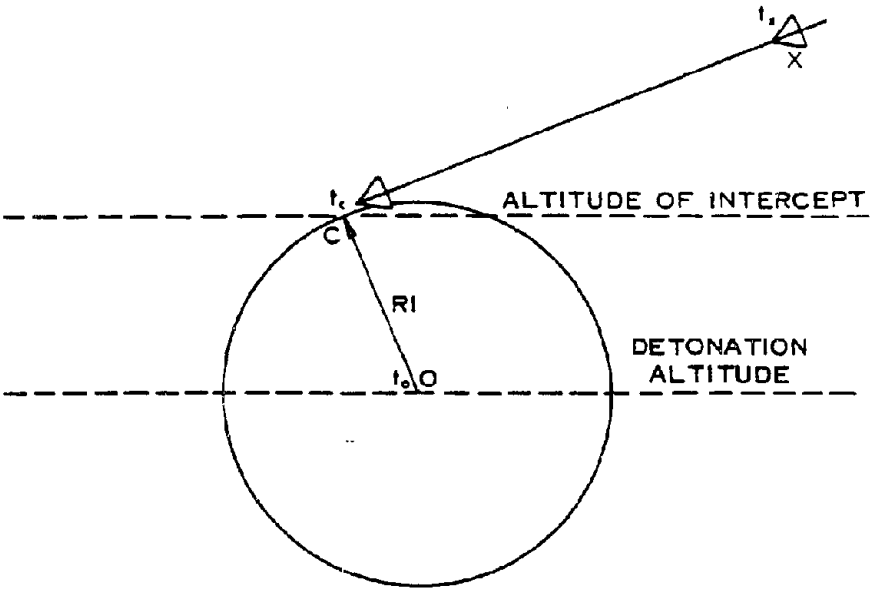

t_o = TIME OF DETONATION

t_c = TIME SHOCK FRONT AND RV ARE AT POINT C

t_x = TIME RV IS AT POINT X

Figure 16-37. [redacted] Determination of Locus of Escape [redacted]

[redacted]

[redacted]

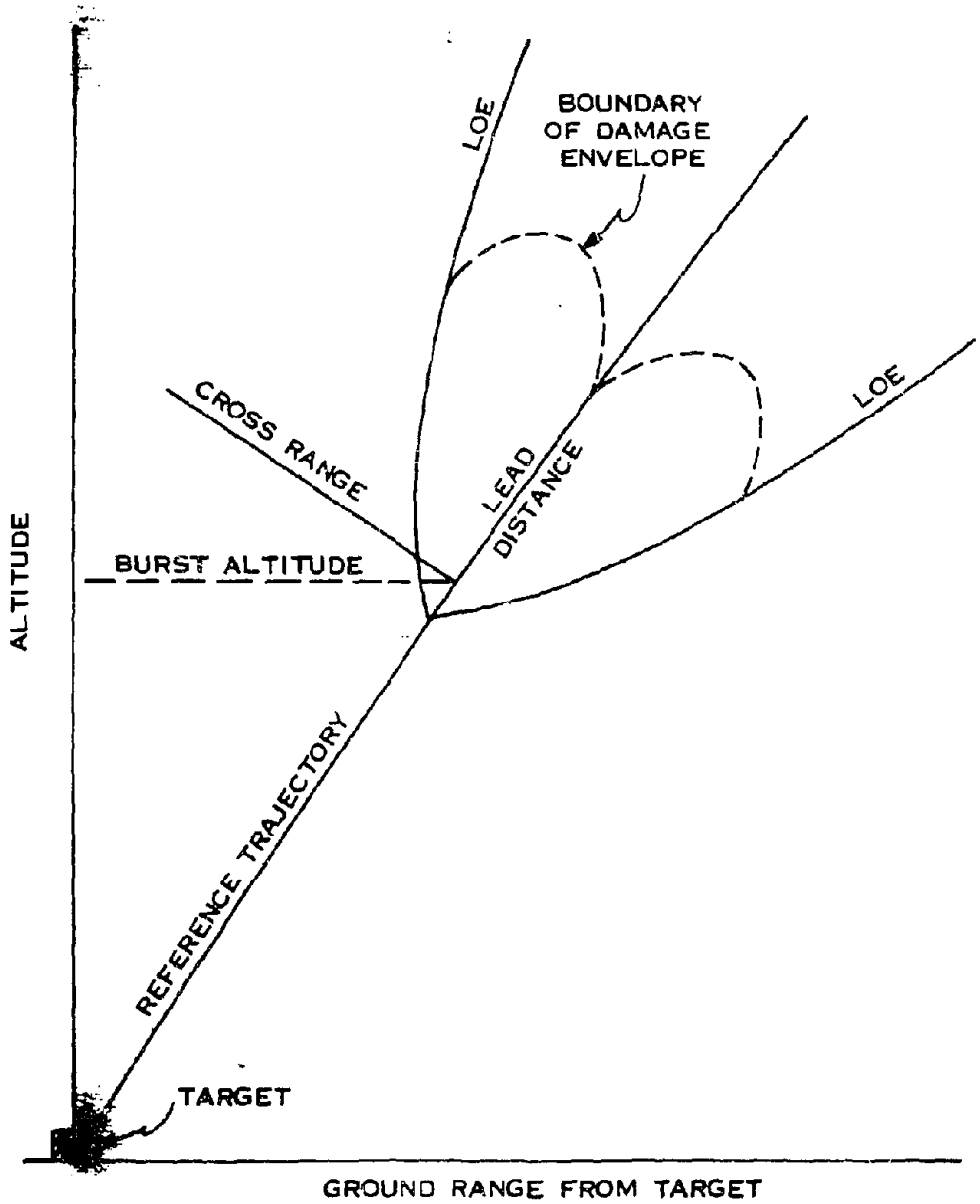

Figure 16-39. [redacted] In-Flight Intercept [redacted]

[redacted]

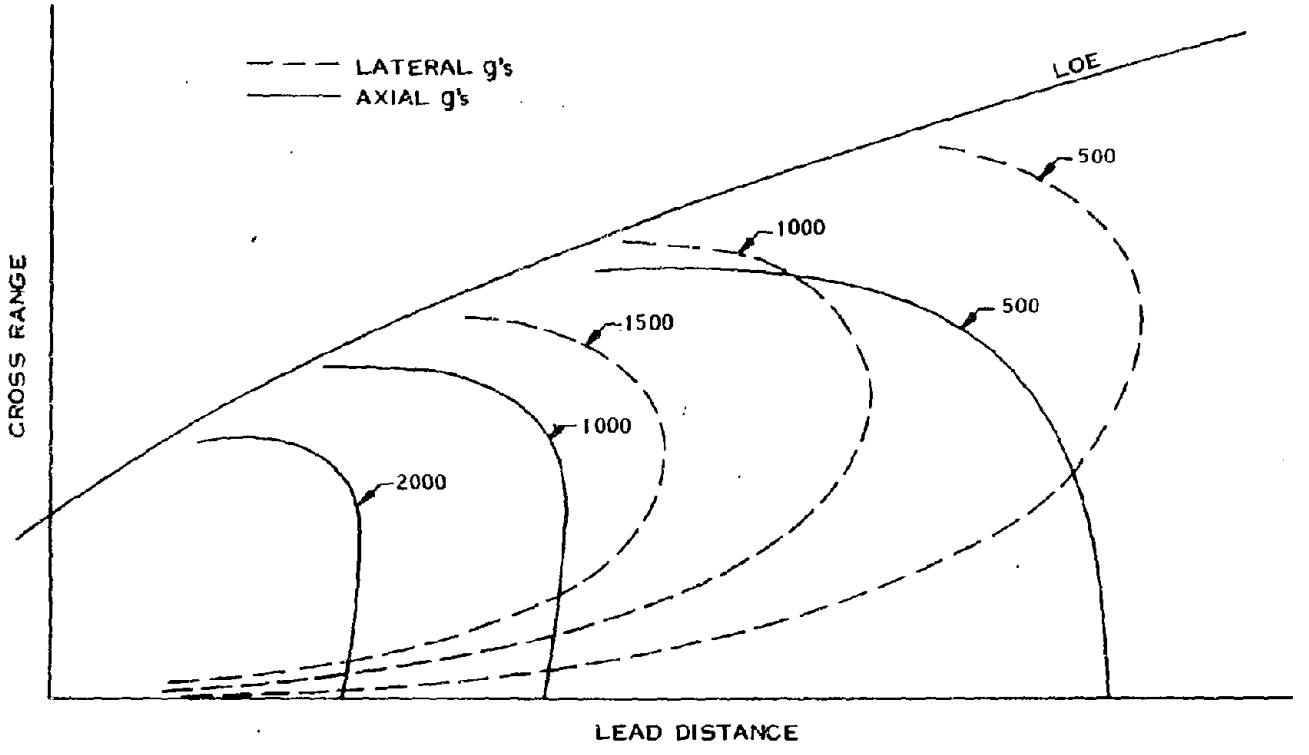

Figure 16-38. [redacted] Qualitative Iso-g Contours [redacted]

[redacted]

[redacted] ABM vehicles (paragraph 16-32). It is evident that damage criteria other than rigid body g levels can be specified to define the damage envelope for a vehicle.

[redacted] RESULTS OF SOME RV BLAST AND THERMAL LOAD AND VULNERABILITY CALCULATIONS [redacted]

[redacted] As pointed out in paragraph 16-13, it is impossible to condense the determination of blast and thermal vulnerability into a generalized methodology suitable for hand computation. The computations are associated too intimately with the design details of the particular *RV* of interest. In order to provide the users of this manual with some understanding of the procedures involved in such computations, some typical calculations are described in the following paragraphs.

16-24 Blast Loads on the RV [redacted]

[redacted] Assume that a reentry vehicle is hardened to survive 200 cal/cm [redacted] incident X-ray environment. The information desired is whether or not the *RV* will be vulnerable to blast and/or thermal effects at any point along the trajectory. The sample vehicle is assumed to have the following parameters.

DNA (b)(3)

- It is a 6° sphere cone configuration.
- The ballistic coefficient is $\beta = 1{,}000$ lb/ft^2.
- Reentry altitude = 400,000 feet.
- Reentry angle = -35°.
- Reentry velocity = 17,000 ft/sec.

Two questions are examined separately to obtain the desired information.

- What blast load (axial and lateral accelerations) accompanies 200 cal/cm^2 incident X-ray exposure at the altitudes of interest from the standpoint of blast?
- What are the minimum axial and lateral rigid body accelerations that will allow blast survival through all altitudes for separation distances equal to the vacuum separation distance for 200 cal/cm^2 incident X-rays [redacted] (the minimum separation during exoatmospheric flight)?

[redacted] Figure 16-40 shows the results of calculation of the axial and lateral rigid body g loads as a function of intercept altitude that would result when the *RV* is initially separated from [redacted] burst so as not to receive more than 200 cal/cm^2 X-ray energy incident on the vehicle. The vacuum separation distance for this X-ray level is about 11,000 feet (Chapter 4), and if the vehicle maintains that separation between altitudes of 40 and 100 kilofeet it will attain maximum g loads at an altitude of 40 kilofeet. The axial load at this altitude is 230 g's and the lateral load is 280 g's. At intercept altitudes less than 40 kilofeet, the rigid body loads will be less for the same separation distance.

[redacted] The axial and lateral loads that would be sustained if the separation distance is such that 200 cal/cm^2 X-ray energy were deposited from [redacted] weapon are also shown in Figure 16-40. The approximate distances are shown as a function of intercept altitude in Figure 16-41.

DNA (b)(3)

[redacted] Figure 16-41 shows near *maximum* separation distance as a function of intercept altitude for the 230 g axial load and the 280 g lateral load. The approximate 200 cal/cm^2 separation distances also are shown as a function of intercept altitude for the [redacted] weapon.

DNA (b)(3)

[redacted] The maximum separation distances for the axial loads were obtained for the near head on interception of the *RV* by the blast wave. The maximum distances for the lateral loads were obtained from the near side on interception, i.e., 65 to 70° measured from the nose of the vehicle.

[redacted] The incident blast overpressures required to induce the g loads are shown in Figure 16-42 for the 230 g axial and 280 g lateral loads of

[redacted] [redacted]

Pages 16-67 through 16-69 DELETED. DNA (b)(3)

[redacted]

[redacted]

Figure 16-41. At 40 kilofeet intercept altitude, a minimum overpressure of 22 psi is required to attain the 230 g axial load. The overpressure required to attain 280 g's laterally is 18.5 psi at 40 kilofeet, and a minimum of 13.5 psi is required above 90 kilofeet altitude.

[redacted] Figure 16-43 shows the curves of g load as a function of maximum separation distance for a 40 kilofeet altitude intercept by a blast wave from [redacted] weapon. It should be noted, from this figure, that extremely large separation distances are indicated if the lateral hardening of an *RV* is less than 100 g's. For yields less than or greater than [redacted] this separation range changes approximately as [redacted]. The approximate nature of this ratio results from the change in the velocity of the vehicle between the points of initial separation and interception.

[redacted] Based on this brief examination of the results of calculation of blast vulnerability, the main conclusion is that rigid body loads of 280 g's axially and 230 g's laterally are compatible with the 200 cal/cm^2 X-ray hardening of the *RV*. Moreover, if the *RV* rigid body response hardness level falls short of these g levels, the blast effects may predominate as a damage mechanism. More specific trajectory/blast cases must be studied to determine the required g loading criteria for balance with a 200 cal/cm^2 X-ray criterion.

16-25 Thermal Radiation Loads on the RV [redacted]

[redacted] A sample investigation has been made of the free field thermal radiation incident on the same *RV* described in paragraph 16-24 as it flies through a nuclear burst in the lower atmosphere. The basic trajectory considered in this study had a reentry velocity 17,000 ft/sec and a flight path angle of -35°. In addition, a limited study was performed for a 19,200 ft/sec/-75° trajectory. Thermal radiation heat loads were computed for head on intercepts of [redacted] burst at 40-, 60-, 80-, and 100-kilofeet burst altitudes. Burst yields of [redacted] and [redacted] were also considered at the 60 kilofeet altitude.

[redacted] The thermal radiation heat flux produced by a nuclear burst can be obtained as a function of distance, direction and time from the radiation/hydrodynamic calculations of Hillendahl that were used to describe the thermal source in Chapter 3 together with the appropriate form factors. These are free field thermal radiation data and do not include any interaction between the vehicle and the radiation field, i.e., the possible attenuation of radiation resulting from an opaque layer of vaporized heat shield material in the flow field surrounding the vehicle was not included (see paragraph 16-31 for a discussion of these "blocking" effects). The total free field heat load to the stagnation point, cone, and base region of the *RV* was determined by integrating the heat flux as a function of time after detonation, assuming a straight line, constant velocity trajectory in the vicinity of the burst.

[redacted] The total radiation heat load for this example is shown in Figures 16-44 through 16-46 as a function of the initial slant range of the vehicle, burst altitude, burst yield, and trajectory. For initial slant ranges less than about 3 to 5 kilofeet, the heat load is very large (35,000 Btu/ft^2) and is essentially independent of location on the vehicle. For a fixed burst yield and initial slant range, the heat load decreases with increasing altitude; conversely, for a fixed burst altitude and initial slant range, the heat load increases with increasing yield. Finally, a higher velocity trajectory increases the heat load for a fixed yield and altitude.

[redacted] The thermal data shown in Figures 16-44 through 16-46 could be used in conjunction with the blast data of paragraph 16-24 to determine the total radiation heat loading as a function of blast loading (rigid body axial load

[redacted]

[redacted]

Page 16-71 Deleted.

[redacted]

[redacted] factors). As a particular example, these data show that, for a 350 kt burst at 40 kilofeet and the 17,000 ft/sec/-35° trajectory, the radiation heat load on the cone associated with a 200 g, head on intercept condition is only 530 Btu/ft^2, whereas for a 300 g intercept condition it is 5,400 Btu/ft^2. This particular example indicates that a 50 percent increase in blast hardness (as measured by the rigid body g criteria) produces an order of magnitude larger thermal environment.

16-26 Description of a Blast/Thermal Vulnerability Determination [redacted]

[redacted] This paragraph continues the description of the sample computations that were described in paragraphs 16-24 and 16-25. The determination of the sample *RV* to blast and thermal effects produced by a nuclear weapon burst is described below.

[redacted] The blast vulnerability analysis of the *RV* is made under the following assumptions:

- 6° sphere cone vehicle with a ballistic coefficient of 1,000 lb/ft^2 (assumed constant for normal reentry).
- Point mass-zero lift trajectories were used in the computations.
- Reentry altitude = 400,000 ft.

[redacted] The blast model used in the computations is considered to be an upper bound to a conventional weapon blast output. Modified Sachs' scaling (see paragraph 2-14) was used in conjunction with curve fits to radius-time-overpressure data. The other peak blast parameters, such as density and particle velocity, are Rankine-Hugoniot values consistent with the scaled overpressures. The environment to which the vehicle is exposed in the interior of the shock front was simulated by assuming constant vehicle velocity during fly through and Sach's scaling curve fits to the interior profiles. It should be noted that, in actual practice, vehicle fly through loading calculations are performed on an electronic computer using the results of detailed radiation/hydrodynamic calculations corresponding to the nuclear device and burst altitude of interest.

[redacted] The vehicle reentry conditions used for this calculation are as follows:

- Case 1
  a. Reentry velocity = 17,000 ft/sec
  b. Reentry angle = -35°
- Case 2
  a. Reentry velocity = 19,200 ft/sec
  b. Reentry angle = -75°

[redacted] The temperature of the heat shield can be an important factor in determining the structural response of the *RV* to blast induced loading because of the possible temperature dependence of some of the structural properties, e.g., elastic modulus and yield stress, at elevated temperatures. For the study discussed here, predictions of the heat shield bulk temperature accounted for ascent heating, normal reentry heating to the burst altitude, and thermal radiation heating from the nuclear burst. The bulk temperature is symbolically related to the heat loads by

$$Q_{ascent} + Q_{reentry} + \alpha\, Q_{radiation} = \rho t \int_{T_{launch}}^{T_{bulk}} C_p\, dT \ \ (\mathrm{Btu/ft^2}),$$

where it has been assumed that the temperature is uniform across the thin ablator skin and that heat losses are negligible compared to heat inputs. In general, considerable caution must be exercised in employing the thin skin-bulk temperature method.

[redacted] The thermal radiation heat flux produced by the nuclear burst was obtained as described in paragraph 16-25. The thermal radiation heat load incident on the vehicle was deter-

[redacted] [redacted]

[redacted]

[redacted]

mined by numerically integrating the flux, as a function of time after detonation, assuming constant vehicle velocity at that altitude and no vehicle spin. It should be noted that, aside from the inherent uncertainties in the free field thermal radiation data, there are additional uncertainties in determining what fraction of the incident thermal radiation is actually absorbed by the ablative surface during the fireball fly through. This is due to a lack of knowledge of the spectral absorptivity of the vehicle surface under these conditions and of the possible attenuation of radiation as a result of an opaque layer of vaporized heat shield material in the flow field surrounding the vehicle.

[redacted] Two basic methods of structural analysis were employed for this sample calculation. The first method involves the application of a finite length, elastic cylinder response solution to determine the dynamic shell stresses resulting from head on intercept loadings. The second method, which was applied to the side on intercept, involved the evaluation of the dynamic response of a lumped parameter, free free beam model subjected to transient blast loadings. In actual practice, the analysis of the structural response of *RV* configurations should employ much more sophisticated and complex methods. The description of these relatively simple methods is included to indicate to the user the general analytical methods that could be used.

[redacted] The results of these two methods of structural analysis depend on assumptions made concerning the blast and thermal environment that the *RV* encounters. In this calculation, the transient aerodynamic loading was developed by using Newtonian theory for pressure magnitudes and distributions (see paragraphs 16-21 and 16-22) combined with a curve-fit exponential time decay obtained by flying an unperturbed trajectory through the blast model. To simplify the calculation, instantaneous engulfment was assumed and shock-on-shock interaction effects were ignored. In addition, the structural response was only examined for blast entrance and for normal reentry conditions. Blast traversal and exit of the vehicle from the blast region were not examined. Thermal loading from normal reentry and nuclear burst thermal radiation were considered for structural response through the bulk skin temperature rise. No attempt was made to evaluate resulting thermal stresses from this high temperature environment; however, the bulk temperature effect was accounted for when choosing material elastic properties and allowables.

[redacted] Three separate bays or ring-stiffened sections of the *RV* were investigated for the head on intercepts. After a few dynamic response calculations were made, it became apparent that Bay L-I (Station 37.5 to Station 49) was the most vulnerable to head on blast loadings; therefore, the results presented are for Bay L-I. The cylinder solution used is a closed form, elastic response code that computes all stresses at both the inside and outside shell fibers at any desired point on the shell.

[redacted] The side on intercept conditions were examined with a lump-parameter, free-free, "Timoshenko" beam model. The bending rigidity was supplied completely by the ablator shell, whereas the mass distribution was made up of both the main shell structure and all internal components. As in the head on studies, the thermal effects were included only in the evaluations of material elastic properties and allowables. Using this lumped-parameter mode, a normal mode solution was employed to determine the complete time history of bending stresses that developed at a number of stations along the missile length from the transient pressure loading that resulted from blast intercept. In all cases, the peak beam bending stresses occurred in a region bounded by Stations 20 and 25.

[redacted] In addition to these two basic tools of structural analysis, i.e., cylinder solution and

[redacted]

[redacted]

[redacted]

[redacted] beam model, a check of shell buckling was made by using the semi-empirical results from the HARTS Program. This check calculation revealed that, if buckling did occur during blast intercept, it probably would be elastic; however, since rather thick walled shells were involved, the calculated critical buckling pressures are very high compared to pressures necessary to cause conditions leading to plastic deformation and rupture.

16-27 Results of the RV Vulnerability Determination [redacted]

[redacted] The results of the structural response study are shown in Figure 16-47 for head on intercept and Figure 16-48 for side on intercept. Figures 16-47 and 16-48 show the allowable stresses and the peak stresses developed from blast entrance loads (characterized by the plotted loads) as a function of initial slant range from a 350 kt burst at an altitude of 40 kilofeet. For the side on intercept cases (i.e., interception by the blast wave normal to the longitudinal axis of the vehicle), the loads are the total g's obtained by vectorially combining the axial and lateral values. For the head on intercept cases, the total loads are the same as the axial loads.

[redacted] The incipient structural damage is indicated in the figures by the intersection of the curve showing peak stress developed with the allowable stress curve. The curve labeled "Developed Stress" indicates the variation with slant range of the peak dynamic stresses developed in the vehicle during blast wave intercept. These curves are shown for both the nominal RV and the 1.2 nominal vehicle, which is the same vehicle with the skin thickness increased by 20 percent. The slant range, stress, and loads are tabulated for each of the points of incipient structural damage.

[redacted] It is apparent that the addition of 20 percent to the skin thickness reduces the vulnerability of the RV by decreasing the slant range for incipient structural damage markedly. It should be recognized that these values of slant range probably are minimum values for the onset of incipient structural damage as a result of the assumptions used in the stress calculations.

[redacted] The thermal response data are shown in Figure 16-49 in terms of the temperature at the aft end of the cone (X/R_N = 19.4) after burst exit as a function of the initial slant range of the vehicle from the burst. These data are the temperatures developed during normal reentry (including ascent heating) to the burst altitude plus the temperature rise caused by the fireball thermal radiation. Beyond initial slant ranges of 16 to 18 kilofeet, the temperatures shown are the normal reentry temperatures at the burst altitude, since the thermal radiation heat load is quite small at these large ranges. The 40-kilofeet burst altitude induces higher temperatures than the 60-kilofeet altitude because of increases in both reentry heating and thermal radiation heating.

[redacted] Two specific temperatures, 2,340°F and 1,750°F, are shown in Figure 16-49. The former is the ablator melt temperature, while the latter is the temperature at which the ablator has low structural strength. Since the bulk temperature generally lies somewhere in between the surface and backface temperatures, surface melting will commence before the bulk temperature reaches 2,340°F, but probably only in small amounts. Of more importance is the fact that if the vehicle emerges from the burst with a bulk temperature greater than 1,750°F at critical structural locations, it probably will not be able to survive the exit blast loads and/or the subsequent reentry loads as it descends through maximum dynamic pressure to impact, i.e., if the thermal radiation heat loads are sufficiently great to result in temperatures of 1,750°F at burst exit, "delayed" structural damage may occur subsequent to the blast entrance, even if the entrance loads are not sufficient to cause damage.

Pages 16-78 and 16-79
Deleted.
DNA (b)(3)

[redacted]

[redacted]

[redacted]

16-28 Summary and Conclusions Concerning RV Vulnerability Calculations [redacted]

[redacted] There are many different ways to summarize the blast/thermal vulnerability of an RV; this subsection employs a bar graph method, whereas the damage envelope method is used in the succeeding subsection to portray ABM Blast/Thermal Vulnerability. The minimum initial slant ranges for structural and thermal damage are summarized in Figure 16-50 for the 17,000 ft/sec/-35° trajectory and 40 kilofeet burst altitude. These data show that the RV is more vulnerable to the side on intercept/structural damage condition than any other condition. The 20 percent increase in ablator thickness reduces the initial slant ranges for damage considerably. The total "g" loading at the slant range for structural damage and the total free field radiation heat load at the slant range for thermal damage also are shown in the figure. It can be seen that there is *no unique* mechanical "g" load or thermal "Q" load that determines when damage occurs. This points out the requirement for more definitive information concerning damage criteria associated with actual RV designs.

[redacted] The separation distance at the burst altitude between two vehicles that were originally at the 130 and 200 cal/cm^2 X-ray separation distances apart in the exoatmospheric [redacted] also are shown in Figure 16-50. It can be seen that if two vehicles were spaced for these X-ray loadings from a 350 kt weapon in the exoatmosphere, and the lead vehicle encountered a direct hit from 350 kt at 40 kilofeet, the trailing vehicle definitely would incur damage if it encountered the blast wave.

DAJP (4)(3)

(S) The foregoing description of the method and results of an RV blast/thermal vulnerability sample calculation was presented to give the user an indication of the important technical aspects that must be included in this type of analysis. Based upon the results, a few rather general conclusions can be drawn:

- It is apparent that the blast/thermal vulnerability of an RV cannot be uniquely expressed in terms of either rigid body "g" load levels or thermal radiation heat loads, but rather is a function of the particular reentry trajectory, intercept geometry, yield of the attacking weapon, and the specific damage mechanism considered.
- Vulnerability loads or damage criteria assigned to a particular RV corresponding to blast or thermal effects may not be compatible with the loads or criteria assigned for other nuclear weapon effects (e.g., X-rays).
- Thermal loads on the RV, resulting from a combination of reentry heating and radiation from the nuclear weapon, can have an important deleterious effect on the material properties (and in turn upon the structural response) of the RV ablator/substructure combination.
- The accurate assessment of RV vulnerability to nuclear weapon effects requires detailed analyses using advanced analytical tools and high-speed electronic computer facilities.

[redacted] ANTIMISSILE (ABM) SYSTEMS [redacted]

[redacted] The assessment of blast and thermal vulnerability of an antimissile (ABM) system presents many of the same problems that were discussed for reentry vehicles; however, ABM systems have some important characteristics that are unique, and these will form the basis for a large portion of the following discussion.

[redacted] There are fundamental differences between the views of the designers of RV's and ABM concerning blast and thermal vulnerability. The designer of an RV may be willing to have his vehicle sustain limited damage if the damage would not degrade the probability of mission success significantly. This willingness to sustain

[redacted] [redacted]

[redacted]

DNA
(b)(3)

Deleted

Figure 16-50. [redacted] Minimum Initial Slant Range for Structural/Thermal Damage at 40 kt Burst Altitude, V_E/γ_E = 17,000 ft/sec/-35° [redacted]

[redacted] [redacted]

[redacted]

[redacted] some level of damage results from the fact that the RV designer usually deals with large numbers of vehicles directed against an array of targets with the objective of insuring that a fraction of the RV's penetrate the defense and reach the targets. The defense, on the other hand, attempts to deny all "leakage" of enemy RV's. Therefore, when considering blast and thermal fratricide damage, the ABM designer usually will not tolerate any degree of damage to the vehicle (i.e., it is designed to be "sure safe"). When assessing the ability of an ABM to defend a target and to kill an enemy RV, however, the objective dictates that the ABM designer achieve a "sure kill" miss distance relative to the incoming RV.

[redacted] Most of the following discussion results from a study to determine the probable damage modes and damage envelopes for the AIRS I and II vehicles (paragraph 16-12) when exposed to blast waves and thermal radiation from nuclear explosions.

[redacted] The scope of the discussion can be summarized as follows:

- Two vehicles are considered, AIRS I and AIRS II. These vehicles nominally represent interceptor vehicles of the SPRINT and SPARTAN class, respectively. Inboard profiles of these vehicles are shown in Figures 16-51 and 16-52.
- Four response modes are considered:
  (1) Shell breathing response to the blast wave.
  (2) Vehicle bending response to the blast wave.
  (3) Internal component damage due to rigid body acceleration produced by the blast wave.
  (4) Material damage produced by the thermal radiation.
- Coupling effects among the damage modes are neglected, except for the inclusion of degradation of material properties that results from heating the material.
- Control surface damage is not considered.
- Each vehicle is assumed to be in a steady state "n"-g maneuver (where n can be zero).

[redacted] The aerodynamic loads initiated by the blast wave must be defined to perform a blast vulnerability analysis. In the definition of the aerodynamic loads imposed on a vehicle traveling at hypersonic speeds when subjected to a strong blast wave, the initial shock-on-shock interactions during the vehicle engulfment by the blast wave present the most difficulty. Recent studies of the response of missile structures to blast loads indicate that the response to the shock-on-shock loads does not contribute significantly to the total response experienced by the missile structure.

[redacted] The response of the structure to blast is separated into shell breathing, vehicle bending, and rigid body acceleration responses. The separation of the total response into uncoupled breathing and bending responses is required since current methods cannot perform the coupled problem; however, this separation is justified to some extent by consideration of the types of damage associated with each response. In shell breathing response, segments of the shell between bulkheads are excited, and the damage is associated with high frequency local shell deformation. In vehicle bending, the damage results from relatively low frequency excitations of the overall structure.

[redacted] Criteria for the yielding and buckling response have been generated primarily from data generated in tests of simple cylindrical and conical bodies subjected to air blast from HE detonations. Studies of damage to the vehicle by bending have neglected the short-duration diffractive loading, which is of little consequence in exciting the long period oscillations associated with bending deformations (except possibly for very low yield weapons). The damage criteria for bending deformations, and the response analysis

[redacted]

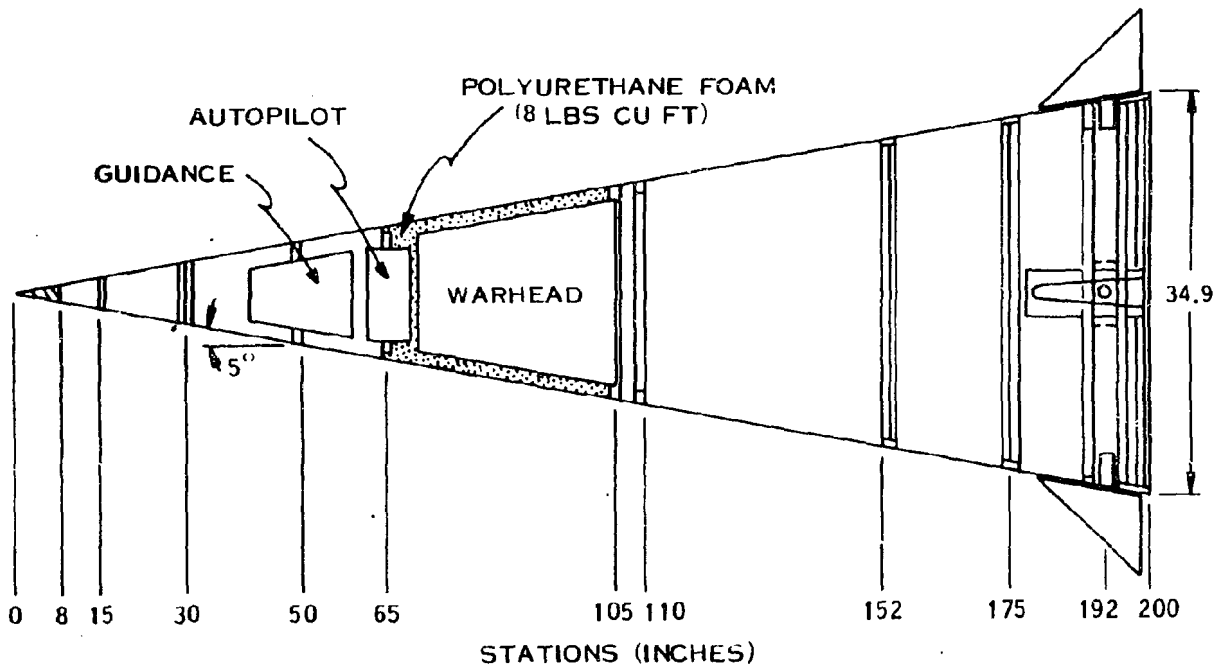

STATION	SKIN THICKNESS	MATERIAL
8 – 30	0.08	2014 – T6 AL
30 – 65	0.125	2014 – T6 AL
65 – 105	0.156	2014 – T6 AL
105 – 200	0.20	FILAMENT-WOUND FIBER GLASS

Figure 16-51. [redacted] Inboard Profile of AIRS I Vehicle [redacted]

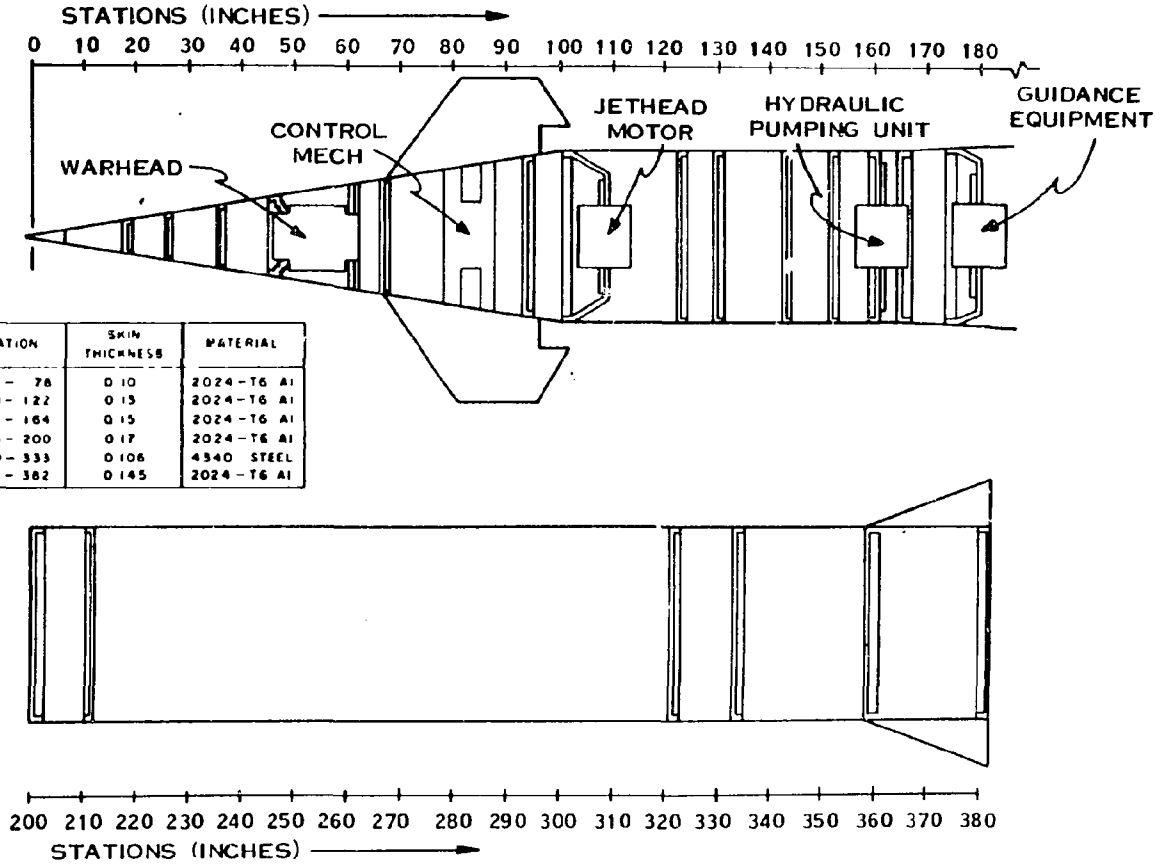

STATION	SKIN THICKNESS	MATERIAL
6 - 78	0.10	2024-T6 Al
78 - 122	0.13	2024-T6 Al
122 - 164	0.15	2024-T6 Al
164 - 200	0.17	2024-T6 Al
200 - 333	0.106	4340 STEEL
333 - 382	0.145	2024-T6 Al

Figure 16-52. [redacted] Inboard Profile of AIRS II Vehicle [redacted]

[redacted]

[redacted] techniques, rely on knowledge developed in similar studies performed for aircraft and launch vehicles in the boost phase.

[redacted] Analysis of response to thermal radiation effects define the mechanisms by which heat is absorbed and distributed throughout the structure, both when the vehicle is outside and inside the fireball. Damage criteria from thermal radiation effects are selected on the basis of the loss of the insulative coverings over the substructure.

[redacted] Blast and thermal radiation effects damage envelopes for both AIRS I and II are presented below. The relative sizes of these envelopes for the various effects on the two representative vehicles and for the encounter condition variations (in yield and altitude) are discussed briefly.

16-29 Shell Breathing Response [redacted]

[redacted] Blast induced pressure loading causes the shell segments of the vehicle between the ring reinforcements to respond in what is usually termed the "breathing mode." Damage occurs in the form of permanent deformation of the skin through the formation of a dented area in the surface of the shell. The primary damage mechanism for the shells is an instability (buckling) of the shell that can occur either when the shell is all elastic or after portions of the shell have become plastic. This damage mechanism can be complicated by the presence of the ablator over the structural shell and by other states of stress and deformation imposed by bending of the vehicle as a result of blast and normal flight loads, or the thermal condition of the vehicle at blast intercept. These interaction problems are not considered.

[redacted] A complete determination of the blast damage to a shell segment that would be required to prevent the AIRS vehicles from performing a specified maneuver requires two separate analyses. The first analysis predicts response levels from threshold to severe post buckling damage, and a second analysis predicts the post damage response: the latter is the response of the "damaged" vehicle to the loads imposed by maneuver. Thus, it is not sufficient to calculate the shell response resulting from the blast loading. A sure-safe criterion also must be established for the actual in-flight conditions in the fratricide mode. The amount of damage that constitutes an "unsafe" level under a known set of environmental conditions must be determined eventually if vulnerability studies are to be considered useful to the military planner.

[redacted] The analyses of the response of critical shell segments of the AIRS I and II vehicles to blast that were selected for this example can only predict the threshold damage level caused by elastic buckling or initial material yielding. Analyses that calculate elastic-plastic response in the post buckling region have only been developed recently for shell response to blast, but experimental data are not sufficiently comprehensive to apply the results to various loading conditions and to different materials. Thus, rather arbitrary criteria must be postulated to relate computed damage levels to "unsafe" conditions for the ABM.

[redacted] The analyses discussed thus far primarily calculate the response of the shell up to threshold damage, i.e., sure-safe levels. These analyses are elastic in nature and cannot be used directly to determine response that includes severe damage. There are three additional elements required before lethality predictions can be made:

- Selection of the applicable analysis: that is, inelastic buckling or yielding (or possibly fracture).
- Definition of damage criteria, i.e., definition of the amount of damage that must occur in the selected damage mode to negate the intended mission of the vehicle.
- Selection of a means to apply the inelastic analysis to the determination of the load

[redacted]

[redacted]

[redacted] level required to produce the amount of damage specified.

16-30 Vehicle Bending Response (U)

[redacted] Discussions of prediction techniques for the response of the AIRS I and AIRS II vehicles to blast in their rigid body and bending degrees of freedom are separated into two parts. First, a formulation of *damage criteria* for these vehicles in bending is discussed for damage to the primary structure and to the internal components. In the second part, analysis that predicts the *structural response* is discussed. The inclusion of critical damage criteria in a computer program for the response analysis results in the capability to determine sure safe envelopes for bending response to blast.

[redacted] A most difficult, but necessary, part of defining damage contours for interceptor missiles in a blast environment is the definition of the amount of damage that must be produced in the primary structure in bending or to internal components to constitute a positive failure of the mission. The approach adopted is to use a simple damage criterion available for interceptor vehicles.

[redacted] Selection of simple damage criteria for an interceptor vehicle undergoing bending deformations requires an understanding of the damage modes involved. The primary bending damage modes possible to the primary structure of a vehicle may be:

- Damage to the joints resulting from tensile stresses in excess of the stresses allowable for the joints.
- Buckling damage to the overall shell structure resulting from combined axial and bending induced normal stresses in the shell.

For this discussion, a damage condition in which the vehicle damage cannot support the loads associated with a specific "n"-g maneuver after buckling was selected tentatively as sufficient.

[redacted] Damage criteria for internal components should involve detailed investigations of the acceleration-time history environment that a component can withstand. In addition, the supports of internal components and the load-carrying ability of the supports must be considered in a comprehensive vulnerability analysis. It is the usual practice to consider an acceleration time-history and to assign a certain peak acceleration value to be critical.

[redacted] In view of a lack of fragility data for the internal components of the AIRS I and II, representative allowable peak acceleration values were selected from information available for design requirements for SPRINT and SPARTAN. These acceleration values are used to demonstrate the procedures involved in determining damage envelopes for internal component damage, but they are not necessarily representative of what the internal equipment mounted inside the vehicles can actually withstand.

[redacted] It is necessary to perform a comprehensive analysis of the blast loading and response of the entire missile structure (including primary and secondary structures) to determine the details of the blast loads imposed upon (and the response of) specific internal components when a missile body is exposed to a nuclear weapon environment. This analysis includes development of a detailed mathematical lumped-mass/spring model of the missile to determine the proper "transfer functions" between the primary structure and the internal component of interest. Calculations that use the mathematical model and the definition of the blast loads imposed on the missile structure during a real encounter lead to the determination of the loads imposed on the internal structures.

16-31 Thermal Radiation Effects [redacted]

[redacted] The establishment of thermal radiation damage criteria for AIRS I and AIRS II required an examination of the individual structures involved.

[redacted]

[redacted]

[redacted] In general, data concerning thermal radiation effects consists of a description of the temperature distribution through the ablator (and substructure material) and the mass ablation rate, both as a function of time and position on the missile. This fundamental information provides the thermal portion of the inputs for a realistic assessment of the overall vehicle performance during and after an encounter with a nuclear burst. The temperature distribution data can be used in a structural analysis to determine the magnitude of the allowable stresses (or strains), thermal stresses, etc. Furthermore, there are usually internal components in the guidance section, fuzing, arming and firing section (FAF), or warhead section that have a fairly low temperature tolerance. The ablation rates also affect the mass distribution and can affect the aerodynamic characteristics of the missile, which can affect its flight characteristics; however, the following discussion is limited to an examination of thermal effects in the ablator and substructure. No concurrent structural and/or trajectory analyses were performed.

[redacted] The principal type of ablation material used on the AIRS I missile is tape-wrapped silica phenolic, which is a silica cloth impregnated with phenolic resin. A detailed theoretical prediction of the thermal response of a charring, melting and vaporizing ablator such as silica phenolic on a high-speed missile that flies through (or near) a nuclear fireball during some portion of its mission involves simultaneous consideration of complex physical and chemical phenomena. The general situation is illustrated in a simplified fashion in Figure 16-53. During normal flight (i.e., preburst or post traversal), the vehicle is heated by forced convection ($\dot{q}_c$) caused by friction forces in the boundary layer on the vehicle (aerodynamic heating). During the fireball traversal phase, the predominant mode of heating is thermal radiation ($\dot{q}_R$) from the high temperature fireball air. In this case, the ablation rates generally are so high that the boundary layer is blown off, and the local flow field (which may be subsonic) is dominated by the ablation vapors. In either case, the heat transfer to the surface causes the ablator to heat, pyrolyze internally, and melt and vaporize at the surface.

[redacted] A realistic thermal analysis for a silica phenolic coated vehicle should consider the following effects:

- Internal heat conduction in the ablator and substructure.
- Pyrolysis of the phenolic resin in the ablator, with the attendant endothermic chemical reactions and pyrolysis gas flow through the char.
- Convective and radiative heat transfer at the ablator outer surface, and the accompanying surface recession that results from melting and vaporization of the silica cloth.
- The interaction of the injected ablation vapors with the local vehicle flow field, especially the absorption of thermal radiation by the vapors (radiation blocking).
- The time dependent nature of the fireball environment, as well as the transient nature of the temperature response of the ablator.
- Variation of all of the effects listed above with location on the body that result in differences in environment, type and/or thickness of ablator, etc.
- Variation of all of the effects with burst encounter conditions.

[redacted] It is convenient to separate the thermal analysis into several basic parts, each of which uses somewhat different techniques of analysis according to the most important physical processes that are treated. This concept can be visualized with the aid of Figure 16-53 and an energy balance at the outer surface of the ablator (denoted by a subscript w).

[redacted]

[redacted]

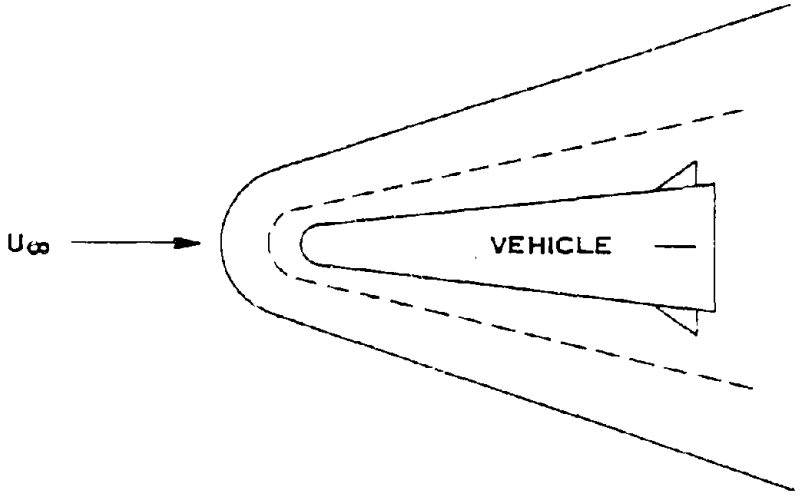

DEFINITION OF TERMS

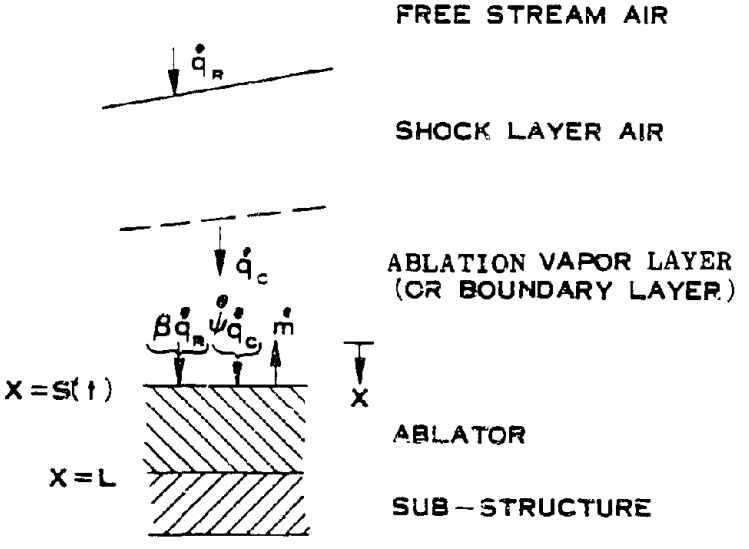

Figure 16-53. [redacted] illustration of Ablation Phenomena [redacted]

[redacted]

[redacted]

[redacted]

$$\psi \dot{q}_c + \beta \dot{q}_R - \epsilon \sigma T_w^4 - \dot{m} \Delta H = \left(-K \frac{\partial T}{\partial x}\right)_w$$

where $\dot{q}_c$ and $\dot{q}_R$ are the free field convective and radiant heating rates, respectively. The term "free field" heating rate denotes that the quantity is computed without regard to ablation effects. Thus, the free field convective heating is computed on the basis of nonblowing boundary layer solutions, while the free field radiative heating is computed on the basis of the fireball flow field being unperturbed by the presence of the vehicle. Therefore, by definition, the free field thermal environment depends only on time and body position for a particular trajectory and encounter condition, and not on the type of ablation material used.

[redacted] The quantities ψ and β are the convective and radiative blocking functions, respectively. They denote the fraction of the free field heating rate that exists at the ablator surface during the actual ablation process. The blocking functions must be obtained from a solution for the local vehicle flow field that accounts for the effects of the injected ablation vapors on the flow field. In general, their values will depend on the level of the free field environment and on the particular ablation material. The quantity $\epsilon \sigma T_w^4$ represents the energy reradiated from the surface, while the term $\dot{m} \Delta H$ represents the energy absorbed in surface melting and vaporization. Finally,

$$\left(-K \frac{\partial T}{\partial x}\right)_w$$

is the heat conducted into the surface of the solid ablator, which in general must be obtained from a solution of the temperature profile in the ablator.

[redacted] The equation simply states that the net convective and radiative heating at the surface, less the energy reradiated and absorbed in melting and vaporization, equals the energy conducted into the ablator. When the net heating rate is sufficiently high to produce surface melting and vaporization, the equation relates the mass ablation rate ($\dot{m}$) to the free field environment and the temperature distribution in the ablator.

[redacted] For the purpose of the present discussion, which is primarily concerned with the thermal effects of a nuclear environment, the overall analysis is separated into two basic parts: fireball radiation and ablation, and the internal temperature and ablation response. The former is essentially multidimensional (around the body) and quasi-steady in nature, since it deals with high temperature flow about a high speed missile, whereas the latter is primarily one dimensional (through-the-thickness) and transient in nature since it deals with heat conduction. The coupling condition (boundary condition) that relates the free field environment and local flow field to the internal response is the energy balance at the surface, i.e., the equation given above.

[redacted] When the results of various theoretical methods are compared there is about a ±50 percent uncertainty in the predictions of the total silica phenolic mass ablated during a nuclear fireball traversal, even among theoretical models that assume full vaporization. If only melting is assumed, the results are at least a factor of five higher, and typically a factor of ten.

[redacted] The condition for thermal damage to the AIRS vehicles was taken to be the time at which 50 percent of the ablator mass was gone; this condition is probably on the conservative side, leading to an upper limit in the size of the vulnerability envelopes.

16-32 ABM Blast/Thermal Vulnerability Envelopes [redacted]

[redacted] The previous paragraphs described techniques of analysis that can be employed to de-

[redacted]

[redacted]

[redacted] fine vulnerability envelopes for the AIRS I and AIRS II vehicles exposed to blast and thermal radiation from nuclear explosions. The vulnerability envelopes for the AIRS vehicles and for two typical encounter conditions are shown in Figures 16-54 through 16-57. In each figure, the vehicle under attack is at the origin (0, 0) flying from left to right. If the attacking weapon is burst inside the envelope, the load on the vehicle will exceed the critical level. Thus, the largest envelope on the graph identifies the "most" critical damage mechanism for the vehicle and the burst condition considered.

[redacted] Figures 16-54 and 16-55 correspond to the AIRS I vehicle in a typical fratricide situation; it is obvious that the size of the critical damage envelopes are very sensitive to the maneuver (or nonmaneuver) condition of the AIRS I. The AIRS II curves in Figures 16-56 and 16-57, indicate envelopes of somewhat different shapes, but the general behavior is similar to AIRS I.

16-33 Conclusions [redacted]

[redacted] The AIRS I and AIRS II vulnerability study produced the following main conclusions:

- The internal component acceleration envelopes are the largest for both AIRS I and AIRS II, but this predominance must be regarded cautiously as a result of the arbitrary nature by which acceleration damage levels were selected for the AIRS internal components.
- Thermal radiation effects appear to be more important for AIRS I than for AIRS II; however, blast effects produce the larger envelopes for both vehicles.
- Thermal radiation effects tend to increase in relative importance for the larger yields and lower intercept altitudes.
- Shell response and bending response damage are of comparable importance for the nonmaneuver condition for both vehicles. For the maneuver condition, however, the shell damage mode is more important than the bending damage mode in defining vulnerability envelopes for both vehicles.
- The maneuver condition modifies the acceleration, bending and shell damage vulnerability envelopes appreciably. In general, the overall areas (or volumes) of these envelopes increase significantly for the maneuver condition.

[redacted] It should be emphasized that the conclusions only apply to the AIRS I and AIRS II vehicles. The foregoing discussion was presented to indicate the types of analyses that must be performed to assess the vulnerability of ABM vehicles to blast and thermal effects. The conclusions could well be significantly different for vehicles of different design.

Pages 16-92 through 16-95
DELETED. DNA (b)(3)

[redacted]

[redacted]

[redacted]

[redacted] BLAST AND THERMAL LETHALITY [redacted]

[redacted] Previous subsections of this section have concentrated on concerns relative to the blast and thermal vulnerability of friendly RV's and ABM's. This subsection will discuss the concern of the defense in the effectiveness of ABM in "killing" an RV. The emphasis shifts from "sure safe" criteria to "sure kill" criteria.

[redacted] The definition of the threat RV vehicles and the details of the free field blast and thermal environments of the ABM are the two primary factors that influence the determination of the kill effectiveness of an ABM system. Calculations of blast kill radii have been performed by various groups for the SPRINT ABM against some representative RV threats. The results of these calculations are described in the following paragraphs.

16-34 Blast and Thermal Free Field Environments [redacted]

DNA (b)(3)

[redacted]

[redacted] Some of the results of these calculations are shown in Figures 16-58 through 16-61 in the form of blast wave parameters at one altitude, e.g., temperature and flow field profile data, at one typical time. These data are essentially self explanatory. They are useful to provide an overview of the environments; however, for detailed vehicle response studies, the principal output of a radiation-hydrodynamics code calculation consists of the radiation-hydrodynamic and field data as a function of radius at a large number of times after burst. These basic data are stored on magnetic tapes (called Usertapes), which allows dissemination of the principal results for use in many studies. This is necessary since blast/thermal effects studies often require that the vehicle be flown through the environment as a function of time, and it is impossible to present environmental data at the vehicle position as a function of time graphically for all possible combinations of vehicles, trajectories, and intercept conditions.

DNA (b)(3)

16-35 ABM Blast Loads on Threat Vehicles (Point Mass) [redacted]

[redacted] The study of ABM blast loads on threat vehicles consisted of computer analyses using a generalized trajectory code, with capabilities of including the free field blast environment provided by the radiation-hydrodynamics Usertapes. A nonrotating spherical earth model with a 1962 atmosphere was used for this calculation. The aerodynamics were computed by Newtonian mechanics, based on the input size and shape data defining a sphere-cone for each vehicle. The reentry conditions for the RV nominal-trajectories were defined in terms of altitude, flight path angle, and reentry velocity. Having computed a flight profile with the specified reentry conditions, the blast fly through runs included trajectory computations that started

[redacted]

[redacted]

[redacted]

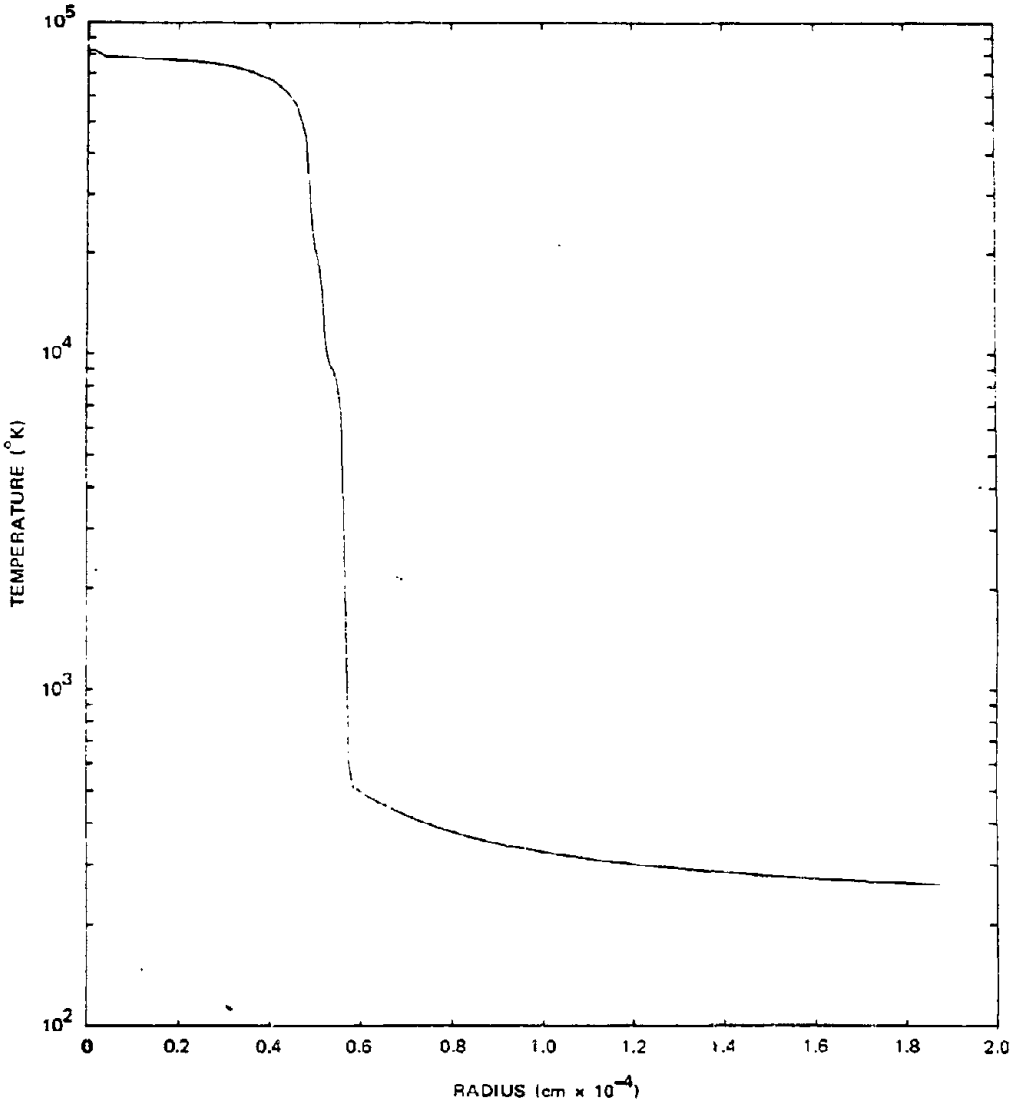

Figure 16-58. [redacted] Computed Temperature Profile, t = 4.64 msec, 30 kilofeet Altitude [redacted]

[redacted]

[redacted]

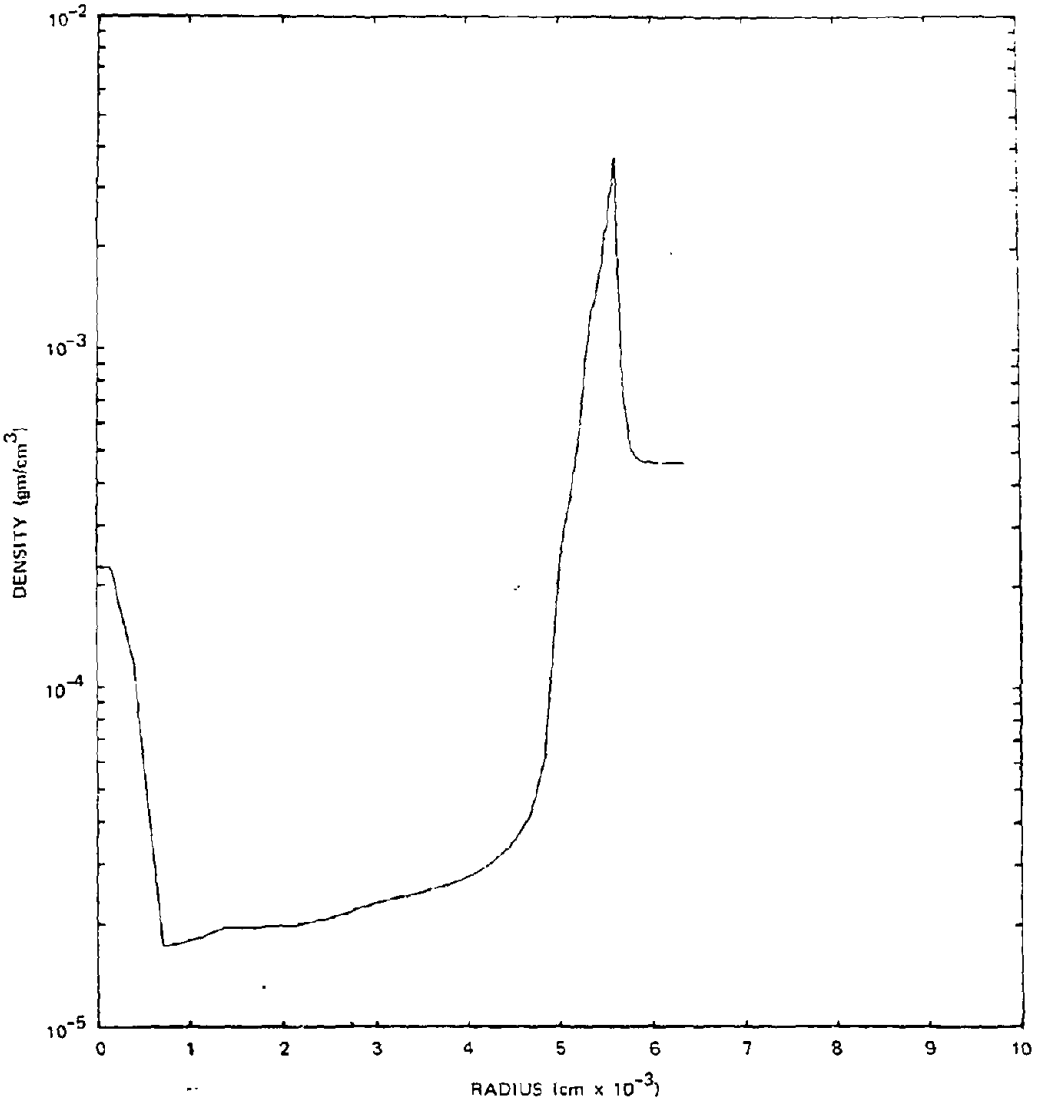

Figure 16-59. [redacted] Computed Density Profile, t = 4.64 msec, 30 kilofeet Altitude [redacted]

[redacted]

[redacted]

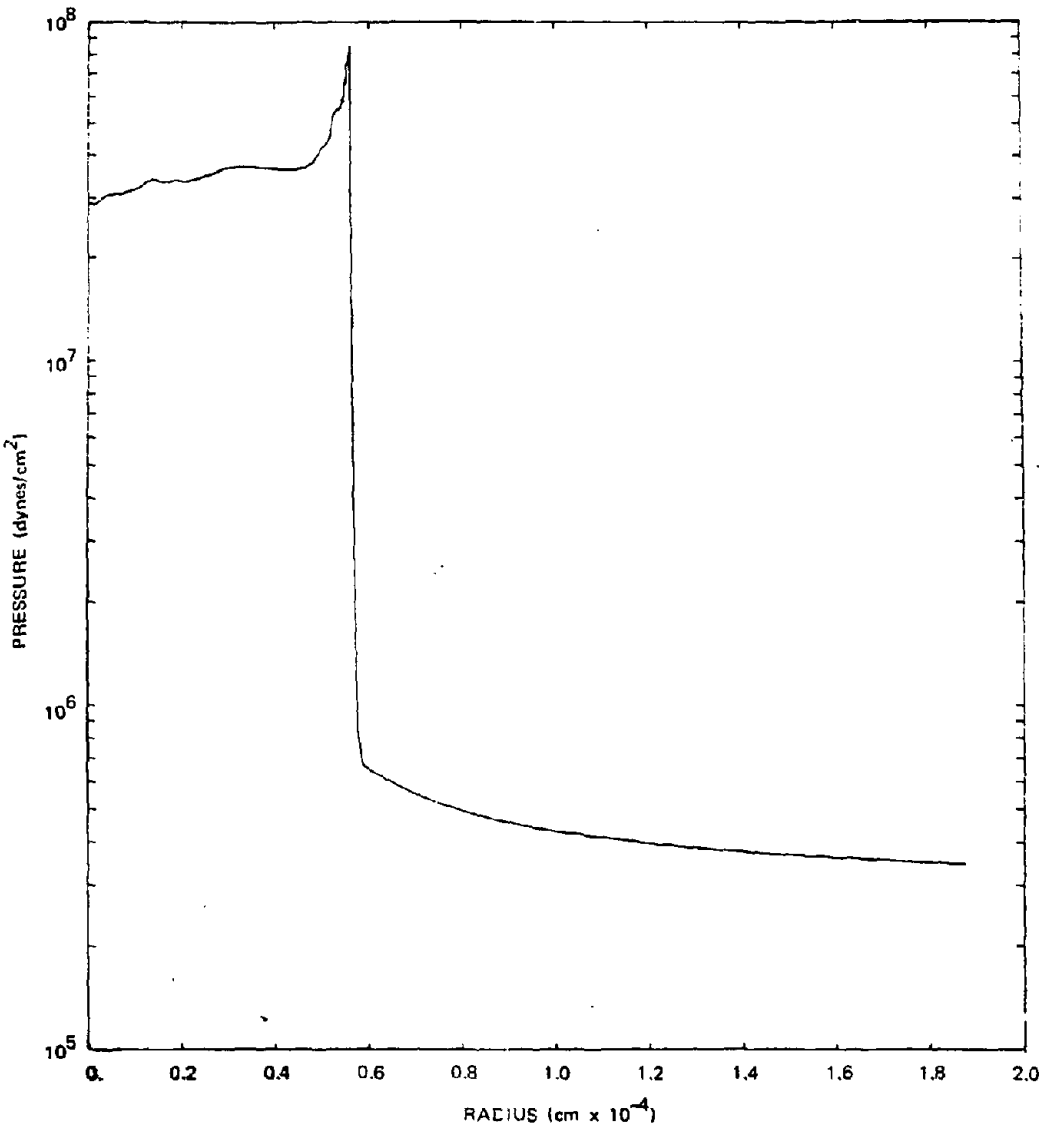

Figure 16-60. [redacted] Computed Static Pressure Profile, t = 4.64 msec, 30 kilofeet Altitude [redacted]

[redacted]

[redacted]

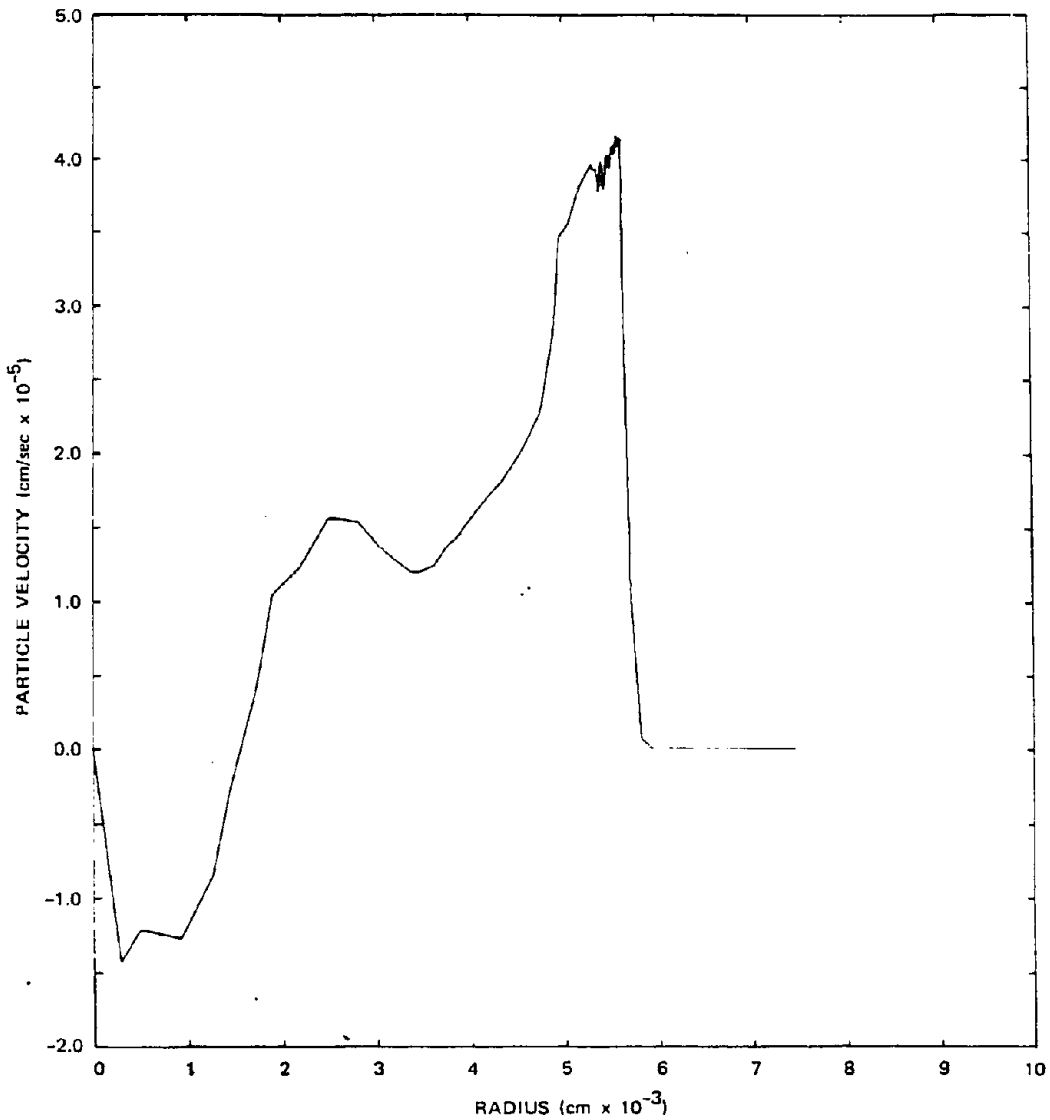

Figure 16-61. [redacted] Computed Particle Velocity Profile, t = 4.64 msec, 30 kilofeet Altitude [redacted]

[redacted]

[redacted]

[redacted] just prior to shock front intercept and terminated within one second. In the dynamic simulation involving interaction between the rapidly changing blast environment and the vehicle trajectory, the environment changes rapidly; changes are measured in microseconds and in inches. The computed dynamic response, nevertheless, is considered to be a valid model.

[redacted] Figures 16-62 through 16-65 provide a graphic portrayal of a sample blast intercept condition. For this one intercept case, four curves are shown: static overpressure, dynamic pressure, static overpressure impulse, and dynamic pressure impulse. All times indicated are measured from the time of blast wave intercept. Twenty-five milliseconds of data are shown in Figure 16-62 while only the first millisecond is shown in Figures 16-63 through 16-65. The values of dynamic pressure impulse are the results of continuous summation from prior trajectory restart conditions, and the measurements must be read relative to a baseline value at time of intercept.

[redacted] The two impulse curves (Figures 16-64 and 16-65) show the relative importance of the dynamic pressure impulse compared to overpressure impulse at early times. The former builds up and levels off extremely quickly while the latter continues to increase. This characteristic is due to the rapid drop in dynamic pressure, whereas the overpressure, plotted for 25 msec, illustrates a considerably slower decay rate.

16-36 Blast Loads on the RV Threat Vehicle [redacted]

[redacted] The time history of surface loading on a threat reentry vehicles were computed from knowledge of the fly through environments (overpressure, dynamic pressure, relative wind angle of attack) and local vehicle aerodynamics.

[redacted] The time history of loading on any part of the RV is found to be the sum of a very short duration dynamic pressure or drag loading, superimposed on a longer duration overpressure loading. (See Figures 16-62 through 16-65 for typical pressure-time histories.)

[redacted] The spatial distributions of these two types of loads on the vehicle surface generally will differ considerably. Blast overpressure results in uniform pressure being applied over the complete vehicle surface, whereas dynamic pressure loadings vary over the vehicle surface, depending on the structural configuration and intercept geometry. These various relationships can be expressed in the following functional form.

$$P(t) = q(t,\alpha,\theta,\psi,\beta) + \Delta p(t)$$

where

- q = dynamic pressure
- Δp = static overpressure
- α = relative wind intercept angle
- ψ,θ = local angles defining structural geometry
- β = circumferential angle on structure measured from windward ray of intercept.

Newtonian aerodynamics were used to determine the peak values of surface pressure resulting from the dynamic pressure environment for all the reentry vehicles that were studied. The structural configurations all were made up of some combination of a sphere nose cap and a conical body. Most of the early structural lethality studies were concentrated on the aft (or weakest) conical shell bay. Shock-on-shock loads were neglected in the analysis.

[redacted] The surface pressure loading on the conical shell elements is computed from the equation on page 16-106.

[redacted]

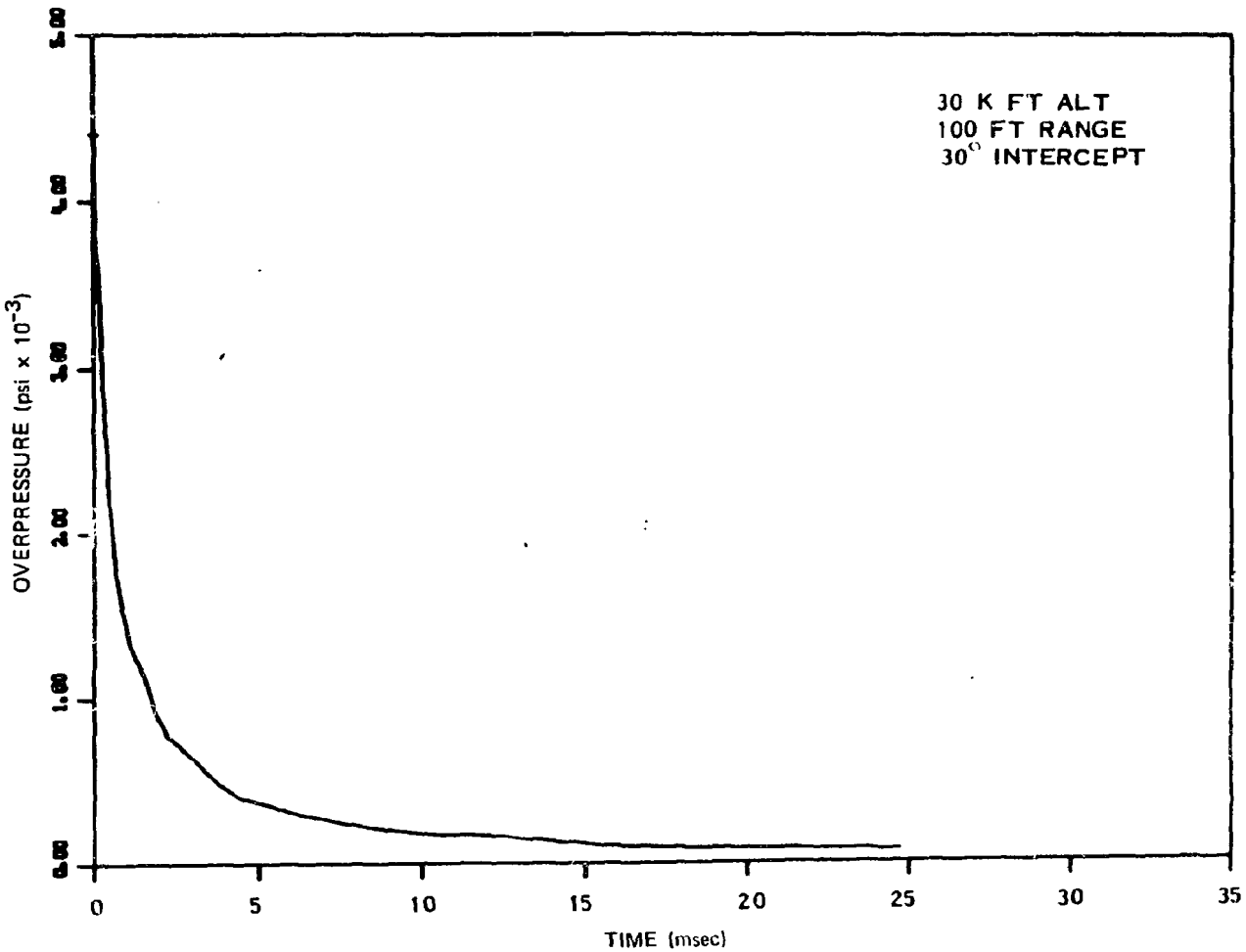

Figure 16-62. [redacted] RV Target A, Static Overpressure as a Function of Time, 30° Intercept [redacted]

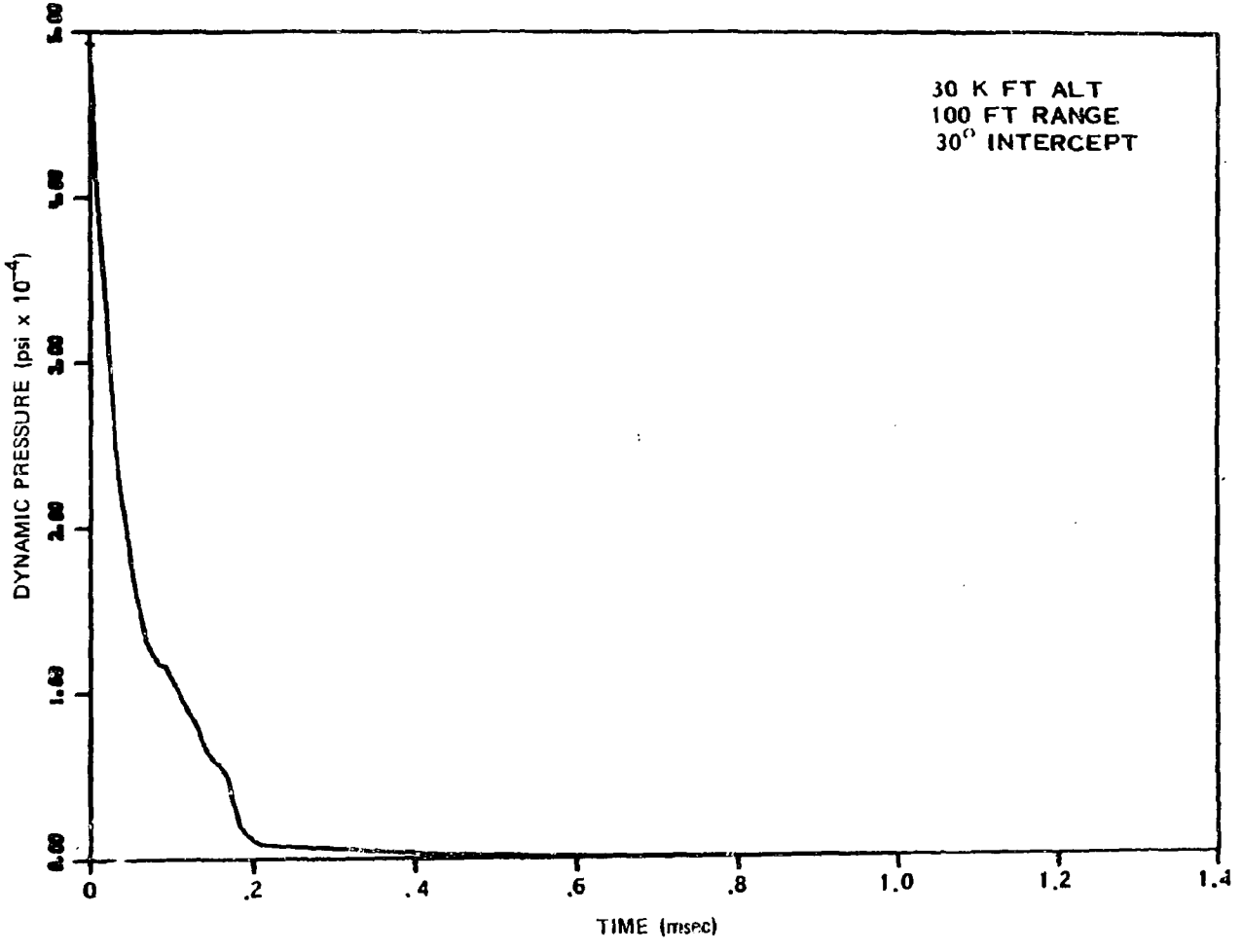

Figure 16-63. [redacted] RV Target A, Dynamic Pressure as a Function of Time, 30° Intercept [redacted]

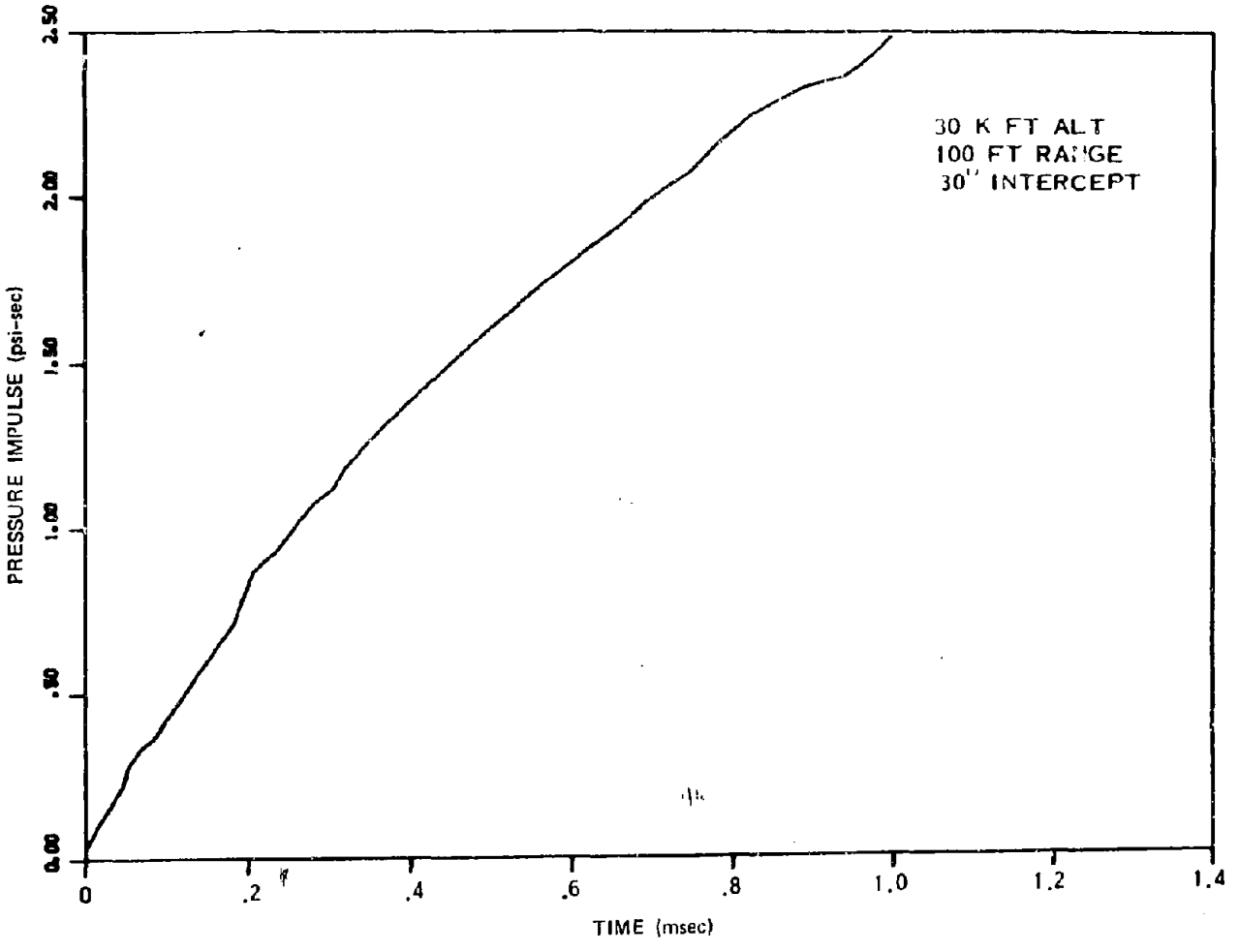

Figure 16-64. [redacted] RV Target [redacted] Static Overpressure Impulse as a Function of Time, 30° Intercept [redacted]

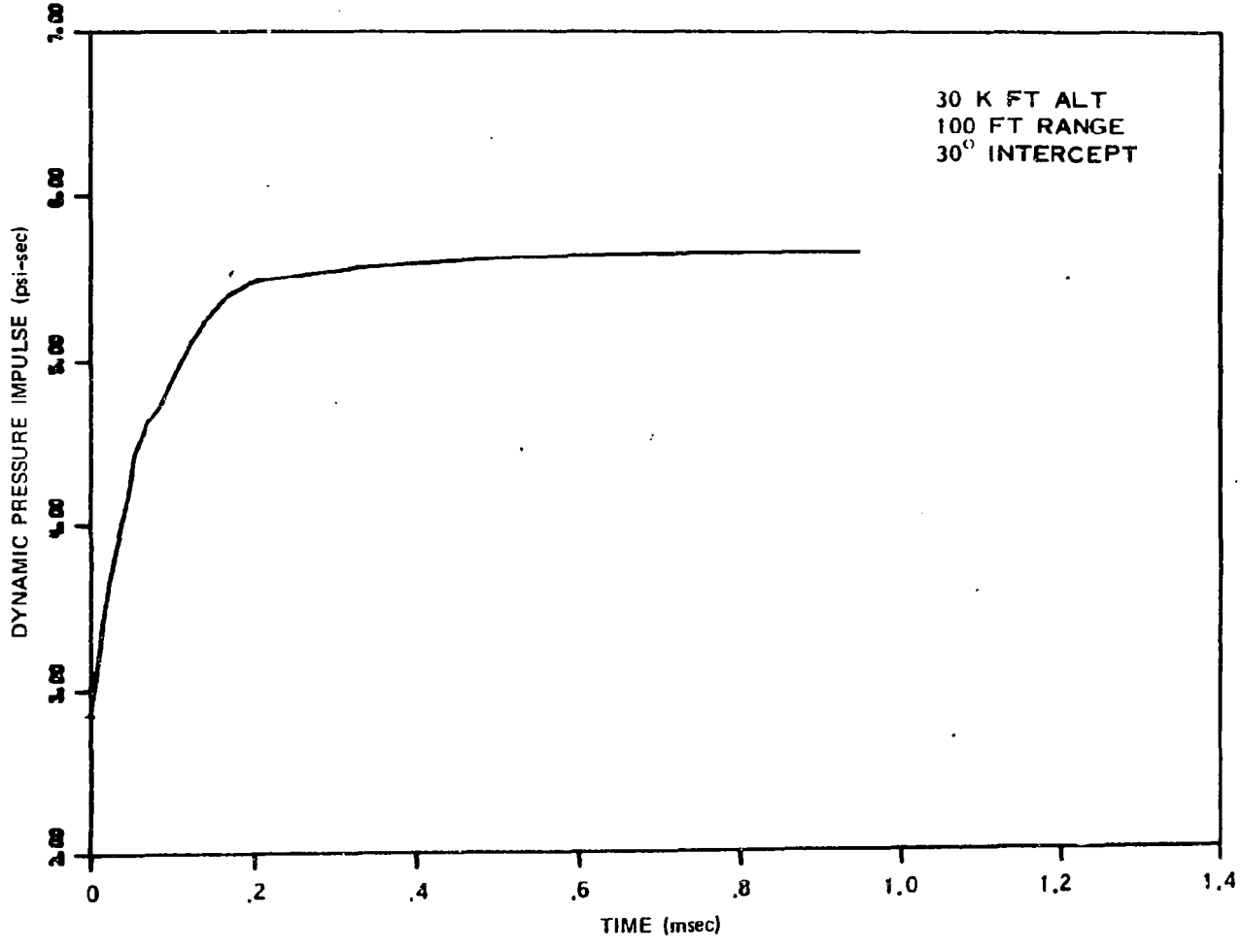

Figure 16-65. [redacted] RV Target [redacted], Dynamic Pressure Impulse as a Function of Time, 30° Intercept [redacted]

[redacted]

[redacted]

$$P(t) = 2q(t)\,(\cos\alpha \sin\theta + \sin\alpha \cos\theta \cos\beta)^2 + \Delta p(t); \qquad -\beta_{max} \leqslant \beta \leqslant \beta_{max}$$

$$P(t) = \Delta p(t) \qquad \beta_{max} \leqslant \beta \leqslant -\beta_{max}$$

where

$$\beta_{max} = \cos^{-1}\left\{1 - \left(\frac{\tan\theta}{\tan\alpha}\right)^2\right\}^{1/2}$$

$$\theta = \text{cone half angle}$$

at the windward ray $\beta = 0$, therefore maximum surface pressure is

$$P(t) = 2q(t)\sin^2(\theta + \alpha) + \Delta p(t),$$

and the impulse at any time, T, at $\beta = 0$ on the cone is

$$I(t) = \int_0^T \left\{2q(t)\sin^2(\theta + \alpha) + \Delta p(t)\right\} dt,$$

where it is noted that $q(t)$ and $\Delta p(t)$ will not, in general, have the same time dependency.

16-37 ABM Blast Kill Radii [redacted]

[redacted] Structural lethality levels of the threat reentry vehicles are evaluated in terms of the blast loadings on the primary structure of the vehicle. In the calculations described here, two categories of lethal loadings were evaluated: (1) Immediate kill, Category 6* and (2) Delayed kill, Category 4. Immediate kill corresponds to load levels sufficient to cause some degree of structural breakup of the metallic subshell. This usually will be accompanied by removal of the ablative covering and severe structural deformation of the remaining subshell. Delayed kill refers to removal of the ablative covering over large portions of the loaded side of the vehicle. In general, this load level also will be sufficient to cause considerable plastic deformation in the vehicle subshell. These definitions of damage are consistent with those recommended by Stanford Research Institute following participation in the HARTS and SPINE experimental programs.

[redacted] One approach used to relate these damage levels to the computed applied loading involves the establishment of a given damage level in terms of the pressure and impulse of the applied surface loading. The equation for a given damage level in the P-I plane is then defined by the following hyperbolic form:

$$\left(\frac{I}{I_o} - 1\right)\left(\frac{P}{P_o} - 1\right) = 1.0.$$

In this equation I_o and P_o are asymptotes corresponding to values of impulsive loading and static pressure loading necessary to induce the specified damage level. Thus, I_o and P_o must be determined for each structure to be studied and for both damage categories, i.e., immediate kill and delayed kill. Although much of the data are consistent with the value 1.0 on the right-hand side of the equation, some data indicate that a value near 3.0 would be more appropriate.

[redacted] For a given structural element, the I_o and P_o asymptotes for a given damage level can be related to computed values of impulse and pressure based on some very simplistic structural analysis techniques. For example, modeling the two layered aft bay shell element as a rigid, perfectly plastic cylinder, the uniform externally applied impulse necessary to cause a permanent

[redacted] Sometimes referred to as "catastrophic damage."

[redacted]

[redacted]

[redacted]

strain, ϵ, in the shell wall is found to be:

$$I = \left\{2\epsilon(\rho_s h_s + \rho_c h_c)(\sigma_{ys} h_s + \sigma_{yc} h_c)\right\}^{1/2},$$

where

ρ_s, ρ_c = mass densities of shell and ablative cover materials,

σ_{ys}, σ_{yc} = yield stress values of shell and ablative cover materials,

h_s = shell thickness,

h_c = ablator thickness.

Under similar assumptions, the value of uniform static pressure necessary to cause material yielding in the shell wall is

$$P_y = \frac{1}{a}\left\{\sigma_{ys} h_s + \sigma_{yc} h_c\right\}$$

where a = average radius of cylinder. The well-known I_{05} parameter for impulsively loaded shells can be obtained by setting $\epsilon = 0.05$.

$$I_{05} = \left\{0.1(\rho_s h_s + \rho_c h_c)(\sigma_{ys} h_s + \sigma_{yc} h_c)\right\}^{1/2}.$$

[redacted] The next step in lethality evaluation is to relate the I_{05} and P_y load levels to load levels corresponding to the Category 6 and Category 4 damage. For the cylindrical or slightly conical shells representative or the aft bay of most threat RV's, these relationships are empirically established based on results obtained from a large number of experimental tests performed during the HARTS, SPINE, and DRIS Programs. Based on the results of these correlations, the following relations were selected to establish the impulsive and quasistatic load level asymptotes for damage Categories 6 and 4.

IMPULSE ASYMPTOTE

Category 4: $I_4 = I_{05}$

Category 6: $I_6 = 2.5\ I_{05}$

QUASISTATIC PRESSURE ASYMPTOTE

Category 4: $P_4 = 0.7\ \frac{a}{L}\ P_{05}$

Category 6: $P_6 = 1.56\ \frac{a}{L}\ P_{05}$

It should be noted that, in the definition of the quasistatic pressure asymptote, the effect of shell length has been included empirically by including the radius-to-length ratio (a/L).

[redacted] Based on the structural lethality estimates described above and the blast environment loading for the various encounter geometries, lethality estimates of the threat RV's can be made. A sample plot is shown in Figure 16-66; the I_{05} and P_{05} (P_y) asymptotes have been determined, and the curves corresponding to the damage asymptotes I_6, P_6 (immediate kill) and I_4, P_4 (delayed kill) are shown. The dashed line shows the damage curve for immediate kill corresponding to the constant in the pressure-impulse equation being equal to 3.0 instead of 1.0.

[redacted] By combining the loads calculated for the various encounters, in terms of pressure and impulse of peak surface loading, with the damage level plot (Figure 16-66), estimates of loads (in terms of slant range and intercept angle) necessary to incur lethal damage can be made for each vehicle. An example of the superposition of the structure load pressures and impulses on the damage definition curves is shown in Figure 16-67. In the figure, different symbols correspond to loads for various intercept angles, and the number adjacent to each symbol defines the value of slant range *at burst time* to which that particular load calculation corresponds.

[redacted]

[redacted]

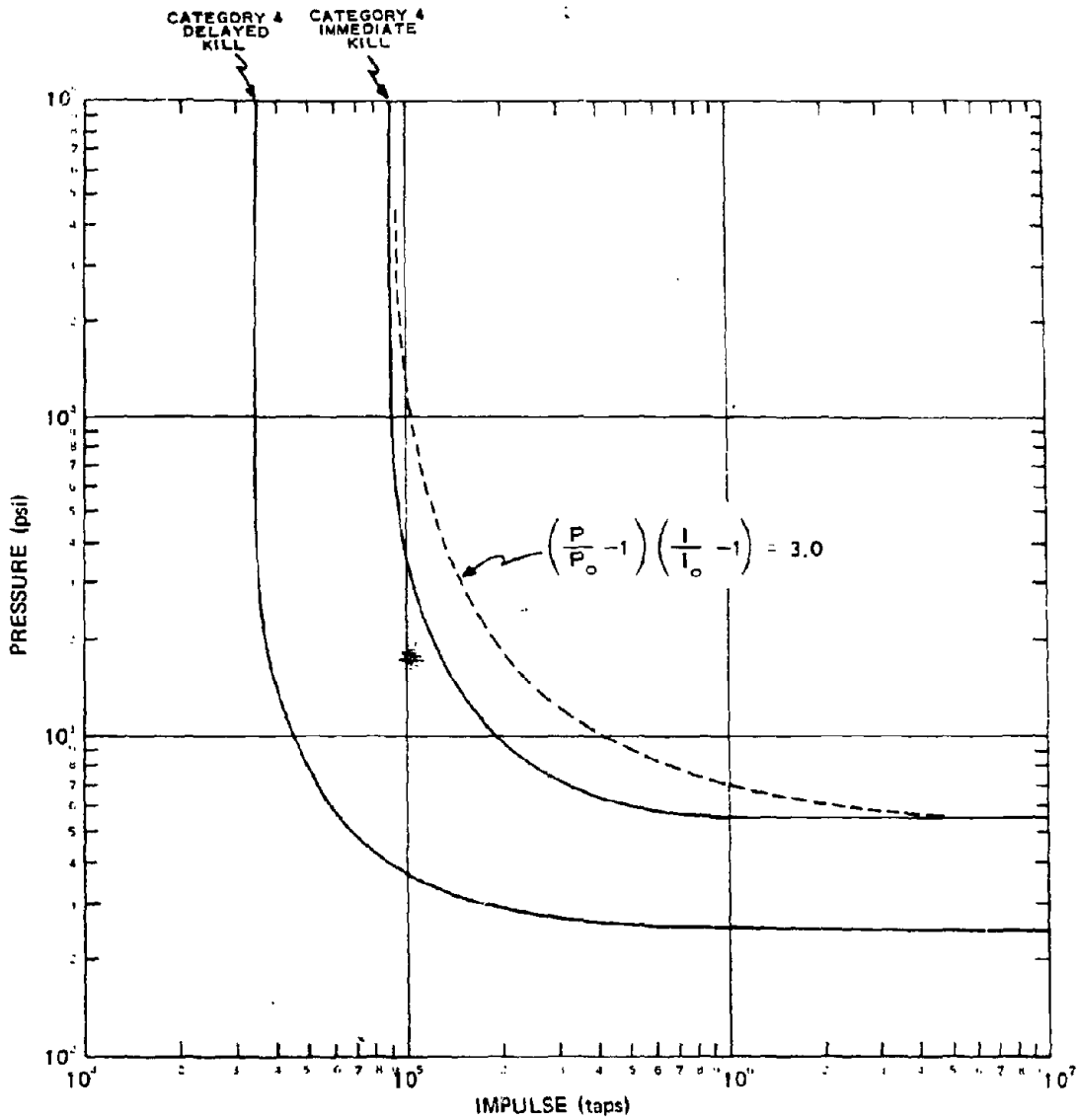

Figure 16-66. [redacted] Pressure-Impulse Damage Levels, RV Target A Configuration, Aft Bay [redacted]

[redacted]

[redacted]

[redacted] By noting where the blast loading points cross the damage level lines in the *P-I* plane, estimates of burst time slant range can be made, for a given intercept angle, that will result in Category 6 immediate kill and Category 4 delayed kill. The following RV kill slant ranges (at burst time) are obtained from the example (Figure 16-67).

DNA (E)(3)

[redacted]

[redacted] It should not be inferred that the *P-I* plot method described above is the only method of analysis that is used to determine blast lethality radii. Some investigators have been successful in computing the structural response of RV's to the derived blast load inputs; however, here experimental data must be used to relate the computed response to damage level, e.g., immediate kill.

16-38 Fireball Thermal Effects on Threat RV's [redacted]

[redacted] Whenever a vehicle intercepts an early time blast wave, it subsequently traverses through (or very near) a high temperature nuclear fireball. Therefore, as one part of a lethality investigation, the thermal effects that would be expected on a threat RV flying through an ABM nuclear fireball would be examined. The calculations for the following example employed the RAD ABLE code. This code uses the free field fireball thermal environment data as read off of a rad-hydro Usertape. The RAD ABLE code formalism assumes that the vehicle flies a constant velocity-straight line trajectory in the vicinity of the burst point. A simplified method is used that accounts for radiation blocking effects in an approximate manner based on detailed stagnation point (rad-hydro) flow field solutions.

[redacted] Figure 16-68 shows a typical history of the ablation rate ($\dot{m}$) and the amount of material ablated

$$\left(m = \int_0^t \dot{m}\, dt \right)$$

for a head on traversal of an ABM explosion at 30 kilofeet altitude. The burst time standoff distance (X_o) of the vehicle was 100 feet in this case.

[redacted]

DNA (E)(3)

[redacted] Figure 16-69 summarizes the results of a number of fireball traversal calculations (similar to those illustrated in Figure 16-67) in the form of total mass ablated at fireball exit as a function of initial standoff distance (X_o) and burst altitude. All of these results are for head on ($X_o > 0$) or tail on ($X_o < 0$) intercepts with

[redacted]

[redacted]

[redacted]

DNA
(b)(3)

Deleted

Figure 16-67. [redacted] SPRINT Blast Loads, RV Target A, 30 kilofeet Altitude, Aft Bay [redacted]

[redacted]

[redacted]

[redacted]

DOE
(b)(3)

Deleted

Figure 16-68. [redacted] Ablation Rate and Mass Ablated as a Function of Time for Target A Threat RV [redacted]

[redacted]

[redacted]

[redacted]

Deleted

Figure 16-69. [redacted] Mass Ablated as a Function of Burst Time Standoff Distance for Target A Threat RV [redacted]

[redacted]

[redacted]

[redacted]

[redacted] no lateral offset (i.e., 0° or 180° intercept angles). [redacted]

DNA
(b)(3)

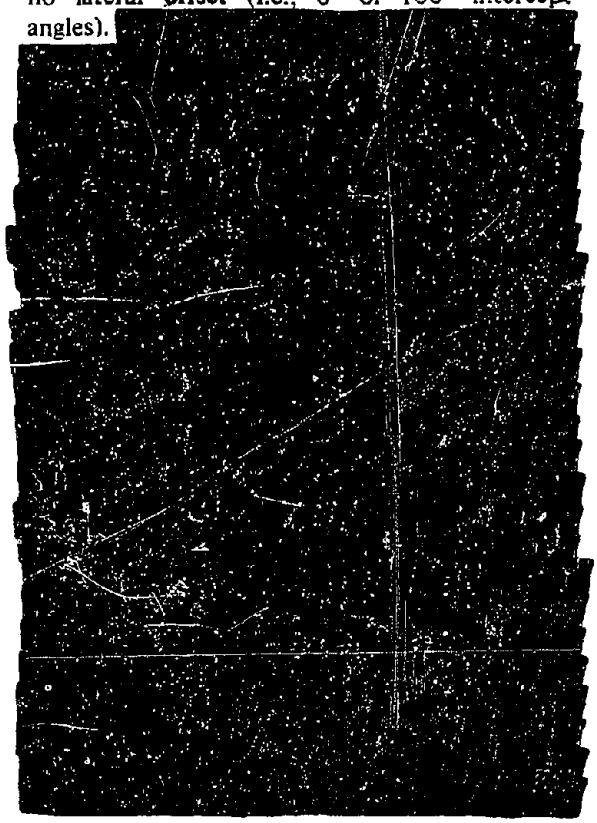

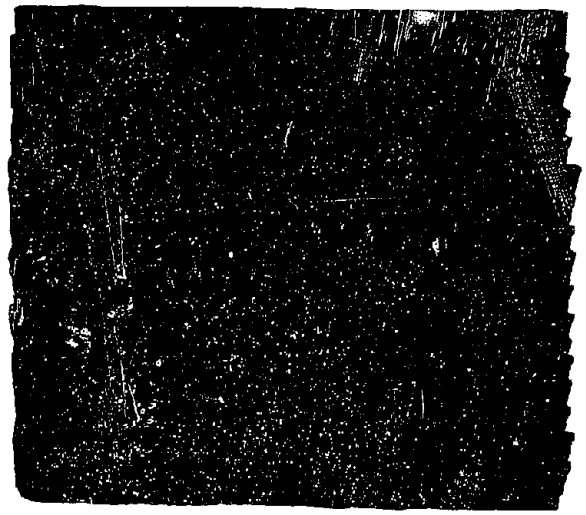

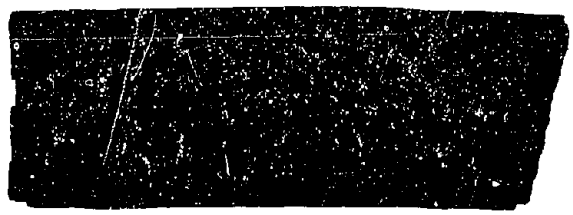

[redacted]

[redacted]

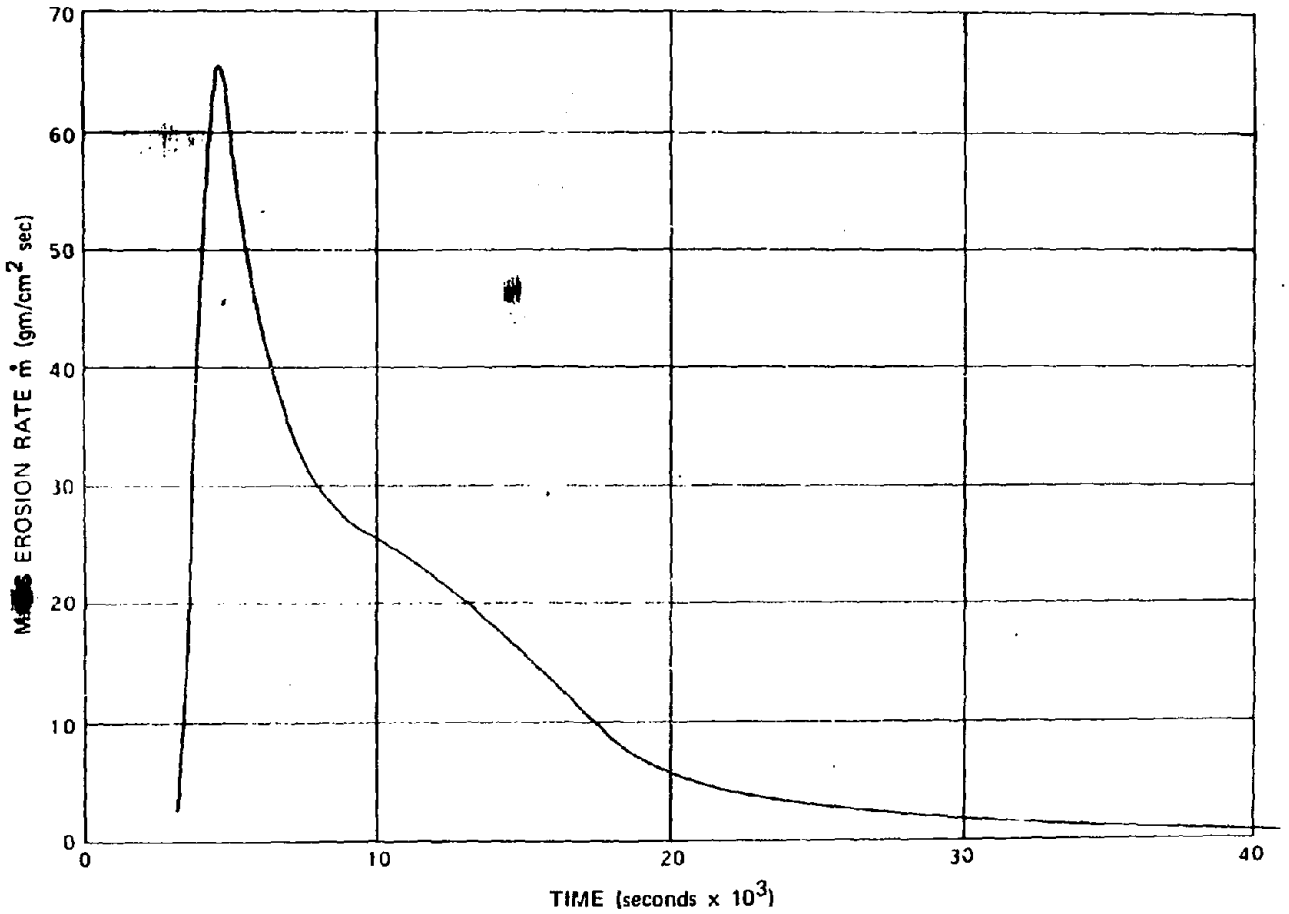

Figure 16-70. Typical Traverse-Mass Erosion Rate History

[redacted]

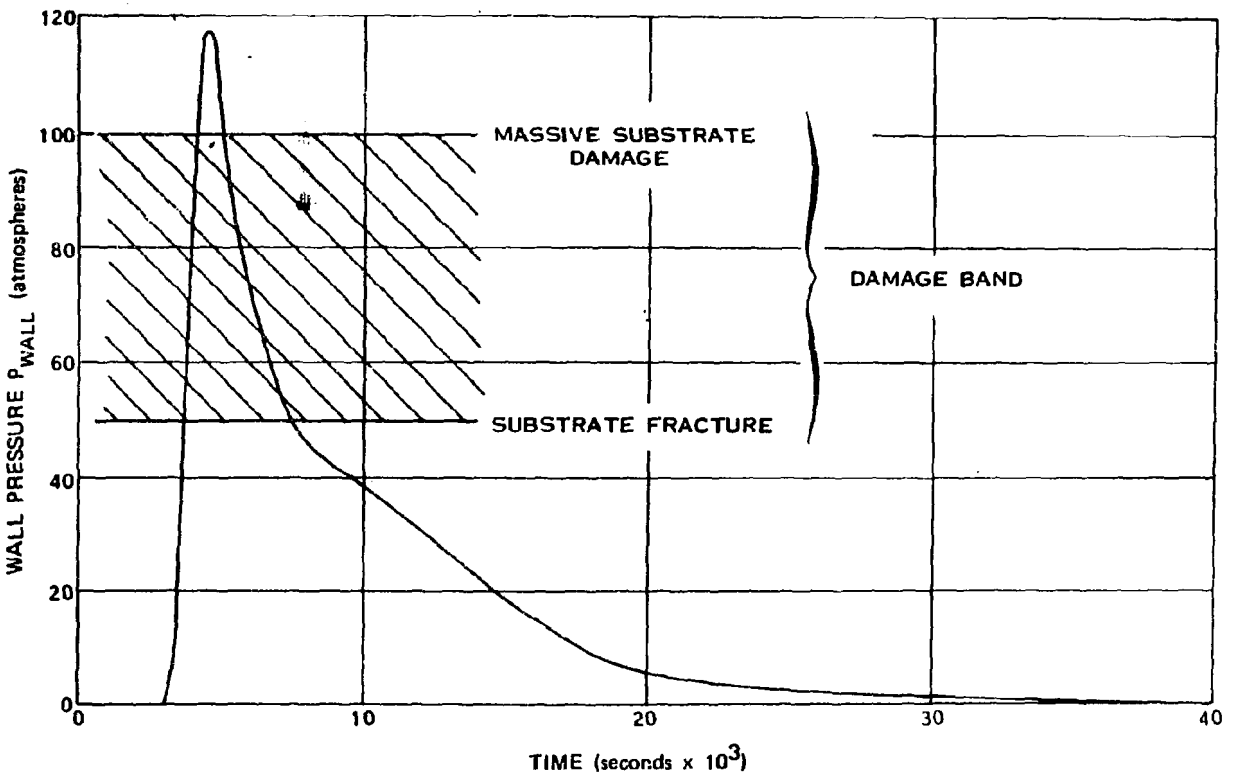

Figure 16-71. [redacted] Typical Traverse-TML History [redacted]

[redacted]

[redacted]

[redacted] BIBLIOGRAPHY [redacted]

Baker, W. E., P. A. Westine, and S. Silverman, *Feasibility Study on Simulating the Structural Response of High Altitude Missiles to Blast Loading*, Final Technical Report AMC-66-8, Southwest Research Institute, San Antonio, Texas, 21 January 1966 [redacted]

Barry, Jr., J. M., *Supplementary Data for the AIRS-II Vehicle* [redacted], Kaman AviDyne TM-25, AMC-66-15, Kaman AviDyne, Burlington, Massachusetts, July 1966 [redacted]

Bryant, E. J., N. H. Ethridge, and M. R. Johnson, *Response of Drag Type Equipment Targets in the Precursor Zone* [redacted], WT1123, Ballistic Research Laboratories, Aberdeen Proving Ground, Maryland, August 1956 [redacted]

Bryant, E. J., and J. D. Day, *Effects of Rough Terrain on Drag-Sensitive Targets* [redacted], WT1408, Ballistic Research Laboratories, Aberdeen Proving Ground, Maryland, 9 November 1959 [redacted]

Criscione, E. S., L. J. Mente, N. P. Hobbs, *Vulnerability of Standard Army Interceptor Systems (AIRS I and II) to Nuclear Weapon Blast and Thermal Radiation Effects* [redacted], AMC-67-18, Kaman AviDyne, Burlington, Massachusetts, April 1967 [redacted]

Eppes, R., Jr., *Review of Experimental Programs for Blast Intercept and Traversal, and Feasibility of Using a Large Bore Gun Facility for Launching Vehicles for Blast Intercept* [redacted], AMSMI-RS-TR-66-12, AMC-66-8, U.S. Army Missile Command, October 1966 [redacted]

Field and Depot Maintenance Manual: Description and Theory of Air Defense Guided Missile XM3E1 [redacted], TM 9-1410-500-35, June 1960 [redacted]

Field and Depot Maintenance Manual: Description and Theory: Guided Missile System Components Organizational Maintenance Test Station AN/MSM-35 (SERGEANT Artillery Guided Missile System) [redacted], Notes on Material NOM 9-4935-303-35/2, November 1961.

Field and Depot Maintenance Manual: Schematics: SERGEANT Artillery Guided Missile XM 15 (SERGEANT Artillery Guided Missile System) [redacted], TM 9-1410-302-35/1, August 1963.

Fraser, W. [redacted] *A Comparison of Experimentally and Theoretically Determined Pressure Distributio[redacted] on a Blast-Loaded Missile Body*, AMC-67-30, Kaman Nuclear, Colorado Springs, Colorado, June 1968 [redacted]

Hardening Technology Studies – I [redacted], LMSC-B130200, Volumes I-IV, Lockheed Missiles and Space Company, Sunnyvale, California, 30 September 1965 [redacted]

[redacted]

[redacted]

[redacted] *Hardening Technology Studies – II* [redacted] LMSC-B130391, Volumes I-IV, Lockheed Missiles and Space Company, Sunnyvale, California, 30 September 1966 [redacted]

Hillendahl, R. W., *Theoretical Models for Nuclear Fireballs* [redacted] DASA 1589-1 through 1589-39, Lockheed Missiles and Space Company, Sunnyvale, California, 1965-1966 [redacted]

Joint Engineer/Service Test SERGEANT Guided Missile System [redacted]. Volume I, U.S. Army Test and Evaluation Command Technical Report 143, November 1963 [redacted]

Johnson, O. T., R. D. Mayerhofer, and W. J. Schuman, Jr., *Effect of Blast Upon Simulated and Actual Missiles (Project 1.4 Operation Snow Ball)* [redacted] Memorandum Report No. 1655, U.S. Army Ballistic Research Laboratories, Aberdeen Proving Ground, Maryland, May 1965 [redacted]

Johnson, O. T., and R. D. Mayerhofer, *Susceptibility and Vulnerability of the Lance Missile System to Nuclear Effects (Blast)* [redacted] BRL-MR-1862, U.S. Army Materiel Command, Ballistic Research Laboratories, Aberdeen Proving Ground, Maryland, August 1967 [redacted]

Johnson, O. T., R. D. Mayerhofer, *Susceptibility and Vulnerability of the SERGEANT Weapon System to Nuclear Effects (Blast)* [redacted] BRL-R-1324, U.S. Army Materiel Command, Ballistic Research Laboratories, Aberdeen Proving Ground, Maryland, June 1966 [redacted]

Kelley, B. E., *LANCE Automet Control System* [redacted] RG-TR-64-3, U.S. Army Missile Command, Redstone Arsenal, Alabama, 25 June 1964 [redacted]

Lindberg, H. E., et al., *Response of Reentry Vehicle-Type Shells to Blast Loads*, LMSC-B130200, Volume IV-C, Stanford Research Institute, Menlo Park, California, for Lockheed Missiles and Space Company, Sunnyvale, California, 30 September 1965 [redacted]

Lindberg, H. E., and G. E. Sliter, *Response of Reentry Vehicle-Type Shells to Transient Surface Pressures*, AFWL-TR-68-56, Stanford Research Institute, Menlo Park, California, June 1969 [redacted]

Logistic Support Plan for the LANCE Missile System [redacted] (Second Revision), U.S. Army Missile Command, Redstone Arsenal, Alabama [redacted]

Mente, K. J., *Standard Research Systems for Army Interceptors* [redacted] TR-35, Kaman AviDyne, Burlington, Massachusetts, July 1965 [redacted]

Mente, K. J., *Supplementary Data for the AIRS-I Vehicle* [redacted] TM-24, Kaman AviDyne, Burlington, Massachusetts, June 1966 [redacted]

[redacted]

[redacted]

[redacted]

Mikami, K., R. D'Amato, *Criteria for the Effect of Damage on the Operational Capabilities of U.S. Army Missile Systems Volume 2, Lance Missile System* [redacted], TR-38, Kaman AviDyne, Burlington, Massachusetts, February 1966 [redacted]

Mikami, K., L. J. Mente, R. D'Amato, *Criteria for the Effect of Damage on the Operational Capabilities of U.S. Army Missile Systems Volume 5, Hawk Missile System* [redacted], TR-38, Kaman AviDyne, Burlington, Massachusetts, July 1966 [redacted]

Muller, J. and D. L. Blank, *SLEDGE Program: Phase I, Feasibility Study* [redacted], DASA-1988, Martin Marietta Corporation (Orlando Division), Orlando, Florida, September 1967 [redacted]

Nicholson, J. E., and J. J. Rossi, *Pressure-Time Histories of Blast Wave Interactions with a Re-Entry Body*, MC-65-163-R1, Mithras, Inc., February 1966 [redacted]

Nicholson, J. E., E. F. Kent, N. Zessoules, and P. H. McIngvale, *A Ballistic Wind Tunnel Test Technique for Measuring Shock-on-Shock Interactions*, MC-66-142-R31, Mithras, Inc., 4 October 1966 [redacted].

Nuclear Radiation Effects Study on LANCE Directional Control Electronics [redacted], RG-TR-64-14, U.S. Army Missile Command, Redstone Arsenal, Alabama, September 1964 [redacted]

Nuclear Weapons Blast Phenomena, Volume I, Source and Development of Blast Waves in Air [redacted], DASA 1200-I, DASIAC, Santa Barbara, California, 1 March 1971 [redacted]

Nuclear Weapons Blast Phenomena, Volume II, Blast Wave Interaction [redacted], DASA 1200-II, DASIAC, Santa Barbara, California, 1 December 1970 [redacted]

Nuclear Weapons Blast Phenomena, Volume III, Air and Subsurface Explosions [redacted], DASA 1200-III, DASIAC, Santa Barbara, California, 1 March 1970 [redacted]

Organizational Maintenance Manual: SERGEANT Artillery Missile XM 15 (SERGEANT Artillery Guided Missile System) [redacted] Notes on Material NOM 9-1410-302-20, May 1962.

Operation and Field Maintenance Manual: General Support Shop Set (GSSS) (SERGEANT Field Artillery Guided Missile System) [redacted], Technical Manual TM 9-4935-305-40/1, July 1963.

Operator and Organizational Maintenance Manual: Guided Missile System. Components Organizational Maintenance Test Station AN/MSM-35 (SERGEANT Artillery Guided Missile System) [redacted], Notes on Material NOM 9-4935-303-12, October 1961.

[redacted]

[redacted]

Operator's Manual: Guided Missile System Components Field Maintenance Test Station AN/MSM-36 (SERGEANT Artillery Guided Missile System) [redacted]. Notes on Material NOM 9-4935-304-10, October 1963.

Operator's Manual, SERGEANT Artillery Guided Missile System [redacted]. Notes on Material NOM 9-1400-300-10, December 1960 [redacted]

Operator and Organizational Maintenance Manual: Air Defense Guided Missile XM3E1 [redacted]. TM 9-1410-500-12, July 1962 [redacted].

Operator and Organizational Maintenance Manual: Emplacement of Hawk Air Defense Guided Missile System [redacted], TM 9-1400-500-12/1, August 1961 [redacted]

Operator's Manual: Description for Hawk Air Defense Guided Missile System [redacted], TM 9-1400-500-10, June 1960 [redacted]

Operator and Organizational Maintenance Manual: SERGEANT Missile Trainer, Device 3G52 (SERGEANT Artillery Guided Missile System) [redacted]. Technical Manual TM 9-6920-130-12, January 1963.

Operator and Organizational Maintenance Manual: Four-Wheel Semitrailer-Mounted Guided Missile Launching Station XM 504 (SERGEANT Artillery Guided Missile System) [redacted]. Notes on Material NOM 9-1440-301-12, October 1961.

Parechanian, H. S., et al., *Dynamic Response Investigation of Simulated R/V Structure – Volume II Impulse and Blast Tests* [redacted], SAMSO TR-69-144, Volume II, McDonnell Douglas Astronautics Company, Santa Monica, California, September 1969 [redacted]

Proceedings: DASA/RAND Hydrodynamic Code Conference [redacted]. DASA-1553, DASA Data Central, General Electric Company, Tempo, Santa Barbara, California, September 1964 [redacted]

Proceedings: DASA Conference on Nuclear Weapons Effects on Re-Entry Vehicles and Interceptor Missiles [redacted], DASA-1651, DASA Data Center, General Electric Company, Tempo, Santa Barbara, California, September 1965 [redacted]

Proceedings: DASA/AFFDL Shock-on-Shock Interaction Conference [redacted], DASA-1674, DASA Data Center, General Electric Company, Tempo, Santa Barbara, California, May 196[redacted]

Proceedings: DASA Anti-Ballistic Missile Blast Vulnerability Conference [redacted], DASA-1744, DASA Data Center, General Electric Company, Tempo, Santa Barbara, California, April 1966 [redacted]

[redacted]

[redacted]

Reck, R. J., and H. E. Lindberg, *Structural Response of the SPINE Reentry Vehicle Models to Blast and Impulsive Loads* [redacted]. AFWL-TR-67-118, Stanford Research Institute, Menlo Park, California and Douglas Aircraft Company, Santa Monica, California, January 1968 [redacted]

Sachs, D. C. and R. E. Keeffe, *An Investigation of Static Blast/Vehicle Intercept Simulation Methods* [redacted]. AMC-67-30, Kaman Nuclear, Colorado Springs, Colorado, November 1967 [redacted]

Sachs, D. C., et al., *An Investigation of Dynamic Blast/Vehicle Intercept Simulation Methods* [redacted]. AMC-67-28, Kaman Nuclear, Colorado Springs, Colorado, August 1967 [redacted]

Schuman, W. J., Jr., *The Response of Cylindrical Shells to External Blast Loading*, BRL Memorandum Report No. 1461, U.S. Army Ballistic Research Laboratories, Aberdeen Proving Ground, Maryland, March 1963 [redacted]

Schuman, W. J., Jr., *The Response of Cylindrical Shells to External Blast Loading, Part II*, BRL Memorandum Report No. 1560, U.S. Army Ballistic Research Laboratories, Aberdeen Proving Ground, Maryland, May 1964 [redacted]

SERGEANT Missile System Operation and Environment Test Program [redacted]. White Sands Missile Range Technical Memorandum 874, White Sands, New Mexico, June 1961 [redacted]

Sieck, D. W., *Stress Analysis of the Hawk I Missile* [redacted]. NA 1-55-10, Volumes I & II, Northrop Aircraft, Inc., [redacted]

Sliter, G. E., et al., *Warhead Optimization for Structural Kill of Re-Entry Vehicles, Lethality Tests of SPINE Vehicles* [redacted] DASA-2215, Stanford Research Institute, Menlo Park, California, July 1969 [redacted]

Sliter, G. E., et al., *Warhead Optimization for Structural Kill of Re-Entry Vehicles* [redacted] DASA-2281, Stanford Research Institute, Menlo Park, California, July 1969 [redacted]

SPRINT Blast Survivability Program-Interim Report [redacted] AMC-4-69(T), Kaman Sciences Corporation, Colorado Springs, Colorado, June 1969 [redacted]

Studies of Blast Simulation Techniques on Re-Entry Vehicles [redacted], AFSWC TDR 62-129, Sandia Corp., Albuquerque, New Mexico, November 1962 [redacted]

Transportation Data for the U.S. Army Hawk Missile System [redacted] AR-150, Raytheon Company Aero/Weapons Division, Andover Plant, Andover, Massachusetts, June 1961.

[redacted]

[redacted]

[redacted]

Wells, [redacted]B. and E. A. Bathke, *Theoretical Methods and Computer Codes for Fireball Ab[redacted]n Effects* [redacted] KN-70-220(R), Kaman Nuclear, Colorado Springs, Colorado, 14 April 1970 [redacted]

Wells, P. B., E. A. Bathke, and D. C. Sachs, *SPRINT Blast and Thermal Environment Calculations* [redacted] KN-70-754(R), Kaman Nuclear, Colorado Springs, Colorado, 2 October 1970 [redacted]

Whitaker, W. A., et al., *Theoretical Calculations of Early Phenomenology – 200 kt at 32 kilometers* [redacted] AFWL-TR-67-68, Air Force Weapons Laboratory, Kirtland Air Force Base, Albuquerque, New Mexico, October 1967 [redacted]

Zvara, J., R. D'Amato, *Criteria for the Effect of Damage on the Operational Capabilities of U.S. Army Missile Systems, Volume I, SERGEANT Guided Missile System* [redacted] TR-38, Kaman AviDyne, Burlington, Massachusetts, February 1966 [redacted]

[redacted]

DTIC
ELECTE
2 MAR 1989
S D
E

AD-A955 401

Chapter 17

RADIO FREQUENCY SIGNAL DEGRADATION RELEVANT TO COMMUNICATIONS AND RADAR SYSTEMS *

INTRODUCTION

Nuclear detonations can affect the performance of radio communication, radar, and other electronic systems that rely on electromagnetic-wave propagation. Usually, the effects will be deleterious although performance may occasionally be enhanced. Applicable nuclear-weapon-induced phenomena are discussed in Chapters 3, 5, and 8. Generally, each system and environmental situation of interest must be examined to determine whether nuclear weapons effects will be important and to what extent they will be important.

Electromagnetic waves propagating along paths entirely below 25 kilometers are not likely to be affected by nuclear-produced disturbances. When a detonation occurs below 25 kilometers, the major degradation region is the fireball, which is limited in extent. When a detonation occurs above 25 kilometers, very little of the weapon radiation penetrates below 25 kilometers and the effects that are produced are short-lived.

Electromagnetic waves propagating along paths above 25 kilometers can be affected severely by nuclear detonations. If the detonation occurs below 25 kilometers, the effects will be minimal, unless the weapon yield is so large that the fission debris is carried well above 25 kilometers. As the detonation altitude is raised above 25 kilometers, propagation disturbances can cover a major portion of a hemisphere; they may last for hours, and they may interfere with systems that depend on the natural ionosphere to reflect or scatter energy, such as HF systems, seriously. The size of the region affected and the duration of the effects on the system decrease with increasing wave frequency for frequencies above a few megahertz. Effects on wave frequencies above a few gigahertz are limited to the fireball region (a few tens to a few hundred kilometers in diameter).

As a result of the very large number of possible interactions between the effects caused by a nuclear burst and the electronic system in its operating environment, problems deriving from the degradation of signals in a nuclear environment are so complex that techniques for calculating signal degradation in nuclear environments are not appropriate for the subject material of this chapter. Such problems are performed most effectively with the aid of computers, using codes such as RANC 4 (see bibliography). Methods for computation of system performance by hand have been devised, but, in general, they are lengthy, even though many simplifications must be included. Some such computations for determining absorption are described in Chapter 8. Analyses of generic systems for selected burst conditions are useful for determining the nature and order of magnitude of effects; however, generalizations from such analyses are not warranted.

* Although the English system of units for measuring distance is given priority throughout most chapters of this manual, wavelengths and other dimensions dealing with electromagnetic wave propagation usually are given in the metric system. Therefore, in this chapter and in Chapter 8, the metric system is used for distance dimensions. Conversion factors from the metric system to the English system are provided in Appendix B.

This document has been approved for public release and sale; its distribution is unlimited.

89 3 02 033

[redacted]

[redacted] As discussed in Chapter 8, considerable uncertainty exists in the prediction of the effects of nuclear weapon bursts on electromagnetic propagation, particularly for burst or propagation conditions different from those for which test data have been obtained. While in general the prediction of weapon effects is more difficult in a multiple-burst environment than for a single burst, system performance may be relatively insensitive to burst parameters; for such cases simple models of the disturbed environment can be used for analysis.

SECTION I

[redacted] DEGRADATION MECHANISMS [redacted]

[redacted] Nuclear weapon effects on electromagnetic propagation are grouped into three degradation mechanisms in this section: attenuation, which defines the change in the amount of electromagnetic energy reaching a given location; interference, which defines the level of noise competing with a received signal; and distortion, which defines the change in information content of a received signal.

[redacted] ATTENUATION [redacted]

[redacted] Attenuation of signals in a nuclear environment derives principally from the phenomena of absorption, scattering, and beam spreading (small angle scattering, i.e., differential refraction or defocusing). In some instances, generally at times after detonation in excess of a few minutes, scattering and beam spreading can be the more important phenomena. For most cases, however, attenuation caused by absorption is regarded as one of the most important effects caused by nuclear detonations (see ELECTROMAGNETIC PROPAGATION IN IONIZED REGIONS in Chapter 8), and it is one of the best understood and most predictable of the effects. There are three principal atmospheric absorption regions caused by a nuclear detonation: the fireball, a region around the fireball, and the D-region of the ionosphere (approximately 50 to 80 km altitude). Figure 17-1 illustrates the absorption regions for several burst altitudes and times after burst.

17-1 Fireball Absorption [redacted]

[redacted] The fireball is generally the most intensely absorbing region. Significant absorption within the fireball can last tens of seconds for frequencies less than about 10 GHz (see paragraph 8-6). Fireball sizes vary from less than a kilometer for small-yield surface bursts to several hundred kilometers for large-yield, high-altitude bursts. The fireball size and location as a function of burst parameters can be determined from Table 8-2 and Figures 8-16 and 8-38. The amount of signal attenuation caused by absorption of signals propagating through the fireball can be determined from Tables 8-3 through 8-7. For many cases of interest in analyzing a system, the duration of attenuation due to fireball absorption is determined by the rise rate of the rising fireball rather than the length of time the fireball remains absorbing.

17-2 Absorption in the Region Around the Fireball [redacted]

[redacted] When the fireball is below the D-region, delayed gamma rays emitted from fission debris in the fireball cause ionization and thus absorption in a small region surrounding the fireball (see paragraph 8-8). The size of the region depends on the burst and propagation parameters; it can extend beyond the fireball for tens of kilometers for frequencies below a few gigahertz. Estimates of signal attenuation can be obtained from Figures 8-42 through 8-48 (Problem 8-6).

[redacted] When the fireball is above the D-region, most of the absorption outside the fireball occurs in the D-region as discussed below.

QUALITY INSPECTED 4

[redacted]

UNANNOUNCED

For
ed
ion
By
Distribution/
Availability Codes
Dist | Avail and/or Special
A-1

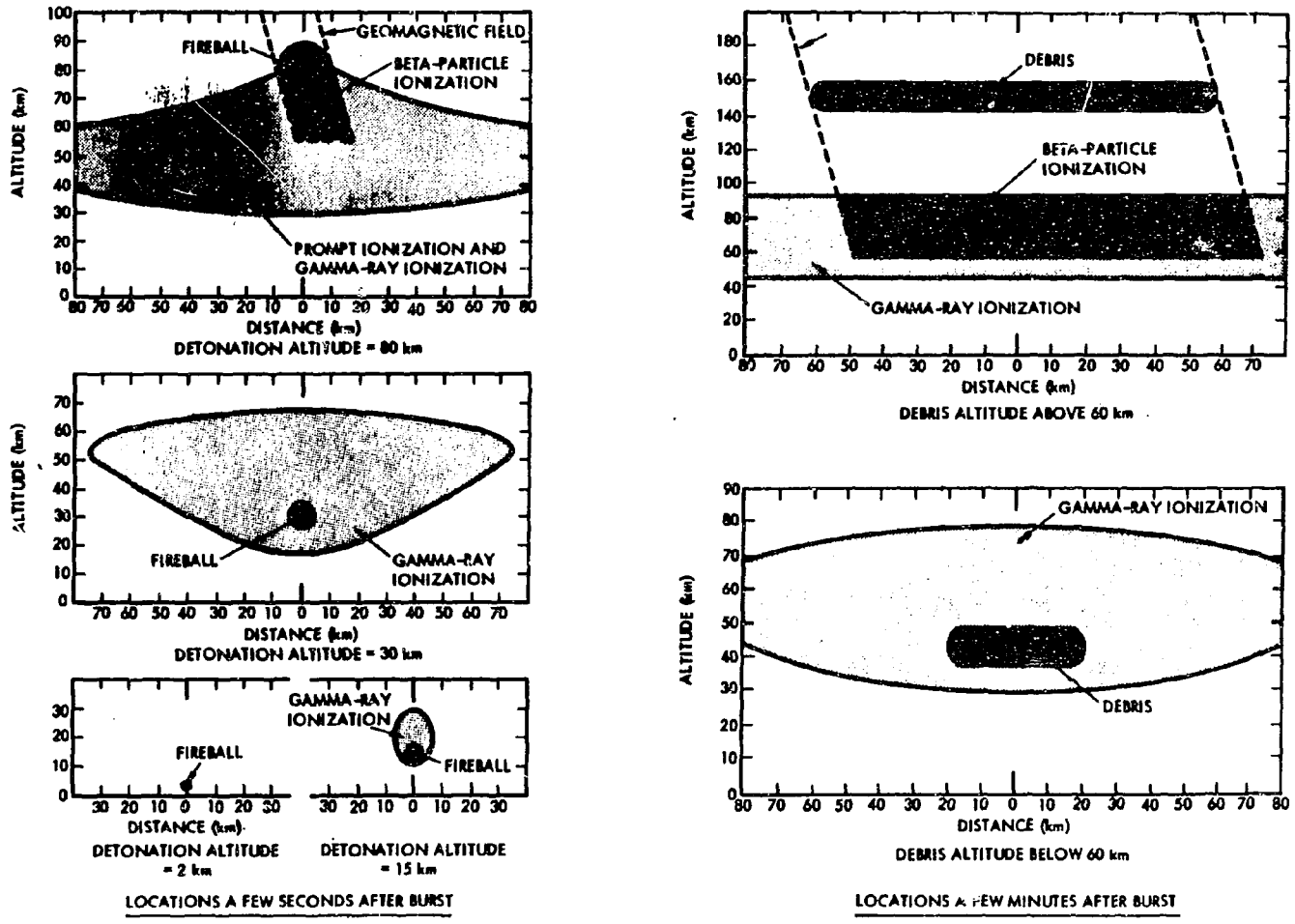

Figure 17-1. Approximate Locations of Ionization Causing Absorption

[redacted]

17-3 D-Region Absorption [redacted]

[redacted] The largest and most persistent absorption region caused by nuclear detonations generally occurs in the D-region. Depending on detonation altitude and weapon yield, both prompt radiation (X-rays and neutrons) and delayed radiation (beta particles and gamma rays) can ionize the D-region and cause absorption (see paragraphs 8-2 through 8-8). For frequencies above a few megahertz, absorption in the D-region is related inversely to the square of the frequency at which the system operates. The extent of D-region ionization caused by prompt radiation depends on the detonation altitude. The size of the ionized region increases from a few tens of kilometers for detonations below the D-region to thousands of kilometers for detonations above several hundred kilometers. The duration of significant absorption caused by ionization resulting from prompt radiation varies from less than a second for 1 GHz and nighttime conditions to tens of minutes for 10 MHz and daytime conditions.

[redacted] Delayed gamma rays are an important D-region ionization source when the fission debris is above about 25 kilometers. The extent of the ionization increases with debris altitude. Large regions (thousands of kilometers in diameter) are affected when the debris is above several hundred kilometers in altitude. The larger ionization regions are primarily of importance for frequencies below a few hundred megahertz. Some of the Compton electrons produced in the burst region by gamma rays are guided by the geomagnetic field and produce ionization in the D-region on the opposite side of the magnetic equator (see paragraph 8-3). The resulting absorption is less intense than that due to gamma ray ionization in the burst region, but it can be important for frequencies in and below the HF band.

[redacted] Beta particles ionize the D-region when the fission debris is above about 60 kilometers. As illustrated in Figure 17-1 and discussed in paragraph 8-3, the size and location of the region ionized by beta-particles depend on the size and location of the debris region and the direction of the geomagnetic field. For each debris region above 60 kilometers there are two beta-particle absorption regions; one in the burst locale and one on the opposite side of the geomagnetic equator. At early times after burst when the debris region is relatively small (less than a few hundred kilometers in radius), beta-particle ionization can cause significant absorption for frequencies below a few gigahertz. At later times, when the debris is dispersed over large regions, the ionization is primarily important in causing absorption for frequencies below a few hundred megahertz.

[redacted] Estimates of D-region absorption caused by prompt and delayed radiation can be obtained from Figures 8-40 through 8-51.

17-4 Absorption of Noise [redacted]

[redacted] Receiving system performance also may be affected if noise normally reaching the system via the ionosphere is absorbed. The noise level of some systems is determined by external sources (atmospheric noise, cosmic noise, or interfering signals from other sources) that propagate energy through the atmosphere. Both the desired signal and the undesired signal may be attenuated. The resulting signal-to-noise ratio depends upon the exact location of terminals, noise source, and weapon-produced ionization.

17-5 Attenuation by Scattering and Beam Spreading [redacted]

[redacted] Attenuation by absorption results when energy from a radio wave is deposited in the propagation medium in the form of heat. A different class of attenuation is that due to scattering of radio energy from the desired direction to other (possibly widely different) directions. A fundamental requirement for scattering is that

[redacted]

the refractive index of the medium be structured. Thus, regions of high electron-density gradient (e.g., fireball boundaries and various regions containing plasma striations) are of prime concern.

Characteristics of the electron-density structure that are important are its strength (i.e., the magnitude of spatial variation) and its size or scale. Generally, the greater the variation (especially in the integral of electron density along the line of sight), the greater the portion of energy scattered, and, the smaller the structure, the wider the scatter cone. The scale, relative to two parameters of the operating system, the wavelength and the Fresnel-zone radius, determine the nature of the attenuation effects associated with this scattering.

As a practical matter, the environments of concern seem to divide naturally, leading to a useful separation of effects into attenuation by scattering and attenuation by signal reduction through beam spreading. The former, loss by scattering, implies scattering at angles that are substantially larger than the system beamwidth. The latter, beam spreading, implies scattering, defocusing, or diffraction at angles comparable to or less than the system beamwidth.

The simplest effects to visualize are those due to structure that is large compared with both the wavelength and the Fresnel zone. These effects are refractive in nature and can be understood on the basis of ray optics. Simple ray bending may apparently displace a radio source from an antenna beam, resulting in attenuation, unless the beam is made to track the source. A patch of enhanced plasma will cause such ray bending in its border regions. In the mid-region of such a patch, the ray bending is minimum, but the radio energy density is actually decreased by defocusing, even if the source is kept in beam center. In effect, the plasma patch acts as a radio-frequency diverging lens. A region of lower-than-average electron density, on the other hand, will act as a converging lens.

A region of plasma-density irregularities (e.g., fireball striations) may act as an ensemble of diverging and converging lenses, producing both attenuation and enhancement of signals. If the scale of the irregularities is small enough to be comparable with the system Fresnel zone at the range of the plasma, then they are too small to produce lenslike focuses, and the propagation must be treated by diffraction theory. The result regarding signal strength, however, still is to produce positive and negative fluctuations. This diffractive scatter can occur even if the irregularities are too weak to produce significant focuses or defocuses; the situation may be viewed intuitively as multipath propagation.

As the irregularity scale becomes smaller, the scatter cone becomes wider and can exceed the system beamwidth. In this case, not only will there be fluctuations in signal strength but also a net attenuation on the average. This net attenuation will occur whether the antenna achieves its directivity by employing a reflecting aperture (e.g., a dish antenna) or from phased elements distributed on the aperture (i.e., a phased array).

In the extreme, when the plasma structure becomes comparable in scale to the system wavelength, the radio energy is backscattered and lost to any receiver on the opposite side of the structured plasma, regardless of its antenna beamwidth. In this case, the attenuation effect is virtually indistinguishable from that due to absorption. Usually, the intensity of very small scale size fluctuations is small so that, although backscatter does occur — leading to radar clutter (paragraph 8-12) — such a small fraction of the energy goes into this phenomenon that the resulting attenuation of the primary beam is quite small. The presence of radar clutter does not necessarily imply that targets cannot be seen on the other side of the scattering region.

[redacted]

17-6 Effects of Reflection [redacted]

[redacted] In addition to absorption, another important cause of signal attenuation in the HF band is loss of reflection from the E- and F-regions of the ionosphere (see TRAVELING DISTURBANCE in Chapter 8). Signals that normally would be returned to the receiver continue on into space. Conversely, burst-induced ionization in the E- and F-regions of the ionosphere may increase the electron density and allow reflection of signals at higher frequencies than normal.

[redacted] INTERFERENCE [redacted]

17-7 Noise [redacted]

[redacted] Thermal noise radiated by the hot fireball can produce receiving-antenna noise temperatures of several thousand degrees Kelvin for tens of seconds to several hundred seconds, depending upon the fireball altitude. A system normally will not experience problems from fireball noise unless the fireball is large enough that the antenna beam is essentially filled by the fireball and that absorption outside the fireball is significant at the frequency of interest.

[redacted] Synchrotron noise may be associated with nuclear bursts that take place at very high altitudes or if the weapon debris rises to very high altitudes. The effect is noticeable only if a large number of electrons are trapped in the geomagnetic field outside the atmosphere. Only very sensitive HF receiving systems with upward-pointing antennas are likely even to detect synchrotron noise, but it may persist for weeks.

17-8 Reflection, Refraction, and Scatter [redacted]

[redacted] Reflection and refraction of electromagnetic (EM) waves can cause unwanted signals to reach the receiver. These signals can mask and distort desired signals. Multipath interference occurs when a desired signal travels two or more paths. The result is severe fading and distortion. HF and VHF systems operating in a nuclear-burst environment may experience unusual multipath conditions due to E- and F-region ionization, causing highly anomalous propagation modes with consequent signal distortion. Reflection from fireball surfaces may, under certain conditions, cause multipath in the UHF band.

[redacted] Signal scattering can occur as a result of irregularities in electron density. A radar signal scattered back to the receiver may mask desired target returns or may produce a false target. Signals from other transmitters may scatter into a receiver, increase the noise level, and mask desired signals. In general, scatter in and above the HF band is caused by fireballs and by beta-particle ionization regions.

[redacted] SIGNAL DISTORTION [redacted]

[redacted] Propagation media disturbances may change the characteristics of a signal and degrade system performance. Frequency shifts, time delays, angle-of-arrival deflection, and polarization rotation are all possible effects (see PHASE EFFECTS in Chapter 8). The results may include reduction of effective system bandwidth and increased error rates when the signal is processed by the system.

[redacted] Range and angular errors may be induced in radar systems by time delay and bending of the propagation direction. Generally, D-region ionization sufficient to produce signal distortion also will produce large absorption levels. At altitudes above the D-region, signal distortion (particularly range and angular errors) may occur at low or moderate absorption levels. Irregularities in electron density in and above the upper part of the D-region can change the direction of propagation and cause fluctuations in the angle of arrival of received signals (scintillation).

[redacted] The significance of a change in signal characteristics depends critically on the signal

[redacted]

processing employed and on the system mission. The effects are most likely to be significant in systems that feature extreme accuracy and sensitivity, and depend upon sophisticated waveform processing.

SECTION II
SYSTEM CHARACTERISTICS AND EFFECTS

Nuclear environments related to the various types of military engagements affect the propagation medium and noise production differently. A detailed analysis of nuclear effects depends on specifying all of the nuclear burst and system parameters, and is beyond the scope of this chapter. However, the kinds of effects and their spatial and temporal extent can be illustrated with a limited number of examples. These examples suggest the general nature of the nuclear effects for most practical cases and will assist in identifying critical system parameters.

VLF AND LF SYSTEMS

17-9 VLF and LF Propagation

Propagation at frequencies below about 1 MHz, i.e., in the VLF, LF, and part of the MF bands, is controlled by the D-region of the ionosphere. Under natural conditions, there is a distinct difference between propagation of VLF (10 to 30 kHz) and LF (30 to 300 kHz). At VLF, the distance between the earth and the ionosphere is only a few wavelengths, and it is natural to think of these two boundaries as the walls of a waveguide. The received field is then the sum of the normal modes that have propagated to the observation point. The quantities of interest are the excitation factor (the relative energy supplied to the mode by the transmitter), the attenuation rate (loss of energy per unit distance), and the phase velocity of each mode. If the ionosphere is less than about three wavelengths from the ground, the modes are almost equally excited, and the most important mode is always the mode of least attenuation. Lowering the ionosphere (which results from weapon-produced ionization) will usually increase the attenuation rate, and will increase the energy in the propagating modes. The effect on the total field strength depends on the trade off of these two effects. The different modes have different phase velocities, so if two modes are of almost equal strength, their sum will vary as a function of distance. The sum will be large where the two components are in phase and small where they are out of phase.

At frequencies above 30 kHz, the distance between the earth and the ionosphere is many wavelengths, and it is more convenient to think of the total field strength as the sum of the direct (or ground) wave, the first-hop skywave (energy reflected once from the ionosphere), the second-hop skywave (energy reflected twice from the ionosphere), etc. This is the same concept used at HF, but there is an important additional consideration. At LF, the downcoming skywaves diffract significantly around the curvature of the earth, so it is necessary to include them at distances that would be considered geometrically impossible at HF.

In the VLF and LF bands, the noise at the receiver is assumed to have an atmospheric source. It therefore depends upon season, time, and geographic location.

17-10 Effects of Nuclear Bursts on VLF and LF Systems

The effects on propagation of VLF and LF signals caused by nuclear detonations result from ionization produced in and below the D-region (see IONIZATION AND DEIONIZATION, Chapter 8). Usually the effects are caused by free electrons, but significant absorption also may result from ions. Depending on weapon type and burst location, prompt radiation (neutrons and X-rays) can produce D-region ioniza-

[redacted]

[redacted] tion in the general vicinity of the burst. Significant D-region ionization also can be produced in the burst region by delayed gamma rays from fission debris if the debris is above 25 kilometers altitude and by beta particles if the debris is above 60 kilometers altitude. Beta particles and Compton electrons (produced by gamma rays) can cause significant ionization in the region magnetically conjugate to the debris location. Under certain circumstances, ionization at locations very distant from the burst may result from neutron-decay betas and the dumping of trapped radiation.

[redacted] Blackout or complete disruption, of VLF and LF communication systems usually requires burst-produced ionization to affect a large portion of the propagation path. Since the propagation paths are typically many thousands of kilometers long, high-altitude detonations or multiple detonations dispersed over the propagation path are required to produce the necessary ionization. Degradation can be caused by reduction of signal amplitude and rapid changes in signal phase. The significance of phase changes to system performance depends critically upon the system characteristics.

[redacted] Usually the greatest change in signal amplitude and phase from preburst conditions occurs for nighttime conditions; however, there are little day-night differences for large weapon yields. Effects are not uniform over the frequency band. When there is sufficient ionization to cause low reflection altitudes, propagation near the lower end of the LF band appears to suffer the least degradation. When the reflection boundary is near normal height but diffuse, propagation near the lower end of the VLF band appears to be affected least. In some cases the ionization distribution along the propagation path is such that low reflection altitudes occur over part of the path and a diffuse reflection boundary over the remainder.

[redacted] In general, the longer the path length, the greater the probability of circuit degradation. Although there is a small probability that the signal-to-noise ratio may be increased, it will generally be reduced. Severe signal reductions can persist for hours, depending on the extent and kind of weapon-produced ionization. Equal reduction of signal and atmospheric noise may not influence system performance until the reduction in noise is so great as to render local receiver noise a determining factor.

[redacted] Phase shifts up to about 1,000 degrees per burst at rates as high as 1 degree per microsecond may occur for each burst. The rate of recovery is usually a few degrees per second. Systems that cannot follow these phase shifts will lose synchronization. Time to reestablish synchronization is very difficult to estimate, but may require tens of minutes or longer.

[redacted] The general effects of nuclear bursts on VLF and LF systems may be summarized as follows:

1. The most severe signal degradation and system outages of longest duration occur for widespread debris environments. This environment may be caused by a large-yield weapon detonated at high altitudes or by multiple detonations distributed over a large area.
2. An ionization impulse resulting from a very-high-altitude (even though low yield) detonation affects a wide area and may degrade LF system performance for tens of minutes. The propagation effects are greater at night than during the day.
3. Single detonations at altitudes below several hundred kilometers produce less severe signal degradation, unless the burst is close to the propagation path. Detonations near the surface (below about 30 km) have the least effect on VLF and LF propagation.

[redacted]

[redacted]

17-11 Spread-Debris Environment [redacted]

[redacted] Following nuclear bursts, debris can be spread over a large area if weapons are detonated above about 50 kilometers at dispersed locations. By assuming the debris to be uniformly distributed, a relatively simple model that provides useful estimates of propagation effects resulting from several bursts is obtained. The ionization affecting VLF and LF propagation is caused by beta and gamma radiation from the fission debris. This ionization can be characterized by the fission yield per unit area and the average age of the debris. Assuming the detonations occur within a few minutes of each other, a parameter w can be defined by

$$w = \frac{W_F}{A} \frac{1}{t^{1.2}},$$

where W_F/A is megatons of fission yield per square kilometer, and t is time after attack in seconds. A value for w of 10^{-7} represents a very severe attack environment. Values of w between 10^{-9} and 10^{-11} are representative of a wide range of attack conditions, and can apply over a considerable area even for relatively light attacks.

[redacted] Figure 17-2 shows the signal attenuation for a 4000 km path. For large values of w, the reflection altitude is low and propagation near the low end of the LF band is least affected. In the range of the more likely w value of 10^{-11} to 10^{-9}, the reflection boundary becomes more diffuse and propagation in the VLF band shows minimum effects. For daytime conditions the LF signal attenuations are somewhat smaller than for nighttime conditions when w is less than about 10^{-11}. Effects similar to those described for propagation beneath the debris occur on the opposite side of the geomagnetic equator as a result of beta-particle and Compton electron ionization (see paragraph 8-3).

[redacted] While the results shown are for that portion of a path under the debris, it should be noted that degradation effects will not be limited to this region. Gamma radiation will increase the size of the ionization region up to several thousand kilometers from the debris boundary. Propagation effects outside the debris region, while significant, depend on the details of the debris-path geometry.

17-12 Effect of a [redacted] 6300-km Burst

[redacted] Prompt radiation from [redacted] burst at 6300-km altitude (one earth radius) produces an impulse of ionization over a very large region. The extent of ionization is determined by the X-ray horizon, [redacted] DNA (b)(1)

[redacted] Figure 17-3 shows the signal attenuation for nighttime conditions on a 4000-km path. The ionization impulse produces a diffuse reflection boundary, and propagation near the lower end of the VLF band is affected less than at the higher end. [redacted] Attenuation caused by prompt radiation is much less in the daytime than at night. DNA (b)(1)

[redacted] The phase advance caused by the ionization impulse (for times greater than 1 second after burst) is shown in Figure 17-4. At the time of the burst, the phase advance is much larger, on the order of thousands of degrees occurring in a few milliseconds. DNA (b)(1)

[redacted]

[redacted]

[redacted]

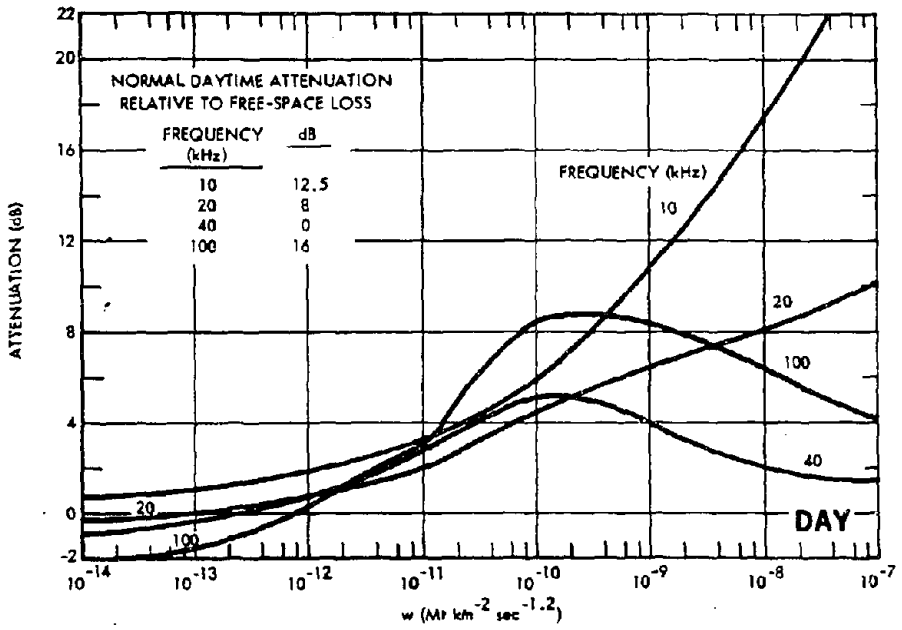

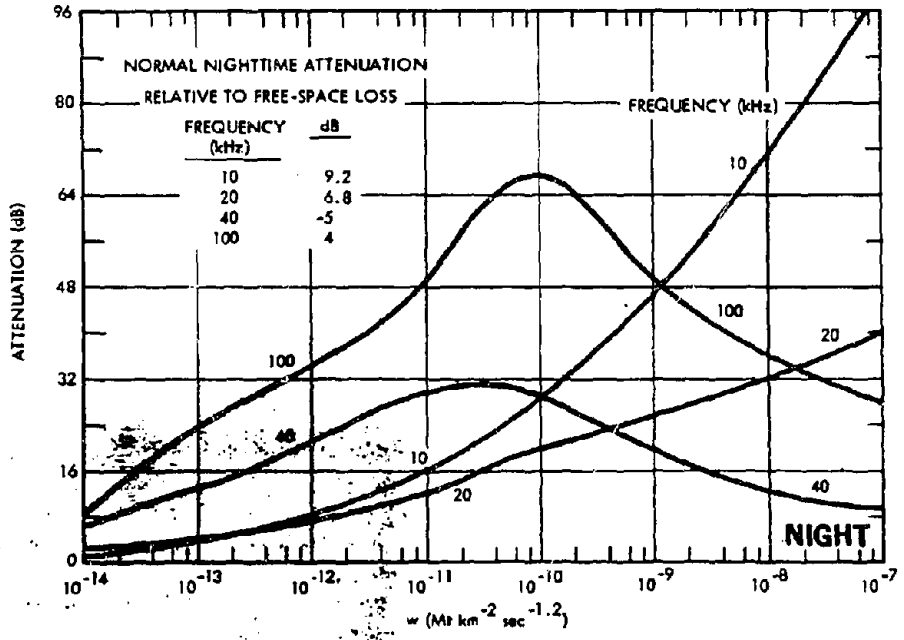

Figure 17-2. [redacted] Attenuation Related to Normal Loss Due to Spread-Debris Environment, 4000-km Path Length [redacted]

PAGES 17-11 THRU 17-12 DELETED DNA(b)(1)

[redacted]

[redacted]

17-13 Effect of Detonations Below About 300 km [redacted]

[redacted] If a nuclear burst occurs below 300 km, the portion of a propagation path that is affected is generally small unless the burst is close to the path. Depending on burst location and detonation altitude, there can be two degradation periods. The first period occurs at or within few minutes of burst time and is caused by prompt radiation and gamma radiation from the fission debris. The second period occurs when the fission debris has spread sufficiently that beta particles produce ionization along the path. In general, degradation is more severe in the LF band than the VLF band. An exception to this rule occurs during the first few minutes after a large-yield burst, which can produce intense ionization along the path that will cause low reflection altitudes.

[redacted] When a nuclear weapon is burst on the surface, ionization is limited essentially to the fireball region until the debris reaches altitudes above about 25 kilometers, where gamma radiation can penetrate the atmosphere. Even then, the extent of ionization affecting propagation is only a few hundred kilometers, and the effects are minimal. A large number of surface bursts, such as might occur during a nuclear war, could produce widespread ionization. Propagation effects similar to those described above for the case where the fission debris has spread to large distances would be expected for such conditions.

[redacted] HF SYSTEMS [redacted]

17-14 HF Propagation [redacted]

[redacted] Propagation at frequencies between about 1 and 60 MHz is supported by the F-region of the ionosphere. Generally speaking, the HF signal is a composite of many signals propagated along ray paths with different geometries. Figure 17-5 is an example of the ray-path geometry of a 4000-km path during the daytime at a single frequency. This multiple ray-path characteristic of HF is very important in any analysis of the susceptibility of a circuit to degradation from nuclear effects. Natural variations in the ionosphere affect the exact ray-path geometry at any specific time.

[redacted] Noise at HF comes from a variety of sources. Noise power in this frequency range has been conventionally calculated as a combination of propagated noise from thunderstorm centers (concentrated mostly in tropical areas) and man-made local noise. Atmospheric noise tends to be dominant at night when ionospheric absorption is less, whereas man-made noise may set the daytime level. Very often, however, the noise level is determined by other interfering signals because of congestion of the HF band. No means have been devised for quantitatively treating this latter and perhaps most important source of noise.

17-15 Effect of Nuclear Bursts on HF Systems [redacted]

[redacted] The most important phenomenon produced by nuclear bursts that affects HF systems is absorption resulting from D-region ionization. The ionization of the D-region is produced by prompt and delayed radiation. The amount of ionization depends on the altitude and the yield of the detonation (see IONIZATION AND DE-IONIZATION in Chapter 8). Persistent absorption results from delayed gamma radiation when the debris is above 25 kilometers, and from beta particles when the debris is above 60 kilometers. Beta particles and Compton electrons can produce significant absorption in the region magnetically conjugate to the debris location. D-region absorption can extend over several thousand kilometers and can be important for hours after burst. For detonations above about 100 kilometers, there are often two distinguishable absorption periods: one, which starts at burst time,

[redacted]

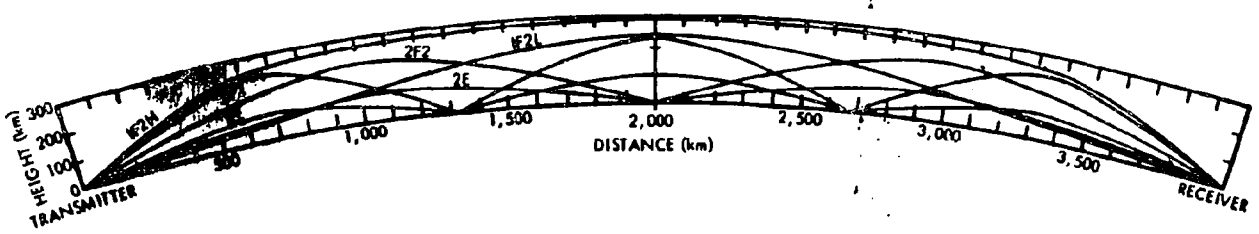

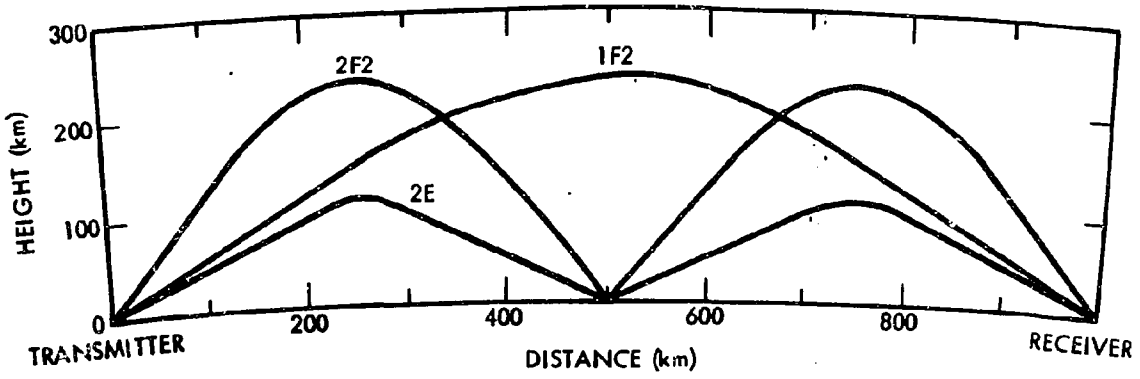

Figure 17-5. Examples of Daytime HF Ray-Path Geometry

[redacted]

[redacted] results from ionization caused by prompt radiation and delayed gamma rays; a second results from ionization caused by beta particles. This latter starts when the fission debris has spread sufficiently that beta particles can ionize the D-region at the location of the propagation path. The duration of absorption depends on weapon yield and design, frequency, and time of day. The duration may vary from a few minutes for a small-yield weapon burst at night to several hours or more for a large-yield weapon burst during the day.

[redacted] Detailed calculations of signal attenuation due to D-region absorption require the determination of the absorption for each ray path connecting transmitter and receiver. The procedures given in Chapter 8 (see Problems 8-5 through 8-7) can be used to determine the absorption when the ray path geometries are specified. Since D-region ionization does not alter ray-path geometry appreciably (see paragraph 8-10, Chapter 8), the pre-burst ray-path geometry can often be used in determining absorption. However, as discussed below, changes produced by the burst in the E- and F-region electron density can alter the number and location of ray paths, and thus can affect absorption calculations.

[redacted] Ionization produced by a nuclear burst and traveling disturbances in the E- and F-regions of the ionosphere can produce significant changes in the E- and F-region electron densities that can last for hours (see TRAVELING DISTURBANCES IN E- AND F-REGIONS OF THE ATMOSPHERE in Chapter 8). Changes in the E- and F-region electron density can result in significant multipath effects by increasing the available ray paths and by introducing off-great-circle propagation paths. The maximum usable frequency (MUF) may be much lower than normal after nighttime detonations for ray paths that pass within several thousand kilometers of the detonation. For certain geometries and burst conditions the MUF may be higher, perhaps up to 60 MHz. Current theoretical models do not provide reliable prediction of the MUF as a function of burst and system parameters. Oblique, frequency-sweep ionospheric sounders may allow determination of usable frequencies during disturbed conditions.

[redacted] While HF system performance usually will be degraded by nuclear bursts (often resulting in complete circuit outage for significant periods of time), there may be factors that tend to minimize the degradation. For example, a reduction in noise or interference may accompany a reduction in signal strength, thus tending to preserve the preburst signal-to-noise ratio. Higher frequency propagation may be possible because of increased E- and F-region ionization, and the higher frequency will be less susceptible to absorption.

[redacted] The general effects of nuclear bursts on HF systems are summarized below:

1. The higher the altitude of detonation, the greater and more widespread are the effects.
2. HF systems can recover from a nuclear attack, with nighttime recovery being much more rapid than daytime.
3. Intermittent propagation may occur even under severe circumstances, but the frequency range is not always predictable.
4. When ionization produced by weapon debris is not widespread (less than about 500 km) and the circuit is longer than a few thousand kilometers, the chances are good that continuous communication can be maintained after recovery from the prompt effects.
5. Multiple bursts occurring at dispersed locations and times can increase the degradation greatly and can reduce the sensitivity of the system to burst location.

The variations in the effects of nuclear bursts on

[redacted]

[redacted]

[redacted]

HF systems are illustrated by the descriptions of several specific examples in the following paragraphs.

17-16 Effect of Surface or Near-Surface Bursts [redacted]

[redacted] Single or closely spaced bursts may occur during attacks against ground targets. Weapon radiation initially is confined to a volume of space near the detonation point, and a fireball is produced that subsequently rises (see paragraph 1-12 and 1-20). Ionization produced by the burst is essentially confined to the fireball region until the fireball carries the fission debris above about 25 kilometers, where gamma radiation can penetrate the atmosphere and produce D-region ionization. The extent of this ionization is a sensitive function of debris altitude. Gamma rays produce ionization over about 200 km horizontal extent for a 1-Mt surface burst, and over about 400 km for a 10-Mt surface burst. Because the area of high absorption is small, multiple rays will be affected only if they have a common D-region intersection. In any situation where the signal propagates over multiple ray paths that are sufficiently separated in the vicinity of the absorbing area, there will be little if any effect. Calculations for long and intermediate path lengths show that it is very difficult to eliminate all propagating frequencies. In some cases it would be necessary to switch to lower rather than higher frequencies to avoid outage, but communications could be maintained.

[redacted] Signal attenuation caused by surface bursts can be severe for short paths since the D-region intersections of the ray paths are close together (see Figure 17-5). Communications on certain frequencies can be disrupted for a period of hours, especially during the day.

17-17 Effect of a [redacted] 30-km Burst [redacted]

DNA (b)(1)

[redacted] A [redacted] device detonated near an altitude of 30 kilometers has potential as a possible penetration aid. The detonation point is sufficiently high that gamma rays will produce moderately widespread ionization even at early times. By 5 minutes after detonation, the debris will have risen [redacted] and beta particles can escape the debris region. Therefore, both gamma rays and beta particles are important ionization sources. [redacted] For a typical burst location, there would be two periods of pronounced absorption; the first would occur during the initial debris rise, and the second would occur when the radiation from the spreading debris reaches critical D-region points. [redacted] Because the region of increased ionization for this example is comparable to the D-region spacing between ray paths, the sensitivity to exact burst position is less critical than it is for surface bursts. The effects are still relatively limited, however, and the communication degradation does depend upon the burst location and the propagation path length. [redacted]

DNA (b)(1)

DNA (b)(1)

DNA (b)(1)

[redacted]

[redacted]

[redacted]

17-18 Effects of a [redacted] 50-km Burst [redacted]

DNA (b)(1)

[redacted] The effects of an extremely large yield weapon can be illustrated by describing the effects of [redacted] at 50 kilometers. Ionospheric effects are widespread and severe in both the burst and the conjugate regions. The debris rises to approximately 150 kilometers in less than 10 minutes, and it spreads to nearly 600 kilometers radius within 15 minutes. Thereafter, the debris radius continues to increase slowly as a result of winds.

[redacted] The relatively high altitude and large yield of such a burst produce immediate and severe effects. [redacted] The size of the absorbing region is large enough that nearly all rays along a given propagation path will be affected simultaneously, causing path orientation and path length within the region to be unimportant. Absorption effects of a similar nature also can be expected in a region on the opposite side of the magnetic equator from the burst centered at the conjugate of the burst point.

DNA (b)(1)

[redacted] The shock wave from a nighttime explosion [redacted] can be expected to reduce the critical frequency of the reflection region [redacted] This condition will probably persist [redacted] after sunrise. [redacted] If the propagation path is offset from the burst, there can be an initial period of absorption as a result of prompt and delayed gamma radiation. This period might be followed by a period of recovery to near normal conditions, and then a second period of absorption would occur as the debris expands and beta particles affect the path. [redacted]

DNA (b)(1)

DNA (b)(1)

17-19 Effect of Multiple Multimegaton 150-km Bursts [redacted]

[redacted] Multiple multimegaton high altitude bursts represent conditions that may result from the employment of a ballistic missile defense system. The most significant effects on HF circuits are widespread prompt ionization, widespread and intense delayed radiation, and F-region modifications. The debris will be distributed over a large altitude region, with some debris reaching altitudes above 1000 kilometers. The geomagnetic field plays an important role in determining late-time debris location (see Problem 8-7, Chapter 8).

[redacted] If multiple multimegaton high altitude bursts occur, HF circuits will be interrupted over a very substantial area, essentially at burst time: [redacted] The duration of the outage for paths at these extreme ranges will be brief. [redacted] The particularly large radius of effects at early times results from the high altitude to

DNA (b)(1)

[redacted]

[redacted]

[redacted]

which the debris rises. Gamma radiation from the debris has a horizon of about 4000 kilometers from the burst points. Eventual expansion of the debris results in secondary outages when beta-particle ionization reaches a given path. In the region around the conjugate of the burst points beta-particle ionization is similar to that produced in the burst region. Compton electrons cause ionization which is less intense than that produced by gamma rays in the burst locale (see paragraph 8-3).

[redacted] The critical frequency of the reflection region probably will be affected out to about 1000 kilometers after many large yield high altitude bursts. Significant electron density enhancement may occur near the detonation points, and electron density depletion may occur at more remote locations [redacted]

DNA (b)(1)

17-20 Effect of a 1-Mt, 250-km Burst [redacted]

[redacted] A 1-Mt weapon burst at an altitude of 250 kilometers will result in significant propagation effects from prompt radiation, delayed radiation, and changes in the F-region. Debris will be distributed over a large altitude region; the geomagnetic field will affect the late-time debris location, with some debris being transported across the geomagnetic equator. Very intense and widespread effects will be produced on the ionosphere; hence there will be degradation of HF communication systems. However, because of the lower yield and somewhat shorter debris rise than in the case discussed in paragraph 17-18, the effects are more dependent on the location and length of the communication path. [redacted] Ionization caused by the betas emitted by the spreading debris from such a burst will result in prolonged outage of HF systems. The lowest frequencies will be out for the longest period of time. [redacted]

DNA (b)(1)

[redacted] During the nighttime, the rapid decay of D-region ionization results in rapid recovery of all HF communication circuits that are not affected by beta ionization. [redacted]

DNA (b)(1)

[redacted] Circuits within several thousand kilometers of the conjugate of the burst point will also experience significant degradation. The absorption caused by beta-particle ionization is similar to that described for the burst region.

[redacted] For this type of high-altitude burst, the E- and F-region electron densities may be increased in the region near the burst. [redacted]

DNA (b)(1)

[redacted]

[redacted]

[redacted] reduced below the MUF at distances beyond 500 kilometers from the burst.

17-21 Effect of a [redacted] 1000-km Burst [redacted]

DNA (b)(1)

[redacted] weapon burst at an altitude of 1000 kilometers would be primarily an anticommunication event. In spite of the small yield, the X-ray output is sufficiently large that even from an altitude of 1000 kilometers, significant ionization would be produced in the lower ionosphere.

[redacted] The radius of effects from such a burst is much greater than individual mode separation distances; thus, the exact ray path position, path length, and orientation are not important for distances less than approximately 2000 kilometers. [redacted]

DNA (b)(1)

[redacted] SATELLITE COMMUNICATION SYSTEMS [redacted]

[redacted] The basic elements of a satellite communication system consist of a ground-terminal transmitter, a satellite-borne repeater, and a ground-terminal receiver. Typically, the satellite-borne equipment provides only the functions of frequency translation and amplification; signal processing and demodulation take place at the ground terminals. Gigahertz frequencies and large bandwidths are typical of satellite communication systems, but some systems may operate in the VHF and lower UHF bands.

17-22 Effects of Nuclear Bursts on Satellite Systems [redacted]

[redacted] The nuclear bursts of primary importance to military satellite communication systems are those that produce an intense ionization region which is intersected by the propagation paths of the relay circuit. One of the principal effects of this ionization is absorption of the propagating signal. The region of significant ray-path absorption for communication satellites operating at several gigahertz is usually confined to the fireball; however, other important absorption regions may exist for some combinations of yield and burst altitude. (See Chapter 8 for a discussion of ionization and absorption regions produced by nuclear detonations.)

[redacted]

DNA (b)(1)

[redacted] D-region ionization produced by prompt and delayed radiation (beta particles and gamma rays) produces absorption that [redacted] depending on propagation frequency, burst altitude, and fission yield. Delayed gamma rays can affect propagation in the VHF band [redacted] The extent of D-region absorption caused by beta particles is determined by the debris expansion, and this absorption can affect propagation in the VHF and UHF bands [redacted]

DNA (b)(1)

[redacted] In modern low-noise receivers, it is often the noise appearing at the terminals of the receiving antenna that will set the limit on the overall performance of the system. As a result, fireball thermal noise can be significant in degrading the performance of satellite communication systems (see ELECTROMAGNETIC RADI-

[redacted]

[redacted]

[redacted] ATIONS in Chapter 8). The amount of electromagentic thermal radiation reaching the receiver antenna depends on the effective fireball temperature at the frequency of interest (a function of temperature and emissivity) and on the amount of attenuation between the fireball and the antenna. Antenna temperature generally will be less than the effective fireball temperature as a result of absorption that occurs outside the fireball and the effect of antenna gain in the direction of the fireball.

DNA (b)(1)

[redacted] The group time delay associated with signal propagation through a plasma usually is frequency dependent. This causes phase distortion of angle-modulated signals (frequency and phase modulation are forms of angle modulation), resulting in what is termed intermodulation noise. This frequency-dependent time delay, or dispersion, also results in envelope distortion for pulse transmission through a plasma. Hence, another effect of burst-produced ionization that may be of importance to angle-modulated multichannel satellite systems of large channel capacities is the intermodulation distortion noise. The strength of this intermodulation noise is determined largely by the integrated electron density along the ray path and the modulation parameters. Typically, it is the late-time, high-altitude fireball ionization that may give rise to this dispersion effect. Similarly, satellite digital-communication systems may encounter pulse distortion when propagating through burst-produced ionization, which in turn may result in large decoding error rates. The dispersive medium may affect pulse amplitude systems because of envelope distortion. The magnitude of the pulse distortion is determined by the integrated electron density along the ray path, the carrier frequency, and the pulse width.

[redacted] Time-variant time delays due to the structured and filament-like behavior of high-altitude fireball striations may be a possible source of degradation to satellite communication systems; no estimate has been made of these effects because of the lack of data from which to scale results. The effects of time-variant time delays would be to introduce channel noise of a nature similar to intermodulation noise or adjacent-channel interference.

17-23 Nuclear Effects on Two Typical Satellite Systems [redacted]

[redacted] Two hypothetical but typical satellite systems have been selected to illustrate many of the problems of satellite communication in a nuclear warfare environment. System A (see Table 17-1) represents a high-volume military communication system. The mission requires continuous coverage between virtually every pair of points on the earth's surface. The system provides a tactical quality of voice communications.

[redacted] System B (see Table 17-2) operates in the UHF band at 400 MHz. It employs an 8-hour circular communications orbit. The power requirements, antenna size, channel capacity, and grade of service provided represent a tactical, transportable communication system.

[redacted] The systems considered employ Frequency Division Multiplex-FM (FDM-FM) as a means of carrier modulation. Voice channels are frequency multiplexed onto a single baseband using subcarriers. This baseband is then applied to a linear frequency modulator to modulate the transmitter RF carrier.

[redacted]

[redacted]

Table 17-1. [redacted] Satellite Communications Link Description, System A [redacted]

System Parameters	Description
Frequency	4 GHz
Channel capacity	300 duplex channels
Baseband	60 to 1300 kHz
Modulation format	FDM-FM
RMS frequency deviation	0.9 MHz
FM threshold	12 dB
Ground antenna	80-foot dish
Ground transmitter power	10 kw
Ground receiver I-F bandwidth	15 MHz
Ground receiver system noise temperature	100°K
Satellite receiver noise figure	10 dB
Satellite antenna (toroidal pattern)	5 dB gain
Satellite transmitter power	25 watts
Satellite altitude (synchronous)	35,788 km

Table 17-2. [redacted] Satellite Communications Link Description, System B [redacted]

System Parameters	Description
Frequency	400 MHz
Channel capacity	12 duplex channels
Baseband	0 to 60 kHz
Modulation format	FDM-FM
RMS frequency deviation	27.4 kHz
FM threshold	12 dB
Ground antenna	30-foot dish
Ground transmitter power	10 kw
Ground receiver I-F bandwidth	0.672 MHz
Ground receiver system noise temperature	250°K
Satellite receiver noise figure	10 dB
Satellite I-F bandwidth	1 MHz
Satellite antenna (toroidal pattern)	-3 dB
Satellite transmitter power	20 watts
Satellite altitude (8-hour circular orbit)	13,896 km

[redacted] Table 17-3 summarizes outage times for the two systems [redacted]

DNA (6)(1)

DNA (6)(1)

[redacted]

[redacted]

Table 17-3. [redacted] Estimated Outage Times for Fireball Intersection of the Propagation Path [redacted]

Deleted

DNA (b)(1)

DNA (b)(1)

[redacted]

Figures 17-6 and 17-7 illustrate [redacted] two [redacted] degradation mechanisms: fireball absorption and fireball noise. Figure 17-6 shows signal-to-noise ratio for Systems A and B [redacted] The fireball is located such that the ray path traverses the fireball when it has stabilized in altitude. Figure 17-6 also shows, for reference, the absorption along the ray path. [redacted]

Figure 17-7 shows signal-to-noise ratio and received noise for Systems A and B [redacted]

[redacted] TROPOSCATTER COMMUNICATION SYSTEMS [redacted]

[redacted] Tropospheric forward-scatter communications are used for communications and military purposes in locations where the nature of the terrain makes other means of highly reliable communication difficult.

[redacted] Figure 17-8 shows the geometry for a troposcatter link. Propagation from transmitter to receiver is via scatter in the common volume in the troposphere.

17-24 Effects of Nuclear Bursts on Troposcatter Systems [redacted]

[redacted] Three potential sources of degradation of troposcatter communication systems are signal absorption, fireball thermal noise, and multipath interference via fireball scattering. [redacted] Since troposcatter systems typically operate between a few hundred MHz and a few GHz, only the regions of intense ionization will produce appreciable signal absorption. The ionization resulting

DNA (b)(1)

PAGES 17-23 THRU 17-24 DELETED
DNA (b)(1)

[redacted]

[redacted]

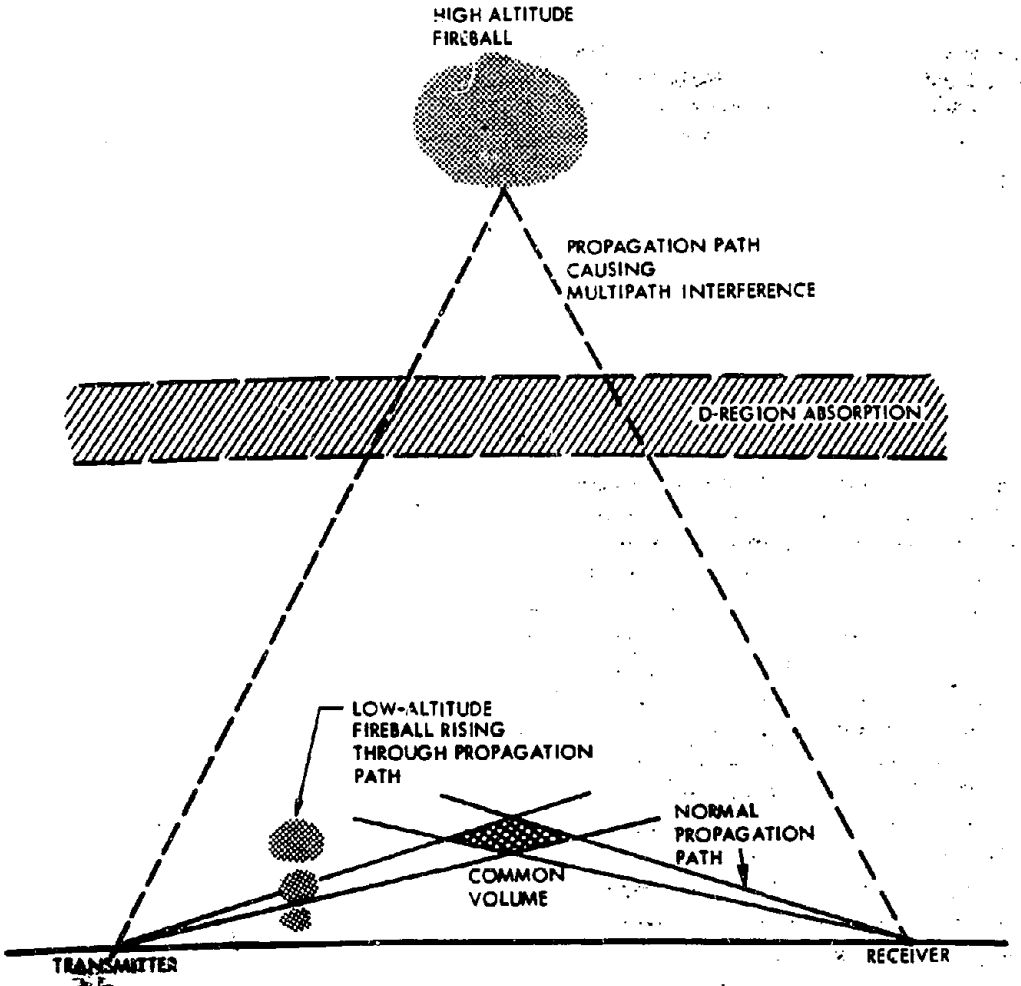

Figure 17-8. [redacted] Illustration of Troposcatter Geometry [redacted]

[redacted]

[redacted]

[redacted] from a low-altitude nuclear burst is largely confined to the immediate vicinity of the fireball; consequently, in order to obstruct troposcatter communications as a result of ray-path absorption, the fireball must be within the scatter path.

DNA (EX1)

[redacted] In low-noise receivers, fireball thermal noise may degrade the performance of troposcatter communication systems significantly. The amount of electromagnetic thermal radiation reaching the receiver antenna depends on the effective fireball temperature at the frequency of interest (a function of temperature and emissivity) and on the amount of attenuation between the fireball and antenna.

DNA (EX1)

[redacted]

[redacted] There are no significant differences between day and night effects for troposcatter systems.

17-25 Nuclear Effects on Three Typical Troposcatter Systems [redacted]

[redacted] Three typical troposcatter communication systems have been selected to illustrate propagation effects for selected weapon environments. System A is representative of a high-quality commercial scatter system; System B is representative of a tactical system; and System C is representative of a long-distance system. The system characteristics are summarized in Table 17-4.

[redacted] Table 17-5 summarizes the effects on the typical systems for several burst environments. There are essentially no differences between day and night effects. The amount of degradation depends on the fireball/debris geometry, which is variable with regard to size, shape, and location. The magnitude of multipath attenuation also depends on the antenna pattern (in the examples, the side-lobe gain was taken to be that of an isotropic antenna).

[redacted] IONOSCATTER COMMUNICATION SYSTEMS [redacted]

[redacted] Ionoscatter systems provide intermediate-distance radio service of 4 to 16 channels of teleprinter and/or a single voice channel. Figure 17-9 shows the geometry for an ionoscatter link. Propagation between transmitter and receiver occurs via scattering from a common volume in the D-region.

[redacted] The ionoscatter system considered here transmits at a continuous low data rate via a scatter signal that is always present, although weak and variable. The ionospheric scatter mode is fundamentally most suitable for low-data-rate teleprinter operations. High-quality voice communications via ionospheric scatter cannot be

[redacted]

[redacted]

Table 17-4. [redacted] Troposcatter Communication Link Description [redacted]

System Parameter	System A	System B	System C
Frequency	2 GHz	900 MHz	400 MHz
Path length	300 km average per hop, 6 hops	150 km, 1 hop	600 km, 1 hop
Channel capacity	120 channels	24 channels	12 channels
Power	10 kw	1 kw	100 kw
Antennas	80-foot dish	18-foot dish	120-foot dish
Antenna height	30 meters	30 meters	30 meters
Diversity	Quad, space	Dual, space	Quad, space
FM threshold	12 dB	8 dB	12 dB
Receiver noise figure	9 dB	9 dB	2.5 dB
Baseband	60-552 kHz	12-108 kHz	12-60 kHz
Modulation format	FDM-FM	FDM-FM	FDM-FM
RMS frequency deviation	362 kHz	63.5 kHz	35.3 kHz
I-F bandwidth	6 MHz	1.3 MHz	775 kHz

[redacted]

achieved with reasonable transmitter power.

[redacted] Ionoscatter systems typically operate at frequencies just above the E- and F-layer MUFs to eliminate multipath reflections and HF interference.

17-26 Effects of Nuclear Bursts on Ionoscatter Systems [redacted]

[redacted] As a result of their reliance on D-layer scattering mechanisms, ionoscatter systems are very susceptible to low-level residual ionization from a nuclear explosion. In view of the very small margin of operation above receiver threshold, usually limited by galactic noise, such systems are vulnerable to abnormal absorption along the scatter path and/or within the scattering volume. Prediction of effects in a nuclear environment is very difficult, because the ionospheric scatter phenomena in the natural environment are not well understood.

[redacted] The low frequencies employed by ionoscatter systems (about 35 to 50 MHz) allow appreciable absorption, even at low levels of residual ionization. Prompt radiation, delayed gammas from fission debris if the debris is above 25 km, and beta particles if the debris is above 60 km can all cause significant D-region ionization. If the debris is above 60 km, the betas will usually be more important than the gammas, and about one-half of the betas will be deposited in the region magnetically conjugate to where the debris is located. [redacted] DNA (b)(

[redacted]

[redacted]

Table 17-5. [redacted] Approximate Extent and Duration of Effects on Troposcatter Communications, Assuming Proper Burst Placement [redacted]

Deleted

DNA (b)(1)

DNA (b)(1) [redacted] Increased E- and F-region ionization caused by prompt radiation and traveling disturbances from a nuclear detonation may result in multipath effects, which decrease the effective bandwidth of ionoscatter circuits. [redacted]

DNA (b)(1) [redacted] Electromagnetic thermal radiation from fireballs is usually not important to ionoscatter systems because of the high ambient-noise environment.

17-27 Nuclear Effects on Typical Ionoscatter Systems [redacted]

[redacted] The ionoscatter system selected as an example uses two-frequency operation: 35 MHz for low transmission loss, and 60 MHz to avoid multipath interference at times of high solar activity.

[redacted] The system parameters are summarized in Table 17-6. For digital communication, the encryption and order of diversity are perhaps the most important parameters that influence system performance. Because of the large variations in system performance with path length, results for 1000-, 1500-, and 2000-km links are considered. The antennas of the system consid-

[redacted]

[redacted]

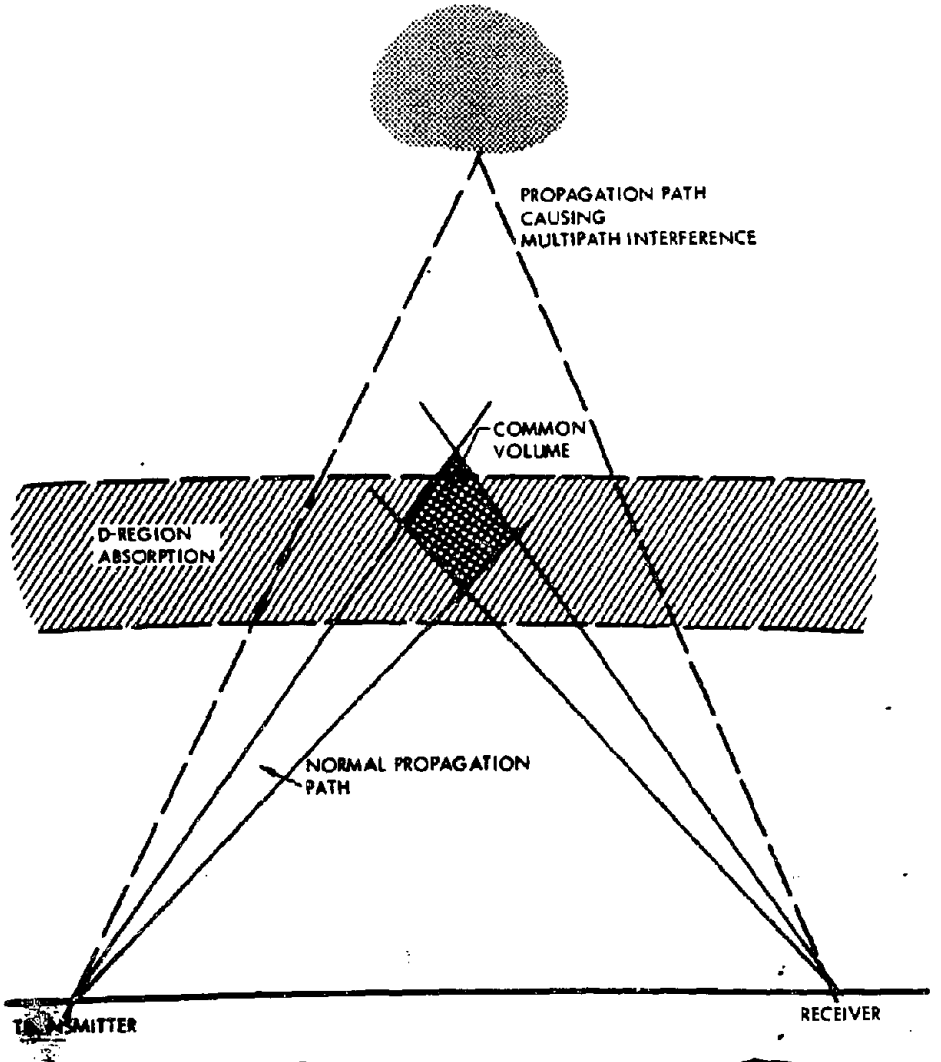

Figure 17-9. [redacted] Illustration of Ionoscatter Geometry [redacted]

[redacted]

[redacted]

Table 17-6. [redacted] Ionoscatter Communications Link Description [redacted]

System Parameters	Description
Frequency	35 or 60 MHz
Path lengths	1,000, 1,500, 2,000 km (three systems)
Channel capacity	16 channels, teletype
Power	60 kw
Antenna gain	19 dB
Antenna 3-dB beamwidths	45 degrees vertical, 11 degrees horizontal
Polarization	Horizontal
Diversity	Dual, space
Receiver noise temperature	450°K
Receiver noise bandwidth	1.2 kHz
Modulation format	TDM-FSK
Frequency shift	6 kHz mark-space
Demodulator	Dual filter, optimal without Doppler spread
Radiated signal element length	1.7 milliseconds
Transmission rate	600 bauds
Coding and synchronization	Standard 5-unit, start-stop neutral code

[redacted]

ered here are aligned along a great-circle path. Each terminal of an ionoscatter link is capable of duplex transmission.

[redacted] Table 17-7 summarizes the effects of several burst environments on the system described in Table 17-6. These effects show a strong dependence on the location of the burst with respect to the normal scatter path and on the scatter path length.

[redacted] Thermal noise from the fireball has negligible effect on this system because of the high cosmic noise levels. Effects of scattering from high-altitude fireballs, field-aligned ionization, or enhanced E- and F-region electron densities that may produce multipath interference are not included in Table 17-7 because the phenomena are not sufficiently understood.

[redacted] The most serious difficulty in predicting ionoscatter propagation characteristics in a nuclear environment is lack of understanding of the mechanisms involved in normal propagation.

[redacted] RADAR SYSTEMS [redacted]

[redacted] Radars are used in a wide variety of missions, including surveillance, target acquisition, navigation, tracking, fire control, discrimination between true targets and decoys, guidance and control, and fuzing. The radars may be ground-based or airborne. Their frequency usually is above the HF band with line-of-sight propaga-

[redacted]

[redacted]

Table 17-7. [redacted] Approximate Outage Times 1000-, 1500-, and 2000-km Ionoscatter Links, Assuming Proper Burst Placement [redacted]

Deleted

DNA (6-X(1))

[redacted]

tion paths. An exception is over-the-horizon radar (OTH or OHR), which operates in the HF band and uses E- and F-region refraction to detect objects at long ranges. Nuclear-weapon effects on over-the-horizon radars correspond to effects on [redacted] systems, described earlier in this section. OTH radars may be used for early detection of targets before detonation of nuclear weapons, and to provide supplementary information to ballistic missile defense radars at later times.

[redacted] The choice of parameters to be used (frequency, radiated power, antenna beam shape, pulse waveforms, etc.) depends on the function intended for the system. Acquisition radars are designed to maximize the initial detection range and angular coverage. These radars generally use lower frequencies than tracking systems and have less stringent requirements for measurement accuracy. Tracking and discrimination radars require high measurement accuracy, and they generally use as high a frequency as

[redacted]

[redacted]

possible. Discrimination radars may use complex waveforms and signal processing to estimate the nature of the incoming object. An important parameter related to radar susceptibility to nuclear-weapon effects is the altitude of the region of space (sometimes called the battle space) from which target echoes are to be received.

[redacted] In view of the different parameters and accuracy requirements for the different types of systems, the significance of weapon effects depends on the radar function. For example, fairly low levels of D-region ionization can cause sufficient absorption to reduce the initial detection range of an acquisition radar without affecting track radars. Levels of clutter, scintillation, and dispersion effects that are too small to affect acquisition radars may degrade discrimination radars seriously.

[redacted] Radars associated with detection of aircraft or surface targets usually will not experience signal degradation, since the propagation paths are below altitudes where persistent or widespread effects are caused by nuclear weapons (about 25 km). Fireballs from surface or air bursts may interdict the propagation path, but the small size of low-altitude fireballs and the relative motion between the rising fireball and the propagation path will usually limit outage to a few seconds. Blast, thermal, and nuclear radiation damage generally will be more significant for such systems when weapons are detonated close enough to interdict the propagation path.

17-28 Ballistic Missile Defense Systems [redacted]

[redacted] Ballistic missile defense (BMD) systems can be categorized conveniently according to the size of the region defended. Area and regional defense systems are designed to protect a large area, such as one or more cities. The functions of detection, tracking, and discrimination of incoming objects are performed at as great a range as possible to allow the area to be defended with a minimum number of radars and interceptor missile sites, and to minimize the damage to the defended area from detonation of intercept weapons. Initial detection ranges are typically a few thousand kilometers (approximately 10 minutes before impact of the incoming object). Intercept of those objects designed as threatening usually is above about 50 kilometers.

[redacted] Hardsite defensive systems are designed to protect a small area, usually hardened against direct damage effects (blast, thermal, etc.). Information concerning threatening objects may be transferred to the system from area defense radars. Since the defended site is hardened, intercept altitudes usually are below 30 kilometers and may be as low as a few kilometers. The system typically is designed to be able to perform acquisition, tracking, and discrimination functions after incoming objects are below 100 kilometers. High-performance interceptor missiles and data handling systems are used.

17-29 Nuclear Effects on Area Defense Systems [redacted]

[redacted] Nuclear weapon effects on area-defense radars may be caused by interceptor weapons (self-blackout) or by penetration aid weapons used by the offense. Although interceptor weapons are designed to minimize propagation effects on defensive radars, the use of a number of interceptor weapons in certain locations can cause significant problems. In the cases of area and regional defense systems, where interceptor detonation altitudes are high, the degradation mechanisms include absorption in the fireball and the D-region, scattering in the fireball and the E- and F-regions, noise, and clutter interference. Scattering and beam spreading can produce attenuation even in the absence of absorption; these propagation effects also produce scintillation of various kinds (amplitude, phase, angle, etc.). Receiver response to these effects will be similar to that associated with multipath. Absorption and scattering appear to be the most significant of the effects.

[redacted]

[redacted]

DNA (b)(1)

[redacted]

Whether the interceptor fireball will interdict the radar propagation path depends on the spacing of incoming objects, the interceptor weapon yield and detonation altitude, and the geometrical relation between the radar and the threat approach azimuth [redacted]

DNA (b)(1)

[redacted] D-region ionization caused by prompt and delayed radiation can be a significant cause of absorption, because for typical geometries the propagation path must traverse the D-region. D-region absorption scales inversely with frequency squared and is essentially negligible for frequencies above a few gigahertz. At a few seconds after burst, the most intense D-region absorption is caused by beta particles. As discussed in paragraph 8-4, the beta-particle ionization region is offset horizontally from the debris region by an amount that is determined by the orientation of the geomagnetic field and the height of the debris above the D-region. Intercept altitudes that place the beta-particle ionization region along the propagation path to successive objects can produce significant signal attenuation as a result of absorption after each intercept burst. Both the location of the ionization region and the propagation path are moving, and the duration of absorption is determined by the length of time the propagation path remains in the beta-particle ionization region. Refraction effects from D-region ionization are generally negligible, unless the level of ionization is large enough to also cause large signal attenuation.

[redacted] Prompt radiation from bursts detonated above about 100 kilometers increases the electron density in the E- and F-regions. The horizontal extent of the affected region depends on the burst altitude, weapon yield, and weapon design. While absorption resulting from E- and F-region ionization outside the fireball is small for radar frequencies, refraction or bending of the propagation path will cause angular errors. Even very small elevation and azimuth errors can result in significant interceptor miss distances.

[redacted] Interference and signal distortion also may be caused by noise (fireball thermal radiation), clutter, dispersion, and scintillation. While noise from fireball thermal radiation does not appear to be a significant problem for military radar systems, the conclusion should be reviewed for specific systems, particularly if low-noise receivers are used. Clutter returns can be orders of magnitude larger than target echoes and may mask the desired echo or appear as false targets. While it appears that antenna side-lobe rejection and doppler discrimination techniques can be used to reject clutter returns, these techniques may increase the data processing required by a substantial amount. Signal distortion caused by dispersion appears to be a secondary effect for acquisition and track radars, but it may degrade the performance of discrimination radars. Scintillation may cause pulse-to-pulse fluctuation in the apparent direction of the target. Computational models for scintillation are currently incomplete.

[redacted] The computational models given in Chapter 8 can be used to estimate fireball absorption for ray paths traversing the fireball or D-region. While effects other than absorption are discussed in Chapter 8, computational models are not given because of the complexity of the scaling. Analysis of radar performance in a nuclear environment usually is done with computer

[redacted]

[redacted]

[redacted]

codes to facilitate the large number of computations required.

[redacted] An example of the results of code calculations is provided below to illustrate the types of effects and the sensitivity of the effects to radar and burst parameters. The example is not intended to model an actual engagement, but it provides representative nuclear environments that might be produced by penetration aid or interceptor weapons. The geometry chosen for the example is shown in Figure 17-10. The threat trajectory (path of an incoming object) is in the direction of the geomagnetic field. One radar is located at the defended target and another is offset from the target to view the incoming object from the side. [redacted]

DNA (b)(1)

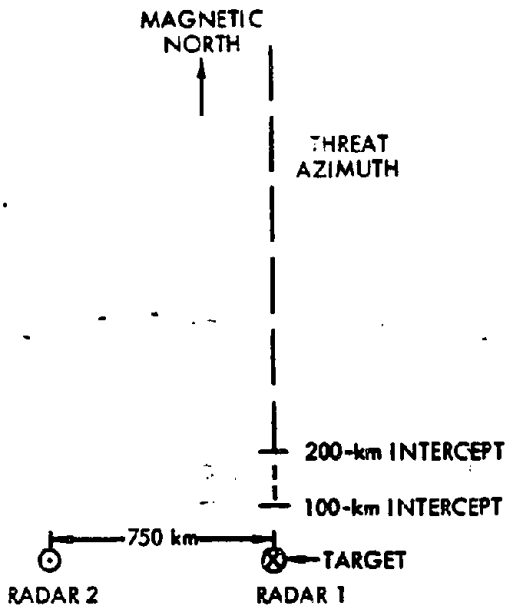

Figure 17-10. (U) Plan View of Radar and Target Geometry (U)

[redacted] As the incoming object approaches the target a series of nuclear bursts are assumed to occur at a fixed altitude on the trajectory. [redacted]

DNA (b)(1)

DNA (b)(1)

Figure 17-11 shows the signal-to-noise ratio and the elevation errors calculated for the radar located at the target. Results are shown for bursts occurring at two detonation altitudes. The propagation path from the radar to the incoming object traverses beta-particle ionization regions. [redacted]

DNA (b)(1)

As previously mentioned, refraction due to E- and F-region ionization can cause angular errors that affect the defense's ability to predict the location of incoming objects and perform intercepts. Figure 17-11 shows the elevation errors computed for the radar located at the target [redacted]

DNA (b)(1)

PAGE 17-35 DELETED
DNA (b)(1)

[redacted]

[redacted]

DNA (b)(1)

[redacted] Figure 17-12 shows the signal-to-noise ratios and elevation errors calculated for the offset radar. Because of the offset, the propagation path does not traverse beta-particle ionization regions or fireball regions, and signal attenuation is due to ionization caused by prompt radiation and delayed gamma radiation. [redacted]

DNA (b)(1)

[redacted] The above example does not show the dependence of system performance on the type of burst, the spacing and number of incoming objects, or the location of the threat azimuth with respect to the geomagnetic field, all of which can be significant. Further, the calculations for the example were based on the assumption that the phenomenology for each weapon was independent of previous weapons. [redacted] It is expected that modifications of burst phenomenology in a sequential-burst environment will be important. Models for such environment are under development (see Appendix E for code listings).

DNA (b)(1)

[redacted] some field simulation has been performed by releasing barium in the ionosphere (at altitudes between 100 and 200 km) in order to produce structured plasmas. The resulting plasma does not produce significant absorption, but it does tend to striate along the geomagnetic field to produce structure [redacted] This permits at least qualitative simulation of scattering effects. [redacted]

DNA (b)(1)

17-30 Nuclear Effects on Hardsite Defense Systems [redacted]

[redacted]

DNA (b)(1)

[redacted] The angular extent of the region obscured by the fireball is shown in Figure 17-13 as a function of detonation altitude for a typical sight line. The solid angle subtended varies as a function of time due to rise and expansion of the fireball (see Problem 8-1, Chapter 8). The magnitude of the variation is not great, however, and the values of solid angle shown in Figure 17-13 are representative of those occurring for the first few tens of seconds after detonation.

[redacted]

DNA (b)(1)

[redacted]

PAGE 17-37 DELETED
DNA (b)(1)

[redacted]

Deleted

DNA (b)(1)

Figure 17-13. [redacted] Solid Angle Obscured by 10-kt Intercept [redacted]

DNA (b)(1)

[redacted] Clutter returns and thermal noise from the fireball are potential degradation mechanisms for area defense systems. The use of narrowbeam antennas and signal processing will generally prevent degradation, but detailed analyses of system performance for specific scenarios and radar geometries are required.

[redacted] Penetration-aid weapons (precursors) detonated between about 20 and 50 kilometers can interfere with detection, track, and discrimination functions, and can reduce the reaction time available to the defense. [redacted] Denial of all information to the defense [redacted] is very difficult [redacted]

DNA (b)(1)

[redacted]

PAGE 17-39 DELETED

DNA (b)(1)

[redacted]

[redacted] BIBLIOGRAPHY [redacted]

Atmospheric Ionization and Effects on Radar and Communications, A Bibliography, DASA 2069, Defense Atomic Support Agency, Washington, D.C., January 1968 [redacted]

Electromagnetic Blackout Handbook (U), Second Edition, Volume I: *Guide to System Effects* [redacted] DASA 1580, Defense Atomic Support Agency, Washington, D.C., December 1964 [redacted]

Electromagnetic Blackout Handbook [redacted] Second Edition, Volume II: *Nuclear Weapons Effects* [redacted] DASA 1580-1, Defense Atomic Support Agency, Washington, D.C., February 1965 [redacted]

Knapp, W. S., and P. G. Fischer, *Aids for the Study of Electromagnetic Blackout*, DASA 2499, General Electric, TEMPO, Santa Barbara, Calif., July 1970 [redacted]

Nuclear Effects on HF Communications Systems [redacted] *Selected Examples*, DASA 1955-1, October 1967; *General Prediction Techniques*, DASA 1955-2, April 1968; Defense Atomic Support Agency, Washington, D.C. [redacted]

Nuclear Effects on VLF and LF Communications Systems [redacted] *Selected Examples*, DASA 1954-1, June 1968; *General Prediction Techniques*, DASA 1954-2, September 1968; Defense Atomic Support Agency, Washington, D.C. [redacted]

Nuclear Effects on Satellite and Scatter Communication Systems [redacted] *Selected Examples*, DASA 1956-1, October 1967; *General Prediction Techniques for Satellite Systems*, Vol. 1, DASA 1956-2, July 1968; *General Prediction Techniques for Scatter Systems*, Vol. 2, DASA 1956-2, October 1968; Defense Atomic Support Agency, Washington, D.C. [redacted]

RANC IV, Computer Simulation of Radar in a Nuclear Environment, Volume I, *Computational Models*, DASA 2497-1; Volume II, *Operational Data*, DASA 2497-2; Volume III, *Appendices*, DASA 2497-3; Defense Atomic Support Agency, Washington, D.C., prepared by General Electric Company-TEMPO, Center for Advanced Studies, Santa Barbara, California, July 1970 [redacted]

Weapon Effects Computer Code Directory, DASA 1727, Special Report 43, DASIAC, Santa Barbara, California, April 1969 [redacted]

Younker, E. L., et al., *VLF/LF Communications During a Major Nuclear Attack* [redacted] SRI 7045, DASA 2369, Stanford Research Institute, Menlo Park, California, September 1969 [redacted]

[redacted]

ADA955402

DTIC
ELECTE
2 MAR 1989
S D
E

AD-A955 402

APPENDIX A

SUPPLEMENTARY BLAST DATA

This appendix consists of two sections. Section I is a collection of equations and data useful in the study of shock waves. Section II contains a description of certain shock wave properties in a way that is intended to convey an understanding of these topics. None of the information in this appendix is required to solve the problems in Chapter 2 concerning blast phenomena or the blast related problems in the chapters of Part II of this manual. This appendix provides supplementary information, useful for solving special problems or for developing a better physical understanding of the phenomena described in Chapter 2.

The shock wave equations presented in this appendix are those that are most likely to be encountered in the study of air blast phenomena, and the concepts that are discussed are those that are most likely to be troublesome to the person who is studying shock wave theory for the first time.

This appendix presupposes a reasonable familiarity with the laws of mechanics and some understanding of how these laws apply to energy and momentum exchange in gases in motion.

SECTION I

MATHEMATICAL DESCRIPTION OF THE SHOCK FRONT

Most mathematical descriptions of shock wave phenomena are focused on the shock front itself since shock front conditions are fairly easy to treat mathematically, but the characteristics of the waveforms that follow the front are not. This limitation is not serious for many types of calculations, because the strength of the shock front is usually the best indicator of the severity of the entire shock wave.

In the absence of direct, simple mathematical techniques, analysis of the shock waveform usually depends on empirical data such as the predetermined shock waveforms shown in paragraph 2-12, Chapter 2. Numerical integration of shock wave problems on a computer provides an alternate method. The computer codes for blast waves from nuclear weapons incorporate the details of weapon configuration, radiation transport, and hydrodynamics; these codes are complex and their characteristics will not be discussed here.

A-1 The Rankine-Hugoniot Equations

A set of three equations governing shock front behavior may be derived from the laws of mechanics. These equations (or any set of three independent equations derived from them) are called the Rankine-Hugoniot equations. They do not completely specify shock front behavior; a fourth equation, the equation of state of the material, is necessary to specify the complete behavior of the shock front. However, these equations have the advantage of being valid for all conditions under which a shock front can occur. They apply equally well to shock waves in solids and in gases.

The equations given below outline the conventional derivation of the Rankine-Hugoniot equations. The same set of equations are derived in Section II in a manner that requires less algebra but more physical reasoning. The three conservation equations that lead to the Rankine-Hugoniot equations involve the so-called jump conditions across a shock front. The parameters involved are illustrated in Figure A-1.

REPRODUCED BY
U.S. DEPARTMENT OF COMMERCE
NATIONAL TECHNICAL
INFORMATION SERVICE
SPRINGFIELD, VA 22161

[redacted]

QUALITY INSPECTED 4

UNANNOUNCED

Accession For
NTIS GRA&I
DTIC TAB
Unannounced
Justification
By
Distribution/
Availability Codes
Dist | Avail and/or Special
A-1

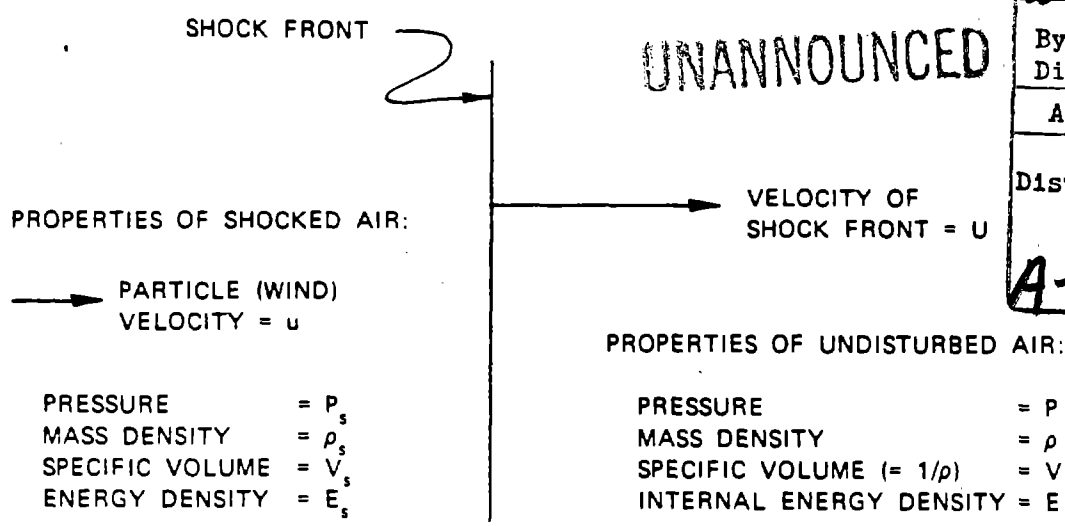

Figure A-1. (U) Change in Air Properties Across a Shock Front [redacted]

[redacted] An equation for the conservation of mass states that the mass of air per unit time overtaken by a unit area of the shock front is equal to the mass of air per unit area per unit time added behind the shock front.

$$\rho U = \rho_s(U - u),$$

where ρ is the ambient air density, U is the shock velocity, ρ_s is the density of the air behind the shock front, and u is the peak velocity of the air behind the shock front.

[redacted] Newton's second law states that force is equal to the rate of change of momentum. The force per unit area acting to accelerate the air entering the shock front is the overpressure, $\Delta p = P_s - P$, where P_s is the absolute pressure behind the shock front and P is the ambient pressure. The mass per unit time that enters a unit area of the shock front is ρU. The change of velocity of the air is u. Thus,

$$\Delta p = P_s - P = \rho U u.$$

[redacted] Conservation of energy requires that the work done while the shock front moves through a unit mass of air, $P_s\ (V - V_s)$, must equal the kinetic energy imparted to the unit mass of air, $u^2/2$, plus the change in internal energy, $E_s - E$, where the various symbols are defined in Figure A-1. Thus,

$$P_s \Delta V = (u^2/2) + (E_s - E),$$

or

$$P_s(V - V_s) = (u^2/2) + (E_s - E).$$

Using the relations $V = 1/\rho$ and $V_s = 1/\rho_s$, a simultaneous solution of these three equations leads to the Rankine-Hugoniot equations in their usual form:

$$E_s - E = \frac{1}{2}(P_s + P)(V - V_s),$$

$$u = \left((P_s - P)(V - V_s)\right)^{1/2},$$

$$U = V\left(\frac{P_s - P}{V - V_s}\right)^{1/2}.$$

[redacted]

[redacted]

A-2 Equation of State of an Ideal Gas [redacted]

[redacted] A gas that is heated at constant volume does not do external work; therefore, all of the thermal energy added to the gas is converted to internal energy. This amount of energy is

$$\Delta E = C_V \Delta T$$

where ΔE is the change in internal energy per unit mass, C_V is the specific heat of the gas at constant volume, and ΔT is the temperature change. By definition, the specific heats of an ideal gas are constant; and the internal energy per unit mass is

$$E = C_V T,$$

where T is absolute temperature.

[redacted] Using the thermodynamic identities $PV = RT$, and $C_P - C_V = R$ (where C_P is specific heat at constant pressure, and R is the universal gas constant) the following equation follows:

$$E = \frac{C_V PV}{C_P - C_V} = \frac{PV}{\gamma - 1}$$

where

$$\gamma = \frac{C_P}{C_V}.$$

Eliminating the variables E_s and E makes it possible to use the Rankine-Hugoniot equations to determine the conditions across a shock front in an ideal gas uniquely.

[redacted] The significance of the quantity γ as it appears in the shock wave equations deserves some explanation. In thermodynamics, γ appears most frequently in equations that involve isentropic compression. For example, γ appears in the equation for sound speed because sound wave pressure fluctuations are isentropic. The presence of γ in shock wave equations is sometimes incorrectly interpreted as implying a relationship between shock wave compression and isentropic compression; actually, γ is a convenient constant relating energy content of a gas to pressure and volume. This fact becomes important in paragraph A-6 where strong shock waves are discussed. Variations in the value of γ must then be considered, and the equations

$$\Delta E = C_V \Delta T, \text{ and}$$

$$E = C_V T$$

cannot hold simultaneously. Conveniently, γ is redefined, so the equation

$$\Delta E = C_V \Delta T$$

still may be used. The meaning of γ as a specific heat ratio is lost, and γ becomes simply a constant in the energy equation.

A-3 Shock Wave Equations for an Ideal Gas (U)

[redacted] From the relation for the speed of sound in ambient air,

$$c = (\gamma P/\rho)^{1/2}$$

and the equation for overpressure,

$$\Delta p = P_s - P$$

the set of shock wave equations shown in Table A-1 can be derived. The equations in the right hand column were obtained by assigning to γ the value 1.4, the value for air at moderate temperatures and pressures.

[redacted] These ideal gas equations apply to shock

[redacted]

[redacted]

Table A-1. [redacted] Shock Wave Equations for an Ideal Gas [redacted]

Equations in General Form:	Equations for $\gamma = 1.4$
Velocity of the Shock Front	
$U = c\left(1 + \frac{\gamma + 1}{2\gamma} \cdot \frac{\Delta p}{P}\right)^{1/2}$	$U = c\left(1 + \frac{6\Delta p}{7P}\right)^{1/2}$
Particle Velocity Behind the Shock Front	
$u = \frac{\Delta p}{\gamma P} \cdot \frac{c}{\left(1 + \frac{\gamma + 1}{2\gamma} \cdot \frac{\Delta p}{P}\right)^{1/2}}$	$u = \frac{5\Delta p}{7P} \cdot \frac{c}{(1 + 6\Delta p/7P)^{1/2}}$
Density Ratio Across the Shock Front	
$\frac{\rho_s}{\rho} = \frac{2\gamma + (\gamma + 1)\Delta p/P}{2\gamma + (\gamma - 1)\Delta p/P}$	$\frac{\rho_s}{\rho} = \frac{7 + 6\Delta p/P}{7 + \Delta p/P}$
Dynamic Pressure Behind the Shock Front	
by definition, $q = \frac{1}{2}\rho_s u^2$	
$q_s = \frac{(\Delta p)^2}{2\gamma P + (\gamma - 1)\Delta p}$	$q_s = \frac{5}{2} \cdot \frac{(\Delta p)^2}{7P + \Delta p}$
Temperature Behind the Shock Front	
$T_s = T\left(1 + \frac{\Delta p}{P}\right)\frac{2\gamma + (\gamma - 1)\Delta p/P}{2\gamma + (\gamma + 1)\Delta p/P}$	$T_s = T\left(1 + \frac{\Delta p}{P}\right)\frac{7 + \Delta p/P}{7 + 6\Delta p/P}$
Peak Reflected Overpressure at Normal Incidence	
$\Delta p_r = 2\Delta p + (\gamma + 1)q$	$\Delta p_r = 2\Delta p\,\frac{7 + 4\Delta p/P}{7 + \Delta p/P}$

[redacted]

[redacted]

[redacted] waves in air provided the shock strength, $\xi = (\Delta p + P)/P = P_s/P$, is not too large. Usually these equations are assumed to hold for shock strengths of about 10 (132 psi overpressure at sea level) or less; note that at high altitudes this limit corresponds to relatively low overpressures, e.g., about 25 psi at 40,000 ft. The equations for high pressure shock waves are given in paragraph A-6.

[redacted] As shown in Figure A-1, the subscript s denotes conditions behind the shock front; the absence of a subscript denotes ambient conditions (the subscript o is reserved for ambient conditions at sea level as in Chapter 2). The overpressure is $\Delta p = P_s - P$; c is the speed of sound in undisturbed air; and γ is the ratio of specific heats C_P/C_V. Other quantities are defined by subheadings in the table.

A-4 Units, Constants, and Conversion Factors [redacted]

[redacted] Since the most commonly used shock wave equations are written in terms of dimensionless ratios, the choice of units is purely a matter of convenience; therefore, there is an inclination to ignore the fact that certain equations must be handled more carefully. Examples of these equations are the Rankine-Hugoniot equations and the dynamic pressure equation. Three consistent sets of units in common use are shown in Table A-2. Conversion factors and sea level values of various parameters are given in the various units in Appendix B.

A-5 Equation of State of Air [redacted]

[redacted] As air is heated by the compression of strong shock waves, the specific heat ratio γ decreases. Therefore, the equation that gives γ in terms of the ratios of the specific heats, which is based on the assumption of a constant γ, is no longer valid. The means of avoiding this problem has already been stated in paragraph A-2: γ_s customarily is *redefined* as that number which gives the correct value for internal energy. Since γ appears frequently in shock wave equations to replace an energy term, the new definition is a convenient one. Note, however, that (except in undisturbed air, where the new and old definitions of γ agree) γ is no longer the specific heat ratio. Therefore, γ should not be used (for example) to calculate sound speed in strongly shocked air.

Table A-2. [redacted] English and Metric Systems of Units [redacted]

Unit	mks	cgs	English
length	meter	centimeter	foot
mass	kilogram	gram	pound
force	newton	dyne	slug
time	second	second	second
pressure	newtons/m^2	dynes/cm^2	pounds/ft^2
density	kg/m^3	g/cm^3	slugs/ft^3
velocity	m/sec	cm/sec	ft/sec
energy	joule	erg	ft-lb

[redacted] Figure A-2 shows the equation of state of air for altitudes up to 240,000 feet. The nearly vertical curves are the Hugoniot curves for air at the indicated altitudes. The Hugoniot curve for a given altitude shows the combinations of peak pressure and peak density that are possible behind a shock front moving into undisturbed air, i.e., into air that is initially at the ambient pressure and density corresponding to that altitude. Curves that show the value of γ assigned to the air just behind the shock front cross the graph as nearly horizontal lines. The curves that cut diagonally across the graph show absolute pressure (not overpressure) just behind the shock front. The ordinate of the graph is shock strength, which was defined in paragraph A-3.

A-6 Equations for Strong Shock Waves in Air [redacted]

[redacted] For shock strengths of 10 or more, accurate calculations must use the nonideal equation

[redacted]

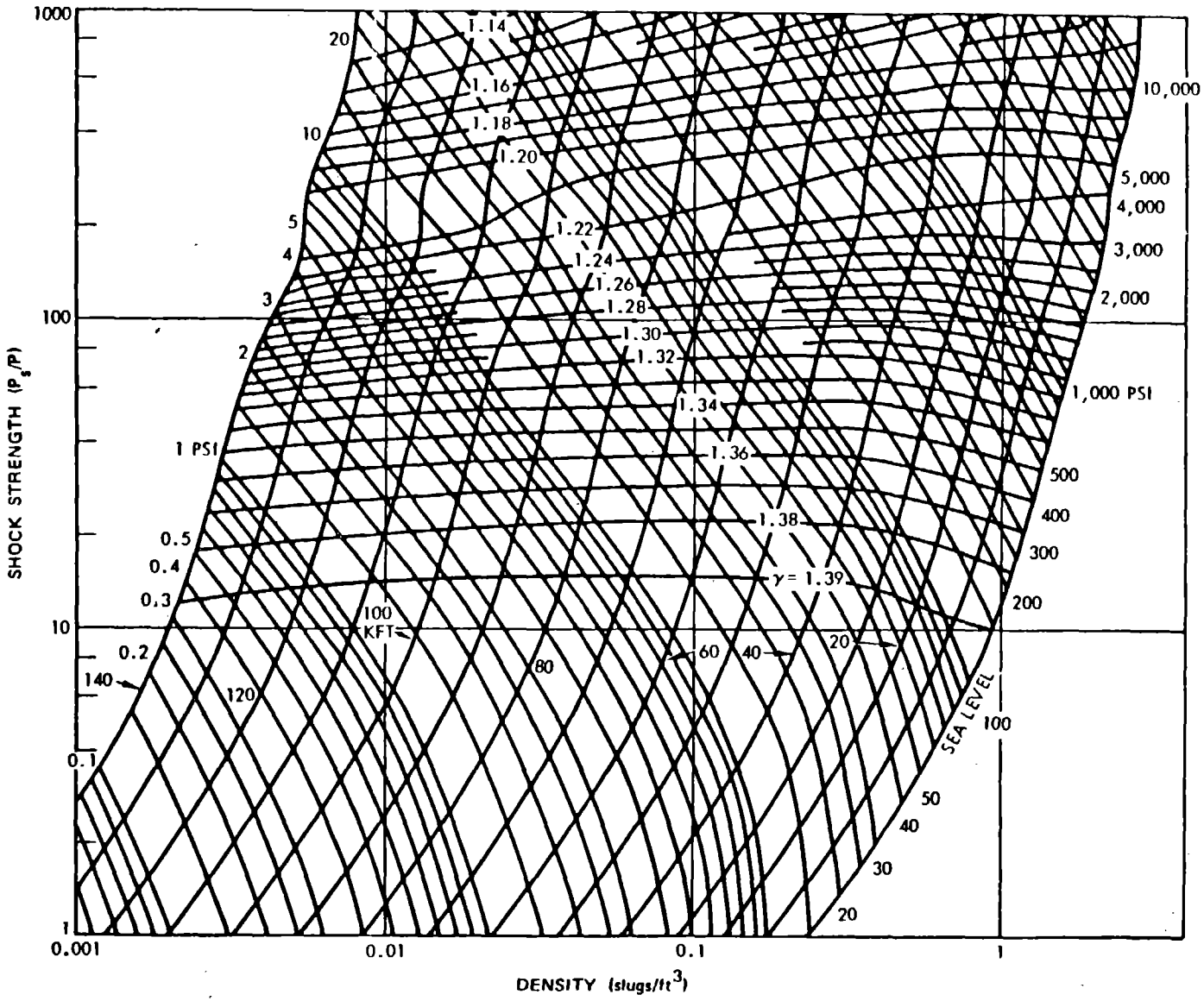

Figure A-2. [redacted] Equation of State Data for Air [redacted]

[redacted]

[redacted]

of state data from Figure A-2. The appropriate shock wave equations are derived in the same manner as those shown in Table A-1. The principal difference is that two values of γ appear, γ for the air ahead of the shock and γ_s for the air just behind the shock front; the values in general are not equal. The shock wave equations for strong shock waves in air are listed in Table A-3. Two approximate velocity equations, accurate to within about 5 percent for shock strengths greater than 5, are shown on the right. As in Table A-1, the subscript s refers to parameters behind the shock front, and symbols with no subscript refer to ambient conditions.

[redacted] Note that shock strength ξ is a direct function of the absolute pressure P_s behind the shock front, rather than of Δp, the overpressure.* A shock strength of 1 therefore represents a vanishingly weak shock wave: and, at sea level, a shock strength of 2 represents an *overpressure* of 14.7 psi. Values for γ_s must be obtained from the equation of state data in Figure A-2.

* [redacted] This definition is not universal; shock strength is defined in some reports as $\Delta p/P$.

Table A-3. [redacted] Equations for Strong Shock Waves [redacted]

Complete Equation:	High-Shock-Strength Approximation:
Velocity of the Shock Front	
$U = c\left(\frac{(\xi - 1)(1 + \mu_s\xi)}{\gamma[\xi(\mu_s - 1) - (\mu - 1)]}\right)^{1/2}$	$U = c\left(\frac{\xi(\gamma_s + 1)}{2\gamma}\right)^{1/2}$
Particle Velocity Behind the Shock Front	
$u = c\left(\frac{(\xi - 1)[\xi(\mu_s - 1) - (\mu - 1)]}{\gamma_o(1 + \mu_s\xi)}\right)^{1/2}$	$u = c\left(\frac{2\xi}{\gamma(\gamma_s + 1)}\right)^{1/2}$
Density Ratio Across the Shock Front	
$\frac{\rho_s}{\rho} = \frac{1 + \mu_s\xi}{\mu + \xi}$	
Dynamic Pressure Behind the Shock Front	
$q_s = \frac{1}{2}P(\xi - 1)\left(\frac{1 + \mu_s\xi}{\mu + \xi} - 1\right)$	

where

$$\mu_s = \frac{\gamma_s + 1}{\gamma_s - 1}, \quad \mu = \frac{\gamma + 1}{\gamma - 1}, \quad \xi = \frac{P_s}{P} = \left(\frac{\Delta p + P}{P}\right), \quad \gamma = 1.4$$

[redacted]

[redacted]

SECTION II

[redacted] PHYSICAL DESCRIPTION OF SHOCK WAVE BEHAVIOR [redacted]

[redacted] Newton's second law, which relates force to the change in momentum that it produces, provides straightforward explanations of many shock wave phenomena. In particular, it explains certain reflection phenomena and the way in which these phenomena determine the forces produced by a blast wave when it strikes a surface or a small object.

[redacted] Acoustic theory also provides explanations of blast phenomena. These explanations are important because they appear frequently in discussions of shock wave reflection. The following discussion relates the acoustic theory explanations with those that are based on Newton's second law.

A-7 Step Function Shock Wave [redacted]

[redacted] In most respects, the properties of the shock front are independent of the shape of the pressure waveform that follows the front. Shock wave phenomena, therefore, can be explained in terms of the simplest possible waveform: a region of completely uniform pressure, density, and particle velocity behind a planar shock front. In such a wave, the shock front usually is considered a mathematical discontinuity, in which the pressure, velocity and other parameters are step functions of position and time.

[redacted] This type of simple shock wave may be generated by the mechanism shown in Figure A-3. A piston moves at constant velocity in a frictionless cylinder (a piston velocity of 431 ft/sec, a number that will be used later for purposes of illustration, produces a shock wave with

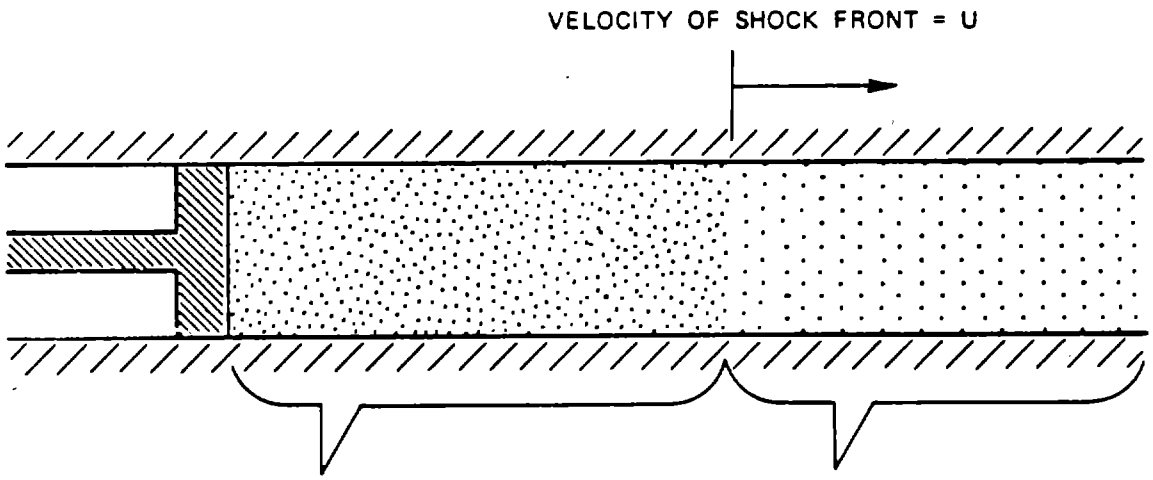

CONDITIONS BEHIND SHOCK FRONT:

PARTICLE (WIND) VELOCITY = u
DENSITY = ρ_s
PRESSURE = P_s
ENERGY PER UNIT MASS = E_s

CONDITIONS IN AMBIENT AIR:

PARTICLE VELOCITY = 0
DENSITY = ρ
PRESSURE = P
ENERGY PER UNIT MASS = E

Figure A-3. [redacted] Idealized Shock Wave [redacted]

[redacted]

[redacted]

[redacted]

an overpressure of 10 psi). The compressed air that constitutes the shock wave is uniform in density, pressure, and velocity.

[redacted] The step function shock wave differs from the blast wave from a nuclear burst in that the latter: (1) becomes weaker as it propagates away from the burst; (2) produces a decaying rather than a constant overpressure after the shock front passes a given point; and (3) has a spherical rather than a planar shock front. However, these differences are unimportant in the development of most of the concepts that apply to the shock front. As a result of its long overpressure duration, the blast wave from a high yield nuclear weapon is in many respects comparable to the idealized shock wave of Figure A-3.

A-8 Shock-Front Formation [redacted]

[redacted] The piston shown in Figure A-3 will require an interval of time to reach its final velocity. While it is accelerating, the pressure at the face of the piston will increase steadily. The pressure wave that the piston generates during this time lacks the abrupt pressure rise characteristic of a shock: however, differences in the velocities of different parts of the pressure wave ultimately will cause a shock front to form. Small pressure disturbances travel at the local speed of sound. In the air compressed by the piston, two factors cause this speed to differ from the speed of sound in ambient air; (1) compression of the air raises the air temperature, thereby increasing the speed of sound; (2) in moving air, pressure disturbances move with a velocity that is the vector sum of the air and sound velocities.

[redacted] As the piston starts to move, it creates an initial pressure disturbance that propagates ahead of the piston (to the right in Figure A-3) with a velocity equal to the velocity of sound in ambient air. By the time the piston reaches its final velocity, it will have produced a pressure wave that can propagate considerably faster than the ambient speed of sound. The wave produced by the high pressure just ahead of the piston soon overtakes the lower pressure wave, and a shock front is formed.

[redacted] After steady-state conditions are reached, the shock front moves at supersonic velocity with respect to the undisturbed air but at subsonic velocity with respect to the air behind the shock front. Ahead of the shock front, there is no early pressure increase to indicate the impending arrival of the shock wave. If such an early pressure wave were present, the shock front would overtake it. Behind the shock front, whatever pressure irregularities that may form can overtake the front and merge with it. The tendency for all pressure gradients to concentrate at the shock front is so strong that moderately strong shock waves in air generate shock fronts that are only a few atomic mean free paths (mfp) thick (at sea level, 1 mfp is about 10^{-5} cm).

A-9 Pressure-Momentum Interaction at a Shock Front [redacted]

[redacted] Before applying Newton's second law to a reflection problem, it will be examined with respect to a step function shock wave shown in Figure A-4. This is a simple problem that requires little more than a sample calculation. It is, however, useful as a preparation for the reflection problem that is discussed below. Numerical values of pressure, density, and velocity, calculated from the equations in Table A-1, appear in the figure.

[redacted] To evaluate Newton's second law, it is necessary to determine the momentum change per unit time and the force that produces the change. If a unit area of the shock front is considered, the force is numerically equal to the shock wave overpressure Δp, which in this example is 10 psi. To obtain a consistent set of units, this pressure must be expressed as 1,440 lbs/ft^2.

[redacted]

[redacted]

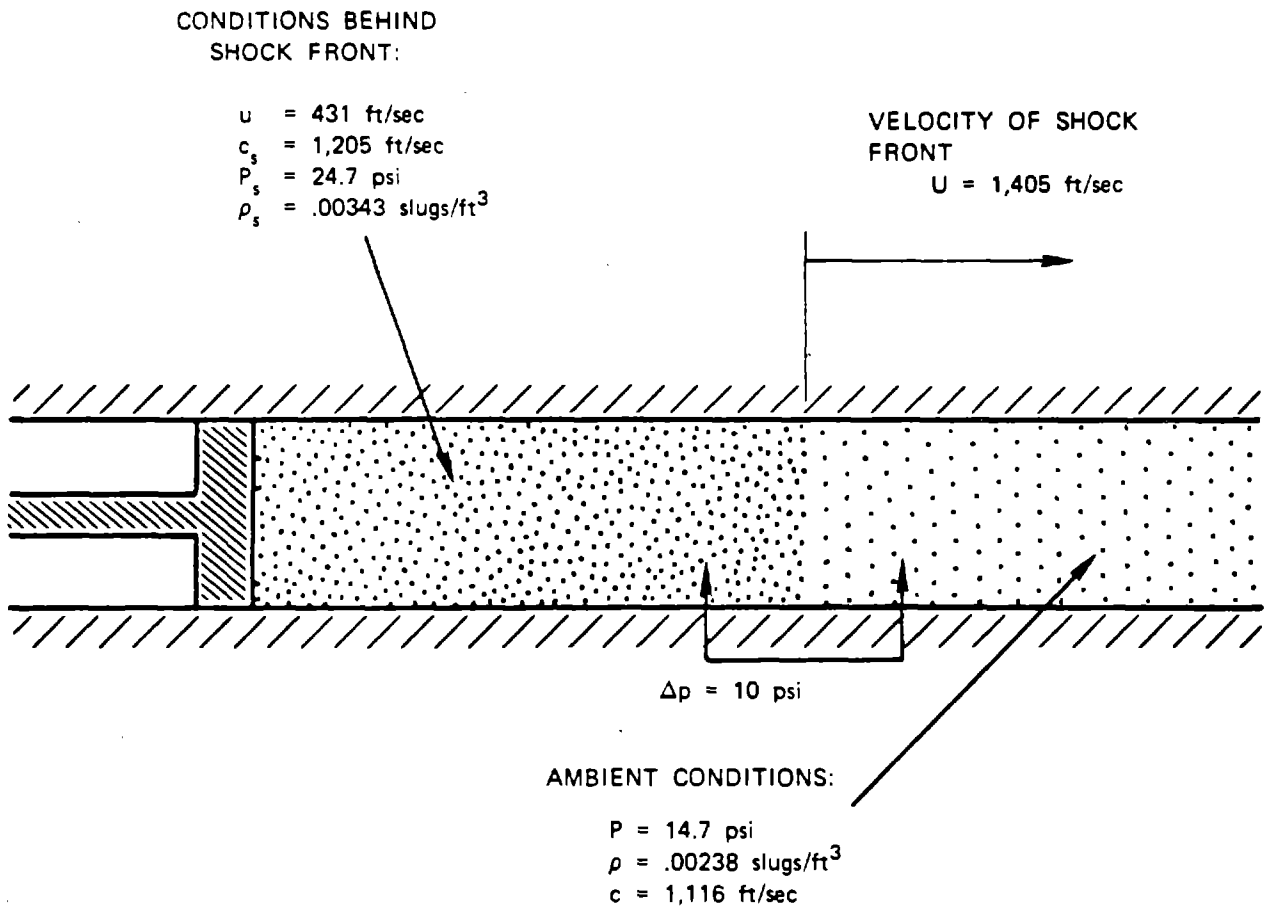

Figure A-4. [redacted] Parameters of a 10 psi Shock Wave [redacted]

[redacted] The mass of air that enters one square foot of shock front area each second is the ambient density, .00238 slugs/ft^3, times the shock front velocity of 1,405 ft/sec. This air is given a velocity of 431 ft/sec as it enters the shock wave. Thus,

$$\Delta p = \rho U u, \text{ or}$$

$$1{,}440 = .00238 \times 1{,}405 \times 431$$

A-10 Normal Reflection at a Solid Barrier [redacted]

[redacted] Figure A-5 shows a 10-psi shock wave that has struck the end of the cylinder and has formed a receding shock wave. Behind the receding shock front, the air is stationary. The velocity change at the reflected shock front has the same magnitude (but the opposite direction) as the velocity change of 431 ft/sec at the incident shock front. However, the pressure jump Δp_1 across the reflected shock front is greater than Δp because more mass per second is involved (see Figure A-5). The difference results principally from the higher density of the air entering the shock wave, but also results from the greater relative velocity, 1,491 ft/sec, between the shock front and the incoming air.

[redacted]

[redacted]

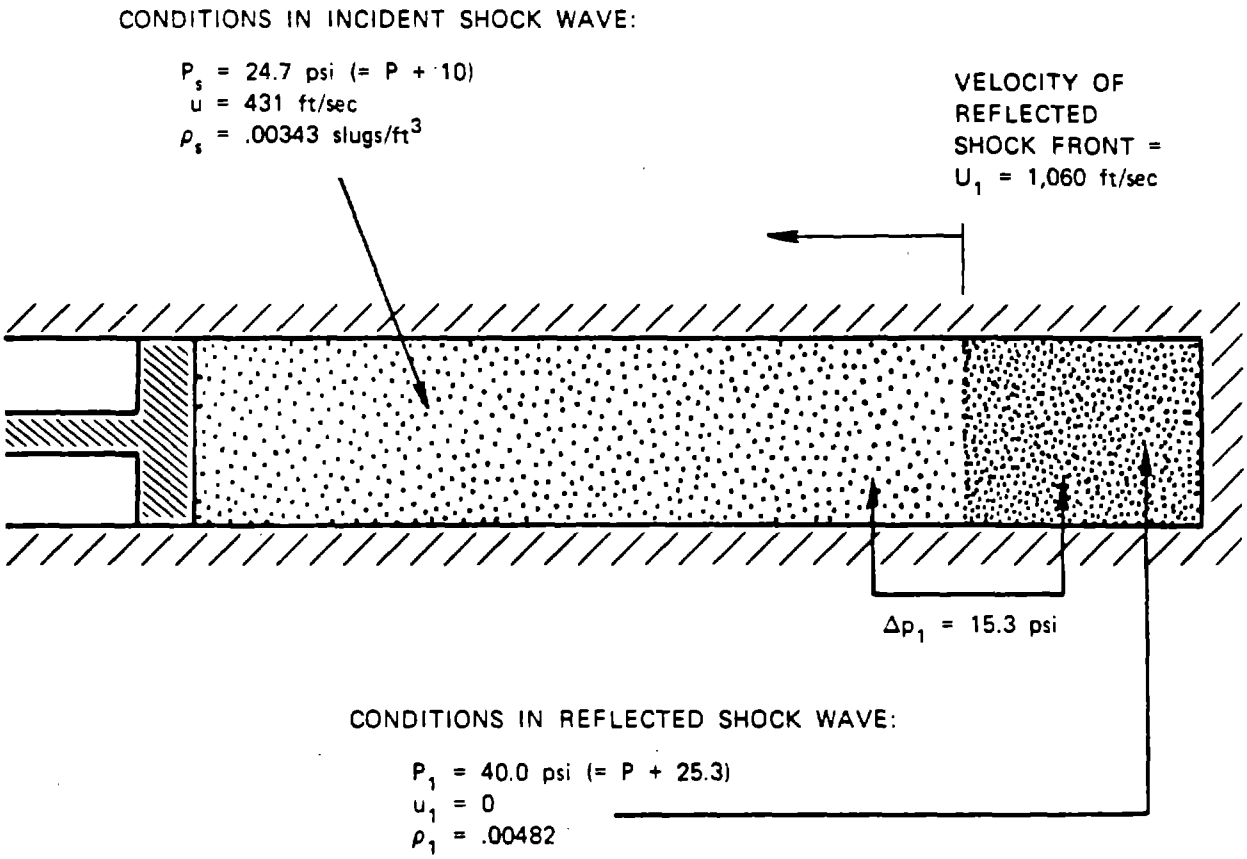

Figure A-5. [redacted] Reflection of a 10 psi Shock Wave from a Solid Barrier [redacted]

[redacted] The equation expressing Newton's second law may be obtained from basic physical principles, or it may be obtained from equations given in Section I by changing the frame of reference to one that is stationary with respect to the air ahead of the reflected shock front.

$$\Delta p = \rho U u,$$

$$15.3 \times 144 = .00343\ (1{,}060 + 431)\ 431,$$

$$2{,}220 = .00343 \times 1{,}491 \times 431$$

[redacted] The reflected overpressure, Δp_r, is the amount by which the pressure at the reflecting surface exceeds ambient pressure. It is the sum of the pressure jumps across the incident and the reflected shock fronts, or 25.3 psi.

[redacted] Acoustic theory often draws on the useful concept of images to explain the shock wave patterns produced at a reflecting surface. The reflecting surface is equivalent to a plane of symmetry. In the foregoing example, the image created by the reflecting surface would be a second piston, moving to the left with a velocity of 431 ft/sec, and located as far to the right of the reflecting surface as the real piston is to the left of it. As the two shock waves of equal strength collide, they produce conditions equivalent to those shown in Figure A-5.

[redacted]

[redacted]

[redacted] Explanation of the strength of the reflected shock front does not follow as readily from acoustic theory as does the basic shock wave pattern. Acoustic theory began with the study of sound waves, which have such low amplitudes that air acts as a linear medium. In such a medium, pressures are additive, and the wave reflected by a perfect reflector has the same amplitude as the incident wave. Shock wave effects are decidedly nonlinear, as is shown in the preceding example.

[redacted] Acoustic theory explains that the pressure jump of 15.3 psi instead of 10 psi at the reflected shock front is caused by the effect of dynamic pressure. Mathematically, this is a convenient explanation. For shock strengths less than about 10, the equations

$$\Delta p_1 = \Delta p + 2.4\ q$$

and

$$\Delta p_r = 2\Delta p + 2.4\ q$$

give correct values for Δp_1, the pressure jump at the reflected shock front and Δp_r, the reflected overpressure. The constant 2.4 is valid for air subjected to low shock strengths. In general, the constant has the value $\gamma + 1$.

[redacted] Physically, however, the explanation is artificial. In the sense that dynamic pressure effects are the effects caused by the momentum of air in motion, Δp_1 is produced entirely by dynamic pressure. The basic acoustic theory fails to predict shock wave phenomena. Predictions are possible only from a modified theory, tailored to fix experimental facts, and experience in using this theory is necessary to use it successfully.

A-11 Pressures on Simple Shapes [redacted]

[redacted] Two examples will be used to illustrate the phenomena that occur when a blast wave interacts with a target.

[redacted] The first example is the steady-state pressure pattern around a sphere placed in the path of the shock wave. Figure A-6 shows the nature of this pattern after the shock front has passed, and equilibrium conditions apply.

[redacted] This problem is more complex than the one discussed in paragraph A-10. The air particles directed exactly toward the center of the sphere reach the stagnation point, a point on the sphere at which the air is brought to rest, and the momentum that these particles give up may be calculated readily. All of the other air particles affected by the sphere behave in a more complicated way. They are slowed down and deflected, but they are not stopped.

[redacted] An order-of-magnitude equation for force may be obtained by assuming that all of the air directed toward the sphere is stopped. The momentum per unit area per unit time di-

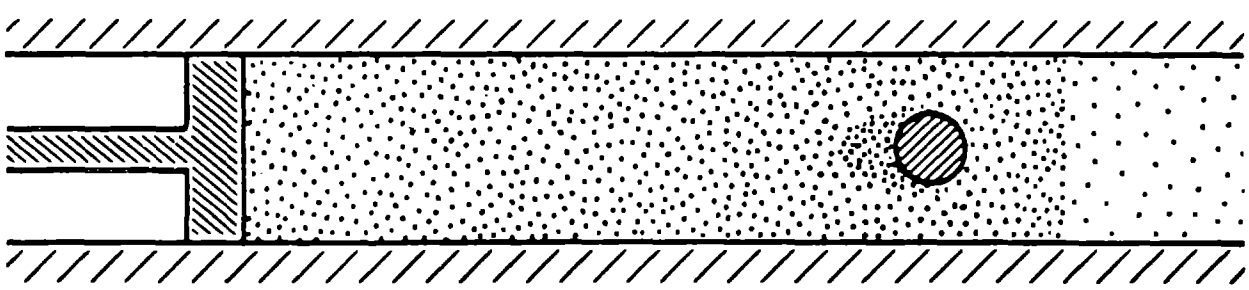

Figure A-6. [redacted] Reflection of a Shock Wave by a Small Object [redacted]

[redacted]

[redacted]

[redacted] rected toward the sphere is $\rho_s u$ (the mass flow per unit area per unit time). Application of Newton's second law shows that the wind pressure is about

$$F/A = \rho_s u^2.$$

A detailed analysis would show that the pressure produced at the stagnation point of a sphere in a moderately strong wind is more closely approximated by dynamic pressure, which has a value that is just half of that given by the previous equation

$$q = \frac{1}{2} \rho_s u^2.$$

[redacted] Therefore, the wind pressure at the stagnation point on the sphere is roughly

$$q = \frac{1}{2} \times .00343 \times (431)^2,$$

$$= 318.58 \text{ lbs/ft}^2,$$

$$= 2.2 \text{ psi}.$$

Total pressure at the stagnation point is about 12.2 psi, the sum of the static overpressure and the dynamic pressure.

[redacted] The important point in this example is that the high pressure region around the object is stationary, not moving forward to meet the oncoming air as was the receding shock wave shown in Figure A-5. Consequently, the rate at which air enters the high pressure region is lower. The rate at which momentum is extracted from incoming air is correspondingly lower. By Newton's second law, the pressure developed is smaller.

[redacted] Acoustically, no reflection is considered to occur in this example. The problem is simply one of an object in an airstream.

[redacted] The second illustration is the transient interaction between a blast wave and a small cube. This type of interaction is largely a combination of those already discussed. For simplicity, the blast wave is assumed to strike one side of the cube head-on. Shortly after the shock front strikes the cube, the reflection process is much like that produced at the closed end of a piston (Figure A-5). A receding shock wave is formed, the mass flow rate into this shock wave is high, and the front face of the cube is subjected to a high reflected overpressure (25.3 psi for a 10 psi incident shock wave).

[redacted] At the edges of the front face of the cube, the layer of compressed air in the receding shock wave is unconfined. It flows outward, around the edges of the cube. This outward flow relieves the high pressure behind the receding shock front. As a result of this pressure relief, the receding shock front loses velocity; consequently, the incoming air gives up its momentum at a decreasing rate. A steady-state flow pattern develops, and the pressure at the front surface of the cube drops to roughly the incident overpressure plus the incident dynamic pressure. The situation is now similar to that shown in Figure A-6.

[redacted] Part of the acoustic explanation is very descriptive. Pressure relief waves form at the edge of the front surface of the cube and propagate inward. Reflections that occur when these relief waves meet increase the rate of flow over the front face and around the edges of the cube. The time required for the steady-state flow pattern to develop is about two or three times that required for a shock wave to travel from the edge of the cube to the center of the front face.

[redacted] The remainder of the acoustic explanation is evident only to a person familiar with acoustic theory or to a person who has previously encountered this particular explanation. It involves understanding: (1) the reflection coefficient of an object becomes small as the wave-

[redacted]

[redacted]

[redacted] length of the incident sound wave becomes large compared with the dimensions of the object; and (2) a pressure waveform has an equivalent spectrum of sound waves of different wavelengths (strictly speaking, the equivalent spectrum requires a linear medium and is only an approximation in strongly shocked air).

[redacted] These acoustic concepts, applied to the problem of reflection from a small cube, predict that the cube will reflect the shock front strongly, but that the reflection coefficient of the cube will decrease rapidly after the shock front passes. The reflected wave weakens by spherical divergence as it propagates away from the cube, and the pressure on the front face of the cube decreases to its steady-state value.

A-12 The Rankine-Hugoniot Equations (Alternate Analysis) [redacted]

[redacted] In the conventional derivation of the Rankine-Hugoniot equations (paragraph A-1), the algebra tends to obscure the physical picture associated with the derivation. The following analysis provides a more intuitive introduction to the subject.

[redacted] *The interaction at the shock front is basically an inelastic collision.* The truth of this statement is evident from the definition of an inelastic collision. It is a collision in which the colliding bodies stick together and move with a common velocity after they collide.

[redacted] The statement given above provides a method to account for the energy exchanges that occur at the shock front. It may be applied most readily if the collision is considered to occur between a very thin layer of unshocked air and the mass of air behind the shock front. The following statement may then be confirmed readily.

[redacted] *The inelastic collision at the shock front is 50 percent efficient in transferring kinetic energy to the incoming air.* A change to the center-of-mass frame of reference is the first step necessary to demonstrate this fact. Since the mass of air being picked up at any instant is infinitesimal, this frame of reference moves with the air behind the shock front. The initial kinetic energy per unit area of the shock front is, in this frame of reference, that of the thin layer of unshocked air approaching the shock front with a relative velocity of u. If its mass is dm, its initial kinetic energy is*

$$d(KE) = \frac{1}{2} u^2 dm.$$

After a completely inelastic collision, the kinetic energy in the center-of-mass frame of reference is zero.† In other words, the amount of energy that is converted from kinetic energy to internal energy in the collision is equal to $d(KE)$.

[redacted] In the original frame of reference (stationary with respect to the unshocked air), $d(KE)$ is equal to the kinetic energy of the thin layer of air after it has become a part of the shock wave. Thus, the kinetic energy imparted to the air and the kinetic energy converted to internal energy by the inelastic collision are equal, i.e., this method of transferring kinetic energy is 50 percent efficient.‡

[redacted] Accounting for all of the work done at the shock front is complicated by an energy ex-

[redacted] A rigorous derivation of the equations governing the inelastic collision of two bodies requires the simultaneous solution of the energy and momentum equations of the system. If a large mass and a very small mass are approaching one another with equal and opposite momenta, the kinetic energy of the larger mass is negligible compared to the kinetic energy of the smaller mass.

[redacted] By definition, total momentum in the center-of-mass frame of reference is zero. Since momentum is conserved in the collision of two bodies, the total momentum remains zero after any collision. After a completely inelastic collision, neither of the colliding bodies is moving with respect to the center of mass; therefore, their final kinetic energy in this frame of reference is zero.

[redacted] Although kinetic energy changes with changes in the frame of reference, the energy loss in an inelastic collision does not.

[redacted]

[redacted]

[redacted] change that is independent of the exchange produced by the inelastic collision. The total work done on a unit mass of incoming air results from the pressure P_s that is behind the shock front moving through the distance required to compress this mass of air from its initial volume V to its final volume V_s.

$$W'_{total} = P_s(V - V_s).$$

One portion of this work is done by the ambient pressure P in displacing the volume $V - V_s$. Since the ambient pressure does not produce a force that has directional characteristics, it has no function in setting the air in motion. This portion of the work only contributes to compression.

$$W'_{comp} = P(V - V_s)$$

The remainder of the work is done by the overpressure $\Delta p = P_s - P$, displacing the volume $V - V_s$. At the shock front, the effect of overpressure is completely directional, and overpressure creates the force that accelerates the air that is overtaken by the shock front. This is the portion of the work that is required to produce kinetic energy by a collision process,

$$W'_{coll} = (P_s - P)(V - V_s).$$

As already demonstrated, half of this work appears as kinetic energy and half as internal energy of the unit mass of air added to the shock front. Note that the work converted to internal energy by the collision process is closely related to W_{comp} in that both contribute to compressing the gas to the volume V_s and, in this way, both increase the internal energy of the air.

[redacted] The energy exchange equations for a unit mass of air entering the shock front follow directly from the discussion in the preceding paragraph. The kinetic energy added to the unit mass of air is

$$\frac{1}{2}u^2 = \frac{1}{2}W'_{coll},$$

$$= \frac{1}{2}(P_s - P)(V - V_s),$$

and the particle (wind) velocity is

$$u = \left((P_s - P)(V - V_s)\right)^{1/2}.$$

The change in internal energy of the unit mass of air is

$$E_s - E = W'_{comp} + \frac{1}{2}W'_{coll}$$

$$= P(V - V_s) + \frac{1}{2}(P_s - P)(V - V_s)$$

$$= \frac{1}{2}(P_s + P)(V - V_s).$$

To obtain the equation for shock front velocity, note that while the air in the shock wave moves into a volume $V - V_s$, the shock front has advanced through a volume V. The ratio of shock front velocity to particle velocity is therefore

$$\frac{U}{u} = \frac{V}{V - V_s}$$

$$U = \left(\frac{V}{V - V_s}\right)\left((P_s - P)(V - V_s)\right)^{1/2}$$

$$U = V\left(\frac{P_s - P}{V - V_s}\right)^{1/2}.$$

The equations for u, $(E_s - E)$, and U are the Rankine-Hugoniot equations given previously in paragraph A-1.

[redacted]

[redacted] *Note:* Although the interaction at the shock front is completely inelastic, the overall reaction of a blast wave in free air is partially elastic. In such a blast wave, the pressure behind the shock front is not constant, but decays with time. The air behind the front expands and returns energy that helps to propagate the shock wave (see footnote to paragraph 2-33, Chapter 2). This fact does not alter the validity of the argument presented above. It simply points out that the inelastic collision at the shock front only describes part of the mechanism of blast wave propagation.

A-13 Dynamic Pressure [redacted]

[redacted] Dynamic pressure is frequently equated to the wind force produced on a target by the high velocity winds in a blast wave, but the relation between force and dynamic pressure is not this simple.

[redacted] One source of confusion is the name which implies a meaning that differs from the correct one. In a compressible fluid, the true meaning of dynamic pressure is limited to the mathematical definition

$$q = \frac{1}{2} \rho_s u^2$$

where ρ_s is mass per unit volume and u is particle velocity behind the shock front. Strictly speaking, q is not a pressure. A body moving along with moving air will not feel a force that is attributable to dynamic pressure. Dynamic pressure is kinetic energy per unit volume. Reasons for calling it a pressure are: (1) it has the dimensions of pressure; and (2) this energy can be used to develop a pressure.

[redacted] A stationary body exposed to a wind will experience pressures that differ at different points on its surface. The highest pressure on the body is the stagnation pressure, which occurs wherever the air is completely stopped by impact with the body. For example, if the body is a sphere, the stagnation pressure occurs at the point on the surface that faces directly into the wind. For an incompressible fluid, stagnation pressure is simply the sum of the free-stream static pressure and the free-stream dynamic pressure. However, for a compressible fluid, such as air, stagnation pressure is the sum of the free-stream static pressure and a quantity called the free-stream *impact pressure.* At low velocities, impact pressure and dynamic pressure are essentially equal, but at velocities that are appreciable compared with sound speed, impact pressure rises above dynamic pressure. When wind speed is equal to sound speed, impact pressure exceeds dynamic pressure by about 28 percent.

[redacted] The forces exerted by strong winds correspond more directly to impact pressures than to dynamic pressure. This suggests that weapons effects calculations should be based on impact pressures rather than on dynamic pressures; but, both in this field and in aerodynamics, dynamic pressures are employed more commonly. The choice is based on conventional practice. In aerodynamic problems, dynamic pressure is used because it may be calculated readily. Wind force on an object is calculated from the equation

$$F_w = C_D q A$$

where C_D is drag coefficient and A is an area related to the size of the object. The drag coefficient is not constant. It is a function of velocity, and its variation absorbs not only the discrepancy between dynamic pressure and impact pressure, but also accounts for the net effect of the complex pressure pattern that forms around an object in an airstream. The product qA, although it has the dimensions of a force, has no direct physical relation to any force exerted by the wind.

[redacted] In weapons effects calculations, dynamic pressure often is as convenient as it is in aerody-

[redacted]

[redacted]

namics: damage criteria for such objects as buildings are established in terms of conventional shock wave parameters, such as overpressure, dynamic pressure, or impulse. Consequently, the stagnation pressure or other actual pressures found at various points on specific structures usually are not calculated unless specific blast loading information is desired. In some cases, the choice of dynamic pressure may not be appropriate for damage criteria. For example, when the air in the blast wave is dust laden (as it is for certain combinations of yield, burst height, ground range, and surface properties), a measurement with a conventional dynamic pressure gauge often is ambiguous. The dust is not necessarily in velocity equilibrium with the air, and the amount of dust is not known. As a result, it is often difficult to calculate the dynamic pressure of air alone from such experimental measurements.

[redacted]

[redacted]

APPENDIX B

USEFUL RELATIONSHIPS[redacted]

B-1 General Equivalents [redacted]

[redacted] One kiloton (kt) is defined to be 10^{12} calories of energy release.* This amount of energy will be released by the complete fission of 0.057 kg (57 grams or 2 ounces) of fissionable material.† Equivalents to this amount of energy in other units are:

- 2.61×10^{25} million electron volts (MeV),
- 4.18×10^{19} ergs,
- 1.16×10^{6} kilowatt-hours,
- 3.97×10^{9} British thermal units.

[redacted] Some equivalents of the complete conversion of mass to energy are:

1 gram mass = 5.61×10^{26} MeV
= 8.99×10^{20} ergs
= 2.15×10^{13} calories

[redacted] The temperature associated with one electron volt is 11,605.9 degrees Kelvin.

B-2 Constants [redacted]

[redacted] Velocity of light: 3×10^{8} m/sec = 3×10^{10} cm/sec.

[redacted] Avagadro's number: 6.023×10^{23} molecules per mole (gram molecular weight).

[redacted] Planck's constant: 6.625×10^{-27} erg-sec.

[redacted] Boltzmann constant: 1.38×10^{-16} erg/°K.

[redacted] ‡Mass of electron: 9.1085×10^{-28} gm.

[redacted] ‡Mass of proton: 1.672×10^{-24} gm.

[redacted] ‡Mass of neutron: 1.675×10^{-24} gm.

[redacted] ‡Mass of alpha particle: 6.64×10^{-24} gm.

[redacted] Loschmidt number: 2.687×10^{19} molecules of ideal gas per cubic centimeter at °C.

[redacted] Electron charge:

4.803×10^{-10} esu = 1.602×10^{-20} emu
= 1.602×10^{-19} coulombs.

B-3 Standard Sea Level Atmosphere [redacted]

[redacted] Pressure = 14.696 psi
= 2,116.22 lb/ft^2
= 1,013.25 millibars
= 101,325. newtons/m^2
= 1,013,250. dynes/cm^2

[redacted] Temperature = 59°F
= 15°C
= 288.15°K
= 518.4°R

[redacted] Density = 2.38×10^{-3} slug/ft^3
= 7.65×10^{-2} lb/ft^3
= 1.225×10^{-3} gm/cm^3
= 1.225 kg/m^3

[redacted] Speed of sound = 1,116.45 ft/sec
= 340.29 m/sec
= 34,029 cm/sec

[redacted] See footnote on page 1-3 for the origin of the definition.

[redacted] This is the energy released by the *fission* of 57 grams of fissionable material. It is *not* the energy that would be released by the conversion of 57 grams mass to energy.

[redacted] Classical rest mass.

[redacted]

[redacted]

[redacted] Gravitational acceleration

= 9.8067 m/sec^2

= 32.1741 ft/sec^2

B-4 Conversions [redacted]

[redacted] Length:

1 ft	= 0.3048 m
	= 30.48 cm
1 m	= 3.281 ft
1 kft	= 0.3048 km
	= 0.1894 mi
	= 0.1645 nm
1 km	= 1,000 m
	= 3,281 ft
	= 3.281 kft
	= 0.6214 mi
	= 0.5396 nm
1 mi	= 5,280 ft
	= 1,760 yds
	= 5.280 kft
	= 1.609 km
	= 0.8684 nm

[redacted] Force:

1 dyne = 1.0197 x 10^{-3} gm (weight)

= 2.2481 x 10^{-6} lb (weight)

1 gm (weight) = 980.665 dynes

= 2.2046 x 10^{-3} lb (weight)

= 1 x 10^{-3} kg (weight)

1 lb (weight) = 4.4482 x 10^5 dynes

= 453.59 gm (weight)

= 0.45359 kg (weight)

[redacted] Pressure:

1 dyne/cm^2 = 1.0197 x 10^{-3} gm/cm^2

= 1 x 10^{-1} newtons/m^2

= 7.5 x 10^{-4} mm mercury (0°C)

= 4.015 x 10^{-4} in. water (4°C)

= 2.089 x 10^{-3} lb/ft^2

= 1.451 x 10^{-5} lb/in.^{2} (psi)

= 1.02 x 10^{-2} kg/m^2

= 1 x 10^{-3} millibars

1 gm (wt)/cm^2 = 980.665 dynes/cm^2

= 980.665 x 10^{-1} newtons/m^2

= 10.0 kg/m^2

= 2.048 lb/ft^2

= 1.422 x 10^{-2} lb/in.^{2} (psi)

= 7.35 x 10^{-1} mm mercury (0°C)

= 0.394 in. water (4°C)

= 980.665 x 10^{-3} millibars

1 lb (wt)/in.^{2} (psi) = 6.895 x 10^4 dynes/cm^2

= 6.895 x 10^3 newtons/m^2

= 703.07 kg/m^2

= 70.307 gm/cm^2

= 51.715 mm mercury (0°C)

= 27.673 in. water (4°C)

= 68.947 millibars

1 millibar = 100 newtons/m^2

= 1,000 dynes/cm^2

= 1.45 x 10^{-2} lb/in.^{2}

= 2.089 lb/ft^2

[redacted] Density:

1 gm/cm^3 = 1,000 kg/m^3

= 3.613 x 10^{-2} lb/in.^{3}

= 62.43 lb/ft^3

= 1.94 slugs/ft^3

1 kg/m^3 = 1 x 10^{-3} gm/cm^3

= 3.613 x 10^{-5} lb/in.^{3}

[redacted]

[redacted]

[redacted]

	= 6.243×10^{-2} lb/ft^3
	= 1.94×10^{-3} slugs/ft^3
1 lb/ft^3	= 1.6018×10^{-2} gm/cm^3
	= 16.018 kg/m^3
	= 5.787×10^{-4} lb/in.^{3}
	= 3.108×10^{-2} slugs/ft^3
1 slug/ft^3	= 0.5154 gm/cm^3
	= 515.4 kg/m^3
	= 1.862×10^{-2} lb/in.^{3}
	= 32.174 lb/ft^3

[redacted] Energy:

1 gm-cal	= 4.184 joules
	= 4.184×10^7 ergs
	= 3.086 ft-lb
	= 3.966×10^{-3} Btu
1 joule	= 1×10^7 ergs
	= 0.239 gm-cal
	= 0.738 ft-lb
	= 9.480×10^{-4} Btu
1 erg	= 1×10^{-7} joules
	= 2.39×10^{-8} gm-cal
	= 7.38×10^{-8} ft-lb
	= 9.48×10^{-11} Btu
1 ft-lb	= 1.356 joules
	= 1.356×10^7 ergs
	= 3.240×10^{-1} gm-cal
	= 1.285×10^{-3} Btu
1 Btu	= 252 gm-cal
	= 1,054 joules
	= 1.054×10^{10} ergs
	= 778 ft-lb

[redacted] Velocity:

1 cm/sec	= 1×10^{-2} m/sec
	= 3.281×10^{-2} ft/sec
	= 2.237×10^{-2} mi/hr
	= 1.942×10^{-2} knots
1 m/sec	= 100 cm/sec
	= 3.281 ft/sec
	= 2.237 mi/hr
	= 1.942 knots
1 ft/sec	= 30.48 cm/sec
	= 3.048×10^{-1} m/sec
	= 6.818×10^{-1} mi/hr
	= 5.921×10^{-1} knots
1 mi/hr	= 44.70 cm/sec
	= 0.4470 m/sec
	= 1.4667 ft/sec
	= 0.8684 knots
1 knot	= 51.48 cm/sec
	= 0.5148 m/sec
	= 1.689 ft/sec
	= 1.152 mi/hr

[redacted] Temperature:

°K	= °C + 273.15
°R	= °F + 459.4
°C	= 5/9 (°F - 32)
°F	= 9/5 °C + 32

[redacted] Wavelength:

1 Å	= 10^{-8} cm
	= 10^{-10} m
	= $10^{-4}\mu$
1μ	= 10^{-4} cm
	= 10^{-6} m
	= 10^4 Å

[redacted]

[redacted]

B-5 Fractional Powers and Dimension Scaling [redacted]

[redacted] Figures B-1 and B-2 provide the information necessary to perform many of the fractional power scaling operations required by equations presented in this manual. The use of these figures is demonstrated in Problem B-1. Figure B-3 is a nomogram that shows the relationships among the height of burst, the horizontal distance, and the slant range. A straight line through any two (known) of these quantities (on the appropriate scale) will pass through the third (unknown) quantity on its scale. The three dimensions must, of course, be in the ~~same~~ appropriate units. The diagram accompanying this nomogram should make its use obvious, and no example is provided. While Figures B-1 through B-3 are plotted accurately, visual interpolation on these figures cannot provide accurate results. If tools such as a slide rule, logarithm tables, or a calculator that can perform fractional power operations are available, users of this manual are encouraged to make use of those tools. Figures B-1 through B-3 are provided for those who desire a reasonable answer in the absence of such tools.

[redacted]

[redacted]

Problem B-1. Use of Fractional Power Curves and Dimension Scaling Nomogram

[redacted] Figure B-1 shows several fractional powers of numbers between 1 and 100,000. The fractional powers are those that are necessary to apply various scaling procedures presented elsewhere.

[redacted] Figure B-2 is a nomogram from which actual dimensions may be obtained from various scaled dimensions for yields from 0.1 kt to 100 Mt. The scaling power for which the scaled dimensions are applicable is indicated at the top of the scale in each case. A straight line connecting a yield with any scaled dimension will cross the actual dimension scale at the proper value according to the scaling which is being used. The dimensions may be in any units for which scaling is given, but the scaled dimension and the actual dimension will always be in the same units.

[redacted] *Example 1* [redacted]

Given: A 500 kt weapon is to be burst at the minimum height of burst at which fallout is not expected. A conservative height of burst is desired.

Find: The actual height of burst at which the weapon is to be detonated.

Solution: From paragraph 5-22, the minimum conservative height of burst for a 500 kt weapon at which fallout is not expected is 180 $W^{0.4}$ ft.

Answer a: From B-1

$$(500)^{0.4} = 12$$

$$180 \times 12 = 2{,}160 \text{ ft.}$$

Answer b: From Figure B-2, a straight line connecting 500 on the yield scale with 180 on the 0.4 power scaled dimension scale crosses the actual dimension scale at 2,160. The desired height of burst is thus 2,160 feet. (*Note:* Conversion from one scaling procedure to another is particularly easy with the nomogram. The line mentioned above crosses the cube root scaled dimension scale at 270. Thus 180 $W^{0.4}$ ft corresponds to 270 $W^{1/3}$ ft for 500 kt.)

[redacted] *Example 2* [redacted]

Given: A ground distance of 2,580 yd from an 80 kt surface burst.

Find: The proper distance to determine overpressure from the 1 kt curves.

Solution: The applicable scaling is (Problem 2-9).

$$\frac{d}{d^1} = W^{1/3}.$$

Answer a: From Figure B-1

$$(80)^{1/3} = 4.3,$$

$$d_1 = \frac{d}{W^{1/3}} = \frac{2{,}580}{4.3} = 600 \text{ yd}$$

$$= 1{,}800 \text{ ft.}$$

Answer b: From Figure B-2, a straight line from 80 on the yield scale through 2,580 on the actual dimension scale intersects the cube root scaled dimension scale at 600. The scaled distance is 600 yards. The proper distance to enter the overpressure charts is 1,800 feet.

[redacted]

[redacted]

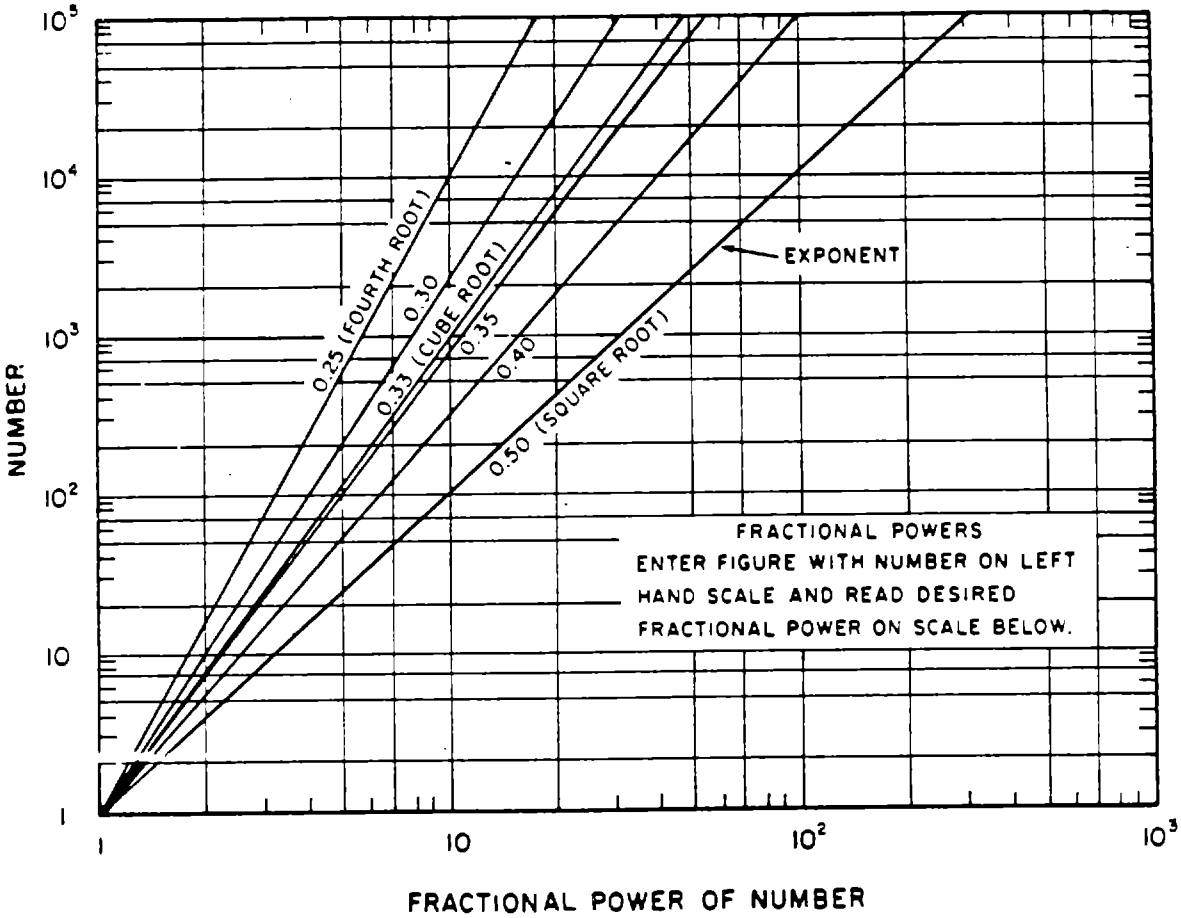

Figure B-1. [redacted] Various Fractional Powers of Numbers [redacted]

[redacted]

[redacted]

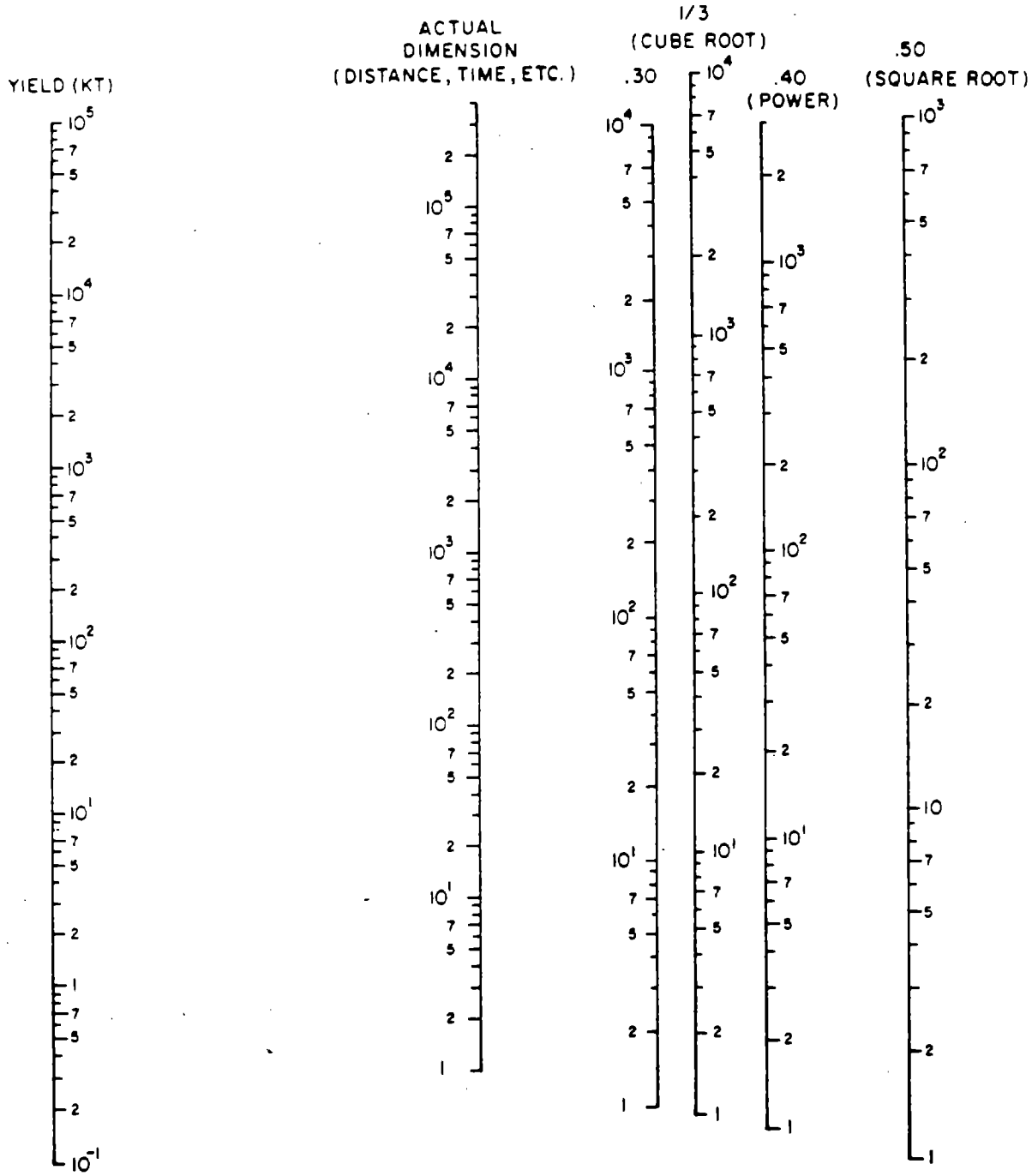

Figure B-2. [redacted] Dimension Scaling Nomogram [redacted]

[redacted]

[redacted]

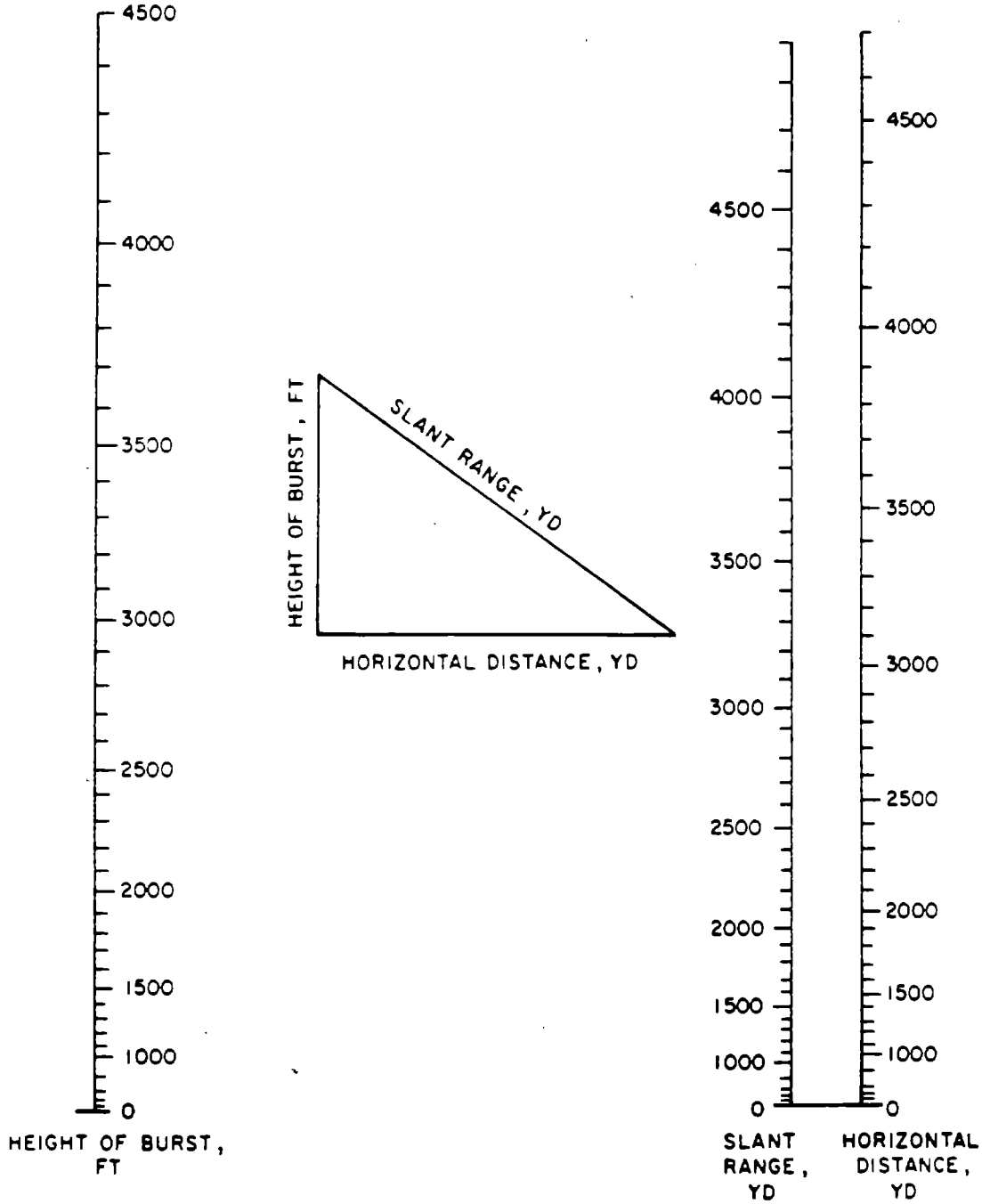

Figure B-3. [redacted] Height of Burst—Horizontal Distance—Slant Range Nomogram [redacted]

[redacted]

[redacted]

APPENDIX C

PROBABILITY CONSIDERATIONS [redacted]

[redacted] The procedures described in Sections I through III of Chapter 11 permit independent calculations of the 50 percent probability of damage to structures, equipment and personnel. Section I of this appendix provides a method for determining the probability of failure for conditions other than those considered in Chapter 11, i.e., where the median or 50 percent probability level of vulnerability differs from the median or 50 percent probability level of input motions or pressures. Section II provides the derivation of some equations used in Section I. Familiarity with Section III, Chapter 2 and Sections I through III, Chapter 11 is presupposed.

[redacted] The discussion herein is related to the intensity of motion (either displacement, velocity, or acceleration) that is required to produce severe damage to equipment or personnel, and to the intensity of input pressures produced by the air shock that will cause severe or moderate damage to both aboveground and belowground structures. The failure of rock openings is also treated in terms of slant range. Either free field values, or values within the structure at the point of support of the equipment, or the response spectrum values, may be used interchangeably as input. In general, the response spectrum values of motion will be used. Different probabilities will be obtained for shock effects depending on the knowledge available pertaining to the type and design of the shock mount.

[redacted] In all cases, the parameters that are dealt with are the intensity of motion, the intensity of overpressures, or the slant range. For motion vulnerability, one of the three elements of motion (displacement, velocity, or acceleration) can be used, depending on which region of the spectrum is involved, without otherwise distinguishing among them. By comparing the median value of input (motion, pressure, or slant range) with the median value of vulnerability, respectively, to motion, overpressure, or slant range as appropriate, the probability of failure or survival of the particular piece of equipment or structure can be obtained directly. When these two levels are equal, the probability of failure is, of course, 50 percent. However, when they are different, the tables and figures provided in this appendix may be used to obtain the probability of failure or of survival.

C-1 Protective Design and Weapon Selection [redacted]

[redacted] In general, all of the parameters governing the response of a structure, including the loading and the structural parameters, are subject to variation and uncertainty. In making a design of a structure to resist certain overpressures, or other inputs, for a particular yield of weapon, the designer ordinarily makes assumptions on the conservative side in all or nearly all of the cases where he has a choice of parameter values. The designer desires to state, with a high degree of confidence, that his structure will withstand an overpressure (the "design" overpressure), or other inputs, specified to him. He will, therefore, choose parameter values sufficiently conservative to assign a high confidence value to his statement, e.g., 90 percent or better.

[redacted] The weapon analyst who is estimating the vulnerability of a structure, on the other hand, can work with an overall variation, which reflects the variation of the individual parameters. The weapon analyst is not bound to the selection of single values for these parameters,

[redacted]

[redacted]

[redacted] because he is not solely interested in being able to state the probability that a single specified input will cause the desired damage, or that a certain input will cause damage with a high degree of confidence. Instead, he must answer the question, given a specified combination of weapon yield and height of burst, and considering the possible variations associated with the structural and weapon parameters, what is the probability that the specified damage will occur.

SECTION I

[redacted] DAMAGE PROBABILITIES [redacted]

[redacted] DAMAGE CAUSED BY MOTION INPUT [redacted]

C-2 Description of Charts for Damage Caused by Motion Input [redacted]

[redacted] Values of the standard deviation σ, stated in terms of a percentage of the mean value m of intensity of motion, are shown in Item 1 of Table C-1. These values represent the combination of variabilities and uncertainties relative to the shock motions as well as to the vulnerability of structures or equipment and personnel. The values apply equally for input displacement in the constant displacement region, or velocity in the constant velocity region and acceleration in the constant acceleration region (see Figures 2-90 and 11-51).

[redacted] Separate values are given for equipment that is not shock mounted and for equipment that is shock mounted. Different values are given for shock mounted equipment to distinguish between equipment where the design of the mount is known, and for two different situations for shock mounted equipment where the design is unknown. In the case where the design is unknown, the type of equipment may be known and therefore some better measure of the vulnerability level can be assessed; alternately, the type of equipment also may be unknown, and major uncertainties must be considered to exist in the data. The values of σ/m given in Items 1a through 1d reflect these degrees of uncertainties.

[redacted] The distributions of the combined vulnerabilities can be considered to be logarithmic normal, and to have the shape corresponding to the typical lognormal curve for the particular values of σ/m listed in Table C-1. The parameters of the lognormal probability distribution and its properties are summarized in Section II of this appendix.

[redacted] Figure C-1 shows the probability distributions for failure or for survival for the various combined values of σ/m stated in Table C-1, plotted as a function of the ratio of the median value of input motion (or input pressure or slant range), b_i, to the median value of vulnerability level of motion (or of pressure vulnerability or of slant range), for the equipment or structure, b_v. Figure C-2 is similar to Figure C-1, except that the ratio σ/m is shown as a function of b_i/b_v for different probability values. Where $b_i = b_v$, i.e., the ratio is unity, the probability of failure is 50 percent. These curves are used to obtain the probability of failure for any other ratio of b_i/b_v; as shown in Section II, these same curves give the probability of survival if the ordinates are taken as b_v/b_i in place of b_i/b_v. Therefore, the probability of failure or of survival can be determined by using the appropriate curve in Figure C-1 or C-2. For example, if a situation exists in which velocity governs the response (in the constant velocity region) and where the equipment is shock mounted (design known) with the mounting being the item in which failure is to be produced, the appropriate σ/m of 100 percent is obtained from Item 1b of Table C-1. With this value, it can be seen that if the median value of input velocity is 2.0 times the vulnerability velocity level, either Figure C-1 or Figure C-2 shows that the probability of failure is about 79 percent.

[redacted]

[redacted]

[redacted] If, however, the acceleration bound governs, and the shock mounting design is unknown but the type is known, Item 1c of Table C-1 shows σ/m to be 150 percent. With this value, if the median input acceleration is 2.0 times the vulnerability level of acceleration, the probability of failure is only 74 percent. To achieve an 85 percent probability of failure for this condition would require that the median value of acceleration be 3.1 times the vulnerability level of acceleration, as shown in Figure C-2.

C-3 Instructions for Motion Input Analyses [redacted]

[redacted] A step-by-step procedure for motion input analysis is given below. Illustrative examples for specific analyses are given in paragraph C-4. It is assumed that b_v is known and b_i for the particular weapon and conditions is assumed for motion inputs and vulnerability. The steps are:

1. Determine the value of σ/m from Table C-1 depending on whether or not an element is shock mounted and on the knowledge of the type and design of the mount.

2. If information other than that given in Table C-1 is available in the form of coefficients of variations of the input motions and of the vulnerabilities, the following equation can be used to obtain the combined σ/m:

$$\frac{\sigma}{m} = \left\{ \left(\frac{\sigma_i}{m_i}\right)^2 + \left(\frac{\sigma_v}{m_v}\right)^2 + \left(\frac{\sigma_i}{m_i}\right)^2 \left(\frac{\sigma_v}{m_v}\right)^2 \right\}^{1/2}.$$

If the parameters are different from those tabulated, and a value of σ/m computed from the above equation is different from any of those shown in Table C-1, enter Figure C-2 with the value of σ/m as abscissa, and read the value of b_i/b_v for a chosen probability of failure P_f (suggest P_f = 90 percent or 95 percent). With this value of b_i/b_v, a line can be plotted on Figure C-1 appropriate to the particular value of σ/m. The value of b_i/b_v is plotted on Figure C-1 as the ordinate at the chosen probability, P_f = 90 percent or 95 percent as the case may be. A line from the plotted point through the 50 percent point (where the other lines intersect) gives the entire curve. Alternately, if the combined value of σ/m is not given in Table C-1 or Figure C-1, Figure C-2 may be used in place of Figure C-1.

3. For the particular value of σ/m determined, read the probability of failure from Figure C-1 using the abscissa at the bottom of the figure, or the probability of survival using the abscissa at the top of the figure for the particular value of b_i/b_v.

4. For the given ratios of σ/m, and for any value of b_i/b_v, the probabilities of failure or of survival are determined as described above; however, Figures C-1 and C-2 also can be used with a ratio of b_v/b_i to give the same probabilities by interchanging P_f, the probability of failure, with P_s, the probability of survival.

5. If a particular probability of failure or survival is desired, the value of b_i/b_v is obtained from Figure C-1 or C-2 for the particular combined value of σ/m, and the desired value of b_i is obtained by trial-and-error for the particular given value of b_v.

C-4 Illustrative Examples for Motion Inputs [redacted]

Example 1 [redacted]

[redacted] Consider the vulnerability of non-shock mounted equipment. The value of b_v is assumed to be 10g at approximately 20 cycles per second. Consider the case in which the spectrum intersection is along a line parallel to a line of constant acceleration.

[redacted] From Table C-1, Item 1a indicates a value of σ/m of 100 percent.

[redacted] For a particular explosion, the acceleration level is determined to be b_i = 7g (by the

[redacted]

[redacted] methods of Section III, Chapter 2). Therefore, the ratio of b_i to b_v is 7/10 = 0.7. From Figure C-1, with b_i/b_v = 0.7 and σ/m = 100 percent, the probability of failure is 33 percent, or the probability of survival is 67 percent. Alternately, b_v/b_i = 1.43. Using this value of b_v/b_i and σ/m = 100 percent, the survival probability is read directly from Figure C-1 or C-2 to be 67 percent.

Example 2 [redacted] For the same conditions as example 1, determine the input acceleration that would be required to produce a 90 percent probability of failure.

[redacted] From Figure C-1 or C-2, a 90 percent probability of failure occurs for σ/m = 100 percent if b_i/b_v = 2.9. This means that an acceleration of 29g will be required to produce 90 percent probability of failure.

Example 3 [redacted] For the same equipment, consider a condition in which the equipment is shock mounted, with a velocity vulnerability of 1,000 in./sec at approximately 4 cycles. Failure is desired in the mounting for a known design of the mount.

[redacted] From Table C-1, Item 1b, σ/m = 100 percent.

[redacted] If the velocity level for the explosion conditions is determined to be 1,500 in./sec, the probability of failure from Figure C-1 or C-2 is 69 percent for b_i/b_v = 1.5 and σ/m = 100 percent.

[redacted] For the same conditions, a 95 percent probability of failure requires a value of b_i/b_v of 4.00, or a value of velocity of approximately 4,000 in./sec.

Table C-1. [redacted] Standard Deviations for Use in Probability Analyses [redacted]

Item	σ/m (percent of mean of reference parameter)	Reference Parameter
1. Shock effects on personnel and equipment:		
a. Not shock mounted	100	Shock motion
b. Shock mounted, design of mount known	100	Shock motion
c. Shock mounted, type of mount known, design unknown	150	Shock motion
d. Shock mounted, type of mount and design unknown	200	Shock motion
2. Aboveground structures or elements flush with ground surface	35	Overpressure
3. Underground structural elements subjected to vertical pressure	65	Overpressure
4. Underground structural elements subjected to horizontal pressure	80	Overpressure
5. Openings in rock	50	Slant range

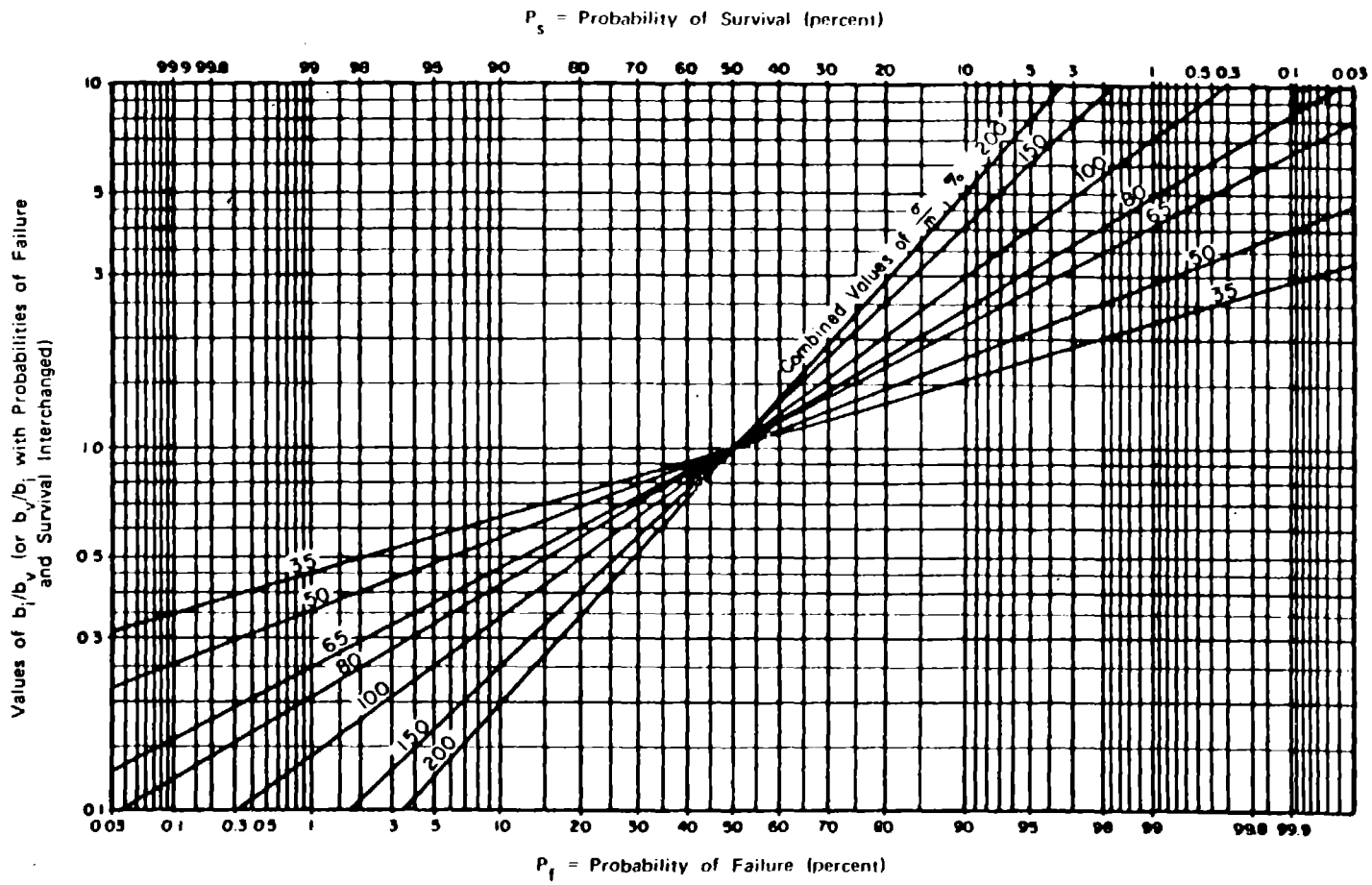

Figure C-1. [redacted] Probability Distributions for Failure or for Survival as Function of Ratio of Median Input Motion b_i to Median Vulnerability Level of Motion b_v [redacted]

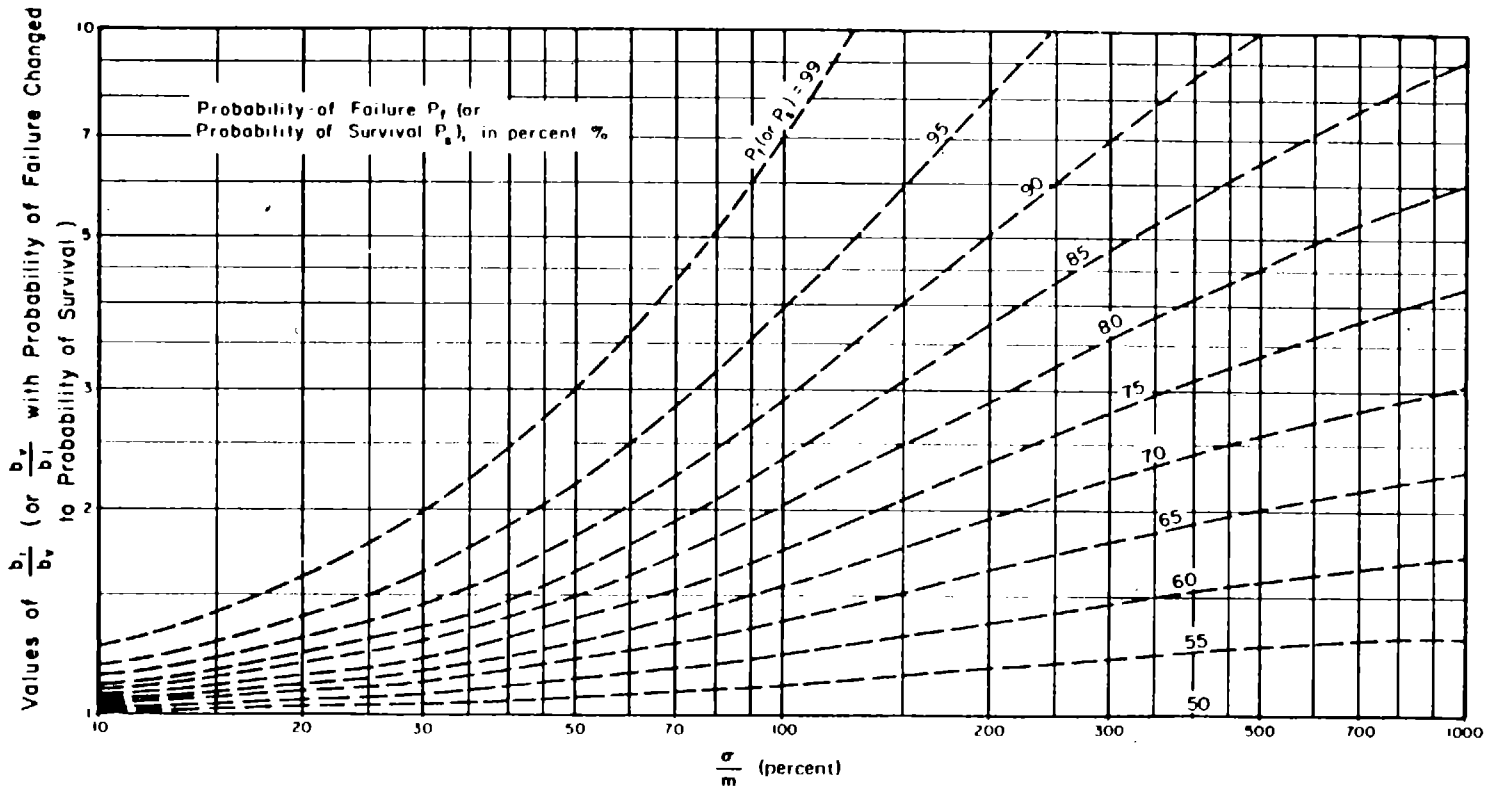

Figure C-2. [redacted] Coefficient of Variation σ/m as Function of b_i/b_v Ratio for Specified Probability of Failure (or of b_v/b_i for Specified Probability of Survival) [redacted]

[redacted]

[redacted] DAMAGE CAUSED BY PRESSURE [redacted]

C-5 Description of Charts for Damage to Surface Structures Caused by Pressure Input [redacted]

[redacted] The probability graphs presented in Figures C-1 and C-2 also apply to failure of surface structures that are sensitive to overpressures or dynamic pressures. In these cases, b_i is the median of the overpressure or dynamic pressure, and b_v is the median vulnerability to overpressure or dynamic pressure. Values of b_i, as a function yield, height of burst, and distance from ground zero may be obtained from the overpressure and dynamic pressure height of burst curves in Section I, Chapter 2.

[redacted] Tables C-2 and C-3 show the median values of overpressure and dynamic pressure respectively, b_v, that correspond to severe damage to the 22 types of structures for which isodamage curves are presented in Figure 11-2 through 11-23. The structures and the types of damage that are considered severe, moderate, or light for each structure are described by number in Table 11-1. Tables C-4 and C-5 show the corresponding overpressures and dynamic pressures, respectively, that provide moderate damage to the same family of structures. Even though the pressure required to produce a stated level of damage to a given structure with a given yield varies somewhat, as shown in the isodamage curves of Chapter 11, the median values presented in the tables are considered to be sufficiently reliable for the calculation of damage probabilities.

[redacted] The ratio σ_i/m_i for the input pressure is assumed to be 20 percent for both overpressure and dynamic pressures, and σ_v/m_v for pressure vulnerability is assigned a value of 30 percent. The combined value may be obtained from the equation given in paragraph C-3:

$$\sigma/m = \left\{\left(\frac{\sigma_i}{m_i}\right)^2 + \left(\frac{\sigma_v}{m_v}\right)^2 + \left(\frac{\sigma_i}{m_i}\right)^2 \left(\frac{\sigma_v}{m_v}\right)^2\right\}^{1/2},$$

$$\sigma/m = \left\{(0.2)^2 + (0.3)^2 + (0.2)^2 \quad (0.3)^2\right\}^{1/2},$$

$$\sigma/m \approx 35 \text{ percent.}$$

With this combined value of σ/m, the probability of failure of a given structure subjected to a specified overpressure or dynamic pressure from a known weapon yield can be determined from Figure C-1 or C-2. For example, consider a diffraction sensitive structure similar to type 11-3 that is subjected to an overpressure of 20 psi from a 3 kt explosion. From Table C-2, the median overpressure vulnerability corresponding to a 3 kt yield is 15 psi. The ratio b_i/b_v is, therefore, 1.333. Using b_i/b_v = 1.333, and σ/m = 35 percent, P_f = 80 percent as the probability of severe structural damage from either Figure C-1 or Figure C-2. The corresponding probability of failure for light to moderate damage of the same structure may be obtained similarly by using the appropriate overpressure vulnerability obtained from Table C-4.

[redacted] To design for a given probability of survival from severe damage from a specified overpressure or dynamic pressure, b_i, and weapon yield, W, enter Figure C-2 with the given P_s to obtain the value of b_v/b_i corresponding to σ/m = 35 percent. The structure should have a median vulnerability equal to the calculated b_v. For example, if the median overpressure from a 30 kt weapon is 10 psi, the design of a structure corresponding to structure type 11-5 with a 70 percent probability of survival from severe damage is determined from Figure C-2, with σ/m = 35 percent and P_s = 70 percent, to be b_v/b_i = 1.25. Hence, the structure must have a median vulnerability of 1.25 b_i = 12.5 psi to achieve a 70 percent probability of survival.

[redacted]

[redacted]

[redacted] To inflict severe damage to a surface structure of known type with a given probability of failure, Figure C-1 or C-2 is entered with this probability to obtain a ratio b_i/b_v corresponding to σ/m = 35 percent. The required median overpressure or dynamic pressure, b_i, is then obtained in terms of b_v from Table C-2 for diffraction sensitive structures or from Table C-3 for drag sensitive structures. A yield that will provide the required pressure input is then selected with the aid of the height of burst curves in Section 1, Chapter 2.

C-6 Description of Charts for Damage to Underground Structures Caused by Pressure Input [redacted]

[redacted] Failure due to vertical overpressures or horizontal pressures must be distinguished for underground structures that are sensitive to soil pressures. Again, b_i is the median of the applied pressure. In this case, the median vulnerability, b_v, to vertical or horizontal pressure is obtained by the procedures discussed in Section II and III, Chapter 11.

[redacted] When using the probability charts, a value of σ/m = 65 percent should be used for structures and structural elements subjected to vertical pressures; however, for structures and structural elements subjected to horizontal pressures, a value of σ/m = 80 percent should be used with appropriate b_i/b_v or b_v/b_i. The procedure for the analysis of the probability of failure or of survival is the same as for aboveground structures. Therefore, the illustrations presented for aboveground structures may be followed.

[redacted] For deep underground openings in rocks that are sensitive to slant range, the quantities b_i and b_v must be expressed in terms of slant range. Similarly, the value of σ/m = 50 percent given in Table C-1 for openings also is expressed in the same term. The computation of probabilities of failure or of survival is again performed with Figure C-1 or Figure C-2. The procedure is the same as described above except that the ratio b_i/b_v or b_v/b_i is the ratio of the slant ranges, and a value of σ/m = 50 percent should be used (Table C-1).

C-7 Instructions for Pressure Input Analyses [redacted]

[redacted] The instructions given in paragraph C-3 pertaining to the use of Figures C-1 and C-2 for motion inputs also apply for pressure inputs. The only difference is in the determination of b_i/b_v and values of σ/m = 65 percent or 80 percent for underground structures sensitive to vertical and horizontal pressures, respectively or 35 percent for aboveground structures. In the case of pressure inputs, the pressure vulnerabilities of a structure are determined from one of the Tables C-2 through C-5 for aboveground structures. For underground structures, these vulnerabilities must be computed as described in Sections II and III of Chapter 11.

1. For a given surface structural type subjected to a specified weapon yield, determine the pressure vulnerability from Table C-2 or C-3 for severe damage, and from Table C-4 or C-5 for light to moderate damage. Tables C-2 and C-4 give the overpressure vulnerability for diffraction sensitive structures, while Tables C-3 and C-5 give the dynamic pressure vulnerabilities for drag sensitive structures. Comparable values for underground structures must be computed by the methods described in Chapter 11.

2. Using appropriate values of σ/m as given in Items 2, 3, and 4 of Table C-1 for aboveground and underground structures, the probabilities of failure or survival can be determined from Figure C-1 or Figure C-2.

C-8 Illustrative Examples for Pressure Inputs [redacted]

Example 1 [redacted]

[redacted] Consider a 5-story conventional reinforced concrete office building of the type de-

[redacted]

[redacted]

[redacted] scribed as Type 11-3 in Chapter 11. Assume that an explosion of 100 kt yield occurs at a height of burst of 1,100 ft. If the building is located at a distance of 4,200 ft from ground zero, the corresponding height of burst and ground distance from a 1 kt explosion would be

$$h_1 = \frac{h}{W^{1/3}} = \frac{1{,}100}{(100)^{1/3}} = 237 \text{ ft},$$

$$d_1 = \frac{d}{W^{1/3}} = \frac{4{,}200}{(100)^{1/3}} = 905 \text{ ft}.$$

From Figure 2-18, the overpressure is 15 psi. From Table C-2, the median vulnerability is 11 psi. Thus b_i/b_v = 15/11 = 1.36. With this value of b_i/b_v, and σ/m = 35 percent, the probability of severe damage is determined from Figure C-1 or Figure C-2 to be approximately 80 percent. To determine the probability of moderate damage, Table C-4 shows the median vulnerability to be 7 psi, and, therefore, b_i/b_v = 15/7 = 2.14. From Figure C-1 or Figure C-2, the probability of moderate damage is 98 percent.

Example 2 [redacted]

[redacted] For the same structure, yield, and height of burst that were used in Example 1, the distance corresponding to 20 percent probability of severe damage may be determined as follows. With σ/m = 35 percent and the probability of survival equal to (1-0.2) = 80 percent, Figure C-2 shows a ratio b_v/b_i = 1.35. Thus b_i = 11/1.35 = 8.15. The median overpressure, therefore, is 8.15 psi. From Figure 2-19, the distance from ground zero corresponding to a height of burst of 237 feet for a 1 kt explosion and 8.15 psi is 1,220 feet. The corresponding distance from a 100 kt explosion is 5,660 feet. The distance for 20 percent probability of moderate damage corresponds to an overpressure of 7/1.35 (Table C-3 and Figure C-2) = 5.18 psi. From Figure 2-19, the distance from ground zero corresponding to a height of burst of 237 feet for a 1 kt explosion and 5.18 psi is 1,650 feet. The corresponding distance from a 100 kt explosion is 7,660 feet.

C-9 System Consideration [redacted]

[redacted] The calculation of probabilities described in the preceding paragraphs pertains to the failure or survival of a single item or component. If the survival or proper performance of a complete piece of equipment or a system requires the survival of every component in the system, the components can be considered to be in series. An example is that of a shock mounted equipment; the satisfactory performance of the equipment requires the survival of the shock mount as well as of the equipment itself. In determining the failure probability or survival probability of a system the two points of view, the designer's and the weapon analyst's, must be distinguished in arriving at conservative estimates of the actual survival probabilities.

[redacted] From the designer's (defensive) point of view, a conservative estimate of the system failure probability is obtained if the failure of the components are assumed to be statistically independent. The probability of failure of the system is:

$$P_f = 1 - (1 - P_{f1})(1 - P_{f2}) \ldots (1 - P_{f(n-1)})(1 - P_{fn})$$

where P_{f1}, P_{f2} . . . P_{fn} are the probabilities of failure of the individual components, which can be determined with the procedure described in the preceding paragraphs.

[redacted] For example, in the case of the shock mounted equipment, if the probability of failure of the shock mount is 30 percent and that of the equipment is 40 percent, the probability of failure of the system is 1 - (0.70)(0.60) = 58 percent.

[redacted]

[redacted]

Table C-2. [redacted] Median Vulnerability to Overpressures Corresponding to Severe Damage of Diffraction Sensitive Structures [redacted]

Weapon Yield	Type of Structure				
	11-2	11-3	11-4	11-5	11-6
	(Median Vulnerability Overpressure, psi)				
30 mt	28	10	5.0	9.0	3.4
10 mt	29	10	5.0	9.0	3.4
3 mt	30	10	5.0	9.0	3.4
1 mt	30	11	5.0	9.0	3.5
300 kt	30	11	5.0	9.0	3.5
100 kt	32	11	5.0	9.5	3.5
30 kt	34	12	5.0	9.5	3.6
10 kt	34	13	5.5	10.0	3.6
3 kt	36	15	5.5	10.0	3.8
1 kt	48	17	5.5	11.0	4.0
[illegible] kt	–	20	6.0	12.0	4.4
0.1 kt	–	22	6.5	12.0	4.8
0.03 kt	–	24	7.0	13.0	5.2
0.01 kt	–	28	7.5	14.0	5.8

[redacted]

Table C-3. [redacted] Median Vulnerability to Dynamic Pressures Corresponding to Severe Damage of Drag Sensitive Structures [redacted]

Weapon Yield	Type of Structure																
	11-7	11-8	11-9	11-10	11-11	11-12	11-13	11-14	11-15	11-16	11-17	11-18	11-19	11-20	11-21	11-22	11-23
	(Median Vulnerability of Dynamic Pressure, psi)																
30 mt	0.8	1.6	2.6	5.0	2.4	5.0	2.6	2.4	2.0	2.0	9.6	5.0	2.8	3.3	2.0	1.4	0.6
10 mt	0.8	1.6	2.6	6.0	2.6	5.0	2.8	2.4	2.0	2.0	10.0	5.0	2.8	3.3	2.0	1.4	0.6
3 mt	0.9	1.8	2.8	7.0	3.0	6.0	3.0	2.6	2.0	2.0	13.0	5.2	2.8	3.3	2.0	1.4	1.0
1 mt	1.0	2.0	3.2	8.5	3.6	7.0	3.4	3.0	2.0	2.0	20.0	6.0	2.8	3.4	2.0	1.4	1.6
300 kt	1.2	2.2	3.6	12.0	4.8	9.0	4.2	3.8	2.5	2.0	48.0	8.0	3.0	4.0	2.0	1.4	2.8
100 kt	1.4	2.6	4.4	18.0	6.0	11.0	5.2	5.0	3.0	2.2		12.0	3.4	5.2	2.2	1.4	4.5
30 kt	2.0	3.6	5.8	34.0	10.0	16.0	7.0	10.0	4.0	2.6	–	20.0	4.0	10.0	2.6	1.4	7.5
10 kt	3.2	5.2	7.5	–	16.0	26.0	10.0	24.0	7.0	3.5	–	40.0	5.2	24.0	3.4	1.6	12.0
3 kt	5.4	7.5	12.0	–	36.0	–	18.0		15.0	5.0		–	7.0	–	4.6	2.0	20.0
1 kt	9.5	13.0	20.0	–	60.0	–	28.0	–	35.0	12.0	–	–	12.0	–	8.0	2.2	32.0
0.3 kt	18.0	26.0	38.0	–	–	–					–		22.0	–	18.0	3.0	55.0
0.1 kt	–	–	–	–	–	–	–	–	–		–	–	–	–		4.0	85.0
0.03 kt	–	–	–	–	–		–	–		–	–		–	–	–	6.0	
0.01 kt	–	–	–	–		–	–	–		–	–	–	–	–	–	9.0	–

[redacted]

Table C-4. [redacted] Median Vulnerability to Overpressures Corresponding to Moderate Damage of Diffraction Sensitive Structures [redacted]

Weapon Yield	Type of Structure				
	11-2	11-3	11-4	11-5	11-6
	(Median Vulnerability Overpressure, psi)				
30 mt	20	6.5	3.4	6.5	2.2
10 mt	20	6.5	3.4	6.5	2.2
3 mt	20	6.5	3.4	6.5	2.2
1 mt	20	6.5	3.4	6.5	2.2
300 kt	20	6.5	3.4	6.5	2.2
100 kt	20	7.0	3.4	6.5	2.2
30 kt	20	7.0	3.4	6.5	2.2
10 kt	20	7.0	3.6	6.5	2.2
3 kt	22	7.5	3.6	6.5	2.2
1 kt	24	8.0	3.6	6.5	2.2
0.3 kt	28	9.0	3.8	7.0	2.4
0.1 kt	–	10.0	4.0	7.5	2.6
0.03 kt	–	11.0	4.2	7.5	2.8
0.01 kt	–	12.0	4.4	8.0	3.0

[redacted]

Table C-5. [redacted] Median Vulnerability to Dynamic Pressures Corresponding to Moderate Damage of Drag Sensitive Structures [redacted]

Weapon Yield	Type of Structure																
	11-7	11-8	11-9	11-10	11-11	11-12	11-13	11-14	11-15	11-16	11-17	11-18	11-19	11-20	11-21	11-22	11-23
	(Median Vulnerability of Dynamic Pressure, psi)																
30 mt	0.6	1.2	2.0	3.4	1.6	3.6	2.0	2.4	2.0	2.0	9.6	5.0	2.8	3.2	2.0	1.4	0.2
10 mt	0.6	1.2	2.0	3.4	1.6	3.6	2.0	2.4	2.0	2.0	10.6	5.0	2.8	3.2	2.0	1.4	0.2
3 mt	0.6	1.2	2.0	3.4	1.6	3.6	2.0	2.4	2.0	2.0	12.0	5.2	2.8	3.2	2.0	1.4	0.4
1 mt	0.6	1.2	2.0	3.6	1.8	3.8	2.0	2.6	2.0	2.0	16.0	5.8	2.8	3.2	2.0	1.4	0.6
300 kt	0.6	1.2	2.0	4.0	2.0	4.0	2.2	2.8	2.0	2.0	26.0	7.4	2.8	3.4	2.0	1.4	1.0
100 kt	0.6	1.2	2.2	4.4	2.0	4.4	2.4	3.2	2.2	2.0	46.0	9.0	3.0	4.0	2.0	1.4	2.0
30 kt	0.6	1.4	2.4	5.4	2.4	5.2	2.6	4.0	2.8	2.2	88.0	14.0	3.4	5.0	2.2	1.4	3.0
10 kt	0.8	1.4	2.6	7.5	3.0	6.0	3.0	6.0	3.6	2.8	–	22.0	4.0	8.4	2.4	1.4	5.0
3 kt	0.8	1.6	3.2	12.0	4.4	9.0	3.6	12.0	6.4	4.2	–	40.0	5.4	18.0	3.4	1.6	8.0
1 kt	1.0	2.0	4.0	20.0	7.5	12.0	5.0	30.0	12.0	6.2	–	–	7.4	36.0	4.6	1.8	13.0
0.3 kt	1.2	3.0	6.0	40.0	13.0	22.0	9.0	–	–	16.0	–	–	10.0	–	6.4	2.2	22.0
0.1 kt	2.2	5.0	10.0	–	20.0	–	16.0	–	–	–	–	–	15.0	–	14.0	2.6	60.0
0.03 kt	–	–	–	–	–	–	–	–	–	–	–	–	–	–	–	3.4	100.0
0.01 kt	–	–	–	–	–	–	–	–	–	–	–	–	–	–	–	4.2	–

[redacted] However, from the weapon analyst's (offensive) standpoint, a conservative estimate of the system failure probability may be obtained if the failure or survival of the components are assumed to be perfectly correlated. In this case, the probability of failure of the system is equal to the largest value among the failure probabilities of the components, or

$$P_f = \max\ (P_{f1}, P_{f2}, \ldots, P_{fn}) .$$

In the example given above for shock mounted equipment, the system failure probability would be 40 percent.

SECTION II

[redacted] DERIVATION OF EQUATIONS USED IN SECTION I [redacted]

[redacted] The treatment used herein is based on the logarithmic normal distribution that was used in Section I. Values were given for the ratio of the standard deviation to the mean of a lognormal distribution, obtained by combining the corresponding quantities for individual parameters governing the distribution.

[redacted] Consider a logarithmic normal distribution for vulnerability, characterized by the parameter σ_v for standard deviation, m_v for mean, b_v for median. Now consider also a logarithmic normal distribution for input having similar parameters, but with the subscript i instead of v. Each case is designated by d_v and β_v or d_i and β_i, respectively, the mean value and standard deviation of the logarithm of the corresponding variate.

C-10 Properties of Lognormal Variates [redacted]

[redacted] For logarithmic normal random variables, the relationships between the above parameters are as follows:

$$m = e^{\alpha + \frac{\beta^2}{2}} ,$$

$$\sigma^2 = m^2 \left(e^{\beta^2} - 1\right), \quad \text{or} \quad \left(\frac{\sigma}{m}\right)^2 = e^{\beta^2} - 1.$$

Thus,

$$\beta^2 = \ln\left[\left(\frac{\sigma}{m}\right)^2 + 1\right]$$

Also,

$$\alpha = \ln\ b$$

where b is the median of the lognormal variable.

C-11 Probability of Failure or Survival [redacted]

[redacted] Assume that the input I and vulnerability V are both logarithmic normal variates with mean and standard deviations m_i, σ_i and m_v, σ_v, respectively, and hence corresponding medians b_i and b_v. The logarithms of the input and vulnerability are therefore individually normal random variables.

[redacted] Failure occurs whenever the vulnerability is less than or equal to the input; or $I/V \geqslant 1.0$. If

$$X = \frac{I}{V},$$

then failure means $X \geqslant 1.0$, or $\ln X = (\ln I - \ln V) \geqslant 0$. Therefore, $\ln X$ is also normal with parameters

$$\alpha = \alpha_i - \alpha_v,$$

and

$$\beta = \left(\beta_v^2 + \beta_i^2\right)^{1/2}.$$

Therefore, the probability of failure P_f is

$$P_f = \frac{1}{\sqrt{2\pi}\,\beta} \int_0^\infty e^{-\frac{1}{2}\left(\frac{\ln X - \alpha}{\beta}\right)^2} d(\ln X).$$

[redacted]

[redacted]

Let

$$y = \frac{\ln X - \alpha}{\beta}.$$

Then

$$dy = \frac{d(\ln X)}{\beta},$$

and

$$P_f = \frac{1}{\sqrt{2\pi}} \int_{-\frac{\alpha}{\beta}}^{\infty} e^{-\frac{1}{2} y^2} \, dy$$

= area of standard normal curve from $-\frac{\alpha}{\beta}$ to ∞.

But

$$\alpha = \alpha_i - \alpha_v = \ln b_i - \ln b_v.$$

Hence,

$$\alpha = \ln \frac{b_i}{b_v},$$

and,

$$\beta = \left(\ln \left[\left(\frac{\sigma}{m} \right)^2 + 1 \right] \right)^{1/2} = \left(\beta_v^2 + \beta_i^2 \right)^{1/2}.$$

Therefore,

$$\ln \left[\left(\frac{\sigma}{m} \right)^2 + 1 \right] = \ln \left[\left(\frac{\sigma_v}{m_v} \right)^2 + 1 \right] \left[\left(\frac{\sigma_i}{m_i} \right)^2 + 1 \right],$$

and

$$\left(\frac{\sigma}{m} \right) = \left(\left(\frac{\sigma_v}{m_v} \right)^2 + \left(\frac{\sigma_i}{m_i} \right)^2 + \left(\frac{\sigma_v}{m_v} \right)^2 \left(\frac{\sigma_i}{m_i} \right)^2 \right)^{1/2}.$$

This is the equation given in paragraph C-3. Therefore, for specified (σ/m), β is a non-negative constant, and

$$P_f = \frac{1}{\sqrt{2\pi}} \int_{\frac{\alpha}{\beta}}^{\infty} e^{-\frac{1}{2} y^2} \, dy$$

$$= \frac{1}{\sqrt{2\pi}} \int_{-\frac{1}{\beta} \ln \left(\frac{b_i}{b_v} \right)}^{\infty} e^{-\frac{1}{2} y^2} \, dy,$$

which gives a linear plot of b_i/b_v with P_f on lognormal probability paper, as shown in Figure C-1.

[redacted] If the ordinates in Figures C-1 and C-2 are expressed in b_v/b_i, it can be shown that the probability of failure in these curves becomes the probability of survival. From the equations given above,

$$P_s = 1 - \frac{1}{\sqrt{2\pi}} \int_{-\frac{1}{\beta} \ln \left(\frac{b_i}{b_v} \right)}^{\infty} e^{-\frac{1}{2} y^2} \, dy$$

$$= \frac{1}{\sqrt{2\pi}} \int_{-\infty}^{\infty} e^{-\frac{1}{2} y^2} \, dy -$$

[redacted]

[redacted]

[redacted]

$$= \frac{1}{\sqrt{2\pi}} \int_{-\frac{1}{\beta}\ln\left(\frac{b_i}{b_v}\right)}^{\infty} e^{-\frac{1}{2}y^2}\, dy$$

$$= \int_{-\infty}^{-\frac{1}{\beta}\ln\left(\frac{b_i}{b_v}\right)} e^{-\frac{1}{2}y^2}\, dy$$

$$= \int_{-\infty}^{\frac{1}{\beta}\ln\left(\frac{b_v}{b_i}\right)} e^{-\frac{1}{2}y^2}\, dy.$$

Since the standard normal distribution is symmetric about the origin, this integral is equal to the integral for P_f. Therefore, the probabilities in Figures C-1 and C-2 become probabilities of survival if the ordinates are replaced by b_v/b_i.

[redacted]

[redacted]

APPENDIX D

[redacted] ABSTRACTS OF DNA HANDBOOKS [redacted]

[redacted] NUCLEAR WEAPONS BLAST PHENOMENA [redacted]

[redacted] *DASA 1200 (Vols. I-V)* (Vol. I, SRD; Vol. II, CRD; Vol. III, SFRD; Vol. IV, to be published; Vol. V, CFRD).

[redacted] *Prepared by:* DASIAC, Santa Barbara, California. Major contributors: Defense Atomic Support Agency, Kaman Nuclear, URS Research Company, Bolt, Beranek, and Newman, and Dikewood Corporation.

[redacted] *Availability:* Volumes I through III through Defense Documentation Center on request through Defense Nuclear Agency, Washington, D.C. 20305. Volume V, limited distribution.

[redacted] DASA 1200 is a source book of air blast data and theory applicable to nuclear explosions occurring in free air, on or near the surface, and beneath the surface. Volume I begins with a detailed description of the nuclear explosion energy source, and presents the theoretical background associated with the formation and propagation of the blast wave in free air. The long range propagation of shock waves is treated in detail. Volume II presents a discussion of blast wave interaction phenomena, including ideal reflection and refraction, ideal diffraction, and nonideal effects. A discussion of topography and shock wave shielding and a section on air blast measurements in the high pressure region also are included. Volume III contains an analysis of and methods for the prediction of the blast phenomena from nuclear weapons burst at moderate altitudes, on the surface, underwater, and underground. Volume IV contains a discussion of the simulation of nuclear air blast phenomena with high explosives. Volume V is a compilation of the measurements of the various blast parameters associated with nuclear weapons at the various nuclear operations. It is planned for limited distribution to scientists and agencies who are working in the field of nuclear weapons blast phenomena.

[redacted] HANDBOOK OF UNDERWATER NUCLEAR EXPLOSIONS [redacted]

[redacted] *DASA 1240* [redacted]

[redacted] *Prepared by:* DASIAC, Santa Barbara, California. Major contributors include NOL, DTMB, Waterways Experiment Station, Naval Civil Engineering Laboratory and the U.S. Naval Radiological Defense Laboratory.

[redacted] *Availability:* Qualified requestors may obtain these documents from the Defense Documentation Center. Each transmittal outside the agencies of the U.S. Government must have prior approval of the Defense Nuclear Agency.

[redacted] The Handbook of Underwater Nuclear Explosions is divided into two parts: Part I, Phenomena, consists of 11 chapters, and Part II, Effects, consists of 13 chapters. Individual chapters and in some cases sections of chapters have been previously published separately.

[redacted] The entire handbook is undergoing revision and will be published in three volumes. The revised Handbook of Underwater Nuclear Explosions will be an authoritative presentation of current knowledge and a reliable source of useful data concerning the phenomena of underwater nuclear explosions. The presentation will include the phenomena of shock wave propaga-

[redacted]

[redacted]

[redacted]

tion, surface waves, underwater cratering, and radioactive debris. The effects of underwater explosions on surface ships, submarines, harbors, and structural installations also will be described.

[redacted] NUCLEAR GEOPLOSICS (A Sourcebook of Underground Phenomena and Effects of Nuclear Explosions) [redacted]

[redacted] *DASA 1285 (Volumes I-V)* [redacted]

[redacted] *Prepared by:* Stanford Research Institute, Menlo Park, California.

[redacted] *Availability:* This document is not approved for open publication or distribution to the Office of Technical Services, Department of Commerce. Qualified requestors may obtain copies of this report from Defense Documentation Center. Foreign announcement and dissemination of this report is not authorized.

[redacted] The Nuclear Geoplosics Handbook contains five volumes: Part I, Theory of Directly Induced Ground Motions; Part II, Mechanical Properties of Earth Materials; Part III, Test Sites and Instrumentation; Part IV, Empirical Analysis of Ground Motion and Cratering; and Part V, Effects on Underground Structures and Equipment.

[redacted] The theory of directly induced ground motion is presented in Part I. The tools and elements required for the study of ground motion effects are discussed. Two analytical solutions of shock propagations are presented. Theoretical predictions (obtained by numerical and analytical methods) are compared with field measurements. The mechanical properties of earth materials are described in Part II. It consists of a preparation of a clear and systematic, but largely qualitative, description of the resistance of earth materials to compression and shear. A summary on stress-strain behavior with very short load durations is included. The basic concepts regarding the mechanical behavior of soil and experimental methods of determining the mechanical properties of soil are described. The physical characteristics of test sites and instrumentation of nuclear and high explosive detonations on which ground motion has been measured are presented in Part III. The discussion of air blast induced ground motion in Part IV relies primarily on experimental evidence. A knowledge of the effects induced in the free field ground motion, the factors influencing these effects, the structure-medium interaction, and the factors influencing interaction is implicit in the study of behavior of underground structures. Part V summarizes these various phenomena as they apply to understanding structures in general and discusses the behavior of equipment mounted within a structure.

[redacted] The book is meant to be an authoritative sourcebook. It is not meant to be a handbook of design specifications.

[redacted] Part II and Part IV are currently under revision. Publication is expected during calendar year 1973.

[redacted] TREE (Transient-Radiation Effects on Electronics) HANDBOOK [redacted]

[redacted] DNA 1420 H-1 (edition 3), DNA 1420 H-2 (edition 3), (1420 H-1, [redacted] 1420 H-2, [redacted]

[redacted] *Prepared by:* Battelle Memorial Institute, Columbus, Ohio

[redacted] *Availability:* Qualified requestors may obtain this document from the Defense Documentation Center. Foreign announcement and dissemination is not authorized.

[redacted] The TREE Handbook consists of two volumes which present information that will be useful to a design engineer who is designing electronic systems for survival in a nuclear-burst environment. The information that is presented covers those areas directly related to electronic parts, circuits, and systems. The

[redacted]

[redacted]

[redacted]

nuclear-burst environment that is covered includes both transient and steady state. It also includes all radiation effects except external EMP. Major areas covered in DNA 1420 H-1 are: the simulated versus burst environment, interaction of transient radiation with matter, discrete semiconductor devices, integrated circuits, capacitors, resistors, miscellaneous electronic materials and devices, circuit hardening, and network analysis techniques. DNA 1420 H-2 discusses the nuclear weapon-burst environment, interaction of transient radiation with matter, system hardening, and internal EMP.

[redacted] The TREE Handbook is updated on a continuing basis.

[redacted] **THEORETICAL MODELS FOR NUCLEAR FIREBALLS** [redacted]

[redacted] *DASA 1589-A, 1589-B, 1589-1 through 1589-39* (1589-A, [redacted] 1589-B, [redacted] 1589-1 through 1589-39, [redacted]

[redacted] *Prepared by:* Lockheed Missiles and Space Company, Sunnyvale, California.

[redacted] The first volume, with parts A and B, describes a radiation hydrodynamic code appropriate for calculation of nuclear fireball phenomenology in the lower atmosphere. Part A describes the code, and part B discusses the results. The FIREBALL code is a one dimensional, spherical, Lagrangian, radiation-hydrodynamics code, which employs a non-grey transport equation to describe the radiation field. The code is used to compute 39 theoretical models for bombs of various explosion yields at various altitudes. These graphical descriptions are the 39 volumes (DASA 1589-1 through 1589-39). Results are compared to experimental measurements made in U.S. field tests.

[redacted] **WEAPONS RADIATION SHIELDING HANDBOOK** [redacted]

[redacted] *DASA 1892-1 through 1892-6* (DASA 1892-1, -2, -3, and -5, [redacted] DASA 1892-4, [redacted] DASA 1892-6, [redacted]

[redacted] *Prepared by:* Oak Ridge National Laboratory, Oak Ridge, Tennessee. Major contributors: Radiation Research Associates and the University of Tennessee.

[redacted] *Availability:* Qualified requestors may obtain these documents from the Defense Documentation Center. Requests for DASA 1892-4 must be on request through Headquarters, Defense Nuclear Agency, Washington, D.C. 20305.

[redacted] DASA 1892-5 (Chapter 2 of the handbook) describes the basic concepts underlying the methods used for weapon radiation shield analyses. These concepts include the quantities used to describe particle populations and the quantities used to describe radiation interactions with materials. The characteristics of the particular radiations produced by weapons, neutrons and gamma rays, are discussed in detail, including their physical properties and their important interactions. The processes by which neutrons and gamma rays are produced also are described. The chapter also discusses the various response functions that are used to convert a radiation field to a biological effect.

[redacted] DASA 1892-3 (Chapter 3 of the handbook) surveys the methods used most frequently to calculate the attenuation of neutrons and gamma rays. Summaries of computer codes based on the various methods also are provided. All of the techniques are either approximate solutions to the Boltzmann equation or are based on kernels obtained from solutions to the equation.

[redacted] DASA 1892-2 (Chapter 4 of the handbook) surveys the work performed to date on

[redacted]

[redacted]

[redacted] the various types of nuclear radiation albedos, particularly as they relate to penetration of air filled openings through radiation shields (ducts, passageways, etc.). This topic is important in that the primary increase in the radiation that penetrates a shield results from such openings and enters primarily as a result of the successive scattering of the radiation from the walls of the openings. Most of the techniques for estimating the transmission through such openings depend on the use of albedos.

[redacted] DASA 1892-1 (Chapter 5 of the handbook) describes effective methods for designing air filled holes in protective structures (access ways, ventillation ducts, other utility pipes, distributed voids resulting from the use of nonhomogeneous material in the structure, etc.) to reduce the amount of radiation that enters the structure.

[redacted] DASA 1892-4 (Chapter 6 of the handbook) describes the various sources of radiation produced by a nuclear explosion and presents techniques for calculating the transport of the radiations from the point of burst to the surface of a shield, i.e., it presents methods for determining source terms for shield attenuation calculations. The emphasis is on initial radiation, i.e., that produced within the first minute following the explosion.

[redacted] DASA 1892-6 (Chapter 7 of the handbook) presents a simplified method for designing (or evaluating) shield covers on single compartment underground structures that will protect against the neutrons and initial gamma rays. Emphasis is given to neutrons. The method is limited to surface or near surface bursts, to weapon yields between 1 kiloton and 20 megatons, and to distances from the burst at which overpressures are between 5 and 100 psi, but no closer than 500 meters.

[redacted] THERMAL RADIATION PHENOMENA [redacted]

[redacted] *DASA 1917 (Volumes 1-6)* (Vols. I-V, [redacted] Vol. VI, [redacted] *Prepared by:* Lockheed Missiles and Space Company, Palo Alto Research Laboratory, Palo Alto, California. Major contributor: The Rand Corporation.

[redacted] *Availability:* Qualified requestors may obtain these documents from the Defense Documentation Center. Volumes I through V are approved for open publication. Volume VI is available only by request through Headquarters, Defense Nuclear Agency, Washington, D.C. 20305.

[redacted] Volume I of the six volume handbook describes the equilibrium thermodynamic properties of high temperature air. The report contains information on air and a mixture of ideal gases in chemical equilibrium: ideal gas properties for monatomic gases, diatomic gases, and polyatomic gases. The effects of interparticle forces on the thermodynamic properties of air, effects of coulomb forces on the thermodynamic properties of air, and equilibrium calculations and results for air are discussed. Tables and graphs of the composition and properties of the atmosphere are included.

[redacted] Volume II presents the theoretical aspects of the equilibrium radiative properties of air. The theory of radiation in hot gases (elementary radiative transfer, theory of radiation, theory of molecular absorption) is described. Spectral and mean absorption coefficients of heated air and spectroscopic properties of six important band systems that contribute to opacity of heated air are included.

[redacted] Tables of the equilibrium radiative properties of air and its constituents are presented in Volume III for a wide range of temperatures and densities. The information contained in the tables is a combination of experimental data and theoretical computation.

[redacted]

[redacted]

[redacted] Volume IV describes the excitation and nonequilibrium phenomena of air that has been subjected to a large amount of radiation. Topics include: absorption and scattering of X-rays and gamma rays; collisions of ions and electrons with air molecules; secondary processes following this excitation (including the creation of various chemical species); X-ray heating and shock heating of air, with special reference to very high energy densities; the approach to composition equilibrium in low and high temperature air; adiabatic, near equilibrium cooling of air and the formulation of a criterion for local thermodynamic equilibrium; nonequilibrium radiative transport and its effect on the total amount and the spectrum of emitted radiation; radiation in tenuous air at high temperatures; and radiation in tenuous air with contaminants at low temperatures.

[redacted] Volume V provides an introduction to radiation hydrodynamics (RH). It contains a discussion of the application of RH to fireballs in the atmosphere. After formulating the basic equations of RH, special attention is given to the radiative transfer problem. Several methods for solving the equations of transfer are touched upon, but special emphasis is placed on the two stream method with a frequency averaging procedure, which is specifically designed for use with finite zone sizes. A version of the fireball code, which uses this approach, is described.

[redacted] Volume VI provides data concerning the interaction of nuclear weapon radiation and debris with the atmosphere. The theoretical analysis of fireball development uses computations based on the equations of radiation hydrodynamics (RH). Various models for simplifying these equations are described, and a summary of codes and calculations based on these models is included. The emphasis of the theoretical discussion is on the status of understanding rather than a detailed quantitative treatment. Yield and altitude scaling laws are developed.

[redacted] **DASA REACTION RATE HANDBOOK**

[redacted] DNA 1948H [redacted]

[redacted] *Prepared by:* General Electric Company, Missile and Space Division, Philadelphia, Pennsylvania. Major contributors: General Electric, TEMPO, University of Pittsburgh, Air Force Cambridge Laboratory, Geophysics Corporation of America, The Rand Corporation, G. C. Dewey Corporation, University of Colorado, General Atomic, Westinghouse Research Laboratories, NASA Ames Research Center, and Air Force Weapons Laboratory.

[redacted] *Availability:* Qualified requestors may obtain this handbook from the Defense Documentation Center.

[redacted] This handbook contains useful, accurate, and reliable information on upper atmospheric chemical and physical processes. Such information is required for the solution of various problems involving military radar and communication blackout. Periodic additions to, and revisions of, this handbook are planned to accomodate new information, revisions of older data, corrections, etc. The material is presented in 19 separate chapters covering pertinent aspects of reaction rate science. Appropriate appendices and illustrations are included.

[redacted] This handbook was issued in March 1973 and is still in process of being completed according to original plans. Several revisions have been made to update the original contents.

[redacted] **NUCLEAR EFFECTS ON VLF AND LF COMMUNICATION SYSTEMS** [redacted]

[redacted] *DASA 1954 (Volumes I and II)* (Vol. I, [redacted] Vol. II, [redacted]

[redacted] *Prepared by:* Institute for Telecommunications Sciences, Boulder, Colorado. Major contributors: General Electric/TEMPO, Illinois Institute of Technology Research Institute.

[redacted]

[redacted]

[redacted] *Availability:* Qualified requestors may obtain these documents from the Defense Documentation Center through Headquarters, Defense Nuclear Agency, Washington, D.C. 20305.

[redacted] This handbook is published in two volumes that describe the effects of nuclear bursts on the propagation of LF and VLF communication systems.

[redacted] The examples presented in Volume I illustrate the approximate duration and extent over which typical systems may experience difficulty. In addition to specific results, a brief tutorial description of the effects of nuclear bursts on radio wave propagation and VLF and LF propagation in natural environments is given.

[redacted] Volume II presents techniques for modeling a relatively wide range of nuclear situations and for predicting how these situations would degrade LF and VLF communications system performance. This volume is intended to be used with Volume I. Together, they provide a basic understanding of nuclear phenomenology and its interrelation with LF and VLF propagation.

[redacted] NUCLEAR EFFECTS ON HF COMMUNICATION SYSTEMS [redacted]

[redacted] *DASA 1955 (Volumes I and II)* [redacted]

[redacted] *Prepared by:* Stanford Research Institute, Menlo Park, California. Major contributors: General Electric/TEMPO, Illinois Institute of Technology Research Institute.

[redacted] *Availability:* Qualified requestors may obtain these documents from the Defense Documentation Center through Headquarters, Defense Nuclear Agency, Washington, D.C. 20305.

[redacted] This handbook is published in two volumes that describe propagation effects of nuclear bursts on HF communication systems.

[redacted] The examples presented in Volume I illustrate the approximate duration and extent over which typical systems may experience difficulty. In addition to specific results, a brief tutorial description of the effects of nuclear bursts on radio wave propagation and HF propagation in natural environments is given.

[redacted] Volume II presents techniques for modeling a relatively wide range of nuclear situations and for predicting how these situations would degrade HF communication system performance. This volume is intended to be used with Volume I. Together they provide a basic understanding of nuclear phenomenology and its interrelation with HF propagation.

[redacted] NUCLEAR EFFECTS ON SATELLITE AND SCATTER COMMUNICATION SYSTEMS [redacted]

[redacted] *DASA 1956-1, 1956-2 Vol. I, 1956-2 Vol. II* [redacted]

[redacted] *Prepared by:* Electromagnetic Systems Laboratories, Sunnyvale, California. Major contributors: General Electric/TEMPO, Illinois Institute of Technology Research Institute.

[redacted] *Availability:* Qualified requestors may obtain these documents from the Defense Documentation Center through Headquarters, Defense, Nuclear Agency, Washington, D.C. 20305.

[redacted] This handbook contains two parts. Part 1 describes the propagation effects of selected nuclear bursts on satellite and scatter communication systems. The examples presented illustrate the approximate duration and extent over which typical systems may experience difficulty. In addition to specific results, a brief tutorial description of the effects of nuclear bursts on radio wave propagation and satellite and scatter propagation in natural environments is given.

[redacted] Part 2, consisting of two volumes, describes the effects of nuclear bursts on the propagation of satellite communication systems

[redacted]

[redacted]

[redacted] (Vol. I) and troposcatter and ionoscatter communication systems (Vol. II). Techniques to model a relatively wide range of nuclear situations and to predict how these situations would degrade the communication systems performance are presented. These volumes are intended to be used with DASA 1956-1. Together, they provide a basic understanding of nuclear phenomenology and its interrelation with propagation to satellites.

[redacted] TREE PREFERRED PROCEDURES (Selected Electronic Parts) [redacted]

[redacted] *DNA 2028H* [redacted]

[redacted] *Prepared by:* Battelle Columbus Laboratories, Columbus, Ohio.

[redacted] *Availability:* Qualified requestors may obtain this document from the Defense Documentation Center.

[redacted] This document provides persons conducting TREE (transient radiation effects on electronics) experiments with recommended procedures which experience has shown to be efficient for determining transient radiation effects on electronic parts. Areas that are covered in detail include: experimental design, experimental documentation, dosimetry and environmental correlation, and preferred measurement procedures for diodes, transistors, capacitors, and microcircuits.

[redacted] HANDBOOK FOR ANALYSIS OF NUCLEAR WEAPON EFFECTS ON AIRCRAFT [redacted]

[redacted] DNA 2048 (Revised March 1976) (DNA 2048 H-[redacted] DNA 2048 H-2. [redacted]

[redacted] *Prepared by:* Kaman Avidyne, Burlington, Massachusetts

[redacted] *Availability:* Qualified requestors may obtain this handbook from the Defense Documentation Center.

[redacted] This handbook and its supplement are designed for use in analyzing conventional nuclear weapon effects on aircraft. DNA 2048 contains a comprehensive review of a large body of available literature pertinent to vulnerability and safety analysis of aircraft subjected to the effects of nuclear explosions. The handbook describes methods for analyzing material velocity, overpressure, thermal radiation and nuclear radiation effects on airplanes and helicopters, including the crew. Sure-safe and sure-kill criteria pertinent to the various weapon effects are presented, as well as the methods to be employed in constructing aircraft sure-safe and sure-kill burst-time volumes. The supplement to DNA 2048 is a handbook of computer programs designed to analyze nuclear weapon effects on aircraft. Detailed methodology for anlyzing material velocity (gust), overpressure, thermal radiation and nuclear radiation effects on airplanes and helicopters, including crew, are presented. Only the computer programs corresponding to the methods of analyzing of DNA 2048 are included, and a full understanding of the programs will require access to DNA 2048.

[redacted] A MANAGEMENT GUIDE TO TREE [redacted]

[redacted] *DNA 2051H* [redacted]

[redacted] *Prepared by:* Batelle Columbus Laboratories, Columbus, Ohio.

[redacted] *Availability:* Qualified requestors may obtain this document from the Defense Documentation Center through Headquarters, Defense Nuclear Agency, Washington, D.C. 20305.

[redacted] This guide is intended primarily for management personnel associated with the development of electronic systems that must survive the transient radiation environment generated by a nuclear explosion. The document is intended to be useful to the manager, whether his background and responsibilities are wholly technical, technically oriented, or wholly administrative. The guide is also a satisfactory primer for engineering and scientific personnel.

[redacted]

[redacted]

[redacted] SUMMARY OF COMMUNICATION SYSTEMS DEGRADATION IN A NUCLEAR ENVIRONMENT [redacted]

[redacted] *DASA 2090* [redacted]

[redacted] *Prepared by:* General Electric/TEMPO, Santa Barbara, California. Major contributor: Illinois Institute of Technology Research Institute.

[redacted] *Availability:* Qualified requestors may obtain this document from the Defense Documentation Center through Headquarters, Defense Nuclear Agency, Washington, D.C. 20305.

[redacted] This report summarizes the degradation of communication systems in a nuclear environment. It is based on the results of a three year program to determine the effects of nuclear detonations on communication systems. The report provides information that will aid in determining whether sophisticated analyses are required to predict degradation.

[redacted] DNA EMP (ELECTROMAGNETIC PULSE) HANDBOOK [redacted]

[redacted] *DNA 2114H-1 (Volume 1), DNA 2114H-2 (Volume 2), DNA 2114H-3 (Volume 3), DNA 2114H-4 (Volume 4),* (Volumes 1, 2, and 4 [redacted]. Volume 3, [redacted] Volume 3 will be issued early in calendar year 1973.

[redacted] *Prepared by:* DASIAC, Santa Barbara, California. Major contributors: Illinois Institute of Technology Research Institute, Mission Research Corporation, American Nucleonics Corporation, Lawrence Livermore Laboratory, U.S. Army Harry Diamond Laboratories, Braddock, Dunn and McDonald, Incorporated, Hughes Aircraft Corporation, Procedyne Corporation, Stanford Research Institute, Sandia Corporation, Air Force Weapons Laboratory, Massachusetts Institute of Technology, Defense Nuclear Agency, General Electric/TEMPO.

[redacted] *Availability:* Qualified requestors may obtain this document from the Defense Documentation Center. Volume 3 must be obtained on request through Headquarters, Defense Nuclear Agency, Washington, D.C. 20305.

[redacted] Volume 1 is designed for the practical electrical engineer. It contains information concerning an overall system evaluation and the practices that should be followed in circuit layout, shielding, grounding, and the use of protective devices for systems that are hardened to EMP. Volume 2 is designed for the theoretical or experimental analyst. It includes an analytic treatment of EMP problems in shielding, antennas, cables, and filters, experimental and analytic information on component degradation, and survey information on test methods and hardware. Volume 3 develops EMP threat criteria and provides an assessment of real system effects. The EMP environment information is presented from a system standpoint. Volume IV contains bibliographic and computer code information. Over 1,000 citations are given for such topics as theoretical calculations and nuclear test data related to the EMP environment and detection, EMP vulnerability analysis for systems and components, EMP protection, internal EMP, test direction and planning, and EMP simulators, sensors, and instrumentation. Current EMP computer codes are described and compared for the topics of environment, internal EMP, and circuit analysis.

[redacted] CORRECTIONS FOR DASA COMMUNICATION HANDBOOK (DASA 1954, 1955, 1956) [redacted]

[redacted] *DASA 2313* [redacted]

[redacted] *Prepared by:* General Electric/TEMPO, Santa Barbara, California.

[redacted] *Availability:* Qualified requestors may obtain this document from the Defense Documentation Center. No foreign dissemination is allowed without approval of Headquarters.

[redacted]

[redacted]

[redacted] Defense Nuclear Agency, Washington, D.C. 20305.

[redacted] This handbook provides a set of corrections to the DASA Communications Handbooks, DASA 1954, 1955 and 1956 (see abstracts of these handbooks above).

[redacted] TREE SIMULATION FACILITIE[redacted]

[redacted] DNA 2432H (Edition 1) [redacted]

[redacted] *Prepared by:* Battelle Memorial Institute, Columbus, Ohio

[redacted] *Availability:* Qualified requestors may obtain this document from the Defense Documentation Center.

[redacted] This handbook characterizes individual pulse reactors, flash x-ray and LINAC facilities on a technical basis for those persons working in the area of transient radiation effects on electronics (TREE). DNA 2432H is arranged to provide the persons who perform TREE experiments with the information concerning facilities which they would require in order to perform an experiment at one of the facilities.

[redacted] X-RAY CROSS SECTION COMPILATION [redacted]

[redacted] *DNA 2433F-1 and -2 and DNA 2433F Supplement* [redacted]

[redacted] *Prepared by:* Kaman Sciences Corporation, Colorado Springs, Colorado.

[redacted] *Availability:* Qualified requestors may obtain this document from the Defense Documentation Center. Requests from other than U.S. government agencies must be made through Headquarters, Defense Nuclear Agency, Washington, D.C. 20305.

[redacted] The experimental X-ray attenuation cross sections for 94 elements between 0.1 keV and 1 MeV, which were obtained for the period from 1920 through 1970, together with exact photoelectric absorption values for hydrogen, are presented in this compilation.

[redacted] Scattering cross sections were calculated by relativistic SCF methods. These were subtracted from the total attenuation data, and the resulting photoelectric and measured photoelectric absorption cross sections from 1 keV to 1 MeV were fit by a least squares procedure to obtain best values. Interpolations were made for elements and energy ranges for which there were no experimental data. From 0.1 keV to between 1 keV and 10 keV nonrelativistic, self-consistent, independent electron theory was used to calculate photoelectric absorption cross sections. Scattering values were added to all photoelectric cross sections to obtain a best set of attenuation cross sections.

[redacted] NUCLEAR ENVIRONMENT DESCRIPTIONS [redacted]

[redacted] *DASA 2491* (CONFIDENTIAL).

[redacted] *Prepared by:* Boeing Company, Seattle, Washington.

[redacted] *Availability:* Qualified requestors may obtain this document from the Defense Documentation Center.

[redacted] The phrase "Nuclear Environment Descriptions" includes: (1) nuclear environment criteria; (2) nuclear effects design specifications; and (3) nuclear effects test specifications. This volume provides an introductory discussion of the three types of nuclear environment descriptions, but it is concerned primarily with the first of these descriptions.

[redacted] The major considerations and procedures required for the development of nuclear environment criteria within a logical system development process are described and illustrated. A standard, comprehensive, understandable format for expressing this description is specified. The material presented is not predicated on the administrative procedures of any one military service and is, therefore, of general applicability.

[redacted]

[redacted]

[redacted] NUCLEAR WEAPON THERMAL RADIATION PHENOMENA [redacted]

[redacted] DNA 2500H [redacted]

[redacted] *Prepared by:* Kaman Sciences Corporation, Colorado Springs, Colorado

[redacted] *Availability:* Volumes 2 and 3 were published in July 1974 and February 1974 respectively. Parts of Volume 1 were completed and published separately in February 1974 as DNA 3220Z, "New Thermal Scaling Laws for Low Altitude Nuclear Bursts (U)," and DNA 3223Z, "Atmospheric Transmission of Nuclear Weapon Thermal Radiation (U)." In November 1977, a draft version of Volume 1 was completed. It is expected to be incorporated into one document and published by mid 1978 under the title *New Thermal Scaling Laws for Bursts Below 30 Kilometers.* All published portions are available for qualified users from the Defense Documentation Center.

[redacted] The DNA Thermal Sourcebook is being prepared as a comprehensive summary of theoretical and experimental information on the prompt thermal radiation environment produced by atmospheric nuclear weapons. This book is designed to provide the latest and most reliable information on thermal environments, including both fireball source characteristics and the transport of the fireball radiation through great distances in the atmosphere. The book does not include the numerous considerations relating to target response, although a short appendix on thermal damage effects will be provided.

[redacted] Volume 1 of this sourcebook will treat the following subjects: nuclear weapon outputs, energy deposition in the atmosphere, the physics of fireballs, radiation-hydrodynamics codes, atmospheric transmission phenomena, weapons test data, comparisons of theory and experiment, and environment prediction methods. Volume 2 provides a complete tabulation of all thermal environment measurements made at all U.S. atmospheric nuclear tests through Operation DOMINIC in 1962. Volume 3 is an extensive bibliography of reports, papers, etc., on the subject of nuclear weapons thermal radiation phenomena.

[redacted] TRAPPED RADIATION HANDBOOK

[redacted] DNA 2524H (Unclassified)

[redacted] *Prepared by:* Lockheed Palo Alto Research Laboratory

[redacted] *Availability:* This document has been approved for public release and sale; its distribution is unlimited.

[redacted] The Trapped Radiation Handbook provides useful information and design data for scientists and engineers engaged in the design of spacecraft systems that must operate in the trapped radiation environment. It contains a compilation of useful charts and graphs and abbreviated derivations of equations and developments of concepts in a wide range of subject matter pertinent to the radiation belts. The handbook is intended to be helpful to scientists who are beginning studies or research in this field as well as to scientists who are actively engaged in magnetospheric research. The following subjects are discussed: the magnetosphere; features and mathematical models of the earth's magnetic field; the motion of charged particles in the field; the properties of the particles in the natural radiation belts; source and loss mechanisms; the artificial radiation belts that have resulted from tests of nuclear devices conducted at high altitudes; the phenomenology of nuclear detonations and beta injection processes; the effects of trapped particles (both natural and fission betas) on materials and devices; the irradiation of circular orbit satellites by trapped particles of the natural environment as well as the environment produced by weapon tests L-values, and an estimated wartime environment; the synchrotron radiation emitted by the trapped electrons; and the vulnerability of oper-

[redacted]

[redacted]

ational systems in the environments mentioned previously.

[redacted] This handbook is updated on a periodic basis. As of September 1977, five changes have been issued.

[redacted] STATUS OF NEUTRON AND GAMMA OUTPUT FROM NUCLEAR WEAPONS [redacted]

[redacted] *DASA 2567* [redacted]

[redacted] *Prepared by:* Science Applications Incorporated, La Jolla, California.

[redacted] *Availability:* Qualified requestors may obtain this document from the Defense Documentation Center on request through Headquarters, Defense Nuclear Agency, Washington, D.C. 20305.

[redacted] This report presents a review and evaluation of existing experiments and calculations of neutron and gamma output spectra and intensities. Comparisons of calculated and measured results for a number of devices are described together with possible explanations for some deviations between the experiment and numerical results. In addition, detailed gamma output calculations were performed for Tambourine, using up-to-date neutron and gamma production cross section data.

[redacted] IMPROVED MODELS FOR PREDICTING NUCLEAR WEAPON INITIAL RADIATION ENVIRONMENTS [redacted]

[redacted] *DASA 2615* [redacted]

[redacted] *Prepared by:* Radiation Research Associates, Inc., Fort Worth, Texas.

[redacted] *Availability:* Qualified requestors may obtain this document from the Defense Documentation Center on request through Headquarters, Defense Nuclear Agency, Washington, D.C. 20305.

[redacted] DASA 2615 presents a review and evaluation of current data and techniques for predicting the initial radiation exposure at or near the ground surface resulting from a nuclear explosion. State-of-art models were then developed for neutron dose, secondary gamma exposure from neutron interactions in the air and ground, and fission product gamma ray exposure occurring during the first minute following a detonation. The neutron and secondary gamma model, based on Straker's discrete ordinates calculations of neutron transport in an air-over-ground geometry and French's first-last collision method for source height effects, yield results for slant ranges up to 4,800 meters from each of 8 different types of weapons. The results may be adjusted for the desired burst height and air density. The fission-product gamma ray model is based on Monte Carlo air transport calculations by Marshall and Wells. It incorporates source spectra, source decay rates, cloud rise approximations, and hydrodynamic enhancement treatments based on the work of a number of previous investigators. The model provides for a wide variety of burst heights and air densities and provides for slant ranges up to 4,800 meters. The models and the incorporated data were validated through extensive comparison with weapon test results and with other calculated and semi-empirical data.

[redacted] THE MODELING OF NUCLEAR CLOUDS [redacted]

[redacted] DASA 2626 [redacted]

[redacted] *Prepared by:* General Research Corporation, Arlington, VA

[redacted] *Availability:* This document is available to qualified users from the Defense Documentation Center.

[redacted] This modeling was performed in response to the need for a systems program to describe the dust particle environment in a nuclear cloud from a detonation on or near the surface. The flowfield during cloud rise was parameterized using a spherical vortex model empirically

[redacted]

[redacted]

[redacted] fit to data from nuclear tests. This work is supplemental to DASA-2304T [redacted] Volume I, "Nuclear Surface Burst Debris [redacted]" as is also the determination of the lofted mass. The cloud dust loading depends on the height-of-burst in a nonlinear manner which is analyzed and modeled empirically. The particle size distribution of the dust in the cloud is that of the crater ejecta and sweep-up modified by the drag forces exerted by the buoyant and convective air flow. Both during rise and after stabilization, the cloud and dust are translated with the ambient wind. The speed and directional shears cause a time dependent cloud shape, which is important to the systems analyst, for whom the model was developed.

[redacted] The spherical model was completed and reported in DNA 2940T [redacted] "Vortex Dust Model for Rising Nuclear Cloud." Some modifications of the post stabilization model was reported in DNA 2745T [redacted] "New Measurements of Visible Cloud Diameter," and DNA 3158F-1 [redacted] "Post-Stabilization Nuclear Dust Cloud," and have been incorporated in the programming of the vortex model.

[redacted] **HANDBOOK OF NUCLEAR WEAPONS AS X-RAY SOURCES** [redacted]

[redacted] *DNA 2866H* [redacted]

[redacted] *Prepared by:* Kaman Sciences Corporation, Colorado Springs, Colorado.

[redacted] *Availability:* Qualified requestors may obtain this document from the Defense Documentation Center.

[redacted] This handbook contains a chronological tabulation of most of the X-ray effects tests that have been conducted by the Department of Defense and the Atomic Energy Commission, as well as a general description of the X-ray spectra and the fluence levels available for experiments on each event. Six illustrative X-ray tests are discussed in some detail. Their X-ray spectra are presented as curves and tabulations and some discussion of their radiation times is given. There is some discussion of the outputs from underground X-ray tests simulating tactical ABM environments.

[redacted] The handbook is not intended to provide all the information required by a person who is not familiar with X-ray effects testing, nor is it for a person whose full time occupation is analysis of X-ray spectra from nuclear weapons. The information is useful to the large majority of the community associated with military effects of X-rays from nuclear weapons. Whether or not this is a "handbook" depends more on the user's definitions than on the author's.

[redacted]

DNA (b)(3)

[redacted] **INSTRUMENTS FOR MEASURING NEUTRON AND GAMMA RADIATION FROM NUCLEAR-WEAPON TESTS** [redacted]

[redacted] *DNA 2888F* [redacted]

[redacted] *Prepared by:* Science Applications Incorporated, La Jolla, California.

[redacted] *Availability:* To be issued during calendar year 1972.

[redacted] DNA 2888 reviews the methods to obtain neutron and gamma ray fluence and spectral data in a nuclear test environment. Approximately forty instruments of those surveyed during this study are described. A complete outline of the experimental techniques employed in these types of measurements is provided, with a description of device input and typical radiation environments encountered during a nuclear test.

[redacted] With few exceptions, only those instruments that have been used in past tests are con-

[redacted]

[redacted]

[redacted] sidered in this report. Instruments to provide neutron and gamma ray dose as a function of time, dose or fluence as a function of energy, and integrated dose were considered. A summary of the relative merits of each instrument is included.

[redacted] THE EFFECTS OF NUCLEAR WEAPONS [redacted]

[redacted] *Prepared and published by:* The U.S. Department of Defense and the U.S. Department of Energy, S. Glasstone and P. J. Dolan, editors.

[redacted] *Availability:* This document may be obtained by contacting the Superintendent of Documents, U.S. Government Printing Office, Washington, D.C.

[redacted] This book presents as accurately as possible, within the limits of national security, a comprehensive summary of information concerning nuclear weapons effects in an unclassified form. The phenomena of air blast, ground and water shock, thermal radiation, and nuclear radiations associated with nuclear explosions are very complex, and descriptions of these phenomena and their related effects are somewhat technical in nature. However, this handbook has been arranged in such a manner as to serve the [redacted] possible range of readers. Most of the chapters are presented in two parts, the first consisting of a general treatment of a particular topic in a less technical manner and the second discussing some of the more technical aspects. The material is so arranged that the reader will experience no loss of continuity by the omission of any or all of the more highly technical sections, but the technical material is available for the use of those who may have need of such information.

[redacted] The third edition of this book was published in December 1977.

[redacted] VORTEX DUST MODEL FOR RISING NUCLEAR CLOUDS [redacted]

[redacted] DNA 2940T [redacted]

[redacted] *Prepared by:* Science Applications, Incorporated, Arlington, VA

[redacted] *Availability:* Qualified users may obtain this document from the Defense Documentation Center.

[redacted] The transport of soil particles after a nuclear detonation on or near the surface is modeled by the vortex flowfield which has a simple mathematical form. By including appropriate particle drag relations and empirically fitting the vortex parameters to both experimental and hydrocode data, a simpler hydrodynamic model (VORDUM) was obtained to predict the soil particle environment. The boundary condition of zero vertical flow velocity at the surface is obtained by using an image vortex moving downward. The VORDUM results are similar to those obtained using the SHELL hydrocode (developed at AFWL). The model has been applied to yields from less than 1 MT to greater than 10 MT. The pancake geometry of the post stabilization model, reported in DASA 2304T [redacted] Volume I, "Nuclear Surface Burst Debris [redacted] was superseded by this description.

[redacted] The post stabilization cloud geometry was improved by the modeling of the late time cloud reported in DNA 3158 F-1 [redacted] "Post-Stabilization Nuclear Dust Cloud."

[redacted] COMMUNICATION SATELLITE SYSTEMS VULNERABILITY TO NUCLEAR EFFECTS – SELECTED EXAMPLES BY FREQUENCY BAND [redacted]

[redacted] DNA 3185H-1 [redacted]

Prepared by: ESL Incorporated

Availability: Qualified requestors may obtain these documents from the Defense Documentation Center. Each transmittal outside the

[redacted]

[redacted]

[redacted] agencies of the U.S. Government must have prior approval of the Defense Nuclear Agency.

[redacted] This document describes communication satellite system vulnerability to propagation disturbance induced by nuclear explosions. Examples of the effects of selected nuclear burst on communication satellite system performance are given by frequency band. The satellite systems analyzed are representative of existing, planned, or proposed systems in seven bands extending from 150 MHz to 14 GHz. The examples presented illustrate the approximate duration and extent over which typical systems may experience difficulty. In addition to specific results, the nuclear effects from the selected weapon environments have been parameterized so that these results can be extended to other systems.

[redacted] Among the effects considered are radio wave absorption, thermal noise, signal dispersion, and propagation time delays. The effect of signal dispersion is considered on systems employing frequency division multiplex-frequency modulation (FDM-FM), and digital systems employing phase shift keying (PSK). While not modeled for the selected examples, the potential effects of phase scintillations on systems employing PSK modulation are shown. Potential effects on systems employing Time Division Multiple Access (TDMA) and Code Division Multiple Access (CDMA) using spread spectrum techniques are discussed.

[redacted] ELECTROMAGNETIC BLACKOUT HANDBOOK [redacted]

[redacted] DNA 3380 H-1, 2, 3 (DNA 3380 H-1, [redacted] DNA 3380 H-2, [redacted] DNA 3380 H-[redacted]

[redacted] *Prepared by:* General Electric Company – [redacted]MPO.

[redacted] *Availability:* Qualified requestors may obtain these documents from the Defense Documentation Center. Each transmittal outside the agencies of the U.S. Government must have prior approval of the Defense Nuclear Agency.

[redacted] This handbook provides source material on nuclear weapon phenomenology, atmospheric processes, and effects of disturbed atmospheric environments on electromagnetic propagation for use in analysis of radar and communications systems. This edition of the handbook is a revision of DASA 1580 and DASA 1580-1 (same title) and replaces those documents. The handbook is divided into seven chapters plus appendices and is published in three volumes. Chapter 1 provides an introduction to nuclear weapon effects on electromagnetic propagation and a summary of communication and radar system performance in nuclear environments. Chapters 2, 3, and 4 present detailed descriptions of weapon radiations and energy deposition in the atmosphere, the phenomenology of heated regions, and atmospheric processes that affect nuclear weapon-induced atmospheric ionization. Chapters 5, 6, and 7 describe electromagnetic propagation effects and weapon-produced noise sources that can have effect on radar and communication systems. The several appendices include material on the properties of the atmosphere and earth's magnetic field, reference material on electromagnetic propagation and thermal radiation, and parametric scaling for weapon-produced regions and effects.

[redacted] ELECTROMAGNETIC PULSE HANDBOOK FOR ELECTRIC POWER SYSTEMS [redacted] December 1974

[redacted] DNA 3466F [redacted]

[redacted] *Prepared by:* Stanford Research Institute, Menlo Park, California

[redacted] *Availability:* Qualified users may obtain this handbook from the Defense Documentation Center.

[redacted] This handbook has been prepared primarily for the power, communications, and systems engineer who must be concerned with the

[redacted]

[redacted]

[redacted] effects of the nuclear electromagnetic pulse on his system. The power engineer should be aware of the effects of EMP on his transmission and distribution system, and the power users must protect their equipment from the pulse conducted into their facilities on the power lines. The commercial power system can be a major path for coupling the EMP into ground-based systems. The power distribution system forms a very large, completely exposed antenna system that is hard-wired into the customer's facility. Thus, extremely high voltages may be developed on the power conductors, and even if the commercial power is not relied on for system survival, these voltages may be delivered to the system either before commercial power is lost, or by the ground or neutral system after transferring to auxiliary power.

[redacted] Considerable research has been performed on EMP coupling to commercial power systems in an effort to characterize the power distribution lines as EMP collectors, and to determine the effects of major components, such as transformers, lightning arresters, and low-voltage wiring, on the penetration of the received signal into ground-based facilities. This research has entailed development and experimental verification of the theory of coupling to transmission lines. This handbook on the interaction of EMP with commercial power systems has been prepared so that designers and systems engineers can benefit from the results of extensive data already accumulated.

[redacted] A POCKET MANUAL OF THE PHYSICAL AND CHEMICAL CHARACTERISTICS OF THE EARTH'S ATMOSPHERE [redacted]

[redacted] DNA 3467H [redacted]

[redacted] *Prepared by:* General Electric Co., Space Sciences Laboratory, P. O. Box 8555, Philadelphia, Pa. based upon information provided by the Bell Telephone Laboratory, the Lockheed Palo Alto Research Laboratory, and the Santa Barbara Research Center. Information was also obtained from "Aid for the Study of Electromagnetic Blackout," DASA 2499 (1970), the DNA "Reaction Rate Handbook, Second Edition," DNA 1948H (1972), and "The Trapped Radiation Handbook" (1971), DNA 2542H.

[redacted] *Availability:* Qualified requestors may obtain the handbook from the Defense Documentation Center or from the National Technical Information Service (NTIS).

[redacted] This pocket manual provides a pocket size compendium of current available knowledge concerning the physical and chemical properties of the earth's ionosphere. It is based principally upon data contained in greater detail in DNA Reaction Rate Handbook, Second Edition (1972), DNA 1948H, as well as the other sources mentioned above. A circular slide rule is normally inserted in the flap of the front cover for convenient calculational use.

[redacted] It is anticipated that as important changes occur in relevant information they will be issued to recipients for inclusion in this pocket manual.

[redacted] AID FOR THE STUDY OF ELECTROMAGNETIC BLACKOUT

[redacted] DNA 3499H [redacted]

[redacted] *Prepared by:* General Electric Company – TEMPO

[redacted] *Availability:* Qualified requestors may obtain this document from the Defense Documentation Center.

[redacted] This report is a revision of DASA 2499 (same title) and replaces that document. The report is a compendium of selected graphs, charts, equations, and relations useful in the analysis of electromagnetic blackout caused by nuclear explosions. Information is provided concerning weapon outputs, ionization source functions, deionization, absorption, phase effects, and noise. The report also contains sections listing atmospheric properties, physical constants, definition of symbols, and a glossary of frequently used terms.

[redacted]

~~CONFIDENTIAL~~

DEPARTMENT OF THE ARMY TECHNICAL MANUAL
DEPARTMENT OF THE NAVY
DEPARTMENT OF THE AIR FORCE
MARINE CORPS PUBLICATIONS

TM 23-200
OPNAV INSTRUCTION 03400.1B
AFL 136-1
NAVMC 1104 REV

CAPABILITIES OF ATOMIC WEAPONS (U)

Prepared by
Armed Forces Special Weapons Project

DEPARTMENTS OF THE ARMY, THE NAVY AND THE AIR FORCE

REVISED EDITION NOVEMBER 1957

~~CONFIDENTIAL~~

WARNING NOTICES

Authority for release of this document to a foreign government must be secured from the Assistant Chief of Staff, Intelligence, Headquarters, Department of the Army.

When this document is released to a foreign government, it is released subject to the following conditions: This information is furnished with the understanding that it will not be released to another nation without specific approval of the United States of America, Department of the Army; that it will not be used for other than military purposes; that individual or corporation rights originating in the information whether patented or not will be respected; and that the information will be afforded substantially the same degree of security as afforded by the United States of America, Department of the Army.

This document contains information affecting the national defense of the United States within the meaning of the Espionage Laws, Title 18 U. S. C., Sections 793 and 794. The transmission or the revelation of its contents in any manner to an unauthorized person is prohibited by law.

Department of the Army Technical Manual
Department of the Navy
Department of the Air Force Manual
Marine Corps Publications

C 1, TM 23-200
OPNAV Instruction 03400.1B, CH-1
AFM 136-1A
NAVMC 1104 REV, CH-1

Capabilities of Atomic Weapons (U)

CHANGES No. 1

DEPARTMENTS OF THE ARMY, THE NAVY, AND THE AIR FORCE
WASHINGTON 25, D.C., *24 June 1960*

TM 23-200/OPNAV Instruction 03400.1B/AFM 136-1/NAVMC 1104 REV, 29 November 1957, is changed as follows:

1. Change the Air Force number to read: **AFM 136-1.**

2. Remove pages v and vi and substitute pages v and vi of Changes Number One.

3. Remove pages xv through xxii and substitute pages xv through xxii of Changes Number One.

4. Remove pages 2-15 through 2-18 and substitute pages 2-15 through 2-18 of Changes Number One.

5. Remove pages 4-1 through 4-8 and substitute pages 4-1 through 4-8 of Changes Number One.

6. Following page 4-16, add pages 4-16a through 4-16d of Changes Number One.

7. Remove pages 4-21 through 4-24 and substitute pages 4-21, 4-22, 4-22a through 4-22d, 4-23, and 4-24 of Changes Number One.

8. Remove pages 9-3 and 9-4 and substitute pages 9-3 and 9-4 of Changes Number One.

9. Remove pages 9-9 through 9-12 and substitute pages 9-9 through 9-12 of Changes Number One.

10. Remove pages I-7 and I-8 and substitute pages I-7 and I-8 of Changes Number One.

11. Remove pages I-29 through I-32 and substitute pages I-29 through I-32 of Changes Number One.

12. Remove pages II-3 and II-4 and substitute pages II-3 and II-4 of Changes Number One.

13. Remove pages 1, 2, 5 through 8, and 11 and substitute pages 1, 2, 5 through 8, 11 and 12 of Changes Number One.

PAGE LOCATOR FOR PHYSICAL PHENOMENA FIGURES AND TABLES*

	Free air	Air	Transition	Land surface	Water surface	Underground	Underwater
BLAST AND SHOCK:							
Altitude Effects	2-9; I-29, 30.	I-29, 30	I-29, 30	I-29, 30	I-29, 30		
Base Surge						2-86	2-94
Crater:							
Depth			2-65, 72	2-65, 72	2-78	2-65, 72	2-78
Lip			2-50	2-50	2-80	2-50	2-80
Profile			2-50	2-50		2-50	
Radius (Diameter)			2-63, 68	2-63, 68	2-76	2-63, 68	2-76
Dynamic Pressure:							
Impulse	I-19						
Peak *vs.* Distance	2-21	2-40, 41	2-40, 41	2-40, 41	2-40		
Versus Time	2-1; I-16, 21.	2-1	2-1	2-1	2-1		
Wave Forms	I-5	I-5	I-5	I-5	I-5		
Ground Shock		2-83	2-83	2-53, 83			
Mach Stem		2-4, 23	2-4, 23				
Overpressure:							
Effect of Rain or Fog	2-43	2-43	2-43	2-43	2-43		
Impulse	I-13	I-24	I-24	I-24	I-24		
Peak *vs.* Distance	2-17	2-30, 32	2-30, 32	2-30, 32; I-32	2-30, I-32	2-47	2-47
Versus Time	2-1; I-15, 16.	2-1	2-1	2-1	2-1		
Wave Forms	I-3	I-3, 27	I-3, 27	I-3, 27	I-3		
Positive Phase:							
Duration	2-19	2-36	2-36	2-36	2-36		
Effect of Cut-Off							2-56, 57
Precursor		2-45	2-12, 45	2-45			
Relations of Various Parameters	*2-3*; I-11	I-11	I-11				
Time of Arrival	2-15	2-26	2-26	2-26	2-26		
Velocity:							
Peak Particle	*2-3*; I-10						
Shock	I-9						
Water Shock							2-59, 89
Water Waves					2-91		2-91
THERMAL:							
Atmospheric Transmissivity	3-14	3-14	3-14	3-14	3-14		
Fireball	3-5	3-5					
Generalized Pulse and Percent Emitted	3-7; 6-15	3-7; 6-15	3-7; 6-15	3-7; 6-15	3-7; 6-15		
Radiant Exposure	3-12, 18	3-18	3-18	3-18	3-18		
Times	3-10	3-10	3-10	3-10	3-10		
Yield *vs.* Altitude	3-12						
NUCLEAR:							
Cloud:							
Diameter	4-84	4-84	4-84	4-84	4-84	4-84	4-84
Height	4-81, 83	4-81, 83	4-81, 83	4-81, 83	4-81, 83	4-81, 83	4-81, 83
Penetration Dose	4-87	4-87	4-87	4-87	4-87	4-87	4-87
Initial Gamma:							
Dose *vs.* Distance	4-14, 15, 16, 16a, 16b, 16c, 16d.	4-14, 15, 16, 16a, 16b, 16c, 16d.	4-10, 11, 12, 13.	4-10, 11, 12, 13.	4-10, 11, 12, 13.	4-19	4-19
Percent *vs.* Time	4-20	4-20	4-20	4-20	4-20		
Shielding (Transmission) Factors	*6-11*; 6-19.	*6-11*; 6-19.	*6-11*; 6-19.	*6-11*; 6-19.	*6-11*; 6-19.	*6-11*; 6-19.	*6-11*; 6-19.

*Page numbers in italics are for tables.

PAGE LOCATOR FOR PHYSICAL PHENOMENA FIGURES AND TABLES*—Continued

	Free air	Air	Transition	Land surface	Water surface	Underground	Underwater
NUCLEAR—Continued							
Neutron:							
Dose, Fission Weapons	4-22a, 22b, 22c, 22d, 23.	4-22a, 22b, 22c, 22d, 23.	4-22a, 22b, 22c, 22d, 23.	4-22a, 22b, 22c, 22d, 23.	4-22a, 22b, 22c, 22d, 23.		
Dose, Thermonuclear Weapons	4-25	4-25	4-25	4-25	4-25		
Flux	12-9	12-9	12-9	12-9	12-9		
Induced Activity	----------	----------	*4-66*; 4-70, 73, 75, 76, 77, 78.				
Transmission Factors	*6-11*	*6-11*	*6-11*	*6-11*	*6-11*		
Fall-Out:							
Contours	----------	----------	4-38, 40, 42, 44, 46, 48.	4-29, 38, 40, 42, 44, 46.	4-38, 40, 42, 44, 46.	4-53, 54, 55, 56, 57.	4-59
Gamma Decay	----------	----------	4-35	4-35	4-35	4-35	4-35.
Shielding (Transmission) Factors	----------	----------	*6-11*; 6-20.	*6-11*; 6-20.	*6-11*; 6-20.	*6-11*; 6-20.	*6-11*; 6-20.
Total Dose	----------	----------	4-61, 63	4-61, 63	4-61, 63	4-61, 63	4-61, 63
GENERAL:							
Atmospheric Conditions	*II-3, 4*; II-9, 10.	*II-3, 4*; II-9, 10.	*II-3, 4*; II-9, 10.	*II-3, 4*; II-9, 10.	*II-3, 4*; II-9, 10.		
Comparison of Phenomena	----------	5-13, 18	5-13, 18	5-13, 18	5-13, 18		
Relative Air Density	*4-2*; II-9	*4-2*; II-9	*4-2*; II-9	*4-2*; II-9	*4-2*; II-9		
Water Vapor Density	II-10	II-10	II-10	II-10	II-10		

PAGE LOCATOR FOR DAMAGE FIGURES AND TABLES*

	Blast	Thermal	Nuclear
Aircraft	9-5, 7, 9, 11	9-11	
Clothing	----------	*12-3*	
Earth-Covered Structures	*7-4, 8*; 7-40, 42, 46		
Electronics Equipment	10-15		
Engineer Equipment	10-21, 23		
Field Fortifications	*7-9*; 7-53, 54, 55		
Forests	*11-2*; 11-7, 8, 9, 10, 11, 12	*11-3, 4*; 11-15	
Land Mines	*10-4*		
Materials	----------	*12-3*; 12-5, 10	
Ordnance Equipment	*10-2*		
Personnel	*6-3*; 6-13, 17	*6-4, 5*; 6-14, 15, 17	*6-7, 11*; 6-17, 19, 20
Railroad Equipment	10-17, 19		
Submarines	*8-2*; 8-10, 11		
Supply Dumps	10-13		
Surface Ships	*8-2*; 8-6, 7, 8		
Surface Structures:			
Bridges	*7-4*; 7-34, 36, 38, 46		
Buildings	*7-3, 4*; 7-14, 16, 18, 20, 22, 26, 28, 30, 32, 45, 46		
Oil Tanks	*7-3*; 7-24, 45		
Tanks and Artillery	10-11		
Tunnels	7-51		
Underwater Mines	8-13, 14, 15		
Urban Areas	----------	*12-1*; 12-5, 6, 7	
Vehicles	10-9		
Subsurface burst damage distance reduction for surface targets	7-49		

*Page numbers in italics are for tables.

CAPABILITIES OF ATOMIC WEAPONS

CHANGES No. 2

DEPARTMENTS OF THE ARMY, THE NAVY AND THE AIR FORCE
WASHINGTON 25, D.C., *3 October 1960*

TM 23-200/OPNAV Instruction 03400.1B/AFM 136-1/NAVMC 1104, REV, 29 November 1957, is changed as follows:

1. Make the following pen and ink changes in Changes No. 1:

a. Page (I). Change item 11 to read: Remove pages I-29 and I-30 and substitute pages I-29 through I-32 Changes No. One.

b. Page (IV). Change Navy distribution to read:

F9 (Station CNO)
H23 (AV Med Ctr)

c. Page v. Change column 1, line 15 to read: 4-22a through 4-22d ..... Change 1
4-23 and 4-24 ..... Change 1
Change column 1, line 16 to read: 4-25 through 4-88 ..... Original
Change column 2, line 9 to read: I-9 through I-28 ..... Original

d. Index. Change page numbers 9 and 10 to read 11 and 12, respectively. Add C 1, 24 June 1960, in the upper inside corners of pages 1, 2, 5 through 8, and renumbered pages 11 and 12.

2. Destroy, according to proper security procedures, the page of the Index issued in Changes No. 1 as page 12. The reverse of page 12 is blank.

3. After necessary action, file the transmittal sheet in the front of the manual for reference.

[AG 461 (9 Aug 60)]

BY ORDER OF THE SECRETARIES OF THE ARMY, THE NAVY, AND THE AIR FORCE:

G. H. DECKER,
General, United States Army,
Chief of Staff.

OFFICIAL:
R. V. LEE,
Major General, United States Army,
The Adjutant General.

G. R. DONAHO,
Rear Admiral, United States Navy,
Assistant Vice Chief of Naval Operations,
Director of Naval Administration.

THOMAS D. WHITE,
Chief of Staff, United States Air Force.

OFFICIAL:
J. L. TARR,
Colonel, United States Air Force,
Director of Administrative Services.

F. L. WIESEMAN,
Major General, U.S. Marine Corps,
Deputy Chief of Staff (Plans).

This publication supersedes TM 23-200/OPNAV INSTRUCTION 003400.1A/AFL 136-4/NAVMC 1104, 1 June 1955, including C 1, 1 April 1956; C 2, 17 October 1956; and C 3, 19 September 1957

PART ONE
PHYSICAL PHENOMENA

SECTION I
INTRODUCTION

1.1 Explosion of a Nuclear Weapon

a. General. An explosion is defined as the sudden release of a large amount of energy in a small space. For high explosives, this energy manifests itself primarily as blast energy, regardless of environmental conditions. In a nuclear explosion, on the other hand, the energy manifests itself in the form of blast, thermal radiation, and nuclear radiation. In addition, the energy released from a nuclear detonation is essentially from a point source, whereas a comparable amount of energy released from a high explosive detonation would require an enormous volume of explosive. Further, the energy released in a nuclear detonation results from a fission process, a fusion process or a combination of the two, while the energy released in a high explosive detonation results from a chemical process which does not affect the nuclei of the atoms involved. In the fission process, heavy atoms are split into pairs of lighter radioactive atoms, whereas in the fusion process two light atoms are combined to form a heavier atom. In both processes, there is a net loss of mass which appears as energy, and there is also an emission of neutrons and gamma rays. The high temperatures resulting from either of these processes in turn cause large pressures to develop, hence rapid expansion and the creation of a shock wave.

b. Energy Partition. Energy partition is defined as the distribution of the total energy released by a nuclear detonation among nuclear radiation, thermal radiation, and blast. Energy partition depends primarily upon environmental conditions, i. e., whether the detonation takes place in air, underground, or underwater. Furthermore, energy partition has meaning only when related to a particular time after detonation. For example, the energy partition of a nuclear detonation in free air under ambient conditions varying from a homogeneous sea level atmosphere to the conditions existing at 50,000 feet altitude is in the proportion of about 50 percent blast, 35 percent thermal, and 15 percent nuclear (5 percent initial radiations, 10 percent in fission products), if evaluated within the first minute. The energy partition of an underground burst, on the other hand, is entirely different. There is a reduction of thermal radiation received at a distance due to the amount of heat used in vaporizing the surrounding soil and a reduction of air blast due to the amount of blast energy used to produce cratering and ground shock.

1.2 Weapon Ratings

a. In order to provide a yardstick for rating the total energy release of a nuclear detonation, it has become the practice to express the total yield of a nuclear device in terms of a TNT energy equivalent. For example, if the total energy of the blast, thermal radiation, and nuclear radiation released by a nuclear weapon is the same as the energy released by the detonation of 1,000 tons of TNT, the nuclear weapon is rated as a 1,000-ton, or 1-kiloton, weapon. When 1 kilogram of U-235 or plutonium undergoes fission nearly one gram (1/450 pound) of matter is converted into energy. This energy expressed in terms of TNT energy equivalence would be the same as for the detonation of 20,000 tons of TNT. Similarly, the fusion of 1 kilogram of deuterium results in the

transformation of 2.65 grams of matter into energy, with an energy release equivalent to that resulting from the detonation of 57,000 tons of TNT.

b. Another method of rating in common usage, and one which is often confused with the rating of *energy* in terms of TNT *energy* equivalence, is the rating of *effects* in terms of TNT *effects* equivalence, i. e., the *effect* of a particular phenomenon of a nuclear detonation expressed in terms of the amount of TNT which would produce the same *effect*. An example of TNT effect equivalence would be the expression of the crater radius of a nuclear surface burst in terms of the amount of TNT which would be required to produce the same radius.

c. For convenience these TNT equivalences are expressed in 1,000 ton or 1,000,000 ton units, KT (kiloton) or MT (megaton), where 1 ton equals 2,000 pounds and the energy content of TNT is defined as 1100 calories per gram.

d. A "nominal" weapon is one the yield of which is 20 KT. The use of this term arose from the approximately 20 KT yields at Hiroshima, Nagasaki, and the Bikini (Crossroads) tests. In some reports nuclear weapons effects data are based on the nominal weapon.

1.3 Data Presentation

This manual is divided into two parts. Part One, *Physical Phenomena*, treats the basic phenomena of blast and shock, thermal radiation, and nuclear radiation resulting from a nuclear explosion in various media and under various conditions. Part Two, *Damage Criteria*, discusses the mechanism of casualty production and damage to military targets, correlating the basic physical phenomena of a nuclear detonation with various defined degrees of damage.

Relatively simple scaling procedures exist for relating the majority of phenomena associated with weapons of one yield to weapons of other yields. For simplicity and convenience in the use of the manual, most physical phenomena data and much of the damage data are presented for 1 KT bursts, from which the phenomena or damage for other yields may be readily obtained by means of the appropriate scaling procedures which are explained wherever their use is required.

An estimate of the degree of reliability accompanies the presentation of nearly all physical phenomena data. This estimated reliability indicates a range of values above and below the curve such that, for a large number of events, 90 percent of the data will fall within this range. Statements regarding reliability of damage data, on the other hand, describe the source and relative quantity of the data. Reliability estimates do not include operational considerations such as aiming error, target intelligence, and height of burst or yield variations.

1.4 Types of Burst

a. General. The medium in which a weapon is burst determines in great measure the relative magnitudes of the various physical phenomena. In particular, large differences result depending upon whether the detonation occurs in air above the surface, at the surface, or beneath the surface. It is often convenient to discuss weapon phenomena by these types of burst.

b. Brief Description of an Air Burst.

(1) *Definition.* An air burst is defined as the explosion of a nuclear weapon at such a height that the weapon phenomenon of interest is not significantly modified by the earth's surface. For example, from a blast standpoint, this height is such that the reflected wave passing through the fireball does not overtake the incident wave above the fireball (heights greater than about 160 $W^{1/3}$ feet $\pm$ 15%, where W is the weapon yield in kilotons). For thermal radiation an airburst occurs at such heights above the surface that the apparent thermal yield viewed from the ground is not affected by surface phenomena, such as heat transfer to the surface, distortion of the fireball by the reflected shock wave, thermal reflection from the surface, etc. (heights above the surface greater than about 180 $W^{0.4}$ feet $\pm$20% for yields of 10 KT to 100 KT, and $\pm$30% for other yields). From the standpoint of fallout, an airburst occurs at such heights that militarily significant local fallout does not result (for yields less than 100 KT, a minimum height of burst of 100 $W^{1/3}$ feet; for yields greater than 100 KT, in the absence of data,

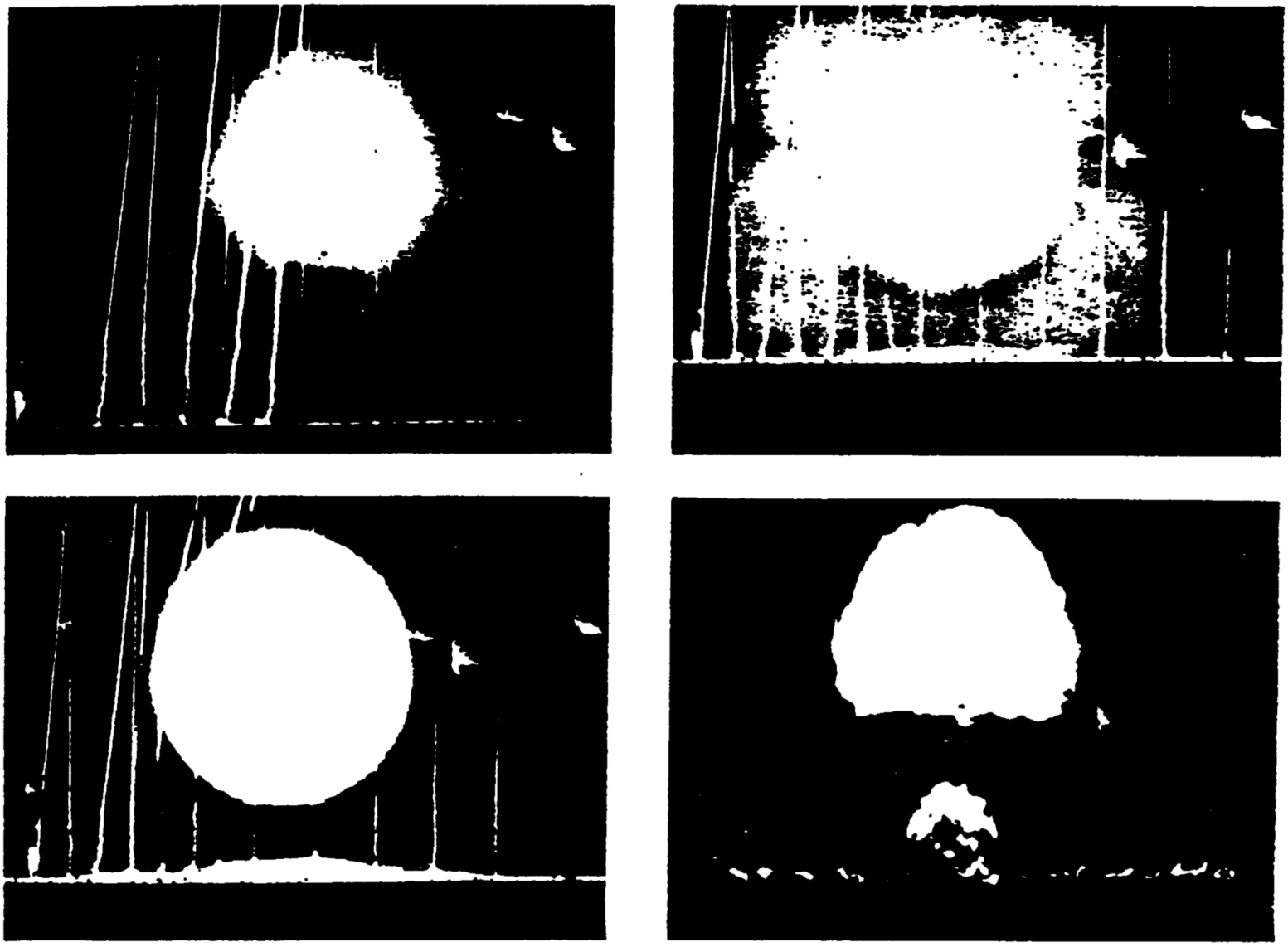

DEVELOPMENT OF AN AIR BURST

the minimum height of burst may be taken conservatively to equal 180 $W^{0.4}$ feet). For certain other phenomena of interest, e. g., neutron induced activity, initial gamma or neutron flux, the height of burst at which the earth's surface fails to produce an effect is difficult or impossible to distinguish.

(2) *Development.* Upon the detonation of a nuclear weapon, there occurs as a direct result of the fission and/or fusion process an emission of neutrons and of electromagnetic radiation in the form of a burst of gamma rays. The nuclear radiations are discussed further in (5) below and section IV.

The tremendous amount of energy created by the nuclear reaction gives rise to extremely high temperatures, which in turn result in the vaporization of the fission products and the components of the weapon, and the emission of additional electromagnetic radiation covering a wide range of wave lengths from infrared through visible to soft X-rays.

Until the temperature falls to about 300,000° K. (540,000° F.), this additional electromagnetic radiation is the most rapid means of energy transfer, and hence is the means by which the surrounding air is heated to incandescence. When the temperature drops below about 300,000° K., a shock wave becomes the primary mechanism for making the surrounding air incandescent. As long as the shock wave is strong enough to

cause the shock-heated air to be luminescent, the boundary of the observable luminous sphere (the fireball) is the shock front. Actually this observable sphere consists of two concentric regions. The inner (hotter) region is a sphere of uniform temperature, surrounded by a layer of shock-heated air at a somewhat lower but still very high temperature.

During the early stages of expansion of the incandescent shock front, the emitted radiant power increases as the luminous sphere increases in size, in spite of the fact that expansion causes a temperature decrease, until a maximum (the first maximum) is reached. At this point, the effect of the rapid rate of decrease in temperature overrides the enhancement of radiant power resulting from the increasing area of the luminous sphere.

Subsequently, further expansion causes a reduction in the radiant power. Eventually the shock front temperature is reduced to a point where the shock front is no longer incandescent; therefore, the rate of emission of radiation from the shock front is negligible. In effect, the shock front has become transparent, and the hotter incandescent inner core would be expected to be observable. Initially, however, the radiation emitted from the inner core is absorbed by compounds formed in the shock heated air, and the radiant power reaches a minimum. As these compounds break down, the radiant power emitted from the inner core begins to pass through, and the inner core becomes the visible source of radiation. Thus, the radiant power increases again. This change in boundary of the observable luminous sphere from the shock front to the incandescent inner core gives rise to the term "breakaway."

As the opacity of the shock-heated air decreases, the apparent temperature as measured from a distance approaches that of the hot gases of the inner core, and the emitted radiant power approaches a second maximum. Further expansion and radiative cooling of the hot gases, however, give rise to a slow decrease in the radiant power. This decrease is so slow, relative to the previous rises and decline, that a large percentage of the total radiant energy emitted is delivered during this period. Finally, the rate of delivery of radiant energy drops to a low value.

The subsequent characteristics of the shock, or blast, wave are discussed in (3) below and section II. The effects of the thermal pulse are discussed in section III.

(3) *Blast wave.* A blast wave is characterized by a sharp rise in pressure, temperature and density at its shock front. Thus, upon the arrival of a blast wave at a given location from the burst point, the sequence of events is a sudden increase in pressure, temperature and density, followed by a subsequent decrease in pressure, temperature and density to values below ambient, and a more gradual return to ambient conditions with the temperature going slightly above ambient. The overall characteristics of the blast wave are preserved over long distances from the burst point, but vary in magnitude with distance. With increase in distance, for example, the maximum pressure in the shock wave decreases, and the length of time over which the blast pressure is above ambient, the "positive phase," increases. In addition, under conditions of high relative humidity (50 percent or higher), the drop in air pressure below ambient lowers the temperature sufficiently to cause condensation of atmospheric moisture to form a large cloud called the Wilson Cloud. When the air pressure again becomes normal, in a matter of seconds, the cloud disappears. Although quite spectacular, the Wilson Cloud always occurs too far behind the shock front to modify the blast effects and too late to reduce the thermal effects appreci-

ably; therefore, the cloud has no military significance.

Also characteristic of a blast wave is the motion of the air away from the burst point during the positive phase and toward the burst point during the negative phase. The pattern of the air motion or air velocity is the same as for the other characteristics, with maximum velocity occurring just behind the shock front and decreasing with distance from the burst point. At 300 yards from the burst point of a 1 KT weapon, the peak wind velocity is about 240 miles per hour.

(4) *Thermal radiation.* The relatively large amount of thermal radiation emitted in a nuclear detonation is one of its most striking characteristics. This radiant energy amounts to approximately one-third of the total energy of an air burst weapon. For a 1 KT weapon most of this radiation is emitted in less than a second, and is sufficient to cause serious burns to exposed personnel and to start fires in some combustible materials out to distances of about a thousand yards.

(5) *Nuclear radiation.* A unique feature of a nuclear explosion is the nuclear radiation released. This consists of gamma rays, neutrons, alpha particles and beta particles. About a third of this energy is emitted within the first second after detonation, the remainder being released from radioactive fission products and unfissioned bomb materials over long periods of time after the burst. Nuclear radiation is primarily an anti-personnel effect, with the penetrating radiations (gamma rays and neutrons) being the most dangerous. Lethal doses of initial gamma radiation from a 1 KT burst are received by exposed personnel out to about 700 yards. Residual nuclear radiation, due either to fallout or to neutron-induced gamma activity, can under certain conditions deny entry into a bombed area for some period of time after a detonation. Nuclear radiation effects on materials and equipment are negligible, except for sensitive photographic materials and certain electronic components.

(6) *Cloud.* Because of its relatively low density compared to ambient conditions, the mass of hot gases comprising the fireball rises. The rate of rise may reach several hundred feet per second, after which it decreases rapidly. As the gases rise, they expand, cool and condense, forming a radioactive cloud which consists largely of water vapor and metallic oxides from the weapon. As the fireball cools, the color changes gradually from red to a reddish brown, and ultimately water vapor from the air condenses sufficiently to produce a white color. As the heated mass of air in the fireball rises, cool air is pulled in from the sides and below, which may cause a doughnut shaped ring to form around the column of hot air. This part of the cloud rolls violently as it rises. The cloud from a 1 KT detonation may reach a height of 5,000 to 10,000 feet above the burst point, after which it is gradually dispersed by the winds.

c. *Brief Description of a Surface Burst.*

(1) *Definition.* A surface burst is defined as the explosion of a nuclear weapon at the earth's surface.

(2) *Development and air blast wave.* When a nuclear weapon is burst at the surface of the earth the sequence of events in the development of the fireball and the formation of the blast wave is the same as that for an air burst, except that the fireball boundary and the shock front are roughly hemispherical. Since the earth's surface is an almost perfect reflector for the blast wave, the resulting blast effects are about the same as for a burst of twice the yield in free air.

(3) *Ground shock.* When a burst takes place on the ground surface, a portion of the energy is directly transmitted to the earth in the form of ground shock. In addition, the air blast wave induces a ground shock wave which at shallow depths has essentially the same mag-

FIGURE 1-2

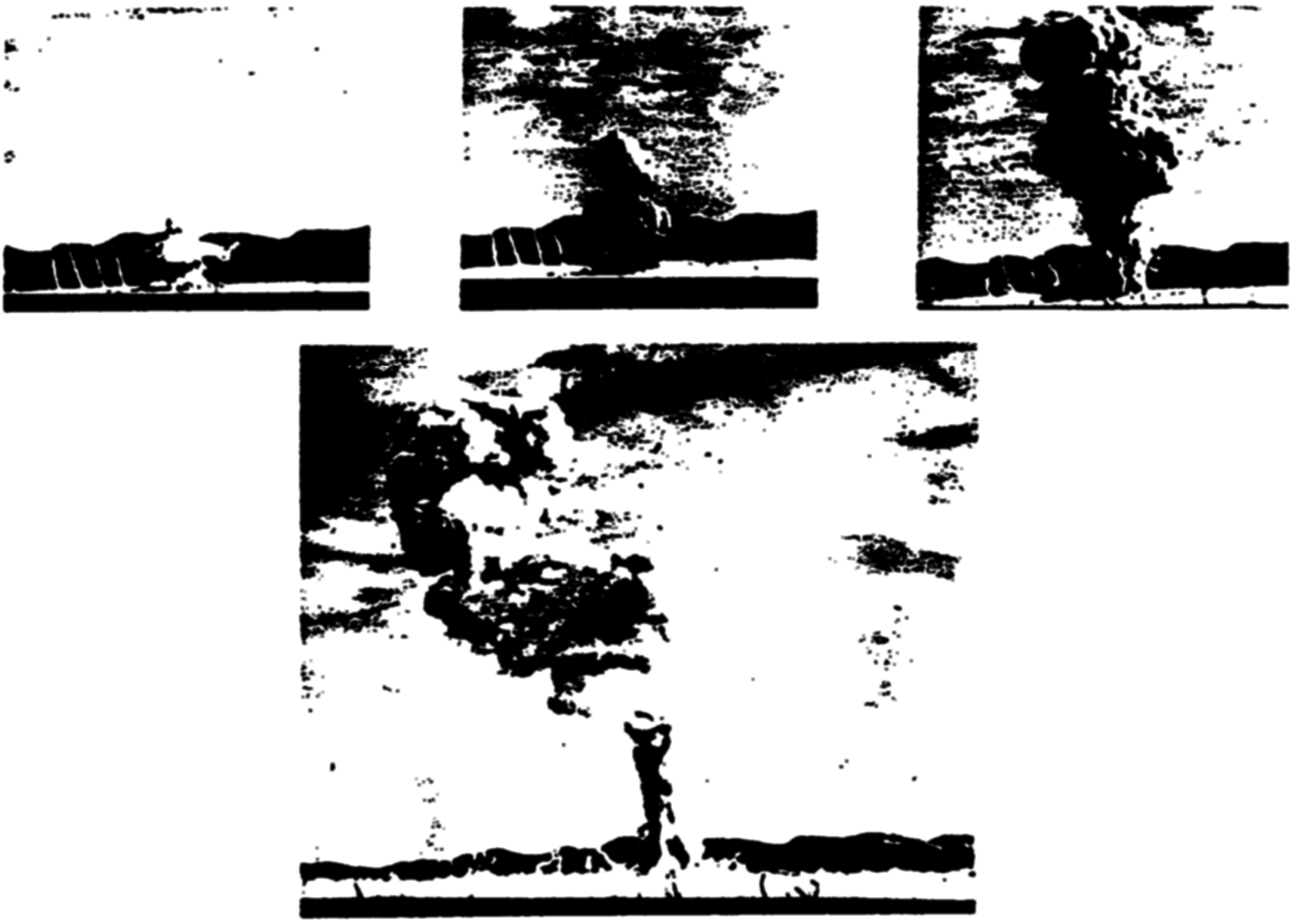

DEVELOPMENT OF A SURFACE BURST

nitude as the air blast wave at the same distance from the burst. The directly transmitted ground shock, although of higher magnitude initially, attenuates faster than the air blast induced shock.

(4) *Crater.* For a burst on land, pressures of hundreds of thousands of pounds per square inch are exerted on the earth's surface, displacing material to form a crater and causing a downward compression of the soil. In addition to the material thrown out and compressed, a considerable quantity of earth is vaporized by the intense heat. A crater approximately 125 feet in diameter and 28 feet in depth is formed by a 1 KT weapon burst on a dry soil surface.

(5) *Thermal radiation.* Because of the heat transfer to the surface, the hemispherical shape of the fireball and the partial obscuration of the fireball by earth or water, the radiant exposure received by surface targets from a nuclear weapon burst on the surface is somewhat less than would be delivered by an air burst nuclear weapon of the same yield.

(6) *Nuclear radiation.*

(*a*) *Initial.* For a small yield weapon, owing largely to absorption by the surface, the initial gamma radiation from a surface burst is somewhat less at the same distance from the burst point than that from a burst of the same yield in free air. For high yield weapons, where hydrodynamic effects become important, a surface burst can be expected to produce as much or more initial gamma radiation as a

burst of the same yield in free air, at the same distance from the burst point.

(*b*) *Residual.* The contamination effects of residual nuclear radiation from a surface burst are very much greater than for an air burst, and hazardous radiological effects are produced over areas much greater than those seriously affected by blast or by thermal radiation. Roughly half of the available radioactivity resulting from a nuclear explosion on land, for example, can be expected to fall out in the general vicinity of the burst point. Dose rate contours near the burst point as great as 10,000 r/hr at $H+1$ hour have been observed at tests, regardless of yield.

(7) *Cloud.* For a burst on the surface, a great quantity of material is thrown out from the point of detonation. As the fireball rises, some material is drawn up under the fireball, forming a stem and sometimes forming a second cloud below the one which develops from the fireball. The stem and cloud(s) continue to rise and follow the course described for an air burst.

(8) *Surface bursts on water.* In general, the phenomena as outlined in (2), (5), (6), and (7) above will occur for a surface burst on water. In addition, the expanding sphere of hot gases depresses the water, causing the formation of a surface wave train and the transmission of a directly coupled shock wave into the water. The expanding air blast wave induces a shock wave in the water, which at shallow depths has essentially the same magnitude as the air blast wave at the same distance from the burst. Although the directly coupled water shock is of higher magnitude initially, it attenuates faster than the air blast induced water shock. As the height of burst increases from zero, depression, surface waves, and directly coupled water shock become smaller in magnitude. The formation of a crater on the bottom as the result of a surface burst in shallow water will depend on the depth of the water, yield of the weapon and other factors. A 1 KT weapon, for example, detonated on the surface of water 50 feet deep with a soft rock bottom, will form a crater 130 feet in diameter and 4 feet deep.

d. Brief Description of a Burst in the Transition Zone Between an Air Burst and a Surface Burst.

(1) *General.* There is a sizable zone above the earth's surface such that, for weapons detonated in the zone, the presence of the earth's surface significantly modifies one or more of the basic weapon phenomena. As the height of burst is successively lowered in this transition zone, the earth's surface plays an increasingly important role in modifying weapon phenomena; there is a gradual transition from the characteristics of an air burst to those of a surface burst. The upper boundary of the transition zone varies depending upon the phenomenon being considered, since the effect of the earth's surface ceases to be of importance at different scaled heights of burst for different phenomena, as mentioned in *b*(1) above and covered in more detail in the discussion of specific weapon phenomena.

(2) *Development.* The development of a burst in the transition zone generally follows the sequence of events described in *b*(2) above for an air burst.

(3) *Blast wave, thermal and nuclear radiation.* From the standpoint of blast, as the height of burst decreases from that of an air burst, peak air overpressures are more and more affected by the blast wave reflected from the surface, until total coalescence of the incident wave and the reflected wave occurs for a surface burst. From the standpoint of thermal radiation, the apparent thermal yield viewed from the ground decreases with increasing distortion of the fireball by the reflected blast wave, until the thermal yield and the fireball shape approach those characteristic of a surface burst. For nuclear radiation, local fall-out becomes increasingly more significant with decreasing height of burst.

and, especially for large yield weapons burst close to the surface, the hydrodynamic enhancement of the initial gamma radiation (see par. 4.2*a*(1)) becomes of considerable importance.

(4) *Ground shock and crater formation.* As the height of burst is lowered, ground shock increases in magnitude. Crater formation commences at a height of burst in the region of $60W^{1/3}$ feet by the mechanism of compression and scouring of the soil. At a height of burst less than about $10W^{1/3}$ feet, the expanding gases from a nuclear detonation form a crater by vaporization, throwing and compressing the soil in an outward direction from the detonation. Below this height of burst, crater radius and depth approach those of a surface burst.

e. Brief Description of an Underground Burst.

(1) *Definition.* An underground burst is defined as the explosion of a nuclear weapon in which the center of the detonation lies at any point beneath the surface of the ground.

(2) *Development.* When an atomic weapon is detonated at a sufficient depth underground, the ball of fire formed is composed primarily of vaporized materials from the bomb and vaporized earth. At shallow depths light from the fireball generally may be seen from the time it breaks through the surface until it is obscured by dust and vapor clouds, a matter of a few milliseconds. The characteristics of the explosion and their related effects depend upon the depth, yield, and soil type. As the depth below the surface is increased, the characteristics depart gradually from those of a surface burst and finally, at depths of the order of 20 feet for a 1 KT detonation, the explosion exhibits the phenomena commonly associated with underground explosions. It is emphasized that the transition from the observed characteristics of a surface burst to those of an underground burst is not sudden, but that the characteristics change gradually.

(3) *Air blast.* Bursts at depths shallow enough to permit significant venting will produce air blast waves similar to those of air or surface bursts. As the depth of burst increases, the magnitude of the air blast will decrease.

(4) *Column, cloud and base surge.* The first physical manifestation of an underground explosion at shallow depths is an incandescence at the ground surface directly above the point of detonation. This is almost immediately followed by large quantities of material being thrown vertically as a consequence of the direct ground shock reflection along the ground surface. Concurrently large quantities of gas are released. These gases entrain additional quantities of material and carry them high into the air in the form of a cylindrical column. As the column rises it fans out and forms a dense cloud. Some of the particles thrown vertically, together with the entrained particles, behave like an aerosol with a density considerably greater than the surrounding air. This aerosol subsequently falls downward in the immediate vicinity of ground zero, and the finer soil particles spread out radially along the ground to form a low dust cloud called the base surge. For a 1 KT weapon burst at a depth of 20 feet, it is estimated that the column will reach a height of approximately 420 feet and a diameter of 660 feet, and the cloud will be 4,400 feet in diameter and 5,000 feet in height. Dimensions of the base surge are discussed in paragraph 2.2. For shallower depths of burst, the column tends to assume the shape of an inverted cone rather than a cylindrical column and has a more pronounced radial throwout. Shallower depths of burst also become less favorable for the formation

SECTION II
BLAST AND SHOCK PHENOMENA

2.1 Air Blast Phenomena

a. General. The shock wave which propagates through air as a consequence of a nuclear explosion is commonly referred to as a blast wave. The head of the blast wave, called the shock front, causes an abrupt rise in both overpressure and dynamic pressure as it passes a given point, as illustrated at point B in figure 2-1. In the case of overpressure, this abrupt rise is followed by a decline to a pressure below ambient and then a gradual return to ambient. The portion of the wave in which the overpressure is above ambient is termed the positive overpressure phase, while the remaining portion, where the pressure is below ambient, is called the negative pressure phase. The decrease in pressure below ambient in the negative phase is usually small in comparison with the increase in pressure in the positive phase.

The dynamic pressure associated with mass motion of air has a positive duration somewhat

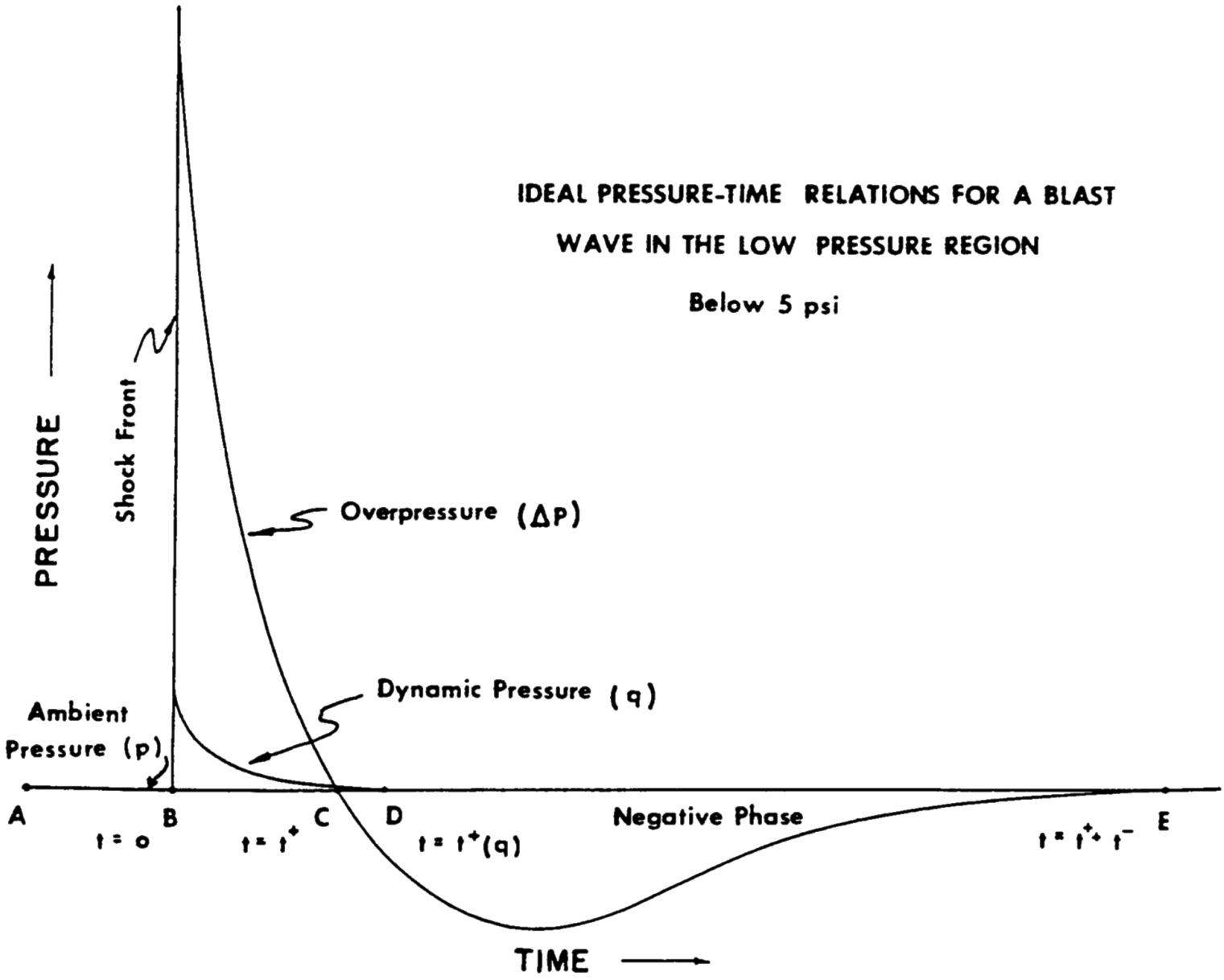

FIGURE 2-6

GROWTH OF THE MACH STEM
(IDEALIZED)

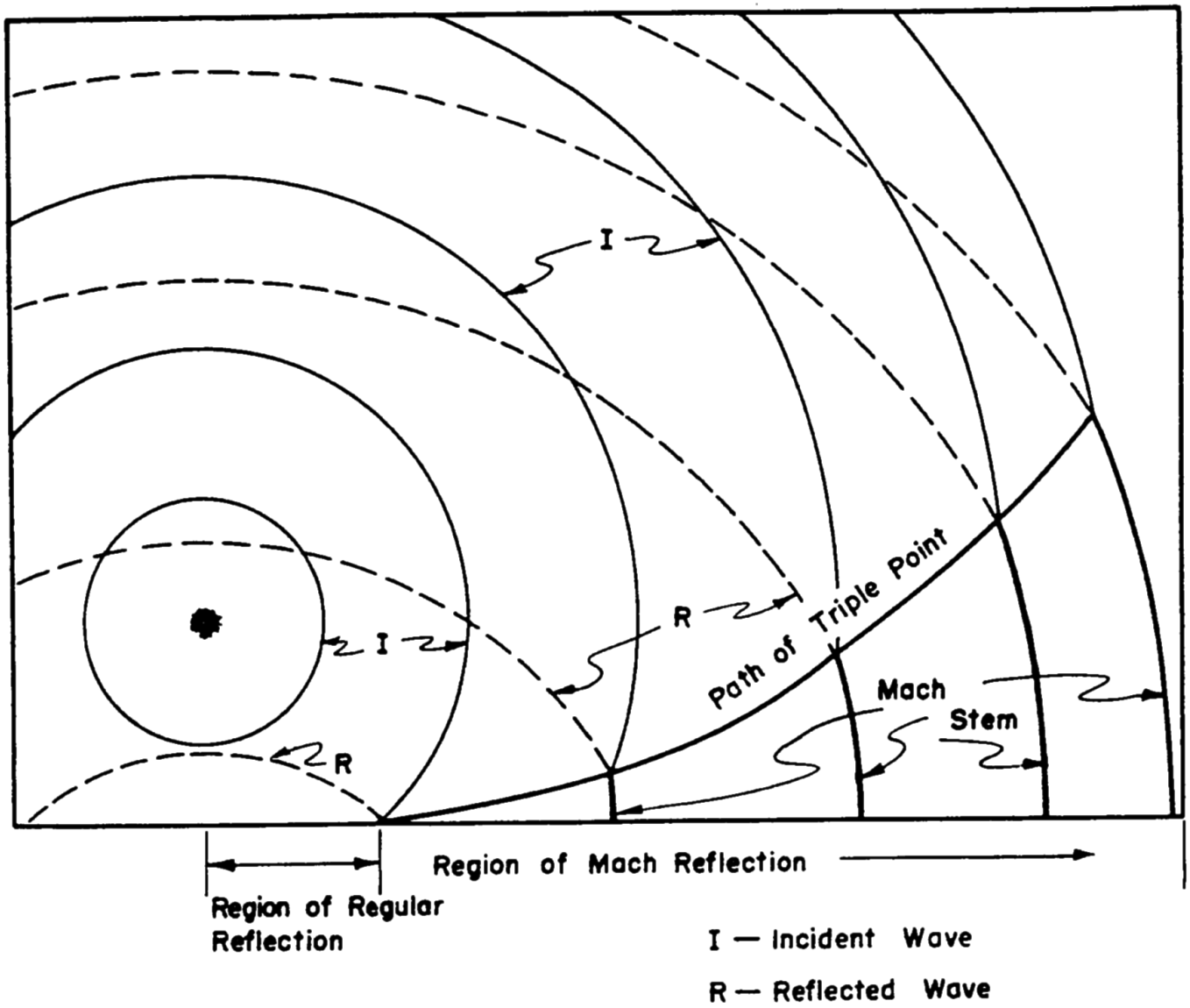

The characteristics of the blast wave at or near the surface, as well as the formation of the Mach stem, are dependent upon yield, height of burst, and the boundary or reflecting surface conditions. The region where the incident and reflected shocks have not merged to form a Mach stem is often referred to as the region of regular reflection; the region where they have merged is referred to as the region of Mach reflection. As the Mach stem travels along the surface, the triple point (the point of intersection of the incident wave, reflected wave, and the Mach stem) rises. The estimated height of the Mach stem as a function of height of burst and distance from ground zero is given in figure 2-7, for a 1 KT burst. The procedure for scaling to other yields is illustrated in the example accompanying this figure. In addition to the fusing of the reflected and incident blast waves to form a Mach stem as just described, that portion of the reflected wave passing through the fireball of a burst in the transition zone will also fuse with that portion of the incident wave directly above the fireball. This fusion is primarily a result of the increased velocity of the reflected wave as it passes through the fireball, and as a consequence, is relatively narrow in lateral extent. As the height of burst varies from the surface to about 160 $W^{1/3}$, the peak overpressures in the fused wave above the fireball vary from those ex-

pected from a particular weapon burst at the earth's surface to those expected from a free air burst of the same weapon. This is primarily the consequence of the spherical divergence of the reflected shock together with the dissipative effect of passing through a heated region.

(*a*) *Good surface conditions.* The preceding description of the reflection process considers the earth's surface as if it were an ideal reflector. For bursts over real target areas, however, the condition and nature of the surface must be considered, since it has been determined that under certain circumstances severe modifications of the blast wave may occur. These modifications are due to the physical characteristics of the surface, which result in thermal and mechanical effects on the blast wave. These effects will be discussed further in *d*(4) below. In a practical sense, the surfaces which most closely approach the ideal are ice, snow and water. These surfaces are considered as "good," since the influence of such surfaces in altering the blast wave is expected to be a minimum. The air blast characteristics for nuclear detonations over such "good" surfaces are presented in figures 2–8A, 2–9, and 2–11A.

(*b*) *Average surface conditions.* As noted above, the characteristics of the blast wave can be appreciably influenced by the type and condition of the surface over which it passes. In many target areas, it is expected that a significant thermal layer will form near the surface prior to shock arrival. The interaction of the incident blast wave with this thermal layer may affect the reflection process to a considerable degree, depending on the intensity of the thermal layer. Thus individual blast wave parameters such as shock velocity, peak overpressure, particle velocity, peak dynamic pressure and duration, as well as arrival times, wave forms and impulse values, will be affected. The nature of these perturbations depends on the height of burst and ground range involved, and to a lesser extent on the yield. They are important for surface bursts, bursts in the transition zone, and air bursts over such surfaces as desert sand, coral, wooded and agricultural areas. In general, severe thermal effects on the blast wave may be expected over such surfaces for burst heights up to 650 $W^{1/3}$ feet, while moderate to light thermal effects may be expected for burst heights between 650 $W^{1/3}$ and 800 $W^{1/3}$. However, these thermal effects are not expected in regions where pressures are below 6 psi for bursts over any surface. Mechanical influences on the blast wave may be present for any pressure level, but their relative importance is considerably less than the thermal effects previously mentioned. A detailed discussion of thermal and mechanical effects is given in *d*(4) below. The air blast characteristics for nuclear detonations over the real surfaces described above are presented in figures 2–8B, 2–10, and 2–11B. These figures should be used as representative for all target areas where surface conditions cannot be considered as *good*.

(2) *Time of arrival.* The time of arrival of the shock front on the surface is given in figure 2–8 as a function of height of burst and ground range for a 1 KT burst in a homogeneous sea level atmosphere. For other yields, cube root scaling applies to burst heights, ground range and time. Figure 2–8A applies to good surface conditions while 2–8B applies to average surface conditions.

(3) *Peak overpressure.*

(*a*) *General.* For given surface conditions, the variation of peak overpressure with distance as a function of the height of burst is presented in "height of burst" curves. Curves for good surface conditions are shown in figure

2–9, while those presented in figure 2–10 are considered appropriate for all other target areas. These figures give distances from ground zero at which various peak overpressures will be attained on the ground surface from a 1 KT explosion at different heights of burst in a homogeneous sea level atmosphere. In order to scale to other yields, the height of burst and the distance at which a given overpressure occurs are multiplied by the cube root of the selected yield. This procedure is illustrated in the example which accompanies these figures. Study of figure 2–10 reveals that if it is desired to obtain the maximum ground range for an overpressure of 10 psi or less, a height of burst should be selected which coincides as nearly as possible with the extreme right projection, sometimes called the "knee," of the desired pressure contour. If the range of an overpressure at the surface greater than 10 psi is of interest, it will be seen that the maximum coverage is obtained from bursts close to the ground (i. e., the extreme right projection of the curve occurs at low heights of burst).

(*b*) *Duration.* The duration of the positive phase of the blast wave at the surface depends upon height of burst, distance from ground zero, yield, and surface conditions. This dependence is illustrated in figure 2–11 for a 1 KT burst at sea level. Figure 2–11A applies to good surface conditions while 2–11B applies to average surface conditions. Accompanying figure 2–11 is the scaling procedure for other yields with an example of its use.

(*c*) *Impulse and wave forms.* The overpressure positive phase impulse is obtained from the area under the positive phase of the overpressure-time curve. The exact value at or near a reflecting surface for a particular range depends on the height of burst and yield, as well as the extent of perturbation of the wave form as noted above. The classical wave form previously discussed for free air overpressures (characterized by an instantaneous rise to a peak value at shock arrival, followed by an exponential decay in some manner dependent upon shock strength) is seldom found along the surface for overpressure levels above 6 psi. Only for such specialized surface conditions as snow, ice and water, where thermal effects on the blast wave are expected to be at a minimum, do the wave forms for higher overpressure levels approach the ideal. Even then, minor mechanical effects may be present; for example, over water the rise time may not be instantaneous and there may be a slight rounding of the peak value of the overpressure wave form. In general, non-ideal overpressure wave forms which reflect precursor action will result for those bursts over such real surfaces as desert sand, coral, wooded and agricultural areas where significant thermal effects on the blast wave may be expected. The variation in the overpressure wave shape depends on height of burst and ground distance. For a detailed discussion of wave form types and overpressure impulse to be expected under various conditions, refer to appendix I. A detailed discussion of the precursor is given in *d*(4) below.

(4) *Dynamic pressure.*

(*a*) *General.* For given surface conditions, the variation of peak dynamic pressure at the surface with range depends on the yield and height of burst. This dependence is shown in the form of height of burst curves, such as those presented in figure 2–12 for 1 KT in a homogeneous sea level atmosphere for good surface conditions. These curves approach the ideal situation where thermal effects on the blast wave are

~~CONFIDENTIAL~~

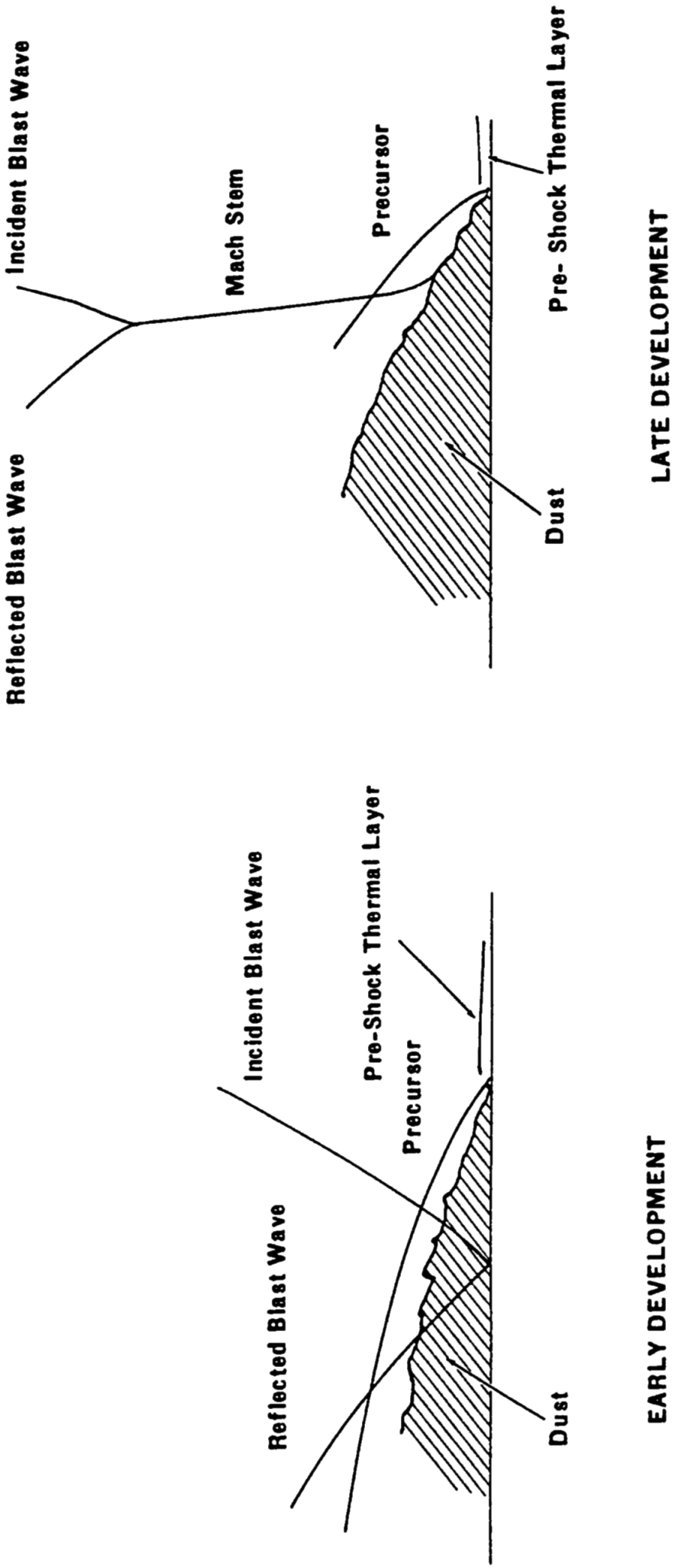

PRECURSOR CHARACTERISTICS

~~CONFIDENTIAL~~

MACH STEM HEIGHT

Figure 2-7 is a plot of ground distance vs. Mach stem height for various heights of burst of a 1 KT detonation in a sea level atmosphere. These curves are for average surface conditions; depending upon the thermal qualities and the roughness of the surface, the triple point rise may be somewhat different from that shown.

Scaling. Distances scale as the cube root of the yield, so that—

$$\frac{H_1}{H_2}=\frac{h_1}{h_2}=\frac{d_1}{d_2}=\frac{W_1^{1/3}}{W_2^{1/3}}$$

where H_1, h_1 and d_1 are Mach stem height, height of burst and ground distance for yield W_1, and H_2, h_2 and d_2 are the corresponding Mach stem height, height of burst and ground distance for yield W_2.

Example.

Given: A 60 KT detonation at 1,000 feet height of burst.

Find:

(*a*) The range at which the Mach stem is 50 feet high.

(*b*) The minimum ground range for which an aircraft at 5,000 feet altitude is in the Mach reflection region.

Solution:

(*a*) The corresponding burst height for 1 KT is—

$$h_1=\frac{1{,}000\times 1}{(60)^{1/3}}=255 \text{ feet.}$$

The corresponding Mach stem height for a 1 KT burst is—

$$H_1=\frac{50\times 1}{(60)^{1/3}}=13 \text{ feet.}$$

From figure 2-7, a Mach stem height of 13 feet is found at 95 yards for a 1 KT burst at 255 feet HOB. For a 60 KT burst, the range is $95\times(60)^{1/3}=$ 370 yards. *Answer.*

(*b*) 5,000 feet altitude for a 60 KT burst corresponds to $\frac{5{,}000}{(60)^{1/3}}=1{,}280$ feet altitude for a 1 KT burst. Interpolating between the 200 feet and 300 feet burst height curves, the ground range for a Mach stem height of 1,280 feet is 810 yards. The corresponding range for a 60 KT burst is $810\times(60)^{1/3}=$ 3,200 yards. *Answer.* This indicates that for the burst condition and altitude specified, an aircraft at ranges greater than 3,200 yards will experience a single shock.

Reliability. The range at which a given Mach stem height occurs as obtained from figure 2-7 is considered to be reliable to ±10 percent for 1 KT and to ±25 percent for 20 MT. This decrease in reliability with increasing yield is a result of the lack of knowledge concerning the effect of atmospheric inhomogeneity on the triple point trajectory. It is suggested that no correction be made for altitude effects; however, when the basic data are applied to high yield air bursts, the results should be treated with somewhat less confidence.

Related material.

See paragraph 2.1.*c*(1).

See also figure 2-6.

FIGURE 2-7

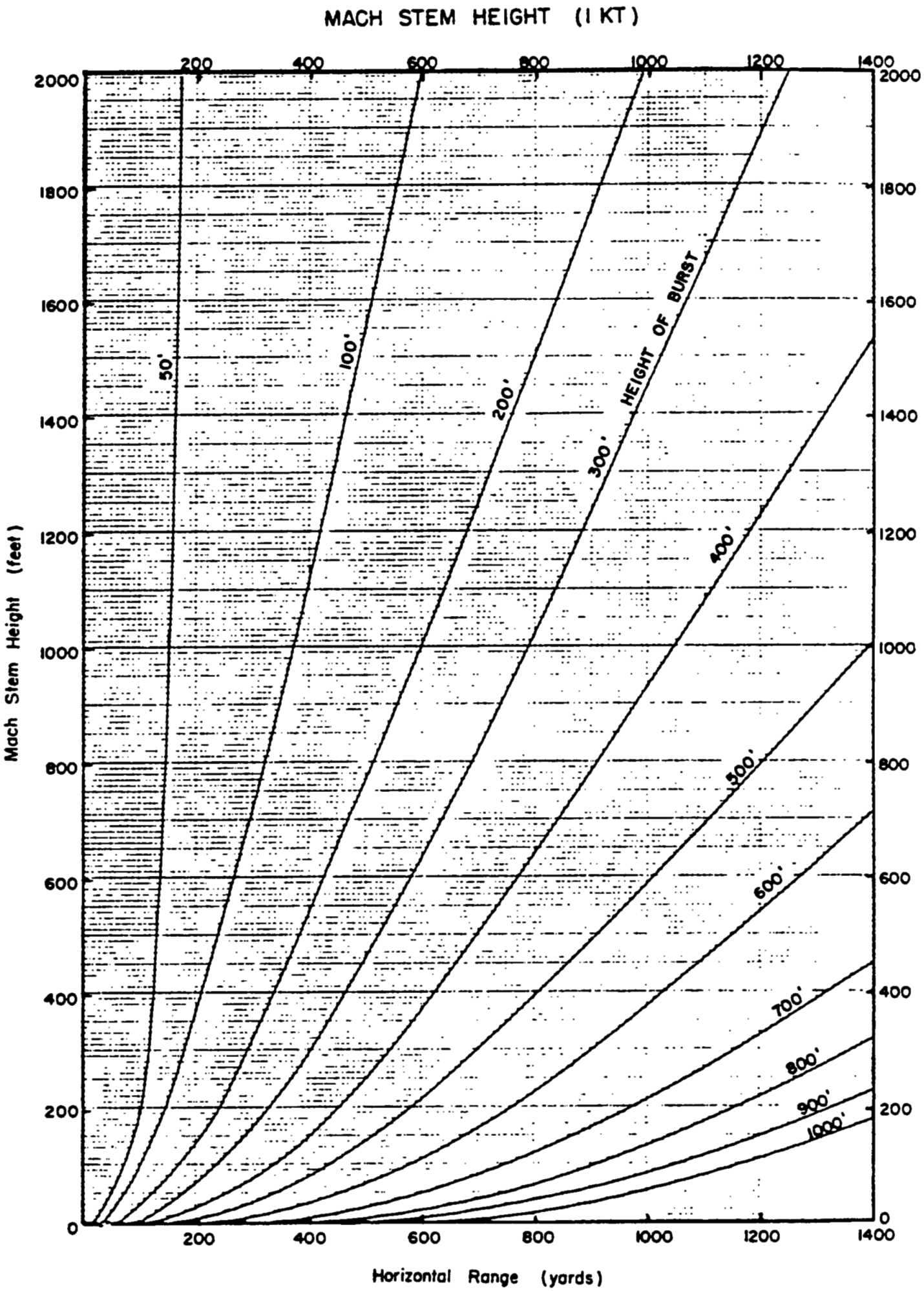

447555 O - 58 - 5

PEAK OVERPRESSURES ON THE SURFACE

(Good and Average Surface Conditions)

Figures 2-9 and 2-10 are families of curves representing peak overpressures on the ground as a function of ground range and height of burst for a 1 KT burst under sea level conditions. The solid lines are based upon experimental data established as a result of full-scale nuclear explosions and the dashed portions are based upon theory and high explosive experiments. The curves in figures 2-9A and 2-9B are considered representative for "good" target surfaces approaching the ideal, while the curves in figures 2-10A and 2-10B are considered appropriate for all other target conditions ("average"). Surface influences are discussed in paragraphs 2.1*c* and *d*(4).

Scaling. The height of burst and the range to which a given peak overpressure extends scale as the cube root of the yield, i. e.,

$$\frac{d_1}{d_2}=\frac{h_1}{h_2}=\frac{W_1^{1/3}}{W_2^{1/3}},$$

where for a given peak overpressure, d_1 and h_1 are ground range and height of burst for W_1 KT, and d_2 and h_2 are the corresponding ground range and height of burst for W_2 KT.

Example.

Given: An 80 KT detonation 2,580 feet above an average surface.

Find: The distance to which 3 psi extends.

Solution: The corresponding burst height for 1 KT is—

$$h_1=\frac{W_1^{1/3}\times h_2}{W_2^{1/3}}=\frac{1\times 2{,}580}{(80)^{1/3}}=600 \text{ ft.}$$

From figure 2-10B, 3 psi extends to 920 yards for a 600 foot burst height for a 1 KT weapon. The corresponding distance for 80 KT is:

$$d_2=\frac{W_2^{1/3}\times d_1}{W_1^{1/3}}=\frac{(80)^{1/3}\times 920}{1}=$$

3,960 yards. *Answer.*

Reliability. The pressures obtained from figures 2-9 and 2-10 are considered to be reliable to ±20 percent for yields of 1 KT to 20 MT. Outside this range of yields the figures may be used with somewhat less confidence.

Related Material.

See paragraphs 2.1*c*(3) and *d*(4).

See also figures 2-3, 2-8, 2-11 through 2-13, and 2-18.

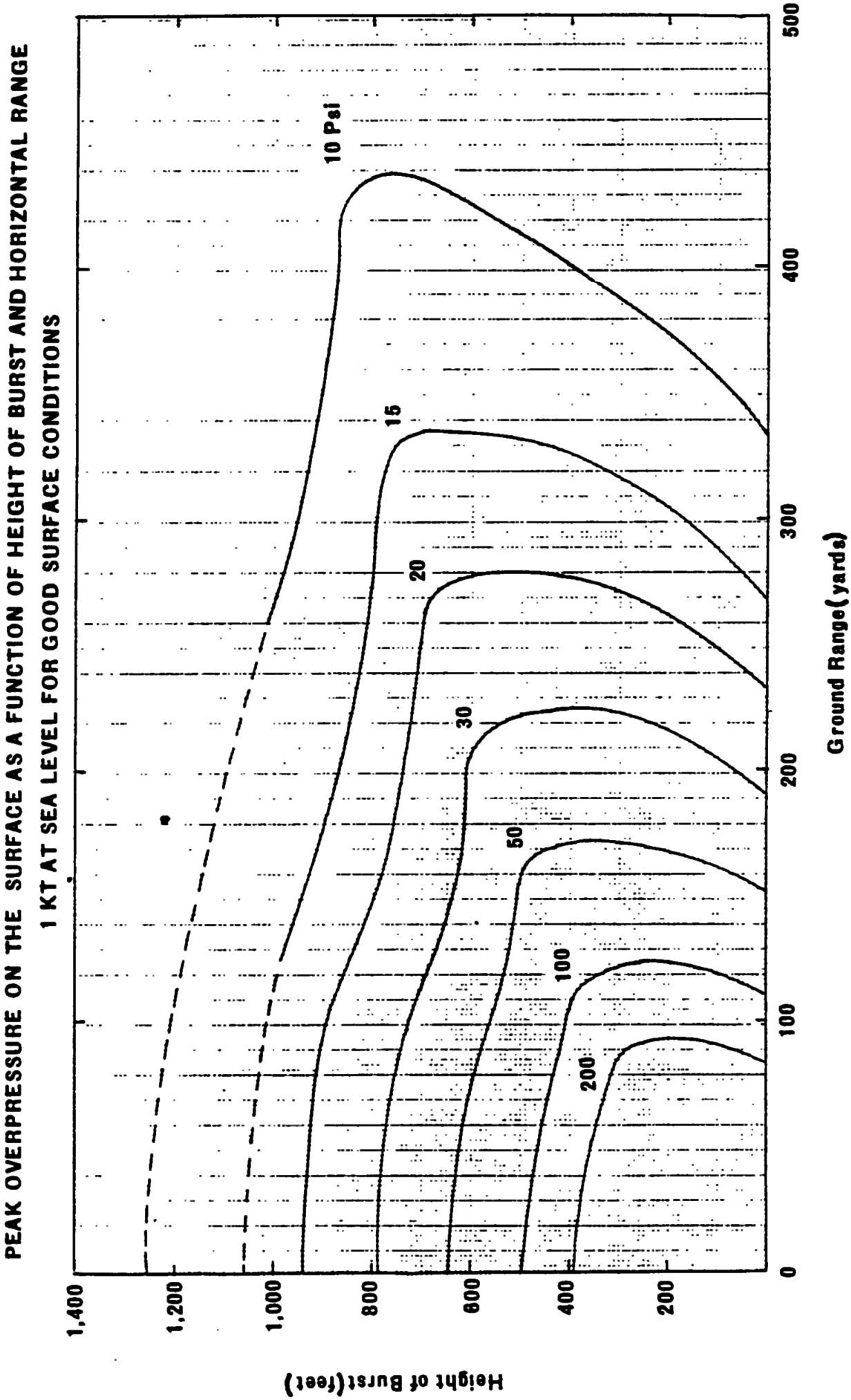
PEAK OVERPRESSURE ON THE SURFACE AS A FUNCTION OF HEIGHT OF BURST AND HORIZONTAL RANGE
1 KT AT SEA LEVEL FOR GOOD SURFACE CONDITIONS
10 Psi
15
20
30
50
100
200
Height of Burst (feet)
1,400
1,200
1,000
800
600
400
200
Ground Range (yards)
0
100
200
300
400
500

FIGURE 2-9B

PEAK OVERPRESSURE ON THE SURFACE AS A FUNCTION OF HEIGHT OF BURST AND GROUND RANGE
1 KT AT SEA LEVEL FOR GOOD SURFACE CONDITIONS

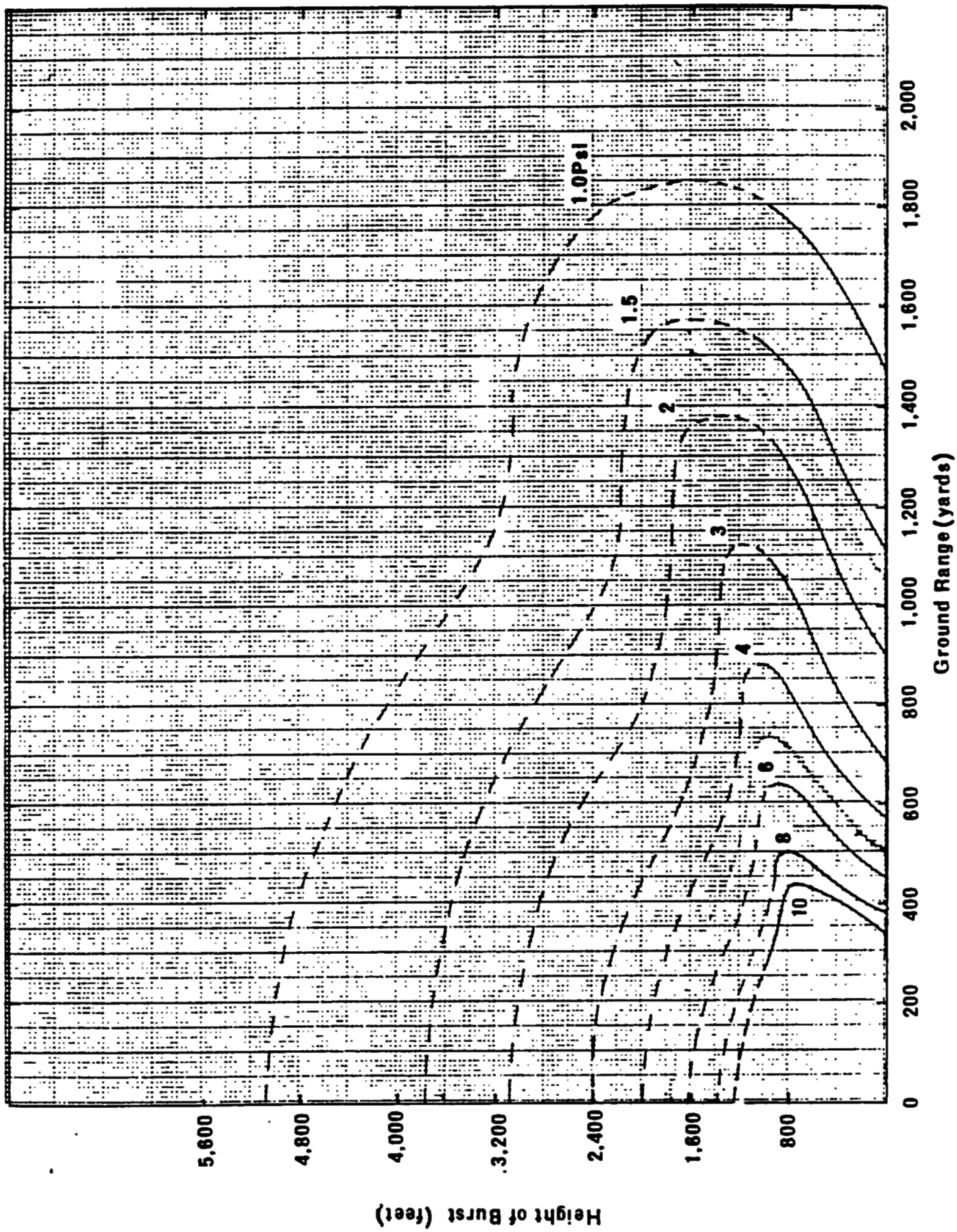

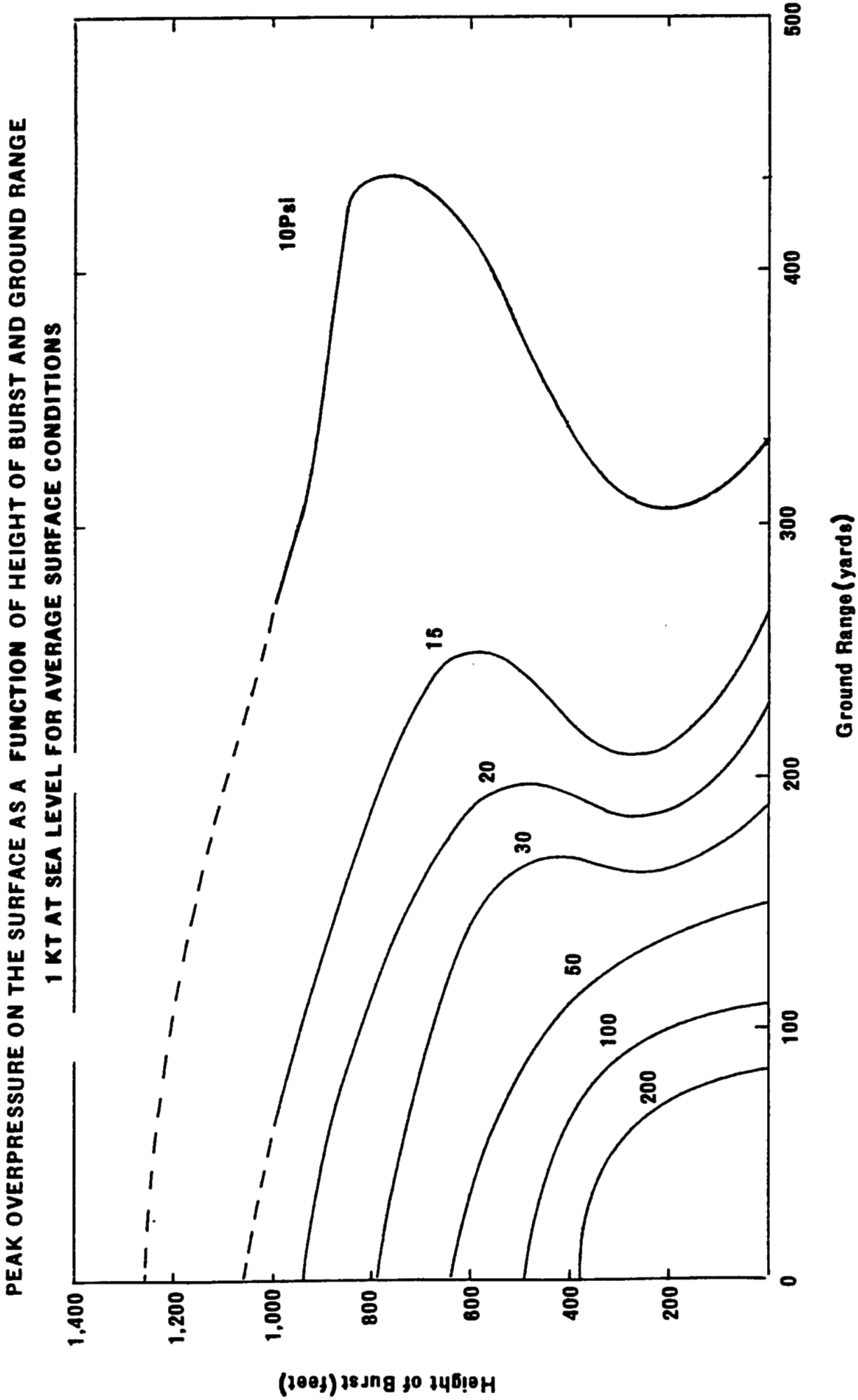
PEAK OVERPRESSURE ON THE SURFACE AS A FUNCTION OF HEIGHT OF BURST AND GROUND RANGE
1 KT AT SEA LEVEL FOR AVERAGE SURFACE CONDITIONS
10Psi
15
20
30
50
100
200
Height of Burst (feet)
1,400
1,200
1,000
800
600
400
200
0
100
200
300
400
500
Ground Range (yards)

FIGURE 2-10B

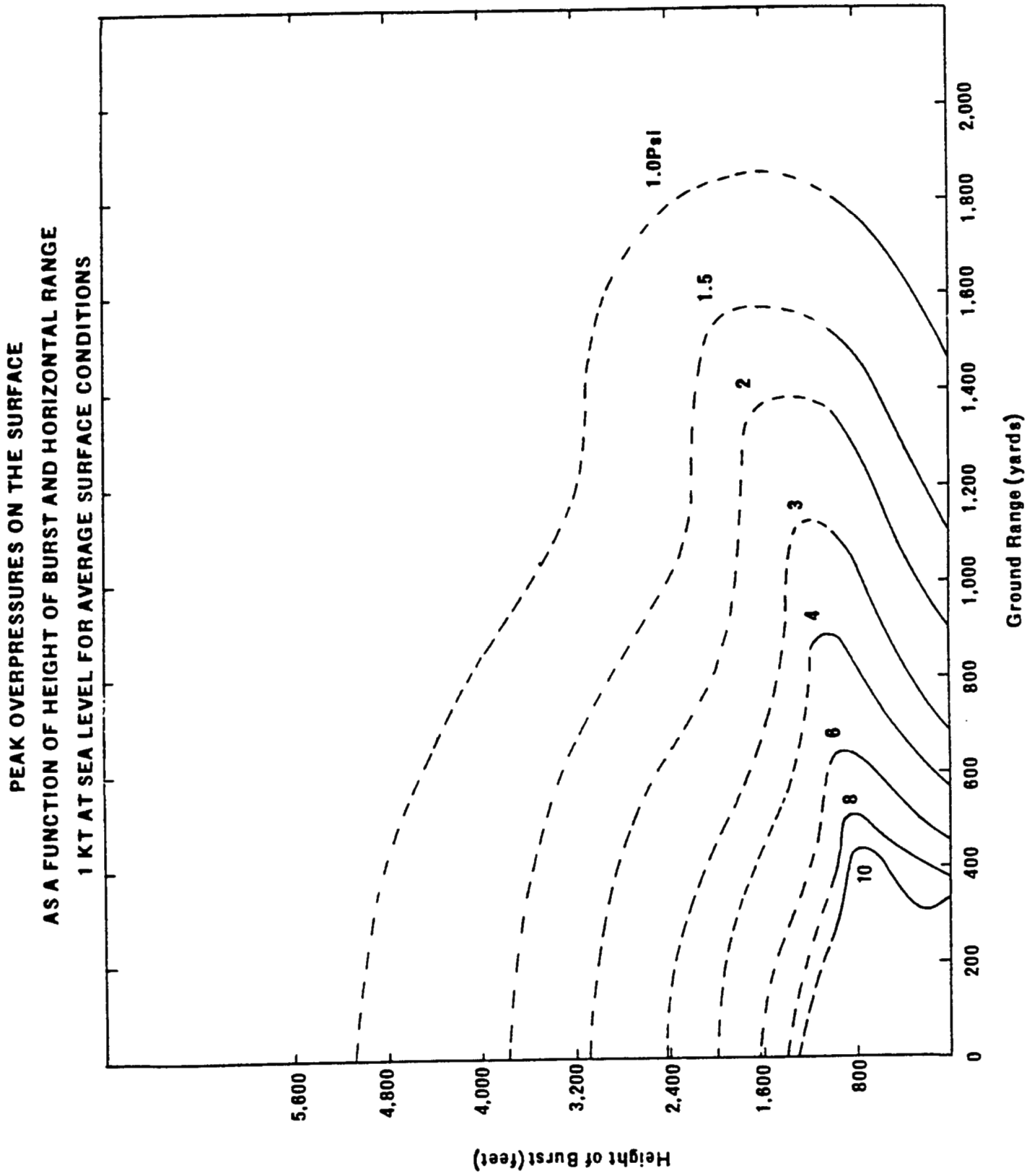
PEAK OVERPRESSURES ON THE SURFACE
AS A FUNCTION OF HEIGHT OF BURST AND HORIZONTAL RANGE
1 KT AT SEA LEVEL FOR AVERAGE SURFACE CONDITIONS
1.0Psi
1.5
2
3
4
6
8
10
Height of Burst (feet)
5,600
4,800
4,000
3,200
2,400
1,600
800
Ground Range (yards)
0
200
400
600
800
1,000
1,200
1,400
1,600
1,800
2,000

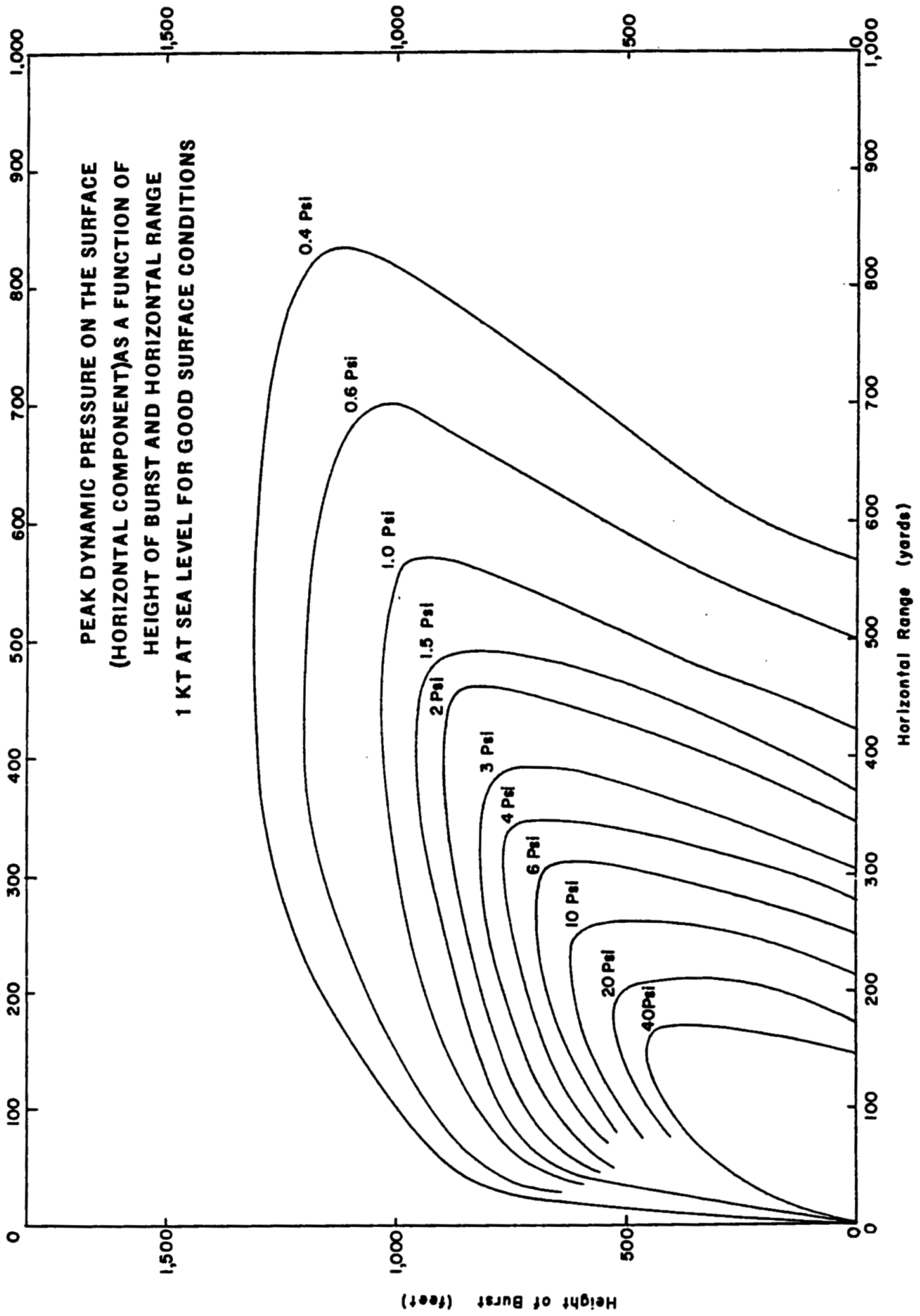
PEAK DYNAMIC PRESSURE ON THE SURFACE
(HORIZONTAL COMPONENT) AS A FUNCTION OF
HEIGHT OF BURST AND HORIZONTAL RANGE
1 KT AT SEA LEVEL FOR GOOD SURFACE CONDITIONS
0.4 Psi
0.6 Psi
1.0 Psi
1.5 Psi
2 Psi
3 Psi
4 Psi
6 Psi
10 Psi
20 Psi
40 Psi
Height of Burst (feet)
Horizontal Range (yards)
0
100
200
300
400
500
600
700
800
900
1,000
1,500

FIGURE 2-13

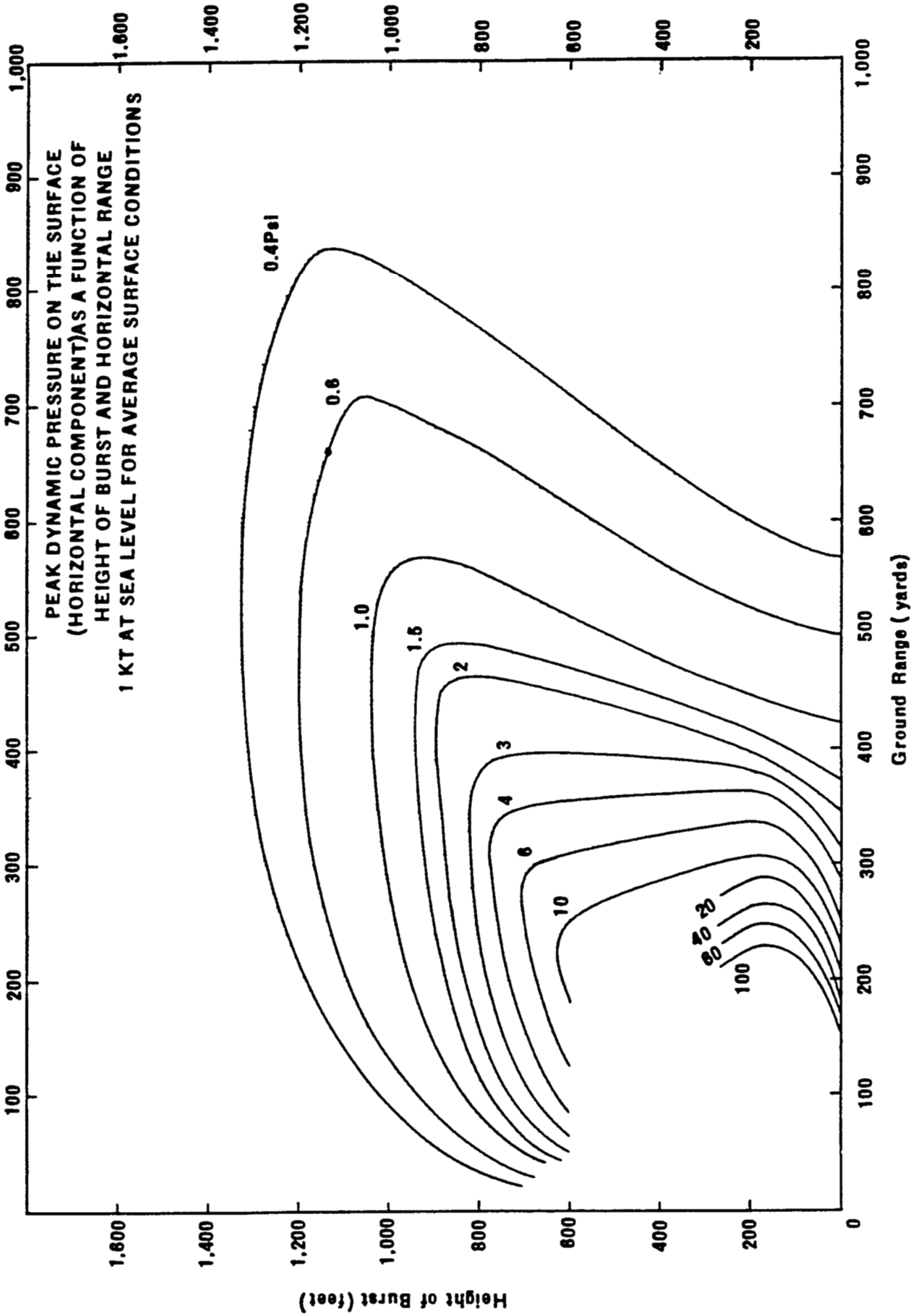
PEAK DYNAMIC PRESSURE ON THE SURFACE
(HORIZONTAL COMPONENT) AS A FUNCTION OF
HEIGHT OF BURST AND HORIZONTAL RANGE
1 KT AT SEA LEVEL FOR AVERAGE SURFACE CONDITIONS
0.4Psi
0.6
1.0
1.5
2
3
4
6
10
20
40
60
100
Ground Range (yards)
Height of Burst (feet)
0
100
200
300
400
500
600
700
800
900
1,000
1,200
1,400
1,600

CONFIDENTIAL

RAIN OR FOG EFFECTS ON PEAK OVERPRESSURE

Figures 2–14A and 2–14B present range correction factors as a function of height of burst and overpressure for a 1 KT detonation in rain or fog. The range to which a given overpressure would extend under normal conditions is multiplied by the correction factor to account for the presence of the rain or fog.

Scaling. Use the relation:

$$\frac{h_1}{h_2}=\frac{W_1^{1/3}}{W_2^{1/3}},$$

where h_1=height of burst for yield W_1, and h_2= the corresponding height of burst for yield W_2.

Example.

Given: A 30 KT burst at 600 feet in a moderate rain.

Find: The distances to which 8 and 30 psi extend on the ground surface under average surface conditions.

Solution: The corresponding burst height for 1 KT is:

$$h_1=\frac{600\times 1}{(30)^{1/3}}=190 \text{ feet.}$$

From figure 2–10, the ground range for 8 psi overpressure is 380 yards and for 30 psi overpressure is 164 yards for a 1 KT burst. The corresponding ranges for a 30 KT burst are 1,200 yards (for 8 psi) and 530 yards (for 30 psi). From figure 2–14A (moderate rain), the correction factors for a burst at 190 feet are 0.9 (for 8 psi) and >0.99 (for 30 psi).

The range to which 8 psi extends in moderate rain is 1,200×(0.9)=1,100 yards. *Answer.*

The reduction in range for 30 psi is negligible; it therefore extends to 530 yards. *Answer.*

Reliability. At a given range obtained in this manner, overpressures are considered to be reliable within ±40 percent.

Related material. See paragraph 2.1.*d*(2). See also figures 2–9, 2–10, and 2–18.

CONFIDENTIAL

FIGURE 2-14A
FIGURE 2-14B

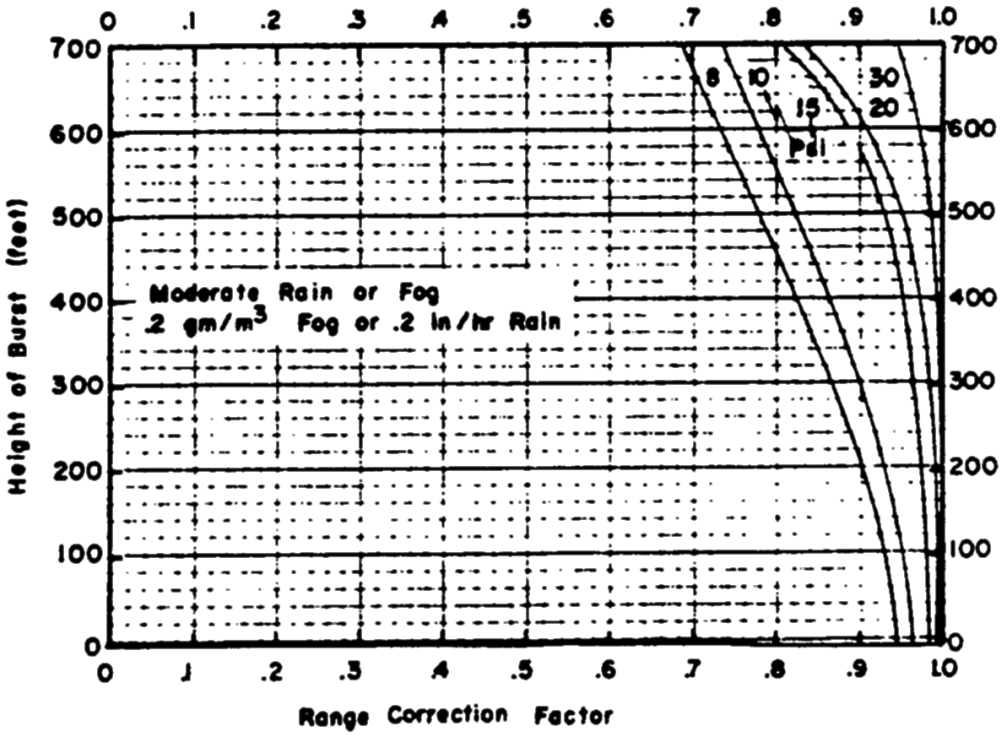

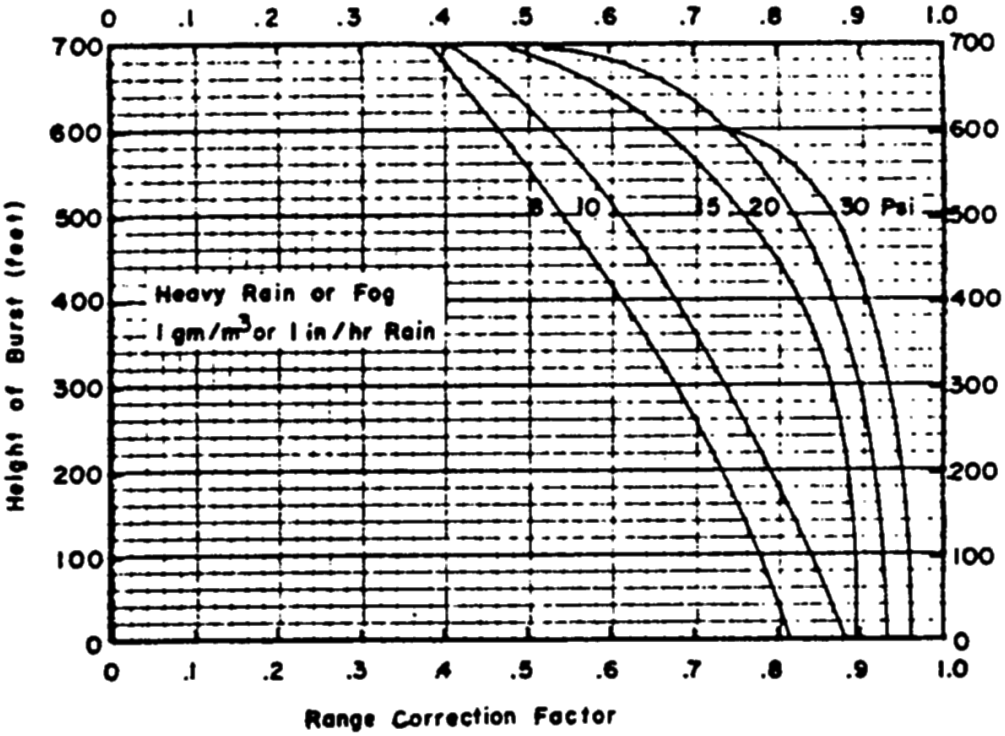

RAIN OR FOG EFFECTS ON PEAK OVERPRESSURE AS A FUNCTION OF HEIGHT OF BURST FOR 1 KT AT SEA LEVEL

CRITERIA FOR PRECURSOR FORMATION

Figure 2–17 gives conditions of burst height and yield for precursor formation over average surfaces, and may be utilized to predict precursor formation if these conditions are known.

Example.

Given: A 100 KT burst at 600 feet over an "average" surface.

Find: Whether or not a precursor may be expected.

Solution: Enter figure 2–17 with a height of burst of 600 feet and a yield of 100 kilotons. The intercept falls within the portion of the figure indicating a precursor will form. *Answer.*

Reliability. Based on data obtained from extensive full scale testing over desert surfaces and limited tests over coral.

Related material.

See paragraphs 2.1*c* and *d*(4), and appendix I. See also figure 2–16.

FIGURE 2-17

CRITERIA FOR PRECURSOR FORMATION(AVERAGE SURFACE CONDITIONS)

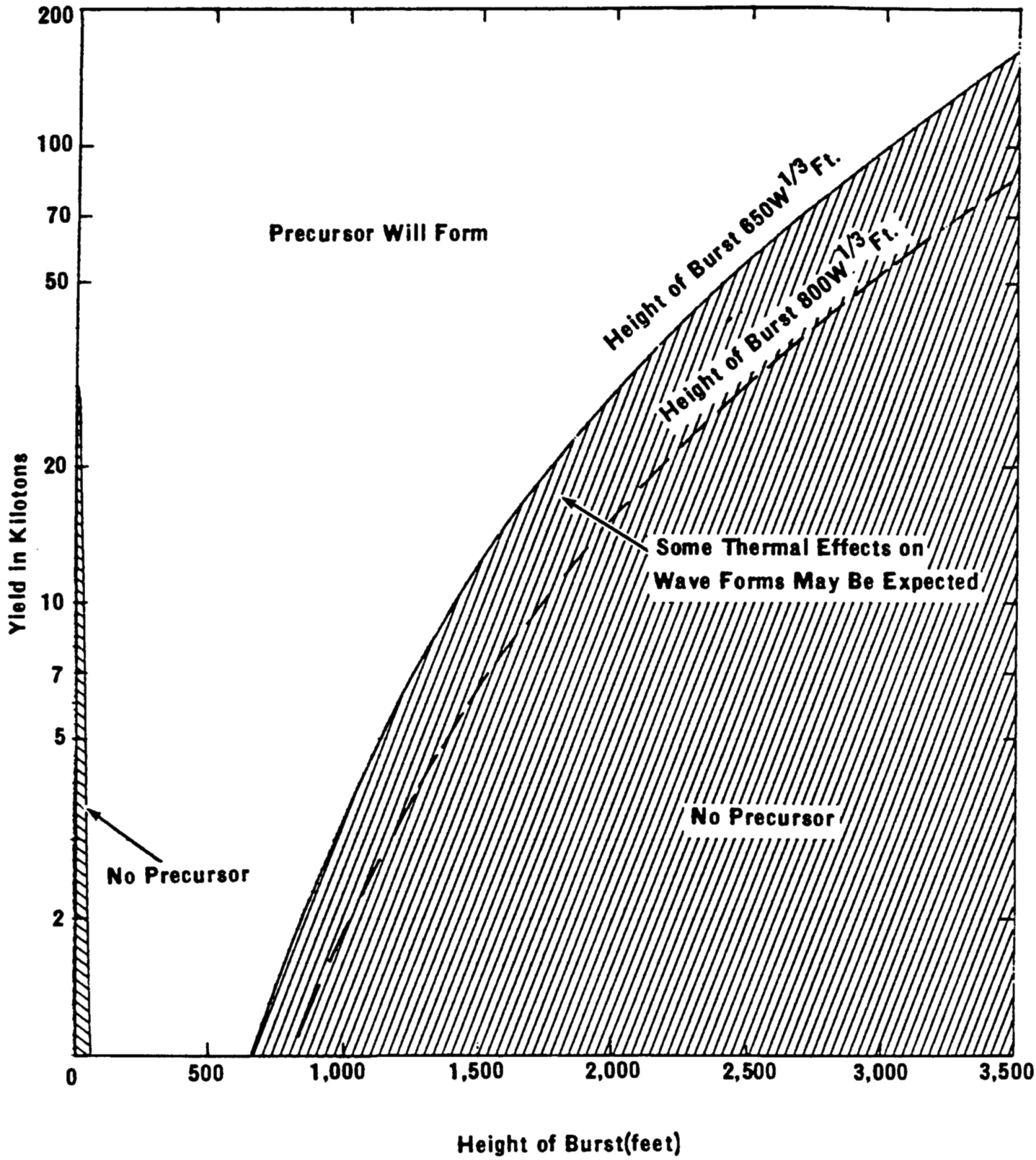

PEAK AIR OVERPRESSURES AT THE SURFACE AS A FUNCTION OF DEPTH OF BURST IN EARTH OR WATER AND HORIZONTAL RANGE

Figure 2-18 is a family of curves representing peak air overpressures on the surface as a function of depth of burst and surface range for a yield of 1 KT.

Scaling. The depth of burst and the range to which a given peak overpressure extends are directly proportional to the cube root of the yield:

$$\frac{d_1}{d_2}=\frac{h_1}{h_2}=\frac{W_1^{1/3}}{W_2^{1/3}}$$

where h_1=depth of burst for yield W_1 KT, h_2=the corresponding depth of burst for yield W_2 KT, d_1=distance to which given overpressure extends for yield W_1 KT, d_2=the corresponding distance to which given overpressure extends for yield W_2 KT.

Example.

Given: A 20 KT weapon burst 60 feet underground.

Find: The peak air overpressure 1,300 yards from surface zero.

Solution: Applying the above scaling to scale to 1 KT,

$$h_1=\frac{W_1^{1/3}\times h_2}{W_2^{1/3}}=\frac{1\times 60}{(20)^{1/3}}=22 \text{ ft},$$

$$\text{and } d_1=\frac{W_1^{1/3}\times d_2}{W_2^{1/3}}=\frac{1\times 1{,}300}{(20)^{1/3}}=480 \text{ yd}.$$

The 22-foot depth line and 480-yard distance line intersect on figure 2-18 at about 4 (± 1) psi. *Answer.*

Reliability. The reliability of pressures taken from figure 2-18 is estimated to be ± 25 percent.

Related material.

See paragraph 2.1*e*.

See also figures 2-9 and 2-10.

FIGURE 2-18

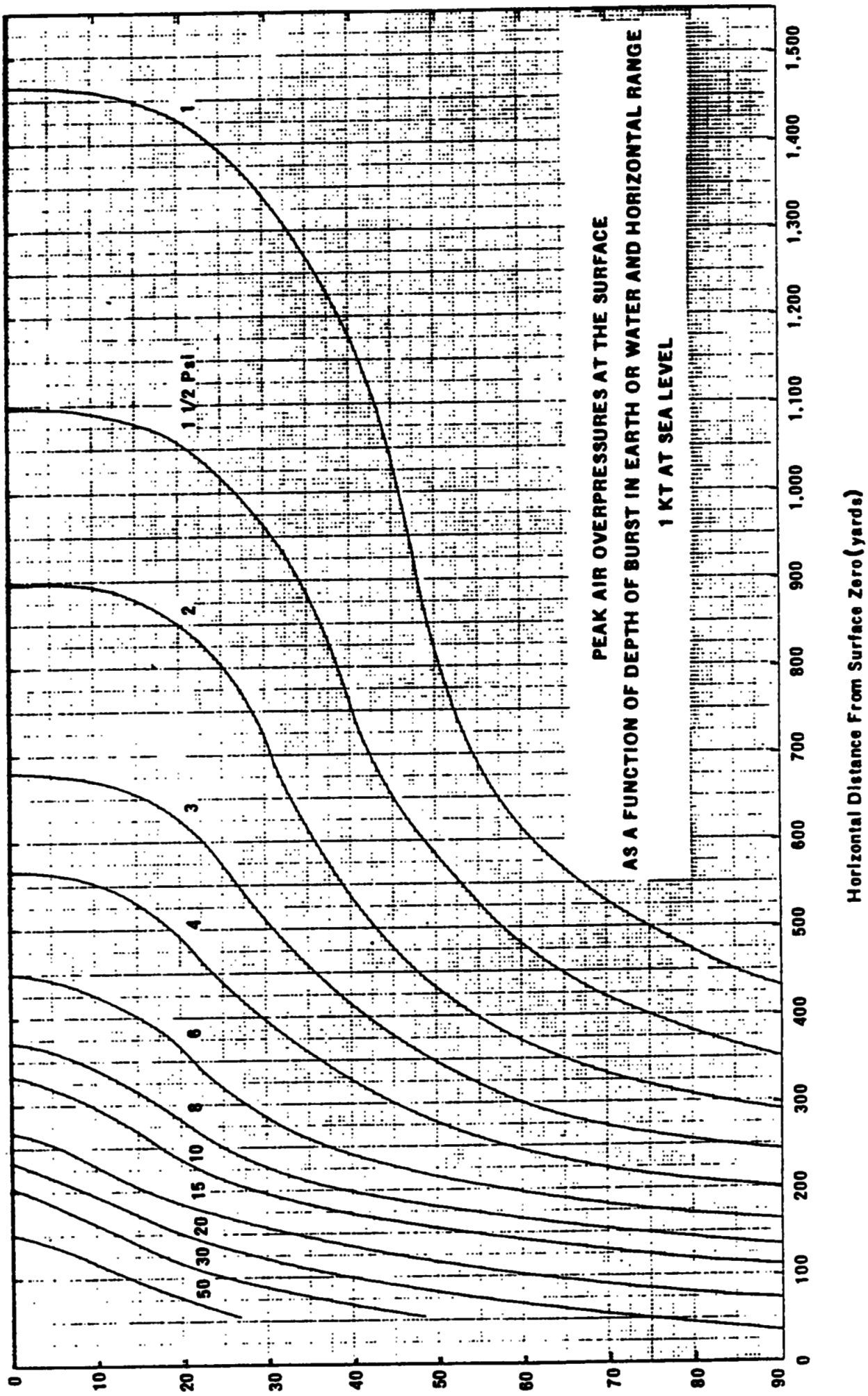
PEAK AIR OVERPRESSURES AT THE SURFACE
AS A FUNCTION OF DEPTH OF BURST IN EARTH OR WATER AND HORIZONTAL RANGE
1 KT AT SEA LEVEL
1
1 1/2 Psi
2
3
4
6
8
10
15
20
30
50
Depth of Burst (feet)
0
10
20
30
40
50
60
70
80
90
Horizontal Distance From Surface Zero (yards)
0
100
200
300
400
500
600
700
800
900
1,000
1,100
1,200
1,300
1,400
1,500

CONFIDENTIAL

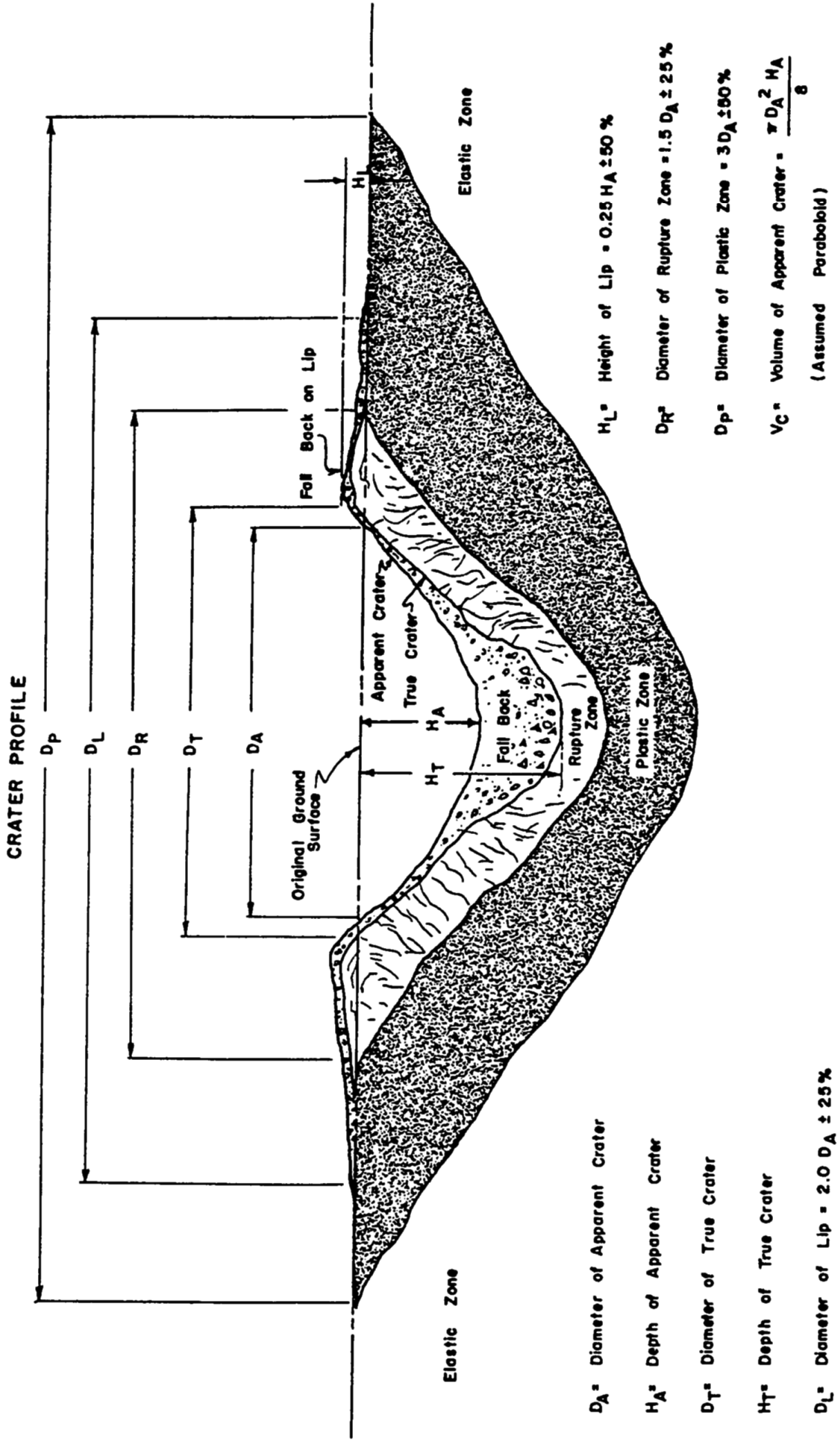

CONFIDENTIAL

depth, and lip height for a burst on the surface and on the bottom in 25, 50, 100, and 200 feet of water. The figures show that the crater dimensions are greater for a bottom burst than for a surface burst. Also for a bottom burst, as the depth of water increases the crater dimensions increase, whereas for a surface burst, as the water depth increases the crater dimensions decrease.

b. Ground Shock.

(1) *General.* The production of ground shock by nuclear explosions is extremely complex, and, in some respects, not well understood. Basically, ground shock may be produced by two separate mechanisms. One mechanism is the sudden expansion of the bubble of gas from a surface or underground explosion which generates a pulse or oscillation in the ground. This is termed "direct ground shock". As this direct shock propagates through the ground, it may be modified by reflections and refractions from underlying bedrock or hard strata, or rarefaction from the air-ground interface. The second mechanism is the production of a ground shock by the air blast wave from a nuclear explosion striking and moving parallel to the ground surface. This is termed "air induced ground shock." For a given burst geometry, except at extremely short ranges, these two forms of ground shock are separated in time. Because the direct ground shock is usually attenuated very rapidly, induced ground shock is more important from the point of view of damage to underground installations, except for extremely close ranges and for deep underground bursts. Figure 2–27A shows in schematic form the relation of these two phenomena in the case of a surface burst. Since sonic velocity is generally higher in ground than in the air, the direct ground shock is indicated as moving faster than the air blast, and consequently faster than the air induced ground shock. Although the direct ground shock and the air blast of a surface or near-surface burst initially propagate approximately together, the velocity of the air blast decreases more rapidly with distance in the higher pressure region than the direct ground shock. Hence, the direct ground shock moves ahead.

Figure 2–27B shows the relation in idealized form of the vertical acceleration caused by the two different forms of ground shock. The direct vertical acceleration is initiated upon arrival of the direct ground shock. The "air blast slap acceleration" is initiated upon the arrival of the air blast which causes a sudden local increase in soil particle acceleration.

The physical mechanisms of major interest in regard to the production of ground shock damage are acceleration, displacement and pressure (or stress). Although extensive measurements have been made, no consistent correlation between these parameters has been found. Each is discussed for both direct ground shock and air induced ground shock in the following paragraphs.

(2) *Direct ground shock.*

(*a*) *Propagation.* The direct ground shock wave produced by a surface or underground burst propagates radially outward from the burst point. For a 1 KT surface or shallow underground burst, in Nevada type soil, propagation velocities on the ground surface are 4,600 feet per second approximately 300 feet from surface zero, and decrease to a more constant 3,500 feet per second approximately 2,500 feet from surface zero. The propagation velocity of ground shock at the surface may increase with distance from the burst due to refraction and reflection from underlying higher velocity strata; and, as the shock reduces to an acoustic wave, the velocity will approach the normal acoustic velocity of the medium near the surface. In sound rock and outside the zone of rupture, the propagation of shock obeys elastic formulae.

FIGURE 2–27A
FIGURE 2–27B

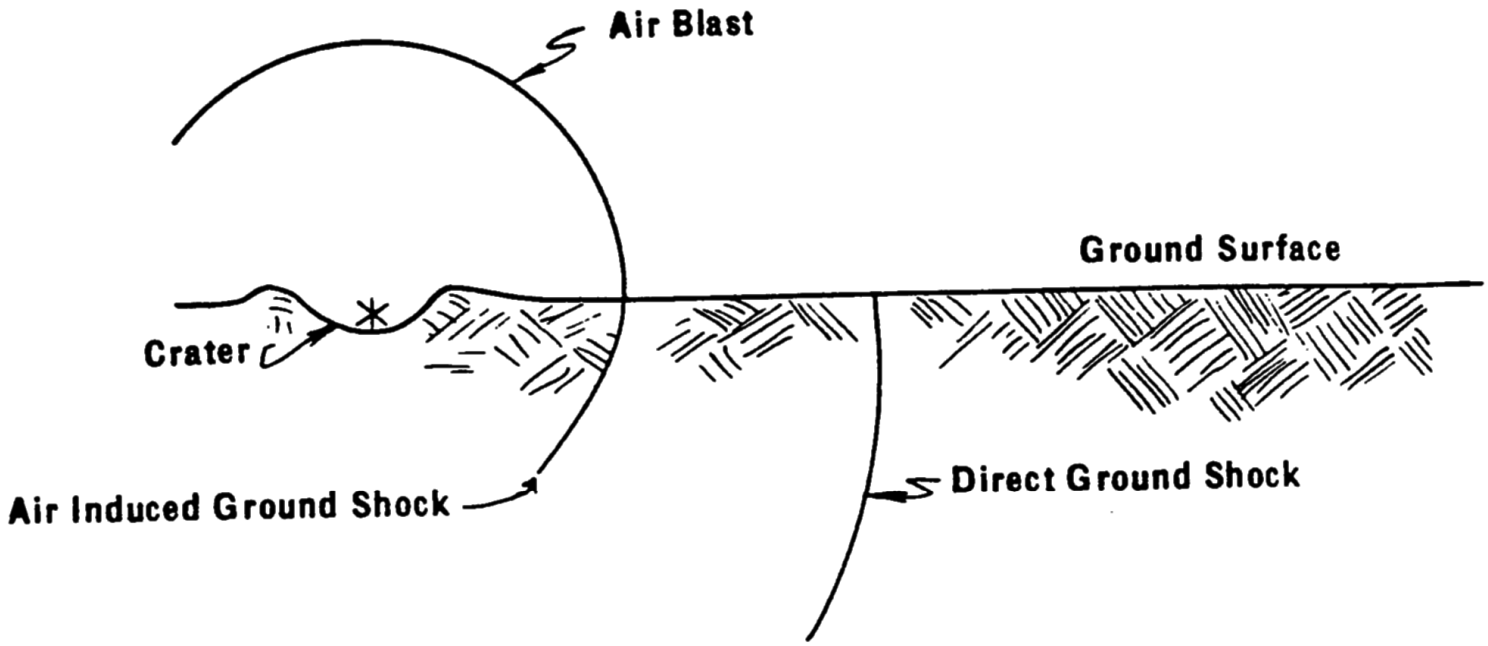

DIRECT AND AIR INDUCED GROUND SHOCK

GROUND ACCELERATION WAVE FORM WITH "SLAP"

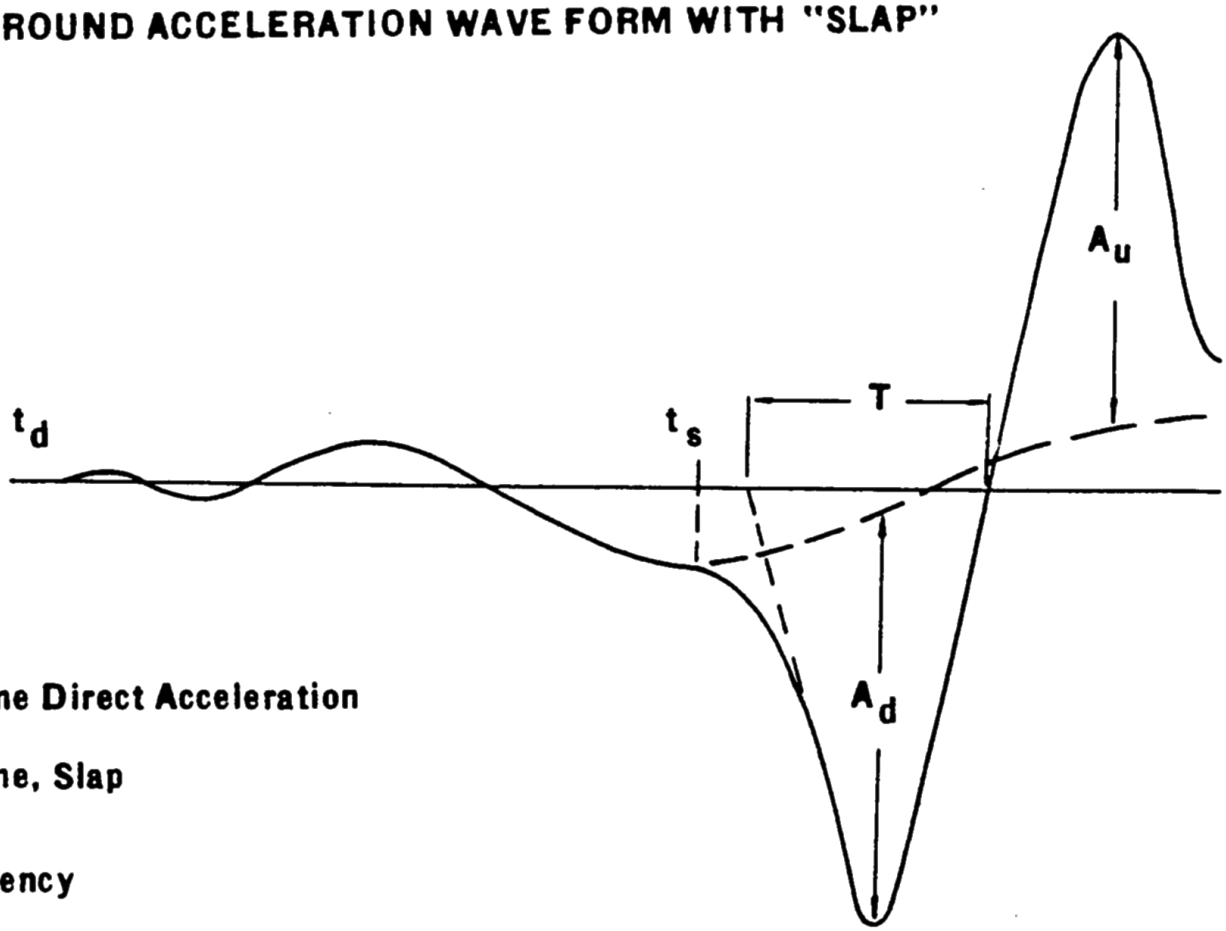

t_d = Arrival Time Direct Acceleration

t_s = Arrival Time, Slap

$\frac{1}{2T}$ = Slap Frequency

A_d = Max. Downward Slap Acceleration

A_u = Max. Upward Slap Acceleration

In such a homogeneous medium (not generally characteristic of surface conditions), there is little attenuation due to internal friction or plastic deformation. Ground shock (compression type wave) in rock is reflected from an air-rock interface as a tensile wave. The intensity of this tensile wave is dependent on shock strength, wave shape, and angle of incidence of the direct shock with the free surface.

(*b*) *Pressure* (*stress*). At any given point air blast or water shock overpressures resulting from a nuclear detonation are equal in all directions, but ground pressures are not. The shear and cohesive strength of the soil change the ground pressure into directional components which differ in magnitude depending upon the direction in which measured. These directional pressure components are termed stress. Under the dynamic loading from a nuclear explosion, the direct ground stresses rise most abruptly in the ground nearest the explosion, whereas at greater distances the peak stresses at any specific point are reduced and the rise times are increased. Stress pulses appear as various combinations of direct ground and air induced shock stresses, depending on arrival time and the range, depth and direction of the measurement. Direct and air induced ground shock stress pulses may coincide at close-in ranges outside the crater, as indicated in (1) above, but will gradually separate with increasing distance along the ground surface until two separate pulses may be detected a few feet beneath the ground surface. The peak stresses from direct ground shock usually attenuate rapidly with distance; however, in highly saturated soils the attenuation of these stresses is less, approaching the attenuation in water (approximately inversely as the range). The stress pulse from the direct ground shock is composed of vibrations of high and low frequencies, the period of which may vary from a few tenths of a second to several seconds. Two hundred feet from a 1 KT underground burst in Nevada type soil, the horizontal earth stress at a depth of 10 feet may be 125 psi; at 250 feet it may be 40 psi; while at 600 feet it may be only 3 psi. A rough comparison of peak stress intensities for various yields at the same distances may be made on the basis of relative crater size.

(*c*) *Acceleration of soil particles*. Acceleration of soil particles may be caused as a direct result of the explosion (direct acceleration), as a result of any shock reflection or refraction from underlying bedrock (indirect acceleration), or as a result of air blast (induced acceleration). Direct and indirect accelerations are generally indistinguishable and together are termed direct or fundamental acceleration. For acceleration values of 1 g or greater measured beyond a range of two crater radii from ground zero the frequency in soil will usually be less than 80 cycles per second for all yields, and for 1 KT the predominant frequencies will be from 3 to 15 cycles per second. In rock, the amplitude of accelerations may be considerably greater and the period may be less than in average soil.

(*d*) *Displacement of soil particles*. Displacement of soil particles is largely permanent within the plastic zone of a crater and transient beyond the plastic zone. For a small, near-surface burst, and at a range of three crater radii, the permanent displacement along the ground surface will probably be less than 0.0003 of a crater radius and the transient displacement will probably be less than 0.001 of a crater radius. A short distance beneath the ground surface, soil particle displacement is usually less than the displacement along the ground surface. Displacements are

appreciably affected by soil types. In wet soils, for example, they may be of the order of ten times greater than the preceding values.

(3) *Air induced ground shock.*

(*a*) *Propagation.* Air induced ground shock propagates outward from the burst with the air blast. The air blast loading may be considered as a moving, non-uniform load that generates a ground shock. The air induced shock in soil quickly attains a velocity that may exceed the air blast velocity; however, the magnitude of any outrunning shock is small and its effects may be ignored. Consequently, as the air blast wave proceeds, the air induced ground shock propagates with a rather complex underground time-of-arrival contour depending on underground shock velocities; but, in general, the ground shock front slopes backward from the air blast shock front as shown in figure 2–27A. Air induced ground shock usually arrives with or after the direct ground shock.

(*b*) *Pressure* (*stress*). Air induced ground stress (pressure) is closely related to direct ground stress (pressure) discussed in (2)(*b*) above. Just below the surface, the air induced shock stresses and durations are approximately equal to the changing positive air blast pressure and duration. These induced ground stresses attenuate gradually with depth and the rise time of the stress pulse increases. The pulse of the air induced ground stress is composed of vibrations of high and low frequencies, the periods of which may vary from a few tenths of a second to several seconds. In general, air induced ground stress is larger than direct ground stress at distances greater than two crater radii for average soils, and for all heights and depths of burst down to about 75 feet for 1 KT.

(*c*) *Acceleration of soil particles.* Air blast induced acceleration maintains its identity in the acceleration pattern and can be separated from the direct shock acceleration. When interactions with other accelerations from reflection and refraction occur, the magnitude is affected markedly and separation is difficult. Upon its arrival, the air blast will cause a sudden local increase in soil particle acceleration termed "air blast slap acceleration" (see fig. 2–27B). For acceleration values of 1 g or greater measured away from ground zero, the predominant frequencies in soil of air blast induced acceleration are 20 to 120 cycles per second. Peak vertical accelerations are larger than peak horizontal (radial) accelerations by an amount approximating 50 percent. Peak accelerations attenuate with depth and are directly proportional to the overpressure and indirectly proportional to the rise time of the pressure pulse in the soil. See figure 2–28 for the relationship of peak accelerations to peak air blast overpressures at a depth of 10 feet.

(*d*) *Displacement of soil particles.* Air induced ground shock causes little permanent horizontal displacement of ground particles beyond two crater radii. When the shock is reflected from vertical soil-air interfaces, local displacement (spalling) of ground particles may occur. Air induced ground shock may cause a vertical displacement of soil particles. Dry Nevada type soil subjected to a peak overpressure of 250 psi has sustained a permanent downward displacement of approximately 2 inches and a transient downward displacement of approximately 8 inches.

c. Column and Base Surge. A general discussion of the column and base surge resulting from an underground burst has been given in paragraph 1.4*e*(4). The maximum column diameter is generally 2 to 3 times the apparent crater diameter and the maximum column height is roughly equal to 400 $W^{1/3}$. The characteristics of the base surge depend upon the depth and yield of burst. The shallowest burst depth at which an earth base

FIGURE 2-30

EFFECT OF CUT-OFF ON THE SHAPE OF THE POSITIVE PULSE

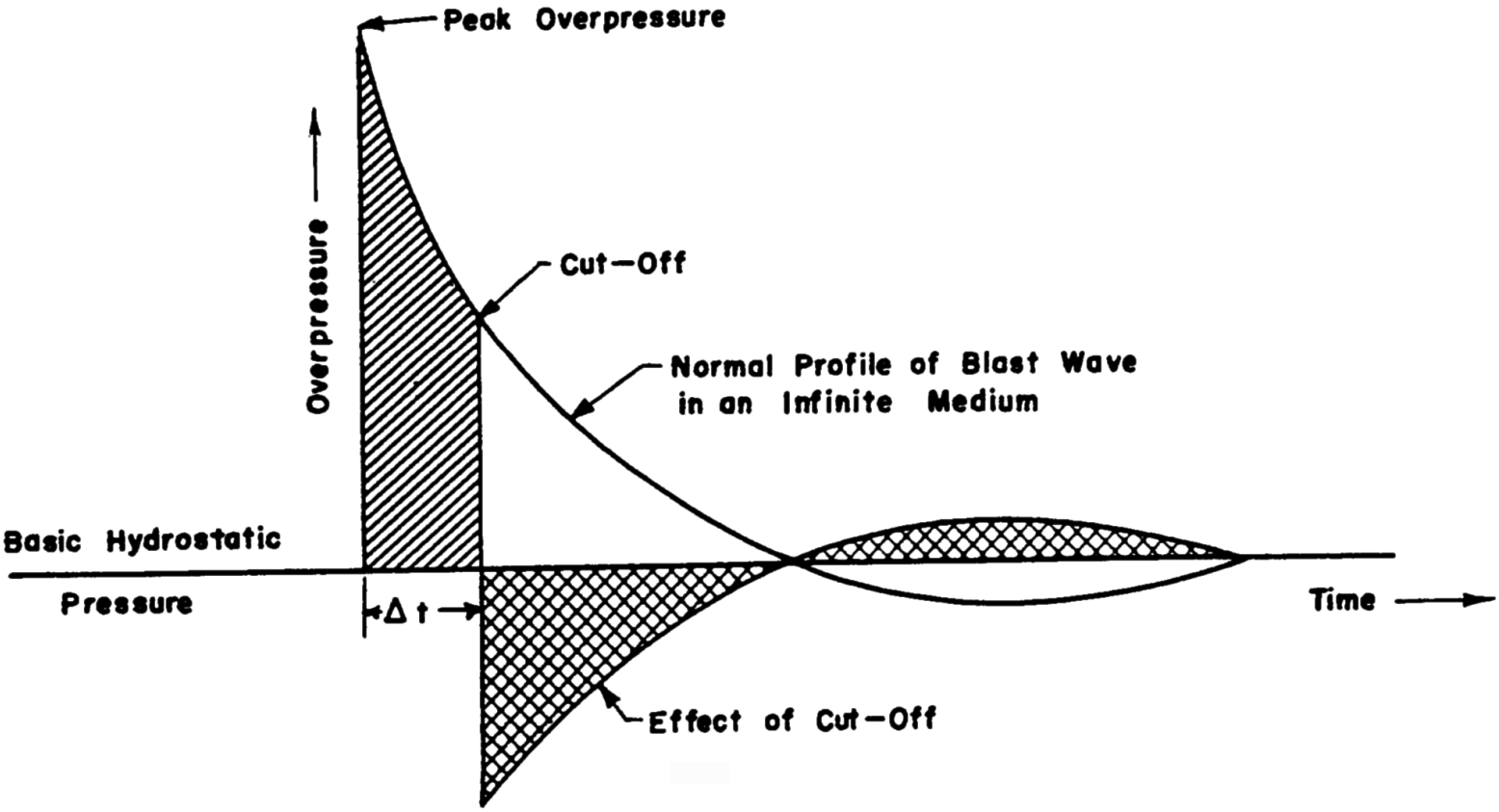

$$(\Delta t \text{ in msec} = \frac{0.4 \times (\text{Bomb Depth in Ft}) \times (\text{Target Depth in Ft})}{\text{Slant Range in Ft.}}$$

surge has been observed is 16 $W^{1/3}$ feet. As the burst depth is increased, the extent of the base surge is expected to increase until a burst depth of about 125 $W^{1/3}$ feet is attained. No further increase in base surge extent is expected below this depth of burst. Figure 2-29 shows the rate of growth of the base surge and maximum radii for various scaled depths of burst.

2.3 Water Shock and Surface Phenomena

a. Water Shock.

(1) *General.* The underwater detonation of a nuclear weapon at a distance from either the water surface or the bottom boundaries produces a shock wave early in the formation of the bubble. This shock wave propagates spherically at the rate of roughly 5,000 feet per second, and is characterized by an instantaneous rise in pressure followed by an exponential decay. In addition to this initial primary shock wave, several subsequent pressure pulses are produced within the water (see par. 1.4*f*(2) and (3)).

(2) *Burst geometry.*

(*a*) *Deep burst in deep water.* When the pressure wave is reflected from the water surface it is reflected as a rarefaction or tensile wave. This reflected rarefaction wave cuts off the tail of the primary compressional shock wave, thereby decreasing the duration of its positive phase. Figure 2-30 shows qualitatively the effect of the reflection wave upon the pressure-time history. The effect of this "cut-off" decreases rapidly with depth of the target in the water; that is, the deeper a target, the less the effect of cut-off for the same depth of detonation. Likewise, the greater the depth of detonation, the less the effect of cut-off for the same target location. The reflection of pressures from the bottom surface is similar to the reflection of pressures from the ground surface for an airburst. A crude approximation of the magnitude and shape of this

WAVE FRONT PROPAGATION IN SHALLOW WATER

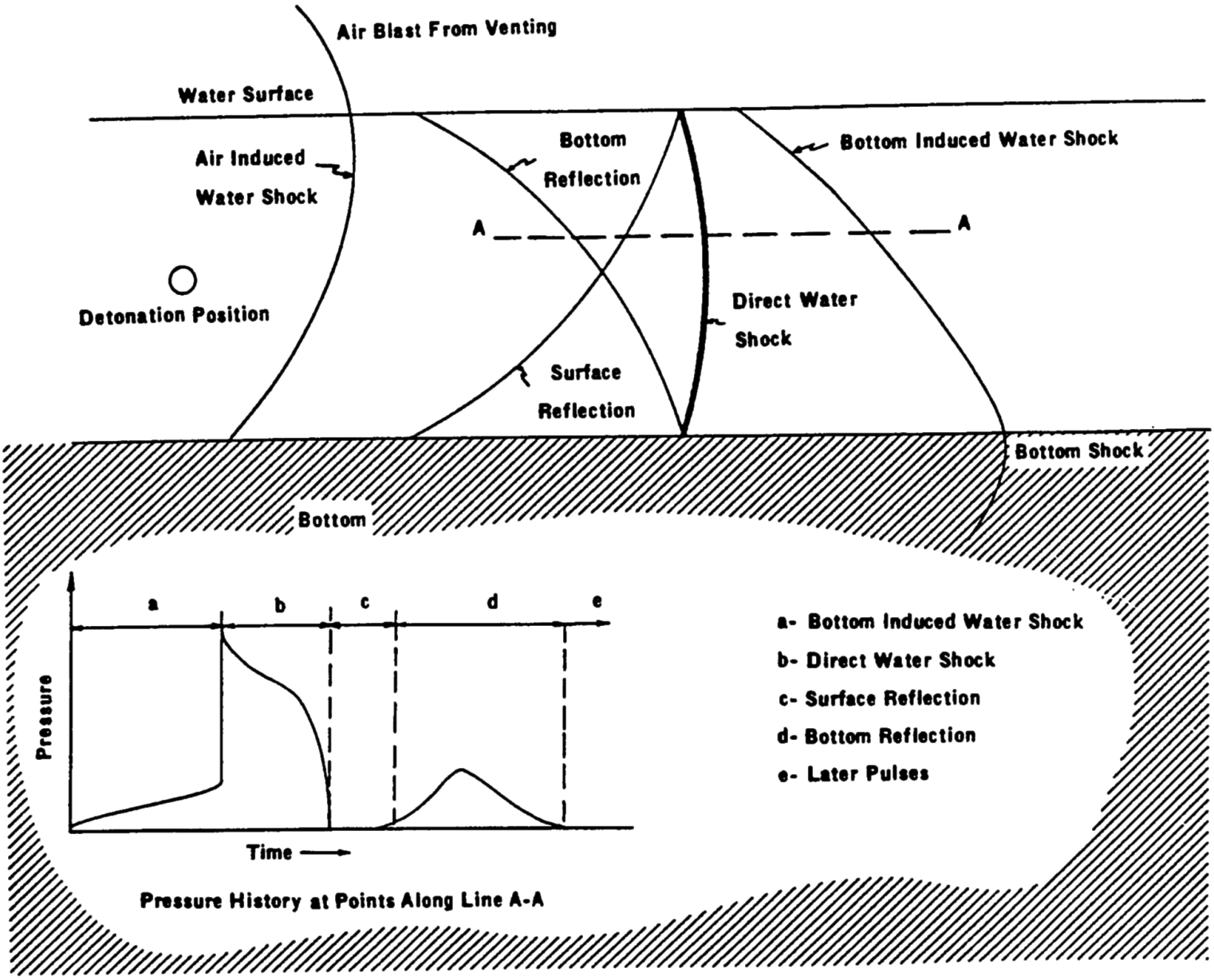

BAKER mately 1,000,000 tons of water were thrown into the air. As the column fell back into the water, there developed on the surface, at the base of the column, a large doughnut-shaped cloud of dense mist. This cloud, called the base surge, formed about 10 seconds after detonation and traveled rapidly outward at an initial velocity greater than 100 feet per second, maintaining an ever-expanding doughnut-shaped form. In the first 100 seconds, the average velocity was 63 feet per second. In 180 seconds, the surge traveled 8,100 feet.

(2) *Deep burst.* If the detonation is at a

WIGWAM depth such that the bubble goes through several oscillations prior to venting, a bushy, ragged plume-like mass of water is thrown into the air by the emerging bubble (see fig. 1–6). The collapse of these plumes generates the base surge. For this deep burst, the first visible surface phenomenon was a very flat spray dome some 7,000 feet in radius and 170 feet in height. Three seconds later a second spray dome emerged out of the first, sending spikes to a height of 900 feet. At 10 seconds the plumes appeared, reaching a height of 1,450 feet and a diameter of 3,100 feet. As the plumes collapsed, a base surge spread out laterally to a cross wind radius of 4,600 feet at 90 seconds and approximately 7,000 feet at 15 minutes.

(3) *Intermediate depths.* At intermediate depths of burst, such that the bubble vents after the first expansion is completed but before several oscillations are completed, the magnitude of the base surge varies in a manner dependent upon the phase of the bubble at venting, together with the motion of the water surrounding the bubble at venting. When the bubble vents in an expanding phase the surge phenomenon is similar to that described for a shallow burst. When the bubble vents in a contracting stage, a tall spire of water is jetted into the air. The base surge resulting therefrom is less dense and of a smaller final radius. However, lack of knowledge of bubble behavior permits only a coarse prediction of the maximum size of base surge.

(4) *Growth.* Figure 2–35A gives the radius of the base surge as a function of time for a 1 KT yield at various depths of burst. Figure 2–35B gives the maximum radius of base surge as a function of yield for several specific depths of burst. Winds cause the surge to travel faster in the direction in which the wind is blowing. Although relative humidity does not affect the initial formation of the base surge, it does influence its subsequent growth and duration. When the relative humidity is significantly less than 70 percent, the extent and duration of the base surge are apt to be less than predicted. A significant increase in extent and duration of the base surge is expected when the relative humidity is appreciably greater than 70 percent.

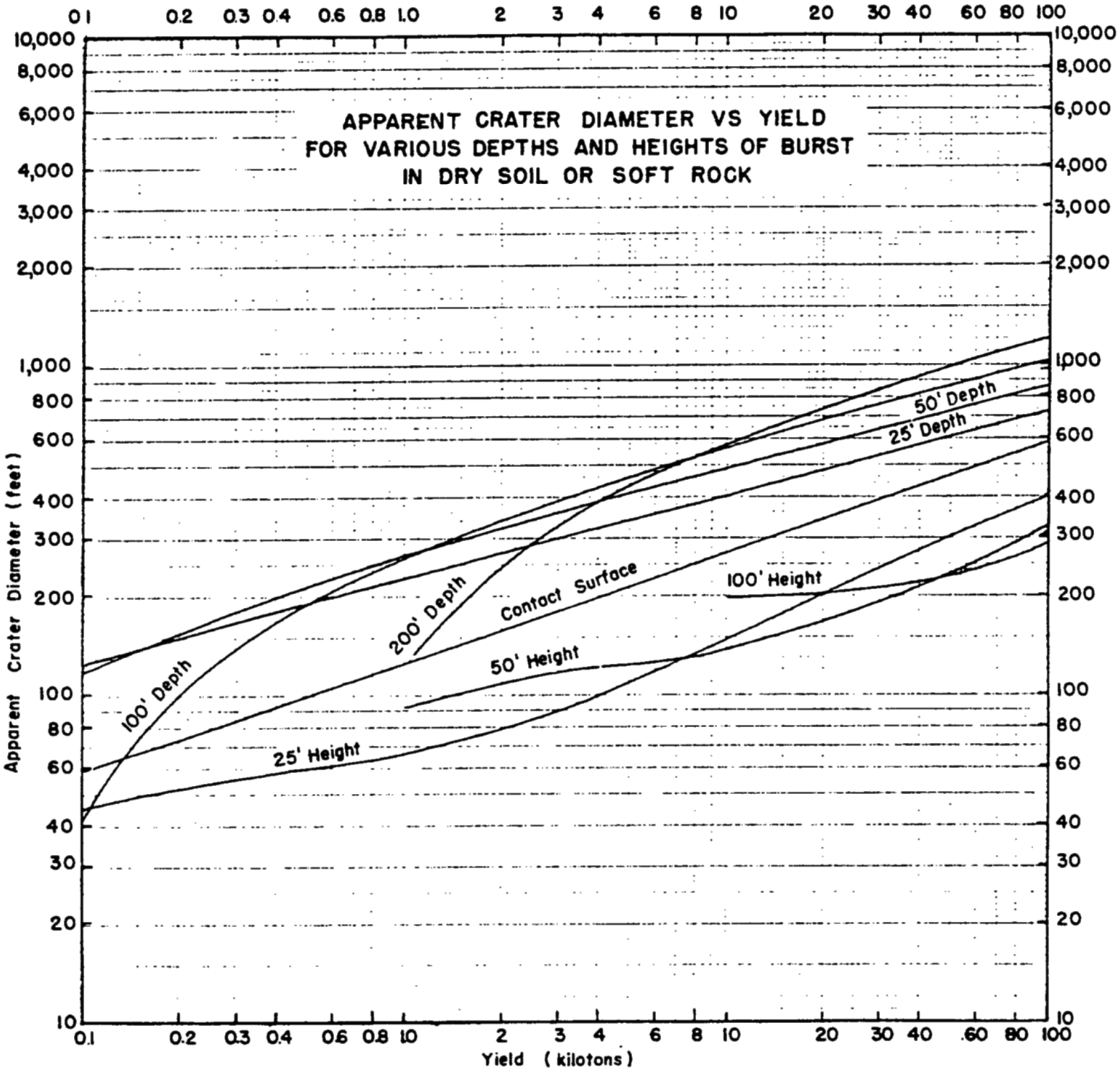
APPARENT CRATER DIAMETER VS YIELD
FOR VARIOUS DEPTHS AND HEIGHTS OF BURST
IN DRY SOIL OR SOFT ROCK
Apparent Crater Diameter (feet)
Yield (kilotons)
0.1
0.2
0.3
0.4
0.6
0.8
1.0
2
3
4
6
8
10
20
30
40
60
80
100
10,000
8,000
6,000
4,000
3,000
2,000
1,000
800
600
400
300
200
100
80
60
40
30
20
10
50' Depth
25' Depth
200' Depth
Contact Surface
100' Height
50' Height
100' Depth
25' Height

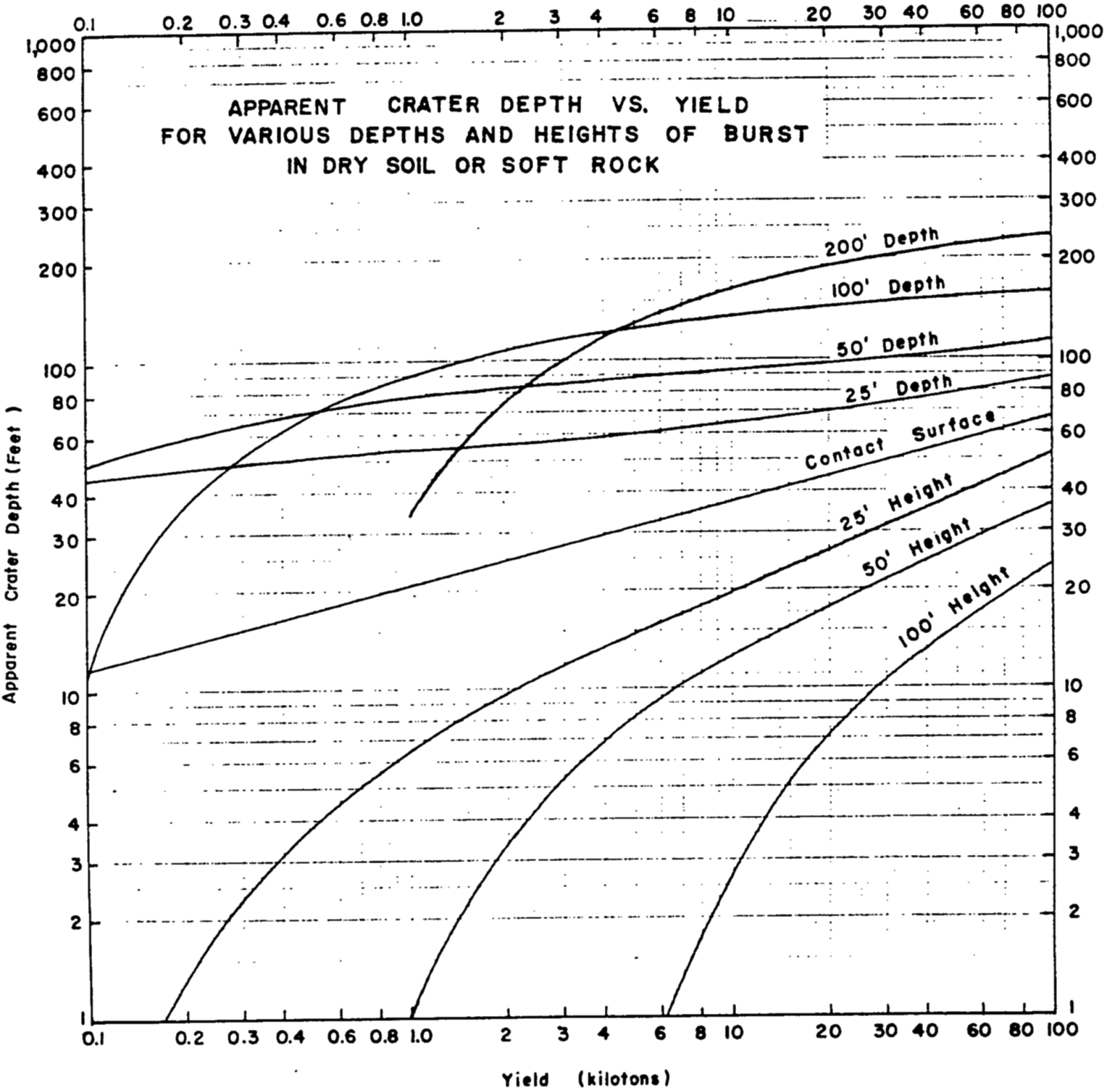
APPARENT CRATER DEPTH VS. YIELD
FOR VARIOUS DEPTHS AND HEIGHTS OF BURST
IN DRY SOIL OR SOFT ROCK
200' Depth
100' Depth
50' Depth
25' Depth
Contact Surface
25' Height
50' Height
100' Height
Apparent Crater Depth (Feet)
Yield (kilotons)
0.1
0.2
0.3
0.4
0.6
0.8
1.0
2
3
4
6
8
10
20
30
40
60
80
100
1,000
800
600
400
300
200
100
80
60
40
30
20
10
8
6
4
3
2
1

FIGURE 2-24B

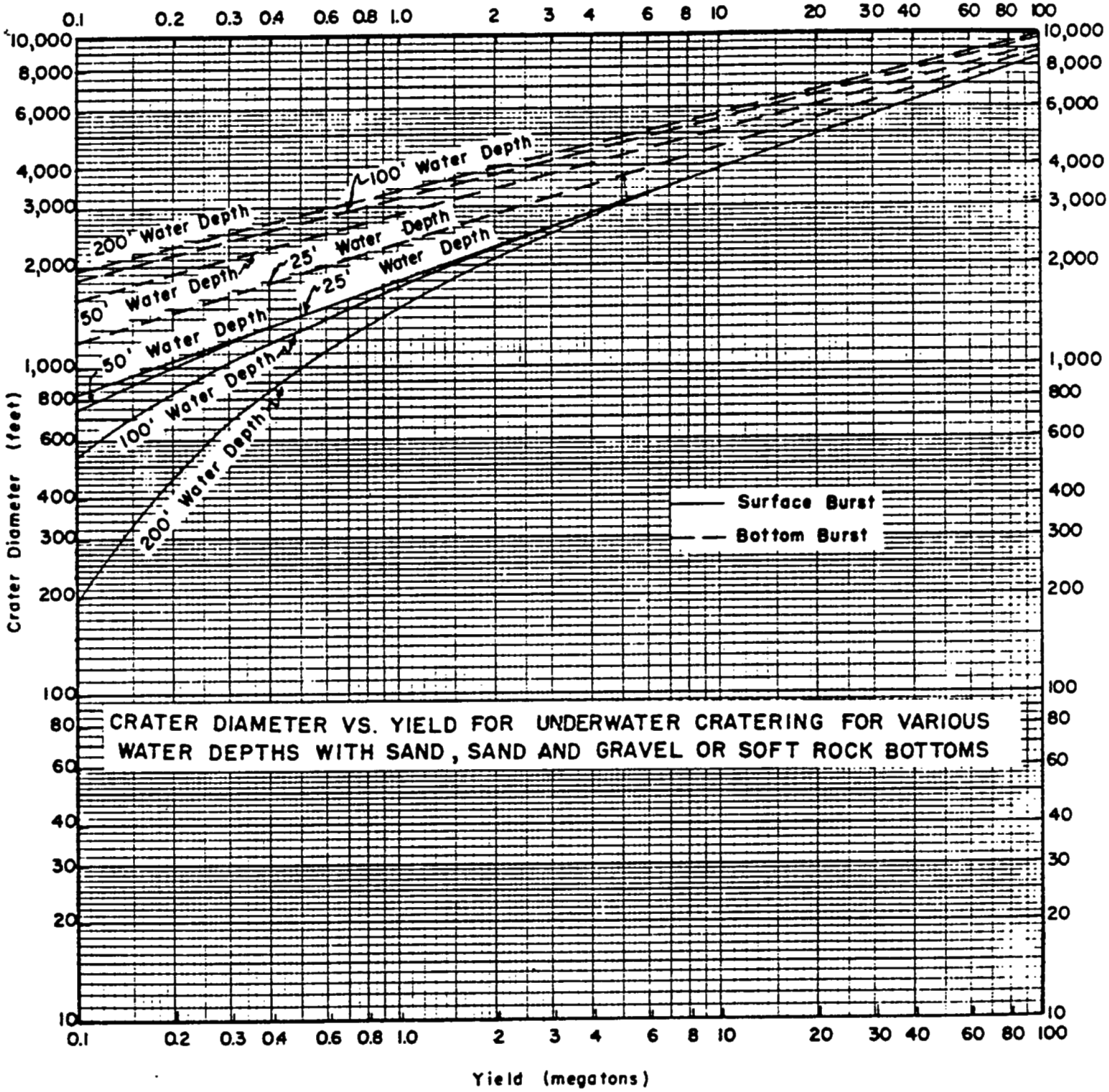
0.1 0.2 0.3 0.4 0.6 0.8 1.0 2 3 4 6 8 10 20 30 40 60 80 100
10,000 8,000 6,000 4,000 3,000 2,000 1,000 800 600 400 300 200 100 80 60 40 30 20 10
Crater Diameter (feet)
100' Water Depth
200' Water Depth
25' Water Depth
50' Water Depth
50' Water Depth
25' Water Depth
100' Water Depth
200' Water Depth
Surface Burst
Bottom Burst
CRATER DIAMETER VS. YIELD FOR UNDERWATER CRATERING FOR VARIOUS WATER DEPTHS WITH SAND, SAND AND GRAVEL OR SOFT ROCK BOTTOMS
Yield (megatons)

FIGURE 2-25B

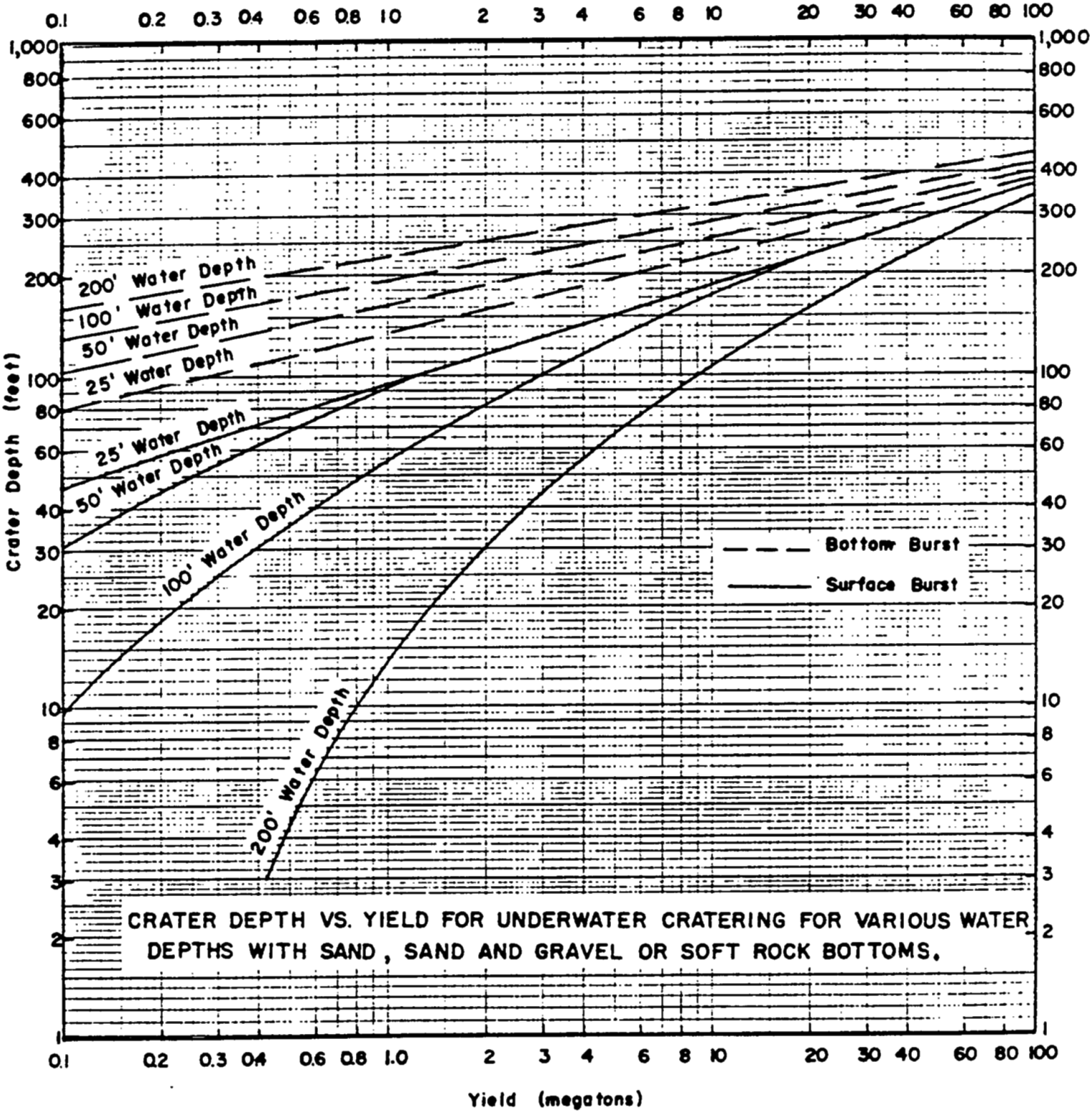

CRATER DEPTH VS. YIELD FOR UNDERWATER CRATERING FOR VARIOUS WATER DEPTHS WITH SAND, SAND AND GRAVEL OR SOFT ROCK BOTTOMS.

FIGURE 2-26B

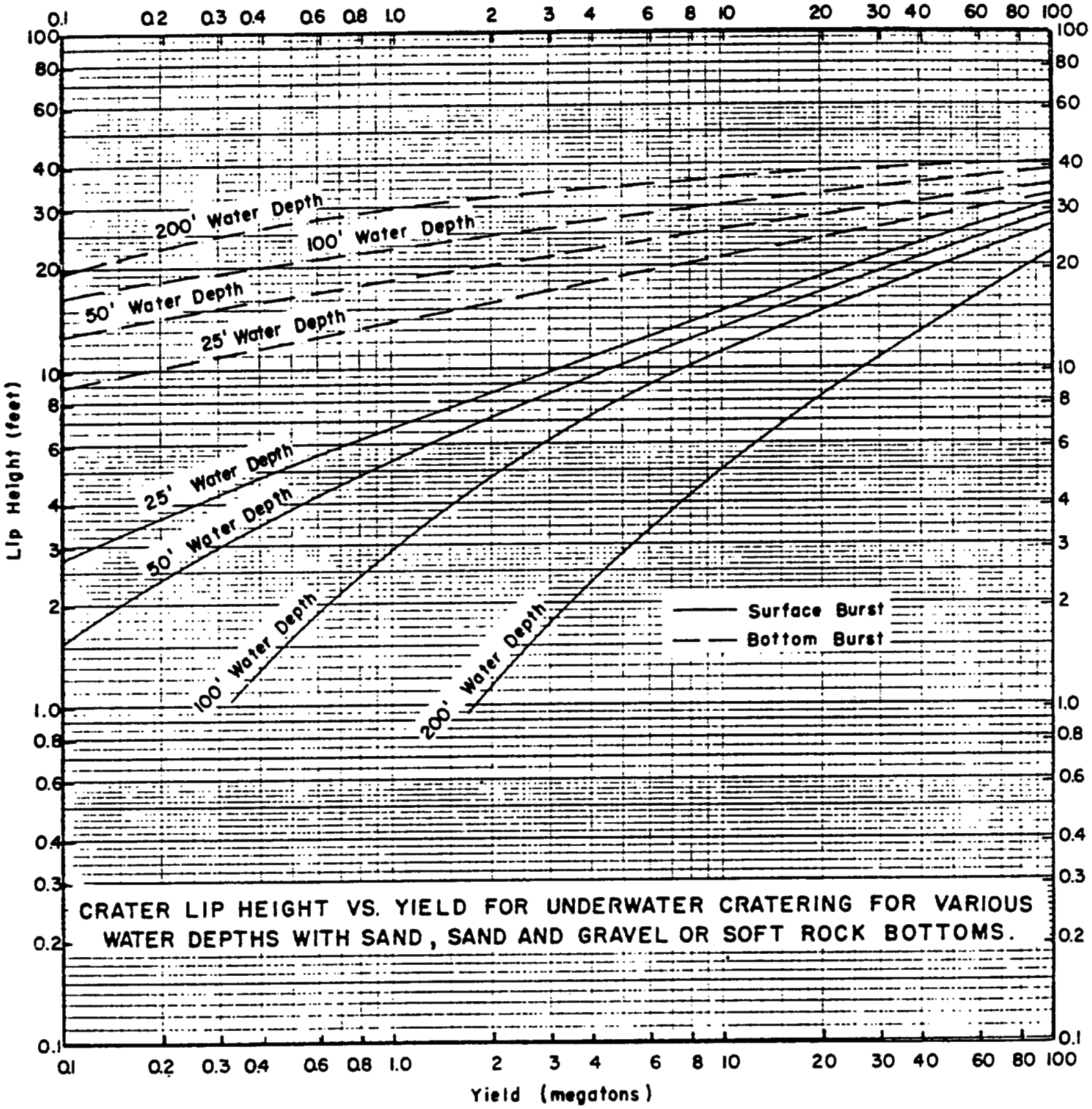

CRATER LIP HEIGHT VS. YIELD FOR UNDERWATER CRATERING FOR VARIOUS WATER DEPTHS WITH SAND, SAND AND GRAVEL OR SOFT ROCK BOTTOMS.

PEAK AIR BLAST INDUCED GROUND ACCELERATION (VERTICAL COMPONENT) VS. PEAK OVERPRESSURE

Figure 2–28 represents the relationship between overpressure and air blast induced ground acceleration. The acceleration shown is the maximum vertical acceleration (upward or downward) measured at a depth of approximately ten feet below the horizontal ground surface in Nevada type soil. Horizontal acceleration can be assumed to be approximately equal to 70 percent of the vertical acceleration. Accelerations measured at a depth of 5 feet may be roughly 150 percent of those indicated and accelerations measured at a depth of twenty feet may be roughly 50 percent of those indicated. Mediums denser than Nevada type soil may experience higher acceleration values and less dense mediums may experience less acceleration. The accelerations shown are applicable only to regions beyond the plastic zone of any crater produced.

Procedure. To determine the acceleration at any range, determine the peak overpressure at that range from figure 2–9 or figure 2–10, whichever is applicable, and read the acceleration directly from the curve.

Example.

Given: An 80 KT detonation at a height of burst of 2,580 feet over an "average" surface.

Find: The vertical ground acceleration at a range of 4,000 yards, 10 feet below the ground surface.

From figure 2–10B the overpressure from an 80 KT burst at 4,000 yards is 3 psi. Reading directly from figure 2–28, the acceleration is 0.2 g. *Answer.*

Reliability. The curve is based on full scale field tests in Nevada type soil. Accelerations obtained from the curve may be high by a factor of two or low by a factor of three even in Nevada type soil. When applied to other soils, the reliability of the curve is reduced.

Related material.

See paragraph 2.2*b*.

FIGURE 2-28

PEAK AIR BLAST INDUCED GROUND ACCELERATION

VERTICAL COMPONENT Vs. PEAK OVERPRESSURE

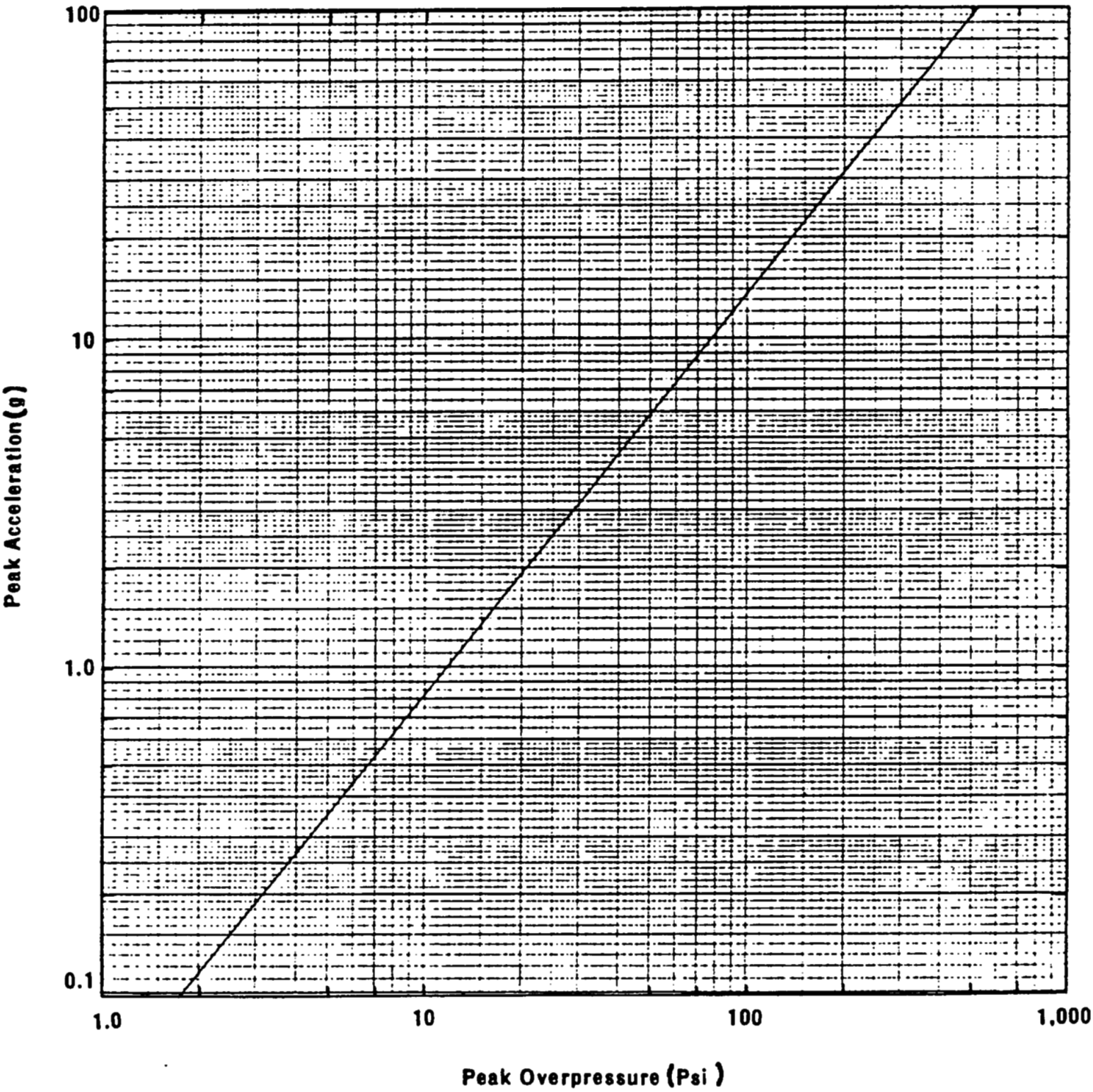

BASE SURGE FOR UNDERGROUND BURSTS

Figure 2–29A gives the expected rate of radial growth of the earth base surge from a 1 KT underground burst; figure 2–29B gives the expected maximum base surge radius vs. yield. Figure 2–29B is based on extrapolation from the maximum base surge radii of the curves in figure 2–29A. Radii obtained from the figures assume no wind, or are crosswind radii. To compute *upwind* or *downwind* base surge radii at a specific time after detonation, add the distance traversed by the wind up to this time to the base surge radius obtained from the figures to obtain the downwind base surge radius, or subtract to obtain the upwind base surge radius.

Scaling. Depth of burst and the maximum radius of the base surge scale as the cube root of yield between scaled depths of burst of 16 $W^{1/3}$ and 125 $W^{1/3}$ feet, or:

$$\frac{h_1}{h_2}=\frac{r_1}{r_2}=\frac{W_1^{1/3}}{W_2^{1/3}}$$

where h_1 and r_1 are depth of burst and base surge radius for yield W_1, and h_2 and r_2 are the corresponding depth of burst and base surge radius for yield W_2.

Time to complete a given percentage of total radial growth of base surge scales as the one-sixth power of the yield for the same scaled depth of burst, or:

$$\frac{t_1}{t_2}=\frac{W_1^{1/6}}{W_2^{1/6}}$$

where t_1=time to complete a given percentage of total radial growth for yield W_1, and t_2=corresponding time to complete the same percentage of total radial growth for yield W_2.

Example.

Given: A 64 KT detonation 65 feet underground.

Find:

(*a*) The maximum base surge radius.

(*b*) The time at which the maximum radius occurs.

Solution: The corresponding depth of burst for 1 KT is:

$$h_1=\frac{W_1^{1/3}\times h_2}{W_2^{1/3}}=\frac{1\times 65}{(64)^{1/3}}=16 \text{ ft.}$$

From figure 2–29A the maximum radius for 1 KT at a 16 foot depth of burst is 2,010 feet and occurs at 180 seconds.

The corresponding radius for 64 KT is:

$$r_2=\frac{r_1\times W_2^{1/3}}{W_1^{1/3}}=\frac{2{,}010\times(64)^{1/3}}{1}=8{,}040 \text{ ft.} \quad \textit{Answer.}$$

This may also be read directly from figure 2–29B.

The time at which this maximum radius occurs is—

$$t_2=\frac{W_2^{1/6}\times t_1}{W_1^{1/6}}=\frac{(64)^{1/6}\times 180}{1}=360 \text{ sec.} \quad \textit{Answer.}$$

Reliability. The data presented in the figure are based on limited full scale testing and extensive HE reduced scale testing.

Related material.

See paragraphs 1.4*e*(4) and 2.2*c*.

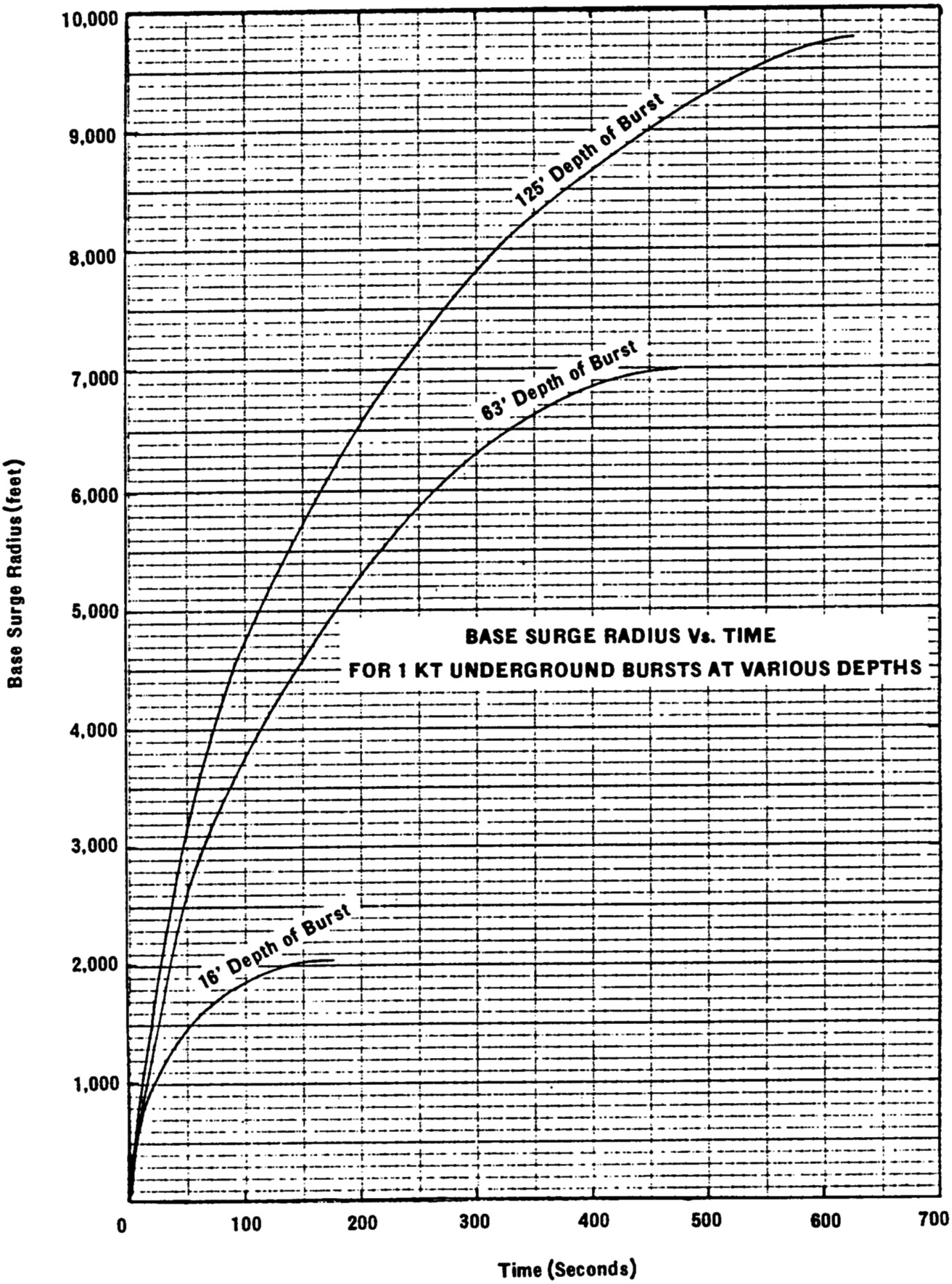
BASE SURGE RADIUS Vs. TIME
FOR 1 KT UNDERGROUND BURSTS AT VARIOUS DEPTHS
125' Depth of Burst
63' Depth of Burst
16' Depth of Burst
Base Surge Radius (feet)
10,000
9,000
8,000
7,000
6,000
5,000
4,000
3,000
2,000
1,000
0
100
200
300
400
500
600
700
Time (Seconds)

BASE SURGE FOR UNDERWATER BURSTS

Figure 2–35A gives the expected radial growth of the water base surge as a function of time after detonation for a 1 KT weapon at various depths of burst. Figure 2–35B gives the expected maximum base surge radius as a function of yield for several specific depth of burst conditions. The maximum base surge is developed from a weapon detonated at approximately the venting depth (250 $W^{1/4}$ ft.). For very shallow depths of burst, less than 10 $W^{1/3}$ feet, the occurrence of a base surge is improbable. Proximity of the bottom to the point of detonation has little effect upon the production of the base surge. For depths of burst between the limits 10 $W^{1/3}$ and 250 $W^{1/4}$ feet, the diameter of the water column producing the base surge is approximately one fourth of the resultant surge radius. With depths of burst below the venting depth of 250 $W^{1/4}$ feet, no such simple relation of the column or plume to the resultant surge exists. Little data or theory is available for base surge predictions at deep depths. A prediction can be made, however, by linear interpolation between the base surge radius of a burst at venting depth and one at a deep scaled depth (650 $W^{1/3}$ feet). A prediction thus made represents the maximum base-surge which could be expected.

Radii obtained from figures 2–35A and 2–35B assume "no wind" conditions. To compute upwind or downward base surge radii for a specific time after detonation, add the distance traveled by the wind up to this time to the "no wind" base surge radius to obtain the downwind base surge radius, or subtract to obtain the upwind base surge radius.

Scaling. Depth of burst and the accompanying maximum radius of the base surge scale as the cube root of yield for depths of burst between 25 $W^{1/3}$ and 250 $W^{1/4}$, or:

$$\frac{h_1}{h_2}=\frac{r_1}{r_2}=\frac{W_1^{1/3}}{W_2^{1/3}},$$

where h_1 and r_1 are depth of burst and base surge radius for yield W_1, and h_2 and r_2 are the corresponding depth of burst and base surge radius for yield W_2.

Time to complete a given percentage of total radial growth of the base surge scales as the one-sixth power of the yield for the same scaled depth of burst, or:

$$\frac{t_1}{t_2}=\frac{W_1^{1/6}}{W_2^{1/6}},$$

where t_1=time to complete a given percentage of total radial growth for yield W_1 and t_2=the corresponding time to complete the same percentage of total radial growth for yield W_2.

Time to reach the maximum base surge radius from a detonation at venting depth or less may also be computed by:

$$t_{max}=2.25r^{1/2}$$

where t_{max}=time to the maximum base surge radius in seconds,

and r=maximum base surge radius in feet.

Examples.

(1) *Given:* A 10 KT detonation at a depth of 150 feet below the water surface.

Find:

(*a*) The maximum base surge radius.
(*b*) Time to maximum base surge radius.
(*c*) The expected base surge radius 1 minute after detonation.

Solution:

(*a*) The maximum base surge radius is read directly from figure 2–35B as 7,200 feet. *Answer.*

(*b*) The venting depth is 250 $W^{1/4}$=440 feet. Since the depth of burst is less than venting, the simplified formula for time to maximum may be used. The time of maximum base surge radius is $t_{max}=2.25\ (7{,}200)^{1/2}=190$ seconds. *Answer.*

(*c*) A 10 KT detonation of 150 feet depth will complete the same percentage of its total radial growth in 60 seconds as a 1 KT detonation will complete at a corresponding scaled time and depth. Using the scaling above, the corresponding depth of burst for 1 KT is—

$$h_1=\frac{W_1^{1/3}\times h_2}{W_2^{1/3}}=\frac{1\times 150}{(10)^{1/3}}=70\text{ ft.}$$

BASE SURGE RADIUS Vs. TIME

FOR 1 KT UNDERWATER BURSTS AT VARIOUS DEPTHS

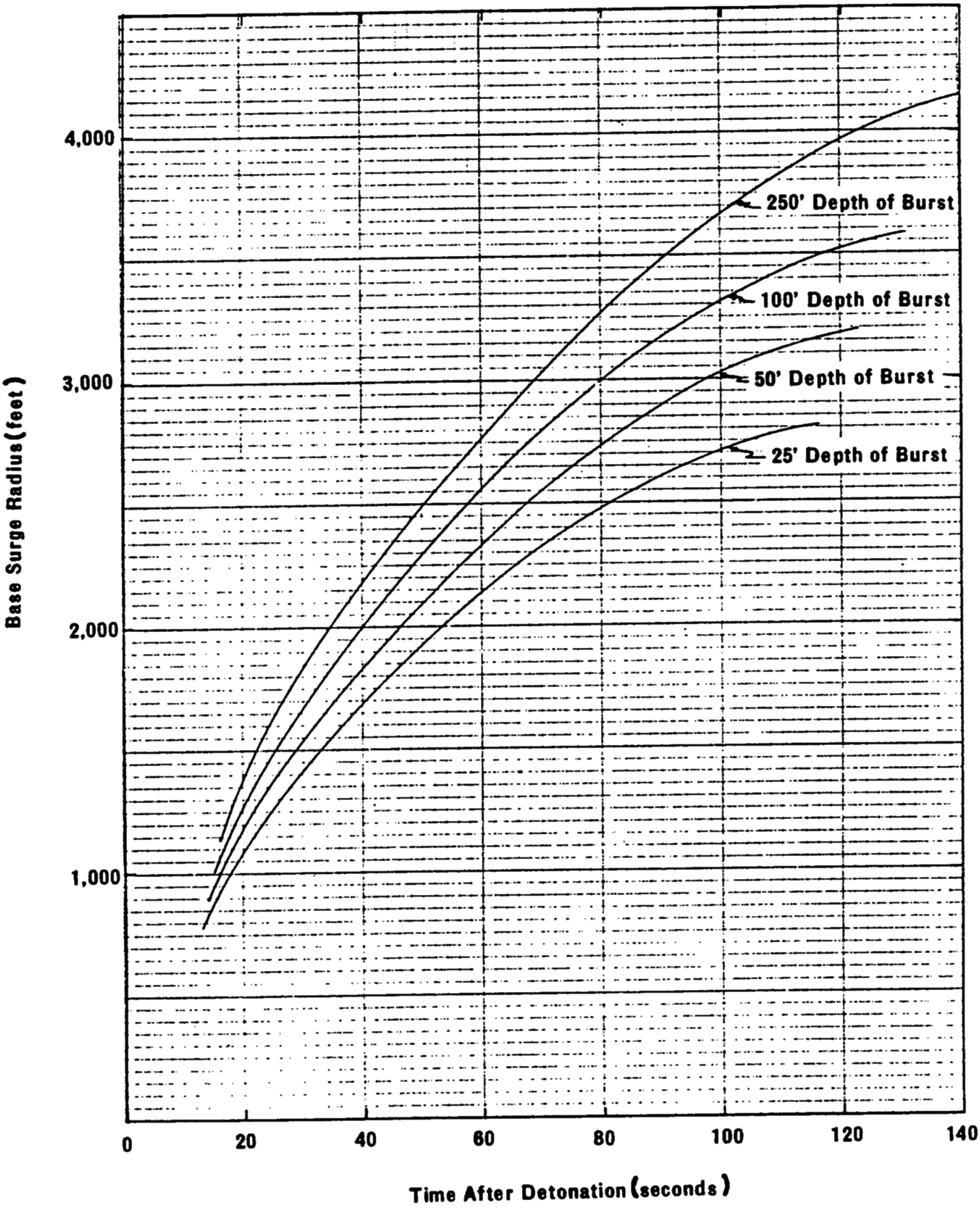

SECTION III
THERMAL RADIATION PHENOMENA

3.1 General

The extremely high temperatures in the fireball result in a large emission of thermal radiation. The relatively large fraction of the total energy of a nuclear detonation which is emitted as thermal radiation is one of its most striking characteristics. This radiant energy amounts to approximately one-third of the total energy of an air burst weapon; it is sufficient to cause serious burns to exposed personnel and to start fires in some combustible materials out to considerable distances. The duration of the thermal radiation emission depends upon the weapon yield, and is longer for the larger yields.

For a surface burst having the same yield as an air burst, the presence of the earth's surface results in a reduced thermal radiation emission and a cooler fireball when viewed from that surface. This is due primarily to heat transfer to the soil or water, the distortion of the fireball by the reflected shock wave, and the partial obscuration of the fireball by dirt and dust (or water) thrown up by the blast wave.

In underground bursts the fireball is obscured by the earth column, and therefore thermal radiation effects are negligible. Nearly all of the thermal radiation is absorbed in fusing and vaporizing the earth.

Thermal radiation from an underwater detonation is increasingly absorbed in vaporization and dissociation of the surrounding medium as the depth of burst is increased. Its direct effects are insignificant for most practical purposes; e. g., for a 20 KT burst in ninety feet of water, thermal effects are negligible.

3.2 Thermal Scaling

a. General. In paragraph 1.4*b*(2) the fireball was described as emitting thermal radiation in a pulse characterized by a rapid rise to a first maximum, a decline to a minimum, another rise to a second maximum and a subsequent final decline. The first phase of this pulse occurs so very rapidly that less than 1 percent of the total thermal radiation is emitted. Consequently, it is the second phase of the pulse which is of interest in weapons effects considerations at altitudes in the lower troposphere.

Throughout, the fireball may be considered to radiate essentially, though not ideally, as a black body, for which the radiant power is proportional to the radiating area and the fourth power of the temperature. After the minimum the radiating radius and area increase relatively slowly, so that the radiant power is predominately determined by the temperature cycle of the fireball. An illustration of the apparent temperature and fireball radius versus time for a 20 KT air burst is shown in figure 3–1. It should be emphasized, however, that the actual radiating area may vary substantially from that of the luminous fireball. Very little quantitative information is available concerning the rate of growth of the fireball following the time at which "breakaway" occurs (approximately 0.015 second for the 20 KT burst shown in figure 3–1). Up to the time of breakaway, however, the radius increases approximately as the 0.4 power of the time after detonation.

b. Thermal Pulse. The shape of the pulse after the radiant power minimum (t_{min}) is sufficiently similar for nuclear detonations that a single curve may represent the time distribution of radiant power emitted (fig. 3–2). This curve has been developed by using ratios. The ratio p/p_{max} is plotted against the ratio t/t_{max}, where p/p_{max} is the ratio of the radiant power at a given time to the maximum radiant power, and t/t_{max} is the ratio of time after detonation to the time to the second thermal maximum for that detonation.

The percent of the total thermal radiation emitted versus the ratio t/t_{max} is also shown on figure 3–2. From this figure it is seen that approximately twenty percent of the total emission occurs up to the time of the second power maxi-

mum, whereas approximately 82 percent is emitted prior to 10 times the time to the second maximum. By this time the rate of delivery has dropped to such a low value that the remaining energy is no longer of significance in damage production.

c. Time scaling. It has been found that both the time to the minimum and the time to the second maximum are proportional to the square root of the weapon yield. Thus, for airbursts at altitudes of burst below about 50,000 feet, the time to the minimum (t_{min}) is 0.0027 $W^{1/2}$ second. The time to the second maximum (t_{max}) is 0.032 $W^{1/2}$ second. (See figures 3–3A and 3–3B. These curves may also be used for surface bursts.) It should be noted that for weapon yields lower than 6 KT the actual values of t_{max} may be as much as 30 percent higher than those given by figure 3–3A. This is caused by the higher mass-to-yield ratio characteristic of low yield weapons. These relations indicate that a one megaton weapon delivers its thermal radiation over a period 32 times as great as does a one kiloton weapon. This can be expected to result in variations in total thermal energy required for a given effect. The significance of the dependence of delivery rate on weapon yield is discussed in the sections dealing with thermal injury and damage.

d. Thermal Yield. Measurements of the total thermal energy emitted for air burst weapons of low yield indicate that this energy is proportional to weapon yield and is about one-third of the total yield. From this and figure 3–2 a scaling procedure for maximum radiant power may be derived. Thus $p_{max}=4W^{1/2}$KT/sec or $4\times10^{12}W^{1/2}$ cal/sec.

Measurements from the ground of the total thermal energy from surface bursts, although not as extensive as those for air bursts, indicate that the thermal yield is a little less than half that from equivalent air bursts. For a surface burst the thermal yield is assumed to be one-seventh of the total yield. For surface bursts, the scaling of the second radiant power maximum (p_{max}) cannot be determined on the basis of available data. Similarly, there are no data which show what the thermal radiation phenomena may be for detonation altitudes in excess of about 50,000 feet. It is expected that the thermal energy may increase with altitude of burst, and figure 3–4 gives a purely theoretical estimate of this increase.

3.3 Radiant Exposure vs. Slant Range

a. Spectral. Characteristics. At distances of operational interest, the spectral (wavelength) distribution of the incident thermal radiation, integrated with respect to time, resembles very closely the spectral distribution of sunlight. For each, slightly less than one-half of the radiation occurs in the visible region of the spectrum, approximately one-half occurs in the infrared region and a very small fraction (rarely greater than 10 percent) lies in the ultraviolet region of the spectrum. The color temperature of the sun and an air burst are both about 6,000° K. A surface burst, as viewed by a ground observer, contains a higher proportion of infrared radiation and a smaller proportion of visible radiation than the air burst, with almost no radiation in the ultraviolet region. The color temperature for a surface burst is about 3,000° K. A surface burst viewed from the air may exhibit a spectrum more nearly like an air burst.

b. Atmospheric Transmissivity. The atmospheric transmissivity ($\overline{T}$) is defined as the fraction of the radiant exposure received at a given distance after passage through the atmosphere, relative to that which would have been received at the same distance if no atmosphere were present. Atmospheric transmissivity depends upon several factors; among these are: water vapor and carbon dioxide absorption of infrared radiation, ozone absorption of ultraviolet radiation, and multiple scattering of all radiation. All of these factors vary with distance and with the composition of the atmosphere. Scattering is produced by the reflection and refraction of light rays by certain atmospheric constituents, such as dust, smoke and fog. Interactions such as scattering which divert the rays from their original paths result in a diffuse, rather than direct, transmission of the radiation. As a result, a receiver which has a large field of view (i. e., most military targets) receives radiation which has been scattered toward it from many angles, as well as the directly transmitted radiation. Since the mechanisms of absorption and scattering are wavelength dependent, the atmospheric transmissivity depends not only upon the atmospheric conditions, but also upon

the spectral distribution of the weapon's radiation. In figures 3–5A and 3–5B the atmospheric transmissivity is plotted as a function of the slant range for air and surface bursts. For each type of burst three sets of atmospheric conditions are assumed. It is believed that these conditions represent the average and the extremes normally encountered in natural atmospheres. These conditions correspond to a visibility of 50 miles and a water vapor concentration of 5 grams/cubic meter; 10 miles visibility and 10 grams/cubic meter water vapor concentration; and 2 miles visibility and 25 grams/cubic meter of water vapor concentration. Curves are presented in appendix I to show under what conditions of ambient temperature and relative humidity the above water vapor concentrations are applicable. The curves of figures 3–5A and 3–5B are plotted to slant ranges equal to one-half the visibility for the three visibility conditions. The reason for this is that the empirical relationships used to obtain the transmissivity values have not been verified for ranges beyond one-half the visibility. As a result, the curves cannot be extrapolated to greater distances with any confidence. If the curves are extended beyond one-half the visibility, there is reason to believe that the values of transmissivity would be too high. Where cloud cover is appreciable or the air contains large quantities of fog or industrial haze, knowledge of the interactions with the radiation is too limited to provide estimates of atmospheric transmissivity.

c. Reflection. If a weapon is burst in the air below a large cloud, the thermal radiation is diffusely reflected downward from the cloud, resulting in greater radiant exposures at a given distance than would be received if no cloud were present. Similarly, if the weapon is burst near the earth's surface, the radiant exposure received at some altitude above the burst (as in the case of an aircraft flying above the detonation) will be greater than that which is received at the same distance on the ground. If the receiver is directly over the burst and the terrain has a high albedo, the reflected radiation from the terrain may be as much as twice the direct radiation. If a reflecting or scattering layer such as a cloud is between the detonation and the target, however, the radiant exposure received will be reduced considerably.

d. Calculation of Radiant Exposure. The radiant exposures at various slant ranges from air and surface burst weapons can be calculated from the following expressions:

$$Q=\frac{3.16\times10^{6}\ W\ (\overline{T})}{D^{2}}\ \text{cal/sq cm (air burst).}$$

and

$$Q=\frac{1.35\times\ 10^{6}\ W\ (\overline{T})}{D^{2}}\ \text{cal/sq cm (surface burst).}$$

where Q=radiant exposure (cal/sq cm)
$\overline{T}$=atmospheric transmissivity
W=weapon yield (KT)
D=slant range (yds).

The values of $\overline{T}$ for both air and surface bursts are obtained from the appropriate curves in figures 3–5A and 3–5B. Curves showing the radiant exposure (Q) as a function of slant range (D) for three atmospheric conditions for both air and surface bursts are shown in figures 3–6A and 3–6B. These curves are plotted for ranges up to one-half the visibility for the reasons explained in *b* above. The surface burst curves differ from the air burst curves for two reasons—the apparent thermal yield when viewed from the surface for a surface burst is lower than that for an air burst, and the spectral distribution of the surface burst is sufficiently different from that of an air burst to require the use of different atmospheric transmissivity curves. Radiant exposure for a burst in the transition zone may be estimated by interpolation between these curves as explained on the instruction page for figures 3–6A and 3–6B. It should be emphasized that these surface burst curves apply to the radiant exposure of *ground* targets. When the surface burst is viewed from the air, as from aircraft, the apparent radiating temperature and the thermal yield will be greater than when viewed from the ground. All of the curves plotted in figures 3–6A and 3–6B are for a total weapon yield of 1 KT. For weapon yields greater or less than 1 KT these radiant exposures should be multiplied by the yield of the weapon in question.

3.4 Other Influences on Thermal Radiation Propagation

a. Topography and Clouds. Propagation of thermal radiation from a nuclear detonation, like that from the sun, is affected by topography and the atmosphere. At close ranges, where the fireball subtends a relatively large angle, the shadowing effects of intervening objects such as hills or trees are less than are experienced with the sun. As discussed earlier, clouds in the atmosphere significantly affect the propagation of radiation through the atmosphere.

b. Fog and Smoke. Where the burst is in the air above a fog covering the ground, a significant fraction of the thermal radiation incident on the fog layer is reflected upward. That radiation which penetrates the fog is scattered. These two effects result in substantial reductions in thermal energy incident on ground targets covered by fog. White smoke screens act like fog in the attenuation of thermal radiation. Reductions as large as 90 percent of incident thermal energies are realized by dense fogs or smoke screens.

c. The Wilson Cloud. The Wilson Cloud, which is sometimes formed in a detonation, does not appreciably affect the thermal radiation incident on a target.

FIGURE 3-1

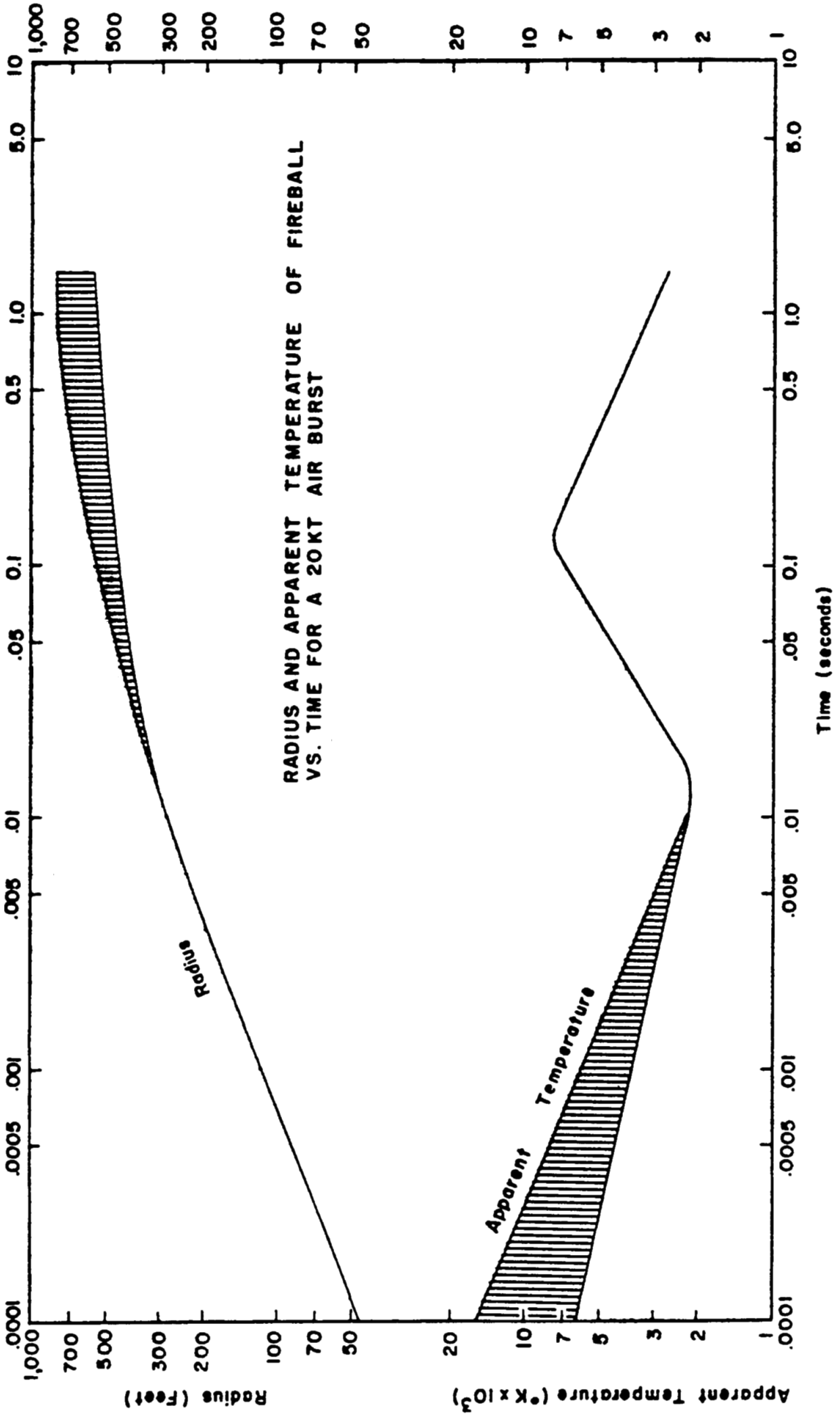
RADIUS AND APPARENT TEMPERATURE OF FIREBALL
VS. TIME FOR A 20KT AIR BURST
Radius
Apparent Temperature
Time (seconds)
Radius (Feet)
Apparent Temperature (°K x 10³)
.0001
.0005
.001
.005
.01
.05
0.1
0.5
1.0
5.0
10
1,000
700
500
300
200
100
70
50
20
10
7
5
3
2
1

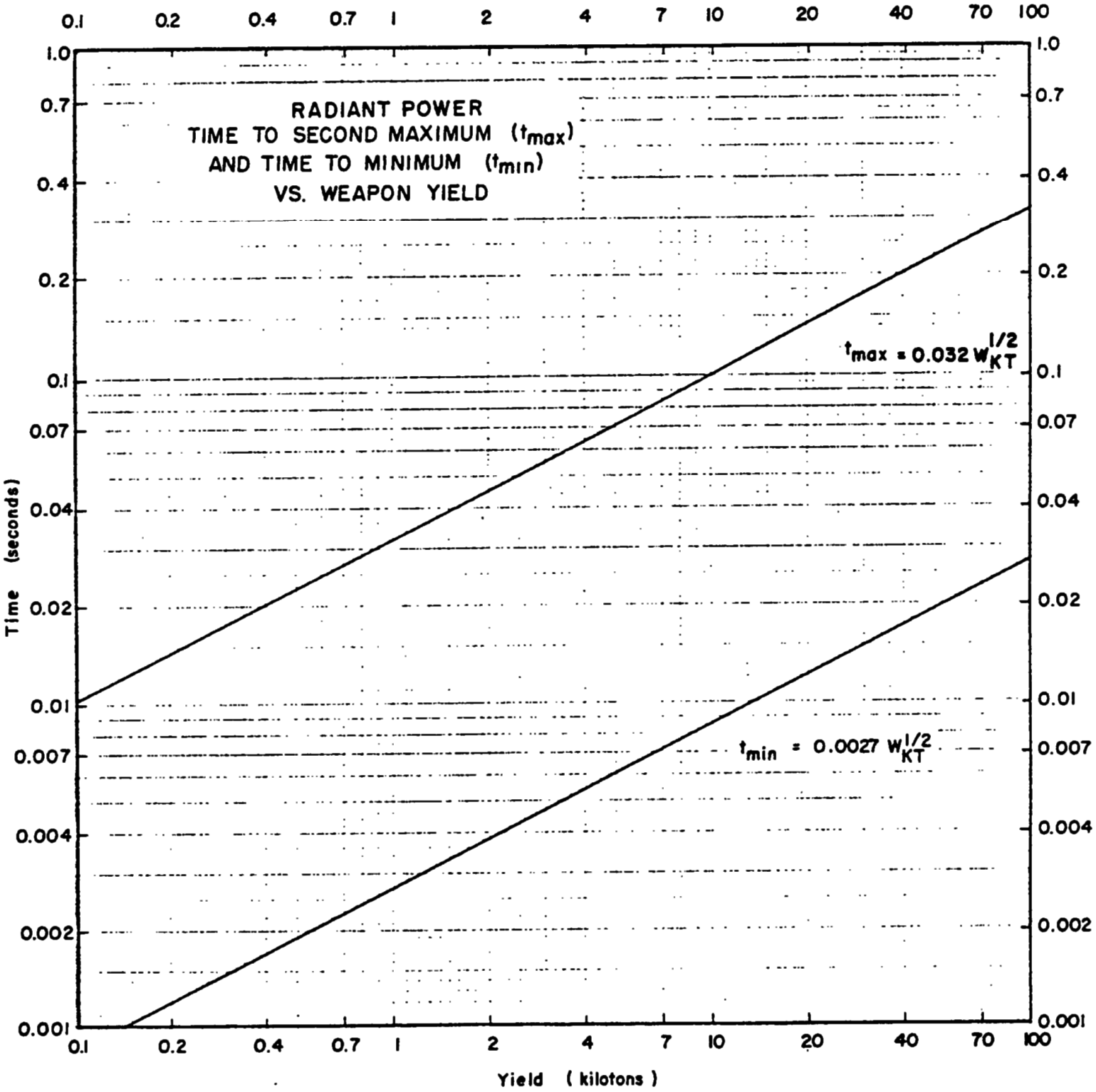
RADIANT POWER
TIME TO SECOND MAXIMUM (t_{max})
AND TIME TO MINIMUM (t_{min})
VS. WEAPON YIELD
$t_{max} = 0.032\ W_{KT}^{1/2}$
$t_{min} = 0.0027\ W_{KT}^{1/2}$
Time (seconds)
Yield (kilotons)
0.1
0.2
0.4
0.7
1
2
4
7
10
20
40
70
100
1.0
0.7
0.4
0.2
0.1
0.07
0.04
0.02
0.01
0.007
0.004
0.002
0.001

ATMOSPHERIC TRANSMISSIVITY

Figures 3–5A and 3–5B give the atmospheric transmissivity versus slant range for three sets of atmospheric conditions for both air and surface burst weapons. These curves are presented for illustrative purposes, since these were used to derive the radiant exposure vs. slant range curves of figures 3–6A and 3–6B.

The differences between the air burst and surface burst curves are caused by the difference in apparent radiating temperatures (when viewed from the ground) and the difference in geometrical configuration of the two types of burst. The three sets of atmospheric conditions represented are:

50 mile visibility and 5 gm/m^3 water vapor.

10 mile visibility and 10 gm/m^3 water vapor.

2 mile visibility and 25 gm/m^3 water vapor.

It is believed that these conditions pertain to the extreme and the average atmospheres which occur naturally.

Reference can be made to the atmospheric water vapor concentration curves in appendix I to ascertain under what conditions of relative humidity and ambient temperature a particular water vapor concentration will occur.

Reliability. The curves of figures 3–5A and 3–5B have not been verified at ranges beyond one-half the visibility and, as a result, are subject to considerably reduced reliability beyond these ranges.

Related material.

See paragraph 3.3*b*.

See also figures 3–6A and 3–6B.

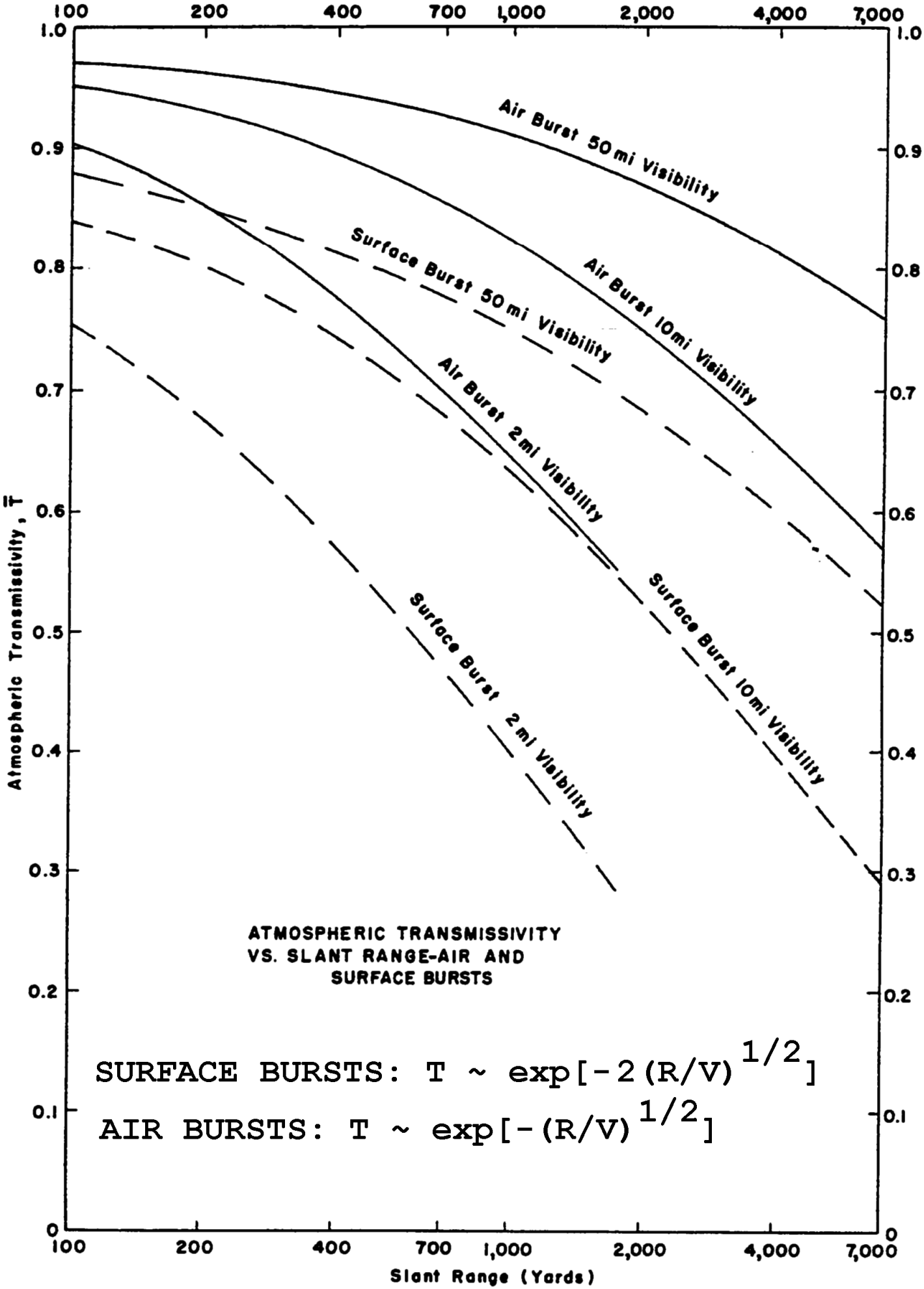

ATMOSPHERIC TRANSMISSIVITY
VS. SLANT RANGE-AIR AND
SURFACE BURSTS

SURFACE BURSTS: $T \sim \exp[-2(R/V)^{1/2}]$

AIR BURSTS: $T \sim \exp[-(R/V)^{1/2}]$

FIGURE 3-5B

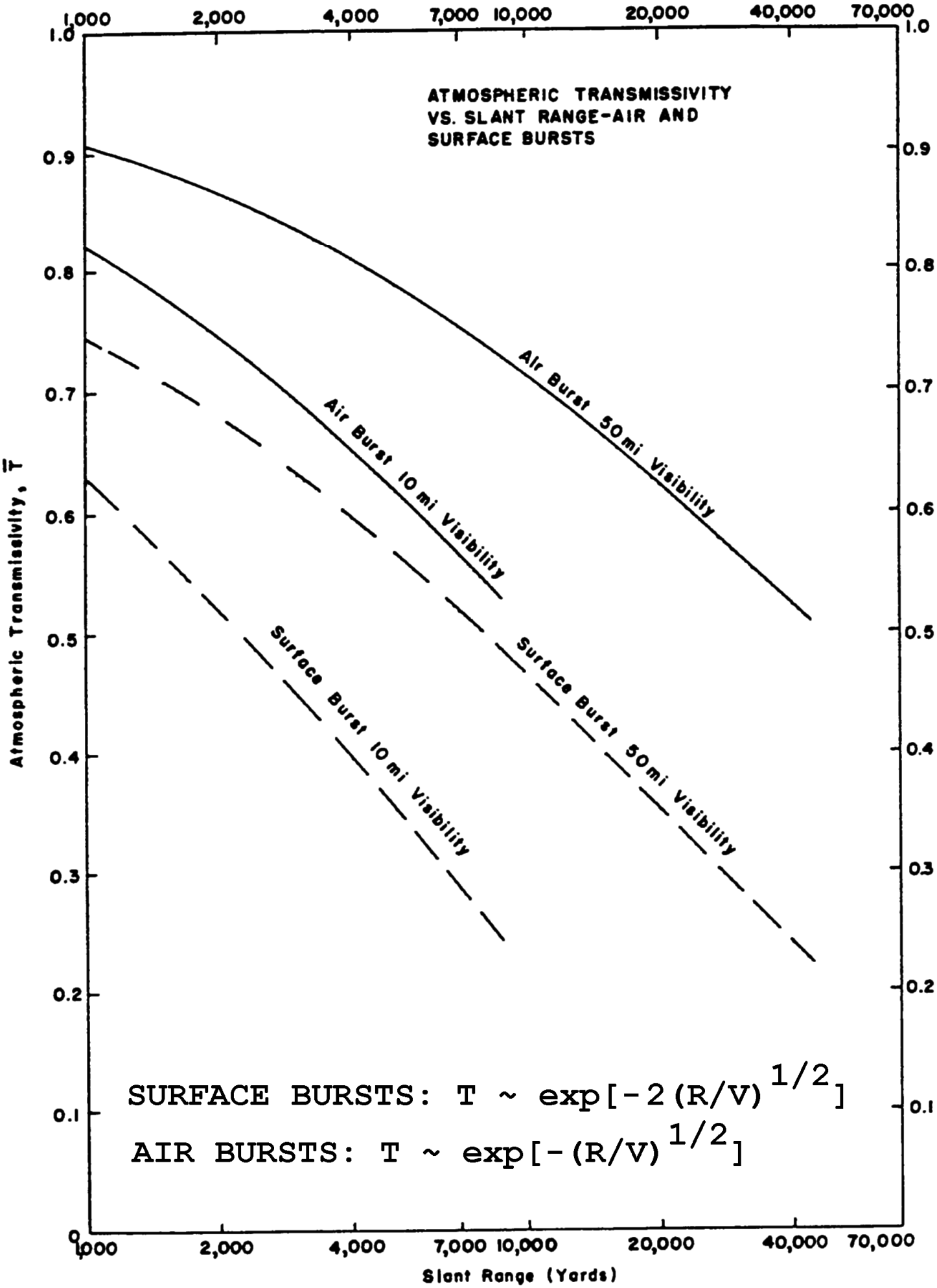
ATMOSPHERIC TRANSMISSIVITY
VS. SLANT RANGE-AIR AND
SURFACE BURSTS
Air Burst 50 mi Visibility
Air Burst 10 mi Visibility
Surface Burst 50 mi Visibility
Surface Burst 10 mi Visibility
SURFACE BURSTS: T ~ exp[-2(R/V)^1/2]
AIR BURSTS: T ~ exp[-(R/V)^1/2]
Atmospheric Transmissivity, T̄
Slant Range (Yards)
1,000
2,000
4,000
7,000
10,000
20,000
40,000
70,000
0
0.1
0.2
0.3
0.4
0.5
0.6
0.7
0.8
0.9
1.0

FIGURE 4-2

INITIAL GAMMA RADIATION DOSE VS SLANT RANGE
SURFACE BURST AND SURFACE TARGET
RELATIVE AIR DENSITY, 1.0

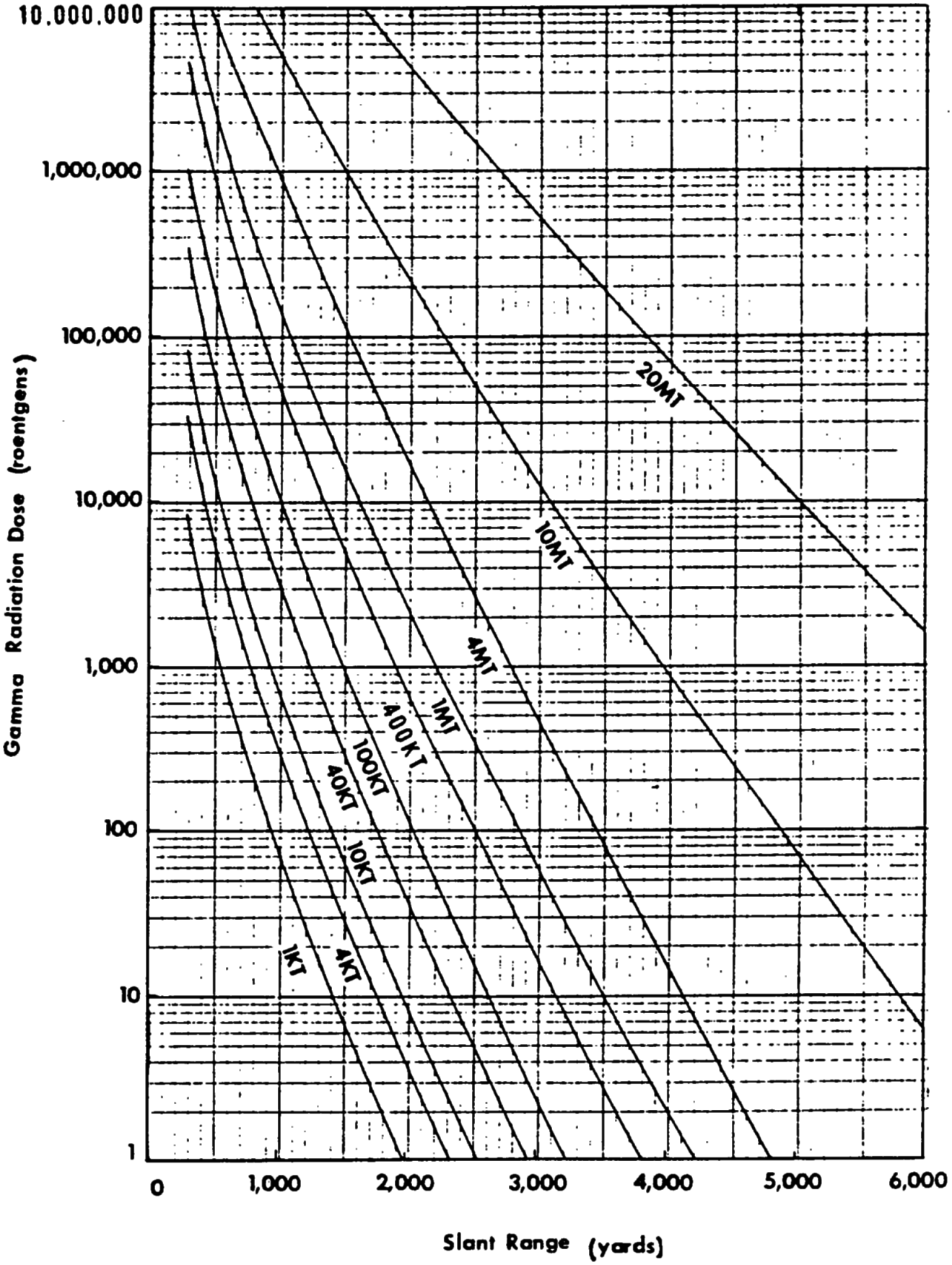

Note: Applicable to other situations as indicated on facing page.

INITIAL GAMMA RADIATION DOSE Vs. SLANT RANGE

SURFACE BURST AND SURFACE TARGET

RELATIVE AIR DENSITY, 0.9

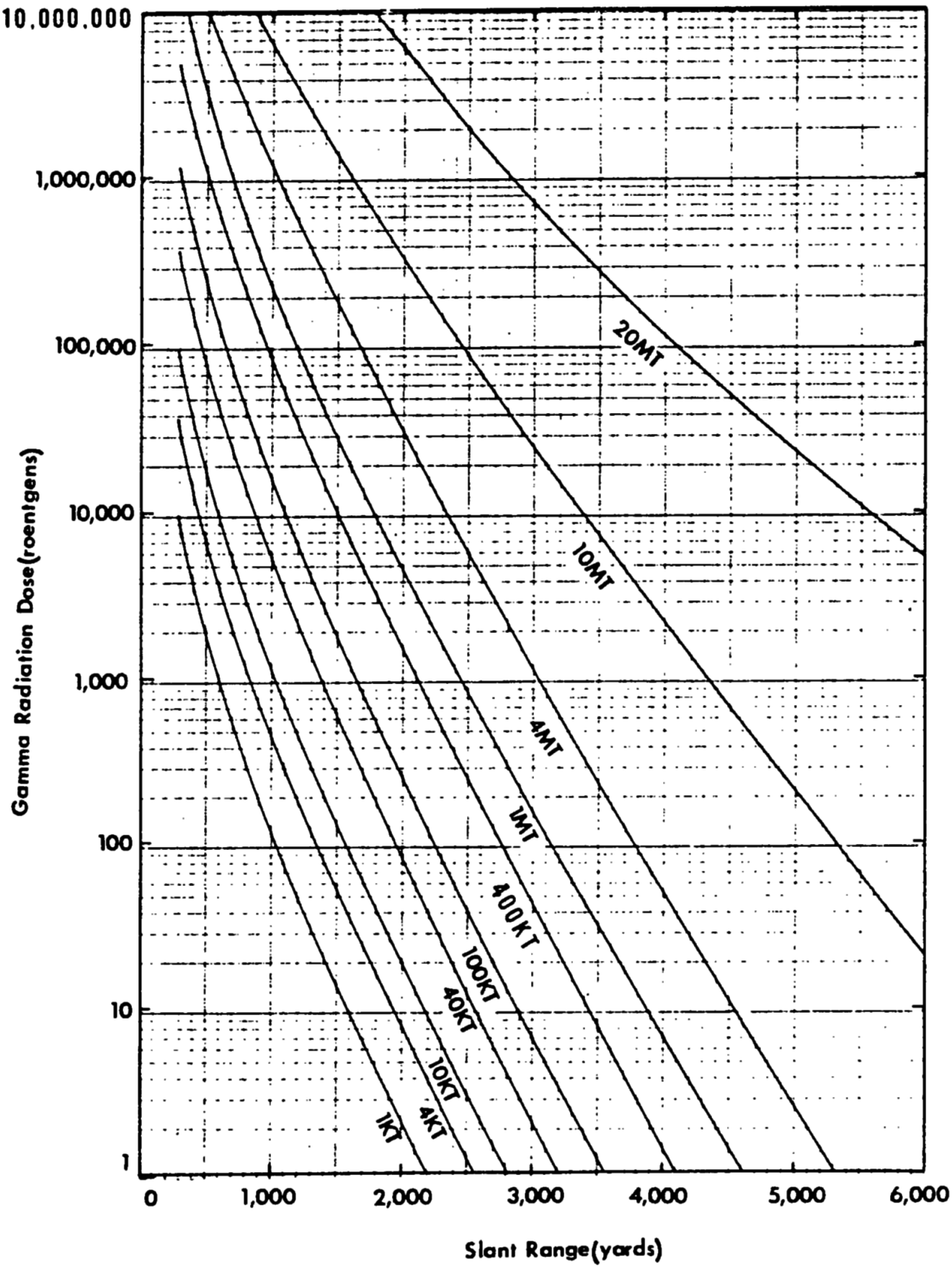

Note:Applicable to other situations as indicated on facing page.

FIGURE 4-8

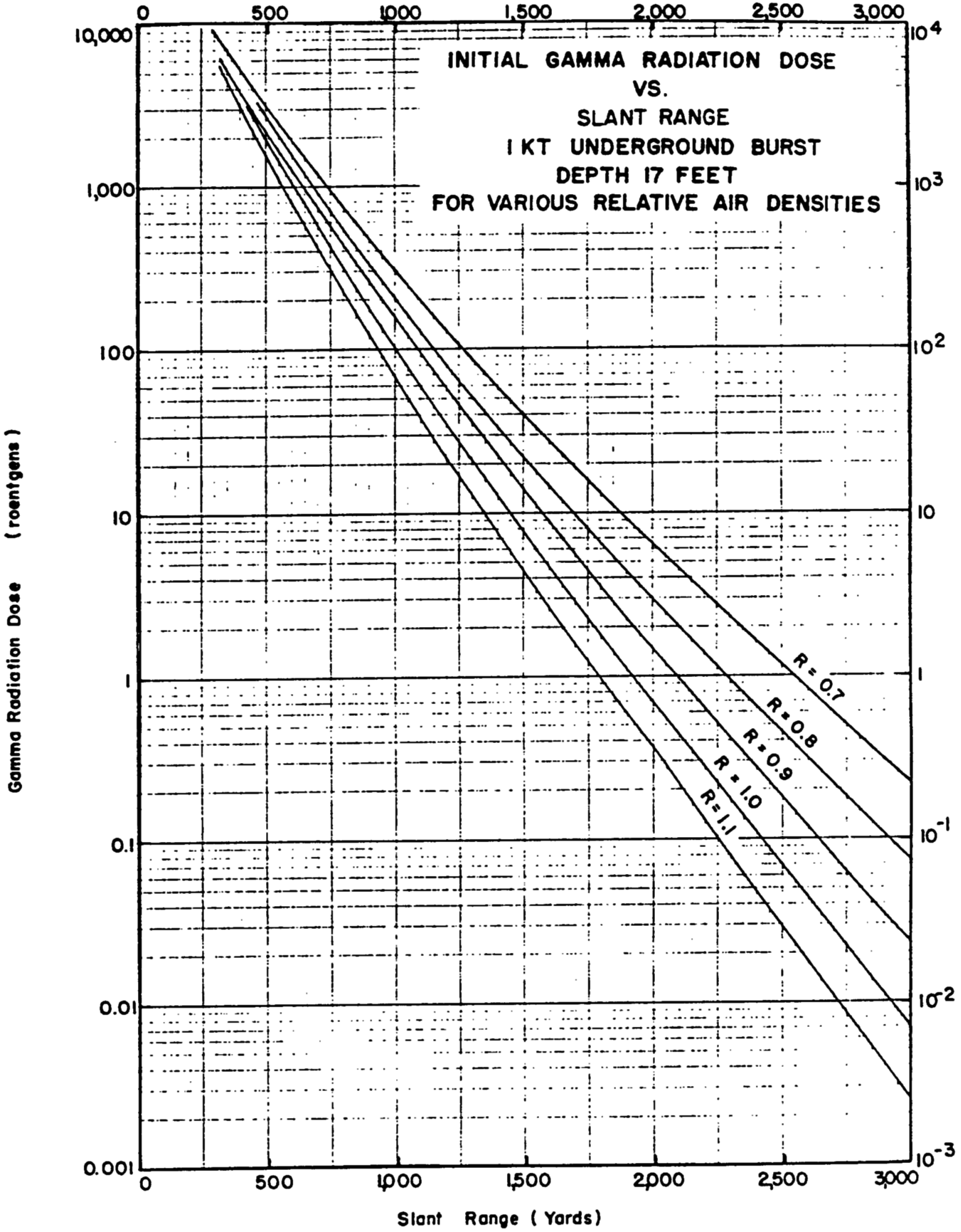
INITIAL GAMMA RADIATION DOSE
VS.
SLANT RANGE
1 KT UNDERGROUND BURST
DEPTH 17 FEET
FOR VARIOUS RELATIVE AIR DENSITIES
R = 0.7
R = 0.8
R = 0.9
R = 1.0
R = 1.1
Gamma Radiation Dose (roentgens)
Slant Range (Yards)
0
500
1,000
1,500
2,000
2,500
3,000
10,000
1,000
100
10
1
0.1
0.01
0.001
10^4
10^3
10^2
10
1
10^{-1}
10^{-2}
10^{-3}

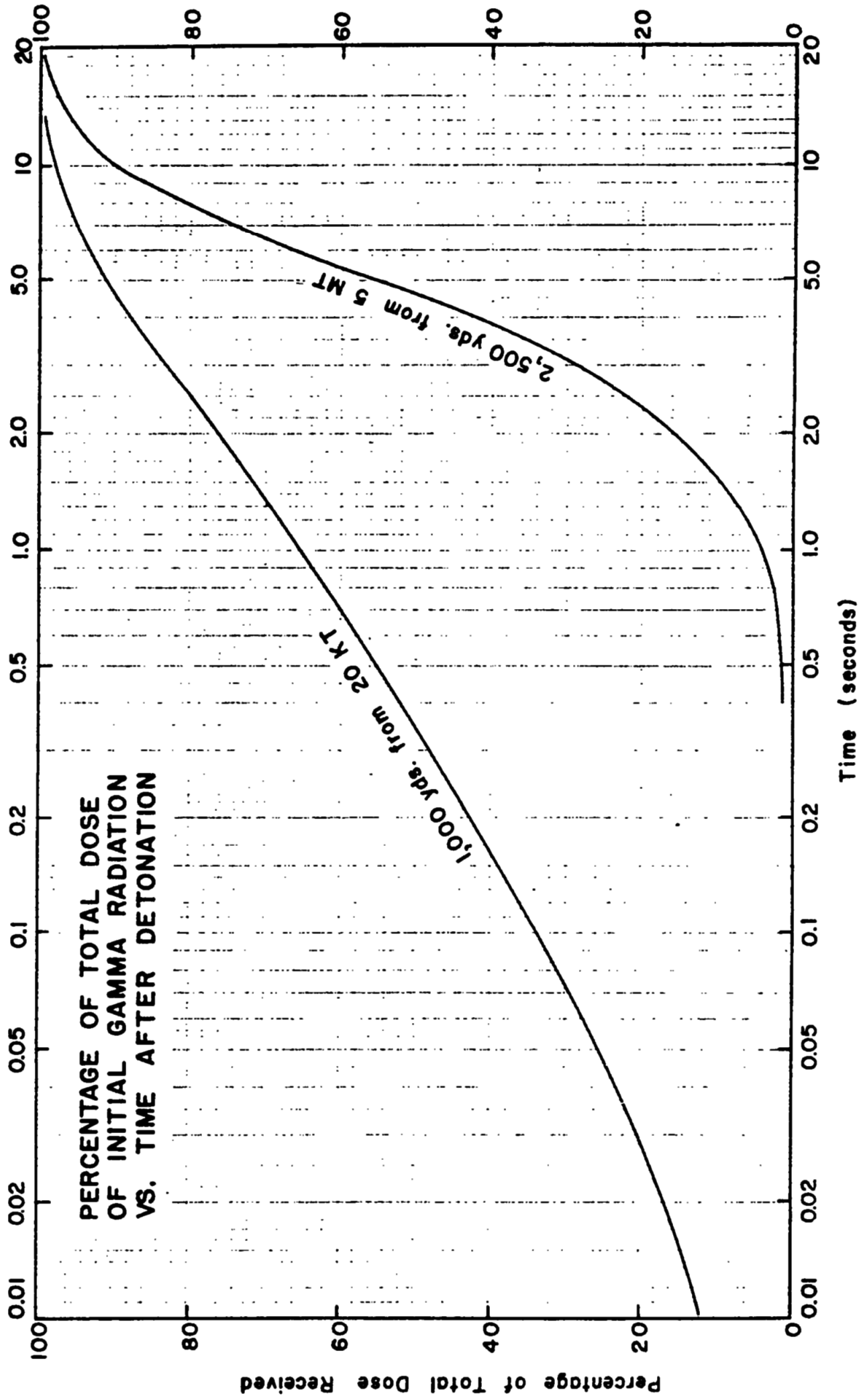
PERCENTAGE OF TOTAL DOSE
OF INITIAL GAMMA RADIATION
VS. TIME AFTER DETONATION
2,500 yds. from 5 MT
1,000 yds. from 20 KT
Percentage of Total Dose Received
Time (seconds)
0.01
0.02
0.05
0.1
0.2
0.5
1.0
2.0
5.0
10
20
0
20
40
60
80
100

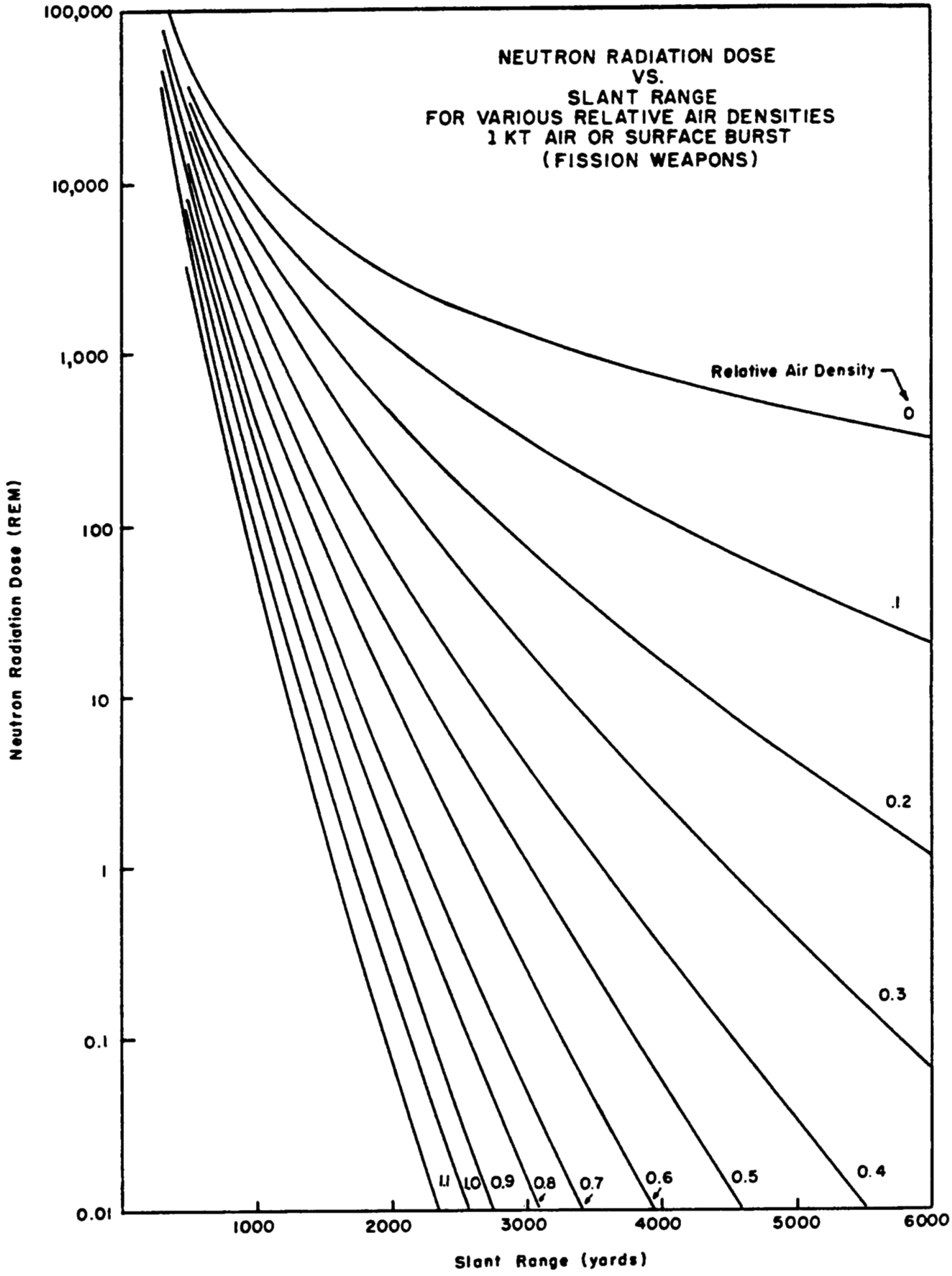
NEUTRON RADIATION DOSE
VS.
SLANT RANGE
FOR VARIOUS RELATIVE AIR DENSITIES
1 KT AIR OR SURFACE BURST
(FISSION WEAPONS)
Relative Air Density
0
.1
0.2
0.3
0.4
0.5
0.6
0.7
0.8
0.9
1.0
1.1
100,000
10,000
1,000
100
10
1
0.1
0.01
1000
2000
3000
4000
5000
6000
Neutron Radiation Dose (REM)
Slant Range (yards)

FIGURE 4-11

NEUTRON RADIATION DOSE VS. SLANT RANGE
FOR VARIOUS RELATIVE AIR DENSITIES
1 MT AIR OR SURFACE BURST (FUSION WEAPONS)

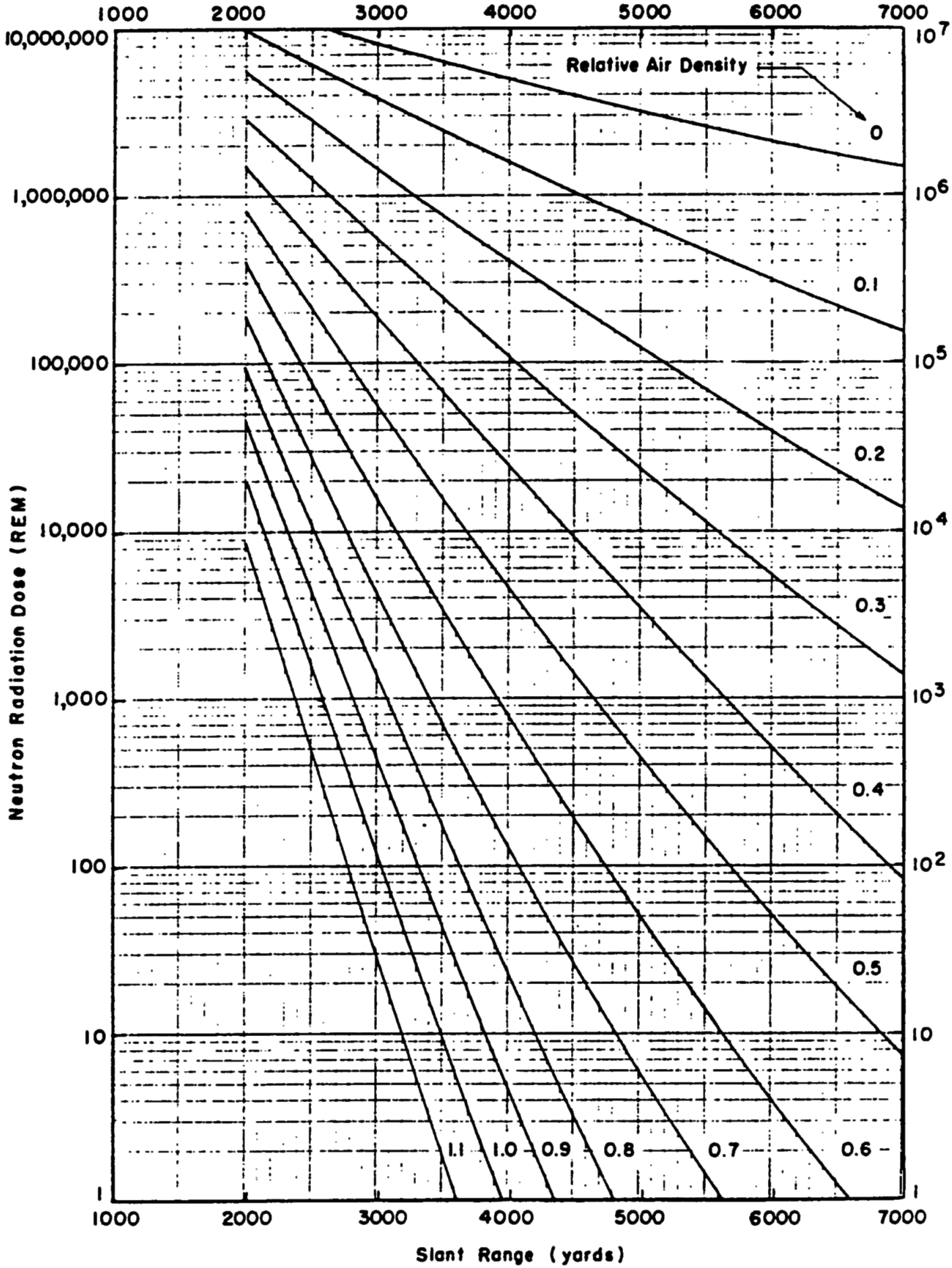

4.3 Residual Radiation

a. General. Most of the damage caused by a nuclear explosion occurs within a few seconds after the detonation; however, there can be a further radiological hazard to personnel, extending over long periods of time. This hazard is most intense when the weapon is detonated at such an altitude that surface particles are drawn into the fireball. The resulting heat transfer changes the physical characteristics of the particles, causing them to become efficient scavengers of the finely divided radioactive remains of the weapon. These radioactive particles then fall under the action of gravity and are spread over a region which is determined by factors such as particle size, cloud height, and wind pattern. The dangerous area covered by this fallout can be of the order of thousands of square miles.

If the altitude of detonation is high enough, the above described interactions with the ground do not occur. The bomb materials will then remain suspended in the atmosphere for very long periods of time and, generally speaking, will settle out in low concentration over much of the earth's surface. This long range settling presents no significant military hazard.

For yields less than 100 KT, the height of burst at which fallout ceases to be a significant military hazard is about 100 $W^{1/3}$ feet. For yields in excess of 100 KT the height of burst at which fallout ceases to be a military hazard is not well defined; however, in the absence of data, the height of burst may be conservatively taken to be 180 $W^{0.4}$ feet.

b. Air Burst. The surface contamination effects of fallout from an air burst weapon are militarily insignificant in most cases, since the bomb cloud carries practically all the radioactive bomb debris to high altitudes. In general, by the time this material can fall back to earth, dilution and radioactive decay will decrease the activity to levels which are no longer important. An exception may occur in the case of a small yield weapon burst in the rain. In this case, the scavenging effect of the precipitation may cause a rain-out of radioactive material which will provide a hazard to personnel located downwind and downhill, and outside the hazard area of initial radiation and other effects. Although the range of weapon yields for which rain-out may become hazardous is not large, quantitative treatment of the problem is difficult. The contamination pattern on the ground depends upon two major dynamic processes, each of which is extremely sensitive to several factors. The major processes are—

(1) The scavenging effect of precipitation on suspended fission products in the atmosphere, and
(2) The flow and ground absorption of rain water after reaching the ground.

Some of the factors which influence the scavenging effect are—

(1) Height and extent of the rain cloud.
(2) Raindrop size and distribution.
(3) Rate of rainfall.
(4) Duration of precipitation.
(5) Position of the nuclear cloud relative to the precipitation.
(6) Hygroscopic character of the fission products.
(7) Solubility of the fission products.
(8) Size of the fission fragments.

The flow and ground absorption of the rain water will, in turn, depend upon such factors as—

(1) Soil porosity.
(2) Drainage features, including rate of drainage.
(3) Degree of soil saturation.

Even in extreme cases, the rainout from an air burst should not be a serious military problem for yields in excess of 20 KT, and for the average case, it should not be a serious problem for yields in excess of 8 KT. Although the weapons of greater yield produce more radioactive material, the updrafts carry the bulk of the material up through the weather to an altitude above the level of precipitation.

Thus, under some circumstances, a rain-out problem may exist; however, it must be evaluated with respect to local conditions. Ditches, puddles and low ground where water collects should be avoided unless survey indicates these areas are safe. Caution should be exercised for a considerable distance downwind and downhill from the burst. So long as drainage is taking place, the rate of decrease in intensity is likely to be greater than decay laws predict.

In addition to rain-out, another contamination mechanism assumes some importance in the case

FIGURE 4-12

GENERALIZED LOCAL CONTOURS FOR RESIDUAL RADIATION

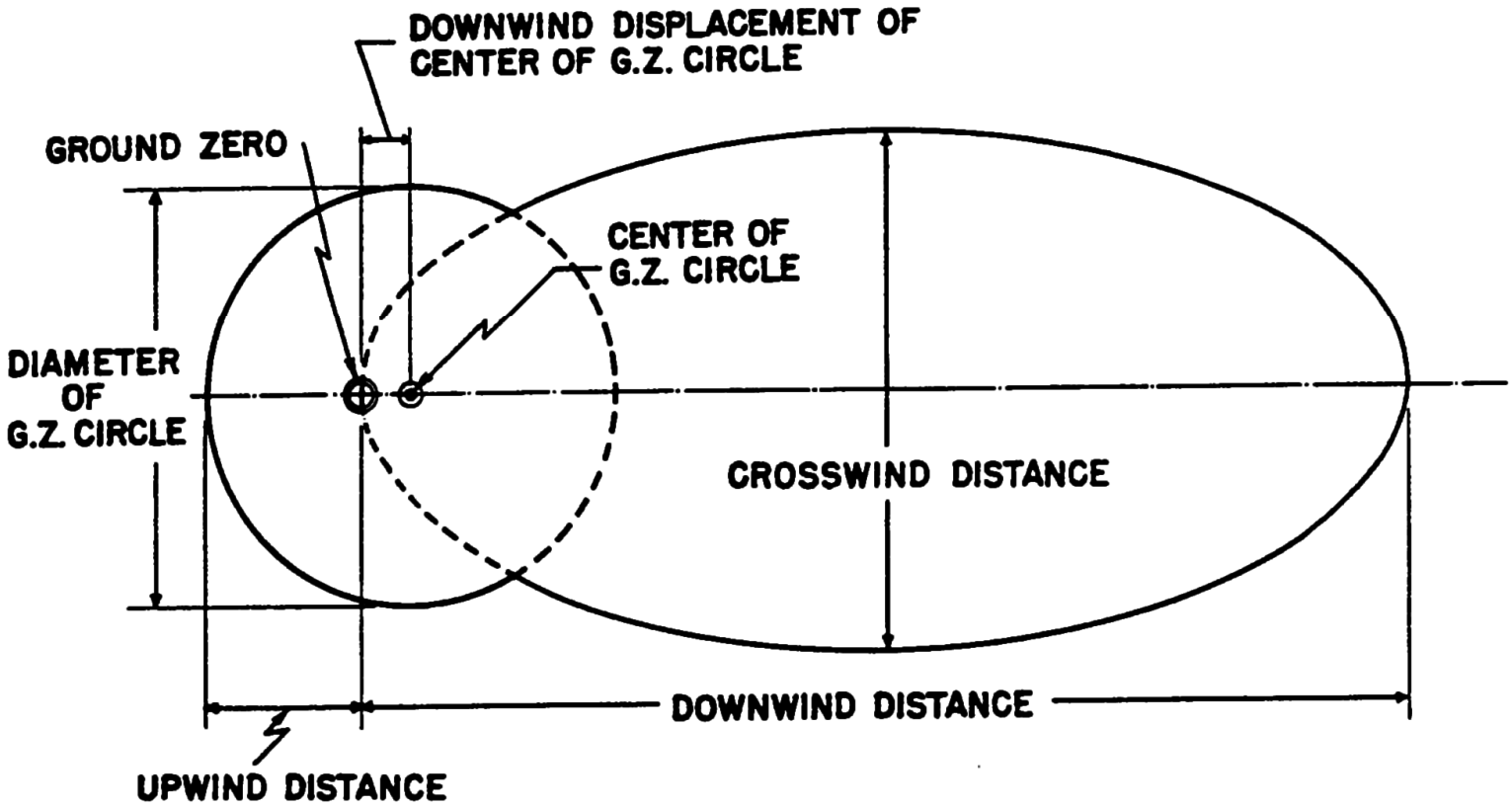

detonation, with a corresponding reduction in the areas of the lower dose rate contours farther out.

(c) *Idealized contours.* In any discussion of the areas affected by residual contamination from fallout, it is convenient to set up a system of contamination dose rate contours which, although simplified and idealized, fit actual contours measured in the field as closely as possible. Figure 4-12 illustrates such a contour system. The "idealized" contour shown consists necessarily of two parts—the ground zero circle, and an elliptical approximation to the downwind component of the fallout. The ground zero circle is formed quite soon after the detonation, largely from heavy particulate matter, throw-out, and soil made active by neutron capture reactions. The parameters which define it are its diameter and the downwind displacement of its center from ground zero. The idealized downwind component, consisting of the fallout proper, is elliptical in shape, and the parameters which define it are its major and minor axes (the downwind and crosswind extent respectively). One end of the ellipse is at ground zero. To define the downwind axis, a simplifying assumption is made—that the downwind direction and extent are determined by a single wind of constant velocity, the so-called "scaling wind." To obtain the scaling wind it is first necessary to obtain the "resultant wind vector" for each of an arbitrary number of equally spaced altitude zones between the top and bottom of the stabilized cloud. Each resultant wind vector is the vector average of all wind vectors for equally spaced altitude intervals from the altitude zone in question down to the surface. The scaling wind is then the vector average of all the resultant wind vectors for the various altitude zones within the cloud. As a rule wide discrepancy from the idealized ellip-

e. Subsurface Burst.

(1) *Underground burst.* A large amount of residual contamination is deposited in the immediate vicinity of the burst point after an underground detonation, because the major portion of the radioactive material falls quickly from the column and cloud to the surface. A very shallow underground burst conforms rather closely to the contamination mechanisms and patterns outlined previously for land surface bursts. As depth of burst is increased, however, a greater percentage of the total available contaminant is deposited as local fallout, until for the case of no surface venting, all of the contamination is contained in the volume of ruptured earth surrounding the point of detonation.

Families of curves are given in figures 4–20 through 4–23 by means of which idealized dose rate contours for a reference time of 1 hour after detonation can be drawn for underground bursts of weapons with yields between 1 KT and 1 MT at a depth of 17 $W^{1/3}$ feet with a 15 knot scaling wind. Multiplying factors are given in figure 4–24 by means of which contour parameters can be estimated for depths other than 17 $W^{1/3}$ feet, down to a limiting depth of 70 $W^{1/3}$ feet. As the depth of burst becomes greater, the contour shapes depart from the idealized pattern, and, particularly in the case of the higher dose rate contours, tend to become more nearly circular. For this reason, the areas obtained by use of the scaling factors from figure 4–24 for burst depths greater than 17 $W^{1/3}$ feet will more nearly represent the actual pattern than will the downwind and crosswind distances for the higher dose rate contours. A more precise scaling is not warranted on the basis of present understanding of the phenomena. For depths of burst greater than 70 $W^{1/3}$ feet, virtually all of the available contamination comes down in the vicinity of the burst point; as burst depth is increased, contours can be expected to decrease in size, with increase in dose rate values in and near the crater. Contours may be drawn for other wind values in the same manner as described for land surface bursts. The contour values given are for an unshielded, open area with substantially level terrain.

(2) *Underwater burst.*

(*a*) *General.* One test at mid-depth in shallow water provided some information on the residual radiation from an underwater detonation. The rather specialized burst conditions make application of the results to specific cases of interest of doubtful validity; however, certain guidelines were established which are applicable and useful in the general case. It was shown that for a ship subjected to fallout radiation, much of the contaminated fallout material drains off the ship into the water, and rapidly becomes relatively ineffective because of the dilution due to mixing in water. For adjacent land areas, residual radiation dose rates about four times as great as on board ship at the same relative position are expected soon after completion of fallout, because dilution and run-off do not occur. For adjacent land areas, the decrease in dose rate with time can be calculated from figure 4–13; however, this cannot be done for ships. As in the case of other types of contaminating bursts, the area of contamination varies considerably with meteorological conditions, particularly with wind.

(*b*) *Harbor burst.* In the case of a nuclear explosion in a comparatively shallow harbor, as in the hold of a ship, more than half of the available radioactivity associated with the device is deposited as local fallout, and large localized high dose rate contours are expected on the adjacent land masses. Although it does not appear feasible to attempt a detailed delineation of contour shapes for a harbor burst on the basis of information available, magni-

tudes of contour areas expected can be given with some confidence. Figure 4–25 indicates expected harbor burst contour areas on adjacent land masses for yields from 1 KT to 1 MT. For yields in the megaton range, contour areas should be estimated from the surface burst curves already presented (fig. 4–14B). To estimate dose rates on the weather decks of anchored ships in a harbor, divide the land-mass values given by four; and for ships alongside a wharf, divide the land-mass values by two.

f. Ground Zero Dose Rates. The residual dose rate curves presented herein make no provision for contours delineating dose rates greater than 3,000 roentgens per hour, except in the case of harbor bursts. Such dose rates occur in "hot spots" rather than over significant areas. The maximum residual radiation dose rates observed on the ground in such hot spots at a reference time of $H+1$ hour, regardless of weapon yield, have been more than 3,000 r/hr and less than 10,000 r/hr for surface burst nuclear weapons. The burst conditions for most of these shots were not truly representative of land shots; hence, there is a large degree of uncertainty regarding the maximum dose rates which may be expected at ground zero under true land surface burst conditions. Higher dose rates may be expected only under certain special circumstances, such as deep underground bursts and bursts in shallow harbors, and are not normally expected for land surface bursts.

g. Total Dose Received. To estimate the dose actually received at a point within an area contaminated by fallout, estimate the time of arrival of fallout at that point (using the scaling wind velocity and the distance from the burst point) and integrate the curve of dose rate as a function of time over the period the individual is within the area. The same procedure is used for the case of a person entering a contaminated area at some time after completion of fallout. Figure 4–26 is presented to facilitate this computation, and can be used to estimate total radiation dose received while in a contaminated area. If, at the time of the explosion, the individual is within the radius of effect of the initial radiation, the acute dose so received must be added to the cumulative residual radiation dose in the manner outlined in paragraph 6.3*b* to obtain the total dose received. If the individual is sheltered, the free field value so obtained should be multiplied by a reduction factor estimated from the degree of shielding involved, as described in paragraph 6.5.

h. Dose Contours. Approximate total dose contours for accumulated doses received during the 48 hours immediately following burst time can be estimated using the appropriate 1-hour dose rate contour curves in conjunction with a scaling factor obtained from figure 4–27. The scaling factor averages the time of arrival effect for 500 roentgen total dose contours using a 15 knot scaling wind, and gives results sufficiently accurate for planning purposes over a range of doses from 100 *r* to 1,000 *r*. This method may be used with somewhat less accuracy for accumulated doses outside this range. It should be recognized that dose and dose rate contours do not have the same shape, although the shapes are sufficiently alike to make this approximate method useful.

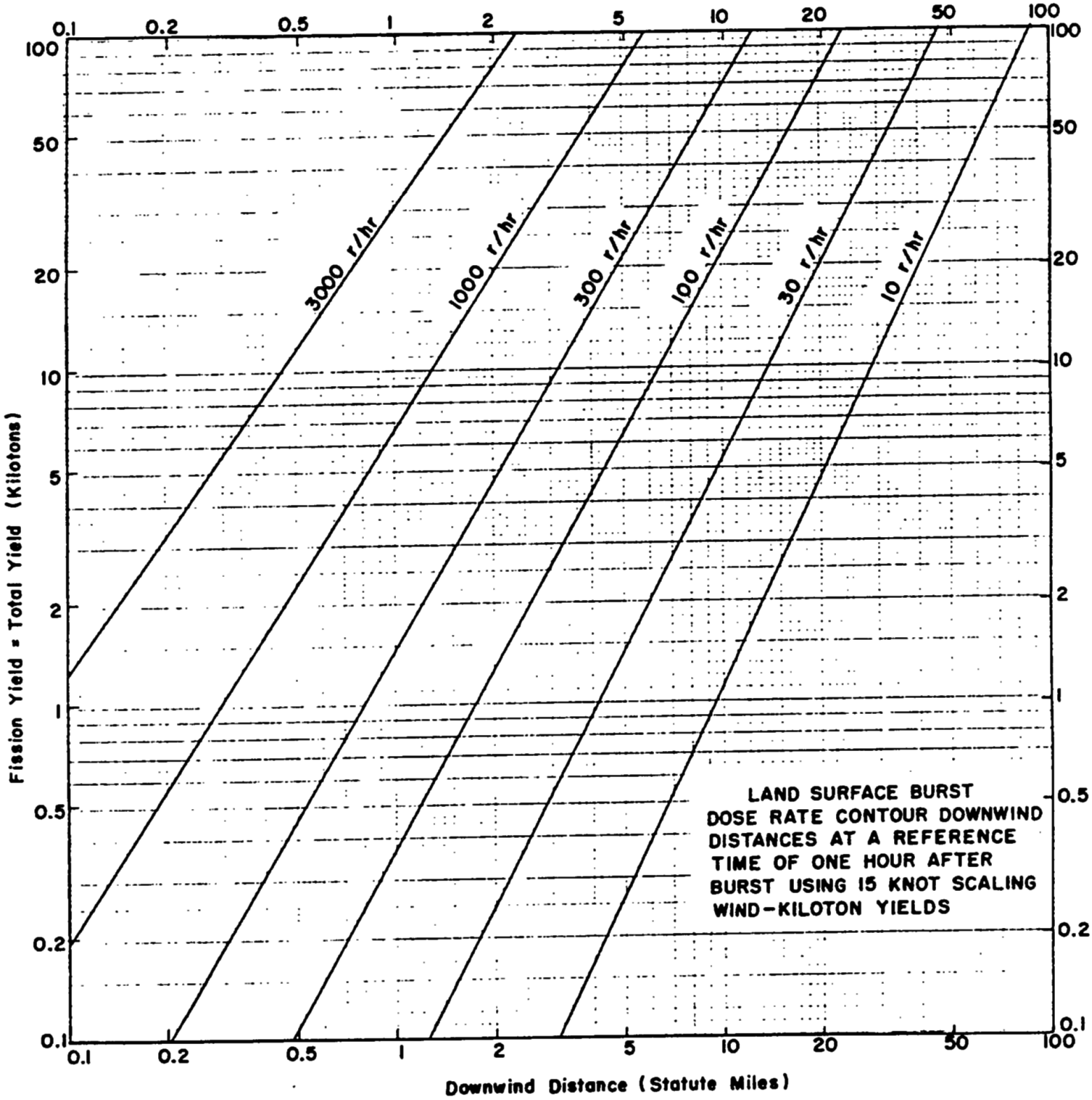
3000 r/hr
1000 r/hr
300 r/hr
100 r/hr
30 r/hr
10 r/hr
LAND SURFACE BURST
DOSE RATE CONTOUR DOWNWIND
DISTANCES AT A REFERENCE
TIME OF ONE HOUR AFTER
BURST USING 15 KNOT SCALING
WIND-KILOTON YIELDS
Fission Yield = Total Yield (Kilotons)
Downwind Distance (Statute Miles)
0.1
0.2
0.5
1
2
5
10
20
50
100

FIGURE 4-15B

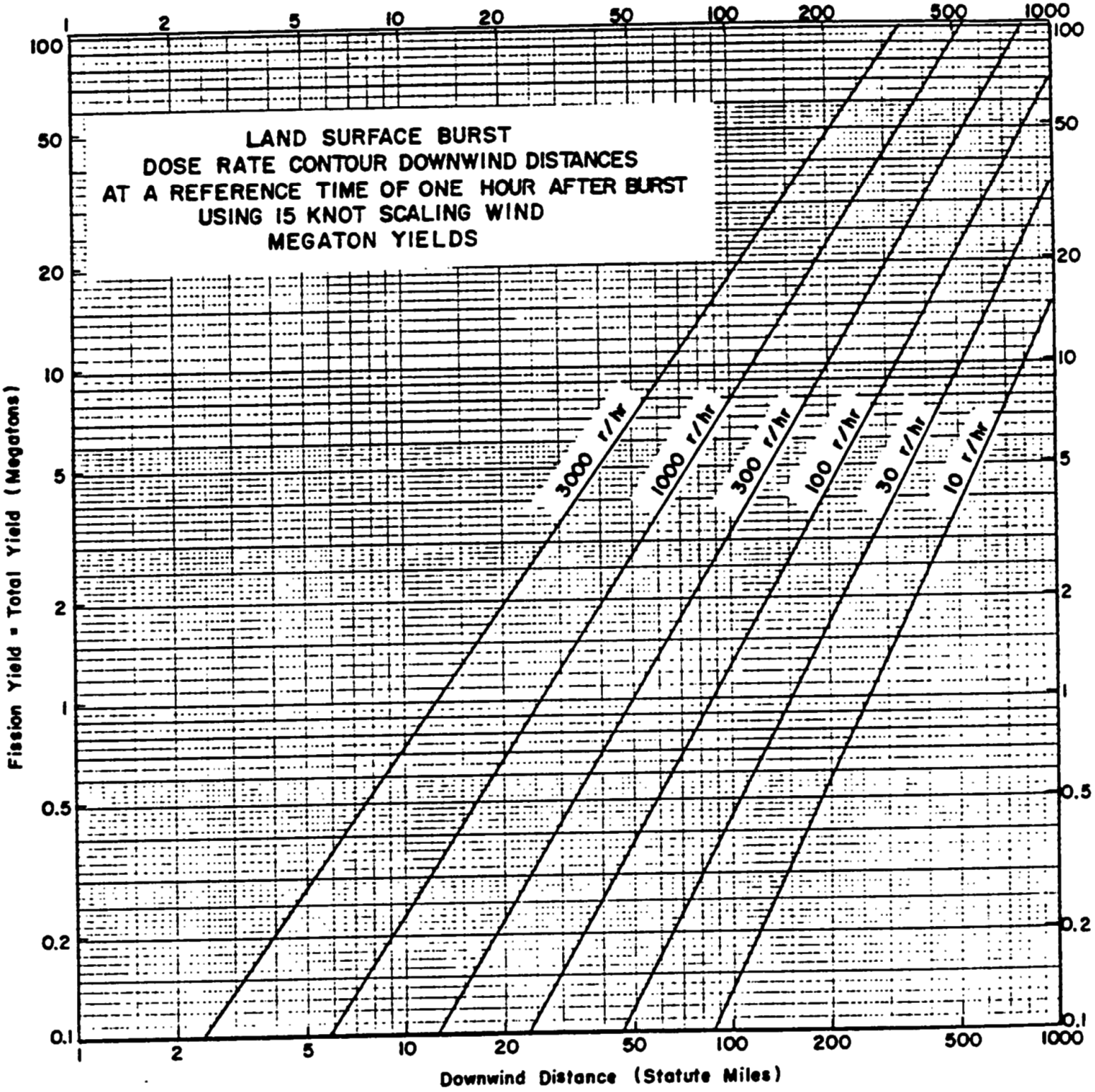
LAND SURFACE BURST
DOSE RATE CONTOUR DOWNWIND DISTANCES
AT A REFERENCE TIME OF ONE HOUR AFTER BURST
USING 15 KNOT SCALING WIND
MEGATON YIELDS
3000 r/hr
1000 r/hr
300 r/hr
100 r/hr
30 r/hr
10 r/hr
Fission Yield = Total Yield (Megatons)
Downwind Distance (Statute Miles)
1
2
5
10
20
50
100
200
500
1000
0.1
0.2
0.5

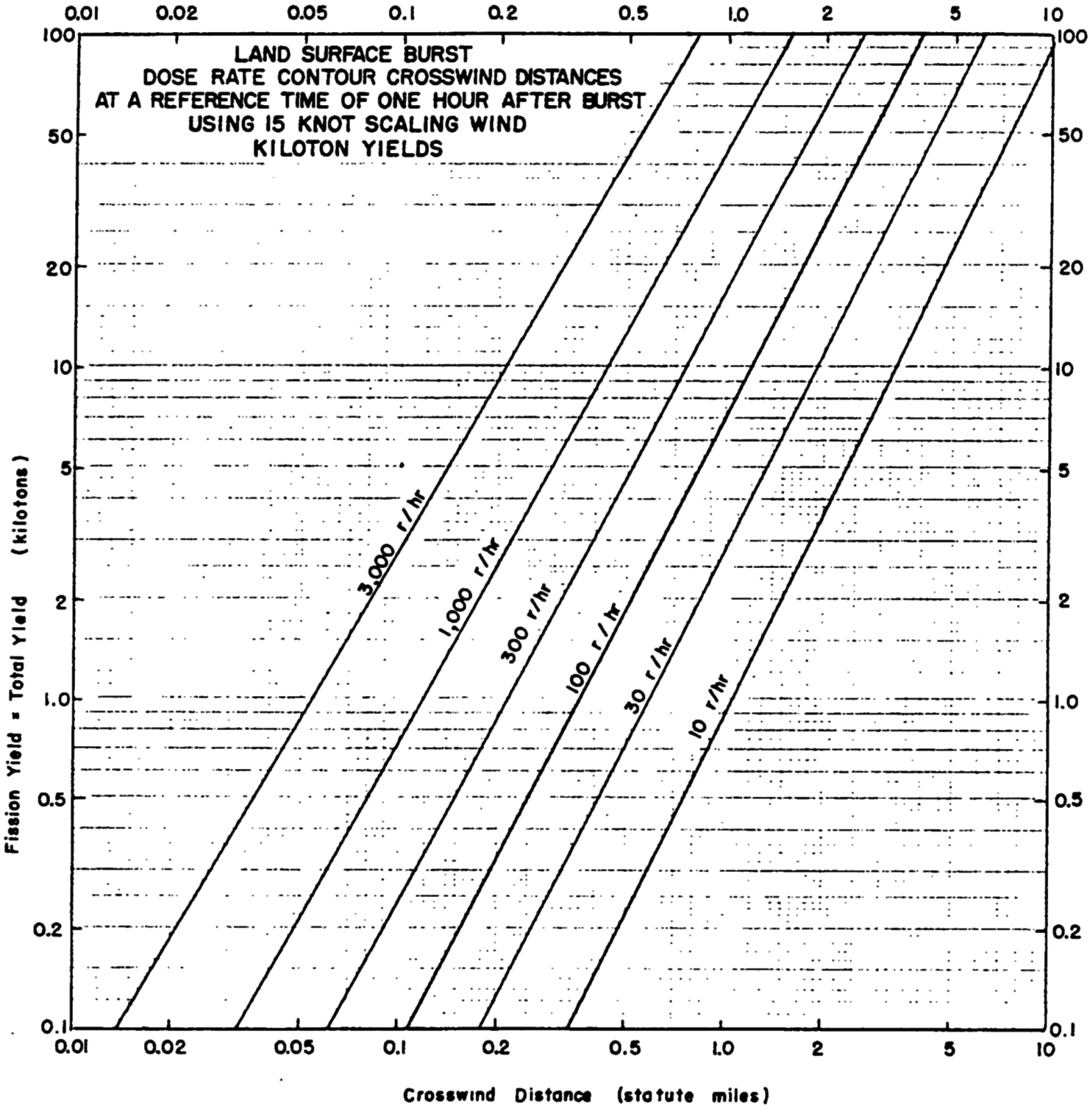
LAND SURFACE BURST
DOSE RATE CONTOUR CROSSWIND DISTANCES
AT A REFERENCE TIME OF ONE HOUR AFTER BURST
USING 15 KNOT SCALING WIND
KILOTON YIELDS
3,000 r/hr
1,000 r/hr
300 r/hr
100 r/hr
30 r/hr
10 r/hr
Fission Yield = Total Yield (kilotons)
Crosswind Distance (statute miles)
0.01
0.02
0.05
0.1
0.2
0.5
1.0
2
5
10
100
50
20
10
5
2
1.0
0.5
0.2
0.1

FIGURE 4-16B

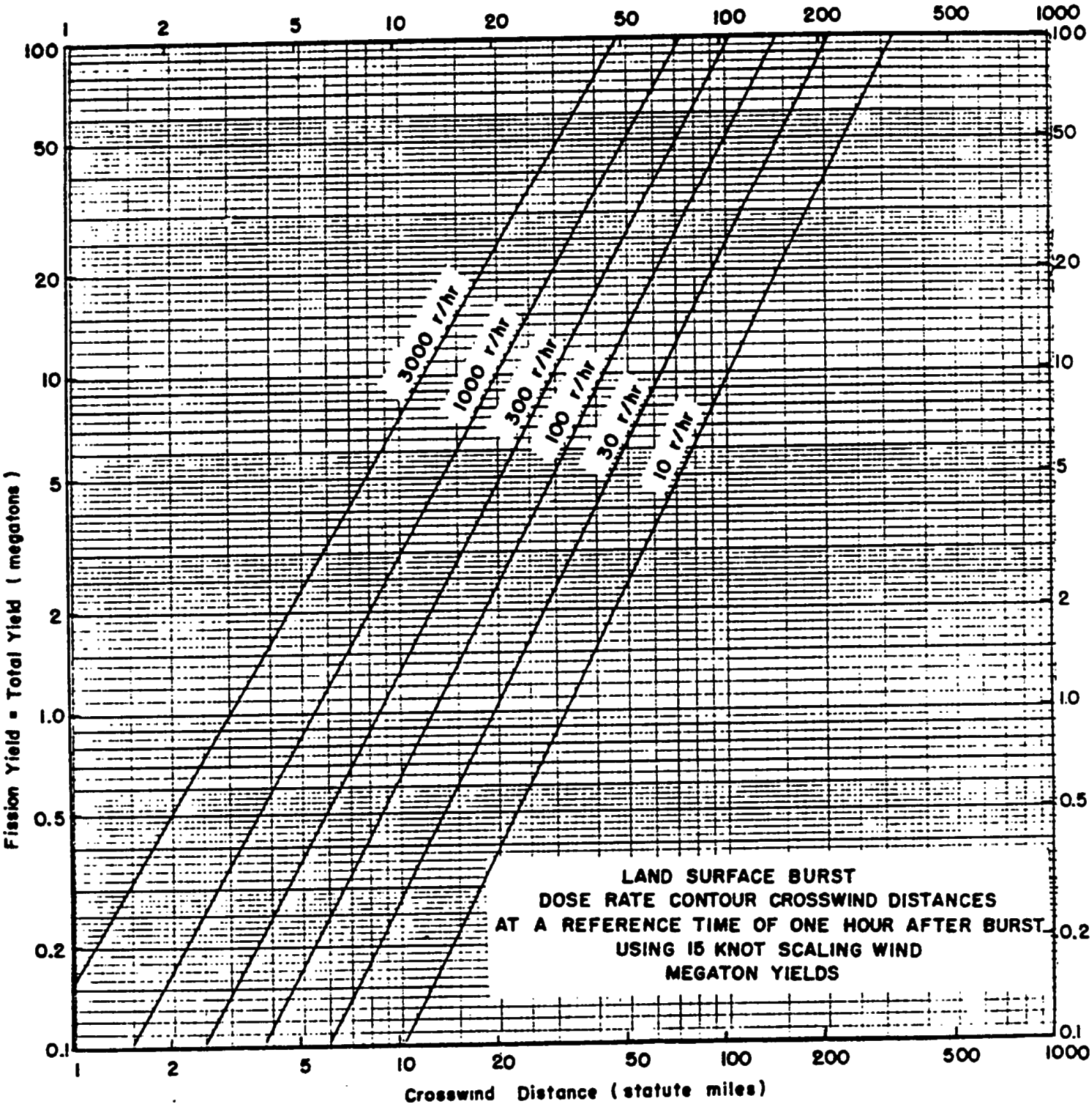
3000 r/hr
1000 r/hr
300 r/hr
100 r/hr
30 r/hr
10 r/hr
LAND SURFACE BURST
DOSE RATE CONTOUR CROSSWIND DISTANCES
AT A REFERENCE TIME OF ONE HOUR AFTER BURST
USING 15 KNOT SCALING WIND
MEGATON YIELDS
Fission Yield = Total Yield (megatons)
Crosswind Distance (statute miles)
1
2
5
10
20
50
100
200
500
1000
0.1
0.2
0.5
1.0

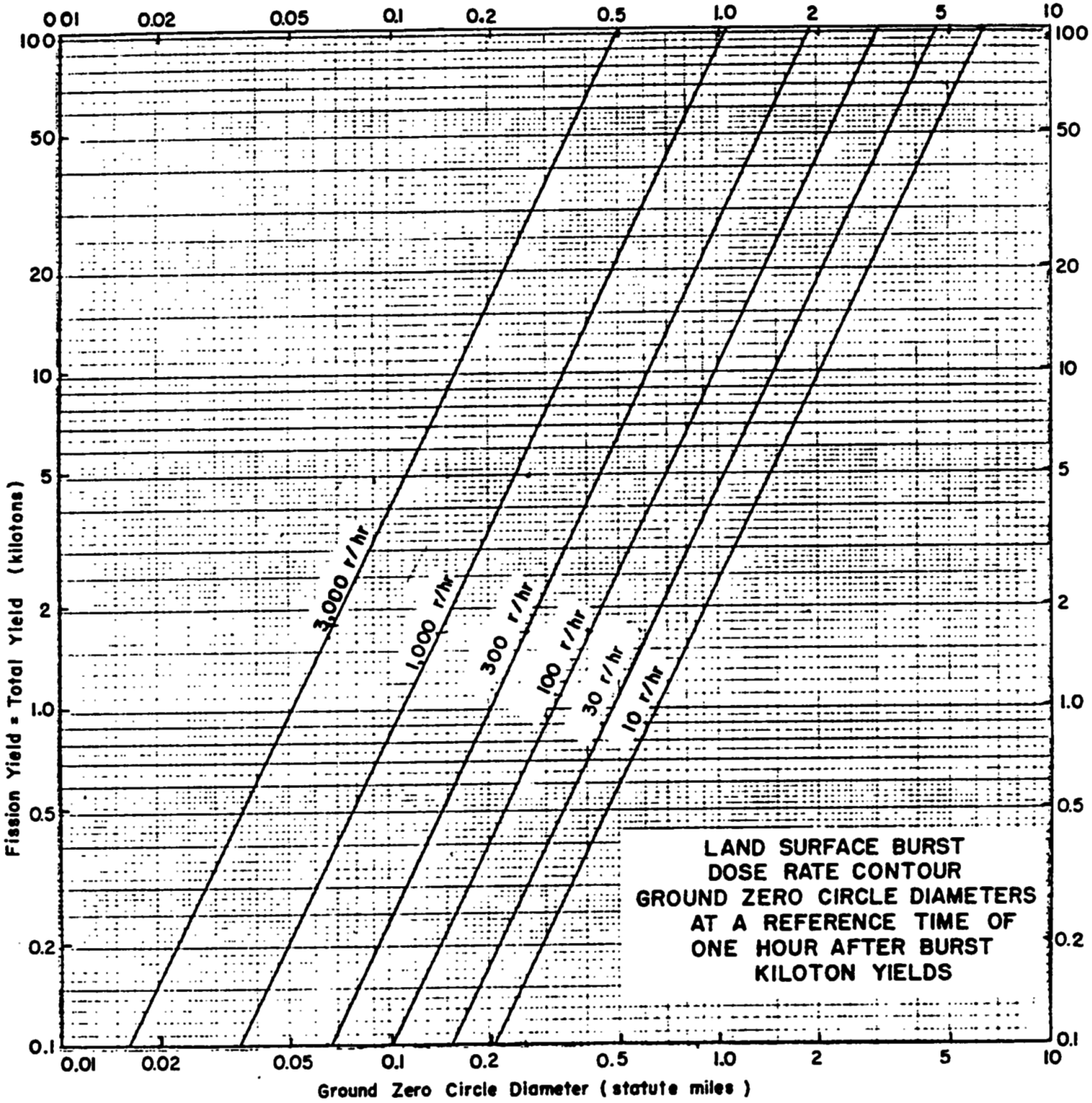
0.01
0.02
0.05
0.1
0.2
0.5
1.0
2
5
10
100
50
20
10
5
2
1.0
0.5
0.2
0.1
3,000 r/hr
1,000 r/hr
300 r/hr
100 r/hr
30 r/hr
10 r/hr
LAND SURFACE BURST
DOSE RATE CONTOUR
GROUND ZERO CIRCLE DIAMETERS
AT A REFERENCE TIME OF
ONE HOUR AFTER BURST
KILOTON YIELDS
Fission Yield = Total Yield (kilotons)
Ground Zero Circle Diameter (statute miles)

FIGURE 4-17B

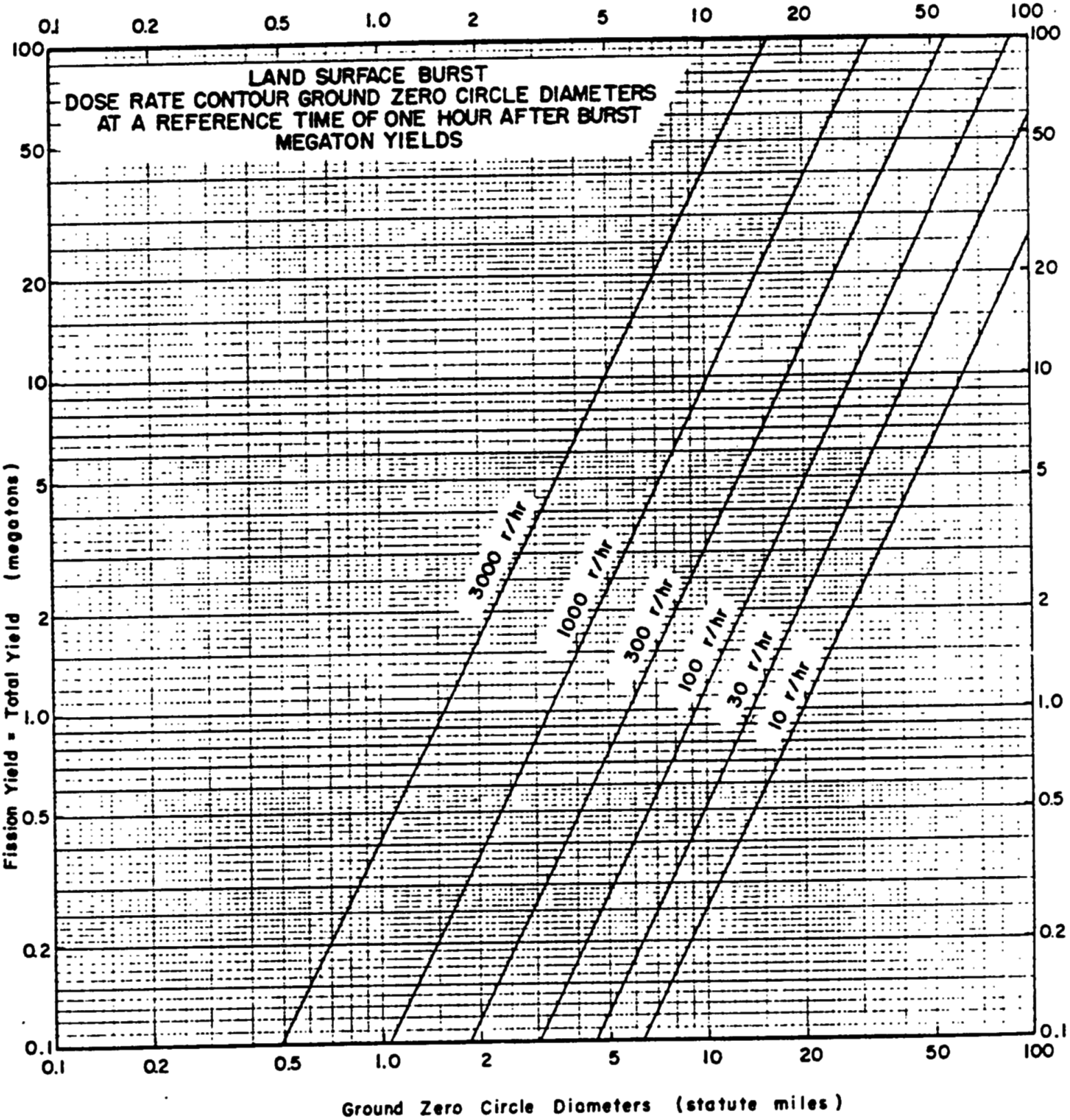
LAND SURFACE BURST
DOSE RATE CONTOUR GROUND ZERO CIRCLE DIAMETERS
AT A REFERENCE TIME OF ONE HOUR AFTER BURST
MEGATON YIELDS
3000 r/hr
1000 r/hr
300 r/hr
100 r/hr
30 r/hr
10 r/hr
Fission Yield = Total Yield (megatons)
Ground Zero Circle Diameters (statute miles)
0.1
0.2
0.5
1.0
2
5
10
20
50
100

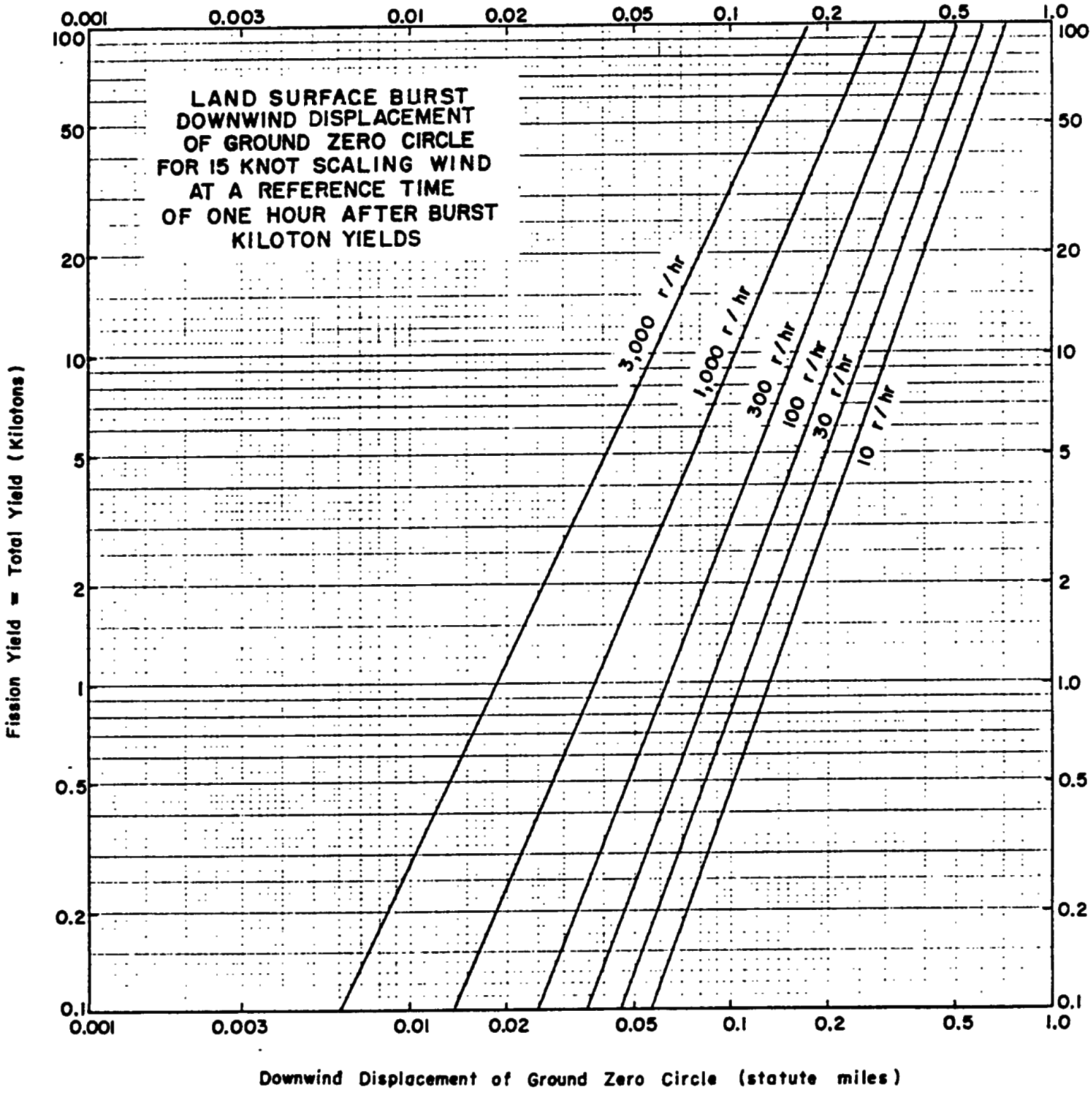
LAND SURFACE BURST
DOWNWIND DISPLACEMENT
OF GROUND ZERO CIRCLE
FOR 15 KNOT SCALING WIND
AT A REFERENCE TIME
OF ONE HOUR AFTER BURST
KILOTON YIELDS
3,000 r/hr
1,000 r/hr
300 r/hr
100 r/hr
30 r/hr
10 r/hr
0.001
0.003
0.01
0.02
0.05
0.1
0.2
0.5
1.0
100
50
20
10
5
2
1
0.5
0.2
0.1
Fission Yield = Total Yield (Kilotons)
Downwind Displacement of Ground Zero Circle (statute miles)

FIGURE 4-18B

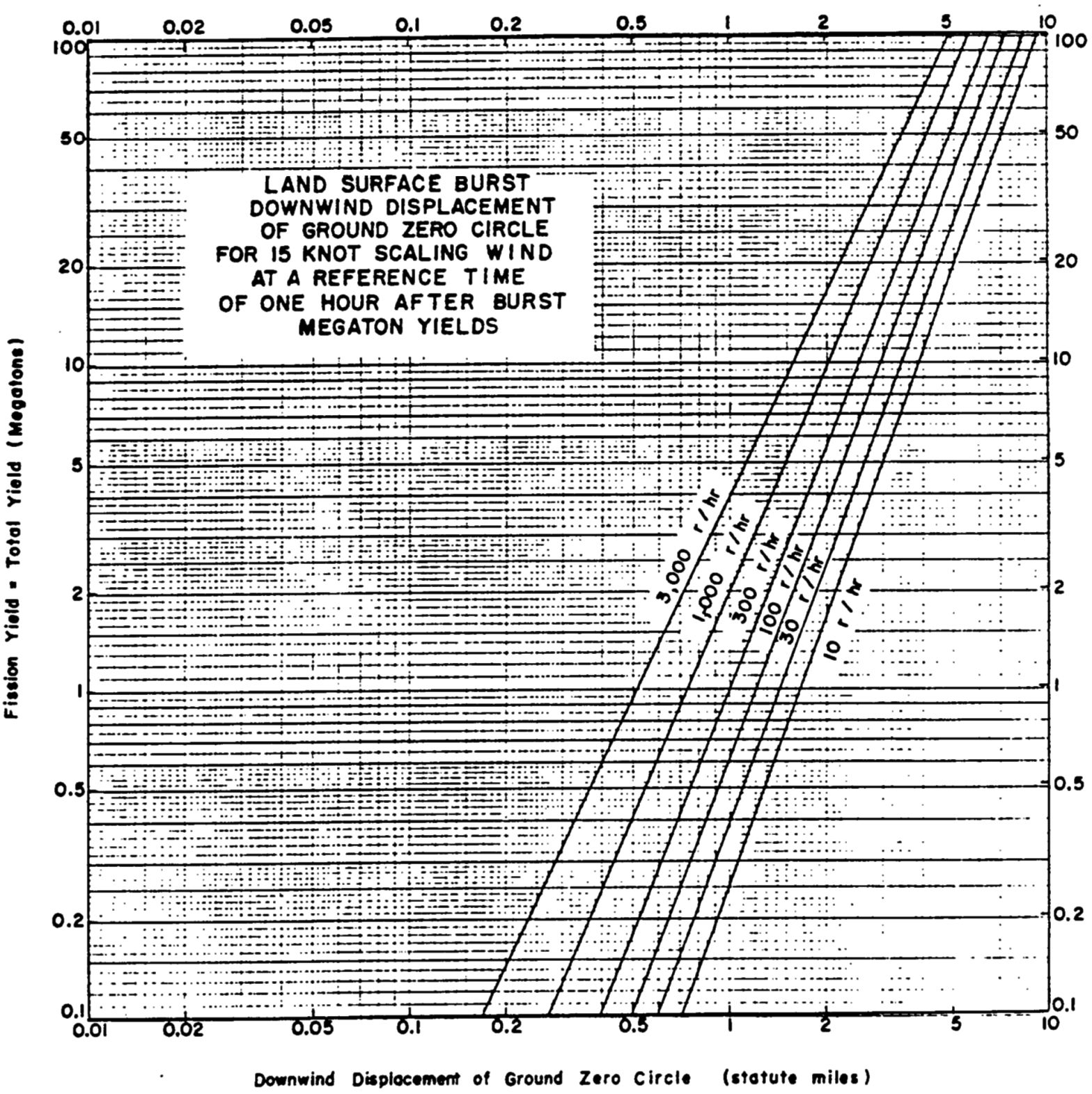
LAND SURFACE BURST
DOWNWIND DISPLACEMENT
OF GROUND ZERO CIRCLE
FOR 15 KNOT SCALING WIND
AT A REFERENCE TIME
OF ONE HOUR AFTER BURST
MEGATON YIELDS
3,000 r/hr
1,000 r/hr
300 r/hr
100 r/hr
30 r/hr
10 r/hr
0.01
0.02
0.05
0.1
0.2
0.5
1
2
5
10
100
50
20
10
5
2
1
0.5
0.2
0.1
Fission Yield = Total Yield (Megatons)
Downwind Displacement of Ground Zero Circle (statute miles)

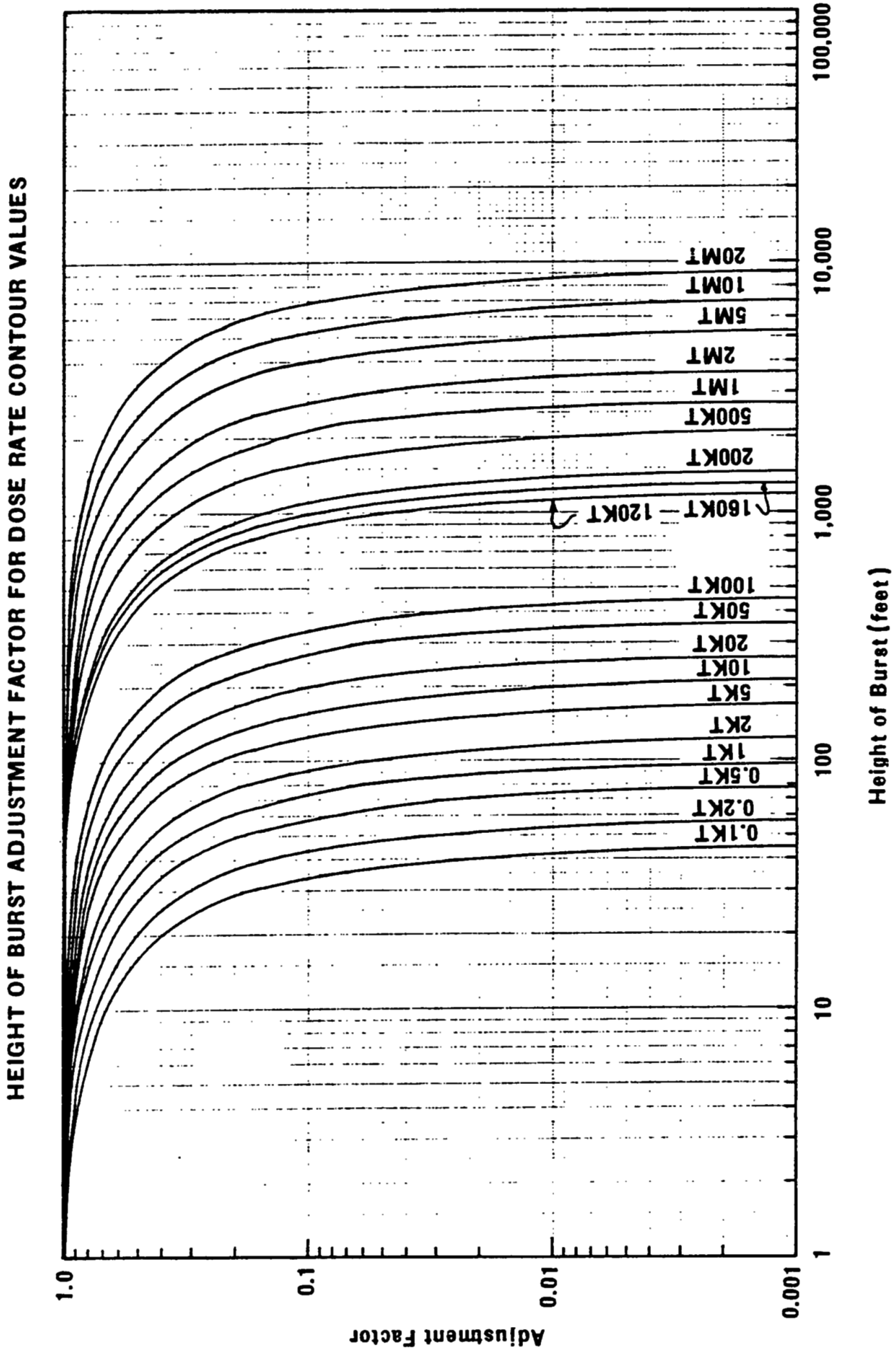
HEIGHT OF BURST ADJUSTMENT FACTOR FOR DOSE RATE CONTOUR VALUES
Adjustment Factor
1.0
0.1
0.01
0.001
Height of Burst (feet)
1
10
100
1,000
10,000
100,000
0.1KT
0.2KT
0.5KT
1KT
2KT
5KT
10KT
20KT
50KT
100KT
120KT
160KT
200KT
500KT
1MT
2MT
5MT
10MT
20MT

FIGURE 4-20

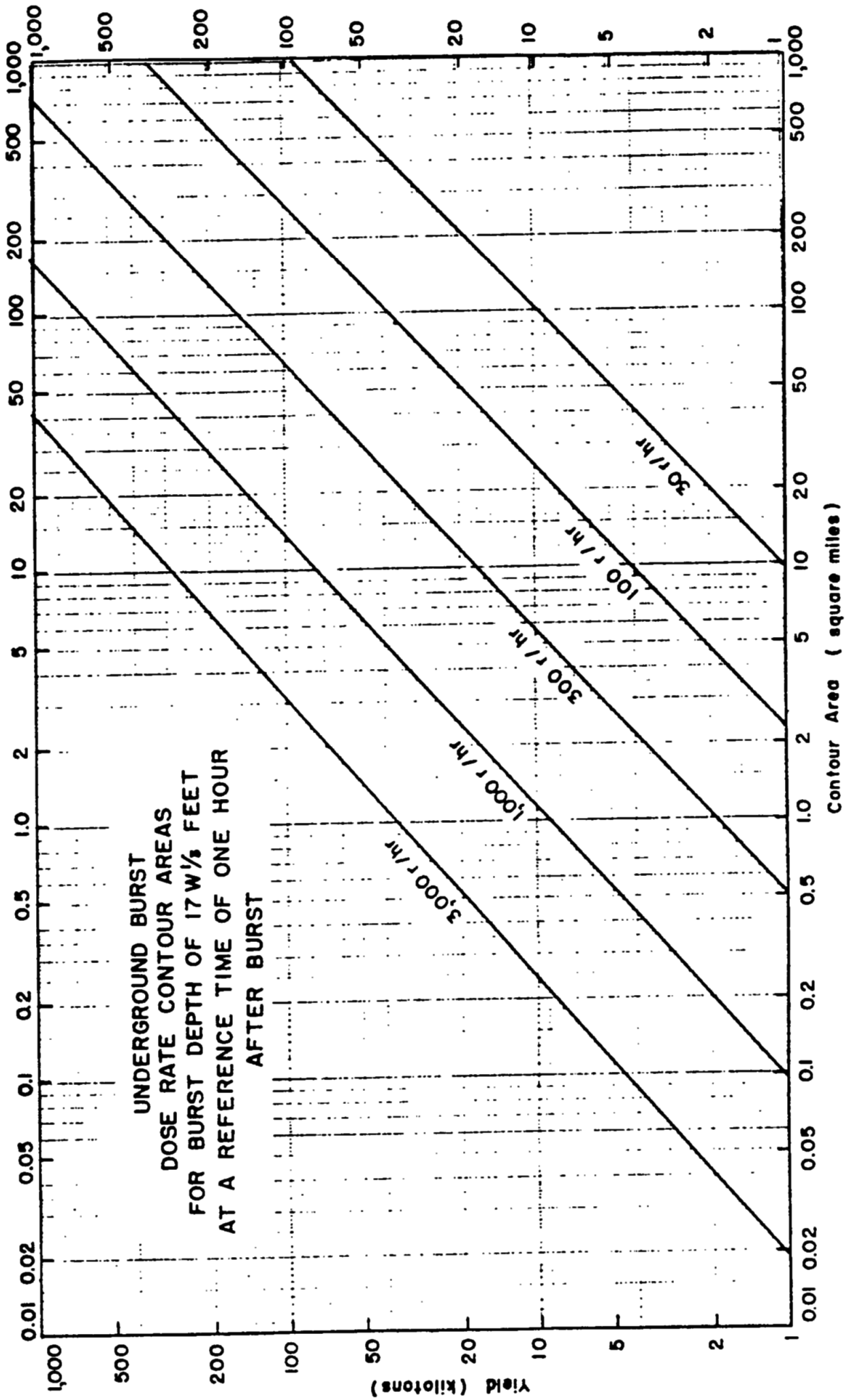
UNDERGROUND BURST
DOSE RATE CONTOUR AREAS
FOR BURST DEPTH OF 17 W^1/3 FEET
AT A REFERENCE TIME OF ONE HOUR
AFTER BURST
30 r/hr
100 r/hr
300 r/hr
1,000 r/hr
3,000 r/hr
Contour Area (square miles)
Yield (kilotons)
0.01 0.02 0.05 0.1 0.2 0.5 1.0 2 5 10 20 50 100 200 500 1,000
1 2 5 10 20 50 100 200 500 1,000

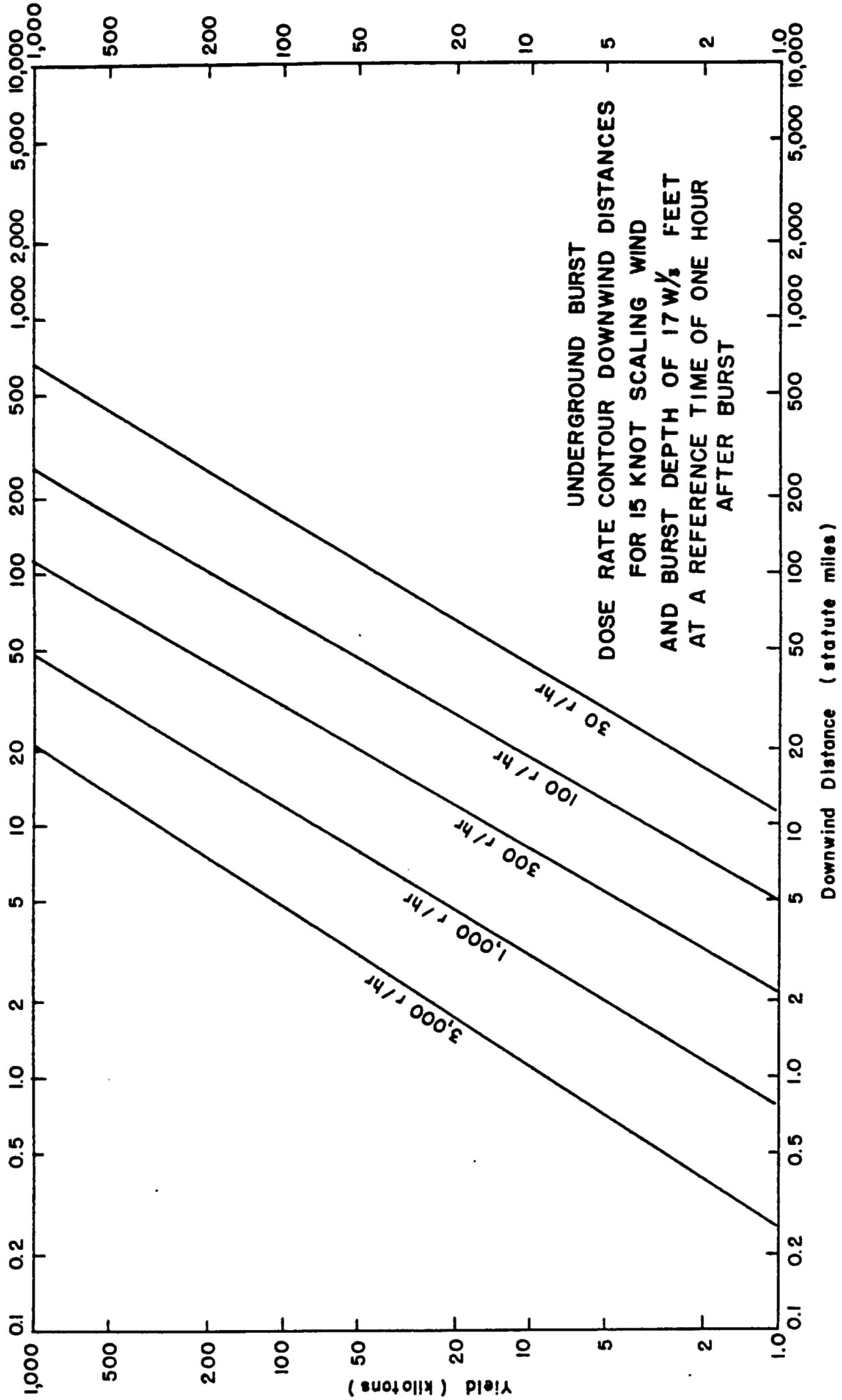
UNDERGROUND BURST
DOSE RATE CONTOUR DOWNWIND DISTANCES
FOR 15 KNOT SCALING WIND
AND BURST DEPTH OF 17 W^1/3 FEET
AT A REFERENCE TIME OF ONE HOUR
AFTER BURST
30 r/hr
100 r/hr
300 r/hr
1,000 r/hr
3,000 r/hr
Downwind Distance (statute miles)
Yield (kilotons)
0.1
0.2
0.5
1.0
2
5
10
20
50
100
200
500
1,000
2,000
5,000
10,000

FIGURE 4-22

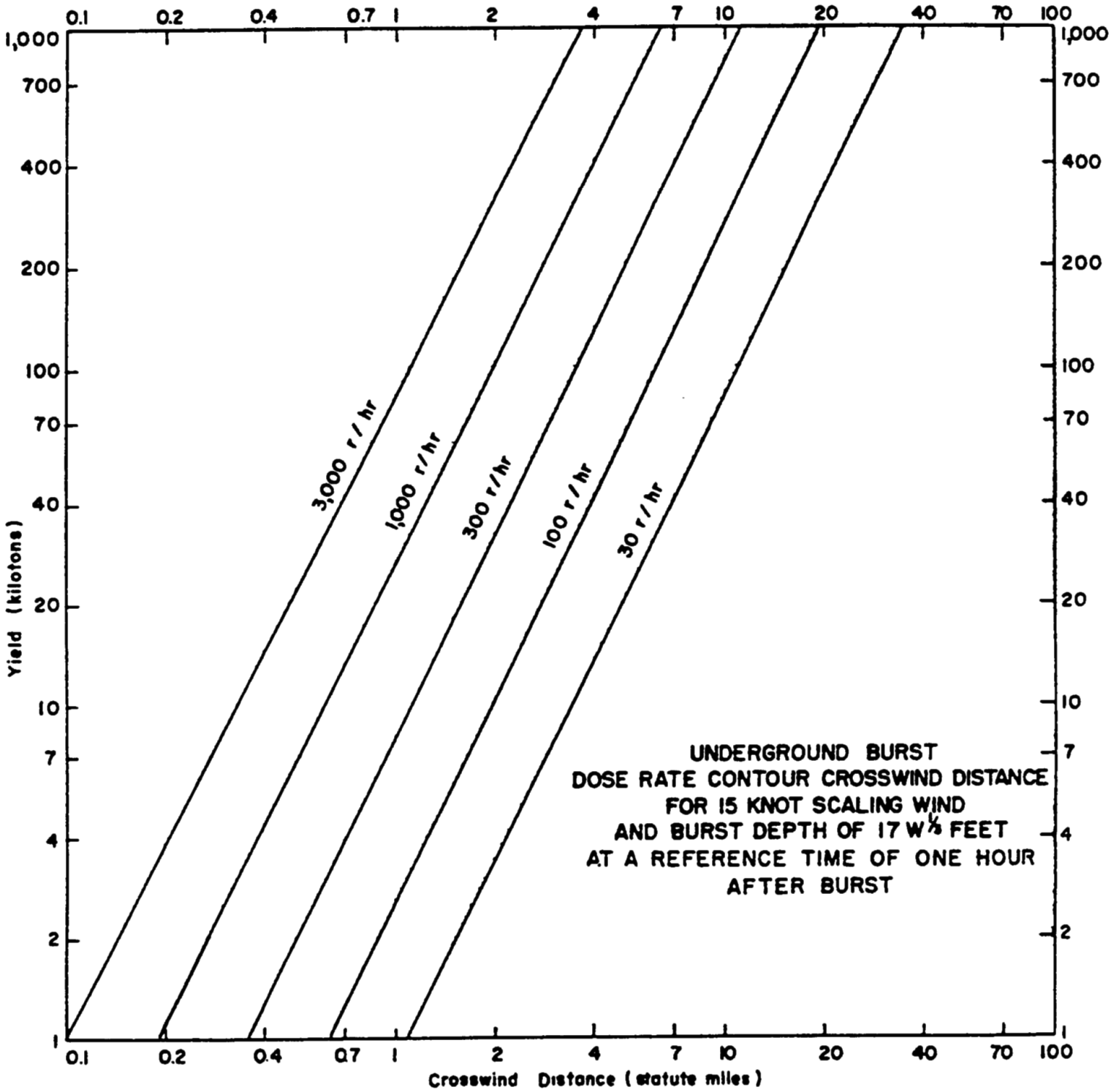
0.1
0.2
0.4
0.7
1
2
4
7
10
20
40
70
100
1,000
700
400
200
100
70
40
20
10
7
4
2
1
Yield (kilotons)
3,000 r/hr
1,000 r/hr
300 r/hr
100 r/hr
30 r/hr
UNDERGROUND BURST
DOSE RATE CONTOUR CROSSWIND DISTANCE
FOR 15 KNOT SCALING WIND
AND BURST DEPTH OF 17 W^1/3 FEET
AT A REFERENCE TIME OF ONE HOUR
AFTER BURST
Crosswind Distance (statute miles)

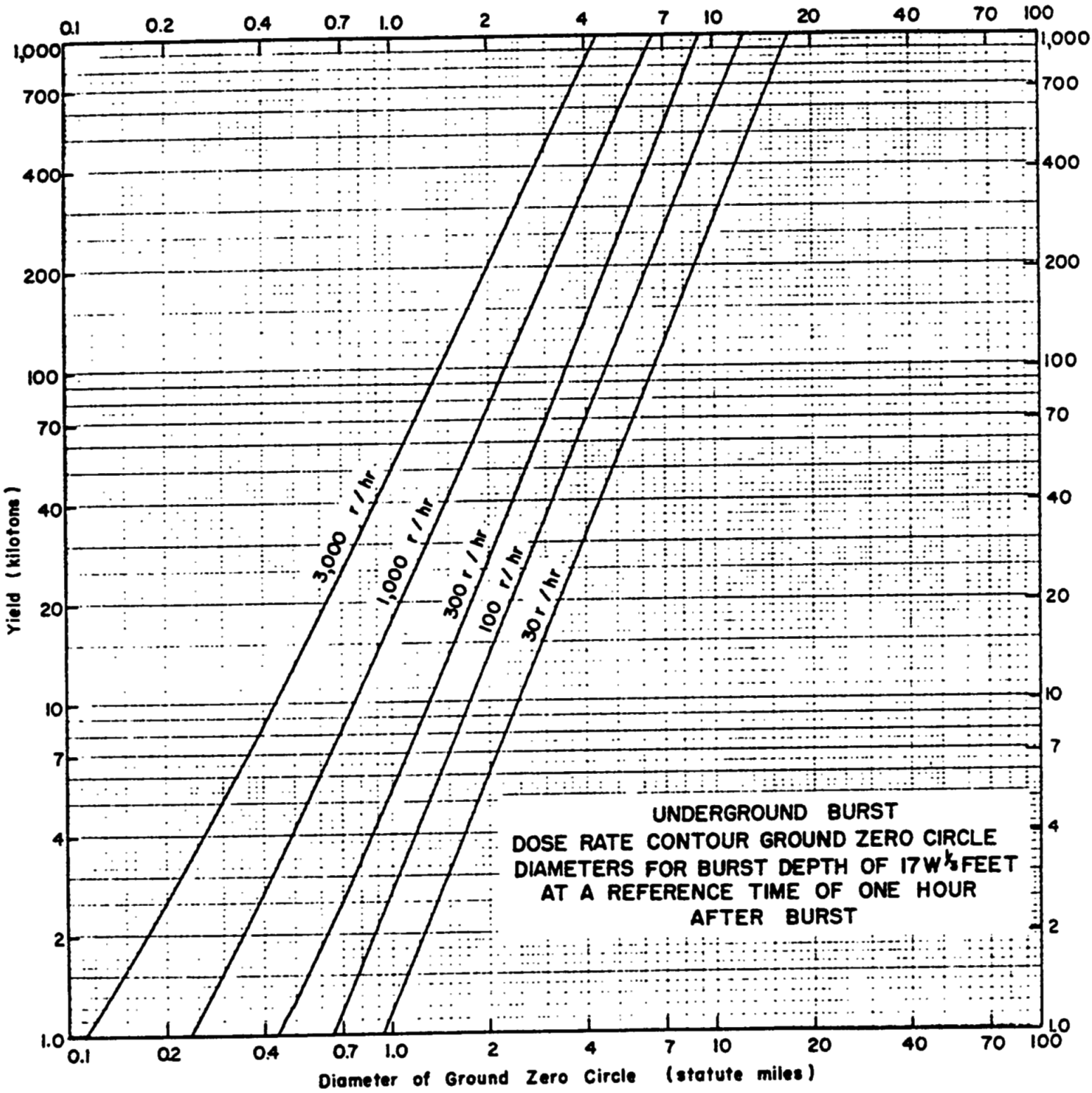
0.1
0.2
0.4
0.7
1.0
2
4
7
10
20
40
70
100
1,000
700
400
200
100
70
40
20
10
7
4
2
1.0
Yield (kilotons)
3,000 r/hr
1,000 r/hr
300 r/hr
100 r/hr
30 r/hr
UNDERGROUND BURST
DOSE RATE CONTOUR GROUND ZERO CIRCLE
DIAMETERS FOR BURST DEPTH OF 17W⅓ FEET
AT A REFERENCE TIME OF ONE HOUR
AFTER BURST
Diameter of Ground Zero Circle (statute miles)

HARBOR BURST DOSE RATE CONTOUR AREAS

Figure 4–25 presents dose rate contour areas to be expected over adjacent land masses at 1 hour after burst time due to residual radiation resulting from bursting nuclear weapons with yields from 1 KT to 1 MT in a shallow harbor. For this purpose, a harbor depth of 30 to 50 feet of water over a mud bottom is assumed, and the burst is assumed to take place a few feet below the water surface, such as in the hold of a ship. The areas given may be assumed to be independent of wind, although specific location of the contaminated areas with respect to the burst point is a sensitive function of wind and other meteorological conditions, as with other types of contaminating bursts. Area magnitudes may be read directly from the curves for those dose-rate values for which curves are provided. Extrapolation to higher or lower dose rate contour values than covered by the families of curves cannot be done accurately and should not be attempted. To obtain dose rate values for times other than $H+1$ hour, multiplying factors from figure 4–13 should be used.

Example.

Given: A 30 KT harbor burst.

Find: The area of effect for dose rates of 1,000 r/hr or greater at $H+1$ hour.

Solution: Reading directly from figure 4–25, the area for a dose rate of 1,000 r/hr or more at $H+1$ hour for a 30 KT harbor burst is 3.4 (± 1.7) square miles. *Answer.*

Reliability. Area magnitudes obtained from these curves for a specific yield are considered reliable within ± 50 percent for the burst conditions indicated.

Related material.

See paragraph 4.3*e*.

See also figure 4–13 and figure 4–26.

FIGURE 4-25

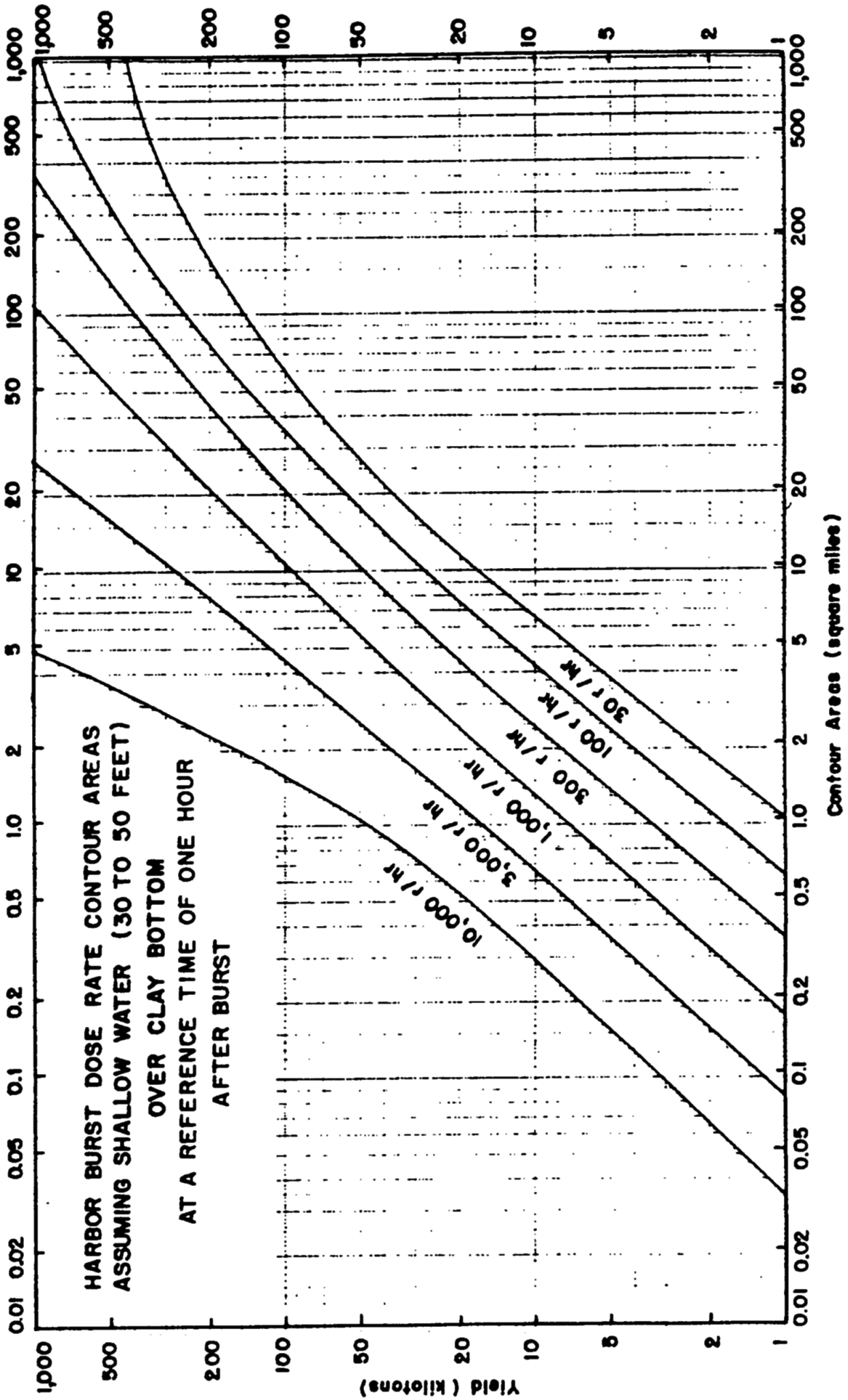
HARBOR BURST DOSE RATE CONTOUR AREAS
ASSUMING SHALLOW WATER (30 TO 50 FEET)
OVER CLAY BOTTOM
AT A REFERENCE TIME OF ONE HOUR
AFTER BURST
30 r / hr
100 r / hr
300 r / hr
1,000 r / hr
3,000 r / hr
10,000 r / hr
Yield (kilotons)
Contour Areas (square miles)
0.01
0.02
0.05
0.1
0.2
0.5
1.0
2
5
10
20
50
100
200
500
1,000
1
2
5
10
20
50
100
200
500
1,000

FIGURE 4-26

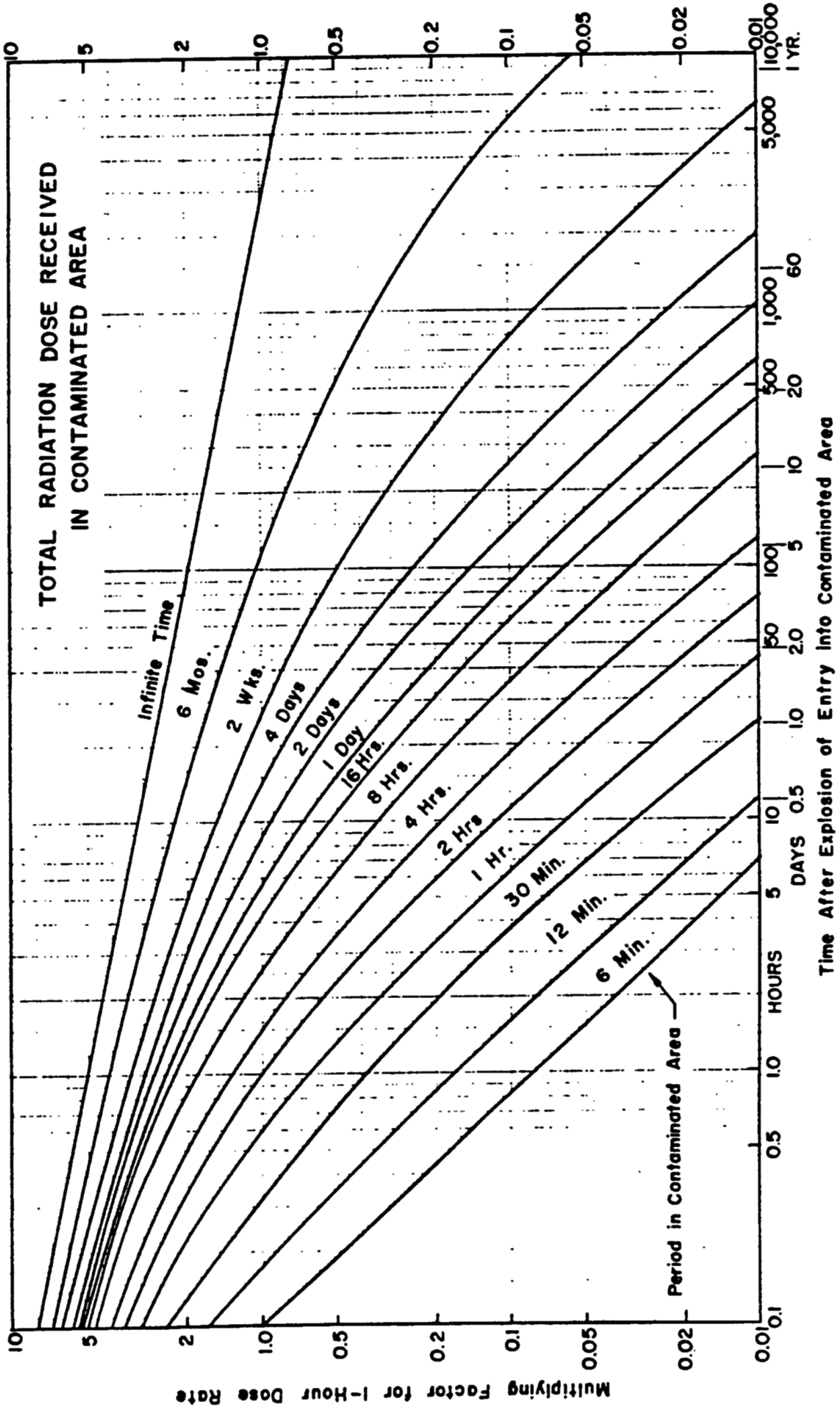
TOTAL RADIATION DOSE RECEIVED
IN CONTAMINATED AREA
Infinite Time
6 Mos.
2 Wks.
4 Days
2 Days
1 Day
16 Hrs.
8 Hrs.
4 Hrs.
2 Hrs
1 Hr.
30 Min.
12 Min.
6 Min.
Period in Contaminated Area
Multiplying Factor for 1-Hour Dose Rate
Time After Explosion of Entry Into Contaminated Area
HOURS
DAYS
1 YR.
10
5
2
1.0
0.5
0.2
0.1
0.05
0.02
0.01
0.1
0.5
1.0
5
10
50
100
500
1,000
5,000
10,000
0.5
1.0
2.0
5
10
20
60

i. Neutron-Induced Activity.

(1) *Air burst.* The neutron-induced gamma activity will depend on soil type as well as weapon type and yield. It is therefore impractical to attempt to define a height of burst above which this effect ceases to be militarily significant.

(2) *Burst in the transition zone.* If a nuclear weapon is detonated at a height of burst above that at which fallout is expected to be a hazard, the radioactivity which is induced in the soil by neutrons can give rise to dose rates of military importance in the vicinity of ground zero. The type, intensity, and energy distribution of the residual activity produced will depend on which isotopes are produced and in what quantity. This, in turn, depends on the number and energy distribution of the incident neutrons and the chemical composition of the soil. Induced contamination contours are independent of wind, except for some wind redistribution of the surface contaminant, and can be expected to be roughly circular.

Four soils have been chosen to illustrate the extent of the hazard which may be expected from induced activity. These soils were selected so as to show wide variations in predicted dose rates; the activity from most other soils should fall within the range of activities presented for these soils. The chemical composition of the selected soils is shown in table 4–2.

The elements which may be expected to contribute most of the induced activity are sodium, manganese and aluminum and small changes in the quantities of these materials can change the activity markedly; however, other elements which capture neutrons can also influence the magnitude of the activity. The elements are listed in table 4–2 in the order of probable importance so far as induced activity is concerned.

Figures 4–28A and 4–28B indicate the manner in which the induced activity is expected to vary with slant range and weapon type. $H+1$ hour dose rates for the four soils may be obtained by multiplying the dose rate obtained from figure 4–28A or 4–28B by the multiplying factor for that soil shown on the facing page of these figures.

In order to calculate the dose rates at times other than one hour after the detonation, decay factors may be taken from figure 4–29 which represents the decay characteristics of the four soils. The decay factors are constants which are multiplied by the value of the dose rate at one hour to give the rate at any other time.

Figures 4–30 through 4–33 are presented to facilitate computation of total dose. Multiplying factors may be obtained from these figures which, when applied to the one hour dose rate for the particular soil, will give the dose accumulated over any of several periods of time for various times of entry into the contaminated area.

When applying the data presented in this section to soils other than the four chosen for illustrative purposes, the activity should be estimated by using the data for the illustrative soil which most closely resembles the soil in question in chemical composition. If none of the illustrative soils resembles the soil in question very closely, the following remarks should be kept in mind. For times less than $H+1/2$ hour aluminum is the most important contributor. For times between $H+1/2$ hour and $H+5$ hours, manganese is generally the most important element. In the absence of manganese, the sodium content will probably govern the activity for this period. Between $H+5$ hours and $H+10$ hours, sodium and manganese content are both important. After $H+10$ hours, sodium will generally be the only large contributor. In the absence of sodium, manganese and aluminum, the activity will probably be low, and will generally be governed by the silicon content. Soil type IV is an example of this latter type.

Table 4–2. Chemical Composition of Illustrative Soils

Element	Percentage (by weight)			
	Soil type I (Liberia, Africa)	Soil type II (Nevada desert)	Soil type III (lava clay, Hawaii)	Soil type IV (beach sand, Pensacola, Fla.)
Sodium	----------	1. 30	0. 16	0. 001
Manganese	0. 008	0. 04	2. 94	----------
Aluminum	7. 89	6. 90	18. 79	0. 006
Iron	3. 75	2. 20	10. 64	0. 005
Silicon	33. 10	32. 00	10. 23	46. 65
Titanium	0. 39	0. 27	1. 26	0. 004
Calcium	0. 08	2. 40	0. 45	----------
Potassium	----------	2. 70	0. 88	----------
Hydrogen	0. 39	0. 70	0. 94	0. 001
Boron	----------	----------	----------	0. 001
Nitrogen	0. 065	----------	0. 26	----------
Sulfur	0. 07	0. 03	0. 26	----------
Magnesium	0. 05	0. 60	0. 34	----------
Chromium	----------	----------	0. 04	----------
Phosphorus	0. 008	0. 04	0. 13	----------
Carbon	3. 87	----------	9. 36	----------
Oxygen	50. 33	50. 82	43. 32	53. 332

Thus, it may be possible to obtain better data for a given soil by using data from a different illustrative soil at each of several times of interest.

If a weapon is burst at such a height as to be in the transition zone from the fallout standpoint, the neutron-induced activity generally can be neglected if the burst height is in the lower three quarters of the fallout transition zone. For weapons burst in the upper quarter of the fallout transition zone the neutron-induced activity may not be negligible compared to fallout. For the cases where fallout dose rate contour parameters, as determined from figures 4–14 through 4–18, are much smaller than those for a burst on the surface, an idea of the magnitude of induced activity may be obtained from figures 4–28 through 4–33. The overall contour values may then be obtained by combining the induced activity and fallout activity. For these cases it must be remembered that fission products and induced activity will decay at different rates. This necessitates a determination of the magnitude of each type of activity for each time of interest.

(3) *Surface and subsurface bursts.* For surface and subsurface bursts, the residual radioactive contamination from fission products is vastly greater than the neutron-induced activity. As a result, neutron-induced activity generally can be neglected for surface and subsurface bursts.

j. Residual Beta Radiation. The discussion of residual radiation has thus far considered only gamma radiation. In general, the hazard due to residual gamma radiation exceeds the beta hazard for all cases except those in which intimate contact with beta-active materials occurs, as in the case of a soldier lying prone in a contaminated area, or for particles falling out directly upon the skin or scalp. For such cases, superficial burns may result, the effect of which is discussed in paragraph 6.3*b*(3).

k. Shielding. The dose rates obtained from the contours described, and the total doses derived therefrom, are free field values which must be reduced if the individual concerned is protected by some degree of shelter. Shielding factors can be estimated from the shielding information given in paragraph 6.5. For example, personnel in the open in a built-up city area would receive 0.7 of the free field dose, while

NEUTRON-INDUCED GAMMA ACTIVITY

Given the weapon type and the slant range from the point of burst to the point of interest, the induced gamma dose rates in the vicinity of ground zero at $H+1$ hour can be estimated using figures 4-28A and 4-28B for bursts over soils similar in composition to any of the soils illustrated in table 4-2. To estimate the dose rate, enter the slant range axis with the slant distance in yards, read the dose rate for the appropriate weapon type, and multiply this dose rate by the appropriate factor for the soil type of interest from the following:

Soil type	*Multiplying factor*
I	0.11
II	1.0
III	12.0
IV	0.0026

Scaling. For yields other than 1 KT multiply the dose rate read from the curve by the yield in KT.

Example.

Given: An average neutron flux 50 KT weapon is burst at a height of 900 feet above soil of type III.

Find: The $H+1$ hour dose rate at ground zero and at 600 yards from ground zero.

Solution: From the average neutron flux weapon curve of figure 4-28A the dose rate at $H+1$ hour at ground zero (300 yd. slant range) is 9 r/hr per KT of weapon yield. The multiplying factor for soil type III is 12. Therefore, the dose rate at ground zero one hour after detonation of a 50 KT weapon over soil type III is:

$$50 \times 12 \times 9 = 5{,}400 \text{ r/hr.} \quad \textit{Answer.}$$

At 600 yards from ground zero the slant range is 670 yards. From the curve, the induced gamma intensity is 0.35 r/hr per KT of weapon yield at this distance. Therefore, the dose rate 600 yards from ground zero one hour after detonation of a 50 KT weapon over soil type III is:

$$50 \times 12 \times 0.35 = 210 \text{ r/hr.} \quad \textit{Answer.}$$

Reliability. Dose rate values taken from the curves for the soils presented are correct to within a factor of 5 for the conditions indicated. For other soils, the data will merely furnish an estimate of the magnitude of the hazard.

Related material.

See paragraph 4.3*i*.

See also figures 4-29 through 4-33.

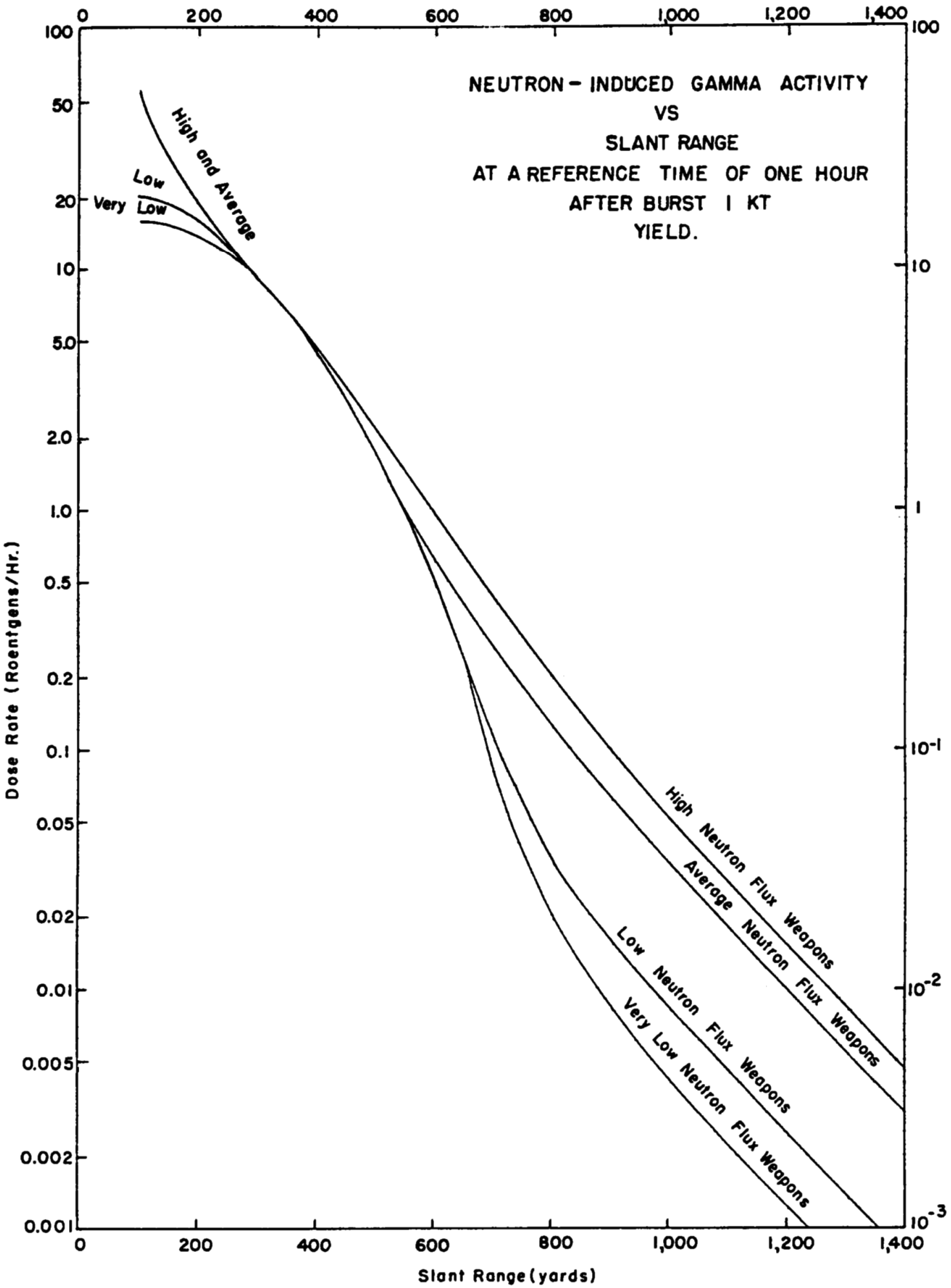
NEUTRON - INDUCED GAMMA ACTIVITY
VS
SLANT RANGE
AT A REFERENCE TIME OF ONE HOUR
AFTER BURST 1 KT
YIELD.
High and Average
Low
Very Low
High Neutron Flux Weapons
Average Neutron Flux Weapons
Low Neutron Flux Weapons
Very Low Neutron Flux Weapons
Dose Rate (Roentgens/Hr.)
Slant Range (yards)
0
200
400
600
800
1,000
1,200
1,400
100
50
20
10
5.0
2.0
1.0
0.5
0.2
0.1
0.05
0.02
0.01
0.005
0.002
0.001
1
10^{-1}
10^{-2}
10^{-3}

FIGURE 4-28B

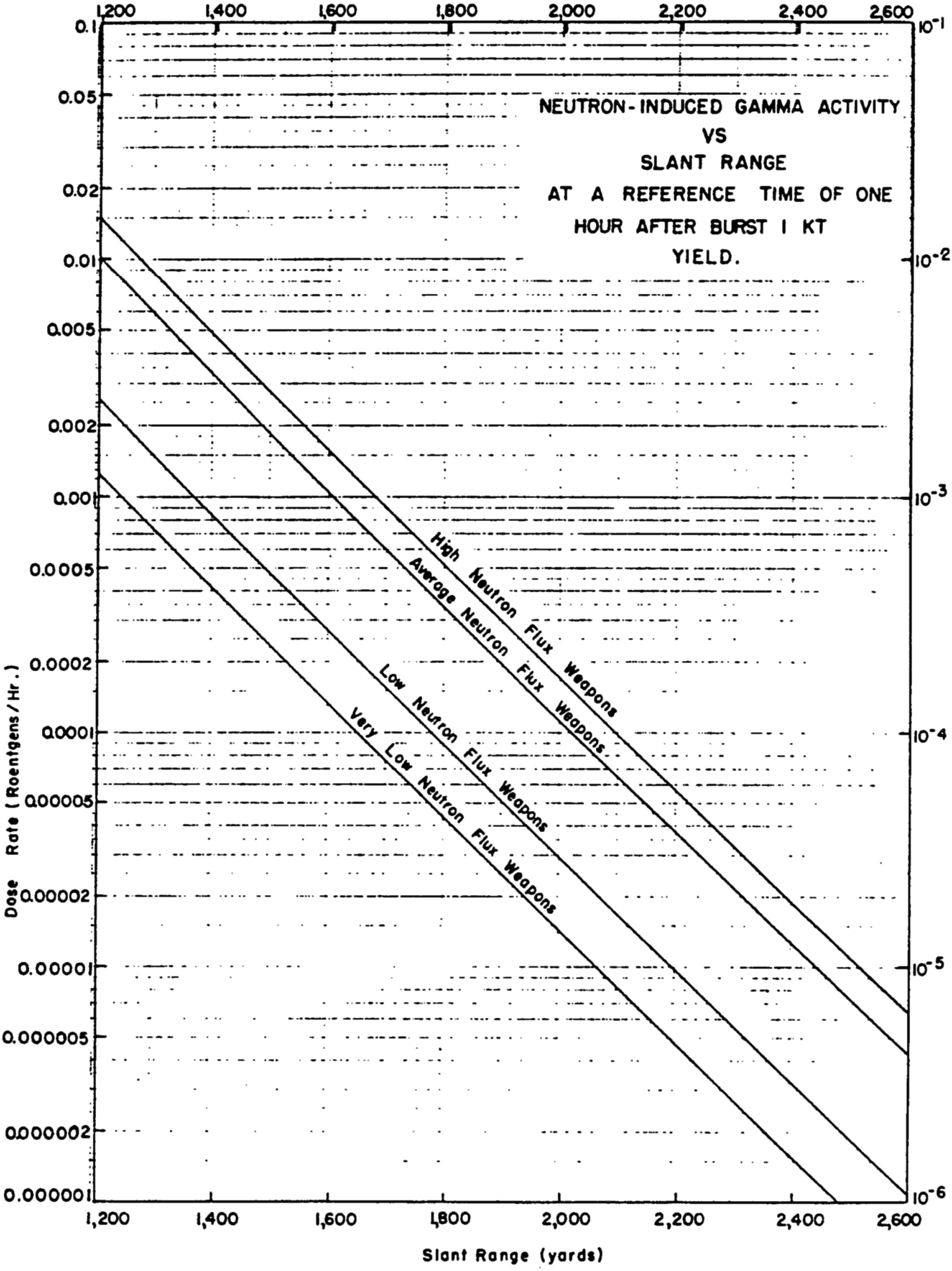
NEUTRON-INDUCED GAMMA ACTIVITY
VS
SLANT RANGE
AT A REFERENCE TIME OF ONE
HOUR AFTER BURST 1 KT
YIELD.
High Neutron Flux Weapons
Average Neutron Flux Weapons
Low Neutron Flux Weapons
Very Low Neutron Flux Weapons
Dose Rate (Roentgens/Hr.)
Slant Range (yards)
1,200
1,400
1,600
1,800
2,000
2,200
2,400
2,600
0.1
0.05
0.02
0.01
0.005
0.002
0.001
0.0005
0.0002
0.0001
0.00005
0.00002
0.00001
0.000005
0.000002
0.000001
10^{-1}
10^{-2}
10^{-3}
10^{-4}
10^{-5}
10^{-6}

FIGURE 4-29

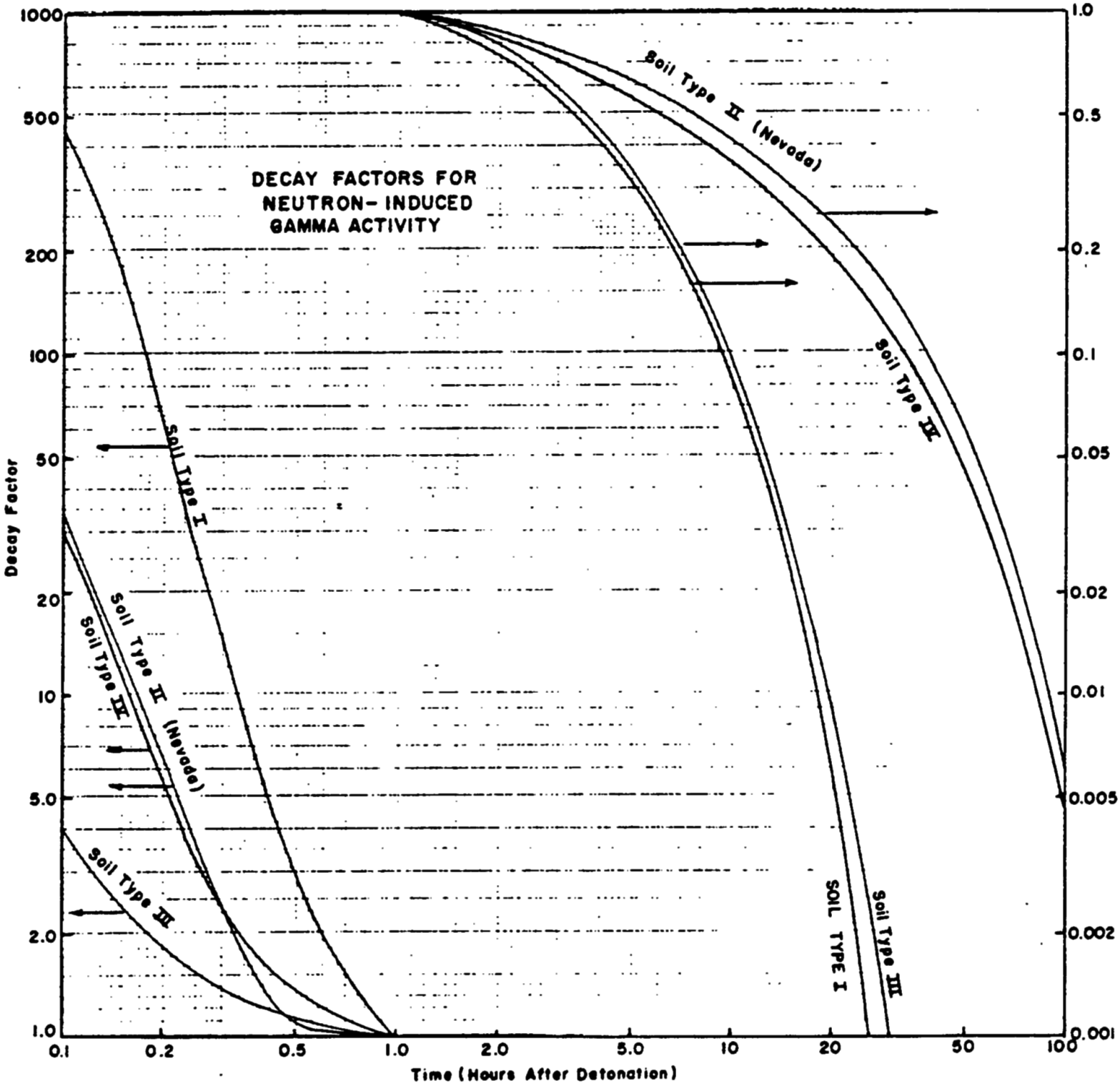
DECAY FACTORS FOR
NEUTRON-INDUCED
GAMMA ACTIVITY
Soil Type II (Nevada)
Soil Type IV
Soil Type I
Soil Type II (Nevada)
Soil Type IV
Soil Type III
SOIL TYPE I
Soil Type III
Decay Factor
Time (Hours After Detonation)
1000
500
200
100
50
20
10
5.0
2.0
1.0
1.0
0.5
0.2
0.1
0.05
0.02
0.01
0.005
0.002
0.001
0.1
0.2
0.5
1.0
2.0
5.0
10
20
50
100

FIGURE 4-37

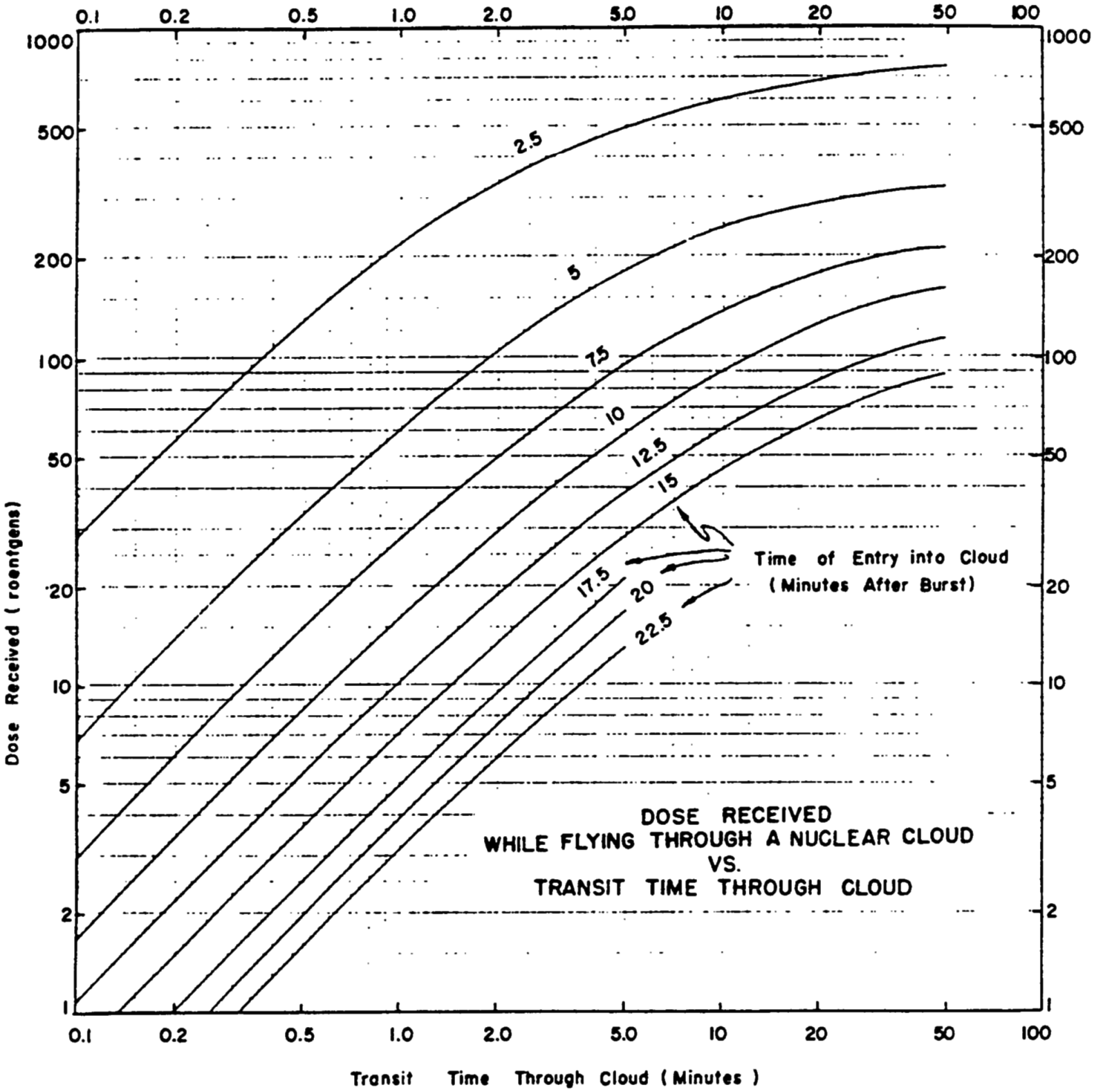
0.1
0.2
0.5
1.0
2.0
5.0
10
20
50
100
1000
500
200
100
50
20
10
5
2
1
2.5
5
7.5
10
12.5
15
17.5
20
22.5
Time of Entry into Cloud
(Minutes After Burst)
DOSE RECEIVED
WHILE FLYING THROUGH A NUCLEAR CLOUD
VS.
TRANSIT TIME THROUGH CLOUD
Dose Received (roentgens)
Transit Time Through Cloud (Minutes)

PHENOMENA AT VARIOUS SCALED BURST HEIGHTS

Figures 5–2A, B, and C show the range from ground zero of various physical phenomena when a burst is on the surface, at a scaled height of 250 $W^{1/3}$ feet, and at a scaled height of 650 $W^{1/3}$ feet, respectively. They are presented primarily for rapid visual comparison of the distance to which the various physical phenomena will extend, and secondarily for a rapid determination of the controlling mechanism of damage at any distance for any yield. From data presented in part one, a similar illustration could be prepared for any scaled or actual burst height.

The significance of the various phenomena curves presented varies with the target being considered. The initial and residual radiation curves are the most significant ones for human targets in the open or in shelters. The values chosen for plotting represent the following:

5 *r*—No obvious effect on personnel.

100 *r*—Non-lethal dose causing sickness in a few personnel, but permitting a unit to remain operationally effective.

450 *r*—Dose lethal within 30 days to 50 percent of personnel exposed.

10,000 *r*—Free field dose which will produce a dose of 100 *r* for personnel within a shelter having a dose transmission factor of 0.01.

The blast and thermal radiation curves cannot be related directly to damage, because of the increasing duration of blast and thermal phenomena with increasing yield and the dependence of the degree of damage sustained on the duration of the damage-producing effect. To assist in relating the curves presented to expected damage, the following table shows the variation with yield of the magnitude of weapon phenomena required to cause various degrees of damage to certain selected targets. (Refer to secs. VI through XII for a more detailed presentation of damage criteria.)

	1 KT	*100 KT*	*10 MT*
Thermal effects:		(*cal/cm²*)	
Second degree bare skin burn	4	5.1	9.1
Newspaper ignition	2.9	5.1	9.1
White pine charring	10	18	32
Thermal effects—Continued	*1 KT*	*100 KT*	*10 MT*
		(*cal/cm²*)	
Army khaki summer uniform destruction	18	31	56
Navy white uniform destruction	34	60	109
Blast effects (in the Mach region):			
Severe damage to overpressure sensitive structures:		(*PSI overpressure*)	
Blast-resistant designed buildings	50	40	35
Reinforced concrete buildings	10.5	9.5	9
Monumental wall bearing buildings	20	15	15
Wood frame housing	3	3	3
Window pane breakage	0.5	0.5	0.5
Severe damage to dynamic pressure sensitive structures:		(*PSI dynamic pressure*)	
Light steel frame single story buildings	4.5	2	0.9
Heavy steel frame single story buildings	6	3	1.5
Steel frame multistory buildings	7.5	2.5	0.9
150′–250′ span truss bridges	50	8	5.5

Some curves are extrapolated beyond data presented in part one, since it is felt that the relationships between phenomena as shown will hold in those regions where there is little supporting knowledge, even though the actual values may be questionable. Since thermal curves are extended beyond one-half the visibility, their interpretation in that region must be approached with caution. In figures B and C, the relative air density would decrease as the actual height of burst is increased in a real case. However, it is held constant for illustrative purposes here. The conversion from slant range to ground range, plus the variation in enhancement of gamma radiation, causes the change in the shape of the radiation curves with change of burst height. Fallout contours are elliptical; only the downwind extent is shown.

Reliability. Varies with the phenomenon of interest. See part one.

Related material.

See paragraph 5.5.

FIGURE 5-2

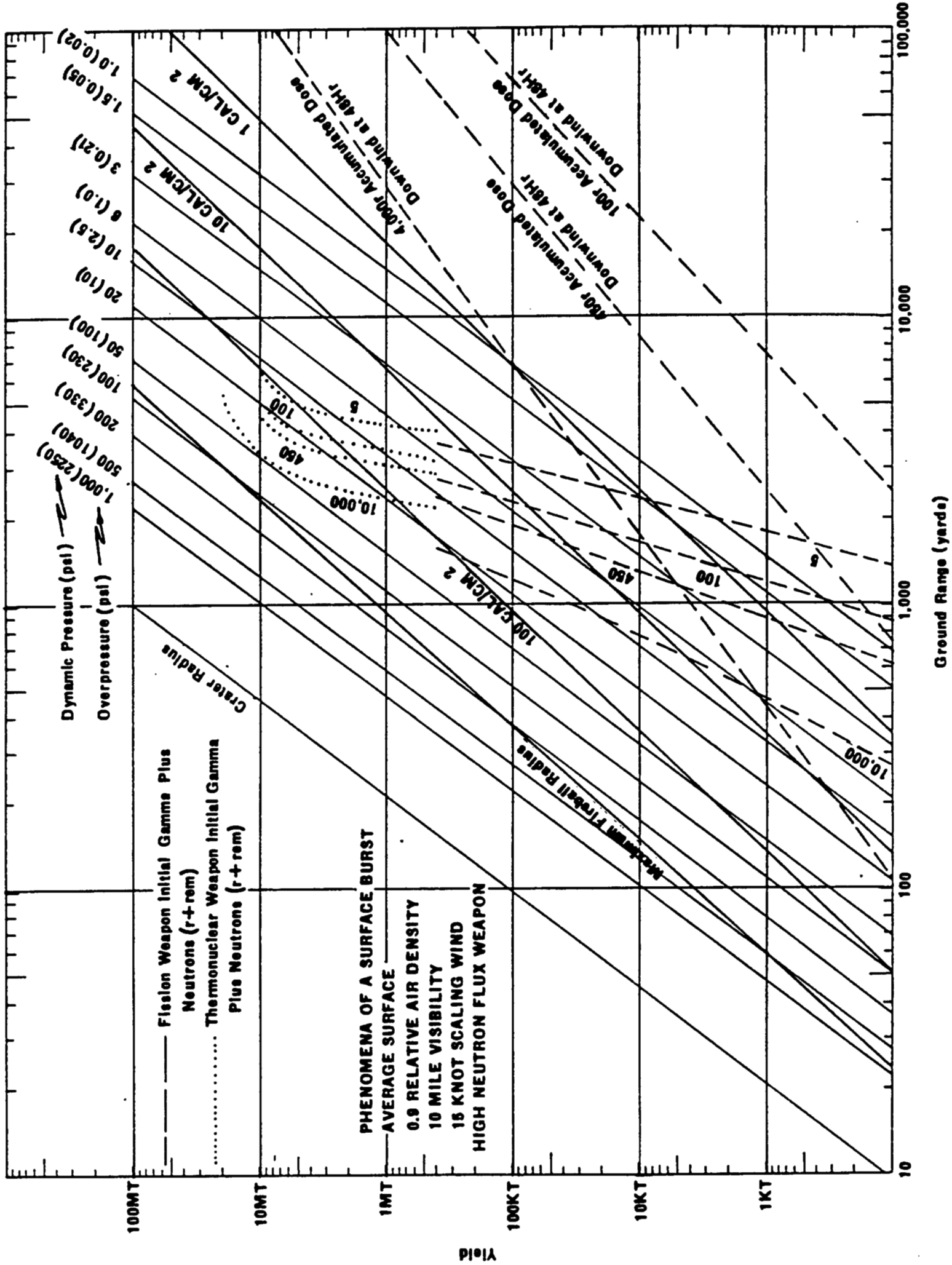
Yield
100MT
10MT
1MT
100KT
10KT
1KT
Ground Range (yards)
10
100
1,000
10,000
100,000
Dynamic Pressure (psi)
Overpressure (psi)
1,000(2250)
500(1040)
200(330)
100(230)
50(100)
20(10)
10(2.5)
6(1.0)
3(0.21)
1.5(0.05)
1.0(0.02)
Crater Radius
Fission Weapon Initial Gamma Plus Neutrons (r+rem)
Thermonuclear Weapon Initial Gamma Plus Neutrons (r+rem)
PHENOMENA OF A SURFACE BURST
AVERAGE SURFACE
0.9 RELATIVE AIR DENSITY
10 MILE VISIBILITY
15 KNOT SCALING WIND
HIGH NEUTRON FLUX WEAPON
Maximum Fireball Radius
100 CAL/CM 2
10 CAL/CM 2
1 CAL/CM 2
10,000
460
100
6
4,000r Accumulated Dose Downwind at 48HR
400r Accumulated Dose Downwind at 48HR
100r Accumulated Dose Downwind at 48HR

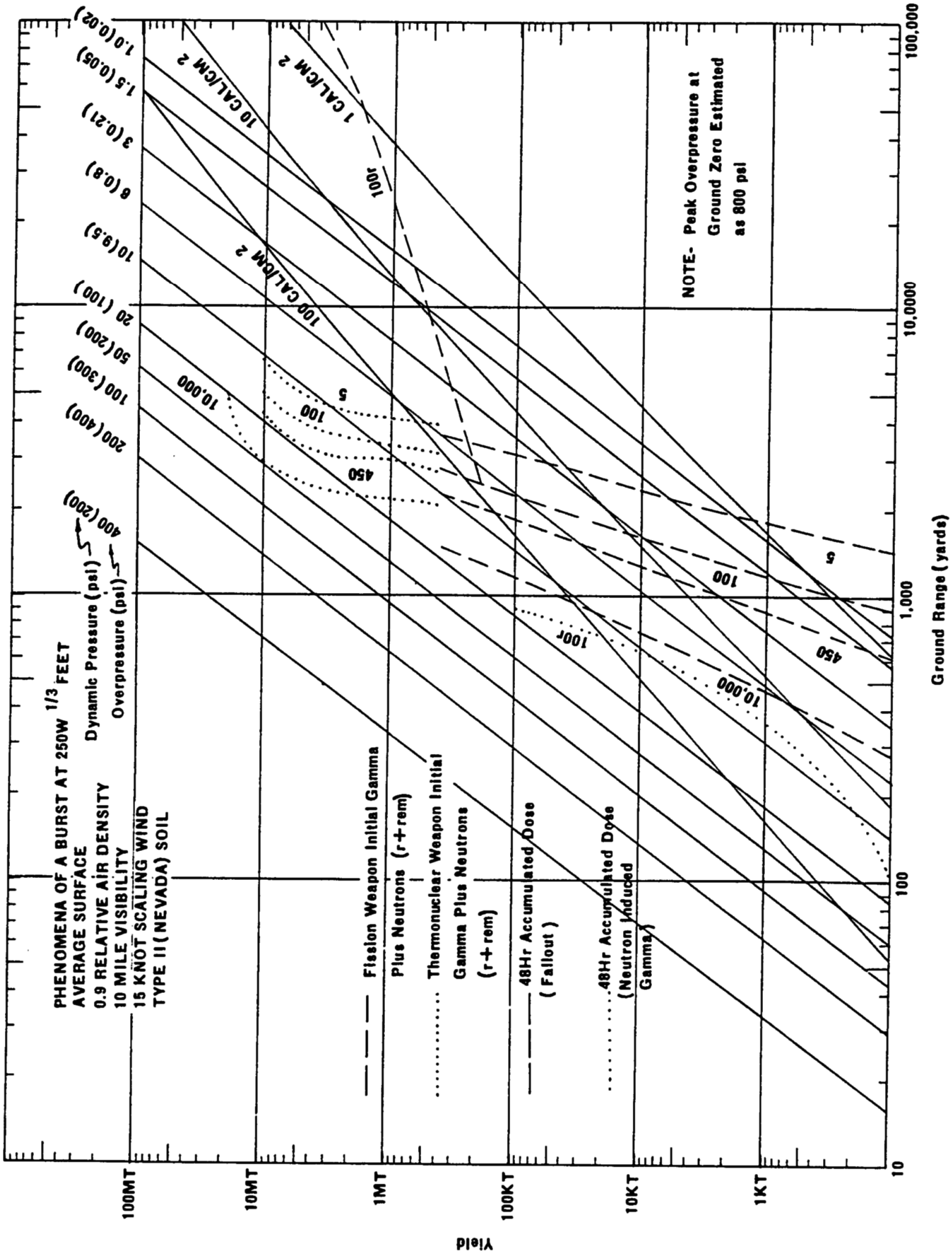
PHENOMENA OF A BURST AT 250W 1/3 FEET
AVERAGE SURFACE
0.9 RELATIVE AIR DENSITY
10 MILE VISIBILITY
15 KNOT SCALING WIND
TYPE II (NEVADA) SOIL
Dynamic Pressure (psi)
Overpressure (psi)
1.0 (0.02)
1.5 (0.05)
3 (0.21)
6 (0.8)
10 (9.5)
20 (100)
50 (200)
100 (300)
200 (400)
400 (200)
10 CAL/CM 2
1 CAL/CM 2
100 CAL/CM 2
100r
5
100
450
10,000
NOTE- Peak Overpressure at Ground Zero Estimated as 800 psi
Fission Weapon Initial Gamma Plus Neutrons (r+rem)
Thermonuclear Weapon Initial Gamma Plus Neutrons (r+rem)
48Hr Accumulated Dose (Fallout)
48Hr Accumulated Dose (Neutron Induced Gamma)
100MT
10MT
1MT
100KT
10KT
1KT
Yield
10
100
1,000
10,0000
100,000
Ground Range (yards)

FIGURE 5-2C

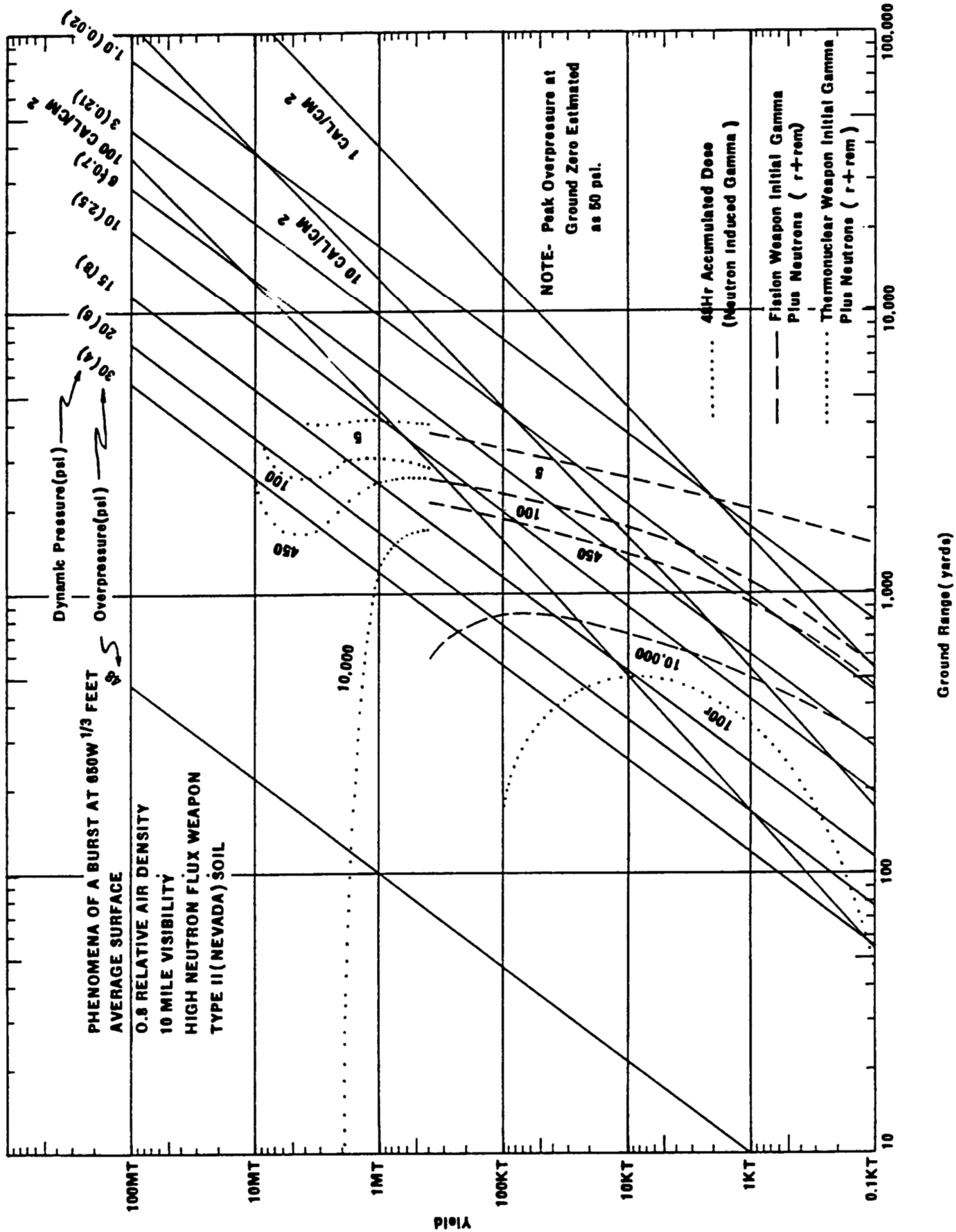

447555 O - 58 - 18

SECTION VI
PERSONNEL CASUALTIES

6.1 Air Blast and Mechanical Injury

a. General. The air blast from a nuclear detonation may cause casualties among human beings in two ways—direct blast injury and indirect blast injury.

b. Direct Blast Injury.

(1) *Crushing forces.* Although the human body is relatively resistant to the crushing forces which result from air blast loading, large pressure differences resulting from blast wave overpressures may cause damage to lungs, abdominal organs and other gas-filled body organs. Based on data obtained from high explosive detonations, it is estimated that on the order of 200 to 300 psi peak overpressure is required to cause death in humans, provided no translational motion occurs. However, the long duration of the overpressure from a nuclear explosion may appreciably lower this peak overpressure criterion. In any event, no crushing injury other than ear drum rupture occurs for a peak overpressure of less than 35 psi. Although ear drum rupture may result from peak overpressures of 7 to 15 psi, this is not considered a disabling injury, and the overall effectiveness of a unit will not be hampered by the occurrence of these injuries. Therefore, since other damage producing effects are overriding at pressures above 35 psi, crushing forces as such need not be considered as a primary mechanism of producing casualties to personnel in the field.

In structures of certain types, such as bomb shelters or permanent type gun emplacements, where adequate shielding exists against thermal and nuclear radiation, the design of the structure may permit the build-up of blast pressure due to multiple reflections. Blast injuries may therefore occur inside even though the free air overpressure outside the structure would not be sufficient to cause injury.

Both ear drum rupture and other bodily damage which may result from overpressure are largely dependent upon the characteristics of the shock front. If the rise time is long, the body organs are subjected to less severe pressure differences and also are able to better adapt themselves to high overpressure. Consequently, the probability of injury is reduced.

(2) *Translational Forces.*

(*a*) *Mechanisms.* The translational force to which an individual exposed to a blast wave is subjected depends primarily on drag forces. Since the human body is relatively small and the blast wave almost immediately envelops it, the diffraction process is short. The translational force may be predicted with reasonable accuracy if the burst position, yield, terrain, and the orientation of the human body are known. Since the translational force applied depends on the exposed frontal surface area of the human body, an individual standing in the open is subjected to much larger translational forces than an individual lying on the ground surface. Thus, assuming a prone position at the instant a nuclear bomb flash is detected is quite effective in reducing the likelihood of injuries resulting from bodily translation. In addition, the translational forces are appreciably reduced for an individual

who is behind a building or in a shelter which is sufficiently blast resistant. The degree of protection afforded by a foxhole against injury resulting from translation is not too well known at present. However, appreciable protection should be provided if the foxhole is deep enough to prevent lifting therefrom.

(*b*) *Criteria for injury.* Although no direct correlation is known between translational motion parameters and injury, it is reasonable to assume that some relationship exists. The initial rate of acceleration, the motions of various parts of the body while being translated, and the nature of the impact, all certainly contribute to injury. Probably most injuries will result from impact. The severity of injury will depend on the nature of the object or objects with which the translated body collides, the nature of the impact, whether glancing or solid, and the velocity at impact. Some individuals may survive a large translation, whereas others may be severely injured or killed by a relatively small translation. Because increased yield results in increased positive phase duration, attainment of velocities sufficient to cause injury on impact will occur for lower peak pressures. The manner of impact likewise depends on the nature of the terrain and surface configuration. If solid impact occurs, it is estimated that body velocities of about 12 feet per second will produce serious injury approximately 50 percent of the time, while collision at about 17 feet per second will result in approximately 50 percent mortality. Figure 6–1 is a plot of burst height vs. ground range at which 50 percent of standing and prone personnel in the open are expected to become direct blast casualties. The curves are drawn for 1 KT and may be scaled to other yields by multiplying the burst heights by the cube root of the yield and the ground distance by the four-tenths power of the yield.

c. *Indirect Blast Injury.*

(1) *General.* Indirect blast casualties result from burial by debris from collapsed structures with attendant production of fractures and crushing injuries, from missiles placed in motion by the blast wave, or from fire or asphyxiation where individuals are prevented from escaping the wreckage.

(2) *Personnel in structures.* A major cause of personnel casualties in cities is structural collapse and damage. The number of casualties in a given situation may be reasonably estimated if the structural damage is known. Table 6–1 shows estimates of casualty production in two types of buildings for several damage levels. Data from Section VII may be used to predict the ranges at which specified structural damage occurs. Demolition of a brick house is expected to result in approximately 25 percent mortality, with 20 percent serious injury and 10 percent light injury. On the order of 60 percent of the survivors must be extricated by rescue squads. Without rescue they may become fire or asphyxiation casualties, or in some cases be subjected to lethal doses of residual radiation. Reinforced concrete structures, though much more resistant to blast forces, produce almost 100 percent mortality on collapse. The figures of table 6–1 for brick homes are based on data from British World War II experience. It may be assumed that these predictions are reasonably reliable for those cases where the population is in a general state of expectancy of being subjected to bombing and that most personnel have selected the safest places in the buildings as a result of specific air raid warnings. For cases of no prewarning or preparation, the number of casualties is expected to be considerably higher. To make a good estimate of casualty production in structures other

than those listed in table 6–1, it is necessary to consider the type of structural damage that occurs and the characteristics of the resultant missiles. Glass breakage extends to considerably greater ranges than almost any other structural damage, and may be expected to produce large numbers of casualties at ranges where personnel are relatively safe from other effects, particularly for an unwarned population.

Table 6–1. Estimated Casualty Production in Structures for Various Degrees of Structural Damage

	Killed outright	Serious injury (hospitalization)	Light injury (No hospitalization)
1–2 story brick homes (high explosive data):	*Percent*	*Percent*	*Percent*
Severe damage	25	20	10
Moderate damage	<5	10	5
Light damage	------	<5	<5
Reinforced-concrete buildings (Japanese data, nuclear):			
Severe damage	100	------	------
Moderate damage	10	15	20
Light damage	<5	<5	15

Note. These percentages do not include the casualties which may result from fires, asphyxiation, and other causes from failure to extricate trapped personnel. The numbers represent the estimated percentage of casualties expected at the maximum range where the specified structural damage occurs. For the distances at which these degrees of damage occur for various yields, see section VII.

(3) *Personnel in vehicles.* Personnel in vehicles may be injured as a result of the response of the vehicle to blast forces. Padding where applicable and the use of safety belts, helmets, and harnesses virtually eliminates this source of casualties, at least within armored vehicles. In the absence of these protective devices, serious lacerations may result from impact with sharp projections within the vehicle interiors. Comparative numbers of casualties are almost impossible to assess in this respect due to the many variables which are involved.

(4) *Personnel in the open.* Missiles translated by the blast wave may be a significant source of injury to exposed personnel. Missiles having low velocities, if of sufficient size, may cause crushing injuries. In contrast, penetrating wounds may be caused by high velocity missiles. The missile density and characteristics are largely a function of the target. Where the target area is relatively clean and there is little material present subject to fragmentation and displacement, fewer injuries from missiles are expected in the open than from debris within structures at comparable distances. When the target complex presents many possible sources of missiles this may not be the case. Personnel in a prone position are less likely to be struck by flying missiles than those who remain standing. Those who succeed in getting into bunkers, foxholes, or in defilade probably will achieve almost complete protection from the flying missile hazard.

6.2 Thermal Injury

a. Introduction. Before attempting to predict the number of thermal casualties which occur in a given situation, it is necessary to recognize the factors which influence the number and distribution of casualties to be expected. These factors include—the distribution or deployment of personnel within the target area, whether proceeding along a road, in foxholes, standing or prone, in the open or under natural cover; orientation with respect to the bomb; clothing, including number of layers, color, weight, and whether the uniform includes helmets, gloves, or other devices which might protect the bare skin, such as flash creams; and natural shielding. These parameters which define the target must be considered along with the factors which define the source of radiation such as yield of the weapon, height of burst, and visibility, as discussed in section III. In many target complexes, a large percentage of thermal casualties may be due to secondary burns. This is particularly true in cities and industrial areas where a major part of the direct radiation may be shielded by intervening structures. Because of the number of factors involved, it is necessary to analyze each particular target situation in order to make realistic predictions of the thermal casualties to be expected.

b. Primary Radiant Energy Burns. Damage to bare skin through the production of burns may be directly related to the radiant exposure and the rate of delivery of the thermal radiation, both of which are yield dependent. For a given total exposure, as the weapon yield increases, the thermal radiation is delivered over a longer period of time and thus at a lower rate. This allows energy loss from the skin surface by conduction to the deeper layers of the skin and by convection to the air. Thus, a given level of damage also is yield dependent. Critical radiant exposures for the production of two degrees of burn on bare skin as a function of yield are presented in figure 6–2 for normal incidence of radiation. Although the data are presented as a single curve, it must be recognized that there will be variations due to factors such as skin color (i. e., darker skin requires a lesser exposure to produce a given severity of burn) and skin temperature (i. e., colder skin as is found in winter or in arctic climates requires a greater exposure to produce the given burn). The curves represent those radiant exposures which will burn 50 percent of any group, including these variants. A first degree burn is defined as one which shows redness; a second degree burn exhibits partial skin destruction or blistering.

c. Burns Under Clothing. Clothing reflects and absorbs much of the thermal radiation incident upon it and thereby protects the wearer against flashburn. In some cases, the protection is complete, but in many cases it is partial in that clothing merely reduces the severity of injury rather than preventing it. At large radiant exposures, there is the additional possibility that the glowing or ignition of the clothing could deliver additional energy to the skin, thereby causing a more severe injury than bare skin would have suffered. There are many factors which contribute to the degree of protection which clothing affords the underlying skin. The thermal resistance of the clothing material itself is probably the most important, as skin burns under undamaged cloth are rarely seen unless the cloth is in close contact with the skin. Other factors are the weight and weave of the fabric; the number of clothing layers worn; the spacing between layers and between the inner layer and the skin; the moisture content, initial temperature, and color of the cloth; the amount and kind of dirt in the cloth; the wind velocity and direction across the surface of the cloth; etc.

The complexity of the interrelations among the above factors makes an accurate prediction extremely difficult. Table 6–2 lists various estimates of radiant exposures required to effect burns under clothing. These values are considered representative of some field conditions, within the limitations due to the varying factors described above.

Table 6–2. Critical Radiant Exposures for Burns Under Clothing

(Expressed in cal/cm² incident on outer surface of cloth)

Clothing	Burn	1 KT	100 KT	10 MT
Summer Uniform	1°	8	11	14
(2 layers)	2°	20	25	35
Winter Uniform	1°	60	80	100
(4 layers)	2°	70	90	120

Note. These values are sensitively dependent upon many variables which are not easily defined (see text), and are probably correct within a factor of two.

d. The Combat Ineffective. A useful term in the discussion of effects of thermal radiation on personnel is "the combat ineffective." A combat ineffective is defined as a person who, because of his injuries, is no longer capable of carrying out his assigned tasks. This is differentiated from the more common term "casualty," which is defined as an individual whose injuries require medical attention. Damage to certain areas of the body produces a greater number of combat ineffectives than damage to other areas. Burns in the area surrounding the eyes which eventually cause the eyes to swell shut, and burns to the hands which lead to loss of mobility are particularly apt to cause ineffectiveness.

If a sufficient portion of the total body area is burned, physiological shock follows and the individual becomes a casualty. When more than 10 to 15 percent of the total body area receives second degree burns or worse, shock may be expected. The efficacy of injuries to the hands and eyes in producing combat ineffectives, coupled with the vulnerability of these parts due to lack of protection under ordinary circumstances, indicates the importance of providing protection for these areas when nuclear attack is likely. Table 6–3 presents estimates of the production of combat ineffectives by various degrees of thermal injury.

Table 6–3. Combat Ineffectives Due to Thermal Injury

	1° burns	2° burns
Both eyes	Combat effective*	Combat ineffective.
Both hands	Combat effective	Combat ineffective.
15% burns excluding hands and eyes.	Combat effective	A few ineffectives (10–15%).
25% burns excluding hands and eyes.	Combat effective	Up to 50% ineffective.

*Some lowering of effectiveness may be expected; however, all should be able to perform combat duties.

e. Thermal Shielding.

(1) *General.* In addition to the protection provided to troops by clothing as discussed above, other possible sources of protection should be considered. Almost any nontransparent material withstands the thermal radiation long enough to afford some shielding to an object behind it. Heavy smoke screens are excellent energy absorbers as described in section III.

Because of the ease of complete shielding from thermal radiation, the amount of forewarning, if any, is of utmost importance to exposed personnel. Covered foxholes or bunkers are excellent thermal shields. The degree to which uncovered foxholes afford protection is related to the height of burst and the distance from ground zero as well as the position of the man within the foxhole. The nearer foxholes offer less protection, since the shadowed portion is a smaller fraction of the total volume. At greater distances from low yield weapons, burns are produced only on those areas subjected to the direct radiation, since reflection from the exposed surfaces of the foxholes may be neglected. Under high megaton burst conditions, a sufficient amount of thermal radiation may be reflected and produce casualties. In highly scattering atmospheres, such as fog or haze, scatter of the radiation into the foxholes could become an important factor. It is important to note than many targets contain openings such as windows in buildings and aircraft, and ports in tanks and ships. While the general target may not be damaged by external thermal radiation, openings in these targets may allow damaging amounts of thermal radiation to fall on personnel inside.

(2) *Evasive action.* Figure 6–3 demonstrates that evasive action against thermal radiation following the detonation of weapons up to 100 KT is not expected to be successful due to the rapid delivery of the thermal pulse. For weapons in the megaton range, the thermal pulse is delivered over a period of seconds. Significant portions of this pulse may be avoided by simple evasive action such as covering exposed hands and face, or dropping to the ground.

f. Specific Effects on the Eye. Effects of thermal radiation on the eye may be divided into two categories—flash blindness, which is a transitory loss of vision; and retinal burns, which constitute permanent injuries to the retina of the eye. In general, under daylight conditions, flash blindness is not an important factor in estimating effects on personnel. If the flash occurs during daylight in the forward field of vision, impairment to precise vision does not persist for more than 2 or 3 minutes. If not in the forward field of vision, no impairment is expected. During darkness, impairment of vision persists for 5 to 10 minutes if the detonation is in the forward field of view, and for 1 to 2 minutes if not. Loss of dark adaptation persists for longer periods. When the fireball is in the forward field of vision and in clear atmospheres, retinal burns and some degree of permanent loss of visual acuity may occur at relatively great distances from the detonation. Retinal burns have occurred in a few individuals located at distances of 2 to 10 miles from the point of detonation and are theoretically possible at distances where the other immediate effects of the weapon are minimal. This loss of vision is more severe if the eye is focused directly on the point of detonation. As

with flash blindness, this effect is likely to be more severe in situations where the eye is dark-adapted.

g. Secondary Flame Burns and Conflagration Effects may be a source of casualties. Secondary flame burns of the hands and face may occur from ignition of clothing. In areas where conflagrations are likely to result from the detonation, large numbers of burn casualties may occur among individuals trapped in the wreckage of burning buildings or structures, or in forest fires. Under circumstances where conflagrations can occur, individuals in shelters may die of asphyxiation, even though otherwise protected from the other casualty producing effects of the nuclear detonation. After a firestorm or a large scale conflagration begins, it is virtually impossible for an individual to leave the shelter and reach safety through the streets of a burning city.

6.3 Nuclear Radiation Injury

a. General. The radiation effects of a nuclear explosion may be divided into two categories; external radiation (from gamma rays, beta particles, and neutrons) and internal radiation (from gamma rays, alpha and beta particles). The end result in cells receiving doses of these nuclear radiations is qualitatively the same. The effects may be acute or delayed. *Only acute effects will be considered here.* Delayed effects, while important, may not be manifest for years and thus will not affect the immediate military situation.

The essential criterion for injury from ionizing radiation is delivery of the radiation to sensitive body tissues. Thus, external beta radiation affects only the skin, while the penetrating gamma rays and neutrons affect critical tissues within the body. With penetrating radiation from external sources the relationship of the free field dosage to biological effect varies according to the amount of shielding interposed between the source and the critical tissues. In fact, the body itself may shield internal organs from external radiation of low energy or from a single direction.

Radiation can be received in a short time or over an extended period. When received in a short time (i. e., in a few days) the effect is essentially independent of dose rate except for extremely large doses of radiation. (See par. 6.3*d* on immediate incapacitation.) When received over a long period of time, either continuously or in repeated doses, biological recovery takes place. This recovery may not be complete, however. It is not possible to specify for the whole body a definite biological recovery rate or a percentage of irreparable damage, since different tissues have different repair rates and different sensitivities to radiation. As an example, the tissue producing one type of white blood cell may repair at the rate of from 2 to 10 percent per day and incur permanent damage of from 10 to 20 percent of the total injury. The skin on the other hand, unless damaged throughout its thickness, may recover functionally 100 percent. Since in the mid-lethal range the state of the blood forming tissues is directly related to survival, it is perhaps reasonable to consider these tissues as representing the whole body response. This is the reason that studies to measure recovery rates and irreparable damage using LD50/30 (the dose lethal to 50 percent of the test population by the end of a 30-day period) as an end point seem to fit an exponential-type function. What is really being measured is a single critical tissue.

b. External Radiation Hazard. The only external radiations of any consequence are gamma rays and neutrons, and under special circumstances, beta particles. During a nuclear explosion the gamma rays and neutrons alone are important, while in a residual fallout field gamma rays and sometimes beta particles must be considered.

(1) *Gamma radiation* received at the time of detonation is biologically instantaneous. It is from an essentially point source, so is less effective than a corresponding free field dose received from an infinite plane source, such as a residual radiation field. The difference may be expressed thus—in humans an acute free field dose of about 600 roentgens from a point source may be equivalent to about 400 roentgens acute free field dose from a bilateral or an extended source. This dose is currently thought to be the amount required to cause about 50 percent of exposed personnel to die within a month. The best estimates of the effects of various dose ranges in humans are presented in table 6–4.

Table 6–4. Probable Effects of Acute Whole Body Radiation Doses

Acute dose (roentgens)*	Probable effect
0 to 50	No obvious effect except possibly minor blood changes.
80 to 120	Vomiting and nausea for about 1 day in 5 to 10 percent of exposed personnel. Fatigue but no serious disability.
130 to 170	Vomiting and nausea for about 1 day, followed by other symptoms of radiation sickness in about 25 percent of personnel. No deaths anticipated.
180 to 220	Vomiting and nausea for about 1 day, followed by other symptoms of radiation sickness in about 50 percent of personnel. No deaths anticipated.
270 to 330	Vomiting and nausea in nearly all personnel on first day, followed by other symptoms of radiation sickness. About 20 percent deaths within 2 to 6 weeks after exposure; survivors convalescent for about 3 months.
400 to 500	Vomiting and nausea in all personnel on first day, followed by other symptoms of radiation sickness. About 50 percent deaths within 1 month; survivors convalescent for about 6 months.
550 to 750	Vomiting and nausea in all personnel within 4 hours from exposure, followed by other symptoms of radiation sickness. Up to 100 percent deaths; few survivors convalescent for about 6 months.
1,000	Vomiting and nausea in all personnel within 1 to 2 hours. Probably no survivors.
5,000	Incapacitation almost immediately. All personnel will be fatalities within 1 week.

*(1) And/or rem in the case of neutrons. See discussion in paragraph 6.3b(2).
*(2) Continuing investigations indicate that these ranges may be low for corresponding effects by a factor of 2.

(2) *Neutrons*, like the gamma rays, are delivered essentially instantaneously at the time of a nuclear explosion. There is some evidence that in animals the size of a man, neutrons are less effective than hitherto supposed because of rapid attenuation in superficial tissues. The following discussion will depend on an understanding of certain units and terms used in the evaluation of biologically hazardous doses of radiation.

The roentgen equivalent physical (rep) is defined as that dose, of any ionizing radiation, which will produce in a unit volume of the irradiated substance, the same energy absorption which would be produced in the same substance by a roentgen of gamma or X-rays. Inasmuch as different radiations, even though producing the same energy absorption per unit volume, have different effectiveness in producing biological injury, the relative biological effectiveness (RBE) of these various radiations must be taken into account. If, for example, it is found that a rep of neutrons causes 30 percent more damage than a rep of gamma rays, it is said that such neutrons have an RBE of 1.3. X-rays produced at 250 KVP (kilo-volt peak) are assigned an RBE of 1.0, and the hazard of the other radiations is measured in terms relative to the effectiveness of X-rays for producing injury. One can then multiply the reps of any other ionizing radiation by the appropriate RBE to get another unit of dose which is directly proportional to the biological damage, i. e., the roentgen equivalent mammal (rem)—

$$(rep) \times (RBE) = (rem).$$

Rem, correctly measured for each type of ionizing radiation, may be added to obtain the total dose. See paragraph 5.4.

Physical dosimetry of neutrons, however, is difficult. The most consistent indicator which responds to the largest biologically important portion of the bomb neutron spectrum is reduction in weight of the spleen and thymus of mice. This measure serves as a basis for comparing gamma rays and neutrons in a biological system in terms of rem. This rem unit applies strictly to this effect, and it may well be that acute effects in man are not predictable on the basis of presently available data.

The curves of neutron dose given in part one, figures 4–10 and 4–11, give the dose directly in rem, an RBE of 1.3 for whole body neutron radiation

having been assumed in preparing the curves. Therefore, the neutron dose in rem determined from figure 4–10 or 4–11 may be added directly to the gamma dose in roentgens obtained from one of the figures 4–1 through 4–8, and the total dose so determined used in conjunction with table 6–4 to estimate the probable overall effects of the immediate nuclear radiations.

(3) *Beta particles.*

(*a*) *General.* Beta particles, as well as gamma rays, constitute an external hazard from residual contamination. In an extended field of fallout radiation the gamma hazard generally far outweighs that from beta particles. However, the beta hazard may become quite important in certain circumstances, such as—

A person receives fallout particles directly on the body, or lies on a contaminated surface.

Personnel are located in a relatively confined area which has been subjected to fallout, and surrounding structures provide shielding from much of the gamma radiation, as would be the case in a narrow city street.

Fallout particles are removed from the extended field into a new environment, but remain in close proximity to personnel.

(*b*) *Effect.* Beta particle penetration is quite limited and may be partially blocked by thin absorbers such as clothing. Due to the limited range of beta radiation, the skin is the only structure directly affected. Mammals may be killed by total surface beta radiation, however. The amount required for an LD50/45 is inversely proportional to the area/mass ratio (i. e., the amount of skin in relationship to the rest of the body). Small mammals are quite sensitive, there being a good correlation between species in this regard. On this basis man *might* require about 40,000 rep over his whole body surface before entering the mid-lethal range.

It should be pointed out, however, that the LD50 is a poor end point for evaluation of a skin damaging process, and that large area injuries would be highly incapacitating, though not necessarily lethal, within a short period of time. A total surface beta injury is an extremely unlikely possibility. The typical human beta injuries from residual contamination are multiple ones, on surfaces directly exposed to the material. These indicate that direct contact is usually necessary for this type of "beta burn".

(*c*) *Decontamination.* Where personnel have been exposed to direct contact with radioactive fallout particles, a few simple measures greatly reduce the probability of development of beta burns. Immediate showering, bathing, or simple removal by brushing off the particulate matter, accompanied by securing shelter and donning clothing of a protective nature (long-sleeved shirts, cover-alls, shoes, etc.) affords sufficient protection against the beta burn hazard. The longer the fallout remains in contact with the skin, the more severe and extensive the beta burn is likely to be.

c. *Internal Radiation Hazard.*

(1) *General.* The hazard associated with the intake of radioactive material into the body is present only in cases where fallout occurs. In such instances radioactive elements may be breathed into the lungs or may be swallowed and absorbed from food and water. The vast majority of the radioactive elements which are inhaled do not remain in the lung, because particles must be within a limited size range to be retained. Only a small fraction of the retained particles are likely to be concentrated and fixed in the lung. Swallowed and inhaled elements must be soluble to become absorbed. Once absorbed, these elements are handled in exactly the same manner as are the cor-

responding non-radioactive elements. Thus, they are eliminated from the body at various rates, with some being concentrated in certain locations for long periods of time. It is this prolonged retention of some radioactive fission products that characterizes the internal hazard.

(2) *Importance.* The significance of internal radiation in terms of *immediate* effects is negligible, since the external gamma hazard in the residual field of fallout contamination is the controlling factor in determining the danger to personnel. The same condition holds for the passage of aircraft through a radioactive cloud. Following the contaminating incident in the Marshall Islands in March 1954, a great quantity of data regarding the hazard associated with internal sources was obtained. In spite of the facts that the Marshallese people lived under conditions where the maximum probability of contamination of food and water supplies existed, and that they took no steps to protect themselves in any way, the degree of internal hazard due to fallout was small.

(3) *Protective measures.* Gas masks, air filters, or even handkerchiefs are effective in removing the particulate matter from inhaled air. Various methods of water decontamination have been proposed and evaluated, resulting in certain effective processes. Distillation, coagulation, filtration, adsorption and ion exchange may all be used advantageously. The Army Engineers' Erdlator units are of particular value. This equipment, which utilizes the processes of coagulation, diatomite filtration and disinfection, is ordinarily used to treat and purify surface waters in the field. When used for radioactive decontamination, a 50–85 percent removal of dissolved gross fission products may be expected when the unit is operated in conventional fashion. The removal can be increased to 93 percent with a clay pre-treatment and to over 99.9 percent with an ion exchange post-treatment. The Mobile Water Purification Unit (Erdlator) may be expected to remove essentially all of the radioactivity present in the form of turbidity or particulates. Canned and covered food and water are not contaminated by fallout. Directly contaminated food may be used when necessary by cutting or scraping off the outer layers.

d. Immediate Incapacitation. There are direct effects of massive, rapidly administered doses of radiation on the vital organs which result in early nausea, vomiting, and loss of ability to perform purposeful actions due to lack of coordination and imbalance. These symptoms may be sufficiently severe to result in immediate incapacitation of an individual to such a degree that he is not able to perform his duties. Experimental animal data indicate the onset of incapacitation by the end of 3 to 7 minutes, but the delay may be even less in the case of very high dose exposures from a nuclear explosion. Extrapolation of experimental data to man in this case is extremely difficult. It appears that on the order of 5,000 roentgens or rem from initial radiation may be sufficient to cause immediate incapacitation, but experimental evidence suggests the possibility of a temporary partial recovery from such doses after about 15 minutes. It is not known whether this partial recovery would result in the individual again becoming combat effective. With doses on the order of 15,000 to 20,000 roentgens, even the transient recovery period is unlikely and death may occur within a few hours.

6.4 Combined Injury

Any combination of moderate but sublethal exposures to thermal or nuclear radiations and/or mechanical injury is expected to produce more casualties or greater lethality than any effect considered singly, due either to additive effects or even to mutually reinforcing (synergistic) effects. Figure 6–4 represents a comparison of the ranges of the three effects considered individually in one situation. Insufficient data precludes the presentation of any summation curve at this time.

6.5 Nuclear Radiation Shielding

a. General. The gamma radiation dosage actually received by an individual is reduced if

absorbing material is located between the individual and the point of detonation. Thus, the dose received by a person behind a building, in a field fortification, in a tank, or in a ship is less, and in some cases much less, than that which would be received in an exposed position at the same distance from the detonation. The shielding under such circumstances is generally discussed in terms of a "dose transmission factor", defined as the ratio of the dose received behind shielding material to the dose which would be received in the absence of the shielding.

b. Initial Radiation. The determining factors in the effectiveness of shielding are the mass of the material between the source of radiation and the target; the energy distribution of the gamma radiation at the target; the distance from the source, which partly determines the gamma energy distribution; the angle of the incident radiation; and the geometry of the shielding itself. Some of these parameters are combined in figure 6–5 to give a series of curves of the dose transmission factor as a function of shielding thickness for various materials. The curves are based on the assumption that the radiation is perpendicular to the slab of shielding material. Since gamma rays are scattered considerably in air, the resultant dose transmission factor holds strictly only for slab shields so large that no radiation can get around the edges. To insure sufficient protection against radiation scattered from all directions, shielding material should be used for all exterior surfaces. The curves of figure 6–5 are applicable for yields between 0.1 KT and 100 KT. For yields above 100 KT, the curves are considered to be a conservative estimate of attenuation of initial gamma radiation (i. e., the transmission is even less than indicated), because the initial spectrum received at the target contains a higher proportion of low energy gamma rays, and is therefore less penetrating. Dose transmission factors are given in table 6–5 for particular situations, such as personnel in tanks, foxholes, houses, buildings, and basements.

c. Residual Radiation. Residual radiation is somewhat less penetrating than initial radiation, as can be seen from the dose transmission curves for residual radiation in figure 6–6. In the case of residual radiation from a contaminated ground surface, the most effective location for shielding material is between the receiver and the contaminated ground, such as the floor of a tank, or the ceiling of an underground shelter. Some shielding against residual radiation is afforded by walls also, since a portion of the radiation received can come horizontally from points up to several hundred yards from the receiver.

Table 6–5. Dose Transmission Factors (Interior Dose/Exterior Dose)

Geometry	Gamma rays		Neutrons [a]
	Initial	Residual	
Foxholes [b]	0.05–0.10	0.02–0.10	0.3
Underground—3 feet	0.04–0.05	0.0002	0.002–0.01
Built-up city area (in open)	.....	0.7	.....
Frame house	0.9	0.3–0.6	0.9–1.0
Basement	0.05–0.5	0.05–0.10	0.1–0.8
Multistory building:			
Upper	0.9	0.01	0.9–1.0
Lower	0.3–0.6	0.1	0.9–1.0
Blockhouse walls:			
9 inches	0.1	0.05	0.3–0.5
12 inches	0.05–0.09	0.01–0.02	0.2–0.4
24 inches	0.01–0.03	0.001–0.002	0.1–0.2
Factory, 200 x 200 feet	.....	0.10–0.20	.....
Shelter, partly above grade:			
With earth cover—2 feet	0.02–0.04	0.005–0.02	0.02–0.08
With earth cover—3 feet	0.01–0.02	0.001–0.005	0.01–0.05
[redacted]			
LVT (Landing Vehicle Tracked)	0.5–0.9	.....	1.0
Battleships and large carriers [c]:			
15% of crew	1.0	1.0	0.8–1.0
25% of crew	0.2	0.1	0.2–0.8
10% of crew	0.05	0.03	0.05–0.2
50% of crew	0.0005–0.005	0.0003–0.003	0.001–0.05
Cruisers and carriers [c]:			
10% of crew	1.0	1.0	0.8–1.0
20% of crew	0.5	0.3	0.4–0.8
30% of crew	0.1–0.3	0.1	0.1–0.4
40% of crew	0.005–0.1	0.003–0.05	0.01–0.1
Aircraft	1.0	.....	1.0
Destroyers, transports, and escort carriers [c]:			
10% of crew	1.0	1.0	0.8–1.0
20% of crew	0.7	0.5	0.6–0.8
30% of crew	0.4	0.2	0.3–0.6
40% of crew	0.1–0.4	0.1	0.1–0.3

[a] Estimated values.
[b] No line-of-sight radiation received.
[c] Crew at General Quarters.

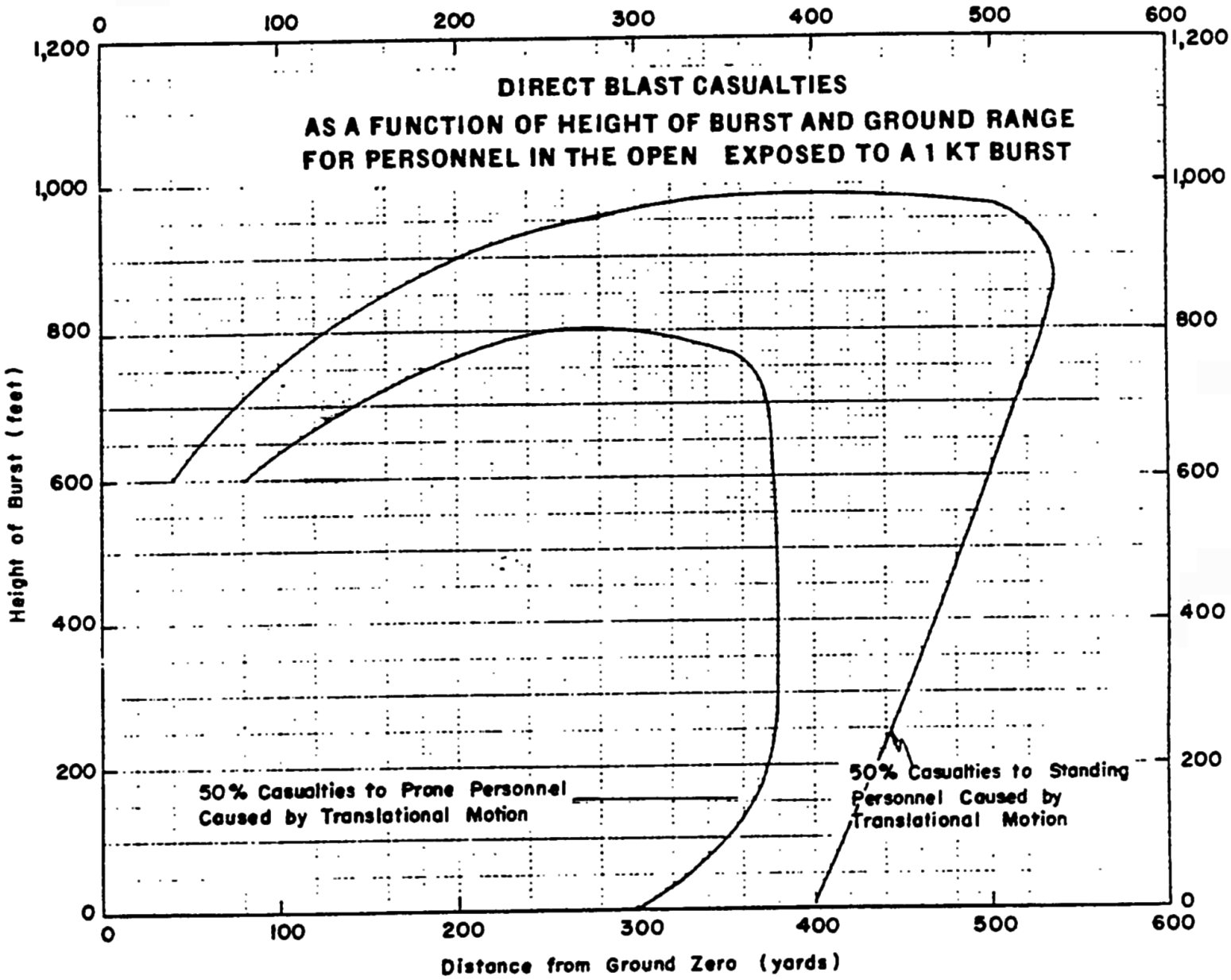
DIRECT BLAST CASUALTIES
AS A FUNCTION OF HEIGHT OF BURST AND GROUND RANGE
FOR PERSONNEL IN THE OPEN EXPOSED TO A 1 KT BURST
Height of Burst (feet)
Distance from Ground Zero (yards)
0
100
200
300
400
500
600
1,200
1,000
800
600
400
200
0
50% Casualties to Prone Personnel Caused by Translational Motion
50% Casualties to Standing Personnel Caused by Translational Motion

FIGURE 6-4

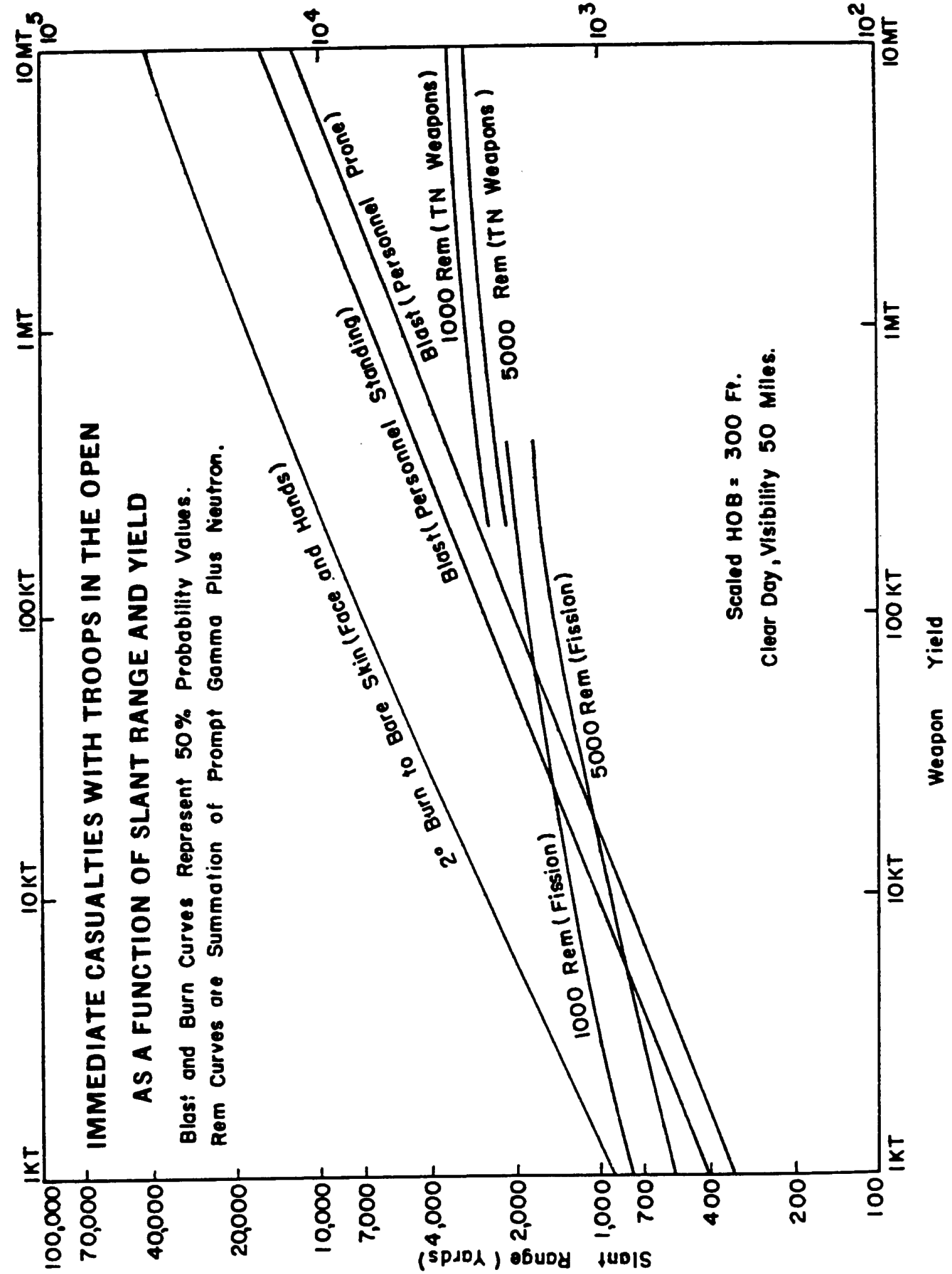
IMMEDIATE CASUALTIES WITH TROOPS IN THE OPEN
AS A FUNCTION OF SLANT RANGE AND YIELD
Blast and Burn Curves Represent 50% Probability Values.
Rem Curves are Summation of Prompt Gamma Plus Neutron.
2° Burn to Bare Skin (Face and Hands)
Blast (Personnel Standing)
Blast (Personnel Prone)
1000 Rem (TN Weapons)
5000 Rem (TN Weapons)
1000 Rem (Fission)
5000 Rem (Fission)
Scaled HOB = 300 Ft.
Clear Day, Visibility 50 Miles.
Weapon Yield
1KT
10KT
100KT
1MT
10MT
Slant Range (Yards)
100,000
70,000
40,000
20,000
10,000
7,000
4,000
2,000
1,000
700
400
200
100

SHIELDING FROM INITIAL AND RESIDUAL GAMMA RADIATION

The curves in figures 6–5 and 6–6 indicate dose transmission factors for bomb initial and residual gamma radiation, respectively, perpendicularly incident upon various thicknesses of earth, water, concrete, iron, and lead. For other materials of known density, the transmission factor may be estimated by interpolation, on a density basis, between the curves given.

Example.

Find: How much concrete would be required to reduce the dose from initial radiation to one one-hundredth the unshielded dose?

Solution: Examine the curve for concrete of figure 6–5. It is seen that the thickness of a slab of concrete required to reduce the dose to 0.01 of its former value is 34 inches. *Answer.*

Reliability. Thicknesses indicated for a given transmission factor are considered reliable within ±20 percent, for conditions outlined in paragraph 6.5.

Densities of Certain Materials
(Expressed in pounds per cubic foot)

Brick, common	120
Clay, dry	63
Clay, damp, plastic	110
Clay and gravel, dry	100
Coal, piled	40–50
Earth, dry, loose	76
Earth, dry, packed	95
Earth, moist, loose	78
Earth, moist, packed	96
Earth, mud, packed	115
Fuel oil	54
Granite	175
Limestone	165
Masonry, stone	150
Sand, gravel, dry packed	100–120
Fir	34
Hemlock	29
Oak	46
Pine, white	26
Pine, yellow	40

Related Material.

See paragraph 6.5. For radiation input data, see figures 4–1 through 4–7 for air and surface burst initial gamma. Figures 4–28 through 4–33, neutron induced gamma activity. Figures 4–14 through 4–19, surface burst residual gamma. Figure 4–8, underground burst, initial gamma. Figures 4–20 through 4–23, underground residual gamma. Figure 4–25, harbor burst, residual gamma.

FIGURE 6-5

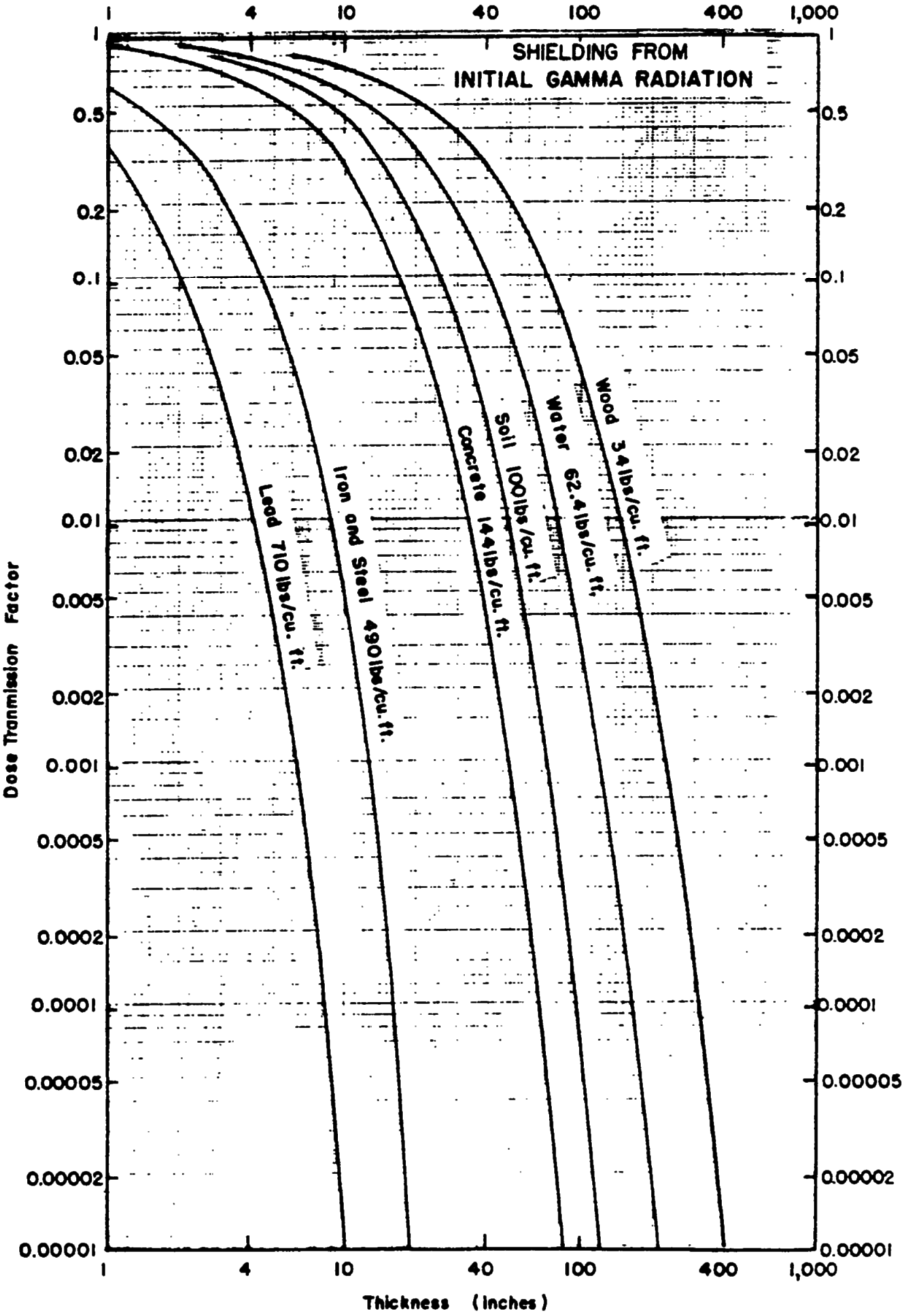
SHIELDING FROM
INITIAL GAMMA RADIATION
Wood 34 lbs/cu. ft.
Water 62.4 lbs/cu. ft.
Soil 100 lbs/cu. ft.
Concrete 144 lbs/cu. ft.
Iron and Steel 490 lbs/cu. ft.
Lead 710 lbs/cu. ft.
Dose Transmission Factor
Thickness (Inches)
1
4
10
40
100
400
1,000
1
0.5
0.2
0.1
0.05
0.02
0.01
0.005
0.002
0.001
0.0005
0.0002
0.0001
0.00005
0.00002
0.00001

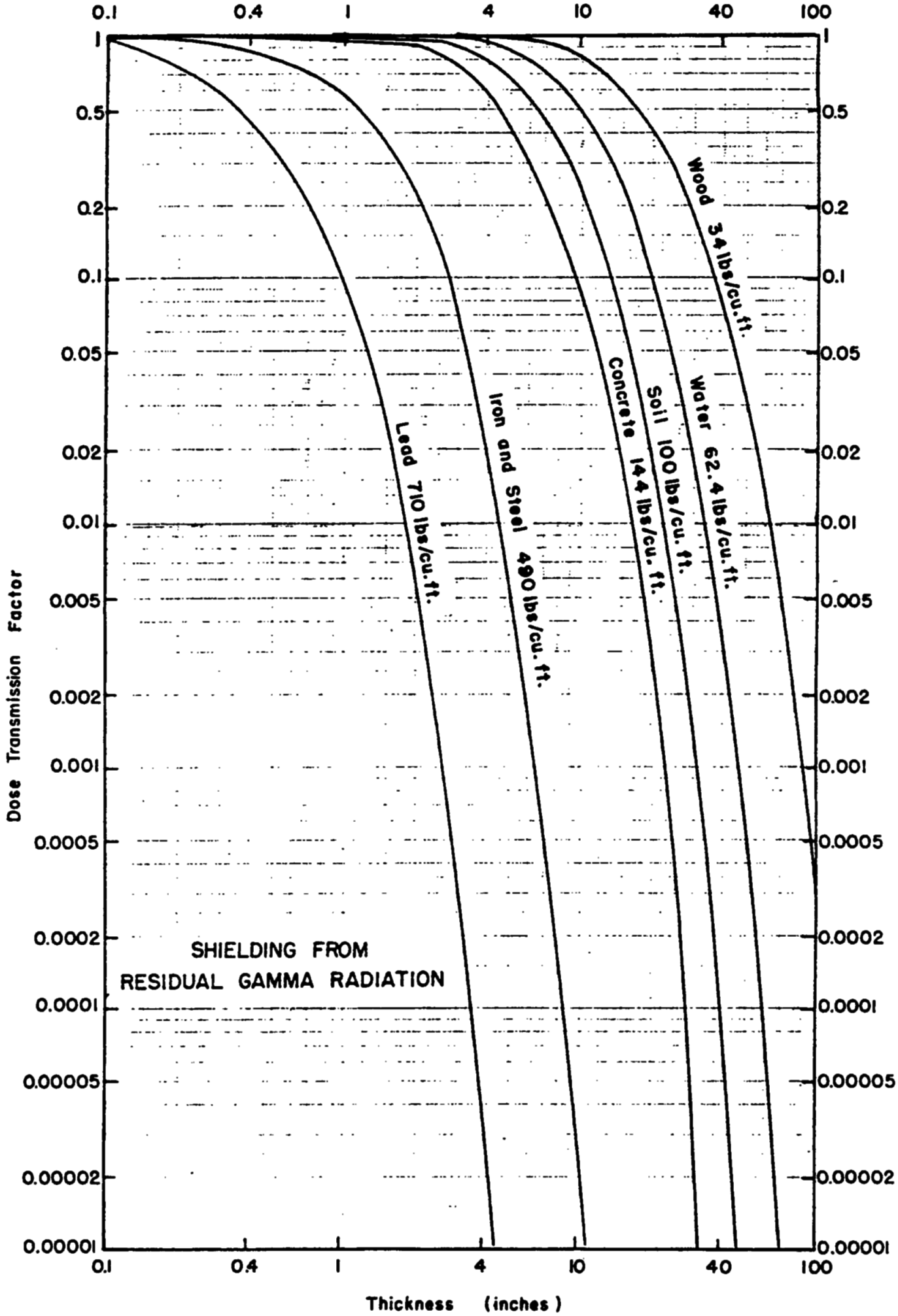
SHIELDING FROM
RESIDUAL GAMMA RADIATION
Wood 34 lbs/cu.ft.
Water 62.4 lbs/cu.ft.
Soil 100 lbs/cu. ft.
Concrete 144 lbs/cu. ft.
Iron and Steel 490 lbs/cu. ft.
Lead 710 lbs/cu.ft.
Dose Transmission Factor
Thickness (inches)
0.1
0.4
1
4
10
40
100
1
0.5
0.2
0.1
0.05
0.02
0.01
0.005
0.002
0.001
0.0005
0.0002
0.0001
0.00005
0.00002
0.00001

ately greater. The effect of non-ideal wave forms on air blast loading is described in paragraph 5.2*b*(1)(*f*).

(2) *Loading during the diffraction phase.* An essentially closed large structure with walls that remain intact throughout most of the load duration is primarily sensitive during the diffraction phase, since most of the translational load is applied during this period. As the blast wave strikes this type structure it is reflected, creating overpressures greater than those incident thereon. Subsequently, the reflected overpressure decays to that of the blast wave. As the blast wave progresses, it diffracts around the structure, eventually exerting overpressures on all sides. Before the blast wave reaches the rear face, overpressures on the front exert translational forces in the direction of blast wave propagation. After the blast wave reaches the rear face, the overpressures on the rear tend to counter the overpressures on the front. For smaller structures, the blast wave reaches the rear face more quickly, so that the pressure differential exists for a shorter time. Thus, the net translational loading resulting from overpressures during the diffraction phase depends primarily on structural dimensions. For some structures where wall failure takes place early in the diffraction phase, only the structural frame may remain during the remainder of the diffraction process, and essentially no load is transmitted to the structural frame through the walls. A longer duration blast wave does not materially change the magnitude of the net translational loading during the diffraction phase or the damage resulting therefrom. In other words, the structure is primarily sensitive to the peak blast wave overpressure. Table 7–1 lists those types of structures which are generally affected primarily by blast wave overpressure during the diffraction phase.

(3) *Loading during the drag phase.* During the diffraction phase, and until the blast wave has passed, dynamic pressures are also exerted on structures. Dynamic pressure loading is commonly called drag loading. In the case of a closed large structure the drag phase loading is small relative to the overpressure loading during the diffraction phase. For smaller structures, the drag phase assumes greater relative importance. For small area components such as the frame of a structure after removal of siding, the translational load applied as a result of the drag phase is much greater than the net translational loading from overpressures during the diffraction phase. For frame buildings with siding removed during the diffraction phase, the drag phase is the predominant factor in producing further damage. Likewise for bridges, the net load during the diffraction phase is applied for an extremely short time, while the drag phase continues until the entire blast wave passes the structure. Because the drag phase duration is closely related to the duration of the blast wave rather than to the overall dimensions of the structure, damage is dependent not only on peak dynamic pressure but also on the duration of the positive phase of the blast wave. Thus damage to this type of structure is dependent on yield as well as peak loading. Table 7–2 lists those types of structures which are primarily sensitive during the drag phase.

(4) *Damage to structures.*

(*a*) *Structural characteristics.* The cases discussed above represent extremes in structural loading. Most structures have characteristics which cause them to be affected by the loading during both the diffraction phase and the drag phase. Some elements of a structure may be damaged more by loading during the diffraction phase; other elements of the same structure may be damaged more by the drag phase. The dimensions and orientation of a structure, together with the number and area of the openings and the rapidity with which wall and roof

about half the dam height is most vulnerable to a surface burst upstream from the dam. An air burst on the downstream side of the dam is the least effective method of producing breaching of concrete gravity dams. Air blast from such a burst or from a burst on top of the dam is a primary damaging agent against powerhouse structures; these should be analyzed according to structural type as in paragraph 7.2.

(2) *Harbor installations.* Air blast is the most important damaging mechanism for most structures around a harbor. Air blast damage to surface structures is discussed in paragraph 7.2. For canal or river locks, where the water level around the gates is low, air blast is effective in making the locks inoperable by damage to the gates.

b. Water Shock. A concrete gravity dam with the reservoir water level higher than about half the dam height is most vulnerable to an underwater burst. As the depth of water increases, the vulnerability of the dam to an underwater burst increases. This is because underwater shock impulse for a given yield weapon at a given distance is greater for greater depths. Only a limited amount of information is available on dam destruction, and scaling laws are not fixed. The following are estimated ranges for damage by a 20 KT underwater burst at mid-depth to full concrete gravity dams (straight or slightly curved in plan):

60 ft. high dam

Cracks are produced at a range of about 300 yards; portions are cracked loose and displaced small distances at a range of about 200 yards.

150-foot high dam

Cracks are produced at a range of about 500 yards; portions are cracked loose and displaced sizable distances at a range of about 200 yards.

500-foot high dam

Cracks are produced at a range of about 1,300 yards; portions are cracked loose and displaced large distances at a range of about 200 yards.

Canal and river locks, where there is a high water level around the gates, are most vulnerable to damage from an underwater burst.

c. Cratering. For earth dams and causeways, the primary damaging mechanism is cratering; for breaching, the dam or causeway should be within the crater. The crater lip formed by an underwater burst in a harbor may create a navigational hazard; however, water erosion may make this hazard temporary. For structures on shore around a harbor, the range for air blast damage is greater than the range of cratering damage to these structures from an underwater burst near the shore. Cratering is the most important damaging mechanism for concrete quay walls and canal and river locks if the structure is within the rupture zone. The crater dimensions formed by an underwater burst can be computed using the procedure given with figures 2–24 through 2–26. Craters from ground surface and underground bursts can be computed from the procedures given in paragraph 2.2. Weapons detonated on the top or at the toe of a concrete gravity dam produce damage to the dam by cratering. The extent of the rupture can be computed by the method given in paragraph 2.2. For a burst on the top of the dam, the extent of rupture determines the amount the water level drops. When the burst is at the toe of the dam the extent of rupture also determines whether the dam loses its stability against overturning. For a detonation in a dam gallery, the extent of damage can be computed as for an underground burst by the method given in paragraph 2.2. Radius of rupture should be taken as 1.5 times the crater depth computed for rock.

d. Water Waves. The many variables involved in predicting damage from wave action require an individual analysis of each target. Among the variables involved are water depth, bottom slope, wave height, wave length, target response characteristics, orientation of target to the wave front, location of target relative to the point of wave breaking, and variation in width of the channel or harbor. Figure 2–34 gives estimated maximum wave height as a function of water depth and burst position. These figures are for a constant depth of water. As the water depth or width of the wave front varies, the wave height also changes. Wave action may cause additional

~~CONFIDENTIAL~~

SEVERE DAMAGE TO M2 OR M4 FLOATING BRIDGES (RANDOM ORIENTATION)
FOR VARIOUS YIELDS AS A FUNCTION OF GROUND RANGE AND HEIGHT OF BURST

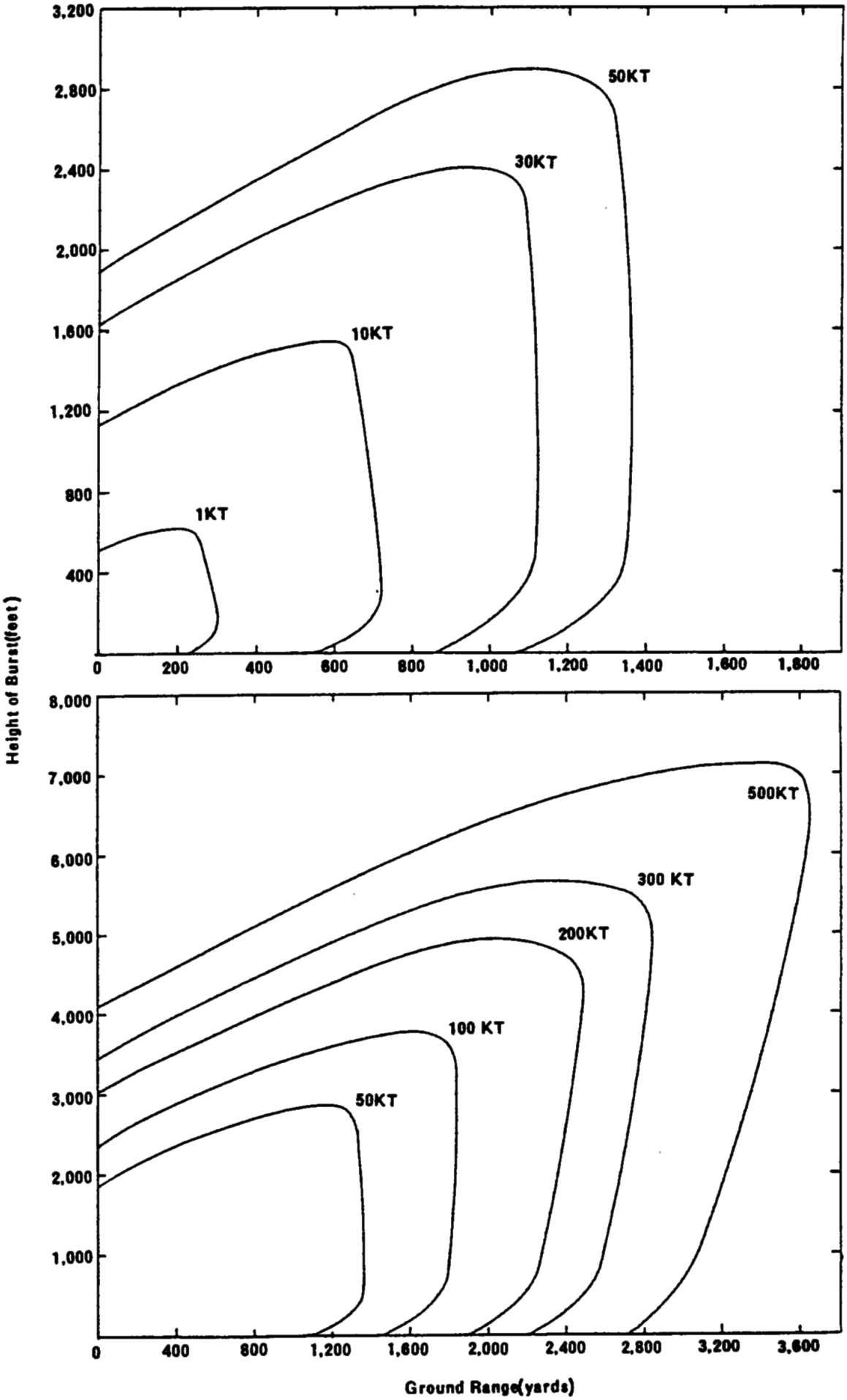

~~CONFIDENTIAL~~

FIGURE 7-13C

SEVERE DAMAGE TO M2 OR M4 FLOATING BRIDGES (RANDOM ORIENTATION)
FOR VARIOUS YIELDS AS A FUNCTION OF GROUND RANGE AND HEIGHT OF BURST

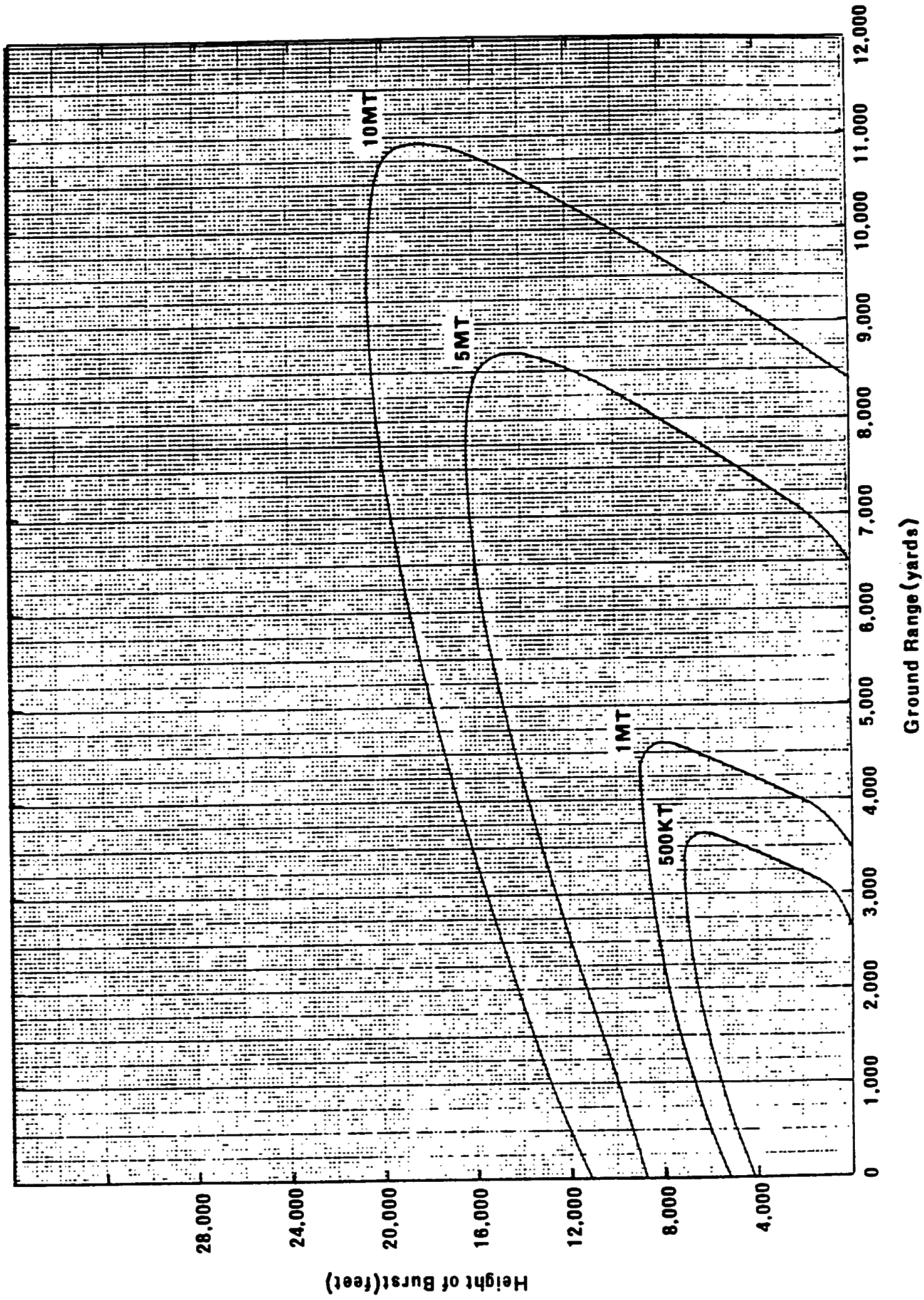

SEVERE DAMAGE TO EARTH COVERED LIGHT STEEL ARCH SHELTER
(10 GAUGE CORRUGATED STEEL WITH 20 TO 25 FOOT SPAN)
BY VARIOUS YIELDS AS A FUNCTION OF HEIGHT OF BURST AND GROUND RANGE

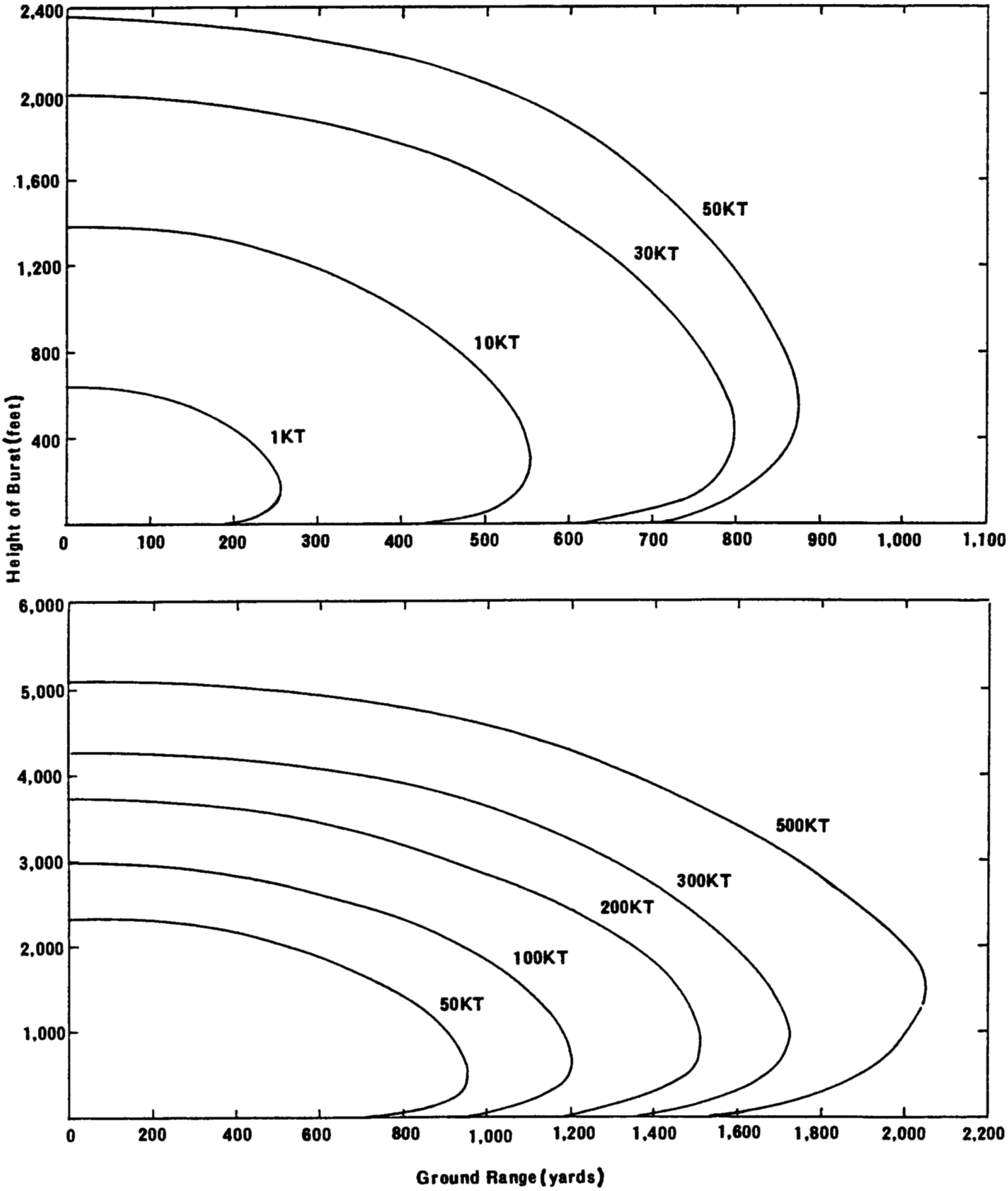

SEVERE DAMAGE TO EARTH COVERED LIGHT STEEL ARCH SHELTER
(10 GAUGE CORRUGATED STEEL WITH 20 TO 25 FOOT SPAN)
BY VARIOUS YIELDS AS A FUNCTION OF HEIGHT OF BURST AND GROUND RANGE

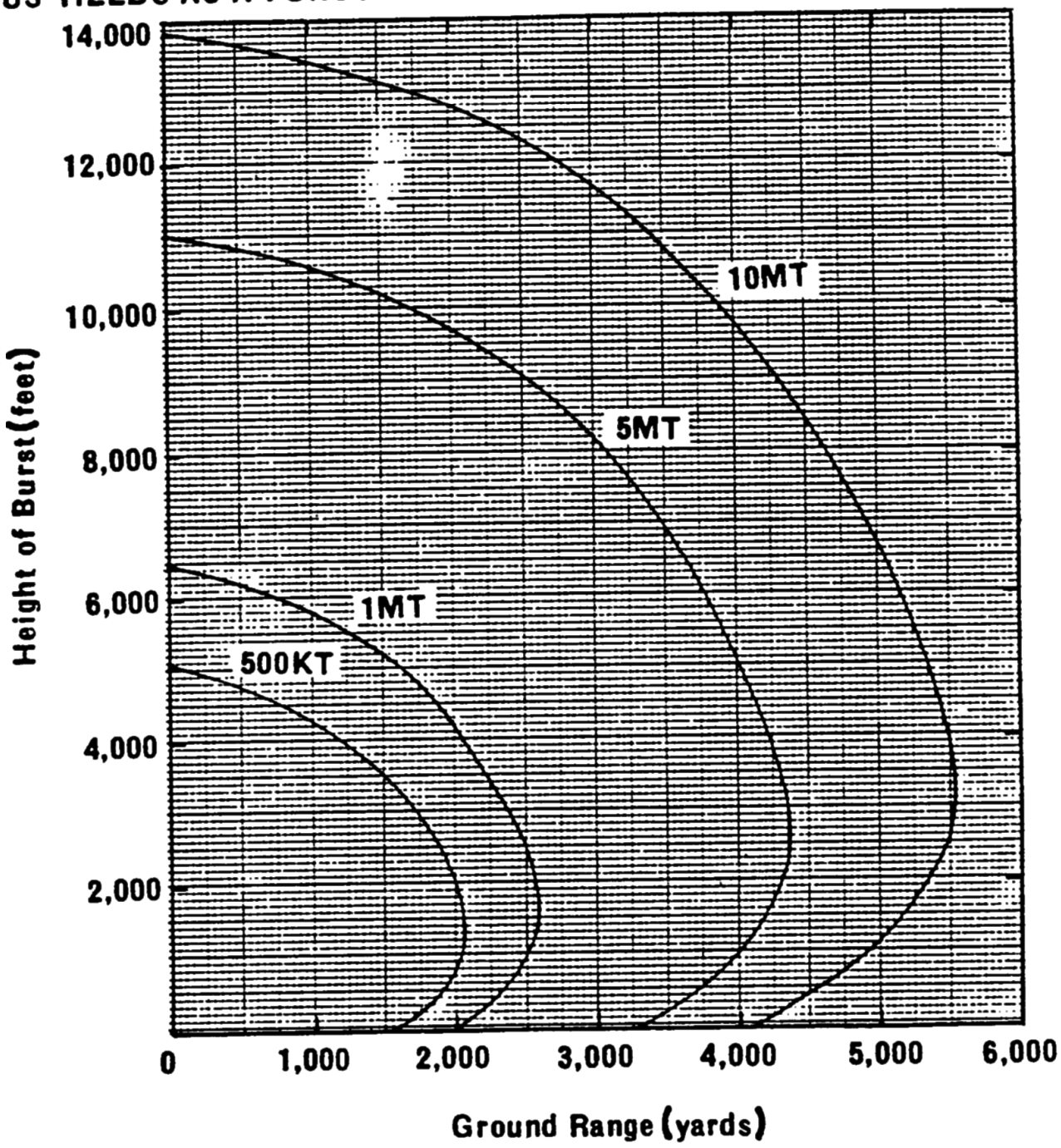

DAMAGE TO FIELD FORTIFICATIONS

Figures 7-20 through 7-22 are a series of plots of height of burst vs. scaled ground range for 50 percent probability of severe, moderate, or light damage to various field fortifications in Nevada type soil scaled to 1 KT. To determine 90 percent or 10 percent probability of damage to structures, lines of probability should be drawn between the indicated 50 percent probability lines. For example, because there is little difference between a line indicating approximately 10 percent probability of severe damage and one indicating 90 percent probability of moderate damage, a single line can represent both and should be drawn midway between the indicated lines for 50 percent probability of severe and moderate damage. To determine the range for 90 percent probability of severe damage use one-half the yield at the same burst height.

The curves in figure 7-22 are based on results of tests run in a *consolidated dry sand and gravel soil*. Trenches and foxholes in damp soil with stable vegetation or dry silty soil will receive moderate and severe damage at ranges less than those shown in figure 7-22. The curves of figure 7-22 are for average rectangular foxholes with the longitudinal axis perpendicular to the direction of air blast propagation. Damage will be equal or less for other orientations.

Scaling. To obtain heights of burst and distances for yields other than 1 KT, use the scaling procedure—

$$\frac{d_1}{d_2}=\frac{h_1}{h_2}=\frac{W_1^{1/3}}{W_2^{1/3}},$$

where d_1 and h_1 are ground distance and height of burst for yield W_1 KT, and d_2 and h_2 are the corresponding ground distance and height of burst for yield W_2 KT.

Example.

Given: A 50 KT burst at an altitude of 1,000 feet.

Find: To what horizontal distance there is a 50 percent probability of severe damage to an unrevetted foxhole in a dry, consolidated sand and gravel soil.

Solution:

$$h_1=\frac{h_2\times W_1^{1/3}}{W_2^{1/3}}=\frac{1{,}000\times 1}{(50)^{1/3}}=270 \text{ feet},$$

the corresponding burst height for 1 KT. From figure 7-22 the ground range for severe damage is 185 yards. To obtain the corresponding ground range for 50 KT:

$$d_2=\frac{d_1\times W_2^{1/3}}{W_1^{1/3}}=\frac{185\times(50)^{1/3}}{1}=680 \text{ yards.}$$

Answer.

Reliability. This figure is based on results of a limited number of full scale tests at which severe, moderate and light damage were observed.

Related material.

See paragraph 7.4.

FIGURE 7-20

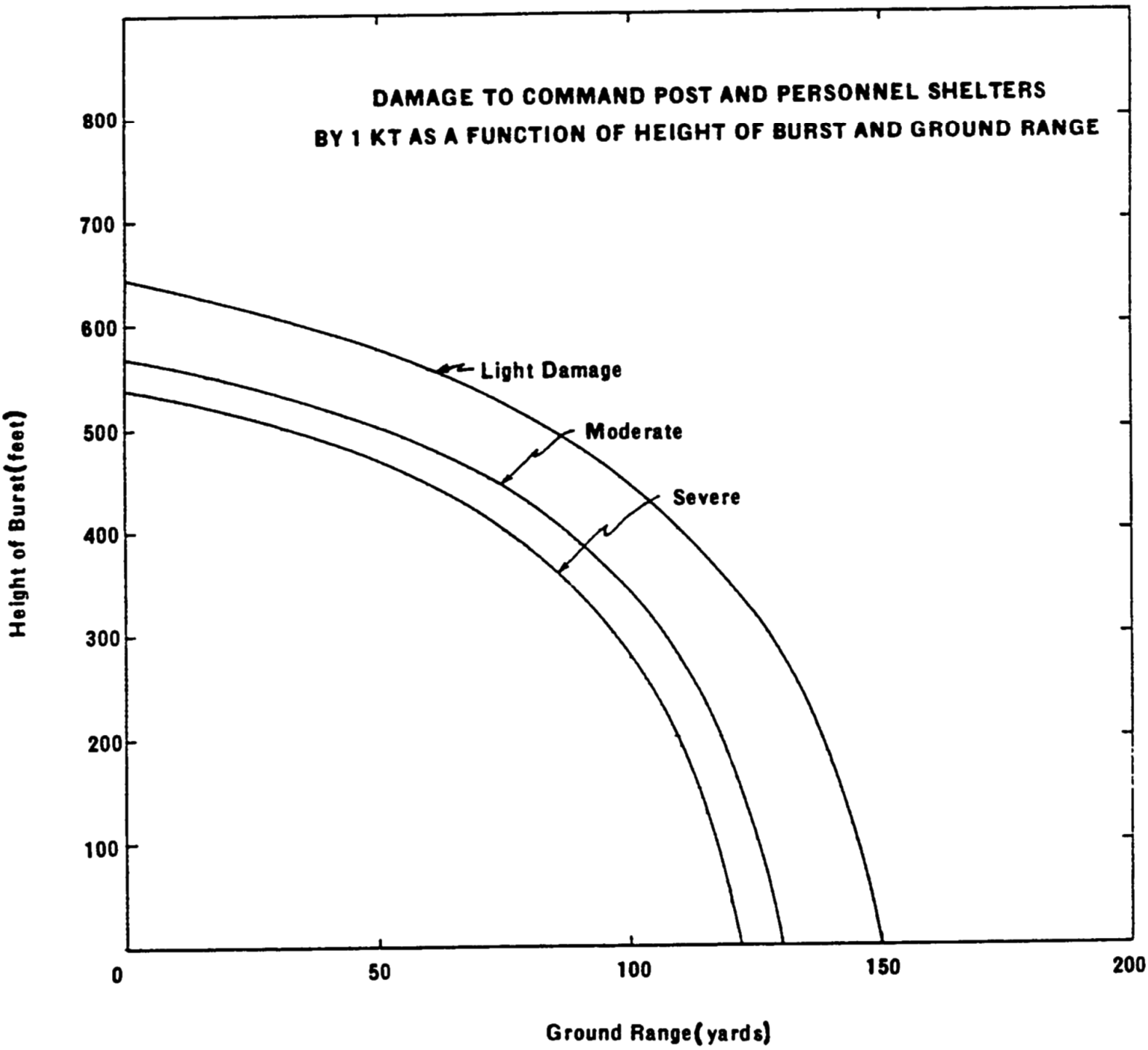
DAMAGE TO COMMAND POST AND PERSONNEL SHELTERS
BY 1 KT AS A FUNCTION OF HEIGHT OF BURST AND GROUND RANGE
Light Damage
Moderate
Severe
Height of Burst(feet)
800
700
600
500
400
300
200
100
0
50
100
150
200
Ground Range(yards)

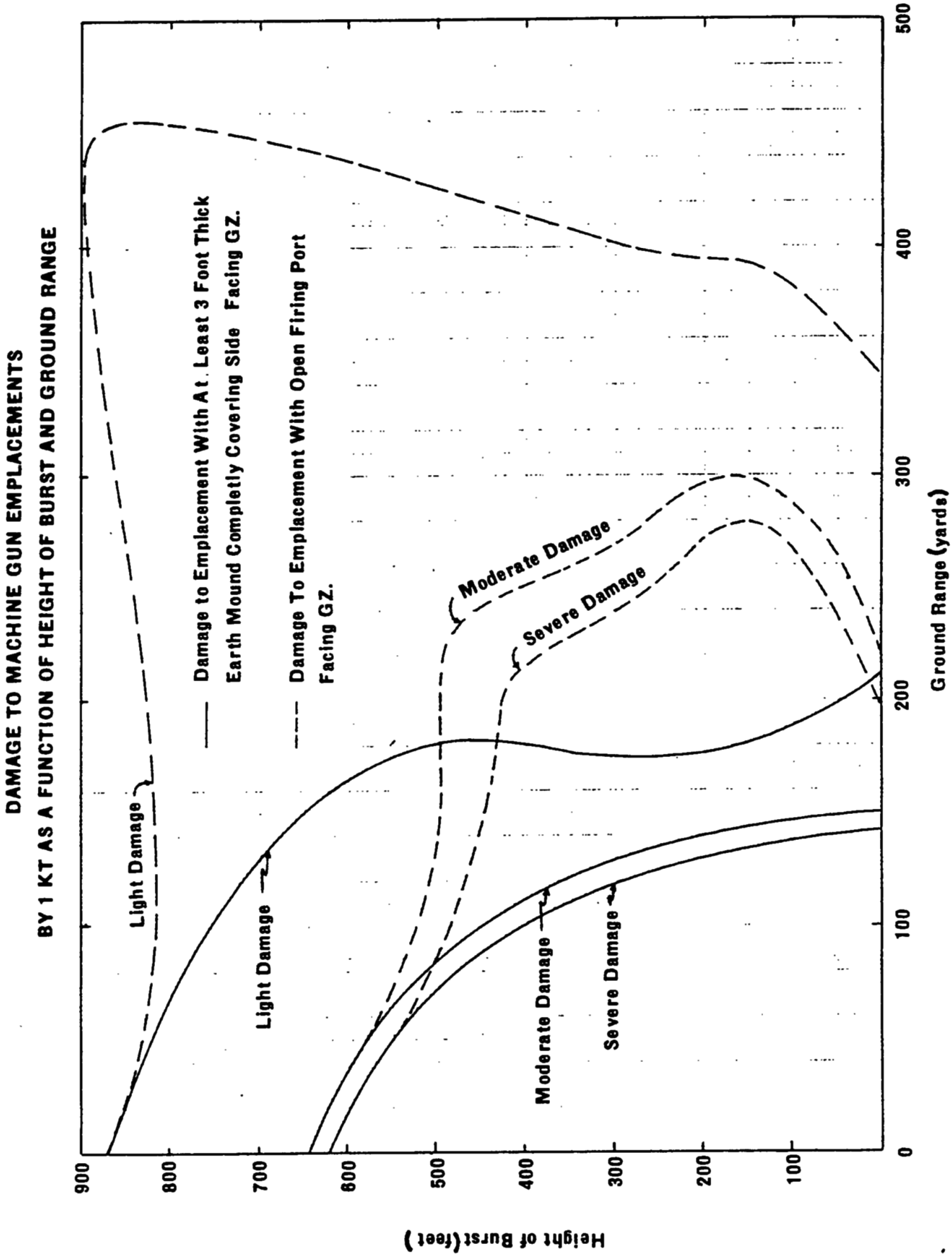

PAGE 7-55 WITHHELD IN ITS ENTIRETY

SECTION VIII
DAMAGE TO NAVAL EQUIPMENT

8.1 General

a. Damage Mechanisms. Mechanical damage to surface ships may be caused by air blast, water shock, and surface wave action. Submerged submarines may be damaged by water shock. Thermal damage to naval vessels and topside equipment is not considered a significant factor, in that it does not of itself cause sinking or immobilization.

b. Damage Classification for Surface Ships. The degree of damage to surface ships and surfaced submarines is separated into three categories—

(1) *Severe damage (probable sinking).* The ship is sunk or is damaged to an extent requiring rebuilding.

(2) *Moderate damage (immobilization).* The ship requires extensive repairs. This includes damage to certain shock sensitive components or their foundations, such as propulsion machinery, boilers, and damage to interior equipment.

(3) *Light damage.* This category includes damage to electronic, electrical, and mechanical equipment; however, the ship may still be able to operate effectively.

c. Damage Classification for Submarines. For submerged submarines two degrees of damage are specified—

(1) *Lethal hull damage.* Pressure hull rupture occurs.

(2) *Interior shock damage (surfacing damage).* Extensive interior damage to equipment, machinery, and piping occurs with immobilization probable. Submarines are forced to surface.

8.2 Surface Ship Damage

a. Water Shock Damage. Water shock is the principal cause of damage to surface ships from underwater explosions. The directly transmitted shock, however, is not the sole damaging mechanism. When the water depth is of the order of 3,000 feet or less for a 1 KT underwater burst, it is possible that the shock wave reflected from the bottom may produce more severe equipment damage at a given range than the direct shock wave, even though the peak pressure of the reflected wave is less. This phenomenon results from the reflected wave propagating in a more vertical direction and hence being more effective in producing vertical velocities in the hull. In addition, certain bottom formations may focus the reflected wave, resulting in local areas of much higher pressures. It is therefore not possible to predict accurately the effects in a given case without extensive knowledge of the bottom structure in the vicinity of the detonation. To estimate the effects of the reflected shock wave in the absence of such knowledge, it is necessary to assume the bottom to be flat and a perfect reflector, and to use the image of the actual burst point as the apparent source of the reflected shock wave.

Refraction of the water shock wave, discussed in paragraph 2.3*a*(4), may act to reduce the range at which a given level of damage occurs. This reduction is not significant, however, except at the ranges for light damage, and the actual magnitude of the reduction depends upon the individual circumstances. Since this range reduction is of a small magnitude when considering severe and moderate damage levels and is in the conservative direction when considering possible effects against weapon delivery vessels, the influence of water shock wave refraction has not been included in the damage curves.

Water shock damage curves for surface ships are presented in figures 8-1 through 8-3. These curves are based upon several criteria. Severe damage to ships with multi-plate side protective systems (cruisers, carriers, etc.) is defined by bottom deflection, while for those with thin skin shells (transports, destroyers, etc.), it is defined by side deflection. Moderate and light damage to all types is related to the bottom plate velocity.

b. Air Blast Damage. As the depth of a burst is decreased, a transition from water shock to air blast as the primary damage-producing mechanism occurs. Peak overpressure is considered a satisfactory parameter for estimating damage to ships from air blast. Peak overpressures of 5 psi cause light damage to most types of surface ships, while overpressures required for severe damage vary from 25 psi for destroyers to 45 psi for battleships. Figures 8–1 and 8–2 present damage ranges for a 1 KT detonation for heights of burst less than 600 feet and depths of burst less than 800 feet, with means of scaling to other yields. A tabulation of peak overpressure required to cause ship damage is given in table 8–1 for use with burst heights greater than those shown in figures 8–1 and 8–2. For such burst heights, distances to which overpressures extend can be obtained from figure 2–17.

Table 8–1. Surface Ship Peak Air Overpressure Damage Criteria

Type of ship	Peak air overpressure (psi)		
	Severe	Moderate	Light
Aircraft carriers	30	20	5
Battleships	45	25	5
Cruisers (heavy)	40	20	5
Cruisers (light) (AA)	30	20	5
Destroyers	25	15	5
Pontoons (for pier construction)	60	------	------
Transports	30	20	5
LST's, landing craft and landing vehicles	25	15	5
Submarines (surfaced)	80	60	------

c. Water Wave Damage. Water waves are a contributing factor in causing damage to surface ships. Wave action may add to the damage to a ship which has already been weakened by air and water shock. The waves may also cause "hogging" damage to ships oriented end-on to the burst, and may cause ships oriented beam-on to the burst to capsize. Small craft may be overturned and sunk or destroyed by wave action.

d. Thermal Damage. Thermal damage to naval vessels and topside equipment is probably limited to superficial scorching of exposed organic surfaces (including paint). Fires are unlikely to originate aboard vessels as the result of thermal radiation from a nuclear explosion, except in cases where severe and probably overriding damage due to blast is also sustained.

8.3 Subsurface Target Damage

a. Submarines.

(1) *Air blast damage.* Air blast damage to surfaced submarines is significant only for the case of surface, transition zone or air bursts. Peak air overpressures of 80 and 60 psi are expected to cause severe and moderate damage, respectively, to surfaced submarines.

(2) *Water shock damage.* Water shock is the controlling damage-producing mechanism for a submerged submarine for any burst position, and also for a surfaced submarine subjected to an underwater burst. The criterion used for estimating lethal hull damage is a function of "excess impulse." This excess impulse is defined as the impulse delivered by that portion of the shock overpressure which is in excess of the static collapse pressure minus the hydrostatic pressure. In deep water when a sharp change in water temperature with depth exists (thermocline) and the weapon is fired in close proximity to this region, refraction may reduce the range for a given degree of damage on the order of perhaps 20 percent. This reduction will only occur when the weapon and the submarine are on opposite sides of the thermocline. For weapons fired well below or above the thermocline, there should be no reduction. Isodamage curves for the hull lethal range and interior shock damage range are presented in figures 8–4 and 8–5 for a submarine with a 600 psi static collapse pressure subjected to a 10 KT and a 30 KT surface or underwater detonation, with methods for scaling to other yields. No account of refraction has been taken in the damage curves presented. Non-linear effects as described in paragraph 2.3 have been incorporated. Initial translational

velocity is the criterion used for prediction of shock damage to submarine equipment.

b. Underwater Mines. Underwater mines are expected to be neutralized when the peak pressure acting on the mines is equal to or greater than the mine case static collapse pressure, or when the mines are within the crater. Figures 8–6 through 8–8 show the neutralization ranges for mines with hydrostatic collapse pressures of 250, 500, and 1,000 psi in depths of water of 50, 100, and 200 feet and for a range of yields from 1 to 100 KT. These curves are computed for mines and burst both on the bottom.

SURFACE SHIP DAMAGE

Figure 8-1 gives estimated ranges for severe damage (probable sinking) plotted as a function of burst height and depth for surface ships for a 1 KT detonation. Figure 8-2 gives the ranges for moderate (immobilization) damage and for light damage as functions of burst height and shallow depths. Figure 8-3 is an extended plot of light damage vs. depth of burst. This latter figure enables an estimate to be made for the effect of the bottom reflection pressures on the predicted light damage range using the assumptions given in paragraph 8.2*a* (i. e., a flat perfect reflector bottom and a burst depth at the image of the actual burst point). For evaluation of light damage, a value should be found for both the direct shock wave and the bottom reflected shock wave and the larger value chosen.

Scaling. For yields other than 1 KT the following relations can be used to estimate ranges for a given degree of damage:

$$\frac{d_1}{d_2}=\frac{W_1^{1/3}}{W_2^{1/3}}=\frac{h_1}{h_2},$$

where d_1=range for a given degree of damage for yield W_1 KT at a depth h_1, and d_2=range for a given degree of damage for yield W_2 KT at depth h_2.

Example.

Given: A 30 KT burst at a depth of 2,000 feet in 5,000 feet of water.

Find:

(*a*) The range at which an aircraft carrier suffers severe damage.

(*b*) The range at which a destroyer suffers light damage.

Solution:

(*a*) The depth of 2,000 feet for a 30 KT burst corresponds for a 1 KT to

$$\frac{h_1}{h_2}=\frac{W_1^{1/3}}{W_2^{1/3}} \text{ or } h_1=\frac{h_2\times(W_1^{1/3})}{W_2^{1/3}}$$

$$h_1=\frac{2{,}000(1)}{(W_2)^{1/3}}=\frac{2{,}000}{(30)^{1/3}}=640 \text{ feet.}$$

From figure 8-1 the range at which an aircraft carrier suffers severe damage from a 1 KT burst 640 feet below the surface is 320 yards.

The range of severe damage to an aircraft carrier for a 30 KT detonation at a depth of 2,000 feet is then

$$\frac{d_1}{d_2}=\frac{W_1^{1/3}}{W_2^{1/3}} \text{ or } d_2=\frac{(d_1)\times(W_2)^{1/3}}{W_1^{1/3}}=$$

$$\frac{(320)\times(30)^{1/3}}{1}=1{,}000 \text{ yards.} \quad \textit{Answer.}$$

(*b*) From either figure 8-2 or 8-3 the range at which a destroyer suffers light damage from the direct shock wave of a 1 KT burst at 640 feet below the surface is 990 yards.

The imaginary burst point from which the bottom reflected shock waves are assumed to come is equal to the depth of the water plus the height of the weapon above the bottom, or 5,000+3,000=8,000 feet for the 30 KT weapon. The corresponding depth for a 1 KT is

$$\frac{h_1}{h_2}=\frac{W_1^{1/3}}{W_2^{1/3}} \text{ or } h_1=\frac{h_2\times W_1^{1/3}}{W_2^{1/3}},$$

$$h_1=\frac{8{,}000\times(1)}{(W_2)^{1/3}}=\frac{8{,}000}{(30)^{1/3}}=2{,}560 \text{ ft.}$$

From figure 8-3 the range at which a destroyer suffers light damage from the shock wave of a 1 KT burst at 2,560 feet is 1,300 yards. Since this is greater than the range noted above (990 yards), the bottom reflected shock wave governs. Hence the range of light damage to a destroyer from a 30 KT burst at a depth of 2,000 feet in 5,000 feet of water is then,

$$\frac{d_1}{d_2}=\frac{W_1^{1/3}}{W_2^{1/3}} \text{ or } d_2=\frac{(d_1)\times(W_2)^{1/3}}{W_1^{1/3}}=$$

$$\frac{(1{,}300)\times(30)^{1/3}}{1}=4{,}000 \text{ yards.} \quad \textit{Answer.}$$

Reliability. Based on limited data. Predictions become less reliable as depth of burst decreases.

Related Material.

See paragraphs 8.1 and 8.2.

See also figures 8-4 and 8-5 for submarine damage.

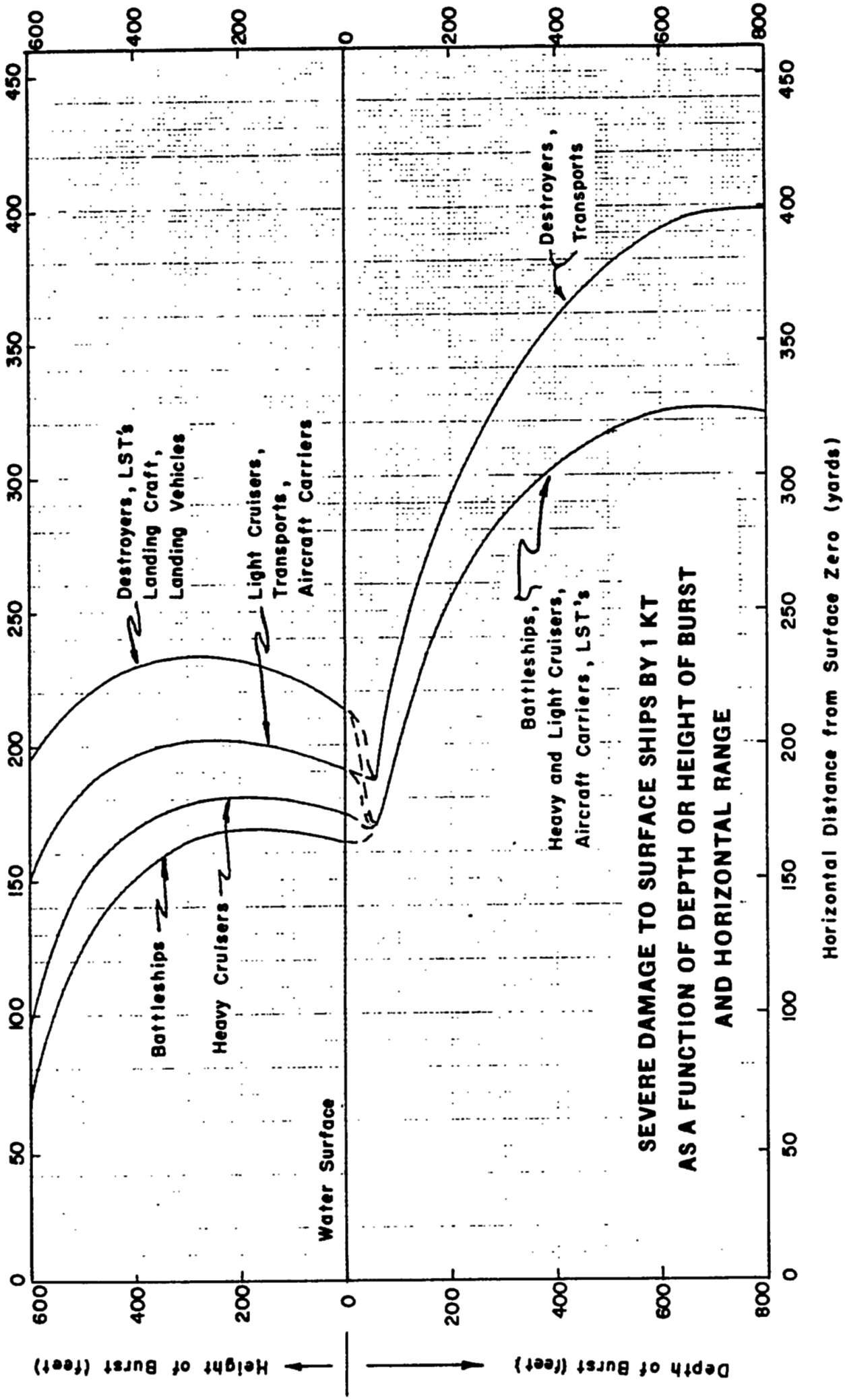
SEVERE DAMAGE TO SURFACE SHIPS BY 1 KT
AS A FUNCTION OF DEPTH OR HEIGHT OF BURST
AND HORIZONTAL RANGE
Destroyers, LST's
Landing Craft,
Landing Vehicles
Light Cruisers,
Transports,
Aircraft Carriers
Battleships
Heavy Cruisers
Destroyers,
Transports
Battleships,
Heavy and Light Cruisers,
Aircraft Carriers, LST's
Water Surface
Height of Burst (feet)
Depth of Burst (feet)
Horizontal Distance from Surface Zero (yards)
0
50
100
150
200
250
300
350
400
450
600
400
200
0
200
400
600
800

FIGURE 8-2

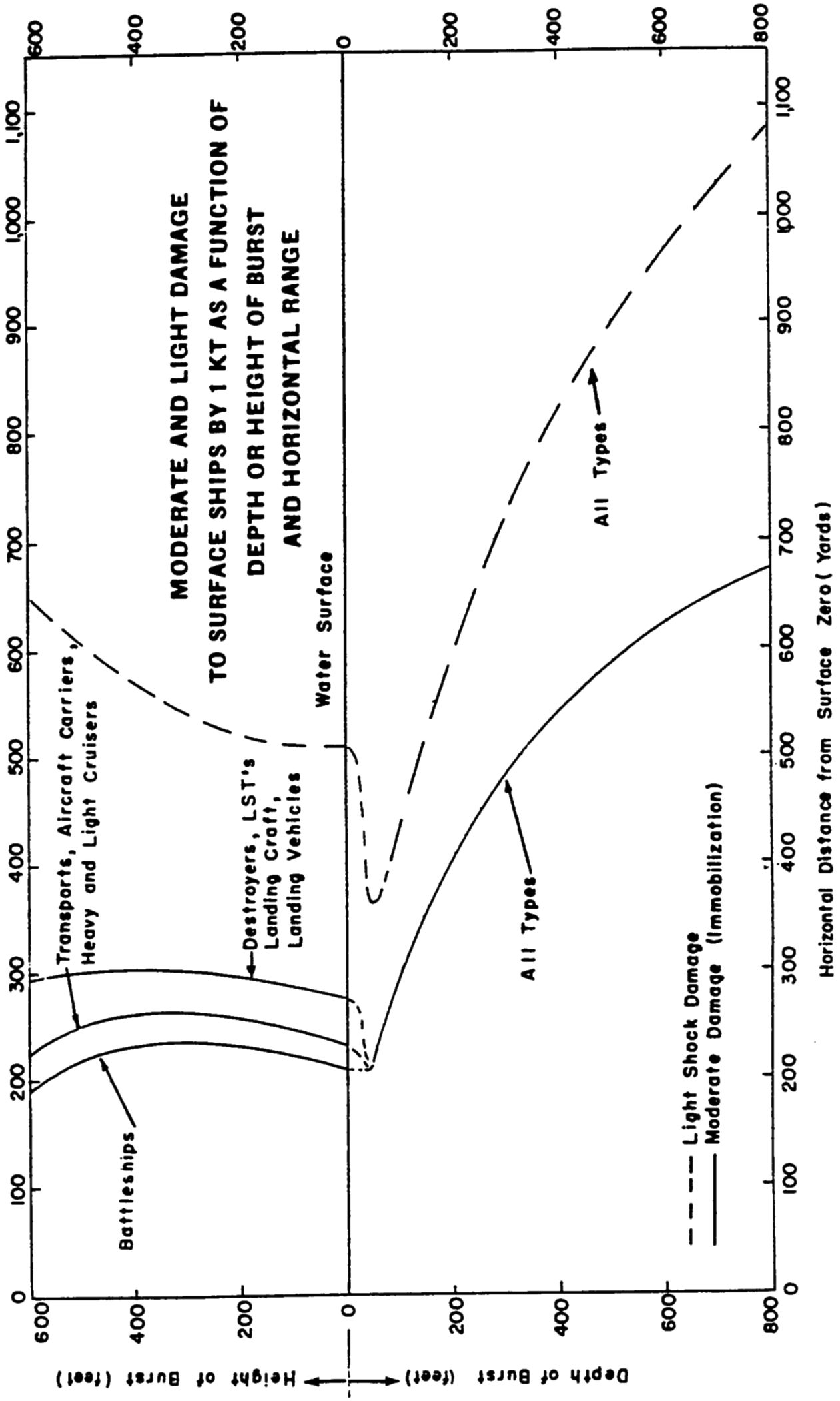

447555 O - 58 - 24

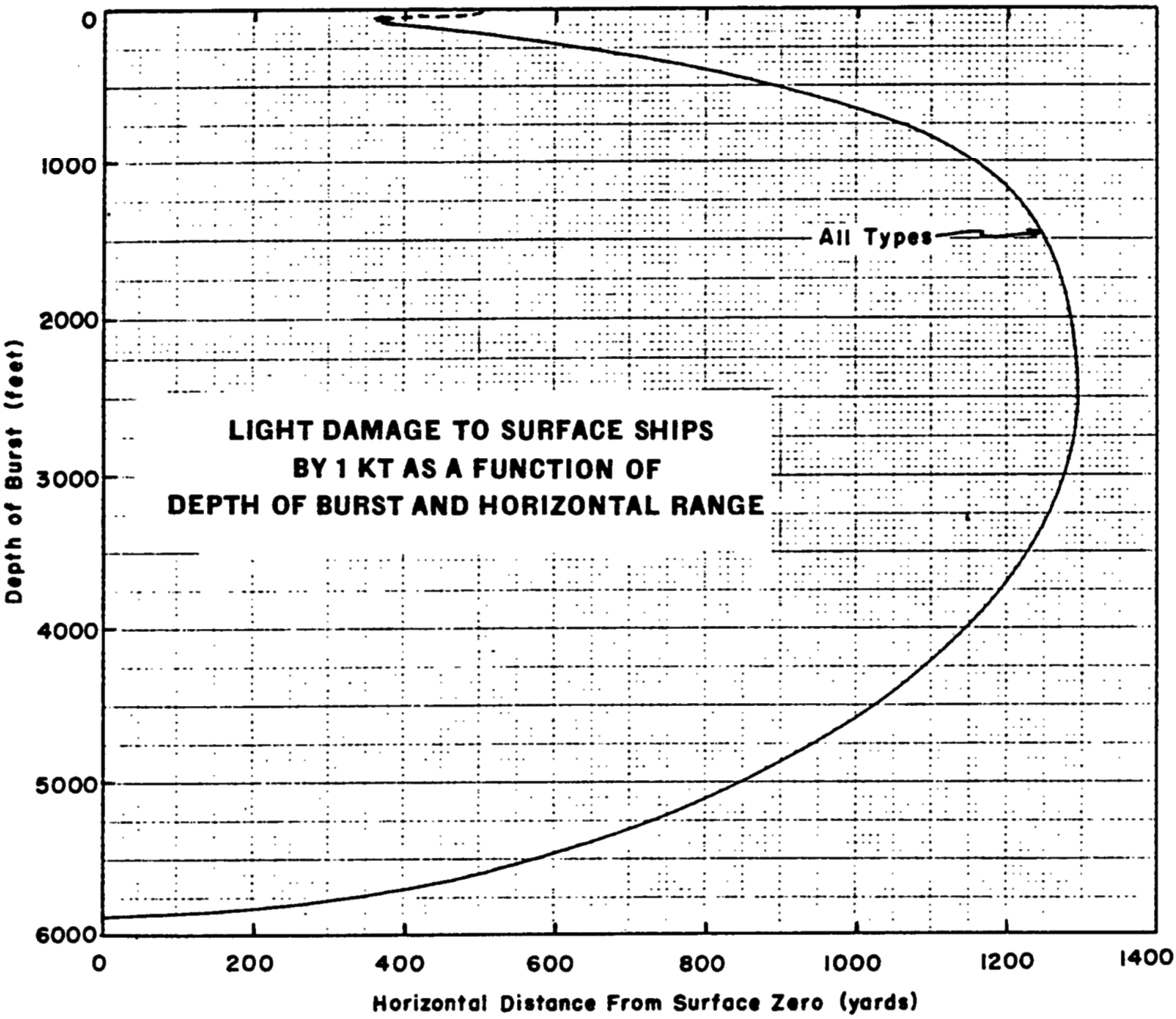
LIGHT DAMAGE TO SURFACE SHIPS
BY 1 KT AS A FUNCTION OF
DEPTH OF BURST AND HORIZONTAL RANGE
All Types
Depth of Burst (feet)
0
1000
2000
3000
4000
5000
6000
0
200
400
600
800
1000
1200
1400
Horizontal Distance From Surface Zero (yards)

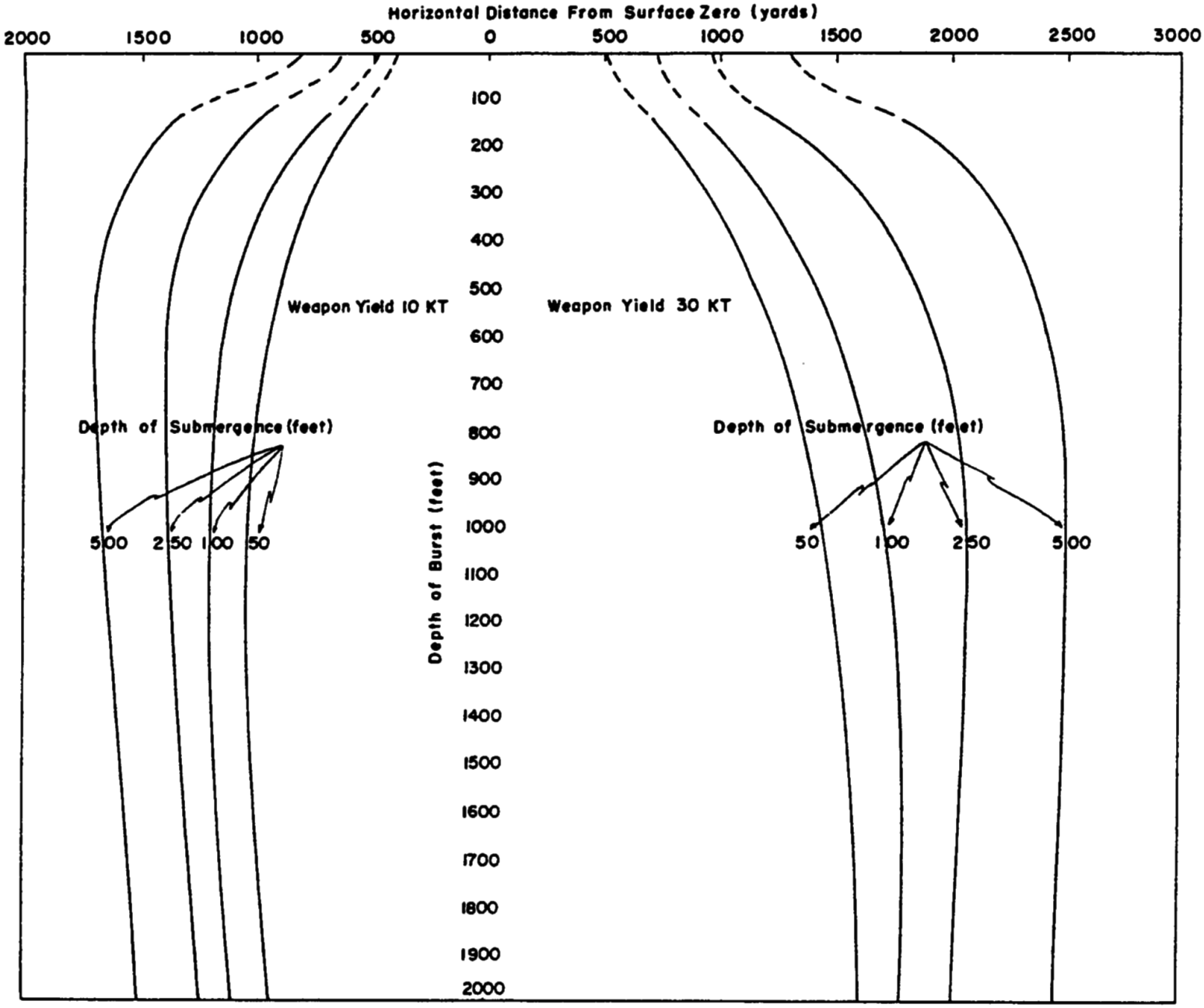

SUBMARINE LETHAL HULL DAMAGE BY 10KT AND 30KT
AS A FUNCTION OF DEPTH OF BURST AND HORIZONTAL RANGE

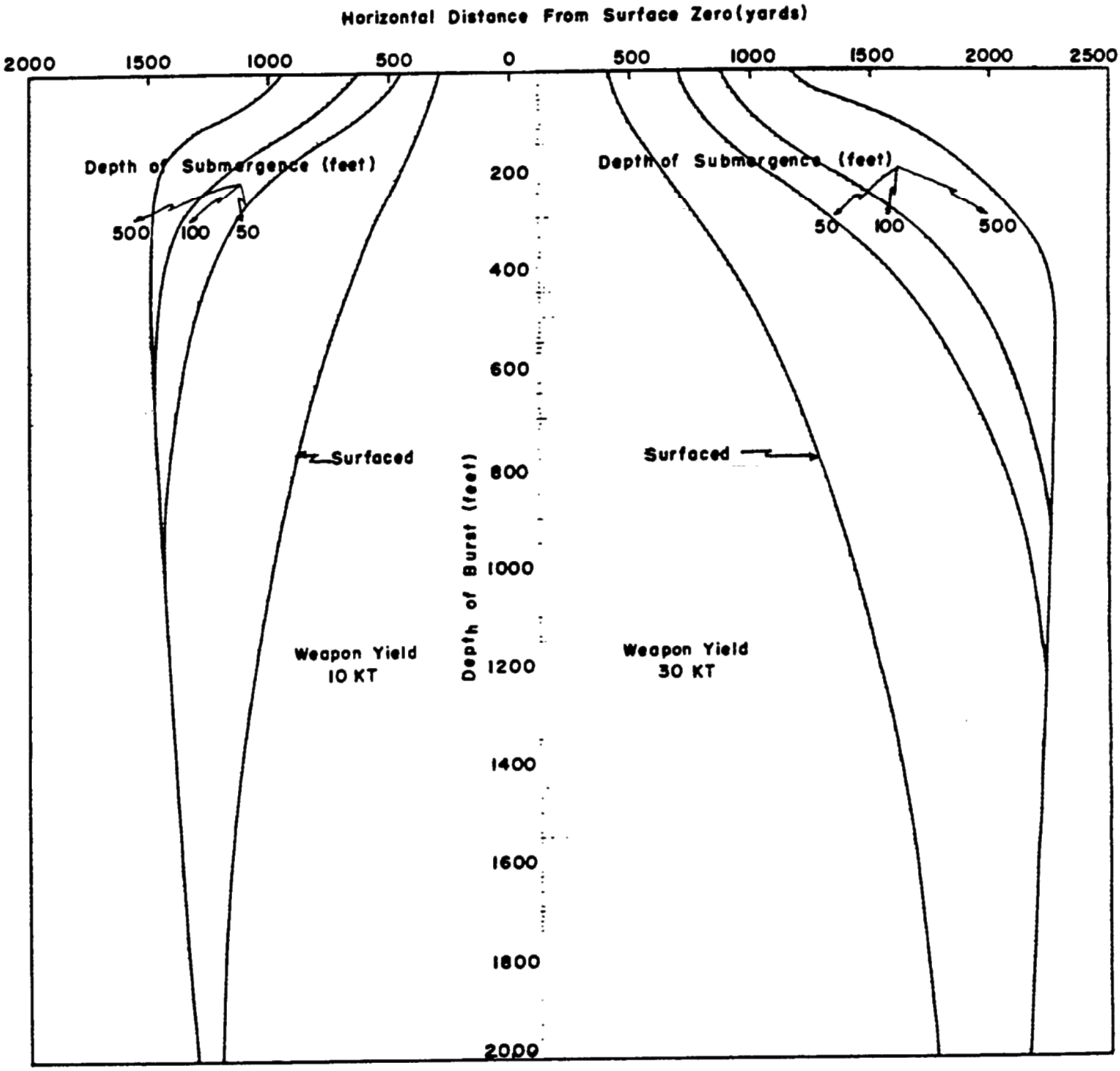

SUBMARINE INTERIOR SHOCK DAMAGE BY 10 KT AND 30 KT
AS A FUNCTION OF DEPTH OF BURST AND HORIZONTAL RANGE

UNDERWATER MINEFIELD NEUTRALIZATION

Figures 8–6 through 8–8 give ranges for underwater minefield neutralization as a function of yield for collapse pressures of 250, 500 and 1,000 psi with both the burst and mines on the bottom. Figure 8–6 is for a 50-foot water depth, figure 8–7 for 100 feet, and figure 8–8 for 200 feet. Linear interpolation between these curves can be used for intermediate water depths and mine case static collapse pressures.

Example.

Given: A 30 KT burst on the bottom in 100 feet of water.

Find The range at which mines with a 500 psi static case collapse pressure located on the bottom are neutralized.

Solution: The range at which the mines are neutralized is taken directly from figure 8–7 to be 400 yards. *Answer.*

Reliability. Based on limited data.

Related Material.

See paragraph 8.3*b*.

FIGURE 8-6

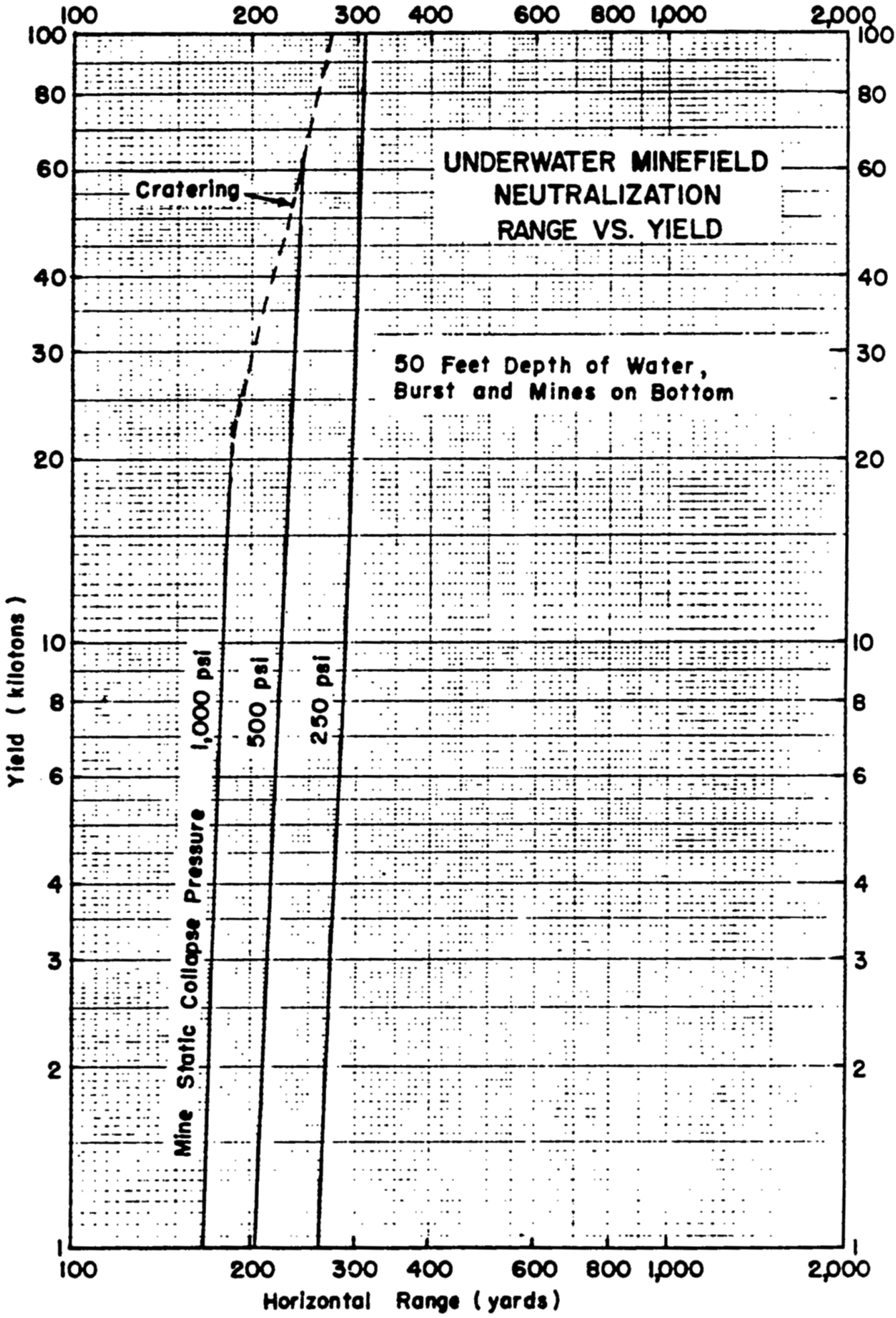
UNDERWATER MINEFIELD
NEUTRALIZATION
RANGE VS. YIELD
50 Feet Depth of Water,
Burst and Mines on Bottom
Cratering
Mine Static Collapse Pressure
1,000 psi
500 psi
250 psi
Yield (kilotons)
Horizontal Range (yards)
100
200
300
400
600
800
1,000
2,000
1
2
3
4
6
8
10
20
30
40
60
80
100

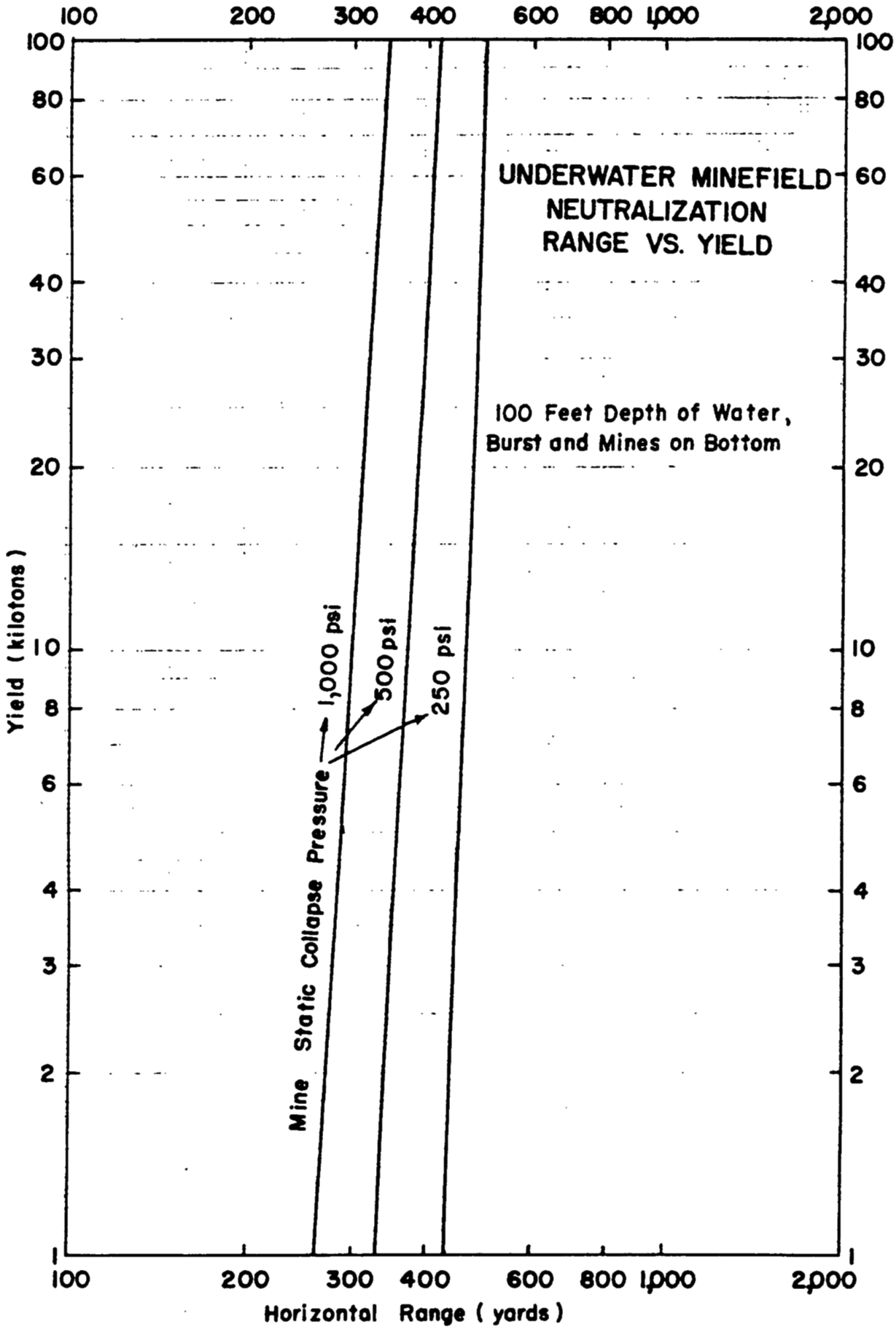
UNDERWATER MINEFIELD
NEUTRALIZATION
RANGE VS. YIELD
100 Feet Depth of Water,
Burst and Mines on Bottom
Mine Static Collapse Pressure
1,000 psi
500 psi
250 psi
Yield (kilotons)
Horizontal Range (yards)
100
200
300
400
600
800
1,000
2,000
1
2
3
4
6
8
10
20
30
40
60
80
100

FIGURE 8-8

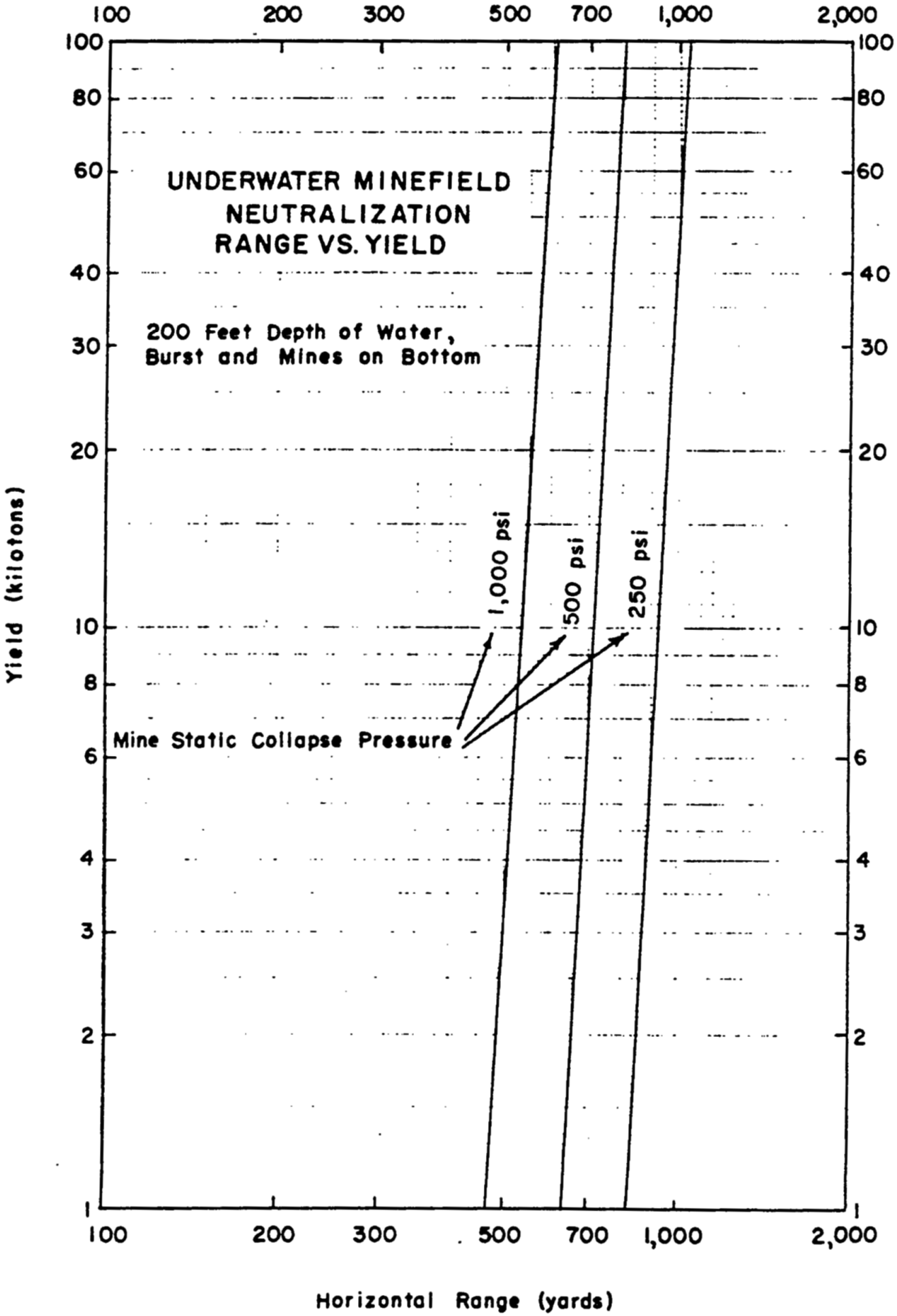
UNDERWATER MINEFIELD
NEUTRALIZATION
RANGE VS. YIELD
200 Feet Depth of Water,
Burst and Mines on Bottom
1,000 psi
500 psi
250 psi
Mine Static Collapse Pressure
Yield (kilotons)
Horizontal Range (yards)
100
200
300
500
700
1,000
2,000
1
2
3
4
6
8
10
20
30
40
60
80
100

SECTION IX
DAMAGE TO AIRCRAFT

9.1 General

Aircraft are relatively vulnerable to the blast and thermal effects of nuclear detonations. Since aircraft are designed within narrow limits for flight and landing loads, the structure can withstand only small additional loads imposed by weapon effects. Blast overpressure on striking an aircraft surface may cause dishing of panels and buckling of stiffeners and stringers. On the side struck by the blast wave, the pressure is increased above the incident intensity by reflection and a diffractive force of short duration is generated. As the wings, empennage, and fuselage are completely enveloped by the blast, further dishing and buckling of skins and structure may result from the crushing effect of the differential pressure between the outside and inside of the aircraft components. Additional damaging loads are also developed by the particle velocity accompanying the blast wave. This particle velocity results in drag loading, which is usually termed "gust loading" with reference to aircraft. The duration of the gust loading is many times that of the diffractive loading, and it develops bending, shear, and torsion stresses in the airfoil and fuselage structures. For aircraft in flight, these stresses are usually the major effect on the aircraft.

The weapon thermal energy which is absorbed by aircraft components can also produce damaging effects. Very thin skins are rapidly heated to damaging temperatures by exposure to the short period thermal flux, because the energy is absorbed by the skin so much more rapidly than it can be dissipated by conduction and convective cooling. Exposed fabric, rubber, and similar materials with low ignition and charring temperatures are vulnerable items which may also initiate extensive fire damage at very low levels of radiant exposure. In recent years, designers of military aircraft have reduced aircraft vulnerability to thermal effects by coating thin skinned materials with low absorptivity paints, by eliminating ignitable materials from exposed surfaces, and by substitution of thicker skins for very thin skins. With these protective measures and design modifications, aircraft can be safely exposed at radiant exposure levels several times those which formerly caused serious damage.

9.2 Parked Aircraft

a. Air Blast. The diffraction phase loading and the drag phase loading have varying relative importance in producing damage to parked aircraft. In general, the diffraction phase is of primary importance in the zones of light and moderate damage. In the zone of severe damage the drag phase assumes more importance. Orientation of the aircraft with respect to the point of burst affects vulnerability considerably. With the nose of the aircraft directed toward the burst, higher weapon effects inputs can be absorbed without damage than for any other orientation. The longer duration of the positive phase of the blast from a large yield weapon may result in some increase in damage over that expected from small yields at the same overpressure level. This increase is likely to be significant at input levels producing severe damage but is not likely to be important at the levels of moderate and light damage. Experiments have shown that revetments provide only slight shielding against blast overpressure and under some conditions reflected pressures within the revetment are higher than corresponding incident pressures. Revetments do provide significant shielding from damage due to flying debris borne by the blast wave. Damage to various types of parked aircraft may be estimated from the curves of figures 9–1, 9–2 and 9–3. Distances to which a given level of damage from a subsurface burst occurs may be derived from figure 7–18 in conjunction with these figures. Quantitative data with respect to high yield influence on damage is not

available. Therefore this influence has not been reflected in the damage curves.

b. Thermal Radiation. A military weapon delivery aircraft properly prepared for its delivery mission with reflective paint and all vulnerable materials shielded from direct thermal radiation will not be damaged by thermal inputs at distances where damage from blast inputs is severe. Other aircraft not so prepared may sustain serious damage at very low thermal levels as a result of ignition of items such as fabric covered control surfaces, rubber and fabric seals, cushions and headrest covers. The radiant exposure levels at which damage to these materials may be expected can be estimated from the data of table 12–2. Aircraft painted with dark paint are especially vulnerable to thermal radiation damage because the dark painted surfaces absorb three to four times the thermal energy that is absorbed by polished aluminum surfaces or surfaces protected with reflective paint. Temporary emergency shielding as provided by trees, buildings, embankments, or similar barriers may be useful for thermal protection of unprepared aircraft, but any of these may increase the blast damage by adding to the flying debris or by multiple reflection of incident overpressures.

9.3 Aircraft in Flight

a. Air Blast. The response of an in-flight aircraft to blast loading is very complex. Factors which influence the response are—

(1) Velocity and altitude of the aircraft.
(2) Orientation of the aircraft with respect to the burst.
(3) Intensity and duration of the overpressure and particle velocity accompanying the blast wave.
(4) Geometry of the aircraft components.
(5) Natural frequency of the aircraft structural components.
(6) Weight and weight distribution at the time of shock arrival.

For weapon delivery aircraft, analytical methods have been developed for predicting response under a variety of flight conditions and for kiloton and megaton yields. These methods require a detailed analysis for each aircraft type. Such analyses have been verified for several aircraft types by observing response at weapon effects tests.

For prediction of weapon effects required to destroy an enemy aircraft in flight, the response problem becomes even more complex. The knowledge of structural behavior and load carrying capacity of aircraft structures in regions above design limit, through ultimate strength to failure, is very limited. Estimates of lethal envelopes for various types of aircraft have been made on the basis of approximate analysis and limited experimental data. Three of these typical envelopes are presented in figure 9–4 to illustrate the general shape and size of regions about a nuclear antiaircraft burst within which an enemy aircraft may be expected to be destroyed by the weapon blast.

b. Thermal Radiation. The radiant exposure of an aircraft in flight varies widely with atmospheric conditions, orientation of the aircraft with respect to the burst, the ground reflecting surfaces, and clouds. Scatter and reflection add to the direct radiation and under some circumstances the thermal energy incident on an aircraft in space may be two to three times that computed at a given slant range from figure 3–6. Conversely, when a heavy cloud layer is between the burst and the aircraft the radiant exposure may be only a fraction of the predicted value for a given range. In other situations, reflected radiation from clouds may contribute significant thermal energy to areas of the aircraft shaded from direct radiation. During weapon effects tests of an aircraft flying in a cloud above the burst, the radiant exposure at the top of the aircraft and its cockpit area was observed to be as much as one-fourth of the direct radiation on the lower surfaces. This experiment demonstrated the need for protection of weapon delivery aircraft from radiant exposure from any direction. For subsonic weapon delivery aircraft which are adequately protected from thermal radiation, the blast loading is usually the limiting effect. However, supersonic aircraft can outrun the shock wave from a delivered weapon, so that thermal inputs determine the minimum safe separation distance of the aircraft and detonation.

DAMAGE TO NON-COMBAT AIRCRAFT

Figure 9–1 presents height of burst vs. ground range curves for light, moderate and severe damage to randomly oriented parked transport airplanes, light liaison airplanes, and helicopters. These curves are drawn for 1 KT and are based on the following definitions of damage and corresponding peak overpressure criteria:

Light Damage--That damage which does not prevent flight of the aircraft, though performance may be restricted thereby. Transport airplanes, 1 psi; light liaison airplanes, ½ psi; helicopters, ½ psi.

Moderate Damage—That damage which requires field maintenance to restore the aircraft to operational status. Transport airplanes, 2 psi; light liaison airplanes, 1 psi; helicopters, 1½ psi.

Severe Damage—That damage which requires depot level maintenance to restore the aircraft to operational status. Transport airplanes, 3 psi; light liaison airplanes, 2 psi; helicopters, 3 psi.

Scaling. Height of burst and ground range for a given degree of damage scale as the cube root of the yield:

$$\frac{h_1}{h_2}=\frac{d_1}{d_2}=\frac{W_1^{1/3}}{W_2^{1/3}},$$

where h_1 and d_1 are height of burst and ground distance for yield W_1, and h_2 and d_2 are the corresponding height of burst and distance for yield W_2.

Example.

Given: A 100 KT weapon is to be burst at optimum height to obtain moderate damage to parked transport airplanes.

Find: The ground range at which moderate damage may be expected and the optimum height of burst.

Solution: From figure 9–1, the optimum height of burst for 1 KT is 1,300 feet. The optimum height of burst for 100 KT is $(100)^{1/3}\times1300=6{,}000$ feet. *Answer.*

Also from figure 9–1, the ground range for moderate damage from a 1 KT burst at a height of burst of 1,300 feet is 1,380 yards. The corresponding ground range for 100 KT is $(100)^{1/3}\times1{,}380=6{,}400$ yards. *Answer.*

Reliability. These curves are based on full scale test data for military bomber and fighter aircraft and detailed analysis of weapons effects on basic structural components. It is considered that they represent the best available estimates, for the aircraft types specified, of distances at which 50 percent of the aircraft parked at that range may be expected to be damaged to the degree specified.

Related Material.

See paragraph 9.2.

See also figures 9–2 and 9–3.

FIGURE 9-1

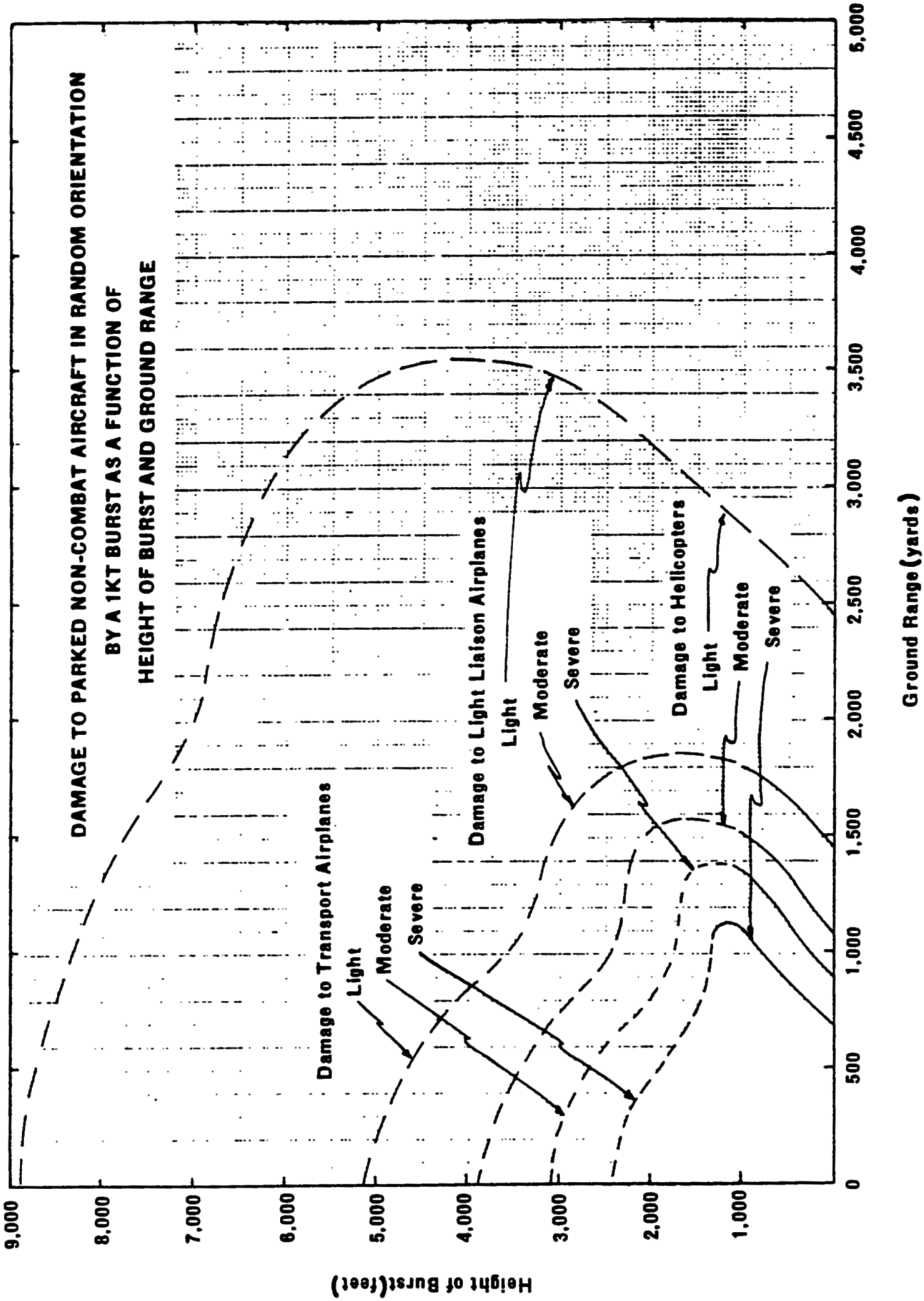
DAMAGE TO PARKED NON-COMBAT AIRCRAFT IN RANDOM ORIENTATION
BY A 1KT BURST AS A FUNCTION OF
HEIGHT OF BURST AND GROUND RANGE
Damage to Transport Airplanes
Light
Moderate
Severe
Damage to Light Liaison Airplanes
Light
Moderate
Severe
Damage to Helicopters
Light
Moderate
Severe
Height of Burst (feet)
9,000
8,000
7,000
6,000
5,000
4,000
3,000
2,000
1,000
Ground Range (yards)
0
500
1,000
1,500
2,000
2,500
3,000
3,500
4,000
4,500
5,000

CONFIDENTIAL

DAMAGE TO PARKED COMBAT AIRCRAFT, RANDOM ORIENTATION

Figure 9–2 presents height of burst vs. ground range curves for light, moderate and severe damage to bomber and fighter aircraft for random orientation. These curves are drawn for 1 KT and are based on the following definitions of damage and corresponding peak overpressure criteria.

Light Damage—That damage which does not prevent flight of the aircraft, though performance may be restricted thereby. Jet bombers, 1½ psi; propeller fighters, 2 psi; jet fighters, 2 psi.

Moderate Damage—That damage which requires field maintenance to restore the aircraft to operational status. Jet bombers, 2½ psi; propeller fighters, 4 psi; jet fighters, 5 psi.

Severe Damage—That damage which requires depot level maintenance to restore the aircraft to operational status. Jet bombers, 4 psi; propeller fighters, 5 psi; jet fighters, 8 psi.

Scaling. Height of burst and ground range for a given degree of damage scale as the cube root of the yield:

$$\frac{h_1}{h_2}=\frac{d_1}{d_2}=\frac{W_1^{1/3}}{W_2^{1/3}},$$

where h_1 and d_1 are height of burst and ground distance for yield W_1, and h_2 and d_2 are the corresponding height of burst and distance for yield W_2.

Example.

Given: A 50 KT burst at ground level.

Find: At what range from ground zero must a jet fighter be parked in order to be no more than lightly damaged.

Solution: From figure 9–2, the distance from ground zero for light damage to jet fighters for a 1 KT burst is 900 yards. The corresponding distance for a 50 KT burst is $900\times(50)^{1/3}=3{,}300$ yards. *Answer.*

Reliability. These curves are based on full scale test data for military bomber and fighter aircraft and detailed analysis of weapons effects on basic structural components. It is considered that they represent the best available estimates, for the aircraft types specified, of distances at which 50 percent of the aircraft parked at that range may be expected to be damaged to the degree specified.

Related Material.

See paragraph 9.2.

See also figures 9–1 and 9–3.

CONFIDENTIAL

FIGURE 9-2

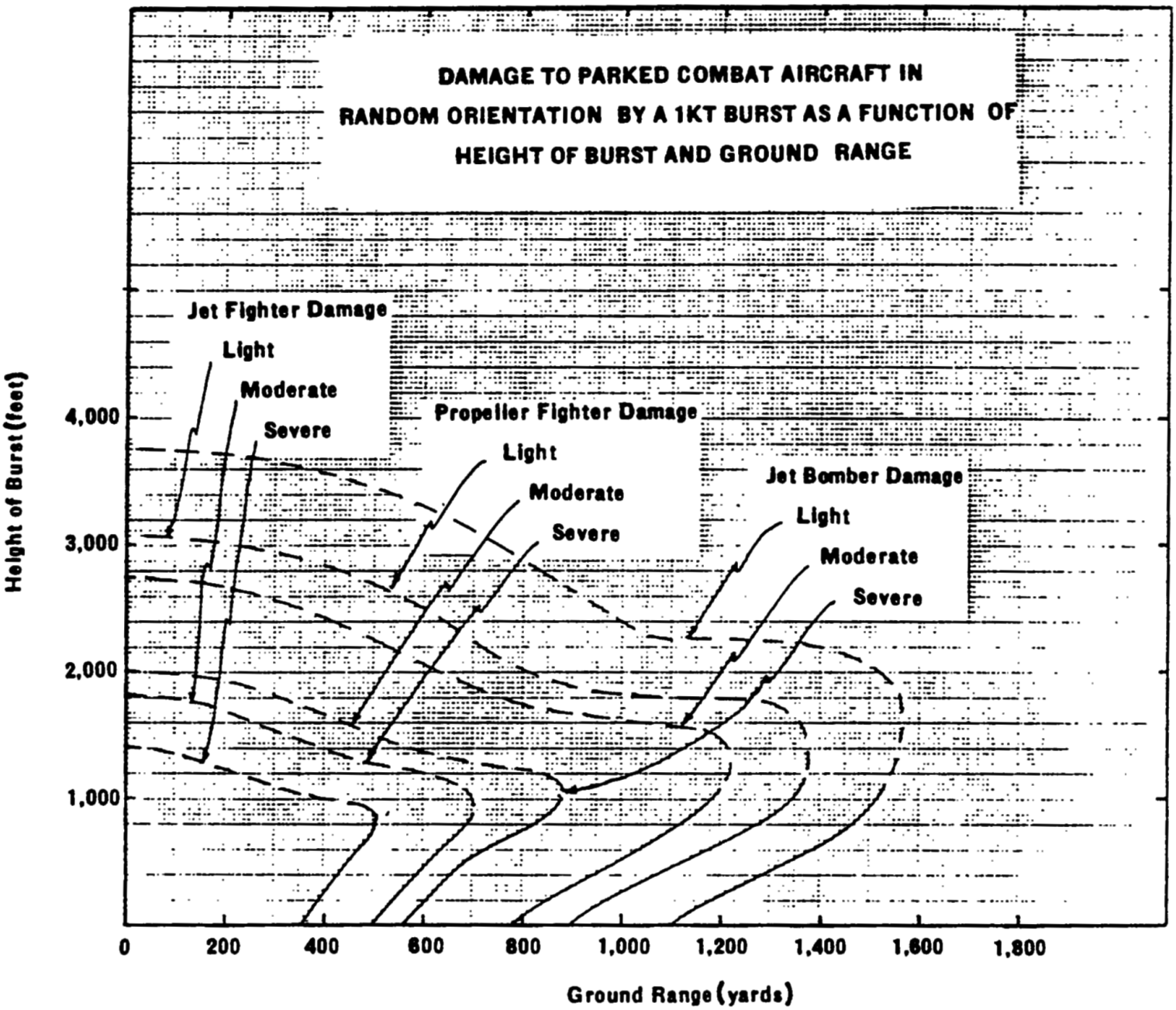
DAMAGE TO PARKED COMBAT AIRCRAFT IN
RANDOM ORIENTATION BY A 1KT BURST AS A FUNCTION OF
HEIGHT OF BURST AND GROUND RANGE
Jet Fighter Damage
Light
Moderate
Severe
Propeller Fighter Damage
Light
Moderate
Severe
Jet Bomber Damage
Light
Moderate
Severe
Height of Burst (feet)
4,000
3,000
2,000
1,000
0
200
400
600
800
1,000
1,200
1,400
1,600
1,800
Ground Range (yards)

DAMAGE TO PARKED COMBAT AIRCRAFT, NOSE-ON ORIENTATION

Figure 9–3 presents height of burst vs. ground range curves for light, moderate and severe damage to bomber and fighter aircraft for nose-on orientation. These curves are drawn for 1 KT and are based on the following definitions of damage and corresponding peak overpressure criteria.

Light Damage—That damage which does not prevent flight of the aircraft, though performance may be restricted thereby. Jet bombers, 2 psi; propeller fighters, 2 psi; jet fighters, 3 psi.

Moderate Damage—That damage which requires field maintenance to restore the aircraft to operational status. Jet bombers, 3 psi; propeller fighters, 5 psi; jet fighters, 7 psi.

Severe Damage—That damage which requires depot level maintenance to restore the aircraft to operational status. Jet bombers, 5 psi; propeller fighters, 7 psi; jet fighters, 9 psi.

Scaling. Height of burst and ground range for a given degree of damage scale as the cube root of the yield—

$$\frac{h_1}{h_2}=\frac{d_1}{d_2}=\frac{W_1^{1/3}}{W_2^{1/3}},$$

where h_1 and d_1 are height of burst and ground distance for yield W_1, and h_2 and d_2 are the corresponding height of burst and distance for yield W_2.

Example.

Given: A 30 KT weapon is burst 4,000 feet above the terrain and a horizontal distance of 2,500 yards from a jet bomber parked nose-on to the burst.

Find: The corresponding 1 KT height of burst and the degree of damage to be expected.

Solution: The corresponding 1 KT height of burst is $\frac{4{,}000}{(30)^{1/3}}=1{,}290$ feet.

The corresponding distance from ground zero is $\frac{2{,}500}{(30)^{1/3}}=800$ yards.

From figure 9–3, moderate to severe damage would be expected at 2,500 yards from ground zero for a 30 KT weapon burst 4,000 feet above the terrain. *Answer.*

Reliability. These curves are based on full scale test data for military bomber and fighter aircraft and detailed analysis of weapons effects on basic structural components. It is considered that they represent the best available estimates, for the aircraft types specified, of distances at which 50 percent of the aircraft parked at that range may be expected to be damaged to the degree specified.

Related Material.

See paragraph 9.2.

See also figures 9–1 and 9–2.

ESTIMATES OF GUSTS AND THERMAL ENVELOPES FOR TYPICAL COMBAT AIRCRAFT

Figure 9-4 presents an estimate, for each of three typical combat aircraft types, of the lethal envelope in the vertical plane containing the flight path. For each diagram, the silhouette represents the position of the aircraft at burst time; a 1 KT burst anywhere within the envelope is expected to destroy the aircraft. The corresponding lethal volume is approximately that within the surface of revolution generated by revolving the envelope shown about the flight path axis. Also indicated on the diagrams are the ranges at which the radiant exposure of the aircraft would be 135 cal/cm^2, an exposure level at which most aircraft would experience some melting of skin panels by thermal radiation from a 1 KT burst.

Scaling and Reliability. Estimates of lethal envelopes for other yields may be made by scaling the ranges to the blast envelopes by the cube root of the yield and the ranges for the 135 cal/cm^2 envelopes by the square root of the yield. The diagrams are presented to illustrate general shapes and sizes of lethal envelopes for aircraft and it is not intended that the numerical data be applied directly to any specific aircraft models.

Related Material.

See paragraph 9.3.

ESTIMATES OF GUSTS & THERMAL ENVELOPES FOR TYPICAL COMBAT AIRCRAFT

1 KT ANTI-AIRCRAFT BURST

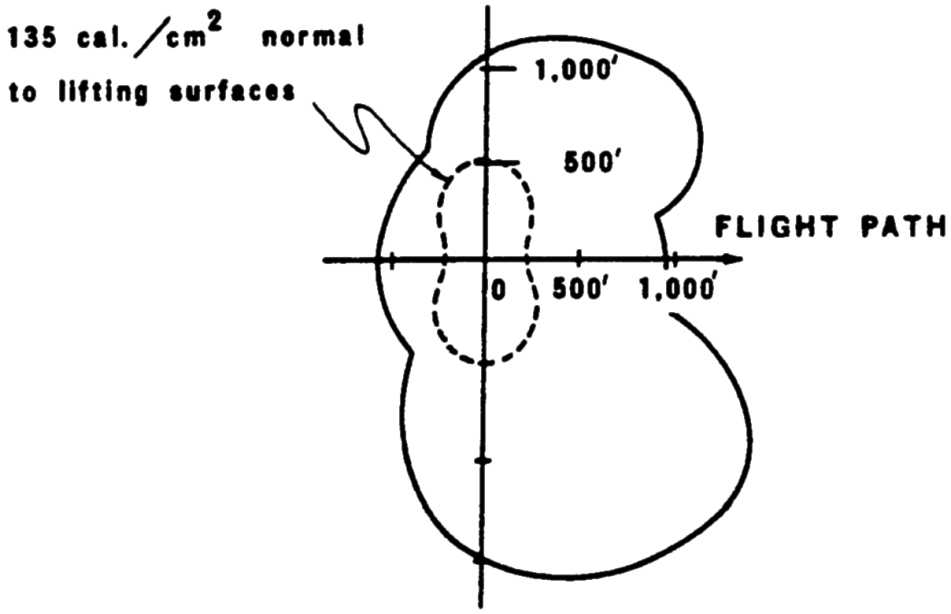

SUBSONIC BOMBER
ALTITUDE 40,000'
SPEED, MACH .9

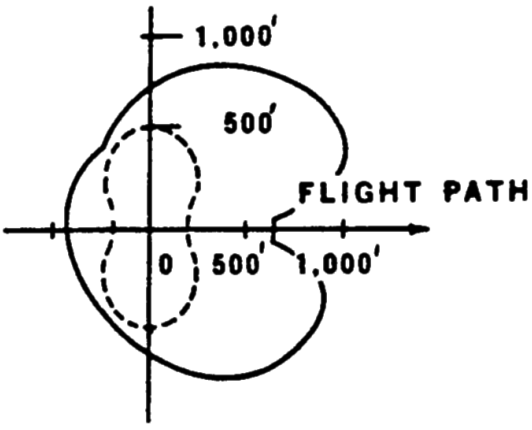

FIGHTER
ALTITUDE 40,000'
SPEED, MACH .95

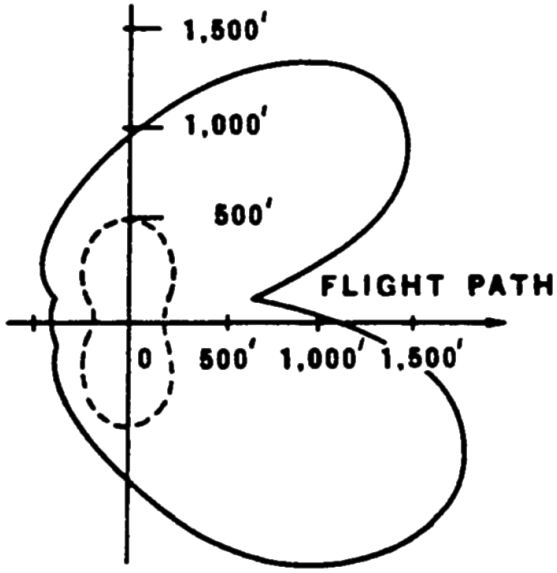

SUPERSONIC BOMBER
ALTITUDE 70,000'
SPEED, MACH 2.5

SECTION XI
FOREST STANDS

11.1 General

Although forests or tree stands may afford troops deployed therein significant protection against certain effects of nuclear weapon detonations (e. g. thermal radiation), the forests themselves are quite vulnerable to some of these effects. Falling limbs and trees create a missile hazard and the resultant debris on the forest floor may impede the movement of troops and most vehicles. In dry, windy weather, forest fires may be initiated by a nuclear weapon detonation, with smoke and flame extending the range of hazardous effects from the bomb itself many times. Forest vulnerability depends on recent local weather history and upon the type of tree stand involved. Forest kindling fuels and types of stands are discussed in detail in the paragraphs which follow.

11.2 Air Blast

a. General. For convenience in discussion of blast effects, forest stands are divided into the following types:

(1) *Type I stand: Improved natural or planted conifer forests of European type.* These forests characteristically grow in regular blocks, usually with definite borders. Tree spacing is uniform with only small patches of ground visible through the canopy from above. Trees are of uniform height (100 to 130 feet) and nearly the same in diameter (14 to 24 inches). Stands of this type are vigorous in appearance and fast growing. Viewed from above the crown canopy appears smooth. Within the stand there usually will be found low stumps resulting from thinning, clear lower stems as a result of pruning, and little or no underbrush, combining to give the interior of the stand a clean park-like appearance, and affording good visibility and easy passage into the forest.

(2) *Type II stand: Naturally occurring, unimproved conifer forests that have developed under unfavorable growing conditions.* Unfavorable growing conditions result from: shallow and/or rocky soil, deficient annual rainfall, short growing season with unfavorable temperatures (i. e., higher latitudes and/or higher elevations), and unfavorable topography such as poorly drained flats or steep slopes. Random tree spacing is characteristic, with trees varying in height (10 to 75 feet) and in diameter (1 to 17 inches). The crown canopy generally has an uneven appearance. Large stands often contain bare areas with irregular borders. The stand itself appears low in vigor. The forest floor within the stand is generally cluttered with dead, fallen trees which, when combined with the persistent dead limbs on the dense growing live stems and the heavy underbrush in the numerous stand openings, impede entrance into the stand and decrease visibility.

(3) *Type III stand: All broadleaf forests and naturally occurring, unimproved conifer forests that have developed under favorable growing conditions.* Favorable growing conditions are associated with: deep, generally rock-free soil, adequate annual rainfall, long growing season with favorable temperatures (i. e., middle latitudes and lower elevations), and favorable topography such as well-drained flats and moderate slopes, or along stream courses. Random tree spacing is characteristic with trees varying in height (30 to 120 feet) and in diameter (2 to 25 inches). The crown canopy generally has an uneven appearance. Large stands often contain bare areas with irregular borders. The stand itself appears high in vigor. The forest floor within the stand may be

cluttered with dead, fallen trees which impede entrance into the stand. Underbrush is light or absent, and visibility is fairly good.

b. Air Blast Damage. Height of burst-damage-distance curves for severe and light damage to forests are presented in figures 11–1 to 11–6. Distances to which a given level of damage from a subsurface burst occurs may be derived from figure 7–18 in conjunction with these figures. Examples of scaling accompany figure 11–1. Tree stand types referred to are those given above. Severe and light damage are defined in terms of length of stems down per acre; approximately 1,500 feet per acre for light damage and 9,000 feet per acre for severe damage. These criteria in terms of percentage of trees broken are shown in table 11–1. The approximate number of trees per acre that may be expected for the three stand types is also shown.

Table 11–1. Percentage of Trees Broken for Light and Severe Damage to Forest Stands

Stand type	Total No. of trees per acre	Trees per acre 6 in. or larger in diameter	Light damage, % trees 6 in. or larger in diameter, broken	Severe damage, % trees 6 in. or larger in diameter, broken
I	75	75	15	95
II	475	260	[a] 10	[a] 65
III	215	200	[b] 10	[b] 60

[a] Majority of damage as uprooted trees.
[b] In broadleaf forests majority of damage as branch breakage and uprooting

11.3 Thermal Radiation

a. General. Under certain conditions, the employment of an air burst weapon over a forest or wildland area may cause fires. During the fire season, even when the burning potential (a measure of probable fire aggressiveness) is low, fires may spread. If fires are started in regions of sufficient fuel density when the burning potential is dangerously high, complete evacuation of personnel and equipment may be necessary. Organized control of the spread of the fire is virtually impossible until changes in weather or fuel availability reduce the burning potential.

b. Ignitions. Wildland fuels are generally a mixture of thin and heavy fuel components. Thin fuels are typified by surface litter and grassland; heavy fuels by fallen branches. The thinnest fuel present determines the exposure required for ignition of the mixture. Heavy fuels do not ignite and continue to burn by themselves; however, thin fuels may serve as the source of a pilot flame which substantially lowers heavy fuel ignition exposure requirements, or thin fuels may spread fire after the end of the thermal pulse. During the fire season, ignitions may be expected in kindling fuels wherever the radiant exposures exceed 2 to 3 cal/cm² for a 1 KT weapon. As the yield increases the minimum radiant exposures for ignition increase as $W^{1/8}$, i. e., 8 to 10 cal/cm² would be required from a 30 MT weapon to ignite the thinnest wildland fuels. These exposures apply to surfaces normal to the direction of radiation; however, wildland fuels rarely present a flat smooth surface. Individual fuel particles are of many shapes and are oriented more or less at random. Consequently, even at low burst altitudes, minimum ignition exposures can be assumed to remain the same, although a reduced number of ignitions is to be expected owing to the increased shielding effect of trees and shrubs. Green leaves and needles on tree crowns smoke and char but do not ordinarily sustain ignition. This smoke production materially reduces the radiant exposure of the ground surface. Ignitions occur in open areas if the dimensions are large enough so that the area is not completely in the shadow of adjacent timber or brush stands. It is estimated that very few ignitions occur within a timber stand in which the tree canopy shades more than 20 percent of the ground surface. Smoldering ignitions are likely to occur in snags and dead limbs on the forest floor. While such ignitions are not an immediate hazard, they may cause fires to break out up to two or three days later, especially if a large amount of blast breakage occurs, opening the stand to the prevailing winds.

c. Fire Seasons. The fire season of an area is primarily a function of the annual rainfall-temperature pattern and its associated vegetation development, and varies widely between geographic locations. Table 11–2 summarizes these conditions for the more important wildland fuels found throughout the world. Once it is determined that fuel conditions meet those prevailing in the fire season, local weather conditions will determine burning potential.

Table 11-2. Condition of Wildland Fuels During Fire Season

Fuel type		Amount and density of fuel required to constitute a fire hazard	Condition during fire season
Grass or heath...	Grassland; dry bracken ferns and other seasonal plants; dry regrowth in previously burned areas.	Uniform grass cover one-half ton or more per acre.	Vegetation nearly cured or dead.
Evergreen brush..	Perennial evergreen shrubs and brush; chaparral; young evergreen growth.	75 percent or more area covered.	15–25 percent by weight of leaves and associated twigs dead.
Deciduous broadleaf forest.	Forest predominantly of trees such as oak, birch, maple, etc., leaves of which die and fall every year.	Ground covered with more or less continuous layer of dead leaves.	Leaves off trees; ground vegetation dead or nonexistent.
Coniferous forest.	Forest of evergreen pines, firs, spruces, etc.; generally the family of needle bearing trees.	Ground covered with more or less continuous layer of dead needles and twigs.	Needles and twigs dry enough to break easily when bent. Grass and other ground vegetation, if present, curing or dead.

d. Kindling Fuels. The majority of thin wildland fuels which serve as kindling material are typed as shown in table 11-3 into four classes corresponding to different minimum exposures required for ignition. Ignition exposures required increase as fuel moisture content increases. Since ignition generally occurs on those surfaces most exposed to the atmosphere, required ignition exposures are a function of relative humidity as shown in figure 11-7. Fires may be blown out by the blast wave, depending on the time interval between ignition and arrival of the shock. Blowout is not expected in overpressure regions below 5 psi for fully exposed fuels. When fires are not blown out, they generally increase in intensity due to action of the blast wind.

Table 11-3. Classes of Thin Wildland Kindling Fuels (Arranged in Order of Decreasing Flammability)

Class	Description
I.....	Broadleaf and coniferous litter—mixture of fine grass, broken leaves and duff, and thin translucent broadleaf leaves.
II.....	Hardwood and softwood punk in various stages of decay.
III.....	Cured or dead grass.
IV.....	Conifer needles and thick, nearly opaque broadleaf leaves.

e. Burning Potential. The principal factors, aside from the fuels present, that influence the burning potential of a forest or wildland area are—the nature of the terrain, the wind speed close to the ground, the relative humidity and the precipitation history. An approximate guide for evaluating the effects of weather on burning potential is given in table 11-4. Fuels seldom burn vigorously, regardless of wind conditions, when the fuel moisture is greater than 16 percent. This corresponds to an equilibrium moisture content for 80 percent relative humidity. About a quarter inch of rain renders fuels temporarily nonflammable and may extinguish going fires in thin fuels. The time required to restore the burning potential to the value prior to the rain may vary from hours to days depending on local weather conditions. Surface fuels in the interior of timber stands are exposed to reduced wind velocities and generally have high fuel moisture due to shading by the canopy.

f. Fire Spread. Under identical weather conditions, concentrations of heavy fuel are more hazardous than thin fuels, even though they tend to reduce local wind speeds and do not respond as rapidly to changes in relative humidity. Trees and heavy limbs on the forest floor may be ignited by an otherwise nonhazardous surface fire. When heavy fuels are present near the borders of standing timber, fire may travel into the tree crowns and continue to crown (spread

Table 11–4. Burning Potential for Light Wildland Fuels During Fire Season (Terrain With Slopes Less Than 20 Percent)

Wind speed at 20 feet above ground in the open	Relative humidity (percent)			
	Below 15	15–40	40–65	65–80
Below 5 knots	Dangerous*	Dangerous	Low*	Low.
5–10 knots	Critical*	Dangerous	Dangerous	Low.
10–15 knots	Critical	Critical	Dangerous	Low.
Above 15 knots	Critical	Critical	Critical	Dangerous.

*Definitions:

Low—irregular fire perimeter, spread greatly affected by local changes in fuel structure and topography, depth of fire small. Fire generally stops at roads and ridge tops. Control action can be on an individual basis.

Dangerous—continuous intense fire front which moves rapidly, frequently spots ahead. Aggressive organized action required to protect personnel and equipment.

Critical—conflagration-type fire, in heavy fuels readily crowns and spots as much as a mile ahead. Requires personnel and equipment to be evacuated from in front and from near the flanks of such fires. Control action effective only when changes in fuel type or burning conditions permit.

Note 1. For heavy fuels, use the classification for the next higher wind speed.
2. For terrain with slopes greater than 20 percent, use the classification for the next higher wind speed.
3. For canopy shading 20 percent of the ground, reduce wind one class and increase relative humidity one class.
4. For full shading, reduce wind two classes and increase relative humidity two classes.

from top to top) even though ground fuel concentrations are low. Pine species are most likely to crown, fir and spruce less likely, and hardwoods least likely. Where large areas of heavy dry fuels are ignited simultaneously, a large whirling fire may develop. Such fires exhibit erratic spread behavior. Whirls may break off the main fire and travel against the prevailing wind. Whenever a strong upward convection column is built up in the case of a heavy fuel fire, the fire may spread very rapidly by "spotting", i. e., by throwing firebrands. Fires started by spotting may travel toward the main fire due to strong indrafts.

FIGURE 11-7

MINIMUM RADIANT EXPOSURE FOR IGNITION OF WILDLAND KINDLING FUELS BY CLASS SCALED TO 1KT

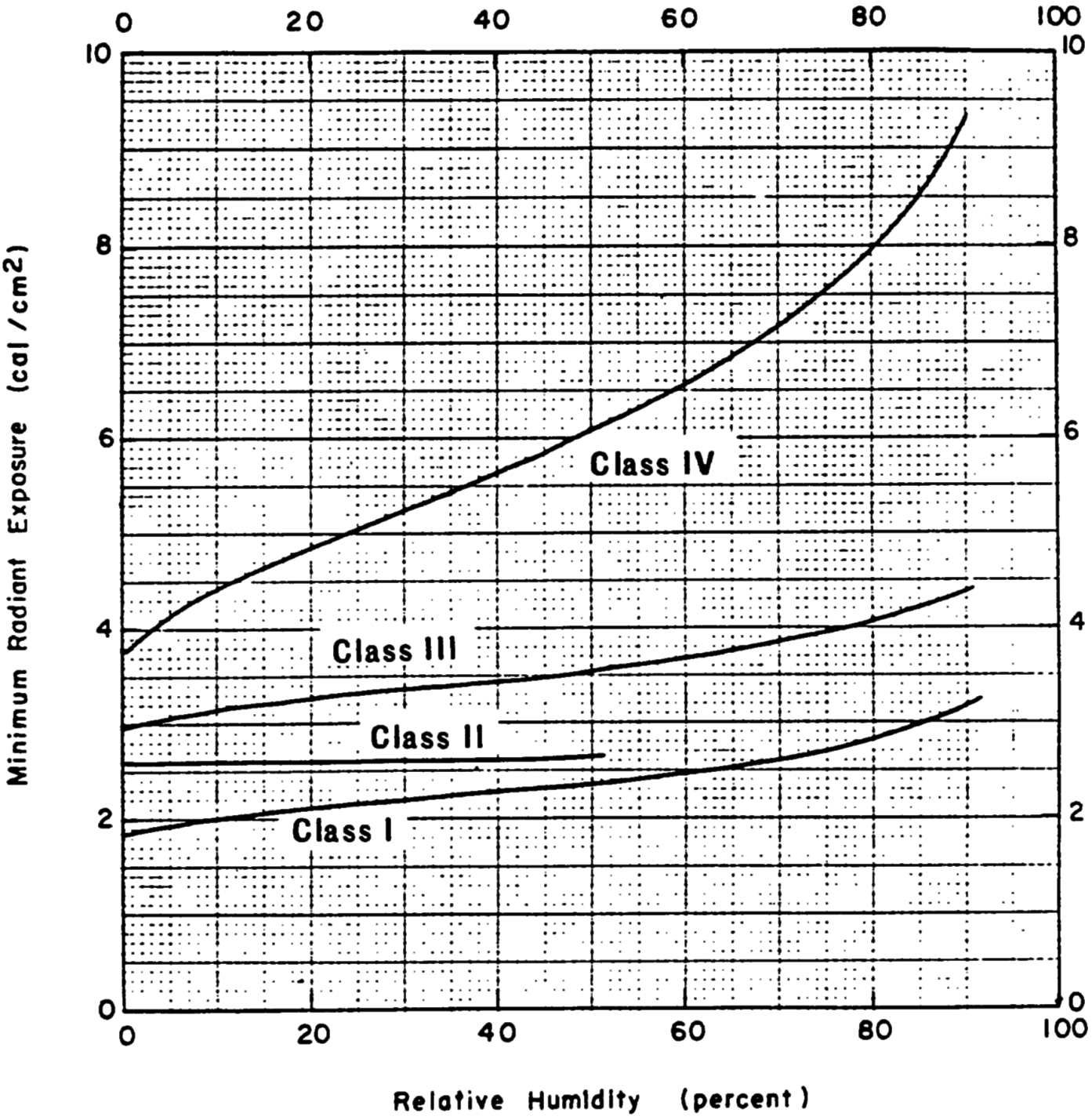

SECTION XII
MISCELLANEOUS RADIATION DAMAGE CRITERIA

12.1 Fire in Urban Areas

a. General. The employment of an air burst weapon over urban areas may produce, in addition to blast damage, mass fires which under proper conditions materially increase the degree and extent of damage. The behavior of such fires, whether they are of primary or secondary origin, follows the pattern of fires in forest and wildland areas. The burning potential for urban areas varies with weather conditions in much the same manner as for wildlands; however, the fire season as such is not as pronounced as in wildlands. During those seasons when weather conditions may reduce exterior potentials to zero, dwellings are usually heated, so that interior fuels are dried out. Fire incidence and subsequent fire buildup depend also upon the amount and distribution of flammable material used in interior furnishing and building construction, the incidence of interior kindling fuels, and the relative cleanliness of the living habits of the population.

b. Ignition Points. A survey of metropolitan areas in the United States indicates that the incidence of exterior ignition points can be correlated with urban land use. Table 12–1 presents a relative tabulation based on exterior kindling fuels. Newspapers and other paper products account for 70 percent of the total, while dry grass and leaves account for another 10 percent in residential areas. Most other exterior kindling fuels are present in small percentages or require radiant exposures in excess of 10 cal/cm^2 for ignition. Weathered and badly checked fences and building exteriors which contain appreciable dry rot constitute an ignition hazard. The tabulation presented in table 12–1 is not representative of European cities and other areas where fuel is at a premium or where extensive use is made of stone, brick, masonry, and heavy timber construction. Multi-story buildings and narrow streets reduce both interior and exterior primary ignitions, since such ignitions are proportional to the amount of sky seen from the location of the probable ignition point.

Table 12–1. Relative Incidence of Ignitions in Metropolitan Areas of the United States by Land Use (Based on Exterior Kindling Fuels)

Land use	Relative incidence
Downtown retail	1.0
Large manufacturing*	1.4
Good residential	1.6
Small manufacturing	3.8
Poor residential	5.2
Neighborhood retail	5.5
Waterfront areas	8.0
Slum residential	11.7
Wholesale	15.1

*May be likened to a typical fixed military installation in the Z. I.

c. Humidity Effects. Since paper is the major exterior kindling fuel and is also an important interior fuel, the extent of ignitions may be estimated from the minimum radiant exposure requirements for this material (fig. 12–1). Thin exterior kindling fuels respond to hourly changes in relative humidity; however, fire buildup and subsequent fire behavior are best estimated from the average daytime relative humidity. Maximum fire effects occur during daily periods of lowest relative humidity, usually mid-afternoon. Guides for estimating urban burning potentials are given in figures 12–2 and 12–3. Where central heating of dwellings is a common practice, interiors are much drier than would be indicated by exterior relative humidities and temperatures. Based on United States experience, interior heating becomes an important factor when the maximum daily temperature drops below 70° F. Where fuel is scarce or expensive, this temperature may drop to 60° F., or even lower.

d. Fire Spread. The rate of fire buildup in urban areas is expected to be slower than for wildlands. The time to maximum fire intensity is less for the relatively high ignition incidence areas of table 12–1 than for those of lower ignition incidence. Aside from weather conditions, the principal factors which influence fire spread are the continuity, size and combustibility of buildings, fuel value of building contents, and

topography. When strong convective action develops and spotting is frequent, the flammability of roof material is an important factor in spread. Spread of the fire front generally occurs by radiation from adjacent buildings; hence, fire stops only when the building spacing becomes great enough to reduce this radiation level below a critical value. This critical spacing is greater for multi-story buildings and varies with building combustibility, but on the average is about 50 to 100 feet.

12.2 Nuclear Radiation Damage

a. Neutron Irradiation.

(1) *Free air neutron flux.* The curves in figure 12–4 show the number of fast neutrons per square centimeter expected per kiloton of yield at various horizontal distances from typical airburst fission weapons detonated at altitudes up to 100,000 feet MSL. It is believed that these curves will give results correct within a factor of five.

(2) *Permanent damage.* Except for photographic film, which is clouded by neutron interaction with particles in the emulsion, and for electronic equipment which utilizes transistors, no permanent damage to equipment results from neutron irradiation. There is evidence that exposure to a neutron flux in excess of 10^{11} neutrons per square centimeter permanently alters the characteristics of transistors. However, any electronic equipment exposed to this flux of neutrons from a nuclear weapon detonation is likely to be severely damaged or destroyed by other effects. Discoloration of glass by neutrons does not occur for fluxes less than about 10^{18} neutrons per square centimeter, and thus can be disregarded as a significant effect.

(3) *Induced activity.* If the neutron flux is sufficiently high, a certain amount of neutron induced gamma activity results for most articles made of steel, due to the manganese which is usually present in commercial steels. The induced activity presents no personnel hazard except for articles exposed within or almost within the fireball, and even then the activity decays so rapidly as to be negligible less than a day after exposure. Significant neutron induced beta activity results in articles made of brass or other copper alloys, if exposed in or near the fireball. The personnel hazard is negligible unless the articles are handled very soon after the detonation. Radioactive decay reduces the activity to negligible levels within a few days.

b. Gamma Radiation. In general, massive quantities of gamma radiation are required to produce any damage to materials, so that damage by some other weapon phenomenon is nearly always more significant. Gamma radiation in excess of 10,000 roentgens can cause deterioration of rubber and other polymers as evidenced by a decrease in breaking strength. Exposure of glass to very high quantities of gamma radiation can produce discoloration. The intensity of radiation required is so great that this may be disregarded as a significant effect. Gamma rays, unlike neutrons, induce negligible radioactivity in materials; therefore, no residual radiation hazard is caused by initial gamma radiation.

c. Electromagnetic Radiation. A large electrical signal is produced by a nuclear weapon detonation. The signal consists of a rather sharp transient signal with a strong frequency component in the neighborhood of 15 kilocycles. Field strengths greater than 1 volt per meter have been detected from megaton yield weapons at a distance of about 2,000 miles. Electronic equipment which responds to rapid, short duration transients can be expected to be actuated by pickup of this electrical noise.

12.3 Thermal Damage to Various Materials

In table 12–2 the critical radiant exposures for specified damage to various materials are shown for three weapon yields. The values presented for fabrics apply for an ambient relative humidity of 65 percent and an ambient temperature of 20° C. For extremely dry conditions the values shown for fabrics should be reduced by 20 percent. For extremely high relative humidities, near 100 percent (at 20° C), the values for fabrics should be increased by 25 percent. If the fabrics are watersoaked, the critical radiant exposures should be increased by 300 percent.

Table 12-2. Critical Radiant Exposure Values for Various Materials

Uniforms	Color	Weight (oz/yd²)	Damage	Critical radiant exposure Q_c (cal/sq cm)		
				1 KT	100 KT	10 MT
Army						
Cotton twill (fatigue)	Green	8	Scorched	3	5	9
			Destroyed	8	14	25
Wool serge (winter service)	OD	9	Scorched	3	6	10
			Destroyed	21	37	66
Wool flannel	OD	11	Scorched	3	5	8
			Destroyed	20	40	70
Wool tropical worsted	Khaki	11	Scorched	6	9	13
			Destroyed	13	20	30
Cotton twill shirt and trousers (summer)	Khaki	6	Scorched	4	6	11
			Destroyed	18	31	56
Navy						
Cotton twill (working)	Khaki	8	Scorched	3	5	8
			Destroyed	15	26	46
Cotton denim (dungaree)	Blue	9	Nap Scorched	6	10	17
			Destroyed	7	13	23
Cotton chambray shirting (working)	Blue	3	Scorched	3	6	11
			Destroyed	7	13	22
Cotton twill (white uniform)	White	8	Scorched	4	8	14
			Destroyed	34	60	109
Wool, Melton, (dress blues)	Blue	16	Scorched	1	16	13
			Destroyed	9	18	28
Wool, Kersey (overcoat)	Blue	30	Scorched	1	2	3
			Destroyed	37	65	110
Wool, serge (officer's uniform)	Blue	14	Scorched	5	9	16
			Destroyed	11	21	37
Wool, tropical worsted (officer's uniform)	Khaki	11	Scorched	5	9	16
			Destroyed	11	20	37
Vinyl resin, combined (rain)	Black	13	Scorched	1	1	2
			Destroyed	5	6	8
Marine Corps						
Cotton poplin shirting	OD	6	Scorched	3	6	10
			Destroyed	10	18	32
Wool elastique (winter)	Green	16	Scorched	2	4	7
			Destroyed	25	45	80
		21	Scorched	5	8	15
			Destroyed	30	54	95
Wool, Kersey (winter)	Green	16	Scorched	2	3	6
			Destroyed	27	48	85
Wool serge	Green	12	Scorched	2	3	6
			Destroyed	16	28	50
Air Force						
Cotton twill shirt (tropical)	Khaki	5	Scorched	6	10	19
			Destroyed	9	15	27
Wool gabardine shirt	Gray	8	Scorched	10	17	28
			Destroyed	14	22	37
Wool gabardine shirt	Blue	8	Scorched	1	2	4
			Destroyed	8	14	25
Nylon—flying jacket	OD	5	Scorched	2	3	6
			Destroyed	7	13	23

Table 12–2. Critical Radiant Exposure Values for Various Materials—Continued

Material	Damage	Critical radiant exposure Q_c, (cal/sq cm)		
		1 KT	100 KT	10 MT
Tent material:				
Canvas, white, 12 oz/yd², untreated	Destroyed	12	21	37
Canvas, OD, 12 oz/yd², flame-proofed	Destroyed	5	9	17
Packaging materials:				
Fibreboard, V2S, BT 350 psi, laminated	Flames during exposure	9	16	29
Fibreboard, V3S, BT 275 psi, laminated	Flames during exposure	7	13	23
Fibreboard, V3C, BT 350 psi, corrugated	Flames during exposure	6	11	19
Fibreboard, W5C, BT 200 psi, corrugated	Flames during exposure	5	10	18
Plywood, douglas fir (¼ in.)	Flames during exposure	9	16	20
Airship material, aluminized, N–113A100, 16 oz/yd²	Aluminum surface discolored	20	35	61
	Aluminum surface destroyed	24	43	75
	Fabric destroyed	27	47	82
Airship material, aluminized, N–113A70, 19.4 oz/yd²	Aluminum surface discolored	10	18	31
	Aluminum surface destroyed	15	27	44
	Fabric destroyed	20	35	61
Airship material, aluminized, N–128A170, 8 oz/yd²	Delaminates	2	4	7
	Fabric destroyed	5	10	17
Doped fabrics (used on some aircraft control surfaces):				
Cellulose nitrate covered with 0.0015″ thick aluminum foil.	Sporadic flaming	60	80	140
Cellulose nitrate, aluminized	Persistent flaming	5	6	10
Plastics:				
Laminated methyl methacrylate	Surface melts	73	120	230
USAF window plastic (½ in.)	Bubbling	240	430	750
Vinylite (opaque), ⅛ in. thick	Dense smoking	3	4	6
	Flaming	20	20	25
Sand:				
Coral	Explosion*	15	27	47
Siliceous	Explosion*	11	19	35
Sandbags: Cotton canvas, dry, filled	Failure	10	18	32
Wood, white pine	0.1 mm depth char	10	18	32
White pine, given protective coating	0.1 mm depth char	40	71	126
Construction materials:				
Roll roofing, mineral surface	Surface melts	8	14	25
	Flaming during exposure	22	40	71
Roll roofing, smooth surface	Surface melts	4	7	12
	Flaming during exposure	9	16	29

*"Popcorning."

It should be emphasized that the values in table 12–2 for uniforms refer to damage to the material itself and are not applicable for predicting skin burns under uniforms.

The above discussion does not include the damage to materials when they come in contact with or are enveloped by the fireball. The heat input under these conditions is many orders of magnitude higher than the cases just discussed. Several of the variables considered as influential factors in determining the amount of surface material lost by an object exposed within a fireball include: type of material, surface curvature, orientation, thermal attenuation by the metallic vapors given off by the object, and spallation.

Figures 12–5A and 12–5B give the material loss from spheres of various materials due to ablation or scaling off of the surface material from contact with or envelopment by the fireball. Data for three types of 10-inch diameter spheres are shown; namely, solid steel, solid aluminum, and solid aluminum with small cylindrical wells filled with ceramic inserts. The one curve in figure 12–5A represents all three types.

FIGURE 12-1

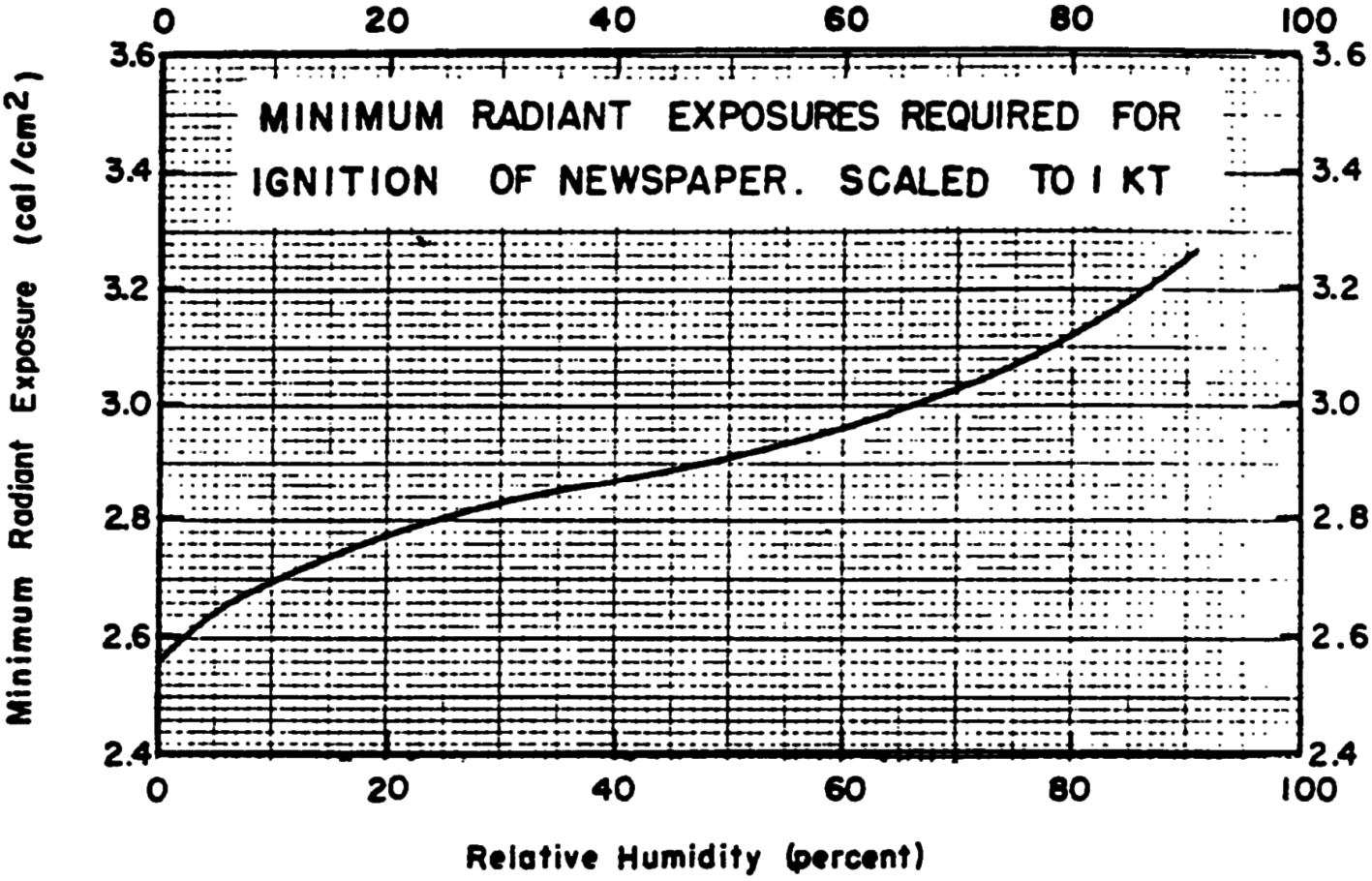

NEWSPAPER IGNITION REQUIREMENTS

Scaling. To find minimum radiant exposures for another yield W at the same relative humidity, multiply the exposures read from figure 12-1 by $W^{1/8}$.

Reliability. Based upon limited empirical data.

Related material.

See paragraphs 12.1*b* and *c*.

See also figure 11-1 for radiant exposures required for wildland kindling fuel ignition.

BURNING POTENTIAL FOR URBAN AREAS

(CENTRAL HEATING NOT IN USE)

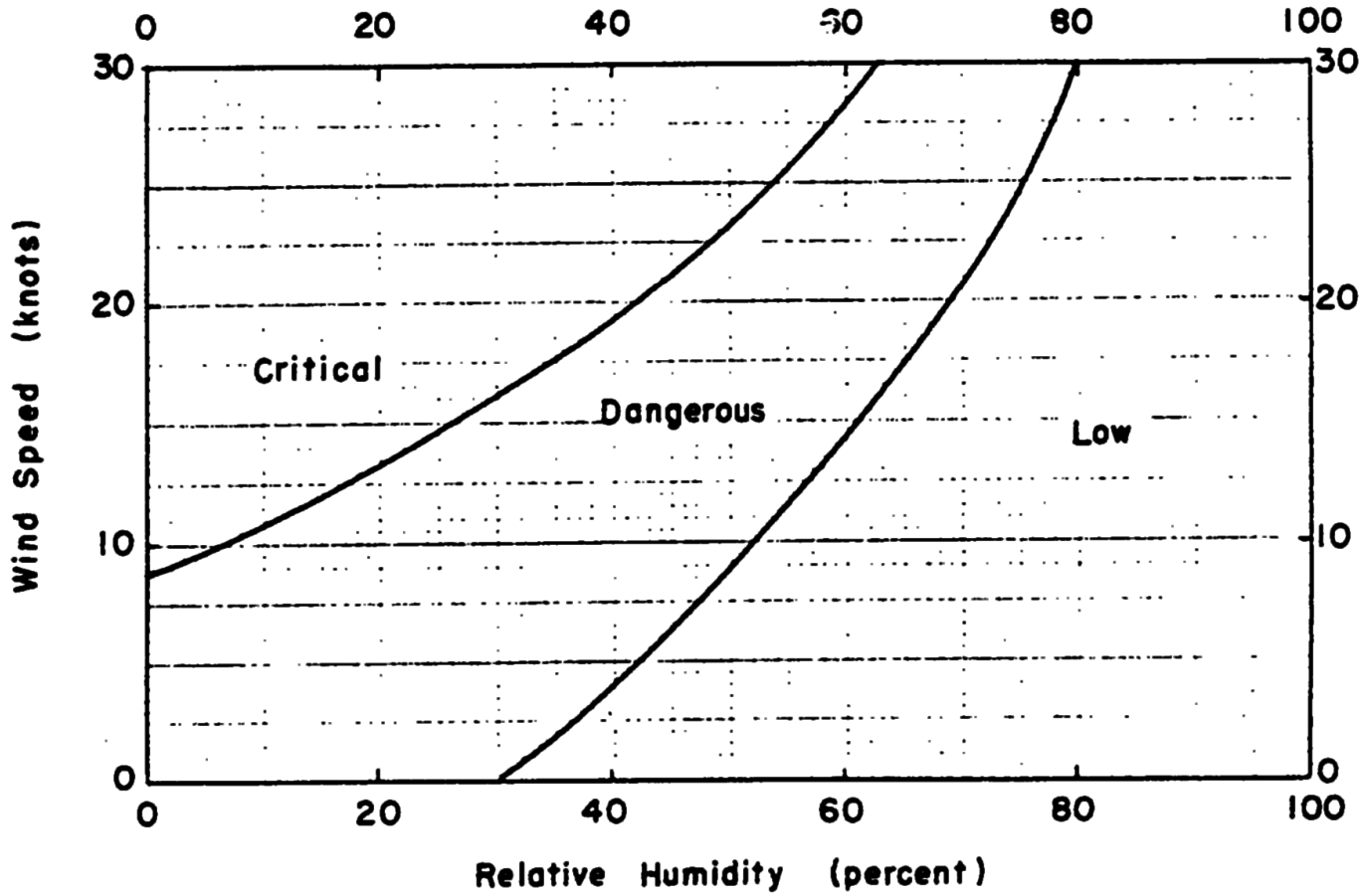

BURNING POTENTIAL FOR URBAN AREAS (CENTRAL HEATING NOT IN USE)

Figure 12–2 represents approximate values of wind speed and average daytime relative humidity conditions corresponding to low, dangerous and critical burning potentials according to the following definitions:

Low. Slow burning fires; fire can be controlled at will. Control action can be on unit structure basis.

Dangerous. Fires burn rapidly; individual building fires combine to form an area fire. Organized action needed to confine fire to area originally ignited.

Critical. Rapid buildup into conflagration-type fires,. high probability of fire storm, spotting frequent and severe. Requires evacuation of fire fighting equipment and personnel; control action effective only at critical breaks in building continuity or density.

Related material.

See paragraphs 12.1*c* and *d*.

See also figure 12–3.

FIGURE 12-3

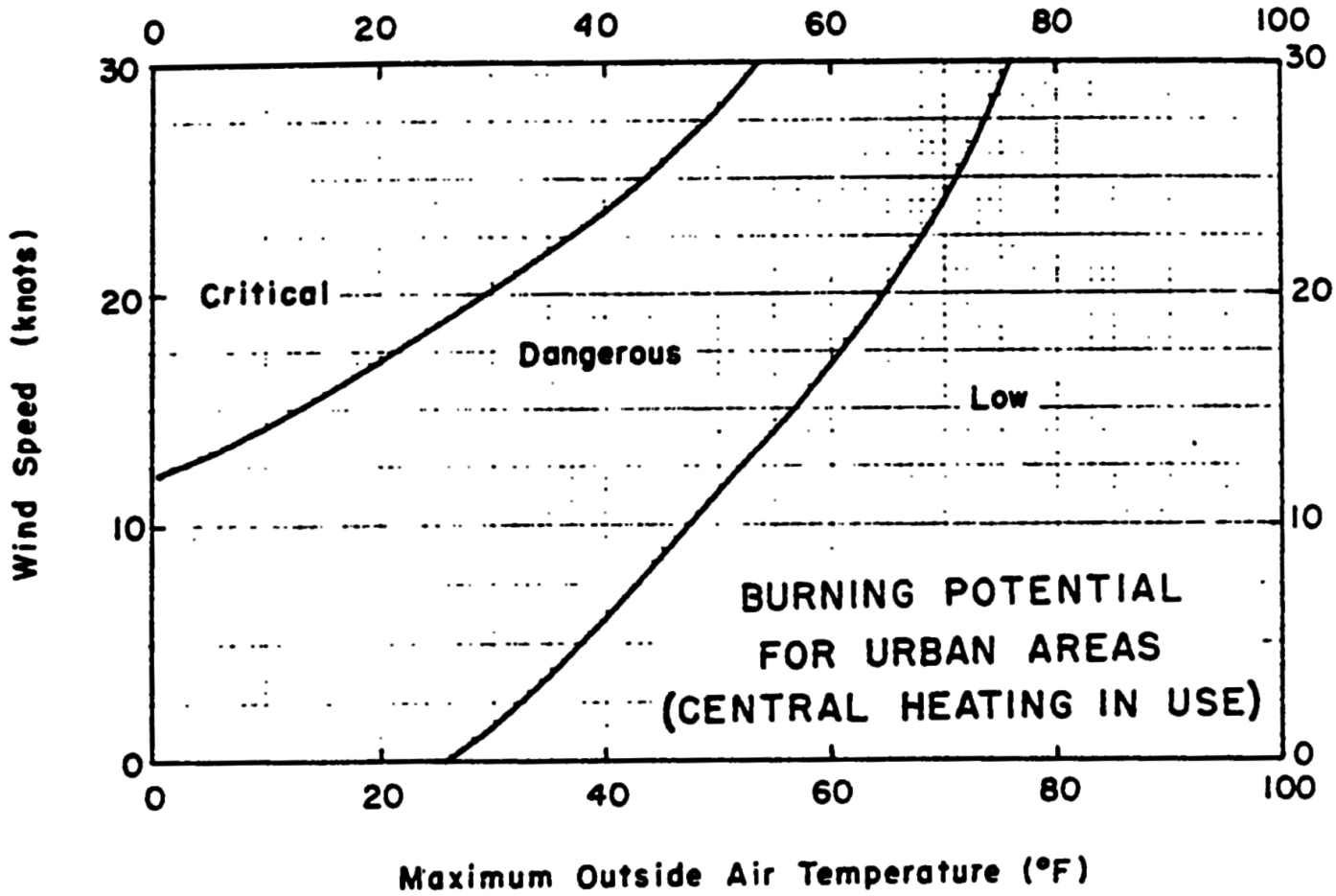

BURNING POTENTIAL FOR URBAN AREAS (CENTRAL HEATING IN USE)

Figure 12–3 shows approximate values of wind speed and maximum outside air temperature conditions corresponding to low, dangerous and critical burning potentials. These burning potentials are defined in the same way as those in figure 12–2.

Note. Temperature must have been below value read on abscissa for at least four consecutive days, with no rain in the previous 24 hours. Snow may be disregarded.

Related material.

See paragraphs 12.1*c* and *d*.
See also figure 12–2.

NEUTRON FLUX FOR A TYPICAL FISSION WEAPON

The curves in figure 12–4 show the number of neutrons per square centimeter per kiloton at various horizontal ranges for different heights of burst of typical fission weapons. The curves are for standard atmospheric conditions. Data are presented in AFSWP–1100, published with a higher security classification, from which neutron flux for specific weapons may be computed.

Scaling. At a given horizontal range and altitude, the neutron flux is proportional to the yield of the weapon.

Example.

Given: A 100 KT air burst at 20,000 feet.

Find: The number of neutrons per square centimeter at a horizontal range of 3,400 yards.

Solution: Reading directly from figure 12–4, the neutron flux from a 1 KT weapon is 10^8 neutrons per cm^2. Since this is a 100 KT burst, 100×10^8 neutrons per $cm^2 = 10^{10}$ neutrons per square centimeter. *Answer.*

Reliability. Neutron flux is dependent upon weapon design. For most fission weapons the curves of figure 12–4 are considered reliable within a factor of 5.

FIGURE 12-4

NEUTRON FLUX FROM TYPICAL FISSION WEAPONS
FOR A 1KT BURST IN A STANDARD ATMOSPHERE
AS A FUNCTION OF BURST ALTITUDE AND HORIZONTAL RANGE

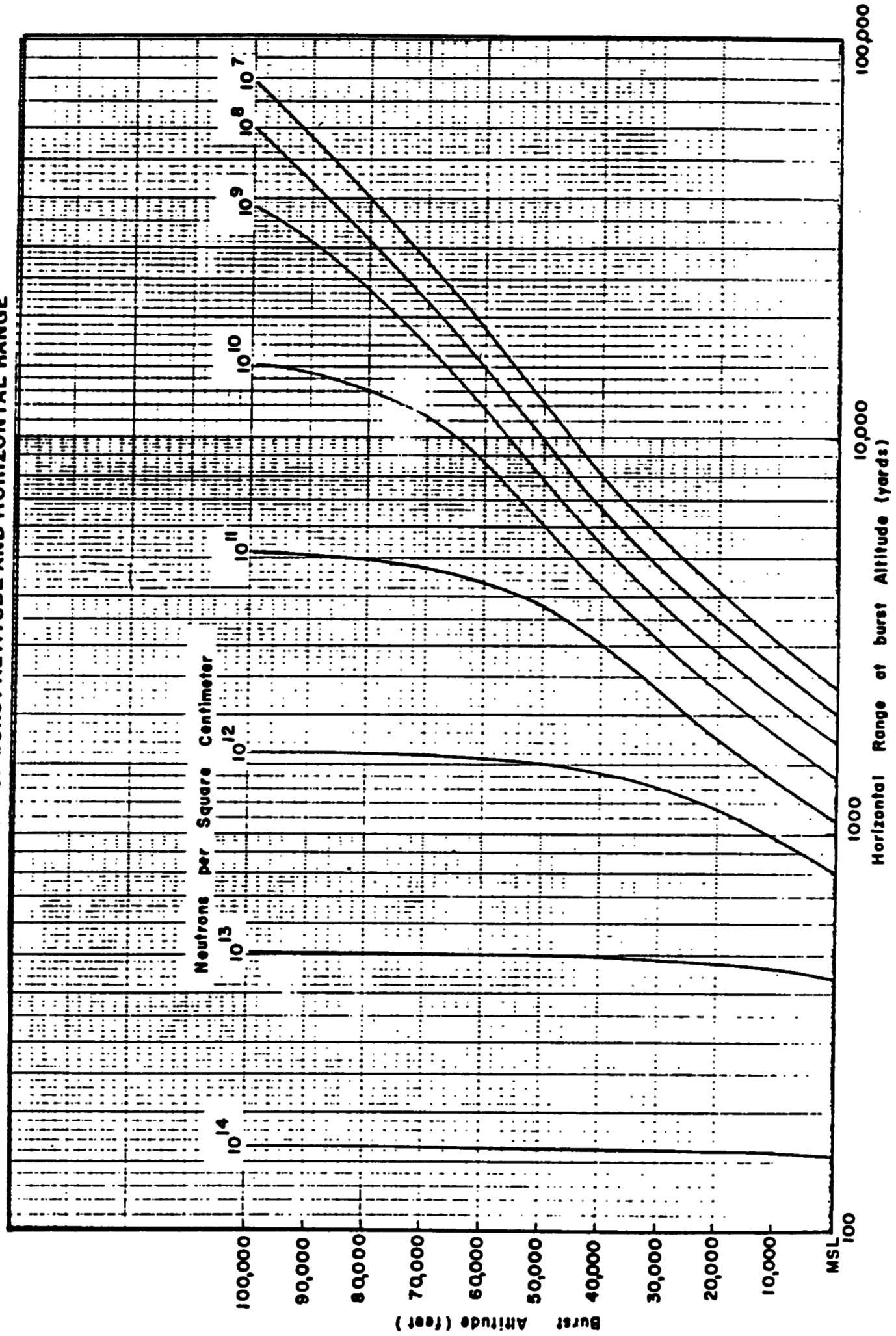

A

WEIGHT LOSS WITH DISTANCE FROM A 23 KT BURST
FOR ALUMINUM, STEEL, CERAMIC INSERT SPHERES

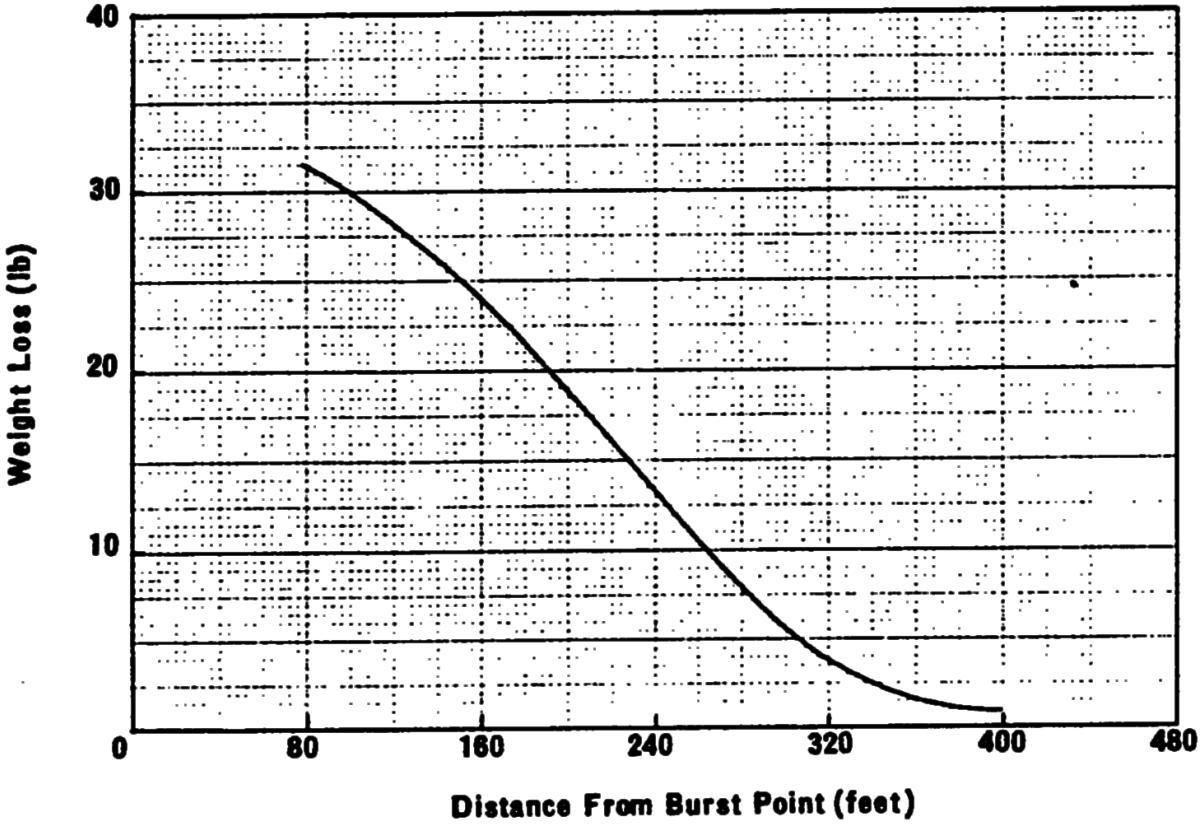

B

REDUCTION OF SPHERE RADIUS WITH DISTANCE FROM A 23 KT BURST
FOR ALUMINUM, STEEL, CERAMIC INSERT SPHERES

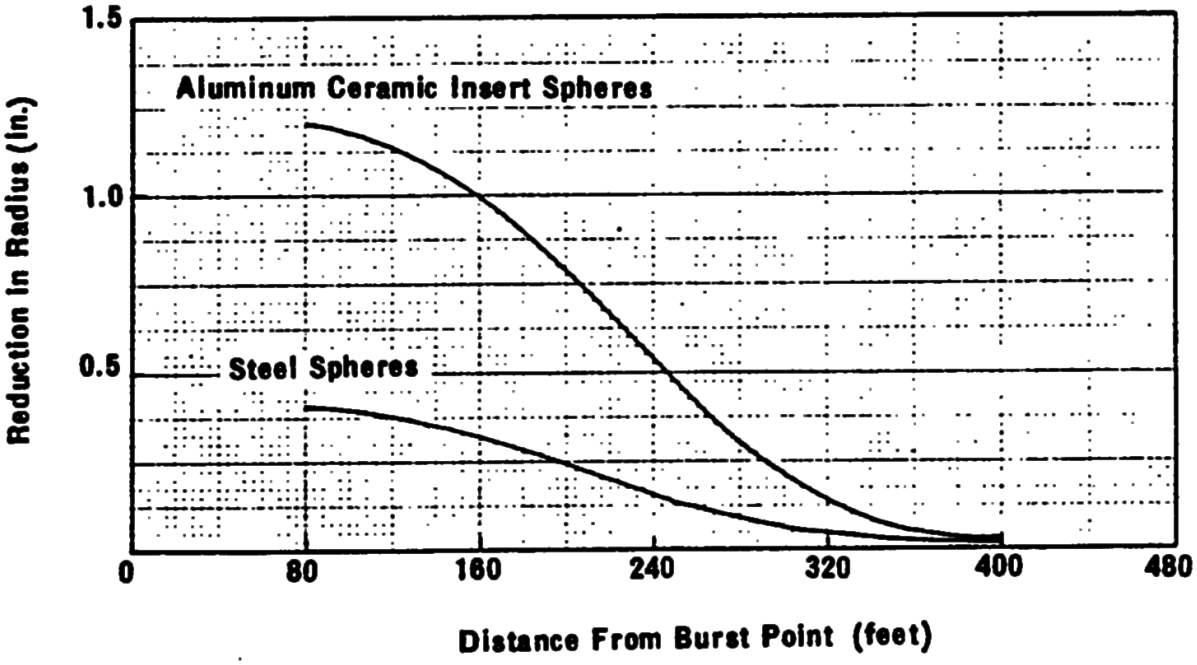

FIGURE I-5

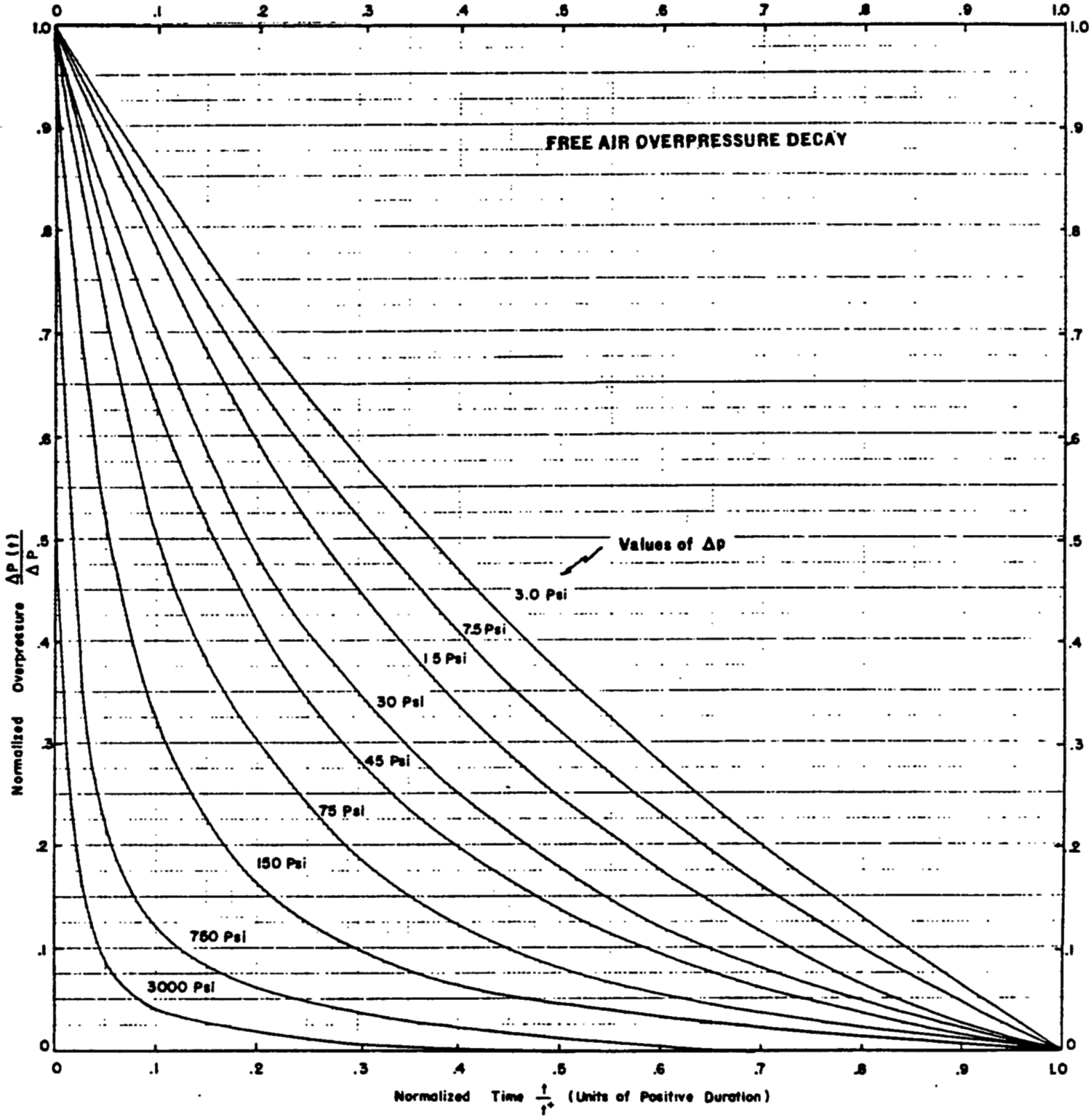
FREE AIR OVERPRESSURE DECAY
Values of Δp
3.0 Psi
7.5 Psi
15 Psi
30 Psi
45 Psi
75 Psi
150 Psi
760 Psi
3000 Psi
Normalized Overpressure ΔP(t)/ΔP
Normalized Time t/t+ (Units of Positive Duration)
0
.1
.2
.3
.4
.5
.6
.7
.8
.9
1.0

FIGURE I-8

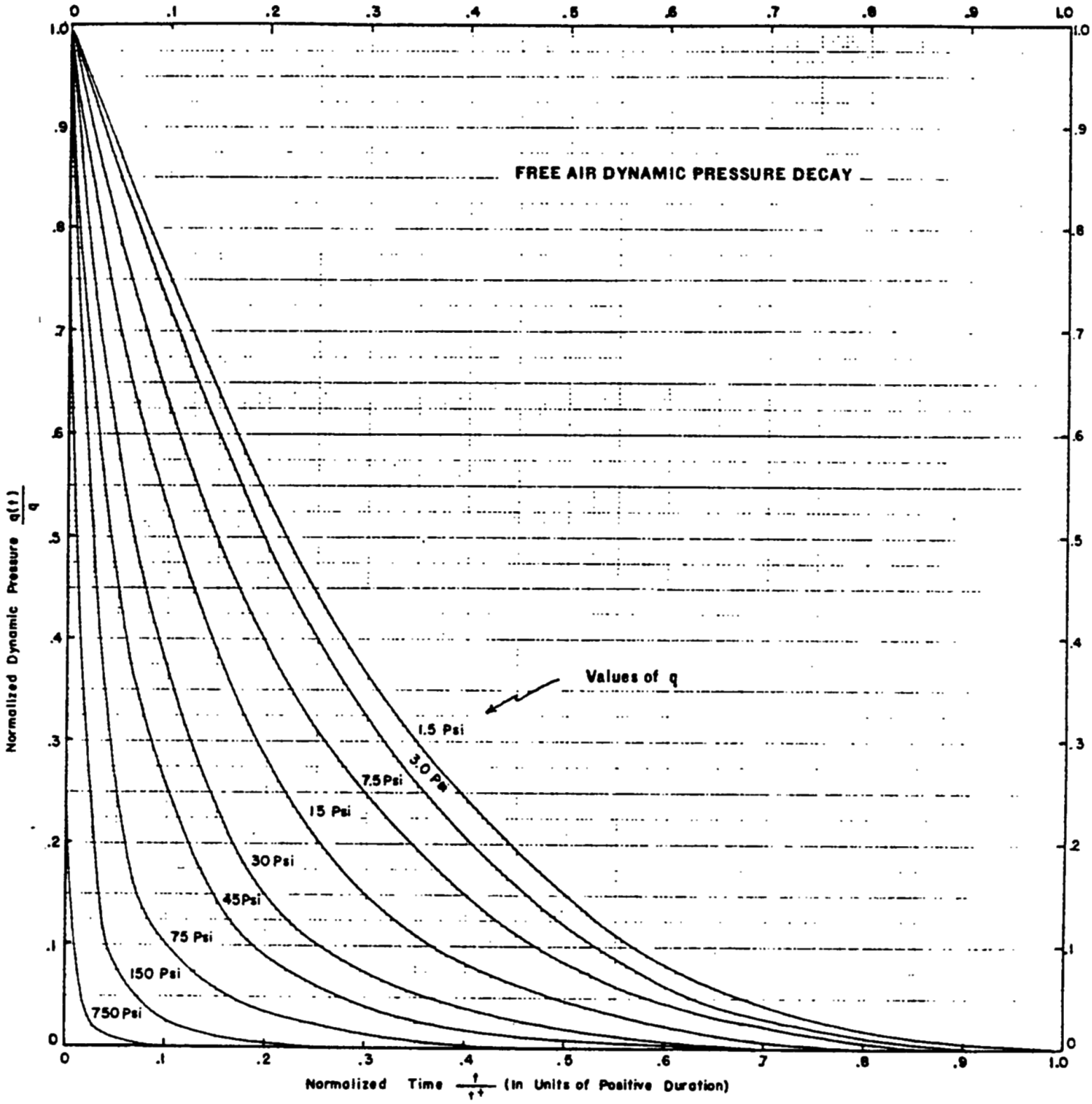
FREE AIR DYNAMIC PRESSURE DECAY
Values of q
1.5 Psi
3.0 Psi
7.5 Psi
15 Psi
30 Psi
45 Psi
75 Psi
150 Psi
750 Psi
Normalized Dynamic Pressure q(t)/q
Normalized Time t/t+ (In Units of Positive Duration)
0
.1
.2
.3
.4
.5
.6
.7
.8
.9
1.0

Second radiant power maximum:

For air bursts under 50,000 feet:

$$P_{max}=4\ W^{1/2}\ KT/\text{sec}=4\ W^{1/2}\times 10^{12}$$

cal/sec (W in KT)

Less than 1 percent of the thermal radiation from a nuclear detonation near sea level is emitted before the radiant power minimum.

II.3. Nuclear

1 KT fission yield makes available 300 megacuries of radioactive fission product gamma activity at a time of one hour after a detonation.

1 curie is that quantity of radioactive material which undergoes 3.7×10^{10} disintegrations per second.

The roentgen is a measure of *quantity of ionization*, and is equivalent to:

83.8 ergs per gram of air; or

1.64×10^{12} ion-pairs per gram of air; or

5.24×10^{7} Mev per gram of air.

0.7 Mev is the approximate mean effective energy for the gamma rays from a residual fission product field.

To obtain the radiation intensity in roentgens per hour three feet above a plane residual fission product field, multiply the concentration of the contaminant in curies per square foot by 120, or in megacuries per square mile by 4.

Total dose in roentgens accumulated to infinite time from one hour after a burst is numerically equal to five times the dose rate in roentgens per hour at $H+1$ hour. (Fission product activity.)

The radioactive decay of gross fission products is approximately exponential with time, so that—

$$I=I_1\ t^{-1.2}$$

where I is the dose rate at any time t, and I_1 is the dose rate at unit time.

The velocity of a thermal neutron ($E=1/40$ ev) is 2,200 meters per second.

Shielding thicknesses in inches required to cut incident gamma radiation by a factor of ten are:

Material	*Initial bomb gamma*	*Residual gamma*
Lead	2.1	1.0
Iron	4.5	2.8
Concrete	18	9.5
Soil	26	14
Water	41	21

As a rough rule of thumb, the area of effect for a given degree of contamination resulting from a nuclear surface burst can be considered directly proportional to the fission yield of the weapon.

Greatest cloud diameter at 9 minutes after burst time (for kiloton yields) is approximately given by—

$$d=10{,}000\ W^{1/3}\ \text{feet}$$

The dose rate inside the bomb cloud is independent of yield (in the kiloton range) and is given by the formula,

$$D=1.31\times 10^{5}t^{-2.06}\ \text{roentgens per hour,}$$

where t is the time after detonation in minutes.

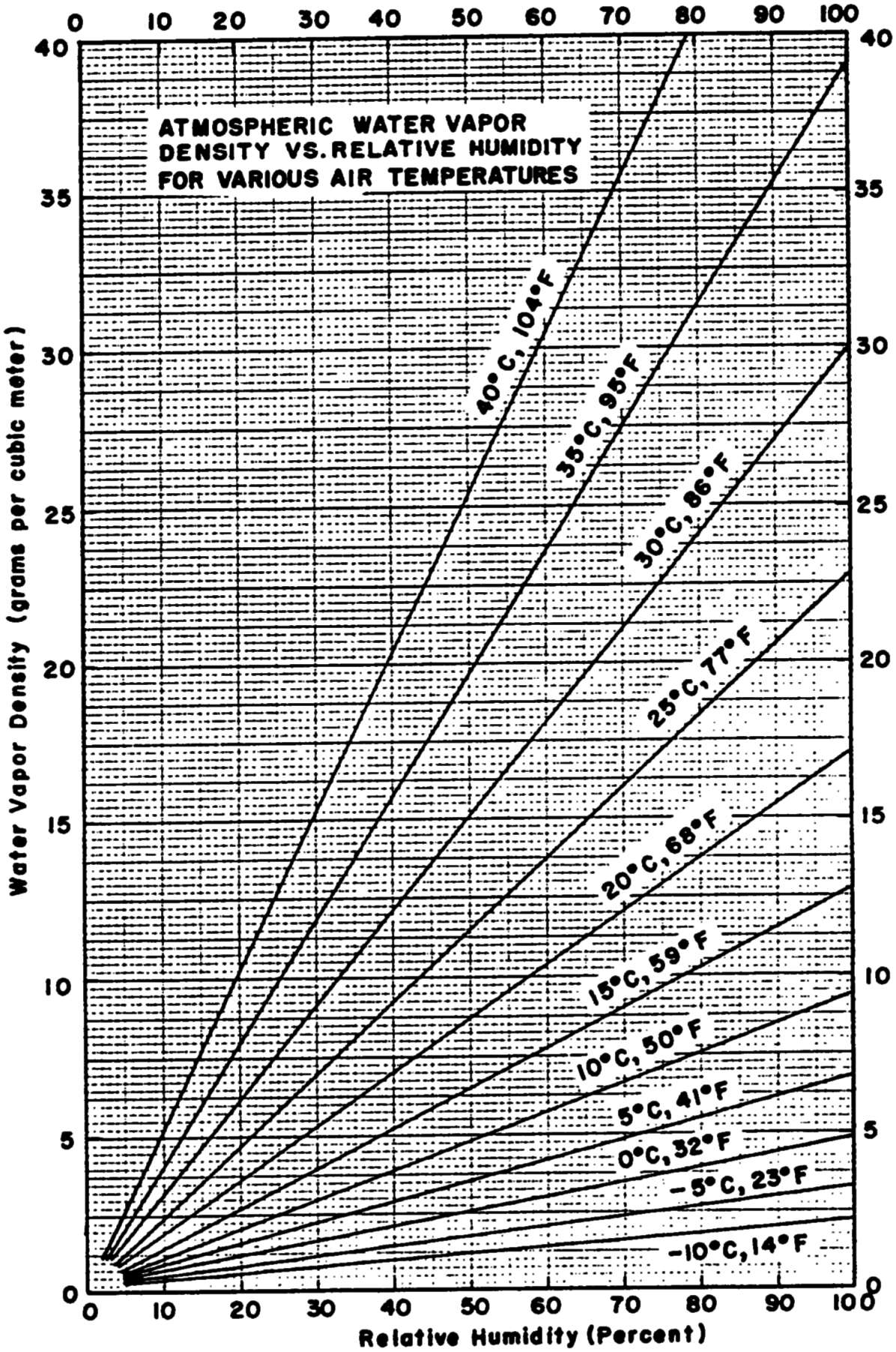
ATMOSPHERIC WATER VAPOR
DENSITY VS. RELATIVE HUMIDITY
FOR VARIOUS AIR TEMPERATURES
40°C, 104°F
35°C, 95°F
30°C, 86°F
25°C, 77°F
20°C, 68°F
15°C, 59°F
10°C, 50°F
5°C, 41°F
0°C, 32°F
-5°C, 23°F
-10°C, 14°F
Water Vapor Density (grams per cubic meter)
Relative Humidity (Percent)
0
5
10
15
20
25
30
35
40
0
10
20
30
40
50
60
70
80
90
100

BIBLIOGRAPHY

The Effects of the Atomic Bomb on Hiroshima, Japan, Volumes I, II, III (Physical Damage Div. of U. S. Strategic Bombing Survey), May 1947 (U).

The Effects of the Atomic Bomb on Nagasaki, Japan, Volumes I, II, III (Physical Damage Div. of U. S. Strategic Bombing Survey), June 1947 (U).

Convective Heating of Air Above an Inorganic Surface Heated by Radiation from a Nuclear Weapon, AFSWP-862, F. M. Sauer and W. Lai (For. Serv.), Nov 55 (C).

Cratering from Atomic Weapons, AFSWP-514 TAR, W. J. Christensen (AFSWP), 29 Jun 56 (SRD).

Curves of Atomic Weapons Effects for Various Burst Altitudes (Sea level to 100,000 ft.), SC-3282 (TR), Cook and Broyles (SC), 9 Mar 54 (SRD).

The Effect of Earth Cover in Protecting Structures Against Blast, AFSWP-357, R. B. Vaile, Jr. (SRI), 30 Sep 54 (CRD).

The Effect of Rain or Fog on Air Blast, NAVORD-2944, G. K. Hartmann (NOL), 1 Aug 53 (S).

Height of Burst for Atomic Weapons, LA-1665, F. B. Porzel (LASL), May 1954, (SRD).

Height of Burst for Atomic Bombs, LA-1406, Francis B. Porzel (LASL), Mar 52 (SRD).

Height of Burst for Nuclear Weapons, RM 1107, H. L. Brode (RAND), 1 June 54 (SRD).

The Interaction of Shock Waves with a Thermal Layer, Robert Varwig and Jay Zemel (NOL), 18 Jun 55 (OUO).

Mach Shock Formation from a Nuclear Detonation, AFSWP-510 TAR, R. J. Hesse and J. R. Kelso (AFSWP), 10 Mar 55 (SRD).

Operation TEAPOT—Underground Shot Base Surge Analysis, AFSWP-876, M. L. Milligan and G. A. Young (NOL), 31 Jan 56 (SRD).

Phenomenology of a High Altitude Atomic Explosion, SC-3363, Shelton (SC), 28 Apr 54 (SRD).

The Precursor—Its Formation, Prediction and Effects, SC-2850 (TR), Frank H. Shelton (SC), 27 Jul 53 (SRD).

A Preliminary Estimate of the Effect of Fog and Rain on the Peak Shock Pressure from an Atomic Bomb, AFCRD AFSG-16, H. P. Gauvin and J. H. Healy (AFCRC), Sep 52 (SRD).

Rain, Fog and Cloud Effects on Blast Damage from Atomic Weapons, SC-3008 (TR), Thomas B. Cook (SC), 22 Oct 53 (SRD).

The Scaling of Base Surge Phenomena of Shallow Underwater Explosions, AFSWP-484, M. L. Milligan and G. A. Young (NOL), 1 May 54 (C).

High Altitude Effects on Blast-Thermal Partition of Energy from Nuclear Explosions, and Associated Scaling Laws, SC-2969 (TR), F. H. Shelton (SC), 15 Sep 53 (SRD).

Contamination Patterns at Operation JANGLE, USNRDL-399, R. K. Laurino and I. G. Poppoff (NRDL), 30 Apr 53 (SRD).

Gamma-Ray Spectral Measurements of Fall-Out Samples from Operation CASTLE, AFSWP-822, C. S. Cook (NRDL), 26 Jan 55 (SRD).

Hazard Due to Beta Radiation from Fission Products Deposited on the Ground After an Atomic Explosion, CREL-529, F. S. Goulding and G. Cowper, Atomic Energy Commission of Canada, Ltd., Jan 53 (U).

Investigation of Gamma Radiation Hazards Incident to an Underwater Atomic Explosion, W. E. Strope (BuShips, DN), 1948 (C).

The Nature of Individual Radioactive Particles. I. Surface and Underground ABD Particles from Operation JANGLE, USNRDL–374, C. E. Adams, I. G. Poppoff, and N. R. Wallace (NRDL), 28 Nov 52 (S).

Radioactive Fall-Out Hazards from Surface Bursts of Very High Yield Nuclear Weapons, AFSWP–507, D. C. Borg, L. D. Gates, T. A. Gibson, Jr., and R. W. Paine, Jr. (AFSWP), May 54 (SRD).

The Residual Radiological Hazard from the Air Detonation of an Atomic Weapon in the Rain, AFSWP–501, L. D. Gates, et al. (AFSWP), May 53 (SRD).

Scaling of Contamination Patterns, Surface and Underground Detonations, NRDL–TR–1, C. F. Ksanda, et al. (USNRDL), Sep 53 (SRD).

Prediction of Neutron-Induced Activity in Soils, AFSWP–518, J. F. Canu and P. J. Dolan (AFSWP), 11 Jun 57 (SRD).

The Combined Effects of Thermal Burns and Whole-Body X-Irradiation on Survival Time and Mortality, AFSWP–470, and 473, 474, 475, E. L. Alpen, et al. (NRDL), May, Oct, 53 (U).

Effect of Nuclear Weapon Yield on Effectiveness of Thermal Energy for Burn Production, AFSWP–734, E. L. Alpen (NRDL), 30 Aug 54 (SRD).

Effects of Spectral Distribution of Radiant Energy of Cutaneous Burn Production in Man and Rat, AFSWP–737, E. L. Alpen, et al. (NRDL), 25 Apr 55 (U).

Heat-Reflecting Textiles as Protective Barriers Against Intense Thermal Radiation, AFSWP–849, R. C. Maggio and T. B. Gilhooly (NML), 25 Mar 55 (U).

Reflectance and Absorptance of Human Skin, AFSWP–840, W. Derksen (NML), 31 Mar 55 (U).

Research Report on the Influence of Air Supply and Air Flow on Burns Behind Irradiated Fabrics, AFSWP–1000, W. L. Derksen and J. J. Bates (NML) (U).

The Effect of Earth Cover in Protecting Structures Against Blast, AFSWP–357A, R. B. Vaile, Jr. (SRI), 30 Sep 54 (CRD).

Field Fortifications Test, Exercise Desert Rock VI, Technical Rpt. 1468–TR (ERDL), 2 Nov 56 (SRD).

The Vulnerability of Parked Army Aircraft to Nuclear Detonations, WADC Tech. Rpt. 56–354, D. H. Whitford (WADC), Jun 56 (SRD).

Exercise Desert Rock I (Hq III Corps, Ft McArthur), Oct 51 (SRD).

Report of Test Exercises Desert Rock II and III (Hq Camp Desert Rock), 15 Dec 51 (SRD).

Exercise Desert Rock IV (Hq Sixth Army), Apr–Jun 1956 (SRD).

Exercise Desert Rock V (Hq Camp Desert Rock), Jan–Jun 53 (SRD).

Damage to Field Military Equipment from Nuclear Detonations, AFSWP–511 TAR, R. J. Hesse (AFSWP), 1 Feb 56 (SRD).

Blast Effects on Forest Stands by Nuclear Weapons, AFSWP–971, W. L. Fons, F. M. Sauer, and W. Y. Pong (For. Serv.), 1957 (C).

Distribution of Primary Ignition Points Following Atomic Attack on Urban Targets-Transient Exterior Fuels, AFSWP–412, G. C. Chandler and Keith Arnold (For. Serv.), Mar 53 (U).

Frequency of Urban Building Fires as Related to Daily Weather Conditions, AFSWP–866, A. R. Pirsko (For. Serv.), Mar 56 (U).

A Method for Estimating Probable Ignitions of Interior Fuels by Atomic Weapon Explosion (Survey of Boston and Detroit), AFSWP–340, H. D. Bruce and L. E. Downs (Forest Products Lab), 1 Feb 56 (SRD).

Primary Ignitions Following Atomic Attack on Urban Targets-Transient Exterior Fuels, AFSWP–413, F. M. Sauer, et al. (For. Serv.), Jun 53 (U).

Remarks on Estimation of the Number of Fires Due to the Ignition of Transient Exterior Kindling Fuels, AFSWP–861, F. M. Sauer (For. Serv.), Oct 55 (U).

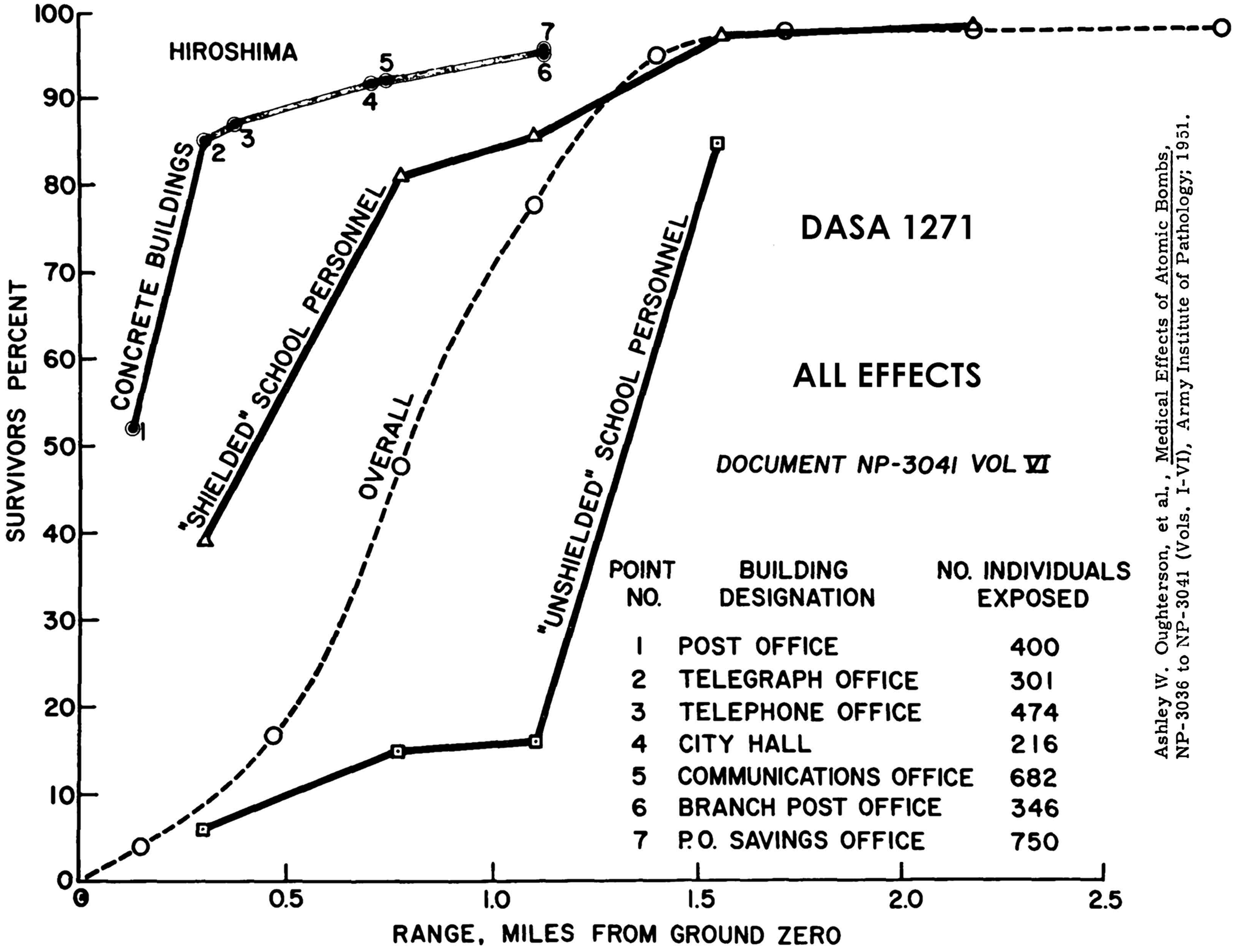

Ashley W. Oughterson, et al., Medical Effects of Atomic Bombs, NP-3036 to NP-3041 (Vols. I-VI), Army Institute of Pathology; 1951.

DC-P-1060

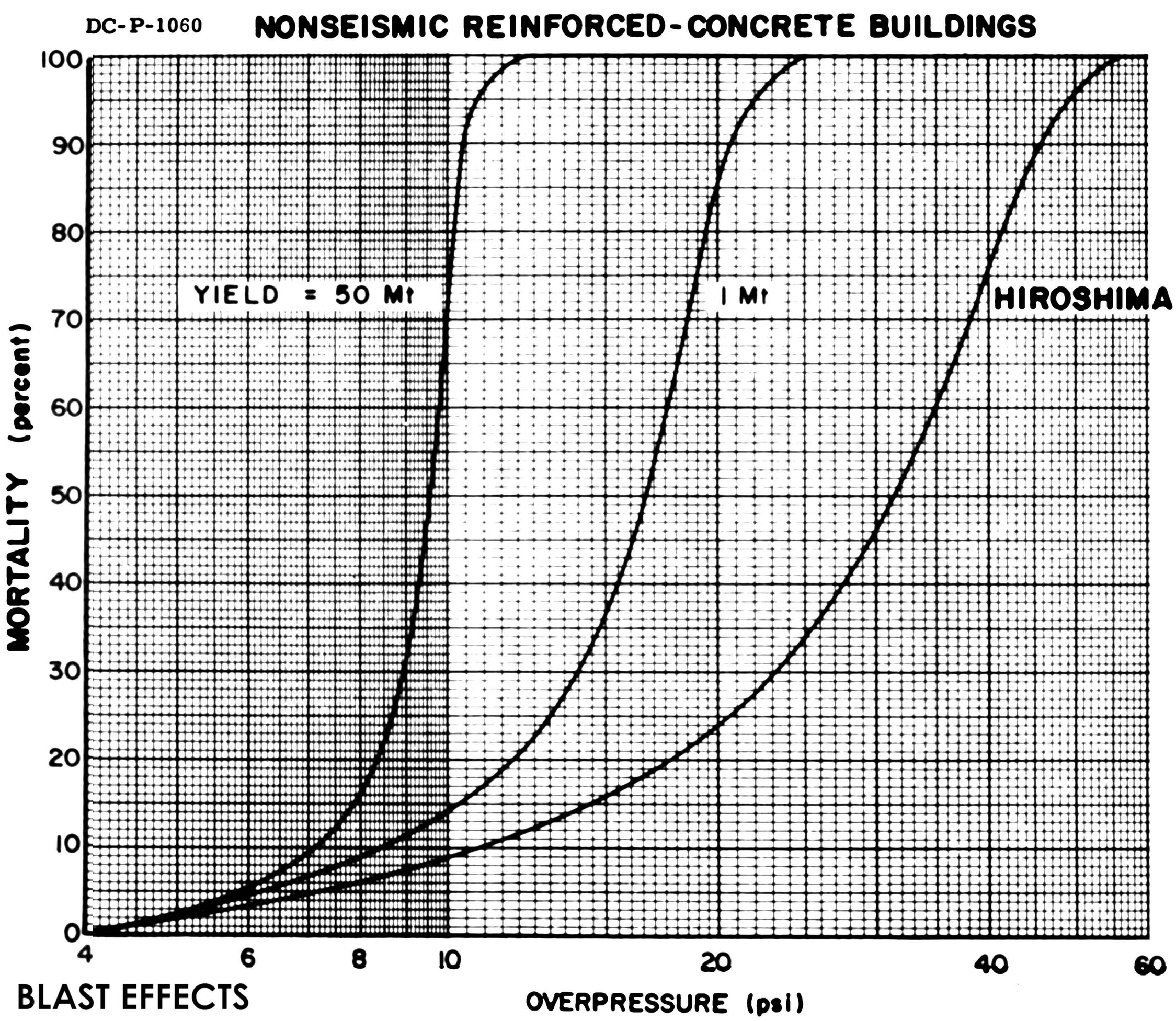

L. Wayne Davis, Donald L. Summers, William L. Baker, and James A. Keller, Prediction of Urban Casualties and the Medical Load from a High-Yield Nuclear Burst, DC-FR-1060, The Dikewood Corporation

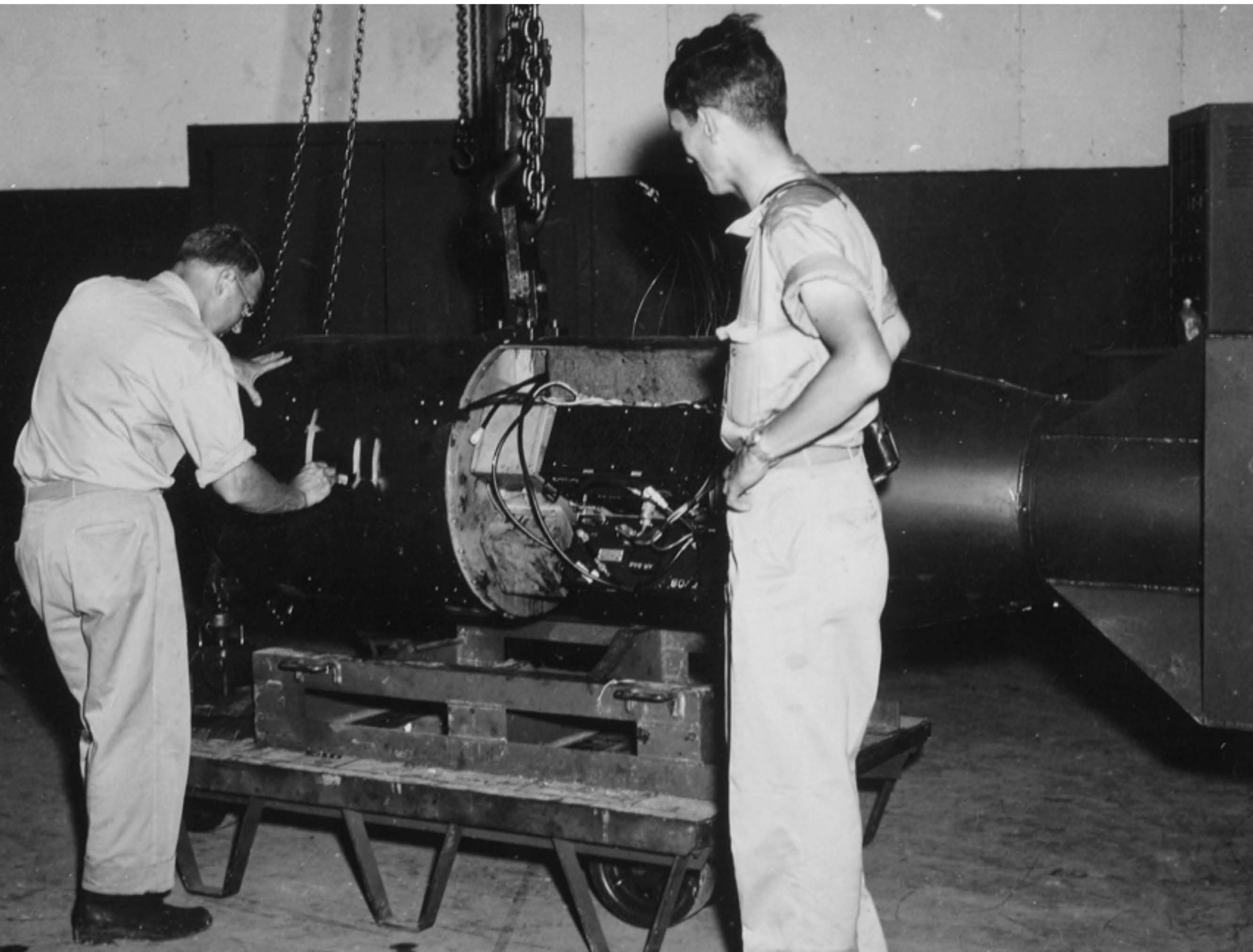

HIROSHIMA BLAST VS. FIRE
8 SEPTEMBER 1945

STEEL FRAME WOODEN BUILDING BURNED OUT, CONCRETE REMAINS INTACT

[redacted]

THE UNITED STATES
STRATEGIC BOMBING SURVEY

THE EFFECTS OF THE ATOMIC BOMB ON HIROSHIMA, JAPAN

Volume I

Physical Damage Division
May 1947

[redacted]

G. CAUSE AND EXTENT OF FIRE

1. Conditions Prior to Attack

The city of Hiroshima was an excellent target for the atomic bomb from a fire standpoint: There had been no rain for three weeks; the city was highly combustible, consisting principally of Japanese domestic-type structures; it was constructed over flat terrain; and 13 square miles (including streets) of the 26.5-square-mile city was more than 5 percent built up (i. e., covered by plan areas of buildings). The remainder of the city comprised water areas, parks and areas built up below 5 percent. Sixty-eight percent of the 13-square-mile area was 27 to 42 percent built up and the 4-square-mile city center was particularly dense, 93.6 percent of it being 27 to 42 percent built up.

a. Fire Department. Public fire equipment had been little improved in anticipation of wartime fires. Private fire equipment had been augmented somewhat but instruction to home occupants in its use had been limited to training in combating incendiary bombs.

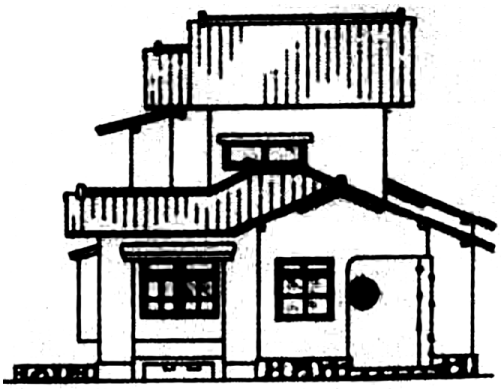

EAST ELEVATION

NORTH ELEVATION

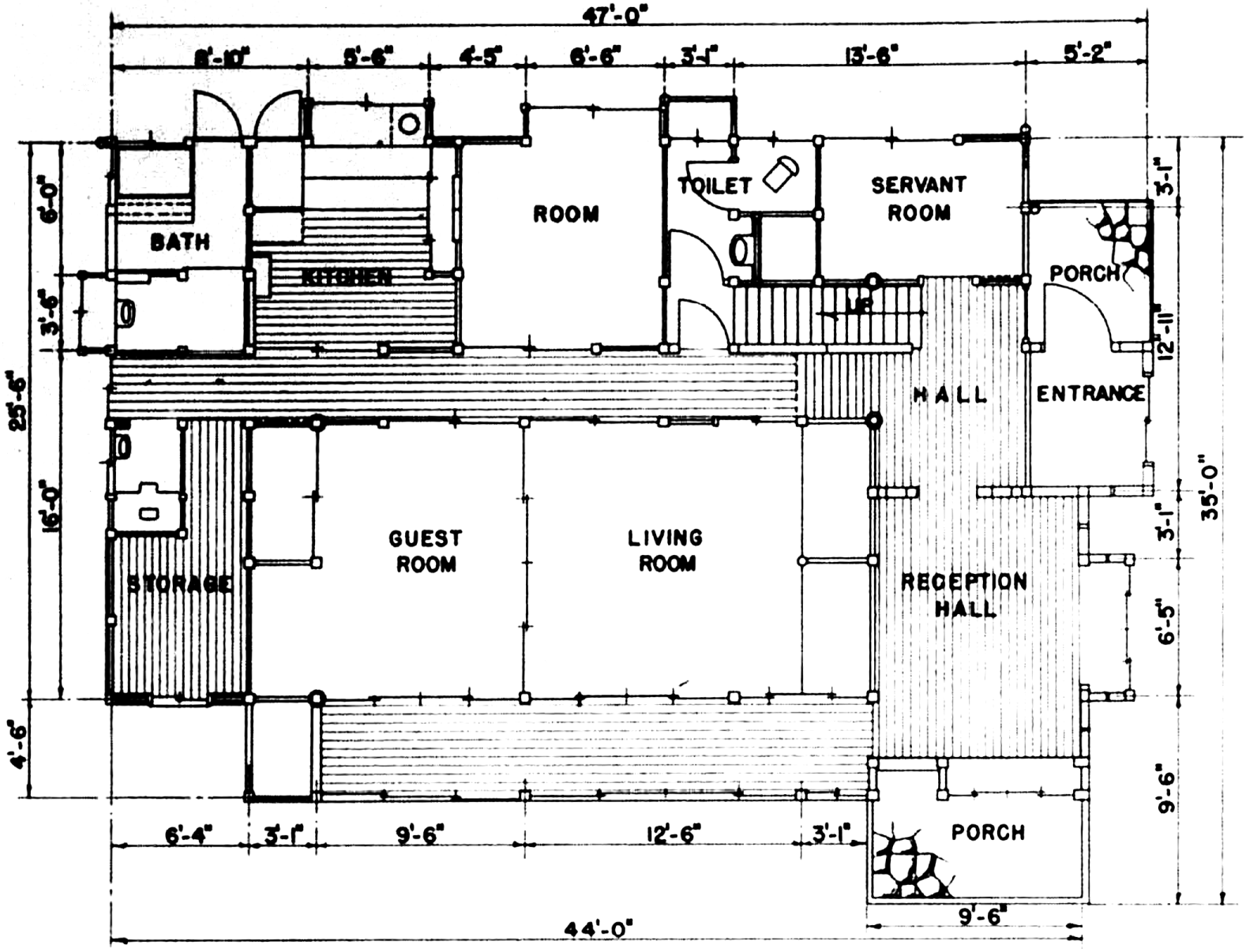

· FIRST · FLOOR · PLAN ·

0' 5'

[redacted]

U.S. STRATEGIC BOMBING SURVEY

TWO-STORY JAPANESE RESIDENCE

FIGURE 6-VII

a. Evidence relative to ignition of combustible structures and materials by heat directly radiated by the atomic bomb and by other ignition sources developed the following: (1) The primary fire hazard was present in combustible materials and in fire-resistive buildings with unshielded wall openings; (2) six persons who had been in reinforced-concrete buildings within 3,200 feet of air zero stated that black cotton black-out curtains were ignited by radiant heat; (3) a few persons stated that thin rice paper, cedarbark roofs, thatched roofs, and tops of wooden poles were afire immediately after the explosion; (4) dark clothing was scorched, and, in some cases, reported to have burst into flame from flash heat; (5) but a large proportion of over 1,000 persons questioned was in agreement that a great majority of the original fires was started by debris falling on kitchen charcoal fires, by industrial process fires, or by electric short circuits.

b. Hundreds of fires were reported to have started in the center of the city within ten minutes after the explosion. Of the total number of buildings investigated 107 caught fire, and, in 69 instances, the probable cause of initial ignition of the buildings or their contents was established as follows: (1) 8 by direct radiated heat from the bomb (primary fire), (2) 8 by secondary sources and (3) 53 by fire spread from exposing buildings.

c. Damage to Rolling Stock. Of the 123 trolley cars operated by the company, 20 percent were damaged by fire and 45 percent by blast. Of the 85 motor busses, fire damaged 21 percent and blast 26 percent. Radiant heat from the bomb ignited cars and busses within 1,500 feet of GZ. Total damage to cars extended a maximum of 5,700 feet from GZ, heavy damage to 8,400 feet and slight damage to 12,500 feet. Busses were totally damaged at 4,000 feet and heavily damaged 5,500 feet from GZ.

d. Damage to Overhead System. Blast and fire damaged 11.4 miles of the overhead transmission system including damage to 500 wood and 100 steel poles. No damage occurred to concrete poles, the nearest of which were 6,000 feet from GZ. Wood poles were damaged at a maximum distance of 4,500 feet from GZ, and steel poles at 3,500 feet. Overhead transmission cable was downed by blast at 8,000 feet.

3. Conditions on Morning of Attack

a. The morning of 6 August 1945 was clear with a small amount of clouds at high altitude. Wind was from the south with a velocity of about 4½ miles per hour. Visibility was 10 to 15 miles.

b. An air-raid "alert" was sounded throughout Hiroshima Prefecture at 0709 hours. Reports of the number of planes causing this alert were conflicting. The governor of the prefecture stated that four B–29s were sighted, while the Kure Naval District reported three large planes.

c. The aircraft apparently came out over Hiroshima from the direction of Bungo Suido and Kunisaki Peninsula, circled the city, and withdrew in the direction of Harima-Nada at 0725 hours. "All-clear" was sounded at 0731 hours.

d. The following circumstances account in part for the high number of casualties resulting from the atomic bomb:

(1) Only a few persons remained in the air-raid shelters after the "all-clear" sounded.

(2) No "alert" was sounded to announce the approach of the planes involved in the atomic-bomb attack.

(3) The explosion occurred during the morning rush hours when people had just arrived at work or were hurrying to their places of business. This concentrated the population in the center of the city where the principal business district was located.

(4) Many persons residing outside the city were present for reasons of business, travel and pleasure.

(5) National volunteer and school units were mobilized and engaged in evacuation operations.

[redacted]

THE UNITED STATES
STRATEGIC BOMBING SURVEY

THE EFFECTS OF THE ATOMIC BOMB ON HIROSHIMA, JAPAN

Volume II

Physical Damage Division

Dates of Survey:

14 October–26 November 1945

Date of Publication

May 1947

[redacted]

A. OBJECT OF STUDY

The object of this fire study was to determine the extent of fire in Hiroshima resulting from the explosion of the atomic bomb on 6 August 1945, and to analyze the contributing factors.

B. SUMMARY

This section presents a picture of factors pertaining to fire in Hiroshima before, during and after the atomic-bomb attack. Part C describes fire conditions prior to the attack and analyzes the effectiveness of precautionary fire measures; Part D relates the story of the fire; Part E presents a detailed analysis of fire in selected fire-resistive, noncombustible, and combustible buildings, and their contents; Part F discusses the cause and extent of fire in bridges; and Part G present conclusions and recommendations.

1. The city of Hiroshima, like other Japanese cities, was poorly prepared to combat a conflagration of large-scale proportions. Private fire equipment had been augmented and home occupants had been given limited instructions and training in combatting incendiary bombs. Public fire equipment had been little improved to fight wartime fires.

2. The public water system was fairly adequate for normal fire conditions, although pressure was very low on dead-end mains at the south end of the city. No improvements had been made for wartime emergencies.

3. The Ota River and its six branches divided the city into nine distinct areas. The river courses and 41,000 feet of firebreak lanes which had been prepared by removing combustible buildings on one or both sides of fairly wide streets formed an extensive network of firebreaks.

4. The city, consisting principally of Japanese domestic structures, was highly combustible and densely built up. Sixty-eight percent of the 13-square-mile city area was 27 to 42 percent built up and the 4-square-mile city center was particularly dense, 94 percent of it being 27 to 42 percent built up. All the large industrial plants were located on the south and southeast edges of the city.

5. Precautionary fire measures were ineffective largely because widespread damage was caused by blast, the populace suffered severe casualties, innumerable fires were started throughout the city on both sides of natural and man-made firebreaks, and the public fire department sustained almost a knock-out blow.

6. One major break occurred in a 16-inch water main when Bridge 29 which carried it was collapsed by blast. This and a large number of breaks in small pipes above ground in collapsed buildings reduced water pressure in the system, but the reservoir never ran dry and lack of water was not a factor in the extent of the fire.

7. The temperature resulting from the explosion of the atomic bomb was of great intensity but of extremely short duration. At ground zero, 2,000 feet from the center of heat, the temperature probably exceeded 3,500° C. for a fraction of a second. Only directly exposed surfaces were flash burned.

8. Evidence relative to ignition of combustible structures and materials by directly radiated heat from the atomic bomb and other ignition sources was obtained by interrogation and visual inspection of the entire city. Six persons who had been in reinforced-concrete buildings within 3,200 feet of air zero stated that black cotton black-out curtains were ignited by flash heat. A few persons stated that thin rice paper, cedarbark roofs, thatched roofs, and tops of wooden poles were afire immediately after the explosion. Dark clothing was scorched and, in some cases, was reported to have burst into flame from flash heat. A large proportion of over 1,000 persons questioned was, however, in agreement that a great majority of the original fires were started by debris falling on kitchen charcoal fires. Other sources of secondary fire were industrial-process fires and electric short circuits.

9. There had been practically no rain in the city for about 3 weeks. The velocity of the wind on the morning of the atomic-bomb attack was not more than 5 miles per hour. A fire storm, including both wind and rain, began to develop soon after the start of the initial fires. The fire wind, which blew always toward the burning area, reached a maximum velocity of 30 to 40 miles per hour 2 to 3 hours after the explosion, and intermittently light and heavy rain fell over the north and west portions of the city.

10. Hundreds of fires were reported to have started in the center of the city within 10 minutes after the explosion.

HIROSHIMA

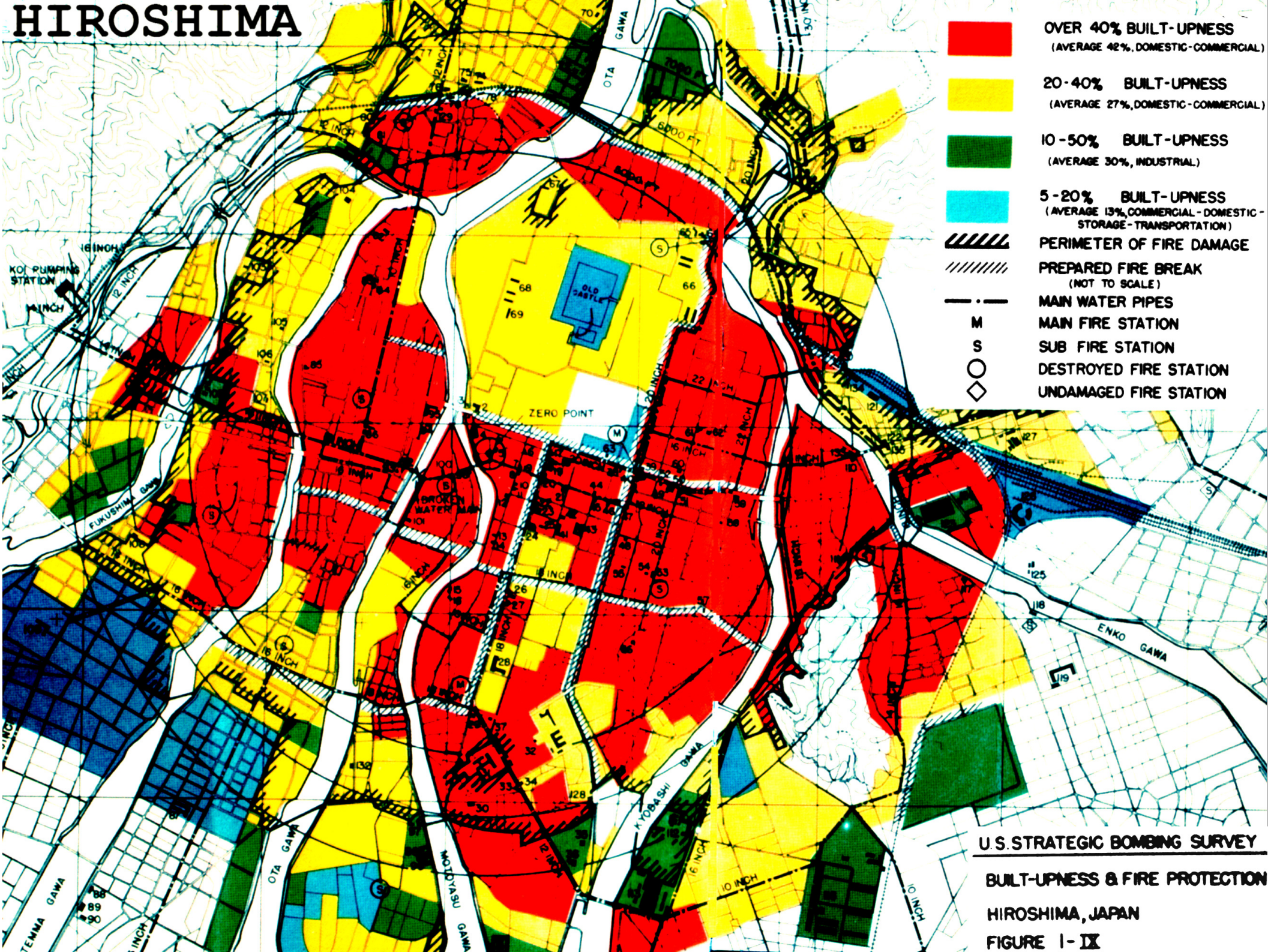
OVER 40% BUILT-UPNESS
(AVERAGE 42%, DOMESTIC-COMMERCIAL)
20-40% BUILT-UPNESS
(AVERAGE 27%, DOMESTIC-COMMERCIAL)
10-50% BUILT-UPNESS
(AVERAGE 30%, INDUSTRIAL)
5-20% BUILT-UPNESS
(AVERAGE 13%, COMMERCIAL-DOMESTIC-STORAGE-TRANSPORTATION)
PERIMETER OF FIRE DAMAGE
PREPARED FIRE BREAK
(NOT TO SCALE)
MAIN WATER PIPES
M MAIN FIRE STATION
S SUB FIRE STATION
DESTROYED FIRE STATION
UNDAMAGED FIRE STATION
OTA GAWA
OLD CASTLE
ZERO POINT
KOI PUMPING STATION
FUKUSHIMA GAWA
ENKO GAWA
KYOBASHI GAWA
MOTOYASU GAWA
TEMMA GAWA
U.S. STRATEGIC BOMBING SURVEY
BUILT-UPNESS & FIRE PROTECTION
HIROSHIMA, JAPAN
FIGURE I-IX

D. THE CONFLAGRATION

1. Start of Fire

a. Source of Evidence. Because of the practically total combustion which prevailed in the burned-over area of 4.4 square miles in the heart of the city, most of the evidence relative to ignition by radiant heat from the bomb and secondary sources of heat was necessarily obtained by interrogation which, wherever possible, was checked by field inspection. Also, since the heaviest casualties occurred closer in, a majority of the persons questioned were 3,000 feet or more from ground zero (GZ) at the time of the explosion. Most people who had been within 2,000 feet of GZ (2,800 feet from air zero) were utterly confused as to what had happened immediately after the detonation and for some time thereafter, although several were located who could give reasonably coherent stories. Because the distance of a point on the ground from air zero (AZ) was important from an ignition standpoint and the distance from GZ was important from a fire spread standpoint, the relationship between the two has been shown on Figure 2.

b. Direct Ignition by the Atomic Bomb. (1) Six persons were found who had been in reinforced-concrete buildings within 3,200 feet of AZ at the time of the explosion and who stated that black cotton black-out curtains were blazing a few seconds later. In two cases it was stated that thin rice paper on desks close to open windows facing AZ also burst into flame immediately, although heavier paper did not ignite. No incidents were recounted to the effect that furniture or similar objects within buildings were ignited directly by radiated heat from the bomb.

(2) Straw-thatched roofs were illegal within the city limits, but a number were erected outside. A few persons stated that they had seen this type of roof burst into flame directly from heat radiated by the bomb but the stories were inconsistent except in two instances where the persons could point to specific building sites. Both of these locations were almost due north of AZ, the first approximately 12,700 feet and the second approximately 13,900 feet. Despite the strong eyewitness accounts of the persons interrogated, there is considerable doubt in the minds of the investigators that these buldings were ignited directly by radiated heat from the bomb. This doubt is predicated chiefly upon three considerations, namely: (1) Buildings, including many with straw-thatched roofs 3,200 feet nearer AZ (10,700 feet), suffered no fire damage; (2) farmers working in an open field only 800 feet beyond (14,700 feet) suffered no burns of any kind although they felt a wave of warm air pass over them almost simultaneously with the sound of the explosion; and (3) the roofs of these buildings collapsed as a result of the blast and may have been ignited by charcoal braziers.

(3) One dwelling which had a cedarbark-shingle covering that was reported ignited by the flash heat from the bomb was found approximately 6,700 feet northeast from AZ and slightly over 200 feet beyond the fringe of the burned-over area. This house was of the frame and stucco type common to the area and was one of several forming a small group within an enclosure formed by an 8-foot masonry and wood wall. All houses within the enclosure had tile-covered roofs, but one of the group also had a small section covered with highly inflammable cedarbark shingles which showed fire damage, although the fire had been extinguished before the entire roof was consumed (Photos 28 and 29). The owners of the property, including a son who was a university graduate, insisted that the roof covering burst into flame immediately with the bomb explosion. Their story could not be shaken. The chief of the fire department stated that he had heard of two or three cases where the cedarbark-covered roofs, also not permitted within the city limits, had been ignited directly by the bomb, and thought the reports credible. A number of buildings with unburned cedarbark roof shingles were found at a rayon plant approximately 11,000 feet southwest from AZ.

(4) About 600 feet east of the dwelling described above and about 365 feet from the nearest burned building, a wood pole which had apparently carried electric wires, probably 220 volts AC, was found with 3 to 4 feet of its top burned off and rather heavy flash burns on the side facing AZ (Photo 30). Several residents of the area stated that this pole had been seen burning about 5 or 10 minutes after the bomb explosion. It is entirely possible that ignition of this pole was caused directly by heat radiation from the bomb. The pole was capped with a light steel plate of dark color and it may be that the steel absorbed sufficient heat and retained it long enough to ignite dry rot which probably was present under the metal cap. An attempt to determine from utility company records whether or not the pole had been burned previously was unsuccessful. Many wood

poles within the fire perimeter were burned, but it is impossible to state with certainty whether the source of ignition was direct heat from the bomb or heat and flying embers from nearby buildings. Other evidence, however, leads to the conclusion that exposed wood was seldom ignited by radiated heat from the bomb.

(5) A cemetery about 2,500 feet from AZ was found cluttered with pieces of very light wood (excellent kindling) which showed no evidence of flash or other burns (Photo 31). It is believed that this debris must have been blown by the blast from the interior or other unexposed portions of structures and this accounts for the lack of flash-burn marks. It is interesting that none of this material was ignited by flying embers, as it was very close to the center of the burned-over area of the city. Photos 32 and 33 also show unburned combustible buildings at 3,800 and 5,000 feet from AZ.

(6) One of the graves in the cemetery was enclosed with a wood fence. The fence was composed of four corner poles extending about 30 inches above the ground and supporting two horizontal pieces, about 12 inches apart. Bamboo pickets (about 1½ by 3/16-inch) were lashed to the fence with vegetable-fibre rope. The corner poles showed deep charring which later proved to have been done according to Japanese custom when they were erected. The horizontal pieces apparently were not charred, but when the lashing for the pickets was removed very definite evidence of flash-burn showed. The bamboo pickets showed light flash-burn marks. The rope lashing for the pickets showed no evidence of having been on fire, but was singed.

(7) At the Red Cross Hospital, 5,300 feet south from AZ, three chairs with backs and seats upholstered with a pile fabric (apparently mohair) were near a window which was exposed to AZ. The backs of the chairs showed moderate to deep singeing except for the lower part which had been shielded by the concrete wall and showed no discoloration. Parts of the seats of the chairs showed light flash-burns where the seats had not been shielded by the chair backs. No part of the upholstery was burned through (Photo 34). Next to the chairs was a varnished wood door which showed definite evidence of flash-burn except for a very small spot adjacent to the door knob which shielded it. The door did not catch fire (Photo 35). A cotton jacket worn by one of the nurses was charred across one breast. The outer material of the jacket was burned away in part, but the padded cotton lining directly underneath was not burned through (Photo 35). The nurse who had worn the jacket was severely injured by the blast and was not available for questioning. It was stated that her body was not burned through the coat. Testimony at the hospital indicated that several coats had burned similarly, but the others could not be produced for examination. Furthermore, nobody at the hospital was certain that these coats had actually burst into flame, and, in fact, the concensus was that they had only smoldered. There was no other evidence of fire in the hospital.

(8) Scores of persons throughout all sections of the city were questioned concerning the ignition of clothing by the flash from the bomb. Replies were consistent that white silk seldom was affected, although black, and some other colored silk, charred and disintegrated. Numerous instances were reported in which designs in black or other dark colors on a white silk kimono were charred so that they fell out, but the white part was not affected. These statements were confirmed by United States medical officers who had been able to examine a number of kimonos available in a hospital. Ten school boys were located during the study who had been in school yards about 6,200 feet east and 7,000 feet west, respectively, from AZ. These boys had flash burns on the portions of their faces which had been directly exposed to rays of the bomb. The boys' stories were consistent to the effect that their clothing, apparently of cotton materials, "smoked," but did not burst into flame. Photo 36 shows a boy's coat that started to smolder from heat rays at 3,800 feet from AZ.

(9) Three automobile trucks, powered with internal combustion motors using fuel generated by burning charcoal (no gasoline or similar volatiles used), which were parked in a clearing about 7,800 feet north from AZ were said to have been ignited immediately after the bomb explosion. Fire damage to the vehicles was total. Conversely, however, a sedan showing no fire damage was examined where it had been abandoned as a result of severe blast damage on a wide street about 5,800 feet southeast from AZ.

(10) A private garden covering an area of slightly over 5 acres and located about 5,000 feet northeast from AZ showed no evidence of having been on fire, although there was some flash-burn damage on the edge of the area facing AZ.

PHOTO 36 IX. Shows partly burned coat of boy who was in open near City Hall (Building 28) 3,800 feet from AZ.

3800 feet from air zero;
3300 feet from ground zero

PROBABILITY OF FIRE SPREAD
IN
VARIOUS AMOUNTS OF BUILT-UPNESS

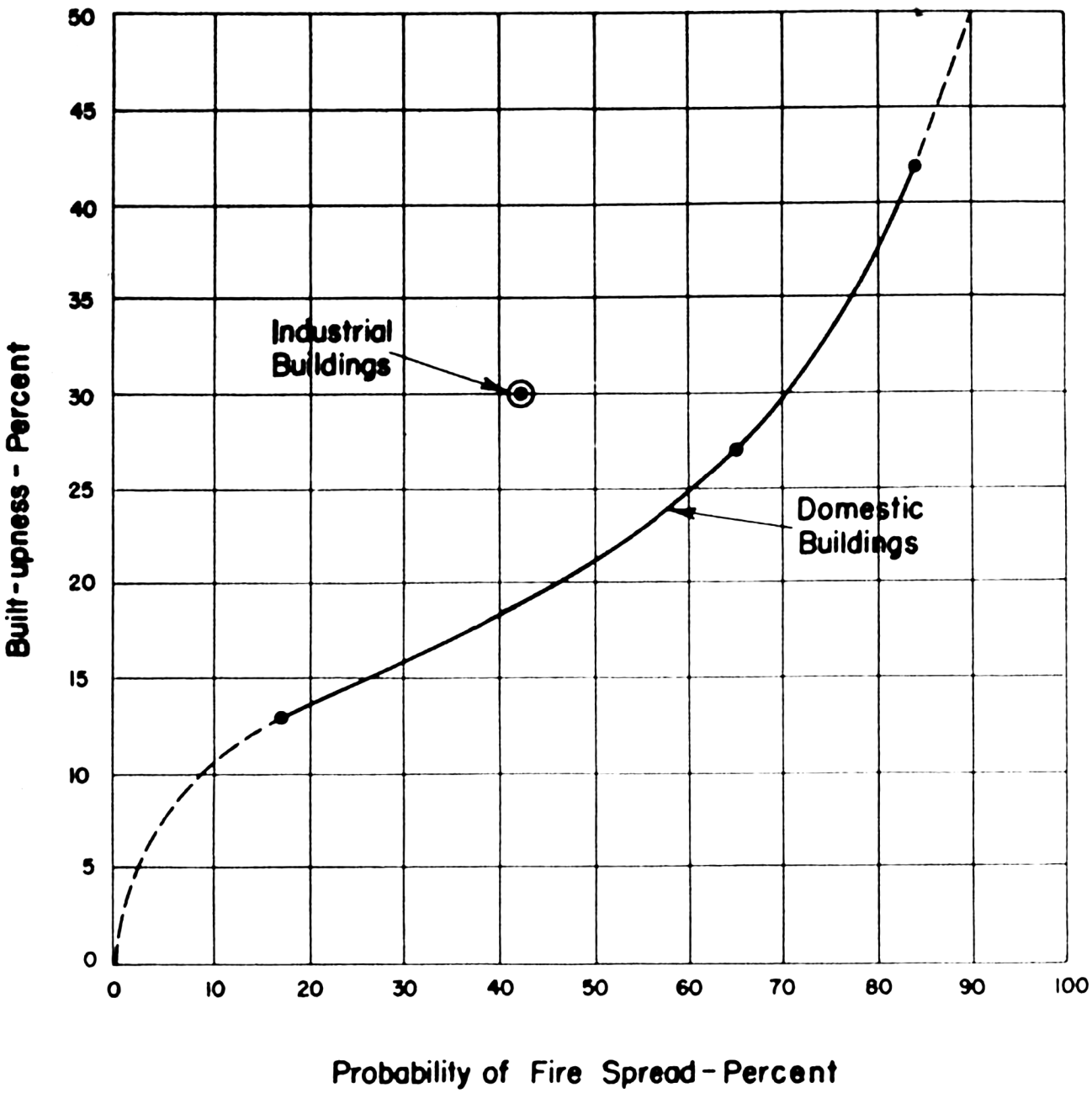

[redacted]

U.S. STRATEGIC BOMBING SURVEY
FIRE SPREAD VS. BUILT-UPNESS
HIROSHIMA, JAPAN
FIGURE 4-IX

[redacted]

PROBABILITY OF FIRE SPREAD ACROSS VARIOUS EXPOSURE DISTANCES

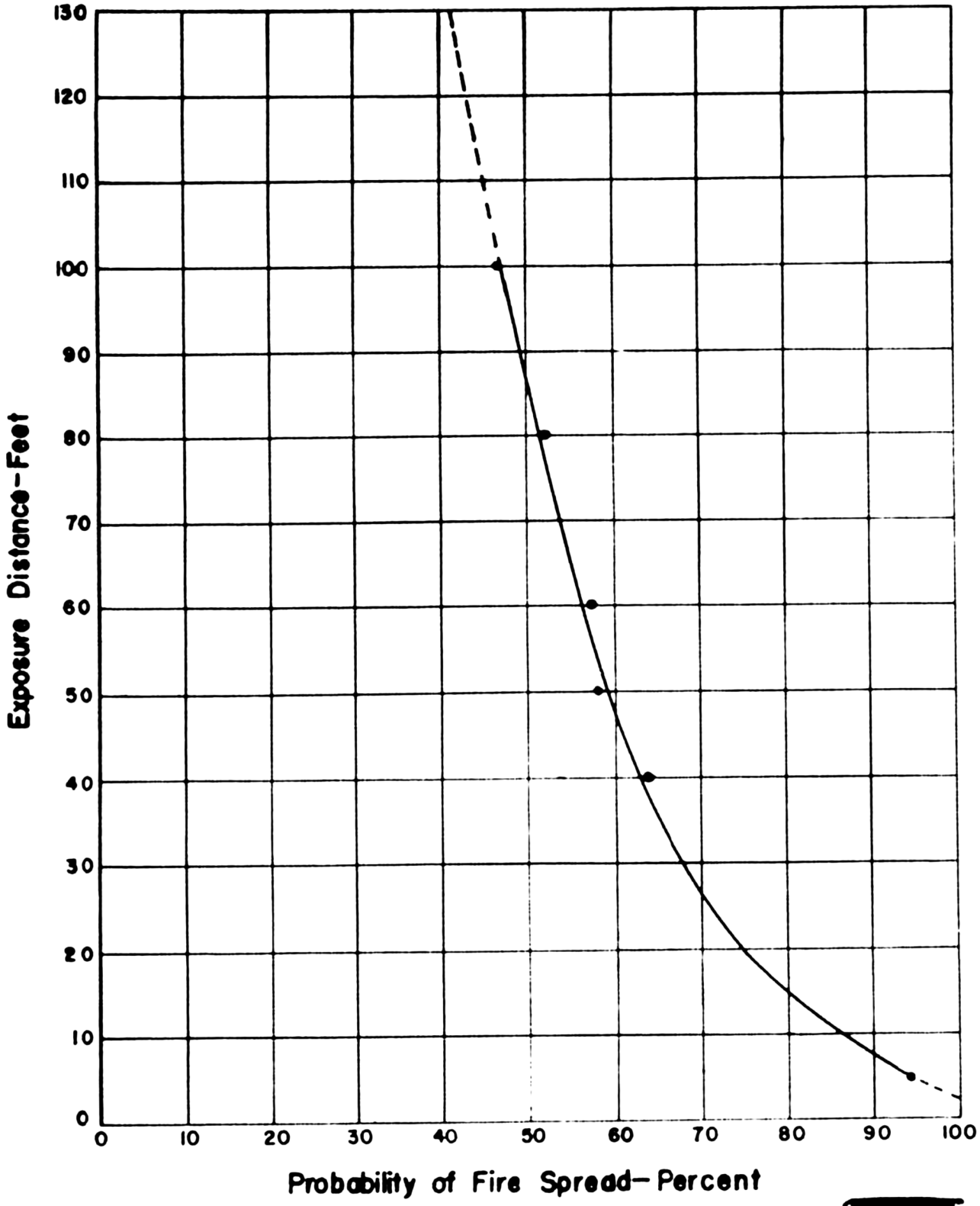

[redacted]

U. S. STRATEGIC BOMBING SURVEY

FIRE SPREAD VS. EXPOSURE DISTANCES
HIROSHIMA, JAPAN
FIGURE 5 - IX

TABLE 5.—*Fire-resistive building data (fire)*

Building No.	Coordinates	Distance from AZ (feet)	Distance from GZ (feet)	Occupancy	Fire shutters on wall openings	Unprotected wall openings exposed to AZ at zero hour	Distance from unprotected wall openings to nearest burned building (feet)	Probable cause of initial ignition	Number of stories	Stories burned (after blast damage)	Areas in thousands square feet: Total floor area	Areas in thousands square feet: Floor area burned	Percent floor area burned
1	4H	2,100	700	Office	No	Yes	0		B-2	1-2	4.2	3.5	83
2	4H	2,100	800	do	No	Yes	20		B-3	60% B, 100% 1-3	27.3	24.3	89
6	5H	2,100	600	do	Yes	Probably no	10	Fire spread	B-3	70% B, 100% 1-3	16.6	15.3	92
7	5H	2,100	600	Bank	Yes	Yes	6	do	2	1-2	5.7	5.7	100
8	5H	2,100	600	do	Yes	Yes	10	do	3	1-3	9.0	9.0	100
9	5H	2,100	600	Office	Yes	Yes	10	do	B-3	1-3	4.9	4.2	86
10	5H	2,100	600	do	Yes	Yes	10	do	2	1-2	2.5	2.5	100
11	5H	2,100	700	do	No	Yes	30		3	1-3	9.8	9.8	100
12	5H	2,100	700	do	No	Yes	10		B-3	B-3	15.8	15.8	100
18	5H	2,200	1,000	Bank	Part	Probably no	10	Fire spread	B-5	B-5	46.4	46.4	100
19	5H	2,200	1,000	do	Yes	Yes	20	Primary	B-4	75% 1-2, 100% 3-4	29.9	25.2	84
20	5H	2,200	1,000	Office	Part	Yes	10		3	1-3	4.5	4.5	100
21	5H	2,300	1,300	Bank	Yes	Yes	15	Primary	2	1-2	7.3	7.3	100
22	5H	2,300	1,100	Office	Part	Yes	10		4	1-4	20.4	20.4	100
23	5H	2,300	1,200	do	No	Yes	10		B-7	1-7	43.3	39.0	90
24	5H	2,400	1,300	Bank	Yes	Yes	25	Fire spread	B-3	5% 2, 100% 3	32.8	5.2	16
25	5H	2,400	1,400	Art museum	Part	Yes	10		2	1-2	5.4	5.4	100
26	5H	3,000	2,300	Office	Part	Yes	10	Primary	B-5	40% B, 100% 1-5	52.0	46.5	88
27	6H	3,100	2,400	Library	Part	Yes	25		4	1-4	13.4	13.4	100
28	6H	3,800	3,300	Office	No	Yes	50	Fire spread	B-4	80% B-1, 100% 2-4	93.4	84.9	91
31	6H	5,300	4,900	Hospital	No	Yes	75	No fire	B-3	None	88.6	0	0
32A	6H	5,100	4,700	Classrooms	No	Yes	25	Fire spread	2	1-2	2.8	2.8	100
32B	6H	5,200	4,800	Library	Yes	No	5	do	2	1-2	3.7	3.7	100
32D	6H	5,000	4,600	Classrooms-laboratories	No	Yes	30	Secondary	3	1-3	103.3	103.3	100
32E	6H	4,700	4,200	Classrooms	No	Yes	30	Fire spread	3	1-3	39.5	39.5	100
32F	6H	5,000	4,600	Laboratory	No	Yes	12	do	1	1	2.0	2.0	100
32G	6H	5,200	4,800	Kitchen	No	Yes	0	do	1	None	3.0	3.0	0
32H	6H	5,300	4,900	Laboratory	No	Yes	6	do	2	1-2	3.8	3.8	100
33	6H	5,600	5,300	Office	Part	Yes	90	do	B-4	None	62.6	0	0
38	5H	2,900	2,100	do	No	Yes	20	do	B-3	B-3	10.4	10.4	100
39	5I	3,200	2,500	do	Part	Yes	10	Primary	4	1-4	32.0	32.0	100
40	5H	3,200	2,500	Department store	No	Yes	50	do	B-7	B-7	78.9	78.9	100
41	5H	2,600	1,700	Classrooms	No	Yes	20		B-3	75% B, 100% 1-3	26.4	25.1	95
43	5H	2,800	2,000	Telephone exchange	Part	Yes	35	Secondary	3	1-3	36.1	36.1	100
44	5H	2,700	1,800	Department store	Yes	Yes	5		3	1-3	4.3	4.3	100
45	5H	2,700	1,800	Bank	Yes	Yes	0		3	1-3	8.0	8.0	100
47	5H	3,100	2,300	Beer hall	No	Yes	20	Fire spread	B-3	1-3	15.3	13.2	86
48	5H	3,300	2,600	Hospital	No	Yes	6		2	1-2	2.9	2.9	100
49	5I	3,600	3,000	Office	Part	Yes	90	Primary	7	1-7	14.7	14.7	100
50	5I	3,600	3,000	Newspaper plant	No	Yes		Fire spread	3	1-3	24.5	24.5	100
51	5I	3,700	3,200	Bank	Part	Yes	40	Primary	B-3	15% B, 100% 1-3	26.7	19.2	72
59	5I	4,500	4,100	Office	Part	Yes	30	Fire spread	B-3	None	16.2	0	
61	5I	4,000	3,400	Radio station	No	Yes	15		2	1-2	8.3	8.3	100
62	5I	4,100	3,600	Residence	No	Yes	0		2	1-2	2.2	2.2	100
64	3I	5,300	4,900	Hospital	No	Yes	30	Primary	B-2	Second only	15.9	5.3	33
65	3I	5,300	4,900	Office	No	Yes	30	Fire spread	4	50% 1-3, 90% 4	83.4	50.0	60
67	3H	5,000	4,600	Munitions storage	Yes	No	125	No fire	1	None	1.7	0	0
74	3H	6,300	6,000	Electrical laboratory	No	Yes	30	Fire spread	B-2	70% B-1, 100% 2	13.2	10.6	80
76	3G	6,200	5,900	Warehouse	Yes	Yes	0	do	1	1	15.9	15.9	100
79	3G	6,100	5,800	do	Yes	Yes	6	do	2	1-2	14.4	14.4	100
85	4G	3,800	3,300	Telephone exchange	Yes	Probably no	125	Secondary	3	25% second only	14.2	1.1	8
86	5G	2,800	2,000	Classrooms	No	Probably no	125	No fire	3	None	11.5	0	0
93	5G	2,500	1,500	Warehouse	Yes	No	0	Fire spread	2	1-2	2.9	2.9	100
95	4G	2,300	1,200	Classrooms	No	Yes	30		B-3	B-3	49.5	49.5	100
96	5G	2,000	400	Clothing store	No	Yes	10		B-3	1-3	12.4	9.3	75
100	5G	2,100	800	Office	No	Yes	0		2	1-2	3.0	3.0	100
101	5G	2,600	1,700	Warehouse	Yes	Probably no	5	Fire spread	2	1-2	4.3	4.3	100
113C	7I	7,700	7,400	Cigarette manufacture	No	Yes	60	No fire	1	None	54.6	0	0
122	5J	6,700	6,400	Bank	Yes	Probably no	5	Fire spread	2	None	5.1	0	0
129	3G	6,000	5,600	do	No	Yes	12	No fire	B-2	None	16.2	0	0
132	6G	5,700	5,400	Warehouse	Yes	No	0	Fire spread	B-1	B-1	15.0	15.0	100
133	5J	6,200	5,900	Mercantile	No	Yes	0	do	4	1-4	3.0	3.0	100
134	4J	6,300	6,000	Office	Yes	Yes	60	do	3	80% 1, 100% 2-3	4.8	4.5	94
135	5J	6,800	6,500	Bank	Yes	Yes	100	No fire	B-2	None	9.0	0	0

SOURCE: USSBS's Secret report, "The Effects of the Atomic Bomb on Hiroshima, Japan," vol. 2 Only 8 of 64 non-wood buildings had thermal flash ignition evidence, 3 had blast damage induced fire, and 28 were ignited by firespread from wood homes.

(4) It was reported that a cotton black-out curtain at an unprotected window in the east stair tower of Building 85 (3,800 feet from AZ) smoked and was scorched by radiated heat from the bomb but it did not burst into flames. All windows other than those in the stair tower were protected by closed steel-roller shutters. There was fire damage in a few telephone relay units in the second story but this was caused by electrical short circuits when debris from windows was blown into the equipment by blast.

(5) A man who was in the third story of building 26 (3,000 feet from AZ) stated that radiated heat from the bomb ignited cotton black-out curtains at unprotected windows in the west wall and thin rice paper on desks. According to his recollection, all stories were afire five minutes after the attack. On the other hand, two men who were working in Building 28 (3,800 feet from AZ) stated that there was no primary fire in this building, the windows of which were not equipped with fire shutters. Black-out curtains at all windows were drawn back and no fires started in them. According to the same men, fire spread into the building by flying brands from the south nearly two hours after the attack.

(10) Fire fighting with water buckets was reported inside only four buildings (24, 33, 59, and 122) and probably prevented extensive fire damage in them. In Building 24, fire was started in contents of a room at the southwest corner of the second story by sparks from trees on the south side about 1½ hours after the attack. Men inside the building extinguished the fire and probably prevented further damage in the first and second stories (Photo 85). A little later, contents in the third story were ignited by sparks from the outside and were totally damaged. This fire was beyond control before it was discovered, but did not spread downward through open stairs. At Building 33, sparks from the west exposure, which burned in early evening, set fire to black-out curtains in the west wall and to waste paper in the fourth story of the northwest section of the building. Twenty persons were on guard in the building awaiting such an occurrence and the fires were quickly extinguished while in the incipient stage. At Building 59 sparks from the south exposure ignited a few pieces of furniture in the first and third stories and black-out curtains in the first story about 2 hours after the attack. These fires were extinguished by men inside and negligible damage resulted. A few window frames in the east and west walls and 2 or 3 desks in the first story of Building 122 were ignited by radiated heat and sparks from the west and northeast exposures. These fires were extinguished quickly and damage was negligible.

A. SUMMARY

1. The atomic bomb detonated at Hiroshima was an extremely effective and powerful blast weapon. Blast effect was essentially similar to that produced by a large charge of high explosive except that it was on a much larger scale; thus, damage was characterized by distortion or crushing of entire buildings rather than collapse of a single truss or rupture of a single wall.

2. Usual blast phenomena such as shielding, reflection, and diffraction were observed. The positive phase of the blast of the atomic bomb is believed to have been of comparatively longer duration that that of high explosives.

3. The primary cause of damage to buildings was blast. In many instances the fire which swept the central portion of the city increased distortion of the building frames, and consumed the combustible contents and interior trim and finish of most of the fire-resistive buildings located within the burned-over area. Blast damage to wood-frame buildings extended well beyond the limits of the burned-over area and it is probable that all wood-frame structures within the burned-over area suffered structural damage initially by blast.

4. The mean areas of effectiveness (MAE) of the atomic bomb for structural damage about ground zero (GZ) and the radii of the MAE's for the several classes of buildings present were computed to be as follows:

	MAE's in square miles	Radii of MAE's in feet
Multistory, earthquake-resistant	0. 03	500
Multistory, steel- and reinforced-concrete frame (including both earthquake- and non-earthquake-resistant construction)	. 05	700
1-story, light, steel-frame	3. 4	5, 500
Multistory, load-bearing, brick-wall	3. 6	5, 700
1-story, load-bearing, brick-wall	6. 0	7, 300
Wood-frame industrial-commercial (dimension-timber construction)	8. 5	8, 700
Wood-frame domestic buildings (wood-pole construction)	9. 5	9, 200
Residential construction	6. 0	7, 300

Of the values listed above, those for wood-frame and residential construction are peculiar to Japan and are not applicable to any other locality.

5. MAE's for similar, high, air-burst atomic bombs against Occidental construction were estimated to be approximately:

	Square miles
Multistory, steel- and reinforced-concrete	0. 06
Very light, steel-frame one-story, low-cost industrial and storage	3. 4
Multistory, load-bearing, brick wall	3. 6
One-story, load-bearing, brick wall	6. 0

MAE values against other types of Occidental construction, including moderate to heavy, steel-frame, industrial construction, could not be estimated because buildings of comparable construction were not present in Hiroshima.

6. Fire was the principal cause of damage to contents. In multistory frame construction fire caused the major part of all contents' damage, suffering only slight to moderate initial damage from blast and debris. Contents in light, steel-frame buildings suffered moderate initial damage from blast and, subsequently, in the burned-over area, almost total damage by fire. Outside the burned-over area there was some exposure damage. Blast and debris were the major causes of damage to contents of brick buildings, additional damage resulting from fire and exposure. Throughout the burned-over area practically all contents of wood-frame buildings were destroyed by fire. Beyond the limits of the fire there was slight to moderate damage to contents from blast, debris, and exposure.

7. Except for multistory, steel- and concrete-frame buildings, contents and structural damage to buildings were generally of similar extent at corresponding distances from air zero (AZ).

8. Had the bomb detonated at a somewhat lower altitude, damage to multistory, steel- and reinforced-concrete frame buildings which were clustered relatively near GZ probably would have been greater. The effect of such an explosion upon the extent of damage to other classes of buildings is uncertain, but probably would not have been great.

9. Comparison of the atomic bomb with high-explosive weapons results, at best, in very rough approximations because of the assumptions necessary. Based upon damage to load-bearing, brick-wall structures, an equivalent bare charge of approximately 4,400 tons of TNT was estimated.

10. Because of the large area through which damage extended, particularly to load-bearing brick construction which constitutes a large proportion of the residential and older industrial sections of occidental cities, the air-burst atomic

TABLE 1.—*Building data, steel- and reinforced-concrete-frame*

[Areas in thousands of square feet]

Building	Grid	Occupancy	Type	Plan area	Stories	Building HE-V	Building fire-V	Distance AZ-(feet)	Total floor area	Building damage—floor area						Content damage	
										Structural damage			Superficial damage		Internal fire	Percent	Cause
										Blast	Fire	Mixed	Blast	Fire			
1	4H	Office	E1	1.7	2	V-1	R	2,100	4.2	1.8					3.5	90	Fire.
2	4H	do	E1	8.3	2/3	V-1	R	2,200	27.3	1.1					24.3	90	Do.
6	5H	do	E1	5.1	3	V-1	R	2,100	16.6						15.3	95	Do.
8	5H	Bank	E1	5.3	1/3	V-1	R	2,100	9.0	5.3					9.0	100	Do.
9	5H	Office	E1	2.1	2/3	V-1	R	2,100	4.9	1.0					4.2	90	Do.
11	5H	do	E1	4.6	3	V-1	R	2,100	9.8	2.1					9.8	100	Do.
18	5H	Bank	E1	10.1	5/2	V-1	R	2,200	45.0	1.9					46.4	100	Do.
19	5H	do	E1	8.8	4	V-1	R	2,200	29.9	2.7					25.2	90	Do.
20	5H	Office	E1	1.5	3	V-1	R	2,200	4.5	.1					4.5	100	Do.
21	5H	Bank	E1	5.5	1/2	V-1	R	2,300	7.3	5.7					7.3	100	Mixed.
22	5H	Office	E1	4.7	4	V-1	R	2,300	20.4	1.6			2.1		20.4	100	Fire.
23	5H	do	E1	5.4	7	V-1	R	2,300	43.3	4.6					39.0	90	Do.
24	5H	Bank	E1	10.6	3	V-1	R	2,400	32.8						5.2	30	Mixed.
26	5H	Office	E1	9.2	5	V-1	R	3,000	52.0				.2		46.5	90	Fire.
27	5H	Library	E1	5.3	2/4	V-1	R	3,100	13.4		0.8				13.4	100	Do.
28	6H	Office	E1	21.3	4	V-1	R	3,800	93.4						84.9	95	Do.
31	6H	Hospital	E1	27.5	3/4	V-1	R	5,300	88.6						0	25	Debris.
32A	6H	Classrooms	E1	1.4	2	V-1	R	5,100	2.8						2.8	100	Fire.
32B	6H	Library	E1	1.9	2	V-1	R	5,200	3.7						3.7	100	Do.
32D	6H	Classroom laboratory	E1	34.4	3	V-1	R	5,000	103.3						103.3	100	Do.
32E	6H	Classrooms	E1	13.2	3	V-1	R	4,700	39.5						39.5	100	Do.
33	6H	Office	E1	11.2	4	V-1	R	5,600	62.6						0	15	Blast-debris.
38	5H	do	E1	2.6	3	V-1	R	2,900	10.4						10.4	100	Fire.
39	5I	do	E1	15.5	3/4	V-1	N/R	3,200	32.0				4.4		32.0	100	Do.
40	5H	Department store	E1	9.9	7	V-1	R	3,200	78.9						78.9	100	Do.
41	5H	Classrooms	E1	7.2	3	V-1	R	2,600	26.4						25.1	95	Do.
43	5H	Telephone exchange	E1	16.3	2/3	V-1	R	2,800	36.1						36.1	100	Do.
44	5H	Department store	E1	2.6	1/3	V-1	R	2,700	4.3	1.7					4.3	100	Do.
47	5H	Beer hall	E1	4.8	3	V-1	R	3,100	15.3						13.2	80	Do.
49	5I	Office	E1	2.1	7	V-1	R	3,600	14.7						14.7	100	Do.
50	5I	Newspaper	E1	10.3	2/3	V-1	R	3,600	24.5						24.5	100	Do.
51	5I	Bank	E1	9.0	1/3	V-1	R	3,700	26.7						19.2	80	Do.
59	5I	Office	E1	4.8	2/3	V-1	R	4,500	16.2						0	10	Blast.
61	5I	Radio station	E1	4.2	2	V-1	R	4,000	8.3						8.3	100	Fire.
62	5I	Residence	E1	1.1	2	V-1	R	4,100	2.2						2.2	100	Do.
64	3I	Hospital	E1	6.8	2	V-1	R	5,300	15.9						5.3	40	Mixed.
65	3I	Office	E1	20.8	4	V-1	R	5,300	83.4						50.0	70	Do.
74	3H	Electrical laboratory	E1	6.6	2	V-1	R	6,300	13.2						10.6	80	Fire.
79	3G	Warehouse	E1	7.7	2	V-1	R	6,100	14.4		9.9			2.3	14.4	100	Do.
85	4G	Telephone exchange	E1	4.8	3	V-1	R	3,800	14.2						1.1	50	Mixed.
86	5G	Classrooms	E1	3.8	3	V-1	R	2,800	11.0						0	30	Debris.
95	4G	do	E1	12.4	3	V-1	R	2,300	49.5	0.5			3.0		49.5	100	Fire.
96	5G	Clothing store	E1	4.1	3	V-1	R	2,000	12.4	3.9					9.3	75	Do.
116A	7J	Warehouse	E1	23.7	3	V-1	R	8,800	71.1						0	0	
116B	7J	do	E1	23.7	3	V-1	R	8,900	71.1						0	0	
116C	7J	do	E1	23.7	3	V-1	R	9,000	71.1						0	0	
116F	7J	do	E1	23.7	3	V-1	R	9,200	71.1						0	0	
122	5J	Bank	E1	2.6	2	V-1	R	6,700	5.1						0	0	
12	5H	Office	E2	4.5	3	V-3	R	2,100	15.8	10.8			0.7		15.8	100	Mixed.
16	5H	Electric substation	E2	1.6	3	V-3	N	3,100	4.1				4.1		2.5	50	Do.
25	5H	Art museum	E2	3.3	2	V-3	R	2,400	5.4	0.3			2.1		5.4	100	Fire.
46	5H	Jewelry store	E2	.9	2	V-3	N/C	2,800	1.9	1.9					1.9	100	Mixed.
48	5H	Hospital	E2	1.5	2	V-3	R	3,300	2.9						2.9	100	Fire.
98	5G	Warehouse	E2	1.5	2	V-3	R	2,500	2.9	2.9					2.9	100	Mixed.
100	5G	Office	E2	1.5	2	V-3	R	2,100	3.0				.1		3.0	100	Fire.
101	5G	Warehouse	E2	2.2	2	V-3	R	2,600	4.3	4.3					4.3	100	Debris.
121	4J	Railroad station	E1	9.0	1/2	V-3	N/C	6,600	14.0	4.9	4.9				14.0	100	Fire.
67	3H	Munitions storage	A2.4	1.7	1	V-4	R	5,000	1.7	1.7					0	10	Exposure.
76	3G	Warehouse	A2.4	15.9	1	V-4	R	6,200	15.9	1.9					15.9	100	Fire.
113C	7I	Cigarette manufacturing.	A1.2	54.6	1	V-4	R	7,700	54.6						0	0	
113D	7I	do	A1.2	54.9	1	V-4	R	7,800	54.9						0	0	
126A	5K	Railroad roundhouse	A2.4	21.1	1	V-4	R	8,900	21.1						0	0	
126B	5K	do	A1.2	11.6	1	V-4	R	9,000	11.6						0	0	

STRUCTURAL DAMAGE BY BLAST
TO
MULTI-STORY, STEEL- AND REINFORCED-CONCRETE-FRAME BUILDINGS
(BASED ON TOTAL FLOOR AREA)

MAE FOR ALL STEEL- & REINF.-CONC.-FRAME BLDGS = 0.05 SQ MI
MAE FOR EARTHQUAKE-RESISTANT BLDGS ONLY = 0.03 SQ MI

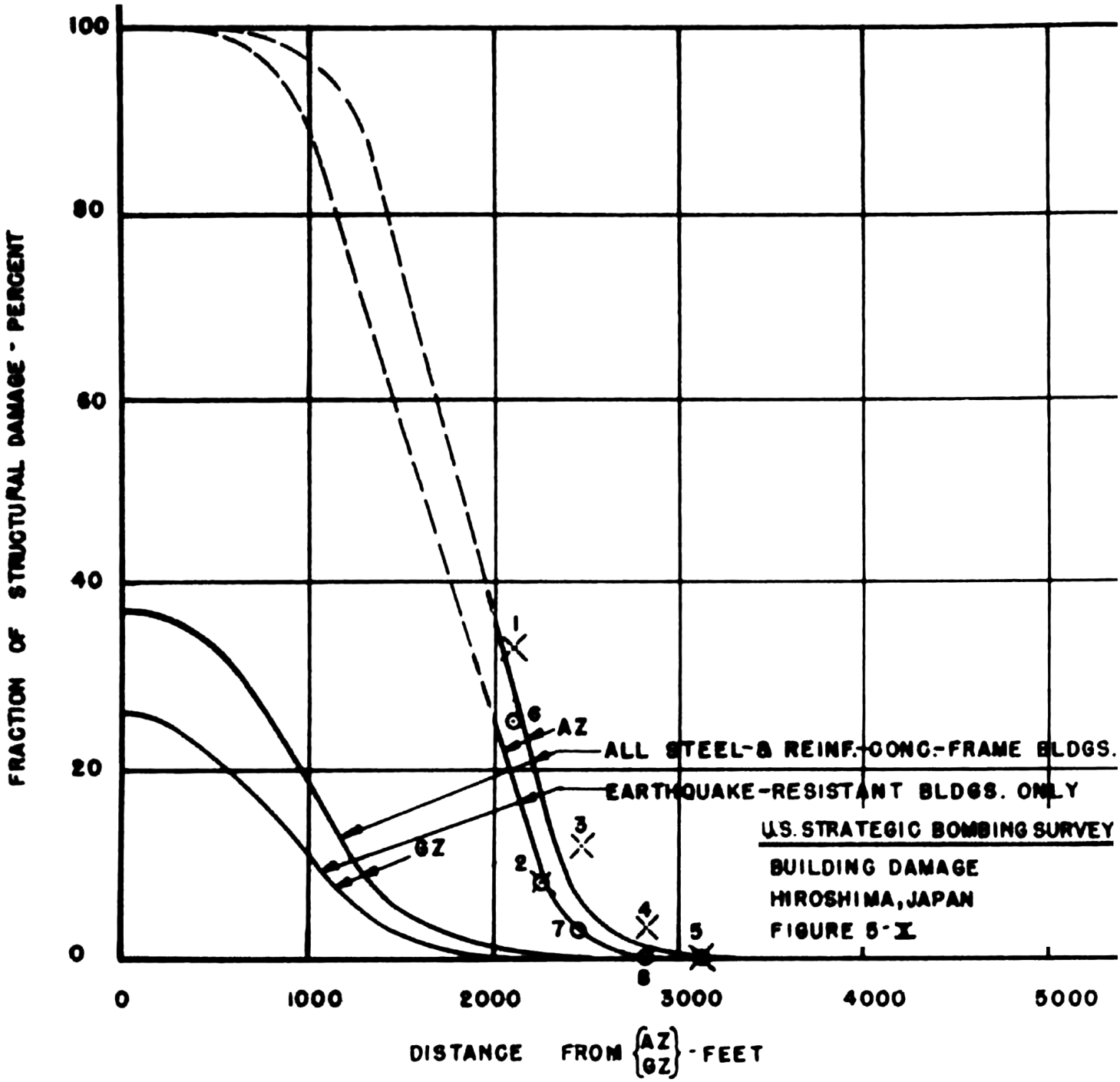

DAMAGE TO CONTENTS

-IN-

[redacted]

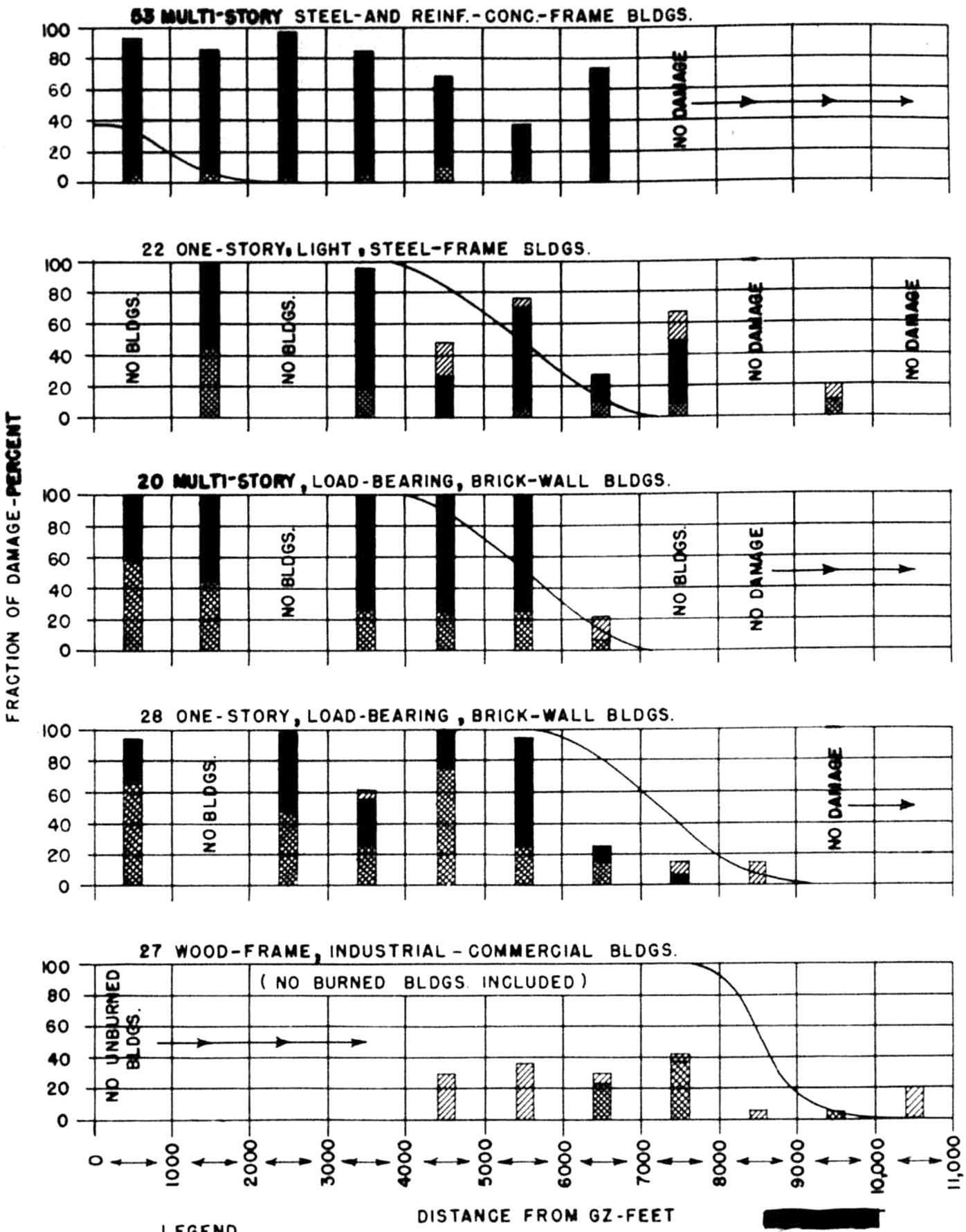

[redacted]

LEGEND

STRUCTURAL DAMAGE BY BLAST

CONTENTS DAMAGE (VALUE LOSS) { FIRE / BLAST & DEBRIS / EXPOSURE

U.S. STRATEGIC BOMBING SURVEY

CONTENTS DAMAGE
HIROSHIMA, JAPAN
FIGURE 10-X

TABLE 7.—*Combustible building data (fire)*

Building Number	Coordinators	Distance from AZ (feet)	Distance from GZ (feet)	Occupancy	Fire shutters on wall openings	Unprotected wall openings exposed to AZ at zero hour	Distance from unprotected wall openings to nearest burned building (feet)	Probable cause of initial ignition	Number of stories	Stories burned (after blast damage)	Areas in thousands square feet: Total floor area	Areas in thousands square feet: Floor area burned	Percent floor area burned
3	4H	2,200	900	Electric substation	No	Yes	40	Secondary	B-1	B-1	3.8	3.8	100
4	5H	2,000	400	Mercantile	No	Yes	15		3	1-3	30.0	30.0	100
5	5H	2,000	100	Hospital	No	Probably no	15		1	1	2.3	2.3	100
13	5H	2,300	1,300	Office	Yes	Yes	10		3	1-3	5.6	5.6	100
14	5H	2,400	1,400	Bank	No	Yes	10		2	1-2	3.1	3.1	100
15	5H	3,000	2,200	Electric repair	No	Yes	0		1	1	6.9	6.9	100
17	5H	2,200	900	Office	No	Yes	0		2	1-2	4.0	4.0	100
29	6H	4,600	4,200	Soy sauce warehouse	No	Yes	5	Fire spread	2	1-2	1.4	1.2	100
30	7H	5,800	5,500	Gymnasium	No	Yes	5	do	1	1	5.8	5.8	100
32C	6H	5,300	4,900	Library	Yes	No	0	do	3	1-3	5.9	5.9	100
34	6H	5,500	5,200	Art museum	Yes	No	0	do	2	1-2	2.4	2.4	100
37	6H	4,600	4,200	Public baths	No	Yes	0	Secondary	1	1	1.2	1.2	100
42	5H	2,600	1,600	Public auditorium	No	Yes	10		2	1-2	11.9	11.9	100
53	5I	3,800	3,200	Warehouse	No	Probably no	10		1	1	.9	.9	100
54	5I	3,700	3,100	Match manufacturing	No	Yes	10		1	1	2.7	2.7	100
55	5H	3,700	3,100	Electrical warehouse	Yes	Yes	5		2	1-2	9.9	9.9	100
57	5I	4,700	4,300	Gymnasium	No	Yes	20	Fire spread	1	1	6.2	6.2	100
60	5I	3,600	3,000	Church	No	Yes	5	do	1	1	3.1	3.1	100
66A	4I	4,500	4,000	Army stores	Yes	Probably no	20	do	2	1-2	19.1	19.1	100
66B	4I	4,400	3,900	do	Yes	Probably no	25	do	2	1-2	19.1	19.1	100
66C	4I	4,600	4,200	do	Yes	Probably no	50	do	2	1-2	19.1	19.1	100
66D	4I	4,800	4,400	do	Yes	Probably no	50	do	2	1-2	19.1	19.1	100
68A	4H	3,200	2,500	do	Yes	Probably yes	60		1	1	14.4	14.4	100
68B	4H	3,300	2,600	do	Yes	Probably yes	60		1	1	14.4	14.4	100
68C	4H	3,500	2,800	Army stores	Yes	Probably yes	60		1	1	14.4	14.4	100
69	4H	3,000	2,300	do	Yes	Probably yes	40		1	1	14.4	14.4	100
70	2H	7,500	7,200	Auditorium	No	Yes	15	Fire spread	1-Bal.	1-Bal.	6.4	6.4	100
71	2H	7,800	7,600	Gymnasium	No	Yes	10	do	1	1	6.4	6.4	100
72	3H	6,500	6,200	Aluminum foundry	No	Yes	15	Secondary	1	20% 1	13.0	2.6	20
77	3G	6,700	6,400	Gymnasium	No	Yes	20	Fire spread	1	1	5.6	5.6	100
80	3G	6,200	5,900	Iron foundry	No	Yes	100	No fire	1	None	6.5	0	0
82	3G	4,400	3,900	Light machine shop	No	Yes	0	do	1	None	9.5	0	0
83	4G	3,900	3,300	do	No	Yes	0		1	1	3.6	3.6	100
84	4G	3,900	3,300	do	No	Yes	0		1	1	7.0	7.0	100
92	5G	2,400	1,300	Bank	Yes	Yes	0		2	1-2	2.9	2.9	100
94	5G	2,300	1,100	Light manufacturing	No	Yes	15		1-Bal	1-Bal.	4.4	4.4	100
97	7G	6,300	6,000	Light machine shop	No	Yes	50	No fire	1	None	3.2	0	0
98A	7G	6,700	6,400	Paper machinery	No	Yes	0	Fire spread	2	2% 2d only	7.5	.1	1
99	7G	6,800	6,500	Office storage	No	Yes	40	No fire	1	None	5.8	0	0
102A	4F	5,300	4,900	Machine shop	No	Yes	25	do	1	None	5.3	0	0
102B	4F	5,300	4,900	do	No	Yes	25	do	1	None	5.9	0	0
102C	4F	5,300	4,900	do	No	Yes	25	do	1	None	13.0	0	0
104	3G	5,400	5,000	Gymnasium	No	Yes	35	do	1	1	3.3	0	0
106	4F	4,400	3,900	Light machine shop	No	Yes	15	do	1	None	2.3	0	0
107	4F	4,200	3,700	Gymnasium	No	Yes	25	Fire spread	1	1	4.8	4.8	100
108	5F	6,200	5,900	Auditorium	No	Yes	25	No fire	1-Bal	None	8.4	0	0
110	5J	6,200	5,900	Bank	Yes	No	0	Fire spread	2	1-2	2.6	2.6	100
111	5J	6,300	6,000	Grain warehouses	No	Probably no	75	do	1	1	30.6	30.6	100
112C	7I	6,900	6,600	Miscellenaous storage	No	Yes	80	No fire	1	None	.9	0	0
112D	7I	6,900	6,600	Light machine shop	No	No	50	do	1	None	.8	0	0
113G	7I	7,400	7,100	Miscellaneous storage	No	Yes	20	do	1	None	4.2	4.2	0
120	4J	6,000	5,700	Printing shop	No	Yes	6	Fire spread	1	1	4.3	4.3	100
128	6H	6,000	5,700	Gymnasium	No	Yes	25	do	1	1	5.8	5.8	100
131B	7H	8,000	7,700	Boiler house	No	Yes	50	do	1	1	5.0	5.0	100

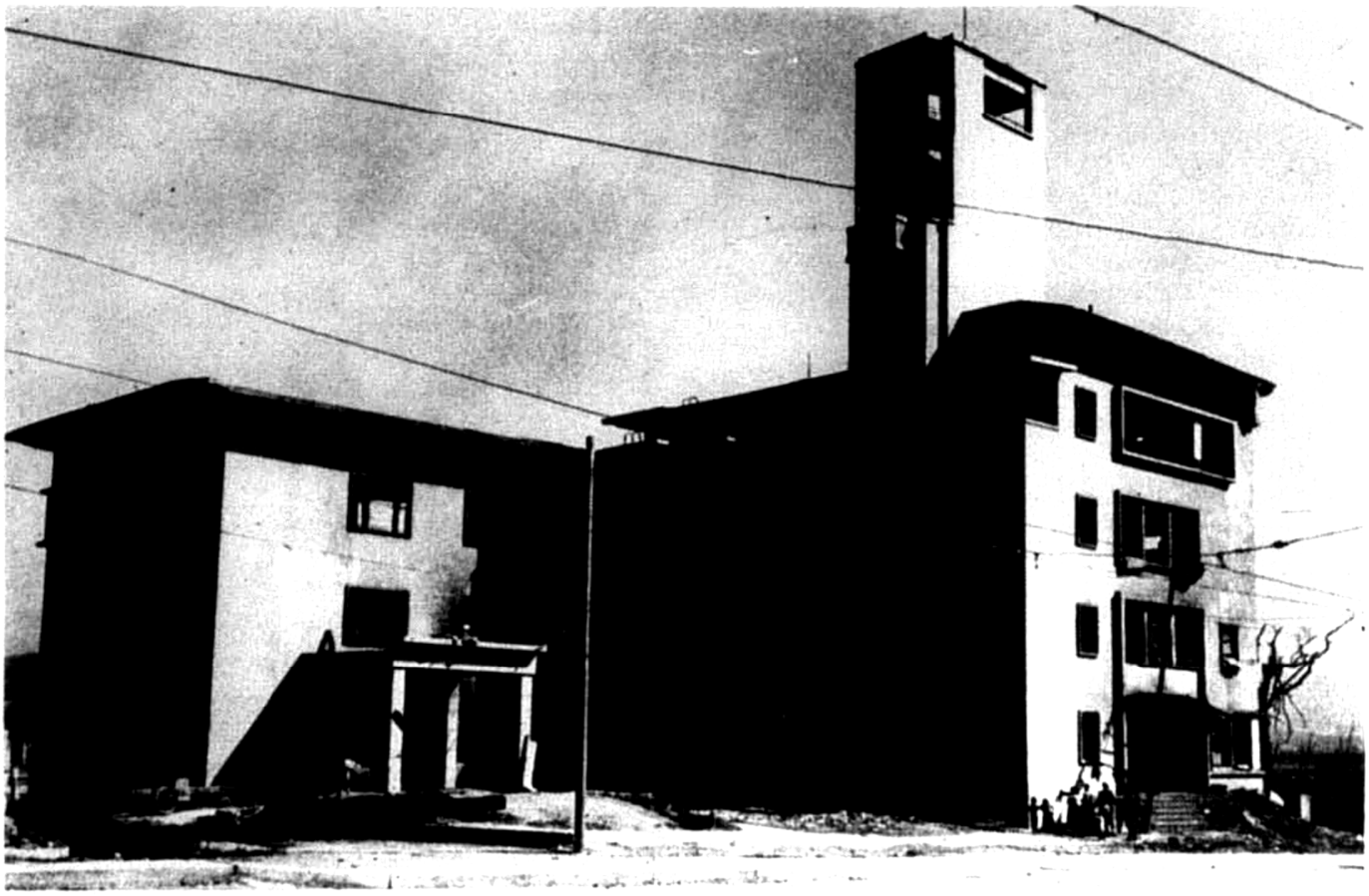

PHOTO 3-XA. Building 2. Looking NE. Note lightning rods on roof were not damaged by blast. Building gutted by fire.

Building No.: 2. Coordinates: 4H. Distance from (GZ): 800, (AZ): 2.100.

NAME: Hiroshima Chamber of Commerce.

CONSTRUCTION AND DESIGN

Type: Reinforced-concrete frame.

Number of stories: 3 and basement. JTG class: E1.

Roof: 5-inch reinforced-concrete slab and beam.

Partitions: Reinforced concrete, major-tile, secondary.

Walls: Reinforced concrete.

Floors: Wood over reinforced-concrete beam and slab.

U. S. STRATEGIC BOMBING SURVEY

PHYSICAL DAMAGE DIVISION

Field Team No. 1, Hiroshima, Japan

BUILDING ANALYSIS

Sheet No. 1

Building No.: 5. Coordinates: 5H. Distance from (GZ): 100, (AZ): 2,000.
NAME: Shima Surgical Hospital.
CONSTRUCTION AND DESIGN
Type: Bearing wall.
Number of stories: 1. JTG class: A 2-3.
Roof: Tile over wood on wood truss.
Partitions: Plaster on wood lath and studs.
Walls: Brick-bearing, 18 inches.
Floors: Wood on wood beams.
Framing: Wall bearing—roof only wood.
Window and door frames: Steel. Ceilings: Unknown.
Condition, workmanship and materials: Excellent.
Compare with usual United States buildings: Greater strength than comparable United States type and occupancy.
OCCUPANCY: Doctor's office and private hospital.
CONTENTS: Office and medical equipment.
DAMAGE to building: Complete destruction. Entire building including walls leveled to the top of the foundation.
Cause: Blast.
To contents: Complete destruction.
Cause: Debris (primary). Combustibles burned.
TOTAL FLOOR AREA (square feet): 2,340. Structural damage: 2,340. Superficial damage: —.
FRACTION OF DAMAGE: Building structural: 100 percent. Superficial: —. Contents: 100 percent.
REMARKS: Of buildings studied this is the nearest to GZ. Destruction was so complete as to preclude obtaining details on roof trusses.
NOTE.—Building damage based on total floor area. Contents damage is fraction of contents seriously damaged.

Sheet No. 2

(Fire Supplement to Sheet No. 1)

Building No.: 5. Fire classification: C.
WALL OPENINGS: Shutters: None.
Shut:
Effect of blast:
FLOOR OPENINGS:

	Enclosed	Fire doors	Automatic	Effect of blast
Stairs:				
Elevators:				

EXPOSURE:

Location	Distance	Firebreak Clearance	Fire Class	Burned	Remarks
N	25′	No	C	Yes	
E	15′	No	C	Yes	
S	20′	No	C	Yes	
W	30′	No	C	Yes	

PROBABLE CAUSE OF FIRE: Not determined.
VERTICAL FIRE SPREAD:
EXTENT OF FIRE: Total floor area: 2,300 square feet. Floor area burned: 2,300 square feet. 100 percent (after blast damage).
REMARKS:

U. S. STRATEGIC BOMBING SURVEY

PHYSICAL DAMAGE DIVISION

Field Team No. 1, Hiroshima, Japan

BUILDING ANALYSIS

Sheet No. 1

Building No.: 6. Coordinates: 5H. Distance from (GZ): 600, (AZ): 2,100.

NAME: Chiyoda Life Insurance Co., Chugoku branch.

CONSTRUCTION AND DESIGN

Type: Reinforced-concrete frame.

Number of stories: Three and basement. JTG class: E1.

Roof: Reinforced-concrete beam and slab-tile covered.

Partitions: Reinforced-concrete, major—metal lath and plaster, minor.

Walls: Reinforced-concrete panels, 10 inches. Reinforced-concrete granite facing.

Floors: Reinforced-concrete beam and slab.

Framing: Reinforced-concrete beam and slab.

Window and door frames: Steel. Ceilings: Wood lath and plaster third floor only.

Condition, workmanship, and materials: Excellent.

Compare with usual United States buildings: Extremely heavy construction, especially beams and columns.

OCCUPANCY: Life insurance office.

CONTENTS: Office equipment.

DAMAGE to building: Minor cracking in roof slab and beams, sash trim windows, etc., destroyed by internal fire—minor damage only.

Cause: Fire.

To contents: Completely destroyed.

Cause: Fire.

Sheet No. 2

(Fire Supplement to Sheet No. 1)

Building No.: 6. Fire classification: R.

WALL OPENINGS: Shutters: Steel rollers.

Shut: Yes.

Effect of blast: Blown in.

FLOOR OPENINGS:

	Enclosed	Fire doors	Automatic	Effect of blast
Stairs:	Part	None		
Elevators:	Yes	Metal	No	Blown in.

EXPOSURE:

Location	Distance	Firebreak Clearance	Fire Class	Burned	Remarks
N	10′	No	C	Yes	
E	15′	No	C	Yes	
S	20′	No	C	Yes	
W	30′	No	C	Yes	

PROBABLE CAUSE OF FIRE: Fire spread from exposures.

VERTICAL FIRE SPREAD: Probably up stairs and elevator.

EXTENT OF FIRE: Total floor area: 16,600 square feet. Floor area burned: 15,300 square feet. 92 percent (after blast damage).

REMARKS: Fire in entire building except about 30 percent of basement.

U. S. STRATEGIC BOMBING SURVEY

PHYSICAL DAMAGE DIVISION

Field Team No. 1, Hiroshima, Japan

BUILDING ANALYSIS

Sheet No. 1

Building No.: 10 Coordinates: 5H. Distance from (GZ): 600, (AZ): 2,100.

NAME: Nippon Life Insurance Co., Hiroshima branch.

CONSTRUCTION AND DESIGN

Type: Load-bearing brick wall.

Number of stories: See drawing. JTG class: F2.

Roof: Reinforced-concrete slab 6 inch (¼-inch bars 6-inch oc by 12 inch oc).

Partitions: Major, 13-inch brick, minor, plaster and wood stud.

Walls: Brick 18- and 4-inch stone trim on front.

Floors: Concrete on earth-wood beams and flooring second floor.

Framing: Reinforced concrete and wood framed second floor.

Window and door frames: Wood. Ceilings: Unknown.

Condition, workmanship, and materials: Fair concrete not of good quality.

Compare with usual United States buildings: Considerably stronger.

OCCUPANCY: Life insurance company.

CONTENTS: Insurance and office equipment.

DAMAGE to building: Roof partially collapsed—remainder depressed and ruptured. Walls cracked and buckled partially collapsed.

Cause: Blast.

To contents: Completely destroyed.

Cause: Debris and fire (about equally).

TOTAL FLOOR AREA: (square feet): 2,500. Structural damage: 2,500. Superficial damage:

FRACTION OF DAMAGE: Building structural: 100 percent. Superficial: —. Contents: 100 percent.

REMARKS: Entire building so out of plumb and cracked as to be in a virtual state of collapse.

Note.—Building damage based on total floor area. Contents damage is fraction of contents seriously damaged.

Sheet No. 2

(Fire Supplement to Sheet No. 1)

Building No: 10. Fire classification: R.

WALL OPENINGS: Shutters: Steel rollers.

Shut: Part.

Effect of blast: Blown in.

FLOOR OPENINGS:

	Enclosed	Fire doors	Automatic	Effect of blast
Stairs:	Yes	Metal	No	Blown in.
Elevators:				

EXPOSURE:

Location	Distance	Firebreak Clearance	Fire Class	Burned	Remarks
N	10′	No	C	Yes	
E	20′	No	C	Yes	
S	30′	No	R	Yes	Building 11 (10′ wall between).
W	30′	No	C	Yes	

PROBABLE CAUSE OF FIRE: Fire spread from exposure.

VERTICAL FIRE SPREAD: Possibly.

EXTENT OF FIRE: Total floor area: 2,500. Square feet floor area burned: 2,500. Square feet: 100 percent (after blast damage).

REMARKS:

U. S. STRATEGIC BOMBING SURVEY

PHYSICAL DAMAGE DIVISION

Field Team No. 1, Hiroshima, Japan

BUILDING ANALYSIS

Sheet No. 1

Building No.: 18. Coordinates: 5H. Distance from (GZ): 1,000, (AZ): 2,200.

NAME: Geibi Bank Co., Hiroshima Branch.

CONSTRUCTION AND DESIGN

Type: Reinforced-concrete frame.

Number of stories: 5 and ½ basement. JTG class: E1.

Roof: Reinforced-concrete slab (metal pan).

Partitions: Reinforced-concrete (5-inch). Wood lath and plaster in rear addition.

Walls: Reinforced concrete (10-inch).

Floors: Reinforced-concrete slabs (metal pan construction).

Framing: Reinforced concrete, heavy haunches.

Window and door frames: Metal. Ceilings: Plaster on concrete.

Condition, workmanship, and materials: Good.

Compare with usual United States buildings: Considerably heavier in structural framing.

OCCUPANCY: Bank and office.

CONTENTS: Bank equipment and furnishings.

DAMAGE to building: Light steel-framed roof over rear addition destroyed by blast. Portion of roof of main building depressed, beams cracked and spalled at haunches and center of span-steel elongated. Minor damage throughout.

Cause: Blast.

To contents: Destroyed.

Cause: Fire.

TOTAL FLOOR AREA (square feet): 46,400. Structural damage: 3,260. Superficial damage:

FRACTION OF DAMAGE: Building structural 7 percent. Superficial: —. Contents: 100 percent.

REMARKS: 1,400 square feet of structural damage shown above was in inferior construction.

Sheet No. 2

(Fire Supplement to Sheet No. 1)

Building No.: 18. Fire classification: R.

WALL OPENINGS: Shutters: Steel rollers in west section and in north wall only of east section.

Shut: Yes.

Effect of blast: Most blown in.

FLOOR OPENINGS:

	Enclosed	Fire doors	Automatic	Effect of blast
Stairs:	Part	Steel rollers	No	None—doors open
Elevators:	Yes	Steel rollers	No	None—doors open

EXPOSURE:

Location	Distance	Firebreak Clearance	Fire Class	Burned	Remarks
N	10′	No	C	Yes	
E	25′	No	C	Yes	
S	20′	No	R	Yes	Building 19 (14-foot wall between).
S	40′	No	C	Yes	14-foot concrete wall between.
W	125′	Yes	C	Yes	

PROBABLE CAUSE OF FIRE: Fire spread from exposure.

VERTICAL FIRE SPREAD:

EXTENT OF FIRE: Total floor area: 46,600 square feet. Floor area burned: 46,400 square feet; 100 percent (after blast damage).

REMARKS: Fires in exposures soon after bomb. This building well afire at 1000 hours.

U. S. STRATEGIC BOMBING SURVEY

PHYSICAL DAMAGE DIVISION

Field Team No. 1, Hiroshima, Japan

BUILDING ANALYSIS

Sheet No. 1

Building No.: 23. Coordinates: 5H. Distance from (GZ): 1,200; (AZ); 2,300.
NAME: Fukoku Building.
CONSTRUCTION AND DESIGN
Type: Steel core reinforced-concrete frame.
Number of stories: 7 and basement. JTG class: E1.
Roof: Reinforced-concrete beam and slab (steel core).
Partitions: Reinforced concrete.
Walls: Reinforced concrete, stone trim.
Floors: Reinforced concrete, wood finish.
Framing: Reinforced concrete.
Window and door frames: Metal. Ceilings: Metal lath and plaster.
Condition, workmanship, and materials:
Compare with usual United States buildings:
OCCUPANCY: First story, commercial. Remainder, office space.
CONTENTS: Office equipment and furnishings, communication equipment second and third floor.
DAMAGE to building: Long-span trusses supporting roof ruptured and roof depressed. Three panels of first floor slab depressed by blast. Minor damage from fire throughout building.
Cause: Blast.
To contents: Almost complete destruction except in basement.
Cause: Fire (primary); some debris damage.
TOTAL FLOOR AREA (square feet): 43,300. Structural damage: 4,600. Superficial damage:
FRACTION OF DAMAGE: Building structural: 11 percent. Superficial: —. Contents: 90 percent.
REMARKS:

NOTE.—Building damage based on total floor area. Contents damage is fraction of contents seriously damaged.

Sheet No. 2

(Fire Supplement to Sheet No. 1)

Building No.: 23. Fire classification: N/R (unprotected steel in roof).
WALL OPENINGS: Shutters: No (wired glass in all windows).
Shut:
Effect of blast: All broken.

FLOOR OPENINGS:

	Enclosed	Fire doors	Automatic	Effect of blast
Stairs:	Yes	Metal and W. G.	No	Part blown off.
Elevators:	Yes	Metal and W. G.	No	Part blown off

EXPOSURE:

Location	Distance	Firebreak Clearance	Fire Class	Burned	Remarks
N	10′	No	R	Yes	Building 22.
E	100′	Yes	C	Yes	
S	25′	No	C	Yes	
W	125′	Yes	C	Yes	

PROBABLE CAUSE OF FIRE: Not determined.
VERTICAL FIRE SPREAD: Probably up stairs, elevator and pipe shaft.
EXTENT OF FIRE: Total floor area: 43,300 square feet. Floor area burned: 39,000 square feet; 90 percent (after blast damage).
REMARKS: Fire throughout building except in basement.

U.S. STRATEGIC BOMBING SURVEY

BUILDING 23
HIROSHIMA, JAPAN GRID 5H
FIGURE 23-X A

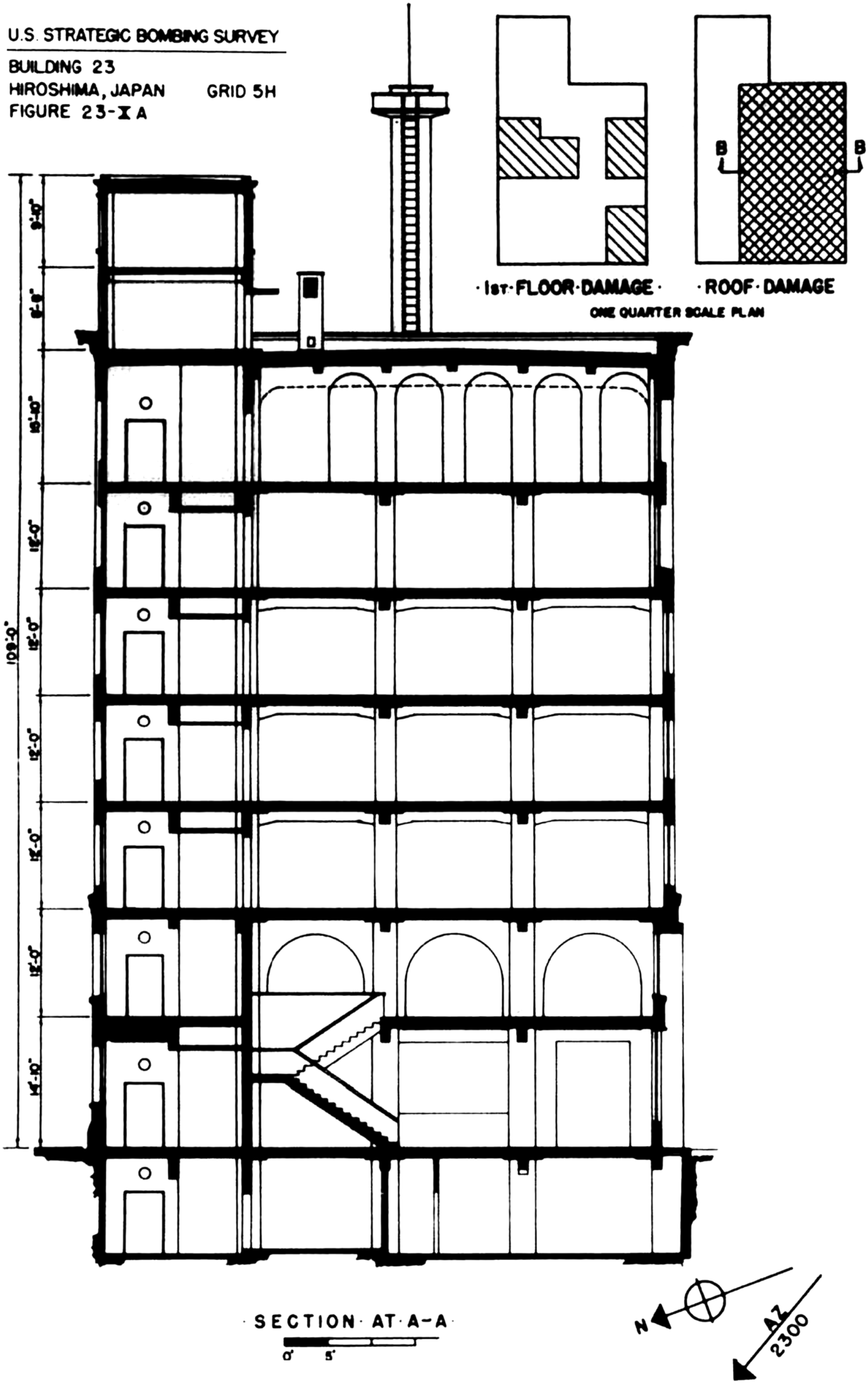

U. S. STRATEGIC BOMBING SURVEY

PHYSICAL DAMAGE DIVISION

Field Team No. 1, Hiroshima, Japan

BUILDING ANALYSIS

Sheet No. 1

Building No.: 24. Coordinates: 5H. Distance from (GZ): 1,300, (AZ): 2,400.

NAME: Bank of Japan, Hiroshima branch.

CONSTRUCTION AND DESIGN

Type: Reinforced-concrete frame (steel core).

Number of Stories: 3 and basement. JTG class: E1.

Roof: Reinforced-concrete beam and slab.

Partitions: Reinforced concrete and wood lath.

Walls: Reinforced concrete (12-inch) and stone (6-inch).

Floors: Reinforced concrete.

Framing: Reinforced concrete.

Window and door frames: Metal (exterior) wood (interior). Ceilings: Plaster on concrete.

Condition, workmanship, and materials: Excellent.

Compare with usual United States buildings: Much stronger—steel core construction.

OCCUPANCY: Bank.

CONTENTS: Bank and office equipment furnishings.

DAMAGE to building: Only minor damage—top story burned out, partitions, sash, trim blown out in two lower stories.

Cause: Fire.

To Contents: Destroyed in third story—moderate debris and blast damage in first and second stories, none in basement.

Cause: Fire and debris (about equally).

TOTAL FLOOR AREA (square feet): 32,800. Structural damage: —. Superficial damage:

FRACTION OF DAMAGE: Building structural: —. Superficial: —. Contents: 30 percent.

REMARKS: Glass removed from skylight (20 by 20 feet) and light steel-frame structure and roof covered with 12 to 18 inches of sand and cinders.

Note.—Building damage based on total floor area. Contents damage is fraction of contents seriously damaged.

Sheet No. 2

(Fire Supplement to Sheet No. 1)

Building No.: 24. Fire classification: R.

WALL OPENINGS: Shutters: Steel rollers.

Shut: Part.

Effect of blast: Blown in.

FLOOR OPENINGS:

	Enclosed	Fire doors	Automatic	Effect of blast
Stairs:	Part	Steel rollers	No	None—doors open.
Elevators:	Yes	Metal and W. G.	No	Bent.

EXPOSURE:

Location	Distance	Firebreak Clearance	Fire Class	Burned	Remarks
N	25′	No	C	Yes	14-foot concrete wall between.
E	25′	No	R	Yes	Building 25 (14-foot wall between).
S	—	No	—	—	No exposure.
W	125′	Yes	C	Yes	

PROBABLE CAUSE OF FIRE: Fire spread from exposures.

VERTICAL FIRE SPREAD: No.

EXTENT OF FIRE: Total floor area: 32,800 square feet. Floor area burned: 5,200 square feet; 16 percent (after blast damage).

REMARKS: Fire only in room at southwest corner of second story and in entire third story. No fire in building right after bomb, but afire at 1000 hours. Fire in room in second story extinguished with water buckets.

U. S. STRATEGIC BOMBING SURVEY

PHYSICAL DAMAGE DIVISION

Field Team No. 1, Hiroshima, Japan

BUILDING ANALYSIS

Sheet No. 1

Building No.: 26. Coordinates: 5H. Distance from (GZ): 2,300, (AZ): 3,000.

NAME: **Chugoku Electric Co.**

CONSTRUCTION AND DESIGN

Type: Reinforced-concrete frame.

Number of stories: 5 and basement and penthouse JTG class: E1.

Roof: Reinforced-concrete beam and slab.

Partitions: Reinforced concrete (6-inch).

Walls: Reinforced concrete (12-inch).

Floors: Reinforced-concrete slab, parquet wood surface 3, 4, 5, and 6 floors.

Framing: Reinforced-concrete beam and slab.

Window and door frames: Metal. Ceilings:

Condition, workmanship, and materials; Excellent.

Compare with usual United States buildings: Considerably stronger.

OCCUPANCY: **Office.**

CONTENTS: Office equipment and furnishings.

DAMAGE to building: One roof slab and girder cracked by blast. Minor damage throughout from blast and fire.

Cause: Blast:

To contents: Severe damage, except in west section of basement and a portion of east section of basement.

Cause: Fire 75 percent. Blast and debris 15 percent.

TOTAL FLOOR AREA (square feet): 52,000. Structural damage: —. Superficial damage: 220.

FRACTION OF DAMAGE: Building structural: —. Superficial: 0.25 percent. Contents: 90 percent.

REMARKS:

Note.—Building damage based on total floor area. Contents damage is fraction of contents seriously damaged.

Sheet No. 2

(Fire Supplement to Sheet No. 1)

Building No.: 26. Fire classification: R.

WALL OPENINGS: Shutters: Steel rollers in north wall of west section only.

Shut: Part.

Effect of blast: Most blown in.

FLOOR OPENINGS:

	Enclosed	Fire doors	Automatic	Effect of blast
Stairs:	No			
Elevators:	Yes	No		

EXPOSURE:

Location	Distance	Firebreak Clearance	Fire Class	Burned	Remarks
N	60′	Yes	C	Yes	
E	35′	No	C	Yes	
SE	10′	No	C	Yes	
S	50′	No	R	Yes	Building 27.
W	150′	Yes	C	Yes	

PROBABLE CAUSE OF FIRE: Direct heat radiation from bomb.

VERTICAL FIRE SPREAD: Possibly upstairs and pipe shaft.

EXTENT OF FIRE: Total floor area: 52,000 square feet. Floor area burned: 46,500 square feet; 88 percent (after blast damage).

REMARKS: Fire throughout building except in 60 percent of basement (no fire in basement of west section and about 25 percent of east section). Man who was in third story stated that he saw cotton blackout curtains in west wall and thin paper on desks catch fire from flash of bomb. Fire was reported to have been in all stories 5 minutes after bomb.

U. S. STRATEGIC BOMBING SURVEY

PHYSICAL DAMAGE DIVISION

Field Team No. 1, Hiroshima, Japan

BUILDING ANALYSIS

Sheet No. 1

Building No.: 28. Coordinates: 6H. Distance from (GZ): 3,300, (AZ): 3,800.

NAME: Hiroshima City Hall.

CONSTRUCTION AND DESIGN

Type: Reinforced concrete, stucco finish.

Number of stories: Four and basement. JTG class: E1.

Roof: Reinforced concrete, tile finish.

Partitions: Reinforced concrete (5-inch) and tile, wood wainscoats in stair halls.

Walls: Reinforced concrete (10-inch).

Floors: Reinforced concrete, cement finish.

Framing: Reinforced concrete.

Window and door frames: Metal. Ceilings:

Condition, workmanship, and materials: Excellent.

Compare with usual United States buildings: Considerably stronger.

OCCUPANCY: Office.

CONTENTS: Furnishings and equipment for office and city administration.

DAMAGE to building: Minor damage only—sash blown out, trim and finish destroyed by fire. Few tile partitions blown out.

Cause: Fire and blast.

To contents: Severely damaged.

Cause: Fire.

TOTAL FLOOR AREA (square feet): 93,400. Structural damage: —. Superficial damage:

FRACTION OF DAMAGE: Building structural: —. Superficial: —. Contents: 75–100 percent.

REMARKS:

Note.—Building damage based on total floor area. Contents damage is fraction of contents seriously damaged.

Sheet No. 2

(Fire Supplement to Sheet No. 1)

Building No. 28. Fire classification: R.

WALL OPENINGS: Shutters: None.

Shut:

Effect of blast:

FLOOR OPENINGS:

	Enclosed	Fire doors	Automatic	Effect of blast
Stairs:	No			
Elevators:				

EXPOSURE:

Location	Distance	Firebreak Clearance	Fire Class	Burned	Remarks
N	—	No	—	—	No exposure.
E	50′	Partial 200′	C	Yes	All exposure burned.
SE	125′	Yes	C	Yes	
W	150′	Yes	C	Yes	

PROBABLE CAUSE OF FIRE: Fire spread from exposure.

VERTICAL FIRE SPREAD: Probably.

EXTENT OF FIRE: Total floor area: 93,400 square feet. Floor area burned: 84,900 square feet; 91 percent (after blast damage).

REMARKS: Fire in entire building except of 20 percent of basement and first story at east end of east section (transverse partitions were noncombustible without openings and there were no combustible construction materials and contents in the corridors at the north wall. Two men who were in building at time of bomb stated that fire spread in from south exposure by flying embers at 1000 hours. Fire started first in the third story. Lower stories may have been ignited later directly by exposure fires.

U. S. STRATEGIC BOMBING SURVEY

PHYSICAL DAMAGE DIVISION

Field Team No. 1, Hiroshima, Japan

BUILDING ANALYSIS

Sheet No. 1

Building No.: 33. Coordinates: 6H. Distance from (GZ): 5,300, (AZ): 5,600.

NAME: **Hiroshima Postal Savings Bureau.**

CONSTRUCTION AND DESIGN

Type: Reinforced-concrete frame.

Number of stories: 4 and basement. JTG class: E1.

Roof: Reinforced concrete, tile finish.

Partitions: Reinforced concrete.

Walls: Reinforced concrete, tile finish.

Floors: Reinforced concrete.

Framing: Reinforced concrete.

Window and door frames: Metal, wood (interior). **Ceilings: Plaster on wood lath—top story. Plaster on concrete—others.**

Condition, workmanship, and materials: Excellent.

Compare with usual United States buildings: Much **stronger.**

OCCUPANCY: **Office.**

CONTENTS: **Office furnishings and equipment.**

DAMAGE **to building:** Minor—**glass blown out, some sash deformed. Hung ceiling in top story 75 percent collapsed.**

Cause: Blast.

To contents: **Slight damage to furnishings and other contents from blast and debris.**

Cause: Blast and debris.

TOTAL FLOOR AREA (square feet): 62,600. Structural damage: —. Superficial damage:

FRACTION OF DAMAGE: Building structural: — Superficial: —. Contents: 15 percent.

REMARKS:

NOTE.—Building damage based on total floor area. Contents damage is fraction of contents seriously damaged.

Sheet No. 2

(Fire Supplement to Sheet No. 1)

Building No.: 33. Fire classification: R.

WALL OPENINGS: **Shutters: Steel rollers in north and east walls only of northeast section.**

Shut: Few only.

Effect of blast: Bent inward slightly.

FLOOR OPENINGS:

	Enclosed	Fire doors	Automatic	Effect of blast
Stairs:	Yes	Metal	No	Part blown off.
Elevators:	Yes	Metal	No	Blown off.

EXPOSURE:

Location	Distance	Firebreak Clearance	Fire Class	Burned	Remarks
NW	150′	Yes	C	Yes	
E	90′	Yes	C	Yes	
S	150′	Yes	C	Yes	
W	150′	Yes	C	Yes	

PROBABLE CAUSE OF FIRE: Fire spread from west exposure.

VERTICAL FIRE SPREAD: None.

EXTENT OF FIRE: Total floor area: 62,600 square feet. Floor area burned: 0 square feet; 0 percent (after blast damage).

REMARKS: Sparks from west exposure ignited cotton black-out curtains in west wall at 2000 hours and waste paper in fourth story of northwest section at 2100 hours. Fires were extinguished with water buckets by 20 fire guards who were stationed inside. Fire damage to contents was negligible. Paper records stored in wood and steel racks in northeast section of building were exposed to direct radiated heat from bomb but did not catch fire.

U. S. STRATEGIC BOMBING SURVEY

PHYSICAL DAMAGE DIVISION

Field Team No. 1, Hiroshima, Japan

BUILDING ANALYSIS

SHEET No. 1

Building No.: 40. Coordinates: 5H. Distance from (GZ): 2,500, (AZ): 3,200.

NAME: Fukuya Department Store.

CONSTRUCTION AND DESIGN:

Type: Reinforced-concrete frame.

Number of stories: 7 and basement and one-half of eighth. JTG class: E1.

Roof: Reinforced-concrete beam and slab (steel trusses over theater).

Partitions: Metal lath and plaster.

Walls: 8-inch reinforced concrete—large windows.

Floors: Wood over reinforced concrete.

Framing: Reinforced concrete (or protected steel).

Window and door frames: Steel. Ceilings: Plaster on concrete.

Condition, workmanship, and materials: Good.

Compare with usual United States buildings: Considerably stronger than comparable United States buildings.

OCCUPANCY: Department store.

CONTENTS: Merchandise on display for sale.

DAMAGE to building: Minor throughout—sash blown out; finish and trim, including floors, burned out. Steel trusses supporting roof over theatre show slight deformation.

Cause: Mixed.

To contents: Destroyed.

Cause: Fire.

TOTAL FLOOR AREA (square feet): 78,900. Structural damage: —. Superficial damage:

FRACTION OF DAMAGE: Building structural: —. Superficial: —. Contents: 90–100 percent.

REMARKS:

NOTE.—Building damage based on total floor area. Contents damage is fraction of contents seriously damaged.

SHEET No. 2

(Fire Supplement to Sheet No. 1)

Building No.: 40. Fire classification: R (north roof on west section).

WALL OPENINGS: Shutters: None.

Shut:

Effect of blast:

FLOOR OPENINGS:

	Enclosed	Fire doors	Automatic	Effect of blast
Stairs:	Part	Metal	No	Blown in or bent.
Elevators:	Yes	Metal	No	Blown in or bent.

EXPOSURE:

Location	Distance	Firebreak Clearance	Fire Class	Burned	Remarks
N	50′	No	R	Yes	Building 39.
E	150′	Yes	C	Yes	
S	180′	Yes	C	Yes	
W	200′	Yes	R	Yes	Building 38.

PROBABLE CAUSE OF FIRE: Direct radiated head from bomb.

VERTICAL FIRE SPREAD: Probably.

EXTENT OF FIRE: Total floor area: 78,900 square feet. Floor area burned: 78,900 square feet; 100 percent (after blast damage).

REMARKS: Three persons who were questioned individually stated that this building was afire immediately or within 20 minutes after the bomb. One man who was in the building at the time stated that cotton blackout curtains in the west wall were smouldering immediately after the bomb. The entire building was afire at 1000 hours.

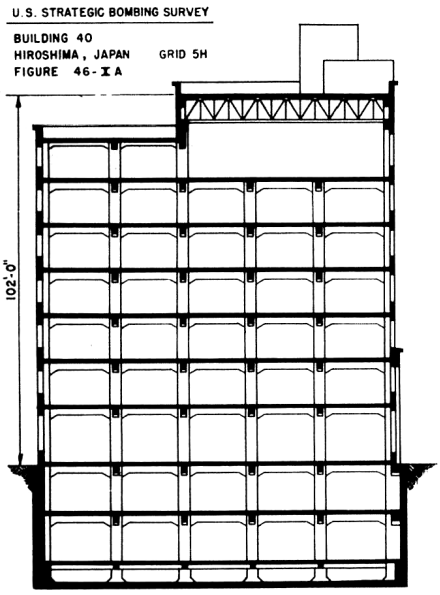

U. S. STRATEGIC BOMBING SURVEY

PHYSICAL DAMAGE DIVISION

Field Team No. 1, Hiroshima, Japan

BUILDING ANALYSIS

Sheet No. 1

Building No.: 47. Coordinates: 5H. Distance from (GZ): 2,300, (AZ): 3,100.

NAME: Hiroshima Kirin Beer Hall.

CONSTRUCTION AND DESIGN

Type: Reinforced-concrete frame.

Number of stories: Three and basement. JTG class: E1.

Roof: Reinforced-concrete beam and slab.

Partitions: 5-inch reinforced concrete.

Walls: 8-inch reinforced concrete integral—large windows.

Floors: 5-inch reinforced-concrete beam and slab.

Framing: Reinforced concrete.

Window and door frames: Steel. Ceilings: Plaster on concrete.

Condition, workmanship, and materials: Good.

Compare with usual United States buildings. Considerably stronger than United States design.

OCCUPANCY: Beer hall.

CONTENTS: Bars, tables, etc.

DAMAGE to building: Minor—sash blown out, finish and trim partly destroyed by fire.

Cause: Mixed.

To contents: Moderate damage from both blast (throwing furnishings around) and fire.

Cause: Mixed.

TOTAL FLOOR AREA (square feet): 15,300. Structural damage: —. Superficial damage:

FRACTION OF DAMAGE: Building structural: —. Superficial —. Contents: 60–80 percent.

REMARKS: Building and contents contained so few combustibles that internal fire was not of great intensity.

Note.—Building damage based on total floor area. Contents damage is fraction of contents seriously damaged.

Sheet No. 2

(Fire Supplement to Sheet No. 1)

Building No.: 47. Fire classification: R.

WALL OPENINGS: Shutters: None.

Shut:

Effect of blast:

FLOOR OPENINGS:

	Enclosed	Fire doors	Automatic	Effect of blast
Stairs:	Part	Metal and glass	No	Bent.
Elevators:	Yes	Metal and glass	No	Blown off.

EXPOSURE:

Location	Distance	Firebreak Clearance	Fire Class	Burned	Remarks
N	—	Yes	—	—	No exposure.
E	20′	No	C	Yes	
S	—	Yes	—	—	No exposure.
W	65′	Yes	C	Yes	

PROBABLE CAUSE OF FIRE: Fire spread from exposures.

VERTICAL FIRE SPREAD: Possibly.

EXTENT OF FIRE: Total floor area: 15,300 square feet. Floor area burned: 13,200 square feet; 86 percent (after blast damage).

REMARKS: Man who worked in building but was not on premises at time of bomb stated that fire spread into building from east exposure about one hour after bomb. Entire building had fire in it except basement. Combustibility of contents was low and very little damage was done to building by fire.

U. S. STRATEGIC BOMBING SURVEY

PHYSICAL DAMAGE DIVISION

Field Team No. 1, Hiroshima, Japan

BUILDING ANALYSIS

Sheet No. 1

Building No.: 49. Coordinates: 5I. Distance from (GZ): 3,000, (AZ): 3,600.
Name: Chūgoku Newspaper.

CONSTRUCTION AND DESIGN

Type: Reinforced-concrete frame.
Number of Stories: 7 and penthouse. JTG class: E1.
Roof: Reinforced-concrete beam and slab.
Partitions: Reinforced concrete—lath and plaster.
Walls: 7-inch reinforced concrete—large windows.
Floors: 6-inch reinforced-concrete beam and slab—small part wood overlay.
Framing: Reinforced concrete (on steel frame).
Window and door frames: Steel. Ceilings: Plaster on concrete.
Condition, workmanship, and materials: Excellent.
Compare with usual United States buildings: Considerably heavier than United States.

OCCUPANCY: **Newspaper office—used in conjunction with Building 50.**

CONTENTS: **Office equipment and supplies.**

DAMAGE to building: **Minor throughout; sash blown in, finish and trim destroyed by internal fire.**
Cause: Fire.

To contents: **Complete destruction.**
Cause: Fire.

TOTAL FLOOR AREA (square feet): **14,700.** Structural damage: **—.** Superficial damage:

FRACTION OF DAMAGE: Building structural: **—.** Superficial **—.** Contents: **100 percent.**

REMARKS: **Contents' damage based upon interrogation as all debris was removed.**

Note.—Building damage based on total floor area. Contents damage is fraction of contents seriously damaged.

Sheet No. 2

(Fire Supplement to Sheet No. 1)

Building No.: 49. Fire classification: R.

WALL OPENINGS: **Shutters: Steel rollers at first to third stories of west wall only.**
Shut: Part.
Effect of blast: Blown in.

FLOOR OPENINGS:

	Enclosed	Fire doors	Automatic	Effect of blast
Stairs:	Yes	No	No	
Elevators:	Yes	Metal		Part blown in.

EXPOSURE:

Location	Distance	Clearance	Firebreak Class	Fire Burned	Remarks
N	150′	Yes	C	Yes	
E and S	0′	No	R	Yes	Building 50 (unprotected openings).
S	185′	Yes	C	Yes	150 feet beyond Building 50.
W	90′	Yes	C	Yes	

PROBABLE CAUSE OF FIRE: Direct radiated heat from bomb.

VERTICAL FIRE SPREAD: Possibly.

EXTENT OF FIRE: Total floor area: 14,700 square feet. Floor area burned: 14,700 square feet; 100 percent (after blast damage).

REMARKS: Man who was in building at time of bomb stated fire broke out in third and fourth stories immediately after bomb flash. Head bookkeeper in bank in Building 51 stated that there was fire in third story of Building 49, 10 minutes after bomb flash.

U. S. STRATEGIC BOMBING SURVEY

PHYSICAL DAMAGE DIVISION

Field Team No. 1, Hiroshima, Japan

BUILDING ANALYSIS

Sheet No. 1

Building No.: 52. Coordinates: 5I. Distance from (GZ): 2,800, (AZ): 3,400.
NAME: Taiyo Theater.
CONSTRUCTION AND DESIGN
Type: Light steel frame.
Number of stories: —. JTG class:
Roof:
Partitions:
Walls:
Floors:
Framing:
Window and door frames: —. Ceilings:
Condition, workmanship, and materials:
Compare with usual United States buildings:
OCCUPANCY:
CONTENTS:
DAMAGE to building: Completely destroyed.
Cause: Mixed.
To contents: Completely destroyed.
Cause: Mixed.
TOTAL FLOOR AREA (square feet): Unknown. Structural damage: —. Superficial damage:
FRACTION OF DAMAGE: Building structural: —. Superficial: —. Contents: — percent.
REMARKS: Mixed construction. Damage too severe to permit analysis of cause of damage or design of structure.

Note.—Building damage based on total floor area. Contents damage if fraction of contents seriously damaged.

Sheet No. 2

(Fire Supplement to Sheet No. 1)

Building No.: 52. Fire classification: C.
WALL OPENINGS: Shutters: None.
Shut:
Effect of blast:
FLOOR OPENINGS:

	Enclosed	Fire doors	Automatic	Effect of blast
Stairs:				
Elevators:				

EXPOSURE:

Location	Distance	Firebreak Clearance	Fire Class	Burned	Remarks
N	0′	No	C	Yes	
E	90′	Yes	R	Yes	
S	0′	No	C	Yes	Buildings 49 and 50.
W	10′	No	C	Yes	

PROBABLE CAUSE OF FIRE: Not determined.
VERTICAL FIRE SPREAD:
EXTENT OF FIRE: Total floor area: — square feet. Floor area burned: — square feet; 100 percent (after blast damage).
REMARKS: This building was excluded from both blast and fire studies.

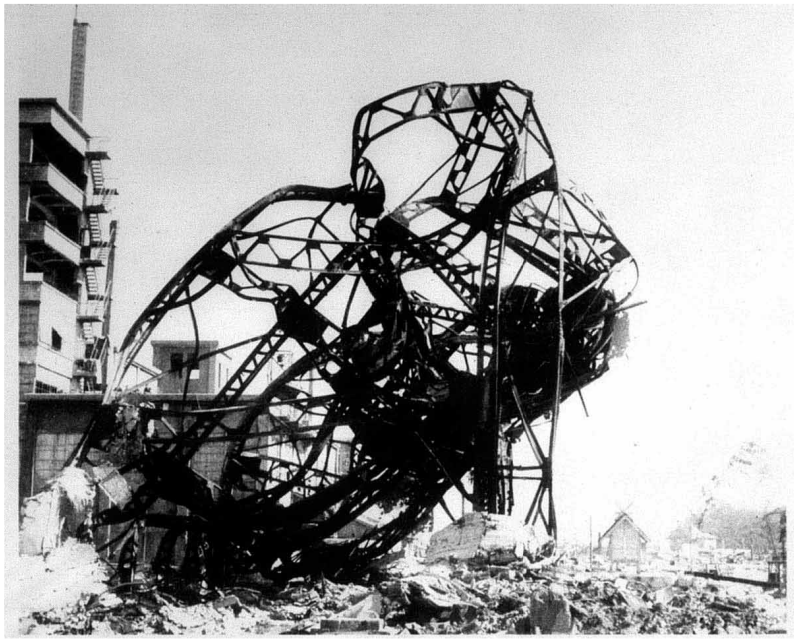

U. S. STRATEGIC BOMBING SURVEY

PHYSICAL DAMAGE DIVISION

Field Team No. 1, Hiroshima, Japan

BUILDING ANALYSIS

Sheet No. 1

Building No.: 59. Coordinates: 5I. Distance from (GZ): 4,100, (AZ): 4,500.

NAME: **Geibi Bank Co., Hiroshima Branch (in use at time of bomb as the Higashi Police Station).**

CONSTRUCTION AND DESIGN

Type: Reinforced-concrete frame.

Number of stories: See sketch. JTG class: E1.

Roof: Reinforced-concrete beam and slab.

Partitions: 7-inch reinforced concrete.

Walls: 8-inch reinforced concrete monolithic—medium window.

Floors: Reinforced-concrete beam and slab—parquet and tile.

Framing: Reinforced-concrete beam and slab.

Window and door frames: Steel. Ceilings: Sheet metal on wood framing.

Condition, workmanship and materials: Good.

Compare with usual United States buildings: Appreciably stronger than United States design.

OCCUPANCY: Police station (office).

CONTENTS: Office equipment.

DAMAGE to building: Minor damage only—sash blown out and hung ceilings partially stripped.

Cause: Blast.

To contents: Slight damage to contents from blast and debris.

Cause: Blast.

TOTAL FLOOR AREA (square feet): 16,200. Structural damage: —. Superficial damage:

FRACTION OF DAMAGE: Building. Structural: —. Superficial: Contents: 10 percent.

REMARKS:

Note.—Building damage based on total floor area. Contents damage is fraction of contents seriously damaged.

Sheet No. 2

(Fire Supplement to Sheet No. 1)

Building No.: 59. Fire classification: R.

WALL OPENINGS: **Shutters: Steel rollers in east wall and third story of south and west walls (wired glass in all windows).**

Effect of blast: Blown in at west wall, bent at south wall.

FLOOR OPENINGS:

	Enclosed	Fire doors	Automatic	Effect of blast
Stairs:	Yes	Metal	No	Bent slightly.
Elevators:				

EXPOSURE:

Location	Distance	Firebreak Clearance	Fire Class	Burned	Remarks
N	150′	Yes	C	Yes	
E	60′	Yes	C	Yes	
S	30′	Partial	C	Yes	All exposures burned.
		100′			
W	60′	Yes	C	Yes	

PROBABLE CAUSE OF FIRE: Fire spread from exposures.

VERTICAL FIRE SPREAD: No.

EXTENT OF FIRE: Total floor area: 16,200 square feet. Floor area burned: 0 square feet; 0 percent (after blast damage).

REMARKS: Sparks from south exposure ignited few pieces of furniture in first and third stories and cotton blackout curtains in first story about 1030 hours. Fires were extinguished with water buckets by people inside. Negligible fire damage resulted. Some of exposing buildings had just been removed prior to the bomb.

U. S. STRATEGIC BOMBING SURVEY

PHYSICAL DAMAGE DIVISION

Field Team No. 1, Hiroshima, Japan

BUILDING ANALYSIS

Sheet No. 1

Building No.: 61. Coordinates: 5I. Distance from (GZ): 3,400, (AZ): 4,000.
NAME: Hiroshima Radio Station:
CONSTRUCTION AND DESIGN
Type: Reinforced-concrete frame.
Number of stories: 2. JTG class: E1.
Roof: Reinforced-concrete beam and slab.
Partitions: 4-inch reinforced concrete ⅜-9 inches O. C.
Walls: 8-inch reinforced concrete—moderate openings.
Floors: Reinforced concrete.
Framing: Reinforced-concrete beam and slab.
Window and door frames: Steel. Ceilings: Unknown.
Condition, workmanship, and materials: Poor, concrete poor, reinforcement exposed in many places, form work poor.
Compare with usual United States buildings: Somewhat heavier than United States design.
OCCUPANCY: Broadcasting studio.
CONTENTS:
DAMAGE to building: Small panel of first floor depressed 4 to 6 inches in front of door. Two non-load-bearing partitions blown out. Minor damage throughout. Sash blown out, trim and finish burned out.
Cause: Blast.
To contents: Completely destroyed.
Cause: Fire (may have been some debris damage).
TOTAL FLOOR AREA (square feet): 8,300. Structural damage: —. Superficial damage: —.
FRACTION OF DAMAGE: Building structural: —. Superficial: —. Contents: 100 percent.
REMARKS: Water pipes in second floor ruptured at one point. General condition and construction of building was very poor.

Note.—Building damage based on total floor area. Contents damage is fraction of contents seriously damaged.

Sheet No. 2

(Fire Supplement to Sheet No. 1)

Building No.: 61. Fire classification: R.
WALL OPENINGS: Shutters: None.
Shut:
Effect of blast:
FLOOR OPENINGS:

	Enclosed	Fire doors	Automatic	Effect of blast
Stairs:	No			
Elevators:				

EXPOSURE:

Location	Distance	Firebreak Clearance	Fire Class	Burned	Remarks
N	60′	Yes	C	Yes	
E	15′	No	C	Yes	
S	80′	Yes	C	Yes	
W	40′	No	C	Yes	

PROBABLE CAUSE OF FIRE: Not determined.
VERTICAL FIRE SPREAD: Possibly.
EXTENT OF FIRE: Total floor area: 8,300 square feet. Floor area burned 8,300 square feet; 100 percent (after blast damage).
REMARKS: Some of exposing buildings were just being removed at time of bomb.

U. S. STRATEGIC BOMBING SURVEY

PHYSICAL DAMAGE DIVISION

Field Team No. 1, Hiroshima, Japan

BUILDING ANALYSIS

Sheet No. 1

Building No.: 86. **Coordinates:** 5G. **Distance from (GZ):** 2,000, **(AZ):** 2,800.

NAME: Kōkō Private Grammar School.

CONSTRUCTION AND DESIGN

Type: Reinforced concrete.

Number of stories: Three. **JTG class:** E1.

Roof: Reinforced-concrete slab.

Partitions: 9-inch brick and 6-inch reinforced concrete.

Walls: Reinforced concrete (8–10 inches).

Floors: Reinforced concrete, wood finish on sleepers.

Framing: Reinforced concrete.

Window and door frames: Wood. **Ceilings:** Wood lath and plaster.

Condition, workmanship, and materials:

Compare with usual united States buildings: Stronger and heavier.

OCCUPANCY: School.

CONTENTS: Classroom furnishings, equipment, and office furnishings.

DAMAGE to building: One roof girder cracked, 9-inch brick partition in first story fractured at ceiling, hung ceiling destroyed. All sash blown out, doors and trim damaged. Outside toilet at west end of building collapsed.

Cause: Blast.

To contents: Furnishings and other contents cut by glass and debris and broken by tumbling around by blast.

Cause: Blast and debris (about equally).

TOTAL FLOOR AREA (square feet): 11,500. **Structual damage:** 500. **Superficial damage:**

FRACTION OF DAMAGE: Building structural: 4 percent. Superficial: —. Contents: 20–40 percent.

REMARKS: Lean-to toilet in which all structural damage occurred, was of weaker construction than rest of building.

Note.—Building damage based on total floor area. Contents damage is fraction of contents seriously damaged.

Sheet No. 2

(Fire Supplement to Sheet No. 1)

Building No.: 86. **Fire classification:** R.

WALL OPENINGS: Shutters: None.

Shut:

Effect of blast:

FLOOR OPENINGS:

	Enclosed	Fire doors	Automatic	Effect of blast
Stairs:	Yes	No		
Elevators:				

EXPOSURE:

Location	Distance	Firebreak Clearance	Fire Class	Burned	Remarks
N	125′	Yes	C	Yes	
E	150′	Yes	C	Yes	Blank wall except fire escape exits.
S	125′	Yes	C	Yes	
W	125′	Yes	C	Yes	Blank wall.

PROBABLE CAUSE OF FIRE: No fire.

VERTICAL FIRE SPREAD:

EXTENT OF FIRE: Total floor area: 11,500 square feet. Floor area burned: 0 square feet; 0 percent (after blast damage).

REMARKS: Extended east-west axis of building would pass approximately through zero point. East wall, which faced zero point was blank except for exit at each story to fire escape. If doors at fire escape were closed at time of bomb, probably the interior of the building was shielded from direct radiated heat from the bomb

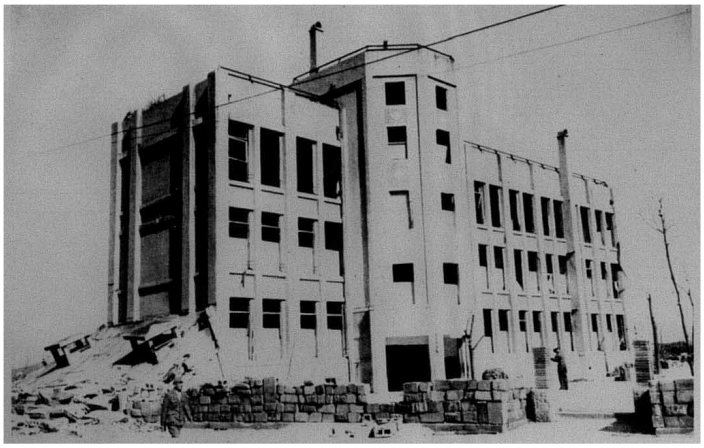

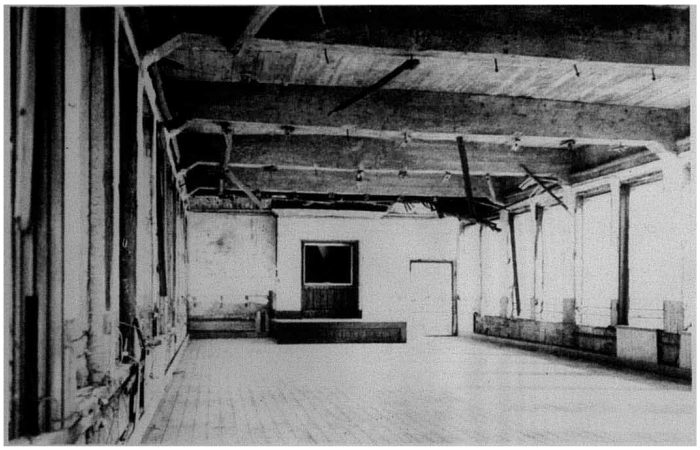

U. S. STRATEGIC BOMBING SURVEY

PHYSICAL DAMAGE DIVISION

Field Team No. 1, Hiroshima, Japan

BUILDING ANALYSIS

Sheet No. 1

Building No.: 87-A. Coordinates: 7F. Distance from (GZ): 8,000, (AZ): 8,200.
NAME: Funairi Grammar School.
CONSTRUCTION AND DESIGN
Type: Wood frame.
Number of stories: Two. JTG class: E2.
Roof: Asbestos cement on wood trusses and wood sheathing.
Partitions: Wood.
Walls: Wood lath and plaster with wood exterior.
Floors: Wood over wood framing.
Framing: Wood.
Window and door frames: Wood. Ceilings: Wood.
Condition, workmanship, and materials: Good, but design rather poor.
Compare with usual United States buildings: Weaker because of very slender columns and poor joints.
OCCUPANCY: Classrooms.
CONTENTS: Classroom furnishing and equipment.
DAMAGE to building: Entire building on verge of collapse, and one wing completely collapsed. Walls and columns facing blast buckled and building displaced away from blast.
Cause: Blast.
To contents: Most of contents were severely damaged by debris and by being overturned and blown about by blast.
Cause: Blast and debris (about equally).
TOTAL FLOOR AREA (square feet): 38,400. Structural damage: 38,400. Superficial damage:
FRACTION OF DAMAGE: Building structural: 100 percent. Superficial: . Contents: 50 percent.
REMARKS: Fire walls were of reinforced concrete.

Note. Building damage based on total floor area. Contents damage is fraction of contents seriously damaged.

Sheet No. 1

Building No.: 87-B. Coordinates: 7F. Distance from (GZ): 8,000, (AZ): 8,200.
NAME: Funairi Grammar School.
CONSTRUCTION AND DESIGN
Type: Light steel frame.
Number of stories: One. JTG class: A2 2.
Roof: Asbestos shingles over wood-sheathing and purlins.
Partitions: None.
Walls: Plaster on wood lath with wood exterior sheathing.
Floors: Wood over wood beams on concrete posts.
Framing: Light steel-trussed arch.
Window and door frames: Wood. Ceilings: None.
Condition, workmanship, and materials: Good.
Compare with usual United States buildings: Slightly lighter design but generally comparable.
OCCUPANCY: School auditorium.
CONTENTS: Lectern, benches, tables, teaching aids.
DAMAGE to building: Roof trusses slightly deformed but probably will be used in place. Most of roofing stripped or displaced. Wall facing blast blown in.
Cause: Blast.
To contents: Slight damage and that primarily due to exposure.
Cause: Exposure.
TOTAL FLOOR AREA (square feet): 4,900. Structural damage: . Superficial damage: 4,900.
FRACTION OF DAMAGE: Building structural: Superficial: 100 percent. Contents: 10 percent.
REMARKS:

Note. Building damage based on total floor area. Contents damage is fraction of contents seriously damaged.

U. S. STRATEGIC BOMBING SURVEY

PHYSICAL DAMAGE DIVISION

Field Team No. 1, Hiroshima, Japan

BUILDING ANALYSIS

Sheet No. 1

Building No.: 95. Coordinates: 4G. Distance from (GZ): 1,200, (AZ): 2,300.

NAME: Honkawa Grammar School.

CONSTRUCTION AND DESIGN

Type: Reinforced concrete.

Number of stories: Three and basement. JTG class E1.

Roof: Reinforced concrete, cement finish.

Partitions: Reinforced concrete (7-inch).

Walls: Reinforced concrete (10-inch).

Floors: Reinforced concrete, wood finish on sleepers.

Framing: Reinforced concrete.

Window and door frames: Metal. Ceilings: Plaster on concrete.

Condition, workmanship, and materials: Excellent.

Compare with usual United States buildings: Stronger.

OCCUPANCY: School classrooms.

CONTENTS: School furnishings and equipment.

DAMAGE to building: Panel walls facing blast buckled. One roof girder structurally damaged and slab depressed. About 15 percent of roof slabs cracked and beams cracked with some spalling but usable in place. All finish, floors and trim burned out, sash and doors blown out.

Cause: Blast.

To contents: Completely destroyed.

Cause: Fire (primary) may have been some debris damage.

TOTAL FLOOR AREA (square feet): 49,500. Structural damage: 500. Superficial damage: 3,000.

FRACTION OF DAMAGE: Building structural: 1 percent. Superficial: 6 percent. Contents: 100 percent.

REMARKS:

Note.—Building damage based on total floor area. Contents damage is fraction of contents seriously damaged.

Sheet No. 2

(Fire Supplement to Sheet No. 1)

Building No.: 95. Fire classification: R.

WALL OPENINGS: Shutters: None.

Shut:

Effect of blast:

FLOOR OPENINGS:

	Enclosed	Fire doors	Automatic	Effect of blast
Stairs:	Part	No		
Elevators:				

EXPOSURE:

Location	Distance	Firebreak Clearance	Class	Fire Burned	Remarks
N	125′	Yes	C		
E	—	No	—	—	No exposure.
S	30′	Partial 150′	C	Yes	All exposures burned
W	100′	Yes	C	Yes	

PROBABLE CAUSE OF FIRE: Not determined.

VERTICAL FIRE SPREAD: Probably.

EXTENT OF FIRE: Total floor area: 49,500 square feet. Floor area burned: 49,500 square feet: 100 percent (after blast damage).

REMARKS:

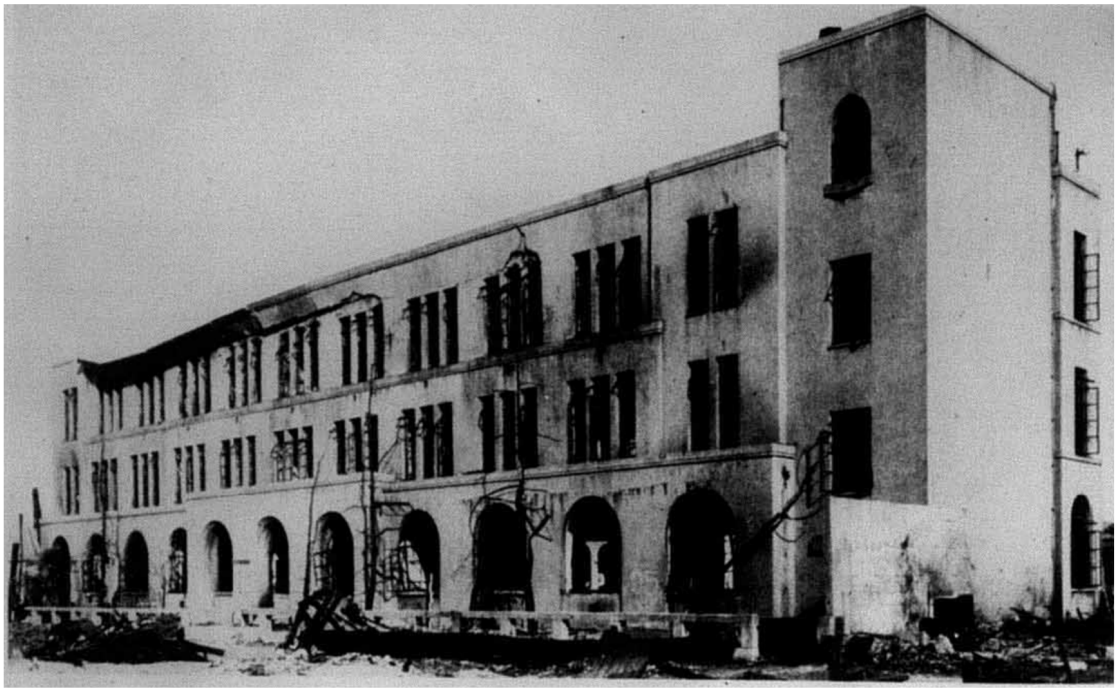

U. S. STRATEGIC BOMBING SURVEY

PHYSICAL DAMAGE DIVISION

Field Team No. 1, Hiroshima, Japan

BUILDING ANALYSIS

SHEET No. 1

Building No.: 96. Coordinates: G5. Distance from (GZ): 400 (AZ): 2,000.

NAME: Taisho Clothing Store.

CONSTRUCTION AND DESIGN

Type: Reinforced concrete.

Number of stories: Three and basement. JTG class: E1.

Roof: Reinforced-concrete slabs, cement finish.

Partitions: Reinforced concrete and wood.

Walls: Reinforced concrete (10-inch), brick panels on first floor.

Floors: Reinforced concrete (wood finish on sleepers, second floor).

Framing: Reinforced concrete.

Window and door frames: Metal. Ceilings: Plaster on concrete.

Conditions, workmanship, and materials: Fair.

Compare with usual United States buildings: Considerable stronger (larger structural members).

OCCUPANCY: Mercantile.

CONTENTS: Merchandise for sale.

DAMAGE to building: All roof slabs depressed, fracturing beams and girders and stretching steel. Panel in east wall buckled, girders in second floor rear cracked and spalled. Ninety percent of parapet demolished. All sash and doors blown out. Finish and trim burned out. No fire in basement.

Cause: Blast.

To contents: Completely destroyed, except in basement.

Cause: Fire (primary cause—probably some debris damage).

TOTAL FLOOR AREA (square feet): 12,400. Structural damage: 3,900. Superficial damage:

FRACTION OF DAMAGE: Building structural: 31 percent. Superficial: —. Contents: 75 percent.

REMARKS:

NOTE.—Building damage based on total floor area. Contents damage is fraction of contents seriously damaged.

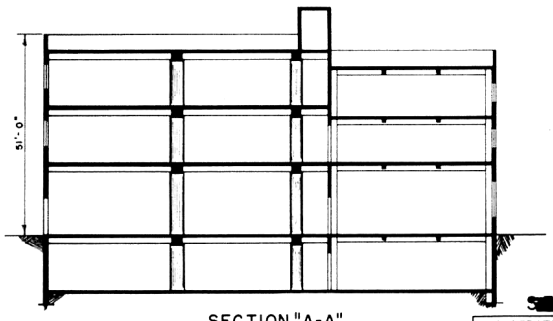

SECTION "A-A"

[redacted]

U.S. STRATEGIC BOMBING SURVEY
BUILDING 96
HIROSHIMA, JAPAN GRID 5H
FIGURE 100-X A

SHEET No. 2

(Fire Supplement to Sheet No. 1)

Building No.: 96. Fire classification: R.

WALL OPENINGS: Shutters: None.

Shut:

Effect of blast:

FLOOR OPENINGS:

	Enclosed	Fire doors	Automatic	Effect of blast
Stairs:	No			
Elevators:				

EXPOSURE:

Location	Distance	Firebreak Clearance	Glass	Fire Burned	Remarks
N	35'	No	C	Yes	
E	10'	No	C	Yes	
S	10'	No	C	Yes	
W	150'	Yes	C	Yes	

PROBABLE CAUSE OF FIRE: Not determined.

VERTICAL FIRE SPREAD: Possibly.

EXTENT OF FIRE: Total floor area: 12,400 square feet. Floor area burned: 9,300 square feet; 75 percent (after blast damage).

REMARKS: Fire throughout building except in basement

U. S. STRATEGIC BOMBING SURVEY

PHYSICAL DAMAGE DIVISION

Field Team No. 1, Hiroshima, Japan

BUILDING ANALYSIS

Sheet No. 1

Building N8.: 100. Coordinates: 5G. Distance from (GZ): 800, (AZ): 2,100.
NAME: Nippon Simple Fire Insurance Co.
CONSTRUCTION AND DESIGN
Type: Reinforced-concrete frame.
Number of stories: 2. JTG class: E2.
Roof: Reinforced-concrete slab and beams.
Partitions: None.
Walls: Reinforced concrete, stucco finish.
Floors: Reinforced-concrete slab, cement finish.
Framing: Reinforced concrete.
Window and door frames: Metal. Ceilings: Plaster on concrete.
Condition, workmanship, and materials: Good.
Compare with usual United States buildings: Comparable.
OCCUPANCY: Office.
CONTENTS: Office furnishings and equipment.
DAMAGE to building: One roof girder cracked and spalled. Sash and doors blown out or deformed. Trim and finish damaged by fire.
Cause: Blast.
To contents: Completely destroyed.
Cause: Fire (probably appreciable blast and debris damage).
TOTAL FLOOR AREA (square feet): 3,000. Structural damage: —. Superficial damage: 80.
FRACTION OF DAMAGE: Building structural: —. Superficial: 3 percent. Contents: 100 percent.
REMARKS:

Note.—Building damage based on total floor area. Contents damage is fraction of contents seriously damaged.

Sheet No. 2

(Fire Supplement to Sheet No. 1)

Building No.: 100. Fire classification: R.
WALL OPENINGS: Shutters: No.
Shut:
Effect of blast:
FLOOR OPENINGS:

	Enclosed	Fire doors	Automatic	Effect of blast
Stairs:	No			
Elevators:				

EXPOSURE:

Location	Distance	Firebreak Clearance	Fire Class	Burned	Remarks
N	0′	No	C	Yes	Door blown off or bent.
E	15′	No	C	Yes	
S	40′	No	C	Yes	
W	0′	No	C	Yes	Blank wall.

PROBABLE CAUSE OF FIRE: Not determined.
VERTICAL FIRE SPREAD: Possibly.
EXTENT OF FIRE: Total floor area: 3,000 square feet. Floor area burned: 3,000 square feet 100 percent (after blast damage).
REMARKS: East wall which faced zero point was blank and it is believed the interior of the building was shielded from direct radiated heat from the bomb.

U. S. STRATEGIC BOMBING SURVEY

PHYSICAL DAMAGE DIVISION

Field Team No. 1, Hiroshima, Japan

BUILDING ANALYSIS

Sheet No. 1

Building No.: 122. Coordinates: 5J. Distance from (GZ): 6,400, (AZ): 6,700.

NAME: Sumitomo Bank Co., Higashi Matsurara Branch.

CONSTRUCTION AND DESIGN

Type: Protected steel frame.

Number of stories: 2. JTG class: E1.

Roof: Reinforced-concrete slab on steel beams.

Partitions: Plaster on metal lath.

Walls: Brick panel—13-inch.

Floors: Reinforced-concrete slab and beams.

Framing: Steel—protected.

Window and door frames: Wood. Ceilings: Plaster on concrete.

Condition, workmanship, and materials: Excellent.

Compare with usual United States buildings: Slightly heavier.

OCCUPANCY: Bank with offices on second floor.

CONTENTS: Office and banking equipment.

DAMAGE to building: Glass blown out, few shutters facing blast deformed.

Cause: Blast.

To contents: None.

Cause:

TOTAL FLOOR AREA (square feet): 5,100. Structural damage: —. Superficial damage:

FRACTION OF DAMAGE: Building structural: —. Superficial: —. Contents:

REMARKS:

Note.—Building damage based on total floor area. Contents damage is fraction of contents seriously damaged.

Sheet No. 2

(Fire Supplement to Sheet No. 1)

Building No.: 122. Fire classification: R.

WALL OPENINGS: Shutters: Steel rollers and hinged shutters.

Shut:

Effect of blast: Part bent in slightly.

FLOOR OPENINGS:

	Enclosed	Fire doors	Automatic	Effect of blast
Stairs:	Yes	No		
Elevators:				

EXPOSURE:

Location	Distance	Firebreak Clearance	Fire Class	Burned	Remarks
N	15'	No	C	Yes	Conn. by C pass metal and W. G. doors stopped fire.
E	200'	Yes	C	Yes	
S	—	Yes	—		No exposure.
W	5'	No	C	Yes	

PROBABLE CAUSE OF FIRE: Fire spread from exposures.

VERTICAL FIRE SPREAD: No.

EXTENT OF FIRE: Total floor area: 5,100 square feet. Floor area burned: 0 square feet; 0 percent (after blast damage).

REMARKS: Fire spread into building from exposures at west wall and northeast corner. Fires were extinguished by people inside and negligible damage was done.

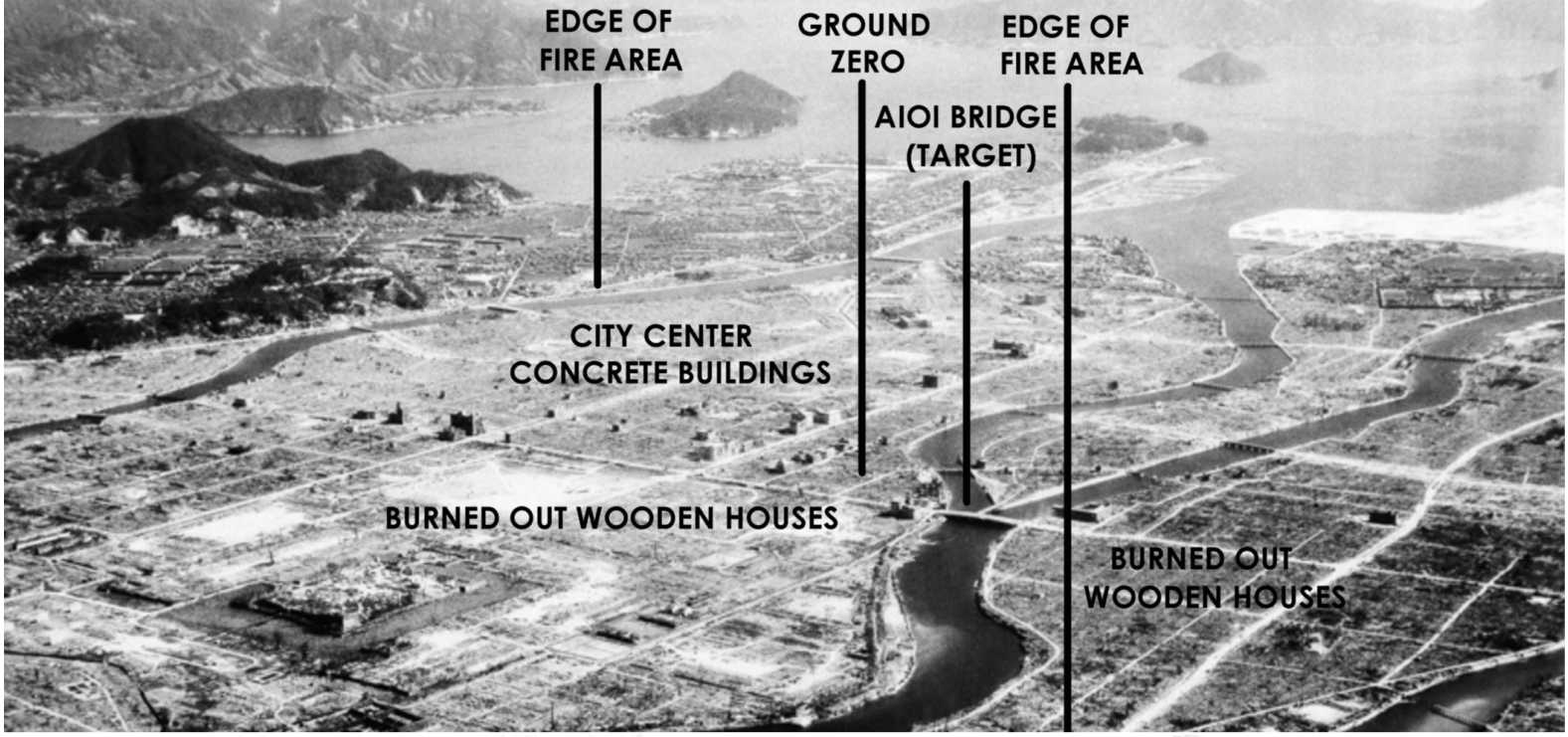
EDGE OF
FIRE AREA
GROUND
ZERO
EDGE OF
FIRE AREA
AIOI BRIDGE
(TARGET)
CITY CENTER
CONCRETE BUILDINGS
BURNED OUT WOODEN HOUSES
BURNED OUT
WOODEN HOUSES

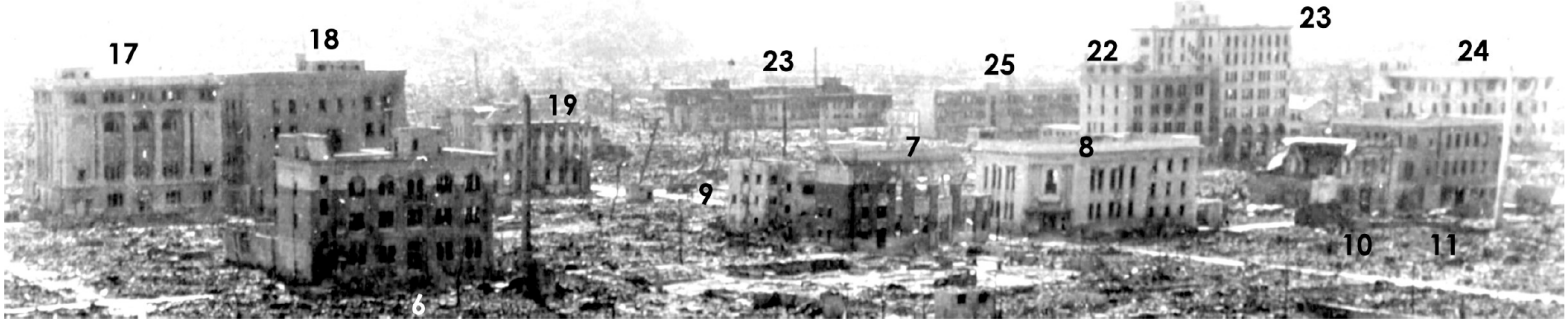
17
18
19
23
25
22
23
24
7
8
9
10
11
6

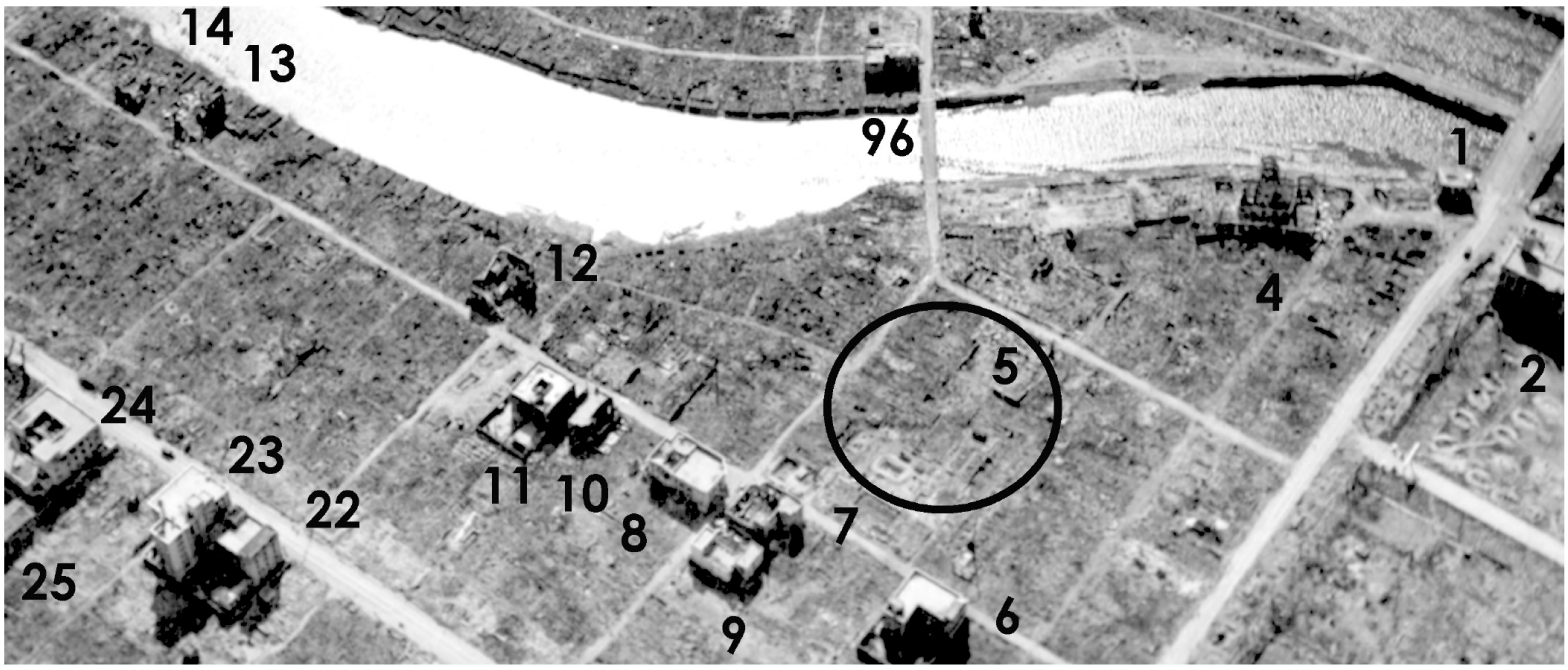
14
13
96
1
12
4
5
2
24
23
22
11
10
8
7
25
9
6

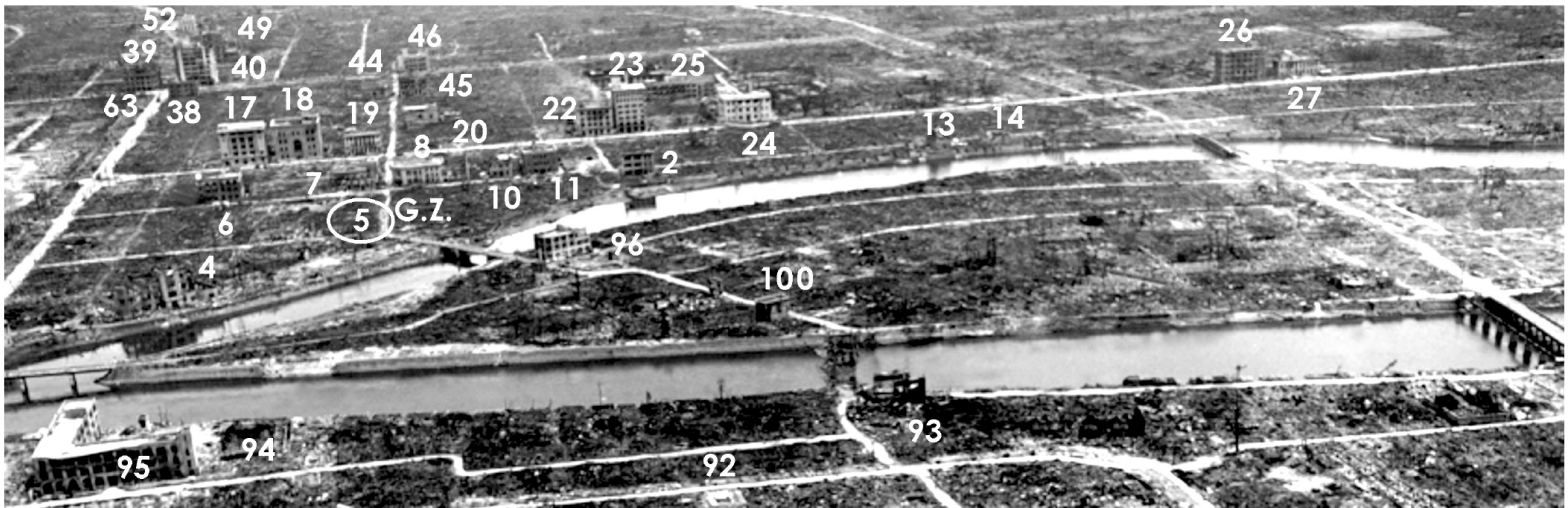
52
49
39
40
44
46
26
63
38
17
18
19
45
23
25
27
22
13
14
8
20
24
2
7
10
11
6
5
G.Z.
96
4
100
93
95
94
92

HIROSHIMA
500 m
Hiroshima Grade School
5th Transport Battalion
5th Field Artillery Regiment
Hiroshima Castle
Imperial Hq
5th Division Hq
Clothing Warehouse
Military Academy
11th Infantry Regiment
Revenue Office
6.3
Regimental Headquarters
NISHI DRILL FIELD
Electric Transformer Station
Division Commander's Quarters
Saibi Grade School
2.6
Military Police
Officers' Club
Dept. Store
TOGIYACHO
Telephone Office
Fish Market
EBISUCHO
Honkawa Grade School
TAKAJO-MACHI
SOKOZAYACHO
NISHI-HIKIMACHI
NISHIKUKENCHO
SHIN-AIOI BASHI
AIOI BASHI
KAJIYA-CHO
Commercial Display Hall
SARUGAKUCHO
SAIKU-MACHI
ABURAYACHO
Canning Factory
NAKAJIMA-HOMMACHI
HONKAWA-BASHI
MOTOYASU-BASHI
Nishio Mat Factory
NISHI JIKATA-MACHI
FIRE LANE
NAKAJIMA-HOMMACHI
Sokan-ji
ZAI-MOKU-CHO
TENJIM-MACHI
ONOMICHICHO
SHIN-BASHI
Kokntai-ji
KOBIKICHO
NAKAJIMA SHIMMACHI
Hotel
Court of Appeals
KO-MACHI
Girls' High School
SHIMONAKACHO
Court
MIKAWACHO
SHIMO-NAGARE KAWACHO
Prefectural Hospital
Electric Substation
Elec Co
School for Blind and Dumb
Bank of Japan
Prefectural Office
ŌTEMACHI
Asano Library
Commercial School
TANAKA-MACHI
Nakajima Grade School
SANTAI-BASHI
Public Hall
Uaiichi Middle School
ATHLETIC FIELD
Sanyo Middle School
Ote Grade School
Hasegawa Knitting Mill
Girls' High School
Fish Market
Commercial School
TAKARAMACHI
Paper Mill
MEIJI-BASHI
City Hall
ZAKOBACHO
Steel
Stone

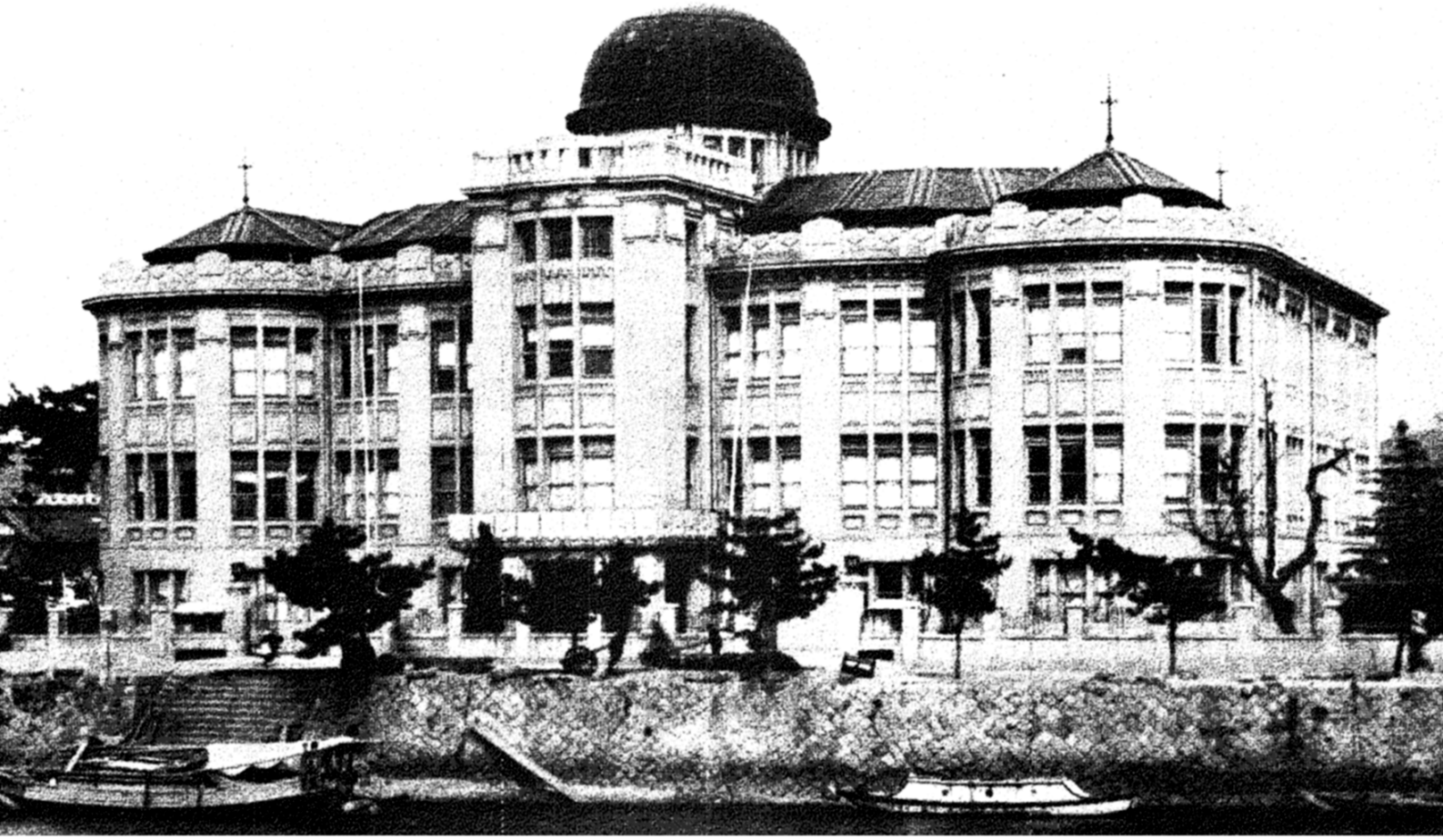

Commercial Museum (300 meters) before and after

1000'

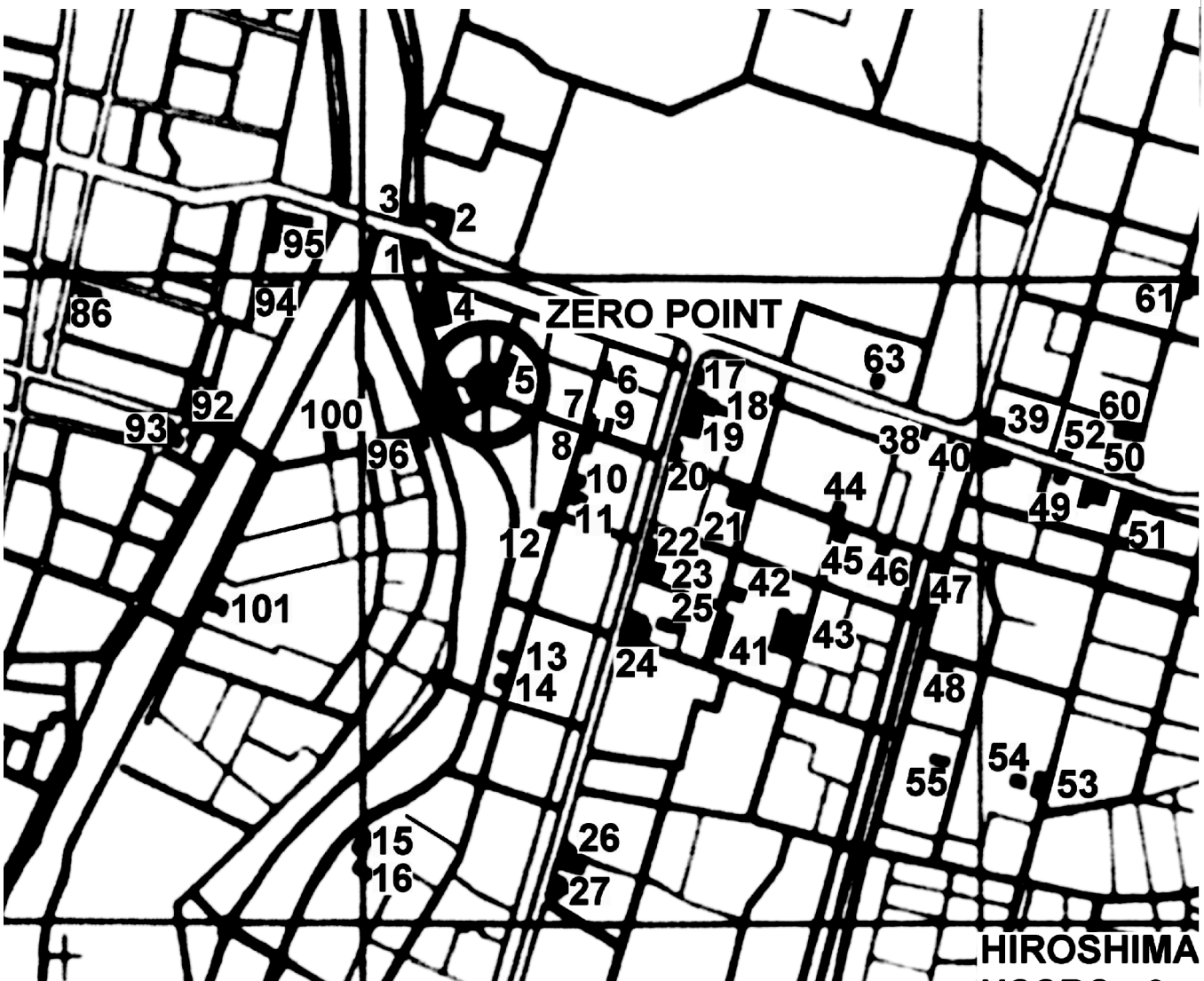
ZERO POINT
HIROSHIMA
1
2
3
4
5
6
7
8
9
10
11
12
13
14
15
16
17
18
19
20
21
22
23
24
25
26
27
38
39
40
41
42
43
44
45
46
47
48
49
50
51
52
53
54
55
60
61
63
86
92
93
94
95
96
100
101

[redacted]

THE UNITED STATES
STRATEGIC BOMBING SURVEY

THE EFFECTS OF THE ATOMIC BOMB ON HIROSHIMA, JAPAN

Volume III

Physical Damage Division

Dates of Survey:

14 October – 26 November 1945

Date of Publication
May 1947

[redacted]

(1,000 ft GZ)
AIOI BRIDGE

HIROSHIMA CITY ELECTRIC RAILWAY AND BUS SYSTEM

U.S. STRATEGIC BOMBING SURVEY
ELECTRIC RAILWAY SYSTEM
HIROSHIMA, JAPAN
FIGURE I-XIII

LEGEND

DAMAGE TO CARS		POLE TYPES
TOTALLY BURNED	22	TYPE 1 – WOOD POLES
HALF BURNED	3	TYPE 2 – STEEL RAIL
SEVERE DAMAGE	23	TYPE 3 – LATTICE STEEL
MODERATE DAMAGE	24	TYPE 4 – BUILT-UP MEMBER
SLIGHT DAMAGE	36	TYPE 5 – CONCRETE POLES
NO DAMAGE	15 — (12 ON MIYAGIMA LINE)	

TROLLEY LINE (RAIL)
DAMAGED OVERHEAD TROLLEY LINES

HIROSHIMA
HIROSHIMA PREFECTURE, HONSHU, JAPAN

CONTOUR INTERVAL 20 METERS
GRID SYSTEM BASED ON 1000 YARD WORLD POLYCONIC GRID

DAMAGE RADII

- LIMIT OF BLAST DAMAGE TO OVERHEAD CABLES (8000')
- LIMIT OF FIRE DAMAGE TO TYPE 1 POLES (6500')
- LIMIT OF BLAST DAMAGE TO TYPE 1 POLES (4500')
- LIMIT OF BLAST DAMAGE TO TYPE 2 POLES (3500')
- LIMIT OF BLAST DAMAGE TO TYPE 4 POLES (3000')

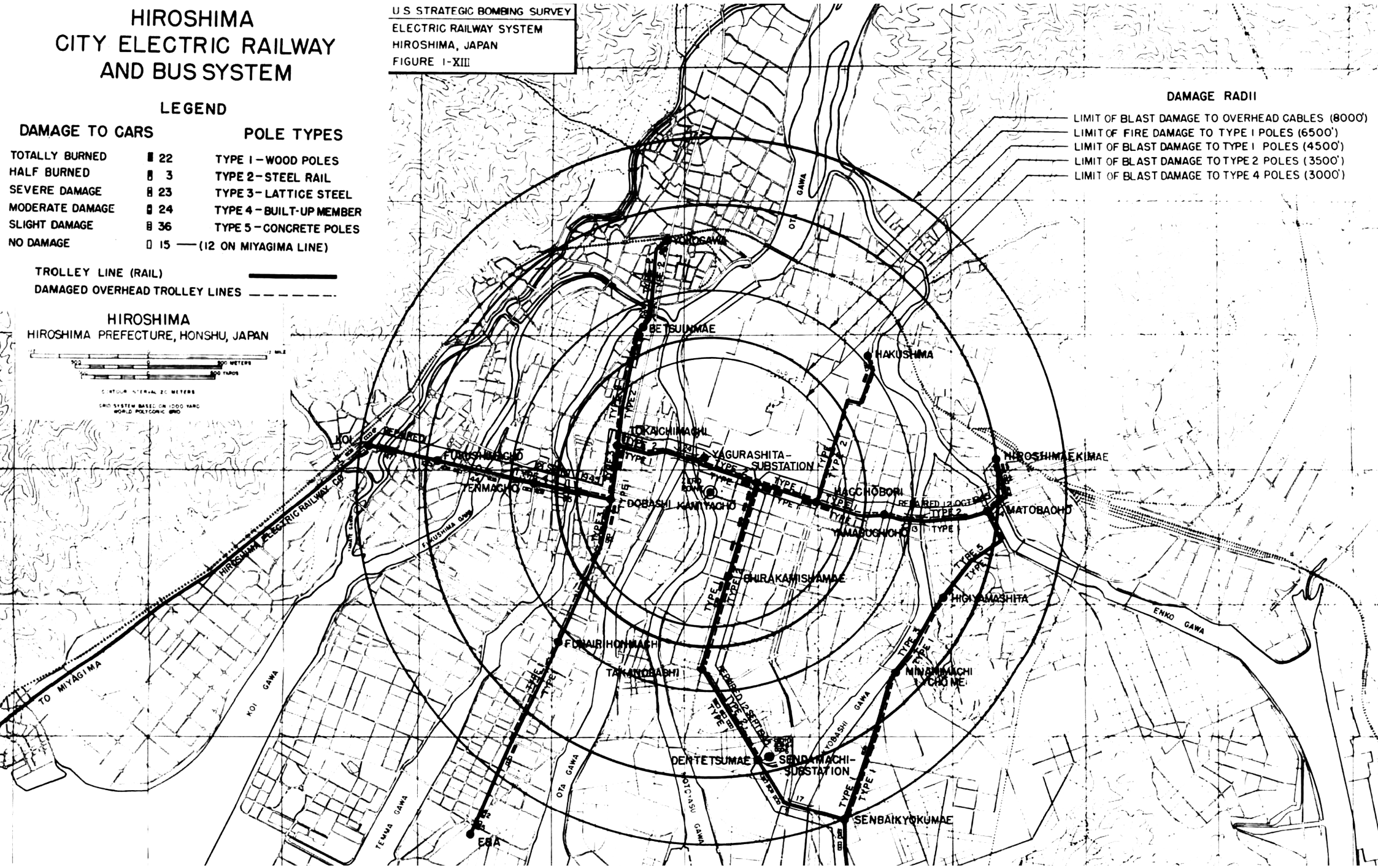

[redacted]

ILLUSTRATION SHOWING THE DERAILING OF FREIGHT TRAIN 377 BY THE ATOMIC BOMB

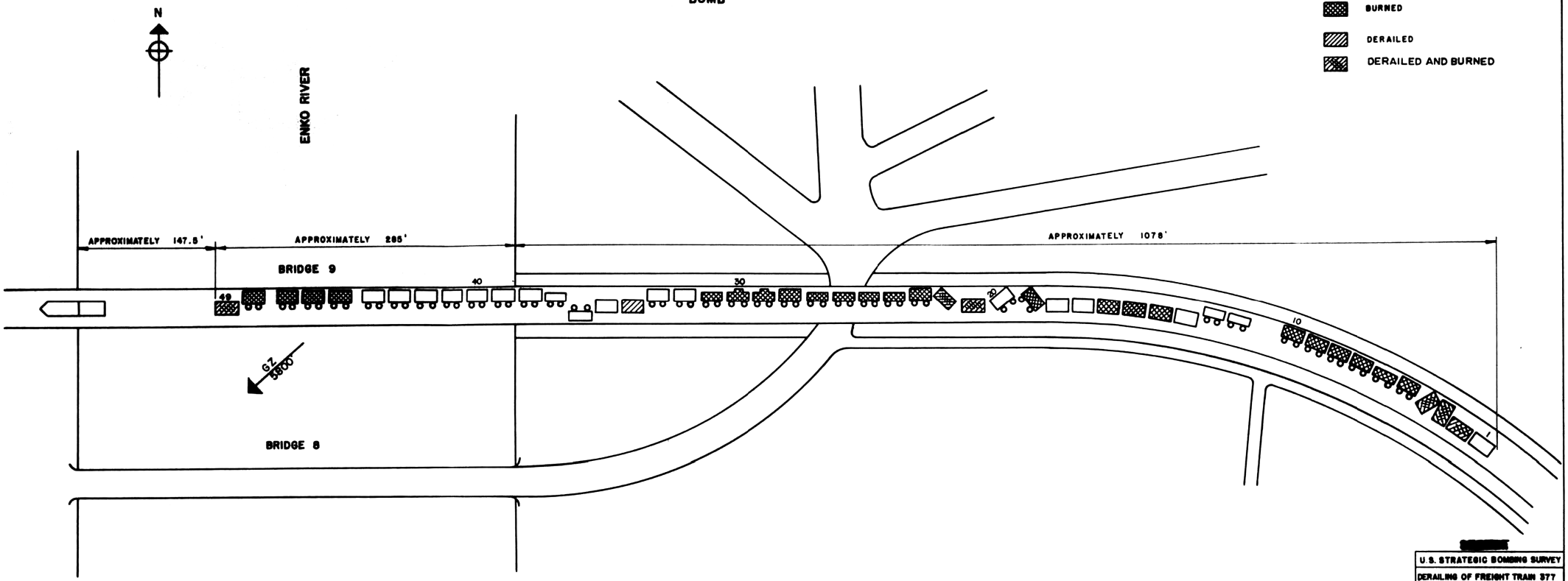

[redacted]

U.S. STRATEGIC BOMBING SURVEY

DERAILING OF FREIGHT TRAIN 377
HIROSHIMA, JAPAN
FIGURE 8 XIII

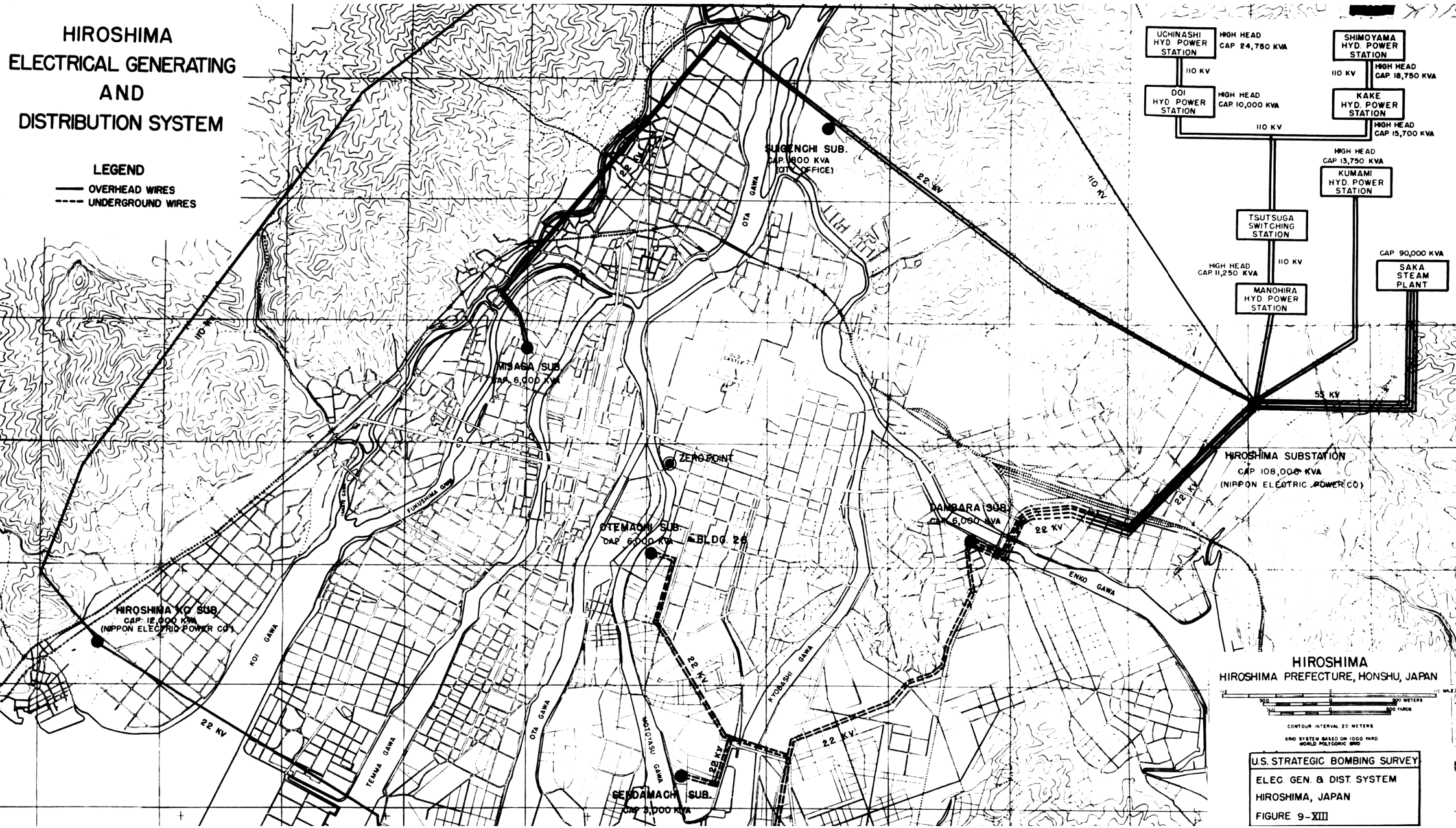
HIROSHIMA
ELECTRICAL GENERATING
AND
DISTRIBUTION SYSTEM
LEGEND
OVERHEAD WIRES
UNDERGROUND WIRES
UCHINASHI HYD. POWER STATION
HIGH HEAD CAP 24,750 KVA
SHIMOYAMA HYD. POWER STATION
HIGH HEAD CAP 18,750 KVA
110 KV
DOI HYD. POWER STATION
HIGH HEAD CAP 10,000 KVA
KAKE HYD. POWER STATION
HIGH HEAD CAP 15,700 KVA
110 KV
HIGH HEAD CAP 13,750 KVA
KUMAMI HYD. POWER STATION
TSUTSUGA SWITCHING STATION
110 KV
HIGH HEAD CAP 11,250 KVA
MANOHIRA HYD. POWER STATION
CAP 90,000 KVA
SAKA STEAM PLANT
55 KV
HIROSHIMA SUBSTATION
CAP 108,000 KVA
(NIPPON ELECTRIC POWER CO)
SUGENCHI SUB.
CAP 1,800 KVA
(CITY OFFICE)
22 KV
110 KV
OTA GAWA
MISAGA SUB.
CAP 6,000 KVA
ZERO POINT
FUKUSHIMA GAWA
OTEMACHI SUB.
CAP 6,000 KVA
BLDG. 26
DANBARA SUB.
CAP 6,000 KVA
ENKO GAWA
HIROSHIMA KO SUB.
CAP 12,000 KVA
(NIPPON ELECTRIC POWER CO)
KOI GAWA
TEMMA GAWA
MOTOYASU GAWA
KYOBASHI GAWA
SENDAMACHI SUB.
CAP 5,000 KVA
HIROSHIMA
HIROSHIMA PREFECTURE, HONSHU, JAPAN
CONTOUR INTERVAL 20 METERS
GRID SYSTEM BASED ON 1000 YARD WORLD POLYCONIC GRID
U.S. STRATEGIC BOMBING SURVEY
ELEC. GEN. & DIST. SYSTEM
HIROSHIMA, JAPAN
FIGURE 9-XIII

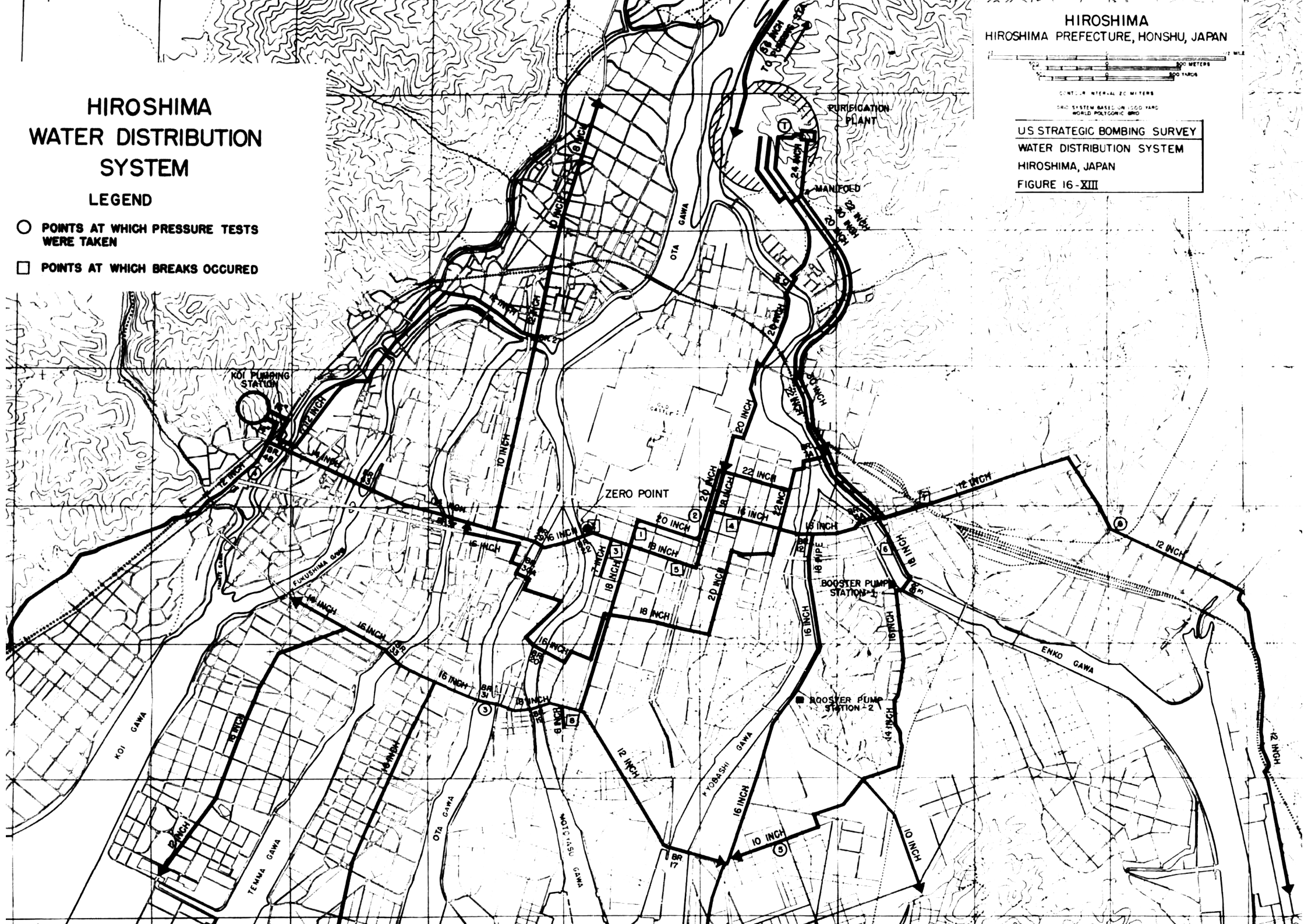
HIROSHIMA
WATER DISTRIBUTION SYSTEM
LEGEND
POINTS AT WHICH PRESSURE TESTS WERE TAKEN
POINTS AT WHICH BREAKS OCCURED
HIROSHIMA
HIROSHIMA PREFECTURE, HONSHU, JAPAN
US STRATEGIC BOMBING SURVEY
WATER DISTRIBUTION SYSTEM
HIROSHIMA, JAPAN
FIGURE 16-XIII
PURIFICATION PLANT
MANIFOLD
KOI PUMPING STATION
ZERO POINT
BOOSTER PUMP STATION #1
BOOSTER PUMP STATION #2
OTA GAWA
KOI GAWA
TEMMA GAWA
FUKUSHIMA GAWA
YOBASHI GAWA
ENKO GAWA
NOTOHASU GAWA

HIROSHIMA

ADA038738

Secondary Fires

Secondary fires are those that result from airblast damage. Their causes include overturned gas appliances, broken gas lines, and electrical short-circuits. McAuliffe and Moll (Reference 1) studied secondary fires resulting from the atomic attacks on Hiroshima and Nagasaki and compared their results with data from conventional bombings, explosive disasters, earthquakes, and tornadoes. Their major conclusion was that secondary ignitions occur with an overall average frequency of 0.006 for each 1000 square feet of floor space, provided airblast peak overpressure is at least 2 psi. The frequency of secondary ignitions appears to be relatively insensitive to higher overpressures.

Based on surveys of Hiroshima and Nagasaki buildings.

FREQUENCY OF SECONDARY IGNITIONS AS A FUNCTION OF BUILDING TYPE

Type of Structure	Frequency of Secondary Ignitions (for each 1,000 square feet of floor area)
Wood	0.019
Brick	0.017
Steel	0.004
Concrete	0.002

MULTIPLYING FACTOR FOR TYPES OF BUILDING OCCUPANCIES

Type of Occupancy	Multiplying Factor
Public	0.4
Mercantile	0.5
Residential	0.5
Manufacturing	1.0
Miscellaneous	10.0

MULTIPLYING FACTOR FOR TIME OF DAY

Time of Day	Multiplying Factor
Night	0.5
Day (other than mealtimes)	1.0
Mealtimes	2.0

1 . Secondary Ignitions in Nuclear Attack, J. McAuliffe and K. Moll, Stanford Research Institute, Menlo Park, California 94025, SRI Project 5106 (AD 625173), July 1965.

15 min. (Enola Gay)
Hiroshima fires merging

0.12 mile from GZ,
Hiroshima

Geibi Bank 250 meters

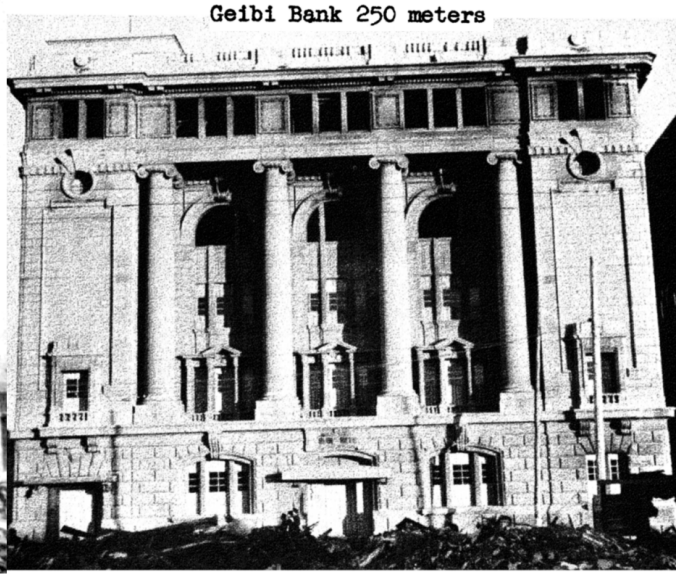

Kirin Beer Hall (2,300 ft GZ)
USSBS building 47

USSBS Hiroshima building 40,
Fukuya Department store 2,500 ft GZ

USSBS Hiroshima building 26
Chugoku Electric Bldg. (700 meters)

790m west of GZ, Hiroshima

Postal Savings Bureau
1 mile

USSBS building 61, J.O.F.K. Hiroshima Broadcasting Station, 900 m from GZ.

City Hall 1100 meters
USSBS Building 28

USSBS Hiroshima Building 65, 1,400 m from GZ.

USSBS Hiroshima Building 31, 1,600 m from GZ.

Red Cross Hospital

USSBS 49
Chugoku
Shimbun
3,000 ft GZ

BANK OF JAPAN BUILDING AFTER ATTACK ON HIROSHIMA

GEIBI BANK CO. BUILDING AFTER ATTACK ON HIROSHIMA

Bank of Japan: USSBS Building 24, 1300 ft from GZ
Geibi Bank Co: USSBS Building 59, 4100 ft from GZ
(Table 5 of USSBS report 92 Hiroshima, v2.)

In both, survivors extinguished fire with water buckets.

(Ref: Panel 26 of the "DCPA Attack Environment Manual", Chapter 3.)

USSBS Report 92, v2 Hiroshima buildings	MAE's in square miles	Radii of MAE's in feet
Multistory, earthquake-resistant	0. 03	500
Multistory, steel- and reinforced-concrete frame (including both earthquake- and non-earthquake-resistant construction)	. 05	700
1-story, light, steel-frame	3. 4	5, 500
Multistory, load-bearing, brick-wall	3. 6	5, 700
1-story, load-bearing, brick-wall	6. 0	7, 300
Wood-frame industrial-commercial (dimension-timber construction)	8. 5	8, 700
Wood-frame domestic buildings (wood-pole construction)	9. 5	9, 200
Residential construction	6. 0	7, 300

OFFICE OF THE AIR SURGEON

NP-3041

MEDICAL EFFECTS OF ATOMIC BOMBS

The Report of the Joint Commission for the Investigation of the Effects of the Atomic Bomb in Japan; Volume VI

By

Ashley W. Oughterson
George V. LeRoy
Averill A. Liebow
E. Cuyler Hammond
Henry L. Barnett
Jack D. Rosenbaum
B. Aubrey Schneider

July 6, 1951
[TIS Issuance Date]

Army Institute of Pathology

UNITED STATES ATOMIC ENERGY COMMISSION
Technical Information Service, Oak Ridge, Tennessee

This document contains information affecting the national defense of the United States within the meaning of the Espionage Act, 50 U. S. C. 31 and 32, as amended. Its transmission or the revelation of its contents in any manner to an unauthorized person is prohibited by law.

RESTRICTED

HIROSHIMA SCHOOL CHILDREN

WORK PARTIES DISTRIBUTION

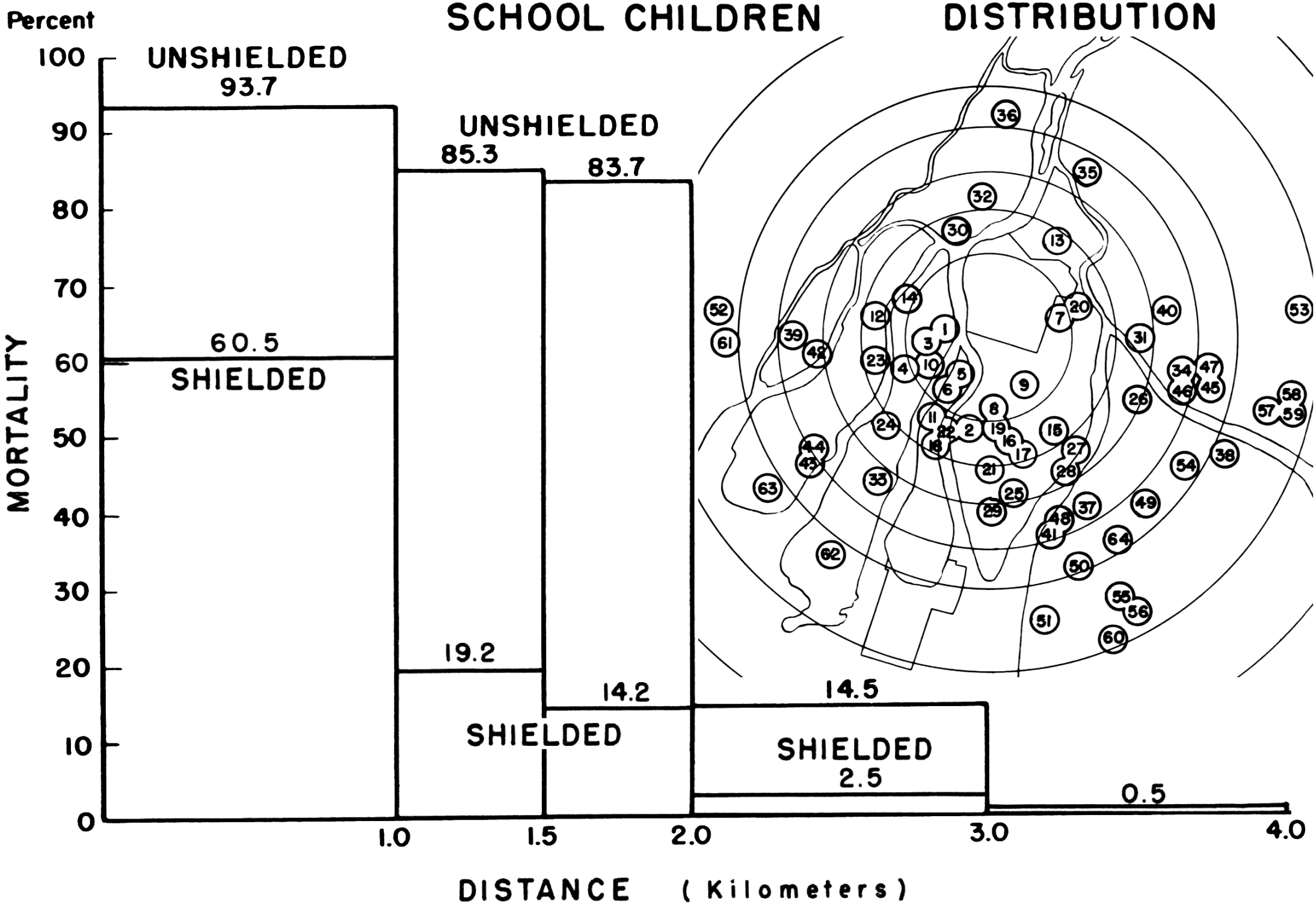

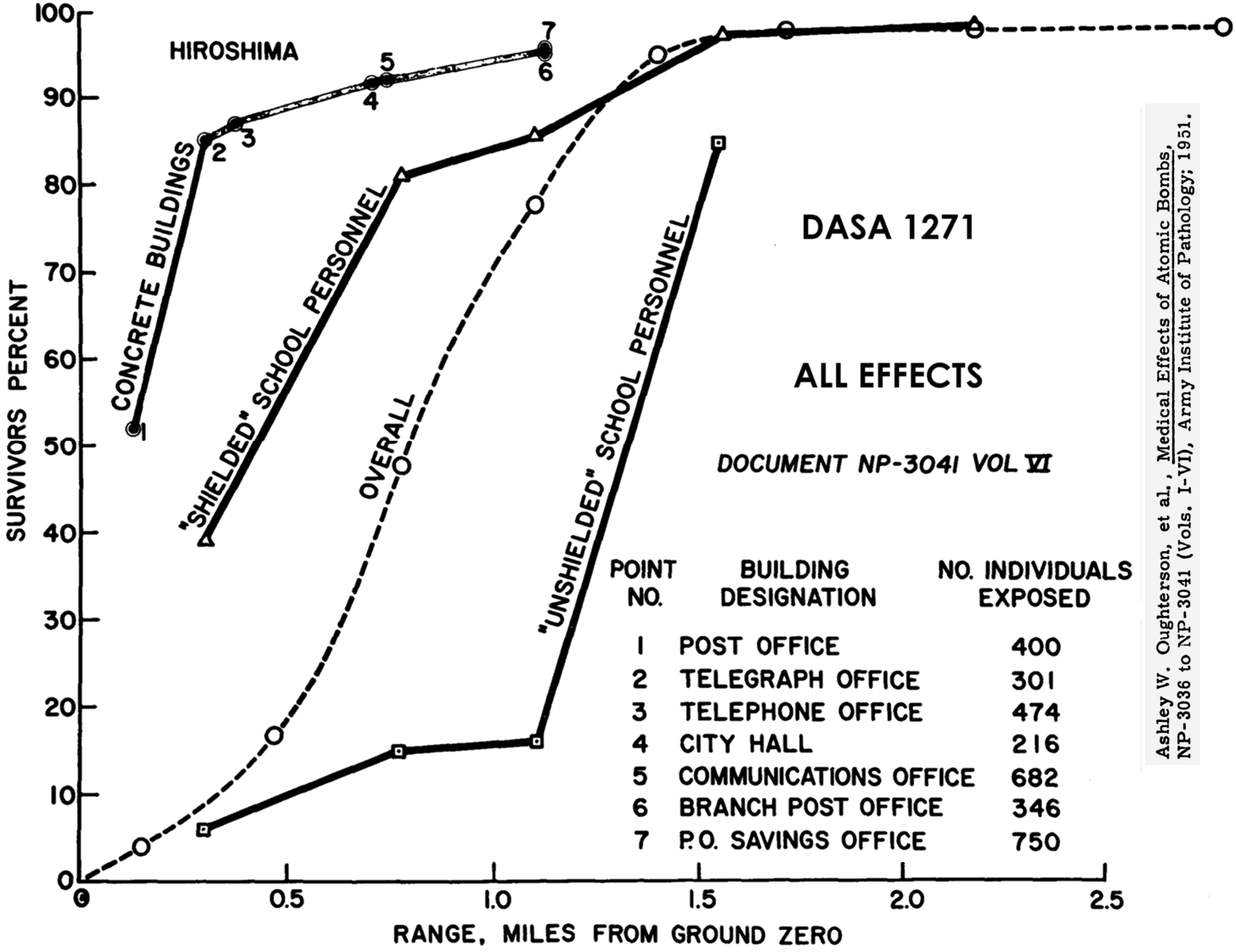

Ashley W. Oughterson, et al., Medical Effects of Atomic Bombs, NP-3036 to NP-3041 (Vols. I-VI), Army Institute of Pathology; 1951.

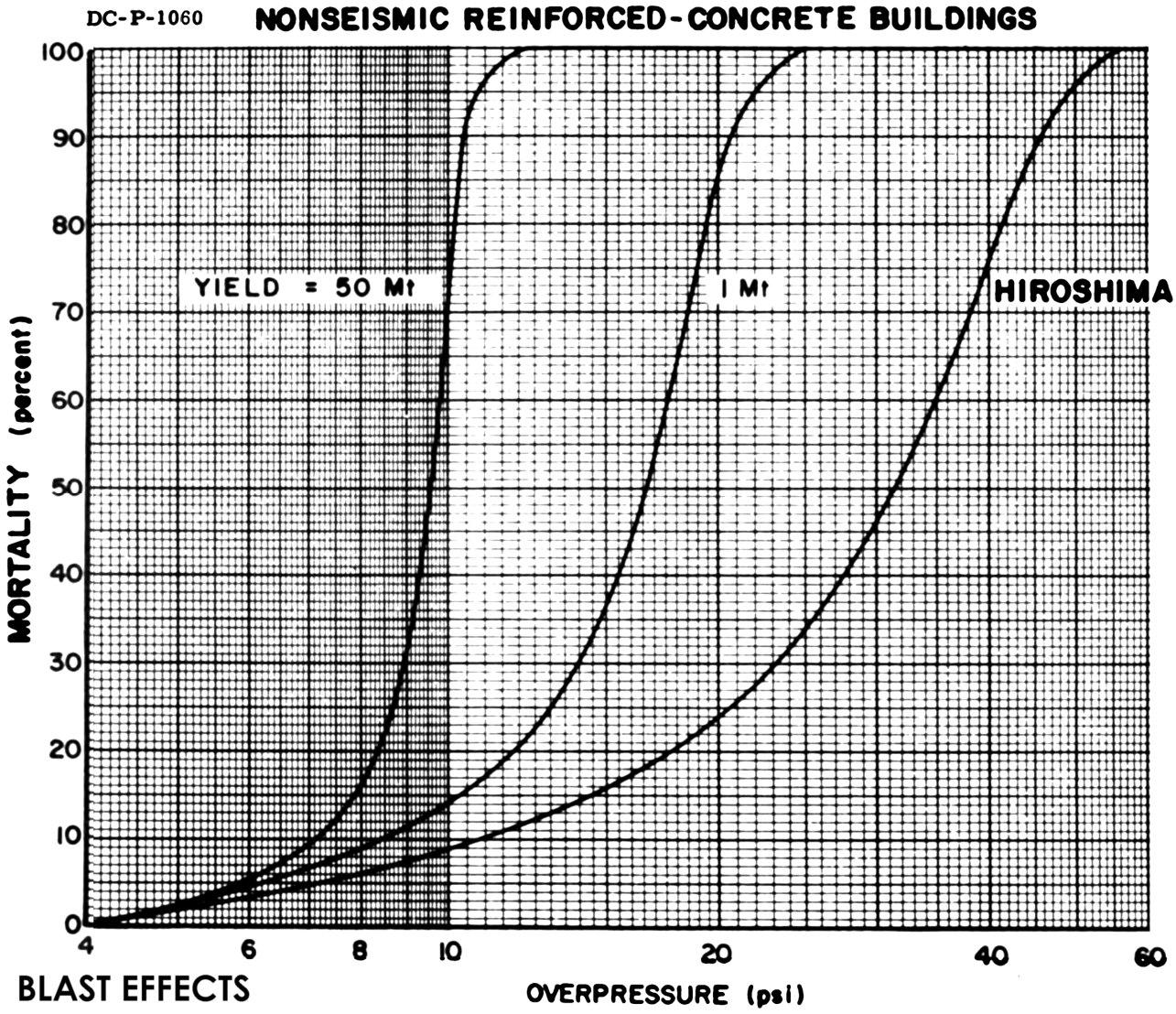

L. Wayne Davis, Donald L. Summers, William L. Baker, and James A. Keller, Prediction of Urban Casualties and the Medical Load from a High-Yield Nuclear Burst, DC-FR-1060, The Dikewood Corporation

MEMORANDUM
RM-3079-PR
1963

403 337

DISASTER AND RECOVERY: A HISTORICAL SURVEY

Jack Hirshleifer

PREPARED FOR:
UNITED STATES AIR FORCE PROJECT RAND

The RAND Corporation
SANTA MONICA • CALIFORNIA

As at Hamburg, people proved tougher than structures. Almost 70 per cent of the buildings in Hiroshima were destroyed, compared with around 30 per cent of population.[1]

The Research Department of the Hiroshima Municipal Office is reported to have estimated the population in the city as 407,000, in Hiroshima (Hiroshima Publishing Company, 1949).

[1]These proportions are the estimates used by the U.S. Strategic Bombing Survey report. The Hiroshima Municipal Office calculations show an even greater disparity, reporting 22 per cent of population killed and missing but some 89 per cent of buildings as destroyed or needing reconstruction (Hiroshima).

On August 7 power was generally restored to surviving areas, and through railroad service commenced on August 8. Telephone service started on August 15. Hiroshima was also not a dead city. The U.S. Strategic Bombing Survey reported that plants responsible for three-fourths of the city's industrial production could have resumed normal operations within 30 days (the newer and larger plants in Hiroshima were on the outskirts of the city, and both physical premises and personnel generally survived).[1] By mid-1949 the population had grown to over 300,000 once more, and 70 per cent of the destroyed buildings had been reconstructed.[2]

---

[1]USSBS, "The Effects of Atomic Bombs at Hiroshima and Nagasaki," p. 8.

[2]Hiroshima.

AIR WAR AND EMOTIONAL STRESS

Psychological Studies of Bombing and Civilian Defense

Irving L. Janis

The RAND Corporation

First Edition

NEW YORK • TORONTO • LONDON
McGRAW-HILL BOOK COMPANY, INC.
1951

CHAPTER 2
EMOTIONAL IMPACT OF THE A-BOMB

UNPREPAREDNESS OF THE POPULATION

At both Hiroshima and Nagasaki, disaster struck without warning. Whether intended so or not, an extraordinarily high degree of surprise was achieved by both A-bomb attacks. At the two target cities, prior to the bombing, there had been relatively little anxiety about the threat of heavy B-29 raids. When the planes carrying the A-bomb arrived over their targets, the population was almost completely unprepared. At the time, not even a light air raid was expected. People were caught at home, at work, out on the city streets, calmly going about their usual daily affairs.

When the first A-bomb was dropped, on August 6, 1945, very few residents of Hiroshima were inside air-raid shelters. An all-clear signal from a previous alert had sounded less than half an hour earlier and the normal routine of community life had resumed. Shortly after eight in the morning, when the explosion occurred, the working-class population was arriving at the factories and shops. Many workers were still out-of-doors en route to their jobs. The majority of school children, along with some adults from the suburbs, were also outside, hard at work building firebreaks as a defense against possible incendiary raids. Housewives, especially in middle-class families, were at home, preparing breakfast. Only a few minutes later, their flaming charcoal stoves were to create hundreds of local fires, adding to a general conflagration of such intensity that even if the assiduous labor of Hiroshima's school children had been completed, the fire storm still would have been beyond control.

At Nagasaki, three days later, the populace had heard only vague reports about the Hiroshima disaster. Here again, people were at

work in factories and offices, tending their homes, engaging in their normal daily activities. A few hours earlier a raid alert had been canceled; before the raid signal could be repeated, the bomb had already exploded. Only 400 people out of a population of close to a quarter of a million were inside the excellent tunnel shelters that could have protected some 75,000 people from severe injury or death.

It is generally recognized that the element of surprise was an important factor contributing to the unprecedented casualty rates at Hiroshima and Nagasaki. Many of those who were exposed to lethal gamma radiation, struck down by flying debris, or trapped in collapsed buildings would not have been killed if they had been warned in time to flee to the outskirts of the city or if they had been in adequate shelters. Thousands of people who were out-of-doors or standing in front of windows would have been protected from incapacitating flash burns if they had been under any sort of cover.[1]

Whether or not they suffered severe injury, those who survived the explosion were also affected by the element of surprise in quite another way. The absence of warning and the generally unprepared state of the population undoubtedly augmented the emotional effects of the disaster. "I was just utterly surprised and amazed and awed." This brief remark, by a newspaper reporter who was living in Nagasaki at the time of the disaster, epitomizes the way in which survivors described the terrifying events to which they were so suddenly exposed.

Of great importance in the predispositional set of the population is the fact that there was not a state of readiness to face danger or to cope with the harsh exigencies of a major catastrophe. The stage was well set for extreme emotional responses to dominate the action. It is against this background of psychological unpreparedness that the emotional impact resulting from the atomic disasters should be viewed.

---

[1] USSBS Report, *The Effects of Atomic Bombs on Hiroshima and Nagasaki*, U.S. Government Printing Office, Washington, D.C., 1946.

(US Strategic Bombing Survey, 1946 report "Effects of the Atomic Bombs on Hiroshima and Nagasaki", page 16)

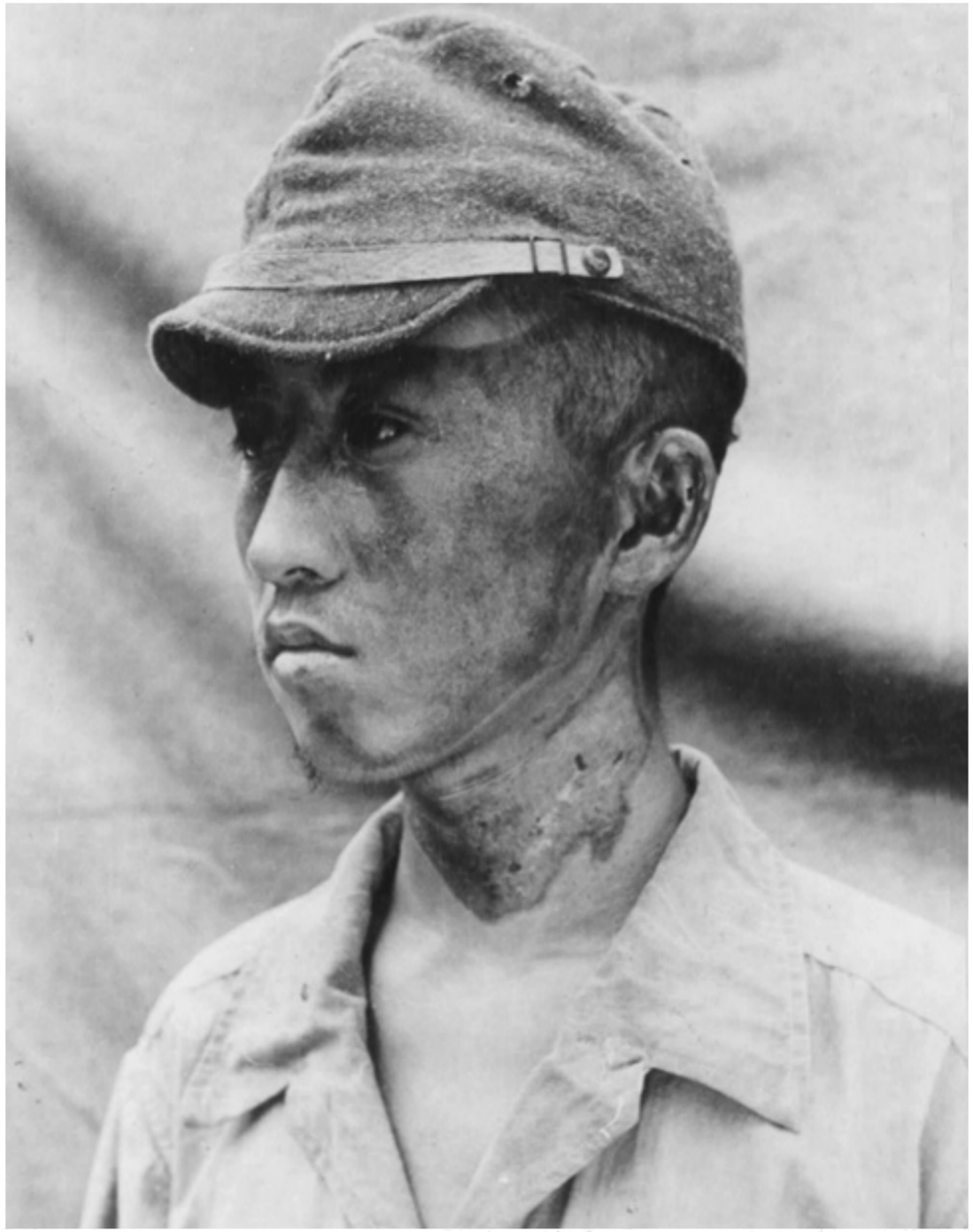

PROTECTION AGAINST RADIANT HEAT. *This patient (photographed by Japanese 2 October 1945) was about 6,500 feet from ground zero when the rays struck him from the left. His cap was sufficient to protect the top of his head against flash burns.*

HIROSHIMA

(Lethal 6.7 cal/sq cm, according to the 1979 US Office of Technology Assessment "Effects of Nuclear War")

The Effects of

Nuclear Weapons

SAMUEL GLASSTONE
Editor

Revised Edition
Reprinted February 1964

Prepared by the
UNITED STATES DEPARTMENT OF DEFENSE
Published by the
UNITED STATES ATOMIC ENERGY COMMISSION
April 1962

For sale by the Superintendent of Documents, U.S. Government Printing Office
Washington 25, D.C. - Price $3.00 (paper bound)

Foreword

This book is a revision of "The Effects of Nuclear Weapons" which was issued in 1957. It was prepared by the Defense Atomic Support Agency of the Department of Defense in coordination with other cognizant governmental agencies and was published by the U.S. Atomic Energy Commission. Although the complex nature of nuclear weapons effects does not always allow exact evaluation, the conclusions reached herein represent the combined judgment of a number of the most competent scientists working on the problem.

There is a need for widespread public understanding of the best information available on the effects of nuclear weapons. The purpose of this book is to present as accurately as possible, within the limits of national security, a comprehensive summary of this information.

Robert S. McNamara

Secretary of Defense

Glenn T. Seaborg

Chairman
Atomic Energy Commission

S. Glasstone, Effects of Nuclear Weapons, 1962:

Explosion yield	*Height of burst (feet)*	*Time after detonation (seconds)*	*Distance from ground zero (miles)*	*Height of stem (feet)*
20 kilotons	1, 760	3	0. 87	185
1 megaton	6, 500	11	3. 2	680

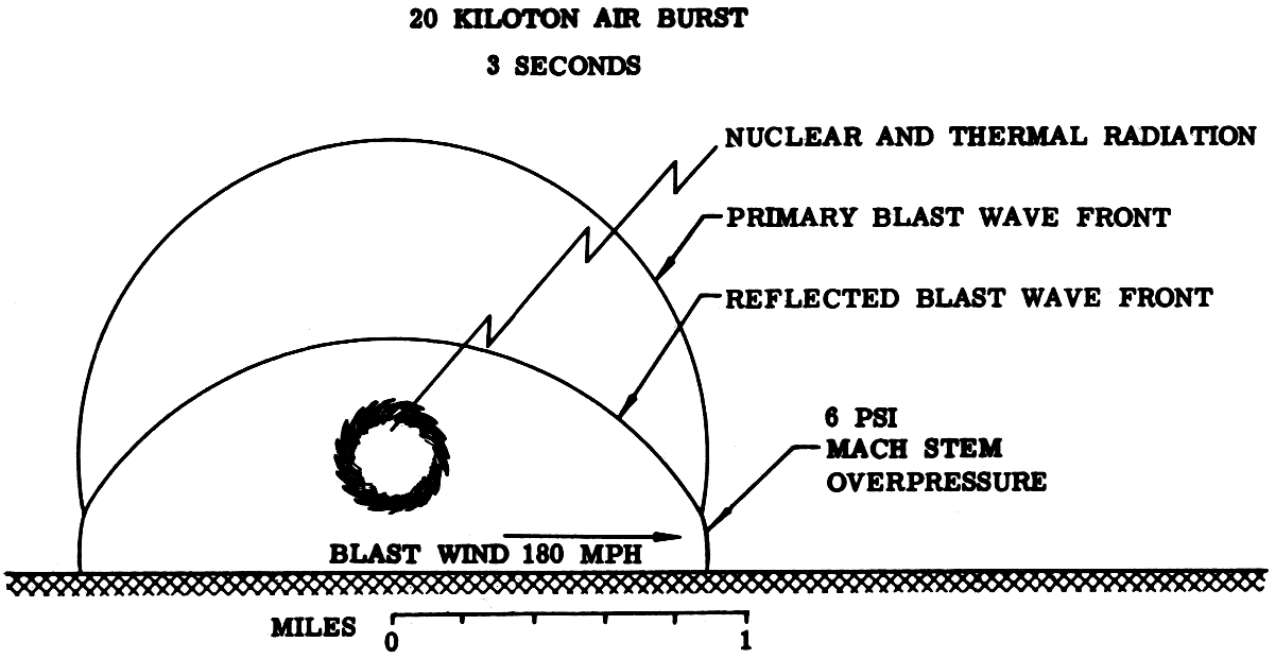

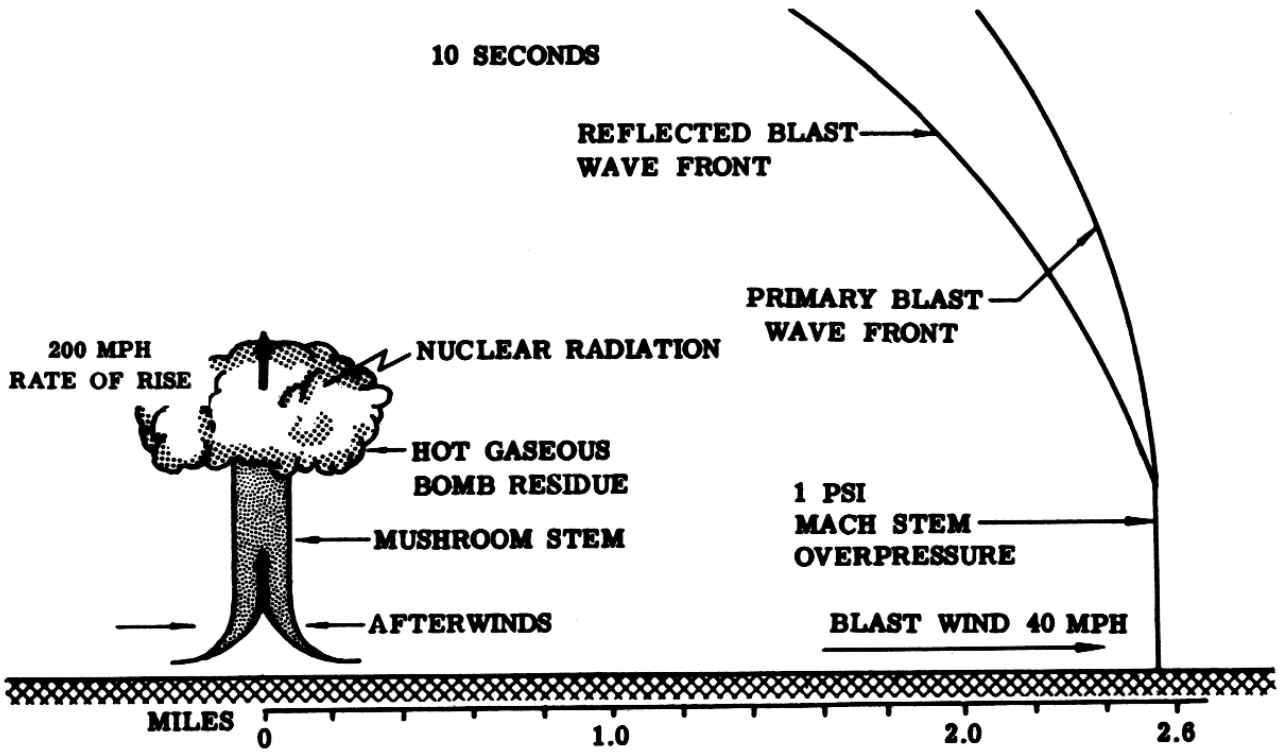

At 10 seconds after a 20-kiloton explosion at an altitude of 1,760 feet the Mach front is over 2½ miles from ground zero, and 37 seconds after a 1-megaton detonation at 6,500 feet, it is nearly 9½ miles from ground zero. The overpressure at the front is roughly 1 pound per square inch, in both cases, and the wind velocity behind the front is 40 miles per hour.

12.11 In Japan, where little evasive action was taken, the survival probability depended upon whether the individual was outdoors or inside a building and, in the latter case, upon the type of structure. At distances between 0.3 and 0.4 mile (530 and 700 yards) from ground zero in Hiroshima the average survival rate, for at least 20 days after the nuclear explosion, was less than 20 percent. Yet in two reinforced-concrete office buildings, at these distances, almost 90 percent of the nearly 800 occupants survived more than 20 days, although some died later from radiation injury.

These facts bring out clearly the greatly improved chances of survival from a nuclear explosion that could result from the adoption of suitable warning and protective measures.

TABLE 12.29—ARRIVAL TIME FOR PEAK OVERPRESSURE

Distance (miles)	*Explosion yield*				
	1 KT	*10 KT*	*100 KT*	*1 MT*	*10 MT*
	(Time in seconds)				
1	4. 3	3. 6	3. 7	2. 5	1. 5
2	9	8. 1	7. 4	6. 5	5. 0

12.35. The major part of the thermal radiation travels in straight lines, and so any opaque object interposed between the fireball and the exposed skin will give some protection. This is true even if the object is subsequently destroyed by the blast, since the main thermal radiation pulse is over before the arrival of the blast wave.

12.36 At the first indication of a nuclear explosion, by a sudden increase in the general illumination, a person inside a building should immediately fall prone, as described in § 12.30, and, if possible, crawl behind or beneath a table or desk or to a planned vantage point.

12. 72 Because of its particulate nature, fallout will tend to collect on horizontal surfaces, e.g., roofs, streets, tops of vehicles, and the ground. In the preliminary decontamination, therefore, the main effort should be directed toward cleaning such surfaces. The simplest way of achieving this is by water washing, if an adequate supply of water is available. The addition of a commercial wetting agent (detergent) will make the washing more efficient. The radioactive material is thus tranferred to storm sewers where it is less of a hazard.

Nevada in 1953.
12 calories per square centimeter

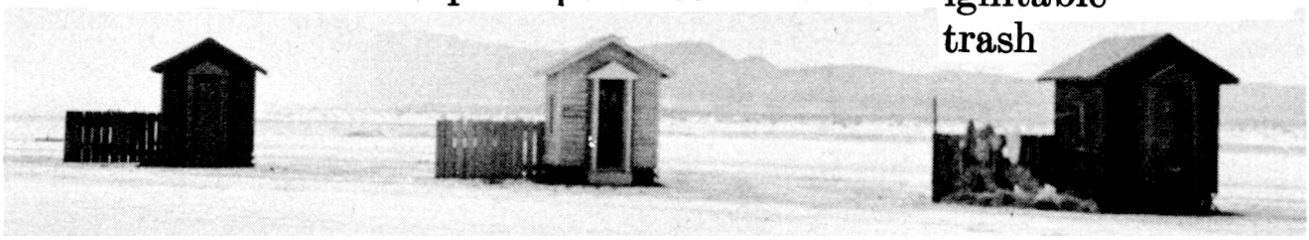

before exposure to a nuclear explosion

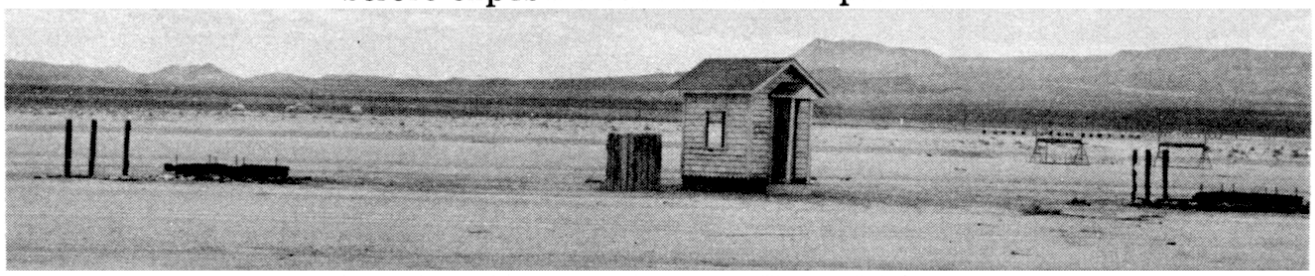

after exposure to a nuclear explosion

7.59 The value of fire-resistive furnishing in decreasing the number of ignition points was also demonstrated in the tests. Two identical, sturdily constructed houses, each having a window 4 feet by 6 feet facing the point of burst, were erected where the thermal radiation exposure was 17 calories per square centimeter. One of the houses contained rayon drapery, cotton rugs, and clothing, and, as was expected, it burst into flame immediately after the explosion and burned completely. In the other house, the draperies were of vinyl plastic, and rugs and clothing were made of wool. Although much ignition occurred, the recovery party, entering an hour after the explosion, was able to extinguish the fires.

7.76 It should be noted that the fire storm is by no means a special characteristic of nuclear weapons. Similar fire storms have been reported as accompanying large forest fires in the United States, and especially after incendiary bomb attacks in both Germany and Japan during World War II. The high winds are produced largely by the updraft of the heated air over an extensive burning area. They are thus the equivalent, on a very large scale, of the draft of a chimney under which a fire is burning. Because of limited experience, the conditions for the development of fire storms in cities are not well known. It appears, however, that some, although not necessarily all, of the essential requirements are the following: (1) thousands of nearly simultaneous ignitions over an area of at least a square mile, (2) heavy building density, e.g., more than 20 percent of the area is covered by buildings, and (3) little or no ground wind. Based on these criteria, only certain sections—usually the older and slum areas—of a very few cities in the United States would be susceptible to fire storm development.

Weapon test report WT-775, Project 8.11b, ENCORE nuclear test, Nevada, 1953:

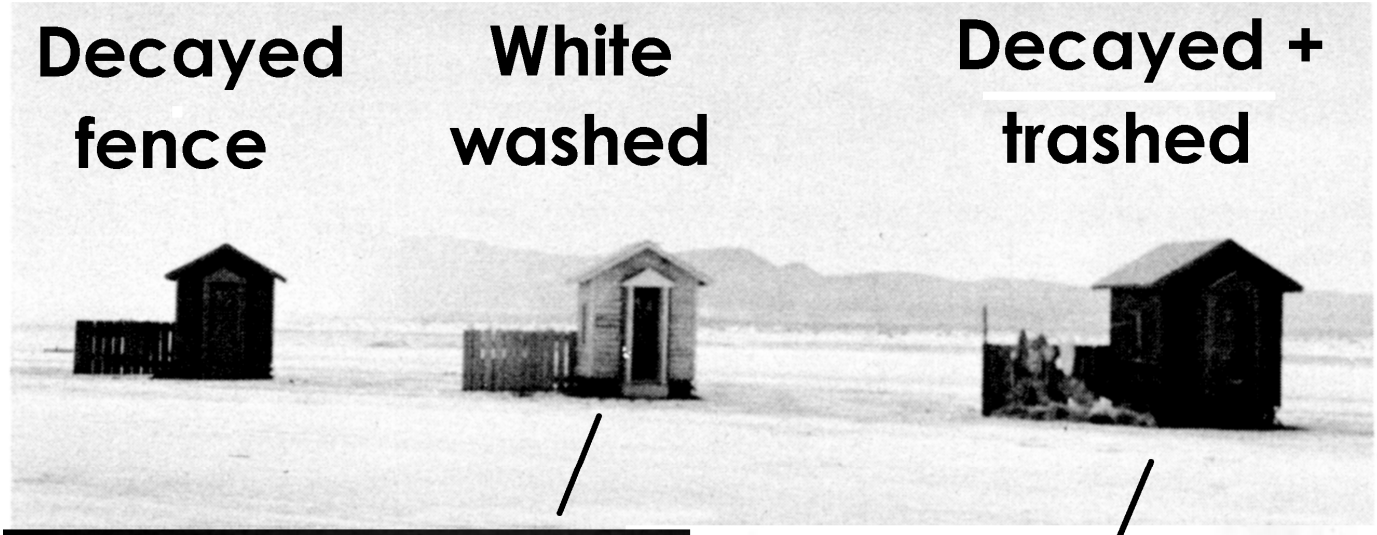

No trash kindling

Trash kindling for fire

6' x 6' wood frame houses

CONFIDENTIAL

WT-774

Copy No. 188 A

Operation UPSHOT-KNOTHOLE

NEVADA PROVING GROUNDS

March - June 1953

Project 8.11a

INCENDIARY EFFECTS ON BUILDING AND INTERIOR KINDLING FUELS

(ENCORE EFFECT REPORT)

27 kt at 2,423 feet altitude, 19% humidity

(DASA-1251) (Note: cities humidity is ~50-80%)

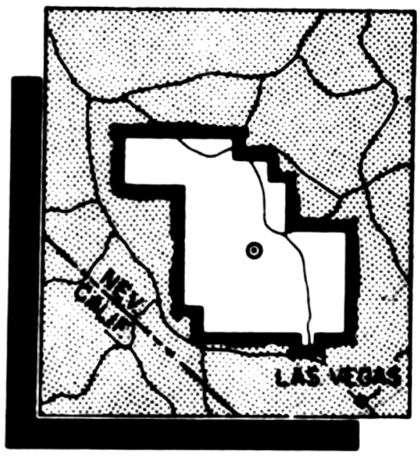

RESTRICTED DATA

This document contains restricted data as defined in the Atomic Energy Act of 1946. Its transmittal or the disclosure of its contents in any manner to an unauthorized person is prohibited.

HEADQUARTERS FIELD COMMAND, ARMED FORCES SPECIAL WEAPONS PROJECT
SANDIA BASE, ALBUQUERQUE, NEW MEXICO

CONFIDENTIAL

Weapon test report WT-774, Project 8.11a, Incendiary effects on buildings and interior kindling fuels

ENCORE test, Nevada, 1953
10' x 12' wooden houses with 4' x 6' windows
17 calories/sq. cm thermal flash

Immediate room flashover during thermal pulse ("Encore effect") in inflammables-filled house while fire-resistant fabrics in other house survived!

LEFT HOUSE: fire-resistant furnishings (woolen rugs and clothes, vinyl plastic draperies)

RIGHT HOUSE: non-fire resistant furnishings plus inflammable magazines and newspapers

Smouldering armchair extinguished 1 hour after detonation, when recovery party arrived at house

---

-17-

We have all had the frustrating experience of trying to light a fire with green, moist, or wet wood. Just as wet wood can't be easily induced to burn, so thick combustibles are not easily ignited. Even a dry two-by-four burns reluctantly and stops burning when taken out of the fire. It is a different matter with a shingle or a bunch of kindling! Density also plays a role, a heavier combustible being harder to ignite than lighter-weight material. Of course, the chemistry of the material to the degree that it influences kindling temperatures and flammability, is an important parameter. Modern plastics tend to smoke and boil - to ablate but not to ignite in sustained burning - while paper trash burns readily.

Just as most materials are not particularly sensitive to the sun's thermal radiation, and are not highly inflammable nor even ignitible, the surfaces exposed to the thermal intensity of a nuclear explosion are generally not given to sustained burning. Very intense heat loads may mar or melt surfaces, may char and burn surfaces while the heat is on, but may snuff out immediately afterward.

-18-

PRIMARY AND SECONDARY FIRES FROM NUCLEAR EXPLOSIONS

Although thermal radiation would start many fires in urban and in most suburban areas, such fires by themselves would seldom constitute a source of major destruction. Outside the region of extensive blast damage, fires in trash piles, in dry palm trunks, in roof shingles, in auto and household upholstery, drapes, or flammable stores are normally accessible and readily controllable. By the very fact that these fires start from material exposed to the incident light, they can be easily spotted and, in the absence of other distractions, can be quickly extinguished. Where the blast effects are severe and damage extensive, little effective fire fighting is likely.

HUMIDITY HAS LESS INFLUENCE ON FINE KINDLING IGNITION ENERGY THAN ON WOOD IGNITION

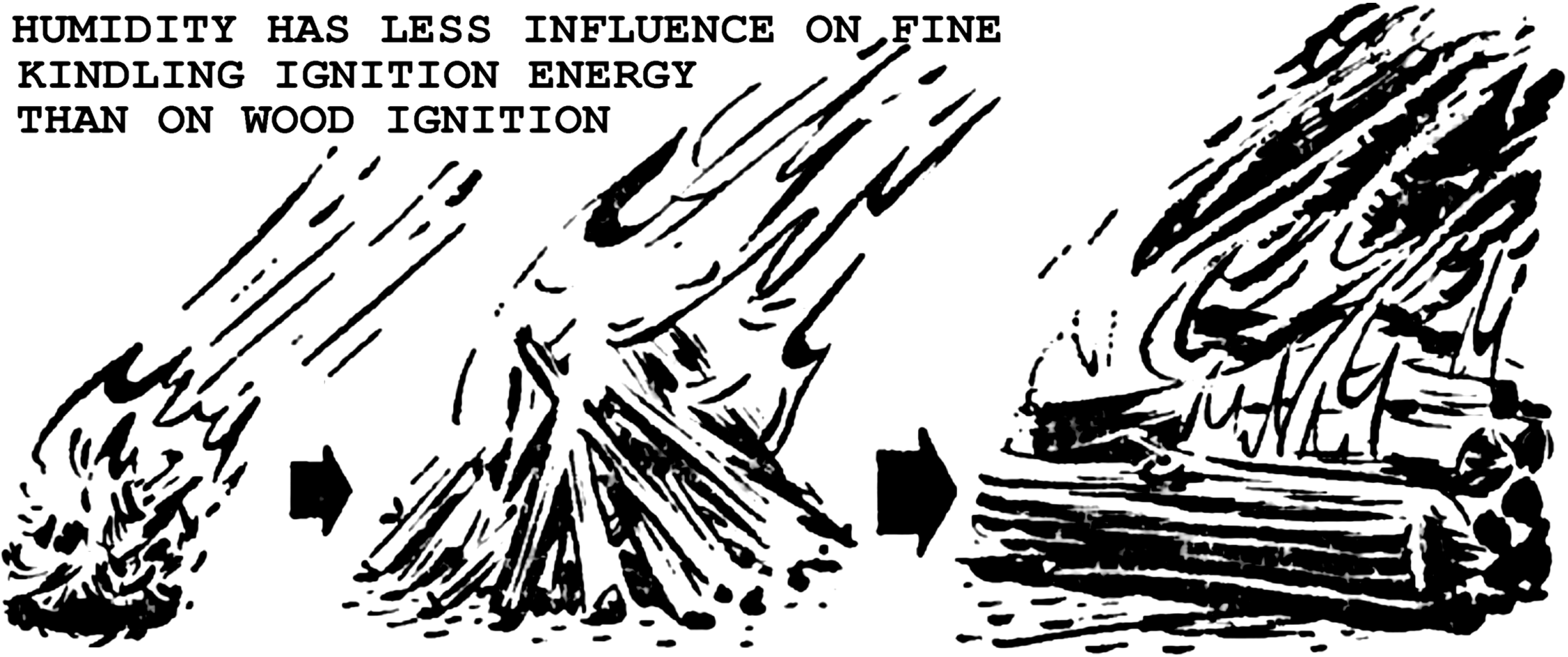

THERMAL PULSE DRIES LEAVES/PAPER

THERMAL PULSE CANNOT PENETRATE 1 MM OF WOOD

THERMAL PULSE IS TOO BRIEF TO DRY OUT WOOD

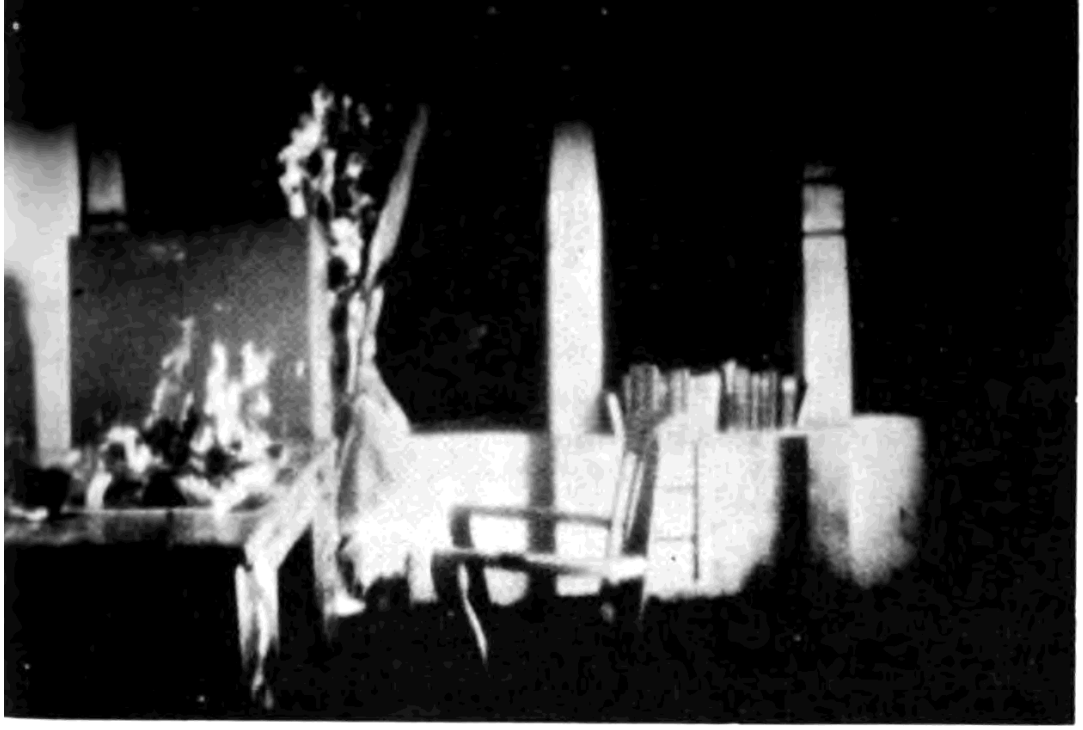

EFFECTS OF 1 PSI OVERPRESSURE ON IGNITIONS

From: Goodale, Effects of Air Blast on Urban Fires
URS 7009–14 Dec. 1970
(AD 723 429)

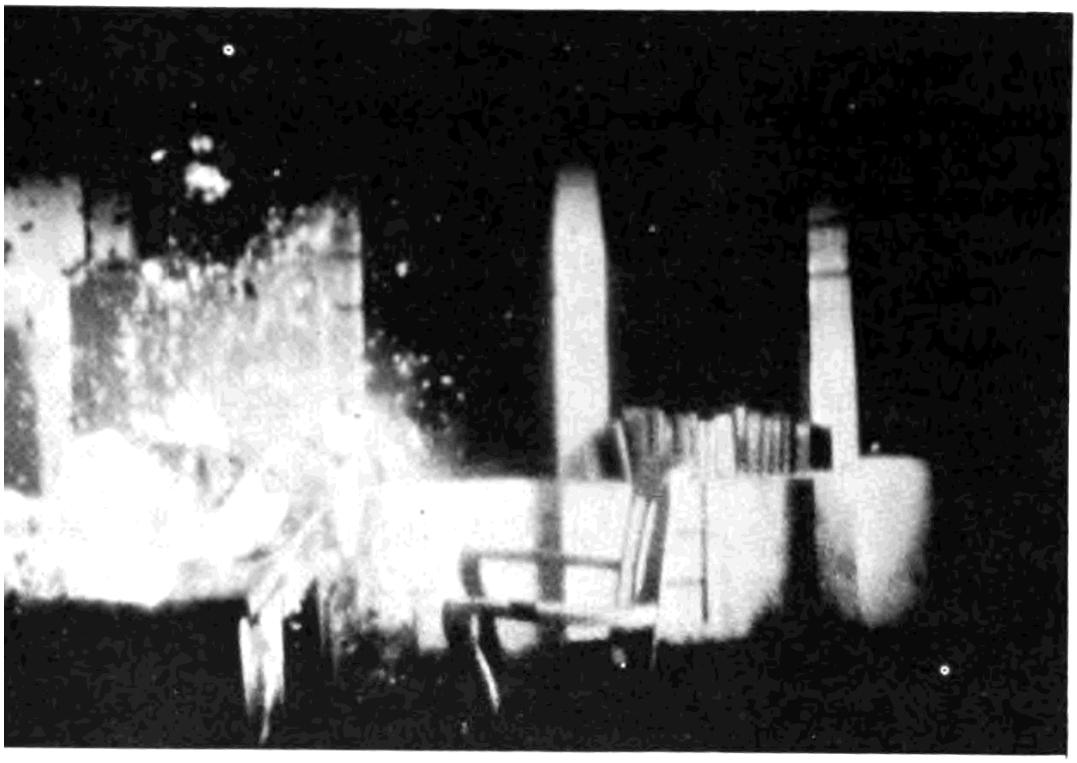

Blast winds both cool burning material and upset flame convection system.

50% of burning curtains are extinguished by 1 psi overpressure

100% are put out by 2.5 psi. Note that burning LIQUIDS in high-wall trays are not put out by blast waves, but this is not relevant to city fires.

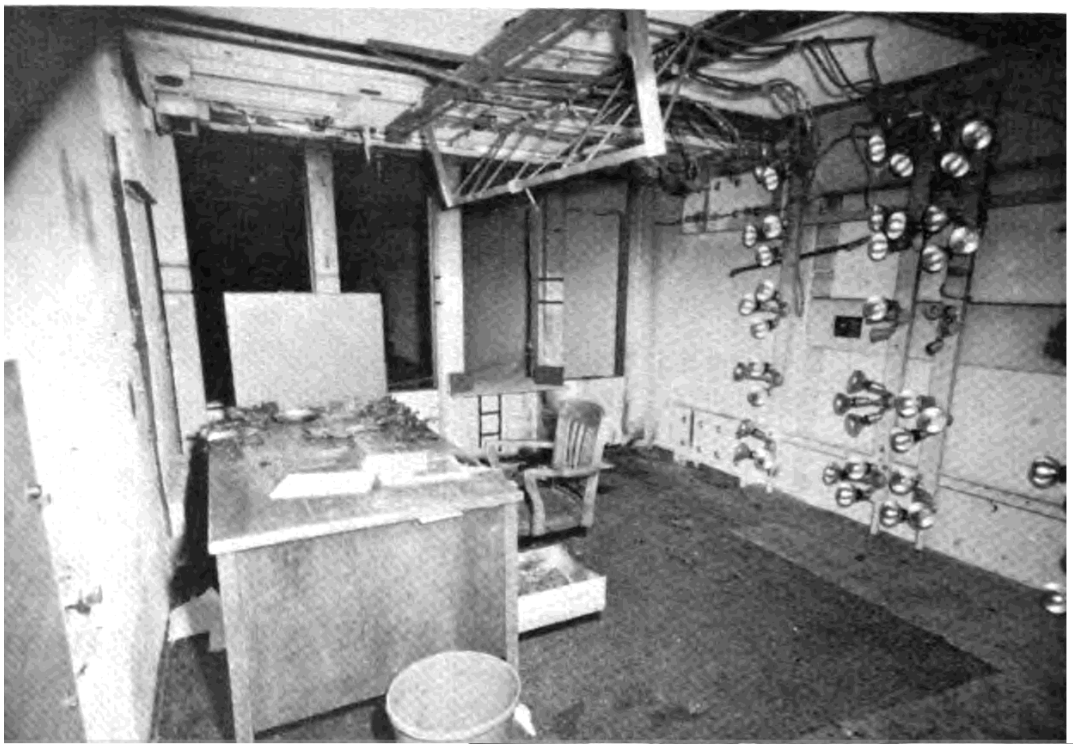

Burning beds can continue to smoulder until extinguished with water.

Operation SAILOR HAT, 0.5 kt shot CHARLIE, at Kahoolawe island, Hawaii, on 16 April 1965. The displacement effects to a standing observer at a peak overpressure of 6 psi (41 kPa) were simulated by using a realistic (fully articulated) dummy.

Operation Snowball, station 10SB, comparison of human dummy with standing goat (proxy)

peak velocity of initially standing 165 lb dummy = 33.7 ft/sec with 20 ft total displacement

(A U.K. dummy lying prone at 9 psi peak overpressure was unmoved in this test)

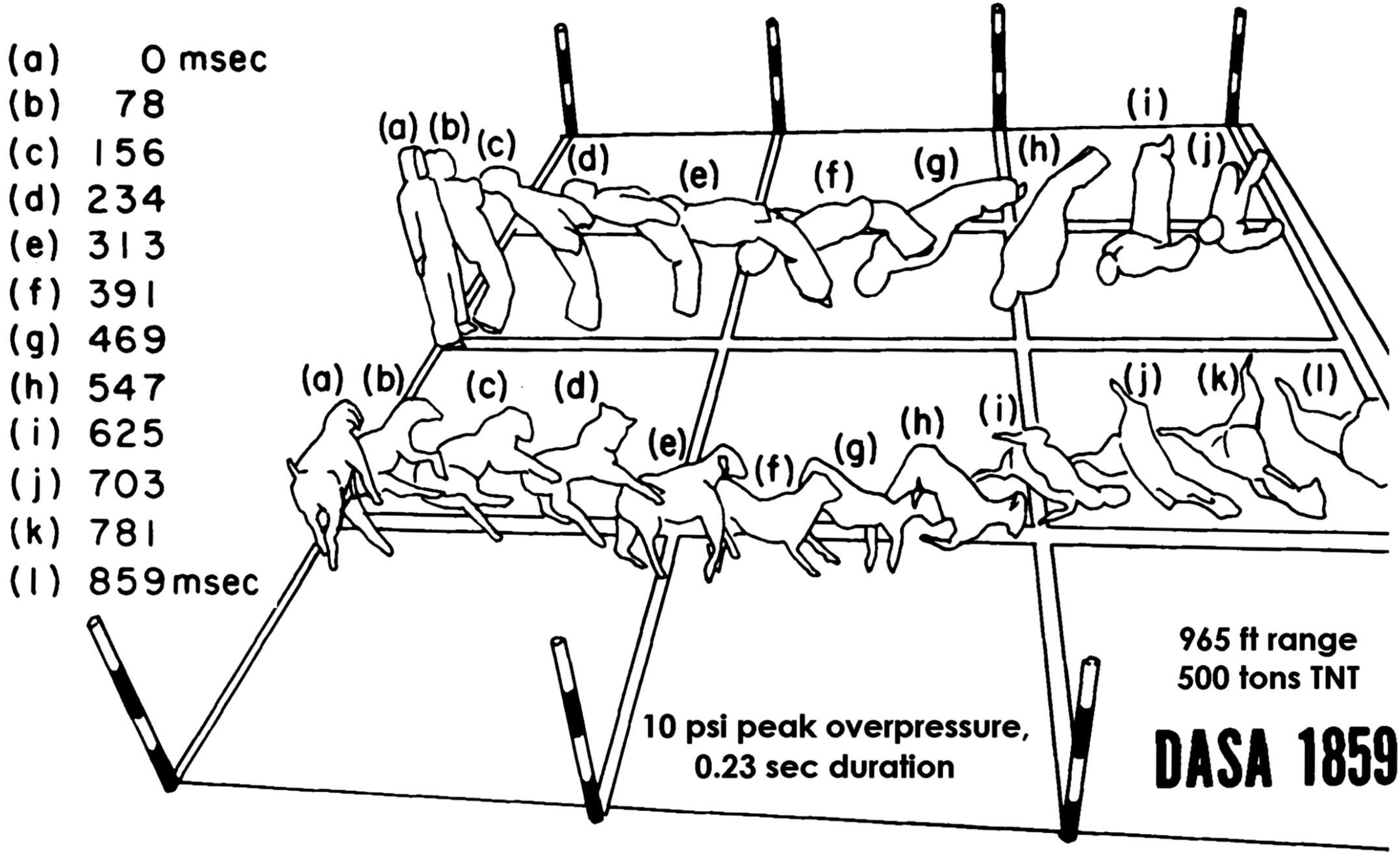

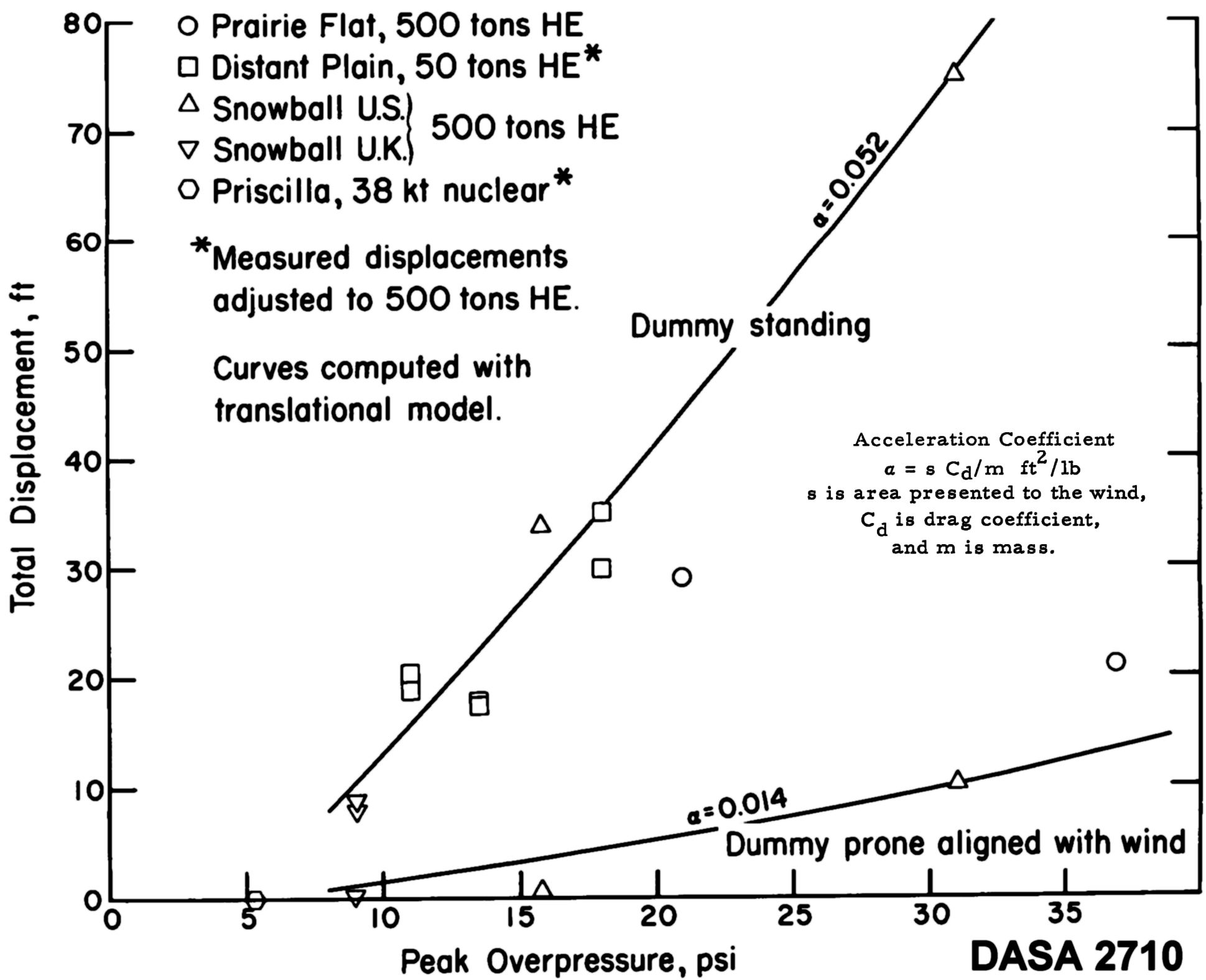
Prairie Flat, 500 tons HE
Distant Plain, 50 tons HE*
Snowball U.S.
Snowball U.K.
500 tons HE
Priscilla, 38 kt nuclear*
*Measured displacements adjusted to 500 tons HE.
Curves computed with translational model.
Dummy standing
a=0.052
Acceleration Coefficient
a = s Cd/m ft2/lb
s is area presented to the wind,
Cd is drag coefficient,
and m is mass.
a=0.014
Dummy prone aligned with wind
Total Displacement, ft
Peak Overpressure, psi
0
10
20
30
40
50
60
70
80
5
15
25
35

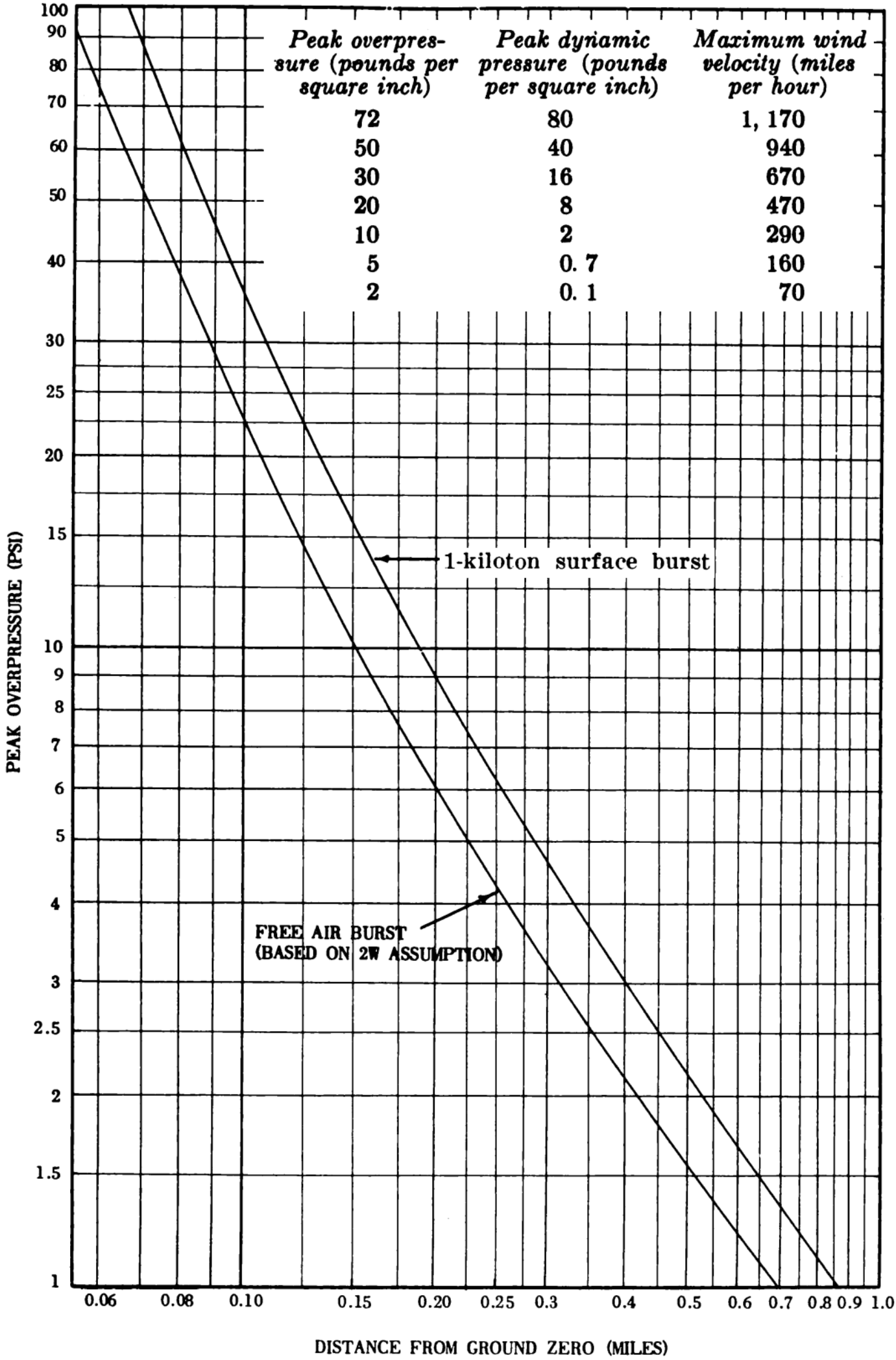

Scaling. For yields other than 1 KT, the range to which a given overpressure extends scales as the cube root of the yield

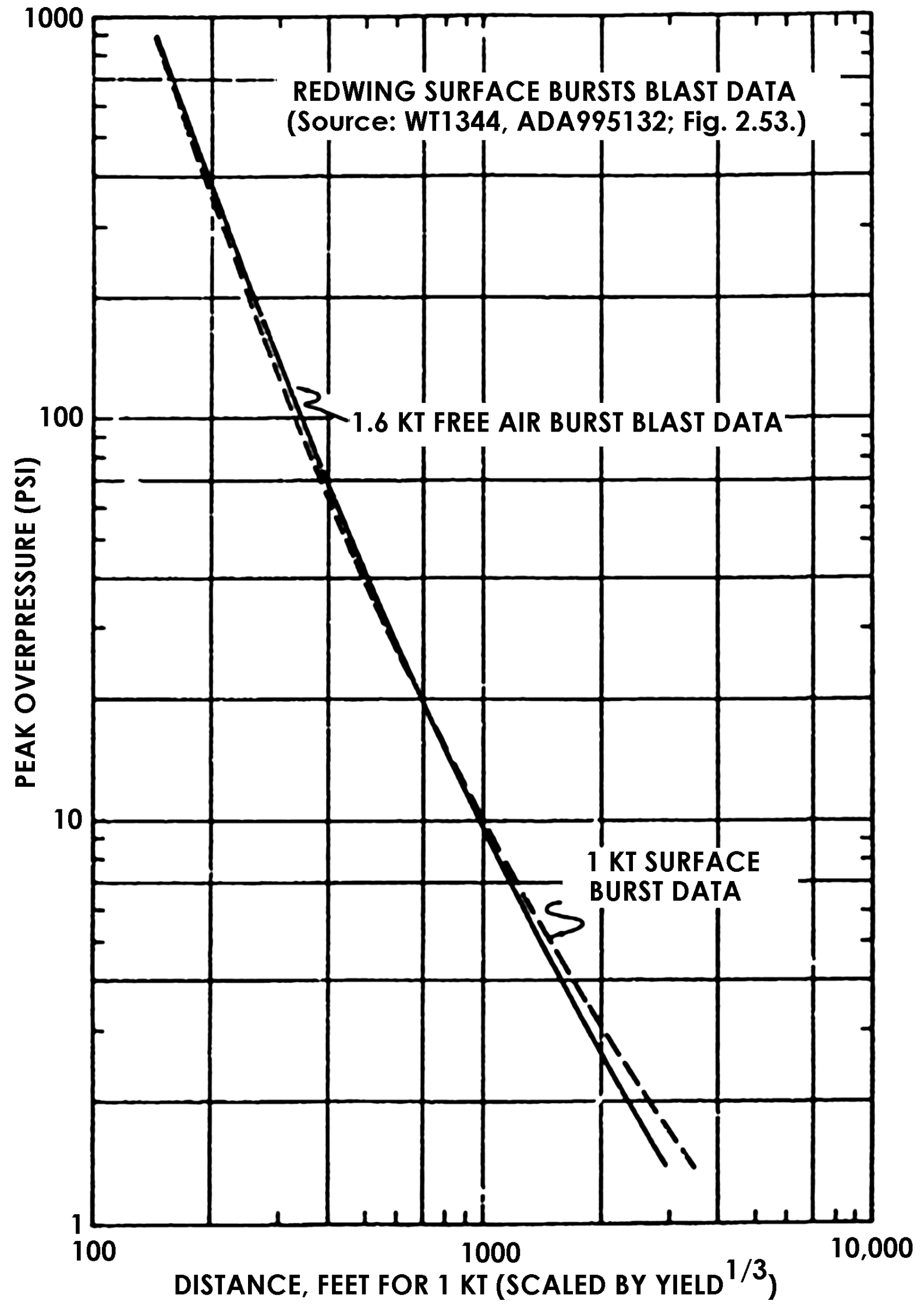
REDWING SURFACE BURSTS BLAST DATA
(Source: WT1344, ADA995132; Fig. 2.53.)
1.6 KT FREE AIR BURST BLAST DATA
1 KT SURFACE
BURST DATA
PEAK OVERPRESSURE (PSI)
1000
100
10
1
100
1000
10,000
DISTANCE, FEET FOR 1 KT (SCALED BY YIELD$^{1/3}$)

WT-1469
and
DASA-1777
AD638342

TEST (BOTH ON 700 FT TOWERS)	37 KT PRISCILLA	44 KT SMOKY	
GROUND RANGE	5320 FT	3406 FT	
Static pressure	5.3 psi	6.6 psi	PRECURSOR
Dynamic pressure	0.7 psi	15.8 psi	
	Movement		
Prone dummy	0	124 ft	PRECURSOR
Upright dummy	21.9 ft	255.7 ft	
	Velocity		
Prone dummy	0		
Upright dummy	21.4 ft/sec max. at 0.45 sec		

Prone dummy after 37 KT PRISCILLA

Upright dummy after 37 KT PRISCILLA

165 lb dummy lying prone at 5.3 psi overpressure from Priscilla was unmoved, but standing dummy was translated 13 ft in air and then rolled for 9 ft.

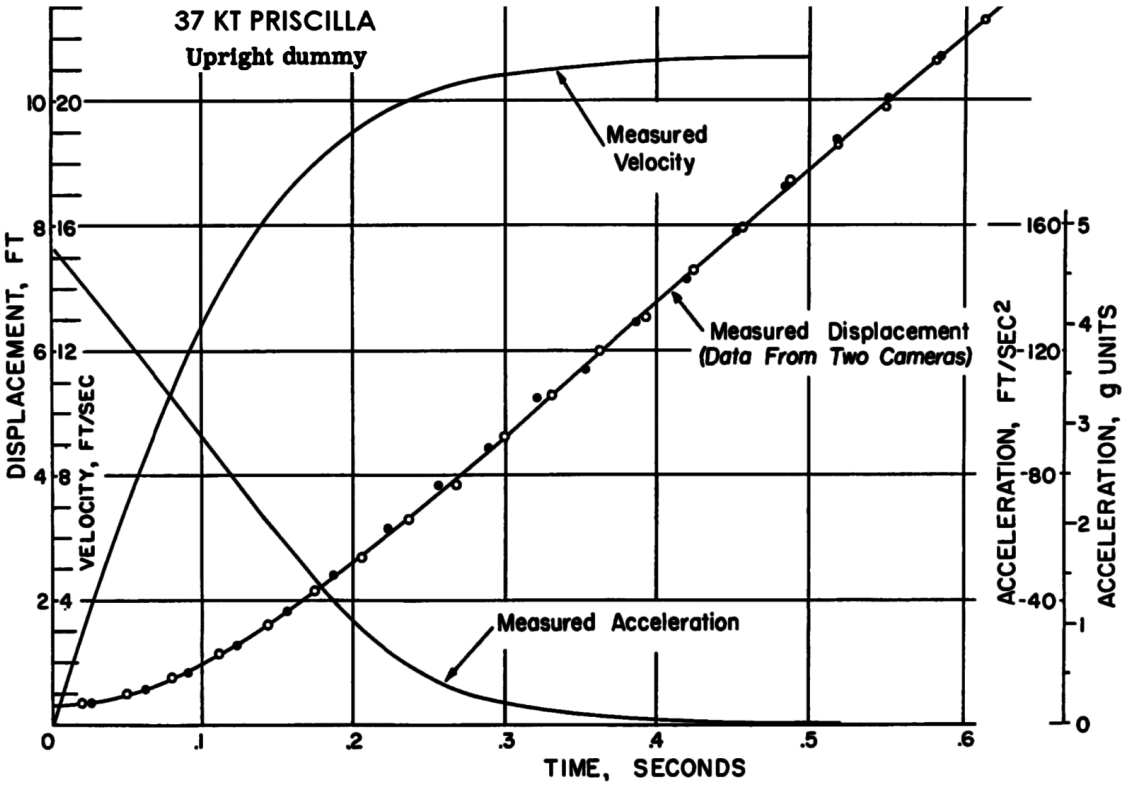

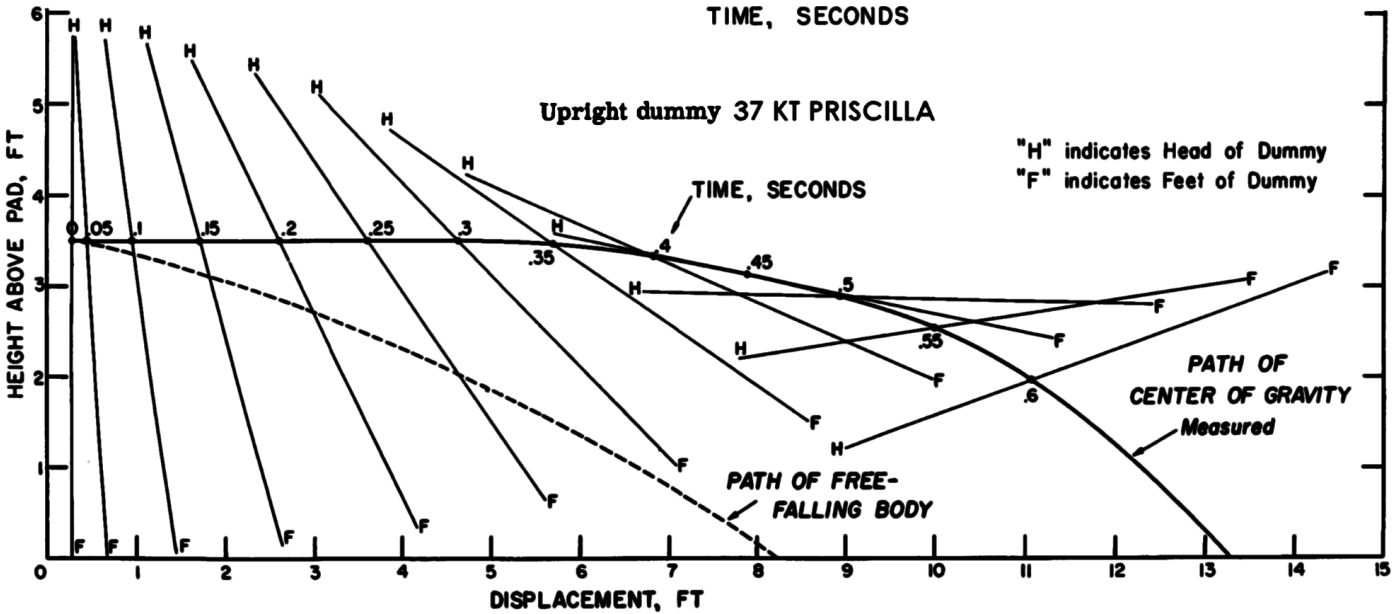

WT-1454

SMOKY 1957 PRECURSOR BLAST WAVEFORM

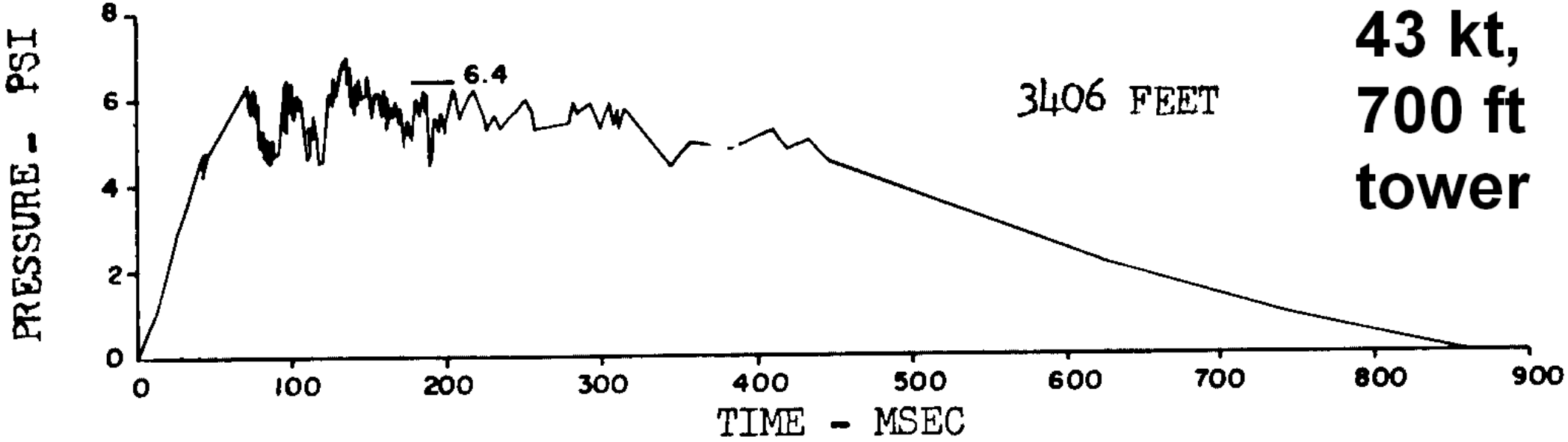

43 kt, 700 ft tower

Fig. 3.109—Blast-line pressure-time; self-recording pressure gauge records.

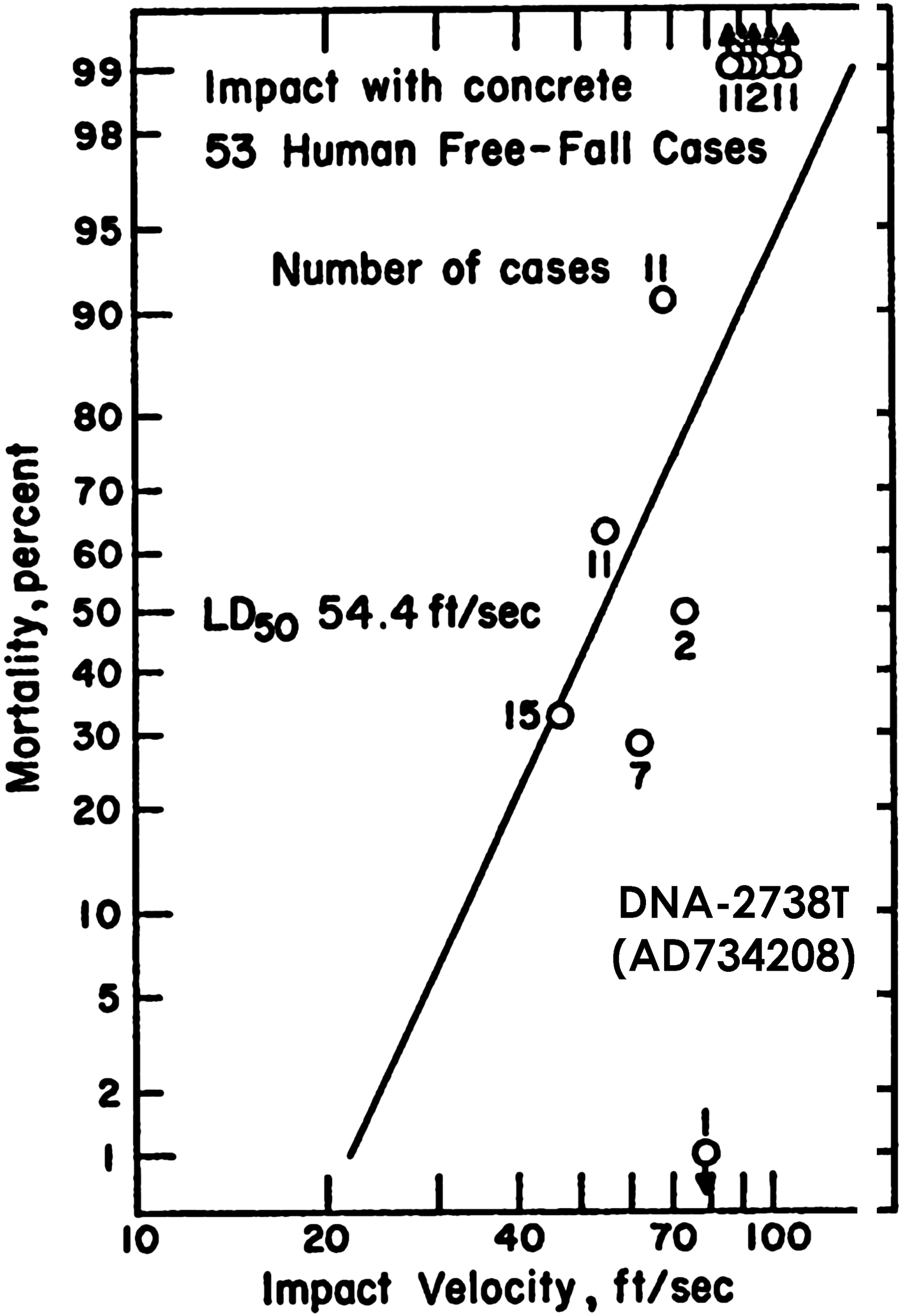
Impact with concrete
53 Human Free-Fall Cases
Number of cases
LD50 54.4 ft/sec
DNA-2738T
(AD734208)
Mortality, percent
Impact Velocity, ft/sec
99
98
95
90
80
70
60
50
40
30
20
10
5
2
1
10
20
40
70
100

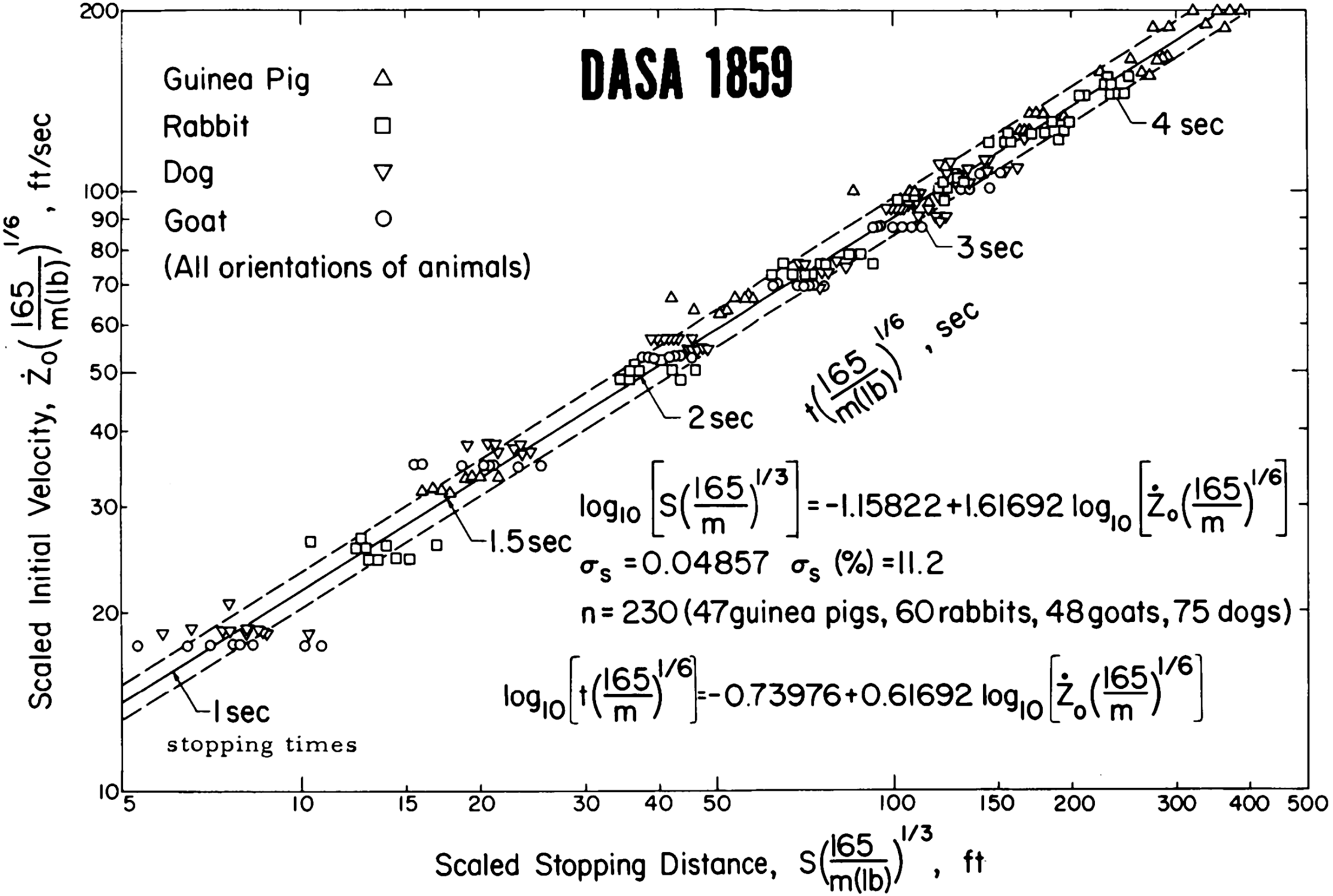
DASA 1859
Guinea Pig
Rabbit
Dog
Goat
(All orientations of animals)
4 sec
3 sec
2 sec
1.5 sec
1 sec
stopping times
$t\left(\frac{165}{m(lb)}\right)^{1/6}$, sec
$\log_{10}\left[S\left(\frac{165}{m}\right)^{1/3}\right] = -1.15822 + 1.61692 \log_{10}\left[\dot{Z}_o\left(\frac{165}{m}\right)^{1/6}\right]$
$\sigma_s = 0.04857$ σ_s (%) = 11.2
n = 230 (47 guinea pigs, 60 rabbits, 48 goats, 75 dogs)
$\log_{10}\left[t\left(\frac{165}{m}\right)^{1/6}\right] = -0.73976 + 0.61692 \log_{10}\left[\dot{Z}_o\left(\frac{165}{m}\right)^{1/6}\right]$
Scaled Initial Velocity, $\dot{Z}_o\left(\frac{165}{m(lb)}\right)^{1/6}$, ft/sec
Scaled Stopping Distance, $S\left(\frac{165}{m(lb)}\right)^{1/3}$, ft
200
100
90
80
70
60
50
40
30
20
10
5
10
15
20
30
40
50
100
150
200
300
400
500

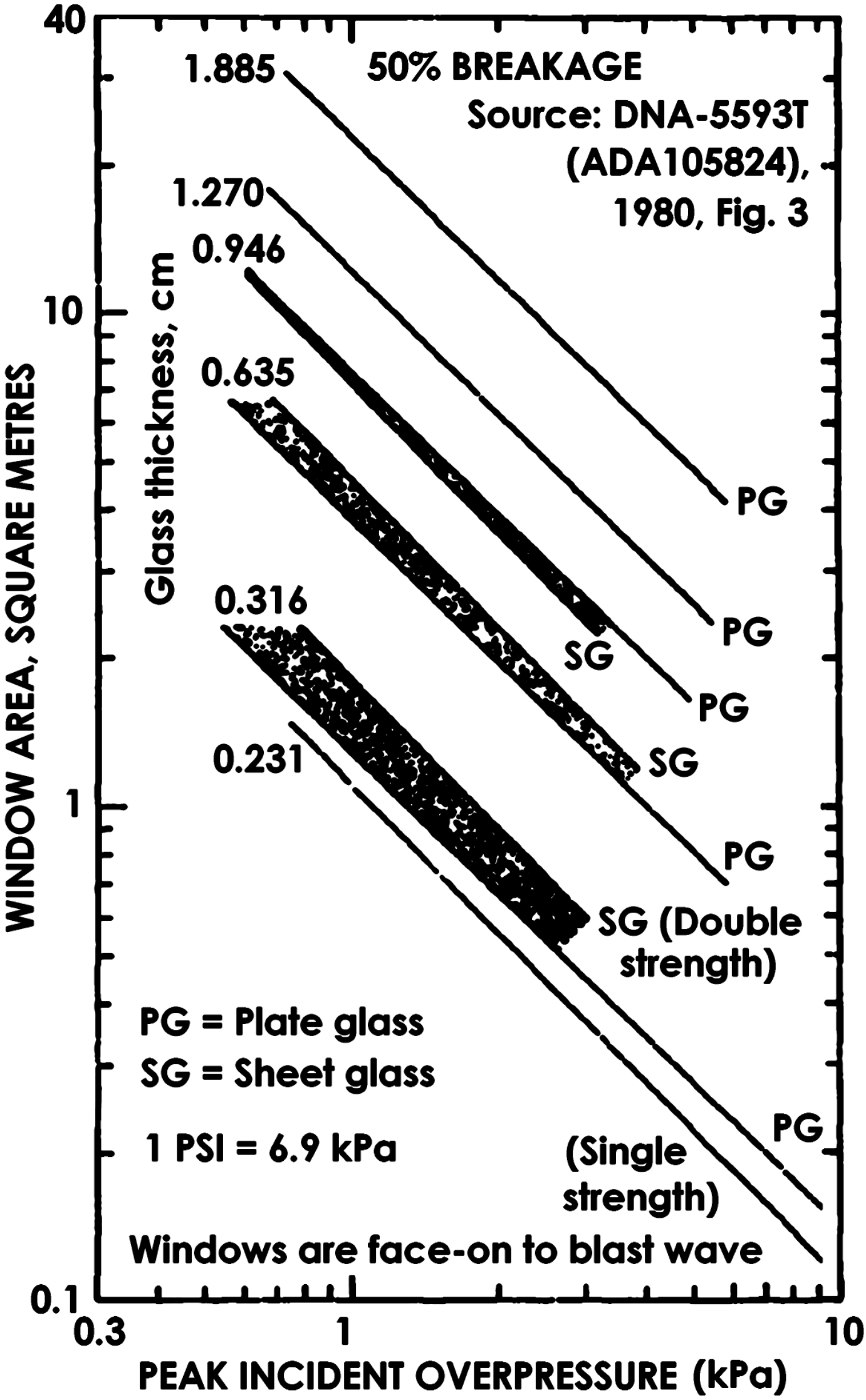
50% BREAKAGE
Source: DNA-5593T (ADA105824), 1980, Fig. 3
1.885
1.270
0.946
0.635
0.316
0.231
Glass thickness, cm
PG
PG
PG
SG
SG
PG
SG (Double strength)
PG
(Single strength)
PG = Plate glass
SG = Sheet glass
1 PSI = 6.9 kPa
Windows are face-on to blast wave
WINDOW AREA, SQUARE METRES
PEAK INCIDENT OVERPRESSURE (kPa)
40
10
1
0.1
0.3
1
10

AECU-3350

UNITED STATES ATOMIC ENERGY COMMISSION

BIOLOGICAL EFFECTS OF BLAST FROM BOMBS. GLASS FRAGMENTS AS PENETRATING MISSILES AND SOME OF THE BIOLOGICAL IMPLICATIONS OF GLASS FRAGMENTED BY ATOMIC EXPLOSIONS

By
I. Gerald Bowen
Donald R. Richmond
Mead B. Wetherbe
Clayton S. White

Table 5.1 Statistical Parameters and Predicted Penetration Data for Missiles from Traps at Various Ranges from Ground Zero

30 kt TEAPOT-APPLE 2 nuclear test, 1955

Distance from Ground Zero, ft	4,700	5,500	10,500
Maximum overpressure, psi	5.0	3.8	1.9
Number of traps	6	2	5
Total number of glass missiles	2129	320	37
Geometric mean missiles mass, gms	0.133	0.580	1.25
Standard geometric deviation in mass	3.01	3.47	3.35
Geometric mean missile velocity, ft/sec	170	168	103
Standard geometric deviation in velocity	1.27	1.25	1.25
Per cent of total missiles expected to penetrate	3.9*	12.8*	0.4*
Average number of missiles per sq ft	100.9	45.5	2.1
Missiles per sq ft expected to penetrate	3.9*	5.3*	0.006*

*Computed from individual evaluation of each missile

AD A105824

DNA 5593T

GLASS FRAGMENT HAZARD FROM WINDOWS BROKEN BY AIRBLAST

E. Royce Fletcher

Flying glass injured to 3.2 km in Hiroshima, 3.8 km in Nagasaki. 3.2 mm thick window glass fragments striking walls 2.1 m behind the windows in nuclear and high explosive tests gave:

10 fragments/m^2 for 6.3 kPa (0.9 psi) overpressure
100 fragments/m^2 for 29 kPa (4.2 psi) overpressure
1,000 fragments/m^2 for 65 kPa (9.4 psi) overpressure

Figure 10

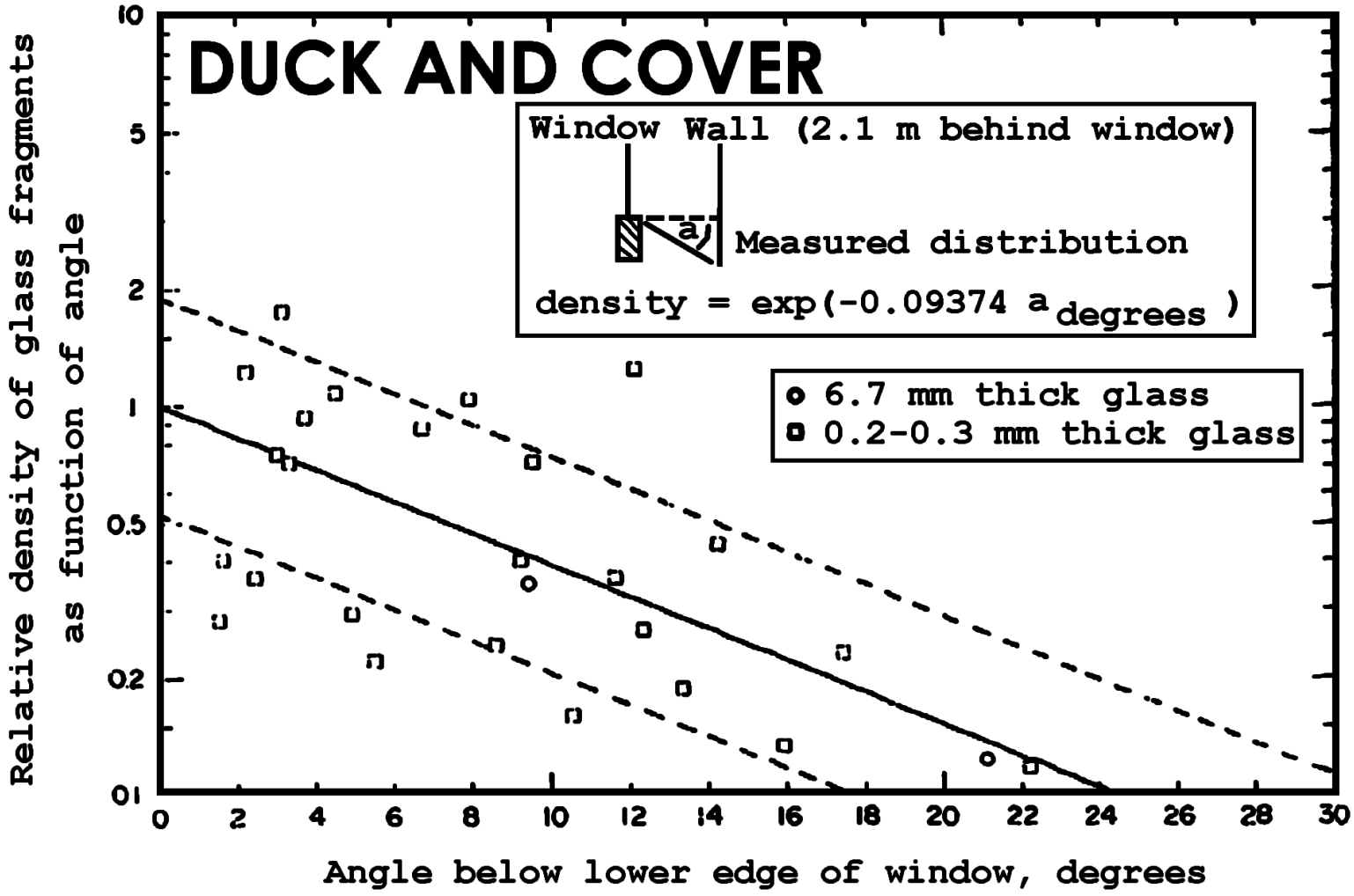

Glass-fragment injuries

Figure 17.

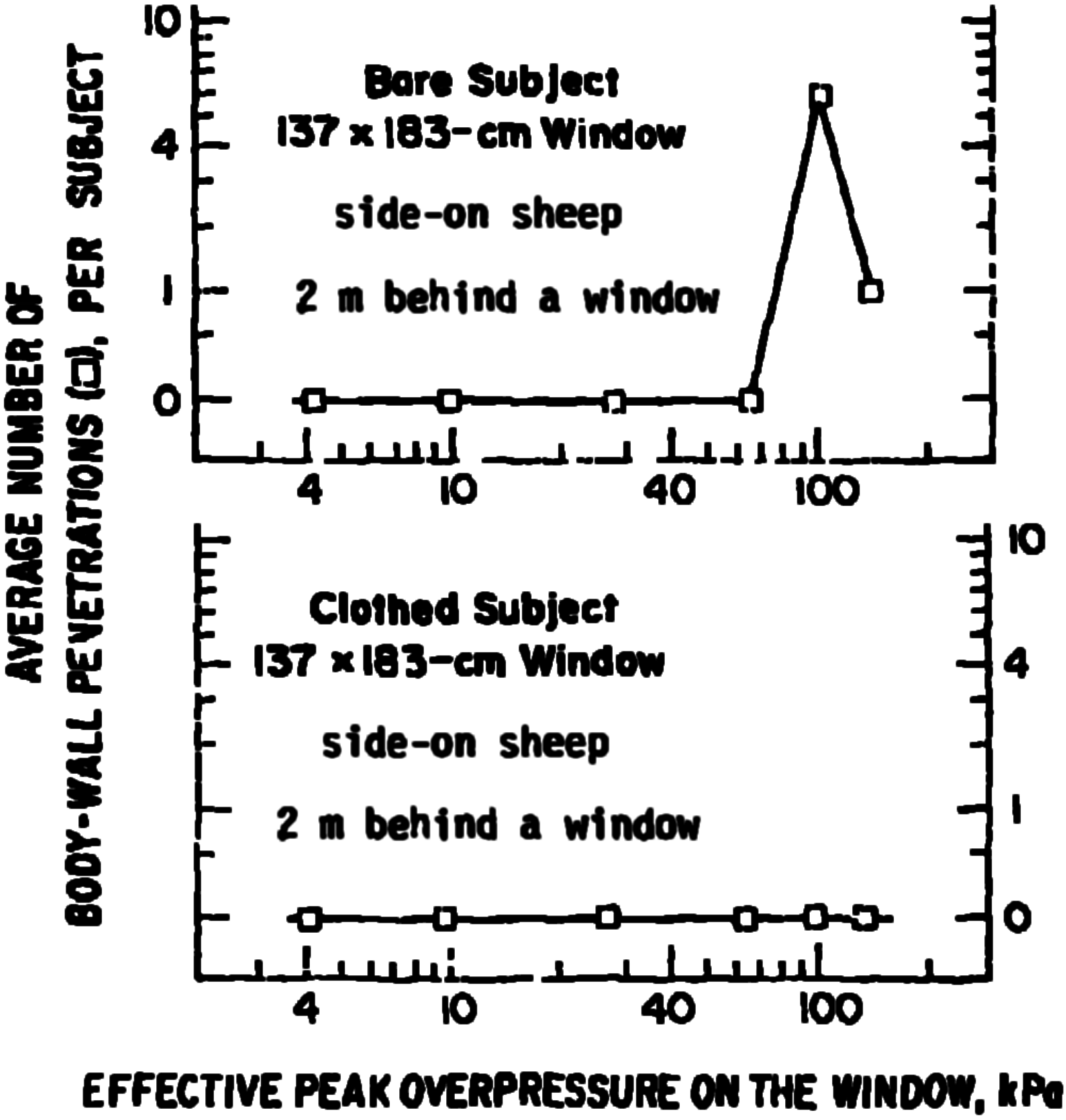

all-cotton tee shirt (145 gm/m^2)

cotton-sateen material (285 gm/m^2)

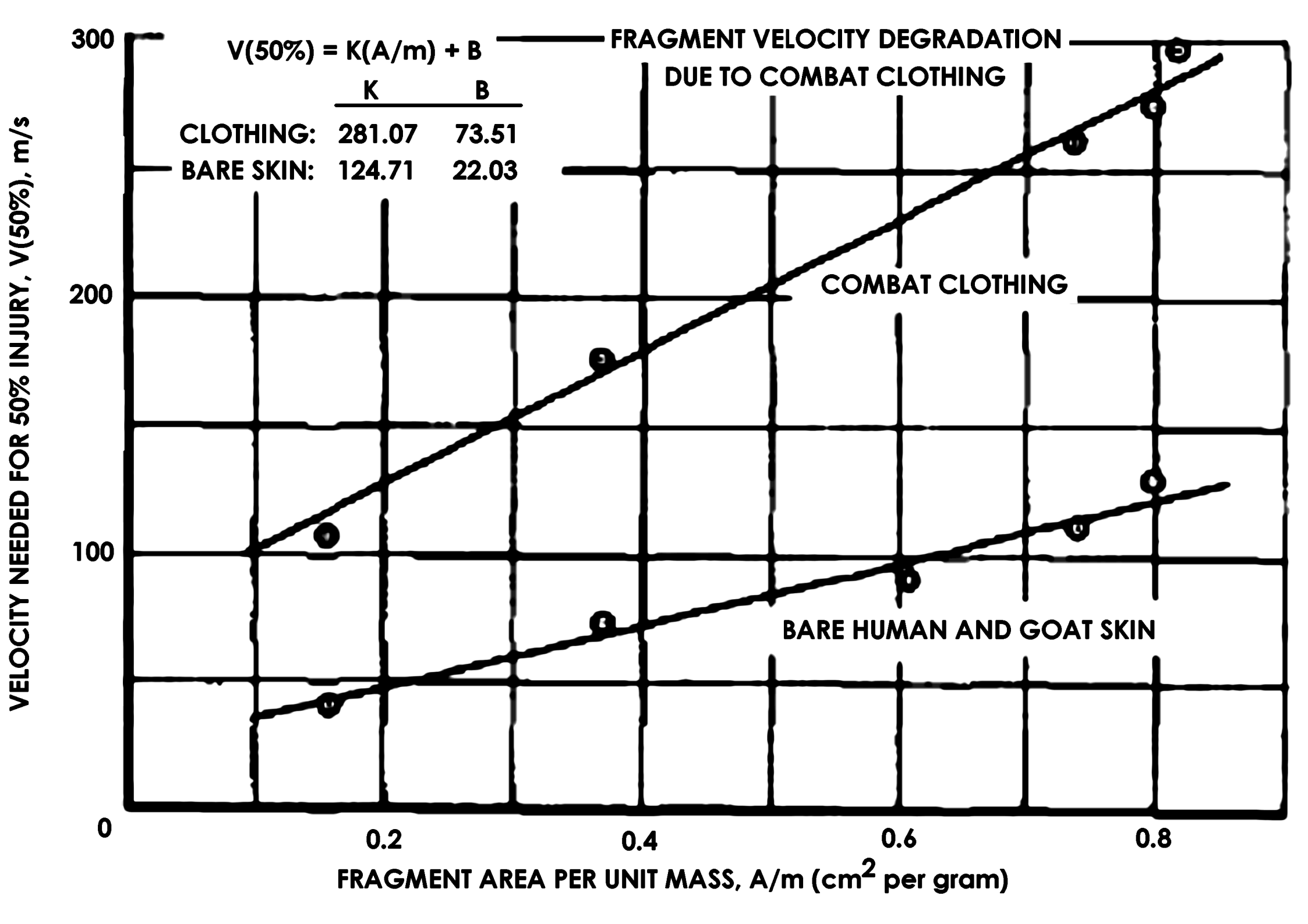
FRAGMENT VELOCITY DEGRADATION
DUE TO COMBAT CLOTHING
V(50%) = K(A/m) + B
K B
CLOTHING: 281.07 73.51
BARE SKIN: 124.71 22.03
COMBAT CLOTHING
BARE HUMAN AND GOAT SKIN
VELOCITY NEEDED FOR 50% INJURY, V(50%), m/s
300
200
100
0
0.2
0.4
0.6
0.8
FRAGMENT AREA PER UNIT MASS, A/m (cm2 per gram)

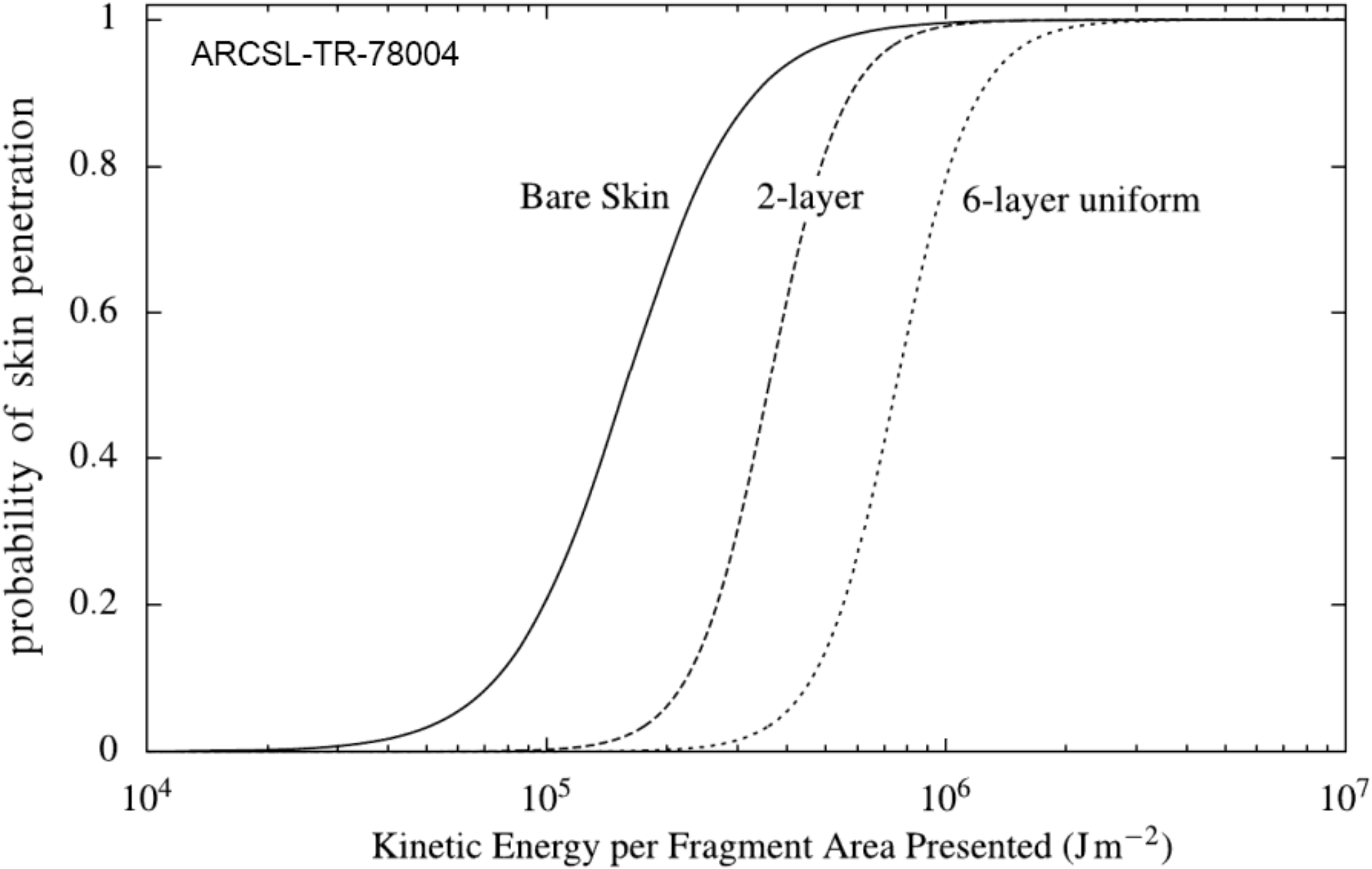

Lewis, James H., *et al, An Empirical/Mathematical Model to Estimate the Probability of Skin Penetration by Various Projectiles,* Technical Report ARCSL-TR-78004, April 1978, US Army Armament Research and Development Command

GLASS PENETRATING ABDOMINAL CAVITY

Mass of glass fragments (grams)	Probability of penetration (percent) 1	50	99
	Impact velocity (ft/sec)		
0. 1	235	410	730
1. 0	140	245	430

GLASS

Peak overpressure (psi)	Median velocity (ft/sec)	Median mass (grams)	Maximum number per sq ft
1. 9	108	1. 45	4. 3
5. 0	170	0. 13	388

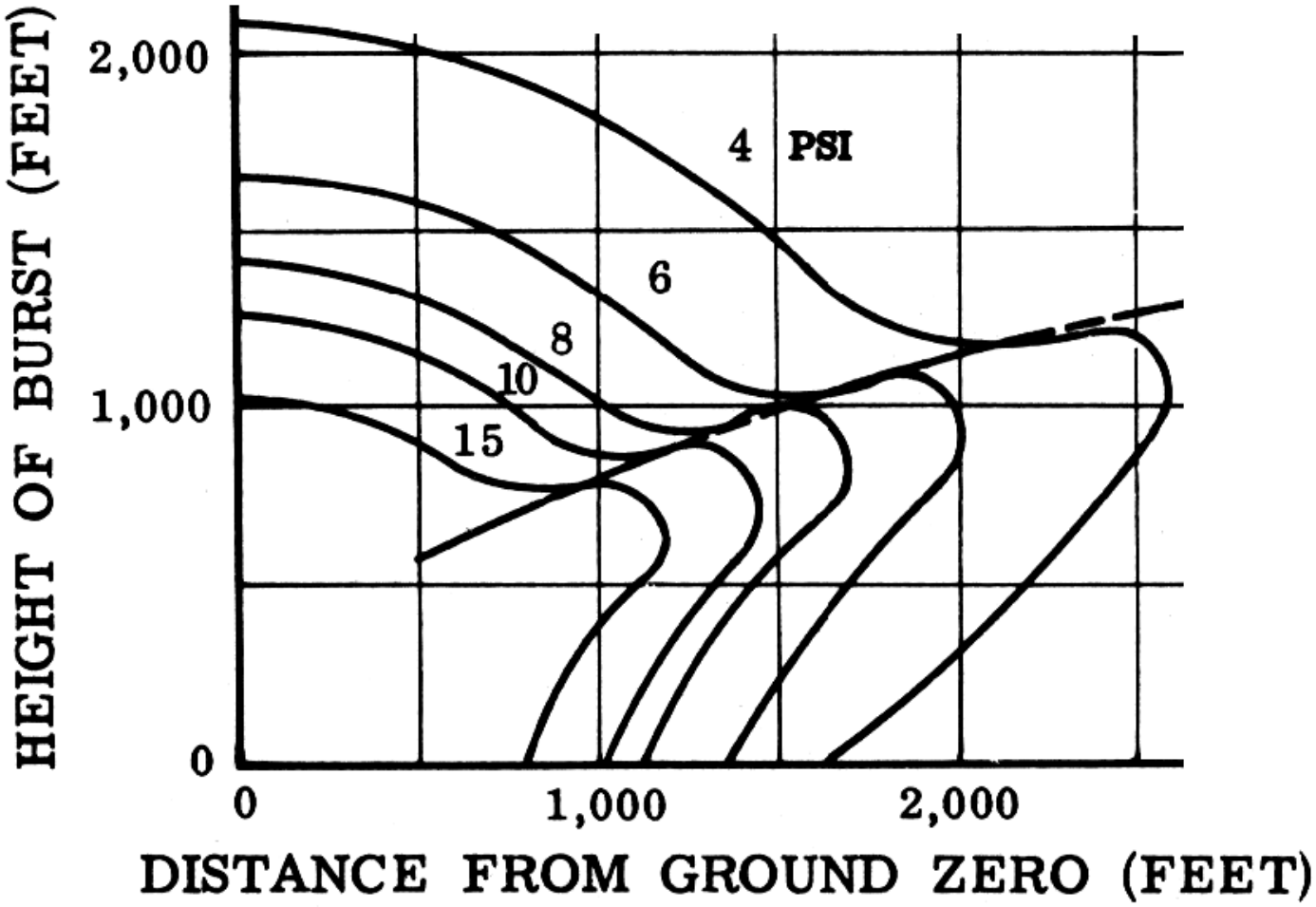

Peak overpressures on the ground for 1-kiloton burst

E. R. Fletcher, et al., "Airblast Effects on Windows in Buildings and Automobiles on the Eskimo II Event", in report AD775580, p. 251. Eskimo II was equivalent to 11 tons of TNT, 22 May 1973. Data below: 1,210 ft (0.54 psi incident, 1.1 psi reflected, 0.158 sec)

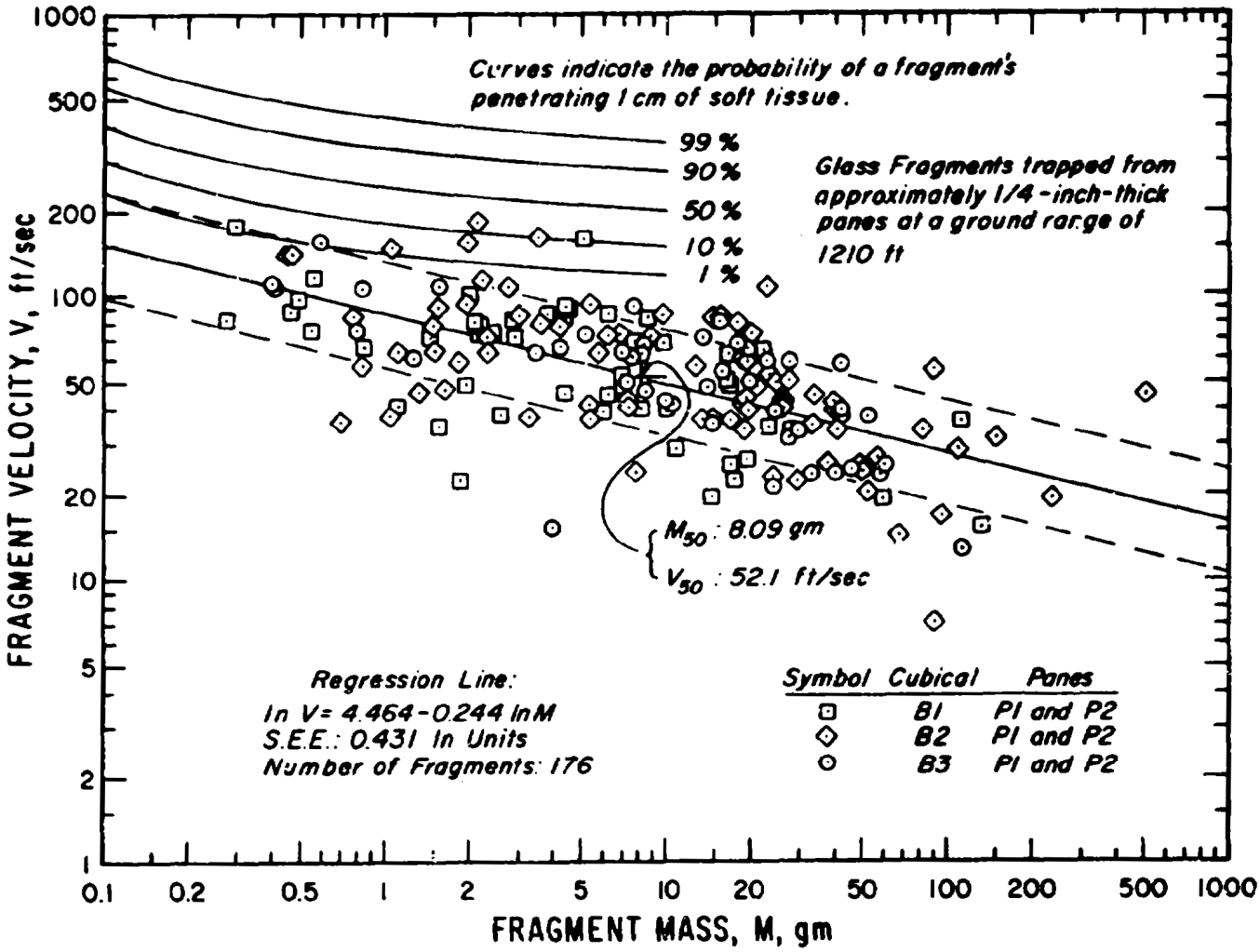

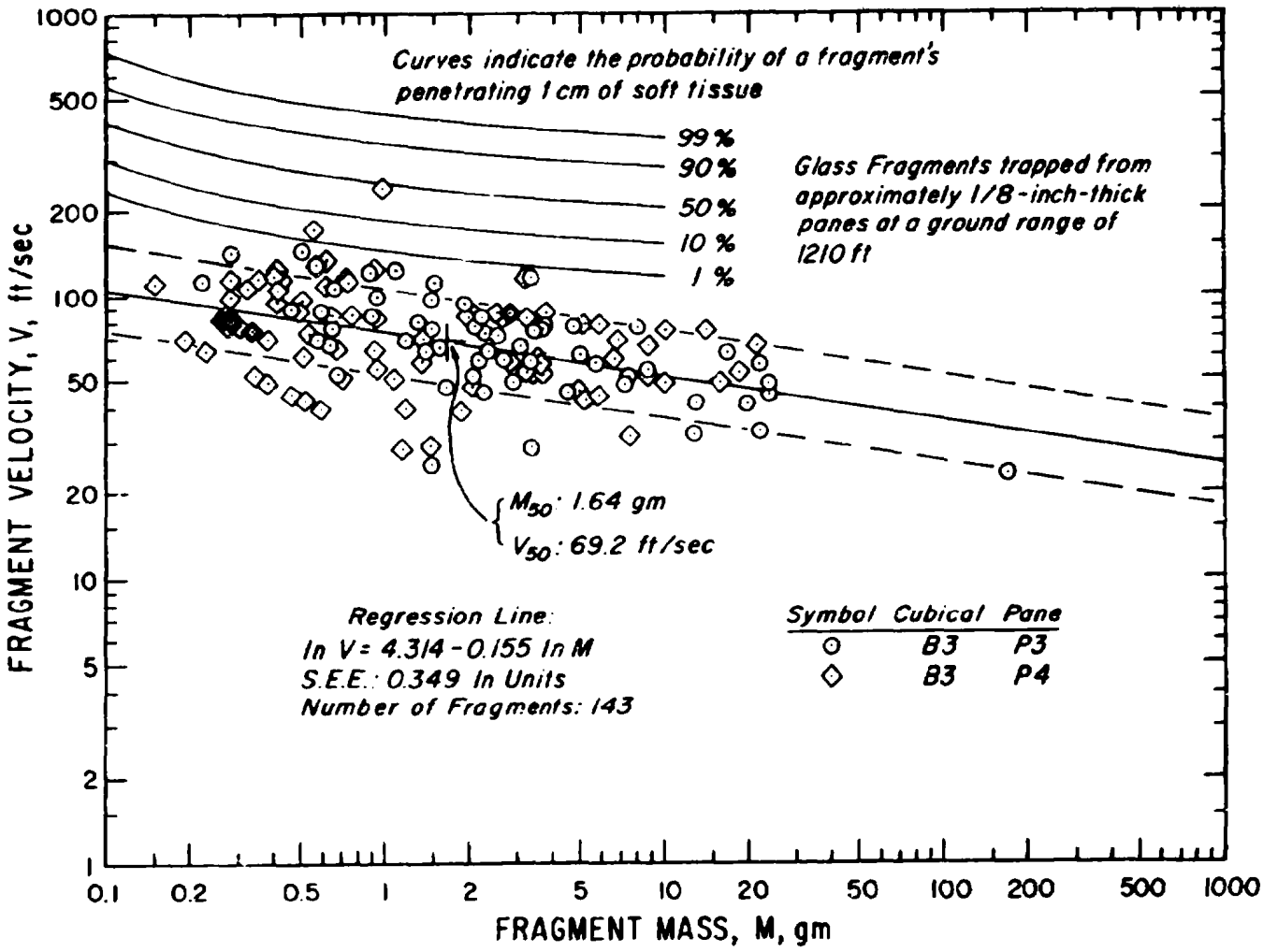

E. R. Fletcher, et al., "Airblast Effects on Windows in Buildings and Automobiles on the Eskimo II Event", in report AD775580, p. 251. Eskimo II was equivalent to 11 tons of TNT, 22 May 1973. Data below: 1,700 ft (0.41 psi incident, 0.83 psi reflected, 0.180 sec)

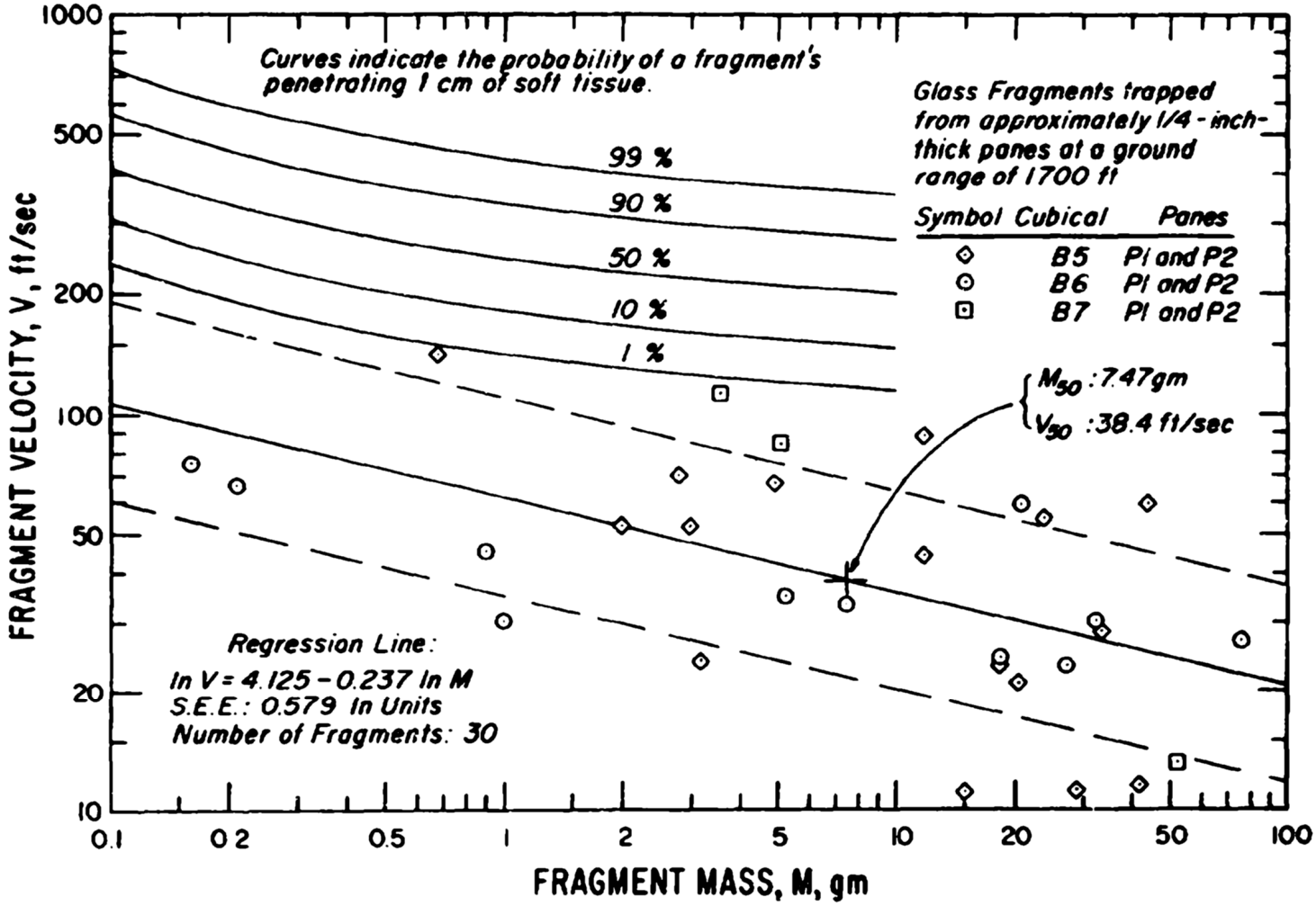

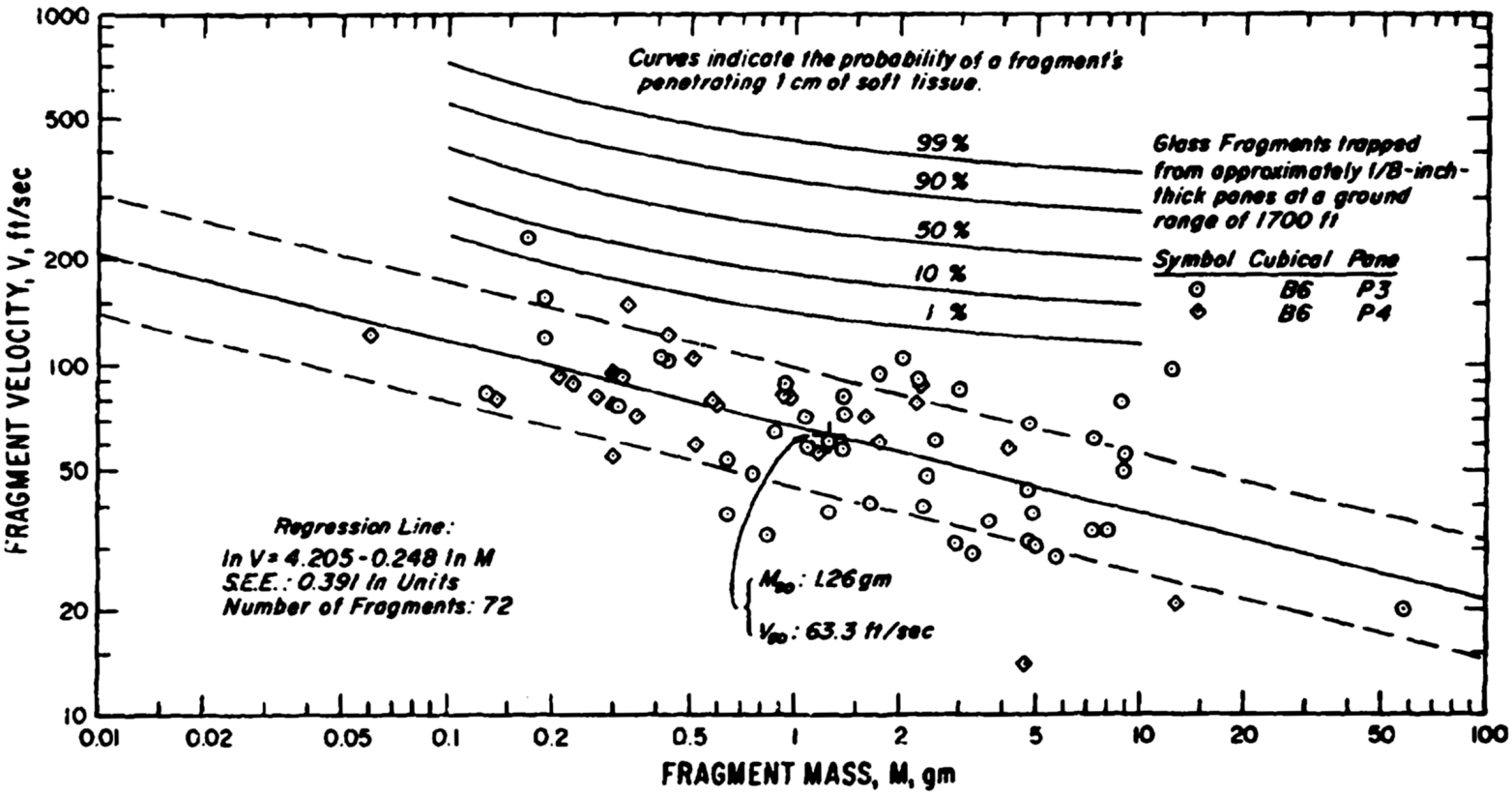

SECONDARY MISSILES GENERATED BY NUCLEAR-PRODUCED BLAST WAVES

A 40-ft concrete-block wall was built 2750 ft from GZ on shot Galileo, 11 kt

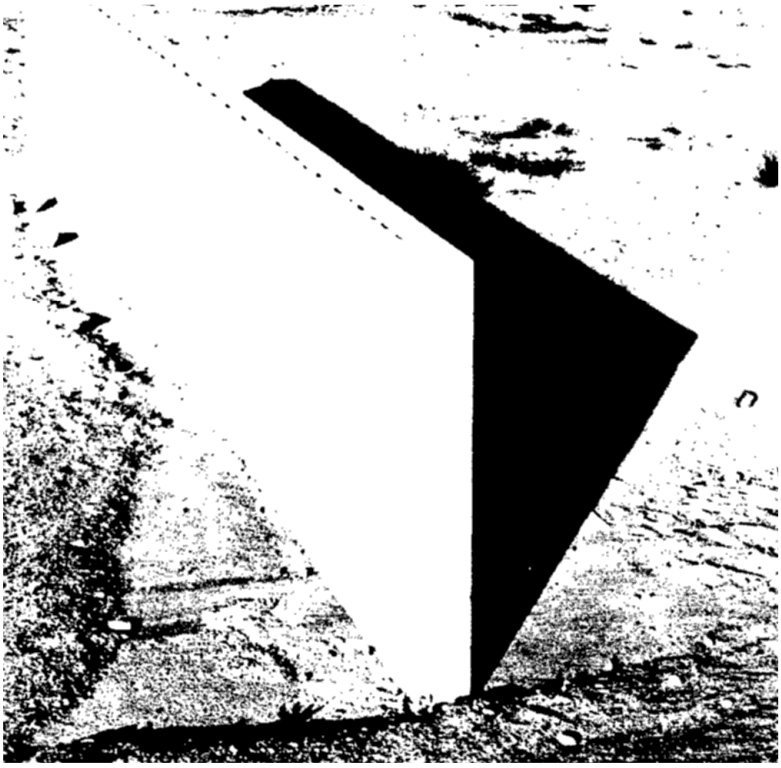

Concrete-block wall (64 in. high, 40 ft long, and 7.5 in. thick) broad side of the wall was oriented toward GZ.

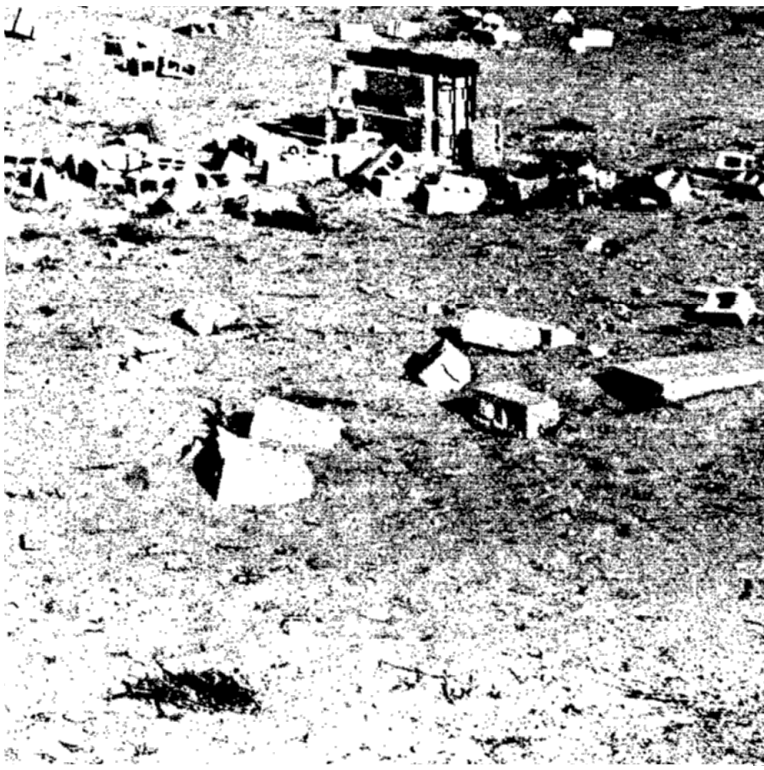

Photograph illustrating the scatter of blocks from the wall 8.4 psi peak overpressure

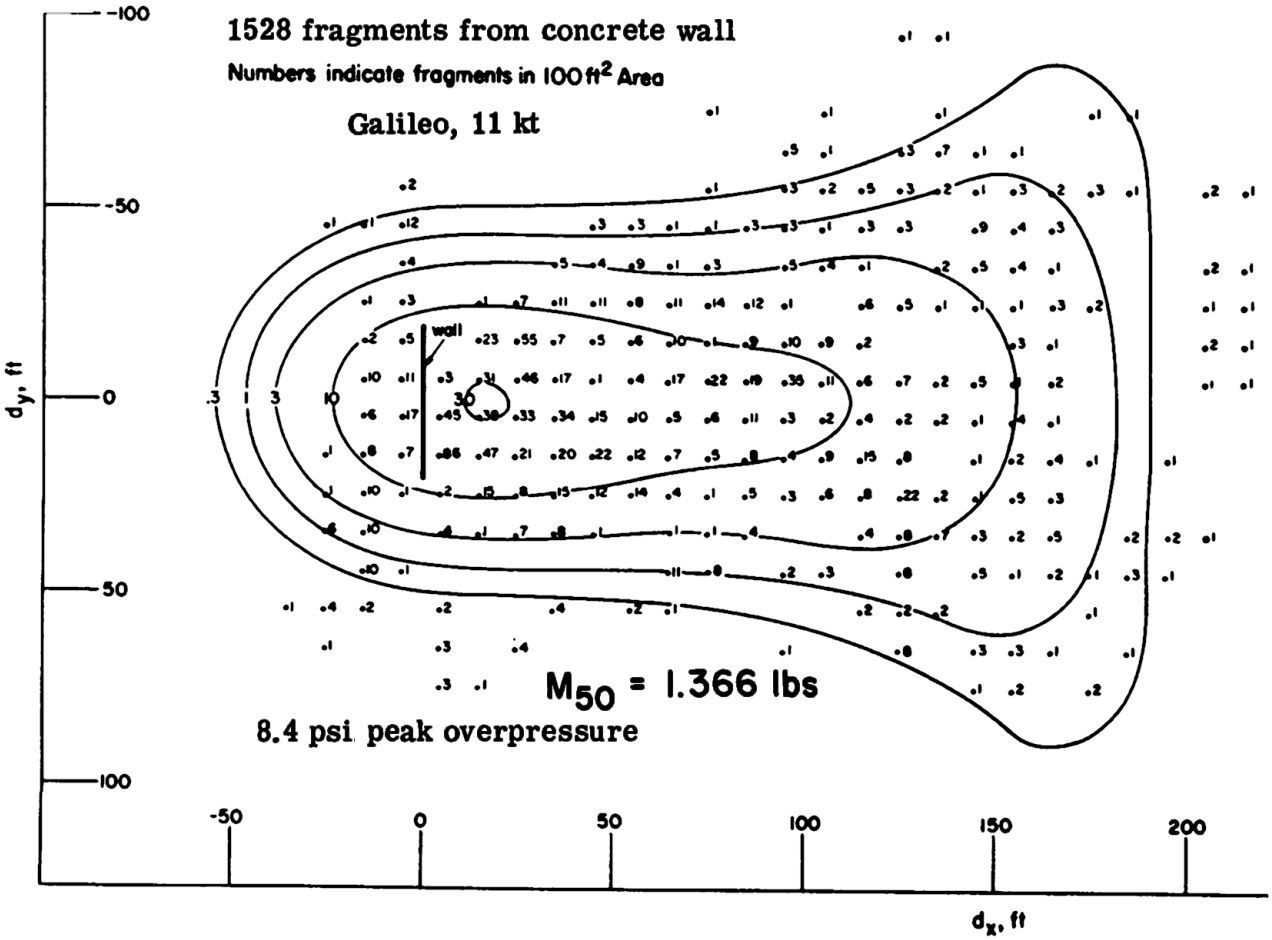

Spatial distribution of all fragments with masses over 0.1 lb from the concrete-block wall.

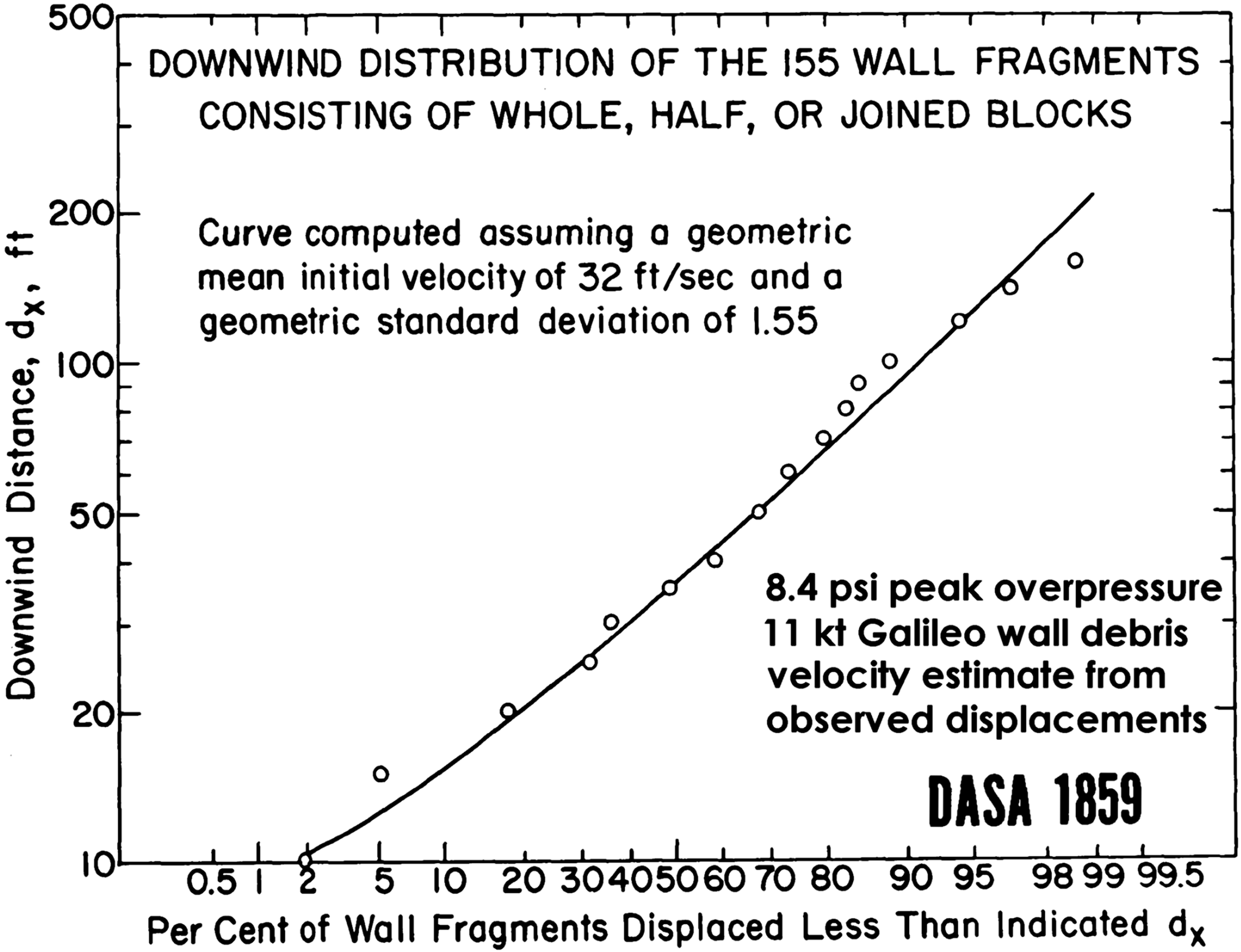
DOWNWIND DISTRIBUTION OF THE 155 WALL FRAGMENTS
CONSISTING OF WHOLE, HALF, OR JOINED BLOCKS
Curve computed assuming a geometric mean initial velocity of 32 ft/sec and a geometric standard deviation of 1.55
8.4 psi peak overpressure
11 kt Galileo wall debris
velocity estimate from
observed displacements
DASA 1859
Downwind Distance, d_x, ft
500
200
100
50
20
10
0.5 1 2 5 10 20 30 40 50 60 70 80 90 95 98 99 99.5
Per Cent of Wall Fragments Displaced Less Than Indicated d_x

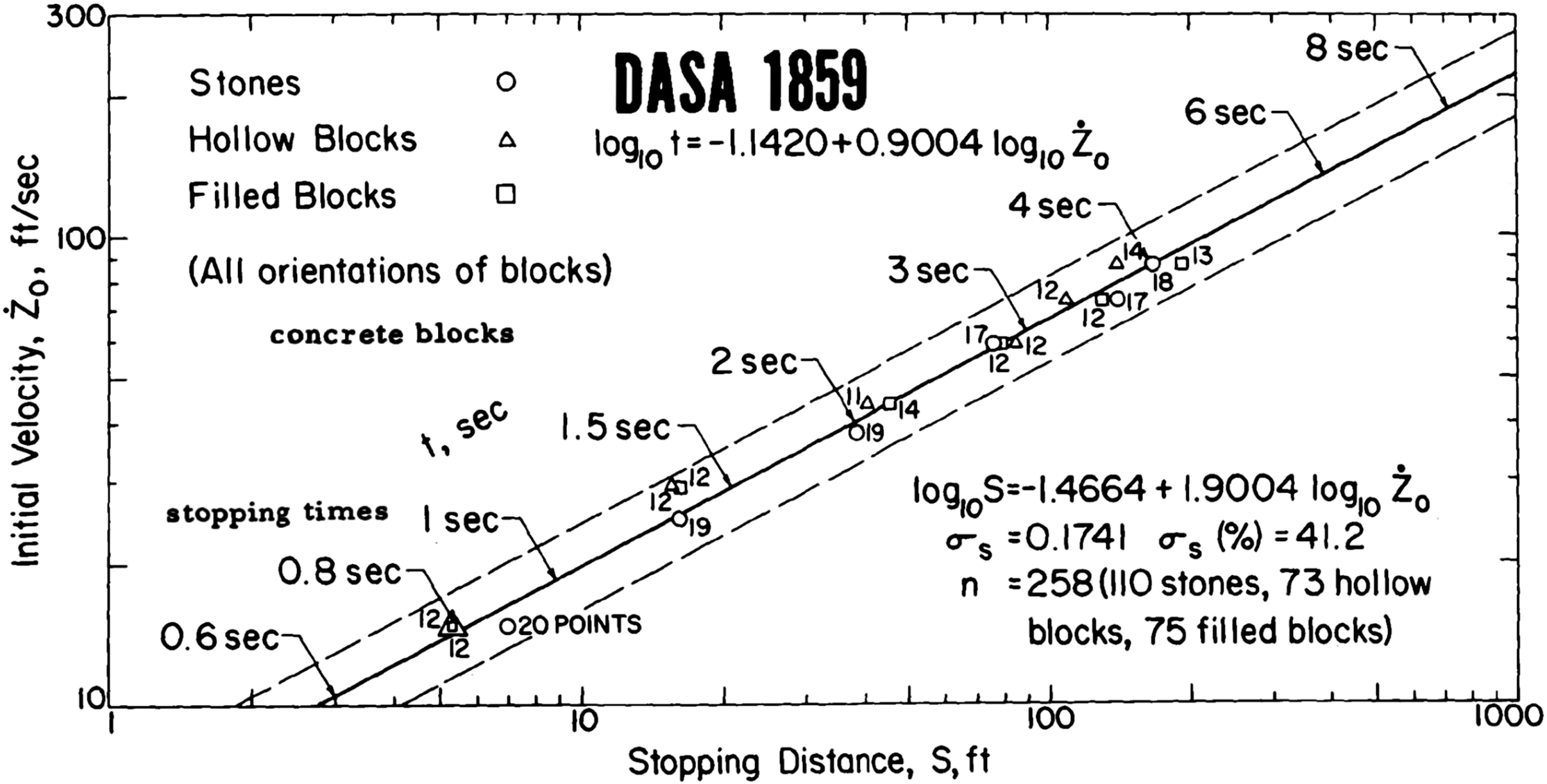
DASA 1859
Stones
Hollow Blocks
Filled Blocks
(All orientations of blocks)
concrete blocks
$\log_{10} t = -1.1420 + 0.9004 \log_{10} \dot{Z}_o$
$\log_{10} S = -1.4664 + 1.9004 \log_{10} \dot{Z}_o$
$\sigma_s = 0.1741$ σ_s (%) = 41.2
n = 258 (110 stones, 73 hollow blocks, 75 filled blocks)
t, sec
stopping times
0.6 sec
0.8 sec
1 sec
1.5 sec
2 sec
3 sec
4 sec
6 sec
8 sec
20 POINTS
Initial Velocity, $\dot{Z}_o$, ft/sec
Stopping Distance, S, ft
300
100
10
1
10
100
1000

Average Minimal Impact Velocities From a 10 lb. Missile Expected to Cause Skull Fracture and Maximal Velocity Without Fracture

Region of blow	Impact velocities expected to fracture the human skull*	
	ft/sec	mph
Maximal without fracture	23.1	15.7
Minimal with fracture	14.6	9.9

*Computed from the data of Gurdjian, et al. using human material

ORNL-TM-3396

NUCLEAR WEAPONS FREE-FIELD ENVIRONMENT RECOMMENDED FOR INITIAL RADIATION SHIELDING CALCULATIONS

J. A. Auxier, Z. G. Burson, R. L. French,
F. F. Haywood, L. G. Mooney, and E. A. Straker

Table 8. Fission-Product Gamma Ray Exposure During the First 60 Seconds from a Typical TN Weapon at a 100-M Burst Height

Slant Range (m)	Shock Arrival (sec)	Percent Before Shock	Percent After Shock
		100 KT	
538	0.3678	13.8	86.2
740	0.8187	20.4	79.6
1030	1.822	36.2	63.8
1446	4.055	63.1	36.9
2097	11.02	95.7	4.3
		300 KT	
771	0.5488	13.7	86.3
1060	1.221	20.5	79.5
1472	2.718	38.6	61.4
2065	6.049	69.8	30.2
2995	16.44	98.8	1.2
		1 MT	
1146	0.8187	11.1	88.9
1576	1.822	18.3	81.7
2190	4.055	38.2	61.8
3075	9.024	75.3	24.7
4458	24.53	99.8	0.2

NUCLEAR WEAPONS FREE-FIELD ENVIRONMENT RECOMMENDED FOR INITIAL RADIATION SHIELDING CALCULATIONS

J. A. Auxier, Z. G. Burson, R. L. French,
F. F. Haywood, L. G. Mooney, and E. A. Straker

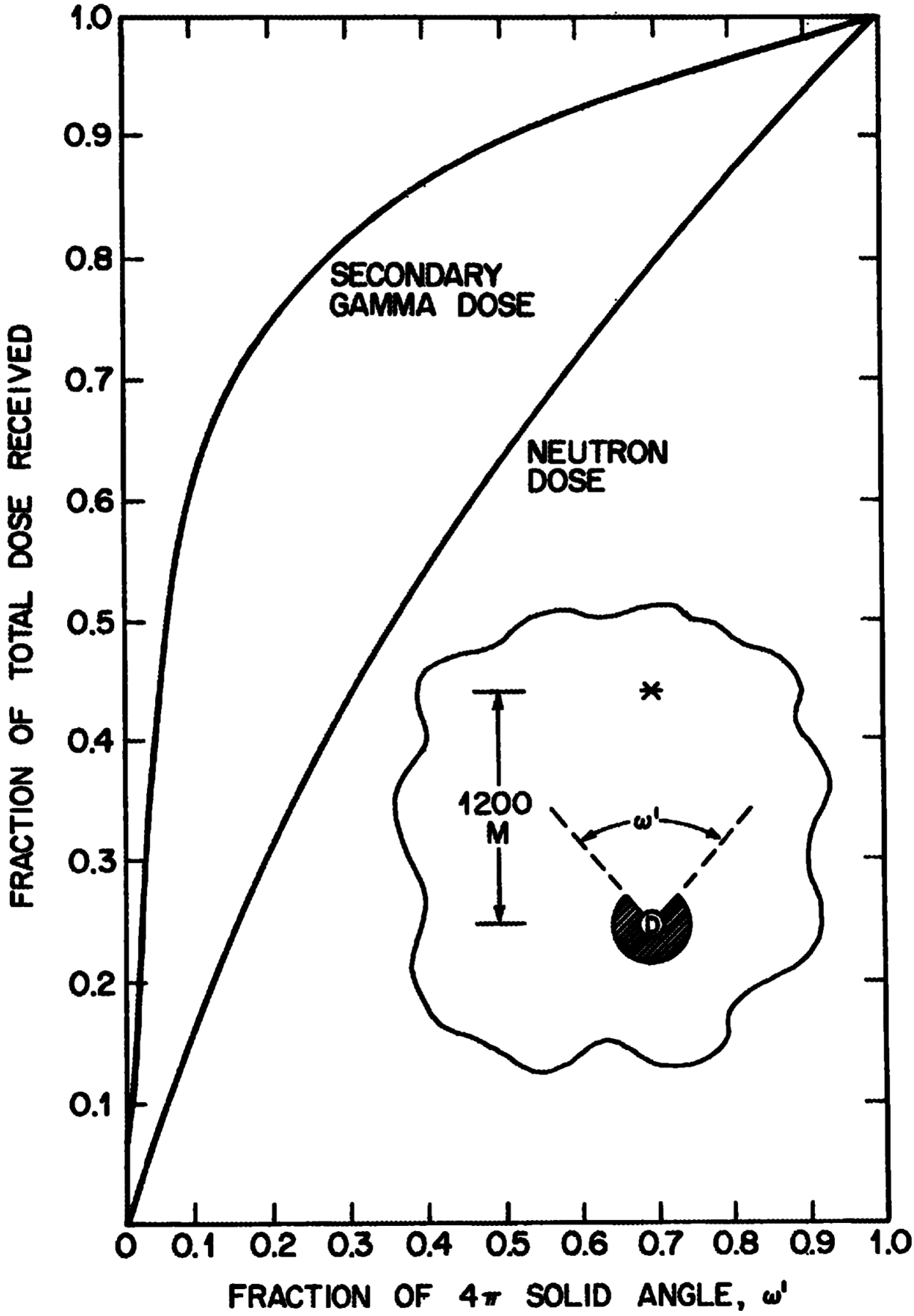

Figure 9. Angular Distribution of Neutron and Secondary Gamma 1200 m from a Thermonuclear Weapon

HIROSHIMA

John Hersey

NEW YORKER *of* 31 *August*, 1946

I

A NOISELESS FLASH

AT exactly fifteen minutes past eight in the morning, on August 6th, 1945, Japanese time, at the moment when the atomic bomb flashed above Hiroshima,

Dr. Terufumi Sasaki, a young member of the surgical staff of the city's large, modern Red Cross Hospital, walked along one of the hospital corridors

He was one step beyond an open window when the light of the bomb was reflected, like a gigantic photographic flash, in the corridor. He ducked down on one knee and said to himself, as only a Japanese would, "Sasaki, *gambare !* Be brave !" Just then (the building was 1,650 yards from the centre), the blast ripped through the hospital. The glasses he was wearing flew off his face; the bottle of blood crashed against one wall; his Japanese slippers zipped out from under his feet—but otherwise, thanks to where he stood, he was untouched.

Dr. Sasaki shouted the name of the chief surgeon and rushed around to the man's office and found him terribly cut by glass.

Starting east and west from the actual centre, the scientists, in early September, made new measurements, and the highest radiation they found this time was 3.9 times the natural "leak."

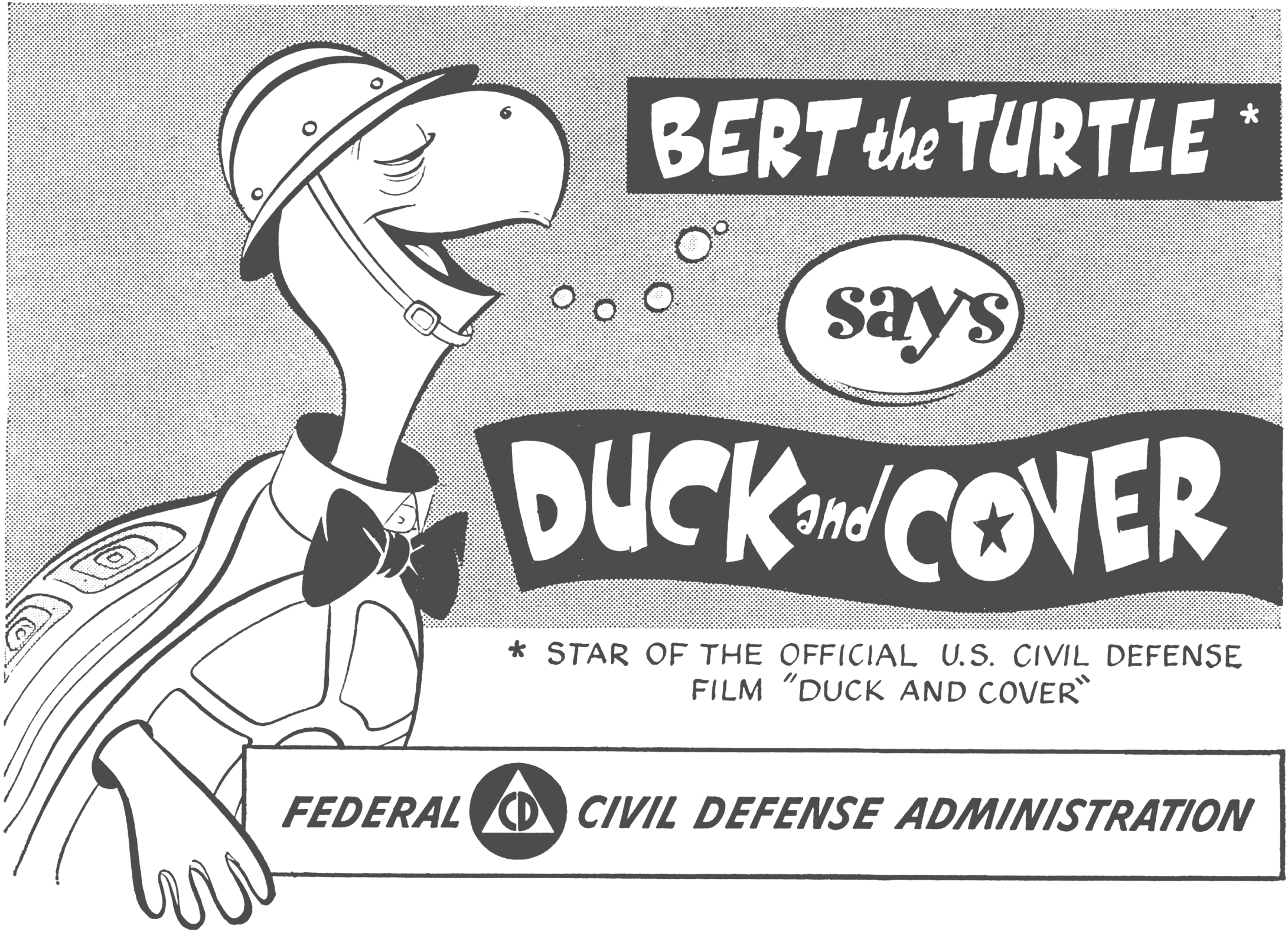
BERT the TURTLE *
says
DUCK and COVER
* STAR OF THE OFFICIAL U.S. CIVIL DEFENSE FILM "DUCK AND COVER"
FEDERAL CD CIVIL DEFENSE ADMINISTRATION

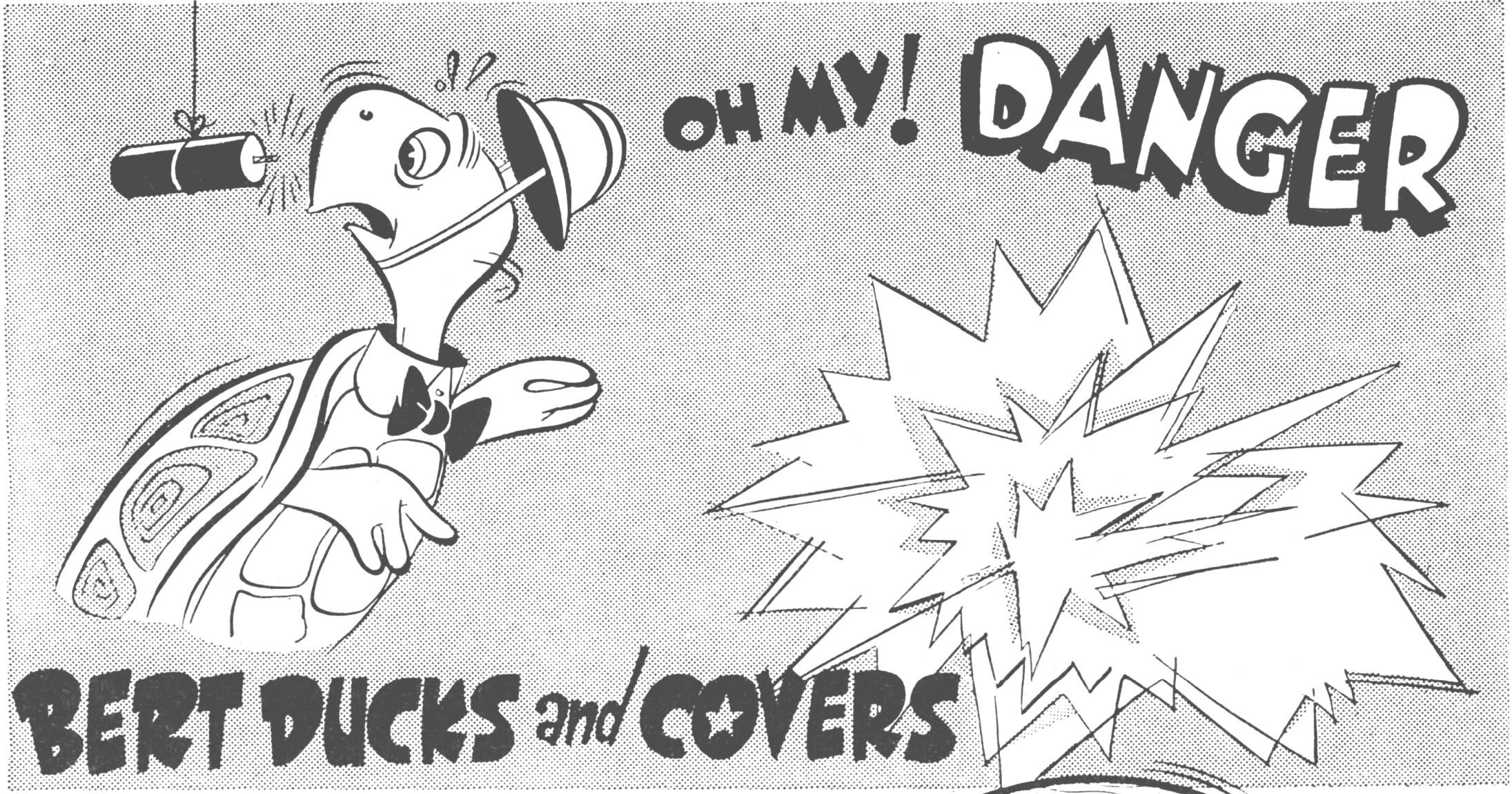

BERT DUCKS and COVERS

HE'S SMART, BUT ***HE*** HAS HIS SHELTER ON HIS BACK..

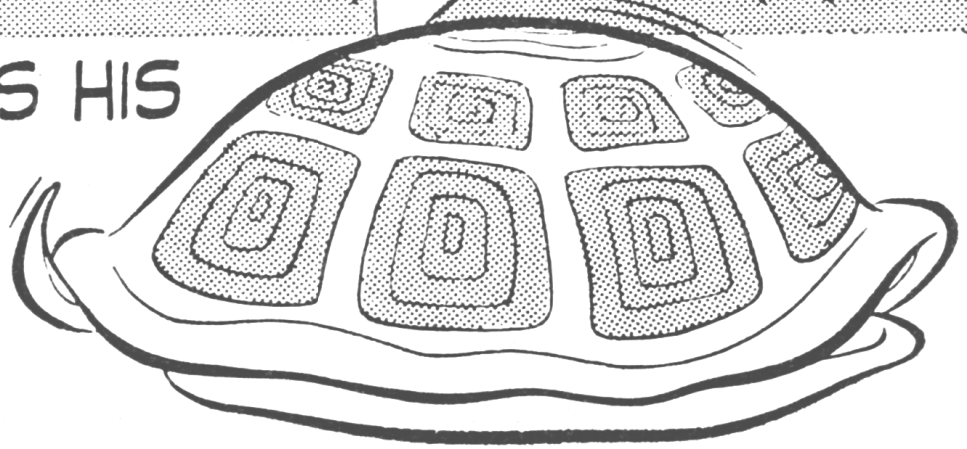

YOU MUST LEARN TO FIND SHELTER

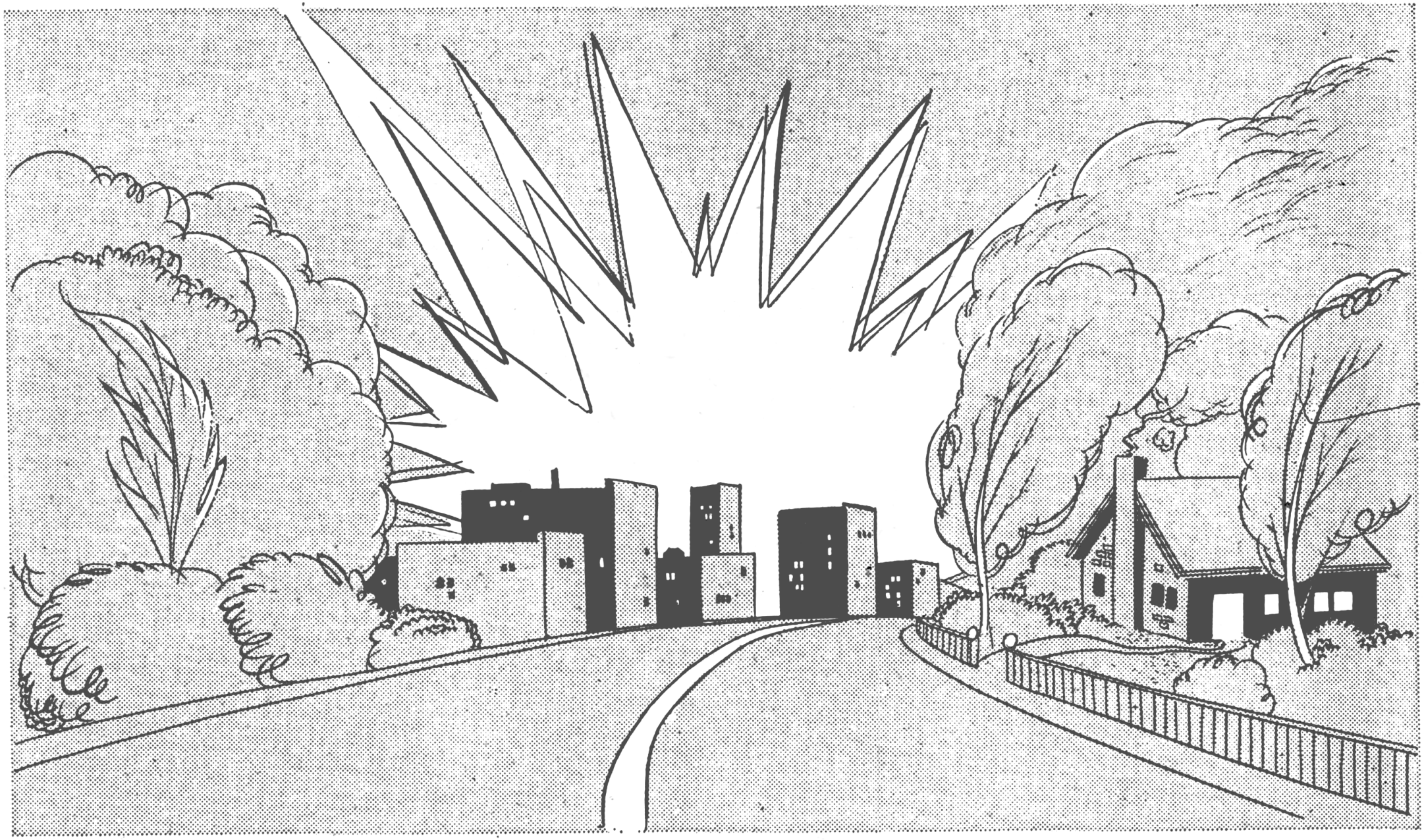

THE ATOMIC BOMB IS A **NEW** DANGER. IT EXPLODES WITH A FLASH BRIGHTER THAN ANY YOU'VE EVER SEEN.

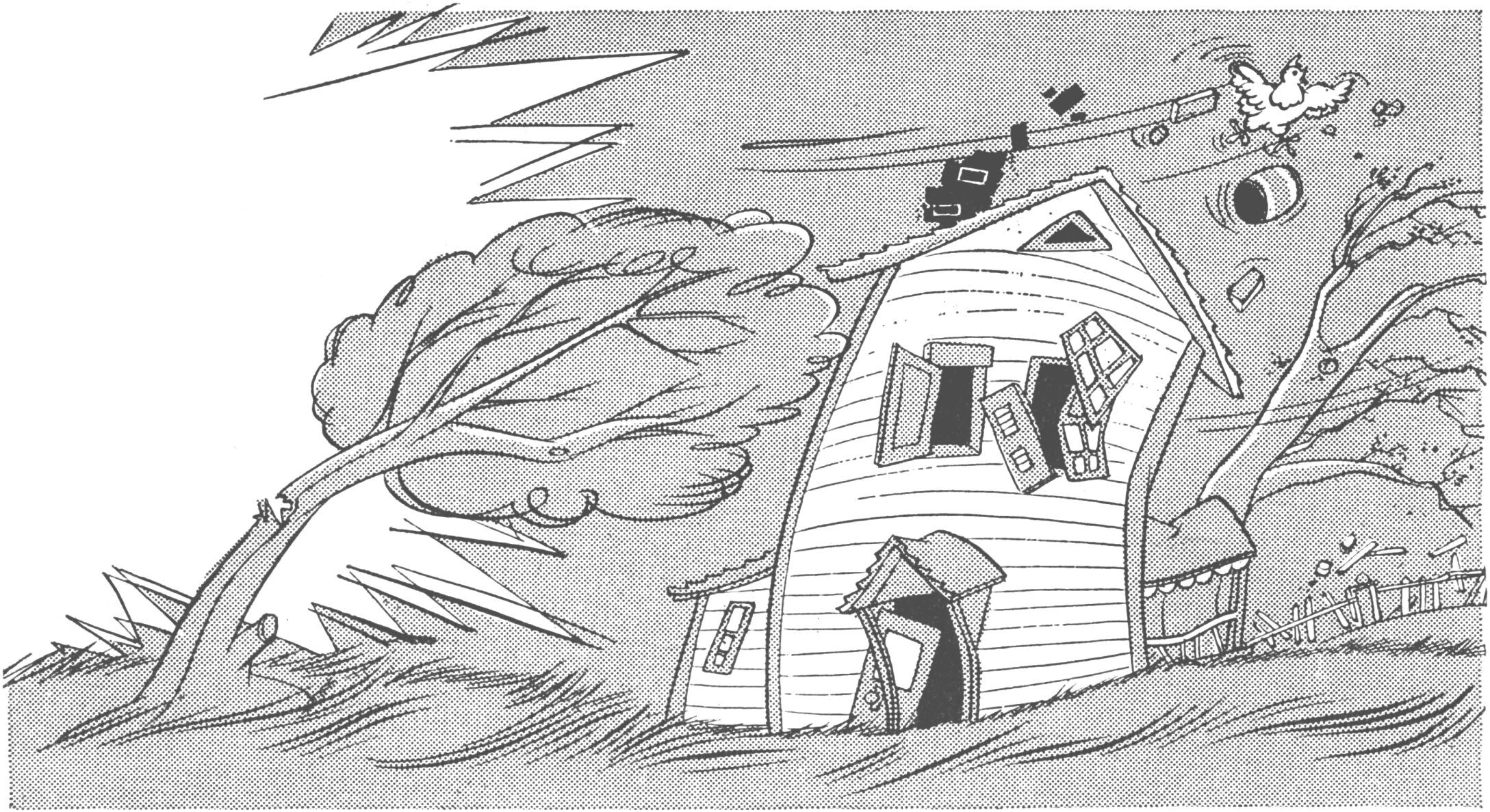

THINGS WILL BE KNOCKED DOWN ALL OVER TOWN, AND, AS IN A BIG WIND, THEY ARE BLOWN THROUGH THE AIR. **YOU** MUST BE READY TO PROTECT YOURSELF.

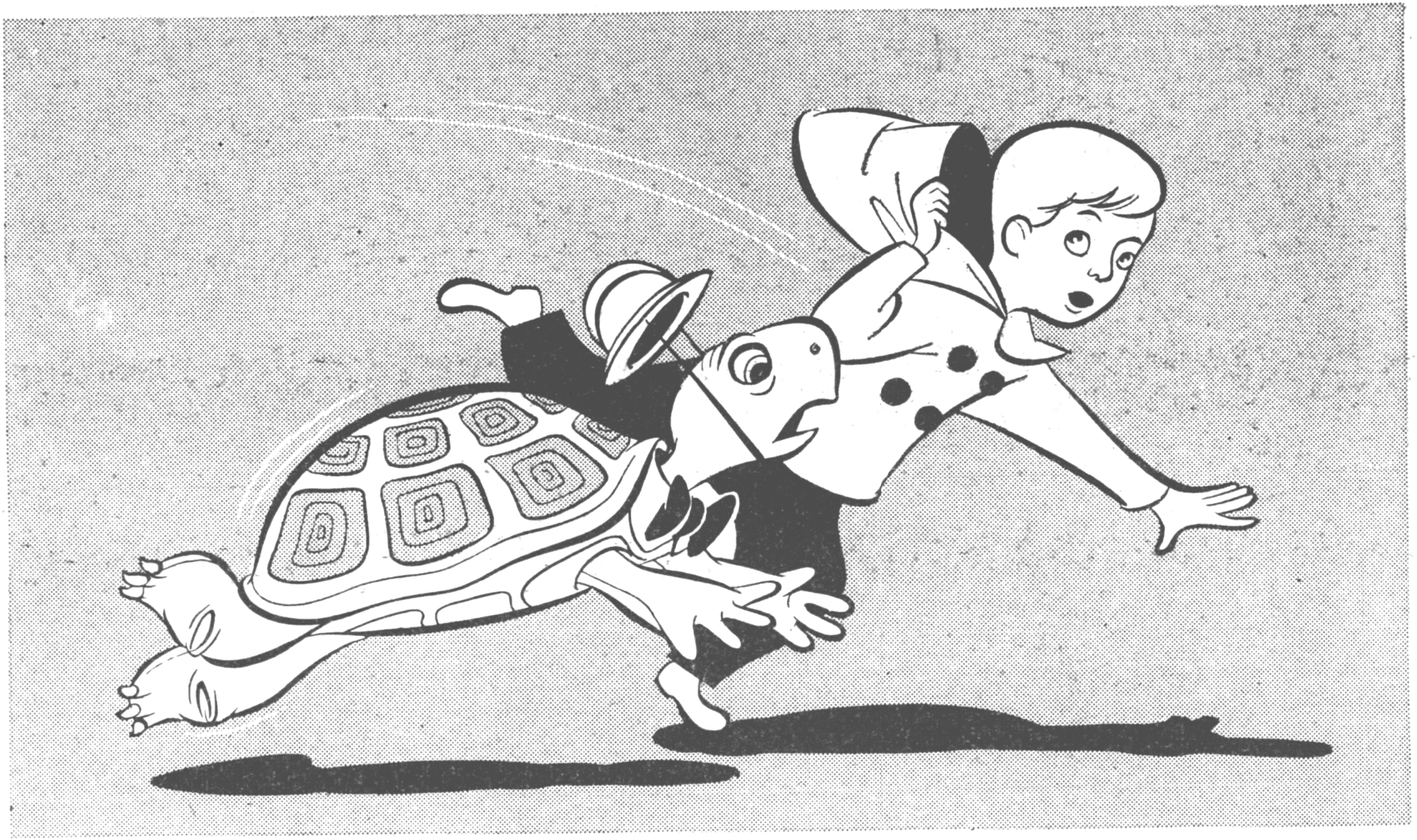

SO, LIKE BERT, YOU **DUCK** TO AVOID
THE THINGS FLYING THROUGH THE AIR...

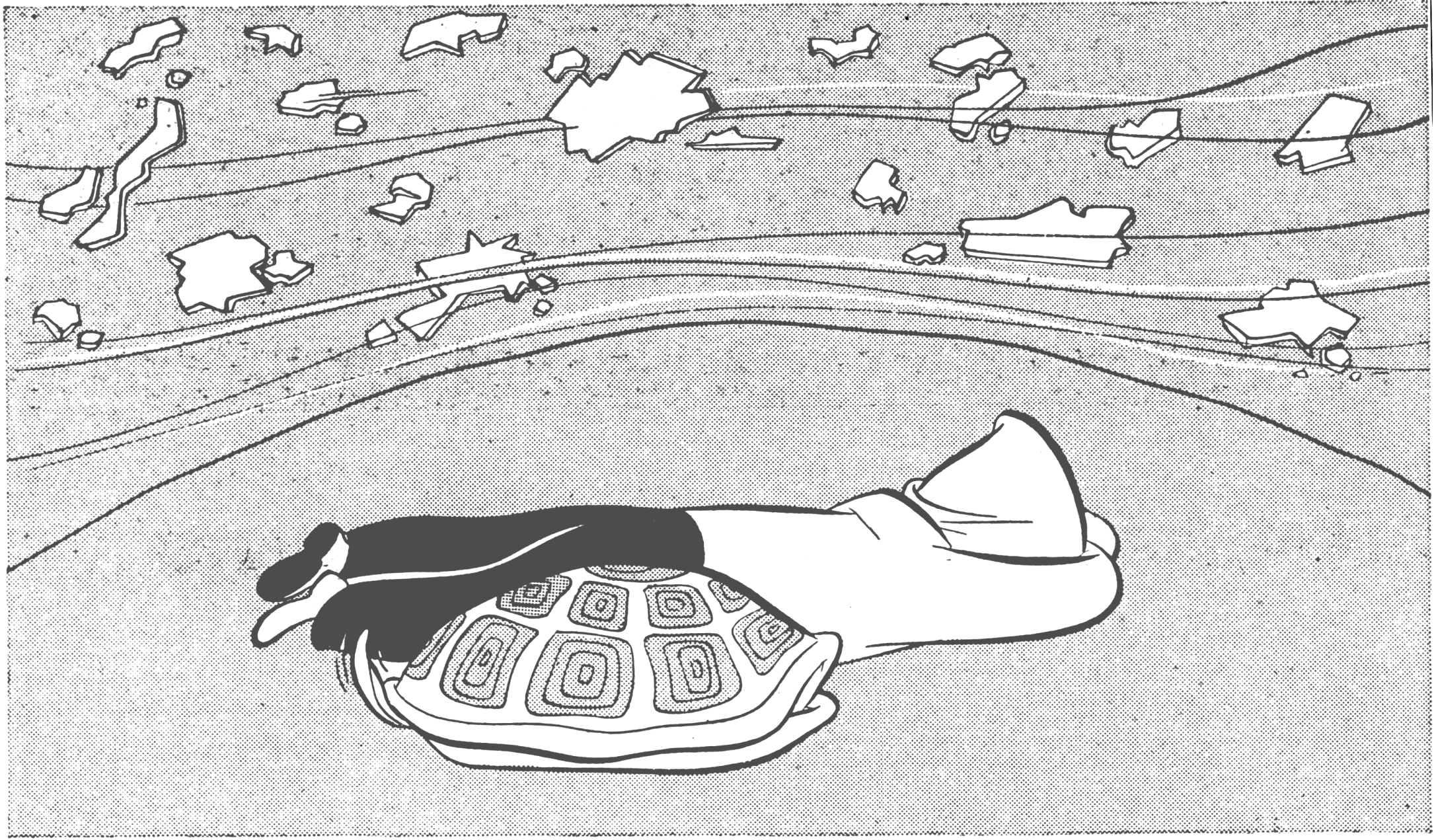

...AND **COVER** TO KEEP FROM GETTING CUT OR EVEN BADLY BURNED.

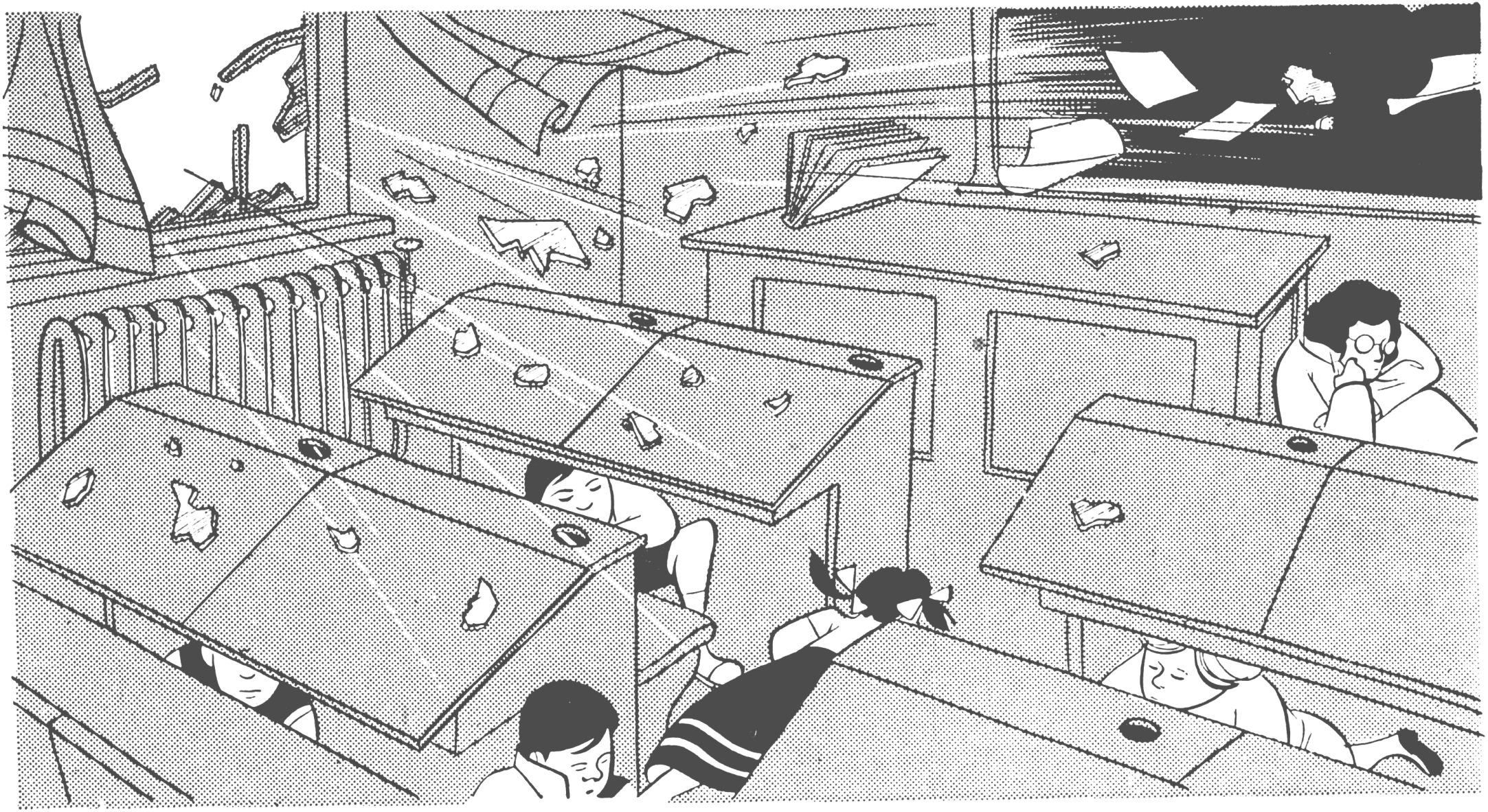

BUT SOMETIMES--**AND THIS IS VERY IMPORTANT**--
THE BOMB MIGHT EXPLODE AND THE BRIGHT FLASH
COME... *WITHOUT ANY WARNING!*

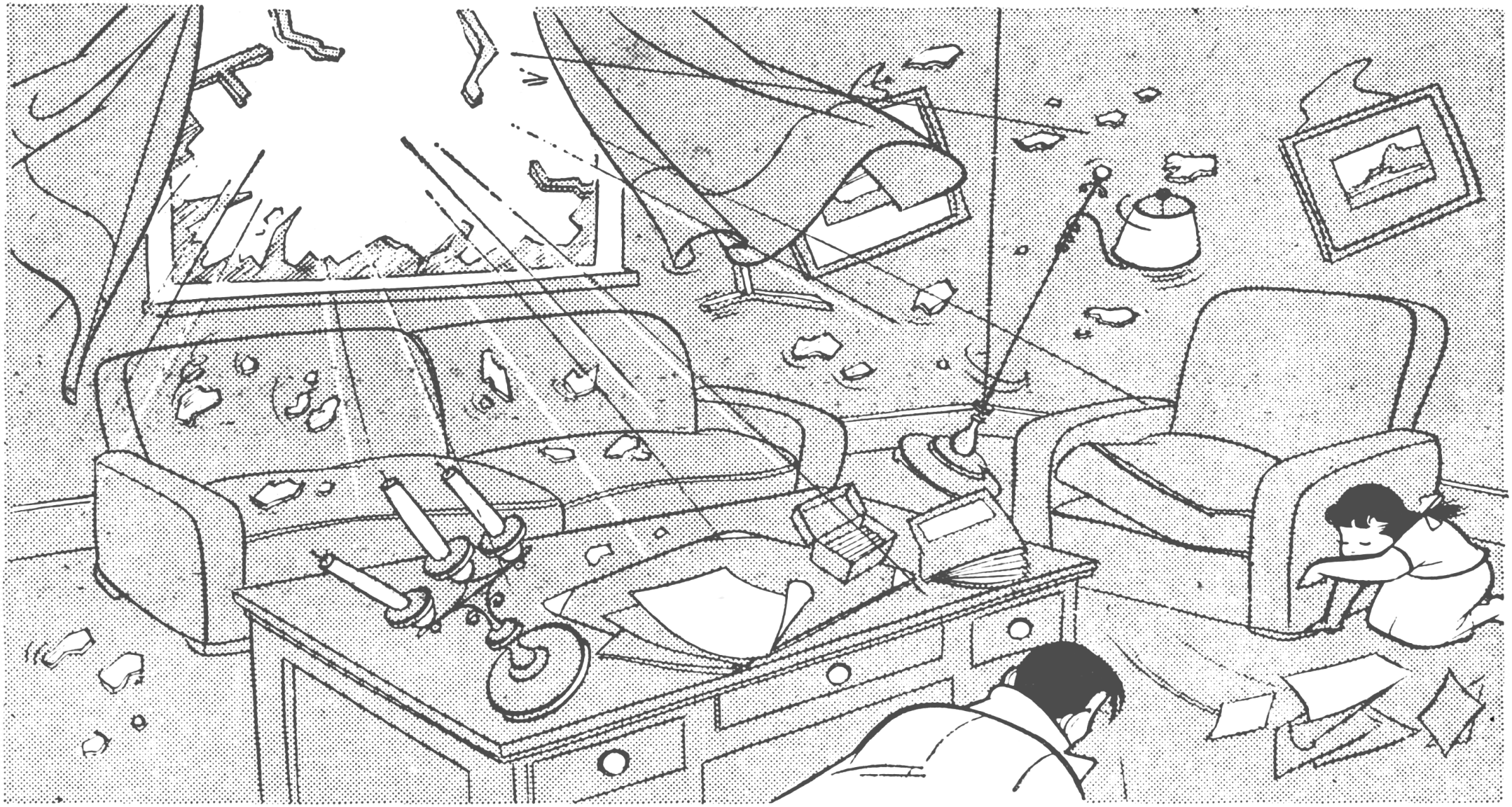

THERE IS ALWAYS **SOMETHING** TO SHELTER YOU-INDOORS, A SCHOOL DESK, A CHAIR, A TABLE. ALWAYS DUCK AWAY FROM WINDOWS AND GLASS DOORS.

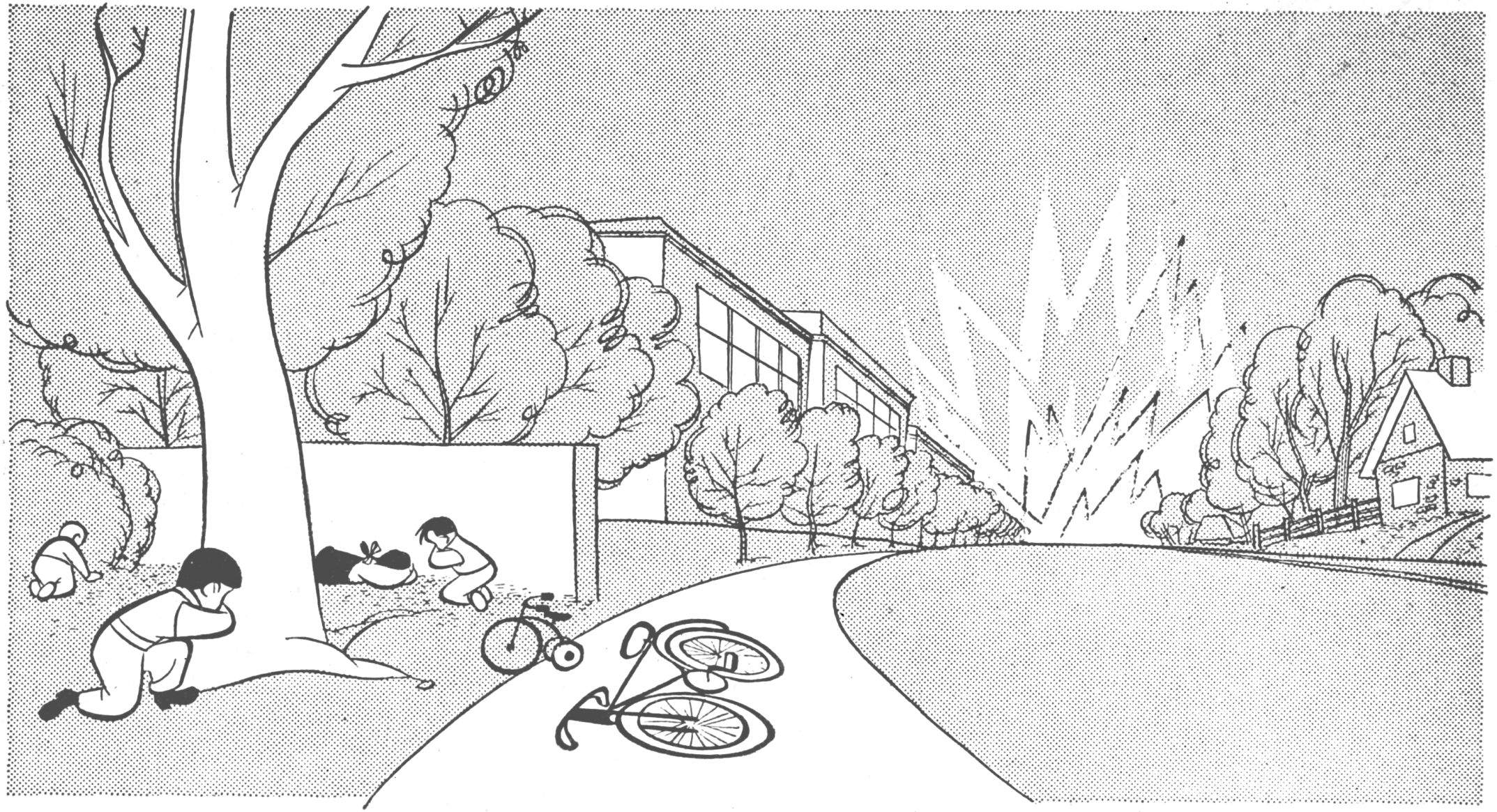

OUTDOORS, DUCK BEHIND WALLS AND TREES. EVEN IN A HOLLOW IN THE GROUND. IN A BUS OR AUTO, DUCK DOWN BEHIND OR UNDER THE SEATS.

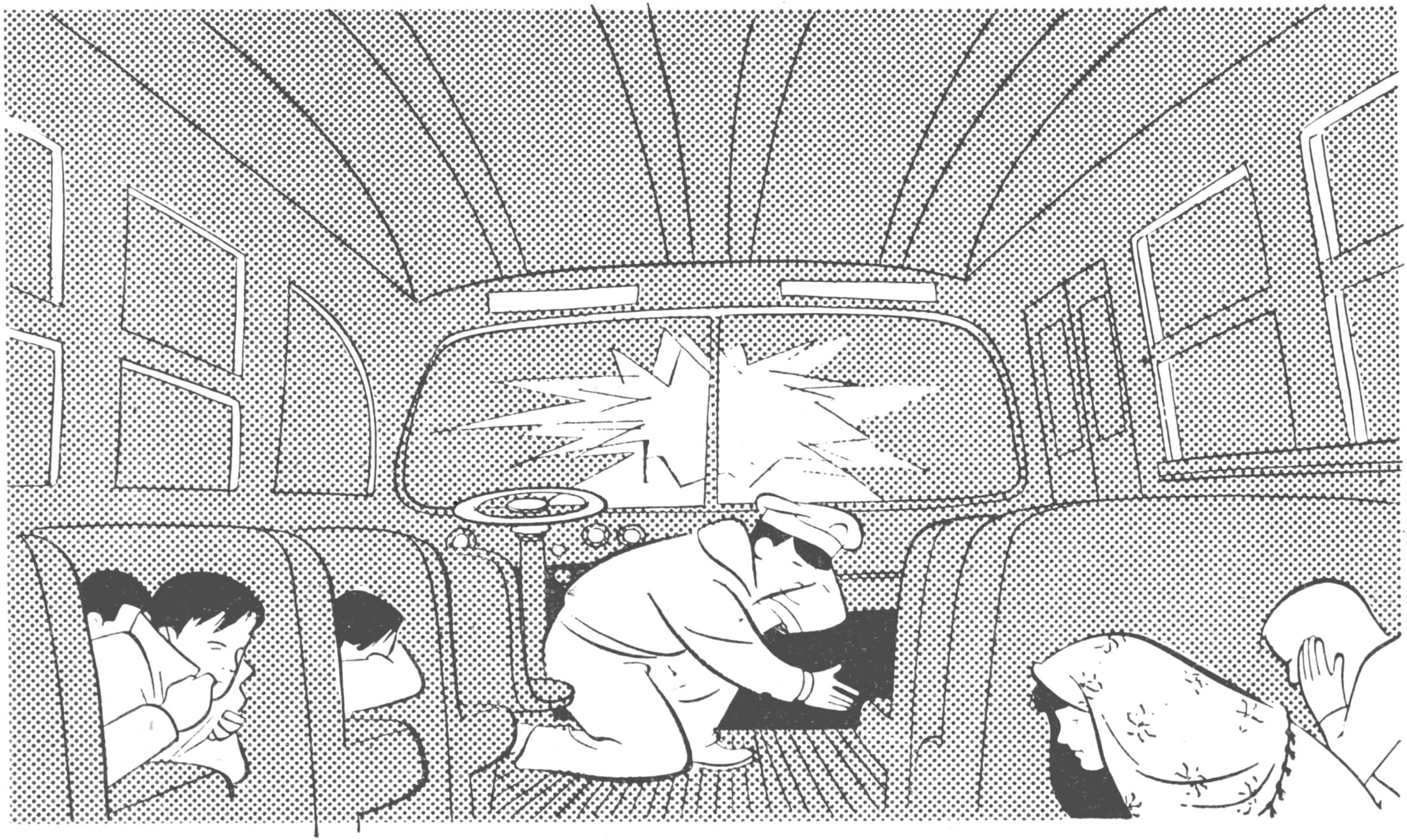

BUT REMEMBER... **DO IT INSTANTLY...**
DON'T STAND AND LOOK. DUCK AND COVER!

cue for survival

OPERATION CUE

A.E.C. NEVADA TEST SITE

MAY 5, 1955

A report by the FEDERAL CIVIL DEFENSE ADMINISTRATION

EFFECTS OF NUCLEAR WEAPONS

BY HAROLD L. GOODWIN,
Director, Atomic Test Operations, FCDA

The time of travel of the shock wave is not generally understood by many persons. The concept of "duck and cover," which would still be of great value in case of attack without warning, is based on the comparatively large time interval between the burst and arrival of the shock wave at a given point.

92

BIOMEDICAL EFFECTS OF THERMAL RADIATION

BY DR. HERMAN ELWYN PEARSE, *Professor of Surgery at the University of Rochester. Consultant to several Government departments, notably the Atomic Energy Commission's Division of Biology and Medicine. Consultant to the Armed Forces Special Weapons Project*

After the Bikini test, I was asked to go to Japan as a consultant for the National Research Council to survey the casualties in Nagasaki and Hiroshima.

140

Then we observed the healing of the wounds, and we found again that the wounds healed in the same manner as those that we had produced in the laboratory. There was some difference in these lesions from the ordinary burns of civil life, but I would predict, from what I learned from experiments, that the difference is on the good side. The burns look worse; they are often charred, but they may not penetrate as deeply, and the char acts as a dressing, nature's own dressing.

142

For example, if you have 2 layers, an undershirt and a shirt, you will get much less protection than if you have 4 layers; and if you get up to 6 layers, you have such great protection from thermal effects that you will be killed by some other thing. Under 6 layers we only got about 50 percent first degree burns at 107 calories.

143

If we can just increase the protection a little bit, we may prevent thousands and thousands of burns.

... For example, to produce a 50-percent level of second-degree burns on bare skin required 4 calories. When we put 2 layers of cloth in contact, it only took 6 calories. But separate that cloth by 5 millimeters, about a fifth of an inch, and it increases the protective effect 5 times. The energy required to produce the same 50-percent probability of a second-degree burn is raised up to 30 calories. So if you wear loose clothing, you are better off than if your wear tight clothing.

144

OSTI ID: 4411414

STUDIES ON FLASH BURNS:

THE PROTECTION AFFORDED BY 2, 4 AND 6 LAYER FABRIC COMBINATIONS

George Mixter, Jr., M. D. and Herman E. Pearse, M. D.

THE UNIVERSITY OF ROCHESTER

ABSTRACT

Fabric interposed between a carbon arc source and the skin of Chester White pigs increased the amount of thermal energy required to cause 2+ burns. For the 2, 4 and 6 layers of fabric studied this increase was 3.6, 38 and over 104 cal/cm^2 respectively when the inner layer of fabric was in contact with the skin. Separation of the inner layer from the skin by 5 mm increased the protective effect of the 2 layer combination from 7.4 to 29 cal/cm^2, provided the outer layer was treated for fire retardation. If the outer layer was not so treated, sustained flaming occurred which in itself added to the thermal burn.

INTRODUCTION

In the past, work in this laboratory has been directed toward a study of flash burns in unshielded skin. It is well known from the atomic bombing in Japan that this type of burn was modified by clothing. A laboratory analysis of the protective effect of fabrics against flash burns was begun (5) by shielding the skin with a few representative fabrics and their combinations.

1. 2 Layers
   a. light green oxford
      knitted cotton underwear
   b. light green oxford (HPM)
      knitted cotton underwear
2. 4 Layers
   olive green sateen
   thin cotton oxford
   wool-nylon shirting
   knitted cotton underwear
3. 6 Layers
   olive green sateen
   thin cotton oxford
   mohair frieze
   rayon lining
   wool-nylon shirting
   knitted wool underwear

5. Morton, J. H., Kingsley, H. D., and Pearse, H. E., "Studies on Flash Burns: The Protective Effects of Certain Fabrics", Surgery, Gynecology and Obstetrics, 94, 497-501 (April 1952).

~~FIDENTIAL~~ ~~UNCLASSIFIED~~

WT-770

Copy No.

AD B951673

TECHNICAL
of the
DEFENSE N
AGENC
AUG

Operation UPSHOT-KNOTHOLE

NEVADA PROVING GROUNDS

March - June 1953

~~CONFIDENTIAL~~ ~~RD~~

~~REGRADED~~

~~BY AUTHORITY OF DA FORM 1575, FCAG~~

Project 8.5

THERMAL RADIATION PROTECTION AFFORDED TEST ANIMALS BY FABRIC ASSEMBLIES

UNCLASSIFIED

BY AUTHORITY OF DA FORM 1575, FCAG 12 274/26

B. Wade 23 Sep 64

~~FORMERLY RESTRICTED DATA~~

~~Handle as~~ Restricted Data in Foreign Dissemination Section 144B, Atomic ~~Energy~~ Act 1954

~~RESTRICTED DATA~~

This document contains restricted data as defined in the Atomic Energy Act of 1954. Its transmittal or the disclosure of its contents in any manner to an unauthorized person is prohibited.

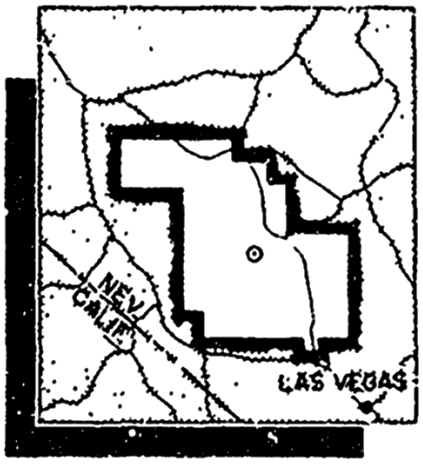

HEADQUARTERS FIELD COMMAND, ARMED FORCES SPECIAL WEAPONS PROJECT
SANDIA BASE, ALBUQUERQUE, NEW MEXICO

~~CONFIDENTIAL~~

UNCLASSIFIED

WT-770

This document consists of 64 pages

No. 196 of 295 copies, Series A

OPERATION UPSHOT-KNOTHOLE

Project 8.5

THERMAL RADIATION PROTECTION AFFORDED TEST ANIMALS BY FABRIC ASSEMBLIES

REPORT TO THE TEST DIRECTOR

by

Alfred Oesterling and Staff

UNCLASSIFIED

REGRADED .....

BY AUTHORITY OF DA Form 1575 FCRG 274/24 2 Aug 63

BY ..... B. W. Oole, 23 Sep 64

~~FORMERLY RESTRICTED DATA~~

Handle As Restricted Data in Foreign Dissemination Section 144B, Atomic Energy Act, 1954

July 1955

~~RESTRICTED DATA~~

~~This document contains restricted data as defined in the Atomic Energy Act of 1954. Its transmittal or the disclosure of its contents in any manner to an unauthorized person is prohibited.~~

Quartermaster Research and Development Laboratories
Army Medical Service Graduate School
Walter Reed Army Medical Center
University of Rochester Atomic Energy Project

~~CONFIDENTIAL~~ UNCLASSIFIED

pigs (Section 3.4). The degree and extent of burns noted beneath these assemblies were less than would have been expected on the basis of previous laboratory experience, especially at the higher calorie levels.

4.1.2 Factors Contributing to the Greater Degree of Thermal Protection in the Field.

There are several conditions encountered in the field, especially at the higher energy levels, but not duplicated in the laboratory (at least not up to the present time) that may account for the fact that like amounts of thermal energy did not produce comparable results in the laboratory and in the field. First, the thermal energy is delivered much more rapidly with the explosion of an atomic bomb than it is in the laboratory. Second, due to smoke obscuration the animals in the field actually received a smaller percentage of the total energy delivered than they did in the laboratory. Third, the blast wave following the explosion tended to extinguish flames and remove char, whereas no such wave was present in the laboratory tests. Fourth, where the heat reached the fabric layer next to the skin, uniform drape (or spacing) provided additional protection in the field.

(1) In comparing field with laboratory results, consideration must be given to irradiance, which expresses the time-intensity of the thermal pulse (cal/cm^2/sec). At the highest calorie levels laboratory irradiances were much lower than field irradiances. The reason for this is that an atomic explosion delivers a high quantity of thermal energy per unit area in a much shorter time than the same quantity can be delivered over a practical exposure area (1.7 cm diam) with existing laboratory equipment. For example, approximately 2 sec are required to deliver 75 cal/cm^2 in the laboratory with the carbon arc operating at peak capacity, an irradiance of 37.5 cal/cm^2/sec. In the field this much energy was delivered at the forward stations in both Shots 9 and 10 in approximately 0.5 sec, an irradiance of 150 cal/cm^2/sec.

Irradiances have been varied within the limits possible in the laboratory, and it has been found that certain levels of thermal energy will produce a more serious lesion if applied slowly than if applied rapidly.[18] Beneath the HW assembly spaced 5 mm from the skin, for example, a 2+ burn was produced when a thermal energy of 17 cal/cm^2 was applied in 2 sec (8.5 cal/cm^2/sec) but no burn, or at the most a mild 1+ burn, resulted when the same energy was applied in 0.5 sec (34 cal/cm^2/sec). With lower irradiances the fabric may be scorched or charred but remain intact and thus act as a heat reservoir from which heat can subsequently be transmitted to the skin. With higher irradiances, laboratory results indicate that all or part of the thermal input may be dissipated by an endothermic decomposition of the fabric. In the field, especially at the closer stations where irradiances exceeded 35 cal/cm^2/sec, conditions were favorable for such dissipation of energy.

(2) Motion pictures of clothed animals, exposed to 50.0 and 33.5 cal/cm^2 on Shots 9 and 10 respectively, showed heavy clouds

of black smoke enveloping the animals within 120 ms of the explosion. There is reason to believe that, in view of the short time within which most of the radiant energy from the explosion was delivered, much of this energy was prevented from reaching the animals by this smoke. In the laboratory tests, because the exposure area was so much smaller and the time of energy application at the high calorie levels so much longer, smoke obscuration appears to be of little or no significance.

(3) The blast wave following the explosion, which has not been duplicated in laboratory applications of thermal energy, has two possible protective effects. First, it can be expected to extinguish flames induced by the radiation in assemblies not treated for fire resistance, thus removing a source of high heat. Although the blast wave may not actually extinguish the flame in all cases,* it can be expected in general to have this effect. Second, the blast wave would tend to remove any char which, if allowed to remain, would act as a heat reservoir and increase the likelihood of a severe burn.

(4) The drape of the uniform may have contributed to a reduction of thermal injury in the field, in the case of the two-layer Hot-Wet assemblies. Laboratory tests upon which estimates of protection in the field were based consisted of the application of energy to fabrics in tight contact with the animal's skin. Other tests on cotton fabrics have indicated that spacing the fabric away from the skin would increase the protection afforded. In the uniforms, although some fabric areas were in close skin contact, many were spaced away in normal drape. This fact undoubtedly gave the uniforms an additional protective value as compared to laboratory tests where fabrics were held in close skin contact.

4.2 THE ROLE OF THE FLAMEPROOFING TREATMENT

One of the major problems designated for study at UPSHOT-KNOTHOLE was to determine whether materials actually did flame under the conditions of the test and, if so, how much protection could be afforded by fire resistant treating the outer layer. The results of the test show conclusively that flaming and probably glow did occur in many instances. The principal value of the fire retardant used in these tests, brominated triallyl phosphate, lay in its prevention of these exothermic reactions. In some cases it also seemed to give additional protection against the primary thermal effects of the explosion, although in other cases the untreated fabrics gave better protection than the treated. The peculiar pebbly, blistered, weeping edema noted in these tests occurred only in pigs wearing the fire resistant uniforms.

---

*The occurrence of persistent flame type burns that require longer to produce (according to laboratory tests) than the blast arrival time may indicate that the blast wave does not always extinguish the flame. On the other hand such burns may have been induced by glow.

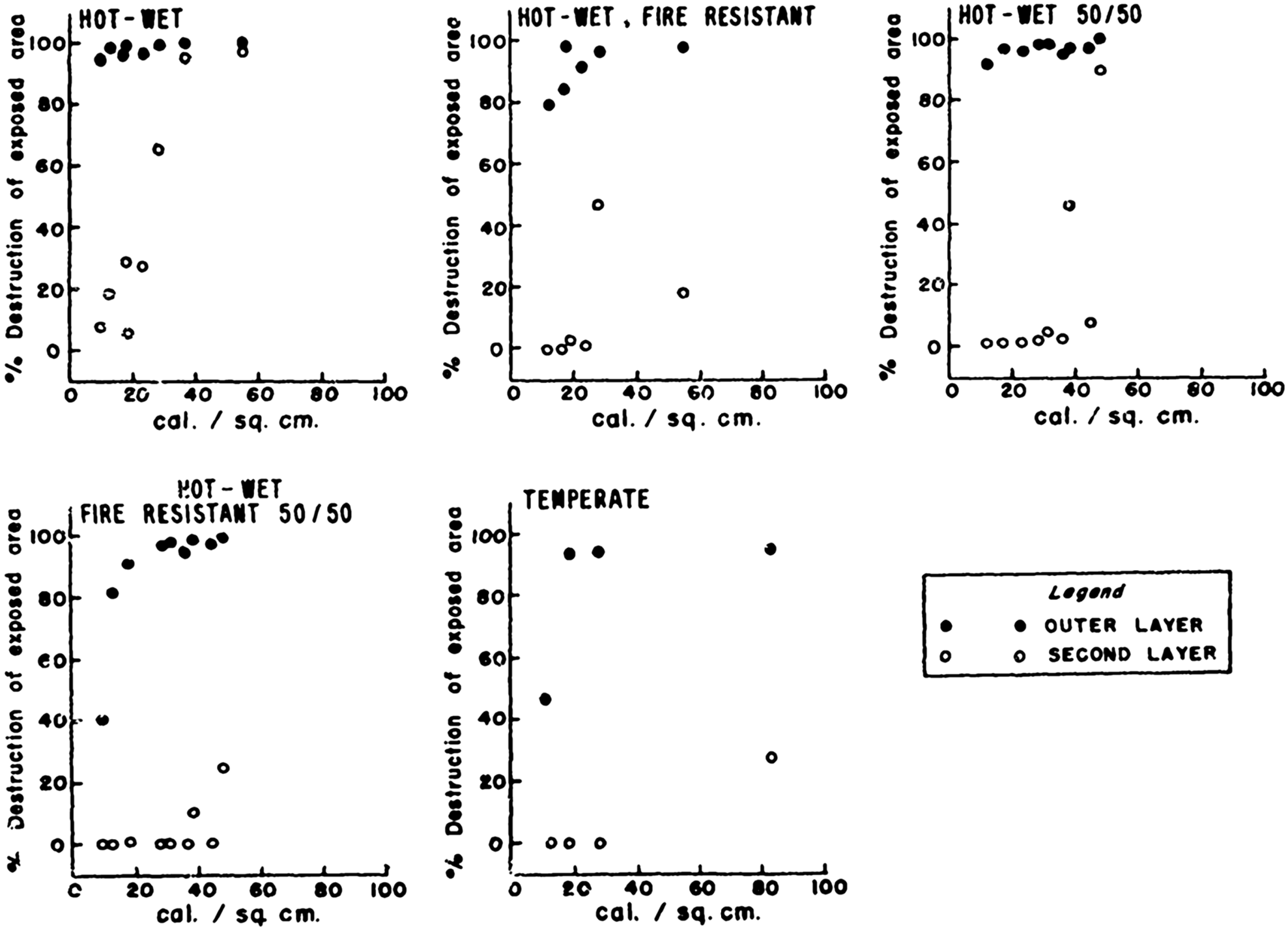

Fig. 3.5 Destruction of Outer and Second Layers of Pigs' Uniforms (Shots 9 and 10)

360876 L
CATALOGED BY: DDC
AS AD No.

WT-1441

This document consists of 50 pages.
No. 175 of 185 copies, Series A

OPERATION

PLUMBBOB

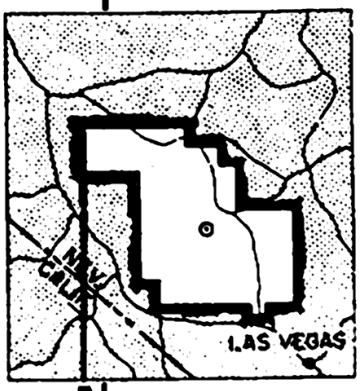

NEVADA TEST SITE
MAY-OCTOBER 1957

TECHNICAL LIBRARY
of the
27 MAY 1965
DEFENSE ATOMIC
SUPPORT AGENCY

AVAILABLE COPY WILL NOT PERMIT
FULLY LEGIBLE REPRODUCTION
REPRODUCTION WILL BE MADE IF
REQUESTED BY USERS OF DDC.

Project 8.2

PREDICTION of THERMAL PROTECTION of UNIFORMS, and THERMAL EFFECTS on a STANDARD-REFERENCE MATERIAL (U)

Issuance Date: May 2, 1960

JUN 7 1965
TISIA D

HEADQUARTERS FIELD COMMAND
DEFENSE ATOMIC SUPPORT AGENCY
SANDIA BASE, ALBUQUERQUE, NEW MEXICO

This material contains information affecting the national defense of the United States within the meaning of the espionage laws Title 18, U. S. C., Secs. 793 and 794, the transmission or revelation of which in any manner to an unauthorized person is prohibited by law.

1.2.2 Comparison of Skin-Simulant Response and Burns to Pigs. The improved NML skin simulant, molded from silica-powder-filled urea formaldehyde, has the thermocouple embedded at a depth of 0.05 cm in order to give burn predictions based on maximum temperature attainment. The basic criterion is a rise of 25 C or more for a second-degree burn to human skin or for a 2+ mild burn to pig skin. This criterion is based on the assumption of (1) the equivalence of a minimal white burn on the rat skin (or a 2+ mild burn in pig skin) to a second-degree burn in human skin, (2) an initial skin temperature of 31 C, and (3) correspondence of the thermal properties of pig, rat, and human skin. The accuracy of such a burn prediction in terms of indicent radiant exposure is estimated to be ± 10 percent. A skin-simulant temperature rise of 20 C or greater is estimated to correspond to a first-degree human burn or a 1+ moderate pig skin burn, and a rise of 35 C is estimated for a third-degree human burn or a 3+ mild pig burn. The latter estimations, probably accurate to ± 20 percent, are based on pig-burn data obtained at the University of Rochester (Reference 6).

TABLE 2.1 RADIANT ABSORPTANCES OF SKIN SIMULANT AND STANDARD FABRICS

Specimen	Radiant Absorptance
Skin simulant, bare	0.72
Skin simulant, blackened	0.95
Poplin, Shade 116, 5-oz/yd^2	0.63
Sateen, gray, 9-oz/yd^2	0.91

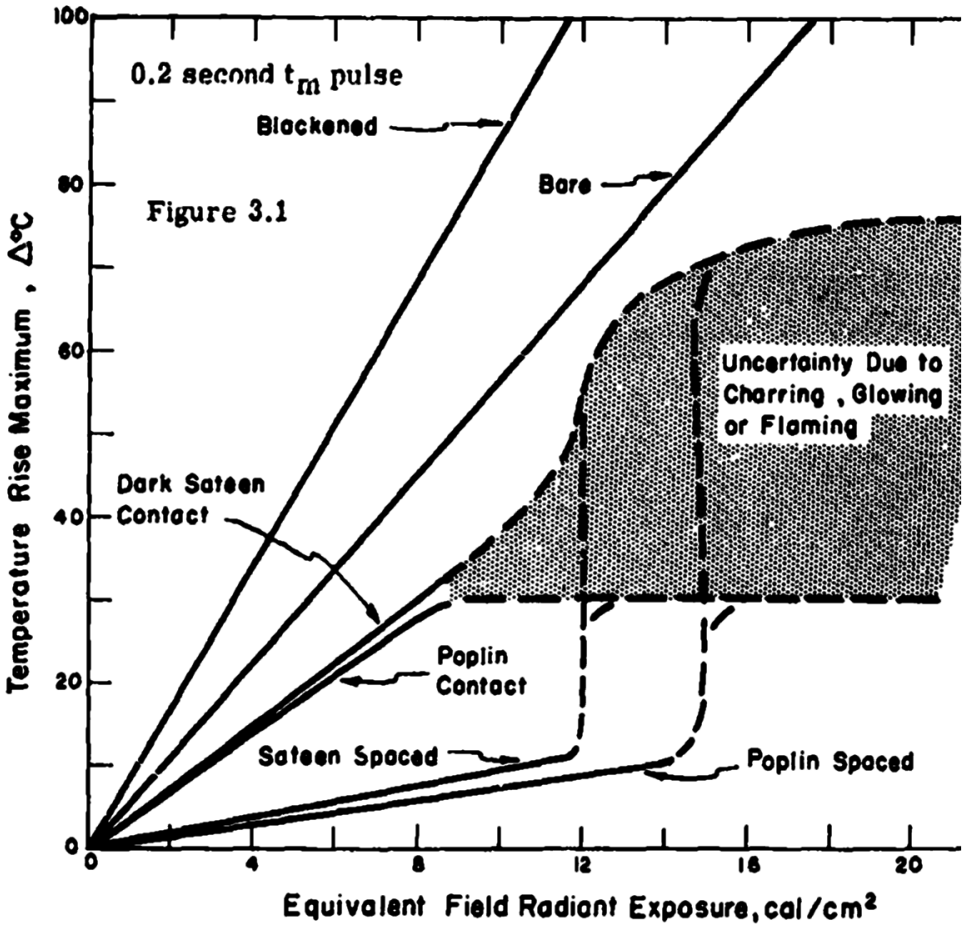

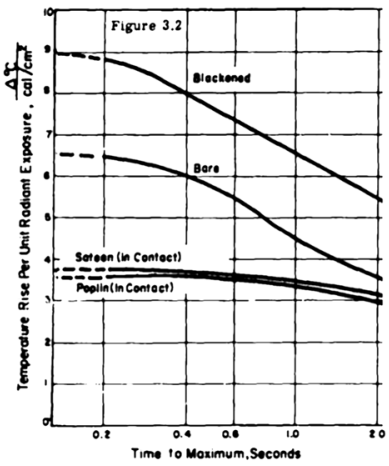

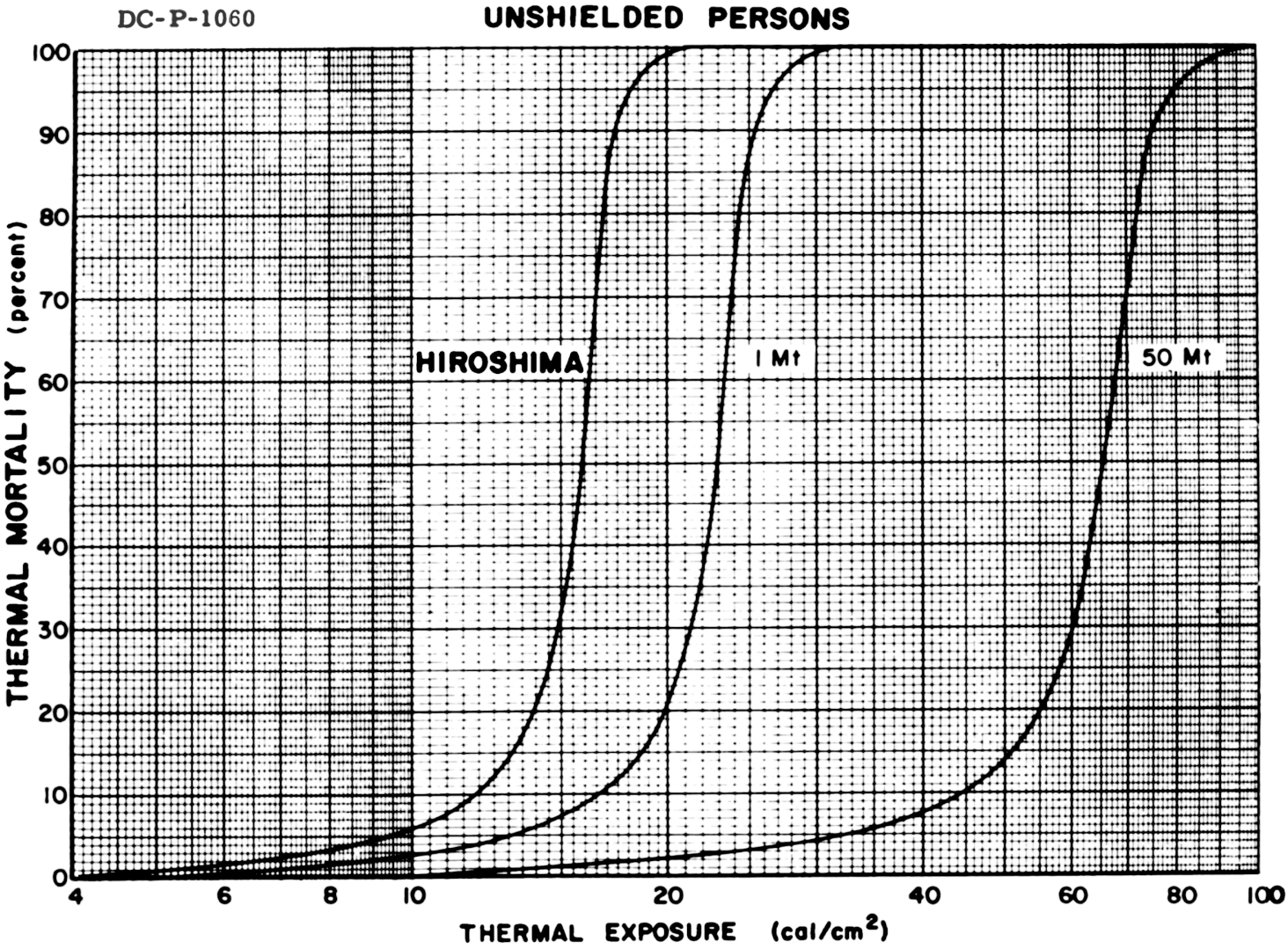

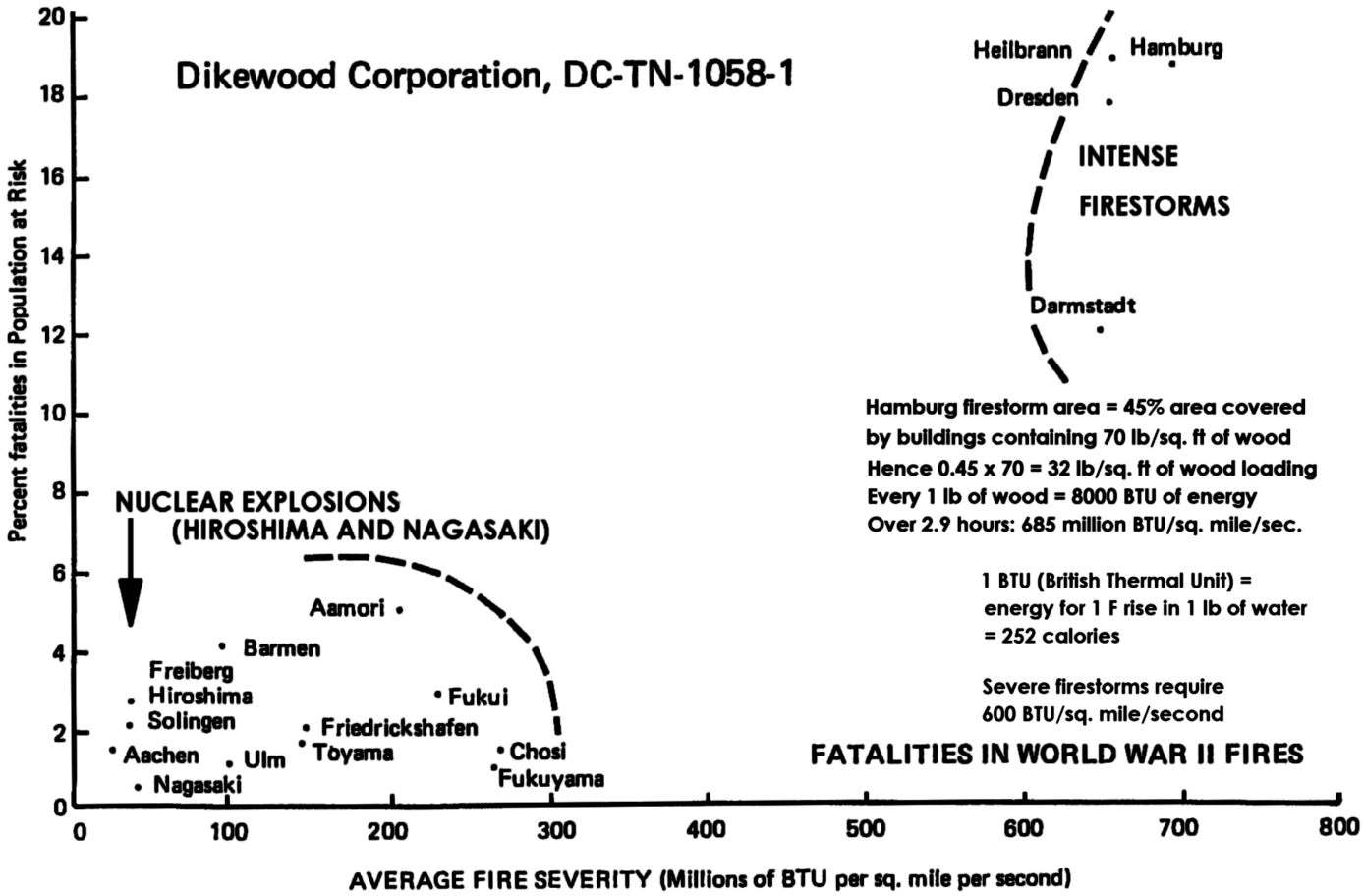

T. E. Lommasson and J. A. Keller, A Macroscopic View of Fire Phenomenology and Mortality Prediction, Proceedings of the Tripartite Technical Cooperation Program, Mass Fire Research Symposium of the Defense Atomic Support Agency, The Dikewood Corporation; October, 1967.

EXPERIENCE OF GERMAN AND JAPANESE AIR RAIDS

Source: AD0642790, p. 8. Basic data: Dirkwood DC-WP-1040-1, AD-827 029/0

City	Lives Lost	Percent of Population	Buildings Destroyed	Area Burned, sq mi
Tokyo	84,000	1.2	300,000	15.8 (total loss)
Hamburg	42,000	2.4	300,000	4.5 (total loss)
				12 (heavy damage)
Kassel	8,700	3.8	33,000	2.9 (total loss)
Darmstadt	8,100	7.4	22,000	1.5
Hiroshima	70,000*	28.0	68,000	4.4 (firestorm area)
Nagasaki	40,000*	17.0	21,000	0.049 (fire only)
				0.864 (fire and blast)

***Guest Korean workers, POWs, and military personnel excluded.**

When water evaporates from the burned surface, cooling results and the body loses heat. The larger the burn wound, the more water loss and the more heat or energy loss.

How Can the Fluid and Heat Losses Be Diminished?

Think Plastic Wrap as Wound Dressing for Thermal Burns

ACEP (American College of Emergency Physicians) News
http://www.acep.org/content.aspx?id=40462

August 2008
By Patrice Wendling
Elsevier Global Medical News

CHICAGO - Ordinary household plastic wrap makes an excellent, biologically safe wound dressing for patients with thermal burns en route to the emergency department or burn unit.

The Burn Treatment Center at the University of Iowa Hospitals and Clinics, Iowa City, has advocated prehospital and first-aid use of ordinary plastic wrap or cling film on burn wounds for almost two decades with very positive results, Edwin Clopton, a paramedic and ED technician, explained during a poster session at the annual meeting of the American Burn Association.

"Virtually every ambulance in Iowa has a roll of plastic wrap in the back," Mr. Clopton said in an interview. "We just wanted to get the word out about the success we've had using plastic wrap for burn wounds," he said.

Dr. G. Patrick Kealey, newly appointed ABA president and director of emergency general surgery at the University of Iowa Hospital and Clinics, said in an interview that plastic wrap reduces pain, wound contamination, and fluid losses. Furthermore, it's inexpensive, widely available, nontoxic, and transparent, which allows for wound monitoring without dressing removal.

"I can't recall a single incident of its causing trouble for the patients," Dr. Kealey said. "We started using it as an answer to the problem of how to create a field dressing that met those criteria. I suppose that the use of plastic wrap has spread from here out to the rest of our referral base."

Although protocols vary between different localities, plastic wrap is typically used for partial- and full-thickness thermal burns, but not superficial or chemical burns. It is applied in a single layer directly to the wound surface without ointment or dressing under the plastic and then secured loosely with roller gauze, as needed.

Because plastic wrap is extruded at temperatures in excess of 150° C, it is sterile as manufactured and handled in such a way that there is minimal opportunity for contamination before it is unrolled for use, said Mr. Clopton of the emergency care unit at Mercy Hospital, Iowa City. However, it's best to unwind and discard the outermost layer of plastic from the roll to expose a clean surface.

UCRL-TR-231593

LAWRENCE
LIVERMORE
NATIONAL
LABORATORY

Thermal Radiation from Nuclear Detonations in Urban Environments

R. E. Marrs, W. C. Moss, B. Whitlock

June 7, 2007

Even without shadowing, the location of most of the urban population within buildings causes a substantial reduction in casualties compared to the unshielded estimates. Other investigators have estimated that the reduction in burn injuries may be greater than 90% due to shadowing and the indoor location of most of the population [6].

We have shown that common estimates of weapon effects that calculate a "radius" for thermal radiation are clearly misleading for surface bursts in urban environments. In many cases only a few unshadowed vertical surfaces, a small fraction of the area within a thermal damage radius, receive the expected heat flux.

6. L. Davisson and M. Dombroski, private communication; "Radiological and Nuclear Response and Recovery Workshop: Nuclear Weapon Effects in an Urban Environment 2007," M. Dombroski, B. Buddemeier, R. Wheeler, L. Davisson, T. Edmunds, L. Brandt, R. Allen, L. Klennert, and K. Law, UCRL-TR-XXXX (2007), in review.

Addendum No. 1

for

DNA 1240H-2, Part 2

HANDBOOK OF UNDERWATER NUCLEAR EXPLOSIONS

21 January 1974

M. J. Dudash
DASIAC
General Electric Company-TEMPO
816 State Street
Santa Barbara, CA 93102

CHAPTER	TITLE	PAGE
	VOLUME 2 – PART 2	
18	SURFACE SHIP PERSONNEL CASUALTIES: EFFECTS OF UNDERWATER SHOCK ON PERSONNEL	18-1

18.7 THERMAL AND NUCLEAR RADIATION EFFECTS ON SURFACE SHIP PERSONNEL

18.7.1 Casualty and Risk Criteria

Table 18-2

CDC NUCLEAR AND THERMAL RADIATION CRITERIA

New Thermal Radiation Criteria

Risk Criteria for Burns Under Summer Uniforms to Warned, Exposed Personnel

	% Incidence	Mechanism	10KT cal/cm^2	100KT cal/cm^2	1000KT cal/cm^2
Negligible	2.5	1° burn	3.1	4.2	5.8
Moderate	5	1° burn	3.7	5.0	6.8
Emergency	5	2° burn	6.3	8.8	12

Time to Ineffectiveness	Casualties due to 2nd Degree Burns			
	% Incidence	10KT cal/cm^2	100KT cal/cm^2	1000KT cal/cm^2
24. hr	50	38	53	73

Personnel Risk and Casualty Criteria for Nuclear Weapons Effects
ACN 4260, U. S. Army Combat Developments Command Institute of Nuclear Studies, August 1971

EFFECTS OF SPECTRAL DISTRIBUTION OF RADIANT ENERGY ON CUTANEOUS BURN PRODUCTION IN MAN AND THE RAT

Research and Development Technical Report USNRDL-TR-46
NM 006-015

25 April 1955

by

E.L. Alpen
C.P. Butler
S.B. Martin
A.K. Davis

U.S. NAVAL RADIOLOGICAL DEFENSE LABORATORY
San Francisco 24, California

For human skin the reflectivities and critical energies for production of a standard burn are the following:

filter "A", $\lambda_{max} = 0.42\mu$, $r = 24.4 \pm 3.5$ per cent, $Q = 3.20 \pm 0.37$ cal/cm^2;

filter "B", $\lambda_{max} = 0.55\mu$, $r = 40.9 \pm 3.8$ per cent, $Q = 3.25 \pm 0.28$ cal/cm^2;

filter "C", $\lambda_{max} = 0.65\mu$, $r = 56.9 \pm 2.5$ per cent, $Q = 9.9 \pm 2.1$ cal/cm^2;

filter "D", $\lambda_{max} = 0.85\mu$, $r = 53.4 \pm 2.2$ per cent, $Q = 14.0 \pm 1.1$ cal/cm^2;

filter "F", $\lambda_{max} = 1.7\mu$, $r = 17 \pm 0.60$ per cent, $Q = 2.50$ cal/cm^2 (approx.).

The ranges shown are standard deviations.

The significance of the optical properties of skin has been discussed and the property of the high transmission of skin in the region 0.7 to 1.0 has been presented.

SUMMARY

The Problem

How does the critical energy for the production of standard burns in both rats and humans vary with the wavelength of radiant energy?

Findings

The critical radiant energy, corrected for spectral reflectance, required for production of standard burns in both rat and human skin varies as much as 4-fold depending on the wavelength.

Proceedings of a Workshop

13 - 14 March 1968

Sponsored

by

The Committee on Fire Research
Division of Engineering
National Research Council

and the

Office of Civil Defense, Department of the Army

Published

by

National Academy of Sciences
Washington, D.C.
1969

Dr. Edward L. Alpen (U. S. Naval Radiological Defense Laboratory): About this question of the spectral dependence of radiant energy, I think Dr. Haynes may have given you the impression that white light does the trick. There is later work which tends to refute that. The work done at Virginia used cut-off filters. The effectiveness of all energy above a certain wave length or below a certain wave length was measured. At the upper end the most effective and the least effective were mixed together and made it appear that infrared was not too good in producing burns. When you subdivide the spectrum, the most effective energy in producing a flash burn is the infrared above about 1.2 microns.

The importance of this, and the only reason I make an issue of it, is that a very important source of flash burn, both in civilian life and under wartime disaster conditions, is radiant energy burns from flaming sources. We have done a great deal of research on this subject for the U. S. Forest Service, because radiant energy burns are important in forest fires.

Energy in the wave lengths of 0.6 to 0.8 micron is about one-eighth as destructive as the rest of the spectrum. But long wave length radiation above one micron is extremely destructive, and the most effective of all.

Dr. Alpen: Anything that shields out radiation above one micron is extremely effective in preventing burns to the skin.

AD0403071

Feasibility

In the typical household, some materials will generally be available for covering windows against thermal radiation. One half roll of aluminum foil would cover about 25 ft^2 and would provide very effective covering for 1 to 2 windows (those most likely to face the blast). Sufficient quantities of either light colored paint, Bon Ami, or whiting would be available in most households to cover windows. Aluminum screens attenuate from 30 - 50% of the thermal radiation and hence screens should be closed or installed.

The amount of water per square foot required to dissipate 25 cal/cm^2 of thermal radiation can quickly be calculated from the heat of vaporization of water (580 cal/gm). Allowing 90% losses due to absorption or spillage, one gallon of water is sufficient to wet 10 ft^2 of material so that it can withstand 25 cal/cm^2 of direct thermal radiation (i.e., the radiation is normal to the material surface at all points). Since the average daily water consumption per service (Reference 3) is about 700 gallons, it is apparent that the wetting of interior flammables (piled up curtains, furniture, etc.) is feasible in most cases when used in conjunction with the other measures.

3. Statistical Abstracts of the United States. Washington: U. S. Government Printing Office, 1962.

HOME OFFICE

SCOTTISH HOME DEPARTMENT

MANUAL OF CIVIL DEFENCE

Volume I

PAMPHLET No. 1

NUCLEAR WEAPONS

LONDON

HER MAJESTY'S STATIONERY OFFICE

1956

The probable fire situation in a British city

35 Japanese houses are constructed of wood and once they were set on fire they continued to burn even when knocked over. In this country only about 10 per cent. of all the material in the average house is combustible, and under conditions of complete collapse, where air would be almost entirely excluded, it is doubtful whether a fire could continue on any vigorous scale.

40 It seems unlikely from the evidence available that an initial density of fires equivalent to one in every other building would be started by a nuclear explosion over a British city. Studies have shown that a much smaller proportion of buildings than this would be exposed to thermal radiation and even then it is not certain that continuing fires would develop. Curtains may catch fire, but it does not necessarily follow that they will set light to the room; in the last war it was found that only one incendiary bomb out of every six that hit buildings started a continuing fire.

From a 10 megaton bomb, with its longer lasting thermal radiation (see paragraph 21), it takes about 20 calories per square centimetre to start fires because so much of the heat (spread out over the longer emission) is wasted by conduction into the interior of the combustible material and by convection and re-radiation whilst the temperature of the surface is being raised to the ignition point. But the distance at which 20 calories per square centimetre can be produced is only 11 miles, so that the scaling factor for a 10 megaton airburst bomb is therefore 11 and not 22.

43 For a ground burst bomb, however, several other factors contribute to a further reduction in the fire range. Apart from an actual loss of heat by absorption into the ground and from the pronounced shielding effect of buildings, the debris from the crater tends to reduce the radiating temperature of the fireball and a greater proportion of the energy is consequently radiated in the infra red region of the spectrum —this proportion being more easily absorbed by the atmosphere.

44 An important point in relation to personal protection against the effects of hydrogen bomb explosions is that because the thermal radiation lasts so long there is more time for people who may be caught in the open, and who may be well beyond the range of serious danger from blast, to rush to cover and so escape some part of the exposure. For example, people in the open might receive second degree burns (blistering) on exposed skin at a range of 16 miles from a 10 megaton ground burst bomb (8×2—see paragraph 24). If, however, they could take cover in a few seconds they would escape this damage. Moreover, at this range the blast wave would not arrive for another minute and a half so that any effects due to the blast in the open (e.g. flying glass, etc.) could be completely avoided.

ADA383988

November 1963
Second printing May 1964

Unclassified Version

SURVEY OF THE THERMAL THREAT OF NUCLEAR WEAPONS

Prepared for:

OFFICE OF CIVIL DEFENSE
DEPARTMENT OF DEFENSE
WASHINGTON 25, D.C.

By: Jack C. Rogers and T. Miller

SRI Project No. IMU-4021

Approved:

Robert A. Harker

ROBERT A. HARKER, DIRECTOR
MANAGEMENT SCIENCES DIVISION

OCD REVIEW NOTICE

This report represents the authors' views, which in general are in harmony with the technical criteria of the Office of Civil Defense. However, a preliminary evaluation by OCD indicates the need for further evaluation of the fire threat of nuclear weapons and formulation of promising research and action programs.

NOTE: discrepancies are due to HUMIDITY differences. ENCORE nuclear test (Nevada desert) humidity was ONLY 19%

Table B-VII

COMPARISON OF ESTIMATES FOR IGNITION ENERGY REQUIREMENTS
(10 mt)

Glasstone (1962) The Effects of Nuclear Weapons		Martin, et al. (1959) Naval Radiological Defense Laboratory		
Material	Cal/cm^2 for Ignition	Material	Cal/cm^2 for Ignition	Ratio of NRDL to ENW
Cotton auto seat upholstery, green, brown, white	16	Heavy cotton draperies, dark color	28	1.75
Wool pile chair upholstery, wine	35 (not sustained)	Wool pile chair upholstery, dark color	25	0.7
Newspaper, single sheet	6	Newspaper, medium printed	40	6.7
		Newspaper, dark areas	30	5.
Kraft paper carton, flat side exposed, used, brown	15	Corrugated Kraft board	40	2.6
Deciduous leaves	12	Walnut leaves	54	4.5
		Beech leaves	36	3.
Coarse grass	16	Harding grass	44	2.7
Ponderosa pine needles, brown	18	Pine needles	50	2.7

Sources: Martin, et al. (1959) and Glasstone (1962).

Martin, S. B., On Predicting the Ignition Susceptibility of Typical Kindling Fuels to Ignition by the Thermal Radiation from Nuclear Detonations, Tech. Report 367, U.S. Naval Radiological Defense Laboratory, San Francisco, Calif., April 1959. (U)

A SURVEY OF THE WEAPONS AND HAZARDS WHICH MAY FACE THE PEOPLE OF THE UNITED STATES IN WARTIME

Harold L. Brode

P-3170

June 1965

Most exposed surfaces in the city are non-combustible and much of the remainder is not ignitable by thermal flash. Although many fires could simultaneously start wherever building interiors are illuminated by the bomb thermal energy, they are not likely to be immediately beyond control, and will often go out unattended as they exhaust the available fuel (as in trash barrels or isolated wood piles or even pieces of paper on tables or floors).

Hanging non-flammable shields over window openings and removing likely fuels from exposed positions could also help.

RAND CORPORATION

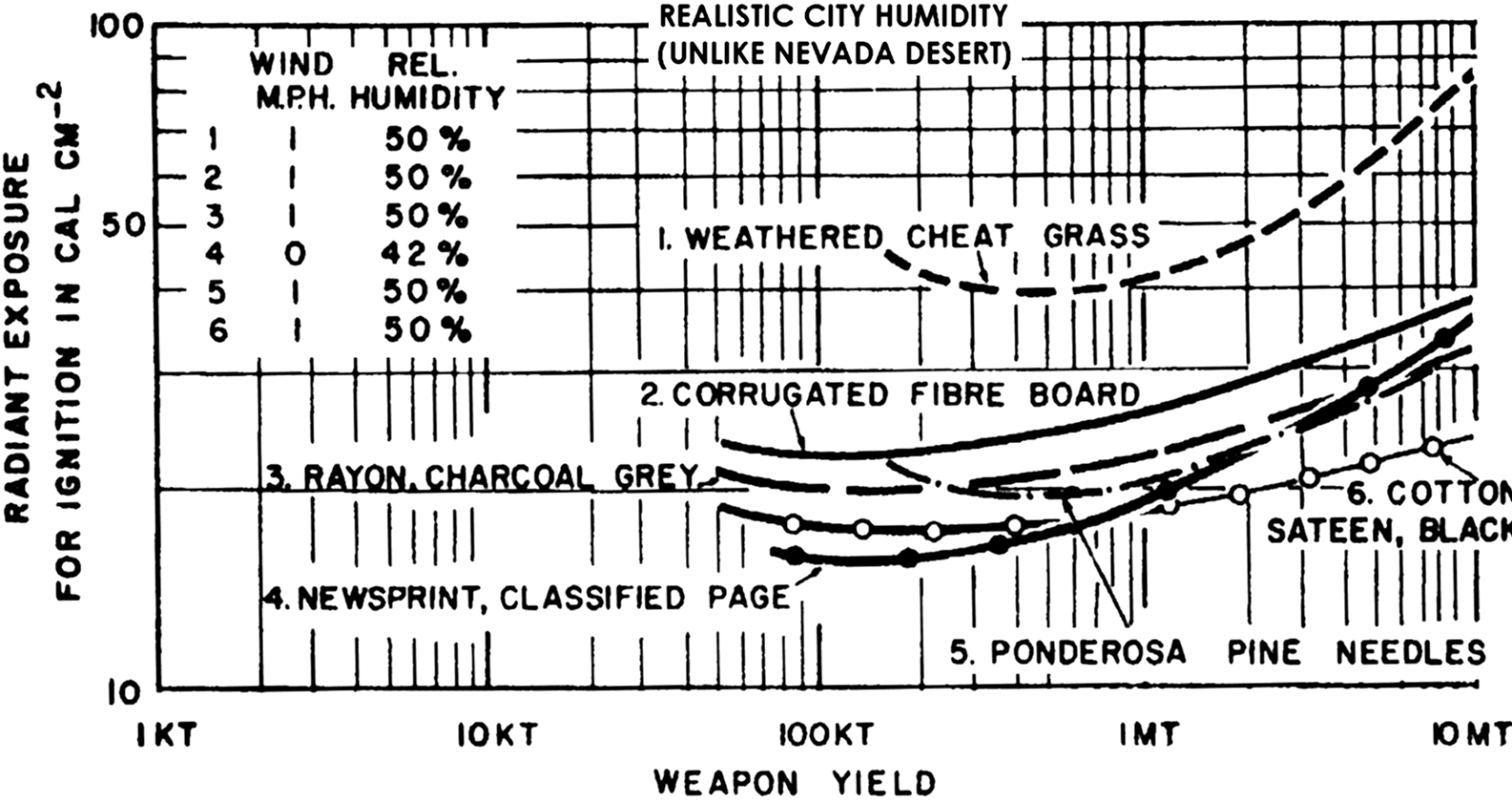

"TECHNICAL OBJECTIVE AW-7, CRITICAL RADIANT EXPOSURES FOR PERSISTENT IGNITION", JULY 1960, J. BRACCIAVENTI & F. DEBOLD AD-249476; DASA-1194

UCRL-TR-231593

Thermal radiation from nuclear detonations in urban environments

LAWRENCE LIVERMORE NATIONAL LABORATORY

June 7, 2007

Even without shadowing, the location of most of the urban population within buildings causes a substantial reduction in casualties compared to the unshielded estimates. Other investigators have estimated that the reduction in burn injuries may be greater than 90% due to shadowing and the indoor location of most of the population [6].

We have shown that common estimates of weapon effects that calculate a "radius" for thermal radiation are clearly misleading for surface bursts in urban environments. In many cases only a few unshadowed vertical surfaces, a small fraction of the area within a thermal damage radius, receive the expected heat flux.

Thermal radiation shadowing in modern high-rise cities

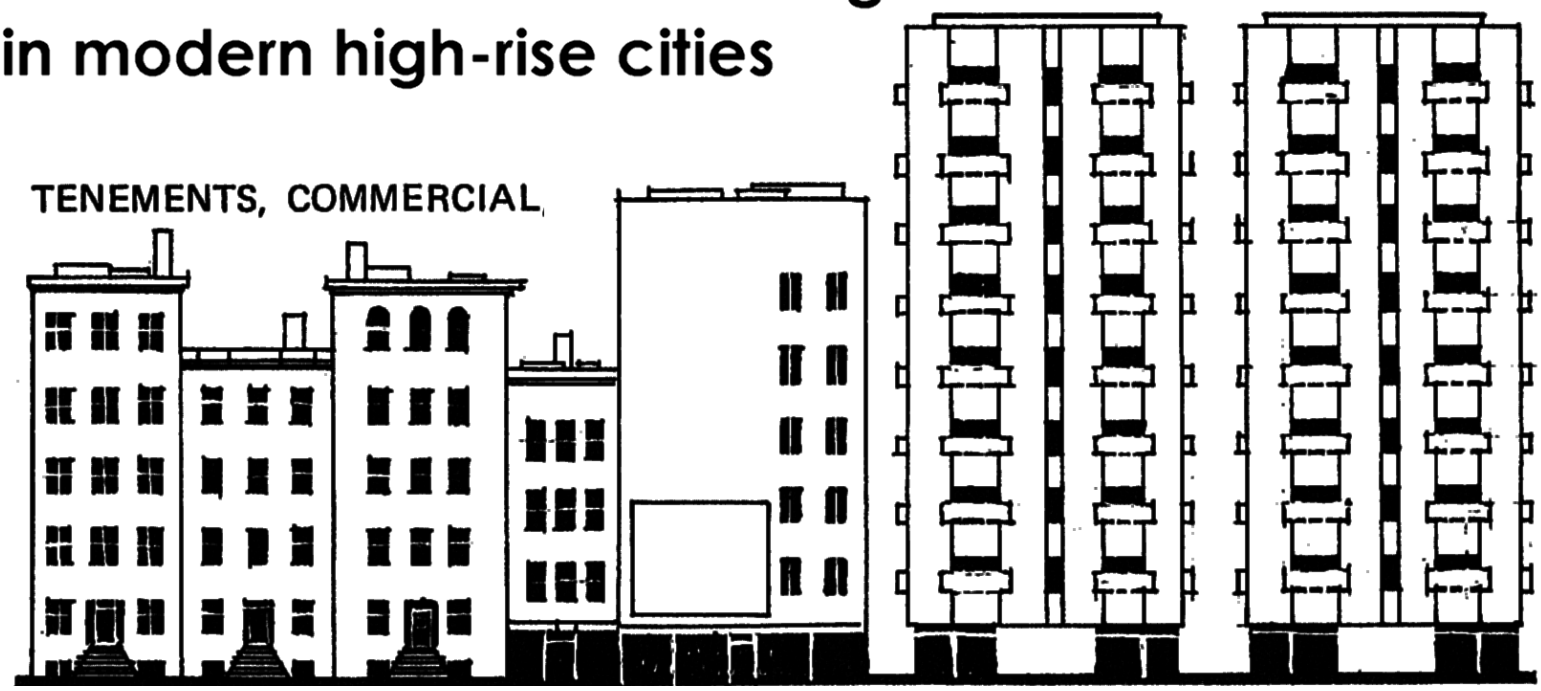

The National Archives
HO 225 /121

HOME OFFICE

SCIENTIFIC ADVISER'S BRANCH

(Paper at Tripartite Thermal Effects Symposium, Dorking, October 1964)

IGNITION AND FIRE SPREAD IN URBAN AREAS FOLLOWING A NUCLEAR ATTACK

G. R. Stanbury

INITIAL FIRE INCIDENCE

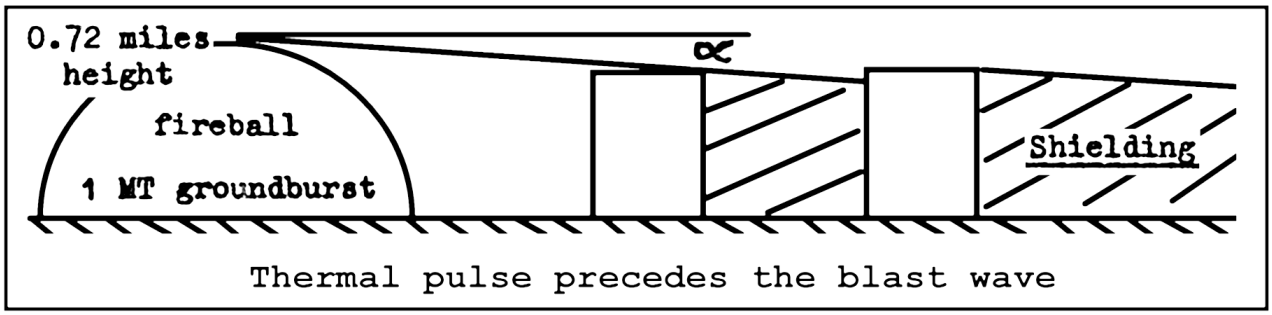

Assuming that buildings on opposite sides of a street which is receiving heat radiation from a direction perpendicular to its length are of the same height we take the average depth of a floor to be 10 ft.

Effect of Shielding: Estimation of the number of exposed floors

Distance from explosion miles	Angle of arrival α^{o}	Width of street (units of 10 ft.)						
		2	3	4	5	6	7	8
3	13½	.5	.5	1	1	1.5	1.5	2
4	10	.5	.5	.5	1	1	1.5	1.5
5	8	.5	.5	.5	.5	1	1	1

SPREAD OF FIRE

From last war experience of mass fire raids in Germany it was concluded that the overall spread factor was about 2; i.e. about twice as many buildings were destroyed by fire as were actually set alight by incendiary bombs

Number of fires started per square mile in the fire-storm raid on Hamburg, 27th/28th July, 1943

102 tons H.E.	48 tons, 4 lb. magnesium	40 tons, 30 lb. gel.
100 fires	27,000 bombs	3,000 bombs
	8,000 on buildings	900 on buildings
	1,600 fires	800 fires
2,500 fires in 6,000 buildings		

However, the important thing to note is that the total number of fires started in each square mile (2,500) was nearly half that of the total number of buildings; in other words, almost every other building was set on fire

When the figure of 1 in 2 for the German fire storms is compared with the figures for initial fire incidence of ~ 1 in 15 to 30 obtained in the Birmingham and Liverpool studies it can only be concluded that a nuclear explosion could not possibly produce a fire storm.

SECONDARY FIRES FROM BLAST DAMAGE IN LONDON

Fire situation from 1,499 fly bombs in the built-up part of the London Region

(Fires from 1 ton TNT V1 cruise missiles, 1944)

	Number of fly bombs	Fly Bombs Caused				
		No fire	Small fire	Medium fire	Serious fire	Major fire
Grand Totals	1,499	804	609	75	7	4

The large proportion started no fires at all even in the most heavily built-up areas.

All these fly bombs fell in the summer months of 1944 which were unusually dry. In winter in this country in residential areas there are many open fires which may provide extra sources of ignition. The domestic occupancy is a low fire risk however, and as the proportion of such property in the important City and West End areas is small this should not introduce any serious error. Moreover, in winter, the high atmospheric humidity and the correspondingly high moisture content of timber would tend to retard or even prevent the growth of fire.

Takata, A.N., Mathematical Modeling of Fire Defenses, IITRI, March 1970, AD 705 388.

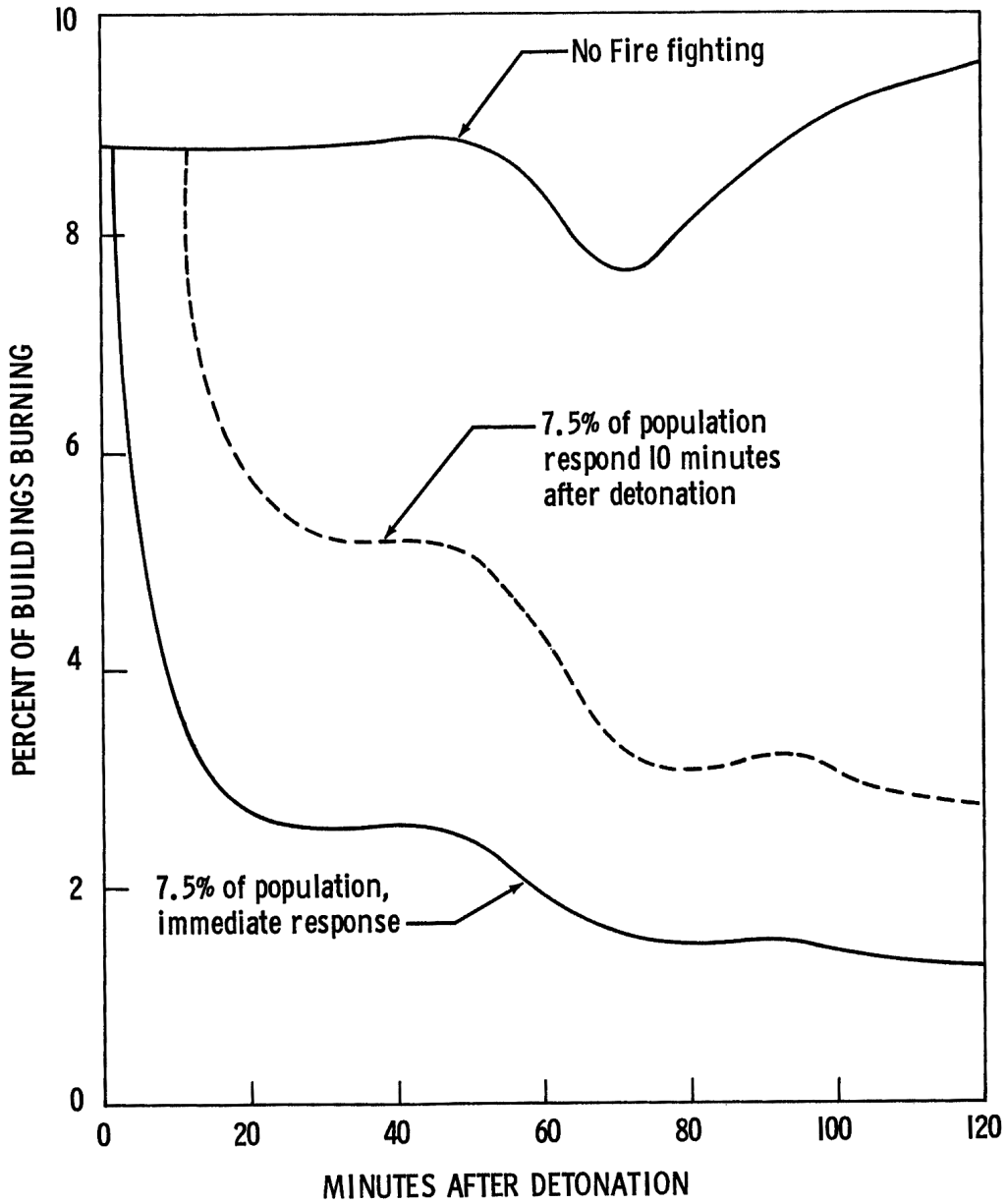

FIRE FIGHTING FOR HOUSEHOLDERS

Folded newspapers may not take fire, but loosely crumpled ones will. The answer? Get rid of trash.

A wet mop or broom will snuff out small fires. So will a burlap bag or a small rug soaked in water.

Buckets of water and sand are essential.

Water is an effective fire fighting agent because it smothers and cools at the same time.

FIRE-BOMBS rained on London

They did not all fall on roads

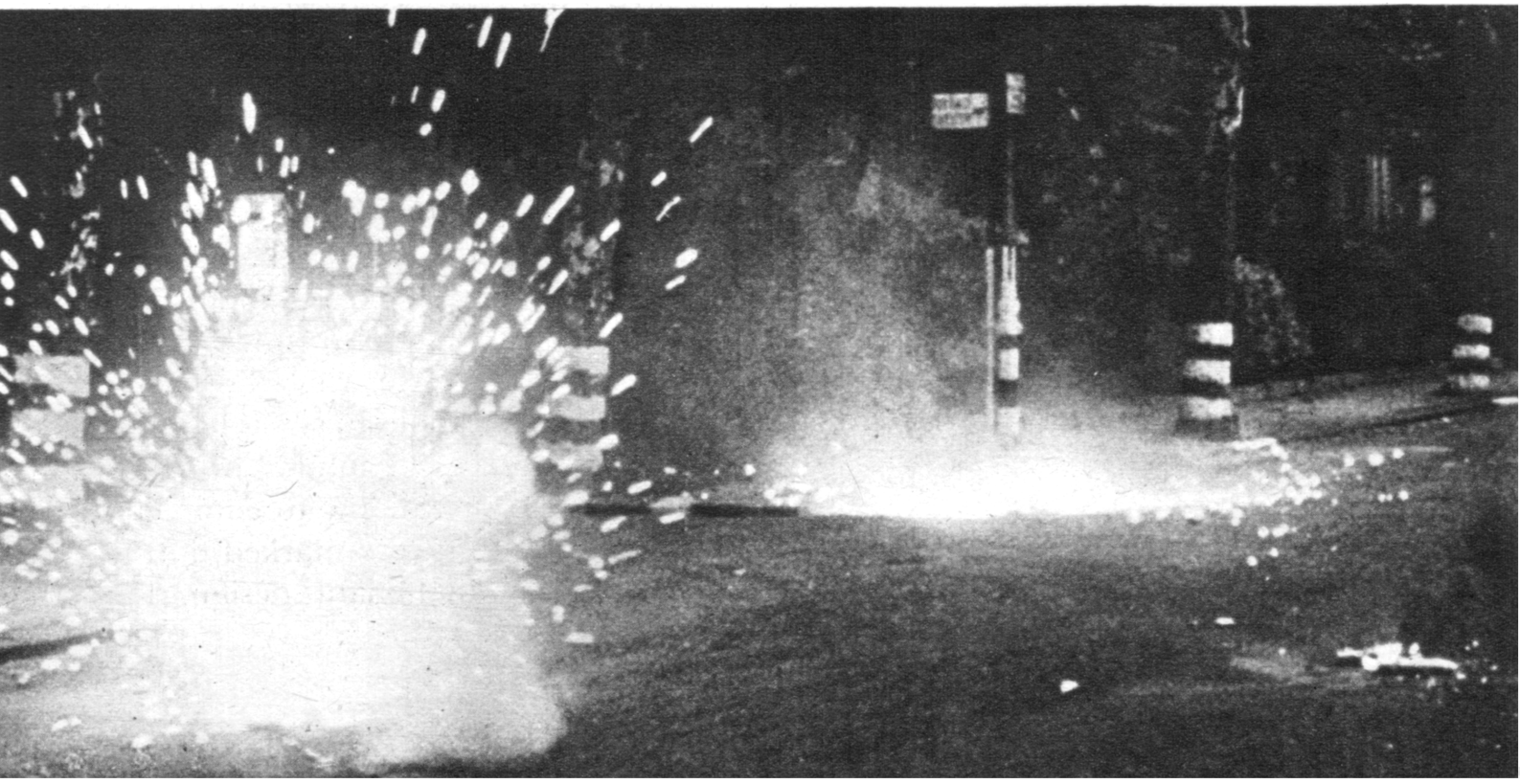

THE LUFTWAFFE SOUGHT A KNOCK-OUT BLOW. The first impact of the attack fell on the docks. The great day raid of 7th September, 1940, which was continued throughout the night and renewed on many nights after, left miles of fires blazing along either bank of the Thames. This is St. Katherine's Dock on the night of 11th September.

Amended Reprint
June, 1940

Crown Copyright Reserved

AIR RAID PRECAUTIONS HANDBOOK No. 9

(*1st edition*)

INCENDIARY BOMBS AND FIRE PRECAUTIONS

Issued by the
Ministry of Home Security

LONDON
PUBLISHED BY HIS MAJESTY'S STATIONERY OFFICE

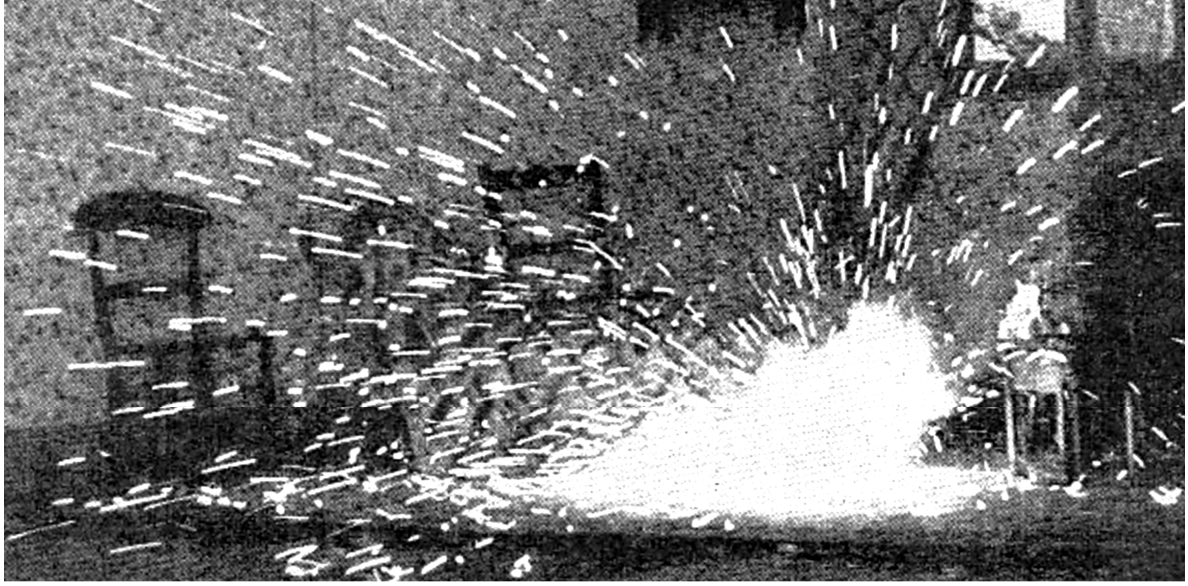

KILO MAGNESIUM INCENDIARY BOMB 15 SECONDS AFTER IGNITION.

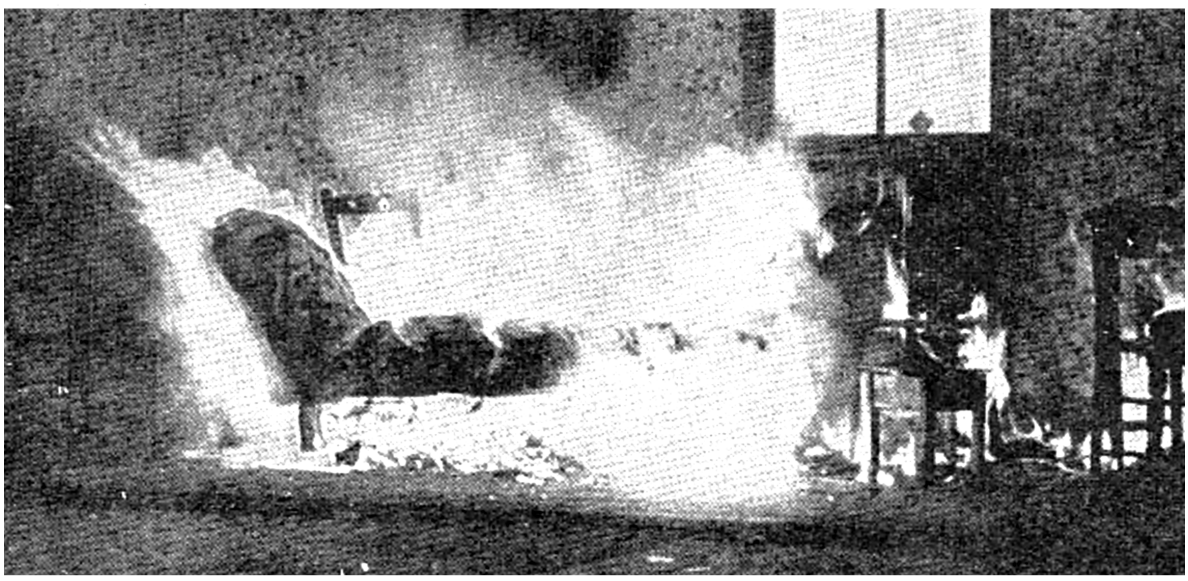

45 SECONDS

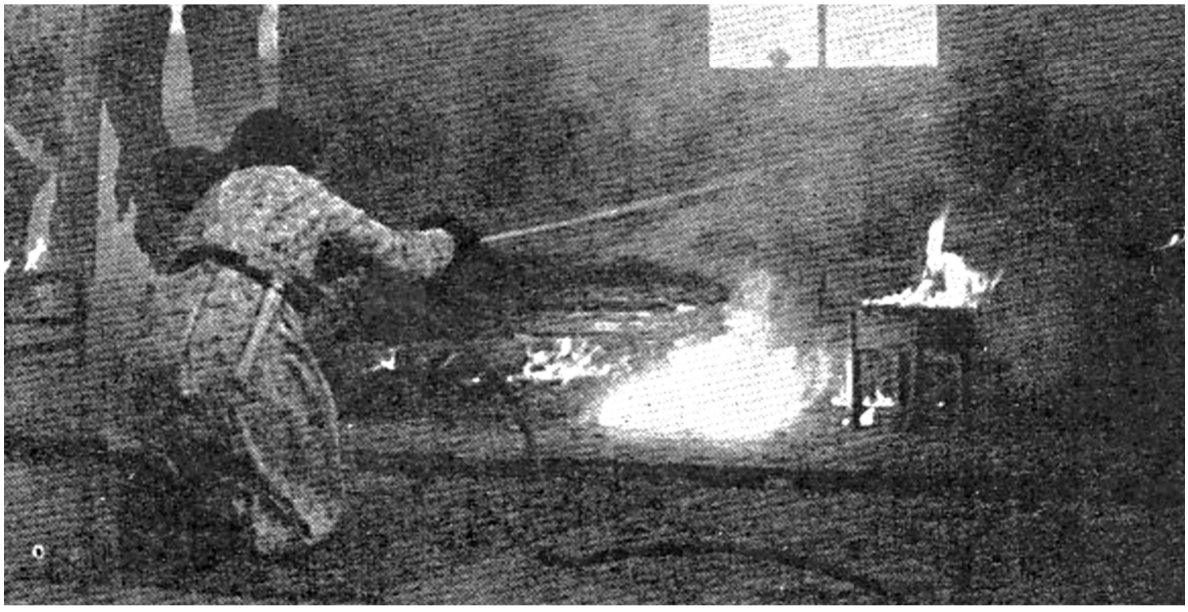

FIRE CONTROLLED BY WATER

Clothing on fire.

Never allow a person whose clothes are on fire to remain standing for a moment. Fatalities nearly always arise from shock of burning about the face and head. If the person starts to run, trip him up at once. Roll him on the floor or in a coat or blanket if you have one handy. If your own clothes catch fire, clap your hand over your mouth, and lie down and roll.

FIG. 1—TYPICAL KILO MAGNESIUM INCENDIARY BOMB.

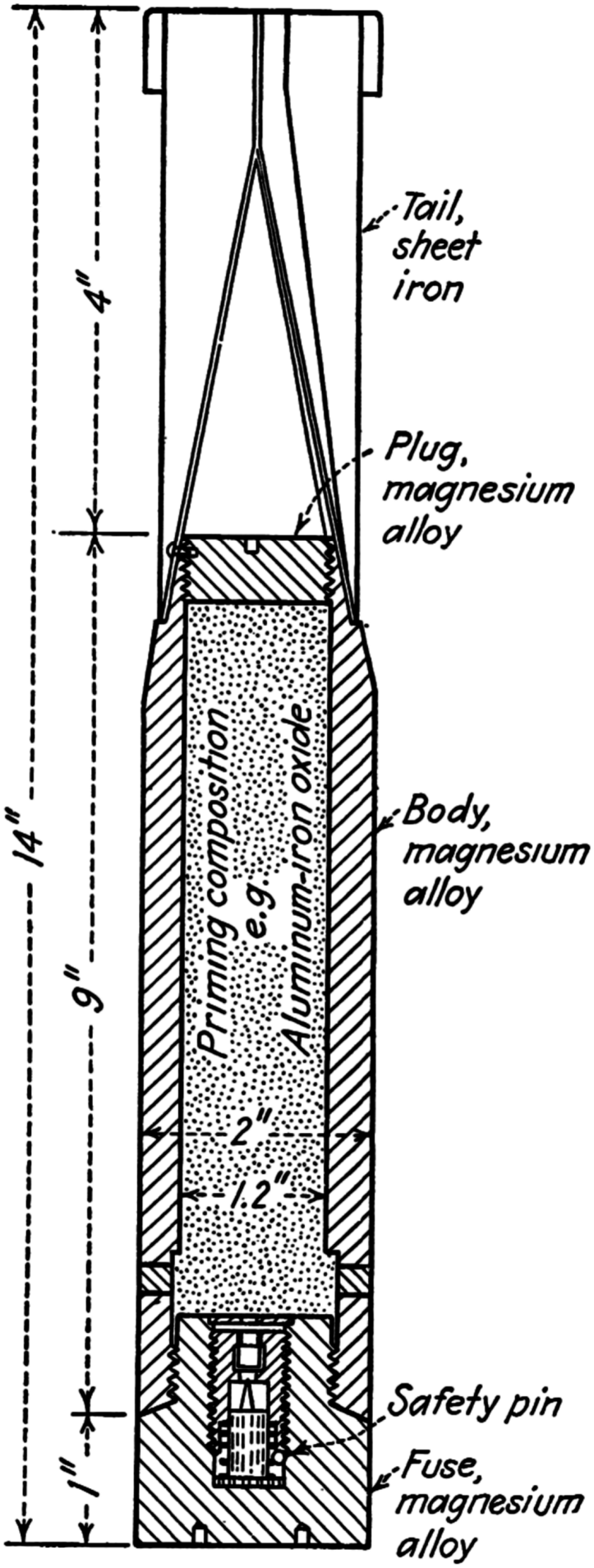

FIG. 2—TYPICAL KILO MAGNESIUM INCENDIARY BOMB. SECTIONAL DRAWING.

Restricted

For Official Use

CIVIL DEFENCE

TRAINING PAMPHLET NO. 2
(3rd Edition)

OBJECTS DROPPED FROM THE AIR

Issued by the Ministry of Home Security

Crown Copyright Reserved

LONDON
HIS MAJESTY'S STATIONERY OFFICE
1944

Price 6d. net

Copies will be sold only on written application by a Clerk to a local authority, a Chief Constable, a principal of a public utility company, or by County Secretaries of the St. John Ambulance Brigade, British Red Cross Society, and St. Andrew's Ambulance Association to H.M. STATIONERY OFFICE at any of the following addresses: York House, Kingsway, London, W.C.2; 13a Castle Street, Edinburgh; 39-41 King Street, Manchester 2; 1 St. Andrew's Crescent, Cardiff; or 80 Chichester Street, Belfast.

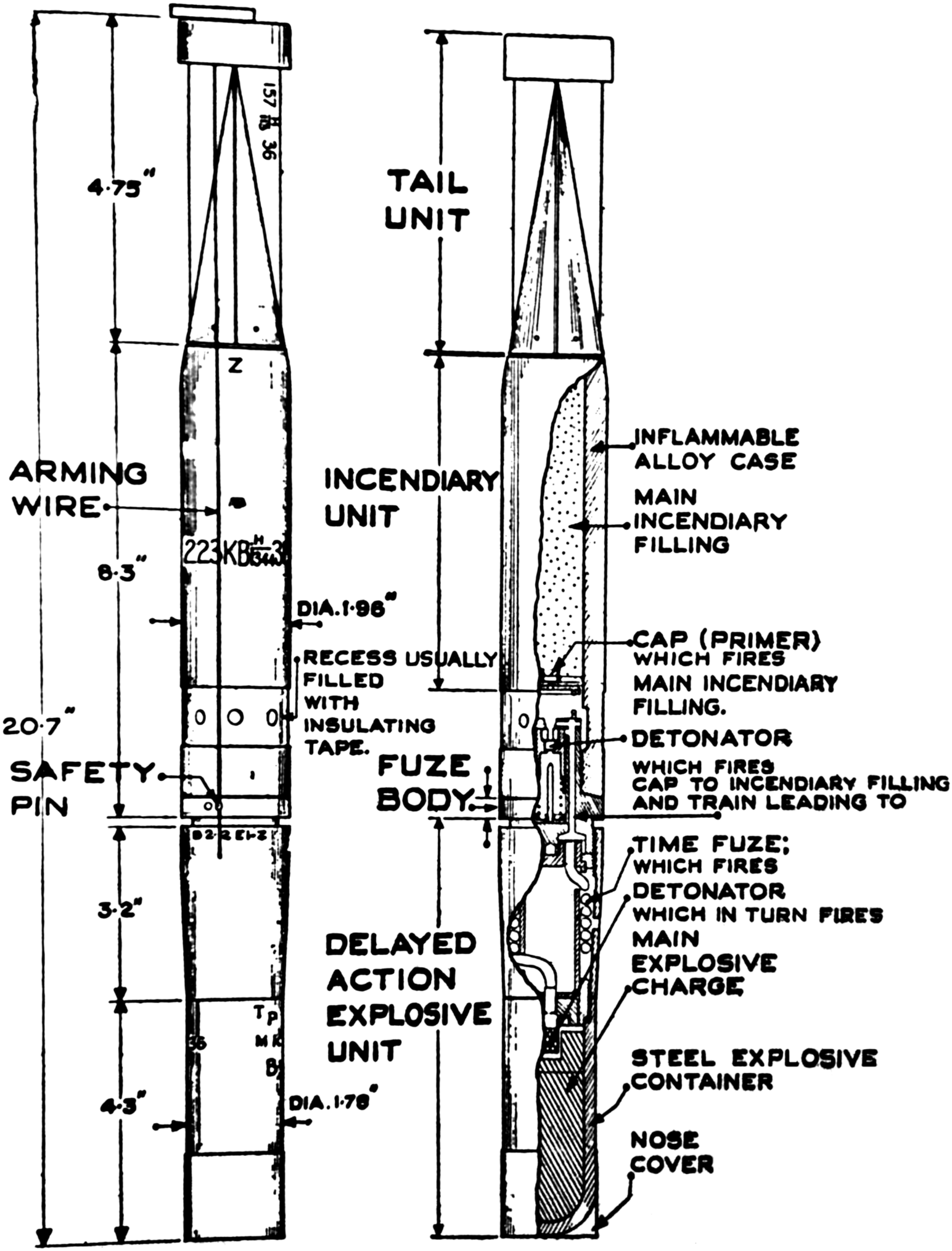

FIGURE 12A.—GERMAN INCENDIARY BOMB WITH EXPLOSIVE NOSE

DOMESTIC NUCLEAR SHELTERS

TECHNICAL GUIDANCE

To obtain some protection from the heat it is necessary to move out of the direct path of the rays from the fireball; any kind of shade will be of some value.

A fire-storm occurred only in an area of several square miles, heavily built up with buildings containing plenty of combustible material and where at least every other building in the area had been set alight. It is not considered that the initial density of fires, equivalent to one in every other building, would be caused by a nuclear explosion over a British city. Studies have shown that due to shielding, a much smaller proportion of buildings than this would be exposed to the heat flash. Moreover, the buildings in the centres of most British cities are now more fire-resistant and more widely spaced than they were 30 to 40 years ago. This low risk of fire-storms would be reduced still further by the control of small initial and secondary fires.

3

A HOME OFFICE GUIDE

P-3026

FIREBALL PHENOMENOLOGY

Harold L. Brode

The RAND Corporation, Santa Monica, California

This paper was prepared for presentation at The Tripartite Technical Cooperation Panel Meeting, Panel N3, held at the Joint Fire Service College, Dorking, England, 5-9 October 1964. The papers are to be published by Defense Atomic Support Agency.

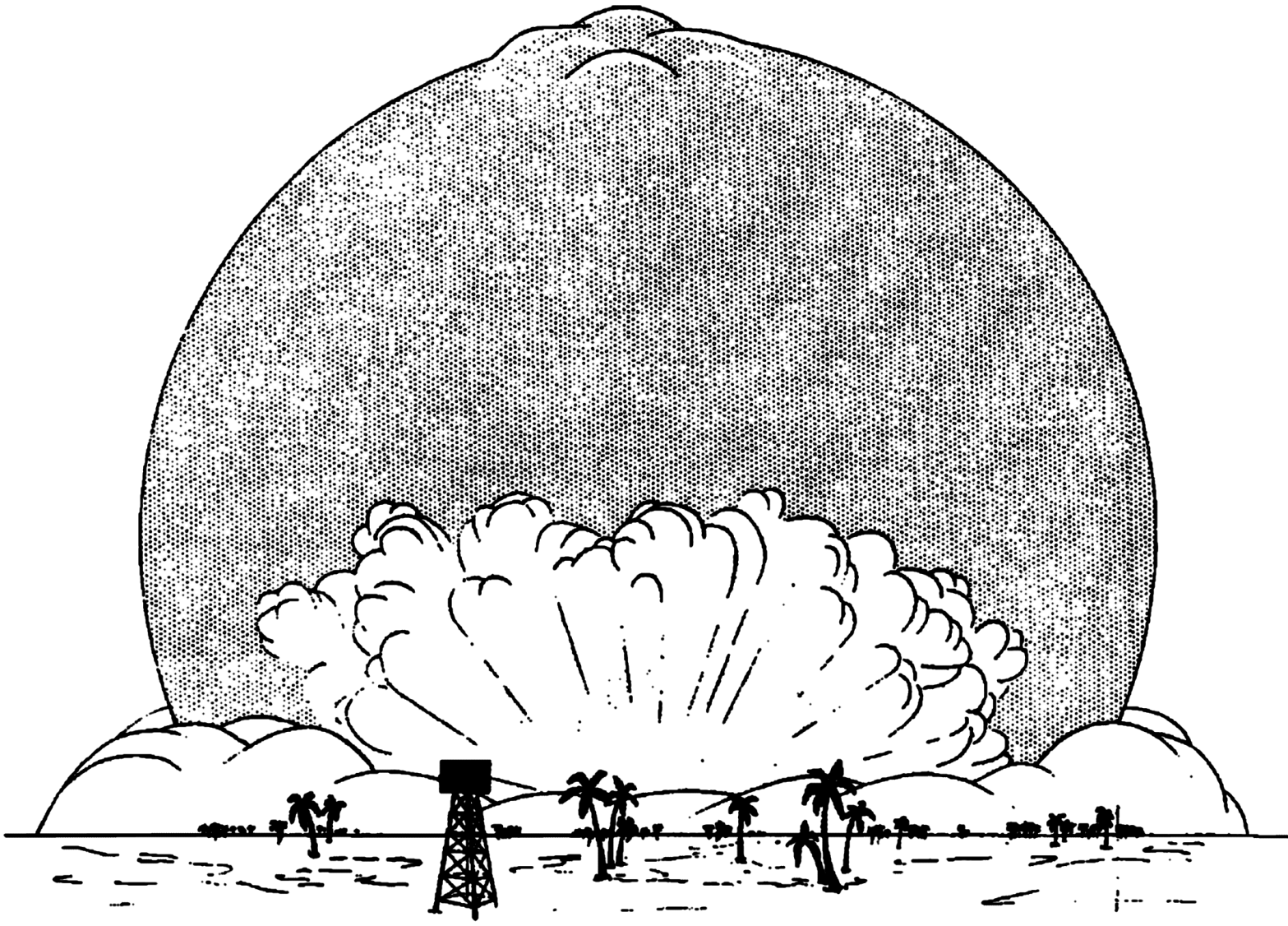

Fig. 20—Surface burst features influencing thermal radiation

Fireball shielding by crater ejecta (1.5 kt Buffalo-2)

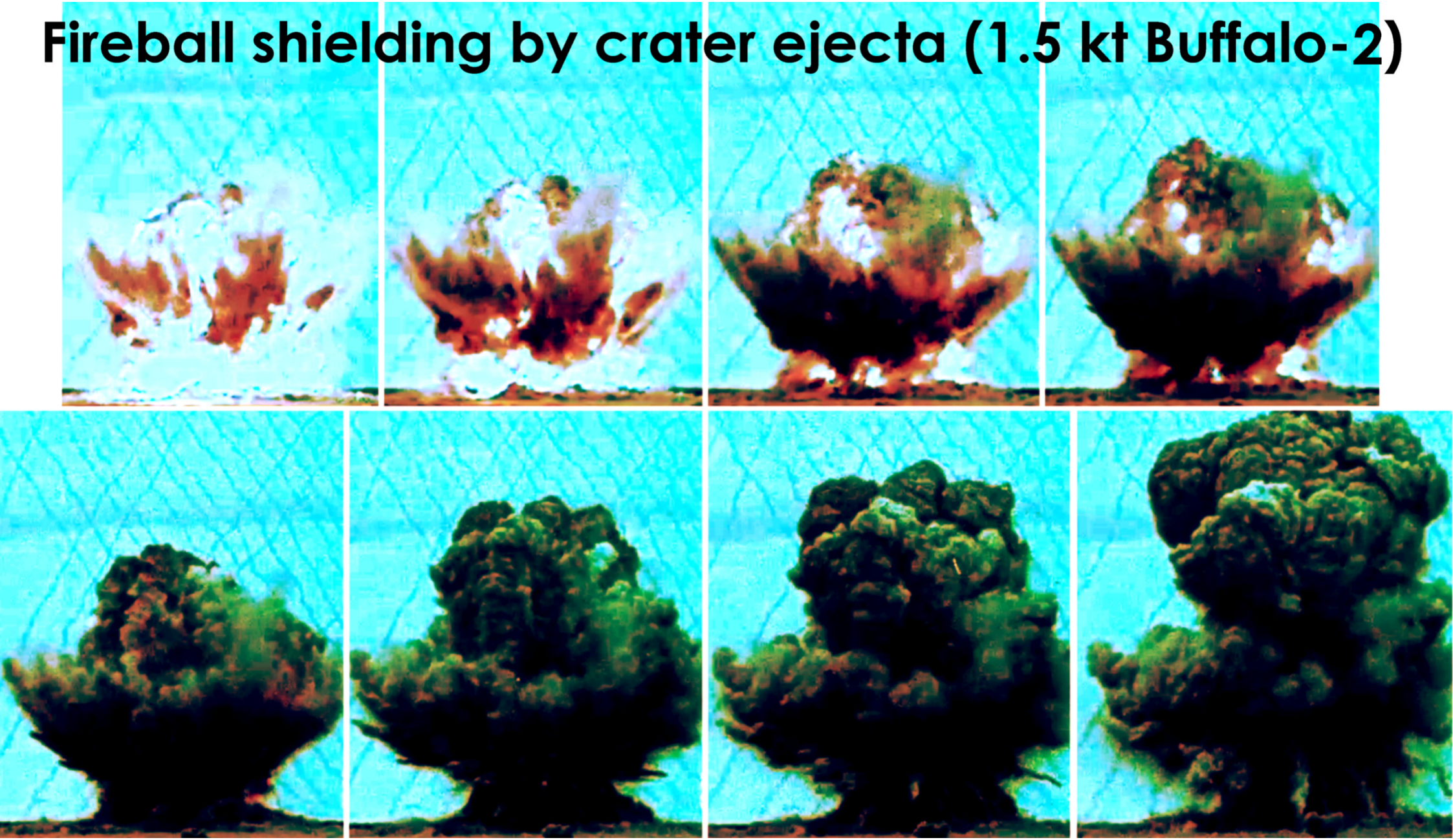

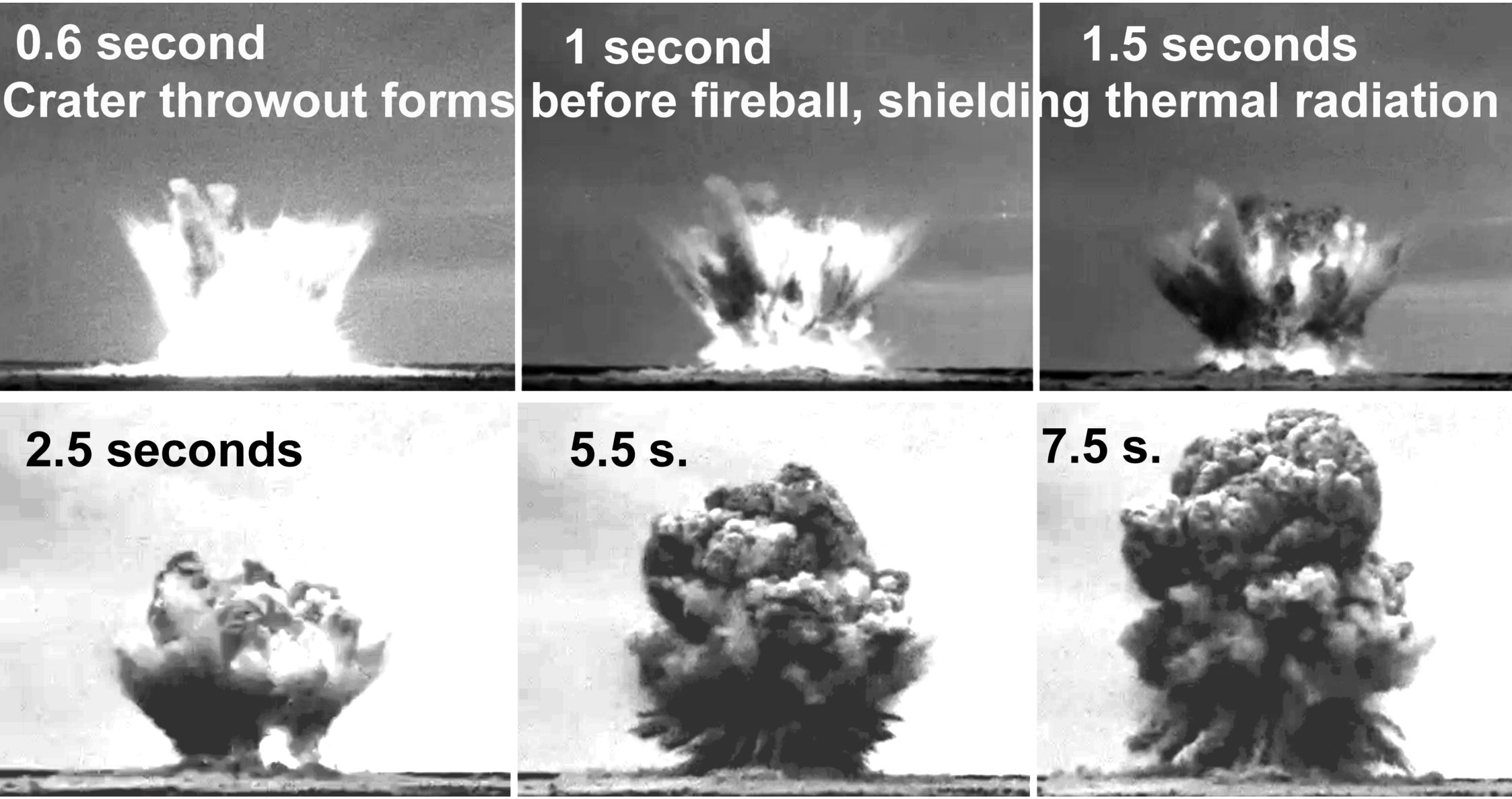

Afterwinds immediately suck in base surge dust from throwout

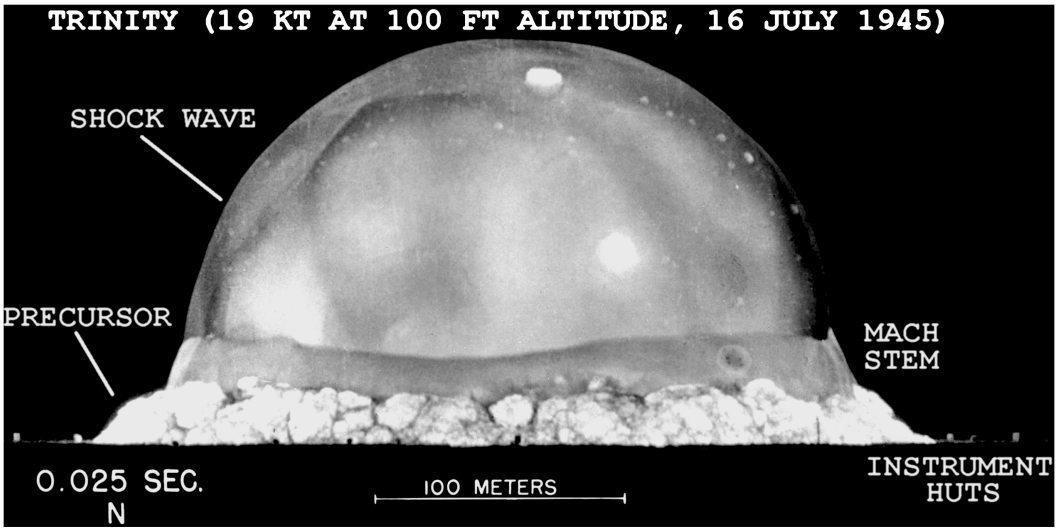
TRINITY (19 KT AT 100 FT ALTITUDE, 16 JULY 1945)
SHOCK WAVE
PRECURSOR
MACH STEM
INSTRUMENT HUTS
0.025 SEC.
N
100 METERS

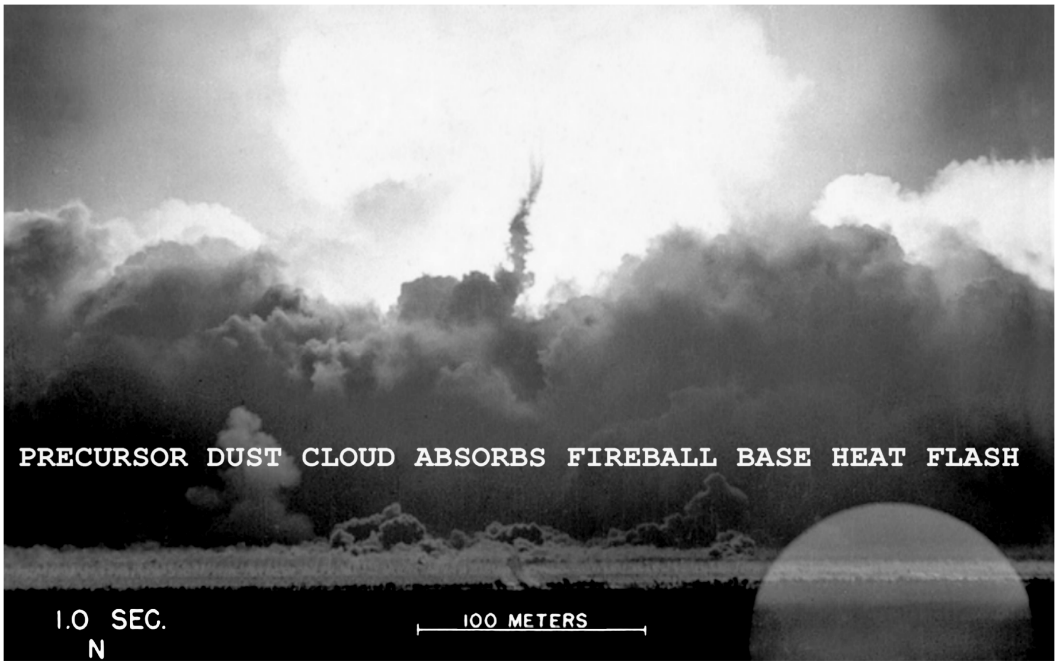
PRECURSOR DUST CLOUD ABSORBS FIREBALL BASE HEAT FLASH
1.0 SEC.
N
100 METERS

TOWER BASE, 1.4 R/HOUR
11 SEPTEMBER 1945

~~CONFIDENTIAL~~

DEPARTMENT OF THE ARMY TECHNICAL MANUAL
DEPARTMENT OF THE NAVY
DEPARTMENT OF THE AIR FORCE
MARINE CORPS PUBLICATIONS

TM 23-200
OPNAV INSTRUCTION 03400.1B
AFL 136-1
NAVMC 1104 REV

CAPABILITIES OF ATOMIC WEAPONS (U)

Prepared by
Armed Forces Special Weapons Project

DEPARTMENTS OF THE ARMY, THE NAVY AND THE AIR FORCE

REVISED EDITION NOVEMBER 1957

~~CONFIDENTIAL~~

Personnel in structures. A major cause of personnel casualties in cities is structural collapse and damage. The number of casualties in a given situation may be reasonably estimated if the structural damage is known. Table 6–1 shows estimates of casualty production in two types of buildings for several damage levels. Data from Section VII may be used to predict the ranges at which specified structural damage occurs. Demolition of a brick house is expected to result in approximately 25 percent mortality, with 20 percent serious injury and 10 percent light injury. On the order of 60 percent of the survivors must be extricated by rescue squads. Without rescue they may become fire or asphyxiation casualties, or in some cases be subjected to lethal doses of residual radiation. Reinforced concrete structures, though much more resistant to blast forces, produce almost 100 percent mortality on collapse. The figures of table 6–1 for brick homes are based on data from British World War II experience. It may be assumed that these predictions are reasonably reliable for those cases where the population is in a general state of expectancy of being subjected to bombing and that most personnel have selected the safest places in the buildings as a result of specific air raid warnings. For cases of no prewarning or preparation, the number of casualties is expected to be considerably higher.

Glass breakage extends to considerably greater ranges than almost any other structural damage, and may be expected to produce large numbers of casualties at ranges where personnel are relatively safe from other effects, particularly for an unwarned population.

Table 6–1. Estimated Casualty Production in Structures for Various Degrees of Structural Damage

	Killed outright	Serious injury (hospitalization)	Light injury (No hospitalization)
1–2 story brick homes (high explosive data):	*Percent*	*Percent*	*Percent*
Severe damage	25	20	10
Moderate damage	<5	10	5
Light damage	------	<5	<5

Note. These percentages do not include the casualties which may result from fires, asphyxiation, and other causes from failure to extricate trapped personnel. The numbers represent the estimated percentage of casualties expected at the maximum range where the specified structural damage occurs.

Personnel in a prone position are less likely to be struck by flying missiles than those who remain standing.

Table 6–2. Critical Radiant Exposures for Burns Under Clothing

(Expressed in cal/cm² incident on outer surface of cloth)

Clothing	Burn	1 KT	100 KT	10 MT
Summer Uniform	1°	8	11	14
(2 layers)	2°	20	25	35
Winter Uniform	1°	60	80	100
(4 layers)	2°	70	90	120

FIGURE 2-6 GROWTH OF THE MACH STEM

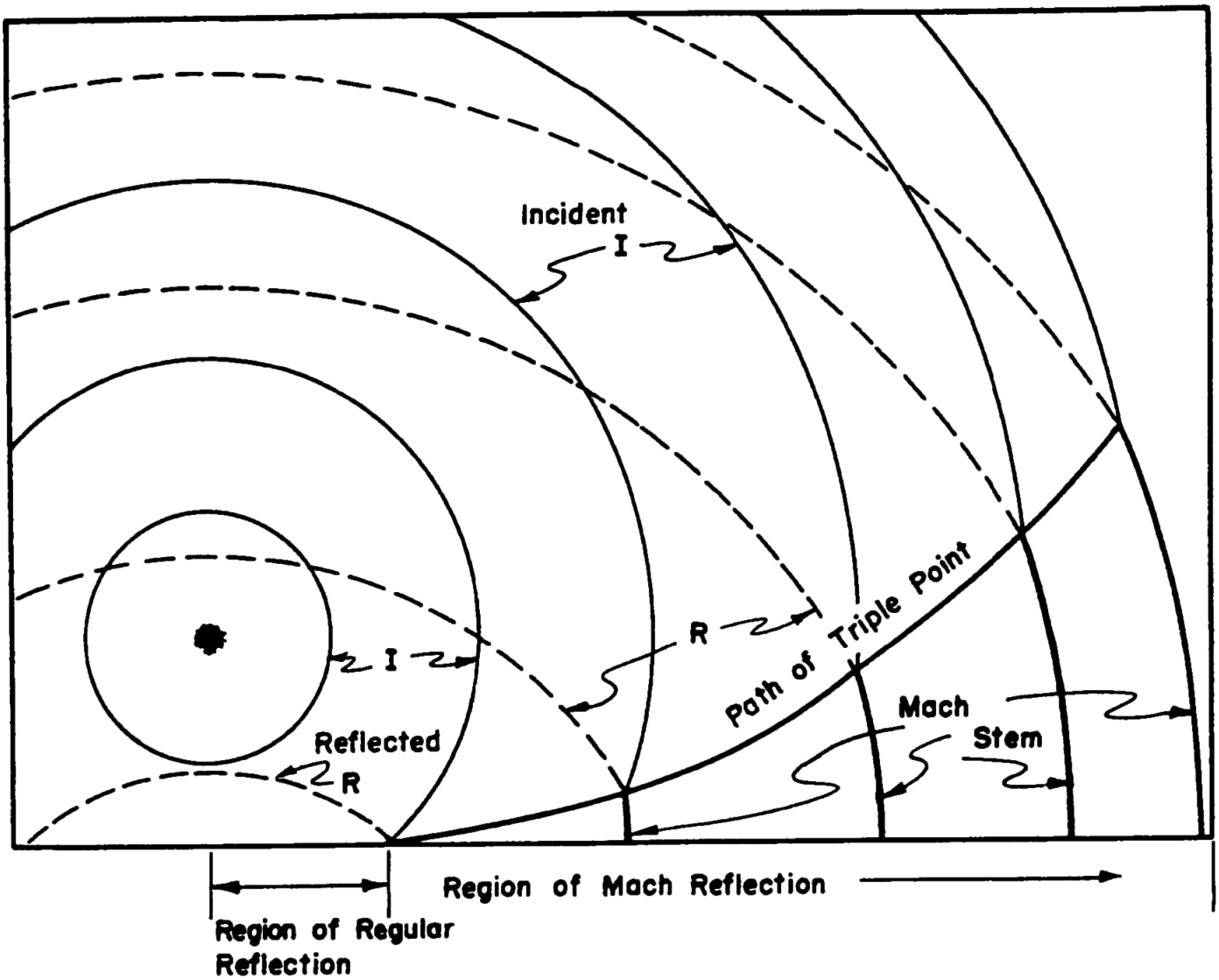

FIGURE 2-7 MACH STEM HEIGHT (1 KT) $\frac{H_1}{H_2}=\frac{h_1}{h_2}=\frac{d_1}{d_2}=\frac{W_1^{1/3}}{W_2^{1/3}}$

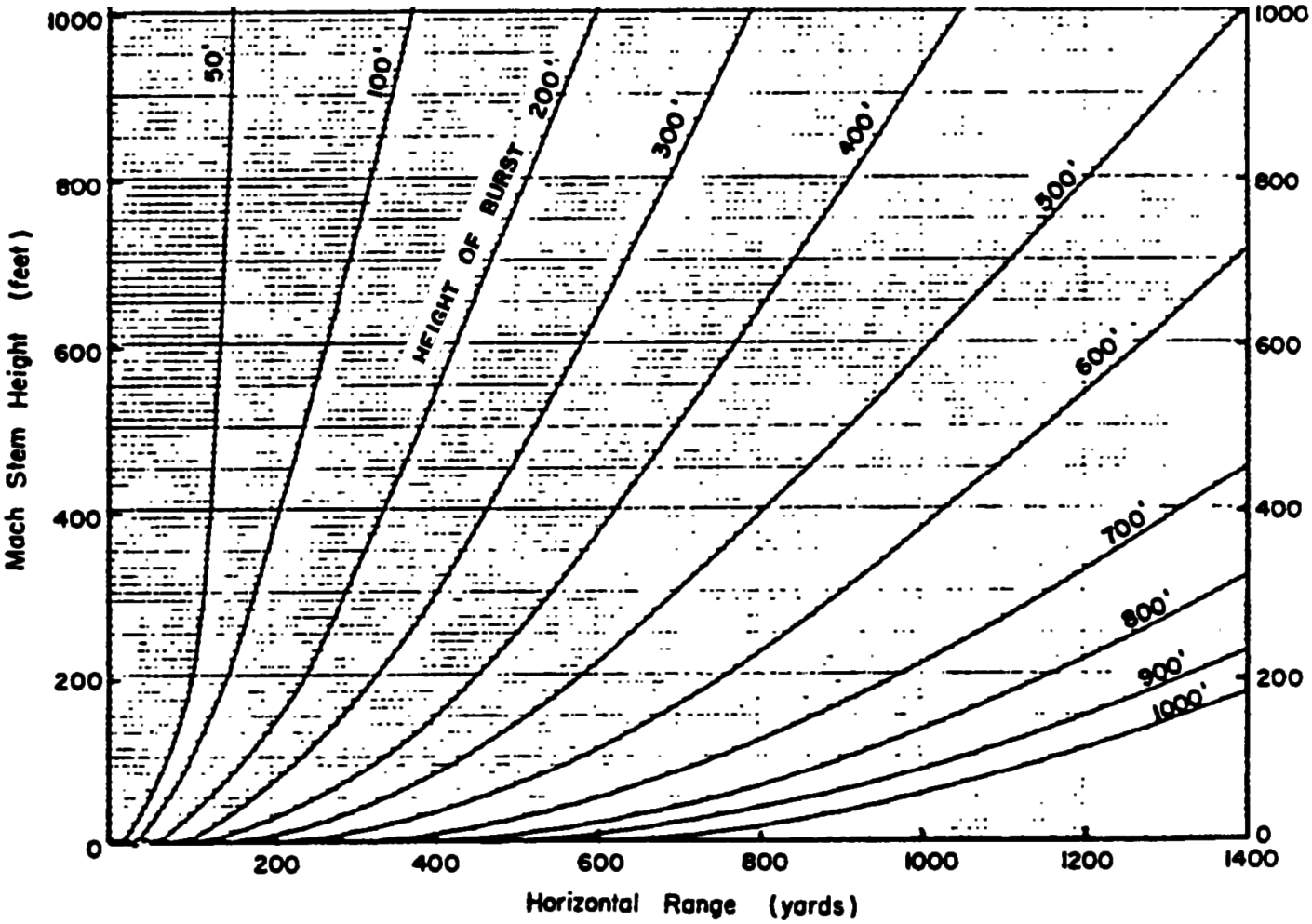

SECTION III
THERMAL RADIATION PHENOMENA

3.1 General

For a surface burst having the same yield as an air burst, the presence of the earth's surface results in a reduced thermal radiation emission and a cooler fireball when viewed from that surface. This is due primarily to heat transfer to the soil or water, the distortion of the fireball by the reflected shock wave, and the partial obscuration of the fireball by dirt and dust (or water) thrown up by the blast wave.

Measurements from the ground of the total thermal energy from surface bursts, although not as extensive as those for air bursts, indicate that the thermal yield is a little less than half that from equivalent air bursts. For a surface burst the thermal yield is assumed to be one-seventh of the total yield.

3.3 Radiant Exposure vs. Slant Range

a. Spectral. Characteristics. At distances of operational interest, the spectral (wavelength) distribution of the incident thermal radiation, integrated with respect to time, resembles very closely the spectral distribution of sunlight. For each, slightly less than one-half of the radiation occurs in the visible region of the spectrum, approximately one-half occurs in the infrared region and a very small fraction (rarely greater than 10 percent) lies in the ultraviolet region of the spectrum. The color temperature of the sun and an air burst are both about 6,000° K. A surface burst, as viewed by a ground observer, contains a higher proportion of infrared radiation and a smaller proportion of visible radiation than the air burst, with almost no radiation in the ultraviolet region. The color temperature for a surface burst is about 3,000° K. A surface burst viewed from the air may exhibit a spectrum more nearly like an air burst.

$$Q=\frac{3.16\times10^6\ W\ (\overline{T})}{D^2}\ \text{cal/sq cm (air burst).}$$

and

$$Q=\frac{1.35\times\ 10^6\ W\ (\overline{T})}{D^2}\ \text{cal/sq cm (surface burst).}$$

where Q=radiant exposure (cal/sq cm)
$\overline{T}$=atmospheric transmissivity
W=weapon yield (KT)
D=slant range (yds).

The differences between the air burst and surface burst curves are caused by the difference in apparent radiating temperatures (when viewed from the ground) and the difference in geometrical configuration of the two types of burst.

50 mile visibility and 5 gm/m³ water vapor.
10 mile visibility and 10 gm/m³ water vapor.

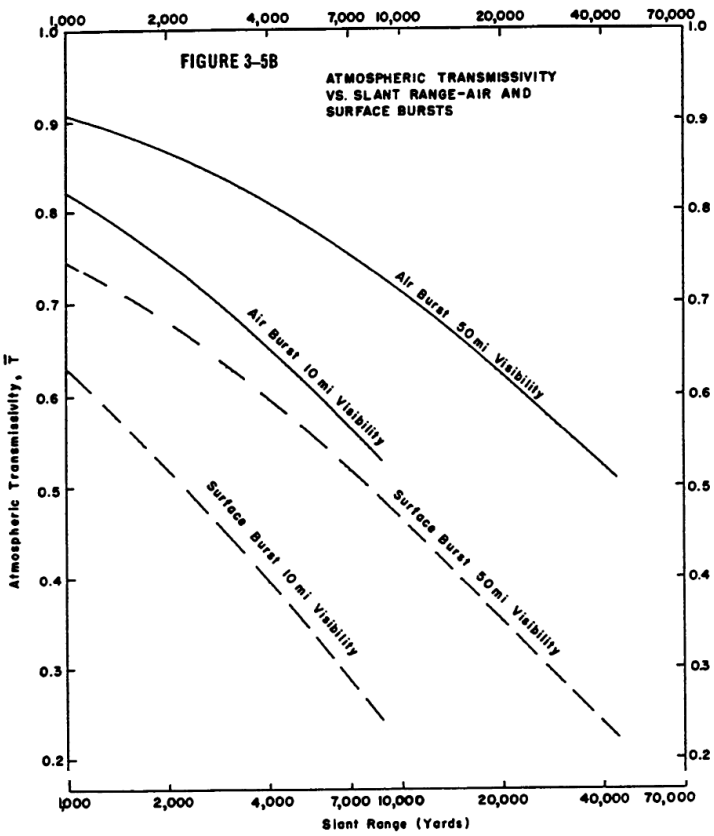

Table 12–2. Critical Radiant Exposure Values for Various Materials

Material	Damage	Critical radiant exposure Q_c, (cal/sq cm)		
		1 KT	100 KT	10 MT
Tent material:				
Canvas, white, 12 oz/yd², untreated	Destroyed	12	21	37
Canvas, OD, 12 oz/yd², flame-proofed	Destroyed	5	9	17
Packaging materials:				
Fibreboard, V2S, BT 350 psi, laminated	Flames during exposure	9	16	29
Fibreboard, V3S, BT 275 psi, laminated	Flames during exposure	7	13	23
Fibreboard, V3C, BT 350 psi, corrugated	Flames during exposure	6	11	19
Fibreboard, W5C, BT 200 psi, corrugated	Flames during exposure	5	10	18
Plywood, douglas fir (¼ in.)	Flames during exposure	9	16	20
Airship material, aluminized, N–113A100, 16 oz/yd²	Aluminum surface discolored	20	35	61
	Aluminum surface destroyed	24	43	75
	Fabric destroyed	27	47	82
Airship material, aluminized, N–113A70, 19.4 oz/yd²	Aluminum surface discolored	10	18	31
	Aluminum surface destroyed	15	27	44
	Fabric destroyed	20	35	61
Airship material, aluminized, N–128A170, 8 oz/yd²	Delaminates	2	4	7
	Fabric destroyed	5	10	17
Doped fabrics (used on some aircraft control surfaces):				
Cellulose nitrate covered with 0.0015″ thick aluminum foil.	Sporadic flaming	60	80	140
Cellulose nitrate, aluminized	Persistent flaming	5	6	10
Plastics:				
Laminated methyl methacrylate	Surface melts	73	120	230
USAF window plastic (½ in.)	Bubbling	240	430	750
Vinylite (opaque), ⅛ in. thick	Dense smoking	3	4	6
	Flaming	20	20	25
Sand:				
Coral	Explosion*	15	27	47
Siliceous	Explosion*	11	19	35
Sandbags: Cotton canvas, dry, filled	Failure	10	18	32
Wood, white pine	0.1 mm depth char	10	18	32
White pine, given protective coating	0.1 mm depth char	40	71	126
Construction materials:				
Roll roofing, mineral surface	Surface melts	8	14	25
	Flaming during exposure	22	40	71
Roll roofing, smooth surface	Surface melts	4	7	12
	Flaming during exposure	9	16	29

*"Popcorning."

FIGURE 12-5B

TEAPOT-MET 1955 ablation of spheres inside fireball

10 inch diameter spheres

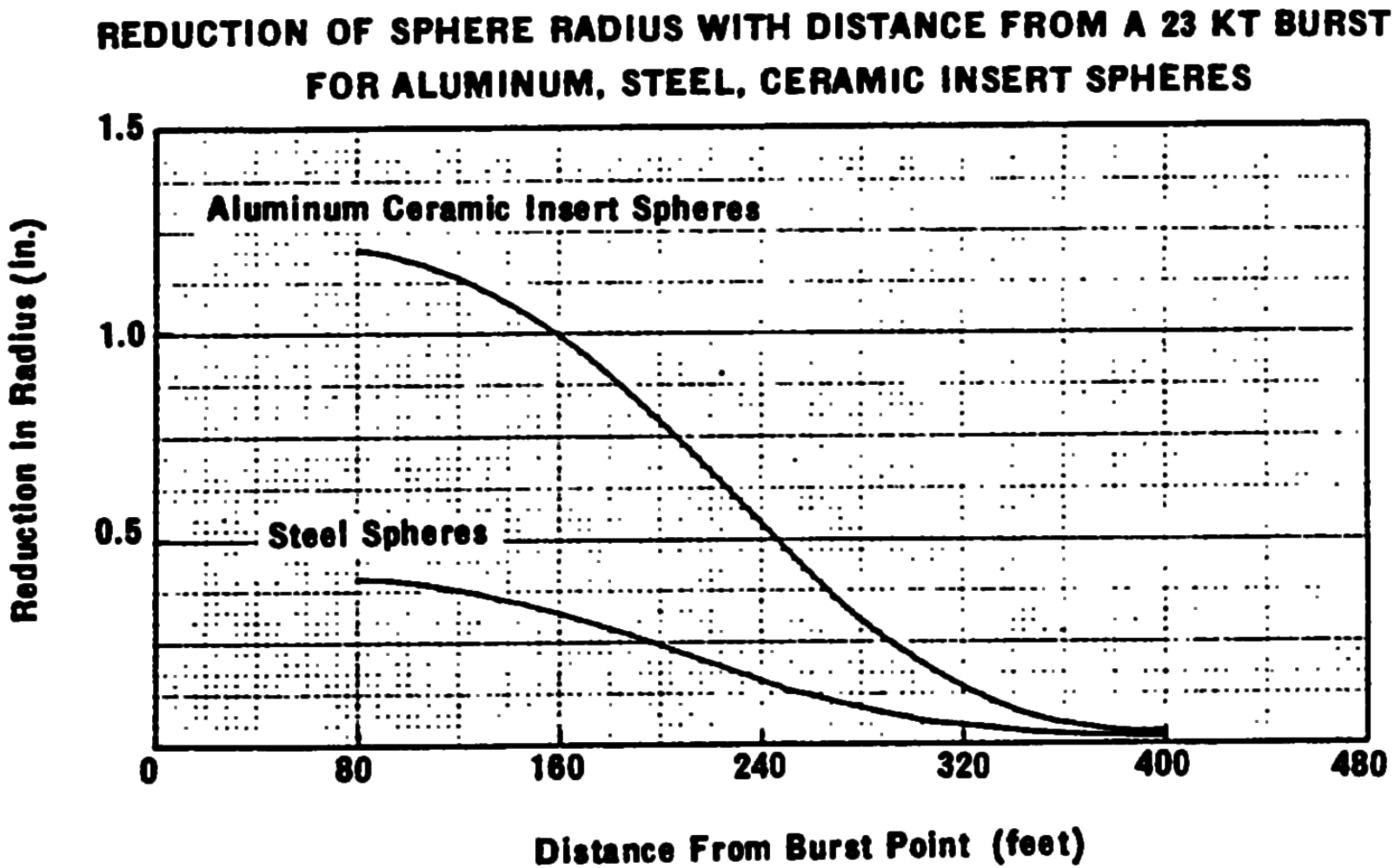

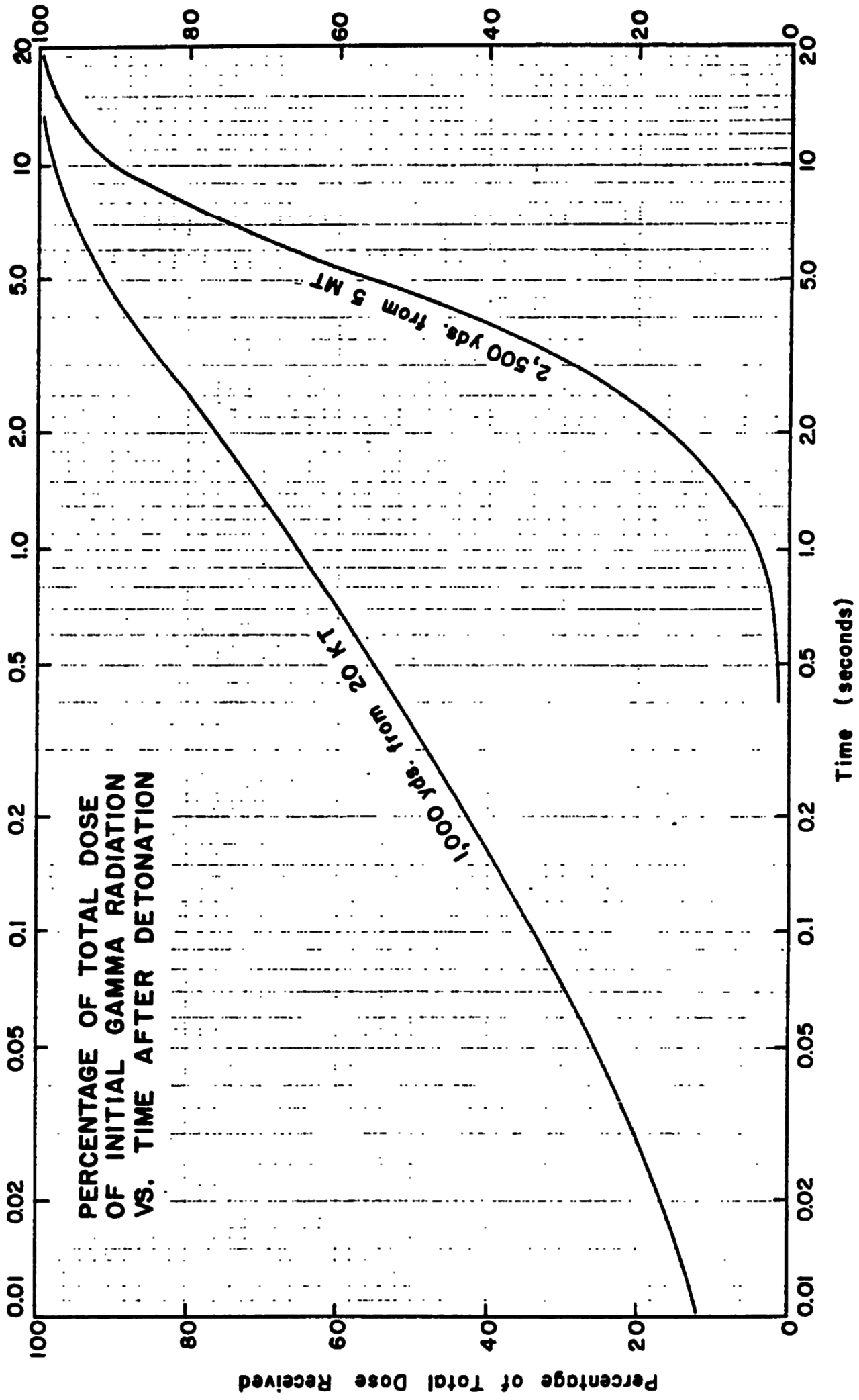
PERCENTAGE OF TOTAL DOSE
OF INITIAL GAMMA RADIATION
VS. TIME AFTER DETONATION
2,500 yds. from 5 MT
1,000 yds. from 20 KT
Percentage of Total Dose Received
Time (seconds)
0.01
0.02
0.05
0.1
0.2
0.5
1.0
2.0
5.0
10
20
0
20
40
60
80
100

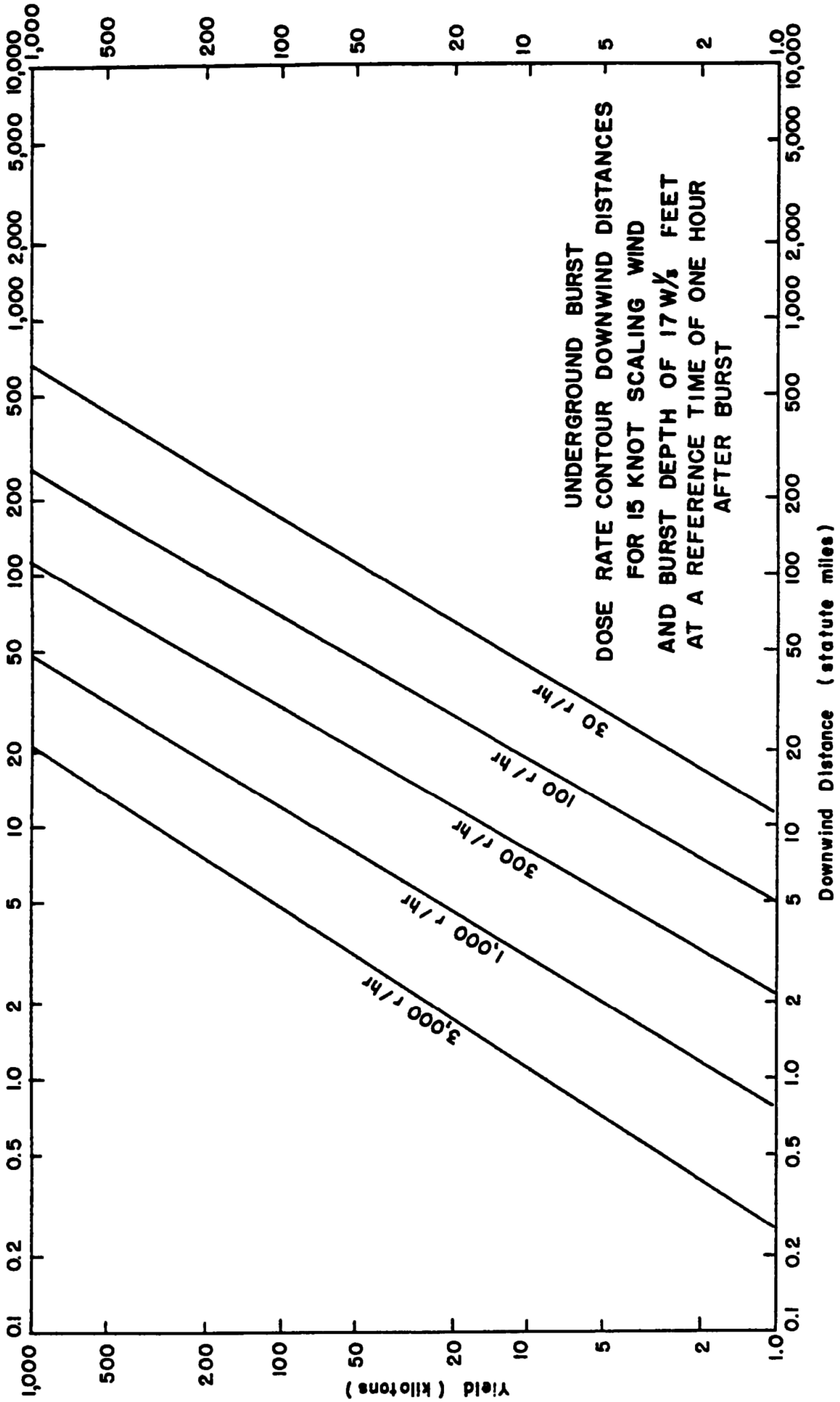
UNDERGROUND BURST
DOSE RATE CONTOUR DOWNWIND DISTANCES
FOR 15 KNOT SCALING WIND
AND BURST DEPTH OF 17 W^1/3 FEET
AT A REFERENCE TIME OF ONE HOUR
AFTER BURST
30 r/hr
100 r/hr
300 r/hr
1,000 r/hr
3,000 r/hr
Downwind Distance (statute miles)
Yield (kilotons)
0.1
0.2
0.5
1.0
2
5
10
20
50
100
200
500
1,000
2,000
5,000
10,000

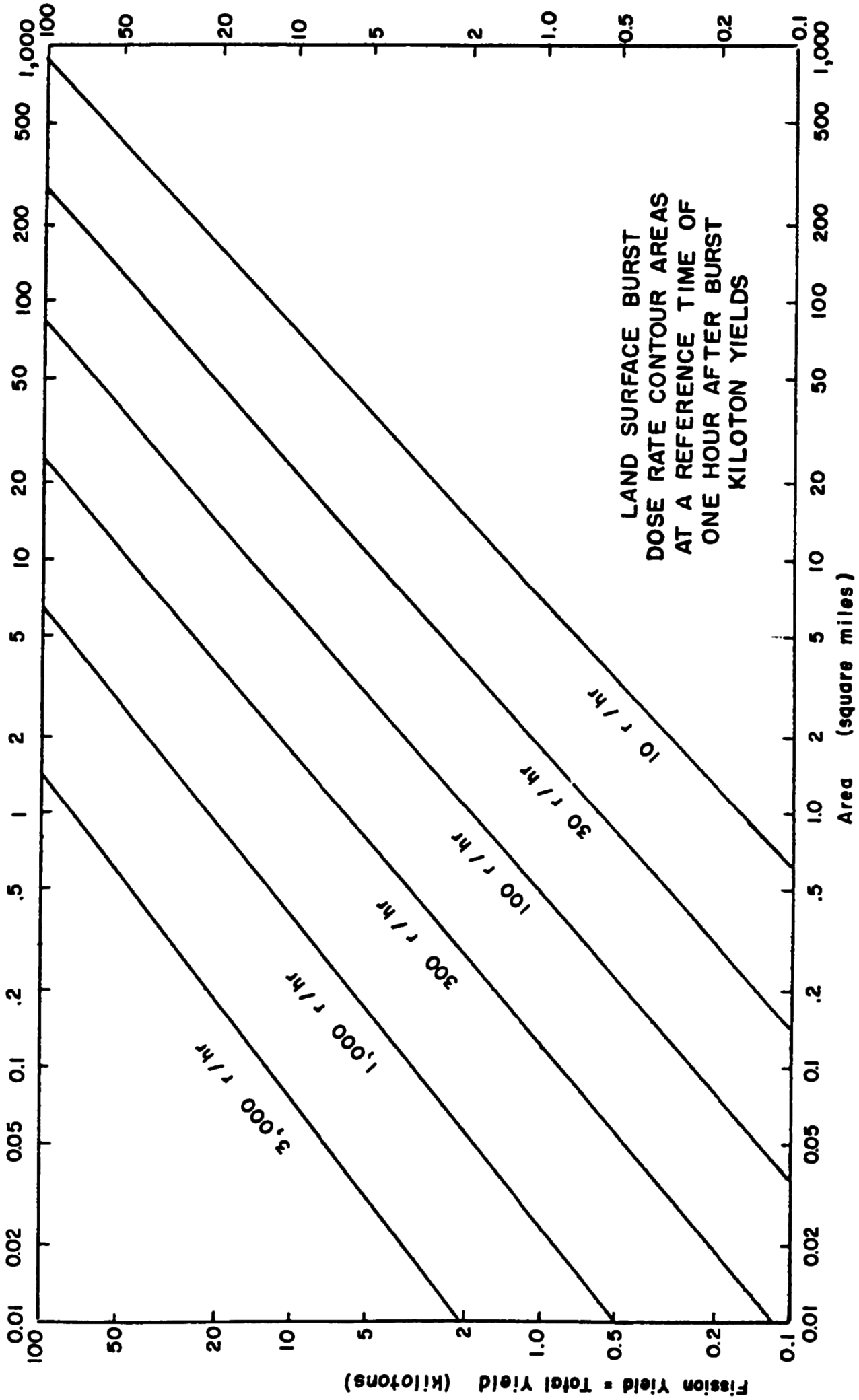
LAND SURFACE BURST
DOSE RATE CONTOUR AREAS
AT A REFERENCE TIME OF
ONE HOUR AFTER BURST
KILOTON YIELDS
10 r / hr
30 r / hr
100 r / hr
300 r / hr
1,000 r / hr
3,000 r / hr
Area (square miles)
Fission Yield = Total Yield (kilotons)
0.01
0.02
0.05
0.1
.2
.5
1
2
5
10
20
50
100
200
500
1,000
0.1
0.2
0.5
1.0
2
5
10
20
50
100

DNA EM-1
PART I

DEFENSE NUCLEAR AGENCY EFFECTS MANUAL NUMBER 1

CAPABILITIES OF NUCLEAR WEAPONS

1 JULY 1972

HEADQUARTERS
Defense Nuclear Agency
Washington, D.C. 20305

DNA EM-1
PART I
CHANGE 2
1 AUGUST 1981

DEFENSE NUCLEAR AGENCY EFFECTS MANUAL NUMBER 1

CAPABILITIES OF NUCLEAR WEAPONS

PART I
PHENOMENOLOGY

HEADQUARTERS
Defense Nuclear Agency
Washington, D.C. 20305

EDITOR
PHILIP J. DOLAN
SRI INTERNATIONAL

FOREWORD

This edition of the *Capabilities of Nuclear Weapons* represents the continuing efforts by the Defense Nuclear Agency to correlate and make available nuclear weapons effects information obtained from nuclear weapons testing, small-scale experiments, laboratory effort and theoretical analysis. This document presents the phenomena and effects of a nuclear detonation and relates weapons effects manifestations in terms of damage to targets of military interest. It provides the source material and references needed for the preparation of operational and employment manuals by the Military Services.

The *Capabilities of Nuclear Weapons* is not intended to be used as an employment or design manual by itself, since more complete descriptions of phenomenological details should be obtained from the noted references. Every effort has been made to include the most current reliable data available on 31 December 1971 in order to assist the Armed Forces in meeting their particular requirements for operational and target analysis purposes.

Comments concerning this manual are invited and should be addressed:

Director
Defense Nuclear Agency
ATTN: STAP
Washington, D. C. 20305

C. H. DUNN
Lt General, USA
Director

Shielding is most effective when the obstacle is between the target and ground zero.

Obstacles that are considered in the assessment of the effects of shielding from air blast are local obstacles, such as ravines, constructed slots, or revetments (the effects of large terrain features on blast waves are discussed in paragraphs 2-38 through 2-41 of Chapter 2). The importance of shielding is well documented. Comparisons of damage between shielded and unshielded vehicles exposed to blast from both nuclear and chemical explosions are available. The effectiveness of an obstacle in shielding a target generally results as much from its capability to reduce the target movement as from its ability to modify the blast environment. Figure 14-8 illustrates this point. When the obstacle is between the blast wave and the target most of the impulse or translational force that induces motion (drag loading) does not act on the target. When the obstacle is "behind" the target, the translational force initially applied to the target is the same as it would have been without an obstacle, but the obstacle not only can modify later translational forces (as a result of shock wave reflection), but it can restrict movement, the major cause of damage. The overpressure effects of crushing and fracturing still occur in both cases, and these effects provide lower limits for damage ground distances.

Most damage resulting from low yield weapons is caused by overpressure impulse rather than translation, even for unshielded targets, and, since overpressure impulse is not altered drastically by shielding, the effects of shielding are relatively minor for such weapons. However, most damage caused to non-shielded targets by higher yield weapons results from the translational effects of dynamic pressure. Since shielding can reduce translational effects substantially, it can be quite effective as a protection from large yield weapons. Damage to shielded targets results largely from overpressure effects, for which damage distances scale as the cube root of the yield ($W^{1/3}$), while damage to unshielded targets results largely from total impulse effects (including those of dynamic pressure), for which damage distances generally scale as $W^{0.4}$. The effects of shielding are illustrated in Figure 14-9, in which damage distances for shielded targets have been scaled as $W^{1/3}$, and those for unshielded targets by $W^{0.4}$.

14-5 Effects of Ground Surface Conditions

Ground surface conditions affect damage in two ways: by modification of the blast parameters; and by modification of target response.

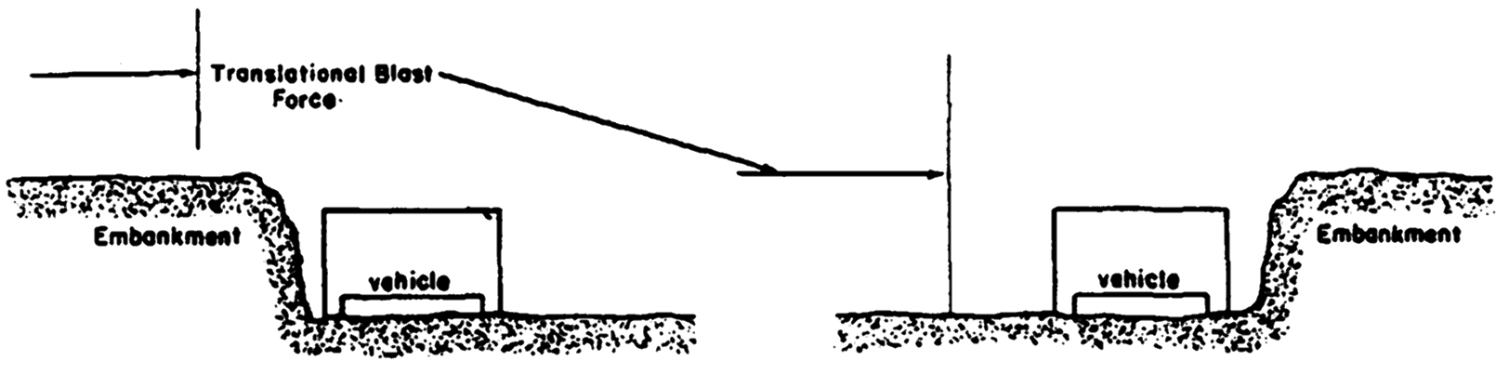

(a) No translation because Translational Force is not applied

(b) No or little translation because embankment restricts movement

Figure 14-8. The Effect of Shielding

Table 10-1 Estimated Casualty Production in Buildings for Three Degrees of Structural Damage

Structural Damage	Percent of Personnel*		
	Killed Outright	Serious Injury (hospitalization)	Light Injury (no hospitalization)
1-2 story brick homes (high-explosive data from England):			
Severe damage	25	20	10
Moderate damage	<5	10	5
Light damage	–	<5	<5
Reinforced-concrete buildings (nuclear data from Japan):			
Severe damage	100	–	–
Moderate damage	10	15	20
Light damage	<5	<5	15

*These percentages do not include the casualties that may result from fires, asphyxiation, and other causes from failure to extricate trapped personnel. The numbers represent the estimated percentages of casualties expected at the maximum range where a specified structural damage occurs. See Chapter 11 for the distances at which these degrees of damage occur for various yields.

A parameter that is useful for calculating thermal response of materials is the characteristic thermal response time τ_o, given by the equation

$$\tau_o = \rho C_p L^2/k \text{ sec},$$

where k is thermal conductivity (cal-sec^{-1} cm^{-1}°C^{-1}), ρC_p is heat capacity per unit volume (ρ = density in g-cm^{-3} and C_p = specific heat at constant pressure in cal-g^{-1}°C^{-1}), and L is the thickness, in centimeters, of the layer of material.

The quantity

$$\alpha = \frac{k}{\rho C_p}$$

is called thermal diffusivity (cm^2/sec). Use of this quantity simplies the previous equation to

9-16

$$\tau_o = \frac{L^2}{\alpha} \text{ sec.*}$$

For any particular material exposed to a rectangular pulse of length τ, the previous equation can be transformed to give a characteristic thickness

$$\delta = \sqrt{\alpha\tau} \text{ cm},$$

for which the characteristic time is equal to the pulse duration. If a thick slab of this material is exposed to a pulse of length τ, the temperature rise at the surface is the same as would be produced by uniformly distributing the absorbed thermal energy in a slab of thickness δ, and the peak temperature rise at depth δ in the thick slab is about half as great as the peak temperature rise at the surface.

For example, consider a block of red pine that is exposed to 15 cal/cm^2 from a rectangular pulse of 3 seconds duration. From Table 9-1,

$$\delta = \sqrt{\alpha\tau} = \sqrt{(24 \times 10^{-3})(3)} = 0.085 \text{ cm}.$$

*This equation is useful, but it is by no means exact. The simplified heat-flow analysis from which this equation is derived neglects the effects of radiation and convection heat losses from the surfaces of the exposed sample. It also assumes an isotropic medium, i.e., a medium whose structure and properties in the neighborhood of any point are the same relative to all directions through the point. It also neglects the changes in thermal properties that occur as the exposed material heats, volatilizes, chars, and bursts into flame.

The heat absorbed by the wood before it begins to scorch is equal to the product of the incident radiant energy, Q, and the absorption coefficient, A.

$$\Delta T_s = \frac{QA}{\rho\delta C_p} = \frac{QA}{\rho C_p \sqrt{\alpha\tau}} = \frac{QA}{\rho C_p \sqrt{\tau k/\rho C_p}}.$$

where ΔT_s is the peak temperature rise at the surface. The parameters that define the thermal pulse may be separated from those that define the material properties, and

$$\Delta T_s = \left(\frac{Q}{\sqrt{\tau}}\right)\left(\frac{A}{\sqrt{k\rho C_p}}\right).$$

For a fixed rectangular pulse, $Q/\sqrt{\tau}$ is a constant, and the equation may be written

$$\Delta T_s = (K)\left(\frac{A}{\sqrt{k\rho C_p}}\right).$$

Sustained ignition only occurs when higher radiant exposures raise the temperature throughout the thickness of the cellulose to a level that is sufficiently high to sustain the flow of combustible gases from breakdown of the fuel. It is difficult to supply sufficient energy with short pulses, since a large amount of the energy that is deposited is carried away by the rapid ablation of the thin surface layer. This transient flaming phenomenon is typical of the response of sound wooden boards to a thermal pulse.

Table 9-1. [redacted] Thermal Properties of Materials [redacted]

Materials	Density, ρ (gm/cm^3)	Specific Heat, C_p ($cal/gm \cdot {}^\circ C$)	Conductivity, k ($cal/sec \cdot cm \cdot {}^\circ C$)	Diffusivity, α (cm^2/sec)
Insulating Materials				
Air	9.46×10^{-4}	0.24	0.55×10^{-4}	0.22
Asbestos	0.58	0.20	4.6×10^{-4}	$40. \times 10^{-4}$
Balsa	0.12	0.4	1.2×10^{-4}	$25. \times 10^{-4}$
Brick (common red)	1.8	0.2	$16. \times 10^{-4}$	$18. \times 10^{-4}$
Celluloid	1.4	0.35	5.0×10^{-4}	$10. \times 10^{-4}$
Cotton, sateen, green	0.70	0.35	1.5×10^{-4}	2.5×10^{-4}
Fir, Douglas-				
spring growth	0.29	0.4	$2. \times 10^{-4}$	$17. \times 10^{-4}$
summer growth	1.00	0.4	$5. \times 10^{-4}$	$12. \times 10^{-4}$
Fir, white	0.45	0.4	2.6×10^{-4}	$14. \times 10^{-4}$
Glass, window	2.2	0.2	$19. \times 10^{-4}$	$43. \times 10^{-4}$
Granite	2.5	0.19	$66. \times 10^{-4}$	$140. \times 10^{-4}$
Leather sole	1.0	0.36	3.8×10^{-4}	$11. \times 10^{-4}$
Mahogany	0.53	0.36	3.1×10^{-4}	$16. \times 10^{-4}$
Maple	0.72	0.4	4.5×10^{-4}	$16. \times 10^{-4}$
Oak	0.82	0.4	5.0×10^{-4}	$15. \times 10^{-4}$
Pine, white	0.54	0.33	3.6×10^{-4}	$18. \times 10^{-4}$
Pine, red	0.51	0.4	$5. \times 10^{-4}$	$24. \times 10^{-4}$
Rubber, hard	1.2	0.5	3.6×10^{-4}	$60. \times 10^{-4}$
Teak	0.64	0.4	4.1×10^{-4}	$16. \times 10^{-4}$
Metals (100°C)				
Aluminum	2.7	0.22	0.49	1.0
Cadmium	8.65	0.057	0.20	0.45
Copper	8.92	0.094	0.92	1.1
Gold	19.3	0.031	0.75	1.2
Lead	11.34	0.031	0.081	0.23
Magnesium	1.74	0.25	0.38	0.87
Platinum	21.45	0.027	0.17	0.29
Silver	10.5	0.056	0.96	1.6
Steel, mild	7.8	0.11	0.107	1.2
Tin	6.55	0.056	0.14	0.38
Miscellaneous Materials				
Ice (0°C)	0.92	0.492	$54. \times 10^{-4}$	$120. \times 10^{-4}$
Water	1.00	1.00	$14. \times 10^{-4}$	$14. \times 10^{-4}$
Skin (porcine, dermis, dead)	1.06	0.77	$9. \times 10^{-4}$	$11. \times 10^{-4}$
Skin (human, living, averaged for upper 0.1 cm)	1.06	0.75	$8. \times 10^{-4}$	$30. \times 10^{-4}$
Polyethylene (black)	0.92	0.55	$8. \times 10^{-4}$	$17. \times 10^{-4}$

If the pulse is of long duration, the ignition threshold rises because the exposed material can dissipate an appreciable fraction of the energy while it is being received. For very long rectangular pulses an irradiance of about 0.5 cal · $cm^{-2} sec^{-1}$ is required to ignite the cellulose. Heat supplied to the material at a slow rate is just sufficient to offset radiative and convective heat losses, while maintaining the cellulose at the ignition temperature of about 300°C.

9-19

Most thick, dense materials that ordinarily are considered inflammable do not ignite to persistent flaming ignition when exposed to transient thermal radiation pulses. Wood, in the form of siding or beams, may flame during the exposure but the flame is extinguished when the exposure ceases.

Table 9-2. [redacted] Approximate Radiant Exposures for Ignition of Fabrics [redacted]

Material	Weight (oz/yd^2)	Color	Effect on Material	Radiant Exposure* (cal/cm^2) t_{max} 0.2 sec	t_{max} 1.0 sec	t_{max} 3.2 sec
Clothing Fabrics						
Cotton	8	White	Ignites	32	48	85
		Khaki	Tears on flexing	17	27	34
		Khaki	Ignites	20	30	39
		Olive	Tears on flexing	9	14	21
		Olive	Ignites	14	19	21
		Dark blue	Tears on flexing	11	14	17
		Dark blue	Ignites	14	19	21
Cotton corduroy	8	Brown	Ignites	11	16	22
Cotton denim, new	10	Blue	Ignites	12	27	44
Cotton shirting	3	Khaki	Ignites	14	21	28
Cotton-nylon mixture	5	Olive	Tears on flexing	8	15	17
	5	Olive	Ignites	12	28	53
Wool	8	White	Tears on flexing	14	25	38
		Khaki	Tears on flexing	14	24	34
		Olive	Tears on flexing	9	13	19
		Dark blue	Tears on flexing	8	12	18
	20	Dark blue	Tears on flexing	14	20	26
Rainwear (double-neoprene-coated nylon twill)	9	Olive	Begins to melt	5	9	13
	9	Olive	Tears on flexing	8	14	22
Drapery Fabrics						
Rayon gabardine	6	Black	Ignites	9	20	26
Rayon-acetate drapery	5	Wine	Ignites	9	22	28
Rayon gabardine	7	Gold	Ignites	**	24†	28†
Rayon twill lining	3	Black	Ignites	7	17	25
Rayon twill lining	3	Biege	Ignites	13	20	28
Acetate-shantung	3	Black	Ignites	10†	22†	35†
Cotton heavy draperies	13	Dark colors	Ignites	15	18	34
Tent Fabrics						
Canvas (cotton)	12	White	Ignites	13	28	51
Canvas	12	Olive drab	Ignites	12	18	28
Other Fabrics						
Cotton chenille bedspread		Light blue	Ignites	**	11†	15†
Cotton venetian blind tape, dirty		White	Ignites	10	18	22
Cotton venetian blind tape		White	Ignites	13†	27†	31†
Cotton muslin window shade	8	Green	Ignites	7	13	19

[redacted] Radiant exposures for the indicated responses (except where marked †) are estimated to be valid to ±25% under standard laboratory conditions. Under typical field conditions the values are estimated to be valid within ±50% with a greater likelihood of higher rather than lower values. For materials marked †, ignition levels are estimated to be valid within ±50% under laboratory conditions and within ±100% under field conditions. For low air bursts, values of t_{max} of 0.2, 1.0, and 3.2 sec correspond roughly to yields of 40 kt, 2 Mt, and 24 Mt, respectively.

** [redacted] Data are not available or appropriate scaling not known.

3-2 Range Effects

As the thermal energy propagates away from the fireball, the divergence that results from the increasing area through which it passes causes the radiant exposure to decrease as the inverse square of the slant range. At a slant range R centimeters from the source, the thermal energy is distributed over a spherical area of $4\pi R^2$. Since the thermal yield in calories is 10^{12} Wf, where W is the yield in kilotons, the radiant exposure at a distance R cm in a clear atmosphere is

$$Q = \frac{10^{12} Wf}{4\pi R^2} \text{ cal/cm}^2.$$

Adding the transmittance factor to the equations given in paragraph 3-2 gives

$$Q = \frac{7.96\ WfT}{R_{km}^2} \text{ cal/cm}^2,$$

$$R_{km} = 2.82 \sqrt{WfT/Q}.$$

3-5

The scattering and absorption properties of the atmosphere depend partly on the wavelength of the radiant energy. Wavelength is often measured in microns (1 micron = 10^{-6} meter), for which the symbol is μ. Wavelengths in the visible spectrum may be identified by the relation between wavelength and color: light with a wavelength of 0.7 μ is red; 0.58 μ light is yellow; and 0.48 μ light is blue. White light is a mixture containing all wavelengths in the visible spectrum, which extends from 0.38 to 0.78 μ. The infrared spectrum consists of radiant energy at wavelengths longer than 0.78 μ, and the ultraviolet spectrum consists of radiant energy at wavelengths shorter than 0.38 μ.

The energy transport properties of atmospheric particles may be expressed in terms of scattering and absorption cross sections, which are fictitious areas that are a measure of the probability that scattering or absorption will occur. Particles that are small compared to the wavelength of light have scattering cross sections that are inversely proportional to the fourth power of the wavelength. Therefore, air molecules scatter light from the extreme blue end of the visible spectrum (wavelength = 0.38 μ) about 16 times as effectively as they scatter light from the red end of the spectrum (wavelength = 0.78 μ).

The sky is blue because most of the scattering at high altitudes is by air molecules, which scatter blue light more efficiently than they scatter other colors of the visible spectrum. A distant mountain appears blue on a clear day for the same reason.

3-7

The principal absorber of thermal energy usually is water vapor, which has strong absorption bands in the infrared spectrum. Dry air transmits infrared energy more efficiently than humid air. Carbon dioxide and other gases present in the atmosphere in small amounts also absorb infrared energy.

Ultraviolet energy is absorbed most strongly at the shorter wavelengths: the limiting wavelength that air in the lower atmosphere will transmit is about 0.2 micron. Ozone, appreciable quantities of which are found between roughly 60,000 and 80,000 feet, absorbs ultraviolet radiation with wavelengths shorter than 0.29 micron. As a result of these absorption bands ultraviolet energy that reaches the earth from the sun is almost entirely limited to the spectral band between 0.38 micron (the violet edge of the visible spectrum) and 0.29 micron.

3-8

The attenuation for light of 0.65 micron wavelength was used to specify $\tau(h)$. This choice was a purely empirical one, used because it brought the calculated values of transmittance into general agreement with experimentally determined values. The wavelength that was selected is attenuated less than is the thermal radiation spectrum as a whole;

For bursts below one-quarter mile and surface targets, a wavelength of 0.55 microns was used together with a buildup factor, as described below.

$$T_d = e^{-2.9\ R/V},$$

where T_d is the transmission coefficient for *direct* flux over a path of slant range R, and V is visual range. As mentioned above, scattered as well as direct flux must be considered. Consequently, transmittance is larger than the transmission coefficient for direct flux and is given approximately by the following empirical equation:

$$T = e^{-2.9\ R/V}\ (1 + 1.9\ R/V).$$

The exponential factor in this equation accounts for energy loss from the direct beam by scattering. The expression in brackets is a buildup factor that accounts for energy scattered toward the target.

When the burst height h is greater than about one-quarter mile, transmittance may be calculated from

$$T = e^{-\gamma(h)\ \frac{16}{V}\ \frac{R}{h}} \qquad 3\text{-}9$$

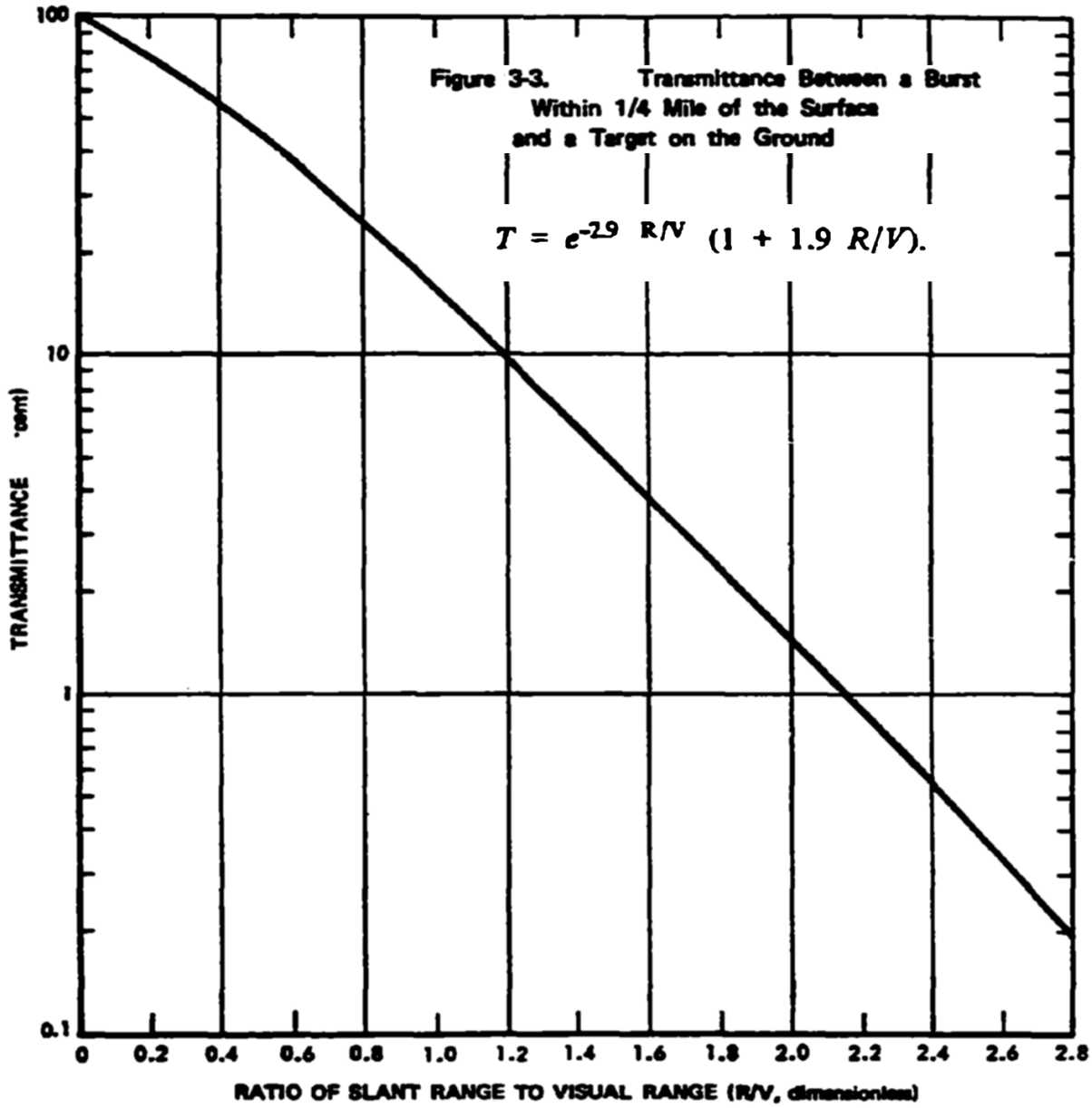

Figure 3-3. Transmittance Between a Burst Within 1/4 Mile of the Surface and a Target on the Ground

Thermal flash on forest leaf canopy produces smoke-screen (in Nevada and Pacific nuclear tests), shadowing dry leaf litter

The high degree of shading by tree crowns and stems for detonations at or below the canopy level often may be offset by scattering of burning debris ignited within the fireball. **15-59**

Fuels seldom burn vigorously, regardless of wind conditions, when fuel moisture content exceeds about 16 percent. This corresponds to an equilibrium moisture content for a condition of 80 percent relative humidity. **15-60**

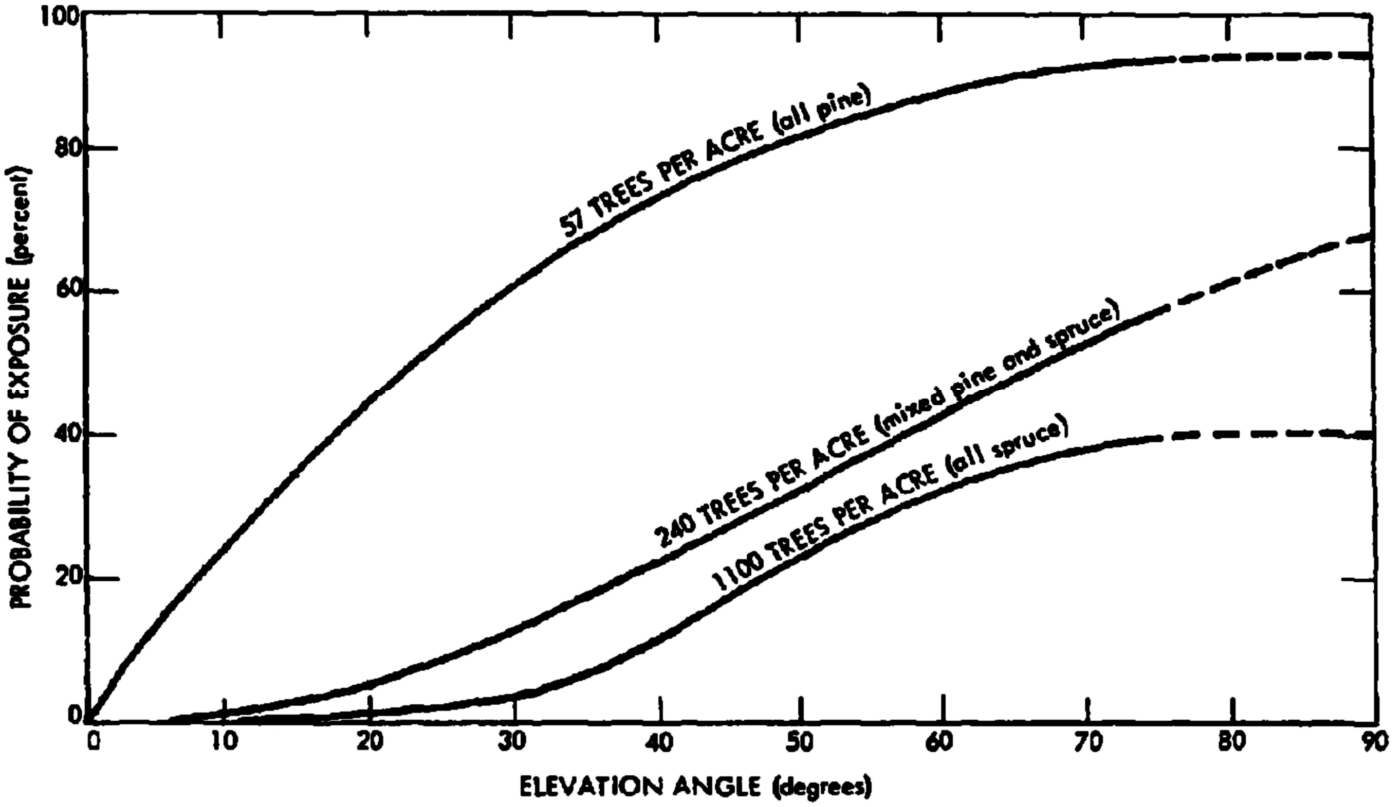

Figure 15-41. Probability of Exposure of Forest Floor for Different Levels of Tree Density

Table 15-13 Burning Durations by Fuel Type

Fuel Type	Violent Burning		Residual Burning		Total Burning Time
	Time (min)	Energy Release (percent)	Time (min)	Energy Release (percent)	
Grass	1.5	90	0.5	10	30 min
Light Brush (12 tons/acre)	2.	60	6.	40	16 hr
Medium Brush (25 tons/acre)	6.	50	24.	50	36 hr
Heavy Brush (40 tons/acre)	10.	40	70.	60	72 hr
Timber	24.	17	157.	83	7 days

Table 15-11 Criteria of "No-Spread" of Fires

Fuel Type	Criteria
All forest fuels	Over 1 inch of snow on the ground at the nearest weather stations.
Grass	Relative humidity above 80 percent.
Brush or hardwoods	0.1 inch of precipitation or more within the past 7 days and: Wind 0-3 mph; relative humidity 60 percent or higher, or Wind 4-10 mph; relative humidity 75 percent or higher, or Wind 11-25 mph; relative humidity 85 percent or higher.
Conifer timber	1. One day or less since at least 0.25 inch of precipitation and: Wind 0-3 mph; relative humidity 50 percent higher, or Wind 4-10 mph; relative humidity 75 percent higher, or Wind 11-25 mph; relative humidity 85 percent or higher. 2. Two to three days since at least 0.25 inch of precipitation and: Wind 0-3 mph; relative humidity 60 percent or higher, or Wind 4-10 mph; relative humidity 80 percent or higher, or Wind 11-25 mph; relative humidity 90 percent or higher. 3. Four to five days since at least 0.25 inch of precipitation and wind 0-3 mph; relative humidity 80 percent or higher. 4. Six to seven days since at least 0.25 inch of precipitation and wind 0-3 mph; relative humidity 90 percent or higher.

shielding from the wind and shading from sunlight by the canopy. The spread or no-spread criteria are summarized in Table 15-11. This table lists the conditions under which fire would not be expected to spread.

The criteria of Table 15-11 have been compared to the records of 4,378 wildland fires. Of the fires for which "no spread" would be predicted, 97.8 percent did not spread; only 40 percent of the fires that were predicted to spread actually did spread (at a rate of 0.005 mph or faster). This failure to spread often may be attributable to lack of fuel continuity around the point of origin.

The criteria of Table 15-11 are considered to be reliable for American forests and suitably conservative to assure a low level of hazard to friendly forces. On the other hand, the criteria are probably not overly conservative to predict conditions for which enemy forces may be denied forested areas because of fire whenever the local weather history and conditions at the time of

14-10 Fire Damage

Damage to equipment by fire is referred to in some damage reports. Although some 20 occurrences have been noted, they involved only a very small percentage of the equipment exposed. Most fires appeared to be secondary in nature, that is, they were not started by direct thermal radiation ignition. Two equipment items were burned during nuclear tests under exposure conditions in which they could have received virtually no thermal radiation. In addition, a 1/4-ton truck exposed at a 100-ton high explosive test (in which thermal radiation was negligible) also burned.

The damage to a 6-kVA generator exposed on a U.K. test is particularly interesting. In the damage report the notation is made, "Fire may have started from fuel from broken carburetor spilling on hot muffler." U.K. practice at nuclear tests was to expose running equipment, that is, the engines were running at the time of the explosion. The six recorded occurrences of fires on U.K. tests represents a considerably larger percentage (about 10 percent) of all U.K. equipment exposed than does the number of fires recorded on U.S. tests. Since this may be due to the U.K. practice of running engines during a test, the incidence of secondary fires in an operational situation may be higher than the U.S. test data indicate.

Seager, E. R. Drake, R. F. C. Butler, *Operation TOTEM Group 12 Report: Effects on a Landrover (car, 5 CWT, 4x4) and Generating Sets* AWRE Report T 79/54(x), FWE-131, Atomic Weapons Research Establishment, Aldermaston, Berks, England, September 1956

SURVIVAL IN FIRE AREAS

The best documented fire storm in history (but not the one causing the greatest loss of life) occurred in Hamburg, Germany during the night of July 27-28, 1943, as a result of an incendiary raid by Allied forces. Factors that contributed to the fire included the high fuel loading of the area and the large number of buildings ignited within a short period of time.

The main raid lasted about 30 minutes. Since the air raid warning and the first high explosive bombs caused most people to seek shelter, few fires were extinguished during the attack. By the time the raid ended, roughly half the buildings in the 5 square-mile fire storm area were burning, many of them intensely. The fire storm developed rapidly and reached its peak in two or three hours.

Many people were driven from their shelters and then found that nearly everything was burning. Some people escaped through the streets; others died in the attempt; others returned to their shelters and succumbed to carbon monoxide poisoning.

Estimates of the number that were killed range from about 40,000 to 55,000. Most of the deaths resulted from the fire storm. Two equally heavy raids on the same city (one occurred two nights earlier; the other, one night later) did not produce fire storms, and they resulted in death rates that have been estimated to be nearly an order of magnitude lower.

More surprising than the number killed is the number of survivors. The population of the fire storm area was roughly 280,000. Estimates have been made that about 45,000 were rescued, 53,000 survived in non-basement shelters, and 140,000 either survived in basement shelters or escaped by their own initiative.

9-25 Causes of Death

The evidence that can be reconstructed from such catastrophes as the Hamburg fire storm indicates that carbon monoxide and excessive heat are the most frequent causes of death in mass fires. Since the conditions that offer protection from these two hazards generally provide protection from other hazards as well, the following discussion is limited to these two causes of death.

Carbon Monoxide. Burning consists of a series of physical and chemical reactions. For most common fuels, one of the last of the reactions is the burning of carbon monoxide to form carbon dioxide near the tips of the flames. If the supply of air is limited, as it is likely to be if the fire is in a closed room or at the bottom of a pile of debris from a collapsed building, the carbon monoxide will not burn completely. Fumes from the fire will contain a large amount of this tasteless, odorless, toxic gas.

During the Hamburg fire, many basement shelters were exposed to fumes. Imperfectly fitting doors and cracks produced by exploding bombs allowed carbon monoxide to penetrate these shelters. The natural positions of many of the bodies recovered after the raid indicated that death had often come without warning, as is frequently the case for carbon monoxide poisoning.

Carbon monoxide kills by forming a more stable compound with hemoglobin than either oxygen or carbon dioxide will form. These latter are the two substances that hemoglobin ordinarily carries through the blood stream. Carbon monoxide that is absorbed by the blood reduces the oxygen carrying capacity of the blood, and the victim dies from oxygen deficiency.

As a result of the manner that carbon monoxide acts, it can contribute to the death of a person who leaves a contaminated shelter to attempt escape through the streets of a burning city. A person recovering from a moderate case of carbon monoxide poisoning may feel well while he is resting, but his blood may be unable

to supply the oxygen his body needs when he exerts himself. After the air raid at Hamburg. victims of carbon monoxide poisoning. apparently in good health. collapsed and died from the strain of walking away from a shelter. It is suspected that many of the people who died in the streets of Hamburg were suffering from incipient carbon monoxide poisoning.

Heat. The body cools itself by perspiration. When the environment is so hot that this method fails. body temperature rises. Shortly thereafter, the rate of perspiration decreases rapidly. and. unless the victim finds immediate relief from the heat, he dies of heat exhaustion. Death from excessive heat may occur in an inadequately insulated shelter: it also may occur in the streets if a safe area cannot be located in a short time.

9-26 Shelters

The results of the Hamburg fire storm illustrate the value of shelters during an intense mass fire. The public air raid shelters in Hamburg had very heavy walls to resist large bombs. Reinforced concrete three feet thick represented typical walls. Some of these shelters were fitted with gas proof doors to provide protection from poison gas. These two features offered good protection from the heat and toxic gases generated by the fire storm.

The public shelters were of three types:

- *Bunkers.* These were large buildings of several shapes and sizes, designed to withstand direct hits by large bombs. The fire storm area included 19 bunkers designed to hold a total of about 15,000 people. Probably twice this number occupied the bunkers during the fire storm, and all of these people survived.
- *Splinterproof Shelters.* These were long single story shelters standing free of other buildings and protected by walls of reinforced concrete at least 2-1/2 feet thick. No deaths resulting from the fire storm were reported among occupants of these shelters. These structures were not gas-proof. Distance from burning structures and low height of the shelters probably provided protection from carbon monoxide.
- *Basement Shelters.* The public shelters that were constructed in large basements had ceilings of reinforced concrete 2 to 5 feet thick. Although reports indicate that some of the occupants of these shelters survived and some did not, statistics to indicate the chance of survival in such structures are not available.
- *Private Basement Shelters.* Private basements were constructed solidly, but most of them lacked the insulating value of very thick walls and the protection of gas-tight construction. Emergency exits (usually leading to another shelter in an adjacent building) could be broken if collapse of the building caused the normal exit to be blocked. As a result of the total destruction in the fire storm area, this precaution was of limited value. Many deaths occurred in these shelters as a result of carbon monoxide poisoning, and the condition of the bodies indicated that intolerable heat followed the carbon monoxide frequently. In some cases, the heat preceded the poisonous gas and was the cause of death. Generally, these shelters offered such a small amount of protection that the occupants were forced out within 10 to 30 minutes. Most of these people were able to move through the streets and escape. Others were forced out later when the fire storm was nearer its peak intensity, and few of these escaped. A few people survived in private basement shelters.

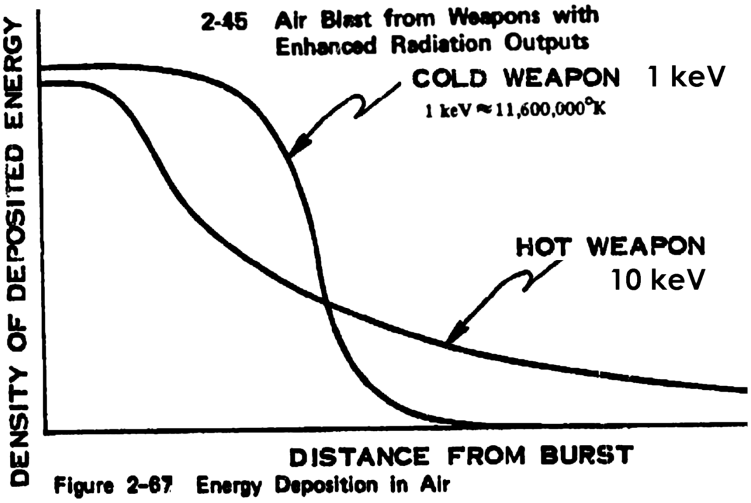

Figure 2-67 Energy Deposition in Air

Rough calculation may be made, however, by applying the following rule of thumb to weapons with enhanced outputs: blast calculations for a given radius may be based on a weapon yield that is equal to the amount of energy contained in the sphere defined by that radius. As this rule implies, the blast wave, as it propagates outward, picks up hydrodynamic energy from the heated air through which it passes.

2-140

THE THERMAL PULSE FROM SPECIAL WEAPONS

As stated in paragraph 2-45, Chapter 2, weapons that have enhanced radiation out-

3-56

puts, i.e., weapons that produce a large fraction of their output in the form of neutrons, gamma rays, or X-rays [redacted] will, in most cases, generate a weaker blast wave than a nominal weapon of the same yield. Similarly, the thermal pulse from such special weapons may be weaker than that from a nominal weapon. The explanation for the reduced thermal output is the same as the explanation for a weaker blast wave: neutrons, gamma rays, and high energy X-rays travel much farther through the atmosphere than the energy from a conventional weapon; therefore, a large portion of the weapon energy may be absorbed by air far from the burst. This air will not become sufficiently hot to contribute effectively to either the blast wave or to the thermal pulse.

[redacted] The terms "nominal weapon" and "conventional weapon" used in the preceding paragraph refer to a nuclear weapon that radiates 70 to 80 percent of its energy as X-rays [redacted] and retains nearly all of the remaining energy as thermal and kinetic energy of the weapon debris (see paragraph 4-4, Chapter 4).

3-17 Effective Thermal Yield of Special Weapons

The modified thermal effects produced by weapons with enhanced outputs may be calculated in terms of an effective thermal yield. This is defined as the yield that a nominal warhead would have in order to radiate the same thermal energy as the special weapon.

3-57

Effective thermal yield is roughly the amount of energy that the nuclear source deposits within a sphere the size of the fireball at the time of the principal minimum. This radius is

$$R_{min} = \frac{29\ W^{0.36}}{(\rho/\rho_o)^{0.22}} \text{ meters,}$$

where W is the weapon yield in kilotons, ρ is the ambient air density at the burst altitude, and ρ_o is the ambient density at sea level.

Energy that is deposited beyond the radius R_{min} is assumed to make a negligible contribution to the energy radiated by the fireball.

Since the size of the fireball is determined by the thermal energy it contains, it would be logical to let W represent effective thermal yield rather than total weapon yield. To do this requires a trial-and-error approach.

3-58

The components of energy deposited within R_{min} of the burst are added together to obtain the effective thermal yield

3-59

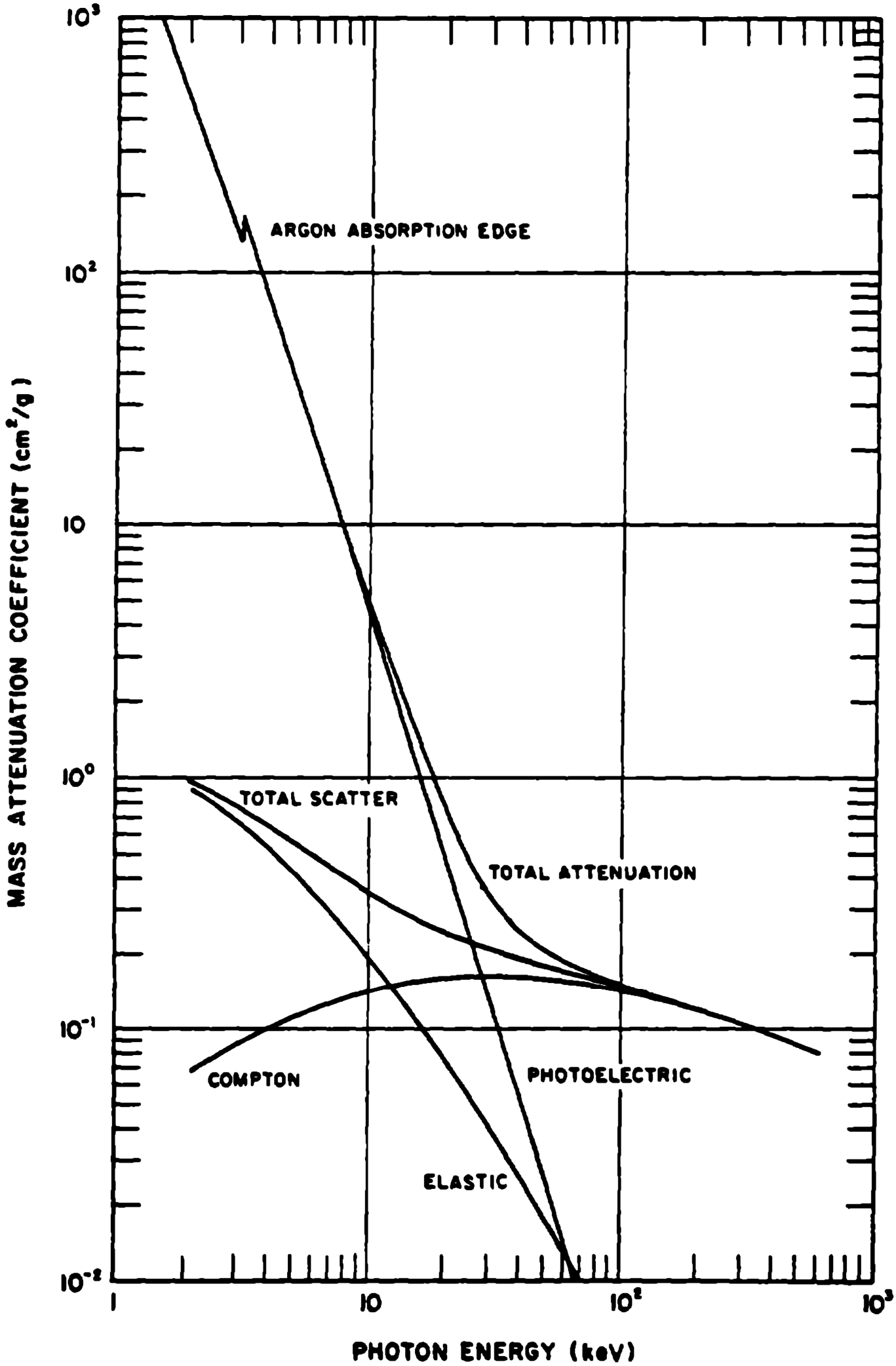

Figure 4-4. Mass Attenuation Coefficients for Air

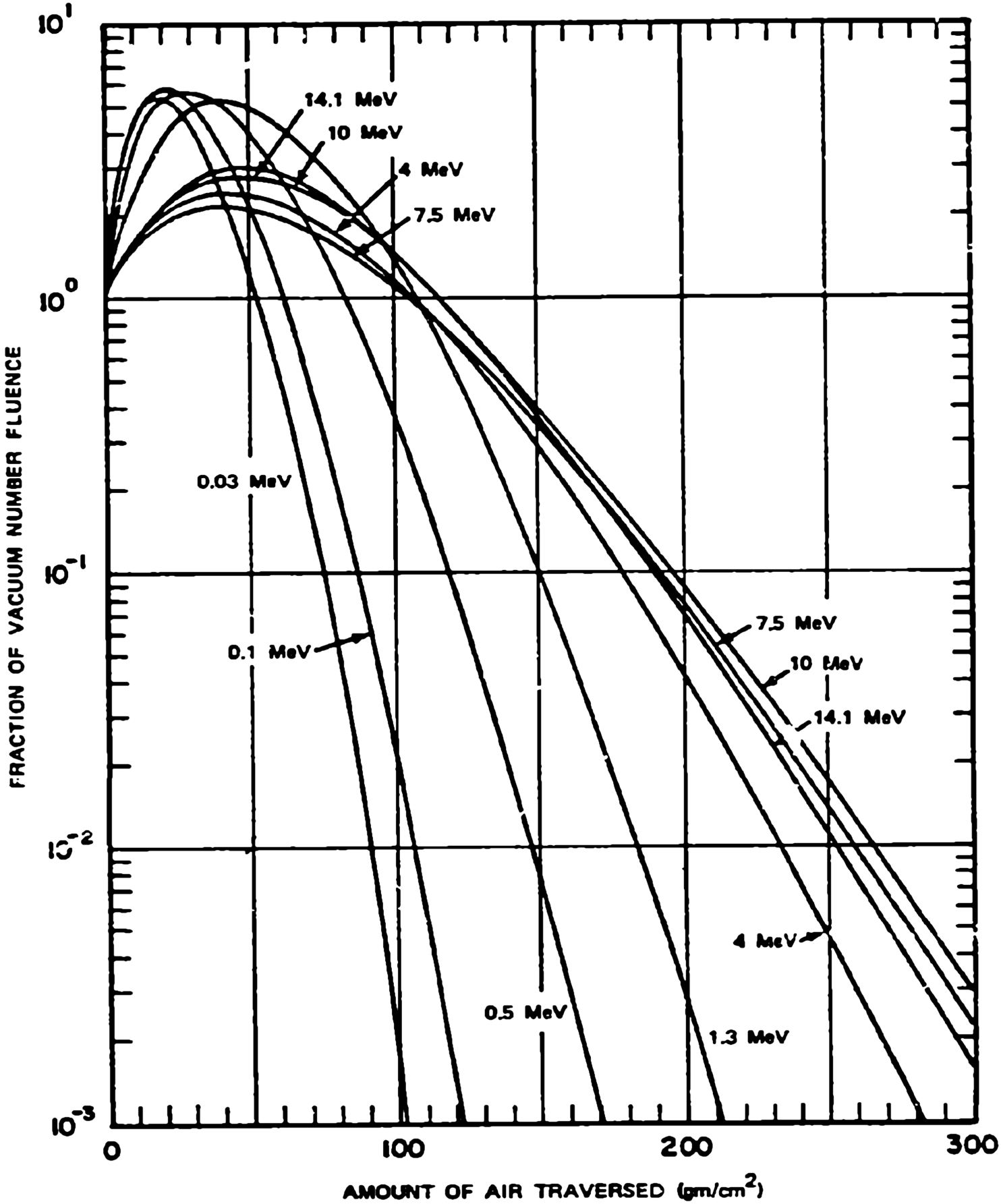

Figure 5-7. Neutron Energy Build-Up Factors for Various Monoenergetic Sources in Homogeneous Air

SECTION V
X-RAY DAMAGE EFFECTS

NTRODUCTION

Nuclear weapons as X-ray sources and the environments they produce are described in Chapter 4.

Cold X-rays (typically 1 to 3 keV black body temperatures) are absorbed in a thin surface layer. At sufficiently high fluence, a short pulse of X-rays can heat the surface rapidly and may cause it to vaporize and blow off. This results in: (1) an impulse imparted to the total structure; and (2) generation of a strong shock wave that propagates into the structure, and which may cause spallation of material at free boundaries and internal fracture of materials and bonds. These latter effects are produced by shock wave propagation through the thickness of a surface structure such as the thermal protection shell of a reentry vehicle. The former effects may produce damage by whole vehicle modes of response to the net impulse.

The hot X-rays are more penetrating. They can cause: (1) thermally generated shock waves in the vehicle structural materials and internal components; (2) melting and vaporization of the substructure: (3) internal deposition of energy in electronic components producing transient or permanent damage (see Chapter 6 and Section 7 of this chapter): or (4) produce internal EMP signals (see Chapter 7).

While some nuclear weapons emit only cold X-rays, all hot X-ray weapons have a cold component. Hence, for exoatmospheric events the hot X-ray effects are accompanied by cold X-ray effects. On the other hand, for endoatmospheric explosions, the cold X-rays have short mean free paths, and the X-ray effects beyond distances of a few tens of meters are produced by hot X-rays alone.

All vulnerability analyses follow similar computational steps:

1. The X-ray energy deposition is computed using known processes for the materials and structure. This energy is assumed most often to be deposited instantaneously.
2. From the calculated energy deposition and the equation of state for the materials in the structure (if known) for the liquid, solid, and vapor phases of the material, a stress wave, which propagates through the surface structure, is calculated.
3. Damage to the surface structure that results from the stress wave (spallation, internal fracturing, delamination and debonding), is determined.
4. The response of the whole structure that results from the impulse imparted to it is determined.

X-RAY ENERGY DEPOSITION CALCULATIONS

The starting point of all X-ray vulnerability analysis is a calculation of the X-ray energy deposition.

9-33 X-ray Cross Sections

The probability of a photon of energy $h\nu$ traversing a distance of absorbing material x is $e^{-\mu x}$, where μ is the linear attenuation coefficient. This probability also can be written as $e^{-(\mu/\rho)\rho x}$, where μ/ρ is the mass attenuation coefficient for the material (see paragraph 4-3). In this representation, μ/ρ is in cm^2/gm and ρx is the thickness in gm/cm^2, i.e., the mass of material in the column of 1 square centimeter cross section and x centimeters long.

If the monoenergic X-ray fluence incident normal (perpendicular) to the material surface is φ_o, the direct fluence after traversing a thickness of absorbing material is

9-68

$$\varphi_{dir} = \varphi_o e^{-(\mu/\rho)\rho x} \text{ cal/cm}^2.$$

Mass attenuation coefficients for the elements beryllium, aluminum, iron, copper, tungsten, and uranium are given in Tables 9-10 through 9-15, and Figures 9-27 through 9-32, respectively. These are representative of metallic materials used in aerospace systems. Mass attenuation coefficients for ablator materials, carbon phenolic and tape-wound silicon phenolic are shown in Figures 9-33 and 9-34, respectively. In these tables and figures, Z is the atomic number, μ_{ce}/ρ is the coherent elastic scattering coefficient, μ_{ie}/ρ is the incoherent Compton elastic coefficient, μ_{is}/ρ is the inelastic Compton coefficient, and μ_p/ρ is the photoelectric coefficient. As designated previously, μ_a/ρ and μ/ρ are the energy absorption coefficient and the total attenuation coefficient.†

9-34 X-ray Energy Deposition and Shine Through Fluences

X-ray energy deposition in a thickness δ at a depth x due to direct fluence photons is given by

$$A'_{dir} = \varphi_o \left[1 - e^{-\left(\frac{\mu_a}{\rho}\right)\rho\delta}\right] e^{-\left(\frac{\mu}{\rho}\right)\rho x}.$$

If $\mu_a\delta << 1$, and if φ_o is in cal/cm^2, this expression can be written as

$$A'_{dir} = \varphi_o \left(\frac{\mu_a}{\rho}\right) \rho\delta \; e^{-\left(\frac{\mu}{\rho}\right)\rho x} \text{ cal/cm}^2.$$

† The symbols K, L_1, L_2, etc., in the tables and figures indicate the binding energies of the various electron shells (see paragraph 4-3, Chapter 4).

Frequently, the absorption is written in terms of cal/gm by dividing out the thickness $\rho\delta$,

$$A_{dir} = \varphi_o \left(\frac{\mu_a}{\rho}\right) e^{-\left(\frac{\mu}{\rho}\right)\rho x} \text{ cal/gm.}$$

This expression for the absorption is in terms of a dose; however, this assumes that very little of the flux is absorbed in the deposition region at depth x, i.e., the deposition region considered is very thin. Clearly, more energy than is in the incident flux cannot be absorbed.

The equation for direct fluence (φ_{dir}) given in paragraph 9-32 can be used to represent a small energy band of photons in X-ray energy spectra such as those tabulated in Table 4-3, Chapter 4, for various black body spectra. The total energy in the direct X-ray fluence after traversing thickness x is obtained by summing over the energy bands.

$$\varphi = \sum_i \varphi_{oi} \, e^{-\left(\frac{\mu}{\rho}\right)_i \rho x} \text{ cal/cm}^2.$$

In a like manner, the total direct fluence X-ray energy absorption at depth ρx is obtained by summing for each energy band.

$$A = \sum_i \left(\frac{\mu_a}{\rho}\right)_i \varphi_{oi} \, e^{-\left(\frac{\mu}{\rho}\right)_i \rho x} \text{ cal/cm}^2.$$

Problems 9-3 and 9-4 illustrate how these equations can be used to calculate approximate values for energy deposition and shine through.

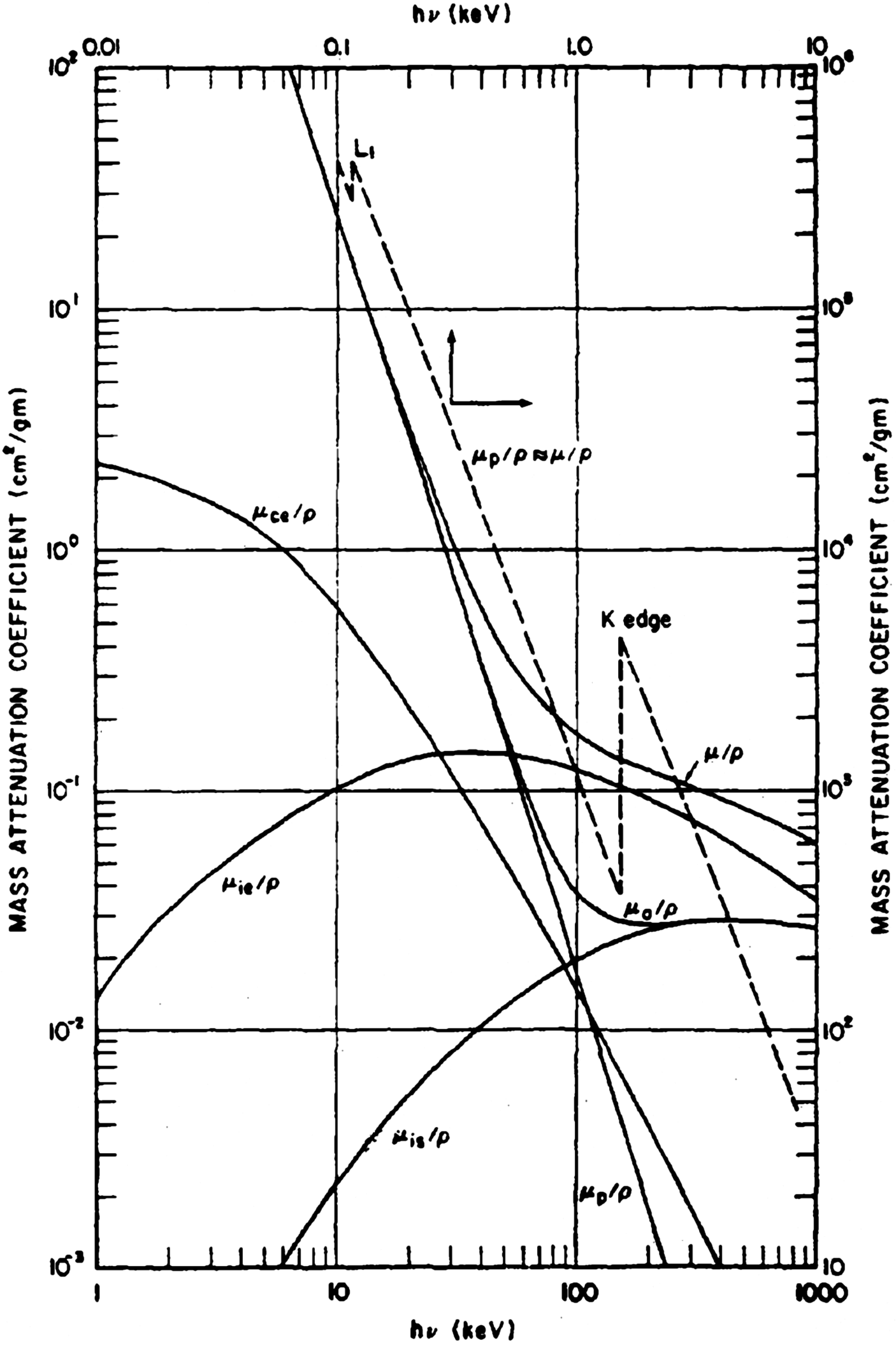

Figure 9-28. Photon Cross Sections in Aluminum

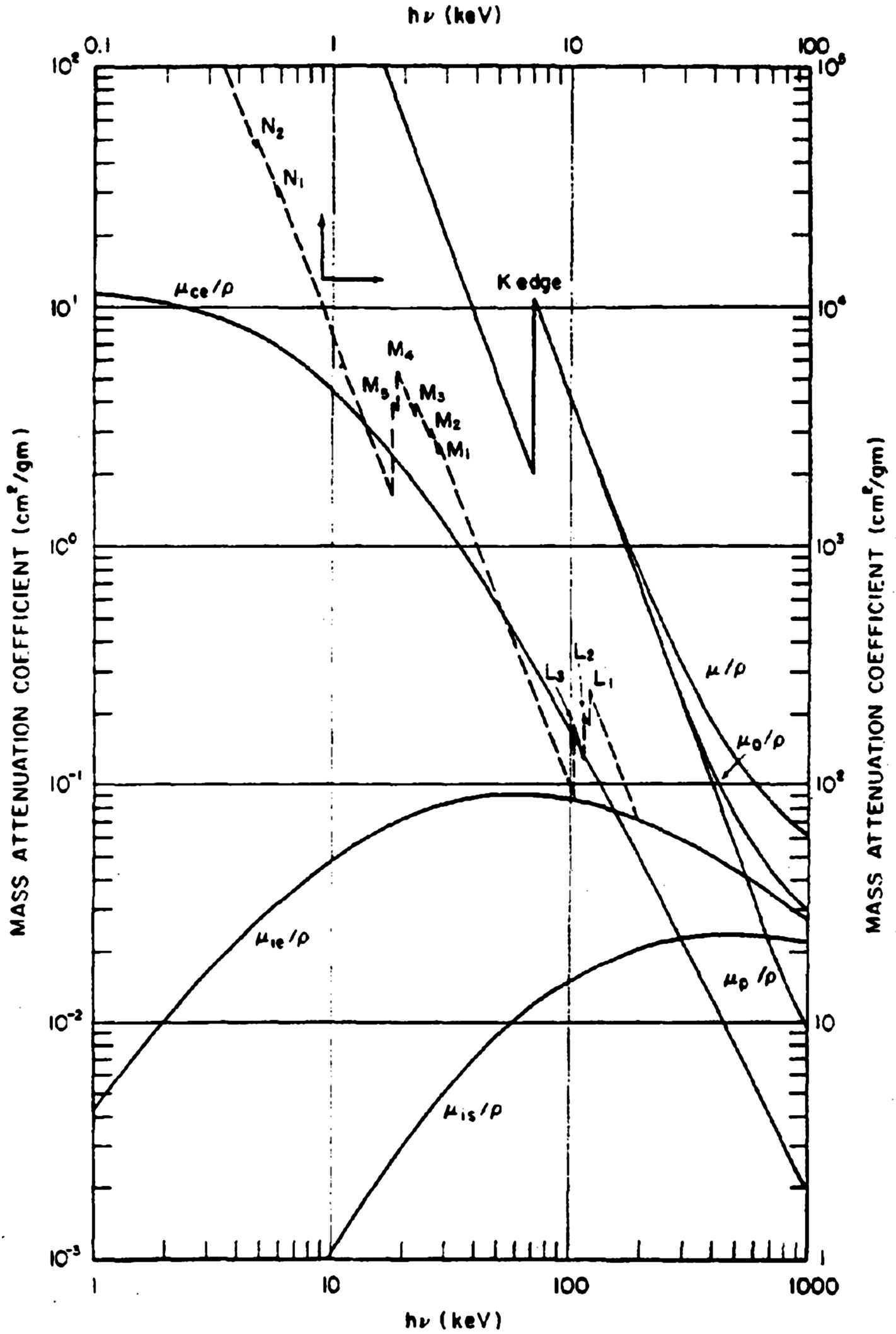

Figure 9-31. Photon Cross Sections in Tungsten

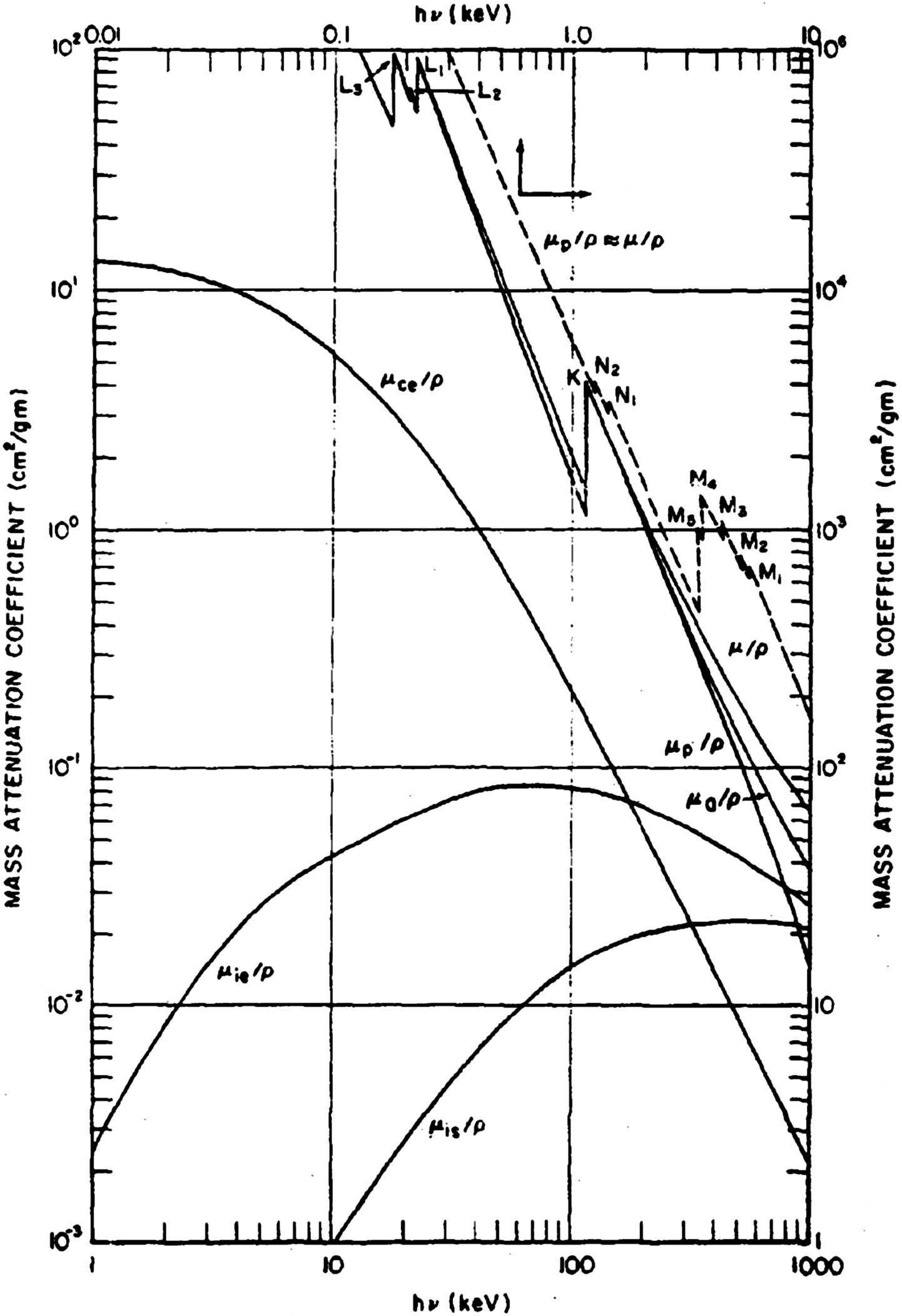

Figure 9-32. Photon Cross Sections in Uranium

9-35 X-ray Energy Deposition Summary

The methods described in paragraphs 9-33 and 9-34 and illustrated in Problems 9-3 and 9-4 allow the calculation of curves that show approximations of energy deposition as a function of depth for black body spectra incident on any material, if the cross sections are known for the material.

INITIAL PRESSURIZATION OF MATERIALS DUE TO X-RAY DEPOSITION

An immediate consequence of the deposition of X-ray energy is the rapid heating of the material. This heating causes an initial pressure distribution as a function of depth in the structure. The initial pressurization generates shock waves that propagate through the thickness of the shell of the structure. The heating can result in a solid material changing phase, that is, melting or vaporizing. The melting and vaporization cause blowoff, which imparts an impulse to the structure and excites whole structure modes of response.

9-36 Phase Changes Induced by X-ray Heating

In most nuclear weapon X-ray environments, the X-ray energy is deposited in a very short time, a few nanoseconds to a few hundred nanoseconds. The material cannot expand appreciably during this time, so the energy deposition process can be considered to occur at a constant volume or at normal material density, ρ_0. Rapid melting and vaporization are accompanied by enormous pressure increases. Values

for enthalpy changes for melting and vaporization for the metals discussed in the previous subsection are given in Table 9-17. These values are for one atmosphere pressure. In most X-ray problems of interest the material is initially at very high pressure, so these values can be considered to be only approximate. This approach is not correct for ablators as a class although it might apply to carbon phenolic in a cold environment. Confining the discussion to metals will not restrict the transfer of principles.*

[redacted] The rising pressure that results from heating at constant density is illustrated in Figures 9-39 and 9-40 where isoenergy lines of aluminum are shown in pressure-density plots. If the internal energy is above the critical energy, 3,016 cal/gm for aluminum, the material can be considered as a vapor. Figure 9-40 shows the high pressure, high energy intercepts with the normal density abscissa (ρ_0 = 2.7 gm/cm^3). The release adiabats for expansion from density ρ_0 to low density and pressure also are shown in this figure. Expansion along the adiabat results in decreasing internal or potential energy as the material develops kinetic energy during "blowoff." For example, a 6,000 cal/gm energy deposition in aluminum at ρ_0 = 2.7 gm/cm^3 results in a pressure of about 1.5 megabars (Mb). The aluminum would expand from that state to low pressure and density, with final internal energy of about 3,000 cal/gm and about 3,000 cal/gm of kinetic energy. The 3,000 cal/gm of internal or potential energy is used to overcome the physical and chemical forces that bind the atoms together in the solid. This leads to the concept of heat of sublimation. The heat of sublimation at absolute zero, E_{so}, is the energy required to form the saturated vapor from the solid at a temperature of absolute zero. Thus, E_{so} does not include any energy of kinetic motion. The energy of sublimation generally is a function of temperature becoming larger for larger deposition energies (temperatures).

* [redacted] The problem of phase changes in a composite heat shield ablator is more complicated since different deposition profiles, material enthalpy, and thermal conductivities are involved in the calculations. While some materials, e.g., tape-wrapped carbon phenolic, may behave like metals in a cold environment, the techniques described here generally are not applicable to the description of the blowoff process in the broad category of composite materials that use three dimension (3-D) weaves for heat shields or for X-ray shields that use dispersed high Z materials for loading.

Table 9-17. [redacted] Enthalpy Change for Selected Metals [redacted] (cal/gm)

Metal-Atomic Weight	To Melt	Through Melt	To Vapor	Through Vapor	Sublimation Energy
Be 9.013	876.0	1,187.0	2,147.0	10,040.0	8,682.0
Al 26.98	160.4	255.3	771.1	3,347.0	2,891.0
Fe 55.85	250.8	315.8	573.0	2,071.0	1,782.0
Cu 63.54	110.0	160.0	336.0	1,481.0	1,275.0
W 183.85	153.9	200.0	304.0	1,353.0	1,110.0
U 238.00	49.0	64.5	171.9	596.1	492.1

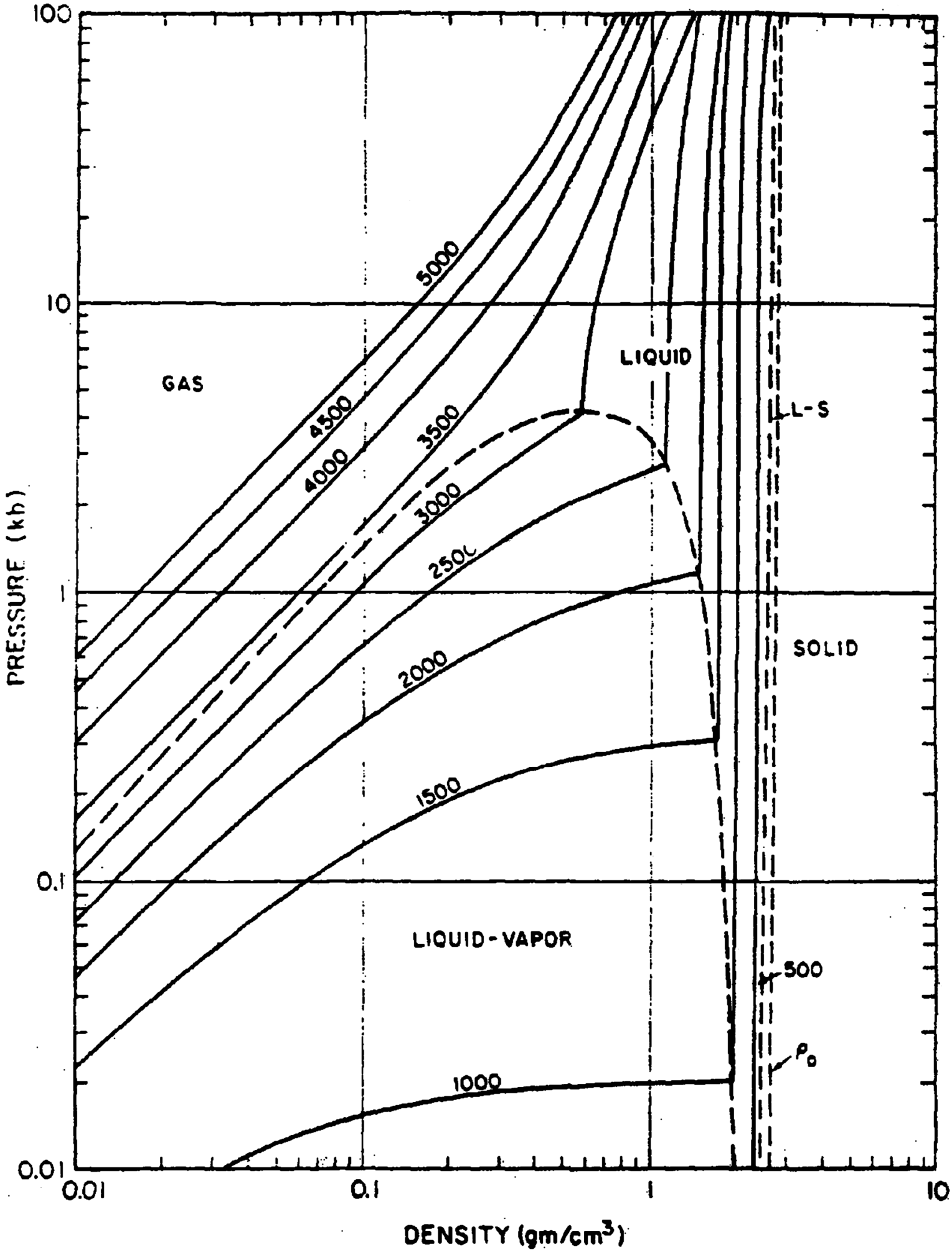

Figure 9-39. Aluminum Isoenergy Lines.
Parameter is Energy in cal/gm

The units for ϵ in the equation given above are energy per unit volume, which have the same dimensions as pressure. Therefore, the energy required in cal/gm for a phase change can be expressed in units of pressure, if the density of the material is specified. If the internal energy, E, is given per unit mass, the relation to ϵ is

$$\epsilon\ (\text{cal/cm}^3) = E\ (\text{cal/gm})\ \rho_o (\text{gm/cm}^3).$$

The value of ϵ in megabars may then be obtained by the relation

$$\epsilon\ (\text{Mb}) = \epsilon\ (\text{cal/cm}^3) \times 4.18 \times 10^7 \left(\frac{\text{erg}}{\text{cal}}\right) \times 1 \left(\frac{\text{dyne} \cdot \text{cm}}{\text{erg}}\right) \times 1 \left(\frac{\text{Mb}}{10^{12}\ \text{dyne/cm}^2}\right)$$

$$\epsilon\ (\text{Mb}) = 4.8 \times 10^{-5}\ \epsilon \left(\frac{\text{cal}}{\text{cm}^3}\right)$$

$$= 4.18 \times 10^{-5}\ \rho_o E \left(\frac{\text{cal}}{\text{gm}}\right).$$

Thus, the previous equation for pressure may be written

$$P\ (\text{Mb}) = G\ \frac{\rho}{\rho_o}\ \epsilon\ (\text{Mb}),$$

or

$$P\ (\text{Mb}) = 4.18 \times 10^{-5}\ G\rho\ E\ (\text{cal/gm}).$$

The enthalpy changes of the metals shown in Table 9-17 in cal/gm are given in Table 9-19.

Table 9-19. [redacted] Enthalpy Changes ϵ (Mb) [redacted]

Metal	ρ_o (gm/cm^3)	To Melt	Through Melt	To Vapor	Through Vapor	Sublimation Energy, E_s
Be	1.85	0.068	0.0918	0.166	0.776	0.671
Al	2.70	0.0181	0.0288	0.087	0.378	0.326
Fe	7.86	0.0824	0.1036	0.188	0.680	0.585
Cu	8.92	0.0410	0.0596	0.125	0.552	0.475
W	19.3	0.124	0.161	0.245	1.092	0.895
U	18.7	0.0383	0.0504	0.134	0.466	0.385

Table 9-20. Pressure Change, P (Mb)
($\rho = \rho_o$, $\eta = 1$)

Metal	G	To Melt	Through Melt	To Vapor	Through Vapor	Sublimation Energy, E_s
Be	1.45	0.099	0.133	0.241	0.12	0.973
Al	2.13	0.0386	0.0613	0.185	0.805	0.694
Fe	1.69	0.139	0.175	0.318	1.15	0.989
Cu	2.00	0.082	0.119	0.250	1.10	0.950
W	1.43	0.177	0.230	0.350	1.56	1.28
U	2.03	0.078	0.102	0.273	0.946	0.782

The pressures associated with these changes at ambient density, i.e., when $\rho = \rho_o$, and P (Mb) = $G\epsilon$ (Mb), are shown in Table 9-20.

From Table 9-20, aluminum has a sublimation pressure of about 0.7 Mb at ambient density, corresponding to sublimation energy of about 2,900 cal gm (Table 9-17). This point is shown in Figure 9-40, labeled E_s at about 3,000 cal gm. Table 9-20 indicates that the pressures associated with vaporization of metals at ambient density are with some exceptions about 1 Mb. A survey of more than 30 common metal elements indicates that an average of 1 Mb for vaporization is a good approximation, especially if the Grüneisen value for the material is uncertain. Since a bar corresponds to 14.7 psi a Mb is the enormous pressure of about 1.45×10^7 psi. Thus, tremendous forces are involved in the pressure gradients associated with metal vaporization at ambient density. Table 9-17 shows that vaporization usually involves several thousand calories per gram of energy. High explosive materials (TNT, etc.) release about 1,000 cal/gm. Therefore, on a mass basis there is more energy associated with metal vaporization than with high explosives. Generally, the thicknesses of material evaporated by X-ray absorption is small, and, the total mass of material that is vaporized generally is small.

SHOCK WAVE PROPAGATION AND DAMAGE PREDICTIONS

The sequence of events for the generation and propagation of a stress wave through the thickness of an aerospace shell and the damage produced is illustrated in Figure 9-41. Cold X-rays are deposited primarily in a relatively thin sheet of material at the front surface (Figure 9-41a). After the energy is deposited a compression wave propagates inward from the front surface, followed by a rarefaction that causes the vapor and liquid to blow off (Figure 9-41b). This rarefaction also may cause a spall of solid material from the front surface (Figure 9-41c). Later the compression wave reflects from the back surface and returns as a rarefaction wave. This rarefaction wave, or the coincidence of this wave with the rearward moving rarefaction may cause the rear surface to spall (Figure 9-41d), or may cause fracturing or debonding. This process occurs within the order of a microsecond and generally is complete before the overall structural motion occurs. The shock effects are

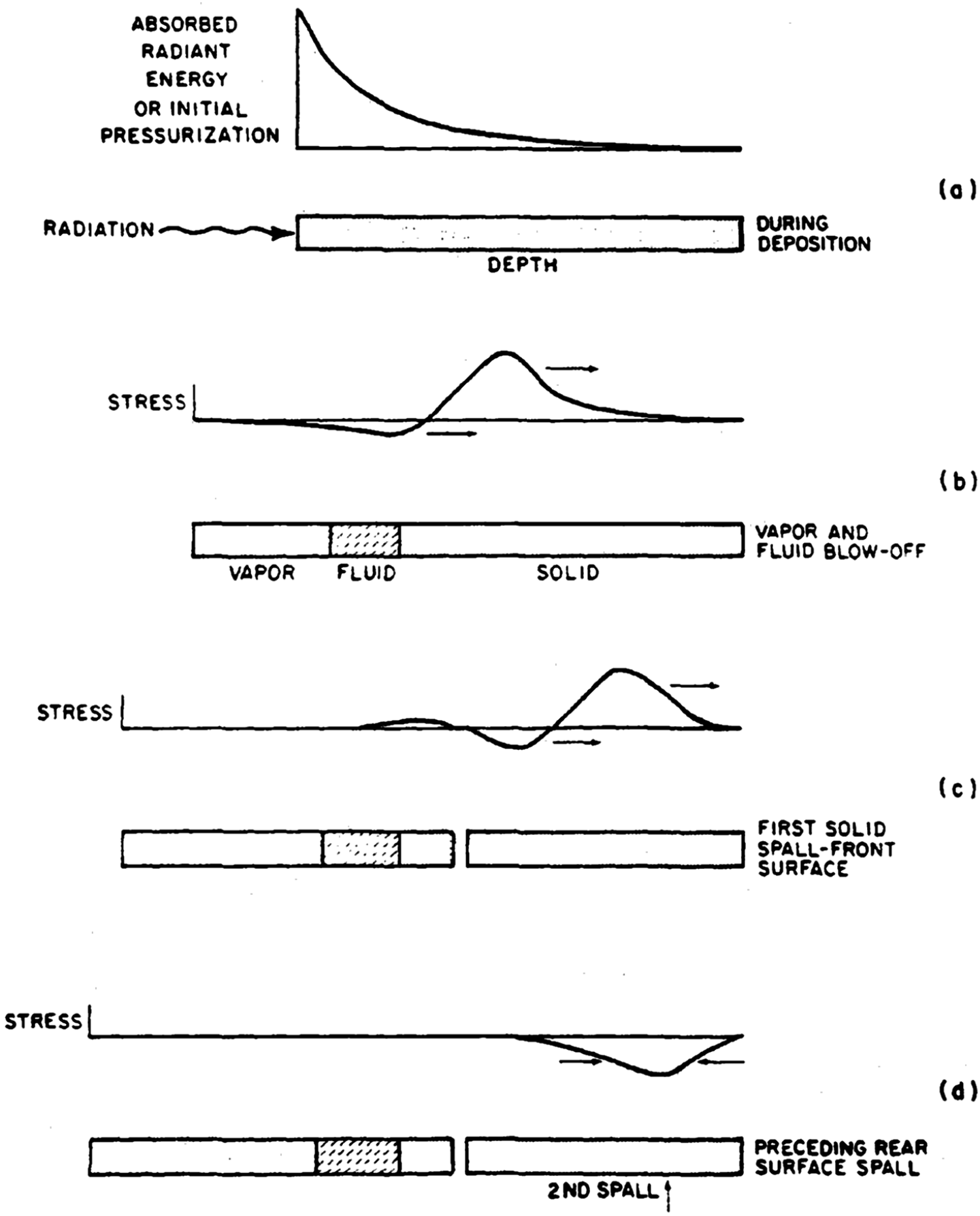

Figure 9-41. Sequence of Spallation Following Radiation Deposition

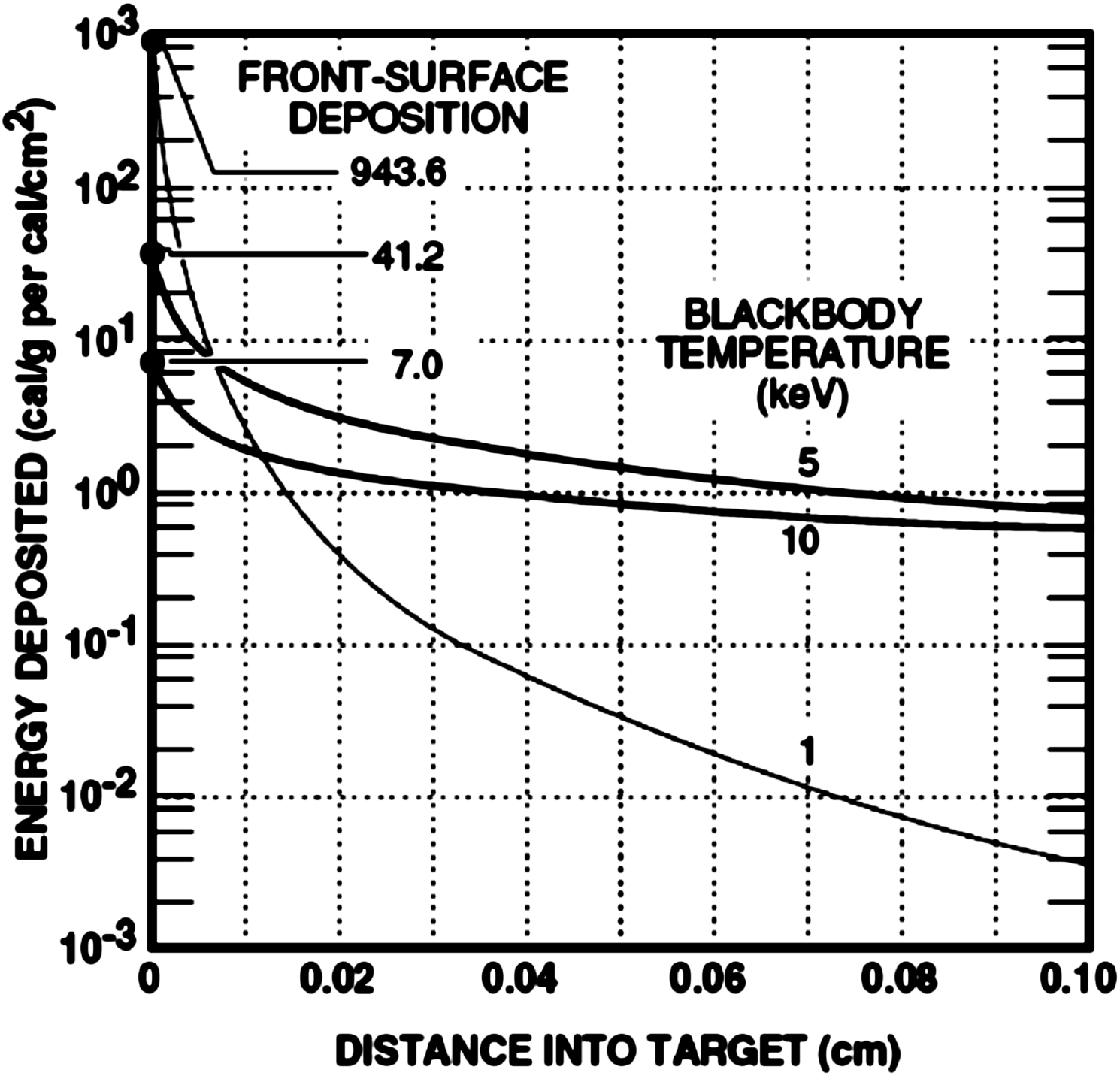

(IMAGE RESTORED TO DELETED IMAGE OF 1989 DECLASSIFIED VERSION OF EM-1 USING THE DECLASSIFIED VERSION OF DIAGRAM IN THE 1996 UNCLASSIFIED JOHN NORTHROP EM-1 EXTRACTS HANDBOOK.)

Figure 9-35. [redacted] Energy Deposited in Aluminum by Black Body Spectra [redacted]

Table 5-3. Representative Types of Nuclear Weapons

Type	Description
I	Subkiloton Fission
II	Pure Fission Implosion
III	Large (physically) Boosted Fission
IV	Small (physically) Boosted Fission
V	Enhanced Neutron Weapon
VI	Gun-Assembly Fission Weapon
VII	Thermonuclear Weapon
VIII	Thermonuclear Weapon

Table 5-1. Weapon Neutron Output Spectra

Neutron Energy (MeV)	Fission Weapon (neutrons/kt)	Thermonuclear Weapon (neutrons/kt)
12.2 -15.0		1.62×10^{22}
10.0 -12.2		8.53×10^{21}
8.18 -10.0	7.32×10^{20}	6.08×10^{21}
6.36 - 8.18	1.27×10^{21}	5.46×10^{21}
4.06 - 6.36	3.00×10^{21}	6.41×10^{21}
2.35 - 4.06	8.90×10^{21}	1.22×10^{22}
1.11 - 2.35	2.52×10^{22}	2.84×10^{22}
0.111 - 1.11	3.84×10^{22}	6.18×10^{22}
0.0033- 0.111	2.22×10^{22}	1.71×10^{23}
Total	9.97×10^{22}	3.16×10^{23}

These spectra are those that were used in the calculation of dose to personnel from weapon types II and VIII, respectively.

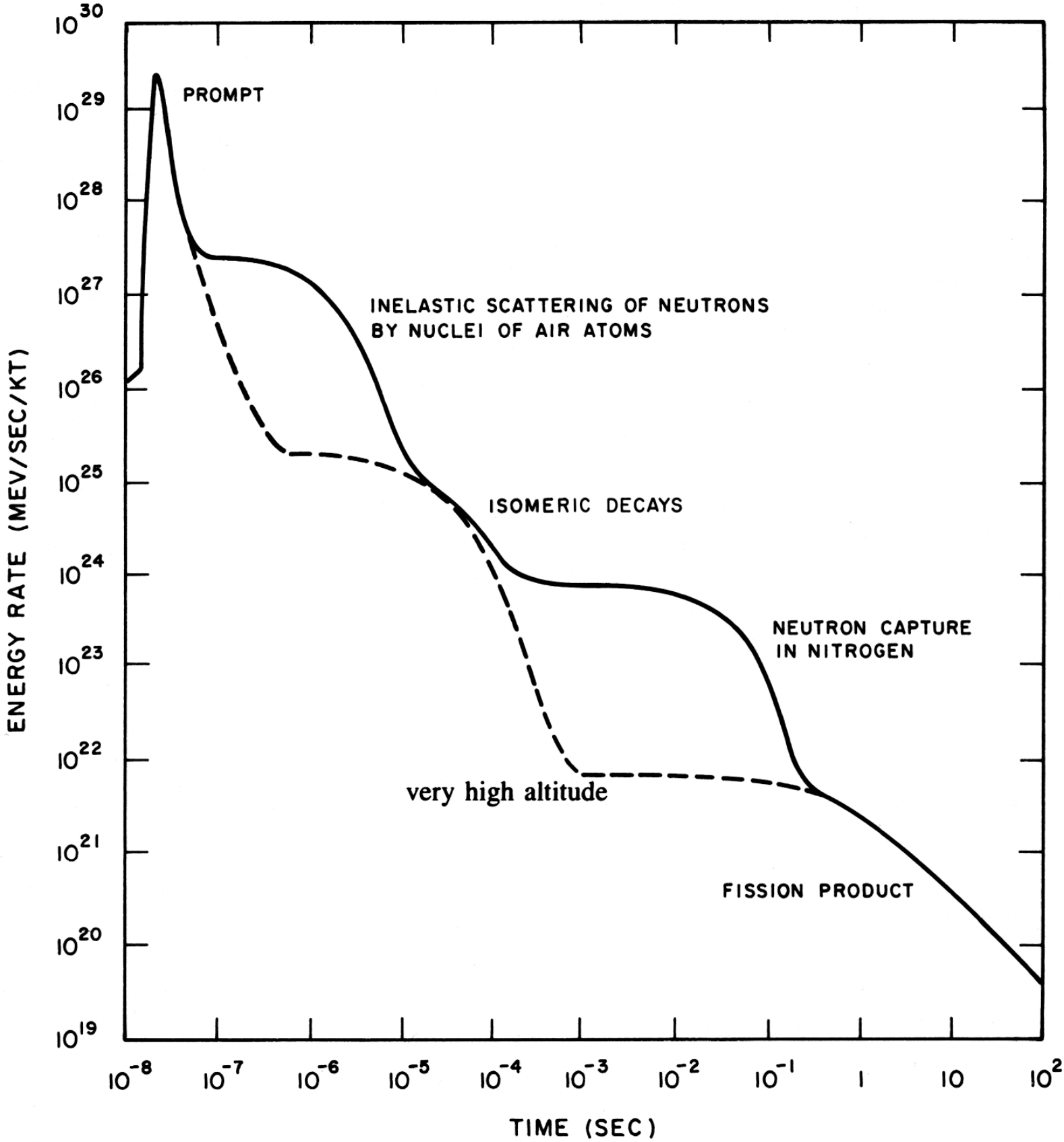

Figure 5-8. Calculated Time Dependence of the Gamma Ray Output from a Large Yield Explosion, Normalized to 1 kt

Table 9-26. [redacted] Failure Thresholds for Typical MOS Digital Microcircuits [redacted]

Designation	Function	Failure Level	
		Gamma, (rads (Si))	Neutron.* (n/cm^2)
SC 1171	NAND gate	2×10^5†	–
MEM 529	Binary element	1.4×10^5‡	–
SC 1171	Binary element	$1. \quad 10^5$‡	–
MEM 501	Shift register	$1. \times 10^5$§	–
MEM 590	Chopper	Not measured**	3×10^{14}
SC 1149	Flip-Flop	Not measured**	8×10^{14}
MC 1155	AND/OR gate	2×10^5 (Cobalt-60)††	
3300	25-bit static shift register	$>5 \times 10^3$ (FXR)‡‡ $>8 \times 10^4$ (TRIGA)‡‡	
3003	100-bit shift register	$>2 \times 10^4$ (FXR)‡‡ $>5 \times 10^4$ (TRIGA)‡‡	
1406	100-bit shift register	$>10^5$ (FXR)‡‡ $<2.5 \times 10^4$ (TRIGA)	
1101	256-random access memory	4×10^4 (FXR) 2×10^4 (TRIGA)	3×10^{11}

* [redacted] Neutron fluence specified as (E > 10 keV, fission).
† [redacted] Supply voltage – 20 volts.
‡ [redacted] Supply voltage – 15 volts.
§ [redacted] Clock voltage – 10 volts.
** [redacted] Supply voltage – 10 volts.
†† [redacted] Type of facility in which test was performed.
‡‡ [redacted] No failures at these levels.

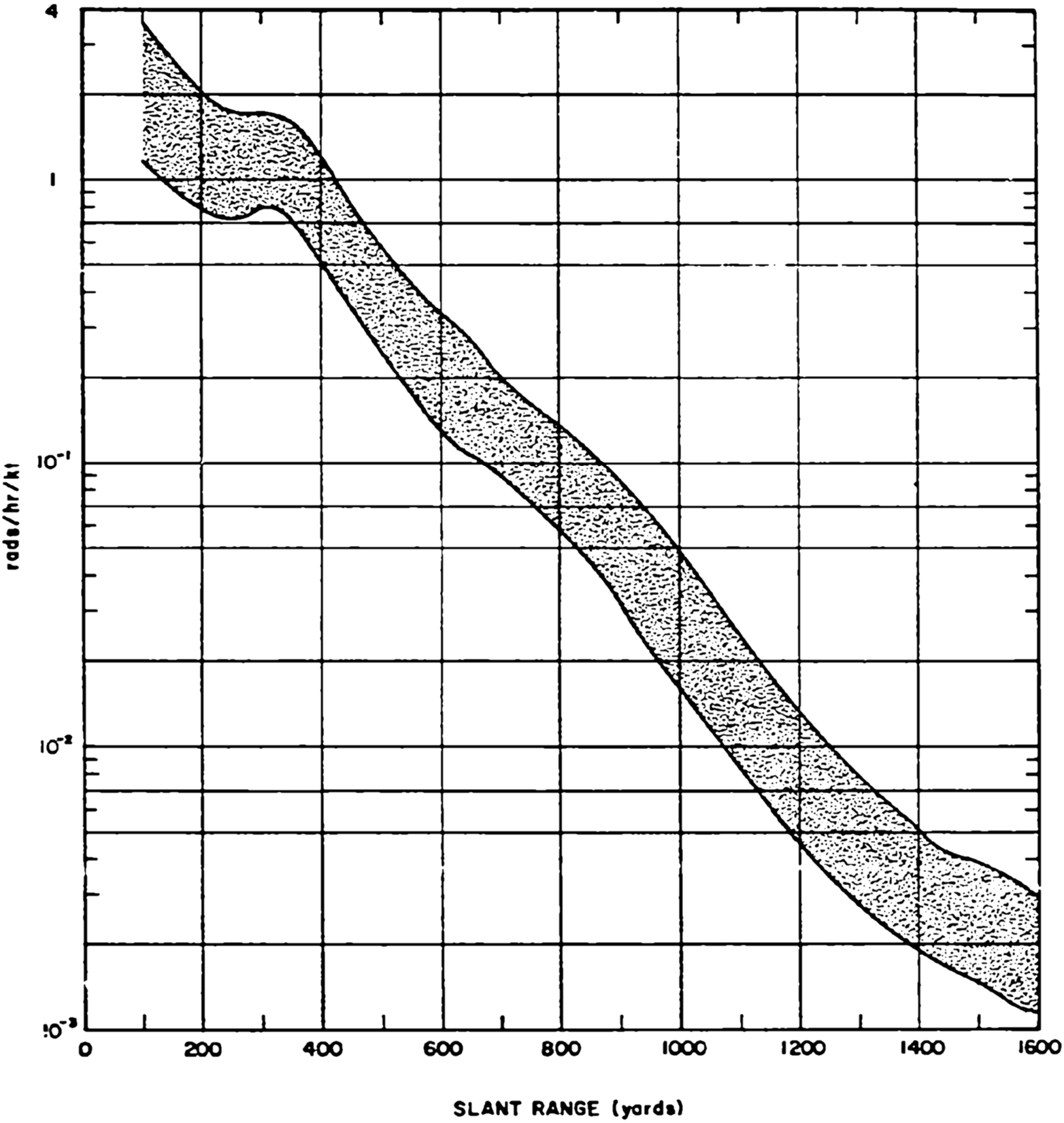

Figure 5-18. Neutron-Induced Gamma Dose Rate as a Function of Slant Range at a Reference Time of 1 Hour After Burst LIBERIA SOIL

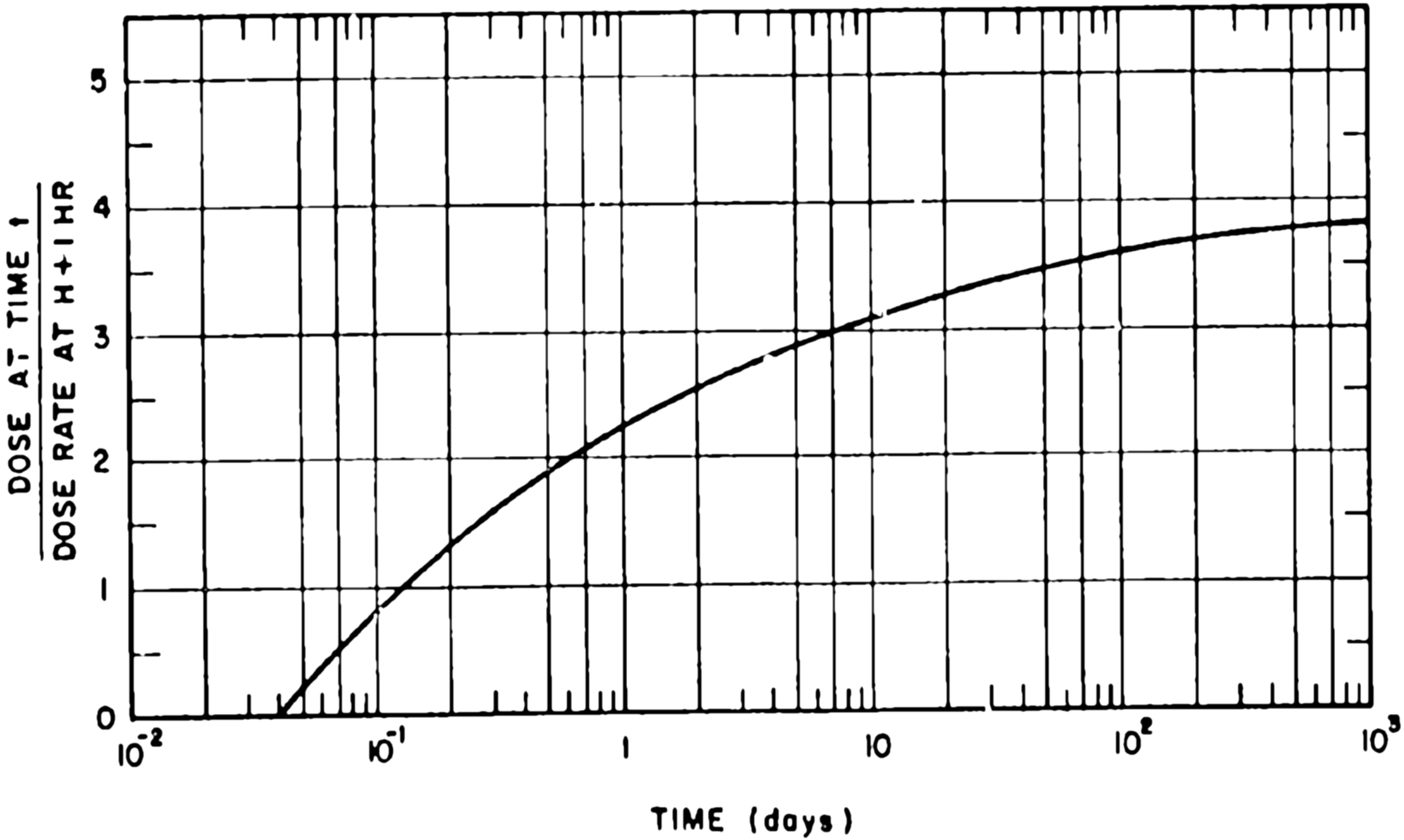

Figure 5-41. [redacted] Normalized Dose Accumulated in a Fallout Contaminated Area from *H* + 1 Hour to *H* + 1,000 Days [redacted]

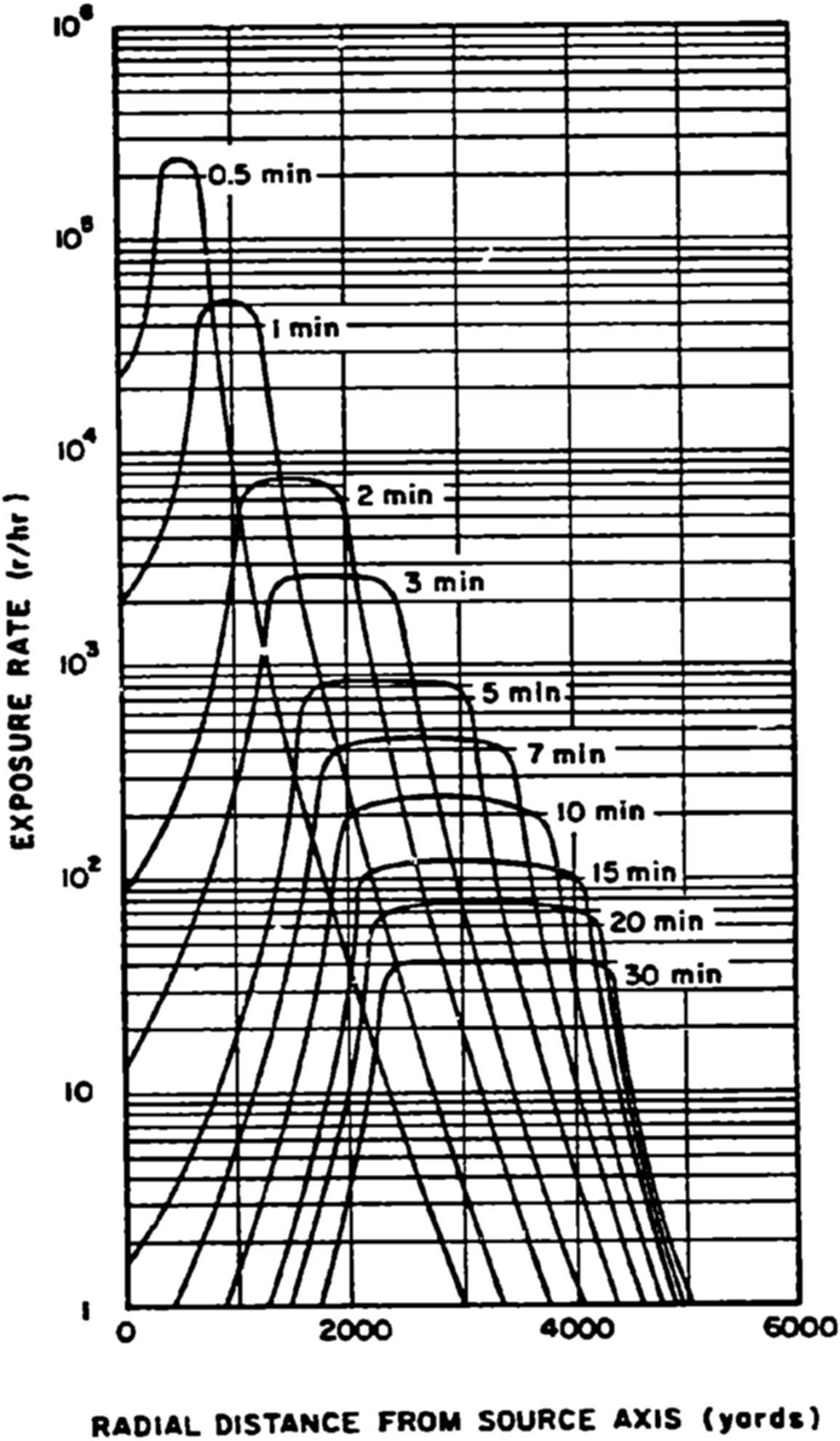

Figure 5-47. [redacted] Base Surge Radiation Exposure Rate 15 Feet Above the Water Surface from a 10 kt Explosion on the Bottom in 65 Feet of Water, No-Wind Environment [redacted]

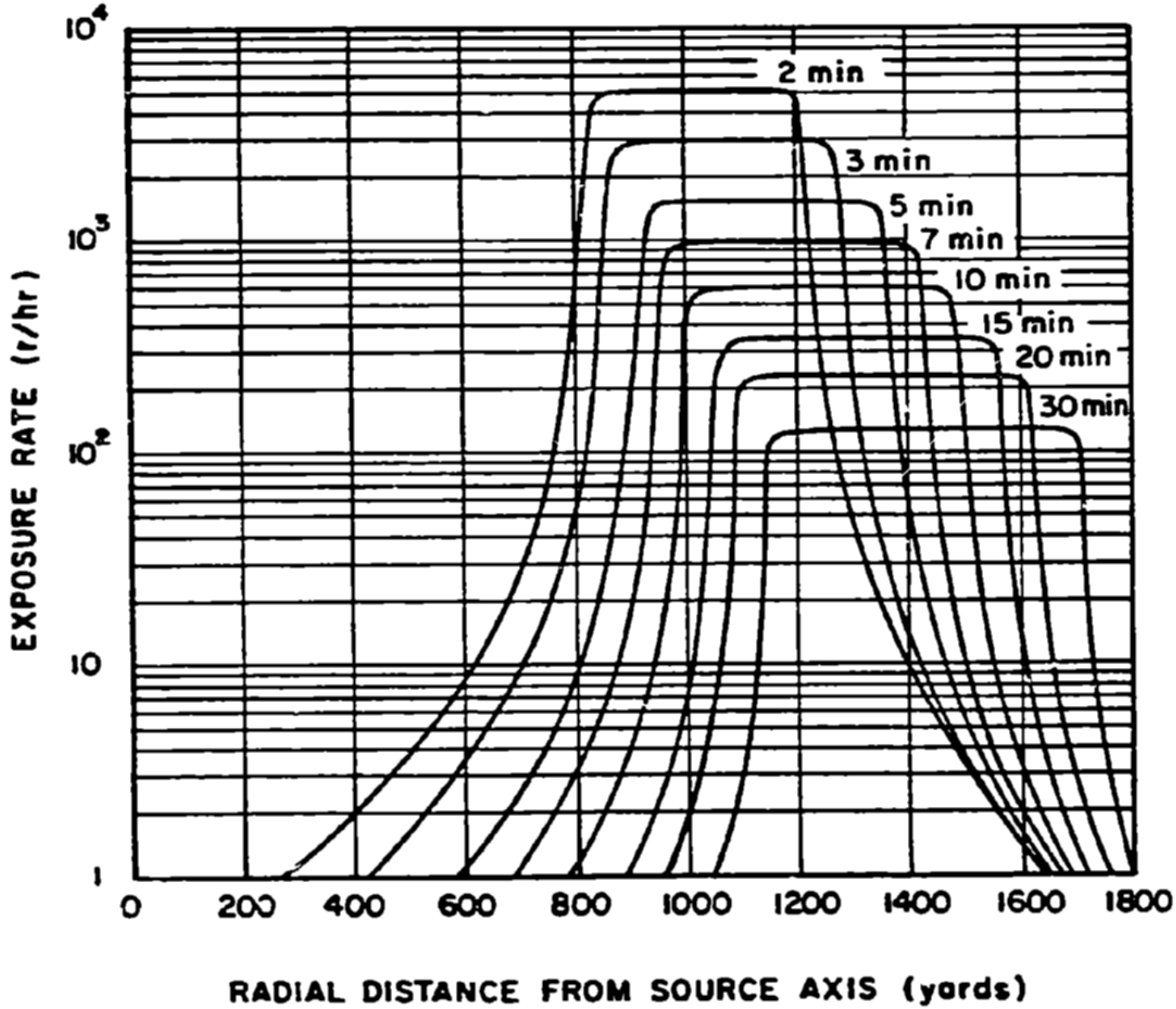

Figure 5-53. Pool Radiation Exposure Rate 15 Feet Above the Water Surface from a 10 kt Explosion on the Bottom in 65 Feet of Water, No-Current Environment

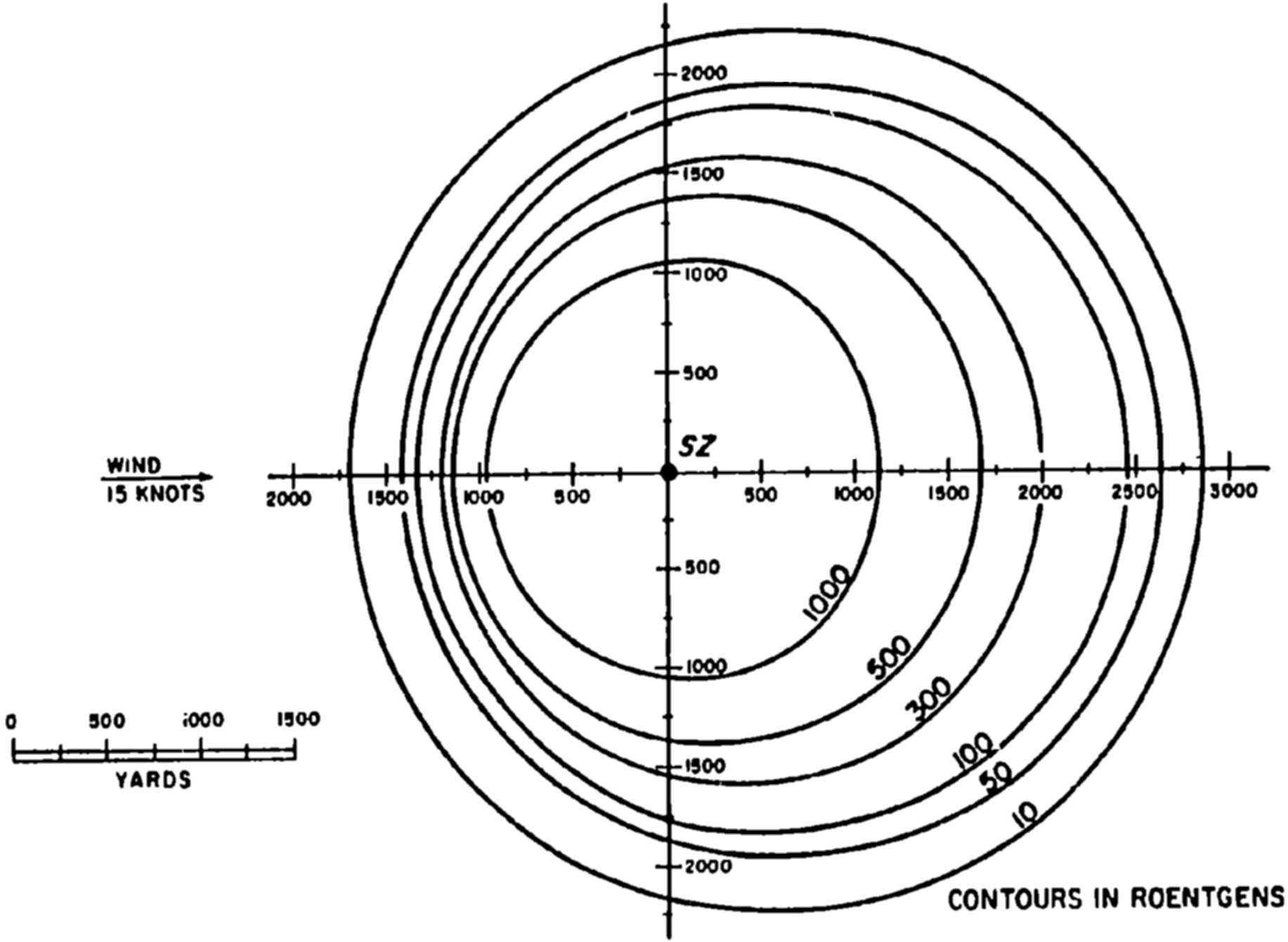

Figure 6-70. Two-Minute Total Exposure 15 Feet Above the Water Surface from 10 kt Explosion at a Depth of 500 Feet in 5,000 Feet of Water, 15 Knot Wind, No-Current Environment

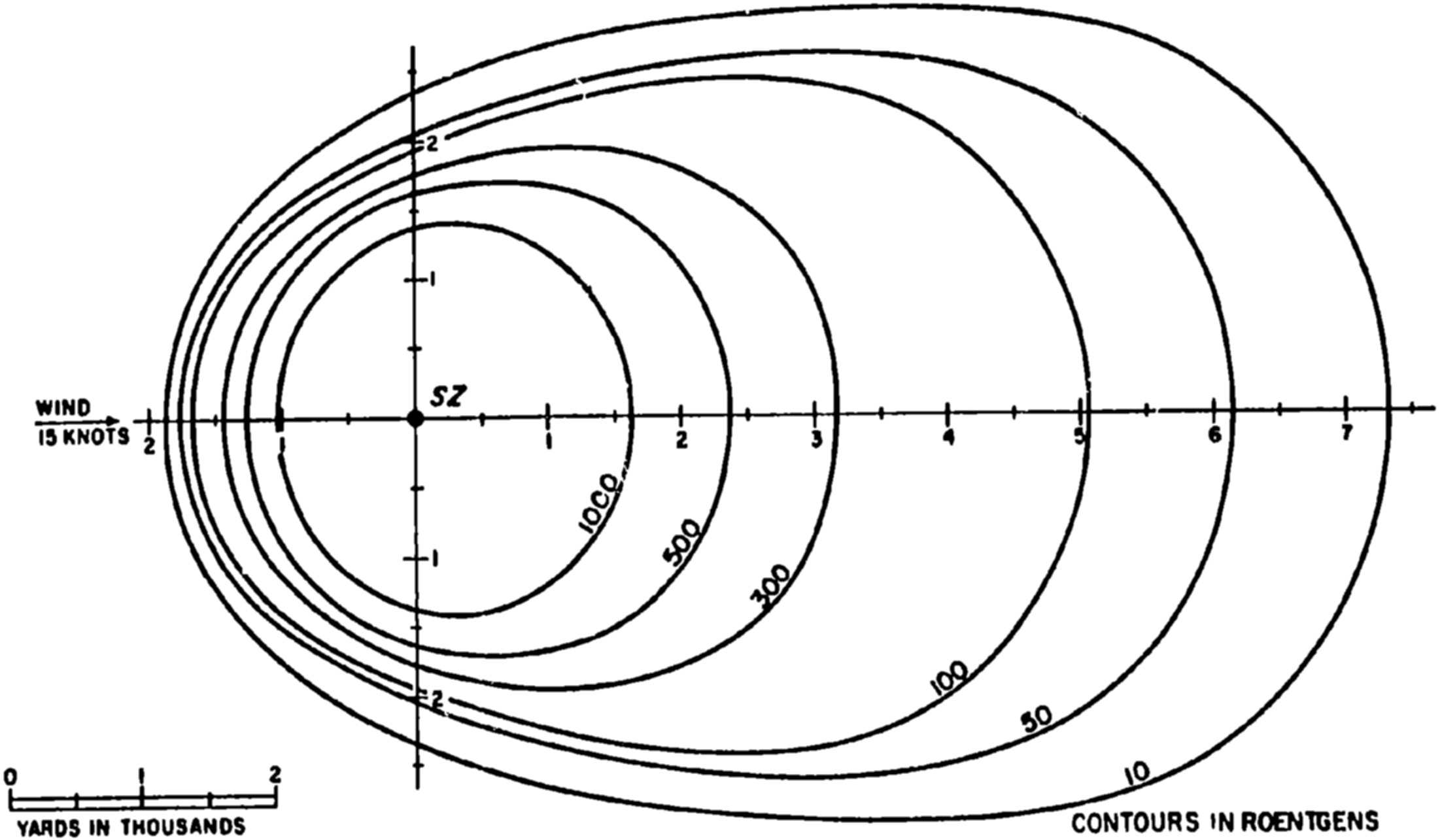

Figure 5-71. [redacted] Ten-Minute Total Exposure 15 Feet Above the Water Surface from a 10 kt Explosion at a Depth of 500 Feet in 5,000 Feet of Water, 15 Knot Wind, No-Current Environment [redacted]

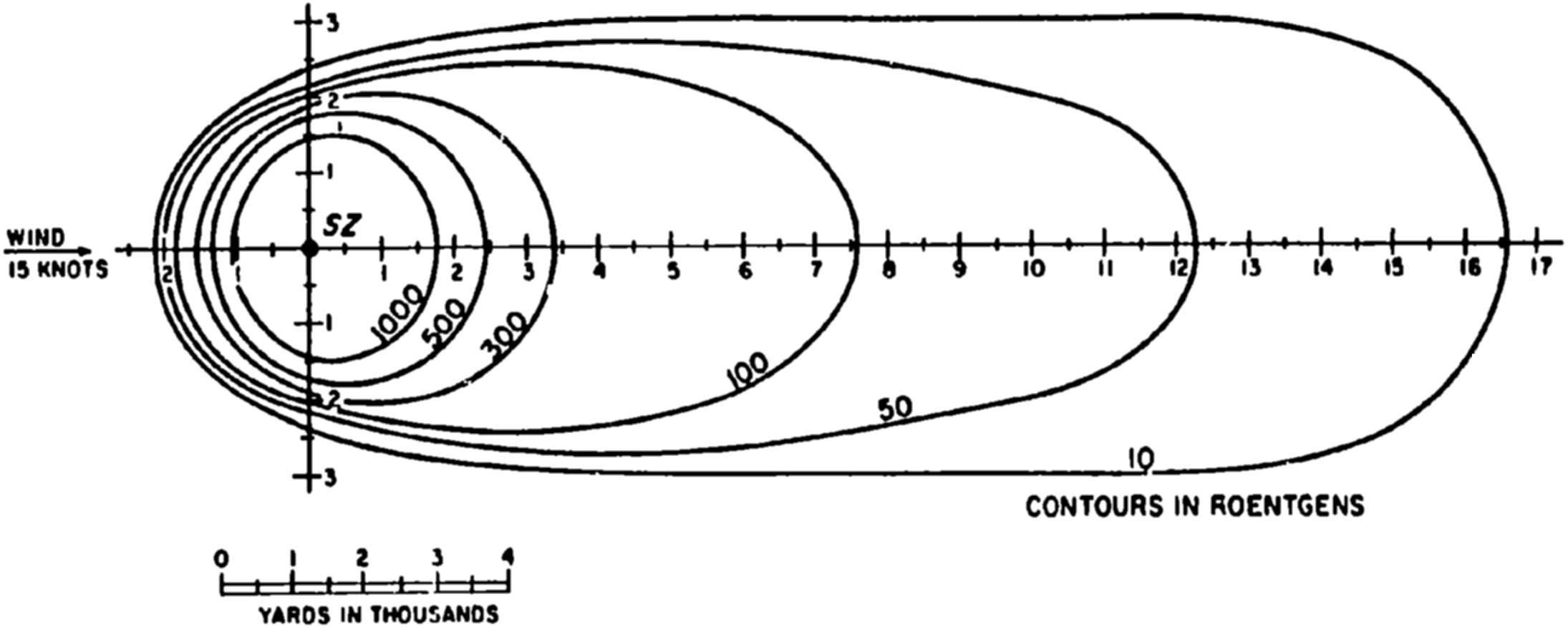

Figure 5-72. [redacted] Thirty-Minute Total Exposure 15 Feet Above the Water Surface from a 10 kt Explosion at a Depth of 500 Feet in 5,000 Feet of Water, 15 Knot Wind, No-Current Environment [redacted]

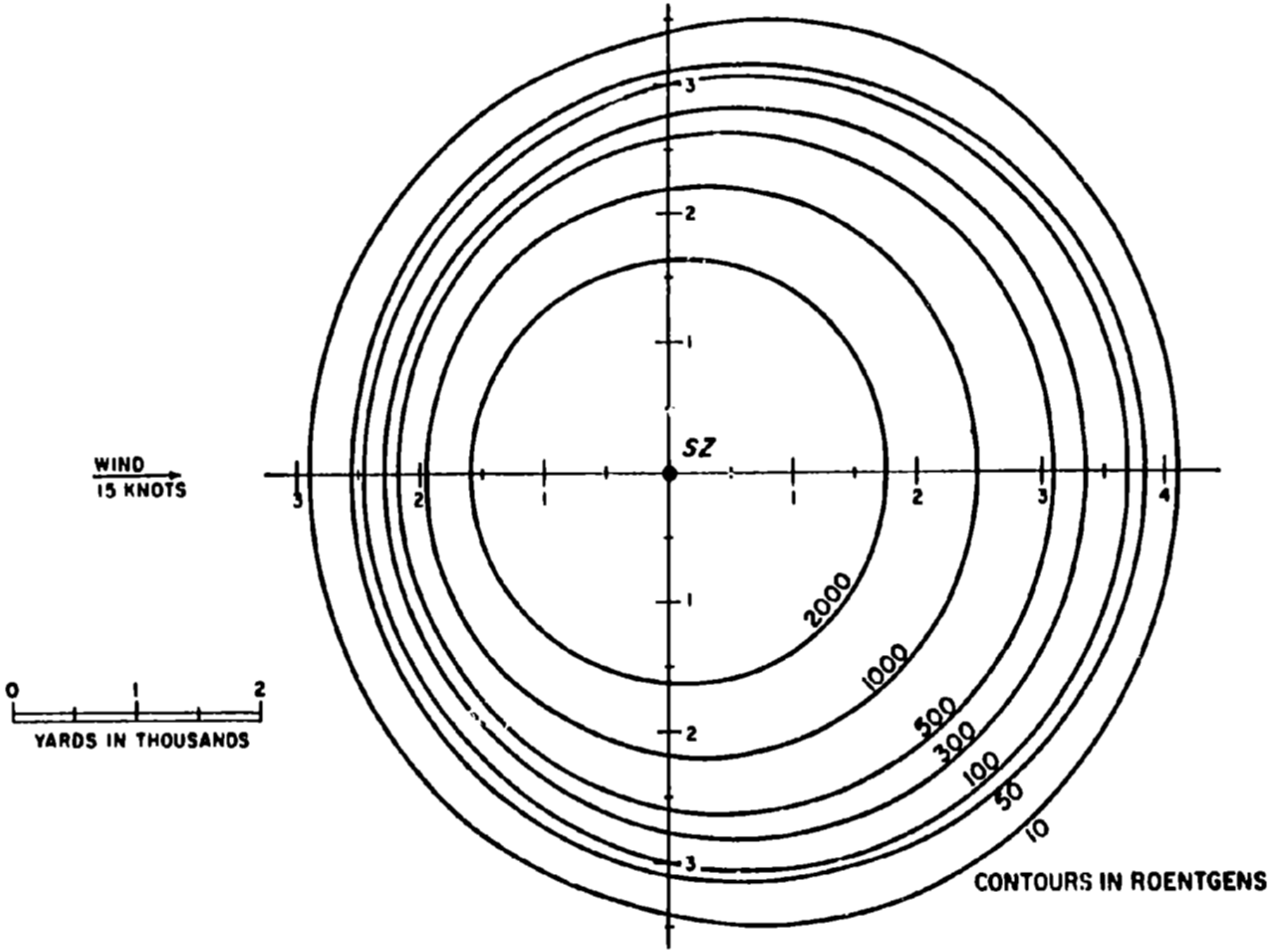

Figure 5-73. [redacted] Two-Minute Total Exposure 15 Feet Above the Water Surface from a 100 kt Explosion at a Depth of 890 Feet in 5,000 Feet of Water, 15 Knot Wind, No-Current Environment [redacted]

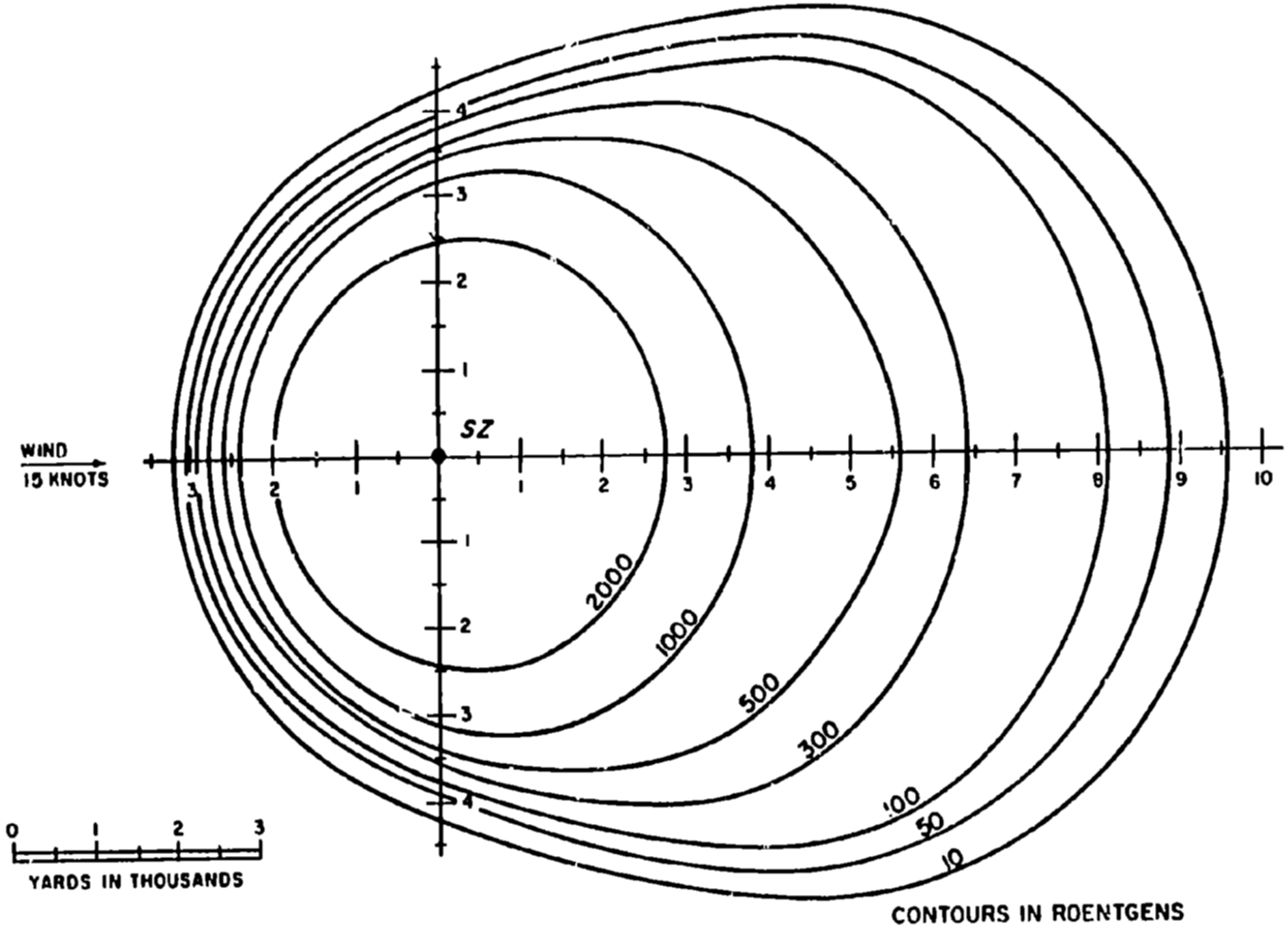

Figure 5-74. [redacted] Ten-Minute Total Exposure 15 Feet Above the Water Surface from a 100 kt Explosion at a Depth of 890 Feet in 5,000 Feet of Water, 15 Knot Wind, No-Current Environment [redacted]

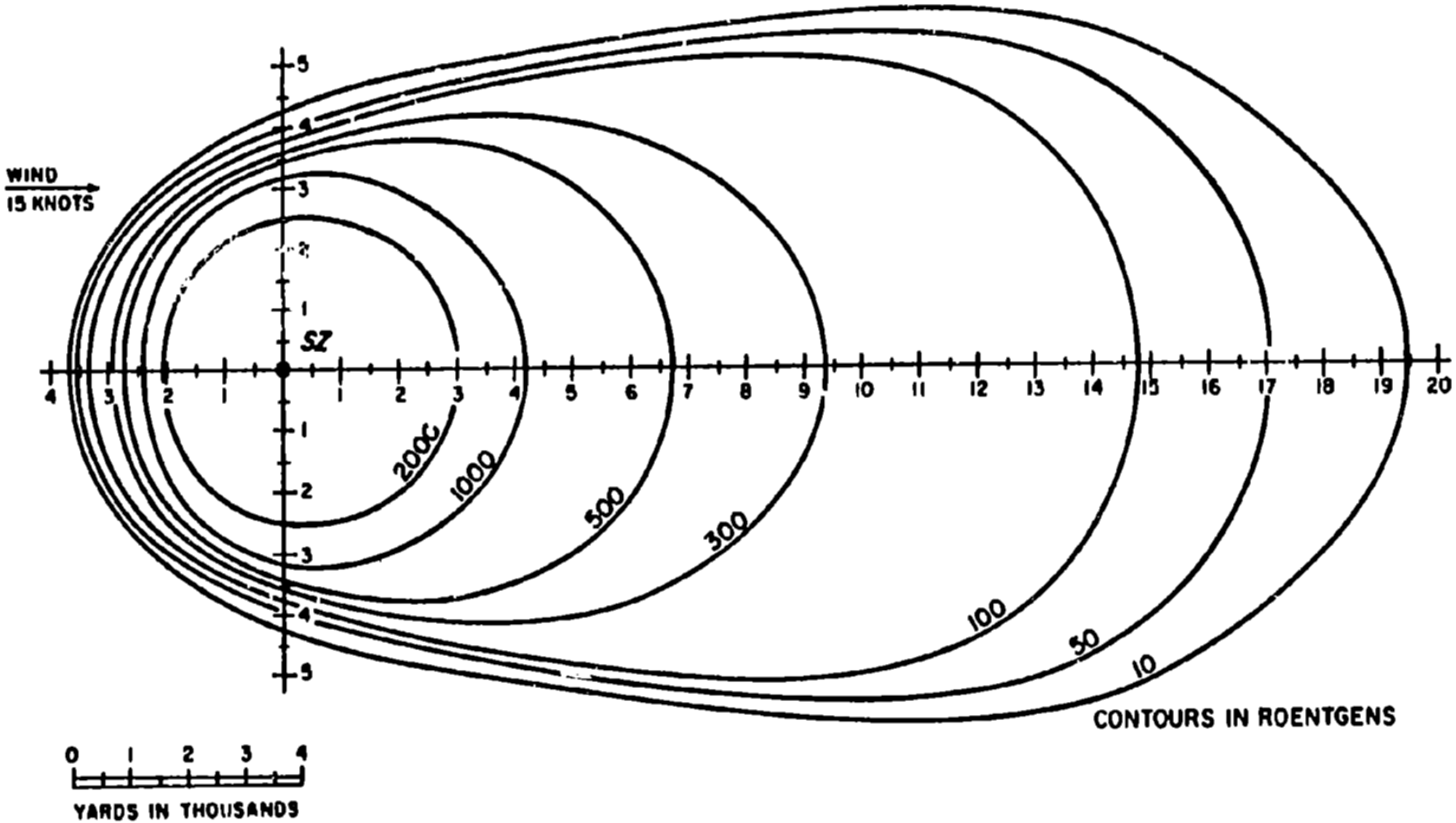

Figure 5-75. [redacted] Thirty-Minute Total Exposure 15 Feet Above the Water Surface from a 100 kt Explosion at a Depth of 890 Feet in 5,000 Feet of Water, 15 Knot Wind, No-Current Environment [redacted]

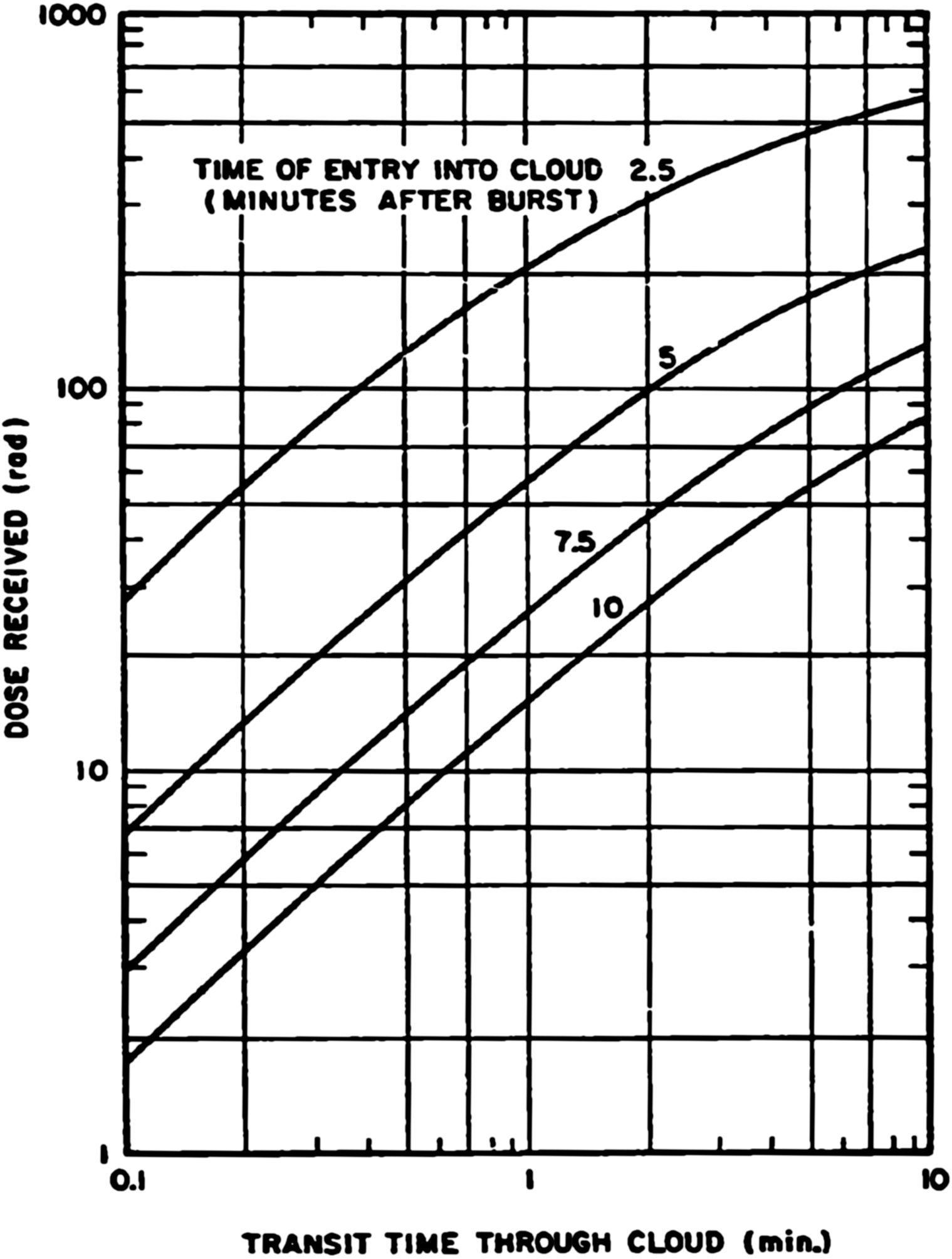

Figure 5-79. Dose Received While Flying Through a Nuclear Cloud as a Function of Transit Time Through the Cloud

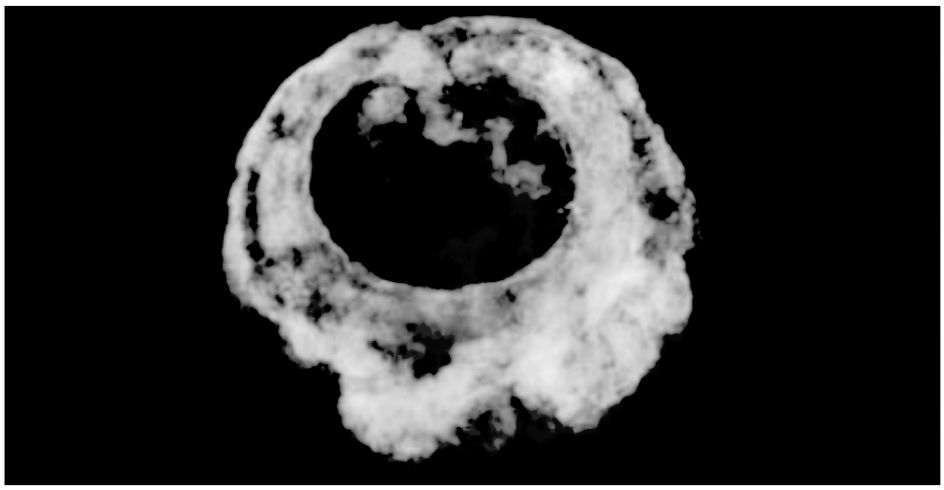

(a) Blue Gill Taken From Burst Locale

50 km altitude

(b) Teak Taken From Maui (1300 km Away)

77 km altitude

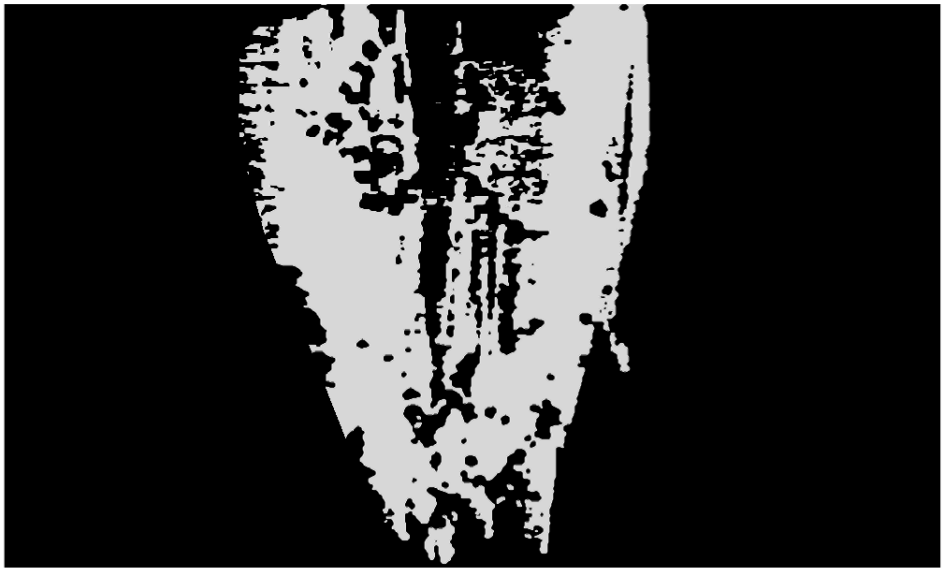

(c) Check Mate Taken From Burst Locale

147 km altitude

The length along the geomagnetic field is about 1,000 kilofeet. The heated air within the fireball is highly ionized, with many striations oriented along the geomagnetic field. (The dark spots within the fireball are rocket trails.)

Figure 1-4. Photographs of High Altitude Bursts, t = 100 sec

Chapter 7

ELECTROMAGNETIC PULSE (EMP) PHENOMENA

The nuclear electromagnetic pulse (EMP) is the time-varying electromagnetic radiation resulting from a nuclear burst. It has a very broad frequency spectrum, ranging from near dc to several hundred MHz.

The generation of EMP from a nuclear detonation was predicted even before the initial test, but the extent and potentially serious degree of EMP effects were not realized for many years. Attention slowly began to focus on EMP as a probable cause of malfunction of electronic equipment during the early 1950s. Induced currents and voltages caused unexpected equipment failures during nuclear tests, and subsequent analysis disclosed the role of EMP in such failures. Finally in 1960 the possible vulnerability of hardened weapon systems to EMP was officially recognized. Increased knowledge of the electric and magnetic fields became desirable for both weapons diagnostics and long-range detection of nuclear detonations. For all these reasons a more thorough investigation of EMP was undertaken.

Theoretical and experimental efforts were expanded to study and observe EMP phenomenology and to develop appropriate descriptive models. A limited amount of data had been gathered on the phenomenon and its threat to military systems when all aboveground testing was halted in 1962. From this time reliance has been placed on underground testing, analysis of existing atmospheric test data, and nonnuclear simulation for experimental knowledge. Extended efforts have been made to improve theoretical models and to develop associated computer codes for predictive studies. At the same time, efforts to develop simulators capable of producing threat-level pulses for system coupling and response studies have been expanded.

This chapter describes the EMP generation mechanism and the resulting environment for various burst regimes. The description is largely qualitative, since the complexity of the calculations requires that heavy reliance be placed on computer code calculations for specific problems. Some results of computer code calculations are presented, but generalization of these results is beyond the scope of this chapter. More complete treatments of the EMP phenomena may be found in the "DNA EMP (Electromagnetic Pulse) Handbook (U)" (see bibliography).

ENVIRONMENT – GENERAL DESCRIPTION

7-1 Weapon Gamma Radiation

The gamma radiation output from a nuclear burst initiates the processes that shape the development of an electromagnetic pulse. The gamma radiation components important in EMP generation are the prompt, air inelastic, and isomeric gammas (see Chapter 5). Briefly, the prompt gammas arise from the fission or fusion reactions taking place in the bomb and from the inelastic collisions of neutrons with the weapon materials. The fraction of the total weapon energy that may be contained in the prompt gammas will vary nominally from about 0.1% for high yield weapons to about 0.5% for low yield weapons, depending on weapon design and size. Special designs might increase the gamma fraction, whereas massive, inefficient designs would decrease it.

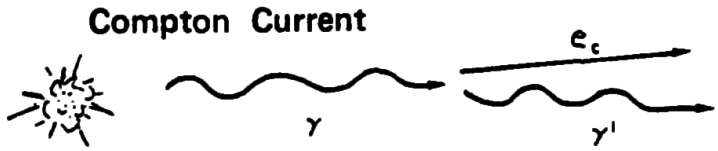

Figure 7-1. (U) The Compton Effect (U)

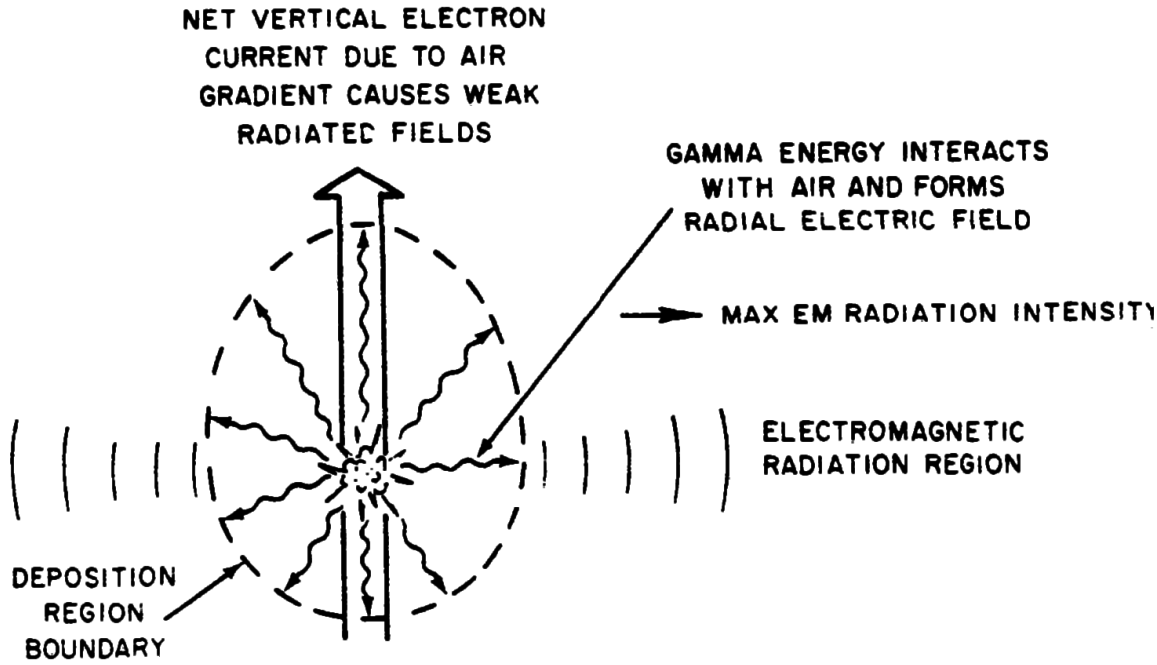

Figure 7-6. Simple Illustration of Air-Burst EMP

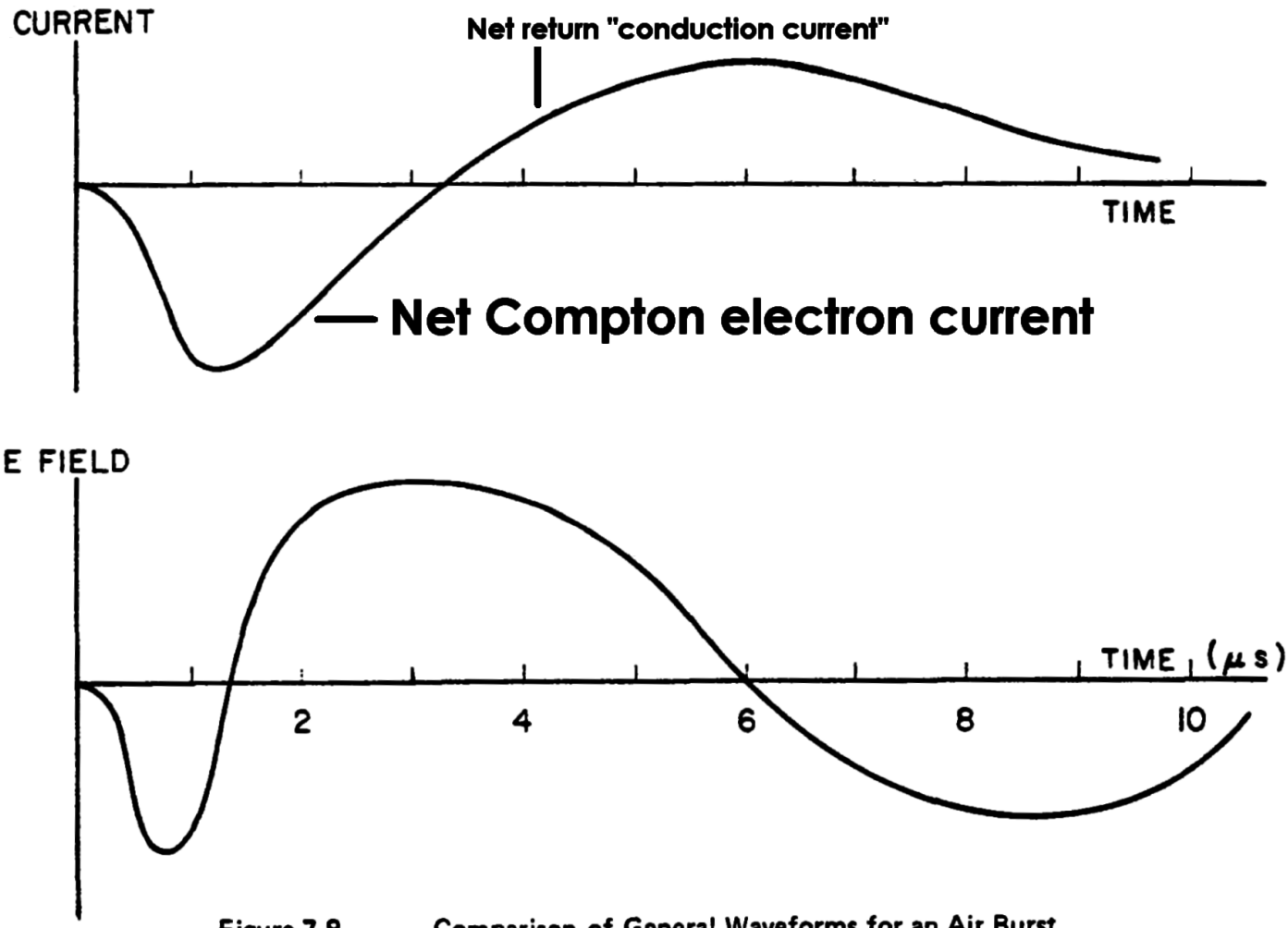

Figure 7-8 Comparison of General Waveforms for an Air Burst

Radiated field is proportional to time-derivative of current

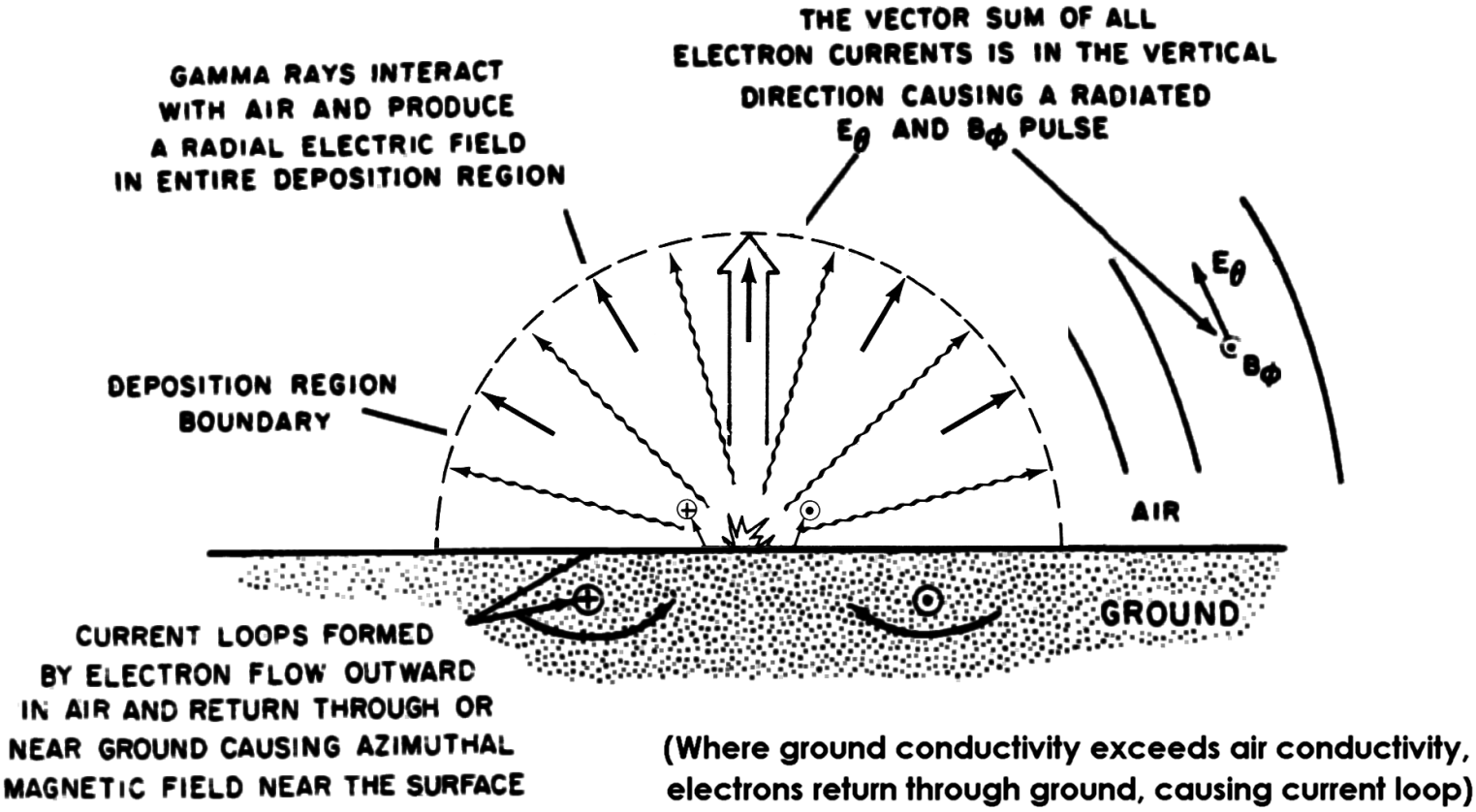

Figure 7-9 Simple Illustration of Surface Burst EMP

The magnitude of the peak value of the radiated electric waveform for a surface burst is a weak function of yield, varying from about 1,300 volts per meter at R_o for a 4.2 TJ (1KT) explosion to about 1,670 volts per meter for a 4.2×10^4 TJ (10 MT) explosion. For most cases, a value of 1,650 volts per meter may be assumed. At ranges along the surface beyond R_o, the peak radiated electric field varies inversely with the distance from the burst. Thus, the magnitude of the peak radiated electric field along the surface may be estimated from the equation

$$E = \frac{R_o}{R} E_o ,$$

where R_o is the range to the beginning of the radiation region, R is the distance along the surface to the point of interest, E_o is the peak value of the radiated field at R_o (assumed to be about 1,650 volts per meter), and E is peak value of the radiated field at R.

10 kilometers from a 1 MT surface burst

$$E = \left(\frac{7.2}{10}\right)(1{,}650) \approx 1{,}200 \text{ v/m.}$$

10 kilometers from a 100 KT surface burst

$$E = \left(\frac{5.8}{10}\right)(1{,}650) \approx 950 \text{ v/m.}$$

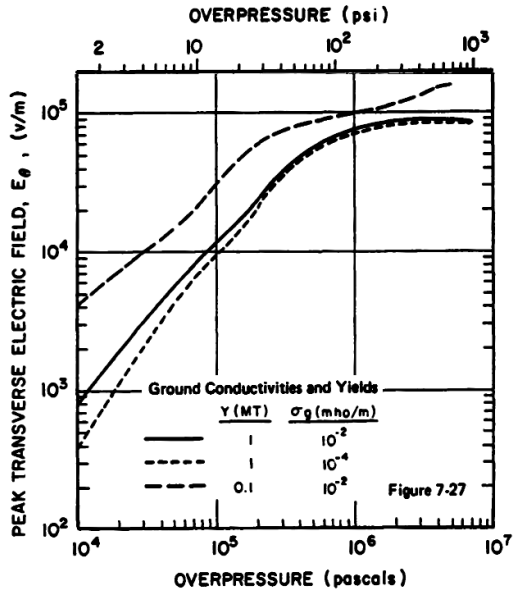

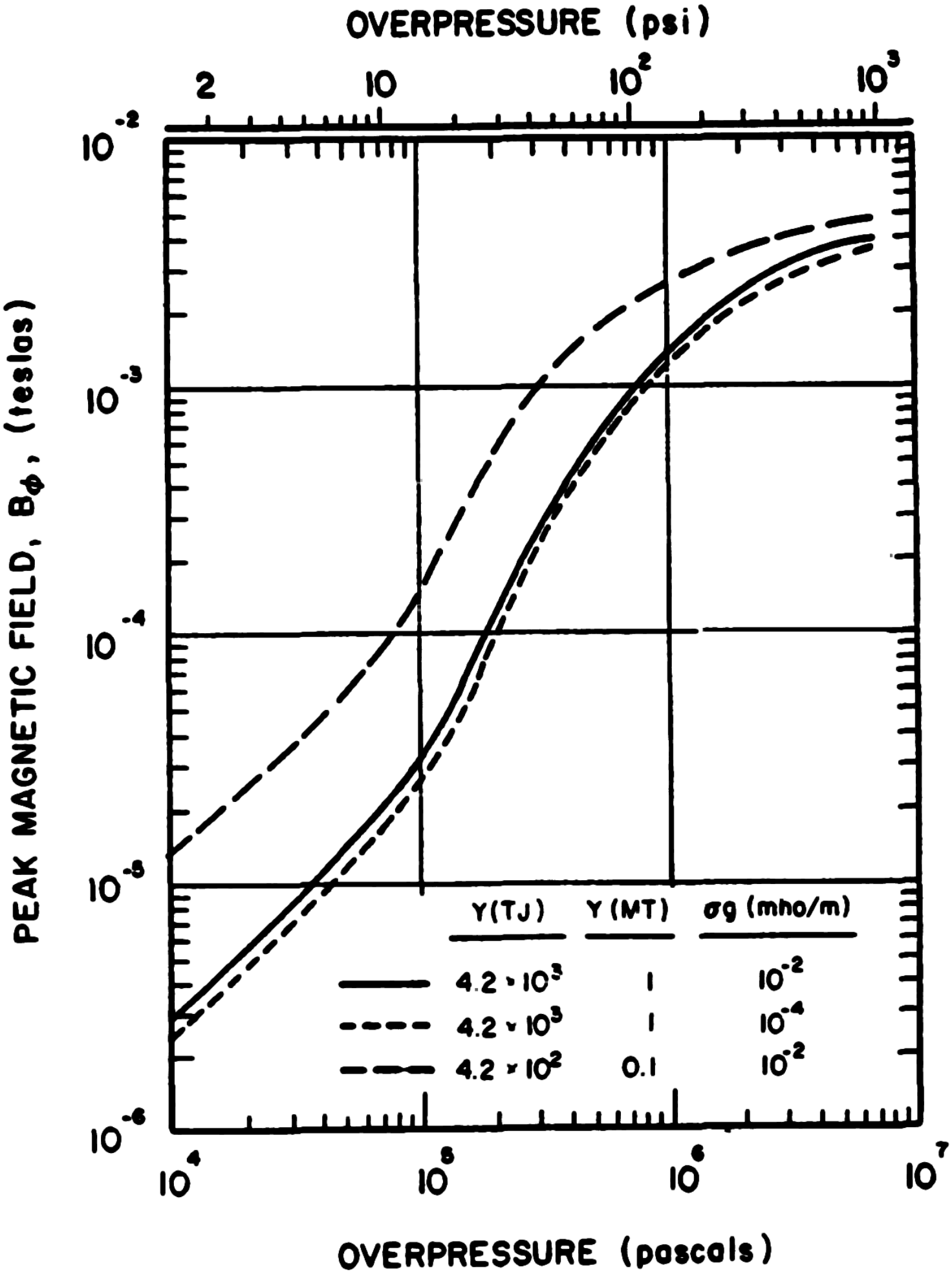

Figure 7-25 Peak Magnetic Field B_ϕ Versus Overpressure for Varying Ground Conductivities and Yields

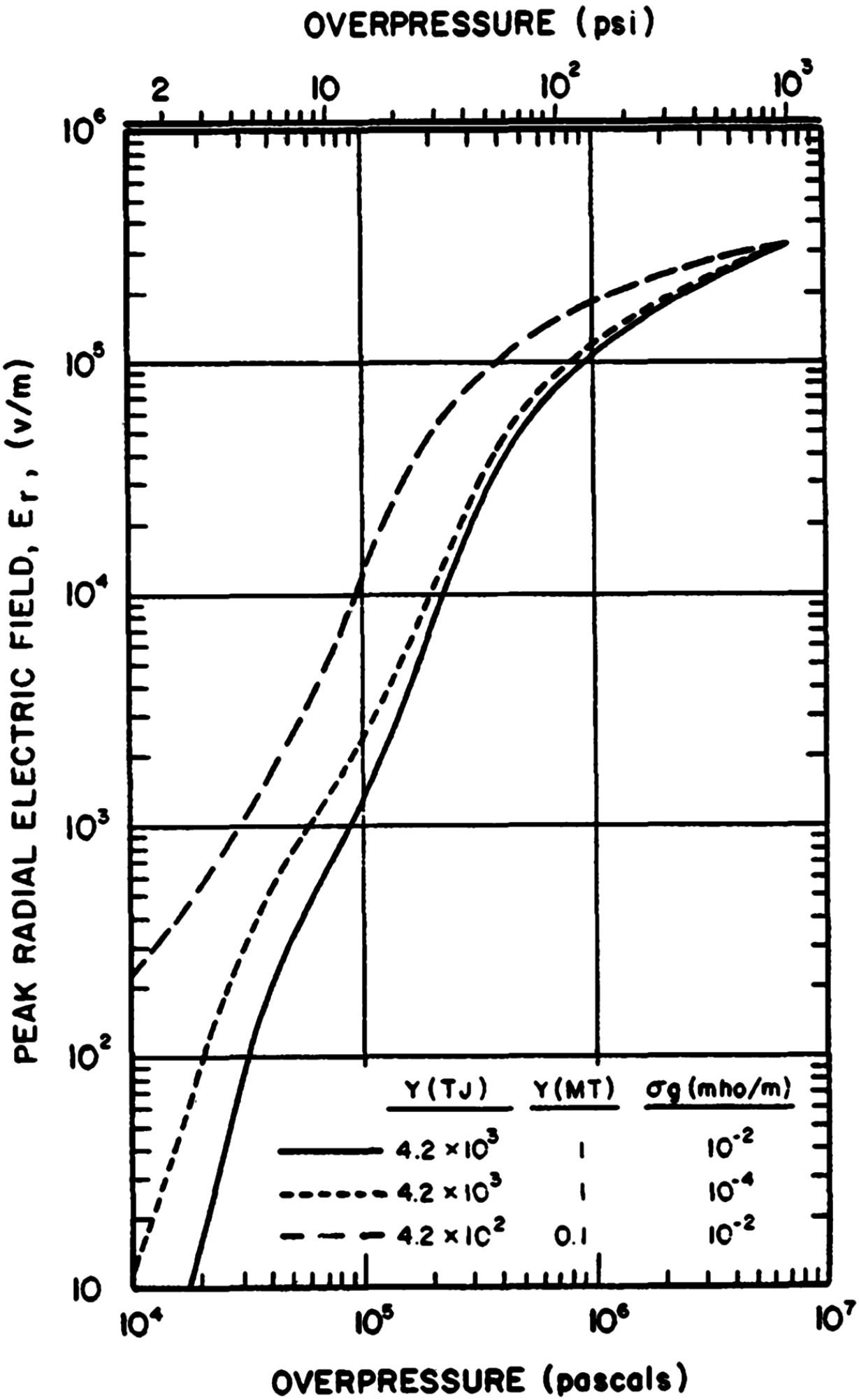

Figure 7-26 Peak Radial Electric Field E_r Versus Overpressure for Varying Ground Conductivities and Yields

SECTION VIII

[redacted] ELECTROMAGNETIC PULSE (EMP) DAMAGE MECHANISMS [redacted]

[redacted] As described in Chapter 7, the nuclear electromagnetic pulse (EMP) is part of a complex environment produced by a nuclear environment. The EMP contains only a very small part of the total energy produced by a nuclear explosion; however, under the proper circumstances, EMP is capable of causing severe disruption and sometimes damage to electrical and electronic systems at distances where all other effects are absent.

[redacted] As with the EMP generation described in Chapter 7, the complexity of the calculation of EMP damage mechanisms requires that heavy reliance be placed on computer code calculations for specific problems, and even these calculations must be supplemented by testing in most cases. Consequently, the information presented herein is largely qualitative and will only serve as an introduction to the subject. More complete treatments of EMP damage mechanisms may be found in the "DNA EMP (Electromagnetic Pulse) Handbook" (see bibliography).

[redacted] Figure 7-18, Chapter 7, provides a matrix that provides some indication of whether EMP constitutes a threat in a given situation relative to the hardness of a system to blast overpressure. This section provides a brief description of EMP energy coupling, component damage, EMP hardening, and testing.

[redacted] ENERGY COUPLING [redacted]

9-56 Basic Coupling Modes [redacted]

[redacted] There are three basic modes of coupling the energy contained in an electromagnetic wave into the conductors that make up an electric or electronic system: electric induction, magnetic induction, and resistive coupling.

[redacted] Electric induction arises as the charges in a conductor move under the influence of the tangential component of an impinging electric field. The overall result is that of a voltage source distribution along the conductor. One such point-voltage source is shown in Figure 9-65 for a simple conducting wire, where the current I is produced as a result of the tangential component $E_{i\ tan}$ of the incident electric field $\bar{E}_i$.

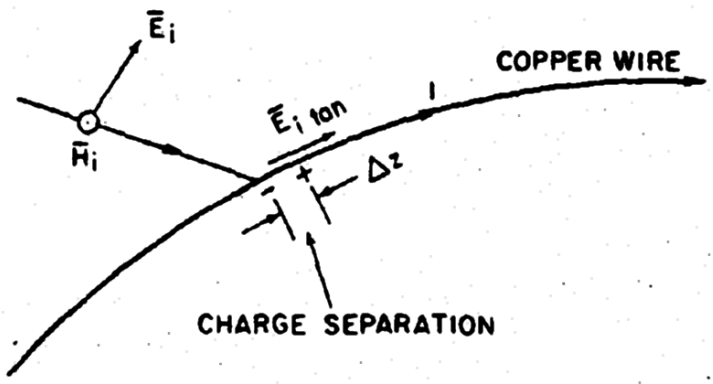

Figure 9-65. [redacted] Electric Induction in a Copper Wire [redacted]

[redacted] Magnetic induction occurs in conductors shaped to form a closed loop when the component of the impinging magnetic field perpendicular to the plane of the loop varies in time, causing charges to flow in the loop. This effect is illustrated in Figure 9-66 for a simple wire loop. Here the magnetic field is shown coming out of the plane of the loop. The loop need not be circular, and magnetic induction may occur with any set of conducting components assembled so as to form a loop.

[redacted] Resistive coupling comes about indirectly as a conductor that is immersed in a conducting medium, such as ionized air or the ground, is influenced by the currents induced in the medium by the other coupling modes. In effect the conductor shares part of the current as an alternate conducting path. This effect is illustrated in Figure 9-67 for the simple case of a

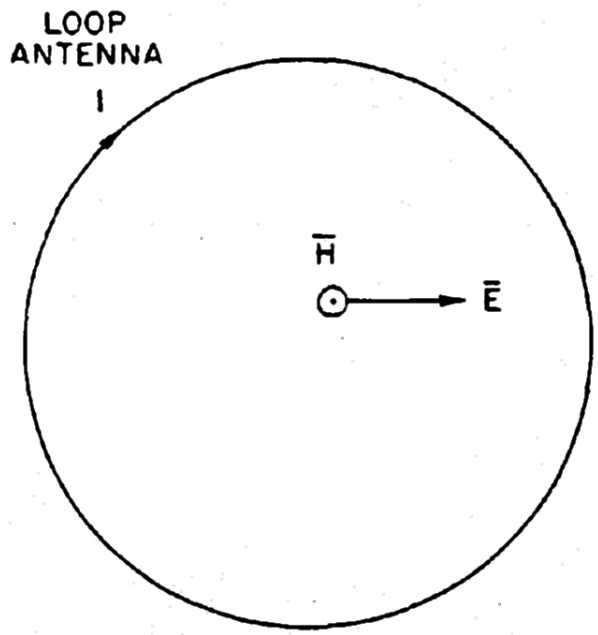

Figure 9-66. [redacted] Magnetic Induction in a Simple Loop [redacted]

[redacted] conductor immersed in the ground. The tangential component of the incident electric field $\bar{E}_i$ induces a current density $\bar{J}$ in the ground. A distributed voltage drop appears along the wire as a result of the current flow in the ground, and this incremental voltage causes current flow I in the wire. Current also may be induced in the wire directly by the tangential component of the refracted electric field, shown as $\bar{E}_g$. The reflected EMP, $\bar{E}_r$, $\bar{H}_r$, is also shown in Figure 9-67. The potential importance of these reflected fields is discussed below.

9-57 Resonant Configurations [redacted]

[redacted] The coupling of energy to a conductor is particularly efficient when the maximum dimension of the conductor configuration is about the same size as the wavelength of the radiation. In this event the voltages that are induced along the conductor at various points are all approximately in phase, so the total voltage induced on the conductor is a maximum. The conductor is said to be resonant, or to behave as an antenna, for

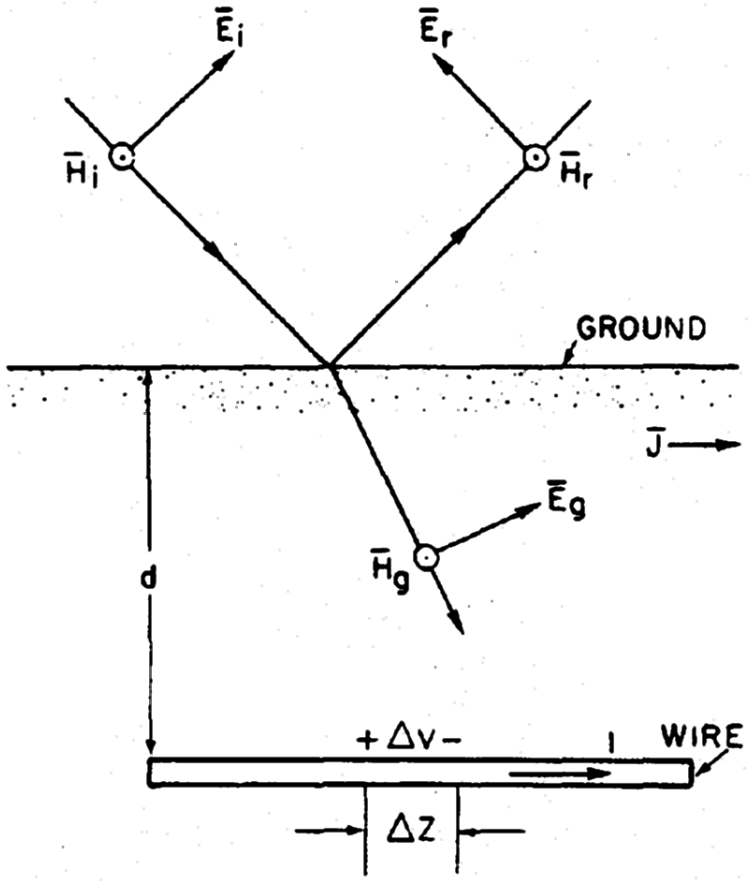

Figure 9-67. [redacted] Resistive Coupling as a Result of Currents in the Ground [redacted]

frequencies corresponding to near this wavelength. Since EMP has a broad spectrum of frequencies (see Chapter 7), only a portion of this spectrum will couple most efficiently into a specific conductor configuration. Thus, a particular system of interest must be examined with regard to its overall configuration as well as its component configuration. Eash aspect will have characteristic dimensions that determine what part of the pulse (strength and frequencies) constitutes the principal threat.

[redacted] Gross system features that are not normally considered antennas, such as structural features, beams, girders, buried cable, overhead conduit or ducting, wings, fuselage, missile skins, and any wall apertures, must be considered to be potential collectors and conductors of energy into the system. In particular, radiation that

Table 9-27. Minimum Observed Joule Energy to Cause Burnout

Type	Minimum Joule Energy	Material	Other Data
2N36	4.0×10^{-2}	Ge	PNP Audio Transistor
2N327A	1.6×10^{-2}	Si	PNP Audio Transistor
2N1041	2.0×10^{-2}	Ge	PNP Audio Transistor
2N1308	5.0×10^{-5}	Ge	NPN Switching Transistors
2N706	6.0×10^{-5}	Si	NPN Switching Transistors
2N594	6.0×10^{-3}	Ge	NPN Switching Transistors
2N398	8.0×10^{-4}	Ge	PNP Switching Transistors
2N240	1.0×10^{-2}	Ge	PNP Switching Transistors
MC715	8.0×10^{-5}	Si	Data Input Gate Integrated Circuit
2N4220	1.0×10^{-5}	Si	RF General Purpose FET
2N4224	3.0×10^{-5}	Si	VHF Amp and Mixer FET
1N3659	8.0×10^{-3}	Si	Automotive Rectifier Diode
1N277	2.0×10^{-5}	Ge	High Speed Switching Diode
1N3720	5.0×10^{-4}		Tunnel Diode
1N238	1.0×10^{-7}	Si	Microwave Diode
2N3528	3.0×10^{-3}	Si	Silicon Controlled Rectifier
67D-5010	1.0×10^{-4}		G.E. Varistar (30-joule Rating)
6AF4	1.0×10^{0}		UHF Oscillator Vacuum Tube
66N8	2.0×10^{0}		General Purpose Triode Vacuum Tube

Table 9-28. [redacted] Minimum Joule Energy to Cause Permanent Degradation Indicated [redacted]

Designation	Minimum Joule Energy	Malfunction	Other Data
Relay	2×10^{-3}	Welded Contact	Potter-Brumfield (539) low-current relay
Relay	1×10^{-1}	Welded Contact	Sigma (IIF) one-ampere relay
Microammeter	3×10^{-3}	Slammed Meter	Simpson Microammeter (Model 1212C)
Explosive Bolt	6×10^{-4}	Ignition	EBW 8 amp for 10 μsec detonator, MK1
Squib	2×10^{-5}	Ignition	Electric Squib. N8 3.5 watts for 5 μsec detonator
Fuel Vapors	3×10^{-3}	Ignition	Propane-air mixture 1.75 mm ignition gap

[redacted] second pulses. Capacitors are also fairly hard components. The approximate energies required for degradation of several common components are shown in Table 9-28.

[redacted] The minimum energy necessary for operational upset is a factor of 10 to 100 less than that which is required to damage the most sensitive semiconductor component. Table 9-29 shows the levels required to cause operational upset to some common components to illustrate this factor.

[redacted] A gross comparison of the energy required to damage several classes of electrical equipment is provided in Figure 9-69.

[redacted] The large range of damage levels emphasizes the fact that it is important to consider EMP damage criteria early during the design stage of any piece of equipment that might be susceptible. It is also important to realize that energy collected in one part of a system may be transmitted to other parts of the system as a result of the currents that are induced. Thus, it is not necessary that the EMP couple directly to a sensitive component; energy coupled to various parts of a system may ultimately reach a particular component in sufficient quantity to cause malfunction. With the current state of the art in EMP vulnerability evaluation, the design and hardening of complicated systems requires the joint efforts of systems engineers and professional EMP effects personnel.

[redacted] EMP HARDENING [redacted]

9-60 System Analysis [redacted]

[redacted] A general approach to the examination

Table 9-29. [redacted] Minimum Joule Energy to Cause Circuit Upset or Interference [redacted]

Designation	Minimum Joule Energy	Malfunction	Other Data
Logic Card	3×10^{-9}	Circuit Upset	Typical logic transistor inverter gate
Logic Card	1×10^{-9}	Circuit Upset	Typical flip-flop transistor assembly
Integrated Circuit	4×10^{-10}	Circuit Upset	Sylvania J-K flip-flop monolithic integrated circuit (SF50)
Memory Core	2×10^{-9}	Core Erasure Via Wiring	Burroughs fast computer core memory (FC2001)
Memory Core	5×10^{-8}	Core Erasure Via Wiring	Burroughs medium speed computer core memory (FC8001)
Memory Core	3×10^{-9}	Core Erasure Via Wiring	RCA medium speed, core memory (269M1)
Memory Core	2×10^{-8}		Minimum observable energy in a typical high-gain subsystem
Amplifier	4×10^{-21}	Interference	Minimum observable energy in a typical high-gain amplifier

[redacted]

of a system with regard to its EMP vulnerability could include the following steps. First information concerning the system components and devices is collected. The information is categorized methodically into physical zones based on the susceptibility and worst case exposure for these items. Using objective criteria, problem areas are identified, analyzed, and tested. Suitable changes are made as necessary to correct deficiencies, and the modified system is examined and tested. The approach may be followed on proposed systems or those already in place, although experience indicates that the cost of retrofitting EMP protection is usually overwhelming.

9-61 Recommended Practices [redacted]

[redacted] Within the scope of this manual it is only possible to mention a few of the practices that may be employed in hardening a system to EMP. The following discussion is intended to convey some impression of the extra effort involved in hardening a system to the EMP rather than to provide a comprehensive treat-

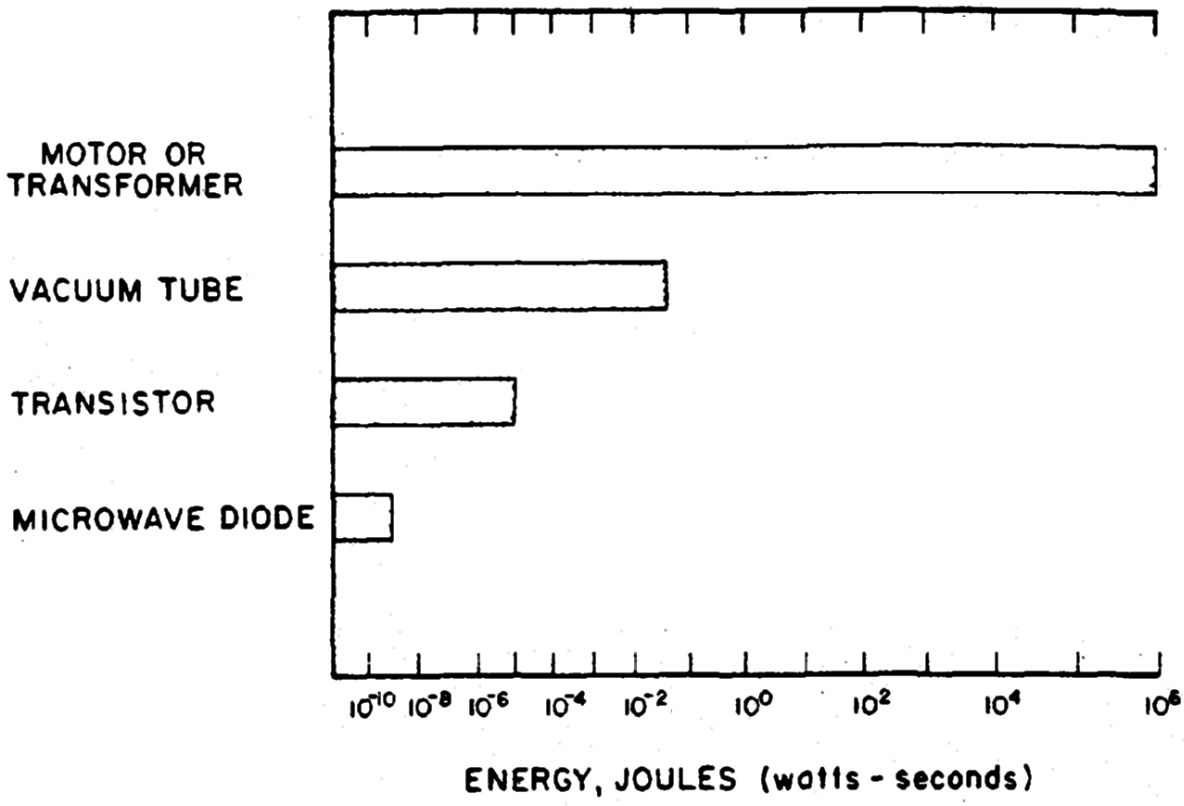

Figure 9-69. [redacted] Energy Required to Damage Various Classes of Equipment [redacted]

ment of what is a highly technical and specialized field.

[redacted] Some general methods for reduction of the EMP environment include geometric arrangement of the equipment, shielding, geographic relocation, and proper grounding.

[redacted] Circuit layout recommendations include the use of common ground points, twisted cable pairs, system and intrasystem wiring in "tree" format (radial spikes) avoiding loop layouts and circuit routes coupling to other circuits, use of conduit or cope trays, and shielded isolated transformers. Avoiding ground return in cable shields is also recommended. Many specific practices carry over from communications and power engineering while many do not. Each must be examined carefully.

[redacted] Good shielding practices include the use of independent zone shields, several thin shields to replace a thick one, continuous shield joints, and keeping sensitive equipment away from shield corners. Avoiding shield apertures, and avoiding the use of the shield as a ground or return conductor is also recommended. The shielding effectiveness of many enclosures frequently is defeated by energy carried by cables or pipes (including water pipes, sewage lines, etc.) into the enclosure.

[redacted] Cabling recommendations include the use of deeply buried intersystem cables (more than 3 feet), shield layer continuity at splices, and good junction box contact. Ordinary braid shielding should be avoided. Cable design represents an extension of shielding and circuit practices from the viewpoint of EMP protection. It is an area where compromises frequently are made in the interests of economy, and thus is an area where professional EMP effects personnel can be

Table 2-9. [redacted] Measured Wave Data from Nuclear Tests [redacted]

NUMBER SERIES SHOT	YIELD	WATER DEPTH AT CHARGE	DEPTH OF BURST	PEAK WAVE* HEIGHT x RANGE	CAVITY RADIUS	$d_w/100(W)^{1/4}$	$HR/2 \times 10^4 \sqrt{W}$
	W (kt) $100(W)^{1/4}$	d_w (ft)	d_b (ft)	HR/2,000 (ft)† min - max	R_c (ft)		min - max
1 HARDTACK UMBRELLA	[redacted]	140	140	[redacted]	[redacted]	[redacted]	[redacted]
2 HARDTACK WAHOO	[redacted]	3,000	500	[redacted]	[redacted]	[redacted]	[redacted]
3 CROSSROADS BAKER	23.5 220	180	90	36 - 60	1,000‡	0.82 Shallow	0.74 - 1.24
4 WIGWAM	32 238	15,000	2,000	118	490†	63 Very Deep	2.08
5 REDWING FLATHEAD	[redacted]	120	0	[redacted]	[redacted]	[redacted]	[redacted]
6 REDWING DAKOTA	[redacted]	140	0	[redacted]	[redacted]	[redacted]	[redacted]
7 REDWING NAVAHO	[redacted]	230	0	[redacted]	[redacted]	[redacted]	[redacted]
8 CASTLE UNION	7,000 916	145	7	232 - 312	1,000†	0.16 Shallow	0.16 - 0.28
9 CASTLE YANKEE	13,500 1,080	220	7	426 - 438	1,000†	0.20 Shallow	0.37 - 0.38

*H is twice the measured height of the peak crest except for shots 8 and 9 where H is the measured height of the first crest from the following trough. H is corrected for uniform water depth = d_b by Green's law.

†Value deduced from measured surface wave train (Kaplan and Wallace, see bibliography) is a lower limit considerably smaller than actual values, which are unknown.

‡Measured values of the column radius (Young, DASA 1240-1(9)), see bibliography.

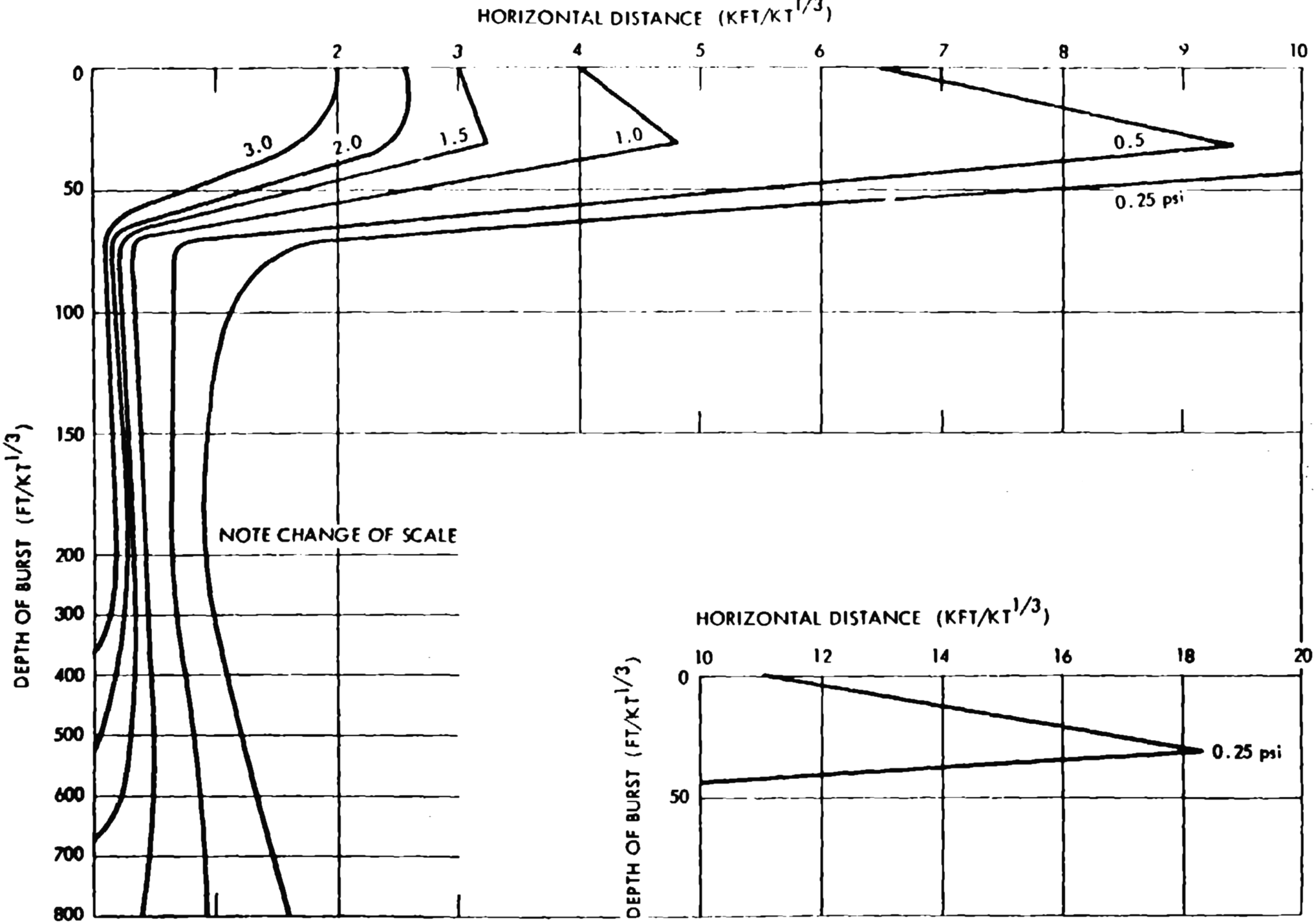

Figure 2-121 Peak Air Blast Overpressure Along the Water Surface from Underwater Nuclear Explosions

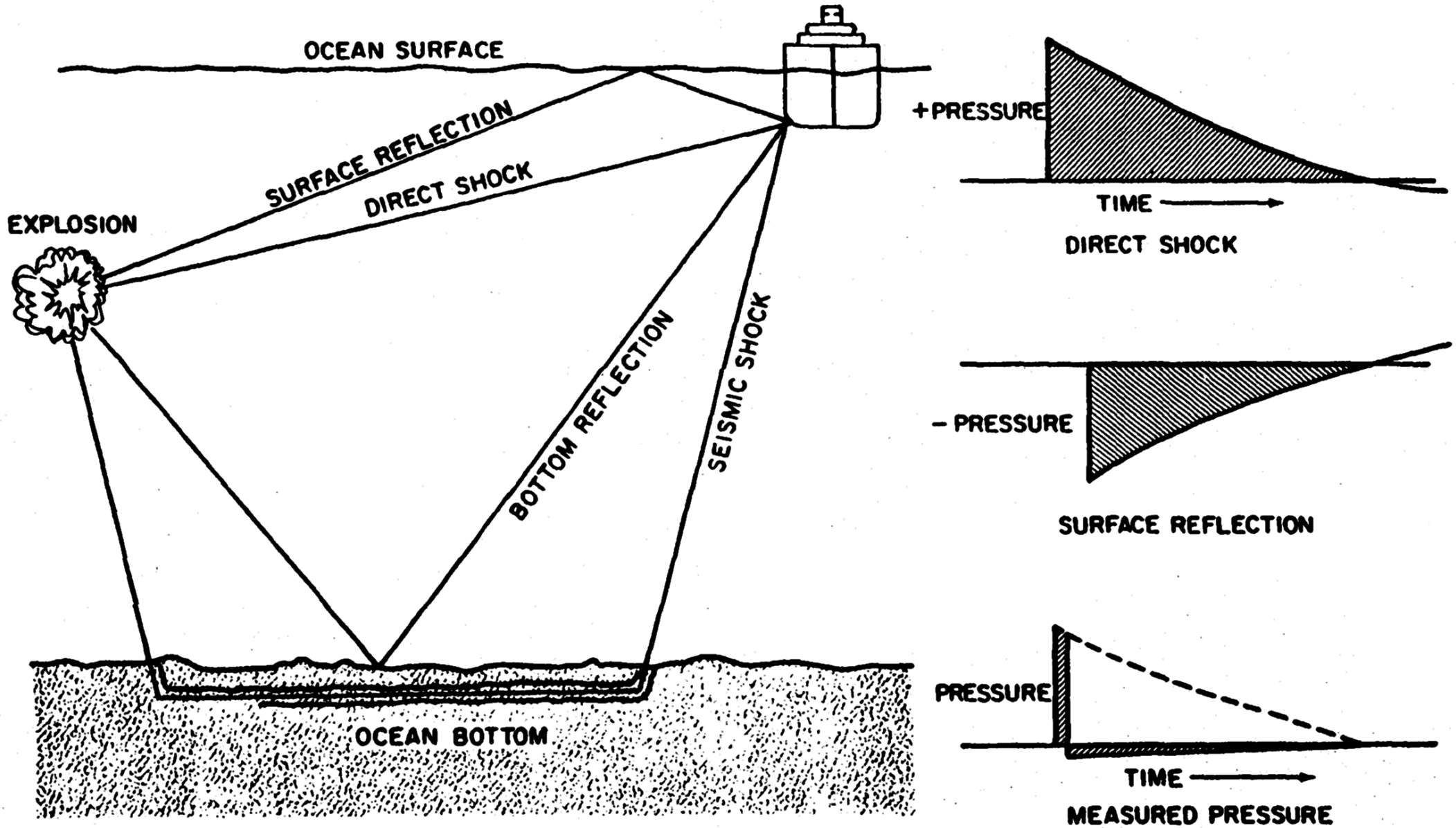

Figure 9-4. Direct and Reflected Shock Waves from an Underwater Burst

July 1973
AD763750
AD763750

DNA 3054F
URS 7049-10, Rev. 1

FOREST BLOWDOWN FROM NUCLEAR AIRBLAST

by

Phillip J. Morris

for

Headquarters
DEFENSE NUCLEAR AGENCY
Washington, D.C. 20305

Contract No. DNA-001-72-C-0021

A sensitivity analysis is performed on a computer model of tree response to airblast loading. This effort was undertaken, with success, to reduce the number of input parameters required by the model to those available to the field commander. Based on the results of this analysis, a new prediction technique was developed which determines the extent of tree blowdown and the resultant effects on troop and vehicle movement. The technique was developed for inclusion in DNA Effects Manual Number 1.

A URS Systems Affiliate

URS RESEARCH COMPANY

Fig. 15-35 in DNA-EM-1 (1972)

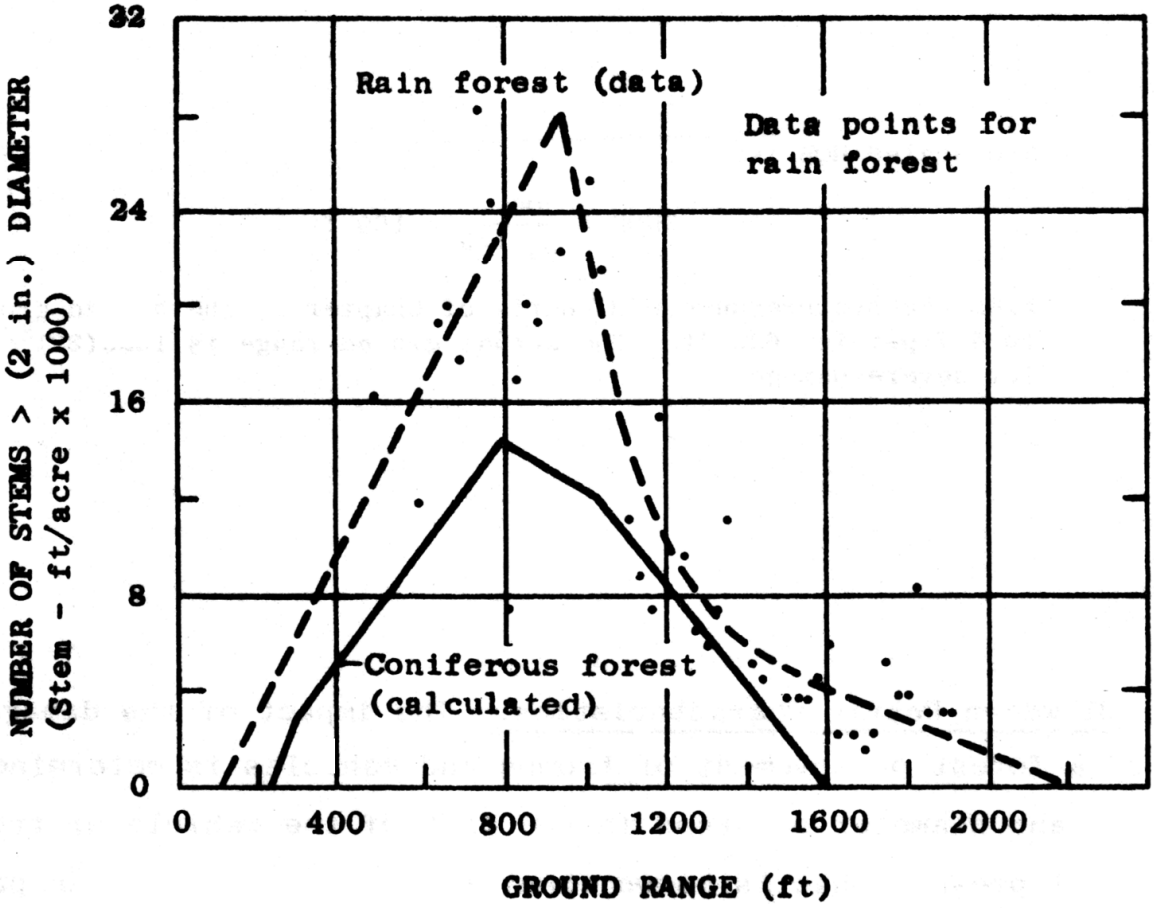

Fig. 15-8. Stem-ft per Acre Comparison Between a Rain Forest and a Coniferous Forest, 1 KT

Fig. 15-36 in DNA-EM-1 (1972)

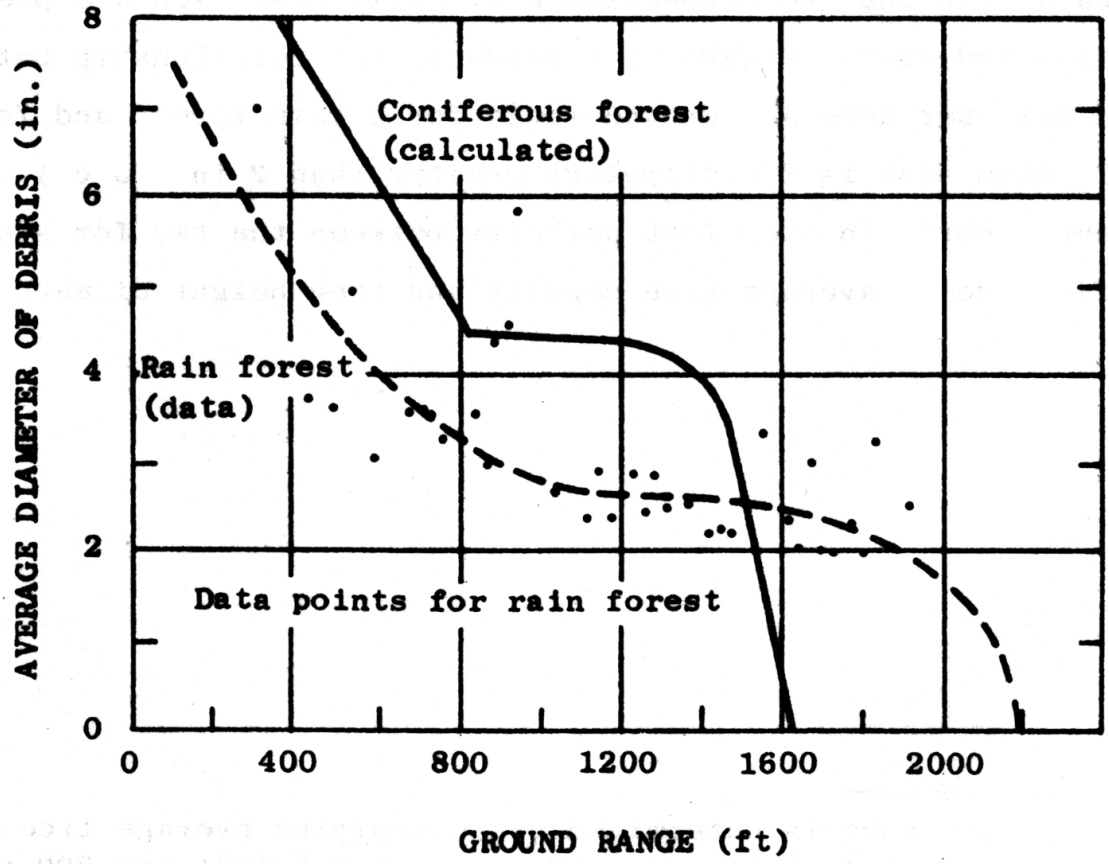

Fig. 15-9. Average Diameter of Stems Down, Comparison Between a Rain Forest and a Coniferous Forest, 1 KT

Fig. 15-46 in DNA-EM-1 (1972)

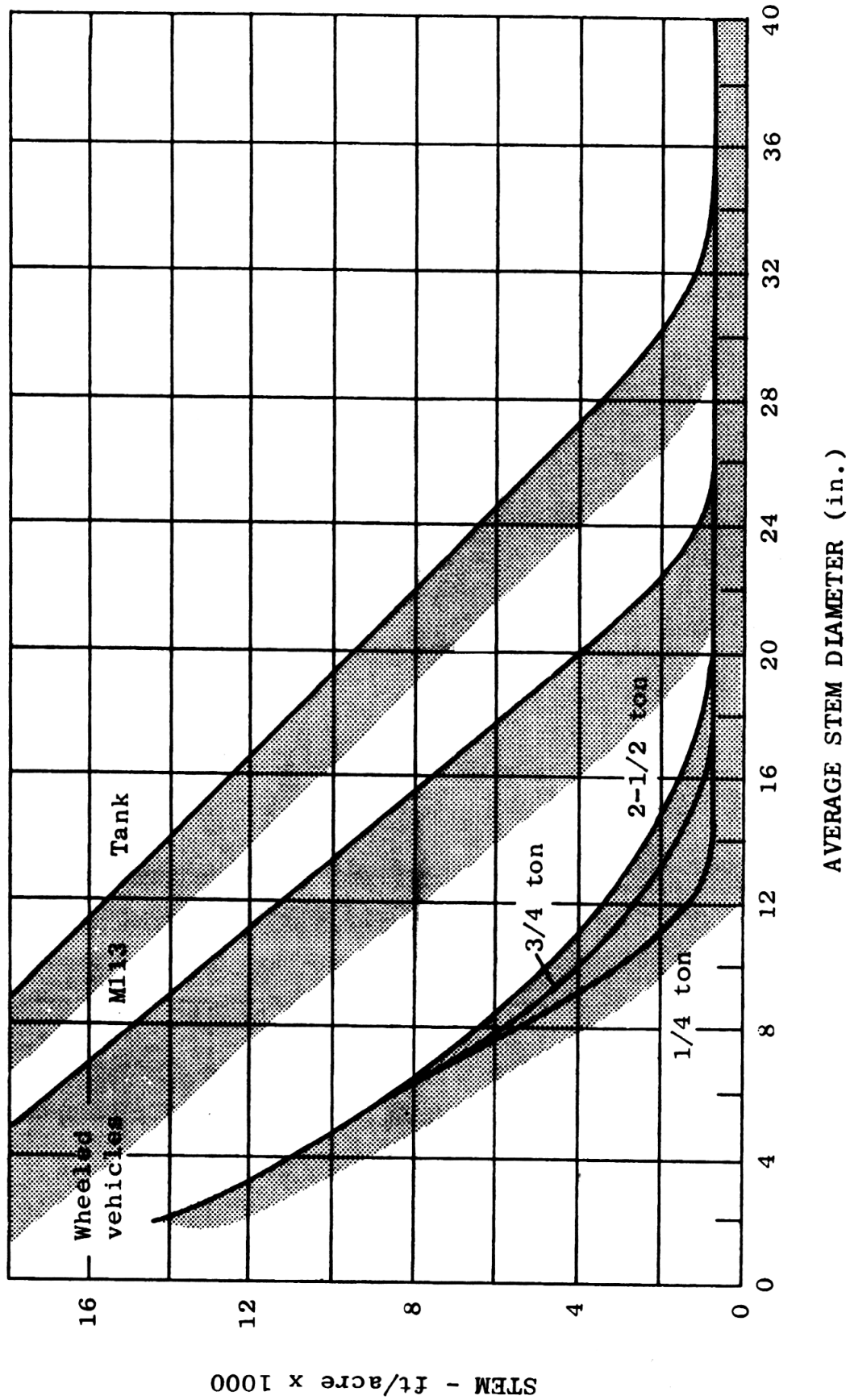

Fig. 15-10. Debris Characteristics Preventing Circumferential Movement of Vehicles

Fig. 15-37 in DNA-EM-1 (1972)

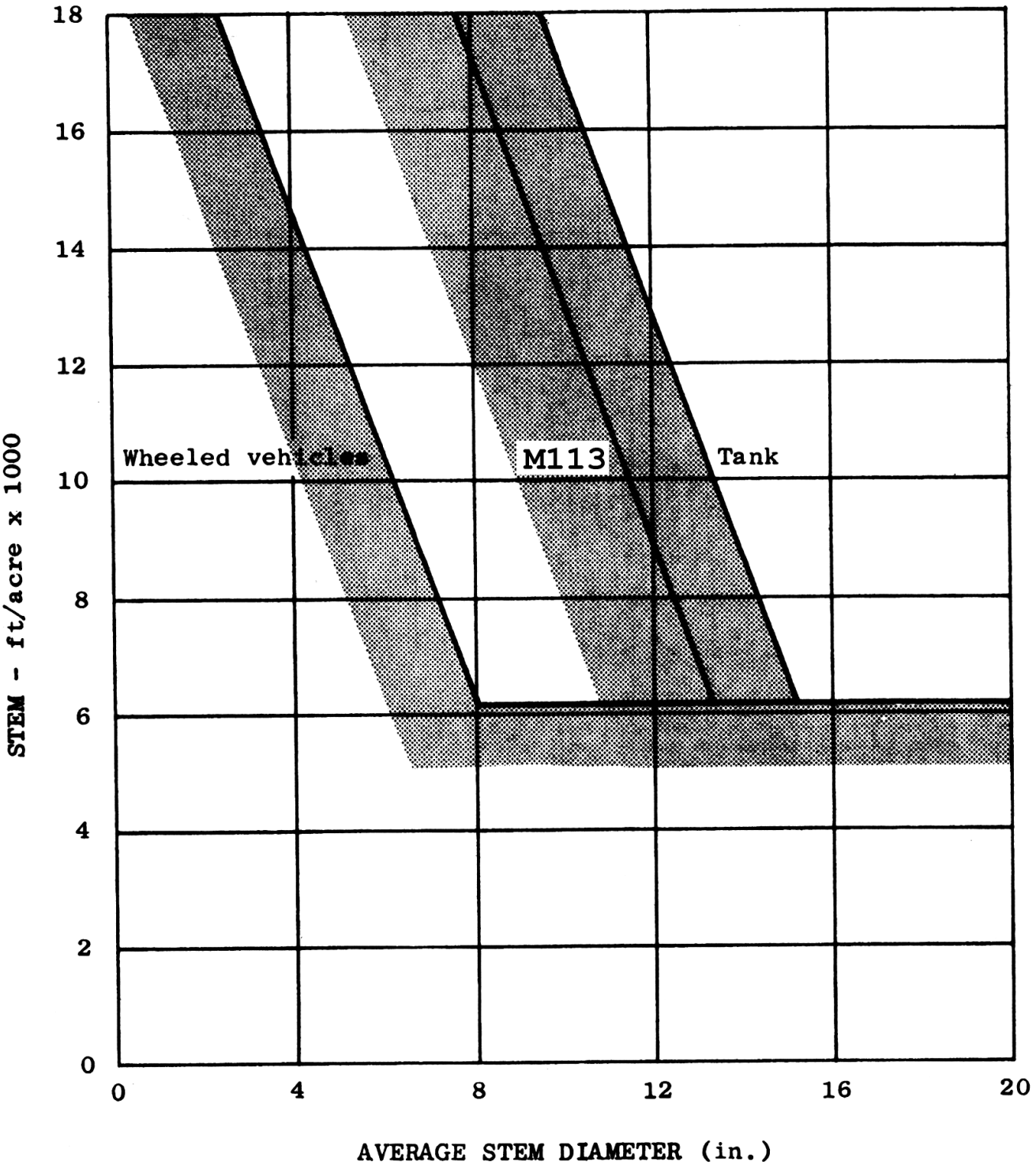

Fig. 15-11. Debris Characteristics Preventing Radial Movement of Vehicles

CONFIDENTIAL

[redacted]

a/11859

TECHNICAL LIBRARY
of the
ARMED FORCES
SPECIAL WEAPONS PROJECT
Mar 55

CONFIDENTIAL

Classification (~~Confidential~~) Changed to
By Authority of Memo, Ch. Security Div. 8-20-52
By G. Hamos 1 OCT 24 1957 Date

HANDBOOK

on

CAPABILITIES

of

ATOMIC WEAPONS

FILE COPY

AD511880 L

DOWNGRADED AT 12 YEAR
INTERVALS; NOT AUTOMATICALLY
DECLASSIFIED. DOD DIR 5200.10

[redacted]

CONFIDENTIAL

10.3 Damage Criteria

10.31 The tables presented in this section show various target items, their criteria for different degrees of damage and pertinent remarks. The items are listed in alphabetical order for each type of military operation. An attempt is made to give the source of the data by use of numbers to the right of the damage criteria. The key of this numbering system is indicated below:

a. Full-scale test data (including Hiroshima and Nagasaki . .(1)

b. Estimates made from scale experiments . . . . . (2)

c. Theoretical analysis . . . . . .(3)

d. Consensus of qualified persons . . . . . .(4)

10.32 For those items not included in Table VIII, select the listed item most similar in those characteristics discussed previously as being the important factors in determining the extent of damage to be expected. Perhaps the most important item to be remembered when estimating effects on personnel is the amount of cover actually involved. This cover depends on several items; however, one factor is all important, namely, the degree of forewarning of an impending atomic attack. It is obvious that only a few seconds warning is necessary under most conditions in order to take fairly effective cover. The large number of casualties in Japan resulted for the most part from the lack of warning.

SECRET

TABLE VIII

PART I. LAND OPERATIONS

ITEM	DAMAGE	AIR SHOCK PSI	GROUND SHOCK ER	THERMAL ENERGY cal/cm^2	REMARKS
Artillery Field (75mm or greater)	Severe	40 (1)	——	——	S: Damage to Gun and Cradle
	Moderate	30 (1)	——	——	M: Damage to Recoil and Carriage
	Light	5 (1)	——	15 (1)	L: Damage to Gun Sights, Paint Scorched
Artillery Field (Less than 75mm)	Severe	25 (1)	——	——	S: Damage to Gun and Cradle
	Moderate	15 (1)	——	——	M: Damage to Recoil and Loading Mechanism
	Light	5 (1)	——	15 (1)	L: Damage to Sights, Paint Scorched
Artillery (AA)	Severe	30 (1)	——	——	S: Damage to Gun and Cradle
	Moderate	20 (1)	——	——	M: Damage to Recoil and Carriage
	Light:	5 (1)	——	15 (1)	L: Damage to Electronic Equipment, Paint scorched
Ammunition in Field Dumps	Severe	10 (1)	——	20 (1)	S: Damage due to Ammo being thrown about and possible fires
	Moderate	3 (1)	——	15 (1)	M: Damage due to displacement, secondary effects and heat
	Light	2 (1)	——	10 (1)	L: Small portion damaged due to secondary effects and heat
Bridges (side on blast)	Severe	20	30 (4)	——	S: Bridge collapses. End on blast requires 60 psi
	Moderate	15	25 (4)	——	M: Bridge Displaced. End on blast requires 45 psi
	Light	—	——	——	

SECRET

SECRET

TABLE VIII
PART II
STRUCTURES

ITEM	DAMAGE	AIR SHOCK PSI	GROUND SHOCK ER	THERMAL ENERGY cal/cm^2	REMARKS
Brick Walls (12-18 inch)	Severe	12 (1)	15 (4)	——	S: Collapse
	Moderate	8 (1)	10 (4)	——	M: Partial collapse & cracking
	Light	3 (1)	6 (4)	——	L: Cracking
Homes Brick	Severe	6 (1)	15 (4)	——	S: Collapse
	Moderate	4 (1)	10 (4)	——	M: Distortion and Cracks
	Light	3 (1)	6(4)	——	L: Plaster & window damage
Homes Wooden Frame	Severe	5 (1)	25 (4)	20 (1)	S: Collapse, Burns
	Moderate	3 (1)	15 (4)	12 (1)	M: Distortion & cracks, may burn
	Light	2 (1)	8 (4)	8 (1)	L: Plaster & window damage, scorched
Multistory Brick Bldg.	Severe	6 (1)	15 (4)	——	S: Collapse
	Moderate	4 (1)	10 (4)	——	M: Structural Damage
	Light	3 (1)	6 (4)	——	L: Plaster & window damage
Oil Tank Farms	Severe	10 (2-4)	——	——	S: Tank collapse. This based on Texas explosion. Fires may break out & destroy entire field.
	Moderate	——	——	——	
	Light	——	——	——	
Reinforced Concrete Bldgs.	Severe	25 (1)	30 (4)	——	S: Collapse
	Moderate	10 (1)	20 (4)	——	M: Structural damage
	Light	3 (1)	15 (4)	——	L: Plaster & window damage
Steel, heavy frame Bldgs.	Severe	18 (1)	20 (4)	——	S: Mass distortion
	Moderate	12 (1)	10 (4)	——	M: Structural Damage
	Light	3 (1)	8 (4)	——	L: Plaster & window damage
Steel, light frame Bldgs.	Severe	10 (1)	15 (4)	——	S: Mass distortion
	Moderate	5 (1)	10 (4)	——	M: Structural Damage
	Light	3 (1)	6 (4)	——	L: Plaster & window damage

SECRET

TABLE VIII
PART III

SEA OPERATIONS

ITEM	DAMAGE	AIR SHOCK PSI	WATER SHOCK *Energy Flux, see Fig. 6.74	Bikini "B" Distance (ft)		REMARKS
Aircraft Carriers	Severe	30 (1)	300(4)	2700(1)	S:	Complete destruction or sunk
	Moderate	20 (1)	200(4)	3000(1)	M:	Immobilized. Failure of primary departments such as elevators. Air shock distorts flight deck.
	Light	5 (1)	100(4)	4500(1)	L:	Scorching & damage to light and electronic equipment.
Battleships	Severe	45 (1)	300(4)	2700(1)	S:	Complete destruction or sunk
	Moderate	25 (1)	200(4)	3000(1)	M:	Immobilized. Failure of primary departments
	Light	5 (1)	100(4)	4500(1)	L:	Scorching & damage to light and electronic equipment.
Cruiser (Heavy)	Severe	40 (1)	300(4)	2700(1)	S:	Complete destruction or sunk
	Moderate	20 (1)	200(4)	3000(1)	M:	Immobilized. Failure of primary departments
	Light	5 (1)	100(4)	4500(1)	L:	Scorching & damage to light and electronic equipment.
Cruiser (light)	Severe	30 (1)	300(4)	2700(1)	S:	Complete destruction or sunk
	Moderate	20 (1)	200(4)	3000(1)	M:	Immobilized. Failure of primary departments.
	Light	5 (1)	100(4)	4500(1)	L:	Scorching & damage to light and electronic equipment.
Destroyers	Severe	25 (1)	300(4)	2700(1)	S:	Complete destruction or sunk
	Moderate	15 (1)	200(4)	3000(1)	M:	Immobilized. Failure of primary departments.
	Light	5 (1)	100(4)	4500(1)	L:	Scorching & damage to light and electronic equipment.

SECRET

SECRET

Effect of irradiation on rate of growth of granulation tissue

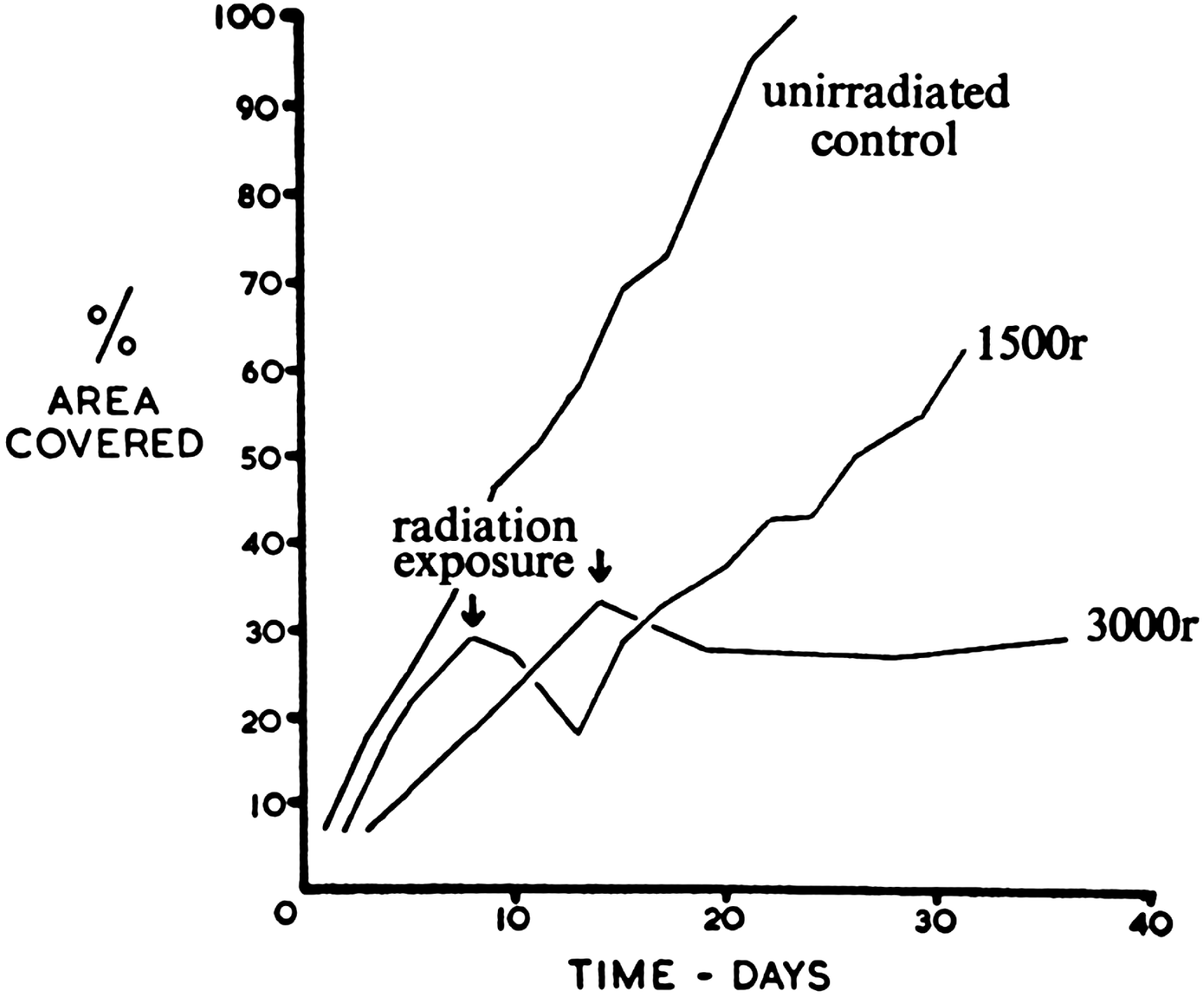

G. H. Blair, H. A. S. van den Brenk, J. B. Walter and D. Slome, "Experimental Study of Effects of Radiation on Wound Healing", in D. Slome, Editor, "Wound Healing: Proceedings of a Symposium 12-13 Nov., 1959, Royal College of Surgeons", Pergamon, 1961, pp. 46-53.

Accession Number : AD0689495

Title : PROCEEDINGS OF A WORKSHOP ON MASS BURNS, 13 - 14 MARCH 1968,

Corporate Author : NATIONAL ACADEMY OF SCIENCES WASHINGTON D C

Personal Author(s) : Walter,Carl W. ; Phillips,Anne W.

Report Date : 1969

Pagination or Media Count : 409

Abstract : This workshop was organized to review the problem of burns, and to marshal data that will permit experts in systems analysis, logistics, mass behavior, and government to apply their skills in planning for the defense of an isolated community that has been largely destroyed by a disastrous fire. Participants have been instructed to focus on the education of a non-medical audience, whose principal interest is civilian defense, and on what to expect from thermal trauma; how to recognize the potential survivors, what measures of self-help can decrease the severity of the illness, how and what to provide in terms of food and water supplies, space and personnel, how to educate the public and train surviving personnel during the weeks or months necessary for the devastated community to reorganize itself and become self-sustaining. (Author)

Descriptors : *BURNS(INJURIES), SYMPOSIA, PATHOLOGY, CASUALTIES, INFECTIOUS DISEASES, CHEMOTHERAPEUTIC AGENTS, TRANSPLANTATION, PROTECTION, THERAPY, RADIATION INJURIES, POPULATION.

Subject Categories : Medicine and Medical Research

Distribution Statement : APPROVED FOR PUBLIC RELEASE

MASS BURNS

Proceedings of a Workshop

13 - 14 March 1968

Sponsored

by

The Committee on Fire Research
Division of Engineering
National Research Council

and the

Office of Civil Defense, Department of the Army

Published

by

National Academy of Sciences
Washington, D.C.
1969

DC-P-1060-1

PREDICTION OF URBAN CASUALTIES AND THE MEDICAL LOAD FROM A HIGH-YIELD NUCLEAR BURST

L. Wayne Davis

Paper
prepared under

Contract No. N0022867C2276
(Work Unit No. 2411H)

Sponsored by

Office of Civil Defense
Office of the Secretary of the Army

through

Technical Management Office
U. S. Naval Radiological Defense Laboratory

Delivered at

Workshop on Mass Burns
National Academy of Sciences
Washington, D. C.
March 13-14, 1968

The Dikewood Corporation
1009 Bradbury Drive, S. E.
University Research Park
Albuquerque, New Mexico 87106

PREDICTION OF URBAN CASUALTIES AND THE MEDICAL LOAD FROM A HIGH-YIELD NUCLEAR BURST

I. INTRODUCTION AND SUMMARY

This work is the result of Dikewood's second iteration at predicting urban casualties due to high-yield nuclear bursts as based on the Japanese nuclear-casualty data from Hiroshima and Nagasaki and on the casualties experienced from the detonation of the ammonium-nitrate fertilizer on board a ship docked at Texas City in 1947. (The first iteration was published in DC-FR-1028, Ref. 1, and DC-FR-1041, Ref. 2.) The Japanese data base has now been more than doubled, and much more information is available on the breakdown of casualties segregated by shielding category. (See DC-FR-1054, Ref. 3.)

Urban casualty predictions are made for nuclear detonations in the yield range from 1 to 50 Mt for scaled burst heights of 0, 300, 585, and 806 feet. (See DC-FR-1060, Ref. 4, to be published.) All casualty curves are given in terms of a reference 12.5-kt surface burst; they must be scaled to the megaton-yield range by the use of scaling curves which are also provided. It is not presently a field manual for easy casualty predictions. Although calculations may be performed by hand, a computer solution is recommended to facilitate the computations for any but the simplest problems. Plans are underway to develop the computer program.

II. CASUALTY CURVES FOR PERSONS IN OR SHIELDED BY STRUCTURES

A. DEVELOPMENT OF "BLAST" MORTALITY CURVES FROM JAPANESE AND TEXAS CITY DATA

A great deal of new information has been gathered concerning the biological effects of the nuclear attacks on Hiroshima and Nagasaki, Japan, during World War II. The data from over 35,000 case histories were collected on magnetic tape, and the results of the analysis were published in DC-FR-1054 (Ref. 3).

The Japanese mortality curves for people in or shielded by structures are plotted as a function of overpressure in Figs. 1 and 2 for Hiroshima and Nagasaki, respectively. These curves are based on a yield for Hiroshima of 12.5 kt burst at a height of 1870 feet (scaled height of 806 feet) and a yield for Nagasaki of 22 kt burst at a height of 1640 feet (scaled height of 585 feet).

The mortality curves from the Texas City disaster of 1947, separated by shielding category, are given as a function of overpressure in Fig. 3. This surface burst* has been estimated to be equivalent to a nuclear yield of 0.67 kt.

The next step was to develop a set of "blast" mortality curves for a reference 12.5-kt surface burst. Of course, the ultimate goal was

---

*Ammonium-nitrate fertilizer exploded within the hold of a ship which was tied up at a pier.

to separate all of the biological damage according to the particular weapons effect which caused it (such as blast, prompt-thermal radiation, or initial-nuclear radiation). Then, each effect could be scaled separately to the higher yield of interest, and the results could be recombined. Joint effects cannot be scaled directly.

For people in or shielded by structures in Japan, the blast and initial-nuclear radiation were the dominant immediate effects. However, when one scales the results to the megaton range, the lethal effects of the initial-nuclear radiation drop out because the blast effects scale to greater ranges. Thus, the blast mortality curves are the set of greatest interest for persons in or shielded by structures. (Similarly, thermal mortality curves are the ones of greatest interest for the outside-unshielded persons.)

By examining a set of theoretical initial-nuclear-radiation mortality curves developed for Hiroshima and Nagasaki and comparing them with the total mortality curves, it could readily be seen that the initial-nuclear radiation played a large role in the deaths of thermally-shielded people located fairly close-in (at the high mortality levels) in the light structures. It is also an important effect even in the concrete structures.

By further comparing the mortality curves for Hiroshima and Nagasaki plotted as a function of overpressure (Figs. 1 and 2), it can

readily be seen that the initial-nuclear radiation was more important or dominant in Hiroshima than in Nagasaki. (It requires more overpressure in Nagasaki to produce the same percent mortality for the equivalent shielding category.) Thus, one would expect the pure blast mortality curves (with no initial-nuclear radiation present) to lie to the right (higher overpressures) of the equivalent Nagasaki curves.

As another boundary condition, the Texas City mortality curves, given in Fig. 3, show the results of blast alone for a lower yield of 0.67 kt. Since a set of blast-mortality reference curves for a 12.5-kt surface burst is the immediate goal, they would appear to lie to the left (lower overpressures) of the equivalent Texas City curves. Of course, this shift is due to the effect of the longer positive-phase duration at the higher yield; it requires less overpressure to produce the same damage at the higher yield. Thus, by scaling the pertinent shielding categories in Texas City up to 12.5 kt and by using the Nagasaki curves as the lower pressure boundaries, the pure blast mortality curves* for the reference 12.5-kt surface burst were developed and are shown in Fig. 4. These blast mortality curves for the reference surface burst are drawn as a smooth function of overpressure since this weapons effects parameter is considered to be the controlling factor in determining the mortality level.

---

*It is felt that any deaths in the Japanese data due to the secondary effects of fire have been eliminated by this process.

FIG. 1

TOTAL MORTALITY CURVES FOR HIROSHIMA

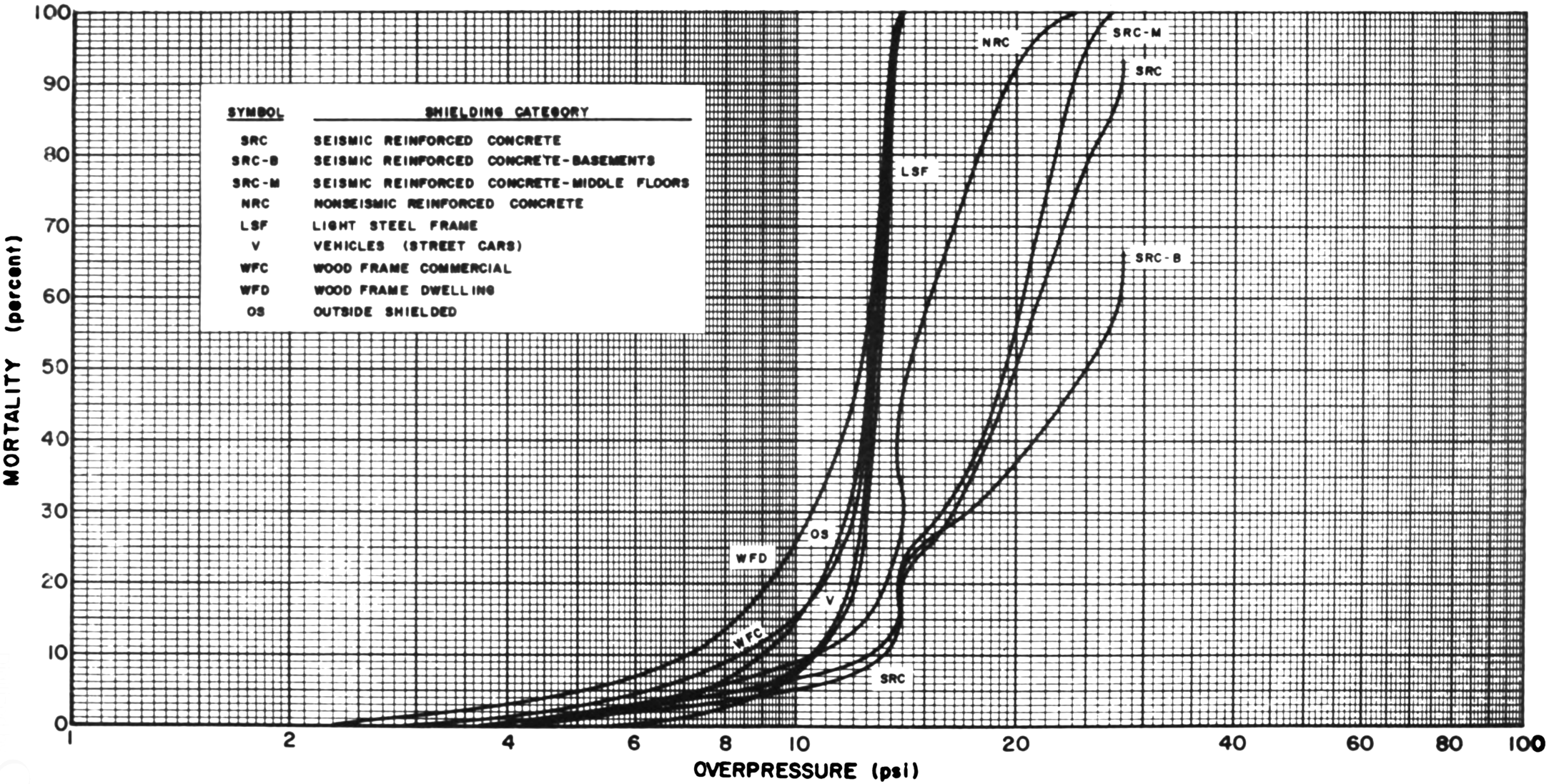

FIG. 2

TOTAL MORTALITY CURVES FOR NAGASAKI

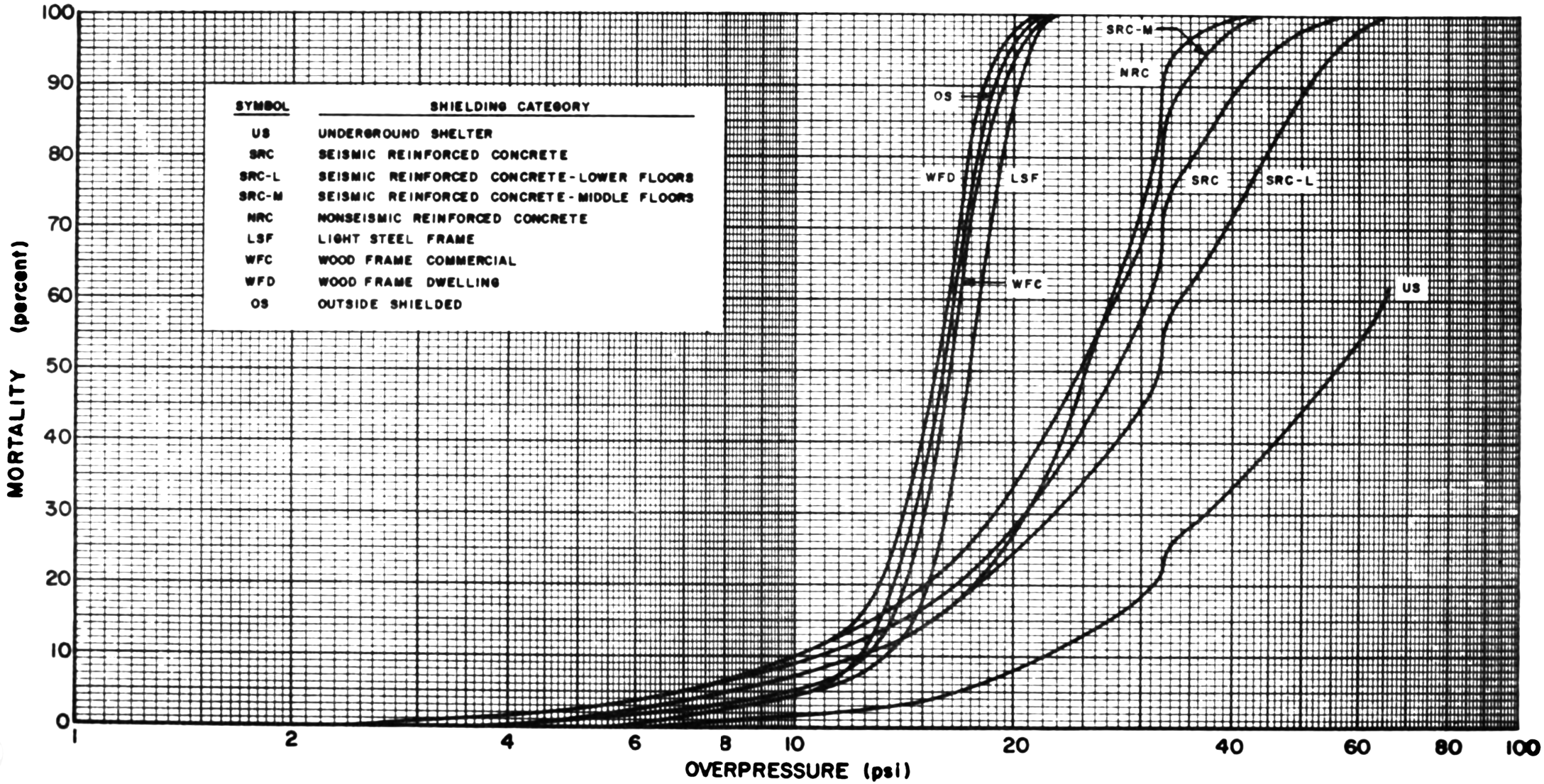

FIG. 3

TOTAL MORTALITY CURVES FOR TEXAS CITY

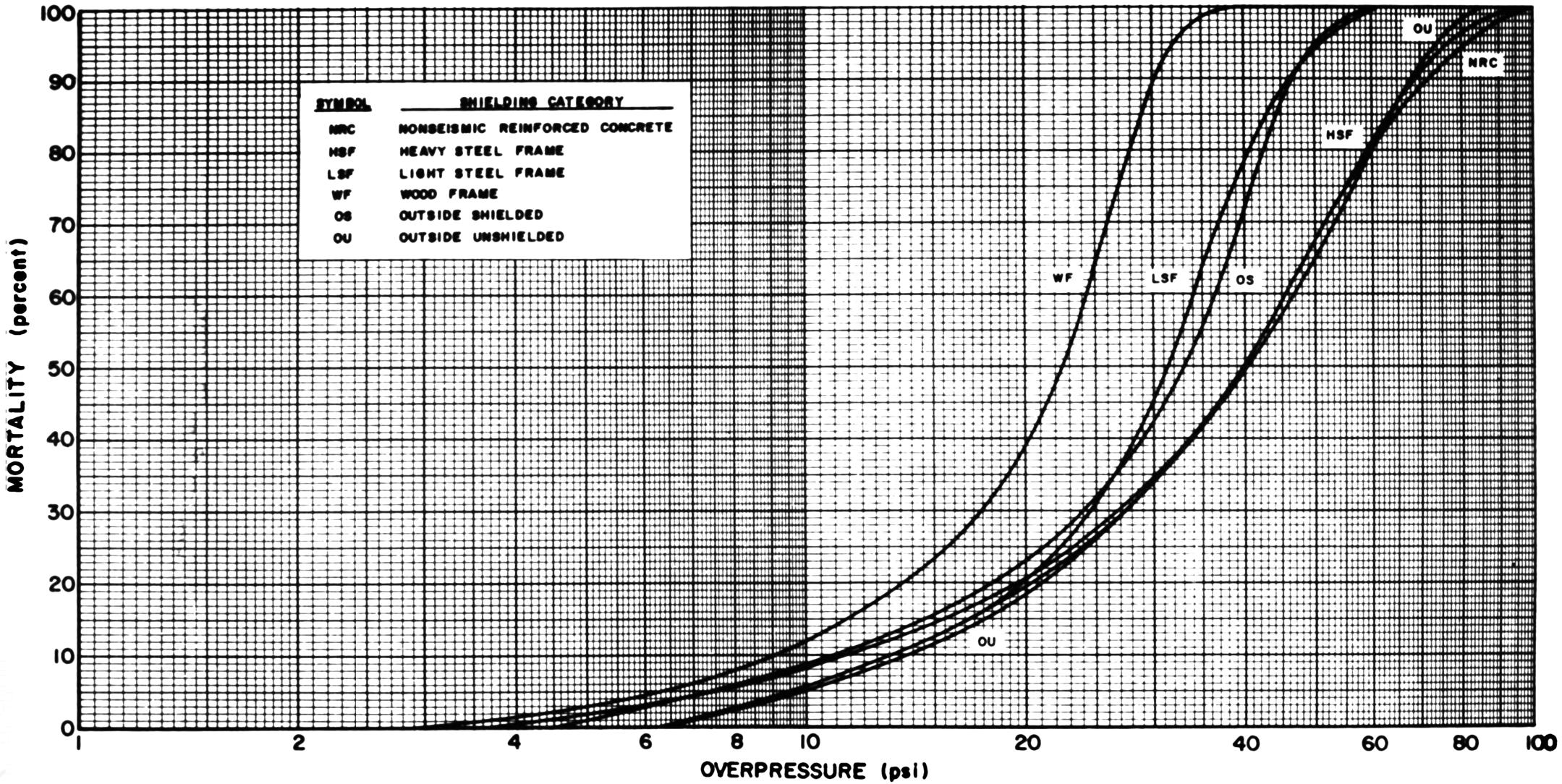

FIG. 4

BLAST MORTALITY CURVES FOR PERSONS IN OR SHIELDED BY STRUCTURES

(12.5-kt SURFACE BURST)

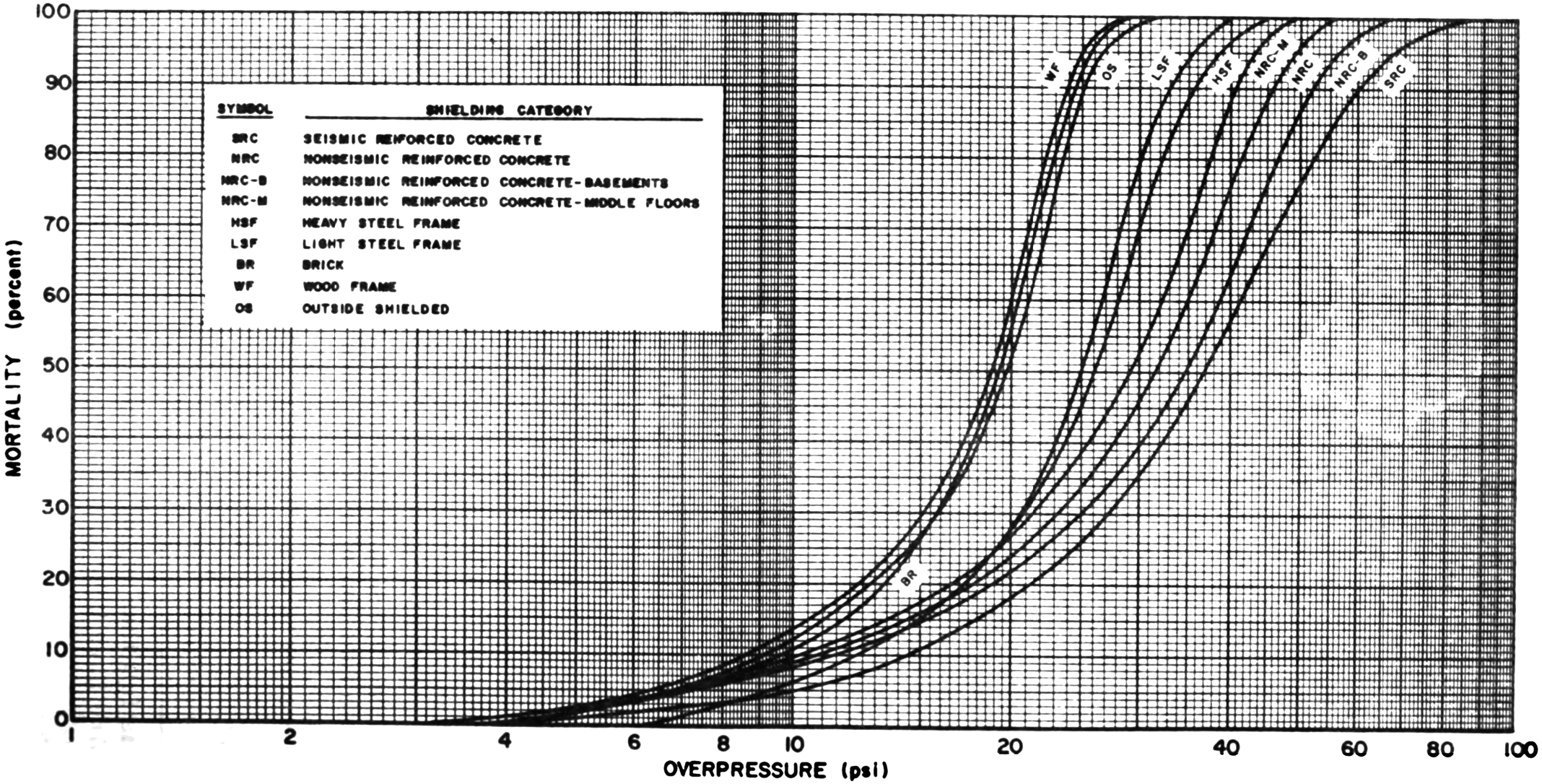

FIG. 7

TOTAL MORTALITY CURVES

FOR NONSEISMIC REINFORCED-CONCRETE BUILDINGS FROM SURFACE BURSTS

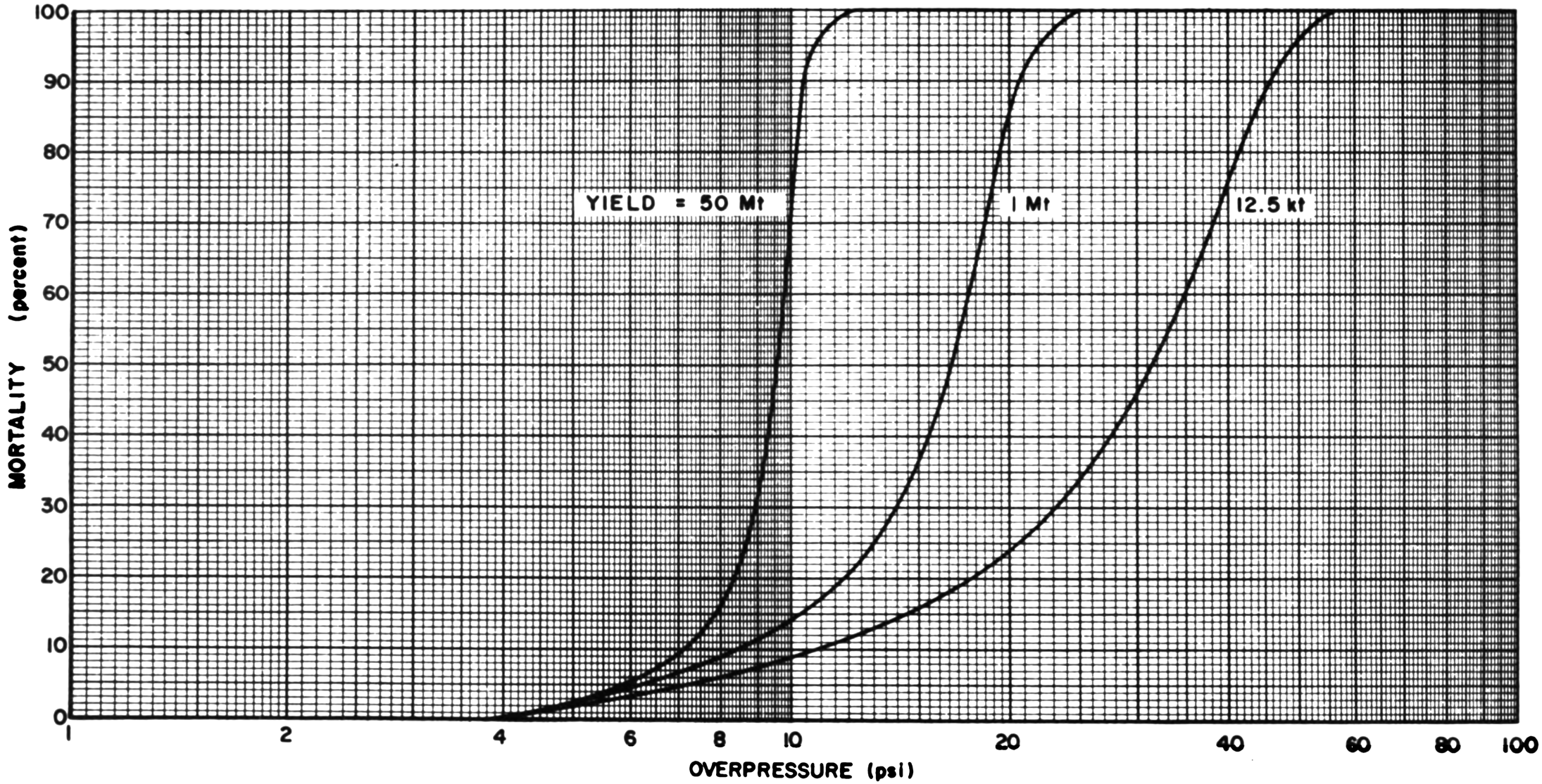

FIG. 10

CASUALTY CURVES VERSUS RANGE FOR NONSEISMIC REINFORCED-CONCRETE BUILDINGS

(5-MT SURFACE BURST)

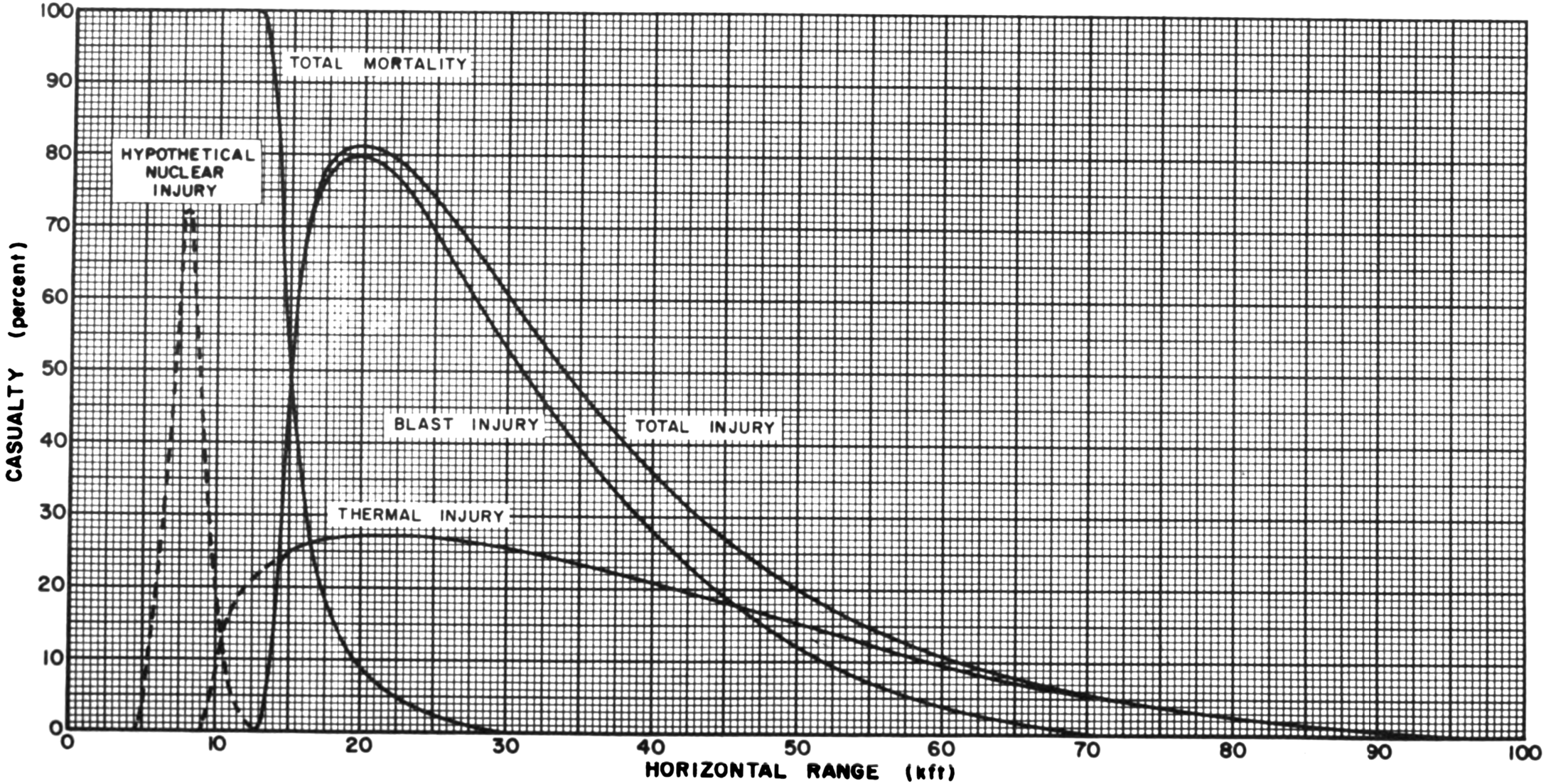

III. PROMPT-THERMAL CASUALTIES FOR OUTSIDE-UNSHIELDED PERSONS

A. PROMPT-THERMAL MORTALITY CURVE FOR OUTSIDE-UNSHIELDED PERSONS

This curve was much easier to develop than the blast mortality curves (complicated by the effects of the initial-nuclear radiation in Japan) since the prompt-thermal radiation producing flash burns was the dominant effect in Japan as well as for high yields for outside-unshielded persons. Since the predictions of the prompt-thermal exposures in Nagasaki did not correlate well with the burns received, apparently caused by problems in determining the transmissivity, only the new Hiroshima data were used to draw the prompt-thermal mortality curve given in Fig. 19 as a function of the prompt-thermal exposure (cal/cm^2) for the 12.5-kt reference burst. This curve, which is also equivalent to the total mortality curve, can be scaled to higher yields according to the method to be described shortly.

B. PROMPT-THERMAL INJURY CURVE FOR OUTSIDE-UNSHIELDED PERSONS

Before drawing the curves for the surviving injured, all of the data from Hiroshima and Nagasaki were replotted as a function of the appropriate weapons effects levels (cal/cm^2 for prompt-thermal injuries). However, the Hiroshima results were considered to be more reliable than the Nagasaki results for prompt-thermal injuries.

FIG. 19

PROMPT-THERMAL CASUALTY CURVES FROM A 12.5-KT SURFACE BURST FOR OUTSIDE-UNSHIELDED PERSONS

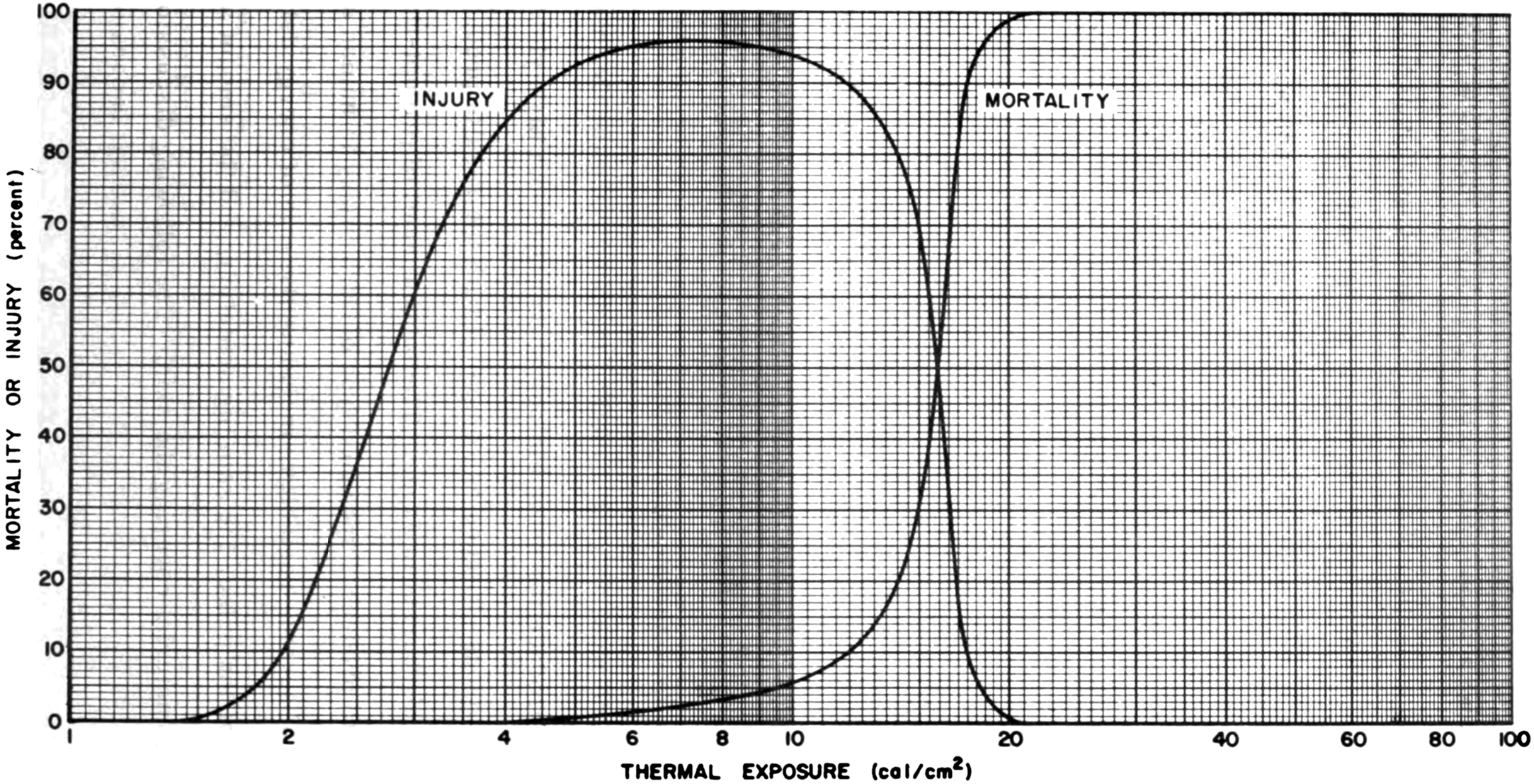

FIG. 24

PROMPT-THERMAL MORTALITY CURVES FROM SURFACE BURSTS FOR OUTSIDE-UNSHIELDED PERSONS

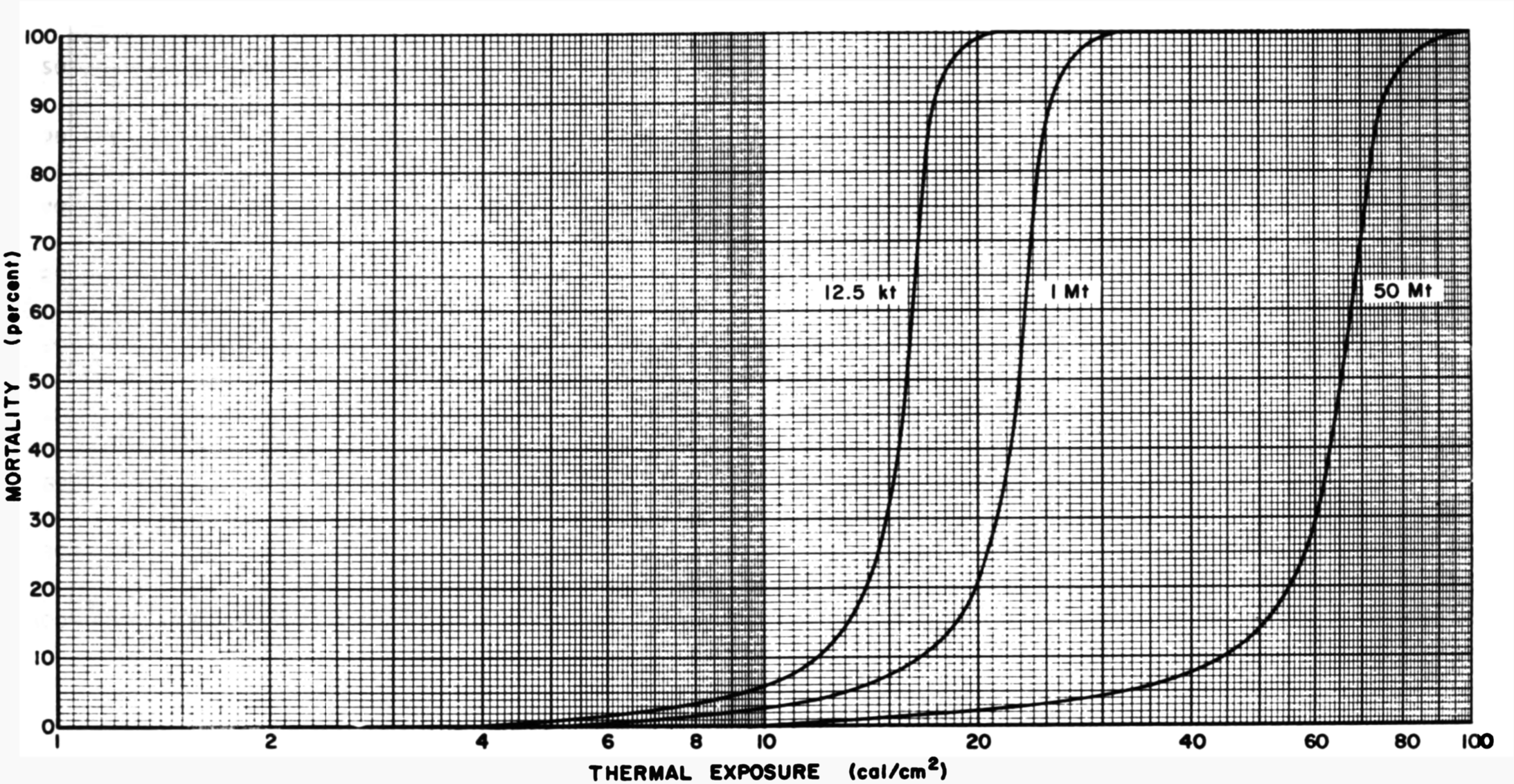

condition for development of firestorms. High ambient winds usually cause conflagrations to develop, as noted above.

B. FIRE MORTALITY CURVES

Fires in nine German cities were analyzed in detail to provide data for the development of fire mortality curves. Similar procedures were applied to the fires caused by the nuclear detonation over Hiroshima. Earlier work in this area indicated a correlation between the peak power density (maximum rate of energy release per unit area of the fire bed) and the percent fire mortality for the population at hazard within the fire area.* The four general groupings of construction or shielding categories given by the curves in Fig. 30 are the result of investigating this correlation (Refs. 14 through 18). The general groupings and breakdowns by shielding category are given below:

1) Heavy Construction
   a) Seismic Reinforced-Concrete Buildings
   b) Nonseismic Reinforced-Concrete Buildings (Basements)

2) Medium Construction
   a) Nonseismic Reinforced-Concrete Buildings (Above Ground)
   b) Heavy Steel-Frame Buildings (Basements)†
   c) Light Steel-Frame Buildings (Basements)†
   d) Heavy Brick Wall-Bearing Buildings (Basements)†

---

*For application of an earlier form of these relationships to historical cases, see Ref. 13.

†If basements are unavailable, this mortality curve probably lies midway between those for medium and light construction.

FIG. 30

FIRE MORTALITY CURVES

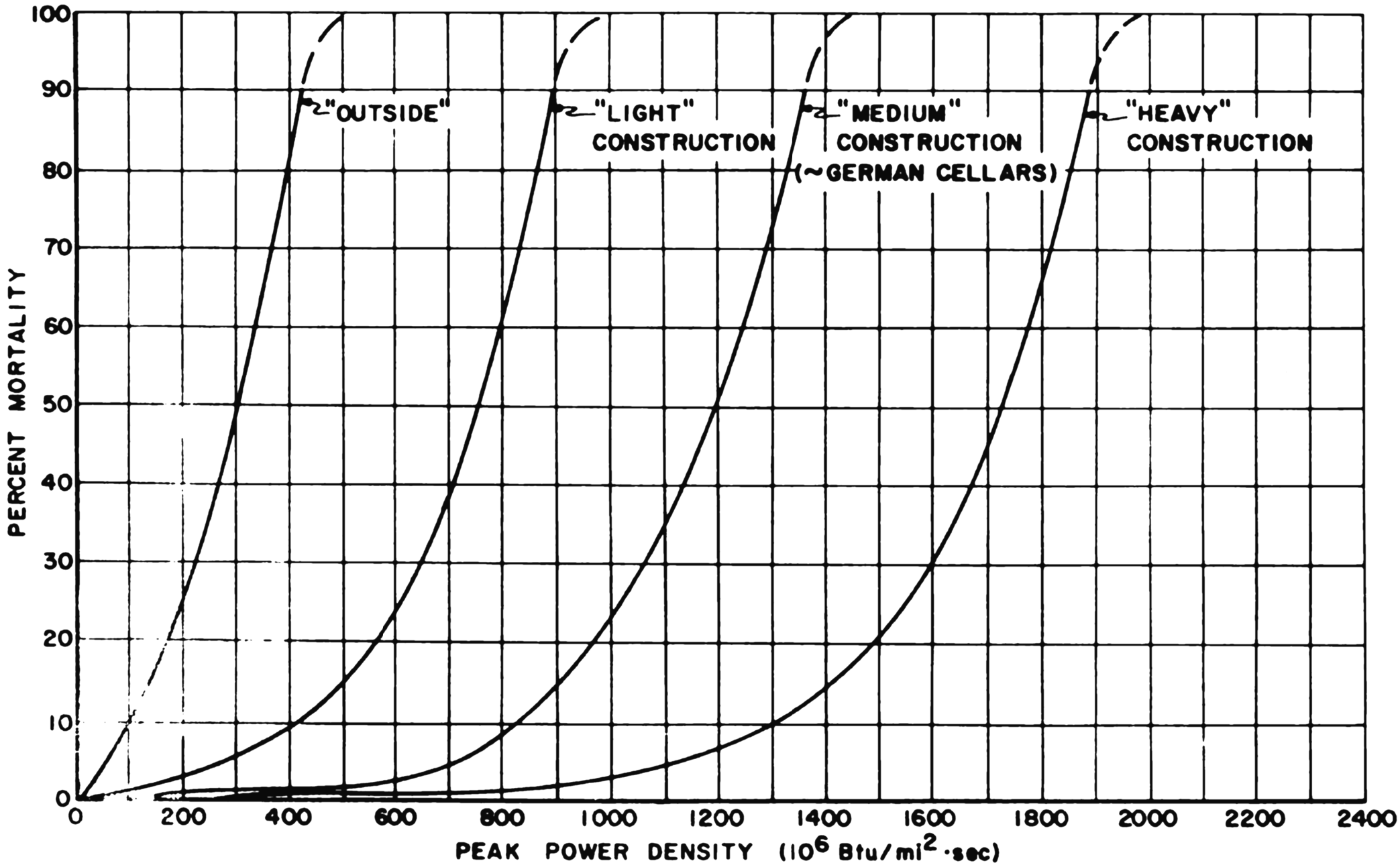

3) Light Construction

a) Brick Residential Buildings

b) Wood-Frame Buildings (Basements)*

4) Outside

a) Outside-Shielded Category

b) Outside-Unshielded Category

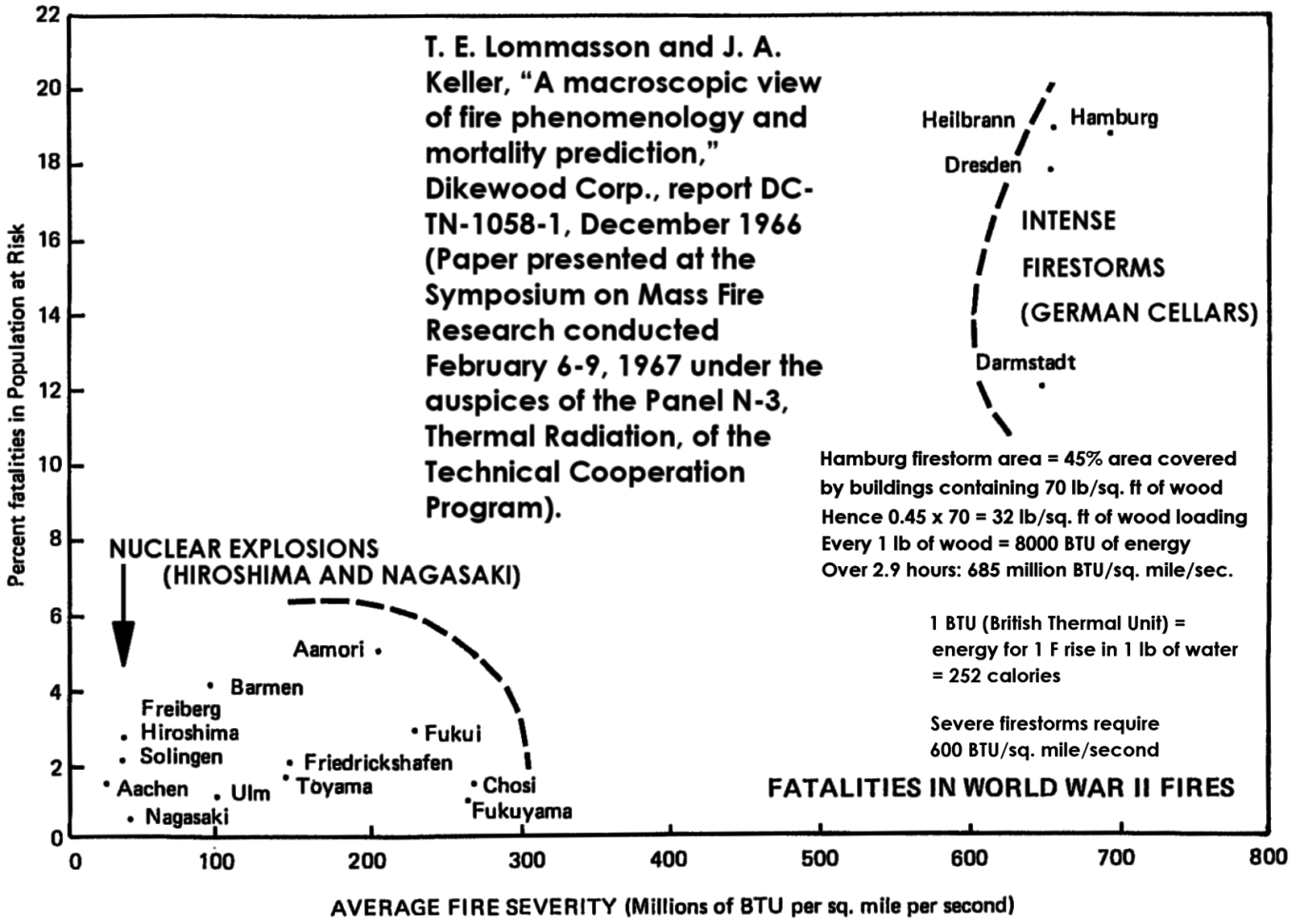

Lommasson and Keller, **A Macroscopic View of Fire Phenomenology and Mortality Predictions**, Dikewood Corporation, DC-TN-1058-1, December 1966.

T. E. Lommasson and J. A. Keller, A Macroscopic View of Fire Phenomenology and Mortality Prediction, Proceedings of the Tripartite Technical Cooperation Program, Mass Fire Research Symposium of the Defense Atomic Support Agency, The Dikewood Corporation; October, 1967.

---

*If basements are unavailable, this mortality curve probably lies midway between those for light construction and the outside category.
between those for medium and light construction.

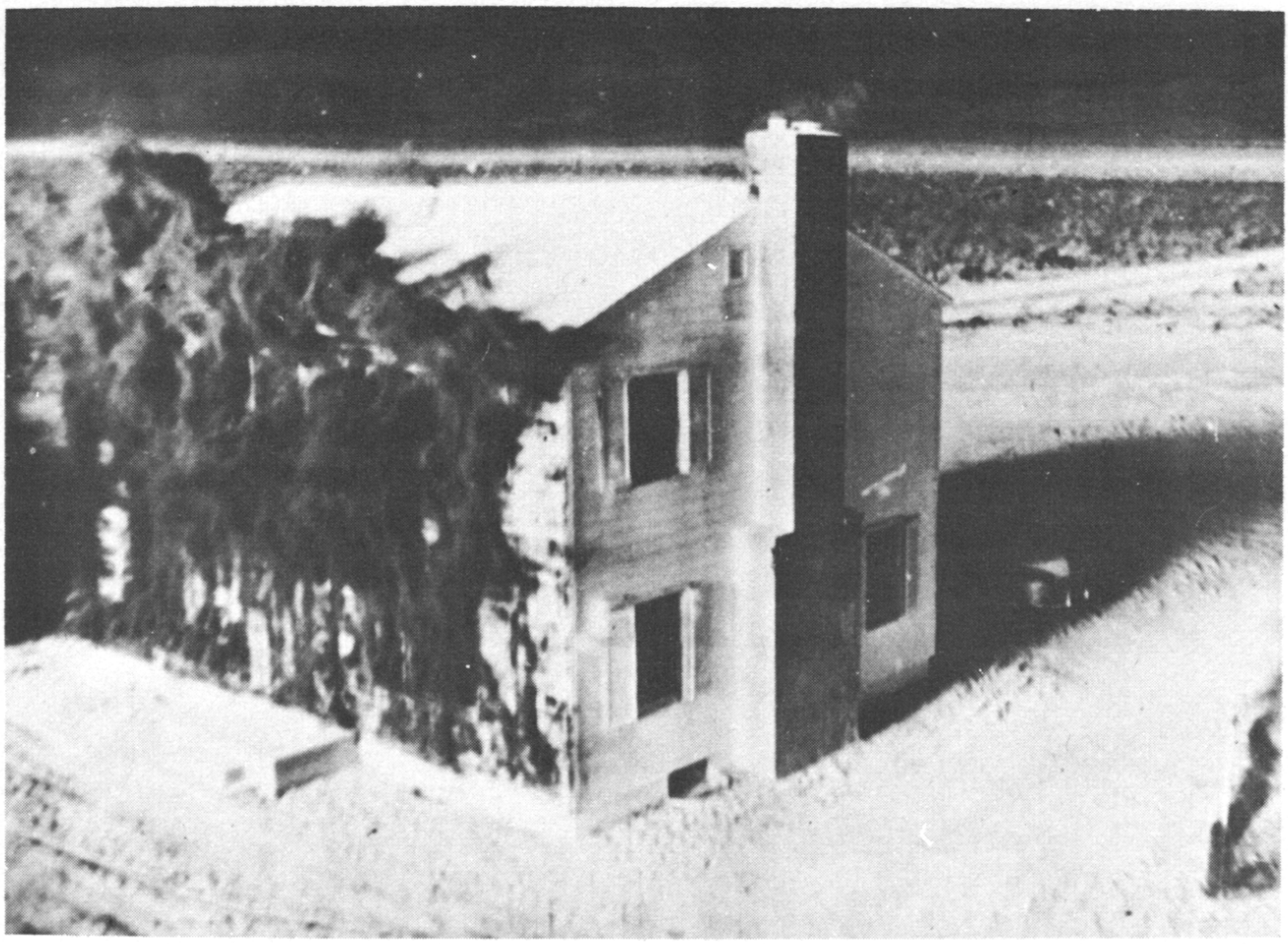

Figure 7.33a. Thermal effects on wood-frame house 1 second after explosion (about 25 cal/sq cm).

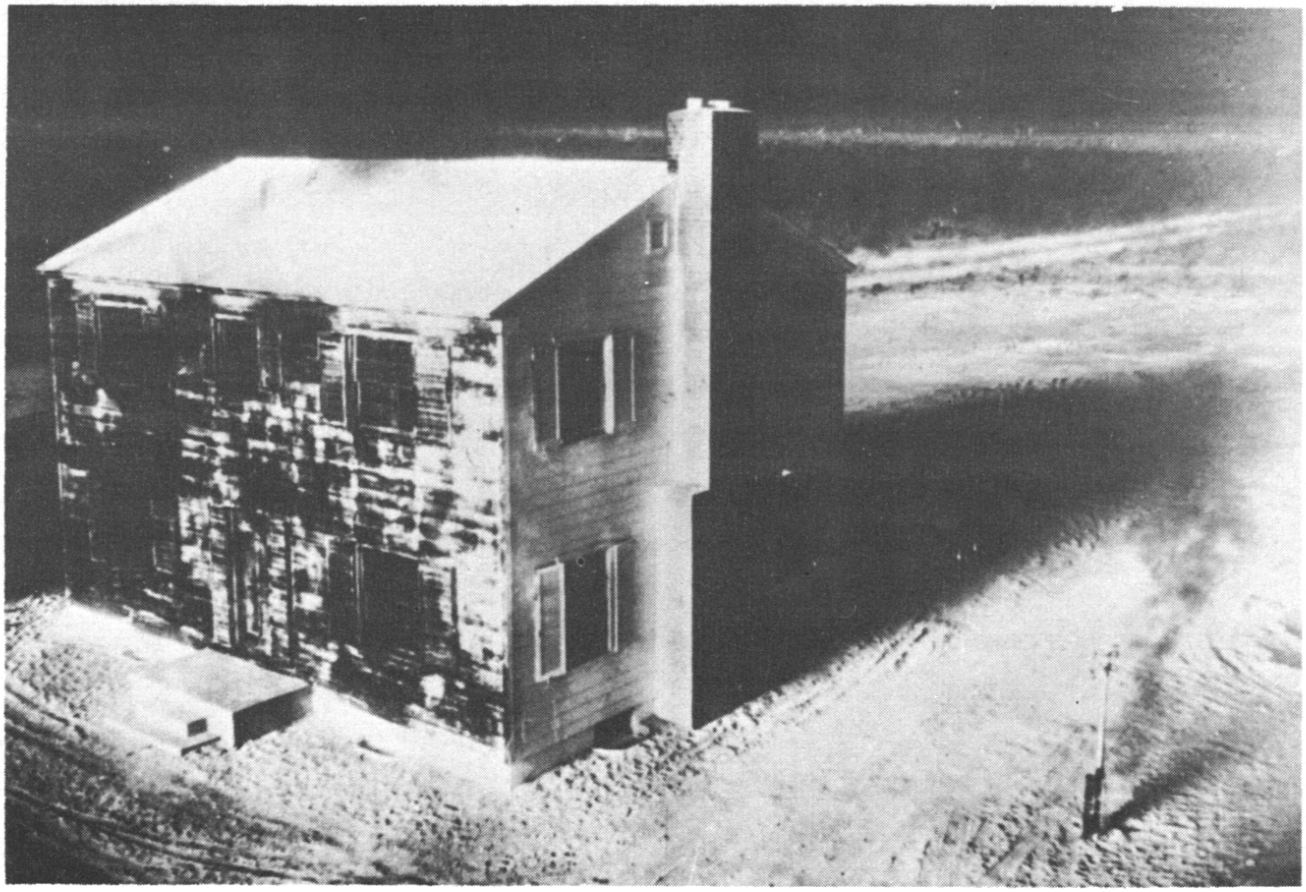

Figure 7.33b. Thermal effects on wood-frame house about ¾ second later.

LIST OF REFERENCES

1. L. Wayne Davis, Donald L. Summers, Milton E. Jenkins, Francis J. Wall, and William L. Baker, Prediction of Urban Casualties from the Immediate Effects of a Nuclear Attack, DC-FR-1028, The Dikewood Corporation; April, 1963. (Classified)

2. L. Wayne Davis, Francis J. Wall, and Donald L. Summers, Development of "Typical" Urban Areas and Associated Casualty Curves, DC-FR-1041, The Dikewood Corporation; April, 1965.

3. L. Wayne Davis, William L. Baker, and Donald L. Summers, Analysis of Japanese Nuclear Casualty Data, DC-FR-1054, The Dikewood Corporation; April, 1966.

4. L. Wayne Davis, Donald L. Summers, William L. Baker, and James A. Keller, Prediction of Urban Casualties and the Medical Load from a High-Yield Nuclear Burst, DC-FR-1060, The Dikewood Corporation; to be published. (Classified)

5. Ashley W. Oughterson, et al., Medical Effects of Atomic Bombs, NP-3036 to NP-3041 (Vols. I-VI), Army Institute of Pathology; 1951.

6. The Effects of the Atomic Bomb on Hiroshima, Japan, Report No. 92 (Vols. I-III), U.S. Strategic Bombing Survey, Physical Damage Division; May, 1947.

7. Effects of the Atomic Bomb on Nagasaki, Japan, Report No. 93 (Vols. I-III), U.S. Strategic Bombing Survey, Physical Damage Division; June, 1947.

8. J. Rotz, et al., Effects of Fire on Structural Debris Produced by Nuclear Blast, URS 639-9, URS Corporation; January, 1965.

9. Willard L. Derksen, et al., Output Intensities and Thermal Radiation Skin Injury for Civil Defense Shelter Evaluation, Special Report for Blast and Thermal Subcommittee of the National Academy of Science, U.S. Naval Applied Science Laboratory; October 16, 1967.

10. Samuel Glasstone (Editor), The Effects of Nuclear Weapons, U.S. Atomic Energy Commission; 1957 and 1962.

11. J. Bracciaventi, W. Derksen, et al., Radiant Exposures for Ignition of Tinder by Thermal Radiation from Nuclear Weapons, Final Report on DASA Subtask 12.009, U.S. Naval Applied Science Laboratory; July 5, 1966.

LIST OF REFERENCES (Continued)

12. S. B. Martin and N. J. Alvares, Ignition Thresholds for Large-Yield Nuclear Weapons, USNRDL-TR-1007, U. S. Naval Radiological Defense Laboratory; April 11, 1966.

13. T. E. Lommasson and J. A. Keller, A Macroscopic View of Fire Phenomenology and Mortality Prediction, Proceedings of the Tripartite Technical Cooperation Program, Mass Fire Research Symposium of the Defense Atomic Support Agency, The Dikewood Corporation; October, 1967.

14. J. A. Keller, A Study of World War II German Fire Fatalities, DC-TN-1050-3, The Dikewood Corporation; April, 1966.

15. R. Schubert, Examination of Building Density and Fire Loading in the Districts Eimsbuettel and Hammerbrook of the City of Hamburg in the Year 1943 (20 volumes, in German), Stanford Research Institute; January, 1966.

16. G. H. Tryon (Editor), Fire Protection Handbook, Twelfth Edition, National Fire Protection Association, Boston; 1962.

17. C. C. Chandler, T. Storey, and C. Tangren, Prediction of Fire Spread Following Nuclear Explosions, PSW-5, U. S. Forest Service, Forest and Range Experiment Station, Berkeley, California; 1963.

18. Kathleen F. Earp, Deaths from Fire in Large-Scale Air Attack, with Special Reference to the Hamburg Firestorm, CD/SA 28, Home Office, Scientific Advisers' Branch, London; April, 1953.

Editorial Comments

If clothing ignites, education should be so thorough that the immediate reaction is "smother the flames."

Every child should be trained to roll on the floor if his clothes catch fire, and every adult should know how to extinguish flames with the nearest material at hand - his own coat, a rug, or a blanket. They should know, in advance of the actual emergency, the importance of bringing the coat (or whatever else they are using) across the face to fend the flames and smoke away from the vital air passages.

37

Dr. Edward L. Alpen (U. S. Naval Radiological Defense Laboratory): About this question of the spectral dependence of radiant energy, I think Dr. Haynes may have given you the impression that white light does the trick. There is later work which tends to refute that. The work done at Virginia used cut-off filters. The effectiveness of all energy above a certain wave length or below a certain wave length was measured. At the upper end the most effective and the least effective were mixed together and made it appear that infrared was not too good in producing burns. When you subdivide the spectrum, the most effective energy in producing a flash burn is the infrared above about 1.2 microns.

The importance of this, and the only reason I make an issue of it, is that a very important source of flash burn, both in civilian life and under wartime disaster conditions, is radiant energy burns from flaming sources. We have done a great deal of research on this subject for the U. S. Forest Service, because radiant energy burns are important in forest fires.

Energy in the wave lengths of 0.6 to 0.8 micron is about one-eighth as destructive as the rest of the spectrum. But long wave length radiation above one micron is extremely destructive, and the most effective of all.

49

Dr. Alpen: Anything that shields out radiation above one micron is extremely effective in preventing burns to the skin.

50

THE BURN SURFACE AS A PARASITE

WATER LOSS, CALORIC DEMANDS, AND THERAPEUTIC IMPLICATIONS

Carl Jelenko, III, M.D.

Department of Surgery

University of Maryland School of Medicine and Hospital

Baltimore, Maryland

Water is Lost through Burned Skin*

A burn may be thought of as a parasite, drawing from its host water, protein, and other substances which the host needs for its survival. An uninjured person who is not perspiring may lose from 1.15 to 2.0 quarts of fluid a day through his lungs and skin,[1,2,4,5,14] depending on the temperature of his environment. The fluid losses from a burn wound are far in excess of those from intact skin and may amount to 2 gallons per day, or more if the burn is large enough.[2,5,6,17,21] If, during the first 48 hours after injury, no more fluid is given to an extensively burned patient than he would need in health, the uncompensated loss of fluid from his circulation may cause shock, and if sufficiently severe, death. After the first 48 hours, the danger of shock is lessened, but inordinate fluid losses will continue from the burn surface.

Heat is Lost Necessitating a High Food Intake

To make matters worse, evaporation of moisture from the wound surface saps not only the body's water stores but its energy stores as well. When water evaporates from the burned surface, cooling results and the body loses heat. The larger the burn wound, the more water loss and the more heat or energy loss.**

*The majority of the paragraph headings in this article were supplied by the editors.

**Although the core temperature of the human body approximates 39.5°C, the body surface averages only 32°C. At any given temperature, water can be evaporated by applying a certain number of heat calories. At 32°C, one gram of water can be evaporated if 0.579 large calories of heat is invested.

How Can the Fluid and Heat Losses Be Diminished?

Unfortunately, we do not possess at present any practical means of reducing the loss of water from a burn to the level of loss from intact skin on a scale suitable for use following a holocaust.

Think Plastic Wrap as Wound Dressing for Thermal Burns

ACEP (American College of Emergency Physicians) News
http://www.acep.org/content.aspx?id=40462

August 2008
By Patrice Wendling
Elsevier Global Medical News

CHICAGO - Ordinary household plastic wrap makes an excellent, biologically safe wound dressing for patients with thermal burns en route to the emergency department or burn unit.

The Burn Treatment Center at the University of Iowa Hospitals and Clinics, Iowa City, has advocated prehospital and first-aid use of ordinary plastic wrap or cling film on burn wounds for almost two decades with very positive results, Edwin Clopton, a paramedic and ED technician, explained during a poster session at the annual meeting of the American Burn Association.

"Virtually every ambulance in Iowa has a roll of plastic wrap in the back," Mr. Clopton said in an interview. "We just wanted to get the word out about the success we've had using plastic wrap for burn wounds," he said.

Dr. G. Patrick Kealey, newly appointed ABA president and director of emergency general surgery at the University of Iowa Hospital and Clinics, said in an interview that plastic wrap reduces pain, wound contamination, and fluid losses. Furthermore, it's inexpensive, widely available, nontoxic, and transparent, which allows for wound monitoring without dressing removal.

"I can't recall a single incident of its causing trouble for the patients," Dr. Kealey said. "We started using it as an answer to the problem of how to create a field dressing that met those criteria. I suppose that the use of plastic wrap has spread from here out to the rest of our referral base."

Although protocols vary between different localities, plastic wrap is typically used for partial- and full-thickness thermal burns, but not superficial or chemical burns. It is applied in a single layer directly to the wound surface without ointment or dressing under the plastic and then secured loosely with roller gauze, as needed.

Because plastic wrap is extruded at temperatures in excess of 150° C, it is sterile as manufactured and handled in such a way that there is minimal opportunity for contamination before it is unrolled for use, said Mr. Clopton of the emergency care unit at Mercy Hospital, Iowa City. However, it's best to unwind and discard the outermost layer of plastic from the roll to expose a clean surface.

EVAPORATION OF WATER FROM 3RD DEGREE BURNS AREAS

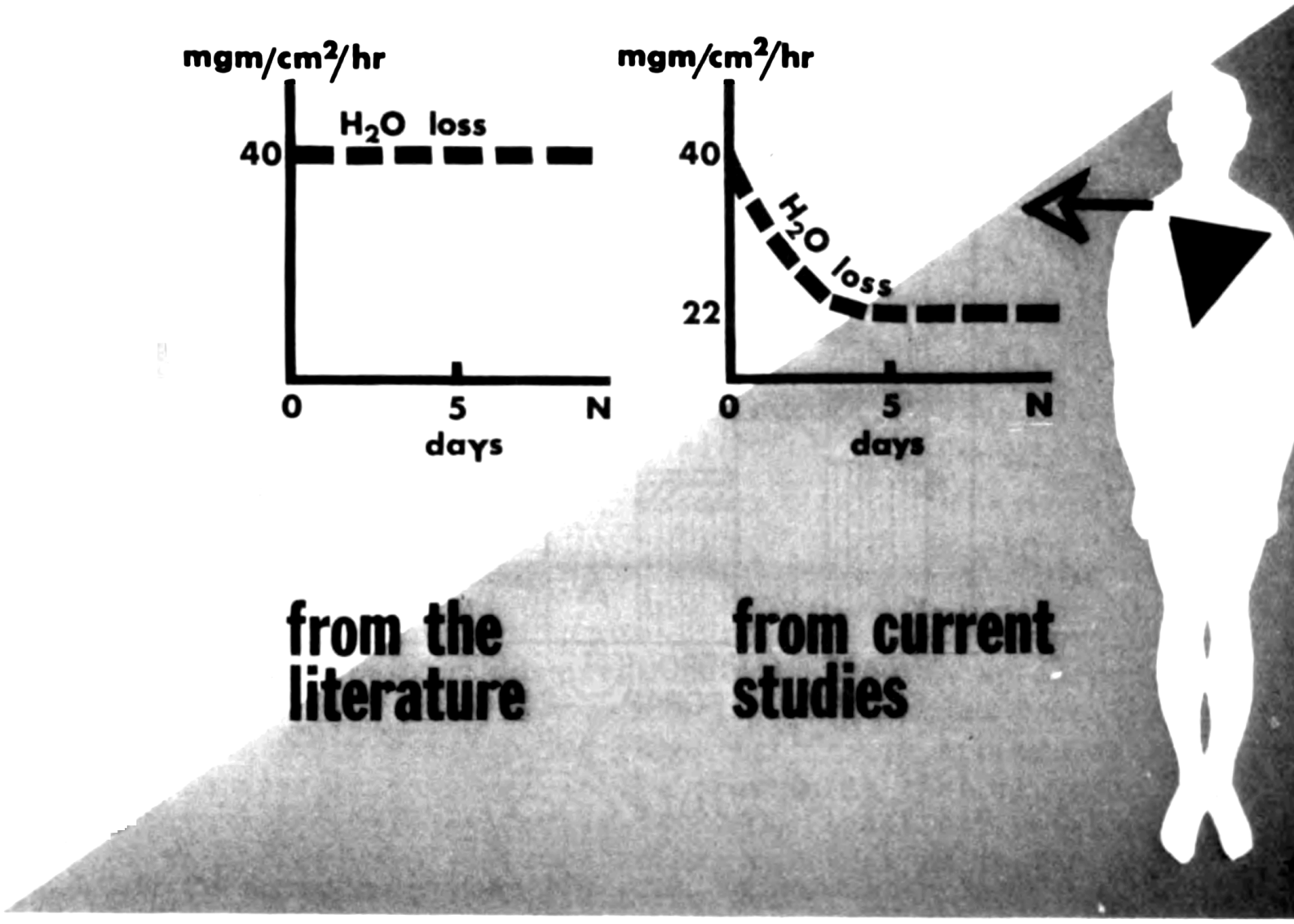

Fig. 2. Schema illustrating the gradual decrease in eschar transmissivity with time.

SOME PRINCIPLES OF PROTECTION AGAINST BURNS FROM FLAME AND INCENDIARY AGENTS

Janice A. Mendelson, M. D., M. M. Sc., (LTC, MC, U. S. Army)*

Chief, Biomedical Department

Biophysics Laboratory

Edgewood Arsenal, Maryland

I. Flame Agents

A. Their Nature

Flame agents are special blends of petroleum products, usually in thickened form, that ignite easily and can be projected to a target. Methods for the throwing of flame were devised by the Greeks in 429 B.C. (Siege of Plataea) when destructive flammable mixtures of pitch and sulfur were used. "Greek fire" composed of pitch, sulfur, and naptha, together with a method of projecting it through brass tubes or in red-hot balls of stone or iron, were developed about 670 A.D. in the arsenals of Constantinople. A type of flame thrower used on ships was constructed, with pressure furnished by a water engine. It is thought by some that this contained an igniting substance (quicklime or phosphide) that acted in the presence of water, but this has not been proven. The Germans in World War I were the first to use flame projectors. All combatting nations developed and used flame throwers extensively in World War II. Fire bombs were first used in the second world war.

M1 (Napalm). M1 thickener is a coprecipitated aluminum soap. The name was derived from the naphthenic and palmitic acids that were its major constituents.

Napalm B, used by the Air Force, is intended as a replacement for the M2 thickener. It is not true napalm, being composed of polystyrene, gasoline, and benzene. It is not a gel, but is a sticky, visco-elastic liquid. It has a longer burning time than the M1, M2, and M4 thickened fuels, and, therefore, possibly better incendiary action.

Unlike the M1, M2, and M4 thickeners, which can be quite easily brushed off the skin, the Napalm B is sticky and the polystyrene itself burns, its burning time being longer than that of the petroleum products. Therefore, this does have the required characteristics to produce more severe burns than unthickened fuel.

B. Defense Against Flame Agents (Protective Coverings)

The primary objective of individual defense against flame[5] is to keep particles of burning fuel off the person. The use of almost any available cover when a flame attack appears imminent is recommended. Troops are instructed to remain covered with no skin exposed until after the flash and flame in the high heat zone have been dissipated and then throw off the cover and remove any burning particles from their clothing. Blankets or items such as an army field jacket have been shown to give real protection. Two thicknesses of the Army shelter half tent will hold burning fuel for more than 10 seconds. Tent canvas and truck tarpaulins which have been treated with fire-resistant material will withstand direct hits with burning fuel and will hold the burning particles for sufficient time (more than 30 seconds) to permit personnel to escape. Foxhole covers improvised of brush with as little as 2 inches of earth on top will successfully withstand burning fuel. The Army plastic poncho is not a satisfactory cover because it melts rapidly and burns when hit with flaming fuel. This would increase the severity of burns received by an individual. Foxholes and weapon positions can be modified to afford adequate protection for anything except a direct hit with a fire bomb.

II. Incendiaries:[19]

A. Their Nature

Incendiary agents are compositions of chemical substances designed for use in the planned destruction of buildings, property, and materiel by fire. They burn with an intense localized heat. They are very difficult to extinguish and are capable of setting fire to materials that normally do not ignite or burn readily. Although there are tactical applications for incendiary munitions, they have played primarily a strategic role in modern warfare. The first practical model of an incendiary artillery shell was developed by the French in 1878.

The mechanics of fire-starting involve three essentials in addition to a source of oxygen: (1) Source of heat acting as a "match" to initiate the fire, (2) A combustible material which serves as the kindling, and (3) The fuel. The incendiary supplies the match and the kindling, and the target supplies the fuel. Modern military incendiaries may be divided into three categories: (1) Oil, (2) Metal, and (3) Combination of oil and metal.

The incendiary bomb (as distinguished from the fire bomb filled with thickened fuel) has been considered a strategic rather than a tactical weapon and has been used mainly against rear-area and supply installations. Incendiary shells and incendiary grenades are primarily tactical weapons, as are the flame munitions (fire bombs and flame throwers). Large incendiary bombs are used against point targets such as air bases and factories. Small incendiary bombs are usually dropped in clusters.

2. Metal incendiaries include those consisting of magnesium in various forms, and powdered or granular aluminum mixed with powdered iron oxide. Magnesium is a soft metal which, when raised to its ignition temperature (623° = 1,150°F), burns vigorously in air. Magnesium has a burning temperature of about 1,982°C (3,600°F) depending upon the rate of heat dissipation, rate of burning, and other factors. Its melting point is 651°C, so it melts as it burns. The liquid metal, burning as it flows, drops to lower levels, igniting combustible materials in its path. Burning stops if oxygen is prevented from reaching the metal or if the metal is cooled below the ignition temperature. Magnesium does not have the highest heat of combustion of the metals, but none of the other metals have been successfully used singly as air-combustible incendiaries. In massive form, magnesium is difficult to ignite. Therefore, a hollow core in the bomb is packed with thermate and an easily ignited mixture which supplies its own oxygen and burns at a very high temperature.[19]

a. Thermite incendiaries.[19] Thermite is essentially a mixture of about 73 per cent powdered ferric oxide (Fe_2O_3) and 27 per cent powdered or granular aluminum. The aluminum has a higher affinity for oxygen than iron has, and if a mixture of iron oxide and aluminum powder is raised to the combustion temperature of aluminum, an intense reaction occurs: $Fe_2O_3+2AL \rightarrow AL_2O_3+Fe$ + heat. Under favorable conditions, the thermite reaction produces temperatures of about 2,200°C (3,922°F). This is high enough to turn the newly formed metallic iron into a white hot liquid which acts as a heat reservoir to prolong and to spread the heat or igniting action.

b. Thermate incendiaries.[19] The thermate mixture composed of thermite with various additives is used as a component in igniter compositions for magnesium bombs and as a filler in incendiary hand grenades. There are several different types of thermate. The more recent ones contain barium nitrate as an oxidizer. The thermate core is ignited by the primer. This burning core then melts and ignites the magnesium alloy body. The incendiary action is localized, since there is little scattering action.

B. Defense Against Incendiaries (Fire Fighting)

Defense against incendiaries, as outlined in a U.S. Army publication[5] is summarized as follows: Incendiary bomb clusters may contain a percentage of high explosive incendiary bombs so precautions should include this possibility. A brick wall offers adequate protection against small explosive incendiary bombs. Incendiary bombs can be scooped up with shovels and thrown into a place where no damage will be done. Sandbags and sandmats can smother bombs and reduce effects of fragmentation. Loose sand helps to smother fires started by the bomb. Whether or not sandbags and sandmats are used, water or fire extinguishers are employed immediately. Water extinguishers should not be used directly on oil, because this tends to spread the fire, but water can be used against incendiaries such as phosphorus. Water confines the spread of the fire by wetting down the surrounding area, but despite some published advice to the contrary,[5] water should not be used on magnesium incendiaries, because of the resulting explosive effect. If hot enough, phosphorus particles ignite when exposed to oxygen in the air. Control them by keeping them covered, preferably with water.

III. White Phosphorus

White phosphorus is often classified as an incendiary, but is actually used primarily as a screening smoke or as an igniter for other munitions. At a sufficiently high temperature, it reacts with air and water vapor to produce a dense cloud of phosphorus pentoxide, a very effective screen. It has two disadvantages for this use. One is that because of its high heat of combustion, it tends to rise in a pillar-like mass, especially in still air. The other is that it is very brittle, and the exploding munitions in which it is used break it into very small particles that burn very rapidly. These disadvantages were somewhat overcome by the development of plasticized white phosphorus (PWP). PWP is produced by melting WP and stirring it into cold water, resulting in a slurry of WP granules about 0.5 mm in diameter. The slurry is then mixed with a very viscous solution of synthetic rubber, thus coating the granules with a film of rubber and separating them from each other. When PWP is dispersed by exploding munitions, it does not break into such small particles, the burning rate is slowed, and the tendency of the smoke to pillar is reduced. Despite the fact that the characteristics of WP and PWP somewhat limit their applications as screening smokes, their military uses include incendiary and anti-personnel effects, because burning particles of WP can start fires in many combustible materials and can produce burns.

IV. Medical Aspects

The one agent about which the most confusion seems to exist is white phosphorus. Its melting point is very low, 44°C (111°F). When it is placed in munitions it is in solid form, and when the munition detonates some will be liquified because of heat.

When white phosphorus is exposed to air, it burns if the temperature is over 34°C (93°F). Burning white phosphorus yields phosphorus pentoxide which combines with water to yield phosphoric acid.

In practice, white phosphorus particles are removed, and the burns treated as any burns. It is often stated or implied that white phosphorus burns are much "more severe" than other burns, but this depends on the method of quantitation and the form of the white phosphorus encountered. Particulate white phosphorus will indeed cause third-degree burns, but these may be scattered small burns. There are few other burns that are combined with explosive fragmentation wounds. Liquid white phosphorus is difficult to remove, penetrates clothing and indeed can cause severe burns. However, unignited particulate white phosphorus can easily be brushed off by the alert individual unless it is partly imbedded.

In 1945, Walker et al., studied the effects of ignited 25 mg. white phosphorus pellets.[29] These burned for about 22 seconds on both glass and the skin of an anesthetized pig. They found that when WP was burned on glass, 79 per cent of the phosphorus was found in the smoke, and when burned on skin, 66 per cent of the phosphorus was in the smoke. The residue on glass contained 9 per cent of the phosphorus as acid, while on the skin, 24 per cent was acid. On glass, about 33 per cent of this acid was orthophosphoric acid, whereas on skin, 93 per cent was orthophosphoric acid. These differences were attributed to available water. About 2.0 mg of the WP was converted to red phosphorus on glass, and about 1.8 mg on skin. An average of 2.7 mg of the phosphorus entered the skin as orthophosphoric acid.

Copper sulfate treatment of white phosphorus injuries and its complication: Traditionally, 5 per cent copper sulfate solution has been applied to white phosphorus injuries. This coats the white phosphorus particles so that they are easily identified and removed, and prevents contact with atmospheric oxygen, so that ignition is prevented. There have been several cases reported of hemolysis* in white-phosphorus-burn patients so treated.

*hemolysis = breakdown of red blood cells

V. Summary

Prompt defensive and corrective action makes a very great difference in the severity of injuries resulting from any of these agents.

References

5. _____, "Chemical, Biological, and Nuclear Defense." Dept. of the Army Field Man., FM 21-40, Hdq., Dept. of the Army, 1966.

6. _____, "Chemical Bombs and Clusters." Dept. of the Army Tech. Man., TM 3-400, Dept. of the Air Force Tech. Order TO 1162-1-1, Depts. of the Army and the Air Force, 1957.

19. _____, "Military Chemistry and Chemical Agents." Dept. of the Army Tech. Man., TM 3-215, Dept. of the Air Force Manual 355-7, Depts. of The Army and Air Force, 1963.

29. Walker, J., Wexler, J. and Hill, M. L. Medical Division Report No. 37. "Quantitative Analysis of Phosphorus-Containing Compounds Formed in WP Burns." Edgewood Arsenal, Md. 1945.

Nihonbashi District in Tokyo after attack of March 9, 1945, with AN-M69 incendiary bombs.

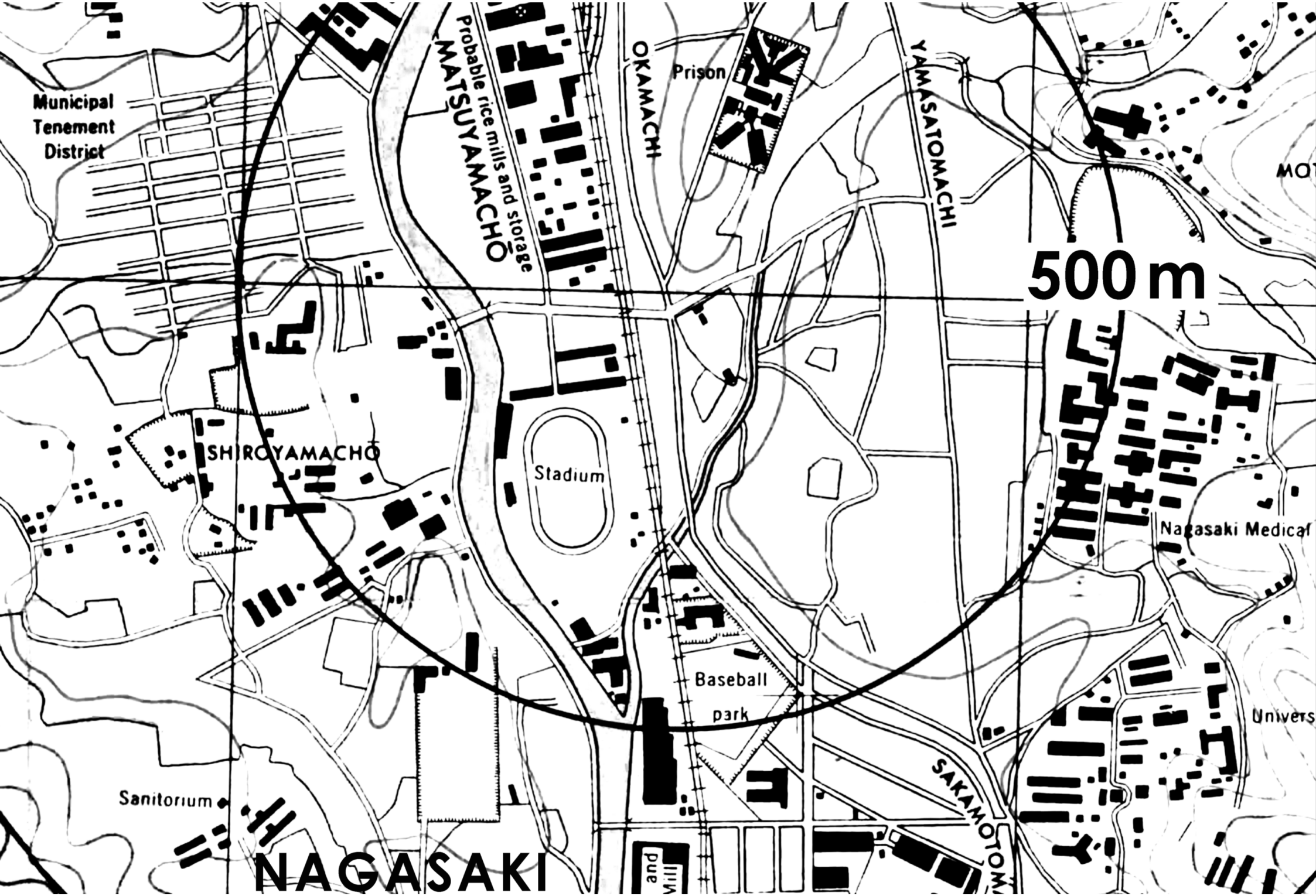
Municipal
Tenement
District
Probable rice mills and storage
MATSUYAMACHO
OKAMACHI
Prison
YAMASATOMACHI
500 m
SHIROYAMACHO
Stadium
Nagasaki Medical
Baseball
park
Univers
SAKAMOTOMA
Sanitorium
NAGASAKI

15
1
2000
12
1000
GROUND ZERO
17
16
20
18
22

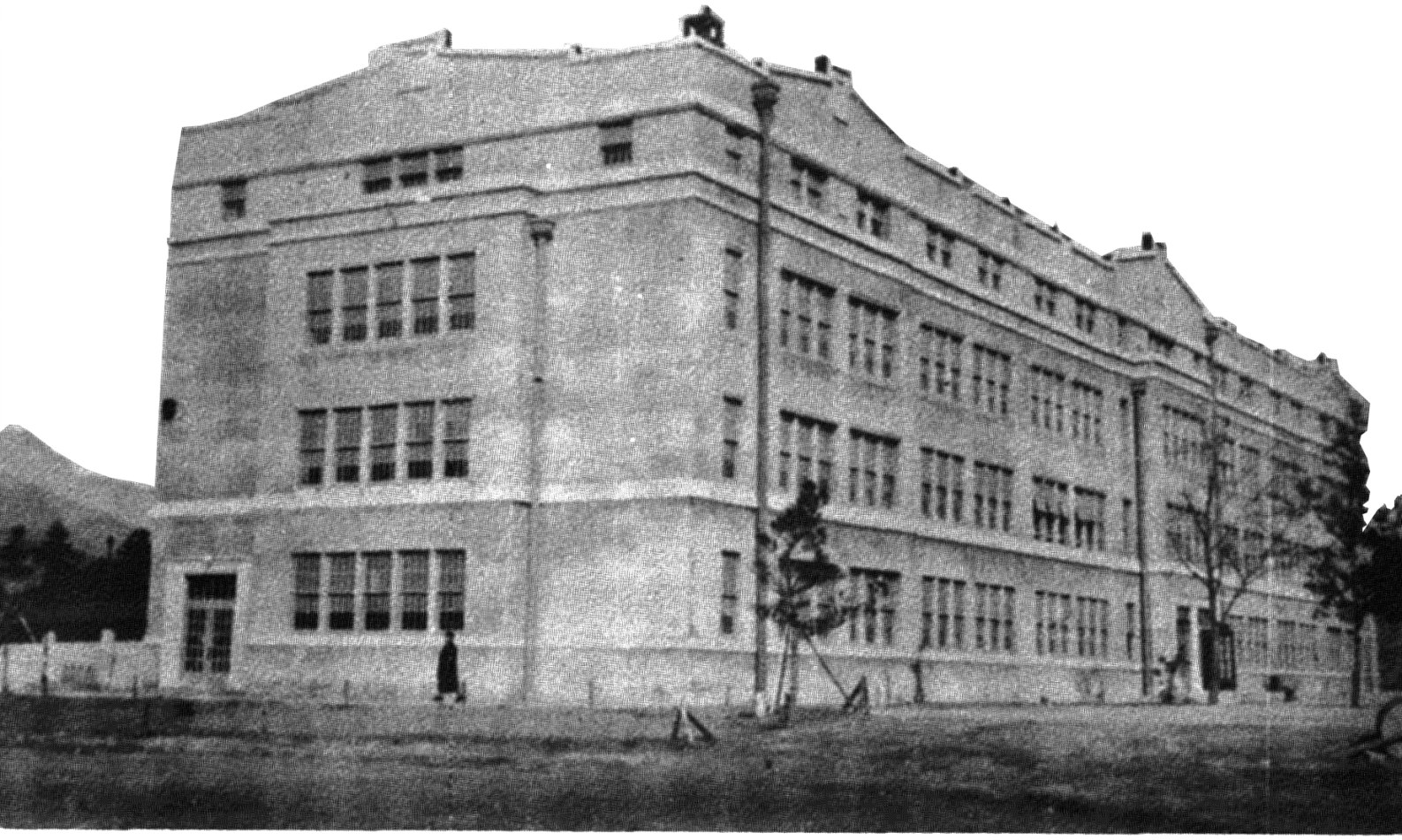

Chinzei Middle School before the explosion.

Chinzei Middle School after the explosion.
500 meters from the center.

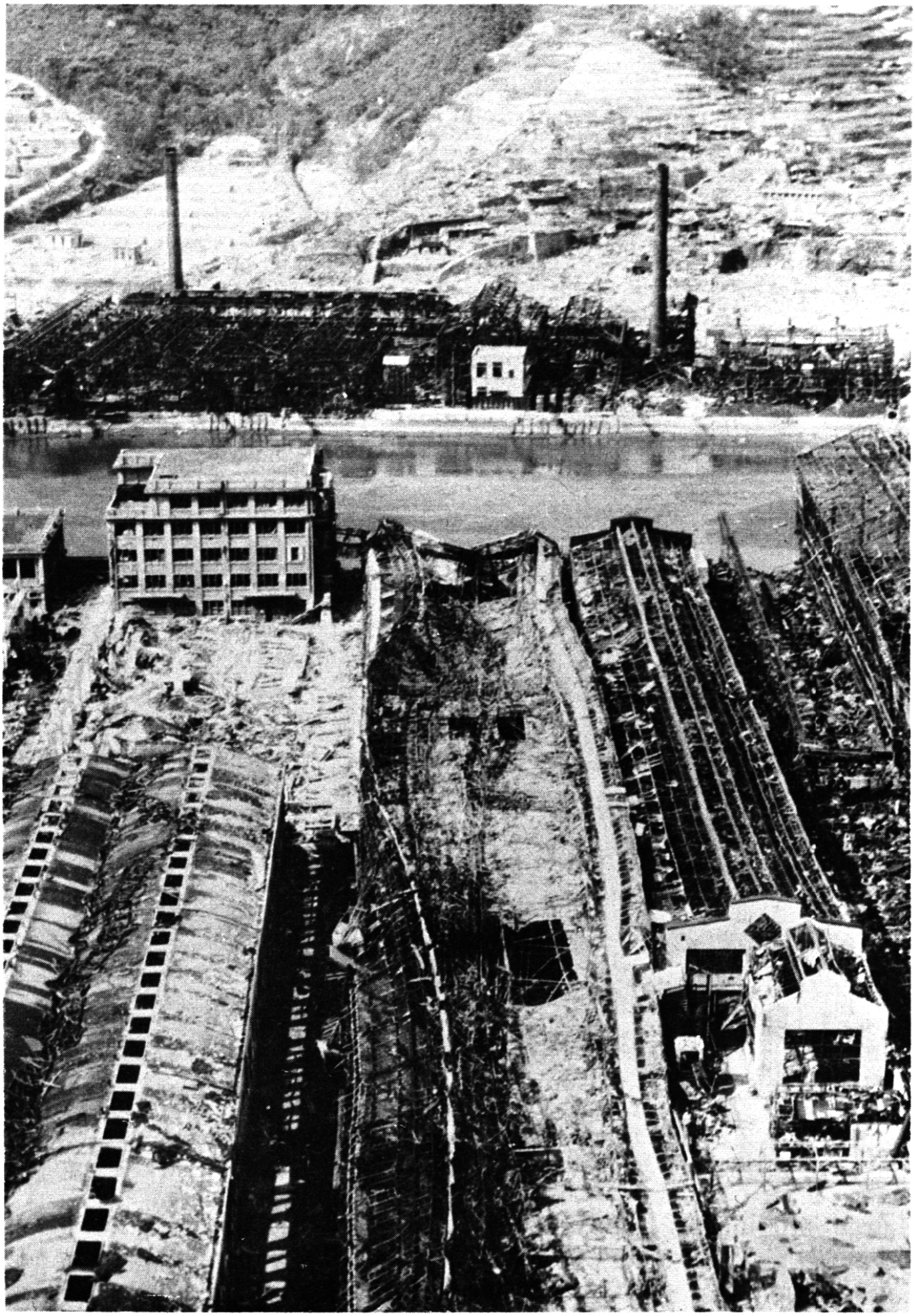

Figure 5.91. At left and back of center is a multistory, steel-frame building (0.85 mile from ground zero at Nagasaki).

Tunnel shelters in hillside, very close to ground zero in Nagasaki, protected the occupants from blast, thermal radiation, and immediate nuclear radiation.

1 2 cms The National Archives ins 1 2
Ref.: HO 225/116 C500594

3rd October, 1963.

~~RESTRICTED~~ 9/89 For Pub

HO 225/116

HOME OFFICE

SCIENTIFIC ADVISER'S BRANCH

CD/SA 116

RESEARCH ON BLAST EFFECTS IN TUNNELS

With Special Reference to the Use of London Tubes as Shelter

by F. H. Pavry

Summary and Conclusions

The use of the London tube railways as shelter from nuclear weapons raises many problems, and considerable discussion of some aspects has taken place from time to time. But - until the results of the research here described were available - no one was able to say with any certainty whether the tubes would provide relatively safe shelter or not.

The more recent research here described showed for the first time that a person sheltering in a tube would be exposed to a blast pressure only about $\frac{1}{3}$ as great as he would be exposed to if he was above ground. (In addition, of course, he would be fully protected from fallout in the tube.)

Large-Scale Field Test ($^1/40$) at Suffield, Alberta

The test is fully described in an A.W.R.E. report(6). The decision of the Canadian Defence Research Board to explode very large amounts of high explosive provided a medium for a variety of target-response trials that was welcome at a time when nuclear tests in Australia were suspended. A.W.R.E. used the 100-ton explosion in 1961 to test, among other items, the model length of the London tube, at $^1/40$th scale, that had already been tested at $^1/117$ scale.

Blast Entry from Stations

There was remarkable agreement with the $^1/117$th scale trials: "maximum overpressure in the train tunnels was of the order of $\frac{1}{3}$rd the corresponding peak shock overpressure in the incident blast. The pressures in the stations were about $^1/6$th those in the corresponding incident blast ..... ".

(6) $^1/40$th Scale Experiment to Assess the Effect of Nuclear Blast on the London Underground System. A.W.R.E. Report E2/62. (Official Use Only.)

100 ton TNT test on 1000 ft section of London Underground tube at Suffield, Alberta, 3 Aug 1961

Atomic Weapons Research Establishment, "1/40th Scale Experiment to Assess the Effect of Nuclear Blast on the London Underground System", Report AWRE-E2/62, 1962, Figure 30. (National Archives ES 3/57.)

200 FT FROM GROUND ZERO	400 FT FROM GROUND ZERO
100 PSI OUTSIDE	20 PSI OUTSIDE
30 PSI IN TUBES	7.2 PSI IN TUBES
15 PSI IN TUBE STATIONS	4.3 PSI IN TUBE STATIONS

Aldwych Underground tube station as Blitz shelter, 8 October 1940

THOSE WHO WENT TO SHELTERS began a new kind of night-life. Some took over the Tubes, camping out in this fashion—Elephant and Castle Station, 11th November, 1940.

ATTENUATION FACTORS FOR GAMMA RAYS FROM FISSION PRODUCTS AS A FUNCTION OF SHIELD THICKNESS FOR INDICATED MATERIALS*

	Shield thickness for indicated materials, in.					
Attenuation factor	Lead (710 lb/cu ft)	Iron and steel (490 lb/cu ft)	Concrete (144 lb/cu ft)	Earth (100 lb/cu ft)	Water (62.4 lb/cu ft)	Wood (Fir) (3.4 lb/cu ft)
2	0.28	0.7	2.5	3.5	4.8	9.2
4	0.64	1.8	6.6	8.9	13	25
10	1.0	2.7	9.7	13	19	36
50	1.6	4.2	14	20	29	55
100	1.9	4.8	16	23	33	62
1,000	2.7	6.8	22	32	45	88
10,000	3.5	8.8	27	39	56	110
100,000	4.3	11	32	46	70	140

*Data from *The Effects of Nuclear Weapons.*

TRINITY GROUND ZERO:
8000 R/hr at 1 hour
1.4 R/hr at
57 days
11 Sept. 1945

Shelter at ground zero, directly under 11 kt Fitzeau nuclear explosion (500 ft tower)

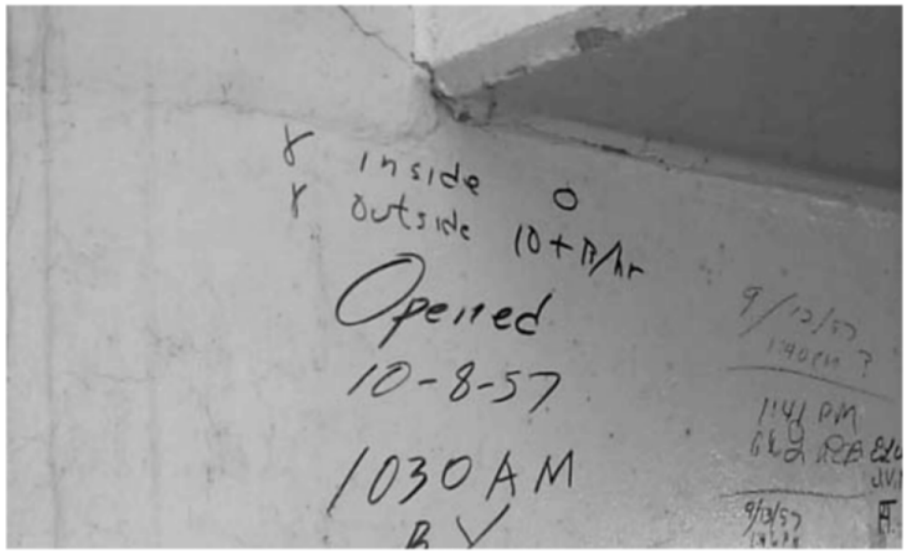

Test fired on 14 September 1957. Shelter was re-entered on 8 October 1957 when outdoor (ground zero) dose rate was down to about 10 R/hr. No fallout entered the concrete shelter, which was protected by a steel dome hatch (above left). Shelter had 5 feet of earth cover, and was depressed 2 feet into the ground by the shock wave. (W. G. Johnson, A Historical Evaluation of the T-3b Fizeau Bunker.)

SANDIA REPORT
SAND2009-3299
Unlimited Release
Printed May 2009

Analysis of Sheltering and Evacuation Strategies for an Urban Nuclear Detonation Scenario

Larry D. Brandt, Ann S. Yoshimura

Executive Summary

A nuclear detonation in an urban area can result in large downwind areas contaminated with radioactive fallout deposition. Early efforts by local responders must define the nature and extent of these areas, and advise the affected population on strategies that will minimize their exposure to radiation. These strategies will involve some combination of sheltering and evacuation actions. Options for shelter-evacuate plans have been analyzed for a 10 kt scenario in Los Angeles.

Results from the analyses documented in this report point to the following conclusions:

- When high quality shelter (protection factor ~10 or greater) is available, shelter-in-place for at least 24 hours is generally preferred over evacuation.
- Early shelter-in-place followed by informed evacuation (where the best evacuation route is employed) can dramatically reduce harmful radiation exposure in cases where high quality shelter is not immediately available.
- Evacuation is of life-saving benefit primarily in those hazardous fallout regions where shelter quality is low and external fallout dose rates are high. These conditions may apply to only small regions within the affected urban region.
- External transit from a low quality shelter to a much higher quality shelter can significantly reduce radiation dose received if the move is done soon after the detonation and if the transit times are short.

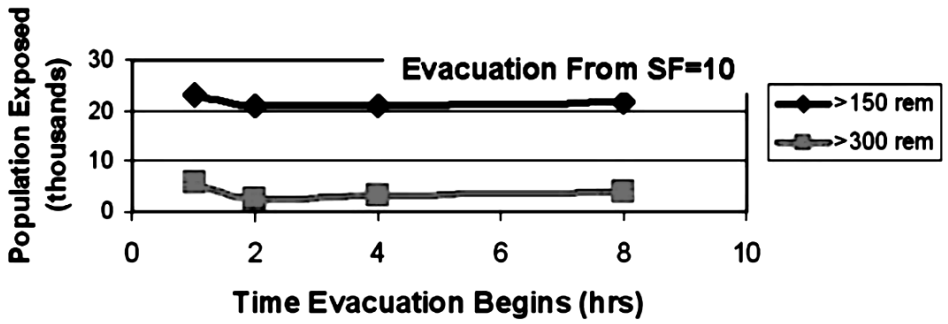

Figure 12. Departure time sensitivities for informed evacuations from shelters with SF=4

Sandia National Laboratories

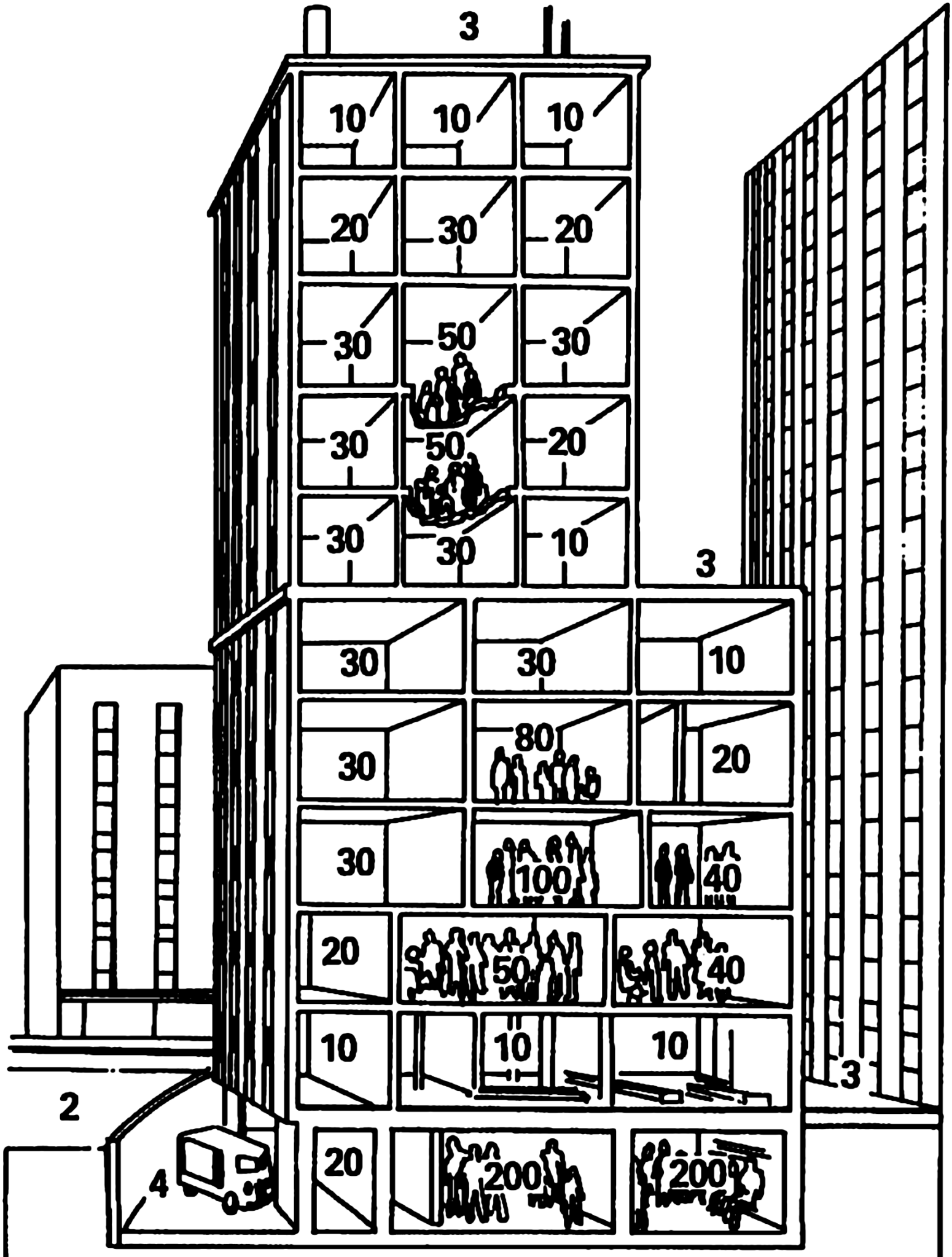

Radiation protection factors in modern city buildings
DCPA Attack Environment Manual, ch. 6, panel 18

RADIOACTIVE FALL-OUT HAZARDS FROM SURFACE BURSTS OF VERY HIGH YIELD NUCLEAR WEAPONS

by

D. C. Borg
L. D. Gates
T. A. Gibson, Jr.
R. W. Paine, Jr.

MAY 1954

HEADQUARTERS, ARMED FORCES SPECIAL WEAPONS PROJECT
WASHINGTON 13, D. C.

e. Passive defense measures, intelligently applied, can drastically reduce the lethally hazardous areas. A course of action involving the seeking of optimum shelter, followed by evacuation of the contaminated area after a week or ten days, appears to offer the best chance of survival. At the distant downwind areas, as much as 5 to 10 hours after detonation time may be available to take shelter before fall-out commences.

f. Universal use of a simply constructed deep underground shelter, a subway tunnel, or the sub-basement of a large building could eliminate the lethal hazard due to external radiation from fall-out completely, if followed by evacuation from the area when ambient radiation intensities have decayed to levels which will permit this to be done safely.

Table II

Total Isodose Contour: 500r from Fall-out to H+50 Hours

Yield (MT)	15	1	10	60
Downwind extent (mi)	180	52	152	340
Area (mi^2)	5400	470	3880	17,900

BIOLOGICAL AND ENVIRONMENTAL EFFECTS OF NUCLEAR WAR

HEARINGS

BEFORE THE

SPECIAL SUBCOMMITTEE ON RADIATION

OF THE

JOINT COMMITTEE ON ATOMIC ENERGY
CONGRESS OF THE UNITED STATES

EIGHTY-SIXTH CONGRESS

FIRST SESSION

ON

BIOLOGICAL AND ENVIRONMENTAL EFFECTS
OF NUCLEAR WAR

JUNE 22, 23, 24, 25, AND 26, 1959

PART 1

Printed for the use of the Joint Committee on Atomic Energy

UNITED STATES
GOVERNMENT PRINTING OFFICE
43338 WASHINGTON : 1959

RADIATION CHARACTERISTICS OF LAND SURFACE BURST FALLOUT

Average γ Energy	8 mi downwind	60 mi downwind
1 hr	--	1.0 mev
2 hr	--	0.95
1/2 day	--	0.60
1 day	--	0.40
1 week	0.25 mev	0.35
1 mo	0.45	0.65

RADIATION CHARACTERISTICS OF WATER SURFACE BURST FALLOUT

Average γ Energy	7 mi downwind	22 mi downwind
1 hr		1.0 mev
2 hr		0.95
1/2 day		0.60
1 day		0.40
1 week		0.35
1 mo		0.65

MYRON HAWKINS:

the induced radiation in uranium 238. We can refer to a British report which indicates that around 60 percent of the total activity at 4 days—activity in this case is the number of disintegrations—is due to the uranium 239 and neptunium 239 that are produced, as the British say, in either large or small weapons. I believe part of the hump on the curves in the early times, say around 4 days, is largely due to this.

Dr. TRIFFET. Yes. I thought this might be an appropriate place to comment on the variation of the average energy. It is clear when you think of shielding, because the effectiveness of shielding depends directly on the average energy radiation from the deposited material. As I mentioned, Dr. Cook at our laboratory has done quite a bit of work on this. What it amounts to is that at one hour the average energy is about one Mev. This appears, by the way, in the tables that are in my written statement but that I did not present orally.

Representative HOLIFIELD. Mev. means?

Dr. TRIFFET. Million electron volts. At 2 hours it drops to 0.95. At a half day, to 0.6. At 1 week it drops to 0.35. Then it begins to go up again. At 1 month, it is 0.65, 2 months 0.65. The meaning of this is simply that there is a period around 1 week when if induced products are important in the bomb, there are a lot of radiations emanating from these, but the energy is low so it operates to reduce the average energy in this period and shielding is immensely more effective.

Strontium 90, for example, has 33-second krypton as its birth predecessor; cesium 137 derives from a fission chain headed up by 22-second iodine, followed by 3.9-minute xenon. Because of their volatile or gaseous ancestry in the fireball or bomb cloud a number of the high-yield fission products are formed in finely divided particles. Some of these are so small that they are not subject to gravitational settling, and in fact they remain suspended in the earth's atmosphere for many years, providing[6] that they reach the stratosphere at the proper latitude. In any event such fission products would be depleted in the local fallout.

For example, the irradiation of uranium^{238} with low Mev. neutrons forms neptunium 239, a 2.3-day radioelement which W. J. Heiman[7] estimates might constitute 50 percent of the residual activity a few days after a bomb detonation.

At higher neutron energies, such as certain types of thermonuclear weapons produce, natural uranium undergoes an (n,2n) reaction which competes with fast fission in U^{238}. The data of R. J. Howerton[8] show that U^{238} has a fission cross section of 0.6 barn from 2 to 6 Mev., thereafter climbing to a plateau value of 1 barn for neutrons up to 14 Mev. At 6.6 Mev. there is a threshold for the (n,2n) reaction and the reaction has a cross section of 1.4 barns in the range of 10 Mev. The ready identification of U^{237} in fallout points to fast fission of U^{238} as a main energy source in high-yield megaton-class weapons.

[6] See E. A. Martell, "Atmospheric Circulation and Deposition of Strontium 90 Debris," Air Force Cambridge Research Center paper (July 1958). See also W. F. Libby, "Radioactive Fallout," speech of Mar. 13, 1959.

[7] Variation of Gamma Radiation Rates for Different Elements Following an Underwater Nuclear Detonation," J. Colloid. Science, 13 (1958), p. 329.

[8] "Reaction Cross Sections of U^{238} in the Low Mev. Range," UCRL 5323 (Aug. 15, 1958).

A. E. R. E. HP/R 2017

ATOMIC ENERGY RESEARCH ESTABLISHMENT

THE RADIOLOGICAL DOSE TO PERSONS IN THE U. K. DUE TO DEBRIS FROM NUCLEAR TEST EXPLOSIONS PRIOR TO JANUARY 1956

By N. G. Stewart, R. N. Crooks, and Miss E. M. R. Fisher

Activity from Neutron Capture

Although several different radioactive elements may be created by the capture of neutrons in materials close to the reacting core of a weapon, the only significant reactions to produce gamma-ray emitters are those associated with the natural uranium which may be used as the tamper material of the bomb.

$$\text{neutron (low energy)} + \text{U-238} \longrightarrow \text{U-239} \longrightarrow \text{Np-239}$$

Chemical analysis of the debris shows that in general about one neutron is captured in this way for every fission that occurs, both in nominal bombs and in thermonuclear explosions. The U^{239} decays completely before reaching the U.K. but at four days after time of burst the Np^{239} disintegration rate reaches a peak relative to that of the fission products and accounts for about 60% of the observed activity at that time.

In addition to this, a smaller number of the neutrons in a thermonuclear explosion undergo an (n,2n) reaction with U^{238} to form 6.7 day U^{237} which is also a (β, γ) emitter.

$$\text{neutron (high energy)} + \text{U-238} \longrightarrow 2 \text{ neutrons} + \text{U-237}$$

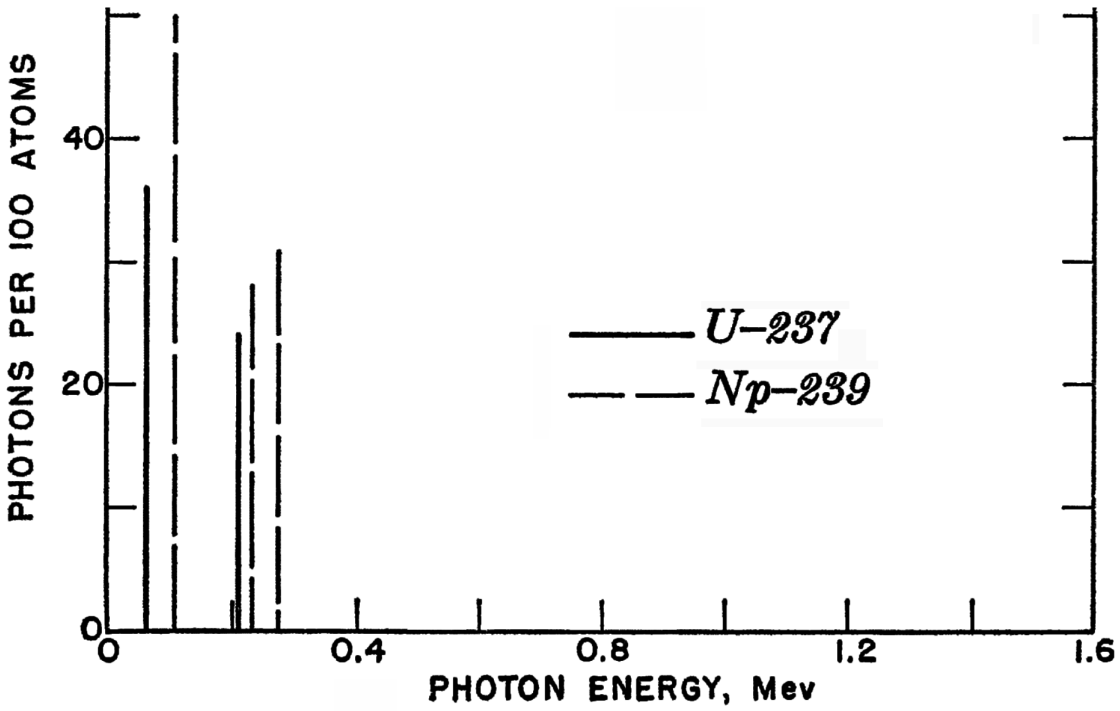

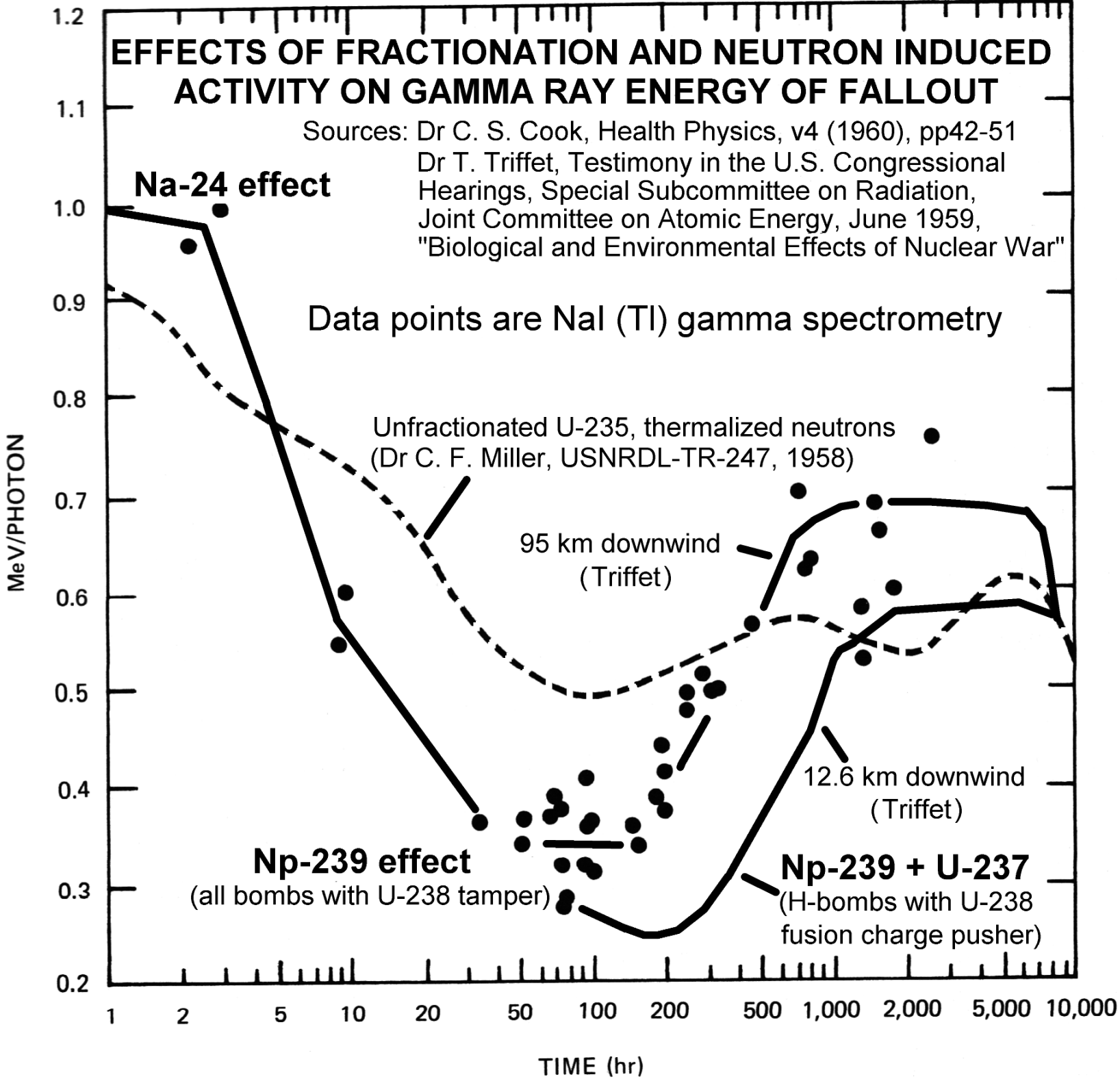
EFFECTS OF FRACTIONATION AND NEUTRON INDUCED ACTIVITY ON GAMMA RAY ENERGY OF FALLOUT
Sources: Dr C. S. Cook, Health Physics, v4 (1960), pp42-51
Dr T. Triffet, Testimony in the U.S. Congressional Hearings, Special Subcommittee on Radiation, Joint Committee on Atomic Energy, June 1959, "Biological and Environmental Effects of Nuclear War"
Na-24 effect
Data points are NaI (Tl) gamma spectrometry
Unfractionated U-235, thermalized neutrons (Dr C. F. Miller, USNRDL-TR-247, 1958)
95 km downwind (Triffet)
12.6 km downwind (Triffet)
Np-239 effect
(all bombs with U-238 tamper)
Np-239 + U-237
(H-bombs with U-238 fusion charge pusher)
MeV/PHOTON
1.2
1.1
1.0
0.9
0.8
0.7
0.6
0.5
0.4
0.3
0.2
1
2
5
10
20
50
100
200
500
1,000
2,000
5,000
10,000
TIME (hr)

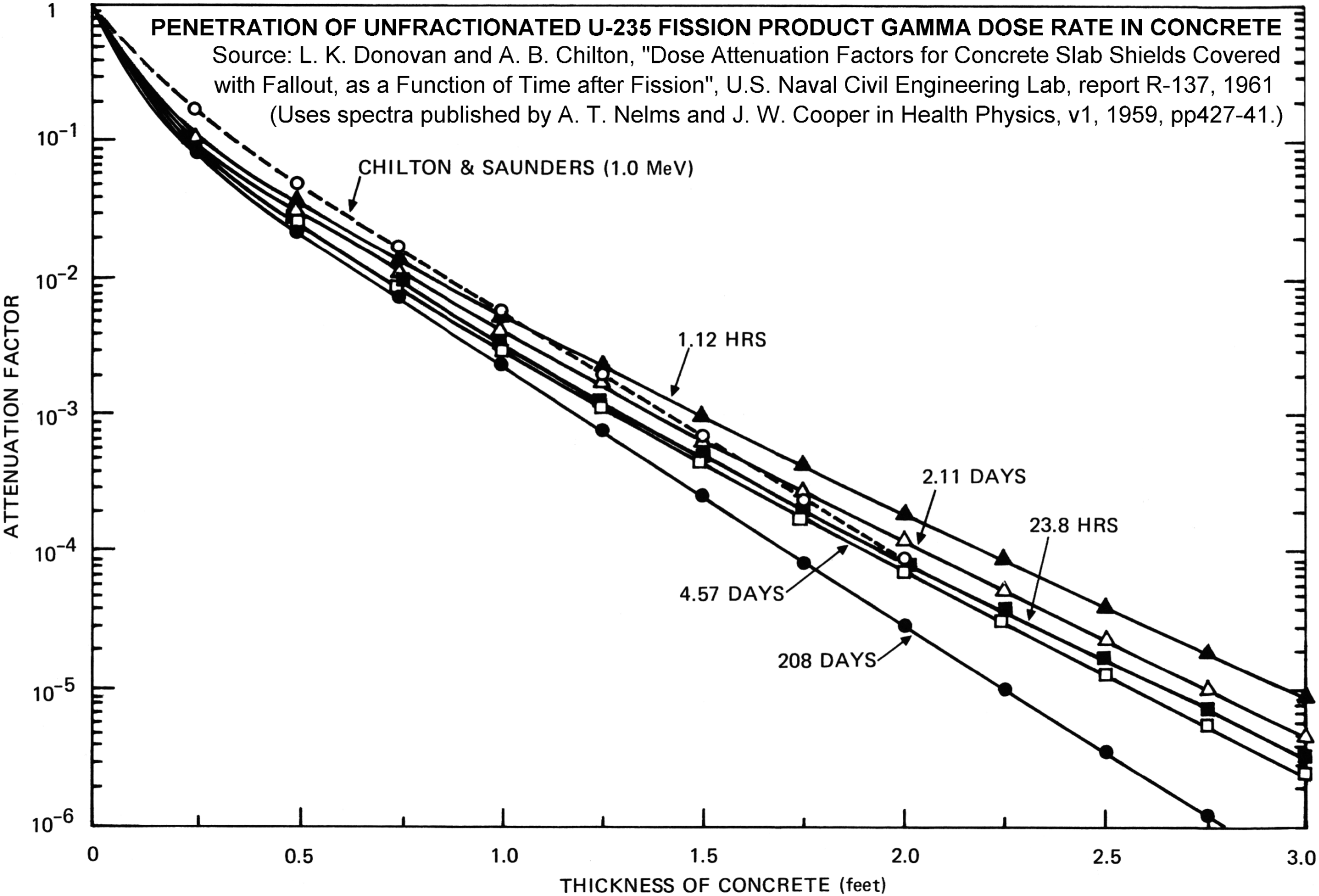
PENETRATION OF UNFRACTIONATED U-235 FISSION PRODUCT GAMMA DOSE RATE IN CONCRETE
Source: L. K. Donovan and A. B. Chilton, "Dose Attenuation Factors for Concrete Slab Shields Covered with Fallout, as a Function of Time after Fission", U.S. Naval Civil Engineering Lab, report R-137, 1961
(Uses spectra published by A. T. Nelms and J. W. Cooper in Health Physics, v1, 1959, pp427-41.)
CHILTON & SAUNDERS (1.0 MeV)
1.12 HRS
2.11 DAYS
23.8 HRS
4.57 DAYS
208 DAYS
ATTENUATION FACTOR
1
10^{-1}
10^{-2}
10^{-3}
10^{-4}
10^{-5}
10^{-6}
0
0.5
1.0
1.5
2.0
2.5
3.0
THICKNESS OF CONCRETE (feet)

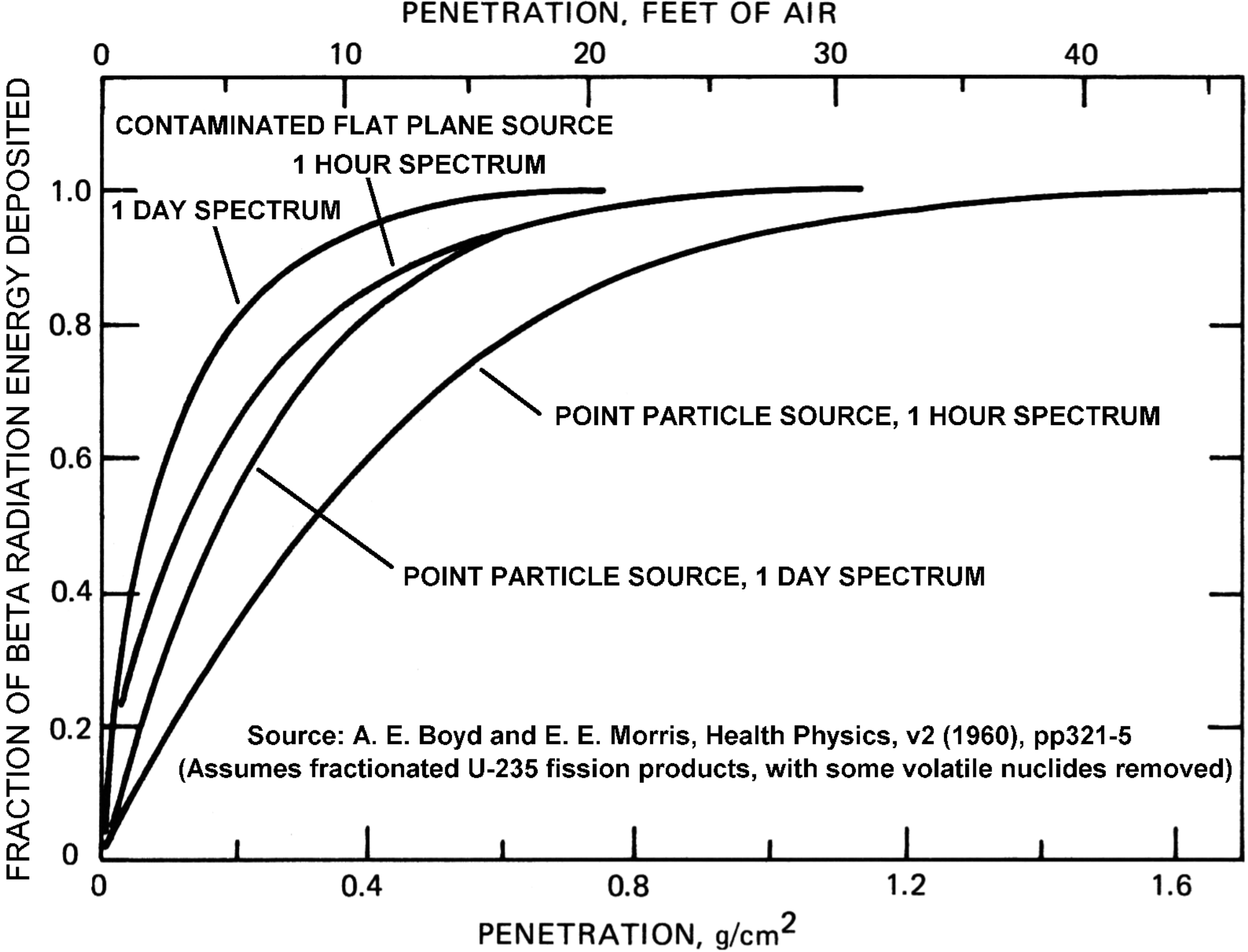
PENETRATION, FEET OF AIR
0
10
20
30
40
CONTAMINATED FLAT PLANE SOURCE
1 HOUR SPECTRUM
1 DAY SPECTRUM
POINT PARTICLE SOURCE, 1 HOUR SPECTRUM
POINT PARTICLE SOURCE, 1 DAY SPECTRUM
Source: A. E. Boyd and E. E. Morris, Health Physics, v2 (1960), pp321-5
(Assumes fractionated U-235 fission products, with some volatile nuclides removed)
FRACTION OF BETA RADIATION ENERGY DEPOSITED
1.0
0.8
0.6
0.4
0.2
0
0
0.4
0.8
1.2
1.6
PENETRATION, g/cm2

F. Titus, Penetration in concrete of gamma radiation from fallout, NBS Report 6143, (Sept. 4, 1958), AEC Report ITR-1477 (Oct. 22, 1957).

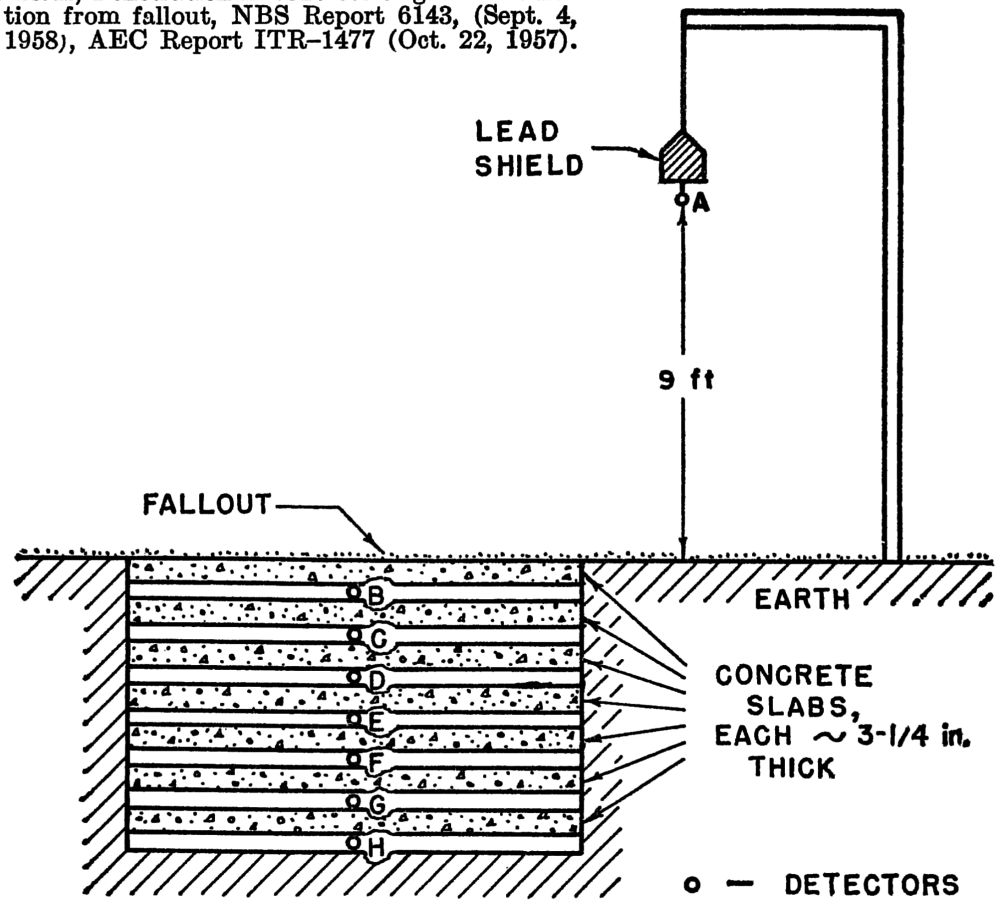

The lead shield prevents fallout material from settling directly on detector "A," while at the same time shielding against the intercepted material

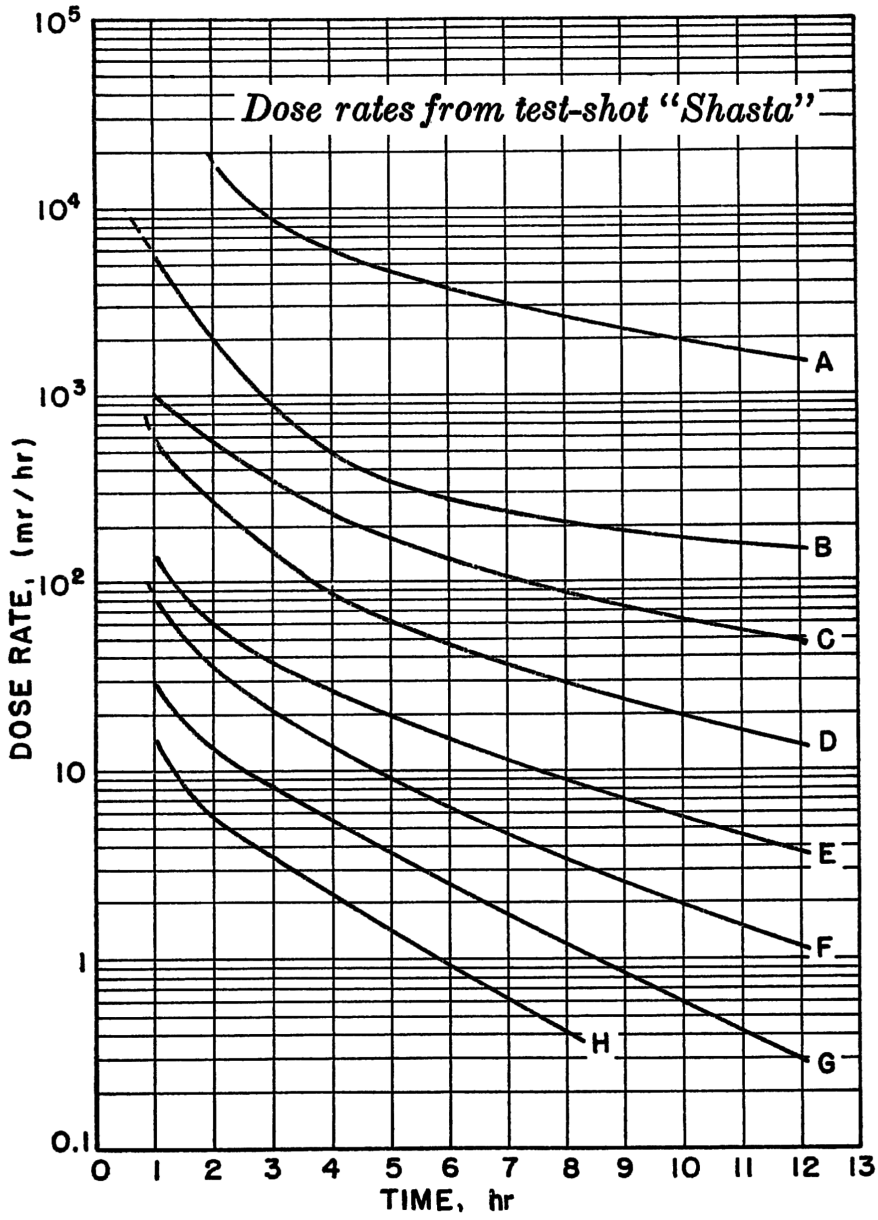

MEAN FALLOUT GAMMA ENERGY FOR LAND BURSTS ZUNI AND TEWA AND AIR BURST CHEROKEE
Terry Triffet and Philip D. LaRiviere, *Characterization of Fallout,* WT 1317 (1961), Table B.21

Test	Mt	Fission	Sample	2 days	3 days	4 days	7 days	10 days	14 days
Aircraft-collected unfractionated cloud samples (no depletion of volatile fission products):									
*Navajo**	4.50	5%	Cloud	0.57	0.48	0.45	0.44	0.53	0.60
Zuni	3.53	15%	Cloud	0.48	0.41	0.42	0.43	0.49	
Tewa	5.01	87%	Cloud		0.40	0.38	0.37	0.46	0.49
*Flathead**	0.365	73%	Cloud			0.34			0.54
Cherokee	3.75	50%	Cloud	0.29	0.30	0.31	0.34	0.42	0.49
*Sea water burst fallout is similar to cloud sample (100 °C droplet condensation prevents fractionation).									
Deposited fractionated land surface burst close-in fallout samples (depletion of volatile fission products):									
Tewa	5.01	87%	YFNB13E56					0.27	0.30
Zuni	3.53	15%	How F-61					0.21	

- Laboratory instrument measurements (ignores degradation due to air scatter of gamma rays). The "clean bombs" *Navajo* and *Zuni* cloud samples include high-energy gamma from sodium-24 (15 hours half life) due to neutron capture by sea salt (NaCl). Low-energy gammas, from Np-239 and U-237 due to neutron capture in U-238, contribute a high proportion of fallout radiation at 4-14 days. Fractionation depletes volatile chains, not Np-239 and U-237, so the mean energy is reduced further.

Spectrum of fission product gamma rays from the thermonuclear neutron fission of U-238 as a function of the degree of fractionation for two different times after detonation (Glenn R. Crocker, *Radiation Properties of Fractionated Fallout; Predictions of Activities, Exposure Rates and Gamma Spectra for Selected Situations,* U.S. Naval Radiological Defense Laboratory, USNRDL-TR-68-134, 27 June 1968, 287 pp.)

Gamma ray energy, MeV	Gamma ray spectrum at 1 hour after burst				Gamma ray spectrum at 1 week after burst			
	Sr-89 abundance (relative to unfractionated fallout)				Sr-89 abundance (relative to unfractionated fallout)			
	10% $R_{89,95} = 0.1$	50% $R_{89,95} = 0.5$	100% $R_{89,95} = 1$*	200% $R_{89,95} = 2$	10% $R_{89,95} = 0.1$	50% $R_{89,95} = 0.5$	100% $R_{89,95} = 1$*	200% $R_{89,95} = 2$
0-0.5	0.396	0.354	0.350	0.304	0.695	0.662	0.678	0.637
0.5-1	0.385	0.379	0.363	0.357	0.262	0.270	0.245	0.265
1-1.5	0.1605	0.1863	0.1914	0.232	0.01339	0.01358	0.01218	0.01273
1.5-2	0.0327	0.0466	0.0558	0.0596	0.0287	0.0519	0.0591	0.0790
2-2.5	0.01628	0.0203	0.0279	0.0290	0.001114	0.001313	0.001268	0.001445
2.5-3	0.00429	0.00717	0.01192	0.01305	0.001372	0.00253	0.00291	0.00388
3-3.5	0.00340	0.00301	0.00267	0.00273	0.0000260	0.0000490	0.0000564	0.0000760
3.5-4	0.001425	0.001187	0.001705	0.00214	0	0	0	0
Total:	1.00	1.00	1.00	1.00	1.00	1.00	1.00	1.00
Relative gamma activity	0.547	0.756	1*	1.25	0.563	0.768	1*	1.12
Mean energy, MeV	0.710	0.767	0.807	0.856	0.444	0.486	0.483	0.526

*Unfractionated ($R_{89,95} = 1$) fission product composition relative gamma activity is normalized to 1 unit/second. The presence of neutron induced activities in U-238 like Np-239, U-240, and U-237 due to non-fission capture is not included, and would further soften the fractionated fallout spectra, since they emit low energy gamma rays.

Measured capture to fission ratios in nuclear tests*

Test shot	*Weapon design*	*Yield*	*Fission %*	*Number of neutron capture atoms per fission*		
				U-239 & Np-239	*U-237*	*U-240 & Np-240*
Jangle-Sugar	U238 reflector	1.2 kt	100	0.59		
Jangle-Uncle	U238 reflector	1.2 kt	100	0.59		
Castle-Bravo	U238 pusher	14.8 Mt	68	0.56	0.10	0.14
Castle-Romeo	U238 pusher	11 Mt	64	0.66	0.10	0.23
Castle-Koon	U238 pusher	110 kt	91	0.72	0.10	
Castle-Union	U238 pusher	6.9 Mt	72	0.44	0.20	0.07
Redwing-Zuni		3.53 Mt	15	0.31	0.20	0.005
Redwing-Tewa		5.01 Mt	87	0.36	0.20	0.09
Diablo	U238 in core**	18 kt	100	0.10		
Shasta	U238 in core**	16 kt	100	0.10		
Coulomb C	U238 in core**	0.6 kt	100	0.03		

* Data is derived from all analyses of aircraft cloud fallout samples and deposited fallout samples in Dr Carl F. Miller, U.S. Naval Radiological Defense Laboratory, report USNRDL-466 (1961), Table 6.
**In these Plumbbob weapon tests, there was no U238 reflector and the only U238 in the bomb was that contained in the fissile core as an impurity.

Measured relationship between the fusion yield of the nuclear explosive and the quantity of neutron-induced activities in the fallout*

Test		*Redwing-Navajo*	*Redwing-Zuni*	*Redwing-Tewa*	
Design		Lead pusher	Lead pusher	U-238 pusher	
Total yield		4.5 Mt	3.53 Mt	5.01 Mt	
% Fission		5	15	87	
% Fusion		95	85	13	
Nuclide	*Half life*	*Abundance of nuclide in bomb fallout, atoms per bomb fission*			*R1***
Na-24	15 hours	0.0314	0.0109	0.00284	1284.7
Cr-51	27.2 days	0.0120	0.0017	0.00030	0.280
Mn-54	304 days	0.10	0.011	0.00053	0.614
Mn-56	2.58 hours	0.094		0.00053	2668
Fe-59	45.2 days	0.0033	0.00041	0.00017	6.19
Co-57	272 days	0.00224	0.0031	0.00018	0.113
Co-58	71 days	0.00193	0.0036	0.00029	3.11
Co-60	5.27 years	0.0087	0.00264	0.00081	0.299
Cu-64	12.8 hours	0.0278	0.0090	0.0023	89.5
Sb-122	2.75 days		0.219***		38.4
Sb-124	60 days		0.073***		6.92
Ta-180	8.15 hours	0.038	0.0411		35.9
Ta-182	114 days	0.038	0.0326	0.01	2.67
Pb-203	52 hours	0.0993	0.050	0.000018	26.0
U-237	6.75 days		0.20	0.20	6.50
U-239	23.5 minutes	0.085	0.31	0.36	173
Np-239	56.4 hours	0.085	0.31	0.36	14.9*+*
U-240	14.1 hours		0.005	0.09	0 (no gamma rays)
Np-240	7.3 minutes		0.005	0.09	150

*Dr Terry Triffet and Philip D. LaRiviere, "Characterization of Fallout, Operation Redwing, Project 2.63," U.S. Naval Radiological Defense Laboratory, 1961, report WT-1317, Table B.22. Data on U-238 capture nuclides is from USNRDL-466, Table 6, in combination with WT-1315, Table 4.1.
**Triffet's 1961 values for the gamma dose rate at 1 hour after burst at 3 ft above an infinite, smooth, uniformly contaminated plane, using an ideal measuring instrument with no shielding from the person holding the instrument, from 1 atom/fission of induced activity, (R/hr)/(fission kt/square stat mile).
***The Zuni bomb contained a lot of antimony (Sb), which melts at 903.7K and boils at 1650K. The abundances of Sb-122 and Sb-124 given in the table are for unfractionated cloud samples; because of the low boiling point of antimony, it was fractionated in close-in fallout, so the abundances of both Sb-122 and Sb-124 in the Zuni fallout at Bikini Lagoon were 8.7 times lower than the unfractionated cloud fallout.
*+*Note that Np-239 at 1 hour after burst is still forming as the decay product of U-239.

Zuni* fallout gamma ray spectrum measured at 10 days after detonation, 13 miles downwind (sample How F-61 GA)

Gamma ray energy (MeV)	% of gamma rays emitted by fallout sample
0.060	15.5
0.105	38.8
0.220	19.4
0.280	9.3
0.330	3.8
0.500	3.9
0.650	3.1
0.750	6.2
Mean energy	**0.218 MeV**

*W. E. Thompson, *Spectrometric Analysis of Gamma Radiation from Fallout from Operation Redwing,* U. S. Naval Radiological Defense Laboratory technical report USNRDL-TR-146, 29 April 1957, Tables 1 and 2. Note that this is the gamma ray spectrum actually measured for a fallout sample placed near the scintillation crystal of a gamma ray spectrometer, so it does not include the further reduction in gamma ray energy that occurs from Compton scattering in the atmosphere.

Krypton-89, krypton-90, and xenon-140, which are present during the formation of the fireball and are precursors for strontium-89, strontium-90, and barium-140, have very little tendency to be incorporated uniformly in the particles during the early stage of formation. These noble gases, when associated with a particle, are deposited unevenly on the surface layers and distributed along with relatively large deposits of inactive debris which were drawn toward the fireball too late to form fused radioactive particles.

14

Both strontium-89 and strontium-90 are examples of radioisotopes having gaseous precursors and are thus subject to a high degree of fractionation.

$$\text{Krypton-89} \xrightarrow[2.6\ \text{min}]{\beta^-} \text{Rubidium-89} \xrightarrow[15\ \text{min}]{\beta^-} \text{Strontium-89}$$

$$\text{Krypton-90} \xrightarrow[33\ \text{sec}]{\beta^-} \text{Rubidium-90} \xrightarrow[\text{V.Short}]{\beta^-} \text{Strontium-90}$$

31

As expected from the earlier discussion, strontium exhibits very definite fractionation. On one series of air samples collected at 40,000 feet at Operation CASTLE after the Bravo shot, the R value for strontium-89 was 0.35. For a fall-out sample collected on land at approximately 80 miles from the burst point, the R value for strontium-89 was 0.14. The R value for strontium-90 using the same fall-out sample was 0.29.

Radioactivity in the Marine Environment (1971), page 13.

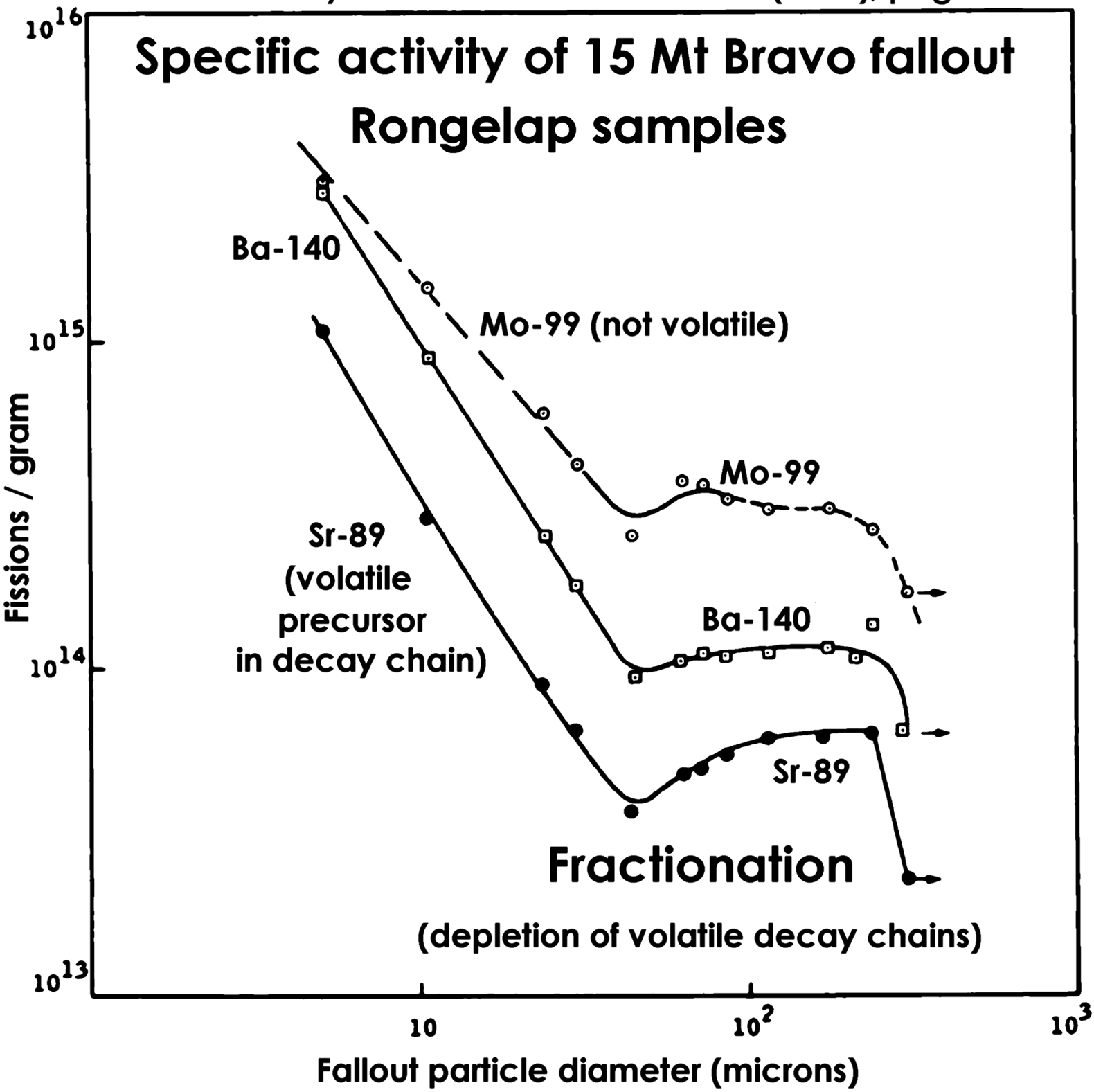

Coral Island Surface Explosion (Equivalent fissions $\times 10^{-14}$ per gram)

Morgenthau *et al.* (1960). **Weapon Test report WT-1319, "Operation Redwing: Land Fallout Studies"**

REDWING-LACROSSE Normalized to 100% fission yield

0.04 Mt Shot Atoll

Platform on reef off Runit Island, Enewetak

$D_g(\mu)$	Chain 99 (^{99}Mo)	Chain 89 (^{89}Sr)	Chain 140 (^{140}Ba)
57	2.5	0.063	0.25
88	4.0	0.074	0.28
125	4.7	0.082	0.30
177	5.7	0.062	0.23
297	4.5	0.044	0.18
594	1.6	0.063	0.24

UNCLASSIFIED

AD232901

Copy No.

RADIOCHEMICAL ANALYSIS OF INDIVIDUAL FALLOUT PARTICLES

Research and Development Technical Report USNRDL-TR-386

17 September 1958

by

J. L. Mackin
P. E. Zigman
D. L. Love
D. MacDonald
D. Sam

U.S. NAVAL RADIOLOGICAL DEFENSE LABORATORY

SAN FRANCISCO 24 · CALIFORNIA

UNCLASSIFIED

TABLE 2 (ZUNI, barge YFNB-29; see Table B8 in WT-1317)

Weight, Activity, and Fission Values for the Sized Fractions From the WHIM Sample (YFNB29, 17 km from ZUNI)

Size Range (μ)	Weight Grams	Weight Percent of Total	Fissions Percent of Total	Fissions Total (10^{14})	Fissions Per Gram (10^{14})
>1000	37.70	41.8	15.8	21.	0.56
500-1000	41.91	46.4	46.0	60.	1.4
250- 500	4.97	5.5	19.8	26.	5.2
100- 250	3.51	3.9	10.7	14.	4.0
50- 100	0.80	0.9	2.3	3.0	3.8
<50	1.38	1.5	5.4	7.1	5.1
Total	90.27			131.	1.5

TABLE 4 (ZUNI: BIKINI/HOW ISLAND, YFNB29, YAG40; TABLE 3.9 IN WT-1317)

Mean Values for Several Quantities, for Altered and Unaltered Particles

Quantity	Melted coral sand Altered: No. of Samples	Altered: Value	Unmelted coral sand Unaltered: No. of Samples	Unaltered: Value
fiss/gm($\times 10^{14}$)	6	3.8 ± 3.1	9	0.090 ± 0.12
Ba^{140}-R value	5	0.090 ± 0.068	8	2.1 ± 1.2
Sr^{89}-R value	7	0.018 ± 0.010	10	0.65 ± 0.17

The data of Table 4 show that the value of fissions/gram was much larger in the altered particles than in the unaltered particles. The R value data indicates that the altered particles were markedly depleted in Ba^{140}-La^{140}, whereas the unaltered particles were enriched in Ba^{140}-La^{140}

R values

With respect to fractionation of radionuclides it has long been accepted that the mass 89 and mass 140 chains which exist for long time periods as noble gases, halogens and alkali metals* would condense late and therefore disproportionate with respect to less volatile elements. On the basis of long-lived gaseous precursors it would be predicted that the altered or melted particles would exhibit low R values for both chains, with the 89 smaller of the two. This was verified by the mean R values given in Table 4, which were 0.090 and 0.018 for the 140 and 89 chains, respectively. The corresponding values for the unaltered particles of 2.1 and 0.65 indicate that this latter class of particles may be important as a scavenger of these nuclides.

It is also of interest to compare R values obtained in this study with values obtained on gross fallout samples. The latter data gave Ba^{140} R values and Sr^{89} R values of 0.10 and 0.04 respectively** in the lagoon samples. The low R values for the gross sample from the lagoon area are similar to R values obtained with altered particles and suggests a lagoon fallout composed primarily of altered particles. This suggestion is supported by the WHIM sample fission/gram data (described above).

* Ba^{140} is formed by the decay of the radioelements Xe^{140} (16-sec half-life) and Cs^{140} (66-sec half-life); Sr^{89} is formed by the decay of the radioelements Kr^{89} (3.16-min half-life) and Rb^{89} (15.4-min half-life).

** P.D. LaRiviere, USERDL, personal communication.

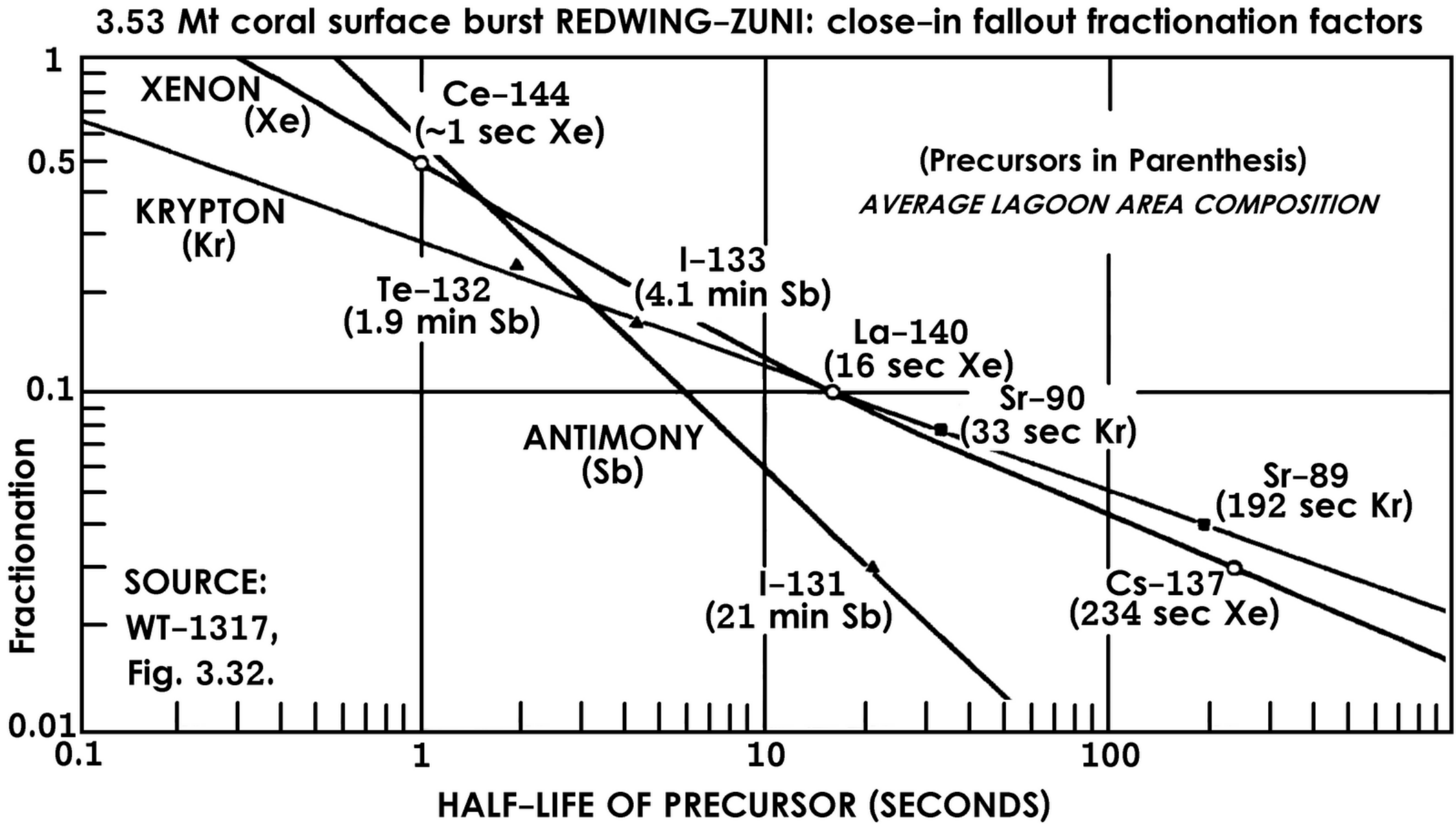
3.53 Mt coral surface burst REDWING–ZUNI: close–in fallout fractionation factors
XENON
(Xe)
KRYPTON
(Kr)
ANTIMONY
(Sb)
Ce–144
(~1 sec Xe)
Te–132
(1.9 min Sb)
I–133
(4.1 min Sb)
La–140
(16 sec Xe)
Sr–90
(33 sec Kr)
Sr–89
(192 sec Kr)
I–131
(21 min Sb)
Cs–137
(234 sec Xe)
(Precursors in Parenthesis)
AVERAGE LAGOON AREA COMPOSITION
SOURCE:
WT–1317,
Fig. 3.32.
Fractionation
1
0.5
0.1
0.01
0.1
1
10
100
HALF–LIFE OF PRECURSOR (SECONDS)

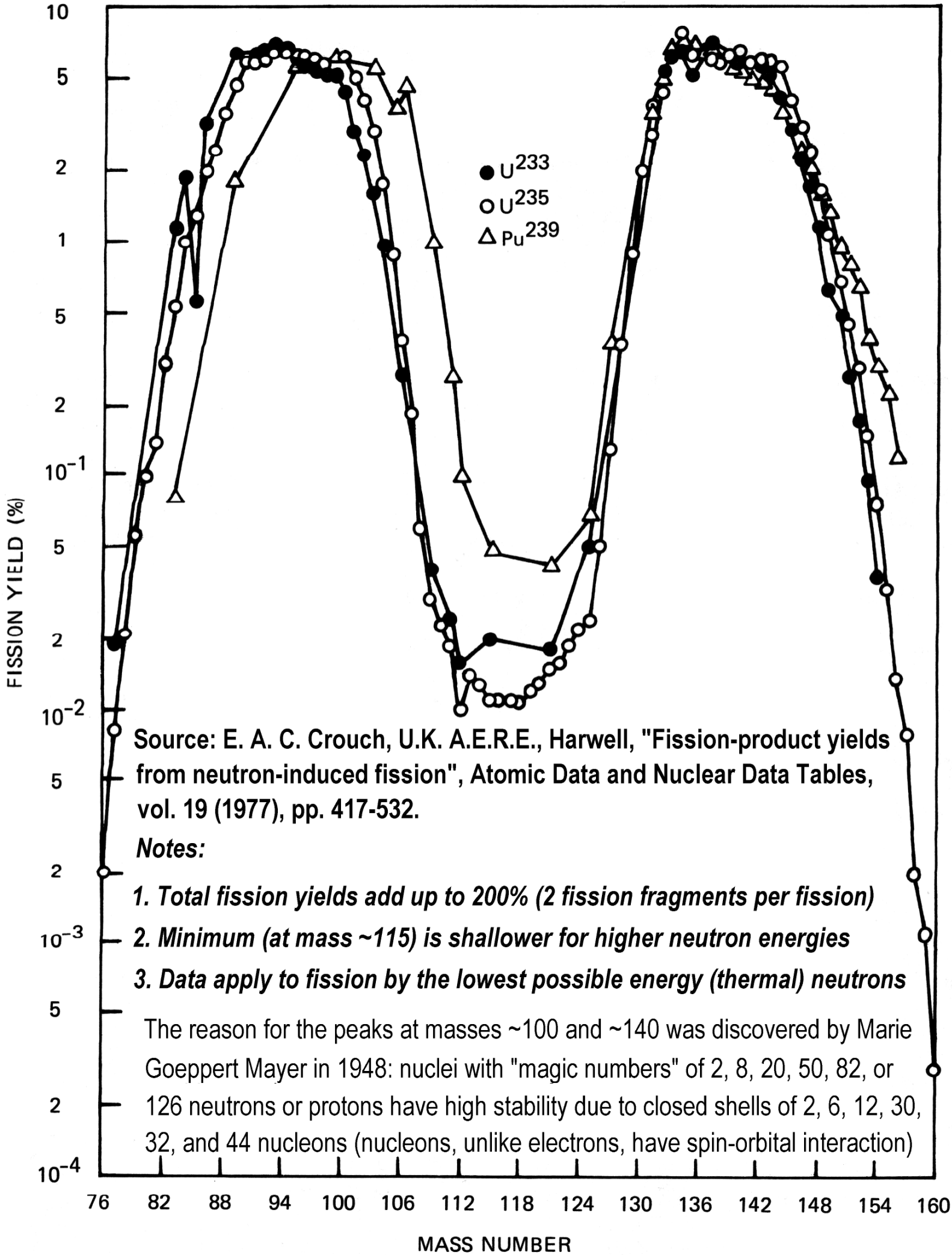

Source: E. A. C. Crouch, U.K. A.E.R.E., Harwell, "Fission-product yields from neutron-induced fission", Atomic Data and Nuclear Data Tables, vol. 19 (1977), pp. 417-532.

Notes:

1. Total fission yields add up to 200% (2 fission fragments per fission)

2. Minimum (at mass ~115) is shallower for higher neutron energies

3. Data apply to fission by the lowest possible energy (thermal) neutrons

The reason for the peaks at masses ~100 and ~140 was discovered by Marie Goeppert Mayer in 1948: nuclei with "magic numbers" of 2, 8, 20, 50, 82, or 126 neutrons or protons have high stability due to closed shells of 2, 6, 12, 30, 32, and 44 nucleons (nucleons, unlike electrons, have spin-orbital interaction)

Source: USNRDL-TR-1009 (curves for Pu-239, U-233 and U-238 by different neutron energies are very similar)

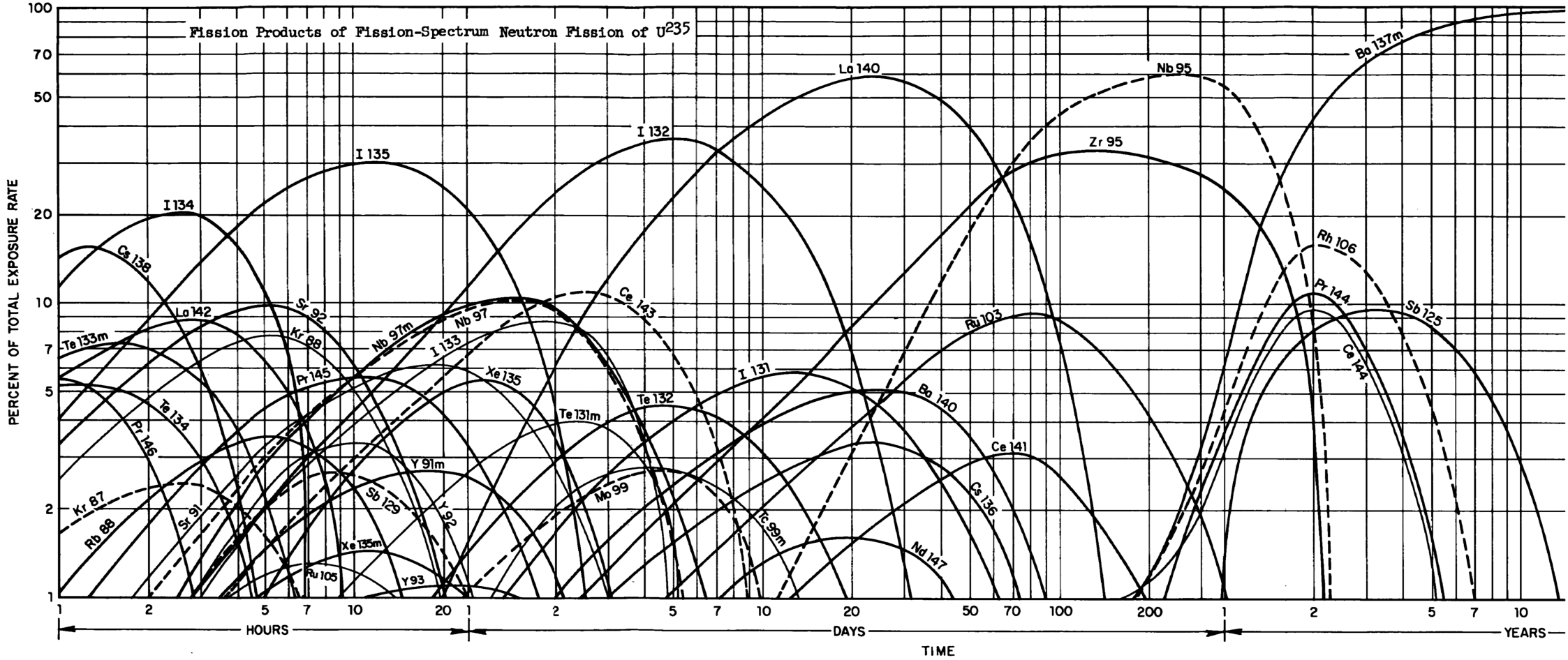

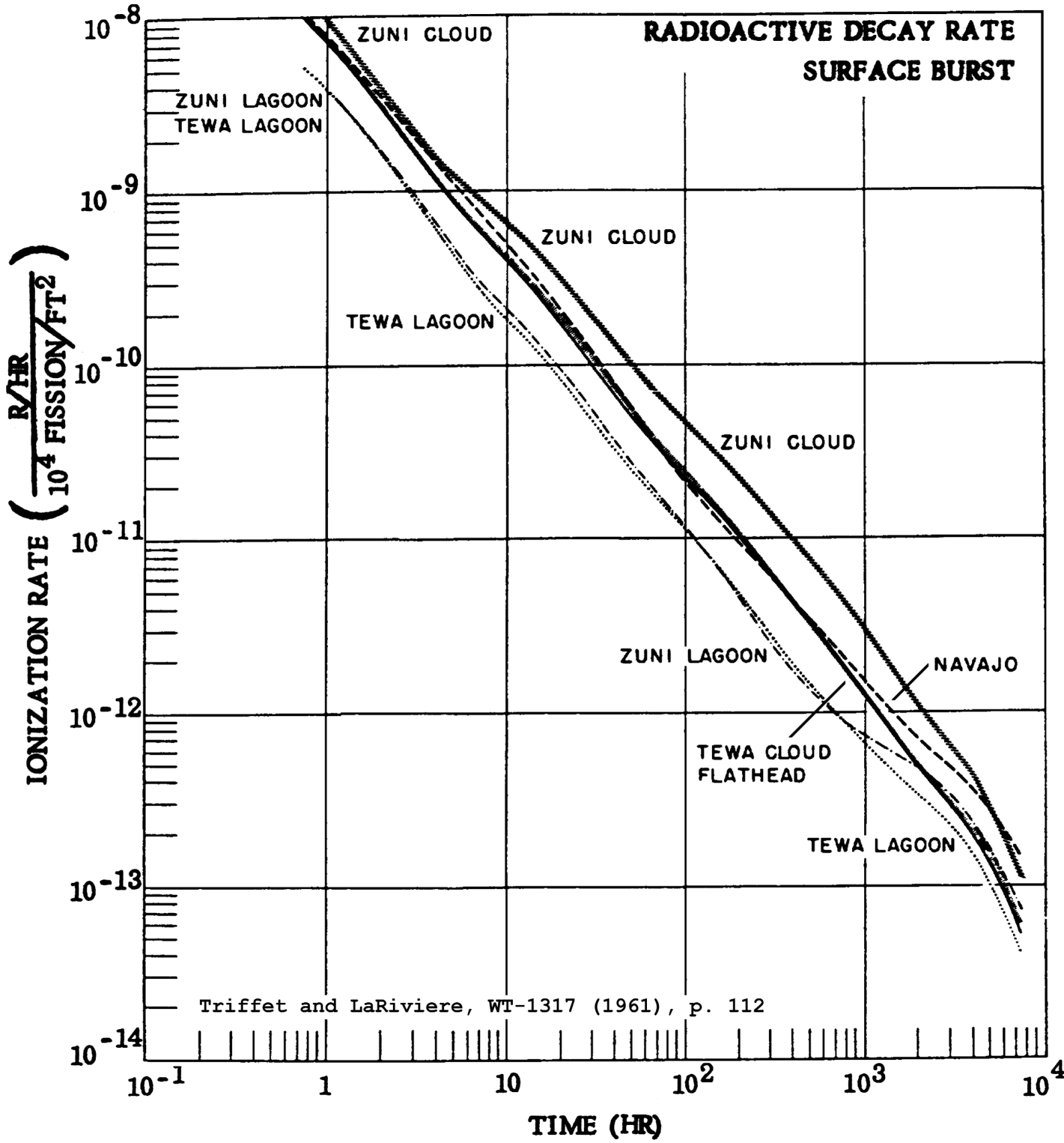
RADIOACTIVE DECAY RATE
SURFACE BURST
ZUNI CLOUD
ZUNI LAGOON
TEWA LAGOON
ZUNI CLOUD
TEWA LAGOON
ZUNI CLOUD
ZUNI LAGOON
NAVAJO
TEWA CLOUD
FLATHEAD
TEWA LAGOON
Triffet and LaRiviere, WT-1317 (1961), p. 112
IONIZATION RATE (R/HR / 10^4 FISSION/FT^2)
TIME (HR)
10^-8
10^-9
10^-10
10^-11
10^-12
10^-13
10^-14
10^-1
1
10
10^2
10^3
10^4

TIR's indicated, on the average, 0.85 ± 25 percent of the survey meter readings

observed/calculated ratio varies from 0.45 at 11.2 hours to 0.66 from 100 to 200 hours, to 0.56 between 370 and 1,000 hours.

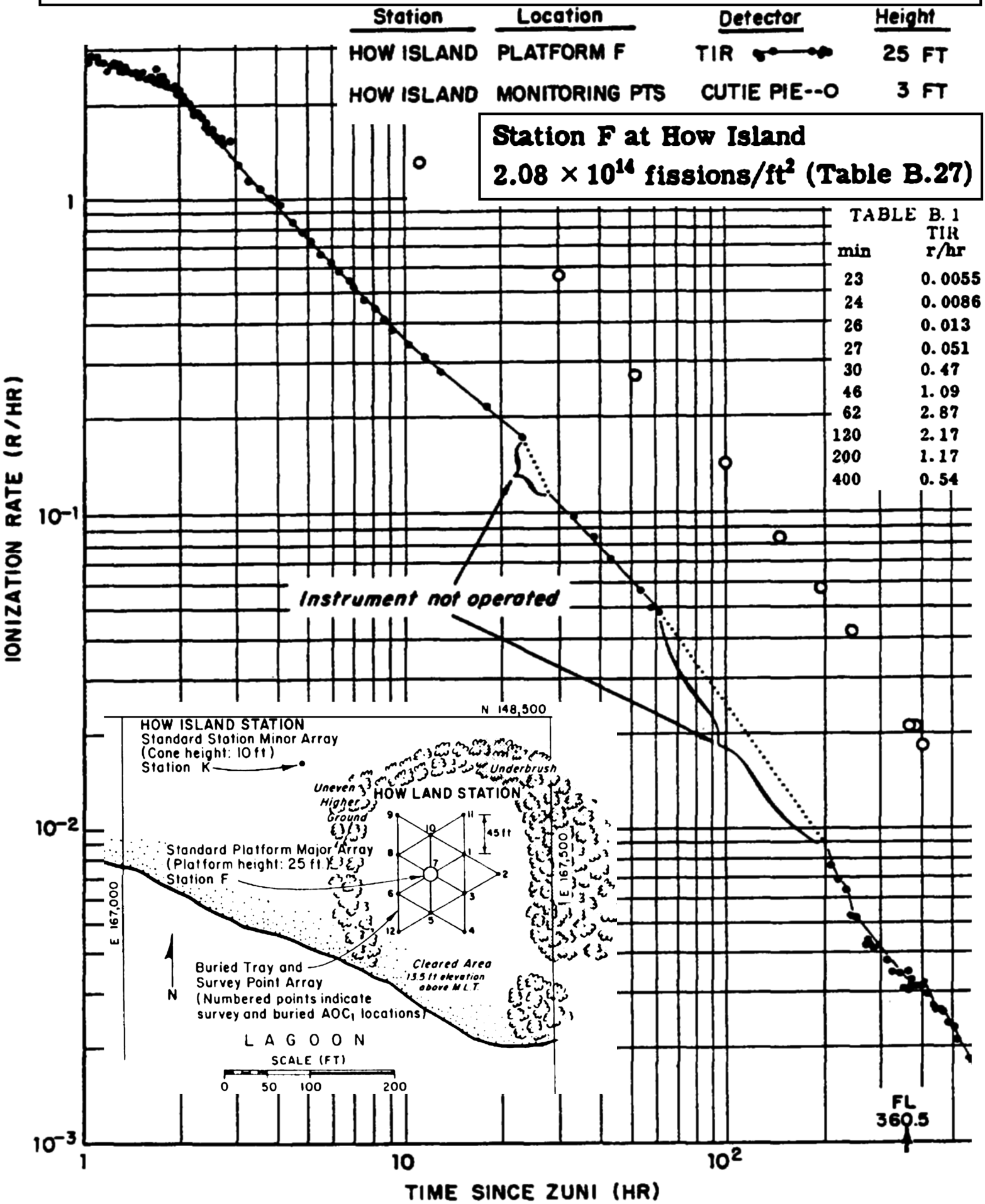

WT-1317

Figure B.7 Gamma-ionization-decay rate, Site How.

LAND SURFACE BURST

A FALLOUT FORECASTING TECHNIQUE WITH RESULTS OBTAINED AT THE ENIWETOK PROVING GROUND

E. A. Schuert, USNRDL TR–139, United States Naval Radiological Defense Laboratory, San Francisco, Calif.

2.36 g/cu cm irregular in shape

Falling speeds (feet/hour)

Altitude	75 μ	100 μ	200 μ	350 μ
0	3,060	5,040	11,700	21,600
20	3,360	5,980	14,400	27,100
40	3,870	6,910	18,600	35,300
60	4,200	7,700	24,400	47,200
80	3,910	6,960	27,800	61,900

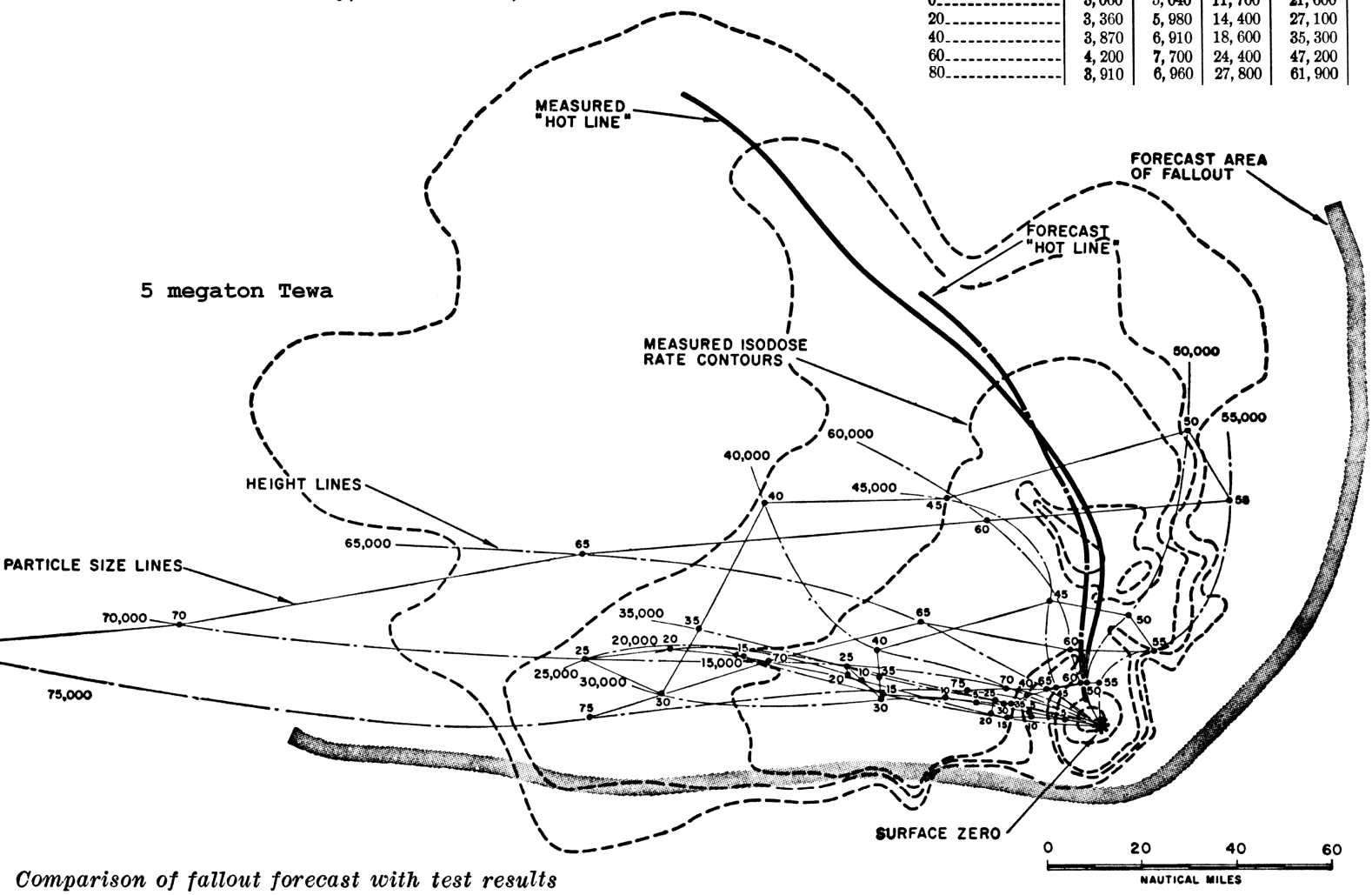

Comparison of fallout forecast with test results

HEIGHT LINE = DESTINATIONS FOR A FIXED HEIGHT OF ORIGIN FOR VARIOUS SIZES
SIZE LINE = DESTINATIONS FOR A FIXED PARTICLE SIZE FROM VARIOUS HEIGHTS
HOT LINE = HEIGHT LINE FROM BASE OF MUSHROOM DISC (MAXIMUM FALLOUT)

5 MT TEWA (87% FISSION), 7.84 STAT. MILES WSW

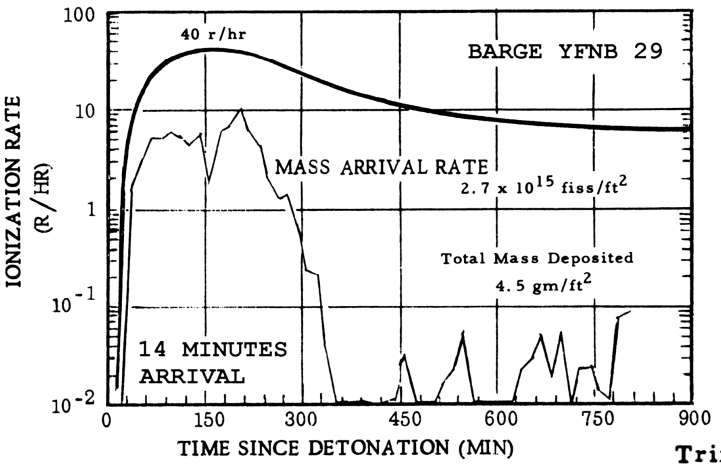

5 MT TEWA (87% FISSION), 59.3 STAT. MILES NW

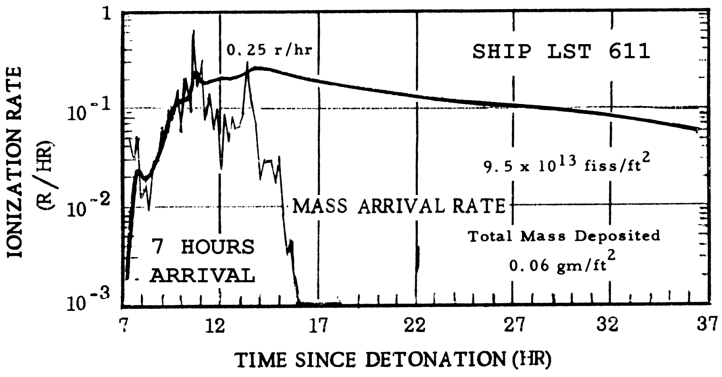

Triffet, T. and LaRiviere, P. D.; Characterization of Fallout

WATER SURFACE BURST

A FALLOUT FORECASTING TECHNIQUE WITH RESULTS OBTAINED AT THE ENIWETOK PROVING GROUND

E. A. Schuert, USNRDL TR–139, United States Naval Radiological Defense Laboratory, San Francisco, Calif.

Time variation of the winds aloft

In most of the observations made at the Eniwetok Proving Ground, the winds aloft were not in a steady state. Significant changes in the winds aloft were observed in as short a period as 3 hours. This variability was probably due to the fact that proper firing conditions which required winds that would deposit the fallout north of the proving ground, occurred only during an unstable synoptic situation of rather short duration.

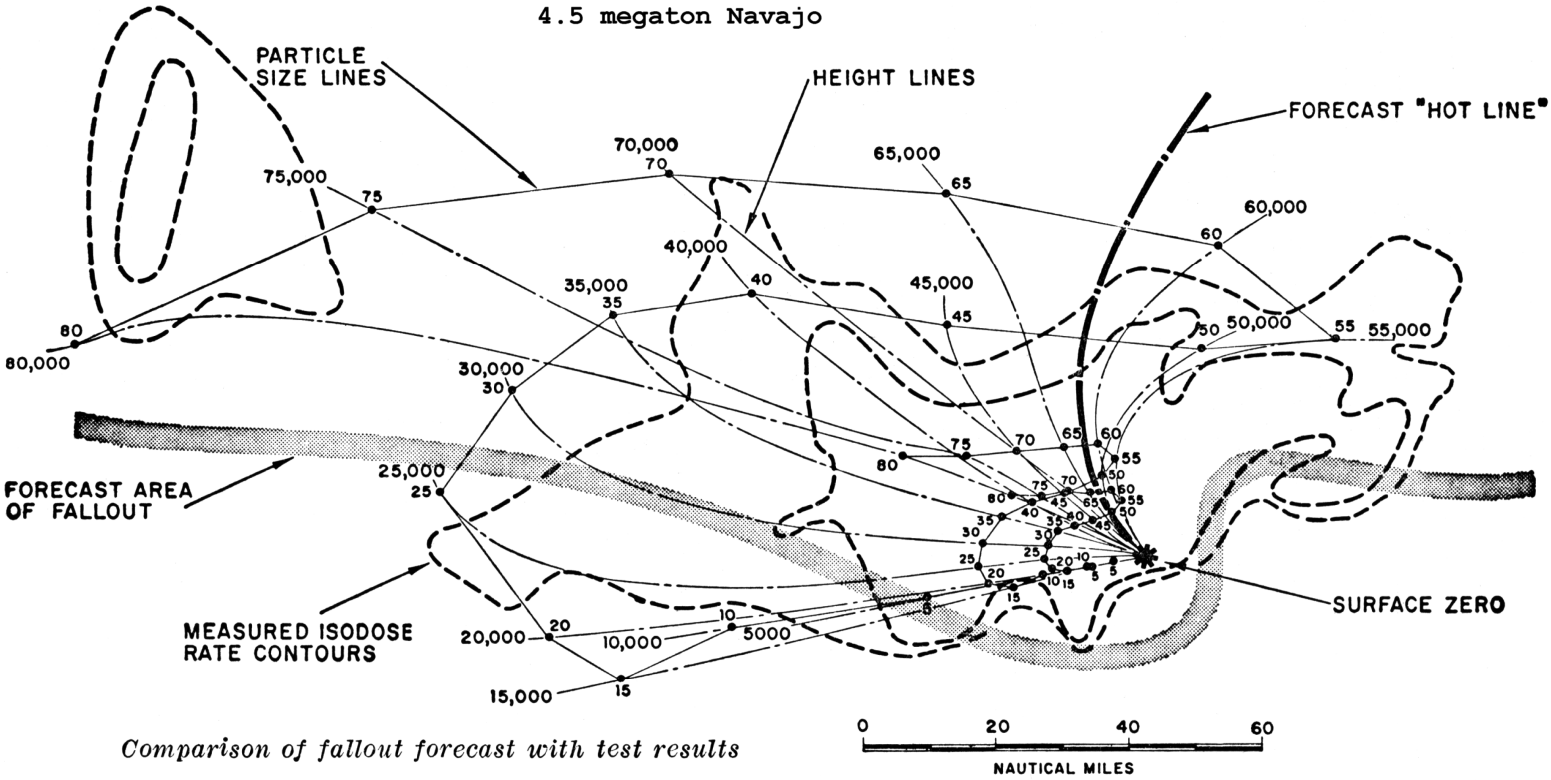

Comparison of fallout forecast with test results

HEIGHT LINE = DESTINATIONS FOR A FIXED HEIGHT OF ORIGIN FOR VARIOUS SIZES
SIZE LINE = DESTINATIONS FOR A FIXED PARTICLE SIZE FROM VARIOUS HEIGHTS
HOT LINE = HEIGHT LINE FROM BASE OF MUSHROOM DISC (MAXIMUM FALLOUT)

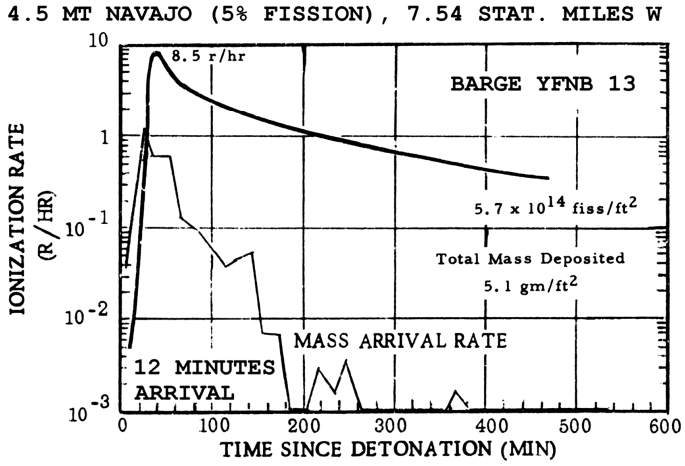

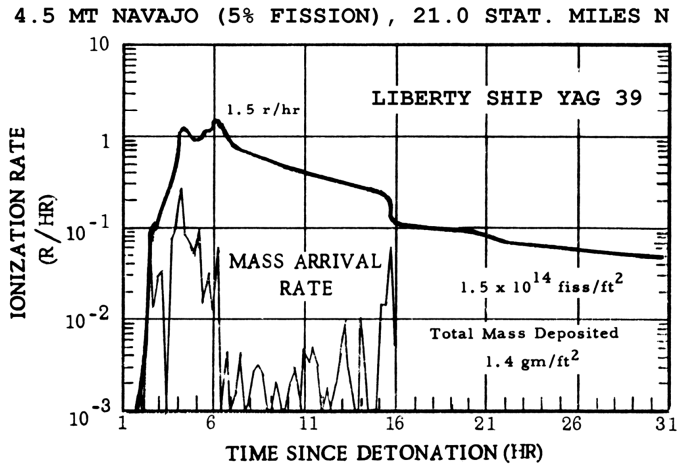

Triffet, T. and LaRiviere, P. D.; Characterization of Fallout, Project 2.63

Carl F. Miller, Fallout and Radiological Countermeasures, SRI, 1963

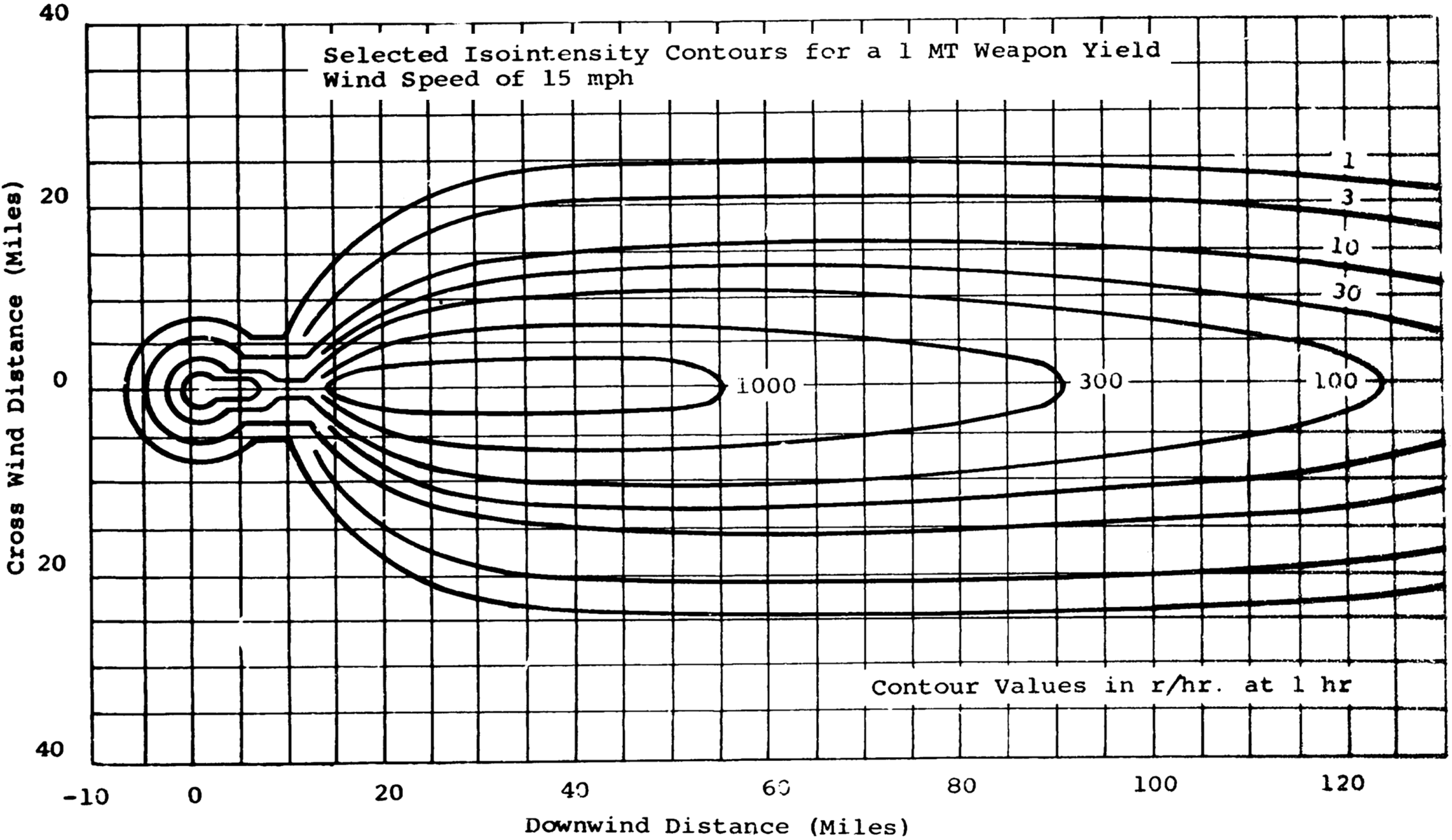

CAR-OVER-TRENCH FALLOUT SHELTER (EXPEDIENT SHELTER HANDBOOK)

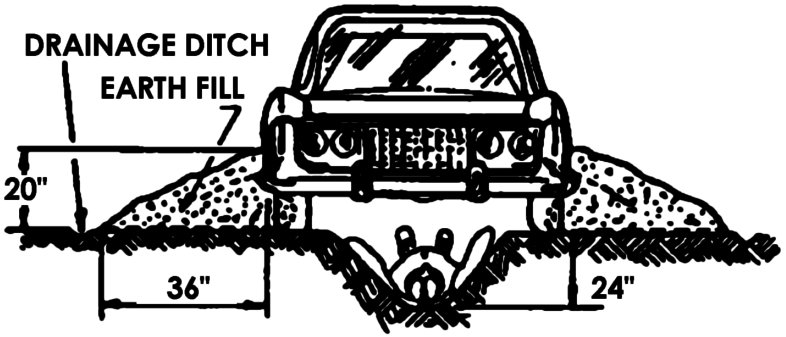

DOORS OR LOGS CAN BE USED IN PLACE OF CAR.

FOR INDOOR SHELTER, USE BAGS OF WATER INSIDE BOXES AROUND & ON TABLE

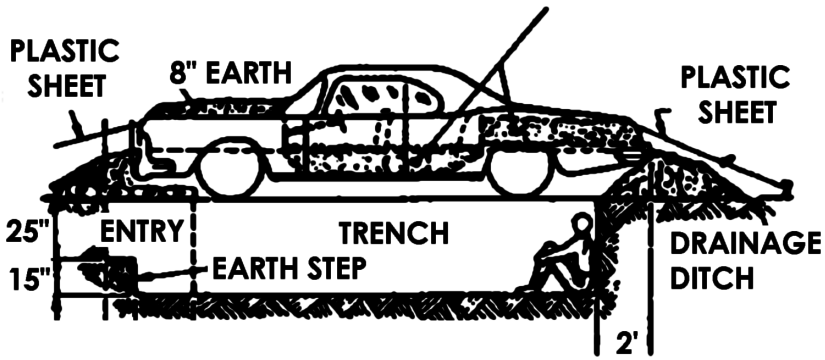

BANK EXCAVATED EARTH 20 INCHES HIGH AROUND CAR

PLACE 8" OF EARTH ON CAR HOOD

DIG SHALLOW DRAINAGE DITCH AROUND FILL

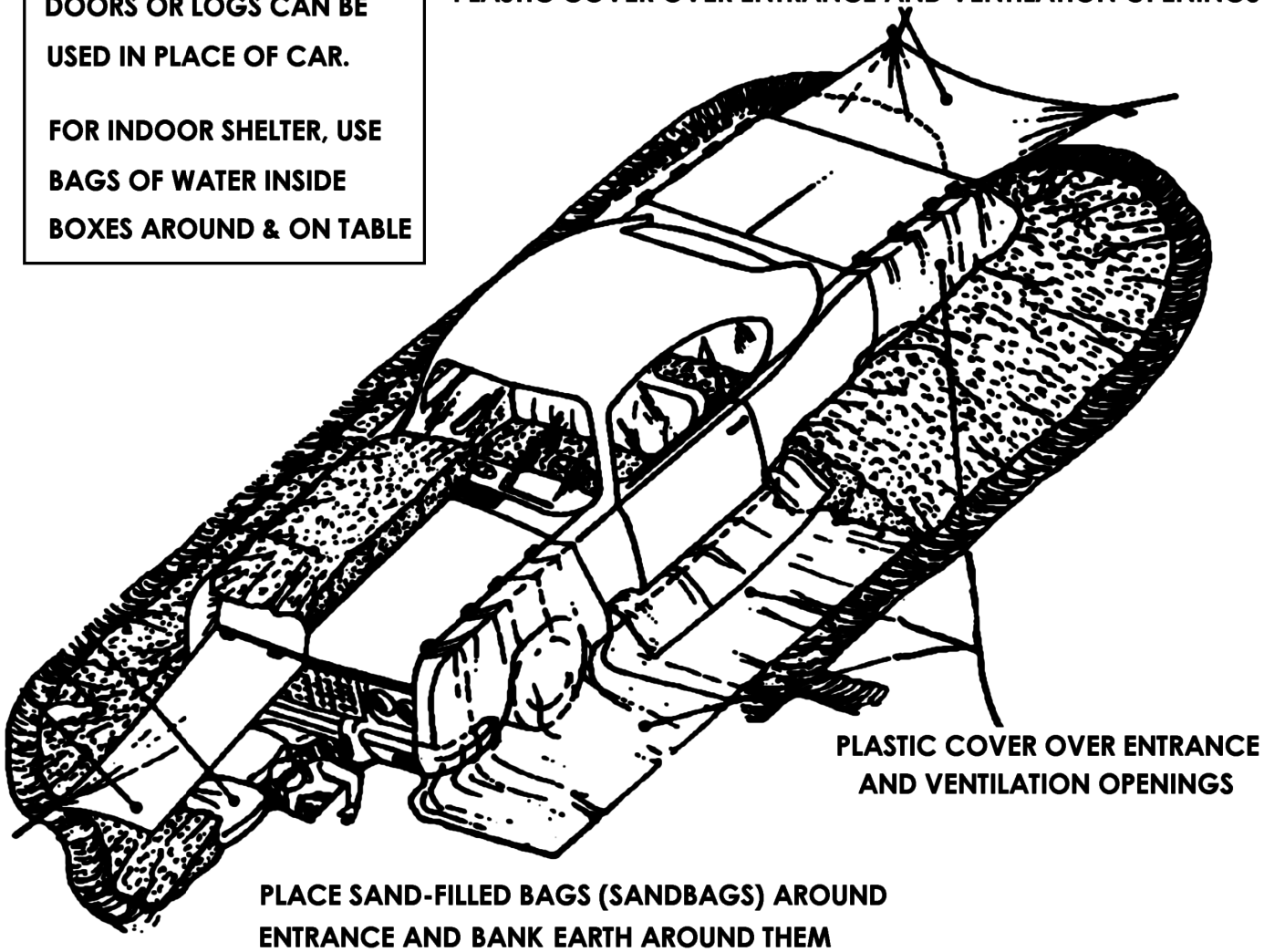

PERSONAL AND FAMILY SURVIVAL

SM-3-11

"...the history of this planet and particularly the history of the 20th Century is sufficient to remind us of the possibilities of an irrational attack, a miscalculation, and accidental war, or a war of escalation in which the stakes by each side gradually increase to the point of maximum danger which cannot be either foreseen or deterred. It is on this basis that civil defense can be readily justified—as insurance for the civilian population in case of enemy miscalculation. It is insurance we trust will never be needed—but insurance which we would never forgive ourselves for foregoing in the event of catastrophe."

— President Kennedy, in May 1961

Remove doors from their hinges and place them over supports

Drinking-water is required for survival. It is also useful as a shielding material. A collapsible children's swimming pool filled with water and located over the best corner of your basement will help improve the fallout protection. A bathtub, if suitably located, can also be used for this purpose.

DEPARTMENT OF DEFENSE

OFFICE OF CIVIL DEFENSE

LIFE

HOW YOU CAN SURVIVE FALLOUT

97 out of 100 people can be saved . . .
Detail plans for building shelters . . .

AND A LETTER TO YOU FROM PRESIDENT KENNEDY

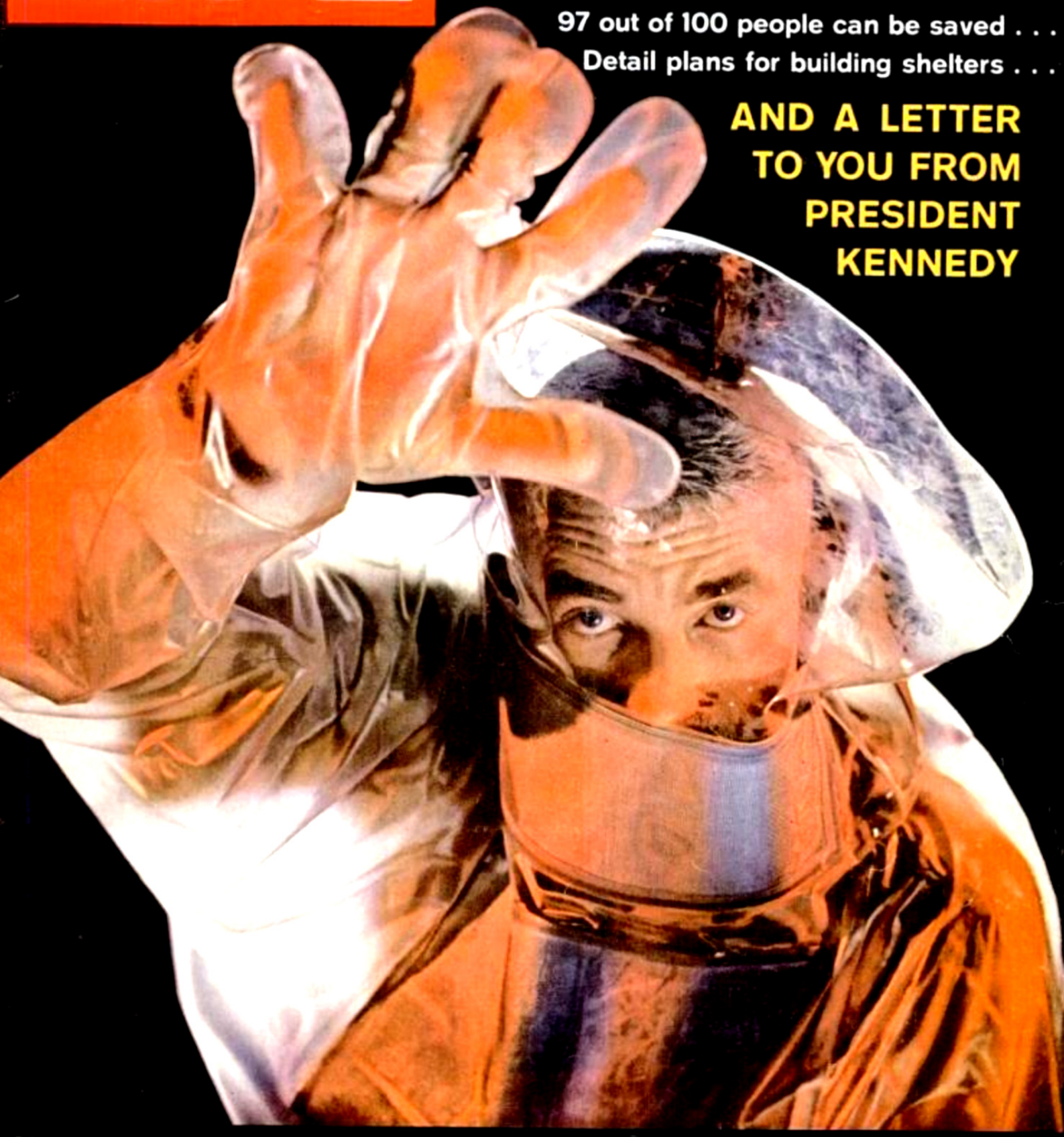

CIVILIAN FALLOUT SUIT

SEPTEMBER 15 · 1961 · 20¢

A MESSAGE TO YOU FROM THE PRESIDENT

The White House
September 7, 1961

My Fellow Americans:

Nuclear weapons and the possibility of nuclear war are facts of life we cannot ignore today. I do not believe that war can solve any of the problems facing the world today. But the decision is not ours alone.

The government is moving to improve the protection afforded you in your communities through civil defense. We have begun, and will be continuing throughout the next year and a half, a survey of all public buildings with fallout shelter potential, and the marking of those with adequate shelter for 50 persons or more. We are providing fallout shelter in new and in some existing federal buildings. We are stocking these shelters with one week's food and medical supplies and two weeks' water supply for the shelter occupants. In addition, I have recommended to the Congress the establishment of food reserves in centers around the country where they might be needed following an attack. Finally, we are developing improved warning systems which will make it possible to sound attack warning on buzzers right in your homes and places of business.

More comprehensive measures than these lie ahead, but they cannot be brought to completion in the immediate future. In the meantime there is much that you can do to protect yourself—and in doing so strengthen your nation.

I urge you to read and consider seriously the contents of this issue of LIFE. The security of our country and the peace of the world are the objectives of our policy. But in these dangerous days when both these objectives are threatened we must prepare for all eventualities. The ability to survive coupled with the will to do so therefore are essential to our country.

John F. Kennedy

Fallout Shelters

YOU COULD BE AMONG THE 97% TO SURVIVE IF YOU FOLLOW ADVICE ON THESE PAGES . . . HOW TO BUILD SHELTERS . . . WHERE TO HIDE IN CITIES . . . WHAT TO DO DURING AN ATTACK

Proceedings of the Symposium
held at Washington, D. C.
April 19-23, 1965 by the
Subcommittee on Protective Structures,
Advisory Committee on Civil Defense,
National Academy of Sciences—
National Research Council

Protective Structures for CIVILIAN POPULATIONS

1966

THE PROTECTION AGAINST FALLOUT RADIATION AFFORDED BY CORE SHELTERS IN A TYPICAL BRITISH HOUSE

Daniel T. Jones
Scientific Adviser, Home Office, London

Protective Factors in a Sample of British Houses (Windows Blocked)

Protective Factor	Percentage of Houses
< 25	36%
25-39	28%
40-100	29%
> 100	7%

"A very much improved protection could be obtained by constructing a shelter core. This means a small, thick-walled shelter built preferably inside the fallout room itself, in which to spend the first critical hours when the radiation from fallout would be most dangerous."(1)

The full-scale experiments were carried out at the Civil Defense School at Falfield Park.(2)

In the staircase construction, the shelter consisted of the cupboard under the stairs, sandbags being placed on treads above and at the sides.

A 93 curies cobalt-60 source was used.

9 in. brick walls The windows and doors were not blocked		contribution r/hr/c/ft^2		Protective Factor
	Position	Ground	Roof	
House only	E2	15.0	8.4	21
Lean-to	E2	10.4	2.4	39
Staircase cupboard:				
Stairs only sandbagged	N2	29.2	5.3	14
Stairs and outer wall sandbagged	N2	16.4	4.6	24
Stairs, outer wall, kitchen wall and corridor partition sandbagged	N2	8.8	1.8	47

1. Six sandbags per tread, and a double layer on the small top landing. 96 sandbags were used.
2. As (1), together with a 4-ft-high wall of sandbags along the external north wall. 160 sandbags were used.
3. As (2), together with 4-ft-high walls of sandbags along the kitchen/cupboard partition wall and along the passage partition. 220 sandbags were used.

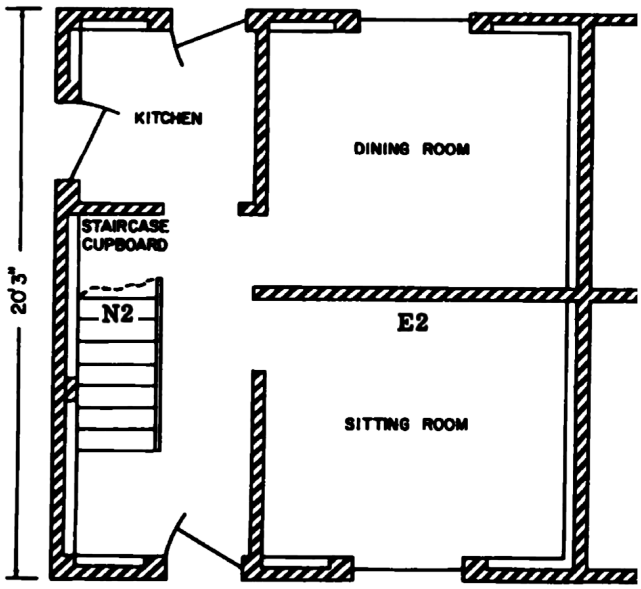

sandbags 24 in. x 12 in. when empty; 16 in. x 9 in. x 4 in. when filled with 25 lb of sand.

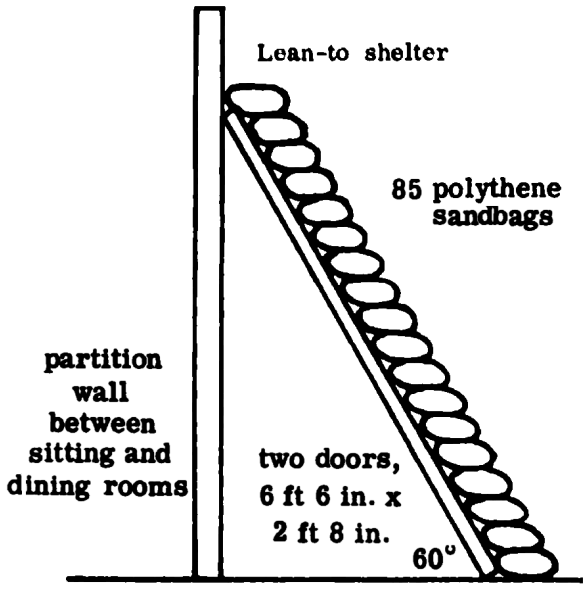

floor area 21 sq ft.

1. Civil Defence Handbook No. 10, HMSO, 1963.
2. Perryman, A. D., Home Office Report CD/SA 117.

BLAST AND OTHER THREATS

Harold Brode
The RAND Corporation, Santa Monica, California

Chemical High-Explosive Weapons

As in past aerial warfare, bombs and missiles carrying chemical explosives to targets are capable of extensive damage only when delivered in large numbers and with high accuracy.

Biological Warfare

Most biological agents are inexpensive to produce; their effective dissemination over hostile territories remains the chief deterrent to their effective employment. Twenty square miles is about the area that can be effectively covered by a single aircraft; large area coverage presents a task for vast fleets of fairly vulnerable planes flying tight patterns at modest or low altitudes. While agents vary in virulence and in their biologic decay rate, most are quite perishable in normal open-air environments. Since shelter and simple prophylactic measures can be quite effective against biological agents, there is less likelihood of the use of biological warfare on a wholesale basis against a nation, and more chance of limited employment on population concentrations —perhaps by covert delivery, since shelters with adequate filtering could insure rather complete protection to those inside.

Chemical Weapons

Chemical weapons, like biological weapons, are relatively inexpensive to create, but face nearly insurmountable logistics problems on delivery. Although chemical agents produce casualties more rapidly, the greater amounts of material to deliver seriously limit the likelihood of their large-scale deployment. Furthermore, chemical research does not hold promise of the development of significantly more toxic chemicals for future use.

Radiological Weapons

The advantages of such modifications are much less real than apparent. In all weapons delivered by missiles, minimizing the payload and total weight is very important. If the total payload is not to be increased, then the inclusion of inert material to be activated by neutrons must lead to reductions in the explosive yield. If all the weight is devoted to nuclear explosives, then more fission-fragment activity can be created, and it is the net difference in activity that must be balanced against the loss of explosive yield. As it turns out, a fission explosion is a most efficient generator of activity, and greater total doses are not achieved by injecting special inert materials to be activated.

The Neutron Bomb

The neutron bomb, so called because of the deliberate effort to maximize the effectiveness of the neutrons, would necessarily be limited to rather small yields—yields at which the neutron absorption in air does not reduce the doses to a point at which blast and thermal effects are dominant. The use of small yields against large-area targets again runs into the delivery problems faced by chemical agents and explosives, and larger yields in fewer packages pose a less stringent problem for delivery systems in most applications. In the unlikely event that an enemy desired to minimize blast and thermal damage and to create little local fallout but still kill the populace, it would be necessary to use large numbers of carefully placed neutron-producing weapons burst high enough to avoid blast damage on the ground, but low enough to get the neutrons down. In this case, however, adequate radiation shielding for the people would leave the city unscathed and demonstrate the attack to be futile.

The thermal radiation from a surface burst is expected to be less than half of that from an air burst, both because the radiating fireball surface is truncated and because the hot interior is partially quenched by the megatons of injected crater material.

SUPERSEISMIC GROUND-SHOCK MAXIMA (AT 5-FT DEPTH)

Vertical acceleration: $\alpha_{vm} \simeq 340\, \Delta P_s/C_L \pm 30$ per cent. Here acceleration is measured in g's and overpressure (ΔP_s) in pounds per square inch. An empirical refinement requires C_L to be defined as the seismic velocity (in feet per second) for rock, but as three fourths of the seismic velocity for soil.

OUTRUNNING GROUND-SHOCK MAXIMA (AT ~10-FT DEPTH)

Vertical acceleration: $\alpha_{vm} \simeq 2 \times 10^5/C_L r^2$ + factor 4 or -factor 2. Acceleration is measured in g's, and r is the scaled radial distance—i.e., $r = R/W^{1/3}$ kft/(mt)$^{1/3}$.

Data taken on a low air-burst shot in Nevada indicate an exponential decay of maximum displacement with depth. For the particular case of a burst of ~ 40 kt at 700 ft, some measurements were made as deep as 200 ft below the surface of Frenchman Flat, a dry lake bed, which led to the following approximate decay law, according to Perret.

$$\delta = \delta_0 \exp(-0.017D),$$

where δ represents the maximum vertical displacement induced at depth D, δ_0 is the maximum displacement at the surface, and D is the depth in feet.

Perret, W.R., Ground Motion Studies at High Incident Overpressure, The Sandia Corporation, Operation PLUMBBOB, WT-1405, for Defense Atomic Support Agency Field Command, June 1960.

MODEL ANALYSIS

Mr. Ivor Ll. DAVIES
Suffield Experimental Station
Canadian Defense Research Board
Ralston, Alberta, Canada

Nuclear-Weapon Tests

In 1952 we fired our first nuclear device, effectively a "nominal" weapon, at Monte Bello, off northwest Australia. To the blast loading from this weapon we exposed a number of reinforced-concrete cubicle structures that had been designed for the dynamic loading conditions, and for which we made the best analysis of response we were competent to make at that time. Our estimates of effects were really a dismal failure. The structures were placed at pressure levels of 30, 10, and 6 psi, where we expected them to be destroyed, heavily damaged with some petaling of the front face, and extensively cracked, respectively. In fact, the front face of the cubicle at 30 psi was broken inwards; failure had occurred along both diagonals, and the four triangular petals had been pushed in. At the 10-psi level, where we had three cubicles, each with a different wall thickness (6, 9, and 12 in.), we observed only light cracking in the front face of that cubicle with the least thick wall (6 in.). The other two structures were apparently undamaged, as was the single structure at the 6-psi level.

In 1957, the first proposals were made for the construction of the underground car park in Hyde Park in London. The Home Office was interested in this project since, in an emergency, the structure could be used as a shelter. Consequently a request was made to us at Atomic Weapons Research Establishment (A.W.R.E.) to design a structure that would be resistant to a blast loading of about 50 psi, and to test our design on the model scale.

Using the various load-deformation curves obtained in this test, an estimate was made of the response of the structure to blast loading. Of particular interest was the possible effect of 100 tons of TNT, the first 100-ton trial at Suffield in Alberta.

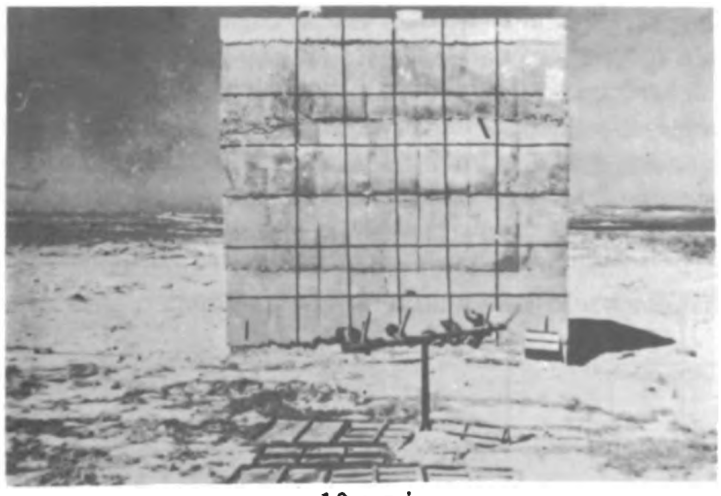

10 p.s.i.

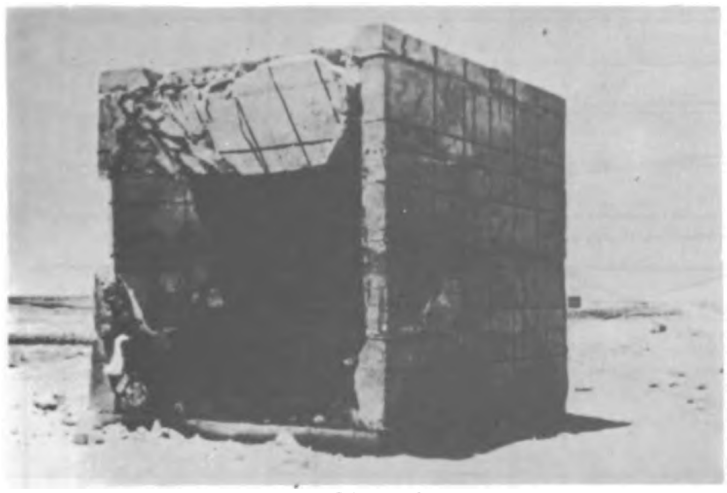

34 p.s.i.

Dynamic tests, Monte Bello cubicles.

A total of seven more models was made; six were shipped to Canada and placed with the top surface of the roof flush with the ground and at positions where peak pressures of 100, 80, 70, 60, 50, and 40 psi were expected. The seventh model was kept in England for static testing at about the time of firing. The results were not as expected. In the field, the four models farthest from the charge were apparantly undamaged; we could see no cracking with the eye, nor did soaking the models with water reveal more than a few hair cracks. The model nearest the charge was lightly cracked in the roof panels and beams, and one of the columns showed slight spalling at the head. This model had been exposed to a peak pressure of 110 psi.

Davies, I. Ll., Effects of Blast on Reinforced Concrete Slabs, and the Relationship with Static Loading Characteristics (U). United Kingdom, Operation BUFFALO - Target Response Tests, AWRE Report T 46/57 (CONFIDENTIAL report), August 1957.

Wood, A. J., The Effect of Earth Covers on the Resistance of Trench Shelter Roofs (U). United Kingdom, Operation BUFFALO-Target Response Target Response Tests, AWRE Report T 47/57 (CONFIDENTIAL report), August 1957.

O'Brien, T. P., Rowe, R. D., and Hance, R. J., The Effect of Atomic Blast on Wall Panels (U). United Kingdom, FWE-36 (CONFIDENTIAL report), April 1955.

Walley, F., Operation TOTEM Group 13 Report: Civil Defense Structures (U). United Kingdom, FWE-111 (CONFIDENTIAL report), May 1957.

Davies, I. Ll., and Thumpston, N. S., The Resistance of Civil Defense Shelters to Atomic Blast (U). United Kingdom, FWE 35 (UNCLASSIFIED report), March 1955.

Davies, I. Ll., The Resistance of Civil Defense Shelters to Atomic Blast: IV Final Report on Experiments with Reinforced Models of Heavily Protective Citadel Shelter Type CD12 (U). United Kingdom, FWE-101 (CONFIDENTIAL report), May 1958.

Davies, I. Ll., Performance Test on Model Garage - Shelter Roof System. SES 100 Ton TNT Trial-Suffield, Alberta, August 1961 (U). United Kingdom, AWRE Report No. E 2/63 (FOR OFFICIAL USE ONLY), March 1963.

Worsfold, W. E., Effects of Shielding a Building from Atomic Blast (U). United Kingdom, FWE-164 (CONFIDENTIAL report), August 1958.

Trimer, A., and Maskell, E. G. B., Operation BUFFALO Target Response Tests - Structures Group Report: The Effect on Field Defenses (U). United Kingdom, FWE-241 (CONFIDENTIAL report), December 1959.

United Kingdom, The Effects of Atomic Weapons on Structures and Military Equipment (U). FWE-8 (SECRET report), July 1954.

HOME OFFICE

SCOTTISH HOME DEPARTMENT

MANUAL OF CIVIL DEFENCE

Volume I

PAMPHLET No. 1

NUCLEAR WEAPONS

LONDON

HER MAJESTY'S STATIONERY OFFICE

1956

Practical protection

88 Large buildings with a number of storeys, especially if they are of heavy construction, provide much better protection than small single-storey structures (see Figure 4). Houses in terraces likewise provide much better protection than isolated houses because of the shielding effect of neighbouring houses.

GOOD PROTECTION

Solidly constructed multi-storeyed building with occupants well removed from fall-out on ground and roof. The thickness of floors and roof overhead, and the shielding effect of other buildings, all help to cut down radiation

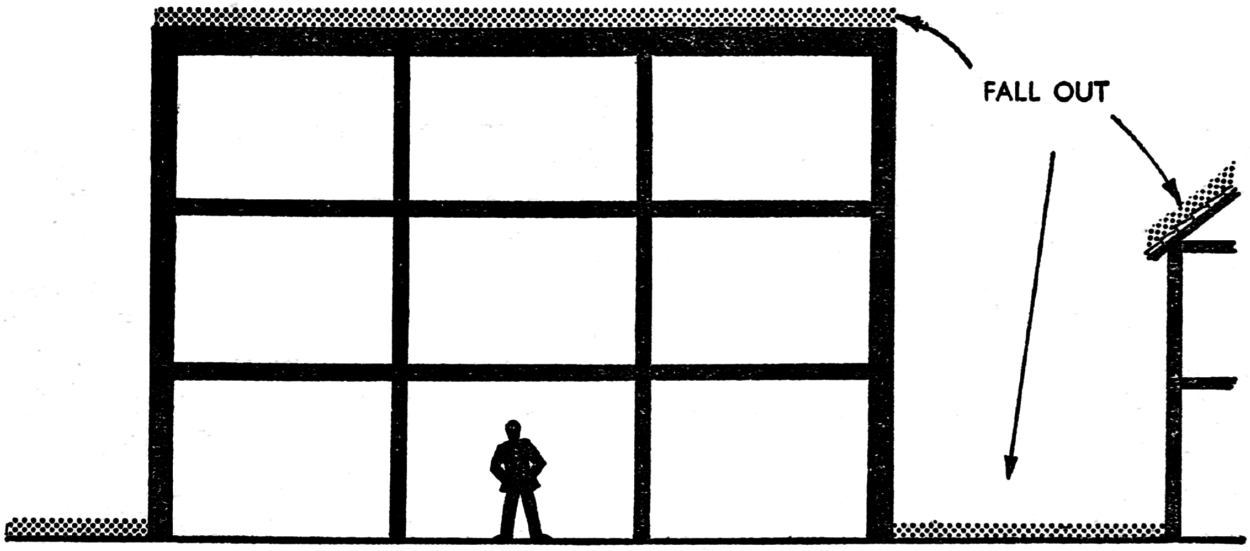

BAD PROTECTION

Isolated wooden bungalow

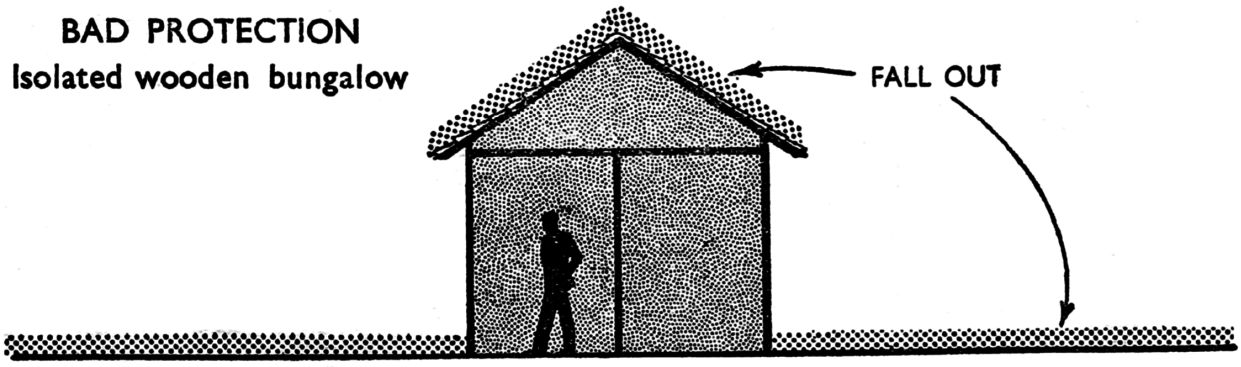

FIGURE 4

Examples of good and bad protection afforded by buildings against fall-out.

89 It is estimated that the protection factor (the factor by which the outside dose has to be divided to get the inside dose) of a ground floor room in a two-storey house ranges from 10 to about 50, depending on wall thickness and the shielding afforded by neighbouring buildings. The corresponding figures for bungalows are about 10–20, and for three-storey houses about 15–100. An average two-storey brick house in a built-up area gives a factor of 40, but basements, where the radiation from outside the house is attenuated by a very great thickness of earth, have protection factors ranging up to 200–300. A slit trench with even a light cover of boards or corrugated iron without earth overhead gives a factor of 7, and if 1 ft. of earth cover is added the

factor rises to 100. If the trench can be covered with 2 or 3 feet of earth then a factor of more than 200–300 can be obtained (see Figure 5).

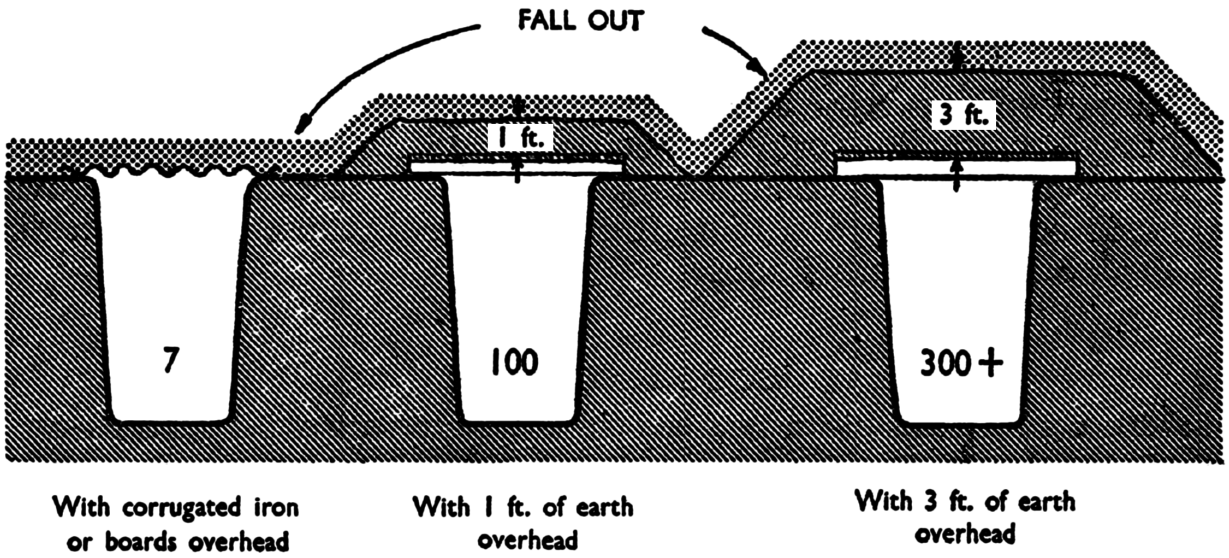

FIGURE 5
Protection factors in slit trenches (the factor by which the outside dose is divided to get the inside dose).

Choosing a refuge room

90 In choosing a refuge room in a house one would select a room with a minimum of outside walls and make every effort to improve the protection of such outside walls as there were. In particular the windows would have to be blocked up, e.g. with sandbags. Where possible, boxes of earth could be placed round an outside wall to provide additional protection, and heavy furniture (pianos, bookcases etc.) along the inside of the wall would also help. A cellar would be ideal. Where the ground floor of the house consists of boards and timber joists carried on sleeper walls it may be possible to combine the high protection of the slit trench with some of the comforts of the refuge room by constructing a trench under the floor.
Once a trap door had been cut in the floor boards and joists and the trench had been dug, there would be no further interference with the peace-time use of the room.

Estimated under-cover doses in the fall-out area

91 Taking an average protective factor of 40 for a two-storey house in a built-up area, the doses accumulated in 36 hours for the ranges referred to in the U.S. Atomic Energy Commission Report (paragraph 84) would have been:—

190 miles downwind		7½r
160	,, ,,	12½r
140	,, ,,	20r

15 Megatons
Bravo 1954

which are all well below the lowest figure of 25r referred to in Table 1. At closer ranges along the axis of the fall-out, the doses accumulated in 36 hours would have been much higher, but over most of the contaminated area—with this standard of protection—the majority of those affected would have been saved from death, and even from sickness, by taking cover continuously for the first 36 hours.

9" solid brick wall British pre-war house design

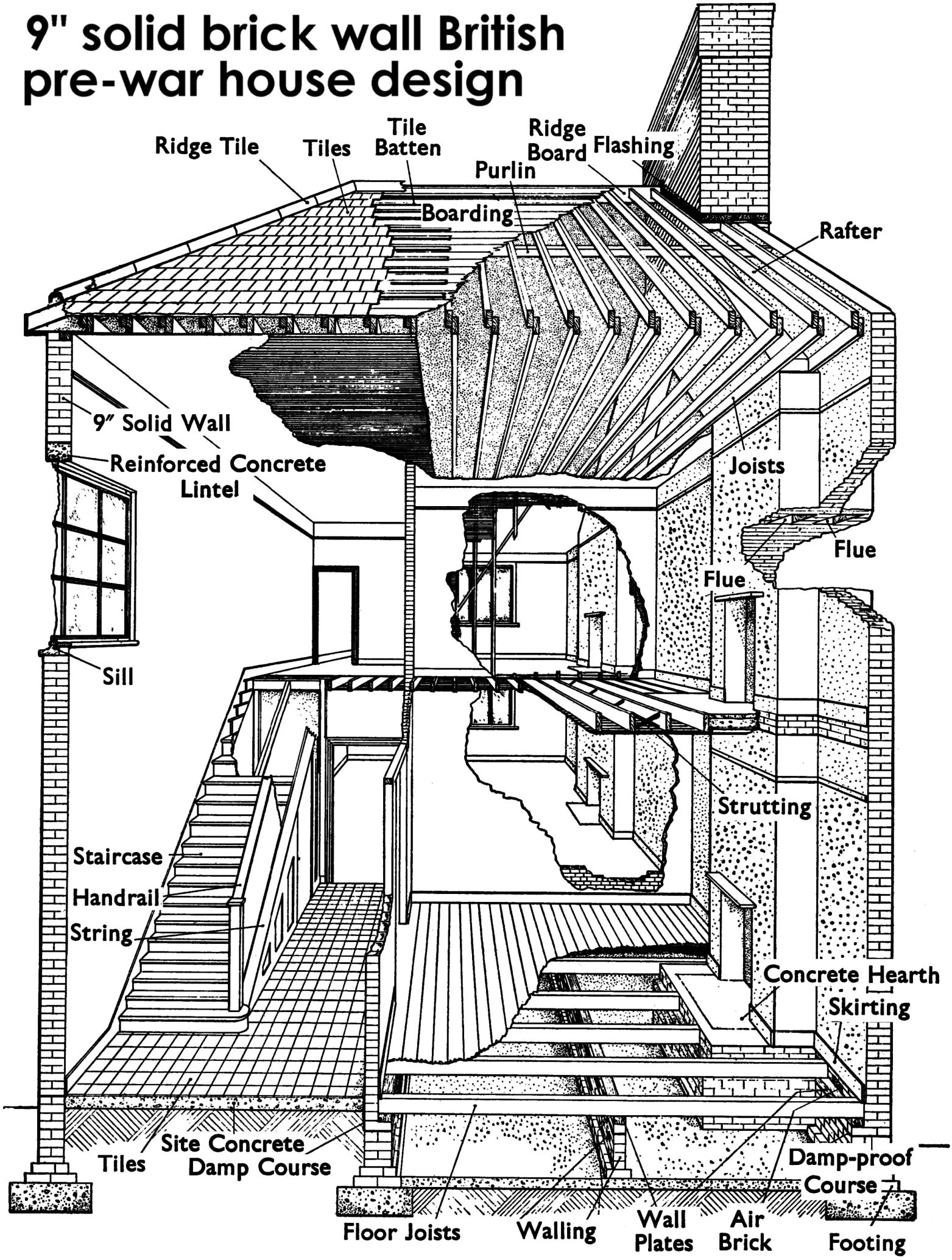

5. Radiation sickness

Assume dose incurred in a single shift (3–4 hours) by the "average" man, over the whole body:—

25 roentgens		—No obvious harm.
100	„	—Some nausea and vomiting.
500	„	—Lethal to about 50 per cent. people (death up to 6 weeks later).
800	„ or more	—Lethal to all (death up to 6 weeks later).

Note: If dose spread uniformly over 2–3 days, then 60 roentgens could be incurred with no more effect than 25 roentgens in a single exposure of 3–4 hours.

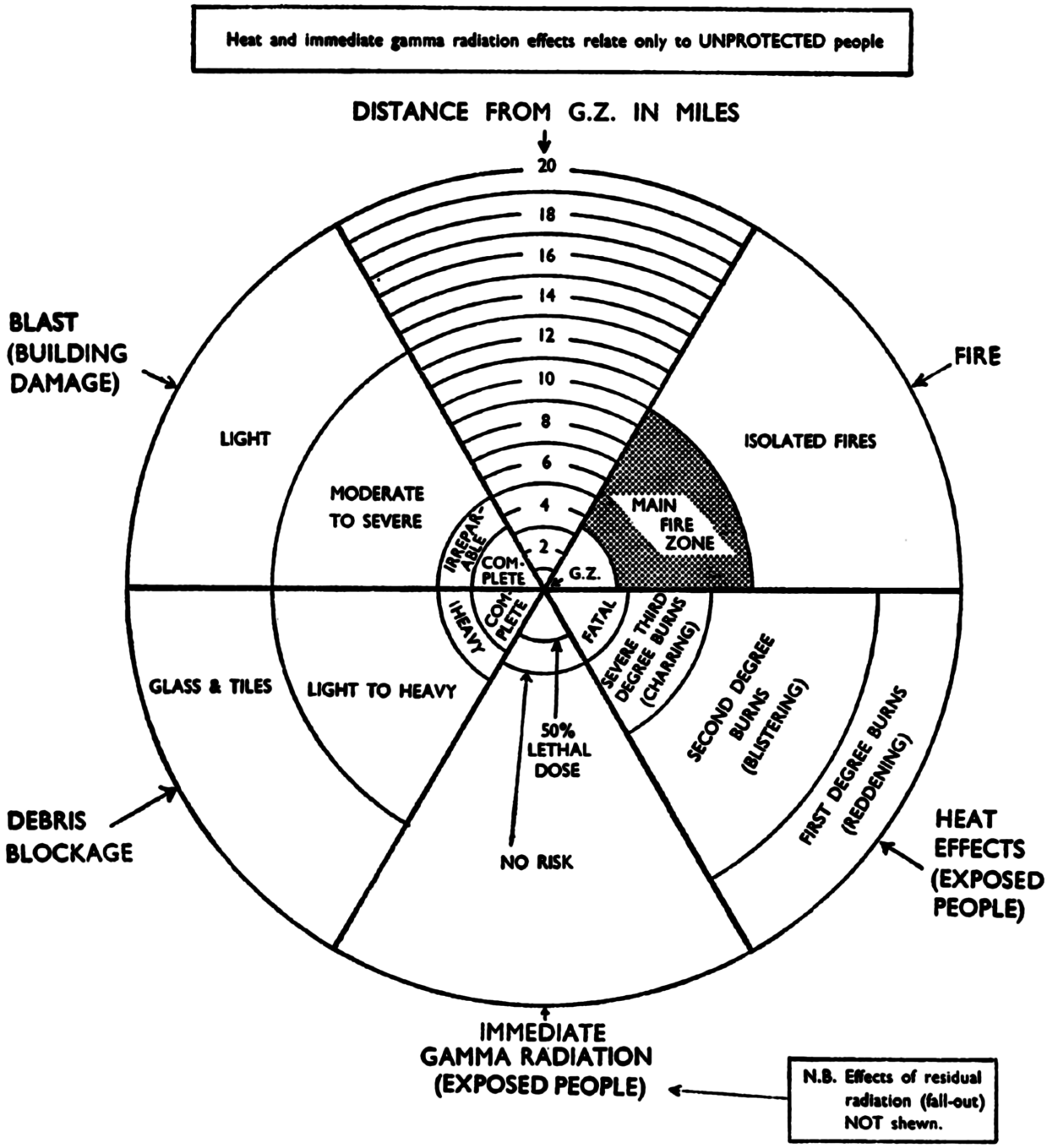

FIGURE 11

Combined effects (excluding residual radioactivity) from a 10 megaton ground burst bomb. Heat and immediate gamma radiation effects relate only to UNPROTECTED people.

HOME OFFICE
SCOTTISH HOME DEPARTMENT

MANUAL OF CIVIL DEFENCE

Volume I

PAMPHLET No. 2

RADIOACTIVE FALL-OUT

PROVISIONAL SCHEME OF PUBLIC CONTROL

LONDON
HER MAJESTY'S STATIONERY OFFICE
1956

Radioactive Fall-out—Summary of Provisional Control Zones

Zone	Definition of Zone Boundaries	Range of Cumulative Doses in open at 48 hours	Summary of permissible and recommended action	Range of Cumulative Doses assuming observance of control rules
W	Outer: Limit of area placed under "Black Warning" (*see* Footnote). Inner: 0·3 r.p.h. at 48 hrs.	Up to 80r	Complete release from refuge as soon as dose-rate fell to 0·3 r.p.h. or, if the rate had not reached that figure, when fall-out was complete.	At 48 hrs. Below 2r
X	Outer: 0·3 r.p.h. at 48 hrs. Inner: 3 r.p.h. at 48 hrs.	80–800r	Qualified release from refuge after 48 hrs.—indoor workers to follow normal occupations, but not to exceed 4 hrs. per day in the open. Outdoor workers to work half shifts for next five days. At the end of this period the zone would be normal, except that all would be advised to be out of doors as little as possible and not in any case to exceed 8 hrs. per day in the open for the next three months.	At 48 hrs. 2-20r At 7 days 6-60r At 5 wks. 12-120r At 3 mths. 14-145r
Y	Outer: 3 r.p.h. at 48 hrs. Inner: 10 r.p.h. at 48 hrs.	800-2,800r	Release from refuge under stringent control after 48 hrs. For the next 12 days people should not leave their refuge for longer than necessary. Time in the open should not exceed 2 hrs. per day and time under cover, but not in refuge, a further 8 hrs. On this basis essential indoor workers should be able to get to their places of work, but outdoor work would remain suspended; a relaxation would be possible after the first fortnight and further easement in another three weeks. For the rest of the first year, however, people in this zone should not exceed 8 hrs. a day in the open.	At 48 hrs. 20-70r At 14 days 50-170r At 5 wks. 70-240r At 3 mths. 95-330r
Z	10 r.p.h. at 48 hrs.	Above 2,800r	All movement outside refuge accommodation in this zone would be dangerous. People should remain in refuge until instructions for clearance were given—they should then leave the zone by the quickest available route if they had means of transport or wait in their refuge to be collected if they had not. The clearance operation might start after 48 hrs. and removal from the zone would be for at least 3 months.	At 48 hrs.—Above 70r

The initial Zone W boundary would be defined by the boundaries of a series of warning districts on the flanks of the fall-out. After 48 hrs. Zone W would for public control purposes have disappeared: its outer boundary would have moved during the period to coincide with the outer boundary of Zone X.

The question of defining an area extending in some places beyond Zone W in which there might be an agricultural hazard is being studied.

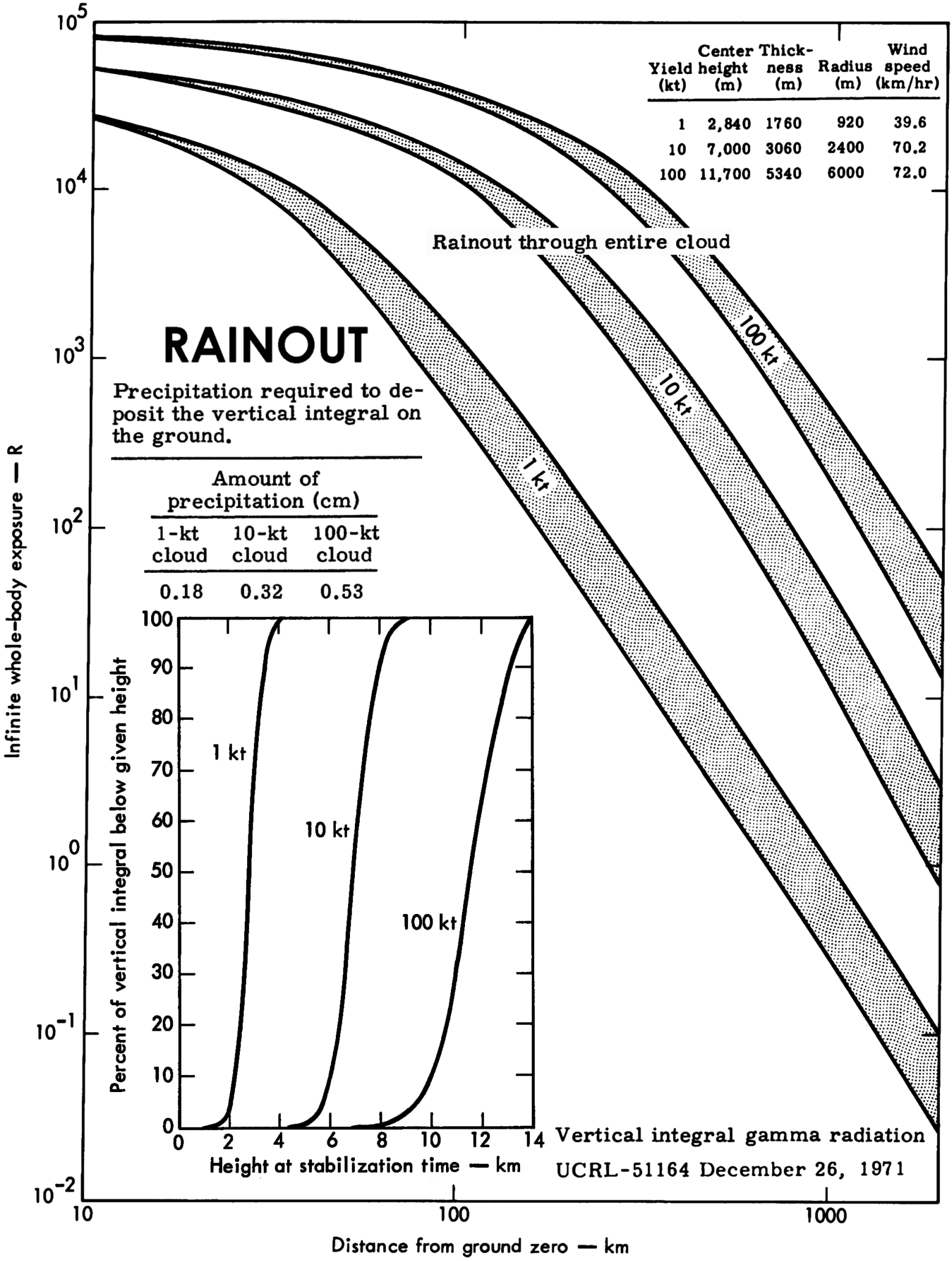
RAINOUT
Precipitation required to deposit the vertical integral on the ground.
Amount of precipitation (cm)
1-kt cloud 10-kt cloud 100-kt cloud
0.18 0.32 0.53
Yield (kt) Center height (m) Thickness (m) Radius (m) Wind speed (km/hr)
1 2,840 1760 920 39.6
10 7,000 3060 2400 70.2
100 11,700 5340 6000 72.0
Rainout through entire cloud
1 kt
10 kt
100 kt
Infinite whole-body exposure — R
Distance from ground zero — km
Percent of vertical integral below given height
Height at stabilization time — km
Vertical integral gamma radiation
UCRL-51164 December 26, 1971

FOR RELEASE AT 4:00 P.M. (E.S.T.)
TUESDAY, FEBRUARY 15, 1955

A REPORT

BY THE UNITED STATES ATOMIC ENERGY COMMISSION

ON THE EFFECTS OF HIGH-YIELD NUCLEAR EXPLOSIONS

FALLOUT PATTERN OF 1954 TEST IN THE PACIFIC

19. Data from this test permits estimates of casualties which would have been suffered within this contaminated area if it had been populated. These estimates assume: (1) that the people in the area would ignore even the most elementary precautions; (2) that they would not take shelter but would remain out of doors completely exposed for about 36 hours; and (3) that in consequence they would receive the maximum exposure. Therefore, it will be recognized that the estimates which follow are what might be termed extreme estimates since they assume the worst possible conditions.

PROTECTION AGAINST FALLOUT

26. In an area of heavy fallout the greatest radiological hazard is that of exposure to external radiation. Simple precautionary measures can greatly reduce the hazard to life. Exposure can be reduced by taking shelter and by utilizing simple decontamination measures until such times as persons can leave the area. Test data indicate that the radiation level, i.e., the rate of exposure, indoors on the first floor of an ordinary frame house in a fallout area would be about one-half the level out of doors. Even greater protection would be afforded by a brick or stone house. Taking shelter in the basement of an average residence would reduce the radiation level to about one-tenth that experienced out of doors.

29. If fallout particles come into contact with the skin, hair or clothing, prompt decontamination precautions such as have been outlined by the Federal Civil Defense Administration will greatly reduce the danger. These include such simple measures as thorough bathing of exposed parts of the body and a change of clothing.

30. If persons in a heavy fallout area heeded warning or notification of an attack and evacuated the area or availed themselves of adequate protective measures, the percentage of fatalities would be greatly reduced even in the zone of heaviest fallout.

Foreword

If the country were ever faced with an immediate threat of nuclear war, a copy of this booklet would be distributed to every household as part of a public information campaign which would include announcements on television and radio and in the press. The booklet has been designed for free and general distribution in that event. It is being placed on sale now for those who wish to know what they would be advised to do at such a time.

May 1980

Protect and Survive

ISBN 0 11 3407289

If Britain is attacked by nuclear bombs or by missiles, we do not know what targets will be chosen or how severe the assault will be.

If nuclear weapons are used on a large scale, those of us living in the country areas might be exposed to as great a risk as those in the towns. The radioactive dust, falling where the wind blows it, will bring the most widespread dangers of all. No part of the United Kingdom can be considered safe from both the direct effects of the weapons and the resultant fall-out.

The dangers which you and your family will face in this situation can be reduced if you do as this booklet describes.

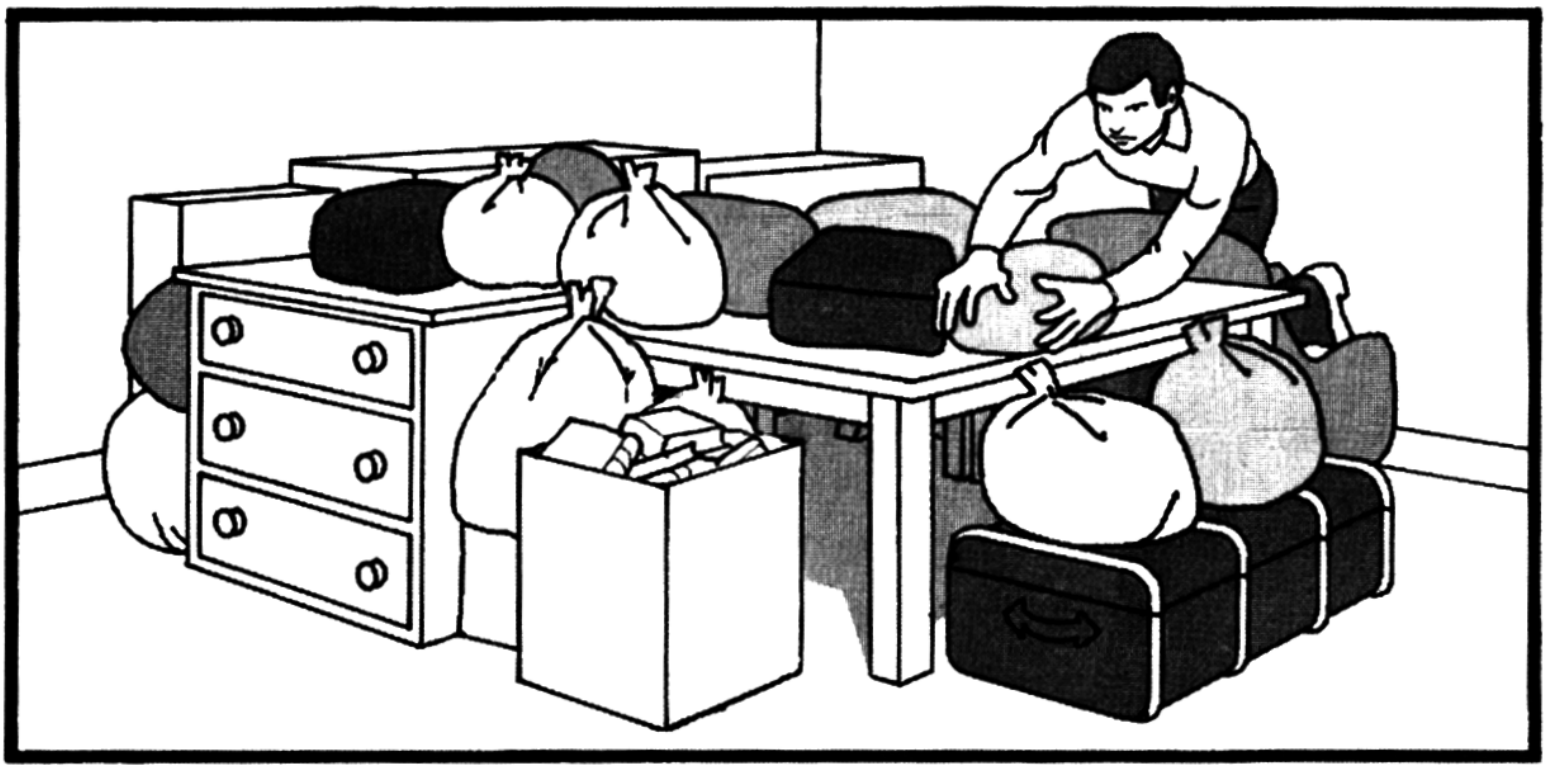

If there is structural damage from the attack you may have some time before a fall-out warning to do minor jobs to keep out the weather – using curtains or sheets to cover broken windows or holes.

If you are out of doors, take the nearest and best available cover as quickly as possible, wiping all the dust you can from your skin and clothing at the entrance to the building in which you shelter.

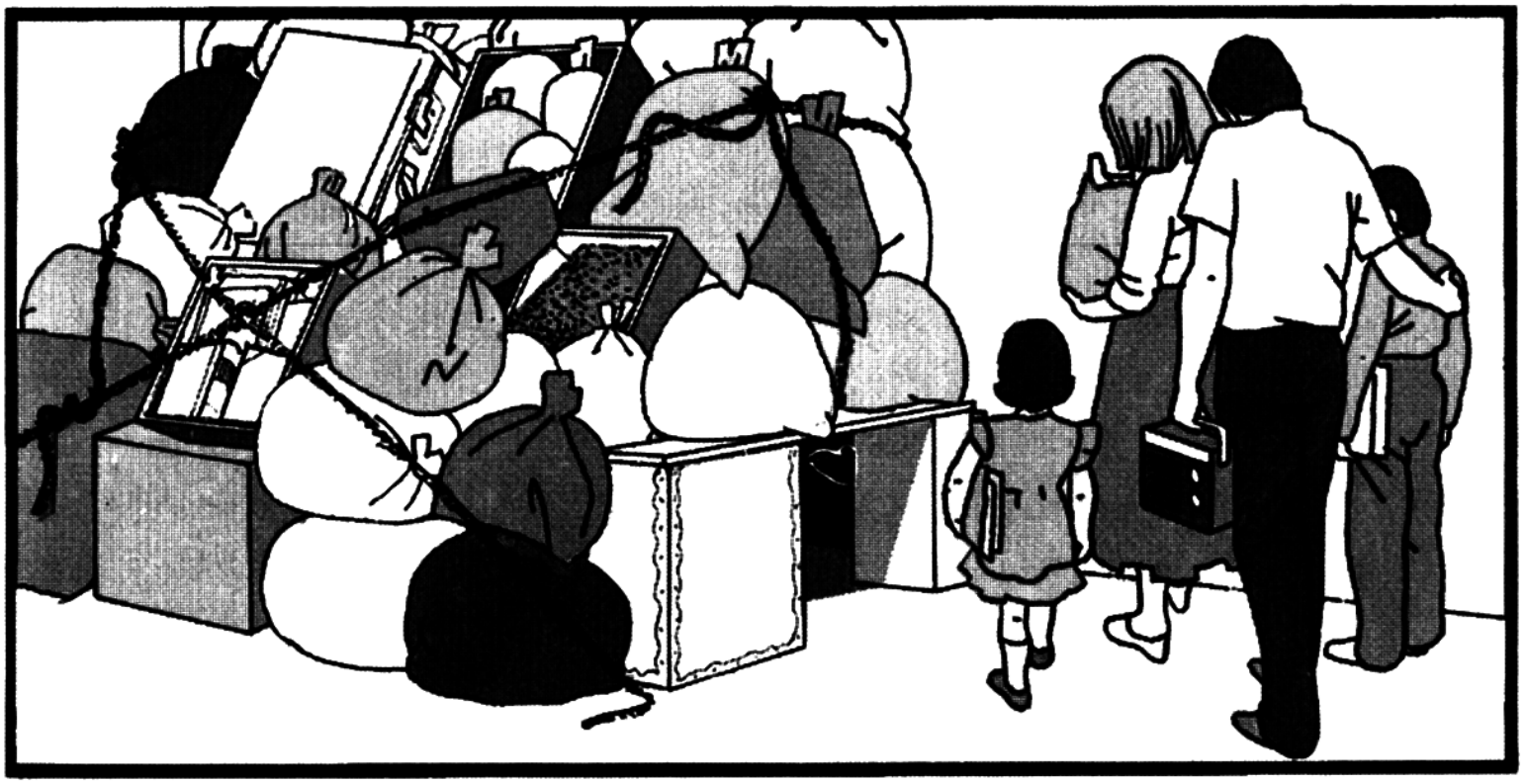

FIRST CASUALTIES OF THE H-BOMB

by DWIGHT MARTIN

Five weeks out of Yaizu, her home port 120 miles southeast of Tokyo, the 99-ton tuna trawler *Fukuryu Maru* ("Fortunate Dragon") hove to at a position 166°30′ east longitude and 11°52′ north latitude. She dropped anchor and cast her nets at 5:30 a.m. on March 1. The *Fortunate Dragon*'s position, though her skipper and crew did not realize it, was 71 miles east-northeast of Bikini atoll and 14 miles outside the boundary of the restricted zone of the U.S. government's atomic testing area.

A calm sea was running and the weather was clear. Sunrise was at 6:09 a.m. and visibility was excellent. The *Fortunate Dragon*'s skipper, 24-year-old Tadaichi Tsutsui, was standing watch on the bridge, and eight crewmen were enthusiastically hauling in their first nets. After nearly three weeks of poor catches near Midway Island, the *Fortunate Dragon* had finally run into luck in more southern waters and her hold was already filled with 16,500 pounds of fat tuna. It was just a few seconds before 6:12 a.m.

"Then," said Crewman Sanjiro Masuda later, "we saw flashes of fire, as bright as the sun itself, rising to the sky. They rose about 10 degrees from the horizon and the sky around them glowed fiery red and yellow.

AT HER DOCK the unfortunate *Fortunate Dragon*, still radioactive, floats untended by crewmen.

"We made port in Yaizu at 6 a.m. on March 14. We were now quite sick and frightened, and we went to see Dr. Toshisuke Oii at Kyoritsu hospital. He said we had severe burns and gave us some white ointment."

But Captain Tsutsui was getting more and more uneasy: "I thought, 'The bomb tests were being conducted over coral reefs. It could be pulverized coral ash, couldn't it?' " He thought some more about *shi no hai*, then ordered the crew to up anchor. The trawler steamed for home, 2,000 miles away.

"On the first night," said Radioman Aikichi Kuboyama, "we were unable to eat our supper. We tried drinking some sake (rice wine) to improve our appetites, but our appetites would not improve and the sake did not make us drunk. We were very depressed. Some of the crew grumbled '*pikadon*' but others said it couldn't be. I think someone said it was probably dust from some volcanic explosion."

LIFE
Vol. 36, No. 13 March 29, 1954

SOME EFFECTS OF

Ionizing Radiation

ON HUMAN BEINGS

from the

Naval Medical Research Institute

Bethesda 14, Maryland

U. S. Naval Radiological Defense Laboratory

San Francisco, California

and

Medical Department

Brookhaven National Laboratory

Upton, New York

Edited by

E. P. Cronkite

V. P. Bond

and C. L. Dunham

A Report on the Marshallese and Americans Accidentally Exposed to Radiation from Fallout and a Discussion of Radiation Injury in the Human Being

UNITED STATES

ATOMIC ENERGY COMMISSION

JULY 1956

Report TID-5358

Extensive lesions in 13 year old boy at 45 days post-exposure. Case 26.

PLATE 5.—*Hyperpigmented raised plaques and bullae on dorsum of feet and toes at 28 days. One lesion on left foot shows deeper involvement. Feet were painful at this time.*

PLATE 8.—*Same case as in Plate 5, six months later. Foot lesions have healed with repigmentation, except depigmented spots persist in small areas where deeper lesions were.*

PLATE 17.—*Epilation in 7 yr. old girl at 28 days. Case 72.*

PLATE 18.—*Same case as in Plate 17, six months after exposure showing complete regrowth of normal hair.*

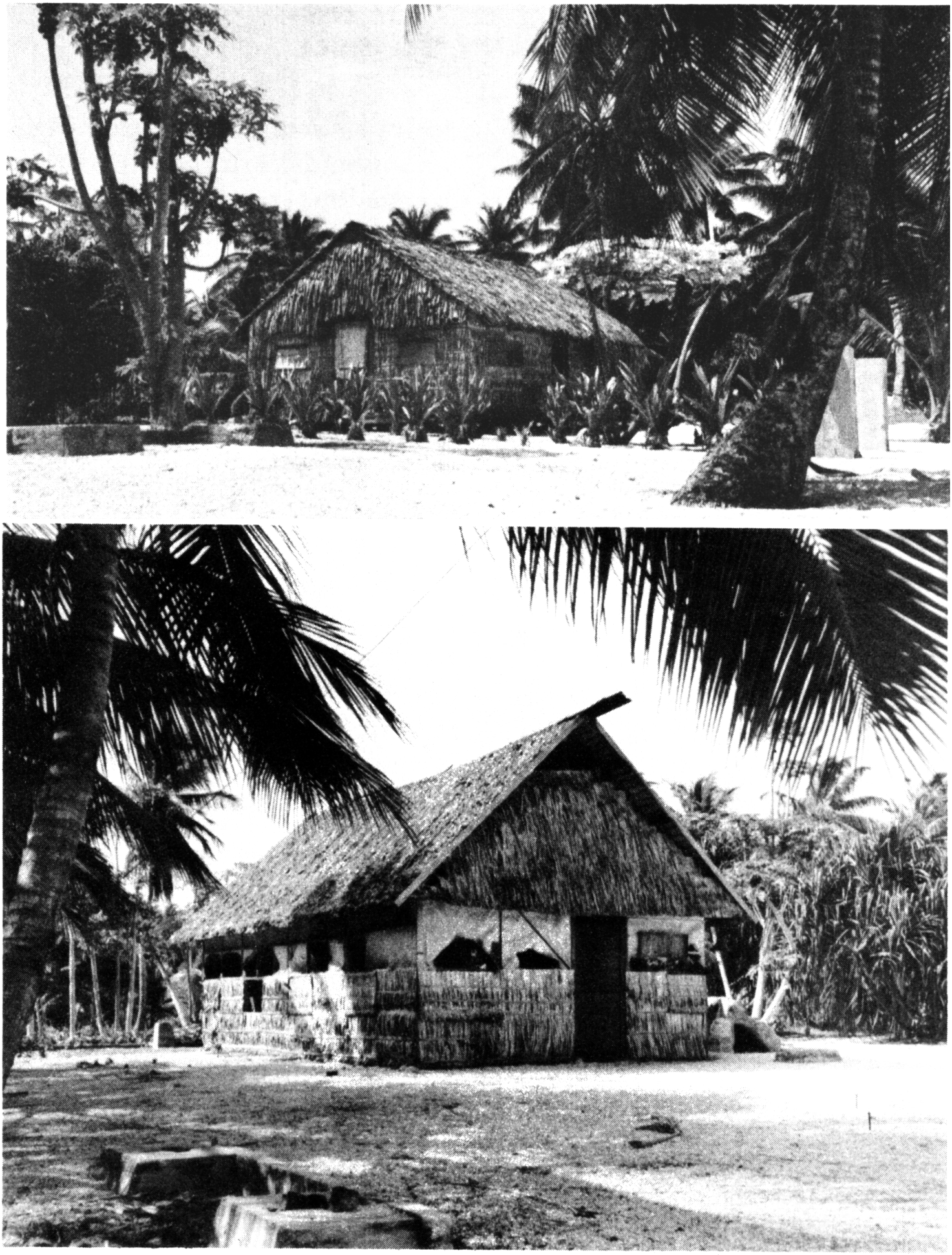

Figure 1.1—*Typical construction of the Marshallese homes to illustrate the exposure environment of the Marshallese and the lack of shielding from gamma radiation.*

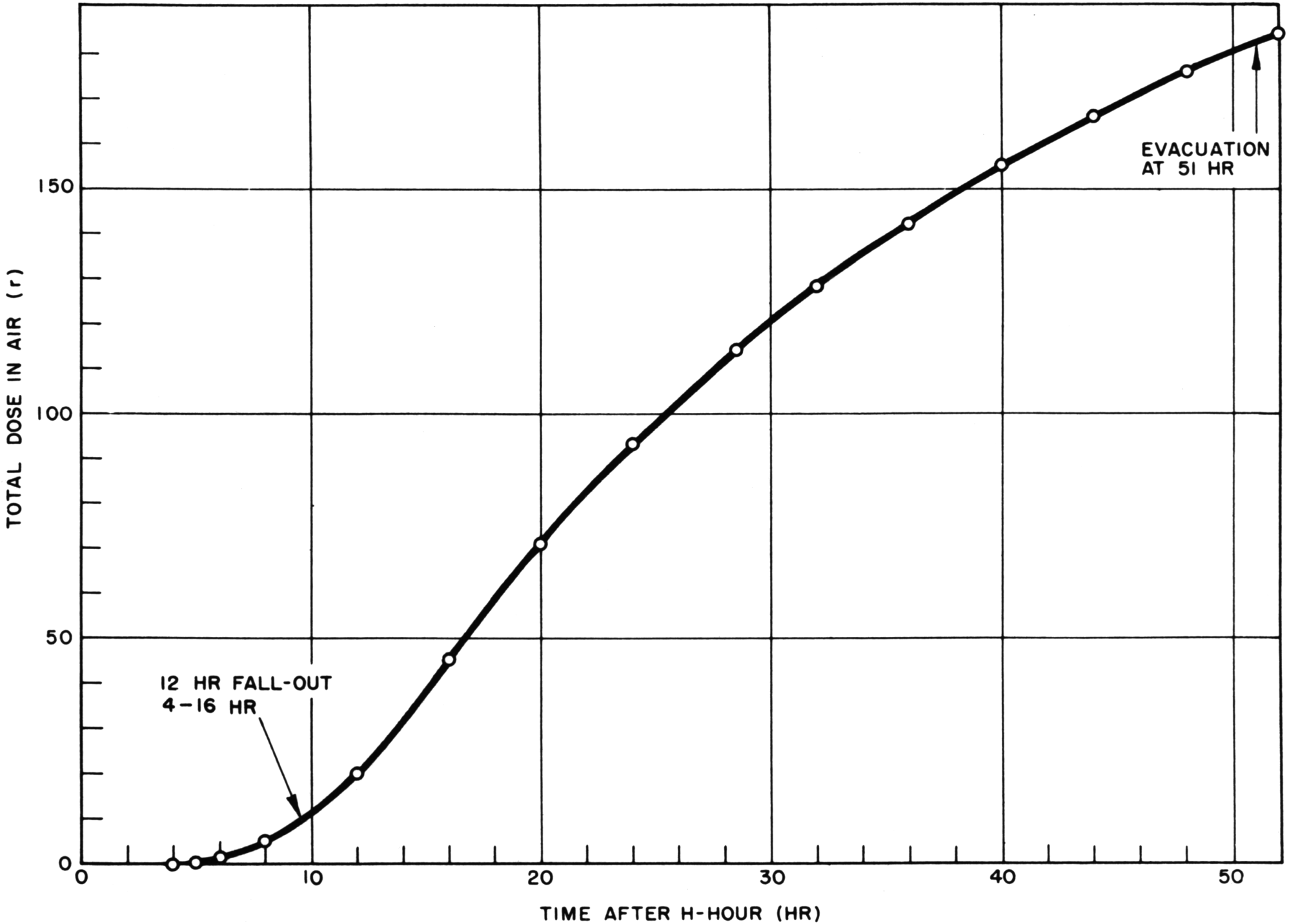

FIGURE 1.3—*The accumulation of gamma dose as a function of time after commencement of fallout on Rongelap*

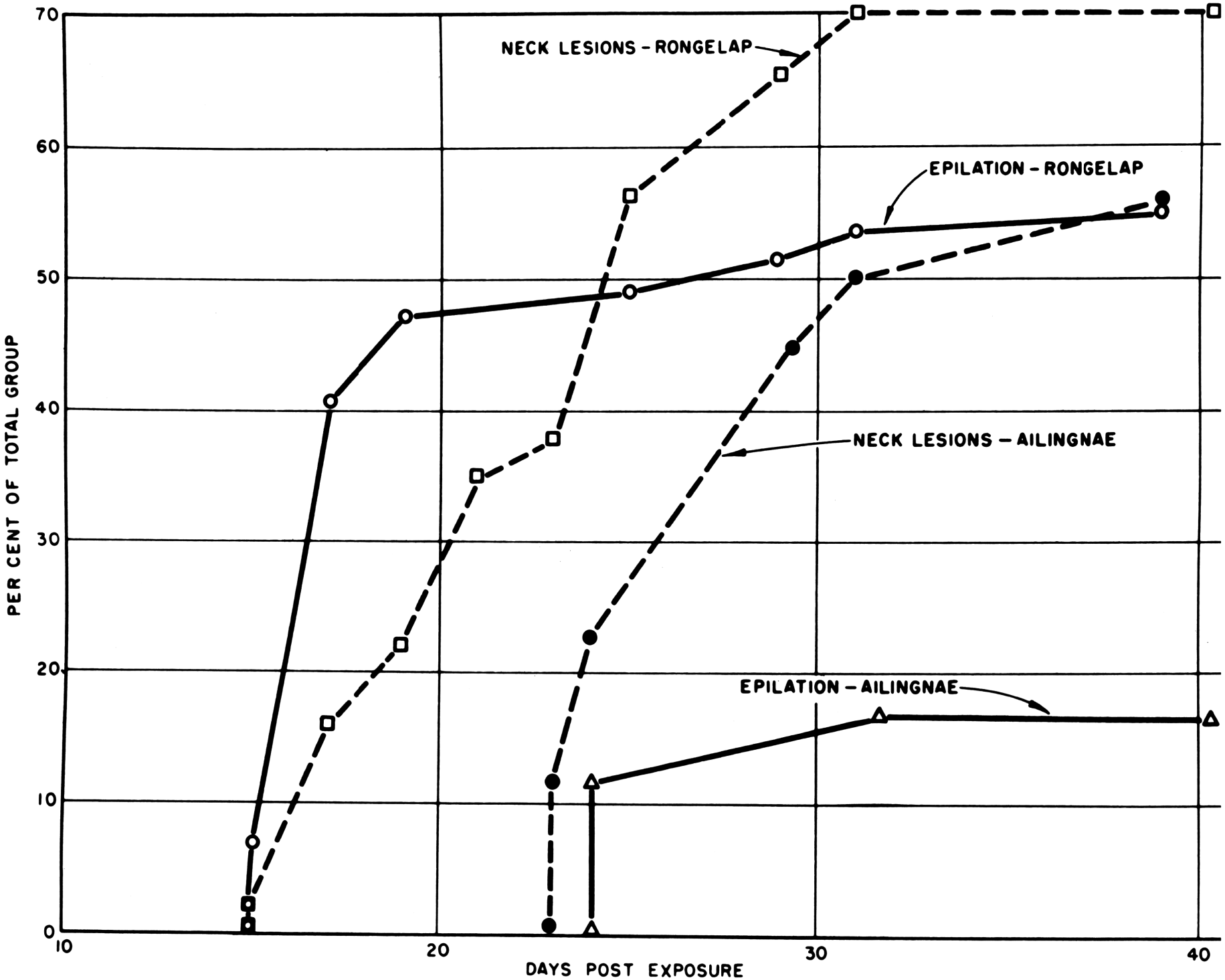

FIGURE 3.1.—*Comparison of the Incidence and Time of Appearance of Epilation and Neck Lesions in the Rongelap and Ailinginae Groups.*

On Rongerik (Group III) a set of film badge readings were obtained which constitute the only direct evidence of total dose. Several badges worn both outdoors and inside lightly constructed buildings on the island read about 50 to 65 r, and one badge which remained outdoors over the 28.5 hour period read 98 r. Another group of badges, kept indoors inside a steel refrigerator, read 38 r.

A long fallout probably would not be uniformly heavy throughout, the first portion being the most intense and the balance decreasing with time. The total phenomenon would thus tend toward the effect of a shorter fallout. This is supported by monitor data from other nuclear events, where initially heavy fallout is reported to produce a peak of air-borne radioactivity soon after arrival, with the airborne activity level then decreasing.

Itching and burning of the skin occurred in 28 percent of Group I (Rongelap), 20 percent of Group II (Ailinginae), 5 percent of Group III (Americans), and none of Group IV (Utirik). Three people in Group I and one in Group II complained of itching and burning of the eyes and lacrimation.

About two-thirds of Group I were nauseated during the first 2 days and one-tenth vomited and had diarrhea. One individual in Group II was nauseated. In Groups III and IV there were no gastrointestinal (GI) symptoms.

Between The 33rd and 43rd post-exposure days, 10 percent of the individuals in Group I had an absolute granulocyte level of 1000 per cubic millimeter or below. The lowest count observed during this period was 700 granulocytes/mm.[3]

Less striking fallout described as "mist-like" was observed on Ailinginae and Rongerik. Fallout was not visible on Utirik, which was contaminated to only a mild degree. The severity of the skin manifestations was roughly proportional to the amount of fallout observed.

Group	Fallout Observed	Skin Lesions and Epilation
Rongelap	Heavy (snowlike)	Extensive.
Ailinginae	Moderate (mistlike)	Less extensive.
Rongerik	Moderate (mistlike)	Slight.
Utirik	None	No skin lesions or epilation.

During the first 24–48 hours after exposure, about 25 percent of the Marshallese in the two higher exposure groups experienced itching and a burning sensation of the skin.

Skin lesions in the lesser exposed Ailinginae and Rongerik groups developed approximately one week after those in the Rongelap group, and were less severe and extensive. The Utirik group did not develop any lesions which could be attributed to irradiation of the skin. The incidence of ulcerating lesions in the different groups reflected the relative severity of the skin injury. Twenty percent of the Rongelap people developed ulcerative lesions while only five percent of the Ailinginae and none of the Rongerik people developed ulcerative lesions. Ninety percent of the Rongelap and Ailinginae groups developed lesions, compared to only forty percent of the Rongerik group. There were more lesions per individual in the Rongelap group than in the Ailinginae or Rongerik groups. A comparison of the incidence and time of appearance of epilation and neck lesions in the two groups is illustrated graphically in Figure 3.1.

a. *Shelter.* Those individuals who remained indoors or under the trees during the fallout period developed less severe lesions.

b. *Bathing.* Small children who went wading in the ocean developed fewer foot lesions. Most of the Americans, who were more aware of the danger of the fallout, took shelter in aluminum buildings, bathed and changed clothes and consequently developed only very mild beta lesions.

c. *Clothing.* A single layer of cotton material offered almost complete protection, as was demonstrated by the fact that lesions developed almost entirely on the exposed parts of the body.

3.54 Factors Favoring the Development of Lesions

a. *Areas of more profuse perspiration.* Lesions were more numerous in areas where perspiration is abundant such as the folds of the neck, axillae, and antecubital fossae.

b. *Delay in decontamination.* There was a delay of 1 or 2 days before satisfactory decontamination was possible.

Table 1.1—Exposed, and Control Unexposed Groups

Group Designation	Total Number In Group	Approximate Time of Commencement of Fallout	Time of Evacuation	Instrument Readings Used in Dose Calculations	Best Estimate of Total Gamma Dose in Air (r)
Group I.—Rongelap	64	H + 4 to 6 hrs.	H + 50 hrs. (16 people) H + 51 hrs. (48 people)	375 mr/hrs., H + 7 days	175
Group II.—Ailinginae	18	H + 4 to 6 hrs.	H + 58 hrs.	100 mr/hrs., H + 9 days	69
Group III.—Rongerik	28	H + 6.8 hrs.	H + 28.5 hrs. (8 men) H + 34 hrs. (20 men)	280 mr/hrs., H + 9 days	78
Group IV.—Utirik	157	H + 22 hrs.	Started at H + 55 hrs. Completed at H + 78 hrs.	40 mr/hrs., H + 8 days	14

Group	Composition	Fallout observed	Estimated gamma dose (rads)	Extent of skin lesions
Rongelap	64 Marshallese	Heavy (snowlike)	175	Extensive
Ailingnae	18 Marshallese	Moderate (mistlike)	69	Less extensive
Rongerik	28 Americans	Moderate (mistlike)	78	Slight
Utirik	157 Marshallese	None	14	No skin lesions or epilation

Proceedings:
SECOND INTERDISCIPLINARY CONFERENCE
ON SELECTED EFFECTS OF A GENERAL WAR

VOLUME II

This Conference was sponsored by the Defense Atomic Support Agency (Contract DASA 01-67-C-0024, NWER Subtask DB003) through the auspices of the New York Academy of Sciences Interdisciplinary Communications Program. It was held at Princeton, New Jersey, during 4-7 October 1967.

DASIAC Special Report 95
July 1969

SESSION II Wright H. Langham 45

LANGHAM: Fallout was predicted for the Trinity test in 1945 by the bomb phenologists, Hershfeider and McGee. Stafford Warren mounted evacuation teams and monitoring teams to cover the potential fallout area. We didn't have to evacuate anybody; we almost did. The arbitrary limit chosen for evacuation was an infinite life-time dose of 50 r. One family approached this limit, and there was much debate as to whether we should evacuate them or not. They weren't evacuated.

SESSION II Theodore B. Taylor 51

TAYLOR: I would like to interject something that you challenged, Staff. You said a moment ago, you can't hear it. Apropos of the Dog Shot, fallout was clearly audible. There were little beads of steel from the tower that condensed, and one heard this constant tinkle, tinkle of steel from the tower hitting the aluminum roofs and then rolling down the gutters and piling up in little piles on the ground.

76 Lin Root DASA 2019-2

ROOT: Mutual Security Agreement—after Korea. It was terribly important that Japan become a responsible member of the organization. The Yoshida cabinet was entirely favorable to the U.S. and it looked as if there would not be too much opposition. Then the fishermen arrived. Demonstrations flared up everywhere. You had the trade unions, three million strong, protesting. The cabinet tried to counteract the anti-American feeling but a tidal wave of anger inundated the country. It was just diminishing when Koboyama died. This was portrayed as a radiation death.

FREMONT-SMITH: This is the fisherman that had the transfusion and the hepatitis?

ROOT: Yes. Japanese doctors give very small blood transfusions, and Koboyama needed a great many.

15-kt Buffalo-1
(AWRE-T28/57, p. 26)

WT-915 Castle-Bravo 15 megaton H-bomb test of 1 March 1954, which contaminated a Japanese tuna trawler and islanders

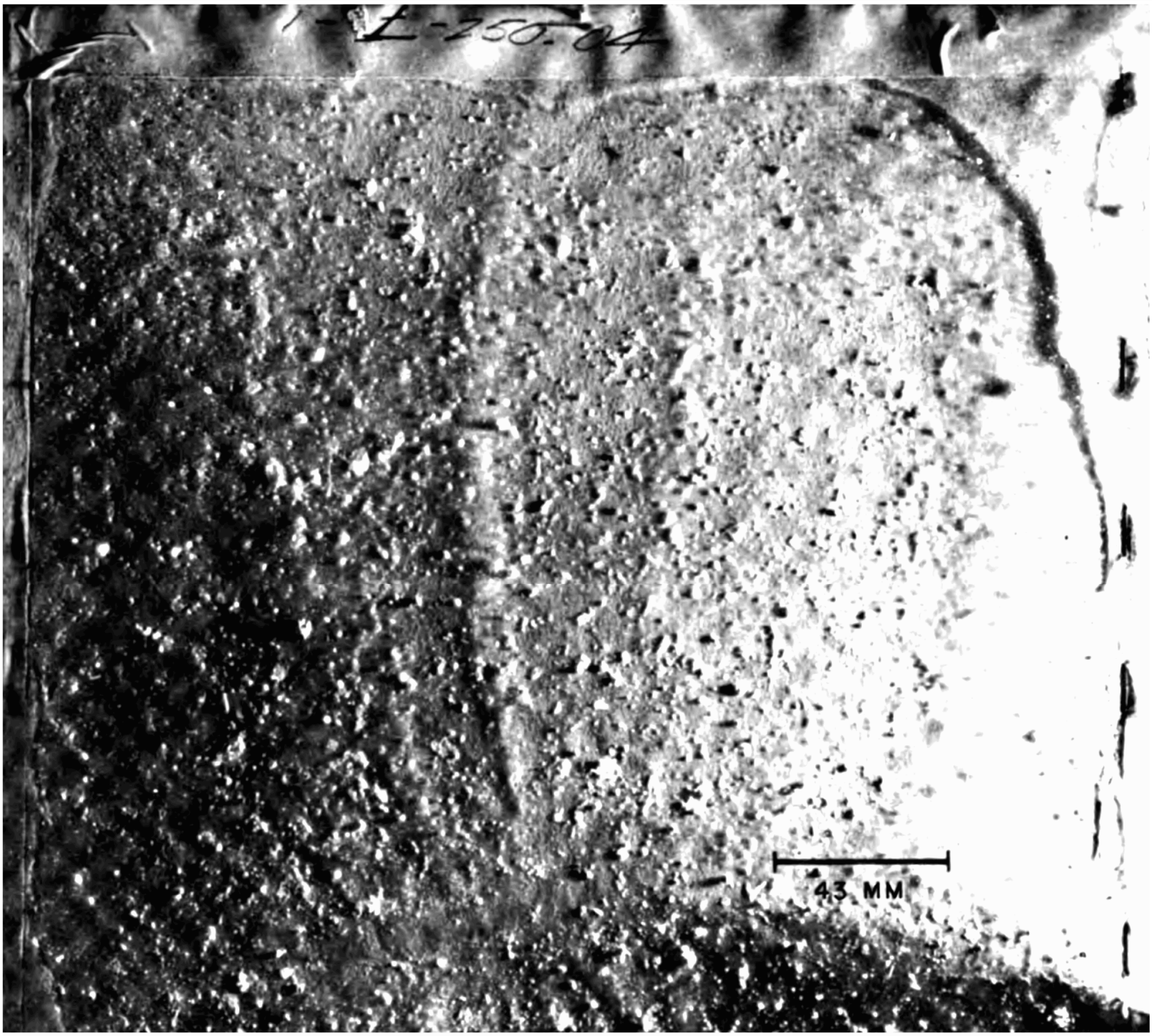

Fig. 5.10 Shot 1, Fallout Particulate, Station 250.04

This is a raft downwind in Bikini Lagoon, which received a land equivalent of 113 R/hr (1 hour reference gamma dose rate), according to Figures 2.2 and 6.1. Land equivalent dose rates were 7 times the raft dose rate in the lagoon.

According to Table 1 in Carl F. Miller's report USNRDL-466, 250.04 received 33.6 (mg/sq ft)/(R/hr at 1 hr) at 59.5 kft. Hence, 3.8 grams/sq ft.

THIN SECTION AND RADIOGRAPH OF A FALLOUT PARTICLE FROM A SMALL-YIELD SURFACE SHOT AT THE NEVADA TEST SITE. THE PARTICLE IS A TRANSPARENT YELLOW-BROWN GLASS WITH MANY INCLUSIONS OF GAS BUBBLES AND UNMELTED MINERAL GRAINS. THE RADIOACTIVITY IS DISTRIBUTED IRREGULARLY THROUGHOUT THE GLASS PHASE OF THE PARTICLE

1.2 KT JANGLE-SUGAR NEVADA SURFACE BURST

C.E. Adams, et al. The Nature of Individual Radioactive Particles. I. Surface and Underground A.B.D. Particles From Operation JANGLE. U.S. Naval Radiological Defense Laboratory Report, USNRDL-374, November 28, 1952

THIN SECTION AND RADIOGRAPH OF AN ANGULAR FALLOUT PARTICLE FROM A LARGE-YIELD SURFACE SHOT AT THE ENIWETOK PROVING GROUNDS. THIS PARTICLE IS COMPOSED ALMOST ENTIRELY OF CALCIUM HYDROXIDE WITH A THIN OUTER LAYER OF CALCIUM CARBONATE. THE RADIOACTIVITY HAS COLLECTED ON THE SURFACE AND HAS DIFFUSED A SHORT DISTANCE INTO THE PARTICLE

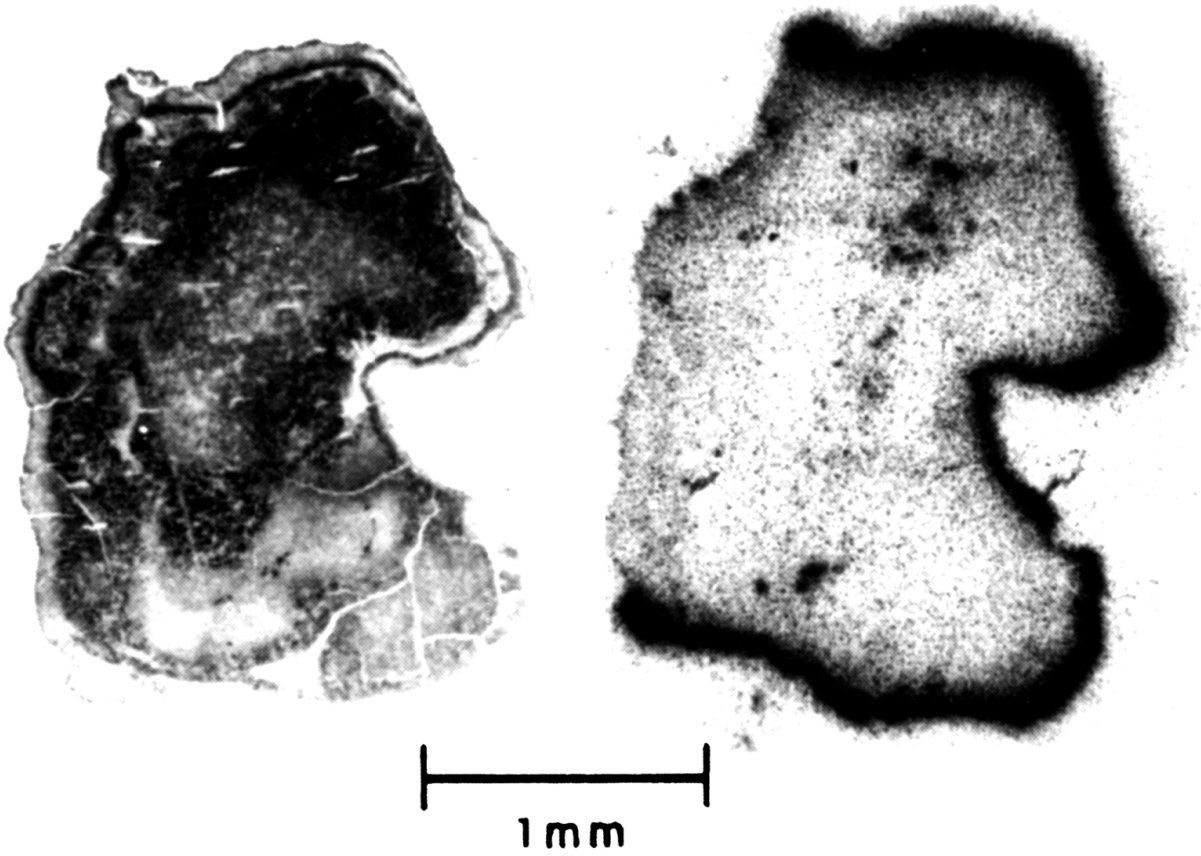

TWO FALLOUT PARTICLES FROM A TOWER SHOT AT THE NEVADA TEST SITE. THE PARTICLE ON THE LEFT IS A PERFECT SPHERE WITH A HIGHLY GLOSSY SURFACE; THE ONE ON THE RIGHT HAS MANY PARTIALLY-ASSIMILATED SMALLER SPHERES ATTACHED TO ITS SURFACE. BOTH PARTICLES ARE BLACK AND MAGNETIC AND HAVE A SUPERFICIAL METALLIC APPEARANCE.

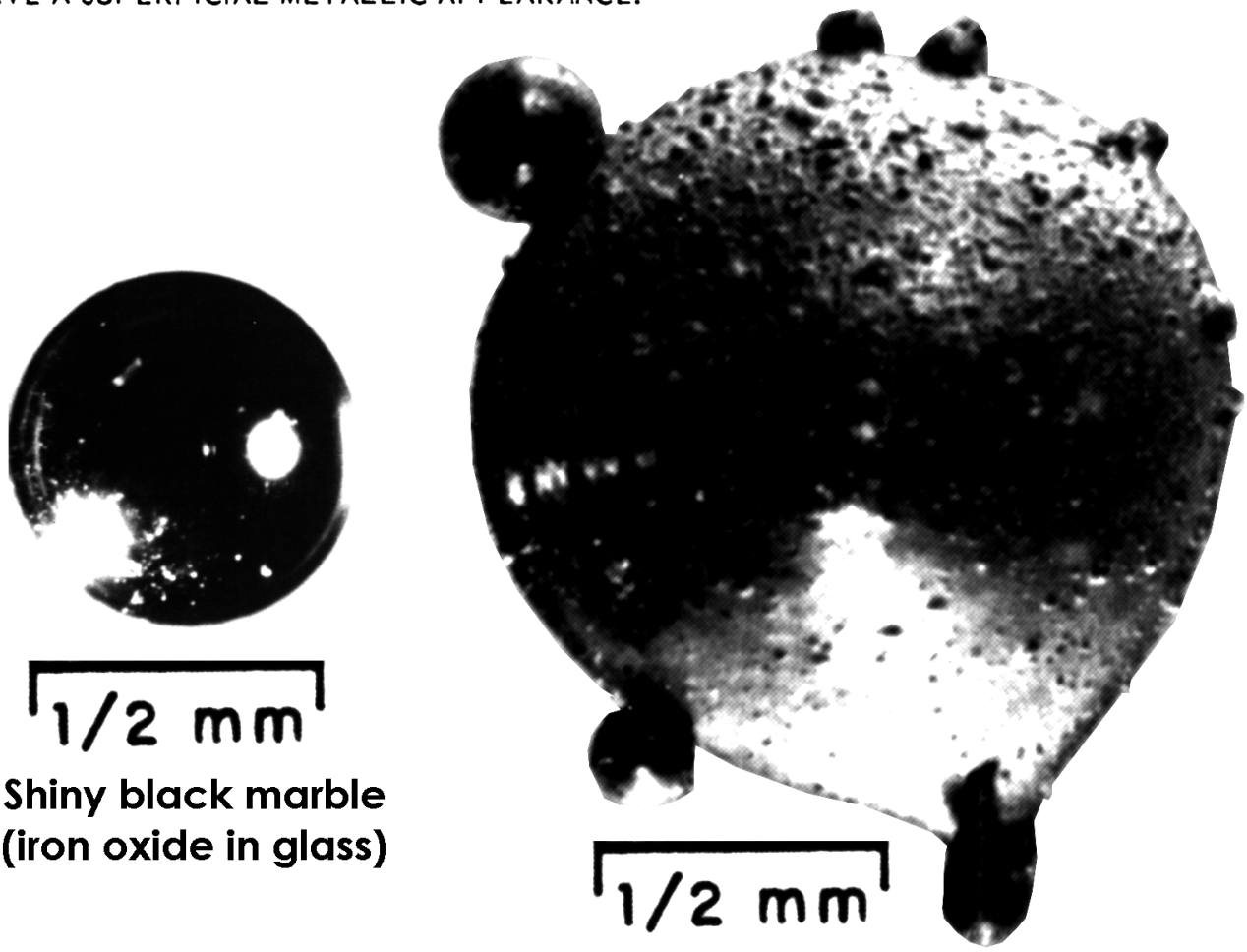

THIN SECTION AND RADIOGRAPH OF A FALLOUT PARTICLE FROM A MODERATE-YIELD TOWER SHOT AT THE NEVADA TEST SITE. THIS PARTICLE IS COMPOSED OF A TRANSPARENT GLASS CORE WITH A DARKLY COLORED IRON OXIDE GLASS OUTER ZONE. MOST OF THE RADIOACTIVITY IS CONCENTRATED IN THE OUTER ZONE

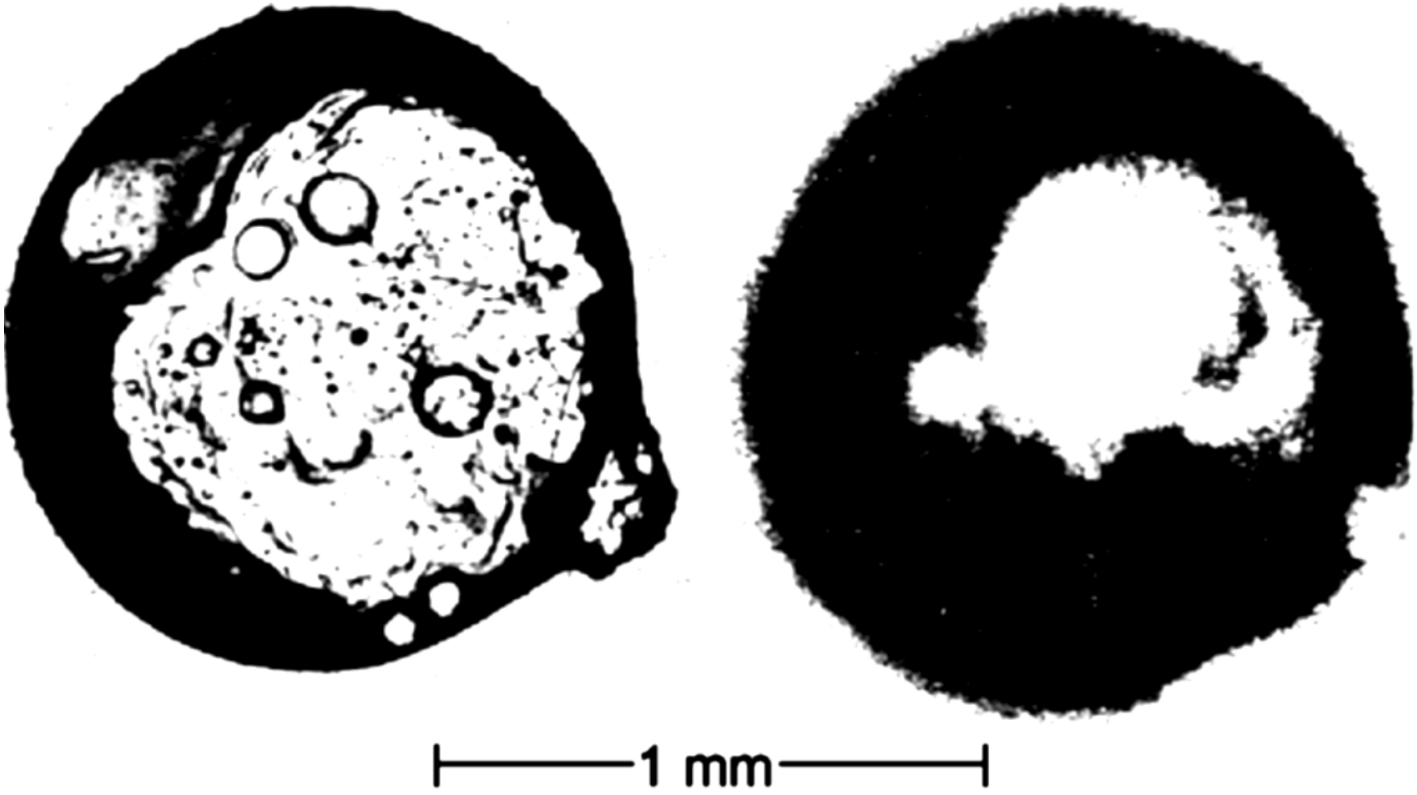

C.E. Adams. The Nature of Individual Radioactive Particles. IV. Fallout Particles From A.B.D. of Operation UPSHOT-KNOTHOLE. U.S. Naval Radiological Defense Laboratory Report, USNRDL-440, February 24, 1954

Road sweeper (fallout radiation removal)

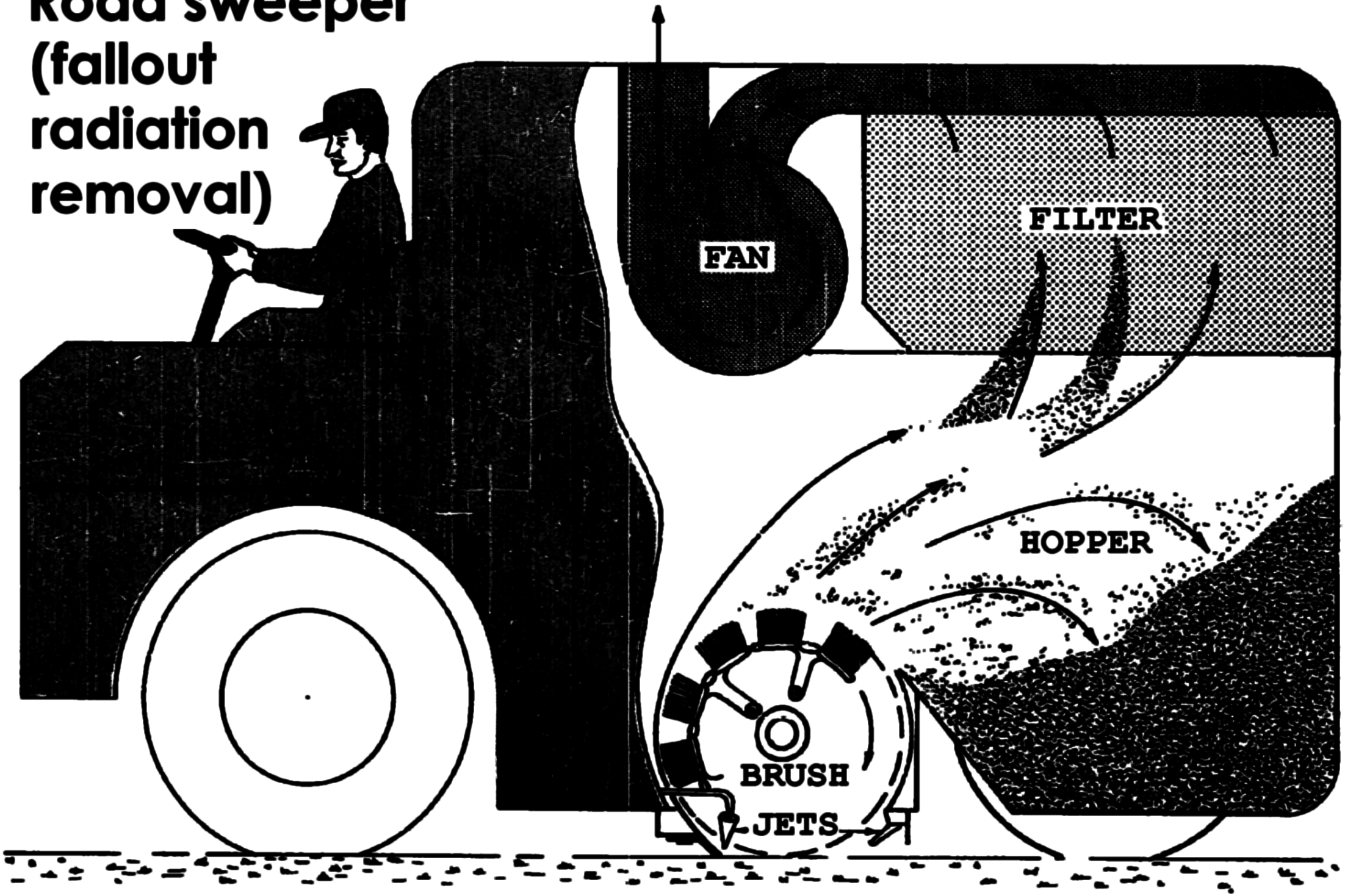

USNRDL-TR-1049
29 July 1966

AD 641480

REMOVAL OF SIMULATED FALLOUT FROM ASPHALT STREETS BY FIREHOSING TECHNIQUES

by

L.L.Wiltshire
W.L.Owen

In general, removal effectiveness improves with increased particle size range and increased mass loading. For the expenditure of an effort of 4 nozzle-minutes (12 man-minutes) per 10^3 ft^2, results ranged as follows:

Particle Size Range (μ)	Nominal Mass Loading (g/ft^2)	Removal Effectiveness (Residual Fraction)
44 - 88	4.0	0.16
	24.0	0.07
350 - 700	4.0	0.005
	24.0	0.003

U.S. NAVAL RADIOLOGICAL DEFENSE LABORATORY

SAN FRANCISCO · CALIFORNIA 94135

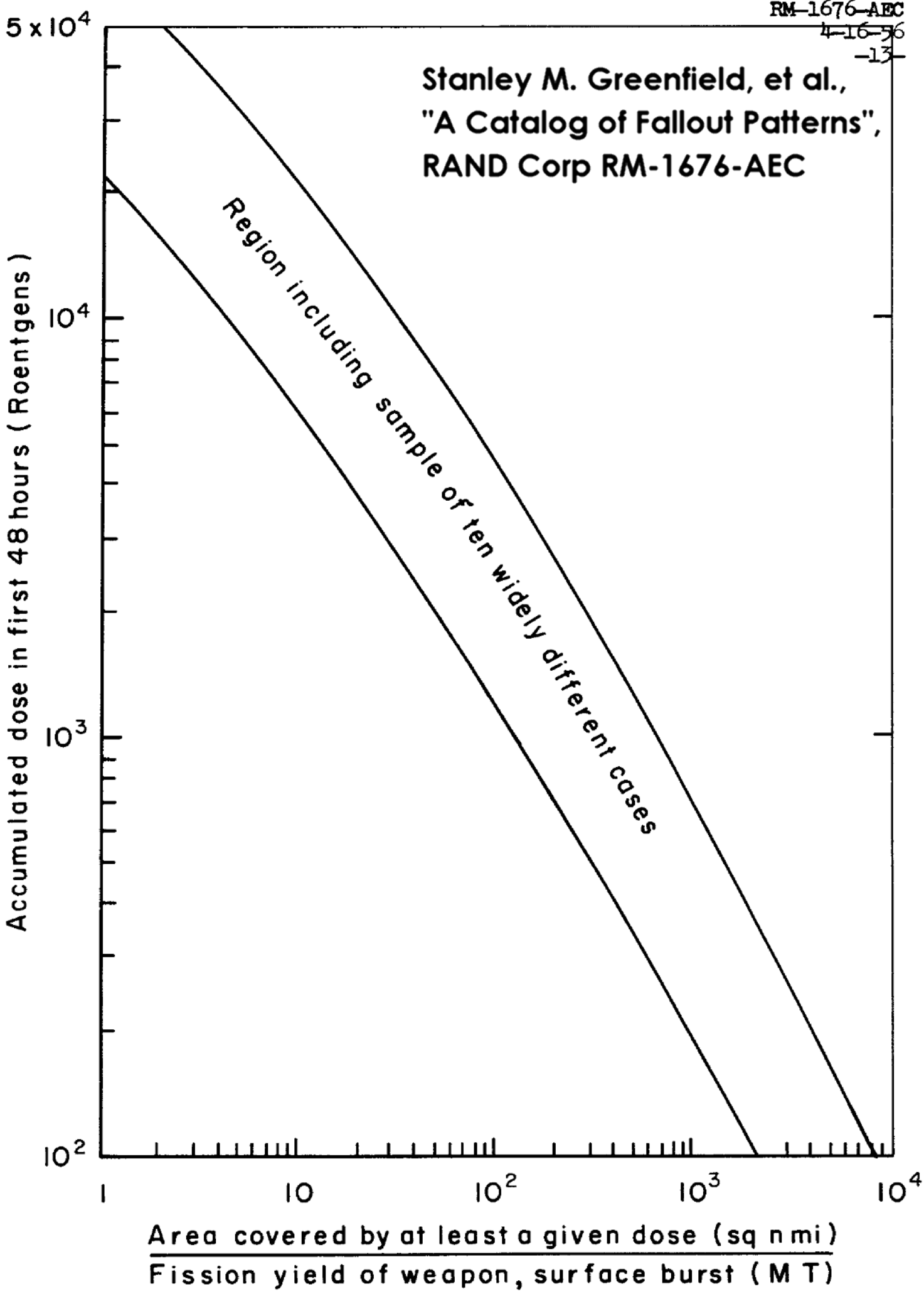

Approximate scaling relationship between 48-hr dose rate and normalized area

AD-A995490

POR-2266 (WT-2266)

TABLE 4.1

AREAS ENCLOSED BY DOSE RATE CONTOURS

Contour Dose Rate, I	Area Within Contour			
	Little Feller I (0.018 kt)	Little Feller II (0.022 kt)	Johnie Boy (0.5 kt)	Small Boy (1.65 kt)
r/hr	mi^2	mi^2	mi^2	mi^2
0.5	0.33	0.827	-	109.83
1.0	0.208	0.469	33.097	61.63
5.0	-	0.070	-	-
10.0	0.032	0.045	3.924	9.057
20.0	-	0.019	-	-
50.0	-	-	0.536	2.954
100.0	0.00478	0.005	0.214	1.200
200.0	-	-	-	0.285
1,000.0	-	-	0.0917	0.092
2,000.0	-	-	-	0.01665
10,000.0	-	-	0.0161	-
17,000.0	-	-	0.00537	-

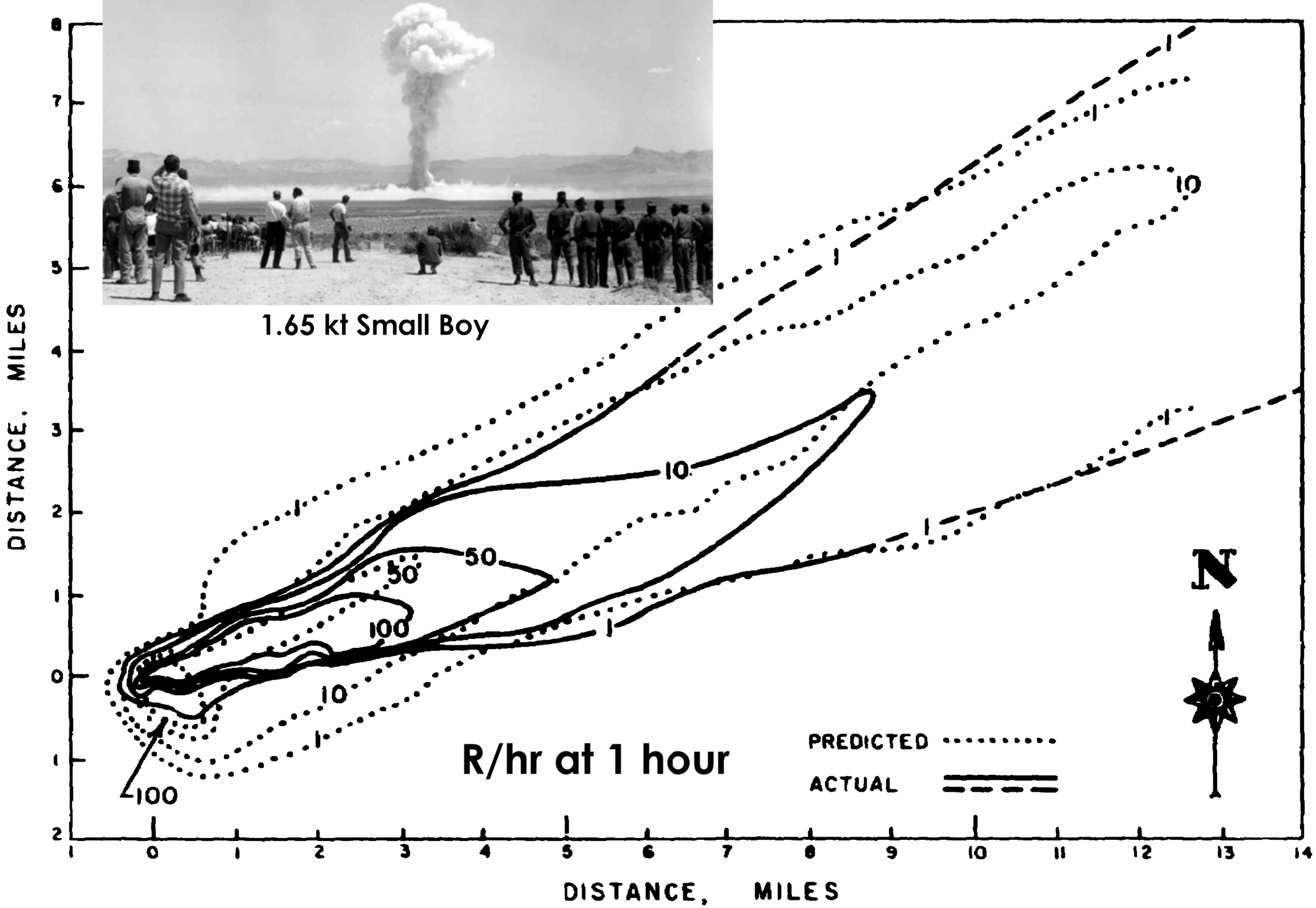

AD-A995490

POR-2266 (WT-2266)

Figure 4.13 Comparison of Ford Instrument Company prediction with observed Small Boy pattern.

Small Boy
14 Jul 1962
TYPE OF BURST AND PLACEMENT:
Tower, over Nevada soil
CLOUD TOP HEIGHT: 19,000 ft MSL
SITE ELEVATION: 3078 ft MSL

Altitude (MSL)	H+5 Minutes Direction	H+5 Minutes Speed
feet	degrees	mph
3,078	135	2.3
4,000	300	1.2
5,000	310	1.2
6,000	330	2.3
7,000	280	2.3
8,000	250	6.9
9,000	240	13.8
10,000	240	18.4
12,000	240	9.2
14,000	240	9.2
15,000	-	-
16,000	240	9.2
18,000	280	16.1
20,000	280	28.8

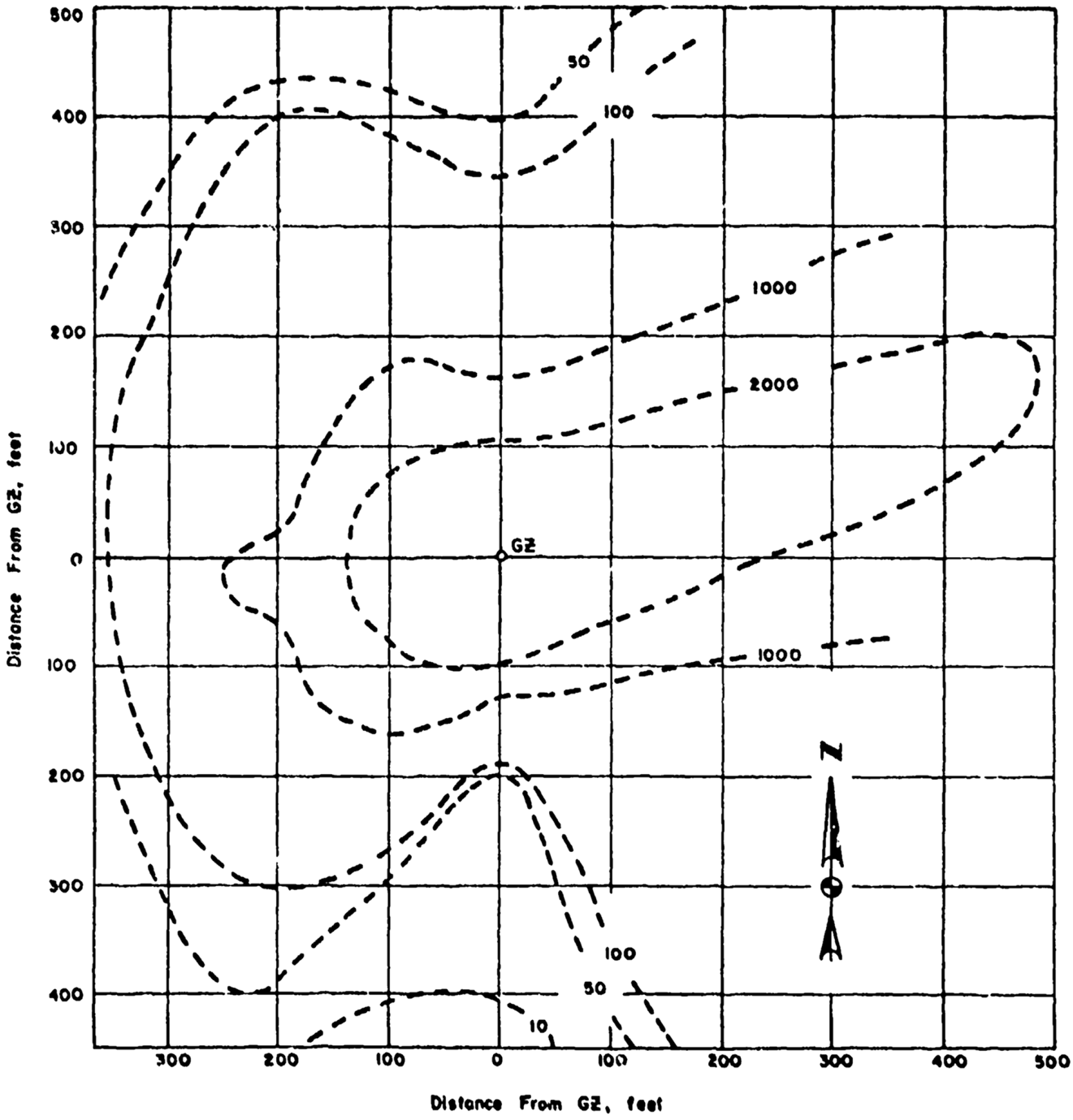

Figure 329. OPERATION SUNBEAM - Small Boy GZ area contours in R/hr at H+1 hour

The contours were corrected to H+1 hour using a decay constant of 1.27.

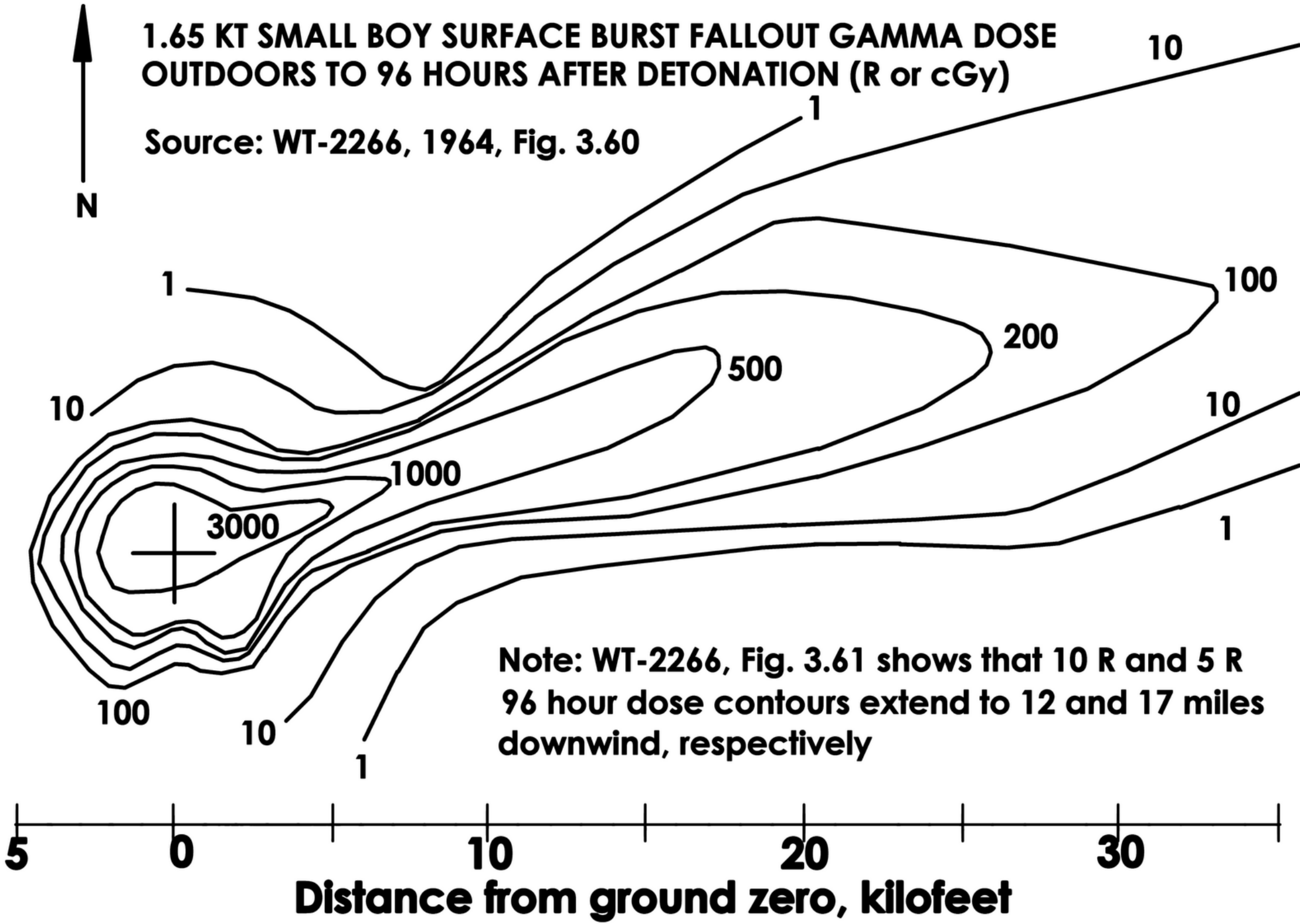
1.65 KT SMALL BOY SURFACE BURST FALLOUT GAMMA DOSE
OUTDOORS TO 96 HOURS AFTER DETONATION (R or cGy)
Source: WT-2266, 1964, Fig. 3.60
N
10
1
1
100
200
500
10
10
1000
3000
1
100
10
1
Note: WT-2266, Fig. 3.61 shows that 10 R and 5 R
96 hour dose contours extend to 12 and 17 miles
downwind, respectively
5
0
10
20
30
Distance from ground zero, kilofeet

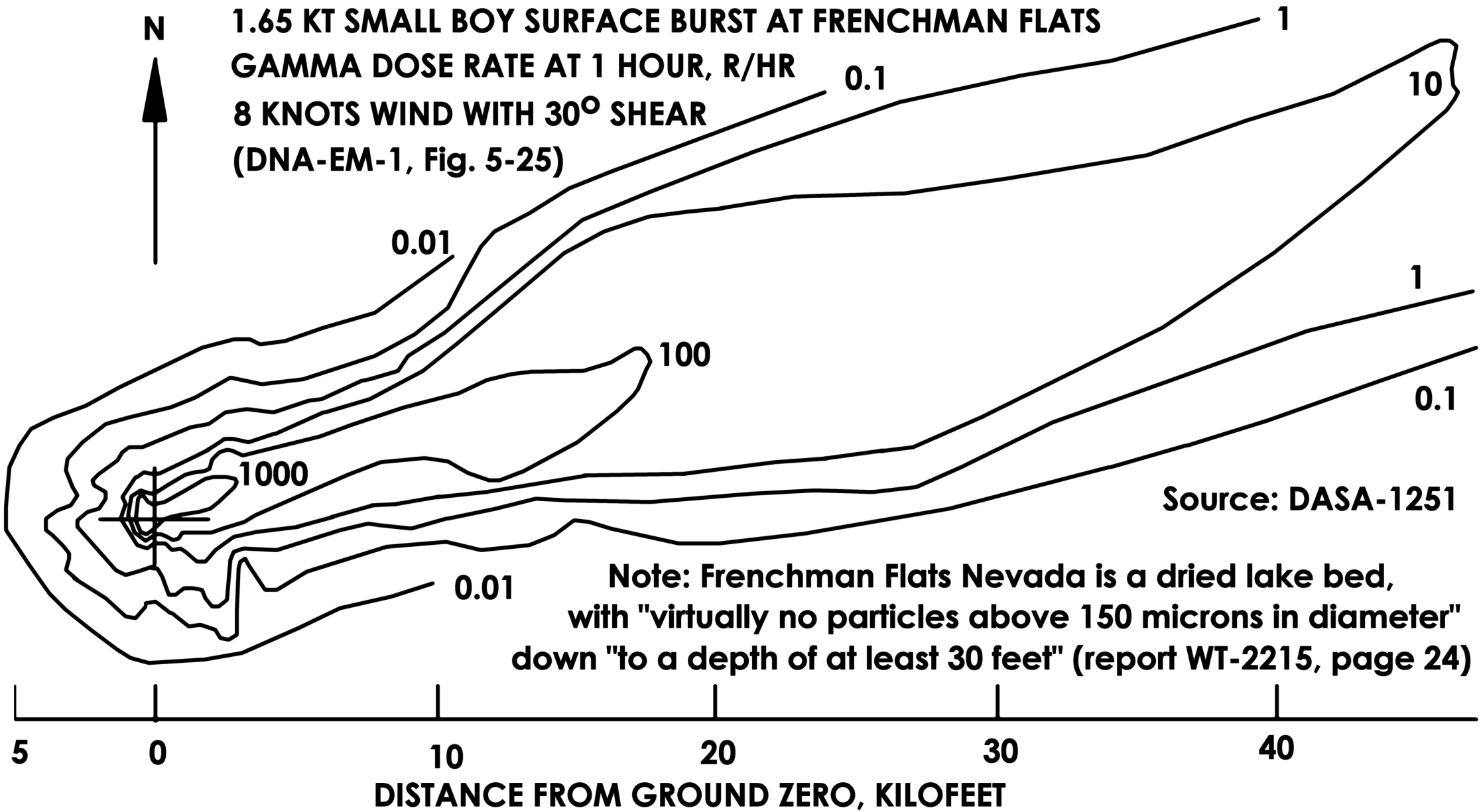
N
1.65 KT SMALL BOY SURFACE BURST AT FRENCHMAN FLATS
GAMMA DOSE RATE AT 1 HOUR, R/HR
8 KNOTS WIND WITH 30° SHEAR
(DNA-EM-1, Fig. 5-25)
1
0.1
10
0.01
1
100
0.1
1000
Source: DASA-1251
0.01
Note: Frenchman Flats Nevada is a dried lake bed,
with "virtually no particles above 150 microns in diameter"
down "to a depth of at least 30 feet" (report WT-2215, page 24)
5
0
10
20
30
40
DISTANCE FROM GROUND ZERO, KILOFEET

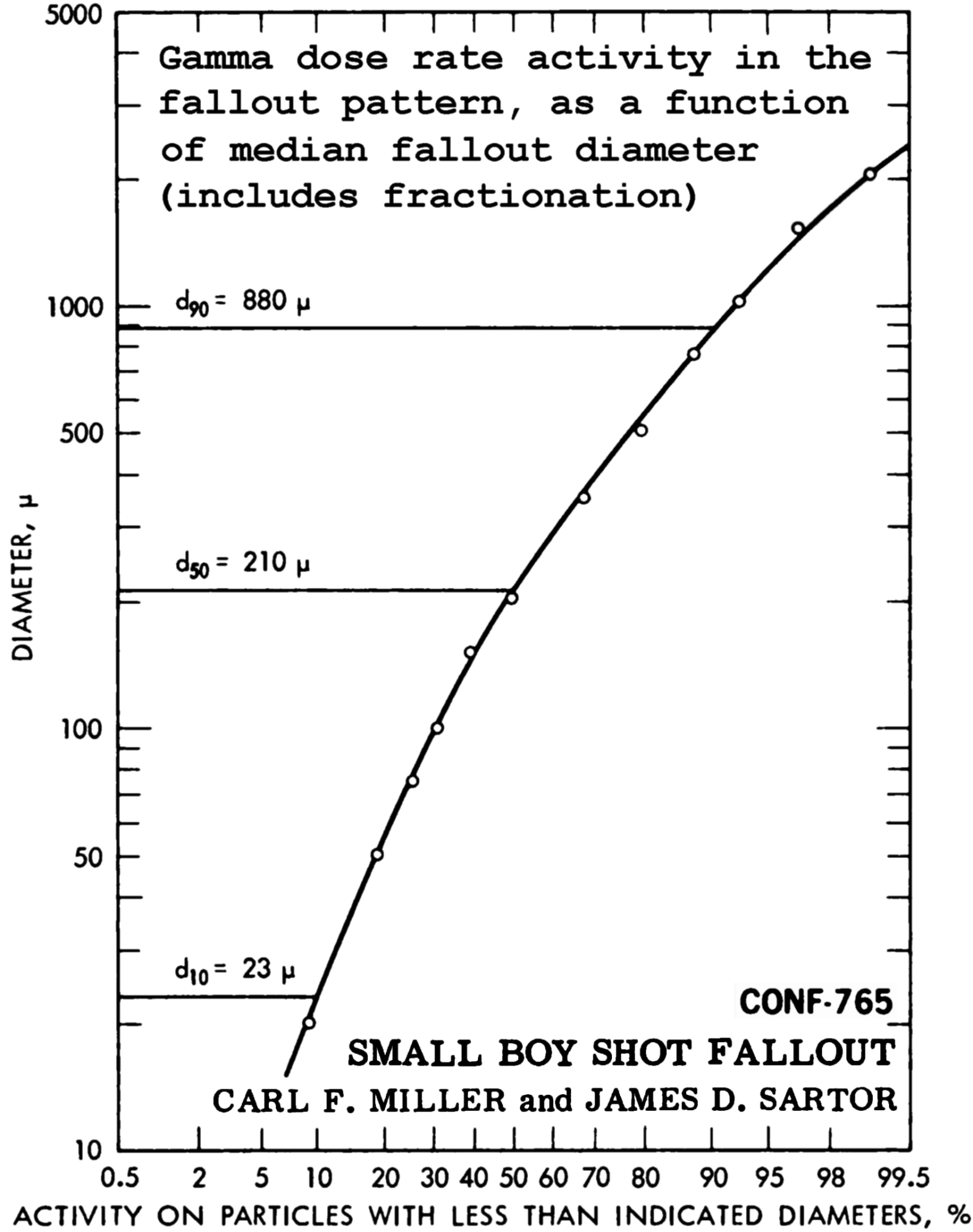
Gamma dose rate activity in the fallout pattern, as a function of median fallout diameter (includes fractionation)
d_{90} = 880 μ
d_{50} = 210 μ
d_{10} = 23 μ
CONF-765
SMALL BOY SHOT FALLOUT
CARL F. MILLER and JAMES D. SARTOR
DIAMETER, μ
5000
1000
500
100
50
10
0.5
2
5
10
20
30
40
50
60
70
80
90
95
98
99.5
ACTIVITY ON PARTICLES WITH LESS THAN INDICATED DIAMETERS, %

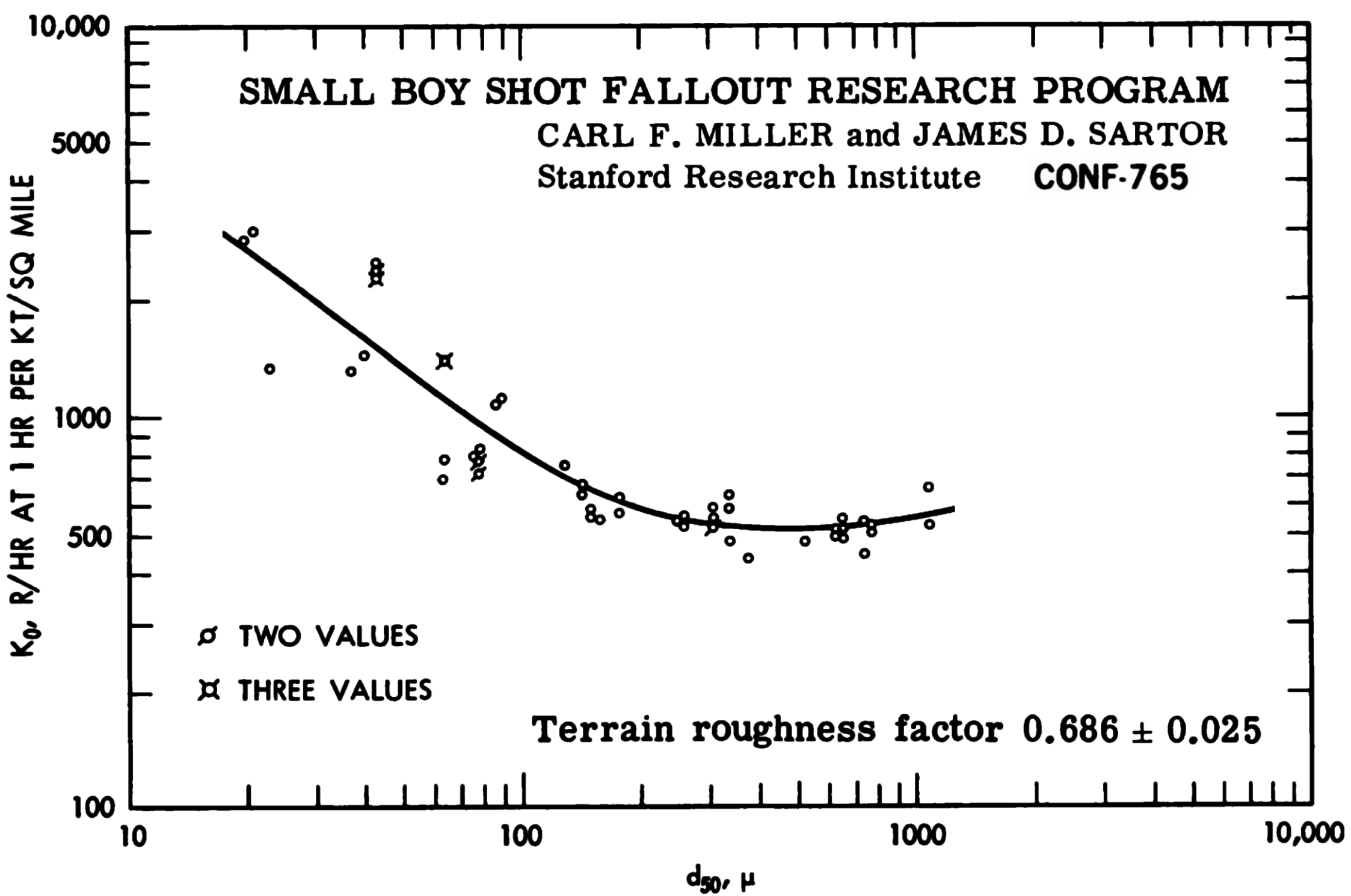

Fractionation effect (factor including terrain shielding)

CONF-765

EARLY FOOD-CHAIN KINETICS OF RADIONUCLIDES FOLLOWING CLOSE-IN FALLOUT FROM A SINGLE NUCLEAR DETONATION

WILLIAM E. MARTIN
University of California at Los Angeles, Los Angeles, California

ABSTRACT

Radiochemical and statistical analyses indicated highly significant correlations between estimates of gamma dose rates and maximum concentrations of ^{89}Sr or ^{131}I in plant samples and in the stomach contents, bone ash, or thyroids of rabbits collected between 15 and 110 miles from ground zero.

Table 1 — AVERAGE GAMMA DOSE RATES, R_0, AND AVERAGE CONCENTRATIONS OF ^{89}Sr IN PLANT SAMPLES AND IN THE BONE ASH OF RABBITS COLLECTED FROM THE SEDAN FALLOUT FIELD

Study areas	Initial gamma dose rates			Days after detonation	Plant samples, pc ^{89}Sr/g (dry)			Rabbit bone ash, pc ^{89}Sr/g (dry)		
	$\bar{x}$	$s\bar{x}$	n		$\bar{x}$	$s\bar{x}$	n	$\bar{x}$	$s\bar{x}$	n
All areas	17.5	±30%	20	5	1436	±32%	20	863	±29%	20
R_0 = mr/hr at 3 ft at H + 24.				15	909	±37%	20	1680	±38%	20
				30	544	±40%	20	2097	±30%	20
				60	313	±32%	20	1389	±34%	20

$\bar{x}$ = mean, $s\bar{x}$ = standard error expressed as a percentage of the mean, and n = number of samples.

Table 2 — AVERAGE CONCENTRATIONS OF ^{131}I IN PLANT SAMPLES AND IN THE THYROIDS OF RABBITS COLLECTED FROM THE SEDAN FALLOUT FIELD

Study areas	Days after detonation	Plant samples, pc ^{131}I/g (dry)			Rabbit thyroids, nc ^{131}I per thyroid		
		$\bar{x}$	$s\bar{x}$	n	$\bar{x}$	$s\bar{x}$	n
All areas	5	3606	±40%	20	221	±28%	19
	15	984	±40%	20	74	±36%	20
	30	113	±27%	20	12	±50%	20

$\bar{x}$ = mean, $s\bar{x}$ = standard error expressed as a percentage of the mean, and n = number of samples.

Our estimates of effective half-lives on plants in the Sedan fallout field, 18 days for ^{89}Sr and 5.0 to 5.5 days for ^{131}I, indicate environmental half-lives (i.e., half-time rates of loss due to all causes other than radioactive decay) of approximately 28 days for ^{89}Sr and 15 days for ^{131}I. Since there was little or no rain in the area of the Sedan fallout field during the period of this study, the environmental half-life of ^{89}Sr on plants can be attributed primarily to wind action that removed particles from foliage or foliage from plants. The shorter environmental half-life of ^{131}I on plants may reflect the combined effects of wind action and sublimation.[1,2]

1. W. E. Martin, Losses of Sr^{90}, Sr^{89}, and I^{131} from Fallout Contaminated Plants, *Radiation Botany*, in press.
2. W. E. Martin, Loss of I^{131} from Fallout-contaminated Vegetation, *Health Phys.*, *9:* 1141-1148 (1963).

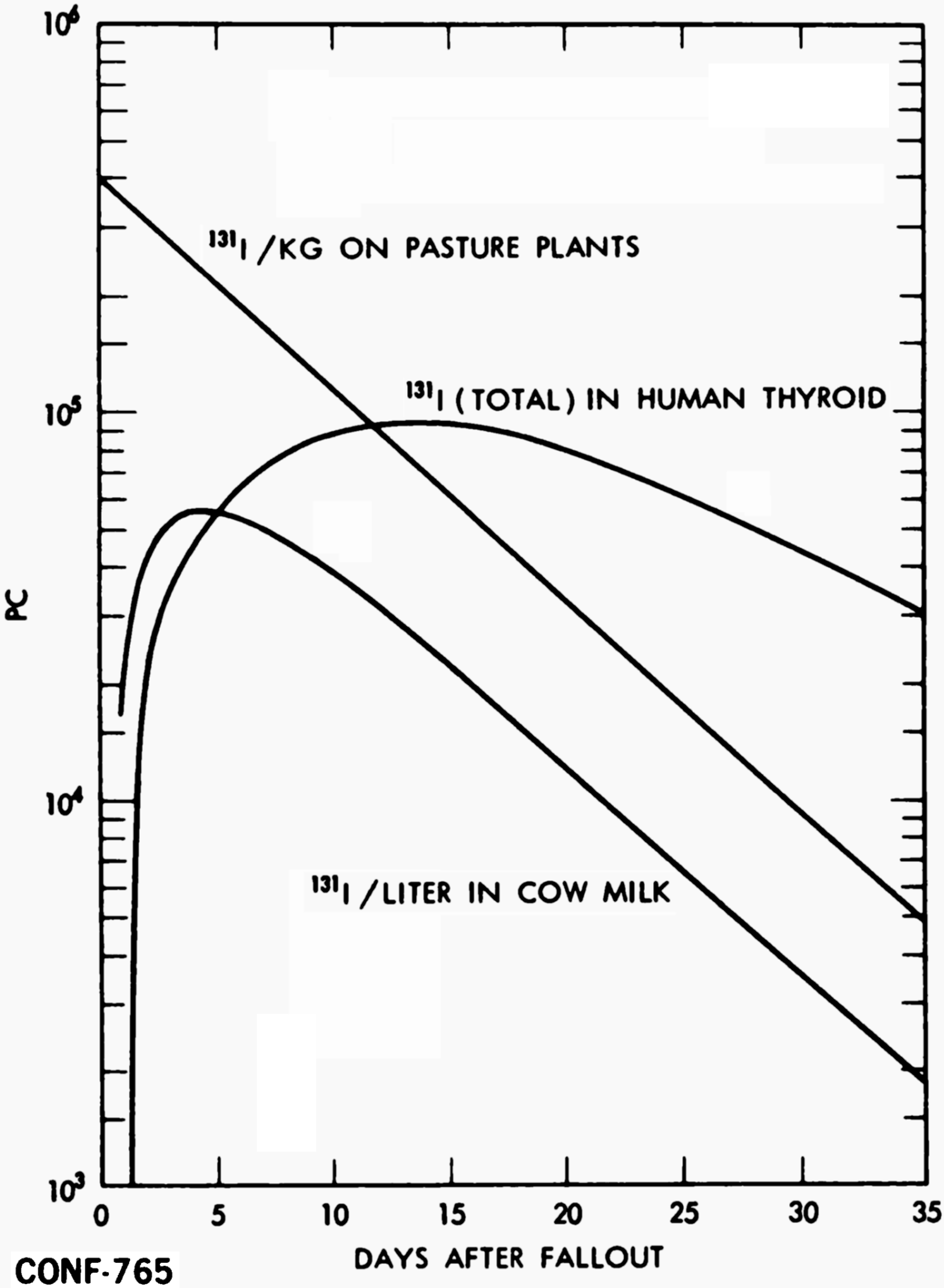

CONF-765

Fig. 8—Hypothetical concentrations of ^{131}I on pasture plants, in cow milk, and in human thyroids following environmental contamination by a single fallout event.

Table 6—SUMMARY OF HYPOTHETICAL VALUES THAT, IF INDICATED BY MEASUREMENTS MADE AFTER ENVIRONMENTAL CONTAMINATION BY A SINGLE FALLOUT EVENT, WOULD IMPLY TOTAL DOSES OF 0.5 REM TO THE SKELETONS OR THYROIDS OF INFANTS CONSUMING 1 LITER OF MILK PER DAY

Hypothetical values	^{89}Sr	^{131}I
Initial concentrations on pasture plants, P_0	61.0 pc/g	13.7 pc/g
Maximum concentrations in milk, M_t	4500 pc/liter	1850 pc/liter
Time after fallout, t_{max}	8 days	4 days
Total intake (to $t = \infty$)	1.60×10^5 pc	2.63×10^4 pc
Maximum concentration in human tissue, H_t	27 pc/g†	1580 pc/g†
Time after fallout, t_{max}	50 days	15 days
Total dose (at $t = \infty$)	0.5 rem†	0.5 rem†

†Based on a 700-g skeleton or a 2.0-g thyroid.

CONF-765

CESIUM-137 AND STRONTIUM-90 RETENTION FOLLOWING AN ACUTE INGESTION OF RONGELAP FOOD

EDWARD P. HARDY, Jr.,* JOSEPH RIVERA,* and ROBERT A. CONARD†
*Health and Safety Laboratory, U. S. Atomic Energy Commission, New York, New York, and †Brookhaven National Laboratory, Upton, New York.

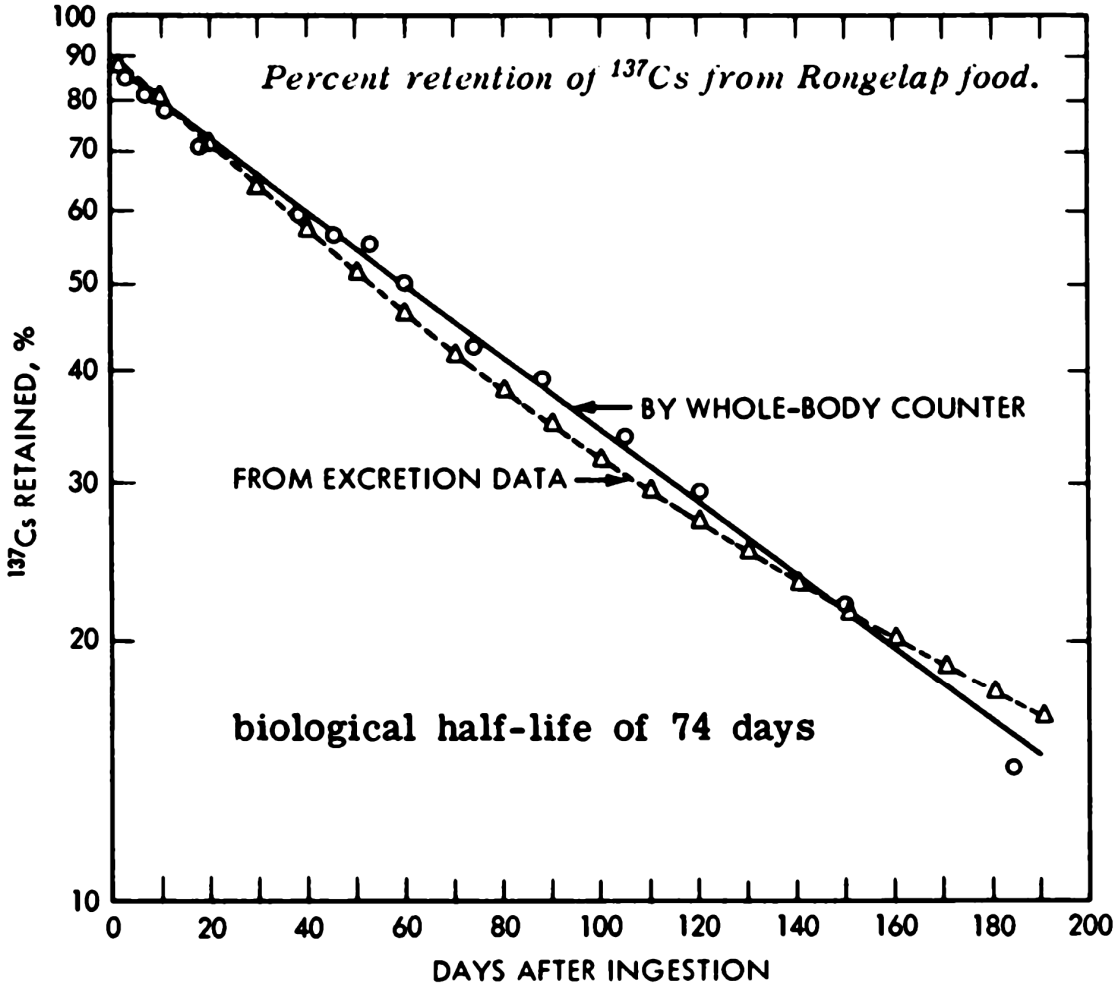

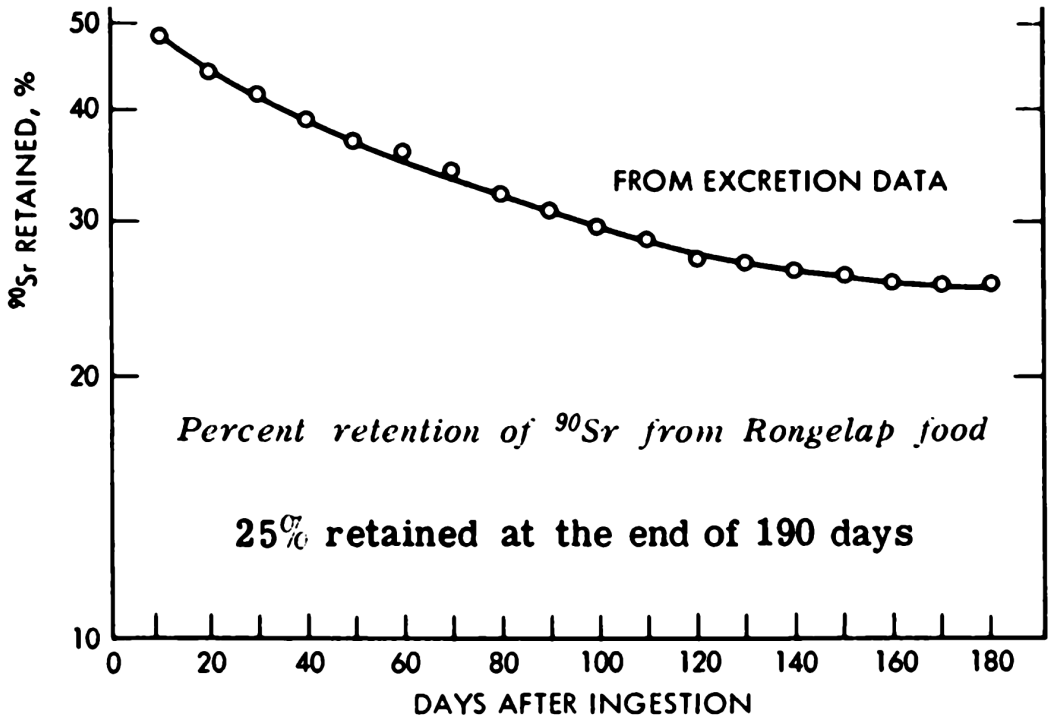

Survival of Food Crops and Livestock in the Event of Nuclear War

Proceedings of a symposium held at
Brookhaven National Laboratory
Upton, Long Island, New York
September 15–18, 1970

Sponsored by
Office of Civil Defense
U. S. Atomic Energy Commission
U. S. Department of Agriculture

Editors

David W. Bensen
Office of Civil Defense
Arnold H. Sparrow
Brookhaven National Laboratory

December 1971

U. S. ATOMIC ENERGY COMMISSION Office of Information Services

THE SIGNIFICANCE OF LONG-LIVED NUCLIDES AFTER A NUCLEAR WAR

R. SCOTT RUSSELL, B. O. BARTLETT, and R. S. BRUCE
Agricultural Research Council, Letcombe Laboratory, Wantage, Berkshire, England

ABSTRACT

The radiation doses from the long-lived nuclides ^{90}Sr and ^{137}Cs, to which the surviving population might be exposed after a nuclear war, are considered using a new evaluation of the transfer of ^{90}Sr into food chains.

As an example, it is estimated that, in an area where the initial deposit of near-in fallout delivered 100 R/hr at 1 hr and there was subsequent worldwide fallout from 5000 Mt of fission, the dose commitment would be about 2 rads to the bone marrow of the population and 1 rad to the whole body. Worldwide fallout would be responsible for the major part of these doses.

In view of the possible magnitude of the doses from long-lived nuclides, the small degree of protection that could be provided against them, and the considerable strain any such attempt would impose on the resources of the community, it seems unrealistic to consider remedial measures against doses of this magnitude. Civil-defense measures should be directed at mitigating the considerably higher doses that short-lived nuclides would cause in the early period.

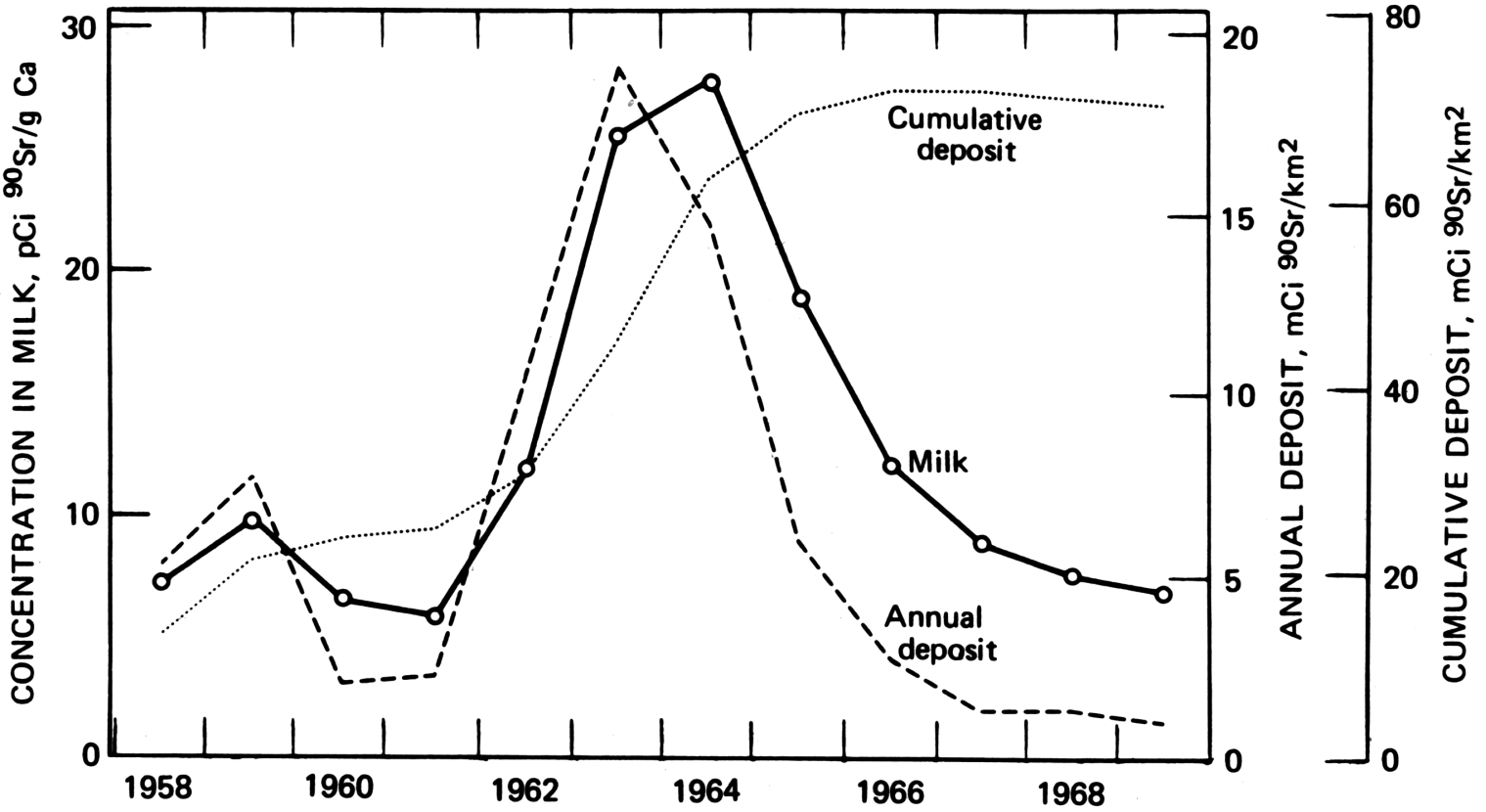

Fig. 1 Strontium-90 in fallout and milk in the United Kingdom

RADIATION EFFECTS ON FARM ANIMALS: A REVIEW

M. C. BELL
UT–AEC Agricultural Research Laboratory, Oak Ridge, Tennessee

ABSTRACT

Hematopoietic death would predominate in food-producing animals exposed to gamma radiation under fallout conditions leaving animal survivors. Gamma-radiation doses of about 900 R would be lethal to 50% of poultry, and about half this level would be lethal for cattle, sheep, and swine. Grazing cattle and sheep would suffer most from combined radiation effects of skin-beta and ingested-beta radioactivity plus the whole-body gamma effects. The $LD_{50/60}$ for combined effects in ruminants is estimated to be at a gamma exposure of around 200 R in an area where the forage retention is 7 to 9%.

Either external parasites or severe heat loss could be a problem in skin irradiated animals. Contrary to early reports, bacterial invasion of irradiated food-producing animals does not appear to be a major problem. Productivity of survivors of gamma radiation alone would not be affected, but, in an area of some lethality, the productivity of surviving grazing livestock would be severely reduced owing to anorexia and diarrhea. Sheltering animals and using stored feed as countermeasures during the first few days of livestock exposure provide much greater protection than shielding alone.

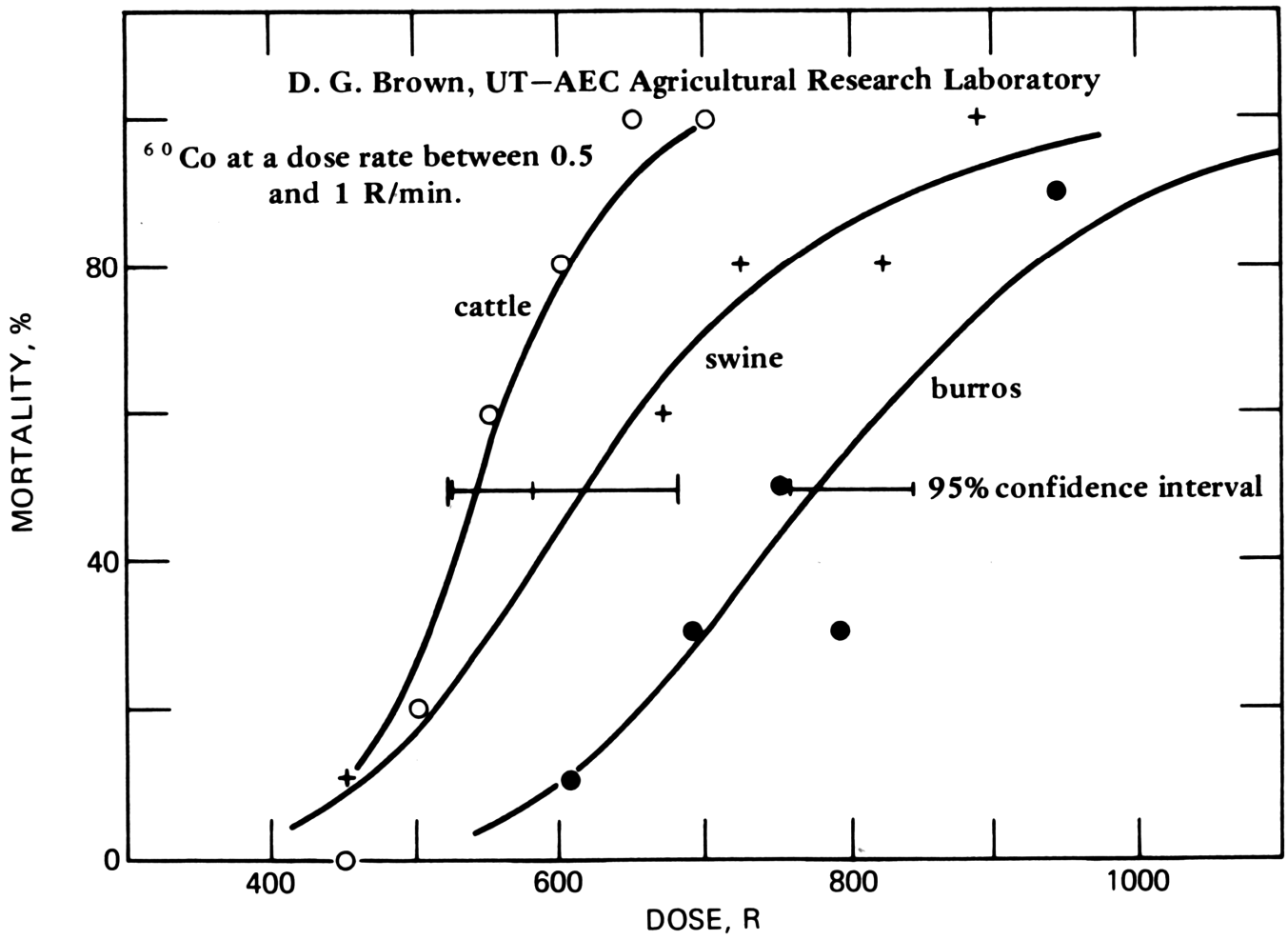

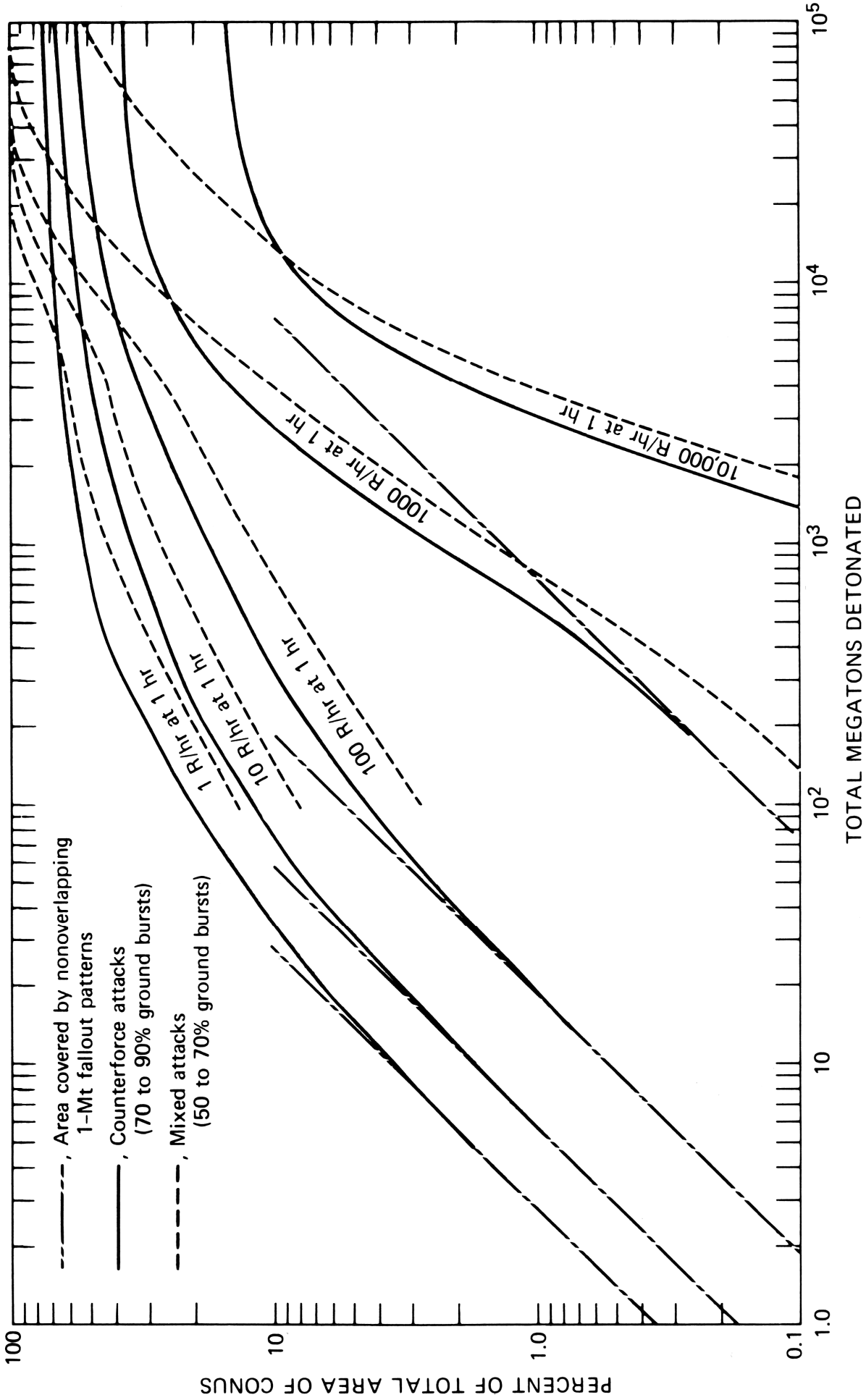

Fig. 1 Percent of area of the continental United States enclosed within selected I_S contours as a function of attack weight (50% fission weapons).

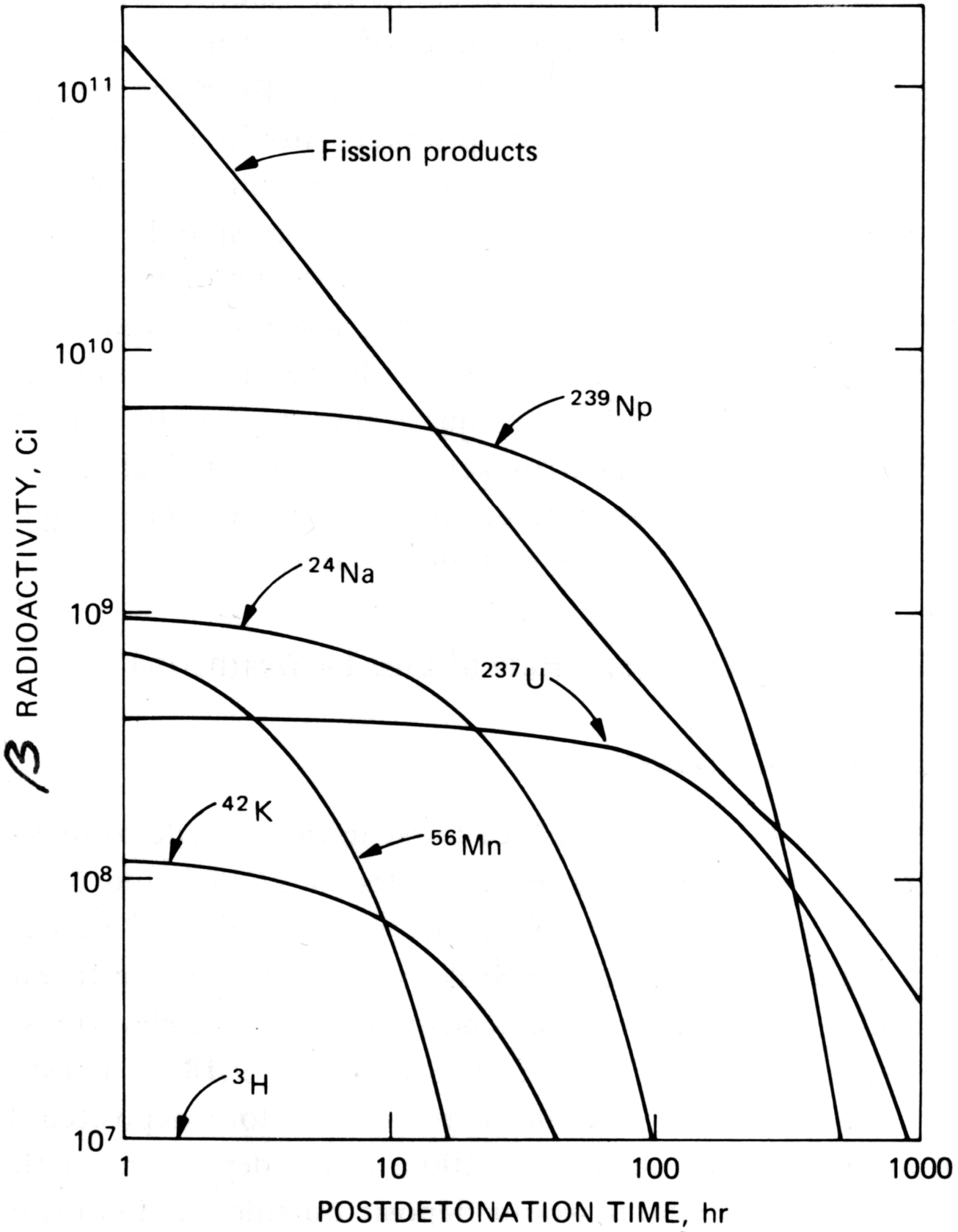

Radioactivity from 1-Mt explosive with a fission-to-fusion ratio of 1.0.

Local Fallout from Nuclear Test Detonations (U), DASA 1251-series (5 volumes with 9 separately-bound parts), by U.S. Army Nuclear Defense Laboratory for the Defense Atomic Support Agency:

Volume I, Indexed Bibliography of United States and British Documents on Characteristics of Local Fallout (U), DASA 1251-1 (AD 329971), 237 pp., 27 June 1961. (C)

Volume II, Compilation of Fallout Patterns and Related Test Data (U):

Part 1 - Trinity Through Redwing (U), DNA 1251-2-1 (AD 349123), 468 pp., August 1963. (SRD)

Part 2 - Plumbbob Through Hardtack (U), DASA 1251-2-2 (AD 329124), 456 pp., August 1963. (SRD)

Part 3 - Nougat Through Niblic (U), DASA 1251-2-3 (AD 371725), 226 pp., March 1966. (SRD)

Supplement, Foreign Nuclear Tests (U), DASA 1251 (AD 358417L), 77 pp., October 1964. (SRD)

Volume III, Annotated Compendium of Data on Physical and Chemical Properties of Fallout (U), DASA 1251-3 (AD 381963L), 770 pp., November 1966. (SRD)

Volume IV, Annotated Compendium of Data on Radiochemical and Radiation Characteristics of Fallout (U):

Part 1 - Specific Activity, Activity-Size Distribution, Decay (U), DASA 1251-4-1 (AD 500919L), 643 pp., September 1968. (SRD)

Part 2 - Radiochemical Composition, Induced Activity, Gamma Spectra (U), DASA 1251-4-2 (AD 523385), 570 pp., 31 May 1972. (SRD)

Volume V, Transport and Distribution of Local (Early) Fallout from Nuclear Weapon Tests (U), DASA 1251-5 (AD 362012), 580 pp., May 1965. (SRD)

1.2 kt JANGLE - Sugar Surface burst 19 Nov 1951

CLOUD TOP HEIGHT: 15,000 ft MSL

CRATER DATA: Diameter: 90 ft Depth: 21 ft

maximum dose rate: 7500 r/hr at H+1 hour at crater lip

Maximum dose rate		Maximum contour distance from GZ (ft)			Contour area (sq mi)		
Value (r/hr)	Distance from GZ (ft)	500 r/hr	300 r/hr	100 r/hr	500 r/hr	300 r/hr	100 r/hr
540	900	2200	4900	12,500	0.05	0.15	0.55

Laurino, R. K., and I. G. Poppoff, 1953: *Contamination patterns at Operation JANGLE.* U. S. Nav. Rad. Def. Lab. Rep. USNRDL-399, 28 pp.

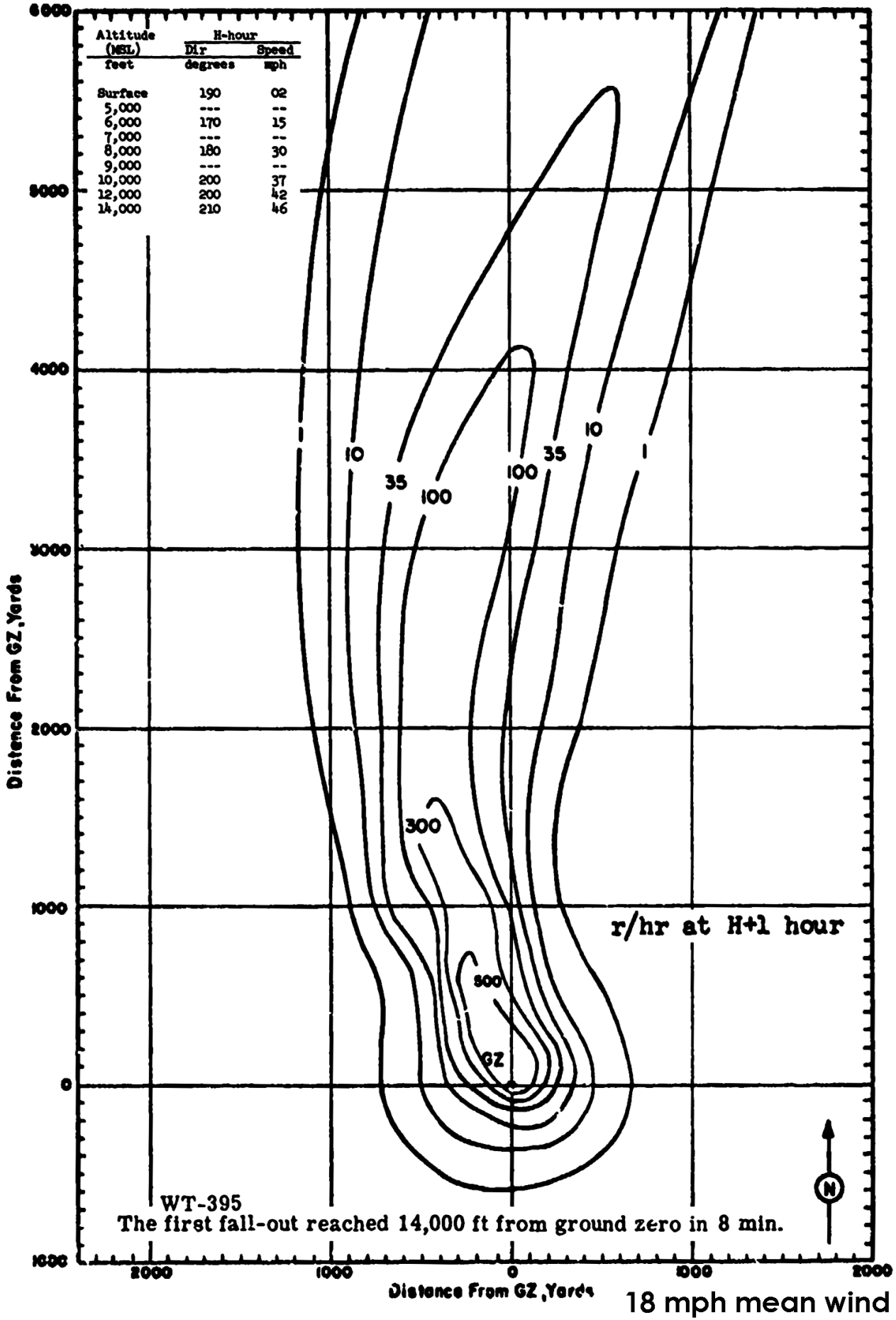

WT-395

The first fall-out reached 14,000 ft from ground zero in 8 min.

18 mph mean wind speed

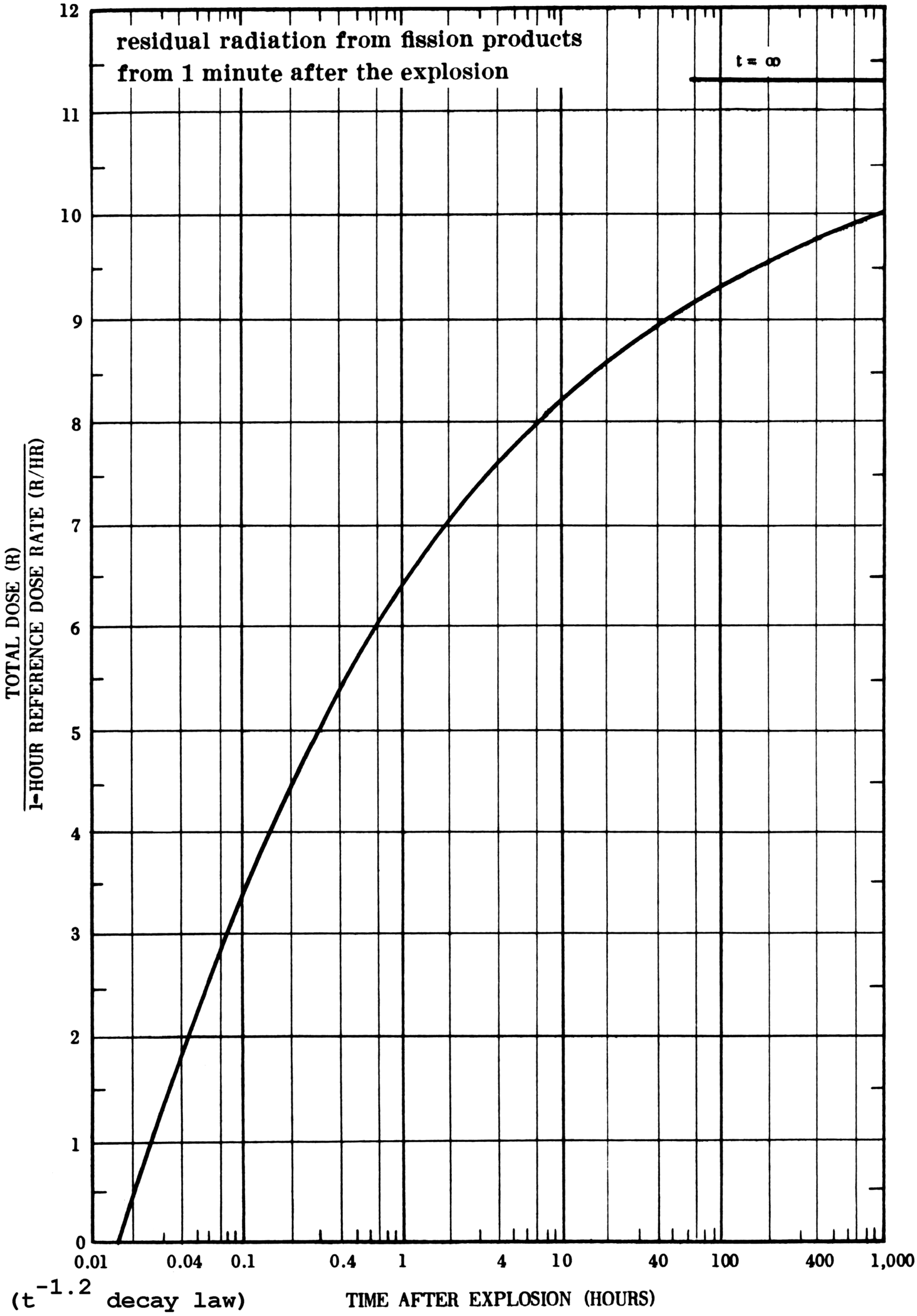
residual radiation from fission products
from 1 minute after the explosion
t = ∞
TOTAL DOSE (R) / 1-HOUR REFERENCE DOSE RATE (R/HR)
0
1
2
3
4
5
6
7
8
9
10
11
12
0.01
0.04
0.1
0.4
1
4
10
40
100
400
1,000
(t^-1.2 decay law)
TIME AFTER EXPLOSION (HOURS)

1.2 kt SUGAR test (Nevada surface burst)

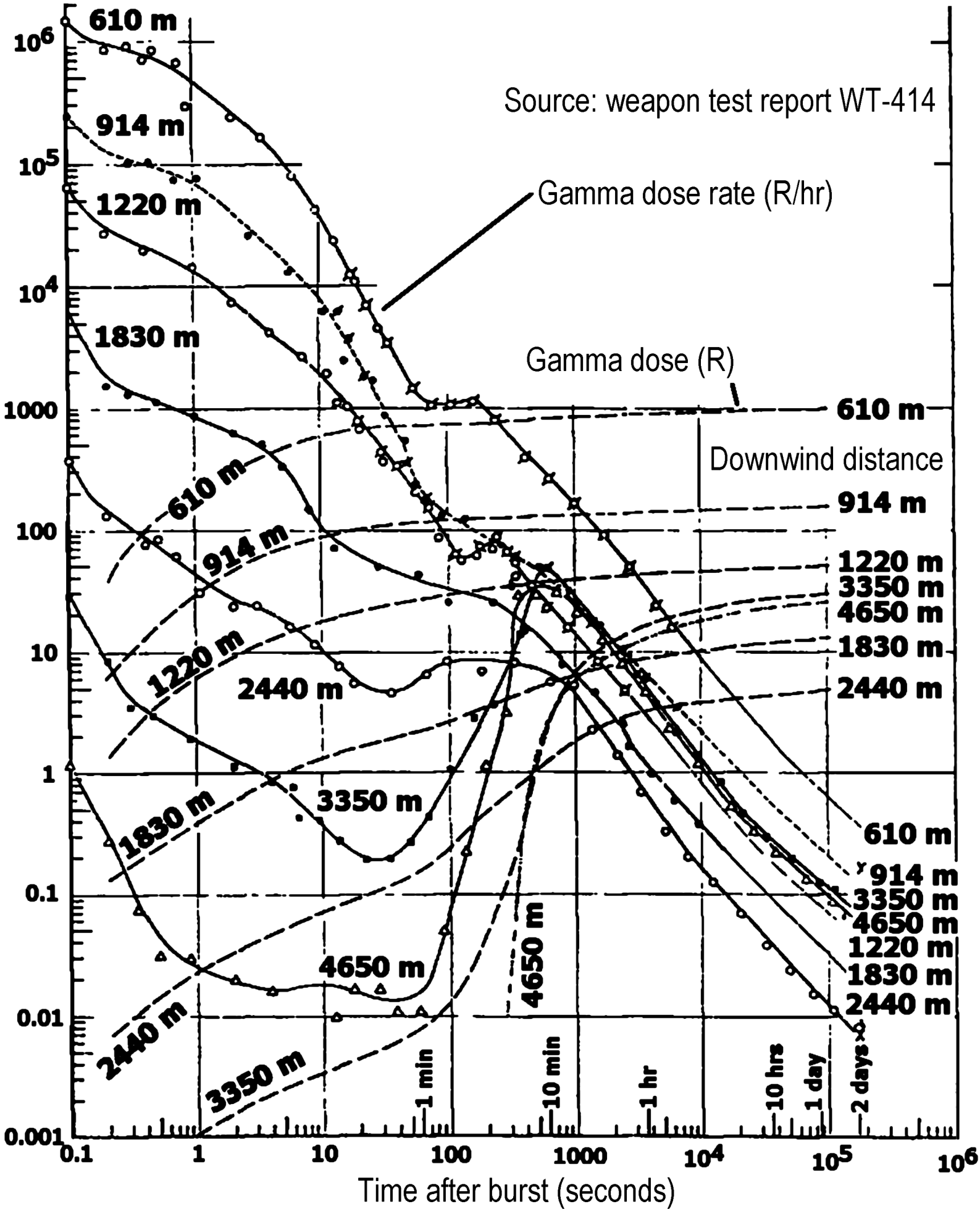

1.2 kt UNCLE test (5.2 m underground, Nevada)

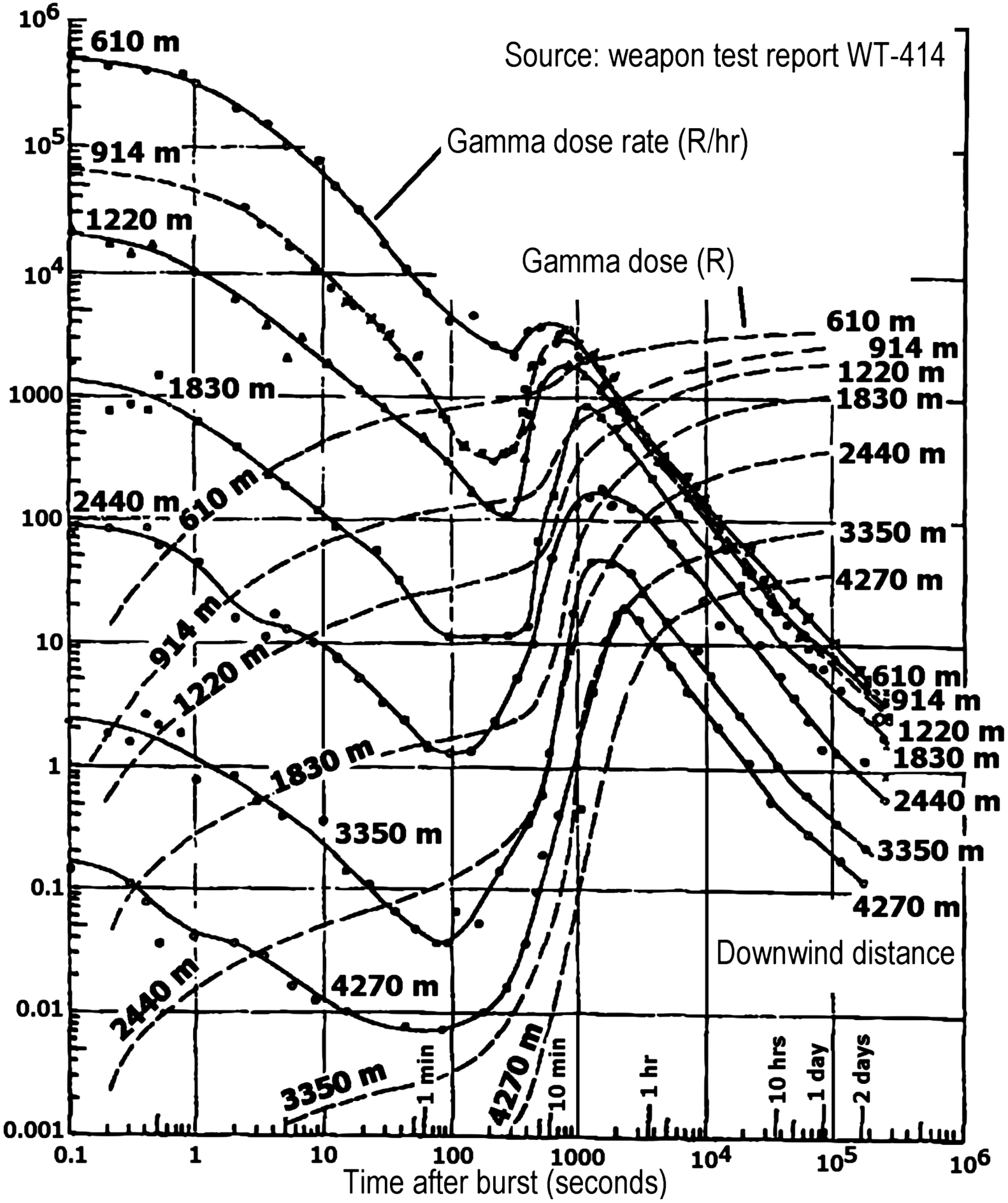

Robbins, Charles; et al. "Airborne Particle Studies, JANGLE Project 2.5a-1." (In: Operation JANGLE, Particle Studies, WT-371-EX, 417 pages.) Army Chemical Center. Washington, D. C.: AFSWP. WT-394-EX. October 1979. 198 Pages. AD/A995 072.

OPERATION JANGLE

Project 2.5a-1

AIRBORNE PARTICLE STUDIES

by

Lt. Col. Charles Robbins
Chemical Corps

Major Hugh R. Lehman
U. S. Air Force

David R. Powers
Chemical Corps

James D. Wilcox
Chemical Corps

July 1952

CHEMICAL AND RADIOLOGICAL LABORATORIES
Army Chemical Center, Maryland

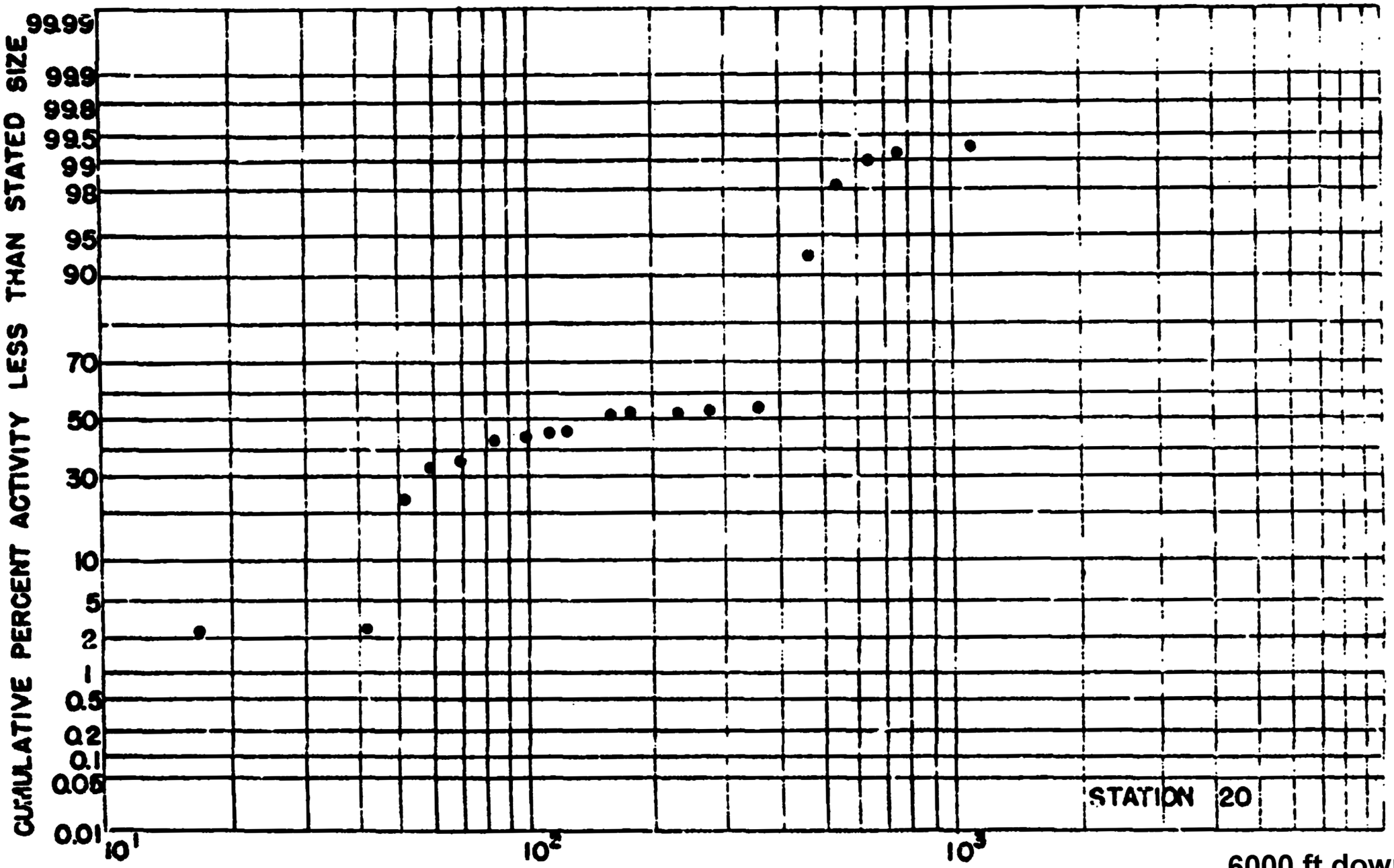

PROJECT 2.5a-1

6000 ft downwind
1.8 km downwind

Fig. 2.24 Fall-out Activity as a Function of Particle Size, Station 20, Surface Shot.

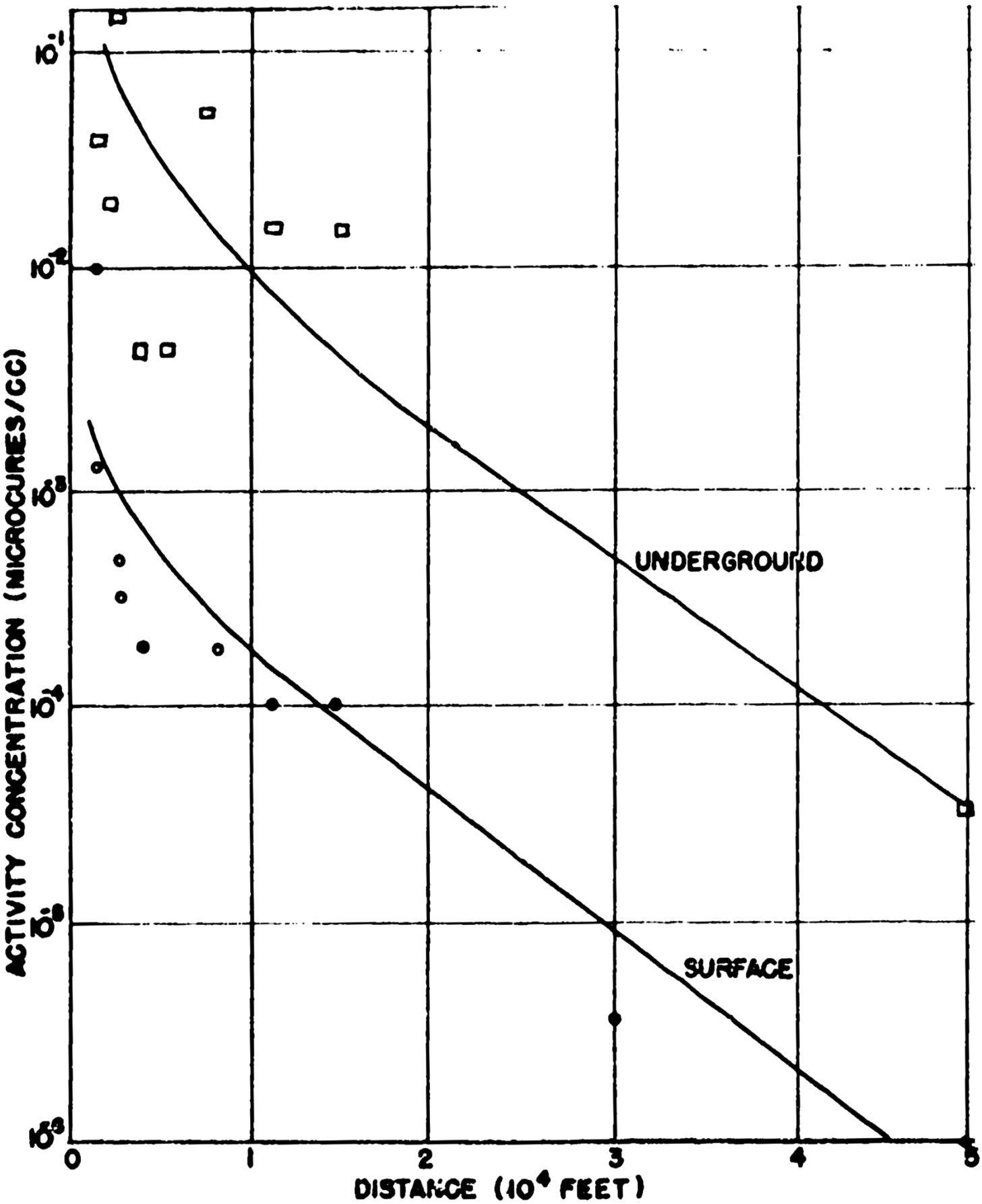

Figure 5.1 Concentration of Activity in the Cloud as a Function of Distance on the Downwind Leg. Filter Sampler Data. Activity was corrected to time at which cloud passed each station.

5.5 STUDY OF FRACTIONATION

5.5.1 Radiochemistry

The data concerning the nuclide activity per unit mass of active material as a function of particle size, which is contained in Table 4.15, provided a method of investigating the mechanism whereby particles acquire activity. The data for Sr^{89} and ZR^{95} have been plotted in Figs. 5.4 and 5.5. Referring to Fig. 5.4, it appears that a straight line with a slope of -1 may be fitted to the data, whereas this is not possible with the data in Fig. 5.5. Allowing for some over-simplification, it appears that the Sr^{89} activity is a function of particle surface, whereas that for Zr^{95} tends to be more of a volume function. Ba^{140} gives a plot similar to the Sr^{89} plot, while Ce^{144} is similar to Zr^{95}. Further study is being made of these data, particularly with respect to the question of whether the activity of Zr^{95} and Ce^{144} is concentrated in a shell rather than a volume. Examination of the decay chains of these four nuclides provides a plausible reason why there should be a difference in the mechanism for acquiring radioactivity. The decay chains are as follows[4]:

$$Kr^{89} \xrightarrow{2.6m} Rb^{89} \xrightarrow{15.4m} Sr^{89}$$

$$Kr^{95} \xrightarrow{short} Rb^{95} \xrightarrow{short} Sr^{95} \xrightarrow{short} Y^{95} \xrightarrow{10.5m} Zr^{95}$$

$$Xe \xrightarrow{16s} Cs \xrightarrow{66s} Ba^{140}$$

$$Xe^{144} \xrightarrow{1s} Cs^{144} \xrightarrow{short} Ba^{144} \xrightarrow{short} La^{144} \xrightarrow{short} Ce^{144}$$

It may be seen that Ba^{140} and Sr^{89} both have gaseous precursors that have half-lives long in comparison with the lifetime of the fireball. Since gases such as krypton and xenon are not significantly subject to adsorption above liquid air temperatures, it is logical to suppose that while the Zr^{95} and Ce^{144} chains passed the rare gas stage early enough to be adsorbed during the particle growth process, no appreciable amount of Kr^{89} and Xe^{140} decayed before the particles had ceased to grow. Hence the Sr^{89} and Ba^{140} activities were confined to the outermost surfaces of the particles.

---

4 C. D. Coryell & N. Sugarman, op cit, pp. 1996-2001.

8.9 INHALATION STUDIES

Dogs and sheep were exposed on the ground surface and in foxholes at distances of 2500 to 6000 feet in the predicted downwind direction from each shot. The purpose of the exposure was to allow the assessment of hazards due to inhalation of radioactive dusts associated with these detonations and to compare internal and external radiation dosages.

Total body activity for animals exposed in the underground test ranged from 2 to 31 microcuries corrected to time of sacrifice. For lung tissue, integrated dosage due to beta emission ranged between 0.2 and 9.0 rep. Radioautographs of lung tissues indicated the presence of a few alpha emitting particles. Bone analyses indicated some uptake of Ba^{140} and Sr^{90}.

The amounts of activity taken up by the combined action of inhalation and ingestion are not considered to be physiologically significant even for animals receiving cumulative external gamma radiation dosages up to several thousand roentgens.

77

9.8 CLOTHING DECONTAMINATION AND EVALUATION OF LAUNDRY METHODS

Standard and special U. S. Army Quartermaster Corps laundering methods and standard laundry equipment were evaluated for field decontamination of clothing and selected fabrics. No clothing worn by personnel became contaminated to a significant degree during this operation. Therefore, this project was carried out with clothing deliberately contaminated with radioactive material from the fall-out area.

The project evaluated the standard and several special laundering formulae, various types of clothing materials, and monitoring instruments (Project 6.7). The significant result of this project is the indication that clothing contamination resulting from work in areas contaminated by atomic bomb detonations will not produce even minor injury to personnel. This conclusion is based on consideration of the data on saturation values of deliberate clothing contamination reduced to one hour after detonation. The resultant exposure to personnel would be less than that required to produce even slight skin irritation (comparable to mild sunburn). Other conditions, such as muddy terrain and much higher specific activity, could increase the amount of contamination received by clothing, but an increase in level of several orders of magnitude would be required to produce injury. In these cases it is certain that routine standards of cleanliness would effectively prevent injury from this cause.

SECRET
Security Information

WT-393
Copy

AD482985

Operation

JANGLE

NEVADA PROVING GROUNDS
OCTOBER-NOVEMBER 1951

Project 2.3-2

FOXHOLE SHIELDING OF GAMMA RADIATION

EACH TRANSMITTAL OF THIS DOCUMENT OUTSIDE THE AGENCIES OF THE U.S. GOVERNMENT MUST HAVE PRIOR APPROVAL OF THE DIRECTOR, DEFENSE ATOMIC SUPPORT AGENCY, WASHINGTON, D.C. 20301.

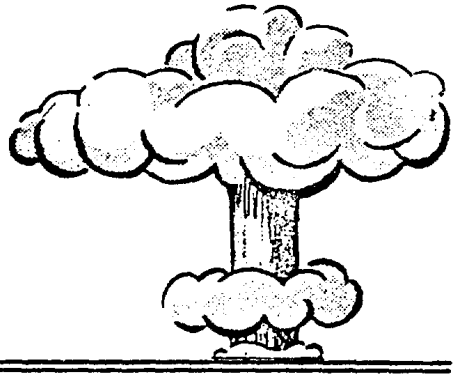

RESTRICTED DATA
ATOMIC ENERGY ACT 1946

ARMED FORCES SPECIAL WEAPONS PROJECT
WASHINGTON D.C.

UNCLASSIFIED

SECRET
Security Information

SECRET
Security Information

PROJECT 2.3-2

TABLE 3.1

Distribution of Gamma Radiation in Foxholes (Surface Burst)

Range (ft)	Location	Two-man Foxhole			One-man Foxhole		Soil Pipe
2000	36" Above Surface		800 r				
	Surface		700				
	16" Below Surface	230	205	415			
	32" Below Surface	24	58	136			
	48" Below Surface	12.8	22	62			
2500	36" Above Surface		230 r				
	Surface		220				
	16" Below Surface	35	60	85			
	32" Below Surface	7	15	26			
	48" Below Surface	4	8.5	13.3			
3000	36" Above Surface		110 r				73 r
	Surface		90			55	
	16" Below Surface	23	36	55	6.8	6.6	10
	32" Below Surface	7.6	12.4	19.4	2.5	2.4	0.5
	48" Below Surface	2.5	4.8	6.7	1.6	1	0
3500	36" Above Surface		41 r				
	Surface		---				
	16" Below Surface	3	---	9.7			
	32" Below Surface	1.6	2.8	3.4			
	48" Below Surface	.54	.99	1.9			
4000	36" Above Surface		17 r				17 r
	Surface		9.6			---	
	16" Below Surface	1.6	3	5.6	---	0.35	---
	32" Below Surface	0.6	1.12	1.62	---	---	0.17
	48" Below Surface	---	0.54	0.57	0.39	---	---
4500	36" Above Surface		9.8 r				
	Surface		4.6				
	16" Below Surface	1	1.8	3.5			
	32" Below Surface	0.5	0.7	1.04			
	48" Below Surface	0.21	0.4	0.57			
5000	36" Above Surface		4.8 r				
	Surface		2.7				
	16" Below Surface	0.6	0.99	2.95			
	32" Below Surface	0.3	0.5	0.75			
	48" Below Surface	0.17	0.2	0.38			

RESTRICTED DATA
ATOMIC ENERGY ACT 1946
SECRET
Security Information

SECRET
Security Information

PROJECT 2.3-2

TABLE 3.2

Distribution of Gamma Radiation in Foxholes (Underground Burst)

Range (ft)	Location	Two-man Foxhole			One-man Foxhole		Soil Pipe
2000	36" Above Surface		3850 r				
	Surface		2300				
	16" Below Surface	1150	--	800			
	32" Below Surface	700	1000	555			
	48" Below Surface	200	200	200			
2500	36" Above Surface		1000 -- 550 r				
	Surface		78				
	16" Below Surface	78	98	115			
	32" Below Surface	43	56	50			
	48" Below Surface	73.4	94	96			
3000	36" Above Surface		175 r				155 r
	Surface		103			75	
	16" Below Surface	30	42	37	20	--	7
	32" Below Surface	22	23	20	15	11	3
	48" Below Surface	43.5	45	54	41	38	3
3500	36" Above Surface		--				
	Surface		48				
	16" Below Surface	12	17	15			
	32" Below Surface	9	10	9			
	48" Below Surface	15	15	22			
4000	36" Above Surface		32 r				28 r
	Surface		22			14	
	16" Below Surface	6	7	15	7	4	2
	32" Below Surface	5	3.4	7.2	3.7	2.8	0
	48" Below Surface	6	8.4	8.6	5	9.8	1.1
4500	36" Above Surface		22 r				
	Surface		10				
	16" Below Surface	4	5	5			
	32" Below Surface	5.8	2.8	2.8			
	48" Below Surface	--	7.7	8.9			
5000	36" Above Surface		73 r				
	Surface		23				
	16" Below Surface	15	15	67			
	32" Below Surface	21.5	22.6	15			
	48" Below Surface	--	21	19			

SECRET
Security Information

RESTRICTED DATA
ATOMIC ENERGY ACT 1946

CHAPTER 5

CONCLUSIONS

5.1 FOXHOLE SHIELDING OF GAMMA RADIATION

5.1.1 Surface Detonation

Standard foxholes provide excellent protection to personnel from the gamma radiation emitted during the detonation of an atomic weapon on the surface of the ground. The results from the comparatively small sized weapon employed in Operation JANGLE show that 2000 feet from the burst, the location of the closest foxhole doses of about 60r were measured at the bottom of a foxhole, less than 10 per cent of the dose measured 3 feet above the surface of the ground. Due to the location of the foxhole in the crosswind direction, the dose at the bottom was caused primarily by scattered prompt radiation plus a small contribution from the residual activity of the fission products on the surface of the ground. In the downwind direction there would be a contribution from matter that falls out from the cloud into the foxhole in addition to the above mentioned. This fall-out will depend on the wind velocity for a given sized weapon, and although it is expected to increase the dose in the foxholes, especially in those located close to the detonation, it is relatively unimportant in comparison to the prompt and residual activity since it can be easily shoveled out of the foxhole in a short time.

5.1.2 Underground Detonation

With the possible exception of those located in the area close to the point of detonation where extensive fall-out occurs, foxholes also provide effective shielding in the case of an underground detonation. Even within this area of extensive fall-out, which at Operation JANGLE extended approximately 2000 feet, the high doses recorded in the foxholes could be greatly reduced by digging out the radioactive matter that fell into the hole. It is highly probable that one-half the doses recorded in the foxholes located within 2500 feet of the detonation at Operation JANGLE were directly attributable to this type of fall-out and most likely a higher percentage at distances greater than 2500 feet.

SECRET
Security Information

RESTRICTED DATA
ATOMIC ENERGY ACT 1946

TOP SECRET UK National Archives PREM 11/560, 12 July 1951

PRIME MINISTER

Clandestine Use of Atomic Weapons

The Chiefs of Staff have been considering the possibility that the enemy might open the next war with an atomic attack on London on the model of the Japanese attack on Pearl Harbour - without warning and before any formal declaration of hostilities. The most effective method of making such an attack would be to drop an atomic bomb from a military aircraft. If the control and reporting system were fully manned and alert in a period of tension, there would be some chance that hostile aircraft approaching this country could be intercepted and driven off. At any rate, there are no special measures, outside the normal measures of air defence, which we could take in peace-time to guard against this type of attack.

2. It is, however, possible that the enemy might use other means of surprise attack with atomic weapons. A clandestine attack could be made in either of the following ways:-

(i) A complete atomic bomb could be concealed in the hold of a merchant ship coming from the Soviet Union or a satellite country to a port in the United Kingdom:

(ii) An atomic bomb might be broken down into a number of parts and introduced into this country in about fifty small packages of moderate weight. None of these packages could be detected by instruments as containing anything dangerous or explosive, and even visual inspection of the contents of the packages would not make identification certain. These packages could be introduced either as ordinary merchandise from Soviet ships, or possibly as diplomatic freight. The bomb could subsequently be assembled in any premises with the sort of equipment usual in a small garage, provided that a small team of skilled fitters was available to do the job.

OPERATION HURRICANE—THE DOSE-RATE CONTOURS OF THE RESIDUAL RADIOACTIVE CONTAMINATION

FIG. 7·2

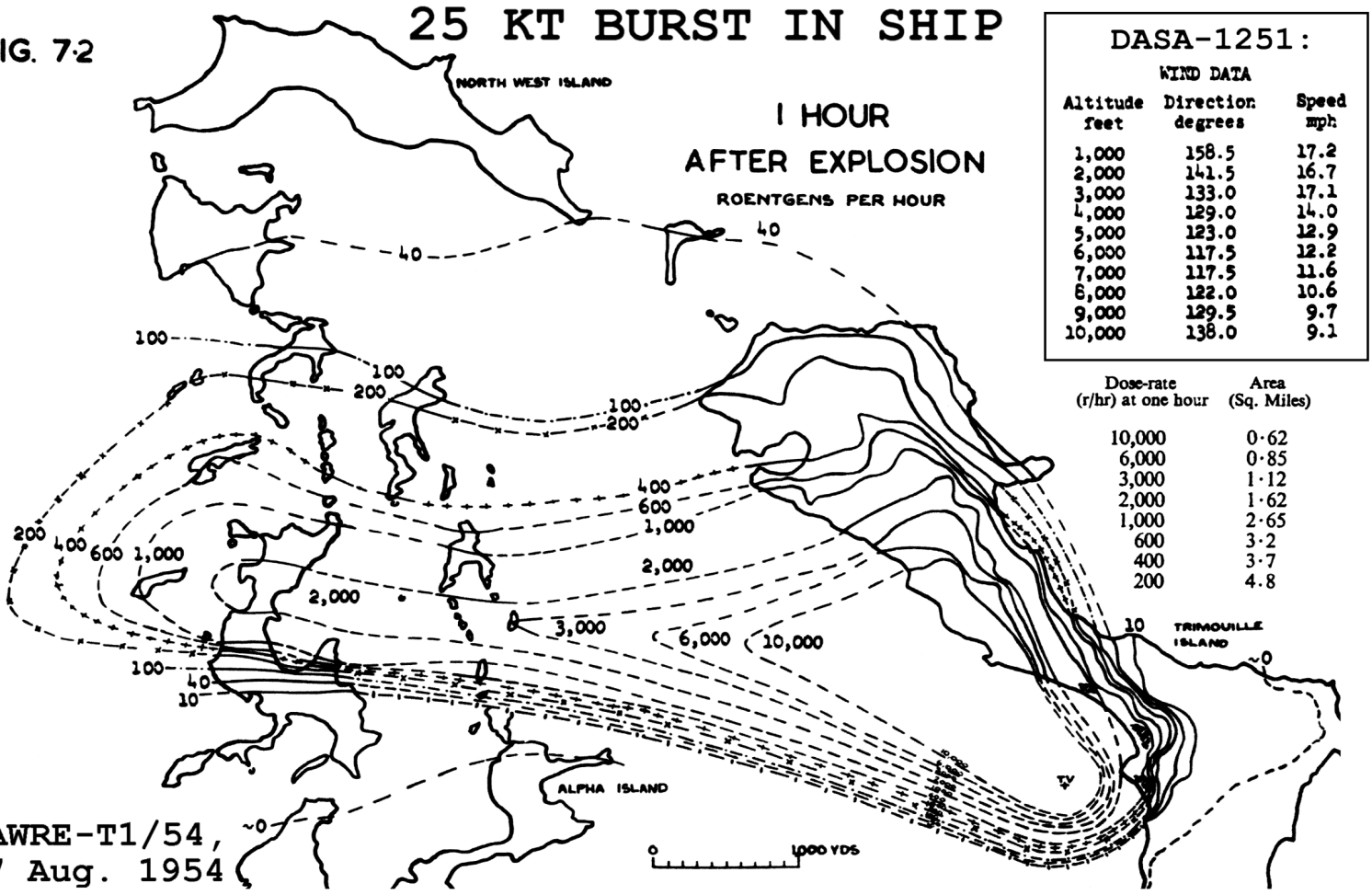

DASA-1251:

WIND DATA

Altitude feet	Direction degrees	Speed mph
1,000	158.5	17.2
2,000	141.5	16.7
3,000	133.0	17.1
4,000	129.0	14.0
5,000	123.0	12.9
6,000	117.5	12.2
7,000	117.5	11.6
8,000	122.0	10.6
9,000	129.5	9.7
10,000	138.0	9.1

Dose-rate (r/hr) at one hour	Area (Sq. Miles)
10,000	0·62
6,000	0·85
3,000	1·12
2,000	1·62
1,000	2·65
600	3·2
400	3·7
200	4·8

AWRE-T1/54,
27 Aug. 1954

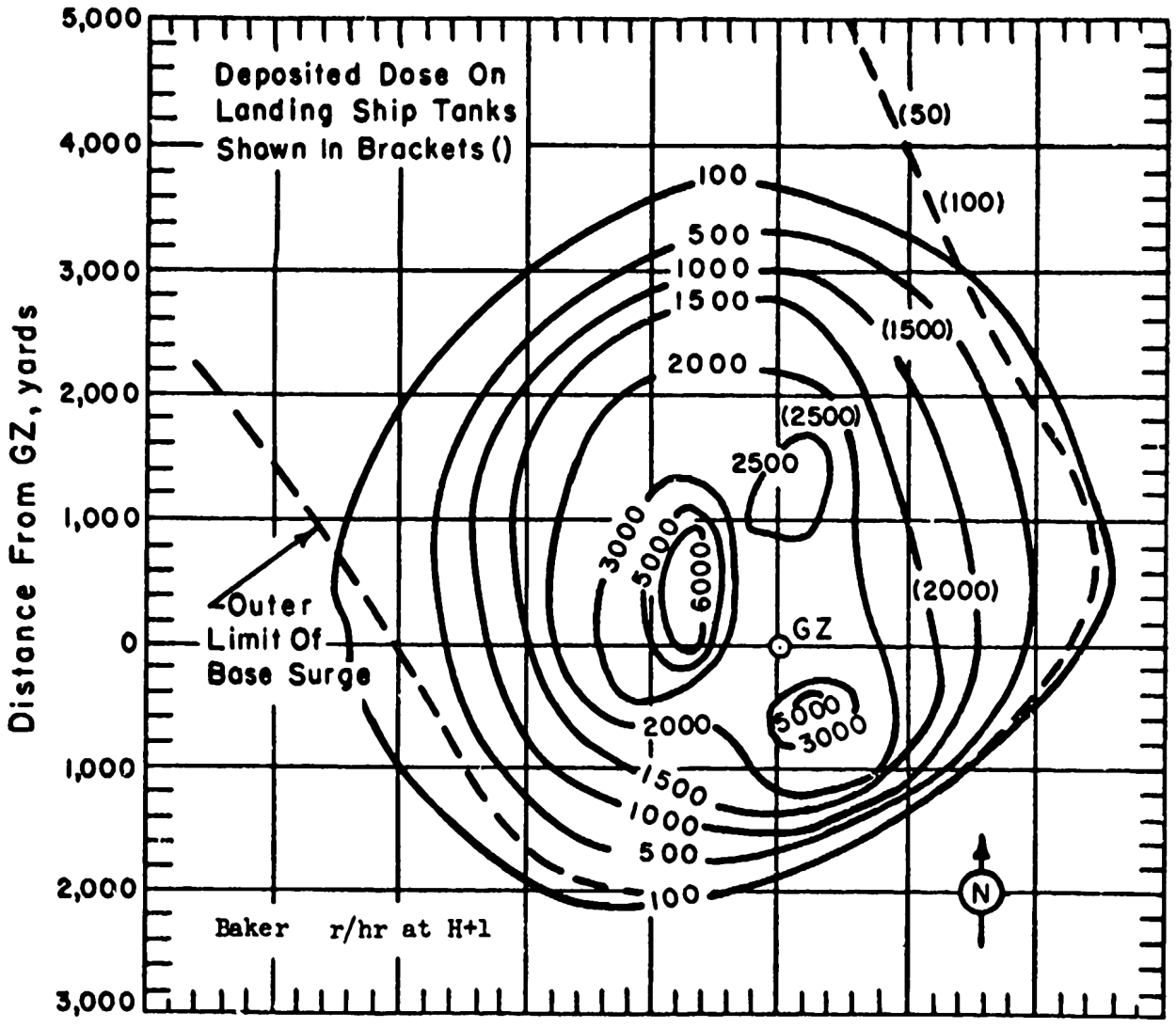

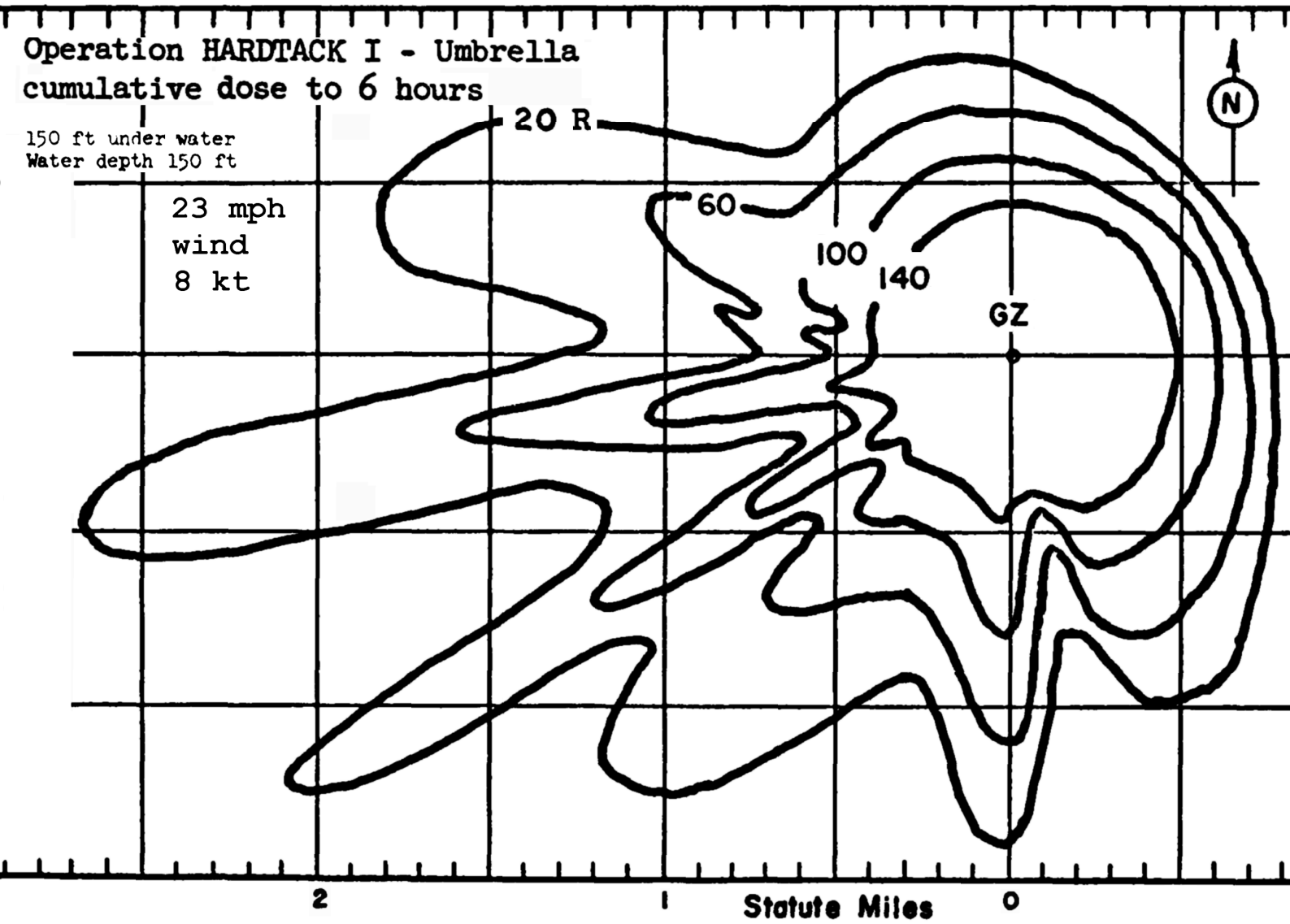
Operation HARDTACK I - Umbrella
cumulative dose to 6 hours
150 ft under water
Water depth 150 ft
23 mph
wind
8 kt
20 R
60
100
140
GZ
N
2
1
Statute Miles
0

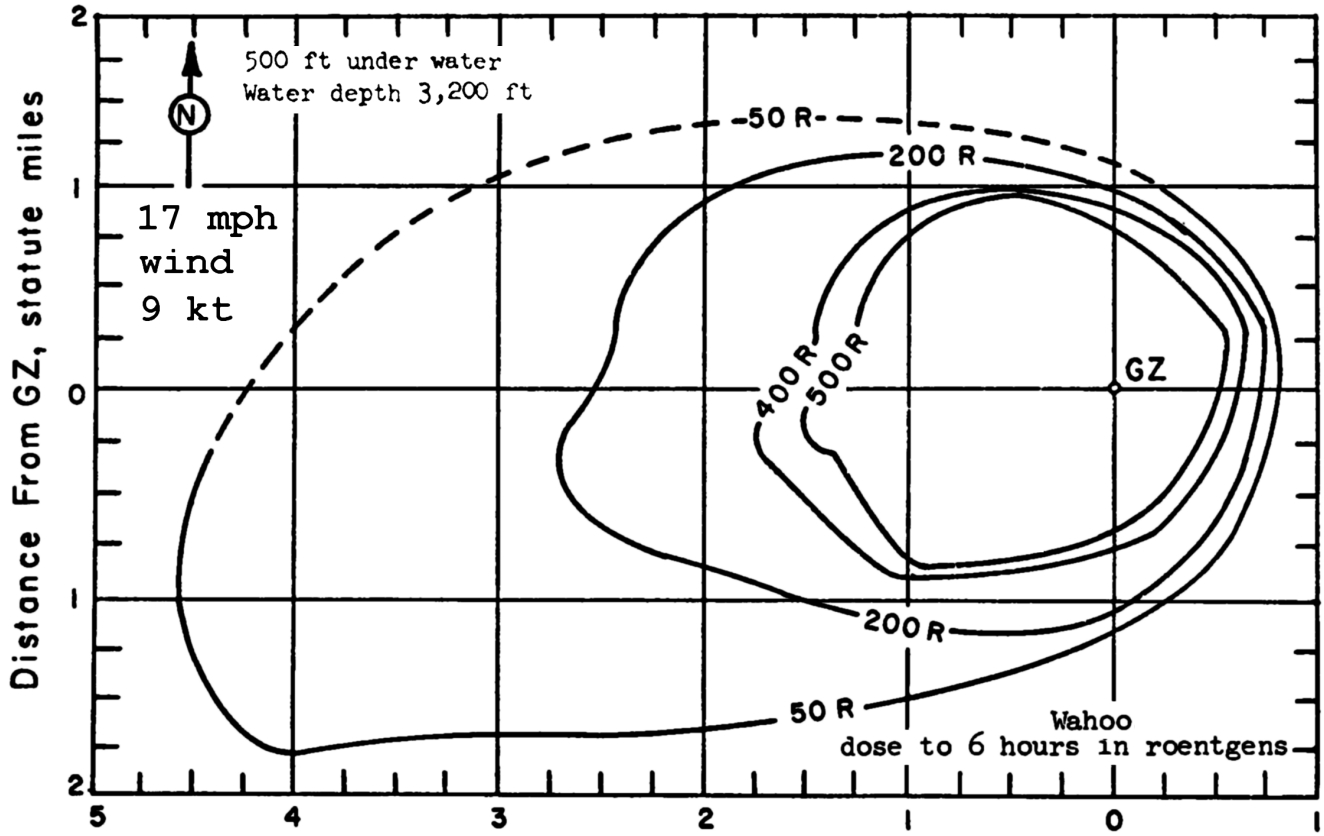
500 ft under water
Water depth 3,200 ft
N
17 mph
wind
9 kt
50 R
200 R
400 R
500 R
GZ
200 R
50 R
Wahoo
dose to 6 hours in roentgens
Distance From GZ, statute miles
2
1
0
1
2
5
4
3
2
1
0
1

WT-1316 (EX)

EXTRACTED VERSION

OPERATION REDWING

Project 2.62a
Fallout Studies by Oceanographic Methods

Pacific Proving Grounds

May - July, 1956

Defense Atomic Support Agency

Sandia Base, Albuquerque, New Mexico

February 6, 1961

NOTICE

This is an extract of **WT-1316, Operation REDWING, Project 2.62a**, which remains classified **Secret/ Restricted Data** as of this date.

Extract version prepared for:

Director
DEFENSE NUCLEAR AGENCY
Washington, D.C. 20305

1 February 1980

Approved for public release; distribution unlimited.

TABLE 2.11

	Navajo	Tewa
Total Yield, Mt	4.50	5.01
Fission proportion	5%	87%

H + 1 Hour Dose Rate (r/hr)	Area (mi^2) Within Contour	
1,000	25	450
500	55	1,050
300	80	1,550
100	310	3,500

Two-day Dose, R	Area (mi^2) Within Contour	
1,000	20	520
500	30	1,050
300	45	1,500
100	350	3,000

CLEAN BOMB: 3.53 MT (15% FISSION) ZUNI

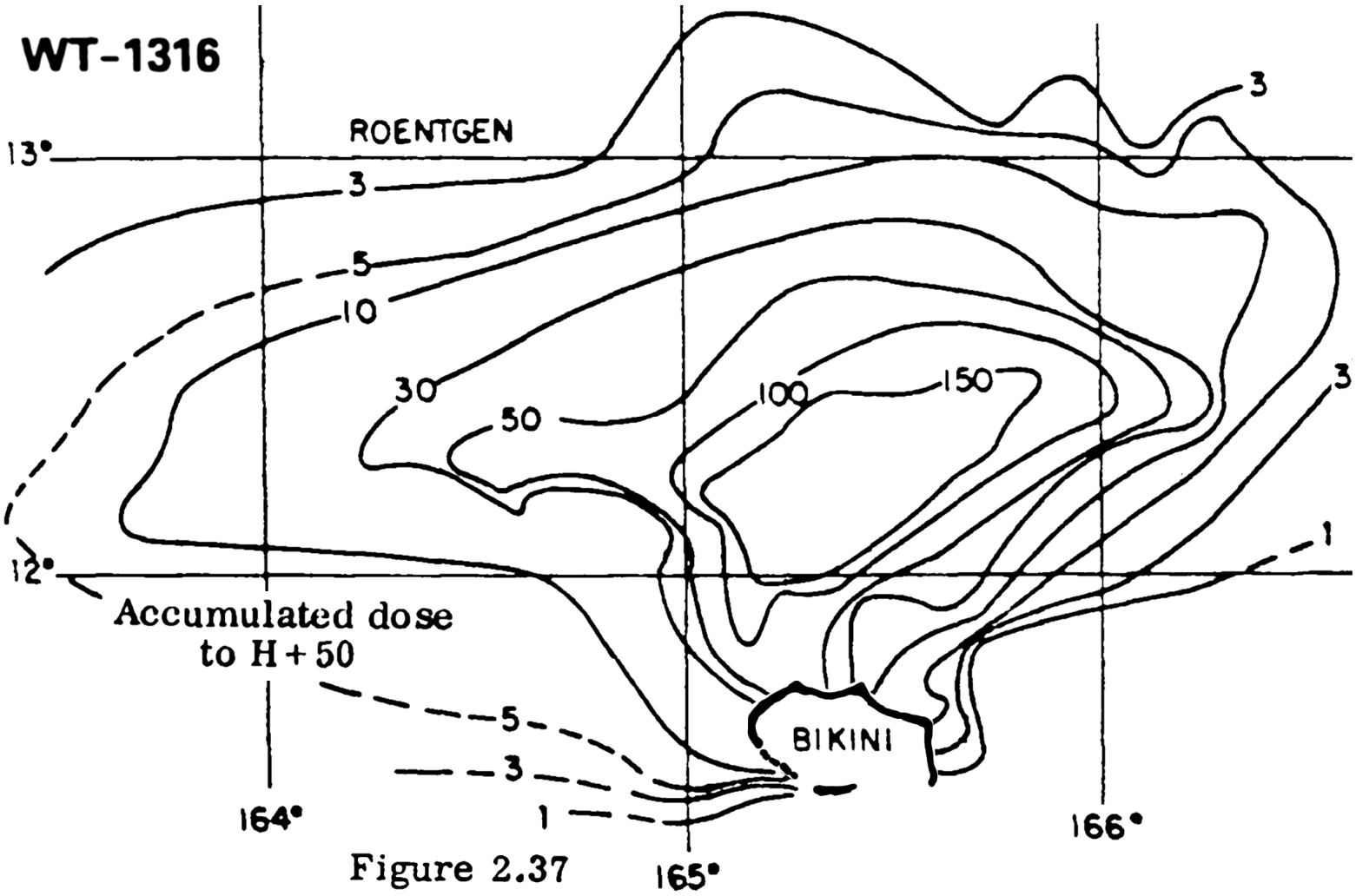

Figure 2.37

DIRTY BOMB: 5.01 MT (87% FISSION) TEWA

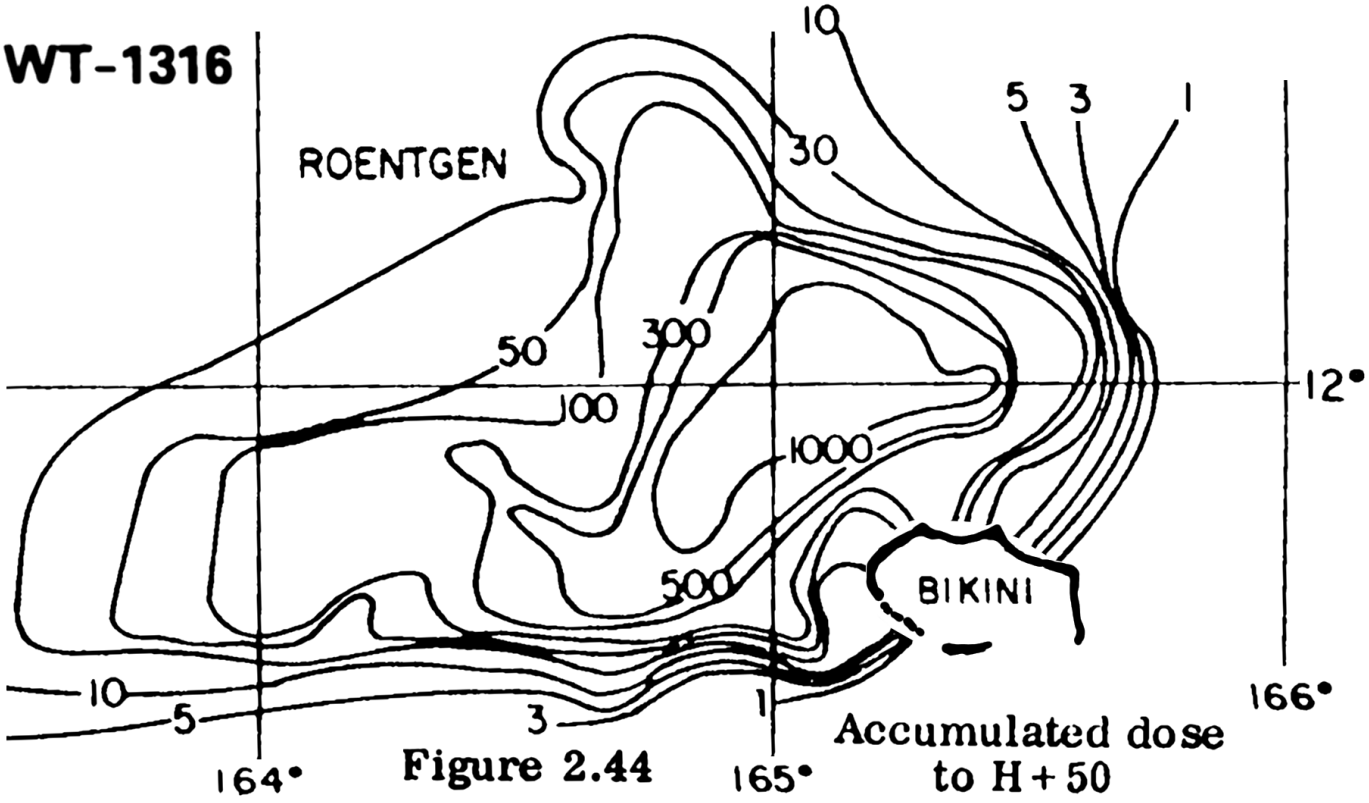

Figure 2.44

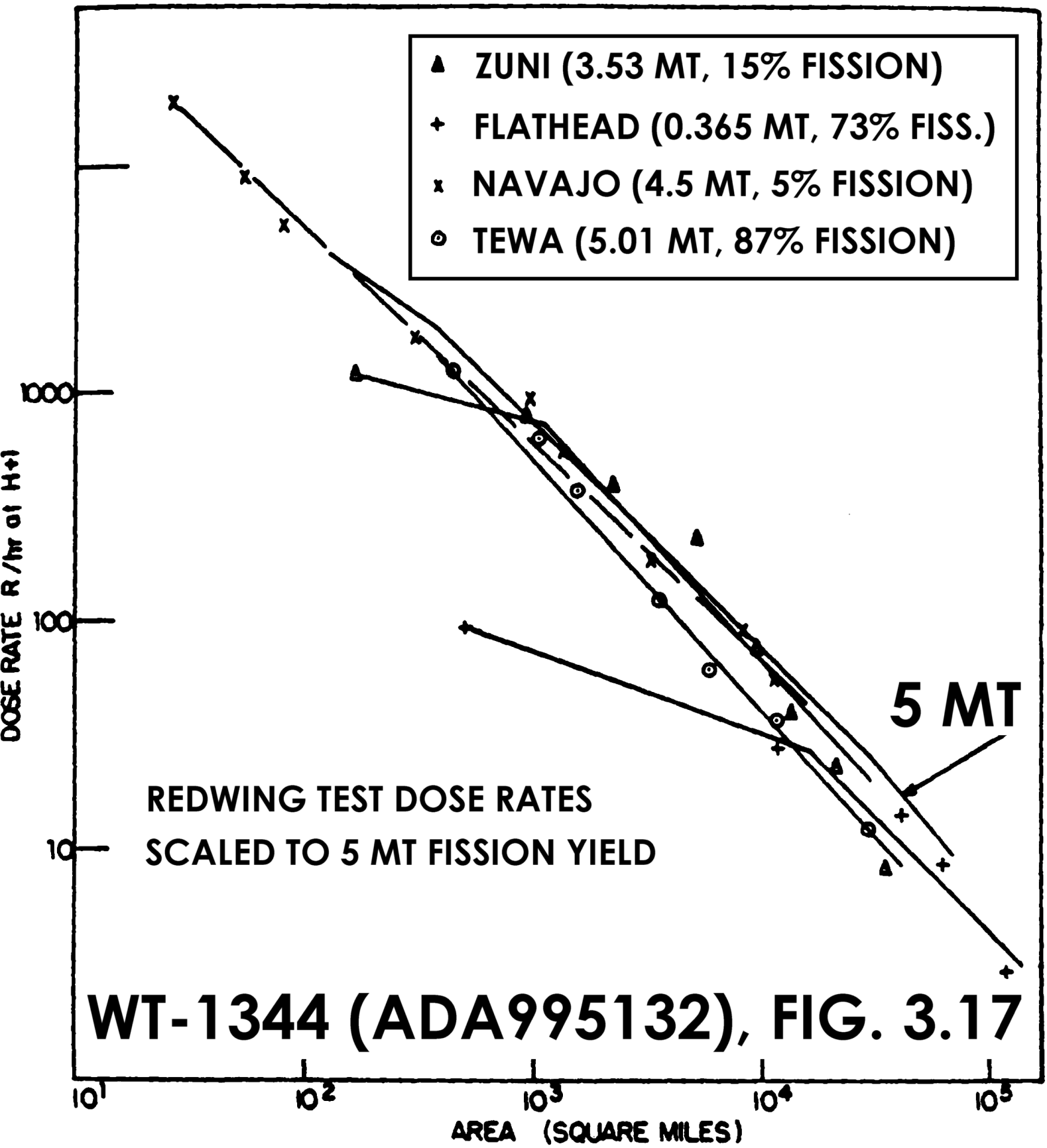
ZUNI (3.53 MT, 15% FISSION)
FLATHEAD (0.365 MT, 73% FISS.)
NAVAJO (4.5 MT, 5% FISSION)
TEWA (5.01 MT, 87% FISSION)
5 MT
REDWING TEST DOSE RATES
SCALED TO 5 MT FISSION YIELD
WT-1344 (ADA995132), FIG. 3.17
DOSE RATE R/hr at H+1
1000
100
10
10^1
10^2
10^3
10^4
10^5
AREA (SQUARE MILES)

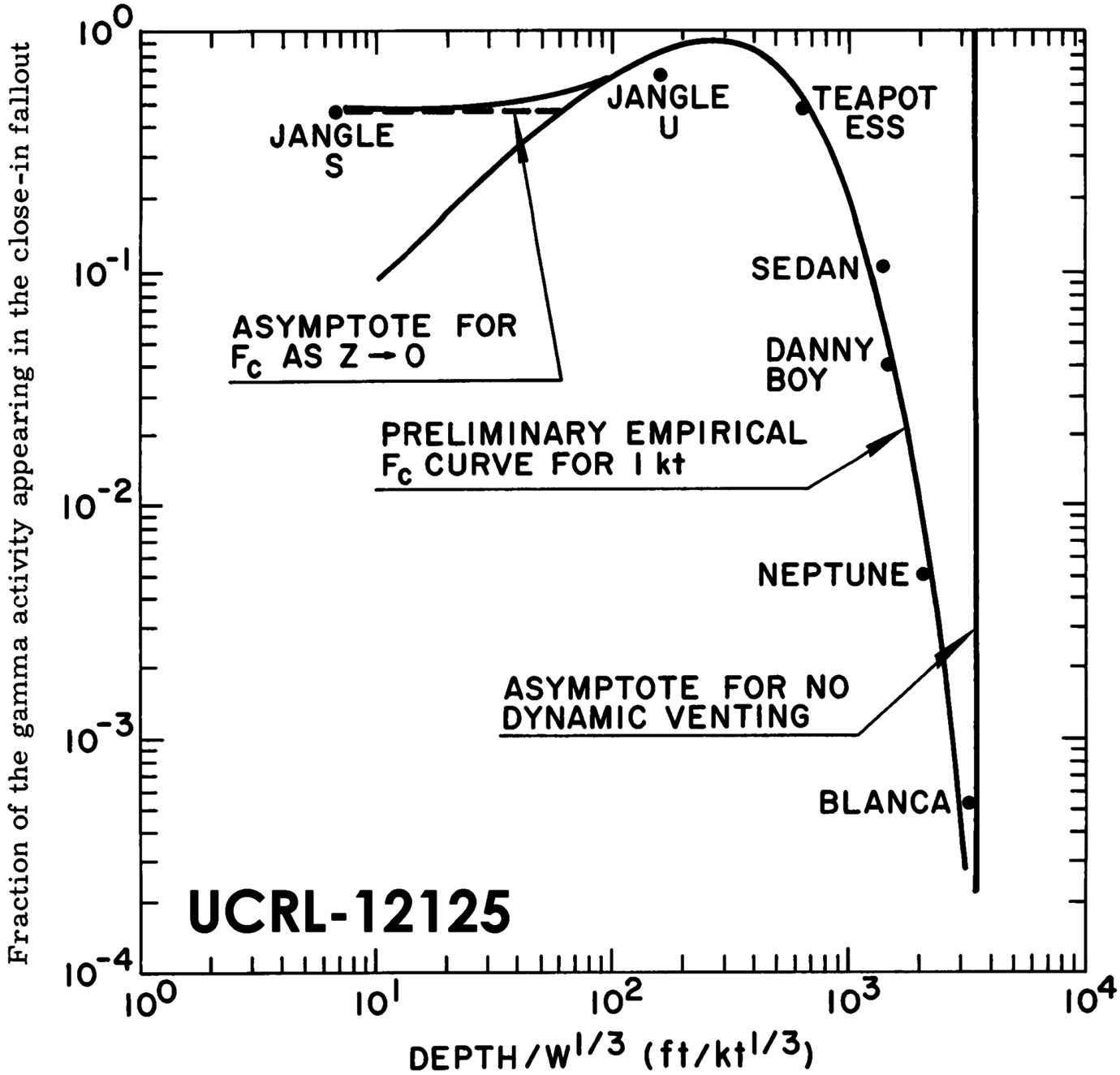

UCRL-12125

Event	W, kt	z, ft	F	Medium
Sedan	100	635	0.10	Alluvium
Teapot ESS	1.2	67	0.46	Alluvium
Jangle U	1.2	17	0.64	Alluvium
Neptune	0.115	100	0.005	Tuff
Jangle S	1.2	0	0.50	Alluvium
Danny Boy	0.43	109	0.04	Basalt
Blanca	19	835	0.0005	Tuff

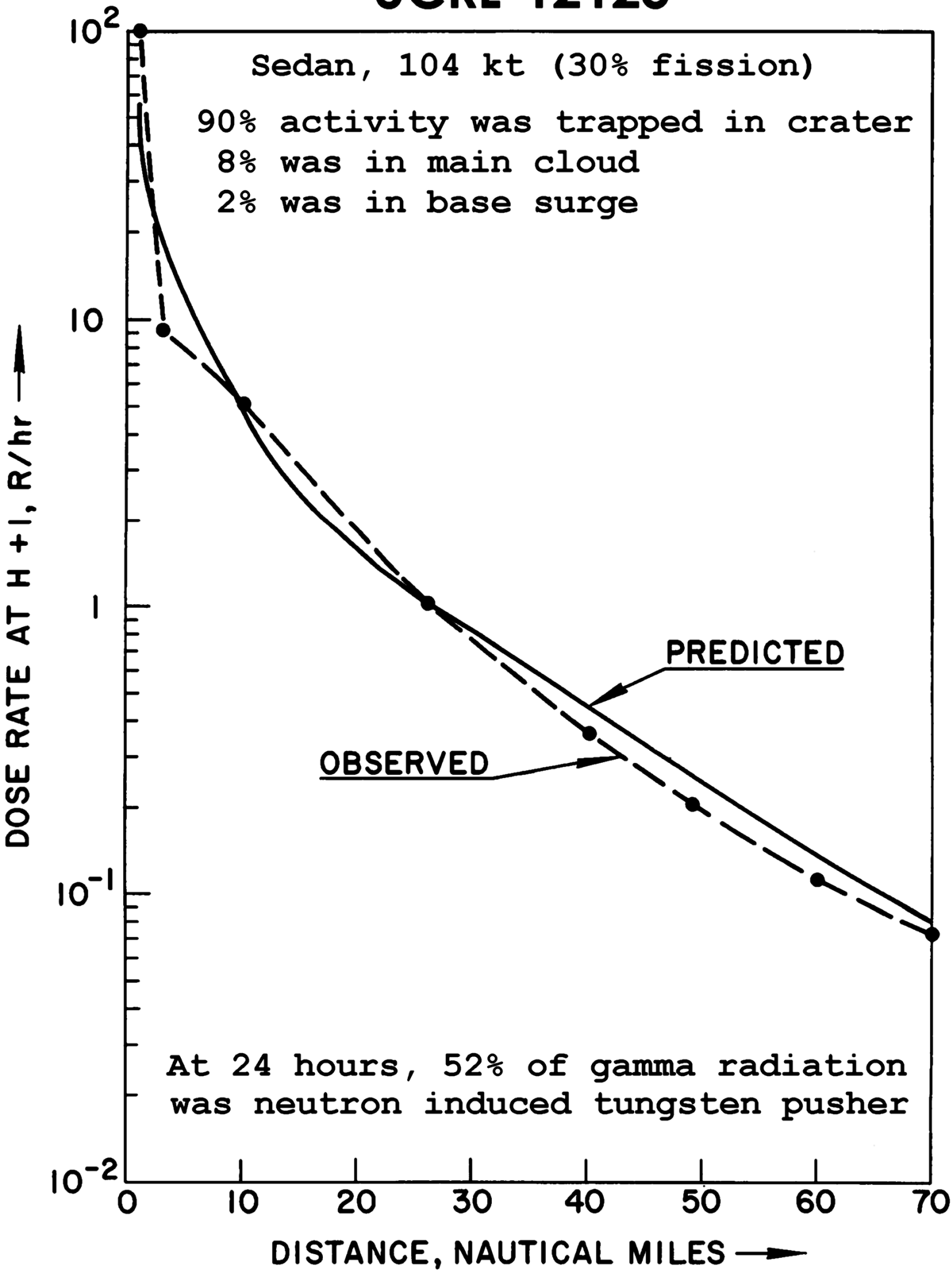
Sedan, 104 kt (30% fission)
90% activity was trapped in crater
8% was in main cloud
2% was in base surge
PREDICTED
OBSERVED
At 24 hours, 52% of gamma radiation was neutron induced tungsten pusher
DOSE RATE AT H +1, R/hr
DISTANCE, NAUTICAL MILES
10^2
10
1
10^{-1}
10^{-2}
0
10
20
30
40
50
60
70

TEAPOT-ESS: 5 SEC. (1.2 KT NUCLEAR TEST AT 67 FEET DEPTH, NEVADA, 23 MARCH 1955)

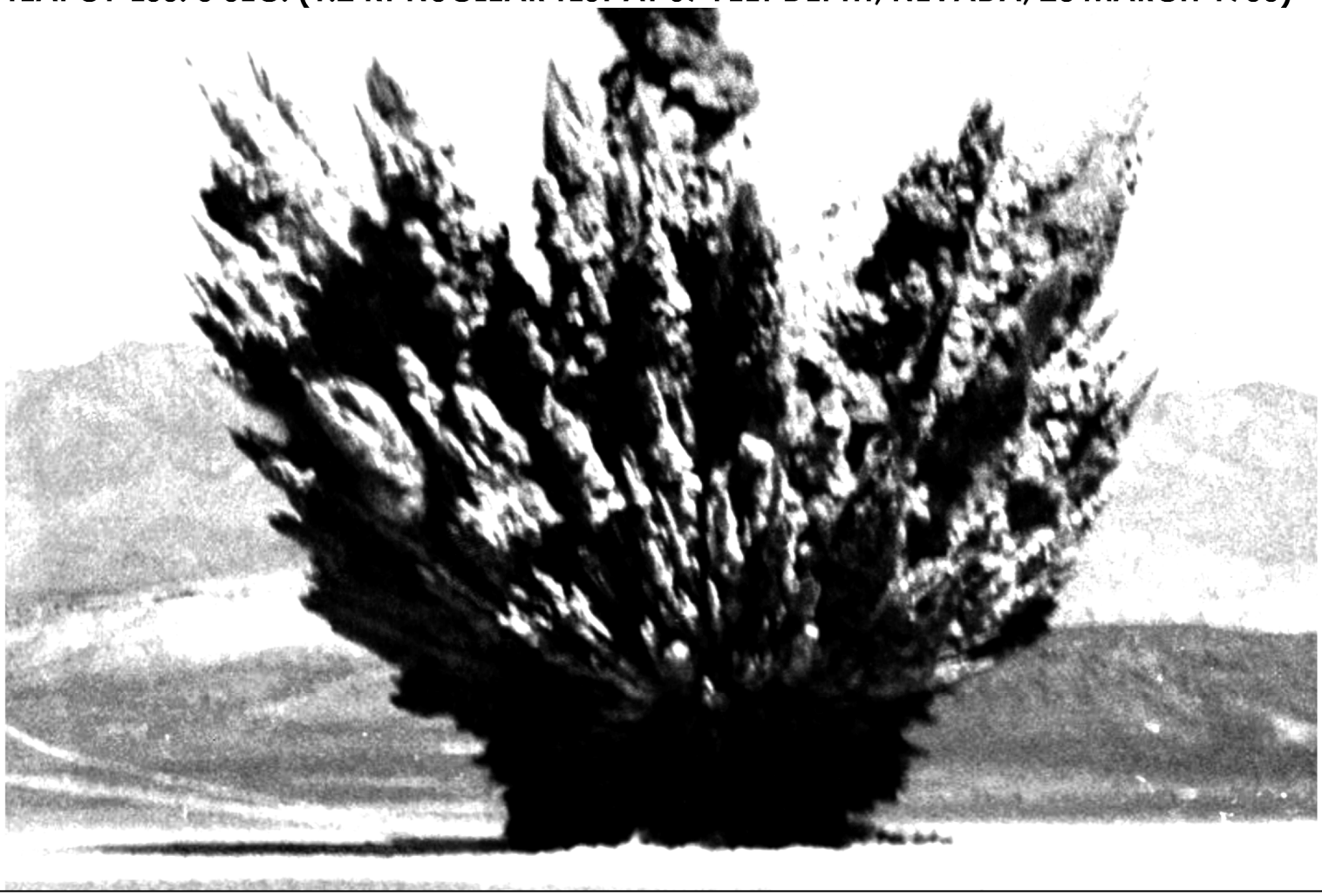

TEAPOT-ESS: 3 MIN. (1.2 KT NUCLEAR TEST AT 67 FEET DEPTH, NEVADA, 23 MARCH 1955)

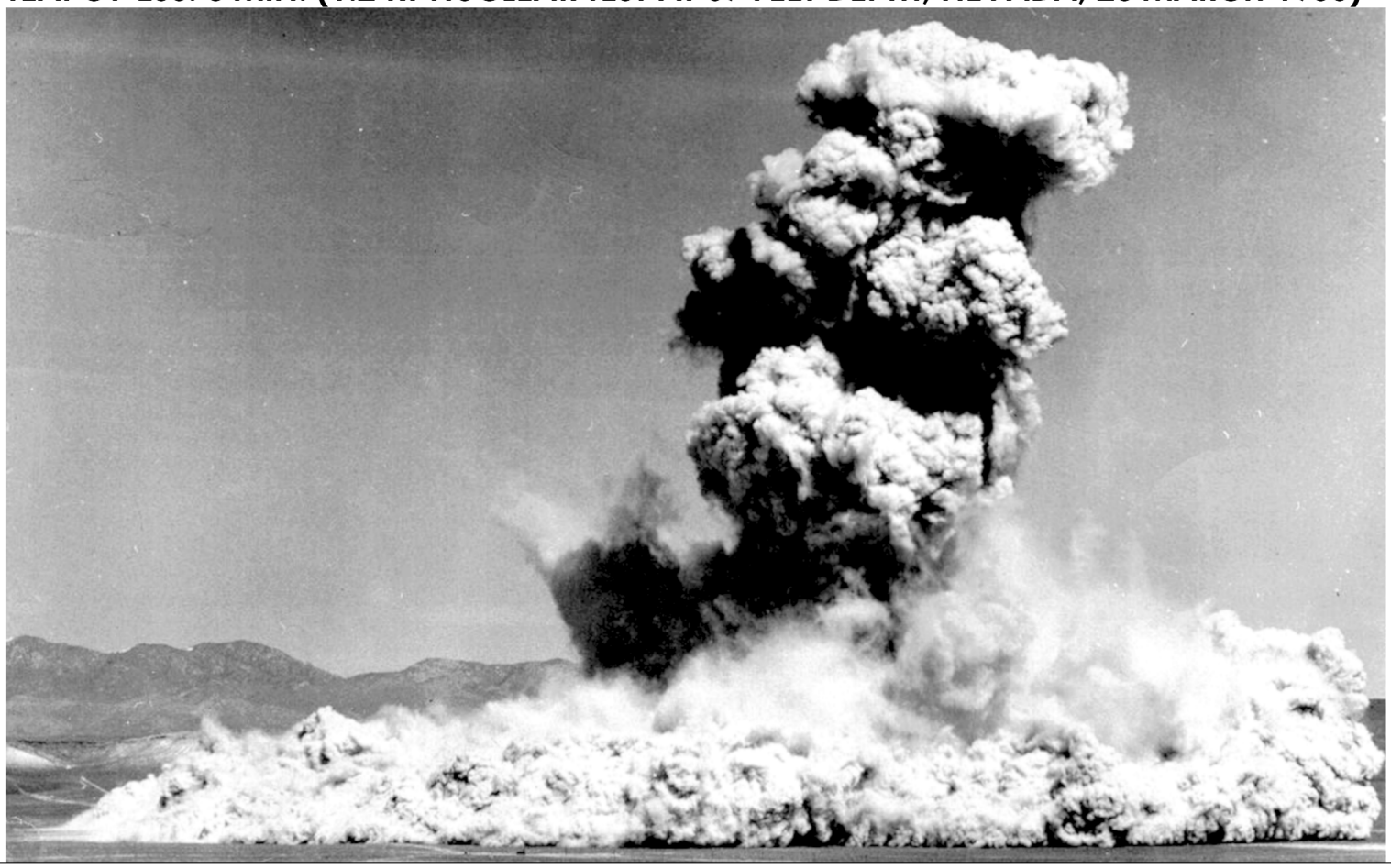

TEAPOT - Ess 23 Mar 1955 **1.2 kt at 67 ft depth, Nevada soil, 20 mph wind**

(Fallout on Banded Mountain spread over slopes, reducing dose rates.)

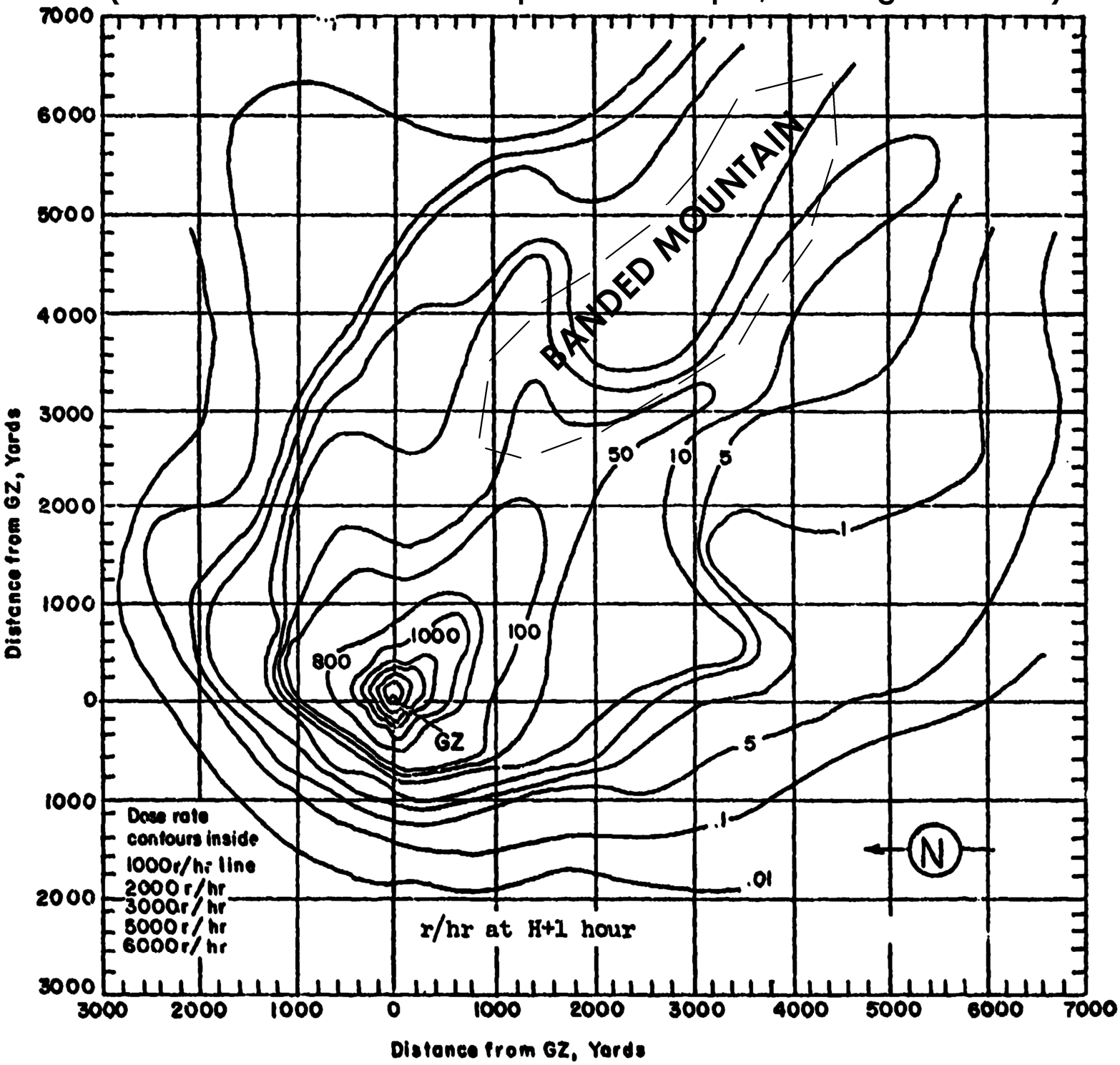

CRATER DATA: Diameter: 292 ft
Depth: 96 ft

HEIGHT OF BURST: -67 ft

Maximum Dose Rate: 6000 r/hr at H+1 hour at crater lip

CLOUD TOP HEIGHT: 12,000 ft MSL

UCRL-51440 (1973)

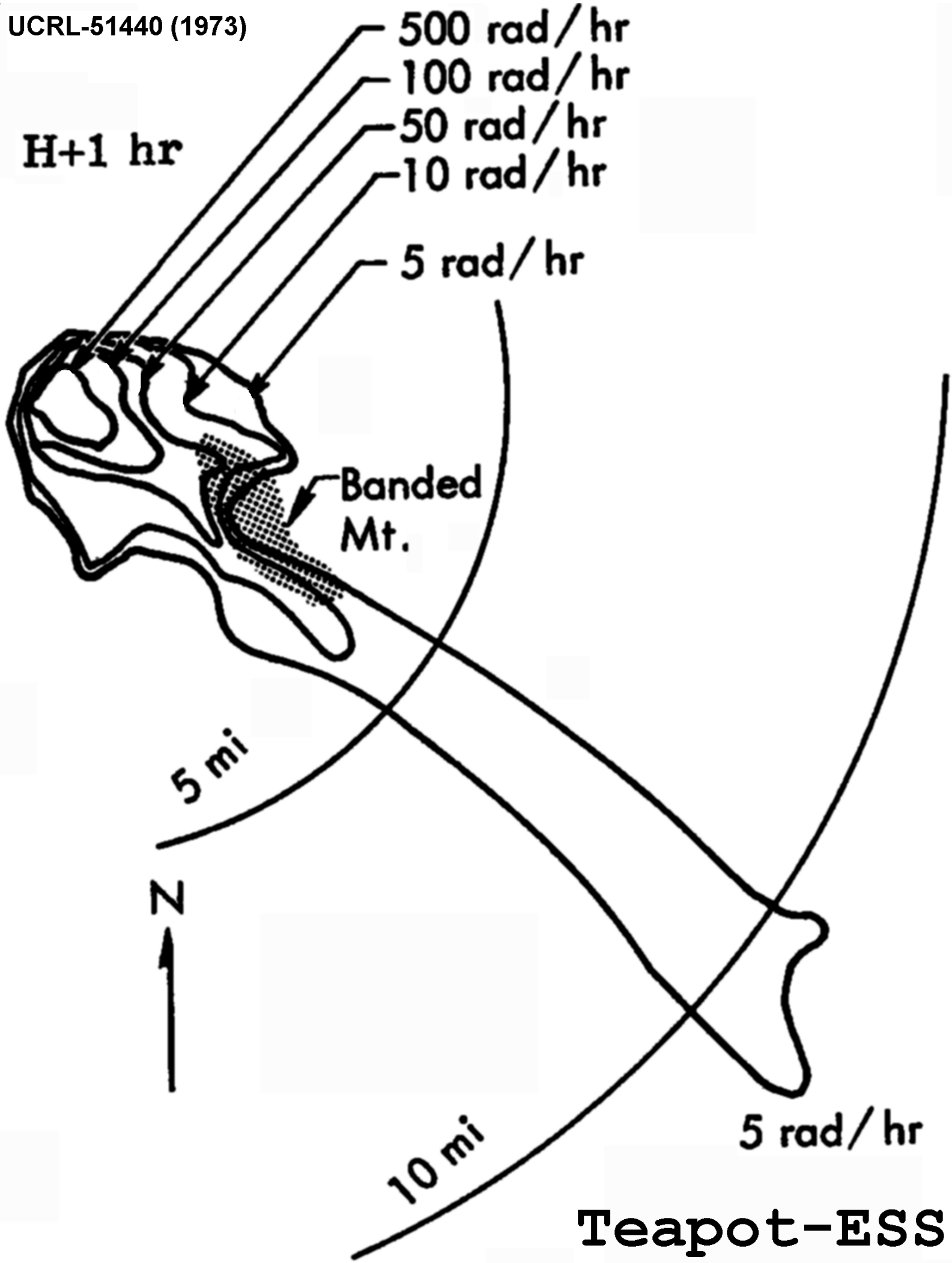

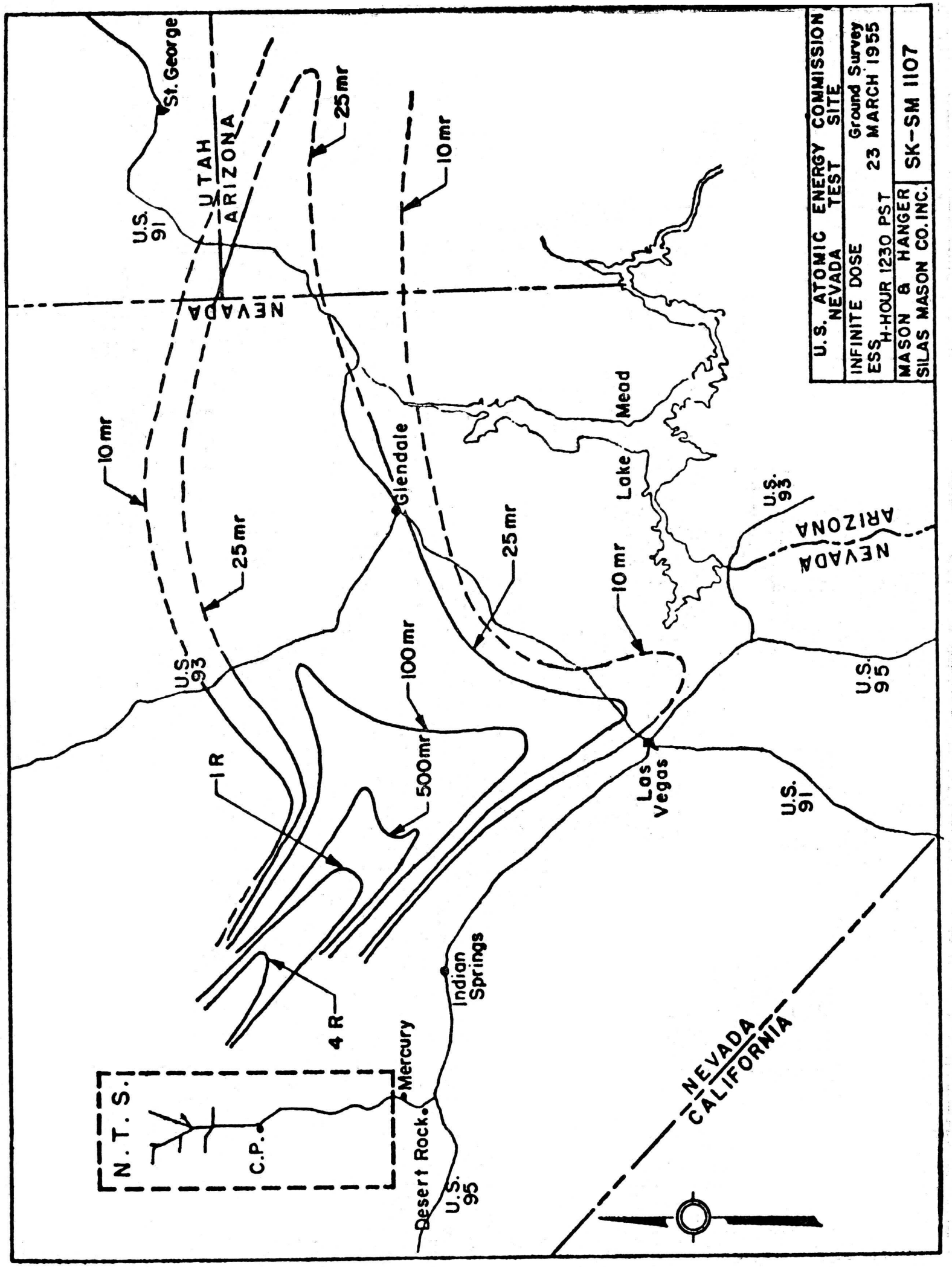
U.S. ATOMIC ENERGY COMMISSION
NEVADA TEST SITE
INFINITE DOSE
ESS
Ground Survey
H-HOUR 1230 PST
23 MARCH 1955
MASON & HANGER
SILAS MASON CO. INC.
SK-SM 1107
St. George
UTAH
ARIZONA
NEVADA
U.S. 91
25 mr
10 mr
Glendale
Mead
Lake
U.S. 93
NEVADA
ARIZONA
U.S. 95
Las Vegas
U.S. 91
100 mr
500 mr
1 R
4 R
Indian Springs
Mercury
Desert Rock
U.S. 95
N. T. S.
C.P.
NEVADA
CALIFORNIA

(May-June 1957 Hearings before Joint Committee on Atomic Energy)

STATEMENT OF DR. W. W. KELLOGG, RAND CORP.

Atmospheric Transport and Close-in Fallout of Radioactive Debris From Atomic Explosions

In the case of an air burst in which the white-hot fireball never reaches the surface, the radioactive fission products never come into close contact with the surface material; they remain as an exceedingly fine aerosol. At first sight this might be thought to be an oversimplification, since there have been many cases in which the fireball never touched the ground, but the surface material was observed to have been sucked up into the rising atomic cloud. Actually, however, in such cases a survey of the area has shown that there has been a negligible amount of radioactive fallout on the ground. Though tons of sand and dust may have been raised by the explosion, they apparently did not become contaminated by fission products.

The explanation for this curious fact prabably lies in a detailed consideration of the way in which the surface material is sucked up into the fireball of an air burst. Within a few seconds from burst time, the circulation in the atomic fireball develops a toroidal form, with an updraft in the middle and downdraft around the outside. Most of the fission products are then confined to a doughnut-shaped region, and may be thought of as constituting a smoke ring. When the surface debris is carried into the fireball a few seconds after the detonation, it passes up along the axis of the cloud, through the middle, and can often be seen to cascade back down around the outside of the cloud. In its passage through the cloud, it has passed around the radioactive smoke ring but has never mixed with it.

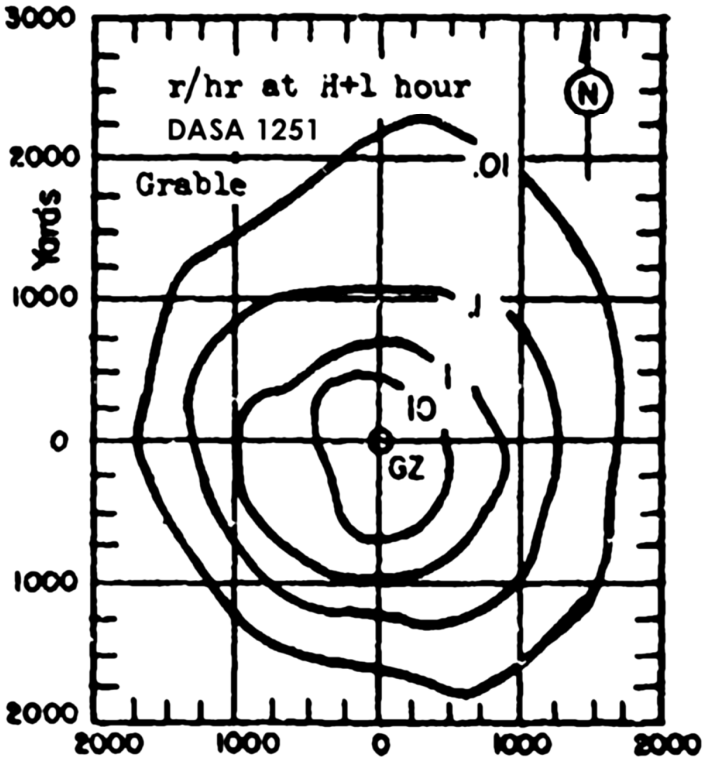

15 kt UPSHOT-KNOTHOLE - Grable 25 May 1953

FIREBALL Radius at 2nd maximum: 557.6

HEIGHT OF BURST: 524 ft

TYPE OF BURST AND PLACEMENT: Airburst of guntype weapon

CLOUD TOP HEIGHT: 35,000 ft MSL

CLOUD BOTTOM HEIGHT: 23,000 ft MSL

ENCORE, 27 KT AIR BURST AT 2,423 FT

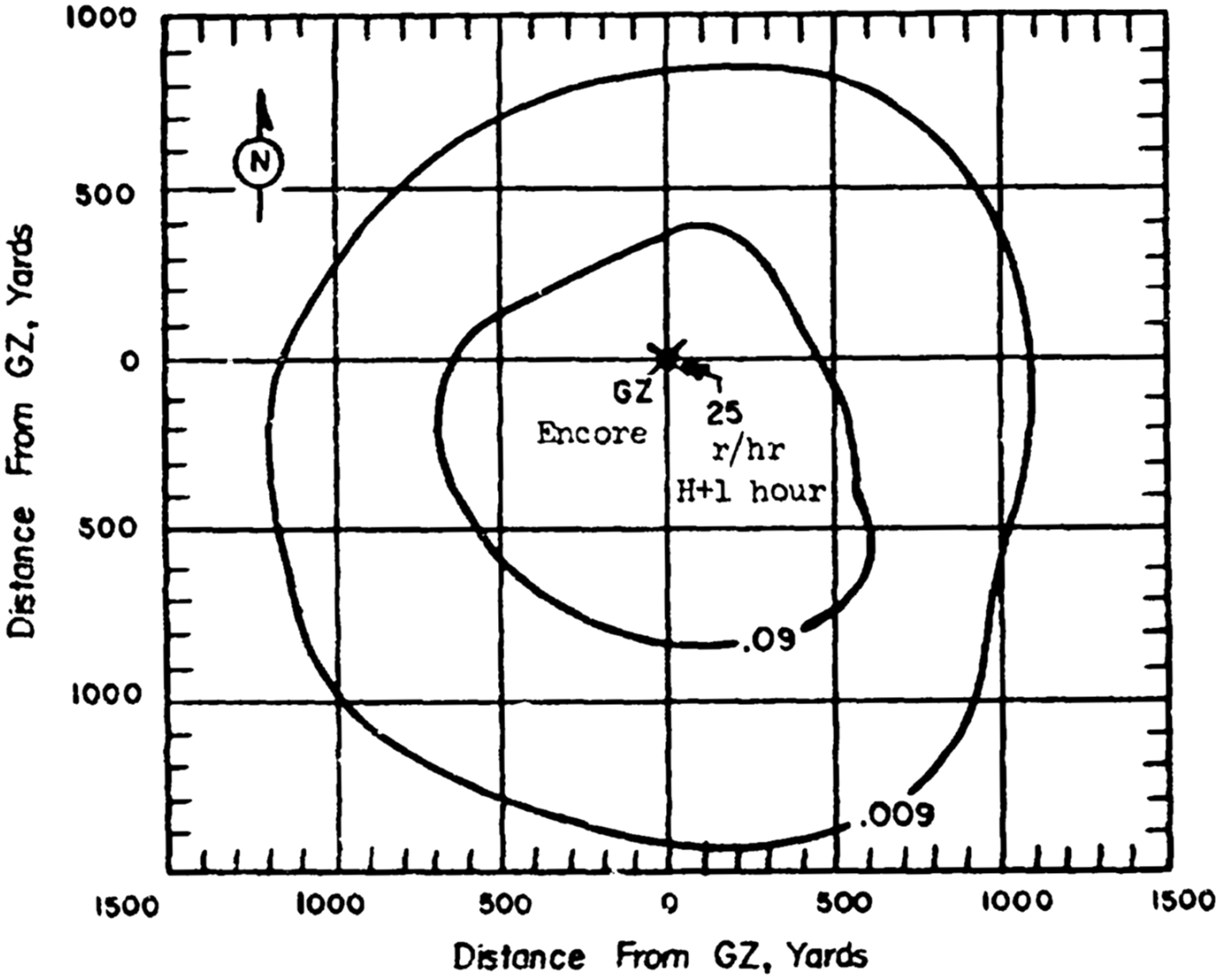

LAPLACE 1 kt 750 ft balloon air burst

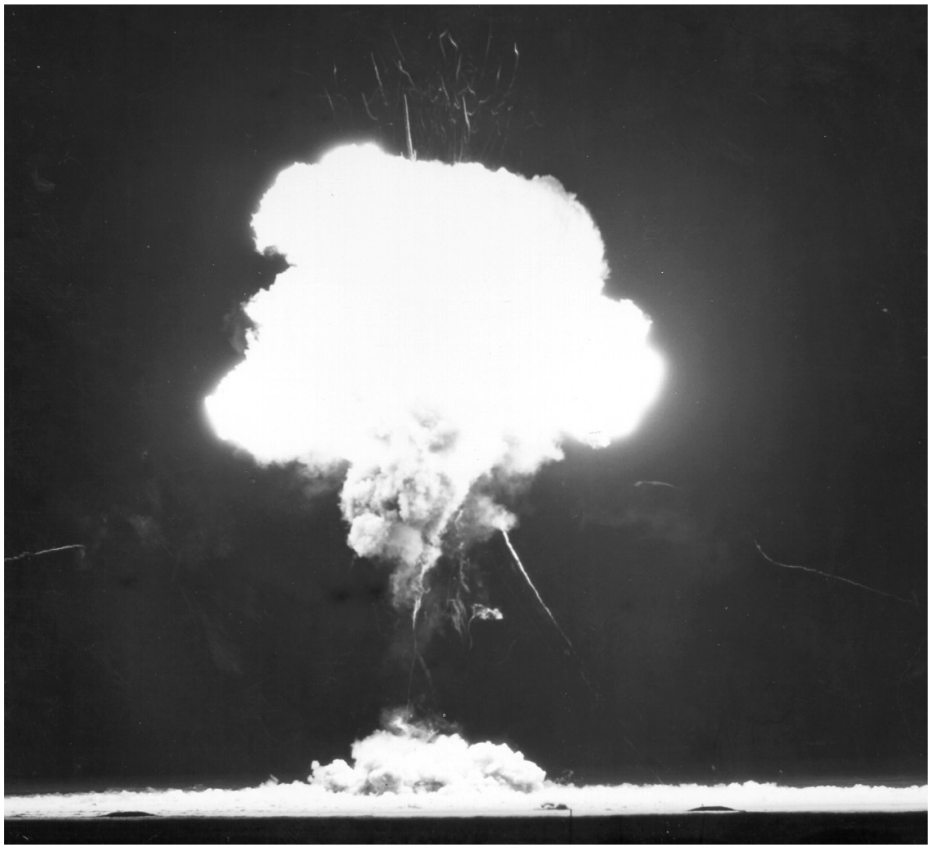

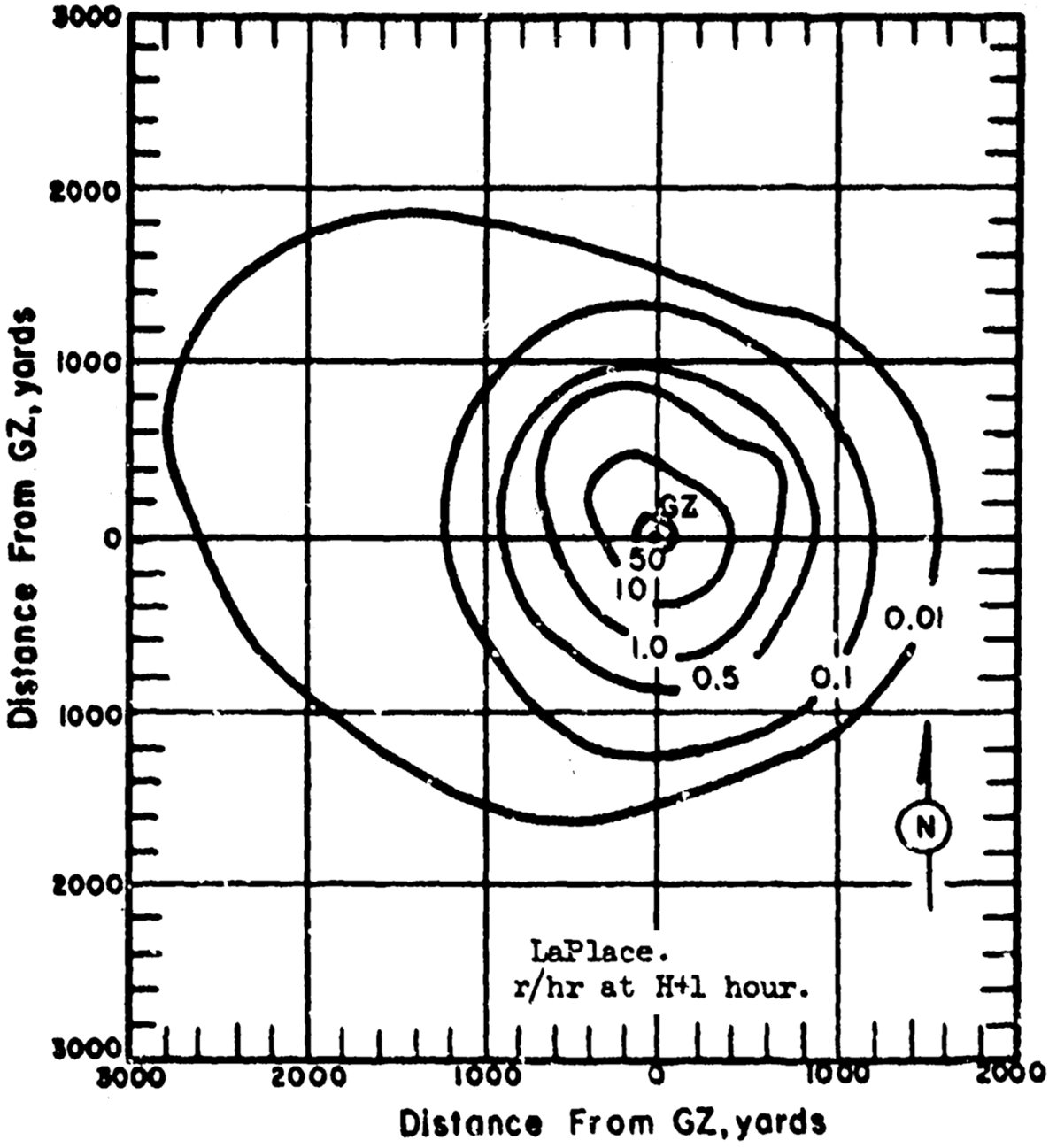

OWENS 9.7 kt 500 ft balloon air burst

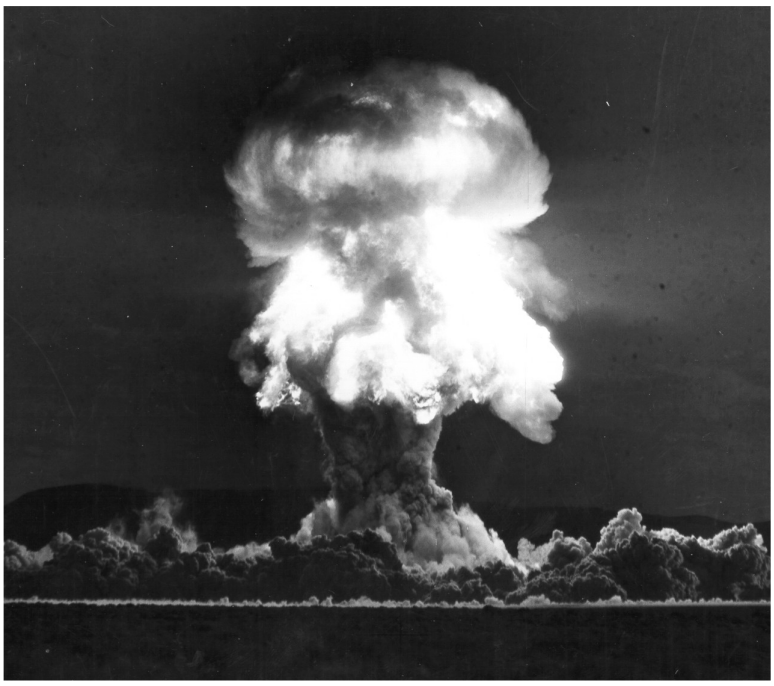

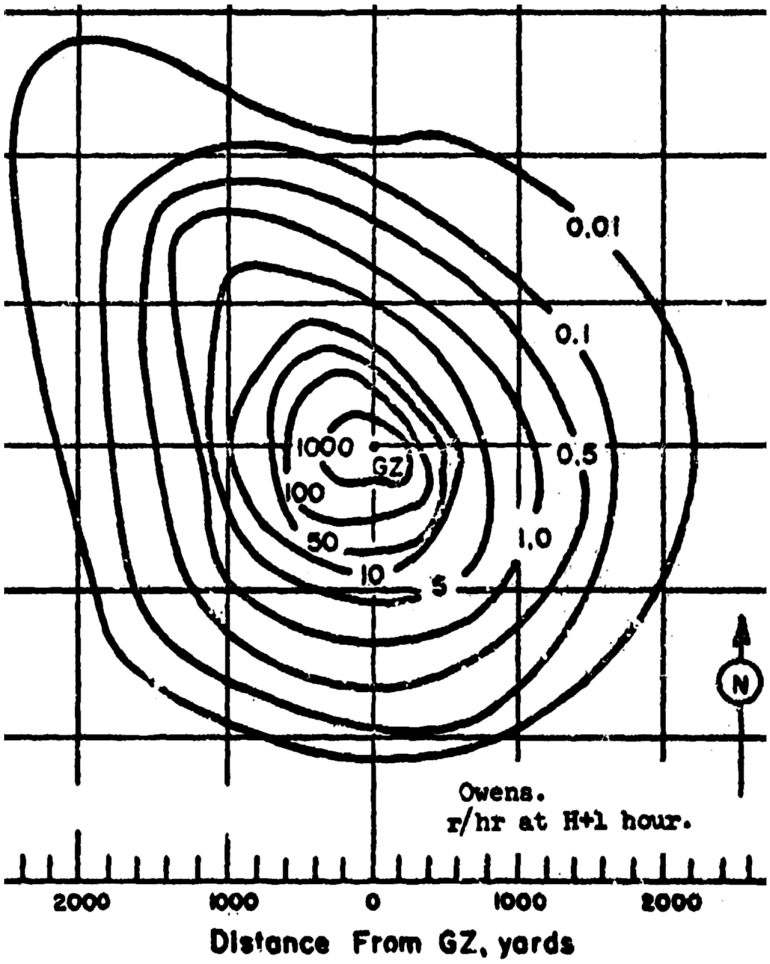

DOPPLER 11 kt 1500 ft balloon air burst

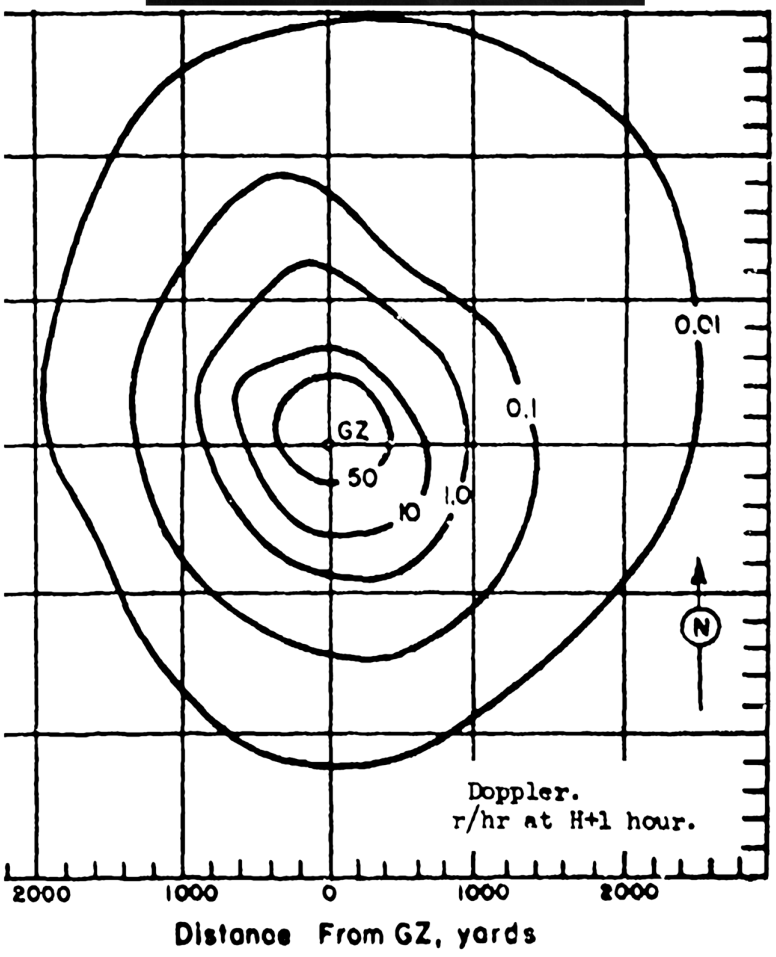

Harold F. Perla and Harry Haller (Holmes and Narver, Inc.), Engineering Study of Underground Highway and Parking Garage and Blast Shelter, ORNL-TM-1381 (March 1966).

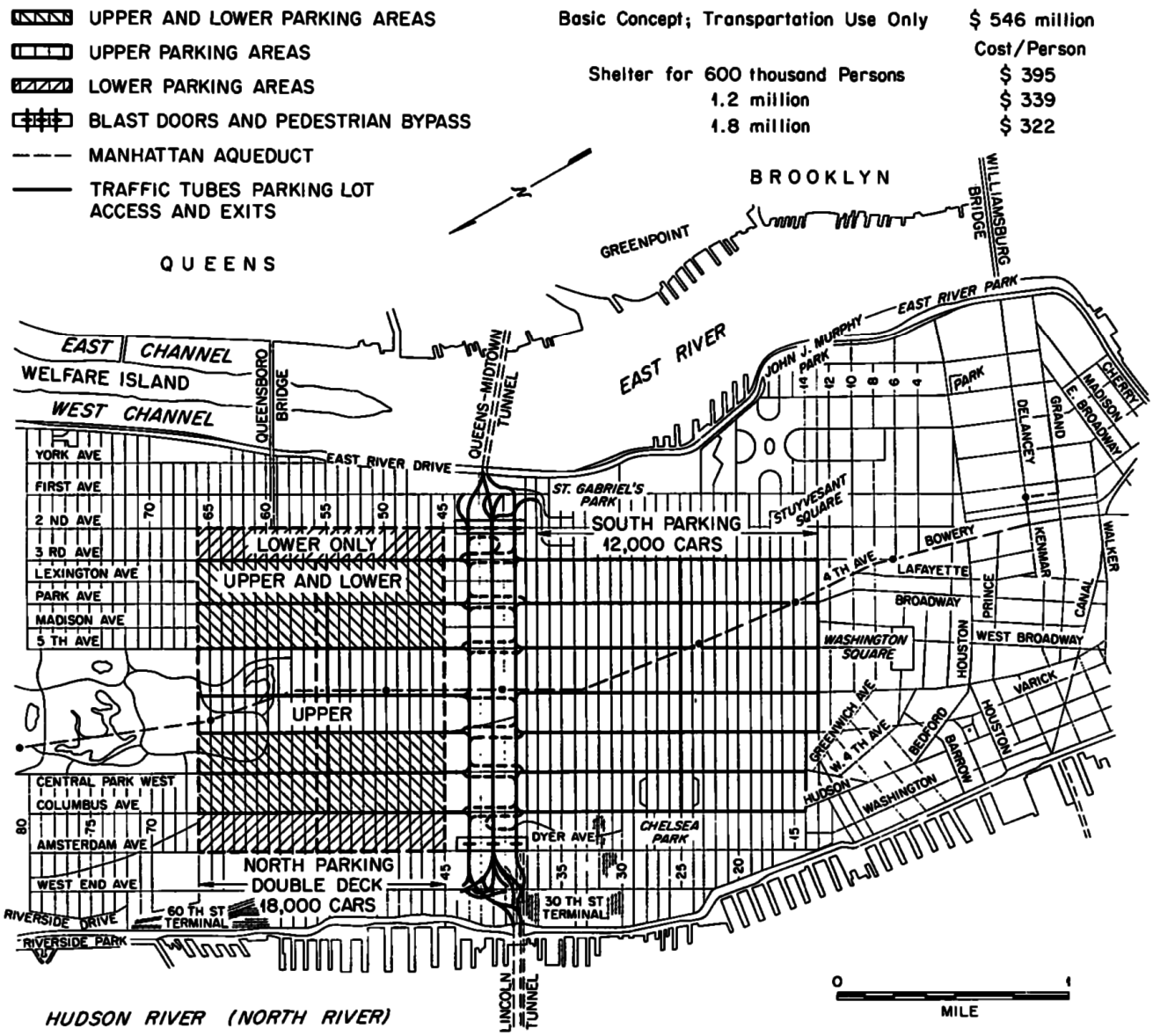

Proposed Dual-Use Shelters for Manhattan.

(Interconnecting Traffic Tubes and Underground Parking Areas)

Report on a Study of Non-Military Defense

July 1, 1958

Report R-322-RC

THE RAND CORPORATION

II. Population Shelters

The first big question that must be raised about non-military defense is whether people can in fact be protected from modern nuclear weapons. Protection involves not only provision of shelters capable of withstanding blast and fallout effects, but also arrangements for getting people into the shelters in response to different kinds of warnings. It should be stated at the beginning that it is impossible to provide reliable protection for all the population, and that the fraction of the population effectively protected depends greatly on the essentially uncertain nature of the enemy attack. There appear to be a number of possibilities for protective systems, however, and under plausible assumptions about the enemy attack and the civilian response, significant—and in some cases dramatic—reductions in civilian casualties appear to be obtainable.

TYPES OF SHELTERS

Improvised fallout shelters, even if only capable of reducing radiation to 1/20 or 1/30 of the radiation outside, could have a significant effect in reducing casualties among people outside the areas of blast damage. There seem to be many possibilities of identifying and preparing such shelters in existing buildings in small cities and towns. For example, a location in the center of the basement of a 40,000-square-foot building (a typical large office, store, or school building) may provide an attenuation to about 1/80. Moreover, a foot of earth gives a reduction to about 1/30, and sandbags distributed in advance could be quickly filled and placed to provide this type of shielding. Even buildings whose structural characteristics provide smaller attenuation factors could be quite useful, with arrangements for washing down or sweeping the roofs and surrounding areas (exposure to carry out the decontamination being rationed among the shelter inhabitants).

Table 2

ESTIMATED LONG-TERM RADIATION AFTER VARIOUS ATTACKS

1500 MEGATONS OF FISSION PRODUCTS (50-CITY ATTACK)

	Average	Maximum	Minimum
Total fallout (kilotons per square mile)	0.4	8.3	0.003
Radiation rate after 90 days with countermeasures[a] (milliroentgens per hour)	0.46	10	0.0035
Cumulative lifetime exposure[a] (roentgens)	3.4	73	0.026
Strontium-90 fallout (curies per square mile)	40	830	0.3
Cumulative lifetime concentration in bone without countermeasures (microcuries)	2	42	0.015

20,000 MEGATONS OF FISSION PRODUCTS (AREA ATTACK)

	Average	Maximum	Minimum
Total fallout (kilotons per square mile)	5.3	36	0.04
Radiation rate after 90 days with countermeasures[a] (milliroentgens per hour)	6.5	43	0.049
Cumulative lifetime exposure[a] (roentgens)	48	310	0.36
Strontium-90 fallout (curies per square mile)	530	3600	4
Cumulative lifetime concentration in bone without countermeasures (microcuries)	26	180	0.2

[a] Assumes that radiation rates are reduced to 1/100 of the level computed with the $r^{-1.2}$ formula, because of decontamination, shielding and time-rationing, and inaccuracy in the formula.

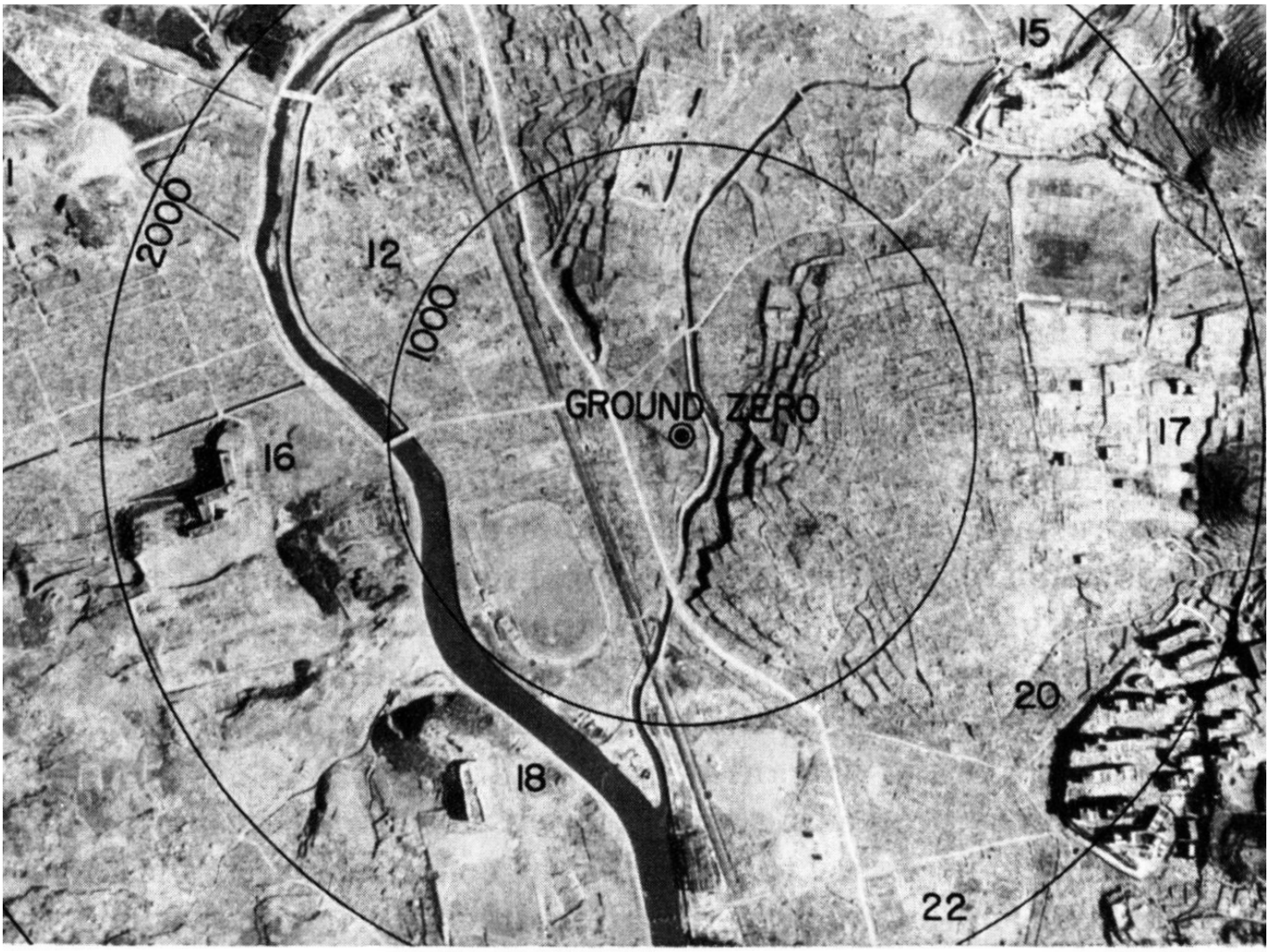

Area around ground zero at Nagasaki before and after explosion (1,000-foot radius circles are shown).

THE EFFECTS OF THE ATOMIC BOMBS AT HIROSHIMA AND NAGASAKI

REPORT OF THE BRITISH MISSION TO JAPAN

PUBLISHED
FOR THE HOME OFFICE AND THE AIR MINISTRY BY
HIS MAJESTY'S STATIONERY OFFICE
LONDON
1946

40. The provision of air raid shelters throughout Japan was much below European standards. Those along the verges of the wider streets in Hiroshima were comparatively well constructed : they were semi-sunk, about 20 ft. long, had wooden frames, and 1 ft. 6 ins. to 2 ft. of earth cover. One is shown in photograph 17. Exploding so high above them, the bomb damaged none of these shelters.

41. In Nagasaki there were no communal shelters except small caves dug in the hillsides. Here most householders had made their own backyard shelters, usually slit trenches or bolt holes covered with a foot or so of earth carried on rough poles and bamboos. These crude shelters, one of which is shown in photograph 18, nevertheless had considerable mass and flexibility, qualities which are valuable in giving protection from blast. Most of these shelters had their roofs forced in immediately below the explosion ; but the proportion so damaged had fallen to 50 per cent. at 300 yards from the centre of damage, and to zero at about ½ mile.

42. These observations show that the standard British shelters would have performed well against a bomb of the same power exploded at such a height. Anderson shelters, properly erected and covered, would have given protection. Brick or concrete surface shelters with adequate reinforcement would have remained safe from collapse. The Morrison shelter is designed only to protect its occupants from the debris load of a house, and this it would have done. Deep shelters such as the refuge provided by the London Underground would have given complete protection.

Photo No. 17. HIROSHIMA. Typical, part below ground, earth-covered, timber framed shelter 300 yds. from the centre of damage, which is to the right. In common with similar but fully sunk shelters, none appeared to have been structurally damaged by the blast. Exposed woodwork was liable to " flashburn." Internal blast probably threw the occupants about, and gamma rays may have caused casualties.

Photo No. 18. NAGASAKI. Typical small earth-covered back yard shelter with crude wooden frame, less than 100 yds. from the centre of damage, which is to the right. There was a large number of such shelters, but whereas nearly all those as close as this one had their roofs forced in, only half were damaged at 300 yds., and practically none at half a mile from the centre of damage.

EARTH ARCHING USED TO STRENGTHEN SHELTERS

ORNL-5037

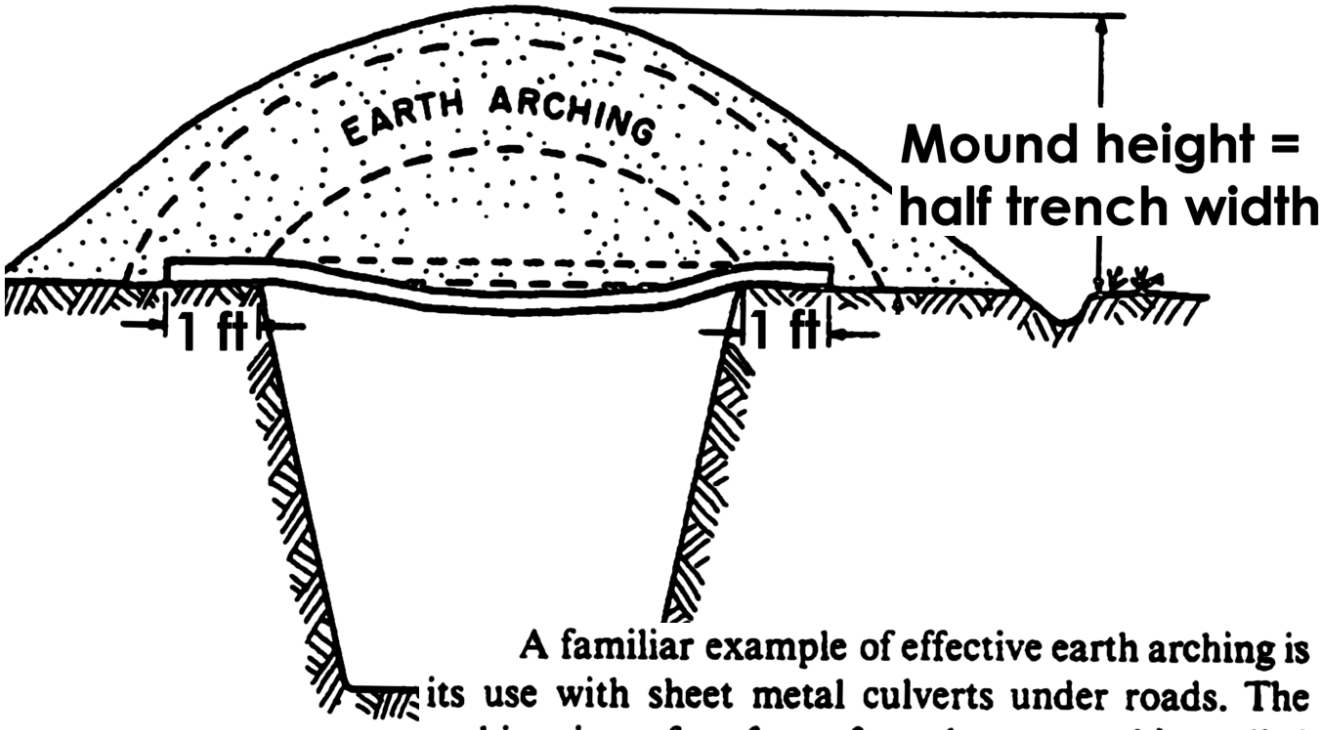

A familiar example of effective earth arching is its use with sheet metal culverts under roads. The arching in a few feet of earth over a thin-walled culvert prevents it from being crushed by the weight of heavy vehicles.

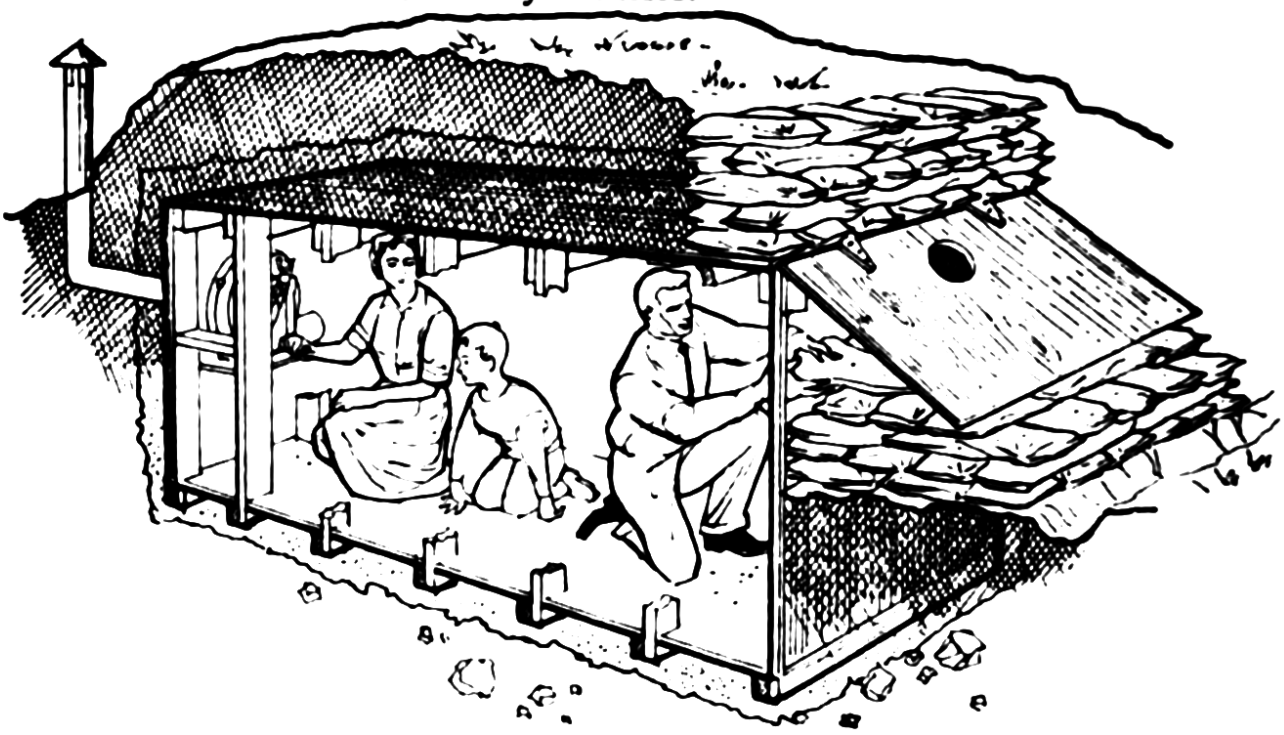

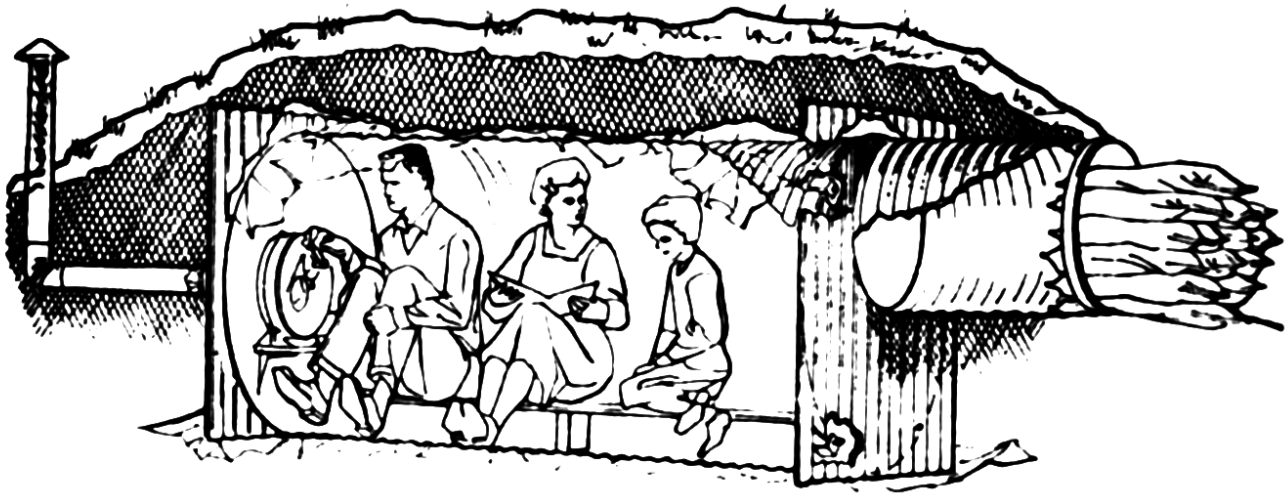

UK NATIONAL ARCHIVES: ES 5/2

ANDERSON SHELTER TESTS AGAINST 25 KT NUCLEAR NEAR SURFACE BURST (2.7 METRES DEPTH IN SHIP)

AWRE-T1/54, 27 Aug. 1954

SECRET—GUARD

ATOMIC WEAPONS RESEARCH ESTABLISHMENT

(formerly of Ministry of Supply)

SCIENTIFIC DATA OBTAINED AT OPERATION HURRICANE

(Monte Bello Islands, Australia—October, 1952)

$$p = \frac{130 \times 10^9}{R^3} + \frac{7 \cdot 7 \times 10^6}{R^2} + \frac{13 \cdot 5 \times 10^3}{R}$$

p is the maximum excess pressure in p.s.i. and R is the distance in feet

Fig. 12.1, Andersons at 1380 ft range from bomb ship shown in the photo, moored 400 yards off shore.

Left: Fig. 12.3, Andersons at 1800 ft after burst. Right: Fig. 12.4, Andersons protected by blast walls at 2760 ft.

12.1. *Blast Damage to Anderson Shelters*

At 1,380 feet, Fig. 12.1, parts of the main structure of the shelters facing towards and sideways to the explosion were blown in but the main structure of the one facing away from the explosion was intact, and would have given full protection. At 1,530 feet, Fig. 12.2, the front sheets of the shelter facing the explosion were blown into the shelter but otherwise the main structures were more or less undamaged, as were those at 1,800 feet, Fig. 12.3.

At 2,760 feet, Fig. 12.4, some of the sandbags covering the shelters were displaced and the blast walls were distorted whilst at 3,390 feet, Fig. 12.5, the effect was quite small. At these distances, the shelters were not in direct view of the explosion owing to intervening sandhills.

13. The Penetration of the Gamma Flash

13.1. *Experiments on the Protection from the Gamma Flash afforded by Slit Trenches*

13.1.1. The experiments described in this section show that slit trenches provide a considerable measure of protection from the gamma flash. From the point of view of Service and Civil Defence authorities this is one of the most important results of the trial.

13.1.2. Rectangular slit trenches 6 ft. by 2 ft. in plan and 6 ft. deep were placed at 733, 943 and 1,300 yards from the bomb and circular fox holes 2 ft. in radius and 6 ft. deep were placed at 943 and 1,300 yards.

The doses received from the flash were measured with film badges and quartz-fibre dosimeters in order to determine the variation of protection with distance, with depth and with orientation of the trench and the relative protection afforded by open and covered trenches.

In general, the slit trenches were placed broadside-on to the target vessel but at 1,300 yards one trench was placed end-on. Two trenches, one at 733 and one at 943 yards were covered with the equivalent of 11 inches of sand.

Table 13.1

Variation of Gamma Flash Dose on Vertical Axis of Trench

Type of trench	Rectangular broadside-on open			Rectangular end-on open	Circular open		Rectangular broadside-on covered	
Distance (yards) ...	1,300	943	733	1,300	1,300	943	943	733
Surface dose (Roentgens)	300	3,000	14,000	300	300	3,000	3,000	14,000
Depth below ground level (inches)								
6 ...	150	1,000	—	230	214	1,200	(75)	—
12 ...	75	430	—	150	120	545	47·6	—
24 ...	33·3	150	584	60	54·5	188	25	(140)
36 ...	23	70	216	31·6	30	86	13	(56)
48 ...	(20)	43	100	20	17·7	48·5	7·7	(31)
60 ...	—	(37·5)	61	13·6	10·7	(33·3)	5	(23)
72 ...	—	—	(46·7)	(8·6)	7	—	(3·5)	—

Entries in brackets are extrapolations or estimates.

Air raid trench
1940

THE NUMBER OF ATOMIC BOMBS EQUIVALENT TO THE LAST WAR AIR ATTACKS ON GREAT BRITAIN AND GERMANY

Summary

During the last war, a total of 1,300,000 tons* of bombs were dropped on Germany by the Strategic Air Forces. If there were no increase in aimi accuracy, then to achieve the same total amount of material damage (to houses, industrial and transportation targets, etc.) would have required the use of over 300 atomic bombs together with some 500,000 tons of high explosive and incendiary bombs for targets too small to warrant the use of an atomic bomb. Increases in accuracy could cause a substantial reduction in this figure of 300 atomic bombs, to as few as 100-150 bombs for very accurate attacks.

1 2 cms The National Archives ins 1 2
Ref.: HO 225/12. C500594

THIS DOCUMENT HAS BEEN
DOWNGRADED TO UNCLASSIFIED
Authority in file ESA 10/4/2
Date 2/12/57 Initials LST

CD 2333

~~SECRET~~

HOME OFFICE

CD/SA 12
Copy. No 5.

OFFICE OF THE CHIEF SCIENTIFIC ADVISER

A COMPARISON BETWEEN THE NUMBER OF PEOPLE KILLED PER TONNE OF BOMBS DURING WORLD WAR I AND WORLD WAR II

BOMB SIZES

=> ≈ 175 kg

For World War II the average bomb weight was between 150 - 200 kg. (R.C. 268, Table 6), whereas for World War I the majority of bombs were 12 or 50 kg.

TABLE 5

Relative safeties in World War II deduced from population and casualty distribution

	In the open	Under cover	In shelter
Population exposure	5%	60%	35%
Location people killed	19%	62%	19%
Relative safety	72%	20%	10%
RELATIVE DANGER!			

(1) A house about 3½ times as safe as in the open.
(2) A shelter about twice as safe as a house.

Table 6 also shows the location of killed which is implied by each of the possible population exposures. The only evidence available on this point is that, for the day raid on June 13th, 1916, in which the total number killed was 59, 69.5% of the people killed in the City were in the open.

HOME OFFICE

AIR RAID PRECAUTIONS

DIRECTIONS FOR THE ERECTION AND SINKING OF THE GALVANISED CORRUGATED STEEL SHELTER

(ANDERSON SHELTER)

February 1939

Crown Copyright Reserved

London family who survived in Anderson shelter during Blitz, when the shelter absorbed the blast (earth was blown off) in 1940

A.R.P. (O) 10

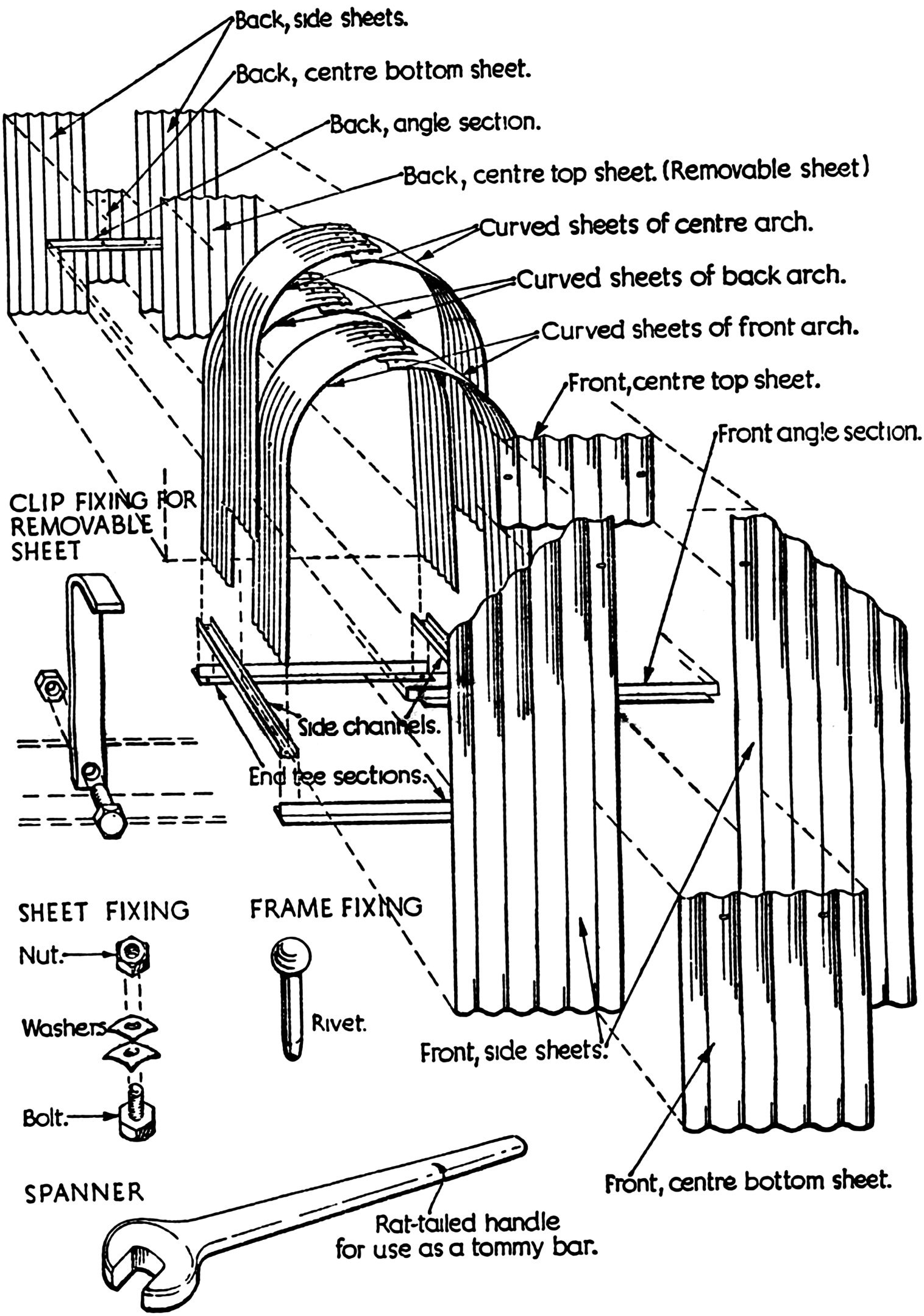

FIG. 3.—THE INDIVIDUAL PARTS.

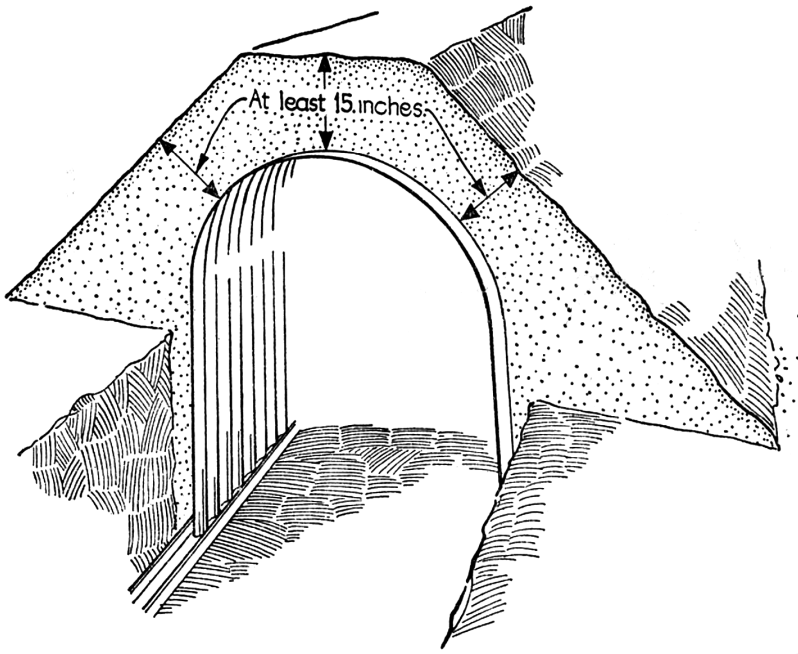

FIG. 4.—STAGE 12. COVERING THE SHELTER WITH EARTH.

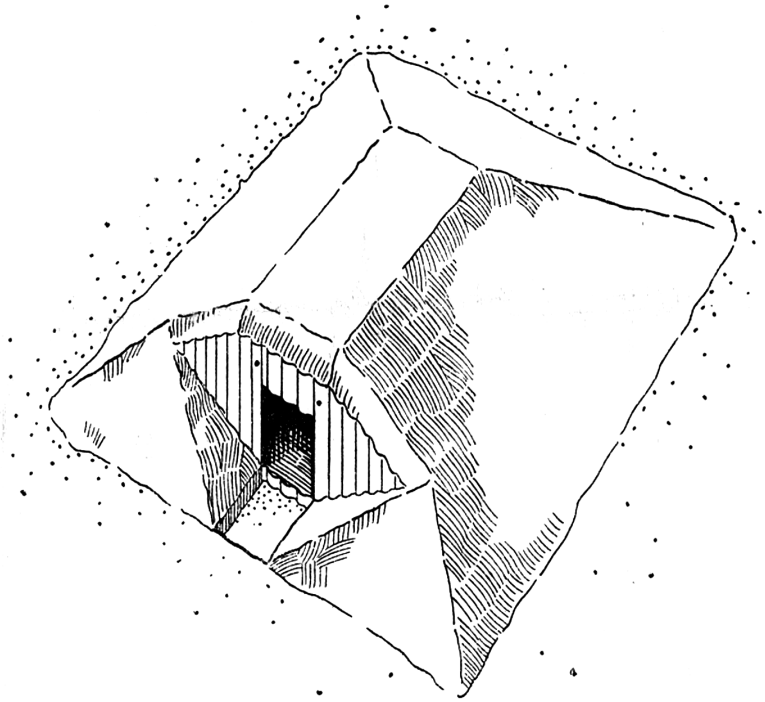

FIG. 4.—STAGE 13. THE SHELTER COMPLETE WITH EARTH COVER.

Anderson shelter survives hit: Norwich 27 April 1942

Anderson shelter survives, Croydon, October 1940

Anderson shelters absorbed the blast energy and were damaged, saving lives.

It cannot be too strongly emphasised that it is most important, from the point of view of reducing casualties as a whole, for everyone in an area under attack to make use of any shelter that is available. Recent research has shown that there would be less fatal casualties if everyone were in relatively poor shelter than if half the population were in shelter twice as good and the other half remained in the open.

THE RISK OF BECOMING A CASUALTY

(Basic Methods of Protection Against High Explosive Missiles - Manual of Basic Training, Civil Defence, vol. 2, Pamphlet 5, H.M.S.O., 1951)

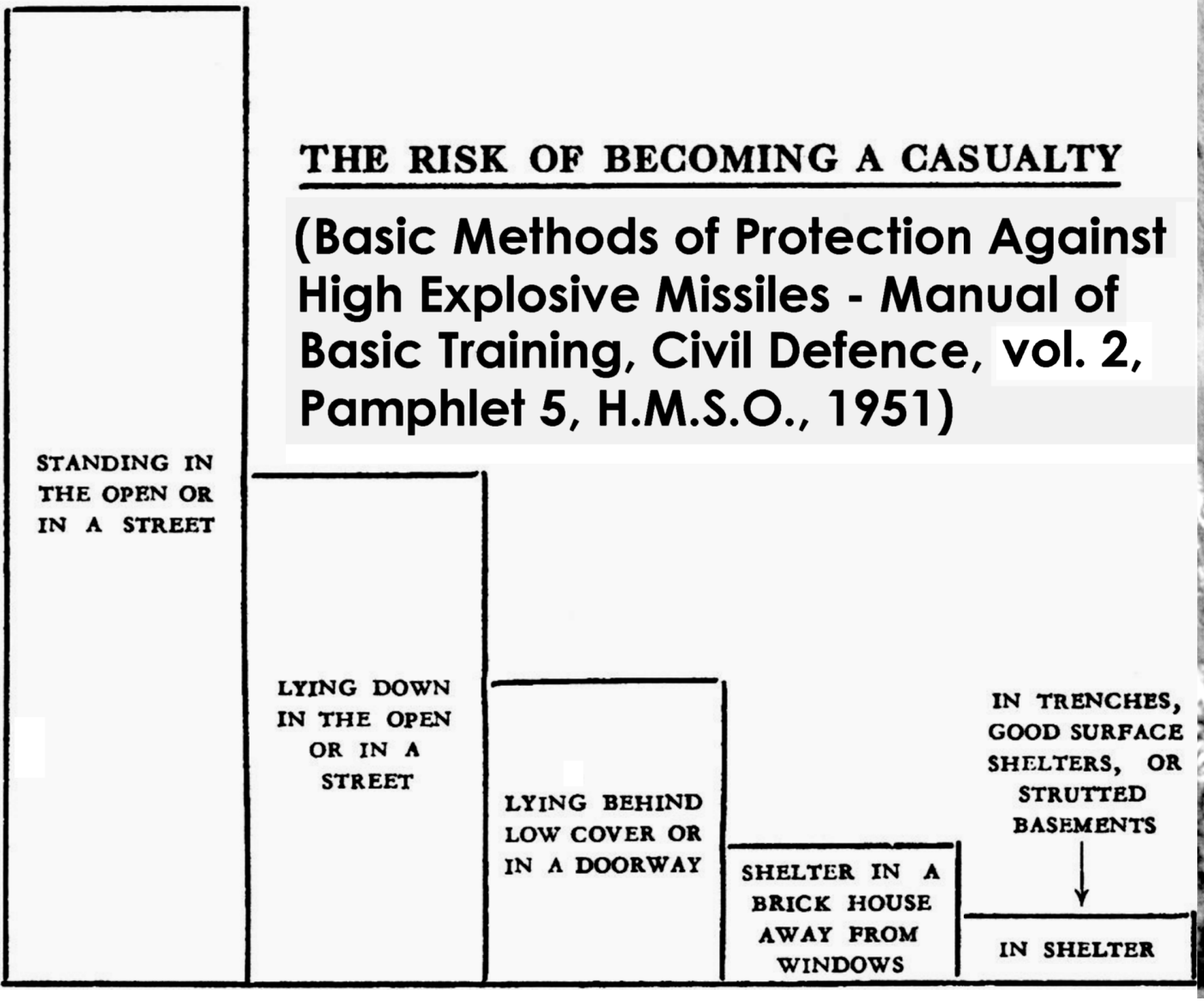

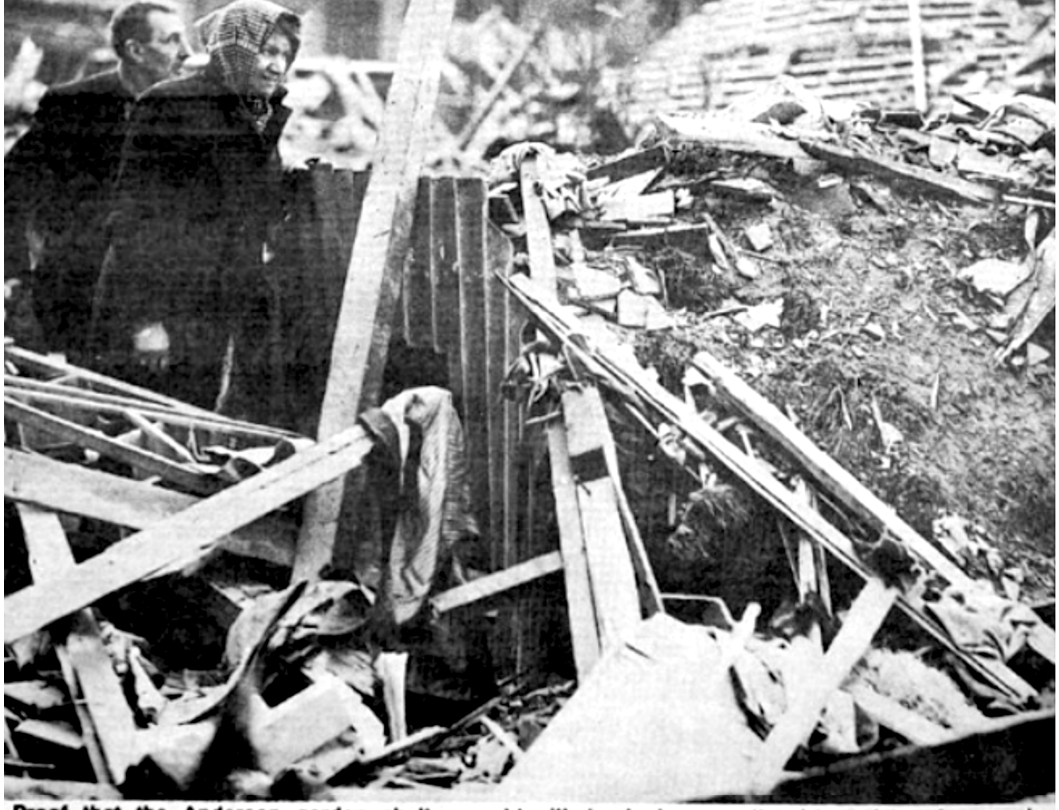

Proof that the Anderson garden shelter could withstand a house collapsing on it can be seen in this picture. Mr. and Mrs. Clague bless their insistence on 'going to ground' when their homes and those of their neighbours were ›duced to rubble.

18 June 1941

Anderson shelter survives at Latham Street, Poplar, London, 1941:

And They Came Out of It Alive . . .

The edge of this bomb crater, 30ft. deep, in a household garden near London, is only 4ft. from the Anderson shelter. But the two people in the shelter during London's six-hour raid—Mrs. Clark and Miss Clark—were unhurt. You see Miss Clark in the picture examining the damage to the structure.

Daily Mirror
28 Aug 1940

UK National Archives: CAB / 67 / 9 / 7

(THIS DOCUMENT IS THE PROPERTY OF HIS BRITANNIC MAJESTY'S GOVERNMENT).

SECRET.

W.P.(G)(41)7. COPY NO. 62

January 15th, 1941.

WAR CABINET.

AIR RAID SHELTER POLICY.

Memorandum by the Minister of Home Security.

---

6. Shelter in the home: The Anderson shelter was originally intended for indoor use but for a number of reasons including the danger of fire an outdoor variant was adopted. Experience has shown that the objections to the indoor use of the Anderson or somewhat similar shelter are not so serious as was thought and two designs have been produced which can be erected indoors without support. These new types, although they may give slightly less protection than a well covered Anderson shelter out of doors, would fill the needs of a large section of the public, especially the middle class. One design allows the use of the shelter as part of the furniture of the room.

7. I regard shelters of this type as of the first importance and wish to provide them on a big scale. Each shelter will use over 3 cwt. of steel and will allow at a pinch two adults and one to two children to sleep inside. For an outlay of about 65,000 tons of steel, as a first instalment, I could therefore produce 400,000 shelters with accommodation for at least 1,000,000 persons. I should wish to complete such a programme within the first three months of production and thereafter at a similar or increasing rate. From enquiries I believe that manufacture can be arranged provided steel is supplied and if the Cabinet approves my policy I shall require their direction that the steel be made available.

10. Conclusions.

I ask for a general endorsement of the policy I have outlined in this paper and in particular for the agreement of my colleagues:

(i) that proposals for building shelters of massive construction should be rejected;

(ii) that steel should be made available to carry out the programme outlined in paragraph 7 for the provision of steel shelters indoors;

(iii) that the limit of income for the provision of free shelter for insured persons should be raised from £250 to £350 per annum.

H.M.

MINISTRY OF HOME SECURITY.

January 15th, 1941.

Morrison Shelters in Recent Air Raids.

National Archives
HO197/24

A report of Ministry of Home Security experts on 39 cases of bombing incidents in different parts of Britain covering all those for which full particulars are available in which Morrison shelters were involved shows how well they have stood up to severe tests of heavy bombing.

All the incidents were serious. Many of the incidents involved direct hits on the houses concerned a risk against which it was never claimed these shelters would afford protection. In all of them the houses in which shelters were placed were within the radius of damage by bombs; in 24 there was complete demolition of the house on the shelter.

A hundred and nineteen people were sheltering in these "Morrisons" and only four were killed. So that 115 out of 119 people were saved. Of these only 7 were seriously injured and 14 slightly injured while 94 escaped uninjured. The majority were able to leave their shelters unaided.

November 1940 design by C. A. Joy, M. Inst. Me. & C. E., Bexley Borough Engineer (UK National Archives: HO 205/257)

ANDERSON SHELTER

(Indoors to avoid groundwater flooding, damp and cold)

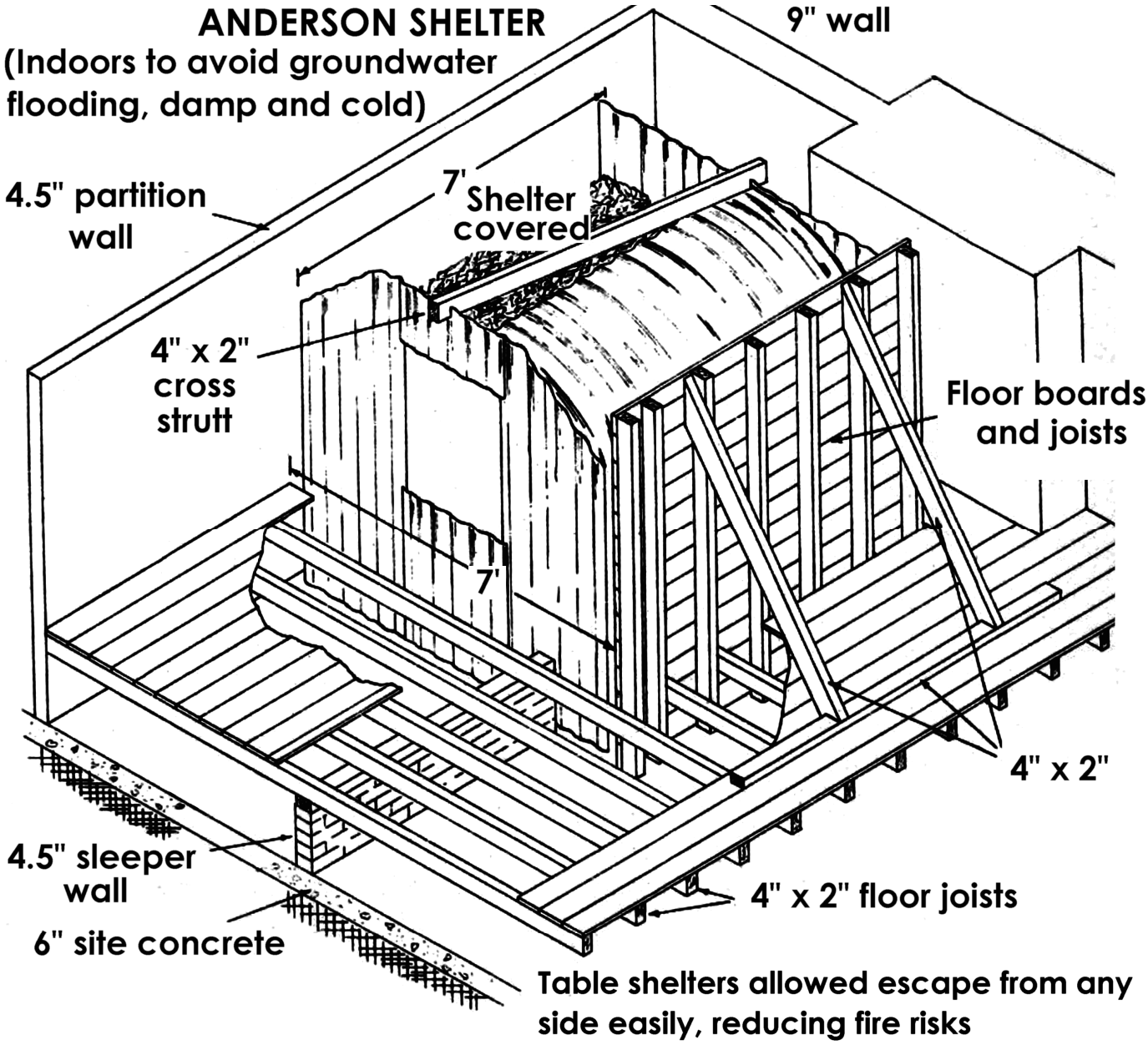

Table shelters allowed escape from any side easily, reducing fire risks

MORRISON SHELTER

(indoor table shelter)

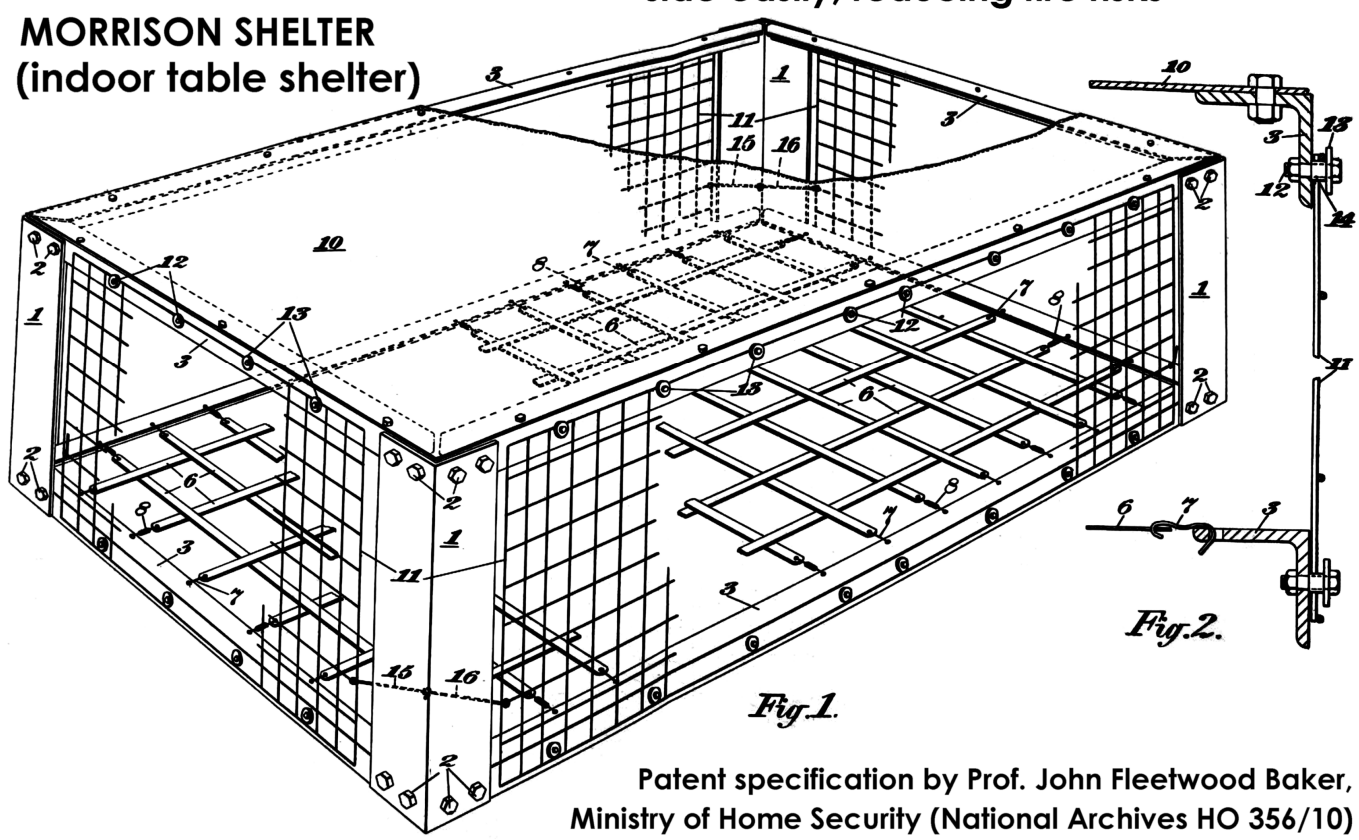

Patent specification by Prof. John Fleetwood Baker, Ministry of Home Security (National Archives HO 356/10)

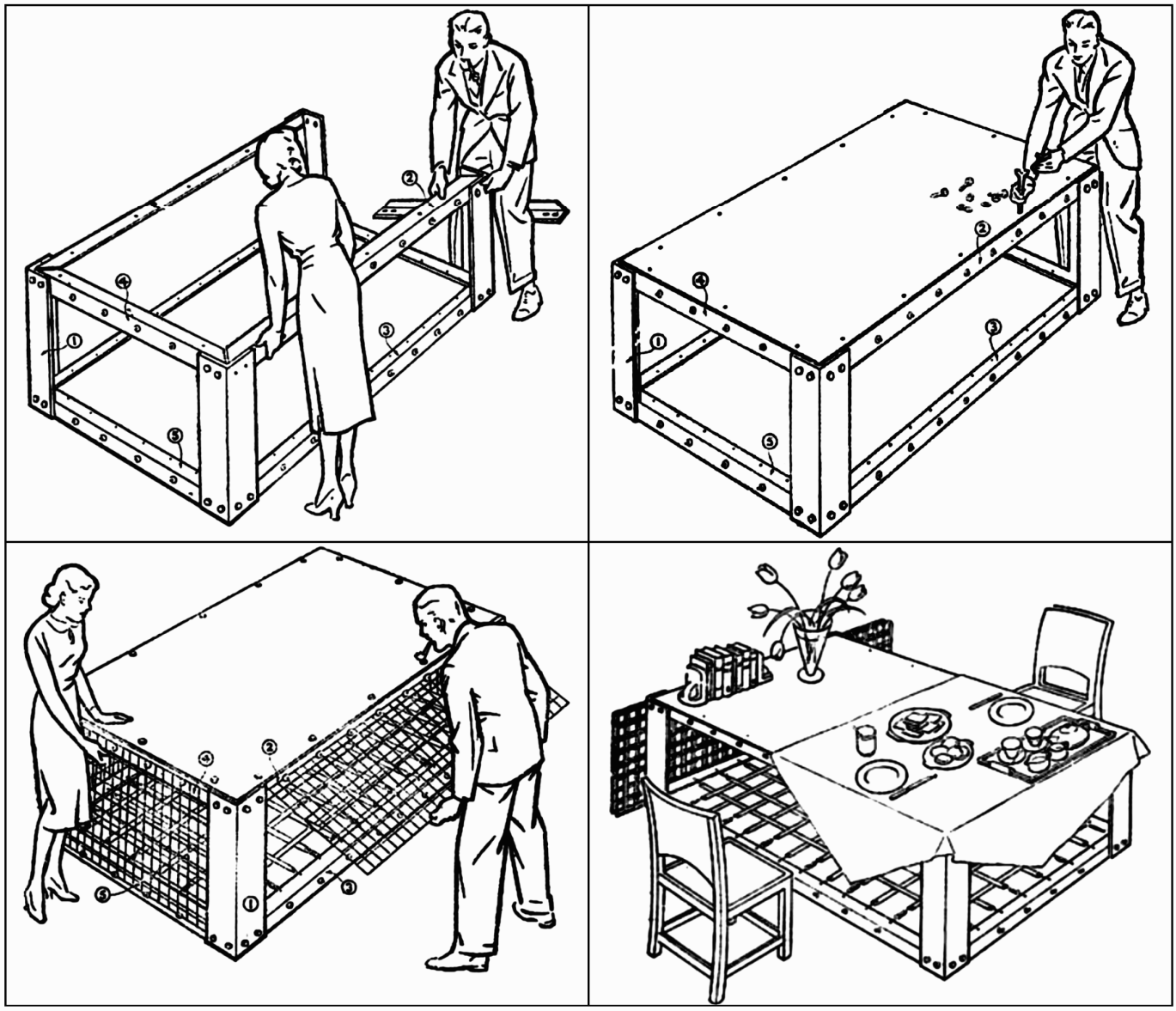

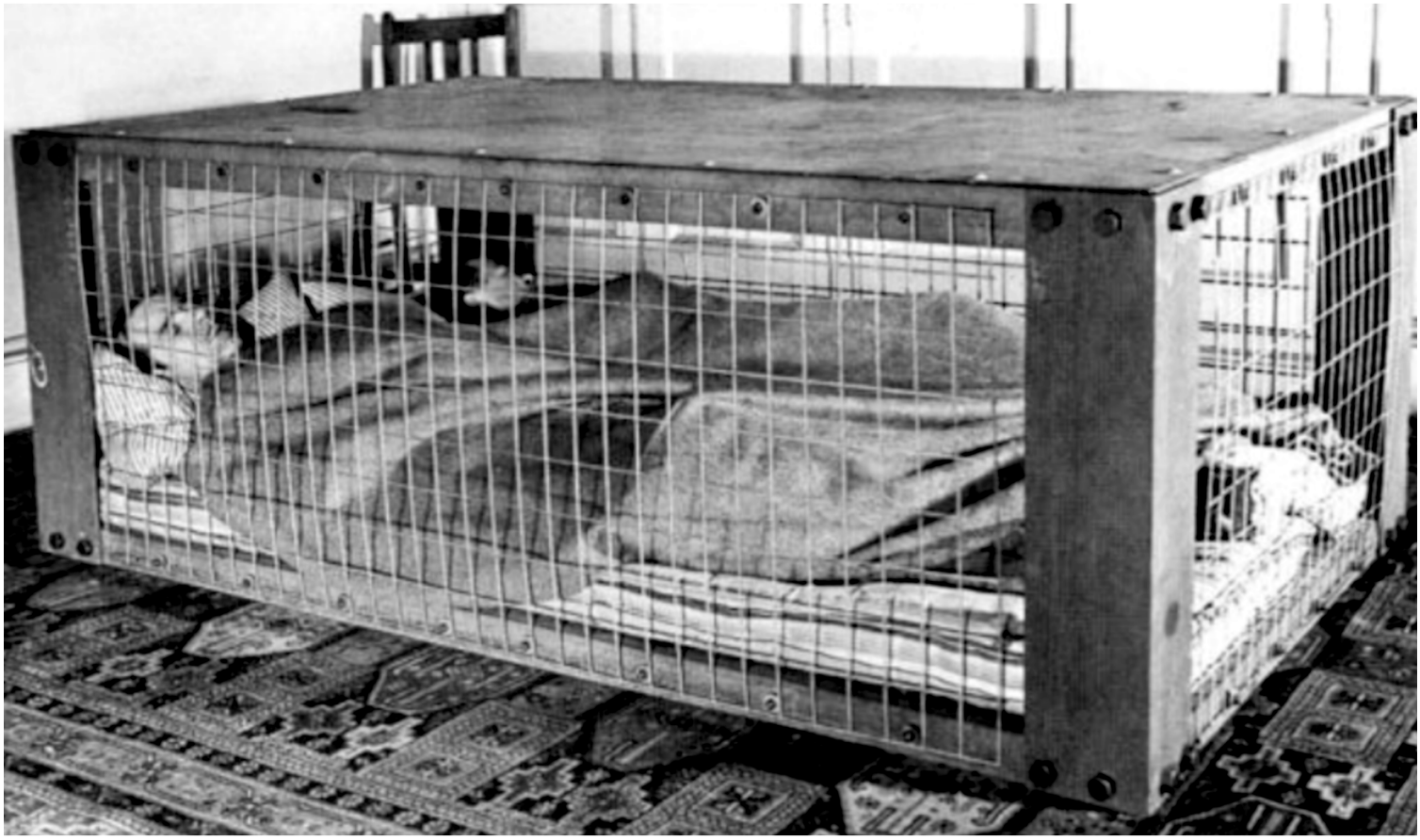

Structural Defense, 1945, by D. G. Christopherson, Ministry of Home Security, RC 450, (1946); Chapters VIII and IX (Confidential). Chapter VIII summarizes the literature on the design and types of British shelters and analyzes their effectiveness.

National Archives
HO 195/16

SHELTER at home

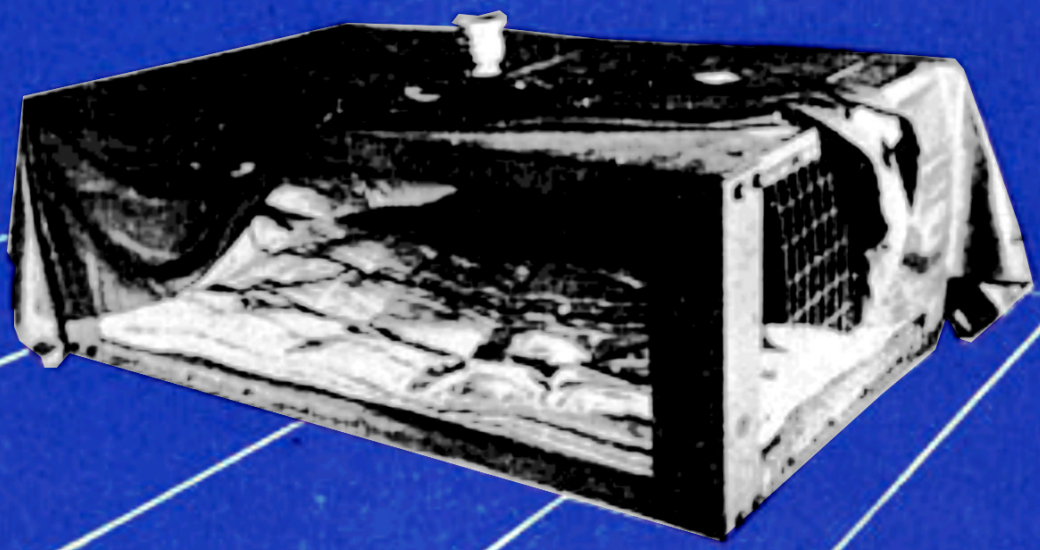

3d.

ISSUED BY THE MINISTRY OF HOME SECURITY
AND PUBLISHED BY H.M. STATIONERY OFFICE

ILLUSTRATION NO. 8.

The house in the upper photograph had a Government steel table shelter in a downstairs room and was blown up to reproduce the effect of a heavy bomb falling near. The whole house collapsed, burying the shelter under débris. In the lower photo the shelter can be seen still intact. It would have been possible for anyone in the shelter to get out unaided.

(Page 11 from the June 1941 UK Ministry of Home Security "Shelter at Home" handbook.)

Morrison shelter survives direct hit in York 1942

HOME OFFICE

THE PROTECTION OF YOUR HOME AGAINST AIR RAIDS

READ THIS BOOK THROUGH
THEN
KEEP IT CAREFULLY

HOW TO CHOOSE A REFUGE-ROOM

Almost any room will serve as a refuge-room if it is soundly constructed, and if it is easy to reach and to get out of. Its windows should be as few and small as possible, preferably facing a building or blank wall, or a narrow street. If a ground floor room facing a wide street or a stretch of level open ground is chosen, the windows should if possible be specially protected (see pages 30 and 31). The stronger the walls, floor, and ceiling are, the better. Brick partition walls are better than lath and plaster, a concrete ceiling is better than a wooden one. An internal passage will form a very good refuge-room if it can be closed at both ends.

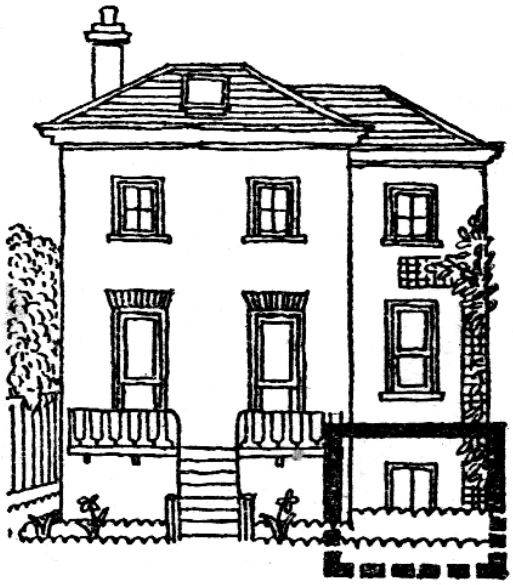

A cellar or basement is the best position for a refuge-room if it can be made reasonably gas-proof

The best floor for a refuge-room

A cellar or basement is the best place for a refuge-room if it can be made reasonably gas-proof and if there is no likelihood of its becoming flooded by a neighbouring river that may burst its banks, or by a burst water-main. If you have any doubt about the risk of flooding ask for advice from your local Council Offices.

Alternatively, any room on any floor below the top floor may be used. Top floors and attics should be avoided as they usually do not give sufficient protection overhead from small incendiary bombs. These small bombs would probably penetrate the roof but be stopped by the top floor, though they might burn through to the floor below if not quickly dealt with.

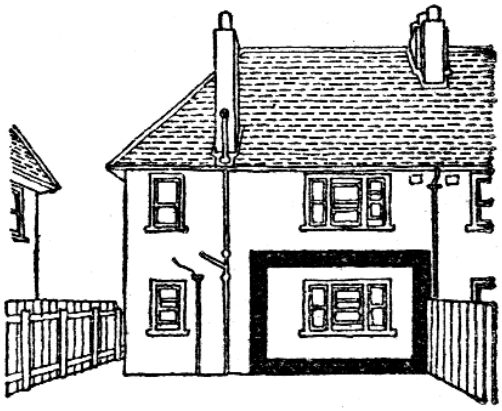

In a house with only two floors and without a cellar, choose a room on the ground floor so that you have protection overhead

Strengthening the room

If your refuge-room is on the ground floor or in the basement, you can support the ceiling with wooden props as an additional protection. The illustration shows a way of doing this, but it would be best to take a builder's advice before setting to work. Stout posts or scaffold poles are placed upright, resting on a thick plank on the floor and supporting a stout piece of timber against the ceiling, at right angles to the ceiling joists, i.e. in the same direction as the floor boards above.

How to support a ceiling

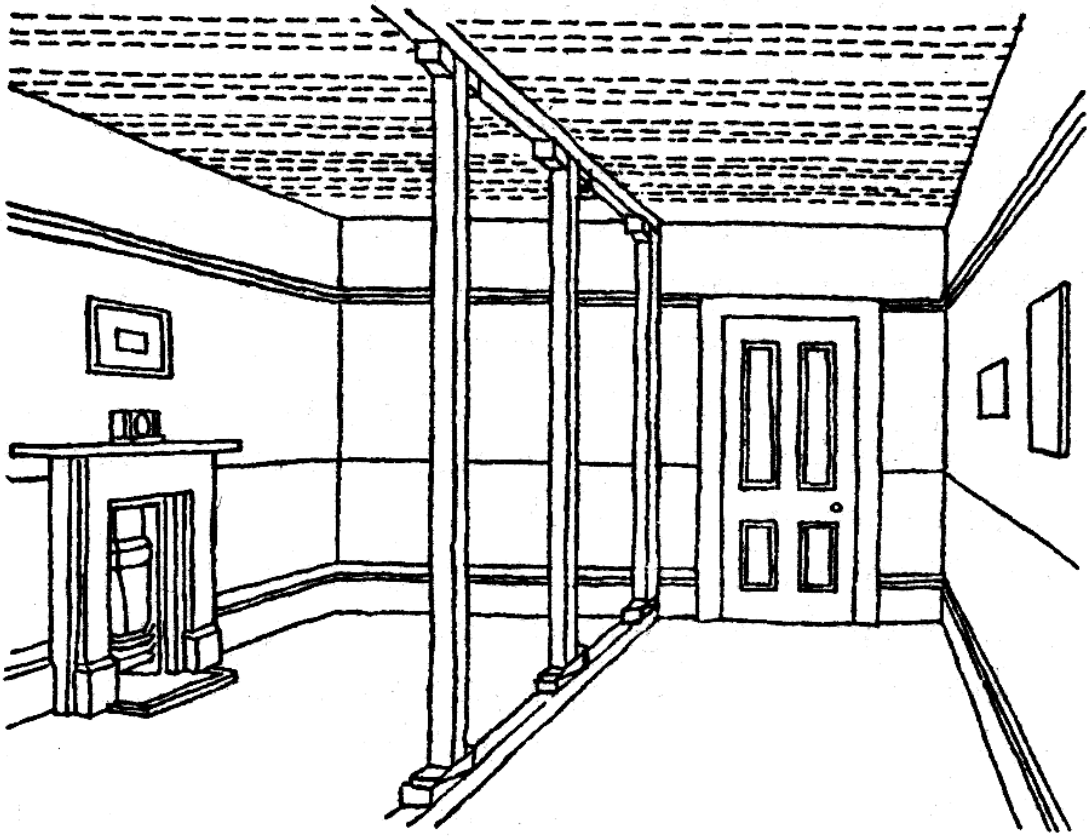

The illustration below shows the detail of how to fix the props

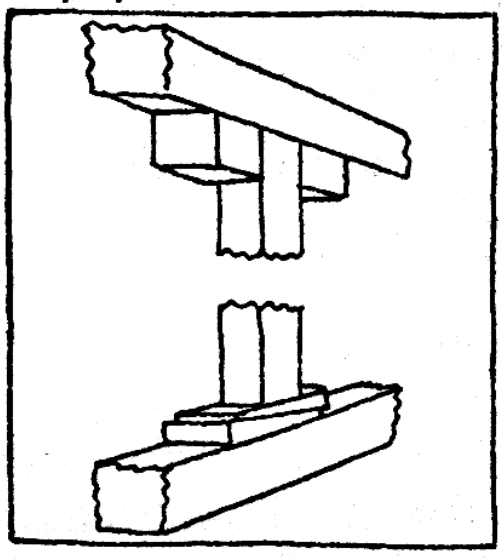

The smaller illustration shows how the posts are held in position at the top by two blocks of wood on the ceiling beam. The posts are forced tight by two wedges at the foot, driven in opposite ways. Do not drive these wedges too violently, otherwise you may lift the ceiling and damage it. If the floor of your refuge-room is solid, such as you might find in a basement, you will not need a plank across the whole floor, but only a piece of wood a foot or so long under each prop.

EXTRA PRECAUTIONS AGAINST EXPLOSIVE BOMBS

TRENCHES. Instead of having a refuge-room in your house, you can, if you have a garden, build a dug-out or a trench. A trench provides excellent protection against the effects of a bursting bomb, and is simple to construct. Full instructions will be given in another book which you will be able to buy. Your air raid wardens will also be able to advise.

SANDBAGS. Sandbags outside are the best protection if your walls are not thick enough to resist splinters. Do not rely on a wall keeping out splinters unless it is more than a foot thick. Sandbags are also the best protection for window openings. If you can completely close the window opening with a wall of sandbags you will prevent the glass being broken by the blast of an explosion, as well as keeping out splinters. But the window must still be sealed inside against gas.

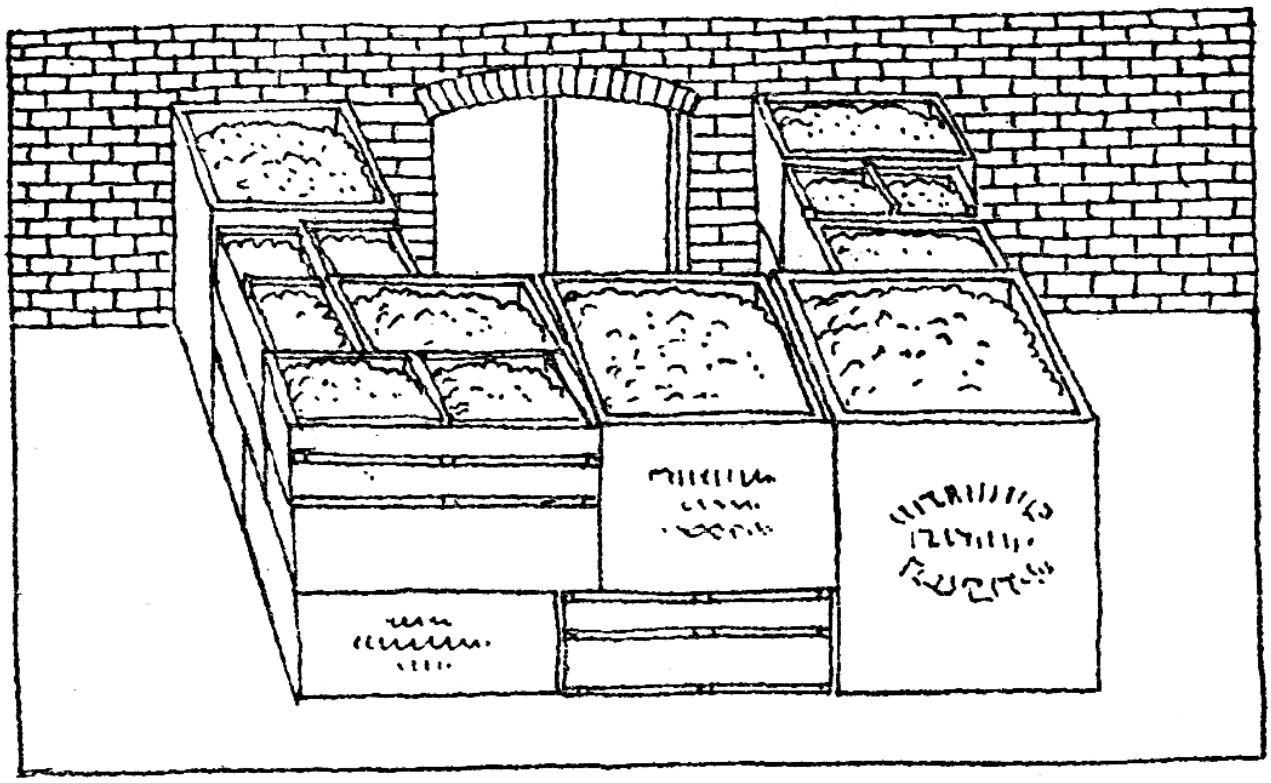

A basement window protected by boxes of earth

Any bags or sacks, including paper sacks such as are used for cement, will do for sandbags. But if they are large, don't fill

UK National Archives: CAB / 67 / 9 / 44

THIS DOCUMENT IS THE PROPERTY OF HIS BRITANNIC MAJESTY'S GOVERNMENT

Printed for the War Cabinet. May 1941.

MOST SECRET. Copy No. 58

W.P. (G) (41) 44.

May 5, 1941.

TO BE KEPT UNDER LOCK AND KEY.

It is requested that special care may be taken to ensure the secrecy of this document.

WAR CABINET.

AIR RAIDS ON LONDON, SEPTEMBER–NOVEMBER 1940.

Memorandum by the Home Secretary and Minister of Home Security.

Framed buildings.

Most valuable information has been gained on the effects of bombs on framed buildings. Such buildings are practically immune to anything but a direct hit. Blast damage from bombs outside is usually confined to windows and internal partitions. Even parachute mines falling immediately outside the building or exploding on the roof produce negligible damage to structure or floors.

Relation of Casualties to Bombs Dropped.

From a knowledge of the number of bombs dropped and the casualties occurring in different boroughs, some idea can be gained of the effectiveness of bombs in producing casualties. The number of casualties per bomb varies widely from 1·59 in the least to 6·94 in the most populated boroughs, but it follows closely the apparent densities of population as shown in figure 1. The number of casualties per bomb is roughly a twelfth of the number of persons per acre, and the number of deaths per bomb about 1/60th of the number of persons per acre. From this it can be deduced that the mean distance at which injury from a bomb is likely to occur is 35 ft., and that at which the bomb is lethal is 15 ft.

The casualties per bomb in Central London fell steadily from an average of 3·7 in September to 2·7 in October and 1·7 in November. This corresponds to the considerable fall in population in most of the boroughs concerned.

Conclusion.

We may now say that we have a good general understanding, both qualitative and quantitative, of the effects of bombs on buildings and on cities. New types of bombs, particularly heavier bombs, may be used, but we can anticipate no startling change in the effects apart from increase in minor damage. With bombing of the present type the results of our work are to show that in urban areas, such as that of the County of London, *for one ton of bombs approximately* 10 *houses will be destroyed or will need pulling down.* 25 *more will be temporarily uninhabitable, and another* 80 *will be slightly damaged.* 80 *people will be made temporarily homeless and* 35 *will lose their homes permanently.* 25 *people, mostly among the latter category, will be wounded, the greater part of them slightly, and* 6 *will be killed or die from wounds.*

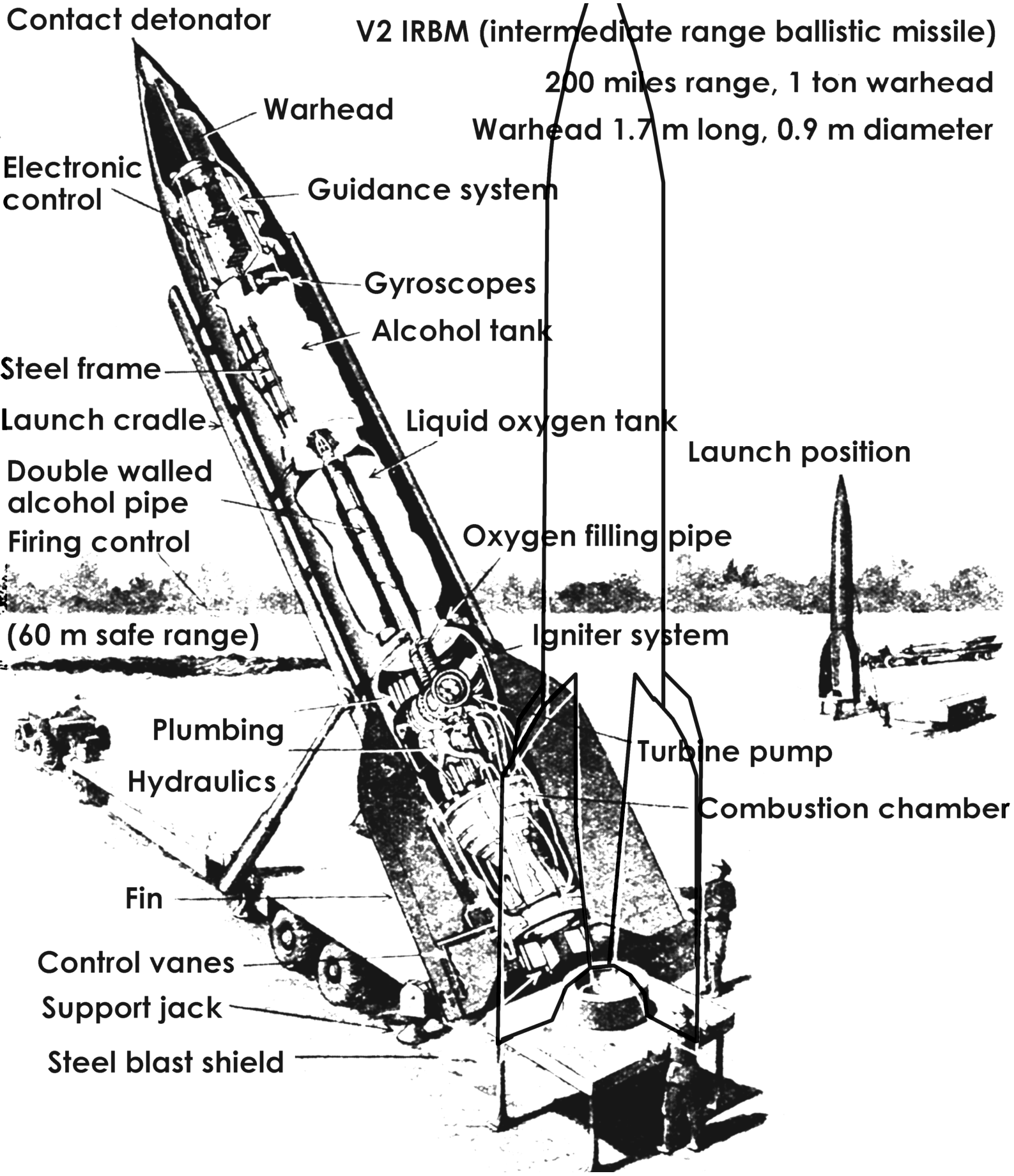
Contact detonator
V2 IRBM (intermediate range ballistic missile)
200 miles range, 1 ton warhead
Warhead 1.7 m long, 0.9 m diameter
Warhead
Electronic control
Guidance system
Gyroscopes
Alcohol tank
Steel frame
Launch cradle
Liquid oxygen tank
Launch position
Double walled alcohol pipe
Firing control
Oxygen filling pipe
(60 m safe range)
Igniter system
Plumbing
Turbine pump
Hydraulics
Combustion chamber
Fin
Control vanes
Support jack
Steel blast shield

Aldwych, 30 June 1944, V1 attack

V-2 ATTACK at Smithfield Market, London, where 110 people were killed and 123 seriously injured when pavements were crowded

CIVIL DEFENCE

RESCUE MANUAL

LONDON
HER MAJESTY'S STATIONERY OFFICE
1952

CHAPTER XI. USE OF HEAVY MECHANICAL PLANT IN RESCUE, DEMOLITION AND CLEARANCE OPERATIONS

In the last war it was found that at major incidents the use of heavy mechanical plant was frequently necessary in support of rescue operations. Such equipment was used to help in the quick removal of debris; to lift heavy blocks of brickwork or masonry; to take the weight of collapsed floors and girders so that voids could be explored and casualties extricated; to haul off twisted steelwork and other debris and to break up sections of reinforced concrete.

In future all these tasks may be required and heavy clearance may have to be effected to enable rescue and other Civil Defence vehicles

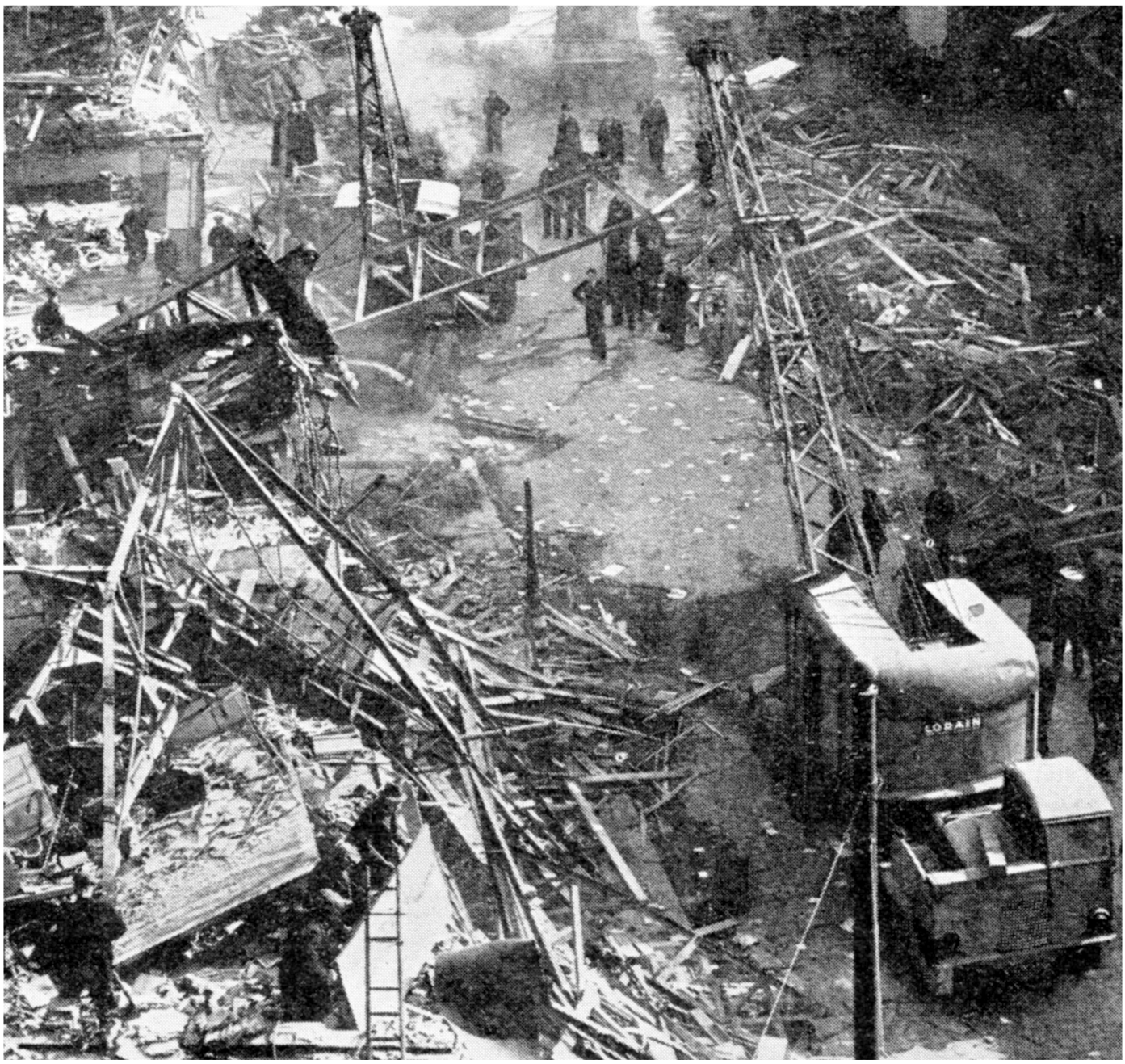

8 March 1945 Fig. 20 **1 ton of TNT equivalent**

Using heavy mechanical plant at the Smithfield Market V.2 incident.

to approach within measurable distance of their tasks. The problem of debris will in fact be a major factor in Civil Defence operations.

Heavy mechanical plant may be required for the following purposes :

(*a*) To assist in the removal of persons injured or trapped. At this stage mainly heavy plant is needed, particularly mobile cranes with sufficient length of boom or jib to reach for long distances over the wreckage of buildings.

(*b*) To force a passage for Civil Defence vehicles and fire appliances to enable them to reach areas where major rescue and other problems exist and require urgent operational action.

(*c*) To take certain safety measures—e.g., to pull down unsafe structures.

(*d*) To clear streets and pavements to help restore communications and to afford access for the repair of damaged mains and pipes beneath the streets.

(*e*) For the final clearance of debris and the tidying of sites. This is a long term and not an operational requirement.

Urgent Rescue Operations

During rescue operations in London in the last war the machines used with great success included heavy 3½-5 ton mobile cranes, mounted on road wheels, with a 30-40 ft. jib ; medium heavy 2-3½ ton mobile cranes, mounted on road wheels, with a 26 ft. jib ; heavy crawler tractor bulldozers ; medium crawler tractor bulldozers ; mechanical shovels and compressors, three stage, mounted on road wheels.

In the case of a large or multiple incident where access was obstructed by considerable quantities of scattered debris, a bulldozer or tractor was first employed in order to clear one or more approaches by which other equipment and personnel could reach the scene of operations.

Next, all debris of manhandling size was loaded into one-yard skips and discharged by the crane into lorries, giving increased manœuvring space to the Services operating on the site.

Heavy mobile cranes were then brought up to the incident where, used under the skilled direction of the rescue party Leader, they were invaluable for removing girders and large blocks of masonry which obstructed access to casualties or persons trapped. The necessary chains and wire ropes for these operations formed part of the standard equipment of the heavy and medium-heavy mobile cranes.

The work was, of course, carried out in close co-operation with the Rescue Parties who also used various forms of light mechanical equipment, such as jacks and ratchet lifting tackle for work in confined spaces.

Compressors sometimes proved valuable for breaking up large masonry such as fallen walls, into sections of a size and weight within the handling and lifting capacity of the cranes. This method was only used when it was known that there were no casualties under the masonry.

HOME OFFICE

SCOTTISH HOME DEPARTMENT

CIVIL DEFENCE HANDBOOK No. 7

Rescue

This Handbook is a revised edition of,

and replaces, the

Civil Defence Rescue Manual

LONDON

HER MAJESTY'S STATIONERY OFFICE

1960

CHAPTER 6

Types of Damage from Modern Air Attack

General Characteristics

6.1 When a nuclear weapon explodes an immense amount of energy is released almost instantaneously and the contents are transformed into a rapidly expanding white hot ball of gas at a temperature as high as that on the sun. From this "fireball" a pulse of intense light and heat is radiated in all directions. The materials in the fireball are also a source of radioactivity in various forms. As the fireball expands and cools, a powerful blast wave develops. As it cools still further, it shoots upwards to a height of many thousands of feet, billowing out at the top to give the appearance of a huge mushroom or cauliflower on its stalk.

6.2 The three forms of energy released in the explosion, namely, light and heat, radioactivity, and blast, all produce effects in different ways and in different proportions according to the position of the explosion in relation to the surface underneath. This chapter, however, deals primarily with the damage caused to buildings by the blast effect.

6.3 With nuclear weapons (as opposed to high explosive weapons), blast pressure rather than "impulse" tends to be the criterion of damage. If the effective blast pressure exceeds the static strength of the structure, failure must be expected. If it is less, no failure can occur however long the duration of the blast. In fact, nuclear bomb blast is more like a strong wind than the sudden blow of high explosive blast, and many of the failures observed at Hiroshima and Nagasaki and in subsequent tests resemble closely the kind of damage that might be done to buildings by a hurricane.

6.4 The scarcity of suction damage from the nominal bombs in Japan was due to the high blast pressures produced and to the fact that these were three or four times as great as the blast suction. With all such large explosions, if a building does not fail from blast pressure it is unlikely to fail under the lower stresses in the suction phase.

Effect of blast on structures

6.5 The type of damage which long duration blast (from nuclear weapons) causes to structures can possibly best be appreciated by considering the forces to which a simple building is subjected during the passage of a horizontal blast wave. When the blast "front" strikes the front wall it is reflected back, and the pressure in the wave front builds up to more than double the original pressure. However, this build-up only lasts for a very short time and is mainly important for large flat surfaces such as walls of big buildings.

Fig. 39 (a). Using a door as a stretcher

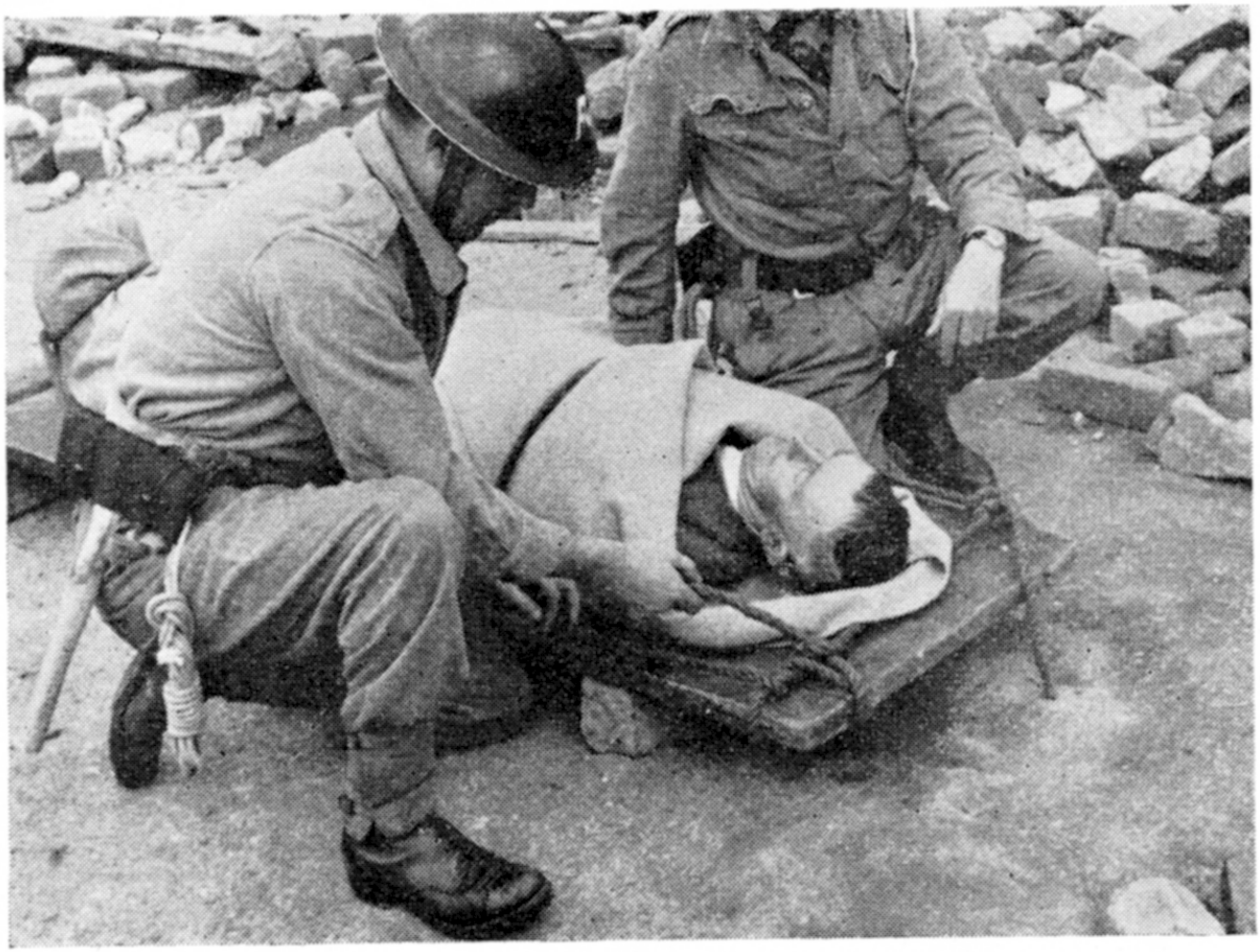

Fig. 39 (b). Using a door as a stretcher

Principles of Levering and Jacking

15.1 The principles of levering and jacking are, in a variety of differing ways, brought into most aspects of rescue work. The purpose of lifting appliances is to gain power so as to lift a large load with a small force suitably applied.

Levers

15.2 The simplest appliance for gaining power is the lever, of which an improvised version made of laminated timber or an ordinary crowbar are most frequently used by rescue workers. There are two principal ways in which a lever can be used, as illustrated in the diagrams. In each case the advantage gained depends on the distance of (A), the centre of the load, and (C) the points where the push or force is applied from (B), the heel or fulcrum.

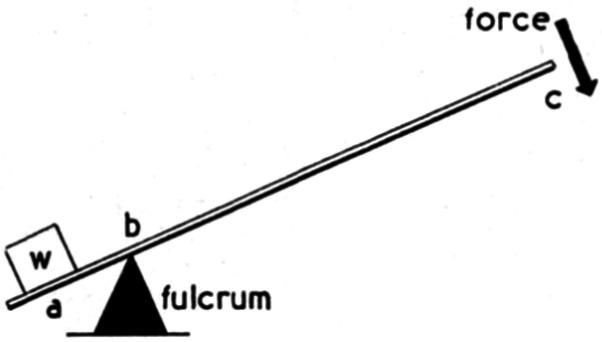

Fig. 68. Lever (downward force)

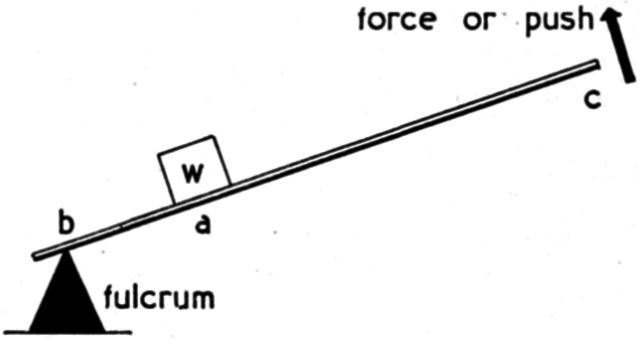

Lever (upward force)

15.3 The relation between the load and the amount of force required to lift it is in the same ratio as the length BC is to AB, where AB and BC are the distances of the weight and the force respectively from the fulcrum. A man using a 10-foot lever and bearing down at C with half his weight, say, 6 stone or 84 lb., against a fulcrum 1 foot from the other end of the lever, can lift a weight of $84 \times 9 = 756$ lb. because the length from fulcrum to hand is nine times the length from pivot to weight. If B is only 6 inches away from the weight the ratio is increased to 19 times its own weight.

Fulcrum blocks

15.4 A fulcrum block should be of wood (hardwood if possible), never of brick or other crushable material. It must be resting on a firm base, which should be as large as possible so as to distribute the weight to be lifted. The fulcrum must be placed as near to the weight as is possible under the circumstances, and it should never be placed at any point where there is a possibility of a casualty being buried immediately below.

In 12 months, 1940-1, the Blitz stray dog Rip (discovered by civil defence rescuers in Poplar, East London after an air raid) sniffed out 100 trapped casualties in London rubble.

Irma. Margaret Griffin used Irma and Psyche to find 233 trapped persons

STANFORD RESEARCH INSTITUTE

STANFORD, CALIFORNIA

June, 1953

Final Report

IMPACT OF AIR ATTACK IN WORLD WAR II: SELECTED DATA FOR CIVIL DEFENSE PLANNING

Evaluation of Source Materials

By

Robert O. Shreve

SRI Project 669

Prepared for
Federal Civil Defense Administration
Washington, D. C.

Approved:

William J. Platt, Chairman
Industrial Planning Research

Weldon B. Gibson, Director
Economics Research Division

For sale by the Superintendent of Documents, U. S. Government Printing Office
Washington 25, D. C. - Price 25 cents

Table 1

Report Outline - USSBS Project

IMPACT OF AIR ATTACK IN WORLD WAR II:
SELECTED DATA FOR CIVIL DEFENSE PLANNING

Division I - PHYSICAL DAMAGE TO STRUCTURES, FACILITIES, AND PERSONS

Volume 1 Summary of Civil Defense Experience
Volume 2 Analytical Studies (Restricted)
Volume 3 Causes of Fire from Atomic Attack (Secret) --VITAL!!

The documents which should be given wide distribution for civil defense use are listed below, with a brief description:

a. USSBS Reports

Effects of the Atomic Bomb on Hiroshima, Japan (3 volumes).

Effects of the Atomic Bomb on Nagasaki, Japan (3 volumes).

These reports constitute two case studies of atomic bombing. Civil defense planners should be aware of the facts these documents record in great detail. Their distribution to all civil defense planners and analysts is highly desirable.

-9-

Effects on Labor in Clydebank of Clydeside Raids of March 1941, (REN 234) USSBS Target Int.(REN 236) Ministry of Home Security

A study of the effects on labor of bombing in a town of 50,000 people in which 76% of houses were rendered uninhabitable, 73% of the population homeless. An equivalent of 65 city days was utilized in the reconstruction.

-22-

Ministry of Home Security
Effects of German Air Force Raids on Coventry (REN 441)

The city, the attack, casualties, repairs and reconstruction (cost), absenteeism, population movements, and housing occupancy. Six pages and charts and graphs. Twenty percent of houses rendered uninhabitable or destroyed, a total reconstruction cost of £ 3,492,000. Average time lost by worker after November raid was eleven days; average after April raid was 7 days. Nine percent of the workers evacuated to points within reach of the city.

Number and Classification of Official Evacuees in Great Britain in 1939 and 1940

900,000 of the 1.5 million returned to the target areas after four months of war.	September, 1939		January, 1940	
	Number	Percentage Distribution	Number	Per cent of Those in September, 1939
1. Unaccompanied school children	826,959	56.1	457,600	55
2. Mothers and accompanied children	523,670	35.5	64,900	12
3. Expectant mothers	12,705	0.9	1,140	9
4. Blind persons, cripples, and other special classes	7,057	0.5	2,440	35
5. Teachers and helpers	103,000	7.0	46,500	45
Total	1,473,391	100.0	572,580	39

Source: R. M. Titmuss, *Problems of Social Policy* (London: H.M. Stationery Office, 1950), pp. 103 and 172.

Effectiveness of Some Civil Defense Actions in Protecting Urban Populations (u)

Appendix B of Defense of the US against Attack by Aircraft and Missiles (u)

ORO-R-17, Appendix B

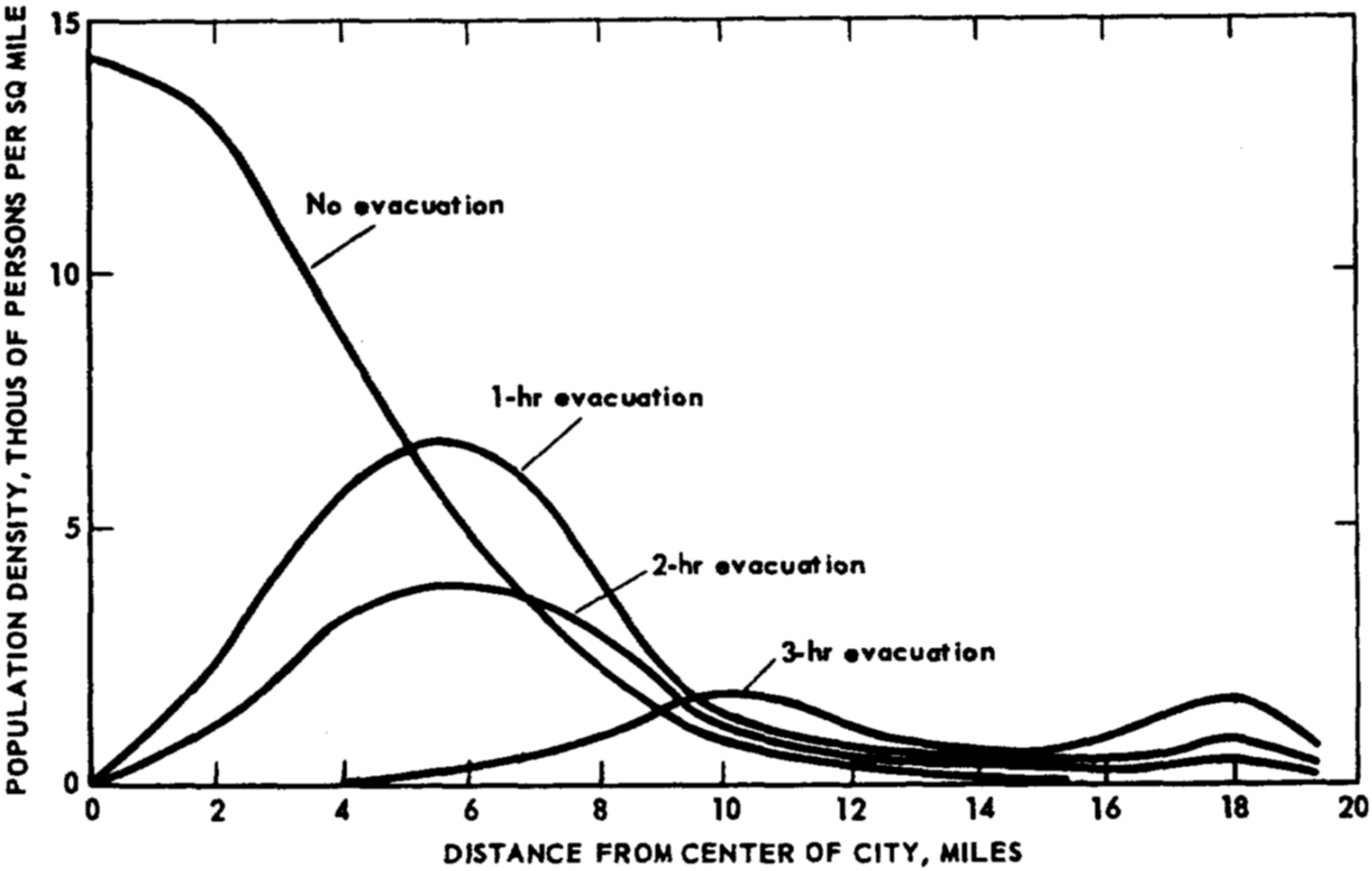

Fig. 10 — Population Density of Washington Target as Function of Distance from Center of City for Three Evacuation Times

William K. Chipman

A publication of the National Security Studies Group
at the University of Wisconsin,
Madison, Wisconsin, May, 1961.

In Britain, by early 1940, the government had issued free, to families of low income, some 2.3 million bomb shelters, enough to shelter over one-fourth of the population. But by the same time -- after Munich had brought home to the British people the peril in which they stood, even after the war had begun -- less than 1000 shelters had been purchased. This was under 0.04 per cent of the total number in place, despite the fact that the shelters were sold at cost.[7]

For protection against chemical and biological attack, our National Plan proposes that protective (gas) masks be made "...available to the people through regulated commercial distribution...."[8] or in a word, sold. That too is nonsense. In Britain, in contrast, the government had decided by 1935 that it would be futile to expect the population to buy their own masks. During the Munich crisis, 38 million gas masks were issued free to the people of Great Britain.[9] The British government of that time could scarcely be called war-minded or over-prepared for war. Still less, it appears, are we prepared in 1961.

---

7. O'Brien, Terence H., Civil Defence, London, HMSO, 1955 at 335. In 1939 the government had decided to issue Anderson (corrugated steel) shelters free to householders with incomes of not over £ 250 a year. Id., 188.

8. OCDM National Plan, Annex 24, "National Biological and Chemical Warfare Defense Plan," at 6.

9. O'Brien, op. cit. supra note 7 at 165.

-- The Argument That Increased Spending for Nonmilitary and Other Defenses May Cause an Economic Decline

A celebrated statesman not many years ago elegantly put (or rather, asserted) the argument for "national bankruptcy":

CHAMBERLAIN IN LATE 1936 WHEN CHANCELLOR OF THE EXCHEQUER

> If we were now to follow [X's] advice and sacrifice our commerce to the manufacture of arms, we should inflict a certain injury on our trade from which it would take generations to recover, we should destroy the confidence which now happily exists, and we should destroy the revenue....[33]

And, a comment on that argument,

> It was held very strongly that financial stability was our fourth, and final, military arm, that we must balance [the national budget], and avoid interference... with trade....[34]

The statement quoted was not made in 1949, when not muscle but fat was being pared from our military budgets. It was not made in 1955 or 1960. It was made, rather, in the 1930's. The statesman who so anxiously viewed the dangers to be apprehended from increased expenditure for arms was Neville Chamberlain. "X" was Winston Churchill. Britain was, if not "generations," at any rate half a generation in paying the bill for Chamberlain's economics. Only recently have her trade, revenue and financial stability recovered from the economies of Stanley Baldwin and Neville Chamberlain.

33. Feiling, Keith, The Life of Neville Chamberlain, London, Macmillan, 1946 at 314. Quotation reproduced by kind permission of the author, MacMillan & Company Ltd. and St. Martin's Press, Inc.

34. Id. at 316.

--The Question of Public Apathy--British Experience Before World War II Compared

The view is often expressed that the population is apathetic, or even hostile, towards nonmilitary defense, and that nothing can be done to develop these defenses until public apathy changes to concern. This view was succinctly put by a member of the House committee which passes on budget requests for OCDM. He said in March, 1959, that, "The Congress is not going to shove something down the throats of the people that they are not interested in. If you did, the Members of Congress would not be here very long."[46]

13

A nation-wide opinion survey by the Institute for Social Research of the University of Michigan, made in 1957, revealed, among other things, that 68 per cent of the population favored planning to evacuate cities, and that 90 per cent favored constructing shelters for people who lived in areas that might be attacked.[47]

Whatever the present reaction of the public might be to a program for nonmilitary defense, it is nearly certain that after a frightening crisis had occurred, the public would not only demand these programs, but would be highly critical of a government which had not taken the necessary action. This, at least, was the experience in Britain.

Munich, however, changed all that. War seemed so imminent that the government ordered day and night digging on trenches in parks and open areas. It issued gas masks to some 38 million citizens.[50] Then, when fitting gas masks and digging trenches had given the citizens personal proof of the threat which hung over them, "Fatalism about providing effective protection against air attack was... replaced by a feeling that this could be done, if the authorities showed enough will and energy."[51]

14

46. U.S. House, Committee on Appropriations, Hearings, Independent Offices Appropriations, 1960, 86th Cong., 1st Sess. (1959) at 486.

47. Pohlenz, D. Dean, "Problems of Civil Defense Preparedness -- A Policy for Today," Washington, Industrial College of the Armed Forces Student Exercise M57-83 (1957) at 33.

49. O'Brien, Terence H., History of the Second World War: Civil Defence, London, HMSO, 1954 at 93, 99 and 104.

50. Id. at 161 and 165.

51. Id. at 166.

Bertrand Russell, for example, wrote in 1959 that,

> On the most favourable hypothesis, [the postwar world] would consist of destitute populations, maddened by hunger, debilitated by disease... incapable of supporting educational institutions, and rapidly sinking to the level of ignorant savages. This, I repeat, is the most optimistic forecast which is in any degree plausible.[61] [Emphasis added.]

This notion of the extinction of civilization, or even of all life, is a comforting one.[63] Most important, it ensures that a nuclear war will never be fought, since no sane (or perhaps even moderately insane) national leader would consider thermonuclear war as an instrument of policy. Also, if there is really nothing that can be done to mitigate the effects of nuclear war, rational men need not trouble themselves about the problems of preparing nonmilitary defenses -- or of paying for them.

The theory that thermonuclear war automatically results in world annihilation has had, and still has, some highly respectable adherents. In 1955, for example, fifty-two Nobel laureates subscribed to the statement that unless all nations renounced the use of force, they would simply "...cease to exist."[64] Writers on disarmament in 1961 continue to point out that it would be impossible to "...protect [civilians not killed by the initial attack on cities] against fallout and starvation,"[65] and that "Proponents of the arms race are willing to risk the destruction of civilized society...."[66]

--The View That National Security Can Best Be Achieved by Buying Only Offensive and Active Defensive Weapons

61. Russell, Bertrand, Common Sense and Nuclear Warfare, London, copyright (C) 1959 by George Allen and Unwin, Ltd., quotation reproduced by kind permission of Simon and Schuster, Inc. The notion of mutual extermination is also alluded to at 32, and the survivors are characterized as starving and debilitated at 26.
62. On Thermonuclear War, 35.
63. Id. at 11.
64. Id. at 9. Compare Bertrand Russell's views, supra note 61.
65. Sohn, Louis B., "Security Through Disarmament," 192 The Nation 159-163 at 159 (February 25, 1961).
66. Melman, Seymour, "The 'Arms-Control' Doctrine," 192 The Nation 114-116 at 116 (February 11, 1961).

Clark, Grenville and Louis B. Sohn, World Peace Through World Law (2d ed.), Cambridge, Massachusetts, Harvard University Press, 1960.

-- The Argument That Nonmilitary Defense Would Destabilize the Balance of Terror

To take any steps to protect the population would be to do them a disservice, since it might make war "thinkable" again. And whatever steps were taken, millions or tens of millions would be sure to die.

A variant of the hostage theory is that if we were to embark on a serious program for nonmilitary defense, we should inescapably spread warmindedness among the American people.[71] Once they were awakened to the possibility, or worse the "thinkability," of war, they would inevitably become more hostile towards the source of the danger, namely, the USSR. They might then be expected, with the American penchant for grasping nettles (those, at any rate, recognized as nettles), to press for a first strike against the Soviet Union.

But other countries, not least the Soviet Union, do have nonmilitary defense programs of substantial value.

It is not, in any case, self-evident that a nonmilitary defense program would have a destabilizing (or unbalancing) effect upon American psychology. If anything, a program which included, for example, building fallout shelters or issuing radiation meters, might, by bringing home the threat of war to the American people in a highly personal way, incline them rather to a sober and pacific than to a war-like psychology. City dwellers might reflect upon the fact that their shelters, at least under any program the United States is likely to undertake in the next five years, would give them not a certainty but only a fair to good chance of survival. Rural residents might reflect upon the prospect of an incursion of refugees from the cities.

---

71. Letter from Dean David F. Cavers, Harvard Law School, New York Times, March 20, 1960, page 10E, column 6. See too Brown, Harrison and James Real, Community of Fear, Santa Barbara, California, Center for the Study of Democratic Institutions, 1960.

This whole problem of psychological response to nonmilitary defense clearly requires detailed study by experts. British experience in the Munich and post-Munich period may not be without relevance.[73]

--Would A Nonmilitary Defense Program Injure Prospects for Arms Control?

Finally, there is the question whether a program for nonmilitary defense is compatible with plans for arms control or even disarmament.

---

the reverse, it should not hazard the success of any arms control or disarmament negotiations in which the Soviets are seriously interested, and it would stabilize any arms control agreement that might be concluded.

73. See, for example, O'Brien, op. cit. supra note 49 at 329 on response to the anti-gas program, and Titmuss, Richard M., Problems of Social Policy, London, HMSO, 1950 at 29-39 on response to evacuation plans and programs.

Thermonuclear war is a grisly topic. It is, however, one about which we would do well to think. The argument might be made that research on war may make it somewhat more likely to occur. It is more probable, however, that the reverse is true, that not thinking about thermonuclear war may make it easier to blunder into one -- or what might be even worse, to lose one.

It would be well indeed if nuclear war would be unmistakably so annihilating as to be unthinkable, at least for sane men, as Bertrand Russell and others hold. But it would be unfortunate if this view prevailed only in the West and not in Moscow and Peiping. There is good evidence that it does not, especially in the latter. There is in any case something of schizophrenia about spending tens of billions each year on thermonuclear weapons and their delivery vehicles and then refusing to think about the ways and conditions in which they might be used, or (more hopefully) the ways in which we can best assure, short of surrender, that they will not be used.

The best study to date is Herman Kahn's On Thermonuclear War, published late in 1960.[77] Most of what follows in this chapter draws heavily upon Kahn's work, though it is impossible to do it justice in so

small a space. He analyzes, so far as possible in a quantitative way, the probable or possible causes, courses and effects of thermonuclear wars which might occur in the next decade. Kahn's work has been bitterly attacked, although to date in no very temperate or reasoned fashion. It has been called "a moral tract on mass murder," "permeated with a bloodthirsty irrationality," and its quantitative approach a "Higher Incoherence."[78] It has been said to show "narrowness of vision," and to have about it an "air of unreality."[79] But coherent criticism, reasoned rather than stated, marked by broadness of vision or an air of reality, has yet to appear, certainly in more than fragmentary form.[80]

77. Kahn, Herman, On Thermonuclear War, Princeton, N.J., Princeton University Press, 1960. On U.S. national strategy see too Rowen, op. cit. supra note 36, and Washington Center of Foreign Policy Research, Johns Hopkins University, Study for Senate Committee on Foreign Relations, Developments in Military Technology and Their Impact on United States Strategy and Foreign Policy, 85th Cong., 1st Sess. (Comm. Print 1959).

78. Newman, James R., "A Moral Tract on Mass Murder," The Washington Post, February 26, 1961, page E7, columns 5-8. The level of coherence of Mr. Newman's critique is best left unstated.

79. Wolff, Robert Paul, "The Game of War," 144 The New Republic (February 20, 1961) 9-13.

80. The usual criticism of Kahn's work is that it does not sufficiently take into account political problems. Careful, or even casual, reading of On Thermonuclear War, however, shows that Kahn has a better grasp of political problems than most of his political-scientist critics have of strategy.

We may expect Soviet or Chinese support for "progressive, revolutionary national liberation wars"[83] in such areas as Algeria or the Congo. We may see guerilla action in Southeast Asia or other areas on the periphery of the "Socialist camp." We may even see limited wars, fought without or perhaps even with tactical nuclear weapons. Soviet missiles may be rattled again, as they have been rattled on behalf of Nasser and Castro. (American missiles might also be rattled, though this seems unlikely during the next few years, at least.) Finally, even negotiations for arms control or disarmament may be devices of cold war conflict, as they have too largely been to date.

What Are We Trying to Deter?

Kahn points out that it is critically important to distinguish between deterring an attack upon the United States and attacks or major provocations at other points, for example, a "squeeze" or even armed attack on Berlin. The same weapons, dispositions of weapons, and strategies do not suffice for both ends.

22

---

83. This was promised in the manifesto issued by the leaders of 81 Communist parties after their meeting in Moscow in late 1960. New York Times, December 7, 1960, pages 14 to 17, with the "progressive revolutionary significance" of "national-liberation wars" noted at page 17, column 7. Premier Khrushchev also adverted to the inevitability of "national liberation wars" in a report delivered January 6, 1961. New York Times, January 19, 1961, page 6, column 4.

84. Berlin was noted as a "seat of international provocation" in the late-1960 manifesto. New York Times, December 7, 1960, page 15, column 2. (Any Western posture other than abject surrender is doubtless "provocative" in the communist lexicon.)

As Kahn has put it, history has a disconcerting way of being "... richer and more imaginative than any scholar."[86]

86. On Thermonuclear War at 557.

23

It is a fearsome thing to contemplate the risk of 10 or 20 or 120 million Americans, or Americans and Britons, being killed in a war, for example, over two and one-half million West Berliners.

24

--Devices to Tide Us Over the Earlier 1960's

The Soviets might not, of course, decide to risk everything, or at any rate a great deal of capital and some millions of their citizens, on our succumbing to postattack coercion. If the Marxist-Leninist dialectic condemns spurning the opportunities offered by history, it also condemns taking excessive risks, a sin termed "adventurism."[109] What can we do to increase the risks to be apprehended from an attack on the United States?

30

---

109. See, for example, Garthoff, Raymond, Soviet Strategy in the Nuclear Age, New York, Praeger, 1958 at 5.

--A $100 Billion Program Including Blast Shelters and Extensive Preparation for Economic Recuperation

The "splendid," $100 billion or more, program is the one which might raise some reasonable Soviet apprehension that we might strike first. This program, including blast shelters into which the urban population could "duck" in a matter of twenty or thirty minutes, would in fact be part of a credible strategic posture allowing us to make a first strike.

(Expensive deep shelters create "Maginot Line" delusions: Hitler simply adapted plans to go around obstructions. Similarly, shelters in Hiroshima were unoccupied due to surprise attack! If you have deep shelters, an enemy will plan surprise attack. It takes 20 min to get into shelters, but only 3 minutes for SLBM submarine missile attack from offshore!)

45

--History and Arms Control

The lessons of history, for what they may be worth, include those of 1914, when Europe stumbled into a major war which no power wanted, as a result of a minor war about which only Austria or Serbia were really serious. As Herman Kahn has pointed out, there are disturbing analogies between the years before 1914 and those in which we now live.[158]

(Wrong: the German Kaiser did WANT war and had been planning since 1912 to use any excuse for starting war, implementing Schlieffen's plan!)

--Arms Control for the 1960's

At all events, it is clear that the problems of arms control must have more intelligent, more intensive, and more sustained attention than they have yet had, if we are to avoid repeating something like the disasters of either 1914 or 1933-1939. Views on the approaches required, as noted above, vary widely.

47

158. Kahn, On Thermonuclear War 368-370.

It would plainly be futile, in view of the vigorous Soviet pacification of Hungary, or of the Chinese liberation of Tibet, to rely upon "world opinion " (whatever that is) to deter violations. . . .

One sanction might be the prospect of a renewed arms race, triggered by the discovery of violations. But this might not deter cheating, particularly if the party bent on violation believed it could secure a commanding position before the injured party could catch up. (Here we might remember the belated but futile efforts of the British to regain air parity, after Hitler's rapid expansion of the Luftwaffe.)[176]

176. See, for the history of that dismal episode in the history of the West, Sir Winston Churchill's The Gathering Storm, chapter 7. Kahn points out that if one side obtained a significant lead because of evasion or rapid rearmament after the agreement broke down, it might then "...feel compelled to perform a great public service by arranging to stop the arms race before a dangerous balance of terror was restored. It could do this most reliably by stopping the cause of the arms race -- its opponent. Most writers ignore this situation...." On Thermonuclear War at 230.

Is Nonmilitary Defense Possible?

If nonmilitary defense is necessary, is it possible? In the discussion to this point, it has been assumed that it is. But can one say, with any measure of confidence, that nonmilitary defenses could in fact ensure the survival of most or all of the population? Even if a shelter program could preserve the lives of most Americans against fallout or even blast, would they emerge into a world worth living in, or indeed, possible to live in? What of the genetic effects of war? Would all children be born deformed? What of leukemia, of cancer, or of a shortened span of life? What of strontium-90? What of the standard of living? Would the survivors, and their descendants, be reduced to grubbing out a wretched existence, with our economy shattered beyond hope of repair? What of the social impact of attack? Could we expect that the survivors, as Bertrand Russell has predicted, would "rapidly sink to the level of ignorant savages"?

54

Further, nonmilitary defense must be designed to cope with widely varying conditions. The nature of the postattack environment would depend upon the weight and pattern of the enemy's attack--which might in turn be influenced by the nonmilitary defense measures we had taken. The areas contaminated by fallout would of course be determined by the winds prevailing on the day of attack, as well as by the enemy's attack pattern. Anti-aircraft and antimissile defenses would also affect the nature of the post-attack environment.

The major systems analyses of nonmilitary defense so far published are the Rand Report and a more detailed work done by Mr. John Devaney's OCDM Operations Research Office, A Preliminary Analysis of Non-Military

55

Defense.[186] Both of these studies give some ground for sober confidence that the United States could survive thermonuclear wars in the 1960's and even beyond, given appropriate levels of nonmilitary defense preparation. But much more detailed research remains to be done. There are still major areas of uncertainty in the performance of nonmilitary defense systems. The principal policy suggestion of the Rand study was therefore that the United States undertake a broad program of research and development on nonmilitary defense problems, to cost some $200 million over two or three years.[187]

186. OCDM, A Preliminary Analysis of Non-Military Defense, Battle Creek, Michigan, 1959.

187. Kahn, Herman, et al., R-322-RC 184 at 44. (This is about fifty times the present OCDM annual research appropriation.) R-322-RC Rand Corporation Report on a Study of Non-Military Defense

--Long-Term Effects of Fallout--Genetic Effects and Life-Shortening, and the Strontium-90 Problem

Even if fallout at first decays rapidly, so that fallout shelters could protect most of the population from immediate death or illness due to radiation, would the longer-term effects of radiation make life as we know it either impossible or insupportable for the survivors? Despite the rapid initial decay of fallout, a relatively small amount of contamination would remain in the environment for a long time. This would include strontium-90, a long-lived isotope produced by nuclear fission.

The Rand Report states that about four per cent of babies are at present stillborn or die shortly after birth, two per cent are malformed and two per cent develop later troubles attributable to genetic defects.[200] If as the result of nuclear war, both parents had been exposed to about 250 roentgens, spread over a long period, their chances of producing a seriously defective living child might increase from four per cent to five per cent.[201]

---

199. Testimony of Dr. James F. Crow, Professor of Genetics, University of Wisconsin, in 1957 fallout hearings, op. cit. supra note 193 at 1013. More recent experiments show that there is a possibility that radiation received over an extended period may not have as much genetic effect as radiation received over a short period. U.S. Congress, Joint Committee on Atomic Energy, Hearings, Fallout from Nuclear Weapons Tests, 86th Cong., 1st Sess. (1959) at 1566.

200. Kahn, et al., op. cit. supra note 184 at 16.

201. Kahn, On Thermonuclear War at 46.

Strontium-90, produced by fission, falls out over crop and pasture lands, is taken up by plants, and can eventually find its way into human bones, where it may cause bone cancer or, in smaller amounts, cause bone lesions and interfere with bone growth, particularly in children.[204]

204. See generally Kahn, On Thermonuclear War at 63-72.

All of these long-term effects of nuclear war are serious, particularly the strontium-90 problem. It appears, however, that with proper preparation, it should be possible to alleviate them. In chapter 2 the subject of decontamination, or removal of radioactive debris, is discussed. In chapter 3 is discussed a scheme suggested by Herman Kahn to ensure that relatively contaminated food be consumed only by older persons, whom it will not much affect, with the least contaminated food reserved for children and pregnant women.

The Rand Report concludes that "...long-term radiation problems are a less critical threat to the survival of a population than the central short-term problem, namely, how to protect a substantial fraction of the population from the immediate disaster of a nuclear war."[205]

---

205. Kahn, et al.,

R-322-RC Rand Corporation Report on a Study of Non-Military Defense at 21.

Economic Recovery from Thermonuclear War

Even if the medical effects of nuclear war might not be insoluble, there remains the problem of economic recovery. Would the survivors be condemned to lives without hope, with standards of living, for most, similar to those of the early years of the industrial revolution?

In the absence of reliable predictions of social response to thermonuclear attack, there is a tendency to lurid speculation. One can too easily visualize society collapsing, with the survivors organizing themselves into robber bands and struggling for the few economic resources remaining, or masses of city dwellers suffering crippling mental breakdown, or mankind rejecting science and technology and reverting to a hunting-and-gathering or at best pastoral existence. Others speculate upon the probability of mass panic or of widespread looting and other criminal behavior.

Just such speculations were made in Britain before the war, and made by sober scientists, government officials and soldiers. The Army Council instructed General Officers Commanding that "the initial preoccupation" of the troops would be "to sustain public morale."[214] At the time of Munich, when evacuation was being considered, "... discussions were held on the question of drafting regular troops into London to keep order and prevent panic. . . ."[215] Gloomiest of all were the predictions of the psychiatrists, who thought that mental casualties might outnumber physical casualties by two or three to one:[216]

> ... the experts foretold a mass outbreak of hysterical neurosis among the civilian population. It was expected that the conditions of life brought about by air raids would place an immediate and overwhelming strain upon the individual. Under this strain, many people would regress to an earlier level of needs and desires. They would behave like frightened and unsatisfied children, and they would demand with the all-or-none vehemence of infants the security, food and warmth which the mother had given in the past.

None of this, of course, occurred. Rather than a dramatic increase in neurosis or mental illness, there was in fact a decrease. Statistics for insanity, suicide, drunkenness and disorderly behavior fell by as much as half.[217] Workers absented themselves from their factories after heavy bombing only when their houses had been damaged or destroyed, and then only for an average of six days.[218]

214. Titmuss, op. cit. supra note 73 at 19.

215. Id. at 30.

216. Id. at 338-339.

217. Id. at 340-341.

218. Id. at 341.

Individual and group protection against chemical attack poses great problems. In World War I, gas was considered one of the most effective means for producing casualties,[117] even though the CW agents used then were far less lethal than the nerve gases developed in Germany prior to World War II. A seven-ton load of nerve gas can reportedly cause casualties over an area fifteen miles wide and twenty-five to fifty miles long, and death over an area of 100 square miles,[119] given weather conditions favorable to the spread of gas clouds.[120] New non-lethal gases are under development, including the so-called psychochemicals, related to compounds used to simulate mental disease, and other incapacitating agents. These agents affect victims by upsetting normal behavior patterns or physiological processes,[121] though their short-term effectiveness appears to suit them more to tactical use against troops than to attack of civilian populations.

117. Rothschild, Brig. Gen. J. "Germs and Gas, the Weapons Nobody Dares Talk About" 218 Harper's Magazine 29 at 30 (June 1959). This article also states, ibid, that 26.8 per cent of AEF casualties were caused by gas. FCDA Technical Bulletin 11-25, "Introduction to Chemical Warfare" (1957) states that mustard gas and other blister gases produced more than 400,000 casualties in the last 16 months of World War I, more than were caused by any other weapon then in use. U.S. House, Committee on Science and Astronautics, Research in CBR, House Report No. 815, 86th Cong., 1st Sess. (1959) states at 4 that some 9 million artillery shells filled with mustard gas produced about 400,000 casualties, which effect was about five times that produced by high explosive shell, on a casualty per ton of shell basis. One should also note that CW casualties in World War I included few deaths. About one-third of U.S. casualties were caused by gas, but only 2 per cent of these died, as compared with 25 percent of nongas casualties. Ibid.

119 U.S. Senate, Committee on Armed Services, Hearings, Civil Defense Program, 84th Cong., 1st Sess. (1955) Part 2 at 800. The 100 square mile figure also appears in ACS, id. at 3.

120. "Inversion" conditions, where air temperatures increase with increase in altitude, are most favorable to the spread of gas clouds, and obtain on clear nights and early mornings until about one hour after sunrise. U.S. Department of the Army, Technical Manual 3-240, Field Behavior of Chemical Agents, Washington, 1951, at 16.

121. U.S. House, Committee on Appropriations, Hearings, Department of Defense Appropriations for 1960, 86th Cong., 1st Sess. (1959) Part 6 at 364-365 and 426-436.

In Great Britain, in contrast, some 44 million masks were distributed by the outbreak of World War II, virtually one per inhabitant, and 1.4 million infants' respirators and 2 million children's masks by January, 1940;[137] 55 million masks are now stockpiled in Britain for issue to civilians.[138] **(They are 1950 designed civilian C7 respirators.)**

Procuring 100 million masks for that part of our population concentrated in urban areas might cost $250 million, at $2.50 per mask, and extensive training in defense against BW and CW would also be required.

137. O'Brien, Terence, Civil Defence, London, HMSO, 1955 at 330. Note that as early as 1935 the British government decided that masks would have to be issued free of charge. Id. at 61.

138. Interview Col. Francis B. Stewart, FCDA (now OCDM), Battle Creek, Michigan, January 30, 1958.

3000 roentgens per hour intensity at one hour
12,000 roentgens outdoor dose in the first year

10,000 r in the first two weeks (emergency phase)
2000 r in the remaining fifty weeks (reclamation phase)

EMERGENCY PHASE (10,000 r)		RECLAMATION PHASE (2000 r)	
Shelter attenuation	10,000 r dose reduced to	Decontamination effectiveness (reduction to)	2000 r dose reduced to
1/100	100	90% (1/10)	200
1/1000	10	99% (1/100)	20

Radiological decontamination involves no very mysterious or sophisticated techniques. In general, fallout material can be swept or flushed off

---

Evacuation

Contrary to popular belief, the effectiveness of tactical evacuation is by no means destroyed by the ICBM. While it is clear that no tactical evacuation could even be started during the 30-minute flight of an ICBM, it is also true, as the Rand Report points out, that cities are not likely to be attacked with the enemy's first ICBM salvo, and it is quite possible that most cities might not be attacked at all.

As Herman Kahn has pointed out, a national evacuation capability could be of the greatest importance in time of international crisis: If the Soviets evacuated their cities, they would have made it highly credible that they were prepared to go to war unless we backed down.[155]

155. Kahn, Herman, On Thermonuclear War, Princeton, N.J., Princeton University Press, 1960 at 213-214, also 132. Objections to evacuation and other nonmilitary defense measures are dealt with at 641-651, with objections bearing on evacuation in particular at 648-651.

The Bureau of Roads in 1956 prepared a report[160] on national evacuation capabilities for 161 urban target areas, containing 90.7 million people, about 55 per cent of the population. The report assumed orderly and disciplined movement, making maximum use of escape routes, and the findings included the following:[161]

(1) In 1 1/2 hours, 32 million persons could be evacuated at least 15 miles from the centers of target areas, over existing highways and streets;

(2) In 4 1/2 hours, 72 million persons could be evacuated at least 15 miles from target area centers;

(3) In 2 hours, 22 million persons could be evacuated at least 25 miles;

(4) In 5 hours, 53 million persons could be evacuated at least 25 miles;

(5) Evacuation of the largest cities within reasonable time limits would not be possible.

In sum, four hours' warning would allow substantial clearance of all but the largest cities, and even in these cities, this warning would allow evacuation of some 9 million of their 48 million inhabitants.[162]

160. Reprinted and discussed in U.S. House, Committee on Government Operations, Hearings, New Civil Defense Legislation, 85th Cong., 1st Sess. (1957) at 111-136.

161. Discussed id. at 124-126.

162. OCDM Operations Research Office, A Preliminary Analysis of Nonmilitary Defense, Battle Creek, Michigan, 1959 at 169.

Since 1956 Great Britain has had a simple scheme for classifying radiation zones by intensity and for evacuating the most dangerous zone, of 1000 r/hr and upwards at H + 1.[171] Such a program is dependent on a monitoring system, so that fallout zones may be delineated and appropriate instructions given their inhabitants. It requires sophisticated and technically competent control, related to the area affected by fallout, not to preattack political subdivisions.

Remedial evacuation also requires detailed arrangements for traffic control, if existing transport within the most dangerous area is relied on for evacuation.

171. Home Office, Radioactive Fall-out, Provisional Scheme of Public Control, London, HMSO, 1956.

The requirement for rescue forces would depend upon the number of survivors trapped or incapacitated in areas which could be approached by rescue teams. OCDM estimated that in the 1446-megaton attack assumed for the 1959 JCAE hearings, 11.5 million people would have been fatally injured by blast and heat effects and 6.3 million nonfatally injured. Fallout would have caused a further 10.7 million fatal and 10.9 million nonfatal injuries.[175] Many of the blast casualties would require to be rescued and, together with fallout casualties, to be transported from the danger area. Other casualty estimates, however, show markedly fewer blast injuries, on the order of one-fourth of those estimated in the JCAE hearings.[176]

(JCAE hearings used gross Hiroshima casualty data, which applies to people watching the B-29 deliver bomb, i.e. no proper "duck and cover" for elayed blast behind windows.)

175. 1959 JCAE Hearings, Effects of Nuclear War, at 651.

176. SRI calculations show only 1.6 million blast casualties from a 1500-megaton attack

177. Note that casualty effects are extrapolated from experience at Hiroshima and Nagasaki, which were attacks with air-bursted kiloton weapons. U. S. Atomic Energy Commission, Effects of Nuclear Weapons, Washington, 1957, at 456. Factors which may affect casualty numbers include yield, height of burst, strength of buildings (or shelters,) and the weather at the time of attack. Ibid. It is interesting to note that prewar British estimates of casualties from aerial attack, based on limited experience from World War I, turned out in the event to have been too high by 6 times.

Finally, fallout would limit rescue operations. Fallout from surface bursts far upwind might make operations impossible, if radiation levels were so high that rescue crews could not work without accumulating harmful radiation doses. Even if rescue groups could approach damaged areas from upwind, rescue of severe blast and burn casualties from within six or nine miles of ground zero would not be possible to a significant extent, since the level of contamination even upwind of a surface burst would be so high as to prevent rescue parties from working in these areas for several days at least, by which time most of the seriously injured would have died.[178] It might be possible, however, to organize rescue operations on the first day from upwind into the areas of lighter damage, perhaps fifteen miles from the center of a 20-megaton burst, where numbers of casualties would have resulted due to burns and partial collapse of frame houses.[179] Rotation of rescue teams could allow exposure to higher radiation intensities, and hence earlier rescue operations, but would increase the requirement for rescue forces. If weapons were airbursted, so that little fallout contamination resulted, rescue forces could enter blast areas soon after the detonation.

(NOTE: severe upwind fallout in the blast damaged area was measured after 10 megaton surface burst MIKE in 1952, see weapon test report WT-615 and AFSWP-507. However, this upwind fallout was a fluke due to the 82-ton steel bomb "case shock" which embedded itself deep into the crater, increasing the activity on large fallout flakes around ground zero. Data from weapons with lighter casings in Castle 1954 and Redwing 1956 disproved the MIKE upwind fallout data for practical, deliverable weapons, WT-1317. MIKE upwind fallout data was given in Glasstone ENW 1957 but was replaced with Redwing upwind fallout data in Glasstone 1962, so light upwind fallout permitted rescue.)

178. U.S. Federal Civil Defense Administration, Survival in Public Shelters, 1957, at 5-9.

179. Id. at 7-8.

The Corps of Engineers analysis of requirements for rescue squads is in U.S. Army Engineer School, Extension Subcourse 321, Civil Defense and Disaster Recovery, Ft. Belvoir, Virginia (May 1958) at 3-3 to 3-4. This document states that about 25 per cent of persons surviving in blast-damaged areas will be lightly trapped and 5 per cent heavily trapped. About 2 man-hours are required to release persons lightly trapped and 20 man-hours for those heavily trapped. Trapped casualties can survive for 4 days, and rescue squads can each produce some 768 man-hours of efficient rescue work in this time. Thus in a city where 100,000 persons remained in blast areas, about 25,000 people would be lightly trapped and 5000 heavily trapped. This would require 65 light rescue squads and 130 heavy squads, each composed of 26 men with appropriate equipment. The total rescue force requirement is thus 5070 persons, or about 50 per 1000 of target area population at the time of detonation.

One promising avenue for reducing vulnerability is to put selected industries underground. The Rand Report suggests that if we had put something like twenty per cent of our manufacturing capital underground by 1970, that economy ought to be able to withstand a 20,000-megaton, 150-city attack somewhat better than our undispersed economy in 1960 could withstand a 1500-megaton, 50-city attack.[252] A 1956 study by the Corps of Engineers discussed in some detail the problems of constructing underground industrial plants. The study pointed out that some sixty per cent of American industry lay in a quadrangle from Boston to Kansas City, and that about two-thirds of existing mine sites, suitable for underground plants, also lay in this quadrangle.[253] Experience both with underground plants in Sweden and Germany and with windowless, fully air-conditioned surface plants in this country indicates that no major personnel problems are likely to arise from working underground.[254]

252. Kahn, Rand Report, op. cit. supra note 62 at 29-30 and 11.

253. U. S. Department of the Army, Corps of Engineers, Underground Plants for Industry, Washington, GPO, 1956 at 7; see too id. at 19.

254. Id. at 37-38 and 7. For discussion of an underground metal processing and fabricating plant in Norway see Skarsgaard, Olav K.," "The Largest Underground Industry in the World." The Fifteen Nations (Number 16) at 124-125.

Prepared by Dr. William Chapman DCPA

July 13, 1979

Mor

CIVIL DEFENSE FOR THE 1980's--CURRENT ISSUES

Presidential Decision (PD) 41, September 1978, established new policies for U.S. civil defense: that it should "enhance deterrence and stability and. . . reduce the possibility that the Soviets could coerce us in times of increased tension," and "include planning for population relocation during times of international crisis." The PD 41 policies are in marked contrast to previous rationales for CD, dating from 1961, which were to the effect that the program should provide "insurance" in the unlikely event of a failure of deterrence.

President Kennedy in 1961:

> But this deterrent concept assumes rational calculations by rational men. And the history of this planet, and particularly the history of the 20th century, is sufficient to remind us of the possibilities of an irrational attack, a miscalculation, an accidental war, or a war of escalation in which the stakes by each side gradually increase to the point of maximum danger which cannot be either foreseen or deterred. It is on this basis that civil defense can be readily justifiable--as insurance for the civilian population in case of an enemy miscalculation. It is insurance we trust will never be needed--but insurance which we could never forgive ourselves for foregoing in the event of catastrophe.18/

18/President John F. Kennedy, "Urgent National Needs, A Special Message to Congress," May 25, 1961.

More light was shed on issues of credibility by a national-sample survey conducted for DCPA in late 1978, involving in-depth interviews with 1620 adult Americans.31/ The results suggest that the public remains favorable in general to civil defense, and is receptive to crisis relocation in particular:

67% believe there could be crisis circumstances under which the President might urge people to evacuate high risk areas

78% believe the U.S. should have crisis relocation plans

70% say that if the President directed relocation, they would comply. (And additional people indicate they might well leave spontaneously, before any direction to do so)

75% believe the nation's communities would be helpful to evacuees

82% believe their own communities would be helpful, if asked to host evacuees. (In fact, 73% say they'd be willing to take evacuees into their own homes)

31/Nehnevasja, Jiri, Issues of Civil Defense: Vintage 1978--Summary Results of the 1978 National Survey, University of Pittsburgh, 1979.

It is significant that on September 1-3, 1939 the British moved some 1.5 million women and children from London and a few other large cities in what was a crisis evacuation, for Britain did not declare war until September 3. (Also of interest are the facts that some 2 million additional persons spontaneously evacuated at their own initiative, and that this was unsuspected at the time by the British government.) It is also worthy of note that in Hurricane Carla, in 1961, between half and three-quarters of a million people were evacuated from Gulf Coast cities without a single fatality or a major reported accident.32/

32/Senate Committee on Banking, Housing, and Urban Affairs, Hearings, Civil Defense, 95th Congress, 2d Session (January 1979) at 51-52.

> In 1939, Hitler attacked Poland, though it appears he calculated (mistakenly) that he had good chances of achieving his objectives without triggering World War II, based upon his earlier successes. In 1941 he attacked the USSR, anticipating the destruction of Bolshevism and not, eventually, of the Third Reich.
>
> In 1941 the leaders of Japan attacked the U.S., not anticipating the defeat of the empire in 1945.

--Presidential Decision 41

At all events, the PD 41 policies lay it down clearly that U.S. civil defense should ". . . enhance deterrence and stability, and contribute to perceptions of the overall U.S./Soviet strategic balance and to crisis stability, and also reduce the possibility that the Soviets could coerce us in times of crisis."

Civil Defense and the Cuban Crisis

In a 1978 interview, Steuart L. Pittman, who was Assistant Secretary of Defense for Civil Defense in 1961 to 1964, pointed out:

> [I]t is interesting that President Kennedy personally raised the civil defense question during the Cuban crisis. He was considering conventional military action against Cuba to knock out the missile sites. I understand he was the only one of the "Committee" to raise the issue of civil defense, which tells us something. He asked whether it would be practical to evacuate Miami and other coastal cities in Florida. . . . I was called into the marathon crisis meeting and had to tell him that it would not be practical; we did not have any significant evacuation plans. . . . The President dropped the idea, but shortly after the crisis was over, his personal concern over his limited civil defense options led him to sign a memorandum directing a significant speedup in the U.S. civil defense preparations. (Emphasis added.)93/

While history seldom repeats itself exactly, it does indeed "tell us something" that in the only overt nuclear confrontation the world has

93/Sullivan, Roger J. et al, The Potential Effects of Crisis Relocation on Crisis Stability, System Planning Corporation, Arlington, Virginia, September 1978 at 152-153.

yet seen, the American President was concerned about civil defense--and that the idea of population relocation during the crisis was one of his specific concerns. Certainly it is clear that in 1962, the notion of vulnerability being stabilizing held little attraction for the Chief Executive.

There is an historical precedent for a relatively rapid buildup of CD capabilities. At the time of the 1938 Munich crisis, Britain had developed civil defense plans but had little capability for actual operations. Spurred by the belief that war had become not only not unthinkable but not unlikely, Britain mounted an intensive effort.

By the time Germany attacked Poland the next September, the British were able to evacuate 1.5 million women and children from major target cities. And by the time of the August 1940 "blitz," the CD system was able to contribute substantially to Britain's ability to "take it" and to continue the war.

Following the Munich crisis, which found Britain as unprepared in civil defense as in all other areas of defense, the working of the civil defense services was reviewed by the House of Commons during a censure debate:

> Members were in a worried and critical mood, and among the charges made it was maintained that the Government had neither policy nor plans for evacuation when the country was on the verge of war. . . . [T]here was much uneasiness in Whitehall.102/

In short, there will be no public outcry for civil defense in normal times. There will be modest political profit, if any, for an Administration proposing enhanced civil defense, or a Congress approving it; the subject is not a congenial one. But should a frightening crisis find civil defense in disarray, the people (and the Congress) would surely demand to know what had been done in "the years that the locust hath eaten."103/

Summary

The PD 41 policies provide that the U.S. civil defense program should enhance deterrence and stability, and reduce the possibility of Soviet coercion during a crisis.

---

* * *

102/Titmuss, Richard M., Problems of Social Policy, HMSO, London, 1950 at 30.

103/Joel 2:25. This phrase, according to Churchill, was used by Sir Thomas Inskip in referring to the period 1931-1935: The Gathering Storm, Houghton Mifflin, Boston, 1948 at 66.

Arguments Against Civil Defense and a Rebuttal

Some of the arguments made against civil defense were parodied as follows in a piece in the Harvard Crimson in 1962:

Recommendations by the Committee for a Sane Navigational Policy:

It has been brought to our attention that certain elements among the passengers and crew favor the installation of lifeboats on this ship. These elements have advanced the excuse that such action would save lives in the event of a maritime disaster such as the ship striking an iceberg. Although we share their concern, we remain unalterably opposed to any consideration of their course of action for the following reasons:

1. This program would lull you into a false sense of security.

2. It would cause undue alarm and destroy your desire to continue your voyage in this ship.

3. It demonstrates a lack of faith in our Captain.

4. The apparent security which lifeboats offer will make our navigators reckless.

5. These proposals will distract our attention from more important things, e.g., building unsinkable ships. They may even lead our builders to false economies and the building of ships which are actually unsafe.

6. In the event of being struck by an iceberg (we will never strike first) the lifeboats would certainly sink along with the ship.

7. If they do not sink, you will only be saved for a worse fate, inevitable death on the open sea.

8. If you should be washed ashore on a desert island, you could not adapt to the hostile environment and would surely die of exposure.

9. If you should be rescued by a passing vessel, you would spend a life of remorse mourning your lost loved ones.

10. The panic caused by a collision with an iceberg would destroy all semblance of civilized human behavior. We shudder at the prospect of one man shooting another for the possession of a lifeboat.

11. Such a catastrophe is too horrible to contemplate. Anyone who does contemplate it obviously advocates it.

HISTORY OF THE SECOND WORLD WAR

Civil Defence

By

T. H. O'BRIEN

The point is of importance for students of the subject in an era in which marked 'progress' has been made in the technique of air warfare by the invention of the atomic bomb. This invention has given fresh currency to the view that 'nowadays every war is different from the one before'—which, if it were valid, would abolish any need to learn the lessons of past experience.

THE WAR OF 1914–1918 9

But in May 1917 the Germans began a series of assaults with twin-engined aircraft, called *Gothas*, which soon became severe. The daylight attack of 13th June on London by fourteen *Gothas* was the worst single attack of the war measured in casualties, which numbered 162 killed and 426 injured; 118 high explosive and incendiary bombs were dropped on the City and the East End.

The Government only gave in gradually and reluctantly to demands for public warnings in London. In July 1917 a system was introduced, under the control of the Commissioner of Police, which to those accustomed to the sirens of 1939–45 may appear somewhat primitive. Warnings were distributed partly by maroons (or sound bombs) fired into the air, and partly by policemen on foot, on bicycles or in cars carrying *Take Cover* placards and blowing whistles or sounding horns.

THE WAR OF 1914–1918 11

during 1914–18 There were in all 103 bombing raids (51 by airships and 52 by aeroplanes); and about 300 tons of bombs were dropped causing 4,820 casualties, 1,413 of which were fatal.

These totals appear small; but when they are broken down into details many different pictures emerge. The two heavy raids on London of June and July 1917, for example, together caused 832 casualties (216 fatal), which amounted to 121 casualties for each ton of bombs dropped; and these casualty figures were to have much significance for the planning authorities of the future.

13 June London raid: 118 bombs, 162 killed, 426 injured.
7 July London raid: 54 killed, 190 injured

121 casualties/ton, 31 killed/ton
(Air raids by twin-engined Gothas began in May 1917)

The Committee of Imperial Defence, created in 1904

In November 1921 the Committee asked the principal Service experts to report on the problem of possible future air attack on the United Kingdom. This report, which appeared the next year, accepted the conclusions of the Air Staff about future air attack, which were briefly as follows.

France's Air Force could drop an average weight of 1,500 tons of bombs on Britain each month by using only twenty bombing days in the month and only fifty per cent of its aircraft. London, which would be an enemy's chief objective, could be bombed on the scale of about 150 tons in the first 24 hours, 110 tons in the second 24 hours, and 75 tons in each succeeding 24 hours for an indefinite period. It was to be anticipated that an enemy would put forth his maximum strength at the outset.

Page 14: on 15 May 1924, the Air Raid Precautions (ARP) Sub-Committee first met, chaired by Sir John Anderson.

THE SCALE OF ATTACK 15

The serious picture thus presented assumed its darkest tones when the Air Staff proceeded to estimate casualties. The 300 tons of bombs dropped in the 1914–18 attacks, the experts pointed out, had caused 4,820 casualties, or 16 per ton of bombs. The 832 casualties of the two big daylight attacks on London in the summer of 1917, however,

produced an average of 121 casualties per ton; and sixteen night raids on London in 1917–18 gave an average of 52 casualties per ton.[1] After weighting these figures with various factors, the experts concluded that 50 casualties (one-third of which would be fatal) per ton formed a reasonable estimate of casualties caused by air attacks of the future on densely-populated areas. For other areas this figure should be reduced in proportion to the actual density of population.

In March 1927 the committee was faced with two matters

Royal Charter incorporating the British Broadcasting Corporation, *Wireless Broadcasting*, Cmd. 2756, 1926.

The Chemical Warfare Research Department had been making experiments to determine how long persons could remain under certain conditions in a 'gas-proof' room; and had prepared a handbook, *The Medical Aspects of Chemical Warfare*, now on sale to the public.

The first of the matters just referred to was a broadcast in February by Professor Noel Baker, on 'Foreign Affairs and How They Affect Us'. This, read in cold print at a distance of twenty years, appears as an attempt to rouse the British public to realisation of the horrors of future war, and to enlist its support for the disarmament negotiations at Geneva. The Professor quoted Mr Baldwin's speech to the Classical Association in the Middle Temple hall, 'Who in Europe does not know that one more war in the West and the civilisation of the ages will fall with as great a shock as that of Rome?' He painted a picture of gas attack from the air in another war and claimed, 'all gas experts are agreed that it would be impossible to devise means to protect the civil population from this form of attack'. The Chemical Warfare Research Department emphatically disputed the accuracy both of the details of the picture and of this general statement. They considered it unfortunate that statements of this nature should have been broadcast to the public, particularly after the Cabinet's decision that the time was not ripe for education of the public in defensive measures.

The committee discussed whether to draw the B.B.C.'s attention to this talk. The Corporation, only a few months old, was then prohibited by the Postmaster-General's instructions from broadcasting 'matter on topics of political, religious or industrial controversy'; but the Post Office representative pointed out this did not mean that his Department was prepared to undertake censoring programmes. The committee, not wishing to incur the obligation to approve in advance all proposed broadcasts relating to their field of study, decided to take no action with respect to the talk in question.

68 *Ch. III: THE A.R.P. DEPARTMENT (1935–1937)*

Gas was the risk most prominently associated in the public mind with future air attack, as was demonstrated a few weeks before the school opened by British reaction to Italy's use of mustard and other gases against Abyssinia.[4]

[4] According to the *Annual Register, 1936* (p. 27), 'feeling in England could hardly contain itself when the Italians were reported to be using poison gas against both soldiers and civilians'.

A final matter which concerned gas-masks belongs perhaps more properly to the topic of public reactions to A.R.P. Early in 1937 some scientific workers at Cambridge University, who described themselves as the 'Cambridge Scientists' Anti-War Group' and their function as that of acting as 'a technical and advisory body to national and international peace movements', published a book attacking the Government's A.R.P. plans.[1] This body had studied the official advice about the 'gas-proofing' of rooms, the civilian mask, and extinguishing incendiary bombs, and then conducted some experiments. It claimed to have shown that the measures officially proposed were ineffective or inadequate, and implied that these constituted deception of the public.

It has been noticed that as 1937 opened the Government was taking steps to make A.R.P. plans more widely known to the public;[2] and this deliberate challenge found a sympathetic echo in various quarters, and caused it some concern. Questions about the Cambridge experiments were asked in Parliament, for example on the occasion of the announcement of the new Wardens' Service; sections of the Press began a critical campaign, and questions were put to officials trying to build up A.R.P. services over the country. The Government's reply was that the experiments were academic (in the sense of removed from reality), and based on fallacious assumptions about the conditions likely to be met in actual warfare.[3] In spite of pressure the authorities refused to engage in technical controversy with the scientists in question and within a few months the agitation subsided. At the close of the year, however, a report on the official experiments (in supervision of which the Chemical Defence Committee had been helped by eminent scientists not in Government employment) was circulated to local authorities and otherwise made public.

---

[1] *The Protection of the Public from Aerial Attack* (Left Book Club Topical Book, Victor Gollancz Ltd, 1937.)

[2] p. 71.

[3] H. of C. Deb., Vol. 320, Col. 1348, 18th February 1937.

A demonstration of how to deal with the light incendiary bomb had been included in the Anti-Gas School curriculum in November 1936; and in February 1937 the Home Office Fire Adviser staged a demonstration at Barnes at which bombs were successfully controlled and fires extinguished by teams of girls with only short training. At an exercise held later at Southampton a group of air raid wardens carried out this function with such success that the Department concluded it must aim to train all householders in the handling of incendiary bombs.

Air Staff had raised their estimate of the weight of bombs which an enemy (now Germany) might drop on Britain during the first stages of an attack from 150 tons *per diem* to no less than 600 tons. The committee proceeded, as their predecessor of 1924 had done, to question the experts and then to accept their hypothesis.[1] The estimate of over 600 tons of bombs *per diem* during the first few weeks (which took account of Britain's various potential forms of counter-offensive) also embraced the possibility of a special bombing effort on the part of the enemy in the first 24 hours which might amount to 3,500 tons. Consideration had to be taken not only of this greatly increased weight of attack but of new methods of attack for which past experience afforded no precedents. The measure offered by the accepted air raid casualty figure of 1914–18 (50 per ton of bombs, 17 of which were killed and 33 wounded) was subject to the *caveat* that modern bombs were more effective. The committee pointed out that an arithmetical computation on this basis for the scale of attack at 600 tons *per diem* would indicate casualties of the order of 200,000 a week, of which 66,000 would be killed.

---

[1] The new estimated scale of attack had been referred to the Home Defence Committee, and was not approved by the Committee of Imperial Defence until 28th October 1937.

ANTI-GAS EQUIPMENT, & OTHER SUPPLIES 139

The 25 million civilian gas-masks accumulated by the opening of 1938 were, from various points of view, one of the most tangible assets of the A.R.P. Service.

SHELTERS; CIVIL DEFENCE ACT, 1939 187

The invention of a practical household shelter—to be quickly known as the 'Anderson'—had transformed the possibilities hitherto envisaged for protection of homes against air attack. The Government had undertaken to supply these shelters, as well as steel fittings for strengthening basements, free to some 2½ million families.

The 'Anderson' had originally been conceived as a shelter to be erected inside the average small working-class home. But the experts soon discarded this idea as open to various objections, including the probability that occupants would be trapped by the fall of their house and killed by fire or escaping coal-gas. During Munich householders had been advised to dig trenches in their yards or gardens, and now, by an extension of this plan, the 'Anderson' was designed as an outdoor or surface shelter. It consisted of fourteen corrugated steel sheets weighing, with other components, about 8 cwt. A corrugated steel hood, curved for greater strength, would be sunk some two feet in the ground and covered with earth or sandbags.

196 *Ch. V: THE NEW ARM OF CIVIL DEFENCE*

The programme for manufacture and distribution by the end of 1939–40 of 2½ million 'Andersons' to protect about 10 million citizens was being steadily carried through.

SHELTERS 371

householders in May in the form of a booklet, *Your Home as an Air Raid Shelter*.[1] This stated that an ordinary soundly-built house would offer very substantial protection; and it gave those unable to build some form of shelter much detailed guidance on the preparation of refuge rooms, the protection of windows and so on.

[1] H.S.C. 98/40, 22nd May 1940.

416 *Ch. X: THE TIDES OF BATTLE*

16 April 1941: heaviest London air raid of WWII:

On the night of 16th-17th some 450 aircraft made the heaviest raid so far on the capital, dropping 446 tons of high explosive and 150 tons of incendiaries and causing more casualties—about 1,180 killed and 2,230 badly injured—than in any previous attack.[1] Over 2,250 fires were started; and the centre and south of the metropolis bore the brunt of the attack.

---

[1] German records show the much higher figures of 685 aircraft, 890 tons of H.E. and 4,200 incendiary canisters dropped. This attack proved the worst on London of the war in terms of weight of bombs dropped, casualties inflicted and the number of fires caused.

438 *Ch. X: THE TIDES OF BATTLE* **1943:**

These occasions apart, the attack was predominantly of the tip and run or—as it was sometimes called—'the scalded cat' variety. The worst single incident of the year took place on 3rd March at Bethnal Green Tube shelter when, ironically enough, no attack was in progress on this particular area. A night attack of moderate proportions was being made on London, and warnings had sounded. A woman among the crowd entering this shelter, encumbered by a baby and a bundle, fell, causing those pressing behind her to tumble in a heap and the death by suffocation of no less than 178 persons. **3 March 1943**

508 *Ch. XII: SHELTERS*

In London a periodical count was made of shelterers, usually once a month; but this took place on a single night which was not necessarily typical. In addition, the population was continually fluctuating owing to evacuation, the call-up to the Forces and war damage. The first shelter census in Metropolitan London, taken early in November 1940, showed that 9 per cent. of the estimated population spent the night in public shelters, 4 per cent. in the Tubes and 27 per cent. in household shelters—in all, only 40 per cent. in any kinds of official shelter. In September and October this proportion was probably a good deal higher. Later, as the London public became accustomed to raids, the figures dropped.

Experience of raids also led to the introduction of an entirely new type of household shelter. 'Andersons', though structurally satisfactory, had not originally been intended for sleeping and became in many cases unfit for winter occupation. Domestic surface shelters were very cramped when used for sleeping and were in some places not popular, and strengthened domestic basements had been neither very successful nor widely used. After night raiding had ceased to be a novelty, many people preferred to stay in their houses rather than to go out of doors even to their own domestic shelters. The 'Anderson', it will be recalled, had at first been envisaged as an indoor shelter. Since many people were now determined to remain in their homes, it had become necessary to introduce some indoor shelter which might reduce the risk of injury from falling masonry and furniture. The fact that many who had hitherto sheltered under their staircases or furniture had been rescued unhurt from the wreckage of houses suggested that extra protection might be given by a light structure on the ground floor.

By the end of 1940 two designs had been produced. The first, later known as the 'Morrison' shelter, had a rectangular steel framework 6 ft. 6 in. long, 4 ft. wide and about 2 ft. 9 in. high. The sides were filled in with wire mesh, the bottom consisted of a steel mattress and the top was made of steel plate an eighth of an inch thick, fastened to the framework by bolts strong enough to withstand a heavy swinging blow. The shelter, which could be used as a table in the daytime, could accommodate two adults and either two young children or one older child, lying down. Experiments showed that it would carry the debris produced by the collapse of two higher floors.

The Prime Minister showed great interest in these shelters the first of which, in fact, were erected in No. 10 Downing Street.[2] In January 1941 the Cabinet approved the manufacture of 400,000, providing protection for perhaps 1,200,000 people.[3]

In February contracts had been placed for 270,000 shelters, and another order for the same number was placed in April (thus exceeding the 400,000 originally approved). Two further orders for 270,000 were placed at the end of July and the end of September.

---

[1] Instructions were given in a pamphlet, *How to put up your Morrison shelter*, on sale to the public.

[2] One with a flat top and one with a curved top were erected in No. 10 Downing Street. The Prime Minister was at first inclined to favour the curved design but he afterwards recognised the advantages of the flat top, which would allow the shelter to be used as a table, and gave his approval to both designs.

[3] It was estimated that each 'Morrison' would use over 3 cwt. of steel, and that about 65,000 tons would be needed for the 400,000 shelters. This proved to be an underestimate since the table shelter, as finally designed, actually weighed 4.43 cwt.

In June a revised version of *Your Home as an Air Raid Shelter* was issued with the title *Shelter at Home.* This included information about three types of shelter which could be put inside refuge rooms—the 'Morrison', a commercially made steel shelter, and a timber-framed structure designed by the Ministry of Home Security.

546 *Ch. XII: SHELTERS*

It was assumed that to be effective in attacks by pilotless aircraft or long-range rockets, shelters would have to be easily accessible. Yet a review of London shelter in the summer of 1943 had shown that large numbers still had no domestic shelter, and that many thousands would be unable to reach a public shelter quickly. Though the obvious solution to the problem was the 'Morrison', production of these had stopped twelve months before; and in order to build up a reserve issue had been discontinued in various areas, including London. At the beginning of October it was decided that another 100,000 'Morrisons' should be manufactured and that the reserves held in Scotland, the North of England, the Midlands and North Wales should be moved to the vicinity of London and to the Reading and Tunbridge Wells Regions, from where they could, if necessary, be used to supply London.

Large-scale redistribution of 'Morrisons' and the procurement of new ones called for a substantial administrative effort. Nonetheless, most reserves were transferred during the autumn, and by the end of January 1944 some 12,000 had deen distributed to London householders. At the beginning of this year, however, preparations for the Allied invasion of Europe began to choke the railways with more important traffic, and it became impossible to transport new shelters from manufacturers in the north of England. This difficulty, combined with delays in the production of spanners and nuts, meant that no new shelters could be delivered before late February or early March, when it was expected that the V-weapon attacks would have begun. Arrangements were made for some to be shipped coastwise to London; but in mid-February the contract for the remaining 'Morrisons' (about 20,000) was cancelled. **V2 THREAT:**

648 *Ch. XV: CHALLENGE OF 'V' WEAPONS*

On 11th September the War Cabinet considered the need for a revival of the plan (known as the 'black move') to evacuate a proportion of the staffs of Government Departments from London. The numbers now involved in such an exodus of the war-expanded Departments would be high, and difficulties of communications, transport, accomodation and billeting again seemed overwhelming; it was, therefore, agreed that the more practical course would be to devise measures such as 'citadel' accommodation to enable essential work to continue in London. The production of the further 100,000 'Morrison' shelters and the work on the reinforcement of street shelters proposed by the Home Secretary were also authorised.

As far as shelter policy was concerned, orders had been placed in September 1943 for an additional 100,000 indoor table shelters and existing stocks were moved into the areas of probable attack. Difficulties of manufacture and transport had led to poor deliveries of 'Morrisons', and it seemed unlikely that more than half of the additional shelters ordered would be available by the time attacks were likely to begin. As the remainder would probably arrive too late to be of any use, contracts for the shelters were to be reduced by about 25,000. On the question of deep Tube shelters it had been agreed earlier that priority in the allocation of space would have to be given to the essential machinery of government. The Ministry of Works worked out a plan to shelter those government staffs not already provided for in the strengthened basements of their own steel-framed buildings. All shelter plans, the reader will recall, were given valuable impetus by the resurgence of 'conventional' attack on London and the south in the 'Little Blitz' of early 1944.

V1 flying bomb: *THE 'V.1' ATTACKS* 659

Flying glass was a special danger and people were warned to take cover on the sound of a bomb diving or the engine stopping, and later on the sounding of imminent danger warnings. The vast damage to houses inevitably caused great domestic upheavals. To begin with there was a definite decline in production in London, due to an increase in the rate of absenteeism, to loss of time in actual working hours through workers taking shelter and to lowered efficiency through loss of sleep and anxiety. The extension of the industrial alarm system and the increase in the labour force repairing damaged property, however, soon reduced these early signs of disturbance. Within a few weeks evacuees were returning to London, shelters were less full and most people were going about their normal tasks as usual.

For the civil defence services the new weapon demanded new tactics. In many ways these attacks were much easier to contend with than ordinary bombing. Firstly, most of the incidents were isolated, so that services could be directed in strength to the affected area without constant competing demands on the personnel at every turn. Secondly, the fall of the bombs could be spotted within a matter of seconds by high-placed observation posts either by night or by day, so that rescue and first aid squads could be on the spot very quickly. Thirdly, the penetrative power of this weapon was slight so that incidents rarely involved the complications of broken gas, electricity or water mains, and there was also little tendency for fires to break out. On the other hand the bombs could fall at any time in crowded thoroughfares; the proportion of casualties in the streets was much higher than ever before while the proportion of trapped casualties was lower. At night time, since there were no German eyes above, the use of artificial light was less restricted and searchlights could be used for rescue work.

APPENDIX IV

Major night attacks on United Kingdom cities and towns from 7th September, 1940 to 16th May, 1941

Target Area	*Number of Major Attacks*[1]	*Tonnages of H.E. Aimed*
London	71	18,291
Liverpool-Birkenhead	8	1,957
Birmingham	8	1,852
Glasgow-Clydeside	5	1,329
Plymouth-Devonport	8	1,228
Bristol-Avonmouth	6	919
Coventry	2	818
Portsmouth	3	687
Southampton	4	647
Hull	3	593
Manchester	3	578
Belfast	2	440
Sheffield	1	355
Newcastle-Tyneside	1	152
Nottingham	1	137
Cardiff	1	115

[1] The enemy's definition of a 'major attack', i.e. one in which 100 tons or more of high-explosive bombs were successfully aimed at the target, has been adopted for this table.

Issued for the Ministry of Home Security
by the Ministry of Information

FRONT LINE

1940-41

The Official Story of the
CIVIL DEFENCE
of Britain

1942
London: His Majesty's Stationery Office

So far was all this from panic that it took three months for the population of the twenty-eight central boroughs to drop by about 25 per cent. from a little over 3,000,000 (the figure before heavy bombing began) to 2,280,000 at the end of November. In a group of the most heavily bombed eastern boroughs the pre-war population of 800,000 had fallen to 582,000 before the blitz began; for four months it had dropped steadily to 444,000; by 31st December a fall of 23 per cent. These figures do not spell panic, and a further substantial fall in 1941, after continuous heavy raiding had ceased, completes the evidence that those who went did so in cold blood, for practical reasons as valid for their hard-pressed city as for their private selves.

But what did all this mean to the average Londoner? In November, inner London (the county) contained some 3,200,000 people. Not more than 300,000 of these were in public shelter of any kind, half of that number at most in those larger shelters on which the limelight shone so exclusively. Nor is this all; in domestic shelter (Andersons, small brick shelters and private reinforced basements) there were no more than

1,150,000 people. Thus of every hundred Londoners living in the central urban areas, nine were in public shelter (of whom possibly four were in "big" shelters), 27 in private shelter, and 64 in their own beds—possibly moved to the ground floor—or else on duty. Particular big shelters, and for a few nights the tubes, were overcrowded, but there was public shelter for twice the number who made use of it. In outer London, with a population of some 4,600,000, there were in November 4 per cent. in public shelter, 26 per cent. in domestic shelter, and 70 per cent. at home or on duty.

In the last great war there had been outbursts of hate against the distant enemy, and shops with German names had been wrecked. This time the citizens did not stop for such things. After the first shock of realisation they found no more need for direct recrimination than does the soldier. Like him, they got on with the job and waited their chance. Neither in this nor in any other way was there a sign of instability; no panic running for shelter, no white faces in the streets (though plenty of taut, grim ones), no nerve disease. In all London, the month of October saw but twenty-three neurotics admitted to hospital. The mind-doctors had rather fewer patients than usual.

BLOCKED ROADS. The morning of 12th May: each raid sets the police still another traffic problem.

ENORMOUS CRATERS. At the Bank, where the road collapsed into the subway beneath. A temporary bridge was thrown right across it.

CITY OF COVENTRY

PREVENTION OF TYPHOID FEVER

In view of present damage to DRAINAGE communications in the City, special precautions against Typhoid Fever are advised:

BOIL ALL DRINKING WATER

The outcome may be seen in the following table, which shows coastal bombing to November, 1941, in round figures.

Town.	*Number of Raids.*	*Civilians Killed.*	*Houses Damaged.*
Fraserburgh ...	18	40	700
Peterhead ...	16	36	700
Aberdeen ...	24	68	2,000
Scarborough ...	17	30	2,250
Bridlington ...	30	24	3,000
Grimsby	22	18	1,700
Gt. Yarmouth ...	72	110	11,500
Lowestoft ...	54	94	9,000
Clacton	31	10	4,400
Margate ...	47	19	8,000
Ramsgate ...	41	71	8,500
Deal	17	12	2,000
Dover	53 (and shelling)	92	9,000
Folkestone ...	42	52	7,000
Hastings	40	46	6,250
Bexhill	37	74	2,600
Eastbourne ...	49	36	3,700
Brighton Hove ...	25	127	4,500
Worthing ...	29	20	3,000
Bournemouth ...	33	77	4,000
Weymouth ...	42	48	3,600
Falmouth ...	33	31	1,100

A PENGUIN SPECIAL

THE PSYCHOLOGY OF FEAR AND COURAGE

BY

EDWARD GLOVER

(Published for Blitz air raids in 1940)

PENGUIN BOOKS

HARMONDSWORTH MIDDLESEX ENGLAND

41 EAST 28TH STREET NEW YORK U.S.A.

Real knowledge, for example, is one of the best antidotes to unreal fear. *Useful action* is also an excellent preventive, and *vigorous preparation to meet real danger* will enormously reduce unreal fear. The strength of a common purpose will do the rest. Knowledge, a common purpose, and preparedness for action. These are the remedies for faintness of heart in the face of danger.

22

Now as to preparation. You may recall that when Napoleon was asked how he was always able to give an instant decision in a crisis, he replied: "Because I constantly prepare every detail in advance." Here is a discipline you can readily cultivate. Always make a point of knowing beforehand *exactly* what you are going to do in an air raid; whether you find yourself in house, street, train, bus or shelter. Have it word perfect.

23

A stray crowd packed into a cinema is likely to panic at the cry of "Fire." There are no common bonds between the people concerned; and there are no leaders. Each one is for himself.

34

Already we have the advantage that we are fighting not only for our lives and homes but for the immemorial cause of human liberty. But that is not enough. Provided we are united with our leaders in a common effort, real danger will never sap our morale. The greatest danger to our morale is unreal fear.

A. R. P.

(Air Raid Precautions)

by

J. B. S. HALDANE, F.R.S.

(Co-inventor of 1915 gas masks)

SEPTEMBER
1938

LONDON
VICTOR GOLLANCZ LTD
1938

keyholes and cracks in the wall or between the floor-boards are to be filled with putty or sodden newspaper.

The windows must be specially protected against breakage by blast or splinters.

(Plastic sheets and duct tape for broken windows)

How far are these precautions effective? In 1937 a committee of the Cambridge Scientists' Anti-War Group published a book[1] in which it was stated that no ordinary room is anywhere near gas-proof.

[1] *The Protection of the Public from Aerial Attack.*

Error of Cambridge Scientists' Anti War Group:

The real criticism is as follows. It is unlikely that there would be a lethal concentration of gas out of doors for a long period. The wind carries gas away, and in cities there are vertical air currents even in calm weather. If many tons of bombs could be dropped in the same small area either at once or in succession this would not be so. But given any sort of defence bombs will be dropped more or less at random.

Suppose we had out of doors during 10 minutes a phosgene concentration of one part in 10,000, which would be fatal in a few breaths to people in the street, the concentration inside would never rise as high as $\frac{1}{15}$ of this value[1] if the leakage time were $2\frac{1}{2}$ hours, which is rather low. (Hence protection factor = 15)

[1] Since 10 minutes is $\frac{1}{15}$ of $2\frac{1}{2}$ hours.

Many of the questions which are asked concerning Air Raid Precautions are unanswerable in the form in which they are put. If I am asked "Does any gas mask give complete protection against phosgene" the only literally true answer is "No." One could not live in a room full of pure phosgene in any of them. And one would be killed if a hundred-pound phosgene bomb burst in the room, even when wearing the very best mask. But one would be safe in a phosgene concentration of one part per thousand, of which a single breath would probably kill an unprotected man. Hence in practice such a mask is a very nearly complete protection.

1. NON-PERSISTENT GASES, such as phosgene. They can be dropped in bombs which burst, and suddenly let loose a cloud of gas, which is poisonous when breathed, but which gradually disperses. If there is a wind the dispersal is very quick; in calm, and especially in foggy weather, it is much slower. These gases can penetrate into houses, but very slowly. So even in a badly-constructed house one is enormously safer than in the open air. Even the cheapest type of gas mask, *provided it fits properly and is put on at once*, gives good protection against them (see Chapter IV).

2. PERSISTENT GASES, such as mustard gas. Mustard gas is the vapour of an oily liquid, which I shall call mustard liquid. So far as I know this has not been dropped from aeroplanes in bombs on any great scale. It was used very effectively by the Italians in Abyssinia, who sprayed it in a sort of rain from special sprayers attached to the wings of low-flying aeroplanes.

If the mustard liquid could be sprayed evenly, things would be far more serious. All the outside air of a large town would be poisonous for several days. But this would only be possible if the spraying aeroplanes could fly to and fro over the town in formation, and at a height of not more than 300 feet or so. A fine rain of mustard liquid would probably evaporate on its way to the ground, or blow away, if it were let loose several thousand feet up in the air. Spraying from low-flying aeroplanes was possible in Abyssinia because the Abyssinians had no anti-aircraft guns and no defensive aeroplanes. It would probably not be possible in Britain.

THE HAMBURG DISASTER. Fantastic nonsense has been talked about the possible effects of gas bombs on a town. For example, Lord Halsbury said that a single gas bomb dropped in Piccadilly Circus would kill everyone between the Thames and Regent's Park. Fortunately, although no gas bombs have been dropped in towns in war-time, there are recorded facts[1] which give us an idea of what their effect would be. On Sunday, May 20th, 1928, at about 4.15 p.m., a tank containing 11 tons of phosgene burst in the dock area of Hamburg.

Casualties occurred up to six miles away. In all 300 people were made ill enough to be taken to hospital, and of these ten died. About fifty of the rest were seriously ill. These casualties are remarkably small.

[1] Hegler, *Deutsche Medizinische Wochenschrift*, 1928, p. 1551.

WHY GAS WAS NOT USED IN SPAIN

In view of the terrible stories as to the effects of gas, many people are surprised that it has not been used in Spain. First, why was it not used against the loyalist army? Secondly, why was it not used against towns? The soldiers had respirators after about February 1937, but were not well trained in their use, and often lost them. Very few civilians had any respirators at all.

Gas was not used in the field for several reasons. The main reason is that the number of men and guns per mile was far less than on the fronts in the Great War. Gas is effective if you have a great deal of it,

but the amount needed is enormous. Thus during the night of March 10-11th, 1918, the Germans fired about 150,000 mustard-gas shells into an area of some twenty square miles south-west of Cambrai. If most of the air in a large area is poisoned the effects are serious. But if a few gas shells are fired or a few cylinders let off, the gas soon scatters and ceases to be poisonous, and a man can often run to a gas-free place, even without a mask, before he is poisoned.

Gas was not used against the towns for this reason, and for another, which is very important. Gas only leaks quite slowly into houses, particularly if there are no fires to make a draught, and draw in outside air; and there is very little fuel in loyal Spain.

PANIC

Panic can be a direct cause of death. If too many people crowd into a shelter, especially one with narrow stairs leading to it, they may easily be crushed to death. In January 1918 fourteen people were killed in this way at Bishopsgate Station in London, and sixty-six were killed in a panic in one of the Paris Underground stations as the result of a false gas alarm.

(Bishopsgate Station incident: 28 January 1918)

BACTERIA AND OTHER MICROBES

It is possible that these will be used in some kind of spray or dust. The difficulty is a technical one. It is easy to disperse many solids as smoke. But this needs heat, and cooked bacteria are harmless. Many

bacteria are killed even by drying. And once bacteria are on the ground they generally stay there. Possibly pneumonic plague or some other air-borne disease might be started by a dust-bomb. Cholera bacilli might be dropped in a reservoir. But they would probably be stopped by filters, and even without this would be likely to die before they reached the houses.

A million fleas weigh very little, and could easily be dropped. In theory they could be infected with plague. In practice this would need a staff of hundreds of trained bacteriologists, and huge laboratories. So with other possible means of infection. Some may very well be tried, if only to create a panic, but I would sooner face bacteria than bombs.

248 A.R.P.

Certain pacifist writers are severely to blame for our present terror of air raids. They have given quite exaggerated accounts of what is likely to happen.

250 A.R.P.

So long as civilian populations are unprotected, criminal States will continue to murder the citizens of their weaker neighbours and to blackmail the stronger.

POISONOUS GASES AND SMOKES 261

PHYSICAL PROPERTIES OF A GAS-CLOUD. Every student of chemistry learns that a heavy gas such as chlorine can be poured from one vessel into another almost like water, whilst a light gas such as hydrogen rapidly rises. Now all the poisonous gases and vapours used in war are heavier than air, so it is thought that they would inevitably flood cellars and underground shelters, and that on the first floor of a house one would not be safe.

262 A.R.P.

But within a short time it would be mixed with many times its volume of air. Now air containing one part in 10,000 of phosgene is extremely poisonous. But its density exceeds that of air by only one part in 4,000.

GAS-MASKS, AND GAS-PROOF BAGS FOR BABIES

THE EARLIEST GAS-MASKS made in 1915, relied on chemical means to stop chlorine, which was the first gas used. A cloth soaked with sodium phenate or various other compounds will stop chlorine on its way through. But it would not stop carbon monoxide, mustard gas, or many other gases. The terrible prospect arose that it would be necessary to devise a new chemical to stop each new gas. There would be a continual series of surprise attacks with different gases, each successful until a remedy was found, and each involving the death of thousands of men.

It is a most fortunate fact that the majority of vapours can be removed from air, not by chemical combination, but by a process called adsorption, which is non-specific. For example lime will stop an acid gas such as carbon dioxide, and woollen cloth soaked in acid will stop an alkaline gas such as ammonia. No single chemical will combine with both.

But charcoal, silica, and various other substances, when properly prepared, will take up vapours of different chemical types. The molecules form a very thin liquid layer on the surface of the adsorbent, as indeed they do on glass or metals. But charcoal is full of pores and has an enormous surface per unit of weight; so it can take up a great deal of gas.

The main characteristic in a vapour which renders it adsorbable is that it should be the vapour of a liquid with a high boiling point. Thus carbon monoxide boils at–190° C, and is hardly adsorbed at all. Phosgene boils at 8° C and is fairly easily adsorbed. Mustard gas boils at 217° C and is very easily adsorbed indeed. This has a lucky consequence. It is quite sure that there are no unknown poisonous gases with a boiling point as low as that of carbon monoxide. For only a substance with very small molecules can have so low a boiling point. And chemists have made all the possible types of very small molecules. It is unlikely that there are any unknown poisonous gases with as low a boiling point as phosgene, though it is just possible. But if there are they will probably be stopped by charcoal. There may very possibly be some vapours of high boiling point more poisonous than mustard gas. But if so I am prepared to bet a thousand to one that charcoal will stop them all.

AD 408 094

FINAL REPORT

11 March 1963

Recovery and Decontamination Measures after Biological and Chemical Attack

This report has been reviewed in the Office of Civil Defense and approved for publication. Approval does not signify that the contents necessarily reflect the views and policies of the Office of Civil Defense.

Contract OCD-OS-62-183

Prepared for
Office of Civil Defense
Department of Defense

by

Science Communication, Inc.
1079 Wisconsin Avenue, N.W.
Washington 7, D. C.

To plan for countermeasures against any weapons one must understand the problem—the nature, the potentials, and the limitations. This research project and the resultant final report were intended to bring together current information most applicable to civil defense. It was particularly intended for those who are responsible for planning preparatory, reclamation and countermeasures effort to minimize the damage from a BW/CW attack.

William J. Lacy
Project Coordinator
Postattack Research

Decontaminants

An important class of decontaminants comprises the common substances or natural influences such as time, air, earth, water, and fire.

Natural Effects

Biological agents are living organisms and tend to die off with time unless they are in a favorable environment with moisture, food, warmth, and other factors necessary for their survival. In addition, most biological organisms are very sensitive to the conditions of temperature and humidity -- and, particularly to the ultra-violet portion of sunlight. Adverse exposure to the elements -- air, sunlight, high temperature, low humidity -- is effective, in fact, against all biological agents except the spore forms of bacterial organisms.

It is generally assumed that in the vegetative form bacteria (as contrasted to the spore form) can persist for less than two hours during daytime and about eighteen hours at night. Since these short-lived bacteria are the most probable agents, outdoor decontamination is usually not called for unless the agent has been identified, either by laboratory tests or by the character of the disease, as one which forms spores or is otherwise known to be persistent.

Appraisal of Biological and Chemical Warfare Protection in the U.S. Field Army. Booz, Allen Applied Research, Inc., June 1961. AD 329 113, (SECRET).

Area-Coverage Capabilities of Bacteriological and Chemical Weapons (U). Tamplin, A.R., Rand Corporation, April 1962. AD 329 207, (SECRET).

Biological Decontamination. Asher, T.M., Naval Biological Laboratory, February 1954. AD 72 485, (SECRET).

Biological Problems Attendant Upon the Application of Bacteriological and Chemical Agents in Limited War (U). Tamplin, A.R., Rand Corporation, RM-2677, June 1961. AD 324 462, (SECRET).

Chemical and Biological Weapons Employment. Department of the Army Field Manual, FM 3-10, February 1962.

Community Reaction to an Accidental Chlorine Exposure - Task Sirocco. Segaloff, Louis, University of Pennsylvania, November 1961. AD 269 681.

Decontamination of Water Contaminated with VX. Lindsten, Don C. and Bauer, Virginia E., U.S. Army Engineer Research and Development Laboratories, Research Report 1630-RR, May 1960. AD 239 310.

Effects of Cooking and Baking Processes on the Sterilization of Food Contaminated with Bacterial Spores. Commissary Research Division, U.S. Naval Supply Research and Development Facility, Final Report Navy Project NT 002 024 (CR 53-89), 1953.

Evaluation of Standard and Modified Laundering Procedures as BW Decontamination Methods. Portner, Dorothy M., Mayo, Elizabeth C. and Surkiewicz, Bernard F., Biological Warfare Laboratories, Technical Memorandum 1-2, March 1959. AD 252 270L.

Field Purification of Water Contaminated by G Agents. Chemical Corps Medical Division Report No. 220, 1949. AD 212 449.

Field Tests of Protective Clothing Exposed to BW Aerosols. Chemical Corps Biological Laboratories, Special Report No. 112, August 1949.

Possible Applications of Bacteriological Warfare to Public Water Supplies. Maloney, John R., Office of Naval Research, November 1959. AD 69 721, (CONFIDENTIAL).

Some Indications of Soviet Views on the Strategic Employment of CW/BW (U). Gouré, Leon, Rand Corporation, RM-2725, March 1961. (SECRET).

Studies on Insect Control (U). U.S. Army Engineer Research and Development Laboratories, Research Report 1656-RR, October 1960. AD 321 975, (CONFIDENTIAL).

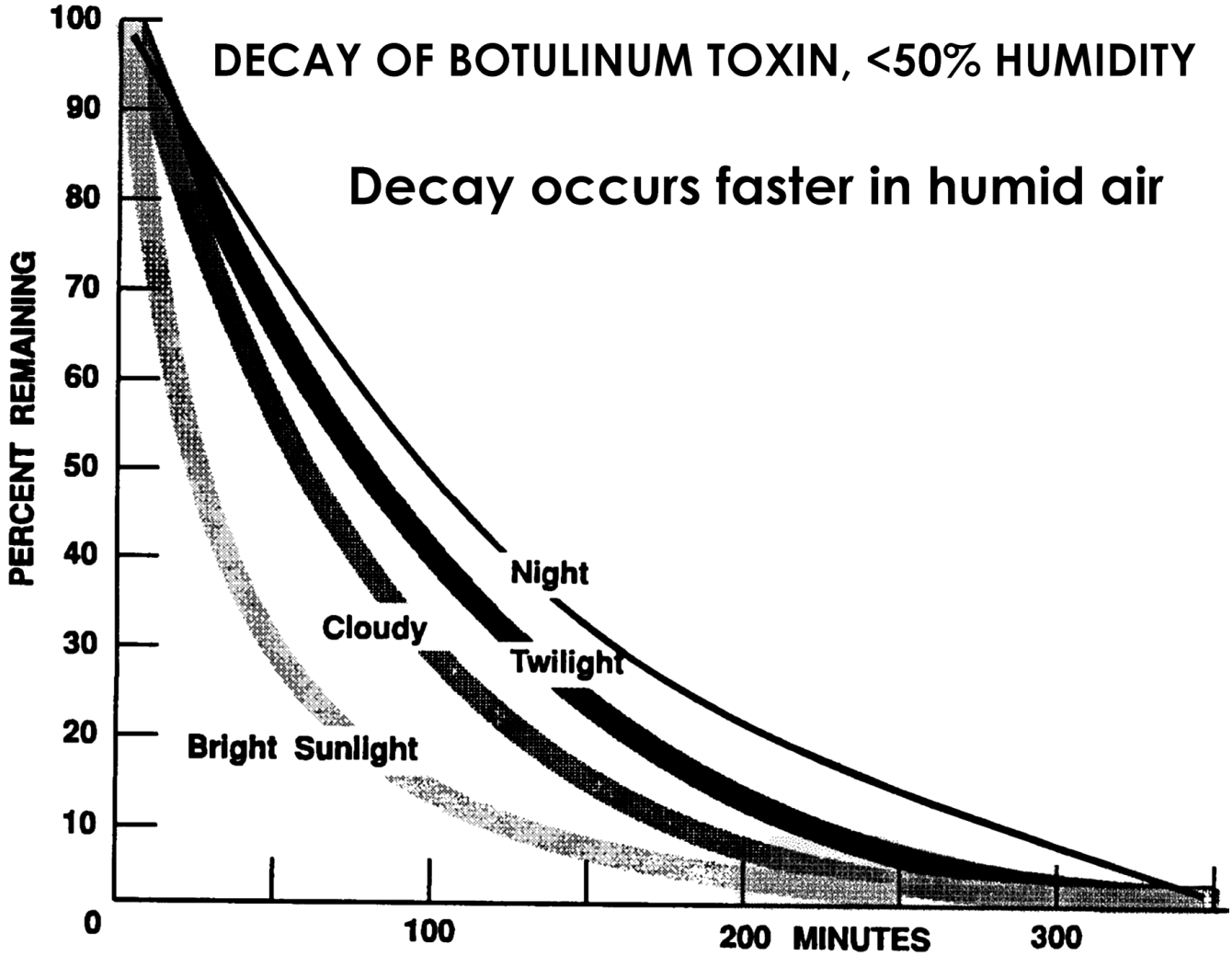

U.S. Army Field Manual FM 3-3 (1992), Fig. B-3.

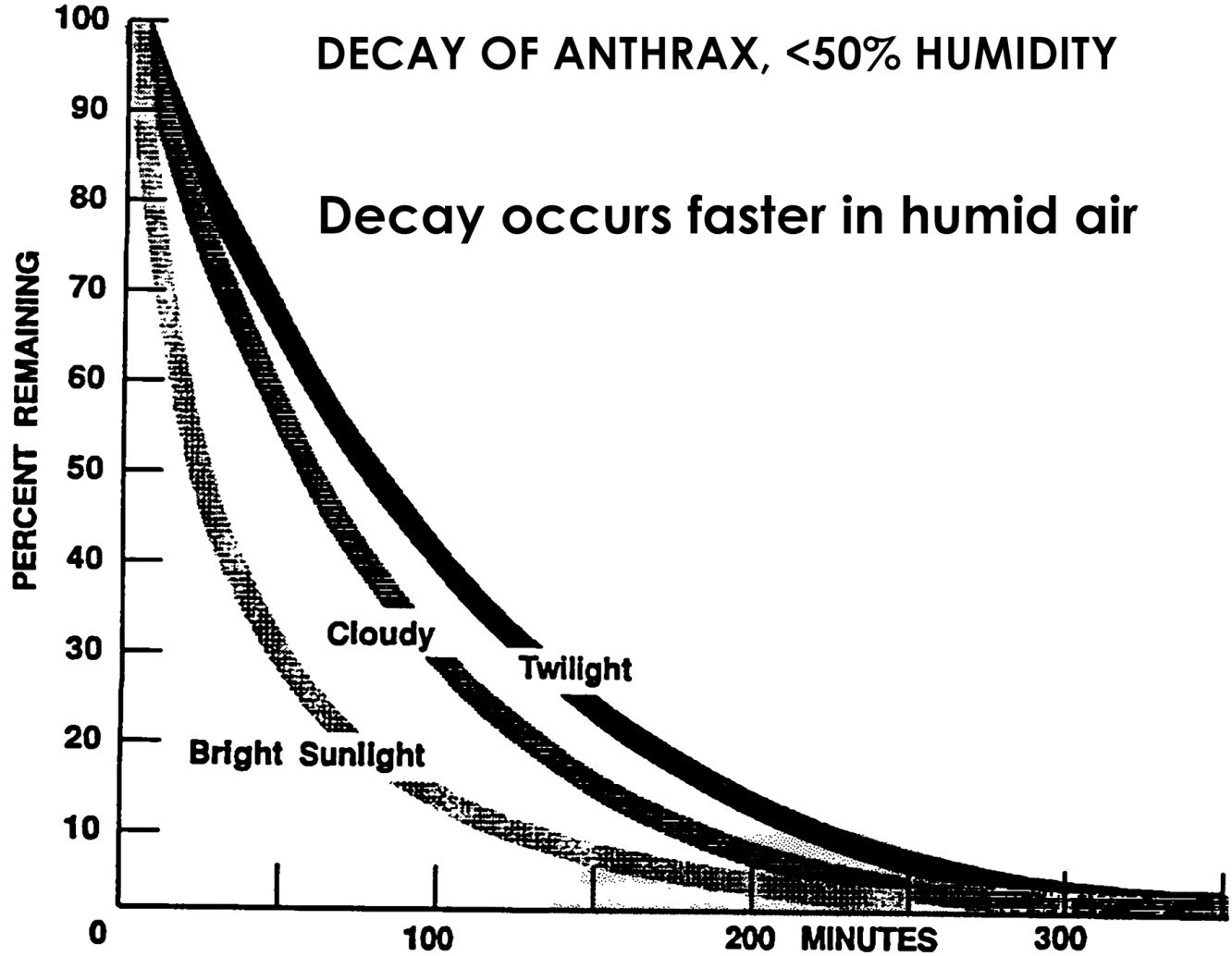

U.S. Army Field Manual FM 3-3 (1992), Fig. B-1.

Chemical and biological contamination avoidance, FM 3-3 (1992)

10 grams/square meter

TABLE 1-2. Chemical Agent Persistency in Hours on CARC Painted Surfaces.

Temperature		GA/ GF[1]	GB[2,3]	GD[2,3]	HD[1]	VX[2,3]
C°	F°					
-30	-22	•	110.34	436.69	••	•••
-20	-4	•	45.26	145.63	••	•••
-10	14	•	20.09	54.11	••	•••
0	32	•	9.44	22.07	••	•••
10	50	1.42	4.70	9.78	12	1776
20	68	0.71	2.45	4.64	6.33	634
30	86	0.33	1.35	2.36	2.8	241
40	104	0.25	0.76	1.25	2	102
50	122	0.25	0.44	0.70	1	44
55	131	0.25	0.34	0.51	1	25

NOTE

1 For grassy terrain multiply the number in the chart by 0.4.
2 For grassy terrain multiply the number in the chart by 1.75.
3 For sandy terrain multiply the number in the chart by 4.5.
• Agent persistency time is less than 1 hour.
•• Agent is in a frozen state and will not evaporate or decay.
••• Agent persistency time exceeds 2,000 hours.

COMPARATIVE VOLATILITY OF CHEMICAL WARFARE AGENTS

Agent	Volatility (mg/m^3) at 25°C
Hydrogen cyanide (HCN)	1,000,000
Sarin (GB)	22,000
Soman (GD)	3,900
Sulfur mustard	900
Tabun (GA)	610
Cyclosarin (GF)	580
VX	10
VR ("Russian VX")	9

Data source: US Departments of the Army, Navy, and Air Force. *Potential Military Chemical/Biological Agents and Compounds*. Washington, DC: Headquarters, DA, DN, DAF; December 12, 1990. Field Manual 3-9. Naval Facility Command P-467. Air Force Regulation 355-7.

SIGNS AND SYMPTOMS REPORTED BY TOKYO HOSPITAL WORKERS TREATING VICTIMS OF SARIN SUBWAY ATTACKS*

Symptom	Number/percentage of the 15 physicians who treated patients at UH		Number/percentage of 472 care providers reporting symptoms at SLI	
Dim vision	11	73%	66	14%
Rhinorrhea	8	53%	No information	
Dyspnea (chest tightness)	4	27%	25	5.3%
Cough	2	13%	No information	
Headache	No information		52	11%
Throat pain	No information		39	8.3%
Nausea	No information		14	3.0%
Dizziness	No information		12	2.5%
Nose pain	No information		6	1.9%

*Data reflect reported survey of self-reported symptomatology of physicians at the University Hospital of Metropolitan Japan emergency department and all hospital workers at Saint Luke's International Hospital exposed to sarin vapors from victims of the Tokyo subway attack.

SLI: Saint Luke's International Hospital

UH: University Hospital

Data sources: (1) Nozaki H, Hori S, Shinozawa Y, et al. Secondary exposure of medical staff to sarin vapor in the emergency room. *Intensive Care Med*. 1995;21:1032-1035. (2) Okumura T, Suzuki K, Fukuda A, et al. The Tokyo subway sarin attack: disaster management, Part 1: community emergency response. *Acad Emerg Med.* 1998;5:613-617. (3) Okumura T, Suzuki K, Fukuda A, et al. The Tokyo subway sarin attack: disaster management, Part 2: Hospital response. *Acad Emerg Med.* 1998;5:618-624.

TABLE 21-3

MANAGEMENT OF MILD TO MODERATE NERVE AGENT EXPOSURES

		Management			
		Antidotes*		**Benzodiazepines (if neurological signs)**	
Nerve Agents	**Symptoms**	**Age**	**Dose**	**Age**	**Dose**
• Tabun • Sarin • Cyclosarin • Soman • VX	• Localized sweating • Muscle fasciculations • Nausea • Vomiting • Weakness/floppiness • Dyspnea • Constricted pupils and blurred vision • Rhinorrhea • Excessive tears • Excessive salivation • Chest tightness • Stomach cramps • Tachycardia or bradycardia	Neonates and infants up to 6 months old	**Atropine** 0.05 mg/kg IM/IV/IO to max 4 mg or 0.25 mg AtroPen† and **2-PAM** 15 mg/kg IM or IV slowly to max 2 g/hr	Neonates	**Diazepam** 0.1–0.3 mg/kg/dose IV to a max dose of 2 mg, or **Lorazepam** 0.05 mg/kg slow IV
		Young children (6 months old–4 yrs old)	**Atropine** 0.05 mg/kg IM/IV/IO to max 4 mg or 0.5 mg AtroPen and **2-PAM** 25 mg/kg IM or IV slowly to max 2 g/hr	Young children (30 days old–5 yrs old)	**Diazepam** 0.05–0.3 mg/kg IV to a max of 5 mg/dose or **Lorazepam** 0.1 mg/kg slow IV not to exceed 4 mg
		Older children (4–10 yrs old)	**Atropine** 0.05 mg/kg IV/IM/IO to max 4 mg or 1 mg AtroPen and **2-PAM** 25–50 mg/kg IM or IV slowly to max 2 g/hr	Children (≥ 5 yrs old)	**Diazepam** 0.05–0.3 mg/kg IV to a max of 10 mg/dose or **Lorazepam** 0.1 mg/kg slow IV not to exceed 4 mg
		Adolescents (≥ 10 yrs old) and adults	**Atropine** 0.05 mg/kg IV/IM/IO to max 4 mg or 2 mg AtroPen and **2-PAM** 25–50 mg/kg IM or IV slowly to max 2 g/hr	Adolescents and adults	**Diazepam** 5–10 mg up to 30 mg in 8 hr period or **Lorazepam** 0.07 mg/kg slow IV not to exceed 4 mg

2-PAM: 2-pralidoxime
IM: intramuscular
IO: intraosseous
IV: intraveneous
PDH: Pediatrics Dosage Handbook
*In general, pralidoxime should be administered as soon as possible, no longer than 36 hours after the termination of exposure. Pralidoxime can be diluted to 300 mg/mL for ease of intramuscular administration. Maintenance infusion of 2-PAM at 10–20 mg/kg/hr (max 2 g/hr) has been described. Repeat atropine as needed every 5–10 minutes until pulmonary resistance improves, secretions resolve, or dyspnea decreases in a conscious patient. Hypoxia must be corrected as soon as possible.
†Meridian Medical Technologies Inc, Bristol, Tenn.
Data sources: (1) Rotenberg JS, Newmark J. Nerve agent attacks on children: diagnosis and management. *Pediatrics*. 2003;112:648–658. (2) Pralidoxime [package insert]. Bristol, Tenn: Meridian Medical Technologies, Inc; 2002. (3) AtropPen (atropine autoinjector) [package insert]. Bristol, Tenn: Meridian Medical Technologies, Inc; 2004. (4) Henretig FM, Cieslak TJ, Eitzen Jr EM. Medical progress: biological and chemical terrorism. *J Pediatr*. 2002;141(3):311–326. (5) Taketomo CK, Hodding JH, Kraus DM. *American Pharmacists Association: Pediatric Dosage Handbook*. 13th ed. Hudson, Ohio; Lexi-Comp Inc: 2006.

TABLE 21-4

MANAGEMENT OF SEVERE NERVE AGENT EXPOSURE

		Management			
		Antidotes*		Benzodiazepines (if neurological signs)	
Nerve Agents	**Severe Symptoms**	**Age**	**Dose**	**Age**	**Dose**
• Tabun • Sarin • Cyclosarin • Soman • VX	• Convulsions • Loss of consciousness • Apnea • Flaccid paralysis • Cardio-pulmonary arrest • Strange and confused behavior • Severe difficulty breathing • Involuntary urination and defecation	Neonates and infants up to 6 months old	**Atropine** 0.1 mg/kg IM/IV/IO or 3 doses of 0.25mg AtroPen† (administer in rapid succession) and **2-PAM** 25 mg/kg IM or IV slowly, or 1 Mark I† kit (atropine and 2-PAM) if no other options exist	Neonates	**Diazepam** 0.1–0.3 mg/kg/dose IV to a max dose of 2 mg, or **Lorazepam** 0.05 mg/kg slow IV
				Young children (30 days old–5 yrs and adults	**Diazepam** 0.05–0.3 mg/kg IV to a max of 5 mg/dose, or **Lorazepam** 0.1 mg/kg slow IV not to exceed 4 mg
		Young children (6 months old–4 yrs old)	**Atropine** 0.1 mg/kg IV/IM/IO or 3 doses of 0.5mg AtroPen (administer in rapid succession) and **2-PAM** 25–50 mg/kg IM or IV slowly, or 1 Mark I kit (atropine and 2-PAM) if no other options exist	Children (≥ 5 yrs old)	**Diazepam** 0.05-0.3 mg/kg IV to a max of 10 mg/dose, or **Lorazepam** 0.1 mg/kg slow IV not to exceed 4 mg
				Adolescents and adults	**Diazepam** 5–10 mg up to 30 mg in 8-hr period, or **Lorazepam** 0.07 mg/kg slow IV not to exceed 4 mg
		Older children (4–10 yrs old)	**Atropine** 0.1 mg/kg IV/IM/IO or 3 doses of 1mg AtroPen (administer in rapid succession) and **2-PAM** 25–50 mg/kg IM or IV slowly, 1 Mark I kit (atropine and 2-PAM) up to age 7, 2 Mark I kits for ages > 7–10 yrs		
		Adolescents (≥ 10 yrs old) and adults	**Atropine** 6 mg IM or 3 doses of 2 mg AtroPen (administer in rapid succession) and **2-PAM** 1800 mg IV/IM/IO, or 2 Mark I kits (atropine and 2-PAM) up to age 14, 3 Mark I kits for ages ≥ 14 yrs		

IM: intramuscular
IO: intraosseous
IV: intravenous

*In general, pralidoxime should be administered as soon as possible, no longer than 36 hours after the termination of exposure. Pralidoxime can be diluted to 300 mg/mL for ease of intramuscular administration. Maintenance infusion of 2-PAM at 10–20 mg/kg/hr (max 2 g/hr) has been described. Repeat atropine as needed every 5–10 min until pulmonary resistance improves, secretions resolve, or dyspnea decreases in a conscious patient. Hypoxia must be corrected as soon as possible. †Meridian Medical Technologies Inc, Bristol, Tenn.

Data sources: (1) Rotenberg JS, Newmark J. Nerve agent attacks on children: diagnosis and management. *Pediatrics*. 2003;112:648–658. (2) Pralidoxime [package insert]. Bristol, Tenn: Meridian Medical Technologies, Inc; 2002. (3) AtroPen (atropine autoinjector) [package insert]. Bristol, Tenn: Meridian Medical Technologies, Inc; 2004. (4) Henretig FM, Cieslak TJ, Eitzen Jr EM. Medical progress: biological and chemical terrorism. *J Pediatr*. 2002;141(3):311–326. (5) Taketomo CK, Hodding JH, Kraus DM. *American Pharmacists Association: Pediatric Dosage Handbook*. 13th ed. Hudson, Ohio: Lexi-Comp Inc; 2006.

French family at Marbache, Meurthe et Moselle, France, September 1918. Gas masks were compulsory in the village, due to nearby gas attacks. Photo is the frontispiece of the October 1921 reprint of Will Irwin's book "The Next War" (Dutton, N.Y., 19th printing Oct 1921; first published April 1921.)

J. Davidson Pratt, "Gas Defence from the Point of View of the Chemist" (Royal Institute of Chemistry, London, 1937): "... during the Great War, French and Flemish ... living in the forward areas came unscathed through big gas attacks by going into their houses, closing the doors - the windows were always closed in any case - and remaining there..."

London 1941 baby gas mask drill

Hand pumped
(asthmatic)
Baby's
Hospital patient's
Police
/warden
Civilian
Soldier's
until 1942
Small child's
(mickey mouse)

An eminent chemist gives the facts about poison gas and air bombing

Breathe Freely!

THE TRUTH ABOUT POISON GAS

by

James Kendall

M.A., D.Sc. F.R.S.

Professor of Chemistry, University of Edinburgh

The civilian has been told that he will have to bear the brunt of another war, that within a few hours from the outset enemy bombers will destroy big cities and exterminate their inhabitants with high explosive, incendiary and gas bombs. What is the truth?

Here, in this book, written in language everyone can understand, is the considered opinion of an authority on chemical warfare.

Breathe Freely !

THE TRUTH ABOUT POISON GAS

JAMES KENDALL

M.A., D.Sc., F.R.S.

Professor of Chemistry in the University of Edinburgh; formerly Lieutenant-Commander in the United States Naval Reserve, acting as Liaison Officer with Allied Services on Chemical Warfare

1938

CASUALTIES IN INITIAL GAS ATTACKS

Gas	*Date*	*Amount Used In Tons*	*Lethal Concentration **	*Non-fatal injuries*	*Deaths*
Chlorine	Apr. 22, 1915	168	5·6	15,000	5,000
Phosgene	Dec. 19, 1915	88	0·5	1,069	120
Mustard	July 12, 1917	125	0·15	2,490	87

(* mg/litre for 10 minutes exposure unprotected)

between September 15 and November 11, 1918, 2,000,000 rounds of gas shell, containing 4,000 tons of mustard gas, were fired against the advancing British troops; our losses therefrom were 540 killed and 24,363 injured. Gas defence had progressed to the point where it took nearly 8 tons of mustard gas to kill a single man !

The first salvo of gas shells often reaches the trenches before the occupants don their masks, whereas the Londoner will receive ample warning of the approaching danger.

The alarmist and the ultra-pacifist love to quote the fact that one ton of mustard gas is sufficient to kill 45,000,000 people. This would indeed be true if the 45,000,000 people all stood in a line with their tongues out waiting for the drops to be dabbed on, but they are hardly likely to be so obliging. One steam-roller would suffice to flatten out all the inhabitants of London if they lay down in rows in front of it, but nobody panics at the sight of a steam-roller.

EVER since the Armistice, three classes of writers have been deluging the long-suffering British public with lurid descriptions of their approaching extermination

These three classes are pure sensationalists, ultra-pacifists and military experts.

perpetrators of such articles may not recognize themselves that what they are writing is almost entirely imaginary, but they do want to get their manuscript accepted for the feature page of the *Daily Drivel* or the *Weekly Wail*. In order to do that, they must pile on the horrors thick, and they certainly do their best

The amount of damage done by such alarmists cannot be calculated, but it is undoubtedly very great.

poison gas has a much greater news value. It is still a new and mysterious form of warfare, it is something which people do not understand, and what they do not understand they can readily be made to fear.

13

The recent film *Things to Come*, in particular, has provided a picture of chemical warfare of the future which shows how simply and rapidly whole populations will be wiped out. Millions of people, perhaps, have been impressed by the authority and reputation of Mr. H. G. Wells into believing that this picture represents the plain truth.

17

EXHIBIT 'B' is the work of the ultra-pacifist. He abominates war and everything connected with war to such an extent that he paints a highly coloured picture of its horrors, in the most extreme Surrealistic style, with the object of frightening the public to the point where they will relinquish, in the hope of escaping war, even the right of self-defence. His motives may be praiseworthy, but his methods are to be deplored.

Tel. No.: VICtoria 6826

Any communication on the subject of this letter should be addressed to—

THE UNDER SECRETARY OF STATE,
HOME OFFICE (A.R.P. DEPT.),
HORSEFERRY HOUSE,
THORNEY STREET,
LONDON, S.W.1.

and the following number quoted:—
701,602/109

HOME OFFICE,
AIR RAID PRECAUTIONS DEPT.,
HORSEFERRY HOUSE,
THORNEY STREET,
LONDON, S.W.1.

31st December, 1937.

SIR,

Experiments in Anti-Gas Protection of Houses

I am directed by the Secretary of State to transmit, for the information of your Council, the annexed Report describing in detail the experiments to which reference was made by the Parliamentary Under Secretary of State in his speech on the second reading of the Air Raid Precautions Bill in the House of Commons on the 16th November.

The experiments were conducted by the Chemical Defence Research Department under the aegis of a special Sub-Committee of the Chemical Defence Committee. That Sub-Committee was composed of eminent experts not in Government employment, and included a number of distinguished University professors and scientists.

I am,
Sir,
Your obedient Servant,
R. R. SCOTT.

The Clerk of the County Council.
The Town Clerk.
The Clerk to the District Council.

Issued to all
County Councils
County Borough Councils (and the Corporation of the City of London)
Metropolitan Borough Councils
Municipal Borough Councils
Urban and Rural District Councils
in England and Wales
Copies sent for information to Chief Officers of Police in England and Wales.

Crown Copyright Reserved

PROTECTION AGAINST GAS

REPORT OF EXPERIMENTS CARRIED OUT BY THE CHEMICAL DEFENCE RESEARCH DEPARTMENT

Handbook No. 1 issued by the Air Raid Precautions Department of the Home Office describes the steps which the public are advised to take in order to protect themselves against the effects of any chemical warfare gases which might be employed by enemy aircraft in time of war.

The gist of these recommendations is:—

First, to go indoors.

Secondly, to arrange for the room into which you go to be made as gas-proof as possible.

Thirdly, to take with you the respirator which will have been issued to you.

Whilst it has never been claimed that any one of these steps by itself will make an individual completely safe, experiments and trials have shown that each of these measures is by itself of considerable value and that when all of them are adopted a very high degree of protection is obtained. An outline is given below of certain typical experiments which have been carried out.

These particular experiments were carried out with four different types of actual war gas. The first four experiments to be described will show the degree of protection that is obtained from each type of gas merely by going indoors and shutting the doors and windows.

As explained in Handbook No. 1*, a chemical warfare gas may be dropped from aircraft either as spray or in bombs. In the former case the liquid drops fall like rain, and it is obvious that by going indoors the public will avoid them. On the other hand, if gas bombs are dropped, people who have gone indoors will avoid being splashed by the chemical in the bomb, and even in an ordinary room they will receive some protection from the gas cloud. The amount of protection obtained in a house which has not been treated in any way can be gathered from the following experiments.

(a) *Protection obtained in a house which has not been treated in any way.*

The house employed was a gamekeeper's cottage with three rooms on the ground floor and three rooms upstairs. It had been unoccupied for about 15 years but was in a reasonable state of repair. It was to a large extent sheltered by belts of

* A.R.P. Handbook No. 1, "Personal Protection against Gas", price 6d. (8d. post free): published by H.M. Stationery Office (see back page).

trees which reduced the strength of the wind in the vicinity of the cottage to about one-eighth of that in the open. In this respect therefore the location of the cottage resembled a house in a town. In one experiment over a ton of actual chlorine gas was released 20 yards from the house so that the wind carried it straight on to the unprotected room. A very strong gas cloud was thus maintained outside the house for about 40 minutes, during which time the gas gradually penetrated to the inside. A fire was burning in the hearth the whole time, and the only measures taken to exclude the gas consisted of closing the doors and windows in the normal way.

Human beings who occupied this unprotected room found that gas penetrated slowly into the room, and after about seven minutes is became necessary for them to put on their respirators. Had these men been outside the house, they would have been compelled to put on their respirators immediately, since otherwise the very intense gas cloud would have caused instantaneous incapacitation and ultimate death.

If the gas, which with its containers weighed about 2½ tons, had been released more quickly, the strength of the gas cloud would have been greater but the time during which the house was enveloped by it would have been correspondingly shorter.

It is important to appreciate properly the severity of this trial. The quantity of gas concentrated on this house could under practical conditions only be obtained by several large bombs dropping very close to the building. The period of exposure to the maximum effects of the gas was also many times longer than would normally be experienced under most practical conditions, since the initial cloud from a gas bomb soon begins to be diluted and dispersed by the action of even quite moderate winds. It is clear that conditions similar to those of the experiment are extremely severe, and are such as would be likely to occur very rarely indeed and to a very small number of houses.

It should also be noted that the cottage used in this experiment had no carpets or other floor coverings. Most of the gas which leaked in came through the spaces between the floor boards, and it is therefore clear that much less would have got into an ordinary room in which there was a carpet, linoleum, or a solid floor.

In another experiment the house was surrounded at a distance of 20 yards by large shallow trays which were filled with mustard gas, the trays being spaced a few yards apart. By this means the vapour given off by the mustard gas was carried on to the house no matter how the direction of the wind varied. As the weather at the time was not very warm, the conditions of the experiment were made more severe by producing a fine spray of mustard gas at a point 10 yards to windward of

the house so that the house was enveloped in the resultant cloud of mustard gas for a period of an hour. The cloud produced in this way was about a hundred times as strong as that caused by the evaporation of the mustard gas from the trays. Animals were placed in an unprotected room in the house and remained there during the spraying period and for a further 20 hours while the house was subjected to the vapour of mustard gas given off from the trays. Observations made upon the animals during the three subsequent days and also post mortem examination showed that none of them was seriously harmed by the mustard gas.

The third type of gas used was tear gas. In this experiment the same cottage was enveloped for an hour in an intense atmosphere of tear gas produced by spraying the gas into the air at a point 10 yards upwind of the house. Men who were stationed 200 yards downwind from the house and in the track of the gas cloud were incapacitated in about a minute, and in some cases in 20 seconds. On the other hand, men who occupied rooms in the house which had received no treatment beyond the closing of the windows and doors found no need to put on their respirators for the first 13 minutes. The tear gas gradually penetrated into these unprotected rooms, although after three-quarters of an hour the strength of the gas inside the house was still very much less than that outside.

In the fourth experiment the cottage was enveloped for 20 minutes in a dense cloud of arsenical smoke. Men occupying an unprotected room of the house found that the arsenical smoke penetrated into the room, but the strength of the cloud inside was much less than that outside. When Civilian respirators were worn in this room, complete protection was obtained. Men who were stationed 200 yards downwind of the house and in the path of the gas cloud were rapidly affected, but when they wore Civilian respirators no effects were felt.

The above four examples clearly demonstrate that, apart from the protection which a house provides against falling airplane spray, some measure of protection is afforded even by an ordinary unprotected room against gas clouds such as are produced by bombs close to the building.

(b) *Protection afforded by a house treated in accordance with Air Raid Precautions Handbook No. 1.*

A brief account will now be given of four further experiments with the same four war gases in order to illustrate the added protection which can be obtained by treating a room in accordance with the instructions given in Air Raid Precautions Handbook No. 1. These experiments were also conducted with the cottage already mentioned. The room selected for treatment was situated on the ground floor on the windward side

of the house so that it was subjected to the full effect of the gas and the wind. It measured about 12 feet square. The Air Raid Precautions instructions for excluding gas were carried out by unskilled men, the official procedure being rigidly followed. As the house was not provided with carpets or other floor covering, it became necessary to seal up the joints between the boards over the whole of the floor of the selected room. This was done by pasting strips of paper along the joints between the floor boards. Some of these strips became displaced by the boots of the men who were inside the room, and an appreciable leakage of gas into the room undoubtedly occurred due to this cause. Two tons of chlorine were released 20 yards from the house, the time of emission being an hour. Animals were placed in the house, some in the " gas protected " room and others in rooms which had received no such treatment. The latter set of animals were killed by the gas which penetrated into the unprotected rooms under these very severe conditions. The animals in the " gas protected " room, however, were unaffected and remained normal, notwithstanding the severity of the trial.

An experiment with mustard gas, similar to that already described, was also carried out after the ground floor room on the windward side of the house had been treated in accordance with the Air Raid Precautions Department's procedure. Animals were placed in the room, which was then subjected to the same exposure of mustard gas spray and vapour as before. At the end of 20 hours the animals were removed and a most thorough examination of them showed no evidence of the effects of the gas at all. Animals placed outside the house during the first hour of the experiment were, of course, very seriously affected. The amount of mustard gas penetrating into the room was also measured by chemical methods and it was found that the amount of gas inside the room was so small that a man could have remained there for the whole 20 hours without its being necessary for him to wear a respirator and without any subsequent ill-effects.

The experiment with tear gas previously described was also performed against the " gas protected " room. A number of men occupied this room and found they were able to remain there without its being necessary for them to put on their respirators at any time during the hours that this very severe experiment lasted.

An experiment with arsenical smoke, similar to that already described, was also carried out against the " gas protected " room. The occupants found that the arsenical smoke penetrated the room to an extent which caused some irritation of the nose and throat and eventually rendered the wearing of respirators desirable to ensure comfort. After putting on the respirator, no

discomfort was felt throughout the remainder of the experiment. Men who left the " gas protected " room wearing their Civilian respirators were able to traverse the densest part of the cloud without discomfort. Under these severe conditions the presence of the arsenical smoke could be detected, but the effects were insignificant.

It is important to appreciate fully the severity of the conditions imposed in the two trials with arsenical smoke. A very high concentration of the irritant smoke was maintained around the house for 20 minutes. Under practical conditions such a high concentration could be produced only by a large and efficiently designed bomb falling close to the building, and then only for a short period. The conditions of the trials were therefore extremely severe and represent a situation which would only rarely be met, and in which only a small number of houses would be involved.

From this second series of experiments it will be seen that treating a room in accordance with the recommendations of the Air Raid Precautions Department does reduce very considerably the amount of gas penetrating into the room, and that a room so treated is correspondingly safer than a room which has received no such treatment.

Indeed, in the case of the experiments with mustard gas and tear gas, the amount of gas which was able to penetrate into the gas protected room was so small that no further measures of protection were necessary.

In the experiment with chlorine, although the amount of gas which entered the treated room was insufficient to injure the animals, human beings who occupied the room during this extremely severe test could smell the gas. They were provided with Civilian respirators, and they found that by putting these respirators on they were completely protected against every trace of gas. Some of these individuals then left the " gas protected " room, passed out of the house, and traversed the lethal cloud of gas which enveloped it. Although they deliberately stood in the densest part of the cloud for some minutes, no trace of the gas passed through their respirators.

Similarly the experiments with arsenical smoke show that although, under the most severe conditions, the cloud may penetrate into the " gas protected " room in sufficient quantity to be detected, or even to cause some irritation, the effects are materially reduced in a room so treated. It is also demonstrated that wearing a Civilian respirator affords complete protection against any smoke which may gain access to the room. The respirator also enabled individuals to pass through an extremely dense cloud of arsenical smoke in complete safety.

The experiments which have been outlined in this statement were purposely designed to represent the most severe conditions likely to be met. The results all combine to show that if the instructions given in Air Raid Precautions Handbook No. 1 are carried out a very high standard of protection is obtained. With regard to the first precaution it has been shown that going indoors and closing the doors and windows affords some measure of protection, even though the room occupied has not been specially prepared. In these circumstances there is ample time to put on the respirator at leisure if this should be necessary. If the second precaution of rendering the room as gas-proof as possible has been carried out, then the occupants will normally be able to remain in complete safety and comfort without further protection. Under the most severe conditions sufficient gas may penetrate such protected rooms to be recognized or even to cause slight irritation. When this occurs the respirator can be put on though in many cases this will be as a matter of convenience and extra precaution rather than real necessity. With regard to the Civilian respirator it has been shown that this will, in conjunction with the above precautions, provide complete safety for any period for which it is likely to be required. It has further been demonstrated that this respirator will enable the wearer to reach a place of safety even if he should for a time be exposed to the most dangerous situation—for example if he is caught out of doors in a gas cloud, or if his gas-protected room becomes damaged and he is compelled to seek shelter elsewhere.

(47178—34 Wt. 3276—235 20,000 12/37 P. St G. 373

LONDON
PRINTED AND PUBLISHED BY HIS MAJESTY'S STATIONERY OFFICE
To be purchased directly from H.M. STATIONERY OFFICE at the following addresses:
Adastral House, Kingsway, London, W.C.2; 120 George Street, Edinburgh 2;
26 York Street, Manchester 1; 1 St. Andrew's Crescent, Cardiff;
80 Chichester Street, Belfast;
or through any bookseller

1937
Price 2*d*. net

S.O. Code No. 34-9999

HOME OFFICE

CIVIL DEFENCE

Manual of Basic Training

VOLUME II

BASIC CHEMICAL WARFARE

PAMPHLET No. 1

LONDON: HIS MAJESTY'S STATIONERY OFFICE
1949

CHAPTER VII

51. COLLECTIVE PROTECTION

Every individual can rely on his respirator for his own protection against war gas, and this is his primary defence, but the protection which is afforded against vapour, by buildings in sound condition, is of considerable value and against liquid and spray is complete.

HOME OFFICE

SCIENTIFIC INTELLIGENCE OFFICERS'

OPERATIONAL NOTES

RESTRICTED

The information given in this document is not to be communicated, either directly or indirectly, to the Press or to any person not authorised to receive it.

Crown Copyright 1965

Mechanism of fallout

Definitions

Wind direction is the direction from which the wind blows, and is given in degrees measured clockwise from north.
E.g. A 270° wind blows from the west.

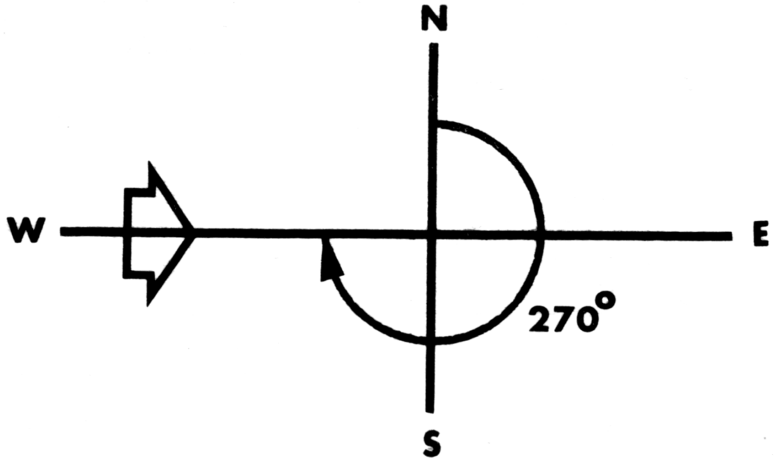

Wind speed is actually measured in knots, but the unit of speed usually used by the SIO is the mile per hour (mph).

1 knot = 1 nautical mile per hour
1 nautical mile = 6080 feet
1 knot = 1.15 mph

N.B. In meteorological forecasts received by the SIO wind speeds will normally be in mph. If a forecast is mistakenly transmitted in knots, then the SIO should transform, using the above relationship. In approximate calculations the difference between a knot and a mile per hour may be neglected.

Winds changing direction with time

(a) If a wind turns clockwise it is said to be veering.
(b) If a wind turns anticlockwise it is said to be backing.

A forecast concerns meteorological data only.

A prediction indicates where fallout may go. It is based on a forecast and on bomb data.

A micron (μ) is one millionth of a metre.
1000 microns = 1 millimetre.

Useful wind data

The following data applies to the 0-60,000, 0-70,000 and 0-80,000 feet mean vector winds.

(a) Variation with speed

Probabilities of occurrence of speeds (all directions)

Speed range (mph)	0-7	7-18	18-35	35+
Percentage probability	4	17	36	43

(b) Variation with direction

Probabilities of directions occurring in 60° sectors (all speeds)

Wind direction (degrees)	0-60	60-120	120-180	180-240	240-300	300-360
Percentage probability	7	4	5	17	41	26

(c) Angular wind shear

This is defined for the present purpose as the angle which includes the directions of all the mean vector winds up to the 0-90,000 feet one, excluding the surface wind. This angle will give a very crude idea of the amount of lateral spreading which might occur in the fallout pattern.

Percentage probability of occurrence of angular shear

Angular shear (degrees)	Mean vector wind speed (mph)				Total
	0 - 7	7 - 18	18 - 35	35 +	
0-15	0	2½	9½	21	33
15-30	½	3½	13	11	28
30-75	½	7	10½	10	28
75 +	3	4	3	1	11
Total	4	17	36	43	100

Mode of decay

Any single radioisotope decays according to an exponential law $N_t = N_o e^{-\lambda t}$, where N_o and N_t are the number of atoms present initially and at time t. λ is a decay constant and can be shown to equal 0.693/T, where T is the half-life of the isotope, i.e. if the activity was originally, say, 8 units, then it will have decayed to 4 units after time T, 2 units after time 2T, 1 unit after time 3T, etc.

Fission products from a nuclear explosion are a mixture of over 200 different radioisotopes with half-lives varying from fractions of a second to many thousands of years. Many of them, moreover, are not produced immediately but are the result of the decay of other nuclides. In addition, the mixture may contain some activity due to neutron activation of the bomb components resulting in the formation of neptunium 239. The decay of this mixture is not exponential and thus cannot be described by a half-life. From nuclear weapons trials it has been found for the first 100 days to follow approximately the $t^{-1.2}$ power law, i.e. $R_t = R_1 t^{-1.2}$, where R_1 and R_t are the dose-rates at 1 hour and t hours after detonation

Factors upsetting normal decay

Probable causes of deviation from the $t^{-1.2}$ decay law are:-

(a) fractionation
(b) neutron activation of soil elements
(c) weathering
(d) rigging or salting of weapons

Fractionation

This is a complex condensation process and is by no means fully understood. Its effect is to give the close-in FO a different composition and hence a different decay from the more distant FO downwind. For example, close-in FO has been found to contain less strontium 90.

Two likely causes of fractionation are:-

(a) as the fireball cools the nuclides with the higher boiling points condense first and do so while the larger particles forming the close-in FO are still present in the cloud. The more volatile nuclides condense later when the larger particles have left the cloud and so tend to contaminate the lighter particles which are carried further downwind.

(b) certain of the fission products are inherently gaseous (e.g. krypton) or have gaseous precursors (e.g. caesium 137). The heavier particles fall out before these nuclides have decayed to non-gaseous daughters capable of condensing on to them. Close-in FO is therefore deficient in these elements. Conversely the smaller particles forming the more distant FO are enriched in them.

Neutron activation of soil elements

For FO to be produced on a substantial scale, the explosion must take place on or near the ground, in which case the radioactivity from the fission products and the bomb materials is supplemented by neutron-induced activity from certain elements in the soil. For the 50% fission weapon this extra activity is small but may be appreciable for the so-called "clean" bomb where possibly only 10% of the total energy is from fission. The number of spare neutrons is doubled and the fission product activity reduced by a factor of 5. Under these circumstances induced activity can become a substantial proportion of the whole. Calculations made on typical UK soils show that the elements most likely to contribute to this activity are sodium and manganese. Under neutron activation these form the gamma emitters sodium 24 and manganese 56. Sodium and manganese are present in soils in varying amounts according to the locality. Sodium, for example, is more abundant in the rock-salt areas of Cheshire and in regions of igneous rock formation. Manganese is fairly uniformly distributed but usually only in small amounts.

If a large quantity of a particular isotope such as sodium 24 is added to a fission product mixture obeying the $t^{-1.2}$ law, the effect is to increase the dose-rate by an amount varying with time. It can be shown that the isotope exerts its maximum proportional effect at a time equal to 1.73 times its half-life. For sodium 24 and manganese 56 the details are:-

Isotope	Half-life (hours)	Time of maximum proportional effect (hours)
Na24	15	26
Mn56	$2\frac{1}{2}$	$4\frac{1}{2}$

For a 10% fission bomb the sodium 24 contribution to the total DR at H + 26 hours could be over 80% for some bomb designs and soil constitutions; the manganese 56 contribution at H + $4\frac{1}{2}$ hours could be over 10%.

Notes on BW and CW

General

Toxicological warfare can consist either of a tactical attack with chemical weapons producing an immediate incapacitating effect, or of a strategic attack with biological weapons which have a delayed effect.

The new Civilian Respirator (C7), with pneumatic tube face fitting which is comfortable for long periods of wearing, affords excellent protection against BW and CW attacks.

BW

In attacks on populations, since the airborne hazard is the main one, only agents of high infectivity and high virulence (i.e. a small number of organisms required to produce infection and cause severe illness), combined with viability for many hours in the atmosphere, are likely to prove effective.

Some representative pathogenic micro-organisms

Bacterial	Anthrax	(lethal, very persistent spores but relatively low infectivity)
	Brucellosis	(incapacitating)
	Tularaemia	(incapacitating or lethal)
	* Rickettsial	Q fever (like typhus)
	* Viruses	Encephalomyelitis (brain fever)
		Smallpox (epidemic)

Personal protection

Respirators and discardible covers for head and body may be used. Extreme personal cleanliness is necessary. Total dosage can be reduced very considerably in a closed room in a house by sealing window cracks and door gaps before the arrival of contamination and ventilating the room fully as soon as it has passed.

Decontamination

Where appropriate the following measures may be taken:-

(a) weathering for a few days will destroy most bacterial agents other than anthrax spores
(b) use of bleach solution
(c) scattering petrol and firing it on open contaminated ground.

CW

Mustard gas and anticholinesterase agents (persistent and non-persistent nerve gases) are the CW agents most likely to be encountered in a tactical battle.

Building/ Vehicle Type	Air Exchange Rate (ACH)	Time Building Is Exposed (hr.)	Time of Occupancy from Cloud Arrival (hr.)	Shielding Factor
Residential Building (Windows Closed)[1]	0.53 0.08-3.24	0.25 0.25	0.25 0.25	15.8 100.7-3.2
Residential Building (Windows Open)[1]	6.4	0.25	0.25	2.0
Nonresidential Building[1]	1.285 0.3-4.1	0.25 0.25	0.25 0.25	6.9 27.3-2.7
Vehicle[1]	36	0.25	0.25	1.1
Mass-Transit Vehicle[1]	1.8-5.6	0.25	0.25	5.1-2.2
Stationary Automobile[2]:				
Windows Closed/No Ventilation	1.0-3.0	0.25	0.25	8.7-3.4
Windows Closed/Fan On Recirculation	1.8-3.7	0.25	0.25	5.1-2.9
Windows Open/No Ventilation	13.3-26.1	0.25	0.25	1.4-1.2
Windows Open/Fan On Fresh Air	36.2-47.5	0.25	0.25	1.1

[1] Ted Johnson, A Guide to Selected Algorithms, Distributions, and Databases used in Exposure Models Developed by the Office of Air Quality Planning and Standards (Chapel Hill, NC: TRJ Environmental, Inc., 22 May 2002), http://www.epa.gov/ttn/fera/data/human/report052202.pdf. Accessed 8 January 2008.

[2] J. H. Park et al., "Measurement of Air Exchange Rate of Stationary Vehicles and Estimation of In-Vehicle Exposure," Journal of Exposure Analysis & Environmental Epidemiology 8, no. 1 (January–March 1998):65-78.

ornl

ORNL/TM-10423

OAK RIDGE NATIONAL LABORATORY

MARTIN MARIETTA

Technical Options for Protecting Civilians from Toxic Vapors and Gases

C. V. Chester

Date Published - May 1988

Prepared for
Office of Program Manager
for
CHEMICAL MUNITIONS
Aberdeen Proving Grounds, Maryland

OPERATED BY
MARTIN MARIETTA ENERGY SYSTEMS, INC.
FOR THE UNITED STATES
DEPARTMENT OF ENERGY

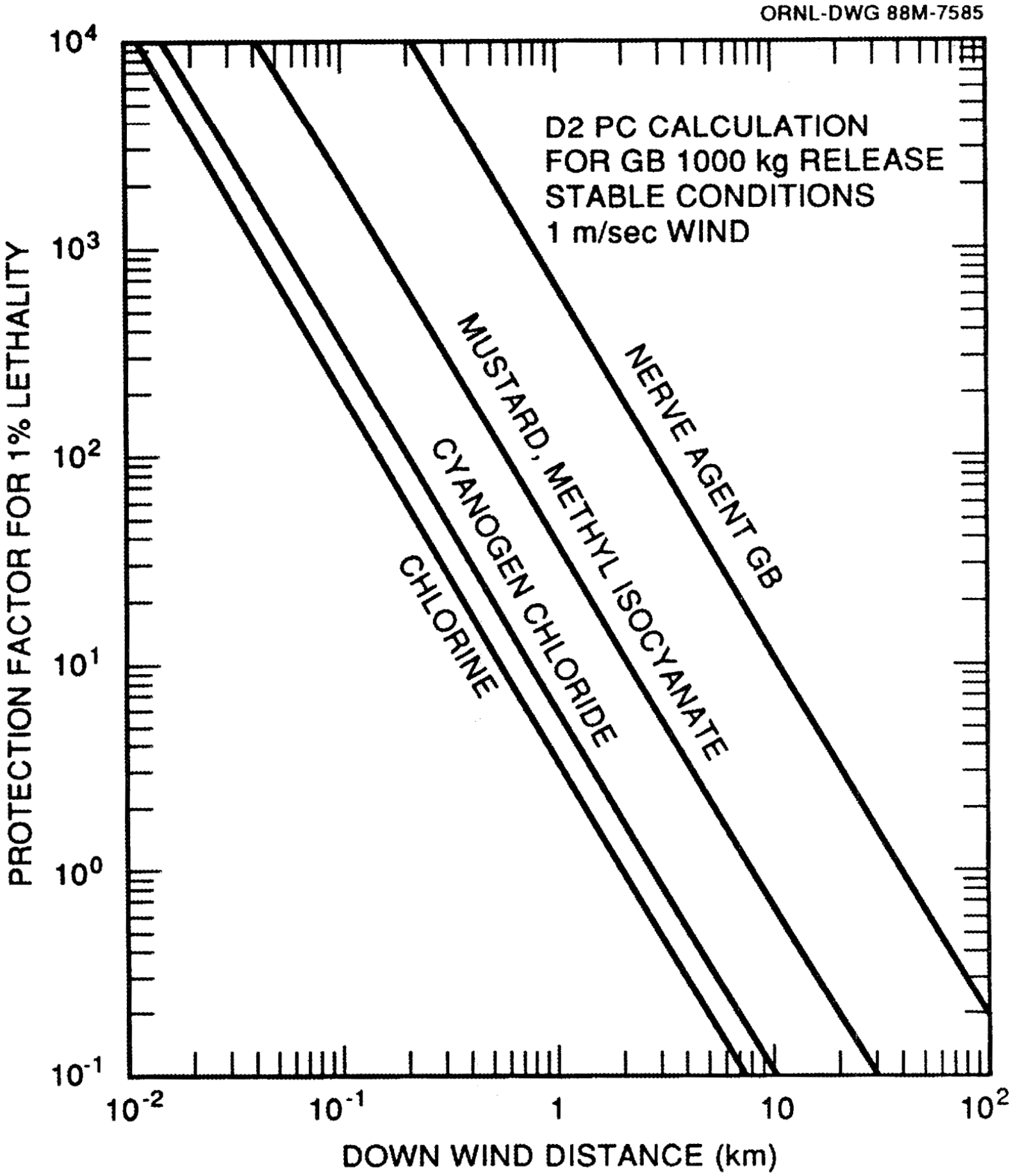

Fig. 1 Dose vs Downwind Distance for Some Very Toxic Gases

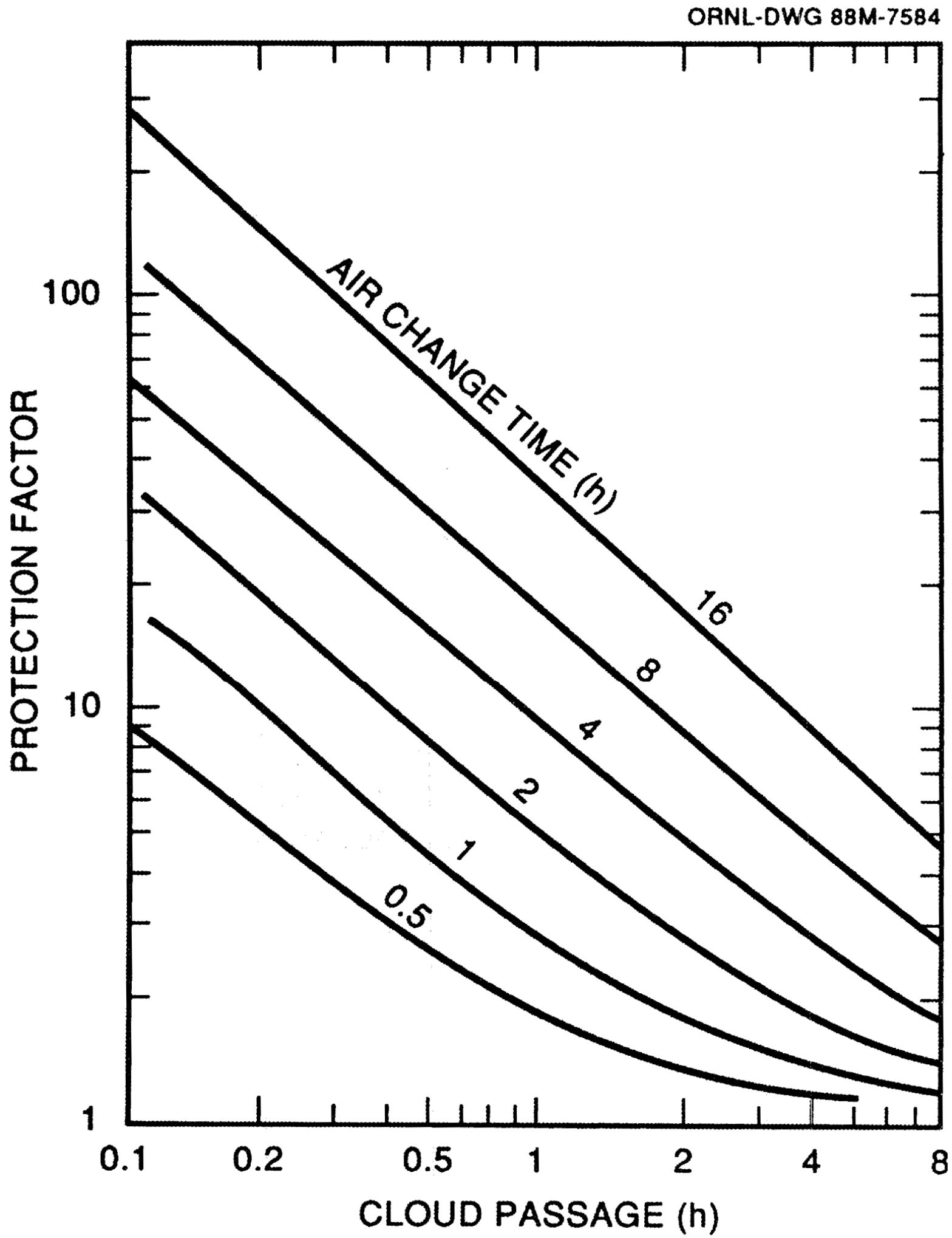

Fig. 2 Protection Factor of Leaky Enclosures

ORNL-DWG 88M-7581

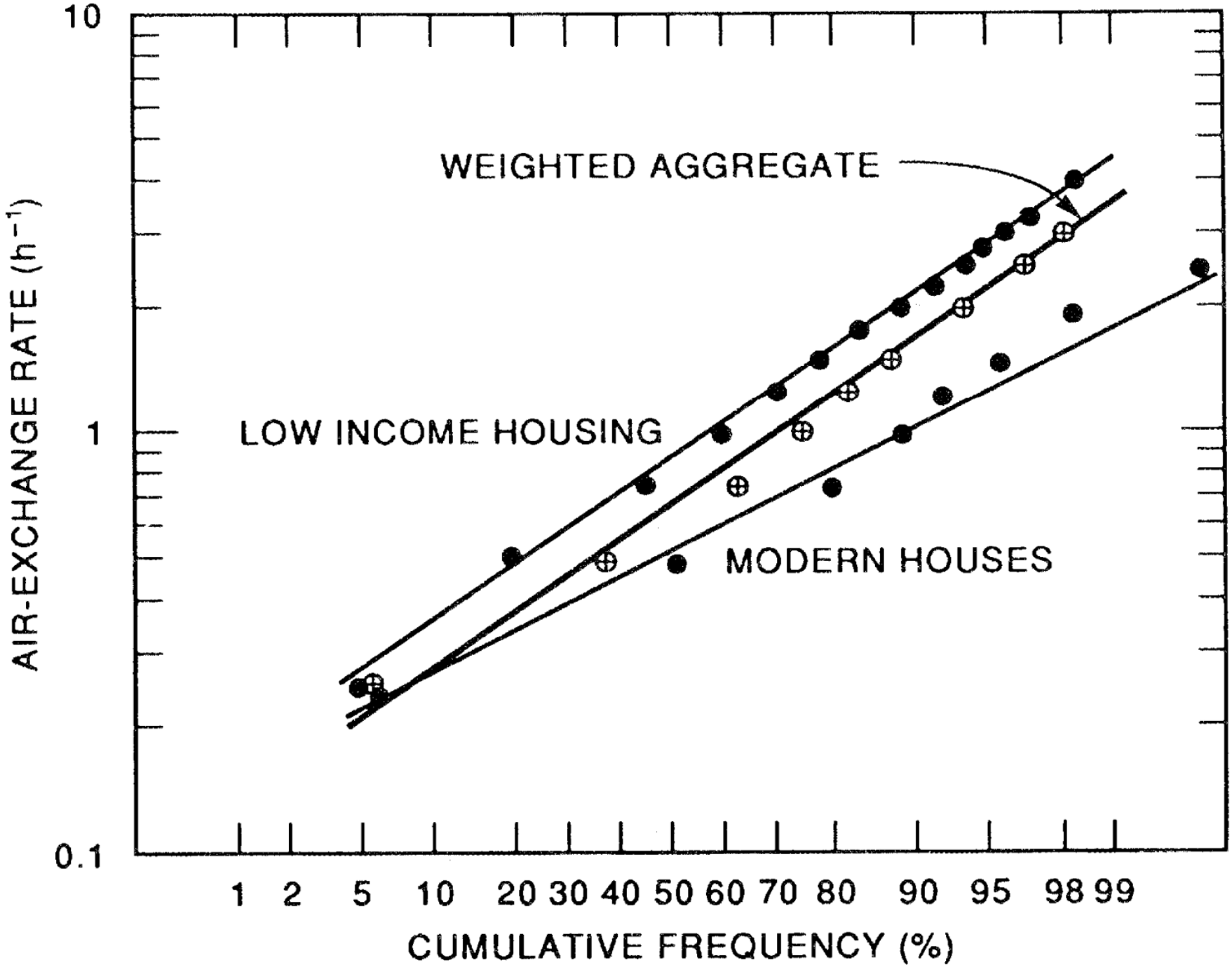

Fig. 3 Infiltration Rates of American Residences

ORNL/TM-2001/154

Energy Division

Will Duct Tape and Plastic Really Work? Issues Related To Expedient Shelter-In-Place

John H. Sorensen
Barbara M. Vogt

Date Published—August 2001

Prepared for the
Federal Emergency Management Agency
Chemical Stockpile Emergency Preparedness Program

Prepared by
OAK RIDGE NATIONAL LABORATORY
Oak Ridge, Tennessee 37831-6285
managed by
UT-BATTELLE, LLC
for the
U.S. DEPARTMENT OF ENERGY
under contract DE-AC05-00OR22725

Although vapors, aerosols, and liquids cannot permeate glass windows or door panes, the amount of possible air filtration through the seals of the panes into frames could be significant, especially if frames are wood or other substance subject to expansion and contraction. To adequately seal the frames with tape could be difficult or impractical. For this reason, it has been suggested that pieces of heavy plastic sheeting larger than the window be used to cover the entire window, including the inside framing, and sealed in place with duct or other appropriate adhesive tape applied to the surrounding wall.

Another possible strategy would be to use shrink-wrap plastic often used in weatherization efforts in older houses. Shrink-wrap commonly comes in a 6 mil (0.006-in.) thickness and is adhered around the frame with double-faced tape and then heated with a hair dryer to achieve a tight fit. This would likely be more expensive than plastic sheeting and would require greater time and effort to install. Because double-faced tape has not been challenged with chemical warfare agents, another option is to use duct tape to adhere shrink-wrap to the walls. Currently, we do not recommend using shrink-wrap plastics because of the lack of information on its suitability and performance.

3. WHY WERE THESE MATERIALS CHOSEN?

Duct tape and plastic sheeting (polyethylene) were chosen because of their ability to effectively reduce infiltration and for their resistance to permeation from chemical warfare agents.

3.1 DUCT TAPE PERMEABILITY

Work on the effectiveness of expedient protection against chemical warfare agent simulants was conducted as part of a study on chemical protective clothing materials (Pal et al. 1993). Materials included a variety of chemical resistant fabrics and duct tape of 10 mil (0.01-in.) thickness. The materials were subject to liquid challenges by the simulants DIMP (a GB simulant), DMMP (a VX simulant), MAL (an organoposphorous pesticide), and DBS (a mustard simulant). The authors note that simulants should behave similarly to live agents in permeating the materials; they also note that this should be confirmed with the unitary agents. The study concluded that “duct tape exhibits reasonable resistance to permeation by the 4 simulants, although its resistance to DIMP (210 min) and DMMP (210 min) is not as good as its resistance to MAL (>24 h) and DBS (> 7 h). Due to its wide availability, duct tape appears to be a useful expedient material to provide at least a temporary seal against permeation by the agents” (Pal et al. 1993, p. 140).

3.2 PLASTIC SHEETING PERMEABILITY

Tests of the permeability of plastic sheeting (polyethylene) challenged with live chemical warfare agents were conducted at the Chemical Defense Establishment in Porton Down, England in 1970 (NATO 1983, p. 133). Agents tested included H and VX, but not GB. Four types of polyethylene of varying thickness were tested: 2.5, 4, 10 and 20 mil (0.0025, 0.004 in., 0.01 in., and 0.02 in.). The results of these tests are shown in Table 1.

Table 1: Permeability of plastic sheeting to liquid agent

	Breakthrough time (h)	
Thickness	VX	H
0.0025	3	0.3
0.004	7	0.4
0.01	30	2
0.02	48	7

Source: NATO 1983, p. 136.

The data shows that at thickness of 10 mil or greater, the plastic sheeting provided a good barrier for withstanding liquid agent challenges, offering better protection against VX than for H. Because the greatest challenge is from a liquid agent, the time to permeate the sheeting will be longer for aerosols and still longer for vapors, but the exact relationship is unknown due to a lack of test data.

NATO Civil Defense Committee 1983. *NATO Handbook on Standards and Rules for the Protection of the Civil Population Against Chemical Toxic Agents*, AC/23-D/680, 2nd rev.

Pal, T., G.Griffin, G. Miller, A. Watson, M. Doherty, and T. Vo-Dinh. 1993. "Permeation Measurements of Chemical Agent Simulants Through Protective Clothing Materials," *J. Haz. Mat.* **33**:123-141.

THE PROTECTION OF THE PUBLIC FROM AERIAL ATTACK

Being

A CRITICAL EXAMINATION OF THE RECOMMENDATIONS PUT FORWARD BY THE AIR RAID PRECAUTIONS DEPARTMENT OF THE HOME OFFICE

by

THE CAMBRIDGE SCIENTISTS' ANTI-WAR GROUP

First published February 12th 1937
Second impression February 12th 1937

LONDON
VICTOR GOLLANCZ LTD
1937

the time taken for the gas to leak out to half its original value was measured in four rooms—the basement of a shop, the dining-room of a semi-detached house, the sitting-room of a Council house and the bathroom of a modern villa. As stated above the leakage half-times for these rooms were $2\frac{1}{2}$, $2\frac{1}{2}$, $3\frac{1}{2}$ and $9\frac{1}{4}$ hours respectively. The reason for the last room being so much better than all the others is that it has steel-frame windows which were sealed with plasticine, painted and tiled walls, and a concrete floor covered with cork tiles.

Note: even a 1 mile wide gas cloud passes in 6 min in 10 miles/hr wind (hence good protection) 41 This property of drifting with the wind is of some importance, for it means that the gas will not remain for long periods in any one place except on still days.

Now it may be objected that, although the "gas-proof" room is not hermetically sealed, it will nevertheless protect the occupants for the two or three hours necessary in case of an attack by a choking gas.

We assume that the gas blows away so quickly that every 10 minutes its concentration is halved. In Engelhard's experiments it took 10 minutes to liberate the gas from its cylinders, so that this assumption is reasonable. Then a person occupying a good "gas-proof" room, the leakage half-time of which (defined on p. 18) is 3 hours, would have breathed a lethal dose of phosgene in 2 hours.

Gas-schutz und Luftschutz, *4*, 174, 1934

Complete lies: bombs are dropped, not cylinders. Engelhard's 1934 article in the Nazi controlled "Gas protection and air protection" journal is enemy propaganda; the Nazis kept the facts secret

As, however, our experiments on the "gas-proof" room illustrate quite clearly that the ordinary dwelling-house is quite incapable of affording protection, it probably will not matter much what a civil population does under a gas and incendiary attack. Nor is it profitable to argue whether the gas or incendiary bomb is the more devastating, as it is necessary to contemplate an air attack in which both will be employed, with a sprinkling of high explosive bombs, which will considerably heighten the "psychological effect." This is the type of attack which people in large towns must expect if war breaks out; our task in this section is to discuss the proposals of the Home Office for dealing with incendiary bombs, remembering that whoever deals with them will require, almost certainly, simultaneous protection against gas. PROVED WRONG!

 PROPAGANDA

extreme lightness and cheapness of the incendiary bomb must be borne in mind. Mr. Noel-Baker cites the case of a single aeroplane carrying a load of less than a ton of bombs which succeeded in starting three hundred fires, and if we take a specimen raid of nine bombers, each carrying a thousand "kilo" bombs, nine thousand of these could be dropped on an area of two square miles. If very generous allowances are made for failures to function and for bombs falling on non-inflammable sites, in an urban area one fifth at least of these bombs should cause fires. This makes one thousand eight hundred fires. The danger of fire spreading over several blocks of buildings as in the San Francisco (1906) and Tokyo (1933) earthquakes, making the centre of the conflagration quite unapproachable by fire brigades is obvious.

To summarise this section, we reach the conclusion:

(*a*) That for individuals the cost of making buildings impenetrable to incendiary bombs is prohibitive.

(*b*) That, bearing in mind the probability of combined incendiary and gas attack, the civilian population will have considerable difficulty in extinguishing fires caused by incendiary bombs in private houses, unless assisted by experts. ← WRONG!

(*c*) That the fires caused by a raid such as is outlined above would very likely be impossible to deal with, even with the improved fire brigade organisation envisaged by the Home Office, because of the probable amalgamation of separate outbreaks into a vast conflagration.

FM 3-10

DEPARTMENT OF THE ARMY FIELD MANUAL

CHEMICAL AND BIOLOGICAL WEAPONS EMPLOYMENT

HEADQUARTERS, DEPARTMENT OF THE ARMY
FEBRUARY 1962

Line	1 Munition	2 Agent	3 Delivery system	4 User	5 Employment data (a) Range (1) (Meters) (2) Maximum	(a) Minimum	(b) Error	(c) Fuze (Capability)
1	Shell, M2A1	HD	4.2-inch Mortar	US ARMY USMC	3,930	180	←Obtain from delivery unit or appropriate firing tables→	M8PD
2	Shell, M360	GB	105-mm Howitzer, M2A1, M2A2, M4, M4A2, M52.	US ARMY USMC	11,140	862		M508PD
3	Shell, M60	HD	105-mm Howitzer, M2A1, M2A2, M4, M4A2, M52.	US ARMY USMC	11,140			M51A5PD
4	Shell, M121	GB	155-mm Howitzer, M1, M1A1, M44.	US ARMY USMC	14,950			M508PD
5	Shell, M110	HD	155-mm Howitzer, M1, M1A1, M44.	US ARMY USMC	14,950			M51A5PD
6	Shell, T__(M121)	VX	155-mm Howitzer, M1, M1A1, M44.	US ARMY USMC	14,950			T76E6VT [1]
7	Shell, M122	GB	155-mm Gun, M2, M53	USMC	23,500			M508PD
8	Shell, M104	HD	155-mm Gun, M2, M53	USMC				M51A5PD
9	Shell, Gas, 175-mm	GB	M107 Gun (SP)	US ARMY	31,500	180		
10	Shell, Gas, 175-mm	VX	M107 Gun (SP)	US ARMY	31,500	180		VT-M514A1
11	Shell, T174	GB	8-inch Howitzer, M2, M2A1, M55.	US ARMY USMC	16,930			M51A5PD
12	Shell, T174	VX	8-inch Howitzer, M2, M2A1, M55.	US ARMY USMC.	16,930			T2061VT
13	Rocket, M55, 115-mm (BOLT)	GB	Launcher, M91	US ARMY USMC.	10,970	2,740		M417PD
14	Rocket, M55, 115-mm (BOLT)	VX	Launcher, M91	US ARMY USMC.	10,970	2,740		T2061VT
15	Warhead, M79, 762-mm (HONEST JOHN).	GB	Rocket, M31A1C Launcher, M386.	US ARMY USMC.	24,960	8,500		T2075 Mech Time
16	Warhead, E19R2, 762-mm (HONEST JOHN).	GB	Rocket, XM50 Launcher, M386.	US ARMY USMC.	33,830	8,500		T2075 Mech Time
17	Warhead, E19R2, 762-mm (HONEST JOHN).	VX	Rocket, XM50 Launcher, M386.	US ARMY USMC.	33,830	8,500		T2075 Mech Time
18	Warhead, E20, 318-mm (LITTLE JOHN).	GB	Rocket, XM51 Launcher, XM80.	US ARMY USMC.	18,290	3,200 [1]		T2075 Mech Time
19	Warhead, E21, (SERGEANT)	GB	Rocket, Launcher	US ARMY	139 km	50 km	304m	Preset Radar
20	Warhead, E21, (SERGEANT)	VX	Rocket, Launcher	US ARMY	139 km	50 km	304m	Preset Radar
21	Bomb, M34A1, 1000-lb, Cluster	GB	Fighter, Bomber	USAF	Range of Aircraft.		←Obtain from delivery unit→	M152E3 Mech Time
22	Bomb, MC-1, 750-lb	GB	Fighter, Bomber	USAF	Range of Aircraft.			M905BD
23	Projectile, 5"/38, MK53, MOD O.	GB	5-inch Gun	US NAVY	16,450			MK29MOD3PD
24	Projectile, 5"/54, MK54, MOD O.	GB	5-inch Gun	US NAVY	19,200			MK30MOD3PD
25	Warhead, Rocket, 5" MK40, MOD O.	GB	Launcher, MK 105 Rocket, M40, MOD O.	US NAVY	4,200			MK30MOD3PD
26	Warhead, Rocket, 5", MK40, MOD O.	HD	Launcher, MK 105 Rocket, M40, MOD O.	US NAVY	4,200			MK30MOD3PD
27	Bomb, MK94, MOD O	GB	Fighter, Bomber	US NAVY	Range of Aircraft.			AN-M103A1ND M195 BD (IMPACT).
28	Bomb, M70A1	HD	Fighter, Bomber	US NAVY	Range of Aircraft.			AN-M158ND (IMPACT).
29	Mine, Land, Chemical, M23	VX	N/A	US ARMY	N/A	N/A	N/A	
30	Mine, Land, Chemical, One-Gallon.	HD	N/A	US ARMY	N/A	N/A	N/A	

See notes at end of figure.

Figure 5. Chemical munitions and delivery systems.

5 Employment data—Continued						6 Functioning and physical characteristics of CML munitions				
(d)		(e)	(f)	(g)	(h)	(a)	(b)	(c)	(d)	(e)
Time for delivery										
(1) Preplanned	(2) Target of opportunity	Organization	Rate of fire per weapon	Height of burst	Diameter (meters) of impact area (single rd) [2]	Weight of munition (kg)	Weight of agent (kg)	Effective weight of agent (kg) [3]	Functioning efficiency of munition (percent)	Agent dissemination efficiency
----------	----------	6 Mort/Plt	30 Rds/2 min	GND	16	10.8	2.72	----------	99	
		8 Mort/Btry	105 Rds/15 min							
----------	1–3 min	6 How/Btry	6 Rds/½ min	GND	27	16.1	.739	----------	99	
			18 Rds/4 min							
----------	1–3 min	6 How/Btry	6 Rds/½ min	GND	11	15.2	1.22	----------	99	
			18 Rds/4 min							
----------	1–5 min	6 How/Btry	3 Rds/½ min	GND	49	45.9	2.95	----------	99	
			12 Rds/4 min							
----------	1–5 min	6 How/Btry	3 Rds/½ min	GND	20	42.0	4.4	----------	99	
			12 Rds/4 min							
----------	1–5 min	6 How/Btry	3 Rds/½ min	20m [1]	----------	45.9	2.95	----------	99	
			12 Rds/4 min							
----------	1–5 min	4 Gun/Btry	2 Rds/½ min	GND	49	45.9	2.95	----------	99	
			8 Rds/4 min							
----------	1–5 min	4 Gun/Btry	2 Rds/½ min	GND	22	43.0	5.31	----------	----------	
			8 Rds/4 min							
		4 Gun/Btry	----------	GND	----------	66.8	6.68	----------	----------	
----------	----------	4 Gun/Btry	----------	GND	----------	66.8	6.04	----------	----------	
----------	½–6 hr	4 How/Btry	6 Rds/4 min	GND	76	97.0	7.12	----------	99	
			10 Rds/10 min							
----------	½–6 hr	4 How/Btry	6 Rds/4 min	20m [1]	----------	97.0	7.12	----------	99	
			10 Rds/10 min.							
----------	30 min	36 Lchr/Bn	45 Rkt/Lchr/15 sec.	GND	46	26.4	4.80	----------	99	
----------	30 min	36 Lchr/Bn	45 Rkt/Lchr/15 sec.	20m [1]	----------	26.2	4.54	----------	99	
----------	15 min	2 Lchr/Bn	2/Hr	Variable	Variable	737	177.5	104.8	95	62 percent.
----------	15 min	2 Lchr/Btry	2/Hr	Variable	Variable	568	210	171	95	86 percent.
----------	15 min	2 Lchr/Btry	2/Hr	Variable	Variable	568	210			
----------	15 min	4 Lchr/Btry	2/Hr	Variable	Variable	119	30			
15 min	120 min	4 Lchr/Bn	2/Day	Intervals of 1,524m.	Variable	744	190			
15 min	120 min	4 Lchr/Bn	2/Day	Intervals of 1,524m.	Variable	744	190			
----------	15 min +flight time.	----------	2–6/Ftr	Variable	170	513	89.6	----------	90	
			4–18/Bmbr.							
----------	15 min +flight time.	----------	2–6/Ftr	GND	127	322	99.9			
			4–27/Bmbr.							
----------	----------	----------	----------	GND	35	25.1	1.47			
----------	----------	----------	----------	GND	40	29.1	2.02			
----------	----------	----------	48 Rkt/Lchr/	GND	49	22.9	2.18			
			1 min							
----------	----------	----------	48 Rkt/Lchr/	GND	----------	----------	----------			
			1 min							
----------	----------	----------	----------	GND	90	222	49.8			
----------	----------	----------	----------	GND	29	58.0	272			
----------	----------	----------	----------	----------	----------	10.50	5.23			
----------	----------	----------	----------	----------	----------	5.45	4.50			

[1] Estimated.

[2] Instantaneous agent area coverage 30 seconds after detonation.

[3] Values are the product of values given in columns 6(*b*), 6(*d*), and 6(*e*). Since values for 6(*e*) are not available, values for 6 (*c*)cannot be computed at this time.

Figure 5.—Continued

Agent—GB.
Wind speed—5 knots (approx 9 km/hr).
Temperature gradient—inversion.
Temperature—60° F. (15.5° C.).
Terrain—open, level, scattered vegetation.
Precipitation—none.
Time limitations on the delivery of agent on target—4 minutes or less.
Casualty level desired—20 percent.

Find: Whether or not the mission can be fired with a 105-mm howitzer battery.

Solution:

(*a*) Using figure 11, convert 20 percent casualties among protected personnel to the corresponding casualty level among unprotected personnel. This is 80 percent.

(*b*) Using the "GB (over 30-sec attack)" column of figure 12, determine the total effects components to be 3.21 as follows:

Inversion	1.09
Wind speed, 9 km/hr	1.00
Temperature, 60° F. (15.5° C.)	.12
Open terrain	.30
No precipitation	.70
	3.21

(*c*) Using figure 13, place a hairline between 80 percent on the percent casualties scale and 12 hectares on the target area scale. On the point of intersection on the reference line, pivot the hairline until it intersects 3.21 on the effects components scale. On the munitions expenditure scale, read 12 as the number of 155-mm equivalents required.

(*d*) To find the number of 105-mm rounds required to fire the mission, multiply 12 by a factor of four (obtain this factor from figure 8); the product is 48 rounds.

(*e*) From figure 9, it is evident that one battery of six howitzers can easily fire the mission if no shift of fires is required. Since the target is twice as large as the dispersion pattern of a 105-mm battery (par. 31*c*(3)(*c*) and 41*d*), a shift of fires should be made. Figure 9 gives a time of 30 seconds for shifting of fires. On this basis the battery could fire twenty-four rounds on half the target in a little less than 30 seconds, take 30 seconds to shift fires, and have ample time to deliver the remaining twenty-four rounds on the other half of the target. The firing should be completed in less than 2 minutes.

Munition	Munition expressed in terms of 155-mm chemical equivalents		
	GB	VX	HD
155-mm Shell	1	1	1
105-mm Shell	0. 25	--------	0. 28
8-inch Shell	2. 40	2. 17	--------
4.2-inch Mortar Shell	--------	--------	. 62
175-mm Shell	2. 1	2. 1	--------
M55 Rocket	1. 6	1. 6	--------
M79 Warhead—HONEST JOHN	60	--------	--------
E19R2 Warhead—HONEST JOHN	71	71	--------
LITTLE JOHN	10	10	--------
SERGEANT	65	65	--------
M34A1 1000-lb Cluster	30	--------	--------
MC1 750-lb Bomb	35	--------	--------
5″/38 Gas Projectile (Navy)	. 50	--------	--------
5″/54 Gas Projectile (Navy)	. 68	--------	--------
5″ Gas Rocket (Navy)	. 74	--------	--------
500-lb Gas Bomb	17	--------	--------
115-lb Gas Bomb (Navy)	--------	--------	6. 2

Figure 7. Munitions expressed in terms of 155-mm chemical equivalents. (The figures given are an estimate of the number of 155-mm howitzer rounds required to give the same effect as one round of the specified munition. Dissemination efficiency has not been considered.)

Munition	Conversion factor		
	GB	VX	HD
155-mm Shell	1	1	1
105-mm Shell	4	--------	3. 6
8-inch Shell	0. 41	0. 45	--------
4.2-inch Mortar Shell	--------	--------	1. 61
175-mm Shell	. 48	. 48	--------
M55 Rocket	. 61	. 61	--------
M79 Warhead—HONEST JOHN	. 017	--------	--------
E19R2 Warhead—HONEST JOHN	. 014	. 014	--------
LITTLE JOHN	. 098	. 098	--------
SERGEANT	. 016	. 016	--------
M34A1 1000-lb Cluster	. 033	--------	--------
MC1 750-lb Bomb	. 029	--------	--------
5″/38 Gas Projectile (Navy)	2. 00	--------	--------
5″/54 Gas Projectile (Navy)	1. 46	--------	--------
5″ Gas Rocket (Navy)	1. 35	--------	--------
500-lb Gas Bomb	. 059	--------	--------
115-lb Gas Bomb (Navy)	--------	--------	. 164

Figure 8. Conversion factors for converting 155-mm munitions to other munitions.

Weapon	Maximum rate (rounds)	Rates of fire for chemical fire missions without shifting or relaying of the piece (rounds)					Estimated time to shift fires
	30 sec	1 min	2 min	4 min	10 min	15 min	
105-mm Howitzer	6	10	14	18	40	60	30 sec
155-mm Howitzer	3	5	7	12	30	40	30 sec
155-mm Gun	2	4	6	8	12	18	60 sec
8-inch Howitzer	1	2	3	6	10	15	60 sec
4.2-inch Mortar	10	16	30 (max)	50	80	105	30 sec
M91 Launcher (M55 Rocket)	45 (15 sec)	Launcher must relocate after firing each ripple.					

Figure 9. Approximate rates of fire for division cannon artillery, mortars, and multiple rockets firing chemical rounds. (Rates of fire for other weapons are given in figure 5.)

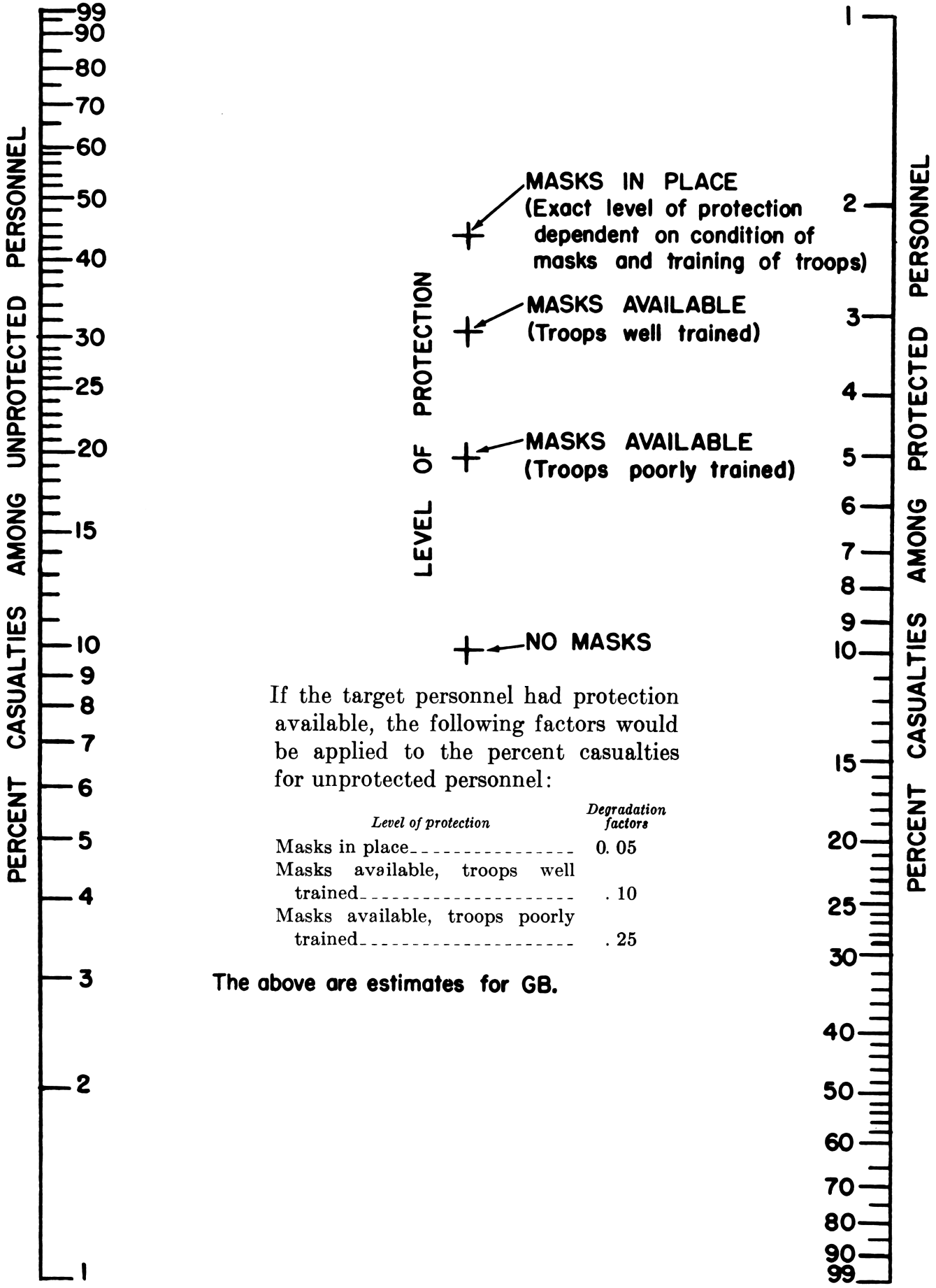

If the target personnel had protection available, the following factors would be applied to the percent casualties for unprotected personnel:

Level of protection	*Degradation factors*
Masks in place	0.05
Masks available, troops well trained	.10
Masks available, troops poorly trained	.25

The above are estimates for GB.

Figure 11. Nomogram for conversion of percent GB casualties for protection of personnel in the target area.

Meteorological and terrain conditions	Effects components			
	GB [2] (surprise attack)	GB (over 30-sec attack)	VX	HD
1. *Temperature Gradient*				
Inversion	0. 67	1. 09	1. 89	0. 69
Neutral	. 57	. 69	1. 89	. 54
Lapse	. 30	. 09	1. 89	. 32
2. *Wind Speed (km/hr)*				
0 to 5	. 20	1. 30	0	. 87
6 to 10	. 50	1. 00	0	. 70
11 to 16	. 70	. 70	0	. 60
17 to 26	. 55	. 30	0	. 48
27 to 52	. 30	0	0	0
3. *Temperature (° F.)*				
a. 0 to 39 (−18° to 4° C.)	0	0	0	----------
40 to 79 (5° to 26° C.)	. 12	. 12	0	----------
80 and up (27° C. and up)	. 23	. 23	0	----------
b. 30 to 49 (−1° to 9° C.)	----------	----------	0	0
50 to 69 (10° to 21° C.)	----------	----------	0	. 70
70 and up (22° C. and up)	----------	----------	0	1. 00
4. *Terrain*				
Open, level, scattered vegetation	. 30	. 30	0	. 30
Rugged, mountainous	0	[1] 0	[1] 0	[1] 0
5. *Precipitation*				
None	. 70	. 70	. 70	0
Moderate rain	0	[1] 0	[1] 0	[1] 0

[1] Estimated.
[2] Tentative figures not yet verified.

Figure 12. Effects components.

Note: paragraph 105 on page 82 states that the "safe entry times" after bio attacks are:

NU (Venezuelan equine encephalitis virus), AB (bovine brucellosis), and UL (tularemia): 2 hrs sun or 8 hrs cloudy
OU (Q fever): 2 hrs sun or 18 hrs cloudy

Cloudy conditions also apply to nighttime

626007 O—62——3

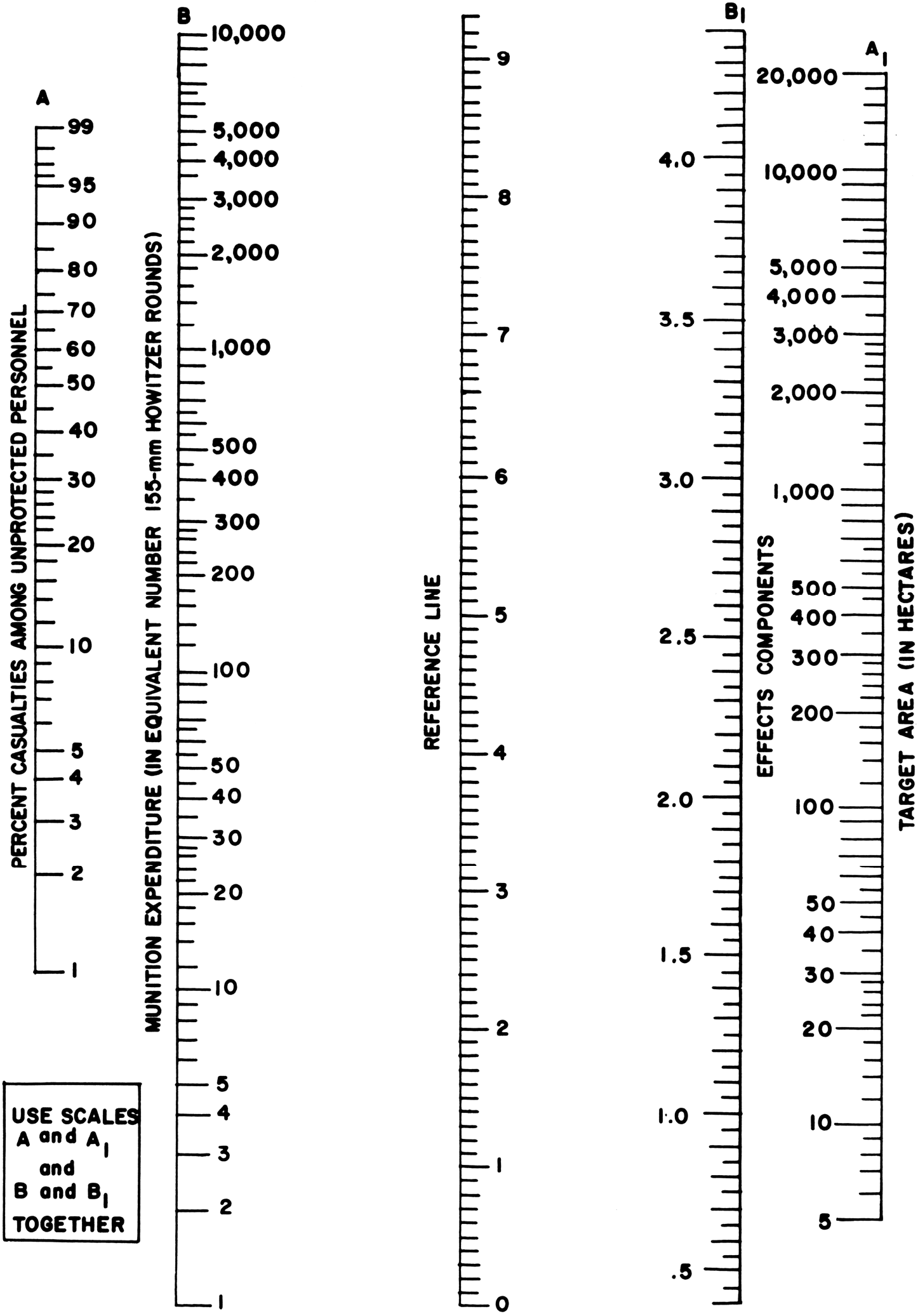

Figure 13. Target area, casualty level, munitions requirement nomogram.

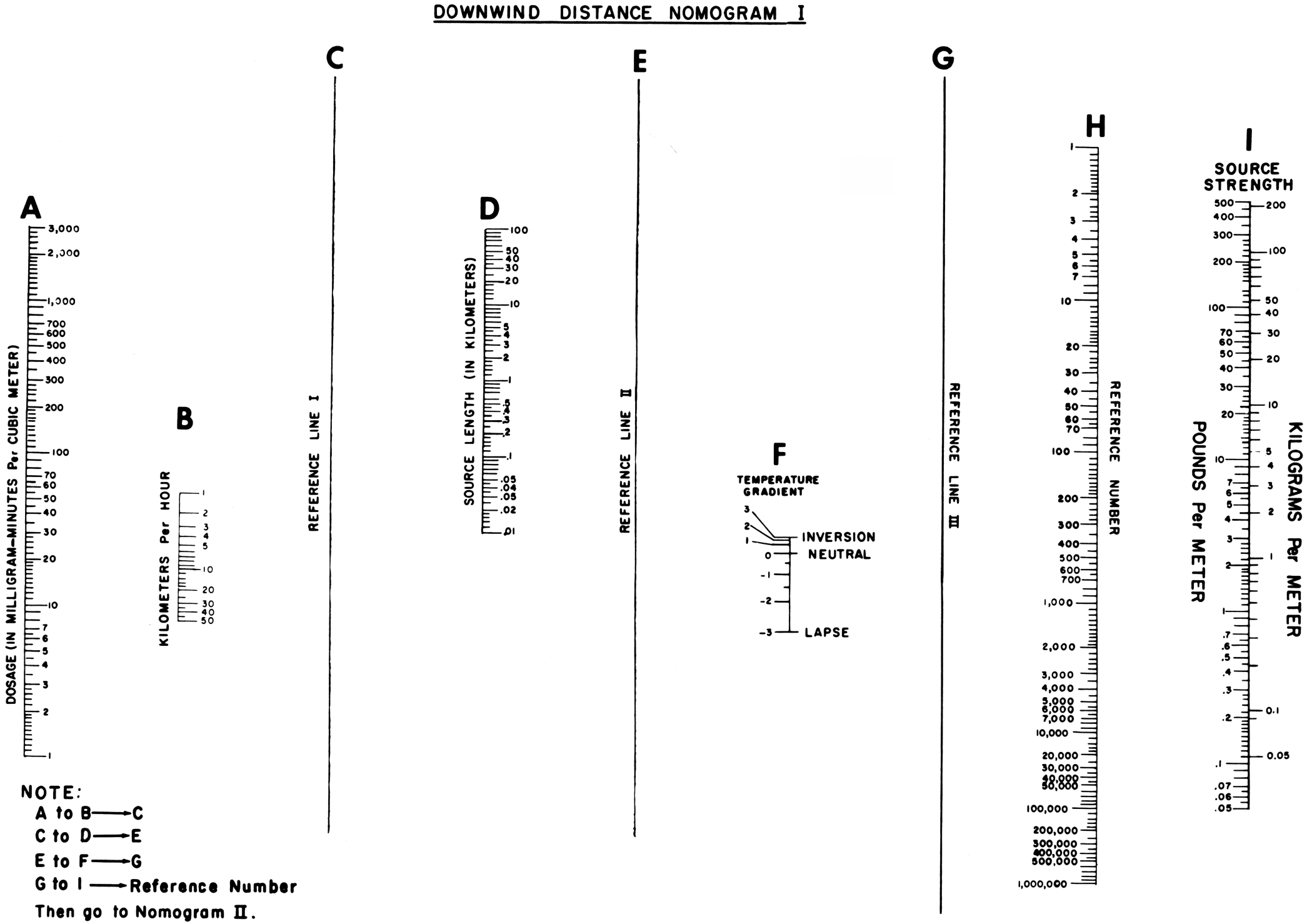

Figure 14. Downwind distance nomogram I.

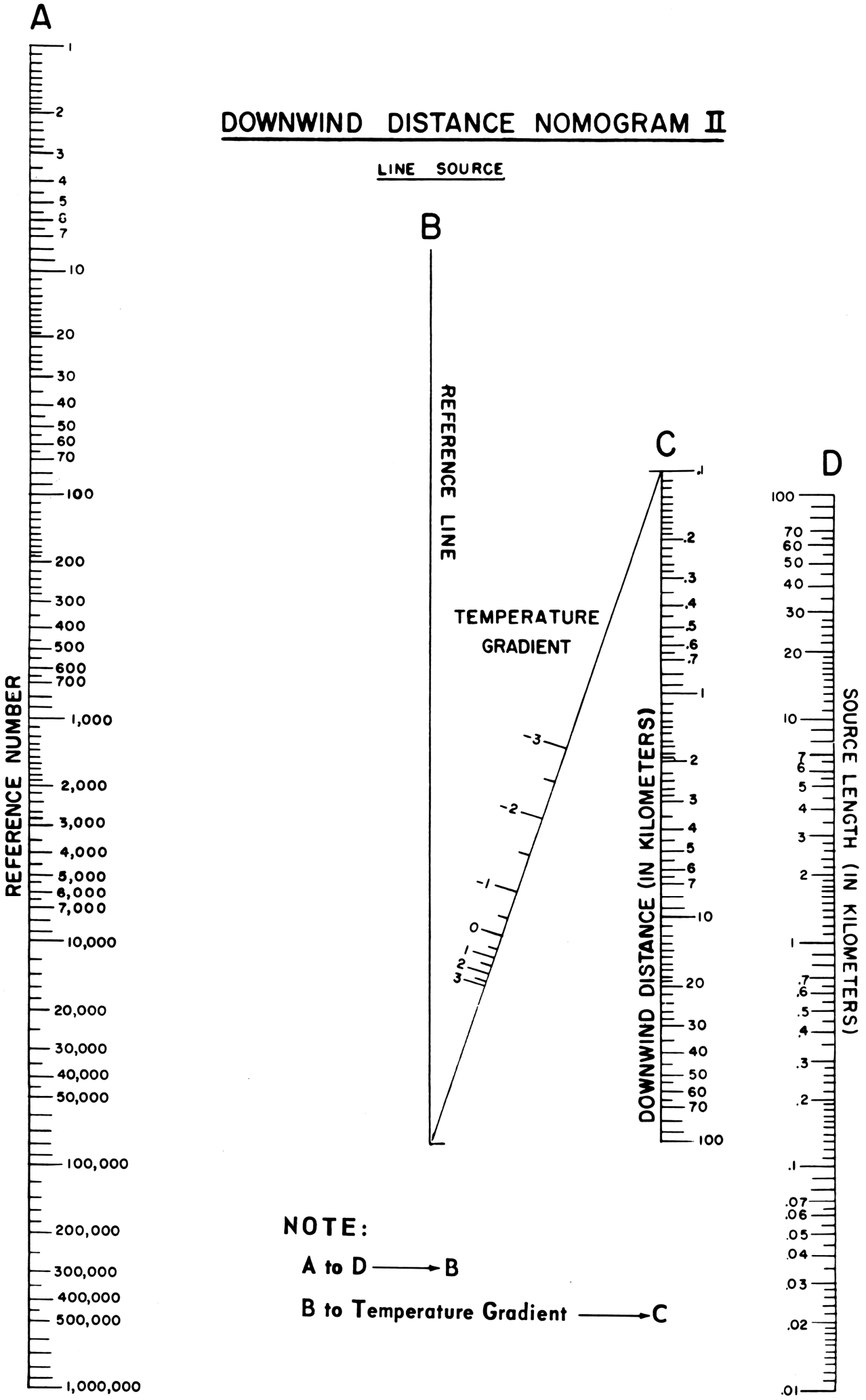

Figure 15. Downwind distance nomogram II.

USACGSC RB 3-1

REFERENCE BOOK

CHEMICAL AND BIOLOGICAL WEAPON EMPLOYMENT

U.S. ARMY COMMAND AND GENERAL STAFF COLLEGE
Fort Leavenworth, Kansas

1 May 1968

This reference book supersedes RB 3-1, 1 May 1967

CHAPTER 2
TOXIC CHEMICAL AGENTS

1. Characteristics and Effects

a. General. The following antipersonnel chemical agents are used for College instruction in chemical weapon employment: nerve agents GB and VX; blister agent HD (mustard); and incapacitating agent BZ. Actual or assumed characteristics of these agents are described in the following paragraphs for instructional purposes only and are summarized in figure 1.

b. Nerve Agent GB. GB is a quick acting, nonpersistent lethal agent that produces casualties primarily by inhalation.

(1) Inhalation effects. Inhaled GB vapor can produce casualties within minutes. As an example, 50 percent of a group of unprotected troops engaged in mild activity, breathing at the rate of about 15 liters per minute, and exposed to 70 milligrams of GB per cubic meter of air for 1 minute will probably die if they do not receive medical treatment in time. This is the median lethal dosage (50) and is expressed as 70 mg-min/m^3. For troops engaged in activities that increase their breathing rate, the median lethal dosage can be as low as 20 mg-min/m^3. The median incapacitating dosage of GB vapor by inhalation is about 35 mg-min/m^3 for troops engaged in mild activity. Incapacitating effects consist of nausea, vomiting, diarrhea, and difficulty with vision, followed by muscular twitching, convulsions, and partial paralysis. Dosages of GB less than the median incapacitating dosage cause general lowering of efficiency, slower reactions, mental confusion, irritability, severe headache, lack of coordination, and dimness of vision due to pinpointing of the eye pupils.

(2) Percutaneous effects. Percutaneous effects refer to those effects produced by the absorption of the agent through the skin. GB vapor absorbed through the skin can produce incapacitating effects. Sufficient GB liquid absorbed through the skin can produce incapacitation or death. The effectiveness of the liquid or vapor depends on the amount absorbed by the body. Absorption varies with the original amount of agent contamination, the skin area exposed and the exposure time, the amount and kind of clothing worn, and the rapidity in removing the contamination and/or contaminated clothing and in decontaminating affected areas of the skin.

(3) Major considerations in the employment of nerve agent GB. The employment of GB is based primarily on achieving casualties by inhalation of the nonpersistent vapor (or aerosol) of the agent. Major considerations in the employment of this agent are:

(a) Time to incapacitate. The onset of incapacitation resulting from inhalation of casualty-producing doses is rapid, the average time being approximately 3 minutes. To allow for the time required for the agent cloud to reach the individual, 10 minutes is used as the mean time to achieve incapacitation. Nonlethal casualties from GB will be incapacitated for 1 to 5 days.

(b) Persistency. Persistency is defined as the length of time an agent remains effective in the target area after dissemination. Nerve agent GB is considered nonpersistent. GB clouds capable of producing significant casualties will dissipate within minutes after dissemination. Some liquid GB will remain in chemical shell or bomb craters for periods of time varying from hours to days, depending on the weather conditions and type of munition. Because of this continuing but not readily discernible threat, GB can also be highly effective in harassing roles by causing exposure to low concentrations of the vapor. Rounds fired sporadically may compel the enemy to wear protective masks and clothing for prolonged periods, thereby impairing his effectiveness as a result of fatigue, heat stress, discomfort, and decrease in perception.

(c) Level of protection. The weapon system requirements for positive neutralization of masked personnel by GB are too great to be supported except for important point or small area targets. A major factor affecting casualties resulting from GB attacks of personnel equipped with masks but unmasked at the time of attack is the time required for enemy troops to mask after first detecting a chemical attack. Therefore, surprise dosage attack is used to establish a dosage sufficient to produce the desired casualties before troops can mask. Casualty levels for surprise dosage attack that are tabulated in the weapon system effects tables (app A) are based on an assumed enemy masking time of 30 seconds. (Refer to FM 3-10 series manuals for operational data for masking times less than 30 seconds.) A total dosage attack is used to build up the dosage over an extended period of time and is normally employed against troops who have no protective masks available. Dosages built up before troops can mask inside foxholes, bunkers, tanks, buildings, and similar structures will generally be less than dosages attained during the same period of time in the open, thereby reducing the effects on occupants from surprise dosage attacks. Total dosage effects are essentially the same inside or outside.

c. Nerve Agent VX. VX is a slow-acting, lethal, persistent agent that produces casualties primarily by absorption of droplets through the skin.

(1) Effects. VX acts on the nerve systems of man; interferes with breathing; and causes convulsions, paralysis, and death.

(2) Major considerations in the employment of nerve agent VX.

(a) General. Agent VX disseminated in droplet (liquid) form provides maximum duration of effectiveness as a lethal casualty threat. VX will remain effective in the target area for several days to a week depending on weather conditions. Because of its low volatility, there is no significant vapor hazard downwind of a contaminated area. Except when disseminated by aircraft spray tanks, meteorological conditions have little effect on the employment of VX, although strong winds may influence the distribution of the agent and heavy rainfall may wash it away or dissipate it.

(b) Employment to cause casualties. Agent VX is appropriate for direct attack of area targets containing masked personnel in the open or in foxholes without overhead protection, for causing severe harassment by the continuing casualty threat of agent droplets on the ground or on equipment, and for creating obstacles to traversing or occupying areas. Casualties produced by agent VX are delayed, occurring at times greater than 1 hour after exposure. Although this agent can be used relatively close to friendly forces, it should not be used on positions that are likely to be occupied by friendly forces within a few days. Because of this continuing hazard, areas in which agent VX has been used should be recorded in a manner similar to minefields or fallout areas so that necessary precautions can be taken.

d. Blister Agent HD. HD, sometimes referred to as mustard, is a persistent slow-acting agent that produces casualties through both its vapor and liquid effects.

(1) Vapor effects.

(a) The initial disabling effect of HD vapor on unmasked troops will be injuries to the eyes. Temporary blindness can be caused by vapor dosages that are insufficient to produce respiratory damage or skin burns. However, skin burns account for most injuries to masked troops. The vapor dosages and the time required to produce casualties (4 to 24 hours) vary with the atmospheric conditions of temperature and humidity and with the amount of moisture on the skin. Depending on their severity, skin burns can limit or entirely prevent movement of the limbs or of the entire body.

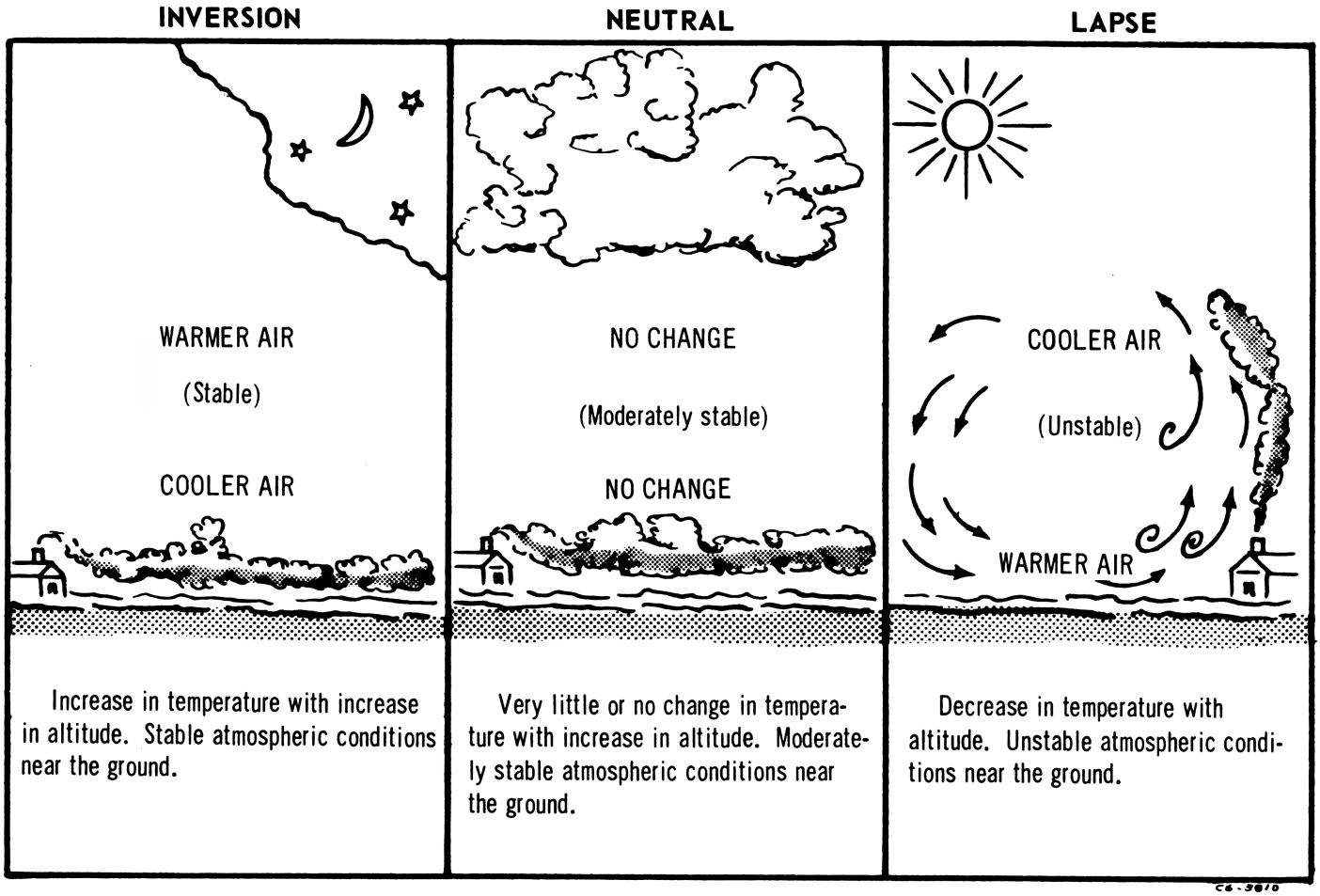

Figure 2. Temperature gradients.

Surprise dosage GB attacks are influenced only slightly by the temperature gradient except when made with the spray tank. Downwind vapor hazards to both enemy and friendly forces will be most significant during inversion and neutral conditions. Employment of VX is not affected by the temperature gradient.

Temperature gradients	Time
1. Inversion	From sunset to sunrise.
2. Neutral	2 hours before sunset to sunset, sunrise to 2 hours after sunrise, or any time windspeed is 15 kmph or greater.
3. Lapse	2 hours after sunrise to 2 hours before sunset.

Figure 3. Estimated times that temperature gradients will prevail. (Use when meteorological data are not available.)

(3) When actual or predicted meteorological conditions are not available for a target analysis, 70° F is used for temperature, 9 kmph is used as windspeed, and the temperature gradient is approximated from figure 3.

d. Windspeed and Direction.

(1) Air moving over the earth's surface sets up eddies, or mechanical turbulences, that act to dissipate a chemical cloud. A condition of calm will limit the merging of the individual gas clouds. Both of these conditions may reduce the effectiveness of a chemical agent attack. High winds increase the rate of evaporation of HD and dissipate chemical clouds more rapidly than low winds. Moderate winds are desirable for chemical employment. Large-area nonpersistent chemical attacks are most effective in winds not exceeding 28 kmph. Small-area nonpersistent chemical attacks with rockets or shell are most effective in winds not exceeding 9 kmph. However, if the concentration of chemical agent can be established quickly, the effects of high windspeed can be partially offset.

CHAPTER 4
EMPLOYMENT OF BIOLOGICAL AGENTS

1. General

a. Antipersonnel biological agents are micro-organisms that produce disease in man. These agents can be used to incapacitate or kill enemy troops through disease. They may cause large numbers of casualties over vast areas and could require the enemy to use many personnel and great quantities of supplies and equipment to treat and handle the casualties. Many square kilometers can be effectively covered from a single aircraft or missile. The search capability of biological agent clouds and the relatively small dose required to cause infection among troops give biological munitions the capability of covering large areas where targets are not precisely located.

b. A biological attack can occur without warning since biological agents can be disseminated by relatively unobtrusive weapon systems functioning at a considerable distance from the target area and relying upon air movement to carry the agent to the target.

c. Biological agents do not produce effects immediately. An incubation period is required from the time the agent enters the body until it produces disease. Some agents produce the desired casualty levels within a few days, whereas others may require more time to produce useful casualty levels. A variety of effects may be produced, varying from incapacitation with few deaths to a high percentage of deaths, depending on the type of agent.

2. Methods of Dissemination

a. The basic method of disseminating antipersonnel biological agents is the generation of aerosols by explosive bomblets and spray devices. Because exposure to sunlight increases the rate at which most biological agent aerosols die and thereby reduces their area coverage, night is the preferable time for most biological attacks. However, if troop safety is a problem, an attack may be made near sunrise to reduce the distance downwind that a hazard to friendly forces will extend. Conversely, to extend the downwind cloud travel and the area coverage from spray attack, a biological agent may be employed soon after sundown.

b. Missile-delivered Biological Munitions. Missile-delivered biological munitions are used for attack of large-area targets. A typical biological missile system consists of the following components:

(1) A missile vehicle and its launching equipment.

(2) A warhead that can be opened at a predetermined height to release biological bomblets over the target area. The warhead is shipped separately for assembly to a missile at the launching site.

(3) A warhead shipping container equipped with a heating-cooling element and a temperature control unit.

(4) Biological bomblets consisting of an agent container and a central burster that functions on impact. The bomblets have vanes that cause them to rotate in flight, thereby achieving lateral dispersion during their free fall and resulting in random distribution as a circular pattern.

c. Aircraft Spray Tank. Biological agents released from an aircraft spray tank cover a large area downwind of the line of release. A typical spray tank consists of the following components:

(1) An agent reservoir section that is shipped separately in an insulated shipping and storage container equipped with a heating-cooling element and a temperature control unit.

(2) A discharge nozzle assembly that can be mechanically adjusted to vary the agent flow rate.

Table 1. Chemical Weapons Data

1	2	3	4	5	6	7	8	9	10	11	12	13
Delivery system	Range (meters)		Agent	Munition	No of weapons per delivery unit	Weapon rate of fire	RT max (meters)[1 2]					Reference (table)
							Fire unit	Total dosage		Surprise dosage		
								Casualty threat		Casualty threat		
	Min	Max						10%	30%	10%	30%	
4.2-in mortar	180	4,500	HD	Cartridge, M2A1	4/Plat	50 rd/3 min 105 rd/15 min						18 19
105-mm howitzer		11,100	GB	Cartridge, M360	6/btry	5 rd/30 sec 30 rd/3 min 66 rd/15 min	1 btry[3]	200	100	100	50	2
							1 bn[3]	300	300	200	100	3
			HD	Cartridge, M60								18 19
155-mm howitzer		14,600	GB	Projectile, M121	6/btry	2 rd/30 sec 12 rd/3 min 24 rd/15 min	1 btry[3]	300	200	100	0	4
							1 bn[3]	500	400	300	100	5
			HD	Projectile, M110								18 19
			VX[4]	Projectile, M121			1 btry[3]	400	200	NA	NA	13
							1 bn[3]	500	400			
8-in howitzer		16,800	GB	Projectile, M426	4/btry	1 rd/30 sec 4 rd/3 min 10 rd/15 min	1 btry[3]	300	200	200	0	6
							1 bn[3]	500	400	300	100	7
			VX[4]				1 btry[3]	400	200	NA	NA	14
							1 bn[3]	500	400			
115-mm multiple rocket launcher, M91	2,740	10,600	GB[4]	Rocket, M55 (THE BOLT)		45 rkt/lchr/15 sec	1 lchr	1,000	750	500	200	8
							3 lchr	1,000	1,000	750	400	
							6 lchr	1,000	1,000	1,000	750	
							9 lchr	1,000	1,000	1,000	1,000	
			VX[4]				1 lchr	300	0	NA	NA	15
							3 lchr	750	300			
							6 lchr	1,000	400			
							9 lchr	1,000	750			
762-mm rocket, Honest John	8,500	38,000	GB[4]	Warhead, M190 (M139 bomblets)	2/btry	2 rkt/lchr/hr	1 lchr	600	600	600	400	9
							2 lchr	600	600	600	400	
Sergeant missile	46,000	139,000	GB[4]	Warhead, M212 (M139 bomblets)	2/bn	2 msl/lchr/hr	1 msl	600	400	600	200	10
							2 msl	600	600	600	400	
Aircraft	Dependent on type aircraft		GB[4]	Bomb, MC-1, 750-lb	Dependent on type aircraft		1 bomb	50				11
							6 bombs	300	200	300	50	
							12 bombs	500	300	400	200	
							24 bombs	500	300	500	300	
			GB[4]	Spray tank, 100-gal			1 spray tank	RT max=750 meters (one-half effective spray release line length)				12
							2 spray tanks					
			VX[4]				1 spray tank	RT max=500 meters (one-half effective spray release line length)				16
			BZ[4]	Bomb, 150-lb								17
				Bomb, 700-lb								

[1]RT max is largest target radius for which indicated casualty threat is tabulated for appropriate fire unit. Division of target into subtargets NOT considered.

[2]All windspeeds, temperature gradients, and protection categories considered.

[3]RT max computed for maximum number of volleys for which data are tabulated.

[4]Weapon system capabilities derived from tables composed of hypothetical data for INSTRUCTIONAL PURPOSES ONLY at the U. S. Army Command and General Staff College. For actual data, refer to FM 3-10.

Table 2. Estimated Fractional Casualty Threat From 105-mm Howitzer, GB Projectile, Battery Fire[1 2]

1	2	3	4	5	6	7	8	9	10	11	12	13	14	15
Target radius–radius of effect (meters)	Range to target (km)	No of volleys	Windspeed[3]											
			4 kmph				9 kmph				28 kmph			
			Surprise[4]	Total dose[5]			Surprise[4]	Total dose[5]			Surprise[4]	Total dose[5]		
				I	N	L		I	N	L		I	N	L
50	<7.5	1	.10	.25	.20	.15	.10	.15	.10	.10				
		2	.20	.45	.40	.30	.15	.30	.25	.20		.10	.05	.05
		3	.30	.60	.60	.35	.30	.50	.45	.30	.10	.20	.15	.10
		4	.30	.75	.70	.45	.30	.55	.45	.35	.10	.25	.20	.10
		5	.35	.90	.85	.55	.35	.60	.50	.40	.15	.30	.25	.15
	>7.5	1	.05	.15	.15	.10	.05	.10	.05	.05				
		2	.15	.30	.25	.15	.10	.20	.15	.10		.05	.05	
		3	.15	.30	.30	.25	.10	.20	.20	.15		.10	.05	.05
		4	.20	.40	.35	.25	.15	.30	.30	.15	.05	.15	.15	.05
		5	.25	.45	.45	.30	.25	.40	.35	.25	.10	.20	.20	.10
100	<7.5	1	.05	.15	.15	.10	.05	.10	.05	.05				
		2	.10	.30	.30	.15	.10	.20	.15	.10				
		3	.15	.40	.35	.20	.15	.25	.25	.15	.05	.10	.05	
		4	.15	.40	.35	.30	.15	.30	.30	.15	.05	.10	.10	.05
		5	.20	.45	.40	.35	.20	.35	.35	.20	.10	.15	.15	.10
	≥7.5	1	.05	.10	.10	.05		.05	.05					
		2	.10	.20	.20	.10	.05	.15	.10	.05				
		3	.10	.25	.25	.15	.10	.15	.15	.10		.05	.05	
		4	.10	.30	.25	.20	.10	.25	.20	.15		.10	.05	
		5	.15	.35	.30	.25	.15	.30	.25	.15	.05	.15	.10	.05
200	Any	1		.05	.05									
		2		.10	.10	.05		.05	.05					
		3	.05	.15	.15	.05		.10	.05					
		4	.05	.15	.15	.10		.10	.10					
		5	.05	.20	.20	.10	.05	.15	.10	.05				

[1] Blank spaces indicate fractional casualties are below 0.05.

[2] If the target is predominately wooded, use a windspeed of 4 kmph and neutral temperature gradient for total dose attack; use a windspeed of 4 kmph for surprise attack.

[3] For windspeeds other than those shown, use data given for the nearest windspeed.

[4] Multiply the figures given in the table by the appropriate factor to obtain the fractional casualties from surprise dose attack:

Troops in open foxholes:	0.7
Troops in covered foxholes or bunkers:	0.6

[5] I=inversion, N=neutral, L=lapse.

DECLASSIFIED

N-13260

INDEX NO. X 28-1

MISCELLANEOUS TARGETS

ATOMIC BOMBS, HIROSHIMA AND NAGASAKI

ARTICLE 1

MEDICAL EFFECTS

REGRADED Declassified per
Secy Defense Memo 5 May 72
BY AUTHORITY OF Auth Declassified w/ Secretary
BY Rosie Koppen
ON 13 Jul 76

JUL 18 1952
DEC 21 1965
DECLASSIFIED

U.S. NAVAL TECHNICAL MISSION TO JAPAN

N-1391 DECLASSIFIED

NS/rkk

U.S. NAVAL TECHNICAL MISSION TO JAPAN
CARE OF FLEET POST OFFICE
SAN FRANCISCO, CALIFORNIA

274500

15 December 1945

[redacted]

From: Chief, Naval Technical Mission to Japan.
To : Chief of Naval Operations.

Subject: Target Report - Atomic Bombs, Nagasaki and Hiroshima.

Reference: (a)"Intelligence Targets Japan" (DNI) of 4 Sept. 1945.

1. Article 1 of the report covering Target X-28 of Fascicle X-1 of reference (a), dealing with medical effects, is submitted herewith.

2. The investigation of the target and the target report were accomplished by Comdr. Shields Warren (MC), USNR, assisted by Lt. Comdr. N. Pace (HC), USNR, and Lieut. R.E. Smith (HC), USNR, and with the assistance of Lt. Col. I.M. Sinclair, AUS, Lt.(jg) H.F. Harsberger, USNR, and Lt.(jg) F.G. McKnight, USNR, as interpreters and translators.

C. G. Grimes
C. G. GRIMES
Captain, USN

[redacted]

DECLASSIFIED

FILE
INTELLIGENCE LIBRARY
1 - JUL 1946
MILITARY BRANCH

27 AUG 1946

Reg # 111 2217

DECLASSIFIED

ATOMIC BOMBS, HIROSHIMA AND NAGASAKI

ARTICLE 1

MEDICAL EFFECTS

"INTELLIGENCE TARGETS JAPAN" (DNI) OF 4 SEPT. 1945

FASCICLE X-1, TARGET X-28, ARTICLE 1

DECEMBER 1945

DECLASSIFIED

U.S. NAVAL TECHNICAL MISSION TO JAPAN

DECLASSIFIED

TABLE OF CONTENTS

Summary ..... Page 1
List of Enclosures ..... Page 2
List of Illustrations ..... Page 3
References ..... Page 4
Introduction ..... Page 5
The Report
Part I General Aspects ..... Page 7
A. HIROSHIMA ..... Page 7
B. NAGASAKI ..... Page 29
C. Effects of the Radiations on the Human Body ..... Page 35
Part II Residual Radioactivity ..... Page 43
Part III Other Aspects of the Atomic Bomb ..... Page 46
Part IV Organization of Research in Nuclear Physics in Japan ..... Page 51
Part V Conclusions ..... Page 51
Part VI Recommendations ..... Page 52

LIST OF ENCLOSURES

(A) Map of HIROSHIMA, with Distances from Hypocenter ..... Page 53
(B) List of Military Installations and Their Losses at HIROSHIMA ..... Page 54
(C) Map of NAGASAKI, with Distances from Hypocenter and with Coordinates ..... Page 57
(D) Map of Damage Area, NAGASAKI ..... Page 59
(E) Census of NAGASAKI, 1 November 1945 ..... Page 61
(F) Summary of Damage of Personnel, NAGASAKI ..... Page 63
(G) Schools Covered in Survey of 373 Girls ..... Page 69
(H) Estimates of School Enrollment, NAGASAKI ..... Page 71
(I) Blood Protein Studies ..... Page 73
(J) Radioactivity at NAGASAKI, Center Area ..... Page 74
(K) Radioactivity at NAGASAKI, Center and NISHIYAMA ..... Page 75
(L) Radioactivity in NAGASAKI Area ..... Page 77
(M) Radioactivity in HIROSHIMA Area ..... Page 79

DECLASSIFIED

DECLASSIFIED

LIST OF ILLUSTRATIONS

Figure 1. Map of HIROSHIMA City ..... Page 18
Figure 2. Area of Devastation in Business Section of HIROSHIMA .... Page 19
Figure 3. Typical Scene Looking North Toward Hypocenter - HIROSHIMA ..... Page 20
Figure 4. View Near Hypocenter - HIROSHIMA ..... Page 21
Figure 5. Healing Second Degree Flash Burns Due to Atomic Bomb .... Page 22
Figure 6. Charred Striped Kimono ..... Page 23
Figure 7. "Shadowing" Effect of Wire on Telephone Pole ..... Page 24
Figure 8. "Shadow" of Bridge Post and Railing on Asphalt Roadway .. Page 24
Figure 9. "Shadow" of Leaf on Charred Telephone Pole ..... Page 25
Figure 10. "Shadow" of Man and Cart on Asphalt Roadway ..... Page 25
Figure 11. View of Bombed Area at NAGASAKI ..... Page 30
Figure 12. Severe Epilation of Man's Scalp ..... Page 38
Figure 13. Partial Epilation of Woman's Scalp ..... Page 38
Figure 14. Partial Epilation of Child's Scalp ..... Page 40
Figure 15. View of SHINKOZEN Hospital Room ..... Page 50

* * * * *

Graph 1. Proportion of Casualties - HIROSHIMA ..... Page 16
Graph 2. Proportion of Damage in 4030 Survivors - HIROSHIMA ..... Page 26
Graph 3. Population Density in 2 Km Radius in HIROSHIMA and NAGASAKI ..... Page 28
Graph 4. Proportion of Casualties - NAGASAKI ..... Page 31
Graph 5. Protection Given by Concrete Buildings in NAGASAKI - 2182 Survivors ..... Page 32
Graph 6. Effects in Open - NAGASAKI - 2182 Survivors ..... Page 33
Graph 7. Menstrual Changes Following Atomic Bomb - NAGASAKI ..... Page 39
Graph 8. Effect on Child-Birth - NAGASAKI 9 Aug. to 15 Nov. 1945 ..... Page 41
Graph 9. Mode of Destruction of Wooden Houses - NAGASAKI ..... Page 49

DECLASSIFIED

DECLASSIFIED

REFERENCES

Japanese Personnel Who Assisted With the Research:

ABE, K. - Ministry of Education
ARAKATSU, B. - Kyoto Imperial University
ARAKAWA, H. - Kyushu Imperial University
ARAKI, T. - Kyoto Prefectural Medical School
ASADA, T. - Osaka Imperial University

CHIN, EIHO - Kyushu Imperial University

FUKUDA, M. - Kyushu Imperial University
FUNAOKA, S. - Kyoto Imperial University

HINO, S. - Tokyo Imperial University
HIRAO, K. - Kyushu Imperial University

IMAMURA, S. - Kyoto Imperial University
ITO, J. - Osaka Imperial University

JINNAKA, S. - Kyushu Imperial University

KAIDA, K. - Kyushu Imperial University
KASHIWADO, T. - Tokyo Imperial University
KIKUCHI, - Osaka Imperial University
KINOSHITA, - Imperial Institute of Science
KISHIMOTO, K. - Tokyo Imperial University
KOGA, S. - Kyushu Imperial University
KONDO, - Kyoto Imperial University
KOYANO, K. - Nagasaki Medical College

MASUYA, T. - Kyushu Imperial University
MENJO, M. - Tokyo Imperial University
MISAO, T. - Kyushu Imperial University
MIYAKE, M. - Tokyo Imperial University

NAGAOKA, S. - Tokyo Imperial University
NARABAYASHI, T. - Yamaguchi Prefectural Medical School
NISHIOKA, T. - Editor, Nagasaki Shimbun
NISHINA, Y. - Imperial Institute of Science

OKAMOTO, K. - Kyoto Imperial University
ONO, K. - Kyushu Imperial University

SAKAI, B. - Kure Naval Hospital
SAWADA, T. - Kyushu Imperial University
SENO, S. - Kyushu Imperial University
SHINOHARA, - Kyushu Imperial University

TSUZUKI, M. - Tokyo Imperial University

URABE, M. - Tokyo Imperial University

YAMAMURA, H. - Tokyo Imperial University
YAMORI, T. - Yamaguchi Prefectural Medical School
YASUYAMA, K. - Rear Admiral, Japanese Naval Medical Corps
YOSHIKAWA, H. - Tokyo Imperial University

DECLASSIFIED

DECLASSIFIED

The explosion was of incredible intensity and of extremely short initial duration (perhaps one micro-second) with a fire-ball lasting up to one second. Nearly the whole electro-magnetic spectrum was apparently emitted, as well as a neutron cloud. Gamma radiation was produced by neutron bombardment of atmospheric nitrogen.

The day was clear, hot and dry, with a light easterly wind, but soon after the explosion showers occurred in the western portions of the city.

The account of Father Siemes is so accurate and graphic that it is given verbatim and will be the only lay account presented for this city.

* * * * *

Eyewitness Account of Father Siemes
(Verbatim)

Up to August 6th, occasional bombs, which did no great damage, had fallen on HIROSHIMA. Many cities roundabout, one after the other, were destroyed, but HIROSHIMA itself remained protected. There were almost daily observation planes over the city but none of them dropped a bomb. The citizens wondered why they alone had remained undisturbed for so long a time. There were fantastic rumors that the enemy had something special in mind for this city, but no one dreamed that the end would come in such a fashion as on the morning of August 6th.

August 6th began in a bright, clear, summer morning. About seven o'clock, there was an air raid alarm which we had heard almost every day and a few planes appeared over the city. No one paid any attention and at about eight o'clock, the all-clear was sounded. I am sitting in my room at the Novitiate of the Society of Jesus in NAGATSUKA; during the past half year, the philosophical and theological section of our Mission had been evacuated to this place from TOKYO. The Novitiate is situated approximately two kilometers from HIROSHIMA, half-way up the sides of a broad valley which stretches from the town at sea level into the mountainous hinterland, and through which courses a river. From my window, I have a wonderful view down the valley to the city. Suddenly - the time is approximately 8:14 - the whole valley is filled by a garish light which resembles the magnesium light used in photography, and I am conscious of a wave of heat. I jump to the window to find out the cause of this remarkable phenomenon, but I see nothing more than that brilliant yellow light. As I make for the door, it doesn't occur to me that the light might have something to do with enemy planes. On the way from the window, I hear a moderately loud explosion which seems to come from a distance and, at the same time, the windows are broken in with a loud crash. There has been an interval of perhaps 10 seconds since the flash of light. I am sprayed by fragments of glass. The entire window frame has been forced into the room. I realize now that a bomb has burst and I am under the impression that it exploded directly over our house or in the immediate vicinity. I am bleeding from cuts about the hands and head. I attempt to get out of the door. It has been forced outwards by the air pressure and has become jammed. I force an opening in the door by means of repeated blows with my hands and feet and come to a broad hallway from which open the various rooms. Everything is in a state of confusion. All windows are broken and all the doors are forced inwards. The book-shelves in the hallway have tumbled down. I do not note a second explosion and the fliers seem to have gone on. Most of my colleagues have been injured by fragments of glass. A few are bleeding but none has been seriously injured. All of us have been fortunate since it is now apparent that the wall of my room opposite the window has been lacerated by long fragments of glass. We proceed to the front of the house to see where the bomb has landed. There is no evidence, however, of a bomb crater; but the southeast section of the house is very severely damaged. Not a door nor a window remains. The blast of air had penetrated the entire house from the southeast, but the house still stands. It is constructed in the Japanese style with a

DECLASSIFIED

DECLASSIFIED

GRAPH I

DISTRIBUTION OF CASUALTIES HIROSHIMA

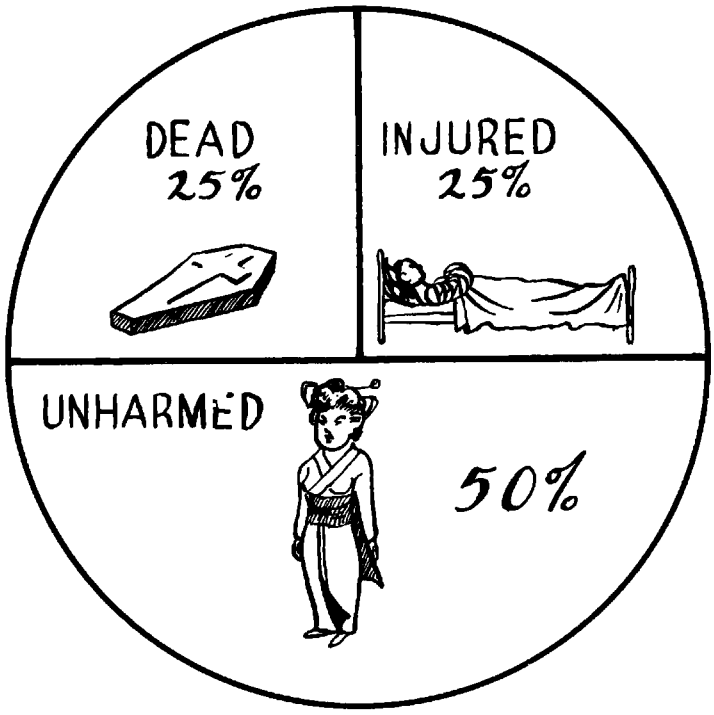

DECLASSIFIED

DECLASSIFIED

Steel frame-work towers and trolley poles close to the hypocenter stood better than those somewhat more distant, which received more lateral force.

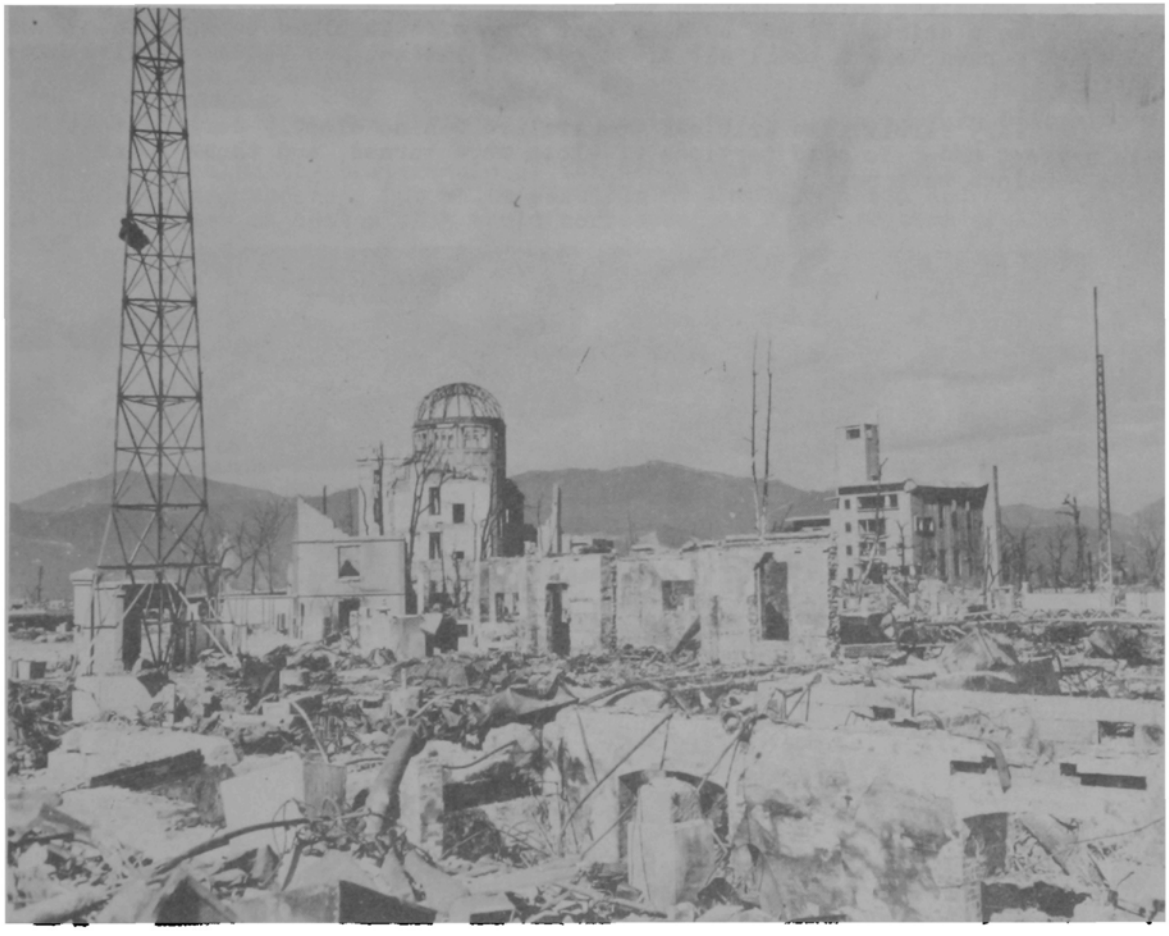

Figure 4

VIEW NEAR HYPOCENTER

Smoke stacks stood throughout the area. The Japanese houses, which had been one or two-story structures of wood with tile roofs, were reduced to ashes and broken tile. Foundations and remnants of metal objects, such as bicycles, sewing machines, or pipes showed amid the general waste. Even at the time of our visit in October, human bones were easily found amid the debris. At the periphery, the wooden structures were crushed, pushed over, or distorted, but were not burned.

DECLASSIFIED

DECLASSIFIED

Practically all persons questioned who had been in the region felt the wave of heat mentioned by Father Siemes in his account. Most of those exposed within four kilometers received flash burns on exposed skin. Lt. Col. Averill Liebow, MC, AUS, has made a careful study of these flash burns, and pointed out numerous instances where a lock of hair, light clothing, the protection afforded by projection of ear, nose or chin served amply to prevent the development of flash burn.

Sometimes burns occurred through that portion of the clothing that was thin, as a shirt. If so, usually that area of skin close to the cloth alone was burned, and a small air space between the two was enough to give protection.

Very rarely, the critical temperature was so clearly defined that skin regions under colored portions of cloth were burned, and those under white portions were not.

Figure 5

HEALING SECOND DEGREE FLASH BURNS DUE TO ATOMIC BOMB

The margins of the burns were sharply defined. If they had not been infected, they healed fairly well.

The hair was sometimes burned off, but usually was intact or had regenerated. Sometimes the sweat glands had been destroyed.

The margins of the healed burns were not only sharply defined, but often accentuated by a narrow zone of pigment loss in the adjacent normal skin, with denser pigmentation over the edge of the scar, fading off centrally.

Some showed keloid formation, but not to a greater extent than in burns due to other causes.

DECLASSIFIED

DECLASSIFIED

Secondary flame burns were usually deeper than the flash burns, and of less extent. These burns or their scars were more rare than flash burns, as those who received them were usually in those regions where most of the people had been killed.

Most of the survivors, as we saw them in October, 1945, showed flash burns of varying extent and/or epilation. A few had hemorrhagic tendencies due to bone marrow injury, and some were found to have anemia, with or without diminution of white blood corpuscles.

Most flash burns when we saw them were healed or healing, and had been of second or third degree.

The more severe burns were producing various contracture deformities.

Rarely, the temperature of the heat wave was such that dark portions of the clothing charred, but white portions of the same cloth did not. (Figure 6) In the case of cotton this would correspond to a temperature of 400° to 450° F.

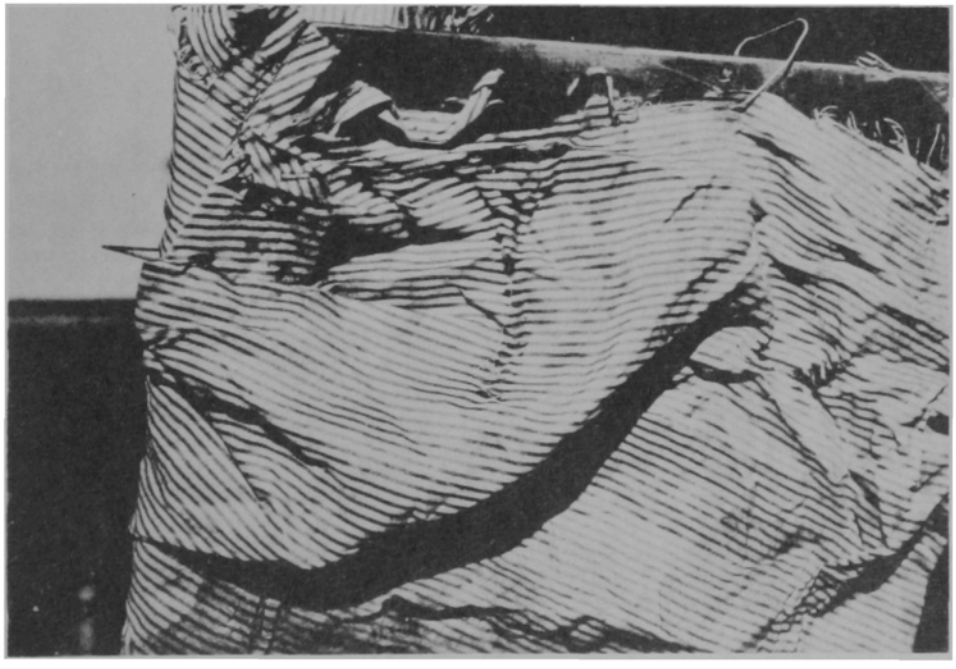

Figure 6

CHARRED

Dark green stripes charred over shoulder nearest bomb explosion; white stripes not charred.

Telephone poles were charred for a considerable distance. Prof. S. IMAMURA of Kyoto Imperial University states that the wood of Cryptomeria Japonica, of which the poles are made, when seasoned, carbonizes at 200°C and ignites at 270°C. We assume this to be expressed in terms of "effective heat."

By "effective heat" we mean that which when maintained for several seconds to a minute will produce a given effect. Even terrific heat applied for an instant, as in the case of the bomb, does not have time for effective transfer of energy.

DECLASSIFIED

DECLASSIFI

It is probable that most fires in the bombed area originated from stoves, electric short-circuits and the like, though this is a matter of conjecture. Some flame burns resulted during the conflagration.

The height and location of the detonating bomb was determined with a high degree of accuracy by the study of shadow silhouettes it produced on various objects by its heat. Japanese investigators had located it approximately within a few days after the explosion.

Sharp lines of "shadow" left where one granite block protected portions of another, where cross-arms or spikes left their shadowing effect on still erect poles, where bridge railings cast "shadows," and other types of "shadows," accurately indicate the center. Examples are shown in Figures 7 and 8.

Lines of blast force, indicated by wrecked buildings, uprooted trees, poles broken or leaning, point radially to the center.

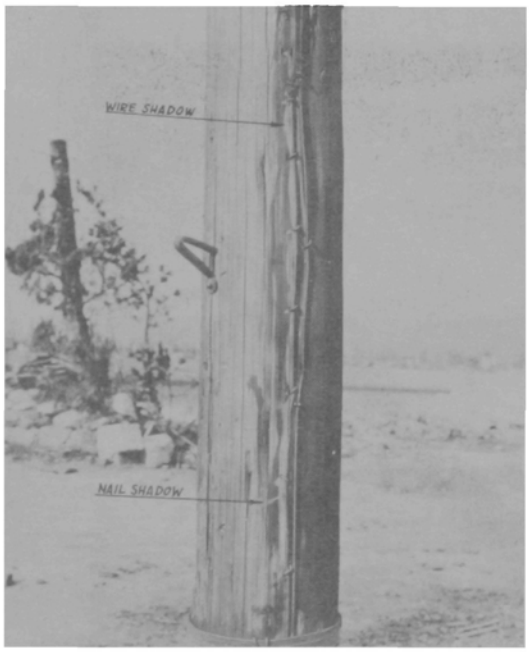

Figure 7

"SHADOWING" EFFECT OF WIRE ON TELEPHONE POLE
(Note sharp line of shielding by nail near bottom.)

Figure 8

"SHADOW" OF BRIDGE POST AND RAILING ON ASPHALT ROAD-WAY

DECLASSIFIED

DECLASSIFIED

The instantaneous character of the explosion is shown by Figure 9 where the leaf sheltered the pole from charring before the blast displaced it. Figure 10 shows where a man was walking, as well as a man and the cart he was pulling. They were pictured in shadow on the asphalt by the heat rays before they were swept away.

Figure 9

"SHADOW" OF LEAF ON CHARRED TELEGRAPH POLE

Figure 10

"SHADOW" OF MAN WALKING (foreground) and (just beyond) that of cart and man pulling it

DECLASSIFIED

DECLASSIFIE

X-28-1

GRAPH 2

EFFECT UPON SURVIVORS

(Sample of 4030)

HIROSHIMA

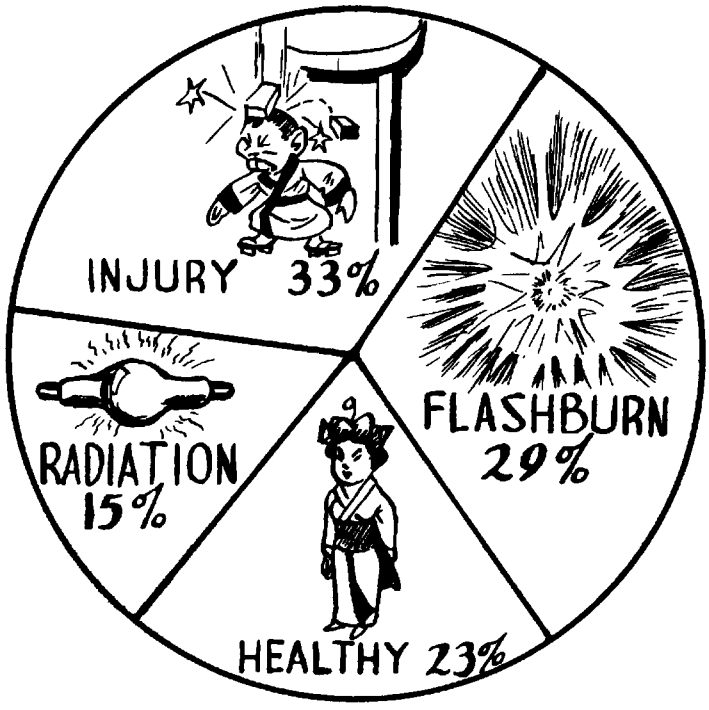

DECLASSIFIED

DECLASSIFIED

GRAPH 4

EFFECTS UPON TOTAL POPULATION

NAGASKI

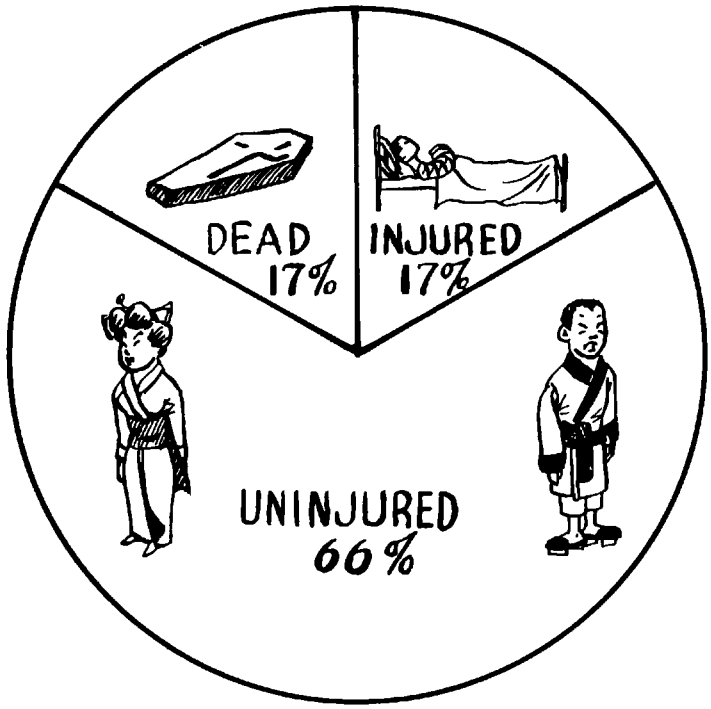

DECLASSIFIED

DECLASSIFIED

X-28-1

GRAPH 5

EFFECT UPON PERSONS SHELTERED BY CONCRETE BUILINGS

(Sample on 2182 survivors)

NAGASAKI

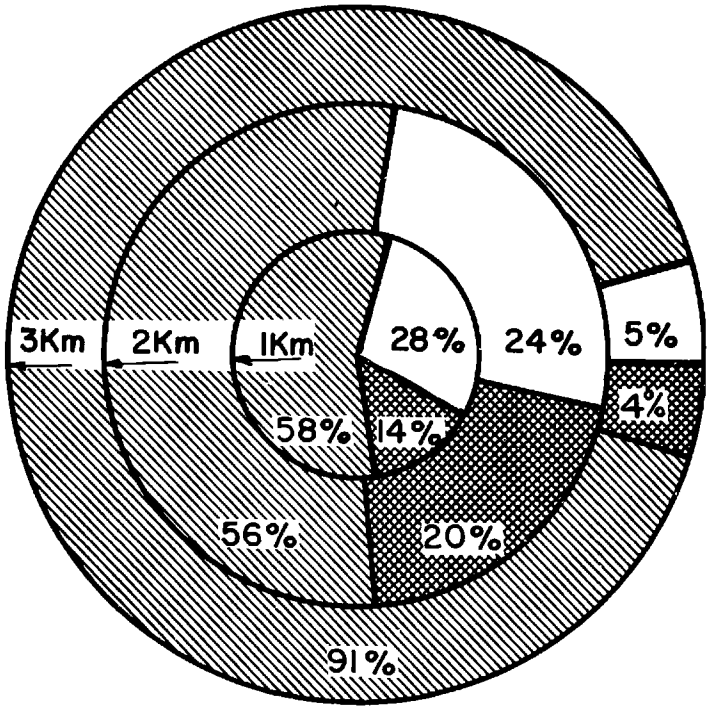

BURN
OTHER INJURY
HEALTHY

DECLASSIFIED

DECLASSIFIED

GRAPH 6

EFFECT UPON PERSONS IN OPEN

(Sample of 2182 survivors)

NAGASAKI

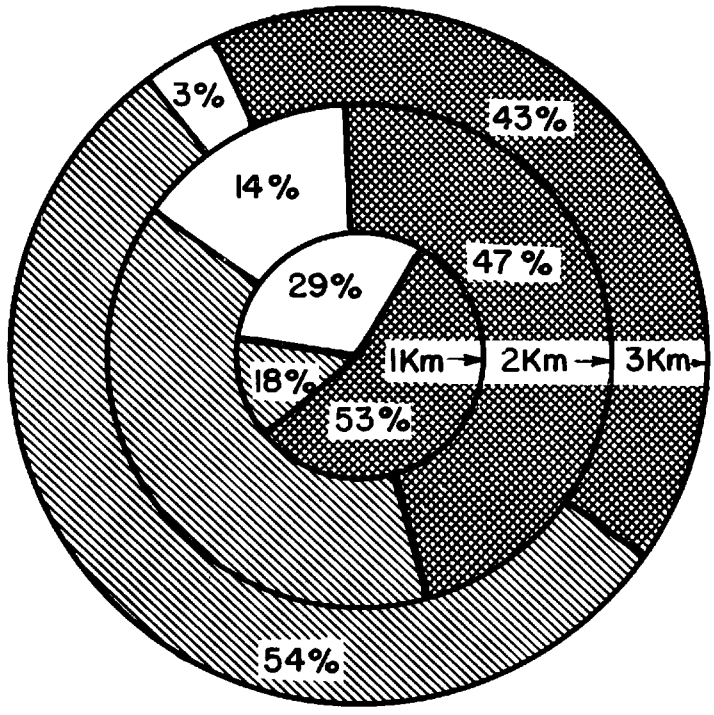

BURN
OTHER INJURY
NORMAL

DECLASSIFIED

DECLASSIFIED

Casualty figures have been difficult to determine. No sound figures of population exist. Lt. Col. LeRoy, Wing Comdr. Bronowski, RAF, associated with the U.S. Strategic Bombing Survey, and Comdr. Warren, (MC), USNR, attempted to assemble these figures, which are believed to be the most accurate available.

POPULATION OF NAGASAKI

	Men	Women	Total
Secret Census, 19 Feb. 1944	137,015	133,098	270,133
Rice Rationing, May 1945 with added military and factory personnel			207,806 260,000+
Census, 1 Nov. 1945*	69,789	72,959	142,748
Rice Rationing, Computed for 1 Nov. 1945			143,617

* See Enclosure (E).

Police permits to leave the city had been granted to 29,313 persons.

The prefectural report of 1 Sept. 1945, gives 23,359 killed, 40,992 injured and 1927 missing.

On the basis of these reports and figures and on our own estimation of casualties, we believe the best approximate figures are: killed 45,000; injured 45,000. See Graph 4.

When it is remembered that only about one-third of the area of the city was in the effective zone of the blast, the lethal power of the bomb can be well appreciated.

In our casualty survey of Nagasaki survivors, 2182 random cases were selected from the 5000 total. These included all cases in the Shinkozen and Omura hospitals. They were grouped in zones of equal distance from the hypocenter, ranging from one to four or more kilometers, and were also classified according to whether they were within concrete, wood, or steel buildings, or in the open. The figures for those in concrete buildings and those in the open are shown in Graphs 5 and 6.

Graph 5 does not mean that 58 percent of those who were in the concrete buildings within a kilometer of the hypocenter survived. Seventy five percent of those in the concrete hospital buildings were killed. But of those who did survive, it means 58 percent suffered no harm, as against 18 percent of those who had been in the open and survived (Graph 6). Probably these 18 percent unharmed were sheltered from the center of explosion by buildings or tile roofs, though technically in the open.

There were three risks to those in concrete buildings. In order of magnitude these were:

1. Fire (most Japanese buildings have wooden trim).

2. Secondary (scattered) radiation.

3. Trauma from glass and other flying debris.

By the time the three kilometer zone was reached, distance alone was a protecting factor, since gamma radiation and infra-red rays both follow the inverse square law. Thus, even in the open, 54 percent of the survivors suffered no harm, and 91 percent of those in concrete buildings were uninjured.

DECLASSIFIED

DECLASSIFIED

GRAPH 8

EFFECTS ON CHILDBIRTH

9 AUGUST TO 15 NOVEMBER 1945

NAGASAKI

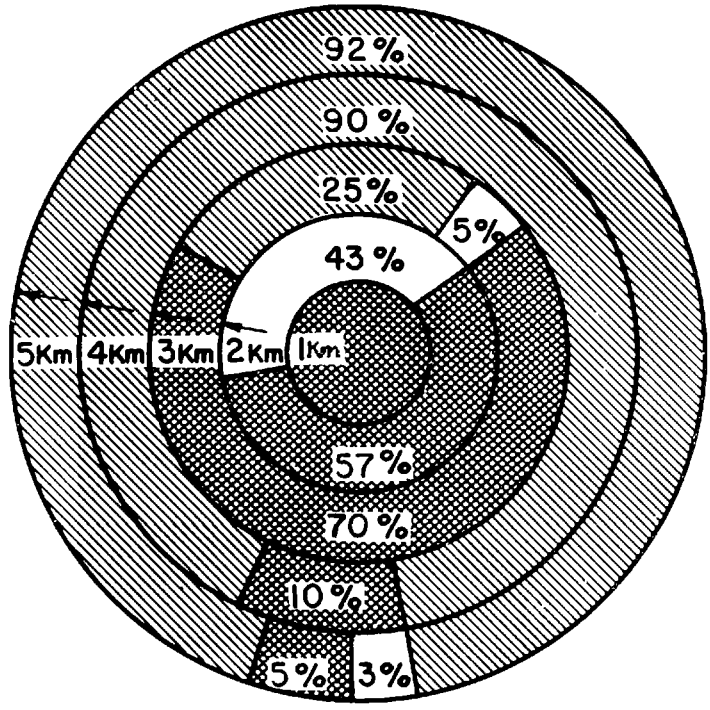

MISSCARRIAGE
PREMATURE
NORMAL

DECLASSIFIED

DECLASSIFIED

Effect on Child-Birth:

Graph 8 demonstrates in startling fashion the disastrous effect of the atomic bomb on pregnancy. These figures are not complete, as it was not possible to contact all obstetricians and midwives. However, it is believed that they are representative. No vital statistics worthy of the name are kept, so no check can be made by this means. Since 9 August 1945, 182 cases had sufficiently accurate records for study. Within two kilometers of the hypocenter there were no normal births. Within one kilometer of the hypocenter, all mothers died. Between one and two kilometers of the hypocenter, half the mothers died.

Outside these zones, between two and three kilometers, a few normal births occurred, and beyond three kilometers the results paralleled the control group.

These miscarriages and premature births were almost all due to hemorrhage into the placenta because of delayed clotting power of the mother's blood.

Effect on the Eyes:

Retinitis occurred in a number of patients. Flame hemorrhages near the macula were most frequent. A few preretina hemorrhages appeared. The hemorrhages resorbed, if they were small, leaving non-pigmented foci in their wake. Rarely was vision seriously impaired.

Lens changes were not noted. Keratitis did not appear as a sequel to the radiation.

Effect on wound healing and growth:

Traumatic injuries and fractures apparently healed about as would be expected under usual conditions.

In children, no evidence of delayed bone growth due to epiphyseal or other radiation injury was seen.

Malnutrition and poor hygiene, both very prevalent in those injured by the bombs, would account for any changes in growth rate that may appear. Careful follow-up of NAGASAKI and HIROSHIMA patients will be needed for some time to check on this point. The period of observation available is too short for a final statement.

Due to wartime privations, the average Japanese child is one centimeter shorter and one kilogram lighter than before the war.

Changes in Blood Chemistry:

1. Blood Proteins. The Japanese population exists on a relatively low margin of protein intake over protein requirement. Consequently, quite early after serious injury with poor or no care, one may see a drop in protein to a level of 5.2 or below with the development of nutritional edema. This nutritional edema clears up usually within a week after the patients are placed on an adequate diet. In the Omura Hospital, where the diet was adequate, nutritional edema and low blood protein levels were extremely rare. In the Shinkozen Hospital, where care and food for the patients was extremely poor, low protein and nutritional edema occurred in a fair number of cases. Most of these recovered within a few days when transferred to the Omura Hospital. A group of cases were studied from 14 to 78 days after the bombing at the Imperial University of Kyushu and it is believed that the determinations are well and carefully done.

DECLASSIFIED

DECLASSIFIED

During use in the field the counter was set at a distance of one meter above the ground by means of a support. Wherever possible the location of each point of measurement was accurately fixed on aerial photo mosaics of the area being surveyed. Adequate photo coverage was available for most of the NAGASAKI measurements. The survey comprised about 1000 individual measurements, 900 in the NAGASAKI area and 100 in the HIROSHIMA area. In addition, a number of earth samples were collected for further study in the United States.

In addition to the physical measurements, a brief evaluation of physiological effects of the residual radiation was made by obtaining case histories and blood studies on some 60 persons residing in the NAGASAKI area of activity, but who were not exposed to the bomb explosion.

Results:

The areas of residual activity at both NAGASAKI and HIROSHIMA were found to be of two types: (1) a well-defined, roughly radially, symmetrical area about the hypocenter of the explosion, and (2) a diffuse and generally larger area displaced some distance from the hypocenter. In the following the term "center" will denote the exact site of the bomb explosion in the air above the gound, and the term "hypocenter" will denote the point on the earth's surface directly beneath the center of the explosion. The geographical areas of residual activity about the hypocenters will be known as the NAGASAKI center area and HIROSHIMA center area, respectively. The geographical area of activity displaced from the hypocenter at NAGASAKI exhibited the highest radiation values near the Nishiyama Reservoir, 2.7 kilometers east of the hypocenter, and will be referred to as the NISHIYAMA area. The corresponding area at HIROSHIMA occurred at the village of TAKASU, 3.2 kilometers west of the hypocenter, and will be termed the TAKASU area.

The geographical distribution of the residual radioactivity at NAGASAKI and HIROSHIMA is shown in a series of four maps. Enclosure (J) shows the distribution of activity in the NAGASAKI center area, Enclosure (K) shows the distribution in the NAGASAKI center and NISHIYAMA areas, Enclosure (L) shows the extent of the activity in the NAGASAKI area, and Enclosure (M) shows the extent of the activity in the HIROSHIMA area. In addition, Table 1 gives a comparison of the size of the NAGASAKI and HIROSHIMA central areas.

Discussion:

It is evident from the map in Enclosure (J) that the residual activity about the hypocenter is roughly radially symmetrical. The departure from true symmetry can be explained in large part by the broken nature of the terrain in this area. It is believed that the elongated nature of the 50μ r/hr contour is in some measure due to the fact that a hill (on which the prison was located) is in the area. Likewise the smaller isolated 50μ r/hr contour occurred on the side of a hill to the southeast of the hypocenter.

There seems to be little doubt that this residual activity was induced from the bombardment of ground material by the neutron and gamma ray shower incident to the explosion. The apparent half-life of the activity here is presumably the resultant of an undetermined number of radioactive isotopes and the complete decay curve is by no means available. On the basis of Japanese measurements made soon after the explosion, the apparent half-life was approximately 10 to 14 days. Sixty to 70 days following the explosion the half-life increased to approximately 90 days in the NAGASAKI center area. This latter value is at present a field approximation and must be taken wi[illegible] [illegible]servation.

DECLASSIFIED

DECLASSIFIED

The activity in the NISHIYAMA area is most certainly the result of fission products deposited from the cloud formed by the explosion. The weather on 9 August 1945 at NAGASAKI was clear and warm with a light west southwest wind. Residents in the NISHIYAMA area tell of the cloud passing over the region and droplets of yellow brown liquid falling after the explosion occurred. The geography of the NISHIYAMA area is such that a range of hills is interposed between the reservoir and the explosion hypocenter. The east side of the NISHIYAMA valley was well out of a direct line from the explosion center. Yet relatively high residual radioactivity was detected in the latter area. Furthermore, definite traces of residual activity were detected on the SHIMABARA Peninsula, some 20 miles to the west of the NAGASAKI hypocenter; and the Japanese reported traces of activity in KUMAMOTO, some 50 miles to the west of the hypocenter.

The radioactive material at NISHIYAMA had a half-life variously estimated to be from 30 to 75 days, and appeared to be made up of distinctly different isotopes from that at the hypocenter. One indication of this came from the different proportion of beta to gamma radiation in the two areas, the beta fraction being much higher at NISHIYAMA than at the center area.

The relative intensity in the two areas is of considrable interest physiologically. At the NAGASAKI center area the residual intensity at the hypocenter on 18 October 1945 was 53μ r/hr which is well below the minimum tolerance dose of 4000μ r/hr. Even assuming a rapid decay directly following the explosion, it is questionable whether physiologically significant residual radioactivity occurred in the center area at any time after the blast. This conclusion was partly verified by interviews with a number of persons who were not exposed to the explosion proper but who entered the explosion area shortly thereafter. They have been residing there almost continuously since that time. Their blood was examined by the Japanese and found to be essentially normal. On interview, they had no physical complaints nor any history of ill effects since 9 August.

The situation at NISHIYAMA was somewhat different. Here many values in excess of 800μ r/hr were obtained, and the highest value measured was 1080μ r/hr. These values were determined about 15 November, some 100 days following the explosion, and are within the order of magnitude of the minimum tolerance dose of 4000μ r/hr. In view of the somewhat shorter apparent half-life at NISHIYAMA, it is possible that physiologically significant radiation was received by the inhabitants of this area for at least a short time after the explosion. Japanese blood studies made in this area about 1 October tend to substantiate this view, as a moderate leukocytocis was observed by these investigators. However, blood studies made on NISHIYAMA residents by NavTechJap Team 11-100 on 16 to 19 November showed a normal blood picture, indicating that complete recovery had apparently occurred. In general, it may be said that there was a possible transitory period of not more than 90 days during which sufficient residual radioactivity remained in the NISHIYAMA area to produce barely perceptible physiological effects.

The maximum radiation intensity measured at HIROSHIMA on 1 November 1945 was 61μ r/hr in the center area. The situation here may be regarded as parrallel to that in the NAGASAKI center area insofar as physiological significance is concerned. It may be concluded that the residual radiation was not physiologically significant following the explosion proper.

The highest measured radiation intensity in the TAKASU area on 1 November 1945 was 28μ r/hr. At least two components of the active material have been isolated by the Japanese, a barium fraction of 13.3 day half-life, and a strontium fraction of 51 day half-life. It is possible, although not probable, that for a short time following the explosion, the residual activity approached physiologically significant levels; however, at present the radiation is not significant.

DECLASSIFIED

DECLASSIFIED

The comparative sizes of the central radioactive areas at NAGASAKI and HIROSHIMA are shown in Table 1. It may be seen from this table that at NAGASAKI the absolute area within each contour is smaller than at HIROSHIMA; and, from the ratio of the corresponding areas at each site, it is evident that this difference is essentially a constant one - the NAGASAKI areas being about 65 percent of those at HIROSHIMA.

An interesting difference between the two explosions lies in the fact that although the NAGASAKI bomb exploded nearer to the ground, roughly 490 meters, as compared with the Japanese estimate of 590 meters at HIROSHIMA, the residual intensity is lower at the center in NAGASAKI than at HIROSHIMA. An explanation for this may be that the two bombs were of different types.

TABLE I
COMPARISON OF AREAS OF RADIOACTIVITY AT NAGASAKI AND HIROSHIMA
(Based on Radioactivity Maps)

Intensity Contour	Major Radius (Meters)		Minor Radius (Meters)		Mean Radius (Meters)		Approx. Area (Km^2)		Ratio of (Areas)	Multiples of 50μ r/hr Area	
	N	H	N	H	N	H	N	H	N/H	N	H
50μ r/hr	100	90	25	60	63	75	.012	.018	.667	1.00	1.00
40μ r/hr	125	140	88	80	106	110	.035	.038	.921	2.92	2.11
30μ r/hr	250	265	138	230	194	248	.118	.193	.611	9.83	10.7
20μ r/hr	350	425	238	313	294	369	.270	.428	.631	22.50	23.8
10μ r/hr	500	510	325	475	413	493	.534	.749	.713	44.5	41.6
5μ r/hr	675	900	475	825	575	858	1.043	2.310	.451	86.9	128.3

N = NAGASAKI H = HIROSHIMA

From the foregoing data it may be concluded that personnel may enter an area under conditions prevailing at HIROSHIMA and the center and peripheral areas at NAGASAKI (aside from NISHIYAMA) without danger immediately after such an atomic bomb has exploded, and remain there indefinitely without harm from radiation. However, a deposit of fission products such as exists at NISHIYAMA may be potentially dangerous up to 60 days or more after the explosion, provided continuous exposure of personnel occurs.

The danger from residual radiation may become real by exploding the bomb at a lower level, increasing the amount of material, or enhancing the activity of reaction.

* * * * *

Part III
OTHER ASPECTS OF THE ATOMIC BOMB

Several points related to the main thesis will be considered below. Since most of these will undoubtedly be taken up by the U.S. Strategic Bombing Survey, they will be given only cursory consideration here.

Effect on Plant Life:

Vegetation was scorched and many trees uprooted within a radius of three to four kilometers both at HIROSHIMA and NAGASAKI. Many trees and shrubs withstood the blast, however, and were only stripped of foliage and lightly scorched. Most of the latter had leafed out again by mid-October and showed no special abnormalities. Root vegetables, as carrots and radish, put out new leaves.

DECLASSIFIED

DECLASSIFIED

Effect on Water:

The center of the bomb at HIROSHIMA was four kilometers from the harbor; the center at NAGASAKI was three kilometers distant. At neither place was a tidal wave produced. The temperature of the water was not observed to change. Fish and shell fish were not killed. Small craft (up to 100 tons) in the rivers and canals within three kilometers of the center were sunk. Vessels in the harbor or at docks were reported not to be damaged seriously, although some plates and beams were sprung.

Effective Types of Shelters:

The simplest type of shelter was effective in protecting personnel from radiation, heat and blast damage. Many small shelters that were made only of 50 centimeters to a meter of earth heaped over bamboo poles did not collapse. People in such shelters at the time of the explosion, even close to the center, were not injured, if the shelter opening was away from the bomb.

At the time the bomb exploded in each city, many people thought all danger had passed and had largely left the shelters.

Shelters of even elaborate types or hillside caves are inadequate, if the mouths are open directly to the center of explosion. Baffling is essential. There were several cases of persons being severely burned within an unbaffled portion of a shelter while those less than two feet away, but behind the baffle, were unharmed.

As will be noted from the body of the report, persons in concrete buildings were partially protected, if not near windows or other openings, but many near the hypocenter received serious or fatal radiation injury as a result of secondary scatter of radiation within the room.

Organization of Relief:

No effective relief organization existed at either HIROSHIMA or NAGASAKI, nor did effective organized help materialize from the central government or other agency. This lack was due to the national disorganization and impending defeat; to the Japanese callousness toward casualties; and to the magnitude of the damage inflicted.

No form of blood bank or reserve of blood or plasma existed.

A striking evidence of the total disorganization was that no effective effort was made other than by the American forces to clear streets, level ruins or even seal off broken water pipes.

Gradually, shacks have been haphazardly built in the ruins by survivors or squatters.

1. HIROSHIMA.

According to Father Siemes, more than 30 hours elapsed before the first official rescue party was on the scene at HIROSHIMA. Emergency care was given patients who could reach hospitals or shelter by themselves or with the aid of friends the first evening, but no organized relief was in evidence. Little could be done for those who reached hospitals or aid stations except to provide some with shelter, water, a little food and emergency care.

Many trapped in the ruins died by fire or shock unnecessarily.

No attempt was made to give blood or plasma transfusions, nor were blood or blood substitutes available. Burns were treated with zinc ointment or

DECLASSIFIED

DECLASSIFIED

GRAPH 9

EFFECT UPON WOODEN HOUSES

NAGASKI

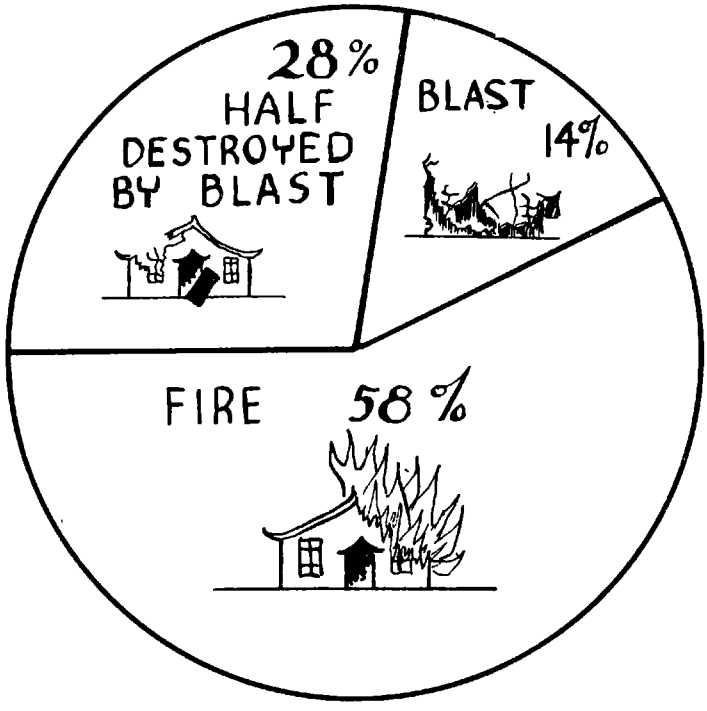

DECLASSIFIED

DECLASSIFIED

SECRET

4. A number of persons died of radiation effects secondary to the explosion, with or without other injury. Many persons within two kilometers of the hypocenter would have died of radiation injury had not death from other causes intervened.

5. Japanese relief organization was non-existent for all practical purposes.

6. Had adequate rescue crews and medical facilities been available, the deaths could probably have been reduced by one-half.

7. Reinforced concrete buildings in general stood the blast adquately. They protected those individuals within them who were not exposed through windows and other openings, although near the hypocenter secondary radiation from floors and walls killed or injured many.

8. Even simple earth air-raid shelters provided adequate protection if baffled.

9. Atomic bombs of the types exploded at HIROSHIMA and NAGASAKI, and at a height of 500 meters or over, create no subterranean disturbance.

10. Atomic bombs of the present type, exploded about 500 meters high in air and at a distance of three or more kilometers from shipping, did not seriously damage vessels of over 100 tons displacement.

11. The effect of exploding atomic bombs in water is totally unknown.

12. Residual radioactivity is not a danger with the atomic bombs as used at NAGASAKI and HIROSHIMA.

13. In order to group atomic bomb radiation casualties with radiation reaction as a whole and to define the characteristic source of the radiation received, it is suggested that they be classified as: Radiation reaction (atomic).

* * * * *

Part VI
RECOMMENDATIONS

1. This report should be publicized widely as soon as national policy with regard to the atomic bomb permits, in order to counteract much of the misinformation that has reached the public.

2. Study of atomic bomb cases should be continued, perhaps at yearly intervals, for at least ten years. Cooperation with Japanese scientists in this is essential.

3. Accurate vital statistics, particularly with regard to births and deaths, should be kept on all persons known to have been within five kilometers of the bomb explosions.

4. Special study should be made of the population of the NISHIYAMA region of NAGASAKI, where residual radioactivity has been relatively high.

5. Joint conferences with the Manhattan Project Group, the Army Medical Group, and this team are desirable to correlate information, guide research, and to issue a complete and authoritative medical report so that all doctors will know how to treat atomic bomb victims, and so that effective relief organizations may be set up to be used in case of need.

DECLASSIFIED

DECLASSIFIED

DECLASSIFIED

LEGEND

(A) EXPLOSION CENTER

(B) AREA TOTALLY DESTROYED AND TOTALLY BURNED

About 2 K.M. East to West
About 3 K.M. North to South
Area about 4.7 S.Q. K.M.

(C) AREA BURNED OUT

About 4 K.M. East to West
About 7 K.M. North to South
Area about 20 S.Q. K.M.

(D) AREA HALF DESTROYED OR PARTLY DAMAGED

About 9 K.M. East to West
About 18 K.M. North to South
Area about 104 S.Q. K.M.

ENCLOSURE (D)

DECLASSIFIED

DECLASSIFIED

ENCLOSURE (E)

POPULATION OF NAGASAKI CITY
Nov. 1, 1945 Census

Age	Men	Women	Total	Age	Men	Women	Total
1	1153	1104	2257	51	723	760	1483
2	1740	1787	3527	52	738	664	1402
3	1674	1584	3258	53	721	636	1357
4	1584	1660	3244	54	684	640	1324
5	1813	1735	3548	55	552	572	1124
6	1553	1491	3044	56	582	554	1136
7	1480	1375	2855	57	551	546	1097
8	1258	1352	2610	58	553	561	1114
9	1452	1330	2782	59	457	507	964
10	1375	1385	2760	60	421	455	876
11	1516	1461	2977	61	403	426	829
12	1470	1453	2923	62	404	404	808
13	1580	1556	3136	63	363	403	766
14	1792	1682	3474	64	303	380	683
15	1774	1781	3555	65	346	420	766
16	1881	1587	3468	66	266	368	634
17	2091	1807	3898	67	278	345	623
18	1939	1654	3593	68	239	296	535
19	1876	1608	3484	69	208	340	548
20	1680	1670	3350	70	190	314	504
21	1717	1508	3225	71	165	222	387
22	1551	1492	3043	72	161	228	389
23	1059	1496	2555	73	132	213	345
24	819	1427	2246	74	105	201	306
25	754	1426	2180	75	111	157	268
26	712	1278	1990	76	58	135	193
27	771	1109	1880	77	81	116	197
28	985	1076	2061	78	67	117	184
29	855	1013	1868	79	48	87	135
30	913	1036	1949	80	38	91	129
31	829	908	1737	81	30	69	99
32	926	943	1869	82	27	48	75
33	834	919	1753	83	26	44	70
34	806	972	1778	84	9	29	38
35	841	955	1796	85	5	28	33
36	850	960	1810	86	7	30	37
37	832	938	1770	87	4	12	16
38	801	894	1695	88	5	13	18
39	878	989	1867	89	5	9	14
40	905	761	1666	90	7	8	15
41	830	856	1686	91	1	4	5
42	921	892	1813	92		7	7
43	867	887	1754	93		3	3
44	882	880	1762	94		1	1
45	851	822	1673	95	1	1	2
46	877	846	1723	96		2	2
47	788	812	1600	97		1	1
48	869	811	1680	98	1		1
49	771	743	1514	99		1	1
50	738	780	1518	Total	69789	72959	142748

DECLASSIFIED

DECLASSIFIED

DECLASSIFIED

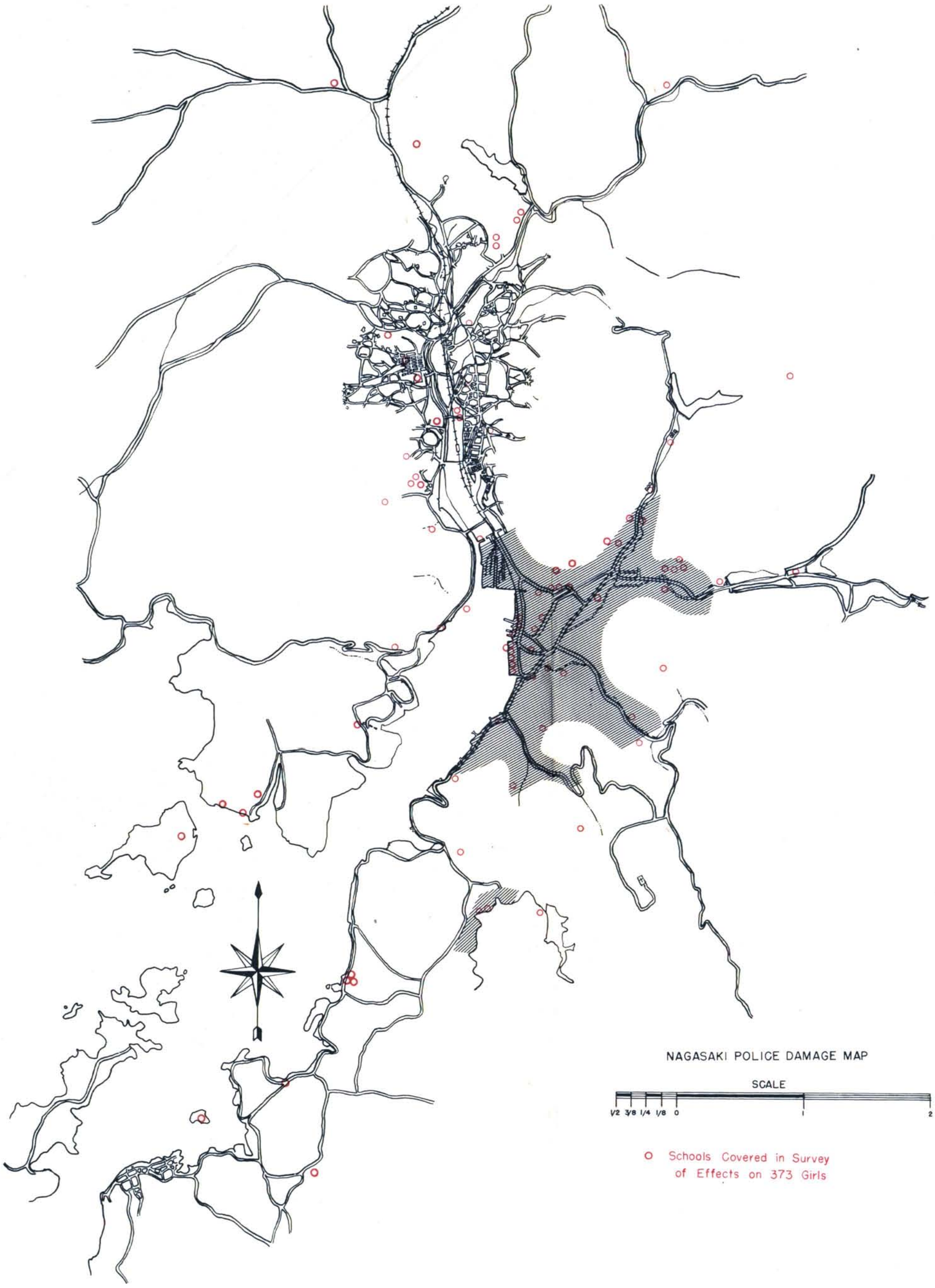

DECLASSIFIED

DECLASSIFIED

ENCLOSURE (H)

TABLE I(H)

ESTIMATES OF SCHOOL ENROLLMENT, NAGASAKI
ATTENDANCE AT SCHOOL
Number of Registered Students by School Districts

School District	Prim.	High	All	July 1945 All	20 Sept. 1945 All	Teachers & Clerks June 1945
SHINKOZEN	592			541	300	20
TOKIYA	760			760	858	24
KOSHIMA	986			986	972	20
KITAOURA	875			859	850	26
ZANZA	932			902	64	26
AKUNOURA	969			969	763	23
ASAHI	864			864	782	24
INASA	906			870	400	33
SHIROYAMA	1324			1324	35	37
YAMAZATO	1581			1581	284	23
NITA	870			865	833	20
MINAMIOURA	796			796	775	29
KATSUYAMA	795	136	931	931	950	27
SAKO	716	289	1005	963	863	17
NAMINOHARA	487	121	608	608	559	
TOMACHI	966	233	1199	1194	1197	25
TATEGAMI	601	148	748	749	783	18
NISHIZAKA	669	174	843	843	223	25
KAMINAGASAKI	901	191	1092	1076	1103	25
IRABAYASHI	1464	141	1605	1583	1687	36
KOGAKURA	323	79	402	410	403	10
DOINOKUBE	763	156	919	904	875	23
KAMINOSHIMA*	256	83	339	303	333	10
KOSAKAKI*	464	83	547	549	554	15
NISHIURAKAMI	1116	195	1311	1311	1015	25
FUCHI		1368	1368	1368	250	38
OURA		617	617	617	592	18
Totals	20976	4014	24990	24746	18670	641

*These two districts appear on map as "KOSAKAKI."

DECLASSIFIED

DECLASSIFIED

ENCLOSURE (H), continued

TABLE II(H)

CASUALTIES AMONG SCHOOL POPULATION
Report Attributed to Nagasaki Prefectural Education Association
19 October 1945

School District	July	Deaths of School Children	Injured or Damaged at home 20 Sept.	
SHINKOZEN	541	13	264	300
TOKIYA	760	7	59	858
KOSHIMA	986	0	54	972
KITAOURA	859	8	35	850
ZENZA (sic)	902	500	370	64
AKUNOURA	969	4	34	763
ASAHI	864	6	345	782
INASA	870	105	981	400
SHIROYAMA	1324	1300	43	35
YAMAZATO	1581	1400	300	284
NITA	865	6	0	833
MINAMIOURA	796	4	13	775
KATSUYAMA	931	17	60	950
SAKA	963	4	65	863
NAMINOHARA	608	4	53	559
TOMACHI	1194	1	320	1197
TATEGAMI	749	2	3	783
NISHIZAKA	843	14	266	223
KAMINAGASAKI	1076	3	34	1103
IRABAYASHI	1583	2	0	1687
KOGAKURA	410	0	0	403
DOINOKUBE	904	0	0	875
KAMINOSHIMA*	303	0	0	333
KOSAKAKI*	549	0	0	554
NISHIURAKAMI	1311	152	387	1015
FUCHI	1368	500	633	250
OURA	617	1	13	592
Totals	24746	4053	4392	18670

*These two districts appear on map as "KOSAKAKI."

DECLASSIFIED

DECLASSIFIED

ENCLOSURE (I)

ENCLOSURE (I)
BLOOD PROTEIN STUDIES KYUSHU IMPERIAL UNIVERSITY

No.	sex	age	days after bomb	w.b.c.	r.b.c. (million)	sed. vel. r.b.c. (mm/1h)	sed. vel. r.b.c. (mm/2h)	tot. prot. (g/100cc.)	non pro. n(mg/100cc.)	albumin (g/100cc.)	globumin (g/100cc.)	albumin globumin	suglob. (g/100cc.)	fibrinogen
1	m	19	14	4000	3.50	65	125	7.4	29	0.9	6.5	0.13	6.5	
			45	9700	6.40	32	62	6.1	39	1.3	4.6	0.32	2.4	
2	f	45	27	3600	1.70	95	138	5.8	28	0.9	5.0	0.06	4.6	
			58	8400	3.20	98	121	6.8	38	0.9	5.6	0.15	2.9	
3	f	46	31	6800	2.50	98	144	5.6	49	0.7	4.9	0.14	4.6	
			51	12800	4.30	6	17	6.0	21	1.5	4.3	0.35	2.1	320
4	f	20	19	1200	2.00	104	154	6.2	48	0.7	5.4	0.13		
			50	8000	4.00	36	51	6.8	32	1.3	3.7	0.35	0.5	314
5	f	20	32	3400	1.90	143	146	6.7	49	2.4	4.2	0.57	2.0	568
			63	11800	4.00	40	92	6.8	35	0.7	5.7	0.12	2.9	578
6	m	20	28	7600	3.60	97	143	7.0	49	0.8	5.9	0.15	0.7	270
			59	6300	4.00	20	46	6.3	22	1.8	4.3	0.42	2.3	491
7	m	52	26	5200	4.40	10	28	4.8	25	0.5	3.6	0.14	0.2	254
			57	4300	2.10	2	7	5.2	32	1.3	3.7	0.35	0.5	314
8	m	24	20	800	2.70	100	136	6.4	25	0.7	5.6	0.12	5.1	
9	m	22	46	4600	3.40	21	53	6.4	28	2.2	4.0	0.35	2.0	639
10	m	43	54	4200	4.60	32	80	6.4	36	1.0	5.1	0.19	1.6	633
11	m	59	56	6600	3.10	131	149	6.9	44	0.2	6.4	0.03	3.5	398
12	m	34	19	6800	2.40	60	120	6.6	38	0.7	5.5	0.13	0.6	227
13	m	30	12	3500	2.70	54	124	5.7	62	1.6	4.2	0.36	1.2	219
14	m	30	26	2400	2.50	40	84	6.3	44	0.8	5.0	0.16	0.1	65
15	m	18	12	3200	2.40	35	112	6.7	53	1.0	5.3	0.19	3.0	407
16	f	18	50	5000	3.60	134	143	6.9	31	1.4	5.3	0.27	3.9	538
17	m	19	78	7400	5.70	20	48	6.9	23	1.3	5.5	0.23	1.2	149
18	f	17	78	6100	4.30	43	84	6.3	26	0.3	5.7	0.05	0.9	
19	f	44	38	7600	3.10	45	96	6.9	36	1.7	4.9	0.38	0.4	
20	m	21	61	7800	4.75	18	48	7.1	27	1.3	5.6	0.23	0.6	496
21	f	17	66	6100	3.30	88	135	7.3	30	1.1	6.0	0.19	1.9	
22	m	16	78	6500	4.10	13	34	7.0	56	1.1	5.4	0.20	0.5	325
23	m	17	78	3300	3.20	36	76	7.6	33	1.5	5.8	0.25	1.5	508
24	f	45	78	5400	2.10	25	52	6.8	31	1.4	5.2	0.27	0.9	393
25	m	16	78	7400	4.30	40	78	5.8	22	0.5	4.9	0.10	0.3	996
26	m	33	78	6200	3.30	35	83	6.7	35	0.7	5.7	0.12	1.5	1022
27	m	19	70	6550	1.91	120		7.5	47	0.5	6.8	0.09	4.5	670
28	f	18	70	8200	3.00	40	65	6.4	43	0.6	5.1	0.12	4.5	302
29	f	17	70	3500	2.40	125	247	6.3	33	0.8	5.2	0.15	4.9	48
30	f	28	70	8600	3.90	25	50	7.0	52	0.6	6.0	0.10	5.2	
31			71	5250		8	15	5.8	35	1.0	4.5	0.22	3.9	142
32	f		71	3900				6.9	49	0.2	6.4	0.03	5.2	417
33	m		71	4000		27	45	5.1	27	0.5	4.4	0.11	3.1	114
34	f		71	3900				6.8	49	0.6	5.9	0.10	3.5	139
35	f		71	4200		50	100	5.1	42	0.3	4.9	0.07	1.9	432
36			71	6450		37	76	6.4	46	0.5	5.6	0.09	1.5	663
37	f		71	7100		50	100	5.4	36	0.1	5.1	0.01	4.0	223
38	f		71	2450		18	50	6.2	14	0.4	5.7	0.07	4.0	259
Standard*														
m since						4	12	7.0	32	4.2	1.8	0.8	0.5	296
f Aug. 9						8	18	6.9	37	4.3	2.4	1.7	0.5	302

*T.Sa J. Med. Assoc., Formosa, 43, 40, 1944

DECLASSIFIED

DECLASSIFIED

ENCLOSURE (J)

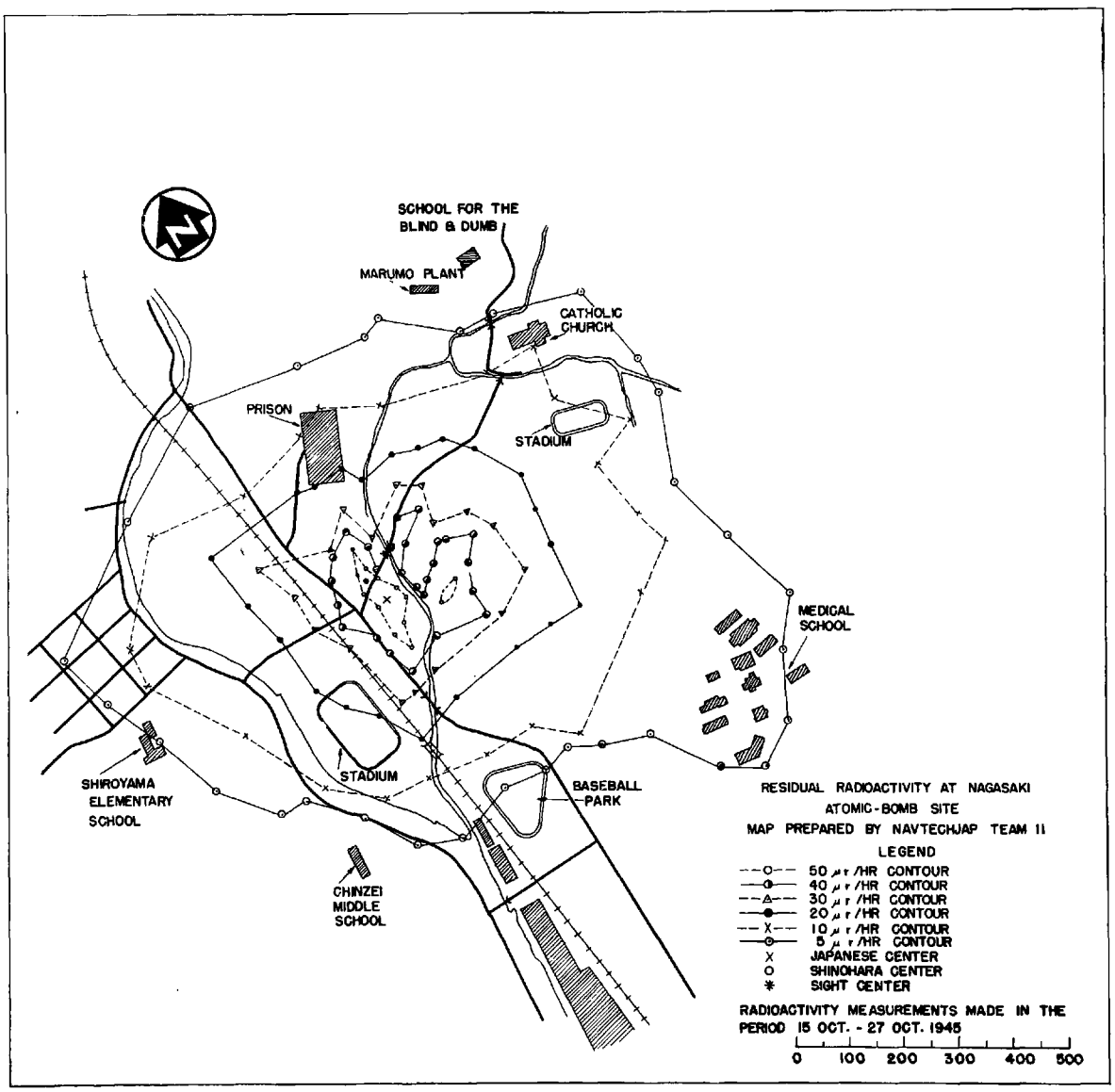

DECLASSIFIED

DECLASSIFIED

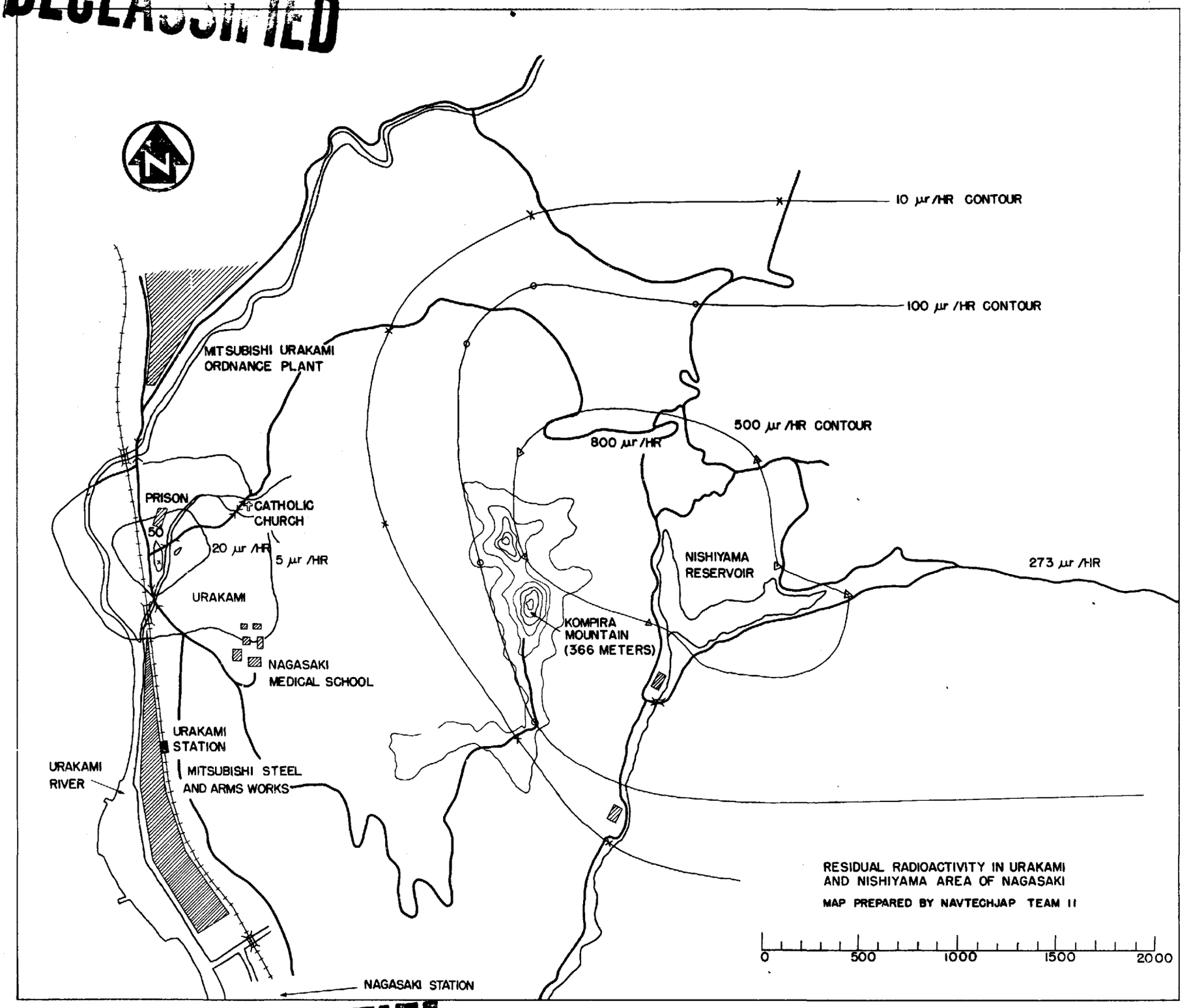

DECLASSIFIED

ENCLOSURE (K)

DECLASSIFIED

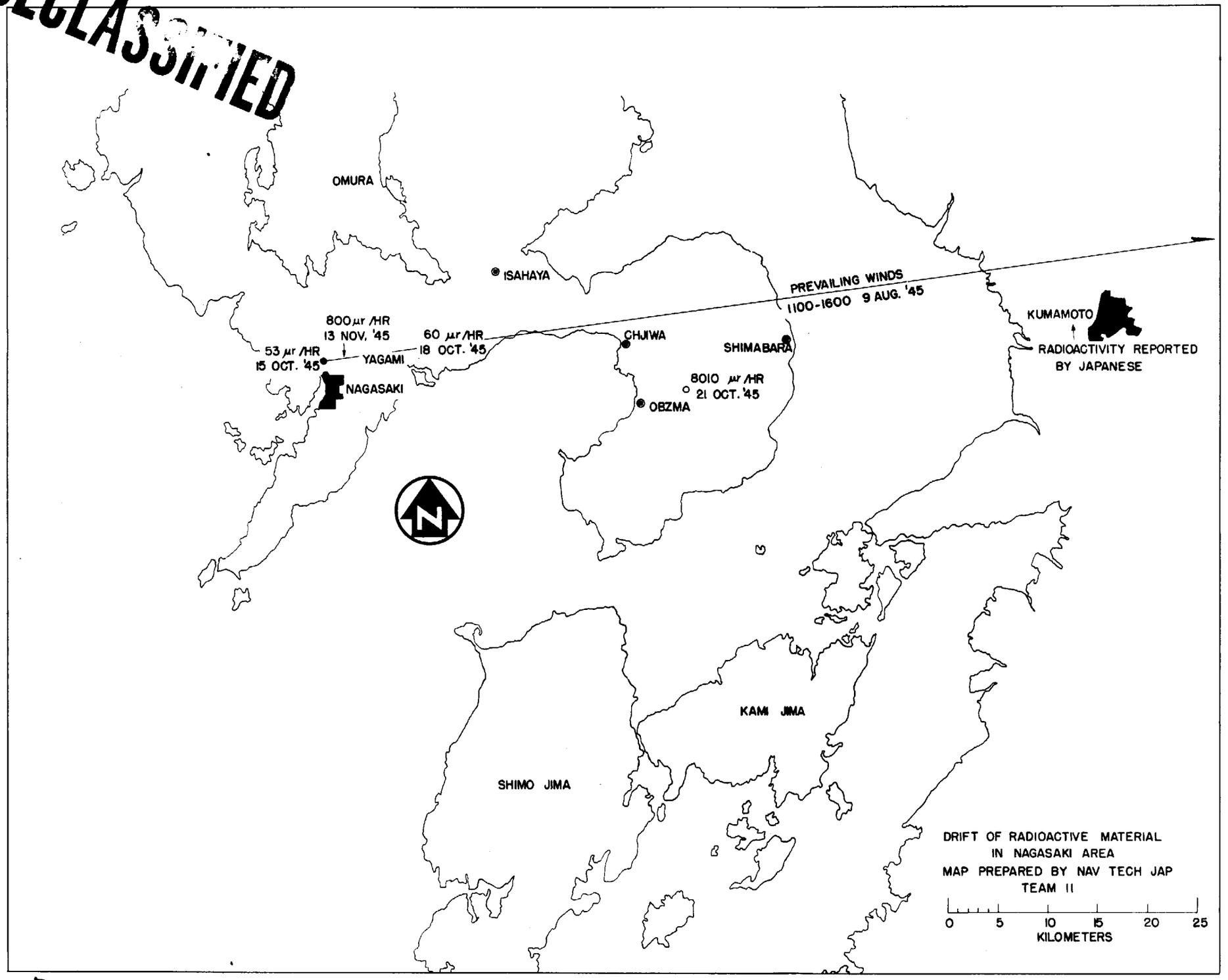

DECLASSIFIED

ENCLOSURE (L)

DECLASSIFIED

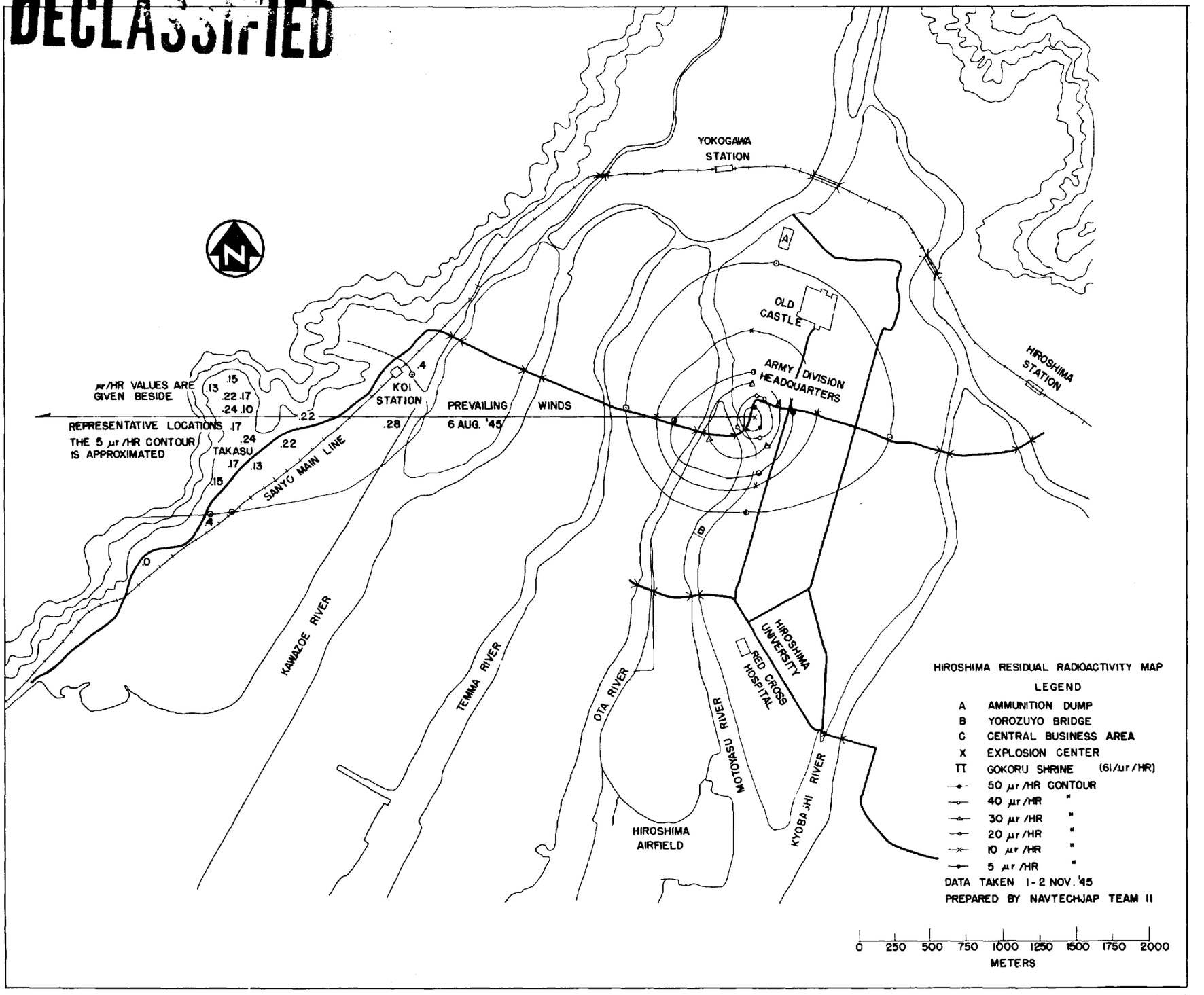

ENCLOSURE (M)

DECLASSIFIED

TMJ
MT
X-28-2

NS/an

U. S. NAVAL TECHNICAL MISSION TO JAPAN
CARE OF FLEET POST OFFICE
SAN FRANCISCO, CALIFORNIA

29 May 1946

SECRET

From: Chief, Naval Technical Mission to Japan.
To : Chief of Naval Operations.

Subject: Target Report - Atomic Bombs, Hiroshima and Nagasaki, Article 2 - Medical Effects, Supplementary Studies.

Reference: (a)"Intelligence Targets Japan" (DNI) of 4 Sept. 1945.

1. Subject report, covering a portion of Target X-28 of Fascicle X-1 of reference (a), is submitted herewith.

2. The report was prepared by Captain Shields Warren, MC (S), USNR.

C. G. Grimes

C. G. GRIMES
Captain, USN

30935

~~SECRET~~

~~Upgraded to T-S by authority of~~
~~CO ltr. 19 Feb '47~~
~~Serial 000740P38~~

Classification cancelled/~~changed to~~ Unclassified
CNO-OP322 by authority of
F2/hga Ser 066:5P32 10 May 1950
Name Title Date
in accordance with AR 380-5.

X-28-2

ATOMIC BOMBS, HIROSHIMA AND NAGASAKI

ARTICLE 2

MEDICAL EFFECTS, SUPPLEMENTARY STUDIES

"INTELLIGENCE TARGETS JAPAN" (DNI) OF 4 SEPT. 1945

FASCICLE X-1, TARGET X-28

MAY 1946

U.S. NAVAL TECHNICAL MISSION TO JAPAN

SUMMARY

MISCELLANEOUS TARGETS

ATOMIC BOMBS, HIROSHIMA AND NAGASAKI - ARTICLE 2
MEDICAL EFFECTS, SUPPLEMENTARY STUDIES

There is no essential difference in the tissue changes produced by the bombs dropped at HIROSHIMA and NAGASAKI.

Atomic bomb injuries may be classified as follows:

1. Air blast injury.

   a. Primary, due to thrust or compression of sonic wave.
   b. Secondary, due to impact with wreckage.

2. Radiation blast injury.

   a. Thermal radiation blast injury.

      (1) Primary, flash burn due to radiant heat.
      (2) Secondary, due to burn from induced fire.

   b. Ionizing radiation blast injury.

      (1) Primary, due to gamma rays and neutrons.
      (2) Secondary, due to induced radiation.
      (3) Tertiary, due to residual radiation.

Changes clearly due to the effect of ionizing radiation blast include lymphoid atrophy, damage to hematopoietic tissue, production of leukopenia, injury to gonadal tissue and epilation.

LIST OF ILLUSTRATIONS

Figure 1. Determination of Hypocentre from Intensity Distribution, NAGASAKI, 27 December 1945.....Page 14

Figure 2. Residual Radioactivity at NAGASAKI, 26 - 29 December 1945..Page 15

Figure 3. Residual Radioactivity at NAGASAKI, 26 - 29 December 1945, Intensity vs. Distance from Hypocentre.....Page 16

Figure 4. Residual Radioactivity at NAGASAKI, 7 January 1946, Intensity vs. Depth at Hypocentre.....Page 17

Figure 5. Residual Radioactivity in NAGASAKI and Environs, 25 December 1945 to 9 January 1946.....Page 18

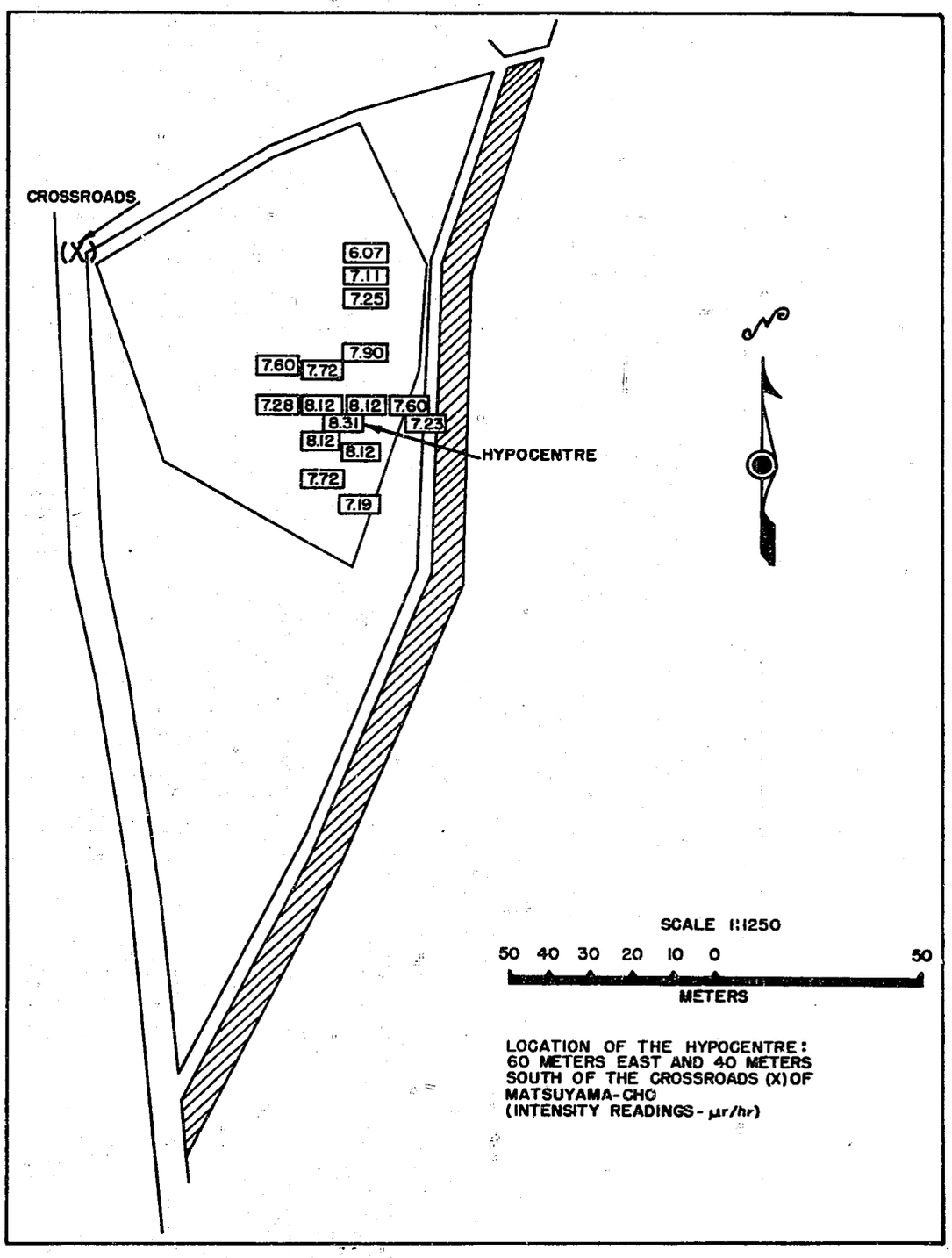

Figure 1

DETERMINATION OF HYPOCENTRE FROM INTENSITY DISTRIBUTION NAGASAKI 27 DECEMBER 1945

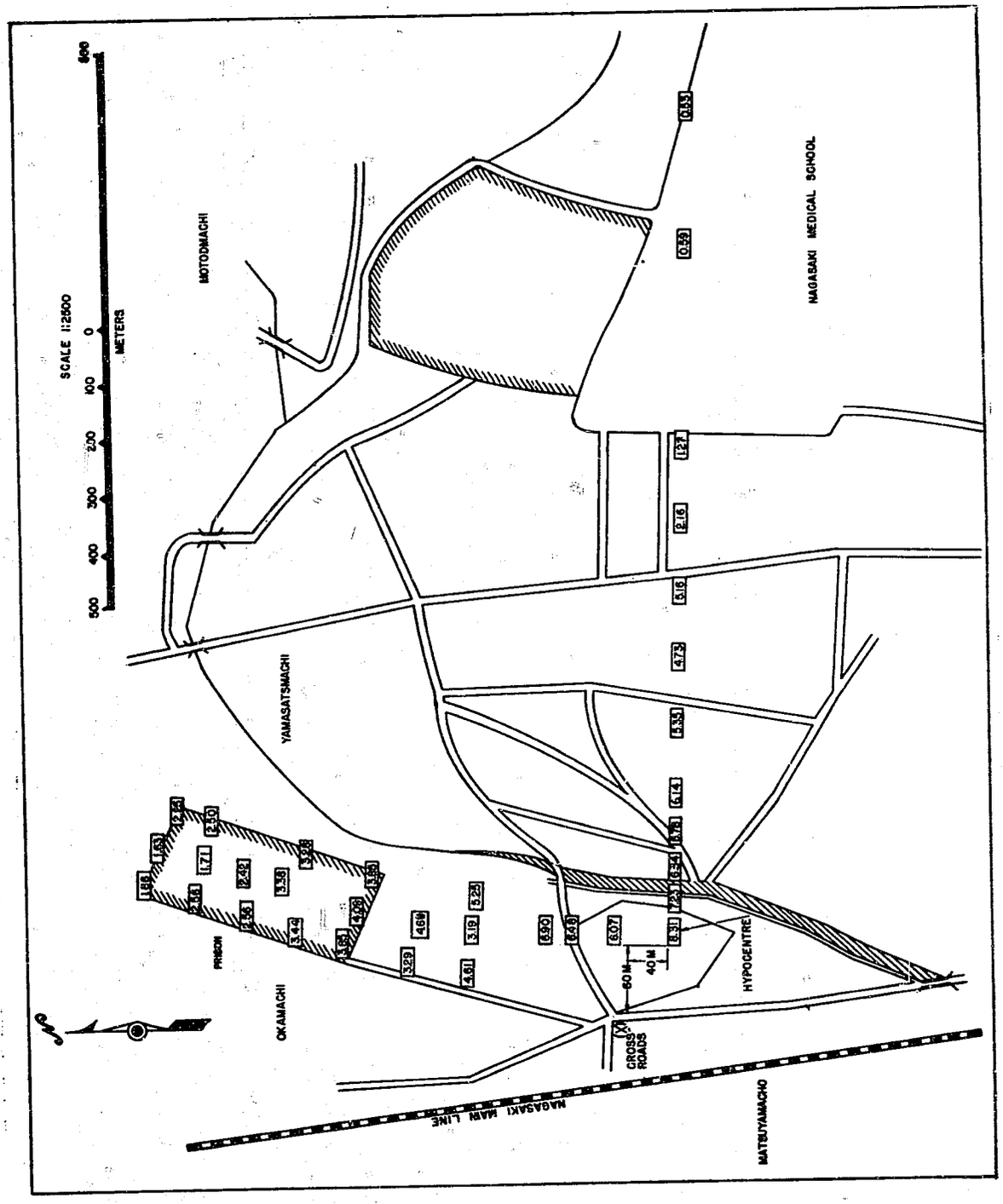

Figure 2

RESIDUAL RADIO-ACTIVITY AT NAGASAKI
(μr/hr) 26-29 DECEMBER 1946

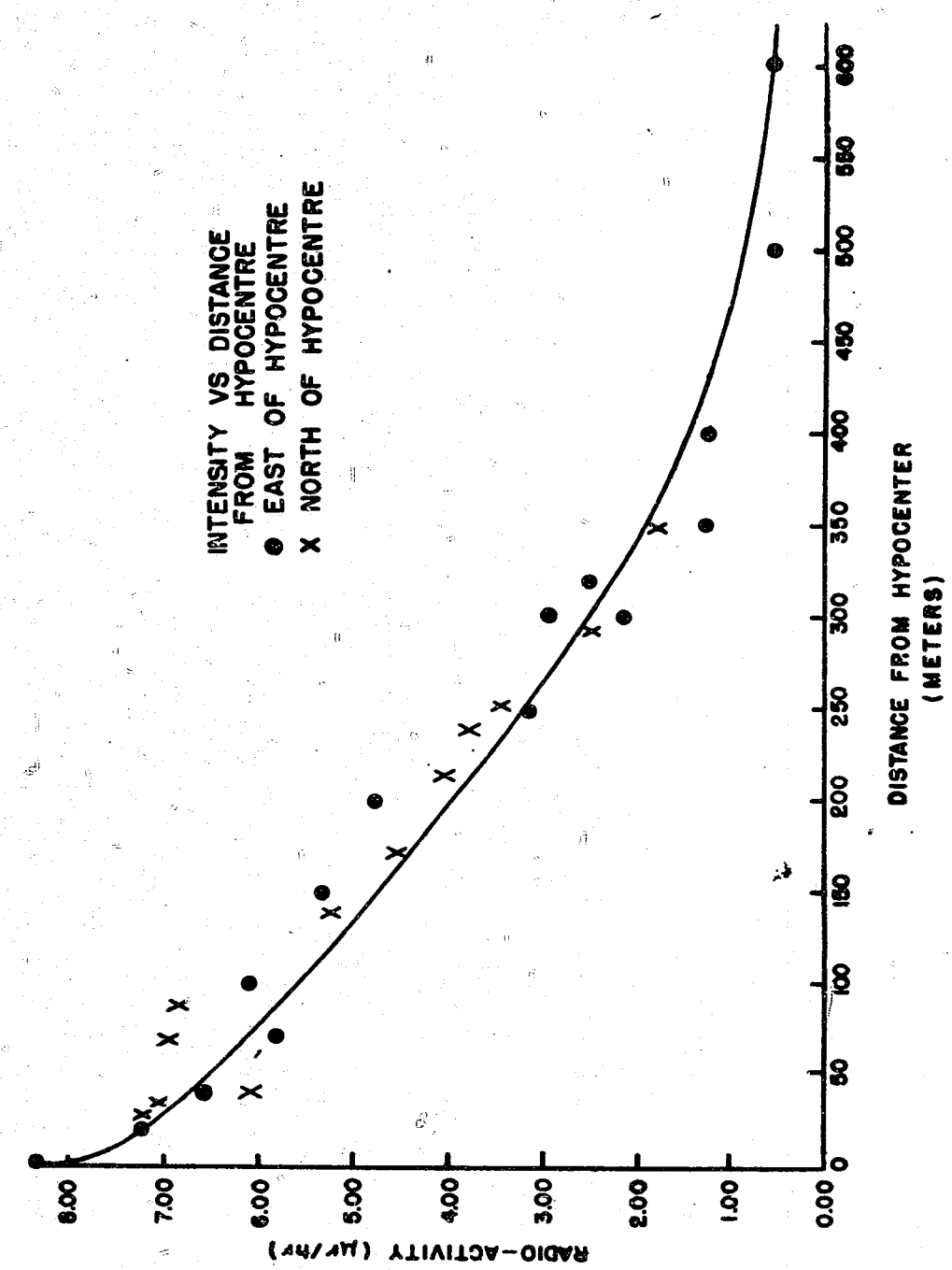

Figure 3

RESIDUAL RADIO-ACTIVITY AT NAGASAKI
26-29 DECEMBER 1946

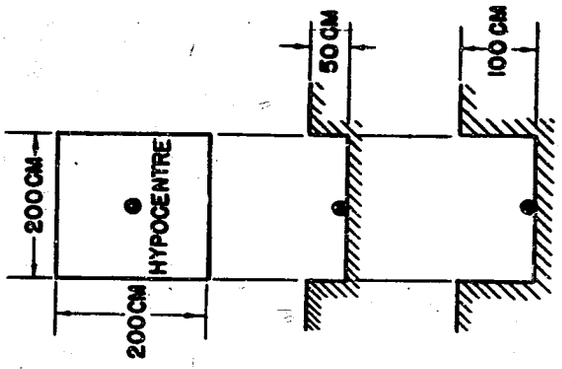

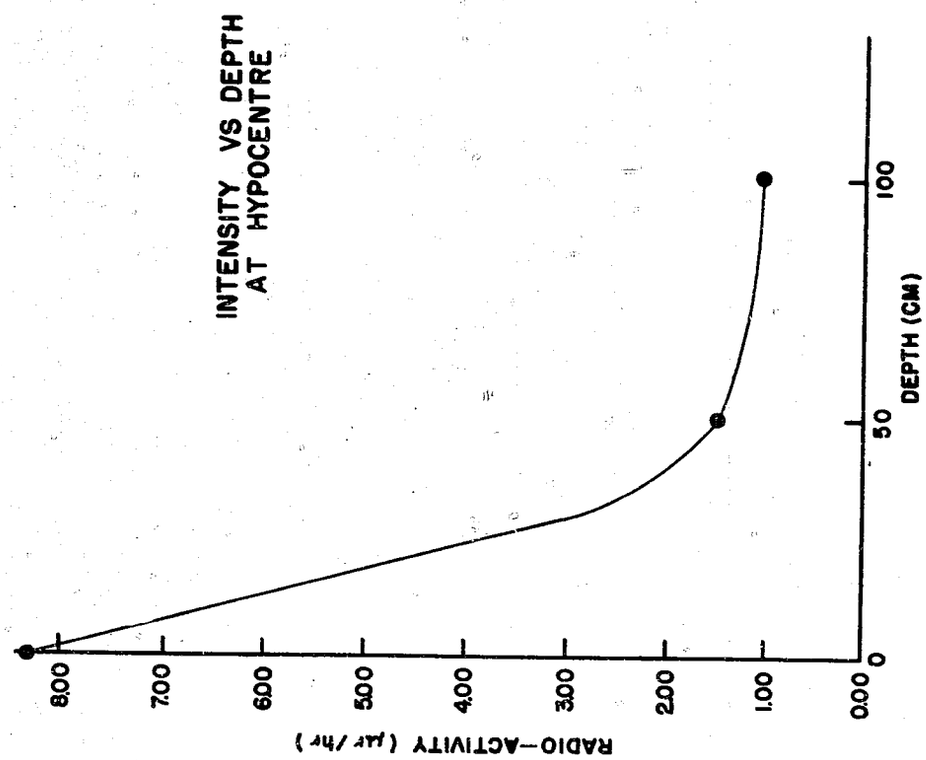

Figure 4

RESIDUAL RADIO-ACTIVITY A
7 DECEMBER 1945

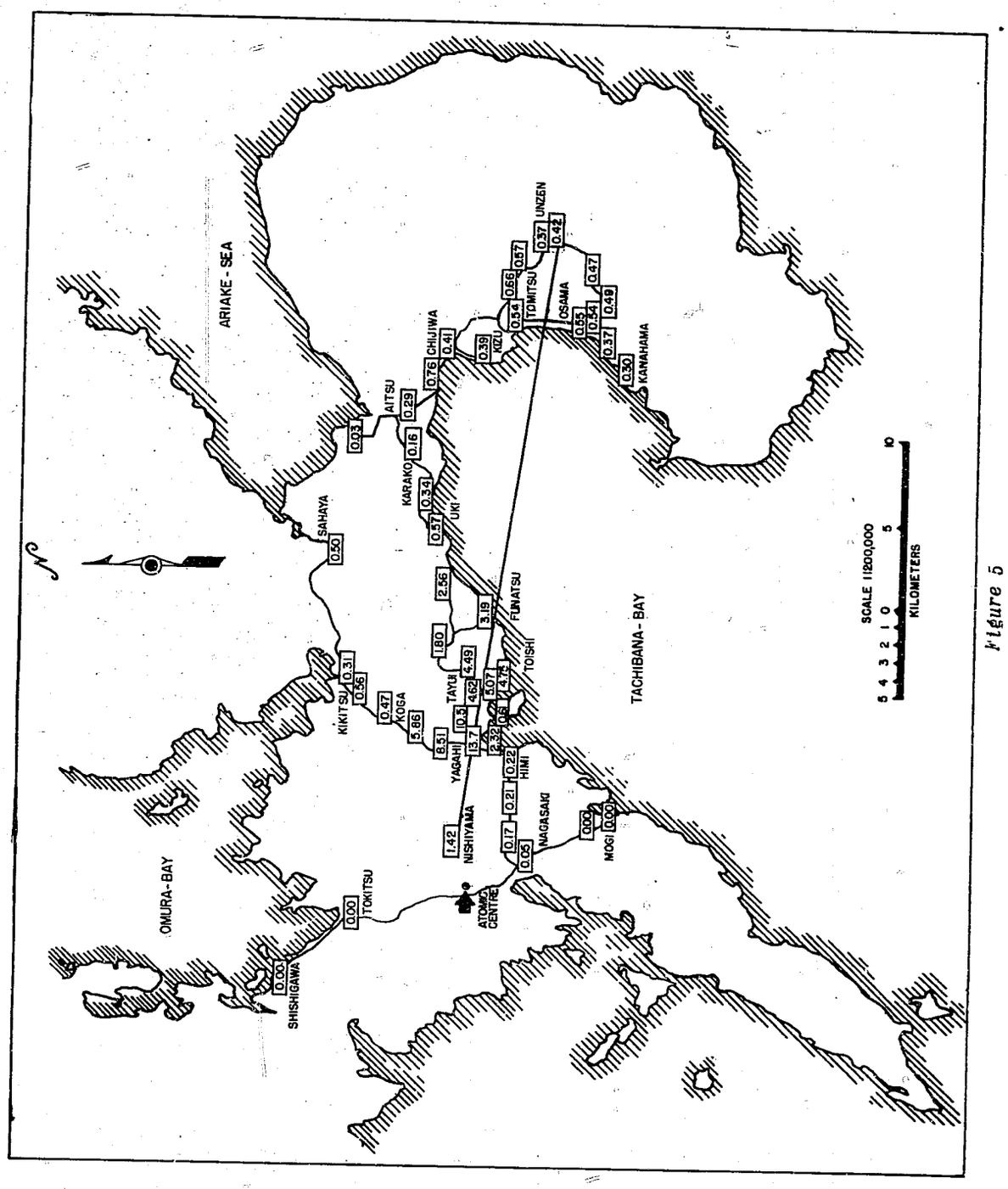

Figure 5
RESIDUAL RADIO-ACTIVITY IN NAGASAKI AND ENVIRONS (μr/hr)
25 DECEMBER 1945 - 9 FANUARY 1946

AD629784

Best Available Copy

RADIOLOGICAL TARGET ANALYSIS PROCEDURES

Code 1

CONTRACT NO. N228-(62479)65421
OCD WORK UNIT NO. 3231C

20050311000

STANFORD RESEARCH INSTITUTE

MENLO PARK, CALIFORNIA

STANFORD RESEARCH INSTITUTE
MENLO PARK, CALIFORNIA

March 1966

RADIOLOGICAL TARGET ANALYSIS PROCEDURES

By: HONG LEE

SRI Project No. MU-5069

CONTRACT NO. N228-(62479)65421
OCD WORK UNIT NO. 3231C

Prepared for:

OFFICE OF CIVIL DEFENSE
DEPARTMENT OF THE ARMY
WASHINGTON, D.C. 20310

Through:

TECHNICAL MANAGEMENT OFFICE
U.S.N.R.D.L.
SAN FRANCISCO, CALIFORNIA 94135

This report has been reviewed in the Office of Civil Defense and approved for publication. Approval does not signify that the contents necessarily reflect the views and policies of the Office of Civil Defense.

REFERENCES

1. Miller, C.F., et al, Introduction to Radiological Defense Planning, Stanford Research Institute, Menlo Park, Calif., May 1965
2. Exposure to Radiation in an Emergency, National Committee on Radiation Protection and Measurement, Report No. 29, University of Chicago, Chicago, Ill., January 1962.
3. Miller, C.F. and P. Loeb, Ionization Rate and Photon Pulse Decay of Fission Products From Slow Neutron Fission of U-235, USNRDL-TR-247, U.S. Naval Radiological Defense Laboratory (USNRDL), San Francisco, Calif., August 1958.
4. Owen, W.L. and J.D. Sartor, Radiological Recovery of Land Target Components--Complex I and II, USNRDL-TR-570, USNRDL, San Francisco, Calif., May 1962.
5. Owen, W.L. and J.D. Sartor, Radiological Recovery of Land Target Components--Complex III, USNRDL-TR-700, USNRDL, San Francisco, Calif., November 1963.
6. Strope, W.E., Evaluation of Countermeasure System Components and Operational Procedures, Operation Plumbbob, Project 323, WT-1464, USNRDL, San Francisco, Calif., September 1959.
7. Lee, H., Estimating Cost and Effectiveness of Decontaminating Land Targets, Vol. I, Estimating Procedure and Computational Technique, USNRDL-TR-435, USNRDL, San Francisco, Calif., June 1960.
8. Spencer, L.V., Structure Shielding Against Fallout Radiation From Nuclear Weapons, National Bureau of Standards (NBS), Monograph 42, June 1962.
9. Barrett, M.J., et al, Transmission of Gamma Radiation Through Thin, Finite Slabs, TO-B 64-44, Technical Operations Research, Burlington, Mass., May 1964.

10. National Fallout Shelter Survey, Phase 2, Computer Printouts, OCD, 1963.

11. Owen, W. L., Radiological Protective Construction, USNRDL-467, USNRDL, San Francisco, Calif., January 1962.

12. Owen, W. L., et al., Performance Characteristics of Wet Decontamination Procedures, Operation Stoneman II, Vol. II, USNRDL-TR-335, USNRDL, San Francisco, Calif., July 1960.

13. Lee, H., et al., Performance Characteristics of Dry Decontamination Procedures, Operation Stoneman II, Vol. III, USNRDL-TR-336, USNRDL, San Francisco, Calif., June 1959.

14. Lee, H., et al., Performance Characteristics of Land Reclamation Procedures, Operation Stoneman II, Vol. IV, USNRDL-TR-337, USNRDL, San Francisco, Calif., January 1959.

15. Taylor, D., et al., Development of Radiological Decontamination Methods and Equipment for Cold Weather Regions, USNCEL, Port Hueneme, Calif., July 1960.

Appendix B

DECONTAMINATION DATA

The available decontamination data are those for roof surfaces, paved surfaces, and unimproved surfaces such as turfed ground, planting areas, and bare ground. The decontamination methods are conveniently separated into the following categories: wet methods, dry methods, and surface-removal methods. Limited data are also available for decontamination in a frigid environment. The wet methods are firehosing and motorized flushing; firehosing is the more versatile. Motorized flushing has three limitations: it can be used only on paved ground areas such as streets and large parking lots; maneuverability is restricted; and motorized flushers are not very available. The only suitably developed large area dry decontamination method to date is motorized sweeping. For special conditions, pavement decontamination may be accomplished by an "air broom," whereby the surface is scoured by air jets but the lifted fallout is permitted to drift downwind. Surface-removal methods are generally applicable for unpaved ground areas. The large area decontamination methods available are motorized scraping, and the combination of motorized grading with motorized scraping. In restricted spaces, large equipment cannot be used effectively and surface removal is limited to drag-type scrapers and hand shoveling. Other methods of reducing radiation effects of contaminated ground areas are plowing and contaminated surface burial. For locations away from plowed or buried areas, the effectiveness of these methods is greater than that indicated.

The selection of decontamination methods for a target complex requires consideration of more than the base data presented but the data will provide a measure of obtainable decontamination effectiveness and the

effort required. The following tables give the expected decontamination performance of various techniques and personnel on surfaces having three fallout mass loadings: Table B-1, 3-men firehose team for tar-and-gravel roofs and composition shingle roofs;[12] Table B-2, firehosing of large paved areas;[12] Table B-3, motorized flushing of pavements;[12] and Table B-4, three dry decontamination methods on pavements.[13] Table B-5 gives the expected performance of various unpaved area reclamation methods; the effort and effectiveness of these methods are independent of mass loading.[4, 14] Table B-6 gives the expected performance of various decontamination methods in a frigid environment.[15]

Table B-1

FIREHOSING OF ROOFS

Standard Intensity (r/hr)	Mass Loading (g/sq.ft)	Unit Effort (man-minutes per 1,000 sq.ft)	Rate per Nozzle (sq.ft/min)	Water Consumption (gal/sq.ft)	Fraction Remaining (F)
* Tar and Gravel - Practically No Slope					
300	10	20	150	0.3	0.6
		30	100	0.45	0.3
		40	75	0.6	0.2
		60	50	0.9	0.1
1000	30	20	150	0.3	0.2
		30	100	0.45	0.1
		40	75	0.6	0.08
		60	50	0.9	0.05
3000	100	20	150	0.3	0.06
		30	100	0.45	0.03
		40	75	0.6	0.02
		60	50	0.9	0.01
+ Composition Shingles - Slope of 1/2.5					
300	10	5	600	0.06	0.09
		10	300	0.12	0.06
		20	150	0.3	0.045
1000	30	5	600	0.06	0.09
		10	300	0.12	0.06
		20	150	0.3	0.04
3000	100	5	600	0.06	0.09
		10	300	0.12	0.05
		20	150	0.3	0.03

* Nozzle pressures 60 to 70 psi.

\+ Nozzle pressures 60 psi when hosing at roof level and 40 to 45 psi when lobbing fire streams from ground level.

Table B-2

FIREHOSING OF PAVEMENTS

Standard Intensity (r/hr)	Mass Loading (g/sq.ft)	Unit Effort (man-minutes per 1,000 sq.ft)	Rate per Nozzle (sq.ft/min)	Water Consumption (gal/sq.ft)	Fractio Remaining (concrete asphal
300	10	15	2000	0.05	0.06
		25	1200	0.08	0.04
		50	600	0.17	0.02
		100	300	0.33	0.015
1000	30	15	2000	0.05	0.06
		25	1200	0.08	0.04
		50	600	0.17	0.02
		100	300	0.33	0.015
3000	100	15	2000	0.05	0.055
		25	1200	0.08	0.035
		50	600	0.17	0.02
		100	300	0.33	0.01

Table B-3

MOTORIZED FLUSHING OF PAVEMENTS
(Conventional Street Flusher) *

Standard Intensity (r/hr)	Mass Loading (g/sq.ft)	Unit Effort equip.-minutes per 10,000 sq.ft	Average Rate (sq.ft/min)	Forward Speed (mph)	Water Consumption (gal/sq.ft)	Fraction Remaining, F	
						Concrete	Asphalt
300	10	1	10,000	15	0.045	0.05	0.06
		2	5,000	7.5	0.09	0.025	0.035
		5	2,000	3	0.22	0.01	0.02
1000	30	1	10,000	15	0.045	0.05	0.055
		2	5,000	7.5	0.09	0.025	0.035
		5	2,000	3	0.22	0.01	0.02
3000	100	1	10,000	15	0.045	0.045	0.05
		2	5,000	7.5	0.09	0.025	0.03
		5	2,000	3	0.22	0.01	0.015

* This machine uses two forward nozzles and one side nozzle under a pressure of 55 psi. One man can operate a flusher, but two are better on older models having manually controlled valves.

Table B-4

SWEEPING OF PAVEMENTS

Method	Standard Intensity (r/hr)	Mass Loading (g/sq.ft)	1st Pass E*	1st Pass F	2nd Pass E*	2nd Pass F	3rd Pass E*	3rd Pass F
Wayne	300	10	11	.09	17	.07	23	.07
450+	1000	30	9	.07	16	.05	20	.03
	3000	100	14	.03	22	.02	--	--
Tennant	300	10	20	.07	30	.02	40	.015
100 ±	1000	30	20	.03	30	.015	40	.011
	3000	100	20	.025	30	.012	40	.010
Air	300	10	16	.03	24	.015	32	.008
Broom #	1000	30	16	.03	24	.01	32	.007
	3000	100	16	.03	24	.009	32	.006

* Effort expended in man/min per 10,000 sq. ft

\+ Conventional motorized sweeper

± Vacuumized motorized sweeper

\# An experimental device consisting of a manifold of air nozzles attached below the rear bumper of a compressor truck.

Table B-5

RECLAMATION OF UNPAVED LAND AREAS

Method	Effort (man-min. per 1000 sq.ft)	Fraction Remaining, F
Motorized Scraping (1 man)		
1st cycle	5-8	0.0016-0.036
2nd cycle	4	0.0002-0.007
Motorized Grading plus Motorized Scraping (2 men)		
1st cycle	10-17	0.015-0.124
2nd cycle	9-17	0.00024-0.0041
Plowing (4-share gang-plow, 1 man)		
continuous	2.5	0.2*
one direction only	4.8	0.2
Earth Filling (3 scrapers, 3 men)		
6" of fill	10-20	0.15
12" of fill	20-40	0.02
18" of fill	40-80	0.002
Scraping - Small drag type	20-50	0.15
Shovel Removal, hand	100-200	0.1-0.15

* Within the plowed area. Away from the plowed area, the effective dose rate fraction is reduced.

Table B-6

PREDICTED PERFORMANCE OF COLD WEATHER RECOVERY MEASURES

Method	Conditions for Application	Average Rate	Fraction Remaining
Skip loading	3 in. and more of snow	12 ton/hr	0.1
Motorized sweeping	Less than 3 in. of snow	10,000 sq.ft/hr per 1 in. of snow depth	
Snow plowing	More than 3 in. of snow mixed with contam.;or less than 3 in. with contam.on top	53 ton/hr, blade type, 625 ton/hr rotary type	0.15
Firehosing	Above 10° F	7500 sq.ft/hr., ground level	0.01
		2000 sq.ft/hr, buildings	0.05
Thawing + Firehosing	Above 10° F	2000 sq.ft/hr, buildings	0.05
Thawing + Scraping	Cohesive soil	9000 sq.ft	0.01

BIBLIOGRAPHY

Adams, C.E. et al, The Nature of Individual Radioactive Particles, I. Surface and Underground ABD Particles from Operation Jangle, USNRDL-374, U.S. Naval Radiological Defense Laboratory (USNRDL), San Francisco, Calif., 1952.

Anxier, J.A. et al, Experimental Evaluation of the Radiation Protection Afforded by Residential Structures Against Distributed Sources, CETO-CEX 58.1, U.S. Atomic Energy Commission (USAEC) Wash., D.C., 1959.

Baran, J.A., Blockhouse Dosage Contributions Resulting From Window-Collimated Ceiling Scattered Fallout Radiation, Dept. of Nuclear Engineering, Kansas State University, Manhattan, Kansas, 1963.

Barrett, M.J. et al, Transmission of Gamma Radiation Through Thin Finite Slabs, TI-B 64-44, Technical Operations Research, Burlington, Mass., May 1964.

Barrett, M.W. and R.L. MacNeil, Dose Rate Distribution in a Compartmental Structure. TO-B 64-1, Technical Operations Research, Burlington, Mass., June 1964.

Barrett, M.J. et al, Experimental Evaluation of Fallout Protection Using Modeling Techniques, TO-B 64-62, Technical Operations Research, Burlington, Mass., July 1964.

Barrett, M.J. and J. Waldman, Experimental Gamma Ray Backscattering by Various Materials, RI-B 63-68, Technical Operations Research, Burlington, Mass., July 1964.

Battle, Joseph, Calculating ERD During a Prolonged Exposure in a Fallout Environment, RM-OU-156-6, Research Triangle Institute, Durham, N.C., June 1964.

Brusse, J.C., A Study of the Infiltration of Radioactive Fallout Particles Into Shelter Spaces through Large Openings, Texas Engineering Experiment Station, College Station, Texas, June 1964.

Cammarano, M.V. et al, A Prototype Civil Defense Manual for Radiological Decontamination of Municipalities, Curtiss-Wright Corp., Caldwell, N.J., May 1964.

Cannell, R.S., LIVE: Plan to Survive a Nuclear Attack, Prentice Hall, New York, N.Y., 1961.

Cannon, E.W., Building Materials as Commonly Used in Existing Urban Buildings in the United States, UCIER, University of California, Berkeley, Cal., January 1958.

Clifford, C.E., Effects of Ground Roughness on the γ Dose from Cs^{137} Contamination, Defense Research Chemical Laboratories, Ottawa, Canada, March 1963.

Cochran, R.W., Scattered Radiation From a Cobalt-60 Source in a Brick Structure, USAF School of Aerospace Medicine, Brooks Air Force Base, Texas, June 1964.

Degelman, L. et al, Evaluation of the Shielding Characteristics of Structures for Simulated Residual Radiation, Dept. of Nuclear Engineering, Pennsylvania State University, University Park, Penna., November 1963.

Donovan, L.K. and A.B. Chilton, Dose Attenuation Factors for Concrete Slab Shields Covered With Fallout As A Function of Time After Fission, USNCEL-TR-137, USNCEL, Port Hueneme, California, June 1961.

Earl, J.R., Land Reclamation, USNRDL-AD-332, USNRDL, San Francisco, Calif., March 1952.

Eisenhauer, C., An Engineering Method for Calculating Protection Afforded by Structures Against Fallout Radiation, NBS-7810, National Bureau of Standards, Washington, D.C., 1963.

Facci, H.A. and M.K. Wood, PARM-Fallout and Decontamination, NREC-36, National Resource Evaluation Center, Washington, D.C., March 1964.

Huddleston, C.M. et al, Ground Roughness Effects On the Energy and Angular Distribution of Gamma Radiation From Fallout, CEX-62.81 Edgerton, Germeshausen and Grier, Inc., Las Vegas, Nevada, July 1964.

Jones, J.L. and J.F. Batter, Experimental Determination of Well-Scattered Radiation Function $G_s(\omega)$, TO-B 63-88 Technical Operations Research, Burlington, Mass., December 1963.

Ksanda, C.F., Gamma Radiations From Contaminated Planes and Slabs, USNRDL-TM-27, USNRDL, San Francisco, Calif., January 1955.

Laurino, R.K., Effectiveness Specifications for Radiological Defense Countermeasures, USNRDL-TR-47, USNRDL, San Francisco, Calif., 1955.

LeDoux, J.C. and L.K. Donovan, Shielding Factors for Underground Shelters of Various Geometric Shapes, USNCEL-TR-080, USNCEL, Port Hueneme, Calif., April 1961.

Lee, H. et al, Performance Characteristics of Land Reclamation Procedures, Operation Stoneman II, Vol. IV, USNRDL-TR-337, USNRDL, San Francisco, Calif., January 1959.

Lee, H. et al, Performance Characteristics of Dry Decontamination Procedures, Operation Stoneman II, Vol. III, USNRDL-TR-336, USNRDL, San Francisco, Calif., June 1959.

Lee, H., Estimating Cost and Effectiveness of Decontaminating Land Targets, Vol. I, Estimating Procedure and Computational Technique, USNRDL-TR-435, USNRDL, San Francisco, Calif., June 1960.

Lee, H., A Method For Determining Mission Reentry Times for Fallout-Contaminated Industrial Complexes, USNRDL-TR-585, USNRDL, San Francisco, Calif., March 1962.

Maloney, J.C. and J.L. Meredith, Cold Weather Decontamination Study, McCoy I, USANDL-TR-24, USANDL, Edgewood Arsenal, Maryland, 1962.

Maloney, J.C. et al, Cold Weather Decontamination Study, McCoy II, USANDL-TR-32, USANDL, Edgewood Arsenal, Maryland, July 1962.

Maloney, J.C. and J.L. Meredith, Simple Decontamination of Residential Areas, McCoy III, USANDL-TR-33, USANDL, Edgewood Arsenal, Maryland, September 1962.

Meredith, J.L. et al, Cold Weather Decontamination Study, McCoy IV, USANDL-TR-58, USANDL, Edgewood Arsenal, Maryland, April 1964.

Miller, C.F., Estimated Effectiveness of Common Decontamination Methods For Paved Areas and Building Surfaces, USNRDL-TR-140, USNRDL, San Francisco, Calif., 1957.

Miller, C.F., Gamma Decay of Fission Products From Slow Neutron Fission of U^{235}, USNRDL-TR-187, USNRDL, San Francisco, Calif., July 1957.

Miller, C.F. and P. Loeb, Ionization Rate and Photon Pulse Decay of Fission Products From Slow Neutron Fission of U-235, USNRDL-TR-247, USNRDL, San Francisco, Calif., August 1958.

Miller, C.F., Theory of Decontamination, USNRDL-TR-460, USNRDL, San Francisco, Calif., July 1958.

Miller, C.F., Analysis of Radiological Decontamination Data Obtained From Field Tests, USNRDL-TR-321, USNRDL, San Francisco, Calif., April 1959.

Miller, C.F., A Theory of Formation of Fallout, USNRDL-TR-425, USNRDL, San Francisco, Calif., 1960.

Miller, C.F., Nuclear War: A Post Attack Picture, Office of Civil Defense, Washington, D.C. (UNPUBLISHED)

Miller, C.F., Fallout and Radiological Countermeasures, Stanford Research Institute, Menlo Park, Calif., January 1963.

Miller, C.F. et al, Introduction to Radiological Defense Planning, Stanford Research Institute, Menlo Park, Calif., May 1965.

Owen, W.L. et al, Performance Characteristics of Wet Decontamination Procedures, Operation Stoneman II, Vol. II, USNRDL-TR-335, USNRDL, San Francisco, Calif., July 1960.

Owen, W.L., Radiological Protective Construction, USNRDL-467, USNRDL, San Francisco, Calif., January 1962.

Owen, W.L. and J.D. Sartor, Radiological Recovery of Land Target Components--Complex I and II, USNRDL-TR-570, USNRDL, San Francisco, Calif., May 1962.

Owen, W.L. and J.D. Sartor, Radiological Recovery of Land Target Components--Complex III, USNRDL-TR-700, USNRDL, San Francisco, Calif., November 1963.

Putz, R.R. and A. Broido, A Computation Method for Gamma Radiation Intensity in the Presence of General Shielding and Source Configurations, UCIER University of California, Berkeley, Calif., December 1957.

Raso, D.J. and S. Woolf, The Dose Resulting From A 1.25 Mev Plane Source Behind Various Arrangements of Iron Barriers, To-B-64-49, Technical Operations Research, Burlington, Mass., June 1964.

Rexroad, R.E. and M.A. Schmoke, Scattered Radiation and Far-Field Dose Rates From Distributed Cobalt-60 and Cs-137 Sources, USANDL-TR-2, USANDL, Edgewood Arsenal, Maryland, September 1960.

Ryan, J.T., An Error Analysis for Total Dose Calculations, RM-156-7, Research Triangle Institute, Durham, N.C., June 1964.

Ryan, J.T. et al, Radiological Recovery Concepts, Requirements and Structures, R-OU-156, Research Triangle Institute, Durham, N.C., October 1964.

Sartor, J.D. et al, Cost and Effectiveness of Decontamination Procedures For Land Targets, Operation Stoneman I, USNRDL-TR-196, USNRDL, San Francisco, Calif., December 1957.

Spencer, L.V., Structure Shielding Against Fallout Radiation From Nuclear Weapons, NBS, Monograph 42, June 1962.

Starbird, A.W. et al, The Effect of Interior Partitions on the Dose Rate in a Multistory Windowless Building, TO-B-63-6, Technical Operations Research, Burlington, Mass., January 1963.

Starbird, A.W. and J.F. Batter, Angular Distribution of Skyshine Radiation At the Surface of A Plane of Fallout Contamination, TO-B 63-40, Technical Operations Research, Burlington, Mass., March 1964.

Strope, W.E. et al, Protection and Decontamination of Land Target and Vehicles, Operation Jangle, Project 6.2, WT-400, DASA, June 1952.

Strope, W.E., Radiological Defense Measures as a Countermeasure System, USNRDL-TR-74, USNRDL, San Francisco, Calif., February 1956.

Strope, W.E., Evaluation of Countermeasure System Components and Operational Procedures, Operation PLUMBBOB, Project 32.3, WT-1464, DASA, August 1958.

Taylor, D. et al, Development of Radiological Decontamination Methods and Equipment for Cold Weather Regions, USNCEL, Port Hueneme, Calif., July 1960.

The Effects of Nuclear Weapons, U.S. Government Printing Office, Washington, D.C., 1957.

Radiological Recovery of Fixed Military Installations, NAVDOCKS-TP-PL-13, April 1958.

Fallout Shelters Survey: Guide for Architects and Engineers, OCD Document NP-10-2, National Plan Appendix Series, May 1960.

Design and Review of Structures For Protection From Fallout Gamma Radiation, DOD-OCD-EN-61-1, October 1961.

Exposure to Radiation in an Emergency, National Committee on Radiation Protection and Measurement, Report No. 29, University of Chicago, Chicago, Ill., January 1962.

National Fallout Shelter Survey, Phase 2, Computer Printouts, OCD, Washington, D.C., 1963.

UNCLASSIFIED
Security Classification

DOCUMENT CONTROL DATA - R&D

(Security classification of title, body of abstract and indexing annotation must be entered when the overall report is classified)

1. ORIGINATING ACTIVITY (Corporate author) STANFORD RESEARCH INSTITUTE Menlo Park, California 94025	2a. REPORT SECURITY CLASSIFICATION Unclassified 2b. GROUP

3. REPORT TITLE

RADIOLOGICAL TARGET ANALYSIS PROCEDURES

4. DESCRIPTIVE NOTES (Type of report and inclusive dates)

5. AUTHOR(S) (Last name, first name, initial)

LEE, Hong

6. REPORT DATE March 1966	7a. TOTAL NO. OF PAGES 94	7b. NO. OF REFS 15
8a. CONTRACT OR GRANT NO. N228-(62479)65421 b. PROJECT NO. OCD Work Unit No. 3231C c. SRI Project No. MU-5069 d. USNRDL TRC-6	9a. ORIGINATOR'S REPORT NUMBER(S) 9b. OTHER REPORT NO(S) (Any other numbers that may be assigned this report)	

10. AVAILABILITY/LIMITATION NOTICES

Distribution of this document is unlimited.

11. SUPPLEMENTARY NOTES	12. SPONSORING MILITARY ACTIVITY Office of Civil Defense Department of the Army Washington, D.C. 20310

13. ABSTRACT

The radiological target analyses in this report consist of a series of analytical procedures for evaluating the residual numbers for shelters and other locations before, during, and after decontamination so that exposure doses may be calculated. These residual numbers are used to provide estimates of (1) shelter stay times, (2) manpower requirements for proposed decontamination, (3) exposure to recovery personnel, (4) decontamination effectiveness requirements, (5) equipment and supplies requirements, and (6) feasibility of plans and schedules for the recovery of vital facilities and living areas. Tables, charts, figures, and sample calculations provide working tools which may be used for civil defense planning and training and similar practical levels of radiological defense preparation.

DD FORM 1 JAN 64 1473

UNCLASSIFIED
Security Classification

CPG 2-1A2
June 1973

DCPA ATTACK ENVIRONMENT MANUAL

CHAPTER 2

WHAT THE PLANNER NEEDS TO KNOW
ABOUT BLAST AND SHOCK

DEFENSE CIVIL PREPAREDNESS AGENCY
DEPARTMENT OF DEFENSE

JUNE 1973

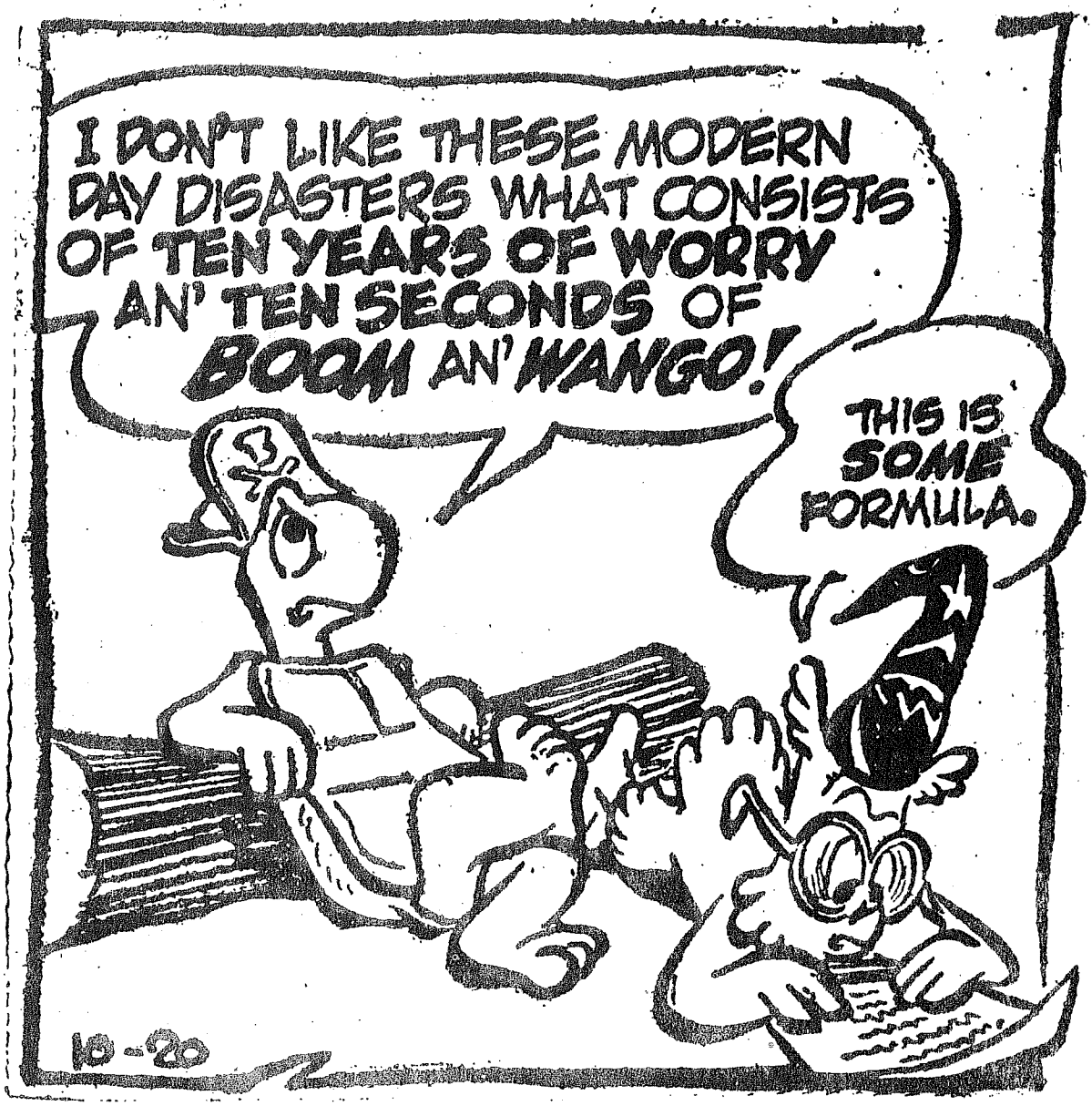

© 1954 Walt Kelly. Courtesy Publishers—Hall Syndicate.

PANEL 1

THE IMPORTANCE OF "LOW" OVERPRESSURES

The fact that civil defense planning is largely concerned with the low overpressure region of the direct effects area should not be interpreted as concern for only a small part of the area affected by blast. Quite the contrary, most of the direct effects area is subjected to "low" overpressures. We have seen that an ability to position the population of the Detroit metropolitan area in basements with a median lethal overpressure of 12 psi would have doubled the survivors of a very heavy attack.

The importance of knowledge about the effects of low overpressure is graphically illustrated in these two sketches. The upper sketch is the picture of direct effects of a 5-MT surface burst that has been presented in OCD literature, including the Federal Civil Defense Guide, for the past 5 years. It shows the limit of light damage as extending to 9 miles from ground zero. The lower sketch is the recent revision of this effects picture. It shows light damage extending to 13 miles. This change more than doubles the direct effects area.

A close comparison of the two sketches reveals that the principal change was a downward shift of 1/2 psi in the overpressure needed to cause damage—from 2.5 psi to 2 psi for moderate damage and from 1.5 psi to 1 psi for light damage. The change came about as the result of experimental work, some of which will be described in this chapter. It is significant that such small changes in knowledge of blast effects can make such large changes in the area of coverage. The implication for emergency planning is that small changes in the vulnerability of people can make large changes in survival. Intelligent use of best available shelter can result in such changes.

And, remember: The area covered by overpressures less than 12 psi constitutes 95 percent of the whole area experiencing at least 1 psi blast.

EFFECTS OF A 5 MT BLAST

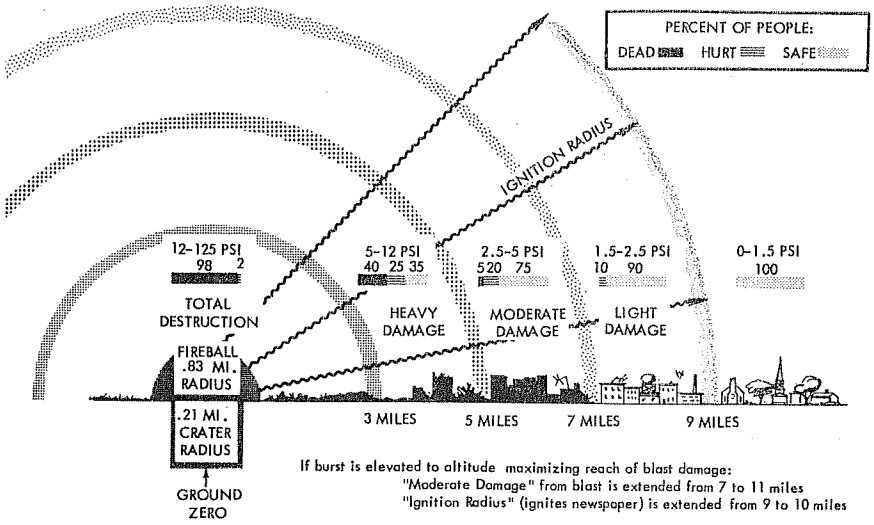

If burst is elevated to altitude maximizing reach of blast damage:
"Moderate Damage" from blast is extended from 7 to 11 miles
"Ignition Radius" (ignites newspaper) is extended from 9 to 10 miles

DIRECT EFFECTS OF 5 MT. BLAST (SURFACE BURST)

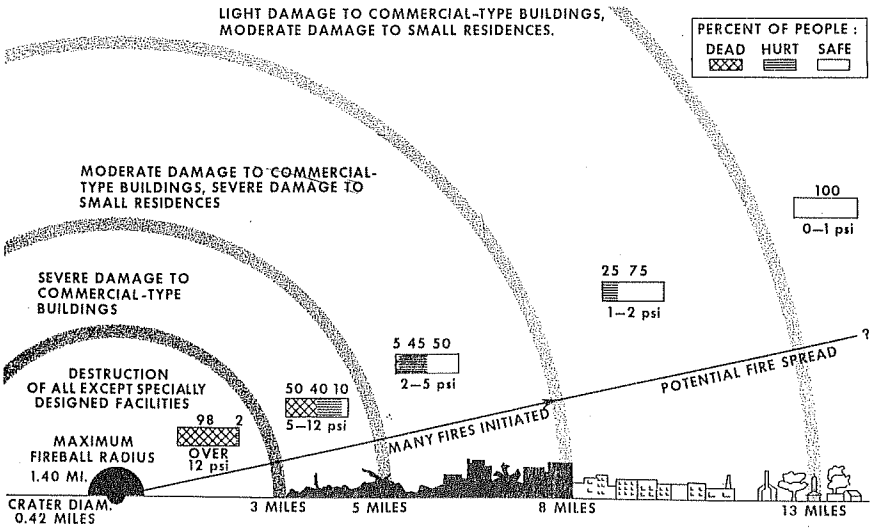

IF BURST IS ELEVATED TO ALTITUDE MAXIMIZING THE REACH OF BLAST DAMAGE, MODERATE DAMAGE FROM BLAST AND INITIAL FIRES ON A CLEAR DAY ARE EXTENDED FROM 8 MILES TO 13 MILES.

BLAST WAVE CHARACTERISTICS
(surface burst)

Peak Overpressure (psi)	Wind Velocity (mph)	Wind Duration for 5-MT Burst (sec)
1	35	9.5
2	70	8.5
5	160	6.8
10	290	6.0
20	470	5.8
30	670	5.6
100	1400	4.3

SUBWAYS, TUNNELS, MINES, AND CAVES

About 12 million fallout shelter spaces have been identified in underground areas, both man-made and natural. Nearly all of these areas offer good blast protection as well. The Soviet Union has emphasized the use of subways as blast shelters in cities. They have provided blast doors in the entrances to the subway station.

Most underground structures are stronger than building basements against blast loading. A recent analysis of a subway station being built in Washington, D.C., indicated that it could withstand an overpressure of 100 psi. Without blast doors, survival might be limited to 30 or 40 psi because of the blast wave entering through entrances and ventilation openings.

Underground subways and tunnels usually contain a large volume of air. When the blast wave enters through relatively small openings into a large-volume space, the blast wave overhead will pass by before the chamber has time to fill. This means that the pressure rise is relatively slow, which increases survival chances, and the overpressure inside may never reach the outside peak overpressure.

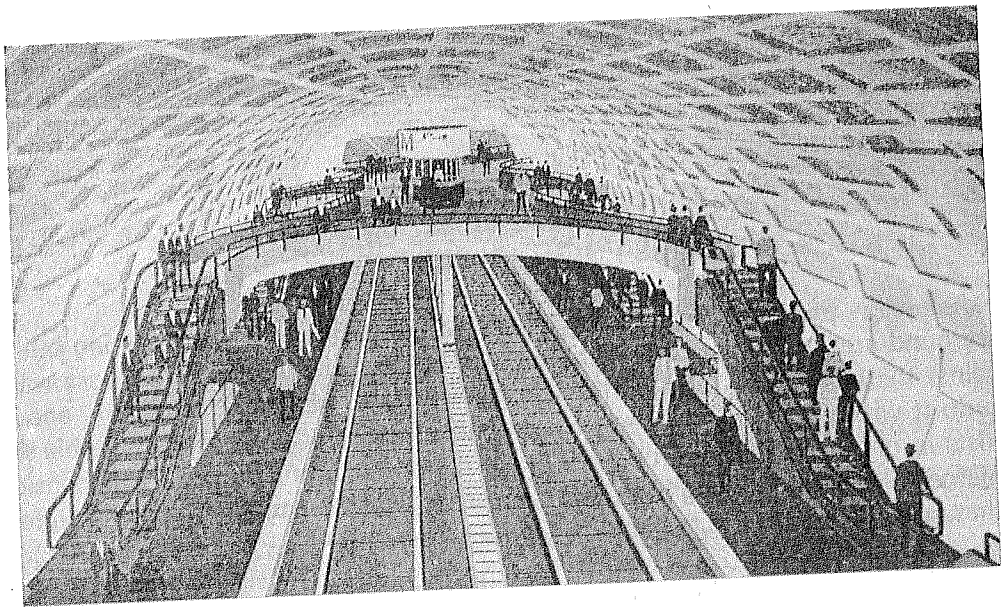

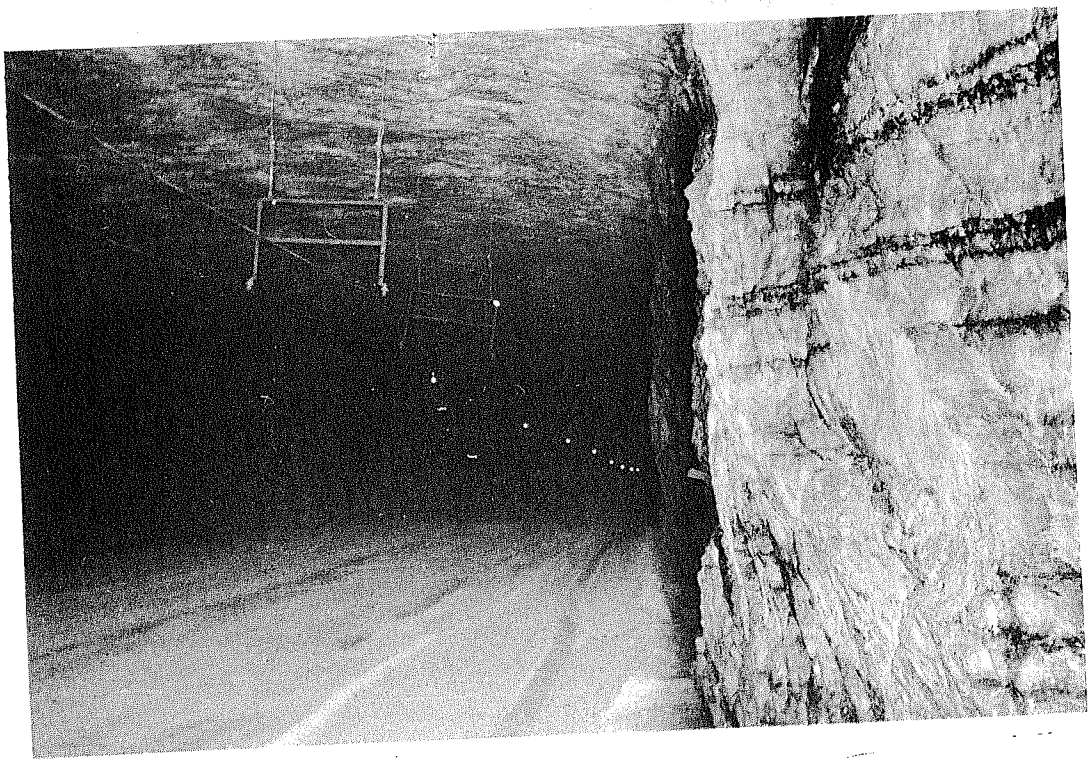

PANEL 18

RELATIVE BLAST PROTECTION

Preference	Description
A	Subway stations, tunnels mines, and caves with large volume relative to entrances.
B	Basements and sub-basements of massive (monumental) masonry buildings.
C	Basements and sub-basements of steel and reinforced-concrete framed buildings having flat slab or slab and beam ground floor construction.
D	First three floors of buildings with "strong" walls.
E	Basements of wood-frame and brick-veneer residences.
F	Fourth and higher floors of buildings with "strong" walls.
G	Basements of steel and reinforced-concrete framed buildings with flat plate ground floor.
H	First three floors of buildings with weak walls, brick buildings and residences
I	Fourth and higher floors of buildings with weak walls.

PROTECTIVE POSTURE FOR BLAST SURVIVAL

As noted previously, being thrown by the blast wind is the main source of injury and death in aboveground locations. Lying down rather than standing up is the preferred protective posture and would save many lives.

In basement areas, the hazard situation is somewhat different. People in basements will be subjected to severe wind forces only for as long as it takes the blast overpressure to fill the basement volume. The blast wave would enter through stairways, ventilation ducts, and other openings. In most basements, the filling process would be complete in several tenths of a second as compared to the several seconds of wind gust aboveground. In the vicinity of the major openings, however, the compressed air behind the shock front will rush into the shelter in the form of a high velocity air jet, as shown in the sketch.

The velocity in the jet can be sufficient to cause impact injury and death for a distance up to 10 times the width of the entranceway. In planning the use of basement areas, this hazard should be taken into account. The best location for people is near the exterior wall of the basement, out of the line of the entranceways. This location also takes advantage of the failure pattern of the ground floor over the basement. Since good basement space will usually be at a premium, people should be close-packed in a sitting position, with children sitting between the legs of adults. This protective posture can be maintained for several hours after the shelter is occupied. If people must be located in more hazardous areas, they should be encouraged to lie prone.

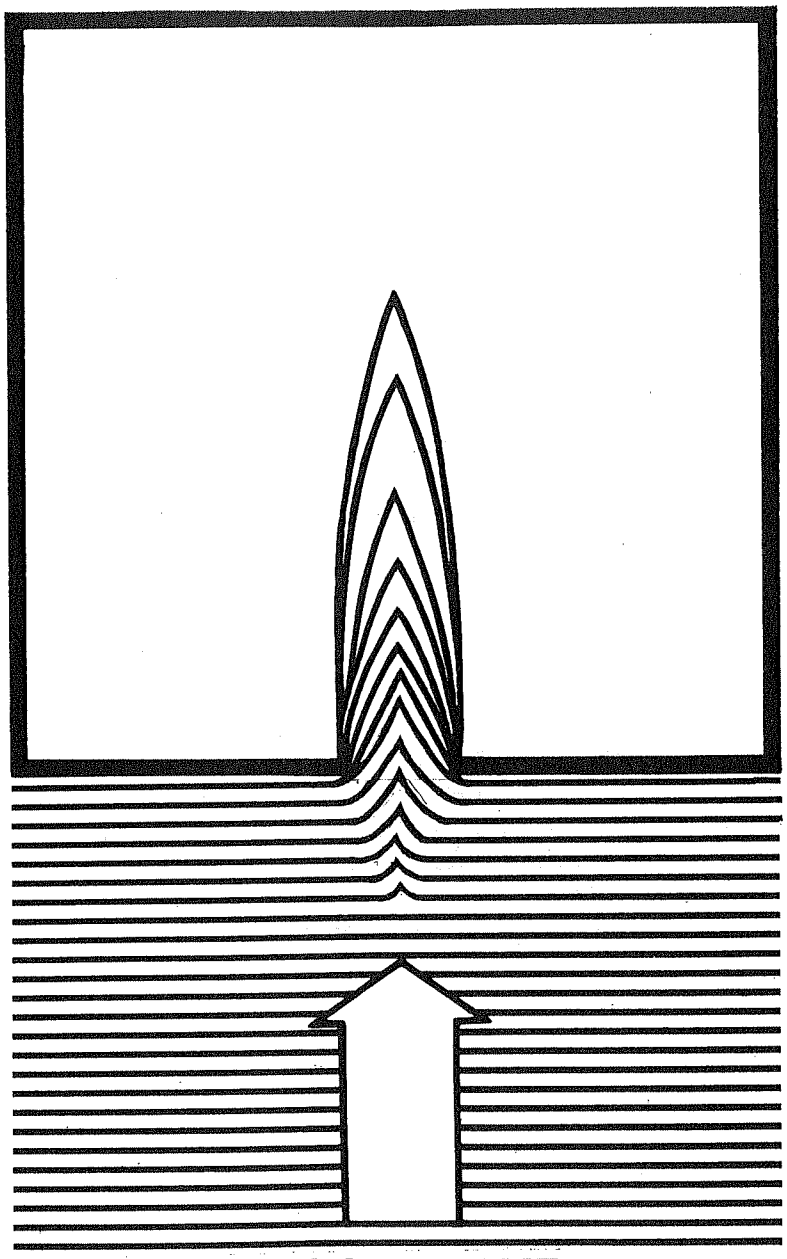

SHOCK WAVE

PANEL 20

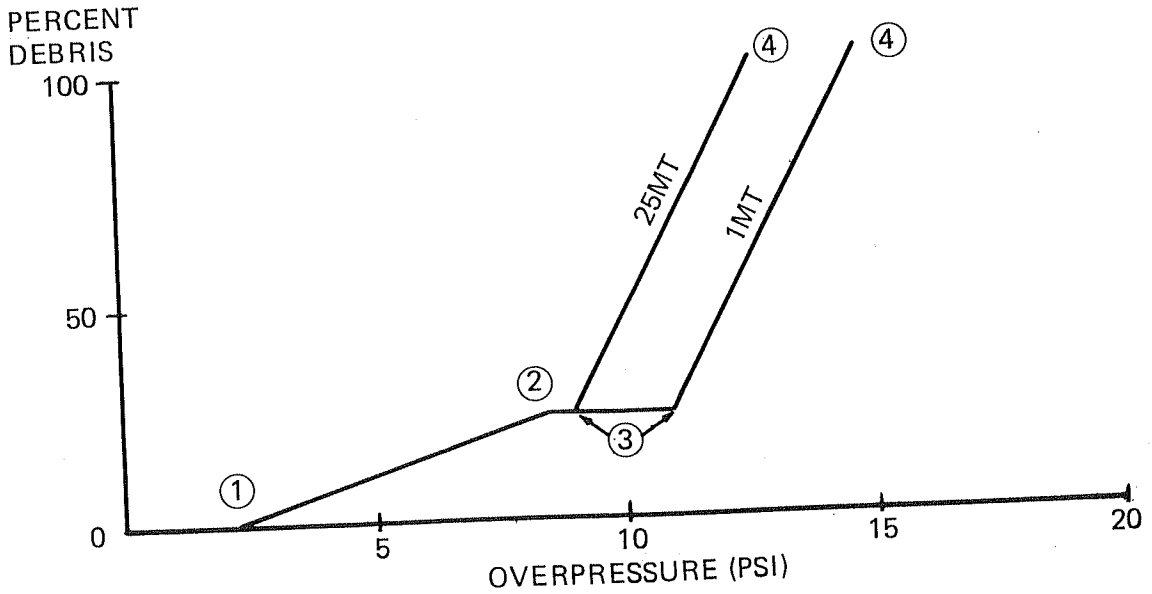

DEBRIS CHART FOR MULTISTORY STEEL OR
R.C. FRAMED BUILDING WITH LIGHT EXTERIOR PANELS

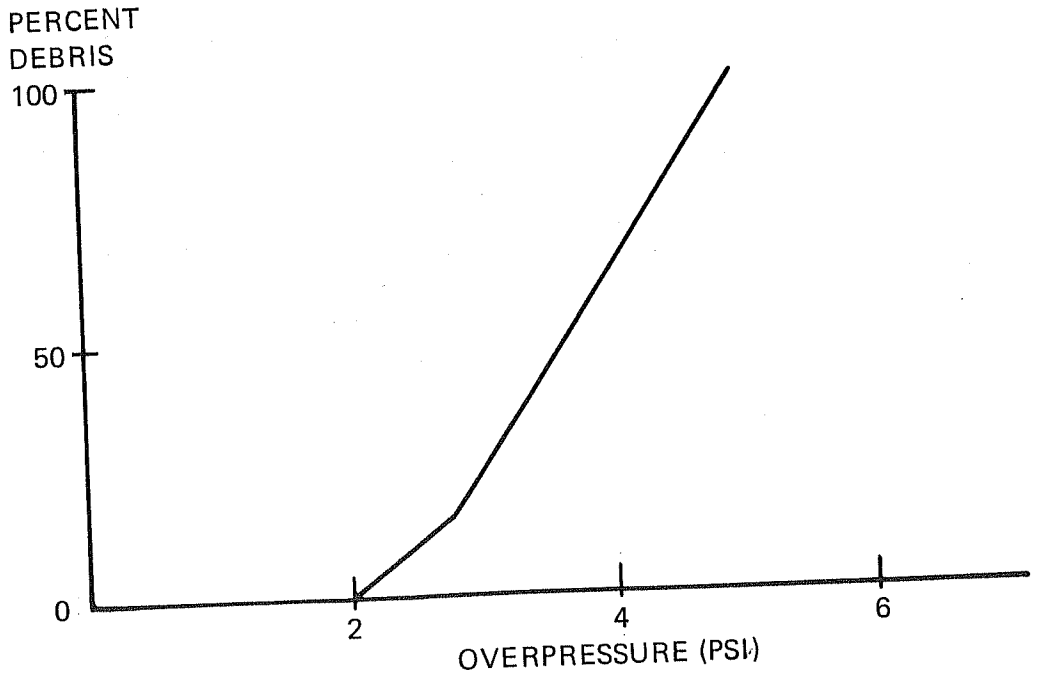

DEBRIS CHART FOR WOOD-FRAME BUILDING

TYPICAL DEBRIS DEPTHS

Building	Average Debris Depth (feet)
One-story Industrial	0.3
Two-story Wood-frame Residence	0.5
One-story Brick Residence	0.5
Three-story Duplex or Row House	3.0
Five-story Steel-frame Apartment House	7.0
Twenty-three-story High-rise Building	33.0

VEHICLE DAMAGE

Type	Moderate Damage (psi)	Inoperable (psi)
Automobiles	3 - 5	5 - 6
Buses	6 - 10	10 - 12
Fire Trucks	6 - 10	10 - 12
Repair Trucks	6 - 10	10 - 12
Earth and Debris Moving Equipment	20 - 30	30 - 35
Truck-Mounted Engineering Equipment	12 - 15	15 - 17
Railroad Cars	15	25
Locomotives	30	80

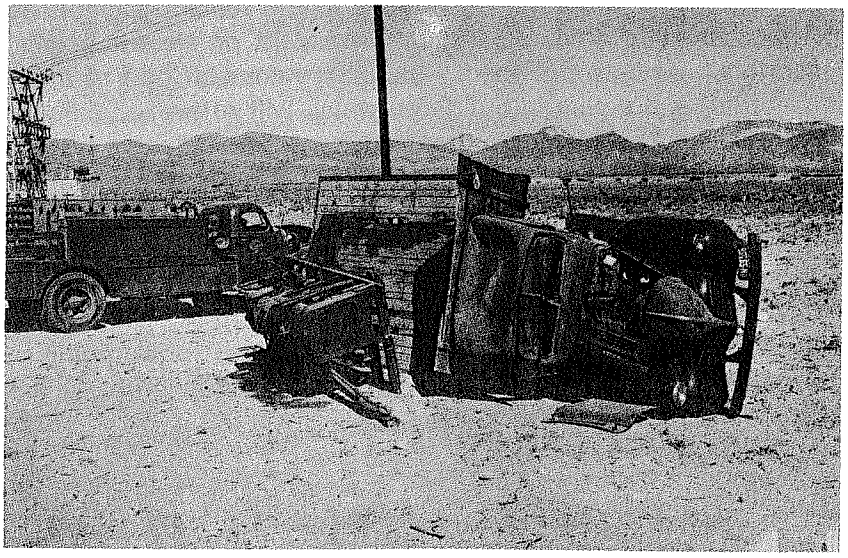

Vehicle damage at 5 psi, Nevada Test Site; both vehicles operable.

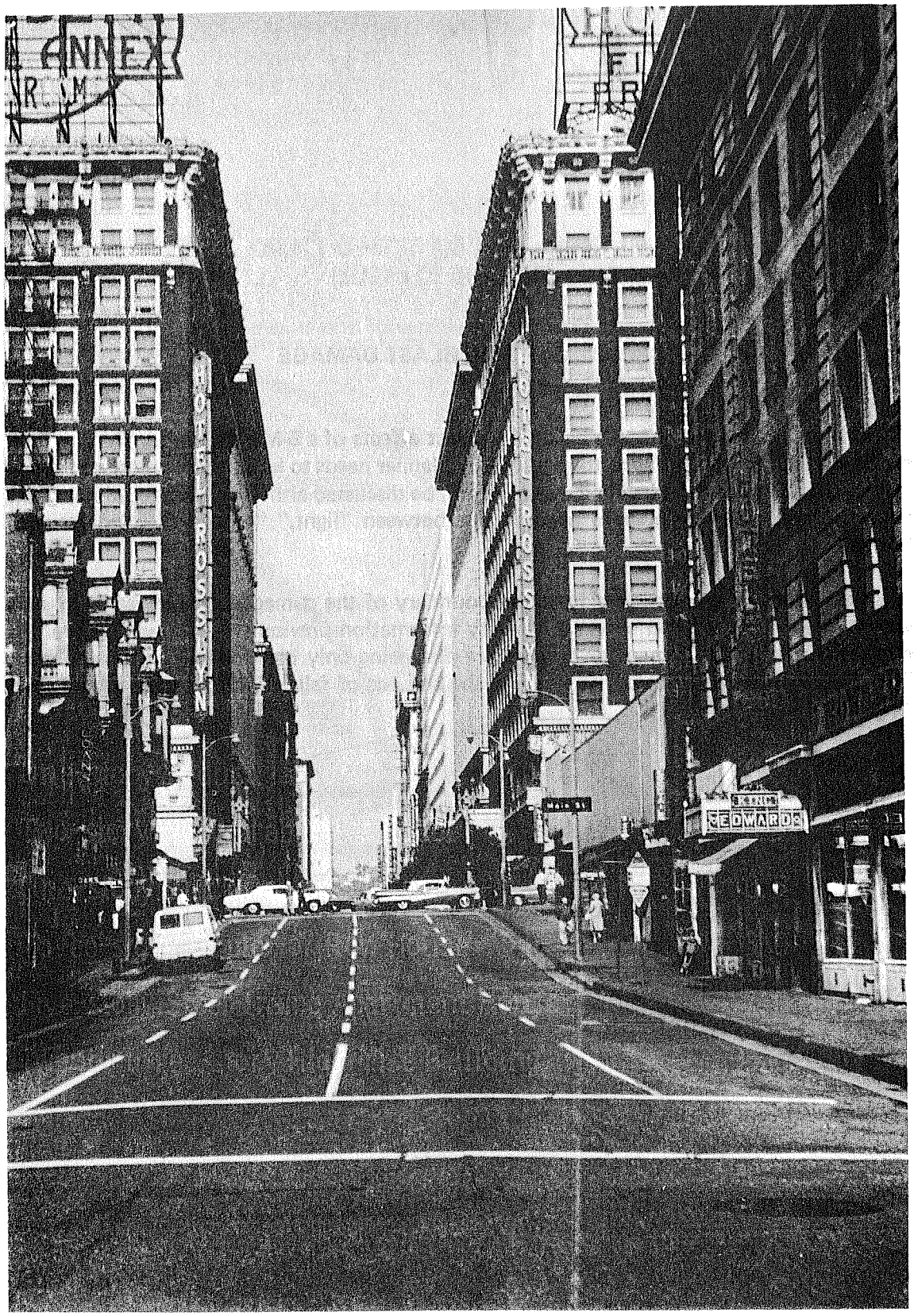

PANEL 32

DIRECT EFFECTS OF 5 MT. BLAST (SURFACE BURST)

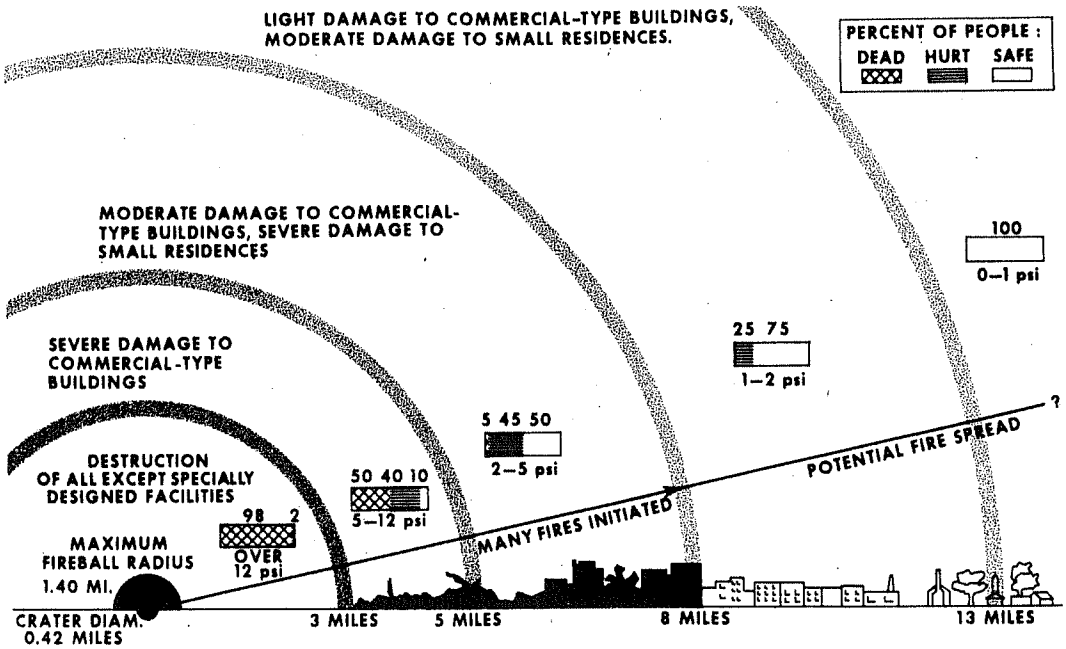

IF BURST IS ELEVATED TO ALTITUDE MAXIMIZING THE REACH OF BLAST DAMAGE, MODERATE DAMAGE FROM BLAST AND INITIAL FIRES ON A CLEAR DAY ARE EXTENDED FROM 8 MILES TO 13 MILES.

PANEL 36

SUGGESTED ADDITIONAL READING

The following sources provide additional background on the material in this chapter:

Effects of Nuclear Weapons, Revised Edition 1964, Glasstone, S., (editor), Chapters III, IV, V, XI, and XII, Superintendent of Documents, GPO.

Andersen, Ferd E., Jr., et al., **Design of Structures to Resist Nuclear Weapons Effects**, ASCE Manual of Engineering Practice No. 42, 345 E. 47th St., New York, New York. 1961.

Davisson, M.T., et al., **Air Force Design Manual**, University of Illinois, AFSWC-TDR-62-138, December 1962, National Technical Information Service, Springfield, Va.

Coulter, G.A., **Flow in Model Rooms Caused by Air Shock Waves**, Ballistic Research Laboratories Memorandum Report 2044, July 1970. (AD 711 885).

Wilton, C., and B. Gabrielson, **Shock Tunnel Tests of Wall Panels**, URS Research Company, January 1972. (AD 747 331).

Wiehle, C.K., and J.L. Bockholt, **Blast Response of Five NFSS Buildings**, Stanford Research Institute, October 1971. (AD 738 547).

Wiehle, C.K., and J.L. Bockholt, **Existing Structures Evaluation, Part IV. Two-Way Action Walls**, Stanford Research Institute, September 1970. (AD 719 306).

White, C.S., **The Nature of the Problems Involved in Estimating the Immediate Casualties from Nuclear Explosions**, CEX 71.1, NTIS, U.S. Department of Commerce, Springfield, Virginia.

Longinow, A., et al., **Civil Defense Shelter Options: Deliberate Shelters**, IIT Research Institute, December 1971. (Volume I, AD 740 174; Volume II, AD 740 175).

CPG 2-1A3
June 1973

DCPA ATTACK ENVIRONMENT MANUAL

CHAPTER 3

WHAT THE PLANNER NEEDS TO KNOW
ABOUT FIRE IGNITION AND SPREAD

DEFENSE CIVIL PREPAREDNESS AGENCY
DEPARTMENT OF DEFENSE

JUNE 1973

LIKELIHOOD OF THERMAL SHIELDING

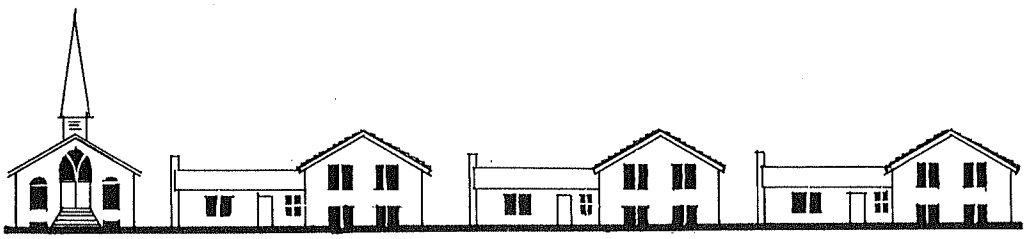

ONE AND TWO FAMILY HOMES **27-34%**

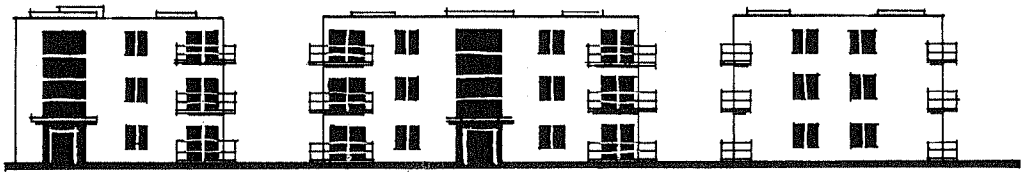

THREE STORY APARTMENTS **46-54%**

TENEMENTS, COMMERCIAL, HIRISE **88-92%**

PANEL 3

EFFECT OF VISIBILITY ON TRANSMISSION OF THERMAL PULSE

Weather	Transmitted Energy
CLEAR DAY (visibility = 12 miles)	100%
LIGHT HAZE (visibility = 6 miles)	70%
MEDIUM HAZE (visibility = 3 miles)	50%
THIN FOG or LIGHT CLOUDS (visibility = 1.2 miles)	30%
HEAVY FOG (visibility less than 1/2 mile)	10%

From Gibbons, M., **Transmissivity of the Atmosphere for Thermal Radiation from Nuclear Weapons**, USNRDL, August 1966, AD 641 481.

COMMON KINDLING FUELS

	WEAPON YIELD (MT)		
	1	5	25
	(calories per square centimeter)		
GROUP I			
Crumpled newspaper, dark picture area	7	9	15
Black lightweight cotton curtains	6	8	11
Dry rotted wood and dry leaves	6	7	10
GROUP II			
Beige lightweight cotton curtains	32	42	55
Kraft corrugated paper carton	19	22	32
White typing paper	30	42	60
Heavy dark cotton drapes	22	27	50
GROUP III			
Upholstered Furniture	28	40	56
Beds	22	34	52

RELATIONSHIP OF BLAST AND HEAT
(Surface Burst on a Clear Day)

BLAST OVERPRESSURE (psi)	HEAT RADIATION (cal. /sq. cm.)		
	1 MT	5 MT	25 MT
1	6	4	2.5
2	21	18	14
5	100	100	105
12	350	440	620
20	560	900	1500

INITIAL FIRES FROM A 5-MT SURFACE BURST IN DETROIT

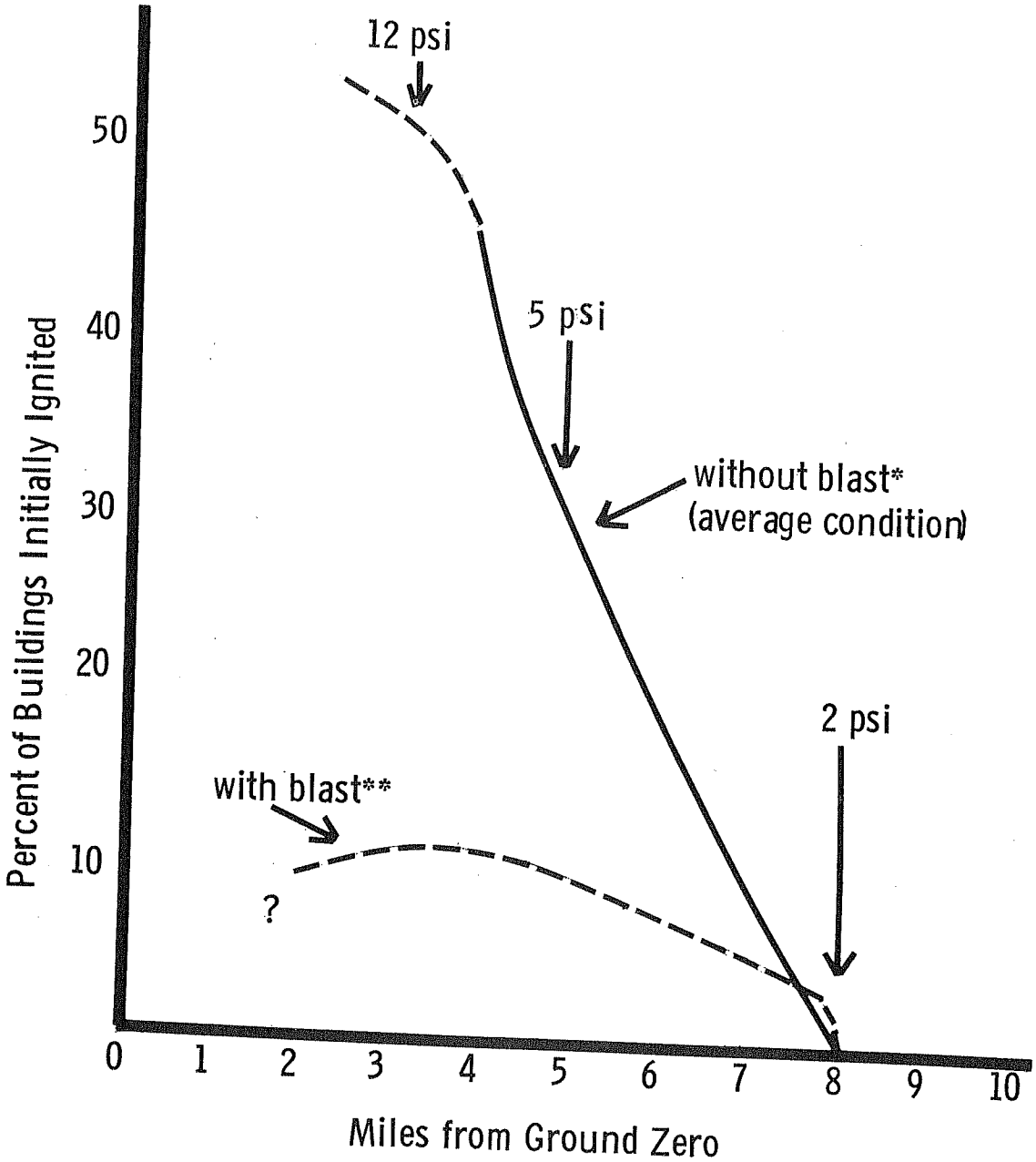

*From Takata and Salzberg, **Development and Application of a Complete Fire Spread Model**, IITRI, June 1963, AD 684 874.

Based on Miller, R.K., et al., **Analysis of Four Models of the Nuclear-Caused Ignitions and Early Fires in Urban Areas, The Dikewood Corporation, August 1970, AD 716 807.

CASUALTIES IN LARGE FIRES

Loss of life in the large fires of World War II was considerable. The term "firestorm," coined by a German journalist, dramatically expressed the awesome nature of some of these mass fires. It took little imagination to transfer the worst of these occurrences to the event of nuclear attack. Numerous writers were led to postulate great areas of fire in which survival was unthinkable.

To gain a more objective understanding of the fire threat, DCPA has sponsored a number of studies of World War II fire experience in considerable detail. One of the results of this analysis is shown here. The loss of life among the population at risk for a large number of war fires was found to be related to the fire severity. The severity of a large fire was expressed in terms of the average heat output as measured in millions of BTU per square mile of fire area per second. [A BTU (British Thermal Unit) is similar to a calorie, being the amount of heat necessary to raise the temperature of a pound of water 1 degree Fahrenheit. A BTU is equal to 252 calories.]

Note that a large number of wartime fires are classed as "group fires." The fire severity ranged up to about 300 million BTU per square mile per second and the loss of life ranged up to 5 percent of the population at risk. Note also that the fires caused by the nuclear detonations at Hiroshima and Nagasaki are among the least severe.

At the other end of the chart are a relatively few war fires labeled "firestorm events." These cases generated a fire severity between 600 and 700 million BTU per square mile per second. The corresponding loss of life ranged between 12 and 20 percent of the population at risk. All of these "firestorms" occurred in German cities.

FATALITIES IN WORLD WAR II FIRES*

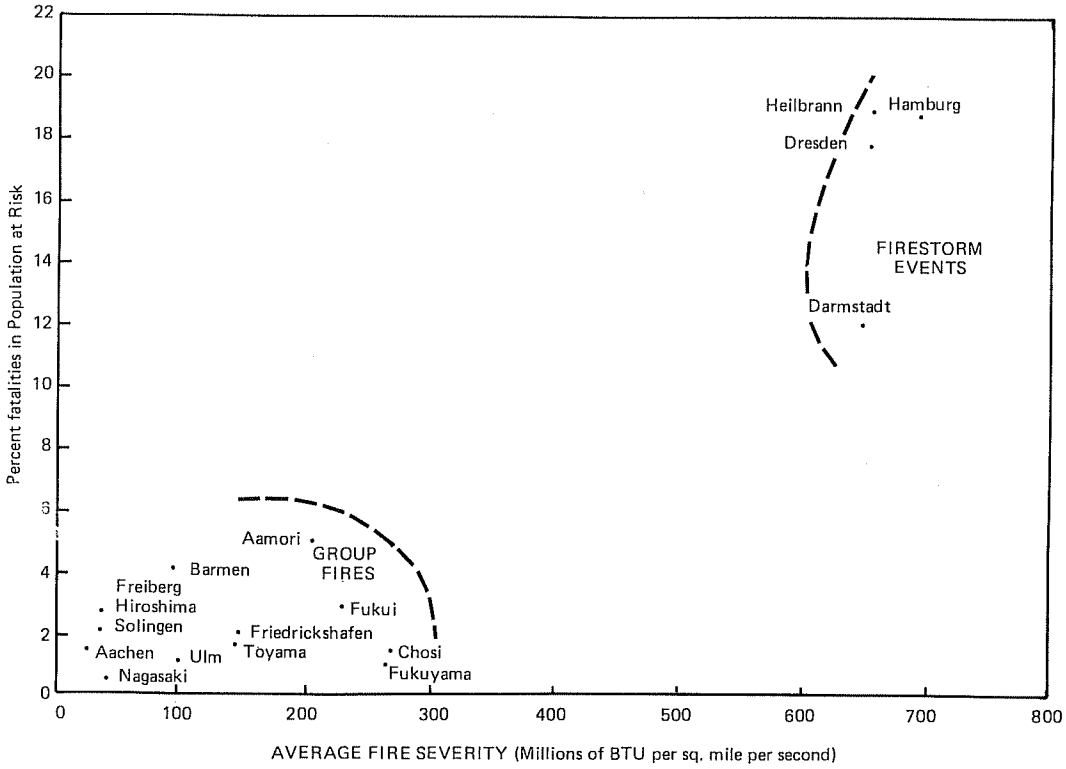

*Lommasson and Keller, **A Macroscopic View of Fire Phenomenology and Mortality Predictions**, Dikewood Corporation, DC-TN-1058-1, December 1966.

FIRESTORM POSSIBILITIES

The marked increase in loss of life found in "firestorm events" focused early attention on the nature of these fires and the necessary conditions for their occurrence. The fire research community is not entirely agreed on what constitutes a firestorm, except in broad qualitative terms. What is generally meant is a mass fire characterized by high-velocity inrushing winds, a well-developed convection or smoke column reaching high into the atmosphere, and little spread beyond the area that contained the initial fires. It has been considered significant that the only clear-cut firestorm events in World War II occurred in German cities, of which the Hamburg fire was the most extreme and the most studied.

Research has been done relating fire-induced inrush wind velocities to the energy release rate of these large fires. In Germany, velocities of 50 miles per hour or greater were associated with firestorms. Winds of 40 mph or less were associated with group fires. Peak fire-induced winds at Hiroshima were estimated to reach 35 mph, which places it well down in the group fire category.

Group fires burn outward with spread from the initial fires determined by the closeness of buildings and the wind conditions prevailing at the time. Firestorms apparently involve rapid spread within the firestorm area to initially unignited structures, aided most probably by the high inrush winds. This one hundred percent involvement in firestorms is confirmed by observer reports.

From 1963 to 1967, OCD participated jointly with the U.S. Forest Service and the Defense Nuclear Agency in a series of mass fire experiments called Operation FLAMBEAU. Slash timber was piled in large arrays representing houses and burned to measure the resulting fire environment. The left-hand picture shows the largest array, occupying 40 acres, before the burn. The right-hand picture shows the array at the height of the burn. Through these tests and other work, it was confirmed that the energy release from a large fire depended on the amount of fuel available, the burning rate of the individual buildings, and the weather conditions at the time of the fire. The table indicates the conditions thought necessary for production of a firestorm.

Since we now estimate that only about 10 percent of the buildings will be ignited by a nuclear detonation, one of the criteria for firestorm conditions, that at least 50 percent be on fire initially, is not met. In other words, present evidence suggests that the most severe nuclear fire situation will be similar to that which occurred in Hiroshima. The information in the next few panels confirms this view.

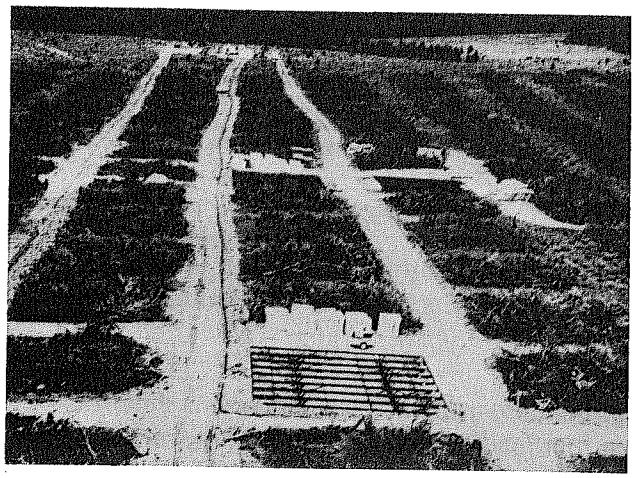

Flambeau plot before burning

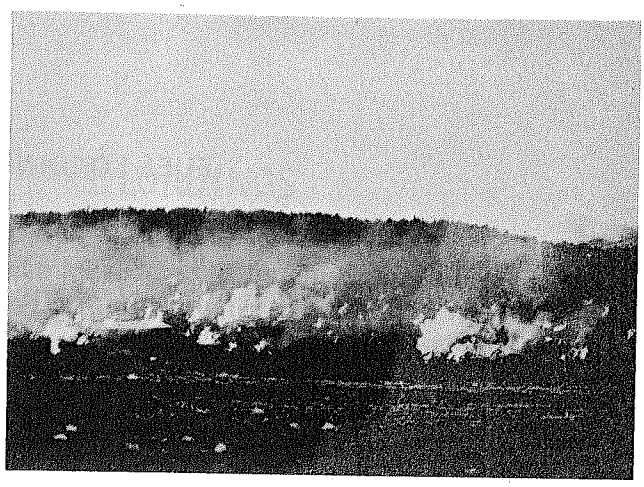

Flambeau plot during burning

CRITERIA FOR PREDICTING FIRESTORMS*

- Greater than 8 pounds of fuel per square foot of fire area.
- Greater than 50 percent of structures on fire initially.
- Surface wind less than 8 miles per hour initially.
- Fire area greater than 0.5 square mile.

*Rodden, R.M., et al, **Exploratory Analysis of Fire Storms**, Stanford Research Institute, 1965, AD 616 638.

FUEL LOADING AND BUILTUPNESS

The total amount of combustibles in a building, including both structure and contents, has an important bearing on the potential severity of fires. Each pound of combustibles typically generates about 8000 BTU upon burning.

An estimated range of fuel loadings in typical building uses or "occupancies" is shown here. Whether a particular structure would have a fuel loading near the high or low end of the range shown depends mainly on the type of construction of the building. For example, the typical combustible contents of residences averages about 3.5 pounds per square foot of floor area, so a total fuel loading near 20 would indicate a home constructed largely of wood whereas a fuel loading of 10 pounds per square foot would be appropriate to brick or other masonry construction.

Similarly, the combustible contents of office and commercial space ranges from 7 to 10 pounds per square foot of floor area. Combustible contents of industrial and storage buildings vary quite widely depending on the nature of the operations involved.

Another important factor in fire growth and spread is the density of construction. This factor is called "building density" or "builtupness" and is expressed usually as the fraction of the total area, including streets, parks, and the like, that is under roof. Typically, the building density in residential tracts ranges from about 10 to 25 percent; that in commercial and downtown areas up to 40 percent. Industrial and storage areas can vary widely in building density. Those with very high density are often referred to as "massive industrial" areas.

The combination of builtupness and fuel loading per square foot of building gives the fuel loading per square foot of fire area. The firestorm area at Hamburg was about 45 percent builtup with buildings having a fuel loading of about 70 pounds per square foot. This would mean about 32 pounds of fuel per square foot of fire area, four times the 8 pounds per square foot estimated as the minimum necessary for firestorm conditions.

In contrast, a residential area 10 percent builtup with single-story wood-frame detached homes would have a fuel loading of only 2 pounds per square foot, well below the criterion.

ESTIMATED RANGE OF FUEL LOADINGS

OCCUPANCY	FUEL LOAD PER STORY* (pounds per square foot)
Hi-Rise Residential (Fire Resistive)	3 - 5
Brick or Frame Residential	10 - 20
Office and Commercial	10 - 40
Industrial	0 - 30
Storage	20 - 80

*Includes building structure and contents.

ESTIMATES OF BURNING TIMES

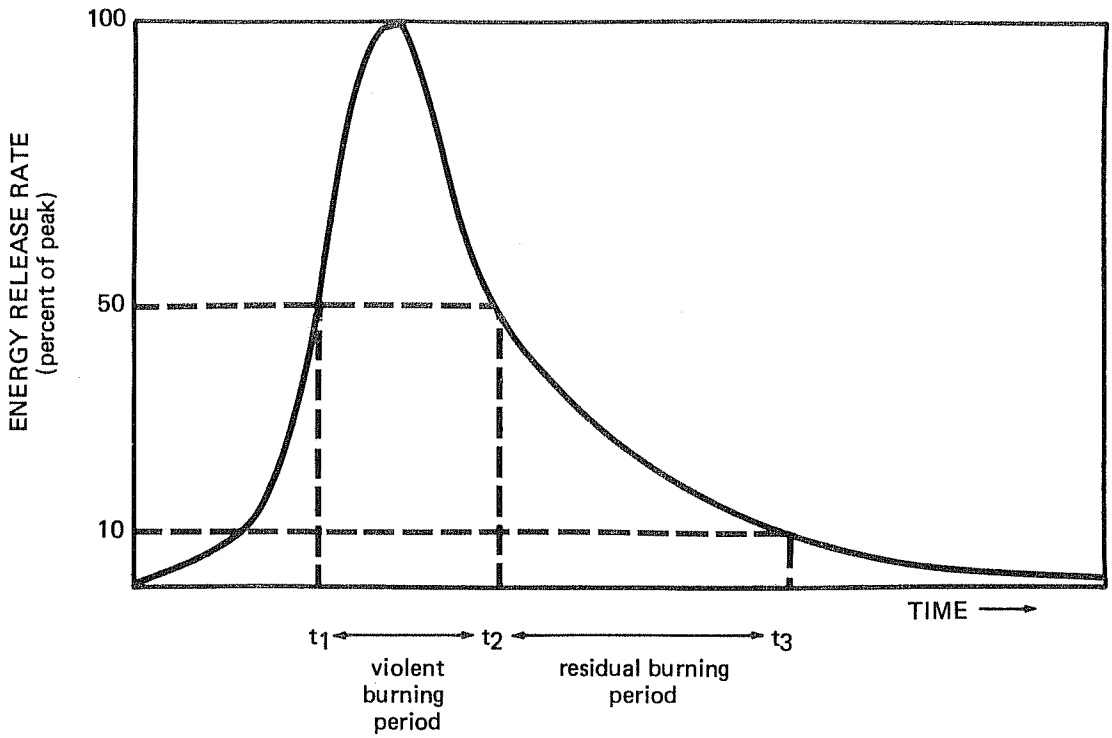

BURNING TIMES FOR URBAN STRUCTURES*

CONSTRUCTION TYPE	VIOLENT BURNING		RESIDUAL BURNING	
	TIME (min.)	ENERGY RELEASE (percent)	TIME (min.)	ENERGY RELEASE (percent)
Light Residential	10	80	12	20
Heavy Residential	13	70	20	30
Commercial	25	60	60	40
City Center and Massive Manufacturing	55	30	120	70

*From Chandler, et al., **Prediction of Fire Spread Following Nuclear Explosions,** Pacific Southwest Forest and Range Experiment Station, U.S. Forest Service, 1963.

FIRE SEVERITY

We have now covered the chief factors involved in estimates of fire severity in nuclear attack. These are: (1) the fuel loading in individual buildings, (2) the builtupness or building density of the area, (3) the burning rate of buildings, and (4) the proportion of buildings burning at the same time. It will be useful to summarize what this information means.

We have already mentioned that, in the Hamburg "firestorm" area, there was a fuel loading of about 32 pounds of fuel per square foot of fire area. Using the heat value of combustibles as about 8000 BTU per pound, and a burning time of 2 hours and 55 minutes for buildings in city centers, we can calculate an average energy release rate, or "power density" as the fire research community prefers to call it, of about 685 million BTU per square mile per second—which is not far from the estimate in the World War II fire casualty chart shown in Panel 10.

At Hamburg, at least 50 percent of the structures were initially set on fire and the burning period was so long that the others also were burning at the same time as those initially on fire. The upper calculation shown here assumes this.

Now, take another example—2-story brick residences, perhaps many row houses, so that the area is 25 percent built-up. As we have seen, such houses might have about 10 pounds of fuel per square foot per story or 20 pounds per square foot for 2-story buildings. At 25 percent builtupness, this would be 5 pounds of fuel per square foot of fire area, less than the "magic number" of 8 pounds previously given as the threshold for possible firestorm events. Using a burning period of 33 minutes (1980 seconds) for "heavy residential" construction and 10 percent of the buildings burning simultaneously, we obtain a fire severity of about 56 million BTU per square mile per second, somewhat higher than that estimated for Hiroshima. In Japan, the burning time of most buildings was short, since there was a great deal of light construction. Only a portion of buildings were burning at the same time, and hence, firestorms did not result. This appears to be the situation in American cities as well and perhaps is the case for all nuclear detonations.

Fire defense can be planned for the fire environment expected in nuclear attack. What measures will be effective can be determined from the details of fire growth and spread described in the next series of panels.

SOME TRIAL CALCULATIONS

The Hamburg Case:

Fire Severity - 8000 BTU per pound of fuel times 32 pounds of fuel per square foot of fire area times 28 million square feet per square mile divided by 10,500 seconds burning time for "city center and massive manufacturing" areas

or

Fire Severity = about 685 million BTU per square mile per second average rate of energy release.

Heavy Residential Case in Nuclear Attack

Fire Severity - 8000 BTU per pound of fuel times 10 pounds of fuel per square foot per story in brick buildings times 2 stories average building height times 0.25 fraction of the area covered by buildings times 28 million square feet per square mile divided by 1980 seconds burning time in "heavy residential" construction times 1/10 of the buildings burning at one time,

or

Fire Severity = about 56 million BTU per square mile per second average rate of energy release.

DOWNTOWN CHICAGO

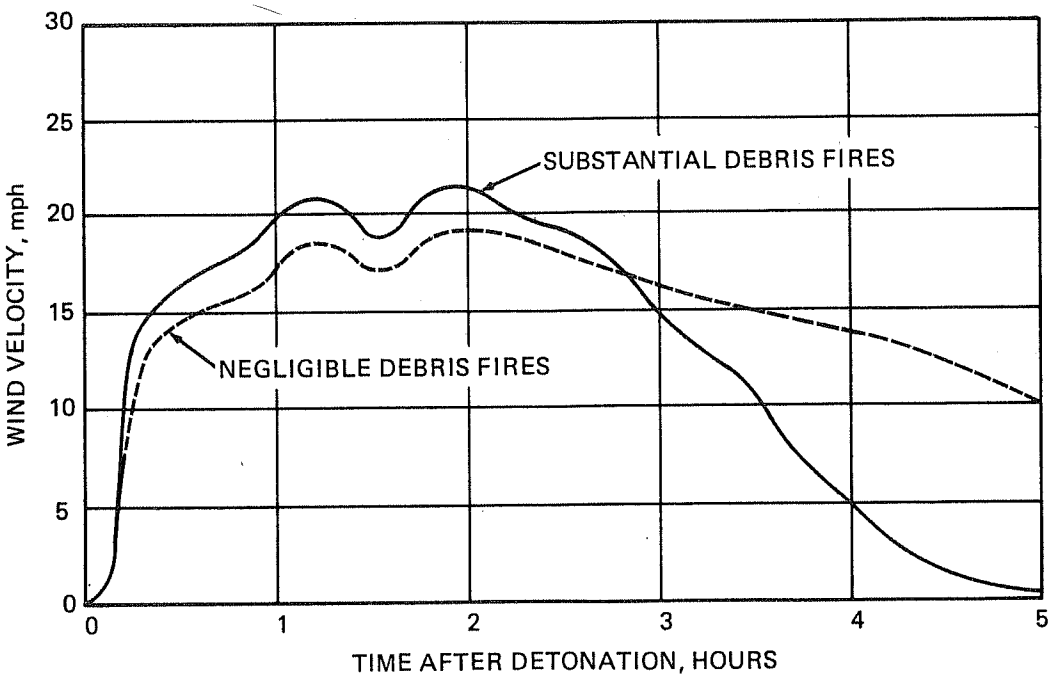

ESTIMATED FIRE WINDS IN CHICAGO LOOP*
(from 5-MT surface burst at 5 miles)

*From Takata, A.N. **Fire Spread in High Density High-Rise Buildings**, IITRI, February 1971, AD 719 731.

FIRE SPREAD BETWEEN BUILDINGS

FIRE SPREAD BY CONVECTION

FIRE SPREAD BY RADIATION

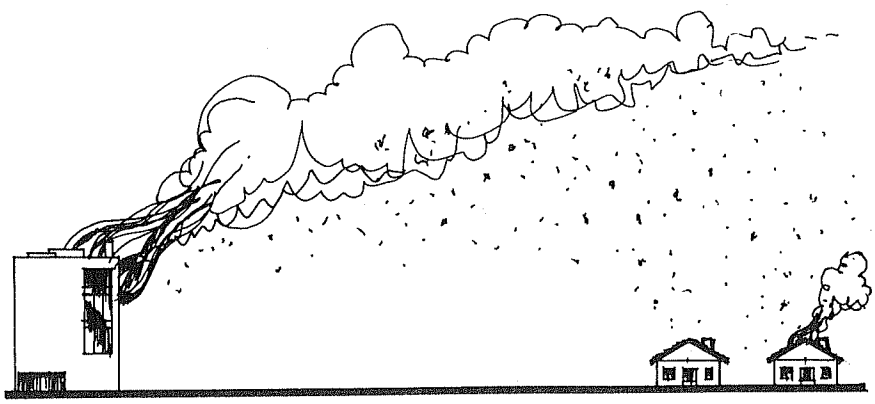

FIRE SPREAD BY FIREBRANDS

FIRE SPREAD IN THE DARMSTADT FIRE*

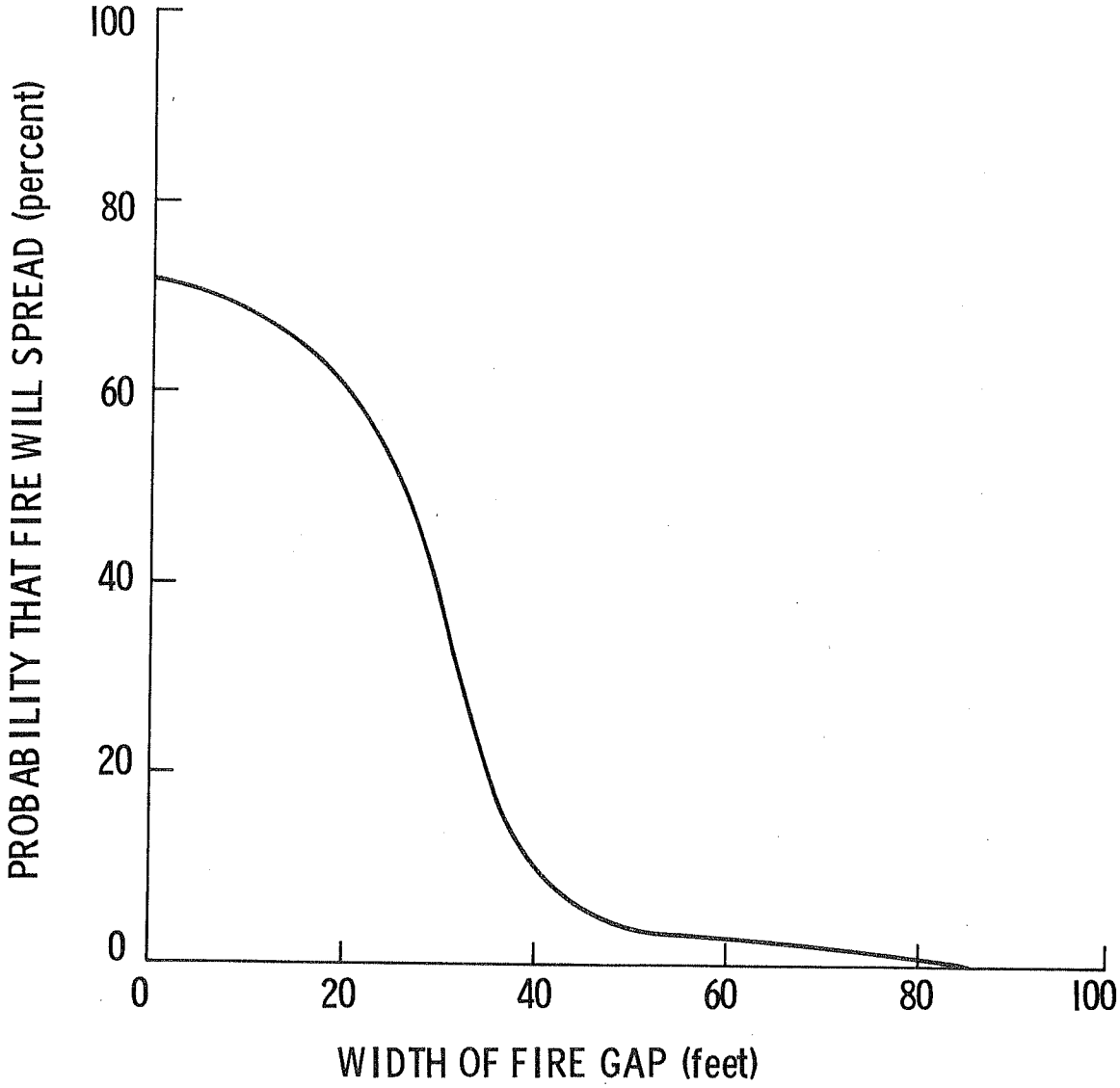

*From Takata and Salzberg, **Development and Application of a Complete Fire-Spread Model**, IITRI, June 1968, AD 684 874.

FIRE SPREAD AT HIROSHIMA*

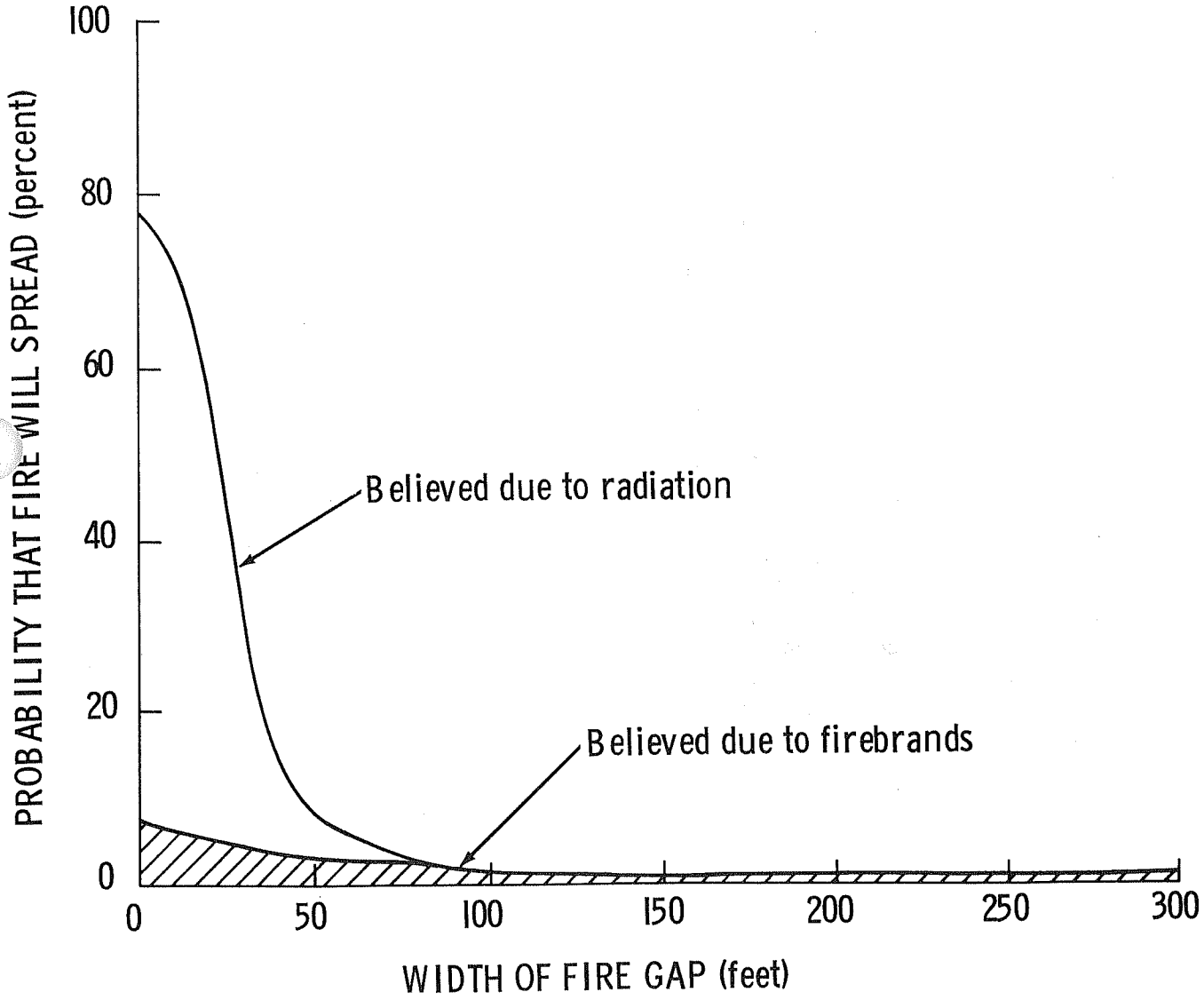

*From Takata and Salzberg, **Development and Application of a Complete Fire-Spread Model**, IITRI, June 1968, AD 684 874.

THE DIMENSIONS OF FIRE SPREAD

To illustrate the overriding importance of fire spread, let us use the example of the 5-MT surface burst at the location shown on the previous panel. For the moment, we will **ignore** two important factors: (1) the **effect of the blast wave on fire ignitions**, and (2) the **effect of any fire countermeasures, either before the attack or after the fires are started.**

For this example, we will assume that all buildings experiencing at least 6 psi blast overpressure are destroyed at the outset. Since most of the buildings with the blast circle shown on Panel 23 are residential or industrial buildings, this assumption is not unrealistic. These immediately destroyed buildings comprise about 14.5 percent of all the buildings in the Detroit area shown on the tract map. Outside the 6-psi line, an additional 3.76 percent of all the buildings are initially ignited.

As can be seen in the table, although less than 4 percent of the undestroyed buildings are initially ignited by the fireball, almost half of the buildings are eventually burned. Together with the nearly 15 percent assumed to be destroyed by blast, almost two-thirds of all buildings are lost by the end of the first day. At 28 hours after detonation, about 1 percent of all buildings are still burning around the periphery of the damaged area, so the destruction shown in the table is not the complete story.

The loss of property due to fire spread dominates the picture, even though a "fire storm" never occurs. Spread by radiation from nearby burning buildings appears to be the most prevalent mechanism, but one should not lose sight of the fact that most of the losses outside the area of high initial ignitions were originated by the firebrands.

We do not know how accurate this picture of the fire spread is, except that it probably represents the upper limit of what might occur without any fire defenses. The reason that it may represent an upper limit is that the effects of the blast wave, ignored here, will generally reduce initial ignitions and may impede fire spread. The main thing that blast effects will provide is additional time to control the fire situation, for even if the initial ignitions do not exceed 10 percent throughout the blast area, these fires can eventually spread as shown here. Thus, if control is not successful in the first few hours, new fires may be set for days following the attack.

Finally, a major implication for operational planning is that mutual aid from nearby localities will have time to play an important role in fire defense.

FIRE SPREAD HISTORY IN DETROIT
(Percent of all buildings ignited and burned*)

TIME (hours)	IGNITED BY FIREBALL	IGNITED BY RADIATION	IGNITED BY FIREBRANDS	TOTAL BURN
0	3.76	—	—	3.76
1	3.76	2.78	—	6.54
3	3.76	8.93	5.50	18.19
10	3.76	17.55	11.50	32.81
28	3.76	28.01	18.16	49.93

* In addition, 14.46 percent of all buildings destroyed by blast, for a total destroyed and burned of 64.39 percent.

From Takata and Salzberg, **Development and Application of a Complete Fire-Spread Model**, Vol. II, IITRI, June 1968, AD 684 874.

SOME JAPANESE EXPERIENCES

One might question at this point whether it is reasonable to assume that the survivors in a "low-risk" shelter facility can suppress ignitions and fires in an area damaged by a nuclear detonation. The most nearly parallel situation and, hence, best evidence comes from the nuclear attack on Hiroshima at the close of World War II. All of the evidence we have cited in this chapter suggests that the fire situation we must expect would be similar to that experienced at Hiroshima.

The upper photograph shows the Hiroshima branch of the Bank of Japan, a 3-story reinforced-concrete frame building of earthquake-resistant design. This building was only 1300 feet from ground zero, where an overpressure of about 18 psi occurred. About 100 people were in the bank at the time, of which about half were killed. Only four of the survivors are said to have been uninjured. Whether because the detonation was high above the building, whether because there were metal shutters at the windows, or whether because of effects of the blast wave, no initial ignitions occurred. About 1-½ hours afterward, a fire started in a room on the second floor from a firebrand. The nearest burning building was only 25 feet distant but the brand was said to come from nearby burning trees on another side. The survivors extinguished the blaze with water buckets, preventing further damage. A little later, a fire was started on the third floor. It was beyond control when discovered and the third floor burned out. But the fire did not spread to the lower floors.

The lower photograph shows another bank building, farther away, that experienced about 8 psi blast overpressure. Again, no initial ignitions were reported. However, at about 10:30 A.M., over 2 hours after the detonation, firebrands from the south exposure ignited a few pieces of furniture and curtains on the first and third stories. The fires were extinguished with water buckets by the building occupants. Negligible fire damage resulted.

These are but two of several examples of successful fire defense taken from the U.S. Strategic Bombing Survey report of events at Hiroshima. If one assumes that Americans can do what the unsuspecting residents of Hiroshima did, self-help measures by shelter fire-guard teams would appear to be effective.

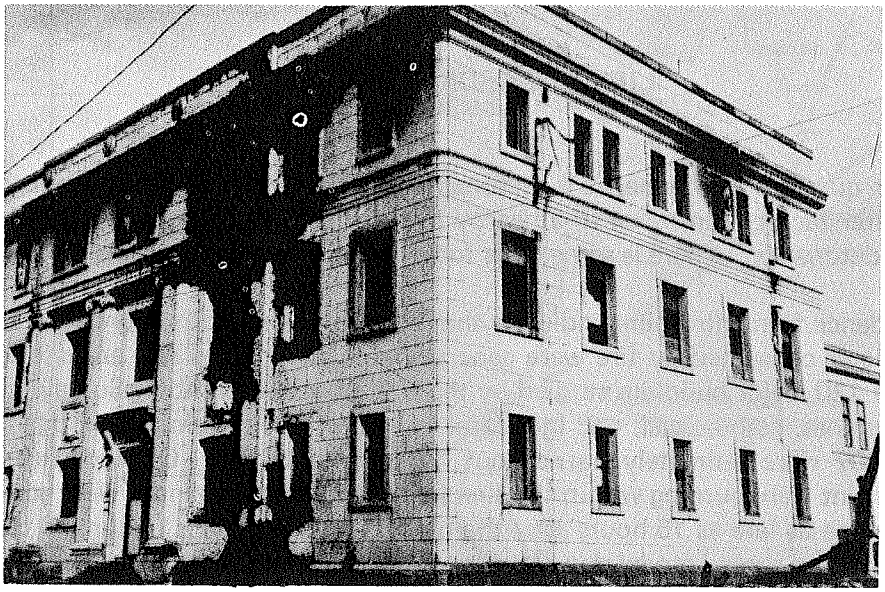

BANK OF JAPAN BUILDING AFTER ATTACK ON HIROSHIMA

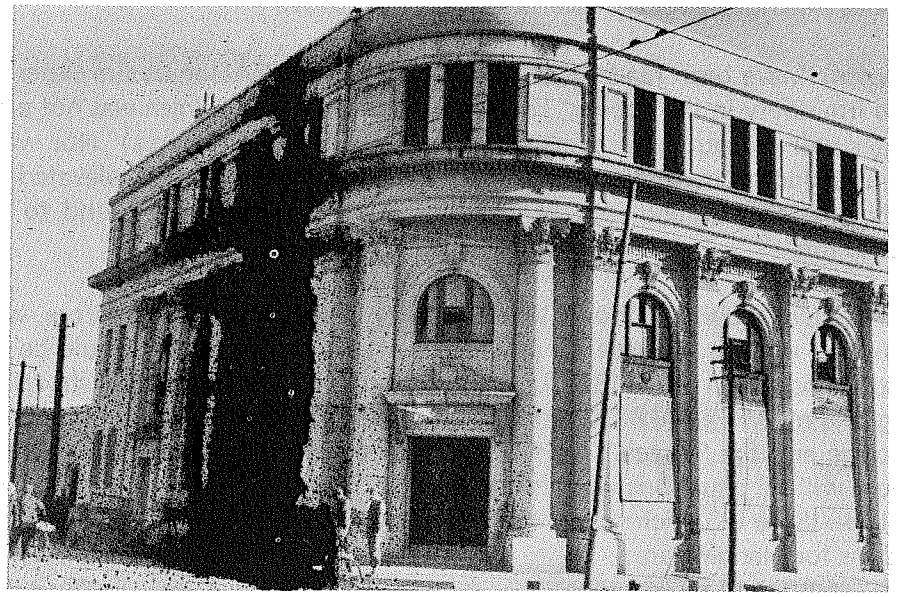

GEIBI BANK CO. BUILDING AFTER ATTACK ON HIROSHIMA

LIFE HAZARDS IN STREETS

Another question is whether it is reasonable to assume that occupants of a threatened high-risk shelter facility can move to a nearby low-risk facility through the damage caused by a nuclear detonation. There is some basis for an answer to this question.

The evidence from Hiroshima indicates that blast survivors, both injured and uninjured, in buildings later consumed by fire were generally able to move to safe areas following the explosion. Of 130 major buildings studied by the U.S. Strategic Bombing Survey (these were hospitals, churches, commercial, and industrial buildings, not the smaller wooden Japanese residences), 107 were ultimately burned out, in total or in part. Of those suffering fire, about 20 percent were burning within the first half hour. The remainder were consumed by fire spread, some as late as 15 hours after the blast. This situation is not unlike the one our computer-based fire spread model described for Detroit (Panel 24).

We have also seen, in Chapter 2, that, except in densely builtup areas of multistory buildings, debris depths will average only a foot or so. This debris would immobilize wheeled vehicles but not pedestrian traffic.

Measurements have been made at the Operation FLAMBEAU mass fire experiments of the hazards to life safety in the streets. It was found that lack of oxygen was not a problem. (Indeed, flames will die out before the air gets too thin for breathing.) Nor was carbon dioxide, a combustion product, found to present a hazard. Heat radiation, elevated air temperatures, carbon monoxide, and lack of visibility due to smoke were found to present a serious threat to life.

The upper chart shows the World War II fatality chart we have seen before, with a line added to show the average fire severity at which mortality in the streets would be expected to become total, based on FLAMBEAU measurements. The table below shows the time period during one of the FLAMBEAU fires when the hazard threshold was exceeded. These fires were intense and the "streets" were only 25 feet wide. Nonetheless, the evidence suggests that there will be situations when people in the streets would be in great peril. These situations will be those in which congested areas with narrow streets are burning violently. The implications for planning are:

(1) Areas where intense conflagrations could occur should be identified in the fire defense plan, and

(2) Decisions to evacuate survivors from these potential conflagration areas should be made as soon as uncontrolled fires are observed, to allow the maximum escape time before radiation intensities, air temperatures, carbon monoxide, and limited street visibility build up to lethal levels.

FATALITIES IN WORLD WAR II FIRES*

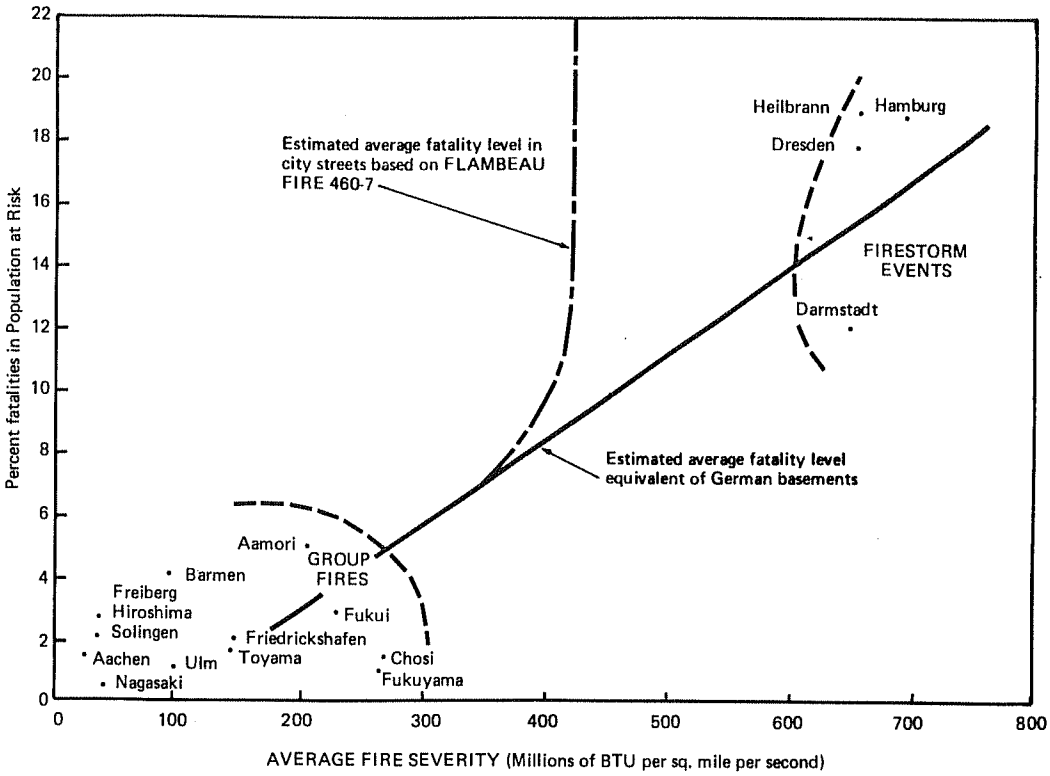

* Lommasson and Keller, DC-TN-1058-1, December 1966

HAZARD PERIODS DURING FLAMBEAU 760-12*

HEAT RADIATION	Over 3 Hours
AIR TEMPERATURE	90 Minutes
CARBON MONOXIDE	80 Minutes
STREET VISIBILITY**	60 Minutes

From Butler, C.P., **Operation Flambeau, Civil Defense Experiment and Support,** USNRDL, June 1968, AD 682 476.

** In addition, smoke conditions causing severe eye pain persisted for about 6 hours.

FIRE HAZARDS IN RESIDENTIAL BASEMENTS

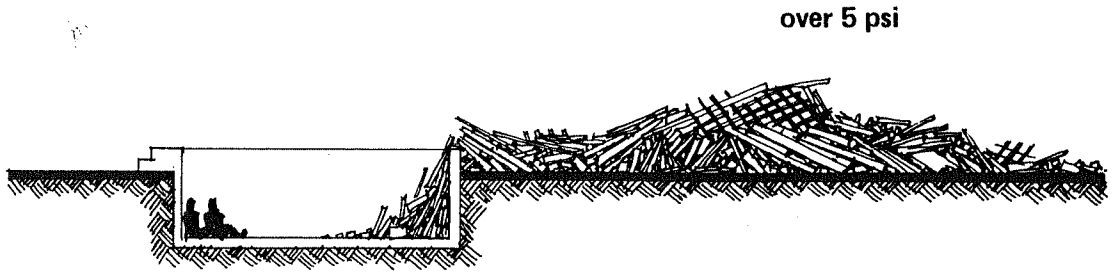

SITUATION OF LEAST FIRE RISK

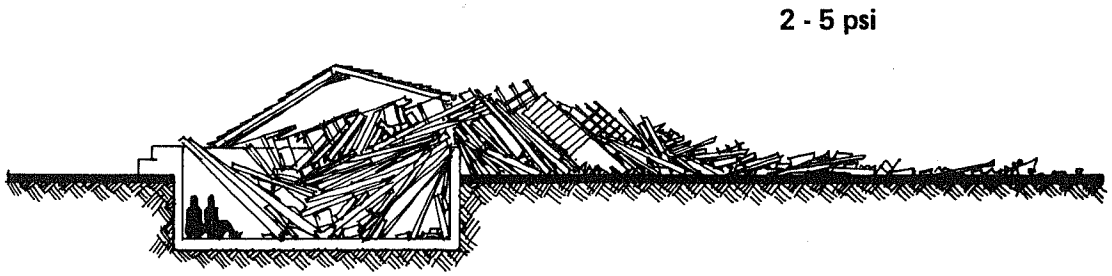

SITUATION OF GREATEST FIRE RISK

FIRE RISK IN LARGE BASEMENTS

Shelters in the basements of large buildings, particularly those described as "good shelters" in Chapter 2, offer a substantial degree of protection against fire. An example from Hiroshima, the Fukoku Building, is shown in the upper photograph. This seven-story reinforced-concrete frame building was near the Bank of Japan building and experienced about 20 psi blast overpressure. Subsequently, the building was gutted by fire. Three panels of the ground floor were depressed by the blast but fire did not penetrate into the basement of the building. This failure of the fire to involve the basement was a common occurrence at Hiroshima.

Since the Hiroshima basements were not occupied as shelters, no evidence exists as to whether heat and noxious gases would have prevented survival inside them. There were numerous instances of loss of life in German basements during the "firestorms," mainly due to excessive heat and carbon monoxide poisoning. On the other hand, the majority of basement occupants in these areas survived. To gain a better understanding of the life hazard in basements, experiments have been conducted for the past several years in a reusable building located in Gary, Indiana. This fire-test facility, shown in the lower photograph, has two stories and a basement. The walls are designed to permit openings to simulate varying degrees of blast damage. Combustibles can be placed in one or both stories to represent the room contents for various occupancies—residential, office, commercial, library, and the like. The ground floor slab can be adjusted in thickness and in tightness to simulate openings that might exist.

Experiments to date indicate toxic gases from most debris fires will not penetrate a ventilated shelter sufficiently to cause a substantial hazard. Heat transmitted through the floor slab can present a serious problem, however. For a slab 5 inches thick, which is a common thickness over basements offering "good" blast protection, the heating reaches an equivalent of four added occupants for every shelter space, given a residential fire loading above. The added heat load would make the basements untenable in a matter of an hour or so. An important finding has been that as little as one-third gallon of water per square foot of floor area applied in the first half hour after the start of a fire on the ground floor will reduce the heating effect to about one-quarter of what it would otherwise be. Since broken water piping in the above-ground part of a large building might very well provide such cooling, basements might remain tenable for considerably longer periods than one hour.

Nonetheless, the potential threat of debris fires on the floor above the basement should be guarded against. In addition to possible preattack measures to reduce the fire loading there, "fire guard" teams should be planned for each shelter facility so that incipient fires can be promptly suppressed.

FUKOKU BUILDING FOLLOWING THE HIROSHIMA ATTACK AND FIRE

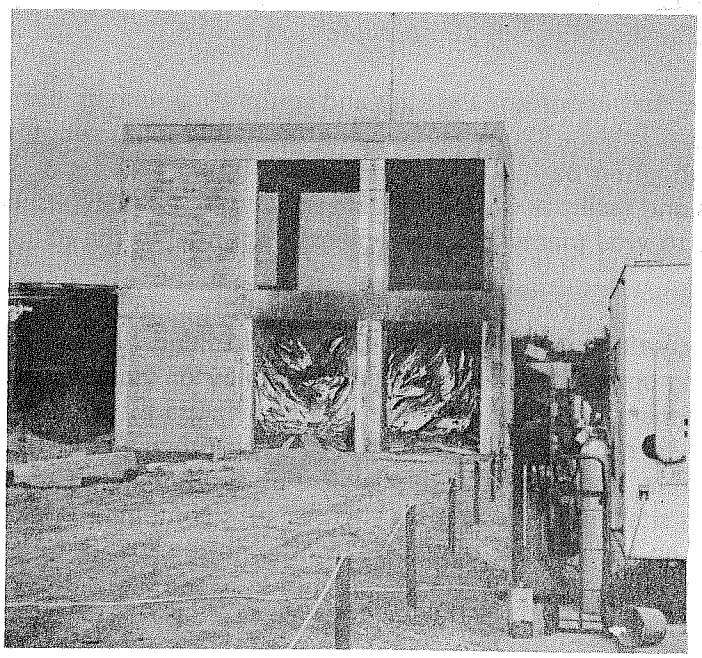

FIRE ABOVE BASEMENT IN GARY FIRE TEST FACILITY

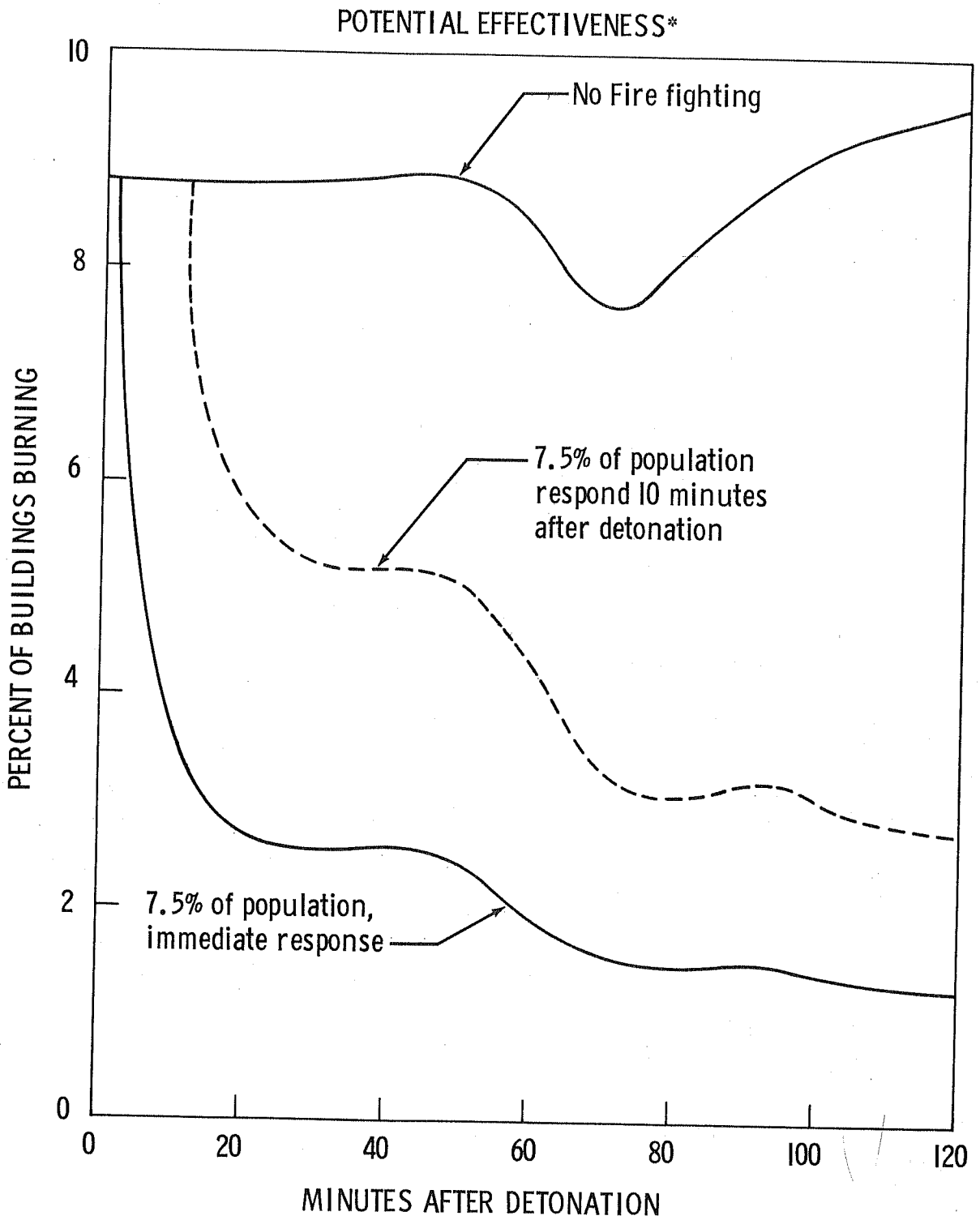

*From Takata, A.N., **Mathematical Modeling of Fire Defenses**, IITRI, March 1970, AD 705 388.

SUGGESTED ADDITIONAL READING

Bond, Horatio (editor), **Fire and the Air War**, National Fire Protection Association, Boston, Mass., 1946.

Fristrom, Robert M., (editor), **Fire Research Abstracts and Reviews**, National Academy of Sciences, Washington, D.C. (published three times a year).

Tryon, George H., (editor), **Fire Protection Handbook**, National Fire Protection Assoc., Boston, Mass. (latest edition).

Committee on Fire Research, National Research Council, **Needs of the Fire Services**, Proceedings of a Symposium, 30-31 October 1968, National Academy of Sciences, Washington, D.C. 1969 (AD 694 056).

Waterman, Thomas E., "Room Flashover, Criteria and Synthesis," **Fire Technology**, Vol. 4, pp 25-31, February 1968.

Committee on Fire Research, National Research Council, **Workshop on Mass Burns**, Proceedings of a Workshop on 13-14 March 1968, National Academy of Sciences, Washington, D.C., 1969 (AD 689 495).

Vodvarka, Frank J., **Urban Burns—Full Scale Field Studies**, IIT Research Institute, Chicago, Illinois, January 1969 (AD 707 454).

Miller, Keith, et al., **Analysis of Four Models of the Nuclear-Caused Ignitions and Early Fires in Urban Areas**, Dikewood Corporation, Albuquerque, N.M., August 1970 (AD 716 807).

Goodale, Thomas, **Effects of Air Blast on Urban Fires**, URS Research Co., San Mateo, California, December 1970 (AD 723 429).

Wiersma, S.J., and Martin, S.B., **Measurements of the Dynamics of Structural Fires**, Stanford Research Institute, Menlo Park, California, August 1971 (AD 732 498).

International Association of Fire Chiefs Development Committee, **Support Assistants for Fire Emergencies**, Instructor Guide Parts A and B, and Student Manual Parts A and B, prepared for the Defense Civil Preparedness Agency, Washington, D.C., July 1971.

Cohn, B.M., Almgren, L.E., and Curless, M., **A System for Local Assessment of the Conflagration Potential of Urban Areas**, Gage-Babcock & Associates, Inc., Westchester, Ill., October 1966 (AD 643 185).

Takata, Arthur N., and Waterman, Thomas E., **Fire Laboratory Tests—Phase II, Interaction of Fire and Simulated Blast Debris**, IIT Research Institute, Chicago, Illinois, February 1972 (AD 743 210).

CPG 2-1A4
June 1973

DCPA ATTACK ENVIRONMENT MANUAL

CHAPTER 4

WHAT THE PLANNER NEEDS TO KNOW
ABOUT ELECTROMAGNETIC PULSE

DEFENSE CIVIL PREPAREDNESS AGENCY
DEPARTMENT OF DEFENSE

JUNE 1973

WHY WORRY ABOUT EMP?

Few people have ever heard of EMP or "radio flash." It might be called the "forgotten" nuclear weapon effect. It was not mentioned in either the 1950 "**Effects of Atomic Weapons**" or the 1957 "**Effects of Nuclear Weapons.**" EMP was first mentioned in a chapter on radio and radar effects in the 1962 version of the "**Effects of Nuclear Weapons**" but the description was brief and no hint was given as to its damaging effects.

One reason for this lack of attention has been that the energy contained in the "radio flash" is much smaller than that in the thermal pulse. We saw in Chapter 3 that where the blast overpressure is 5 psi, the thermal energy is about 100 calories per square centimeter. At the same distance from a surface burst, the radio flash energy is equivalent to much less than one calorie per square centimeter.

We know that sunlight can be focused by a magnifying glass so as to ignite paper. If magnifying glasses or their equivalent were common in target areas, we would need to be concerned about very low levels of thermal radiation in nuclear attack. Fortunately, this is not the case. But natural energy collectors for radio frequencies are widespread. They magnify the weak "radio flash" somewhat as a magnifying glass does sunlight.

Anyone who has hooked up an old radio to a bedspring knows that almost any metallic object can collect energy from radio waves. Any long wire can pick up the energy in the electromagnetic field and then deliver it in the form of current and voltage pulses to the attached equipment. The larger or longer the conductor, the greater the amount of energy collected. For example, the short antenna of an automobile radio will collect less energy than a large broadcast station transmitting antenna. Typical collectors of EMP energy include long exposed cable runs, piping or conduit, large antennas, metallic guy wires, power and telephone lines, and even shallow-buried pipes and cables, long runs of electrical wiring in buildings, and the like. Sufficient energy can be collected by these means to cause damage to attached electrical and electronic equipment.

EMP FROM A 5–MT SURFACE BURST

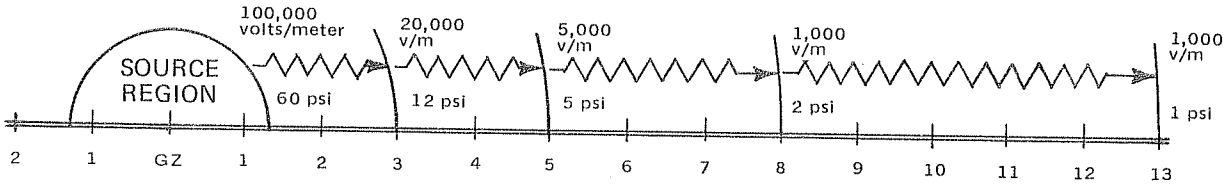

DISTANCE FROM GZ, MILES

COMPARISON OF ELECTROMAGNETIC FIELDS

SOURCE	INTENSITY (volts per meter)
EMP	UP TO 100,000
RADAR	200
RADIO COMMUNICATION	10
METROPOLITON "NOISE"	0.1

Source: Defense Nuclear Agency

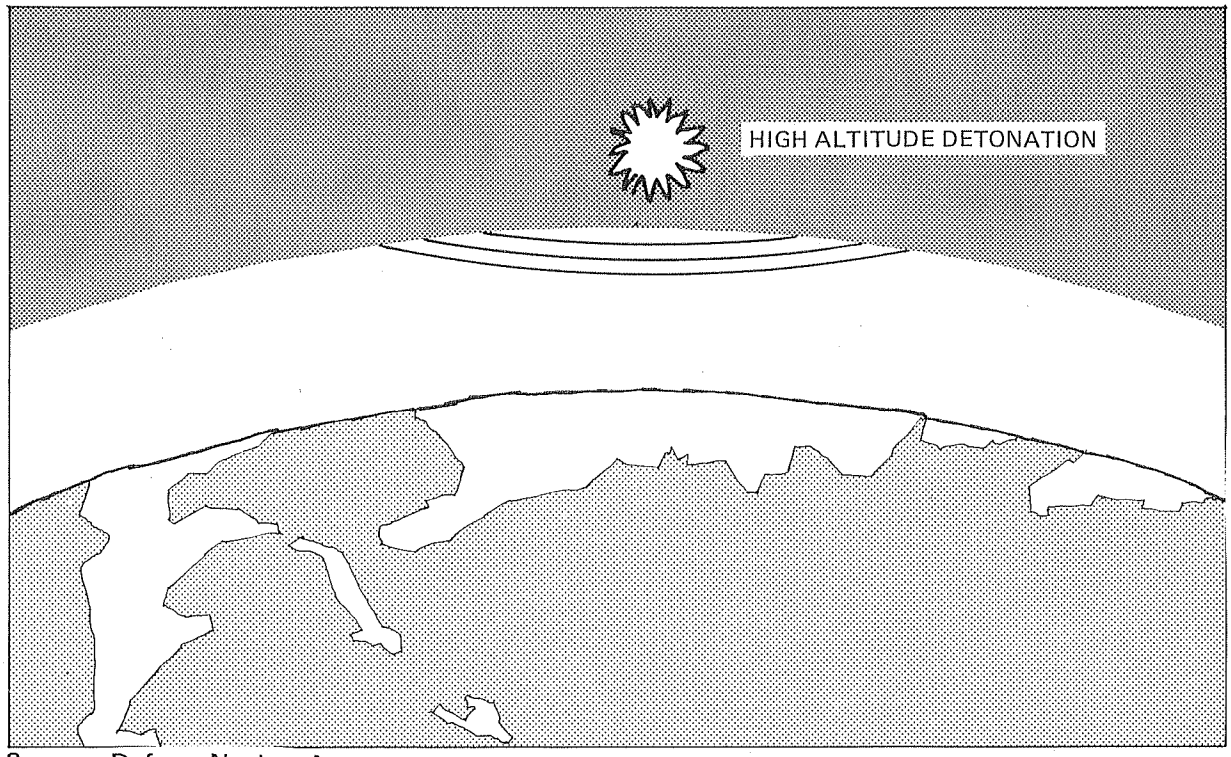

Source: Defense Nuclear Agency

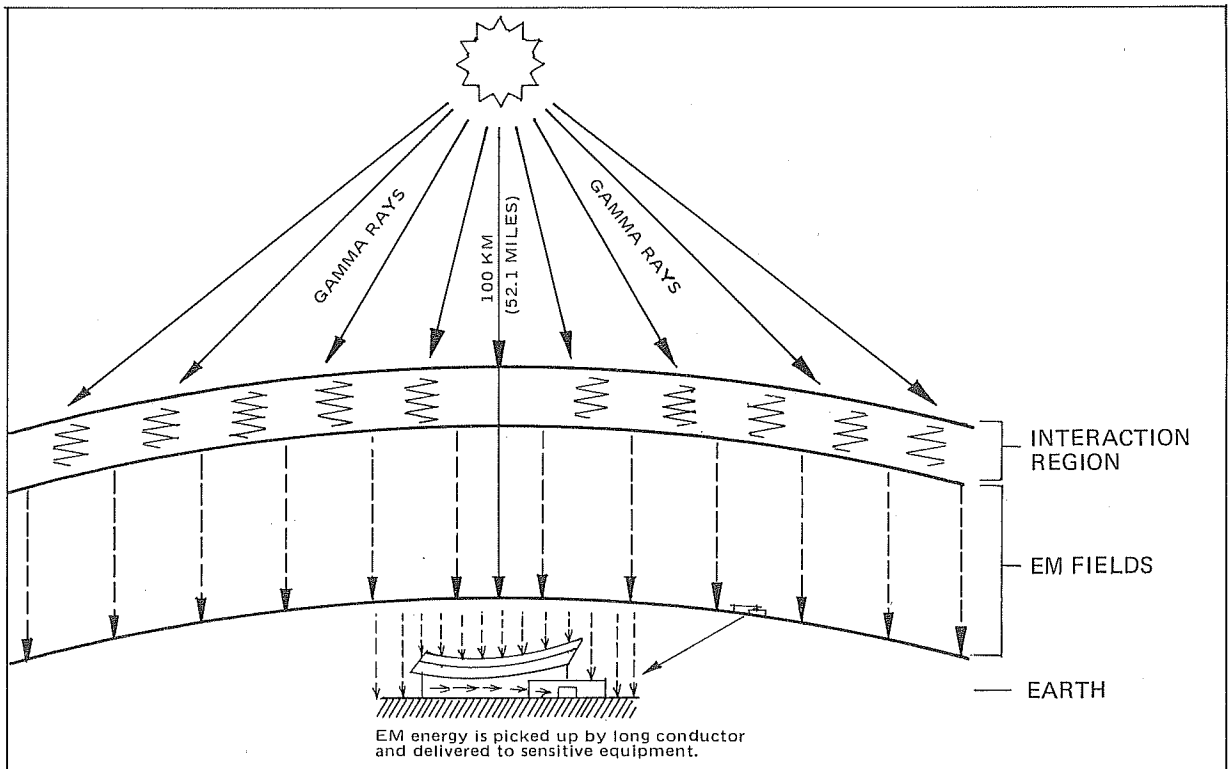

EMP ENERGY FROM HIGH ALTITUDE BURST.

PANEL 4 From Survive, November-December 1969.

EMP COVERAGE

In the case of an exoatmospheric burst, blast damage does not occur and other effects are minor except for the EMP. The source region at 12½ to 25 miles above the earth's surface can be quite large, perhaps a thousand miles in diameter. As a consequence, the radiated fields from this source region can cover a substantial fraction of the earth's surface.

A typical high-altitude burst over Omaha, Nebraska, is shown here. Within the circle passing through Dallas, Texas, ground-level fields of a few tens of thousands of volts per meter would be created. The outer circle shows that a few kilovolts per meter would occur everywhere within the contiguous 48 states.

That these pulses can cause damage to electrical and electronic equipment is not a matter of scientific theory. The failure of approximately 30 strings of street lights on Oahu at the time of the Starfish detonation about 750 miles away over Johnson Island was the most publicized effect during the weapons test series Operation FISHBOWL in 1962.

High-altitude bursts are no longer unlikely. The deployment of those ballistic missile defenses permitted by the recent treaty with the Soviet Union would include the use of megaton-yield warheads to intercept incoming weapons outside the atmosphere. Even if this were not in prospect, the effectiveness of EMP in interrupting communications would make it probable that some of the thousands of warheads discussed in Chapter 1 would be used for this purpose.

An implication for operational planning is that a potential EMP threat must be anticipated in every locality during the first minutes and perhaps hours after a nuclear attack is initiated.

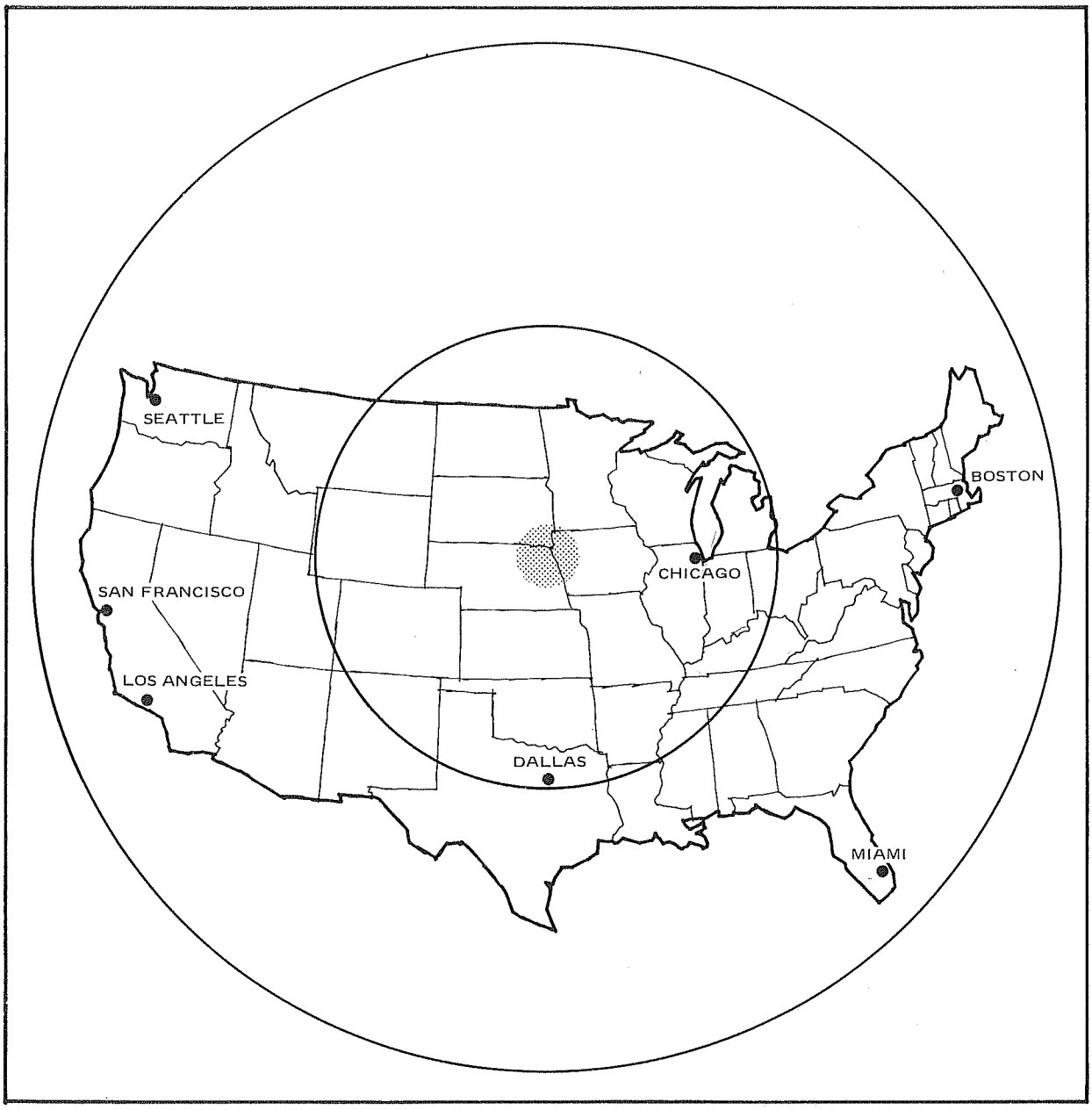

EMP GROUND COVERAGE OF HIGH ALTITUDE BURSTS

Source: Defense Nuclear Agency

PANEL 5

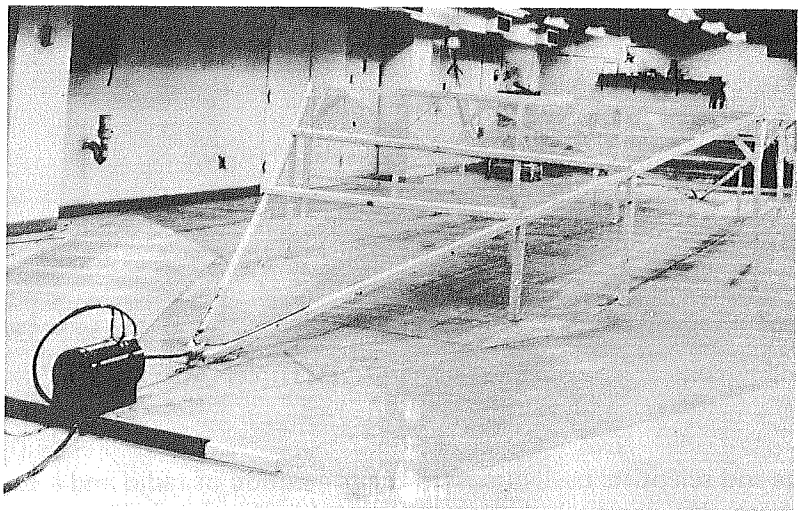

ONE TYPE OF EMP SIMULATOR

IITRI Laboratory photograph.

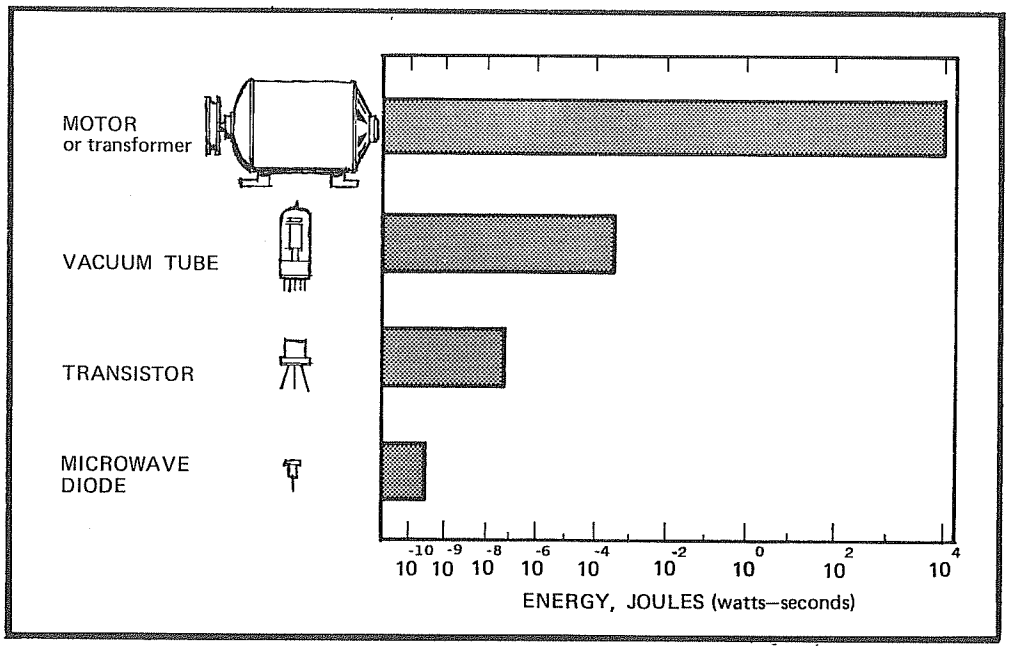

SENSITIVITY OF VARIOUS COMPONENTS

NOTE: 300 feet of wire can absorb about 1/10 to 40 joules of energy depending on orientation and proximity to other conductors.

Source: Defense Nuclear Agency

PANEL 6

TIME HISTORY
COMPARISON WITH LIGHTNING

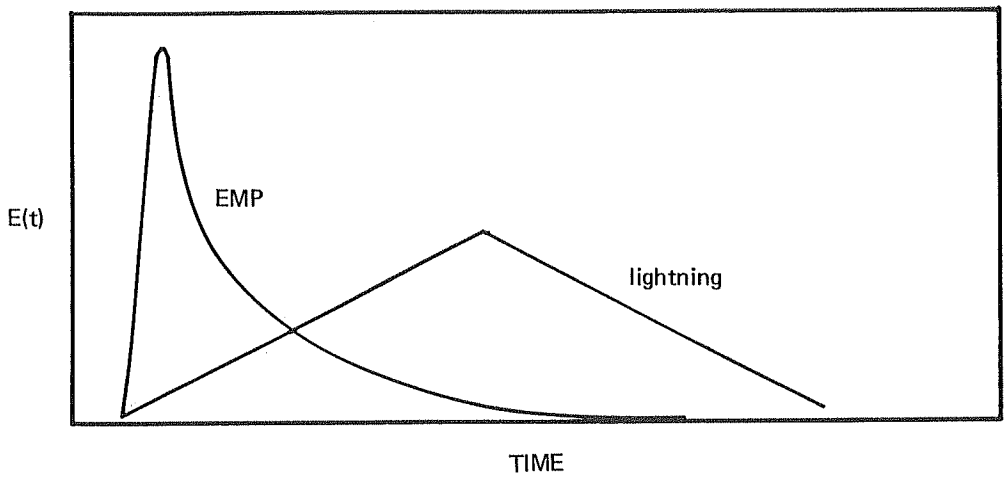

NOTE: Rapid rise of EMP pulse

Source: Defense Nuclear Agency

SPECTRUM COMPARISON

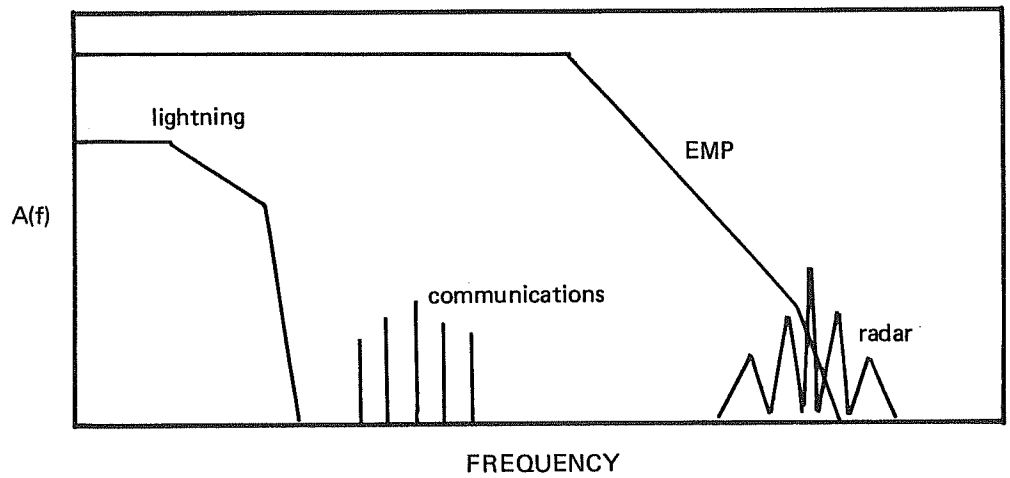

NOTE: Broad frequency range of EMP

Source: Defense Nuclear Agency

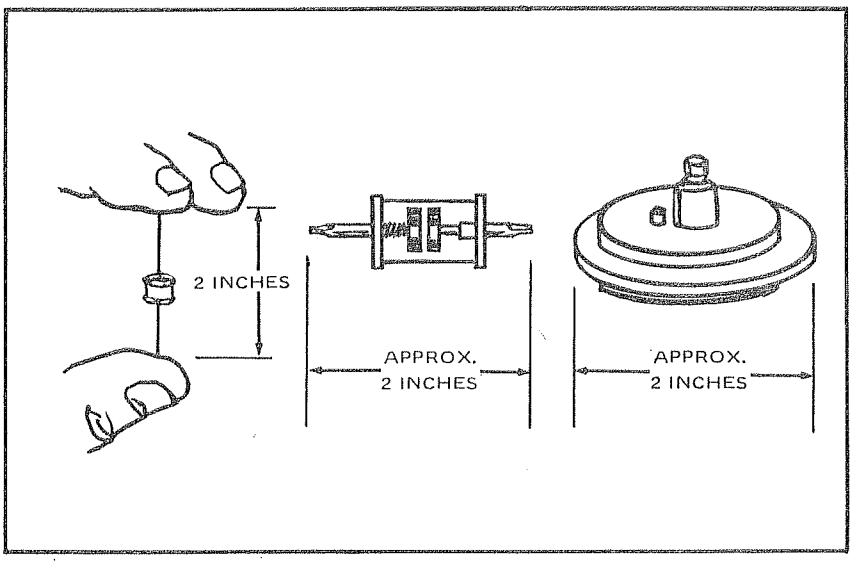

GAS-GAP SURGE ARRESTOR (also called spark-gaps)

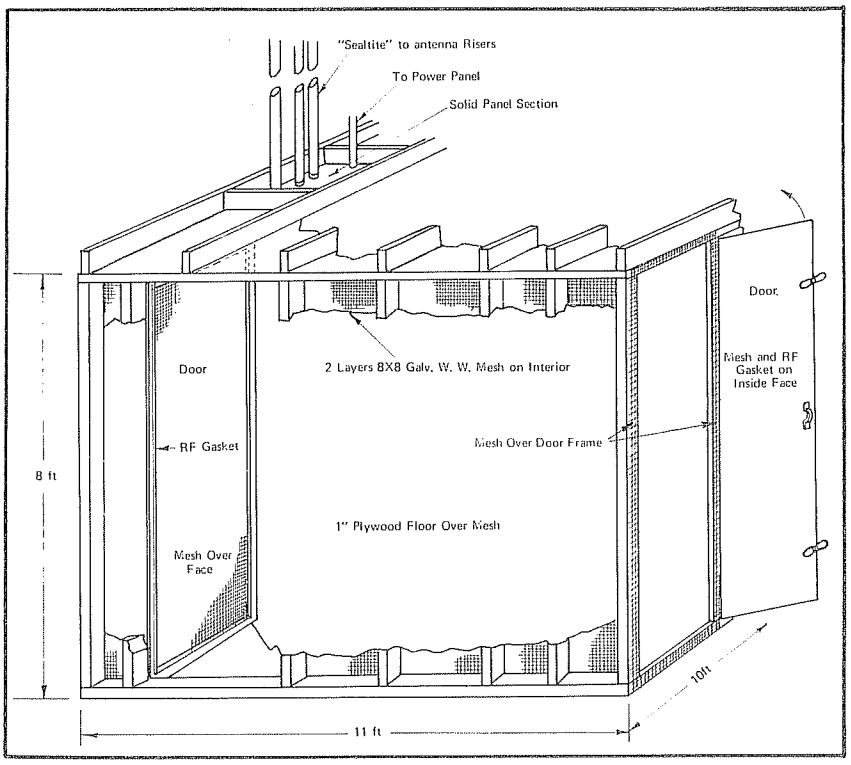

SHIELDED BOX

PANEL 12

SUSCEPTIBILITY TO RADIO BLACKOUT

Radio Band	Frequencies	Example	Effects
LF	30 - 300 KHZ	DIDS	Least affected
MF	300 - 3000 KHZ	EBS	Some distant interference
HF	3000 - 30,000 KHZ	RACES	Many hours
VHF	30,000 KHZ - 300 MHZ	High-band Public Safety	Few seconds to minutes
UHF	300 - 3000 MHZ	TV, Latest Public Safety	Little effect
SHF	3 - 30 GHZ	Microwave and Satellite	Virtually no effect

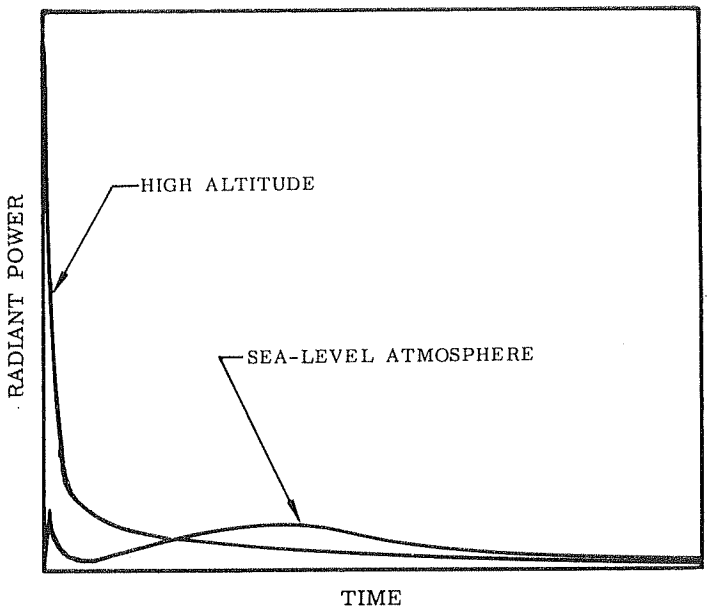

COMPARISON OF RATES OF THERMAL ENERGY RELEASE FOR MEGATION WEAPONS

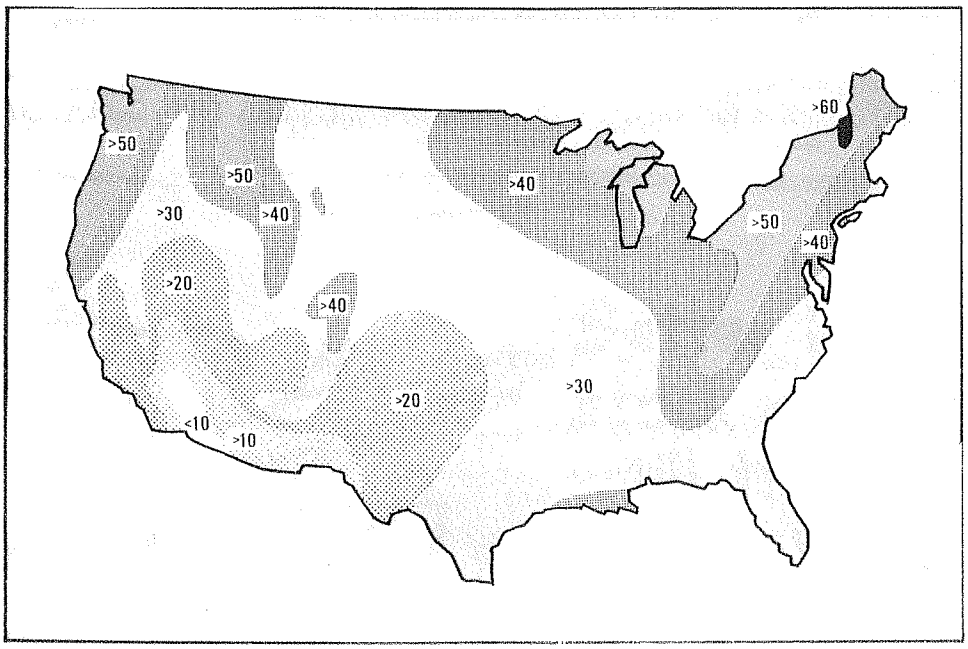

PERCENTAGE OF ANNUAL "OPAQUE" CLOUDINESS

PANEL 15

SUMMARY

One final point should be made about EMP effects. We do not have to concern ourselves about the effects upon people as we did in Chapters 2 and 3. Without considerable focusing, the EMP energy is totally harmless to living things. Standing in the open, one would literally not feel a thing with respect to the strongest EMP pulse. However, the energy collected in a long wire might cause electrocution or a burn, if a person were touching it at the time. Such conditions are not generally expected.

With respect to the protection of communications and electrical equipment, recent research results have been incorporated into the following publications:

EMP Threat and Protective Measures, DCPA TR-61, August 1970.

EMP Protection for Emergency Operating Centers, DCPA TR-61A, May 1971.

EMP Protective Systems, DCPA TR-61B, revised July 1972.

EMP Protection for AM Radio Broadcast Stations, DCPA TR-61C, May 1972.

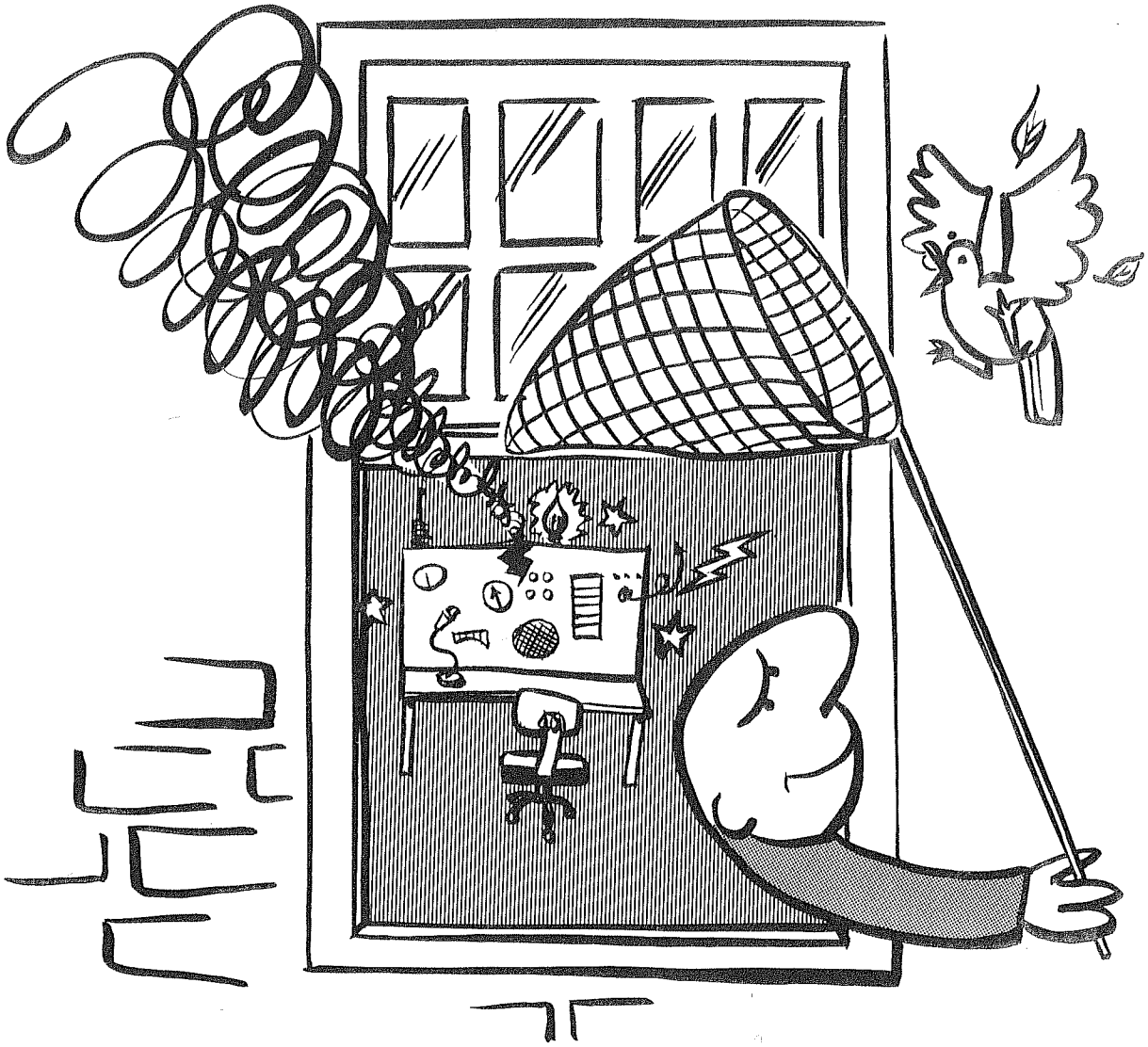

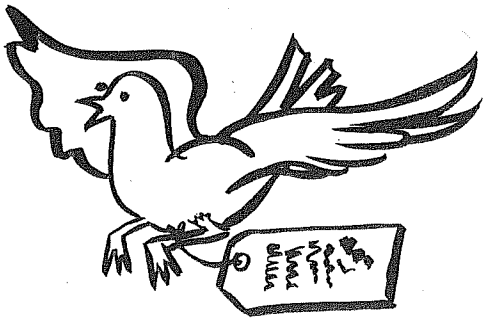

Better lay in a stock of bird seed --till the EMP threat is over.

Courtesy of Don Clark, U.S. Naval Civil Engineering Laboratory.

CPG 2-1A5
June 1973

DCPA ATTACK ENVIRONMENT MANUAL

CHAPTER 5

WHAT THE PLANNER NEEDS TO KNOW
ABOUT INITIAL NUCLEAR RADIATION

DEFENSE CIVIL PREPAREDNESS AGENCY
DEPARTMENT OF DEFENSE

JUNE 1973

SOMATIC AND GENETIC EFFECTS

The statements shown here were made in 1967 by Dr. Charles L. Dunham, Chairman of the Division of Medical Sciences, National Research Council. He was summarizing the views of the professional community at a symposium on the consequences of a nuclear war in which about 3500 megatons were assumed to be detonated in the United States. As we saw in Chapter 1, an attack perhaps twice as heavy could be delivered today. In the larger war, the number of survivors would be less but the average radiation dose received by the survivors would be much the same as Dr. Dunham's assumption of 200R. The first quotation refers to the late somatic effects discussed in the previous panel. For perspective, about 20,000 new cases of leukemia are diagnosed each year in the U.S. About 69,000 deaths occurred from lung cancer in 1971, most due to smoking.

The second quotation refers to the genetic effects—those affecting future generations. Genetic injury does not affect the health of exposed individuals in any way and can be detected only by statistical studies of their descendents. So far, searches for evidence of abnormalities in children conceived after one or both of the parents were irradiated have been unsuccessful. Using pessimistic assumptions, calculations have been made that suggest that major defects in newborn babies of succeeding generations might increase to 5 percent from the present rate of 4 percent, assuming that all parents received a dose of 200 to 250R following attack.

Both somatic and genetic effects are believed to be directly related to the dose received by the surviving population. Thus, if by effective civil defense planning, the protection provided the population could be doubled, the numbers shown here would be cut in half.

PANEL 7

GENERAL PREDICTIONS*

"20,000 additional cases per year of leukemia during the first 15 or 20 years postattack followed by an equal number of cases of miscellaneous cancers, added to the normal incidence in the next 30 to 50 years, would constitute the upper limiting case. They would be an unimportant social, economic, and psychological burden on the surviving population."

"The genetic effects would be lost as at Hiroshima and Nagasaki, in all the other 'background noise.'"

*From **Proceedings of the 1967 Symposium on Postattack Recovery from Nuclear War,** National Academy of Sciences, April 1968 (AD 672 770).

RELATIONSHIP OF BLAST AND INITIAL NUCLEAR RADIATION

(Near-Surface and Surface Bursts)

Blast Overpressure (psi)	Nuclear Radiation (Roentgens)		
	1 MT	5 MT	25 MT
1	Neg.	Neg.	Neg.
2	Neg.	Neg.	Neg.
5	Neg.	Neg.	Neg.
12	280 (260)*	7 (7)	Neg.
20	3600 (3200)	430 (420)	10 (10)

*Values in parentheses are for surface bursts.

TYPICAL INR PROTECTION FACTOR RANGES RELATIVE TO BLAST PROTECTION

Blast Preference	Description
A	Subway stations, tunnels, mines, and caves with large volume relative to entrances. (10 - 10,000)
B	Basements (10 - 100) and sub-basements (100 - 1000) of massive (monumental)masonry buildings.
C	Basements (10 - 100) and sub-basements (100 - 1000) of steel and reinforced-concrete framed buildings having flat slab or slab and beam ground floor construction.
D	First three floors of buildings with "strong" walls. (2 - 5)
E	Basements of wood-frame (4 - 8) and brick veneer residences. (5 - 10)
F	Fourth and higher floors of buildings with "strong" walls. (1 - 5)
G	Basements of steel and reinforced-concrete framed buildings with flat plate ground floor. (10 - 100)
H	First three floors of buildings with weak walls, brick buildings and residences. (2 - 5)
I	Fourth and higher floors of buildings with weak walls. (1 - 5)

THE POSSIBLE USE OF "SMALL" WEAPONS

In Chapter 1 we alerted the emergency planner to the fact that there has been and likely will continue to be a trend toward larger numbers of smaller-yield nuclear weapons fitted on missiles as multiple warheads. We noted that many U.S. missile systems have already been modified in this fashion and that the Soviets may be beginning to do so.

Some of the motivation to use multiple warheads has stemmed from a perceived need to complicate the task of developing ballistic missile defense systems, commonly called ABM systems, by providing many separate incoming warheads. But this objective is not the whole motivation Although the total megatonnage that can be delivered in the form of multiple warheads is substantially less than that delivered as single weapons, the sum of the separate direct effects areas are very much the same. The blast effects would be somewhat lessened; the thermal effects would be somewhat increased. As we shall see, the relative effects of initial nuclear radiation are greatly increased, so that survival in ordinary structures may be limited by the lack of initial radiation protection. Since many smaller detonations may cover a sprawling metropolitan area more efficiently or permit more effective attack against separated industrial facilities, airports, and other key targets, the trend toward warheads in the kiloton-yield range may continue despite agreements to limit the deployment of missile defense systems.

Small-yield nuclear weapons in the range of tens to hundreds of kilotons also may differ from large megaton-range weapons in the nuclear processes employed in creating an explosive release of energy. About half the energy in large-yield weapons comes from fission of heavy elements like uranium. The remainder comes from fusion of light elements, such as hydrogen. Small-yield weapons may use only the fission process, as was the case at Hiroshima and Nagasaki. In describing large-yield weapons, we have assumed 50 percent fission yield. In describing small weapons, we will assume 100 percent fission yield.

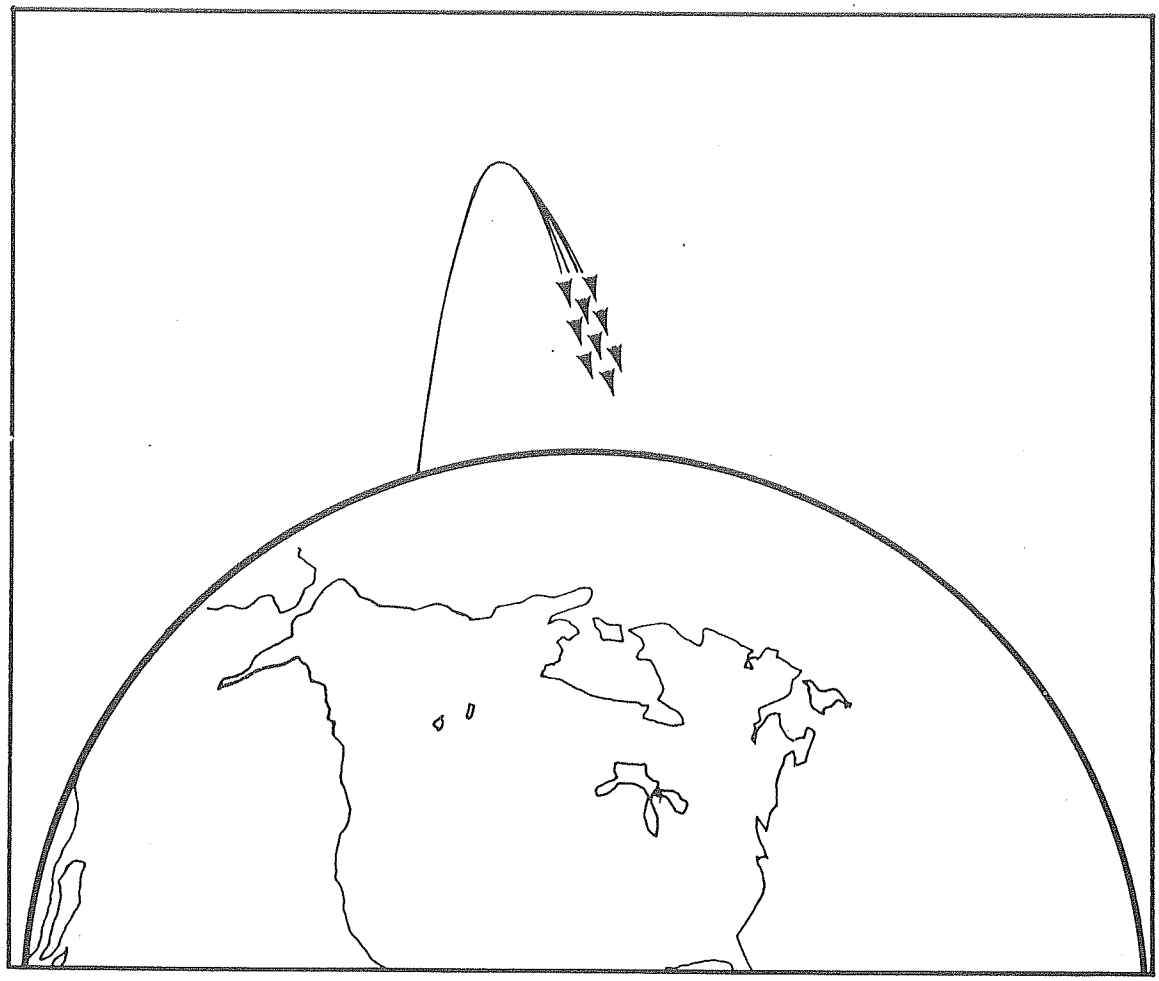

PANEL 10

INITIAL NUCLEAR RADIATION FROM "SMALL" WEAPONS

When the explosive power of a nuclear weapon is changed, the extent of blast overpressure varies as the cube root of the change in explosive power. Thus, the extent for a 5-KT detonation is 1/10 that of a 5-MT detonation (one that has 1,000 times more explosive power) and the extent for a 40-KT detonation is 1/5 that of a 5-MT burst. The extent of initial nuclear radiation is reduced somewhat but not nearly as much as are the blast overpressures. Consequently, the INR exposure becomes increasingly large at a given overpressure as the weapon yield is reduced, as shown here.

At these short ranges (5-psi overpressure occurs at a mile or two from ground zero), neutrons are an important constituent of initial nuclear radiation in addition to gamma radiation. Whereas gamma radiation is electromagnetic radiation, neutrons are extremely tiny particles of matter ejected from the nuclei of atoms involved in the nuclear detonation. Neutrons have about the same effectiveness in causing biological damage as gamma rays. The use of Rem (Roentgen-equivalent-man) in the table merely signals that radiation other than gamma radiation is contributing to the exposure.

For 40-KT detonations, initial nuclear radiation is significant in the moderate damage region (2 to 5 psi). Further, our imaginary person in the open at 10 psi (about 7/10 mile from Ground Zero) is exposed to about 8000 Rem. The protection afforded by a residential basement (5 to 10 IPF) would be insufficient. Only the better parts of large building basements, sub-basements, and subways would permit survival.

At higher yields (over 100 KT), INR doses in the area of severe damage would not be as high but basement protection would be essential and survival possibilities are clearly limited by the initial nuclear radiation exposure.

RELATIONSHIP OF BLAST AND INITIAL NUCLEAR RADIATION

(Near-Surface Bursts)

Blast Overpressure (psi)	Nuclear Radiation (Rem)		
	40 KT	100 KT	1 MT
1	1	Neg.	Neg.
2	5	Neg.	Neg.
5	560	170	Neg.
12	10,000	5,500	280
20	34,000	23,000	3,600

WHAT HAPPENED AT HIROSHIMA

At Hiroshima, casualties were the result of a combination of the three major "direct" effects (blast, thermal radiation, and initial nuclear radiation) but blast and thermal radiation seemed to be the dominant causes. The weapon was relatively small (about 12 KT) and exploded very high (about 1900 feet) relative to its size. It was a clear morning with a large number of people in the streets at the time. The maximum blast overpressure was about 30 psi on the ground directly under the bomb and the initial nuclear radiation dose there was about 26,000 Rem. However, the initial nuclear radiation exposure reduces rapidly with increased distance from the weapon. Both the overpressures and INR doses for several distances at Hiroshima are shown in this bar chart.

At 8-psi blast overpressure, where more than half the people in Japanese houses were killed, the initial nuclear radiation exposure was about ½ percent of its maximum or 155 Rem, too low to cause death. If the weapon had been detonated nearer the ground (within a few hundred feet), initial nuclear radiation would have been a more important cause of death than either blast or thermal radiation. For example, at 8 psi, the initial nuclear radiation exposure in the houses would have been 2800 Rem.

In discussing the threat of initial nuclear radiation, we have assumed that surface or near-surface detonations would occur. If this is not the case, this threat will be greatly diminished.

BLAST AND INR* AT HIROSHIMA

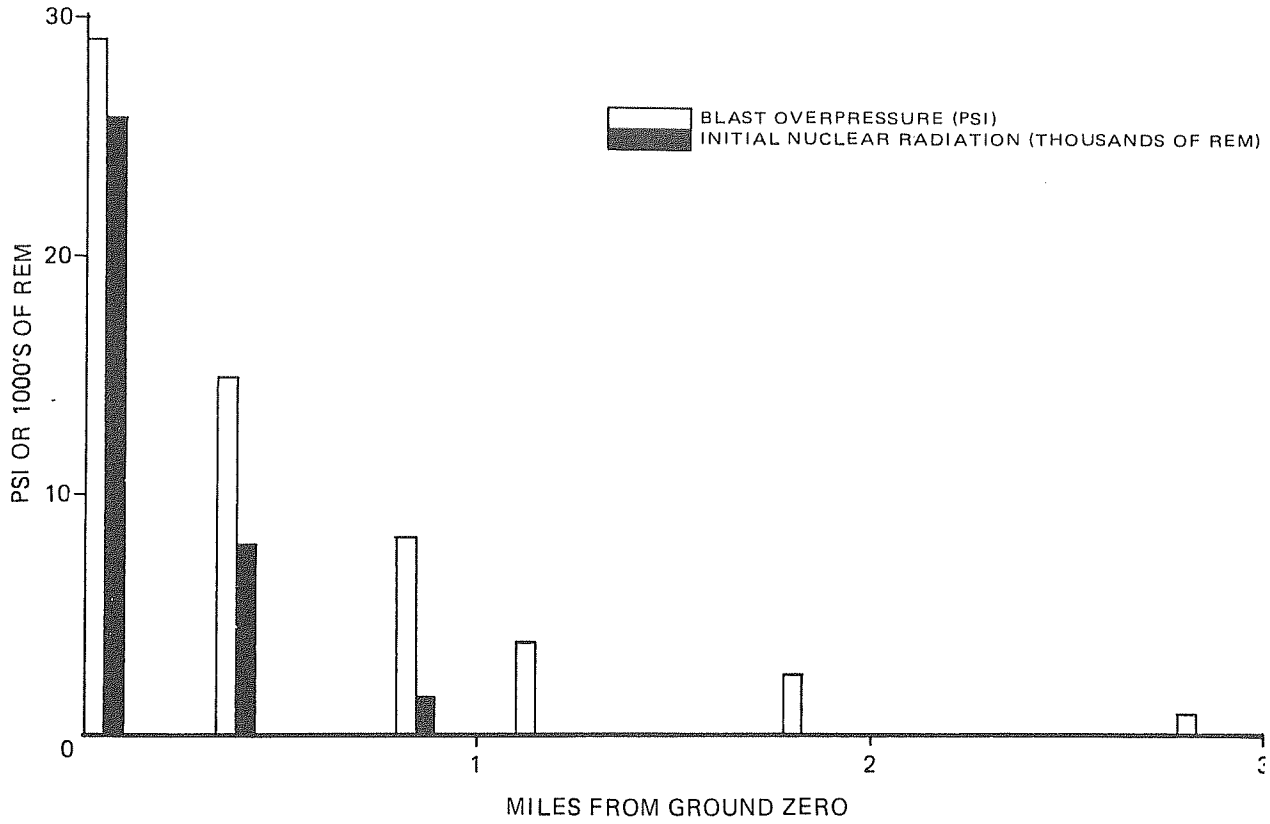

*From Auxier, J.A., et al., **Free-field Radiation-dose Distributions from the Hiroshima and Nagasaki Bombings,** Health Physics, Vol. 12, 1966.

PANEL 12

SUGGESTED ADDITIONAL READING

Effects of Nuclear Weapons, Revised Edition 1964, Glasstone, S., (editor), Chapters II VIII, and XII, Superintendent of Documents, GPO.

French, R.L., and Mooney, L.G., **Initial Radiation Exposure from Nuclear Weapons,** Radiation Research Associates, Inc., Report RRA-T7201, July 1972 (AD 745-906).

National Committee on Radiation Protection, **Exposure to Radiation in an Emergency,** Report No. 29, January 1962.

Proceedings of the 1967 Symposium on Postattack Recovery from Nuclear War, National Academy of Sciences, April 1968 (AD 672-770).

Auxier, J.A., et al, **Free-field Radiation-dose Distributions from the Hiroshima and Nagasaki Bombings,** Health Physics Vol. 12, 1966.

CPG 2-1A6
June 1973

DCPA ATTACK ENVIRONMENT MANUAL

CHAPTER 6

WHAT THE PLANNER NEEDS TO KNOW
ABOUT FALLOUT

DEFENSE CIVIL PREPAREDNESS AGENCY
DEPARTMENT OF DEFENSE

JUNE 1973

CLOUD FALLOUT

(5 MT Surface Detonation)

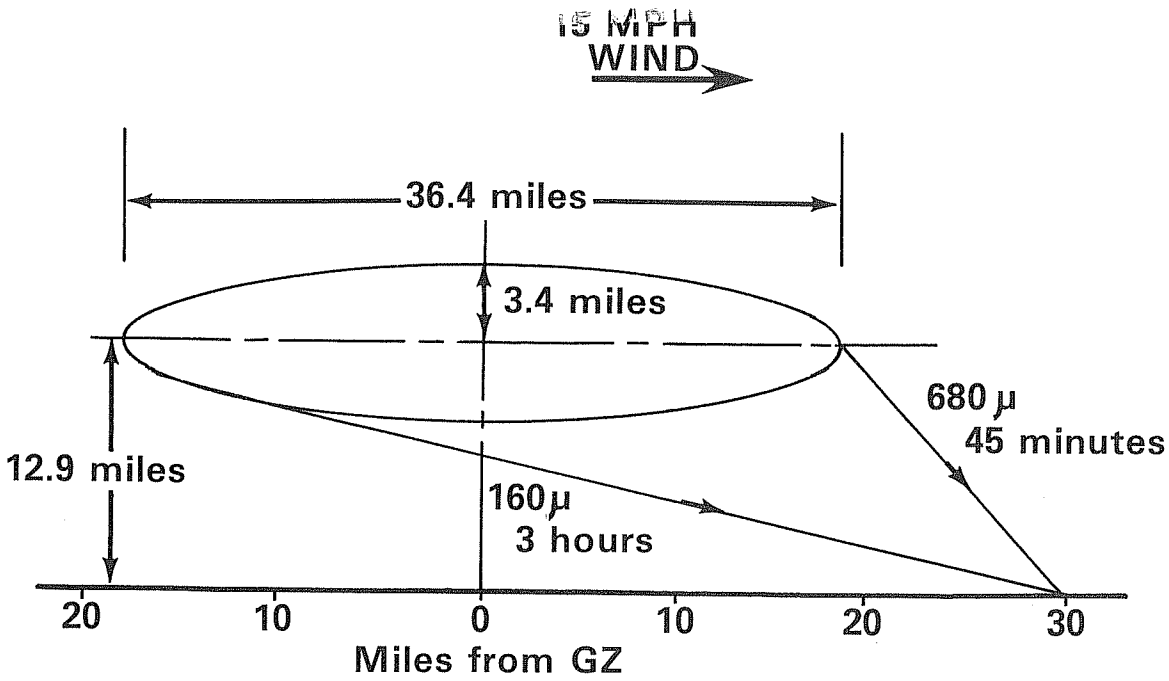

MASS DEPOSITION PATTERN
(5 MT SURFACE BURST)

EFFECTIVE
WIND SPEED 15 MPH

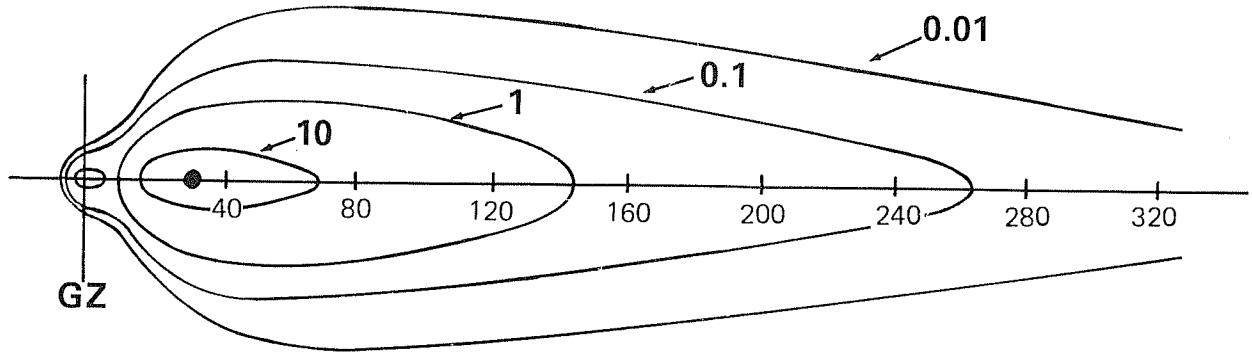

- Distances in miles
- Contours in grams per square foot

PEAK DOSE-RATE PATTERN
(5 MT Surface Burst)

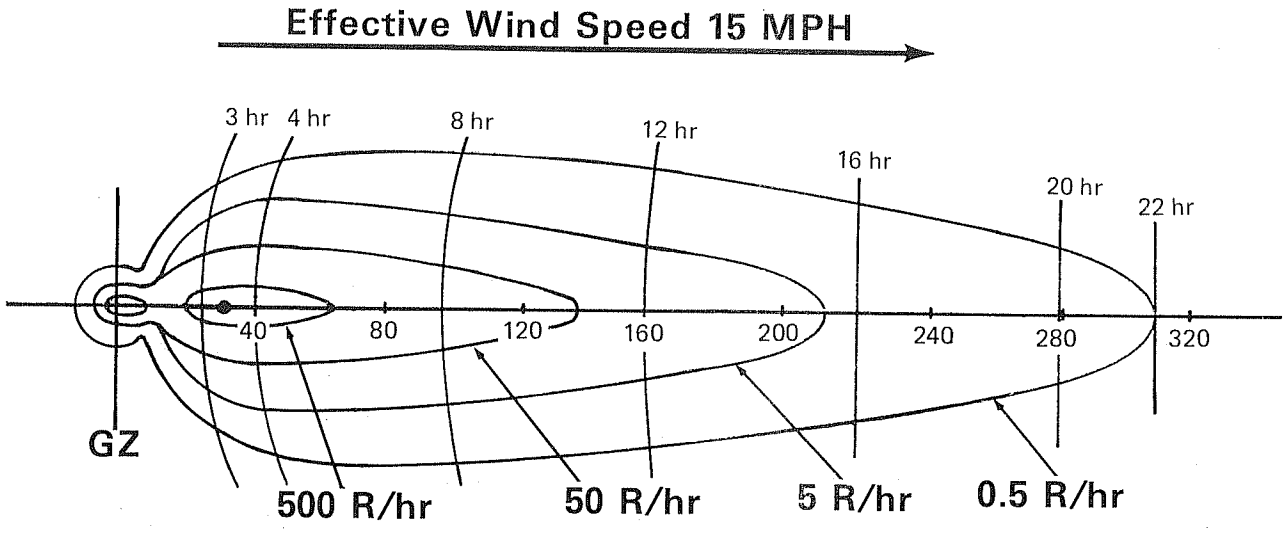

- Distances in miles
- Contours in roentgens per hour (true ionization rate at three feet above a smooth infinite plane)
- Vertical curves show peaking time in hours after detonation
- Fission yield 50%.

FALLOUT SITUATION AT 30 MILES DIRECTLY DOWNWIND FROM 5 MT SURFACE BURST

(15 MPH WIND SPEED)

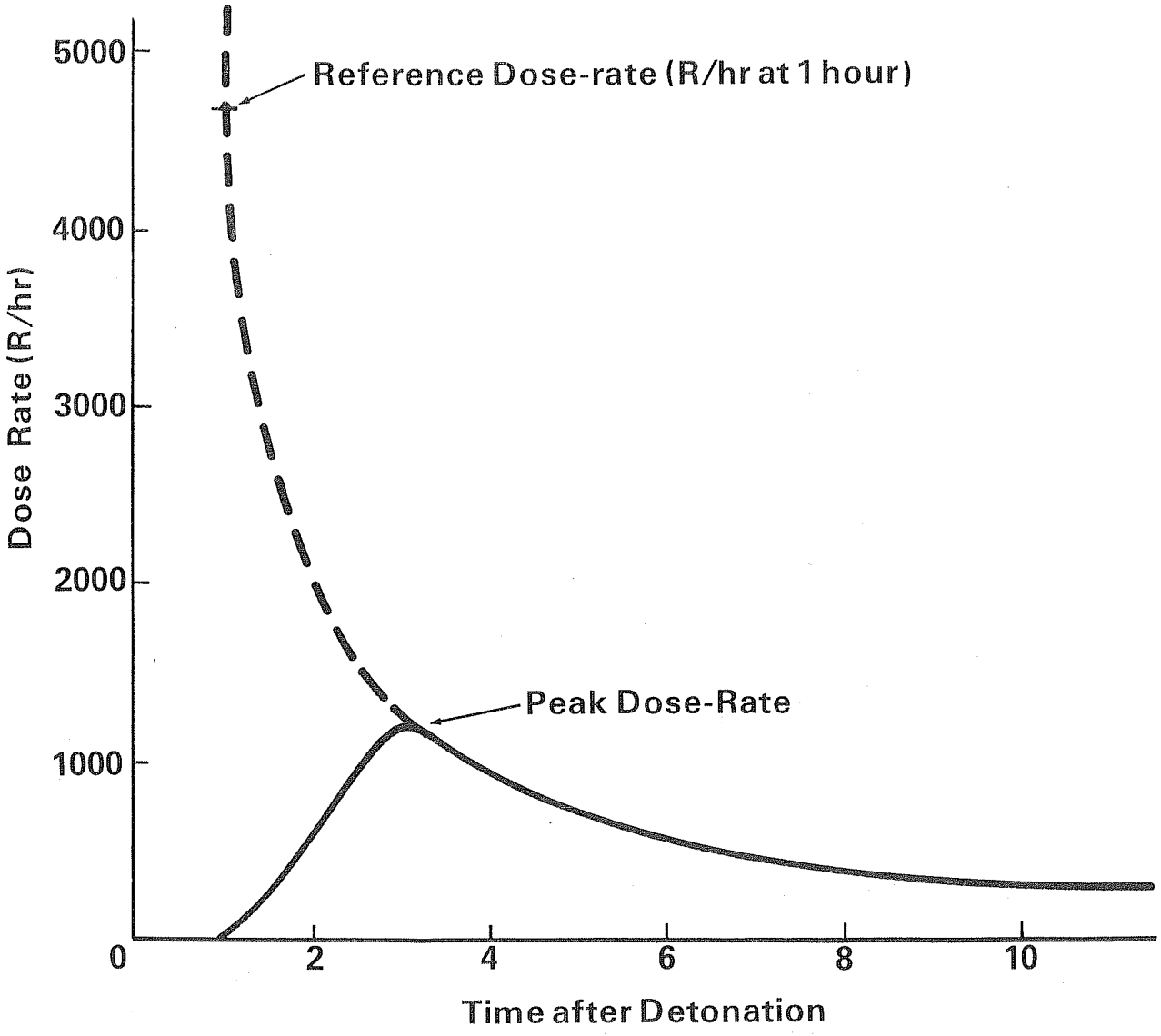

PANEL 14

DOSE-PENALTY TABLE

Roentgen Exposure Dose in Any / Acute Effects	1 Week	1 Month	4 Months
Medical Care Not Needed	150	200	300
Some Need Medical Care Few if Any Deaths	250	350	500
Most Need Medical Care 50% + Deaths	450	600	*

*Little or no practical consideration.

DOSES AT 30 MILES DOWNWIND

(5-MT surface burst; 15 MPH wind)

Time	In Open	In Shelter 46	In Shelter 76
1 Week	11,400	248	150
1 Month	13,500	294	178
4 Months	15,000	326	197

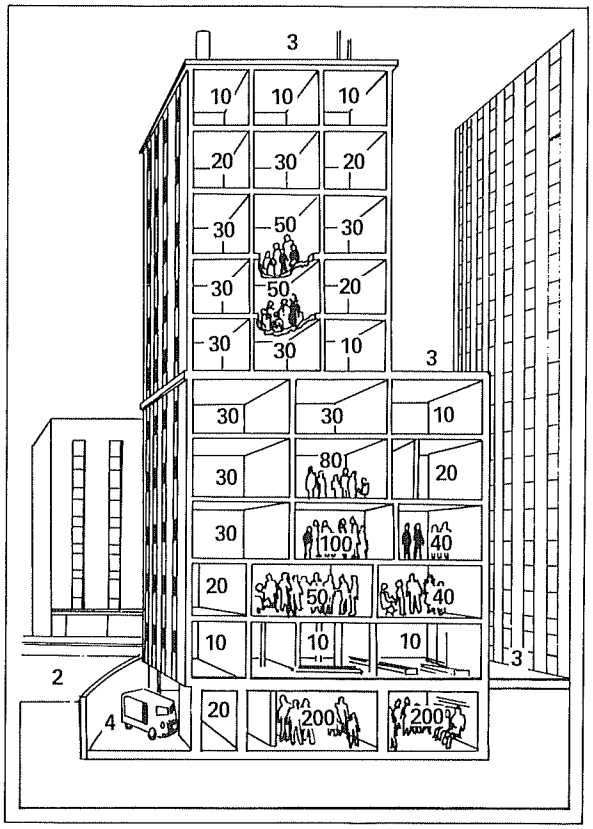
3
10
10
10
20
30
20
30
50
30
30
50
20
30
30
10
3
30
30
10
30
80
20
30
100
40
20
50
40
10
10
10
3
2
4
20
200
200

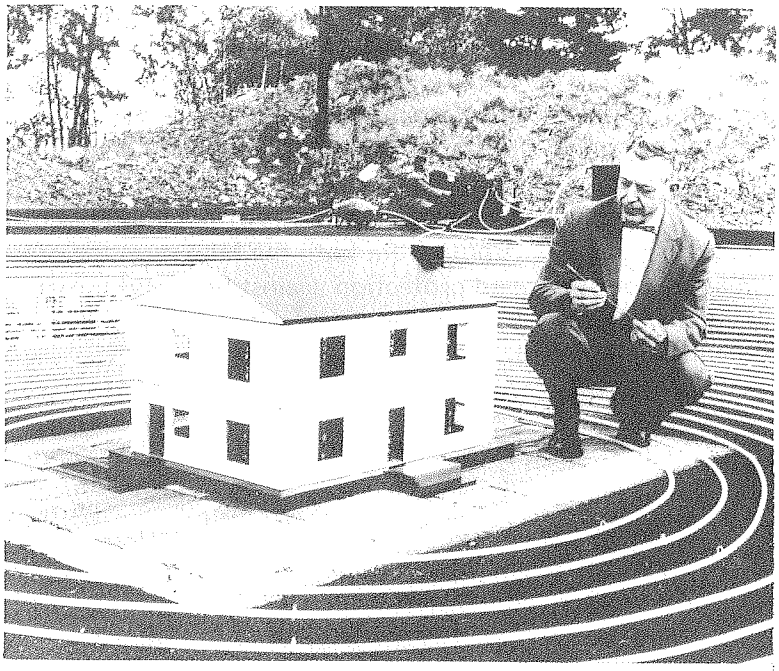

PANEL 18

TYPICAL FALLOUT PROTECTION FACTOR RANGES

RELATIVE TO BLAST PROTECTION

Blast Preference	Description
A	Subway stations, tunnels, mines, and caves with large volume relative to entrances. (1000 - 10,000)
B	Basements ans sub-basements of massive (monumental) masonry buildings. (100 - 1000)
C	Basements and sub-basements of steel and reinforced-concrete framed buildings having flat slab or slab and beam ground floor construction. (100 - 1000)
D	First three floors of buildings with "strong" walls. (20 - 80)
E	Basements of wood-frame and brick-veneer residences. (10 - 50)
F	Fourth and higher floors of buildings with "strong" walls. (20 - 100)
G	Basements of steel and reinforced-concrete framed buildings with flat plate ground floor. (100 - 200)
H	First three floors of buildings with weak walls, brick buildings and residences. (20 - 80)
I	Fourth and higher floors of buildings with weak walls. (20 - 100)

ONE-WEEK DOSE AFTER LARGE ATTACK FOR VARIOUS PROTECTION FACTORS

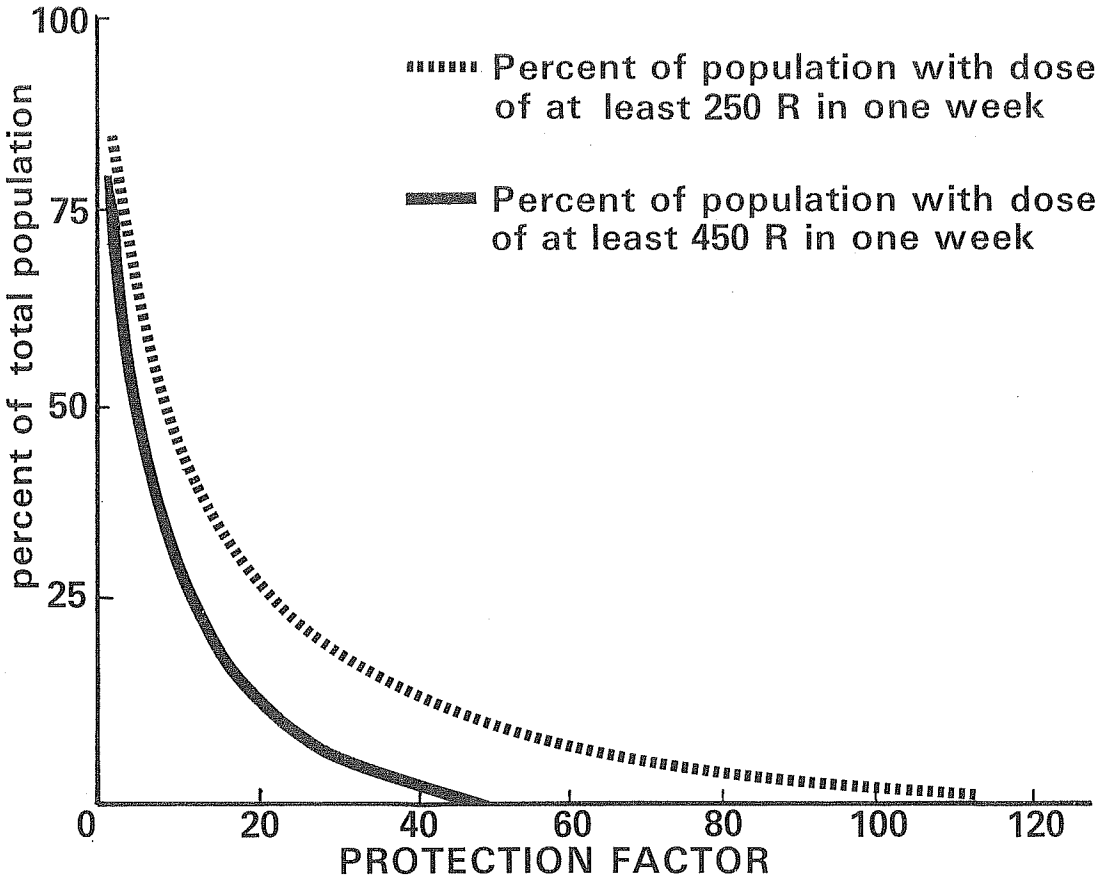

PANEL 20

PROTECTION IN RESIDENTIAL BASEMENTS

We noted in Chapter 2 that home basements could play an important role in improving survival from blast effects. They can also play an important role in providing protection against fallout radiation. In most parts of the country outside of the downtown areas of cities, the amount of fallout shelter identified in the National Fallout Shelter Survey (NFSS), which is located in large buildings, is insufficient for the population that needs shelter.

About half the homes in the United States have basements, but, as shown on this map, they tend to be concentrated in the northern part of the country. A small proportion of homes have basements in the South, Southwest, and Far West sections. Even these could be of great value if neighbors shared with neighbors. The average residential basement has an area greater than 1000 square feet. The standard shelter space in the NFSS buildings is 10 square feet. The usual emergency housing space allotment in peacetime natural disasters is 40 square feet. Thus, from 25 to 100 persons could be sheltered in the average home basement, if necessary.

The fallout protection afforded by home basements can be estimated in the following way:

(1) Single-story homes with average basement wall exposures (i.e., above ground) less than 2 feet will provide at least PF 20 throughout the basement.

(2) Homes with 2 or more stories and 2 feet or less average basement wall exposure will provide at least PF 40 throughout the basement.

(3) Single-story homes with average basement wall exposure greater than 2 feet can be improved to PF 20 by sandbagging the exposed walls or mounding earth against them.

(4) Similarly, multi-story homes with basement wall exposure greater than 2 feet can be improved to PF 40 by sandbagging or mounding earth.

Generally, fallout protection in home basements is least in the center of the basement and greatest in the corners and along the walls.

PERCENTAGE OF HOMES WITH BASEMENTS

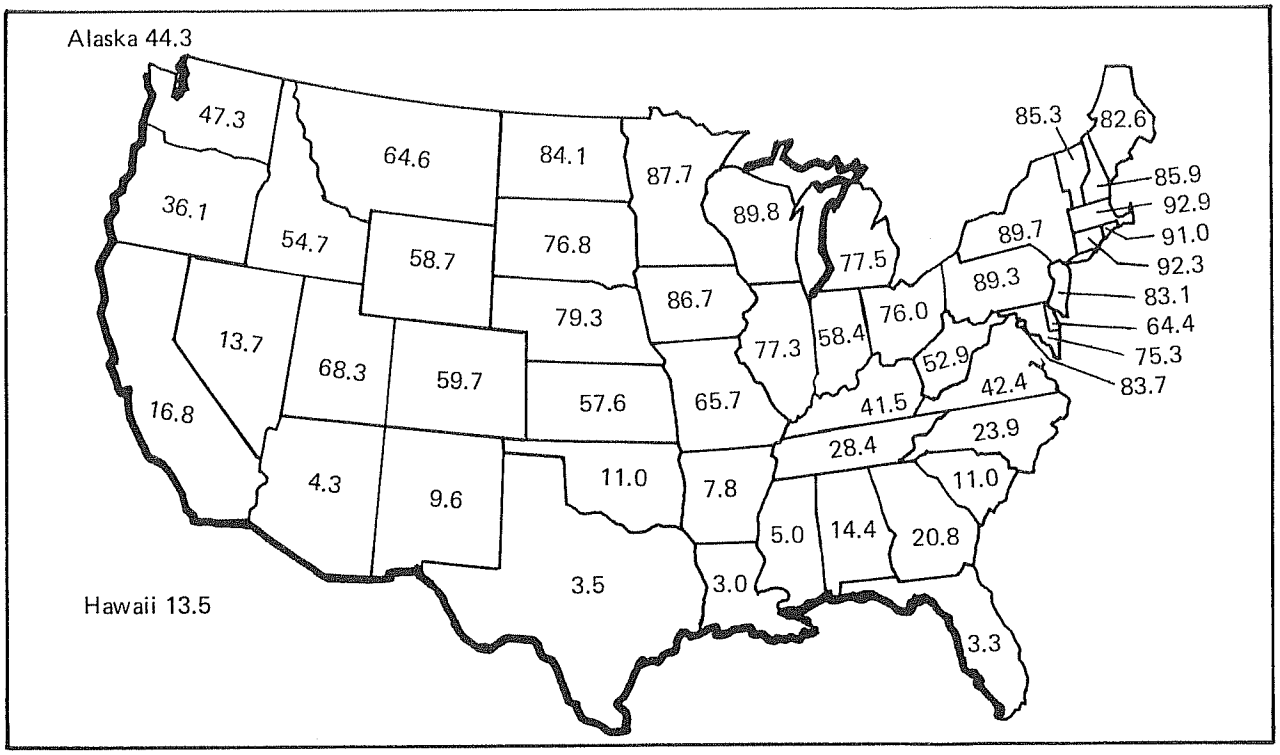

PANEL 21

FALLOUT PATTERNS
(PEAK DOSE RATES AND TIME OF PEAK) FOR 15 MPH EFFECTIVE WIND

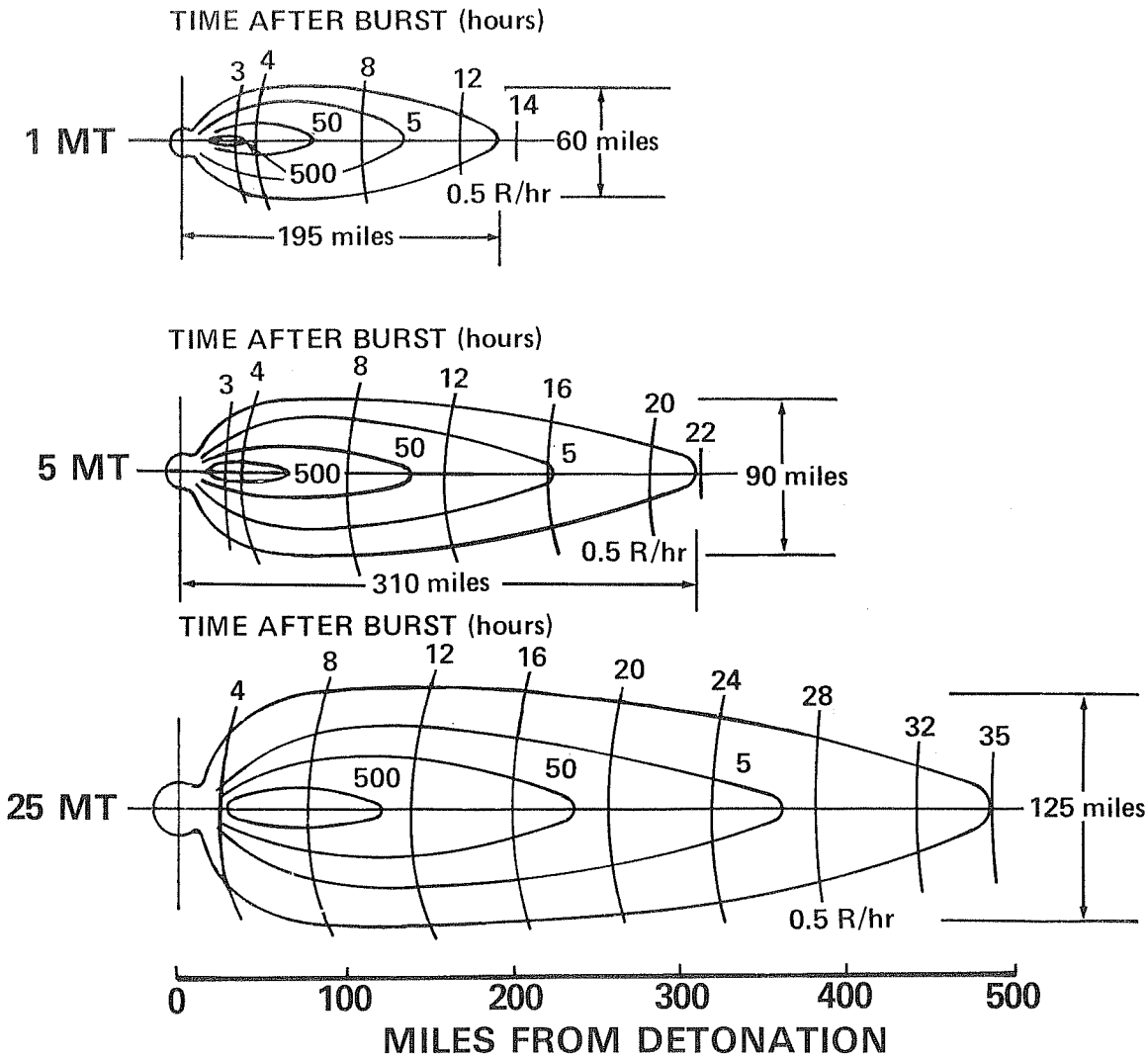

DOSE IN ROENTGENS TO KILL HALF THE ANIMALS IN BARNS, PENS, OR PASTURE*

Animal	In Barn (R)	In Open Pen (R)	On Pasture (R)
Cattle	500	400	170
Sheep	400	320	240
Pigs	660	(550)**	(400)
Horses	670	(600)	(350)
Poultry	850	(780)	(730)

*From current Department of Agriculture estimates.

**Parentheses indicate no experimental data available.

GAMMA DOSE IN ROENTGENS TO REDUCE CROP YIELD BY 50 PERCENT*

Crops	YD-50 Dose
Peas, Broadbeans	less than 1000R
Rye, Barley, Onion	1000 to 2000R
Wheat, Corn, Oats, Cucumber	2000 to 4000R
Peanut, Alfalfa, Fescue, Sorghum	4000 to 6000R
Cotton, Sugar Cane, Melons, Celery	6000 to 8000R
Soybeans, Beets, Broccoli, Red Clover	8000 to 12,000R
Rice, Turnips, Sweet Potatoes, Strawberries	12,000 to 16,000R
Squash	16,000 to 24,000R

*Based on estimates in NATO document AC/25-WP/79, **The Effects of Radioactive Fallout on Food and Agriculture**, November 1972.

EFFECTS ON THE HUMAN ECOSYSTEM

The study of the interrelationships among members of a community of animals and plants is called **ecology** and the community itself is usually referred to as an **ecosystem.** Today's environmentalists tend to call the human ecosystem, the "ecology." Concern has been expressed since the development of nuclear weapons that a nuclear war might have a catastrophic effect on the biological environment insofar as it affects humans. The concerns have stemmed mainly from the perceived characteristics of fallout and the radiations emanating from it.

In his novel, **On the Beach**, Neville Shute had to invent an impossible kind of fallout, one that did not settle out or undergo significant radiological decay, in order to cause the end of mankind. Others, not intending fiction, have forecast a new Ice Age or, alternatively, the melting of the polar ice caps, raising the level of the oceans to flood the eastern United States—and most of the populated part of the rest of the world. Which should occur depends on the presumed particle size and shape of that part of the fallout that is injected into the stratosphere and mesosphere (Panel 7). Particle clouds circling the earth could upset the earth's heat balance. Whether the earth would cool off or heat up would depend on whether the dust particles interfered with the sunlight striking the earth more or less than it interfered with the heat loss to outer space. Large volcanic eruptions offer the closest natural analogy. It is said that the huge eruptions of 1815, involving quantities of volcanic dust equivalent to the detonation of 50,000 MT or more, may have been responsible for an unusually cool summer the following year, some 13 degrees below normal. Indeed, the three major historic volcanic eruptions were all followed by exceptionally cold years. But only one year was affected. It has been concluded that the earth's climate is exceptionally stable despite severe temporarily imbalancing effects. Continued pressure of change over decades and centuries are required to produce an Ice Age.

Similarly, observation that insect predators, such as birds, are more vulnerable to fallout radiation has led to predictions that the insects will inherit the earth after a nuclear war. Analysis shows, however, that heavy fallout areas are rarely more than 50 to 100 miles from areas of negligible fallout. Since the population of the various species is controlled largely by food supply, there would be a rapid invasion of predators into the temporarily insect-rich areas. In sum, no nuclear attack can induce gross and permanent changes in the "balance of nature" anything like those that human civilization has already produced through agriculture and urbanization.

On the other hand, there could be ecological changes that might require governmental control action in the early postwar years. World-wide fallout could increase rainfall over normal amounts by acting as a "cloud-seeding" mechanism. This would have adverse effects in flood-plain areas but would delay the onset of fire hazard from radiation-killed trees in areas of moderate-to-heavy fallout. Failure to log dead trees (which would be useful for housing and firewood) would sooner or later result in forest fires and erosion damage. Over a period of several years, silting could destroy the usefulness of reservoirs and irrigation works. Finally, degraded sanitation and public health measures in damaged urban areas could create conditions favorable to outbreaks of disease-carrying insect and rodent populations. All these consequences are subject to human planning, intervention, and control.

IMPLAUSIBLE CATASTROPHES

1. End of all life on the planet Earth.
2. A new Ice Age.
3. Melting of the polar ice caps.
4. Insects inherit the Earth.

MORE LIKELY ECOLOGICAL CONSEQUENCES

1. Temporarily increased rainfall.
2. Fire hazard in dead pine forests.
3. Longer-term threat of increased erosion and silting.
4. Outbreaks of disease-carrying insects and rodents in damaged urban areas.

FALLOUT IN THE DAMAGED AREA

Most of the fallout from megaton-yield nuclear detonations is carried tens to hundreds of miles by the wind before it is deposited on the ground. For this reason, we have emphasized the fallout environment outside the area of blast damage and fire. Fallout from surface bursts will also occur in the direct-effects area, making firefighting, rescue, and medical aid more difficult and urgent. The next six panels describe the fallout threat in the damaged area, as defined by the Miller fallout model. Weapons test data supporting these estimates are quite limited.

Fallout does not arrive immediately in the damaged area. Particles begin to fall from the rising fireball when the rate of cloud rise decreases to less than the falling velocity of the particles. The time of arrival of first fallout from the mushroom stem is shown in the table for 1-, 5-, and 25-MT detonations.

The somewhat complex pattern below the table shows the time of arrival of close-in fallout for the example 5-MT surface burst used previously. Fallout arrives almost simultaneously at 22 minutes after burst over nearly all of the direct effects area. (For reference, the extent of 2-psi blast overpressure is shown as a dotted circle.) Thereafter, fallout progresses downwind at the assumed effective wind speed of 15 miles per hour, reaching a distance of about 16 miles at one hour after detonation. For other wind speeds, the distances shown would obviously be different.

One might ask how it could be that fallout would not arrive at 16 miles downwind until one hour after detonation when, in Panel 9, we saw that fallout arrived 30 miles downwind at 45 minutes after burst. The reason is that the point at 30 miles, shown by a black dot, is in the cloud fallout region, not the stem fallout region. In the upwind portion of the cloud fallout region, fallout from the bottom of the cloud arrives before that from the main portion of the cloud. The earliest arrival of cloud fallout is beyond 30 miles and arrival times increase toward ground zero. Fallout arrival at 25 miles is later than at 30 miles, increasing to about one hour inside 20 miles where cloud and stem fallout arrive almost simultaneously. Therefore, stem fallout arrival times are not shown beyond one hour.

EARLIEST FALLOUT ARRIVAL

Weapon Yield	Fallout Arrival Time
1 MT	16 Minutes
5 MT	22 Minutes
25 MT	30 Minutes

FALLOUT ARRIVAL FOR 5 MT BURST

(15 MPH WIND SPEED)

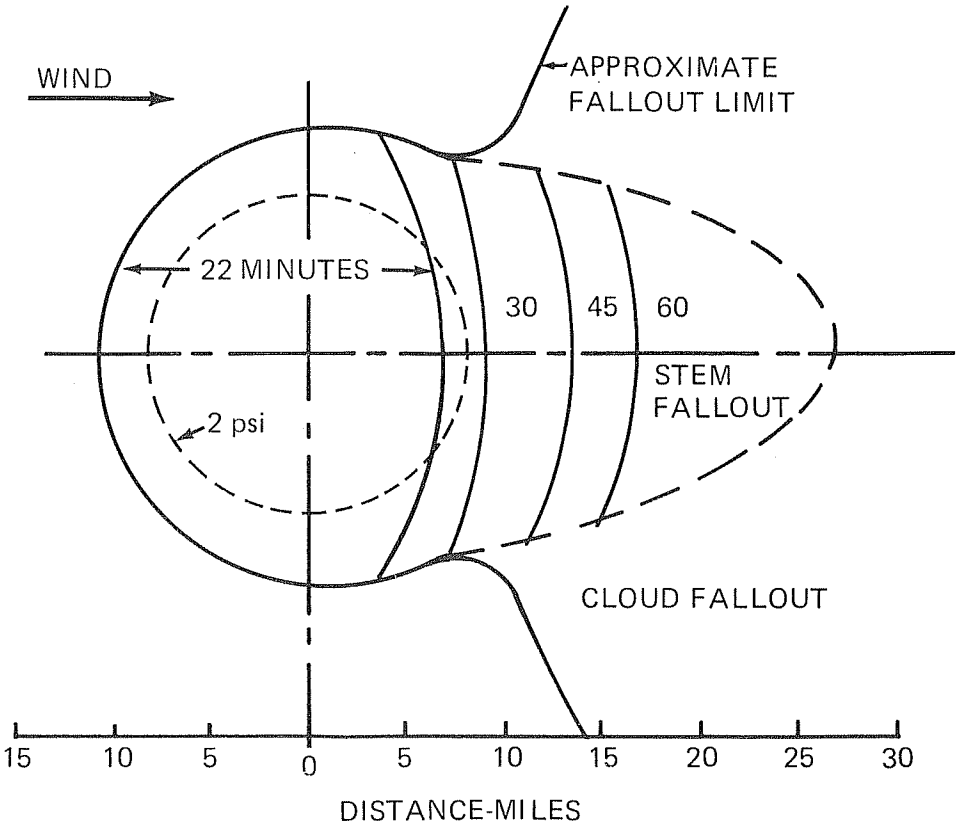

PANEL 29

EARLY OPERATIONAL DOSES

Although fallout will arrive in the damaged area within 15 to 30 minutes after detonation, fallout radiation exposures during the critical first hour will generally be nominal. The region affected by the doses defined in the Dose Penalty Table of Panel 15 is shown here. This region is confined to a small downwind area in the moderate and severe damage areas. There is a small area astride the 12-psi circle where exposures in the first hour would be in excess of 450R. Practically all of the area where suppression of smouldering ignitions, fire-fighting, rescue, and medical aid would be urgent tasks would experience outside doses of less than 150R during the first hour.

The doses shown are not those that would be received over a smooth, infinite plane. As we saw in Panel 16, exposures under actual operating conditions would be lower than the smooth, infinite-plane case because real surfaces are rough and of limited extent. Debris caused by blast damage would make most of the damaged area quite "rough." How "rough" these areas might be can be appreciated by reviewing Panels 35 and 36 of Chapter 2.

For this example, it has been assumed that the "real world" exposures would be about one-third those predicted for the smooth, infinite-plane situation. This is probably a conservative estimate of the effect of blast damage, and actual exposures would likely be even lower. Radiation exposures would vary even more widely than suggested by Panel 16. To aid in control of such exposures, at least one member of each emergency team should be equipped with a dosimeter.

One additional point to be considered is that, although gamma radiation exposures might be nominal during the first hour, fallout would be occurring during most of this period. Emergency teams should be dressed to avoid accumulation of fallout particles on the skin. A "Man-from-Mars" suit is not necessary. A coat with hood or hat and gloves are desirable. The usual fireman's "running gear" is excellent for the purpose.

DOSE DURING THE FIRST HOUR
(5MT SURFACE BURST -15 MPH WIND)

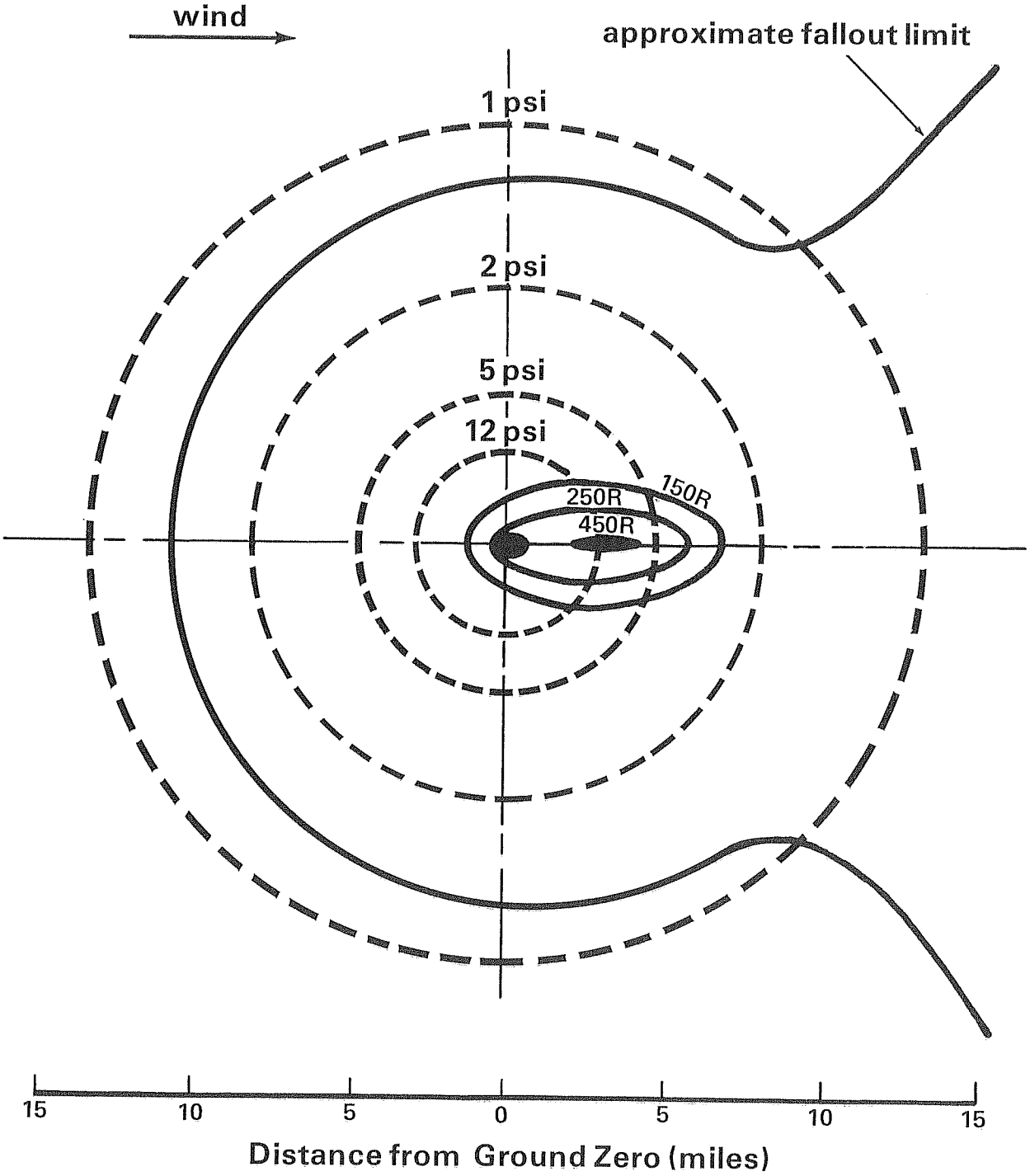

PANEL 30

LATER OPERATIONAL DOSES

Urgent tasks of fire defense, rescue, medical aid, and remedial movement of people from threatened shelters may require continued operations beyond the first hour after a detonation. Shown here are the areas in which 150R, 250R, and 450R doses might be expected during the first two hours (upper sketch) and first four hours (lower sketch). The assumption as to the roughness of the debris-strewn area is the same as in the previous panel.

At two hours, the area enclosed by the 450R dose contour extends from about 1 mile upwind to about 8½ miles downwind and is about 4 miles wide at its widest. By the end of four hours, this area extends from 1½ miles upwind to 10 miles downwind and is 5 miles wide. As can be seen, doses above 150R are likely only in the downwind sector of the damaged area and affect less than one-third of the potential fire area.

In contrast to the situation in the cloud fallout area further downwind, the dose rate in the stem fallout area will peak well before the cessation of fallout. This is because of the rapid decay of radioactivity at early times. The dose rate can be expected to peak within the first hour throughout most of the damaged area. Only a small part of the subsequent dose is received during the "buildup period." Hence, the observed peak dose rate can be used to guide emergency operations. For example, where the dose rate peaks at, say, 125 R/hr, the anticipated dose in the first two to four hours is predicted to be about 125R. Similarly, if the CD V-715 goes off-scale on the high range (greater than 500 R/hr), potentially lethal outside exposures are to be anticipated. Since the direction of down-wind fallout may not be related to the observed surface winds, use of radiation measurements is to be preferred in operational planning.

DOSE DURING FIRST TWO HOURS

(5 MT SURFACE BURST-15 MPH WIND)

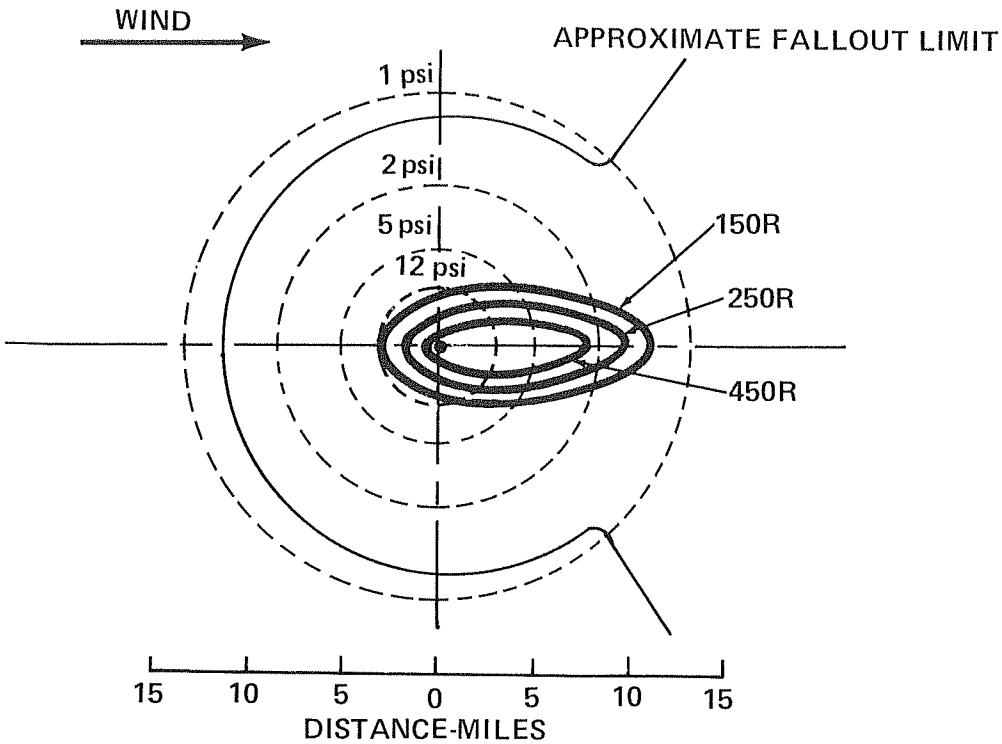

DOSE DURING FIRST FOUR HOURS

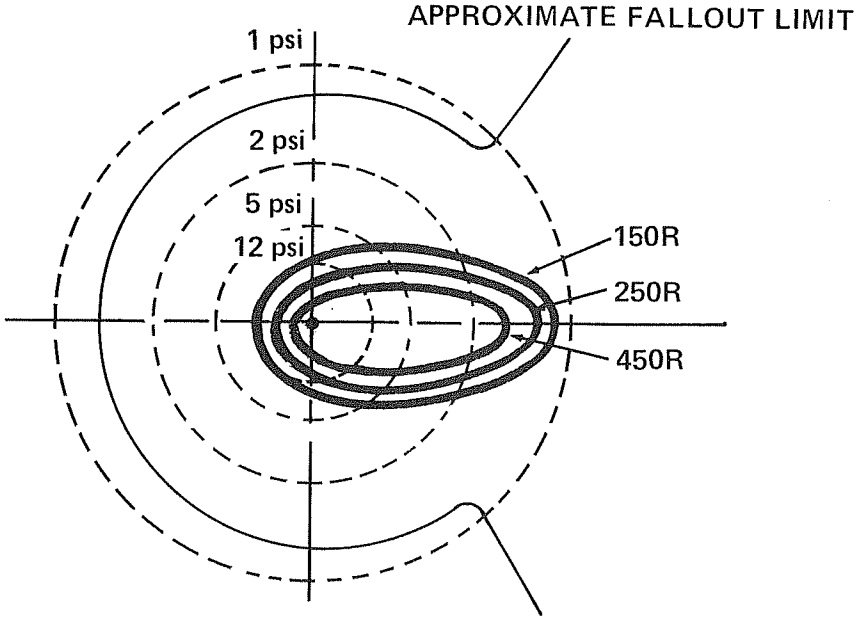

PANEL 31

EFFECT OF FIRES ON FALLOUT DEPOSITION

In Chapter 3, the fire environment in the damaged area was described. Mass fires are marked by "in-rush" winds and a rising "convection column" above the fires. Theoretical analyses of convection columns above large-scale fires indicate that the updraft from even moderate rates of heat output exceeds the falling velocities of most fallout particles. It would appear, then, that convection columns induced by fires set by the detonation could have an effect on the fallout pattern.

A time lapse occurs between the time of ignitions and the time when massive fires can be burning. Experience from World War II incendiary raids indicates this time period may vary from 25 to 45 minutes. The effect of the nuclear blast wave in suppressing ignitions to a smouldering condition would increase this time delay substantially. Thus, it is unlikely that the fires resulting from a megaton-yield surface burst would alter significantly the deposition of stem fallout in the damaged area.

Analyses and experiments have been done to assess the effect of well-established fires on fallout deposition from the cloud or from later fallout from upwind detonations. The main experiments were conducted in the low-velocity wind tunnel shown here. Gas burners were used to simulate the fire area and simulated fallout was introduced upwind of the fire near the top of the wind tunnel. As predicted by theory, the fire updraft buoyed up the fallout, causing it to fall much further downwind than otherwise would be the case. There was also much lateral dispersion of the fallout so the effect would be to lower markedly the high dose rates in the downwind area and increase somewhat the lower dose rates over a much larger area.

Other experiments conducted in the mid-1950s showed that rapidly burning fires in already contaminated areas as small as one tenth of an acre resulted in removal of perhaps a third of the deposited fallout, and the removed material was dispersed so that there was no significant concentration in any other region. This process may have some effect in further reducing radiation hazards during firefighting operations.

LOW-VELOCITY WIND TUNNEL USED IN FIRE-FALLOUT EXPERIMENTS*

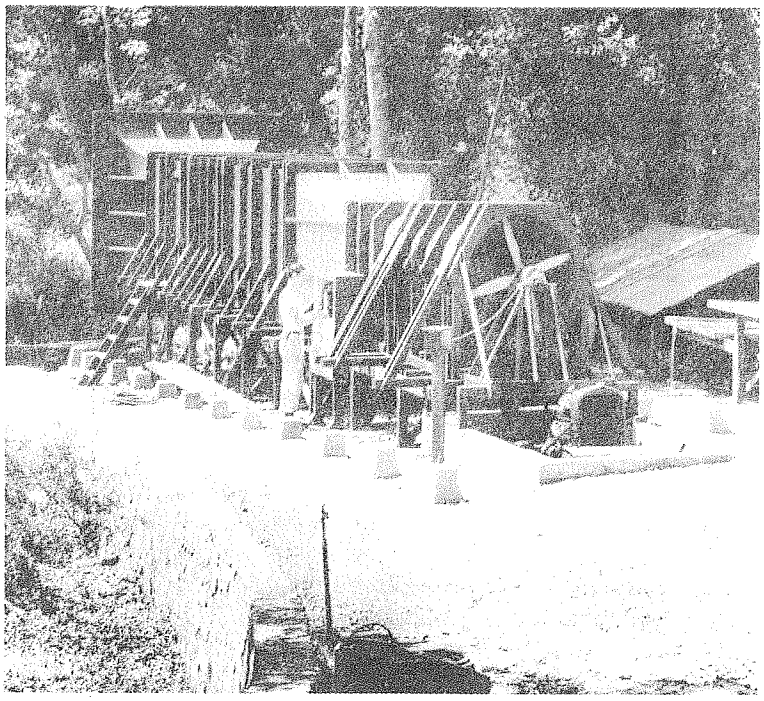

* From Broido, A., and McMasters, A.W., **The Influence of a Fire-Induced Convection Column on Radiological Fallout Patterns**, California Forest and Range Experiment Station, Forest Service, U.S. Department of Agriculture, February 1959. (Library of Congress PB 149923)

EFFECT OF DAMAGE ON FALLOUT PROTECTION

The fallout protection afforded by buildings (Panel 18) is estimated on the basis that the roof and surrounding ground areas are uniformly contaminated with fallout and that fallout does not lodge on the sides of the buildings nor do fallout particles penetrate into the interior of the building. In effect, the calculation is made as if the fallout fell vertically onto the surfaces below. In the real world, winds or breezes are blowing near the ground most of the time. If windows were broken or walls blown in, some fallout could penetrate into the interior of buildings.

A number of calculations have been made of the effect of "fallout ingress" on the protection afforded by buildings. These estimates have been necessarily highly idealized and are not very useful. The small amount of experimental evidence available does indicate, however, that large reductions in fallout protection are not to be expected in most instances.

The best evidence comes from the volcano fallout in Costa Rica described in Panel 12. Shown here is a fallout situation where most of the wall is open. Visible fallout is concentrated in a band about 20 inches wide below the sill. (The devices shown are for collecting fallout and measuring air movement.) Measurements indicated that the deposition near the sill was about 5 percent of that on the ground in the open and about 1 percent elsewhere in the corridor. Other measurements near smaller open windows indicated deposition near the windows of about 1 percent of the exterior amounts. Calculation of the effect of this amount of ingress on the mid-floors of tall buildings indicate a reduction of about 5 percent in the protection factor (e.g., 38 PF rather than 40 PF). Measurements under covered walkways where both sides were completely open indicated that as much as one-tenth of the outside deposit level could be deposited. Thus, where walls are completely blown in as shown in the upper sketch of Panel 14 in Chapter 2, the protection factor in the middle floors could be reduced by perhaps 10 percent or more (e.g., 35 PF rather than 40 PF).

The deposition of building debris on the floor above basements would tend to increase the protection below in most cases.

The most serious degradation of fallout protection due to blast damage would occur in residential basements and the basements of other lightly constructed buildings under the circumstance where the building is blown clear of the basement (lower sketch in Panel 12 of Chapter 2). Fallout would be deposited in the basement, reducing the protection factor from 20 to 40 down to about 4 or 5. It would be necessary for basement occupants to prop sections of flooring or walls against the basement wall, lean-to fashion, and to cover the lean-to with nearby pieces of masonry for fallout protection. This need is another reason why it may be desirable to plan for group occupancy of residential basements in urban areas rather than single families.

OPEN CORRRIDOR ON THIRD FLOOR OF SCHOOL CONTAMINATED BY FALLOUT-LIKE VOLCANIC DEPOSIT IN COSTA RICA*

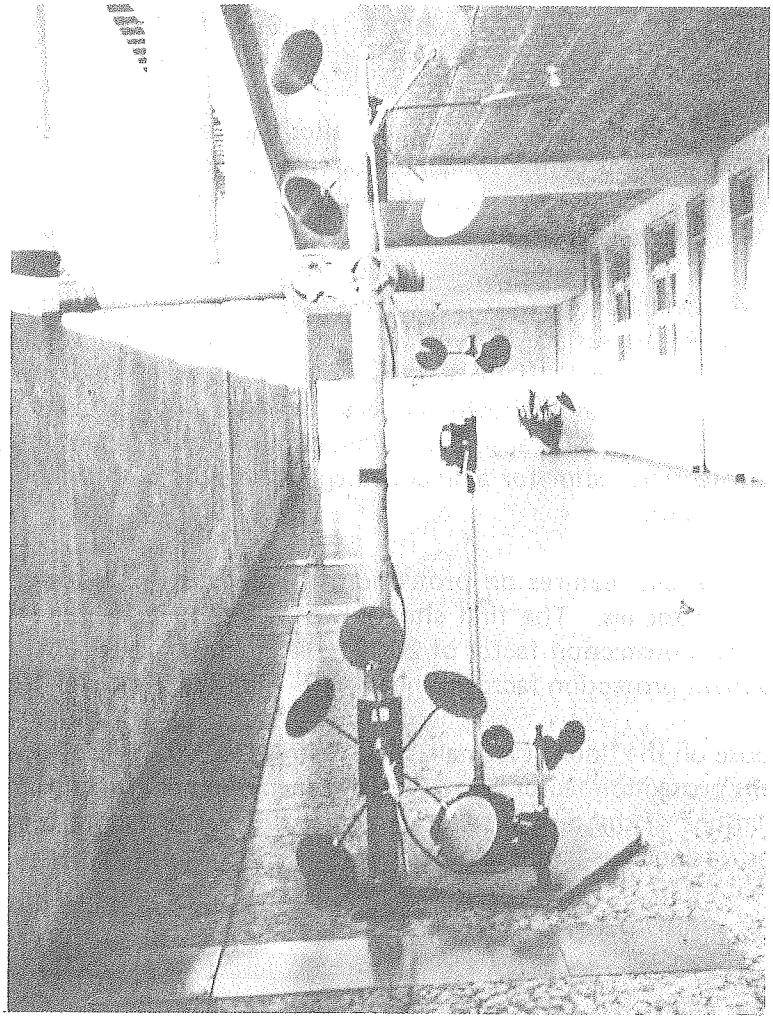

* From Clark, D.E., Jr., and Sartor, J.D., **Operation Ceniza-Arena: Techniques for the Measurement of Deposition and Redistribution of Fallout Around Structures**, Stanford Research Institute Project No. MU-5779, December 1966. (AD 647 242)

WHAT ABOUT HILLS?

Protection factor calculations assume that fallout is deposited on smooth plane surfaces. In Panel 16, the effect of the roughness of real surfaces was discussed, but again in terms of level terrain. The question might be raised as to the effect of prominent terrain features, such as hills and valleys.

The upper sketches show the protection afforded a person standing in the open on smooth surfaces. When the surface is level, we have the standard unprotected location for which the protection factor is 1. If the person were on top of a small, steep hill that falls away in all directions (the example shown here is a hemisphere with a diameter of 100 feet), the PF is increased to nearly 2 because the hill hides much of the fallout beyond the immediate area. The protection factor for a small, steep depression is not much improved over the infinite-plane situation.

The effect of terrain features on protection in basements is much more marked, as shown in the lower sketches. The first situation shows a home basement on a smooth, infinite plane having a protection factor of 20. The same house on top of a small, steep hill would have a basement protection factor of nearly 70. Many rural houses are built on hills.

The same house on the floor of a small, steep depression would also have a substantially increased basement protection factor. However, not many homes are built in such locations. In general, undulations of the terrain tend to restrict the area of fallout that can contribute to radiation exposure and thus improve protection.

EFFECT OF TERRAIN FEATURES

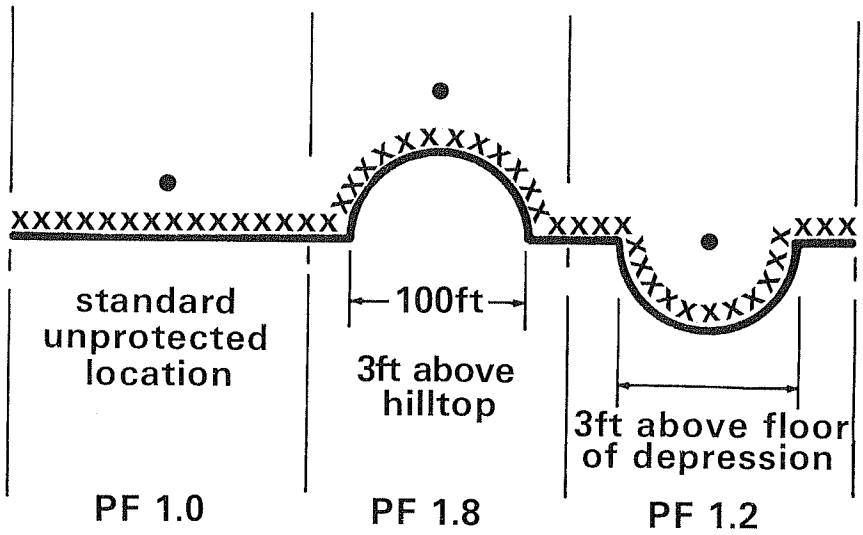

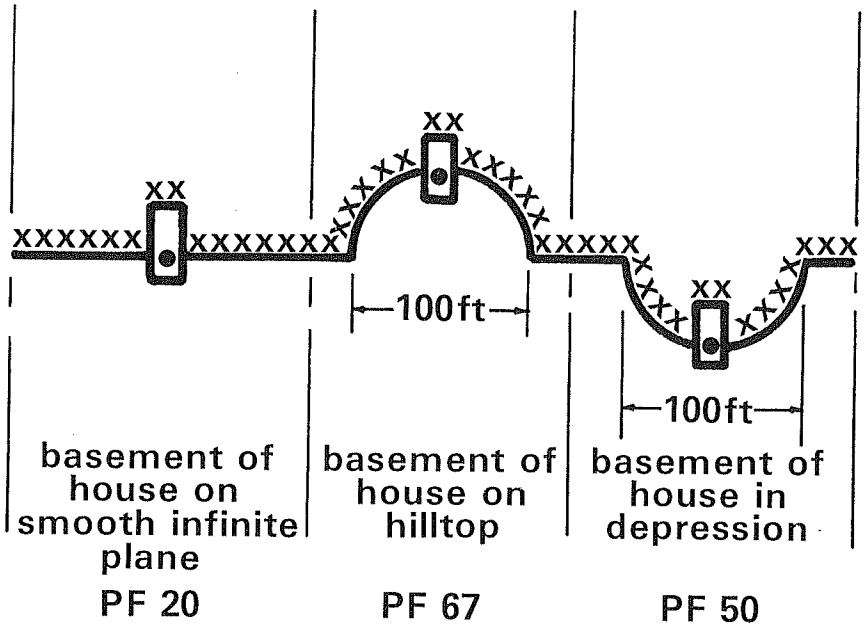

A NOTE ON DECONTAMINATION

Surfaces on which fallout particles have fallen are called **contaminated** surfaces. Being sand-like material, fallout can be cleaned from most surfaces by readily available means. The process of removing fallout particles from exposed surfaces and disposing them where they cannot harm people is called **radiological decontamination**. Paved areas can be decontaminated with firehoses, street flushers, or with street sweepers. Roofs can be decontaminated with firehoses. Unpaved areas can be decontaminated by scraping off or plowing under the top layer of soil.

As shown in this sketch, half of the radiation received at a point 3 feet above a large, smooth, unbroken surface comes from fallout within 50 feet. On rough surfaces, the area contributing half the exposure is much less. In an area covered with 6 inches of debris, a depth indicated in Chapter 2 as quite common, half the radiation comes from fallout within about 10 feet.

The sketch shows that three-quarters of the radiation comes from fallout within 200 feet on smooth surfaces (100 feet or less on rough or debris-strewn surfaces). But at least 10 percent of the exposure comes from fallout radiation originating many hundreds of feet away. This suggests that, if large reductions of exposure are desired, not only must the work or living area be decontaminated but also a "buffer zone" around it to a distance of several hundred feet in most instances.

For this reason, decontamination as a measure to improve the fallout protection of people in shelter is not generally practical except, possibly, for the sweeping up of visible fallout near broken windows or near entrances to a shelter area. Decontamination can be important, however, in speeding postattack recovery in fallout areas. Hence, decontamination is covered in more detail in Chapter 8.

DOSE CONTRIBUTION vs DISTANCE

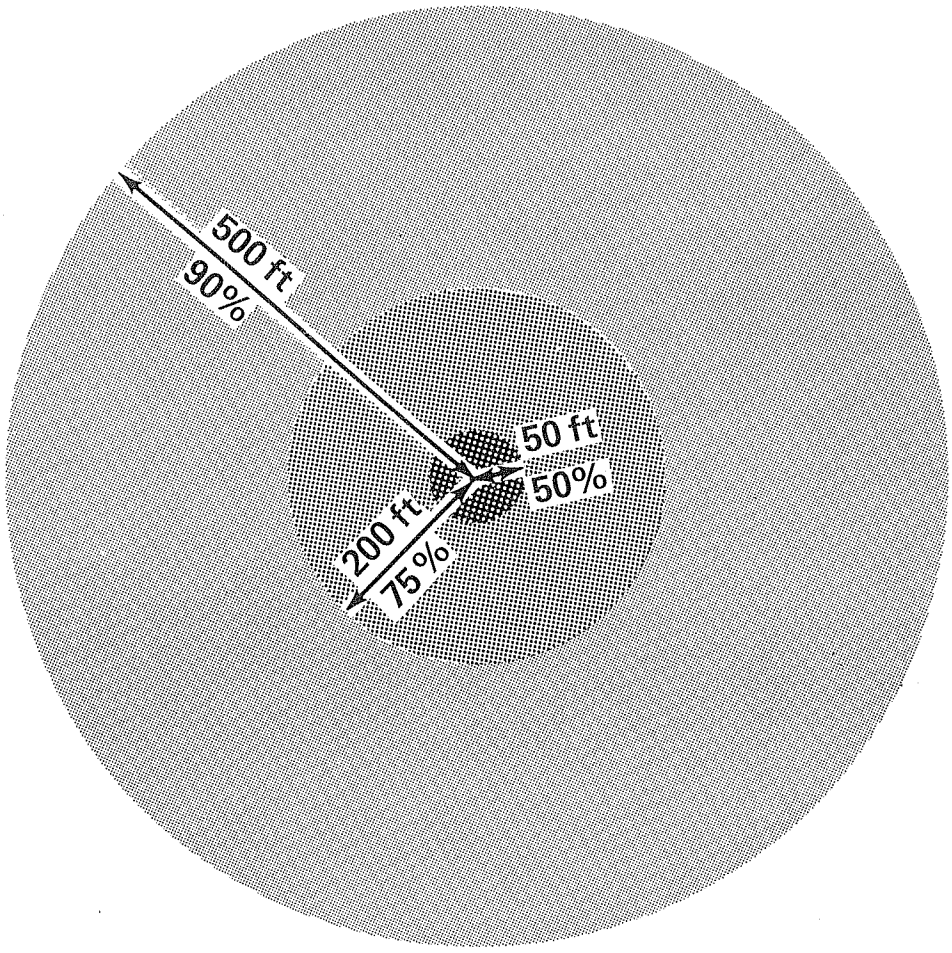

WHAT ABOUT BOATS?

The fact that a large part of the radiation from fallout comes from contaminated areas a considerable distance away has suggested that boats and ships located on bodies of water (lakes, rivers, and bays) might provide good fallout protection. Fallout particles will settle rather quickly to the bottom. Three to five feet of water will provide ample shielding from this fallout. Thus, if a boat is anchored or lying at least several hundred feet offshore, nearly all of the radiation exposure will come from fallout actually deposited on the boat. Most fishing and pleasure boats are quite small, and the protection factor from being on the water would be about 4 or 5, better than in a house but not as good as most home basements.

The protection can be greatly improved by rigging a tarpaulin or awning over cockpit areas and shaking or sluicing the canvas to dislodge the fallout particles when visible deposits appear. Exposed decks can also be sluiced by hose or bucket. Thus, a combination of lying offshore and early decontamination can generally result in an equivalent protection factor of 20 to 40. If no better fallout protection is available, boats may be considered in localities where they are plentiful.

Ships may also be useful in many circumstances. They can carry large numbers of people. Because they are larger than boats, the radiation levels from fallout deposited on the decks more nearly approaches the level that would occur on shore. The steel construction will offer significant shielding but prompt decontamination is also necessary to achieve a reasonable amount of fallout protection. The topside areas of ships are readily flushed off. Most naval ships and some merchant ships have washdown equipment to accomplish rapid decontamination. A washdown system in action is shown here.

PHOTOGRAPH OF USS KITTY HAWK UNDER WASHDOWN
(Courtesy of Office of Chief of Naval Operations)

FACTS ABOUT RADIATION AND FALLOUT

During the average lifetime, every person receives about 10 Roentgens of ionizing radiation from nature and about an equal amount additionally from dental and chest X-rays and even the luminous dials of wrist watches. Yet radiation effects and fallout remain mysterious and misunderstood threats to both the average citizen and government employee. Emergency planning should include informing the public on the basic facts shown here if an unwarranted paralysis of action during a fallout emergency is to be avoided. The basis for these statements is contained in the panels of this chapter and those of Chapter 5.

SOME BASIC FACTS

1. Everyone receives some radiation exposure in peacetime. It is when large doses are absorbed in a short period that sickness or death results.

2. Radiation sickness is neither contagious nor infectious. But people made sick by radiation are temporarily more susceptible to infection.

3. Radiation exposures that cause sickness are much lower than those that cause death. Being sick does NOT indicate that one is necessarily going to die.

4. Fallout radiation cannot make anything radioactive. Fallout itself consists of sand-like particles too large to be inhaled.

5. Dangerous amounts of fallout can generally be seen but special instruments are needed to measure the danger of radiation exposure.

6. Radiation exposure can be kept below sickness levels by using good fallout shelter; by delaying outside activities until decay has reduced the exposure rate; and by limiting the time of exposure on urgent tasks.

7. No one should thirst or starve for fear of contaminated water or food. Illness can be caused as readily by malnutrition and poor sanitation as by radiation injury.

SUGGESTED ADDITIONAL READING

The following sources provide additional background on the material in this chapter:

Effects of Nuclear Weapons, Revised Edition 1964, Glasstone, S., (editor), Chapters 1, 2, 6, 9, 10, and 11, Superintendent of Documents, GPO.

National Committee on Radiation Protection, **Exposure to Radiation in an Emergency**, Report No. 29, January 1962.

Miller, C.F., **Fallout and Radiological Countermeasures, Volumes I and II**, Stanford Research Institute, January 1963. (Vol. I—AD 410 522, Vol. II—AD 410 521)

Casarett, A.P., **Radiation Biology**, Prentice-Hall, 1968.

Upton, A.C., **Radiation Injury: Effects, Principles, and Perspectives**, University of Chicago Press, 1969.

Bensen, D.W., and Sparrow, A.H.,(editors), **Survival of Food Crops and Livestock in the Event of Nuclear War**, No. 24 of AEC Symposium Series, CONF-700909, December 1971.

Radiological Defense Textbook, SM-11.22.2, Office of Civil Defense, June 1968.

Radiological Health Handbook, U.S. Department of Health, Education and Welfare, Public Health Service, Rockville, Maryland 20852, January 1970.

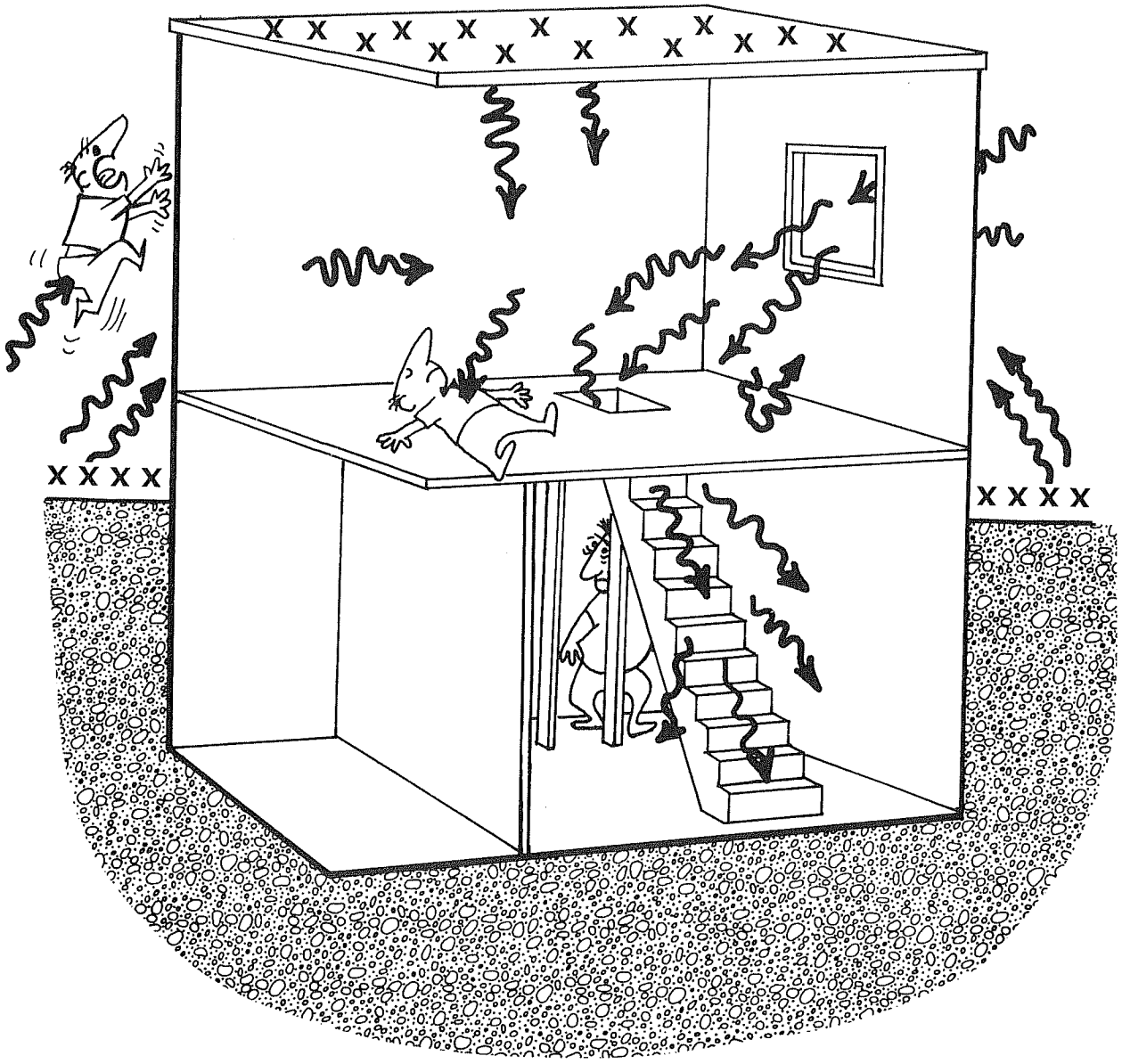

PANEL 38

CPG 2-1A8
June 1973

DCPA ATTACK ENVIRONMENT MANUAL

CHAPTER 8

WHAT THE PLANNER NEEDS TO KNOW ABOUT
THE POST-SHELTER ENVIRONMENT

DEFENSE CIVIL PREPAREDNESS AGENCY
DEPARTMENT OF DEFENSE

JUNE 1973

NINE BARRIERS TO WELL-BEING*

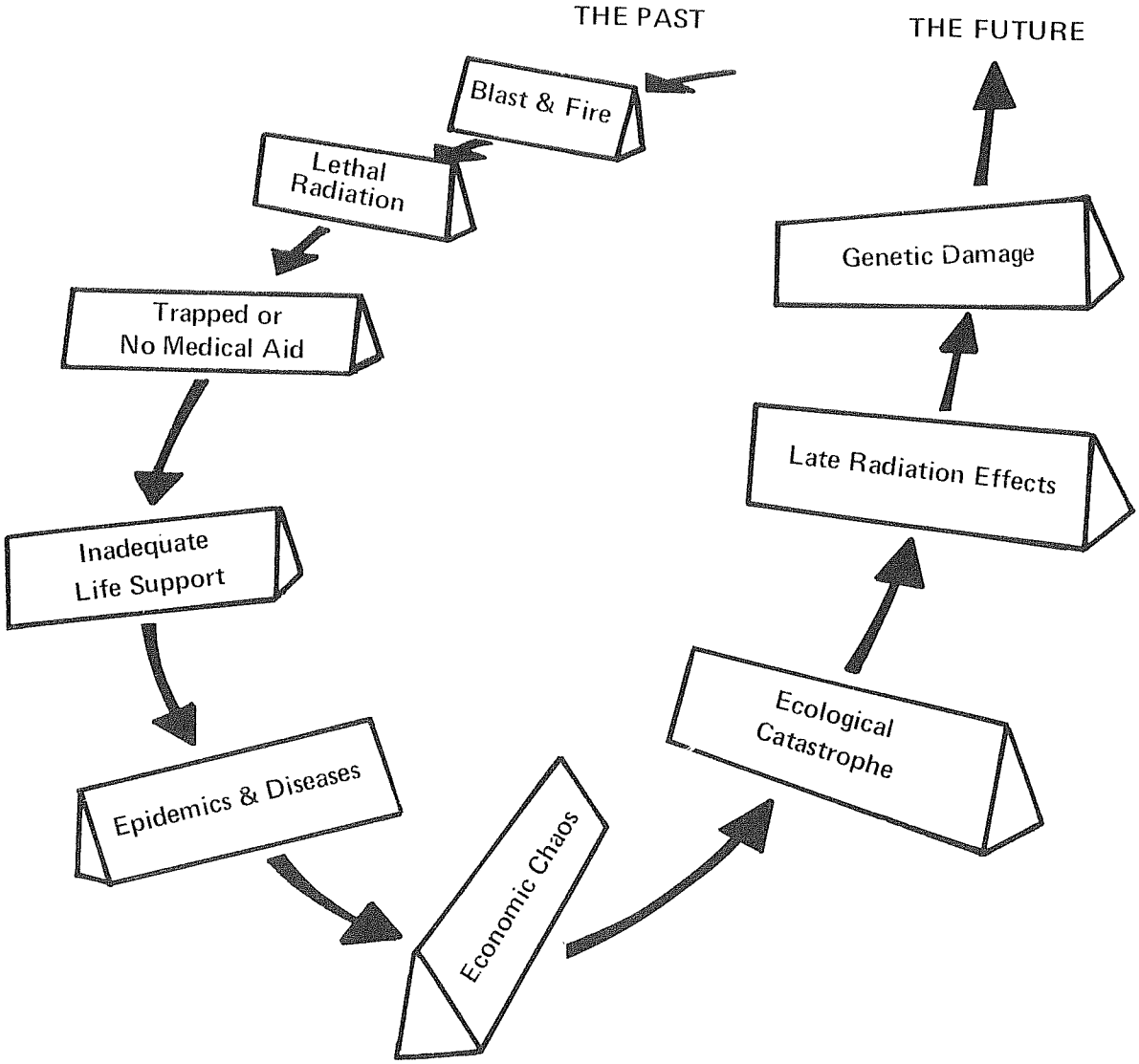

*Based on Greene, J.C., **The Case for Civil Defense**, DCPA Research Report No. 16, 1972 (AD 758 452).

PRIORITY NEEDS*

1. People would need leadership.
2. People would need information.
3. People would need reassurance.
4. People would need instructions.

*From Allnutt, Bruce C., **A Study of Consensus on Psychological Factors Related to Recovery from Nuclear Attack**, Human Sciences Research, Inc., May 1971. (AD 730 360)

DETROIT URBANIZED AREA

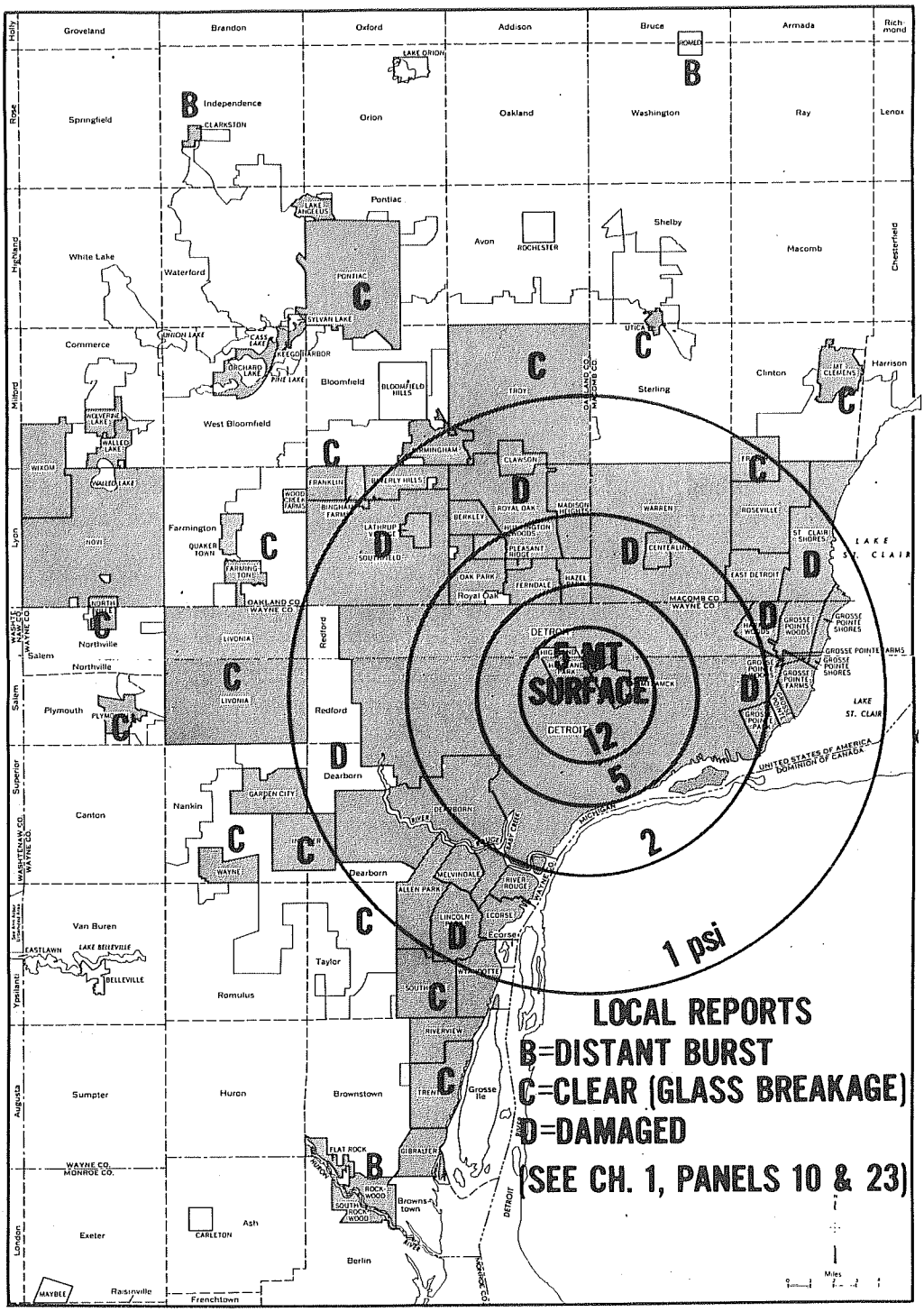

PANEL 4

THE FALLOUT CONSTRAINT

Gamma radiation from fallout is the attack effect that may persist in the post-shelter environment in amounts sufficient to cause injury or death. Studies of possible attacks in which fallout-producing surface bursts are assumed to occur indicate that, by one week after the last detonation, no part of the U.S. would be in a HIRAD situation (dose rate in excess of 50 R/hr).

The example fallout map shown here indicates the areas of the United States in which dose rates at the end of the first week could restrict post-shelter operations, as estimated by the Miller fallout model for the winds of a particular Spring day. An attack is assumed in which a portion of the weapons, amounting to about 2500 megatons, is detonated on the surface to cause fallout. In the clear areas, the dose rates at the end of the first week are estimated to be less than 0.1 R/hr (100 mR/hr). The dose rates in the lined area would range from 0.1 R/hr to 1R/hr. The black areas would have dose rates between 1R/hr and 10 R/hr. There are several stippled areas on the map where the one-week dose rates would be over 10 R/hr.

Time would further reduce the fallout radiation hazard. Using the 7-10 Rule discussed in Chapter 6, seven weeks after the attack the lined areas would become clear, the black areas would become lined areas, and the stippled areas would be black areas. To achieve a further factor-of-10 reduction would require, according to the rule, another seven-fold passage of time (49 weeks, or nearly one year after attack). Actually, increasingly rapid decay after six months and the effects of weathering would leave few, if any, areas outside the bomb craters above 100 mR/hr at year's end.

If the people are instructed and guided to limit exposures so as to avoid post-shelter radiation sickness, the principal effect of fallout radiation during the early months would be to delay the accomplishment of recovery activities. Delay would occur for several reasons. Recovery workers would need to restrict their exposure outside shelter to a shorter work-week in most cases. Survivors most able to participate in the recovery work force would be those in the best fallout shelters or those coming from areas experiencing little fallout, there by limiting the size of the work force. Survivors manifesting symptoms of radiation sicknes during the first week would have to remain in shelter or be transported to less-contaminate areas. It can be seen from the map that the distances to be traveled from heavy fallout are to areas of much lower hazard are not great in most instances.

EXAMPLE FALLOUT MAP
(DOSE RATES AT ONE WEEK)

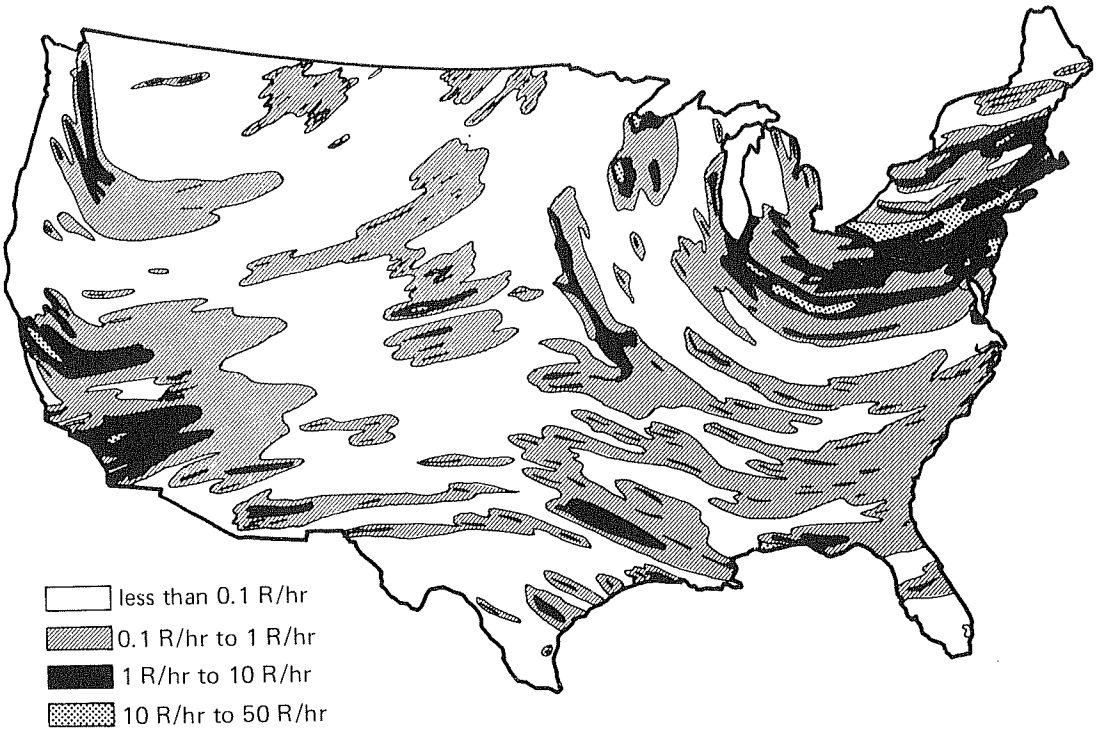

PANEL 5

DECONTAMINATION

As noted in Chapter 6, the delays caused by fallout radiation can be reduced greatly by decontamination, a process in which the deposited fallout is removed from surfaces and placed where it can no longer irradiate people. Thus, if 90 percent of the fallout material affecting a workplace could be removed in the first few weeks, a situation would be created that would not occur otherwise until many months later. Halving the dose rate would permit recovery workers to work twice as long as would otherwise be the case.

Outside damaged areas, decontamination can be accomplished using a variety of common methods. Flushing fallout particles from roofs and paved surfaces and into the storm drains by means of a firehose has been found to remove over 90 percent of the fallout material. An hour's work by three men with a firehose will clean 1800 square feet of roof or 15,000 square feet of paved area. Motorized street flushers and street sweepers are more effective on paved areas and three to five times faster. Open ground areas can be scraped by earth-moving equipment: scrapers, graders, or bulldozers. These methods typically remove a slice of native soil amounting to several hundred times as much as the thin coating of fallout removed with it. The scrapings must be dumped at a remote corner of the cleared area. With room to maneuver, these methods are as effective as the paved area methods and almost as fast.

In damaged areas, widespread debris will complicate the decontamination process. If water pressure has been restored, the preferred decontamination procedure is to fire-hose an area 30 to 50 feet in radius around the debris-clearing equipment, flushing the exposed fallout down into or under the debris piles. Then, the street or area can be cleared of debris, and the remaining fallout in the cleared area can be flushed into the drains. Without water, debris removal must occur first, followed by motorized sweeping or vacuuming of the fallout.

Because of the specialized equipment and operator skills required by most decontamination techniques, widespread decontamination of whole cities does not appear practical during the first month or so. Decontamination will be useful to permit key utility plants, staging areas, and supply warehouses to be operated safely in the first weeks after attack. Later, a large part of the population can be usefully employed in mass clean-up efforts, using household brooms, garden hoses, and shovels. Calculations have shown that such efforts can result in significant reductions in population exposure to radiation over the long term.

SOME DECONTAINATION OPERATIONS*

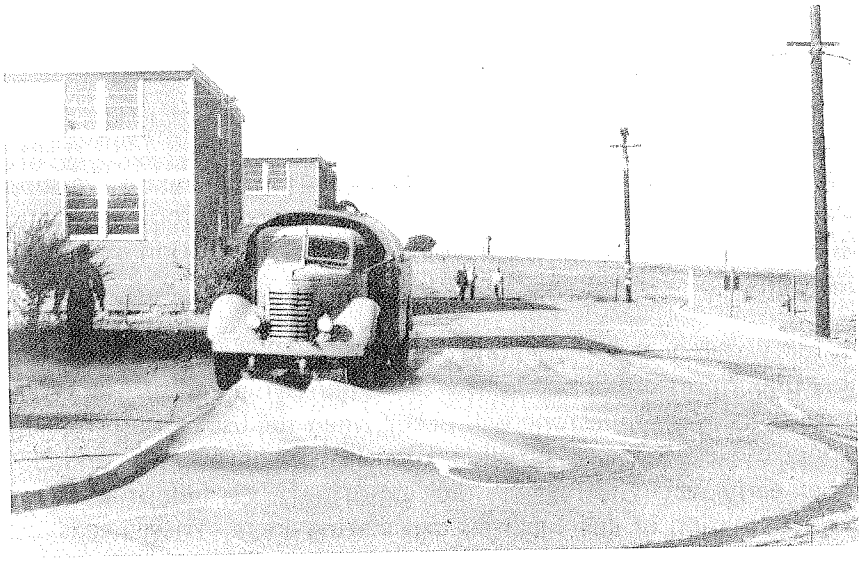

Decontaininating with a street flusher

Removing fallout from an unpaved area.

*From Owen, W.L., and Sartor, J.D., **Radiological Recovery of Land Target Components - Complex III**, U.S. Naval Radiological Defense Laboratory, November 1963 (AD 433 141).

NATIONAL FOOD SUPPLY*

	Days Supply**
Farm Crops in the Field (Grains only on July 1st)	1163
Grain Stocks	
Food Processors and Private Storage	457
Government (CCC) Inventory	103
Farm Animals (Cattle, Hogs, Poultry)	105
Food Processors and Interstate Warehouses	45
Local "Secondary" Resources of Food (Wholesalers, Retailers, and Households)	25
Grand Total	1898***

*Based on 1969 data in A.F. Shinn, **Vulnerability of the U.S. Food Supply and Food Distribution to Nuclear Attack**, Oak Ridge National Laboratory, 1969.

**Assumes 3000 calories daily for 203 million people.

***Neglecting crops in the field and farm animals leaves 630 days of supply or nearly two years of food, mostly grain.

EMERGENCY HOUSING

To the extent that people have survived the attack environment, both direct effects and fallout, the areas where they were sheltered may continue to offer adequate protection against the elements. We saw in Chapter 2 that people can survive blast and fire effects better than houses. Thus, millions of homeless survivors can be expected after a nuclear attack. Some portion of these will have been driven from untenable shelters during the emergency period and will have had to seek shelter elsewhere. Nonetheless, providing of emergency housing is unlikely to be as urgent in the post-shelter environment as would be assuring the survivors that water will be available for drinking and personal hygiene and that no family or small group need forage on their own for the next meal.

Post-shelter emergency housing will be important to plan for not only for health reasons but also for morale purposes. Just as the opportunity to take a bath is likely to mark an early postattack milestone, so will the opportunity to sleep once more in a bed in the privacy of one or more rooms assigned to a family. As shown in this chart, such relative comfort is likely through use of only surviving housing units because Americans presently enjoy housing accommodations that are quite roomy compared to those in many other countries of the world.

A measure of adequacy in emergency housing would likely be the criterion of 40 square feet per person used following peacetime disasters. This is four times the DCPA shelter space allotment but far short of the space normally available in U.S. housing units, the majority of which have five or more rooms. In areas nearby nuclear detonations, a major repair task will be to cover in various ways the window openings that have been blown out by the blast wave. In fallout areas, occupancy of emergency housing during the first month may require converting multi-story office buildings into dormitories by bringing beds from the less protective residences or decontamination and intensive use of selected multi-unit dwellings until the rest of the housing can be safely used. In any event, occupancy of emergency housing will entail the restoration of electric power, water, and the availability of fuel for heating and cooking.

Ultimately, the housing destroyed in the attack will have to be replaced to the extent the survivors require it. A standard of housing approaching the preattack situation is consistent with recovery goals and with the need to assure the public of the return of private property to its rightful owners at the earliest possible time and the replacement of losses through some system of loss sharing. This is a longer-term matter that will be planned for at the Federal level in conjunction with recovery of industrial production.

HOUSING SPACE IN VARIOUS COUNTRIES*

Place	Persons per Room	Relative to U. S.
United States	0.6	1.0
Canada, United Kingdom	0.7	1.2
France, West Germany	0.9	1.5
Puerto Rico, Italy	1.1	1.8
Czechoslovakia, Finland	1.3	2.2
Soviet Union, Greece	1.5	2.5
Poland, Yugoslavia, China	1.7	2.8
India, Guatemala	2.6	4.3

* From United Nations Statistical Yearbook, 1971.

ONE PROJECTION OF ECONOMIC RECOVERY*

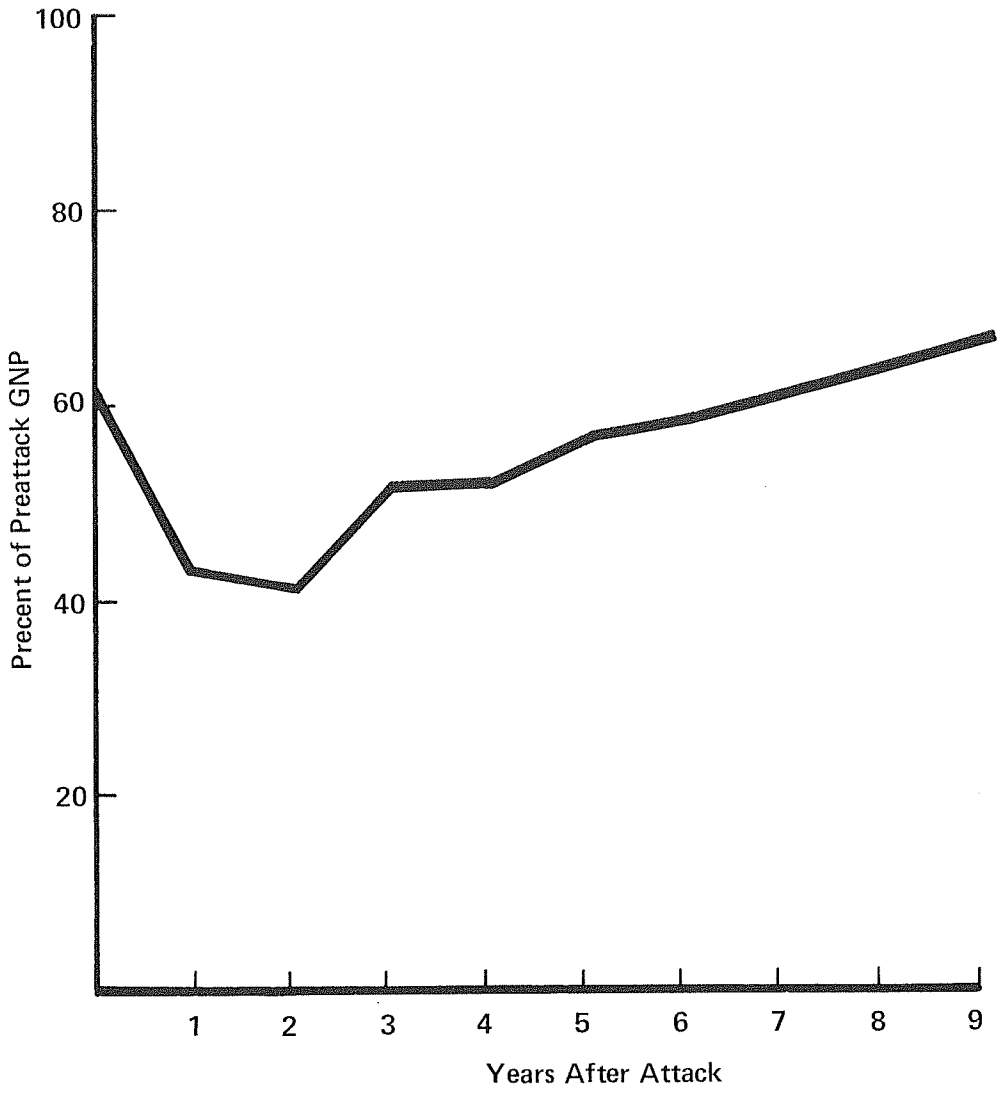

*From Dresch, F.W., and Baum, S., **Analysis of the U.S. and USSR Potential for Economic Recovery Following a Nuclear Attack,** Stanford Research Institute, October 1972 (AD 755 552).

CRISIS ACTIONS FOR ECONOMIC RECOVERY

A period of extreme crisis could provide both the time and the sense of urgency that would be necessary for taking action to improve the prospects for postattack economic recovery. Local government, working cooperatively with local industry, could make the essential peacetime plans without which the task of implementing crisis actions would be much more difficult. Mobilization during times of international tension is compatible with current estimates of a low probability of sudden attack (see Chapter 1).

Many major corporations have made peacetime arrangements for protected alternate corporate headquarters. In a crisis, most other businesses could relocate essential records and management personnel outside the large cities. Management will recognize such plans as insurance that they can "stay in business."

Hundreds of billions of dollars of economic assets are located in potential target areas in the form of finished inventories, parts, and specialized equipment. In a crisis, many of these resources could be loaded on trucks, railroad cars, and delivery vehicles and removed from the area where they could be placed in temporary open storage or parked in the loaded vehicles. Equipment and parts needed to sustain production, should this be necessary, could be buried later on the premises to protect them against blast and heat damage. This could be done in a few hours' time in many instances. Delicate and irreplaceable control equipment should be wrapped in plastic before burial. Machine tools and bulky equipment that cannot be moved can be made less vulnerable to damage by sandbagging and other protective measures so that they could be recovered even if the building is demolished. A large proportion of business assets could be preserved with the use of these measures.

Facilities outside the cities for bulk storage of fuels, chemicals, grains and other essential commodities could be brought at full capacity despite seasonal demands. As noted in the next panel, fuel, fertilizers, and pesticides will be of particular importance in assuring early recovery of agricultural production. Needless to say, expedient fallout shelter should be planned for at industrial and supply facilities that are intended for continued operation or for early postattack use.

Finally, government can contribute to early economic recovery by offering RADEF equipment and crisis training and by preparing plans and materials for implementing rationing and other control measures.

CRISIS PREPARATIONS*

- Remove records and management to safer locations.
- Relocate valuable equipment and inventories.
- Bury critical movable items.
- Protect machine tools and special equipment.
- Augment inventories of fuel, chemicals, and other stocks outside urban areas.
- Accelerate production and safe stockpiling of essential survival items.
- Provide shelter and alternate locations for work force and dependents.
- Expand RADEF capabilities outside urban areas.
- Mobilize postattack control measures.

---

*Based in part on Rockett, F.C., and Brown, W.M., **Crisis Preparations for Postattack Economic Recovery,** Hudson Institute, July 1966 (AD 639 387).

AGRICULTURAL PRODUCTION

In his major study, **Economic Viability After Thermonuclear War: The Limits of Feasible Production,** Rand economist Sidney G. Winter, Jr., came to this conclusion: "If measures could be devised and preparations made to assure that agriculture would not be drastically altered, then it appears that all other economic problems could be managed." Dr. Winter was considering attacks of the size that could now be delivered at a time when lack of knowledge about fallout created a grave uncertainty as to how much farmland would remain suitable for growing crops. As discussed in Chapter 6, this is no longer believed to represent a serious problem. Nonetheless, recovery of agriculture remains crucial to post-attack viability.

In the United States, less than 5 percent of the population produces peacetime surpluses on a fraction of the arable land. This means that agriculture is dependent on other sectors of the economy to support its mechanized and intensive operations. The most critical needs are fuel and fertilizer. Without petroleum products, field crop production would be virtually impossible. All major food and feed crops are mechanically planted and harvested. Livestock, which accounts for nearly half the caloric value of the food produced, depends on the availability of feed, which is itself dependent on petroleum. The petroleum refining industry, which is highly concentrated, is potentially vulnerable. However, the use of farm machinery is seasonal and petroleum storage on or near farms is substantial. Post-attack, a greater share of the surviving fuel could be directed to agriculture and plans should be made to allocate petroleum to those areas where immediate use of machinery is essential and where high yields are to be expected.

It has been estimated that about one half of U.S. food production can be attributed to applied fertilizers. Lack of fertilizers can be accommodated partially by emphasizing crops and farm regions not requiring fertilizer and by bringing more land under cultivation. The latter course, however, requires more fuel. Nitrogen is the principal nutrient required. Nitrogen production facilities are located throughout the country and considerable excess capacity exists today. Sufficient production is expected to survive a major nuclear attack.

Major field crops are grown without pesticides in many places. Lack of pesticide availability would be most strongly felt in the yields of potatoes, fruits, and vegetables. Irrigation is also important for these crops, as well as for rice and sugar beets. Availability of electricity is most critical to dairy and poultry production.

Studies have shown that capabilities for transportation, storage, and food processing of basic agricultural commodities should survive as well or better than food production, except for wholesale warehousing. Good management, based on adequate plans, appears to be the key to recovery of food production.

CRITICAL NEEDS FOR FOOD PRODUCTION*

- Fuel and Lubricants
- Fertilizer
- Pesticides
- Seeds
- Irrigation and Drinking Water
- Equipment and Parts
- Feed
- Electricity
- Transportation, Storage, and Processing

*From Brown, S.L., et al., **Agricultural Vulnerability to Nuclear War,** Stanford Research Institute, February 1973. (AD 765 725)

ECOLOGICAL DEFENSE

In Chapter 6, Panel 28, the possibilities of ecological catastrophe were discussed. Speculation that the attack environment might cause drastic upsets in the "balance of nature" have assumed that changes that exist for a relatively short time can induce permanent ecological damage. This is not borne out by experience. For example, some of the atolls in the South Pacific have experienced repeated direct effects and fallout from weapons tests comparable to the worst that could occur in a nuclear war. As these illustrations show, the tropical ecosystem has survived and recovered. The native population has returned to live on Bikini and Rongelap Atolls. Long-term consequences require continuous pressure over centuries of time, of which the impact of human habitation is the outstanding example.

Some significant consequences that may well occur as part of the post-shelter environment are also discussed in Chapter 6. These potential ecological consequences (one cooler growing season, temporarily increased rainfall, fire in dead pine forests, increased erosion and silting, and outbreaks of insect and rodent pests) could have an indirect effect on agriculture and forestry.

Trees, especially pines, are vulnerable to fallout radiation. The loss of a forest can be regained only after many decades. Dead trees are a valuable resource for wood products if they are harvested. If not harvested, they become a refuge for insect pests and plant diseases. They become a fire hazard. Forest fires destroy both trees and ground litter, resulting in increased surface runoff and erosion, excessive silting of streams, reservoirs, and irrigation works, loss of water for crops, and loss of crop yield. Prompt harvesting and reforestation are postattack actions needed to control these consequences.

Fallout radiation effects on insects and wild animals could affect agricultural production. For example, bees are essential to the pollination of certain agricultural crops, particularly fruits. A large reduction in the natural population of birds and preying insects could produce severe crop infestation by parasitic insects. But man is not helpless. He can move bee colonies where they are needed. He can import or otherwise assist the repopulation of fallout areas with beneficial species. All of these actions could well be called, "ecological defense."

A BATTERED ISLAND

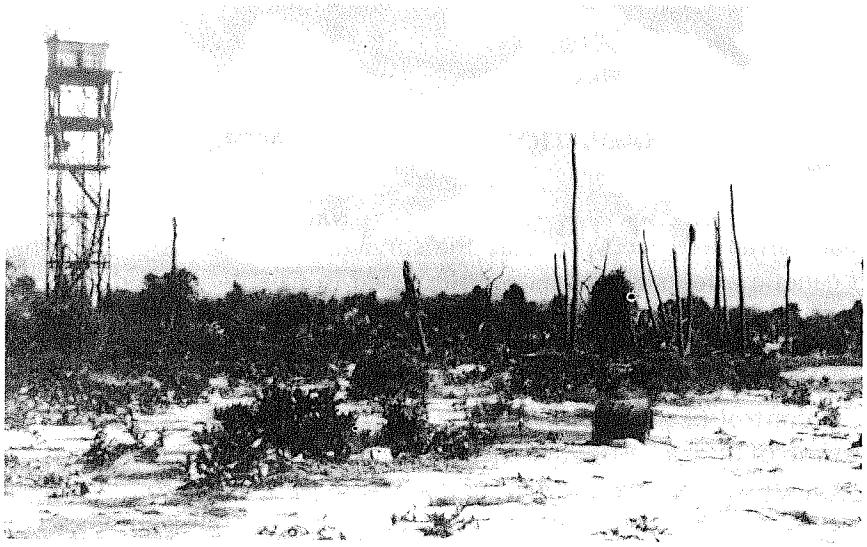

Bikini Island, November 1955

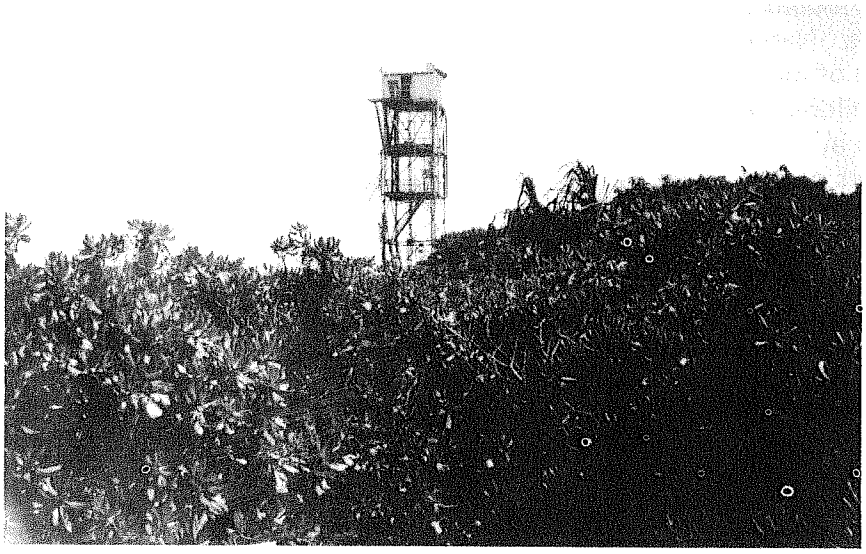

View of same area as above in 1967. Some coconut trees had reached 20 feet and were bearing fruit.

RADIATION EXPOSURE CONTROL

The final barriers to recovery that the survivors must surmount are the possible late somatic and genetic effects of irradiation discussed in Chapters 5 and 6. The key to these problems is good radiation exposure control. Exposure control in the post-shelter environment will be greatly aided by the advice of trained Radiological Defense Officers.

Exposure control begins, however, with effective warning and sheltering of the population at the time of attack. Effective sheltering involves the use of the **best** available fallout shelter, not just those that meet some minimum criterion, such as PF 40. That is, the planner must be concerned not only with preventing lethal exposures but also with keeping the radiation **burden** of the survivors as low as possible. To this end, a protection factor of 400 is vastly better than a protection factor of 40. Crisis plans to build expedient shelters (Chapter 7) and to improve the protection in existing shelter areas can contribute to exposure control.

People should be encouraged and instructed to remain in shelter as long as possible in fallout areas. Naturally, this advice must be balanced against the need to get on with the urgent tasks of recovery. But many, especially children, are not needed for these early tasks outside. Children and young adults should be given maximum protection to minimize genetic damage in subsequent generations. Late radiation injury is of minimal concern to those over 40 years of age. Even so, the shelter areas should be used as off-duty quarters for the workers.

An important control measure during the first month after attack will be to limit the intake of radioactive iodine by children (see Chapter 6, Panel 25). They should be provided with stocked water or water from wells or areas of low contamination and kept from drinking contaminated milk.

Even in areas of moderate fallout, decontamination will be important to limit the continued exposure to radiation over the months and years ahead. In the process, the necessary radiation exposure should be spread among the able-bodied survivors by rotation and work shifts so that the radiation burden of individuals is kept as low as possible.

ELEMENTS OF EXPOSURE CONTROL

- Make sure there is a RADEF person on the staff who is well-trained and qualified.
- Make use of best available fallout shelter.
- Keep the population in shelter as long as possible.
- Preferentially protect children and young adults.
- Use shelters for lodging after "shelter emergence."
- Provide children with uncontaminated drinking water for the first month.
- Decontaminate living and working areas.
- Spread the necessary radiation exposure among the work force.
- Keep on decontaminating.

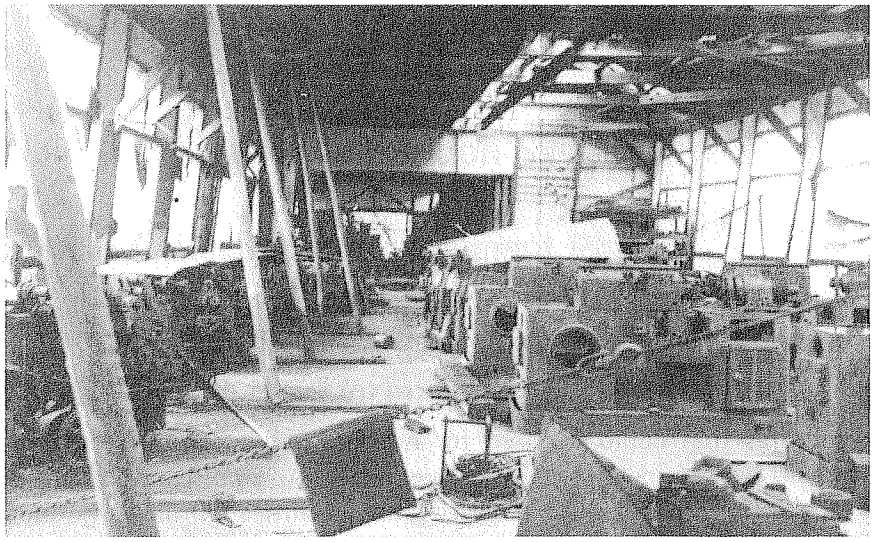

Undamaged machine tools at Hiroshima. Sheet metal is being used to protect against weathering.

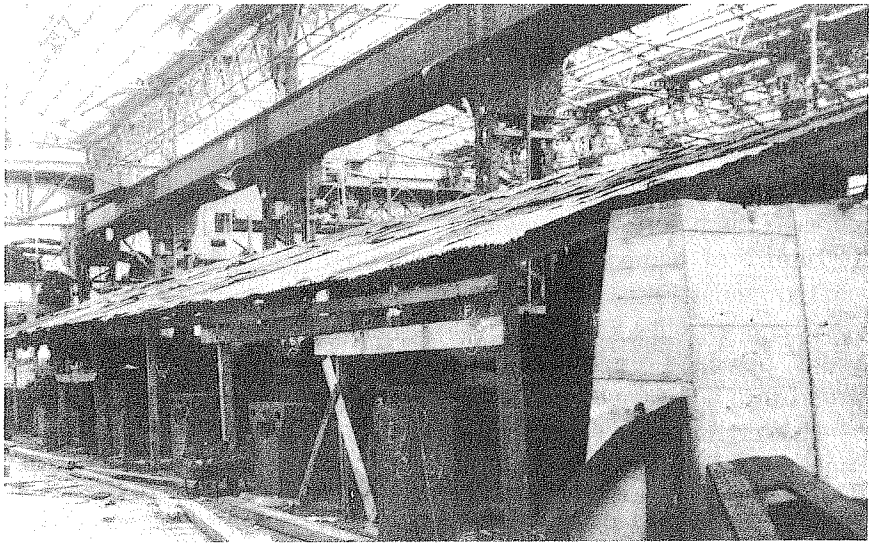

Arrangement of temporary weather protection in Nagasaki industrial plant.

POSTNUCLEAR ATTACK STUDIES

STUDY	YEAR	FOR	ESTIMATED LOSSES POPULATION	ESTIMATED LOSSES INDUSTRY
The Rand Study	1958	USAF	35%	55%
The SRI Study	1963	DoD	42%	45%
PAVUS-75	1967	Army	45%	35%
DAL-67	1967	DoD	45%	42%
PONAST II	1973	JCS	46%* 11%**	63%

* With present civil preparedness capability.
** With crisis relocation and expedient fallout shelter.

SUGGESTED ADDITIONAL READING

Proceedings of the 1967 Symposium on Postattack Recovery from Nuclear War, National Academy of Sciences, April 1968. (AD 672 770)

Goen, R.L., **The Magnitude of Initial Postattack Recovery Activities**, Stanford Research Institute, December 1971. (AD 741 389)

Bensen, D.W., and Sparrow, A.H., **Survival of Food Crops and Livestock in the Event of Nuclear War**, U.S. Atomic Energy Commission, December 1971. (CONF 700-909)

Van Horn, W.H., et al., **Repair and Reclamation of Gas and Electric Utility Systems**, URS Research Co., July 1967. (AD 665 307)

Walker, F.E., **Estimating Production and Repair Effort in Blast-Damaged Petroleum Refineries**, Stanford Research Institute, July 1969. (AD 697 717)

Staackmann, M., et al., **Damage to the Drug Industry from Nuclear Attack and Resulting Requirements for Repair and Reclamation**, URS Research Co., July 1970. (AD 714 304)

Fernald, O.H., **Critical Industry Repair Analysis, Food Industry**, Advance Research, Inc., April 1965. (AD 614 908)

Pyecha, J.N., et al., **Postattack Medical Care Measures of Effectiveness**, Research Triangle Institute, September 1971. (AD 730 945)

PHOENIX RISING FROM THE ASHES

PANEL 31

CPG 2-1A9
June 1973

DCPA ATTACK ENVIRONMENT MANUAL

CHAPTER 9

APPLICATION TO EMERGENCY
OPERATIONS PLANNING

DEFENSE CIVIL PREPAREDNESS AGENCY
DEPARTMENT OF DEFENSE

JUNE 1973

"Plans are worthless, but planning is everything. . . . keep yourself steeped in the character of the problem you may one day be called upon to solve--or to help to solve."

President Dwight D. Eisenhower, 1957

THE UNCERTAINTIES OF RISK

Chapter 1 also emphasized the need for contingency planning to develop operational readiness in each locality to cope with the range of attack environments that could reasonably occur. Subsequent chapters made clear that in areas remote from the sites of nuclear detonations, only fallout was a hazard to life and EMP a threat to electronic and electrical equipment. The direct effects of nearby detonations—blast, fire, and initial nuclear radiation—posed a threat as well. Nuclear emergency operations would be more complex and demanding in these "risk" areas.

It would be advantageous to know in advance where nuclear detonations will occur in event of war. Emergency planning would be much simpler. But the uncertainties will not permit more than a judgment that some localities are more at risk than others, and, of course, no weapon has been made perfectly reliable or accurate. Hence, no place can be "written off" as certain of devastation. For another thing, we do not know how many enemy weapons would be burst on or near the surface. Hence, we do not know how severe the fallout threat will turn out to be. Of course, we do not know what the winds will be like and, thus, where the significant fallout will occur. And, finally, we do not know what targets an enemy will select.

Perhaps the most authoritative statement of Soviet targeting doctrine is contained in the Russian book, **Military Strategy**, by Marshal V.D. Sokolovsky, where it is stated:

> "The targets in a modern war will be the enemy's nuclear weapons, his economy, his system of government and military control, and also his army groups and his navy in the theaters of military operation."

This listing is repeated several times in this book. People as such are never mentioned as a legitimate target. But, as this chart shows, U.S. industry is mainly located in the larger cities—and that is where much of the population lives as well. That is why it was argued in Chapter 1, Panel 14, that all localities needed to plan for the possibility of potentially serious fallout radiation exposure, and those near important military and industrial facilities needed to plan for direct weapons effects as well.

PANEL 2

INDUSTRIAL CONCENTRATION

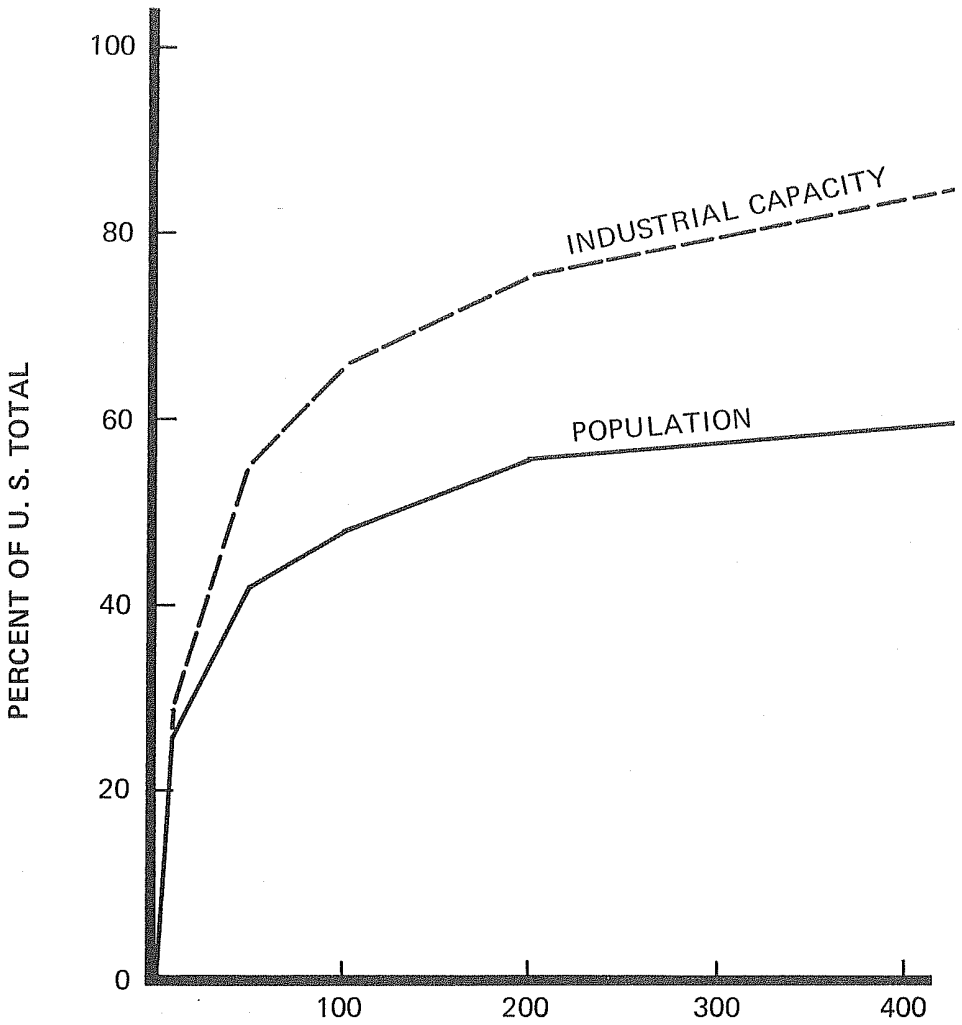

Number of U.S. populated areas.
(Ranked by population from largest to smaller.)

PANEL 2

BRAVO COMES AFTER ALFA

ALFA is the first letter in the international phonetic alphabet. BRAVO is the second letter. We use ALFA to denote an emergency plan based on protecting the population in place—where they normally live. BRAVO plans are based on relocating masses of the population from the places of highest risk (cities, in nuclear attack planning; coastal areas in hurricane planning) in advance of attack or disaster. This table shows how the population might be located if a BRAVO relocation had occurred as compared with that shown in Chapter 1, Panel 14. Clearly, preattack dispersal and evacuation could save millions of lives.

Evacuation was the basic civil defense plan in the 1950s when nuclear weapons could be delivered only by bomber aircraft. Several hours could be expected after detection of the aircraft before nuclear detonations could occur in U.S. cities. Evacuation planning concentrated on means to move city-dwellers out of the cities during this short time interval. The deployment of ballistic missiles made evacuation after attack warning impractical, and means for protection of the population in-place were given much consideration.

By the time of the Cuban Missile Crisis of 1962, it had become accepted that a "bolt-out-of-the-blue" surprise attack was highly unlikely. Evacuation of cities during a crisis appeared feasible. But planning for this contingency was de-emphasized because strategic warning indicators were notoriously ambiguous, and because a decision to evacuate cities might not be compatible with the President's objective of resolving the crisis short of nuclear conflict.

However, in the past few years, crisis evacuation has emerged as the basis for Soviet civil defense. Other countries, such as Sweden and Norway, publish evacuation and other defense plans in their telephone books as guidance for the populace. Plans to evacuate our cities if the Soviets should do so—BRAVO plans—are now important if the President is to have additional time to negotiate the differences that generated the crisis. Nonetheless, the carrying-out of such plans will remain uncertain. Therefore, the strategy of protection in place, by shelter in existing buildings, remains the primary basis for nuclear emergency operations planning and will be considered first in this chapter. That is, A comes before B!

1 2 cms The National Archives ins 1 2
Ref.: Prem 11/563 C503799

SECRET

DR. PENNEY'S DRAFT BROADCAST

Recorded: 30 October 1952

When the planning began, a lot of thought was given to deciding which type of explosion would provide information and experience of the greatest value. Purely scientific measurements are most easily made when the weapon is placed at the top of a high tower, but there were other weighty considerations. The Civil Defence authorities in this country badly needed more data about atomic explosions and, accordingly, the test was planned to get as much novel information as possible for Civil Defence. The decision was made to explode the weapon in a ship moored near land, thus simulating an explosion in a port. The ship was to be equipped as a scientific transmitting station, sending out by radio a vast number of measurements about the nuclear explosion before the equipment was destroyed. More scientific apparatus was to be placed on the land to record other phenomena such as blast, heat and radioactivity.

Many comments have been made about the shape of the cloud, and how different it was from the 'mushroom' cloud with the very high stem shown in most American pictures of atomic explosions. The great weight of the mud and water in the cloud at Monte Bello kept it from rising very far.

The experiment went according to plan and the scientific records were complete. We know what happened and we can give to the Civil Defence authorities an accurate description of their problems. As you know, the explosion threw water, mud and rock into the air and on to the nearby land, causing severe radioactive contamination, and that it was necessary to measure this contamination and to recover records in the contaminated area.

1 2 cms The National Archives ins 1 2
Ref.: Prem 11/563 C5037799

Outward Telegram from Commonwealth Relations Office

TO: U.K. HIGH COMMISSIONER IN AUSTRALIA

(SENT: 01.00 hours, 22nd October 1952)

CYPHER
IMMEDIATE

No. 848 SECRET

Prime Minister Winston Churchill's Statement to House of Commons, 23 October 1952.

HURRICANE

My immediately preceding telegram.

Following is text of Prime Minister's statement. Begins.

The object of the test was to investigate the effects of an atomic explosion in a harbour. The weapon was accordingly placed in H.M.S. "PLYM", a frigate of 1,450 tons, which was anchored in the Monte Bello Islands.

2. Conditions were favourable and care was taken to wait for southerly winds so as to avoid the possibility of any significant concentration of radio-active particles spreading over the Australian mainland.

3. Specimen structures of importance to civil defence and to the Armed Services were erected at various distances. Instruments were set up to record the effect of contamination, blast, heat flash, gamma ray flash and other factors of interest.

4. The weapon was exploded in the morning of the 3rd October.

5. Thousands of tons of water and of mud and rock from the sea bottom were thrown many thousands of feet into the air and a high tidal wave was caused. The effects of blast and radio-active contamination extended over a wide area. H.M.S. "PLYM" was vaporised except for some red hot fragments which were scattered over one of the Islands and started fires in the dry vegetation.

G.R. TOP SECRET

Take All of Clandestine use of weapon Part 2

PRIME MINISTER

At the "Apex" Committee on Wednesday you asked me to let you have a report on the risk that an enemy might explode an atomic bomb in a ship in one of our ports and on difficulties of countering this risk.

I attach the report below on this question which I submitted to Mr. Attlee in July, 1951. As you will see, the Chiefs of Staff had then asked me to arrange to have the matter further considered by the civil Departments concerned; but I had come to the conclusion that matters could not be advanced further by this means and I suggested that Mr. Attlee should discuss the problem with the Foreign Secretary and the Minister of Defence. This he was unable to do before the Election. Since then I have taken no further initiative to raise the matter since I myself believe that this is a risk against which we cannot at present take, in normal times, any effective precautions.

Norman Brook.

R. 28th March, 1952

TOP SECRET

PRIME MINISTER

Clandestine Use of Atomic Weapons

The Chiefs of Staff have been considering the possibility that the enemy might open the next war with an atomic attack on London on the model of the Japanese attack on Pearl Harbour - without warning and before any formal declaration of hostilities. The most effective method of making such an attack would be to drop an atomic bomb from a military aircraft. If the control and reporting system were fully manned and alert in a period of tension, there would be some chance that hostile aircraft approaching this country could be intercepted and driven off. At any rate, there are no special measures, outside the normal measures of air defence, which we could take in peace-time to guard against this type of attack.

2. It is, however, possible that the enemy might use other means of surprise attack with atomic weapons. A clandestine attack could be made in either of the following ways:-

(i) A complete atomic bomb could be concealed in the hold of a merchant ship coming from the Soviet Union or a satellite country to a port in the United Kingdom:

(ii) An atomic bomb might be broken down into a number of parts and introduced into this country in about fifty small packages of moderate weight. None of these packages could be detected by instruments as containing anything dangerous or explosive, and even visual inspection of the contents of the packages would not make identification certain. These packages could be introduced either as ordinary merchandise from Soviet ships, or possibly as diplomatic freight. The bomb could subsequently be assembled in any premises with the sort of equipment usual in a small garage, provided that a small team of skilled fitters was available to do the job.

3. It is difficult at any time to take practical and effective measures against this type of danger. It would be less difficult, of course, in a period immediately before the outbreak of a war which the

public had come to regard as inevitable - the period which we call the Precautionary Stage. But the enemy might prefer to make such a move in a period of comparative calm, when he might assume that less attention would be paid to security risks of this kind.

The only possible measures which could be taken to reduce this risk are control of shipping and closer supervision of diplomatic freight.

Control of Shipping

4. For effective security against this risk all suspect shipping would have to be kept at least 5,000 yards distant from any worth-while target - e.g. from London, Liverpool, Glasgow, Southampton, Bristol and Hull. There are in theory four possible ways of doing this:-

(a) Trade Attraction. All Russian ships carrying bulk cargoes on Government account could be diverted to minor ports, by specifying that that was where the consignee desired delivery of the goods. This would be regarded as discrimination against Russian ships and would invite inconvenient reprisals. It would be expensive. And it would not cover Russian ships carrying cargo ordered on private account.

(b) Diversion by Order. The Admiralty could take power to regulate the movements of all vessels, as they had in the war under Defence Regulation 43. They could then divert all ships of any kind suspected of carrying Russian cargo to minor ports. By a liberal use of this power, the diversion could be made effective; but the discrimination against Russian and satellite shipping would be so blatant that it might well end in the complete stoppage of all trade with the Iron Curtain countries.

(c) Off-shore Discharge. All Russian, Polish and Roumanian ships approaching the major ports could be instructed to discharge their cargoes at off-shore anchorages. This method would lead to retaliation. Moreover, it is hardly practicable; for grain is the main commodity carried by Russian ships and we do not possess the floating elevators which would be necessary for off-shore discharge of grain cargoes at all major ports.

(d) Port and Transit Control. In the Precautionary Stage we propose to introduce a scheme by which all ships approaching the country would be met and escorted to determined ports and anchorages. Under this control

suspect ships could be diverted away from the main target areas; but the control would only be practicable in the Precautionary Stage when there would be a much reduced volume of United Kingdom and Allied shipping, and enemy shipping would be likely to keep as far away as possible from United Kingdom ports. It would be impracticable to bring this system into force at a time of normal trade with Russia and satellite countries.

5. Any action of the kind discussed in the preceding paragraph would involve some element of open discrimination against the Soviet Union; it would invite retaliation in some form; and it would probably have serious political and economic consequences. Moreover, even if those consequences could be accepted, this type of action could not completely exclude the risk. For even, if it were possible by this type of action to keep all Russian, Polish and Roumanian ships away from the main target areas, the enemy could, if he were so minded, defeat all these precautions by chartering an innocent-looking ship of another flag and using it for a clandestine atomic attack or by placing his bomb in crated merchandise consigned to this country by a neutral vessel normally trading to a U.K. port.

Supervision of Diplomatic Freight

6. If the enemy wished to introduce an atomic bomb into this country in parts and assemble them here, as suggested in paragraph 2(ii) above, the parts would probably be consigned to the Soviet Embassy in London as diplomatic freight. A foreign Embassy has an absolute right to receive by diplomatic courier correspondence which is exempt from any examination by the territorial authorities. It has a further right to import certain things without paying Customs duty, but the territorial authorities are entitled to verify that diplomatic freight and diplomatic bags are not being abused as a method of importing things which are neither documents nor things which the Embassy has a right to import without paying Customs duty. It would therefore be permissible for us to open the Soviet diplomatic bag or to examine diplomatic freight for this purpose, provided that this were done in the presence of a member of the Soviet Embassy and that no attempt was made to open seals on any documents in envelopes. There would, however, be serious risks in doing so. We should invite immediate reprisals, which might involve widespread interference with our arrangements for supplying our own diplomatic missions behind the Iron

Curtain. In an exchange of discourtesies like this, we should normally have more to lose than to gain. Action of this kind could not fail to increase international tension. These disadvantages are certain. The gain, on the other hand, would be problematical; for we understand that, even if packages were opened and subjected to expert inspection, it could not be established with certainty that the contents were not parts of an atomic bomb.

7. Although it may be impracticable to prevent the importation of parts of an atomic bomb into this country, whether as diplomatic freight or otherwise, it is just possible that we might be able to detect the preparation for its assembly. This process would probably be directed and controlled through the Soviet Embassy in London, and it might be possible by increased vigilance to detect suspicious movements of vehicles to and from the Embassy. That is a point which we should like to examine further. It is of course by no means certain that we should be able by this means to secure, until it was too late, any positive indication that a bomb was being assembled here.

Conclusion

8. It is clear that it would be practicable for the Russians to introduce an atomic bomb into this country by clandestine methods. It is equally clear that there is no certain method of preventing them from doing so. The most that we could secure, by taking any of the measures discussed in this minute, would be to make their task more difficult. And the adoption of any of these measures would involve considerable risks and serious political and economic difficulties. This being so, it seems legitimate to ask whether the Russians would think it worth while to adopt these elaborate clandestine methods of launching an atomic attack when a military aircraft might do the job more effectively for them. An even larger question is whether the Russians would think it was worth their while to invite immediate retaliation by atomic attack against themselves so long as the advantage in numbers of atomic bombs remains overwhelmingly with the Americans.

9. The Chiefs of Staff have already arranged for an official working party (comprising representatives of the interested civil Departments) to consider means of guarding against this risk, and the possible

counter-measures discussed in this minute were all suggested in the report of this working party. The Chiefs of Staff have now asked me to arrange for further Departmental examination of these proposals and for any necessary submission to Ministers. For the reasons indicated in this minute I am very doubtful whether the increased security which might be obtained by adopting any of these measures could outweigh the very serious disadvantages, political and economic, which would be entailed. I have therefore thought it desirable to seek your guidance in the matter before asking Departments to undertake the work of assessing those disadvantages. You may like to discuss the problem with the Foreign Secretary and the Minister of Defence; but I suggest that, for the moment, it would be preferable that it should not be discussed in any wider group of Ministers.

(Signed) NORMAN BROOK

12th July, 1951

1 2 cms The National Archives ins 1 2
Ref.: Prem 11/565 C5037799

Prime Minister

As requested in your letter I attach a note showing the principal events leading up to the dropping of the atomic bombs at Hiroshima and Nagasaki.

I think this account answers all the questions you asked - if you want further details I will try ~~and~~ to unearth them.

CHERWELL

28th January, 1953.

Mr Littlejohn has sent the originals to Miss Sindee to keep with the book papers.
29/1.

EVENTS LEADING UP TO THE USE OF THE ATOMIC BOMB, 1945

On March 21, 1944, Sir John Anderson suggested that the Tube Alloys programme should be mentioned to the Service Ministers and to the other Ministers concerned but you minuted "I do not agree". Sir John Anderson was perturbed by your decision and I am fairly certain that in the spring of 1945 he made another attempt to persuade you to bring the matter to Cabinet and that I supported him. No papers bearing on this can however be found. In the event, it seems, the question was never discussed at Cabinet or in the Defence Committee.

2. In September 1944 Sir John Anderson minuted you annexing a report which included the information that a bomb (equivalent to 20,000 - 30,000 tons of T.N.T.) would "almost certainly" be ready by August 1945. On my return from America in November 1944, I gave you further details about the work they were doing and said that it was hoped a bomb would be ready some time the following summer.

3. In the winter of 1944/5 so far as I recollect I mentioned to you that some doubts had arisen about the initiation of the detonation of the plutonium bomb but that there was no anxiety about the U.235 bomb. But I well remember telling you in the spring of 1945 that I thought the successful explosion of a bomb was 90 to 95% certain but that the people actually working on it considered it 99% certain.

4. In April 1945 Lord Wilson telegraphed to Sir John Anderson that the Americans proposed to make a full scale test in the desert in July and to drop a bomb on the Japanese in August and I told you about this.

5. On May 2 Sir John Anderson minuted you that he had had some details from Lord Wilson of the American intentions for the operational use of the bomb and requested your approval of his proposal that Lord Wilson should tell General Marshall that you had been consulted and would want to be kept informed. On May 21 you agreed that Wilson should speak to Marshall "in a tactful and friendly way";

you thought that the machinery for reaching a joint decision would emerge from this talk. Discussions took place and it was agreed that in order to fulfil the Quebec Agreement the concurrence of H.M.G. should be recorded at a meeting of the Combined Policy Committee.

6. On June 29 Sir John Anderson reminded you of the American intentions about which I had told you. In this minute he requested authority to instruct our representatives to give the concurrence of H.M.G. in the decision to use the bomb against the Japanese. You initialled this minute on July 1. On July 4 Lord Wilson formally gave the concurrence at a meeting of the C.P.C

7. A minute from Ricketts to Sir John Anderson's Secretary dated July 2 reads:

"Lord Cherwell told me this evening that in initialling the Chancellor's minute of the 29th June on the Operational Use of T.A., the Prime Minister had wished it to be understood that he would expect to discuss this matter with President Truman at TERMINAL, though he was anxious that nothing should be done by us to retard the use of the T.A. weapon."

8. A report on discussions at Potsdam records:

"Mr. Stimson described the results of the recent test to the Prime Minister and the Prime Minister confirmed the agreement given by Field Marshal Wilson at a meeting of the Combined Policy Committee to the use of the weapon within the next few weeks against the Japanese."

9. It must be remembered that until the actual explosin in the desert in New Mexico there was great scepticism in military and political circles about the efficacy of the new form of explosive. Certainly nobody thought it would end the war. And in fact it is doubtful to what extent it did so. As you know it has now been proved that the Japanese asked the Russians to convey an offer accepting the Potsdam terms of unconditional surrender to the Allies on August 2. The Russians did not pass on this message. Had they done so, it might well be that the bombs on Hiroshima and Nagasaki would not have been dropped. Whether the fact that they were dropped did more than induce the Japanese to make a direct offer of surrender to the Americans is therefore questionable.

8
END

10. In retrospect it seems unlikely that the atom bombardment could have forced the Japanese to surrender before the planned invasion of the Home Islands in November 1945, had they not - unknown to us - been already at the point of collapse. For the Americans could not have dropped much more than two bombs a month for the rest of the year. But of course the Japanese did not know this.

28th January, 1953

UK NATIONAL ARCHIVES: ES 5/3

Misc./P (54) 29
27th August, 1954

DEPARTMENT OF ATOMIC ENERGY

ATOMIC WEAPONS RESEARCH ESTABLISHMENT

SCIENTIFIC DATA OBTAINED AT OPERATION HURRICANE

TOP SECRET SECTION OF DIRECTOR'S REPORT

Issued by
Ministry of Defence,
London, S.W. 1.

27th August, 1954

DEPARTMENT OF ATOMIC ENERGY

ATOMIC WEAPONS RESEARCH ESTABLISHMENT

(formerly of Ministry of Supply)

OPERATION HURRICANE—THE DOSE-RATE CONTOURS OF THE RESIDUAL RADIOACTIVE CONTAMINATION

(Monte Bello, Australia—October, 1952)

TOP SECRET SECTION OF DIRECTOR'S REPORT

Summary

This section of the report on scientific data obtained at Operation Hurricane gives the dose-rate contours of the residual radioactive contamination resulting from the detonation of the first British atomic weapon which was exploded under conditions representing a ship-borne attack on a port.

The main body of the report, issued separately, covers other aspects of the contamination, as well as the air blast, gamma flash, thermal radiation and underwater shock.

The results given in the present section imply that the residual contamination due to the deposited fission products provides a major contribution to the effect of a weapon detonated in this way.

Approximate estimates suggest that the area in which a median lethal dose of 400 roentgens of gamma radiation could be received may be increased by the contamination by a factor of from two to four.

7.8. *The Dose-rate Contours of the Residual Radioactive Contamination*

7.8.1. The numbering of this sub-section follows that of the main report in which Section 7 deals with the residual contamination.

7.8.2. From an examination of the day-to-day radiological survey measurements at various points on the different islands and by the application of the gross decay relationship given in section 7.3. of the main report, a set of dose-rate contours at 1 hour after the explosion has been constructed as shown in Fig. 7.2. These are shown dotted over the sea areas because although the dose-rates in these regions would be the same as over land immediately after fall-out, the rapid dispersal of the contamination (see section 7.6.) in the sea would soon reduce the radiation dose-rate there to a negligible quantity. The dose-rate on a ship in these regions would, of course, be the same as on land until decontamination had been effected.

It will be seen that the radiation dose-rate from deposited fission products would be very high on land near an atomic explosion in a ship.

7.8.3. The areas within the various contours and the equivalent radii are given below in comparison with radii derived from figures given in " The Effects of Atomic Weapons " for an airburst at 100 feet over land.

TABLE 7.4.

Dose-rate (r/hr) at one hour	Monte Bello Weapon Area (Sq. Miles)	Monte Bello Weapon Equivalent Radius (Feet)	Low Air-burst over Land. Radius (Feet)
10,000	0·62	2,350	—
6,000	0·85	2,750	200
3,000	1·12	3,150	450
2,000	1·62	3,800	525
1,000	2·65	4,850	575
600	3·2	5,350	600
400	3·7	5,750	700
200	4.8	6,500	850

Since the lethal distance from the gamma flash, corresponding to the median lethal dose of 400r, is about 4,000 feet in both cases, it appears that whereas for a low airburst over land the lethal area is not likely to be appreciably increased by the contamination, the area due to a weapon exploded under the same conditions as at Monte Bello is likely to be considerably increased by the activity of the deposited fission products.

Approximate estimates suggest that the area in which a median lethal dose of gamma radiation is received may be increased by the contamination by a factor of 2 to 4 depending on the degree of screening afforded by buildings and the time taken to get out of the contaminated area.

7.8.4. A comparison may also be made between the contamination from the Monte Bello weapon and that which would be expected on land areas near to an underwater atomic explosion such as the one at Bikini Test Baker. The areas within the 50 r/hr contour from the Monte Bello weapon and from the underwater burst at Bikini Test Baker, for which estimates are given in Figure 8.101 of " The Effects of Atomic Weapons," are about equal. Within the 400 r/hr contour the area from the Monte Bello weapon is larger by a factor of about 3 to 4 while for regions of heavier contamination the areas within its contours will apparently be even greater relative to the Bikini weapon.

7.8.5. A further radiological survey was made in November, 1953, 405 days after the explosion and the islands were found to be still highly radio-active.

Although in some places drifting sand had materially reduced the gamma radiation compared with that in places where the soil surface was held by vegetation, in general, despite some 16 inches of rain and a cyclone in early 1953, there was no apparent evidence of the accelerated decay of fission products due to weathering.

From readings taken at certain points immediately after the trial and again in November, 1953, the decay factor from 1 hour to 405 days after the explosion was found to be 200,000. By applying this factor to the various readings obtained during this second survey, gamma dose-rate contours at one hour were constructed. These were found to be very similar in shape and size to those shown in Fig. 7.2. which are based on observations made during the period immediately following the explosion.

FIG. 7·2 DOSE-RATE CONTOURS

1 HOUR AFTER EXPLOSION

~~TOP~~ SECRET

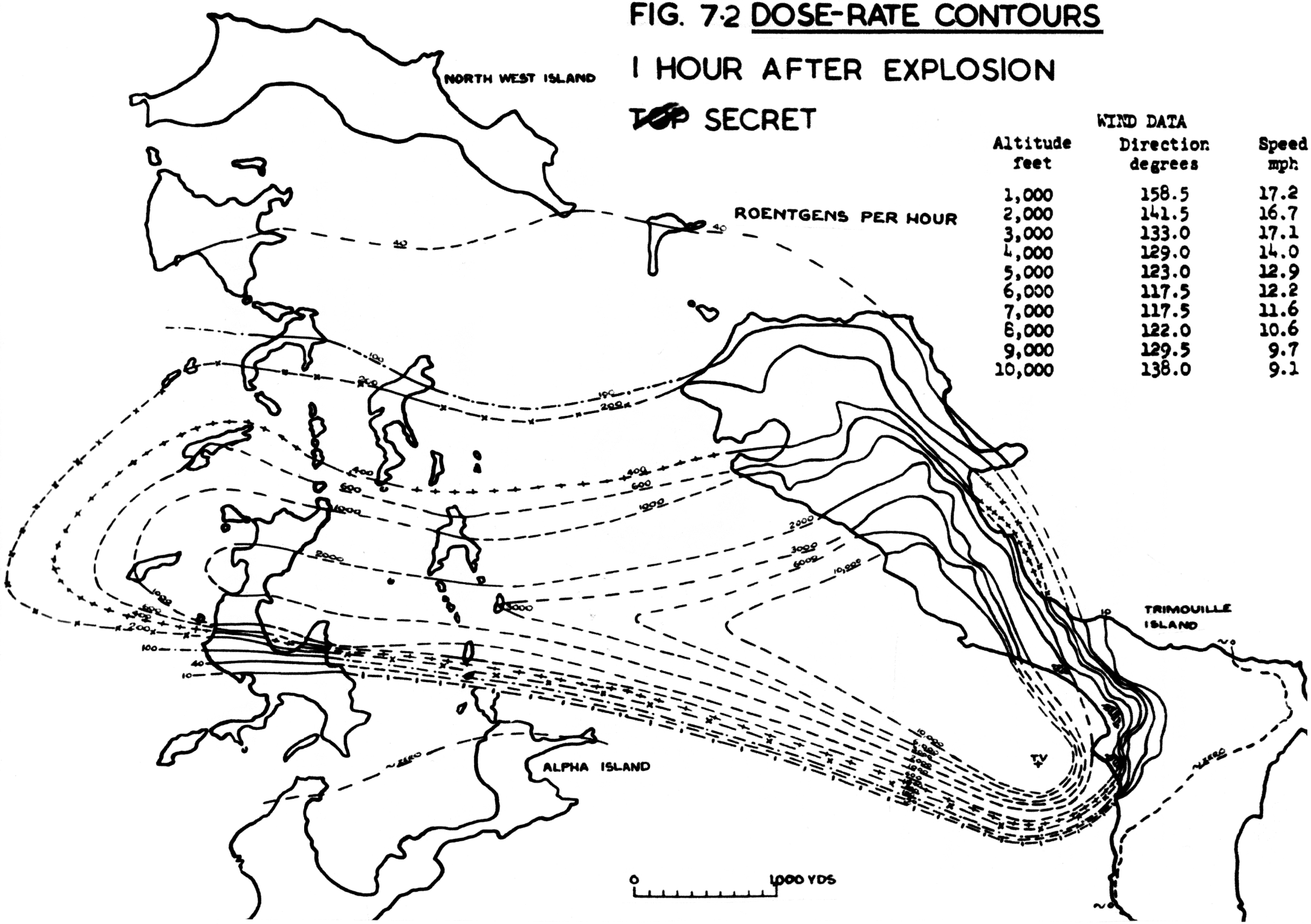

WIND DATA

Altitude feet	Direction degrees	Speed mph
1,000	158.5	17.2
2,000	141.5	16.7
3,000	133.0	17.1
4,000	129.0	14.0
5,000	123.0	12.9
6,000	117.5	12.2
7,000	117.5	11.6
8,000	122.0	10.6
9,000	129.5	9.7
10,000	138.0	9.1

UK NATIONAL ARCHIVES: ES 5/2

AWRE-T1/54 (27 AUGUST 1954)

DEPARTMENT OF ATOMIC ENERGY

ATOMIC WEAPONS RESEARCH ESTABLISHMENT
(formerly of Ministry of Supply)

SCIENTIFIC DATA OBTAINED AT OPERATION HURRICANE
(Monte Bello Islands, Australia—October, 1952)

DIRECTOR'S REPORT

Summary

This report summarises data on the external effects observed in the trial of the first British atomic weapon, which was exploded under conditions representing a ship-borne attack on a port.

Briefly, it may be said, in reviewing the general physical effects, that the air blast and gamma flash effects were comparable with those for an air burst but the thermal radiation effects were very much less. The underwater shock was much less than that from an underwater burst. Some general information on the residual contamination is given, but data on the extent of the contamination forms the subject of a separate section not generally available.

The report describes the conditions under which the trial was conducted, the measurements made of the physical phenomena produced by the detonation of the weapon, and gives brief descriptions of the results.

Information is given concerning the behaviour of Anderson shelters, of certain reinforced concrete cubicles, of a model ship's funnel, of a compartment representing a deckhouse, and various aircraft components. Data are also given for the penetration of gamma rays into slit trenches, concrete cubicles and Anderson shelters; for the effect of thermal radiation on various materials and service equipment; and for possible contamination (and decontamination) of personnel, equipment, ships and food stored in open dumps. The report also includes the results of experiments on the absorption of radio-elements by biological systems.

Regraded by A.W.R.E. on ....10-1-61.....

From SECRET ATOMIC GUARD

to SECRET

PART I.—BASIC SCIENTIFIC MEASUREMENTS

1. Trial Conditions and Effects Observed

1.1. The trial was carried out in the Monte Bello Islands lying about 50 miles off the North-West coast of Australia. Fig. 1.1 gives a map of these islands.

The weapon was exploded at 9·30 a.m., local time, on October 2nd, 1952, in H.M.S. *Plym*, a frigate lying in a shallow channel about 400 yards offshore from Trimouille Island. The depth of water was about 40 feet and the weapon centre was 9 feet below the water line. The conditions of burst were thus representative of a ship-borne attack on a port.

1.2. The variation of wind speed and direction was obtained by means of a balloon ascent one hour after burst. At ground level the wind was southerly (175°) with a speed of 17 knots. With increasing height it changed through east to become slightly north of east (77°) at 6,000 feet with a speed of 10 knots. The change in direction with height was then rapidly reversed so that the wind was practically due south again at 8,000 feet after which it changed gradually to about south-westerly at 12,000 feet and finally to westerly at 20,000 feet. Thus the wind was coming straight off the mainland up to about 8,000 feet after which it blew roughly parallel with the coast line. The speed decreased steadily up to 7,000 feet and then increased. The results are displayed in Fig. 1.1.

1.3. The main control centre was located at H 1 at the southern end of Hermite Island. Other key points, including A4, N4 and T4, will be referred to in connection with particular measurements.

1.4. The basic scientific measurements which were made covered all aspects which might be likely to have practical importance. One aspect, namely the thermal radiation, proved to have definitely less importance than it would have had in the case of an airburst bomb. The blast, gamma radiation and the contamination were the major effects at the observation sites.

The various measurements are considered in detail in the following pages, starting with a description of the phenomena (fireball and water column) photoghaphed from a distance immediately after the detonation of the bomb. The air blast, gamma flash, thermal radiation and contamination which reached the observation posts are then considered, followed by the underwater shock, the crater in the sea-bed and the earth movements observed on the shore of Trimouille Island.

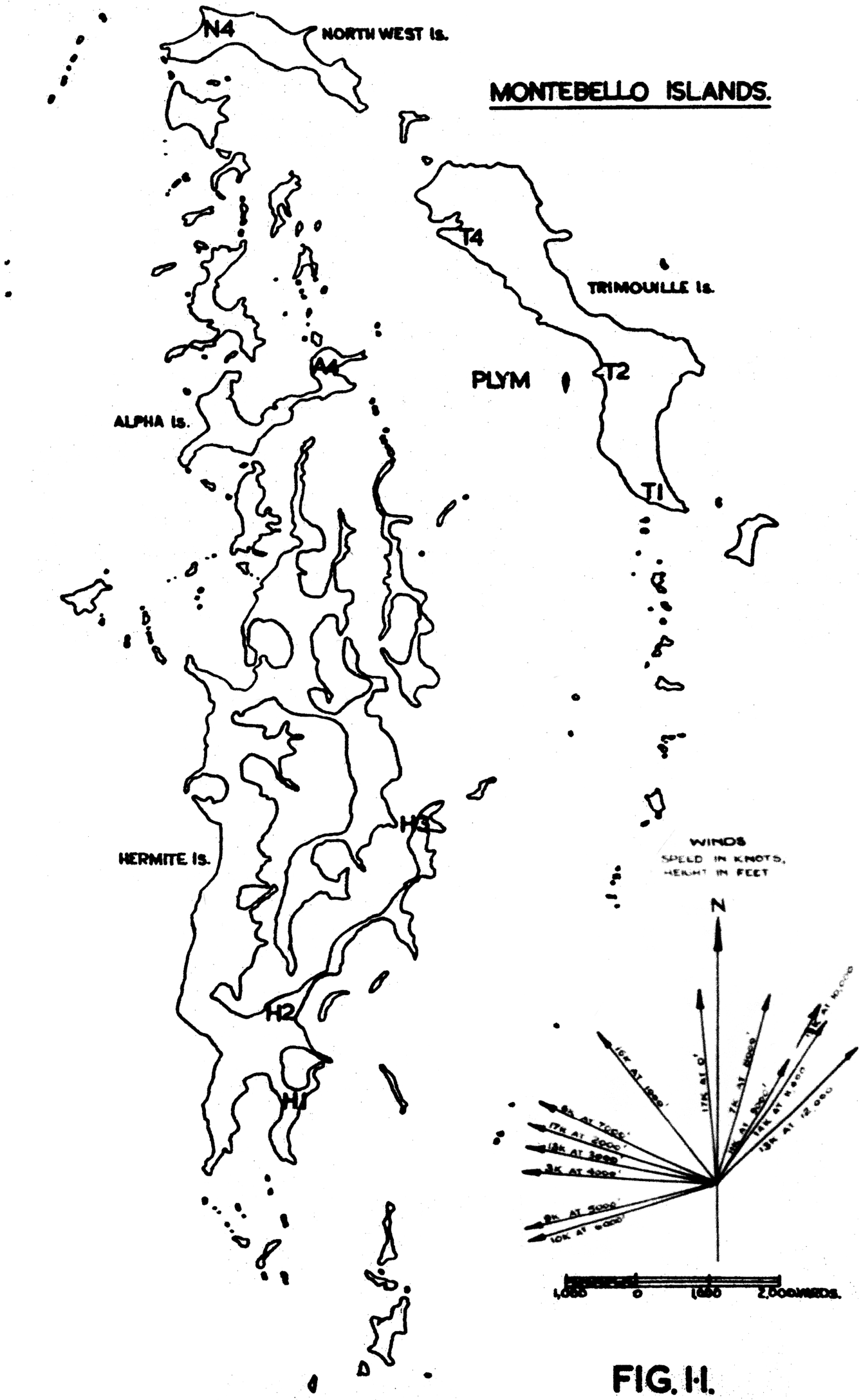
MONTEBELLO ISLANDS.
N4
NORTH WEST Is.
T4
TRIMOUILLE Is.
A4
PLYM
T2
ALPHA Is.
T1
H3
HERMITE Is.
H2
H1
WINDS
SPEED IN KNOTS,
HEIGHT IN FEET
N
16K AT 1000'
17K AT 0'
7K AT 8000'
10K AT 8000'
14K AT 9000
12K AT 10,000
13K AT 12,000
8K AT 7000'
17K AT 2000'
18K AT 3000'
3K AT 4000'
8K AT 2000'
10K AT 6000'
1,000
0
1,000
2,000 METRES.

FIG. 11.

2. The Fireball

2.1. The fireball was first observed from H 1 with the Kerr cell camera at 23 microseconds after explosion as a faint segment of a circle on the water-line of *Plym*. Within the accuracy of measurement, it appeared to emerge from the point on the ship's side nearest to the weapon. Fig. 2.1 shows successive stages in the development of the fireball up to 3·75 milliseconds. In the early frames the bows of the target vessel can be seen silhouetted against a portion of the fireball which has emerged from the far side of the ship.

2.2. Fig. 2.2 shows the variation with time of the height of the top of the fireball above the weapon centre. The time t is taken from the arrival of the first gamma radiations. In the early stages, for about the first 1·5 milliseconds, this height varies approximately as $t^{\frac{1}{2}}$, after which it follows a more familiar $t^{\frac{2}{3}}$ relation up to about 100 milliseconds. The increase in the diameter of the fireball on the water-line is given graphically in Fig. 2.3. The variation of the diameter of the best fitting hemisphere fits this very closely although the fireball was far from hemispherical.

2.3. At 41 milliseconds the shock wave commenced to separate from the fireball which at this stage had a height of 650 feet and a diameter at the water-line of 1,000 feet. It eventually attained a diameter of 1,700 feet in 0·6 seconds after which it started to contract leaving an inner ball 1,400 feet in diameter after about 3½ seconds. The configuration of the fireball at these later stages was rather indistinct owing to the water present in the ball itself and thrown up from the water surface by the underwater shock. As the fireball contracted it left a dark zone which appeared brown in the colour photographs. This darkening extended into the zone behind the shock wave up to a diameter of 2,500 feet and was presumably due to the presence of nitrogen dioxide.

(Annotations to PDF report version are in this typeface)

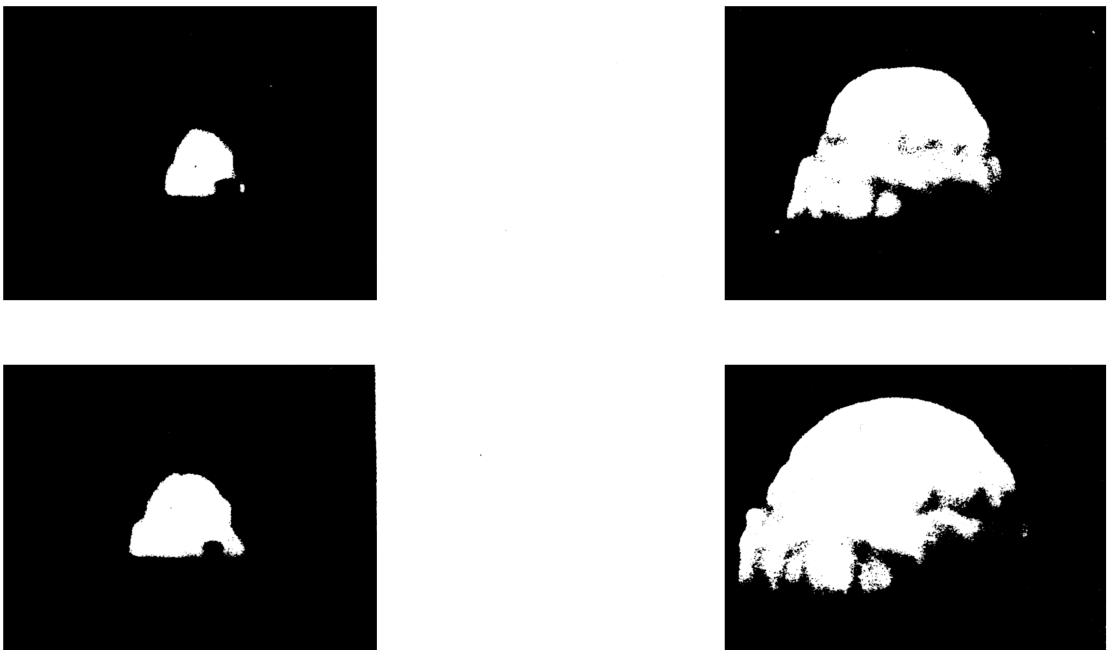

3.75 millisec

Fig. 2.1, Kerr cell camera photos of fireball emerging from far side of ship. Bows of ship are visible as dark region in the lower right of the fireball.

FIG. 2·2 RISE OF FIRE BALL.

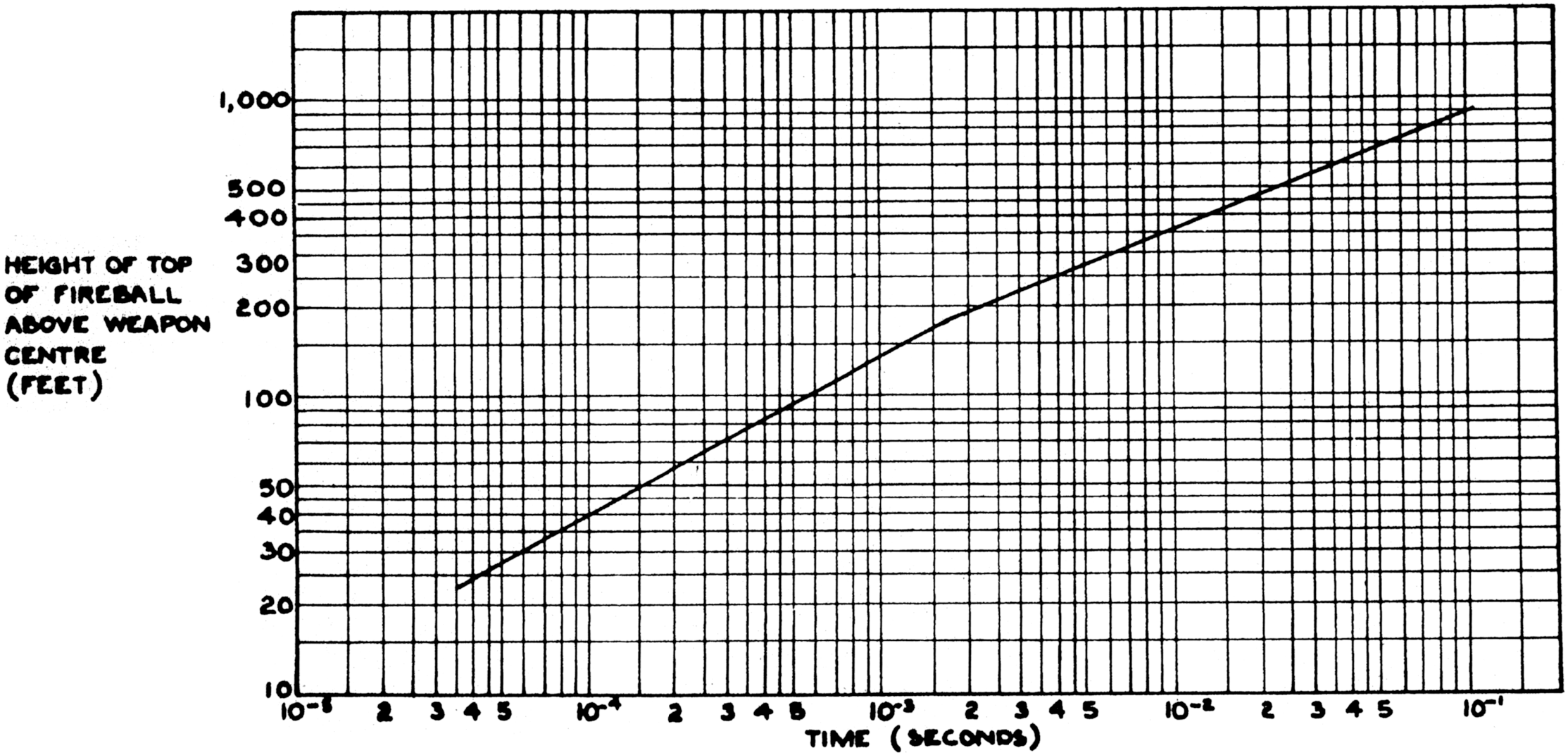

FIG. 2·3 EXPANSION OF FIREBALL ON WATERLINE.

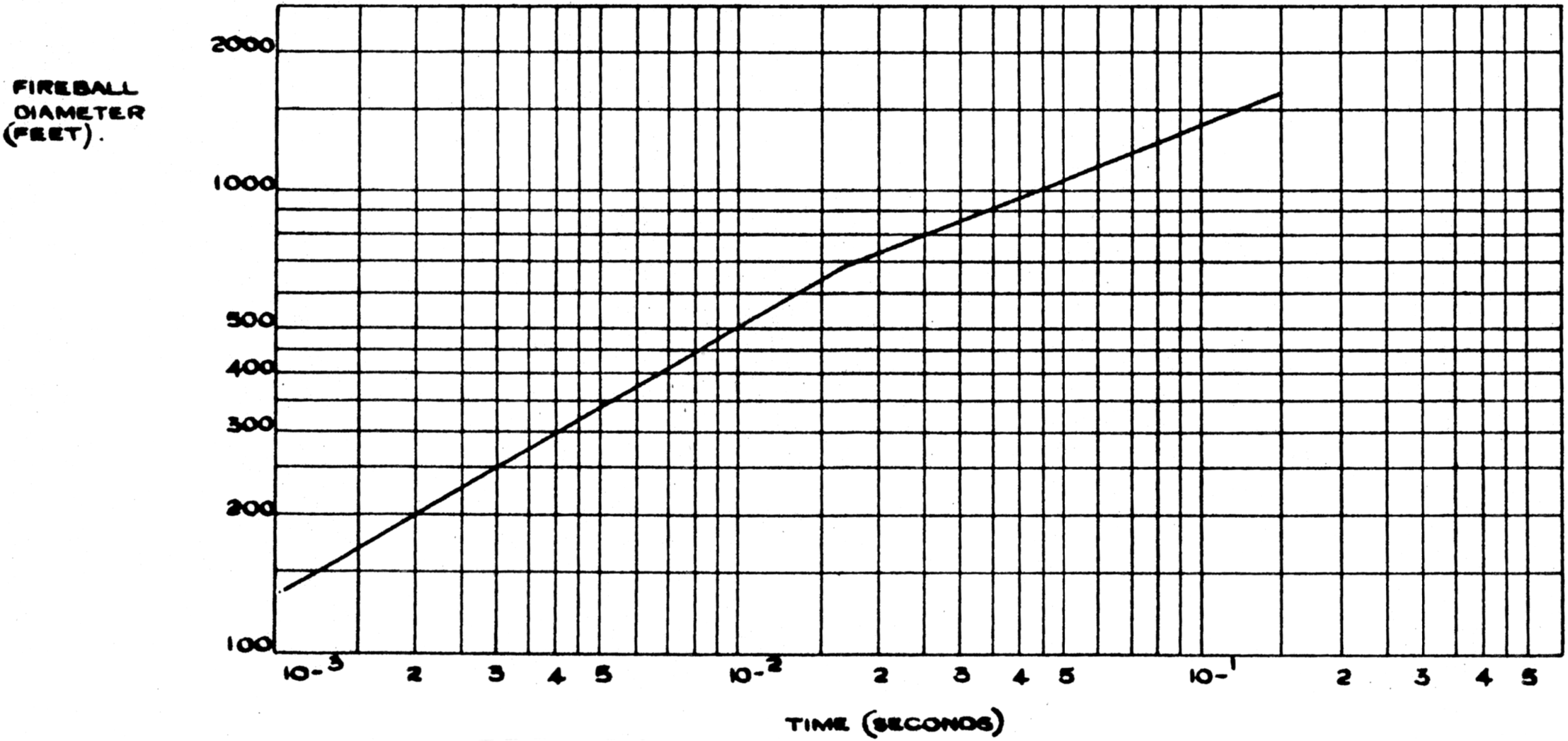

3. The Water Column and the Cloud

3.1. Water was first observed from H 1 emerging from the fireball at an angle of about 60° to the horizontal after about 0·1 seconds, Fig. 3.1. Its height above sea level at this stage was about 650 feet and its vertical component of velocity was 350 feet per second.

Fig. 3.1, 0.1 second. Water plumes begin to emerge from fireball due to the underwater bubble expansion and cratering.

Plumes of mixed water and black ferrous oxide from ship emerge at 1-2 seconds from the top of the fireball, which cools and fades out at 3 seconds. Last photo is at 5 seconds after burst.

3.2. Fall-out commenced from the side of the column but this did not spread far and was probably not important. The more widespread fall-out came from the bottom of the cloud and fell with an initial velocity of about 65 feet per second reaching sea-level at about 1 minute after the explosion, Figs. 3.8 and 3.9, and continuing for at least ten minutes.

3.4. The top of the cloud rose very roughly as $t^{\frac{1}{3}}$ having a height of about 1,800 feet at 1 second and reaching a maximum of about 10,000 feet at 4 minutes, when its ascent was substantially stopped by a temperature inversion.

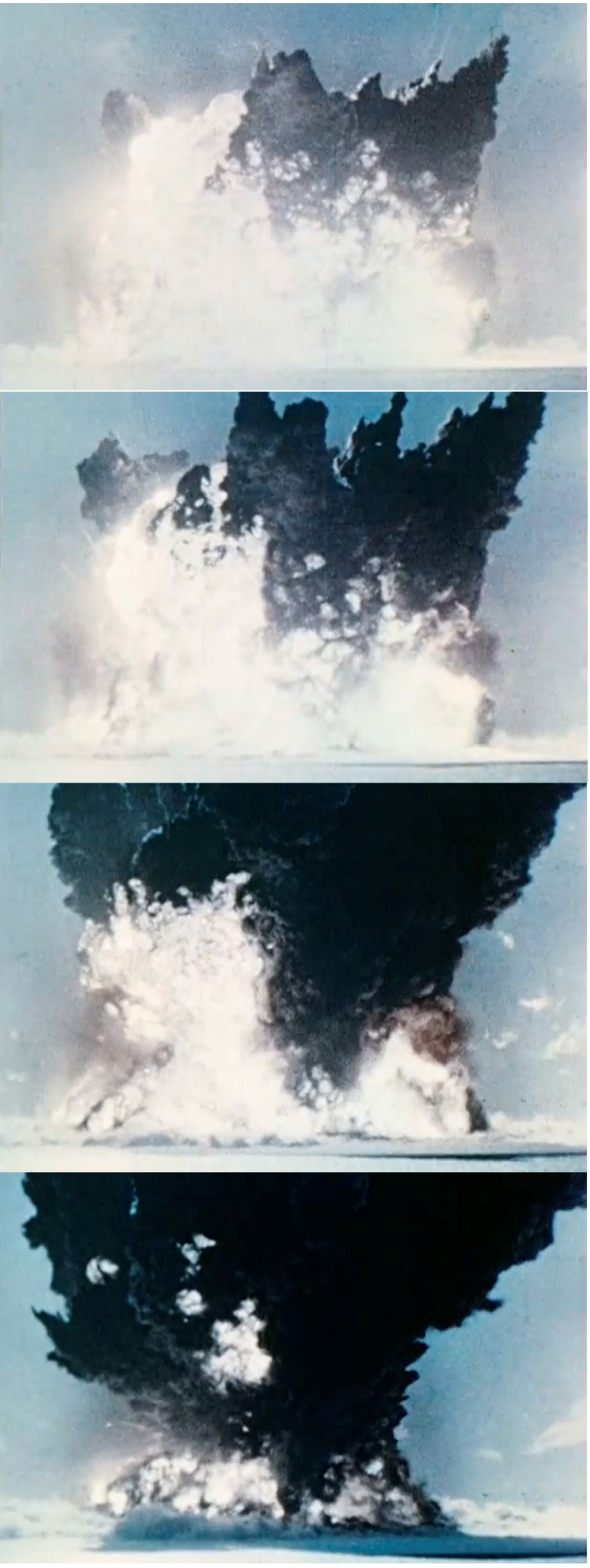

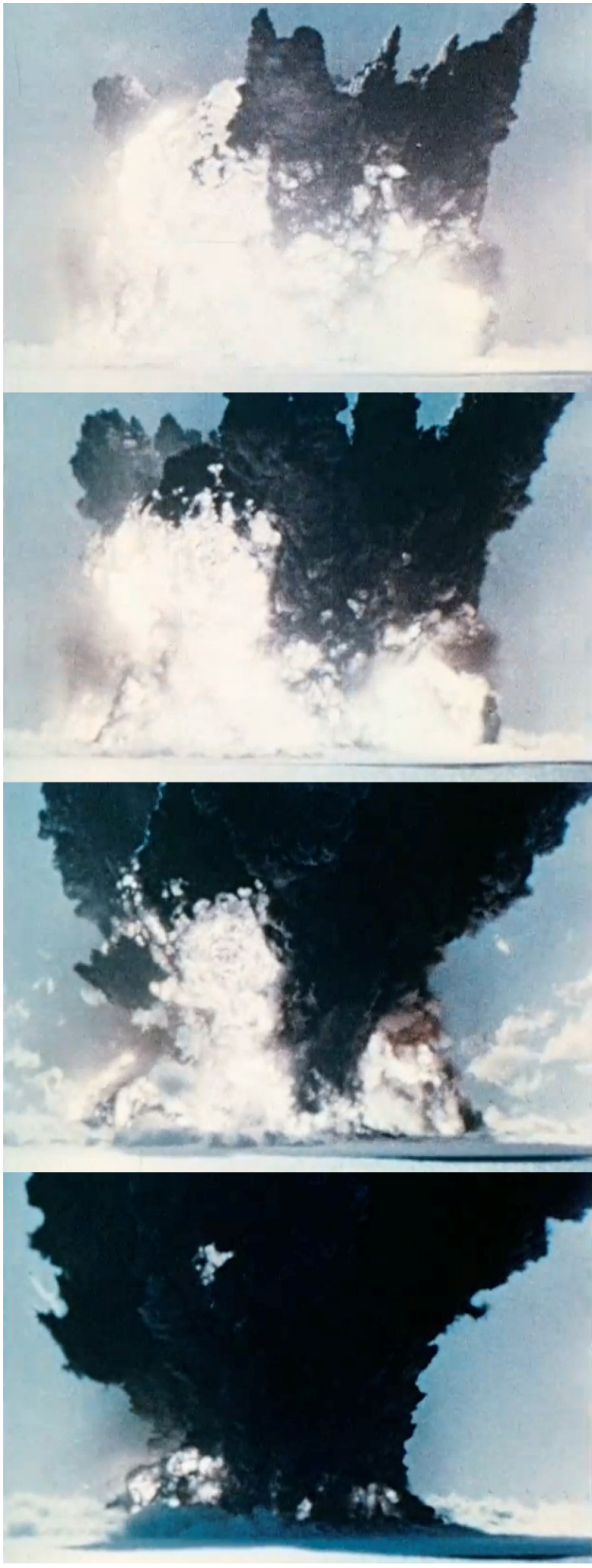

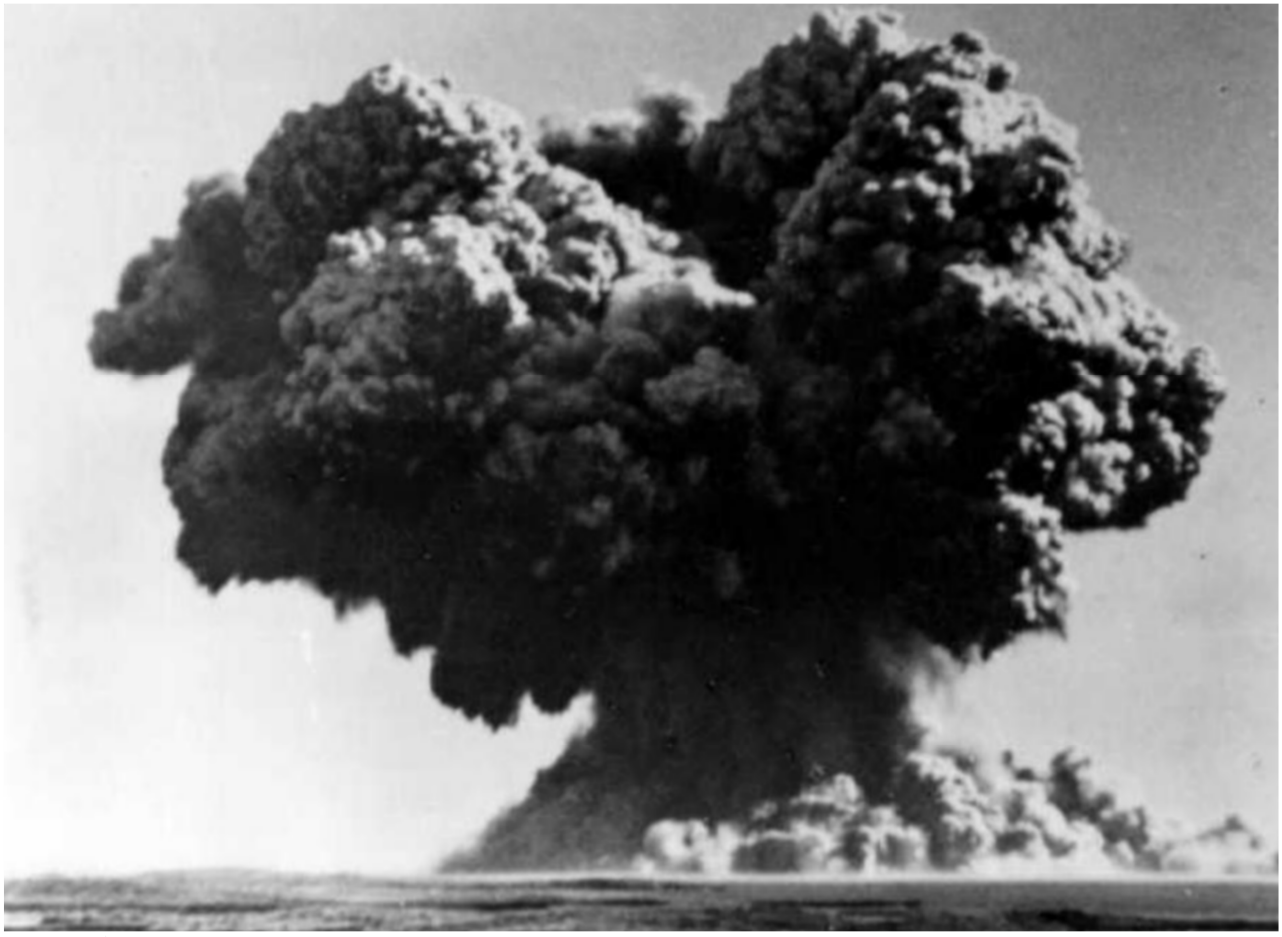

Fig. 3.8, cloud and base surge at 30 seconds. Water is falling from base of mushroom cloud at 65 ft/sec, and reached surface at 1 minute after burst. The base surge fallout was trivial.

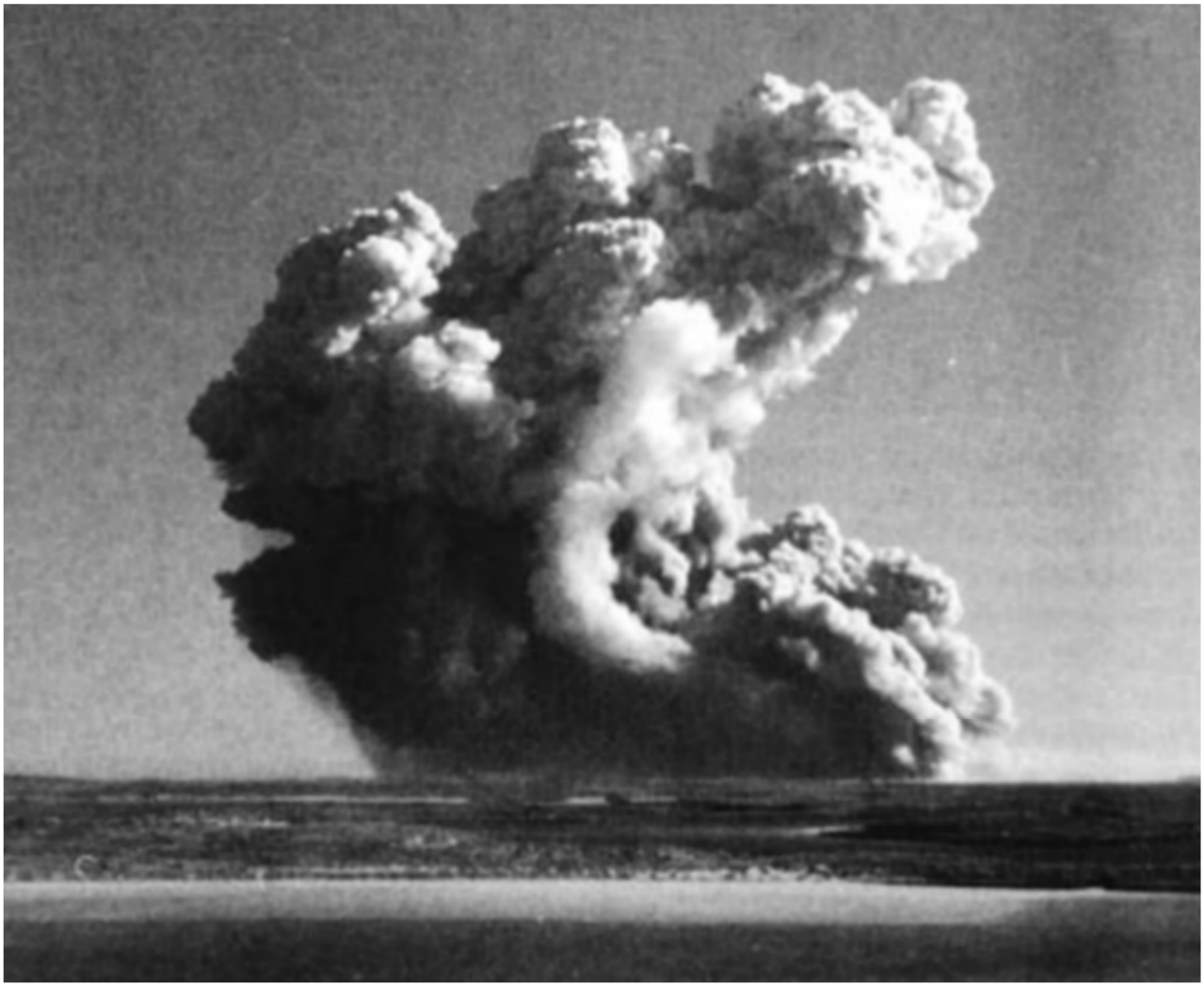

Fig. 3.10, cloud and base surge at 2.5 minutes after burst.

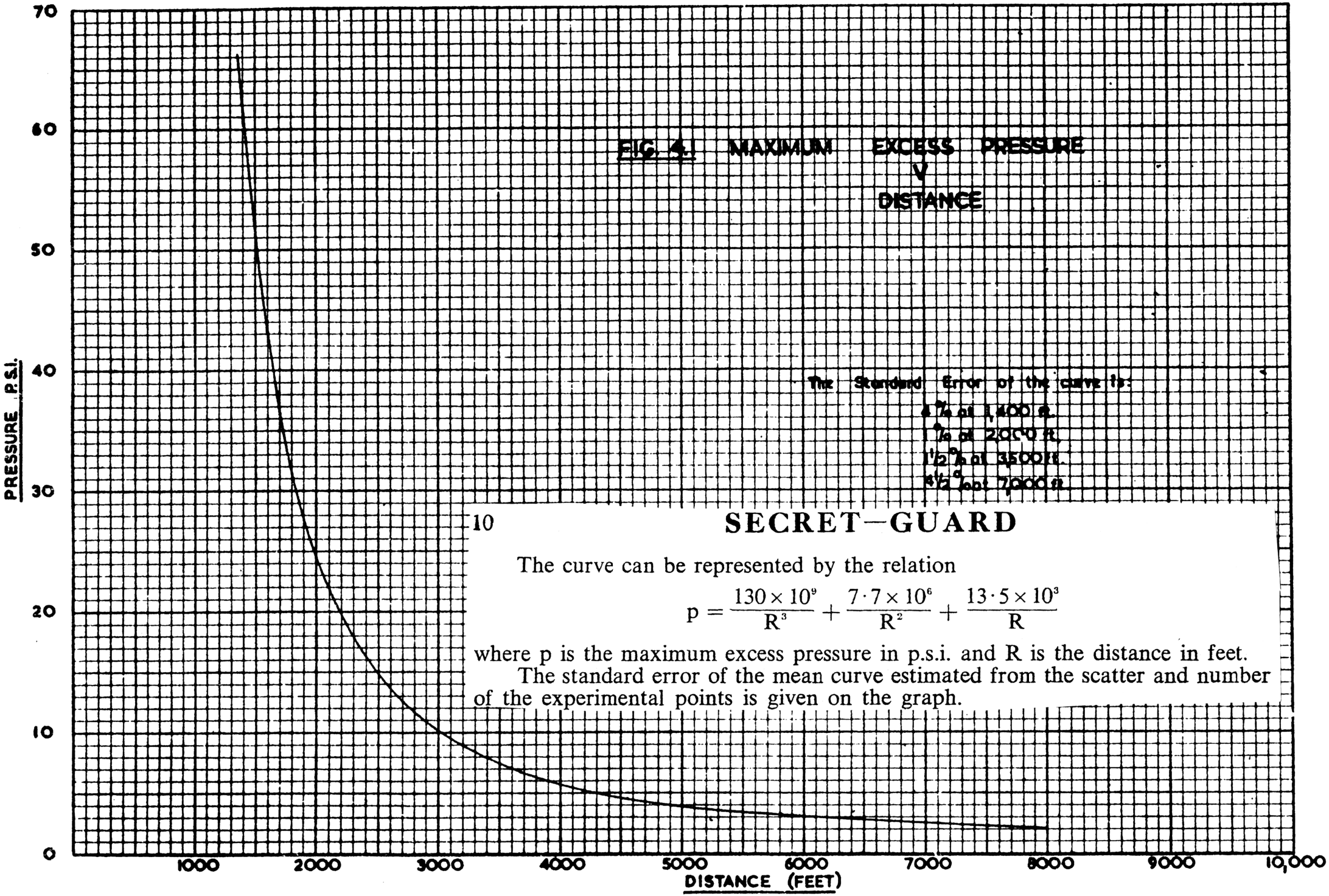

The curve can be represented by the relation

$$p = \frac{130 \times 10^9}{R^3} + \frac{7 \cdot 7 \times 10^6}{R^2} + \frac{13 \cdot 5 \times 10^3}{R}$$

where p is the maximum excess pressure in p.s.i. and R is the distance in feet.

The standard error of the mean curve estimated from the scatter and number of the experimental points is given on the graph.

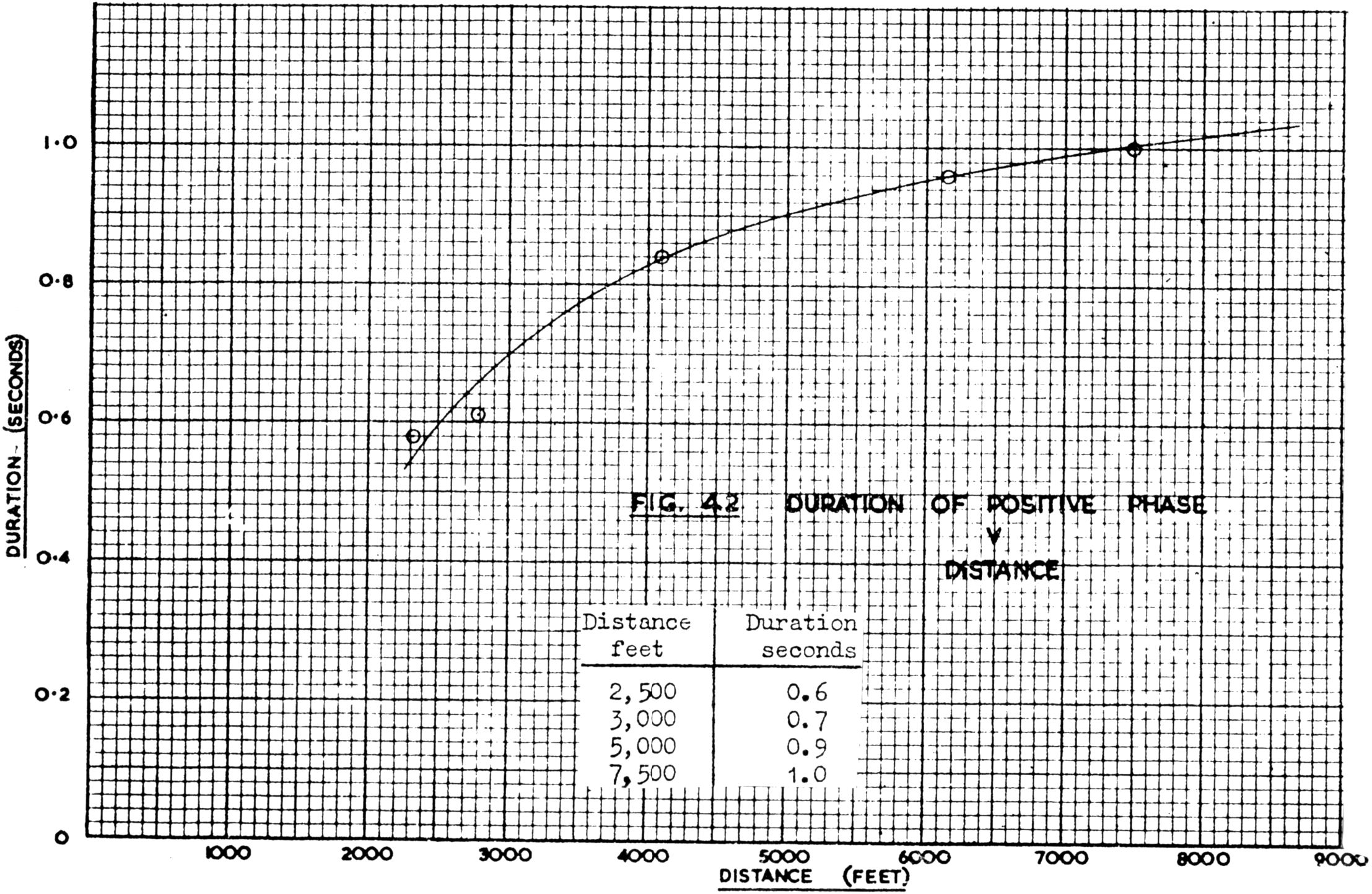

FIG. 42 DURATION OF POSITIVE PHASE
v
DISTANCE

Distance feet	Duration seconds
2,500	0.6
3,000	0.7
5,000	0.9
7,500	1.0

5. The Gamma Flash

5.1. The initial radiation or gamma flash comes from the rising cloud of radioactive material following the explosion and is normally confined to the first minute although most of it is received in the first second or two.

5.2. *The Variation of Gamma Flash Dose with Distance*

The total initial dose from the gamma flash was recorded by film badges placed at over 100 sites. Because of the unexpected magnitude and extent of the fall-out, many of the films were in the fall-out area and were completely blacked-out. Altogether 35 reliable readings of the dose were obtained; for these there was either a free optical path or only slight shielding, there was no fall-out and dosage readings were given by at least two different emulsions. From these readings the dosage/distance curve down shown in Fig. 5.1 was obtained. The general accuracy of the results is considered to be of the order ±10 to 15 per cent. The shielding effect of relatively small contours (of the order 30–60 ft.) was quite considerable; thus sites at equal distances from the explosion received doses that differed by as much as 50 per cent. depending on whether they were on a reverse or forward slope.

The doses received at given distances were about one half of those given for an air-burst weapon in the United States publication "The Effects of Atomic Weapons," but the distance at which a given dose was received was only about 10 per cent. less. Thus the ship's structure and the small depth of water above the point of burst did not have a very important effect in reducing the intensity of the initial radiation.

Measurements of the variations of dose-rate with time were made using flux-meters. Because of the long time-constant of the pen recorders used with them, the recording of the gamma flash was not entirely satisfactory but it was possible to use the results to obtain the approximate percentage of the total dose as a function of time. The results so obtained are given below in Table 5.1:—

Table 5.1

Time after Detonation (seconds)	*Percentage of total Dose Received*
0·05	30
0·10	50
1·0	80
10	90
60	99·5

These results indicate that about 80 per cent. of the total dose was received within one second of detonation, which is higher than the value of 50 per cent. generally quoted for an air-burst bomb and which suggests that only a small reduction in the dose received would be likely to result from evasive action.

The reason why a greater proportion of the total dose was received in the first second than would have been the case with an air-burst bomb is that the water and crater debris thrown up gave some protection after one second.

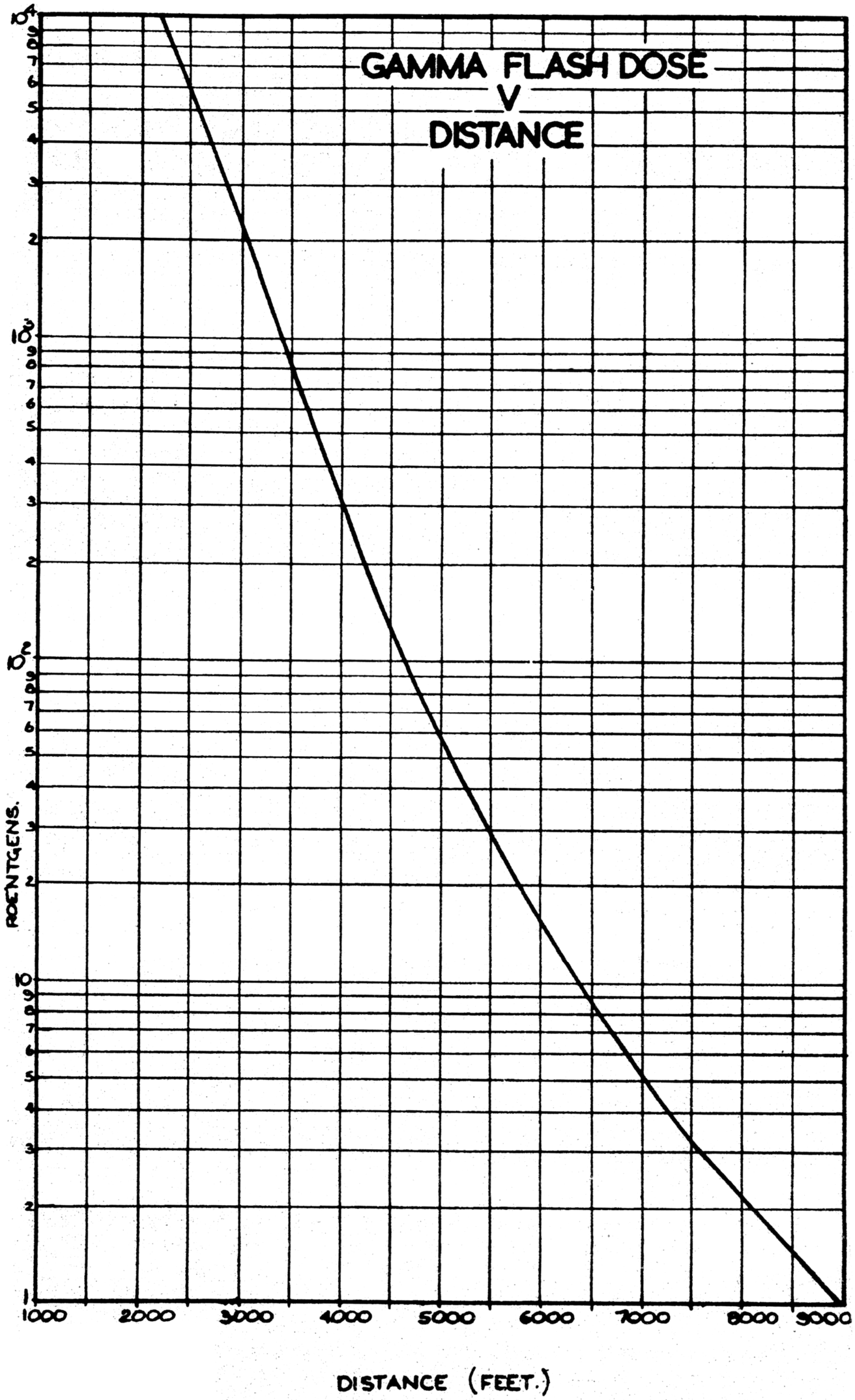
GAMMA FLASH DOSE
V
DISTANCE
ROENTGENS.
DISTANCE (FEET.)
1000
2000
3000
4000
5000
6000
7000
8000
9000

FIG. 5-1

6. Thermal Radiation

6.1. A number of methods were used to measure the total heat radiated by the fireball and the variation with time of the intensity of the radiation in a number of wave-bands and at various distances from the explosion.

6.2. *Variation of Intensity with Time*

6.2.1. Photo-electric recorders and photographic film recorders were used to obtain the variation of total intensity with time at 35,530 feet (H 1) and 10,630 feet (A4), the sun being used for calibration purposes. From these records, the curves shown in Fig. 6.1 have been derived showing the variation of the thermal radiation flux per unit area, at any distance D metres in an absorption free atmosphere. Also from these records the variation of temperature of the radiating surface has been estimated and the results are shown in Fig. 6.2.

6.2.2. Similar observations were made by staff of the Royal Naval Scientific Service using a photographic film intensity recorder designed at the Admiralty Material Laboratory. With this instrument the variation of intensity with time in nine wave-bands was recorded. The estimated total thermal output over the first 15 milliseconds of the flash in the range of wave-lengths, 3,850 A° to 6,650 A°, given by this method is in good agreement with the value derived from the experiments described in the previous paragraph.

6.2.3. The experiments referred to above show that the thermal radiation occurred in two peaks with a minimum at 25 milliseconds. In the first peak the energy was concentrated mainly in the shorter wave-lengths, whereas during the second peak it was mainly in the longer wave-length region. The total duration was quite short, about 1 second compared with 3 seconds normally quoted for an air-burst, suggesting that the water spout very quickly shielded the observation points from the heat radiation.

6.3. *Integrated Radiation Output*

6.3.1. The total thermal radiation output is of direct interest since, in general, when the rate of energy is high, as it is in the case of an atomic weapon, the damage produced is dependent largely on the total quantity of energy received.

6.3.2. In one experiment the total energy at three distances was determined from the rise in temperature of blackened copper discs exposed to the flash. From the three results obtained allowance was made for atmospheric absorption and a value of $0 \cdot 36 \times 10^{12}$ calories was derived for the point source of energy which at any distance in free space would give the same thermal intensity as the fireball. The absorption coefficient of $0 \cdot 075$ Km.$^{-1}$ corresponded to a visibility of 33 miles.

6.3.3. A second method, used by staff of the Royal Naval Scientific Service, was developed at the Admiralty Materials Laboratory and employed a photochemical actinometer. This method gave results for the total energy output per sq. cm. at 3,220 and 4,630 feet in two wave-bands in the violet and near ultra-violet which for reasons which are not yet understood, were considerably higher than those given by the other methods.

6.3.4. A number of indicators designed by the Army Operational Research Group of the War Office incorporated heat sensitive papers drawn across slits. It was intended to use these to record the variation of intensity with time but, owing to the somewhat inadequate time resolution possible with the apparatus the shape of the intensity time curve obtained is probably not significant. However, the value deduced from the records for the *total* energy received at 4,024 feet was $1 \cdot 52$ calories/cm.^{2}, which is the same as would be given at that distance in free space by a point source of $0 \cdot 31 \times 10^{12}$ calories.

6.3.5. From the observations given by the photo-electric recorders, it is estimated that the total thermal energy released to the atmosphere in the first peak, *i.e.*, in the first twenty milliseconds, was $0 \cdot 05 \times 10^{12}$ calories with an equal amount lost into the ground. The total of $0 \cdot 1 \times 10^{12}$ calories in the first twenty milliseconds may be compared with a release in free air of $0 \cdot 36 \times 10^{12}$ calories for the whole flash. The overall thermal energy released from an air-burst nominal weapon is generally quoted as $6 \cdot 7 \times 10^{12}$ calories. $0 \cdot 36 \times 10^{12}$ Calories is 1·8% of 20 kt yield

1 kt = 10^{12} cal.

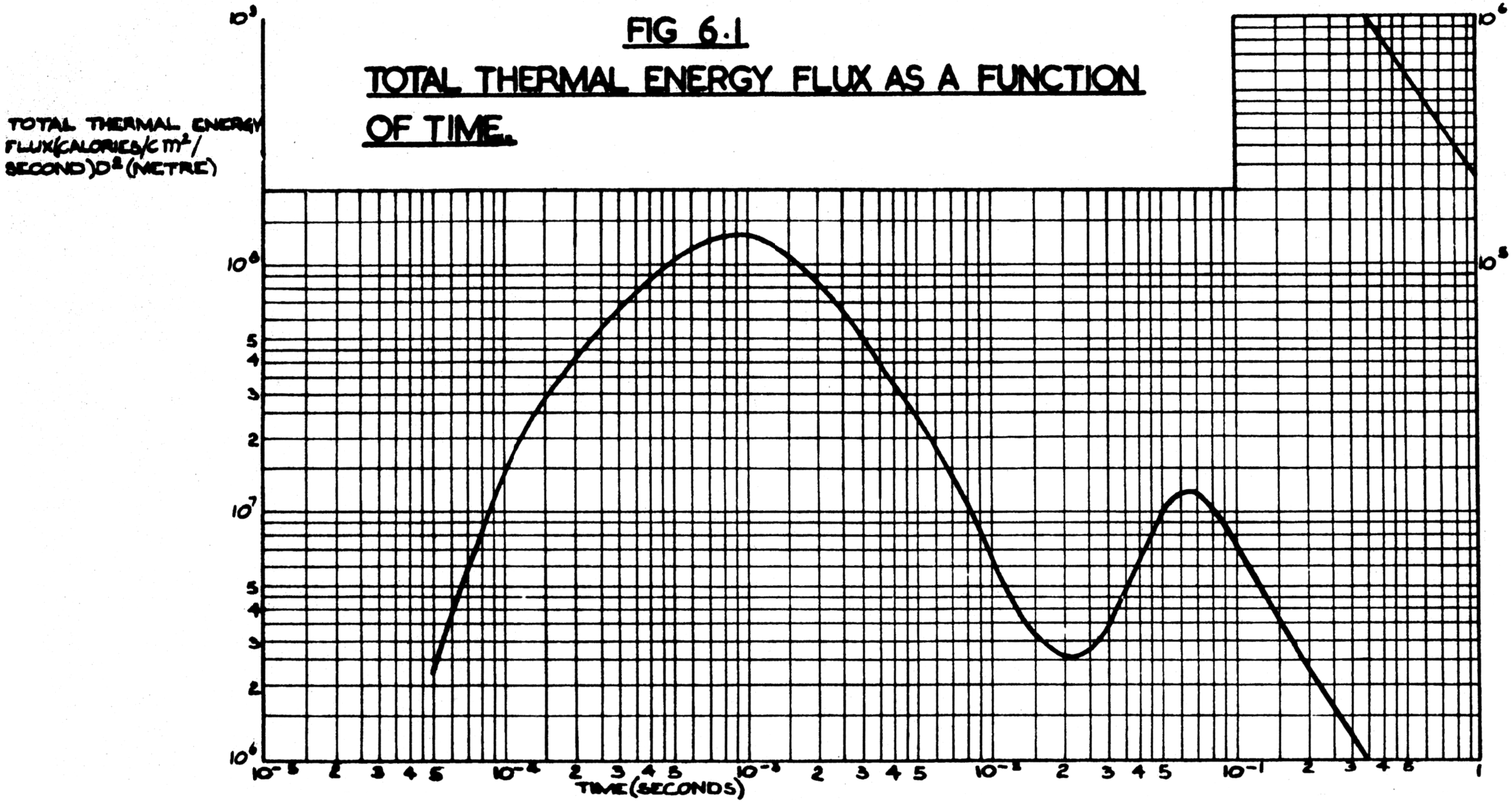

FIG 6.1

TOTAL THERMAL ENERGY FLUX AS A FUNCTION OF TIME.

RADIATING TEMPERATURE,
NOT AVERAGE FIREBALL TEMPERATURE!

FIG. 6·2

ESTIMATED FIREBALL TEMPERATURE.

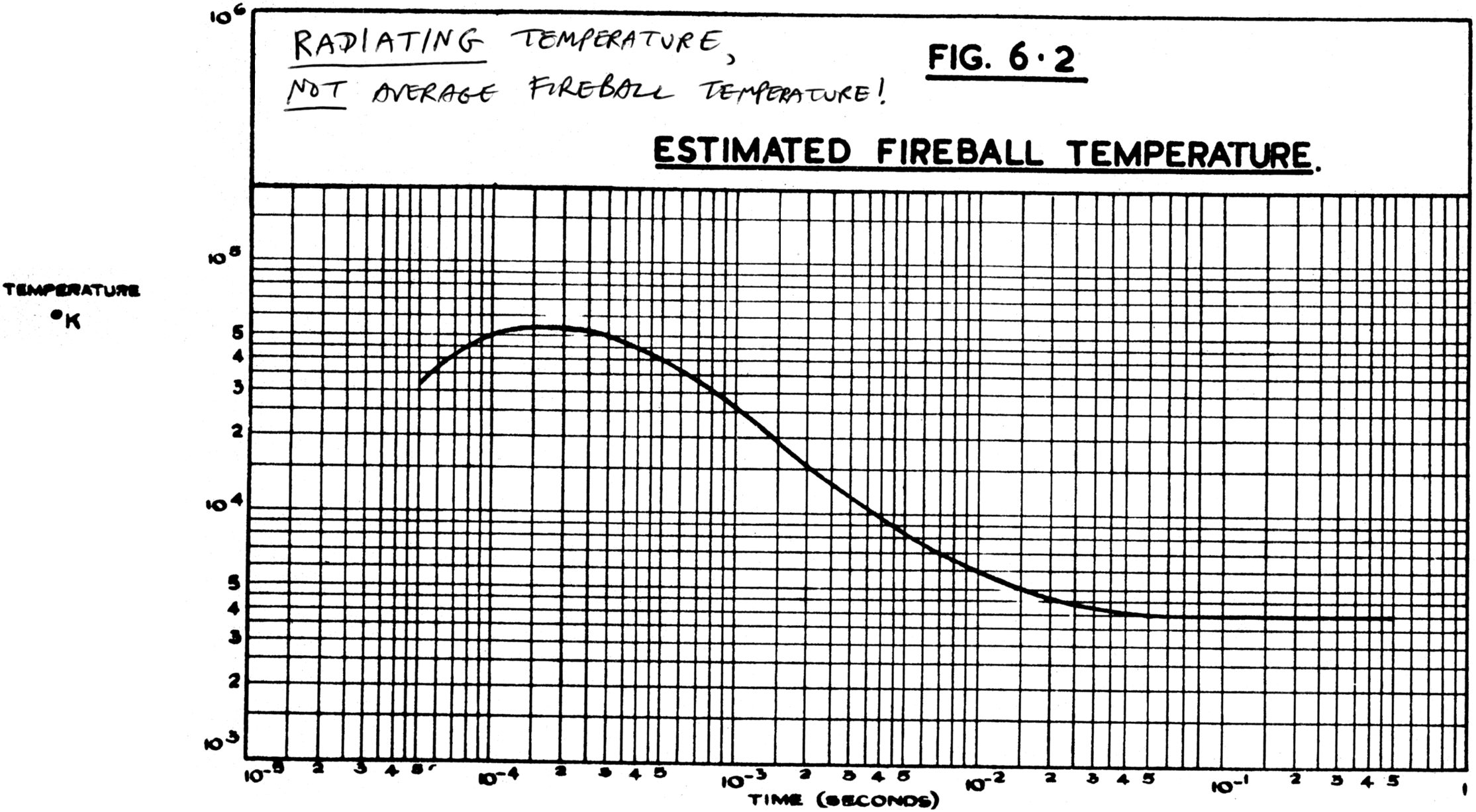

7. The Residual Contamination

7.1. Residual contamination is due to the deposition of radioactive fission products, and lasts indefinitely with decreasing intensity.

7.2. *Dose Rates during the First Twelve Hours*

Continuous records of the dose-rate r of the gamma radiation from the residual contamination were made at various distances during the period 0 to 10 hours from the time of detonation. These were intended to give the time of arrival of the fall-out and the value of the exponent x in the relation $^{dr}/_{dt} = k\ t^{-x}$ over the first twelve hours.

For this purpose fluxmeters of the ionisation chamber variety were used in conjunction with pen recorders. These were protected from the effects of the blast by hermetically sealed steel casings about ¼-inch thick and were shielded from the sun by a horizontal steel plate also ¼-inch thick. It was estimated that the observed radiation doses should be increased by 25 per cent. to allow for the effect of these shields.

The time of arrival of the fall-out in the downwind areas of widespread contamination was approximately proportional to the distance from the explosion and a period of about one minute was required for each 2,500 feet of distance. This time clearly depends on the meteorological conditions obtaining at the time and is thus not of general application.

The measured decay factor varied over the fall-out area but a mean value of 1·45 is considered reasonable, *i.e.*, the dose-rate over the first twelve hours is proportional to $t^{-1.45}$.

7.3. *The Gross Decay Law up to 1000 Hours*

For later periods up to about 1000 hours dose-rate measurements were made by survey teams using portable monitors. The decay factors obtained at various points over the area were in fair agreement. Since the terrain varied from rock to very sandy areas, this agreement suggests that wind erosion was slight, perhaps merely resulting in a continual shifting of the active dust over a restricted region, and implies that the loss in intensity was due almost entirely to radioactive decay.

The dose-rate values have all been reduced to correspond to a dose of 1 roentgen per hour at H+1 (one hour after the explosion) and the results are shown graphically in Fig. 7.1. It will be seen that the results for the later times do not fit well with the results up to 12 hours and there is quite a pronounced scatter in the period 100 to 200 hours. It has been found from experiments carried out since the trial that, as the survey meters are dependent on the photon energies of the gamma rays up to 0·2 Mev, the readings given by these monitors are likely to have been too high by a factor of as much as 1·3. By reducing the dose-rates by a factor 1·3 the curve II of Fig. 7.1 is obtained which joins up with the curve for times up to 10 hours very much better.

It may be seen that:—

(i) for the first twelve hours the dose-rate varied at $t^{-1.45}$;
(ii) between 12 and 100 hours, the decay was proportional to about $t^{-1.2}$;
(iii) between 100 and 200 hours, the decay was slower and very roughly as $t^{-1.0}$;
(iv) after 200 hours, it was rapid and varied as $t^{-1.6}$.

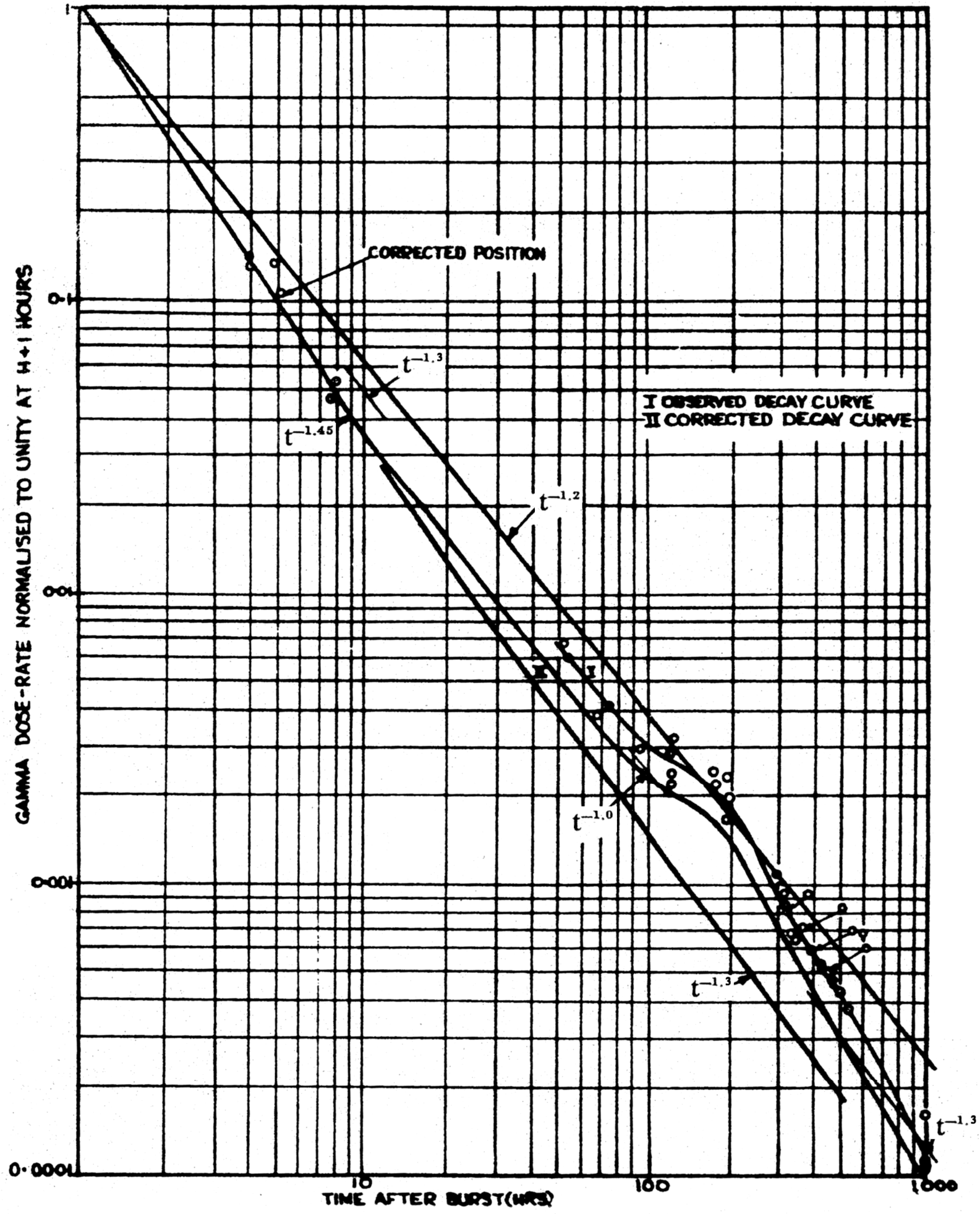

FIG.7·1 DECAY OF GAMMA DOSE-RATE WITH TIME.

(NORMALISED TO UNITY AT H+1 HOUR)

7.4. *Variation of Dose-rate with Height*

Observations were made of the variation of the dose-rate with height above the ground in order to determine whether the dose-rate on the ground could be inferred from measurements made by an aircraft flying at a known height above the ground.

The important practical conclusion was reached that dose-rates obtained by helicopter survey at a given height above a location will enable an estimate to be made of the dose-rate on the ground. The observed dose-rate at 100 feet should be multiplied by 2·5 and that at 500 feet by 10 to obtain the ground level value.

7.5. *Air-borne Contamination and the Inhalation Hazard*

Measurements were made to obtain data on the inhalation hazard in areas of heavy contamination and to assess its magnitude relative to the external hazard from the deposited activity. Samples of air were taken during the period following the explosion by means of standard air samplers working on the vacuum cleaner principle. The air was drawn through a filter paper of which the activity was subsequently measured, and the total volume passed was recorded on an anemometer. The air sampled was that which would have been inhaled by a man walking alone. In three cases it was arranged for dust to be stirred up by walking up and down in windward of the sampler while the sampling was in progress. A visible dust deposit was collected on the filter papers in consequence.

The results of these measurements are given in Table 7.1.

TABLE 7.1

Date	*Time*	*Activity of Sample Microcuries/c.c.*	*Dose rate of Contamination on Ground Milliroentgens/hr.*	*Ratio of Activity to Dose rate*
D-day	H+1 hour	$1\cdot9 \times 10^{-4}$	$1\cdot7 \times 10^{7}$	$1\cdot1 \times 10^{-11}$
D-day	H+2 hours	$1\cdot9 \times 10^{-4}$	$6\cdot1 \times 10^{6}$	$3\cdot1 \times 10^{-11}$
D-day	H+3 hours	$5\cdot7 \times 10^{-6}$	$3\cdot5 \times 10^{6}$	$1\cdot6 \times 10^{-12}$
D-day	H+4 hours	$5\cdot1 \times 10^{-6}$	$2\cdot3 \times 10^{6}$	$2\cdot2 \times 10^{-12}$
D+8		$6\cdot2 \times 10^{-10}$	1	6×10^{-10}
D+8		$6\cdot8 \times 10^{-9}$	8	$8\cdot5 \times 10^{-10}$
D+8		$7\cdot2 \times 10^{-8}$*	65	$1\cdot1 \times 10^{-9}$
D+8		$8\cdot8 \times 10^{-8}$*	15	$5\cdot9 \times 10^{-9}$
D+8		$1\cdot7 \times 10^{-7}$*	200	$8\cdot6 \times 10^{-10}$
D+8		$3\cdot1 \times 10^{-9}$	7·2	$4\cdot3 \times 10^{-10}$
D+16		$1\cdot36 \times 10^{-8}$	25	$5\cdot4 \times 10^{-10}$
D+16		$1\cdot14 \times 10^{-8}$	15	$7\cdot6 \times 10^{-10}$
D+16		$1\cdot88 \times 10^{-8}$	200	$9\cdot4 \times 10^{-11}$
D+18		$7\cdot2 \times 10^{-7}$	1,000	$7\cdot2 \times 10^{-10}$
D+18		$1\cdot5 \times 10^{-7}$	450	$3\cdot3 \times 10^{-10}$
D+18		$5\cdot1 \times 10^{-8}$	100	$5\cdot1 \times 10^{-10}$
D+18		$4\cdot9 \times 10^{-8}$	150	$3\cdot3 \times 10^{-10}$

* Dust stirred up by walking to windward of sampler.

There appears to be an approximate relationship between the dose-rate given by the contamination of the ground and the airborne activity associated with it. This relationship is 7×10^{-10} microcuries/c.c. per milliroentgen/hour under the particular conditions existing at Monte Bello. From this the values given in Table 7.2 are obtained for the total activity that would be inhaled while various integrated external doses were received.

TABLE 7.2

External Dose Received	*Fission Products Inhaled*
1 milliroentgen	$8\cdot7 \times 10^{-4}$ microcuries
100 ,,	$8\cdot7 \times 10^{-2}$,,
1 roentgen	0·87 ,,
25 ,,	22 ,,
50 ,,	44 ,,
100 ,,	87 ,,
400 ,,	348 ,,

8. Underwater Shock Measurements

By means of mechanical gauges underwater shock measurements were made over the range 900 to 3,600 feet by staff of the Naval Construction Research Establishment of the Admiralty. Very few positive results were obtained because of the very low value of the underwater pressures.

Five different types of gauge were used, of which only one type gave measurable records. This was a 6-inch copper diaphragm gauge suspended at half-depth, 22 feet, and consisting of a heavy steel cylinder approximately 10 inches long with a 0·2-inch thick annealed copper diaphragm bolted on to each end. The mean deflection of the two diaphragms of each gauge was used to assess the dynamic peak pressure from the calibration curves.

Measurable deflections were obtained at only the two nearest distances, *i.e.*, 960 and 1,185 feet. The values obtained are shown in the Table 8.1 below in comparison with values given by similar gauges in Test Baker at Bikini where the bomb was fired at half-depth in water 200 feet deep.

Table 8.1

	Pressure (p.s.i.)	
Distance	*Monte Bello*	*Bikini Test B*
5,000	...	150
4,000	...	260
3,000	Negligible	490
2,000	Negligible	950
1,185	20	...
960	270	...

The very low underwater pressures obtained indicate that in an explosion in a ship and very near the water-line little of the energy is transmitted to the water as a pressure wave and that, in shallow water, the quantity of energy that does enter the water in this way is very rapidly attenuated by the surface cut-off action.

If a pressure criterion is applicable it appears, by comparison with observed damage to ships at Bikini, that slight to medium underwater damage to surface ships would occur between 800 and 1,000 feet and no material damage beyond 1,000 feet whilst a submarine, submerged at half-depth, might be sunk or seriously damaged at 800 feet and yet only slightly damaged at 1,000 feet. Judging from the results of Test Able at Bikini, at 1,000 feet the damage from air blast would cause almost total destruction to all but capital ships. Thus for a near-surface burst in very shallow water, the distance for structural safety of surface ships and surfaced submarines is likely to be determined by air blast.

9. Crater

The crater formed in the sea-bed was a shallow saucer-shaped depression some 1,000 feet across and 20 feet deep at the centre with a lip averaging 4 feet in height. Its contour was determined by a survey of the sea-bed in the vicinity of the burst, before and after the trial, by means of echo soundings along six diametrical lines, 30 degrees apart and intersecting approximately in the position of the weapon. Fig. 9.1 shows the mean depth change between the two surveys over the six diametrical lines as a function of distance from the centre.

Before the explosion the sea-bottom in this region was a coarse sand composed of crushed coral, and for about 500 feet on each side of the weapon position it was fairly flat, differences from the mean depth not exceeding some 5 to 8 feet. It was at first thought that there was a layer of mud above the coral because of a black deposit which was found on objects in the fall-out area. This has since been identified at the Admiralty Materials Laboratory as being composed of 90 per cent. magnetic oxide of iron and 10 per cent. ferrous oxide and is therefore the remains of H.M.S. *Plym* and not mud.

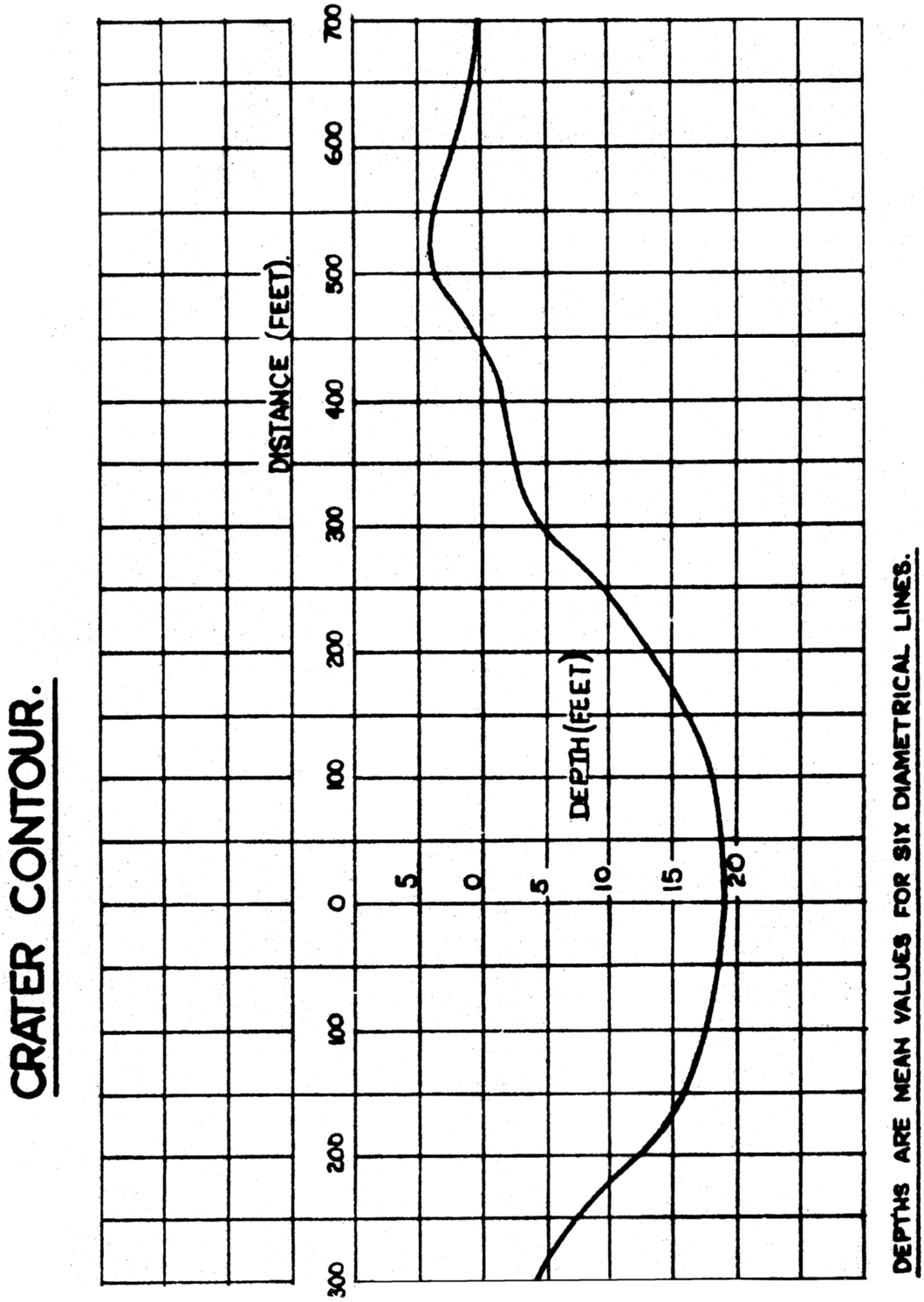

FIG. 9·1

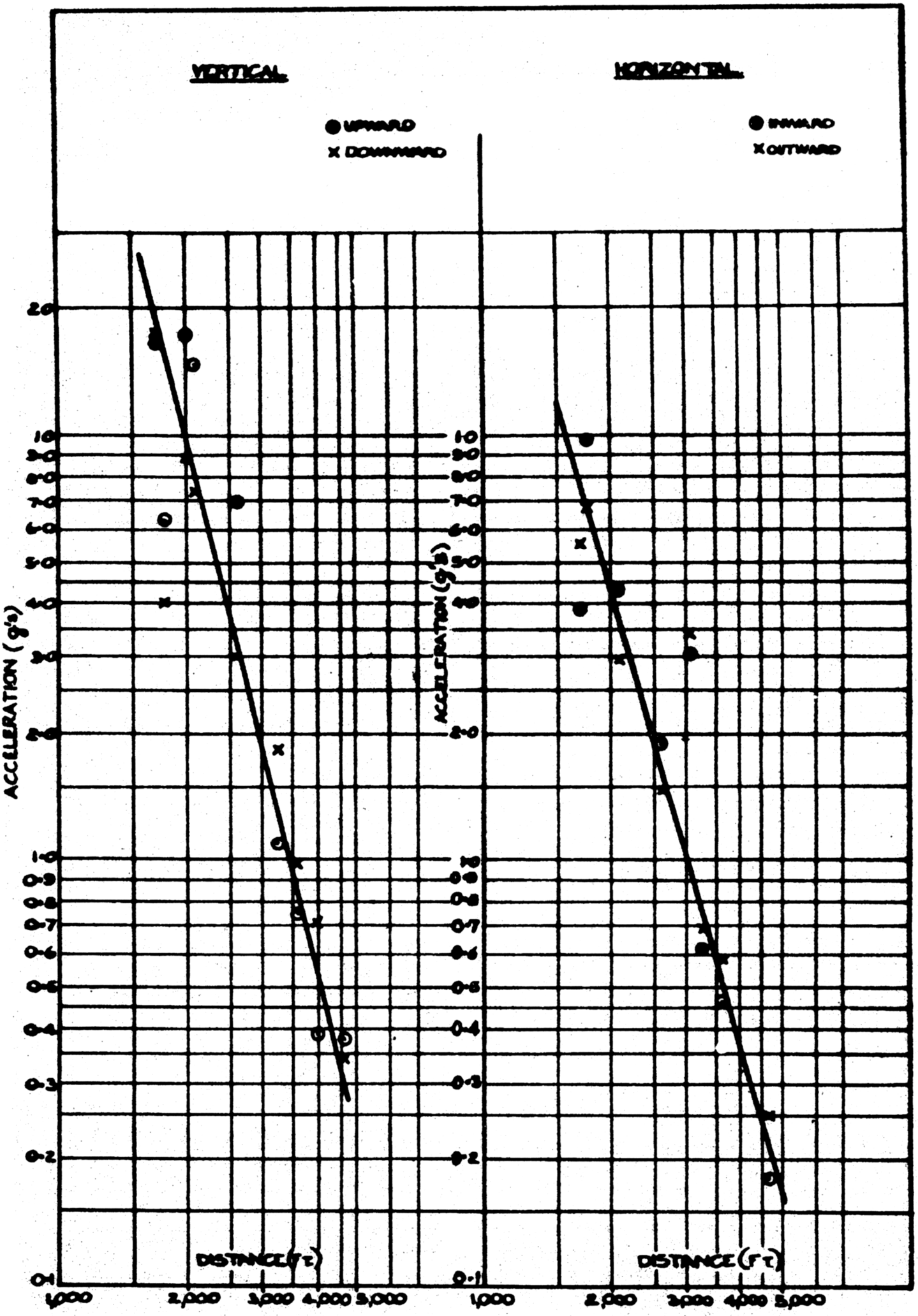

FIG. 10·1. MAXIMUM ACCELERATIONS.

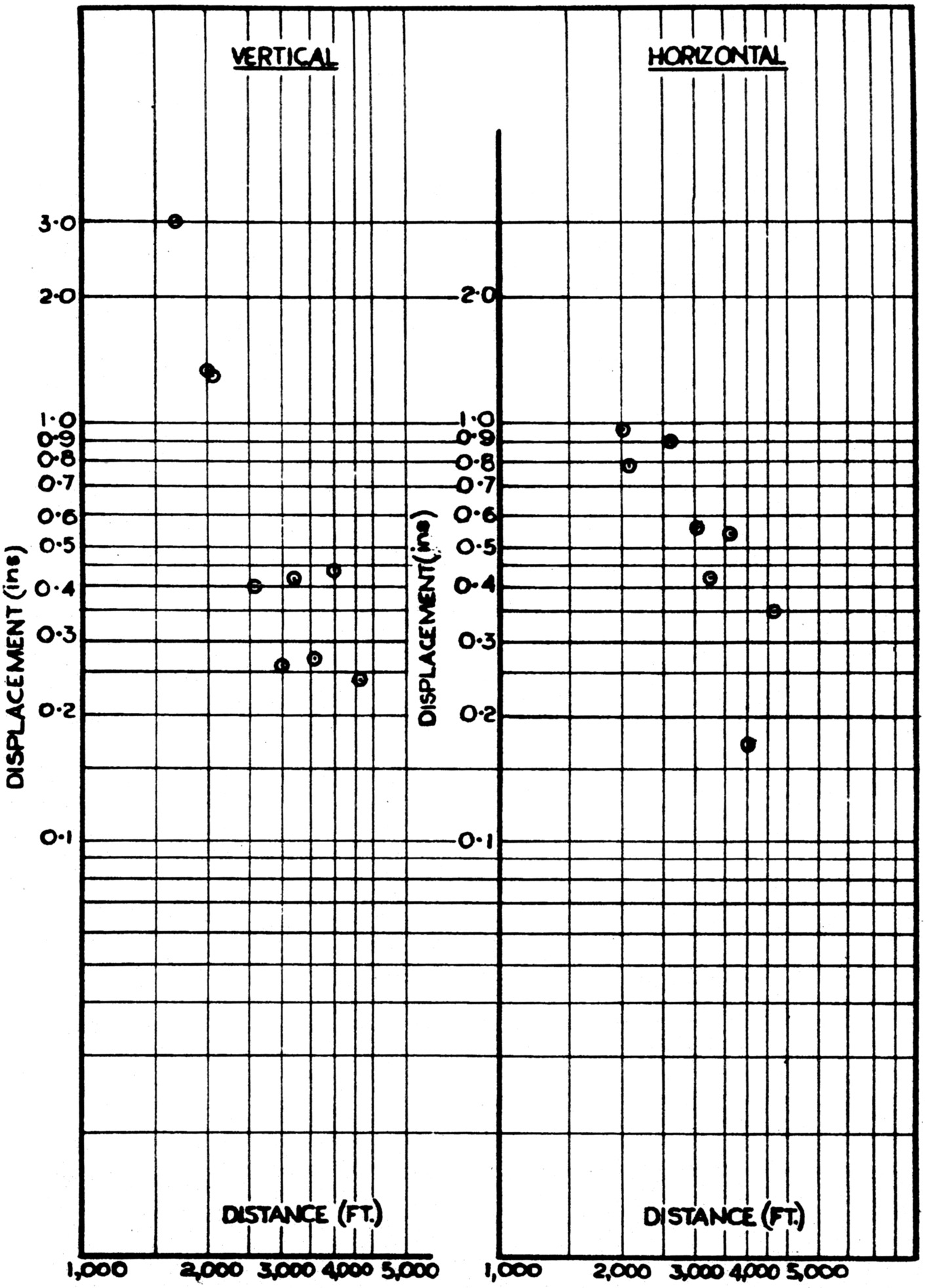

PEAK TO PEAK MAXIMUM DISPLACEMENTS.

FIG. 10·2

12. Blast Effects

12.1. *Blast Damage to Anderson Shelters*

12.1.1. In accordance with certain requirements of the Chief Scientific Adviser to the Home Office, fifteen Anderson shelters were erected, three at each of five sites situated, on Trimouille Island, more or less due West of the explosion at distances of 1,380, 1,530, 1,800, 2,760 and 3,390 feet. In each group one shelter was placed with its entrance facing the explosion, one with the entrance facing away from the explosion and one sideways to it.

The shelters were erected with a blast wall shielding the entrance, by the normal procedure laid down by the Ministry of Works, there being a difference from the usual practice in this country in that the covering of the shelter and the filling of the blast wall, instead of being earth, consisted of sandbags filled with fine dune sand, the only material available. The shelters were sunk with their floors about 4 feet below ground level; the thickness of the sandbags averaged 18 inches directly over the top of the roof arch to about 3 ft. 6 ins. at ground level at the sides. The blast wall was from 2 ft. to 2 ft. 6 ins. thick contained within sheets of corrugated iron and was placed about 3 feet from the shelter.

12.1.2. In the groups of shelters at 1,380, 1,530 and 1,800 feet, the sandbags covering them were almost entirely blown away and the blast walls were destroyed.

At 1,380 feet, Fig. 12.1, parts of the main structure of the shelters facing towards and sideways to the explosion were blown in but the main structure of the one facing away from the explosion was intact, and would have given full protection. At 1,530 feet, Fig. 12.2, the front sheets of the shelter facing the explosion were blown into the shelter but otherwise the main structures were more or less undamaged, as were those at 1,800 feet, Fig. 12.3.

At 2,760 feet, Fig. 12.4, some of the sandbags covering the shelters were displaced and the blast walls were distorted whilst at 3,390 feet, Fig. 12.5, the effect was quite small. At these distances, the shelters were not in direct view of the explosion owing to intervening sandhills.

12.2. *Maximum Pressures Inside Anderson Shelters*

Measurements of the maximum pressures inside the Anderson shelters were obtained using the toothpaste tubes referred to in paragraph 4.1.

The results obtained are summarised below in Table 12.1.

Table 12.1

Distance from Burst (Feet)	*Maximum Excess Pressure in Incident Blast* (p.s.i.)	*Maximum Pressure Inside Shelter* (p.s.i.) *Door towards Burst*	*Door sideways to Burst*	*Door away from Burst*
1,530	48	38	27	40·5
1,800	31·5	28	21	28
2,760	12	16	7	13·5
3,390	8	8·5	4	5·5

No results were obtained at the nearest distance of 1,380 feet.

12.3. *Blast Damage to Concrete Cubicles*

12.3.1. A number of concrete cubicles designed by the Ministry of Works were erected to obtain some information on the failure of reinforced concrete structural units under the action of the blast from an atomic bomb.

12.3.2. *Details of the Cubicles*

The original intention was to construct nine cubicles with internal dimensions of 12 feet and with wall and roof thicknesses of 6, 9 and 12 inches respectively. They were all designed to resist a uniform transverse load of 300 lbs./sq. ft. (2·1 p.s.i.), adopting conventional elastic theory. It was intended that one cubicle

Fig. 12.1, Andersons at 1380 ft range from bomb ship shown in the photo, anchored 400 yards off shore.

Left: Fig. 12.3, Andersons at 1800 ft after burst. Right: Fig. 12.4, Andersons protected by blast walls at 2760 ft.

of each thickness should be placed at distances where the peak excess hydrostatic pressure in the blast was expected to be 6, 10 and 25 p.s.i.

It transpired, however, that there was only sufficient time available at the site to construct five cubicles. Moreover, in order to permit the use of 1¼ inch aggregate, the proposed 6-inch and 9-inch walls had to be modified to 6¾ and 9¾ inches respectively.

The cubicles were situated as follows:—

TABLE 12.2

Distance (Feet)	*Peak Hydrostatic Pressure in the Incident Blast* (p.s.i)	*Wall Thickness* (Inches)		
1,815	31		9¾	
2,970	10	6¾	9¾	12
3,975	6		9¾	

The reinforcement of MS rods to British Standard Specification 785 and the cement, Ferrocrete Rapid Hardening, were shipped from the United Kingdom. The aggregate was obtained by crushing local rock to a maximum size of 1¼ inches. The rock had a granular surface, a bulk density of only 72·5 lbs. per cu. ft., and was very weak. Chemically it consisted mainly of calcium carbonate.

The sand was obtained from the beach nearby; it was somewhat fine, 70 per cent. passing through a No. 25 sieve. The concrete was made using sea water.

Normal methods of construction were adopted throughout, the walls being cast in 3-ft. lifts. Compaction was done with tamping rods.

The mix used was 1 part cement, 1·4 parts sand, 2·8 parts aggregate (all by volume) with a water/cement ratio of 0·48. This was a richer mix than would normally be used for concrete made with ballast aggregate but it was found to be necessary, owing to the poor quality of the local aggregate, in order to obtain a suitable strength combined with reasonable workability. The density of the concrete so obtained averaged only 133 lbs. per cu. ft. Tests on bin cubes at 7 days gave a crushing strength ranging generally between 2,000 and 3,000 p.s.i. Tests on plain concrete beams gave a modulus of rupture varying from about 300 to 500 p.s.i.

12.3.3. *Description of Damage*

There were no indications that any of the cubicles was tilted or translated bodily.

The only cubicle that sustained any serious damage was the one at 1,815 feet in which the wall facing the explosion was completely destroyed, a large portion of it being pushed inwards and hurled against the rear wall. There were some instances of failure of the reinforcement in this panel, but, in the main, failure of the concrete caused collapse, the concrete being either stripped from the bars or failing in bond, the latter being very evident along the bottom edge. Figs. 12.6 to 12.9 show this cubicle before and after the explosion.

The two side walls were left slightly bowed outwards and showed typical fine cracks from the corners to the centre. There was some failure at the construction joints near the front edges of these walls, as shown in Fig. 12.8. The extent of the bowing was not measured but its magnitude was estimated as about 1 inch. It could not be ascertained whether or not these walls had been first deflected inwards and then, after the failure of the front wall, pushed outwards.

The roof showed some cracks which roughly followed the line of the inside faces of the walls and there was failure above the inside edge of the front wall. Only a few hair cracks could be found in the rear wall.

At 2,970 feet the cubicles with 6¾ and 9¾-inch walls showed some fine hair cracks which did not extend to the inner surface, a typical example being shown in Figs. 12.10 and 12.11.

The cubicle with 12-inch walls showed no indication of any damage and the same applies to the one with 9¾-inch walls at 3,975 feet.

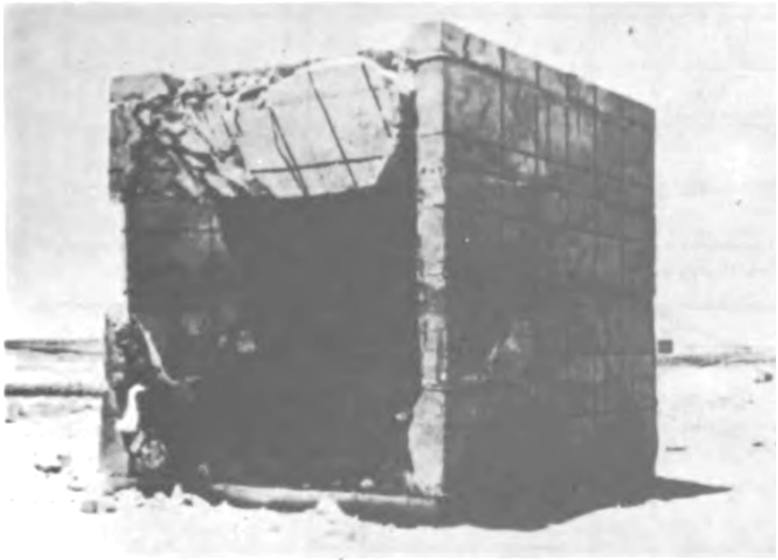

Fig. 12.6 and Fig. 12.7. Concrete cubicle at 1815 ft.

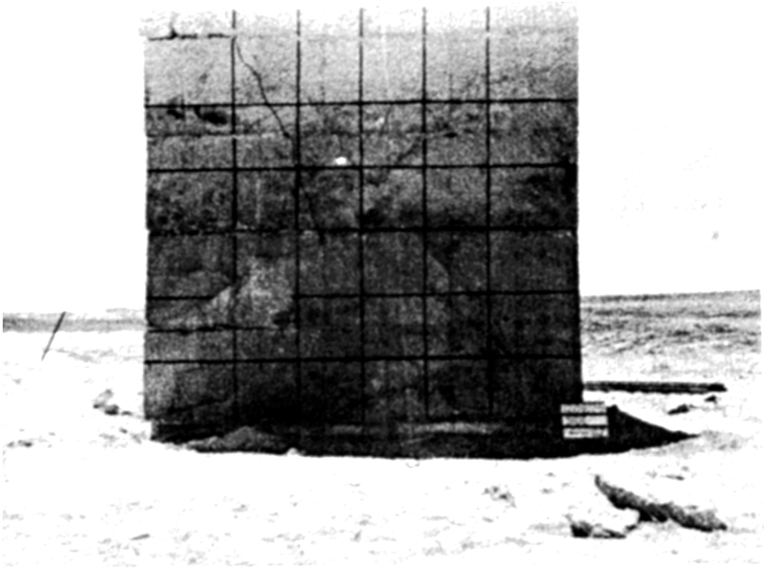

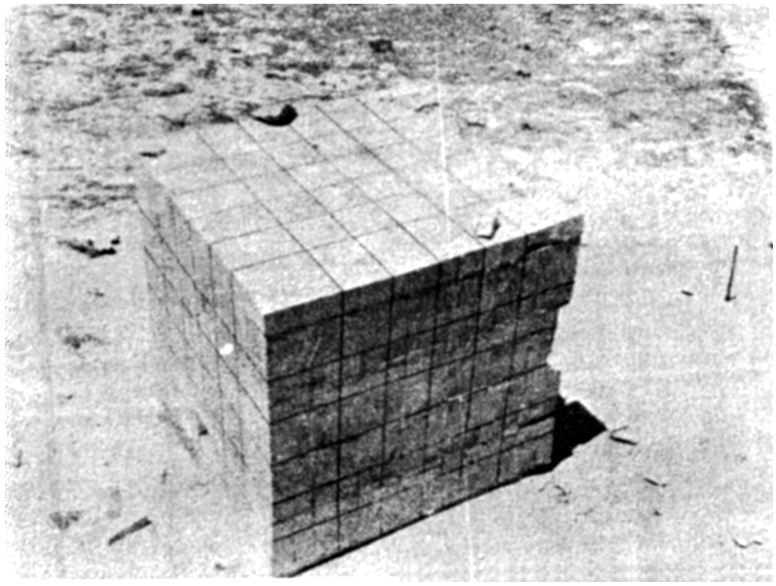

Fig. 12.8 and Fig. 12.9. Concrete cubicle at 1815 ft.

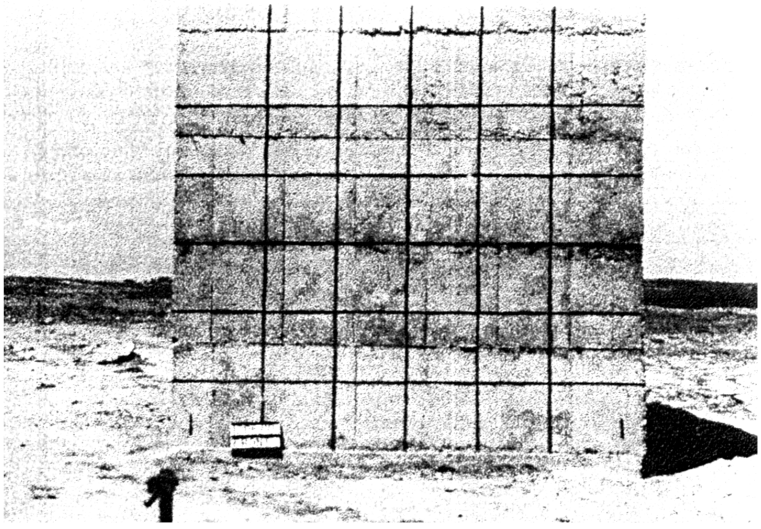

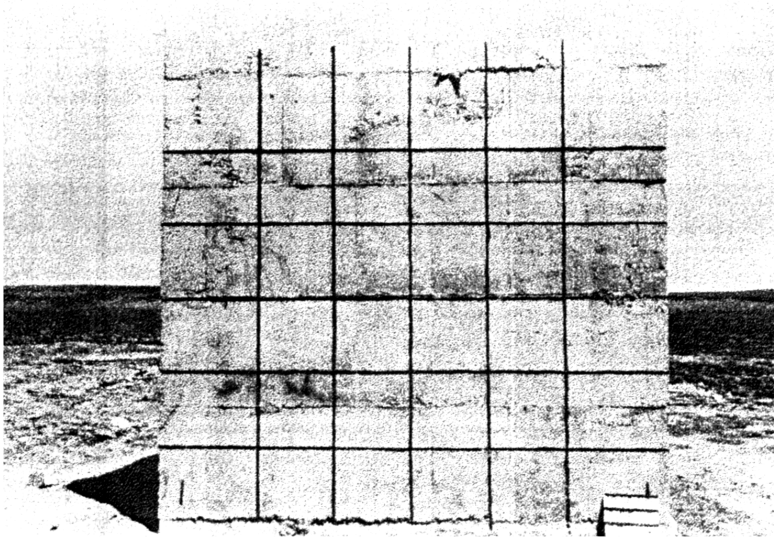

Fig. 12.10 and Fig. 12.11. Concrete cubicle at 2970 ft

13. The Penetration of the Gamma Flash

13.1. *Experiments on the Protection from the Gamma Flash afforded by Slit Trenches*

13.1.1. The experiments described in this section show that slit trenches provide a considerable measure of protection from the gamma flash. From the point of view of Service and Civil Defence authorities this is one of the most important results of the trial.

13.1.2. Rectangular slit trenches 6 ft. by 2 ft. in plan and 6 ft. deep were placed at 733, 943 and 1,300 yards from the bomb and circular fox holes 2 ft. in radius and 6 ft. deep were placed at 943 and 1,300 yards.

The doses received from the flash were measured with film badges and quartz-fibre dosimeters in order to determine the variation of protection with distance, with depth and with orientation of the trench and the relative protection afforded by open and covered trenches.

In general, the slit trenches were placed broadside-on to the target vessel but at 1,300 yards one trench was placed end-on. Two trenches, one at 733 and one at 943 yards were covered with the equivalent of 11 inches of sand.

13.1.3. A few results were obtained to show the variation of dose in a horizontal plane inside a trench and these indicated that the dose at a given depth is not likely to differ from that measured on the vertical axis by a factor greater than 2·5 even at the remote ends. Such differences are insignificant compared with those accompanying a change in depth so that the degree of protection can be assessed simply from the dose received on the vertical axis of the trench. A summary of the results obtained is given in Table 13.1. The surface doses are taken from the mean curve for the gamma flash dose given in Fig. 5.1.

13.1.4. From these experiments the following general conclusions may be drawn:—

(*a*) Open slit trenches, nominally 6 ft. × 2 ft. × 6 ft. deep provide a considerable degree of protection from the gamma flash and this increases with depth but at a decreasing rate.

(*b*) The approximate doses received by a man standing erect on the vertical axis of such a trench, averaged for all orientations of the trench are given below:—

Distance in yards ...	1,300	943	733
Dose in Roentgens	55	240	1,070

Thus personnel protected in this way would receive the median lethal dose of 400r at about 850 yards compared with just under 1,300 yards when exposed on the surface.

(*c*) Personnel lying prone in open slit trenches 3 ft. or more in depth should not receive the median lethal dose even as close as 733 yards.

(*d*) A top cover equivalent to one foot of earth reduces the dose experienced inside a trench by a factor of about 5 so that, under these conditions, median lethal dose for a man standing erect would be received at a distance of about 650 yards.

(*e*) The dose received on the vertical axis of trenches of rectangular cross-section and which had random orientation, do not differ greatly from those on the vertical axis (at the same depth) of cylindrical trenches of the same area of cross-section.

(*f*) This experimental data, showing how great is the protection afforded by slit trenches, provides one of the most important results of the trial from the point of view of Service and Civil Defence authorities.

TABLE 13.1

Variation of Gamma Flash Dose on Vertical Axis of Trench

Type of trench	Rectangular broadside-on open			Rectangular end-on open	Circular open		Rectangular broadside-on covered	
Distance (yards) ...	1,300	943	733	1,300	1,300	943	943	733
Surface dose (Roentgens)	300	3,000	14,000	300	300	3,000	3,000	14,000
Depth below ground level (inches)								
6 ...	150	1,000	—	230	214	1,200	(75)	—
12 ...	75	430	—	150	120	545	47·6	—
24 ...	33·3	150	584	60	54·5	188	25	(140)
36 ...	23	70	216	31·6	30	86	13	(56)
48 ...	(20)	43	100	20	17·7	48·5	7·7	(31)
60 ...	—	(37·5)	61	13·6	10·7	(33·3)	5	(23)
72 ...	—	—	(46·7)	(8·6)	7	—	(3·5)	—

Entries in brackets are extrapolations or estimates.

13.2. *The Penetration of the Gamma Flash into Anderson Shelters and Concrete Cubicles*

13.2.1. Film badges were used to measure the gamma flash dose inside Anderson shelters and concrete cubicles. The latter were erected primarily to study the effect of blast on reinforced concrete panels but because of their regular shape and appropriate range of panel thickness were well adapted for the study of gamma-ray penetration.

In the Anderson shelters, the floors of which were situated at a depth of 3 ft. below ground level, four film badges were disposed, two above ground level and two below. Four badges were also placed in the concrete cubicles, along the horizontal axis of symmetry pointing towards the weapon, (*a*) in the centre of the cube, (*b*) against the front wall, (*c*) against the rear wall and (*d*) at a distance of one foot from the front wall.

13.2.2. The results of these measurements are summarised in Tables 13.2 and 13.3 together with estimates of the dose received outside the cubicles.

The results for Anderson shelters show considerable scatter but some broad conclusions can be drawn. It is clear that for a burst near ground level, the dose below ground level was about half that above ground, but this would not necessarily apply to an airburst, where more of the radiation would come through the roof. The shelter as a whole was quite effective in reducing the dose and the median lethal dose of 400r would be received at about 2,400 ft. below ground level and at about 2,700 ft. above, as compared with 3,900 feet in the open. The advantage of getting down on the floor is further illustrated by the fact that at 2,700 ft. the dose received at floor level would be only 150r which may be regarded as generally non-lethal, whereas the median lethal dose would be received above ground level.

The results for the cubicles indicate complete protection against lethal effects of radiation, *i.e.*, a dose of 100–150r, inside a reinforced concrete structure with walls 12 inches thick at about 3,300 ft. and for 6¾-inch wall thickness in the region of 3,900 ft. where the dose in the open would be the median lethal dose of 400r.

TABLE 13.2

Gamma Flash Doses in Anderson Shelters

Distance (Feet)	*Estimated Dose Outside* (r)	*Average Dose Inside* (r) *Above Ground Level*	*Below Ground Level*
1,380	75,000	N.R.	10,500
1,530	47,000	11,000	5,500
1,800	30,000	7,000	2,000
2,760	4,000	150	100
3,390	1,200	30	15

TABLE 13.3

Gamma Flash Dose inside Concrete Cubicles

Distance (ft.)	Estimated dose outside (*r*)	Dose inside (*r*)			Average dose inside (*r*)
		Wall thickness (inches)	Position of badge (see text)	Dose	
2,970	2,800	6¾	*a*	410	460
			b	455	
			c	430	
			d	545	
		9¾	*a*	260	270
			b	—	
			c	230	
			d	322	
		12	*a*	185	190
			b	220	
			c	158	
			d	195	
3,975	380	9¾	*a*	35	50
			b	62	
			c	46	
			d	58	

The front of the cubicle at 1,800 ft. was blown in and the badges were exposed to radiation from the fall-out.

14. THE EFFECT OF HEAT FLASH ON MATERIALS

14.1. Samples of cloth, service clothing and equipment, black-out materials and temperature indicating lacquers were set out at various distances from the weapon. This work was organised by staff of the Scientific Adviser to the Army Council, of the Home Office and of the Admiralty. Owing to the small amount of heat radiated by explosion under the particular conditions of the test, very few positive thermal effects were obtained.

14.2. A preliminary report from the Scientific Adviser to the Army Council gives the following observations:—

(i) Some scorching of cloth samples set up on panels at 500 yards was observed.

(ii) No effects were observed on the following:—

Samples of R.A.F. flying clothing exposed at 1,000 and 1,500 yards.

Norman battle-dress or combat suits with respirators and steel helmets exposed at 1,000, 1,200 and 1,400 yards.

Gas capes and pouches at 1,000 yards and beyond.

Black-out materials, treated and untreated, fully exposed and behind clear and white-washed glass, together with temperature indicating lacquers on mild-steel plates at 1,000 yards and beyond.

Pieces of fibre-board and dummies representing the human arm covered with shirt and battledress serge at ranges of 1,000 yards and above.

(iii) Samples of black-out material and heat-indicating lacquer exposed at 500 yards received heavy contamination and have not yet been fully examined.

14.3. A service respirator face-piece, a civil defence respirator face-piece, a civilian respirator and a children's respirator were exposed at six positions between 450 yards and 1,000 yards. At all sites severe blast damage occurred and at the nearest nothing of the masks was recovered. At the other distances, *i.e.* between 500 and 1,000 yards, where in some cases only parts of the respirators were found, there was no sign of flash burn.

14.4. For one of the Naval ABC trials, canvas wallets, on to which were sewn samples of different types of naval clothing, were set up at twelve points between 750 and 3,500 yards from the explosion. The results were almost entirely negative, the only material affected being IA8 blue serge which had a very slight surface scorch at 750 yards.

15. Contamination and Decontamination

15.1. The results and conclusions quoted here can be applied only to the type of conditions experienced at Monte Bello, *i.e.*, to a dry dusty location or to dry debris resulting from the destruction of buildings. They also apply to reconnaissance, rather than rescue or other dust-raising operations, with entry to the contaminated area after fall-out has occurred and any fluid fall-out has dried. The contamination will then be tightly absorbed on to the dust particles and decontamination is then largely achieved by removing the dust. Contamination from direct fluid fall-out was found to be strongly absorbed by the surface and its removal was very difficult.

15.2. *Protective Clothing*

15.2.1. For the use of personnel entering contaminated areas a standard issue was made of protective clothing. This consisted of cotton singlet and trunks, woollen socks, a combination suit, rubber undergloves, cotton overgloves, half wellington boots, a light service respirator and a hat, something like a trilby. The combination suit had double legs from just below the knee, the inner one being caught under the foot by means of a loop. The sleeves were double from the elbow, the inner sleeve being retained in place by a loop passing over the thumb. Both the inner leg and inner arm had elastic around the bottom. A sweat-rag was worn round the neck. The following notes are given to illustrate the lessons learned and conclusions reached, not always unanimous, concerning its protective value and general usefulness.

15.2.2. *Suits*

General opinion agreed that the combination suit was surprisingly comfortable although for use in a hot climate a lighter colour would have been preferable. The material was splash-proof but not water-proof and its weave seemed to be a fair compromise between reasonable ventilation and the need to keep out contaminated dust. It was generally effective in preventing body contamination but where the dust was rubbed or pressed in, *e.g.*, at the knees or elbows or round the legs when pushing through the long spinifex grass, it penetrated the suit and contamination of the skin resulted. Thicker material or the use of long pants or vests with sleeves would prevent this but would be impracticable for hot climates. Elastic at the bottom of the legs and sleeves is liable to be damaged during laundering and tapes would have been preferable.

15.2.3. *Sweat-rags*

The sweat-rags used were not of the type expected and made only a defective seal. They allowed perspiration to trickle on to the shoulders and thus caused contamination which was sometimes difficult to remove. The necessity for a sweat-rag would be obviated by the use of a hood as recommended later.

15.2.4. *Headgear*

The hats provided were unsuccessful as they did not prevent dust-borne and air-borne contamination from collecting on the exposed parts of the head and face. It was clear that only a hood would prevent head contamination.

15.2.5. *Respirators*

Although it was found that the respirators provided could be worn for long periods, heavy work was rendered difficult by condensation of perspiration inside the mask. It was felt generally that for fire or dust-raising operations, it is highly desirable to have some form of respirator and for trials purposes these should be worn in all significantly contaminated areas. Further investigation on the most suitable type is clearly required, *e.g.*, a light industrial dust mask and eye-shield might be adequate.

15.2.6. *Gloves*

Owing to the heat the rubber gloves were unpleasant to wear and were liable to be torn in heavy work. They were also surprisingly difficult to decontaminate. A plastic impregnated material might be more suitable, or alternatively the use of two separate expendable gloves, *e.g.*, a light cotton close-fitting underglove and a heavier reinforced overglove. Experience with the suit and underwear showed that two layers of material would prevent contamination and at the same time allow reasonable ventilation and sweat absorption. Two gloves were found to be necessary at Monte Bello when records were being recovered from contaminated regions, but for general use it would probably be better to have a single glove if a suitable material could be found.

15.2.7. *Boots*

The rubber half-wellingtons used in conjunction with a double trouser leg (one inside the boot and one outside) were effective in reducing foot contamination. Their disadvantage lay in the difficulty of decontaminating them which was accentuated by the matt finish and the indented pattern of the sole of those supplied. A boot with a high gloss would probably be easier to decontaminate or an expendable overboot might be considered.

15.3. *Body Contamination*

15.3.1. *Removal of Body Contamination*

During the three weeks following the burst about 940 man-sorties were made into the contaminated areas. All personnel who had worn protective clothing had to take a shower, as a matter of routine procedure, although many, *e.g.*, boats crews, had not entered areas of appreciable contamination. No records were kept of the number of cases where there was no appreciable contamination before the first shower. In only 18·4 per cent. of cases was further treatment necessary.

The effectiveness of the various treatments is summarised below:—

Treatment	*Percentage*
No significant contamination after first shower ...	81·6
Contamination removed by re-wash only	5·5
Contamination removed with titanium dioxide and Teepol* followed by re-wash	8·3
Further treatment with potassium permanganate and re-wash	3·7
Release, after preceding treatments, with slight residual contamination	0·9

* Later precipitated chalk and Teepol.

Personnel who were released with slight contamination lost much of it within two days.

The heaviest contamination was found on members of a party which was engaged in a variety of activities in the worst contaminated area of Trimouille. They registered a gamma activity of between 3 and 6 milli-roentgens per hour. The total dose rate in the area in which they worked was between 5 and 10 roentgens per hour and the total gamma dose received by each person was about 3r. Even in these cases the first shower-bath removed the bulk of the activity.

15.3.2. *Location of Body Contamination*

The following summary shows the number of instances in which contamination was found on the various parts of the body after the first shower:—

Neck	*Face*	*Hair*	*Knees and Legs*	*Hands*	*Shoulders*	*Arms*	*Chest*	*Feet*
91	67	67	54	27	10	7	3	1

The location of the contamination varied with time. For example, about seven days after the burst, entry into areas of heavy contamination was possible and an increased number of contaminated knees and legs was caused by pushing through knee-deep vegetation. Later the boats became contaminated and this was spread to the knees and legs by sitting on the decks.

15.4. *Decontamination of Equipment*

15.4.1. *General Procedure*

The procedure adopted fell into three main classes

(i) depending on complexing action involving the use of citric and other acids to form soluble complexes with certain of the fission products which are less easily absorbed on surfaces;

(ii) normal cleansing action with wetting agents such as Teepol and degreasing agents such as trichlorethylene, Butex and Irgalon, which may also have valuable complexing actions;

(iii) absorption with fine powders such as titanium oxide or precipitated chalk which present large effective surface areas.

15.4.2. *Decontamination of Instruments*

Loose dry contamination was first removed by cleaning by means of a dry rag or by vacuum cleaning. It was found to be important not to wet the surfaces before this was complete, for it the surface were wetted the fission products tended to be carried in solution on to the surface and to be strongly absorbed. When time allowed, dry cleaning was followed by storage to allow further decay of radioactivity.

If wet treatment was necessary, the procedure consisted in first rinsing with fresh water, and following it, if necessary, with a mixture of 5 per cent. citric acid and 1 per cent. Teepol in equal parts. Precipitated chalk was also used.

It was found to be important that electronic equipment for use in the field should be completely watertight so that it can be washed down. Rubber seals should be designed so that the minimum crevice is left into which contamination can lodge and so that joints can easily be remade after servicing. All surfaces should be as smooth as possible and recesses, screw holes, slots and knurled knobs avoided. Even then everything should be done to prevent contamination of monitoring instruments and the use of expendable covers or bags, is strongly recommended.

Experience with a ciné camera illustrates the difficulty of removing contamination due to direct fluid fall-out. This camera was not recovered until the fifth day and even though the surfaces appeared clean there was heavy contamination which was only reduced by about 20 per cent. after practically all the various treatments had been tried at a prohibitive cost in time. It was finally cleaned in the United Kingdom by complete removal of the black instrument finish.

It was also found to be practically impossible to decontaminate the fabric instrument carrying cases and haversacks by any simple process such as scrubbing. It is clear that expendable cases made of plastic or plastic-impregnated material with smooth surfaces are required for this purpose.

15.4.3. *Decontamination of Boats*

By the end of the operation the outer surfaces of the boat hulls were not seriously contaminated as the contaminated water had dispersed and the hulls had been cleansed by much passing through clean water. Cordage, canvas and bare wood fittings which retained radioactive products were finally jettisoned. Contamination of decks was never high, and at the end of the operation was removed by scrubbing and hosing after which the boats were hoisted at the davits and left for the radioactivity to decay.

15.5. *Contamination of Ships*

Some build-up of contamination occurred in certain parts of the engine room of the Health Ship due to the circulation of contaminated sea water. In the circulator and the weed trap the dose-rate rose to a higher level than that in the water outside and reached a value as high as 6 mr/hr. It was concluded that contamination of the engine room will be the limiting factor in assessing the level of water contamination into which a ship may be permitted to sail. At Monte Bello the contamination level was never serious and would not have restricted operations.

15.6. *Special Decontamination Trials*

15.6.1. *Trial of Decontamination under Service Conditions*

The steel deckhouse, referred to in section 12.6 under blast effects, received a heavy dose of contamination which gave a dose-rate of 6 r/hr after 19 days.

As part of the Naval ABC trials, decontamination was done by two naval parties, each of which, using a portable pump, hosed down for fifteen minutes with sea-water, three minutes for each bulkhead and three for the roof.

Two removable steel plates were fitted to the deckhouse. One was removed before decontamination and one after and both were sent to the health ship for measurements of the beta and gamma activity. These measurements indicated that the effect of the hosing down was to reduce the gamma activity by 60 per cent. and the beta activity by 70 per cent.

15.6.2. *Reduction of Contamination by the Water Spray Method*

In another Naval ABC trial, an attempt was made to protect surfaces painted with naval light grey weatherwork paint from contamination by spraying with water during exposure to fall-out. The operation commenced shortly before the explosion and continued throughout the fall-out period. One set of samples was sprayed with sea-water and one with a mixture of sea-water and 0·1 per cent. of citric acid. A third set was unsprayed and was used as a control. All samples were inclined at an angle of 30° to the horizontal to minimise the effect of blast and heat.

One set of samples was in a region of heavy fall-out, the dose-rate after 18 days being 5 r/hr. This corresponds to about 10,000 r/hr at 1 hour after burst, a dose-rate which is comparable with that at the centre of a base surge.

Measurements of beta plus gamma activities showed that the activity of samples sprayed with plain sea-water was only 11 per cent. of that of unsprayed samples whilst the use of sea-water and 0·1 per cent. of citric acid reduced the activity to only 4 per cent. of that of unsprayed samples.

15.6.3. A further Naval ABC trial was performed to determine the merits of various surface finishes and materials in regard to ease of decontamination. Small squares (3 inch) of a variety of paints, lacquers, instrument finishes and miscellaneous materials of Service interest were set out in the fall-out area in horizontal frames. At two sites the samples were lightly contaminated by dry fall-out. This fall-out is the type of contamination to be expected from dust distributed by an atomic explosion or carried by the smoke from fires. It is also the type to be expected when civil defence squads enter contaminated areas. Tests showed that about one half of this could be removed from smooth surfaces by rubbing with a dry cloth but complete cleansing required wet treatments. This work is still proceeding.

At a third site liquid fall-out occurred and samples were mottled with a black deposit of contamination which proved to be the remains of H.M.S. *Plym*. The main problem here is to find to what extent and by what process the finishes and materials contaminated by direct fall-out can best be decontaminated. This work is still proceeding at the Admiralty Research Laboratory.

It may be mentioned that the control samples which were used in the spraying tests at the same site and which were inclined at an angle of 30° were completely free of the black fall-out, indicating its very fluid nature. This emphasises the advantage of effective draining of ships' decks and superstructures.

15.7. *Contamination of Stored Food*

15.7.1. At the request of the Ministry of Food a trial was performed by the Home Office representatives to see the effect of an atomic burst on food stored temporarily on a dockside or in dock buildings severely damaged by previous attack, particularly with a view to estimating what proportion of such food could be recovered and made fit for human consumption. Three dumps of food were set up on Trimouille their contents being given in Table 15.1. It should be remembered that the results obtained must be related to the dose-rate rather than the distance since the position at which a given level of contamination was received at Monte Bello was determined by the particular wind conditions obtaining at the time.

15.7.2. At one site, the activity at one hour after burst was estimated to be 100 r/hr. There was no sign of fluid fall-out at this site. Considerable damage was done by blast and some samples were destroyed by fires which almost certainly were started by pieces of red hot metal from the target vessel rather than by heat flash. The activity in samples inside containers varied from 1/20th to 1/2,000th of that on the outsides of the containers which was of the order of 20 micro-curies per sq. cm.

At a second site, there was no appreciable fall-out in the region of the food dump and no disturbance of the food-stuffs by blast or fire.

At the third site, the estimated activity at one hour after the explosion was about 250 r/hr and there was evidence of heavy liquid fall-out in the form of black cloudy rain which covered the upper surfaces of the various packages with black spots giving the surfaces an overall activity of about 50 micro-curies per sq. cm. None of this discolouration penetrated to the inside surfaces of any of the covers. The activity of samples of the contents of the various packages was between 1/10th and 1/100th of that on the outside. The activity of the samples at this site was about ten times that in the samples at the first site although the ground contamination was only 2·5 times as great. This illustrates the greater penetrating power of liquid fall-out. It is also evident that the penetration through woven materials was about ten times that through paper and plywood. In the worst case (of woven sacks) only one-tenth of the activity deposited by the fall-out found its way into the upper layer of food and this activity was of the same order as that stated in Civil Defence Technical Bulletin TB–11–8 to be the permissible emergency level in water and food (0·9 microcuries per cc.) for consumption over a period of ten days.

15.7.3. It is therefore concluded that under heavy contamination of the type which occurred in this test a very high proportion of food exposed in dumps such as those tested would be fit for human consumption. Special care would be required in the handling and disposal of the covers. These considerations, of course, apply to dry atmospheric conditions. It is possible that, if there were heavy rain at the time, penetration through the covers would be much greater.

15.8. *Radiation Hazard, inside a Compartment, due to External Contamination*

Measurements of the gamma dose-rate inside and outside the ¼-inch steel plate deckhouse used for the decontamination experiments described in section 15.6.1 showed that the dose-rate inside the compartment was 25 per cent. lower than that outside. The readings obtained before and after decontamination of the outside of the deckhouse were the same showing that the contamination on the actual deckhouse made only an insignificant contribution to the level of radiation inside.

15.9. *Radiac Instruments*

Tests under service conditions were made of many types of dose-rate meter and personal dosimeters. A report on appropriate ones has been made to the Radiac Panel.

TABLE 15.1

Contents of Food Dumps

Commodity	Weight	Container
Flour	3 × 140 lb. bags	Finely-woven jute
	3 × 140 lb. bags	Cotton
	3 × 140 lb. bags	Nylon
	2 × 56 lb. bags	5-ply paper, bitumen-lined
Wheat	5 × 180 lb. sacks	Jute
	3 × 180 lb. sacks	Cotton
	2 × 56 lb. bags	Paper, 5-ply, bitumen-lined
	2 × 56 lb. bags	Paper, no lining
Carcase Meat ...	1 Carcase of mutton, total weight 50 lb. ...	Wrapped in cotton
Sugar	1 × 160 lb. sack	Jute
	1 × 160 lb. sack	Cotton
	1 × 56 lb. case containing 28 × 2 lb. cartons	Fibreboard
	28 × 2 lb. cartons	Cardboard, unwrapped
Tea	1 × 120 lb. chest	Plywood—metal foil-lined
	56 × ½ lb. packets	Paper, no outer wrapping
Canned Meat ...	24 × 6 lb. tins (360 lb. gross)	
Fats	1 × 64 lb. cases	Wood—paper-lined
	28 × ½ lb. packs	Paper—exposed
	28 × ½ lb. packs	Paper inner—fibreboard outer
Rice	2 × 114 lb. bags	Jute
	1 × 114 lb. bags	Cotton
Potatoes ...	2 × 1 cwt.	Jute sacks
	2 cwts.	Buried in soil
Cabbage ...	1 cwt. (2 × 56 lb.)	String bags

16. BIOLOGICAL INVESTIGATIONS

16.1. *Introduction*

Previous atomic explosions have provided information about injuries from blast effects, heat and prompt nuclear radiations, but relatively few data are available about the biological hazards of fall-out. The purposes of these investigations, undertaken at the instance of the Medical Research Council, were therefore to observe the Monte Bello explosion from the point of view of all medical effects, in a general way, and to scrutinise those of the fall-out in particular.

The following questions were selected for special study:—

(*a*) Would radio-iodine exist in the *fall-out on the ground* or in a vapour state? The absence of radio-iodine would not only influence ground radiation doses by some 20 per cent. in the first few days, but also the rate of decay of fall-out at this time.

(*b*) Would the iron and debris present during the quenching of the fire ball absorb the fission products and interfere with their availability to plants and animals? This would influence all risks due to radio-active elements lodging in tissues, especially bone, after inhalation or swallowing fall-out.

Investigations were conducted at the trial, and later in laboratories in the United Kingdom. In particular, samples of fission products were collected after the explosion and flown back to the United Kingdom for plant and animal studies.

16.2. *Studies in Relation to Operational Problems*

16.2.1. *Availability and Absorption of Radio-elements by Biological Systems*

Various animals and fish were caught within seven days of the explosion. Radio-iodine was recognised in the thyroid of a severely contaminated rat. The radioactive decay of all other tissues examined, including bones, suggested the absorption of a diversity of radio-elements by biological systems. Radio-iodine also appeared to be available to, and concentrated by, seaweed in the lagoon.

These results indicated that previous assumptions about the constitution of the mixed fission products on the ground are applicable to calculations of the intensity of radiation fields and their decay rates there in the early days after the explosion. The absorption of radio-iodine and other fission products revealed that the presence of iron and debris had not completely eliminated biological hazards due to swallowing or inhaling them and made necessary the quantitative studies of uptake described in Sections II and III below, and more experiments at the trial.

16.2.2. *Contamination and Decontamination of Vegetation*

It was found that the radioactive contamination of leaves was particulate, and, in worst cases, it could be recognised as black spots, visible to the naked eye; this could be of assistance to radiological monitors.

As up to 66 per cent. of the radioactive contamination could be removed by washing vegetation for 10 minutes, some measure of salvage of vegetables might be achieved, and such washing would be worth while in the absence of radiological monitoring, or until this could be completed. There appeared to be very little selection of the radio-elements removed from vegetation by water or detergents. Heavy rain cannot be expected to effect the complete decontamination of the surface of vegetation. A rough estimate suggests that 60–90 per cent. would be removed by heavy precipitation. Radio-elements from the fall-out, blackened with debris, which fell to the North of the Target Vessel, were absorbed by plants and recognised in leaf veins. However, this internal contamination was small by comparison with that adhering to the surface of leaves.

16.2.3. *Inhalation of Fission Products by Human Beings*

Inhalation could be another route of entry for fission products into animals and man. At various times, men entered the radioactive areas without respirators and it was possible to find traces of radioactivity in their urine within a few days. In an experiment designed to utilise a situation which arose fortuitously, it was possible to secure convincing evidence that such radioactivity in urine had been due to the inhalation of fission products, rather than by other possible routes of entry. These, and other, results indicated that respirators were effective barriers against the inhalation of fission products from this atomic weapon.

The amounts of radioactivity found in the urine subjects collected for 30 hours after exposure without respirators ranged up to 25×10^{-3} microcuries. These small amounts had some rough correlation with the radiation dose from the fission products on the ground. These results were in general agreement with previous predictions as between the uptake by inhalation, and the surface radiation intensity. Although only traces of radioactivity were found in men exposed to the fall-out several days after the explosion, it would seem advisable to wear a respirator while the fall-out settled.

It may be of some operational significance to record that, as expected, the urine of a man who inadvertantly bathed in and swallowed mildly contaminated water (2 milli-r/hr at 3 feet) did not contain measurable radioactivity.

16.2.4. *Protective Clothing: Thermal Stress*

Men working in radioactive areas wore dark-coloured protective garments. The first parties to return to the Health Ship on D-day showed many features of thermal stress including intense thirst, marked irritability and tremor. Investigations were initiated. Men wearing the protective clothing in solar radiation with wind speeds of 9–10 knots, shade temperature of 77–86° F. and Relative Humidities of 61, lost up to 16 lbs. The mean 4-hour sweat rates ranged from 2–4 litres on various days. A sweat rate of 4 litres per hour is approximately the general upper limit of tolerance. It is concluded that the thermal stress of protective clothing deserves consideration.

16.2.5. *Decontamination Procedures—Time Involved*

After returning from radioactive areas, all men were monitored, decontaminated by washing and remonitored. The average times taken for the various procedures were measured, as follows:—

(*a*) Being undressed down to underwear and socks ...	61	seconds
(*b*) Preliminary monitoring	169	„
(*c*) Showering	390	„
(*d*) Drying	126	„
(*e*) Second Monitoring	164	„

In the case of personnel still contaminated—

(*f*) Application of decontaminating chemicals	60	„
(*g*) Second shower—usually to neck	235	„
(*h*) Second drying	120	„

Some men needed 5 showers to pass the (very low) tolerance at final monitoring.

These times do not include waiting periods. It must be emphasised that they apply to men insulated by protective clothing. The times would be greater for uninjured persons not in protective clothing escaping after an attack. It is clear that great time losses would accrue in the general confusion whether such persons were left to fend for themselves, or if cleansing were organised. Decontamination would certainly have to be organised for all casualties, with ensuing delays in evacuation, sorting and treating them.

16.3. *Botanical Investigations of Material Collected at Monte Bello*

16.3.1. *Introduction*

The objects of the investigations were:—

(*a*) To make some measure of the degree of contamination of the ground by radio-elements of biological significance.
(*b*) To discover the fraction of the deposited radioactivity which consisted of such radio-elements.
(*c*) To determine the extent to which such radio-elements were available to plants.
(*d*) To discover how various soils might influence this availability.
(*e*) To assess the effect of rain upon the movement of fission products into the soil.

16.3.2. *Materials Used in these Investigations*

The materials which became available for study were:—

(*a*) Esparto grass filters contaminated with airborne fission products.
(*b*) Cotton gauze sheets, 1 yard square, collected from T 2 on D+3.
(*c*) Miscellaneous plant samples collected from Gardenia, Primrose, North East and Trimouille Islands within three weeks of the explosion.

These materials became available in the United Kingdom 9, 13 and 48 days after the explosion. The majority of tests were conducted with aqueous extracts of the filters and the cotton gauze sheets, neither of which were contaminated by the blackened fall-out. However, it should be pointed out that it is highly unlikely that practical agriculture would be considered soon after an attack in areas visibly contaminated. The long-term problems in such an area are under study.

16.3.3. *Degree of Radioactive Contamination of the Ground*

The mean contamination levels by radio-elements of biological significance on the cotton gauze samples examined were, as microcuries per cm.^{2}, ^{140}Barium: 0·89, ^{89}Strontium: 0·007, ^{131}Iodine: 0·99, ^{106}Ruthenium: 0·013. All these values have been extrapolated back to the day of the explosion, at which time they exceed the levels judged to be tolerable for cattle grazing by factors of 10 to 2,000.

16.3.4. *The Fraction of Total Radioactivity on the Ground which Consisted of Radio-elements of Biological Significance*

The solubility of fission products in water and aqueous carrier solution was regarded as a useful index of biological significance. 60 per cent. of the total activity in the cotton gauze samples, and 80 per cent. of that in the esparto grass filters, were soluble in this way.

Analysis of the radio-elements in these solutions several weeks after the explosion revealed that, as calculated back to the day of the explosion, ^{131}Iodine was predominant and ^{140}Barium, ^{89}Strontium and ^{106}Ruthenium were also present: the proportions were approximately 600 : 175 : 15 : 3, respectively. Traces of other Rare Earths were also identified.

16.3.5. *Absorption of Radio-elements by Plants*

The absorption of the radio-elements in an aqueous extract of cotton gauze was studied.

(*a*) *Water Culture.*—Barley and cabbage were grown in the aqueous extracts, alone and with various nutrients and concentrations of calcium ions. In 12 days, Barley took up 20 per cent. of the radio-barium present, 10 per cent. of the radio-strontium, 12 per cent. of the radio-iodine and 8 per cent. of the radio-ruthenium from the aqueous extract alone. Cabbage took up rather less ruthenium and rather more of the other radio-elements studied. After 21 days, the uptake was somewhat increased. Smaller amounts of barium and strontium were absorbed in the presence of calcium ions. It may also be noted that very little of the ruthenium or iodine was transferred from the roots to the shoots.

(*b*) *Soil Culture.*—Wheat was grown in soil from Wytham and Cannock Chase to which aqueous extracts of the contaminated gauzes had been added. After 150 days, the radioactive content of the whole plants was less than 1 per cent. of the total activity added, and probably less than 0·5 per cent. of the original total fission products in the gauze. The radioactivity in the wheat shoot was greater by a factor of 3, in those growing in Cannock Chase soil. This is believed to be related to the lower calcium content of this soil, 0·6 mEq. per cent. as opposed to 17·2 mEq. per cent. in the case of Wytham soil.

Important for future laboratory studies is the finding in parallel experiments that the absorption and behaviour of carrier-free ^{90}Sr was in every way similar to the same element in the mixed fission products.

16.3.6. *The Effect of Rain upon the Movement of Fission Products into Soil*

One hundred days after the explosion, aqueous extract of fission products was added to the surface of soils in 12-inch high cylinders, and the mixture exposed to natural rainfall for a further 80 days.

Eighty-eight per cent. of these soluble fission products were retained in the top 1 inch of the Wytham soil, and 68 per cent. in the top 1 inch of the Cannock Chase soil.

Of the traces of radioactive material leached through the 12 inches of soil, over 90 per cent. was as ^{106}Ruthenium, which therefore may be regarded as the radio-element most likely to migrate from contaminated areas into the water table and so drain away.

16.3.7. *Summary of Botanical Investigation*

The results show that after the Monte Bello explosion, contamination of the ground occurred which was at dangerous levels for agriculture in places where the fall-out was not visible to the naked eye.

The presence on the ground of radio-iodine, and other radio-elements of biological importance, was confirmed, as was their availability to plants. However, apart from the risks of animals and human beings eating vegetation contaminated directly on the surface, a variety of factors in Nature tended to diminish the risks to be expected from eating fresh crops of vegetation growing in the fall-out area after the Monte Bello explosion.

Sixty per cent. of the fission products which lay invisible on the ground in the highly contaminated region of Trimouille were soluble, and may be considered

as of biological significance. Although plants growing in water culture might take up as much as 50 per cent. of these soluble fission products in 21 days, in the more practical experiments, wheat shoots grown for 150 days in soil to which soluble fission products had been added contained less than 1 per cent. of the radioactivity applied (*i.e.*, about 0·5 per cent. of the total fission products). This low fraction of fission products absorbed may be related to the fact that almost all the fission products were trapped in the top inch of soil, even after exposure to rain for 80 days. Thus the percentage uptake might be higher with shallow-rooted plants such as grass.

The retention of fission products in the upper layers of soil precludes their rapid removal from contaminated areas by rain. Less than 5 per cent. of the fission products were leached through 12 inches of soil between D+120 and D+200. Ruthenium constituted most of this leached fraction. Fortunately Ruthenium was not absorbed readily by plants; less than 1 per cent. of ^{106}Ruthenium in water cultures found its way into the shoots of barley and cabbage plants growing therein for 12 days.

These results agree with the findings at the trial that internal contamination in plants is much less than direct surface contamination. Under the conditions of these experiments the expected uptake of fission products by new crops growing in contaminated soil would be no higher than 1 per cent., and new crops growing in areas draining contaminated zones, probably less than 0·05 per cent. More investigations are needed before these data can be used to determine accurate safety levels. In particular, it is necessary to establish the percentage of radioactivity in plants which can be absorbed by animals and man as a result of ingesting crops containing such radio-elements as the latter will select from the soil.

These investigations are being pursued.

16.4. *Zoological Investigations with Material Collected at Monte Bello*

16.4.1. *Introduction*

The purpose of these investigations was to confirm and extend, both qualitatively and quantitatively, those made on animals at the trial. Particular attention was paid to the proportion and chemical identification of fission products taken up by various tissues.

16.4.2. *Materials and Methods*

The samples investigated were:—

(*a*) Airborne fission products collected on esparto grass filters. These and aqueous extracts thereof were fed to 4 rabbits 200–859 hours after the explosion.

(*b*) Aqueous extracts of "invisible" fall-out from T 2 on Trimouille as prepared for the botanical experiments, containing 15–20 per cent. of the total radioactivity present in the fall-out. This was fed by pipette to 11 guinea-pigs 200–400 hours after the event.

(*c*) Blackened earth and sedge-like herbage collected inland from Main Beach on Trimouille. These, and aqueous extracts thereof, were fed to guinea-pigs and 6 rabbits 1,300–2,500 hours after the event.

The animals were sacrificed at various times after being fed, dissected, and digests prepared of excreta, intestines, muscles, liver, kidneys, thyroid, and bones. These digests were investigated in an M.6.H. liquid counter.

16.4.3. *Results of Examining Tissue Digests for Radioactivity*

(*a*) *General.*—Computations comparing the total radioactivity given to that detected in the excreta and tissues showed that recovery was within the limits of the errors in methods of feeding. A large proportion (usually more than 50 per cent.) of the radioactivity given appeared in the fæces and bowel contents and a small percentage was detected in the urine. The findings in all tissues except the thyroid and bones were of more interest than practical significance: after early sacrifice the livers, kidneys and muscles contained small percentages of relatively rapidly decaying fission products.

More detailed investigations were directed towards the findings in the thyroid gland, the skeleton, the former because of its value in providing information about radioactive iodine, the latter because of the clinical importance of injury to the blood-forming cells from bone-seeking fission products.

(*b*) *Thyroids.*—Up to 2·4 per cent. of the radioactivity in the samples fed within 2 weeks of the explosion could be traced in the thyroid gland.

On D+10 the thyroid from an animal fed with airborne fission products showed a decay compatible with a mixture of ^{132}I and ^{131}I. The decay of other thyroid glands was always with an 8 day half life. presumably due to ^{131}I.

15–20 per cent. of the radio-iodine in the aqueous extracts of invisible fall-out from T 2 fed to animals could be found in their thyroids after 24 hours.

It was therefore concluded that radio-iodine was present not only in the airborne cloud, but also in the *invisible* fall-out, and that it was water soluble and available for absorption by guinea-pigs and rabbits; it did not prove feasible to investigate the presence and availability of radio-iodine in the *black* fall-out.

(*c*) *Bones.*—The outstanding feature of these studies was the variation in the percentage of radio-activity deposited in the bones after feeding different samples of fission products. The average percentages were:—

Airborne Fission Products	8 per cent.
Aqueous Extracts of Invisible Fall-out	14 per cent., *i.e.*, some 3 per cent. of the total activity on the ground.
Blackened Fall-out ...	0·2 per cent.

The counts of all skeletal digests showed an early rise, which could be attributed to ^{140}Lanthanum being formed from ^{140}Barium. The subsequent decay could have been explained by various mixtures of ^{140}Ba and ^{89}Sr, but chemical analysis revealed the presence of various Rare Earths as well: Cerium, Yttrium and Praseodymium have been identified.

More detailed studies showed that, after feeding airborne fission products and aqueous extract of invisible fall-out, the proportion of Barium and Strontium in bones was roughly the same as in the material given. In contrast, after feeding material contaminated with blackened fall-out—where the percentage deposition in bone was so small (0·2 per cent.)—the absorption of Barium and Strontium was even more severely curtailed than that of Rare Earths.

16.4.4. *Supplementary Experiments*

The low absorption after feeding blackened fall-out and the very small percentage deposition in skeletons are obviously of interest not only in respect of a possible atomic attack, but also in the event of accidental exposures to mixed fission products in atomic energy programmes.

Some possible factors responsible for the diminished deposition in bones are as follows:—

(*a*) The presence of Magnesium Sulphate in the Monte Bello sand.
(*b*) The presence of Calcium ions in the Monte Bello sand; both these facts were known from previous soil analysis.
(*c*) The presence of iron from the target vessel.

Because low absorption was found using black fall-out but absent using extracts of the invisible fall-out which was mixed with Monte Bello sand at T 2, interest was naturally aroused in the possible rôle of iron in interfering with the absorption of Barium and Strontium as well as Rare Earths.

In an experiment with guinea-pigs fed radio-Barium/Lanthanum solution with minimal carrier, it was shown that 5 mg. spectroscope-pure Iron oxide half an hour before feeding would reduce deposition in the skeleton by a factor of 3. When the same treatment was also continued twice a day for 3 days after feeding, the deposition in the skeleton was reduced by a factor of 10.

These studies continue.

T 1/53

AWRE – T1/53

[redacted]

22/10/84 . SCD 4668 refers

COPY No. 15
14 PAGES

NATIONAL ARCHIVES
ES5/1

MINISTRY OF SUPPLY

ATOMIC WEAPONS RESEARCH ESTABLISHMENT

REPORT No. T 1/53
(HURRICANE)

B. 0134

DECLASSIFIED FOR PR
BY AWE ALDERMASTON

TOP SECRET
THIS DOCUMENT IS THE PROPERTY OF H.B.M. GOVERNMENT, and is intended only for the personal information of
Report Copy
and of those officers under him whose duties it affects. He is personally responsible for its safe custody and that its contents are disclosed to these officers and to them only.
The document will be kept in a locked safe when not in actual use.

A.W.R.E.
Aldermaston Berks.

[redacted]

May, 1953

3.2 Blast Damage

3.2.1 Anderson Shelters

Standard Anderson Shelters, with sandbag covering and blast wall construction were located at 460, 510, 600, 920 and 1,130 yards from ground zero. Mean blast pressures, in pounds/sq. inch, recorded inside the shelters are shown in the following table.

Distance (yds.)	Presentation		
	Front	Side	Rear
460	NR	NR	NR
510	38	27	40
600	28	21	28
920	16	7	14
1130	8.5	4	5.5

Front presentation implies blast wall facing towards event.
Rear " " " " " away from event.
Side " " shelter side on to event.

Shelters at 460, 510 and 600 yards suffered damage including demolition of blast walls, removal of sandbag covering and some displacement of the corrugated iron.

At 920 and 1,130 yards the shelters suffered relatively little damage.

Civil defence authorities consider that there might have been some 50% survival from blast damage of personnel in shelters at 460 yards and some 90 per cent at 600 yards, fatal casualties being mainly due to secondary blast effects (e.g. debris) and not to direct effects on the person of the blast pressure itself. The front presentation appears the most hazardous, due to the collapse of the blast wall into the shelter. At such distances, however, the survival from the effects of gamma flash would have been virtually nil. (MORE EARTH COVER IS NEEDED FOR RADIATION.)

At 920 and 1,130 yards there would have been no casualties from blast, and incidentally, little risk from the effect of gamma flash.

3.2.2 Concrete Cubicles

Reinforced concrete cubicles, 12 feet cube were exposed to the blast. There were three types of cubicle, varying in wall thickness and the mesh of reinforcement. The following table gives some details:-

Thickness of Wall and Roof	Mesh of Reinforcement		Dia. of Rods (mild steel)
	Walls	Roof	
$6\frac{3}{4}$"	9"	$7\frac{1}{2}$"	$\frac{5}{8}$"
$9\frac{3}{4}$"	$6\frac{1}{2}$"	$4\frac{1}{2}$"	$\frac{3}{8}$"
12"	9"	$5\frac{1}{2}$"	$\frac{3}{8}$"

The concrete was a mixture of 1 cement, 1.4 sand and 2.8 of $1\frac{1}{4}$ inches aggregate (parts by volume). The aggregate was of local rock and rather soft and weak. The water/cement ratio was 0.5. This produced a crushing strength of 6 inches cubes of over 2,000 p.s.i. in 7 days.

The cubicles faced the event squarely. In the rear wall was a tapered opening about 2 feet high × 1 foot 6 inches broad into which a pile of four tapered blocks fitted to close this entrance prior to the explosion.

A $9\frac{3}{4}$ inch wall thickness cubicle was 600 yards from the explosion. Its front wall failed and was pushed inside the cubicle. The side walls were fractured and had a slight outward bowing (about 1 inch). The rear wall had minor hair cracks. The roof showed cracks along the line of the inside of the side walls and had failed completely along the line of the front wall.

At 990 yards, $6\frac{3}{4}$ inch and $9\frac{3}{4}$ inch walled cubicles showed fine hair cracks. There was no damage to the 12 inch walled cubicle at this distance, nor to one with a $9\frac{3}{4}$ inch wall at 1,320 yards.

In all cases the tapered blocks closing the rear entrance had been thrown outwards.

4. Water Shock

The underwater shock was relatively feeble, and significant recordings were obtained at two points only. The results were:-

Depth of gauges - 22 feet.

Distance from weapon (feet)	Pressure p.s.i.
960	270
1185	20
1380	~0

Compare to air blast peak overpressures.

6. Fires

Some outbreaks of fire took place amongst the parched grass-like vegetation on Trimouille. It appeared that these were not due to radiant heat from the weapon, but arose from ignition by hot fragments of H.M.S. Plym. The inference is that the water column formed an effective shield against the direct thermal effects of the radiation.

7. The Gamma Flash

7.1 The Dose - Distance Relationship

The decay of short lived fission products from the weapon gives rise to an intense pulse of gamma radiation. A large proportion of the dose from this is received in a few seconds. Figure 4 shows the total dose (recorded by films) as a function of distance from the weapon.

7.2 Gamma Energies

In applying these results to shielding problems (using for example the methods given by Liston and Cave, HER Report H13/51) it would be desirable to know what assumed energy of photon would give the right answer. Naturally, the actual gamma ray flux consists of a continuous spectrum of a quite unpredictable nature.

The spectrum will of course vary with the distance from the weapon, largely due to Compton scatter. No data are available from the trial which can lead to an estimation of these spectra. The trend of the dose distance curve is similar to that which would be calculated on the assumption that the original photons were all of about 3 Mev energy; one must be careful not to draw any further conclusions from this statement.

Concrete cubicles of wall thickness $6\frac{3}{4}$ inches, $9\frac{3}{4}$ inches and 12 inches at 900 yards appeared, from somewhat incomplete data, to give the same reduction of dose inside as they would from a parallel gamma beam of about 1 Mev photons. At 1,320 yards a cubicle with a $9\frac{3}{4}$ inch wall appeared to reduce the dose by an amount equivalent to the reduction expected from a parallel $1\frac{1}{2}$ Mev beam. This latter result implies an energy higher than $1\frac{1}{2}$ Mev at 900 yards, and does not appear to be consistent with a value of 1 Mev at 900 yards. The difference between the results might be within the errors inherent in experiment and calculation.

UNITED STATES
ATOMIC ENERGY COMMISSION
Washington 25, D. C.

FOR RELEASE AT 4:00 P.M. (E.S.T.)
TUESDAY, FEBRUARY 15, 1955

A REPORT

BY THE UNITED STATES ATOMIC ENERGY COMMISSION

ON THE EFFECTS OF HIGH-YIELD NUCLEAR EXPLOSIONS

1. Considerable information on the effects of the explosions of atomic weapons has been made public by the Government since the first nuclear detonations in 1945. The handbook, "The Effects of Atomic Weapons", published in 1950, is being revised and brought up to date to include the effects of thermonuclear weapons, as a result of the most recent tests at the Pacific Proving Grounds. References to the effects of thermonuclear explosions have been made in several official statements, beginning with Chairman Strauss' description of the phenomenon of "fallout" at a White House news conference on March 31, 1954. The following statement is designed to condense and correlate information, some of which already has been made public and other portions of which have been of a classified nature until now.

2. The effects of nuclear tests are evaluated for civil defense planning as well as for military and technological purposes. So long as nuclear weapons are in possession of any unfriendly power, the Commission believes the American public will wish to be as fully informed as possible as to the nature and extent of the dangers of nuclear attack and of the protective measures that can be taken by individuals and communities to avoid or minimize those dangers if we should be attacked.

BLAST AND HEAT EFFECTS

7. The effects of blast and heat from a nuclear explosion are relatively localized. One A-bomb of the earliest type equivalent to 20,000 tons of TNT (20 kilotons) would produce blast sufficient to destroy or damage severely residences within a radius of more than one mile from the point of burst. Within a radius of about a mile and a half, residences would be so damaged as to be unusable without repairs. A principal hazard to human beings would come from flying and falling debris and from fires due to such causes as broken gas and electric lines or overturned stoves. The area in which injuries to human beings would be caused by blast, therefore, would be about the same as the area of damage to structures.

8. The United States, as announced previously, has developed fission bombs many times as powerful as the first A-bombs, and hydrogen weapons in the ranges of millions of tons (megatons) of TNT equivalent. For these larger weapons, the blast effects can be calculated approximately by means of a scaling law, namely, the distance at which a given blast intensity is produced varies as the cube roots of the yields of the explosions.

9. Similarly, the heat and burn effects of nuclear explosions can be estimated from accumulated data. These effects, of course, are influenced by prevailing atmospheric conditions. The time element also is a prime factor. Very large weapons deliver heat over an appreciably greater period of time than smaller weapons. A given quantity of heat from a high-yield weapon, delivered over a longer period of time, will produce somewhat less severe burns than the same quantity of heat from a nominal detonation.

PROTECTION AGAINST BLAST AND HEAT

10. The hazard from both burn and blast effects in the outer affected areas would be reduced greatly by shelter. Clothing or almost any kind of shelter would reduce the danger of direct burns, although there might be some danger of clothing and structures becoming ignited. Also, shelter would materially reduce the hazard of blast injury by affording protection against flying or falling debris.

FALLOUT PATTERN OF 1954 TEST IN THE PACIFIC

16. The very large thermonuclear device fired at the Bikini Atoll on March 1, 1954, was exploded on a coral island. Coral consists of calcium carbonate, thus the detonation's radioactivity was spread by particles consisting largely of unslaked lime which, during the hours of descent, was slaked by moisture in the atmosphere. These particles ranged between 1/1000th and 1/50th of an inch in diameter and were, on the average, somewhat adhesive. The prevailing winds were westerly so the bomb cloud moved generally to the east and deposited the radioactive particles in varying amounts over an elliptical or cigar-shaped area. About 160 (statute) miles down-wind from the point of burst the early fallout was observed in the form of fine particles which looked like snow. Fallout began there about eight hours after the detonation and continued for several hours.

17. The roentgen is the commonly accepted unit of measurement of radiation dosage. A dose of about 25 roentgens of radioactivity received by a person over a brief space of time will produce temporary changes in the blood. A dose of some 100 roentgens received in a short interval may produce nausea and other symptoms of radiation sickness. About 450 roentgens delivered over a day or so might be fatal to approximately half of the persons so exposed. However, because of the body's repair processes, a total radiation dose which would be serious if incurred in a few minutes would produce much less effect if spread over a period of years. These statements may be helpful in understanding the data which follow.

18. The test explosion, at ground surface, contaminated a cigar-shaped area extending approximately 220 statute miles down-wind and varying in width up to 40 miles. In addition, there was a contaminated area up-wind and cross-wind extending possibly 20 miles from the point of detonation. Data was collected from 25 points on 5 atolls located from 10 to 330 miles down-wind (generally east) from Bikini Atoll. Due to an unexpected shift in the direction of the prevailing winds in the higher altitudes, the fallout missed the observation rafts that had been placed farther north previous to the test firing. The estimated contour of the pattern of fallout is, therefore, based only in part on data obtained from actual measurements and partly on extrapolation, i.e., calculations based on known data, including factual information obtained during previous tests of smaller devices.

19. Data from this test permits estimates of casualties which would have been suffered within this contaminated area if it had been populated. These estimates assume: (1) that the people in the area would ignore even the most elementary precautions; (2) that they would not take shelter but would remain out of doors completely exposed for about 36 hours; and (3) that in consequence they would receive the maximum exposure. Therefore, it will be recognized that the estimates which follow are what might be termed extreme estimates since they assume the worst possible conditions.

20. On the basis of our data from this and other tests, it is estimated that, following the test explosion on March 1, 1954 there was sufficient radioactivity in a down-wind belt about 140 miles in length and of varying width up to 20 miles to have seriously threatened the lives of nearly all persons in the area who did not take protective measures. During the actual tests, of course, there were no people in this zone. Inside Bikini Atoll at a point 10 miles down-wind from the explosion it is estimated that the radiation dosage was about 5000 roentgens for the first 36 hour period after the fallout. The highest radiation measurement outside of Bikini Atoll indicated a dosage of 2300 roentgens for the same period. This was in the northwestern part of the Rongelap Atoll, about 100 miles from the point of detonation. Additional measurements in Rongelap Atoll indicated dosages, for the first 36 hour period, of 2000 roentgens at 110 miles, 1000 roentgens at 125 miles, and, farther south, only 150 roentgens at 115 miles from Bikini.

21. Some distance farther from the point of detonation, at about 160 miles down-wind and along the axis of the ellipse, the amount of radioactivity would have seriously threatened the lives of about one-half of the persons in the area who failed to take protective measures. It is estimated that the radiation dosage at that point was about 500 roentgens for the first 36 hour period.

22. Near the outer edge of the cigar-shaped area, or approximately 190 miles down-wind, it is estimated that the level of radioactivity would have been sufficient to have seriously threatened the lives of 5 to 10 percent of any persons who might have remained exposed out of doors for the first 36 hours. In this area the radiation dosage is estimated at about 300 roentgens for the first 36 hour period.

23. Thus, about 7,000 square miles of territory down-wind from the point of burst was so contaminated that survival might have depended upon prompt evacuation of the area or upon taking shelter and other protective measures.

24. At a distance of 220 miles or more down-wind, it is unlikely that any deaths would have occurred from radioactivity even if persons there had remained exposed up to 48 hours and had taken no safety measures.

25. The estimates cited above do not apply uniformly throughout the contaminated area inasmuch as the intensity of radioactivity within a region of heavy fallout will vary from point to point due to such factors as air currents, rain, snow, and other atmospheric conditions. Because of this and because most persons, if given sufficient warning, probably would evacuate the area or take shelter and other precautionary measures, the actual percentage of deaths could reasonably be presumed to be considerably smaller than these extreme estimates.

PROTECTION AGAINST FALLOUT

26. In an area of heavy fallout the greatest radiological hazard is that of exposure to external radiation. Simple precautionary measures can greatly reduce the hazard to life. Exposure can be reduced by taking shelter and by utilizing simple decontamination measures until such times as persons can leave the area. Test data indicate that the radiation level, i.e., the rate of exposure, indoors on the first floor of an ordinary frame house in a fallout area would be about one-half the level out of doors. Even greater protection would be afforded by a brick or stone house. Taking shelter in the basement of an average residence would reduce the radiation level to about one-tenth that experienced out of doors. Shelter in an old-fashioned cyclone cellar, with a covering of earth three feet thick, would reduce the radiation level to about 1/5000, or down to a level completely safe, in even the most heavily contaminated area. Designs of shelters of simple yet effective construction have been prepared by the Civil Defense Administration and are available to the public.

27. Radioactive material deposited during fallout may or may not be visible but would be revealed by radiation

detection instruments such as Geiger counters. Any falling dust or ash that can be seen down-wind within a few hours after a nuclear explosion should be regarded as radioactive until measured by a radiation detection instrument and found to be harmless.

28. Care should be taken to avoid the use of solid foods or liquids that may contain fallout particles.

29. If fallout particles come into contact with the skin, hair or clothing, prompt decontamination precautions such as have been outlined by the Federal Civil Defense Administration will greatly reduce the danger. These include such simple measures as thorough bathing of exposed parts of the body and a change of clothing.

30. If persons in a heavy fallout area heeded warning or notification of an attack and evacuated the area or availed themselves of adequate protective measures, the percentage of fatalities would be greatly reduced even in the zone of heaviest fallout.

FALLOUT FROM NEVADA TESTS

31. Only relatively small nuclear test explosions are conducted at the Nevada Test Site, in contrast to the tests of high-yield thermonuclear devices at the Pacific Proving Grounds. In Nevada, as well as in the Pacific, all tests are planned for times when forecast weather conditions minimize the possibility of fallout hazard. Methods of forecasting weather patterns in these areas are improving steadily. High air bursts at the Nevada Test Site have produced no significant fallout; heavy fallout from near-surface explosions has extended only a few miles from the point of burst. The hazard has been successfully confined to the controlled area of the Test Site. The highest actual dose of radiation at an off-site community has been estimated to be less than one-third of the greatest amount of radiation which atomic energy workers are permitted to receive each year under the Atomic Energy Commission's conservative safety standards.

INTERNAL RADIATION EFFECTS

32. Several basic facts should be kept in mind in evaluating the hazard from fallout radiation. First, radiation

is not a new phenomenon created by the explosions of fission and thermonuclear weapons. Since the beginning of life, living things have been exposed constantly to radiation from natural sources. Cosmic rays from space constantly pass through our bodies. We are exposed to "background" radiation from radium and radon in the soil, water and air. Our bodies have always contained naturally radioactive potassium and carbon.

33. As pointed out earlier, detonations of all atomic weapons produce radioactivity, a portion of which is carried to high altitudes and over great distances in the form of fine particles. The percentage of this radioactivity which travels beyond the relatively near area of the explosion depends largely on the conditions under which the bomb is fired, the percentage being higher for in-the-air bursts where the fireball does not touch the earth's surface. The most widespread radioactivity is produced only by the longer-lived fission products, since the radioactivity of the shorter-lived products decays and disappears before the particles come down to earth in a matter of days, weeks, months, and even years. The longer-lived radioactive products may be distributed over the entire earth. However, as the particles are carried farther and farther to remote areas, the possibility of significant amounts of fallout decreases.

RADIOSTRONTIUM FALLOUT

34. One of the most biologically important radioactive substances found in fallout is strontium-90. It has a long lifetime--nearly 30 years on the average. Radiostrontium has a chemical similarity to calcium and, therefore, when taken into the body it has a tendency to collect in the bones. Radiostrontium can enter the body in two ways -- by inhaling or by swallowing. Normally, the amount inhaled would be small compared with the amount one might swallow. Fallout material deposited directly on edible parts of plants may be eaten along with the plants, but washing the plants before they are eaten would remove most of this radioactive material. However, rainfall carrying the radiostrontium down to earth may deposit it in the soil where it can be taken up, in part, by plants and incorporated into plant tissues, later to be eaten by humans or by grazing animals which, in turn, provide food for humans.

35. Since the start of nuclear tests, careful measurements have been made of the distribution of radiostrontium over the earth's surface, in the soils, in plants and animal tissues, in the oceans, in rain, in the atmosphere and in all forms in which it might be expected to occur. The results of this study are reassuring. The amount of radiostrontium now present in the soil as a result of all nuclear explosions to date would have to be increased many thousand times before any effect on humans would be noticeable.

RADIOIODINE FALLOUT

36. Among the shorter-lived fission products involved in the study of internal radiation, the most biologically important is radioiodine-131 with an average life of only 11.5 days. Even though this product may be widely spread after a nuclear explosion, the possibility of serious hazard is limited by its relatively short life. Like the non-radioactive form of the element, it concentrates in the thyroid gland and, in excessive quantity, conceivably could damage the thyroid cells.

37. Scientists of the Atomic Energy Commission have estimated that the average exposure of people in the United States from radioiodine in the fallout from the entire series of tests in the spring of 1954 was only a few percent of the annual dose that can be received year after year and still have no noticeable effects.

38. These two isotopes -- radiostrontium and radioiodine -- constitute the principal internal hazards from the radioactivities produced by the detonations of atomic weapons, both fission and thermonuclear. The Atomic Energy Commission has been engaged for three years in a broad study of the radioactive forms of these isotopes and conducts year-round monitoring of these radioactivities in many locations. Any accumulation of these materials can be detected with great sensitivity so that ample warning of potential hazard could be given long before any actual danger occurred from test detonations. The amounts of radiostrontium and radioiodine which have fallen outside the areas near the test sites as a result of all atomic tests up to nov are insignificant compared to concentrations that would be considered hazardous to health.

GENETIC EFFECTS OF RADIATION

39. One other effect of radiation must be considered in evaluating the long-range possibilities of hazard from nuclear detonations. This is the possible genetic effect upon the germ cells which transmit inherited characteristics from one generation to another. At our present stage of genetic knowledge, there is a rather wide range of admissible opinion on this subject.

40. In general, the total amount of radiation received by residents of the United States from all nuclear detonations to date, including the Russian and British tests and all of our own tests in the United States and the Pacific, has been about one-tenth of one roentgen. This is only about 1/100th of the average radiation exposure inevitably received from natural causes by a person during his or her reproductive lifetime. It is about the same as the exposure received from one chest x-ray.

41. The medical and biological advisers of the Atomic Energy Commission believe that the small amount of additional exposure of the general population of the United States from our nuclear weapons testing program will not seriously affect the genetic constitution of human beings. Nevertheless, we are continuing our thorough study of the entire question and will continue to report our findings to the American people.

SUMMARY

42. The Atomic Energy Commission hopes that the information on nuclear weapons effects contained in the foregoing report will never be reflected in human experience as the result of war. However, until the possibility of an atomic attack is eliminated by a workable international plan for general disarmament, the study and evaluation of weapons effects and civil defense protection measures must be a necessary duty of our government.

43. Inevitably, a certain element of risk is involved in the testing of nuclear weapons, just as there is some risk in manufacturing conventional explosives or in transporting inflammable substances such as oil or gasoline on our streets and highways. The degree of risk must be balanced against the great importance of the test programs to the security of

the nation and of the free world. However, the degree of hazard can be evaluated with considerable accuracy and test conditions can be controlled to hold it to a minimum. None of the extensive data collected from all tests shows that residual radioactivity is being concentrated in dangerous amounts anywhere in the world outside the testing areas.

44. In the event of war involving the use of atomic weapons, the fallout from large nuclear bombs exploded on or near the surface would create serious hazards to civilian populations in large areas outside the target zones. However, as mentioned in the foregoing Report, there are many simple and highly effective precautionary measures which must be taken by individuals to reduce casualties to a minimum outside the immediate area of complete or near-complete destruction by blast and heat. Many of these protective measures, such as shelter and decontamination procedures, have been detailed by the Federal Civil Defense Administration.

cue

FOR SURVIVAL

OPERATION CUE

A. E. C. NEVADA TEST SITE

MAY 3, 1955

A REPORT BY THE

FEDERAL CIVIL DEFENSE

ADMINISTRATION

EFFECTS OF NUCLEAR WEAPONS

BY HAROLD L. GOODWIN,
Director, Atomic Test Operations, FCDA

A great deal of information has been released over the past several years on the effects of atomic explosions, yet many of these effects are still poorly understood by the general public. For that reason, the principal effects of a nuclear explosion are reviewed, with a brief discussion of factors of particular importance to civil defense.

This entire section is based on informaton available in published sources. There is a widespread but erroneous view that most information on the effects of nuclear explosions is classified, and hence is not available to the general public. Information that exists only in classified form generally is information which deals with refinements of weapons effects. A considerable amount of gross information on any major effect is available in a number of publications.

The best reference in this field is still the basic handbook, *The Effects of Atomic Weapons.* Despite the fact that this useful work was first published in 1950, queries daily to the Federal Civil Defense Administration indicate that it has not been widely studied or understood. A thoughtful reading will be of value to any person with civil defense responsibility. A revision, now in process, may be issued in the next few months.

The time of travel of the shock wave is not generally understood by many persons. The concept of "duck and cover," which would still be of great value in case of attack without warning, is based on the comparatively large time interval between the burst and arrival of the shock wave at a given point.

It takes several seconds for the shock wave of a nominal bomb to reach a point 2 miles from the burst. A person who moved promptly at the first light of the detonation would have time to get under or behind a convenient piece of furniture, or other protection. At greater distances there would be even more time.

This time lapse between the detonation and arrival of the shock wave was graphically demonstrated to persons watching from the observer areas in the Test Site. The detonation takes place, a phenomenon without sound from the viewpoint of the observer. So much time elapses between the detonation and arrival of the shock wave that observers sometimes forget that the shock wave is on its way and the loud bang of its arrival finds them unprepared. Persons are frequently startled and have even been pushed off balance by the shock wave. The pause between a lightning flash and the thunder is comparable.

The question may be asked, how will one know when a burst has gone off if the sound does not arrive for some time? The answer is that the light from the explosion is its own warning.

BIOMEDICAL EFFECTS OF THERMAL RADIATION

BY DR. HERMAN ELWYN PEARSE, *Professor of Surgery at the University of Rochester. Consultant to several Government departments, notably the Atomic Energy Commission's Division of Biology and Medicine. Consultant to the Armed Forces Special Weapons Project*

After the Bikini test, I was asked to go to Japan as a consultant for the National Research Council to survey the casualties in Nagasaki and Hiroshima. Being a surgeon, I was greatly impressed with the magnitude of the medical problem from burns and wounds very largely caused by flying missiles. They constituted roughly 85 percent of the casualties in Japan.
140

In Japan it was an August day, the people were lightly clothed, and they were out in the open.
141

Then we observed the healing of the wounds, and we found again that the wounds healed in the same manner as those that we had produced in the laboratory. There was some difference in these lesions from the ordinary burns of civil life, but I would predict, from what I learned from experiments, that the difference is on the good side. The burns look worse; they are often charred, but they may not penetrate as deeply, and the char acts as a dressing, nature's own dressing. The scab solidifies, and the healing process goes on under that scab, after which the scab is sequestrated, and the healed surface is revealed beneath.
142

I didn't care what happened to the fabrics; I wanted to know what happened to the man under the fabric. So we conceived this idea, that the important factor in studying clothing was what happened under the clothing; how it shielded the animal with cloth of different composition, weight, texture, weave, and color. We have made a great many studies both in the laboratory and in the field on this problem of the protective effect of clothing....

For example, if you have 2 layers, an undershirt and a shirt, you will get much less protection than if you have 4 layers; and if you get up to 6 layers, you have such great protection from thermal effects that you will be killed by some other thing. Under 6 layers we only got about 50 percent first degree burns at 107 calories.
143

If we can just increase the protection a little bit, we may prevent thousands and thousands of burns.

... For example, to produce a 50-percent level of second-degree burns on bare skin required 4 calories. When we put 2 layers of cloth in contact, it only took 6 calories. But separate that cloth by 5 millimeters, about a fifth of an inch, and it increases the protective effect 5 times. The energy required to produce the same 50-percent probability of a second-degree burn is raised up to 30 calories. So if you wear loose clothing, you are better off than if your wear tight clothing.
144

UR-261

Health and Biology

THE UNIVERSITY OF ROCHESTER
Atomic Energy Project
P. O. Box 287, Station 3
Rochester 20, New York

DOE Information Bridge (online): OSTI ID: 4411414

Contract W-7401-eng-49

* * *

STUDIES ON FLASH BURNS: THE PROTECTION AFFORDED BY 2, 4 AND 6 LAYER FABRIC COMBINATIONS

by:

George Mixter and Herman E. Pearse

Division: Special Programs

Division Head: H. A. Blair

Section: Flash Burn

Section Head: H. D. Kingsley

Submitted by: Henry A. Blair, Director

Date of Report: 6/4/53

STUDIES ON FLASH BURNS:

THE PROTECTION AFFORDED BY 2, 4 AND 6 LAYER FABRIC COMBINATIONS

by

George Mixter, Jr., M. D. and Herman E. Pearse, M. D.

ABSTRACT

Fabric interposed between a carbon arc source and the skin of Chester White pigs increased the amount of thermal energy required to cause 2+ burns. For the 2, 4 and 6 layers of fabric studied this increase was 3.6, 38 and over 104 cal/cm^2 respectively when the inner layer of fabric was in contact with the skin. Separation of the inner layer from the skin by 5 mm increased the protective effect of the 2 layer combination from 7.4 to 29 cal/cm^2, provided the outer layer was treated for fire retardation. If the outer layer was not so treated, sustained flaming occurred which in itself added to the thermal burn.

INTRODUCTION

In the past, work in this laboratory has been directed toward a study of flash burns in unshielded skin. It is well known from the atomic bombing in Japan that this type of burn was modified by clothing. A laboratory analysis of the protective effect of fabrics against flash burns was begun (5) by shielding the skin with a few representative fabrics and their combinations.

1. 2 Layers
   a. light green oxford
      knitted cotton underwear
   b. light green oxford (HPM)
      knitted cotton underwear
2. 4 Layers
   olive green sateen
   thin cotton oxford
   wool-nylon shirting
   knitted cotton underwear
3. 6 Layers
   olive green sateen
   thin cotton oxford
   mohair frieze
   rayon lining
   wool-nylon shirting
   knitted wool underwear

5. Morton, J. H., Kingsley, H. D., and Pearse, H. E., "Studies on Flash Burns: The Protective Effects of Certain Fabrics", Surgery, Gynecology and Obstetrics, 94, 497-501 (April 1952).

~~CONFIDENTIAL~~

DEPARTMENT OF THE ARMY TECHNICAL MANUAL
DEPARTMENT OF THE NAVY
DEPARTMENT OF THE AIR FORCE
MARINE CORPS PUBLICATIONS

TM 23-200
OPNAV INSTRUCTION 03400.1B
AFL 136-1
NAVMC 1104 REV

CAPABILITIES OF ATOMIC WEAPONS (U)

Prepared by
Armed Forces Special Weapons Project

DEPARTMENTS OF THE ARMY, THE NAVY AND THE AIR FORCE

REVISED EDITION NOVEMBER 1957

~~CONFIDENTIAL~~

c. *Indirect Blast Injury.*

(1) *General.* Indirect blast casualties result from burial by debris from collapsed structures with attendant production of fractures and crushing injuries, from missiles placed in motion by the blast wave, or from fire or asphyxiation where individuals are prevented from escaping the wreckage.

(2) *Personnel in structures.* A major cause of personnel casualties in cities is structural collapse and damage. The number of casualties in a given situation may be reasonably estimated if the structural damage is known. Table 6–1 shows estimates of casualty production in two types of buildings for several damage levels. Data from Section VII may be used to predict the ranges at which specified structural damage occurs. Demolition of a brick house is expected to result in approximately 25 percent mortality, with 20 percent serious injury and 10 percent light injury. On the order of 60 percent of the survivors must be extricated by rescue squads. Without rescue they may become fire or asphyxiation casualties, or in some cases be subjected to lethal doses of residual radiation. Reinforced concrete structures, though much more resistant to blast forces, produce almost 100 percent mortality on collapse. The figures of table 6–1 for brick homes are based on data from British World War II experience. It may be assumed that these predictions are reasonably reliable for those cases where the population is in a general state of expectancy of being subjected to bombing and that most personnel have selected the safest places in the buildings as a result of specific air raid warnings. For cases of no prewarning or preparation, the number of casualties is expected to be considerably higher. To make a good estimate of casualty production in structures other than those listed in table 6–1, it is necessary to consider the type of structural damage that occurs and the characteristics of the resultant missiles. Glass breakage extends to considerably greater ranges than almost any other structural damage, and may be expected to produce large numbers of casualties at ranges where personnel are relatively safe from other effects, particularly for an unwarned population.

Table 6–1. Estimated Casualty Production in Structures for Various Degrees of Structural Damage

	Killed outright	Serious injury (hospitalization)	Light injury (No hospitalization)
1–2 story brick homes (high explosive data):	*Percent*	*Percent*	*Percent*
Severe damage	25	20	10
Moderate damage	<5	10	5
Light damage	------	<5	<5
Reinforced-concrete buildings (Japanese data, nuclear):			
Severe damage	100	------	------
Moderate damage	10	15	20
Light damage	<5	<5	15

Note. These percentages do not include the casualties which may result from fires, asphyxiation, and other causes from failure to extricate trapped personnel. The numbers represent the estimated percentage of casualties expected at the maximum range where the specified structural damage occurs.

Personnel in a prone position are less likely to be struck by flying missiles than those who remain standing.

6–3

Table 6–2. Critical Radiant Exposures for Burns Under Clothing

(Expressed in cal/cm² incident on outer surface of cloth)

Clothing	Burn	1 KT	100 KT	10 MT
Summer Uniform	1°	8	11	14
(2 layers)	2°	20	25	35
Winter Uniform	1°	60	80	100
(4 layers)	2°	70	90	120

6–4

Morrison Shelters in Recent Air Raids.

A report of Ministry of Home Security experts on 39 cases of bombing incidents in different parts of Britain covering all those for which full particulars are available in which Morrison shelters were involved shows how well they have stood up to severe tests of heavy bombing.

All the incidents were serious. Many of the incidents involved direct hits on the houses concerned a risk against which it was never claimed these shelters would afford protection. In all of them the houses in which shelters were placed were within the radius of damage by bombs; in 24 there was complete demolition of the house on the shelter.

A hundred and nineteen people were sheltering in these "Morrisons" and only four were killed. So that 115 out of 119 people were saved. Of these only 7 were seriously injured and 14 slightly injured while 94 escaped uninjured. The majority were able to leave their shelters unaided.

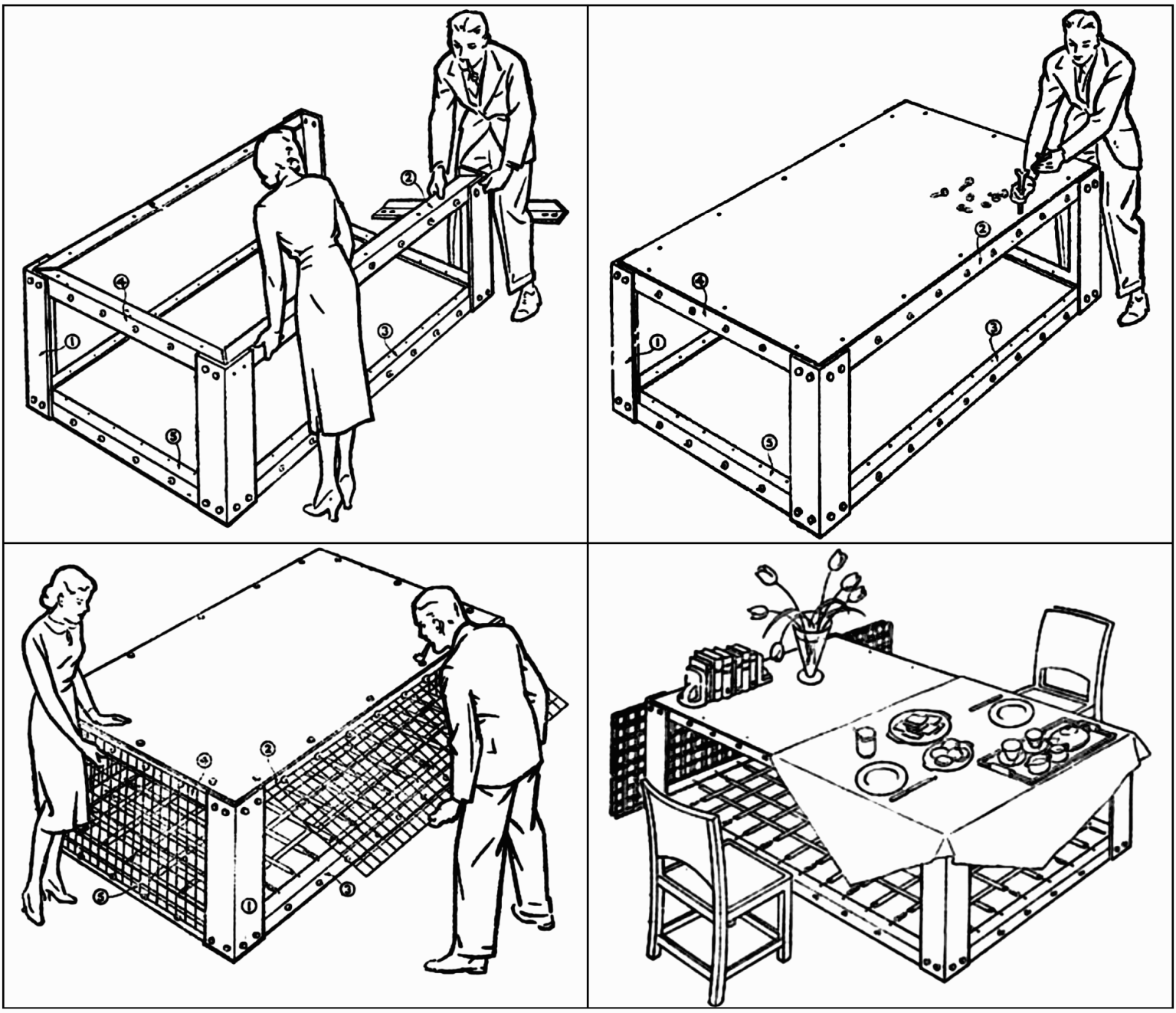

SOURCE: http://www.nationalarchives.gov.uk/education/homefront/bombing/pdf/shelter.pdf

The Morrison shelter was invented in 1941 and proved highly convenient and effective.

UK National Archives: CAB / 67 / 9 / 7

(THIS DOCUMENT IS THE PROPERTY OF HIS BRITANNIC MAJESTY'S GOVERNMENT).

SECRET.

W.P.(G)(41)7. COPY NO. 62

January 15th, 1941.

WAR CABINET.

AIR RAID SHELTER POLICY.

Memorandum by the Minister of Home Security.

---

6. Shelter in the home: The Anderson shelter was originally intended for indoor use but for a number of reasons including the danger of fire an outdoor variant was adopted. Experience has shown that the objections to the indoor use of the Anderson or somewhat similar shelter are not so serious as was thought and two designs have been produced which can be erected indoors without support. These new types, although they may give slightly less protection than a well covered Anderson shelter out of doors, would fill the needs of a large section of the public, especially the middle class. One design allows the use of the shelter as part of the furniture of the room.

7. I regard shelters of this type as of the first importance and wish to provide them on a big scale. Each shelter will use over 3 cwt. of steel and will allow at a pinch two adults and one to two children to sleep inside. For an outlay of about 65,000 tons of steel, as a first instalment, I could therefore produce 400,000 shelters with accommodation for at least 1,000,000 persons. I should wish to complete such a programme within the first three months of production and thereafter at a similar or increasing rate. From enquiries I believe that manufacture can be arranged provided steel is supplied and if the Cabinet approves my policy I shall require their direction that the steel be made available.

10. Conclusions.

I ask for a general endorsement of the policy I have outlined in this paper and in particular for the agreement of my colleagues:

(i) that proposals for building shelters of massive construction should be rejected;

(ii) that steel should be made available to carry out the programme outlined in paragraph 7 for the provision of steel shelters indoors;

(iii) that the limit of income for the provision of free shelter for insured persons should be raised from £250 to £350 per annum.

H.M.

MINISTRY OF HOME SECURITY.

January 15th, 1941.

UK National Archives: CAB / 67 / 9 / 44

THIS DOCUMENT IS THE PROPERTY OF HIS BRITANNIC MAJESTY'S GOVERNMENT

Printed for the War Cabinet. May 1941.

MOST SECRET. Copy No. 58

W.P. (G) (41) 44.

May 5, 1941.

TO BE KEPT UNDER LOCK AND KEY.

It is requested that special care may be taken to ensure the secrecy of this document.

WAR CABINET.

AIR RAIDS ON LONDON, SEPTEMBER–NOVEMBER 1940.

Memorandum by the Home Secretary and Minister of Home Security.

Framed buildings.

Most valuable information has been gained on the effects of bombs on framed buildings. Such buildings are practically immune to anything but a direct hit. Blast damage from bombs outside is usually confined to windows and internal partitions. Even parachute mines falling immediately outside the building or exploding on the roof produce negligible damage to structure or floors.

Relation of Casualties to Bombs Dropped.

From a knowledge of the number of bombs dropped and the casualties occurring in different boroughs, some idea can be gained of the effectiveness of bombs in producing casualties. The number of casualties per bomb varies widely from 1·59 in the least to 6·94 in the most populated boroughs, but it follows closely the apparent densities of population as shown in figure 1. The number of casualties per bomb is roughly a twelfth of the number of persons per acre, and the number of deaths per bomb about 1/60th of the number of persons per acre. From this it can be deduced that the mean distance at which injury from a bomb is likely to occur is 35 ft., and that at which the bomb is lethal is 15 ft.

The casualties per bomb in Central London fell steadily from an average of 3·7 in September to 2·7 in October and 1·7 in November. This corresponds to the considerable fall in population in most of the boroughs concerned.

Conclusion.

We may now say that we have a good general understanding, both qualitative and quantitative, of the effects of bombs on buildings and on cities. New types of bombs, particularly heavier bombs, may be used, but we can anticipate no startling change in the effects apart from increase in minor damage. With bombing of the present type the results of our work are to show that in urban areas, such as that of the County of London, *for one ton of bombs approximately* 10 *houses will be destroyed or will need pulling down.* 25 *more will be temporarily uninhabitable, and another* 80 *will be slightly damaged.* 80 *people will be made temporarily homeless and* 35 *will lose their homes permanently.* 25 *people, mostly among the latter category, will be wounded, the greater part of them slightly, and* 6 *will be killed or die from wounds.*

1 2 cms The National Archives ins 1 2
Ref.: HO 225/12. C500594

THIS DOCUMENT HAS BEEN
DOWNGRADED TO UNCLASSIFIED
Authority in file ESA 10/4/2
Date 2/12/57 Initials LST

CD 2333

~~SECRET~~

HOME OFFICE

CD/SA 12
Copy. No 5.

OFFICE OF THE CHIEF SCIENTIFIC ADVISER

A COMPARISON BETWEEN THE NUMBER OF PEOPLE KILLED PER TONNE OF BOMBS DURING WORLD WAR I AND WORLD WAR II

BOMB SIZES

=> ≈ 175 kg

For World War II the average bomb weight was between 150 - 200 kg. (R.C. 268, Table 6), whereas for World War I the majority of bombs were 12 or 50 kg.

TABLE 5

Relative safeties in World War II deduced from population and casualty distribution

	In the open	Under cover	In shelter
Population exposure	5%	60%	35%
Location people killed	19%	62%	19%
Relative safety	72%	20%	10%
RELATIVE DANGER!			

(1) A house about 3½ times as safe as in the open.
(2) A shelter about twice as safe as a house.

Table 6 also shows the location of killed which is implied by each of the possible population exposures. The only evidence available on this point is that, for the day raid on June 13th, 1916, in which the total number killed was 59, 69.5% of the people killed in the City were in the open.

THE EFFECTS OF THE ATOMIC BOMBS AT HIROSHIMA AND NAGASAKI

REPORT OF THE BRITISH MISSION TO JAPAN

PUBLISHED
FOR THE HOME OFFICE AND THE AIR MINISTRY BY
HIS MAJESTY'S STATIONERY OFFICE
LONDON
1946

Photo No. 17. HIROSHIMA. Typical, part below ground, earth-covered, timber framed shelter 300 yds. from the centre of damage, which is to the right. In common with similar but fully sunk shelters, none appeared to have been structurally damaged by the blast. Exposed woodwork was liable to " flashburn." Internal blast probably threw the occupants about, and gamma rays may have caused casualties. See paragraph 40.

Photo No. 18. NAGASAKI. Typical small earth-covered back yard shelter with crude wooden frame, less than 100 yds. from the centre of damage, which is to the right. There was a large number of such shelters, but whereas nearly all those as close as this one had their roofs forced in, only half were damaged at 300 yds., and practically none at half a mile from the centre of damage. See paragraph 41.

1 2 cms The National Archives ins 1 2
Ref.: HO 225/116 C500594

~~RESTRICTED~~ 9/89 For PRO

3 OCTOBER 1963

HO 225/116

HOME OFFICE

SCIENTIFIC ADVISER'S BRANCH

CD/SA 116

RESEARCH ON BLAST EFFECTS IN TUNNELS

With Special Reference to the Use of London Tubes as Shelter

by F. H. Pavry

Summary and Conclusions

The use of the London tube railways as shelter from nuclear weapons raises many problems, and considerable discussion of some aspects has taken place from time to time. But - until the results of the research here described were available - no one was able to say with any certainty whether the tubes would provide relatively safe shelter or not.

This research, consisting of a series of model experiments, has demonstrated that the risk from blast in the tubes would be less than the risks above ground. The results are considered to be consistent enough to provide a good estimate of full-scale conditions, and reliable enough to be used as a basis for Home Office shelter policy regarding the London tube railways.

Introduction

When the Advisory Group on Structural Research for Civil Defence was formed in 1957, the Chairman recommended that a study of the effects of blast on tunnels should be one of the main research projects. The relevant paragraphs of his proposals(1) for a research programme were:-

> "In any consideration of tunnels as shelter the crucial problem is the entry of blast, either through existing openings or from a crater formed by a ground-burst bomb. It is particularly important to know if the collapse of a tunnel by earth shock would prevent the blast from entering it, and also whether the collapse would provide a seal against the entry of water from the crater. It is probable that some data could be derived from model experiments using H.E. charges. But it is for consideration whether the results would be so conclusive that the behaviour of full-size tunnels when damaged by megaton weapons could be forecast with the confidence that a major shelter programme would demand."

At the second meeting(2) the Group agreed that model experiments with H.E. charges would be worthwhile, and that the Atomic Weapons Research Establishment (A.W.R.E.) should carry out this research, which has now been accepted by the Advisory Group as successfully completed. A summary record of the progress follows.

~~RESTRICTED~~

100 ton TNT test on 1000 ft section of London Underground tube at Suffield, Alberta, 3 Aug 1961

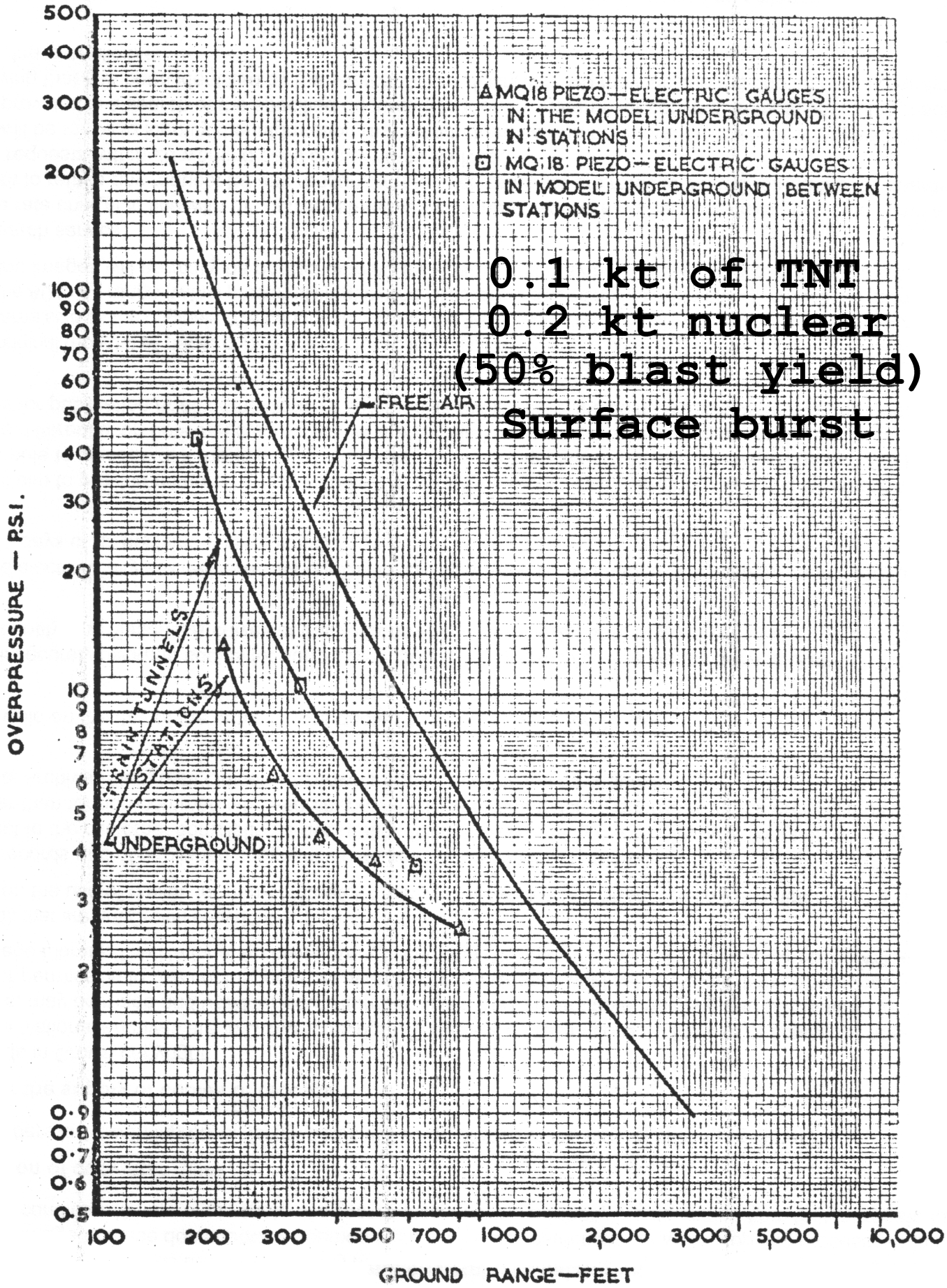

Atomic Weapons Research Establishment, "1/40th Scale Experiment to Assess the Effect of Nuclear Blast on the London Underground System", Report AWRE-E2/62, 1962, Figure 30. (National Archives ES 3/57.)

These trials are described in a preliminary report(5) prepared for the Advisory Group by A.W.R.E. It was shown that the blast pressure inside a tunnel system, having openings at intervals to ground level, is less than the pressure at ground level at any distance from the explosion, by a factor of about 3. This reduction in pressure was apparently caused by the station entrances acting as expansion chambers. This observation was of outstanding significance to the consideration of London tubes as shelter.

All previous research on blast in tunnels - and a great amount of work was done on this in the last war - had been conducted with blast entering the open end of a tunnel without side openings. This research had shown that the blast, once it had got into a tunnel, tended to travel great distances without appreciable diminution. This had, therefore, led to the general belief that the London tubes could be death traps rather than shelters.

The more recent research here described showed for the first time that a person sheltering in a tube would be exposed to a blast pressure only about $\frac{1}{3}$ as great as he would be exposed to if he was above ground. (In addition, of course, he would be fully protected from fallout in the tube.)

In fact A.W.R.E. carried out two further tests, with more accurate scaling of station volumes based on more detailed information from the London Transport Executive. A full report on all four tests is in preparation.

These later tests showed that the pressure in station tunnels was only about 1/6th of the ground-level pressure, but that the reduction was not so great in the smaller-diameter train tunnels.

At this stage the Advisory Group were reasonably satisfied that this problem - of blast entry from stations - had been solved. But the other major question of blast entry direct from the crater remained in doubt, on account of the very small scale of the tests to date. Therefore, when the opportunity arose of testing at a really large scale at Suffield, Canada, it was naturally accepted.

Large-Scale Field Test (1/40) at Suffield, Alberta

The test is fully described in an A.W.R.E. report(6). The decision of the Canadian Defence Research Board to explode very large amounts of high explosive provided a medium for a variety of target-response trials that was welcome at a time when nuclear tests in Australia were suspended. A.W.R.E. used the 100-ton explosion in 1961 to test, among other items, the model length of the London tube, at 1/40th scale, that had already been tested at 1/117 scale.

Blast Entry from Stations

There was remarkable agreement with the 1/117th scale trials: "maximum overpressure in the train tunnels was of the order of $\frac{1}{3}$rd the corresponding peak shock overpressure in the incident blast. The pressures in the stations were about 1/6th those in the corresponding incident blast ..... ". In comparing the results at the two scales it was noted that the pressures in the train tunnels (between stations) was higher at Suffield than at the smaller scale; this may, the report suggests, have been due to some blast entry from the crater at Suffield.

Blast Entry from the Crater

There may - as has just been noted - have been some entry of blast at the crater. But the all-important fact is that it was nowhere enough to bring the pressure in the tunnel up to more than a $\frac{1}{3}$rd of the free-air pressure (see fig. 30 reproduced, and attached to this note.) From this, and from a detailed study of tunnel rings ejected by the explosion over a wide area, it can be concluded that the instantaneous crushing of the tube near the crater sealed it against the entry of any significant blast pressure.

Air Flow in Stations

The Report indicates that there would be turbulence generated by blast entry at stations and that there would be a danger to occupants there, on account of blast "windage" acting on them and on missiles that could injure them. This danger would be less in the train tunnels between stations.

Conclusion

The Advisory Group discussed the Suffield Test on tunnels on Nov. 1st 1962, and concluded that model experiments have successfully demonstrated that the risks from blast inside the London tubes would be less than above ground. The Group considered that the results obtained were consistent enough to provide as good an estimate of full-scale effects from megaton weapons as was likely to be obtainable, and that the Chairman could advise the Home Office confidently on the basis of these results. The Group accepted that there would be a risk of casualty-producing air flow in stations, but decided to defer a decision on whether further research on this problem would be profitable. The Chairman said that he would first convey the results of the completed research to the Shelter Division of the Home Office before asking the Group whether it was worth studying this remaining, but less important, problem.

3rd October, 1963.

References

(1) Advisory Group on Structural Research for Civil Defence

Note by Chairman on the Structural Research Programme for Shelters. SAB/SG(57)6. (Restricted)

(2) Notes of Meeting on 15th May 1957. SAB/SG(57)2nd Minutes (Confidential)

(3) The Entry of Air Blast from Craters into Tunnels. A.W.R.E. Report E1/59 (Official Use Only)

(4) The Effect of Tunnel Blockage on Shock Waves .... SAB/SG(58)6 (Confidential)

(5) Model Experiments on the Entry of Blast into the London Underground System, Interim Report on Rounds 1 and 2. SAB/SG(59)4 (Confidential)

(6) 1/40th Scale Experiment to Assess the Effect of Nuclear Blast on the London Underground System. A.W.R.E. Report E2/62. (Official Use Only.)

The Effects of

Nuclear Weapons

SAMUEL GLASSTONE
Editor

Prepared by the
UNITED STATES DEPARTMENT OF DEFENSE
Published by the
UNITED STATES ATOMIC ENERGY COMMISSION
June 1957

For sale by the Superintendent of Documents, U. S. Government Printing Office
Washington 25, D. C. - Price $2.00 (paper bound)

Foreword

This handbook, prepared by the Armed Forces Special Weapons Project of the Department of Defense in coordination with other cognizant government agencies and published by the United States Atomic Energy Commission, is a comprehensive summary of current knowledge on the effects of nuclear weapons. The effects information contained herein is calculated for yields up to 20 megatons and the scaling laws for hypothetically extending the calculations beyond this limit are given. The figure of 20 megatons however is not to be taken as an indication of capabilities or developments.

CHARLES E. WILSON
Secretary of Defense

LEWIS L. STRAUSS
Chairman
Atomic Energy Commission

THE FEDERAL CIVIL DEFENSE ADMINISTRATION commends this publication as the definitive source of information on the effects of nuclear weapons for the use of organizations engaged in Civil Defense activities. Its detailed treatment of the physical phenomena associated with nuclear explosions provides the necessary technical background for development of countermeasures against all nuclear effects of Civil Defense interest.

VAL PETERSON
Administrator
Federal Civil Defense Administration

TABLE 3.11

OVERPRESSURE, DYNAMIC PRESSURE, AND WIND VELOCITY IN AIR AT SEA LEVEL

Peak overpressure (pounds per square inch)	*Peak dynamic pressure (pounds per square inch)*	*Maximum wind velocity (miles per hour)*
72	80	1, 170
50	40	940
30	16	670
20	8	470
10	2	290
5	0. 7	160
2	0. 1	70

3.12 At a given location, the dynamic pressure changes with time in a manner somewhat similar to the change in the overpressure, but the rate of pressure decrease behind the shock front is different. This may be seen from Fig. 3.12 which indicates qualitatively how the two pressures vary in the course of the first second or so following arrival of the shock front.

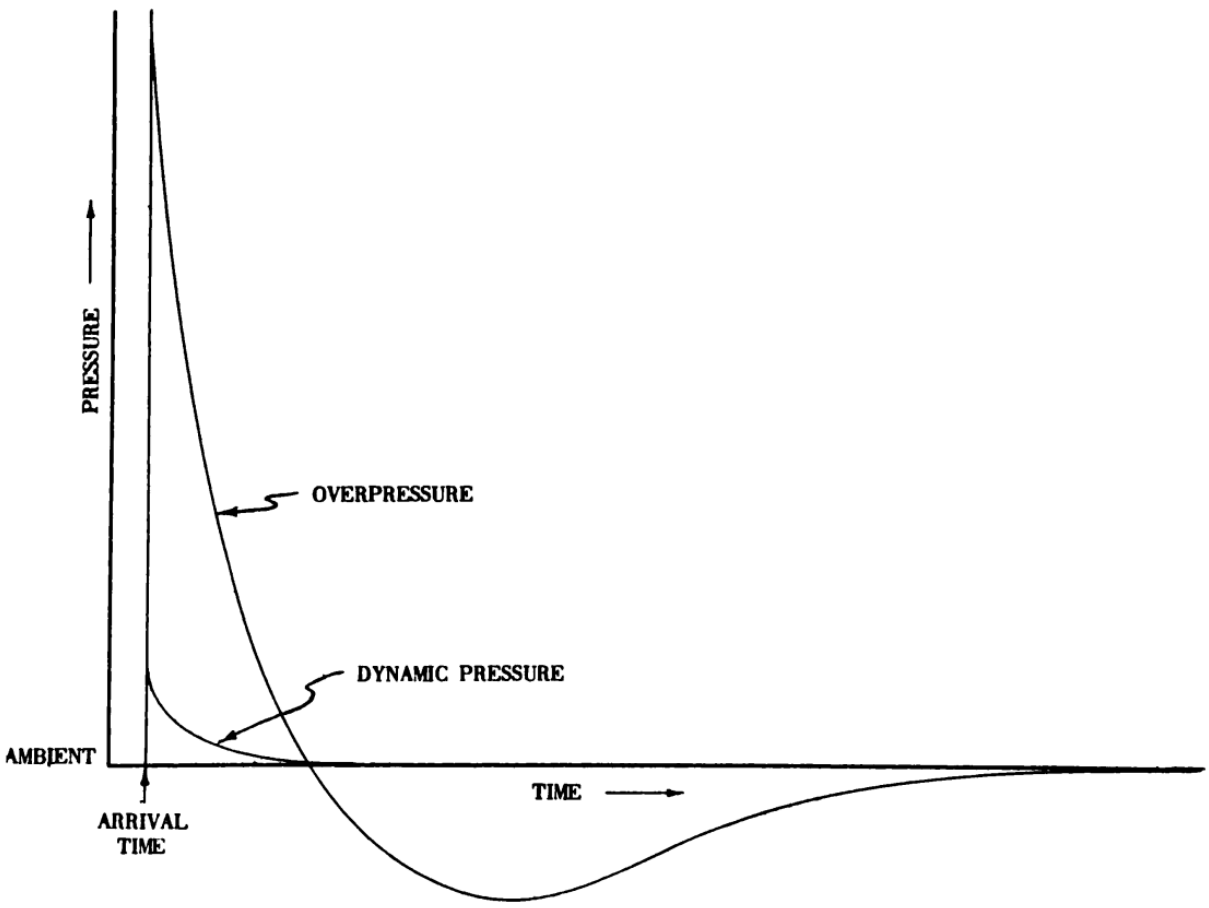

Figure 3.12. Variation of overpressure and dynamic pressure with time at a fixed location.

Ductility

3.73 The term ductility refers to the ability of a material or structure to absorb energy inelastically without failure; in other words, the greater the ductility, the greater the resistance to failure. Materials which are brittle have poor ductility and fail easily.

3.74 There are two main aspects of ductility to be considered. When a force (or load) is applied to a material so as to deform it, as is the case in a nuclear explosion, for example, the initial deformation is said to be "elastic." Provided it is still in the elastic range, the material will recover its original form when the loading is removed. However, if the "stress" produced by the load is sufficiently great, the material passes into the "plastic" range. In this state the material does not recover completely after removal of the stress, that is to say, the deformation is permanent, but there is no failure. Only when the stress reaches the "ultimate strength" does failure, i. e., breakage, occur.

3.75 Ideally, a structure which is to suffer little damage from blast should have as much elasticity as possible. Unfortunately, structural materials are generally not able to absorb much energy in the elastic range, although many common materials can take up large amounts of energy in the plastic range before they fail. The problem in blast-resistant design, therefore, is to decide how much permanent (plastic) deformation can be accepted before a particular structure is rendered useless. This will, of course, vary with the nature and purpose of the structure. Although deformation to the point of collapse is definitely undesirable, some lesser deformation may not seriously interfere with the continued use of the structure.

3.76 It is evident that ductility is a desirable property of structural materials required to resist blast. Structural steel and steel reinforcement have this property to a considerable extent. They are able to absorb large amounts of energy, e. g., from a blast wave, without failure and thus reduce the chances of collapse of the structure in which they are used. Steel has the further advantage of a higher yield point (or elastic limit) under dynamic than under static loading.

3.77 Although concrete alone is not ductile, when steel and concrete are used together, as in reinforced-concrete structures, the ductile behavior of the steel will usually predominate. The structure will then have considerable ductility and, consequently, resistance to blast. Without reinforcement, masonry walls are completely lacking in ductility and readily suffer brittle failure, as stated above.

The curves show the variation of peak overpressure with distance for a 1 KT surface burst and for a 1 KT free-air burst (based on the $2W$ assumption in § 3.94) in a standard sea level atmosphere.

Scaling. For yields other than 1 KT, the range to which a given overpressure extends scales as the cube root of the yield, i. e.,

$$d = d_0 \times W^{1/3},$$

where, for a given overpressure,

d_0 is the distance from the explosion for 1 KT,

and

d is the distance from the explosion for W KT.

Example

Given: A 1 MT surface burst.

Find: The distance to which 2 psi extends.

Solution: From Fig. 3.93 the cube root of 1000 is 10. From Fig. 3.94a, a peak overpressure of 2 psi occurs at a distance of 0.53 mile from a 1 KT surface burst. Therefore, for a 1 MT surface burst,

$$d = d_0 \times W^{1/3} = 0.53 \times 10 = 5.3 \text{ miles.} \quad \textit{Answer}$$

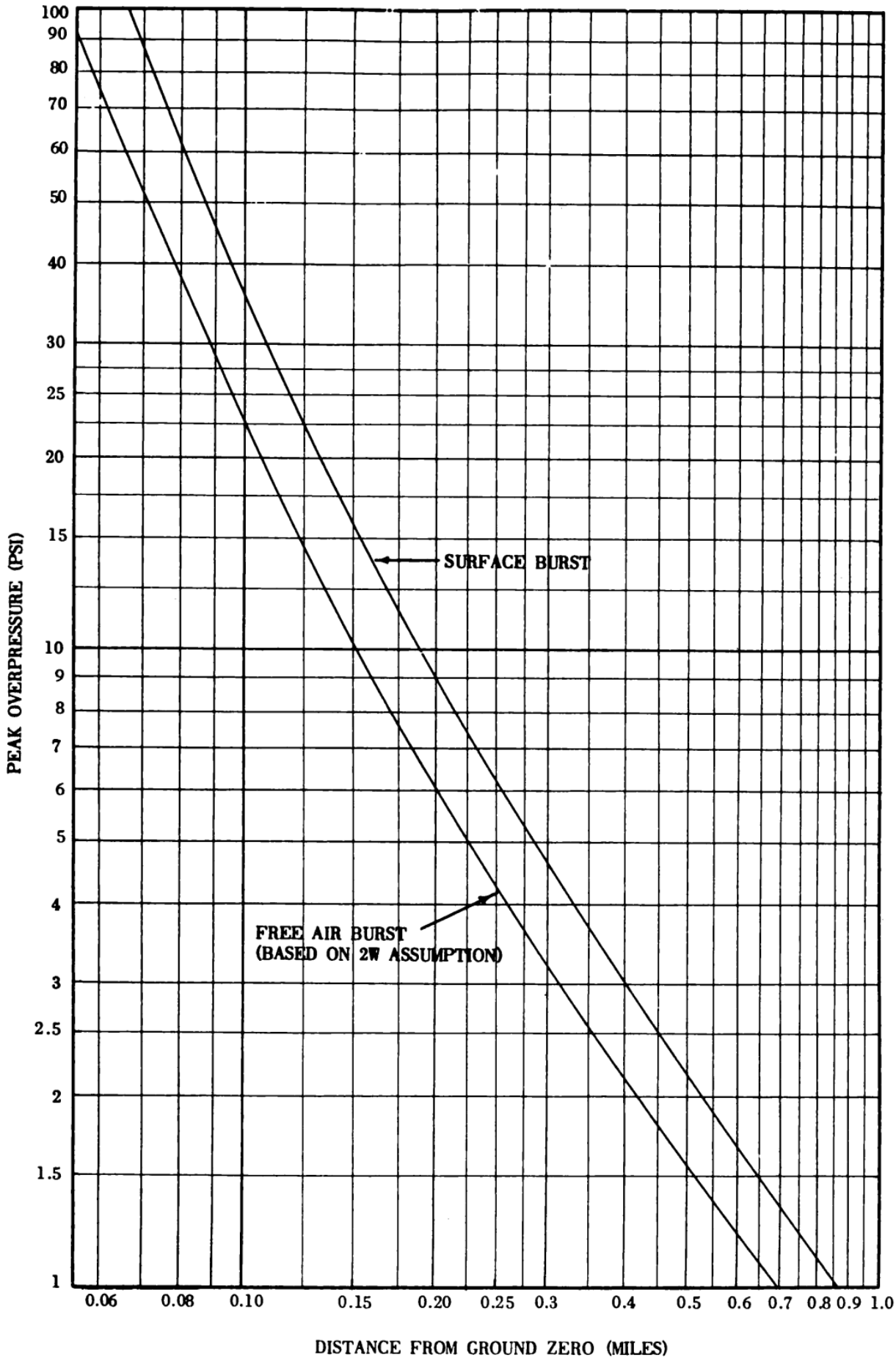

Figure 3.94a. Peak overpressure for a 1-kiloton surface burst and free air burst.

TABLE 6.12

DAMAGE CRITERIA FOR SHALLOW BURIED OR EARTH COVERED SURFACE STRUCTURES

Type of structure	Damage class	Peak overpressure (psi)	Nature of damage
Light, corrugated steel arch, surface structure (10-gage corrugated steel with a span of 20 to 25 feet) with 3 feet of earth cover over the crown.	A	35–40	Complete collapse.
	B	30–35	Collapse of portion of arch facing blast.
	C	20–25	Deformation of end walls and arch, possible entrance door damage.
	D	10–15	Possible damage to ventilation system and entrance door.
Light, reinforced-concrete surface or underground shelter with 3 feet minimum earth cover. (Panels 2 to 3 inches thick, with beams spaced on 4-foot centers.)	A	30–35	Collapse.
	B	25–30	Partial collapse.
	C	15–25	Deformation, severe cracking and spalling of panels.
	D	10–15	Cracking of panels, possible entrance door damage.

6.13 An illustration of B-type damage to a 10-gage corrugated steel-arch, earth-covered, surface structure is shown in Fig. 6.13. It will be noted that about half of the arch has collapsed. This failure was attributed primarily to the dynamic pressure acting on the forward slope of the earth mound.

6.14 The peak overpressure for the complete collapse of the corrugated steel-arch structure, with 3 feet of earth cover, is given in Table 6.12 as 35 to 40 pounds per square inch. However, it has been estimated that if this structure had been completely buried, so that no earth mound was required, an overpressure of 40 to 50 pounds per square inch would have been necessary to cause it to collapse. This increase in the required overpressure is due to the fact that the dynamic pressure is minimized under these conditions. It may be mentioned

Figure 6.13. B-type damage to earth-covered 10-gage corrugated steel structure.

that, using standard engineering techniques, it is possible to design underground structures which will withstand blast overpressures in excess of 100 pounds per square inch at the surface (see Chapter XII).

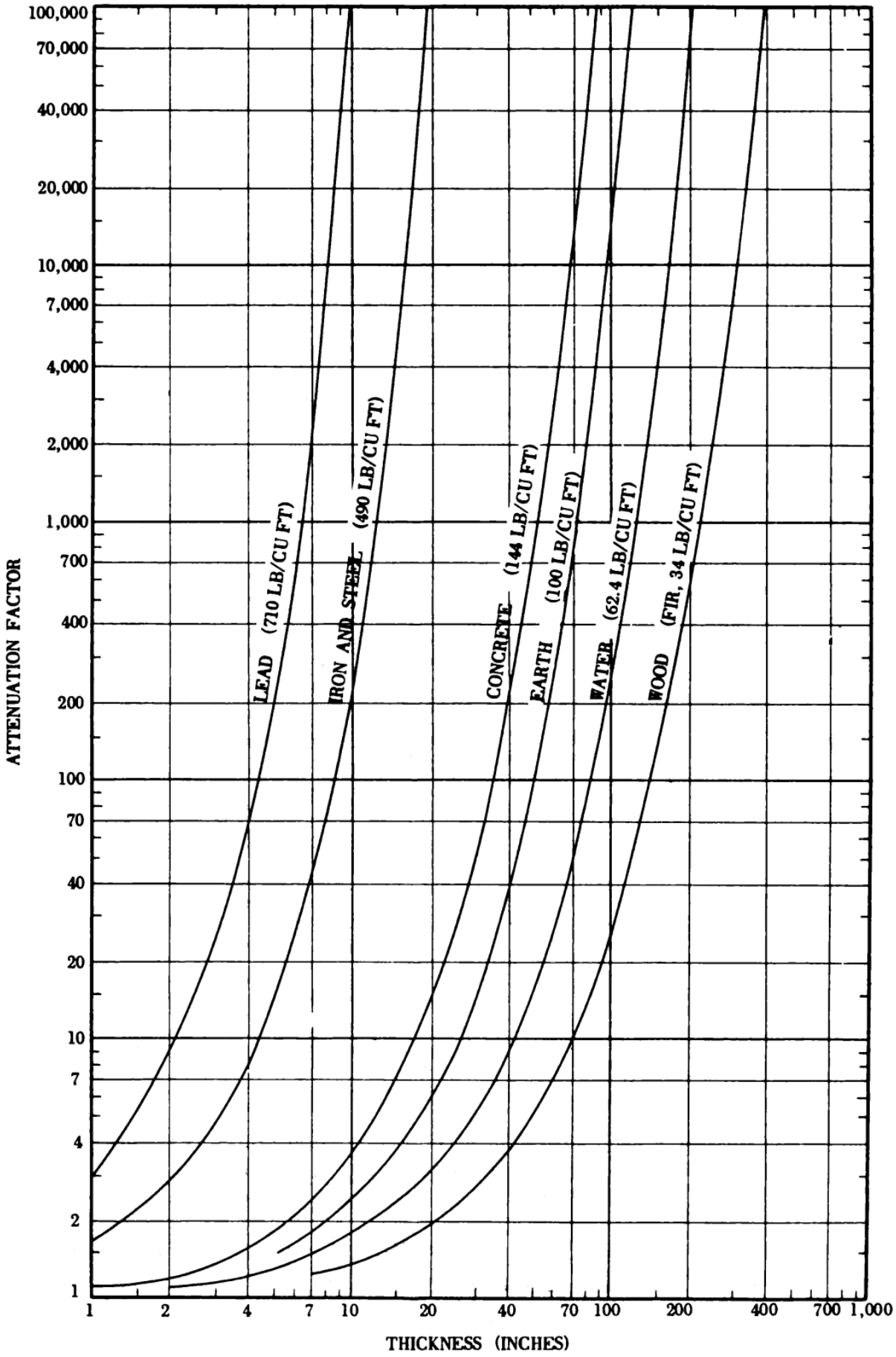

Figure 8.47. Attenuation of initial gamma radiation.

HOME OFFICE

SCOTTISH HOME DEPARTMENT

MANUAL OF CIVIL DEFENCE

Volume I

PAMPHLET No. 1

NUCLEAR WEAPONS

LONDON

HER MAJESTY'S STATIONERY OFFICE

1956

CONTENTS

	Paragraphs	Pages
INTRODUCTION		1
CHAPTER I. Features of Nuclear Explosions		2
General characteristics	1–3	2
Types of Burst		
An airburst	4–6	2
A burst on or near the ground	7–10	3
An underground burst	11–13	3–4
A surface or very shallow water burst	14–15	4
An underwater burst	16–19	4
CHAPTER II. The Fire Risk		5
Thermal radiation	20–23	5
Effects on people	24–27	5–6
Primary fires	28	6
Secondary fires	29–30	6–7
Fire precautions	31–34	7
The probable fire situation in a British city	35–36	7
The possibilities of a fire storm	37–41	7–8
Scaling laws	42–44	8–9
CHAPTER III. Nuclear Radiation Hazards		10
General		
Alpha, beta, gamma rays, and neutrons	45–50	10
The Immediate Danger from Nuclear Radiation	51–52	11
Gamma Rays		
Description	53–55	11
Penetration of materials	56–59	11–12
Effect on living organisms	60–64	12–13
The immediate gamma dose from a nominal bomb ...	65–66	13–14
The immediate gamma dose from a hydrogen bomb...	67	14
Neutrons		
Description	68	14
Effect on materials	69–70	14
Effect on living organisms	71	15
The Delayed Danger from Nuclear Radiation		
Fall-out and induced radioactivity	72–76	15–16
Radioactive decay	77	16
Radioactive poisoning	78–79	16–17
The residual radiation hazard from a nominal bomb.	80	17
The residual radiation hazard from a hydrogen bomb.	81	17
Contamination in the devastated area	82	18
Contamination in the undamaged area	83–84	18
Protection Against Fall-out		
Factors involved	85	35
(*a*) Distance	86	35
(*b*) Shielding	87	36
Practical protection	88–89	37
Choosing a refuge room	90	38
Estimated under-cover doses in the fall-out area ...	91	38
Problems of control in the fall-out area	92–93	38–39

30 Research into the causes of fire in Hiroshima and Nagasaki, combined with a study of the secondary fire risk from the flying bomb damage in this country during the last war has shown that with nuclear attack the secondary fire risk is likely to be small compared with the primary risk of direct ignition by thermal radiation.

Fire precautions

31 Although the fire risk even from a nominal bomb is always serious, targets in this country, where the great majority of buildings are of brick, stone or concrete, are less vulnerable to fire than were those in Japan, where most of the buildings were of wood. Moreover, if people do what they can to keep heat radiation out of buildings, the risk of fire can be further reduced, although these precautions would be effective only beyond the central area of blast destruction (see Chapter IV).

32 It might be advisable to brick up certain windows of important buildings, but since the thermal radiation has no great penetrating power, any opaque screen, especially a white one, will keep it out: the simple process of whitewashing windows will keep out about 80 per cent. of the heat. The windows may be broken by the blast wave but as this travels more slowly it arrives after the thermal radiation is over (except of course in the central area of blast destruction), whether the bomb is a hydrogen bomb or an atomic bomb.

33 Another obvious fire precaution is the removal of all readily combustible material from the direct path of any heat radiation that could possibly enter windows or other openings.

34 Both these precautions apply only to those windows and other openings that have a direct view of some part of the sky. In a built-up area they would apply more particularly to the windows of upper floors; even for a high airburst, in a closely built-up area one building shields another to a considerable extent.

The probable fire situation in a British city

35 Within ½ mile of an airburst nominal bomb the heat flash is very intense indeed, but in this area there would be almost complete destruction of buildings by blast, and this would tend to impede the development of fire. This did not happen in Japan because most Japanese houses are constructed of wood and once they were set on fire they continued to burn even when knocked over. In this country only about 10 per cent. of all the material in the average house is combustible, and under conditions of complete collapse, where air would be almost entirely excluded, it is doubtful whether a fire could continue on any vigorous scale. The main fire zone will be around this central area of heavy destruction, in the region where buildings are damaged but standing sufficiently to allow free burning. For a nominal bomb, this zone is likely to reach as far as 1¼ miles.

36 The range of ignition is affected to some extent by the state of the atmosphere and on a dull misty day will be reduced, although it is impossible to say precisely to what degree.

The possibilities of a fire storm

37 The chief feature of a fire storm is the generation of high winds which are drawn into the centre of the fire area to feed the rising column of hot air and flames. These in-rushing winds prevent the spread of fire outwards, but ensure the almost complete destruction by fire of

everything within the fire area. This inevitably increases the number of casualties, since it becomes impossible for people to escape by their own efforts because they succumb to the effects of suffocation and heat stroke.

38 The Hiroshima bomb (but not the Nagasaki one) caused a fire storm. A fire storm occurred in Hamburg and possibly also in several other German cities as a result of accurate and very dense attacks with incendiary and high explosive bombs by the R.A.F. Information on the subject is limited, but it has been fairly well established that during these particular raids on Germany half the buildings in the target area were set on fire in about half an hour. In such circumstances it seems that nothing can prevent all the fires from joining together into one mass fire engulfing the whole area.

39 Whether a fire storm develops depends also on the nature of the target; where there are tall buildings closely packed together with plenty of combustible material to burn, the risk is much greater than in areas less densely built up.

40 It seems unlikely from the evidence available that an initial density of fires equivalent to one in every other building would be started by a nuclear explosion over a British city. Studies have shown that a much smaller proportion of buildings than this would be exposed to thermal radiation and even then it is not certain that continuing fires would develop. Curtains may catch fire, but it does not necessarily follow that they will set light to the room; in the last war it was found that only one incendiary bomb out of every six that hit buildings started a continuing fire. Moreover after a nuclear explosion the large and almost completely flattened central area would counteract the development of a fire storm, since one essential requirement seems to be a continuous mass of fire over a large area. It is unlikely, therefore, that a fire storm would develop after a nuclear attack on a British city, though the possibility cannot be ruled out. The risk can be reduced by clearing or partially clearing the top floors of buildings which are likely to be exposed to the heat radiation, and by adopting the other precautions mentioned above.

41 There would, however, in any case be many serious fires and fire areas.

Scaling laws

42 For more powerful bombs the total heat output is roughly proportional to the power of the bomb, so that a 10 megaton bomb, which is 500 times more powerful than a nominal bomb, radiates 500 times as much heat. Because of the inverse square law, the distance at which a given amount of heat is received (measured per unit area of receiving surface) varies as the square root of the power of the bomb. For example, if a nominal airburst bomb produces 5 calories per square centimetre at 1 mile, a 10 megaton airburst bomb will produce the same amount at 22 miles ($22=\sqrt{500}$). However, although at 1 mile from a nominal bomb an intensity of 5 calories per square centimetre would ignite easily combustible materials and start fires, it would not do so at 22 miles from a 10 megaton bomb because the heat is applied more slowly. From a 10 megaton bomb, with its longer lasting thermal radiation (see paragraph 21), it takes about 20 calories per square centimetre to start fires because so much of the heat (spread out over the longer emission) is wasted by conduction into the interior of the combustible material and by convection and re-radiation whilst the

temperature of the surface is being raised to the ignition point. But the distance at which 20 calories per square centimetre can be produced is only 11 miles, so that the scaling factor for a 10 megaton airburst bomb is therefore 11 and not 22.

43 For a ground burst bomb, however, several other factors contribute to a further reduction in the fire range. Apart from an actual loss of heat by absorption into the ground and from the pronounced shielding effect of buildings, the debris from the crater tends to reduce the radiating temperature of the fireball and a greater proportion of the energy is consequently radiated in the infra red region of the spectrum —this proportion being more easily absorbed by the atmosphere. The magnitude of this absorption effect is not known with certainty, but it is important in hydrogen bomb explosions because of the longer ranges involved and because—as later explained in paragraph 81—the likelihood of ground bursts has been increased with the advent of the hydrogen bomb. For all these reasons it has been estimated that the scaling factor for the fire range for a ground burst 10 megaton bomb is about 8. This will mean a fire ring extending from about 3½ to 10 miles instead of, as in the case of a nominal airburst bomb, from ½ to 1¼ miles. Isolated fires may occur at greater distances, depending on the combustibility of material within buildings, but it is impossible to apply precise scaling laws to such haphazard incidents.

44 An important point in relation to personal protection against the effects of hydrogen bomb explosions is that because the thermal radiation lasts so long there is more time for people who may be caught in the open, and who may be well beyond the range of serious danger from blast, to rush to cover and so escape some part of the exposure. For example, people in the open might receive second degree burns (blistering) on exposed skin at a range of 16 miles from a 10 megaton ground burst bomb (8×2—see paragraph 24). If, however, they could take cover in a few seconds they would escape this damage. Moreover, at this range the blast wave would not arrive for another minute and a half so that any effects due to the blast in the open (e.g. flying glass, etc.) could be completely avoided.

Practical protection

88 Large buildings with a number of storeys, especially if they are of heavy construction, provide much better protection than small single-storey structures (see Figure 4). Houses in terraces likewise provide much better protection than isolated houses because of the shielding effect of neighbouring houses.

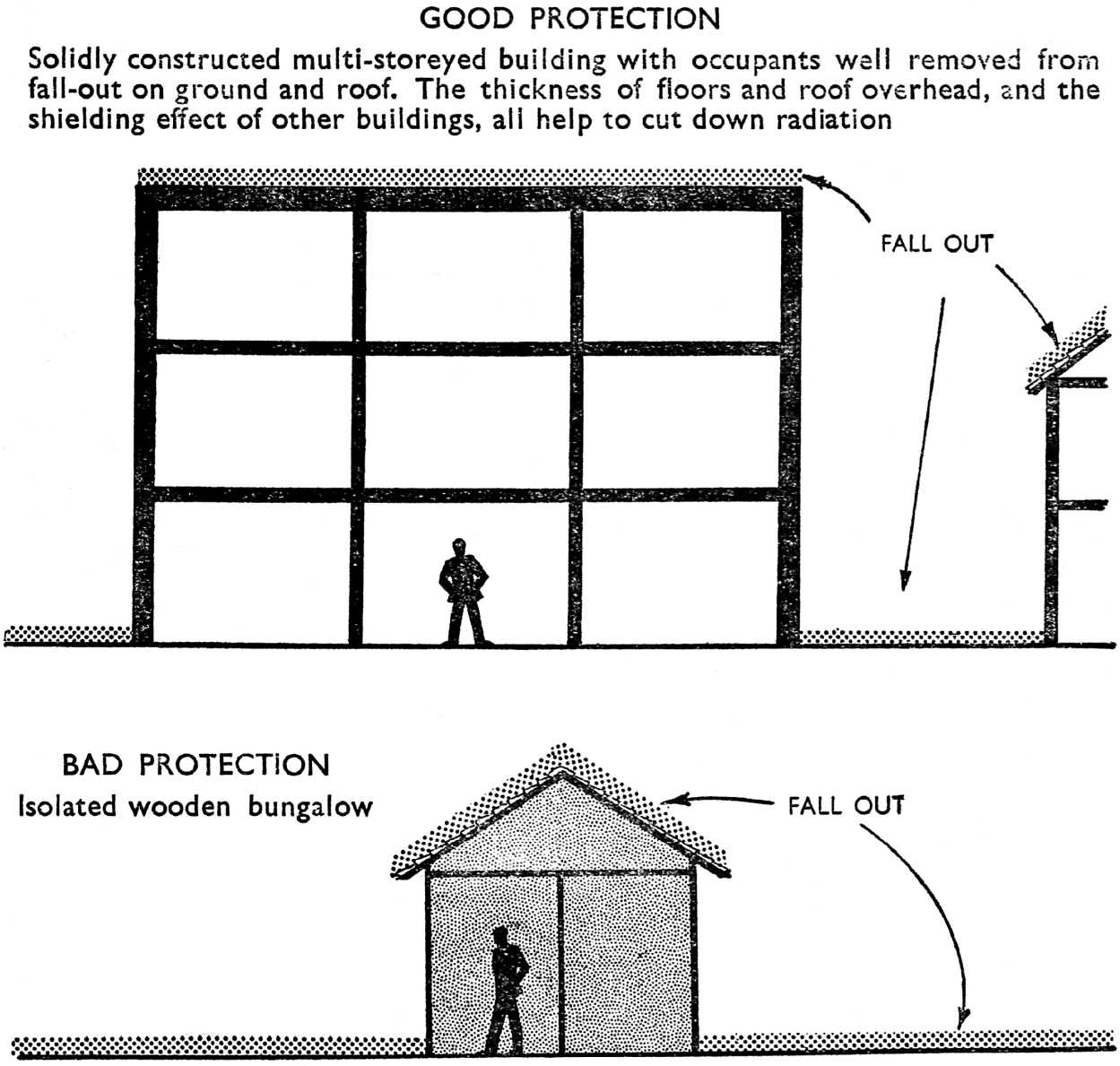

FIGURE 4

Examples of good and bad protection afforded by buildings against fall-out.

89 It is estimated that the protection factor (the factor by which the outside dose has to be divided to get the inside dose) of a ground floor room in a two-storey house ranges from 10 to about 50, depending on wall thickness and the shielding afforded by neighbouring buildings. The corresponding figures for bungalows are about 10–20, and for three-storey houses about 15–100. An average two-storey brick house in a built-up area gives a factor of 40, but basements, where the radiation from outside the house is attenuated by a very great thickness of earth, have protection factors ranging up to 200–300. A slit trench with even a light cover of boards or corrugated iron without earth overhead gives a factor of 7, and if 1 ft. of earth cover is added the

factor rises to 100. If the trench can be covered with 2 or 3 feet of earth then a factor of more than 200–300 can be obtained (see Figure 5).

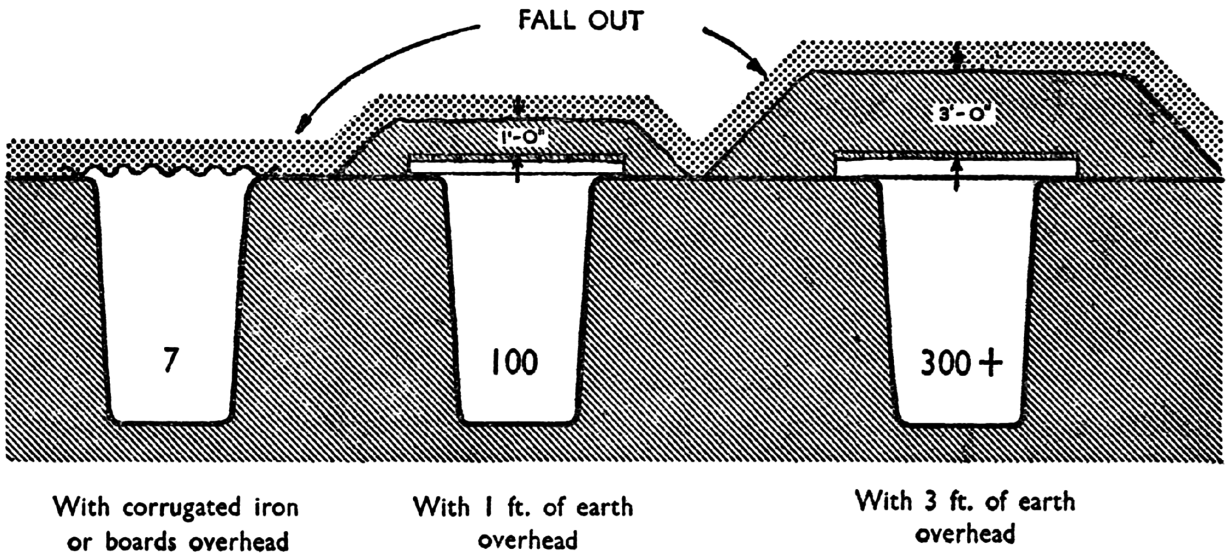

FIGURE 5
Protection factors in slit trenches (the factor by which the outside dose is divided to get the inside dose).

Choosing a refuge room

90 In choosing a refuge room in a house one would select a room with a minimum of outside walls and make every effort to improve the protection of such outside walls as there were. In particular the windows would have to be blocked up, e.g. with sandbags. Where possible, boxes of earth could be placed round an outside wall to provide additional protection, and heavy furniture (pianos, bookcases etc.) along the inside of the wall would also help. A cellar would be ideal. Where the ground floor of the house consists of boards and timber joists carried on sleeper walls it may be possible to combine the high protection of the slit trench with some of the comforts of the refuge room by constructing a trench under the floor.
Once a trap door had been cut in the floor boards and joists and the trench had been dug, there would be no further interference with the peace-time use of the room.

Estimated under-cover doses in the fall-out area

91 Taking an average protective factor of 40 for a two-storey house in a built-up area, the doses accumulated in 36 hours for the ranges referred to in the U.S. Atomic Energy Commission Report (paragraph 84) would have been:—

190 miles downwind		7½r
160	,, ,,	12½r
140	,, ,,	20r

15 Megatons
Bravo 1954

which are all well below the lowest figure of 25r referred to in Table 1. At closer ranges along the axis of the fall-out, the doses accumulated in 36 hours would have been much higher, but over most of the contaminated area—with this standard of protection—the majority of those affected would have been saved from death, and even from sickness, by taking cover continuously for the first 36 hours.

5. Radiation sickness

Assume dose incurred in a single shift (3–4 hours) by the "average" man, over the whole body:—

25 roentgens		—No obvious harm.
100	„	—Some nausea and vomiting.
500	„	—Lethal to about 50 per cent. people (death up to 6 weeks later).
800	„ or more	—Lethal to all (death up to 6 weeks later).

Note: If dose spread uniformly over 2–3 days, then 60 roentgens could be incurred with no more effect than 25 roentgens in a single exposure of 3–4 hours.

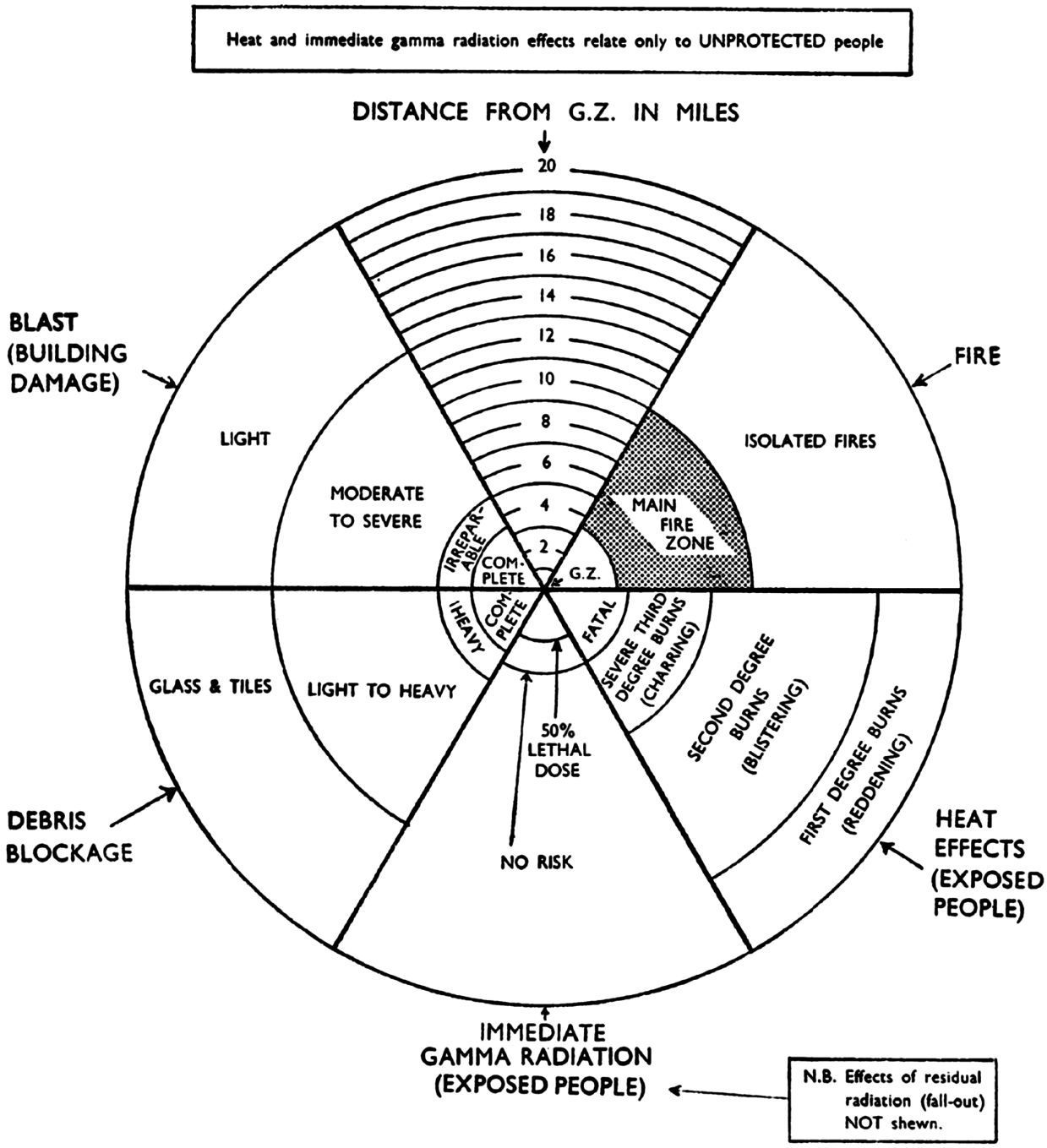

FIGURE 11

Combined effects (excluding residual radioactivity) from a 10 megaton ground burst bomb. Heat and immediate gamma radiation effects relate only to UNPROTECTED people.

A Fallout Forecasting Technique With Results Obtained at the Eniwetok Proving Ground

E. A. Schuert, USNRDL TR–139, United States Naval Radiological Defense Laboratory, San Francisco, Calif.

ADMINISTRATIVE INFORMATION

The work described herein is a part of the research sponsored by BuShips and the United States Army and locally designated as program 2, problem 3, phase 3. Its technical objective is AW–7 and it is described on RDB card NS 081–001.

SUMMARY

The problem: A fallout forecasting technique is needed to qualitatively describe the fallout hazard resulting from nuclear detonations. This technique should have such flexibility that its employment is valid for field use.

Findings: A summary of the latest experimental and theoretical considerations has resulted in the development of a technique whose complexity is dependent on the required accuracy of the results desired. This technique has been satisfactorily tested at the Eniwetok Proving Grounds for land surface and water surface bursts.

Particle size distribution in source model

All particle sizes were assumed at all elevations within the cloud except the lower two-thirds of the stem. However, to obtain agreement with past fallout measurements and with the optical diameter of the mushroom, it was necessary to fractionate the particle size distribution radially within the cloud. Otherwise, the computed fallout area about ground zero would be too large. The fractionation was specified as follows: particles of 1,000 microns in diameter and larger were restricted to the inner 10 percent of the mushroom radius or approximately the stem radius; those from 500 to 1,000 microns in diameter were limited to the inner 50 percent of the cloud radius. Since the relation of activity to particle size is some function of the particle diameter this fractionation tends to concentrate the activity about the axis of symmetry of the cloud.

Falling speeds (feet/hour)

J. M. Dallavalle, Mircomeritics, Pittman Publishing Corp., 1948.

Altitude	75 μ	100 μ	200 μ	350 μ	Altitude	75 μ	100 μ	200 μ	350 μ
0	3,060	5,040	11,700	21,600	65	4,190	7,480	26,100	51,100
5	3,120	5,240	12,300	22,900	70	4,110	7,320	27,600	55,200
10	3,200	5,480	12,900	24,100	75	4,010	7,150	28,100	59,700
15	3,270	5,750	13,700	25,500	80	3,910	6,960	27,800	61,900
20	3,360	5,980	14,400	27,100	85	3,800	6,770	27,100	67,800
25	3,470	6,160	15,300	28,800	90	3,720	6,640	26,500	71,300
30	3,570	6,380	16,300	30,800	95	3,620	6,470	25,800	77,300
35	3,720	6,640	17,500	33,000	100	3,550	6,340	25,300	80,200
40	3,870	6,910	18,600	35,300	105	3,470	6,180	24,800	75,800
45	4,040	7,200	19,800	37,800	110	3,400	6,050	24,000	74,200
50	4,210	7,520	21,400	40,600	115	3,330	5,930	23,700	72,600
55	4,420	7,860	23,200	44,600	120	3,260	5,800	23,400	71,100
60	4,200	7,700	24,400	47,200					

Experimental data from past tests at Eniwetok Atoll indicated that the particles were irregular in shape and had a mean density of 2.36 g/cu cm.

Time variation of the winds aloft

In most of the observations made at the Eniwetok Proving Ground, the winds aloft were not in a steady state. Significant changes in the winds aloft were observed in as short a period as 3 hours. This variability was probably due to the fact that proper firing conditions which required winds that would deposit the fallout north of the proving ground, occurred only during an unstable synoptic situation of rather short duration.

The forecasting technique described was employed by the fallout program at the Eniwetok Proving Ground to satisfy certain project requirements. One project had three ships equipped to collect fallout and their positions had to be determined for most efficient collection; another sampled the ocean for fallout; while another made an aerial survey of the contaminated area. The navigational schedules for these latter projects were based on the forecast fallout pattern. Operations were controlled through the program control center aboard the task force command ship where the forecasts were prepared.

The meteorological data was received from the weather ship at Bikini Atoll as well as from weather stations at Rongerik Atoll and Eniwetok Atoll. Furthermore all forecasts made by the task force weather central at Eniwetok Atoll were usually available aboard the command ship by facsimile through the ships weather station.

Upper air measurements were made at Bikini, Rongerik, and Eniwetok Atolls every 3 hours starting at H—24 hour and continuing until H+24 hour for any given detonation. The frequency of observations was usually increased during the period from H—6 to H—2 hours. The altitudes reached on the wind runs were remarkably high and gave perhaps the best set of winds-aloft measurements to date. The average termination altitude was approximately 90,000 feet with many runs over 100,000 feet. Such excellent coverage of the winds aloft was a major help in the fallout forecasting.

Fallout forecasts were made every 3 hours starting at H—24 hour using the *measured* winds available at the time. This process was continued up to shot time and from then on the technique of correcting for time variation was employed every 3 hours until the fallout event was completed. It was not feasible to correct for space variation and vertical motions during this period because of lack of time and data.

Fallout plots

The fallout forecasts determined at the weapons-test operation were based entirely on measured data and quantitatively considered time variation of the wind. No space variation corrections or computed values of vertical motions were employed in their construction.

A and B were land-surface detonations, C and D were water-surface shots.

The comparison is excellent for all shots except B.

SUMMARY

The fallout forecasting technique described in this report was successfully employed for both land surface and water surface detonations at the Eniwetok Proving Ground. With known meterological data such a technique will successfully qualify the area of fallout and indicate qualitatively the relative intensity of radiation.

"Height lines" are deposit locations for all particles falling from a fixed altitude within the mushroom cloud. "Size lines" are deposit locations of a fixed particle size from various altitudes. A height line from the base of the mushroom disc is the "hot line".

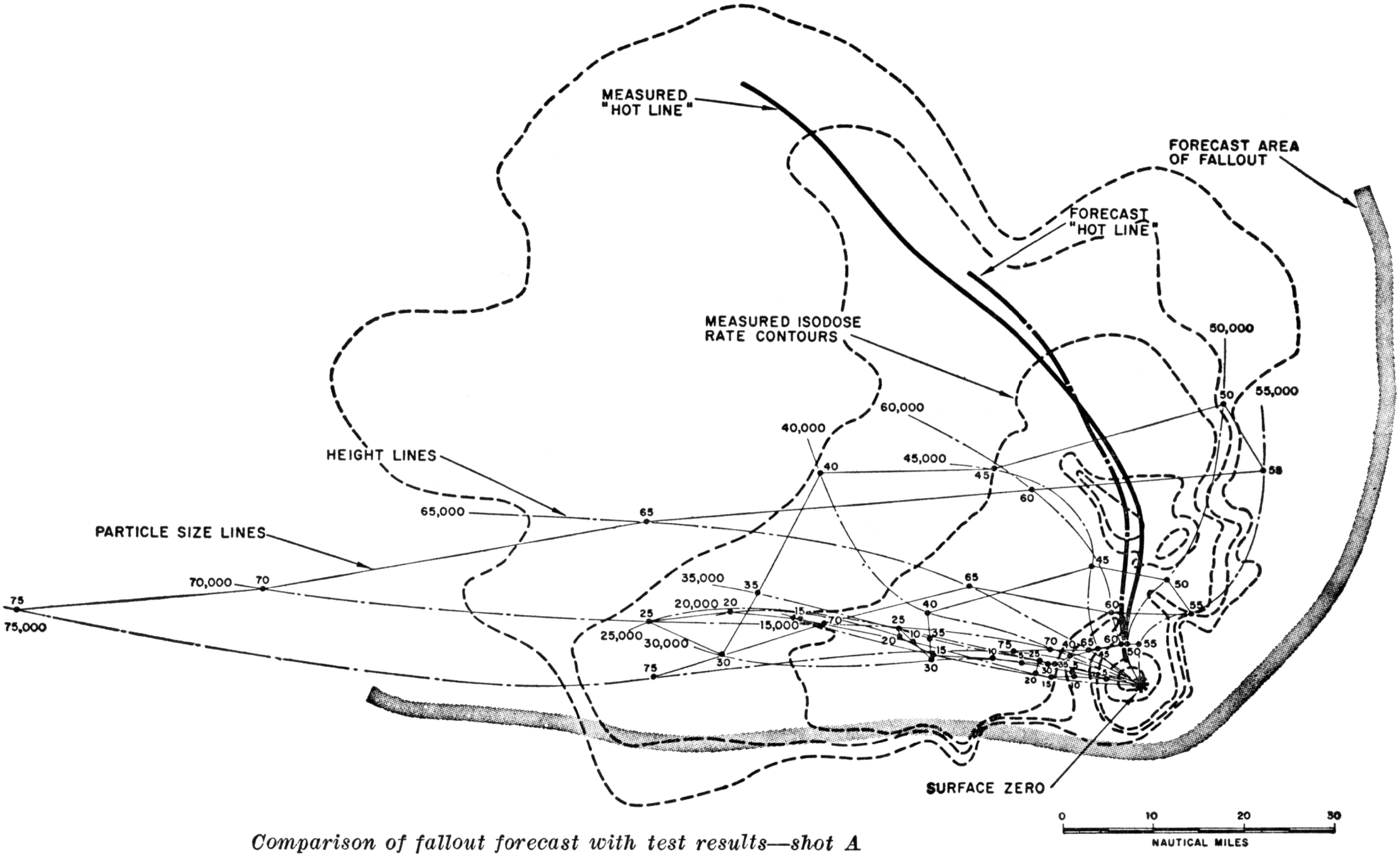

Comparison of fallout forecast with test results—shot A

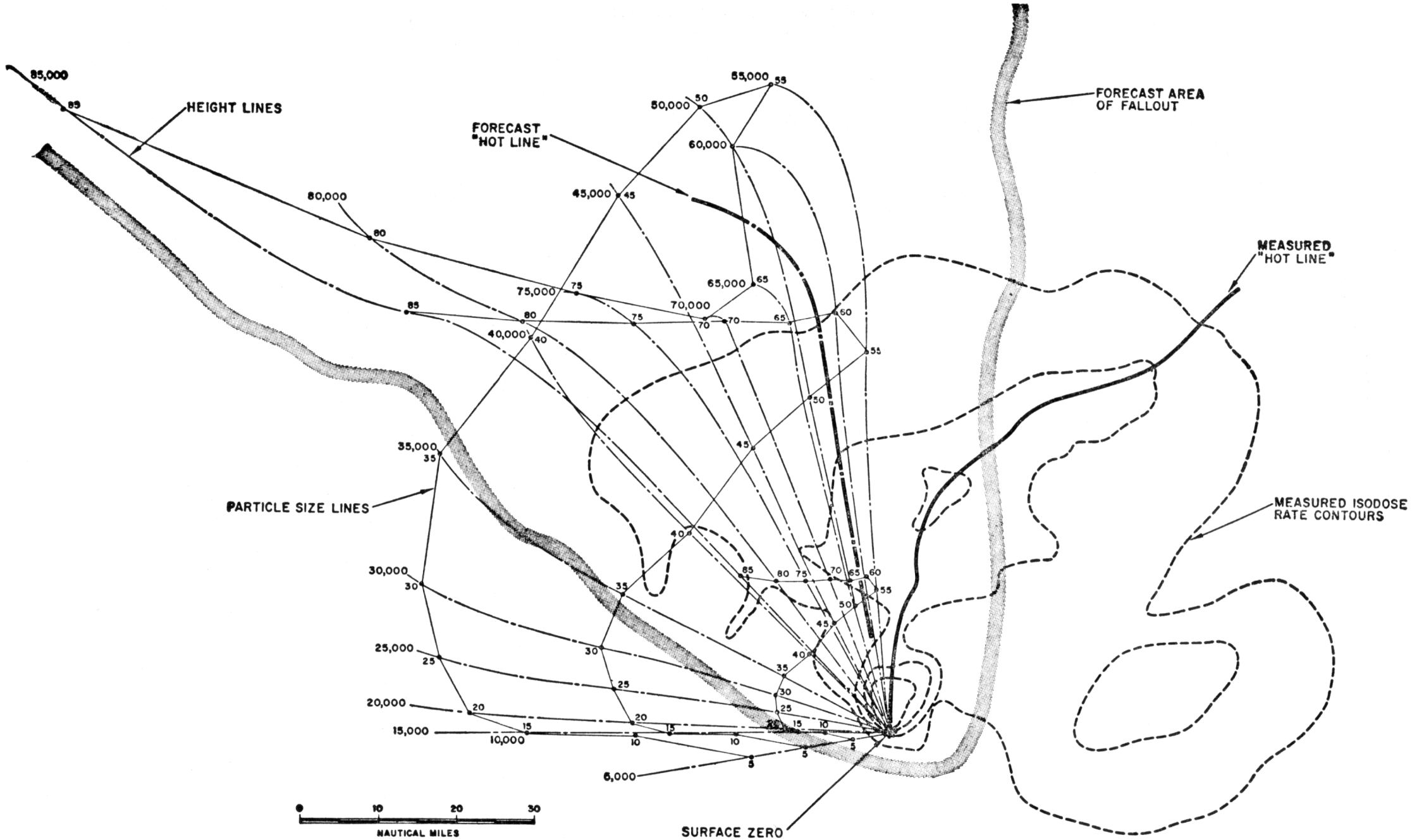

Comparison of fallout forecast with test results—shot B.

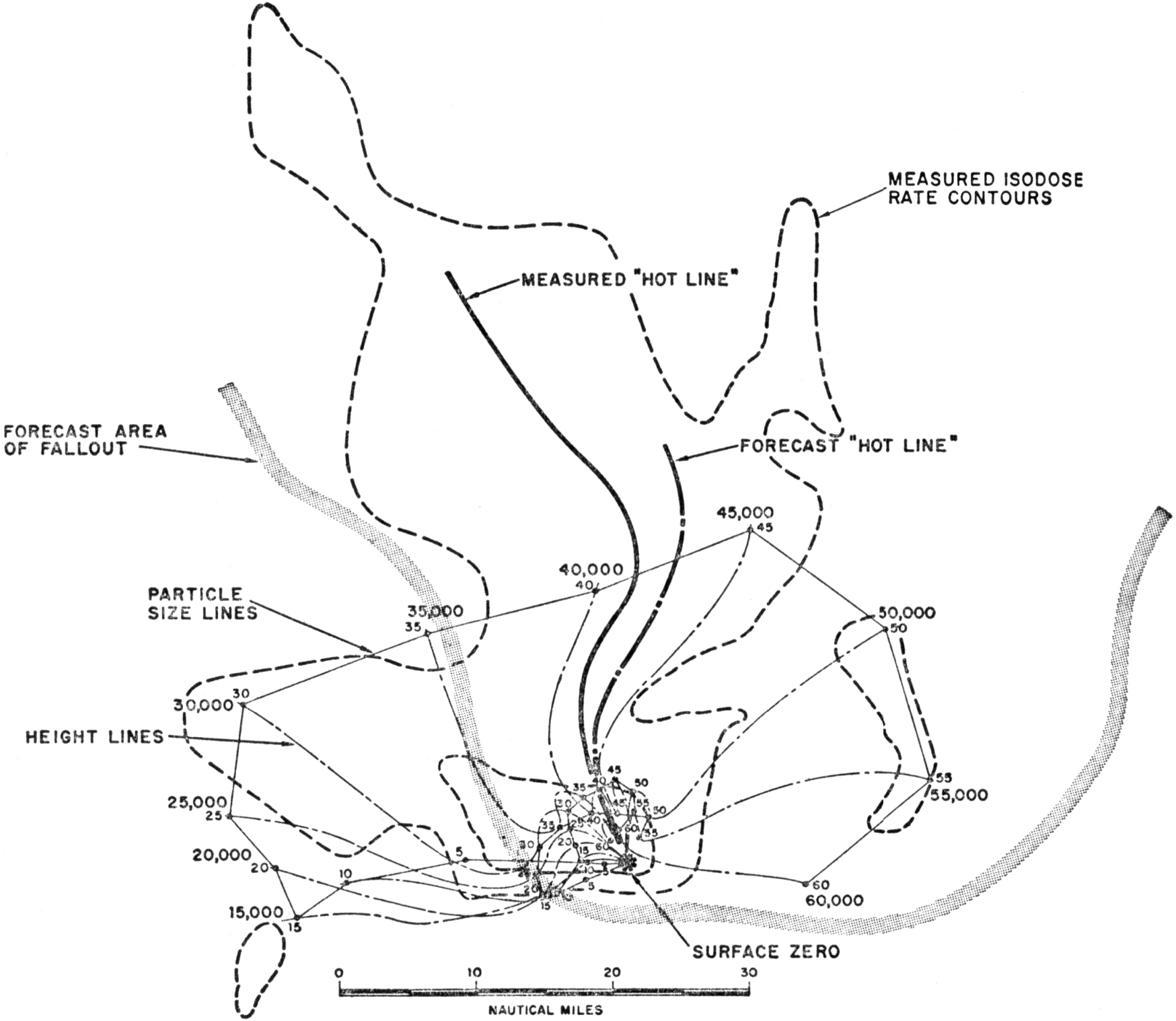

Comparison of fallout forecast with test results—shot C.

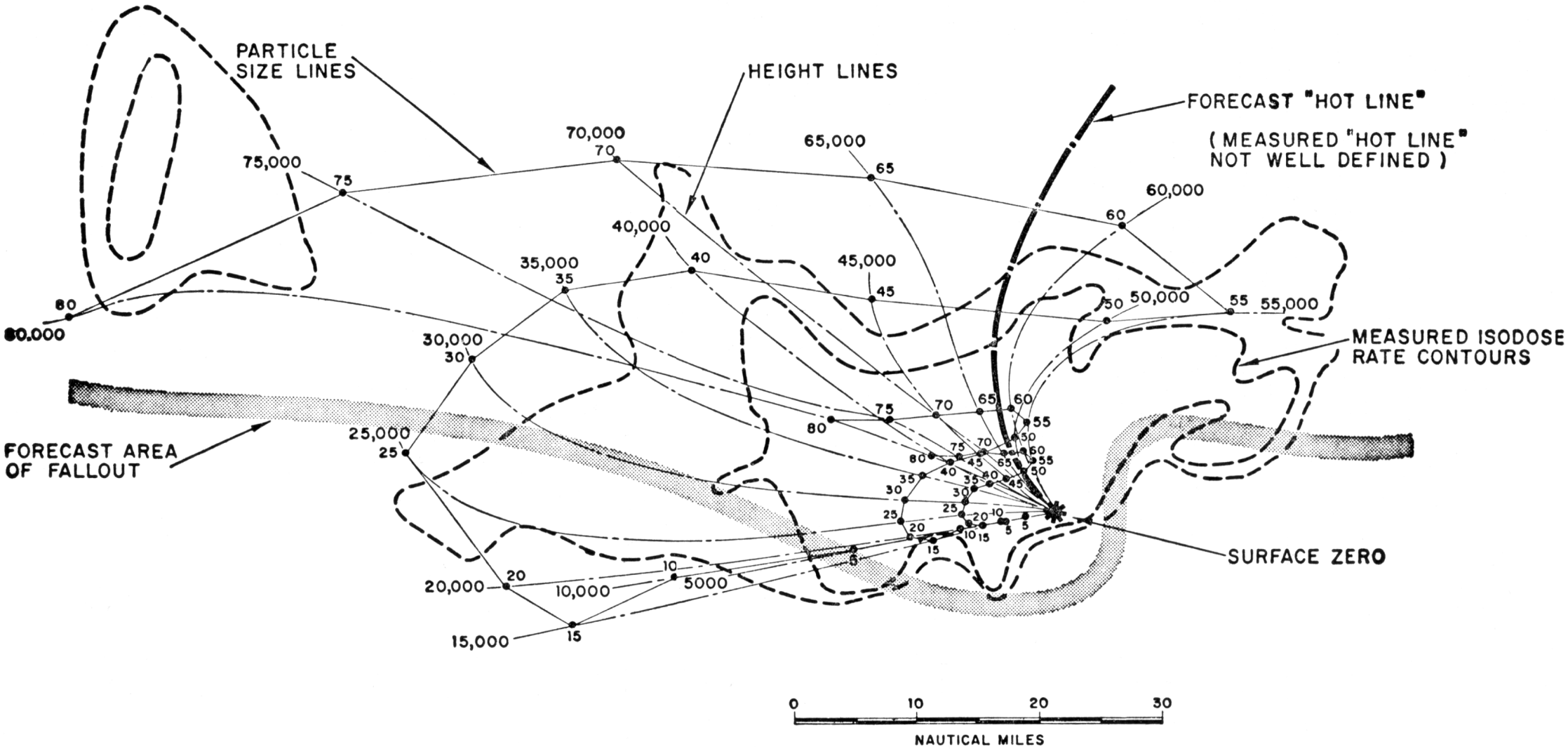

Comparison of fallout forecast with test results—shot D.

SECRET

WT-615

This document consists of 84 pages
No. 254 of 265 copies, Series A

Report to the Scientific Director

NATURE, INTENSITY, AND DISTRIBUTION OF FALL-OUT FROM MIKE SHOT

By

W. B. Heidt, Jr., LCDR, USN
E. A. Schuert
W. W. Perkins
R. L. Stetson

U. S. Naval Radiological Defense Laboratory
San Francisco, California
April 1953

RESTRICTED DATA

This document contains restricted data as defined in the Atomic Energy Act of 1946. Its transmittal or the disclosure of its contents in any manner to an unauthorized person is prohibited.

SECRET
SECURITY INFORMATION

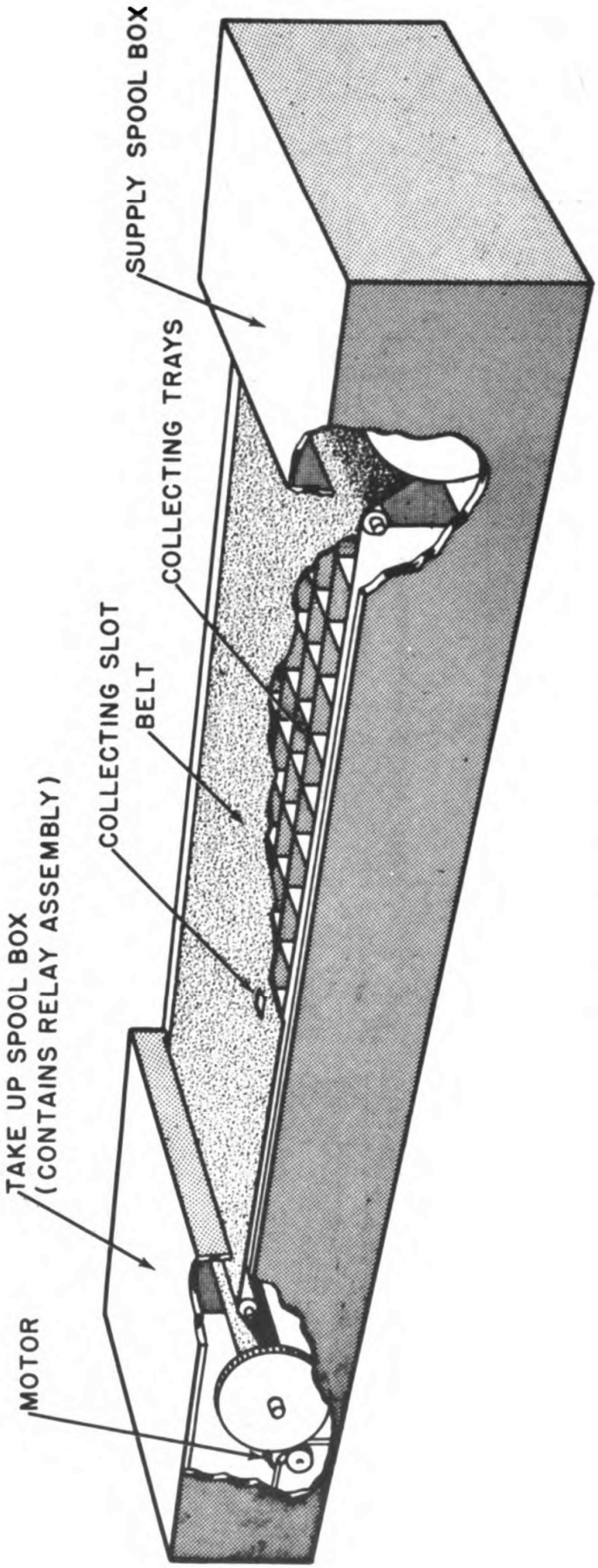

Fig. 3.2—Differential fall-out collector.

RESTRICTED DATA—SECRET—SECURITY INFORMATION

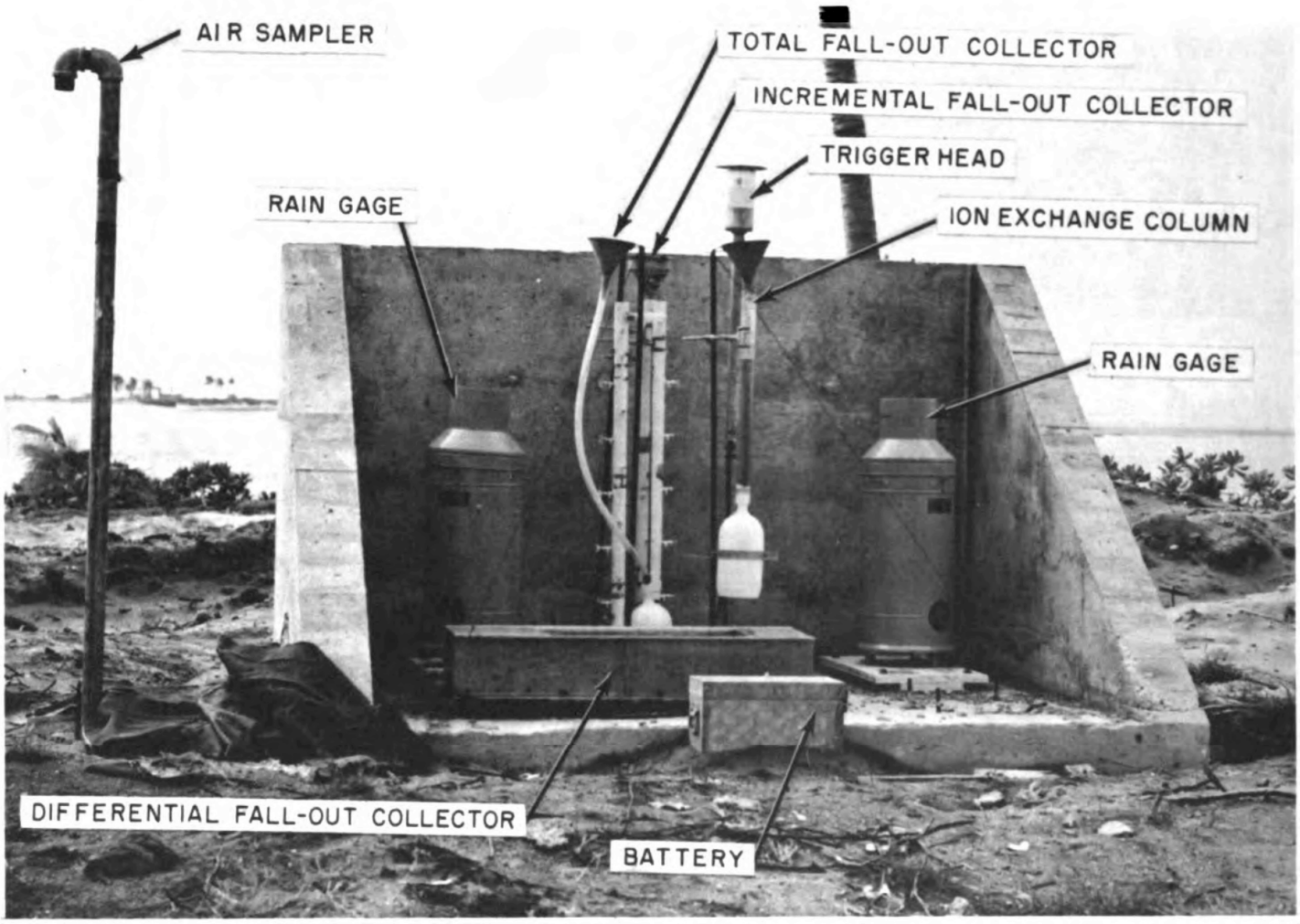

Fig. 3.8—A typical land station.

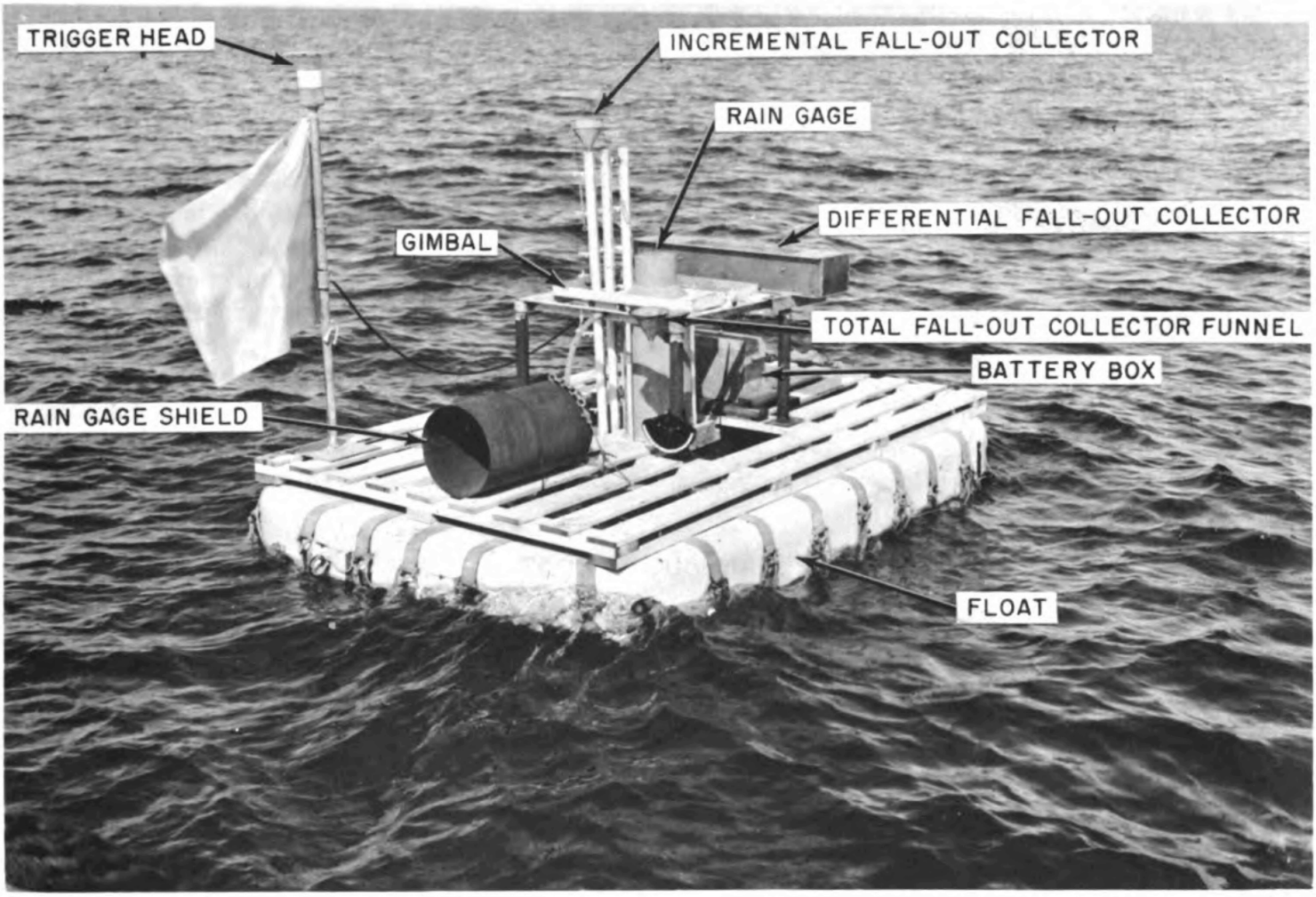

Fig. 3.9—A typical lagoon station.

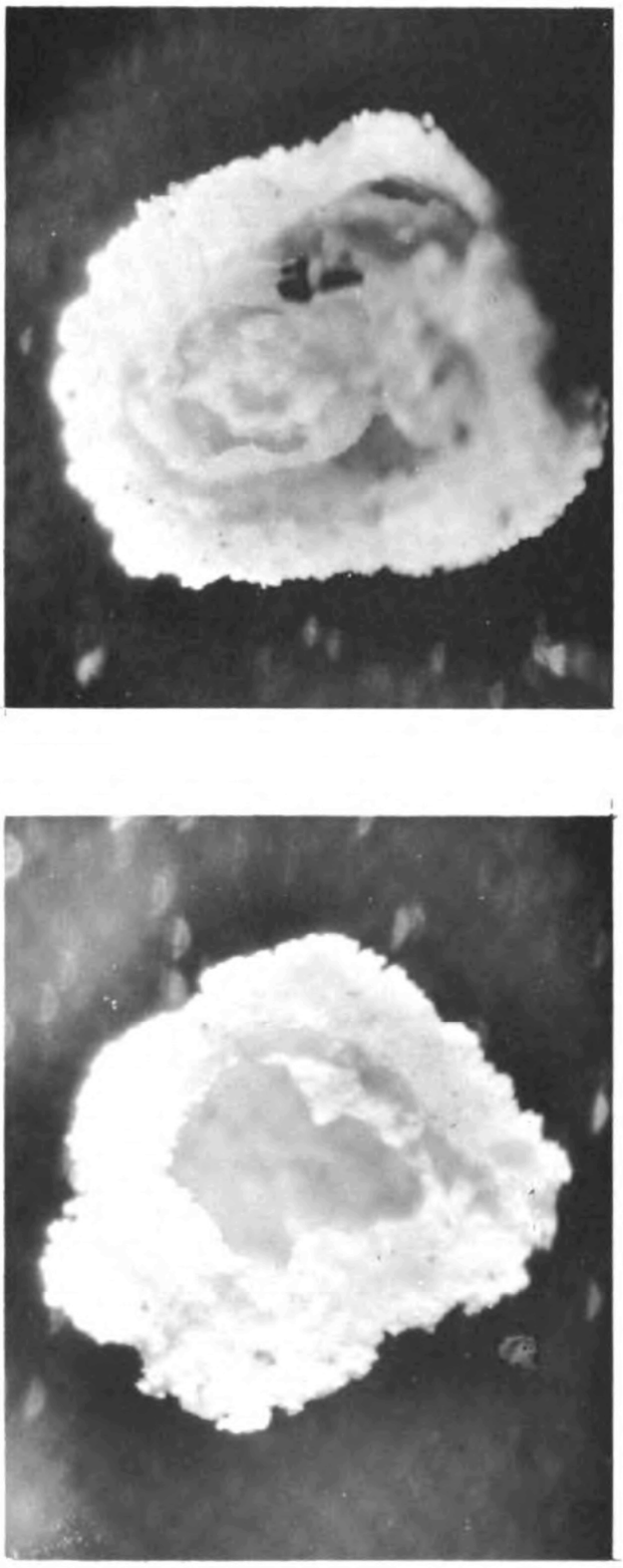

1,000
MICRONS

Fig. 4.4—Inverted view of typical particles removed from life-float decking.

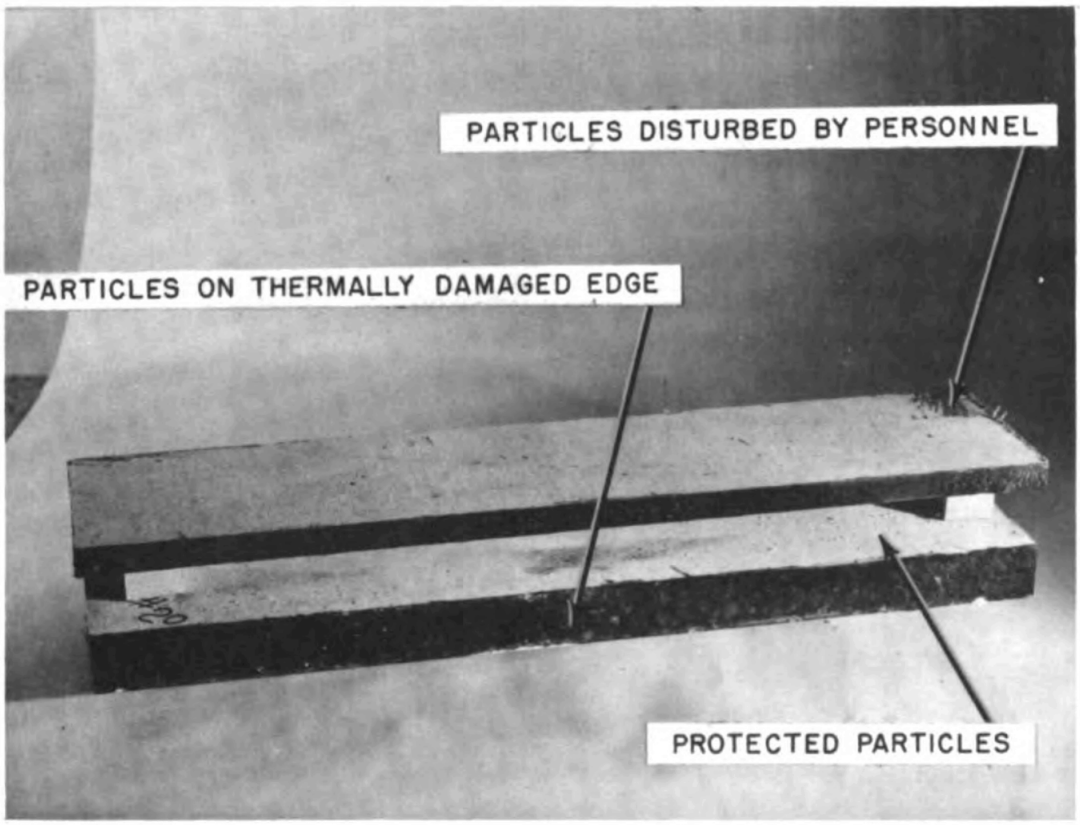

Fig. 4.5—Typical life-float section.

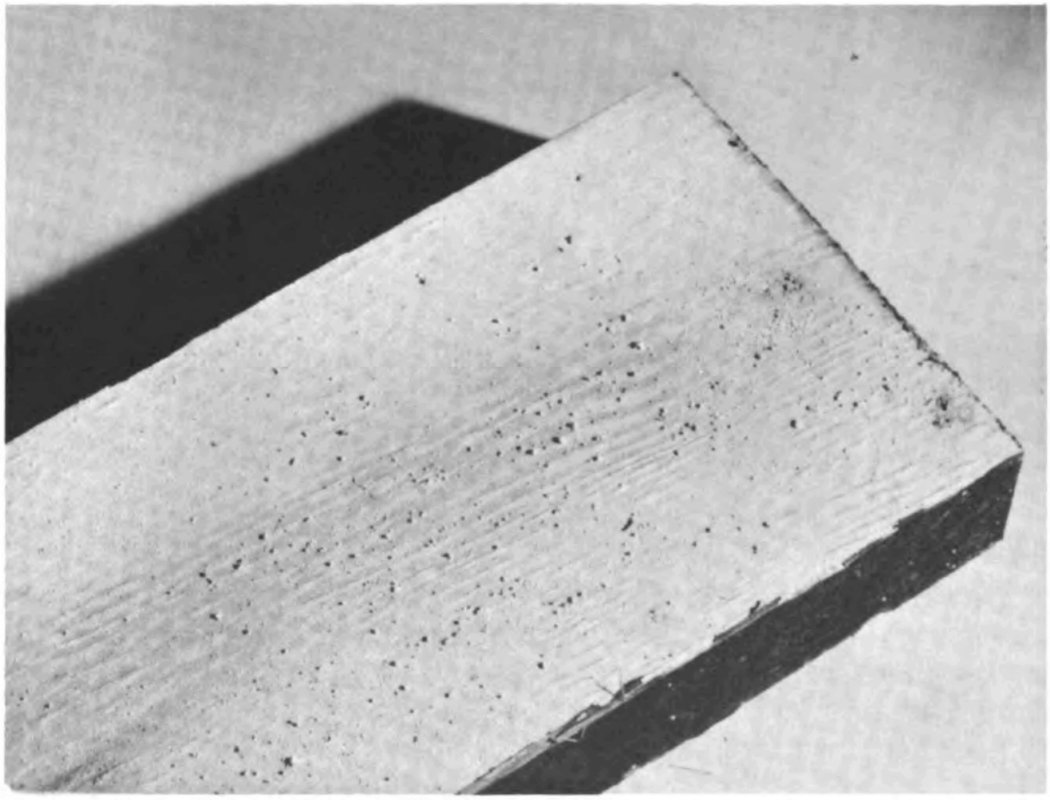

Fig. 4.6—Particle deposition on life-float decking (lower deck of Fig. 4.5).

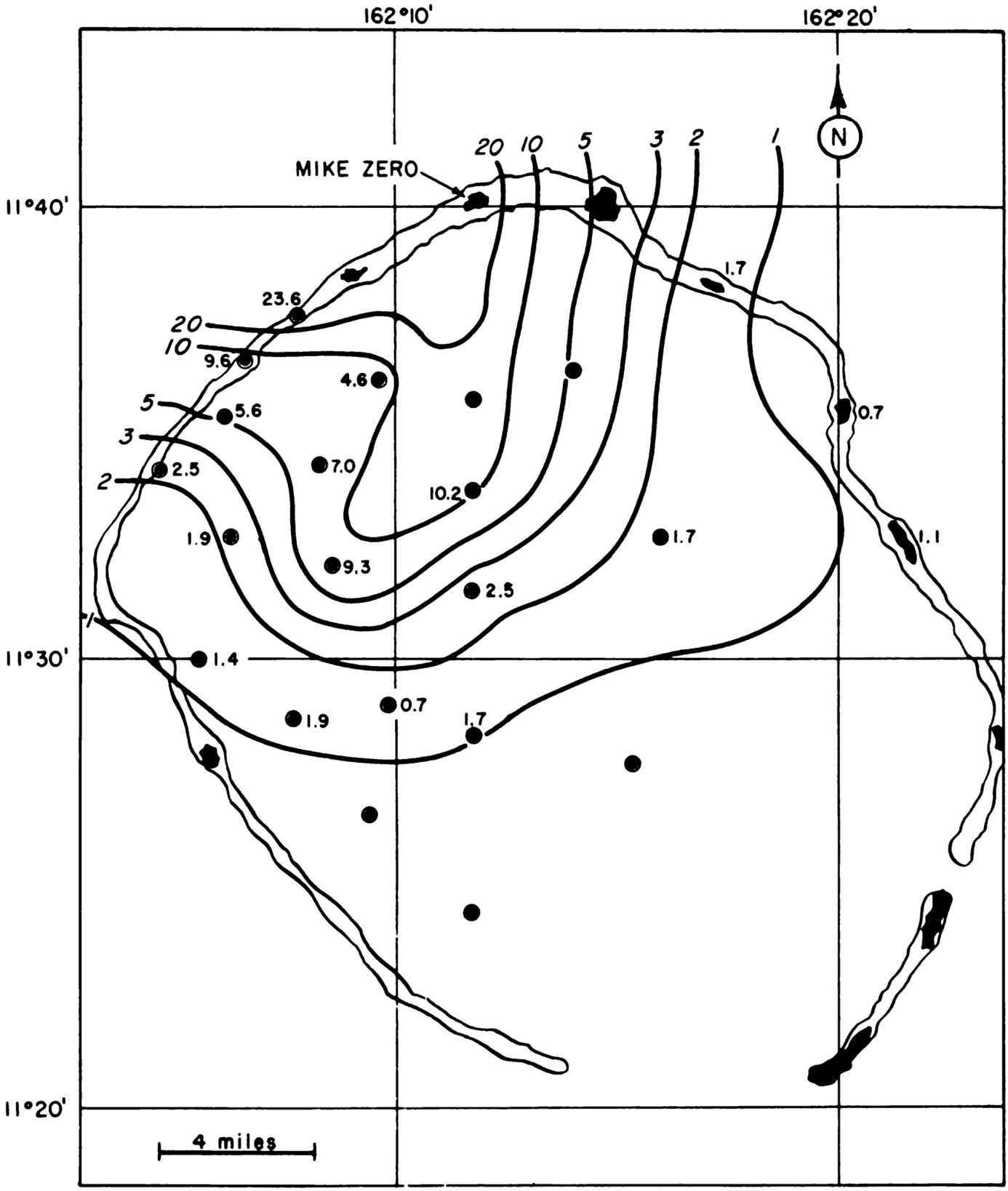

Fig. 4.8—Mass distribution of fall-out (g/sq ft).

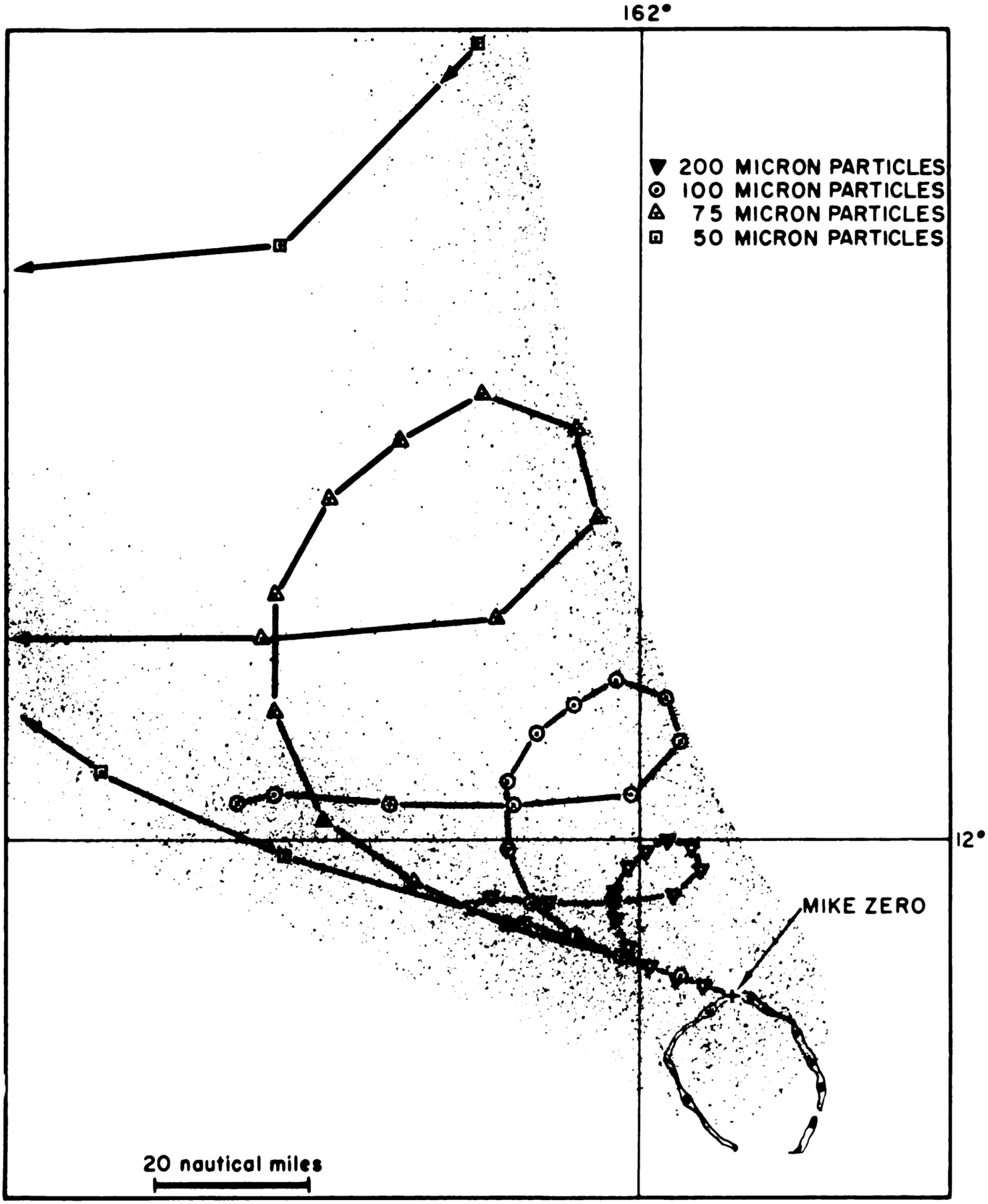

Fig. 6.1—Predicted area of primary fall-out.

WT-915

This document consists of 172 pages

No. 238 of 240 copies, Series A

OPERATION CASTLE

Project 2.5a

DISTRIBUTION AND INTENSITY OF FALLOUT

REPORT TO THE SCIENTIFIC DIRECTOR

by

R. L. Steton
E. A. Schuert
W. W. Perkins
T. H. Shirasawa
H. K. Chan

This document regraded
From SECRET
To UNCLASSIFIED
Date 14 July 82
Authority DNA LTR, 6/14/82
Robert W. Ring

January 1956

[redacted]

U. S. Naval Radiological Defense Laboratory
San Francisco 24, California

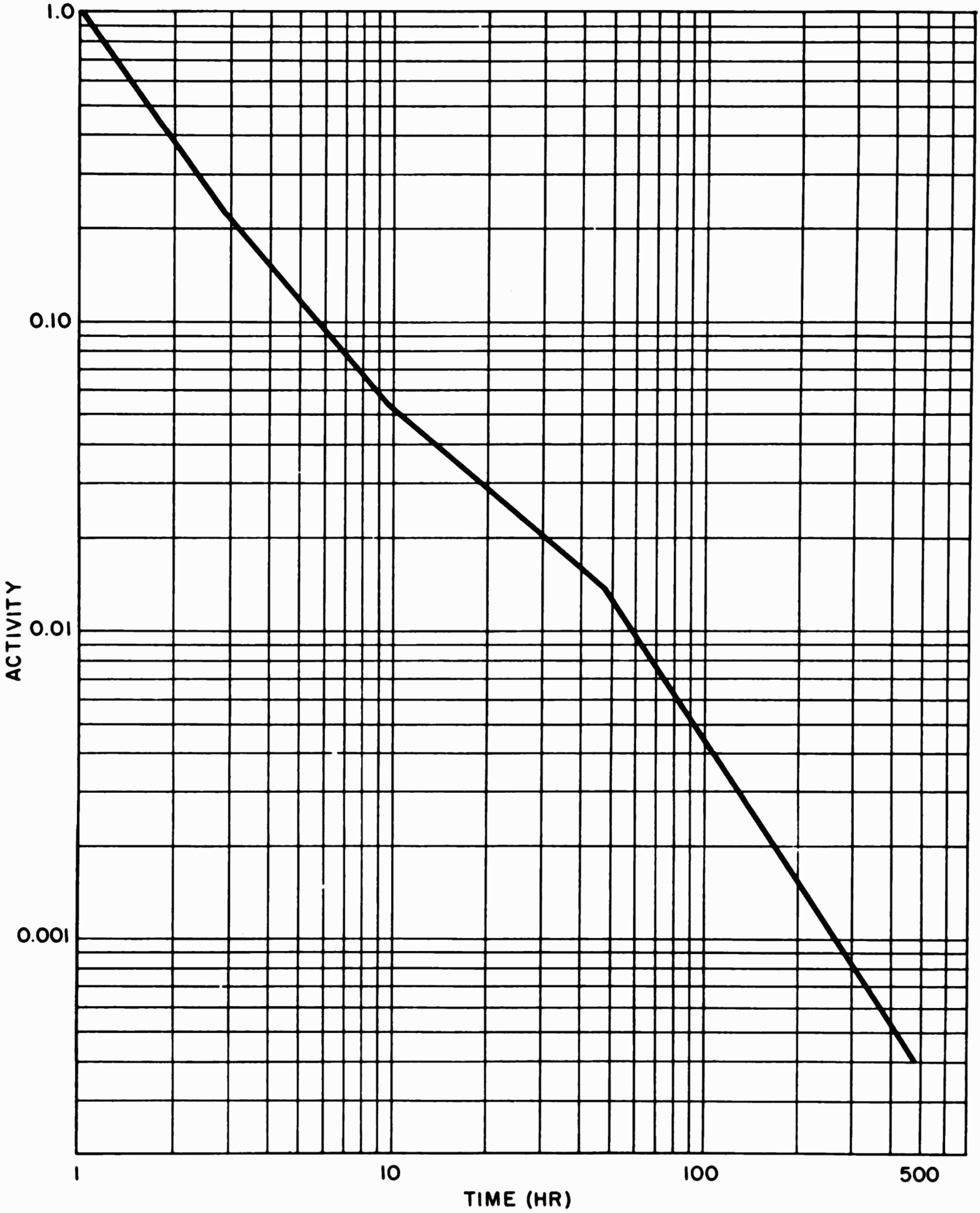

Fig. 5.3 Composite Gamma Ionization Decay Curve

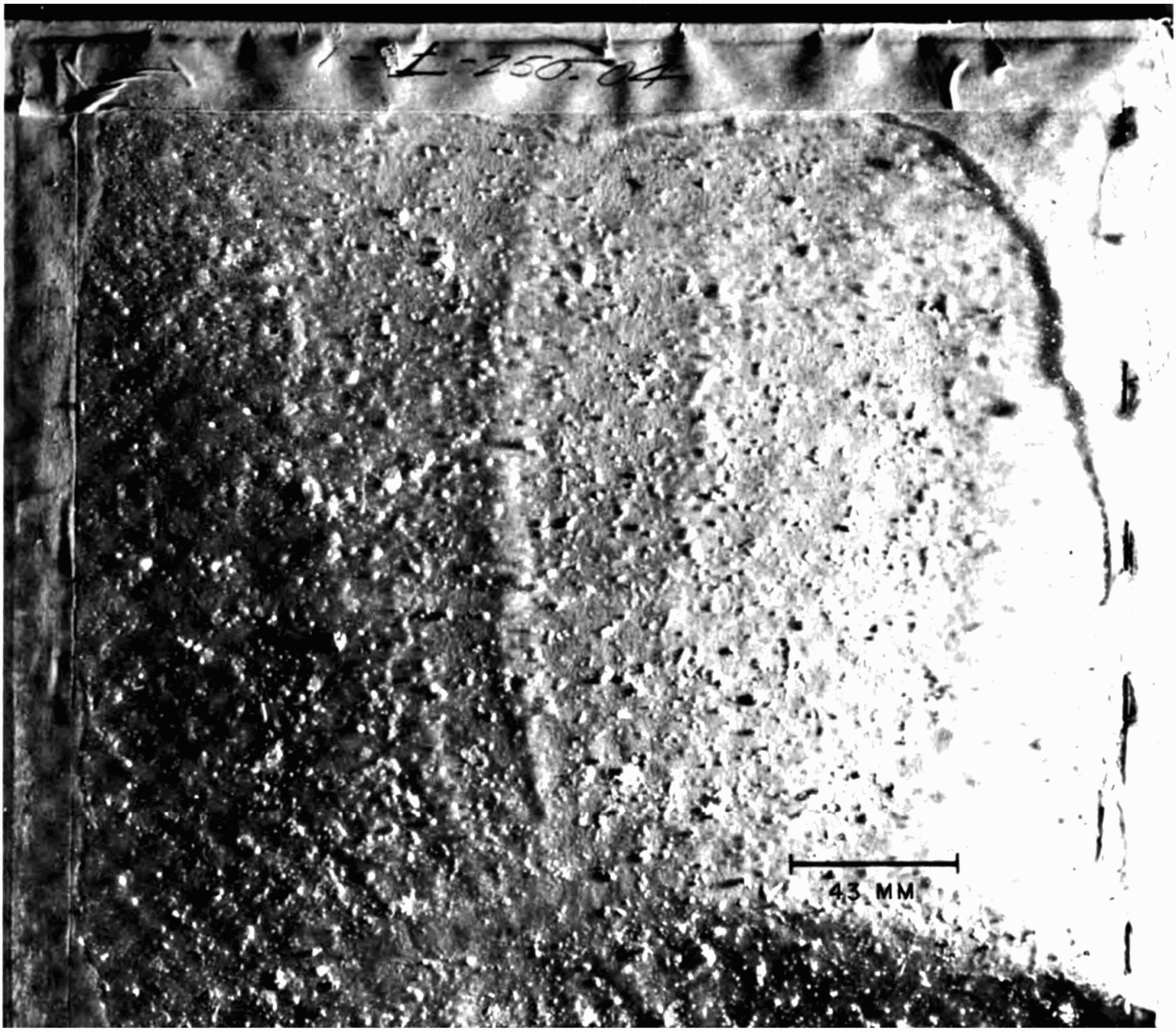

Fig. 5.10 Shot 1, Fallout Particulate, Station 250.04

This is a raft downwind in Bikini Lagoon, which received a land equivalent of 113 R/hr (1 hour reference gamma dose rate), according to Figures 2.2 and 6.1. Land equivalent dose rates were 7 times the raft dose rate in the lagoon.

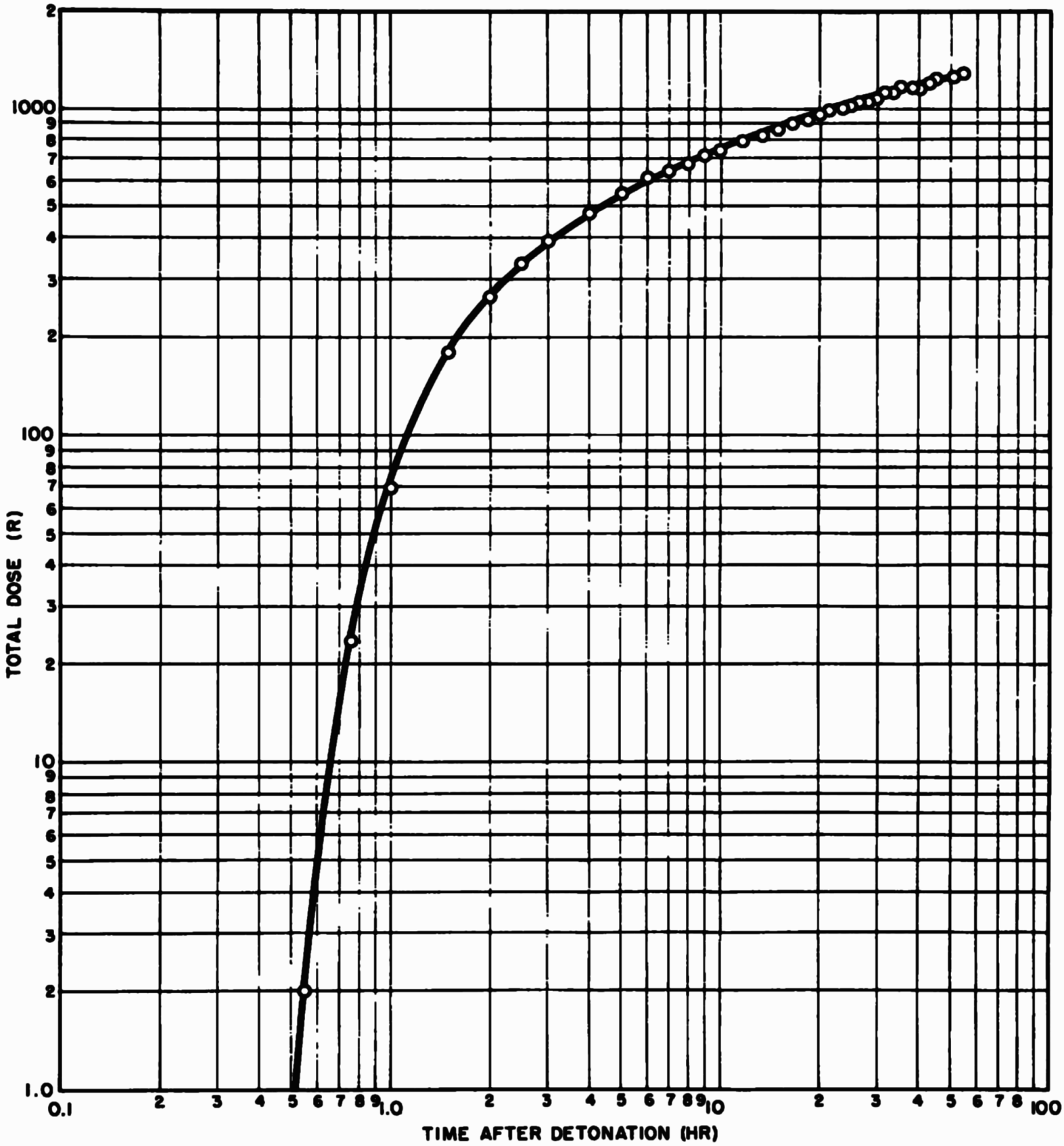

Fig. 5.11 Shot 1, Integrated Gamma Dose, Station 251.03

Bikini (How) Island in Bikini Atoll, which received a land equivalent of about 725 R/hr gamma at 1 hour reference time, according to Figures 2.2 and 6.1.

[redacted]

UNCLASSIFIED

SANITIZED VERSION

TECHNICAL ANALYSIS REPORT - AFSWP NO. 507-SAN

RADIOACTIVE FALL-OUT HAZARDS FROM SURFACE BURSTS OF VERY HIGH YIELD NUCLEAR WEAPONS, Sanitized Version

by

D. C. Borg
L. D. Gates
T. A. Gibson, Jr.
R. W. Paine, Jr.

WEAPONS EFFECTS DIVISION

This Armed Forces Special Weapons Project Technical Analysis Report is a staff study prepared for the Chief, AFSWP on a subject of military interest. The conclusions may be modified as new data become available.

Reproduced From
Best Available Copy

MAY 1954

HEADQUARTERS, ARMED FORCES SPECIAL WEAPONS PROJECT
WASHINGTON 13, D. C.

[redacted]

Declassified WITH DELETIONS BY DNA,
Chief, ISTS and DOE for FOIA 96-032
Date: 2/22/96

Statement A
Approved for public release;
Distribution unlimited.

19991108 122

UNCLASSIFIED

DISTRIBUTION STATEMENT A
Approved for Public Release
Distribution Unlimited

[redacted]

Fig. A TOTAL DOSE FROM TIME OF FALL OUT TO H+50

Idealized Fall-out Contours for a 15 MT Land-surface Burst with a 15 Knot Effective Wind

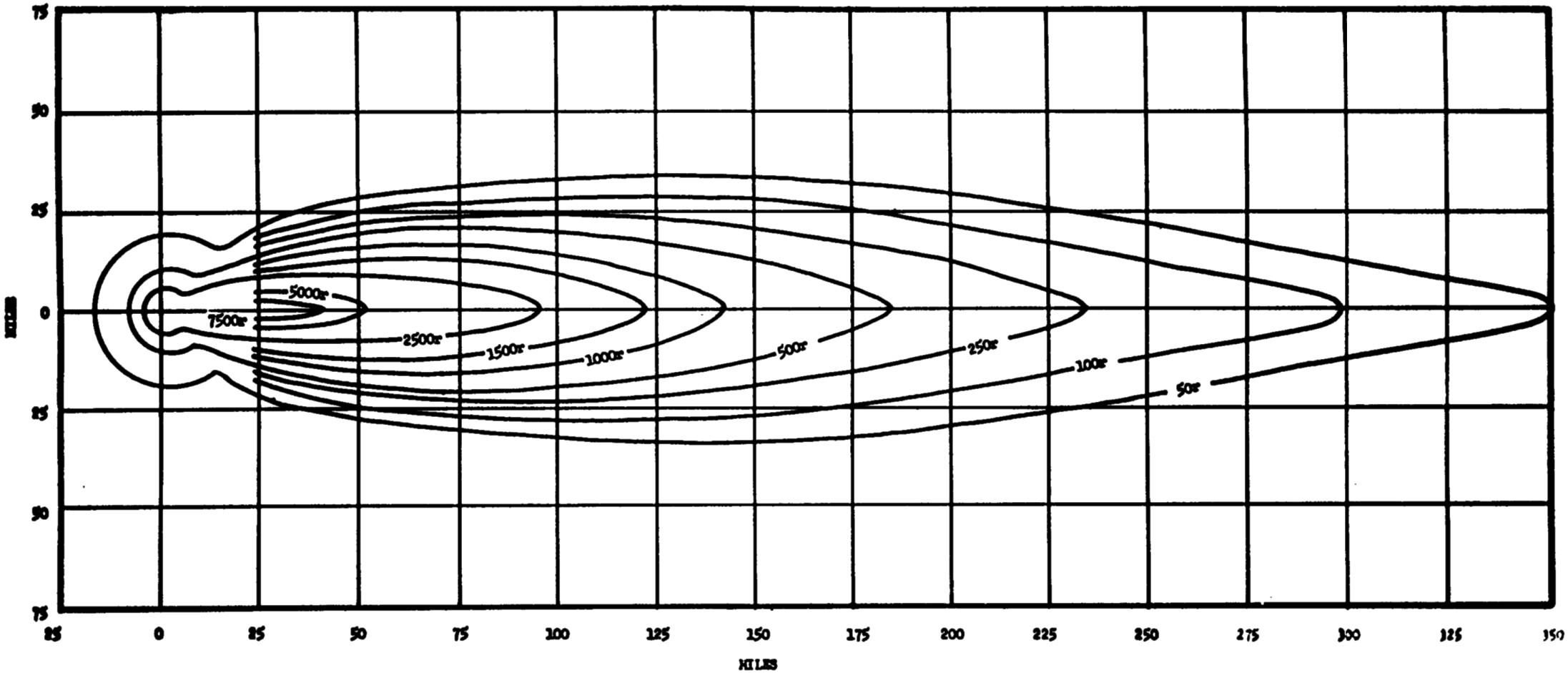

[redacted]

[redacted]

The shielding afforded by an ordinary frame house may effectively reduce the size of the hazard areas by a factor of about two, and a basement shelter by a factor of ten or more. Virtually complete protection against the lethal effects of radioactive fall-out can be obtained if personnel have protection equal to or better than that afforded by a simple underground shelter with at least three feet of earth cover, and if they are evacuated after a week or ten days in such a shelter.

One may draw the following conclusions from this analysis:

a. Very large areas, of the order of 5,000 square miles or more, are likely to be contaminated by the detonation of a 15 megaton yield weapon on land surface, in such intensities as to be hazardous to human life.

b. The fact that a large percentage of the radiologically hazardous area will lie outside the range of destructive bomb effects for normal wind conditions, extending up to several hundred miles downwind, makes the radiological fall-out hazard a primary anti-personnel effect.

c. Accurate pre-shot prediction of the location of the hazardous area with respect to the burst point is virtually impossible without extensive wind data at altitudes up to about 100,000 feet, owing to the sensitive wind-dependence of the distribution mechanism.

d. The fall-out contaminant can be expected to decay at such a rate that all but the most highly contaminated areas could be occupied by previously unexposed personnel on a calculated risk

basis within a few days after the contaminating event; and even these highly contaminated areas may then be entered briefly by decontamination teams.

e. Passive defense measures, intelligently applied, can drastically reduce the lethally hazardous areas. A course of action involving the seeking of optimum shelter, followed by evacuation of the contaminated area after a week or ten days, appears to offer the best chance of survival. At the distant downwind areas, as much as 5 to 10 hours after detonation time may be available to take shelter before fall-out commences.

f. Universal use of a simply constructed deep underground shelter, a subway tunnel, or the sub-basement of a large building could eliminate the lethal hazard due to external radiation from fall-out completely, if followed by evacuation from the area when ambient radiation intensities have decayed to levels which will permit this to be done safely.

g. It is of vital importance for individuals in hazardous areas to seek optimum shelter at once, since the dosage received in the first few hours after fall-out has commenced will exceed that received over the rest of a week spent in the contaminated area.

Table II

Total Isodose Contour: 500r from Fall-out to H+50 Hours

Yield (MT)	15	1	10	60	* 60
Downwind extent (mi)	180	52	152	340	(307)
Crosswind axis (mi)	40	12	34	70	
GZ circle radius (mi)	11.5	3.85	9.7	21	
GZ circle displacement (mi)	3.5	1.2	3	5.75	
Area (mi^2)	5400	470	3880	17,900	(16,250)
Area of true ellipse (mi^2)	(5650)	(491)	(4055)	(18,700)	

* Using Part D, Chapter II.

[redacted]

Table VII

Minimum Dosages Within Areas
For City Decontamination
15 MT Surface Burst

Case When Decontamination Takes 2.2 Days and Starts at H+2 Days

AREA	1000 mi^2	3000 mi^2	5000 mi^2	8000 mi^2
Damage dose after staying in best average shelter (fall-out time to H+2 days)	160 r	65 r	40 r	23 r
Damage dose during decontamination effort received by 66% of population which is engaged (H+2 days to H+4.2 days)	120 r	50 r	30 r	17 r
Total Damage dose received up to H+4.2 days	280 r	115 r	70 r	40 r
Acute biological effect	LD/1 SD/55	None	None	None

Case When Decontamination Takes 13 Days and Starts at H+6 Days

AREA	1000 mi^2	3000 mi^2	5000 mi^2	8000 mi^2
Damage dose before decontamination begins when in best average shelter (fall-out time to H+6 days)	240 r	110 r	60 r	30 r
Damage dose during decontamination effort received by 60% of population which is engaged (H+6 Days to H+19 days)	(No additional damage dose received due to biological recovery)			
Total damage dose received up to H+19 days	240 r	110 r	60 r	30 r
Acute biological effect	SD/25	None	None	None

[redacted]

Proceedings of the Symposium
held at Washington, D. C.
April 19-23, 1965 by the
Subcommittee on Protective Structures,
Advisory Committee on Civil Defense,
National Academy of Sciences—
National Research Council

Protective Structures for CIVILIAN POPULATIONS

1966

MODEL ANALYSIS

Mr. Ivor Ll. DAVIES
Suffield Experimental Station
Canadian Defense Research Board
Ralston, Alberta, Canada

Nuclear-Weapon Tests

In 1952 we fired our first nuclear device, effectively a "nominal" weapon, at Monte Bello, off northwest Australia. To the blast loading from this weapon we exposed a number of reinforced-concrete cubicle structures that had been designed for the dynamic loading conditions, and for which we made the best analysis of response we were competent to make at that time. Our estimates of effects were really a dismal failure. The structures were placed at pressure levels of 30, 10, and 6 psi, where we expected them to be destroyed, heavily damaged with some petaling of the front face, and extensively cracked, respectively. In fact, the front face of the cubicle at 30 psi was broken inwards; failure had occurred along both diagonals, and the four triangular petals had been pushed in. At the 10-psi level, where we had three cubicles, each with a different wall thickness (6, 9, and 12 in.), we observed only light cracking in the front face of that cubicle with the least thick wall (6 in.). The other two structures were apparently undamaged, as was the single structure at the 6-psi level.

In 1957, the first proposals were made for the construction of the underground car park in Hyde Park in London. The Home Office was interested in this project since, in an emergency, the structure could be used as a shelter. Consequently a request was made to us at Atomic Weapons Research Establishment (A.W.R.E.) to design a structure that would be resistant to a blast loading of about 50 psi, and to test our design on the model scale.

Using the various load-deformation curves obtained in this test, an estimate was made of the response of the structure to blast loading. Of particular interest was the possible effect of 100 tons of TNT, the first 100-ton trial at Suffield in Alberta.

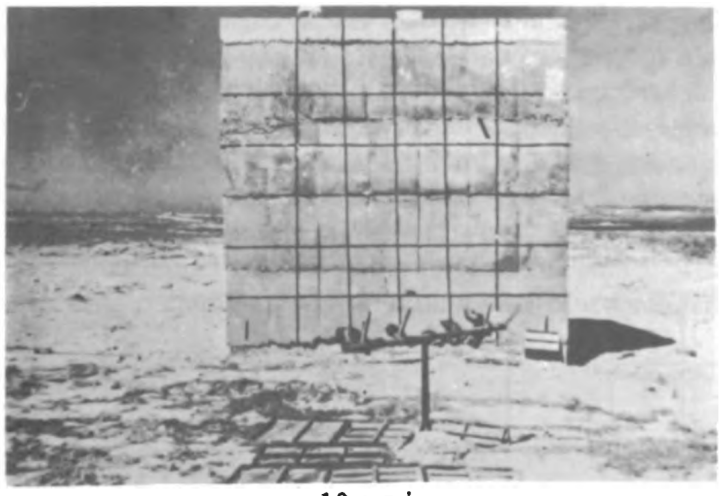

10 p.s.i.

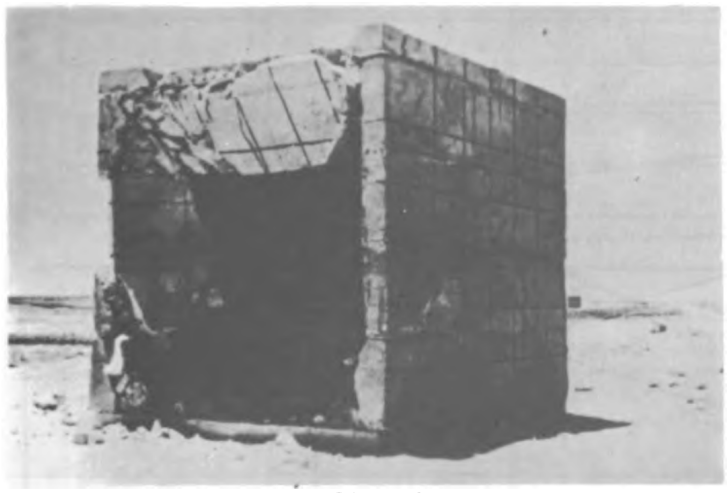

34 p.s.i.

Dynamic tests, Monte Bello cubicles.

A total of seven more models was made; six were shipped to Canada and placed with the top surface of the roof flush with the ground and at positions where peak pressures of 100, 80, 70, 60, 50, and 40 psi were expected. The seventh model was kept in England for static testing at about the time of firing. The results were not as expected. In the field, the four models farthest from the charge were apparantly undamaged; we could see no cracking with the eye, nor did soaking the models with water reveal more than a few hair cracks. The model nearest the charge was lightly cracked in the roof panels and beams, and one of the columns showed slight spalling at the head. This model had been exposed to a peak pressure of 110 psi.

BLAST AND OTHER THREATS

Harold Brode
The RAND Corporation, Santa Monica, California

Chemical High-Explosive Weapons

As in past aerial warfare, bombs and missiles carrying chemical explosives to targets are capable of extensive damage only when delivered in large numbers and with high accuracy.

Biological Warfare

Most biological agents are inexpensive to produce; their effective dissemination over hostile territories remains the chief deterrent to their effective employment. Twenty square miles is about the area that can be effectively covered by a single aircraft; large area coverage presents a task for vast fleets of fairly vulnerable planes flying tight patterns at modest or low altitudes. While agents vary in virulence and in their biologic decay rate, most are quite perishable in normal open-air environments. Since shelter and simple prophylactic measures can be quite effective against biological agents, there is less likelihood of the use of biological warfare on a wholesale basis against a nation, and more chance of limited employment on population concentrations —perhaps by covert delivery, since shelters with adequate filtering could insure rather complete protection to those inside.

Chemical Weapons

Chemical weapons, like biological weapons, are relatively inexpensive to create, but face nearly insurmountable logistics problems on delivery. Although chemical agents produce casualties more rapidly, the greater amounts of material to deliver seriously limit the likelihood of their large-scale deployment. Furthermore, chemical research does not hold promise of the development of significantly more toxic chemicals for future use.

Radiological Weapons

The advantages of such modifications are much less real than apparent. In all weapons delivered by missiles, minimizing the payload and total weight is very important. If the total payload is not to be increased, then the inclusion of inert material to be activated by neutrons must lead to reductions in the explosive yield. If all the weight is devoted to nuclear explosives, then more fission-fragment activity can be created, and it is the net difference in activity that must be balanced against the loss of explosive yield. As it turns out, a fission explosion is a most efficient generator of activity, and greater total doses are not achieved by injecting special inert materials to be activated.

The Neutron Bomb

The neutron bomb, so called because of the deliberate effort to maximize the effectiveness of the neutrons, would necessarily be limited to rather small yields—yields at which the neutron absorption in air does not reduce the doses to a point at which blast and thermal effects are dominant. The use of small yields against large-area targets again runs into the delivery problems faced by chemical agents and explosives, and larger yields in fewer packages pose a less stringent problem for delivery systems in most applications. In the unlikely event that an enemy desired to minimize blast and thermal damage and to create little local fallout but still kill the populace, it would be necessary to use large numbers of carefully placed neutron-producing weapons burst high enough to avoid blast damage on the ground, but low enough to get the neutrons down. In this case, however, adequate radiation shielding for the people would leave the city unscathed and demonstrate the attack to be futile.

The thermal radiation from a surface burst is expected to be less than half of that from an air burst, both because the radiating fireball surface is truncated and because the hot interior is partially quenched by the megatons of injected crater material.

SUPERSEISMIC GROUND-SHOCK MAXIMA (AT 5-FT DEPTH)

Vertical acceleration: $\alpha_{vm} \simeq 340\, \Delta P_s/C_L \pm 30$ per cent. Here acceleration is measured in g's and overpressure (ΔP_s) in pounds per square inch. An empirical refinement requires C_L to be defined as the seismic velocity (in feet per second) for rock, but as three fourths of the seismic velocity for soil.

OUTRUNNING GROUND-SHOCK MAXIMA (AT ~10-FT DEPTH)

Vertical acceleration: $\alpha_{vm} \simeq 2 \times 10^5/C_L r^2$ + factor 4 or -factor 2. Acceleration is measured in g's, and r is the scaled radial distance—i.e., $r = R/W^{1/3}$ kft/(mt)$^{1/3}$.

Data taken on a low air-burst shot in Nevada indicate an exponential decay of maximum displacement with depth. For the particular case of a burst of ~ 40 kt at 700 ft, some measurements were made as deep as 200 ft below the surface of Frenchman Flat, a dry lake bed, which led to the following approximate decay law, according to Perret.

$$\delta = \delta_0 \exp(-0.017D),$$

where δ represents the maximum vertical displacement induced at depth D, δ_0 is the maximum displacement at the surface, and D is the depth in feet.

Perret, W.R., Ground Motion Studies at High Incident Overpressure, The Sandia Corporation, Operation PLUMBBOB, WT-1405, for Defense Atomic Support Agency Field Command, June 1960.

THE PROTECTION AGAINST FALLOUT RADIATION AFFORDED BY CORE SHELTERS IN A TYPICAL BRITISH HOUSE

Daniel T. Jones
Scientific Adviser, Home Office, London

Protective Factors in a Sample of British Houses (Windows Blocked)

Protective Factor	Percentage of Houses
< 25	36%
25-39	28%
40-100	29%
> 100	7%

"A very much improved protection could be obtained by constructing a shelter core. This means a small, thick-walled shelter built preferably inside the fallout room itself, in which to spend the first critical hours when the radiation from fallout would be most dangerous."(1)

The full-scale experiments were carried out at the Civil Defense School at Falfield Park.(2)

In the staircase construction, the shelter consisted of the cupboard under the stairs, sandbags being placed on treads above and at the sides.

A 93 curies cobalt-60 source was used.

9 in. brick walls The windows and doors were not blocked		contribution r/hr/c/ft^2		Protective Factor
	Position	Ground	Roof	
House only	E2	15.0	8.4	21
Lean-to	E2	10.4	2.4	39
Staircase cupboard:				
Stairs only sandbagged	N2	29.2	5.3	14
Stairs and outer wall sandbagged	N2	16.4	4.6	24
Stairs, outer wall, kitchen wall and corridor partition sandbagged	N2	8.8	1.8	47

1. Six sandbags per tread, and a double layer on the small top landing. 96 sandbags were used.
2. As (1), together with a 4-ft-high wall of sandbags along the external north wall. 160 sandbags were used.
3. As (2), together with 4-ft-high walls of sandbags along the kitchen/cupboard partition wall and along the passage partition. 220 sandbags were used.

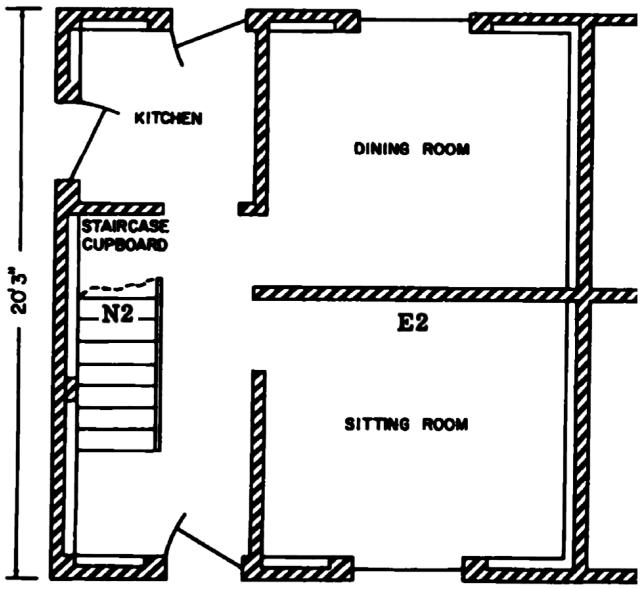

sandbags 24 in. x 12 in. when empty; 16 in. x 9 in. x 4 in. when filled with 25 lb of sand.

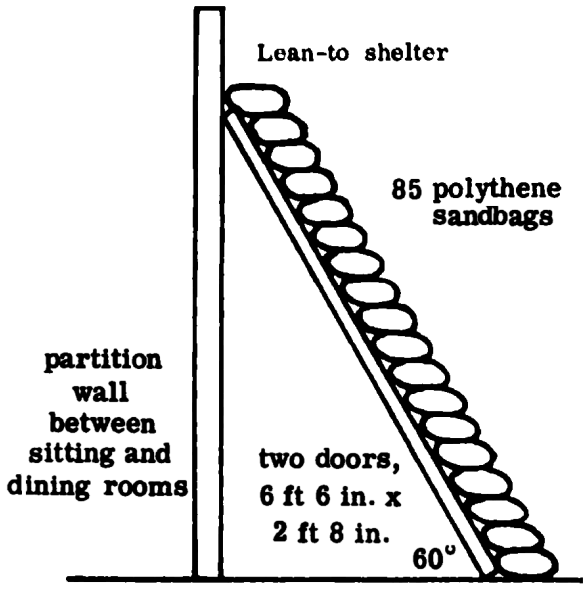

floor area 21 sq ft.

1. Civil Defence Handbook No. 10, HMSO, 1963.
2. Perryman, A. D., Home Office Report CD/SA 117.

Foreword

If the country were ever faced with an immediate threat of nuclear war, a copy of this booklet would be distributed to every household as part of a public information campaign which would include announcements on television and radio and in the press. The booklet has been designed for free and general distribution in that event. It is being placed on sale now for those who wish to know what they would be advised to do at such a time.

May 1980

Protect and Survive

ISBN 0 11 3407289

If Britain is attacked by nuclear bombs or by missiles, we do not know what targets will be chosen or how severe the assault will be.

If nuclear weapons are used on a large scale, those of us living in the country areas might be exposed to as great a risk as those in the towns. The radioactive dust, falling where the wind blows it, will bring the most widespread dangers of all. No part of the United Kingdom can be considered safe from both the direct effects of the weapons and the resultant fall-out.

The dangers which you and your family will face in this situation can be reduced if you do as this booklet describes.

Use tables if they are large enough to provide you all with shelter. Surround them and cover them with heavy furniture filled with sand, earth, books or clothing.

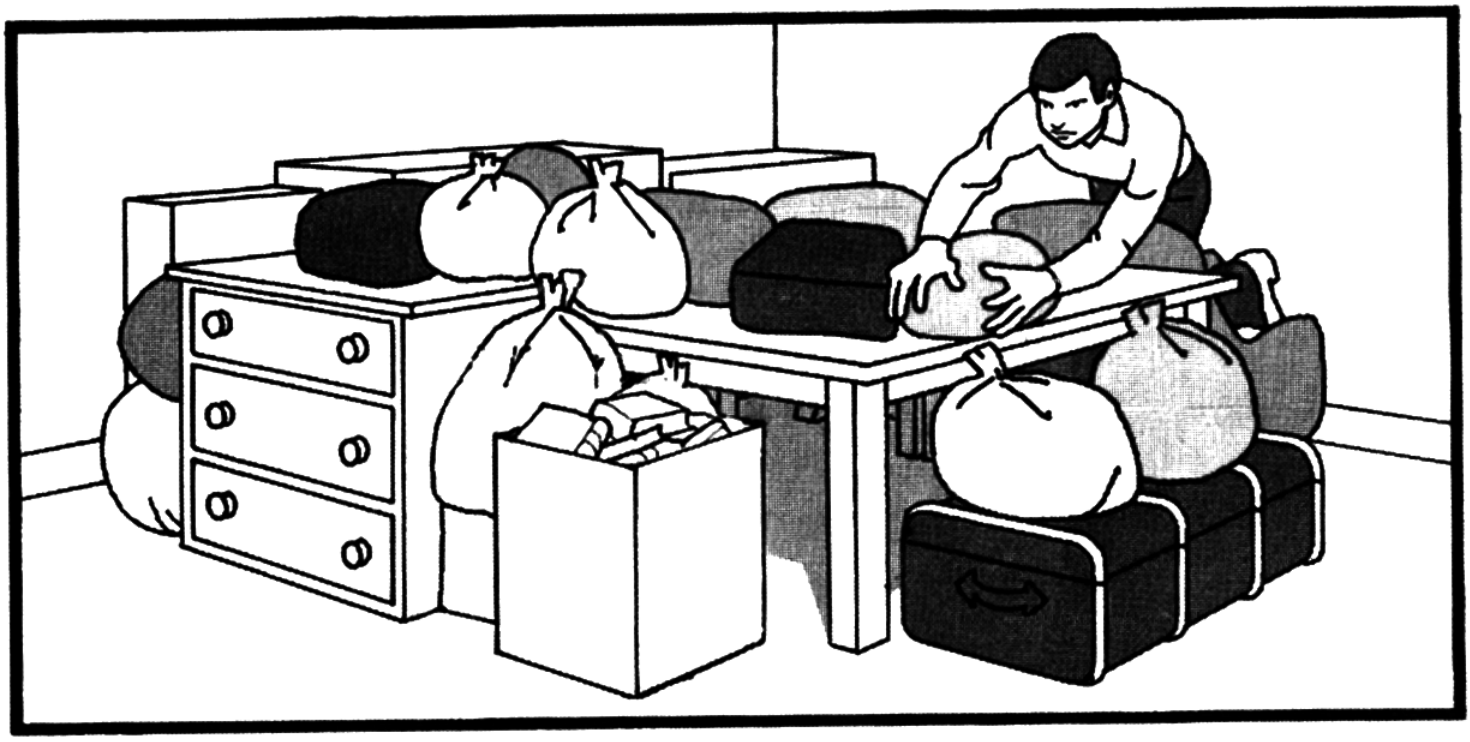

Use the cupboard under the stairs if it is in your fall-out room. Put bags of earth or sand on the stairs and along the wall of the cupboard. If the stairs are on an outside wall, strengthen the wall outside in the same way to a height of six feet.

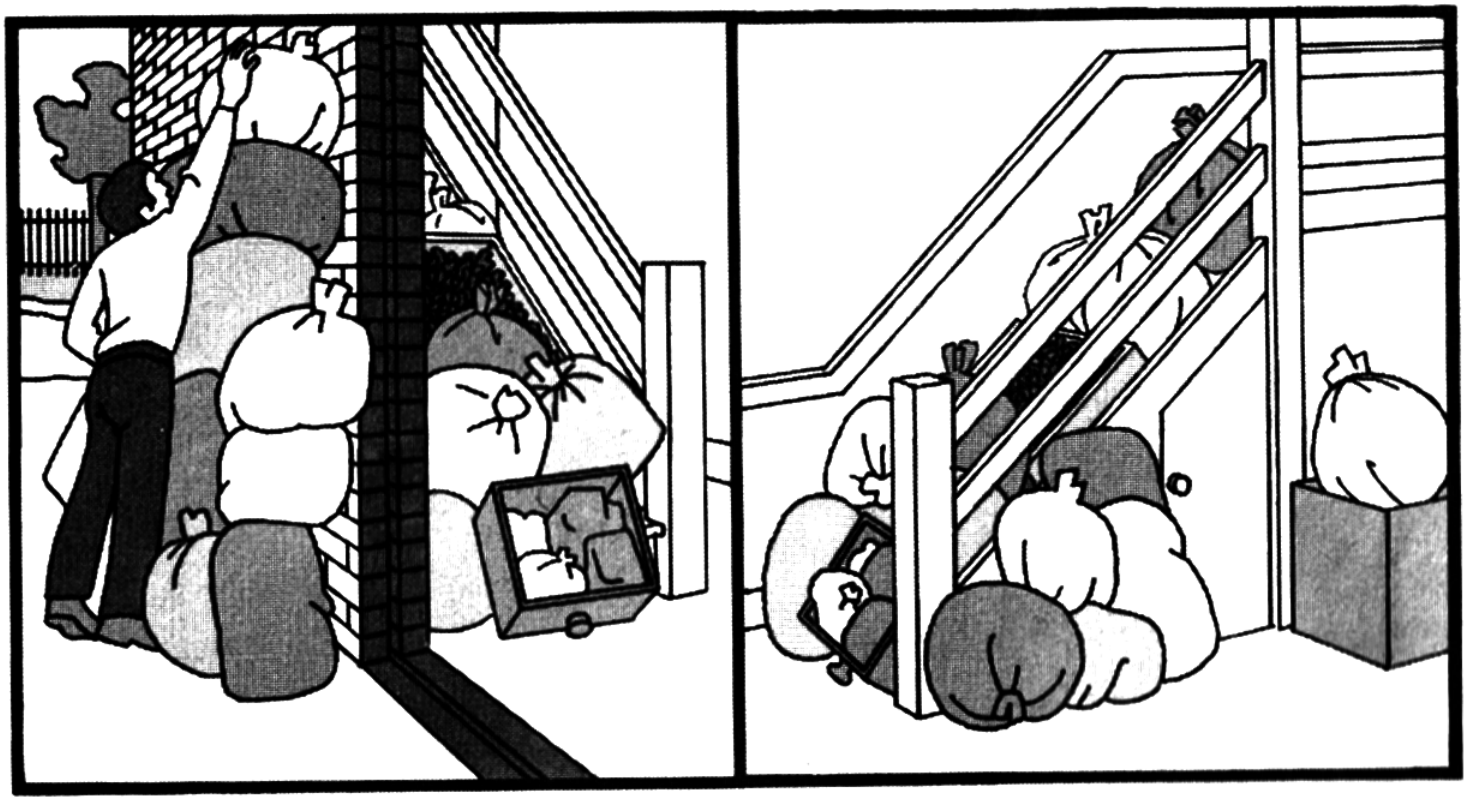

What to do after the Attack:

After a nuclear attack, there will be a short period before fall-out starts to descend. Use this time to do essential tasks. This is what you should do.

Do not smoke.

Check that gas, electricity and other fuel supplies and all pilot lights *are* turned off.

Go round the house and put out any small fires using mains water if you can.

If anyone's clothing catches fire, lay them on the floor and roll them in a blanket, rug or thick coat.

If there is structural damage from the attack you may have some time before a fall-out warning to do minor jobs to keep out the weather – using curtains or sheets to cover broken windows or holes.

If you are out of doors, take the nearest and best available cover as quickly as possible, wiping all the dust you can from your skin and clothing at the entrance to the building in which you shelter.

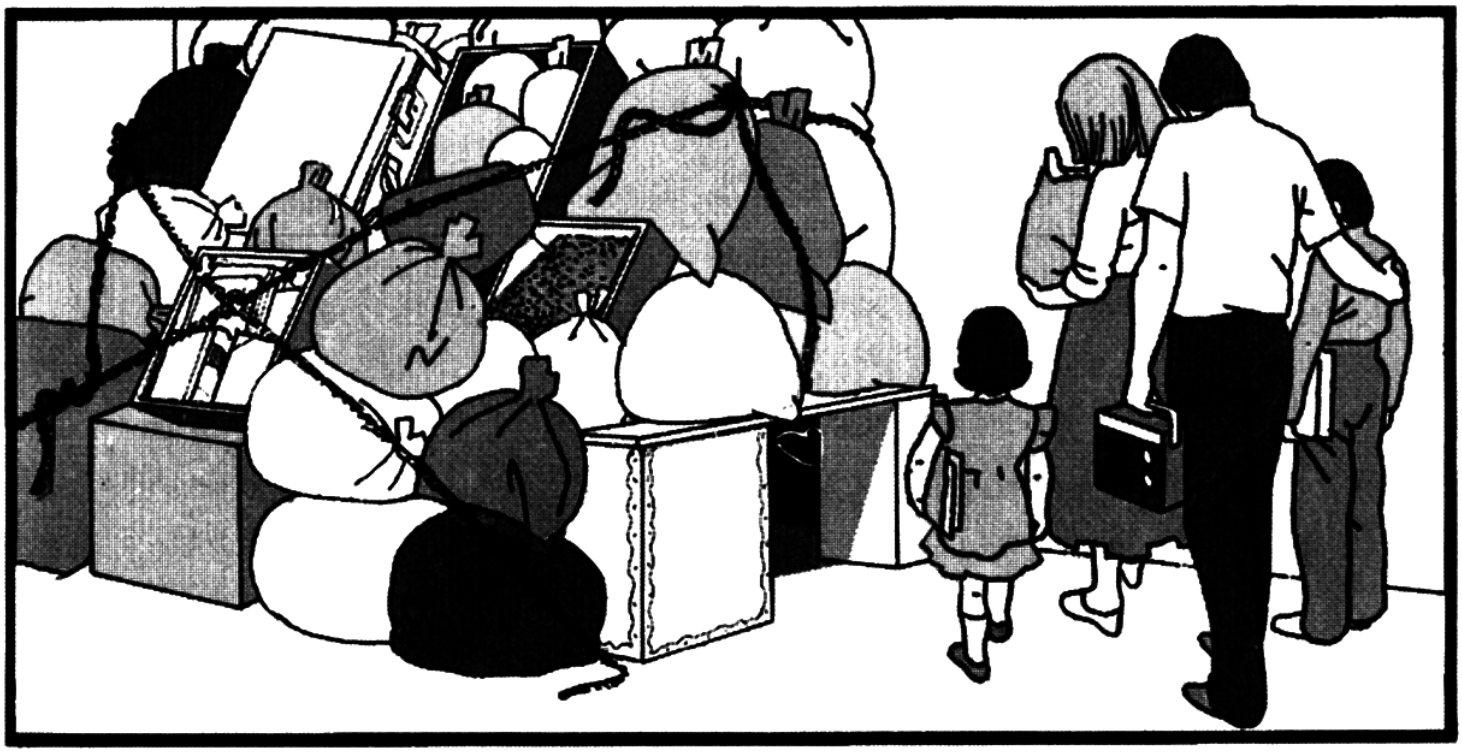

1 2 cms The National Archives ins 1 2
Ref.: HO 225 /121 C500594

SEPTEMBER 1964

HOME OFFICE

CD/SA 121

SCIENTIFIC ADVISER'S BRANCH

IGNITION AND FIRE SPREAD IN URBAN AREAS FOLLOWING A NUCLEAR ATTACK

G. R. Stanbury

INITIAL FIRE INCIDENCE

For a 1 MT groundburst bomb the height of the top of the fireball above ground is about 0.72 miles. Because this distance is large compared with the height of most buildings, the exposed upper floors do actually see a large part of the fireball and not just the top of it, but in assuming that the radiation is just as intense from the top as from the middle we were overestimating the fire risk.

On the above basis the following table gives the number of exposed upper floors (to the nearest ½ floor) for a range of distances from the explosion and a range of street widths.

Effect of Shielding: Estimation of the number of exposed floors

Assuming that buildings on opposite sides of a street which is receiving heat radiation from a direction perpendicular to its length are of the same height

Thermal pulse precedes the blast wave

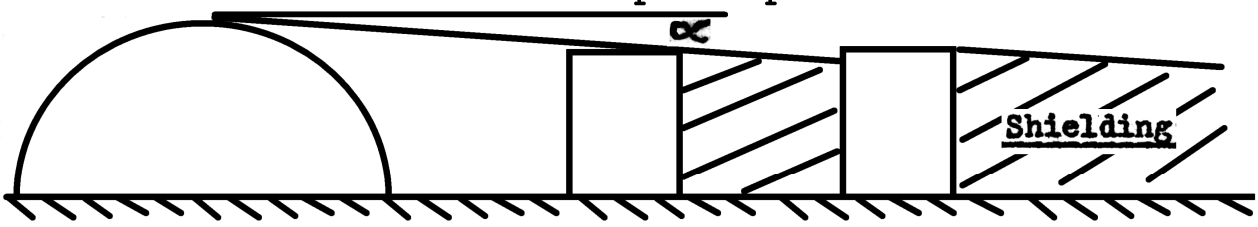

Distance from explosion miles	Angle of arrival α°	tan α	Width of street (units of 10 ft.)						
			2	3	4	5	6	7	8
1	35	.72	1.5	2	3	3.5	4.5	5	6
1½	26	.48	1	1.5	2	2.5	3	3.5	4
2	20	.36	.5	1	1.5	2	2	2.5	3
3	13½	.24	.5	.5	1	1	1.5	1.5	2
4	10	.18	.5	.5	.5	1	1	1.5	1.5
5	8	.15	.5	.5	.5	.5	1	1	1

we take the average depth of a floor to be 10 ft.

Angle between heat flash and street (degrees)	90-75	75-60	60-45	45-30	30-15	15-0
Proportion of heat flash entering windows %	99	92.5	80	60	40	14

SPREAD OF FIRE

From last war experience of mass fire raids in Germany it was concluded that the overall spread factor was about 2; i.e. about twice as many buildings were destroyed by fire as were actually set alight by incendiary bombs

Number of fires started per square mile in the fire-storm raid on Hamburg, 27th/28th July, 1943

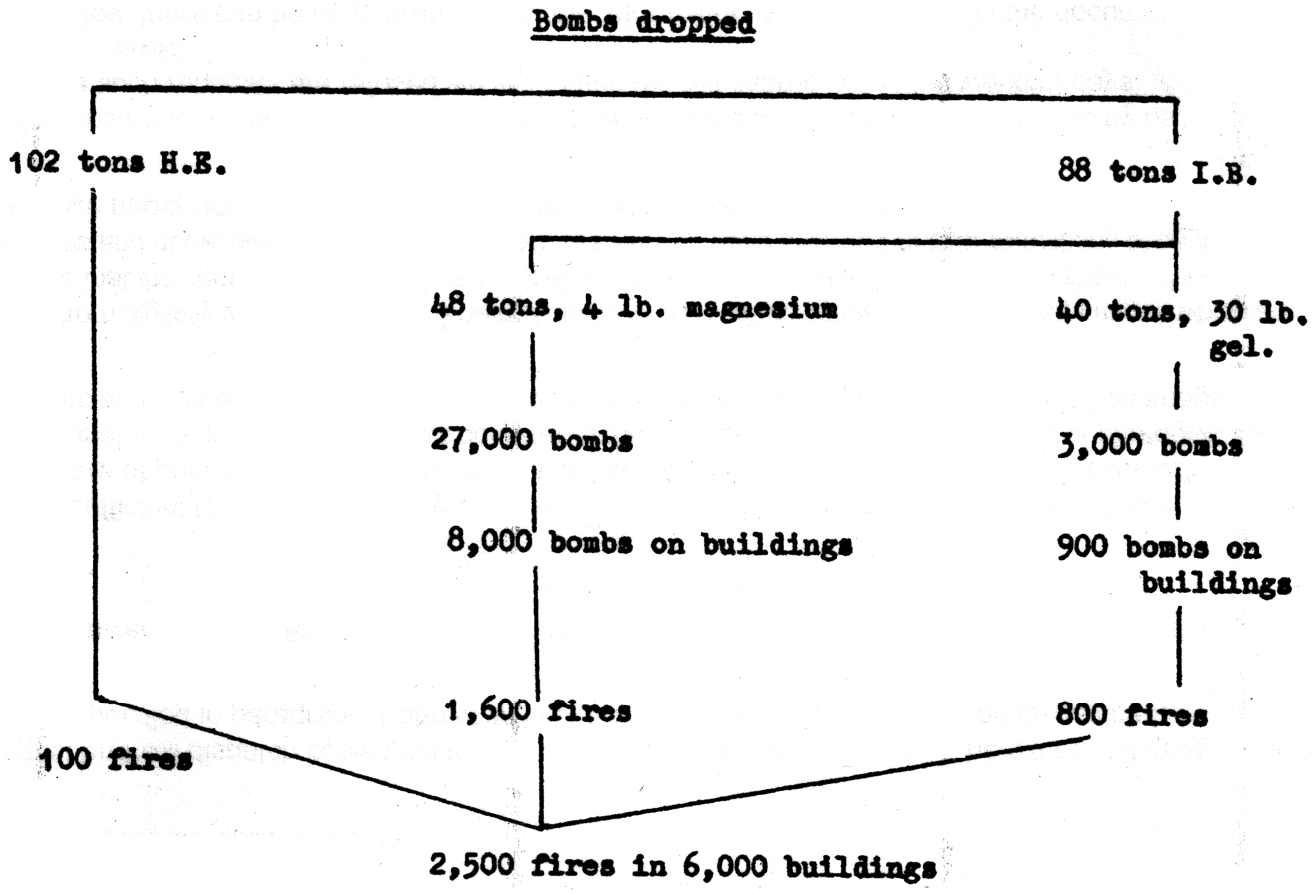

However, the important thing to note is that the total number of fires started in each square mile (2,500) was nearly half that of the total number of buildings; in other words, almost every other building was set on fire during the raid itself. When this happened no fire-fighting organisation, however efficient could hope to prevent the fires from joining together and engulfing the whole area.

When the figure of 1 in 2 for the German fire storms is compared with the figures for initial fire incidence of ∿ 1 in 15 to 30 obtained in the Birmingham and Liverpool studies it can only be concluded that a nuclear explosion could not possibly produce a fire storm.

Fire situation from 1,499 fly bombs in the built-up part of the London Region

WWII VI high explosives (1 ton TNT warhead) (cruise missiles)

Where dropped	Number of fly bombs	Fly Bombs Caused				
		No fire	Small fire	Medium fire	Serious fire	Major fire
City	119 ~~199~~	47	49	17	4	2
West-End	33	8	22	2	-	1
Closed Residential	430	207	203	20	-	-
Open Residential	804	478	296	28	2	-
Docks	113	64	39	8	1	1
Grand Totals	1,499	804	609	75	7	4

Discussion of results

Two important points emerge from a study of these results:-

(i) The small proportion of fly bombs - less than 20% - which started fires of any greater category than "small" even in the most heavily built-up areas; and

(ii) The large proportion which started no fires at all even in the most heavily built-up areas.

All these fly bombs fell in the summer months of 1944 which were unusually dry. In winter in this country in residential areas there are many open fires which may provide extra sources of ignition. The domestic occupancy is a low fire risk however, and as the proportion of such property in the important City and West End areas is small this should not introduce any serious error. Moreover, in winter, the high atmospheric humidity and the correspondingly high moisture content of timber would tend to retard or even prevent the growth of fire.

In order to determine how many fly bombs are equivalent to one nominal atomic bomb one method is to compare the areas over which a given category of house damage is produced by each. If we do this for a $\frac{3}{8}$th mile air burst as at Hiroshima, the result is that 1 atomic bomb does as much damage as about 1,200 fly bombs.

This in itself is not a serious fire situation and it is doubtful whether it could ever give rise to a fire storm. In Hamburg 2,500 fires were started per square mile by a bomb density (combined H.E. and I.B.) of 2oo tons per square mile, and for the area of destruction produced by an atomic bomb this would correspond to a total of about 10,000 fires.

LAWRENCE
LIVERMORE
NATIONAL
LABORATORY

UCRL-TR-231593

Thermal Radiation from Nuclear Detonations in Urban Environments

R. E. Marrs, W. C. Moss, B. Whitlock

June 7, 2007

An obvious next step (left for future work) would be a calculation of burn injuries and fires. Even without shadowing, the location of most of the urban population within buildings causes a substantial reduction in casualties compared to the unshielded estimates. Other investigators have estimated that the reduction in burn injuries may be greater than 90% due to shadowing and the indoor location of most of the population [6].

We have shown that common estimates of weapon effects that calculate a "radius" for thermal radiation are clearly misleading for surface bursts in urban environments. In many cases only a few unshadowed vertical surfaces, a small fraction of the area within a thermal damage radius, receive the expected heat flux.

In future work, our code could be extended to tally the total surface area receiving various amounts of heat, and to account for reflected radiation.

References

1. *The Effects of Nuclear Weapons*, edited by S. Glasstone and P. J. Dolan, U S Dept. of Defense (1977).

2. "RADFLO Physics and Algorithms," E. M. D. Symbalisty, J. Zinn, and R. W. Whitaker, LA-12988-MS (September, 1995).

3. "The Development and Testing of the Air Transport of Radiation Code Version 6 (ATR6)." D. C. Kaul et al., DNA-TR-91-237 (November, 1992).

4. *Handbook of Nuclear Weapon Effects (EM-1)*, J. Northrop, DSWA (1996).

5. http://www.esri.com/

6. L. Davisson and M. Dombroski, private communication; "Radiological and Nuclear Response and Recovery Workshop: Nuclear Weapon Effects in an Urban Environment 2007," M. Dombroski, B. Buddemeier, R. Wheeler, L. Davisson, T. Edmunds, L. Brandt, R. Allen, L. Klennert, and K. Law, UCRL-TR-XXXX (2007), in review.

Takata, A.N., **Mathematical Modeling of Fire Defenses**, IITRI, March 1970, AD 705 388.

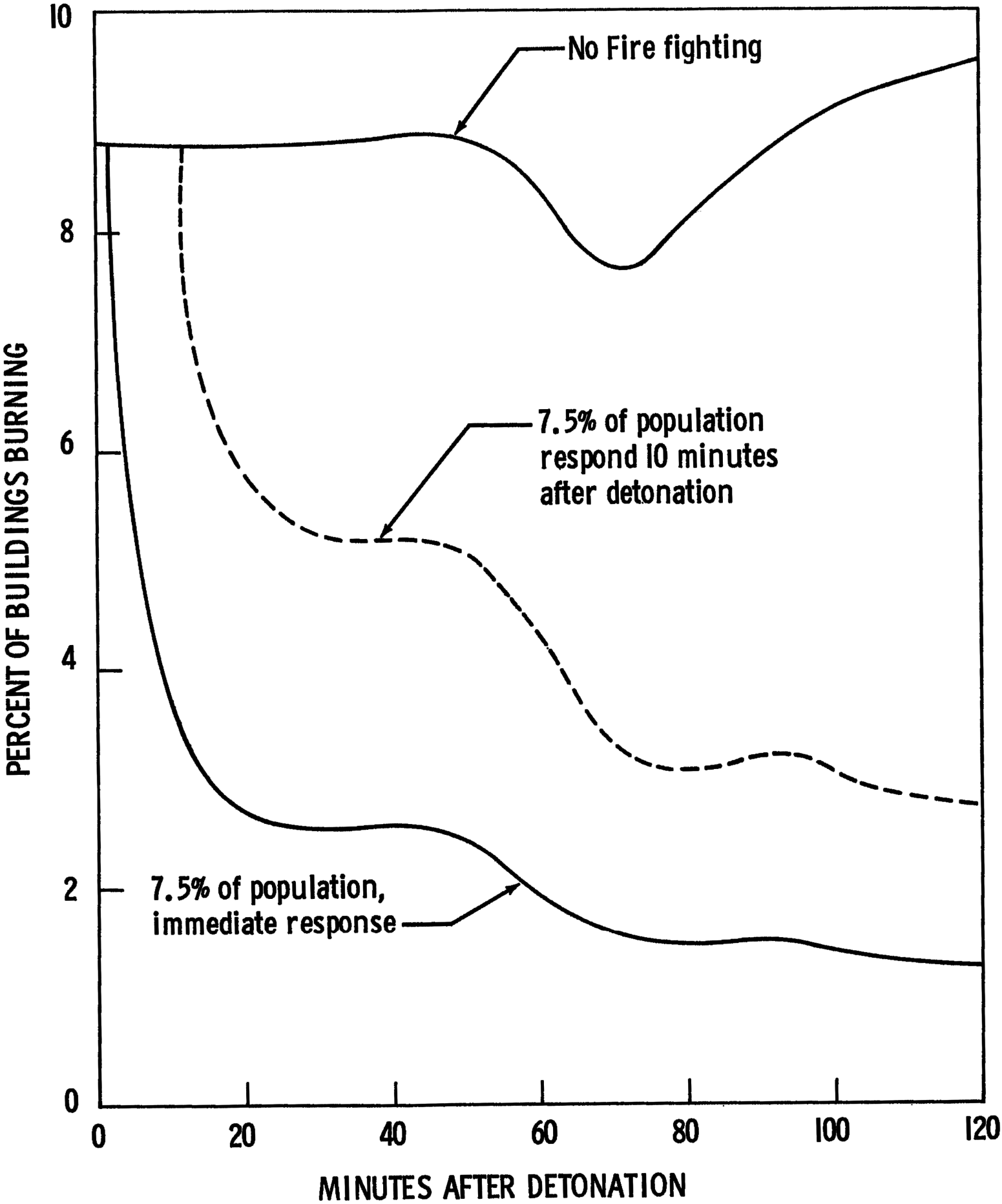

The Effects of

Nuclear Weapons

SAMUEL GLASSTONE
Editor

Revised Edition
Reprinted February 1964

Prepared by the
UNITED STATES DEPARTMENT OF DEFENSE
Published by the
UNITED STATES ATOMIC ENERGY COMMISSION
April 1962

For sale by the Superintendent of Documents, U.S. Government Printing Office
Washington 25, D.C. - Price $3.00 (paper bound)

Foreword

This book is a revision of "The Effects of Nuclear Weapons" which was issued in 1957. It was prepared by the Defense Atomic Support Agency of the Department of Defense in coordination with other cognizant governmental agencies and was published by the U.S. Atomic Energy Commission. Although the complex nature of nuclear weapons effects does not always allow exact evaluation, the conclusions reached herein represent the combined judgment of a number of the most competent scientists working on the problem.

There is a need for widespread public understanding of the best information available on the effects of nuclear weapons. The purpose of this book is to present as accurately as possible, within the limits of national security, a comprehensive summary of this information.

Robert S. McNamara

Secretary of Defense

Glenn T. Seaborg

Chairman
Atomic Energy Commission

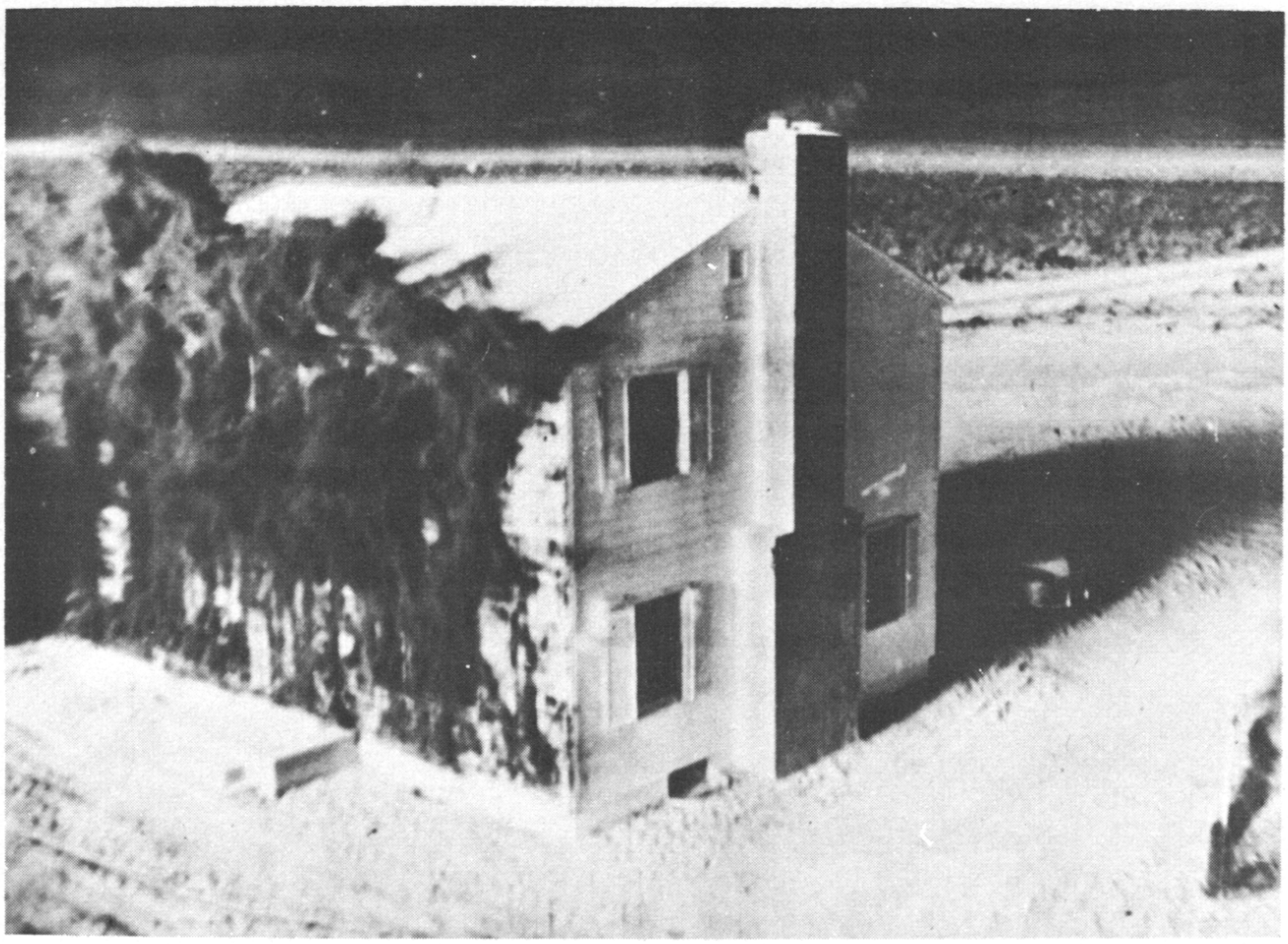

Figure 7.33a. Thermal effects on wood-frame house 1 second after explosion (about 25 cal/sq cm).

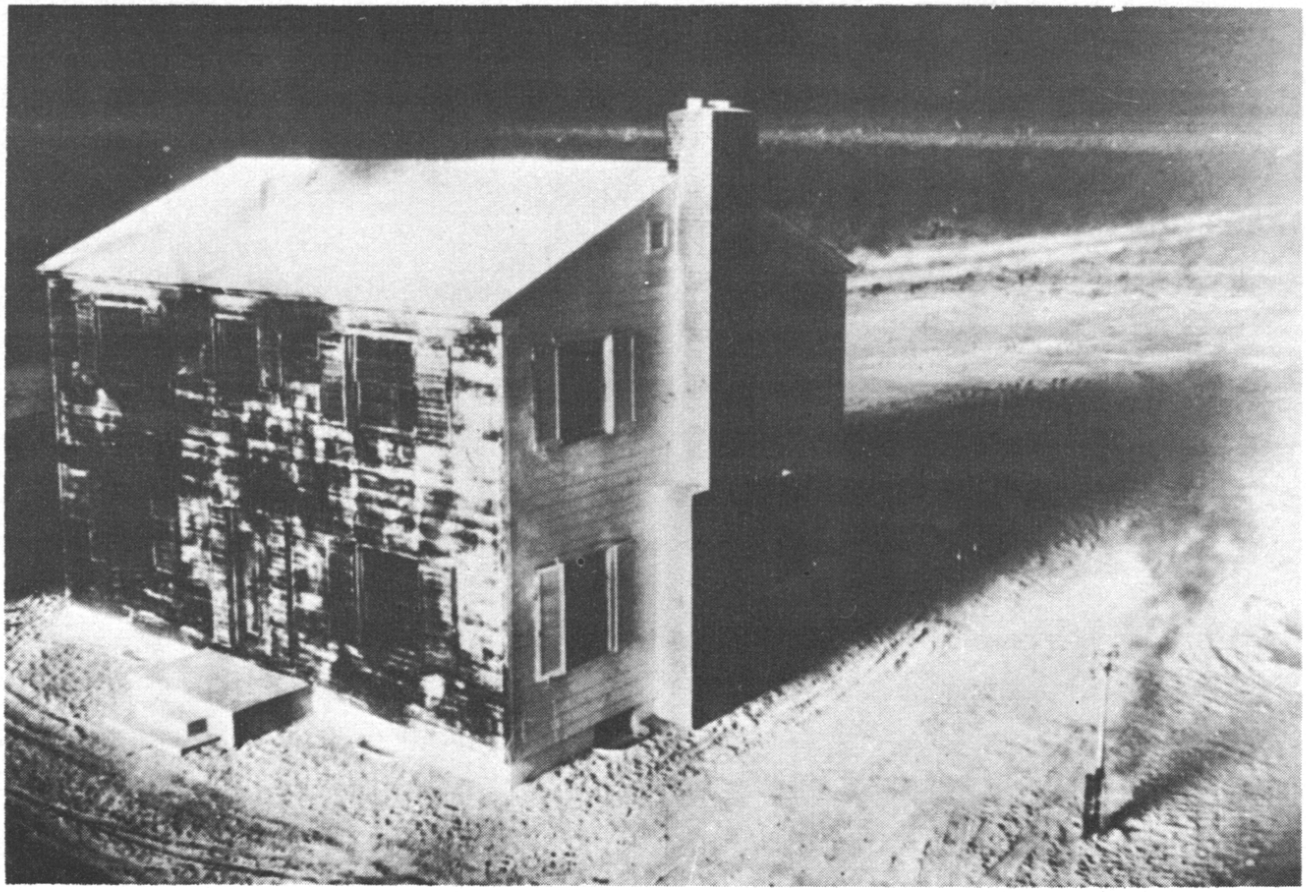

Figure 7.33b. Thermal effects on wood-frame house about ¾ second later.

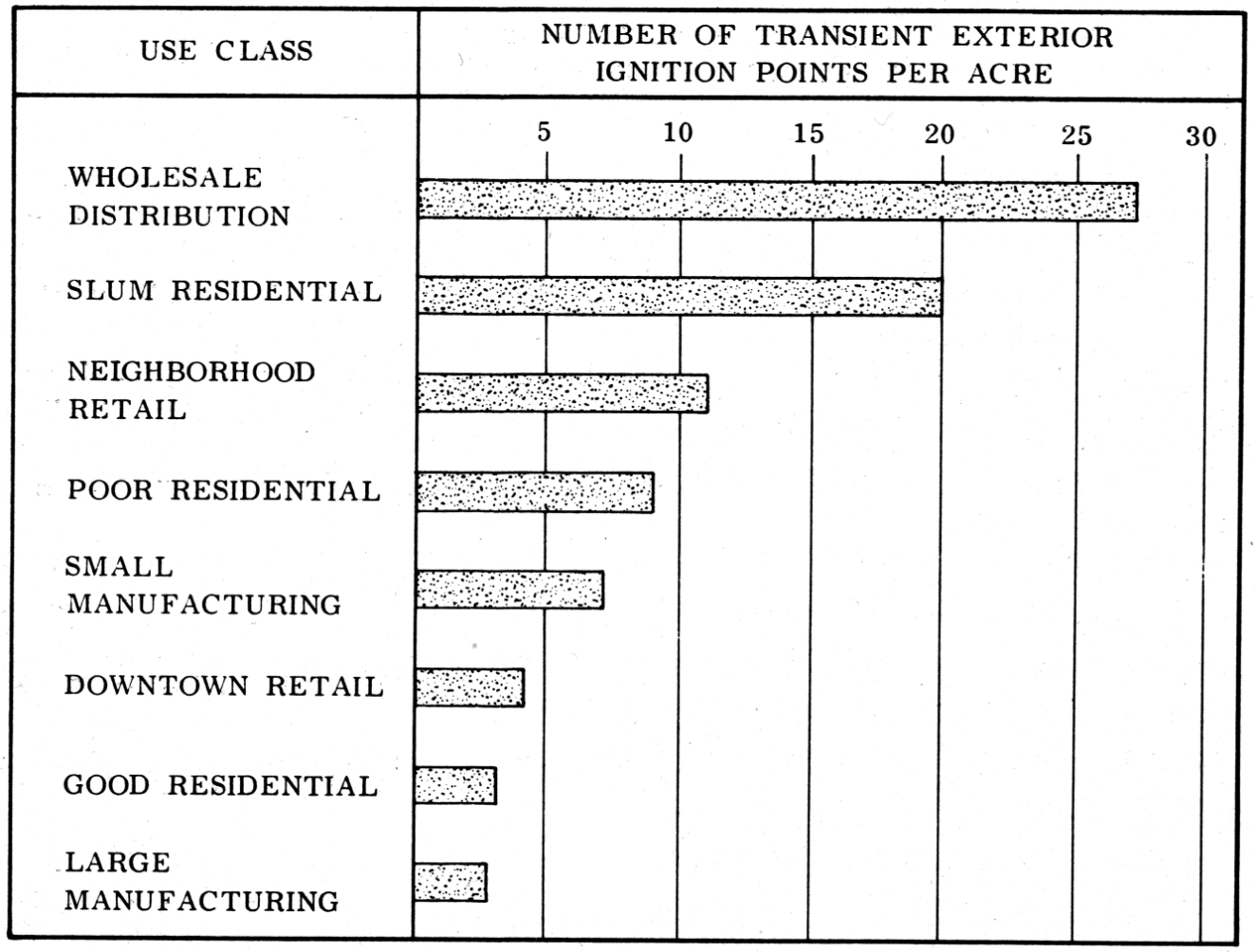

Figure 7.55. Frequency of exterior ignition points for various areas in a city

the formation of a significant fire, capable of spreading, will require appreciable quantities of combustible material close by, and this may not always be available.

7.57 The fact that accumulations of ignitable trash close to a wooden structure represent a real fire hazard was demonstrated at the nuclear tests carried out in Nevada in 1953. In these tests, three miniature wooden houses, each having a yard enclosed with a wooden fence, were exposed to 12 calories per square centimeter of thermal radiation. One house, at the left of Fig. 7.57, had weathered siding showing considerable decay, but the yard was free from trash. The next house also had a clean yard and in addition, the exterior siding was well maintained and painted. In the third house, at the right of the photograph, the siding, which was poorly maintained, was weathered, and the yard was littered with trash.

7.58 The state of the three houses after the explosion is seen in Fig. 7.58. The third house, at the right, soon burst into flame and was burned to the ground. The first house, on the left, did ignite but it did not burst into flame for 15 minutes. The well maintained house in the center with the clean yard suffered scorching only. It is of interest to recall that the wood of a newly erected white-painted

Figure 7.57. Wooden test houses before exposure to a nuclear explosion, Nevada Test Site.

Figure 7.58. Wooden test houses after exposure to a nuclear explosion.

house exposed to about 25 calories per square centimeter was badly charred but did not ignite (see Fig. 7.33b).

7.59 The value of fire-resistive furnishing in decreasing the number of ignition points was also demonstrated in the tests. Two identical, sturdily constructed houses, each having a window 4 feet by 6 feet facing the point of burst, were erected where the thermal radiation exposure was 17 calories per square centimeter. One of the houses contained rayon drapery, cotton rugs, and clothing, and, as was expected, it burst into flame immediately after the explosion and burned completely. In the other house, the draperies were of vinyl plastic, and rugs and clothing were made of wool. Although much ignition occurred, the recovery party, entering an hour after the explosion, was able to extinguish the fires.

7.76 It should be noted that the fire storm is by no means a special characteristic of nuclear weapons. Similar fire storms have been reported as accompanying large forest fires in the United States, and especially after incendiary bomb attacks in both Germany and Japan during World War II. The high winds are produced largely by the updraft of the heated air over an extensive burning area. They are thus the equivalent, on a very large scale, of the draft of a chimney under which a fire is burning. Because of limited experience, the conditions for the development of fire storms in cities are not well known. It appears, however, that some, although not necessarily all, of the essential requirements are the following: (1) thousands of nearly simultaneous ignitions over an area of at least a square mile, (2) heavy building density, e.g., more than 20 percent of the area is covered by buildings, and (3) little or no ground wind. Based on these criteria, only certain sections—usually the older and slum areas—of a very few cities in the United States would be susceptible to fire storm development.

12.35. The major part of the thermal radiation travels in straight lines, and so any opaque object interposed between the fireball and the exposed skin will give some protection. This is true even if the object is subsequently destroyed by the blast, since the main thermal radiation pulse is over before the arrival of the blast wave.

12.36 At the first indication of a nuclear explosion, by a sudden increase in the general illumination, a person inside a building should immediately fall prone, as described in § 12.30, and, if possible, crawl behind or beneath a table or desk or to a planned vantage point. Even if this action is not taken soon enough to reduce the thermal radiation exposure greatly, it will minimize the displacement effect of the blast wave and provide a partial shield against splintered glass and other flying debris. An individual caught in the open should fall prone to the ground in the same way, while making an effort to shade exposed parts of the body. Getting behind a tree, building, fence, ditch, bank, or any structure which prevents a direct line of sight between the person and the fireball, if possible, will give a major degree of protection. If no substantial object is at hand, the clothed parts of the body should be used to shield parts which are exposed.

DOMESTIC NUCLEAR SHELTERS

TECHNICAL GUIDANCE

A HOME OFFICE GUIDE

Government bookshops

49 High Holborn, London WC1V 6HB
13a Castle Street, Edinburgh EH2 3AR
41 The Hayes, Cardiff CF1 1JW
Brazennose Street, Manchester M60 8AS
Southey House, Wine Street, Bristol BS1 2BQ
258 Broad Street, Birmingham B1 2HE
80 Chichester Street, Belfast BT1 4JY

Government publications are also available through booksellers

© Crown copyright 1981
Second Edition 1982

Prepared by the Home Office and the Central Office of Information 1981
Printed in England for Her Majesty's Stationery Office by Hobbs the Printers of Southampton

ISBN 0 11 340777 7 (2462) Dd717557 C40 1/82 G381

Introduction

This manual of technical guidance on the design of domestic nuclear shelters has been prepared by a working group set up by the Emergency Services Division of the Home Office. The working group was asked to consider designs of nuclear shelters which could be made available to members of the public in the United Kingdom who might wish to purchase and install shelters for the use of themselves and their families.

The working group realised that the range of designs which it might produce would not be exhaustive. However, it was aware of the need to give technical guidance to professional engineers to assist them in producing reliable shelter designs. Thus the first three chapters of this book are written to give such guidance.

The other four chapters of the book give detailed designs of five shelters. These five cover a range of types which are applicable to different sorts of houses; they also cover a wide price range. These designs are not intended to be exhaustive, and as explained in the text, the working group is already giving attention to other designs, particularly those which might be incorporated into existing or new houses and also underground shelters of shapes other than box-like and using materials other than concrete. It is planned to publish details of this work at a later date.

The members of the working group are:

Mr J C Cotterill, *Chairman*	Scientific Advisory Branch, Home Office
Dr J R Stealey	Scientific Advisory Branch, Home Office
Mr A Lindfield	Scientific Advisory Branch, Home Office
Mr K A Day	F6 Division, Home Office
Mr R W T Haines, C Eng	Directorate of Works, Home Office
Mr H G S Banks, C Eng	Directorate of Works, Home Office
Mr M Connell, C Eng	Directorate of Civil Engineering Services Property Services Agency, Department of Environment
Mr S Bell, C Eng	Directorate of Civil Engineering Services Property Services Agency, Department of Environment
Mr S England, C Eng	Directorate of Mechanical and Electrical Engineering Services Property Services Agency, Department of Environment
Mr I Leys	Atomic Weapons Research Establishment, Ministry of Defence Foulness
Major I C T Ingall	HQ United Kingdom Land Forces Wilton, Wilts.
Mr R Million, *Secretary*	F6 Division, Home Office

Any enquiries concerning this manual should be addressed to the Home Office, F6 Division, and not to individual members of the working group.

To obtain some protection from the heat it is necessary to move out of the direct path of the rays from the fireball; any kind of shade will be of some value. In shelter design, any materials affording protection against ionising radiation or blast will give more than adequate protection against the heat. However it is important to ensure that no exposed parts of the shelter (such as the facings of doors) are made of flammable materials. In the case of shelters made from plastic materials such as GRP (glass reinforced plastic) it is essential that no surfaces should be exposed to the heat pulse. It is unlikely that such plastic materials would catch fire, but they may melt or distort. Since the blast wave follows the heat pulse, such distorted areas may result in lowered blast resistance.

It is considered unlikely that the heat flash from a nuclear explosion would give rise to fire-storms. In the last war, fire-storms were caused in the old city of Hamburg as a result of heavy incendiary attacks and at Hiroshima but not at Nagasaki. A close study of these cities and of German cities where fire-storms did and did not occur revealed several interesting features. A fire-storm occurred only in an area of several square miles, heavily built up with buildings containing plenty of combustible material and where at least every other building in the area had been set alight. It is not considered that the initial density of fires, equivalent to one in every other building, would be caused by a nuclear explosion over a British city. Studies have shown that due to shielding, a much smaller proportion of buildings than this would be exposed to the heat flash. Moreover, the buildings in the centres of most British cities are now more fire-resistant and more widely spaced than they were 30 to 40 years ago. This low risk of fire-storms would be reduced still further by the control of small initial and secondary fires.

There are two main hazards from a large area of fire to the occupants of shelters. One is the transmission of heat through the earth and shelter wall. In most cases this would make for discomfort rather than danger, particularly in underground shelters. The major danger is the possibility that the gaseous products of combustion, mainly carbon dioxide and perhaps carbon monoxide, might be drawn into the shelter. These dangers may be mitigated by taking advantage of the fact that the arrival of fallout is unlikely to occur for about half an hour after the explosion and a fallout warning will be given (for details see the booklet *Protect and Survive*). The intervening time might be used to try to extinguish or damp down any nearby fires. This may not be possible in many cases where a fallout warning has already been given based on ground bursts further upwind than the local bomb.

Crater formation and ground shock

When a nuclear weapon bursts near the ground much of the energy is expended in making a crater. At the same time a shock wave is transmitted outwards through the ground.

Crater formation

A large amount of vapourised or pulverised material is sucked up by the ascending fireball. Larger amounts are gouged out and deposited on the perimeter of the crater making an elevated lip roughly equal in width to the radius of the crater itself. The size of the crater, for a weapon of given power, will depend on the nature of the ground and

Fig. 6 *Approximate ranges of blast damage to UK houses (from 1 MT groundburst)*

Designation	Radial distance	Overpressure	Effect	Death/injury
A ring	Up to 2.5 km (1½ mi)	77 kPa plus. (11 psi)	Houses totally destroyed	High probability of death or serious injury
B ring	2.5 to 3.5 km (1½ to 2¼ mi)	77 to 42 kPa (11 to 6 psi)	Houses irreparably damaged	About 10% killed; 35% trapped; others injured
C ring	3.5 to 9 km (2¼ to 5½ mi)	42 to 10 kPa (6 to 1.5 psi)	Houses with moderate to severe damage	About 25% trapped or seriously injured at inner edge of ring
D ring	9 to 14 km (6 to 9 mi)	10 to 5 kPa (1.5 to 0.75 psi)	Houses lightly damaged	No deaths; few injuries expected

(WWII house damage vs injury data)

The debris problem

From Fig. 6 it can be deduced that the problems of debris around buried shelters might be serious in some locations near to ground zero. It is important that entrances or escape hatches and ventilation pipes where included should be as far as possible from nearby buildings — at least a distance equal to one-half the height (measured to the eaves) of the nearest building.

Trees are very vulnerable to long duration blast waves and in some areas these might cause obstruction to shelter entrances. The blast from a 1 MT groundburst would blow down 90 per cent of trees at a distance of 6 km (3¾ miles), 30 per cent at 7 km (4½ miles) and cause damage to branches out to 10 km (6¼ miles).

Initial nuclear radiation (INR)

Neutrons and gamma rays are emitted instantaneously by a nuclear explosion and these are followed by the gamma radiation from the intensely radioactive products in the fireball. This radiation is called initial nuclear radiation and is defined as that radiation emitted within one minute after detonation. In fact most of this hits the ground within a few seconds since the rapid rise of the fireball quickly takes the gamma rays and neutrons out of range. The phenomenon of initial nuclear radiation is very complex and not completely understood, but four facts are of importance for shelter design.

1. Range of INR

The intensity of INR falls off very rapidly with distance. The dose of INR received by a person in the open 2.5 km (1½ miles) from a 1 MT burst would give only a 50 per cent chance of survival. At 2.8 km (1¾ miles) the dose received would be negligible. At those distances, of course, anyone in the open would be killed by the blast. One important difference between kiloton and megaton weapons is the relationship between blast and INR ranges. With the smaller kiloton weapons the range of INR extends beyond the range of lethal blast; the reverse is true for megaton weapons. The Hiroshima and Nagasaki weapons were in the kiloton range and produced lethal INR effects. Fig. 7 gives the approximate exposures in roentgens of INR at locations where the blast overpressures are significant. Shelters designed to withstand a given overpressure should also be designed to protect against this level of INR. Overpressures are given in kiloPascals (psi).

Fig. 7 *Exposures of INR from surface burst (in roentgens)*

Overpressure	315 (45)	105 (15)	77 (11)	42 (6)	10 (1.5)	5 (0.75)
100 KT	300,000	20,000	9000	500	<1	<1
1 MT	70,000	1,000	250	2	<1	<1
10 MT	20,000	15	<1	<1	<1	<1
20 MT	9,000	1	<1	<1	<1	<1

Exposure would be lower from air bursts of the same weapon power. The figures given refer to thermonuclear weapons with 50 per cent fission yield. These figures may vary from 25 per cent to 150 per cent of the values given in the chart.

2. Shielding for INR

INR has greater energy and penetration than the radiation from fallout. The intensity of both INR and fallout radiation are reduced in proportion to the density of the shielding material. This can be expressed in terms of the 'half-value thickness' which is the thickness of a particular shielding material required to halve the radiation dose-rate. The approximate half-value thicknesses of some shielding materials against INR are given in Fig. 8.

Fig. 8 ***Half-value thicknesses of shielding materials***

	Against INR		Against fallout radiation	
	mm	(inches)	mm	(inches)
Steel	38	(1.5)	18	(0.7)
Concrete	152	(6.0)	56	(2.2)
Earth	190	(7.5)	84	(3.3)
Water	330	(13.0)	122	(4.8)
Brickwork	157	(6.2)	71	(2.8)

The half-value thicknesses of these materials against fallout radiation are given for comparison. They will be referred to later.

3. Slant incidence of INR

Most of the INR from a nuclear explosion arriving at a given point comes in a direct line from the fireball. There is a certain amount of scattering known as 'skyshine' which means that some initial gamma radiation might be received by a person shielded by a barrier from the light and heat flash (see Fig. 10). The amount of scattering of initial gamma radiation depends upon a number of factors, but probably amounts to about 10 per cent of that in the main beam. This means that though an underground or semi-sunk shelter might be shielded from the major part of the initial gamma radiation a certain amount could be received through the roof or sides of the shelter (if semi-sunk) by what is known as 'angular distribution'. However this benefit of shielding by nearby buildings cannot be taken into account in calculating the protection afforded by a shelter since the location of the source of the initial gamma radiation cannot be known.

4. Rate of emission of INR

The rate of delivery of initial nuclear radiation has some relevance to actions that might be taken immediately after a nuclear burst. Fig. 9 gives the percentage of initial gamma radiation dose received as a function of time for 20 KT and 5 MT air bursts. It can be seen that in the former case about 65 per cent and in the latter case 5 per cent of the total initial gamma radiation dose is received during the first second. In the case of the higher yield weapon it can be seen that if some shelter could be obtained within one second of seeing the explosion flash, such as by falling prone behind some substantial object, it could make the difference between life and death. Such an action would also help to prevent the translational effect of the blast.

Residual radiation from fallout

Nature of fallout

Fallout from a groundburst weapon consists of molten and solidified particles of earth on to which the radioactive products of the detonation have condensed. It has the consistency of fine to coarse sand particles with size varying from 20 to 700 micrometres. Particles smaller than about 20 micrometres would most probably remain in the stratosphere and come down as late fallout weeks, months, or even years later; by this time their radioactivity would have decayed considerably. The fall times from various heights of particles of various sizes are given in Fig. 11.

The time taken for fallout to be deposited in any one place varies from about half an hour close to the explosion to many hours further downwind. It is particularly important that people get under some kind of cover during this period to avoid fallout particles getting on the skin. Anyone who is caught out during fallout deposition should certainly cover the head and exposed skin and remove the contaminated clothing before entering shelter. No special protective clothing is required since no kind of clothing will prevent the gamma radiation from fallout reaching the body. If anyone has to emerge from shelter after the fallout has been deposited on the ground it would be useful to wear waterproof boots and gloves with a coat over the indoor clothing. Again these should be removed before re-entering the shelter. Any exposed skin should be washed after any contact with fallout particles.

Fig. 9 ***Percentage of total initial gamma dose received***

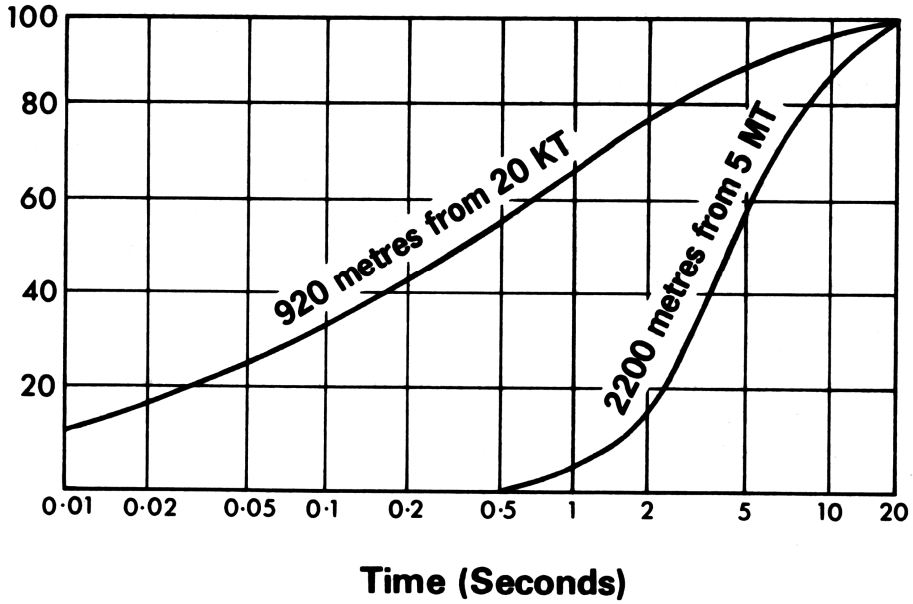

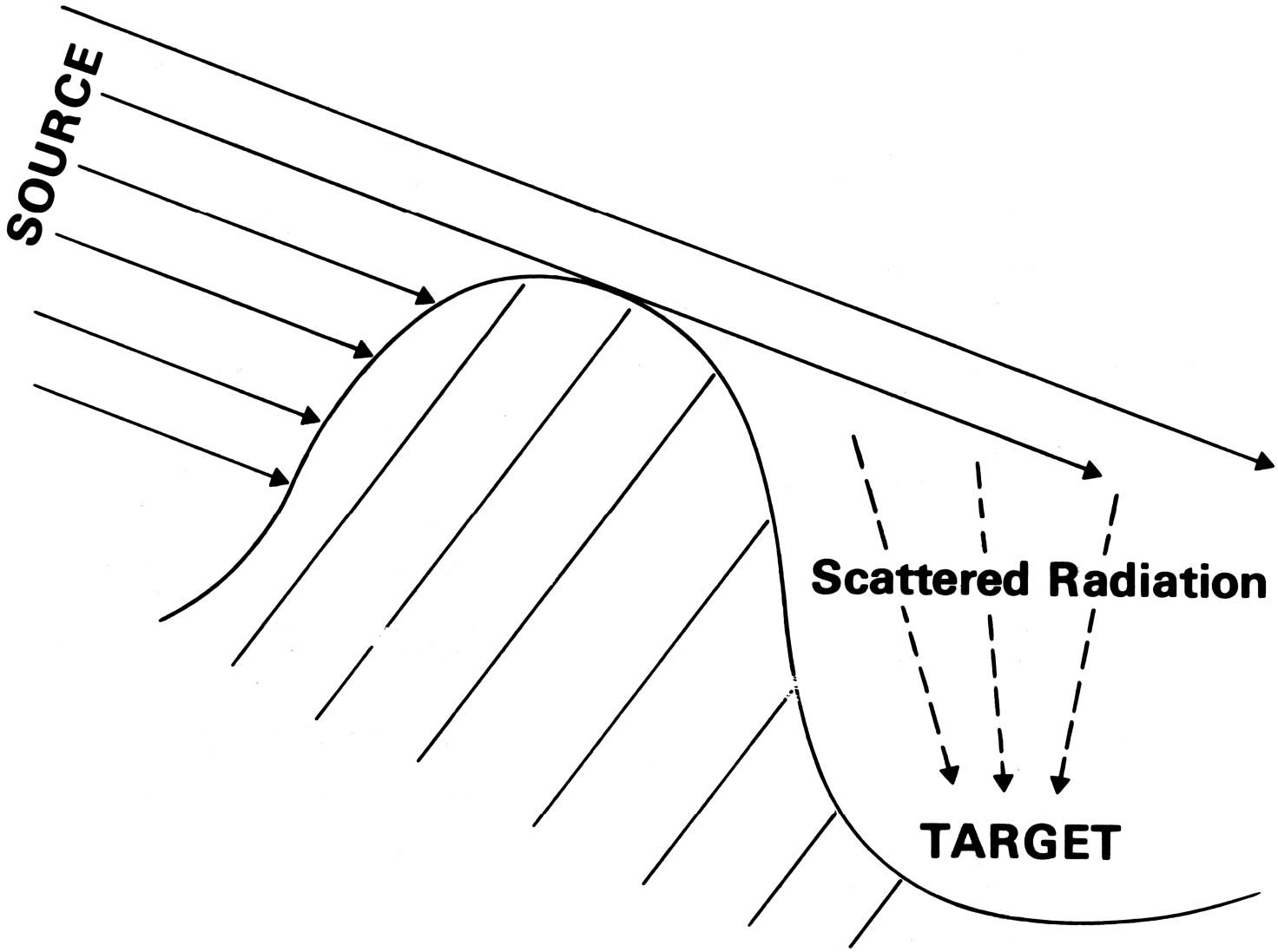

Fig. 10 ***Target exposed to scattered gamma radiation from a nuclear burst***

The nature of fallout particles has an influence on the filtration requirements for shelters. If the air coming into the shelter follows a tortuous path such as is provided by an inverted U shape or a cowl over the air intake, the need for filtration is minimised, if not entirely eliminated. The fallout particles will tend to fall to the earth rather than be carried along by the air current into the air duct. In any case the fallout particles are in the air for a limited period of time in the early hours after the burst so that if filtration is thought desirable, it need only be for that limited time. It would however be better to avoid drawing air into the shelter whilst the fallout is being deposited, if it is possible to know when this is taking place.

If a filter is incorporated into shelter design two points should be considered. The first is that a coarse filter is all that is necessary; a fine filter runs the risk of becoming blocked by ordinary atmospheric dust with resultant reduction of air supply. The second point is that if a filter is likely to become contaminated with radioactive dust then it should be placed outside the shelter.

Protection from fallout radiation

Protection against the radiation from fallout can be achieved in three ways. Consideration must be given to *duration* of exposure, *distance* from the fallout, and *density* of materials between the person and the fallout.

Duration. The damage caused by radiation to the body is cumulative (although the body does show a capability of some recovery). Thus it is important to reduce the time of exposure to radiation. In addition to this the radioactivity from fallout decays in a predictable manner by what is known as the '7/10 law'. Thus a dose rate of 1000 roentgens per hour at one hour after burst will decay to 100 roentgens per hour at seven hours after burst and 10 roentgens per hour at 49 hours (or two days) after burst and so on. This rapid decay means that, except in very severely contaminated areas, it is unlikely that anyone would have to stay continuously in shelter for two or three weeks. Local authorities will tell people when the intensity of the radiation has fallen to levels which make it safe to emerge from shelter for one or more hours. This time, which will gradually increase, can be used to ventilate the shelter better and attend to necessary tasks.

Distance. Protection can be achieved too by keeping as far away from the fallout as possible. A person standing on ground evenly contaminated by fallout would receive half his radiation dose from a circle of about 7.5 metres around him. Thus the floor of an underground shelter or a position in a house as far as possible from the roof and outside walls offers the best protection.

Density. The most important way of reducing the intensity of radiation is by sheltering behind some dense material. As explained, the level of radiation is reduced as it passes through any material but the greater the density of the material, the greater the reduction. The thickness of some materials required to reduce the intensity of fallout radiation to one half were given in Fig. 8. Glass gives little or no protection against radiation and many light materials, such as clothing, bedding etc., afford little protection. However, shelters can be constructed from such materials as glass reinforced plastic (GRP) which does not give much protection itself but can be buried in the ground; the earth cover then will give protection. A layer of 375 mm (15 inches) of earth or 250 mm (10 inches) of concrete over a shelter area would reduce the intensity of the radiation inside the shelter to 1/100th of the intensity outside. This reduction is called a protective factor (PF). A method for calculating protective factors is given in Chapter 2. It is designed for calculating the PFs of buildings. When applied to buried shelters the table dealing with penetration through the roof may be all that is needed.

Fig. 11 ***Time in hours for rough particles of different sizes to fall to the ground from specific heights***

Particle diameter in microns	**500**	**350**	**200**	**100**	**75**	**50**
Falling from metres (feet)						
25,000 (80,000)	1.6	2.3	4.5	12	22	49
18,000 (60,000)	1.3	2.0	3.7	9.5	17	36
12,000 (40,000)	1.0	1.5	2.8	6.8	12	25
9,000 (30,000)	0.8	1.2	2.2	5.3	9	19

Further comments on protection against INR and fallout radiation

From Fig. 7 it can be seen that a person on the outer edge the 'A' ring at 77 kPa (11 psi) from a one megaton explosion might receive a dose of about 250 rads INR. This would not in itself be lethal and even some rudimentary shelter would reduce the dose. At this same point the proportion of the population in houses surviving though injured might be about 40 per cent. Nearer to the point of burst the survivors would be fewer but the INR higher. It is in fact in the areas where blast shelters can give the greatest saving of life that INR becomes important, and so must be protected against. As a general rule, shelters designed to protect against 77 kPa (11 psi) and above should also give protection against INR. In most cases however, the required thicknesses of earth, concrete, etc. to give blast protection will also give the required INR protection.

Fig. 12 gives a comparison of the protective factors against INR gamma, neutrons and fallout radiation of some typical buildings. The data has been taken from *Effects of Nuclear Weapons* and the choice has been made of those buildings which are reasonably comparable with structures in the UK. The wide range of values is due partly to uncertainty in the data (since some have been calculated and others derived from weapons trials) and partly to the fact that protection to some extent is determined by the position in the building where the protective factor is measured.

Fig. 12 ***Protective factors of various buildings against initial gamma, neutron and fallout gamma radiation***

Structure	Initial gamma	Neutrons	Fallout gamma
1 metre underground	250–500	100–500	5000
Shelter partly above ground:			
with 600 mm earth	15–35	12–50	50–200
900 mm earth	50–150	20–100	200–1000

Classification of shelters

Summary of effects of nuclear weapons

From this brief review of the effects of nuclear weapons we can list the order of events from the detonation of a weapon. These are:

(a) Light and heat flash – immediate, and lasting some seconds.

(b) Initial nuclear radiation – following within one second of the commencement of the light flash.

(c) Blast wave – following from about a half second to several seconds after the light and heat flash.

(d) Fires – these may have been ignited by the heat flash but would be either extinguished or increased in intensity by the wind from the blast wave.

(e) Fallout – about one half hour to several hours after burst.

Protection against all these effects can be summed up by stating that distance from the source of the hazard and density of shielding materials give the best, and indeed the only, means of avoiding serious injury or death. The two major hazards in this list are blast and radiation. Adequate protection against these two will include protection against the others. It can indeed be said that adequate protection against blast will usually involve protection against radiation. The reverse however is not true. In spite of this, however, it is worthwhile looking at the need for protection in the whole of the United Kingdom.

Considerations arising from the probable attack pattern

In section 1.1.1 reference was made to the fact that an expected attack pattern on the United Kingdom might use 200 megatons on about 80 targets. If we now make an assumption that this attack would be in the form of 100 weapons of 1 MT airbursts and 100 weapons of 1 MT groundbursts we can use the information given in Fig. 6 to indicate the probability of areas being subject to various effects.

On this assumption, we should find that about 2.2 per cent of the land area of the UK would be subject to overpressures in the 'A' ring of 77 kPa (11 psi) and above about 1.8 per cent would be subject to overpressures of between 42 and 77 kPa (6-11 psi) in the 'B' ring and about 10 per cent of the land area would be subject to overpressures of between 10 and 42 kPa (1.5 to 6 psi). The rest of the land area, about 85 per cent, would be subject to blast in the D ring of 5 to 10 kPa (0.75 to 1.5 psi) or to no blast at all. Blast effects in the D ring will cause minor damage to buildings and no lethalities. It is impossible to determine the extent of the total D ring areas since many of these will overlap from adjacent bombs. Any part of the country might be subject to radiation from fallout.

There is of course no certainty of where the weapons will fall – and city centres are not necessarily the prime targets – but this consideration leads us to group shelters into various types and assess the probability of survival in given circumstances. It should of course be obvious that within about 450 metres (1500 feet) of a 1 MT groundburst no shelter can give any hope of protection. But the following grouping of shelters has some cogency.

Fig. 13 ***Classification of shelters***

	Type 1 Improvised	**Type 2 Indoor Kit**	**Type 3 Outdoor Kit**	**Type 4 Purpose built**
Blast protection kPa (psi)	Up to 10 (1.5)	Up to 42 (6)	Up to 77 (11)	In excess of 77 (11)
Fallout radiation protection	Not less than 40	Not less than 70	Not less than 200	In excess of 300. This type must also protect against INR
'Safety distance' from 1 MT airburst km (miles)	11.5 (7)	5 (3)	3.3 (2)	3.3 (2) for 77 kPa (11 psi) 3 (1.8) for 105 kPa (15 psi) 2 (1.2) for 315 kPa (45 psi) shelter
Ventilation	Natural	Natural or forced	Forced	Forced
Site of installation	In house† or garden	In house	In garden. Sectional for access through house	In garden. Appropriate access to garden necessary (See 1.3.4)
Forethought and planning	During crisis period. Some materials can be prepared in advance	Obtain in peace-time. Install in crisis period	Obtain in peace-time. Install in peace-time or crisis period. (2-3 days needed for installation (see 6.5)	Install in peace-time using professional advice and help.
Habitability	Not very comfortable. Suitable for few days occupancy. May be damp. Floor covering desirable	Able to sit up but not stand. May be able to use parts of house depending on radiation and damage situation	Rather cramped for 6 people; advance planning can improve comfort	Can be made very comfortable and habitable
Approximate expected cost (1980 prices)	Nominal if local materials used. Scaffold frame about £250	Kit: £500–£800 Bricks: £300	Kit: £900–£1800 Plus installation costs*	£6000–£10,000

*Installation costs will vary with nature of soil and nature of access to garden.
†E.g. The measures described in *Protect and Survive*.

Further comments on Home Office shelter designs

Chapters 4 to 7 of this book give details of the Home Office shelter designs and, where appropriate, detailed instructions for construction. It will be useful however to discuss here the reasons why this range of shelters has been chosen. Other designs are under consideration and it is planned to make details of these available later.

Limitations related to houses and gardens

In making recommendations for shelters it has been necessary to keep in mind the varying needs governed by the types of housing in the United Kingdom. Very roughly housing can be divided into the following groups:

a. Detached or semi-detached houses where there is appropriate access to the rear garden. (About 34%).
b. Semi-detached and terrace housing where there is no access to the rear garden, except through the house. (About 20%).
c. Houses with no rear garden. Such houses usually have a passage between the rows of terraces with access to a back yard. (About 25%).
d. Multi-storey blocks of flats. (About 12%).
e. Flats resulting from the conversion of 2, 3 and 4 storey houses. There is usually some garden space available attached to such property. (About 7%).
f. Bungalows, usually with accessible gardens. (About 2%).
g. Caravans.

The shelter types in Fig. 13 are designed for use in these housing groups as follows:

Type 1 Groups a, b, c, f, possibly d, e and g.
Type 2 Groups a, b, c, f, possibly d.
Type 3 Groups a, b, f, possibly e.
Type 4 Groups a and f.

It will be seen that all groups of housing are covered except possibly for d and only minimally for e and g. Further consideration will be given to shelter provision for those in group d and also upper storeys of group e. However, we believe that one or more of our shelter types will be suitable for installation in the majority of the houses in the country.

Type 1 shelters

A 'core shelter' for use inside a house has already been described in *Protect and Survive.* Its life-saving potential should not be minimised. The details of the two improvised shelters in Fig. 13 are given in later chapters. The construction of these shelters has been carried out by volunteers satisfactorily. They were given a short time to read the instructions before carrying out the work. Although these are all designated improvised shelters, some thought can be given in advance to the procurement of materials for their construction, thereby eliminating the need to remove doors, etc. from the house.

Type 2 shelters

This type is designed for houses where there is no suitable ground attached to the house on which to install a shelter. It is in essence a 'core shelter' which will protect the occupants from the debris of a house that is severely damaged. The radiation protection factor is obtained by shielding it with bricks, blocks, sand, furniture, books, bags of soil, etc. It is designed to withstand the debris from a two- or three-storey house falling on it. However, it is probable that the debris from a three-storey house may make it difficult for the occupants to dig themselves out. The 'blast protection' indicated is that at which most houses would receive irreparable damage and there would be a considerable amount of debris on the shelter.

The details of this shelter are given in Chapter 5. This is not the only possible shape; further studies are underway which should result in different designs of the 'Indoor kit-type' shelter.

Fig. 27 *Typical end-of-terrace house*

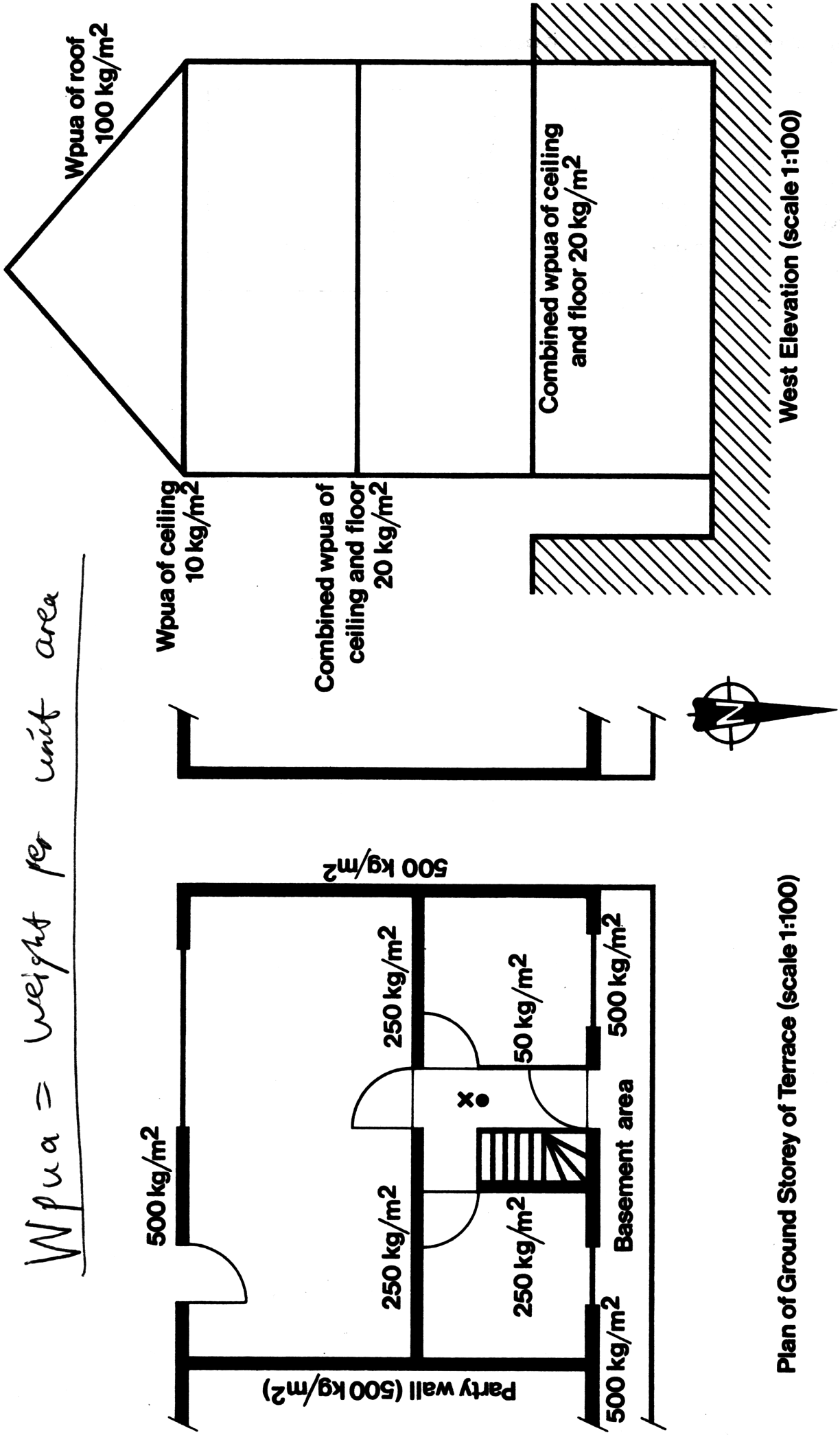

Chapter 5
Indoor kit shelter design

"Morrison Shelter" of 1941 (indoor steel table shelter)

General

This chapter gives information about an indoor shelter suitable for erection in homes that have basements or rooms that can be converted into a fallout room. It can be used as the 'inner refuge' referred to in the Home Office booklet *Protect and Survive* and anybody considering purchasing or using such a shelter should read *Protect and Survive* and be totally familiar with its contents.

The shelter will accommodate two adults and two small children. Two or more shelters can be placed together to gain more shelter area.

It should be stored in a clean dry place, ready for erection if required, *and could be used for other purposes, e.g. a workbench in a garage or garden shed.*

Shelter details

The indoor kit-type shelter is shown in Fig. 64.

A specialist steelwork fabricator will need to cut, weld, paint and drill bolt holes for the steel parts. However, once the units have been manufactured the shelter can be erected by unskilled labour. (Two persons two hours each.) Steelwork shop fabrication drawings are given in section 5.11, a steelwork specification in 5.10 and a guide to putting up the shelter in 5.12.

The basic unit has been designed to be capable of sustaining the debris load resulting from the complete collapse of a typical two-storey house, and when surrounded with brickwork, sandbags or other protective materials it will provide good protection against fallout.

Location of shelter

Where the shelter can be used

In two-storey houses and the lower floors of blocks of flats of substantial reinforced concrete or steel-framed construction, in areas where the density of building is comparatively low.

Where the shelter should not be used

1. Houses that have more than two storeys.

2. On the upper floors of houses or any ground floor that has a basement directly below it.

3. Blocks of flats having load bearing brickwork, blockwork or precast concrete panel construction.

4. The top two floors of a block of flats.

5. Lightly clad buildings.

Location of shelter in fallout room

As explained in *Protect and Survive* the shelter should be placed within the fallout room. Choose the place furthest from the outside walls and from the roof, or the room which has the smallest amount of outside wall or openings. The entrance should be positioned facing a solid internal wall wherever possible (see Fig. 65). A gap of 600 mm should be left between the outside of the fallout protection around the shelter and the walls of the fallout room to facilitate emergency escape.

The shelter should be placed on the most solid base available. When the shelter is to be placed on a suspended ground floor, this floor may require strengthening by providing additional piers, walls or props to support the floor joists.

Protecting the shelter against fallout radiation

Fallout protection to the shelter can be obtained by surrounding it with dry-laid brickwork, blockwork, sandbags, or heavy furniture filled with sand, earth or books (see Figs. 66 and 67). Recommended thicknesses of shielding materials are given in the following table:

Fig. 61 ***Recommended thicknesses of shielding materials***

	Thicknesses		
	To sides		To top
	Sides facing external walls	Sides facing solid internal walls	
Brickwork	1½ bricks (343 mm)	1 brick (225 mm)	4 courses bricks (260 mm)
Dense blockwork	1½ blocks (330 mm)	1 block (225 mm)	3 courses blocks (300 mm)
Sandbags	350 mm	250 mm	300 mm

If bricks or blocks are used they should be dry-laid, but closely packed and bonded so as to stagger the joints as much as possible. Suggested bonding is shown in Fig. 68.

Fallout room

External windows and doors in the room containing the shelter should be blocked up with material of the same weight as the surrounding wall. A 600 mm by 600 mm dry-laid area should be left within the blocked-up area to provide an escape exit.

For shelters protected as described, protective factors are given in the following table:

Fig. 62 ***Approximate protective factor***

House type	Protective factors	
	House with all exterior windows blocked	House with exterior windows blocked plus shelter and bricks
Terraced: traditional	15	260
modern	11	140
Semi-detached: traditional	12	210
modern	9	130
Detached: traditional	10	180
modern	8	110

Provision of emergency escape tunnel

Materials

Use tables, doors and other items of heavy furniture to form an emergency escape tunnel. As for *ad hoc* shelters, other structural commodities might be utilised for building escape tunnels. Fig. 69 shows how scaffold poles could be used for the purpose.

Location of escape tunnel

The escape route should be planned so that it emerges near to an opening in an external wall. If external openings are blocked up, a weaker escape knock-out area (e.g. dry-laid bricks or blocks 600 mm by 600 mm) should be provided.

Tools and materials required

For construction

16 mm and 10 mm spanners (1 open, and 1 ring, of each).
Steel lever for lining up holes.
Work gloves.

For shelter

Recommended quantities of materials for fallout protection are given in the following table. (Figures in table for entrance shielding wall, but do not consider materials required for blocking up openings in external walls.)

Fig. 64 ***Indoor kit-type shelter***

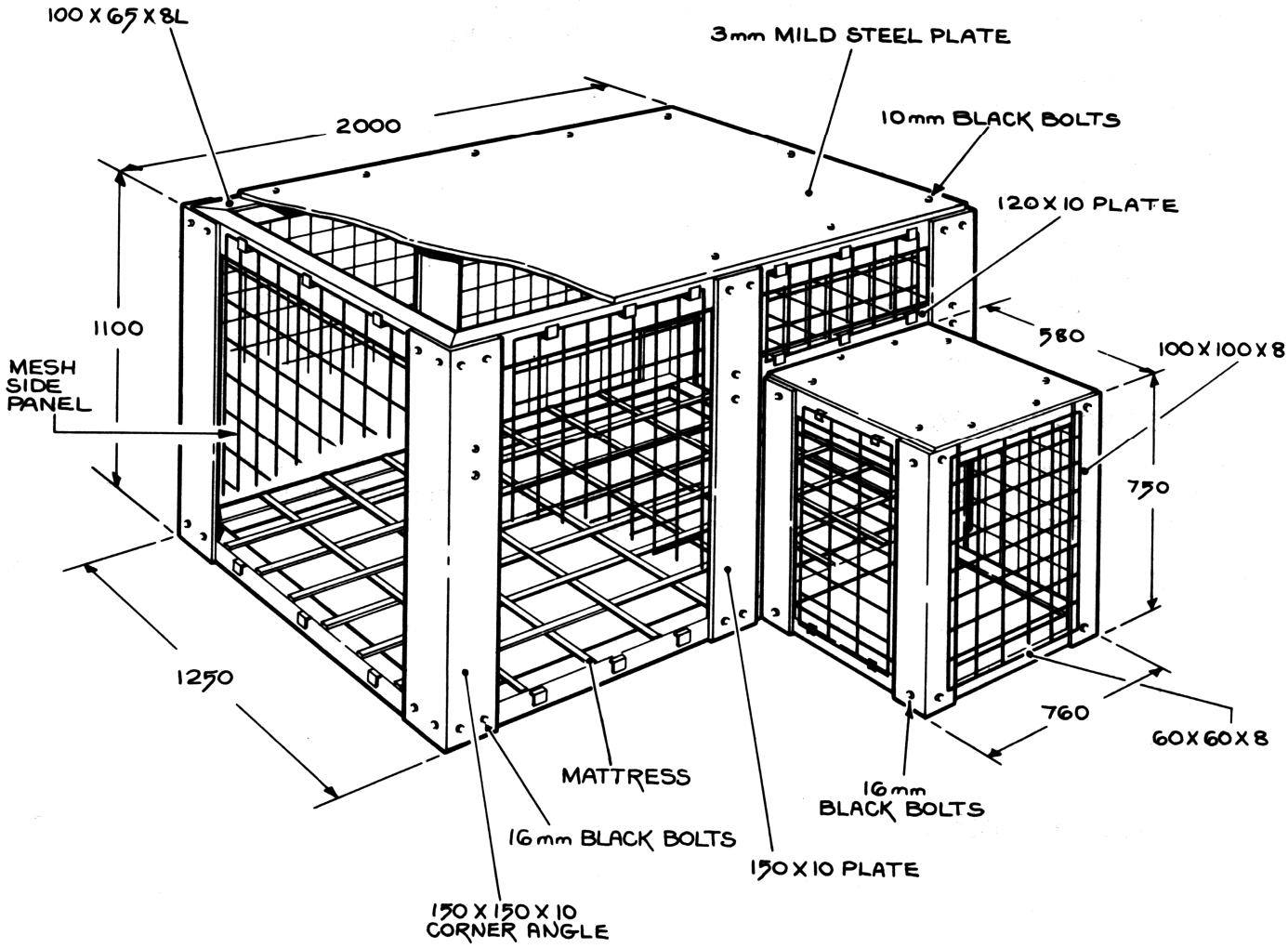

Fig. 65 ***Location of shelter***

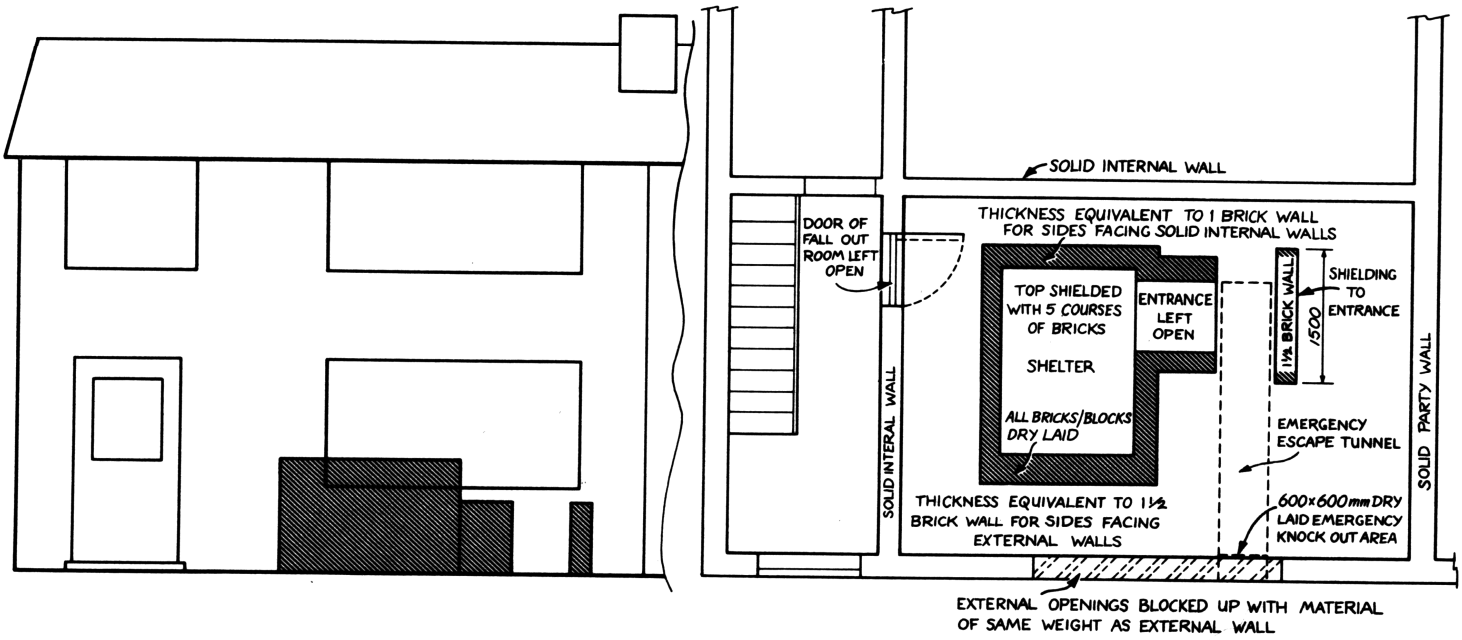

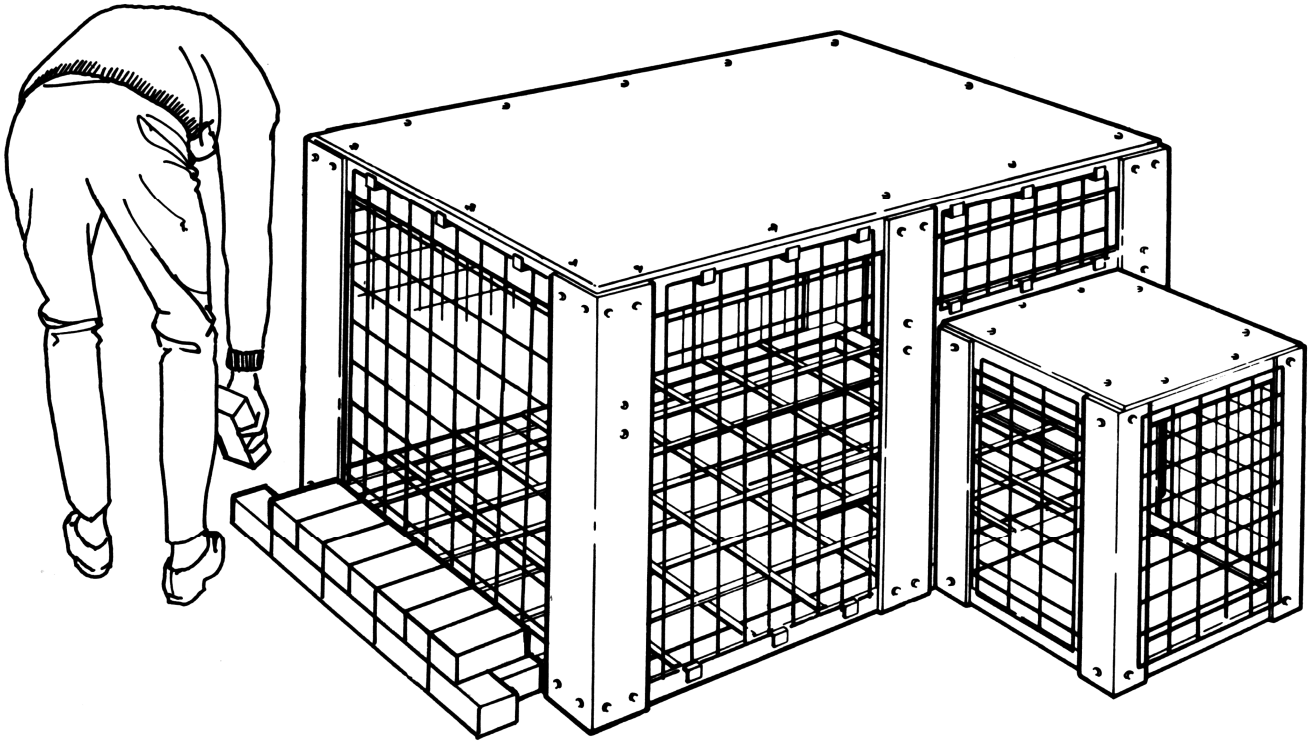

Fig. 66 ***Shelter surrounded with bricks***

Fig. 67 ***Shelter surrounded with sandbags***

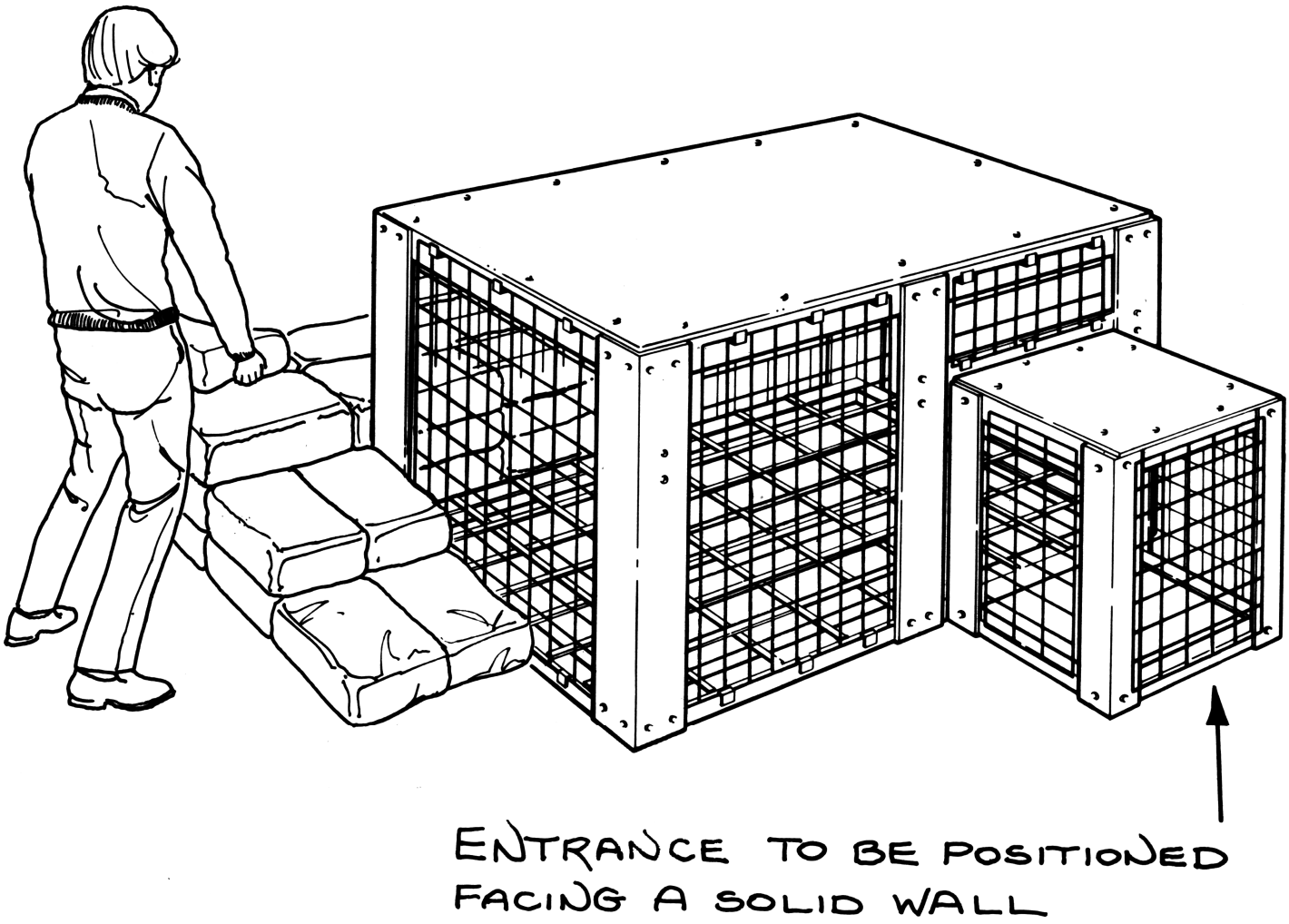

Fig. 79 ***Erection drawings***

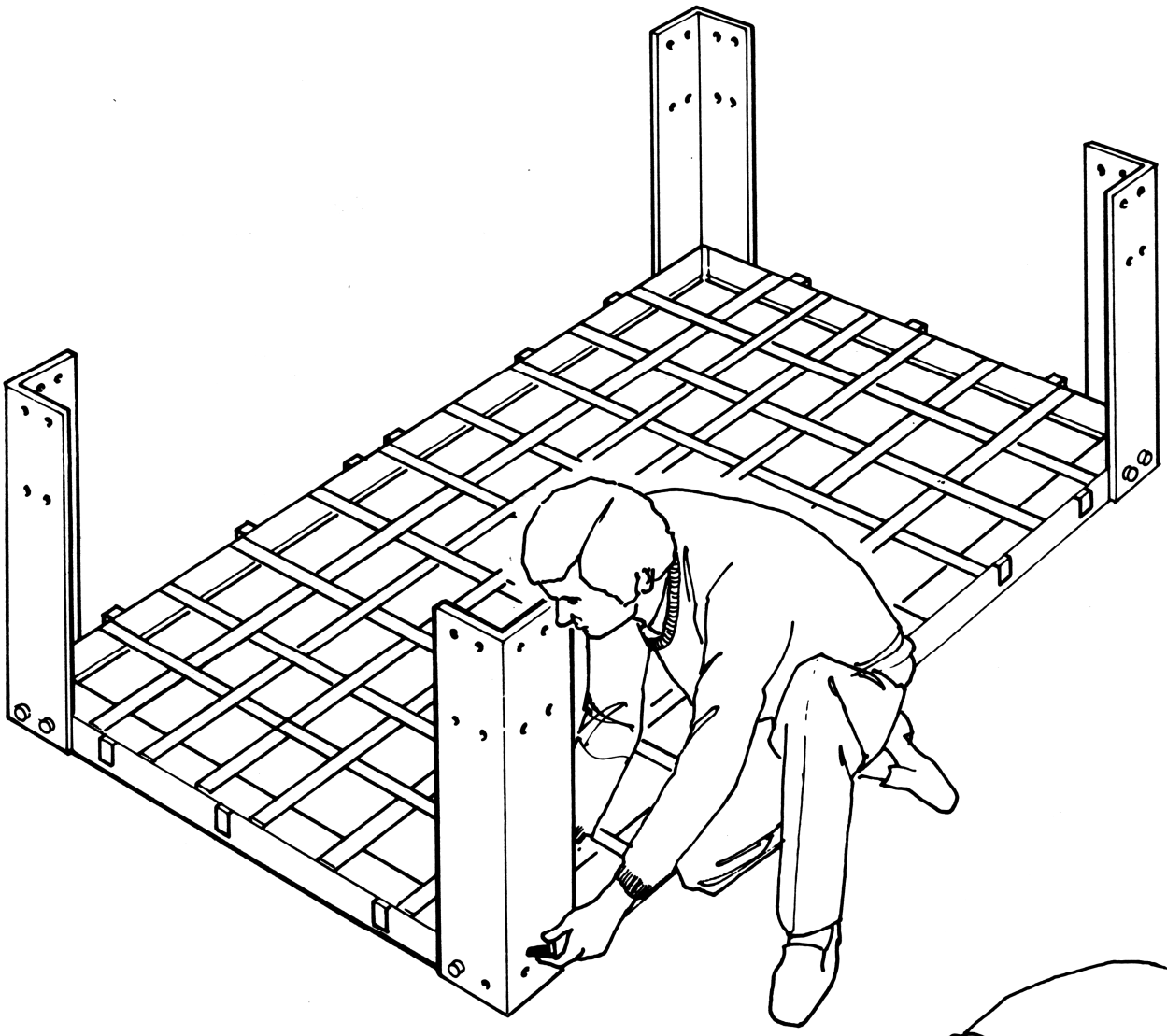

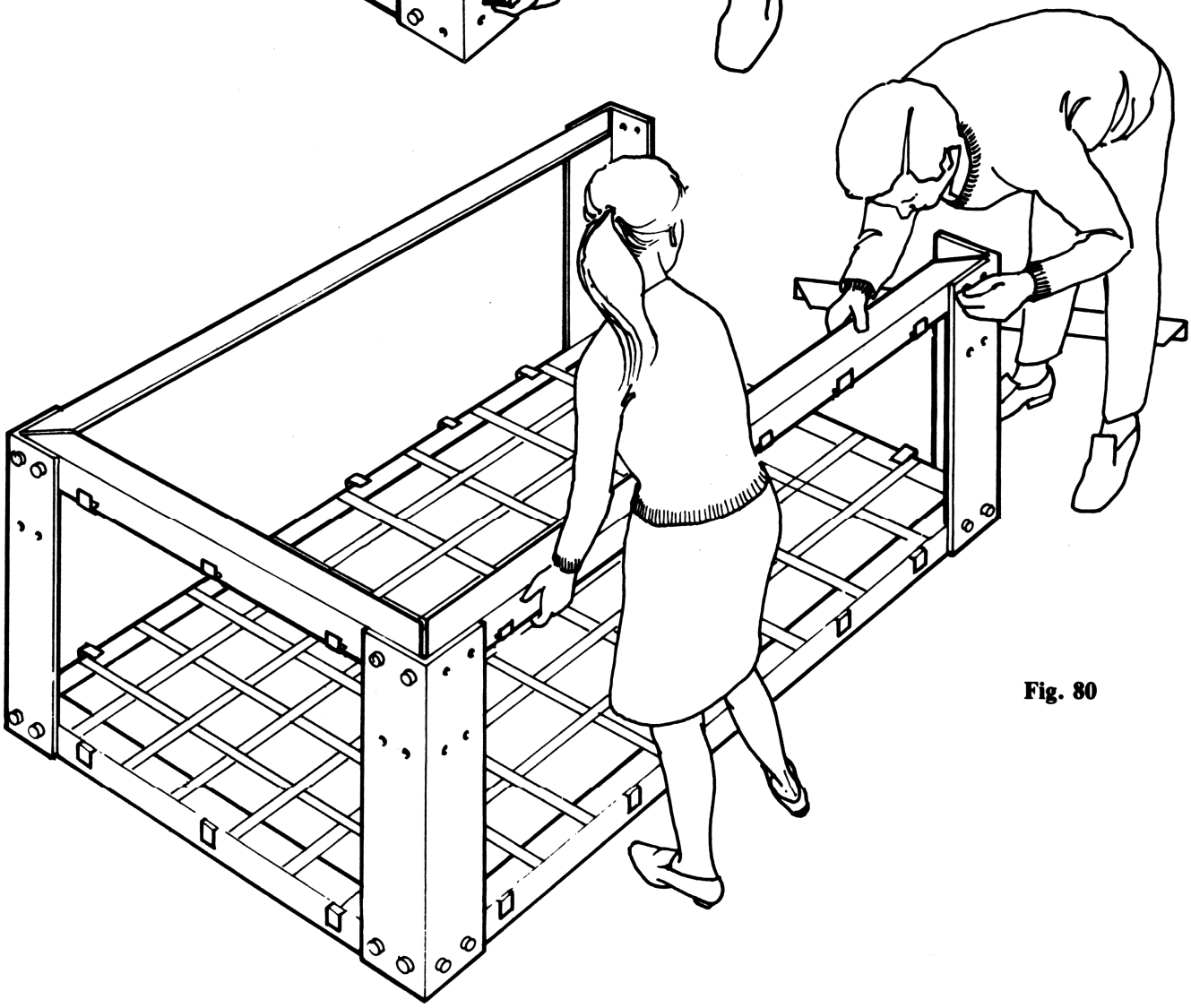

Fig. 80

Fig. 81

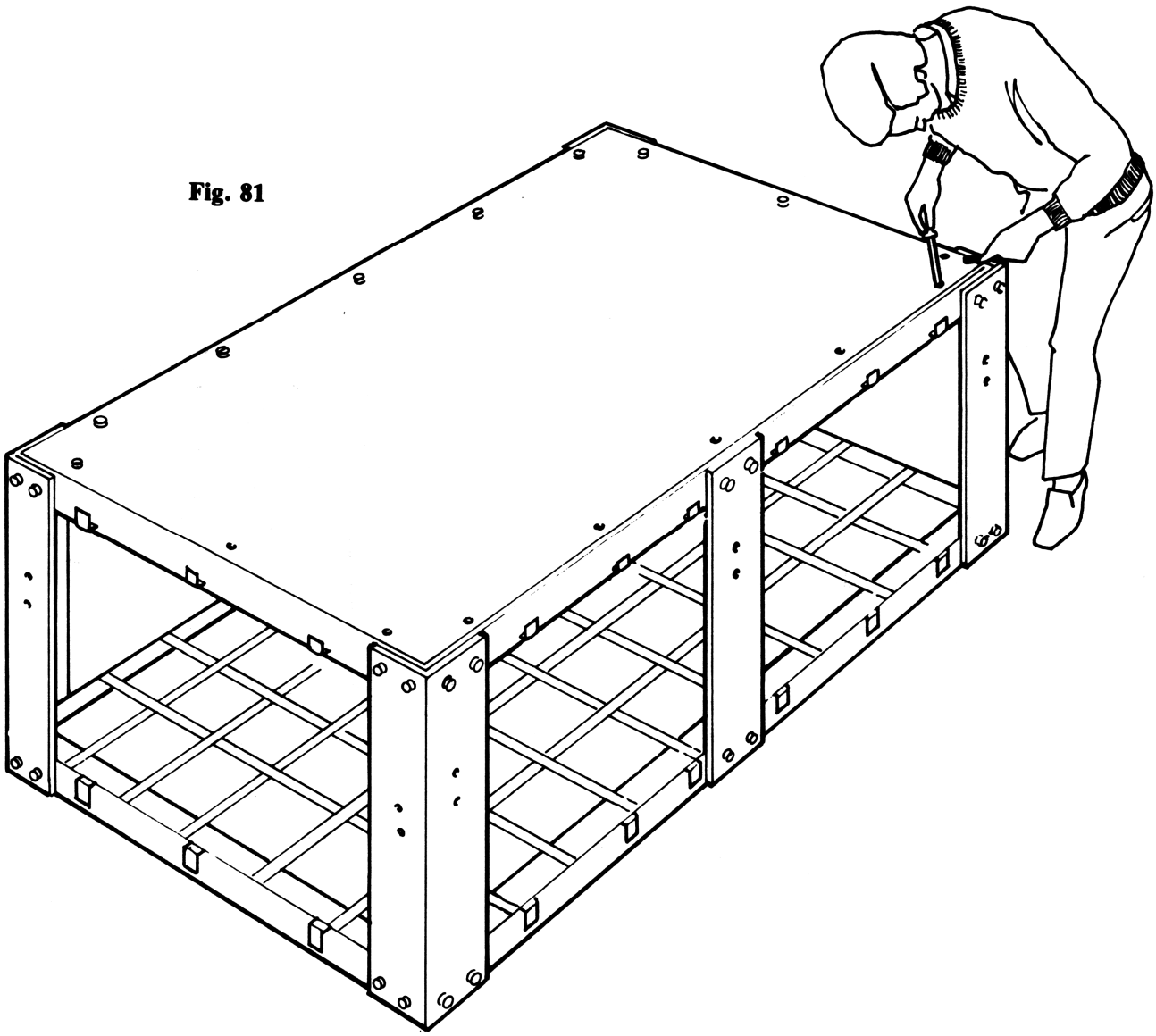

Fig. 82

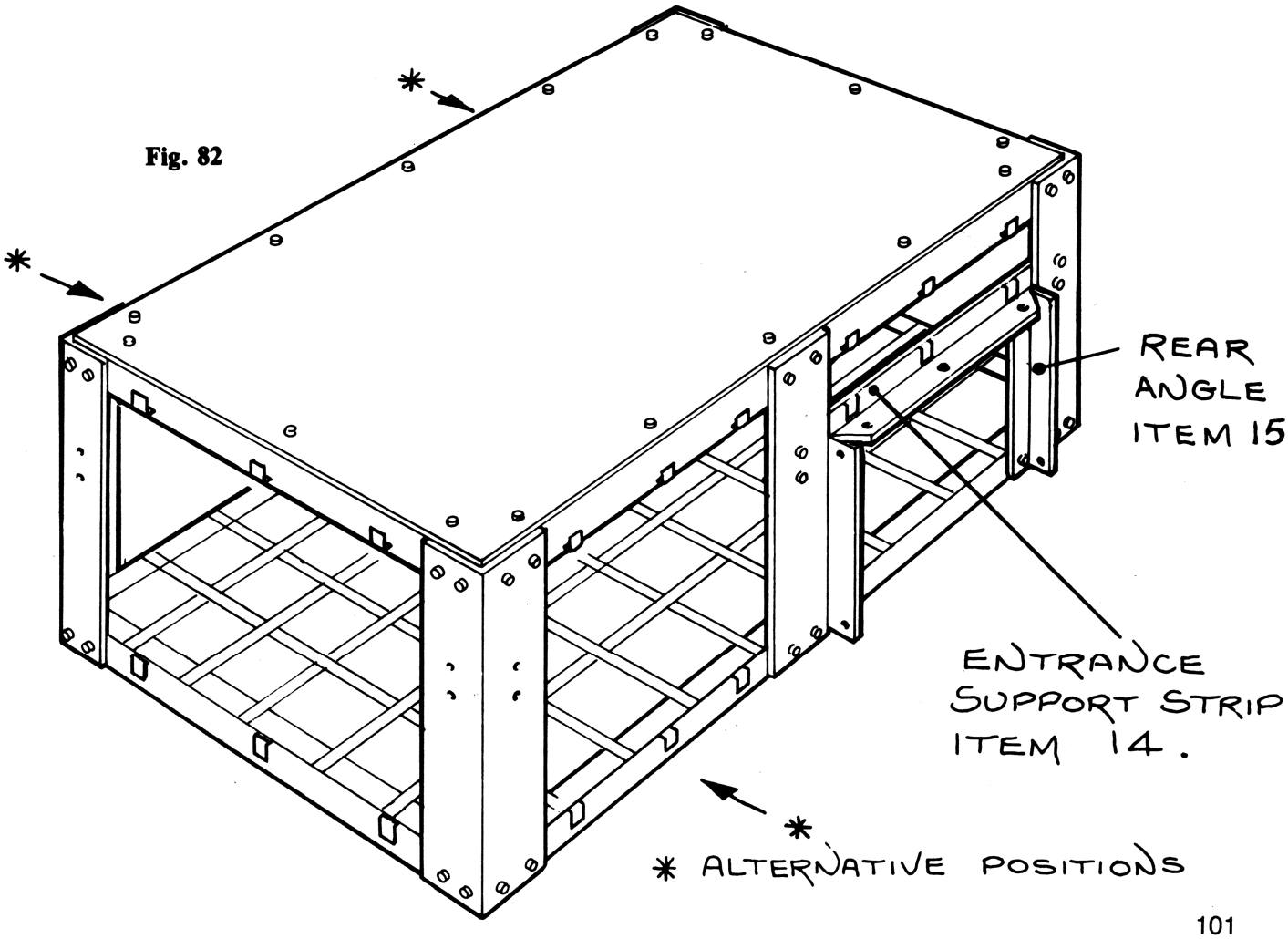
REAR ANGLE ITEM 15
ENTRANCE SUPPORT STRIP ITEM 14.
* ALTERNATIVE POSITIONS

CAR-OVER-TRENCH FALLOUT SHELTER (EXPEDIENT SHELTER HANDBOOK)

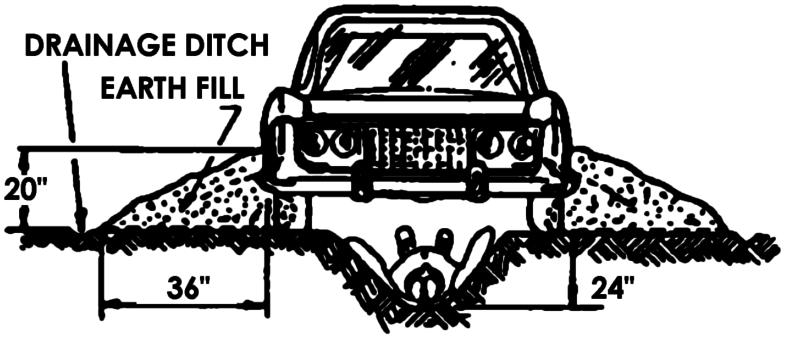

DOORS OR LOGS CAN BE USED IN PLACE OF CAR.

FOR INDOOR SHELTER, USE BAGS OF WATER INSIDE BOXES AROUND & ON TABLE

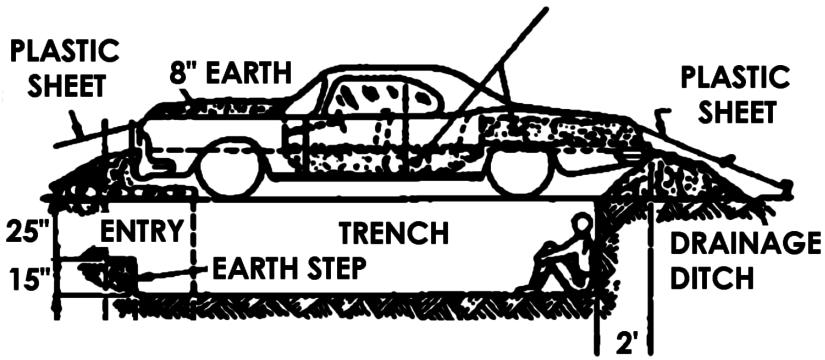

BANK EXCAVATED EARTH 20 INCHES HIGH AROUND CAR

PLACE 8" OF EARTH ON CAR HOOD

DIG SHALLOW DRAINAGE DITCH AROUND FILL

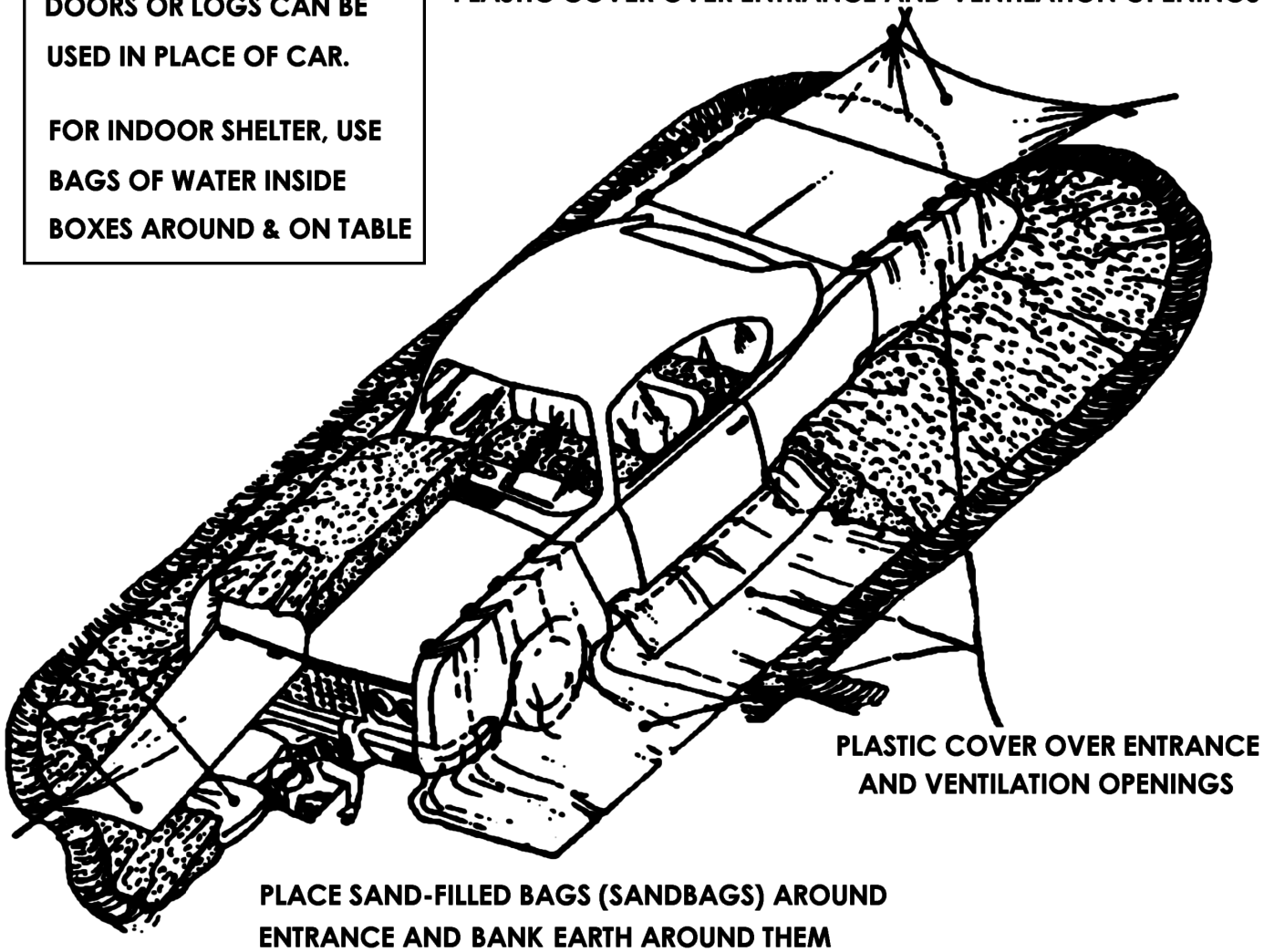

HOME OFFICE

THE PROTECTION OF YOUR HOME AGAINST AIR RAIDS

READ THIS BOOK THROUGH
THEN
KEEP IT CAREFULLY

Why this book has been sent to you

If this country were ever at war the target of the enemy's bombers would be the staunchness of the people at home. We all hope and work to prevent war but, while there is risk of it, we cannot afford to neglect the duty of preparing ourselves and the country for such an emergency. This book is being sent out to help each householder to realise what he can do, if the need arises, to make his home and his household more safe against air attack.

The Home Office is working with the local authorities in preparing schemes for the protection of the civil population during an attack. But it is impossible to devise a scheme that will cover everybody unless each home and family play their part in doing what they can for themselves. In this duty to themselves they must count upon the help and advice of those who have undertaken the duty of advice and instruction.

If the emergency comes the country will look for her safety not only to her sailors and soldiers and airmen, but also to the organised courage and foresight of every household. It is for the volunteers in the air raid precautions services to help every household for this purpose, and in sending out this book I ask for their help.

Samuel Hoare

HOW TO CHOOSE A REFUGE-ROOM

Almost any room will serve as a refuge-room if it is soundly constructed, and if it is easy to reach and to get out of. Its windows should be as few and small as possible, preferably facing a building or blank wall, or a narrow street. If a ground floor room facing a wide street or a stretch of level open ground is chosen, the windows should if possible be specially protected (see pages 30 and 31). The stronger the walls, floor, and ceiling are, the better. Brick partition walls are better than lath and plaster, a concrete ceiling is better than a wooden one. An internal passage will form a very good refuge-room if it can be closed at both ends.

A cellar or basement is the best position for a refuge-room if it can be made reasonably gas-proof

The best floor for a refuge-room

A cellar or basement is the best place for a refuge-room if it can be made reasonably gas-proof and if there is no likelihood of its becoming flooded by a neighbouring river that may burst its banks, or by a burst water-main. If you have any doubt about the risk of flooding ask for advice from your local Council Offices.

Alternatively, any room on any floor below the top floor may be used. Top floors and attics should be avoided as they usually do not give sufficient protection overhead from small incendiary bombs. These small bombs would probably penetrate the roof but be stopped by the top floor, though they might burn through to the floor below if not quickly dealt with.

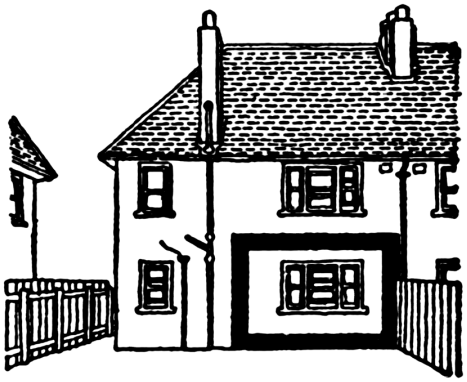

In a house with only two floors and without a cellar, choose a room on the ground floor so that you have protection overhead

How to seal up the door

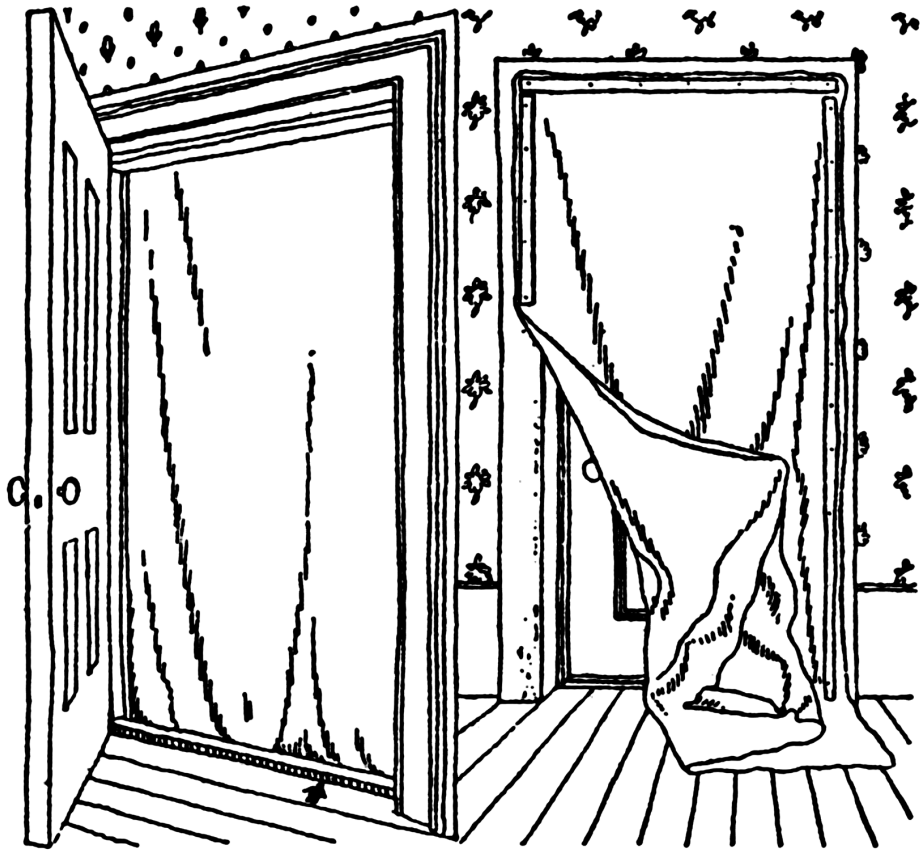

Doors which have to be opened and closed should be sealed against gas. This is how to do it.

Nail a piece of wood, padded with felt, to the floor so that the door, when closed, presses tightly against it. Take care not to nail this piece of wood on the wrong side of the door so that it cannot be opened. Strips of felt may also be nailed round the inside of the door to exclude draughts. Fix a blanket outside the door if the door opens inwards, or inside the door if the door opens outwards, with strips of wood. The top of the blanket should be fixed to the top of the door frame. One side of the blanket should be fastened down the whole length of the door frame, on the side where the hinges are, by means of a strip of wood nailed to the frame. The other side of the blanket should be secured not more than two feet down, so that a flap is left free for going in and out. Arrange the blanket so that at least 12 inches trails on the floor to stop air from blowing underneath it. See illustration above. If the blanket is kept damp during an air raid, it will give better protection.

Strengthening the room

If your refuge-room is on the ground floor or in the basement, you can support the ceiling with wooden props as an additional protection. The illustration shows a way of doing this, but it would be best to take a builder's advice before setting to work. Stout posts or scaffold poles are placed upright, resting on a thick plank on the floor and supporting a stout piece of timber against the ceiling, at right angles to the ceiling joists, i.e. in the same direction as the floor boards above.

How to support a ceiling

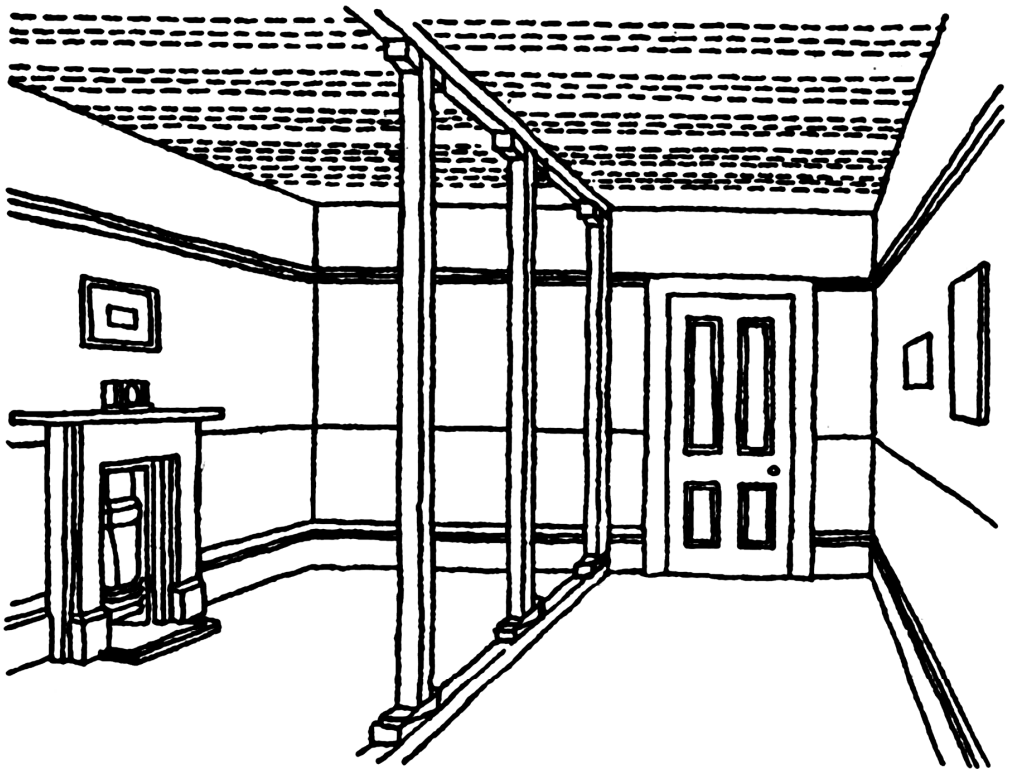

The illustration below shows the detail of how to fix the props

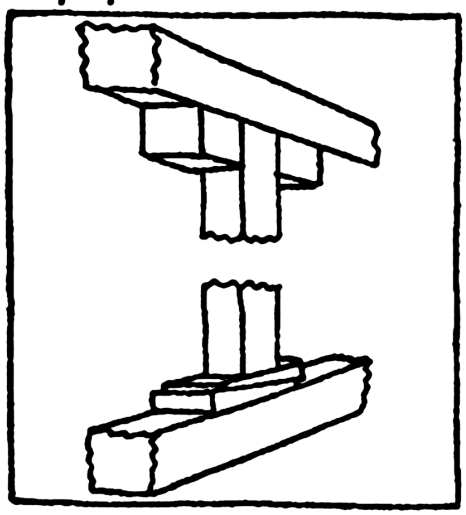

The smaller illustration shows how the posts are held in position at the top by two blocks of wood on the ceiling beam. The posts are forced tight by two wedges at the foot, driven in opposite ways. Do not drive these wedges too violently, otherwise you may lift the ceiling and damage it. If the floor of your refuge-room is solid, such as you might find in a basement, you will not need a plank across the whole floor, but only a piece of wood a foot or so long under each prop.

How to deal with an incendiary bomb

You can tackle a small incendiary bomb yourself (better if you have someone to help you) if you will follow these directions. You will also be able to get proper instruction about it.

The bomb will burn fiercely for a minute or so, throwing out burning sparks, and afterwards less fiercely. It will set fire to anything inflammable within reach. You should try to deal with it before it has caused a big fire.

Before you can get close enough to do anything, you will probably have to cool down the room with water, preferably with a line of hose. (See page 20 for a simple hand pump.)

There are two ways of dealing with the bomb itself.

1 It can be controlled by means of the Stirrup Hand Pump (see page 20), with a *spray* of water which, although it does not extinguish the bomb, makes it burn out quickly and helps to prevent the fire spreading. Water must *not* be used on a bomb in any other way.

2 If it has fallen where you can get at it, it can be smothered with dry sand or earth. A bucket full of sand or earth is enough to cover and control a small bomb. The best method of applying it is by the Redhill sand container and scoop (see page 19); but a bucket will do if you have a long-handled shovel to use with it.

   Immediately the bomb is smothered, shovel or scoop it into the sand container or bucket and take it out of doors. If a bucket is used, 2 or 3 inches of sand or earth must be kept in the bottom to prevent the bomb burning through.

Remember that the bomb might burn through the floor before you have had time to remove it, and you might have to continue to deal with it on the floor below.

ACT PROMPTLY. PROMPT ACTION MAY BE THE MEANS OF SAVING LIVES. PROMPT ACTION WILL SAVE PROPERTY. PROMPT ACTION WILL PREVENT SERIOUS DAMAGE. PROMPT ACTION WILL DEFEAT THE OBJECT OF THE RAID.

EXTRA PRECAUTIONS AGAINST EXPLOSIVE BOMBS

TRENCHES. Instead of having a refuge-room in your house, you can, if you have a garden, build a dug-out or a trench. A trench provides excellent protection against the effects of a bursting bomb, and is simple to construct. Full instructions will be given in another book which you will be able to buy. Your air raid wardens will also be able to advise.

SANDBAGS. Sandbags outside are the best protection if your walls are not thick enough to resist splinters. Do not rely on a wall keeping out splinters unless it is more than a foot thick. Sandbags are also the best protection for window openings. If you can completely close the window opening with a wall of sandbags you will prevent the glass being broken by the blast of an explosion, as well as keeping out splinters. But the window must still be sealed inside against gas.

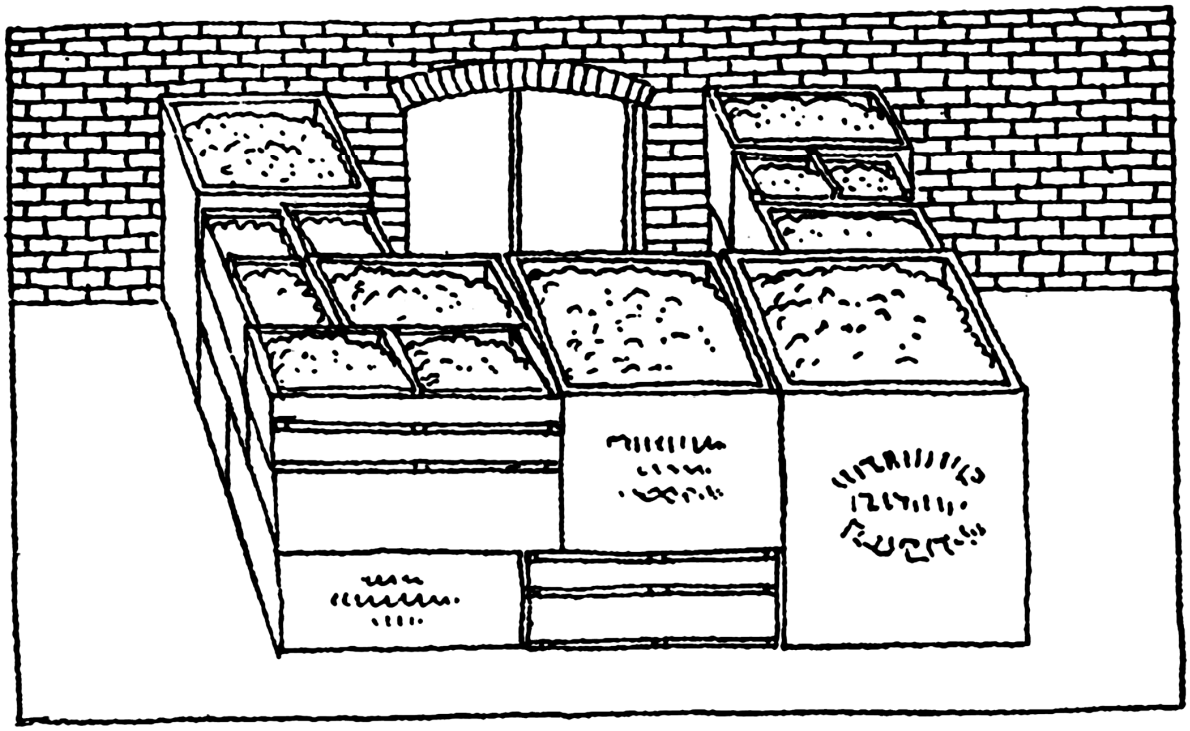

A basement window protected by boxes of earth

Any bags or sacks, including paper sacks such as are used for cement, will do for sandbags.

ALL persons involved in accidents suffer from shock, whether or not they suffer physical injury. Shock is a disturbance of the nervous system. It varies in its severity. The signs of shock are faintness, paleness, weak pulse, and weak breathing.

TREATMENT OF SHOCK

1 Place the patient flat on his back on a bed or a rug or on cushions. If you think a bone may be broken do not move the patient more than can be helped.

2 Loosen the clothing at the neck, chest and waist to make the breathing freer.

3 Cover the patient warmly with rugs and blankets. In cases of shock the body loses heat. A hot-water bottle is helpful, but take care that it does not lie in contact with the skin.

4 Give hot drinks. If you cannot make hot drinks, give cold water *in sips*. But only if the patient is conscious and able to swallow.

5 Soothe the patient by speaking reassuring words in a calm voice and in a confident way.

TREATMENT OF WOUNDS

The first thing to do is to stop the bleeding and to keep the wound clean. This can be done by covering it with a clean dressing bound on tightly. Do not touch a wound with your fingers because of the risk of poisoning from dirt. Treat the patient for shock in addition to attending to the wound, because the loss of blood, if the wound is serious, and the pain do in themselves cause shock.

WOUNDS IN THE HEAD AND BODY

1 Cover the wound with a clean folded handkerchief or a double layer of dry lint.

2 Apply another handkerchief or a layer of cotton wool as a pad to distribute the pressure over the wound.

3 Tie the dressing in position with a bandage, a strip of linen, or a necktie. This can be done quite firmly, unless there is any foreign body, especially glass, in the wound, or unless the bone is broken. In this case the dressing should be tied on lightly.

4 Treat the patient for shock.

ornl

ORNL/TM-10423

OAK RIDGE NATIONAL LABORATORY

MARTIN MARIETTA

Technical Options for Protecting Civilians from Toxic Vapors and Gases

C. V. Chester

Date Published - May 1988

Prepared for
Office of Program Manager
for
CHEMICAL MUNITIONS
Aberdeen Proving Grounds, Maryland

OPERATED BY
MARTIN MARIETTA ENERGY SYSTEMS, INC.
FOR THE UNITED STATES
DEPARTMENT OF ENERGY

Table 1. Chemical Agent Toxic Properties[1]

Agent	Volatility (mg/m^3, 25^oC)	Median Lethal Concentration X Time (mg/m^3 *min)		Median Incapacitation Concentration X Time (mg/m^3 *min)
		Respiratory	Percutaneous	
Chlorine (CL)	2.2×10^7	19,000	-	1,800
Phosgene (CG)	4×10^6	3,200	-	1,600
Hydrogen Cyanide (AC)	1×10^6	2,000-4,500	-	>2,000
Cyanogen Chloride (CK)	1×10^6	11,000	-	7,000
Sulfur Mustard (HD)[2]	920	1,500	10,000	200
Nitrogen Mustard (HN-1)	2,000	1,500	20,000	200
Lewisite (L)[2]	6,000	1,200-1,500	100,000	300
Mustard Lewisite (HL)	4,200	1,500	>10,000	200
Tabun (GA)[2]	610	400	40,000	300
Sarin (GB)[2]	22,000	100	15,000	35-75
Soman (GD)	3,900	100	1,000	35-75
VX[2]	10.5	100	1,000	50
Methyl Isocyanate		1500		

[1]Taken from U.S. Department of the Army (1975) and WHO (1970).

[2] Chemical agents in the stockpile to be destroyed in this program.

DISTANCE AND ATMOSPHERIC DISPERSION

As a toxic cloud moves downwind it mixes with ever increasing amounts of air, becoming larger and more dilute. Diffusion of the vapor vertically and at right angles to direction of motion reduces the exposure to someone standing in the path of the cloud. Diffusion forward and backwards along the direction of travel in general does not reduce the amount inhaled by someone in the path of the cloud.

The rate of vertical and lateral mixing of the toxic cloud with the surrounding air can vary enormously depending on weather conditions. A bright, sunshiny day promoting convection of the atmosphere close to the ground will cause rapid vertical mixing. A turbulent wind will promote lateral mixing. High windspeeds also reduce the time that a person is immersed in a passing cloud and directly reduces the amount they will inhale for given quantity going by. The worst conditions providing the greatest threat to people at the greatest distance downwind occur under conditions of light, steady winds, a clear night with cooling of the ground to cause vertical stability in the atmosphere and the existence of a temperature inversion not too far above the ground to trap the chemical close to the ground. Conditions very close to these were responsible for the large casualties at the Bhopal incident in India.

Figure 1 shows the downwind hazard from clouds of 1000 kilograms of each of several toxic gases moving at 1 meter per second (approx. 2 miles per hour) in a highly stable atmosphere (Pasquill type E). These conditions also assume an inversion at 750 meters. Calculations use the Army's D2PC code (Whitacre et al, 1986). The dependent variable in Fig. 1 is given as the protection factor offered by protective measures required to prevent 99 percent of the fatalities at each location downwind. For example for GB, to keep the dose down to 1 percent fatalities at 1 kilometer downwind, the population would have to have masks or other protection giving a protection factor of a little less than 700. The

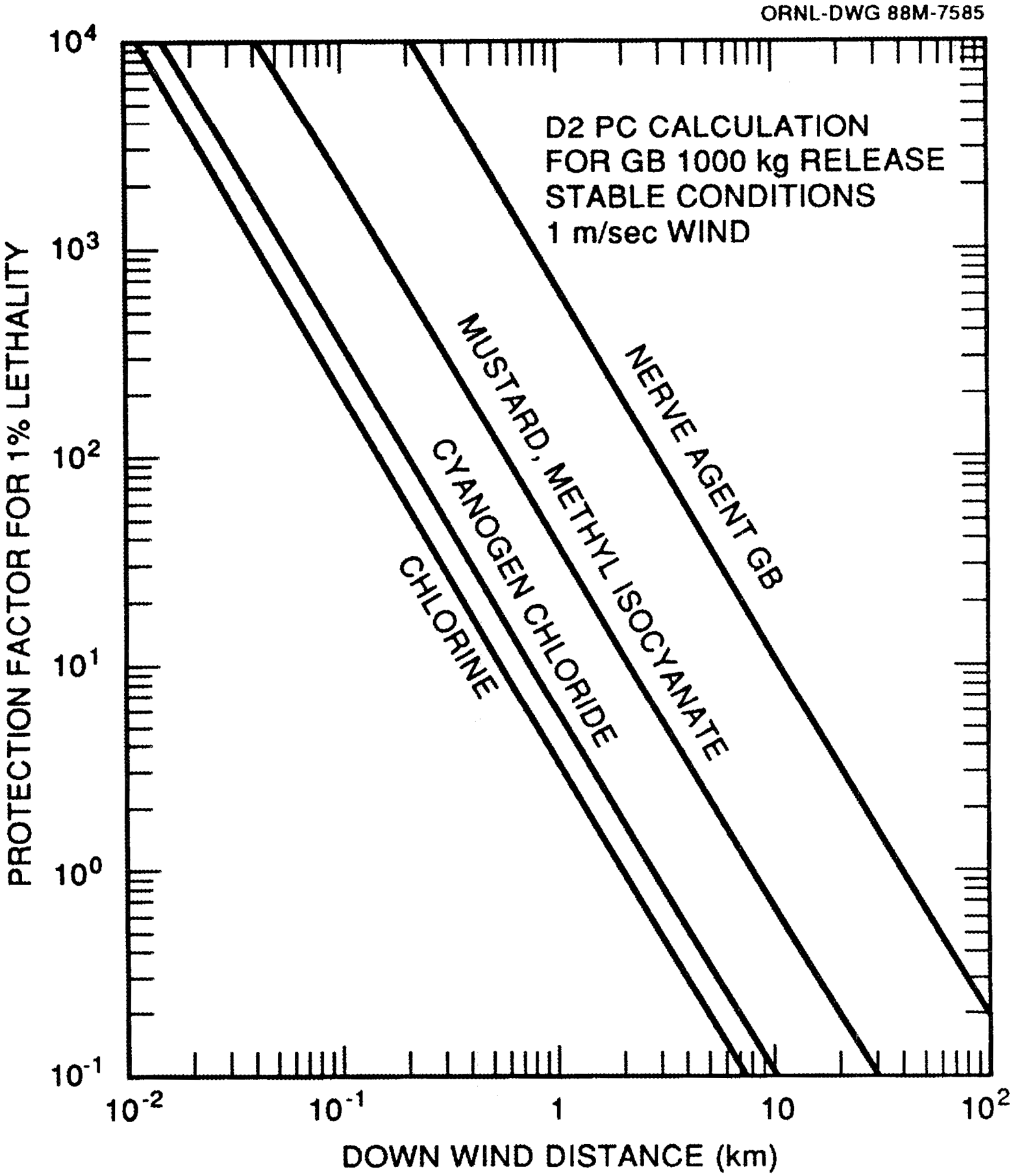

Fig. 1 Dose vs Downwind Distance for Some Very Toxic Gases

protection factor is the ratio of the dose people would get with no mask compared to what they would get if they were wearing a gas mask.

As can be seen from Fig. 1 the requirement for gas masks diminishes rapidly as one gets further away from the point of release of a quantity of agent. Under sunny conditions with a higher wind speed the requirement for protection would decrease even more rapidly. For the purposes of this study, these relatively pessimistic meteorological conditions (1.0 m/s. wind velocity, type E stability, inversion at 750 m) will be assumed in all cases.

EVACUATION

Evacuation is a way of increasing the distance between the population and a hazard and is the countermeasure to toxic chemical releases with which there is the most experience. Sorensen and his colleagues have reviewed the subject thoroughly (1987). It is very effective for slowly (few hours) developing hazards and in areas where emergency plans employing evacuation have been developed. Slowly developing chemical hazards can include a relatively small leak of a volatile toxic chemical, a large spill of a low volatility but highly toxic substance, or a progressive accident (e.g. fire) which doesn't at first cause release of toxic chemicals but has the potential of spreading to nearby equipment, tanks or drums containing toxics. Where small areas are threatened, evacuation can be quite effective.

Situations where taking shelter may be preferable to evacuating include quick release of small quantities of volatile toxic chemicals, or circumstances where an evacuation is likely to result in a traffic jam. This latter is a possibility where the area at risk is large, the population density is high, and the time available is short.

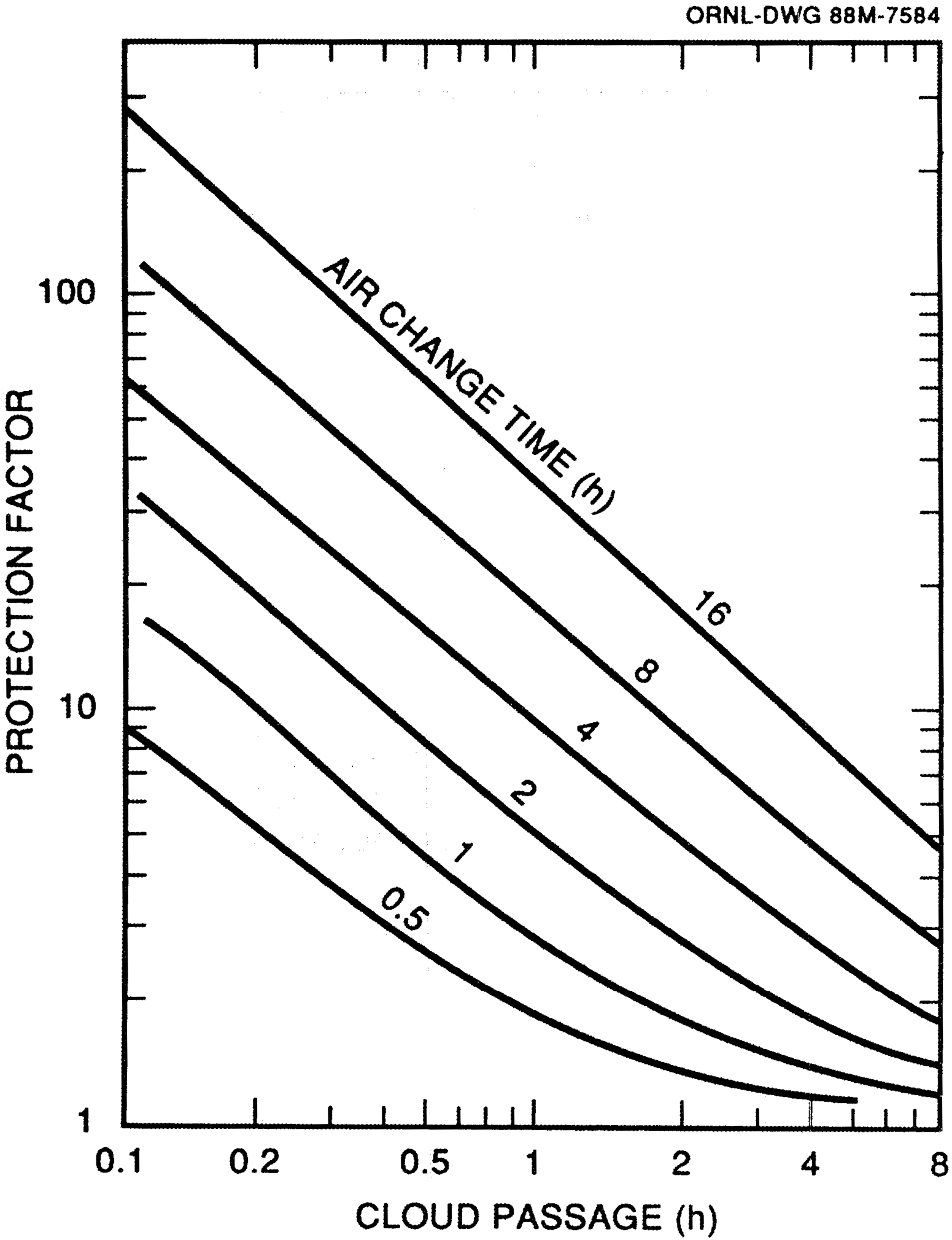

Fig. 2 Protection Factor of Leaky Enclosures

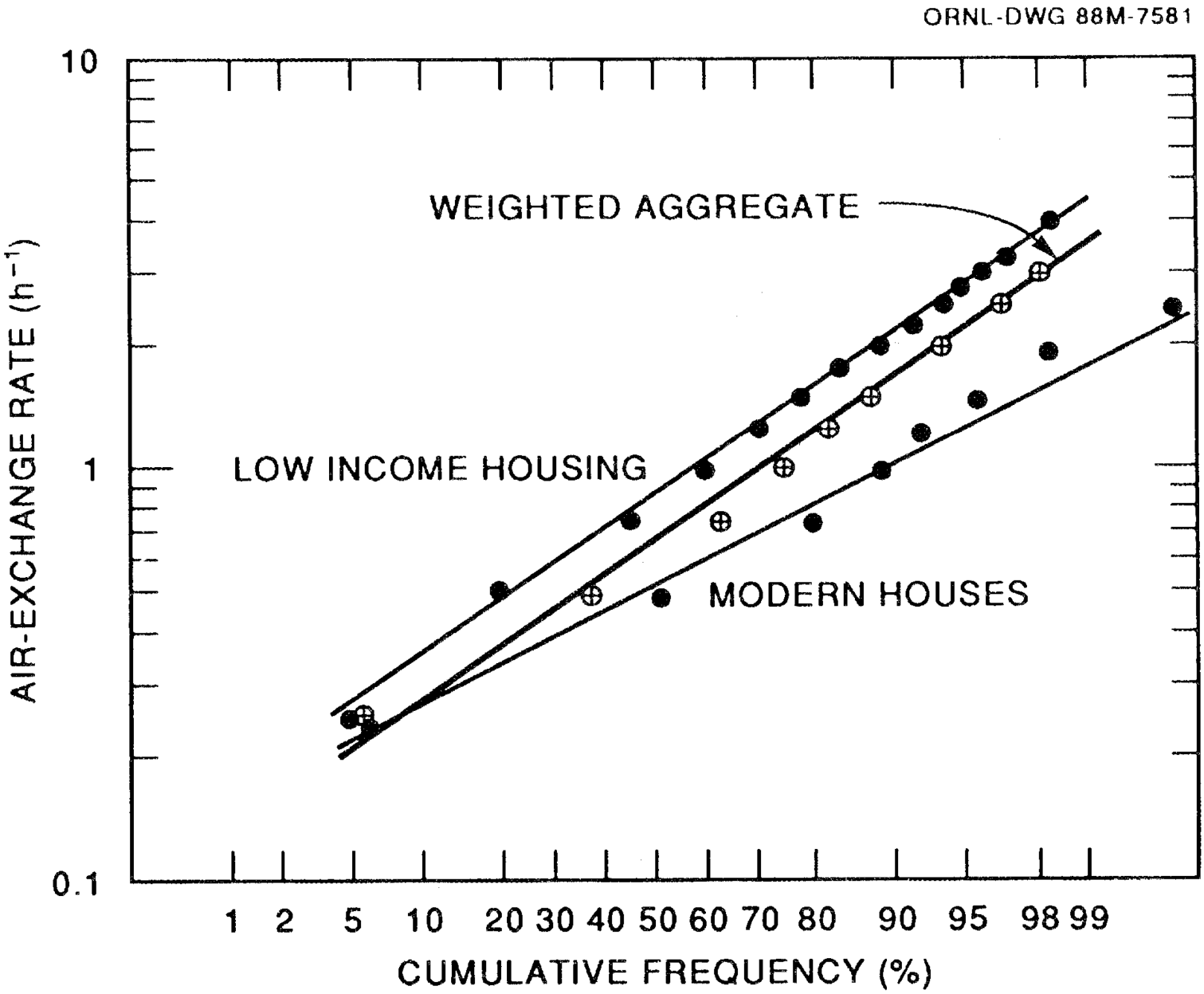

Fig. 3 Infiltration Rates of American Residences

Sorensen, J.H., 1988, Evaluation of Warning and Protective Action Implementation Times for Chemical Weapons Accidents, ORNL-TM/10437, Oak Ridge National Laboratory, Oak Ridge, TN 37831.

U.S. Department of the Army 1975, Military Chemistry and Chemical Compounds, FM3-9/AFR 355-7.

Whitacre, G.C. et al, Personal Computer Program for Chemical Hazard Prediction (D2PC), U.S. Army Chemical Research and Development Center, Aberdeen Proving Ground, MD.

Wilson, D. J. 1987, Stay Indoors or Evacuate to Avoid Exposure to Toxic Gas, Emergency Preparedness Digest (Canada) 14 no. 1.

World Health Organization, 1970, Health Aspects of Chemical and Biological Weapons, Geneva, Switzerland.

ORNL/TM-2001/154

Energy Division

Will Duct Tape and Plastic Really Work? Issues Related To Expedient Shelter-In-Place

John H. Sorensen
Barbara M. Vogt

Date Published—August 2001

Prepared for the
Federal Emergency Management Agency
Chemical Stockpile Emergency Preparedness Program

Prepared by
OAK RIDGE NATIONAL LABORATORY
Oak Ridge, Tennessee 37831-6285
managed by
UT-BATTELLE, LLC
for the
U.S. DEPARTMENT OF ENERGY
under contract DE-AC05-00OR22725

Expedient sheltering involves the use of common materials to enhance the safety of a room inside a building against the impacts of a chemical plume. The central premise behind taping and sealing with duct tape and plastic is to reduce airflow into a room. Vapors penetrate into a room through cracks and openings in the walls, floors and ceilings, around doors and windows, and through openings for ducts, light fixtures, fans, pipes, electrical outlets, chimneys, door handles, and locks. The goal of taping and sealing is to significantly reduce infiltration at these points.

Expedient sheltering was suggested by NATO (1983) using the term "ad-hoc shelter" to protect civilian populations from chemical warfare agent exposure. The concept was to use plastic sheeting to seal off a room by fashioning a simple airlock at the entrance to the room and sealing off doors, windows or louvered vents. The NATO guidelines also stressed the need for rapid exit from the ad-hoc shelter once the plume had passed to avoid further exposure (NATO 1983, p. 143).

This strategy was further developed by the Israeli Civil Defense in the mid-1980s to protect the public against a chemical weapons attack (Yeshua 1990). The tape and seal strategy was in place when the Gulf War occurred in 1991 and received considerable media attention. The Israeli strategy was to have citizens prepare a "safe room" in their house or apartment with the use of weatherization techniques to permanently reduce infiltration. Citizens were also instructed to take expedient measures, such as sealing

doors and windows with plastic sheets, in the event of a chemical weapons attack. The use of plastic over a window was developed to reduce air infiltration and to provide a vapor barrier in the event of glass breakage from bomb explosions. A modification of the Israeli strategy was proposed for use in CSEPP (Sorensen 1988; Rogers et al. 1990).

Although vapors, aerosols, and liquids cannot permeate glass windows or door panes, the amount of possible air filtration through the seals of the panes into frames could be significant, especially if frames are wood or other substance subject to expansion and contraction. To adequately seal the frames with tape could be difficult or impractical. For this reason, it has been suggested that pieces of heavy plastic sheeting larger than the window be used to cover the entire window, including the inside framing, and sealed in place with duct or other appropriate adhesive tape applied to the surrounding wall.

Another possible strategy would be to use shrink-wrap plastic often used in weatherization efforts in older houses. Shrink-wrap commonly comes in a 6 mil (0.006-in.) thickness and is adhered around the frame with double-faced tape and then heated with a hair dryer to achieve a tight fit. This would likely be more expensive than plastic sheeting and would require greater time and effort to install. Because double-faced tape has not been challenged with chemical warfare agents, another option is to use duct tape to adhere shrink-wrap to the walls. Currently, we do not recommend using shrink-wrap plastics because of the lack of information on its suitability and performance.

3. WHY WERE THESE MATERIALS CHOSEN?

Duct tape and plastic sheeting (polyethylene) were chosen because of their ability to effectively reduce infiltration and for their resistance to permeation from chemical warfare agents.

3.1 DUCT TAPE PERMEABILITY

Work on the effectiveness of expedient protection against chemical warfare agent simulants was conducted as part of a study on chemical protective clothing materials (Pal et al. 1993). Materials included a variety of chemical resistant fabrics and duct tape of 10 mil (0.01-in.) thickness. The materials were subject to liquid challenges by the simulants DIMP (a GB simulant), DMMP (a VX simulant), MAL (an organoposphorous pesticide), and DBS (a mustard simulant). The authors note that simulants should behave similarly to live agents in permeating the materials; they also note that this should be confirmed with the unitary agents. The study concluded that “duct tape exhibits reasonable resistance to permeation by the 4 simulants, although its resistance to DIMP (210 min) and DMMP (210 min) is not as good as its resistance to MAL (>24 h) and DBS (> 7 h). Due to its wide availability, duct tape appears to be a useful expedient material to provide at least a temporary seal against permeation by the agents” (Pal et al. 1993, p. 140).

3.2 PLASTIC SHEETING PERMEABILITY

Tests of the permeability of plastic sheeting (polyethylene) challenged with live chemical warfare agents were conducted at the Chemical Defense Establishment in Porton Down, England in 1970 (NATO 1983, p. 133). Agents tested included H and VX, but not GB. Four types of polyethylene of varying thickness were tested: 2.5, 4, 10 and 20 mil (0.0025, 0.004 in., 0.01 in., and 0.02 in.). The results of these tests are shown in Table 1.

Table 1: Permeability of plastic sheeting to liquid agent

	Breakthrough time (h)	
Thickness	VX	H
0.0025	3	0.3
0.004	7	0.4
0.01	30	2
0.02	48	7

Source: NATO 1983, p. 136.

The data shows that at thickness of 10 mil or greater, the plastic sheeting provided a good barrier for withstanding liquid agent challenges, offering better protection against VX than for H. Because the greatest challenge is from a liquid agent, the time to permeate the sheeting will be longer for aerosols and still longer for vapors, but the exact relationship is unknown due to a lack of test data.

In Fig. 1 we plot the data in Table 1 to determine the nature of the relationship between thickness and breakthrough time. The data suggest a somewhat linear relationship, thus allowing some interpolation for various thickness of plastic sheeting. For reference, commercially available sheeting is typically sold at 0.7, 1, 1.2, 1.5, 2, .2.5, 3, 4, 6, and 10 mil. although thicker material is available (up to 100 mil). Plastic painter drop cloths are sold between 0.5 and 2 mil.

4. HOW HAVE THEY PERFORMED IN TESTS OR REAL EVENTS?

Although the “safe room” strategy was used in the many scud missile attacks against Israel in the Gulf War, no chemical agents were released during these attacks. Sheltering has been recommended as a protective action in several chemical releases in the United States and Canada. Some anecdotal information exists about sheltering effectiveness in those events, but no empirical studies of actual effectiveness in a real event have been conducted. Such data would be extremely difficult to capture. Two sets of experiments have been conducted on the effectiveness of in-place sheltering (Rogers et al. 1990; Blewett et al. 1996).

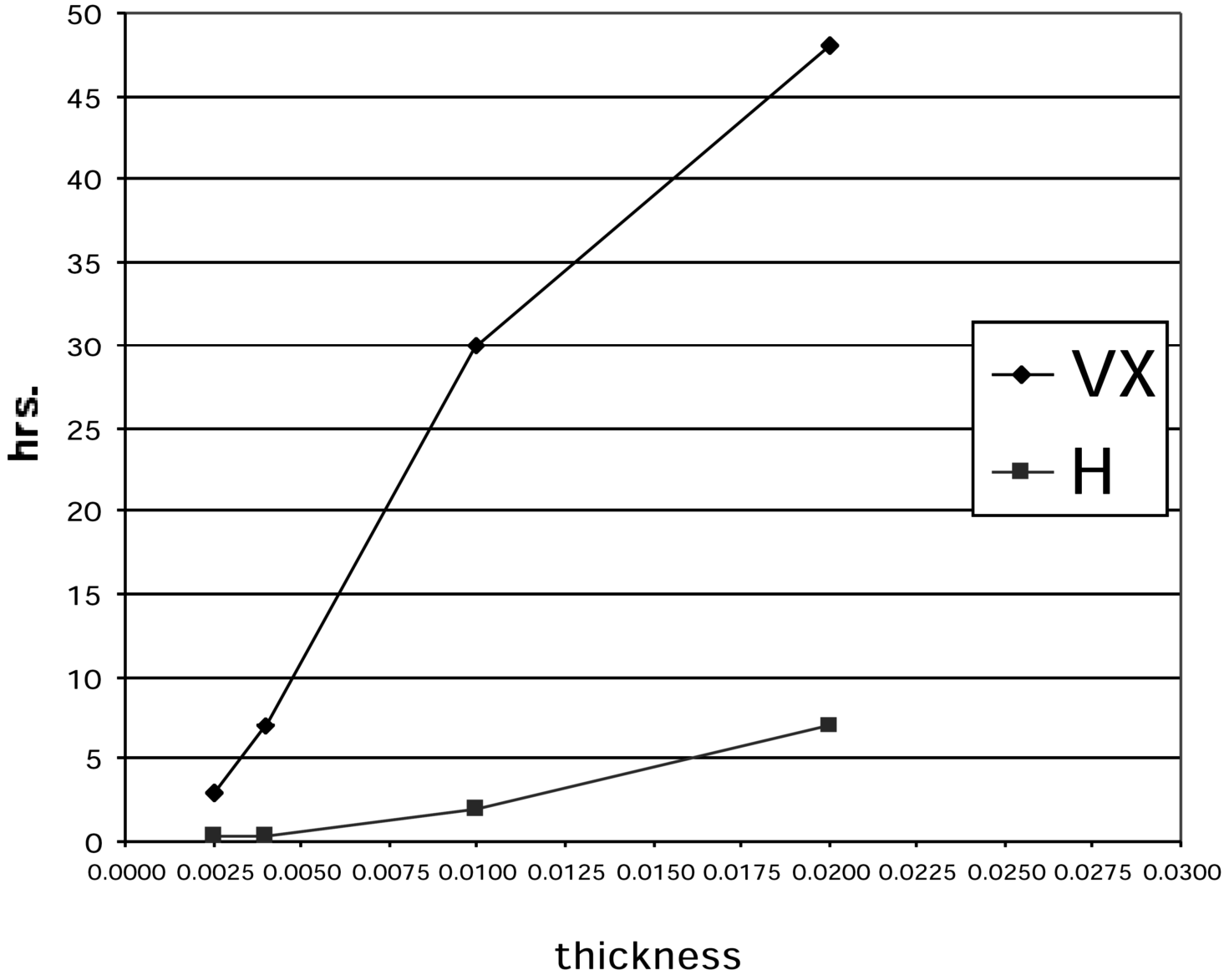

Fig. 1. Breakthrough as a function of the thickness of plastic sheeting.

The results of the two sets of experiments or trials using tracer gas methods provide some insight into the effectiveness of expedient sheltering. These trials were conducted in the vicinity of Oak Ridge, TN., in the late 1980s and Edgewood, MD in the mid 1990's. The Oak Ridge tests involved 12 single-family homes. The trials measured the air exchange for the whole house, the expedient room (mainly bathrooms) with a towel against the door, and the bathroom fully taped and sealed by a household member. Materials used included duct tape, flexible insulation cord, and plastic sheeting. In each test, subjects were given written instructions and checklists, but were left to make the decision how to seal the room.

Infiltration or air exchange is measured by the number of air changes per hour (ach). The average air exchange rate for the houses tested in the Oak Ridge trials was 0.45 ach. The bathrooms with a towel averaged only 0.94 ach. The fully sealed bathrooms averaged

0.33 ach, a reduction of 0.61 ach or 65% (0.61/0.94). One factor not assessed in the study was the air exchanged between the sealed room and the whole house versus the sealed room and the outside. If one assumes that the air exchanged by the room is mostly with the rest of the house, an added protection factor would be achieved because the contaminated air concentrations outside the house are reduced by mixing with air in the whole house and then reduced again in the expedient room. If it is assumed that most of the exchange is between the room and the outside, little added protection beyond that provided by the room would be achieved.

The tests in Edgewood, Maryland, involved 10 residential buildings and 2 mobile homes. Three types of rooms were tested: bathrooms with windows, windowless bathrooms, and walk-in closets. The expedient measures were applied by technicians, and the doors were taped from the outside of the room. A total of 36 trials were performed using different configurations of protection. The results (Table 2) show the air exchange rate for the whole house and for the room in which the expedient measure(s) was applied. The most aggressive strategy (Method 2) proved to be fairly effective, reducing average air exchange rates to between 0.15 and 0.21 ach.

Table 2: Results of Edgewood trials

Room and method	Average house ach	Average room ach
Bathroom—no expedient measures	0.29	0.27
Method 1: Bathroom—wet towel and taped vent	0.28	0.23
Method 2: Bathroom—door taped, plastic sheet on window, wet towel and taped vent	0.32	0.21
Windowless bathroom—no expedient measures	0.37	0.29
Method 1: Windowless bathroom—wet towel and taped vent	0.33	0.29
Method 2: Windowless bathroom—door taped, wet towel and taped vent	0.34	0.15
Walk in closet—no expedient measures	0.39	0.28
Method 1: Walk in closet—wet towel and taped vent	0.44	0.30
Method 2: Walk in closet—door taped, wet towel and taped vent	0.21	0.15

A good way of examining the numbers in the table is to compare the baseline case (door closed with no expedient protection) to the case with the greatest amount of expedient protection (Method 2). For the bathroom, the ach dropped from 0.27 to 0.21 (22%). For the windowless bathroom, the ach dropped from 0.29 to 0.15 (48%). For the closet, the ach dropped from 0.28 to 0.15 (46%).

The results of the two studies are consistent. Both studies showed a reduction of average air exchange rates from expedient protective measures. In some of the specific rooms tested such measures substantially reduced air infiltration into the sealed room when compared to the unsealed room. Infiltration was reduced in one trial by 90% in the

Oak Ridge study and by 57% in Edgewood study. In addition, fairly low air exchanges were achieved in some of the specific expedient room trials (0.11 ach in both studies). The effectiveness of individual trials varied. In the Oak Ridge study, the lowest reduction was 13% and highest air exchange rate was 0.58 ach. In the Edgewood study, the highest air exchange rate for the most aggressive strategy (Method 2) was 0.31 ach. The greater variability in the Oak Ridge data likely results from the variability in the way individuals implemented the taping and sealing, which was more uniform in the Edgewood study because taping was done in a consistent manner by a skilled technician.

5. TIMING OF EXPEDIENT SHELTER

In the ORNL study (Rogers et al. 1990), the time to implement the expedient protection was recorded. Overall times ranged between 3 and 44 min in total, with a mean of 19.8 min. The time to close up the house was relatively short, with a mean of 3.2 min with a range of 1 to 6 min. Times to tape and seal ranged between 2.3 and 38.6 min, with a mean of 16.7 min. These data are shown in Fig. 2.

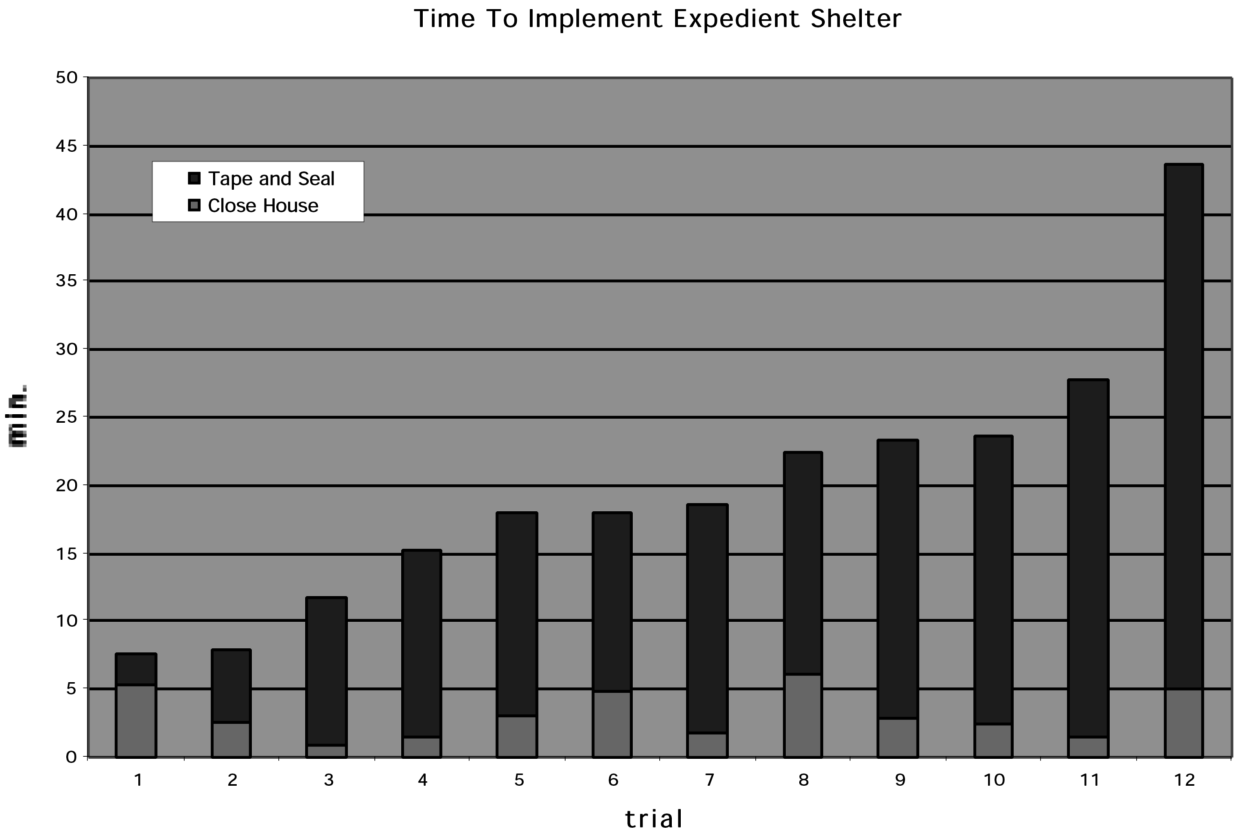

Fig. 2: Expedient shelter trial times.

8. REFERENCES

Blewett, W. K., D. W. Reeves, V. J. Arca, D. P. Fatkin, and B. D. Cannon 1996. *Expedient Sheltering in Place: An Evaluation for the Chemical Stockpile Emergency Preparedness Program*, ERDEC-TR-336, Edgewood Research, Development, and Engineering Center, Aberdeen Proving Ground, Md.

NATO Civil Defense Committee 1983. *NATO Handbook on Standards and Rules for the Protection of the Civil Population Against Chemical Toxic Agents*, AC/23-D/680, 2nd rev.

Pal, T., G.Griffin, G. Miller, A. Watson, M. Doherty, and T. Vo-Dinh. 1993. "Permeation Measurements of Chemical Agent Simulants Through Protective Clothing Materials," *J. Haz. Mat.* **33**:123-141.

Rogers, G. O., A. P. Watson, J. H. Sorensen, R. D. Sharp, and S. A. Carnes. 1990. *Evaluating Protective Actions for Chemical Agent Emergencies*, ORNL-6615, Oak Ridge National Laboratory, Oak Ridge, Tenn.

Sorensen, J. H. 1988. *Evaluation of Warning and Protective Actions Implementation Times for Chemical Weapons Accidents*, ORNL/TM-10437, Oak Ridge National Laboratory, Oak Ridge, Tenn.

Yeshua, I. 1990. *Chemical Warfare: A Family Defense Manual*, Centre for Educational Technology, Ramat Aviv, Israel.

U.S. Department of the Army and Federal Emergency Management Agency. 1996. Planning Guidance for the Chemical Stockpile Emergency Preparedness Program, Washington, D.C.

CATALOGED BY DDC
AS AD No. 408094
408094

FINAL REPORT

11 March 1963

Recovery and Decontamination Measures after Biological and Chemical Attack

This report has been reviewed in the Office of Civil Defense and approved for publication. Approval does not signify that the contents necessarily reflect the views and policies of the Office of Civil Defense.

Contract OCD-OS-62-183

Prepared for
Office of Civil Defense
Department of Defense

by

Science Communication, Inc.
1079 Wisconsin Avenue, N.W.
Washington 7, D. C.

To plan for countermeasures against any weapons one must understand the problem—the nature, the potentials, and the limitations. This research project and the resultant final report were intended to bring together current information most applicable to civil defense. It was particularly intended for those who are responsible for planning preparatory, reclamation and countermeasures effort to minimize the damage from a BW/CW attack.

William J. Lacy
Project Coordinator
Postattack Research

Decontaminants

An important class of decontaminants comprises the common substances or natural influences such as time, air, earth, water, and fire.

Natural Effects

Biological agents are living organisms and tend to die off with time unless they are in a favorable environment with moisture, food, warmth, and other factors necessary for their survival. In addition, most biological organisms are very sensitive to the conditions of temperature and humidity -- and, particularly to the ultra-violet portion of sunlight. Adverse exposure to the elements -- air, sunlight, high temperature, low humidity -- is effective, in fact, against all biological agents except the spore forms of bacterial organisms.

It is generally assumed that in the vegetative form bacteria (as contrasted to the spore form) can persist for less than two hours during daytime and about eighteen hours at night. Since these short-lived bacteria are the most probable agents, outdoor decontamination is usually not called for unless the agent has been identified, either by laboratory tests or by the character of the disease, as one which forms spores or is otherwise known to be persistent.

The persistent, low-volatile, agents such as the liquid nerve agents (V-agents) and the blister gases present the principal chemical decontamination problem. Even these evaporate in time. The speed of evaporation and dissipation is enhanced by higher temperatures and wind. Thus, if it is possible to avoid the area or the use of contaminated objects for a reasonable length of time, decontamination may be unnecessary. Such periods might run from hours to a few days, depending on the degree of contamination and weather conditions. In cold weather the agents will persist for longer periods.

Water

Next to weathering, the most important natural decontaminant is water, used either to remove the agent, with or without soap or detergents to assist, or by boiling. One caution -- water used to wash away contamination becomes contaminated and must be disposed of accordingly. Boiling destroys most chemical agents and all biological agents. When it is feasible, boiling is one of the most generally desirable methods -- particularly for household use by individuals.

Earth and fire, the other natural decontaminants, would have relatively little application in civil defense BW/CW decontamination operations. Earth may be used to cover contamination temporarily to keep it out of contact with people while natural processes either dissipate or destroy the agent. This involves substantial effort with bulldozers and earth-moving equipment and usually is neither practical or necessary.

Chemical Decontaminants

These are preferred when they are available. Chemical decontaminants fall in two classes -- those which destroy or neutralize the agents, and those which simply assist in their removal.

The principal decontaminants which destroy or neutralize are:

- Chlorine-containing materials, such as calcium hypochlorite (HTH) and sodium hypochlorite solutions. Many household disinfectants available under various brand names -- Clorox, Purex, etc. -- are sodium hypochlorite solutions.
- Alkalies, such as caustic soda (lye) and sodium carbonate (washing soda, or soda ash).

The chlorine-containing materials, in proper concentrations, are effective against both biological and chemical agents. As solutions they are used to decontaminate surfaces, as in washing off sealed food containers; for decontaminating cotton fabrics by soaking or addition during the washing process; and for sterilizing water. Hypochlorite solutions have the disadvantage of corroding metals and so must be rinsed off thoroughly.

The hypochlorites -- calcium and sodium -- are the preferred decontaminants for blister gases and liquid nerve agents. For most such applications they are used as solutions but for vertical surfaces or porous surfaces a "whitewash" of calcium hypochlorite (HTH), hydrated lime, and water (called a "slurry") is more effective

Appraisal of Biological and Chemical Warfare Protection in the U.S. Field Army. Booz, Allen Applied Research, Inc., June 1961. AD 329 113, (SECRET).

Area-Coverage Capabilities of Bacteriological and Chemical Weapons (U). Tamplin, A.R., Rand Corporation, April 1962. AD 329 207, (SECRET).

Biological Decontamination. Asher, T.M., Naval Biological Laboratory, February 1954. AD 72 485, (SECRET).

Biological Problems Attendant Upon the Application of Bacteriological and Chemical Agents in Limited War (U). Tamplin, A.R., Rand Corporation, RM-2677, June 1961. AD 324 462, (SECRET).

Chemical and Biological Weapons Employment. Department of the Army Field Manual, FM 3-10, February 1962.

Community Reaction to an Accidental Chlorine Exposure - Task Sirocco. Segaloff, Louis, University of Pennsylvania, November 1961. AD 269 681.

Decontamination of Water Contaminated with VX. Lindsten, Don C. and Bauer, Virginia E., U.S. Army Engineer Research and Development Laboratories, Research Report 1630-RR, May 1960. AD 239 310.

Effects of Cooking and Baking Processes on the Sterilization of Food Contaminated with Bacterial Spores. Commissary Research Division, U.S. Naval Supply Research and Development Facility, Final Report Navy Project NT 002 024 (CR 53-89), 1953.

Evaluation of Standard and Modified Laundering Procedures as BW Decontamination Methods. Portner, Dorothy M., Mayo, Elizabeth C. and Surkiewicz, Bernard F., Biological Warfare Laboratories, Technical Memorandum 1-2, March 1959. AD 252 270L.

Field Purification of Water Contaminated by G Agents. Chemical Corps Medical Division Report No. 220, 1949. AD 212 449.

Field Tests of Protective Clothing Exposed to BW Aerosols. Chemical Corps Biological Laboratories, Special Report No. 112, August 1949.

Possible Applications of Bacteriological Warfare to Public Water Supplies. Maloney, John R., Office of Naval Research, November 1959. AD 69 721, (CONFIDENTIAL).

Some Indications of Soviet Views on the Strategic Employment of CW/BW (U). Gouré, Leon, Rand Corporation, RM-2725, March 1961. (SECRET).

Studies on Insect Control (U). U.S. Army Engineer Research and Development Laboratories, Research Report 1656-RR, October 1960. AD 321 975, (CONFIDENTIAL).

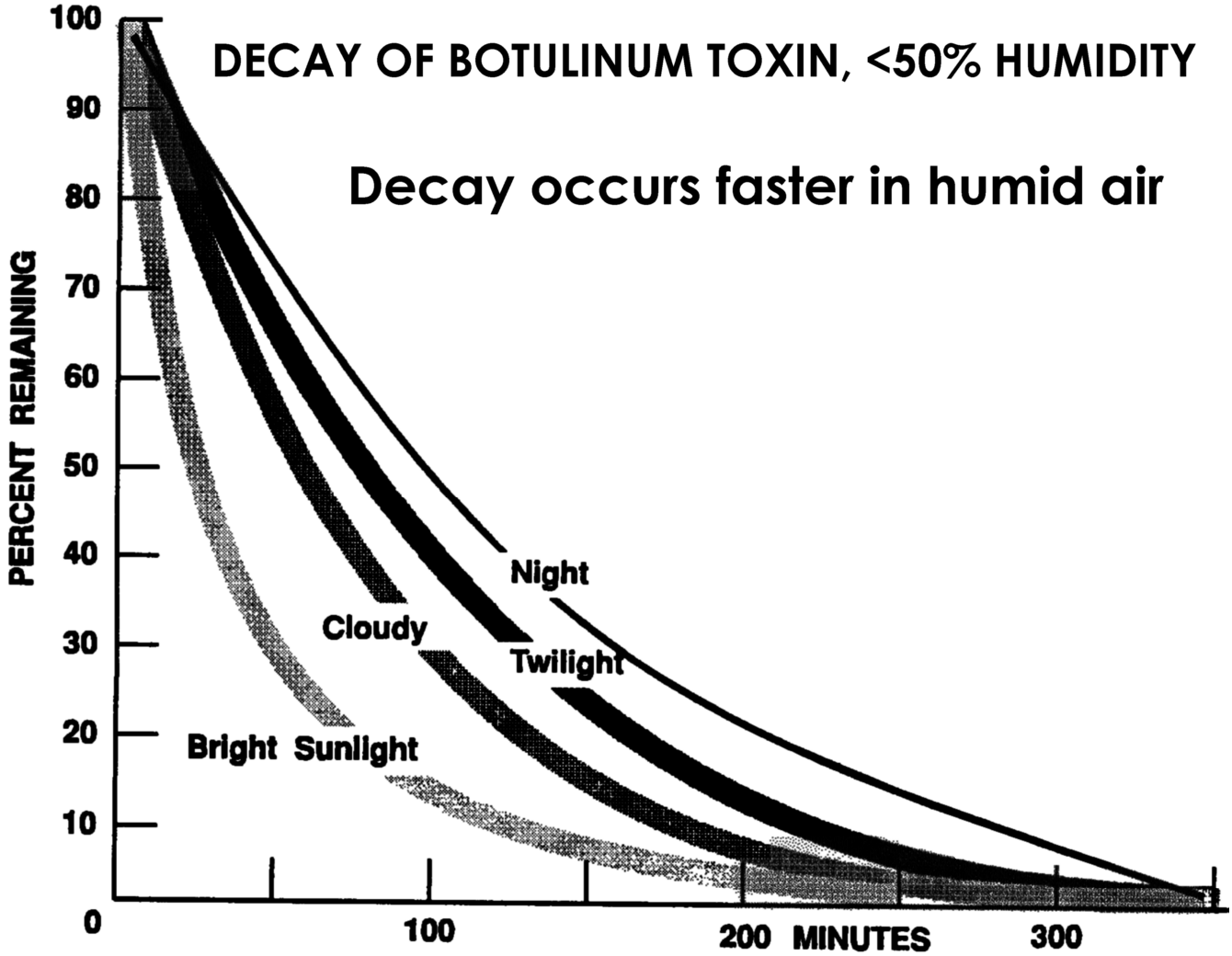

U.S. Army Field Manual FM 3-3 (1992), Fig. B-3.

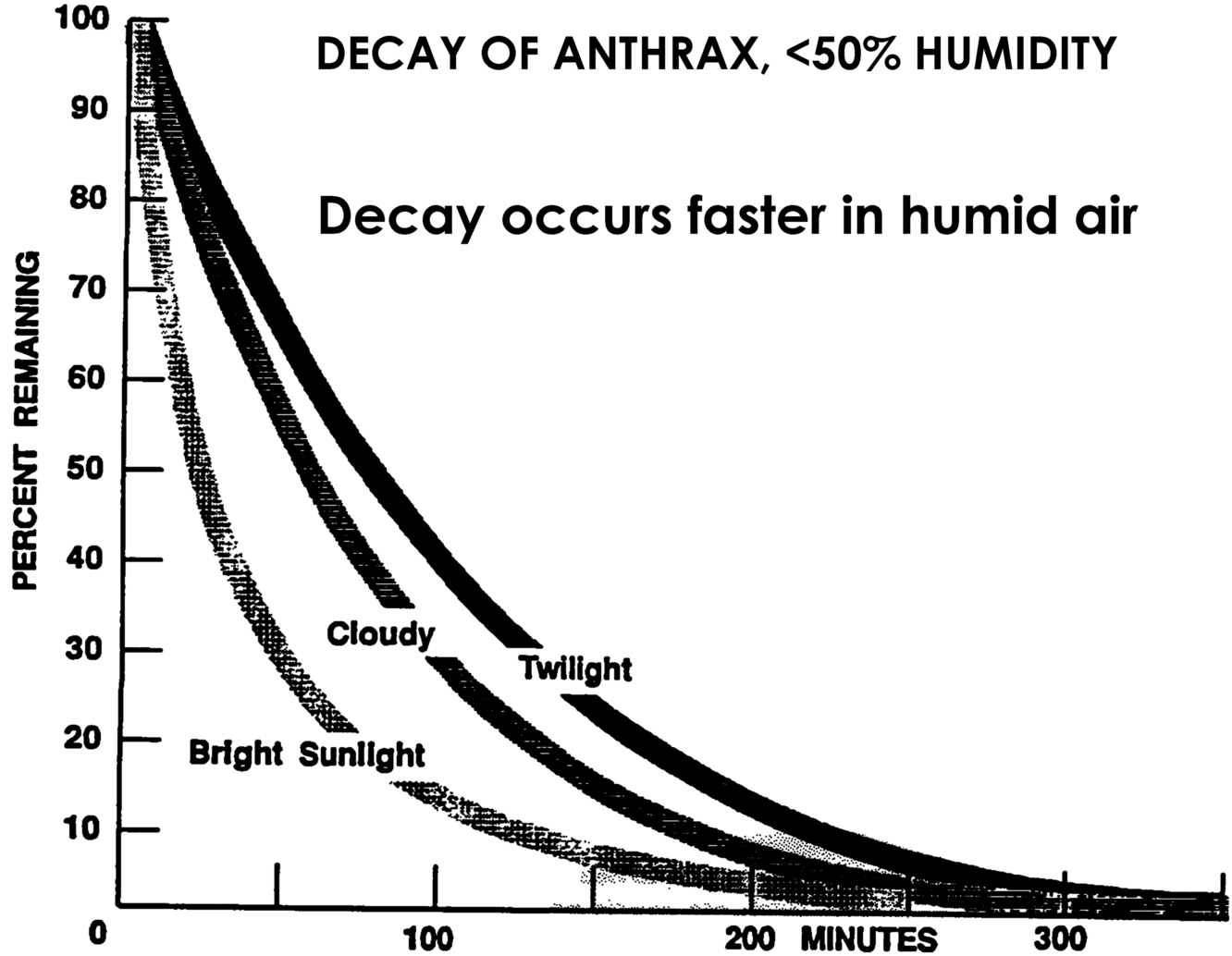

U.S. Army Field Manual FM 3-3 (1992), Fig. B-1.

- Basic decontamination procedures are generally the same no matter what the agent. Thorough scrubbing with large amounts of warm soapy water or a mixture of 10 parts water to 1 part bleach (10:1) will greatly reduce the possibility of absorbing an agent through the skin.

Sealing a Room

- Close all windows, doors, and shutters.
- Seal all cracks around window and door frames with wide tape.
- Cover windows and exterior doors with plastic sheets (6 mil minimum) and seal with pressure- sensitive adhesive tape. (This provides a second barrier should the window break or leak).
- Seal all openings in windows and doors (including keyholes) and any cracks with cotton wool or wet rags and duct tape. A water-soaked cloth should be used to seal gaps under doors.
- Shut down all window and central air and heating units.

Suggested Safehaven Equipment

- Protective equipment—biological/chemical rated gas masks, if available; waterproof clothing including long-sleeved shirts, long pants, raincoats, boots, and rubber gloves.
- Food and water—a 3-day supply.
- Emergency equipment—flashlights, battery-operated radio, extra batteries, can or bottle opener, knife and scissors, first aid kit, fire extinguisher, etc.
- Most chemical and biological agents that present an inhalation hazard will break down fairly rapidly when exposed to the sun, diluted with water, or dissipated in high winds.

United States Department of State Publication No. 11162
Bureau of Diplomatic Security
Reprinted July 2004

United States Department of State
Bureau of Diplomatic Security

Responding to a Biological or Chemical Threat

IN THE UNITED STATES

In 1995, the Aum Shinrikyo, a Japanese religious cult, launched a large-scale chemical attack on the Tokyo subway system. The attack focused on four stations using Sarin gas, a potent chemical warfare nerve agent. Twelve people were killed but the attack fell far short of the apparent objective to inflict thousands of casualties. Subsequent investigation by authorities revealed that the cult had previously conducted several unsuccessful attacks against a variety of targets using other chemical agents and the biological agents botulism toxin and anthrax.

More recently, the incidents of anthrax contamination in the United States served to illustrate the viability of this type of terrorist threat. Again, the attacks fell short of mass casualties, but some deaths did occur and the fear and disruption caused by a few positive anthrax findings were crippling. The U.S. Government continues working to meet the potential consequences of such attacks.

ORNL-6615

EVALUATING PROTECTIVE ACTIONS FOR CHEMICAL AGENT EMERGENCIES

by

G. O. Rogers
A. P. Watson
J. H. Sorensen
R. D. Sharp
S. A. Carnes

Date Published–April 1990

Prepared for the
U.S. DEPARTMENT OF THE ARMY
Office of the Assistant Secretary,
Installations, Logistics and Environment
under Interagency Agreement DOE No. 1769-1354-A1
and
FEDERAL EMERGENCY MANAGEMENT AGENCY
Office of Natural and Technological Hazards
under Interagency Agreement No. 1457-B106-A1

Prepared by the Oak Ridge National Laboratory
Oak Ridge, Tennessee 37831
operated by
Lockheed Martin Energy Research
for the
U.S. DEPARTMENT OF ENERGY
under Contract No. DE-AC05-84OR21400

APPENDIX G
INSTRUCTIONS FOR IMPLEMENTING EXPEDIENT SHELTER IN CHEMICAL EMERGENCIES

Entering your dwelling or other buildings and following a few simple procedures can reduce exposure to released toxic chemical. These instructions can help you implement a series of actions to increase your protection. The series includes six basic steps:

1. preparing your dwelling to provide protection,
2. selecting an appropriate room within your dwelling to provide maximum shelter,
3. assembling the necessary materials needed to complete the procedures,
4. sealing a room within the dwelling to provide additional protection,
5. remaining in the shelter until notified that the hazard has passed, and
6. vacating the shelter upon plume passage.

Because each house is in some ways unique, you may need to adapt these procedures to your particular home. These instructions order the activities in terms of what is most important in obtaining maximum protection. Therefore, we recommend that you follow these steps in sequence wherever possible. Time is critically important to ensure adequate protection, so implement each step as quickly as you can without making mistakes and continue to the next step as soon as possible.

G.1. Preparing Your Dwelling

The objective is to prepare your dwelling to provide the maximum reduction of airflow from outside to inside. These preliminary steps also provide some protection while you carry out the procedures.

1a. Go or stay indoors.
1b. Close all exterior doors and windows (close storm windows if this can be done quickly). Don't forget garage doors in integral or attached garages as well as doors normally left open for ventilation.
1c. Close all interior doors.
1d. Turn off central heat/air conditioning fans, ceiling fans, kitchen hood fans, and circulating fans.

G.2. Selecting the Appropriate Room

The objective is to select the room that is best suited to reducing overall air infiltration while <u>having at least 10 square feet of floor area per person.</u> Under hot and humid conditions more space is advisable to avoid conditions that might lead to heat prostration within the shelter. Moreover, room air conditioners that recirculate internal

air may be used to create more comfortable shelter conditions. For example a 5 × 8 foot room has 40 ft^2, which would be appropriate for sheltering up to 4 people. This step can be completed in advance. If you have already preselected the room to provide maximum shelter, skip to Sect. G.3 below.

2a. The best room is a relatively small, has no outside walls, and is on the ground floor.
2b. If 2a is not available; select a small room with no windows.
2c. If 2a and 2b are not available: select the room with the smallest number of windows and doors.
2d. Avoid rooms with window air conditioners, windows that leak, vents to outside such as automatic dryer vents, and circulation vents.
2e. Do not select rooms with exhaust vents that automatically start when the light is turned on. These exhaust fans force external air into the room.
2f. If all the above elements are the same for two rooms, choose the room that is free of plumbing fixtures, because such fixtures increase the potential airflow and will require sealing as described in Sect. G.4 below.

G.3. Assembling Materials and Resources

This stage of the procedures is designed to collect all the needed materials to reduce the airflow as much as possible in the room you selected in Sect. G.2 above. This step can be performed ahead of time. Place the following materials in the selected room.

3a. the expedient shelter kit provided;
3b. verify that the kit still has the tape, plastic sheet, scissors, clay, and screwdriver;
3c. obtain a large towel (at least bath-towel size);
3d. a ladder, stool, or chair if required to seal any ceiling vents or the tops of windows and doors;
3e. a radio or television or other communication device (preferably portable) to let you to know when the plume has passed so you can exit at an appropriate time; and
3f. if the selected room does not have plumbing, drinking water and sanitary facilities (a covered bucket or other vessel containing approximately 1 cup of chlorine bleach).

G.4. Taping and Sealing

This set of procedures is designed to identify and seal the major sources of airflow between the room you have selected and the rest of the house, as well as restrict the flow of any toxic chemical that may be outside. These steps are sequenced to eliminate larger sources of air exchange first, so they should be implemented in the order listed whenever possible.

4a. Assemble people to be protected in the selected room and close the door. If windows were not closed as instructed in Sect. G.1 above, do so now.

4b. Jam the towel under the entire width of the door, sealing the whole area between the bottom of the door and the floor.

4c. VENTS: <u>If there are no vents, skip to step 4d below</u>. Locate any vents associated with the heating system, fan vents which are sometimes located in bathrooms, or vents to other rooms or to the outside such as dryer vents. Then, tape over small vents repeatedly, overlapping the tape to form a complete seal. For large vents, cut a piece of plastic sheeting large enough to cover the vent, place it over the vent, and tape the plastic loosely in place at the corners. Tape the plastic along each edge to ensure a complete seal. Repeat for each vent in the room.

4d. WINDOWS: <u>If there are no windows, skip to step 4e below</u>. If there are any broken or cracked windows, apply tape or cling-wrap over glass. Locate all leak points (any joints in the window frame, where movable parts of the frame come together), apply cling-wrap to each leak point. Then, cut a piece of plastic sheeting large enough to cover window and window frame, place it over the window and frame, and tape the plastic loosely in place at the corners. Tape the plastic along each edge to ensure a complete seal.

4e. Before you complete the seal on the door, check all supplies to ensure that you have enough material to completely seal the door. <u>Do not open the door unless you clearly have inadequate materials to complete the seal</u>; breaking the door seal will substantially reduce the protection provided by the refuge.

4f. DOOR: Tape along each edge of the door to seal off airflow, beginning with the parts you can reach from the floor and proceeding to the upper parts that may require the use of a ladder, stool, or chair. Place and tape cling-wrap over each hinge and the door handle.

4g. PLUMBING FIXTURES: <u>If there are no plumbing fixtures, skip to step 4h below</u>. Use putty or clay around all pipes that penetrate walls, ceiling, or floor (both intake and drainage pipes). To apply clay or putty, pull back the pipes decorative sealing ring (use screwdriver if necessary), wrap enough clay or putty around the pipe to fill any gaps between the wall and the pipe, and reset the decorative ring in clay by pressing the ring firmly against wall. Repeat for all pipe entry and exit points.

4h. CABINETS: <u>If there are no built-in cabinets such as sink cabinets, linen closets, or medicine cabinets, skip to step 4i below</u>. Close the cabinet doors and tape them closed according to the procedures described for doors in step 4f above. Note that, because cabinet hinges and handles are smaller than those on doors, tape will probably cover these areas adequately. Then, tape or use cling-wrap along all joints where the cabinet meets the wall. Pay particular attention to kickplates below cabinets, by checking the underside for holes and gaps. Smaller gaps may need to be plugged with clay.

4i. ELECTRICAL FIXTURES: Locate all electrical fixtures, including outlets, switch boxes, and lights. If a light is recessed or if it cannot be sealed without

turning it off, it will have to remain unsealed because covering a light without turning it off may start a fire. Put tape over the outlet boxes, and use cling-wrap or tape to cover all switch boxes. Put cling-wrap over light fixtures not in use. (Some light fixtures contain fans that run continuously with the light in the room. These fans should be turned off as early as practical; if they cannot be turned off, a different room should be selected as instructed in Sect. G.2 above.)

4j. CHECKING YOUR WORK: After, you have completed the procedures to seal the room you have selected, check each area you sealed by slowly passing your hand in front of all potential leak areas. If you can feel air flowing, try to seal it better. We do not recommend that you remove any previous seals, but you may want to add plastic sheeting over sealed areas or tape them more securely.

G.5. Remaining in Shelter

The objective of this stage is to relax as much as possible and wait to be notified of the appropriate time to exit the shelter.

5a. Shelter occupants should be as comfortable as possible; they should stand or move around as little as possible.
5b. Remain calm and relax; doing so adds additional protection by reducing your respiration rate.
5c. Turn on communication device so you can be contacted when it is safe to exit the shelter.
5d. Ask each occupant to periodically check for airflows near them. If any are discovered, seal them by following the above procedures.
5e. Wait for notification of plume passage.

G.6. Vacate Shelter

The objective of this step is to exit the shelter when the plume passes by and to avoid any further cumulative exposure.

6a. Put on protective clothing.
6b. Open all windows and doors.
6c. Evacuate to reception center for medical evaluation and decontamination.

EXPEDIENT SHELTER INSTRUCTION CHECKLIST

1. Prepare your dwelling to provide protection.

1a. Go or stay indoors.
1b. Close all exterior doors and windows.
1c. Close all interior doors.
1d. Turn off fans.

2. Select an appropriate room within your dwelling to provide maximum shelter, <u>having at least 10 square feet of floor area per person</u>.

2a. Choose a relatively small room with no outside walls on the ground floor.
2b. If not available: select a small room with no windows.
2c. If not available: select the room with the fewest windows and doors.
2d. Avoid rooms with window air conditioners, windows that leak, vents to the outside, and circulation vents whenever possible.
2e. Avoid rooms with plumbing fixtures whenever possible.

3. Assemble the necessary materials.

3a. Use the expedient shelter kit provided;
3b. Verify that its contents are complete;
3c. Large towel of at least bath-towel size;
3d. Ladder, stool, or chair if necessary;
3e. Radio, television, or other communication device;
3f. Drinking water and covered container with chlorine bleach for sanitary purposes.

4. Seal a room in the dwelling to provide additional protection.

4a. Enter the selected room and close the door.
4b. Jam the towel under the door.
4c. Seal vents.
4d. Seal windows.
4e. Check all supplies; replace if necessary.
4f. Seal door.
4g. Seal plumbing.
4h. Seal cabinets.
4i. Seal electrical fixtures.
4j. Check you work; reseal where necessary.

5. Remain in the shelter until notified that the plume has passed.

5a. Get as comfortable as possible.
5b. Remain calm, relax, and stay immobile.
5c. Turn on communication device.
5d. Periodically check for airflows in the shelter.
5e. Wait for notification of plume passage.

6. Vacate shelter.

6a. Don protective clothing.
6b. Open all windows and doors.
6c. Evacuate.

ORNL/TM-2001/153

Energy Division

Expedient Respiratory and Physical Protection: Does a Wet Towel Work to Prevent Chemical Warfare Agent Vapor Infiltration?

John H. Sorensen
Barbara M. Vogt

Date Published—August 2001

Prepared for the
Federal Emergency Management Agency
Chemical Stockpile Emergency Preparedness Program

Prepared by
OAK RIDGE NATIONAL LABORATORY
Oak Ridge, Tennessee 37831-6285
managed by
UT-BATTELLE, LLC
for the
U.S. DEPARTMENT OF ENERGY
under contract DE-AC05-00OR22725

1. INTRODUCTION

Several public information efforts in the Chemical Stockpile Emergency Preparedness Program (CSEPP) advocate the use of wet towels to (1) seal a door jam against the infiltration of chemical vapors and (2) provide expedient respiratory protection.

A wet towel has been a common respiratory protection practice for fires to reduce inhalation of soot and smoke, but will this strategy protect against chemical vapors? Using a wet towel to reduce infiltration of chemicals into a room by sealing the gap between the floor and the door is frequently cited in the shelter-in-place (SIP) literature (see Blewett et al. 1996).

The purpose of this paper is to examine the effectiveness of such measures to reduce exposure to vapors from chemical warfare agents. This evaluation includes an examination of the physical and the psychological effectiveness of these measures. Little research has been conducted to examine the effectiveness of expedient protection against chemical vapors and aerosols. More is known about the penetration of aerosols than vapor. In this paper, we summarize the research to date and offer several recommendations for CSEPP.

2. PREVIOUS RESEARCH ON EXPEDIENT PROTECTION

The first documented research on expedient respiratory protection was conducted by Guyton et. al. (1959). They performed a series of tests to determine whether common household items provided respiratory protection against a release of radiological or biological aerosols. The materials they tested included

- a man's cotton handkerchief,
- a women's cotton handkerchief,
- cotton clothing material,
- muslin bed sheet,
- cotton shirt,
- rayon slip,
- cotton terry bath towel, and
- toilet paper.

In total, 18 variations of the 8 materials were tested. The tests performed used human subjects who inhaled *B. globigii* (a bacteria aerosol) through the various materials into a mouthpiece collector. The results of the testing indicated that 5 of the variations had filtration efficiency of greater than 85%. These included a folded (16 and 8 thickness) or crumpled handkerchief, 3 thickness of toilet paper, and a bath towel folded in half. Tests

were performed on wetted items, but the efficiency was lower than for dry items. In addition, only the bath towel was feasible to breath through when wet. No testing for vapor protection was performed.

A series of experiments was performed by the Harvard School of Public Health in the early 1980's (Cooper, Hinds, and Price 1981; 1983; Cooper et al. 1983a,b; Price, Cooper, and Yee 1985). These efforts sought to build on the work of Guyten et al. by examining the penetration of expedient materials by particle size and by examining penetration by vapors. Materials similar to those in the earlier studies were used; but instead of human subjects, several test chambers were designed. Mineral oil was used for the aerosol tests and methyl iodide and iodine were used in the vapor tests. Methyl iodide is a difficult vapor to capture, while iodine, a highly reactive gas, was chosen because it is readily removed by wet filtration, thus setting the upper boundary for effectiveness against a gas.

The first set of tests examined the effectiveness of the materials in filtering the aerosols and vapors. For aerosols, the reductions by a factor of 30 were achieved with the dry materials across the range of aerosol sizes. Reductions by a factor of five were achieved with wet materials. No filtration was achieved with dry materials for both vapors. As predicted, wet materials had no effectiveness for methyl iodide but were effective in filtration of iodine vapors (60 % filtration) (Cooper, Hinds, and Price 1981; 1983).

Additional experiments were performed using a manikin to evaluate aerosol leakage around the protective materials assessed in the first experiments. These tests showed that the leakage rates around the edges of the expedient materials (in addition to the leakage of the materials), ranged as high as 63%. The study concluded that holding expedient materials over the face would not provide significant protection against aerosols due to the leakage problem. The study also concluded that some material, such as a panty hose, was needed to secure the expedient protective materials around the mouth and nose in order to minimize leakage (Cooper et al. 1983a,b). Although vapors were not included in this study, it is reasonable to assume that leakage around the perimeters of the materials would also be problematic for vapors.

Additional tests were performed with aerosols in the extremely small particle size range (Price, Cooper, and Yee 1985). These tests, as with the other aerosol tests, are not relevant for civilian protection in CSEPP SIP actions because of the extremely low likelihood of aerosol contamination off-post.

A major concern in all studies was the ability to inhale through the expedient materials. This proved problematic for all wet materials except for wet toweling. For the thick dry materials, such as the folded handkerchief—which was the most effective filter, breathing comfortably would be possible for only short periods of time.

Additional work on the effectiveness of expedient protection against chemical warfare agent simulants was conducted as part of a study on chemical protective clothing materials (Pal et al. 1993). Materials included a variety of chemical-resistant fabrics and duct tape. The materials were subject to liquid challenges by the simulants DIMP (GB

simulant), DMMP (VX simulant), MAL (organoposphorous pesticide), and DBS (mustard simulant). The study concluded that "Duct tape exhibits reasonable resistance to permeation by the 4 simulants, although its resistance to DIMP (210 min) and DMMP (210 min) is not as good as its resistance to MAL (>24 h) and DBS (> 7 h). Due to its wide availability, duct tape appears to be a useful expedient material to provide at least a temporary seal against permeation by the agents" (Pal et al. 1993, p. 140).

3. ADDITIONAL CONSIDERATIONS

Expedient respiratory protection may have social-psychological benefits as well as problems that need to be examined as well.

Problems

Expedient respiratory protection can cause or exacerbate problems by

- deterring oral communications among a family in a sheltered room and communications are very important in a SIP situation,
- deterring taping a room if people attempt to use expedient respiratory protection from the onset of SIP,
- being an additional resource for a SIP kit or materials that would need to be located at the time of a SIP warning,
- hampering driving ability during evacuation because of impairment of hand use and possible visual difficulty, and
- causing hyperventilation in some people with a tendency to be claustrophobic about impediments to breathing.

Benefits

Expedient respiratory protection can also

- have a placebo effect, making people believe they are safe while they are in a SIP and
- reinforcing the concept of proactive protection during SIP.

Overall, it appears that the non-physical benefits of expedient respiratory protection do not exceed the potential problems. However, it will be important to communicate to the public that expedient respiratory protection is beneficial in other emergency situations (such as a fire or for volcanic ash).

4. RECOMMENDATIONS FOR CSEPP

Respiratory protection for civilians has never been considered a viable option for population protection in the CSEPP. Problems of storage, ability to effectively don respirators, and questionable fit have been primary factors in rejecting this option. Expedient respiratory protection seems to offer little benefit for population protection.

Because chemical warfare agent vapors are not reactive with water—or, in some cases, not very soluble, even if easily hydrolyzed (Munro et al. 1999)—it is unlikely that wetted towels will provide significant respiratory protection while a person is sheltering in place. In no case would it be recommended that people attempt to evacuate through a vapor plume with or without expedient respiratory protection. Because of the physical ineffectiveness of the practice and the fact that the social-psychological benefits do not outweigh the social-psychological problems, we recommend that expedient respiratory protection should not be used in CSEPP protective action strategies.

Furthermore, we believe that using wet towels as a vapor barrier at the bottom of a door should be discouraged in favor of using duct tape to seal the bottom of doors. A wet towel provides no vapor filtration; and while it will reduce infiltration, its effectiveness in doing so is not known. A towel wetted with a 0.5% solution of hypochlorite (a 1:9 dilution of household bleach) may provide some protection. A hypochlorite solution is an effective decontaminant for nerve agent vapors and would provide dual protection, both physical and chemical (Munro et al. 1990). Taping the bottom of the door will still likely provide greater infiltration reduction and is recommended as the current method for use in SIP for CSEPP.

5. ACKNOWLEDGEMENTS

The authors thank Rob Weiss and Bill Blewett, Soldier and Biological Chemical Command, and Nancy Munro, Oak Ridge National Laboratory, for their comments on the draft of this paper.

6. REFERENCES

Blewett, W. K., D. W. Reeves, V. J. Arca, D. P. Fatkin, and B. D. Cannon 1996. *Expedient Sheltering in Place: An Evaluation for the Chemical Stockpile Emergency Preparedness Program*, ERDEC-TR-336, Edgewood Research, Development, and Engineering Center, Aberdeen Proving Ground, Md.

Cooper, D. W., W. C. Hinds, and J. M. Price 1981. *Expedient Methods of Respiratory Protection,* NUREG/CR-2272, Sandia National Laboratory, Albuquerque, N.M

Cooper, D. W., W. C. Hinds, and J. M. Price 1983. "Emergency Respiratory Protection with Common Materials," *Am. Ind. Hyg. Assoc. J.* **44**(1):1-6.

Cooper, D.W., W. C. Hinds, and J. M. Price, R. Weker, and H. S. Yee 1983a. "Common Materials for Emergency Respiratory Protection: Leakage Tests with a Manikin," *Am. Ind. Hyg. Assoc. J.* **44**(10):720-26.

Cooper, D. W., W. C. Hinds, J. M. Price, R. Weker, and H. S. Yee 1983b. "Expedient Methods of Respiratory Protection II: Leakage Tests," NUREG/CR-2958, Sandia National Laboratory, Albuquerque, N.M.

Guyton, N. G., H. M. Decker, and G. T. Anton 1959. "Emergency Respiratory Protection Against Radiological and Biological Aerosols*," A.M.A. Arch. Ind. Hlth.* **20**(Aug.):91-95.

Munro, N. B., A. P.Watson, K. R. Ambrose, and G. D. Griffin 1990. "Treating Exposure to Chemical Warfare Agents: Implications for Health Care Providers and Community Emergency Planning," *Env. Hlth. Persp.* **89**: 205-15.

Munro, N. B., S. S. Talmage, G. D. Griffin, L. C. Waters, A. P. Watson, J. F. King, and V. Hauschild 1999. "The Sources, Fate, and Toxicity of Chemical Agent Degradation Products," *Env. Hlth. Persp.* **107**:933-974.

Pal, T., G. D. Griffin, G. Miller, A.P. Watson, M. L. Doherty, and T. Vo-Dinh 1993. "Permeation Measurements of Chemical Agent Simulants Through Protective Clothing Materials," *J. Haz. Mat.* **33**:123-41.

Price, John M., Douglas W. Cooper, and H. S. Yee 1985. "Expedient Methods of Respiratory Protection III: Submicron Particle Tests and Summary of Quality Factors," NUREG/CR-3537, Sandia National Laboratory, Albuquerque, N.M.

FM 3-10

DEPARTMENT OF THE ARMY FIELD MANUAL

CHEMICAL AND BIOLOGICAL WEAPONS EMPLOYMENT

HEADQUARTERS, DEPARTMENT OF THE ARMY
FEBRUARY 1962

FIELD MANUAL
No. 3-10

HEADQUARTERS,
DEPARTMENT OF THE ARMY
WASHINGTON 25, D.C., *20 February 1962*

CHEMICAL AND BIOLOGICAL WEAPONS EMPLOYMENT

		Paragraphs	Page
CHAPTER 1.	INTRODUCTION	1-4	3
2.	PRINCIPAL FACTORS AFFECTING CHEMICAL AGENT EMPLOYMENT		
Section I.	Introduction	5	7
II.	Methods of dissemination	6, 7	7
III.	Meteorological factors	8-13	7
IV.	Terrain conditions	14-16	10
CHAPTER 3.	CONCEPTS OF EMPLOYMENT	17-22	11
4.	CHEMICAL MUNITIONS AND DELIVERY SYSTEMS	23-28	15
5.	CHEMICAL TARGET ANALYSIS AND FIRE PLANNING	29-39	19
6.	COMPUTATIONS INVOLVING MUNITIONS REQUIREMENTS, AREA COVERAGE, AND PERCENT CASUALTIES.		
Section I.	Detailed method	40-43	25
II.	Rapid method	44, 45	35
CHAPTER 7.	TROOP SAFETY		
Section I.	General	46-51	37
II.	Troop safety calculations	52-58	39
CHAPTER 8.	COMMAND AND STAFF ACTIONS		
Section I.	Planning	59-66	47
II.	Chemical ammunition supply	67, 68	48
CHAPTER 9.	FACTORS AFFECTING THE EMPLOYMENT OF BIOLOGICAL AGENTS		
Section I.	Introduction	69, 70	51
II.	Meteorological and terrain conditions	71, 72	52
III.	Methods of dissemination	73, 74	52
CHAPTER 10.	CONCEPTS OF EMPLOYMENT	75-77	55
11.	BIOLOGICAL TARGET ANALYSIS AND EFFECTS ASSESSMENT		
Section I.	Target analysis procedure	78-87	57
II.	Target analysis computations	88-95	61
III.	Sample problems	96-100	64
CHAPTER 12.	TROOP SAFETY	101-106	81
13.	COMMAND AND STAFF ACTIONS		
Section I.	Planning	107-114	85
II.	Biological ammunition supply	115-117	87
APPENDIX I.	REFERENCES		91
II.	SAMPLE FORMAT—CBR WEATHER FORECAST		92
III.	CONVERSION SCALES		93
IV.	FORMAT FOR CHEMICAL TARGET ANALYSIS		94
V.	EXAMPLE ANALYSIS OF CHEMICAL TARGETS		95
GLOSSARY			109

CHAPTER 1

INTRODUCTION

1. Purpose

This manual provides guidance to commanders and staff officers in the employment of chemical and biological weapons. It contains a brief summary of background knowledge of chemical and biological agents and munitions and the procedures to be followed in planning their employment.

2. Scope

a. General. Considerations are limited to chemical and biological agents and delivery systems that are type-classified or expected to be type-classified during the period ending December 1965. The chemical agents are nerve agent GB, nerve agent VX, and blister agent HD. The agent delivery means are artillery and mortar shells, rocket and missile warheads, aircraft bombs, and spray devices. FM 3–10A contains the classification and characteristics of biological agents and information on biological munitions and delivery systems. Troop safety considerations are presented. This manual is applicable to nuclear and nonnuclear warfare.

b. Chemical Agents. Chapters 3 through 8 contain a discussion of chemical agents and their characteristics; factors affecting the employment of chemical agents; chemical munitions and delivery systems and the concepts for their employment; and target analysis, fire planning, and logistical considerations. Methods of chemical target analysis presented are suitable for fire planning and casualty assessment at all echelons of command having chemical fire planning and assessment responsibilities.

c. Biological Agents. Chapters 9 through 13 contain a discussion of biological agents and their characteristics; factors affecting the employment of biological agents; biological munitions and delivery systems and the concepts of their employment; and target analysis, effects assessments, and logistical considerations. Only the antipersonnel effects of biological agents are considered. The methods of biological weapons target analysis presented are suitable for biological fire planning and casualty assessment. The unique character of biological munitions supply and field management is presented.

d. Reliability. The data and procedures presented in this manual have been extracted or derived from official studies and from research and development documents. The potential performance of materiel is based on field trial data with simulants and selected live agents and on theoretical calculations and assumptions developed from mathematical models. The procedures are therefore subject to change as may be required by future developments or refinements. It should be noted that the flow of a chemical or biological agent cloud over the terrain cannot be predicted with a high degree of precision. This is due principally to the inability to predict accurately the prevailing atmospheric conditions of the area under consideration with respect to the diffusion and dissipation of an agent cloud. Nevertheless, the methods and procedures presented here provide information with sufficient accuracy to be used with reasonable confidence.

e. User Comments. Users of this manual are encouraged to submit recommended changes or comments to improve the document. Comments should be keyed to the specific page, paragraph, and line of the text in which change is recommended. Reasons should be provided for each comment to insure understanding and complete evaluation. Comments should be forwarded direct to the Commandant, U.S. Army Chemical Corps School, Fort McClellan, Ala.

3. The Role of Chemical Agents in Military Operations

a. Chemical weapons increase the flexibility of the integrated weapons systems and place at the commander's disposal a highly effective means of conducting antipersonnel operations.

b. In the conduct of military operations involv-

ing chemical weapons, some factors that should be considered are—

(1) The chemical agents discussed herein do not destroy materiel. On the contrary, they allow the physical preservation of industrial complexes, cultural institutions, lines of communications, and other facilities and materiel that may be useful to friendly forces or that merit preservation for political or economic reasons.

(2) Chemical munitions do not produce physical obstacles to maneuver, since they cause minimal destruction, blowdown, rubble, and similar barriers. Agents that produce a persistent effect, however, will create a hazard to friendly troops.

(3) Chemical agents may be employed to produce a variety of effects ranging from harassment to lethality.

(4) Toxic chemical clouds penetrate fortifications and similar structures that are not airtight.

(5) Because of their area coverage effect, chemical agents, used in mass, are particularly effective in attacking targets whose location is not precisely known.

(6) Chemical munitions are particularly effective for producing casualties among dug-in personnel who are not provided with chemical protection.

(7) Chemical agents increase the flexibility of the entire spectrum of firepower available to the commander.

(8) Chemical agents may be used to follow up and exploit advantages gained by other means.

(9) Because the effectiveness of chemical agents on the target is influenced by the type and quantity of agent employed and by the method of dissemination, meteorological factors, conditions of the target, and protection and training of enemy troops, it is difficult to predict the results of employment accurately.

(10) Chemical agents may produce hazards to friendly forces because of residual contamination and cloud movement.

4. Chemical Agents

a. The following three type-classified chemical agents provide commanders flexibility in their employment of chemicals.

(1) Nerve agent GB is a rapid-acting lethal agent that is used primarily for respiratory effects against unprotected personnel and for surprise attack against personnel having masks available.

(2) Two agents are used in circumventing the protective mask.

(*a*) VX is a slow-acting lethal nerve agent when absorbed percutaneously. If inhaled as an aerosol or vapor, VX acts as rapidly as GB and is more toxic.

(*b*) HD is a slow-acting casualty agent with a limited lethal effect. It attacks the skin in liquid or vapor form and is also effective by inhalation.

b. The following figures describe GB and HD in more detail. Detailed information on VX is contained in FM 3–10A. More comprehensive data on chemical agents are in TM 3–215.

1. Primary use	Nonpersistent, rapid-acting lethal agent used primarily for respiratory effect.
2. Average time to incapacitation	15 minutes after exposure to an incapacitating dosage; for lethal dosages, death in 5 minutes after appearance of symptoms if untreated.
3. Duration of incapacitation	1 to 5 days for return to duty. (30 to 60 days for return to normal blood cholinesterase level.)
4. Signs and symptoms	Tightness of chest, pinpointing of eye pupils, dimness of vision, excessive sweating, drooling; followed by tension, giddiness, tremors, confusion, slurred speech, weakness, convulsions, and death.
5. Physiological effects	Nerve poison; slow detoxification by body (60 days); effects of successive small dosages considered cumulative for short periods of time (weeks).
6. Route of entry	Inhalation; percutaneous entry by liquid or high vapor concentration is unlikely in the field because of the high dosage required.
7. Protection	Mask against vapor; protective clothing against liquid agent.
8. Limitations	Mask offers adequate protection against vapor for trained and warned personnel.
9. Duration of hazard	The area in and around shell or bomb craters will be contaminated and will remain a hazard to unprotected personnel for periods ranging from 6 hours to several days.
10. Physical properties	Clear, colorless, odorless liquid; freezing point minus 56° C (−69° F.); boiling point 147° C (297° F.); evaporates at approximately the same rate as water.

Figure 1. Characteristics of nerve agent GB.

1. Primary use	To cause delayed casualties by liquid and vapor effect on the skin and eyes and by vapor effect through the respiratory system.
2. Average time to incapacitation	Eye effect 3 to 12 hours; skin effect 3 to 24 hours.
3. Duration of incapacitation	Eye effect 1 to 7 days; skin effect 1 to 4 weeks.
4. Signs and symptoms	Inflammation of eyes; redness of skin; blistering; ulceration.
5. Physiological effects	Produces blisters and destroys tissues.
6. Route of entry	Skin absorption of vapor or liquid and inhalation of vapor.
7. Protection	Mask, ointment, and protective clothing.
8. Limitations	Limited effectiveness in freezing weather; greater dosages are required for casualty production than are required with GB or VX.
9. Duration of hazard	36 hours to several days. See figure 2.1d.
10. Physical properties	Clear oily liquid with garliclike odor; moderately volatile; freezing point 14° C. (57° F.); boiling point 228° C. (442° F.).

Figure 2. Characteristics of blister agent HD.

Times given indicate approximate time after contamination that personnel may operate in the area

Task	Terrain	Protection (Based on expenditures between 240 and 1,200 pounds of HD per hectare)			
		With protective clothing and wearing masks		Without protective clothing [1]	
		Temperature		Temperature	
		16°–27° C. (60°–80° F.)	Above 27° C. (80° F.)	16°–27° C. (60°–80° F.)	Above 27° C. (80° F.)
		Hours	*Hours*	*Days*	*Days*
TRAVERSAL [2] (Walking across area up to 2 hr)	Bare soil, sand, or short grass	0	0	[3] 1½	[3] 1½
	Low vegetation	4	2	[3] 1½	[3] 1½
	High vegetation, including jungle and heavy woods.	12	6	[3] 4	[3] 2
ADVANCE UNDER FIRE (Contact with ground, 1 hr; total time in area, 2 hr).	Bare soil or low vegetation	24	8	[3] 3	[3] 2
	High vegetation, including jungle and heavy woods.	48	24	[3] 6	[3] 4
OCCUPATION (Without hitting ground, 24 hr)	Bare soil or low vegetation	1	1	[4] 4	[4] 3
	High vegetation, including jungle and heavy woods.	1	1	[4] 4	[4] 3
OCCUPATION (Involving advance under fire, 24 hr).	Bare soil or low vegetation	24	8	[4] 4	[4] 3
	High vegetation, including jungle and heavy woods.	48	24	[4] 6	[4] 4

[1] For men walking in a contaminated area for 2 hours without protective clothing, the limiting factor is the vapor.
[2] For men with protective clothing, when traversal is made in daylight and areas of heavy contamination can be avoided or decontaminated, the times can be reduced to about one-half of those indicated above.
[3] Wearing masks.
[4] Not wearing masks.

Figure 3. Duration of HD hazard in target area.

Additional micrometeorological characteristics of the zone of operations are obtained through the following methods:

(1) Aerial reconnaissance and observations.
(2) Ground reconnaissance and observations.
(3) Observations of fog, smoke, and dust in the zone of operations.
(4) Field expedient methods for obtaining micrometeorological data in the vicinity of the target area.
(5) Statistical studies of weather in the theater of operations.

b. A suggested format for transmission and recording of basic weather data is illustrated in appendix II. It is emphasized that in chemical target analysis, the weather predictions are required for a period of time after the attack as well as for the time of the chemical attack.

c. Normally, Air Weather Service detachments are stationed at field army, corps and division headquarters. From these sources a target analyst may obtain weather data and weather briefings, or he may request detailed operational and planning forecasts and climatological information.

10. Temperature

The rate of evaporation of chemical agents increases as the temperature rises. High temperatures cause personnel to perspire more freely, thus opening the pores of the skin and accelerating penetration of the skin by the agent. At low temperatures, extra layers of clothing increase the barrier to the skin.

11. Temperature Gradient

The temperature gradient is an expression of the difference in air temperature at two levels. In the United States Army, it is determined by subtracting the air temperature (Fahrenheit) measured one-half meter above the ground from the air temperature 2 meters above the ground. The three characteristic conditions that are associated with the temperature gradient follow:

a. Lapse. A decrease in air temperature with an increase in height is known as a *lapse* condition. Such a condition normally exists on a clear or partially clear day and is characterized by heat turbulence. It is the least desirable condition for chemical operations because of rapid dissipation of agent clouds.

b. Inversion. An increase in air temperature with an increase in height is known as an *inversion* condition. This condition exhibits a minimum of turbulence and usually exists on a clear or partially clear night or early morning. This is the most desirable condition for chemical operations since the agent cloud tends to remain in the cooler layers of the air near the ground.

c. Neutral. A condition intermediate between lapse and inversion is known as a *neutral* condition. Such a condition prevails when there are small differences in temperature at the two levels and usually exists on heavily overcast days or nights, and shortly after sunrise and near sunset.

12. Wind

The wind is also an important weather element affecting the field behavior of chemical clouds. Of the wind characteristics, velocity and direction have greatest influence. Both characteristics are influenced by terrain and temperature gradient.

a. Velocity. Air moving over an irregular surface sets up eddies, or mechanical turbulence. This turbulence is similar to heat turbulence in that it acts to dissipate a chemical cloud. High wind velocities also cause the agent cloud to pass rapidly over the target area, thus reducing the exposure time. Some air movement is desired to blend the individual clouds of agent formed by each shell burst into a uniform cloud covering the target. Ideal wind velocities for chemical operations are 3 to 9 knots (approximately 6 to 16 kilometers per hour). Wind velocities in excess of 16 knots (approximately 30 kilometers per hour) are not suitable for nonpersistent effects.

b. Direction. Wind directs the travel of a chemical cloud. This fact must be considered in the release of an agent for coverage of a particular target and in the determination of the downwind hazard to friendly troops. The wind direction is the direction from which the wind blows and is expressed in terms of azimuth in mils or degrees.

13. Precipitation

Precipitation has an adverse effect on the behavior of chemical agents, since rain will wash away the liquid agent contamination and snow will cover it. Precipitation also washes agent vapors or aerosol clouds from the air and destroys some agents by hydrolysis.

Line	1 Munition	2 Agent	3 Delivery system	4 User	5 Employment data (a) Range (1) (Meters) (2) Maximum	(a) Minimum	(b) Error	(c) Fuze (Capability)
1	Shell, M2A1	HD	4.2-inch Mortar	US ARMY USMC	3,930	180	←Obtain from delivery unit or appropriate firing tables→	M8PD
2	Shell, M360	GB	105-mm Howitzer, M2A1, M2A2, M4, M4A2, M52.	US ARMY USMC	11,140	862		M508PD
3	Shell, M60	HD	105-mm Howitzer, M2A1, M2A2, M4, M4A2, M52.	US ARMY USMC	11,140			M51A5PD
4	Shell, M121	GB	155-mm Howitzer, M1, M1A1, M44.	US ARMY USMC	14,950			M508PD
5	Shell, M110	HD	155-mm Howitzer, M1, M1A1, M44.	US ARMY USMC	14,950			M51A5PD
6	Shell, T__(M121)	VX	155-mm Howitzer, M1, M1A1, M44.	US ARMY USMC	14,950			T76E6VT [1]
7	Shell, M122	GB	155-mm Gun, M2, M53	USMC	23,500			M508PD
8	Shell, M104	HD	155-mm Gun, M2, M53	USMC				M51A5PD
9	Shell, Gas, 175-mm	GB	M107 Gun (SP)	US ARMY	31,500	180		
10	Shell, Gas, 175-mm	VX	M107 Gun (SP)	US ARMY	31,500	180		VT-M514A1
11	Shell, T174	GB	8-inch Howitzer, M2, M2A1, M55.	US ARMY USMC	16,930			M51A5PD
12	Shell, T174	VX	8-inch Howitzer, M2, M2A1, M55.	US ARMY USMC.	16,930			T2061VT
13	Rocket, M55, 115-mm (BOLT)	GB	Launcher, M91	US ARMY USMC.	10,970	2,740		M417PD
14	Rocket, M55, 115-mm (BOLT)	VX	Launcher, M91	US ARMY USMC.	10,970	2,740		T2061VT
15	Warhead, M79, 762-mm (HONEST JOHN).	GB	Rocket, M31A1C Launcher, M386.	US ARMY USMC.	24,960	8,500		T2075 Mech Time
16	Warhead, E19R2, 762-mm (HONEST JOHN).	GB	Rocket, XM50 Launcher, M386.	US ARMY USMC.	33,830	8,500		T2075 Mech Time
17	Warhead, E19R2, 762-mm (HONEST JOHN).	VX	Rocket, XM50 Launcher, M386.	US ARMY USMC.	33,830	8,500		T2075 Mech Time
18	Warhead, E20, 318-mm (LITTLE JOHN).	GB	Rocket, XM51 Launcher, XM80.	US ARMY USMC.	18,290	3,200 [1]		T2075 Mech Time
19	Warhead, E21, (SERGEANT)	GB	Rocket, Launcher	US ARMY	139 km	50 km	304m	Preset Radar
20	Warhead, E21, (SERGEANT)	VX	Rocket, Launcher	US ARMY	139 km	50 km	304m	Preset Radar
21	Bomb, M34A1, 1000-lb, Cluster	GB	Fighter, Bomber	USAF	Range of Aircraft.		←Obtain from delivery unit→	M152E3 Mech Time
22	Bomb, MC-1, 750-lb	GB	Fighter, Bomber	USAF	Range of Aircraft.			M905BD
23	Projectile, 5"/38, MK53, MOD O.	GB	5-inch Gun	US NAVY	16,450			MK29MOD3PD
24	Projectile, 5"/54, MK54, MOD O.	GB	5-inch Gun	US NAVY	19,200			MK30MOD3PD
25	Warhead, Rocket, 5" MK40, MOD O.	GB	Launcher, MK 105 Rocket, M40, MOD O.	US NAVY	4,200			MK30MOD3PD
26	Warhead, Rocket, 5", MK40, MOD O.	HD	Launcher, MK 105 Rocket, M40, MOD O.	US NAVY	4,200			MK30MOD3PD
27	Bomb, MK94, MOD O	GB	Fighter, Bomber	US NAVY	Range of Aircraft.			AN-M103A1ND M195 BD (IMPACT).
28	Bomb, M70A1	HD	Fighter, Bomber	US NAVY	Range of Aircraft.			AN-M158ND (IMPACT).
29	Mine, Land, Chemical, M23	VX	N/A	US ARMY	N/A	N/A	N/A	
30	Mine, Land, Chemical, One-Gallon.	HD	N/A	US ARMY	N/A	N/A	N/A	

See notes at end of figure.

Figure 5. Chemical munitions and delivery systems.

5 Employment data—Continued						6 Functioning and physical characteristics of CML munitions				
(d)		(e)	(f)	(g)	(h)	(a)	(b)	(c)	(d)	(e)
Time for delivery										
(1) Preplanned	(2) Target of opportunity	Organization	Rate of fire per weapon	Height of burst	Diameter (meters) of impact area (single rd) [2]	Weight of munition (kg)	Weight of agent (kg)	Effective weight of agent (kg) [3]	Functioning efficiency of munition (percent)	Agent dissemination efficiency
----------	----------	6 Mort/Plt	30 Rds/2 min	GND	16	10.8	2.72	----------	99	
		8 Mort/Btry	105 Rds/15 min							
----------	1–3 min	6 How/Btry	6 Rds/½ min	GND	27	16.1	.739	----------	99	
			18 Rds/4 min							
----------	1–3 min	6 How/Btry	6 Rds/½ min	GND	11	15.2	1.22	----------	99	
			18 Rds/4 min							
----------	1–5 min	6 How/Btry	3 Rds/½ min	GND	49	45.9	2.95	----------	99	
			12 Rds/4 min							
----------	1–5 min	6 How/Btry	3 Rds/½ min	GND	20	42.0	4.4	----------	99	
			12 Rds/4 min							
----------	1–5 min	6 How/Btry	3 Rds/½ min	20m [1]	----------	45.9	2.95	----------	99	
			12 Rds/4 min							
----------	1–5 min	4 Gun/Btry	2 Rds/½ min	GND	49	45.9	2.95	----------	99	
			8 Rds/4 min							
----------	1–5 min	4 Gun/Btry	2 Rds/½ min	GND	22	43.0	5.31	----------	----------	
			8 Rds/4 min							
		4 Gun/Btry	----------	GND	----------	66.8	6.68	----------	----------	
----------	----------	4 Gun/Btry	----------	GND	----------	66.8	6.04	----------	----------	
----------	½–6 hr	4 How/Btry	6 Rds/4 min	GND	76	97.0	7.12	----------	99	
			10 Rds/10 min							
----------	½–6 hr	4 How/Btry	6 Rds/4 min	20m [1]	----------	97.0	7.12	----------	99	
			10 Rds/10 min.							
----------	30 min	36 Lchr/Bn	45 Rkt/Lchr/15 sec.	GND	46	26.4	4.80	----------	99	
----------	30 min	36 Lchr/Bn	45 Rkt/Lchr/15 sec.	20m [1]	----------	26.2	4.54	----------	99	
----------	15 min	2 Lchr/Bn	2/Hr	Variable	Variable	737	177.5	104.8	95	62 percent.
----------	15 min	2 Lchr/Btry	2/Hr	Variable	Variable	568	210	171	95	86 percent.
----------	15 min	2 Lchr/Btry	2/Hr	Variable	Variable	568	210			
----------	15 min	4 Lchr/Btry	2/Hr	Variable	Variable	119	30			
15 min	120 min	4 Lchr/Bn	2/Day	Intervals of 1,524m.	Variable	744	190			
15 min	120 min	4 Lchr/Bn	2/Day	Intervals of 1,524m.	Variable	744	190			
----------	15 min +flight time.	----------	2–6/Ftr	Variable	170	513	89.6	----------	90	
			4–18/Bmbr.							
----------	15 min +flight time.	----------	2–6/Ftr	GND	127	322	99.9			
			4–27/Bmbr.							
----------	----------	----------	----------	GND	35	25.1	1.47			
----------	----------	----------	----------	GND	40	29.1	2.02			
----------	----------	----------	48 Rkt/Lchr/	GND	49	22.9	2.18			
			1 min							
----------	----------	----------	48 Rkt/Lchr/	GND	----------	----------	----------			
			1 min							
----------	----------	----------	----------	GND	90	222	49.8			
----------	----------	----------	----------	GND	29	58.0	272			
----------	----------	----------	----------	----------	----------	10.50	5.23			
----------	----------	----------	----------	----------	----------	5.45	4.50			

[1] Estimated.

[2] Instantaneous agent area coverage 30 seconds after detonation.

[3] Values are the product of values given in columns 6(*b*), 6(*d*), and 6(*e*). Since values for 6(*e*) are not available, values for 6 (*c*)cannot be computed at this time.

Figure 5.—Continued

Agent—GB.
Wind speed—5 knots (approx 9 km/hr).
Temperature gradient—inversion.
Temperature—60° F. (15.5° C.).
Terrain—open, level, scattered vegetation.
Precipitation—none.
Time limitations on the delivery of agent on target—4 minutes or less.
Casualty level desired—20 percent.

Find: Whether or not the mission can be fired with a 105-mm howitzer battery.

Solution:

(*a*) Using figure 11, convert 20 percent casualties among protected personnel to the corresponding casualty level among unprotected personnel. This is 80 percent.

(*b*) Using the "GB (over 30-sec attack)" column of figure 12, determine the total effects components to be 3.21 as follows:

Inversion	1.09
Wind speed, 9 km/hr	1.00
Temperature, 60° F. (15.5° C.)	.12
Open terrain	.30
No precipitation	.70
	3.21

(*c*) Using figure 13, place a hairline between 80 percent on the percent casualties scale and 12 hectares on the target area scale. On the point of intersection on the reference line, pivot the hairline until it intersects 3.21 on the effects components scale. On the munitions expenditure scale, read 12 as the number of 155-mm equivalents required.

(*d*) To find the number of 105-mm rounds required to fire the mission, multiply 12 by a factor of four (obtain this factor from figure 8); the product is 48 rounds.

(*e*) From figure 9, it is evident that one battery of six howitzers can easily fire the mission if no shift of fires is required. Since the target is twice as large as the dispersion pattern of a 105-mm battery (par. 31*c*(3)(*c*) and 41*d*), a shift of fires should be made. Figure 9 gives a time of 30 seconds for shifting of fires. On this basis the battery could fire twenty-four rounds on half the target in a little less than 30 seconds, take 30 seconds to shift fires, and have ample time to deliver the remaining twenty-four rounds on the other half of the target. The firing should be completed in less than 2 minutes.

Munition	Munition expressed in terms of 155-mm chemical equivalents		
	GB	VX	HD
155-mm Shell	1	1	1
105-mm Shell	0. 25	--------	0. 28
8-inch Shell	2. 40	2. 17	--------
4.2-inch Mortar Shell	--------	--------	. 62
175-mm Shell	2. 1	2. 1	--------
M55 Rocket	1. 6	1. 6	--------
M79 Warhead—HONEST JOHN	60	--------	--------
E19R2 Warhead—HONEST JOHN	71	71	--------
LITTLE JOHN	10	10	--------
SERGEANT	65	65	--------
M34A1 1000-lb Cluster	30	--------	--------
MC1 750-lb Bomb	35	--------	--------
5″/38 Gas Projectile (Navy)	. 50	--------	--------
5″/54 Gas Projectile (Navy)	. 68	--------	--------
5″ Gas Rocket (Navy)	. 74	--------	--------
500-lb Gas Bomb	17	--------	--------
115-lb Gas Bomb (Navy)	--------	--------	6. 2

Figure 7. Munitions expressed in terms of 155-mm chemical equivalents. (The figures given are an estimate of the number of 155-mm howitzer rounds required to give the same effect as one round of the specified munition. Dissemination efficiency has not been considered.)

Munition	Conversion factor		
	GB	VX	HD
155-mm Shell	1	1	1
105-mm Shell	4	--------	3. 6
8-inch Shell	0. 41	0. 45	--------
4.2-inch Mortar Shell	--------	--------	1. 61
175-mm Shell	. 48	. 48	--------
M55 Rocket	. 61	. 61	--------
M79 Warhead—HONEST JOHN	. 017	--------	--------
E19R2 Warhead—HONEST JOHN	. 014	. 014	--------
LITTLE JOHN	. 098	. 098	--------
SERGEANT	. 016	. 016	--------
M34A1 1000-lb Cluster	. 033	--------	--------
MC1 750-lb Bomb	. 029	--------	--------
5″/38 Gas Projectile (Navy)	2. 00	--------	--------
5″/54 Gas Projectile (Navy)	1. 46	--------	--------
5″ Gas Rocket (Navy)	1. 35	--------	--------
500-lb Gas Bomb	. 059	--------	--------
115-lb Gas Bomb (Navy)	--------	--------	. 164

Figure 8. Conversion factors for converting 155-mm munitions to other munitions.

Weapon	Maximum rate (rounds)	Rates of fire for chemical fire missions without shifting or relaying of the piece (rounds)					Estimated time to shift fires
	30 sec	1 min	2 min	4 min	10 min	15 min	
105-mm Howitzer	6	10	14	18	40	60	30 sec
155-mm Howitzer	3	5	7	12	30	40	30 sec
155-mm Gun	2	4	6	8	12	18	60 sec
8-inch Howitzer	1	2	3	6	10	15	60 sec
4.2-inch Mortar	10	16	30 (max)	50	80	105	30 sec
M91 Launcher (M55 Rocket)	45 (15 sec)	Launcher must relocate after firing each ripple.					

Figure 9. Approximate rates of fire for division cannon artillery, mortars, and multiple rockets firing chemical rounds. (Rates of fire for other weapons are given in figure 5.)

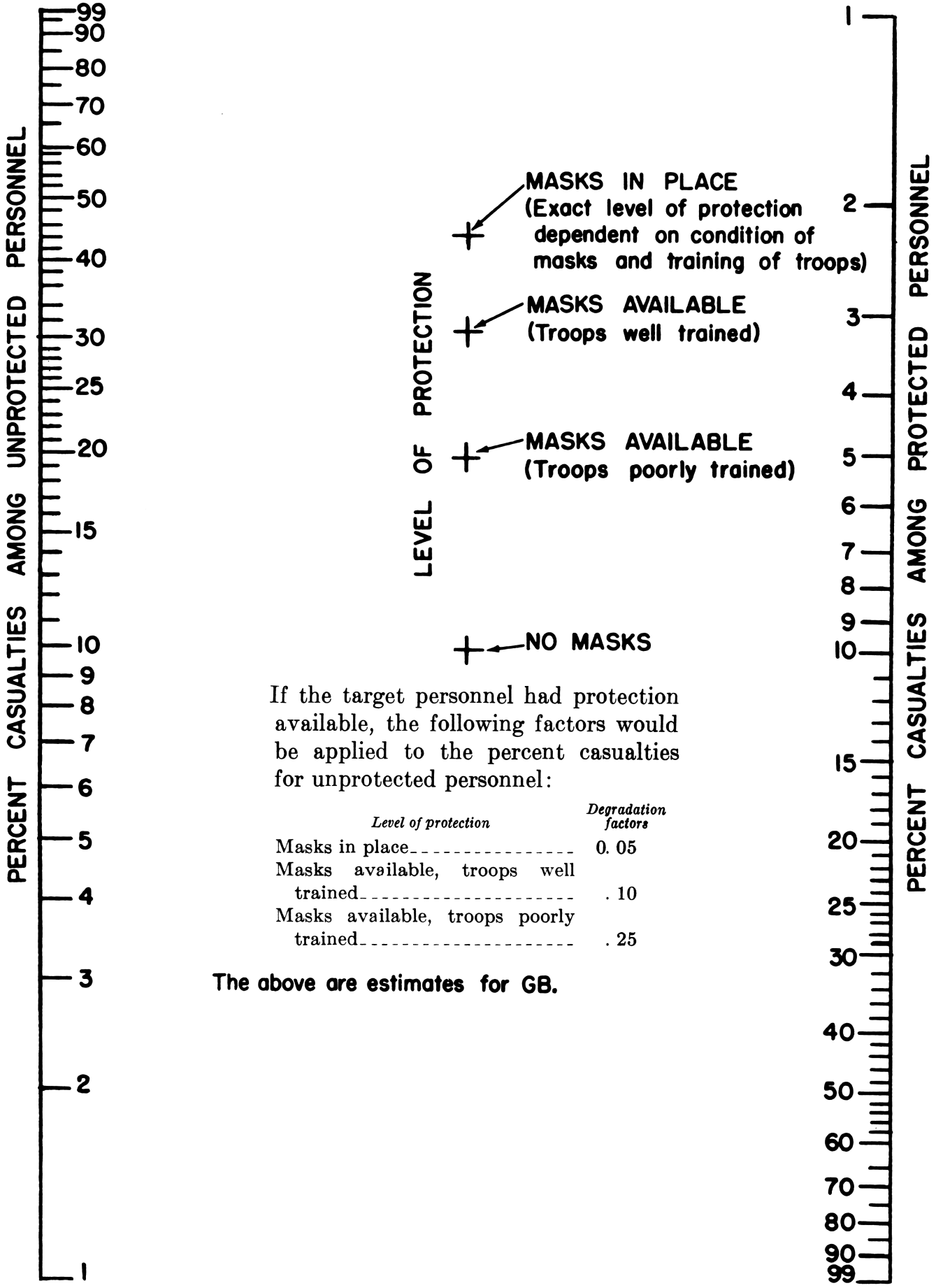

If the target personnel had protection available, the following factors would be applied to the percent casualties for unprotected personnel:

Level of protection	*Degradation factors*
Masks in place	0.05
Masks available, troops well trained	.10
Masks available, troops poorly trained	.25

The above are estimates for GB.

Figure 11. Nomogram for conversion of percent GB casualties for protection of personnel in the target area.

Meteorological and terrain conditions	Effects components			
	GB [2] (surprise attack)	GB (over 30-sec attack)	VX	HD
1. *Temperature Gradient*				
Inversion	0. 67	1. 09	1. 89	0. 69
Neutral	. 57	. 69	1. 89	. 54
Lapse	. 30	. 09	1. 89	. 32
2. *Wind Speed (km/hr)*				
0 to 5	. 20	1. 30	0	. 87
6 to 10	. 50	1. 00	0	. 70
11 to 16	. 70	. 70	0	. 60
17 to 26	. 55	. 30	0	. 48
27 to 52	. 30	0	0	0
3. *Temperature (° F.)*				
a. 0 to 39 (−18° to 4° C.)	0	0	0	----------
40 to 79 (5° to 26° C.)	. 12	. 12	0	----------
80 and up (27° C. and up)	. 23	. 23	0	----------
b. 30 to 49 (−1° to 9° C.)	----------	----------	0	0
50 to 69 (10° to 21° C.)	----------	----------	0	. 70
70 and up (22° C. and up)	----------	----------	0	1. 00
4. *Terrain*				
Open, level, scattered vegetation	. 30	. 30	0	. 30
Rugged, mountainous	0	[1] 0	[1] 0	[1] 0
5. *Precipitation*				
None	. 70	. 70	. 70	0
Moderate rain	0	[1] 0	[1] 0	[1] 0

[1] Estimated.
[2] Tentative figures not yet verified.

Figure 12. Effects components.

Note: paragraph 105 on page 82 states that the "safe entry times" after bio attacks are:

NU (Venezuelan equine encephalitis virus), AB (bovine brucellosis), and UL (tularemia): 2 hrs sun or 8 hrs cloudy
OU (Q fever): 2 hrs sun or 18 hrs cloudy

Cloudy conditions also apply to nighttime

626007 O—62——3

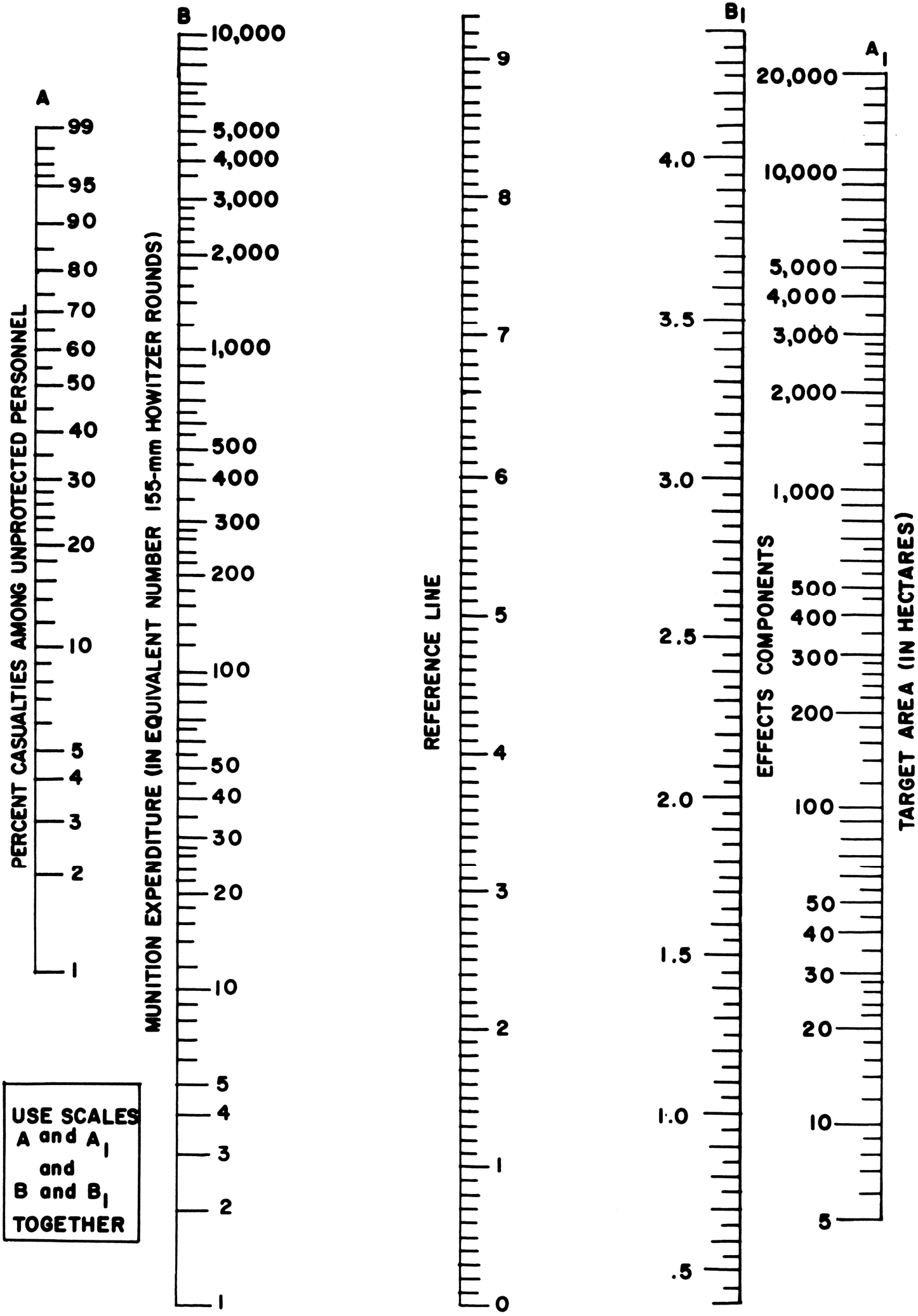

Figure 13. Target area, casualty level, munitions requirement nomogram.

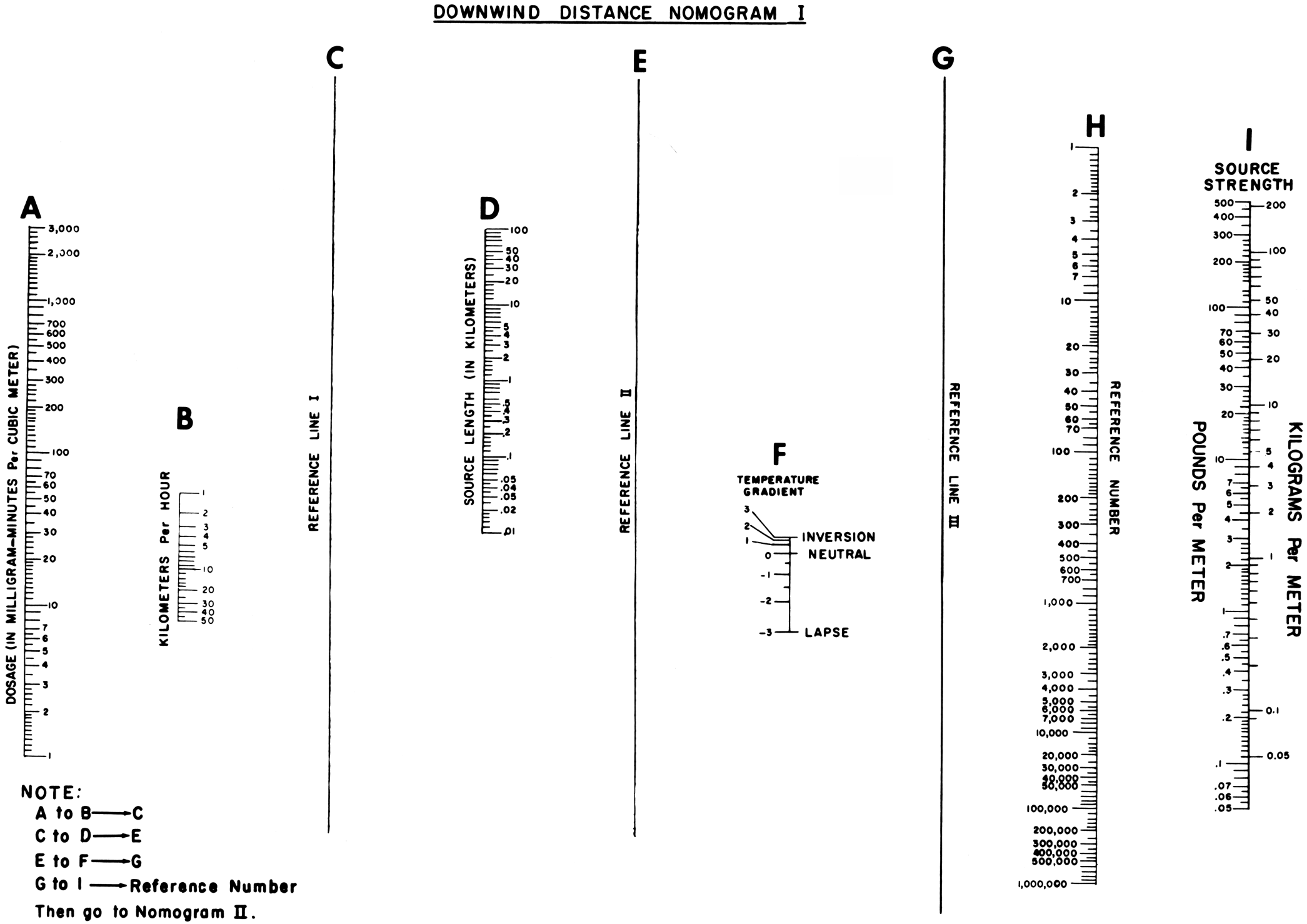

Figure 14. Downwind distance nomogram I.

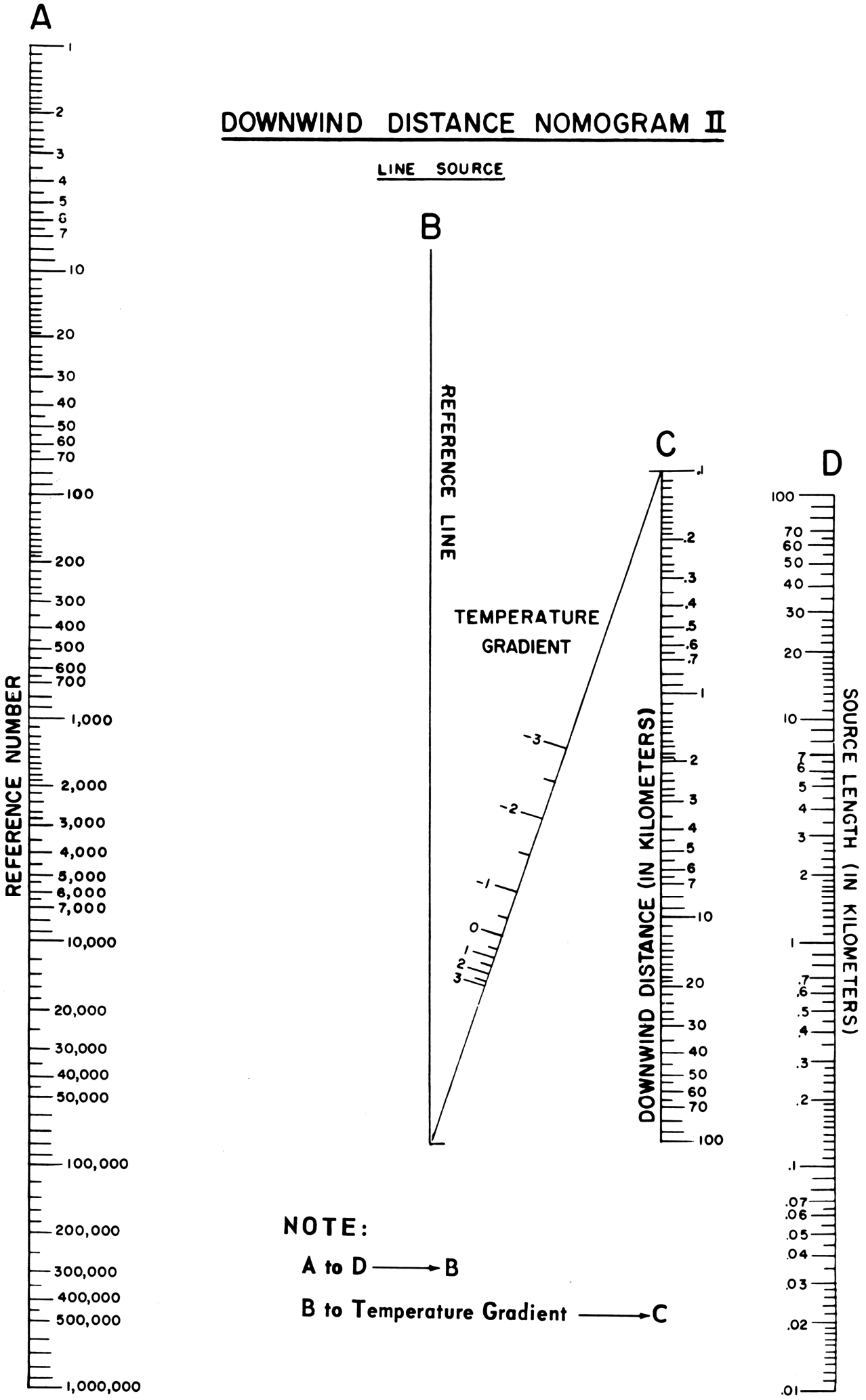

Figure 15. Downwind distance nomogram II.

USACGSC RB 3-1

REFERENCE BOOK

CHEMICAL AND BIOLOGICAL WEAPON EMPLOYMENT

U.S. ARMY COMMAND AND GENERAL STAFF COLLEGE
Fort Leavenworth, Kansas

1 May 1968

This reference book supersedes RB 3-1, 1 May 1967

CHAPTER 2
TOXIC CHEMICAL AGENTS

1. Characteristics and Effects

a. General. The following antipersonnel chemical agents are used for College instruction in chemical weapon employment: nerve agents GB and VX; blister agent HD (mustard); and incapacitating agent BZ. Actual or assumed characteristics of these agents are described in the following paragraphs for instructional purposes only and are summarized in figure 1.

b. Nerve Agent GB. GB is a quick acting, nonpersistent lethal agent that produces casualties primarily by inhalation.

(1) Inhalation effects. Inhaled GB vapor can produce casualties within minutes. As an example, 50 percent of a group of unprotected troops engaged in mild activity, breathing at the rate of about 15 liters per minute, and exposed to 70 milligrams of GB per cubic meter of air for 1 minute will probably die if they do not receive medical treatment in time. This is the median lethal dosage (50) and is expressed as 70 mg-min/m^3. For troops engaged in activities that increase their breathing rate, the median lethal dosage can be as low as 20 mg-min/m^3. The median incapacitating dosage of GB vapor by inhalation is about 35 mg-min/m^3 for troops engaged in mild activity. Incapacitating effects consist of nausea, vomiting, diarrhea, and difficulty with vision, followed by muscular twitching, convulsions, and partial paralysis. Dosages of GB less than the median incapacitating dosage cause general lowering of efficiency, slower reactions, mental confusion, irritability, severe headache, lack of coordination, and dimness of vision due to pinpointing of the eye pupils.

(2) Percutaneous effects. Percutaneous effects refer to those effects produced by the absorption of the agent through the skin. GB vapor absorbed through the skin can produce incapacitating effects. Sufficient GB liquid absorbed through the skin can produce incapacitation or death. The effectiveness of the liquid or vapor depends on the amount absorbed by the body. Absorption varies with the original amount of agent contamination, the skin area exposed and the exposure time, the amount and kind of clothing worn, and the rapidity in removing the contamination and/or contaminated clothing and in decontaminating affected areas of the skin.

(3) Major considerations in the employment of nerve agent GB. The employment of GB is based primarily on achieving casualties by inhalation of the nonpersistent vapor (or aerosol) of the agent. Major considerations in the employment of this agent are:

(a) Time to incapacitate. The onset of incapacitation resulting from inhalation of casualty-producing doses is rapid, the average time being approximately 3 minutes. To allow for the time required for the agent cloud to reach the individual, 10 minutes is used as the mean time to achieve incapacitation. Nonlethal casualties from GB will be incapacitated for 1 to 5 days.

(b) Persistency. Persistency is defined as the length of time an agent remains effective in the target area after dissemination. Nerve agent GB is considered nonpersistent. GB clouds capable of producing significant casualties will dissipate within minutes after dissemination. Some liquid GB will remain in chemical shell or bomb craters for periods of time varying from hours to days, depending on the weather conditions and type of munition. Because of this continuing but not readily discernible threat, GB can also be highly effective in harassing roles by causing exposure to low concentrations of the vapor. Rounds fired sporadically may compel the enemy to wear protective masks and clothing for prolonged periods, thereby impairing his effectiveness as a result of fatigue, heat stress, discomfort, and decrease in perception.

(c) Level of protection. The weapon system requirements for positive neutralization of masked personnel by GB are too great to be supported except for important point or small area targets. A major factor affecting casualties resulting from GB attacks of personnel equipped with masks but unmasked at the time of attack is the time required for enemy troops to mask after first detecting a chemical attack. Therefore, surprise dosage attack is used to establish a dosage sufficient to produce the desired casualties before troops can mask. Casualty levels for surprise dosage attack that are tabulated in the weapon system effects tables (app A) are based on an assumed enemy masking time of 30 seconds. (Refer to FM 3-10 series manuals for operational data for masking times less than 30 seconds.) A total dosage attack is used to build up the dosage over an extended period of time and is normally employed against troops who have no protective masks available. Dosages built up before troops can mask inside foxholes, bunkers, tanks, buildings, and similar structures will generally be less than dosages attained during the same period of time in the open, thereby reducing the effects on occupants from surprise dosage attacks. Total dosage effects are essentially the same inside or outside.

c. Nerve Agent VX. VX is a slow-acting, lethal, persistent agent that produces casualties primarily by absorption of droplets through the skin.

(1) Effects. VX acts on the nerve systems of man; interferes with breathing; and causes convulsions, paralysis, and death.

(2) Major considerations in the employment of nerve agent VX.

(a) General. Agent VX disseminated in droplet (liquid) form provides maximum duration of effectiveness as a lethal casualty threat. VX will remain effective in the target area for several days to a week depending on weather conditions. Because of its low volatility, there is no significant vapor hazard downwind of a contaminated area. Except when disseminated by aircraft spray tanks, meteorological conditions have little effect on the employment of VX, although strong winds may influence the distribution of the agent and heavy rainfall may wash it away or dissipate it.

(b) Employment to cause casualties. Agent VX is appropriate for direct attack of area targets containing masked personnel in the open or in foxholes without overhead protection, for causing severe harassment by the continuing casualty threat of agent droplets on the ground or on equipment, and for creating obstacles to traversing or occupying areas. Casualties produced by agent VX are delayed, occurring at times greater than 1 hour after exposure. Although this agent can be used relatively close to friendly forces, it should not be used on positions that are likely to be occupied by friendly forces within a few days. Because of this continuing hazard, areas in which agent VX has been used should be recorded in a manner similar to minefields or fallout areas so that necessary precautions can be taken.

d. Blister Agent HD. HD, sometimes referred to as mustard, is a persistent slow-acting agent that produces casualties through both its vapor and liquid effects.

(1) Vapor effects.

(a) The initial disabling effect of HD vapor on unmasked troops will be injuries to the eyes. Temporary blindness can be caused by vapor dosages that are insufficient to produce respiratory damage or skin burns. However, skin burns account for most injuries to masked troops. The vapor dosages and the time required to produce casualties (4 to 24 hours) vary with the atmospheric conditions of temperature and humidity and with the amount of moisture on the skin. Depending on their severity, skin burns can limit or entirely prevent movement of the limbs or of the entire body.

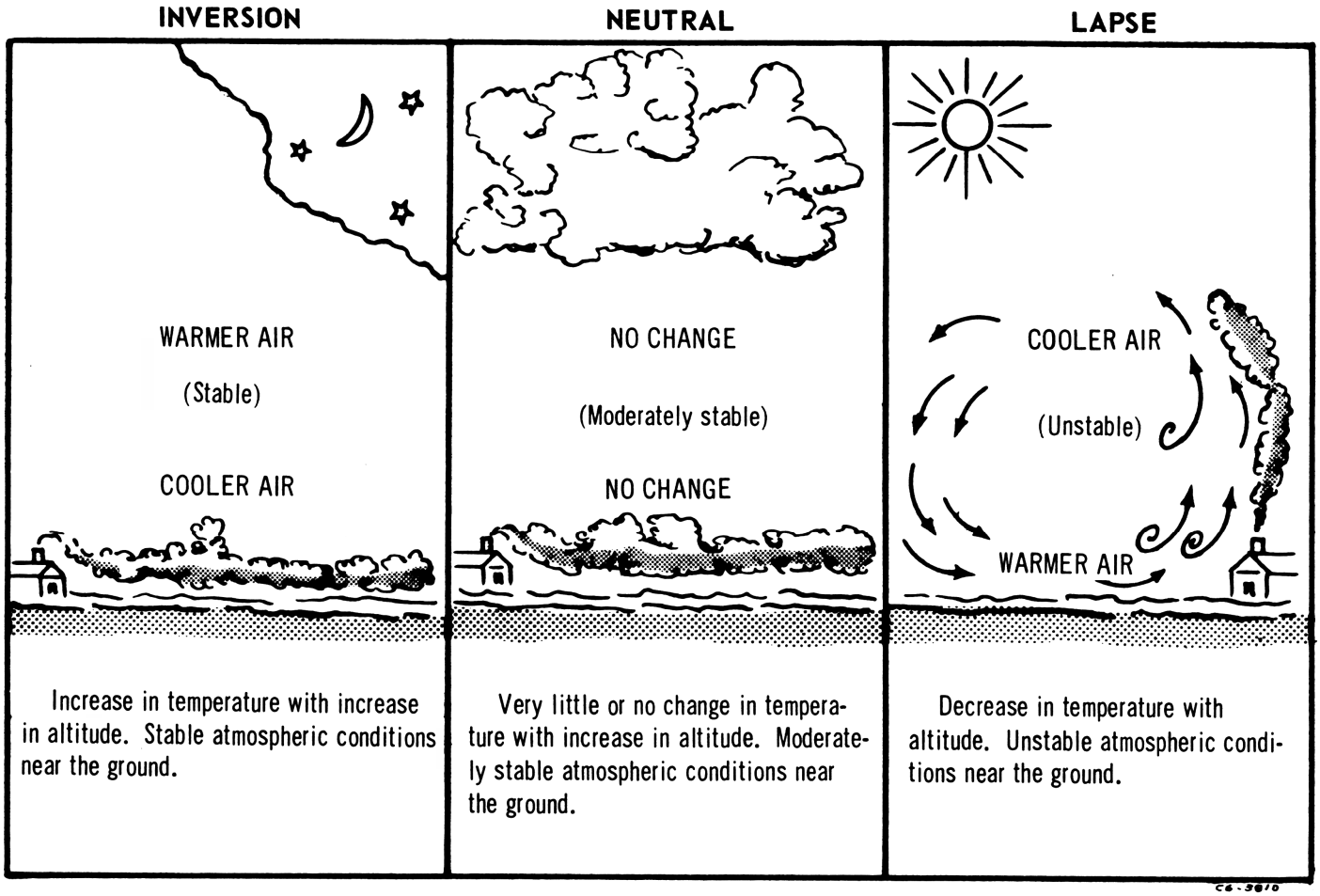

Figure 2. Temperature gradients.

Surprise dosage GB attacks are influenced only slightly by the temperature gradient except when made with the spray tank. Downwind vapor hazards to both enemy and friendly forces will be most significant during inversion and neutral conditions. Employment of VX is not affected by the temperature gradient.

Temperature gradients	Time
1. Inversion	From sunset to sunrise.
2. Neutral	2 hours before sunset to sunset, sunrise to 2 hours after sunrise, or any time windspeed is 15 kmph or greater.
3. Lapse	2 hours after sunrise to 2 hours before sunset.

Figure 3. Estimated times that temperature gradients will prevail. (Use when meteorological data are not available.)

(3) When actual or predicted meteorological conditions are not available for a target analysis, 70° F is used for temperature, 9 kmph is used as windspeed, and the temperature gradient is approximated from figure 3.

d. Windspeed and Direction.

(1) Air moving over the earth's surface sets up eddies, or mechanical turbulences, that act to dissipate a chemical cloud. A condition of calm will limit the merging of the individual gas clouds. Both of these conditions may reduce the effectiveness of a chemical agent attack. High winds increase the rate of evaporation of HD and dissipate chemical clouds more rapidly than low winds. Moderate winds are desirable for chemical employment. Large-area nonpersistent chemical attacks are most effective in winds not exceeding 28 kmph. Small-area nonpersistent chemical attacks with rockets or shell are most effective in winds not exceeding 9 kmph. However, if the concentration of chemical agent can be established quickly, the effects of high windspeed can be partially offset.

CHAPTER 4
EMPLOYMENT OF BIOLOGICAL AGENTS

1. General

a. Antipersonnel biological agents are micro-organisms that produce disease in man. These agents can be used to incapacitate or kill enemy troops through disease. They may cause large numbers of casualties over vast areas and could require the enemy to use many personnel and great quantities of supplies and equipment to treat and handle the casualties. Many square kilometers can be effectively covered from a single aircraft or missile. The search capability of biological agent clouds and the relatively small dose required to cause infection among troops give biological munitions the capability of covering large areas where targets are not precisely located.

b. A biological attack can occur without warning since biological agents can be disseminated by relatively unobtrusive weapon systems functioning at a considerable distance from the target area and relying upon air movement to carry the agent to the target.

c. Biological agents do not produce effects immediately. An incubation period is required from the time the agent enters the body until it produces disease. Some agents produce the desired casualty levels within a few days, whereas others may require more time to produce useful casualty levels. A variety of effects may be produced, varying from incapacitation with few deaths to a high percentage of deaths, depending on the type of agent.

2. Methods of Dissemination

a. The basic method of disseminating antipersonnel biological agents is the generation of aerosols by explosive bomblets and spray devices. Because exposure to sunlight increases the rate at which most biological agent aerosols die and thereby reduces their area coverage, night is the preferable time for most biological attacks. However, if troop safety is a problem, an attack may be made near sunrise to reduce the distance downwind that a hazard to friendly forces will extend. Conversely, to extend the downwind cloud travel and the area coverage from spray attack, a biological agent may be employed soon after sundown.

b. Missile-delivered Biological Munitions. Missile-delivered biological munitions are used for attack of large-area targets. A typical biological missile system consists of the following components:

(1) A missile vehicle and its launching equipment.

(2) A warhead that can be opened at a predetermined height to release biological bomblets over the target area. The warhead is shipped separately for assembly to a missile at the launching site.

(3) A warhead shipping container equipped with a heating-cooling element and a temperature control unit.

(4) Biological bomblets consisting of an agent container and a central burster that functions on impact. The bomblets have vanes that cause them to rotate in flight, thereby achieving lateral dispersion during their free fall and resulting in random distribution as a circular pattern.

c. Aircraft Spray Tank. Biological agents released from an aircraft spray tank cover a large area downwind of the line of release. A typical spray tank consists of the following components:

(1) An agent reservoir section that is shipped separately in an insulated shipping and storage container equipped with a heating-cooling element and a temperature control unit.

(2) A discharge nozzle assembly that can be mechanically adjusted to vary the agent flow rate.

Table 1. Chemical Weapons Data

1	2	3	4	5	6	7	8	9	10	11	12	13
Delivery system	Range (meters)		Agent	Munition	No of weapons per delivery unit	Weapon rate of fire	RT max (meters)[1 2]					Reference (table)
							Fire unit	Total dosage		Surprise dosage		
								Casualty threat		Casualty threat		
	Min	Max						10%	30%	10%	30%	
4.2-in mortar	180	4,500	HD	Cartridge, M2A1	4/Plat	50 rd/3 min 105 rd/15 min						18 19
105-mm howitzer		11,100	GB	Cartridge, M360	6/btry	5 rd/30 sec 30 rd/3 min 66 rd/15 min	1 btry[3]	200	100	100	50	2
							1 bn[3]	300	300	200	100	3
			HD	Cartridge, M60								18 19
155-mm howitzer		14,600	GB	Projectile, M121	6/btry	2 rd/30 sec 12 rd/3 min 24 rd/15 min	1 btry[3]	300	200	100	0	4
							1 bn[3]	500	400	300	100	5
			HD	Projectile, M110								18 19
			VX[4]	Projectile, M121			1 btry[3]	400	200	NA	NA	13
							1 bn[3]	500	400			
8-in howitzer		16,800	GB	Projectile, M426	4/btry	1 rd/30 sec 4 rd/3 min 10 rd/15 min	1 btry[3]	300	200	200	0	6
							1 bn[3]	500	400	300	100	7
			VX[4]				1 btry[3]	400	200	NA	NA	14
							1 bn[3]	500	400			
115-mm multiple rocket launcher, M91	2,740	10,600	GB[4]	Rocket, M55 (THE BOLT)		45 rkt/lchr/15 sec	1 lchr	1,000	750	500	200	8
							3 lchr	1,000	1,000	750	400	
							6 lchr	1,000	1,000	1,000	750	
							9 lchr	1,000	1,000	1,000	1,000	
			VX[4]				1 lchr	300	0	NA	NA	15
							3 lchr	750	300			
							6 lchr	1,000	400			
							9 lchr	1,000	750			
762-mm rocket, Honest John	8,500	38,000	GB[4]	Warhead, M190 (M139 bomblets)	2/btry	2 rkt/lchr/hr	1 lchr	600	600	600	400	9
							2 lchr	600	600	600	400	
Sergeant missile	46,000	139,000	GB[4]	Warhead, M212 (M139 bomblets)	2/bn	2 msl/lchr/hr	1 msl	600	400	600	200	10
							2 msl	600	600	600	400	
Aircraft	Dependent on type aircraft		GB[4]	Bomb, MC-1, 750-lb	Dependent on type aircraft		1 bomb	50				11
							6 bombs	300	200	300	50	
							12 bombs	500	300	400	200	
							24 bombs	500	300	500	300	
			GB[4]	Spray tank, 100-gal			1 spray tank	RT max=750 meters (one-half effective spray release line length)				12
							2 spray tanks					
			VX[4]				1 spray tank	RT max=500 meters (one-half effective spray release line length)				16
			BZ[4]	Bomb, 150-lb								17
				Bomb, 700-lb								

[1]RT max is largest target radius for which indicated casualty threat is tabulated for appropriate fire unit. Division of target into subtargets NOT considered.

[2]All windspeeds, temperature gradients, and protection categories considered.

[3]RT max computed for maximum number of volleys for which data are tabulated.

[4]Weapon system capabilities derived from tables composed of hypothetical data for INSTRUCTIONAL PURPOSES ONLY at the U. S. Army Command and General Staff College. For actual data, refer to FM 3-10.

Table 2. Estimated Fractional Casualty Threat From 105-mm Howitzer, GB Projectile, Battery Fire[1 2]

1	2	3	4	5	6	7	8	9	10	11	12	13	14	15
Target radius–radius of effect (meters)	Range to target (km)	No of volleys	Windspeed[3]											
			4 kmph				9 kmph				28 kmph			
			Surprise[4]	Total dose[5]			Surprise[4]	Total dose[5]			Surprise[4]	Total dose[5]		
				I	N	L		I	N	L		I	N	L
50	<7.5	1	.10	.25	.20	.15	.10	.15	.10	.10				
		2	.20	.45	.40	.30	.15	.30	.25	.20		.10	.05	.05
		3	.30	.60	.60	.35	.30	.50	.45	.30	.10	.20	.15	.10
		4	.30	.75	.70	.45	.30	.55	.45	.35	.10	.25	.20	.10
		5	.35	.90	.85	.55	.35	.60	.50	.40	.15	.30	.25	.15
	>7.5	1	.05	.15	.15	.10	.05	.10	.05	.05				
		2	.15	.30	.25	.15	.10	.20	.15	.10		.05	.05	
		3	.15	.30	.30	.25	.10	.20	.20	.15		.10	.05	.05
		4	.20	.40	.35	.25	.15	.30	.30	.15	.05	.15	.15	.05
		5	.25	.45	.45	.30	.25	.40	.35	.25	.10	.20	.20	.10
100	<7.5	1	.05	.15	.15	.10	.05	.10	.05	.05				
		2	.10	.30	.30	.15	.10	.20	.15	.10				
		3	.15	.40	.35	.20	.15	.25	.25	.15	.05	.10	.05	
		4	.15	.40	.35	.30	.15	.30	.30	.15	.05	.10	.10	.05
		5	.20	.45	.40	.35	.20	.35	.35	.20	.10	.15	.15	.10
	≥7.5	1	.05	.10	.10	.05		.05	.05					
		2	.10	.20	.20	.10	.05	.15	.10	.05				
		3	.10	.25	.25	.15	.10	.15	.15	.10		.05	.05	
		4	.10	.30	.25	.20	.10	.25	.20	.15		.10	.05	
		5	.15	.35	.30	.25	.15	.30	.25	.15	.05	.15	.10	.05
200	Any	1		.05	.05									
		2		.10	.10	.05		.05	.05					
		3	.05	.15	.15	.05		.10	.05					
		4	.05	.15	.15	.10		.10	.10					
		5	.05	.20	.20	.10	.05	.15	.10	.05				

[1] Blank spaces indicate fractional casualties are below 0.05.

[2] If the target is predominately wooded, use a windspeed of 4 kmph and neutral temperature gradient for total dose attack; use a windspeed of 4 kmph for surprise attack.

[3] For windspeeds other than those shown, use data given for the nearest windspeed.

[4] Multiply the figures given in the table by the appropriate factor to obtain the fractional casualties from surprise dose attack:

Troops in open foxholes:	0.7
Troops in covered foxholes or bunkers:	0.6

[5] I=inversion, N=neutral, L=lapse.

Table 17. BZ Munitions Requirements

1	2	3	4	5	6
Munition	Casualty level[2]	Area coverage[1] (square kilometers)			
		Windspeed[3]			
		8 kmph		16 kmph	
		Temperature gradient		Temperature gradient	
		Inversion	Neutral	Inversion	Neutral
150-lb bomb	.40	.05	.02	.03	.01
	.75	.03	.01	.02	.009
700-lb bomb	.40	.20	.07	.09	.04
	.75	.10	.04	.05	.03

[1]Area coverages are for one bomb.

[2]Casualty levels are for personnel without masks available. For personnel with masks available, multiply casualty levels by 0.7.

[3]For windspeeds other than those shown, use data given for the nearest windspeed.

NOTE: The above table is composed of hypothetical munitions and data for INSTRUCTIONAL PURPOSES ONLY at the U. S. Army Command and General Staff College. For actual data, refer to FM 3-10.

Table 18. HD Ammunition Expenditure for Vapor Effect (50 Percent Coverage of Target Area)[1 2]

Desired effect[3]	Exposure time (hours)	Rounds required per hectare																																				
		4.2-inch mortar (cartridge M2A1)												105-mm howitzer (cartridge M60)												155-mm howitzer and gun (projectiles M110 and M104)											
		Windspeed (kmph)												Windspeed (kmph)												Windspeed (kmph)											
	Temperature (°F)	6			9			15			26			6			9			15			26			6			9			15			26		
		Temperature gradient[4]												Temperature gradient[4]												Temperature gradient[4]											
	55° 70° 85° 100°	I	N	L	I	N	L	I	N	L	I	N	L	I	N	L	I	N	L	I	N	L	I	N	L	I	N	L	I	N	L	I	N	L	I	N	L
Cause eye irritation to troops without masks.	1 ½ ¼ ⅛	10	14	16	11	21	22	15	22	26	20	24	29	22	24	27	24	34	39	39	44	46	32	53	65	8	10	10	9	11	12	10	12	13	11	14	16
	2 1 ½ ¼	6	8	9	8	12	14	12	13	16	17	21	24	18	22	23	20	22	27	29	32	34	26	39	51	6	8	9	8	10	11	9	11	12	10	12	14
	4 2 1 ½	6	6	8	8	9	10	9	10	13	13	16	20	16	17	20	17	18	20	20	22	24	22	29	39	4	5	6	6	8	9	8	9	10	9	10	12
	8 4 2 1	4	6	6	6	8	9	8	9	11	12	13	15	12	15	17	13	12	17	15	20	22	18	27	36	4	5	5	5	6	8	6	8	9	8	9	11
	16 8 4 2	4	5	5	5	8	9	8	8	10	10	11	13	10	12	13	10	11	15	12	17	20	15	24	34	4	4	4	4	5	6	5	6	8	5	8	10
Disable masked troops (sweating in humid weather).	1 ½ ¼ ⅛	35	46	52	39	53	63	46	63	80	59	77	108	70	83	108	77	95	121	95	123	166	108	157	243	20	28	30	23	32	36	26	39	44	32	46	58
	2 1 ½ ¼	20	29	33	24	35	40	30	45	56	41	59	69	42	54	63	47	63	84	66	89	102	82	108	192	12	17	20	15	22	24	18	27	34	24	36	46
	4 2 1 ½	15	21	24	17	27	33	24	35	42	30	47	65	27	36	45	32	47	62	48	64	84	64	88	162	10	13	16	11	18	20	15	20	27	18	29	33
	8 4 2 1	11	17	18	13	21	26	17	28	38	27	45	63	18	29	34	24	38	47	33	53	76	54	83	138	6	10	12	9	13	16	12	17	24	16	23	33
	16 8 4 2	9	14	16	11	18	22	16	24	33	24	42	58	15	23	27	18	32	42	30	51	66	48	72	120	5	9	11	8	11	15	11	15	22	15	20	29
Disable masked troops (dry weather).	1 ½ ¼ ⅛	64	83	95	72	95	114	86	113	144	108	144	198	128	154	174	144	174	212	189	...	...	202	...	...	36	48	53	41	56	63	46	66	78	59	83	105
	2 1 ½ ¼	36	52	58	44	62	72	57	81	101	71	120	125	75	98	128	89	113	147	111	156	180	148	198	288	21	28	33	26	36	41	38	54	63	42	65	84
	4 2 1 ½	26	35	41	30	46	56	45	62	76	57	86	119	50	64	81	59	86	111	88	118	153	117	165	256	15	21	26	18	28	33	26	36	45	33	50	66
	8 4 2 1	18	27	30	23	35	44	32	50	68	50	81	114	33	50	58	45	65	84	62	95	138	101	154	240	11	16	18	13	21	26	22	33	40	28	42	56
	16 8 4 2	13	21	26	18	30	40	29	46	60	42	72	108	26	39	45	34	56	72	54	84	120	84	132	193	9	12	15	11	18	21	18	30	36	24	38	46

[1]For open terrain. For heavily wooded terrain or jungle, multiply the figure obtained by 0.5 to obtain the appropriate expenditure.

[2]Blank spaces indicate excessive expenditures.

[3]An average of 50 percent casualties is expected among all troops who remain in the target area for the times specified.

[4]I = inversion, N = neutral, L = lapse.

[redacted]

S/C

DEPARTMENT OF THE ARMY FIELD MANUAL — FM 3-10B

NAVAL WARFARE INFORMATION PUBLICATION — NWIP 36-4

DEPARTMENT OF THE AIR FORCE MANUAL — AFM 355-9

MARINE CORPS MANUAL — FMFM 11-3B

EMPLOYMENT OF CHEMICAL AGENTS (U)

This copy is a reprint which includes current pages from Changes 1.

[redacted]

[redacted]

DEPARTMENTS OF THE ARMY, THE NAVY AND THE AIR FORCE

NOVEMBER 1966

[redacted]

[redacted]

CHAPTER 1

INTRODUCTION

Section I. GENERAL

1. (U) Purpose

This manual provides classified data on chemical agents and on the capabilities and effects of chemical munitions. When used in conjunction with its unclassified counterpart, FM 3-10/NWIP 36-2/AFM 355-4/FMFM 11-3, Employment of Chemical and Biological Agents, it provides guidance in planning the employment of chemical munitions.

2. (U) Scope

This manual contains classified data on lethal agents VX and GB and incapacitating agent BZ; munitions effects tables; and predicted effects of ground-fired and air-released munitions utilized to disseminate these agents. As a joint publication, it discusses all appropriate chemical munitions of the U.S. Army, Navy, Air Force, and Marine Corps. Unclassified HD chemical munitions expenditure tables and guidance in chemical target analysis and casualty estimation are given in FM 3-10/NWIP 36-2/AFM 355-4/FMFM 11-3.

3. (U) Reliability

Data contained in this manual are based on proving ground tests and field tests, analytical studies of such data, and predictions extrapolated from mathematical models.

4. (U) Army, Navy, Air Force, and Marine Corps User Comments

Users of this manual are encouraged to submit recommended changes or comments to improve the manual. Comments should be keyed to the specific page, paragraph, and line of the text in which the change is recommended. Reasons for each comment should be provided to insure understanding and complete evaluation. Comments should be forwarded direct to the Commanding Officer, U.S. Army Combat Developments Command CBR Agency, Fort McClellan, Ala. 36205, with an information copy to the cognizant service doctrinal development agency.

Section II. ANTIPERSONNEL CHEMICAL AGENTS

6. ~~(S)~~ (U) Incapacitating Agent BZ

This agent is disseminated as an aerosol to produce physical and mental effects when inhaled. The effects are temporary, and recovery is normally complete. There may be permanent ill effects in a few instances among the very young, the aged, and the infirm, or when massive dosages are received.

a. Tactical Employment. BZ is employed against carefully selected targets to incapacitate enemy troops when the use of lethal or destructive munitions is undesirable. This agent may be particularly useful in situations where adequate protective equipment is normally not available to enemy troops or where the status of training or mask discipline is poor, such as in counter-insurgency operations.

b. Limitations. BZ has the following limitations:

(1) The white agent cloud produced by pyrotechnic mixtures acts as a visible alarm.

(2) BZ may be defeated by improvised respiratory protection such as a folded cloth over mouth and nose.

(3) The effects are not immediate but require an average onset time of about 3 to 6 hours.

(4) There is no known antidote to treat affected friendly personnel.

c. Median Incapacitating Dosage (ICt_{50}). This is about 110 mg-min/m^3 for man engaged in mild activity (breathing rate of 15 liters/min).

d. Physiological and Psychological Symptoms. The symptoms listed below will become more intense as the dosage received increases. They also vary according to the inherent characteristics of each individual exposed to the agent. Because of the many variables involved, estimation of the percentage and type of casualties produced from a BZ attack is difficult. Approximations for the occurrence of ultimate casualties among unmasked personnel are 5 percent in 2 hours, 50 percent in 4½ hours, and 95 percent in 9½ hours.

(1) Symptoms likely to appear in 30 minutes to 3 hours: dizziness, extreme drowsiness, dryness of the mouth, and increased heartbeat.

(2) Symptoms likely to appear in 3 to 5 hours: restlessness, involuntary muscular movement, near vision impairment, and physical incapacitation.

(3) Symptoms likely to appear in 6 to 10 hours: hallucinations, lack of muscular coordination, disorientation, and difficulty in memory recall.

e. Duration of Incapacitation. The duration of incapacitation varies with the dosage received—from 24 hours to 5 days.

f. Duration of Effectiveness. Under average meteorological conditions in the open, the aerosol is normally effective for only a few minutes after dissemination, since the fine BZ particles travel

27. (U) CBU-5B/M43 750-Pound BZ Cluster Bomb

Both the U.S. Air Force CBU-5B and the U.S. Army M43 750-pound cluster bombs contain 57 M138 BZ-filled bomblets. The U.S. Army M43 cluster is designed for delivery by aircraft at low speeds. When modified and equipped with a suitable fairing for streamlining purposes, an internal arming wire system, and a strengthened tail fin, it is then designated the CBU-5B and can be delivered by high-performance aircraft.

a. Operational Concepts. The BZ cluster bomb is used on carefully selected targets against enemy personnel when the use of lethal chemical or destructive weapon systems is militarily or politically undesirable. See paragraph 6 for additional data.

b. Characteristics. The cluster contains about 85 pounds of agent BZ and employs two tail mechanical time fuzes. To function properly, the cluster must be released above 6,200 feet so as to allow the cluster to open at approximately 4,500 feet. The M138 bomblet contains four canisters, each with three-fourth pound of agent-pyrotechnic mixture (50/50 ratio), and an "all-ways" impact fuze. The bomblet is *not* self-dispersing.

c. Capabilities. The cluster delivers M138 bomblets over an elliptical impact area having a cross section of approximately 100 by 200 meters when released at heights above 6,200 feet. One cluster can cover about 12,000 square meters (1.2 hectares) with an incapacitating total dosage of BZ (110 mg-min/m^3) under neutral temperature gradient and in a wind speed between 2 and 10 knots; under lapse temperature gradient conditions, the area coverage will be smaller. Under optimum delivery conditions, the area coverage for one cluster is expected to range from 15,000 to 20,000 square meters. Field tests indicate that wind speed has only minor effects upon area coverage.

d. Operational Considerations. Refer to the appropriate technical order/flight manual to determine aircraft loads (see para 16*d*).

Field Manual
No 3-6

Air Force Manual
No 105-7

Fleet Marine Force Manual
No. 7-11-H

HEADQUARTERS
DEPARTMENT OF THE ARMY
DEPARTMENT OF THE AIR FORCE
UNITED STATES MARINE CORPS
Washington, DC, 3 November 1986

FIELD BEHAVIOR OF NBC AGENTS (INCLUDING SMOKE AND INCENDIARIES)

Table of Contents

Preface ii

Chapter 1. Chemical Agents 1-1
- Basic Characteristics 1-1
- Vapors and Aerosols 1-9
- Liquids 1-12

2. Smoke and Incendiaries 2-1
- Smoke 2-1
- Incendiaries 2-8

3. Biological Agents and Nuclear Detonations 3-1
- Biological Agents 3-1
- Nuclear Detonations 3-3

Appendix A. Air Weather Service A-1

B. Units of Measure B-1

C. Weather C-1

Glossary Glossary-1

References References-1

Index Index-1

DISTRIBUTION RESTRICTION: Approved for public release; distribution is unlimited.

DISPERSION CATEGORY	ATMOSPHERIC DESCRIPTION	TRADITIONAL ATMOSPHERIC CONDITIONS
1	Very Unstable	Lapse
2	Unstable	Lapse
3	Slightly Unstable	Neutral
4	Neutral	Neutral
5	Slightly Stable	Neutral
6	Stable	Inversion
7	Extremely Stable	Inversion

Figure 1-1. Atmospheric stability categories and conditions.

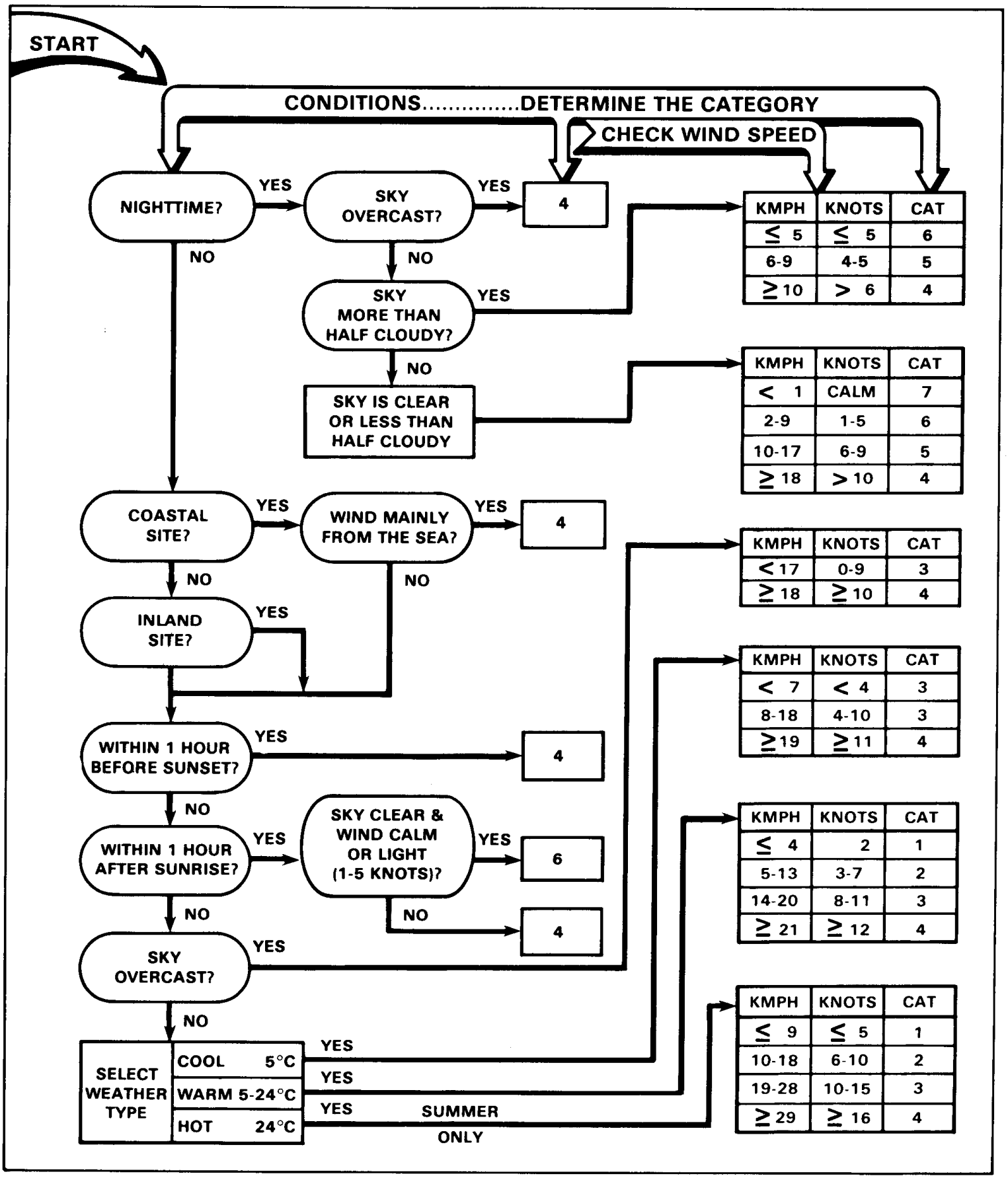

Figure 1-2. Stability decision tree.

Page 1-14 states that the mixed air layer height is 50-100 m on a clear, calm night, just before 400 m before sunrise, and 2 km on a hot summer day

Table 1-3. Center line dosages at different distances downwind for different dispersion categories and wind speeds for a unit source. 100 kilograms of GB

STABILITY CATEGORY	Wind Speed	DOWNWIND DISTANCE IN KM							
		.5	1	2	4	6	10	20	30
		DOSAGES (mg-min/M³)							
1	1	57.82	10.960	2.4820	1.2070	.8048	.48290	.24140	.16100
	3	19.15	3.628	.8224	.3998	.2665	.15990	.07995	.05330
	5	11.47	2.174	.4928	.2396	.1597	.09582	.04791	.03194
2	3	65.93	16.480	4.121	1.0300	.4671	.22840	.11360	.07575
	6	32.86	8.215	2.054	.5135	.2328	.11380	.05663	.03775
	10	19.75	4.938	1.235	.3087	.1400	.06843	.03404	.02269
3	3	172.60	46.26	12.400	3.321	1.5370	.5825	.18010	.11510
	7	73.86	19.79	5.302	1.421	.6576	.2492	.07703	.04925
	12	43.09	11.55	3.094	.829	.3837	.1454	.04494	.02874
4	3	572.4	170.20	50.590	15.040	7.398	3.0260	.8997	.44450
	8	213.9	63.61	18.910	5.622	2.765	1.1310	.3363	.16620
	16	107.1	31.84	9.467	2.814	1.384	.5662	.1683	.08318
5	2	1,837.0	606.0	199.90	65.94	34.470	15.220	5.021	2.6250
	5	736.2	242.9	80.12	26.43	13.810	6.101	2.012	1.0520
	9	408.7	134.8	44.47	14.67	7.668	3.387	1.117	.5839
6	1	10,080.0	3,691.0	1,351.0	494.50	274.70	131.00	47.930	26.630
	3	3,339.0	1,222.0	447.4	163.80	90.96	43.37	15.870	8.818
	5	2,001.0	732.4	268.1	98.12	54.51	25.99	9.5120	5.284
7	HIGHER DOSAGES THAN ABOVE								

Table 1-4. Summary of favorable and unfavorable weather and terrain conditions for tactical employment of chemical agent vapor or aerosol. (The stability condition listed for the south slope is for the northern hemisphere; due to solar loading on the slope, the situation would be reversed for the southern hemisphere.)

FACTOR	UNFAVORABLE	MODERATELY FAVORABLE	FAVORABLE
Wind	Artillery employment if speed is more than 7 knots. Aerial bombs if speed is more than 10 knots.	Steady, 5 to 7 knots, or land breeze.	Steady, less than 5 knots, or sea breeze.
Dispersion Category	Unstable (lapse).	Neutral.	(Stable) inversion.
Temperature	Less than 4.4°C.	4.4° to 21.1°C.	More than 21.1°C.
Precipitation	Any.	Transitional.	None.
Cloud Cover	Broken, low clouds during daytime. Broken, middle clouds during daytime. Overcast or broken, high clouds during daytime. Scattered clouds of all types during daytime. Clouds of vertical development.	Thick, low overcast. Thick, middle overcast.	Broken, low clouds at night. Broken, middle clouds at night. Overcast or broken, high clouds at night. Scattered clouds of all types at night. Clear sky at night.
Terrain	Hilltops, mountain crests. South slopes* during daytime.	Gently rolling terrain. North slopes at night.	Even terrain or open water.
Vegetation*	Heavily wooded or jungle.	Medium dense.	Sparse or none.

*Cloud dissemination occurs above the canopy.

Chemical and biological contamination avoidance, FM 3-3 (1992)

10 grams/square meter

TABLE 1-2. Chemical Agent Persistency in Hours on CARC Painted Surfaces.

Temperature		GA/ GF[1]	GB[2,3]	GD[2,3]	HD[1]	VX[2,3]
C°	F°					
-30	-22	*	110.34	436.69	**	***
-20	-4	*	45.26	145.63	**	***
-10	14	*	20.09	54.11	**	***
0	32	*	9.44	22.07	**	***
10	50	1.42	4.70	9.78	12	1776
20	68	0.71	2.45	4.64	6.33	634
30	86	0.33	1.35	2.36	2.8	241
40	104	0.25	0.76	1.25	2	102
50	122	0.25	0.44	0.70	1	44
55	131	0.25	0.34	0.51	1	25

NOTE

1 For grassy terrain multiply the number in the chart by 0.4.
2 For grassy terrain multiply the number in the chart by 1.75.
3 For sandy terrain multiply the number in the chart by 4.5.
* Agent persistency time is less than 1 hour.
** Agent is in a frozen state and will not evaporate or decay.
*** Agent persistency time exceeds 2,000 hours.

REFERENCE BOOK
3—2*

U.S. ARMY COMMAND AND GENERAL STAFF COLLEGE
Fort Leavenworth, Kansas, *25 July 1983*

CHEMICAL WEAPONS EMPLOYMENT DATA

Page

CHAPTER 1

Appendix E. Target Analysis Methods ..... 1—1

Section I. General Methodology for Chemical Target Analysis ..... 1—1

Introduction to Target Analysis ..... 1—1

Defining the Target ..... 1—3

Selecting an Agent and Delivery System ..... 1—9

Quick Reference Guide ..... 1—10

Aim-Point Adjustment ..... 1—12

Munitions Requirement ..... 1—12

Terms for Safety Distance Calculations ..... 1—13

Troop Safety Distance Calculations ..... 1—14

Example Problems for MSD ..... 1—14

Downwind Vapor Hazard Distance ..... 1—15

Chemical Target Analysis Worksheet ..... 1—16

II. GB Target Analysis ..... 1—17

GB Delivery Systems ..... 1—17

GB Casualty Effects Tables ..... 1—17

Example Problems Using Agent GB ..... 1—18

III. VX Target Analysis ..... 1—23

VX Artillery Delivery Systems ..... 1—23

VX Spray Tank ..... 1—23

VX Casualty Effects Tables ..... 1—25

Example Problems Using Agent VX ..... 1—26

IV. HD Target Analysis ..... 1—29

HD Munitions Requirements Tables for Vapor Effects ..... 1—29

Procedures Used to Determine HD Munitions Requirements ..... 1—30

Downwind Hazard for Troop Safety (HD Vapor) ..... 1—32

Example (HD) Downwind Hazard Distance Problem ..... 1—32

Munitions Requirement for HD Liquid Contamination ..... 1—33

*This reference book replaces RB 3—2, 8 July 1981, for all resident and nonresident programs.

Section X
Spray Tank/VX

AIM POINT & FLIGHT PATH ADJUSTMENTS
VARIABLE DELIVERY TECHNIQUES

DELIVERY SYSTEM	TANKS/AIRCRAFT	AIRCRAFT SPEED*
Refer to Air Force & Navy Publications	Minimum 1 Maximum 2	450 Knots Centered Delivery

$$\text{Altitude of Spray Release Line} = \frac{\text{Windspeed - Height Product (VWH)}}{\text{Windspeed in Knots}}$$

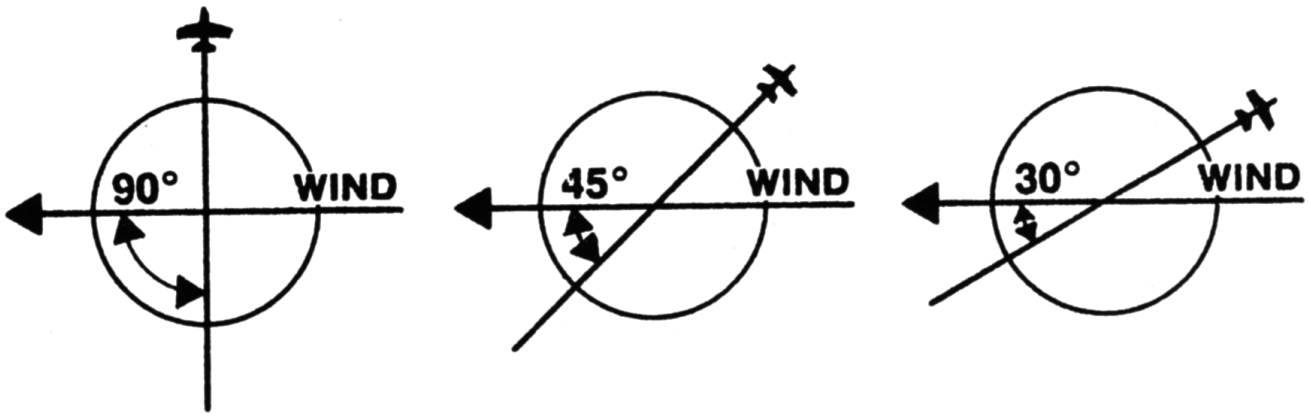

FLIGHT PATH IN RELATION TO WIND DIRECTION

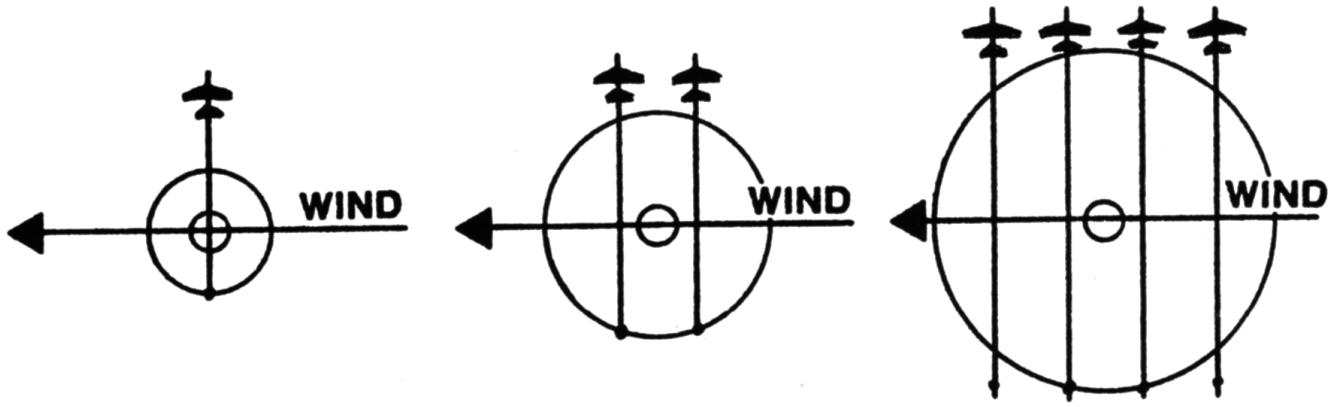

500-M TARGET RADIUS | 1,000-M TARGET RADIUS | 1,500-M TARGET RADIUS

Flight path Initiation point is leading edge of target Target center

*Used on all tables in this section.

Table I-79. Spray Tank/VX Aim Point & Flight Path Adjustments

Spray Tank/VX

Expected Fraction of Casualties

PROTECTION CATEGORY: A (NO MASK OR PROTECTIVE CLOTHING)
CASUALTIES WITHIN: 1/2 HOUR

FLOW RATE	WIND ANGLE	TARGET RADIUS (Meters)	WINDSPEED-HEIGHT PRODUCT (VWH) 500 NO. AIRCRAFT 1	500 2	500 4	750 NO. AIRCRAFT 1	750 2	750 4	1000 NO. AIRCRAFT 1	1000 2	1000 4	2000 NO. AIRCRAFT 1	2000 2	2000 4	3000 NO. AIRCRAFT 1	3000 2	3000 4
ONE TANK AT HALF FLOW	90°	500	.06	.15	.20	.17	.37	.60	.25	.46	.68	.25	.43	.60	.19	.35	.50
		1000	.01	.04	.10	.06	.15	.31	.09	.19	.45	.09	.20	.45	.09	.20	.45
		1500	–	.02	.07	–	.06	.14	–	.06	.19	–	.06	.22	–	.08	.23
	45°	500	.04	.11	.23	.13	.29	.61	.20	.41	.69	.22	.41	.64	.21	.37	.57
		1000	.01	.04	.11	.04	.10	.23	.07	.16	.36	.08	.19	.42	.08	.19	.42
		1500	–	–	.07	–	.06	.12	–	.08	.18	–	.08	.20	–	.08	.22
	30°	500	.02	.07	.16	.10	.23	.48	.15	.32	.64	.17	.36	.62	.18	.35	.57
		1000	–	.03	.08	.03	.09	.20	.06	.13	.29	.07	.15	.34	.07	.16	.36
		1500	–	–	.04	–	.04	.09	–	.06	.14	–	.08	.18	–	.08	.20
TWO TANKS AT HALF FLOW	90°	500	.08	.17	.30	.22	.46	.69	.34	.55	.69	.31	.50	.65	.25	.43	.60
		1000	.01	.05	.11	.10	.19	.41	.13	.29	.61	.15	.33	.53	.18	.35	.51
		1500	.01	.03	.10	.05	.11	.25	.07	.17	.38	.09	.20	.46	.09	.22	.49
	45°	500	.06	.13	.28	.18	.37	.71	.27	.50	.71	.30	.50	.67	.29	.47	.62
		1000	.02	.06	.13	.06	.14	.31	.11	.24	.51	.13	.29	.60	.15	.32	.63
		1500	–	.02	.08	.03	.09	.20	.06	.14	.31	.07	.17	.38	.08	.19	.42
	30°	500	.04	.09	.39	.13	.29	.73	.20	.41	.69	.23	.44	.63	.24	.43	.57
		1000	.01	.04	.10	.05	.11	.26	.09	.19	.41	.10	.23	.51	.12	.26	.56
		1500	–	.01	.06	.02	.07	.14	.04	.11	.24	.06	.13	.29	.07	.15	.34

PROTECTION CATEGORY: A (NO MASK OR PROTECTIVE CLOTHING)
CASUALTIES WITHIN: 1 HOUR

FLOW RATE	WIND ANGLE	TARGET RADIUS (Meters)	WINDSPEED-HEIGHT PRODUCT (VWH) 500 NO. AIRCRAFT 1	500 2	500 4	750 NO. AIRCRAFT 1	750 2	750 4	1000 NO. AIRCRAFT 1	1000 2	1000 4	2000 NO. AIRCRAFT 1	2000 2	2000 4	3000 NO. AIRCRAFT 1	3000 2	3000 4
ONE TANK AT HALF FLOW	90°	500	.08	.20	.27	.25	.50	.70	.36	.57	.69	.33	.53	.64	.28	.48	.58
		1000	.02	.06	.15	.10	.22	.47	.16	.34	.65	.19	.39	.65	.22	.40	.63
		1500	–	.04	.09	–	.10	.23	–	.12	.34	–	.15	.41	–	.21	.42
	45°	500	.06	.14	.30	.19	.40	.71	.28	.52	.72	.31	.52	.68	.30	.49	.64
		1000	.02	.06	.14	.07	.15	.33	.11	.25	.52	.14	.29	.55	.16	.32	.54
		1500	–	.02	.07	–	.08	.19	–	.13	.34	–	.16	.38	–	.19	.43
	30°	500	.04	.10	.22	.14	.30	.63	.21	.43	.69	.24	.45	.65	.25	.45	.59
		1000	.01	.04	.10	.05	.12	.27	.09	.19	.41	.10	.23	.48	.12	25	.49
		1500	–	.01	.05	–	.06	.14	–	.11	.24	–	.14	.31	–	.16	.37
TWO TANKS AT HALF FLOW	90°	500	.11	.24	.41	.32	.57	.74	.39	.59	.72	.35	.55	.69	.29	.47	.66
		1000	.03	.08	.19	.13	.28	.58	.21	.43	.72	.27	.49	.71	.31	.51	68
		1500	.01	.05	.14	.07	.16	.37	.12	.26	.56	.16	.34	.66	.19	39	.67
	45°	500	.08	.17	.37	.23	.48	.75	.35	.57	.72	.35	.55	.68	.32	.51	.65
		1000	.03	.08	.17	.09	.20	.42	.16	.34	.67	.20	.42	.71	.24	.47	.71
		1500	.01	.03	.10	.05	.13	.28	.09	.20	.44	.12	.26	.55	.14	.30	60
	30°	500	.05	.13	.51	.17	.37	.74	.26	.50	.71	.28	.49	65	.28	.48	.64
		1000	.02	.05	.13	.07	.16	.34	.12	.26	.55	.16	.33	.67	.18	38	.69
		1500	–	.02	.07	.03	.10	.20	.07	.15	.35	.10	.19	.43	.10	23	.48

Table I-80. Spray Tank/VX Expected Fraction of Casualties

PROTECTION CATEGORY: **A** (NO MASK OR PROTECTIVE CLOTHING)
CASUALTIES WITHIN: **ULTIMATE**

FLOW RATE	WIND ANGLE	TARGET RADIUS (Meters)	WINDSPEED-HEIGHT PRODUCT (VWH) 500 NO. AIRCRAFT 1	500 2	500 4	750 NO. AIRCRAFT 1	750 2	750 4	1000 NO. AIRCRAFT 1	1000 2	1000 4	2000 NO. AIRCRAFT 1	2000 2	2000 4	3000 NO. AIRCRAFT 1	3000 2	3000 4
ONE TANK AT HALF FLOW	90°	500	.14	.31	.43	.39	.62	.74	.39	.59	.69	.35	.55	.65	.30	.50	.60
		1000	.05	.12	.26	.18	.38	.69	.30	.54	.73	.35	.56	.70	.36	.56	.68
		1500	--	.06	.15	--	.21	.42	--	.31	.56	--	.34	.59	--	.41	.59
	45°	500	.10	.23	.49	.30	.56	.75	.39	.60	.72	.36	.56	.68	.33	.53	.65
		1000	.04	.10	.22	.12	.26	.53	.19	.39	.63	.23	.43	.61	.26	.44	.59
		1500	--	.06	.12	--	.16	.33	--	.27	.54	--	.35	.62	--	.41	.65
	30°	500	.07	.16	.36	.22	.45	.74	.30	.54	.69	.31	.52	.65	.30	.50	.60
		1000	.03	.07	.16	.09	.20	.42	.14	.29	.55	.16	.34	.56	.18	.35	.55
		1500	--	.04	.09	--	.12	.25	--	.20	.45	--	.27	.55	--	.33	.59
TWO TANKS AT HALF FLOW	90°	500	.18	.38	.64	.43	.64	.75	.39	.59	.73	.35	.55	.70	.30	.50	.67
		1000	.06	.15	.30	.21	.45	.74	.35	.59	.73	.39	.60	.71	.39	.59	.69
		1500	.04	.09	.22	.13	.28	.60	.22	.46	.72	.30	.54	.74	.34	.56	.72
	45°	500	.13	.28	.58	.35	.60	.75	.40	.61	.72	.36	.56	.68	.34	.53	.65
		1000	.05	.11	.27	.16	.33	.66	.27	.52	.75	.33	.57	.73	.37	.59	.72
		1500	.03	.06	.16	.10	.21	.44	.16	.34	.65	.21	.42	.69	.24	.46	.68
	30°	500	.09	.20	.72	.26	.51	.74	.33	.56	.74	.32	.53	.70	.31	.50	.67
		1000	.04	.09	.20	.12	.26	.54	.20	.41	.73	.25	.49	.74	.29	.53	.73
		1500	.02	.04	.12	.07	.16	.32	.12	.25	.52	.15	.30	.60	.17	.34	.61

Table I-81. Spray Tank/VX Expected Fraction of Casualties

HD DOSAGE REQUIREMENTS

HD DOSAGES mg/minute/cubic meter			PERSONNEL PROTECTION CATEGORY	CASUALTY EFFECTS	DEGREE OF DISABILITY	ONSET TIME	DURATION
HOT[1]	WARM[2]	COOL[3]					
50	50	50	"A" no mask or protective clothing	No significant injury; maximum safe dosage	--	--	--
100	100	100		Eye damage of threshold military significance	PARTIAL	6-24 HR	1-3 DAYS
200	200	200		Temporary blindness	TOTAL	3-12 HR	2-7 DAYS
100	150	400	"B" or "C" with no protective clothing	No significant injury; maximum safe dosage	--	--	--
200	300	1,000		Skin burns of threshold military significance	PARTIAL	2-12 DAYS	1-2 WEEKS
500	1,000	2,000 to 4000		Severe genital burns	PARTIAL TO TOTAL	2-7 DAYS	1-4 WEEKS
750	2,000 to 4,000	4,000 to 10,000		Severe generalized burns	PARTIAL TO TOTAL	4-12 HRS About 24 HRS	3-4 WEEKS 1-2 WEEKS
			"D" mask with protective clothing	HD IS NOT RECOMMENDED FOR USE IN THIS PROTECTION CATEGORY.			

[1]Hot, humid; above 80°F; sweating skin
[2]Warm; 60°-80°F; skin not wet with sweat
[3]Cool; 40°-60°F; cool, dry skin

Table I-85. HD Munitions

HD Contamination Replenishment Time (Rate Factors)

TERRAIN FACTOR **X** WINDSPEED FACTOR **X** GROUND SURFACE TEMPERATURE FACTOR **X** TEMPERATURE GRADIENT FACTOR[2] (STABILITY) **=** TIME (HOURS) FOR 50% EVAPORATION OF HD

FACTORS

TERRAIN	WINDSPEED[1] (knots)	GROUND SURFACE TEMPERATURE (°F)	TEMPERATURE GRADIENT[2]
OPEN GRASSLAND = 1	1 = 3.1 2 = 1.8 3 = 1.3 4 = 1.0		INVERSION = 1.2
FOREST OR JUNGLE = 1	5 = 0.8 6 = 0.7 7 = 0.6 9 = 0.5 11 = 0.4	50° = 4.0 60° = 2.5 70° = 1.6 80° = 1.0 90° = 0.6 100° = 0.4 110° = 0.3 120° = 0.2	NEUTRAL = 1.0
BARREN SOIL OR SAND = 2	14 = 0.3 18 = 0.3		LAPSE = 0.7

[1]at 2 meters high in the open
[2]in the open

Table I-96. HD Contamination Replenishment Time (Rate Factors)

Approximate Duration of Hazard in Contaminated Terrain

TASK	TERRAIN	APPROXIMATE TIME AFTER CONTAMINATION THAT PRESCRIBED TASKS MAY BE PERFORMED WITH NEGLIGIBLE RISK[1] (Not wearing protective clothing)[2]			
		BLISTER AGENT (HD) TEMPERATURE[3]		NERVE AGENT (VX-GB) UNIFORM[4]	
		WARM (70°-85°F)	HOT (80°-100°F)	SUMMER	WINTER
		WEARING MASKS			
TRAVERSAL[5] (Walking across area 2 hours or less	Bare soil or low vegetation[6] (except sand)	36 HOURS	36 HOURS	5 HOURS	2 HOURS
	High vegetation, including jungle and heavy woods	4 DAYS	2 DAYS	28 HOURS	10 HOURS
		NOT WEARING MASKS[7]			
OCCUPATION (Without hitting ground 24 hours)	Bare soil or low vegetation[6] (except sand)	4 DAYS	3 DAYS	32 DAYS	13 DAYS
	High vegetation, including jungle and heavy woods	4 DAYS	3 DAYS	32 DAYS	13 DAYS
OCCUPATION (Involving advance under fire 24 hours)	Bare soil or low vegetation[6] (except sand)	4 DAYS	3 DAYS	32 DAYS	13 DAYS
	High vegetation including jungle and heavy woods	6 DAYS	4 DAYS	50 DAYS	18 DAYS

[1]These times are safe-sided for troop safety.
[2]Leather combat boots treated with protective dubbing or rubber combat boots are worn.
[3]Effects of blister agent vary significantly with temperature. Mustard freezes in temperatures below 60°F and can present a hazard when the temperature rises.
[4]Protection from V-agent and thickened G-agent varies significantly with layers of clothing worn.
[5]For personnel walking for 2 hours in an area contaminated by blister agents, the limiting factor is the vapor hazard. If only a few minutes are required for traversal of the area, the task can be initiated at earlier times than those given.
[6]Times shown are not applicable to sand, which will hold chemical agents for longer periods of time than those given.
[7]The data refer to approximate times at which personnel could occupy contaminated areas without having to wear protective masks for protection against vapor hazard.

Table I-97. Approximate Duration of Hazard in Contaminated Terrain

WARNING
This table is intended as a guide only.
Chemical agent detectors must be used to determine the extent of actual contamination and vapor hazards.

83-(RB 3-2)-3625—8635—25 Jul 83

Table 5-2. Potential Biological Warfare Agents.

Microorganism	Mode of Transmission	Incubation Period (Days)[2]	Mortality Rate (Percent)2	Vaccine ([3])	Treatment ([4])
Bacteria					
Bacillus Anthracis (Anthrax)	A, D[9], I	1-7	5-1005	+	E[6]
Francisella Tularensis (Tularemia)	A, D[9], I, V	1-10	<30	+ +	E
Yersinia Pestis (Plague)	A, V	2-6	25-1007	+ + +	E[6]
Vibrio Cholerae (Cholera)	I	1-5	15-90	+ + +	E
Corynebacterium Diptheriae (Diptheria)	A, D[9]	2-5	5-12	+ + +	E
Salmonella Typhi (Typhoid Fever)	I	6-21	7-14	+ + +	E
Rickettsiae					
Rickettsia SPP (Spotted fevers group)	V	6-15	10-40	+ + +	E
Rickettsiae (Endemic or flea-borne typhus)	V	6-14	2-5	N	E
Rickettsia (Rocky Mountain spotted fever)	V	3-10	30 (approx)	N	E
Coxiella Burnetii (Q fever)	A, I	14-21	<1	+ +	E

[1] Transmission can be by aerosol-A, direct contact-D, ingestion-I, and/or vector-V.
[2] Incubation periods and mortality rates vary according to a number of factors (such as ability of the host to resist infection, infective dose, portal of entry, and virulence of the microorganism).
[3] + indicates vaccine available but of questionable value; + + indicates vaccine available, but mainly used in high risk individuals; + + + indicates vaccine used extensively; N indicates no vaccine available.
[4] E indicates effective treatment available; N indicates no specific treatment.
[5] The mortality rate is lower when the agent enters through the skin; higher when it enters through the respiratory tract.
[6] Treatment must be initiated in the earliest stage of the pulmonary form to be effective.
[7] The 25 percent represents mortality due to bubonic form; 100 percent represents mortality due to pneumonic form.
[8] Mosquitoes are thought to be the primary vectors, but this has not been proven.
[9] Direct contact refers to being bitten by a rabid animal, which is the usual means of transmission, or coming into contact with a rabid animal.

Table 5-2. Potential Biological Warfare Agents (continued).

Microorganism	Mode of Transmission	Incubation Period (Days)[2]	Mortality Rate (Percent)2	Vaccine ([3])	Treatment ([4])
Viruses					
Eastern Equine Encephalitis (EEE)	V[8]	4-24	60 (Approx)	N	N
Venezuelan Equine Encephalitis (VEE)	V[8]	4-24	<1	+ +	N
Japanese B Encephalitis	V (Mosquito)	5-15	10-80	+ +	N
Russian SpringùSummer Encephalitis (RSSE)	V (Tick)	7-14	3-40	+	N
Yellow Fever	V (Mosquito)	3-6	5-40	+ + +	N
Dengue Fever	V (Mosquito)	4-10	<1	+	N
Pox Virus					
Variloa Virus (Smallpox)	A, D[9]	7-16	10-25	+ + +	N
Hantaan Virus (Hemorrhagic Fever with Renal Syndrome)	A, V				
Phlebovirus (Rift Valley Fever)	V (Mosquito)	4-6	<1	N	N
Nairovirus (Crimean-Congo Hemorrnagil Fever)	V (Tick)	3-7			
Bunyavirus (LA Crosse)	V (Mosquito)				
Phlebovirus(Sandfly)	V (Sand fly)	3-6			

[1] Transmission can be by aerosol-A, direct contact-D, ingestion-I, and/or vector-V.
[2] Incubation periods and mortality rates vary according to a number of factors (such as ability of the host to resist infection, infective dose, portal of entry, and virulence of the microorganism).
[3] + indicates vaccine available but of questionable value; + + indicates vaccine available, but mainly used in high risk individuals; + + + indicates vaccine used extensively; N indicates no vaccine available.
[4] E indicates effective treatment available; N indicates no specific treatment.
[5] The mortality rate is lower when the agent enters through the skin; higher when it enters through the respiratory tract.
[6] Treatment must be initiated in the earliest stage of the pulmonary form to be effective.
[7] The 25 percent represents mortality due to bubonic form; 100 percent represents mortality due to pneumonic form.
[8] Mosquitoes are thought to be the primary vectors, but this has not been proven.
[9] Direct contact refers to being bitten by a rabid animal, which is the usual means of transmission, or coming into contact with a rabid animal.

Table 5-3. Threat Toxins.

Type of Toxin	Means of ID	Symptoms in Man	Effects on Man	Rate of Action	How Normally Disseminated	Protection Required	Decontamination
Mycotoxins	None	Vomiting, eye and skin irritation, dizziness, bloody diarrhea, and blisters.	Can incapacitate or kill, depending on concentration.	Rapid	Dusts, droplets, aerosols, smokes, or covert means	Protective mask and protective clothing	Soap and water, bleach, M258-series kit, STB and DS2
Enterotoxins	None	Severe vomiting and diarrhea, painful cramps, and weakness	Primarily incapacitates, assuming proper first aid is conducted	Same as above	Same as above	Same as above	Same as above
Botulinum Toxin	None	Double vision, weakness, difficulty in speech and swallowing, and respiratory paralysis	Kills	Delayed	Same as above	Same as above	Same as above

POTENTIAL MILITARY CHEMICAL/BIOLOGICAL AGENTS AND COMPOUNDS, US Army FM 3-11.9, 2005

Table G-4. Toxicity Estimates for CW Agents

ROE		Liquid (mg/70 kg man)		Inhalation/Ocular ($mg\text{-}min/m^3$)			Inhalation (mg/m^3)	Ocular ($mg\text{-}min/m^3$)		Percutaneous Vapor ($mg\text{-}min/m^3$)			
		Lethal (LD_{50})	Severe (ED_{50})	Lethal (LCt_{50})	Severe (ECt_{50})	Mild (ECt_{50})	Odor Detection (EC_{50})	Severe (ECt_{50})	Mild (ECt_{50})	Lethal (LCt_{50})		Severe (ECt_{50})	
Endpoints										Moderate	Hot	Moderate	Hot
Choking Agents	CG	-	-	1,500 (2-60)	-	-	6 S	-	-	-	-	-	-
	DP	-	-	1,500P (10-60)	-	-	4 S	-	-	-	-	-	-
Nerve Agents	GA	1,500	900	70 (2)	50 (2)	0.4 (2)	-	-	-	15,000 (30-360)	7,500P (30-360)	12,000 (30-360)	6,000P (30-360)
	GB	1,700	1,000	35 (2)	25 (2)	0.4 (2)	-	-	-	12,000 (30-360)	6,000P (30-360)	8,000 (30-360)	4,000P (30-360)
	GD	350	200	35 (2)	25 (2)	0.2 (2)	-	-	-	3,000 (30-360)	1,500P (30-360)	2,000 (30-360)	1,000P (30-360)
	GF	350	200	35 (2)	25 (2)	0.2 (2)	-	-	-	3,000 (30-360)	1,500P (30-360)	2,000 (30-360)	1,000P (30-360)
	VX	5	2	15 (2-360)	10 (2-360)	0.1 (2-360)	-	-	-	150 (30-360)	75P (30-360)	25 (30-360)	12P (30-360)
	Vx	NR											
Blood Agent	AC	-	-	2860P (2)	NR		34 S	-	-	-	-	-	-
	CK	-	-	NR	NR		12 S	-	-	-	-	-	-
	SA	-	-	7,500P (2)	-	-	-	-	-	-	-	-	-
Blister Agents	HD	1400	600	1,000 (2)	-	-	0.6 – 1 S	75 (2-360)	25 (2-360)	10,000 (30-360)	5,000P (30-360)	500 (30-360)	200 (30-360)
	HN-1	1400P	600P	1,000P (2)	-	-	-	75P (2)	25P (2)	10,000P (30)	5,000P (30)	500P (30)	200P (30)
	HN-2	1400P	600P	1,000P (2)	-	-	-	75P (2)	25P (2)	10,000P (30)	5,000P (30)	500P (30-360)	200P (30-360)
	HN-3	1400P	600P	1,000P (2-360)	-	-	-	75P (2-360)	25P (2-360)	10,000P (30-360)	5,000P (30-360)	500P (30-360)	200P (30-360)
	HT	1400P	600P	1,000P (2-360)	-	-	-	75P (2-360)	25P (2-360)	10,000P (30-360)	5,000P (30-360)	500P (30-360)	200P (30-360)
	L	1400P	600P	1,000P (2-360)	-	-	8 S	75P (2-360)	25P (2-360)	5,000 - 10,000P (30-360)	2,500 - 5,000P (30-360)	500P (30-360)	200P (30-360)
	HL	1400P	600P	1,000P (2-360)	-	-	2 S	75P (2-360)	25P (2-360)	10,000P (30-360)	5,000P (30-360)	500P (30-360)	200P (30-360)

COMPARATIVE VOLATILITY OF CHEMICAL WARFARE AGENTS

Agent	Volatility (mg/m^3) at 25°C
Hydrogen cyanide (HCN)	1,000,000
Sarin (GB)	22,000
Soman (GD)	3,900
Sulfur mustard	900
Tabun (GA)	610
Cyclosarin (GF)	580
VX	10
VR ("Russian VX")	9

Data source: US Departments of the Army, Navy, and Air Force. *Potential Military Chemical/Biological Agents and Compounds*. Washington, DC: Headquarters, DA, DN, DAF; December 12, 1990. Field Manual 3-9. Naval Facility Command P-467. Air Force Regulation 355-7.

SIGNS AND SYMPTOMS REPORTED BY TOKYO HOSPITAL WORKERS TREATING VICTIMS OF SARIN SUBWAY ATTACKS*

Symptom	Number/percentage of the 15 physicians who treated patients at UH		Number/percentage of 472 care providers reporting symptoms at SLI	
Dim vision	11	73%	66	14%
Rhinorrhea	8	53%	No information	
Dyspnea (chest tightness)	4	27%	25	5.3%
Cough	2	13%	No information	
Headache	No information		52	11%
Throat pain	No information		39	8.3%
Nausea	No information		14	3.0%
Dizziness	No information		12	2.5%
Nose pain	No information		6	1.9%

*Data reflect reported survey of self-reported symptomatology of physicians at the University Hospital of Metropolitan Japan emergency department and all hospital workers at Saint Luke's International Hospital exposed to sarin vapors from victims of the Tokyo subway attack.

SLI: Saint Luke's International Hospital

UH: University Hospital

Data sources: (1) Nozaki H, Hori S, Shinozawa Y, et al. Secondary exposure of medical staff to sarin vapor in the emergency room. *Intensive Care Med*. 1995;21:1032-1035. (2) Okumura T, Suzuki K, Fukuda A, et al. The Tokyo subway sarin attack: disaster management, Part 1: community emergency response. *Acad Emerg Med.* 1998;5:613-617. (3) Okumura T, Suzuki K, Fukuda A, et al. The Tokyo subway sarin attack: disaster management, Part 2: Hospital response. *Acad Emerg Med.* 1998;5:618-624.

TABLE 21-3

MANAGEMENT OF MILD TO MODERATE NERVE AGENT EXPOSURES

		Management			
		Antidotes*		**Benzodiazepines (if neurological signs)**	
Nerve Agents	**Symptoms**	**Age**	**Dose**	**Age**	**Dose**
• Tabun • Sarin • Cyclosarin • Soman • VX	• Localized sweating • Muscle fasciculations • Nausea • Vomiting • Weakness/floppiness • Dyspnea • Constricted pupils and blurred vision • Rhinorrhea • Excessive tears • Excessive salivation • Chest tightness • Stomach cramps • Tachycardia or bradycardia	Neonates and infants up to 6 months old	**Atropine** 0.05 mg/kg IM/IV/IO to max 4 mg or 0.25 mg AtroPen† and **2-PAM** 15 mg/kg IM or IV slowly to max 2 g/hr	Neonates	**Diazepam** 0.1–0.3 mg/kg/dose IV to a max dose of 2 mg, or **Lorazepam** 0.05 mg/kg slow IV
		Young children (6 months old–4 yrs old)	**Atropine** 0.05 mg/kg IM/IV/IO to max 4 mg or 0.5 mg AtroPen and **2-PAM** 25 mg/kg IM or IV slowly to max 2 g/hr	Young children (30 days old–5 yrs old)	**Diazepam** 0.05–0.3 mg/kg IV to a max of 5 mg/dose or **Lorazepam** 0.1 mg/kg slow IV not to exceed 4 mg
		Older children (4–10 yrs old)	**Atropine** 0.05 mg/kg IV/IM/IO to max 4 mg or 1 mg AtroPen and **2-PAM** 25–50 mg/kg IM or IV slowly to max 2 g/hr	Children (≥ 5 yrs old)	**Diazepam** 0.05–0.3 mg/kg IV to a max of 10 mg/dose or **Lorazepam** 0.1 mg/kg slow IV not to exceed 4 mg
		Adolescents (≥ 10 yrs old) and adults	**Atropine** 0.05 mg/kg IV/IM/IO to max 4 mg or 2 mg AtroPen and **2-PAM** 25–50 mg/kg IM or IV slowly to max 2 g/hr	Adolescents and adults	**Diazepam** 5–10 mg up to 30 mg in 8 hr period or **Lorazepam** 0.07 mg/kg slow IV not to exceed 4 mg

2-PAM: 2-pralidoxime
IM: intramuscular
IO: intraosseous
IV: intraveneous
PDH: Pediatrics Dosage Handbook

*In general, pralidoxime should be administered as soon as possible, no longer than 36 hours after the termination of exposure. Pralidoxime can be diluted to 300 mg/mL for ease of intramuscular administration. Maintenance infusion of 2-PAM at 10–20 mg/kg/hr (max 2 g/hr) has been described. Repeat atropine as needed every 5–10 minutes until pulmonary resistance improves, secretions resolve, or dyspnea decreases in a conscious patient. Hypoxia must be corrected as soon as possible.

†Meridian Medical Technologies Inc, Bristol, Tenn.

Data sources: (1) Rotenberg JS, Newmark J. Nerve agent attacks on children: diagnosis and management. *Pediatrics*. 2003;112:648–658. (2) Pralidoxime [package insert]. Bristol, Tenn: Meridian Medical Technologies, Inc; 2002. (3) AtropPen (atropine autoinjector) [package insert]. Bristol, Tenn: Meridian Medical Technologies, Inc; 2004. (4) Henretig FM, Cieslak TJ, Eitzen Jr EM. Medical progress: biological and chemical terrorism. *J Pediatr*. 2002;141(3):311–326. (5) Taketomo CK, Hodding JH, Kraus DM. *American Pharmacists Association: Pediatric Dosage Handbook*. 13th ed. Hudson, Ohio; Lexi-Comp Inc: 2006.

TABLE 21-4

MANAGEMENT OF SEVERE NERVE AGENT EXPOSURE

		Management			
		Antidotes*		Benzodiazepines (if neurological signs)	
Nerve Agents	**Severe Symptoms**	**Age**	**Dose**	**Age**	**Dose**
• Tabun • Sarin • Cyclosarin • Soman • VX	• Convulsions • Loss of consciousness • Apnea • Flaccid paralysis • Cardio-pulmonary arrest • Strange and confused behavior • Severe difficulty breathing • Involuntary urination and defecation	Neonates and infants up to 6 months old	**Atropine** 0.1 mg/kg IM/IV/IO or 3 doses of 0.25mg AtroPen† (administer in rapid succession) and **2-PAM** 25 mg/kg IM or IV slowly, or 1 Mark I† kit (atropine and 2-PAM) if no other options exist	Neonates	**Diazepam** 0.1–0.3 mg/kg/dose IV to a max dose of 2 mg, or **Lorazepam** 0.05 mg/kg slow IV
				Young children (30 days old–5 yrs and adults	**Diazepam** 0.05–0.3 mg/kg IV to a max of 5 mg/dose, or **Lorazepam** 0.1 mg/kg slow IV not to exceed 4 mg
		Young children (6 months old–4 yrs old)	**Atropine** 0.1 mg/kg IV/IM/IO or 3 doses of 0.5mg AtroPen (administer in rapid succession) and **2-PAM** 25–50 mg/kg IM or IV slowly, or 1 Mark I kit (atropine and 2-PAM) if no other options exist	Children (≥ 5 yrs old)	**Diazepam** 0.05-0.3 mg/kg IV to a max of 10 mg/dose, or **Lorazepam** 0.1 mg/kg slow IV not to exceed 4 mg
		Older children (4–10 yrs old)	**Atropine** 0.1 mg/kg IV/IM/IO or 3 doses of 1mg AtroPen (administer in rapid succession) and **2-PAM** 25–50 mg/kg IM or IV slowly, 1 Mark I kit (atropine and 2-PAM) up to age 7, 2 Mark I kits for ages > 7–10 yrs	Adolescents and adults	**Diazepam** 5–10 mg up to 30 mg in 8-hr period, or **Lorazepam** 0.07 mg/kg slow IV not to exceed 4 mg
		Adolescents (≥ 10 yrs old) and adults	**Atropine** 6 mg IM or 3 doses of 2 mg AtroPen (administer in rapid succession) and **2-PAM** 1800 mg IV/IM/IO, or 2 Mark I kits (atropine and 2-PAM) up to age 14, 3 Mark I kits for ages ≥ 14 yrs		

IM: intramuscular
IO: intraosseous
IV: intravenous

*In general, pralidoxime should be administered as soon as possible, no longer than 36 hours after the termination of exposure. Pralidoxime can be diluted to 300 mg/mL for ease of intramuscular administration. Maintenance infusion of 2-PAM at 10–20 mg/kg/hr (max 2 g/hr) has been described. Repeat atropine as needed every 5–10 min until pulmonary resistance improves, secretions resolve, or dyspnea decreases in a conscious patient. Hypoxia must be corrected as soon as possible. †Meridian Medical Technologies Inc, Bristol, Tenn.

Data sources: (1) Rotenberg JS, Newmark J. Nerve agent attacks on children: diagnosis and management. *Pediatrics*. 2003;112:648–658. (2) Pralidoxime [package insert]. Bristol, Tenn: Meridian Medical Technologies, Inc; 2002. (3) AtroPen (atropine autoinjector) [package insert]. Bristol, Tenn: Meridian Medical Technologies, Inc; 2004. (4) Henretig FM, Cieslak TJ, Eitzen Jr EM. Medical progress: biological and chemical terrorism. *J Pediatr*. 2002;141(3):311–326. (5) Taketomo CK, Hodding JH, Kraus DM. *American Pharmacists Association: Pediatric Dosage Handbook*. 13th ed. Hudson, Ohio: Lexi-Comp Inc; 2006.

Sarin (GB)

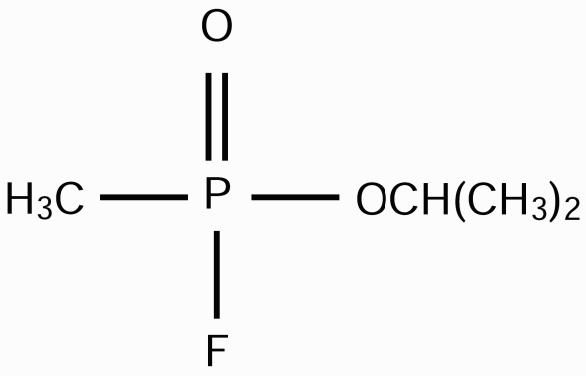

Soman (GD)

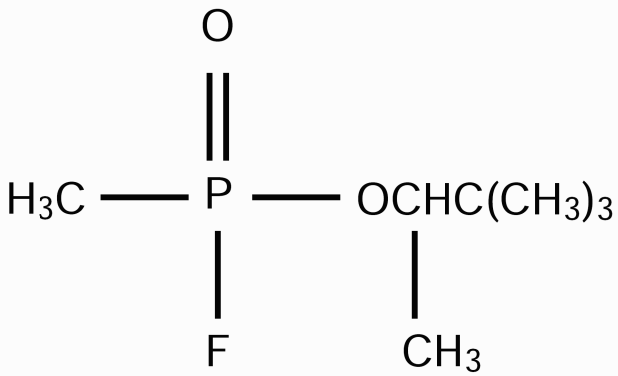

Cyclosarin (GF)

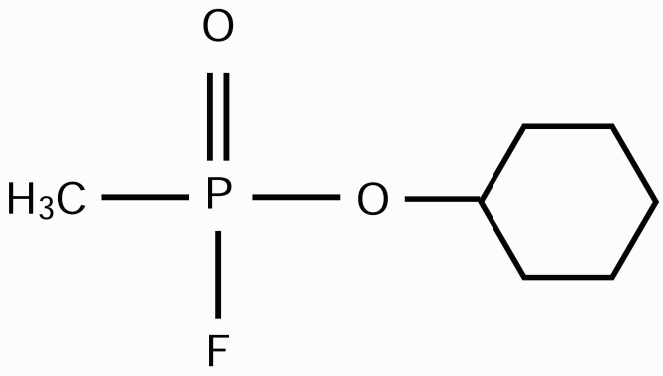

Tabun (GA)

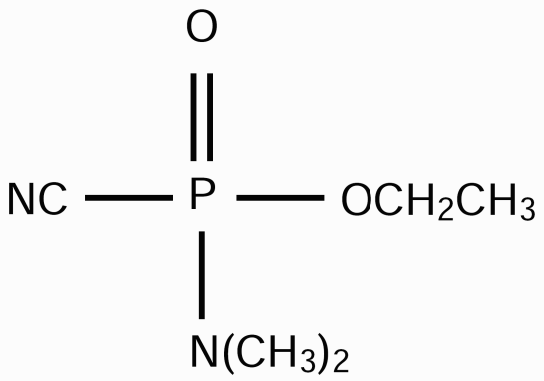

VX

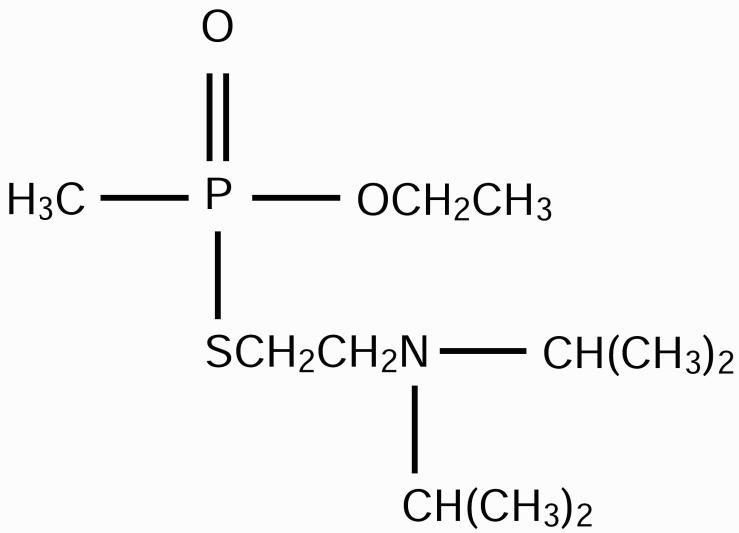

Russian VX

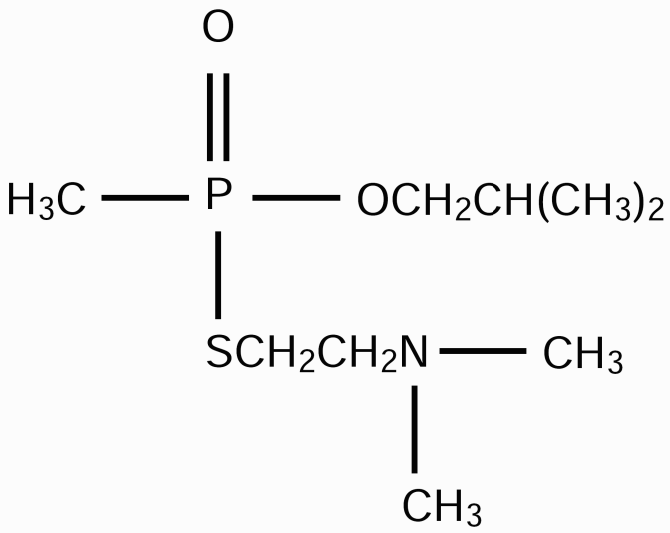

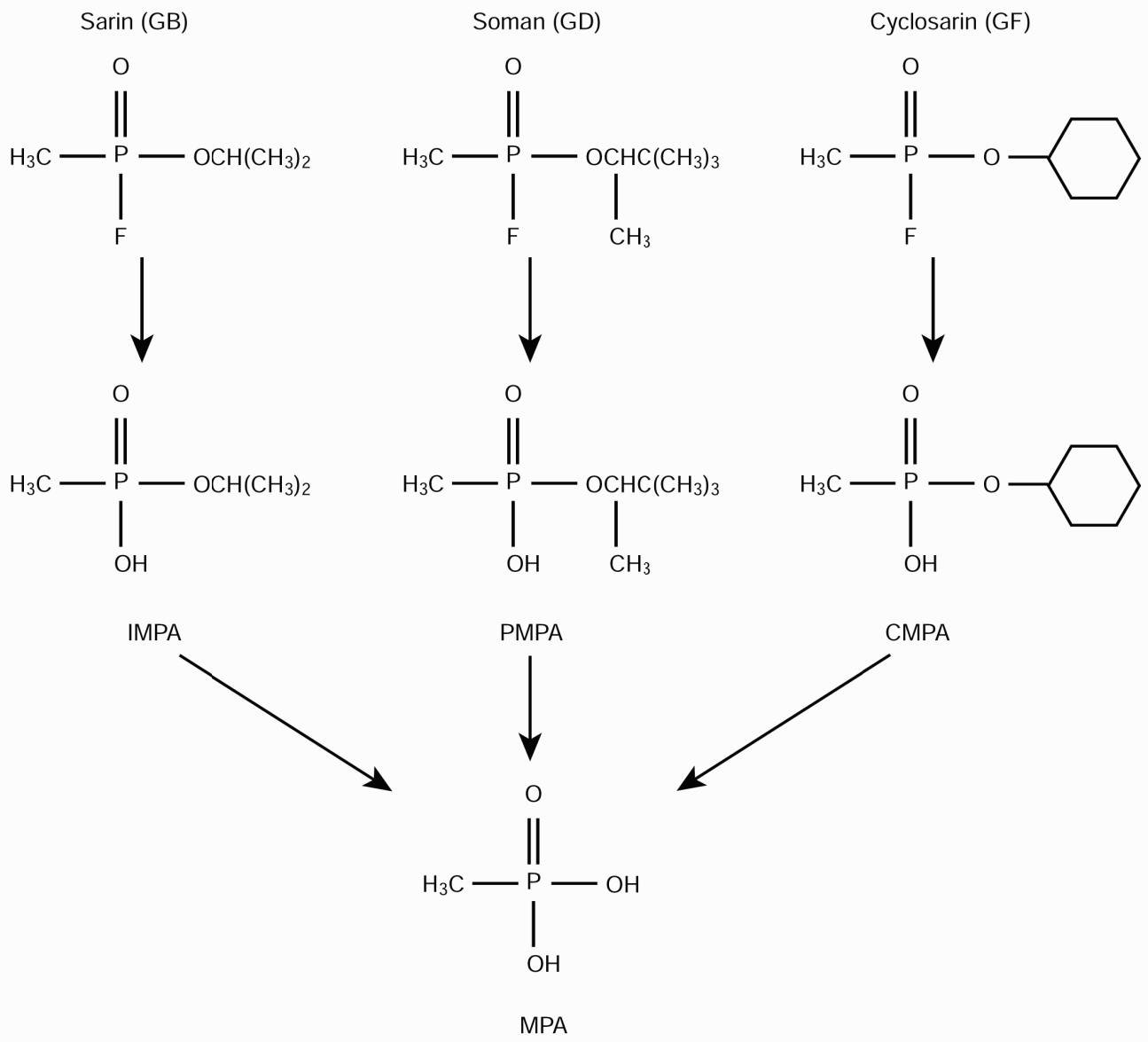

Fig. 22-2. Hydrolysis pathway of sarin (GB), soman (GD), and cyclosarin (GF). Hydrolysis pathway of nerve agents proceeds through the alkyl methylphosphonic acids IMPA, PMPA, and CMPA to MPA. Analysis of the alkyl methylphosphonic acids allows identification of the parent agent, while assay of MPA is nonspecific.
CMPA: cyclohexyl methylphosphonic acid
IMPA: isopropyl methylphosphonic acid
MPA: methylphosphonic acid
PMPA: pinacolyl methylphosphonic acid

STANFORD RESEARCH INSTITUTE
MENLO PARK, CALIFORNIA
SRI

42522

January 1963

Volume I

FALLOUT AND RADIOLOGICAL COUNTERMEASURES

Prepared for:

OFFICE OF CIVIL DEFENSE
DEPARTMENT OF DEFENSE
WASHINGTON, D.C.

By: Carl F. Miller

SRI Project No. IM-4021

Approved:

Robert A. Harker

ROBERT A. HARKER, DIRECTOR
MANAGEMENT SCIENCES DIVISION

This report has been reviewed in the Office of Civil Defense and approved for publication. Approval does not signify that the contents necessarily reflect the views and policies of the Office of Civil Defense.

CONTENTS

1 THE NATURE OF FALLOUT 1

1.1 Background 1

1.2 A General Description of Fallout 3

1.3 Characteristic Types of Fallout 4

1.4 Potential Hazards from Fallout 4

1.5 Radioactive Decay 7

1.6 The Standard Intensity and Contour Properties 9

Chapter 1 References 11

2 FORMATION OF FALLOUT PARTICLES 13

2.1 General Definition of the Process 13

2.2 Mass-Chain Yields for the Fission of U-235, U-238 and Pu-239 17

2.3 The Structure and Composition of Individual Fallout Particles 28

2.3.1 Low Yield, Surface Shot, Silicate Soil 28

2.3.2 Low Yield, Underground Shot, Silicate Soil 31

2.3.3 Large Yield, Surface Shot, Coral 37

2.3.4 Tower Shot, Silicate Soil 38

2.3.5 Tower Shot, Coral Soil 41

2.3.6 Surface Shot, Ocean (Sea Water) 45

2.3.7 Inferences on Fallout-Particle Formation Processes 48

2.4 Properties of Small Fallout Particles from Detonations at Weapons Tests 72

2.5 Redistribution of Deposited Fallout 78

2.6 The Collection and Retention of Fallout Particles by Plant Foliage 81

Chapter 2 References 93

CONTENTS

3 A THERMODYNAMIC MODEL OF FALLOUT FORMATION 97

3.1 The Condensation Process 97
3.1.1 Gas-Liquid Phase Condensation 99
3.1.2 Gas-Liquid Phase: Material Balance Constraints and Fractionation Numbers 106
3.1.3 Gas-Liquid Phase Condensation--Particle-Size Effects 111

3.2 The Dependence of Fireball Parameters on Weapon Yield and Time After Detonation 115

3.3 Estimates of Fireball Parameters for a Model Surface Burst on a Soil Consisting of Silicate Minerals 133

3.4 Process for Estimating the Concentration of Liquid Soil in the Fireball of a Model Surface Burst and the Fractionation Numbers of the Radionuclides 146

3.5 Computing the Decay Rates of Fission Product Mixtures . . . 177

Chapter 3 References 201

4 DISTRIBUTION OF FALLOUT PARTICLES FOLLOWING A NUCLEAR DETONATION 203

4.1 General Description of the Fallout Distribution Process . . . 203
4.1.1 The Particle Source Geometry 203
4.1.2 The Particle Fall Trajectory 203
4.1.3 Radiological Factors 204

4.2 Mathematical Descriptions of the Fallout Distribution Process 204
4.2.1 Scaling Methods 204
4.2.2 Mathematical Models 204

4.3 Descriptive Features of a Simplified Fallout Scaling System for Land Surface Detonations 206
4.3.1 General Description of the Scaling Method 206
4.3.2 Particles Falling from Cloud Altitudes 207
4.3.3 Particles Falling from Stem Altitudes 211
4.3.4 Methods for Estimating the Dynamics of the Fallout Deposition 220
4.3.5 Estimation of Ionization Rate and Exposure Dose . . . 223

Chapter 4 References 227

CONTENTS

5 CORRELATION OF SCALING MODEL PARAMETERS WITH OBSERVED FALLOUT-PATTERN FEATURES 220

5.1 General Description of Fallout Patterns from Land Surface Detonations 220

5.2 General Conditions to Which the Source Data Apply 231

5.3 Scaling Functions for Fallout Pattern Features of Interest . . 232
5.3.1 Intensity Ridge Near Ground Zero 232
5.3.2 Location of the Downwind Standard Intensity Contour for Fallout from Stem Altitudes 237
5.3.3 Stem Pattern Half-Width 239
5.3.4 The Distance to Fallout Pattern Features for Fallout from Cloud Altitudes 239
5.3.5 The Intensity Levels of Pattern Features for Fallout from Cloud Altitudes 241
5.3.6 The Maximum Pattern Width 243
5.3.7 Areas and Fraction of Total Activity Within Intensity Contours 245

5.4 Summary of Derived Idealized Fallout Pattern Scaling Functions 249

5.5 Illustrative Computations for the Use of the Simplified Fallout Scaling System 255
5.5.1 Construction of Idealized Fallout Patterns 255
5.5.2 Fallout Arrival Rate and Exposure Dose During Fallout Arrival 259
5.5.3 Method for Estimating the Particle Sizes in the Fallout at a Given Location 270

5.6 The Effect of Cross-Wind Shear on the Fallout Pattern Scaling System 288

5.7 Comparison of Several Fallout Pattern Computations 295

Chapter 5 References 299

6 IONIZATION RATE CONTOUR RATIOS AND COMPOSITION OF FALLOUT 301

6.1 Definition and Use of Ionization Rate Contour Ratios 301

6.2 Dependence of the Mass Contour Ratio on Detonation Conditions and Other Parameters 302

CONTENTS

6.2 Continued
6.2.1 Dependence on Weapon Type and Yield 302
6.2.2 Dependence on Downwind Distance from Shot Point 304
6.2.3 Dependence on Height or Depth of Burst 326
6.2.4 Mass Contour Ratio for Fallout from a Surface Detonation on Deep Sea Water 327
6.2.5 Mass Contour Ratio for Fallout from Detonations in Harbors 330
6.2.6 Mass Contour Ratio for Fallout from a 1-MT Detonation at Several Detonation Geometries 335

6.3 Fission-Product and Fraction-of-Device Contour Ratios 338

6.4 Foliage-Contamination Factor Contour Ratio 339
6.4.1 Insoluble-Nuclide Fractions 341
6.4.2 Soluble-Nuclide Fractions 342
6.4.3 Variation of the Foliage-Contamination Factor with Particle Size 342

Chapter 6 References 349

ILLUSTRATIONS

Figure		Page
2.1	Thin Sections and Radiographs of Some Fallout Particles from a Small-Yield Surface Shot at the Nevada Test Site	29
2.2	Thin Section and Radiograph of a Fallout Particle from a Small-Yield Surface Shot at the Nevada Test Site	33
2.3	Thin Section and Radiograph of an Angular Fallout Particle from a Large-Yield Surface Shot at the Eniwetok Proving Ground	34
2.4	Section of a Fallout Particle from a Large-Yield Surface Shot at the Eniwetok Proving Ground	35
2.5	Thin Section and Radiograph of a Spherical Fallout Particle from a Large-Yield Surface Shot at the Eniwetok Proving Ground	37
2.6	Two Fallout Particles from a Tower Shot at the Nevada Test Site	39
2.7	Thin Section and Radiograph of a Fallout Particle from a Moderate-Yield Tower Shot at the Nevada Test Site	40
2.8	Thin Section and Radiograph of a Fallout Particle from a Moderate-Yield Tower Shot at the Eniwetok Proving Ground	43
2.9	Thin Section and Radiograph of a Fallout Particle from a Moderate-Yield Tower Shot at the Eniwetok Proving Ground	44
2.10	Photomicrograph of a Dichromate Reagent Film of an Individual Liquid Fallout Particle from a Large-Yield Barge Shot at the Eniwetok Proving Ground	46

ILLUSTRATIONS

Figure		Page
2.11	Electronmicrograph of the Radioactive Solids in the Liquid Fallout Particles from a Large-Yield Barge Shot at the Eniwetok Proving Ground	47
2.12	Calculated Fraction of Mass Chains 89, 90, 137, and 140 Condensed as a Function of Time after Fission with Indicated Non-condensing Elements	64
2.13	Plot of Calculated r_0 (A) Values for Mass Numbers 90, 137, and 140 against Those of Mass Number 89 for the Assumption that Only the Alkali Metal Elements and Alkaline Earth Elements in the Chain Condense	65
2.14	Reduction in the Ionization Rate at the Center of 10th Street and at the Center of the Plaza, Camp Parks, California	82
2.15	Accumulated Distribution of Number of Particles Having Different Diameters on Foliage	83
2.16	Distribution of Activity as a Function of Particle Diameter for Local Collections of Fallout from Tower-Mounted Detonations	86
3.1	Fraction of Nitrogen Molecules Dissociated as a Function of Temperature and Total Pressure	122
3.2	Fraction of Oxygen Molecules Dissociated as a Function of Temperature and Pressure	123
3.3	The Calculated Variation of n/W, P_s, n_s/n, and n_s/W with Assumed Values of T_s(s) for the Model Surface-Burst Fireball	140
3.4	Comparison of Calculations of the Activity and Photon Emission Rate of the Fission Products from 14-Mev Neutron Fission of U-238 with Those from 8-Mev Neutron Fission of U-238 Given as a Ratio of the Two with Time after Fission	183

ILLUSTRATIONS

Figure		Page
3.5	The Gross Air Ionization Rate Fractionation Number, r_{fp}, Relative to the Ionization Rate of the Fission Products from Thermal Neutron Fission of U-235, for the Fission Product Mixtures from Other Fissile Nuclides and Neutron Energies	185
3.6	The Gross Air Ionization Rate Fractionation Number, r_{fp}, Relative to the Ionization Rate of the Fission Products from Thermal Neutron Fission of U-235, for the Fission Product Mixtures from Other Fissile Nuclides and Neutron Energies	186
3.7	The Number of Photons per Disintegration for the Normal Mixture of Fission Products from 8-Mev Neutron Fission of U-238	188
3.8	The Average Energy of the Photons from the Normal Mixture of Fission Products from 8-Mev Neutron Fission of U-238	189
3.9	The Relative Response of the AN/PDR-39(T1B) Portable Radiac Held by a Man at 3 Feet above an Extended Plane Area Contaminated with Fission Products from Thermal Fission of U-235	191
3.10	Variation of r_{fp} with Time after Fission for the Fractionated Mixture of Fission Products from 8-Mev Neutron Fission of U-238	193
3.11	The Observed Variation of r_{fp} with Time after Fission for Close-in Fallout from a Low Tower Shot at the Nevada Test Site	195
5.1	Schematic Outline for the Intensity Profile Downwind from Ground Zero along the Axis of the Fallout Pattern (y = 0) as Used in the Simplified Fallout Pattern Scaling System	233
5.2	Intensity-Distance Plots for Construction of an Idealized Fallout Pattern for a 1-MT Yield Surface Detonation for a Wind Speed of 15 mph	257

ILLUSTRATIONS

Figure		Page
5.3	Idealized Fallout Pattern for a 1-MT Yield Surface Burst for a Wind Speed of 15 mph and 100 Percent Fission	258
5.4	First Estimate of the Dependence of $K_0(1)\ A_\alpha$ on α for a 1-MT Surface Detonation and Wind Speed of 15 mph	260
5.5	Variation of $K_0(1)A_\alpha(\alpha)$ with α at $X = 1.87 \times 10^5$ ft for $W = 10^3$ KT and a Wind Speed of 15 mph	262
5.6	Time of Arrival of the Various Particle Groups Designated by α For a Wind Speed of 15 mph	267
5.7	Rate of Activity Deposition on the Ground as a Function of α at $X = 1.87 \times 10^5$ ft, for $W = 10^3$ KT and a Wind Speed of 15 mph	268
5.8	Rate of Fallout Arrival as a Function of Time after Detonation at $X = 1.87 \times 10^5$ ft for $W = 10^3$ KT and a Wind Speed of 15 mph	269
5.9	Variation of Ionization Rate with Time after Detonation at $X = 1.87 \times 10^5$ ft for $W = 10^3$ KT and a Wind Speed of 15 mph	270
5.10	Variation of α_{max} and α_{min} with Downwind Distance for a 1-MT Yield Surface Detonation and Wind Speed of 15 mph	273
5.11	First Estimate of $K_0(1)A_\alpha$ as a function of $\bar{\alpha}$ for Fallout from Stem Altitudes for a 10^3 KT Yield Surface Burst and a Wind Speed of 15 mph	275
5.12	Variation of the Ionization Rate with Time after Detonation at $X = 3.36 \times 10^4$ ft for $W = 10^3$ KT and a Wind Speed of 15 mph	278
5.13	Vertical Component of the Velocity for Spherical Particles Falling from Various Altitudes to Sea Level	280

ILLUSTRATIONS

Figure		Page
5.14	Accumulated Activity Distribution as a Function of Particle Size at X = 3.35 x 10^4 ft and 1.87 x 10^5 ft Downwind from the 1-MT Yield Surface Burst for a Wind Speed of 15-mph	286
5.15	Comparison of the Gross Activity Distribution on Particles of Various Diameters Derived from the Simplified Fallout Model to Distributions Used in Other Mathematical Fallout Models	287
5.16	Plot of Particle Fall Trajectory Components Relative to Estimated Pattern Center Line for Castle Bravo Winds	292
5.17	Variation of the Calculated Infinite Ideal Plane Standard Intensity with Downwind Distance (Center Line of Pattern) for a 10-MT Yield Surface Detonation (100 percent Fission)	297
6.1	Calculated Ionization Rate as a Function of Time after Detonation for Assumed Condensations up to 60,174 and 406 Seconds after Fission of Fission Products from 8-Mev Neutron Fission of U-238 and an Assumed Surface Burst Total Yield of 14-MT	314
6.2	Estimated Percent of the Fission Product Activity in r/hr at 1 hr from the Fission Products Condensed on Particle Groups with α Values (15-mph Wind Speed) Less than a Stated Value	320
6.3	Proposed Curve for the Variation of f(α) with α for a 15-mph Wind Speed	324
6.4	Proposed Mass Correction Curve to the Mass Contour Ratio as a Function of the Nuclear Scaled Depth of Burst	328
6.5	Proposed Crater Depth Correction Curve for the Mass Contour Ratio as a Function of the Nuclear Scaled Depth	332
6.6	Variation of σ_L with Calculated Values of σ_0	345
6.7	Variation of the Median Particle Diameter of Fallout on Foliage with σ_0 of the Deposited Fallout	347

TABLES

Number		Page
2.1	Fractional Chain Yields for Mass 89 for U-235 Fission	18
2.2	Fractional Chain Yields for Mass 140 for U-235 Fission	19
2.3	Cumulative Mass-Chain Yields of Fission Products	20
2.4	Calculation of Relative Activity Ratios from Kimura's Data on Coral Fallout[28]	51
2.5	Percentage Activities in Ion Exchange Peaks of Different Chemical Groups in Coral Fallout Sample[28]	53
2.6	Summary of Estimated Fractionation Numbers for Beta-Emitting Nuclides in Coral Fallout from No. 5 Fukuryu Maru at D+21 and D+25	54
2.7	Radiochemical Data on Coral Type Fallout Particles from a Large Yield Surface Detonation	57
2.8	Summary of Fractionation Numbers for Mass Numbers 89 and 140 in Coral Fallout Particles	61
2.9	Summary of Fractionation Numbers Relative to Mass Number 89 for Coral and Seawater Fallout Corrected for Appropriate Fission Yields	65
2.10	Comparison of Empirical Fractionation-Correlation Parameters with Those Estimated for Condensation of Alkali and Alkaline Earth Elements of Mass Chains 90, 132, 137, and 140, at Specified Times after Fission	70
2.11	Relative Radioelement Concentrations in Jack Rabbit Bone Tissue at about 20 Days after Detonation of Shot Smoky, Operation Plumbbob, in 1957	75
2.12	Average Fractionation Numbers of Radionuclides in Fallout from Tower- and Balloon-Supported Detonations at the Nevada Test Site	77
2.13	Gross Solubility of Activity from Small Fallout Particles	77

TABLES

Number		Page
2.14	Gross Solubility of Activity from Small Fallout Particles Lodged on Plant Foliage	79
2.15	The Size Distribution and Amount of Fallout Particles Lodged on the Foliage of Different Species of Plants	87
2.16	Collection and Retention of Fallout by Some Forage Crops	88
2.17	The Decontamination of Fallout Particles from Foliage	89
2.18	Summary of Averaged Foliage Contamination Factors for Native Foliage Exposed to Fallout from Tower- and Balloon-Mounted Detonations at the Nevada Test Site	91
3.1	Thermal Properties of Nitrogen and Oxygen as Ideal Gases	124
3.2	The Change in Energy Content and Number of Moles of Gas in Heating 1 Mole of Air as an Ideal Gas from 290°K and 1 Atmospheric Pressure to T°K at Pressures of 1 to 20 Atmospheres	126
3.3	Summary of Values of the Fireball Energy and Gas Content Related to Total Pressure, Volume, and Temperature for Heating Air from 298°K to 8300°K	127
3.4	Summary of Values of n_T/W and p_2 for the Model Air Burst	136
3.5	Thermal Data for Ideal Soil Constituents of Composition $Na_2O \cdot Al_2O_3 \cdot 6SiO_2$	138
3.6	Summary of Calculations for $T_2(s)$ Based on the Assumption of Equal Vapor Densities at the Second Temperature Maximum for the Model Air- and Surface-Burst Fireballs	139
3.7	Summary of Fireball Conditions at the Second Temperature Maximum for the Model Surface Burst of Different Yields Using Eq. 3.132 for $T_2(s)$	141
3.8	Summary of Some Fireball Parameter Values for Various Yields of the Model Surface Burst	147
3.9	Summary of Fireball Parameters and Thermal Data for the 14-MT Yield Model Surface-Burst Fireball	149
3.10	Summary of Estimates of $n(\ell)/V$ for the Model Surface Burst of Different Yields at the Time the Fireball Temperature is 1673°K	153

TABLES

Number		Page
3.11	Summary of Estimates of n(r)/V or n(m)V Based on Fission Content of Fallout	156
3.12	Summary of Empirical Constants for Vaporization Reactions of Fission Products and Other Elements	160
3.13	Summary of Raoult's Law Constants for the Gaseous Species of the Fission Product and Other Elements at 1673° K	166
3.14	Calculated Partial Pressures and Equilibrium Partial Pressures of Some of the More Abundant Fission Product Elements Dispersed Uniformly in the Model Surface-Burst Fireball at 1673° K for a Fission Yield of 14-MT	167
3.15	Summary of $r_n(A)$ Values at 9 and 60 Seconds after Fission for Fission Product Nuclides that Contribute to the Gross Activity at 45.8 Minutes and Longer Times after Fission	169
3.16	Summary of Disintegration Multipliers for the Fission Product and Other Radionuclides[a]	171
3.17	Decay of Normal Fission Products from U-235, U-238, and Pu-239	175
3.18	Summary of H+1 Ionization Rates of Normal Fission Products[a]	187
3.19	Early-Time Ionization Rate, Photon Energy Emission Rate, and Average Photon Energy for Fission Products from Thermal Neutron Fission of U-235	192
3.20	Ionization Rate for Fission Products Condensed on Ideal Soil at 1400°C at 9 Seconds (84-KT) and 60 Seconds (14-MT) after Fission of U-238 (8-Mev Neutrons) and Ratio to That for the Normal Mixture from Fission of U-235 (Thermal Neutrons)	194
3.21	Activity from U-237 for 10^4 Atoms at Zero Time[a]; C(237) = 1	197
3.22	Activity from U-239 for 10^4 Atoms at Zero Time[a]; C(239) = 1	198
3.23	Activity from Np-239 for 10^4 Atoms of U-239 at Zero Time[a]; C(U-239) = 1	199
3.24	Activity from Np-240 for 10^4 Atoms of U-240 at Zero Time[a]; C(U-240) = 1	200

TABLES

Number		Page
4.1	Values of Stem and Fireball-Cloud Geometry Constants for Several Weapon Yields	214
5.1	Equation Parameter Values for the Variation of $\Delta z_{u,n}$ with Wind Speed and Derived Values of $K_{u,n}\bar{A}_f$	237
5.2	Summary of the Relative Wind Speed Shear Factor $S(v_w)$, for the Fallout Pattern Maximum Half-width and Associated Standard Ionization Rate, for Several Wind Speeds	244
5.3	Summary of Fallout Pattern Features and Fallout Scaling System Parameter Values for an Assumed Effective Wind Speed of 15 mph	254
5.4	Comparison of Fallout Pattern Data for a 1-MT Yield Obtained from the Simplified Scaling System Functions and from the ENW Methods	256
5.5	Calculation of Fallout Arrival Rate at $X = 1.87 \times 10^5$ feet, $y = 0$, from a 1-MT Surface Burst for a Wind Speed of 15 mph	261
5.6	Summation of Fallout Rates for α Groups Arriving at the Same Time and Accumulation of Activity and Exposure Dose during the Fallout Period	264
5.7	First Estimate of $K(1)\bar{A}'_\alpha$ as a Function of α for a 1-MT Yield Surface Detonation	274
5.8	Calculated Arrival Times and Dose Rates during the Fallout Period and up to 1.5 hour at the Downwind Distance of 6.8 Miles from a 1-MT Surface Detonation	276
5.9	Diameters of Spherical Particles for Various α Groups Falling at 1.87×10^5 feet and 3.85×10^4 feet Downwind from a 1-MT Yield Surface Detonation Assuming a Wind Speed of 15 mph	284
5.10	Wind Data and Particle Fall Trajectory Components for Jangle "S" Shot	289

TABLES

Number		Page
5.11	Summary of "Equivalent" Uniform Wind Shear from Relative Pattern Spread for the Simple Fallout Scaling System Patterns (Wind Speed of 15 mph)	293
5.12	Ratio of Areas within Stated Standard Intensity Contours for Fallout Patterns Computed	295
6.1	Summary of Fission Product Nuclide $r_i'(A)$ Values for 84-KT and 14-MT Yield Surface Detonations	307
6.2	Equation Constants for Air Ionization Rates from 0.75 to 1.12 Hours after Fission and Fraction of the Total Ionization Rate at H+1 from Fission Products Condensed on Particles at Given Times after Detonation of an 84-KT and a 14-MT Yield Land Surface Burst	311
6.3	Calculated Ionization Rates of Condensed Fission Product Mixtures from U-238 (8-Mev Neutrons) Fission at Selected Condensation Times	313
6.4	Fractionation Numbers for U-238 (8-Mev Neutrons) Fission Products Relative to the Normal Mixture of U-235 (Thermal Neutrons) Fission Products as Calculated for the End of the First Period of Condensation and at 405 Seconds after Detonation	318
6.5	Computation of Particle Size Parameters for Various Condensation Times of the 84-KT and 14-MT Yield Land Surface Detonations	319
6.6	Calculation of $f(\alpha)$ from M_r (1) Data from Operation Jangle Shot "S"	322
6.7	Computation of S_a for Several Detonation Conditions of a 1-MT Fission Weapon	336
6.8	Computation of M_r^{λ} (1) for Several Detonation Conditions of a 1-MT Yield Fission Weapon at Selected Downwind Distances	337
6.9	Summary of Shot Conditions for Estimating the Median Particle-Diameter Designator	343
6.10	Calculation of α_0 for Some Fallout Locations from Shots Apple II and Smoky	344

Table 2.8

SUMMARY OF FRACTIONATION NUMBERS* FOR MASS NUMBERS 89 AND 140 IN CORAL FALLOUT PARTICLES

Particle Description	GIC/f at H+70 (ma/f)x10[9]	R_{99}^{89}	R_{99}^{140}	R_{99}^{140}/R_{99}^{89}
A. Fused Particles				
WS	18.8	0.024	0.015?	0.625
S	18.8	0.012	0.030	2.50
YS	25.2	0.20	-	-
YS	26.9	0.026	0.028	1.08
S	29.0	0.0058?	0.018?	3.14
YI	32.8	0.046	0.14	3.04
YS	34.7	0.023	-	-
YI	35.0	0.041	0.14	3.41
WI	38.8	0.114	0.32	2.81
WI	40.7	0.23	-	-
WS	58.0	0.040	0.20	5.00
Geometric Mean	-	0.050(±150%)	0.10(±180%)	-
B. Irregular Particles				
WI	54.9	1.31	0.62	0.473
WI	75.7	0.64	1.8	2.81
WI	88.6	0.36	-	-
GI	93.1	0.82	2.7	3.29
WI	120	1.0	4.0	4.00
WI	126	1.7	2.6	1.53
I	142	0.52	0.89	1.71
WI	203	2.3	3.6	1.56
GI	218	2.3	4.0	1.74
Geometric Mean	-	1.05(±98%)	2.19(±94%)	-

R_{99}^{89} (U-238 fission) = 1.54xR_{99}^{89} (U-235 fission)

R_{99}^{140} (U-238 fission) = 1.17R_{99}^{140} (U-235 fission)

? Questionable values, not used to calculate means.

Table 2.14

GROSS SOLUBILITY OF ACTIVITY FROM SMALL FALLOUT PARTICLES LODGED ON PLANT FOLIAGE

Plant Type	Distance From Ground Zero (miles)	Fraction Dissolved[a] in 0.1N HCL
1. Shot Apple I (14 KT on 500 ft. Tower)		
Artemisia (Sagebrush)	12	0.20
Ephedra (Mormon tea bush)	40	0.27
Ephedra (Mormon tea bush)	80	0.15
Juniperus (Juniper)	165	0.32
	Average:	0.24
2. Shot Met (22 KT on 400 ft. Tower)		
Larrea (Creosote bush)	20	0.26
Larrea (Creosote bush)	55	0.08
Medicago (Alfalfa)	140	0.14
	Average:	0.16
3. Shot Apple II (29 KT on 500 ft. Tower)		
Triticum (wheat)	7	0.10
Triticum (wheat)	40	0.17
Triticum (wheat)	106	0.35
	Average:	0.24

a. Based on beta count-rate measurements.

Figure 2.14
REDUCTION IN THE IONIZATION RATE AT THE CENTER OF 10TH STREET AND AT THE CENTER OF THE PLAZA, CAMP PARKS, CALIFORNIA, AS A FUNCTION OF THE WIND VECTOR (sum of the products of wind speed · time) FOR WINDS IN EXCESS OF 10 MPH OVER A 10-DAY PERIOD. THE TAGGED PARTICLES WERE 150 TO 300 MICRONS IN DIAMETER

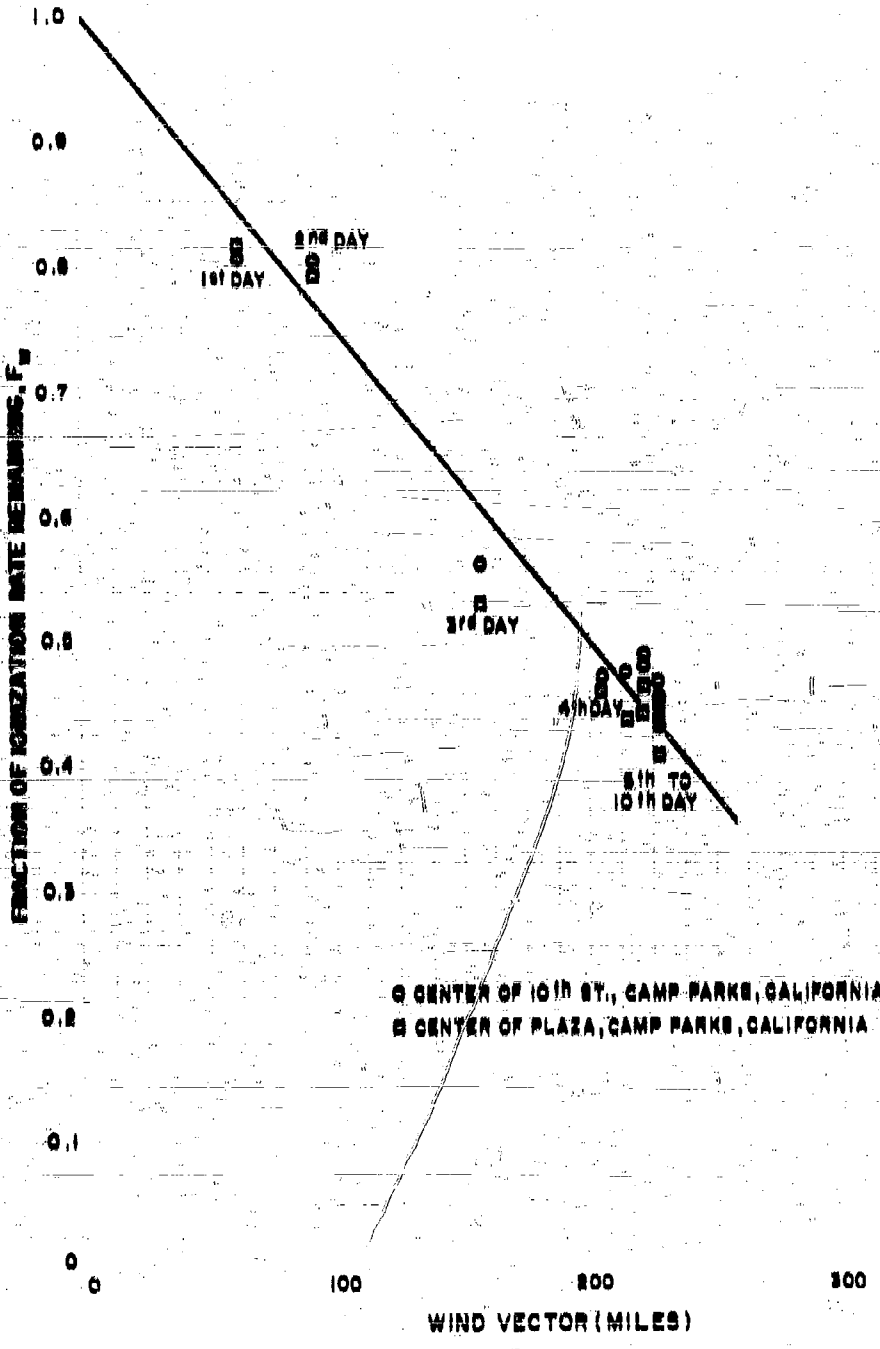

Figure 2.15
ACCUMULATED DISTRIBUTION OF THE NUMBER OF PARTICLES WITH DIFFERENT DIAMETERS ON FOLIAGE

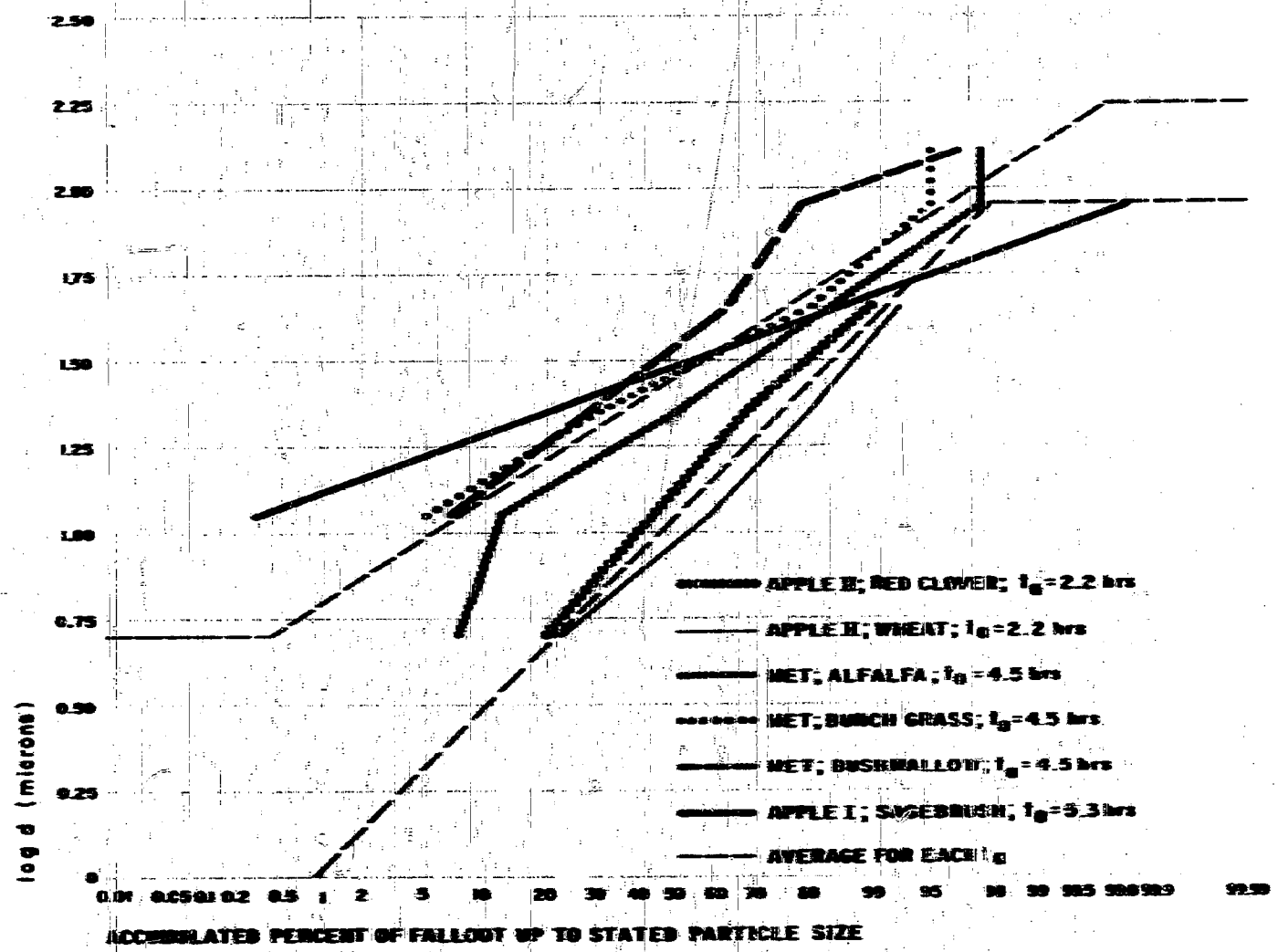

Figure 2.16
DISTRIBUTION OF ACTIVITY AS A FUNCTION OF PARTICLE DIAMETER FOR LOCAL COLLECTIONS OF FALLOUT FROM TOWER-MOUNTED DETONATIONS

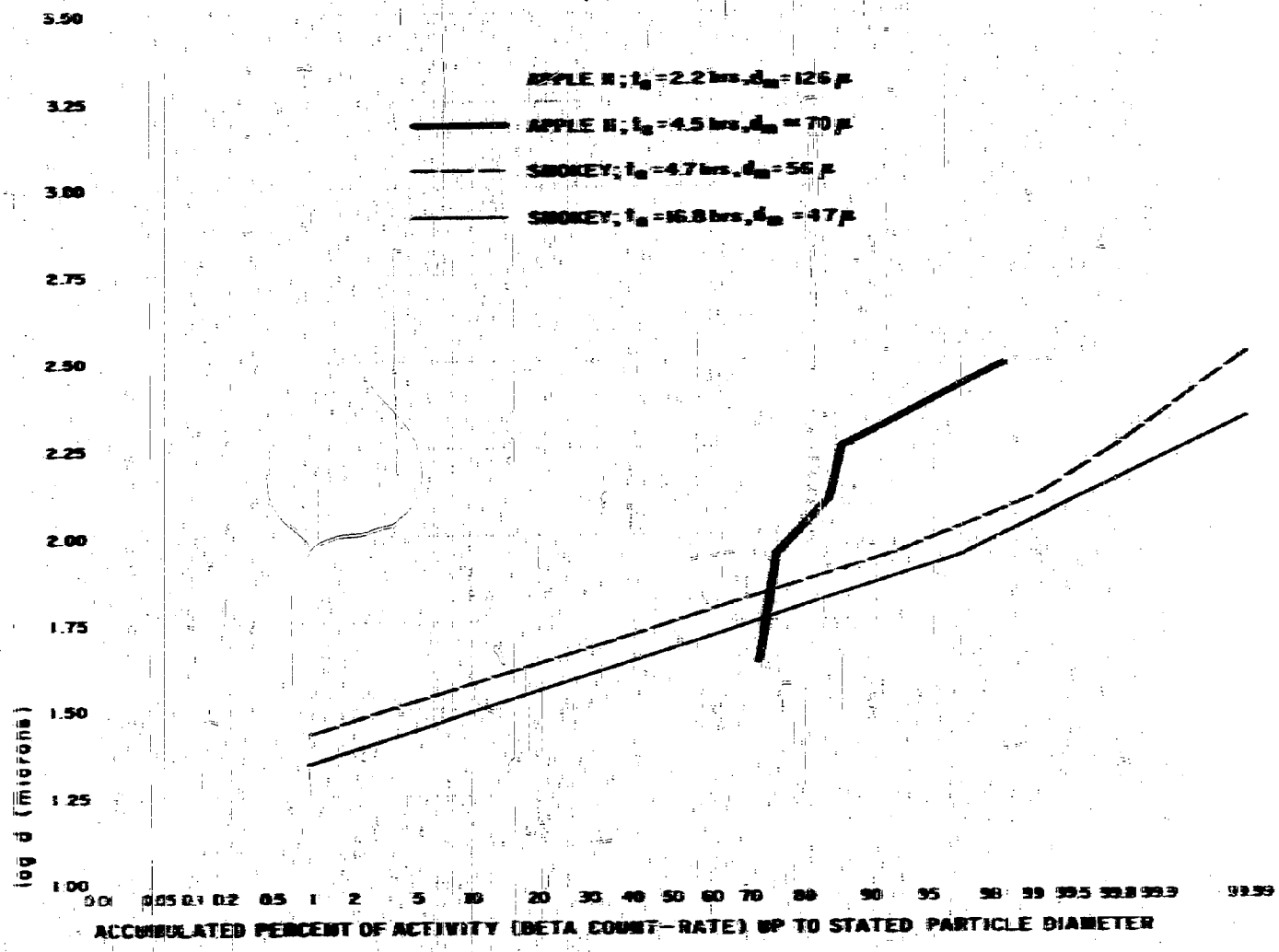

Table 2.17

THE DECONTAMINATION OF FALLOUT PARTICLES FROM FOLIAGE

Plant	Distance From Ground Zero (miles)	Fraction of Gross Activity Remaining on the Foliage After Decontamination*		
		Reagent		
		Water	0.1N HCL	5% EDTA
1. Shot Met (22 KT on a 400 ft. Tower)				
Larrea (Creosote bush)	29	0.52	0.34	0.33
Lepidium (Peppergrass)	58	0.19	0.10	0.05
Artemisia (Sagebrush)	149	0.64	0.51	0.46
2. Shot Apple II (29 KT on a 500 ft. Tower)				
Broad-leaf annual	7	0.022	0.18	0.28
Coleogyne (Black brush)	7	0.28	0.18	0.58
Triticum (wheat)	45	0.18	0.10	0.19
Artemisia Spinescens (Sagebrush)	45	0.32	0.16	0.17
Artemisia Tridentata (Sagebrush)	48	0.33	0.20	0.14
Chrysothamnus (Rabbit brush)	48	0.38	0.29	0.10
Atriplex (Shadscale)	106	0.26	0.26	0.21
Chrysothamnus (Rabbit brush)	106	0.40	0.26	0.11

a. Based on beta count-rate measurements

Table 2.17 (concluded)

Leaf Surface Properties
Larrea – very-resinous Lepidium – glabrous and glaucous Artemisia – dense, matted, unbranched hairs and glands Broad-leaf annual – smooth, veined, sparse hairs Coleogyne – dense, fine hairs Triticum – rows of short hairs, parallel to veins Chrysothamnus – dense, soft, wooly hairs Atriplex – scurfy surface Ephedra – scale-like, muricated branches Juniperus – scale-like, imbricated Oryzopsis – sparse, barb-like hairs Sphaeralcea – dense, stellate hairs Trifolium (clover) – rough, with scattered, unbranched hairs

Table 2.18

SUMMARY OF AVERAGED FOLIAGE CONTAMINATION FACTORS FOR NATIVE FOLIAGE EXPOSED TO FALLOUT FROM TOWER- AND BALLOON-MOUNTED DETONATIONS AT THE NEVADA TEST SITE

Shot	Distance from Ground Zero (miles)	$10^{n} \alpha_L$ (fissions/gm of dry plant / fissions/ft² of total fallout)	$10^{n} \alpha_L^{*}$ (fissions/gm of dry plant / fissions/ft² of ≈44μ fallout)
Tesla, 1955	12	0.008	2.23
	60	0.418	2.21
	79	0.453	2.20
	96	0.524	2.09
Apple I, 1955	12	0.355	2.78
	40	0.522	2.36
	80	0.465	2.02
Met, 1955	20	0.025	13.04
	80	2.37	18.00
	140	2.05	18.23
Apple II, 1955	7	0.002	2.90
	48	0.720	2.32
	106	0.97	2.00
Priscilla, 1957[a]	7	4.80	5.00
	84	2.28	7.27
	129	5.12	6.42
	154	5.20	6.46
	190	4.80	6.16
Diablo, 1957	12	1.91	23.5
	15	1.79	30.0
	20	1.63	17.8
	40	0.25	12.2
	62	12.0	10.5
Shasta, 1957	15	1.52	11.6
	44	1.87	7.72
	76	2.81	5.03
	172	5.10	0.42
Smoky, 1957	48	0.460	2.98
	80	0.370	2.52
	100	0.250	2.85

Table 2.18 (concluded)

Shot	Distance from Ground Zero (miles)	$10^{n}\ a_{T_L}$ $\left(\frac{\text{fissions/gm of dry plant}}{\text{fissions/ft}^2\text{ of total fallout}}\right)$	$10^{n}\ a'_{T_L}$ $\left(\frac{\text{fissions/gm of dry plant}}{\text{fissions/ft}^2\text{ of } \approx 44\mu\text{ fallout}}\right)$
	130	0.520	2.70
	150	1.40	3.12
	175	1.20	2.00
	200	0.002	3.28

a. Balloon-mounted detonation

In order to estimate the number of additional moles of air that have entered the fireball between t_2 and $28.0t_2$, it is assumed that the internal pressure of the fireball at $28.0t_2$ is very close to 1 atmosphere. With this assumption and that of the perfect-gas law, the number of moles of gas in the 14-MT fireball at 60 seconds is

$$n_T = 1.35\times10^7 W \text{ moles} \tag{3.159}$$

The net gain in air molecules, neglecting the small amount of other gases, is

$$\Delta n = n_T - n_0 = 1.11\times10^7 W \text{ moles} \tag{3.160}$$

On this basis, about 80 percent of the fireball gas molecules at 60 seconds is from the air that entered after t_2. The energy required to heat this air from 298°K to 1673°K is

$$Q_4 = 8.90\times10^{10} W \text{ cals} \tag{3.161}$$

Since the energy changes for all processes must equal zero, the remaining amount not accounted for is

$$Q_5 = 8.73\times10^{10} W \text{ cals} \tag{3.162}$$

Assuming that this remainder is utilized to heat and melt soil, the amount of soil that could be liquified (at the melting temperature) plus that condensed from the vapor is

$$\begin{aligned} n(\ell) &= 3.83\times10^5 W + 5.51\times10^4 W \text{ moles} \\ &= 4.38\times10^5 W \text{ moles} \end{aligned} \tag{3.163}$$

Therefore at 1673°K, or 60 seconds after detonation of the 14-MT model surface burst, the gross concentration of the liquid soil is

$$n(\ell)/V = 2.37\times10^{-7} \text{ moles/cm}^3 \tag{3.164}$$

The results of similar computations of $n(\ell)/V$ at 1673°K for values of W from 1- to 10^5-KT are summarized in Table 3.10. Over this large range in yields, the $n(\ell)/V$ values for the model surface burst vary only from about 1.8×10^{-7} to 2.5×10^{-7} moles of soil/cm³. The fractions of the energy required to melt these amounts of soil range from 7.5 to 9.2 percent of the total. For a low yield tower shot, Adams[5] estimated that about 3 percent of the energy was used in heating the soil and tower materials. Since it is expected that a larger fraction of the energy would be utilized in a surface burst, the two estimates are in relative agreement.

208°K and, of course, the energy balance equations do not specify the origin of the gas atoms. Some of the additional air certainly comes from the volume swept out above the fireball as it rises; also, some must enter from the bottom along with the column of soil particles that is formed by the updrafts. The latter is particularly noticeable on the periphery of the columns of the larger yield detonations.

Some estimate of the amount of the crater material that is involved in the formation of $n(\ell)$ can be made, using the crater radius given above and the crater depth, $25W^{1/3}$ feet, as given in ENW. For the crater volume, a cone shape is used, which is somewhat more typical of the shape of craters from the larger yield nuclear weapons than the ellipsoid of revolution of ENW. Taking 110 lb/cu. ft for the soil density gives

$$M_0 = 5.11\times10^{11}\,W^{0.917}\,\text{gm} \tag{3.166}$$

for the amount of soil removed from the crater (yields in the MT range leave no crater lip). The range in the mass of $n(\ell)$ from 1-KT to 10^3-KT according to the model surface burst fireball (mol. wt. 524) is 1.93×10^{11}W gms to 2.35×10^{11}W gms; with the crater mass of Eq. 3.166, the corresponding range in the percentage of the crater mass that forms $n(\ell)$ is from 3.8 percent to 12 percent, respectively. In terms of the model, these are the fractions of the crater mass that have entered the fireball up to 1.0 and 122 seconds after detonation, providing no significant amounts of melted soil have fallen out of the fireball volume during this period.

It is clear that the $n(\ell)/V$ ratios, as calculated, assume that many soil particles have entered the fireball and that none have left. If a large number of particles have been ejected from the fireball during the period when the liquid soil can exist, then the computed values of $n(\ell)/V$ are too large. However, the assumption that only an insignificant fraction of the particles leave the fireball during the period when the more refractory fission products condense should be valid because of the short times involved. If it is further assumed that the mixing in the volume is rather uniform and that equilibrium conditions exist between the liquid particles and vapor, then estimates can be made of $n(\ell)$ (or of $n(s)$ if complete condensation of all the elements does not occur at temperatures above the melting point of the carrier) from observed values of the concentration of fission product elements in fallout.

The condensation of the more refractory fission-product elements occurs independently of the state of the carrier material. All that is required is the presence of a macroscopic condensed phase, liquid or solid, on which the vapor can condense. When complete condensation of one or more of the fission product

Figure 3.7
NUMBER OF PHOTONS PER DISINTEGRATION FOR THE NORMAL MIXTURE OF FISSION PRODUCTS FROM 8-Mev NEUTRON FISSION OF U-238

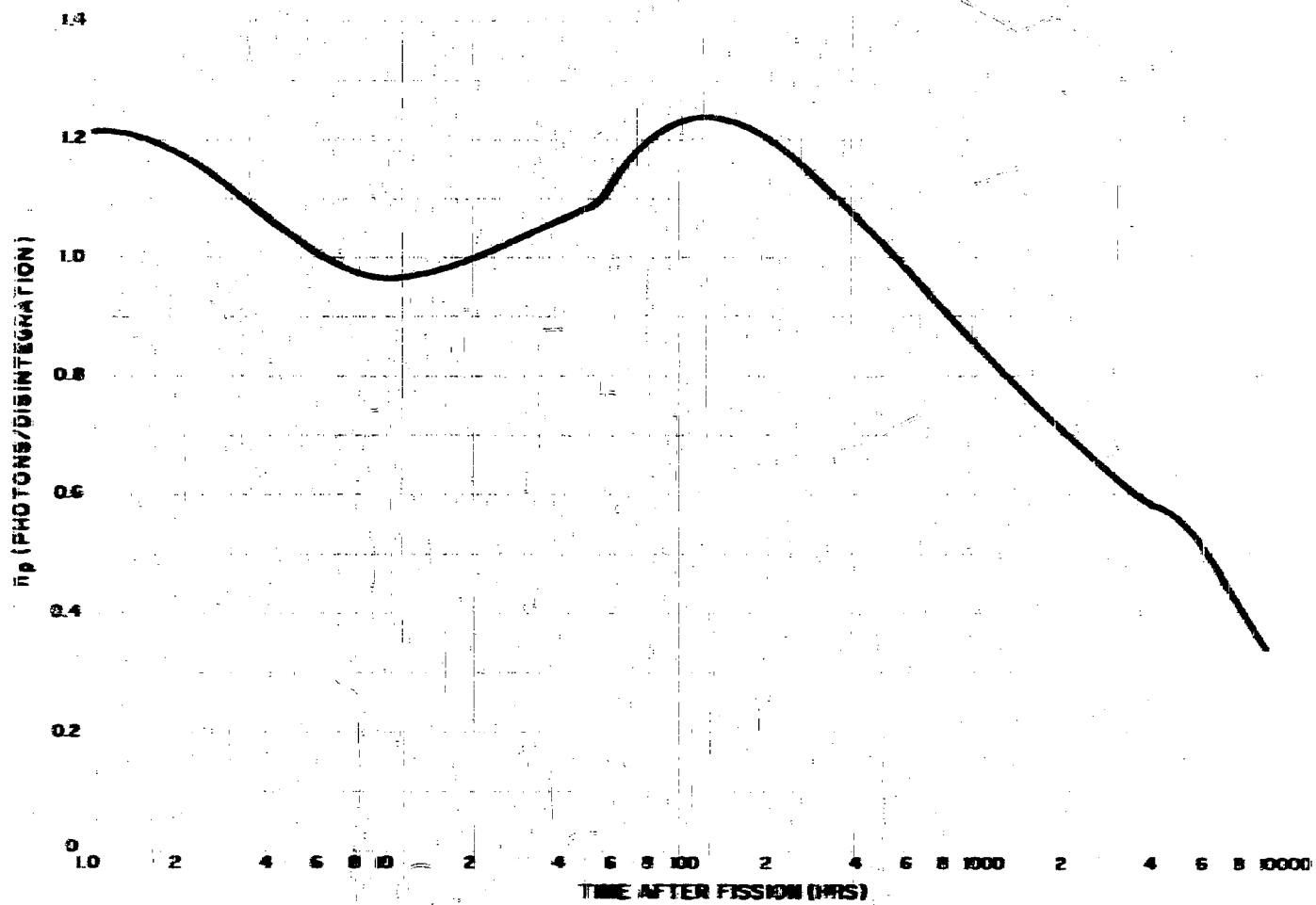

Figure 3.8
AVERAGE ENERGY OF THE PHOTONS FROM THE NORMAL MIXTURE OF FISSION PRODUCTS FROM 8-Mev NEUTRON FISSION OF U-238

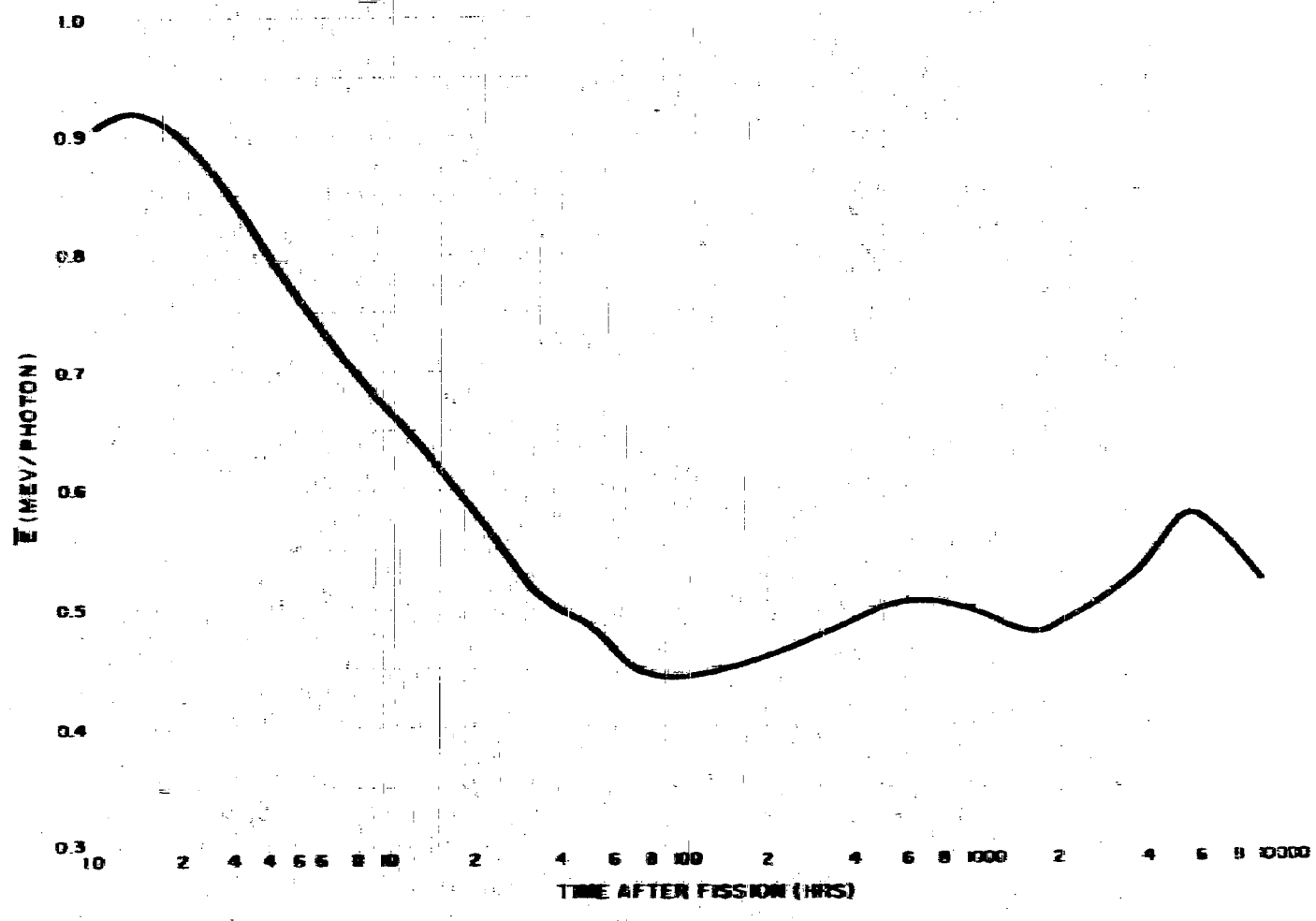

The ratio of the response of an AN/PDR 39(TIB) radiac held by a man at about 3 feet above a uniform distribution of fission products over a plane area to the calculated air ionization rate is shown in Figure 3.9 as a function of time after fission. The instrument, for the indicated response, is held by a man and is calibrated with a Co-60 standard source.[15] The ratio varies from about 73 to 77 percent; most of the reduction in the ionization rate measured is due to attenuation of the gamma rays by the person holding the instrument and by the batteries and other dense materials near the ion chamber of the instrument.

The only estimates of the ionization rate of mixed fission products at early times after fission available are those for the products of thermal neutron fission of U-235. The data, and calculations of the gamma energy release, from these fission products at early times, after fission have been summarized by Zigman and Mackin.[16] This summary of the gamma ray abundances is converted to the ionization rates, photon energy emission rate, and average photon energies given in Table 3.19. To adjust the ionization rate values calculated from the data of Zigman and Mackin to those of Table 3.17 at 45.5 minutes, the former were increased by 22.5 percent; this adjustment provides a smooth join of the ionization rate decay curve from the early to the later times.

The computed ionization rates for the fission product elements condensed in the liquid of the ideal soil when it solidifies at 1400°C (end of the first period of condensation) for times of 9 seconds (84-KT) and 60 seconds (14-MT) are given in Table 3.20 for 8-Mev neutron fission of U-238. Also given are the r_{f_n} values, with respect to the normal fission-product mixture from thermal neutron fission of U-235. The variation in Figure 3.10 of the computed values of r_{f_n} with time after fission shows that the dependence of the fractionation on times of condensation of 9 seconds and 60 seconds (84-KT and 14-MT, respectively) is not large, but that between about 2 hours and 4000 hours after fission the mixture from the lower yield is more highly fractionated.

The minimum in the curve at 2 hours is due to major depletions in Cs and Te, whereas the minimum at about 200 hours is due to depletions in I-131 and Ba-140 - La-140. The maximum in the curve, at 3500 hours, results from the high abundance of Zr-95 - Nb-95, and the peaks at times longer than 10,000 hours are due to the high yields of the rare earth elements from U-238 fission products with respect to the U-235 fission products.

The observed variation in r_{f_n} with time after fission as measured with a standard ionization chamber, is shown in Figure 3.11 for the fallout from a low tower shot.[20] The observed r_{f_n} value at 1 hour after detonation is very close to the values computed for the larger yields and with the exception of some details in the curve that may be due in part to the response characteristics of the ion chamber and, in part, to the type of fission, the calculated curves follow the trend of the observed curve quite well.

Figure 3.9
RELATIVE RESPONSE OF THE AN/PDR-39(T1B) PORTABLE RADIAC HELD BY A MAN AT 3 FEET ABOVE AN EXTENDED PLANE AREA CONTAMINATED WITH FISSION PRODUCTS FROM THERMAL NEUTRON FISSION OF U-235

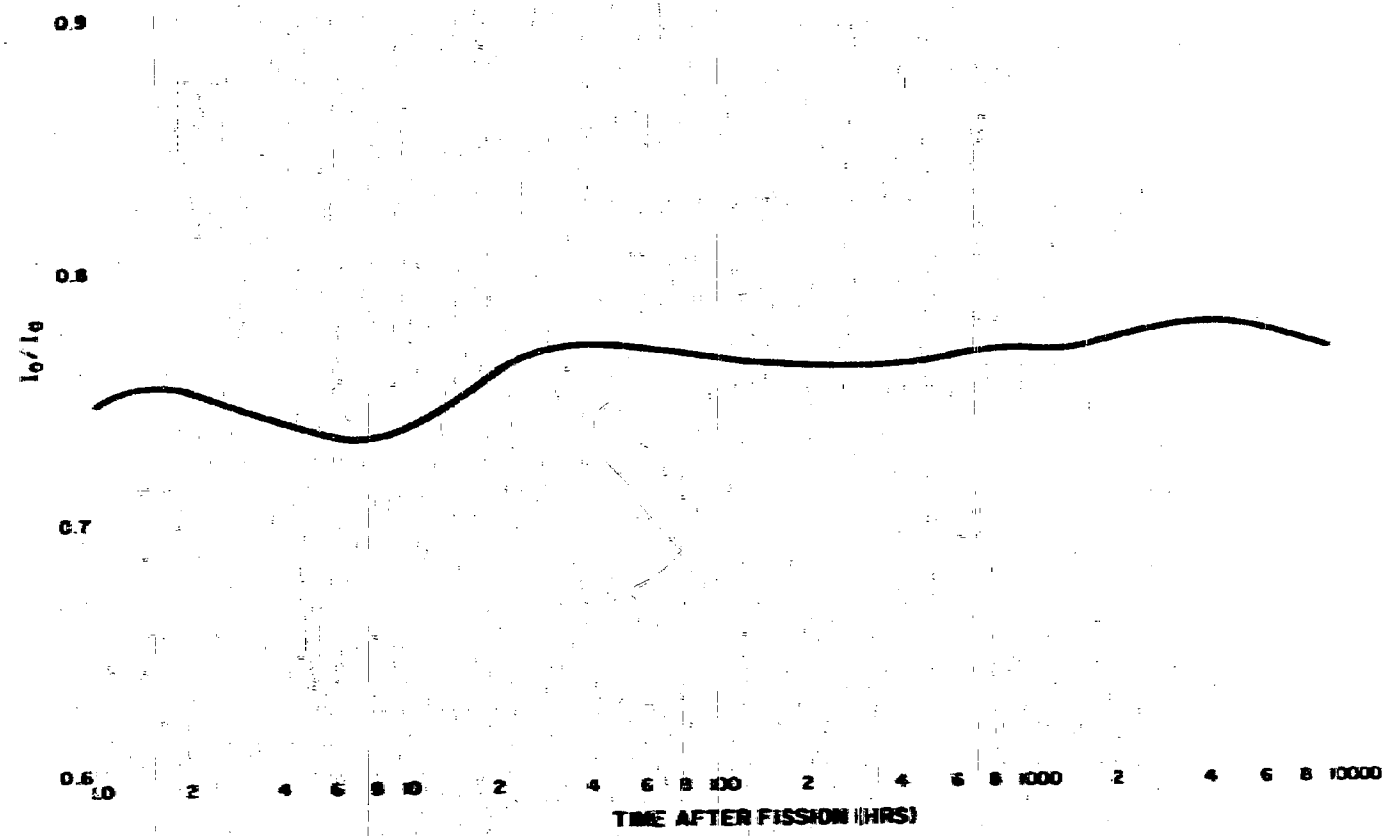

Table 3.10

EARLY-TIME IONIZATION RATE, PHOTON ENERGY EMISSION RATE, AND AVERAGE PHOTON ENERGY FOR FISSION PRODUCTS FROM THERMAL NEUTRON FISSION OF U-235

Time After Fission (secs)	Air Ionization Rate (10^{-13} r/hr)/(fission/sq ft)	Photon Energy Emission Rate (Mev/sec)/(10^4 fissions)	Average Photon Energy (Mev/photon)
1	25,600	5,020	1.150
1.5	19,800	3,940	1.178
2	16,600	3,300	1.200
3	12,700	2,530	1.235
4	10,300	2,060	1.262
6	7,530	1,510	1.296
9	5,280	1,060	1.328
13	3,820	768	1.348
19	2,680	541	1.363
28	1,840	368	1.375
41	1,250	252	1.384
60	840	168	1.390
88	560	112	1.393
129	373	74.3	1.390
189	250	49.1	1.376
277	166	32.0	1.355
406	109	20.6	1.308
595	70.2	13.5	1.245
870	45.5	8.65	1.170
1250	28.5	5.42	1.074
1870	17.9	3.28	0.992
2750	10.5	1.92	0.958
4050	6.65	1.24	0.970
5900	4.15	0.776	0.964

Figure 3.10
VARIATION OF τ_{fp} WITH TIME AFTER FISSION FOR THE FRACTIONATED MIXTURE OF FISSION PRODUCTS FROM 8-Mev NEUTRON FISSION OF U-238

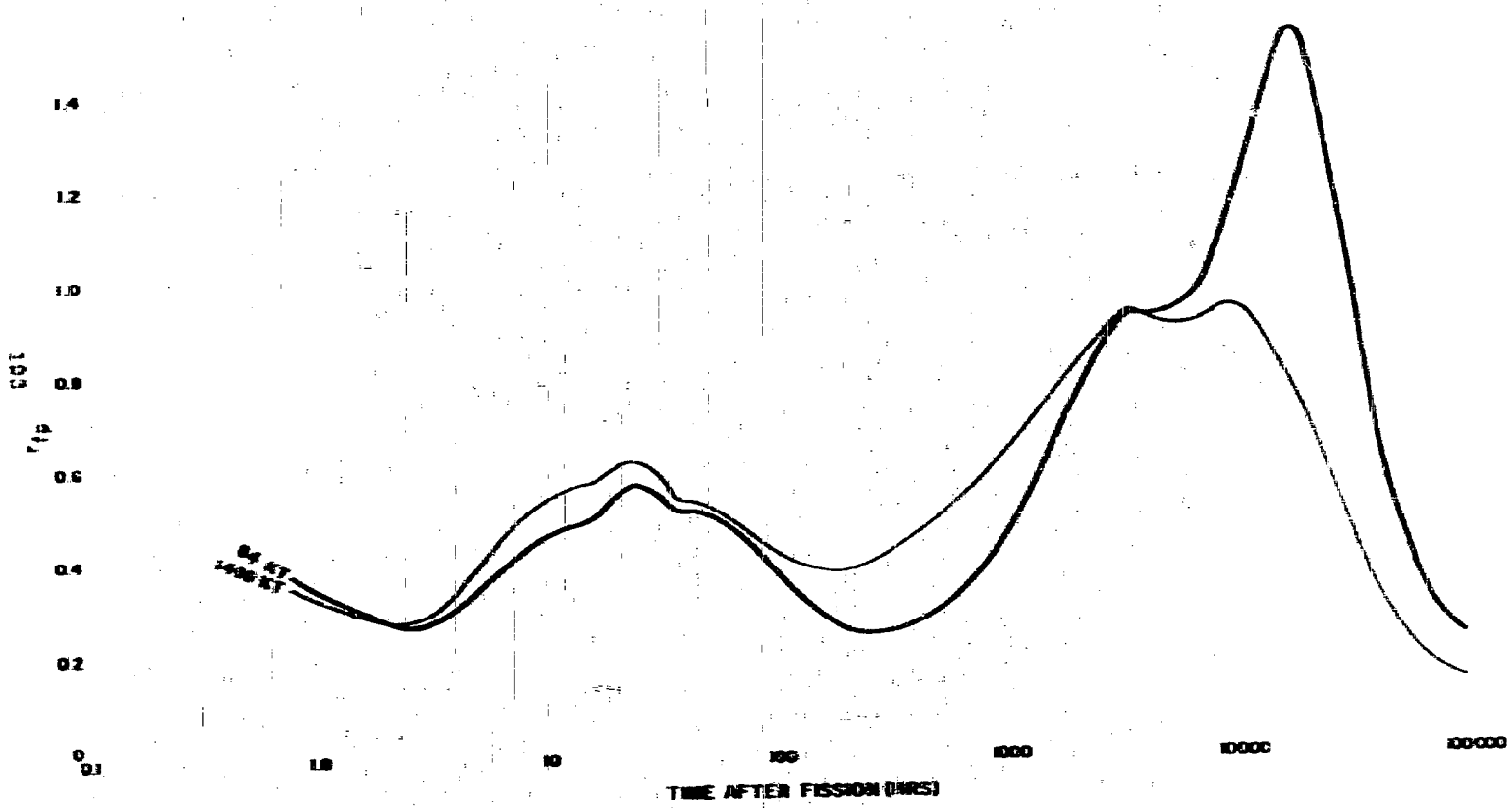

Figure 3.11
OBSERVED VARIATION OF r_{Sr} WITH TIME AFTER FISSION FOR CLOSE-IN FALLOUT FROM A LOW TOWER SHOT AT THE NEVADA TEST SITE

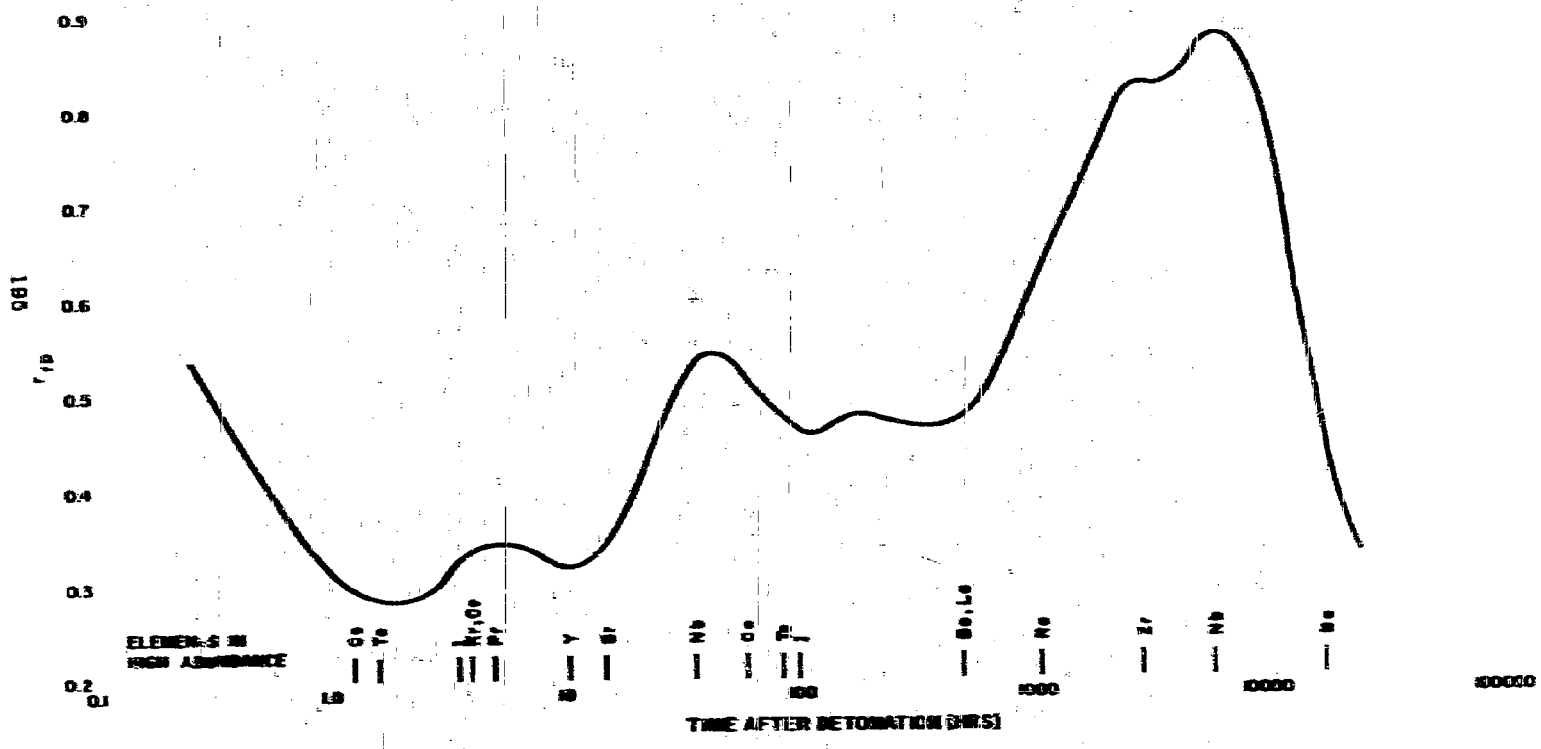

For an r_{ip} of 33 percent at H+1, the ionization rate at 1 hour per KT per sq mi. would be 1100 for the mixture of fission products condensed up to the indicated times. If the fallout also contained neutron-induced activities that contribute at H+1, the ratio would be higher. The important likely (or possible) induced activities are those produced from neutron captures by U-238 as was found by Kimura[7], Mackin[8], Freiling[22] and also reported by Stewart, Crooks and Fischer[21].

The activities and ionization rates of the possible product nuclides, for a yield of 10^4 atoms at zero time and up to 100 days later, are summarized in Tables 3.21 to 3.24. For the case in which the tabulated activities are associated with the activities from 10^4 fissions, they are equivalent to a yield of one product-nuclide for each fission. Thus, for the case where one of the neutrons from each fission event results in a (n, γ) reaction with U-238, the ionization rate from the products U-239 and Np-239 at H+1 would be 0.357×10^{-13} r/hr per fission or about 180 r/hr per KT/sq mi. The ratio for the gross mixture is then 1070 r/hr at 1 hour per KT/sq mi.

If the relative yield of U-237 was that found by Kimura[7], namely 0.15 atoms per fission, the additional activity at H+1 would be 0.0020×10^{-13} r/hr per fission or about 1 r/hr per KT/sq mi. A yield of 0.15 atoms per fission of U-240, however, would give a contribution at H+1 of about 20 r/hr per KT/sq mi. If this occurred, the ratio for the mixture would be 1300 r/hr at 1 hour per KT/sq mi. The observed ratio for this mixture of radionuclides in fallout particles on an open real terrain would be less than this value, due to both the instrument response mentioned above and to shielding by the roughness of the terrain. If it is assumed that the instrument response to the final mixture is about the same as it is for the normal mixture of fission products, then a value of about 75 percent (see Figure 2.9) would be appropriate for the AN/PDR-39(TIB) or similar radiac instrument. An effective terrain attenuation of 75 percent with respect to the ideal smooth plane would give an observed value for the ratio of about 780 r/hr at 1 hour per KT/sq mi. This is lower than the value, 1240, obtained from the data of the ENW.

Additional discussions of how the condensation process may proceed at times longer than the end of the first period of condensation, and of how the radioactive composition can vary with particle size and downwind distance, are given in Chapter 6.

Chapter 4

DISTRIBUTION OF FALLOUT PARTICLES FOLLOWING A NUCLEAR DETONATION

4.1 General Description of The Fallout Distribution Process

4.1.1 The Particle Source Geometry

A very simple descriptive statement of the fallout process might be that a cloud of particles is formed rapidly as the result of an explosion and that this cloud is then dispersed by the wind and by the force of gravity acting on the particles to return them to the earth. Most investigators concerned with the distribution of fallout assume that the visible volume occupied by the nuclear cloud and stem above the point of detonation within a few minutes after explosion more or less defines the volume source of the fallout particles[1].

Anderson[2], however, considers a moving source volume which might be described as the air volume swept through by the rising fireball and stem. In either case the source volumes for the particles depend on total yield and, if other than surface detonations are considered, on the height or depth of burst. The yield dependent parameters which are used to define the particle source geometry include the cloud height, cloud thickness and radius, and, occasionally, the stem geometry. Anderson's studies include consideration of the time dependence of these parameters.

One important additional factor that is usually considered is the distribution, or spatial concentration, of the particles in the volume, and qualitative considerations have been given to internal circulations of the particles by several investigators.[3]

4.1.2 The Particle Fall Trajectory

The fall trajectory of a particle depends on its own properties and on meteorological factors. The various aspects of these factors have been discussed by Schuert,[4] Anderson[2] and others[1]. The major properties that influence a particle's fall rate through the atmosphere are its density, diameter or size, and shape. The major meteorological factors are the wind speed and direction, and the air density and viscosity.

The two air properties, of course, are dependent on the air pressure and temperature and these, in turn, change with altitude. The wind speed and direction are also highly variable quantities since each has both spatial and time variations. The vertical motions of the air and particle-group diffusion can influence the fall trajectory of particles, but are usually not taken into account in the study of the fallout distribution process.

4.1.3 Radiological Factors

The major radiological factors in the fallout distribution process are the fission yield and the variation with particle size of the gross radioactivity carried by particles of a given size. The first essentially determines the total radioactivity available for distribution on the particles; the second involves the distribution of that radioactivity among particles of different sizes.

Additional factors, such as neutron induced radioactivity, fractionation, and the biological availability of single fission-product elements, have not yet been incorporated into studies of the fallout distribution process in a systematic way by most investigators and fallout model designers.

4.2 Mathematical Descriptions of the Fallout Distribution Process

4.2.1 Scaling Methods

The original attempt to describe and/or predict the end result of the fallout distribution process--the fallout pattern--was made by C.F. Kaanda and coworkers in 1953[5]. The original scaling method was based on the work of Laurino and Poppoff[6] which described some fallout patterns from Operation Jangle in 1951 from low yield devices. The original scaling method was intended for predictions or estimates of fallout patterns from yields possibly as high as 10-KT. In 1955[7] the method was expanded to include yields in the megaton range, without adequate explicit experimental documentation. This method was subsequently included in ENW.[8] In some studies of fallout effects a scaling system is to be preferred over a complex mathematical model. Therefore, a scaling method for estimating fallout patterns is described in Section 4.3.

4.2.2 Mathematical Models

Mathematical models attempt to establish quantitative values for the several factors mentioned in Section 4.1 and to compute the activity deposited on the ground at various locations usually with use of electronic computers. The general approach used and the organizations and investigators involved in the

development and testing of these models up to 1957 is described in some detail by Kellogg.[1] Later developments include the work by Anderson,[9,10] by Pugh and Galiano,[10] by Callahan, et al[11] and by Rapp,[12] to mention a few of the unclassified reported studies. A general comment on the results might be that none of the models agree with each other in several details, and that none of the models reproduce very accurately all of the few data in the yield range of 1-KT to 15-MT that are experimentally available.

The exact causes of the differences among the various models are difficult to isolate for at least two reasons: 1. Each model is different from any other in several of its assumptions about parameter values or in its manner of handling the many variables mathematically. 2. The reports describing the models generally do not include sufficient detailed information regarding the minor assumptions and the methods used in making the computations. If the input data in the mathematical models were all more reliably established experimentally, many of the differences among them would disappear. Whether better agreement with observations resulted would still have to be established.

Nonetheless, many of the features of the mathematical models are used in Section 4.3 which describes the derivation of a simplified scaling method. A few of the parameter values used in several of the mathematical models are discussed there to better describe the over-all process of fallout distribution as it might take place. In Chapter 6 some general concepts are described that could be utilized to derive a more refined mathematical model of fallout than is presently available. Some possible improvements in the treatment of the problem are also touched upon in this chapter.

In most mathematical models, after selecting the values of the source geometry, trajectory, and radiological factors, the computation is carried out by dividing the source geometry for each of several particle size ranges into horizontal discs of finite thickness. The location on the ground where these "particle discs" land, under the influence of the ascribed meteorological conditions, is then calculated. All the activity at each of a series of coordinate points is then summed, according to the number of different discs that land at the point and the amount of activity assigned to each disc.

So short a summary of the work on the mathematical models should not be interpreted to mean that the efforts in the development of the mathematical models have been small and unfruitful. On the contrary, much has been learned about the fallout process through them, and most of the concepts employed by many of the mathematical model developments are covered in the remainder of this chapter. But to describe all the work and all the details of each model currently in use is not considered to be within the scope of this discussion.

Figure 5.12
VARIATION OF THE IONIZATION RATE WITH TIME AFTER DETONATION AT X = 3.35 · 10^4 FT FOR W = 10^3 KT AND A WIND SPEED OF 15 MPH

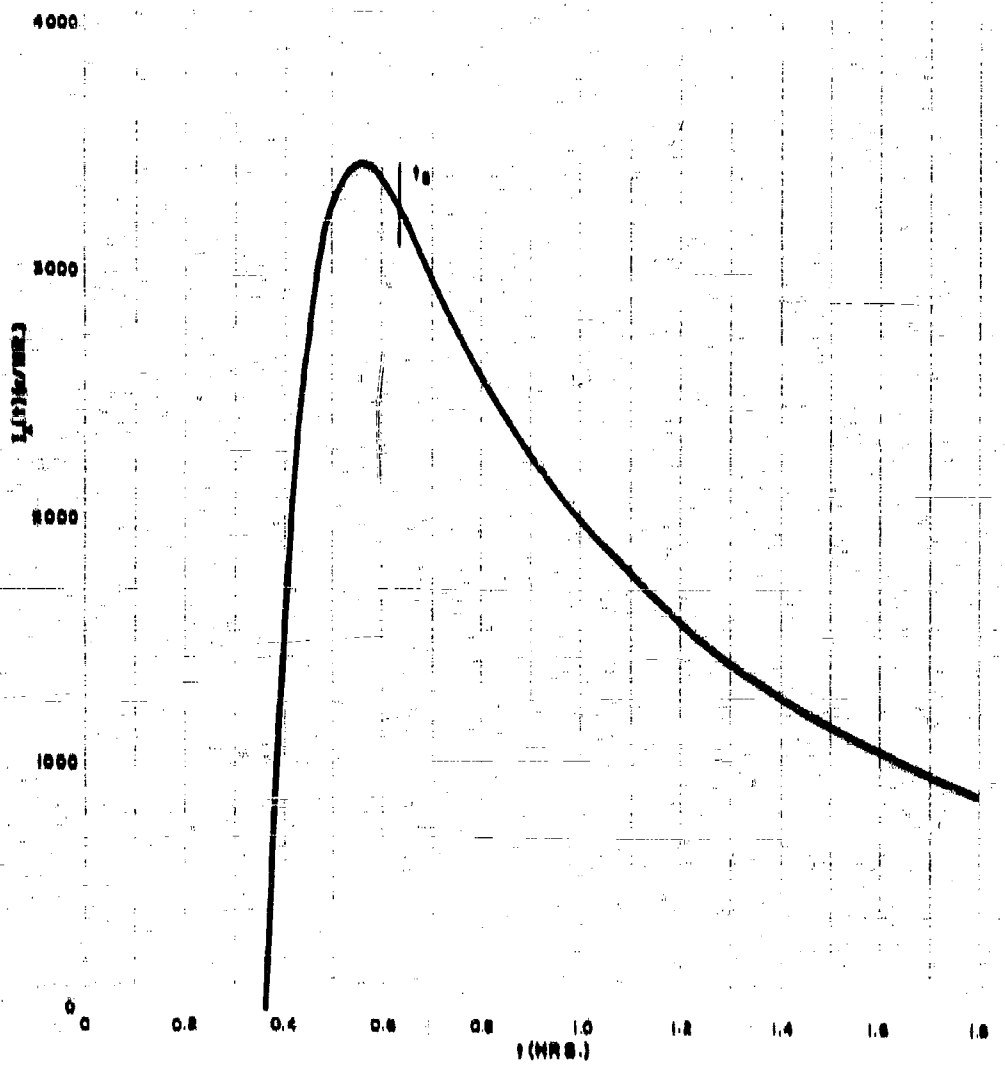

Figure 5.16
PLOT OF PARTICLE FALL TRAJECTORY COMPONENTS RELATIVE TO ESTIMATED PATTERN CENTER LINE FOR CASTLE BRAVO WINDS

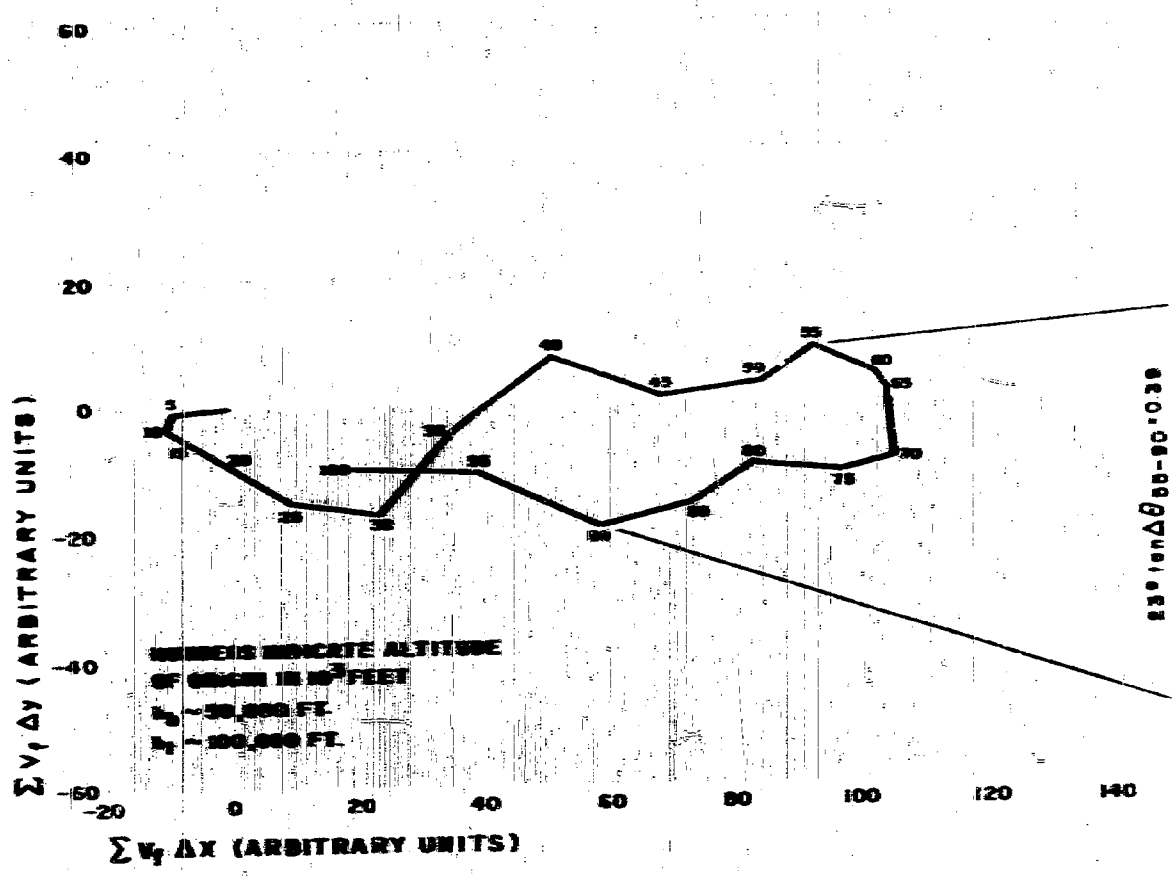

CHAPTER 6 REFERENCES

1. LaRiviere, P.D., Early-Time Gamma Ray Properties of U-235 Gross Fission Products, USNRDL-TM-80, 1958.

2. Clark, D.E., and A.D. Anderson, Private communication, USNRDL, July 1960.

3. Pugh, G.E., and R.J. Galiano, An Analytic Model of Close-In Deposition of Fallout for Use in Operational-Type Studies.

4. Research Memorandum No. 10, Weapons Systems Evaluations Group, 1959.

5. Ferber, Gilbert J., and Jerome L. Heffter, A Comparison of Fallout Model Predictions With a Consideration of Wind Effects, U.S. Weather Bureau, 1961.

6. Batton, E.S., D.L. Inglehart, and R.H. Rapp, Derivation of Two Simple Methods for the Computing of Radioactive Fallout, RM-2500, 1960.

7. Nagler, K.M., L. Machta, and F. Pooler, Jr., A Method of Fallout Prediction for Tower Bursts at the Nevada Test Site, TID-5489, OTS, Department of Commerce, Washington 25, D.C., 1955.

8. U.S. Government, Nuclear Weapons Employment Handbook, Air Force Manual 200-8, 1961 (Classified).

9. The Effects of Nuclear Weapons, U.S. Government Printing Office, Washington, D.C., 1957.

10. Anderson, A.D., Scaling Relations for Fallout Dose-Rate Patterns from Land Surface Nuclear Bursts, USNRDL-TR (in publication, 1961).

Chapter 6

IONIZATION RATE CONTOUR RATIOS AND COMPOSITION OF FALLOUT

6.1 Definition and Use of Ionization Rate Contour Ratios

These contour ratios are defined as the ratio of the surface density of some property of fallout to the ionization rate at 3 feet above an extended open area covered with fallout. The three fallout properties of most interest in radiological countermeasures are:

1. The mass of fallout per unit area,
2. The number of atoms or moles of fission products per unit area, and
3. The fraction of the weapon yield deposited per unit area.

At a given location in the fallout area, the contour ratios for these quantities are defined by

$$M_r(t) = \frac{m_s}{I_s(t)} \tag{6.1}$$

$$FP_r(t) = \frac{n_{fp}}{I_s(t)} \tag{6.2}$$

and

$$FD_r(t) = \frac{FD}{I_s(t)} \tag{6.3}$$

where $M_r(t)$ is the mass contour ratio, m_s is mass of fallout per unit area at the location, $FP_r(t)$ is the fission product or activity contour ratio, n_{fp} is the number of atoms or moles of fission products per unit area, $FD_r(t)$ is the fraction of device contour ratio, FD is the fraction of device per unit area, and $I_s(t)$ is the observed ionization rate.

Knowledge of the values of these contour ratios makes possible estimates of the amount of fallout particles, fission products, or other components of the weapon that are present, given the level of the ionization rate. These estimates are necessary in the design of realistic experiments using synthesized fallout materials, in the operational use of radiological counter measures, and in general evaluations of radiological hazards from fallout.

The reverse procedure is equally useful; knowledge of the chemical or physical behavior of particles or of the fission-product elements as a function of their surface density can, through the contour ratios, be associated with the level of the radiation hazard. For example, decontamination data based on the mass of particles can be readily converted into reduction in radiation hazard by means of the contour ratio. Use of the contour ratios and their scaling functions allows extrapolation of a modest amount of experimental data to innumerable operational cases because the contour ratios are not constants; they are point functions whose value depends on many variables. Thus a single value of m_x, for example, may be associated with many values of $I_x(t)$.

The final use of the contour ratios is to permit estimates of m_x, n_{ip}, and FD to be made, for use in radiological countermeasure operations, from observations of $I_x(t)$. In such estimates, additional information is required, along with the value of $I_x(t)$, before a reliable estimate of the quantity of interest can be made. This particular use of the contour ratio may be the only method available for estimating one of the desired quantities when fallout areas are monitored with portable survey instruments. The additional information needed for these estimates is discussed in the following paragraphs.

6.2 Dependence of the Mass Contour Ratio on Detonation Conditions and Other Parameters

6.2.1 Dependence on Weapon Type and Yield

Because the mass contour ratio is inversely proportional to the specific activity of fallout, its value or range of values must depend on the amount of radioactive materials produced in the detonation. The fission product yield is proportional to BW where B is the ratio of fission to total yield; hence, for the usual amount of induced activities, the total area activity from Eq. 4.74, is

$$I_x(t)\,\text{Area} = 5.46\times10^{10}\left[r_x(1) + 0.010\right] BW \text{ r/hr at 1 hr-sq ft} \qquad (6.4)$$

where $r_x(1)$ is the gross ionization rate fractionation number at H+1 and 0.010 is the ratio of the ionization rate from a nominal yield of induced activities to that of the fission products (both at H+1). The multiplier, 5.46×10^{10} r/hr at

1 hr per R/T/sq ft, contains an instrument response and a terrain roughness attenuation factor. The value of r_x (1) will vary with downwind distance, or particle size, as well as with time after detonation. The value of the ratio, 0.010, for the induced activities will depend on the construction materials of the weapon, the environmental elements at the point of detonation, and, to some degree, on the height of burst and on the values of B. For example, if B is very small (the definition of the so-called "clean" bomb), then the relative induced activity yield could be much higher than is indicated by the 0.010 of Eq. 6.4. Except for the possible dependence of r_x (1) and induced activity ratio on yield, the total area activity of Eq. 6.4 is directly proportional to W.

If it is assumed that the total crater mass becomes uniformly mixed with the radioactive material in the fallout formation, then the expected maximum value of M_r (1) should be given by $M_v/(I_x$ (1)xAren) which (from Eqs. 3.166 and 6.4) is

$$\overline{M_r(1)_{max}} = \frac{93.6W^{-0.083}}{\left[B\ r_x(1) + 0.019\right]} \frac{\text{mg/sq ft}}{\text{r/hr at 1 hr}} \tag{6.5}$$

If, on the other hand, it is assumed that only the soil that is melted at 1400°C, as in the case of the ideal surface burst, becomes uniformly mixed with the radioactive elements, then only the mass equivalent of the n(ℓ) moles of liquid soil would be considered. The yield dependence of this quantity, from Table 2.18, can be represented by

$$n(\ell) = 1.92\times10^{11}\ W^{1.018}\ \text{mg soil} \tag{6.6}$$

On the average, the mass represented by n(ℓ) should result in an expected minimum value of M_r (1), which is

$$\overline{M_r(1)_{min}} = \frac{3.52W^{0.018}}{B\left[r_x(1) + 0.019\right]} \frac{\text{mg/sq ft}}{\text{r/hr at 1 hr}} \tag{6.7}$$

The two limiting values of M_r (1) indicate that (1) the dependence on the total yield should be rather small, (2) the values are inversely proportional to the fraction of fission yield of the detonation, and (3) the real values are most likely to be in the range 1 to 100 (mg/sq ft)/(r/hr at 1 hr) for B=1. With respect to the fraction of fission yield, B, the type of weapon is apparently a more important parameter in determining the value of M_r (1) than is the yield itself. Because both melted and unmelted particles are found in fallout, more soil is involved in the fallout formation process than is indicated by n(ℓ), but the amount involved should certainly be less than that removed from the whole (apparent) crater -- even for the larger yield where essentially no crater lip remains.

Actually, the values of M_r (1) show a tendency to decrease with yield that is more or less proportional to the apparent crater mass. Therefore, the crater mass per KT associated with fallout formation, $m(\sigma, W)$, is assumed to have the form

$$m(\sigma, W) = f(\sigma) W^{-0.083} \text{ mg/KT} \qquad (6.8)$$

where $f(\sigma)$ is the mass per kiloton of yield for each particle group to be evaluated from available measurements of M_r (1). With the assumed dependence of $m(\sigma, W)$ on yield, the relative abundance of melted particles increases with yield, since $n(\ell)$ increases with yield, and the average value of M_r (1) decreases with yield.

6.2.2 Dependence on Downwind Distance from Shot Point

The variation of M_r (1) with downwind distance from shot point is best considered in terms of the particle group size parameter, σ. To represent this dependence r_x (1) is redesignated r_σ (1) for evaluation as a function of both σ and the yield. Appropriate values of r_σ(1) along with observed values of M_r (1) are then used to evaluate $f(\sigma)$.

In estimating r_σ (1), the assumption is made that an abundance of solid surface (as particles) is present in the rising fireball and cloud at all times to facilitate the condensation of the gaseous radioactive species. With this condition, the amounts of each element condensed during the second period of condensation may be estimated by the method outlined in Chapter 2. In the simple process where all the particles are present at the end of the first period of condensation, differences in the radioactive composition on the various particles at a later time can occur only if some of the particles are removed from the volume before further condensation occurs. The particles that remain in the volume the longest time, providing a large number are always present, will then condense more of the volatile radioactive elements. In the fallout formation process, where the larger particles are falling out or leaving the gas volume at earlier times, the fraction of total available activity that is condensed on particles of various sizes should increase with decreasing particle size. Hence the fraction of the total activity condensed up to a given time after detonation should be described by an accumulative distribution curve that increases to a stated amount for a given particle size, or σ value for a group of particles. Such a representation cannot consider discrete values of the fraction condensed for a given particle size but may be given in terms of an average value for each of the particle groups.

Table 6.6

CALCULATION OF $f(\alpha)$ FROM $M_r(1)$ DATA FROM OPERATION JANGLE SHOT "S"

X (ft)	$M_r(1)$ $\left(\frac{\text{mg/sq ft}}{\text{r/hr at 1 hr}}\right)$	α_{min}	α_{max}	$\bar{\alpha}$	$r_\alpha(1)$	$(r_\alpha(1)+0.010)$	$f(\alpha)$ (mg/KT)
280	24,000	0.382	0.474	0.428	0.100	0.110	1.31×10^{14}
860	815	0.415	0.625	0.550	0.550	0.100	7.96×10^{12}
1,110	155	0.516	0.680	0.598	0.100	0.200	1.77×10^{12}
1,720	105	0.620	0.800	0.710	0.258	0.272	1.56×10^{12}
1,940	505	0.685	0.860	0.750	0.280	0.290	0.22×10^{12}
2,600	22.5	0.770	1.00	0.885	0.345	0.304	4.47×10^{11}
2,820	22.0	0.804	1.04	0.922	0.362	0.381	4.70×10^{11}
3,040	47.8	0.85	1.09	0.970	0.387	0.400	10.0×10^{11}
3,480	31.8	0.924	1.18	1.052	0.430	0.440	7.80×10^{11}
3,600	26.0	0.96	1.25	1.005	0.448	0.407	6.58×10^{11}
5,010	37.1	1.00	1.27	1.135	0.470	0.470	9.00×10^{11}
7,400	17.8	1.65	1.98	1.805	0.625	0.644	6.08×10^{11}
9,120	17.8	1.94	2.32	2.130	0.687	0.670	6.98×10^{11}
12,000	19.6	2.60	3.00	2.80	0.605	0.714	5.90×10^{11}

The variation of the function, $f(\alpha)$, with α can be indicated in a very general sort of way by making an analogy between what may occur in the fallout formation process to what should occur in an idealized condensing system. If the idealized system consists of a group of suspended drops in equilibrium with a dissolved gas, the concentration of the condensing gas should be the same in all particles whose diameter is larger than a few tenths of a micron. For these particles, the concentration is independent of the particle diameter and, therefore, independent of the parameter, α.

In a system where the particles are rapidly heated and cooled over a short period of time, only the surface of the particles having diameters larger than the same size will be melted; these larger particles should, in a given period of time, condense amounts of vapor that are proportional to their surface area or to the square of their diameters. The same result should occur for particles of all sizes that do not melt at all. If the particles are very large, only part of the surface may be melted (see discussion in Chapter 2); the amount that is condensed will not be proportional to their surface area.

Thus, in an ideal system where particles are exposed for the given period of time to a uniform concentration of condensing gas, the ratio of the particle mass to the amount condensed on each particle (m/a) should: (1) remain constant for smaller liquid particles; (2) be proportional to the particle diameter, d, for the larger surface-melted particles and for all solid particles, and (3) increase more rapidly than the particle diameter for very large partially-melted particles.

However, in the fallout formation process some of the smaller liquid particles can remain in the gas volume after they solidify, and condense material on their surfaces in addition to that contained in their volumes; these particles could carry more activity than would be indicated by (1) above. Smaller particles, with diameter less than about 80 microns, have terminal fall velocities proportional to the square of their diameter (Stokes' law). For These, the particle diameter is proportional to $\sqrt{v_w/\alpha}$. Hence, for a mixture of small spherical (previously melted) and irregular particles, the ratio, (m/a), should not decrease with α more rapidly than does $1/\sqrt{\alpha}$. If the amount of small unmelted particles that enter the cloud at late times is large, it would be possible for the average value of (m/a) actually to increase with α. For particles with diameters from about 80 to 1000 microns that have fall velocities roughly proportional to their diameter, their diameters are proportional to v_w/α. The dependence of the ratio, (m/a), for these particles on α should lie between being proportional to α and $1/\alpha$.

If $f(\alpha)$ roughly follows this admixture of behaviors, it should decrease very rapidly with α at low values of α; also, its rate of decrease with α should also decrease with the value of α. At high values of α, $f(\alpha)$ may decrease slowly with α, have a constant value, or even pass through a minimum and increase again.

In Figure 6.3 a proposed curve for the variation of $f(\alpha)$ with α is shown; it is based mainly on the Jangle "B" data. The slope of the curve from α=0.1 to 0.9 was determined with the aid of single-particle activity data of fallout from low tower detonations where the specific activity was roughly proportional to the diameter of the particles and, for larger sizes comparable to α values less than 0.1, increased less and less rapidly with size. The line from α= 0.9 to 20 was based on a geometric mean value of the plotted data in the range α= 0.88 to 2.8, and on several values of M_r (1) from higher yield detonations which, when corrected by use of Eq. 6.12, gave a mean value of $f(\alpha)$ of 1×10^{11} and an average α value of 20. No data were available for estimating $f(\alpha)$ at α values larger than 20; hence a constant value of 1×10^{11} was assumed for α values larger than 20.

The lack of available data for establishing more accurate values of $f(\alpha)$ at the higher α values is not of too much concern for many uses of $f(\alpha)$ because of the lower levels of fallout that are associated with the smaller particles. This lack of data is of much more concern in evaluating the longer-

Figure 6.3
PROPOSED CURVE FOR THE VARIATION OF f(z) WITH z FOR A 15-MPH WIND SPEED

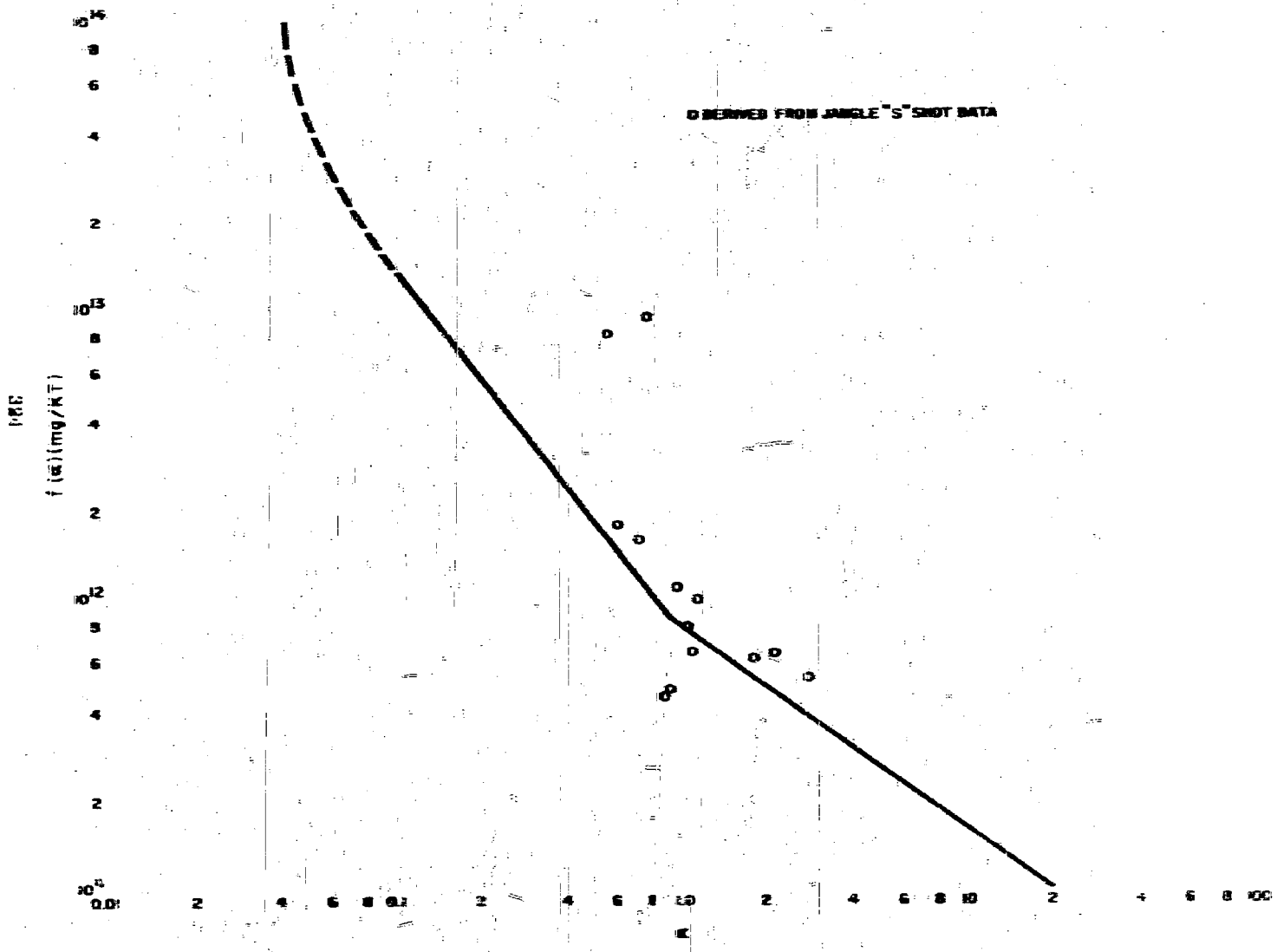

term hazards that are associated with the uptake of certain long-lived radioelements by plants and animals, since much of the surface-condensed, biologically available elements will be carried by the smaller particles.

The mathematical expressions for portions of the proposed function for $f(\alpha)$ are

$$f(\alpha) = 7.46\times10^{11}\ \alpha^{-1.25}\ \text{mg/KT, or}$$
$$= 5.33\times10^{-19}\ \alpha^{-1.25}\ \text{mg/fission,}\quad \alpha = 0.1 \text{ to } 0.9 \tag{6.13}$$

and

$$f(\alpha) = 7.90\times10^{11}\ \alpha^{-0.690}\ \text{mg/KT, or}$$
$$= 5.64\times10^{-19}\ \alpha^{-0.690}\ \text{mg/fission,}\quad \alpha = 0.9 \text{ to } 20 \tag{6.14}$$

$$f(\alpha) = 1.0\times10^{11}\ \text{mg/KT, or}$$
$$= 7.14\times10^{-19}\ \text{mg/fission,}\quad \alpha < 20 \tag{6.15}$$

in which the wind speed associated with the α values is approximately 15 mph.

The general equation for estimating $M_r(1)$ for a land surface burst, from the above treatment of the data, is

$$M_r(1) = \frac{f(\alpha)W^{-0.083}}{D(1)q_x B\left[r_\alpha(1)I_{fp}(1) + I_i(1)\right]} \tag{6.16}$$

in which $f(\alpha)$ is the ideal (or unfractionated) inverse specific activity in mg/fission, $D(1)$ is an instrument response factor, q_x is the terrain attenuation factor, B is the ratio of fission to total yield, $r_\alpha(1)$ is the gross fission-product ionization rate fractionation number at H+1, $I_{fp}(1)$ is the true air ionization rate at H+1 at 3 feet above an ideal plane uniformly contaminated with the radionuclides from a normal (unfractionated) mixture of fission products at a surface density equivalent to one fission per sq ft, and $I_i(1)$ is the true air ionization rate per fission contributed by induced activities.

By substituting 0.75 for $D(1)$, 0.75 for q_x, 0.94×10^{-13} (r/hr at 1 hr)/(fission/sq ft) for $I_{fp}(1)$, and 0.13×10^{-13} (r/hr at 1 hr) (fission/sq ft) for $I_i(1)$, the mass contour scaling function for the land surface burst is

$$M_r(1) = \frac{1.83\times10^{11}\ f(\alpha)W^{-0.083}}{B\left[r_\alpha(1) + 0.019\right]}\ \frac{\text{mg/sq ft}}{\text{r/hr at 1 hr}} \tag{6.17}$$

6.2.3 Dependence on Height or Depth of Burst

When an explosive charge is detonated below the surface of the ground, the apparent crater volume increases in size until a maximum amount of soil is thrown out. As the charge depth increases beyond this point, the amount of soil thrown out begins to diminish and, at some depth, the explosive force is no longer sufficient to break through the surface of the ground. When the height of burst is increased, the apparent crater from the explosion rapidly decreases until no crater is formed.

However, in nuclear explosions, the updraft of air following the rising fireball usually forms a column of loosened soil particles even when no real crater is formed. The height of burst at which the local fallout becomes insignificant occurs for detonations in which the rising dust column just fails to catch up with the rising cloud. Instead of specifying the requirement for entrainment of soil particles to form fallout, ENW gives a fireball radius of $180W^{0.4}$ feet as the minimum height of burst for negligible fallout; this height is supposedly associated with the height for contact of the fireball with the earth's surface.

Since the gross specific activity of the fallout for surface detonations has been found to be more or less proportional to the mass of soil removed from the crater, it seems that the same trend should occur with change of depth or height of burst. Thus, the value of $M_r(1)$ is expected to increase with depth of burst and decrease with height of burst, at least if the depths and/or heights of burst are not large. As the depth of burst becomes very large, only a small amount of activity should escape with most of the radioactivity remaining in or beneath the crater; that which does escape is on very small particles which could be dispersed over relatively large areas, so that no high levels of fallout would occur. However, the specific activity of those very small particles may still be higher than it is for the particles from detonations at intermediate depths.

As the height of burst is increased (by small distances) the smaller amounts of loosened (or melted) soil particles would result in increases in the specific activity of the fallout. However, as the height of burst becomes large, the size of the particles that can actually enter the cloud decreases. Since those that enter do so at later times (because of the height involved), and since, by this time, the concentration of the condensing radioactivity has decreased, due to both expansion of the cloud and depletion by vapor condensation to form very small solid particles, the amount of radioactivity collected by each soil particle that enters the fireball or rising cloud should be small. Therefore the specific activity of particles in the fallout should first increase and then decrease as the height of burst increases.

A proposed curve for a mass correction to M_r (1) is shown in Figure 6.4 in which the mass-correction factor, K_λ, is defined by

$$M_r^\lambda(1) = M_r(1)/K_\lambda \tag{6.18}$$

where $M_r^\lambda(1)$ is the mass contour ratio at the nuclear-scaled depth given by

$$\lambda_N = h/W^{1/3} \tag{6.19}$$

and h is the depth of burst (-h is the height of burst) and W is the total yield in KT rather than in pounds of TNT as usually defined.

The point at $K_\lambda = 0.3$ was obtained, from the M_r (1) data of Reference 4 for the Operation Jangle "U" shot, by comparing the measured values with those from the Jangle "S" shot at the same downwind distance. At the larger heights of burst one of the two points was derived from the specific activity and contour ratio data of fallout from a tower detonation; the other point was derived from the specific activity data of fallout from a balloon detonation. The values of K_λ are ratios of the average values of M_r^λ (1) in each case. The remainder of the curve was determined from high-explosive crater-volume data.

In using the proposed curve, the assumption is implied that the crater volume or mass that forms fallout varies as $W^{0.917}$ for all heights and depths of burst represented by the curve. This assumption is valid, within the accuracy of most crater data, for a fairly wide variation in soil type media, and for λ_N values between about -100 and +75. In estimating M_r^λ(1) for a low air-burst or shallow underground-burst, M_r (1) at selected values of the downwind distance is to be computed for the same yield surface-burst and then corrected by use of Eq. 6.18. This procedure is indicated because K_λ was determined by comparison to the M_r(1) values at the same downwind distances. However, without methods for correcting the fallout contours themselves for height or depth of burst, the contour ratio M_r^λ(1), is of less immediate general use than M_r (1).

6.2.4 Mass Contour Ratio for Fallout from a Surface Detonation on Deep Sea Water

No unclassified data are available from which M_r(1) for sea water detonations can be computed; however, rough estimates may be made, using the data in ENW, if it is assumed that (1) the mass of water thrown up is proportional to the yield, (2) K_λ holds for a detonation in water as well as in soil, and (3) fractional mixing of the environmental materials and fission

Figure 6.4
PROPOSED MASS CORRECTION CURVE TO THE MASS CONTOUR RATIO AS A FUNCTION OF THE NUCLEAR SCALED DEPTH OF BURST

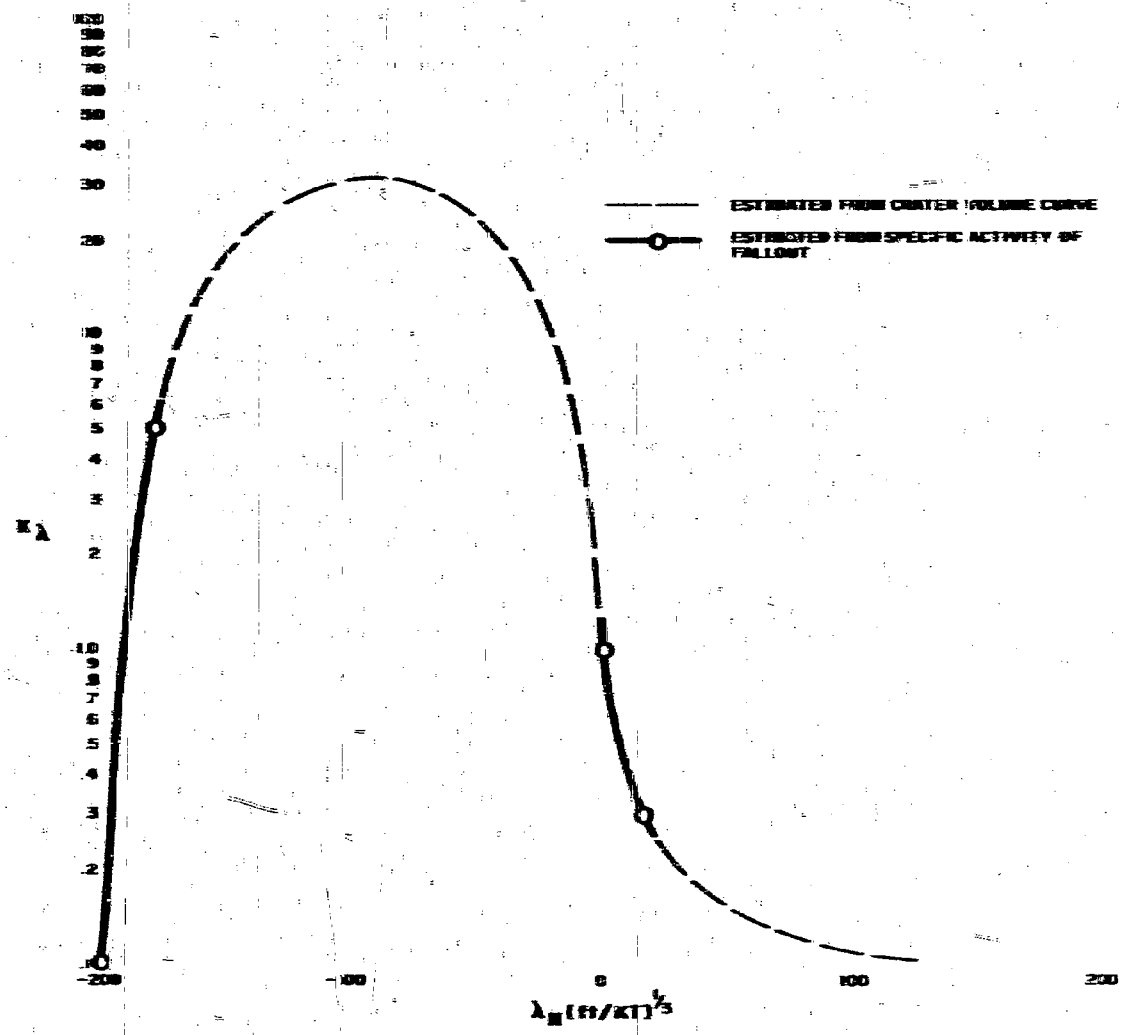

products is larger for a water shot. In ENW, p. 45, it is estimated that approximately 10^{9} tons of water were ejected into the air by the 20-KT Bikini Baker detonation. This is equivalent to 4.5×10^{18} mg/KT. Taking the depth of burst as approximately half the depth of the lagoon, K_λ is about 0.21. Therefore, the amount of water thrown up for a sea water surface detonation may be approximated by

$$M_w = 9.6\times10^{19}\ W \text{ mg sea water.} \tag{0.20}$$

If α_T is used to estimate an average value of $f(\alpha)$ for the fallout from a land-surface detonation, the fractional mixing of the soil can be estimated from $f(\alpha)/M_s$ which, from Figure 6.3 and Eq. 3.100, is found to be approximately given by $0.14W^{-0.014}$, or about 10 to 14 percent of the total soil thrown out of the crater. For the surface water burst, the fractional mixing was assumed to be about 50 percent of the water thrown up or about 3 to 5 times larger than that of the surface land detonations.

Because the end of the first period of condensation for a water shot occurs at about 0°C, very little fractionation of the fission products (with possible exception of the rare gas elements) should occur, especially for the larger yield detonations. This longer period of condensation for the water before the final sea water fallout particles are formed by vapor condensation should result in more thorough mixing of the water and the fission products, as well as in rather uniform concentrations of the radioactive elements in all fallout particles or drops. For these reasons, $f'(\alpha)$ for the water shots was taken to be independent of α, or droplet size, and equal to 4.5×10^{18} mg/KT or 0.4×10^{11} mg/fission. The mass contour ratio, in terms of the mass of original sea water, is then

$$M_r(1) = \frac{3.4\times10^{-11}}{D(1)q_{1x}\ B\left[1_{fp}(1) + 1_i(1)\right]}\ \frac{\text{mg sea water/sq ft}}{\text{r/hr at 1 hr}} \tag{0.21}$$

where no fractionation of the radionuclides in the fallout is assumed.

The no-fractionation assumption is essentially valid for yields greater than about 5-MT. For lower yields than this, a gross estimate of the gross fractionation number for a surface water detonation, $r'_\alpha(1)$, can be made from a log-normal distribution curve of $r'_\alpha(1)$ in which the cumulative distribution curves passes through $r'_\alpha(1) = 0.8$ at $\alpha = 1$, and through $r'_\alpha(1) = 0.9$ at $\alpha = 100$ (see dotted line of Figure 6.2). The simple fallout scaling system for the land surface burst can be used to provide a gross estimate of the fallout areas from sea water detonations. No large or experimentally observed significant differences in the areas of heavy fallout at sea have been found between the land and sea types of detonations for large yields.

For sea water fallout that is deposited on land areas where the previous values of D(1) and q_s apply, the mass contour ratio for the fallout of a large yield detonation on the surface of the water reduces to

$$M_r(1) = \frac{85}{B} \frac{\text{mg sea water/sq ft}}{\text{r/hr at 1 hr}} \qquad (0.23)$$

When completely dried, the sea water salt residue, at 3.3 percent of the initial sea-water mass, is only 2.8/B(mg/sq.ft.)/(r/hr at 1 hr).

Because the fallout drops apparently fall most of the distance from the high altitude in the solid state through temperatures where the sublimation pressure of the water is rather low, the change in droplet-size with time is probably rather slow. At the lower and warmer altitudes, where the particles exist in the liquid state, they either grow larger or decrease in size by evaporation, depending on the relative humidity of the surrounding air. Thus, the true value of M_r (1) for the arriving particles could be almost as low as the 2.8/B value or could be even larger than the 85/B value. In dry (warm) climates and over land areas where the M_r (1) value of the arriving material would be low, the fallout pattern would extend much farther downwind than would be estimated from use of the simple fallout scaling system for land surface detonations. This is simply because the droplets, decreasing in size and density as the water evaporates, would be carried to greater distances and dispersed over a larger area. Under these conditions, the deposit levels would all be decreased.

0.2.5 Mass Contour Ratio for Fallout from Detonations in Harbors

The mass contour ratio from detonations in shallow water should depend on (a) the height or depth of the burst point with respect to the water surface, (b) the depth of the water, and (c) the effective depth of the crater in the bottom of the harbor. Equations for estimating the contour ratio were derived from the assumption of proportional mixing of the soil and water contained in a set of assumed cone-shaped crater volumes.

For detonations in which the water depth, d_w, is small enough so that a significant amount of bottom material is removed, the crater depth, as measured from the surface of the water to the bottom of the crater in the harbor bottom, is assumed to approach the crater depth of a detonation in dry soil. Using the data of ENW (p.213) for a land surface detonation, the crater depth is given by

$$d_0 = \frac{25W^{0.25}}{\delta_\lambda} \text{ ft} \qquad (0.23)$$

where δ_λ is the ratio of the crater depth for a surface burst to the crater depth for a burst at the nuclear scaled depth, λ_N. An estimating curve for δ_λ, based on high-explosive data, is shown in Figure 6.6.

It is convenient to use the mass solid-to-liquid ratio, designated S, as a composition variable for the relative amounts of harbor bottom material and sea water as the two major constituents of this type of fallout. The same relative mixing ratios of the total material removed from the soil craters and the water volumes lifted up to form fallout are assumed to occur in the harbor detonation as occur for each type of shot separately; the ratios would then depend on the relative masses of water and soil that are drawn up. Accordingly, the ratios (of the masses of each constituent) would be roughly proportional to $f(\sigma)W^{-0.085}/f'(\sigma)$; the proportionality factor itself must be related to the initial amounts of soil and water dislocated by the detonation. The initial amounts of each constituent involved must, in turn, depend on the depth of the water and the size of the crater in the harbor bottom.

Data are not available for establishing the proportionality factor on an empirical basis, so geometrical considerations were used to develop a model for estimating its values. The geometrical crater-shapes assumed were two inverted cones both having the same radius, R, at the water surface. The height of the cone involving the harbor bottom material is the depth of the water, d_w plus the depth of the crater in the harbor bottom, d_c^s. With this geometry, the volume of the harbor bottom material (solids) removed is

$$V_s = (\pi/3)R^2(d_c^s)^3/(d_c^s + d_w)^2 \qquad (6.24)$$

where R, for a land surface detonation, according to ENW, is $0.2W^{1/3}$ ft.

The depth (or height) of the cone for the water component, d_c', was taken to be equal to the depth of the water involved in the explosion for the case in which the water is sufficiently deep so that no crater is formed in the harbor bottom. For this geometry, the volume of water involved is

$$V_L = (\pi/3)R^2\left[d_c' - (d_c' - d_w)^3/(d_c')^2\right] \qquad (6.25)$$

By assuming the ratio of the bulk density of the bottom material to that of the sea water to be 2, the proportionality factor is given by

$$S_0 = \frac{2(d_c^s)^3}{d_c'(d_c^s + d_w)^2\left[1 - (d_c' - d_w)^3/(d_c')^3\right]} \qquad (6.26)$$

Figure 6.5
PROPOSED CRATER DEPTH CORRECTION CURVE FOR THE MASS CONTOUR RATIO AS A FUNCTION OF THE NUCLEAR SCALED DEPTH

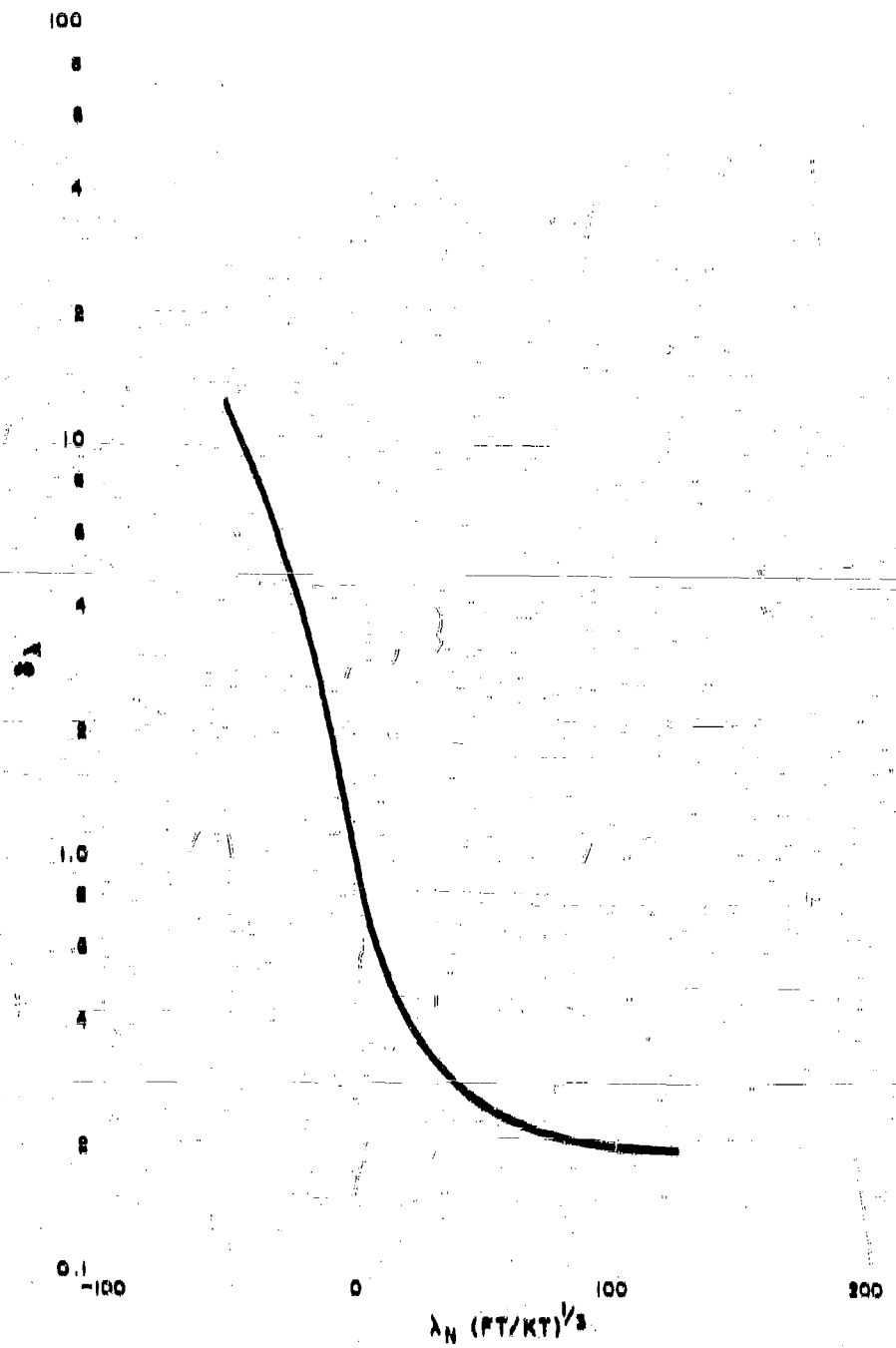

Since d_0'' should decrease with depth of water, a first-order approximation of d_0'' may be obtained from a function of the form

$$d_0'' \quad d_0^{*} \left[1 - d_0(W) d_w\right] \tag{6.27}$$

where $d_0(W)$ is a yield dependent parameter that must be evaluated from available data. It was not possible to evaluate $d_0(W)$ from the data of ENW (pp.226 and 227) because, for yields of about 10-KT and greater, that data gives larger craters in a harbor bottom (clay mud) under water than for a land surface detonation. Because such results are not in accord with observations, the data in ENW are presumably extrapolated incorrectly from high explosive data; hence they are not directly applicable to the higher yield nuclear explosions. Correcting some of the ENW data to an equivalent nuclear yield (see Chapter 2 for fraction of energy in blast) gives

$$d_0(W) \approx 0.017 W^{-0.16} \text{ ft.} \tag{6.28}$$

The appropriate value of d_0' is obtained from Eq. 6.27 for the water depth at which d_0'' becomes zero; for a water surface detonation this is

$$d_w = d_0^{*} \approx 59 W^{0.16} \text{ ft.} \tag{6.29}$$

From Eq. 6.29, the value of d_0' obtained by assuming the involvement of a hemispherical volume of water is $56W^{1/3}$ ft. On the other hand, if the shape of the water volume thrown up is assumed to be the same as that of a crater in soil, then d_0', from a linear increase in all the soil crater dimensions to the volume of the water removed, would be $38W^{0.270}$ ft. Thus the value of d_0' found for Eq. 6.29 suggests that the ratio of the radius to the depth for the water "crater" increases more rapidly with yield than it does for a crater in dry soil.

With S_0 defining the solid-to-liquid ratio weighting factor, the liquid mass fraction weighting factor is $1/(1 + S_0)$ and the solid mass fraction weighting factor is $S_0/(1 + S_0)$. With these weighting factors, the total mass of material for the mixture per unit of yield for the fallout from a harbor detonation on the surface of the water, is

$$f_{s,f}(\alpha) = \frac{f(\alpha) + S_0 f(\alpha) W^{-0.083}}{1 + S_0} \tag{6.30}$$

The solid-to-liquid mass ratio at a given location in the fallout area is, then,

$$S = \frac{S_0 f(\alpha) W^{-0.083}}{f(\alpha)} \tag{6.31}$$

and the mass contour ratio for this harbor detonation type of fallout may be estimated from

$$M_r(1) = \frac{7.1 \times 10^{-24} f_{sf}(\alpha)}{d(1) q_x K_\lambda B \left[r_\alpha^*(1) I_{fp}(1) + I_i(1) \right]}, \tag{6.32}$$

for $I_{fp}(1)$ and $I_i(1)$ in (r/hr at 1 hr)/(fission/sq ft), $f_{sf}(\alpha)$ in mg/KT, and in which $r_\alpha^*(1)$ is the gross fractionation number for the slurry.

For shot geometries where S_0 has values less than about one, a large amount of water and sea water salts are present in the fireball. Under such conditions the use of the $r_\alpha(1)$ values for fallout from a surface land detonation is not appropriate--even for the solid fraction--because of differences in vapor pressures between the oxides and hydroxides of many of the fission product elements. However, as the water content decreases (S_0 becomes larger) the use of $r_\alpha(1)$ for the solids becomes more applicable, and, as the S_0 values decrease, the $r_\alpha'(1)$ values for the water fallout apply. To account, in gross way, for these interactions, it is suggested that $r_\alpha^*(1)$ be estimated from

$$r_\alpha^*(1) \approx \frac{r_\alpha(1) + S_0 r_\alpha'(1)}{1 + S_0}, \quad S^0 > 1 \tag{6.33}$$

and

$$r_\alpha^*(1) \approx r_\alpha'(1), \quad S^0 < 1 \tag{6.34}$$

For large-yield detonations (W > 1-MT) on the surface of the harbor water (where $r_\alpha'(1)$ is essentially unity for all α, S_0 is less than unity, and D(1), q_x, $I_{fp}(1)$, and $I_i(1)$ have the standard values), the mass contour ratio is

$$M_r(1) = \frac{1.8 \times 10^{-11} (4.8 \times 10^{18} + S_0 f(\alpha) W^{0.083})}{(1 + S_0) B} \; \frac{\text{mg slurry/sq. ft.}}{\text{r/hr at 1 hr}} \tag{6.35}$$

and, for lower yields, the multiplier would be $1.83 \times 10^{11} \cdot F_{\lambda}^{1}(1) + 0.02$ instead of 1.8×10^{11}.

Because the f(e)values were derived from data on fallout from land surface detonations, and because the simple fallout model applies only to land surface detonations, use of the scaling functions at other depths of burst will introduce errors among the distance, standard intensity, and particle size parameters. These errors should, of course, increase as the nuclear scaled depth (or height) shifts farther away from zero.

For burst heights or depths that are a small deviation from a surface burst, the error in the extent of the fallout pattern itself should not be large since the cloud heights and size are not very sensitive to either height or depth of burst or type of media at the point of detonation. However, the value of the mass contour ratio is very sensitive to the depth of burst; this is indicated by the rapid change of K_{λ} and δ_{λ} with λ_N when λ_N is small. Considering the general trends and accuracy of the source data, the fallout model scaling functions for a surface detonation could be used, without significant increases in error for all types of detonations characterized by λ_N values up to ±5, and it is likely that consistent errors would become increasingly large for λ_N values larger than ±10. By use of K_{λ} and δ_{λ}, however, the scaling function for $M_r^{\lambda}(1)$ values appears to be as reliable as the original data up to λ_N values of ±20.

6.2.6 Mass Contour Ratio for Fallout from a 1-MT Detonation at Several Detonation Geometries

To illustrate the use of the scaling functions for the mass contour ratio and how its value depends on the various parameters, computations for $M_r^{\lambda}(1)$ were made for: (1) a land surface detonation, (and detonations on the) (2) water surface, and (on the) (3) water bottom, for depths of 20, 50, and 100 feet. The calculation results for S_n are shown in Table 6.7.

The value of d_r^{λ} indicates that, for water depths in excess of about 180 feet, the fallout, from a surface detonation, would be a pure-sea water type of fallout. It may be noted that d_r^{λ} has been corrected for depth of burst by $1/\delta_{\lambda}$ in the same way as d_r and d_r^{λ}.

For computing $M_r(1)$, the parameters B, q_x, and D(1) were taken to be 1.0, 0.75 and 0.75, respectively. With these values, the mass contour ratio scaling function becomes

$$M_r^{\lambda}(1) = \frac{1.26\times10^{-33} f_{NI}(\alpha)}{K_{\lambda}\left[6.93\times10^{-13} r_{\sigma}^{*}(1) + 0.13\times10^{-13}\right]^{S_0 - 1}} \qquad (6.36)$$

and

$$M_r^{\lambda}(1) = \frac{1.83\times10^{-11} f_{NI}(\alpha)}{K_{\lambda}}, \quad S_0 < 1 \qquad (6.37)$$

Table 6.7

COMPUTATION OF S_0 FOR SEVERAL DETONATION CONDITIONS OF A 1-MT FISSION WEAPON

Depth of Burst (ft)	λ_N	d_w (ft)	δ_{λ}	K_{λ}	d_0 (ft)	d_0^{*} (ft)	d_0' (ft)	S_0
0	0	20	1.0	1.0	140	124	178	0.40
20	2.0	20	0.90	0.86	150	138	198	0.80
0	0	50	1.0	1.0	140	101	178	0.808
50	5.0	50	0.74	0.60	189	136	240	1.20
0	0	100	1.0	1.0	140	61	178	0.108
100	10.0	100	0.57	0.47	246	108	312	0.272

The $M_r^{\lambda}(1)$ values at various downwind distances are given in Table 6.8.

The values for $r_{\sigma}^{*}(1)$ were calculated by use of Eq. 6.33 for S_0 = 0.40, 0.80, and 1.20. At distances where both stem and cloud fallout occur, the overall $M_r^{\lambda}(1)$ values were calculated by multiplying the individual ratios by the respective I values, adding the masses obtained, and then dividing the total by the sum of the two I values.

Selection of the surface-water and bottom detonations was made so as to give the spread in $M_r^{\lambda}(1)$ values for detonations anywhere in the water layer; this spread is not large for 20 and 50 foot depths, but at 100 foot the spread is

Table 6.8

COMPUTATION OF M_r^{λ} (I) FOR SEVERAL DETONATION CONDITIONS OF A 1-MT YIELD FISSION WEAPON AT SELECTED DOWNWIND DISTANCES

X (10^5 ft)	$\bar{\sigma}$ or σ_m	r_m(I)	I (r/hr at 1 hr)	$f(\sigma)M^{-0.5m}$ (10^{21} mg/KT)	M_r^{λ} (I) (mg slurry/sq ft) / (r/hr at 1 hr)						
					S_m = =	S_m = 1.93	S_m = 3.89	S_m = 0.908	S_m = 1.20	S_m = 0.103	S_m = 0.272
0.1	6.48	0.124	9000	*0.5	133	102	121	82.7	135	81.0	155
0.2	0.90	0.30	9000	5.56	31.7	57.3	65.4	76.8	102	80.1	151
0.3	1.18	0.48	3100	3.55	14.3	41.8	45.1	75.0	85.5	79.9	150
0.4	1.46	0.57	930	3.38	10.7	35.7	39.0	74.2	78.8	79.7	149
0.5	1.94	0.63	(280)	2.90							
0.5	0.96	0.36	(0.5)	4.37	8.32	32.9	35.8	73.6	75.6	79.7	149
0.6	2.19	0.66	(65)	2.60							
0.6	1.15	0.47	(60)	4.06	10.3	35.3	38.6	74.1	49.0	79.8	149
0.8	2.38	0.79	(7.7)	2.14							
0.8	1.54	0.58	(1600)	3.30	10.2	34.9	38.1	74.2	73.8	79.7	149
1.0	1.92	0.64	1020	2.84	7.83	32.0	35.6	73.6	75.3	79.7	149
1.52	2.92	0.70	2520	2.13	5.42	28.8	31.2	72.8	70.6	79.5	149
2	3.84	0.72	1040	1.76	4.45	27.4	29.3	72.4	69.1	79.5	148
3	5.76	0.74	520	1.34	3.22	26.4	28.5	72.0	67.5	79.4	148
4	7.67	0.75	530	1.09	2.58	25.7	27.7	71.5	67.1	79.4	147
5	9.58	0.76	265	0.942	2.21	25.5	27.0	71.5	66.1	79.4	147
6	11.5	0.76	140	0.835	1.95	25.2	26.8	71.2	66.1	79.4	147
7	13.4	0.76	72	0.744	1.74	24.7	26.5	71.2	65.8	79.4	147
8	15.4	0.77	38	0.677	1.58	24.7	26.2	71.0	65.8	79.4	147
9	17.3	0.77	20	0.632	1.47	24.5	26.0	71.0	65.6	79.4	147
10	19.2	0.77	10	0.581	1.35	24.5	26.0	71.0	65.5	79.4	147
11	21.1	0.77	5.4	0.564	1.31	24.5	26.0	71.0	64.8	79.4	147
12	23.0	0.77	2.8	0.564	1.30	24.5	26.0	71.0	64.8	79.4	147
13	24.9	0.77	1.5	0.564	1.30	24.5	26.0	71.0	64.8	79.4	147
13.6	26.1	0.77	1.0	0.564	1.30	24.5	26.0	71.0	64.8	79.4	147

about a factor of 3. The large change in $M_F(1)$ from dry-soil fallout to that for the fallout from a detonation on the surface of 20 feet of water is, of course, due to the larger amounts of water thrown up. No absolute accuracy can be stated for any of the numbers for the harbor-shot fallout; however, the values for the water-surface detonations are more accurate, taken relative to each other, than are the absolute values of the mass contour ratios.

6.3 Fission-Product and Fraction-of-Device Contour Ratios

Since two fission-product atoms are produced in each fission event, there are 3.32×10^{-24} moles of fission products formed per fission, or 0.405 moles of fission products produced per kiloton of yield. The distribution of these products over an extended area would result in an air ionization rate at 3 feet above the area given by i_{fp} (t) in r/hr per fission/sq ft. Thus the fission-product contour ratio for a fractionated mixture, including induced activities, from a land surface detonation, is given by

$$FP_F(1) = \frac{3.32 \times 10^{-24} \Sigma_{jA} r_{jA}(\alpha)}{D(1) q_x \left[r_\alpha(1) i_{fp}(1) + i_i(1) \right]} \quad \frac{\text{moles fp/sq ft}}{\text{r/hr at 1 hr}} \qquad (6.38)$$

where $r_{jA}(\alpha)$ is the fraction of each nuclide condensed on the particle group designated by α relative to the total number of fissions, and is defined by

$$r_{jA}(\alpha) = \frac{1}{2} \left[r_0(A) + r_0'(A) \right] y_A \qquad (6.39)$$

in which r_0 (A) is the fraction of the mass chain for a given element (or chain mass number) condensed when the particles were in the liquid state, r_0' (A) is the fraction condensed on the surface of the particles of size α, y_A is the yield of the mass chain in atoms per fission, and the factor 2 is for the total yield of 2 atoms per fission. If no fractionation occurs the sum of the $r_{jA}(\alpha)$ for all α is unity.

Using the standard values of D(1), q_x, and i_i (1), FP_F (1) is given

$$FP_F(1) = \frac{8.51 \times 10^{-18} \Sigma_{jA} r_{jA}(\alpha)}{\left[r_\alpha(1) + 0.019 \right]} \qquad (6.40)$$

For non water or barob-type fallout, $r_\alpha(1)$ is replaced by r_{tr} (1) or r_{tr}'(1); thus the value of FP_F (1) is dependent on the conditions of detonation only through the gross fractionation number.

The fraction-of-device contour ratio, in terms of the total number of fission events, is

$$FD_r(1) = \frac{7.1\times10^{-24}}{D(1)q_x BW\left[r_\alpha(1)i_{fp}(1) + i_i(1)\right]} \text{ (r/hr at 1 hr-sq ft)}^{-1} \qquad (6.41)$$

or, for the standard values of D(1), q_x, and $i_i(1)$,

$$FD_r(1) = \frac{1.83\times10^{-11}}{BW\left[r_\alpha(1) + 0.019\right]} \qquad (6.42)$$

The fraction-of-device contour ratio has two uses. The first is that it is used to estimate the surface density of constituents that are assumed to mix uniformly with the more refractory fission products. The second is that it is used in conjunction with observed fallout patterns when the latter are integrated for the total fraction of the weapon contained within a stated ionization rate contour. The use of both contour ratios is illustrated in Chapter 7, Volume II.

For a land surface burst, the average concentration of the fission products is estimated from the ratio of FP_r (1) to M_r (1); this is

$$C_{fp} = \frac{1.12\times10^{-24} BW^{0.083} \Sigma_{jA} r_{jA}(\alpha)}{f(\alpha)} \quad \frac{\text{moles fp}}{\text{mg fallout}} \qquad (6.43)$$

6.4 Foliage-Contamination Factor Contour Ratio

In Chapter 2, the foliage contamination factor, a_L, was defined as the ratio of the number of fissions in the fallout on foliage per gram of dry plant (or foliage) to the number of fissions in the total deposited fallout, per sq ft of soil. Also, the foliage surface density, w_L, (subject to contamination) was defined as the grams of dry foliage per sq ft of soil. Therefore, the foliage-contamination factor contour ratio is defined by

$$FC_r(t) = \frac{a_L w_L}{K_\alpha(t)} \quad \frac{\text{fissions on foliage/ft}^2 \text{ of soil area}}{\text{r/hr}} \qquad (6.44)$$

The contour ratio, evaluated as of H + 1, is

$$FC_r(1) = \frac{a_L w_L}{K_\alpha(1)} \quad \frac{\text{fissions on foliage/ft}^2 \text{ of soil area}}{\text{r/hr at 1 hr}} \tag{6.45}$$

where

$$K_\alpha(1) = 1.90\times10^{-18}\left[r_\alpha(1) + 0.019\right] \quad \frac{\text{r/hr at 1 hr}}{\text{fission/ft}^2} \tag{6.46}$$

when the standard values of D(1) and q_α are used. It is seen that multiplication of FC_r (1) by I(1) gives the number of fissions on foliage per sq ft of soil area.

The "zero-time" number of atoms of a given radionuclide (at least for the end member of a mass chain) in the fallout is given by

$$N_A^0 = Y_A\, FC_r(1) I(1) \quad \frac{\text{atoms on foliage}}{\text{ft}^2 \text{ of soil area}} \tag{6.47}$$

in which Y_A is the mass chain yield in atoms per fission of mass number A.

The major interest in the contamination of foliage by fallout is related to the fact that the consumption of the foliage by animals and humans may produce an internal radiological hazard. Therefore, generalization and extensions of the foliage contamination factor data from tower-and balloon-detonation fallout are needed for making estimates of the potential biological availability of the radionuclides in the fallout from other types of nuclear explosions and for various foliage contamination conditions.

When contaminated foliage is consumed, some of the radionuclides or some fraction of each nuclide ingested is dissolved in the stomach fluids; the remainder stays with the particles and pass through the digestive tract. Many of the dissolved nuclides are assimilated into the blood and concentrate in specific body organs. The factors involved in this distribution and the methods for estimating the resulting internal doses are given by K.Z. Morgan and others.[7]

However, methods are needed for estimating the relative amount of each nuclide that is soluble in the stomach fluids. Evaluations of the internal hazard can be made (for fallout conditions in a nuclear war, for example) from the generalizations of the foliage contamination factor together with estimates of the solubilities of the radionuclides.

The amount of radioactive nuclides that pass through the digestive tract may be considered separately because a large fraction of certain radionuclides in the fallout will be insoluble. For these radionuclides, only the gross amounts passing through need be considered. However, for the case of the assimilation of the soluble nuclides in other body organs, each radionuclide must be considered separately.

6.4.1 Insoluble-Nuclide Fractions

A gross estimate of the radioactivity of insoluble nuclides passing through the digestive tract from ingestion of contaminated foliage can be made if it is assumed that the gross solubility of the radioactivity is the same in the stomach as it is in 0.1N HCL. If the soluble fraction of the gross activity is defined as S(t), the number of moles of fission product atoms ingested that pass through the digestive tract with the particles is given by

$$FP_g = 3.32\times10^{-24}\left[1 - S(t)\right] A_F C_p(t) \quad \frac{\text{moles of fission products}}{\text{day}} \tag{6.48}$$

where A_F is $FC_r(t)f(t)$ in fissions on foliage/ft² of soil area, and $C_p(t)$ is in ft² of foliage consumed/day. Equation 6.48 can be written in terms of dis/sec, as

$$FP_g = \left[1 - S(t)\right] A_F C_p(t) a_{fp}(t) \quad \frac{\text{dis/sec}}{\text{day}} \tag{6.49}$$

where a_{fp} (t) is in dis/sec per fission at the time, t, after detonation. It may be noted that if C_p (t) is defined in terms of grams of dry foliage per day, w_f may be eliminated from the definition of FC_r (t) in Eqs. 6.44 and 6.45.

Theoretical estimates of the fractional amount of insoluble activities may be made from the data of Chapter 4 if it is assumed that all the fission-product nuclides on the exterior surface of the particles dissolve in the stomach fluids. The fraction not dissolved is then given by the r_n (A) values for each of the fission-product nuclides. If these fractionation numbers are redefined as r_{jA}, where j designates the element and A the mass number (isotope), then Eqs. 6.48 and 6.49 can be written as

$$FP_g = A_F C_p(t) \Sigma_{jA} r_{jA} N_{jA}(t) \quad \frac{\text{moles of fission products}}{\text{day}} \tag{6.50}$$

and

$$FP_{jA} = A_F C_a(t) N_{jA}(t) a_{jA}(t) \quad \frac{\text{dis/sec}}{\text{day}} \tag{6.51}$$

where $N_{jA}(A)$ is the number of atoms of element j with the mass number A per fission at the time, t, after fission, and $a_{jA}(t)$ is the activity in dis/sec per fission of the nuclide (the indices A and j define the nuclide in terms of its mass number and its atomic number, or elemental designation).

6.4.2 Soluble-Nuclide Fractions

The solubility in digestive fluids of each element, radionuclide, carried by the fallout particles deposited on edible foliage must be known before estimates of the amounts of each that concentrate in the tissue of (specific) body organs can be made. If the nuclide solubilities in 0.1 normal HCl solution are the same as in digestive fluids, then measurements of the solubilities in the acid can be used in such estimates. If the solubility in the 0.1 normal HCl solution is defined as S_j for the jth element, the amount and radioactivity of the ith radionuclide (of element j) dissolved is

$$N^*_{jA} = 1.66\times10^{-24} A_F C_a(t) S_j N_{jA}(t) \quad \text{moles/day} \tag{6.52}$$

and

$$a^*_{jA} = A_F C_a(t) S_j a_{jA}(t) \quad \frac{\text{dis/sec}}{\text{day}} \tag{6.53}$$

in which S_j is the fraction of element j that is soluble. Theoretical upper-limit values of $N^*_{jA}(t)$ and a^*_{jA} can be estimated by substituting the appropriate values of $r'_n(A)$, redefined as r'_{jA}, given by Eq. 6.9 for S_j.

It should be emphasized that, for general applicability, the values of $S(t)$ and S_j must be known as a function of particle-diameter. For the smaller particles, the values of $R_n(A)$, or r_{jA}, are independent of particle size but the values of $r'_n(A)$, or r'_{jA}, are not.

6.4.3 Variation of the Foliage-Contamination Factor with Particle Size

The values of a_I and $K_\sigma(t)$ depend on particle size. The dependence of the latter on the particle-size designator, σ, is represented by Eq. 6.46. The dependence of a_I on σ was derived from the data of Romney and coworkers[6] presented in Chapter 2.

The values of σ that are applicable to the various measured values of n_1 were calculated from

$$\sigma_n = X/h \qquad (6.54)$$

where X is the distance from ground zero and h is the mid height of the cloud. The values of σ_n can be used to estimate the median particle-diameter of the particles deposited at the distance X by the methods described in Chapter 5. When v_f (the fall velocity) can be determined for the median particle diameter, as obtained from particle-size data, then the 15 mph value of σ_n can be determined from

$$\sigma_n = 22.0/v_f \qquad (6.55)$$

for v_f in feet per second. The values of h and other data, for the detonations for which values of n_1 are available, are given in Table 6.9.

Table 6.9

SUMMARY OF SHOT CONDITIONS FOR ESTIMATING THE MEDIAN PARTICLE DIAMETER DESIGNATOR

Shot	Yield (KT)	Height of Burst (feet)	h (feet)	Type of Shot
Tesla	7	500	24,000	Tower
Apple I	14	500	27,000	Tower
Met	22	400	35,500	Tower
Apple II	29	500	38,500	Tower
Priscilla	37	700	34,500	Balloon
Diablo	17	500	20,000	Tower
Shasta	17	500	24,000	Tower
Smoky	44	700	32,000	Tower

The values of the median particle size, with respect to the distribution of activity on the particles, for two locations each on Shots Apple II and Smoky, along with the computations of σ_n, are given in Table 6.10. The σ_n values calculated by the two methods are nearly the same.

Table 6.10

CALCULATION OF α_0 FOR SOME FALLOUT LOCATIONS FROM SHOTS APPLE II AND SMOKY

Shot	X (miles)	d_m (microns)	v_f (ft/sec)	α_0 X/h	α_0 22.0/v_f
Apple II	7	-	-	0.000	(0.000)
	48	120	3.24	0.58	0.50
	100	70	1.00	14.5	15.8
Smoky	132	50	0.94	21.8	23.4
	206	47	0.67	34.0	32.8
	259	-	-	42.8	(41.8)

The values of a_{L_t} given in Table 2.18 (see Chapter 2) are plotted in Figure 6.6 as a function of α_0 values computed by use of Eq. 6.54. This set of data for the retention of fallout by native plants, is widely scattered; however, the general trend of the values of a_{L_t} from individual shots is to increase with increasing α_0. Part of the difference in the observed variation of a_{L_t} with α from one detonation to another is undoubtedly due to the fact that differences in wind speed occurred. Other causes of the differences in the variation with α could be due to differences in humidity conditions and in the predominant types of foliage that were collected for analyses.

The values of a_{L_t} calculated from the data of Table 2.16 (see Chapter 2) for the forage crops (clover, alfalfa, wheat, and mixed grasses) are plotted in Figure 6.6 as a function of the α_0 values that were corrected to an average wind speed of 15 miles per hour (see Table 6.10). Since the absolute accuracy of the source data is probably not better than 50 percent, a single line was drawn through the plotted data, neglecting one point. The suggested representation of a_{L_t} for these four forage crops is therefore given by

$$a_{L_t} = 9.5\times10^{-6}(\alpha_0 - 0.34); \quad \alpha_0 \geq 0.34 \qquad (6.56)$$

The complete representation of the foliage contamination factor contour ratio for evaluation at 1H1 hour is then

$$FC_r(1) = \frac{2.44\times10^{6} w_{L_t}(\alpha_0 - 0.34)}{(r_0(1) + 0.019)}; \quad \alpha_0 \geq 0.34 \qquad (6.57)$$

The value of $FC_r(1)$ for α_0 values less than 0.34 is taken to be zero.

Figure 6.6
VARIATION OF a_L WITH CALCULATED VALUES OF a_0

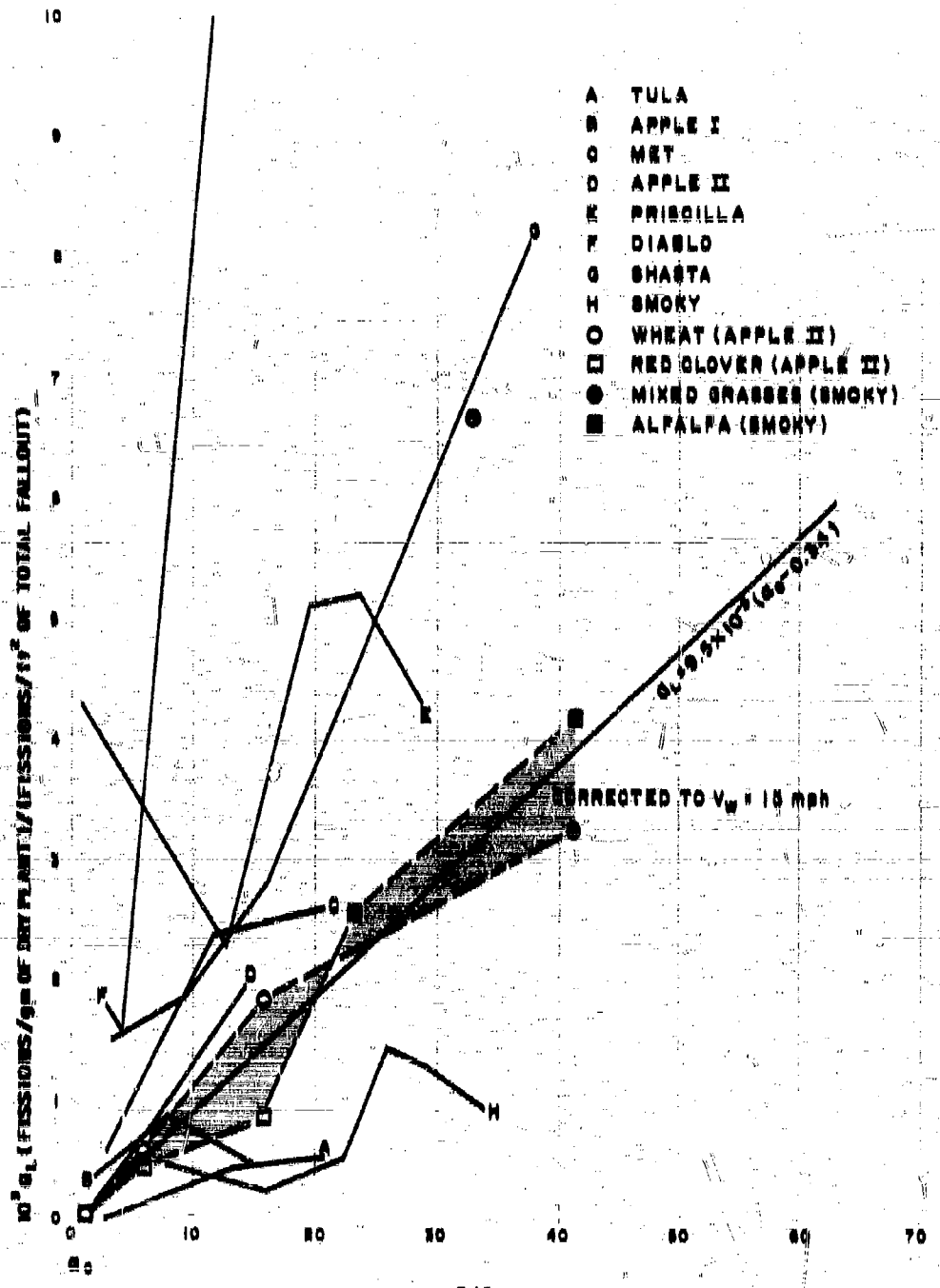

If it is assumed that the surface densities of the clover and wheat foliage in the flats used on Apple II detonation were higher than the average for such crops, then a range of values of w_L may be suggested. These are:

Red Clover	:	w_L = 5 to 25 gm. dry plant/ft^2 of soil surface
Wheat	:	w_L = 10 to 40 gm. dry plant/ft^2 of soil surface
Alfalfa	:	w_L = 10 to 80 gm. dry plant/ft^2 of soil surface
Mixed Grasses	:	w_L = 5 to 25 gm. dry plant/ft^2 of soil surface

Wide variations in w_L from these ranges might occur in various sections of the country.

The fraction of the total fallout that is retained on foliage can be estimated from the product $a_L w_L$. Thus, for a w_L value of 20, the fraction retained is 1.9×10^{-2} (α_0 = 0.84). In Table 6.8, the value of α_0 at the 1 r/hr at 1 hr contour farthest downwind from ground zero is 26.1; at this location, $a_L w_L$ is then 0.049, or about 5 percent, and the calculated value of $r_\alpha(1)$ is 0.77. Hence, from Eq. 6.57, the value of $FC_r(1)$, is 1.6×10^{11} (fissions on foliage/ft^2 of soil area)/(r/hr at 1 hr).

Estimates of the median size (or size-range) of particles retained on foliage may be made if the variation with α_0 of the median diameter of the particles in the deposited fallout is known. In Figure 6.7 the values of the median diameters of the fallout lodged on foliage, taken from Table 2.15, are plotted as a function of α_0. For these data, the median diameter of the fallout particles on the foliage increases with α_0; thus, the median diameter of the retained fallout increases as the median diameter of the deposited fallout decreases.

Clearly this trend in the median diameter of the retained particles with α_0 could not continue indefinitely since at some point, when the diameters of the deposited fallout particles become very small, all the particles could be retained by the foliage. To illustrate this aspect, calculated values of the median diameter (d_m) for the deposited fallout are also plotted as a function of α_0 in Figure 6.7. Extrapolation the linear representation of the data for d_m of the foliage-retained particles as a function of α_0 to the curve for d_m of the deposited fallout gives a maximum value of about 57 microns.

The various functional representations of the foliage contamination factor contour ratio, as derived from the data of Romney and coworkers[9], are based on information obtained from nuclear detonations of tower and balloon-mounted devices. However, in the treatment of that data the emphasis was placed on the particular mathematical functions that could be used in making estimates of internal hazard from fallout produced by land-surface detonations.

Figure 6.7
VARIATION OF THE MEDIAN PARTICLE DIAMETER OF FALLOUT ON FOLIAGE WITH σ_0 OF THE DEPOSITED FALLOUT

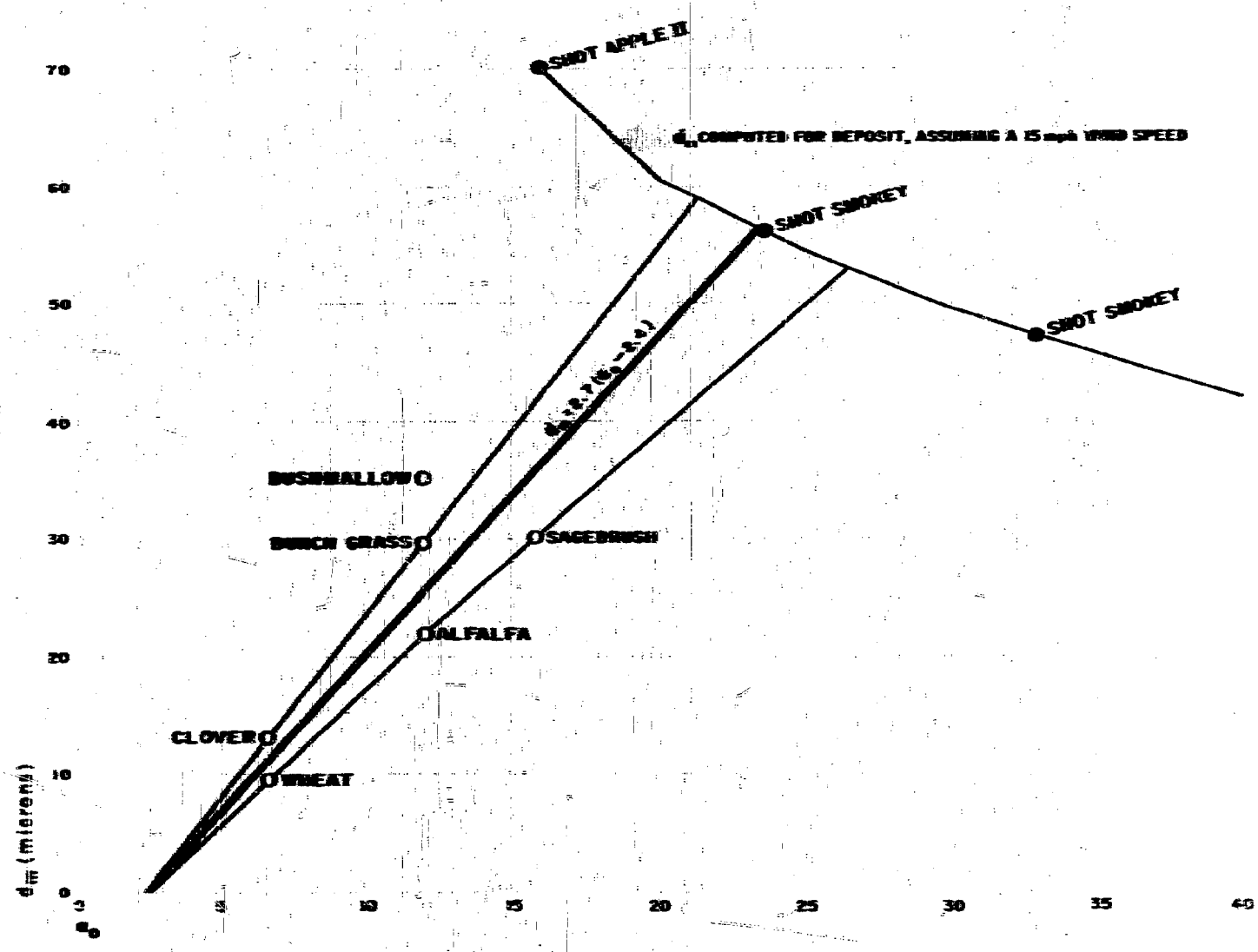

This application should be valid for any condition of detonation since the same physical phenomena must be involved in particle retention by foliage irrespective of the source of the depositing particles. When more data become available, the proposed representations of the processes can be altered to be either more specific for different types of foliage or otherwise more complicated depending on the observed variations in the data.

CHAPTER 6 REFERENCES

1. Bolles, R.C., and N.E. Ballou, Calculated Abundances of U-235 Fission Products, USNRDL-456, 1956.

2. Miller, C.F., and P. Loeb, Ionization Rate and Photon Pulse Decay of Fission Products From the Slow Neutron Fission of U-235, USNRDL-TR-247, 1958.

3. Strope, W.E., Evaluation of Countermeasure System Components and Operational Procedures, Operation Plumbbob WT-1404, 1958.

4. Miller, C.F., Analysis of Fallout Data, I. The Jangle "S" and "U" Shot Fallout Patterns, USNRDL-TR-220, Del. 1959.

5. Morgan, K.Z., et al., Report of ICRP Committee II on Permissible Dose For Internal Radiation (1959), Health Physics, Vol. 3 (1960).

6. Romney, E.M., R.G. Lindberg, H.A. Hawthorne, B.G. Bystrom, and K.H. Larson, Health Physics (to be published).

Wind
  crosswind area, 244
  direction effects, 202, 237, 300, 382
  downwind location, 9, 63-91, 112, 195, 217, 227-245, 276-304, 362-370
  shear, 228, 242, 290, 301
  upwind location, 360
  vector, 81, 218
  velocity, 80, 202, 205, 218, 235, 242, 292
Wittman, J.P., 38
Work-effort, see Effort
World War II, 361
WSEG, 293, 294, 297

--X--

X-rays, 4, 8, 204

--Y--

Yield, weapon
  attack level, 366-367
  effects, 8, 27, 45, 56, 62, 67, 87, 101-115, 135-139, 157, 165, 183, 202-204, 230, 305, 327, 397, 355-366, 381, 392
  independent, 17, 67, 197

--Z--

Zone, Black, 356
Zigman, P., 56, 180, 195, 223

Best Available Copy

STANFORD RESEARCH INSTITUTE

MENLO PARK CALIFORNIA

Regional Offices and Laboratories

Southern California Laboratories
820 Mission Street
South Pasadena, California

Washington Office
808 17th Street, N.W.
Washington 6, D.C.

New York Office
270 Park Avenue, Room 1770
New York 17, New York

Detroit Office
The Stevens Building
1025 East Maple Road
Birmingham, Michigan

European Office
Pelikanstrasse 37
Zurich 1, Switzerland

Representatives

Honolulu, Hawaii
Finance Factors Building
195 South King Street
Honolulu, Hawaii

London, Ontario, Canada
85 Wychwood Park
London 14, Ontario, Canada

London, England
15 Abbotsbury Close
London W. 14, England

Milan, Italy
Via Macedonio Melloni 40
Milano, Italy

Tokyo, Japan
911 Iino Building
22, 2-chome, Uchisaiwai-cho, Chiyoda-ku
Tokyo, Japan

Best Available Copy

AD 634901

THE CONTAMINATION BEHAVIOR OF FALLOUT-LIKE PARTICLES EJECTED BY VOLCANO IRAZU

SRI Project
No. MU-5779

April 1966

Prepared by:

Carl F. Miller

Contract No. N228-(62479)69928
OCD Subtask No. 3119A

STANFORD
RESEARCH
INSTITUTE

MENLO PARK
CALIFORNIA

Prepared for:

OFFICE OF CIVIL DEFENSE
DEPARTMENT OF THE ARMY
WASHINGTON, D.C. 20310

Through:

Technical Management Office
U.S.N.R.D.L.
San Francisco, California 94135

This report has been reviewed by the Office of Civil Defense and approved for publication. This approval does not signify that the contents necessarily reflect the views and policies of the Office of Civil Defense.

Figure 1

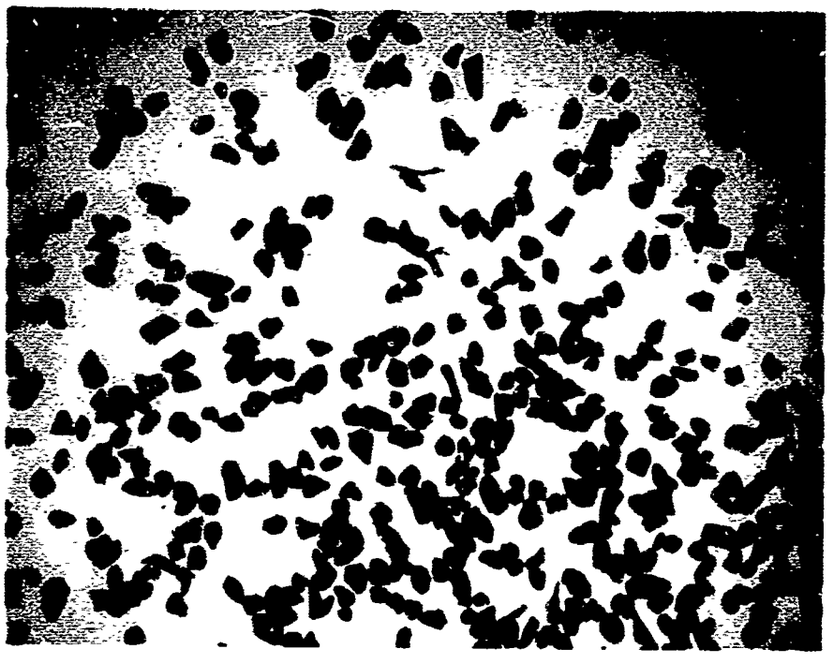

FALLOUT PARTICLES FROM A LOW-YIELD NEAR-SURFACE NUCLEAR DETONATION

Particle Size Range: 44 to 88 microns (mag 30X)

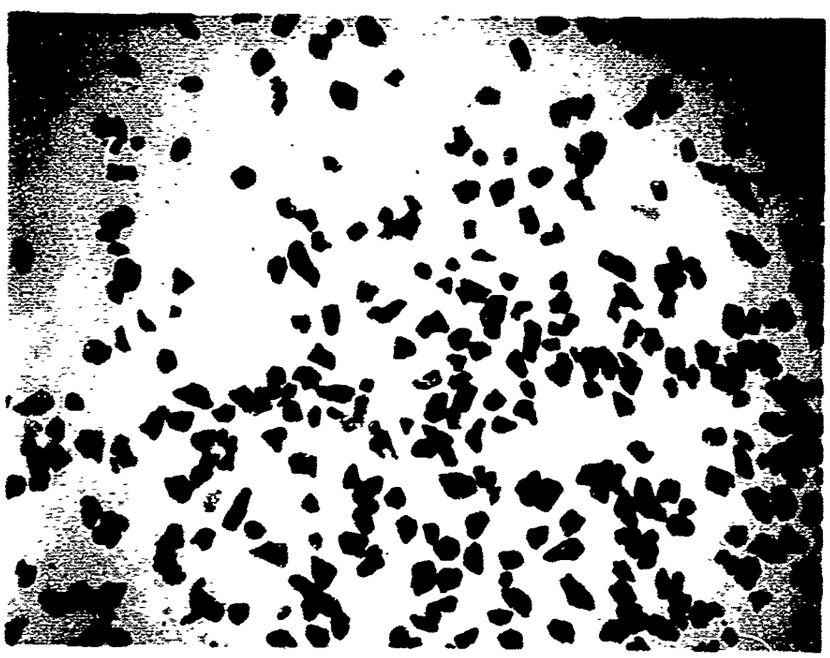

FALLOUT PARTICLES FROM AN ERUPTION OF VOLCANO IRAZU

Figure 2

FALLOUT PARTICLES FROM A LOW-YIELD NEAR-SURFACE NUCLEAR DETONATION

Particle Size Range: 88 to 175 microns (mag 30X)

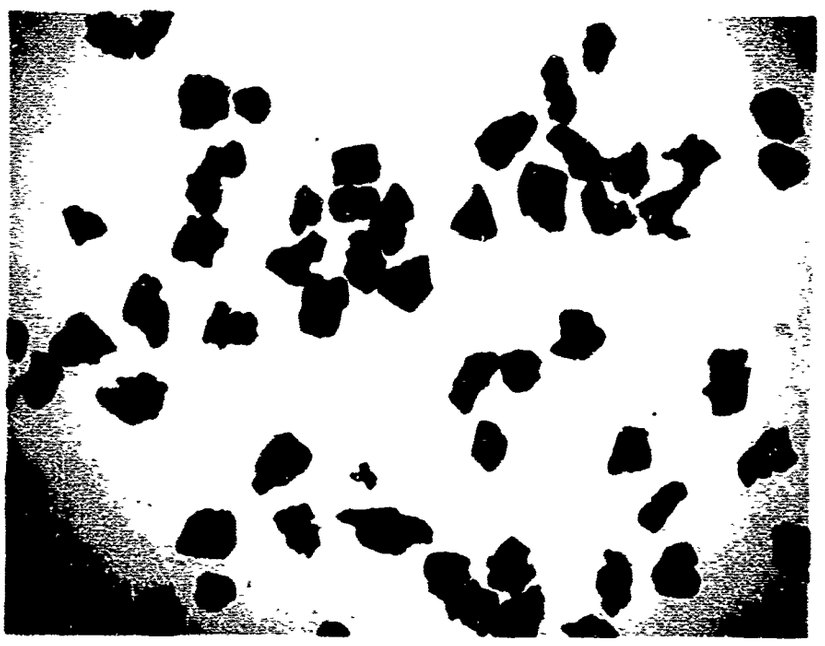

FALLOUT PARTICLES FROM AN ERUPTION OF VOLCANO IRAZU

Figure 26

CONTAMINATION OF PEOPLE

The first sensation by humans in a particle shower was the impact of the particles on the nose and forehead. Local fallout particles from nuclear detonations are generally too large to enter the nose by normal breathing, and this was also true of the volcanic particles at distances up to about 30 miles from the volcano where the deposit levels were readily observed and measurable. After a few minutes of exposure, the second sensation was a gritty feeling on the lips and between the teeth. Next noticed was a disturbance in the scalp--especially for people with short haircuts.

Figure 44

CONTAMINATION OF VEGETATION: OAT AND WHEAT HEADS

Translocation of radionuclides from nuclear weapon fallout particles to the seeds could occur at any stage before the seeds ripen, and in the flowering stage, beta radiation might inhibit pollinization. The wheat seeds are protected from contamination more than the barley seeds by the husks around the individual seed grains. Data from fallout tests show that the translocated radionuclides are not distributed uniformly in the wheat grains; of the small amount that penetrates through the husk, only a low fraction passes through the seed skin. After milling, most of the remaining radionuclides are separated from the flour along with the bran.

Figure 45

CONTAMINATION OF VEGETATION: BROADLEAF GRASSES

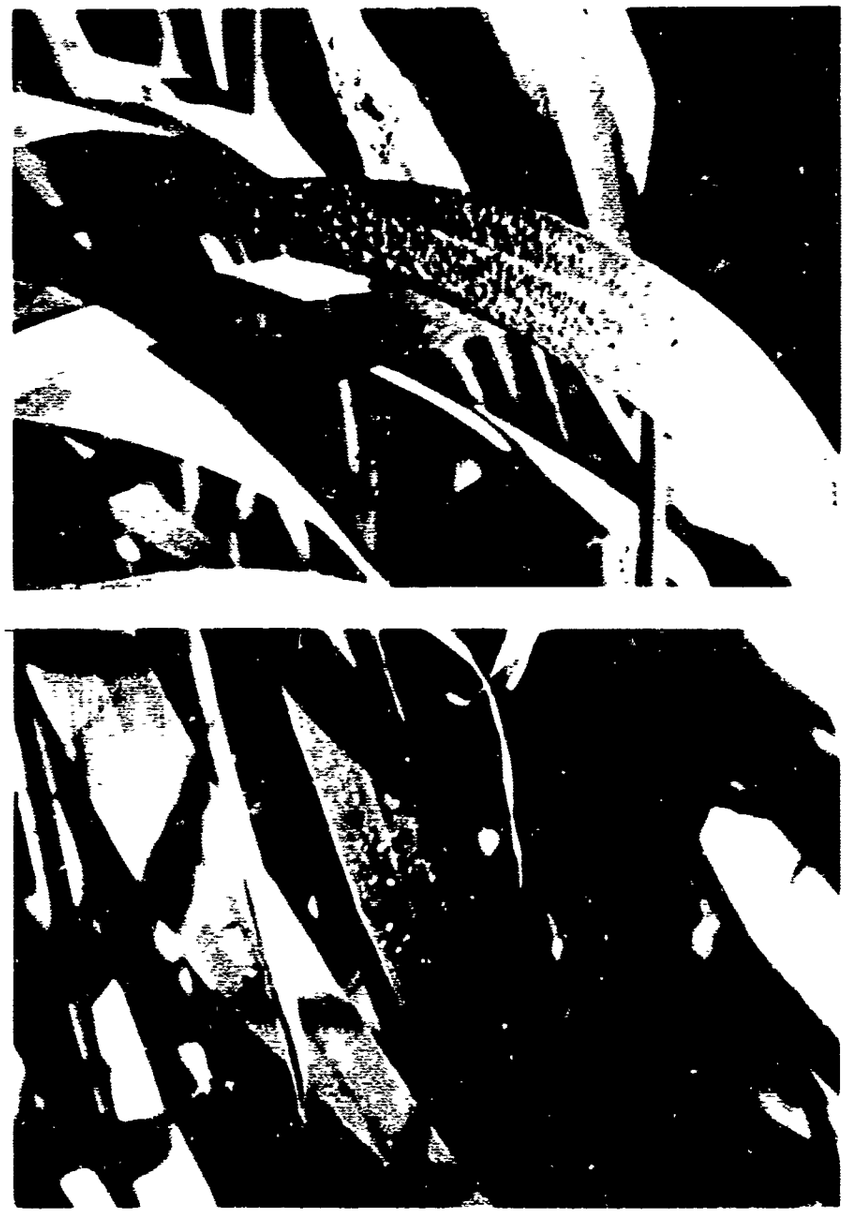

Broad-leafed oat grass was partially cleaned by heavy dew. On the bottom, mud balls and clean dewdrops are shown in an early stage of drying in the morning sun. On the top, the mud balls on the horizontal portion of the leaf were almost fully dried. The portion of the leaf with the steep slope was cleaned by the drainage of the dew-drops. The initial contamination of most vegetation under damp conditions (presence of dew) was about twice that under dry conditions, given the same wind conditions, despite the loss of particles when the dew was very heavy.

Figure 46

COSTA RICAN DECONTAMINATION METHODS: ROOFS

Although the wind and rain kept the exposed corrugated iron sheet roofs relatively clean, wind-protected roof areas collected a relatively large amount of the particles and were not cleaned by wind action. These areas were occasionally cleaned by sweeping. This cleaning job was left to the property owner to accomplish. The material was swept off the roof, as shown in this figure, and onto the street and sidewalk. After the roof was cleaned, the material on the sidewalk was generally swept into the gutter in a pile. Some of the house owners and shop owners collected the sweepings in large barrels and garbage cans for later pickup by municipal crews.

Figure 47

COSTA RICAN DECONTAMINATION METHODS: ROOFS

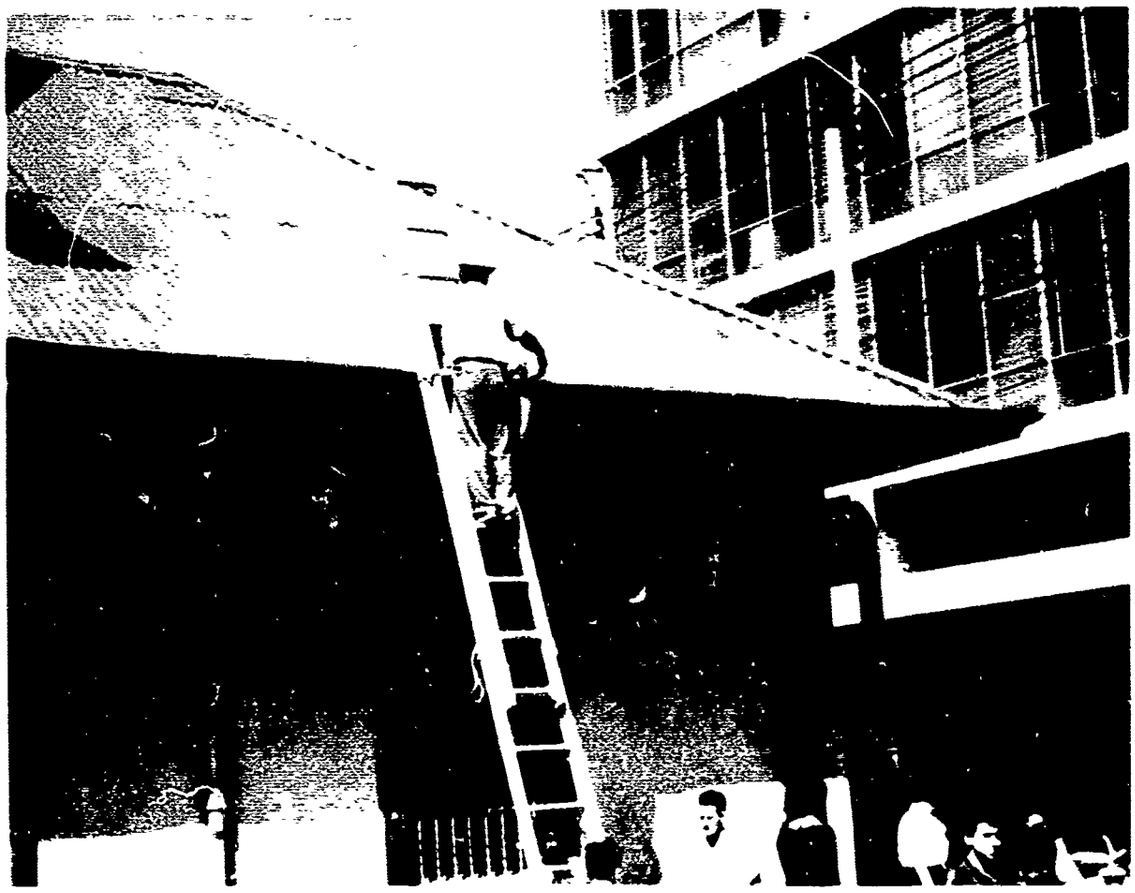

Most of the roof gutters were cleaned by hand, using a small can to scoop the particles from the gutter. They were then dumped into a large bucket which, when full, was lowered to the sidewalk with a rope. In some of the downtown areas, a vacuum cleaner attached to a large metal drum (as a collecting container) was used to clean the gutters.

Figure 48

COSTA RICAN DECONTAMINATION METHODS: ROOFS

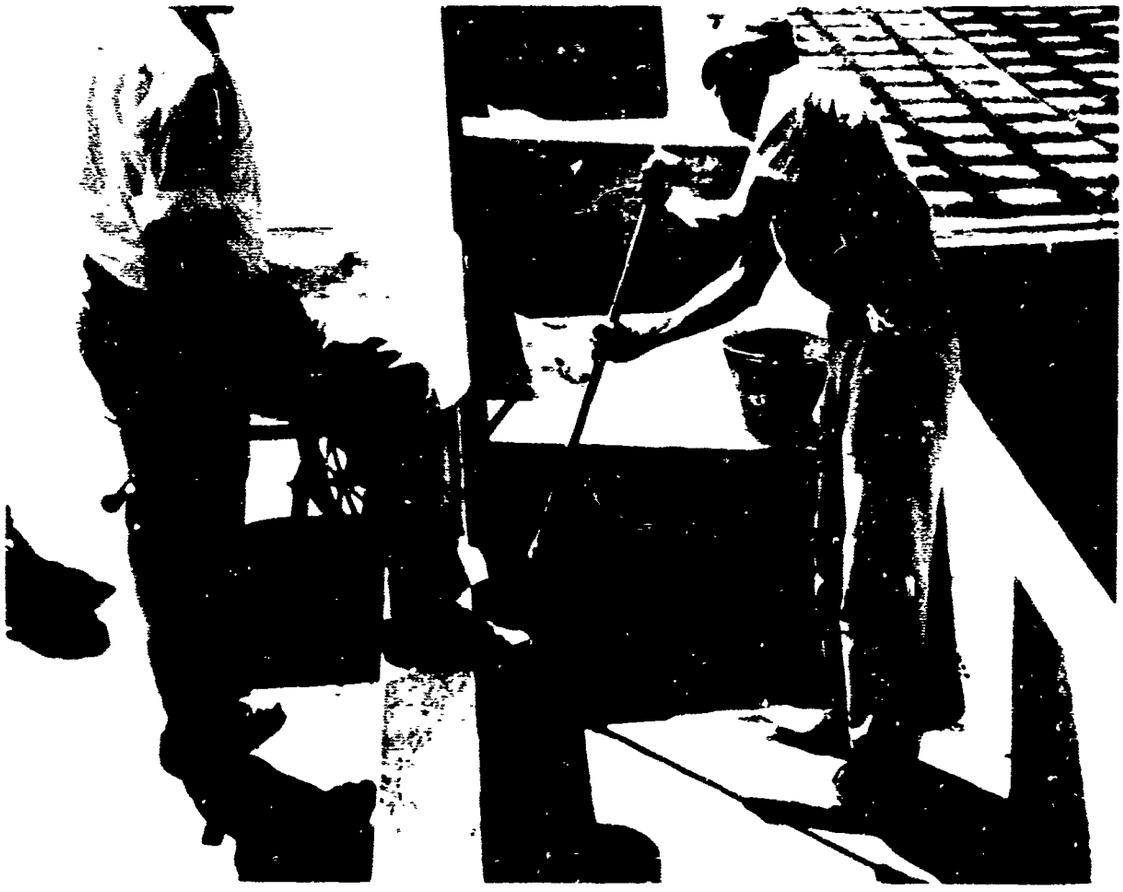

Broom, shovel, pail, and wheelbarrow were used to clean parapeted flat roofs. For small areas, such as shown in this figure, the material was put into the wheelbarrow, transported to the edge of the roof, and dumped onto the ground (or street) below.

With a limited water supply, some variation of the described techniques would be suitable for decontamination of roofs in the postattack period following a nuclear war. Where water is available, roofs would be more effectively cleaned by fire-hosing, using trained crews under controlled scheduling of the exposure of the crews to radiation.

SECRET
Security Information

CONFIDENTIAL

WT-393
Copy

UNCLASSIFIED

This document has been released by the Division of Military Application for authorized distribution within the Atomic Energy Commission.

Operation

JANGLE

NEVADA PROVING GROUNDS
OCTOBER-NOVEMBER 1951

Project 2.3-2

FOXHOLE SHIELDING OF GAMMA RADIATION

EACH TRANSMITTAL OF THIS DOCUMENT OUTSIDE THE AGENCIES OF THE U.S. GOVERNMENT MUST HAVE PRIOR APPROVAL OF THE DIRECTOR, DEFENSE ATOMIC SUPPORT AGENCY, WASHINGTON, D.C. 20301.

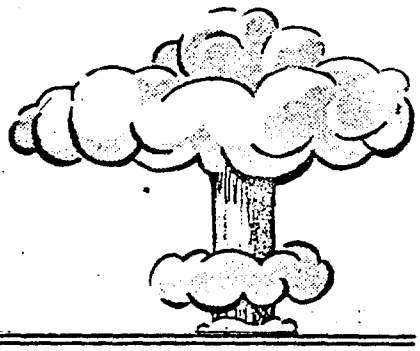

RESTRICTED DATA
ATOMIC ENERGY ACT 1946

ARMED FORCES SPECIAL WEAPONS PROJECT
WASHINGTON, D.C.

UNCLASSIFIED

604-001

CONFIDENTIAL

SECRET
Security Information

CONFIDENTIAL

SECRET
Security Information

This document has been released by the Division of Military Application for authorized distribution within the Atomic Energy Commission.

UNCLASSIFIED

~~This document consists of 29 plus 4 pages (counting preliminary pages)~~

18 AEC

19 WT-393

N643062

21 Report on OPERATION JANGLE,

PROJECT 2.3-2

6 FOXHOLE SHIELDING OF GAMMA RADIATION,

by

10 THOMAS G. WALSH.

11 27 June 1952,

12 21p.

Classification cancelled (or changed to CONFIDENTIAL)
by authority of Ltr fr. Capt. J.W. Gratton, DASA, dated 7/4/57
by 88 TIE, date 10/6/59

ENGINEER RESEARCH AND DEVELOPMENT LABORATORIES

UNCLASSIFIED

SECRET
Security Information

RESTRICTED DATA
ATOMIC ENERGY ACT 1946

CONFIDENTIAL

038050

CONFIDENTIAL

SECRET
Security Information

PROJECT 2.3-2

ABSTRACT

This project was designed by the Corps of Engineers to evaluate the protection afforded by foxholes against the gamma radiation emitted by atomic weapons detonated on the surface and beneath the ground. Film dosimeters were used to measure total gamma ray doses at different depths in one and two-man foxholes as well as in soil pipes sunk into the ground. The film dosimeters were contained in National Bureau of Standards' type holders and responded to gamma radiation of energy greater than 120 Kev. In the report, all doses are given in terms of roentgens and a reading of 650r (roentgens) is taken as the lethal dose; that is, the dose which will cause death to nearly 100 ~~per cent~~ % of exposed personnel.

The major conclusions of this experiment, based on the data obtained in the above manner, follow:

1. Standard foxholes, as described in FM 5-15, provide excellent protection to personnel from the gamma radiation emitted during the detonation of an atomic weapon on the surface of the ground. The results show that the doses in the bottom of such foxholes located in the crosswind direction during Operation JANGLE were less than 10 per cent of the surface doses at identical locations. Since the foxholes were located outside of the major fall-out pattern, the complete dose measured was due to scattered prompt radiation. If the foxholes had been located downwind, however, the doses would have been higher, since fall-out into the foxhole and scattered radiation from the contamination on the surface would contribute more significantly to the total dose. There are indications that these contributions will not materially change the per cent of surface-received radiation reaching trained personnel in the bottom of the foxholes. An increase of surface contamination will increase the surface dose as well as the dose at the bottom of the foxhole, thereby maintaining the ratio between the two. The contaminated matter that falls into the foxhole can easily be removed by occupying personnel before it has time to increase the doses received to any great extent.

2. Except in those areas covered by extensive fall-out, foxholes also provided affective shielding in the case of the underground detonation of Operation JANGLE. The doses at the bottom of the foxholes varied from about 24 to 38 per cent of the surface doses at distances greater than 2500 feet from the burst. A great portion of this

SECRET
Security Information

RESTRICTED DATA
ATOMIC ENERGY ACT 1946

004-006

dose, about 90 per cent, was obviously due to radioactive matter that fell into the foxhole, because the doses measured in the holes during the surface shot were approximately 10 per cent of those measured during the underground shot of identical yield. It is expected that both bursts contributed equally to the doses as far as prompt radiation is concerned.

3. The doses obtained from the detonation of atomic weapons on the surface or underground receive contributions from prompt gamma radiation, radiation emanating from column and cloud, and from residual activity due to fall-out of radioactive matter. No base surge activity was evident.

4. The complete doses at the bottom of the foxholes after the surface burst of this operation were attributable to scattered prompt radiation in addition to a small contribution from the column and cloud; no material contribution from fall-out or residual activity was evident. This lack of effect undoubtedly resulted from the location of the foxholes in the crosswind direction. If the foxholes had been located downwind, there would have been a material contribution from fall-out and residual activity. It is not expected that this would falsify the conclusions drawn in this report on the effectiveness of foxholes as protection for personnel against gamma radiation. (See conclusion 1, above.)

5. The major portion of the total dose measured at the bottom of the foxholes after the underground burst apparently came from fall-out matter in the foxhole. Contamination on the surface of the ground surrounding the foxhole contributed only about 10 per cent to the doses at the bottom of these structures, and prompt radiation could not contribute more than evidenced in the surface burst since both weapons were the same size. Yet, in all cases the doses were considerably higher during the underground detonation, leading to the obvious conclusion that matter falling into the foxholes played the most important role. Also, the doses in the two and one-man foxholes were equal, although the two man foxhole had twice the opening area. If the column or cloud activity contributed greatly to these doses, it could be expected that the doses in the two-man foxhole would be about twice as great as those in the one-man structure.

RESTRICTED DATA
ATOMIC ENERGY ACT 1946

007.

SECRET
Security Information

PROJECT 2.3-2

TABLE 3.1

Distribution of Gamma Radiation in Foxholes (Surface Burst)

Range (ft)	Location	Two-man Foxhole			One-man Foxhole		Soil Pipe
2000	36" Above Surface		800 r				
	Surface		700				
	16" Below Surface	230	205	415			
	32" Below Surface	24	58	136			
	48" Below Surface	12.8	22	62			
2500	36" Above Surface		230 r				
	Surface		220				
	16" Below Surface	35	60	85			
	32" Below Surface	7	15	26			
	48" Below Surface	4	8.5	13.3			
3000	36" Above Surface		110 r				73 r
	Surface		90			55	
	16" Below Surface	23	36	55	6.8	6.6	10
	32" Below Surface	7.6	12.4	19.4	2.5	2.4	0.5
	48" Below Surface	2.5	4.8	6.7	1.6	1	0
3500	36" Above Surface		41 r				
	Surface		---				
	16" Below Surface	3	---	9.7			
	32" Below Surface	1.6	2.8	3.4			
	48" Below Surface	.54	.99	1.9			
4000	36" Above Surface		17 r				17 r
	Surface		9.6			---	
	16" Below Surface	1.6	3	5.6	---	0.35	---
	32" Below Surface	0.6	1.12	1.62	---	---	0.17
	48" Below Surface	---	0.54	0.57	0.39	---	---
4500	36" Above Surface		9.8 r				
	Surface		4.6				
	16" Below Surface	1	1.8	3.5			
	32" Below Surface	0.5	0.7	1.04			
	48" Below Surface	0.21	0.4	0.57			
5000	36" Above Surface		4.8 r				
	Surface		2.7				
	16" Below Surface	0.6	0.99	2.95			
	32" Below Surface	0.3	0.5	0.75			
	48" Below Surface	0.17	0.2	0.38			

RESTRICTED DATA
ATOMIC ENERGY ACT 1946

SECRET
Security Information

SECRET
Security Information

PROJECT 2.3-2

TABLE 3.2

Distribution of Gamma Radiation in Foxholes (Underground Burst)

Range (ft)	Location	Two-man Foxhole			One-man Foxhole		Soil Pipe
2000	36" Above Surface		3850 r				
	Surface		2300				
	16" Below Surface	1150	--	800			
	32" Below Surface	700	1000	555			
	48" Below Surface	200	200	200			
2500	36" Above Surface		1000 -- 550 r				
	Surface		78				
	16" Below Surface	78	98	115			
	32" Below Surface	43	56	50			
	48" Below Surface	73.4	94	96			
3000	36" Above Surface		175 r				155 r
	Surface		103			75	
	16" Below Surface	30	42	37	20	--	7
	32" Below Surface	22	23	20	15	11	3
	48" Below Surface	43.5	45	54	41	38	3
3500	36" Above Surface		--				
	Surface		48				
	16" Below Surface	12	17	15			
	32" Below Surface	9	10	9			
	48" Below Surface	15	15	22			
4000	36" Above Surface		32 r				28 r
	Surface		22			14	
	16" Below Surface	6	7	15	7	4	2
	32" Below Surface	5	3.4	7.2	3.7	2.8	0
	48" Below Surface	6	8.4	8.6	5	9.8	1.1
4500	36" Above Surface		22 r				
	Surface		10				
	16" Below Surface	4	5	5			
	32" Below Surface	5.8	2.8	2.8			
	48" Below Surface	--	7.7	8.9			
5000	36" Above Surface		73 r				
	Surface		23				
	16" Below Surface	15	15	67			
	32" Below Surface	21.5	22.6	15			
	48" Below Surface	--	21	19			

SECRET
Security Information

RESTRICTED DATA
ATOMIC ENERGY ACT 1946

6 2 014

SECRET

(18) AEC (19) WT-728

This document consists of 262 pages

No. 217 of 275 copies, Series A

(21) Report on

OPERATION UPSHOT-KNOTHOLE

Project 3.9

(6) # FIELD FORTIFICATIONS

~~REPORT TO THE TEST DIRECTOR~~

by

(10) Allan R. Fowler and Daniel R. Muller

(11) Dec 54

(12) 262 p.

December 1954

EACH TRANSMITTAL OF THIS DOCUMENT OUTSIDE THE AGENCIES OF THE U.S. GOVERNMENT MUST HAVE PRIOR APPROVAL OF THE DIRECTOR, DEFENSE ATOMIC SUPPORT AGENCY, WASHINGTON, D.C. 20301.

ATA

This document contains restricted data as defined in the Atomic Energy Act of 1954. Its transmittal or the disclosure of its contents in any manner to an unauthorized person is prohibited.

Classification cancelled (or changed to ...) by authority of Defense Atomic Support Agency, DASA Bulletin 11-16-60. by J. R. Nelson TISOR, date 1-13-61

Engineer Research and Development Laboratories
Fort Belvoir, Virginia

SECRET

1.2.2 Exercise DESERT ROCK I(1)

This exercise was conducted at the Nevada Proving Grounds in the fall of 1951 in conjunction with BUSTER-JANGLE. The objective of this exercise was "to test current doctrines to the extent afforded, to determine the effect of an atomic weapon on equipment and materiel, to indoctrinate personnel, test their psychological reaction during the tactical employment of the weapon, and to the degree possible to determine what physical protective measures can be taken against the weapon."

As a part of that exercise, all normal types of tactical field fortifications were constructed and exposed at ranges from 1000 to 5000 yd from ground zero. Film badges and JS-1 thermal indicators were installed in emplacements to roughly indicate the amount of nuclear and thermal radiation received. Animals were placed at ground level, below ground level, and in shelters. From the test, an evaluation of damage to emplacements was made. Through the use of test animals and indicators, an estimate of the probable effects on personnel under varying conditions of shielding was made. The test conditions were estimated as 21.5 KT at a height of burst of 1417 ft giving 6 psi, 40 cal/cm^2, and 700 r incident at 1020 yd from ground zero.

It was concluded that: "An atomic weapon of the yield employed in Exercise DESERT ROCK and detonated at similar height will cause very few, if any, casualties beyond 1000 yd from ground zero, when personnel and equipment are well dug in on the battlefield and alerted to a possible attack. Physical protective measures currently employed by our forces are adequate to include normal field fortifications, revetments of all types, and present types of military equipment."

1.2.3 Exercises DESERT ROCK II and III(2)

These exercises were conducted at the Nevada Proving Grounds during the fall of 1951 in conjunction with BUSTER-JANGLE to supplement Exercise DESERT ROCK I. They were to obtain information relative to the effects of surface and underground nuclear explosions on typical army field emplacements, equipment and materiel, and to determine (insofar as possible) the probable effects on personnel.

As a part of these exercises, a few special and a multitude of standard army field emplacements were positioned from 100 to 1000 yd from ground zero and instrumented with film badges. These included revetted and unrevetted emplacements, both with and without overhead cover. From the tests, evaluations of the gross damage to the emplacements were made and the results of the gamma radiation measurements presented.

Exercise DESERT ROCK II, conducted with an estimated 1.1 KT surface burst, included the following general results: "The most distant revetted emplacement which collapsed to an appreciable degree was foxhole No. 3 at 280 yd. The most distant unrevetted foxhole which suffered serious damage was foxhole No. 9 at 515 yd. The average emplacement reduced the (gamma) dosage to 10 per cent of the dosage in the open at the same distance; indications were that overhead cover increased the protection from gamma radiation to a small degree."

SECRET – RESTRICTED DATA

Exercise DESERT ROCK III, conducted with an estimated 1.1 KT burst at 17 ft below ground surface, included the following general results: "In this test, the most distant revetted emplacement which collapsed to an appreciable degree was the two-man foxhole with overhead cover at 412 yd. The most distant unrevetted emplacement which suffered severe damage was the two-man foxhole without overhead cover at 566 yd. A substantial amount of the initial radiation following the underground shot came from the low radioactive cloud which covered the test positions. ...Along the NE line of positions, the average foxhole gave roughly 75 per cent protection from the radiation. Along the S line of positions, the average emplacement gave roughly 85 per cent protection. The per cent protection apparently depends upon how close the center of the cloud comes to a particular foxhole or emplacement."

General conclusions from the two tests are: "It is felt that the results of DESERT ROCK Exercises I, II, and III provide adequate information as to the protection afforded by normal field emplacements in this type of terrain and soil. Normal field emplacements provide about 80 per cent protection against the nuclear radiation effects of surface and underground bursts. Specially designed field emplacements for atomic warfare are not justified."

1.2.4 Exercise DESERT ROCK IV(3)

Exercise DESERT ROCK IV, the U. S. Army designation for its participation in TUMBLER-SNAPPER, was held at the Nevada Proving Grounds during the months of April, May, and June of 1952. In general, the mission of Exercise DESERT ROCK IV was a continuation of the missions of the previous three Exercises DESERT ROCK. While the principal mission of the exercise was the indoctrination of troops and observers, attention was also given to blast and thermal effects on troop equipment, materiel, emplacements, and live animals.

The exercise included fortification display areas at ground ranges between 200 and 3500 yd for Shots 3, 4, 6, and 8. The fortifications were of the normal tactical type. Animals, film badges, and equipment and materiel were placed both inside and outside of the emplacements.

Damage effects were presented in the form of tables and photographs in the report, with emphasis placed on the damage to equipment and materiel.

There was little discussion of the damage to fortifications. Applicable results and conclusions were: "Lethal effects of gamma radiation on sheep in foxholes up to 550 yd from ground zero, and lethal effects of gamma radiation on sheep above ground surface up to 900 yd from ground zero. Severe blast damage on surface of ground up to 1700 yd from ground zero (for Shots 3, 6, and 8). Troops in average hasty entrenchments at a range of 1700 yd from ground zero are believed safe from all effects of the size burst used in this exercise, provided they are 'down' at the time of burst." (Refers to Shot 4, 22 KT, 1050 air burst.)

SECRET – RESTRICTED DATA

1.2.5 Exercise DESERT ROCK V(4)

Although Exercise DESERT ROCK V was conducted at the Nevada Proving Grounds concurrently with Project 3.9, UPSHOT-KNOTHOLE, and therefore does not actually fall into the category of background, their final report has been published and is summarized here for purposes of continuity of the overall DESERT ROCK work. The following quotations should explain the scope of the fortification study made in this exercise: "In general, the mission of Exercise DESERT ROCK V was a continuation of the four previous Exercises DESERT ROCK. The principal mission of the exercise was the orientation and indoctrination of troop observers and troop participants."

Two special features of this exercise were groups of volunteer officers who occupied trenches at the closest range any known personnel have been exposed in a training situation, and the preparation of target damage estimates by instructors of the Special Weapons Course, C&GSC, for comparison with the actual damage evaluations.

The fortification layouts were extensive, ground ranges varying from 100 to 3500 yd for Shots 1, 2, 5, 7, 8, 9, and 10. Other than normal type trenches and weapon emplacements, the layouts included several types of heavily constructed bunkers. Fortifications were instrumented with film badges in NBS holders and, to a lesser degree, with passive type thermal indicators. There was extensive exposure of animals (sheep), both inside and outside of the fortifications. From the tests, the gross effects on equipment, materiel, fortifications, and animals along with the predicted effects on these items were presented in tabular form. The results of gamma and thermal radiation measurements were also presented.

The applicable general conclusions of the exercise are illustrated in the following paragraphs:

Selected officer volunteers, capable of calculating effects of atomic weapons, were positioned in trenches at 2000 yd for Shots 5 and 7, and at 2500 yd for Shot 2. The location of the trench in each case was based upon the determination of a safe distance by the volunteers using data from TM 23-200, dated 1 October 1952. The volunteer officers concluded that a trench 6 ft deep and unrevetted gave adequate protection under the given conditions, that there was no discomfort from blast or thermal effects, and that ground shock, at this distance, was not of sufficient magnitude to be of any concern.

On all shots, a diagram of the equipment display area was forwarded to the Command and General Staff School, Ft. Leavenworth, Kansas, in order that instructors of the Special Weapons Course could predict damage based on the layout of the display area, the expected KT yield, and the predicted weather. From comparing these estimates with actual damage and from the results of the officer volunteer program, it was concluded that "atomic weapons effects data found in TM 23-200, dated 1 October 1952, can be used by qualified officers to determine safe troop positions and to predict damage to equipment, emplacements, and personnel as the result of an atomic weapon detonation."

SECRET - RESTRICTED DATA

1.2.6 Report of the Protection Afforded by Field Fortifications Against Gamma Radiation from an Airburst Atomic Bomb, RANGER

This test is reported in WT-201, along with other studies made at RANGER. Because this test was essentially duplicated by a later test at BUSTER, which is summarized in Section 1.2.8 below, further discussion here is considered unnecessary.

1.2.7 Blast Injuries in Foxholes, GREENHOUSE(5)

This experiment was conducted as part of the atomic weapons tests at Eniwetok in 1951. The following paragraphs are totally or in part extracted from the report and should adequately describe the experiment:

Sixteen dogs protected in foxholes were exposed in pairs to the Item Shot in GREENHOUSE. The foxholes were of a uniform size, plywood lined, and fitted with instruments to measure blast, temperature, and ionizing radiations. They were dug 4 ft deep in coral at ranges of 400, 600, 800, 1000, 1250, and 1500 yd from zero point.

Post shot inspection showed that the two foxholes at 400 yd were about one-third filled with coral rubble. In one of these, the wall toward ground zero was pushed in about 20 degrees from the vertical, scorched on both sides at one-third the distance to the floor, and had three holes burned completely through. The foxholes at 600 yd held lesser amounts of coral stones and rubble. The plywood reinforcing walls held satisfactorily at these and all other more distant stations. Peak ground level overpressures were estimated to be about 100 psi and 30 psi, at 400 yd and 600 yd, respectively.

The blast gages used within the foxholes failed to yield useful data.

The clock mechanism in the (temperature) recorders failed in all but the two most distant stations. A definite increase in temperature (within the foxholes) was evident at 1250 and 1500 yd. Since the recorders were shielded from direct thermal radiation, it may be assumed that this represents a rise in temperature of the ambient air. Temperature increase was greater in the center of the holes than on the proximal wall. The temperature rise at 1250 yd was greater than at 1500 yd. Inasmuch as the greatest temperature rise was approximately 10 degrees (Fahrenheit), this phenomenon would have no biological significance to men or animals located near the bottom of the hole.

It was concluded that: "Under the conditions of this experiment and with the exception of the 400 yd station, the foxholes provided effective shelter against thermal and secondary blast injuries.

"With the observed brain damage not classified as a true primary blast injury, it appears that all the foxholes except the 400 yd station were protected against critical primary blast injury.

"At and beyond 1250 yd, the total gamma ray and neutron exposure in the bottom half of the foxholes was below lethal limits for the dog. Throughout the range of distance involved in these studies, the total gamma-ray and neutron dosages at the surface were in the supposedly lethal or seriously incapacitating range for dogs and man."

It was recommended that: "A thorough program with a high priority should be planned and carried out to determine the optimum designs for emergency field shelters. Animal exposures should be part of this program."

1.2.8 The Protective Effects of Field Fortifications Against Neutron and Gamma Ray Flux, BUSTER(6)

"This experiment was designed by the Corps of Engineers to evaluate the protection afforded by field fortifications against the nuclear radiations from atomic weapons." The experiment was conducted at the Nevada Proving Grounds in the fall of 1951 as Project 2.6 of BUSTER.

The experimental procedure was as follows: Standard two-man foxholes were constructed in Area 7 of the Nevada Proving Grounds at 300 yd intervals from 100 to 2200 yd from the expected ground zero of the Baker, Charlie, and Dog detonations. Each foxhole was instrumented in 10 different positions with gamma film detectors. Slow neutron detectors were placed along the center vertical axis in those foxholes which were located within 1300 yd of ground zero and fast neutron detectors in the same positions in those foxholes closer than 1000 yd. In addition, there were two-man foxholes with concrete covers and open one-man foxholes constructed adjacent to those located at distances of 400, 1000, and 1600 yd from ground zero. Also, at these specific distances, a soil pipe 48 in. long and 6 in. in diameter was sunk flush with and perpendicular to the surface of the earth. The concrete-covered foxholes were instrumented in the same manner as the open two-man foxholes, but the one-man foxhole and the soil pipe were instrumented only along the central vertical axis at depths of 16, 32, and 48 in. with gamma detectors. No neutron detectors were employed in the one-man foxholes.

Some of the more important results and conclusions of the test are presented in the following paragraphs.

"On the average, the dosages at the bottom of the fortifications were approximately 12 per cent of those at the surface. It is interesting to note that the percentage decrease at the various depths was essentially constant, despite the variation in the size of the detonations. Therefore, if the surface dosage at a point or the approximate size of the weapon were known, it is possible from this information to predict accurately exposures to personnel in open fortifications.

"Comparison of the exposures in the two-man and the one-man fortifications indicates that the exposures at different depths were directly proportional to the solid angle formed at the point of measurement by the opening of the fortifications, for distances greater than approximately 1500 ft from ground zero.

"Comparison of the exposures recorded in the concrete-covered fortification with those in the uncovered showed that the 15 in. concrete slab decreased measured dosages by a factor of about 16. This factor was calculated by considering the results in the two-man fortifications located at slant ranges of approximately 1800 and 3350 ft.

"The gamma radiation emitted during a detonation should be considered the primary nuclear hazard to personnel exposed to the burst of

SECRET - RESTRICTED DATA

this weapon. The range of the neutrons is such that they do not contribute greatly to the dosage except at those distances from a burst where the gamma radiation is already extremely dangerous.

"Analysis of the data obtained from the slow neutron detectors indicated that the neutron flux at different depths in open fortifications was essentially the same as that on the surface." (There was a marked decrease in slow neutron flux in the fortification with the 15 in. concrete cover.)

"The flux of fast neutrons, those whose energies were greater than 3 Mev, decreased with the depth of the fortification. Again, the marked decrease in the flux beneath the concrete slab was found in all cases."

1.2.9 F. C. D. A. Family Shelter Evaluation, BUSTER(7)

The Federal Civil Defense Administration family shelter evaluation under Project 9.1a, BUSTER, was designed to develop information on the degree of protection from atomic explosions afforded by simple structures which could be built by the average householder with available materials.

A total of 29 simple structures spaced 25 ft apart were built along an arc 1200 ft from the target point. Eighteen of the structures were the covered-trench type; five, metal-arch; four, wood-arch; and two, the basement lean-to type. Structural strength, materials, amount of earth cover, elevation, and orientation were varied for test purposes. The shelters were instrumented with gamma film badges, improvised deflection devices, and peak pressure recording land mine fuses.

The shelter structures were subjected to Shots Baker, Charlie, and Dog. From the tests, peak overpressures, thermal radiation, and gamma radiation readings were recorded. The effects of the explosions on the shelters were listed separately to assist in evaluating their reaction to each shot. Recorded data and structural damages were summarized in tabular form.

Some of the more important results and conclusions of the test are presented in the following paragraphs.

"Large quantities of earth cover were removed by each explosion. Amounts of cover blown off by Shot Baker varied from 30 to 60 per cent of the total cover. These quantities varied with elevation of structures with respect to natural grade. Partly above-grade shelters were affected to a greater extent. This undesirable reaction was serious, for it not only affected protection against radiation but also resistance of the structures to blast.

"Additional test data are needed on the reaction of earth cover. The test results do not show the effect of earth-arch action or whether the resistance of the mass of the earth cover contributed to the ability of structures to withstand blast. However, results did show that damage to structures was less severe when protected by even a small amount of cover. This was particularly evident where entrance structures were poorly protected but survived when covered. It appeared that if earth cover were below natural grade it would not be greatly affected by blast. Thus, lowering grade level of shelters would add considerably to their safety.

SECRET - RESTRICTED DATA

"The reaction of the earth cover affected not only the structural resistance of the shelters, but also their ability to protect against radiation. Reduced cover on the second and third explosions greatly increased radiation dosages within the shelters. Test structures were located sufficiently close to the three explosions to receive the shock an appreciable interval before all gamma radiation was absorbed.

"The entrances of all structures were considerably weaker than the shelters proper...practically all above-grade entrance construction was demolished and blown away. Debris thrown into the shelters was trapped in entrances and would not have injured occupants. It did block access to many of the shelters, and escape would have been hazardous. Some of the damage to the entrances was superficial and did not affect the protective value of the shelters, but all should be redesigned to provide resistance comparable with the capabilities of the rest of the structures.

"Scorching of parts of the entrance panels not directly exposed to the blast indicated the possibility of heat reflection of some magnitude. However, even in the shelter where the entrance side faced the blast, there was no evidence of heat entering the shelter proper.

"Wood shelters offered good resistance to blast provided they were properly protected by earth cover. They did not burn, and their resiliency permitted them to absorb shock without failing completely.

"The results obtained from the substitution of materials were satisfactory. Chicken wire and tarpaper sheathing for the sides of shelters were adequate where the spacing of supporting members was not too great."

1.2.10 AEC Communal Shelter Evaluation, BUSTER(8)

This test was conducted at the Nevada Proving Grounds in the fall of 1951 as Project 9.1b of BUSTER. The objectives of this test were to assess the effects of atomic bombs of various yields detonated in air at varying distances on a communal shelter of the design described herein, and to recommend to the Commission on the basis of the observed results a communal shelter design, deemed adequate within the limits of certain assumed risks, for construction as required at AEC facilities.

Since the test structure was a cylindrical, combination concrete and steel-pipe shelter of large dimensions, most of the results of the test are not applicable to field fortifications within the scope of this report. Those results that are applicable (such as the removal of earth cover affecting gamma radiation dosages within the shelter) do not materially differ from those presented in the preceding section of this report--1.2.8. For these reasons, as well as for purposes of brevity, further discussion of this test is not deemed necessary.

1.2.11 Hasty Type Air Raid Shelters, TUMBLER(9)

This experiment was conducted at the Nevada Proving Grounds in the spring of 1952 as a part of TUMBLER. The scope of the test is illustrated in the following quotations: "The necessity of providing

SECRET - RESTRICTED DATA

for the protection of personnel in the event of an enemy air attack against Sandia Base presents the problem of constructing adequate shelters in a short time with the facilities available to the Base Engineer. The degree of protection afforded against an atomic explosion by a trench shelter capable of being put in rapidly with powered ditchers gave rise to the desire of testing such a shelter under actual conditions." A test was set up with a primary objective: "...to determine the relative protection afforded personnel by an uncovered 'Z' shaped trench shelter versus that afforded by a covered 'Z' shaped trench shelter."

Two trench shelters, both unrevetted, one covered and one uncovered, were constructed at each of four positions located such that the actual ranges resulted as 625 ft, 1550 ft, 2725 ft, and 4925 ft from ground zero for Shot 4. "The main or middle portion of the trench shelter was dug approximately 25 to 30 ft long and 24 to 26 in. wide in both the covered and uncovered shelters. The arms forming the entrances varied from 8 ft to 11 ft in length, and were dug to a depth of 2 ft at their outer edge and sloped to the level of the floor of the main trench. One series of trenches was dug to a depth of 5 ft, and another series to a depth of 6 ft. The cover was constructed of 2 in. wood planking overlapping the sides of the main trench by at least 2 ft and overlaid with the spoil taken from the trench. The shelters were instrumented by the use of clothed dummies and film badges to observe the effects of blast and thermal radiation and to measure the value of nuclear radiation. From the test, the incident effects at the ranges listed above were tabulated as: 68 psi, 350 cal/cm^2, 77,000 r; 18.5 psi, 145 cal/cm^2, 18,000 r; 8.8 psi, 60 cal/cm^2, 3030 r; and 3.9 psi, 20 cal/cm^2, 183 r, respectively.

Some of the more important conclusions of the test are presented in the following paragraphs.

"The covered trench shelter affords greater protection against atomic effects, particularly gamma radiation, than does the uncovered trench shelter.

"In the region of 8 psi overpressure (Position 3), both shelters afford protection against blast pressure; but the measured nuclear radiation in the uncovered shelter of from 600 r to 800 r would have been fatal to occupants. The additional shielding afforded by the cover of spoil reduced this radiation to a range of from 80 r to 175 r, which is not considered to be a lethal dose. Protection from gamma appears to be the paramount problem in the shelter design; since, in the case of the shelters tested here, protection against blast and thermal effects apparently was greater than the protection against prompt gamma radiation.

"Soil structure is a major factor determining how well the shelter walls will withstand the effects of a blast. At Position 2, where the soil structure was fairly good, the shelter held at 18.5 psi overpressure; whereas, at Position 4, where the soil structure was poor, the sides of the shelter gave way at only 3.9 psi overpressure.

"The shape of the earth mound forming the cover should be broad and flat. The peaked mound of the covered shelter at Position 2 was greatly lowered; while the flat, low mound formed from the spoil of the uncovered shelter at that position was only slightly altered by the blast.

SECRET - RESTRICTED DATA

"Total thermal radiation estimated from observations of clothed dummies and charred wood is highly inadequate and not reliable."

It was recommended that: "If more detailed information on thermal radiation and blast effects on shelters of this type is desired, a more extensive program of instrumentation should be used in conjunction with a future test."

SECRET - RESTRICTED DATA

CHAPTER 2

EXPERIMENT DESIGN

2.1 TEST STRUCTURES

2.1.1 General Description

Fifty simplified structures were used to represent 12 command posts, 19 machine gun emplacements, and 19 two-man foxholes. All of the structures included revetment and overhead cover, the structure frames following timber bridge nomenclature and consisting of posts, caps, stringers, revetment, and top filler. The structures were varied in strength and materials for purposes of comparison. Table 2.1 shows the extent of variation of materials for each structural component. This variation is further illustrated in Tables 3.1 through 3.3, which show the particular materials used in each structure. Along with the variation in strength and materials, two types of construction were used. These consisted of the continuous-stringer type and the spaced-stringer-with-top-filler type and are illustrated in Figs. 2.1 through 2.6.

TABLE 2.1 - Variation in Materials

Component	Material
Post	8" x 8" timber 4" x 4" timber 2" x 4" timber
Cap	8" x 8" timber 4" x 4" timber 2" x 4" timber
Stringer	4" x 4" timber 2" x 4" timber 1" x 6" timber
Revetment	4" x 4" timber 1" x 6" timber 5/8" plywood corrugated iron

SECRET - RESTRICTED DATA

TABLE 2.1 - Variation in Materials (Continued)

Component	Material
Revetment(cont'd)	chicken wire and burlap chicken wire and pasteboard pasteboard
Top Filler	1" x 6" timber 5/8" plywood corrugated iron chicken wire and burlap chicken wire and pasteboard pasteboard

The construction of the command posts is shown in Figs. 2.1 and 2.2. The figures show an underground side view, with the near wall and post removed. The command posts were constructed with their stringers at grade level. The overall inside dimensions were 6 ft x 6 ft x 6 ft. The overall dimensions of the cover were 9 ft x 9 ft overlain with about 2 ft of loose earth. The entrance excavation protruded 6 ft from the wall of the structure and was 2 ft wide, with three 2 ft steps cut down to the command post proper. The sizes and spans of the timbers and the various materials used for each component in each command post are included in Table 3.1.

The construction of the machine gun emplacements is shown in Figs. 2.3 and 2.4. The figures show a partially underground rear view, with a portion of the rear wall and posts cut away. The stringers were 1½ ft above grade level, and the overall dimensions of the cover were 8½ ft x 10 ft overlain with about 1 ft of loose earth and sandbags. The overall inside dimensions were 5½ ft long x 7 ft wide x 6 ft tall. The entrance excavation protruded 6 ft from the rear wall and was 2 ft wide and 2 ft deep, leaving a 2 ft step down to the floor of the emplacement. The sizes and spans of the timbers and the various materials used for each component in each machine gun emplacement are included in Table 3.2.

The construction of the two-man foxholes is shown in Figs. 2.5 and 2.6. The figures show an underground corner view, with portions of the walls cut away. The overall inside dimensions of the foxholes were 2 ft long x 6 ft wide x 5½ ft tall. The stringers were 1 ft above grade level, and the cover had overall dimensions of 5 ft x 9 ft overlain with about ½ ft of loose earth and sandbags. On some of the foxholes, not shown, the cover had no overhang reducing the dimensions to 2 ft x 6 ft. The timber sizes and spans and the materials used in each foxhole are included in Table 3.3.

2.1.2 Instrumentation

Peak pressure measurements were made both outside and inside one command post, one machine gun emplacement, and one two-man foxhole with indenter peak pressure gages furnished by the Naval Ordnance Laboratory (NOL). This instrumentation was actually a part of the overpressure multiplication study, and the details are presented in Part II.

SECRET - RESTRICTED DATA

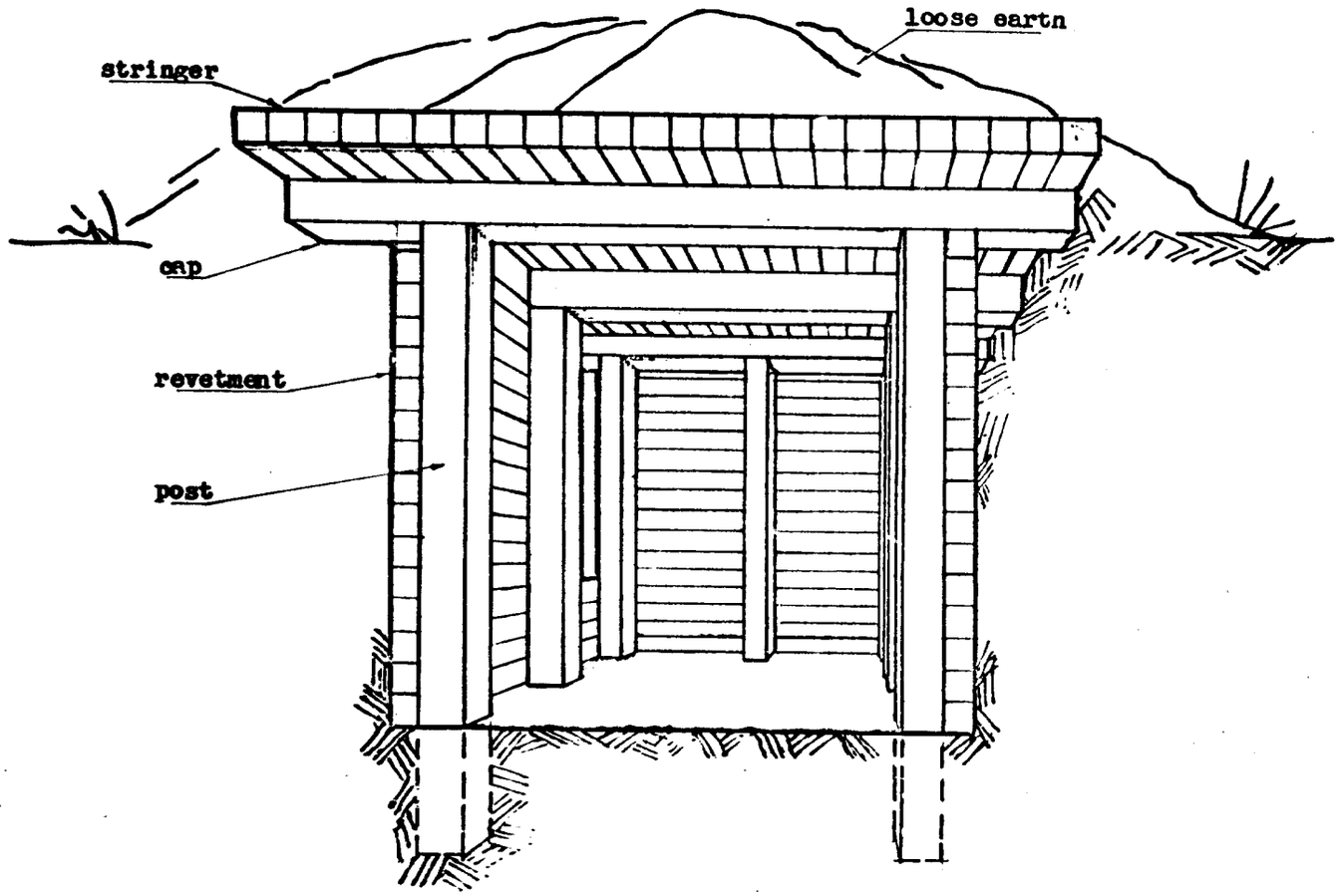

Fig. 2.1 Command Post with Continuous Stringers

SECRET – RESTRICTED DATA

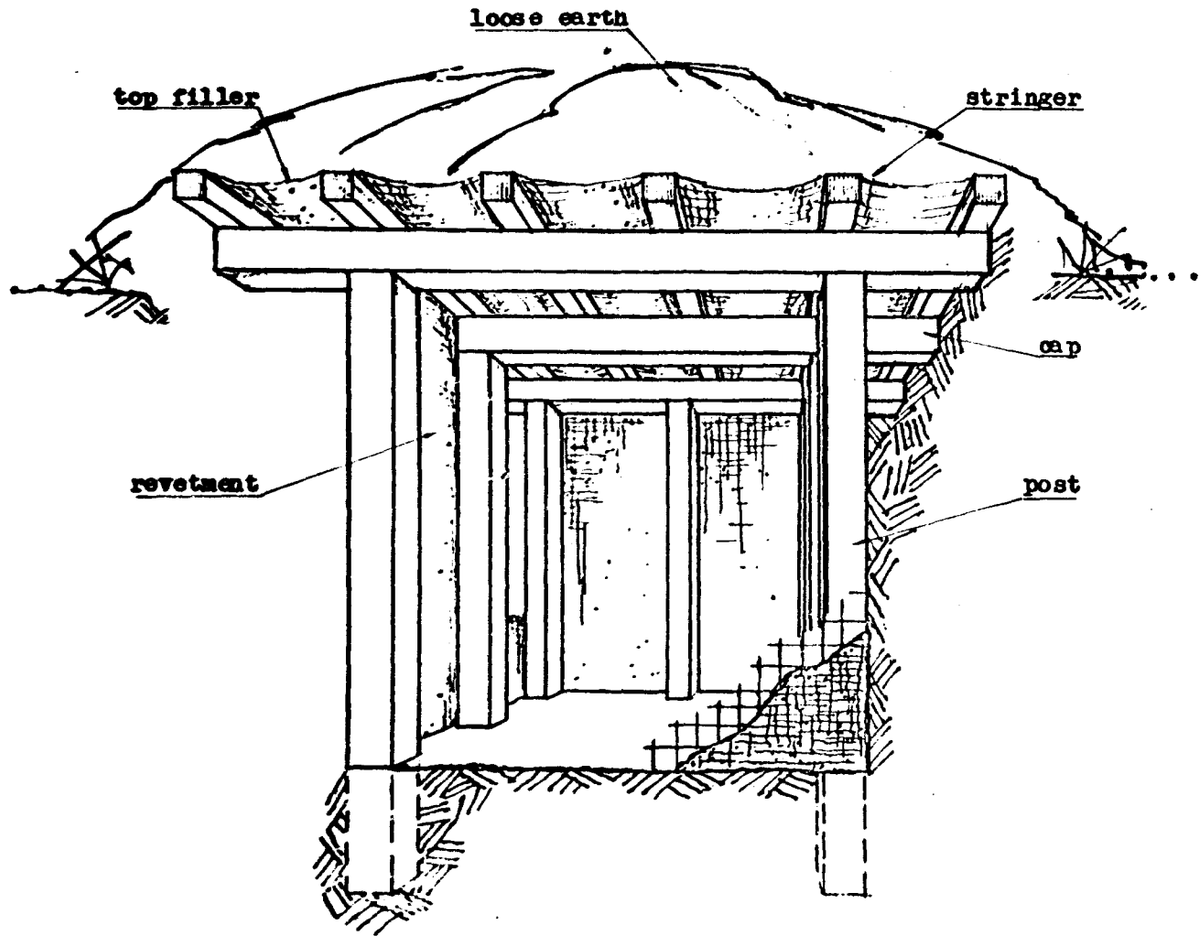

Fig. 2.2 Command Post with Spaced Stringers and Top Filler

SECRET - RESTRICTED DATA

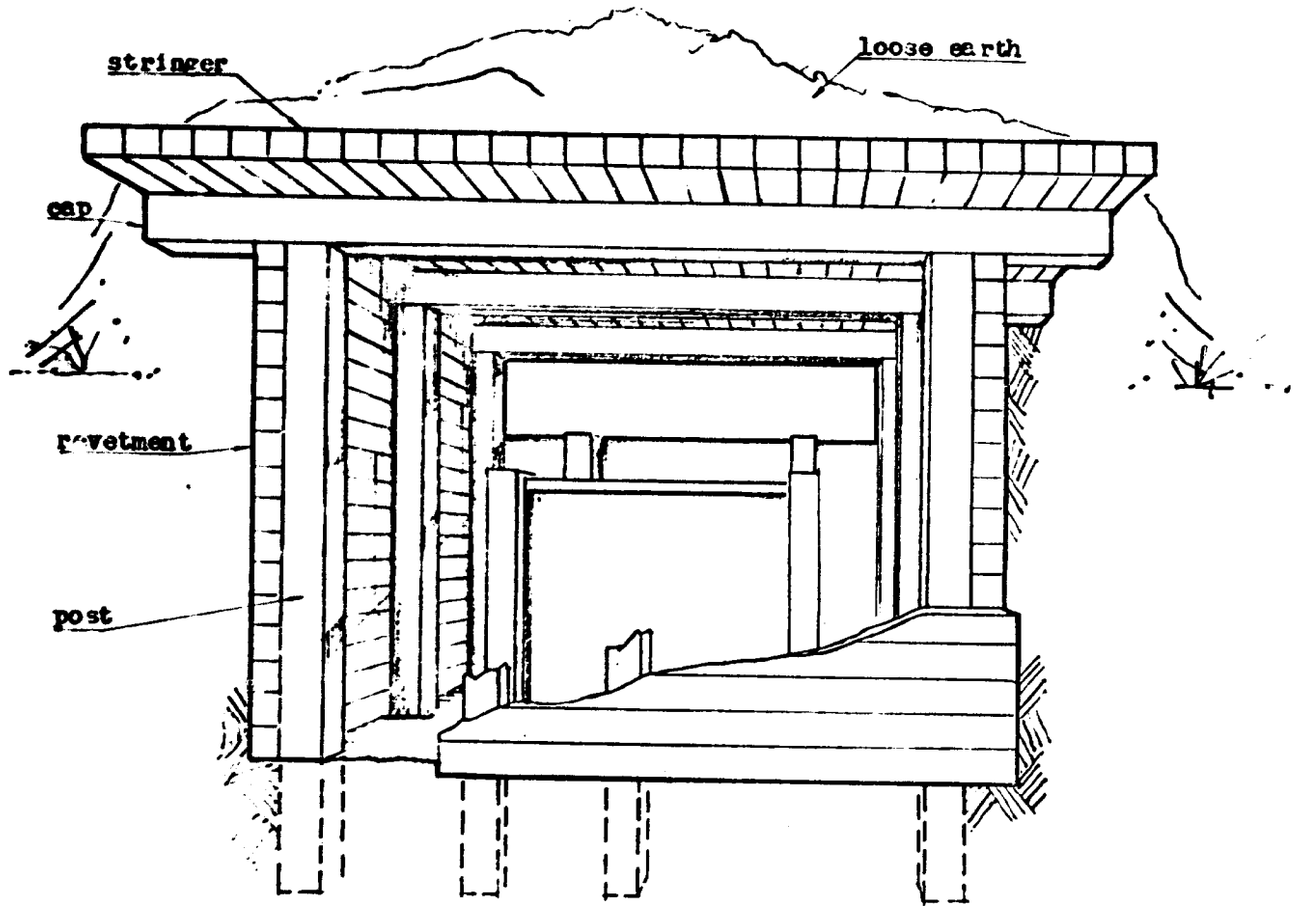

Fig. 2.3 Machine Gun Emplacement with Continuous Stringers

SECRET - RESTRICTED DATA

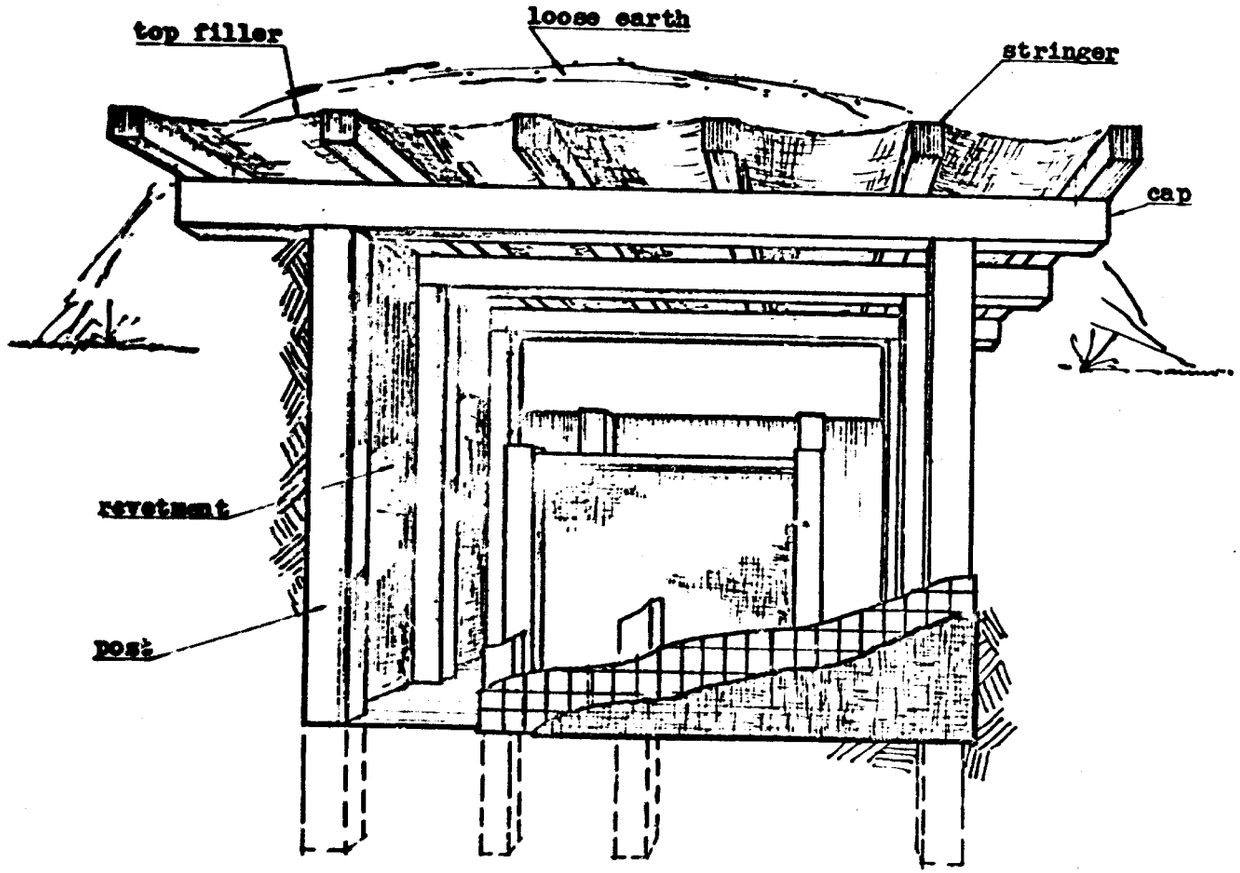

Fig. 2.4 Machine Gun Emplacement with Spaced Stringers and Top Filler

SECRET – RESTRICTED DATA

2.2 TEST PROCEDURE

2.2.1 Site Layout

The test structures were constructed by personnel from the 412th Engineer Construction Battalion. Fifty structures were divided between three areas--Area 3.9-A at 500 ft, Area 3.9-B at 1500 ft, and Area 3.9-C at 4000 ft from target ground zero. The exact location of the areas is shown in Appendix A, and the detailed distribution of the structures in each area is shown in Appendix B.

2.2.2 Shot Participation

It was anticipated that all areas would be exposed to Shot 9 and Shot 10. The plan was to rehabilitate the structures after Shot 9.

2.2.3 Recording the Effects on Structures

The effects on the test structures were recorded by preshot and postshot photography supplemented with postshot inspection notes. The photography was furnished by Program 9, AFSWP.

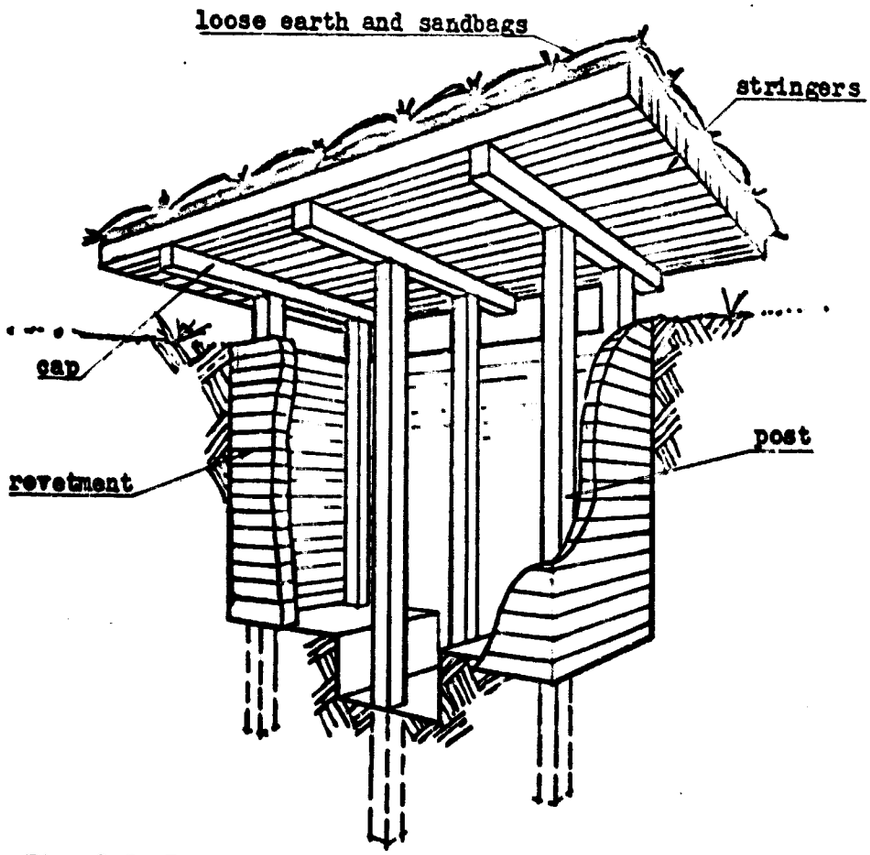

Fig. 2.5 Two-man Foxhole with Continuous Stringers

SECRET - RESTRICTED DATA

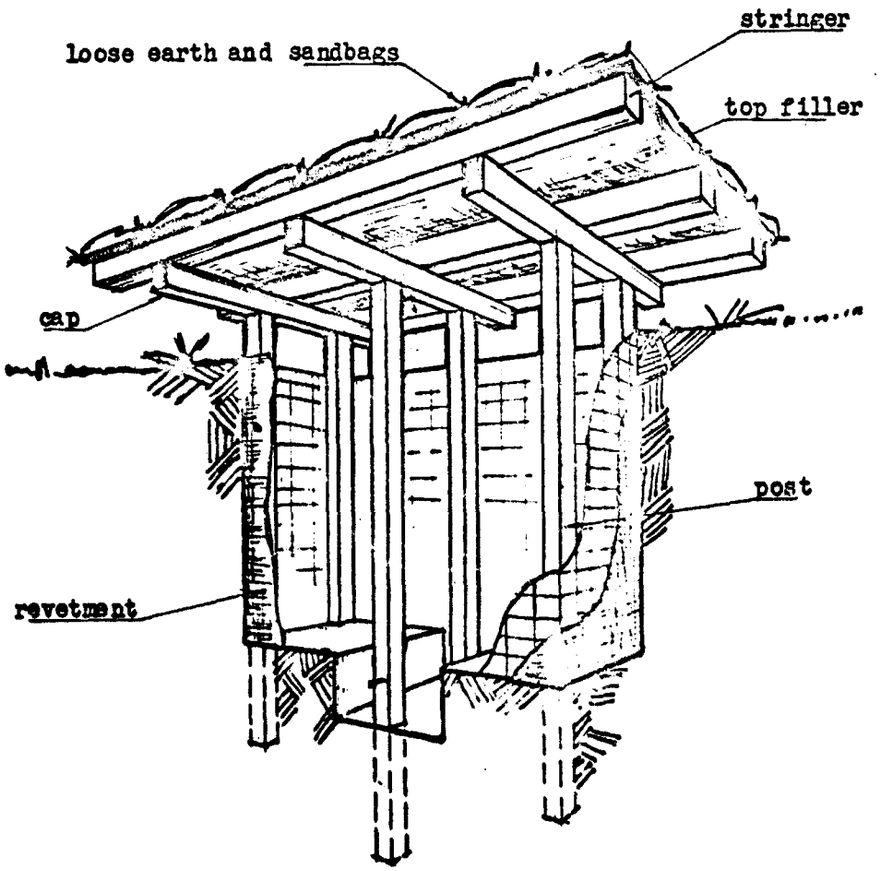

Fig. 2.6 Two-man Foxhole with Spaced Stringers and Top Filler

SECRET – RESTRICTED DATA

CHAPTER 3

RESULTS

3.1 INTRODUCTION

3.1.1 Shot Participation

Shot 9, 8 May 1953, was a 26 KT air burst at a height of 2423 ft with the actual ground zero located 837 ft south and 15 ft west of target ground zero. Shot 10, 25 May 1953, was a 14.9 KT air burst at a height of 524 ft with the actual ground zero located 139 ft south and 86 ft west of target ground zero.

All three areas were exposed to Shot 9. The actual ground zero for this shot was located between and to one side of Areas 3.9-A and 3.9-B; and, as a result, the peak overpressures and peak dynamic pressures were changed from those expected in these areas. Area 3.9-C was little affected by this miss of target ground zero.

Since the damage to the structures from Shot 9 was not severe and the 412th Engineers had a heavy work load between shots, it was decided that only Area 3.9-A be restored for Shot 10 and that Areas 3.9-B and 3.9-C be policed. The work order was interpreted by the construction personnel to mean that Areas 3.9-B and 3.9-C be removed. As a result, only Area 3.9-A was exposed to Shot 10. The miss in target ground zero for Shot 10 resulted in Area 3.9-A being about 350 ft rather than the planned 500 ft from actual ground zero. This substantially increased the expected pressures.

3.1.2 Tabulation of Effects on Structures

Tables 3.1 through 3.3 break down the effects of Shot 9 into the effects on each component of each structure. The effects of Shot 10 are not tabulated, since the damage was so complete that they are better described. The tables are explained as follows: The ranges and approximate peak overpressures are actual values, not expected values. The timber sizes are designated sizes, the actual dimensions being somewhat smaller since finished timber was used.

SECRET – RESTRICTED DATA

TABLE 3.1 - Effects on Command Posts, Shot 9

Fort. No.	Ground Range (ft)	Peak Over-Pressure (psi)	Stringers		Caps		Posts		Revetment & Top Filler	
			No.-Size-Span	Eval.	No.-Size-Span	Eval.	No.-Size	Eval.	Type	Eval.
1	650	25	30-4"x4"-3'	0	2-8"x8"-3' 1-8"x8"-6'	0 0	8-8"x8"	0	4"x4"	0
2	620	25	30-4"x4"-3'	0	2-8"x8"-3' 1-8"x8"-6'	0 0	8-8"x8"	0	4"x4"	0
3	590	25	30-4"x4"-3'	0	2-8"x8"-3' 1-8"x8"-6'	0 0	8-8"x8"	0	4"x4"	0
4	560	25	5-4"x4"-3' 1-4"x4"-3'	0 S	2-4"x4"-3' 1-4"x4"-6'	S M	8-4"x4"	0	Cor.I.	00
18	700	23	4-4"x4"-3' 2-4"x4"-3'	0 M	2-4"x4"-3' 1-4"x4"-6'	0 X	8-4"x4"	0	Cor.I.	00
19	700	23	4-4"x4"-3' 2-4"x4"-3'	0 M	2-4"x4"-3' 1-4"x4"-6'	0 M	8-4"x4"	0	Cor.I.	00
20	700	23	5-4"x4"-3' 1-4"x4"-3'	0 M	2-4"x4"-3' 1-4"x4"-6'	0 M	7-4"x4" 1-4"x4"	0 S	Plyd.	00
21	700	23	3-4"x4"-3' 1-4"x4"-3'	0 M	2-4"x4"-3' 1-4"x4"-6'	0 X	8-4"x4"	0	CW&B	00
22	750	23	4-4"x4"-3' 2-4"x4"-3'	0 M	2-4"x4"-3' 1-4"x4"-6'	0 M	8-4"x4"	0	1"x6"	00
35	3890	8	6-4"x4"-3'	0	2-4"x4"-3' 1-4"x4"-6'	0 0	8-4"x4"	0	CW&B	00
36	3890	8	6-4"x4"-3'	0	2-4"x4"-3' 1-4"x4"-6'	0 0	8-4"x4"	0	1"x6"	00
37	3890	8	4-4"x4"-3' 1-4"x4"-3'	0 X	2-4"x4"-3' 1-4"x4"-6'	0 X	8-4"x4"	0	CW&B	00

0 - undamaged; S - slightly damaged or cracked; M - moderately damaged or cracked and bent;
X - severely damaged or broken.

SECRET - RESTRICTED DATA

TABLE 3.2 - Effects on Machine Gun Emplacements, Shot 9

Fort. No.	Ground Range (ft)	Peak Over-pressure (psi)	Stringers		Caps		Posts		Revetment & Top Filler	
			No.-Size-Span	Eval.	No.-Size-Span	Eval.	No.-Size	Eval.	Type	Eval.
5	650	25	30-4"x4"-2½'	0	1-8"x8"-3½' 2-8"x8"-7'	0 0	7-8"x8"	0	4"x4"	00
6	620	25	30-4"x4"-2½'	0	1-8"x8"-3½' 2-8"x8"-7'	0 0	7-8"x8"	0	4"x4"	00
7	590	25	30-4"x4"-2½'	0	1-8"x8"-3½' 2-8"x8"-7'	0 0	7-8"x8"	0	4"x4"	00
8	560	25	30-4"x4"-2½'	0	1-8"x8"-3½' 2-8"x8"-7'	0 0	7-8"x8"	0	4"x4"	00
9	650	25	30-4"x4"-2½'	0	1-4"x4"-3½' 2-4"x4"-7'	0 0	8-4"x4"	0	4"x4"	00
10	620	25	5-4"x4"-2½'	0	1-4"x4"-3½' 2-4"x4"-7'	0 X	8-4"x4"	0	Cor.I.	MO
11	590	25	5-4"x4"-2½'	0	1-4"x4"-3½' 2-4"x4"-7'	0 S	8-4"x4"	0	Plywd.	00
23	750	23	30-4"x4"-2½'	0	1-4"x4"-3½' 3-4"x4"-7'	0 X	8-4"x4"	0	4"x4"	00
24	750	23	5-4"x4"-2½'	0	1-4"x4"-3½' 2-4"x4"-7'	0	8-4"x4"	0	Cor.I.	MO
25	750	23	5-4"x4"-2½'	0	1-4"x4"-3½' 2-4"x4"-7'	0 X	8-4"x4"	0	Plywd.	00
26	800	23	7-4"x4"-2½'	0	1-4"x4"-3½' 2-4"x4"-7'	0 0	7-4"x4"	0	CW&B	SX
27	800	23	7-4"x4"-2½'	0	1-4"x4"-3½' 2-4"x4"-7'	0 X	7-4"x4"	0	CW&B	MS
28	800	23	7-4"x4"-2½'	0	1-4"x4"-3½' 2-4"x4"-7'	0 0	8-4"x4"	0	CW&B	MM
29	800	23	24-1"x6"-2½'	0	1-4"x4"-3½' 2-4"x4"-7'	0 X	8-4"x4"	0	1"x6"	00

SECRET - RESTRICTED DATA

TABLE 3.2 - Effects on Machine Gun Emplacements, Shot 9(Continued)

Fort. No.	Ground Range(ft)	Peak Over-pressure (psi)	Stringers		Caps		Posts		Revetment & Top Filler	
			No.-Size-Span	Eval.	No.-Size-Span	Eval.	No.-Size	Eval.	Type	Eval.
34	3890	8	5-4"x4"-2½'	O	1-4"x4"-3½' 2-4"x4"-7'	O O	8-4"x4"	O	CW&B	OX
38	3940	8	5-4"x4"-2½'	O	1-4"x4"-3½' 2-4"x4"-7'	O O	8-4"x4"	O	CW&B	OM
39	3940	8	5-4"x4"-2½'	O	1-4"x4"-3½' 2-4"x4"-7'	O O	8-4"x4"	O	CW&B	OM
40	3940	8	4-4"x4"-2½' 1-4"x4"-2½'	O M	1-4"x4"-3½' 2-4"x4"-7'	O X	8-4"x4"	O	CW&B	OO
41	3940	8	20-1"x6"-2½'	O	1-4"x4"-3½' 2-4"x4"-7'	O O	8-4"x4"	O	1"x6"	OO

O - undamaged; S - slightly damaged or cracked; M - moderately damaged or cracked and bent;
X - severely damaged or broken.

SECRET - RESTRICTED DATA

TABLE 9.3 - Effects on Two-Man Foxholes, Shot 9

Fort. No.	Ground Range (ft)	Peak Over-pressure (psi)	Stringers		Caps		Posts		Revetment & Top Filler	
			No.-Size-Span	Eval.	No.-Size-Span	Eval.	No.-Size	Eval.	Type	Eval.
12	560	25	3-4"x4"-3'	0	3-4"x4"-2'	0	6-4"x4"	0	4"x4"	0,0
13	650	25	3-4"x4"-3'	0	3-4"x4"-2'	0	6-4"x4"	0	4"x4"	0,0
14	650	25	2-4"x4"-3'	0	3-4"x4"-2'	0	6-4"x4"	0	4"x4"	0,0
15	620	25	3-4"x4"-3'	0	3-4"x4"-2'	0	6-4"x4"	0	1"x6"	0,0
16	590	25	3-4"x4"-3'	0	3-4"x4"-2'	0	6-4"x4"	0	4"x4"	0,0
17	620	25	3-2"x4"-3'	0	3-2"x4"-2'	0	6-2"x4"	0	CW&PB	0,0
30	850	23	14-4"x4"-3'	0	3-4"x4"-2'	0	6-4"x4"	0	Plywd.	0
31	850	23	4-2"x4"-3'	0	3-2"x4"-2'	0	6-4"x4"	0	CW&B	S,0
32	850	23	4-2"x4"-3'	0	3-2"x4"-2'	0	6-2"x4"	0	CW&PB	M,0
33	850	23	16-2"x4"-3'	0	3-2"x4"-2'	0	6-2"x4"	0	1"x6"	0
42	3990	8	3-4"x4"-3'	0	3-4"x4"-2'	0	6-4"x4"	0	CW&B	0,0
43	3990	8	2-4"x4"-3'	0	3-4"x4"-2'	0	6-4"x4"	0	CW&B	0,0
44	3990	8	3-2"x4"-3'	0	3-2"x4"-2'	0	6-2"x4"	0	P.Bd.	0,X
45	3990	8	3-2"x4"-3'	M	3-2"x4"-2'	0	6-2"x4"	0	CW&PB	0,S
46	4040	8	3-2"x4"-3'	0	3-2"x4"-2'	0	6-2"x4"	0	CW&PB	0,X
47	4040	8	3-2"x4"-3'	0	3-2"x4"-2'	0	6-2"x4"	0	1"x6"	0,0
48	4040	8	3-4"x4"-3'	0	3-4"x4"-2'	0	6-4"x4"	0	CW&B	0,0
49	4040	8	3-2"x4"-3'	0	3-2"x4"-2'	0	6-2"x4"	0	CW&PB	0,S
50	4070	8	3-2"x4"-3'	0	3-2"x4"-2'	0	6-2"x4"	0	1"x6"	0,0

0 - undamaged; S - slightly damaged or cracked; M - moderately damaged or cracked and bent;
X - severely damaged or broken.

SECRET - RESTRICTED DATA

3.1.3 Photography

Preshot and postshot photographs of all test structures for both Shot 9 and Shot 10 are presented in Appendix C. The photographs are considered important because they constitute the only real and impartial record of the test. All of the damaged elements in any emplacement are shown in the photographs.

3.2 EFFECTS ON COMMAND POSTS

3.2.1 Effects of Shot 9

As shown in Table 3.1, most of the damage was confined to the failure of the center 4" x 4" caps and stringers at midspan. The evaluation of the damage to top fillers in the table does not take into consideration that small portion covering 4 ft of the entranceway. In general, the entrances were about half filled with loose earth; and the top filler immediately over the entrance was crushed inward enough to make access to the fortification difficult. It appeared that some of the loose earth mound covering the fortifications was removed by the blast. In most cases, the volume of the mounds was reduced by about one-fifth.

3.2.2 Effects of Shot 10

The peak overpressure in Area 3.9-A was approximately 300 psi, extrapolated value. All of the command posts were severely damaged. About one-fourth of the 8" x 8" posts failed in compression; most of the posts were displaced, and some appeared to have been driven slightly into the ground. The center 8" x 8" caps were broken and the two end caps severely shattered, showing 1 in. deep impressions where they had rested on the posts. About one-half of the 4" x 4" stringers were broken, the remainder suffering no apparent damage other than being removed from position. It appeared that the covers had been partly blown down into the fortifications and partly scattered about the area. Even though there were many undamaged timbers, all of the cover timbers were separated, no cover remaining even partly intact. The fortification excavations were about half filled with loose earth and rubble. The 4" x 4" timber revetments were bowed in, but the timbers retained their same relative positions and were not damaged. One command post of relatively light construction, 4" x 4" timbers and corrugated iron, was completely destroyed.

3.3 EFFECTS ON MACHINE GUN EMPLACEMENTS

3.3.1 Effects of Shot 9

As shown in Table 3.2, most of the damage to structural members was confined to the failure at midspan of the two front 4" x 4" caps. The evaluation of the damage to revetments and top fillers is problematic, because the damage seemed to be as attributable to poor construction as to lack of strength in the materials. In Area 3.9-A where the

SECRET - RESTRICTED DATA

peak dynamic pressure was about 0.7 psi, most of the loose earth and sandbags covering emplacements remained in place and there was little damage to revetments and top fillers, which were strongly constructed. In Area 3.9-B where the peak dynamic pressure was about 0.9 psi, the revetments and top fillers of emplacements utilizing chicken wire and burlap were damaged and the loose earth and sandbags covering these emplacements were half removed. In Area 3.9-C where the peak dynamic pressure was about 1.6 psi, the top fillers of emplacements utilizing chicken wire and burlap were damaged and the burlap, loose earth, and sandbags covering these emplacements were almost totally removed. In one case in this area, the entire cover, including 4" x 4" stringers and 1" x 6" top filler, was moved intact about 4 ft toward ground zero. The entrance excavations in all three areas were about half filled with displaced and ruptured sandbags and loose earth.

3.3.2 Effects of Shot 10

The three emplacements having 4" x 4" timber structural frames were destroyed beyond recognition. The four emplacements utilizing 8" x 8" timbers for posts and caps and 4" x 4" timbers for stringers and revetment were destroyed but still recognizable. Confining the discussion to the latter four emplacements, a few useful observations can be made. The superstructures were entirely removed, leaving the excavations almost filled with scrambled timbers, loose earth, and rubble. A few of the 8" x 8" posts remained undamaged; and, where the posts had remained, the 4" x 4" timber revetments were relatively undamaged and in position. The walls of the emplacements were pushed inward, reducing the dimensions somewhat below the original dimensions. There were a multitude of undamaged 4" x 4" timbers strewn in and about the emplacements, some of which must have been stringers and others part of the revetments. It appeared that if the posts had held, the 4" x 4" timber revetments would have held also. In general, damage to the machine gun emplacements was more severe than the damage to command posts of the same timber size construction.

3.4 EFFECTS ON TWO-MAN FOXHOLES

3.4.1 Effects of Shot 9

As shown in Table 3.3, there was no appreciable damage to the individual structural members of the foxholes. In Areas 3.9-A and 3.9-B, there was little damage to top fillers and most of the loose earth and sandbags covering the foxholes remained in place. In these areas, a few of the 2" x 4" posts were driven farther into the ground, allowing the covers to slant. In Area 3.9-C, the foxholes having the more substantial revetments and top filler, 1" x 6" lumber, suffered no damage other than the removal of loose earth and sandbags. Foxholes with lighter revetments and top filler, chicken wire and burlap or pasteboard, suffered considerable derangement of their superstructure. In some cases, the timbers forming the cover were pulled apart at their joints; and, in other cases, the whole cover frame was displaced, pulling the posts out of position. The top filler materials, sandbags, and loose earth were

SECRET - RESTRICTED DATA

removed. In general, the earth walls of the foxholes would have held even if they had not been revetted.

3.4.2 Effects of Shot 10

The only thing that remained of the foxholes was the 4" x 4" revetment timbers and a few 4" x 4" posts. Most of the foxholes were completely filled in, but two were still open enough to indicate the process of failure. It appeared that the two 6 ft walls had been moved inward uniformly, reducing the original 2 ft dimension of the foxholes to about 8 in. in these two cases and completely closing the foxholes in all other cases. Other than this, the revetment timbers of the two partially open foxholes were relatively undamaged and retained their same relative position.

3.5 GENERAL OBSERVATIONS

3.5.1 Gross Effects of Thermal Radiation

The incident thermal energies in the areas varied from 40 to 160 cal/cm^2 for Shot 9. All of the exposed sandbags were burned and had spilled their contents. In many instances, this loose earth was spilled into the entrances of the test structures. Only a few timbers were burned severely, and there were no significant fires continuing after the shock wave had passed. Of some significance was the heavy scorching of the underneath side of burlap top filler and the inside of chicken wire and burlap revetted back walls of the machine gun emplacements in Area 3.9-B. The foxholes utilizing chicken wire and burlap were similarly damaged.

3.5.2 Joints and Fastenings of Structure Components

Foxholes and machine gun emplacements experienced forces from the high winds which resulted in the removal or dislocation of various members and parts. Individual timbers were not damaged, but only disjoined. Because of the structure design, the quality of workmanship going into the joints and fastenings largely determined the extent to which a particular emplacement was damaged.

SECRET - RESTRICTED DATA

CHAPTER 4

DISCUSSION

4.1 OVERHEAD COVER

4.1.1 Test Results, Shot 9

The structural damage done to command post cover was a result of the action of the blast induced air pressure difference between the top and bottom sides of the cover, hereafter called diffraction type loading for brevity. In seven of the nine command posts having 4" x 4" caps and stringers, the center cap failed in bending at midspan, increasing the span for stringers which then failed. Estimating the time required for the average pressure within the command post to reach its effective peak to be in excess of 90 msec(10), and considering that within the one instrumented command post the maximum peak overpressure measured was 0.7 as great as that measured outside at ground level, it can be seen that there was a significant pressure differential between the top and underside of the cover. Since there was no serious damage to the top fillers or 4" x 4" posts, and there was evidence that the stringers failed only as a result of cap failure, the center cap proved to be the limiting member in the structure.

Structural damage to machine gun emplacement covers was in part a result of diffraction-type loading. In 6 of 15 emplacements having 4" x 4" caps, the center and front cap failed in bending at midspan. On a percentage basis, only half as many machine gun emplacements as command posts suffered cap failure. Coupling this observation with the fact that the maximum peak overpressure measured within the machine gun emplacement was twice that measured within the command post, one would suspect that the machine gun emplacement cover was subjected to a lighter load because of the relieving pressure reaching a significant value in a shorter time. However, when all factors are considered, including the short response time of the timbers, the implication is not certain when based on this test alone. Since there was no other serious damage to the machine gun emplacement cover resulting from diffraction-type loading, the center and front cap proved to be the limiting members in the structure.

Other than a few instances of posts being driven slightly farther into the ground, showing that there was a definite downward push on the cover, there was little evidence of diffraction loading on foxhole covers.

SECRET - RESTRICTED DATA

The maximum peak overpressure measured inside the instrumented foxhole was about the same as that measured outside at ground level.

Although the dynamic pressures (wind pressures) were small, 0.7 to 1.6 psi, their effect on cover was in evidence. For the command posts, the damage was limited to the removal of part of the loose earth cover; whereas, for machine gun emplacements and foxholes, whose cover structure was above grade level, the effects were multiple. Generally speaking, the dynamic pressures were effective in tearing the cover materials apart from each other where they were joined, blowing away the loose materials, and moving whole covers or parts thereof out of position. The effects were most severe on those emplacements having chicken wire and burlap top filler.

The gross effect of thermal radiation on the cover structure of the fortifications was not severe. An examination of the test structures showed that there was no serious fire hazard and that the few fires that had been started were either blown out or left in a smouldering state by the blast. All of the exposed sandbags were severely burned and ruptured, and were of little value for holding loose earth in place. The sandbags having a small amount of earth covering them were not damaged. Examination of the covers to machine gun emplacements and foxholes showed that thermal radiation had reflected from the ground and scorched the underneath side of the burlap used in chicken wire and burlap top filler. This was particularly noticeable because of the design left on the burlap by the shielding effect of the chicken wire. No threshold values for thermal radiation effects on the materials are available from this test.

4.1.2 Test Results, Shot 10

Of all parts of the fortifications that had originally been above natural grade level, little or nothing remained in place. The covers to machine gun emplacements and foxholes could not be identified after the shot. Although the covers to command posts stood up better than the others, none remained intact; and the manner of failure was at best a matter of conjecture. It appeared that the 8" x 8" center caps had failed first in horizontal shear then in bending at midspan, and that the end caps had failed in horizontal shear only with a beginning failure in either bending or vertical shear. About one-fourth of the 8" x 8" timber posts failed in compression, a few were driven slightly farther into the ground, and most were left leaning inward to some degree. The large number of scattered and undamaged 4" x 4" timbers showed the inadequacy of designing for conventional forces.

4.1.3 Generalization of Past Results

The following generalizations applicable to overhead cover can be made from the results and conclusions of past tests:

Damage to structures is less severe when they are covered by even a small amount of earth. Wood shelters offer good resistance to blast provided they are properly protected with earth cover. They do not burn, and their resiliency permits them to absorb considerable shock without failing completely. As the elevation of a shelter is increased

SECRET – RESTRICTED DATA

with respect to natural grade level, larger amounts of earth cover are subject to removal; and there is a reduction in the shelter's resistance to blast, as well as increase in the measured gamma radiation doses.

The covered shelter affords greater protection against atomic effects, particularly gamma radiation, than does the uncovered shelter. For air bursts, overhead cover greatly reduces the gamma radiation doses within fortifications; whereas, for surface bursts, the reduction directly attributable to overhead cover is less. The first limit in the protection afforded by covered shelters has been gamma radiation.

Although the gold neutron flux does not decrease appreciably with depth in an open fortification, there is a marked decrease in fortifications having a concrete cover. Sulphur neutron flux does decrease with depth in open fortifications and is further reduced in fortifications having a concrete cover.

4.1.4 Generalization of the Present Results

The following generalizations can be made from the observation of the effects on overhead cover in this test:

Fortification covers located flush with grade level are primarily damaged by diffraction-type loading. When located above grade level, cover components may be seriously disarranged by the dynamic pressure; however, the physical breaking of timbers and materials themselves is still a result of diffraction loading on the cover. Disarrangement begins to appear at dynamic pressures as low as 0.7 to 1.6 psi, and is dependent upon the design and the quality of workmanship going into the joints and fastenings.

For both above and below grade covered fortifications, the longer spanned, horizontal supporting members limit the strength of the cover's resistance to diffraction loads. The posts supporting these caps are relatively invulnerable to damage from loads on the cover; and, if the soil is at all stable, they are better sunk into the soil than set on timber footings or spreaders. Light top filler materials, such as chicken wire and burlap or pasteboard, corrugated iron, 5/8" plywood, and 1" x 6" lumber, when supported at about 2½ ft intervals and covered with loose earth, are not seriously damaged by the diffraction load on the cover at a peak overpressure of 25 psi.

There is no serious fire hazard created by using timbers and other lighter materials in fortifications. The primary damage from thermal radiation is the burning of directly exposed sandbags. Those sandbags covered with small amounts of loose earth are not damaged.

4.2 REVETMENT

4.2.1 Test Results, Shot 9

The revetments were constructed with a few inches of very loose, fine earth backfill between them and the solid earth walls. Although this loose material may have acted as a buffer, the effect was not apparent.

Generally speaking, all kinds of revetments held up well, there being no failure directly attributable to a lack of strength in the

SECRET – RESTRICTED DATA

materials themselves. The chicken wire and burlap, chicken wire and pasteboard, and corrugated iron revetments showed a tendency to bulge inward, but not rupture. There were several instances in which these types of revetments pulled loose from their supporting timbers; however, in each instance, examination showed that they had not been well attached. The plywood revetments did not bulge inward as much as the others and were affected less by the quality of workmanship. The 1"x6" and 4"x4" timber revetments were not damaged at all by the blast. Considering general strength, simplicity of quality construction, and dependability, the 1"x6" and 4"x4" timber revetments proved to be superior to other types.

While the lighter materials were successfully used for the revetment of the main walls of the fortifications, they proved to be unsatisfactory, and in some cases hazardous, when used as revetment for the gun mount platforms in the machine gun emplacements. Only the 1"x6" and 4"x 4" timber revetments held these earth platforms in place satisfactorily.

4.2.2 Test Results, Shot 10

All revetments except those constructed from 4"x4" timbers failed completely. The 4"x4" timber revetments were supported by posts at about 3 ft intervals which yielded to varying degrees to the lateral earth forces. Although the 4"x4" revetment timbers bowed in accordingly, they did not break; and each wall remained intact. It appeared that had the posts remained rigid and unmoved, the 4"x4" timber revetments would have held satisfactorily.

4.2.3 Generalization of Past Results

There is little information available from past tests on the reaction of various types of revetment to an atomic explosion. It has been generally concluded that all normal types of revetment are adequate for military use, that revetments permit fortifications to hold up at much closer distances to ground zero than do the unrevetted fortifications, and that soil structure is a major factor determining how well unrevetted walls will withstand a blast. One-inch lumber and chicken wire and tarpaper revetments have been used successfully at ranges where the peak air overpressure was about 15 psi.

4.2.4 Generalization of the Present Results

Diaphragm type revetments such as those constructed from chicken wire and burlap, chicken wire and pasteboard, corrugated iron, and plywood may be successfully used at ranges from air bursts where the peak air overpressures are about 25 psi provided that care is taken to attach them well to supports spaced about 2½ ft apart and provided that they are not depended upon to add strength or stability to the overall basic structure.

Considering general strength, simplicity of quality construction, and dependability, the 1"x6" and 4"x4" timber revetments are superior to the others. Rigidly supported at about 3 ft intervals, a 4"x4" timber revetment appears to have sufficient strength to stand up at a range from

SECRET - RESTRICTED DATA

an air burst where the peak air overpressure is of the order of 300 psi.

4.3 ENTRANCES AND APERTURES

4.3.1 Results

The entrances to the machine gun emplacements and command posts used in this test were purposely kept simple and direct. More elaborate entrance construction would not have added much to the value of the overall test; because, structurally, entrances fall within the revetment and overhead cover study and otherwise are tied in with protection from physiological effects. Although simple and unrevetted, the entrances used in this test did lend weight to various observations made in the tests summarized in Chapter 1. To save repetition, generalizations of the effects on entrances are not presented here but are incorporated into the discussion in the following section in that they substantiate the emphasis placed on some of the past observations.

The machine gun emplacements were constructed such that there was no chance of direct thermal radiation entering the firing aperture in Area 3.9-B. However, the thermal radiation entering this aperture after reflecting from the ground in front of the emplacements was of sufficient intensity to burn burlap on the back walls inside the fortifications.

4.3.2 Generalization of Past Results

The entrance construction of most structures has been considerably weaker than the structure proper and has been almost invariably the limiting factor in blast resistance.

Scorching of parts of entrances not directly exposed to thermal radiation has indicated reflection of some magnitude; however, those entrances requiring reflections of thermal radiation to enter the structure proper have successfully shielded the interior from high values of thermal radiation.

Directly exposed sandbags burn and rupture, spilling their contents. The use of such sandbags adjacent to entrances has invariably resulted in the partial filling of the entrances with loose earth and damaged sandbags.

Cutting an entrance into a covered fortification can remove a great deal of the earth shielding against gamma radiation and can greatly reduce the nuclear radiation protection otherwise offered by the addition of overhead cover.

4.4 GENERAL OBSERVATIONS

The importance of proper design and high quality construction is highly magnified by the nature of the forces resulting from an atomic explosion; and, if the construction plans for a structure do not adequately present all detail, improvisations on the part of the constructors are not likely to be in favor of the structure's resistance to atomic effects.

SECRET - RESTRICTED DATA

CHAPTER 5

CONCLUSIONS AND RECOMMENDATIONS

5.1 CONCLUSIONS

The following conclusions represent a consolidation of the more certain observations made in past reports with those made in this test. Conclusions concerning damage probability are presented in Appendix G.

5.1.1 Overhead Cover

The covered shelter affords greater protection against atomic effects, particularly nuclear radiation, than does the uncovered shelter. For air bursts, overhead cover greatly reduces gamma radiation doses within fortifications; whereas, for surface and subsurface bursts, the reduction directly attributable to overhead cover is less. In general, the lethal radius of nuclear radiation has been greater than the lethal radius of other effects in both open foxholes and covered shelters.

As the elevation of the cover is increased with respect to the natural grade level, large and increasing amounts of loose earth are subject to removal; and there may result an appreciable increase in the measured gamma doses within the structure, since in many situations the blast wave passes before all of the nuclear radiation is absorbed.

The effect of blast on overhead cover construction depends upon, among other things, the structure's elevation with respect to natural grade level. Fortifications that have their total profile flush with grade level are subject to loads which tend to rupture the longer spans of the horizontal supporting members by pushing downward on the cover; whereas, those fortifications having their cover structure above grade level are not only subject to this diffraction load but are also subject to drag type loads which tend to disarrange and remove entire cover structures or parts thereof.

Light top filler materials such as chicken wire and burlap or pasteboard, corrugated iron, plywood, and 1 in. lumber, when supported at about 2½ ft centers and covered with loose earth, are sufficiently strong to withstand diffraction loads on the cover to fortifications at a peak overpressure of 25 psi. However, as pointed out above, the members acting as supports for these materials are subject to failure.

SECRET - RESTRICTED DATA

Posts used to support the cover are relatively invulnerable to damage and, if the soil is at all stable, are better sunk into the soil than set on footings or spreaders.

Overhead cover structure suffers less damage from diffraction loads when covered with earth. Although the exact physical nature of the phenomenon has yet to be resolved, it can be stated generally that earth effectively adds mass to supporting members, increasing the time of response to impact loads; and, if of substantial thickness, it effectively absorbs some of the energy of the blast wave. The results of a recent study of earth cover should be consulted when they become available (11).

5.1.2 Revetment

Because of the unknown nature of the transmission of a shock wave through earth and of the loading of structures by such a wave, required revetment strength is based more on experience than theoretical calculation. Soil structure has been a major factor determining how well unrevetted walls withstand a blast; however, it has not yet been shown to affect success of revetted walls. In general, the forces applied to revetments have been considerably less effective than those applied to cover structure by a blast, and relatively light revetment construction has been successful.

Light filler materials, such as chicken wire and burlap or pasteboard, corrugated iron, and plywood, when supported at about 2½ ft intervals, are sufficiently strong for revetting purposes at ranges where the peak air overpressure is 25 psi. However, they cannot be depended upon to add strength or stability to the overall structure; and they are subject to failure resulting from a lack of quality workmanship on the ties between them and their supporting structure. Considering general strength, simplicity of construction, and dependability, these materials are inferior to 1"x6" and 4"x4" timber.

5.1.3 Entrances and Apertures

The protection from nuclear radiation afforded by covered fortifications can be reduced by entrances and other apertures. By removing part of an earth wall, an entrance can remove a great deal of the earth normally shielding against nuclear radiation, and thus substantially depreciate the additional nuclear radiation protection otherwise offered by the use of overhead cover. The inclusion of firing apertures necessitates that a covered fortification be partially above grade and complicates the problem of obtaining effective earth cover.

Scorching of parts of fortifications not directly exposed to thermal radiation has indicated reflections of some magnitude. However, by constructing entrances to require at least two reflections of thermal radiation to enter the structure proper, the interior of a fortification can be successfully shielded from high values of thermal radiation.

The use of directly exposed sandbags adjacent to entrances results in the partial filling of the entrances with loose earth spilled from burned sandbags.

There is a tendency to slight the design and construction of

SECRET - RESTRICTED DATA

entrances. Aside from nuclear and thermal radiation considerations, entrance construction has been generally the weakest point of blast resistance in past tests. Structurally, entrances fall within the revetment and overhead cover study, and their proper construction is as important as that of any other part of a fortification.

5.1.4 General

There is no serious fire hazard created by using timber and other lighter materials in fortifications. The primary damage from thermal radiation is the burning of exposed sandbags, which are then of no value for holding their contents in place. Those sandbags covered with small amounts of loose earth are not damaged.

The importance of proper design and high quality construction are highly magnified by the nature of the forces resulting from an atomic explosion; and, if the construction plans for a structure do not adequately present all detail in a simple and direct manner, improvisations on the part of the constructors are not likely to be in favor of the structure's resistance to atomic effects.

Although large quantities of field fortifications have been subjected to atomic exposions, most of these were part of the DESERT ROCK Exercises, whose mission did not include obtaining detailed effects information but was pointed toward troop indoctrination and orientation. Practically all of the certain quantitative measurements made inside fortifications in the past are confined to gamma radiation--most other instrumentation being either unsuccessful or non-existent.

5.2 RECOMMENDATIONS

That the information presented in this report be included in appropriate field manuals for use in reducing the vulnerability of field fortifications to the effects of atomic weapons.

That no future tests be conducted on standard (FM 5-15) field fortifications for the purpose of obtaining qualitative information on their vulnerability to atomic weapon effects.

That balanced fortification designs be made by competent personnel who are familiar with the nature of the forces and radiation phenomena resulting from an atomic weapon detonation. As used here, "balanced fortification design" is intended to imply a design which reaches its limits in protection from all atomic effects, including structural failure of all parts of the fortification itself, at approximately the same range from the explosion, and in which there is a weighted compromise between atomic protection, conventional weapons protection, and practical military requirements such as drainage, limited materials, and simplicity of construction.

That, in the event suitable balanced designs are evolved, acceptance of these improved fortifications be held subject to final testing. That, in testing these finished designs, the construction of the test fortifications be closely supervised by those who are to analyze the results, that their interior be well instrumented for air pressure, gamma radiation, neutron flux, and thermal radiation, and that they be located at such distances from the explosion that their actual limit in structural strength and protection from atomic effects is realized.

SECRET – RESTRICTED DATA

PART II

PRESSURE MEASUREMENTS IN FIELD FORTIFICATIONS

CHAPTER 6

INTRODUCTION

6.1 OBJECTIVES

The objectives of Part II of Project 3.9 were as follows:

1. To determine the magnitude of overpressure build-up within open two-man foxholes, a command post, a machine gun emplacement, and a covered foxhole.
2. To observe the pressure-time characteristics of the blast wave within two-man foxholes such that a preliminary understanding of the method of the overpressure build-up is achieved.
3. To discuss the variables that were observed affecting the overpressure build-up in emplacements.

6.2 BACKGROUND

The reflection characteristics of pressure waves incident on plane surfaces have been studied extensively in the region of Mach reflection. Los Alamos Scientific Laboratory has published reports (12, 13) which include experimental and theoretical investigations of these phenomena. The mechanism of shock front propagation over a rectangular opening below a plane surface has been investigated by Ballistic Research Laboratories(14) and Princeton University(15). These investigations form the basis of much of the theory of this report.

Prior to UPSHOT-KNOTHOLE, there were no field test results published showing either peak pressures or pressure-time variation in field fortifications.

6.3 THEORY

The mechanism of reflection of a blast wave from a plane surface is described in The Effects of Atomic Weapons, where it is shown that the reflection coefficient (ratio of reflected to incident overpressure) of a blast wave on a rigid surface is a function of the incident overpressure and the angle of incidence. This is shown in Fig. 6.1, which was adopted from The Effects of Atomic Weapons. The incident overpressures used in the figure were chosen to be close to those which

SECRET - RESTRICTED DATA

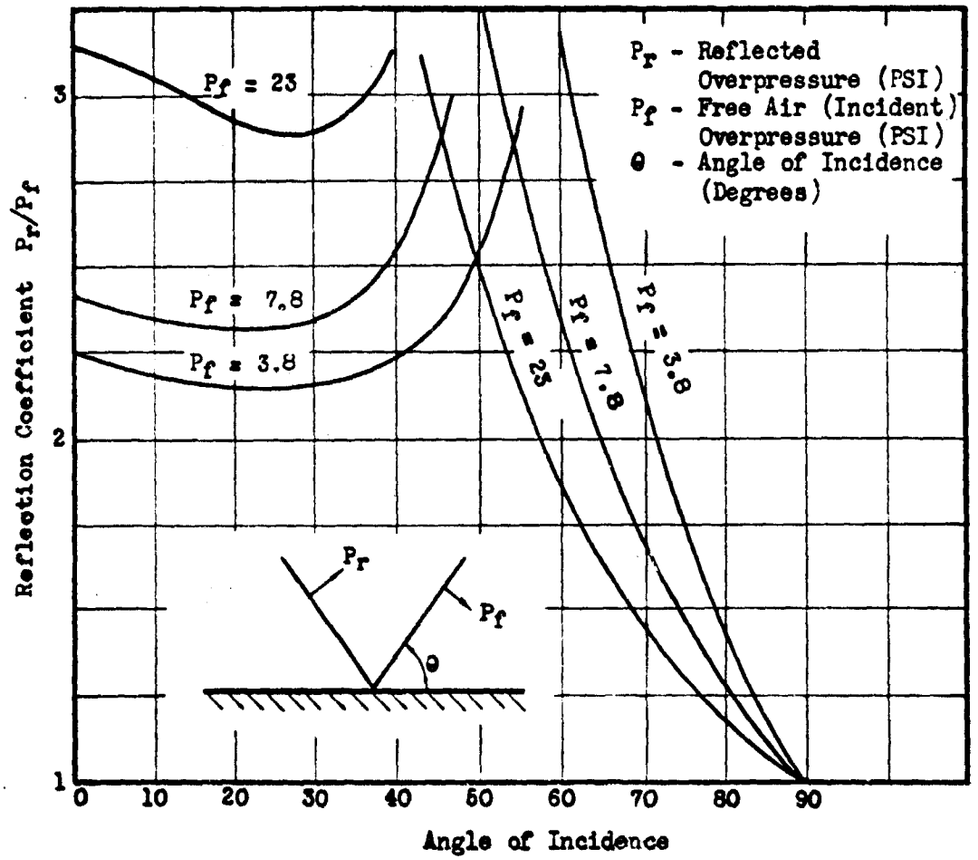

Fig. 6.1 Relation Between Incident Overpressure, Angle of Incidence, and Reflected Overpressure

were experienced during the test. Each curve shows a discontinuity at some point which seems to be a peak. The area to the right of this discontinuity is the region of Mach (irregular) reflection, while the left exhibits regular reflection. The curve is experimental; and, as more information becomes available, the discontinuities may be minimized. It serves to illustrate, however, that reflection coefficients of more than three can be expected under certain conditions.

Figure 6.2 is a cross section of a foxhole-type cavity showing the passage of a blast wave across a point "A" which is significant because it is in the same relative position as the Wiancko pressure-time gages used in this experiment. This and the following figures were based on shadowgraphs of shock tube studies made by BRL. Figure 6.3 shows the blast wave advanced slightly further and illustrates the passage of a second (reflected) blast wave, over the point "A." Figure 6.4 shows the blast wave in a further stage of advancement. Figures 6.5 and 6.6 illustrate how two more distinct reflected waves pass through the point "A." It follows that the time-overpressure relation in the cavity should have characteristics similar to Figure 6.7.

SECRET - RESTRICTED DATA

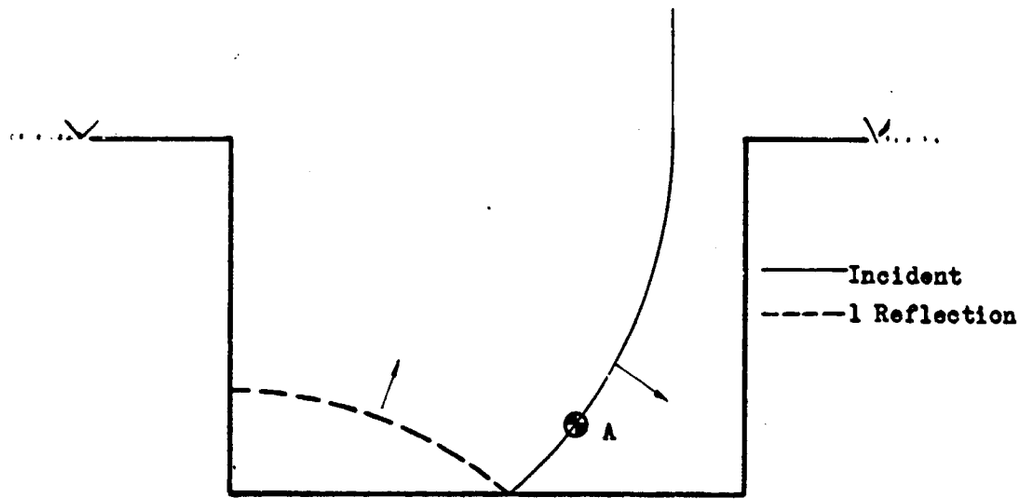

Fig. 6.2 Propagation of Pressure Waves in Foxhole - Time 1

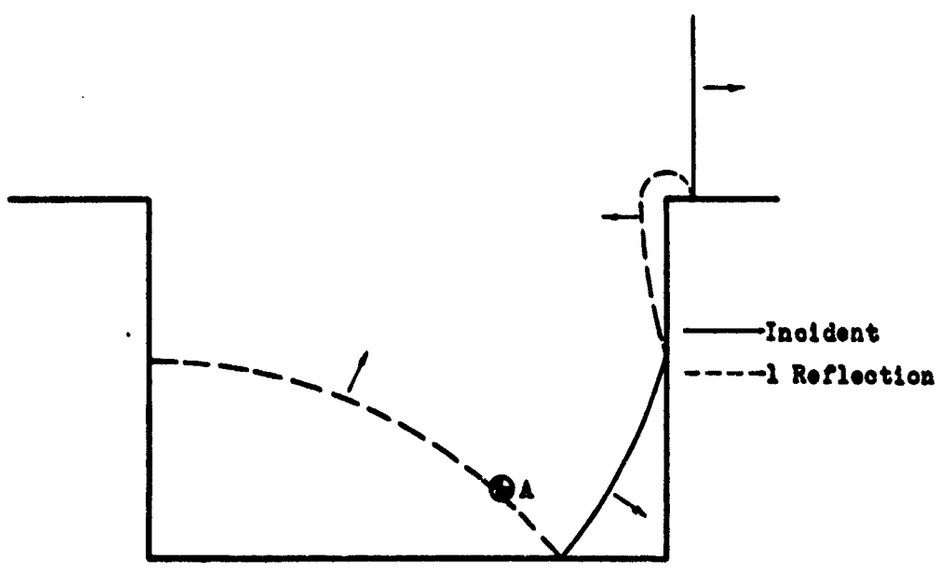

Fig. 6.3 Propagation of Pressure Waves in Foxhole - Time 2

SECRET - RESTRICTED DATA

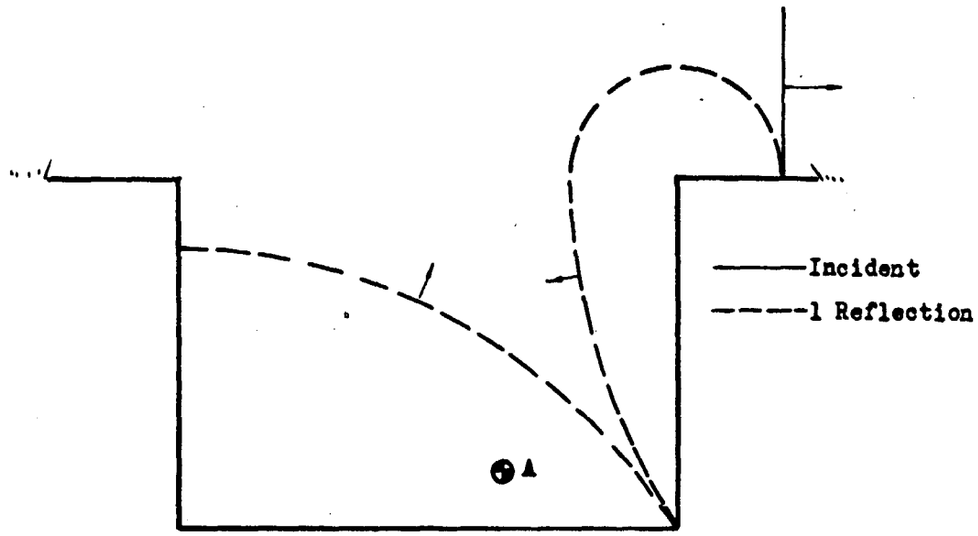

Fig. 6.4 Propagation of Pressure Waves in Foxhole - Time 3

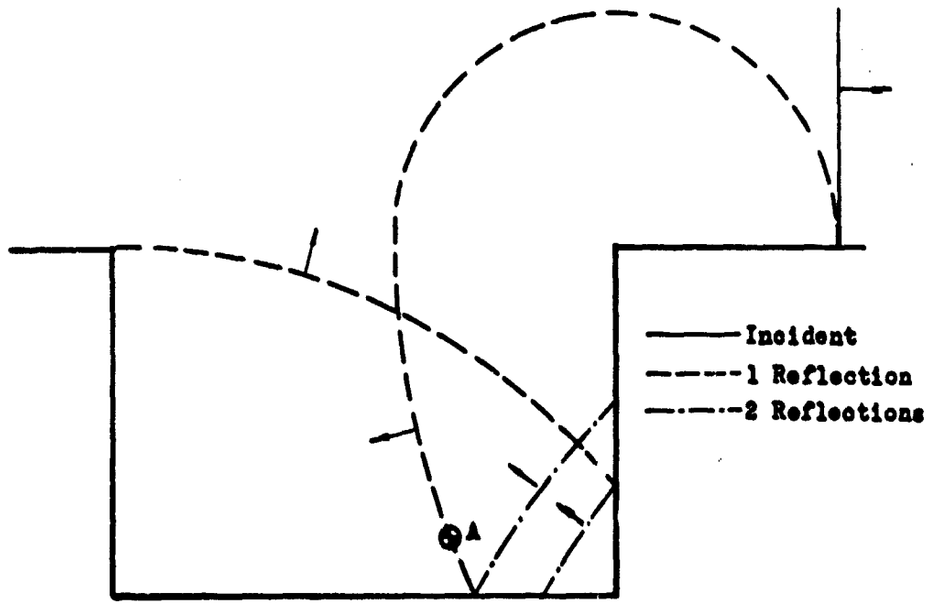

Fig. 6.5 Propagation of Pressure Waves in Foxhole - Time 4

SECRET - RESTRICTED DATA

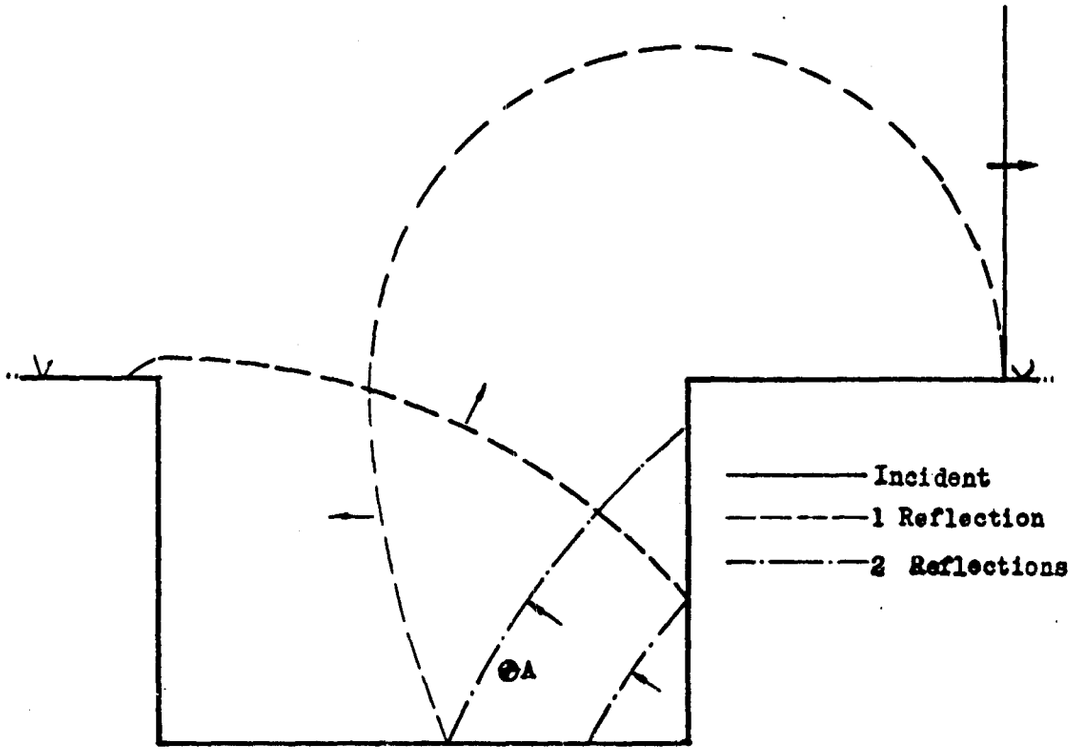

Fig. 6.6 Propagation of Pressure Waves in Foxhole - Time 5

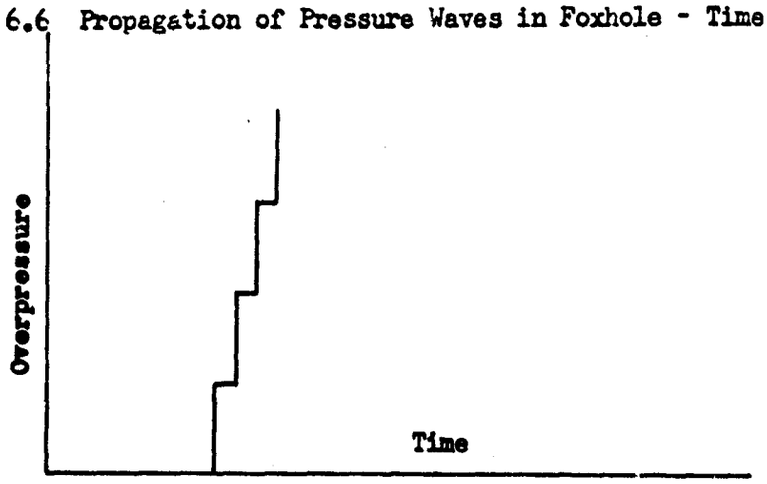

Fig. 6.7 Ideal Time-Overpressure Relationship in Cavity

The magnitude and time of the various steps in Fig. 6.7 depend upon such variables as the angle of incidence, incident overpressure, dimensions and aperture-volume relationship of the cavity, and position of point "A." The various surface irregularities, surfaces which are not perfect reflectors, and the interaction with the sidewalls will also tend to modify the shape of the curve. Because of the dependence of the wave propagation on the above-mentioned factors, the reflections shown in Figs. 6.2 to 6.6 give only an idealized representation of an actual situation.

SECRET - RESTRICTED DATA

CHAPTER 7

EXPERIMENT DESIGN

7.1 TEST STRUCTURES

The test facilities for Part II of Project 3.9 consisted of eight structures: four uncovered 2' x 4' x 6' foxholes; one 2' x 4' x 6' foxhole in which the aperture was two-thirds covered; and one each command post, machine gun emplacement, and covered foxhole. The latter three were concurrently used for the blast section of Project 3.9, and their physical appearance is fully described therein. They were emplacements 20, 25, and 30, respectively.

A diagram of the test site layout is given in Appendix A. The position of emplacements 20, 25, and 30 is given in Appendix B.

7.2 INSTRUMENTATION

Indenter peak pressure gages(10) developed and supplied by NOL, were used to obtain the peak overpressure in all of the emplacements.

Wiancko pressure-time gages (16,17) were used to obtain the time dependence of the overpressure as received in the foxholes. These were supplied and calibrated, and the traces were interpreted by NOL.

Pressure-time, scratch gages were used in the foxholes during Shot 10. They were supplied, calibrated, and their traces were interpreted by BRL.

Diagrams showing the placement of each gage are given in Figs. 8.1 to 8.8. The figures are placed, as a convenience to the reader, with their corresponding data sheets.

SECRET - RESTRICTED DATA

CHAPTER 8

RESULTS

8.1 INTRODUCTION.

The positions of the indenter, scratch, and Wiancko gages for each foxhole and emplacement are given in Figs. 8.1 to 8.8, which are development drawings of the emplacements. The small, numbered circles each represent an indenter gage position. The larger circles, with such notations as S-1 or W-1, represent scratch and Wiancko gages respectively. No dimensions are shown in the figures; however, they were drawn to scale to facilitate the exact location of the gage positions.

8.2 PRESENTATION OF DATA

Tables 8.1 to 8.8 are the results of all of the gage readings from each emplacement. The definitions of the headings of the tables are as follows:

Pgl - Ground level overpressure (psi).

d - Average of a series of readings of the diameter of the indentation in copper disk (millimeters).

k - Calibration factor - 82.6 psi/d^2.

Pmax - Maximum overpressure - kd^2 (psi).

Figures 8.9 to 8.24 are the pressure time curves obtained from the Wiancko and scratch gages. Their peak overpressures are given in Tables 8.1 to 8.5.

SECRET - RESTRICTED DATA

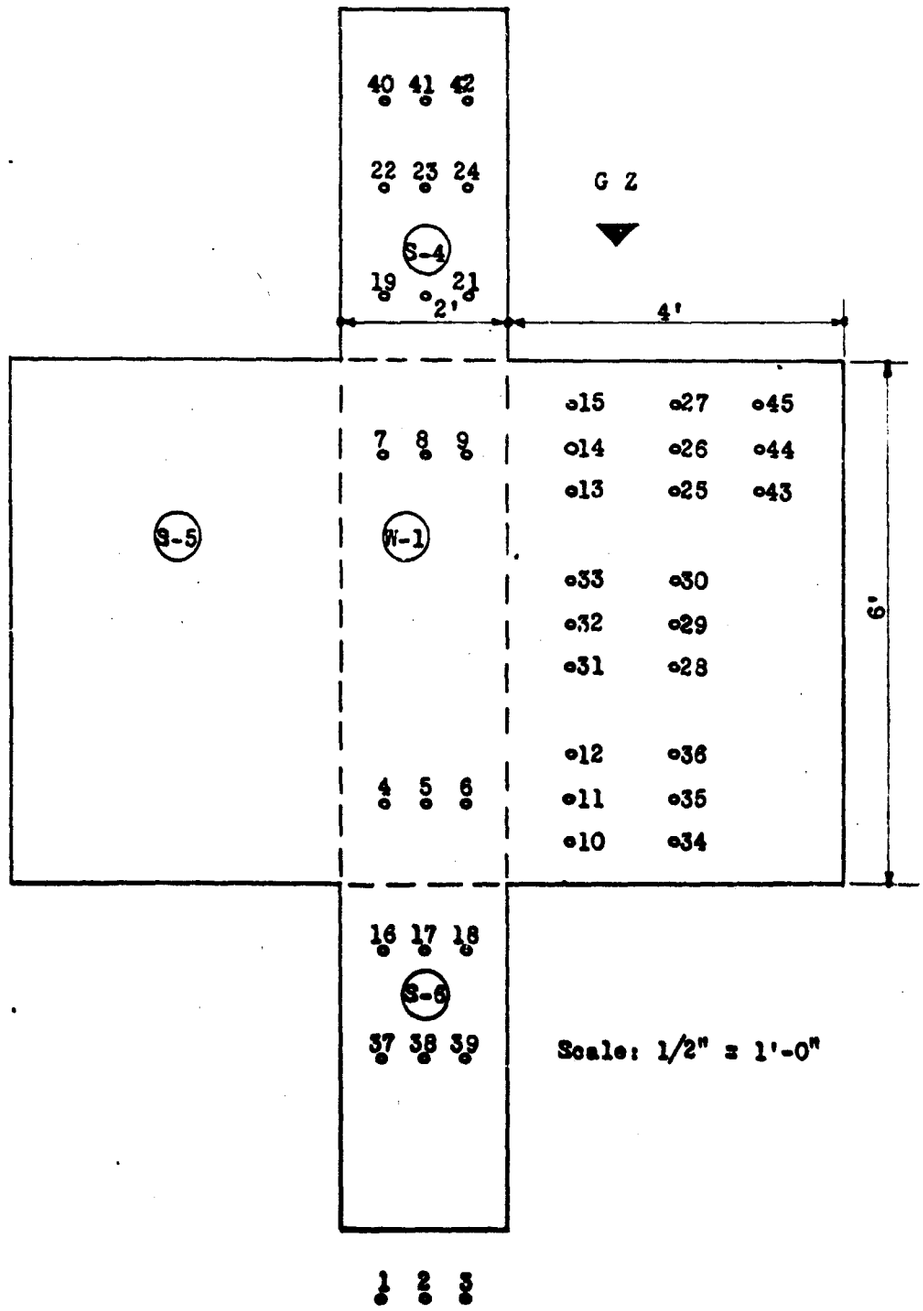

Fig. 8.1 Gage Positions - Foxhole 1

SECRET - RESTRICTED DATA

TABLE 8.1 - Overpressure Readings in Foxhole 1

Ground Level Overpressure: Shot 9 - 7.8 psi; Shot 10 - 4.6 psi

Gage Position	Shot 9				Shot 10			
	d	dave	Pmax	Pmax/Pgl	d	dave	Pmax	Pmax/Pgl
1	0.299				0.251			
2	0.287	0.307	7.8	*1.00	0.234	0.237	4.64	*1.01
3	0.335				0.225			
4	0.379				0.306			
5	0.386	0.389	12.5	1.60	0.474	0.305	7.68	1.67
6	0.401				0.303			
7	0.405				0.304			
8	0.389	0.397	13.0	1.67	0.299	0.300	7.44	1.62
9	0.398				0.297			
10	0.337				0.312			
11	0.432	0.385	12.2	1.56	0.308	0.310	7.94	1.72
12	0.387				0.309			
13	0.411				0.302			
14	0.621	0.493	20.1	2.57	0.439	0.347	10.0	2.17
15	0.448				0.299			
16	0.334				0.321			
17	0.378	0.379	11.9	1.53	0.304	0.296	7.25	1.58
18	0.376				0.263			
19	0.412				0.293			
20	0.418	0.414	14.1	1.81	0.312	0.300	7.44	1.62
21	0.412				0.296			
22					0.301			
23					0.304	0.305	7.85	1.71
24					0.311			

* Gage positions 1, 2, and 3 were at ground leve

SECRET – RESTRICTED DATA

TABLE 8.1 (Continued) - Overpressure Readings in Foxhole 1

Gage Position	Shot 9				Shot 10			
	d	dave	Pmax	Pmax/Pgl	d	dave	Pmax	Pmax/Pgl
25					0.302			
26					0.307	0.298	7.34	1.60
27					0.286			
28					0.303			
29					0.381	0.349	10.1	2.20
30					0.362			
31					0.295			
32					0.299	0.291	7.00	1.52
33					0.278			
34					0.356			
35					0.238	0.293	7.09	1.54
36					0.284			
37					0.275			
38					0.321	0.296	7.25	1.58
39					0.291			
40					0.273			
41					0.265	0.284	6.67	1.45
42					0.313			
43					0.293			
44					0.292	0.293	7.09	1.54
45					0.302			
W-1	-	-	14.6	1.87	-	-	N.G.	-
S-1					-	-	8.1	1.76
S-2					-	-	9.0	1.96
S-3					-	-	8.7	1.89

SECRET - RESTRICTED DATA

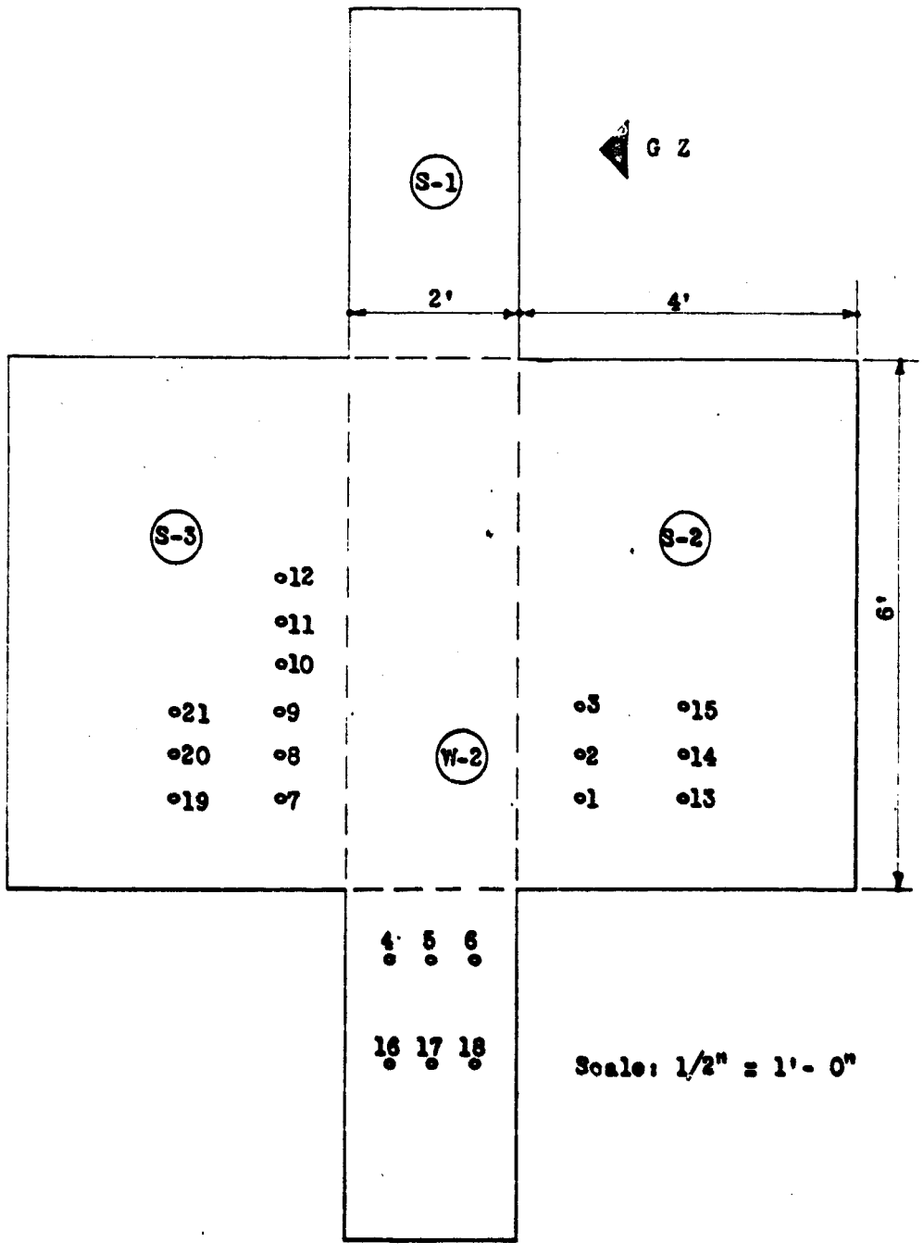

Fig. 8.2 Gage Positions - Foxhole 2

SECRET - RESTRICTED DATA

TABLE 8.2 - Overpressure Readings in Foxhole 2

Ground Level Overpressure: Shot 9 - 7.8 psi; Shot 10 - 4.6 psi

Gage Position	Shot 9				Shot 10			
	d	dave	Pmax	Pmax/Pgl	d	dave	Pmax	Pmax/Pgl
1	0.375				0.300			
2	0.397	0.380	11.9	1.53	0.293	0.294	7.14	1.55
3	0.367				0.288			
4	0.382				0.301			
5	0.433	0.401	13.3	1.70	0.243	0.261	5.64	1.22
6	0.389				0.240			
7					0.281			
8					0.301	0.290	6.95	1.51
9					0.284			
10	0.370							
11	0.378	0.374	11.5	1.47				
12	0.373							
13					0.276			
14					0.285	0.286	6.75	1.47
15					0.296			
16					0.285			
17					0.284	0.288	6.85	1.49
18					0.295			
19					-			
20					0.303	0.284	6.67	1.45
21					0.265			
W-2	-	-	13.9	1.78	-	-	7.9	1.72
S-1					-	-	8.8	1.91
S-2					-	-	9.1	1.98
S-3					-	-	8.5	1.85

SECRET - RESTRICTED DATA

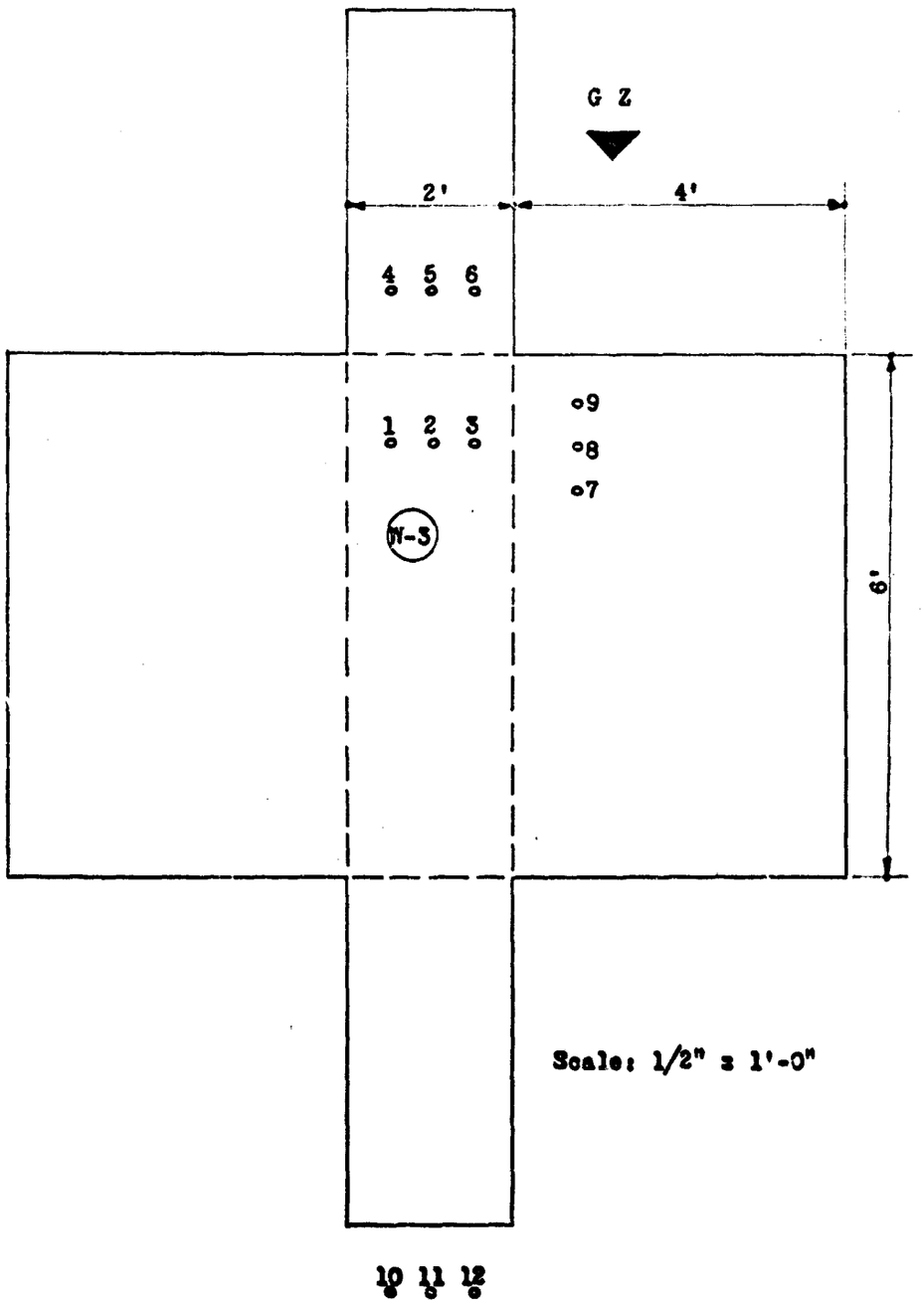

Fig. 8.3 Gage Positions - Foxhole 3

SECRET - RESTRICTED DATA

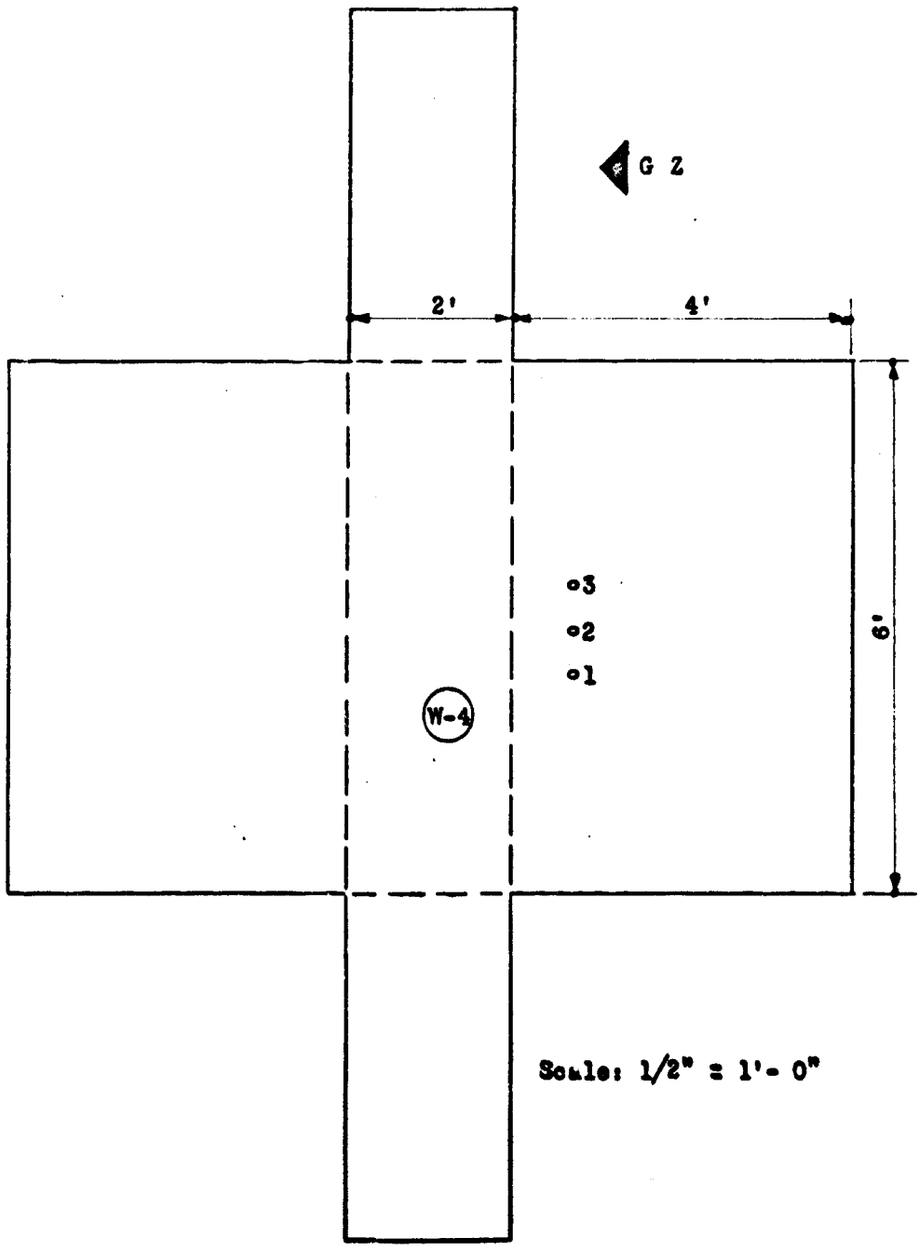

Fig. 8.4 Gage Positions - Foxhole 4

SECRET – RESTRICTED DATA

TABLE 8.3 - Overpressure Readings in Foxhole 3

Ground Level Overpressure: Shot 9 - 3.8 psi; Shot 10 - 1.8 psi

Gage Position	Shot 9				Shot 10			
	d	dave	Pmax	Pmax/Pgl	d	dave	Pmax	Pmax/Pgl
1	0.270							
2	0.273	0.270	6.0	1.58				
3	0.268							
4	0.259							
5	0.275	0.270	6.0	1.58				
6	0.275							
7	0.262							
8	0.285	0.270	6.0	1.58				
9	0.263							
10	0.219							
11	0.215	0.218	3.92	*1.04				
12	0.220							
W-3	-	-	6.2	1.63	-	-	3.0	1.67

* Gage positions 10, 11, and 12 were at ground level.

TABLE 8.4 - Overpressure Readings in Foxhole 4

Ground Level Overpressure: Shot 9 - 3.8 psi; Shot 10 - 1.8 psi

Gage Position	Shot 9				Shot 10			
	d	dave	Pmax	Pmax/Pgl	d	dave	Pmax	Pmax/Pgl
1	0.265							
2	0.283	0.275	6.3	1.66				
3	0.277							
W-4	-	-	6.3	1.66	-	-	2.8	1.55

SECRET - RESTRICTED DATA

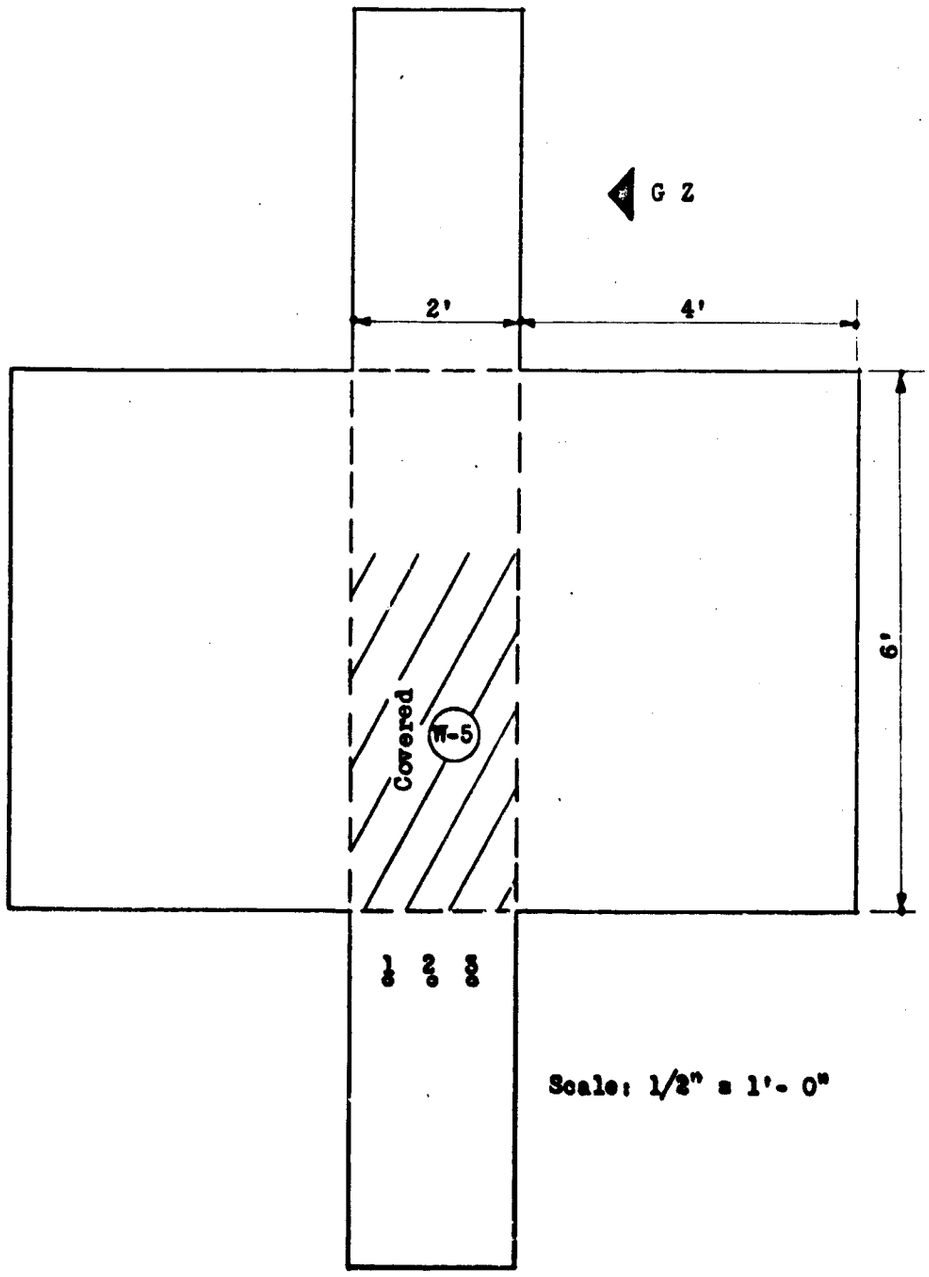

Fig. 8.5 Gage Positions - Foxhole 5 (2/3 Covered)

SECRET - RESTRICTED DATA

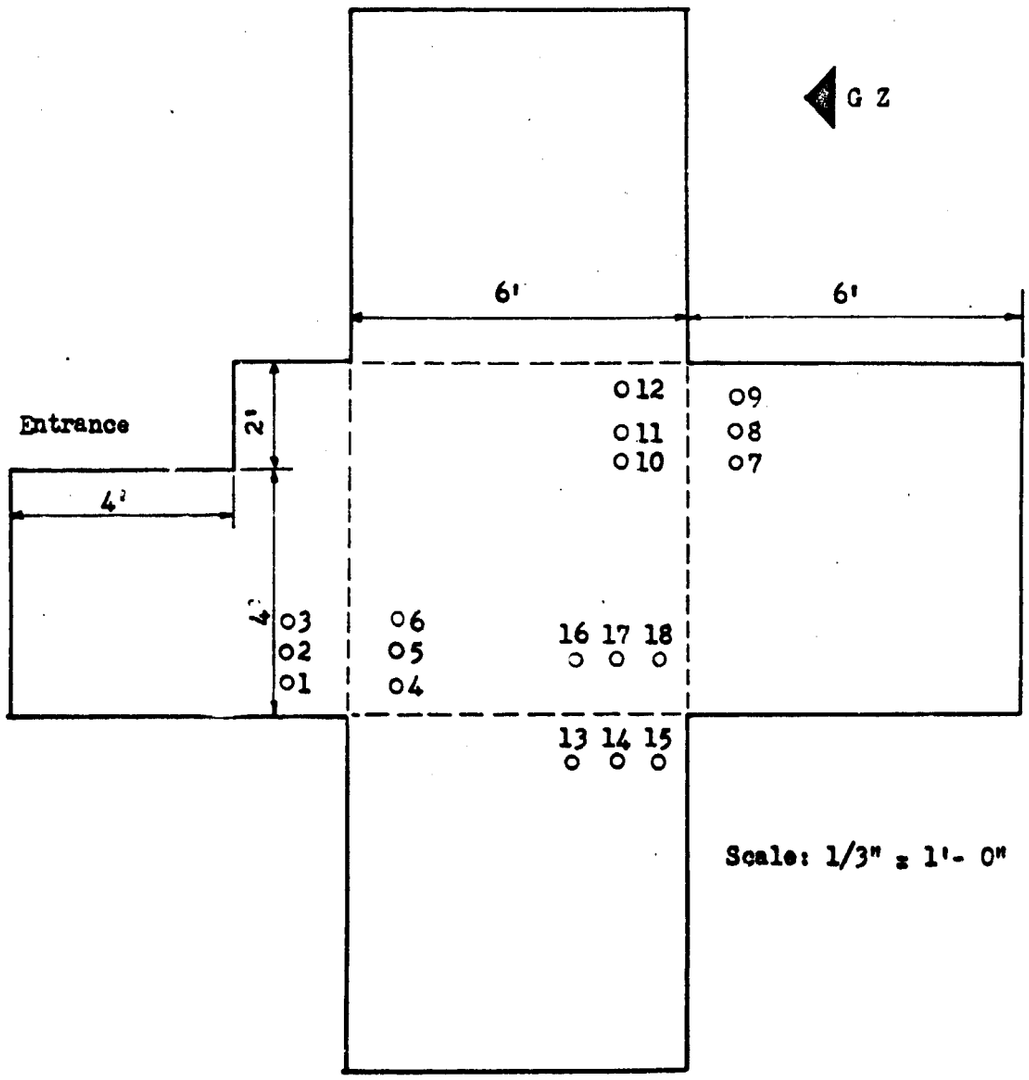

Fig. 8.6 Gage Positions - Command Post

SECRET - RESTRICTED DATA

TABLE 8.5 - Overpressure Readings in Foxhole 5 (2/3 Covered)

Ground Level Overpressure: Shot 9 - 3.8 psi; Shot 10 - 1.8 psi

Gage Position	Shot 9				Shot 10			
	d	dave	Pmax	Pmax/Pgl	d	dave	Pmax	Pmax/Pgl
1	0.249							
2	0.242	0.242	4.8	1.26				
3	0.235							
W-5	-	-	5.5	1.45	-	-	2.8	1.55

TABLE 8.6 - Overpressure Readings in Command Post

Ground Level Overpressure: 23 psi

Gage Position	Shot 9				Shot 10			
	d	dave	Pmax	Pmax/Pgl	d	dave	Pmax	Pmax/Pgl
1	0.457							
2	0.430	0.442	16.1	0.700				
3	0.440					Not Used		
4	0.427							
5	0.440	0.434	15.5	0.675				
6	0.434							
7	0.454							
8	0.462	0.449	16.7	0.725				
9	0.432							
10	0.438							
11	0.420	0.422	14.4	0.625				
12	0.408							
13	0.448							
14	0.430	0.435	15.6	0.678				
15	0.426							
16	0.453							
17	0.420	0.438	15.9	0.691				
18	0.441							

SECRET - RESTRICTED DATA

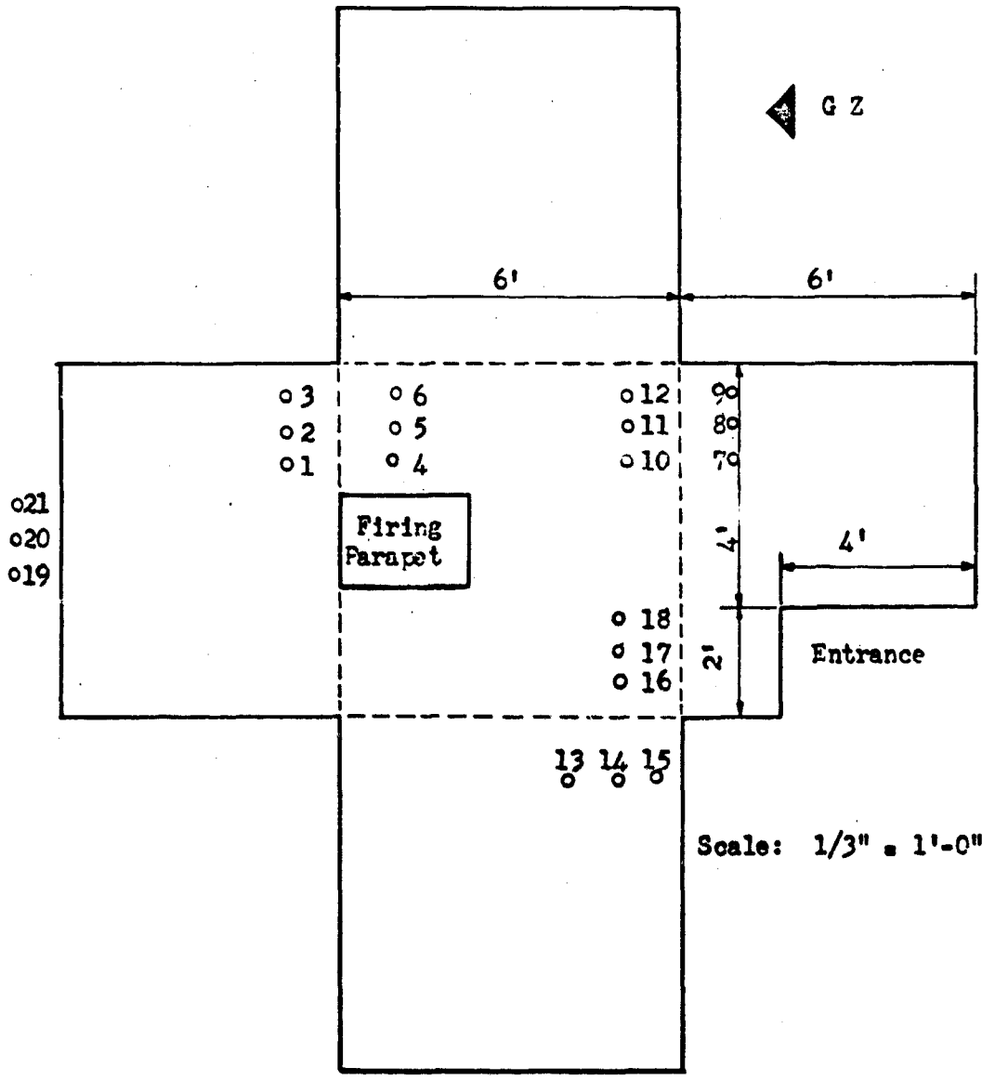

Fig. 8.7 Gage Positions - Machine Gun Emplacement

SECRET - RESTRICTED DATA

TABLE 8.7 - Overpressure Readings in Machine Gun Emplacement

Ground Level Overpressure: 23 psi

Gage Position	Shot 9				Shot 10			
	d	dave	Pmax	Pmax/Pgl	d	dave	Pmax	Pmax/Pgl
1	0.557							
2	0.572	0.555	25.4	1.10				
3	0.537					Not Used		
4	0.577							
5	0.571	0.572	27.0	1.17				
6	0.568							
7	0.619							
8	0.605	0.639	33.7	1.47				
9	0.692							
10	0.578							
11	0.561	0.573	27.1	1.18				
12	0.579							
13	0.535							
14	0.536	0.545	24.5	1.07				
15	0.563							
16	0.531							
17	0.555	0.547	24.7	1.08				
18	0.556							
19	0.529							
20	0.518	0.529	23.0	*1.00				
21	0.541							

* Gage positions 19, 20, and 21 were at ground level.

SECRET - RESTRICTED DATA

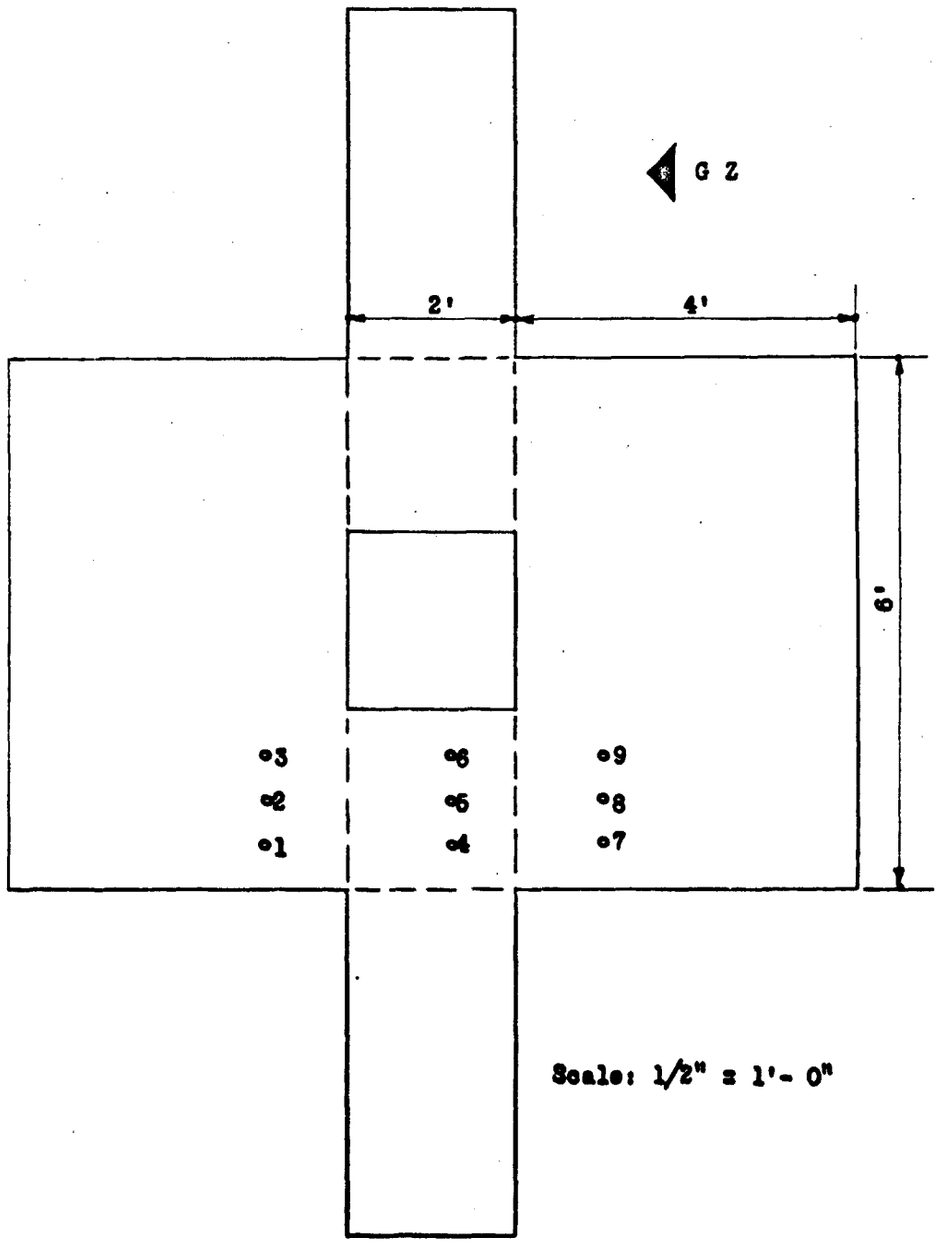

Fig. 8.8 Gage Positions - Foxhole (Covered)

SECRET - RESTRICTED DATA

TABLE 8.8 - Overpressure Readings in Covered Foxhole

Ground Level Overpressure: 23 psi

Gage Position	Shot 9				Shot 10			
	d	dave	Pmax	Pmax/Pgl	d	dave	Pmax	Pmax/Pgl
1	0.528							
2	0.531	0.528	23.0	1.00				
3	0.526					Not Used		
4	0.536							
5	0.545	0.537	23.8	1.04				
6	0.529							
7	0.528							
8	0.545	0.532	23.4	1.02				
9	0.523							

SECRET - RESTRICTED DATA

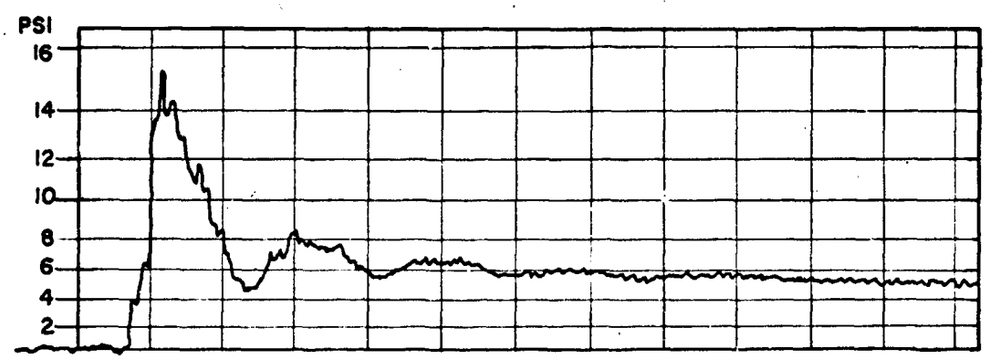

Fig. 8.9 NOL Wiancko Gage Record Shot 9, Foxhole 1

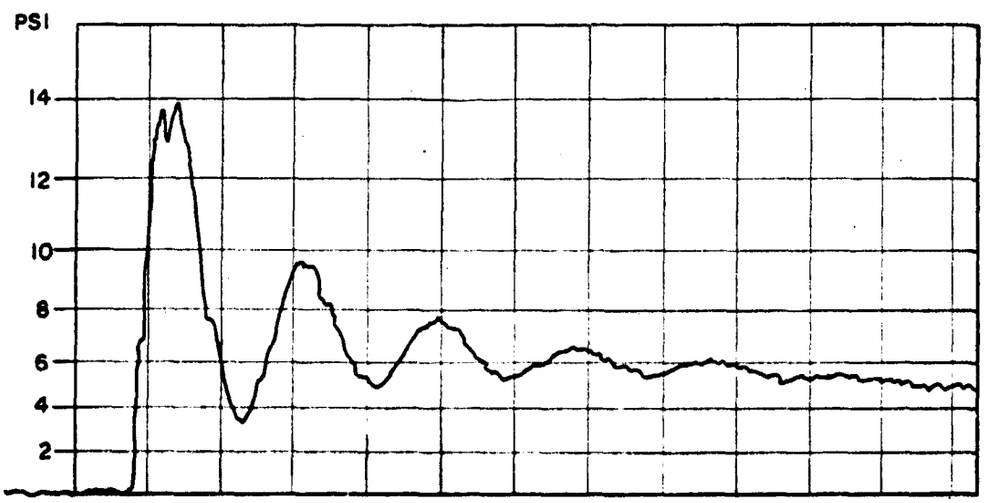

Fig. 8.10 NOL Wiancko Gage Record Shot 9, Foxhole 2

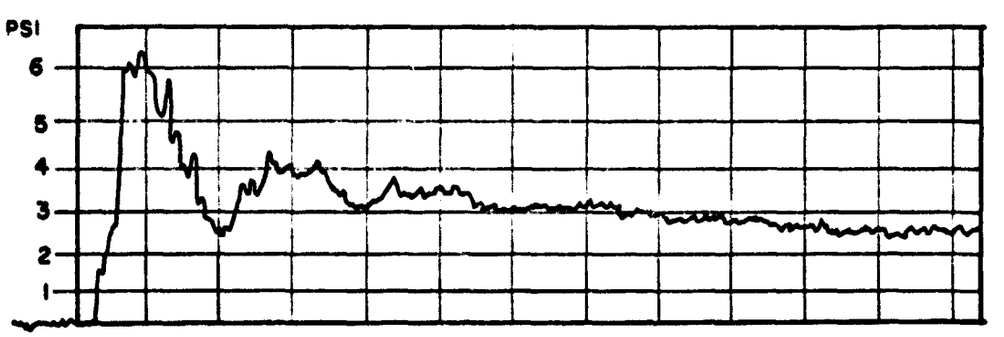

Fig. 8.11 NOL Wiancko Gage Record Shot 9, Foxhole 3

SECRET - RESTRICTED DATA

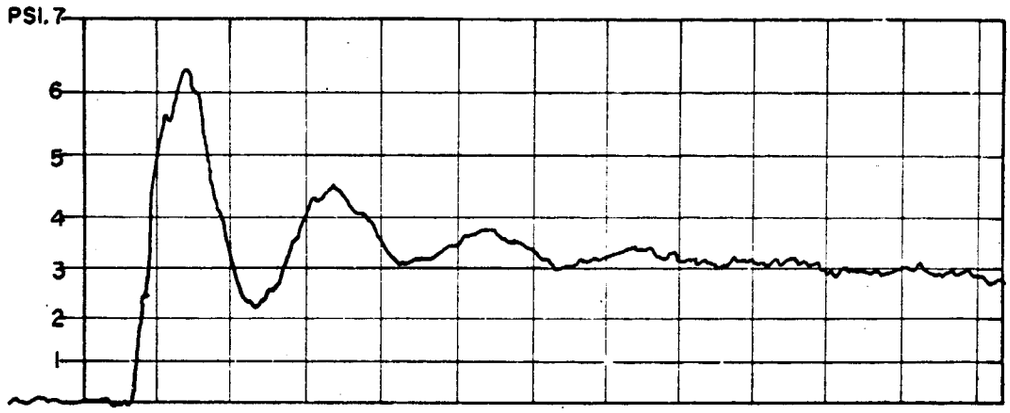

Fig. 8.12 NOL Wiancko Gage Record Shot 9, Foxhole 4

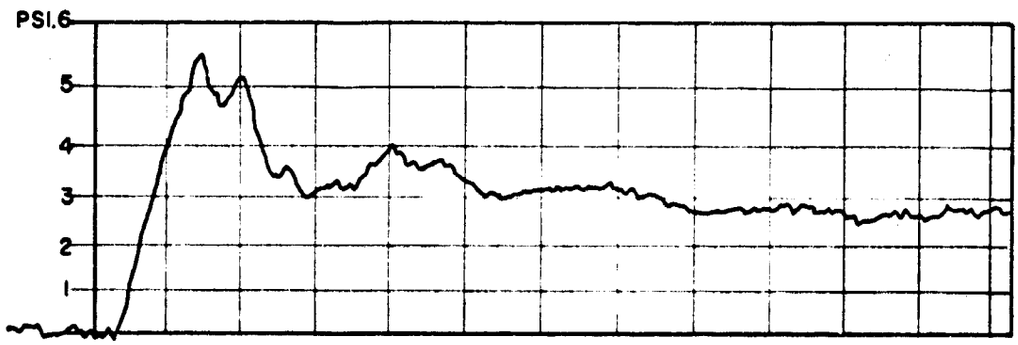

Fig. 8.13 NOL Wiancko Gage Record Shot 9, Foxhole 5

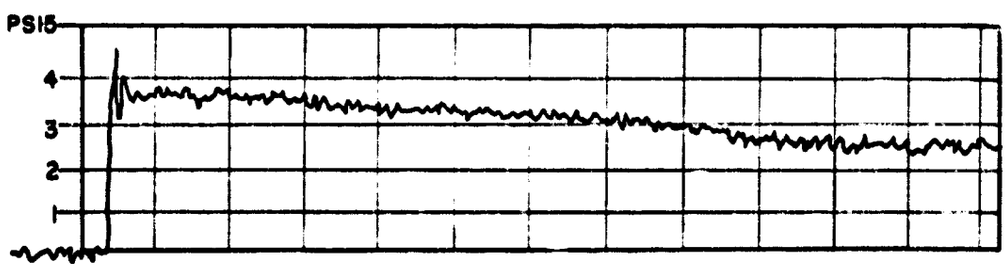

Fig. 8.14 NOL Wiancko Gage Record Shot 9, 7000 ft Ground Level

SECRET - RESTRICTED DATA

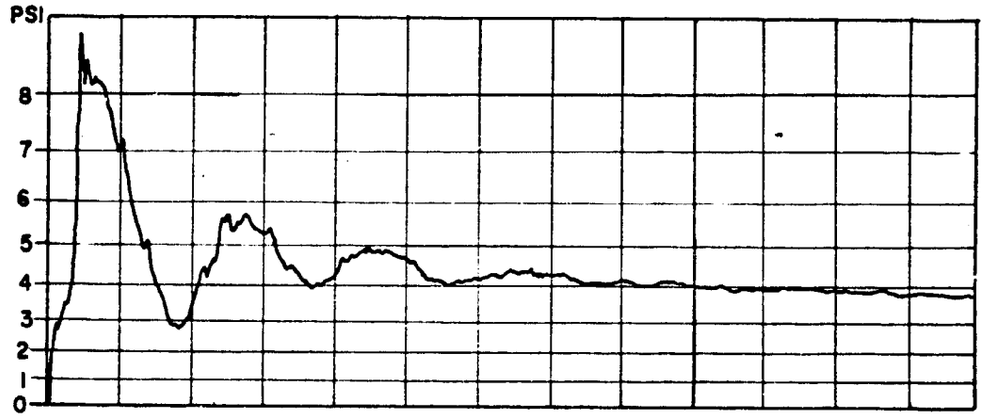

Fig. 8.15 NOL Wiancko Gage Record Shot 10, Foxhole 1

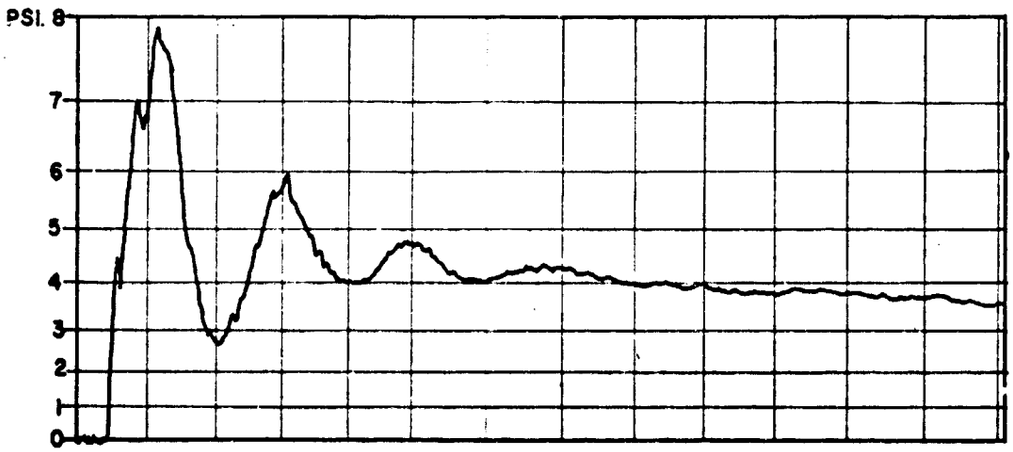

Fig. 8.16 NOL Wiancko Gage Record Shot 10, Foxhole 2

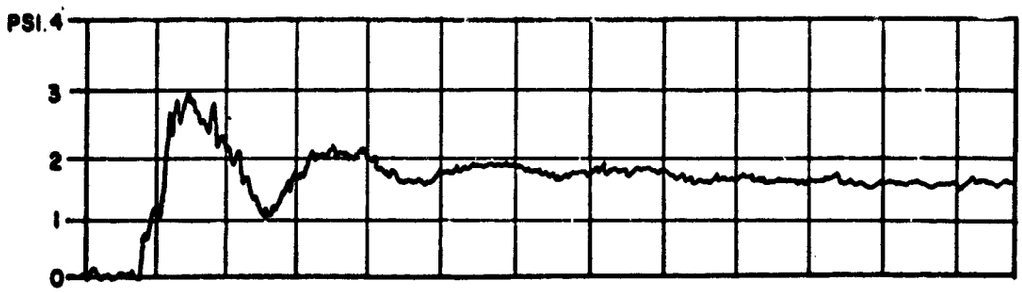

Fig. 8.17 NOL Wiancko Gage Record Shot 10, Foxhole 3

SECRET - RESTRICTED DATA

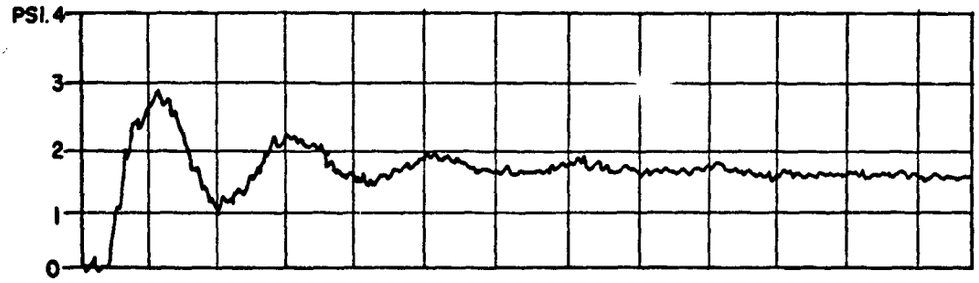

Fig. 8.18 NOL Wiancko Gage Record Shot 10, Foxhole 4

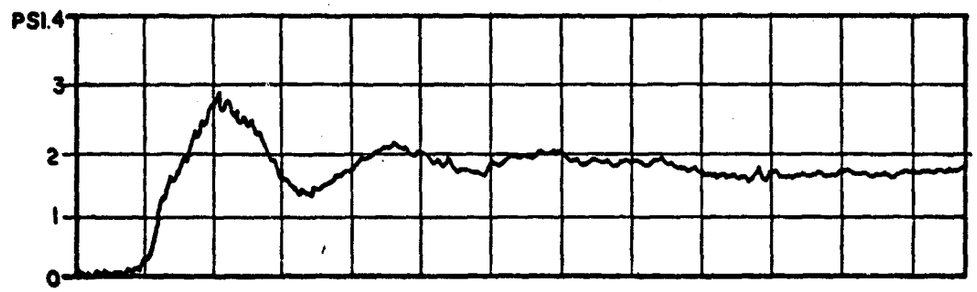

Fig. 8.19 NOL Wiancko Gage Record Shot 10, Foxhole 5

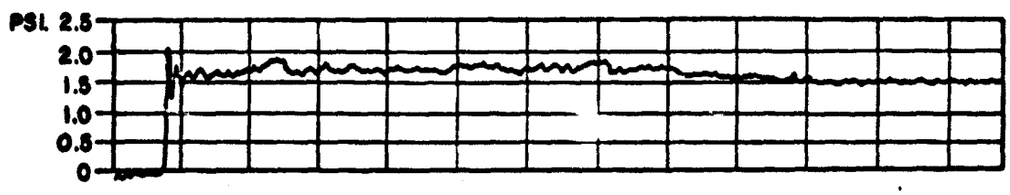

Fig. 8.20 NOL Wiancko Gage Record Shot 10, 7000-ft Ground Level

SECRET - RESTRICTED DATA

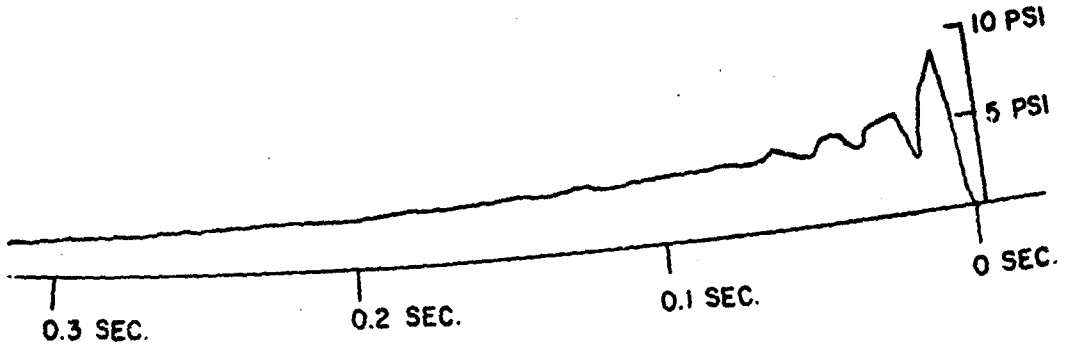

Fig. 8.21 BRL Scratch Gage Record Shot 10, Position S-4, Foxhole 1

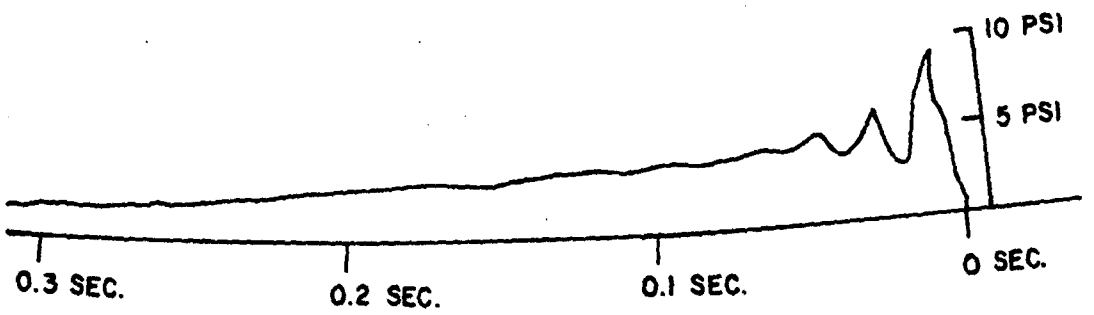

Fig. 8.22 BRL Scratch Gage Record Shot 10, Position S-6, Foxhole 1

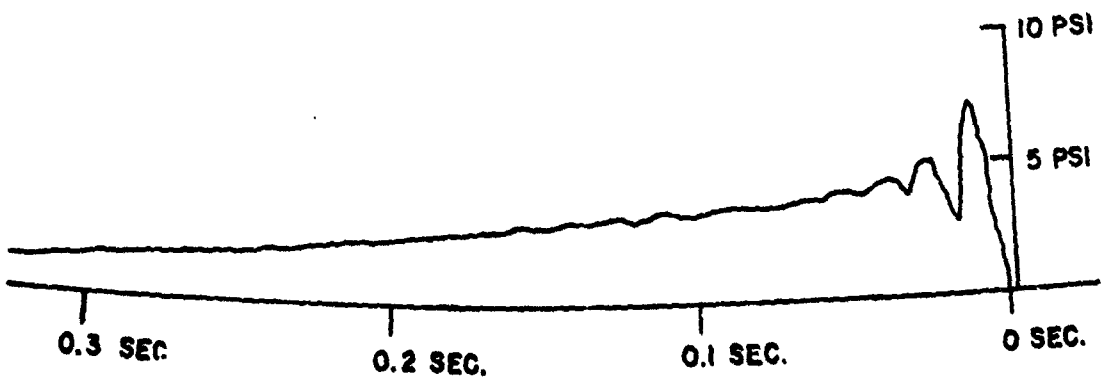

Fig. 8.23 BRL Scratch Gage Record Shot 10, Position S-2, Foxhole 2

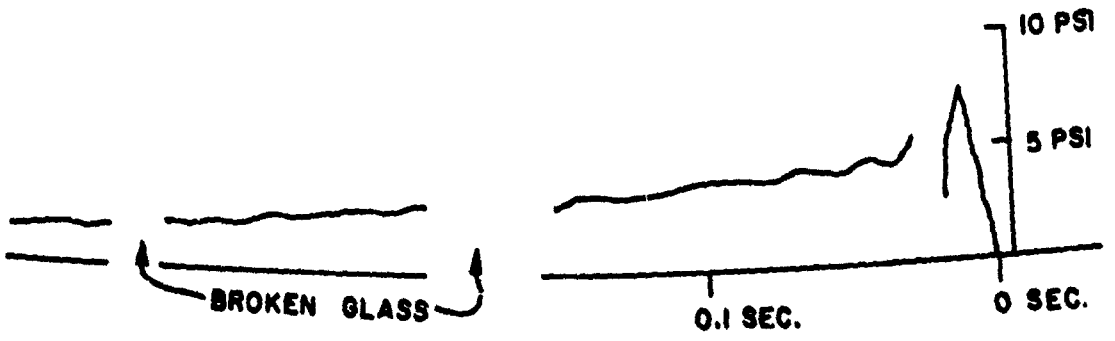

Fig. 8.24 BRL Scratch Gage Record Shot 10, Position S-3, Foxhole 2

SECRET - RESTRICTED DATA

CHAPTER 9

DISCUSSION

9.1 INTRODUCTION

To attain a complete understanding of the nature of overpressure multiplication (build-up) in a field fortification, it is necessary to determine such things as the effect of the size, geometry, and orientation of the emplacement; of the overpressure region in which the emplacement is exposed; of a partial cover; of an object, such as a soldier, in the emplacement; and of the material of the walls and floor. The design of this experiment included an insufficient amount of instrumentation to isolate these with certainty. Certain trends in multiplication and response of the instruments are indicated, and an introductory attempt is made to determine the significance of covers on the emplacement.

The function of a field fortification is to protect the individual soldier. Therefore, the results of this type of experiment should be integrated with the physiological effects of the overpressure on the individual soldier. Until this can be accomplished, the protective value of field fortifications from shock phenomena cannot completely be determined.

9.2 INSTRUMENTATION

9.2.1 Wiancko Gages

The traces of the Wiancko pressure-time gages given in Figs. 8.9 to 8.20 are of sufficient definition to enable a general verification of the predicted method of overpressure build-up in the emplacement.

Ideally, the overpressure build-up in an emplacement should follow the characteristics shown in Fig. 6.7, showing three and possibly more distinct "steps" in the process. Examination of the Wiancko gage traces reveals that the initial build-up is indeed characterized by a series of "steps." Each trace for both shots for foxholes 1 to 4 (those that were uncovered) shows at least two of these steps, the presence of which indicates that method of build-up described in the theory section of this report is valid, at least to the point where the third or possibly fourth pressure wave travels past the instrument.

SECRET - RESTRICTED DATA

The rise times from first initiation of the shock wave to the highest peak varied from 5 to 10 milliseconds (ms), differing considerably from the almost instantaneous build-up recorded at the surface. The duration of the first pulse was 10 to 20 ms, depending upon the emplacement. It is important to determine whether rise times and durations of this magnitude are physiologically dangerous.

The significance of the oscillatory nature of the traces after the initial peak is not known; however, certain general observations about them can be made. The period of the oscillations for each foxhole, whether oriented parallel or perpendicular to the blast, was between 16 and 22 ms, with most near 20 ms. The oscillations in the 2/3 covered emplacement were less evident than those recorded in the uncovered emplacement.

9.2.2 Scratch Gages

For Shot 10, foxholes 1 and 2 were further instrumented with scratch gages such that a pressure-time record on the walls of the emplacement could be obtained. The exact location of these gages is given in Figs. 8.1 and 8.2.

The traces of the scratch gages shown in Fig. 8.21 to 8.24 compare favorably with the Wiancko gage traces, insofar as the peak pressure and times of the peaks are concerned. The sensitivity of these gages, however, was not sufficient to record the "steps" in the initial rise. Some slight variation in the time of the initial peaks was observed from gage to gage. It is felt that this was caused by the location of the gages in the emplacement. The gages S-1 and S-5 failed to operate except for recording the peak overpressure.

9.2.3 Indenter Gages

The indenter gages were used to augment the overpressure determinations made by the Wiancko and scratch gages, in order to determine whether any areas of unusually high overpressure existed at any point within the emplacements. For Shot 9, all of the emplacements were instrumented; while, for Shot 10, foxholes 1 and 2 were instrumented extensively with no indenter gages in the additional emplacements.

The peak overpressure values, as measured with the indenter gages, tended to remain relatively even throughout the emplacements. Where there was a considerable increase at some point, it is uncertain whether the extreme multiplication was caused by a high overpressure or some flaw in a gage; because the increase was often not demonstrated for both shots in the same emplacement or in emplacements in the same orientation. In all cases, the average of all the peak overpressures as measured by the indenter gages was within ± 15 per cent of that measured by the Wiancko gage. It is felt that indenter gages were sufficiently accurate and consistent for this experiment.

9.3 INTERPRETATION

Table 9.1 is a condensation of the data obtained from the Wiancko gages relating the overpressure multiplication, incident overpressure,

SECRET – RESTRICTED DATA

TABLE 9.1 - Summary of Data*

Emplacement	Overpressure Multiplication		Incident Overpressure (psi)		Aperture (ft^2)	Volume (ft^3)	Aperture / Volume
	Shot 9	Shot 10	Shot 9	Shot 10			
Foxhole 1	1.87	-	7.8	4.6	12	48	0.25
Foxhole 2	1.78	1.72	7.8	4.6	12	48	0.25
Foxhole 3	1.63	1.67	3.8	1.8	12	48	0.25
Foxhole 4	1.66	1.55	3.8	1.8	12	48	0.25
Foxhole 5	1.45	1.55	3.8	1.8	4	48	0.083
Command Post	0.682	-	23	-	4	250	0.016
M. G. Emplacement	1.15	-	23	-	-	-	-
Foxhole (covered)	1.02	-	23	-	-	-	-

* Based on Wiancko gage results for foxholes 1 to 5 and indenter gage results for Command Post, M. G. Emplacement, and foxhole (covered).

SECRET - RESTRICTED DATA

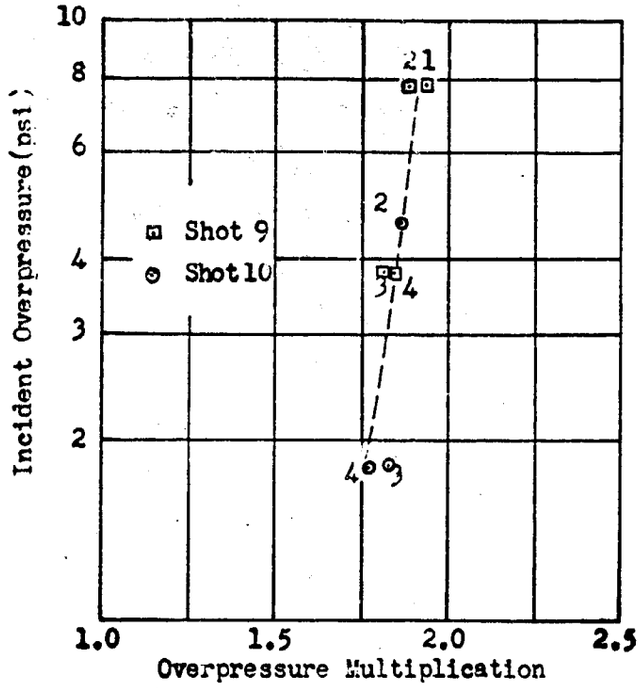

Fig. 9.1 Overpressure Multiplication Plotted as a Function of Incident Overpressure

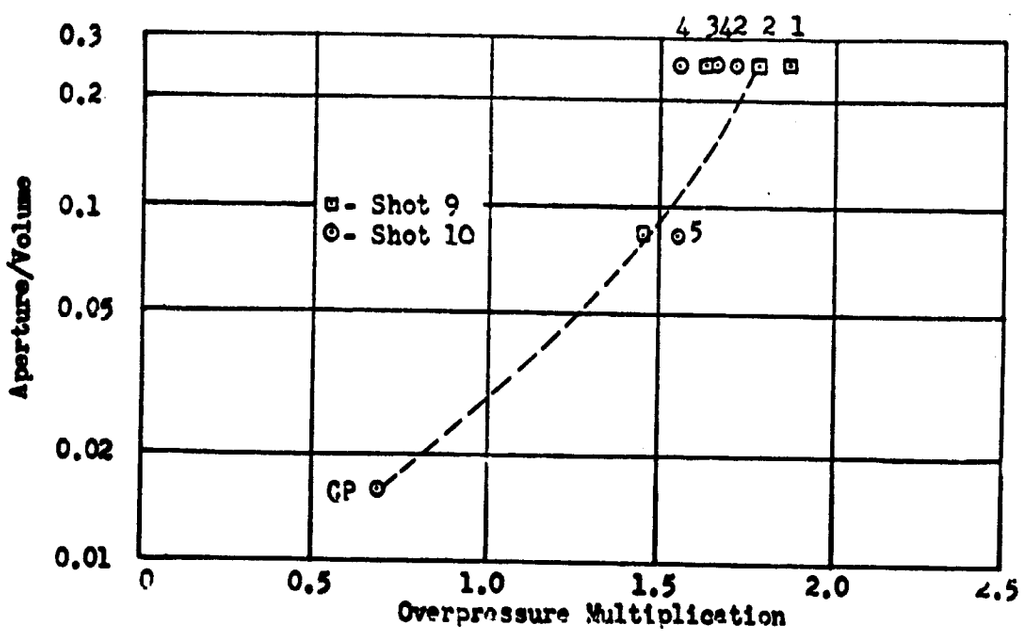

Fig. 9.2 Overpressure Multiplication Plotted as a Function of Aperture/Volume

SECRET – RESTRICTED DATA

aperture, volume, and the aperture-volume ratio for each emplacement. Data from the machine-gun emplacement and covered foxhole are not included in the subsequent discussion, because it was deemed that the type of cover used on these was not consistent with those used on the other emplacements. The remaining data give an indication of the importance of some of the parameters which affect the overpressure multiplication.

Plotting overpressure multiplication as a function of incident overpressure (Fig. 9.1) indicates--at least, in a preliminary nature--that the multiplication will increase with increased incident overpressure. Before a more reliable curve can be established, however, it is necessary to obtain a greater range of points on the graph.

Figure 9.2 shows the overpressure multiplication plotted as a function of aperture-to-volume ratio. The points are connected by a dotted line which serves only as an indication of the trend. A more definite relation could not be established; because, as is seen in Fig. 9.1, the overpressure multiplication is also a function of incident overpressure. Had there been more command posts and type 5 (2/3 covered) emplacements placed at various overpressure regions, it may have been possible to draw a series of curves similar to the dotted one shown in Fig. 9.2, each for a different incident overpressure.

The available data illustrate, however, that the overpressure multiplication within these emplacements is related to the aperture-to-volume ratio such that, as the aperture-to-volume ratio increases, the overpressure multiplication will also increase.

SECRET - RESTRICTED DATA

CHAPTER 10

CONCLUSIONS AND RECOMMENDATIONS

10.1 CONCLUSIONS

During this test, the overpressure multiplication as measured by the Wiancko gages in the open two-man foxholes was between 1.87 and 1.55; and the corresponding values for 2/3 covered two-man foxholes were between 1.45 and 1.55.

Instrumentation on the walls and floors of these foxholes indicates few overpressures unusually higher or lower than those indicated above.

A method of overpressure build-up in a foxhole has been predicted and verified with fair certainty.

The principal variables concerning overpressure multiplication in an emplacement are the incident overpressure and aperture-to-volume ratio.

10.2 RECOMMENDATIONS

Until the physiological significance to a human of overpressure with properties similar to those shown in the Wiancko gage traces is determined, it is recommended that no further full-scale field tests of these phenomena be attempted.

If further testing, whether laboratory or field, is warranted on the basis of the considerations delineated above, it is recommended that more data be obtained to fully determine the effects of incident overpressure and aperture-to-volume ratio on the overpressure multiplication, and that an attempt be made to determine whether orientation, materials of the walls and floor of the emplacement, and some object in the emplacement will markedly change the overpressure multiplication.

SECRET - RESTRICTED DATA

PART III

REFLECTED THERMAL RADIATION IN FOXHOLES

CHAPTER 11

INTRODUCTION

11.1 OBJECTIVES

The objectives of Part III of Project 3.9 were to measure the thermal radiation from an atomic bomb in the shadowed portion of a standard, 2' x 4' x 6', two-man foxhole; and to determine a method of scaling such that the reflected thermal energy in a foxhole may be predicted for any atomic weapon yield, height of burst, distance from ground zero, and reflectance of exposed wall.

11.2 BACKGROUND

During the DESERT ROCK operations(18), much work but little correlation was done to illustrate the gross effects of a nuclear detonation on field fortifications. These emplacements, in general, were constructed to illustrate effects graphically to the troops participating in the operation, with little or no attempt at instrumentation or recording of results. The blast and overpressure sections of this report have attempted to obtain more definite information on blast effects.

Measurements have been made of the gamma radiation intensity and the neutron flux in a standard two-man foxhole(6,19).

The protective value of standard field emplacements from thermal radiation has been illustrated qualitatively in the DESERT ROCK operations, and it has been generally agreed that adequate protection is afforded except in extreme conditions where a large portion of the emplacement is directly exposed. In a quantitative sense NML instrumented one foxhole with passive thermal indicators for one shot of the BUSTER series. Eighteen cal/cm^2 were received on the directly exposed wall, but little measurable reflected energy was received on the unexposed walls or floor(20).

Little more than this was known about the reflected thermal energy within an emplacement, which indicated a need to determine this quantity, and to develop means of scaling this information to many conceivable operational conditions.

SECRET - RESTRICTED DATA

11.3 THEORY

The successful completion of an experiment of this type depends upon achieving a balance between the actual conditions experienced by the soldier in combat and modifications which are necessary to provide convenient, reliable experimental measurements. During the conduct of the field test, these modifications should be kept at a minimum, providing accurate operations are not impaired.

To accomplish the objectives, a series of foxholes representative of the basic type of emplacement most used in combat were instrumented. They were lined with aluminum which was treated with an "Alzak" process, giving the surface high diffuse reflectance characteristics(21). (Averages 70.7 per cent over the 400 to 1100 micron wavelength range.) This material was chosen because polar reflectance curves of sand and soil indicate that they are essentially diffuse reflectors, and the walls of the foxhole should have similar reflectance characteristics(22). Aluminum was used because it was desirable to have a reflector whose characteristics would remain unchanged through the entire thermal pulse. This generally would not be the case for paints or most otherwise suitable diffusely reflecting surfaces.

Briefly, a diffuse reflector is one in which the energy intensity measured at any angle from the normal to the reflecting surface is proportional to the cosine of this angle multiplied by the intensity of the reflected energy in the normal direction. In mathematical form:

$$I_\theta = I_n \cos \theta$$

where I_θ = energy intensity at angle θ from the normal to the surface

and I_n = energy intensity in normal direction to the surface.

SECRET – RESTRICTED DATA

CHAPTER 12

EXPERIMENT DESIGN

12.1 GENERAL

A series of 22 two-man foxholes instrumented to measure thermal energy were exposed to Shots 9 and 10. Each was lined with aluminum sheet, the surface of which was treated to be a diffuse reflector, and was oriented for each shot such that the direct thermal energy was incident either 1 ft, 2 ft, 3 ft, or 4 ft down the directly exposed wall, or 2 ft across the floor. This was accomplished by placing all foxholes (except those used for calorimeters and scaling) in the same immediate area and orienting each one in the ground at an angle such that the desired amount of back wall was directly exposed as shown in Figs. 12.1 and 12.2. The area around the foxholes was subsequently stabilized to minimize preshock dust, an effect which will vary considerably with soil conditions.

12.2 TEST SITE LAYOUT

Eighteen foxholes were placed 4000 ft from estimated ground zero on the East-West blast line, two were placed at 6000 ft, and one at 8000 ft from planned ground zero on the Forest Service Line.

A diagram of all Project 3.9 emplacements is given in Appendix A.

12.3 INSTRUMENTATION

Each foxhole was instrumented with an array of passive indicators placed to provide measurements of the thermal energy distribution for each orientation (area of back wall exposed). For those emplacements in which the long (6 ft) edge was perpendicular to a radial line from the bomb, measurements were taken along a vertical line 1 ft from the directly exposed wall. When the long (6 ft) side was parallel to a radial line from the bomb, measurements were made along vertical lines 1½ ft, 3 ft, 4 ft, and 4½ ft from the directly exposed wall and along horizontal lines 1 ft, 2 ft, and 3 ft from the top of the foxhole. To eliminate shielding of the passive indicators by the supporting frame, a series of foxholes were often necessary for each orientation. The purpose of each is given in Appendix E, and was the same for each shot.

SECRET - RESTRICTED DATA

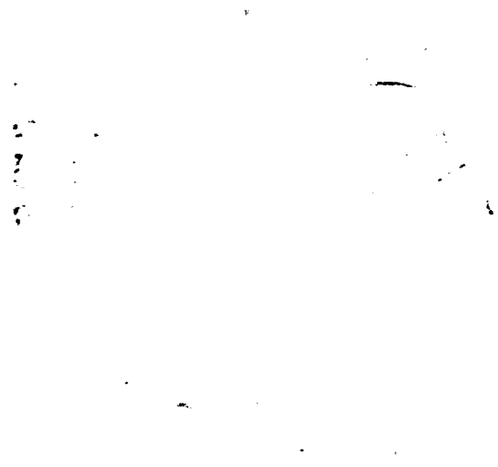

Fig. 12.1 Foxhole 63 A

Fig. 12.2 Foxhole 70 A

SECRET – RESTRICTED DATA

Furthermore, at the 6000 ft and 8000 ft stations, calorimeters were utilized to measure the reflected thermal energy. They were placed parallel to the passive indicators in order to obtain a direct comparison with the total energy as measured by the passive indicators.

12.4 THERMAL INDICATORS

The passive indicators consisted of carbon paper, M-6 liquid vesicant detector paper, black matt paper, cherry bond paper, and buff bond paper which were developed and supplied by NML. These react to various thermal energies from 0.45 cal/cm^2 for the M-6 liquid vesicant detector paper to 14 cal/cm^2 for the buff bond paper. They were cut into $\frac{1}{2}$ in. wide x 12 in. long strips and mounted with cellophane tape on $\frac{1}{4}$ in. x 3 5/8 in. x 12 in. plywood panels. With the necessary space between passive indicator strips for firebreaks, it was possible to mount four strips per plywood panel. The panel assembly was then painted with an acryloid gloss type fire-resistant paint exposing eight evenly spaced $\frac{1}{4}$ in x 3/4 in. "windows" per indicator strip. For certain applications, panels 9 1/8 in. long and 2 in. long were assembled.

The calorimeters were supplied by the Naval Radiological Defense Laboratory. They consisted essentially of a suitably mounted disk-shaped blackened copper energy receiver with a thermocouple soldered to its unexposed face(23). With appropriate recording devices, it was possible to obtain the time-temperature characteristics of the copper disk during exposure. This could then be converted to a curve giving the total energy received as a function of time.

SECRET – RESTRICTED DATA

CHAPTER 13

RESULTS

13.1 DATA ANALYSIS

The reflected thermal energy as measured in the foxholes was made independent of the direct thermal energy by representing, wherever there was a passive indicator reaction, the reaction energy as a fraction of the direct thermal energy. Thus, if the indicator reaction energy was 5.6 cal/cm^2, and the direct energy was 40 cal/cm^2, the fraction is then 5.6 cal/cm^2/40 cal/cm^2 = 0.140. In this manner, the data obtained from corresponding foxholes for Shots 9 and 10 were combined into a single set of data.

It was necessary to compensate for variations in wall area caused by slight errors in orientation of emplacements and the difference between actual and planned ground zero. Accordingly, if the exposed area was planned to be 2 ft^2, but was actually 1.5 ft^2, the fraction at each indicator reaction point was multiplied by 2 ft^2/1.5 ft^2 = 1.33 to give the fraction had 2 ft^2 been exposed. In addition, this figure was then multiplied by a constant factor (1/Reflectance of aluminum = 1/0.707 = 1.42) to give the fraction of incident energy had the reflectance of the walls been unity. Appendix F gives the complete thermal data.

13.2 PASSIVE INDICATORS

Figs. 13.1 to 13.12 give the fraction of incident energy within the foxhole as a function of distance from exposed wall at a particular depth or as a function of depth at a particular distance from the exposed wall.

13.3 CALORIMETERS

In each case, the calorimeters were placed in the foxholes such that direct comparison of the total energy as measured by the calorimeters and the passive indicators could be made. The reflected thermal energy, as measured by the calorimeters along with their position in the foxholes, is given in Tables 13.1 and 13.2 and Figs. 13.14 and 13.15.

SECRET – RESTRICTED DATA

13.4 MAGNITUDE OF INTERREFLECTION

Figure 13.13 gives the fraction of incident energy as a function of distance from the directly exposed wall for the 3 ft depth in the foxhole. In this emplacement, all of the walls (except that which was directly exposed) were coated with a low reflectance, flat black paint.

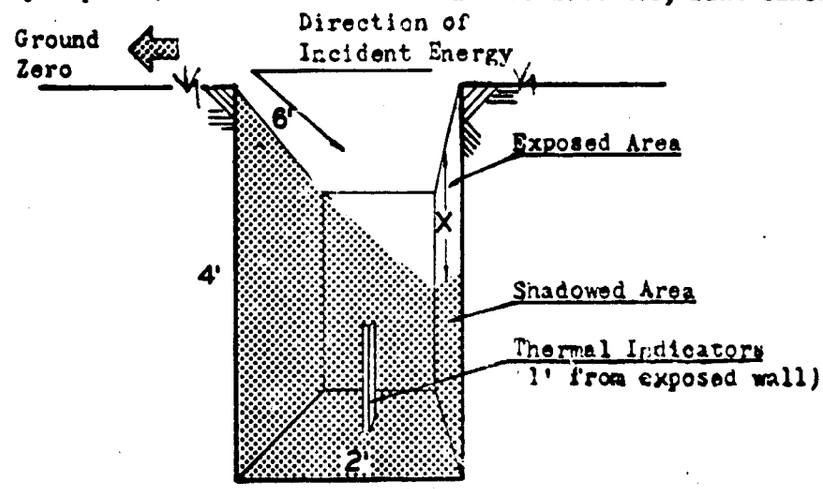

Foxhole Cross Section

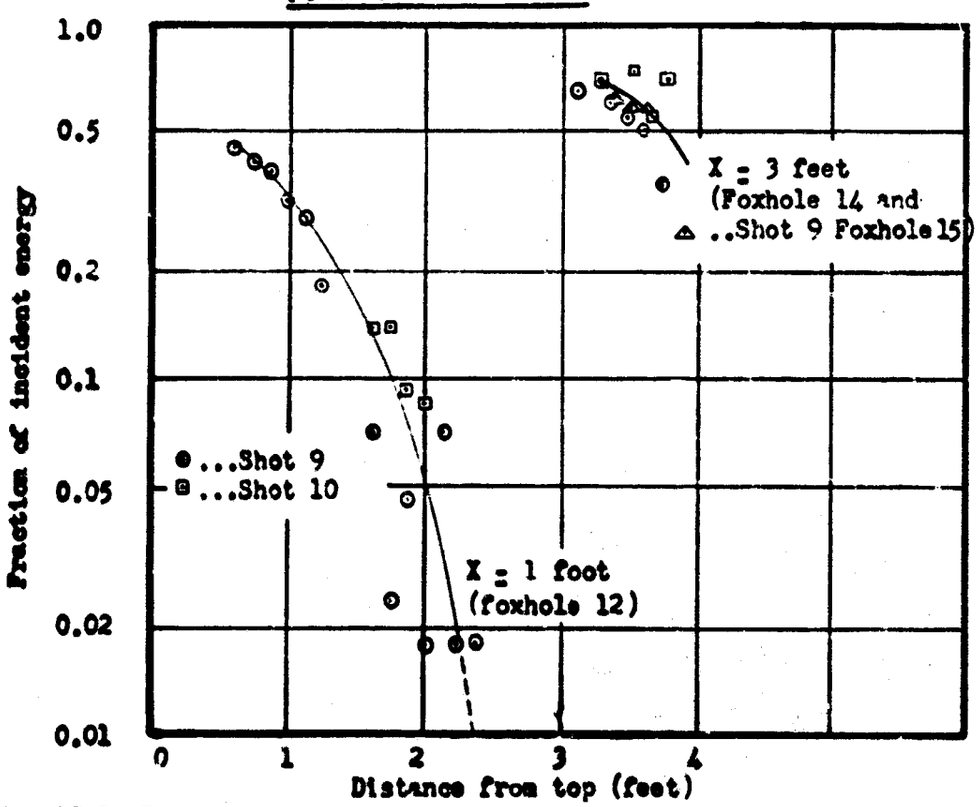

Fig. 13.1 Fraction of Incident Thermal Energy as a Function of Depth in Foxhole

SECRET – RESTRICTED DATA

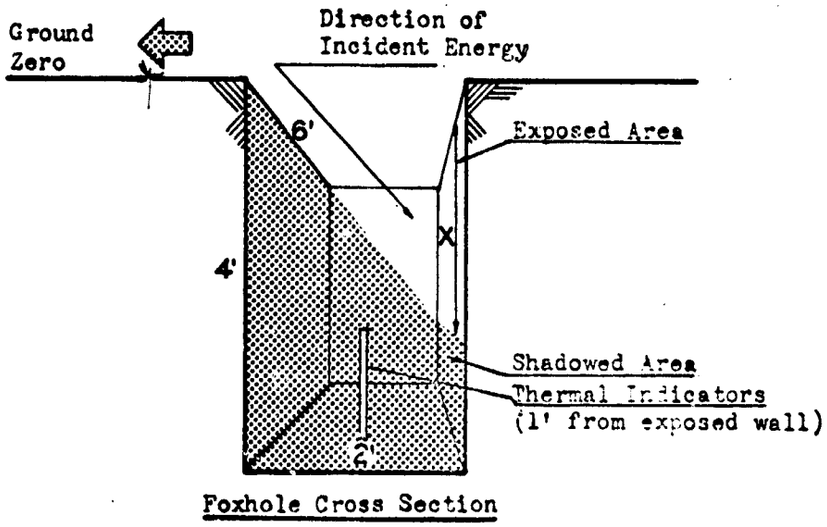

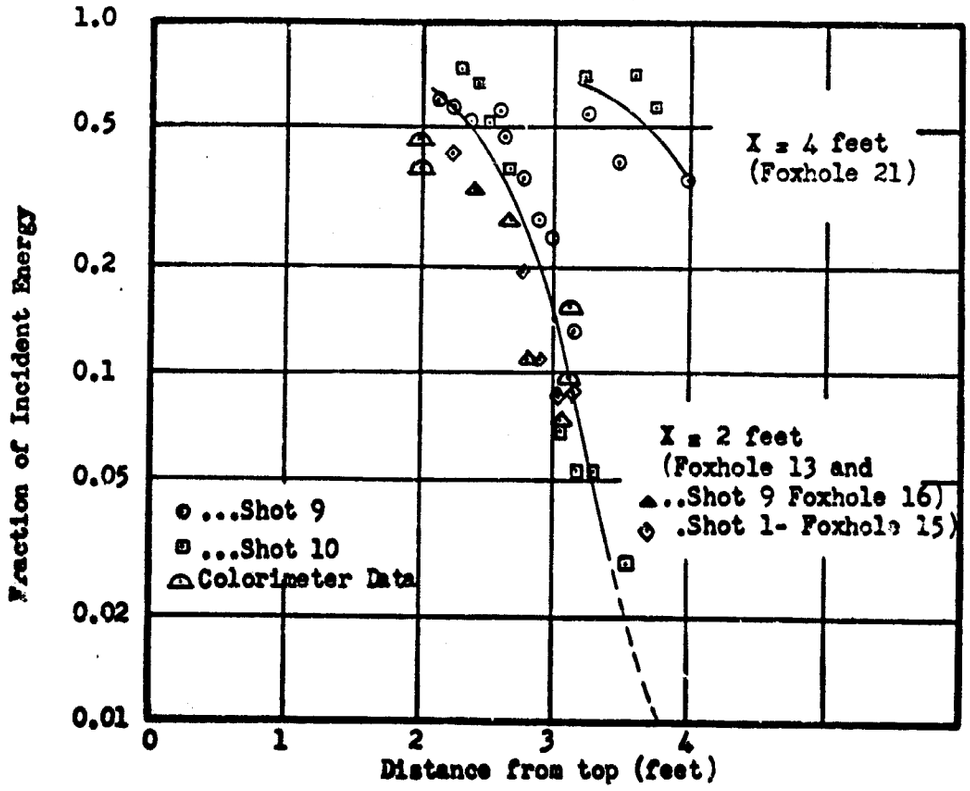

Fig. 13.2 Fraction of Incident Thermal Energy as a Function of Depth in Foxhole

SECRET – RESTRICTED DATA

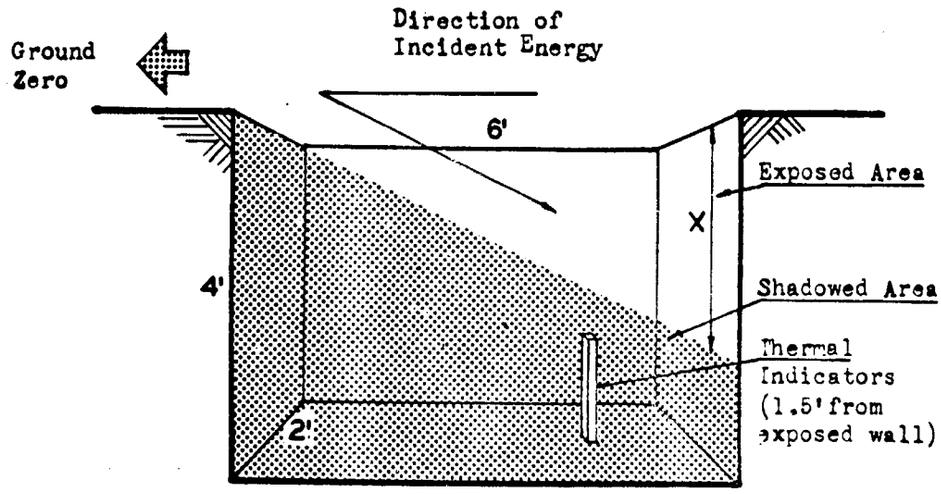

Foxhole Cross Section

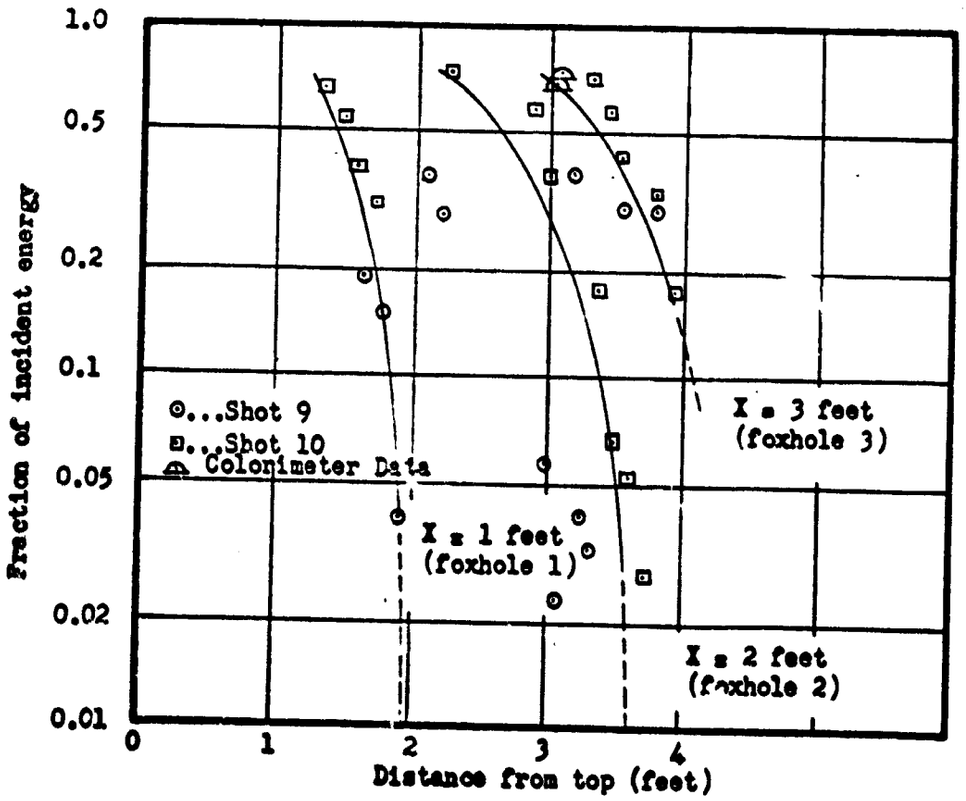

Fig. 13.3 Fraction of Incident Thermal Energy as a Function of Depth in Foxhole

SECRET – RESTRICTED DATA

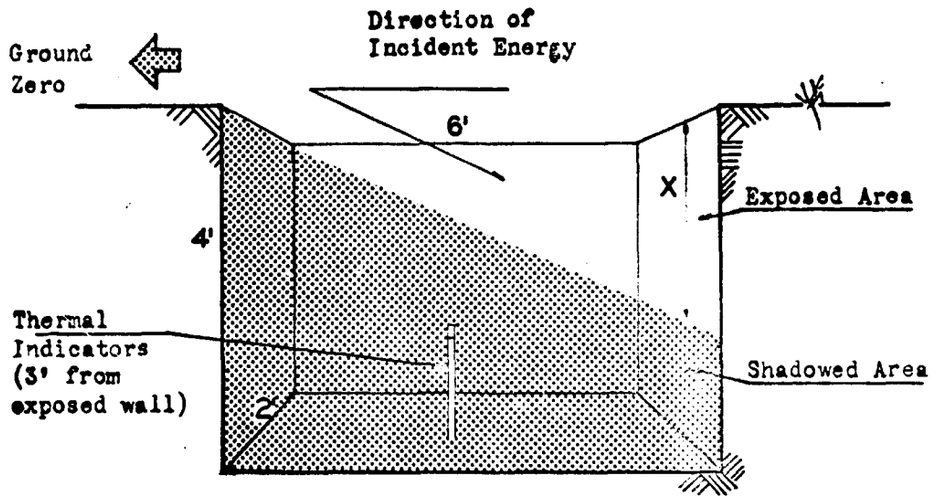

Foxhole Cross Section

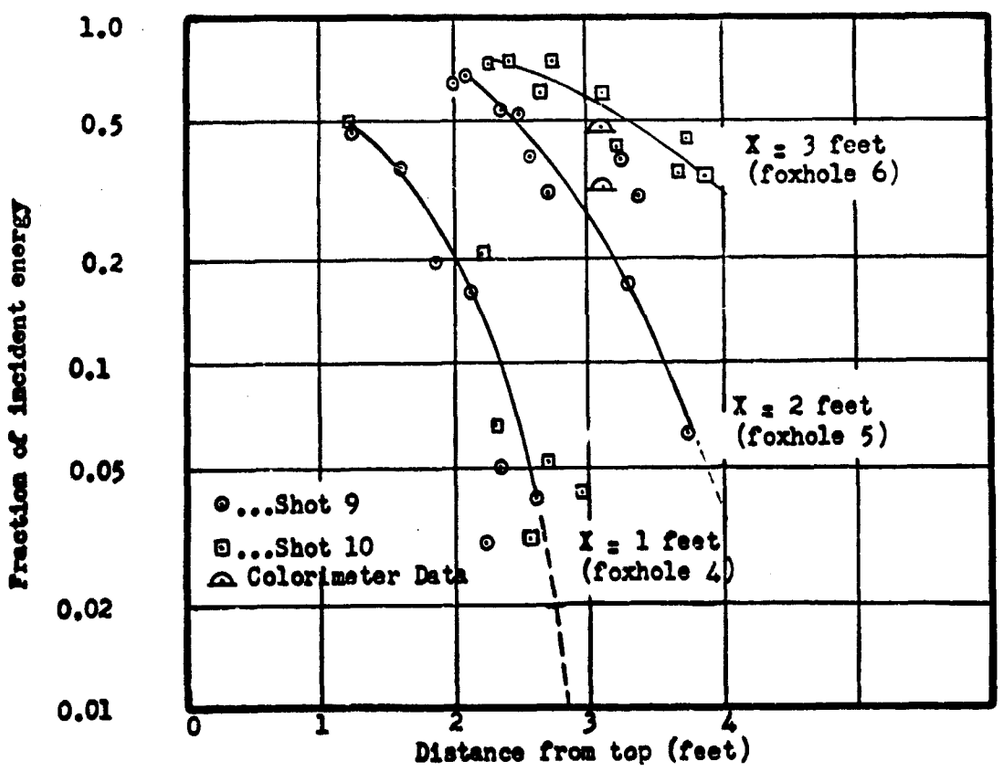

Fig. 13.4 Fraction of Incident Thermal Energy as a Function of Depth in Foxhole

SECRET – RESTRICTED DATA

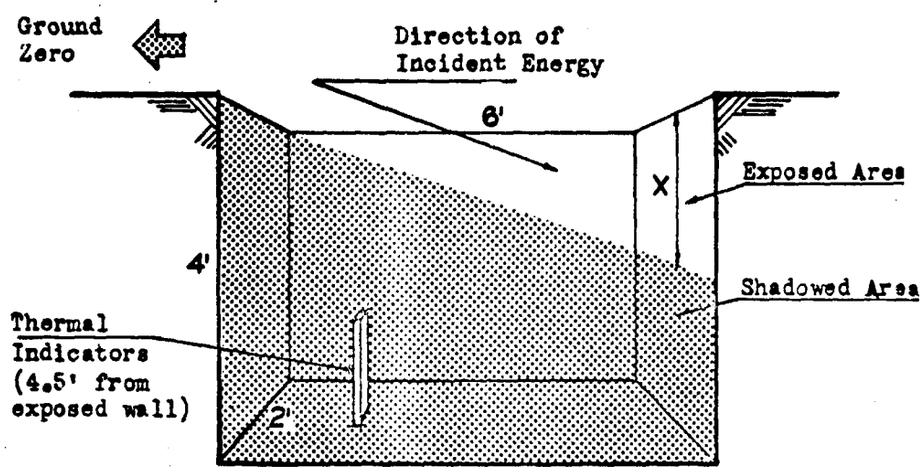

Foxhole Cross Section

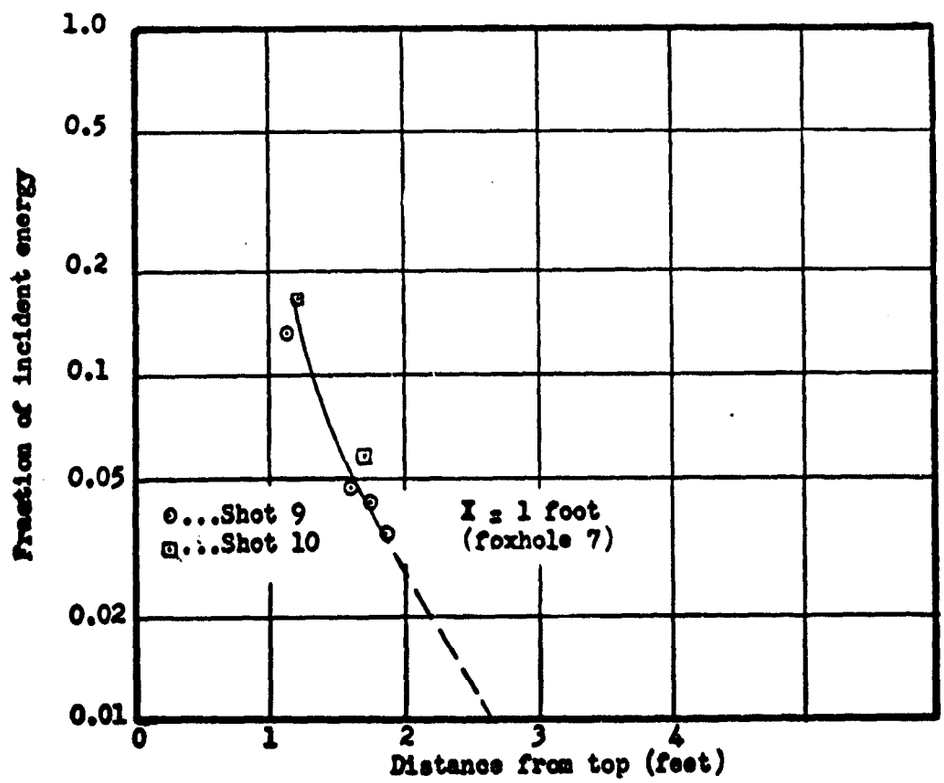

Fig. 13.5 Fraction of Incident Thermal Energy as a Function of Depth in Foxhole

SECRET – RESTRICTED DATA

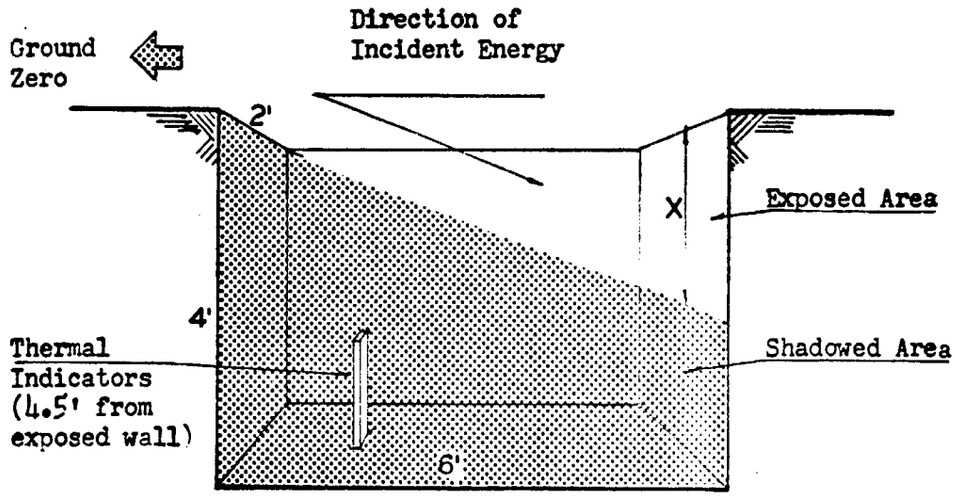

Foxhole Cross Section

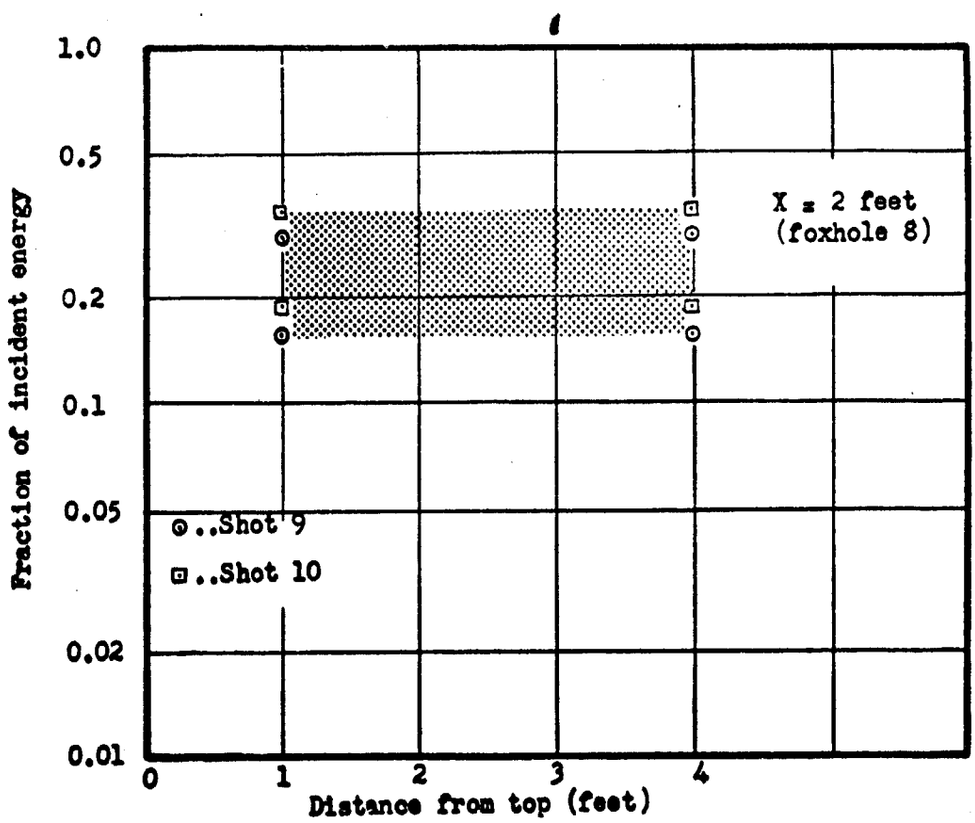

Fig. 13.6 Fraction of Incident Thermal Energy as a Function of Depth in Foxhole

SECRET – RESTRICTED DATA

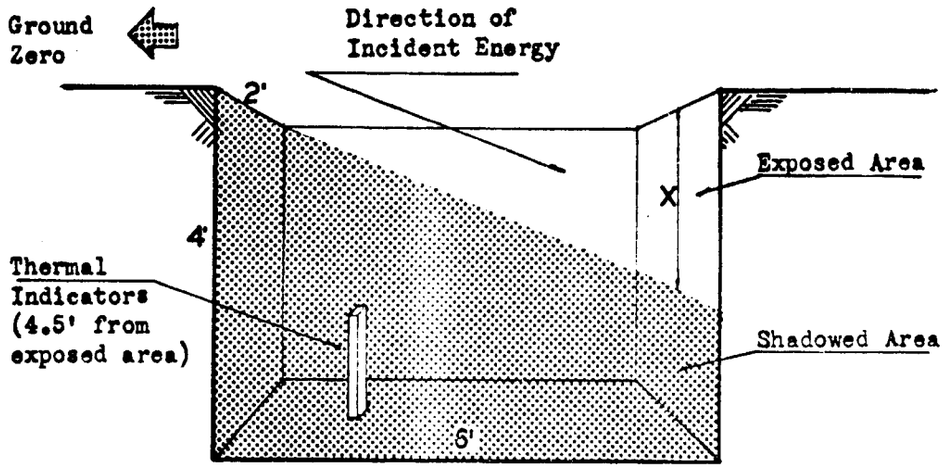

Foxhole Cross Section

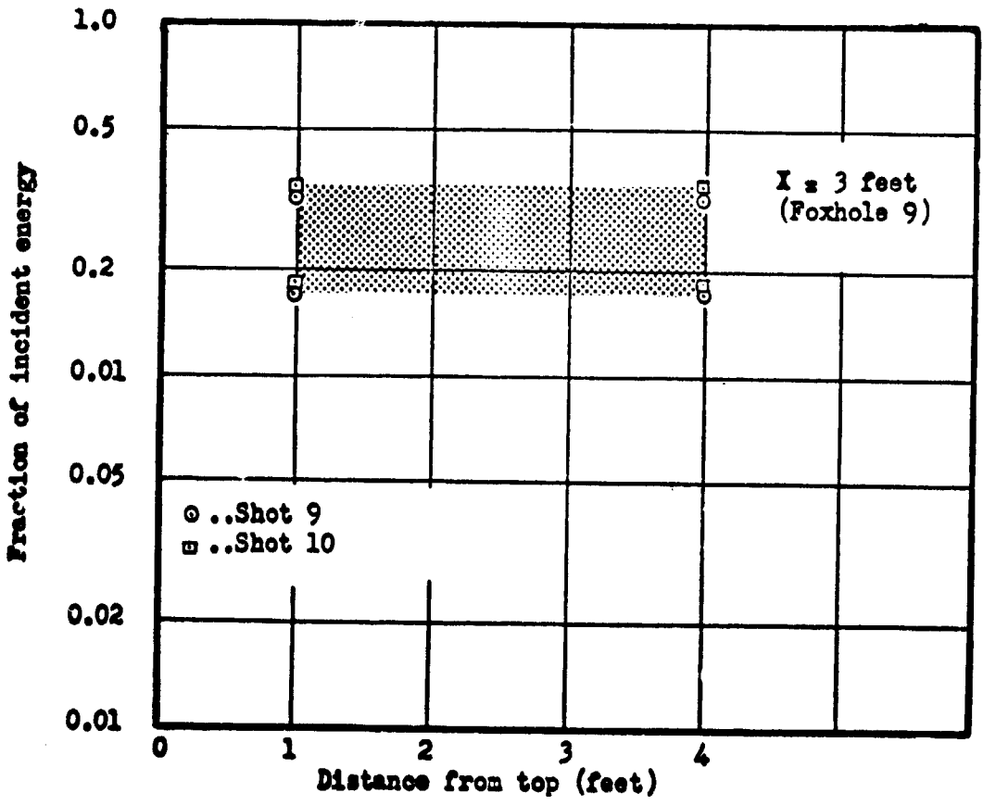

Fig. 13.7 Fraction of Incident Thermal Energy as a Function of Depth in Foxhole

SECRET – RESTRICTED DATA

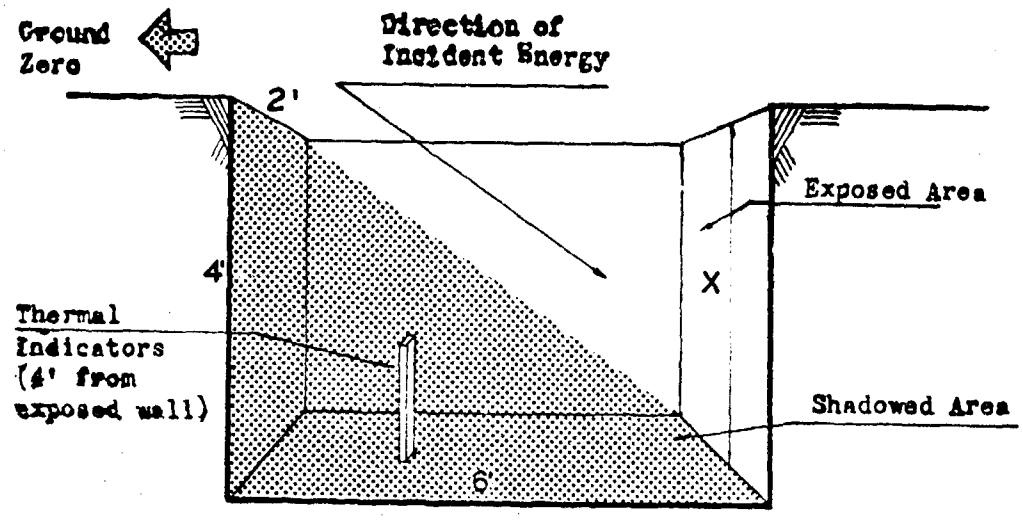

Foxhole Cross Section

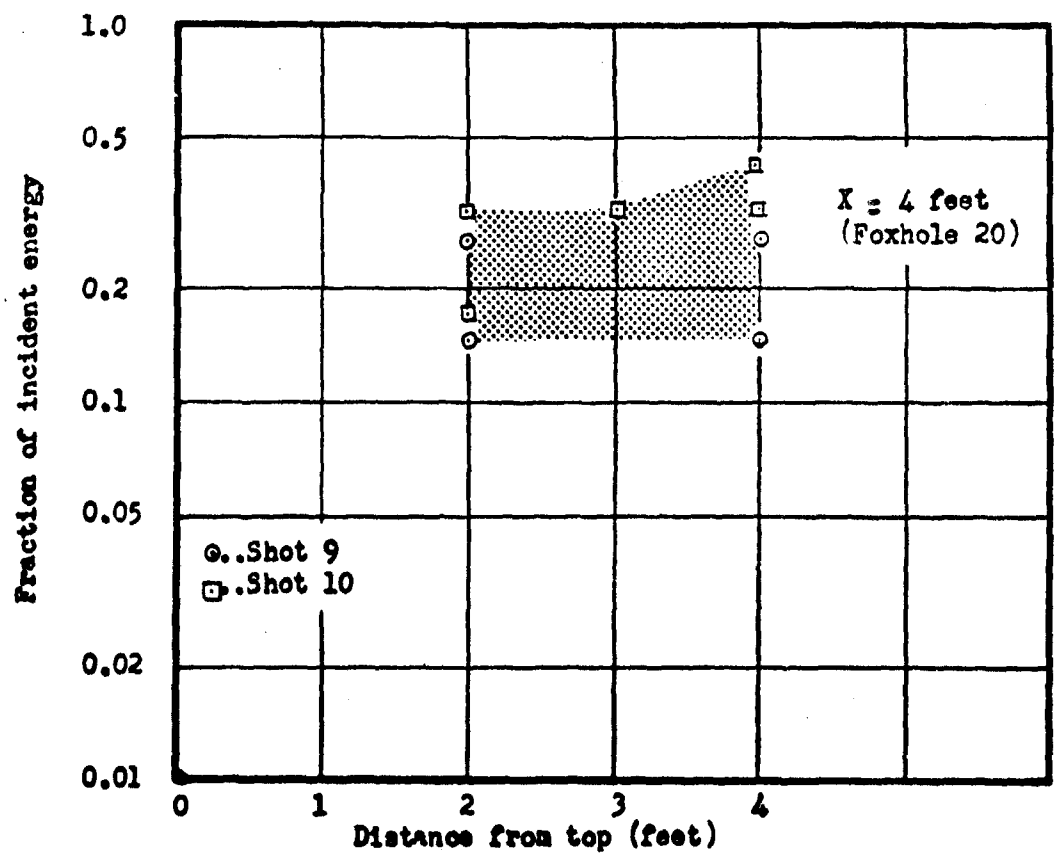

Fig. 13.8 Fraction of Incident Thermal Energy as a Function of Depth in Foxhole

SECRET – RESTRICTED DATA

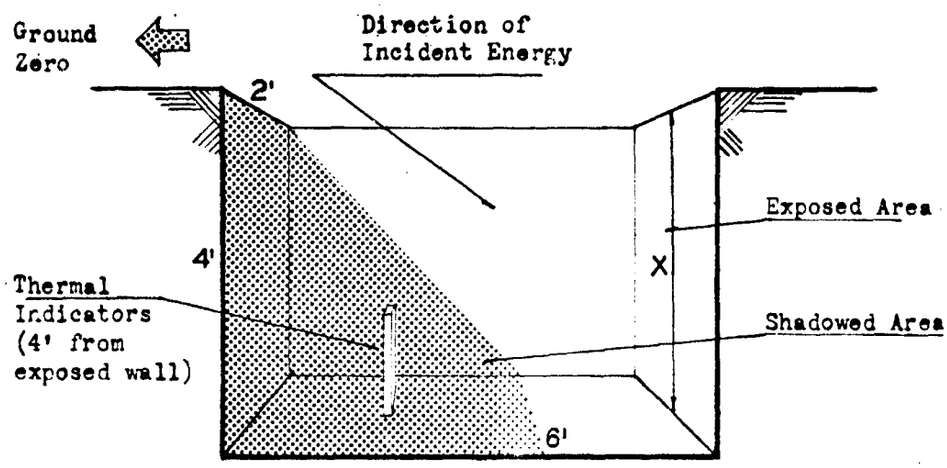

Foxhole Cross Section

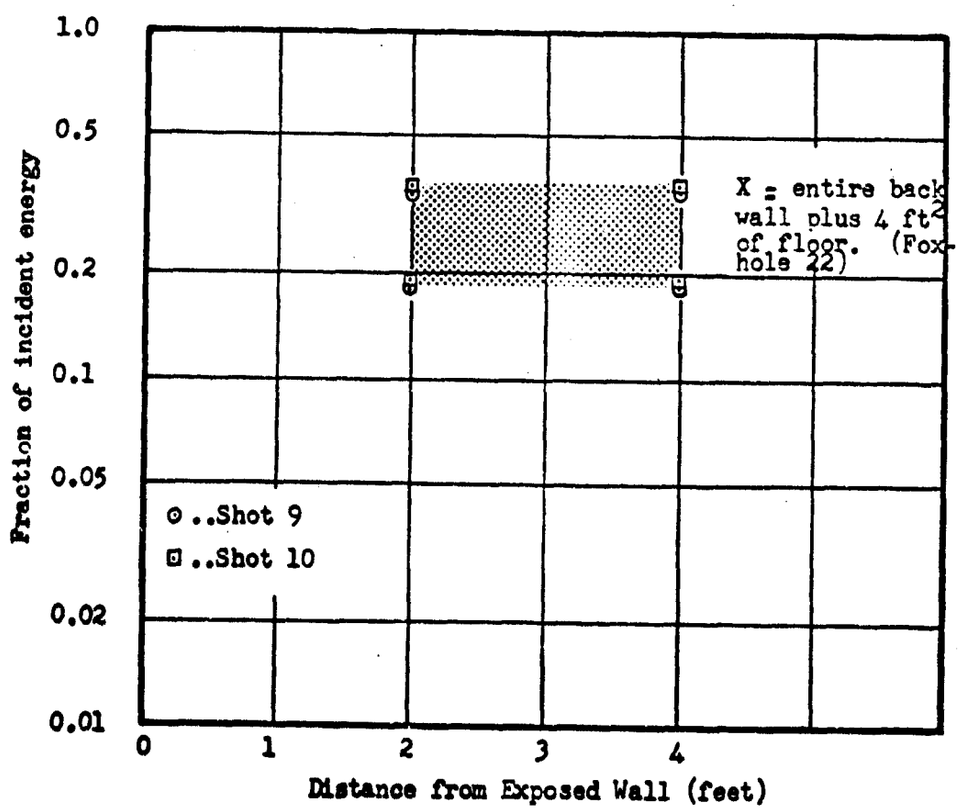

Fig. 13.9 Fraction of Incident Thermal Energy as a Function of Depth in Foxhole

SECRET – RESTRICTED DATA

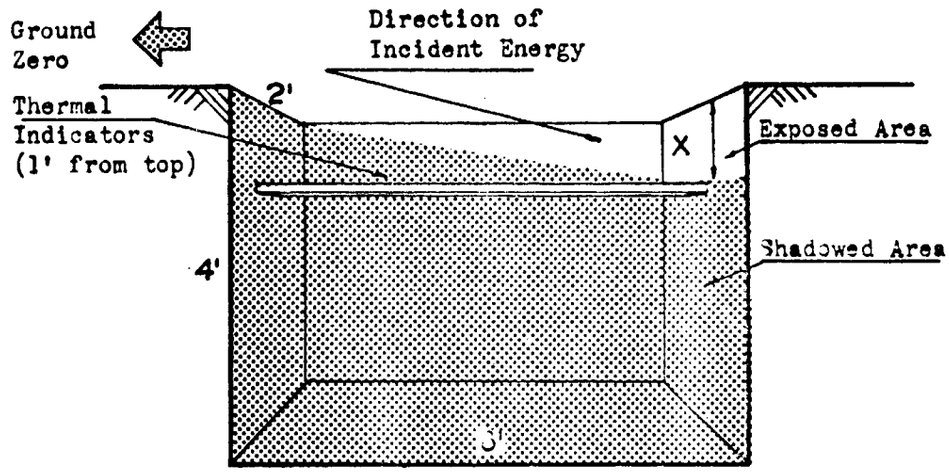

Foxhole Cross Section

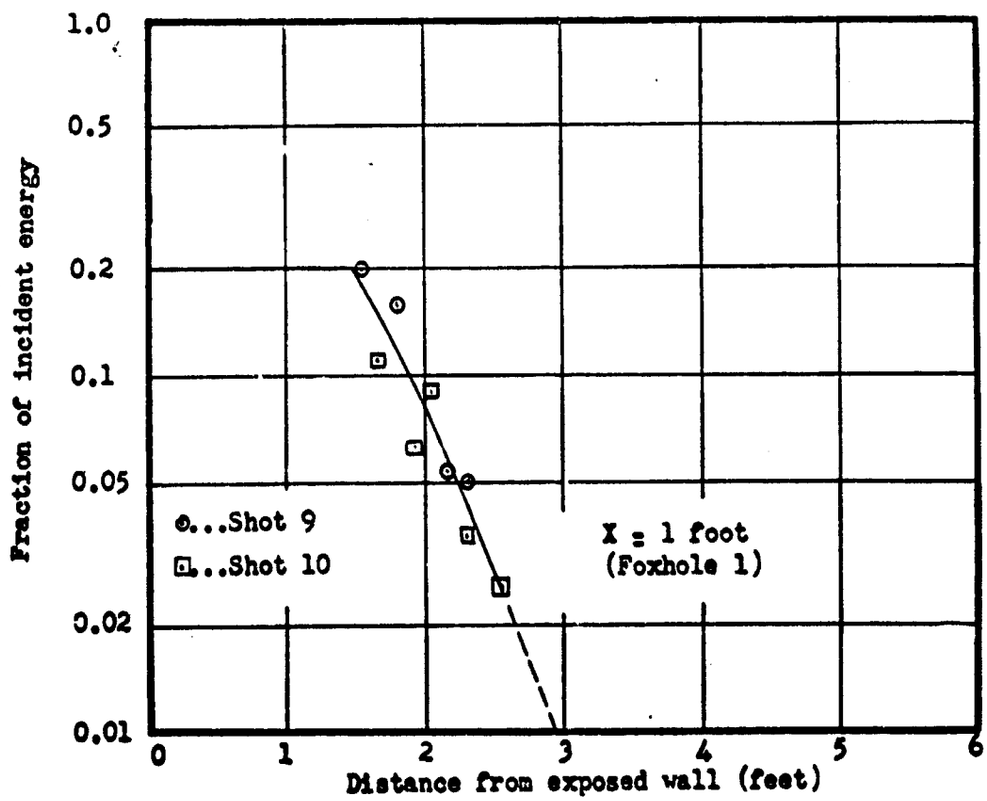

Fig. 13.10 Fraction of Incident Thermal Energy as a Function of Distance from Exposed Wall

SECRET – RESTRICTED DATA

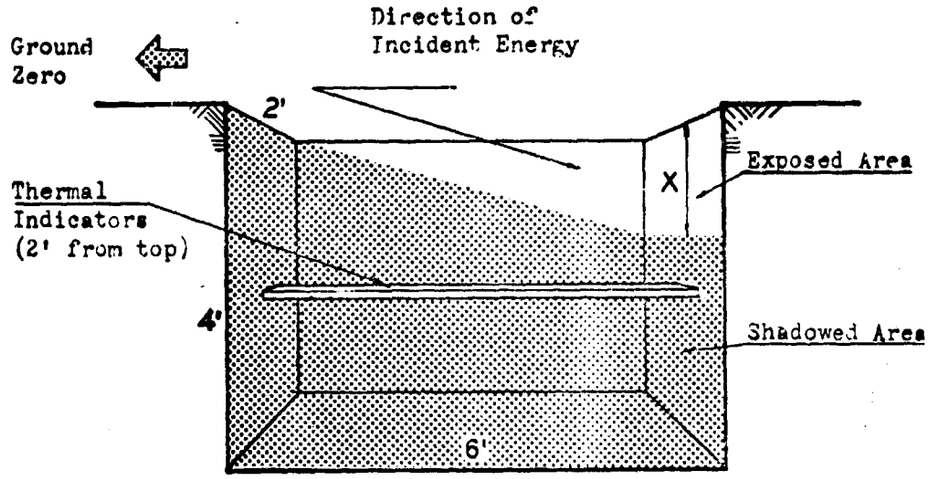

Foxhole Cross Section

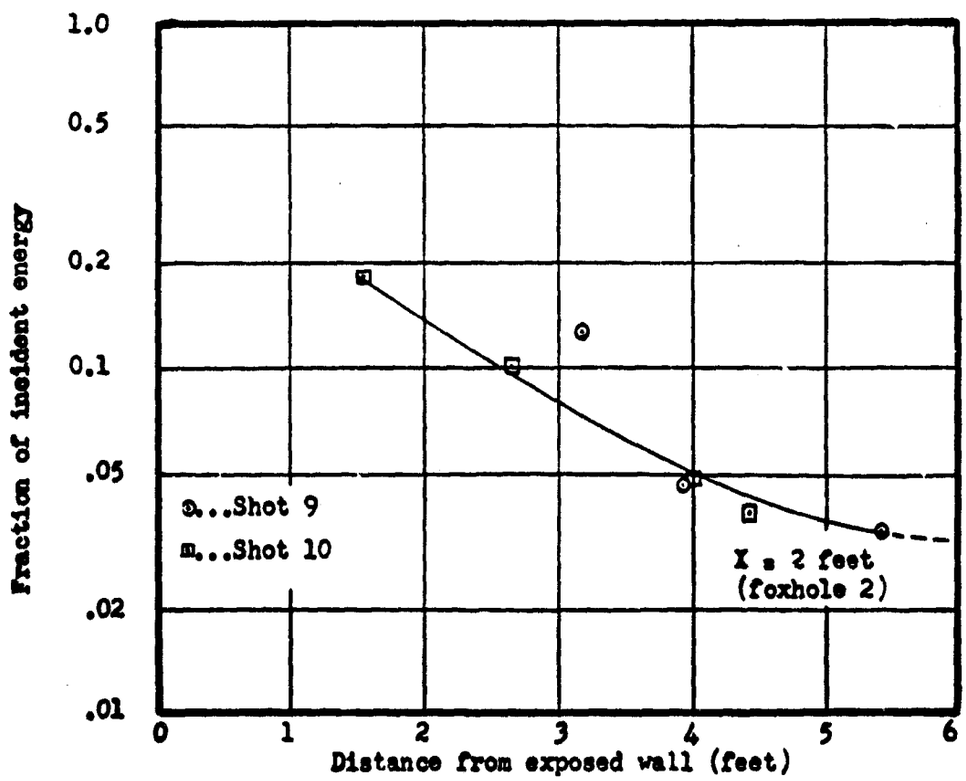

Fig. 13.11 Fraction of Incident Thermal Energy as a Function of Distance from Exposed Wall

SECRET – RESTRICTED DATA

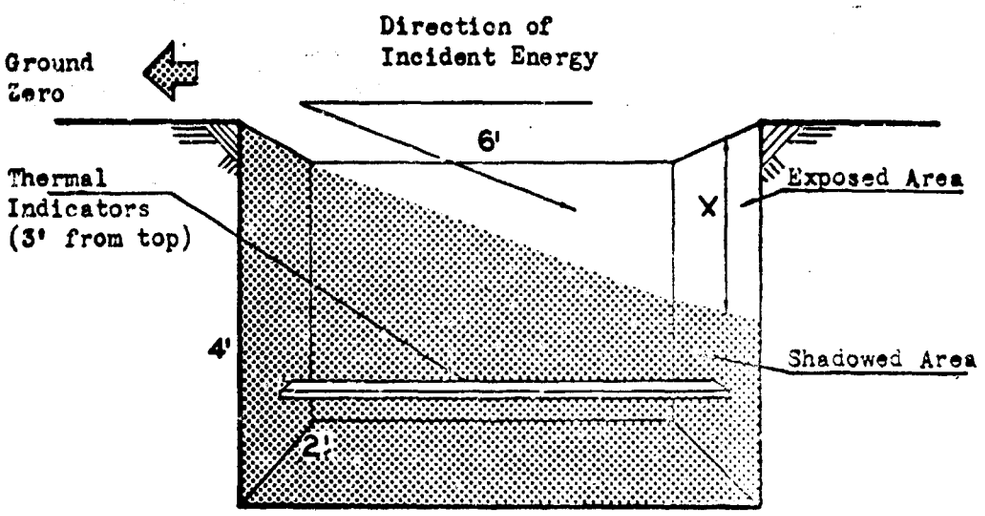

Foxhole Cross Section

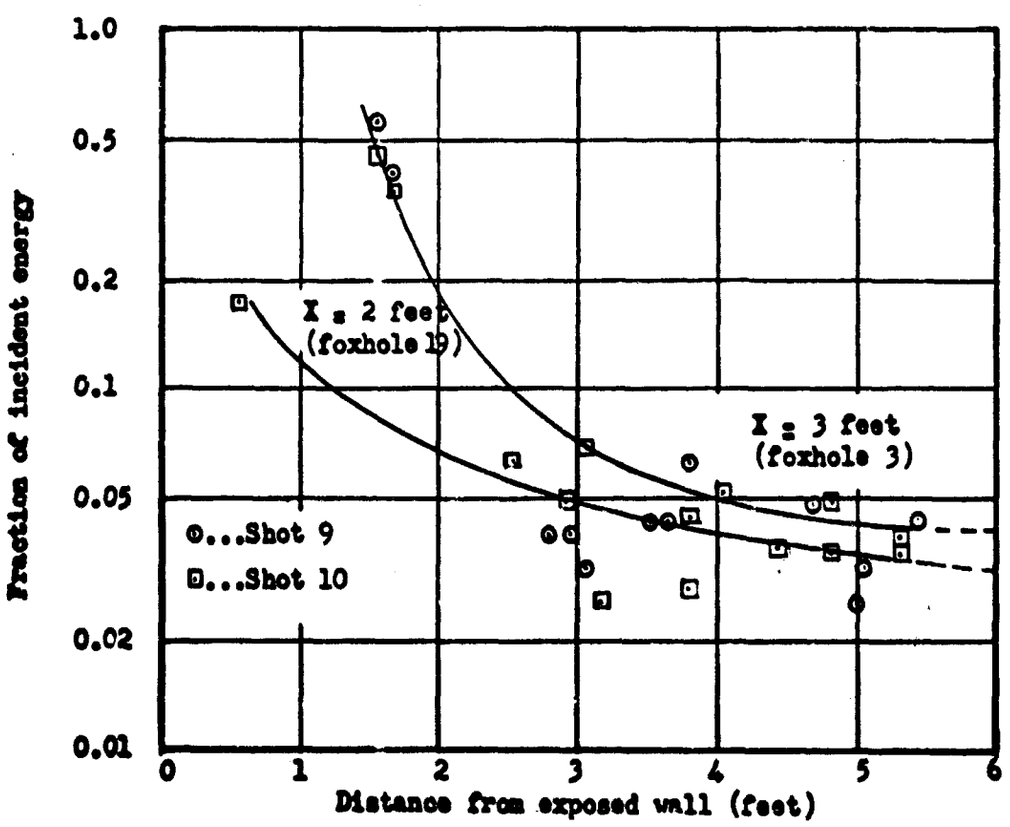

Fig. 13.12 Fraction of Incident Thermal Energy as a Function of Distance from Exposed Wall

SECRET – RESTRICTED DATA

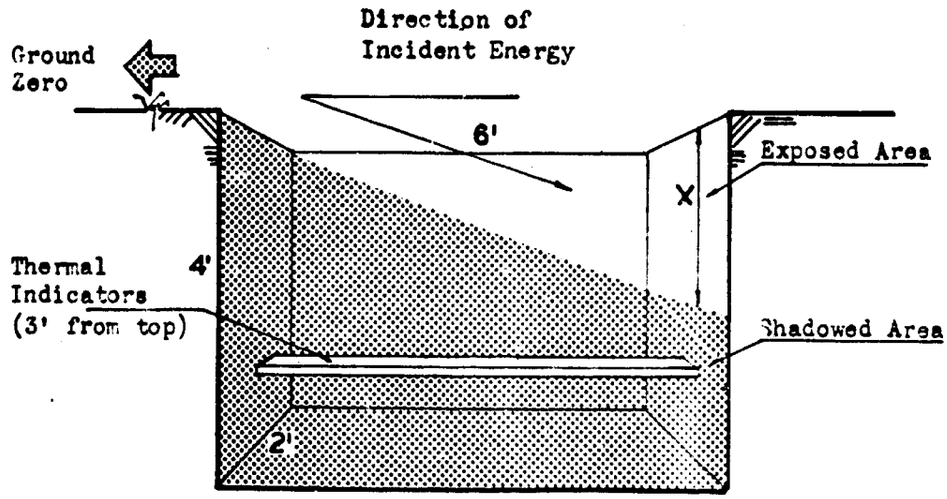

Foxhole Cross Section

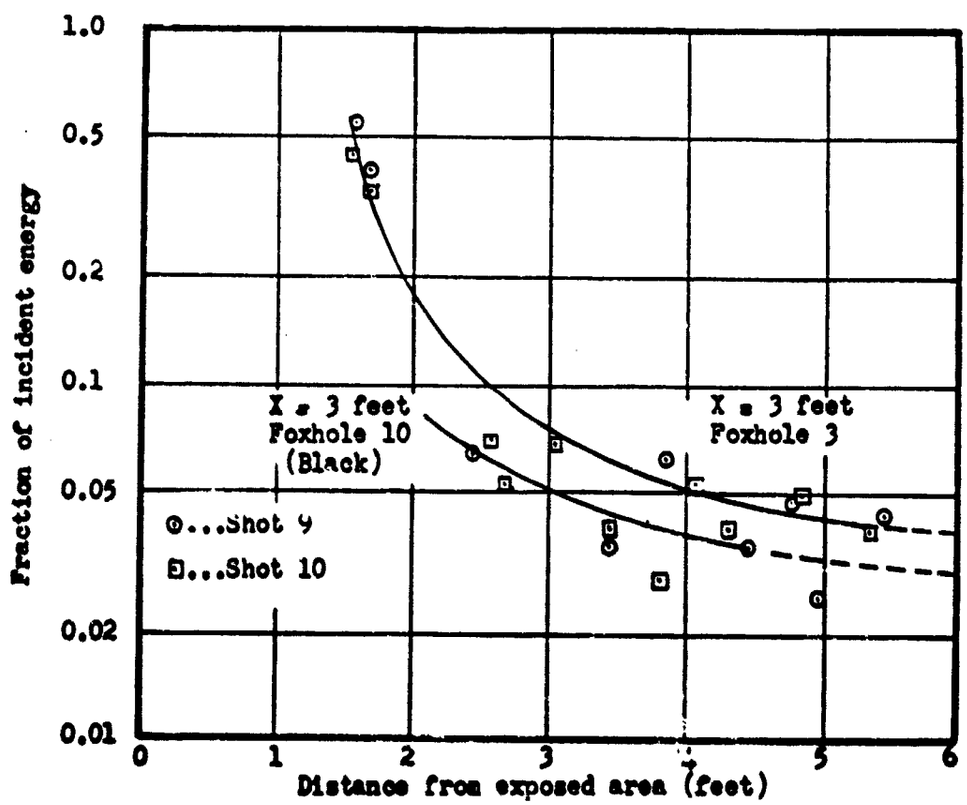

Fig. 13.13 Fraction of Incident Thermal Energy as a Function of Distance from Exposed Wall

SECRET – RESTRICTED DATA

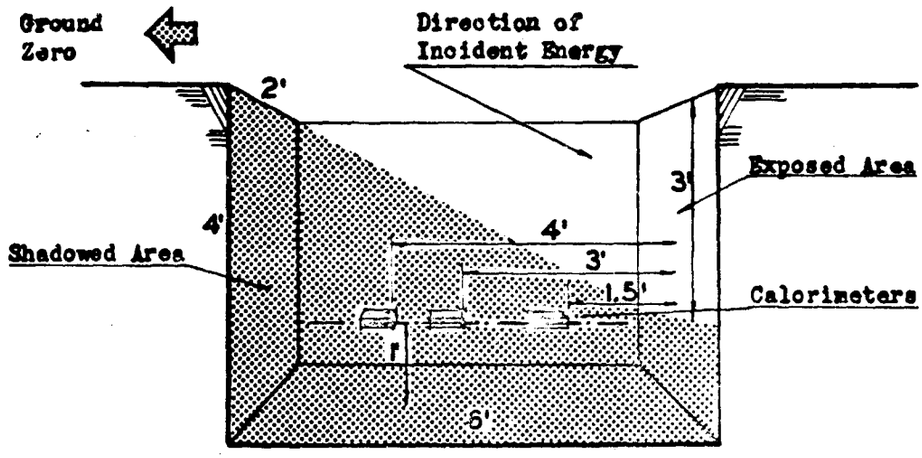

Fig. 13.14 Foxhole Cross Section

TABLE 13.1 - Calorimeter Results

Shot	Distance From Top	Distance From Exposed Wall	Energy	Fraction	Correction Factor	Corrected Fraction
9	3'	1.5'	8.85	.402	1.76	.708
	3'	3.0'	4.04	.183		.322
	3'	4.0'	3.70	.168		.296
	3'	1.5'	5.20	.452	1.64	.741
	3'	3.0'	3.36	.292		.479
	3'	4.0'	2.04	.170		.279

SECRET – RESTRICTED DATA

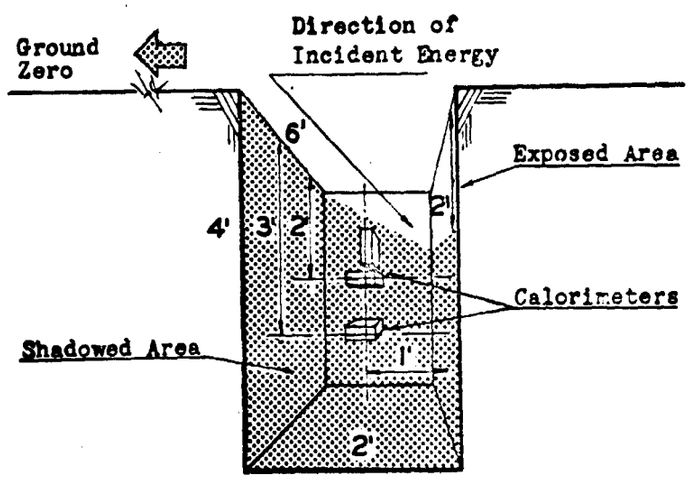

Fig. 13.15 Foxhole Cross Section

TABLE 13.2 - Calorimeter Results

Shot	Distance From		Energy	Fraction	Correction Factor	Corrected Fraction
	Top	Exposed Wall				
9	2	1	3.37	.280	1.46	.409
	3	1	1.35	.112		.164
	*2	1	2.12	.177		.258
10	2	1	1.54	.257	1.74	.447
	3	1	0.32	.053		.092
	*2	1	1.04	.173		.301

* Calorimeters facing directly upward.

SECRET - RESTRICTED DATA

CHAPTER 14

DISCUSSION

14.1 GENERAL

The data as given in Figs. 13.1 to 13.12 enable the prediction of the reflected thermal energy distribution in a foxhole for the following conditions:

1. Long (6 ft) edge parallel to a radial line from the bomb and 2, 4, 6, or 8 ft^2 of the back wall directly exposed which corresponds to the direct energy incident 1, 2, 3, or 4 ft, respectively, down the back wall.
2. Long (6 ft) edge parallel to a radial line from the bomb and 8 ft^2 of the back wall plus 4 ft^2 of the floor directly exposed. This was considered the most extreme exposure conceivable, still permitting a man to crouch in the shadowed portion of the foxhole.
3. Long (6 ft) edge perpendicular to a radial line from the bomb and 6, 12, 18, or 24 ft^2 of the back wall directly exposed which corresponds to the direct energy incident 1, 2, 3, or ft respectively down the back wall.

14.2 ANALYSIS OF RESULTS

14.2.1 Vertical Receivers

In those foxholes in which the receivers were oriented vertically with respect to the foxhole, the data curves for each receiver position are characterized by the same general shape. See Appendix D. This is evident in all but Fig. 13.6 to 13.9, which are the curves for the receiver 4.0 ft or 4.5 ft from the directly exposed wall. For these cases, the apparent discrepancy can be resolved by considering the fact that the indicators when placed along a line at this distance from the directly exposed wall are such that the distance between the directly exposed wall and the receivers is only slightly changed as the receiver depth is increased to 4 ft. As a consequence, the energy at the receivers varied slightly, and the data could only be represented as a band.

For each other receiver location (1 ft, 1.5 ft, or 3 ft from the directly exposed wall), the curves have a similar shape; and the

SECRET - RESTRICTED DATA

author feels that, when any other intermediate area is exposed, the energy distribution may be obtained for these conditions by careful and discreet interpolation.

The location of each individual curve indicates that the position of the receiver relative to the directly exposed source (wall) is the main factor in determining the energy received by the receivers. Of lesser importance, within limits, is the area of source and also the angle of incidence of the direct energy on the source (exposed wall).

14.2.2 Horizontal Receivers

The curves in this case have maximum fractional values near the source which are considerably lower than the case for vertical receivers. They all tend to decrease as distance from the source increases.

When 2 ft^2 of the wall were directly exposed and the receivers were placed along a line 2 ft and 3 ft from the top of the foxhole, there were no indicator reactions capable of being interpreted, which indicates that the energy received in this area was too low to be measured reliably by the passive indicators. However, it may be concluded that the fraction is at least less than 0.0510 when the receivers are 2 ft from the foxhole top, and less than 0.0300 when the receivers are 3 ft from the top.

14.2.3 Calorimeters

It was anticipated that a direct comparison of the calorimetric and passive indicator data could be made. However, since the aperture of the calorimeters used was 90°, and the aperture of the passive indicators was essentially 180°, a direct comparison is not meaningful. The calorimetric results in Table 13.2 are plotted with the passive indicator data in Fig. 13.2. Here, the calorimeter "saw" essentially only 3.14 ft^2 of the exposed wall; while, actually, 12 ft^2 of the wall was exposed. The decrease of measured energy is not directly proportional to these areas, because the source (exposed wall) immediately in front of the receiver contributes a proportionally greater amount of the total received energy.

When the long (6 ft) side is parallel to a radial line from ground zero, there is better correlation. Here, the calorimeters were further from the exposed wall, and they could "see" almost all of the exposed area. The data from these calorimeters are plotted for comparison with the passive indicator results on Figs. 13.3 and 13.4.

Comparison of the calorimeter results as measured in the foxholes with similar calorimeter measurements taken of the direct thermal energy indicates essentially no change in the shape of the thermal pulse. This eliminates the possibility of an excessive amount of dust obscuration or reflection of thermal energy from dust above the emplacement which would negate the passive indicator results.

14.3 MAGNITUDE OF INTERREFLECTION

It was felt that the high reflectance of the foxhole walls would cause some increase in the received energy because of interreflection from one wall to another. In an attempt to measure the magnitude of

SECRET – RESTRICTED DATA

this effect, a foxhole was constructed in which the walls (except the one which was directly exposed to the incident radiation) were coated with a low reflectance, flat black paint. Fig. 13.13 gives the data from this foxhole and for a corresponding aluminum lined foxhole, and shows that the energy received by the black foxhole is lower by a factor of approximately 30 per cent when the receivers are relatively far from the source and is lower by a factor of approximately 40 per cent when the receivers are closer to the directly exposed wall. It must be noted that the data are of limited extent and may not be conclusive for other receiver positions.

The actual magnitude of interreflection will depend upon the reflectance of the emplacement walls, increasing as the reflectance increases.

14.4 SCALING

Part of the objective of this test was to provide scaling laws such that the information presented herein would be applicable to all field conditions. Using data from foxholes 11, 15, and 16, and the data from both shots for corresponding foxholes, the average deviation when calculated with respect to the fraction of incident energy is 0.054, and is 0.190 ft when calculated relative to the distance from the top or exposed wall. This indicates that the results, when obtained under different conditions, are reproducible.

14.5 APPLICATION

The reflected thermal energy distribution in a foxhole may be determined for the conditions within the limit of the experiment by using the following formula:

$E = PFI$

E = the desired energy in the foxhole

P = the reflectance of the walls of the foxholes

F = the fraction of incident energy as determined from Figs. 13.1 to 13.12

I = the direct incident energy

The reflectances of some typical soils and materials is given in Table 14.1.

TABLE 14.1 - Reflectances of Typical Materials

Material	Reflectance	Source
Loam, sandy	0.24	1
Earth, moist	0.08	1
Marl, argillaceous	0.16	1
Snow	0.93	1
Yucca Flat sand	approx 0.30	2
Frenchman Flat sand	approx 0.25	2
Pine	0.53	3
Oak	0.35	3
Birch	0.35	3
Walnut	0.23	3

1. Handbook of Chemistry and Physics, Chem. Rubber Pub. Co., 32 ed., pages 2444, 2445.
2. The Thermal and Optical Properties of Nevada Sand, Naval Material Laboratory, May 1952, CONFIDENTIAL.
3. Journal of the Optical Society of America, April 1948.

SECRET – RESTRICTED DATA

CHAPTER 15

CONCLUSIONS AND RECOMMENDATIONS

15.1 CONCLUSIONS

The thermal energy distribution in a two-man foxhole can be predicted using the data given in Figs. 13.1 to 13.12 and the methods of scaling shown in Chapter 14.

The data from foxholes 11, 15, and 16 and the data from both shots for corresponding foxholes indicate that scaling to reasonable operational conditions of height of burst, distance from ground zero, and yield is valid.

The thermal energy distribution in foxholes, as well as in other types of emplacements, can be predicted by using the methods, and within the limitations, of Appendix D.

If the reflectance is one third or less, a man will receive less than 10 per cent of the direct thermal radiation if he is in the shadowed portion of his foxhole at least 1 ft below the limit of the direct thermal radiation on the exposed wall.

15.2 RECOMMENDATIONS

It is recommended that this experiment be considered conclusive unless a requirement is shown for the thermal energy distribution in an emplacement of markedly different geometry, such as a case where the directly exposed wall is not perpendicular to a radial line from ground zero, or unless a requirement is shown for data of greater detail or extent.

With its limitations in mind, it is recommended that the method described in Appendix D for determining the energy received in an emplacement be considered for general use.

SECRET - RESTRICTED DATA

PART IV

GAMMA RADIATION IN FOXHOLES

CHAPTER 16

INTRODUCTION

16.1 OBJECTIVE

The objective of Part IV of Project 3.9 was to instrument a 2' x 4' x 6' two-man foxhole for prompt gamma radiation such that the angular dependence of the instrumentation is determined.

16.2 BACKGROUND

Under Project 2.6, BUSTER, a series of two-man foxholes were instrumented to measure prompt gamma radiation; and the results were subsequently published in the final report(6). Among the conclusions were: the exposure for troops at the bottom of foxholes would be about 12 per cent of that received by unprotected troops in the same location; air-scattered gamma radiation contributed from 80 to 90 per cent of the total intensity at the bottom of the foxhole. This information was based on film badges (the prompt gamma radiation instrumentation) which were placed vertically with respect to the foxhole.

Shortly prior to UPSHOT-KNOTHOLE, the question was posed as to whether the orientation of the film badges in the foxholes would markedly change the concepts of fortification protection described in the Project 2.6, BUSTER report. To answer this question, one two-man foxhole was instrumented with film badges which were placed vertically, horizontally, and at a 45° angle with respect to the foxhole.

16.3 DISCUSSION

The basis of this experiment was to justify the method of instrumentation and the assumptions used in Project 2.6, BUSTER. Therefore, this experiment is primarily concerned with the angular dependence of film badges, rather than the protection afforded by field fortifications.

Theoretically, the response of a film badge which is placed at various angles to parallel gamma radiation will depend upon the angle of incidence of the radiation and should follow the familiar cosine relation

$$I_\theta = I_n \cos \theta$$

SECRET – RESTRICTED DATA

where I_n is the amount of incident radiation measured normal to the direction of incident radiation, the θ (called the angle of incidence) is the angle between the direction of the incident radiation and the normal to the badge; and I_θ is the amount of incident radiation measured at the angle θ. Thus, as θ increases from 0° to 90°, the value of I_θ will decrease from a maximum equal to I_n to zero.

It was discovered in BUSTER that the majority (80-90 per cent) of the radiation received at the bottom of a foxhole could be attributed to that which is scattered, and that this radiation comes essentially from the top of the foxhole. Accordingly, most of the radiation received by the films near the bottom of the foxhole was at a high angle of incidence. This, it was felt, would cause the films to read too low. Ellery Storm of Los Alamos Scientific Laboratory made an investigation and concluded that an average correction factor of 1.5 would compensate for a high angle of incidence(24). Further speculation about this effect was made; and it was postulated that the radiation values obtained in BUSTER may be too low, even though the 1.5 correction factor is applied. The objective of this experiment was to investigate this assumption.

SECRET - RESTRICTED DATA

CHAPTER 17

INSTRUMENTATION

17.1 FILM BADGES

Standard dosimeter film packets using DuPont types 554 insensitive and 558 insensitive films were used as the gamma radiation detectors. The type 554 insensitive film was used to detect gamma radiation intensities to about 200 roentgens, while the type 558 insensitive was utilized to detect gamma radiation intensities to about 1000 roentgens.

For field exposure, the badges were mounted in National Bureau of Standards film holders.

17.2 CALIBRATION

Since the film badges were placed horizontally, vertically, and at a 45° angle with respect to the foxhole, it was necessary to calibrate the films at a series of angles of incidence. This was accomplished by using a Co_{60} source and rotating the films to the desired angle. It was determined that the calibration curves as obtained from the Co_{60} source were sufficiently accurate to be used with no further modification for the radiation range of interest in this test.

Comparison of the calibration curves indicated that the angular dependence of the exposure of the badge was not as critical as would be postulated on the basis of the cosine law. The calibration data were not of sufficient detail to verify any relationship between the exposure of the film and the angle of incidence of the radiation.

It was felt that the materials of the NBS holder tend to scatter and, to some extent, attenuate the incident radiation.

17.3 TEST SITE

One foxhole, 4000 ft from expected ground zero, along the East-West blast line was utilized for this experiment. The film badges were placed, numbered, and oriented as shown in Figs. 17.1 and 17.2.

Shot 9 was used for the exposure.

SECRET - RESTRICTED DATA

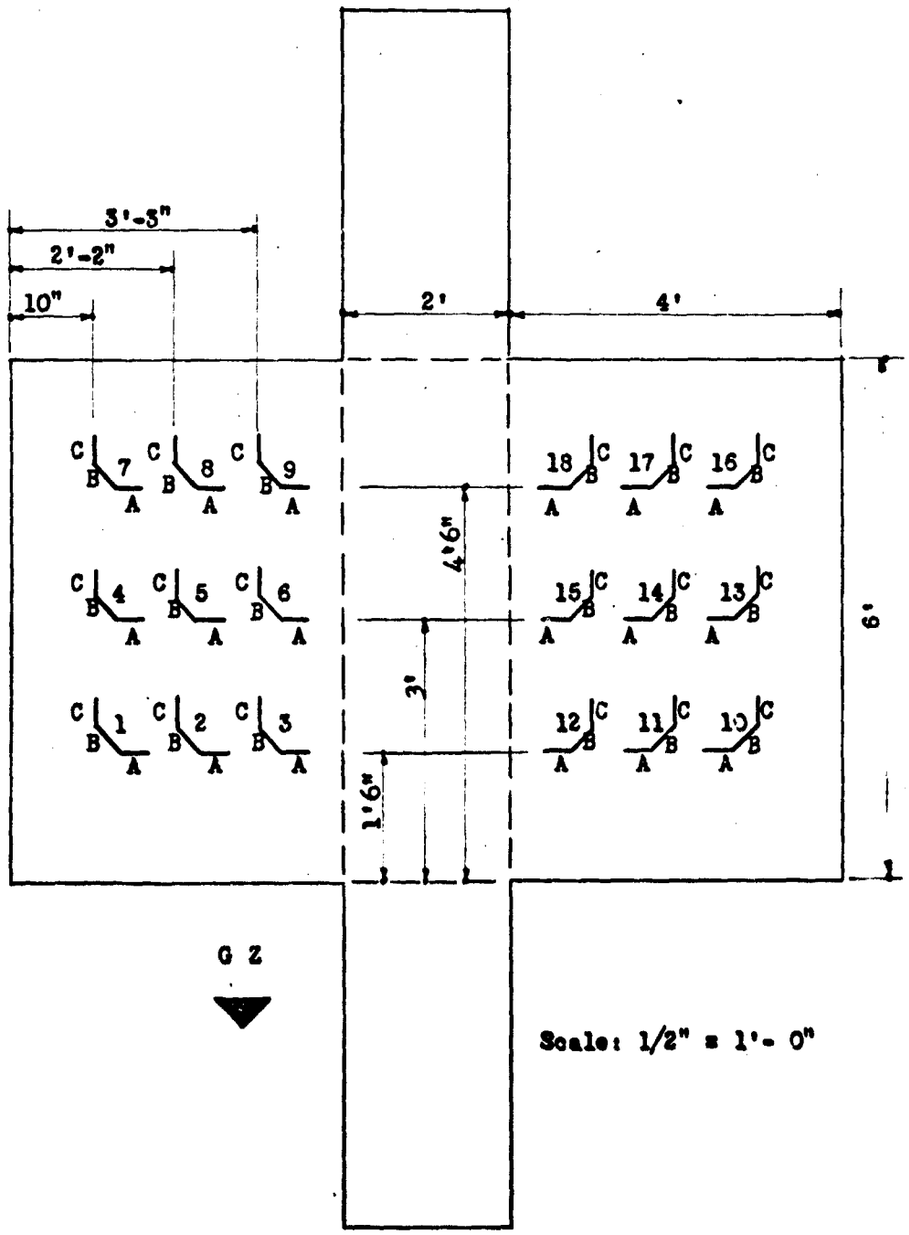

Fig. 17.1 Numbering of Film Badge Locations

SECRET - RESTRICTED DATA

Fig. 17.2 Photograph of Foxhole

SECRET – RESTRICTED DATA

CHAPTER 18

RESULTS

18.1 METHODS OF ANALYSIS

The film badges used during BUSTER were placed vertically with respect to the foxhole and calibrations were made with the film placed at a zero degree angle of incidence (the film was perpendicular to the incident energy). In order to obtain a direct comparison, all of the films used in this test which were placed in position A (vertical with respect to the foxhole) were read from calibration curves made at a zero degree angle of incidence.

It was determined during BUSTER that 80-90 per cent of the radiation received near the foxhole bottom was scattered in from the top. Therefore, the films placed in positions B (45° angle) and C (horizontal) in groups 2, 3, 6, 9, 11, 12, 15, and 18 effectively received most of the incident radiation at an angle that is formed approximately by a line drawn from the upper front edge of the foxhole to the film and the normal to the film. Thus, each of these films was characterized by an angle of incidence. Calibration curves for these angles were drawn and the amount of radiation was obtained. These data, and the per cent difference between positions A and B and A and C, are given in Tables 18.1 and 18.2.

It was felt that the remaining groups received essentially all of their radiation directly, i.e., unscattered. Calibration curves obtained at the angles of incidence on the film of the direct radiation from the bomb were used to obtain the radiation values for positions B and C. Position A was evaluated as discussed earlier in this chapter. These data, and the per cent difference between positions A and B and positions A and C are given in Tables 18.3 and 18.4. The overall average per cent difference between positions A and B and positions A and C is given in Table 18.5.

All of the above data have been corrected to give the radiation value had each film of a group (horizontal, vertical, and at a 45° angle) been at exactly the same point.

SECRET - RESTRICTED DATA

18.2 DISCUSSION OF RESULTS

Position A was chosen as the basis for comparison in Tables 18.1 to 18.5, because this orientation was used during BUSTER. It was necessary to obtain a direct comparison between film badge readings obtained as they were during BUSTER and film badge readings taken at other orientations during this test.

Calibration of the film badges at the angles and by the methods described above provides a direct comparison between data which have been obtained in the most accurate manner available and the data which are in question.

It can be noted by an investigation of Tables 18.1 to 18.4 that there is little significant difference between the radiation values of a group whether obtained horizontally, vertically, or at a 45° angle. This difference becomes even less significant when the 20 per cent error of the film is considered. There is a tendency, however, for the radiation values obtained from the horizontal and 45° angle film badges to be slightly higher than those obtained from the vertical film badge.

TABLE 18.1 - Data from Film Badges Receiving Scattered Radiation

Film Type - 554 Insensitive

Position	Exposure (Roentgens)			Difference Between A and B(%)	Difference Between A and C(%)
	A	B	C		
2	26	16	23	38	12
3	15	16	17	7	13
6	19	23	19	21	0
9	23	22	33	4	43
11	33	38	40	15	21
12	15	18	16	20	7
15	28	32	28	12	0
18	80	67	65	16	19

TABLE 18.2 - Data from Film Badges Receiving Scattered Radiation

Film Type - 558 Insensitive

Position	Exposure (Roentgens)			Difference Between A and B(%)	Difference Between A and C(%)
	A	B	C		
2	29	25	42	14	45
3	12	15	15	25	25
6	17	23	24	35	41
9	22	28	33	27	50
11	34	47	48	38	41
12	15	19	17	27	13
15	35	33	47	6	34
18	67	68	84	1	25

SECRET - RESTRICTED DATA

TABLE 18.3 - Data from Film Badges Receiving Direct Radiation

Film Type - 554 Insensitive

Position	Exposure (Roentgens)			Difference Between A and B(%)	Difference Between A and C(%)
	A	B	C		
1	143	239	90	67	37
4	175	169	173	3	1
5	36	40	46	11	28
7	195	201	194	3	1
8	55	56	58	2	5
10	190	186	199	2	5
13	225	220	240	2	7
14	81	94	90	16	11
16	225	250	260	11	16
17	168	161	181	4	8

TABLE 18.4 - Data from Film Badges Receiving Direct Radiation

Film Type - 558 Insensitive

Position	Exposure (Roentgens)			Difference Between A and B(%)	Difference Between A and C(%)
	A	B	C		
1	126	166	175	32	39
4	153	-	199	0	30
5	40	62	54	55	35
7	161	185	220	15	37
8	52	66	68	27	31
10	182	225	225	24	24
13	300	245	260	18	13
14	82	93	100	13	22
16	270	250	310	7	15
17	152	230	172	51	13

TABLE 18.5 - Overall Average Per Cent Difference

Film	Average Percent Difference Between A and B	Average Percent Difference Between A and C
554 Insensitive	14	13
558 Insensitive	24	30

SECRET - RESTRICTED DATA

CHAPTER 19

CONCLUSIONS AND RECOMMENDATIONS

19.1 CONCLUSIONS

The angular orientation of film badges used to measure the gamma radiation in a foxhole is not a critical factor in determination of the total dose.

19.2 RECOMMENDATIONS

It is recommended that the angular orientation of film badges be considered not to affect the conclusions of Project 2.6, BUSTER.

SECRET - RESTRICTED DATA

BIBLIOGRAPHY

1. Exercise DESERT ROCK I, October 1951 (SECRET)
2. Exercise DESERT ROCK II AND III, November 1951 (SECRET)
3. Exercise DESERT ROCK IV, April-June 1952 (SECRET)
4. Exercise DESERT ROCK V, January-June 1953 (SECRET)
5. Blast Injuries in Foxholes, GREENHOUSE, WT-8, (SECRET-RD)
6. The Protective Effects of Field Fortifications Against Neutron and Gamma Ray Flux, BUSTER Project 2.6, WT-383 (SECRET-RD)
7. F.C.D.A. Family Shelter Evaluation, BUSTER Project 9.1a, WT-359 (SECRET-RD)
8. A.E.C. Communal Shelter Evaluation, BUSTER Project 9.1b, WT-360 (SECRET-RD)
9. Hasty Type Air Raid Shelters, TUMBLER, WT-560, (SECRET-RD)
10. A Copper Indenter Gage for the Measurement of Air Blast Peak Pressure, Naval Ordnance Laboratory, NAVORD 2192, 10 July 1951 (UNCLASSIFIED)
11. Final Report of Project 3.8, UPSHOT-KNOTHOLE WT-727 (SECRET-RD)
12. Height of Burst For Atomic Bombs, Los Alamos Scientific Laboratory, 3 August 1949 (SECRET)
13. Effects of Atomic Weapons, Los Alamos Scientific Laboratory, September 1950 (UNCLASSIFIED)
14. Two - Dimensional Diffraction of Plane Shock Waves Over a Rectangular Opening, Ballistic Research Laboratories (UNCLASSIFIED)
15. Diffraction of a Shock Wave Over a Rectangular Notch, Princeton University, February 1954 (UNCLASSIFIED)
16. Evaluation of Wiancko and Vibration Gages and Development of New Circuitry for Atomic Blast Measurements, Project 1.1a-1, WT-784
17. Development of Pressure-time and Peak Pressure Recorders for Atomic Blast Measurement, Project 1.1a-2, WT-785
18. Foxhole Shielding of Gamma Radiation, Jangle, Project 2.3-2, WT-393, (SECRET-RD)
19. The Effect of Thermal Radiation on Water 1a, BUSTER Project 2.4.2, WT-311, (SECRET-RD)
20. Specifications for Alcoa Lighting Sheet and Alzak Reflectors, Aluminum Company of America
21. The Thermal and Optical Characteristics of Nevada Sand, Naval Material Laboratory, May 1952 (CONFIDENTIAL)
22. Thermal Radiation From a Nuclear Detonation, TUMBLER - SNAPPER Project 8.3, WT-543, (SECRET-RD)
23. The Response of Film to X-Radiation of Energy up to 10 MEV, Los Alamos Scientific Laboratory, LA-1220, (UNCLASSIFIED)
24. The Construction of Damage Curves From Test Data, Sandia Corporation, SC-3209(TR), January 1954 (CONFIDENTIAL)

UNCLASSIFIED

SECURITY CLASSIFICATION OF THIS PAGE (When Data Entered)

REPORT DOCUMENTATION PAGE

READ INSTRUCTIONS BEFORE COMPLETING FORM

1. REPORT NUMBER
WT-1677 (EX)

2. GOVT ACCESSION NO.

3. RECIPIENT'S CATALOG NUMBER

4. TITLE (and Subtitle)
Operation HARDTACK - Projects 2.9/2.12b
Gamma Dose From Very-Low-Yield Bursts

5. TYPE OF REPORT & PERIOD COVERED

6. PERFORMING ORG. REPORT NUMBER
WT-1677 (EX)

7. AUTHOR(s)
J. C. Maloney
M. Morgenthau

8. CONTRACT OR GRANT NUMBER(s)

9. PERFORMING ORGANIZATION NAME AND ADDRESS
U.S. Army Chemical Warfare Laboratories
Army Chemical Center
Maryland

10. PROGRAM ELEMENT, PROJECT, TASK AREA & WORK UNIT NUMBERS

11. CONTROLLING OFFICE NAME AND ADDRESS
Headquarters Field Command
Defense Atomic Support Agency
Sandia Base, Albuquerque, New Mexico

12. REPORT DATE
August 24, 1960

13. NUMBER OF PAGES

14. MONITORING AGENCY NAME & ADDRESS(if different from Controlling Office)

15. SECURITY CLASS. (of this report)
UNCLASSIFIED

15a. DECLASSIFICATION/DOWNGRADING SCHEDULE

16. DISTRIBUTION STATEMENT (of this Report)
Approved for public release; unlimited distribution.

17. DISTRIBUTION STATEMENT (of the abstract entered in Block 20, if different from Report)

18. SUPPLEMENTARY NOTES
This report has had the classified information removed and has been republished in unclassified form for public release. This work was performed by Kaman Tempo under contract DNA001-79-C-0455 with the close cooperation of the Classification Management Division of the Defense Nuclear Agency.

19. KEY WORDS (Continue on reverse side if necessary and identify by block number)
Operation HARDTACK
Gamma Dose

20. ABSTRACT (Continue on reverse side if necessary and identify by block number)
Project 2.9 participated in Shot Quince and Shot Fig with the following objectives: (1) to document the initial gamma dose versus ground range and (2) to measure the total gamma dose received at a point as a function of time, at distances of military interest, for a fractional-kiloton nuclear surface burst. Project 2.12b participated in Shot Hamilton and Shot Humboldt with the following objectives: (1) to provide gamma-dose measurements in support of the biomedical Project 4.2 and (2) to document the initial gamma dose versus ground range.

DD FORM 1 JAN 73 1473 EDITION OF 1 NOV 65 IS OBSOLETE

UNCLASSIFIED

SECURITY CLASSIFICATION OF THIS PAGE (When Data Entered)

ABSTRACT

Project 2.9 participated in Shot Quince and Shot Fig with the following objectives: (1) to document the initial gamma dose versus ground range and (2) to measure the total gamma dose received at a point as a function of time, at distances of military interest, for a fractional-kiloton nuclear surface burst.

Project 2.12b participated in Shot Hamilton and Shot Humboldt with the following objectives: (1) to provide gamma-dose measurements in support of the biomedical Project 4.2 and (2) to document the initial gamma dose versus ground range. In addition, secondary objectives of this project were to document residual radiation intensities and to determine the field gamma-decay rate.

These objectives were accomplished by measuring the dose with film badges which were exposed at various ranges and azimuths, observing the dose on the film badges of the incremental-gamma-dose recorders (Emmett devices), and by field surveys with portable instruments.

Project 4.2 was furnished gamma-dose information for their stations.

The following conclusions are based on the results from Shots Fig, Hamilton, and Humboldt and apply to fractional-kiloton-yield devices tested:

1. Initial gamma doses in the 300 to 900 yard range may be extrapolated from TM 23-200 data with confidence, for surface bursts.

2. An air burst will deliver at least twice the initial gamma dose of a surface burst for the same yield, at distances up to 300 yards from detonation. At greater distances the difference between the doses received from the air burst and the surface burst decreases, and the doses become nearly equal to 1,000 yards.

3. Lethal doses (600 r) of initial gamma radiation are received at approximately 150 yards from the point of detonation the 7.8-ton Humboldt low air burst, while the delivery crews, in the open, would receive 15 r of initial gamma radiation at ranges 575 yards respectively.

4. The observed variation of gamma dose with azimuth for the surface burst is probably caused by the contribution of dose from the transient cloud.

5. The residual gamma fields produced by low air bursts detonated on wooden towers are very small, less than 200 yards radius after 15 minutes, for the 10 r/hr isodose line. This field is due to fission-product radiation, probably from contaminated tower materials.

6. The alpha-contamination levels from low air bursts at distances greater than 100 yards are considered to be an insignificant hazard.

TABLE 1 SHOT DATA

Shot	Burst Height	Support	Yield	Air Temp	Relative Humidity	Atmospheric Pressure	Relative Air Density
	ft		tons	C	pct	mb	
Quince	0	Ground					
Fig	0	Ground		30	77	1,007	0.90
Hamilton	50	Wooden Tower	1.17 ± 0.06	15.7	31	891	0.83
Humboldt	25	Wooden Tower	7.8 ± 0.7	7.4	46	885	0.85

TABLE 2 STATION LOCATIONS, SHOTS QUINCE AND FIG

Station Number	Type	Distance	Azimuth	Station Number	Type	Distance	Azimuth
		yds	deg			yds	deg
South Line				West Line			
35	Land	30	143	W-1	Land	30	233
1	Land	90	135	10	Land	86	242
13	Land	99	150	W-2	Land	100	233
14	Land	198	150	11	Land	103	205
36	Land	200	165	W-3	Buoy	247	233
15	Land	293	150	W-4	Buoy	344	233
16	Land	400	147	W-5	Buoy	444	233
17	Land	497	147	W-6	Buoy	603	233
18	Land	596	147	W-7	Buoy	817	233
19	Land	723	145	W-8	Buoy	1,040	232
20	Land	805	145				
21	Land	873	145	Balloon Line			
				B-1	Balloon	121	165
North Line				B-2	Balloon	133	165
6	Land	100	330	B-3	Balloon	173	165
7	Land	100	315	B-4	Balloon	227	165
8	Land	100	300	B-5	Balloon	283	165
5	Land	105	350	B-6	Balloon	347	165
24	Land	199	330	B-7 *	Balloon	410	165
23	Land	200	315				
22	Land	200	300	Emmett Station			
26	Land	298	319	E-1	Emmett	100	324
25	Land	301	330	E-2	Emmett	200	323
27	Land	401	315	E-3	Emmett	200	304
28	Land	402	329	E-4	Emmett	400	322
30	Land	500	328				
29	Land	501	315	Miscellaneous Stations			
32	Land	601	329	3	Land	40	61
31	Land	602	315	4	Land	49	16
34	Land	701	330	2	Land	60	85
33	Land	711	315	12	Land	100	180
				9	Land	101	270

* Station destroyed.

RESULTS

Project 2.9 participated in Shots Quince and Fig, which were surface detonations of fractional-kiloton nuclear devices on Site Yvonne at EPG. Project 2.12b participated in Shots Hamilton and Humboldt, which were tower detonations of similar devices at the Nevada Test Site.

Shot Quince.

Shot Hamilton. Participation was successful in Shot Hamilton, a 1.17-ton shot on a 50-foot wooden tower. All Emmett devices functioned properly and all film-badge stations were recovered.

Film calibration, station recovery, field surveying, and film processing proceeded according to plan. The same calibration source used for Shot Fig was available for this event. However, an accident during film development resulted in the loss of data from the project film-badge stake station and Emmett devices. A defective safe light in the dark room fogged the

films to the extent that interpretation of density was impossible. However, all open-field stations of Project 4.2 in three directions were instrumented by Project 2.12b. Each of the stations had a direct line of sight to ground zero and provided enough data points to meet the objective of documenting initial gamma dose versus distance.

All open-field data were corrected the same as for Shot Fig and appear in Figure 11. The doses in vehicles, open foxholes, and some offset foxholes were corrected for neutron and station-shielding effects. However, most offset foxholes and all $^2/_3$-covered foxholes were not adequately instrumented for neutron measurements, and the data had to be left in the raw form.

Gamma dose versus distance, corrected to a relative air density of 0.9, is tabulated in Table 5 and plotted in Figure 12. Gamma doses at all Project 4.2 stations are tabulated in Table 7 for the test-condition relative air density of 0.83. Alpha-survey data is tabulated in Table 8.

The 10 r/hr isodose lines as determined from field surveys were irregular star-shaped curves inclosing very small areas as shown in Table 9. No evidence of a downwind highly radio-

active (hot) line was found. The minimum and maximum distances of these curves from ground zero at various times are tabulated in Table 9. The gamma decay followed the usual fission-product decay law with an average exponent of −1.1 from H+10 minutes to H+1 day. Reference 13, the report of the field-survey group, contains a multitude of data sheets, curves, and iso-dose plots of the data.

Shot Humboldt. Participation was successful in Shot Humboldt, a 7.8-ton shot on a 25-foot wooden tower. Since this event was moved at the last minute to a different ground zero than planned, effort was limited to instrumenting Project 4.2 stations with film badges plus a few hasty gamma-field surveys.

The film badges were recovered within a few minutes after detonation by a coordinated effort of this project and Projects 2.12a and 4.2. Instrumentation, and the two APC vehicles, were dragged out of the ground-zero area by pulling cables.

The open-field data were corrected the same as for Shot Fig. See Figure 11. The doses in

vehicles and foxholes were corrected for neutron and station-shielding effects.

Gamma dose versus distance, corrected to a relative air density of 0.9, is tabulated in Table 5 and plotted in Figure 12. Gamma doses at all Project 4.2 stations are tabulated in Table 10 for the test-condition relative air density of 0.85.

The 10 r/hr isodose lines, as determined from field surveys, were roughly circular with radii of 200 yards or less. There was no evidence of a downwind hot line. The minimum and maximum distances that these curves extended from ground zero at various times are tabulated in Table 9. Since field surveying had to be concluded by H+7 hours, only limited experimental data was obtained on field decay. These data only suggest that the contamination decayed according to the fission-product law. Reference 13 contains all survey data obtained for this event.

DISCUSSION

Although the film badges were in all cases exposed for more than 1 minute, it is felt that the data in Figure 12 represents initial gamma dose or a combination of initial dose and dose caused by the passage of the low cloud. Some close-in stations for all three events were affected by

TABLE 6 EMMETT GAMMA DOSES

Time Interval	Dose at Station			
	100 yd, 325 deg	200 yd, 325 deg	200 yd, 305 deg	400 yd, 325 deg
min	r	r	r	r
0 to 0.05	3,200	390	360	19
0 to 0.25	3,500	280	390	79
0 to ½	4,100	700	260	54
0 to 1	2,700	450	*	11
½ to 1½	580	89	110	0
1 to 2	120	5.8	5.3	0
1½ to 2½	14	0	1.8	0
2 to 3	3.8	0	0	0
2½ to 3½	3.6	0	0	0
3 to 4	1.3	0	0	0
3½ to 4½	2.9	0	0	0
4 to 5	1.5	0	0	0
4½ to 5½	1.4	0	0	0
5 to 6	0	0	0	0

* Defective film badge

residual fields.

the Hamilton and Humboldt low air bursts, the values beyond 100 yards approximated straight lines. The best least-squares fit for these lines was calculated and extrapolated to 100 and 1,000 yards.

the open-field results of Shots Hamilton and Humboldt were adjusted to a 1-ton yield for comparative purposes. Predicted gamma doses were calculated from Equation 1 for a 1-ton yield. Gamma

doses scaled from 1-kt curves in TM 23-200 (Reference 12) to a 1-ton yield agreed with these calculations.

All open-field test results (adjusted to 1-ton yield) were divided by the predicted 1-ton yield (calculated and scaled) data for each 100-yard distance from detonation, and plotted as a function of distance in Figure 13. From the curves in this figure, it is possible to note trends in the variation of test results from predictions.

The doses from the low air bursts were higher than predicted surface-burst values by a factor of two for close-in distances (100 to 300 yards). This is in keeping with the theory that initial dose from a surface burst is reduced by 50 percent compared to an equivalent air burst. Many basic references (such as References 7 and 12) indicate that surface and near-surface bursts produce the same initial gamma dose. Figure 13 shows that the low air-burst doses do approach the surface-burst doses at distances in excess of 1,000 yards. This phenomenon would favor the use of a low air burst rather than a surface burst for tactical employment, as there would be a bonus in the higher target dose. Figure 12 illustrates this bonus quite well. The 7.8-ton low air burst (Shot Humboldt) delivered as much gamma dose within 400 yards of ground zero, Lethal doses (600 r) were received at approximately 150 yards from detonation The delivery crews, in the open, would receive only 15 r or less of initial gamma radiation at a range of 600 yards.

For the case of an air burst and a surface burst having the same yield, it can be seen from Figure 13 that at distances within 300 yards from detonation, the air burst delivered at least

TABLE 7 SHOT HAMILTON GAMMA DOSES AT PROJECT 4.2 STATIONS

Relative air density = 0.83

Station	Slant Distance	Corrected Dose	Uncorrected Dose
	yd	r	r
Doses in the Open, South Line			
100 S	101.3	350	
200S	200	67	
I	225	49	
II	245	39	
III	265	32	
IV	285	26	
300 S	300	22	
VI	325	18	
VIII	365	12	
400 S	400	9.4	
X	405	9.0	
XII	445	6.7	
XIV	485	5.0	
500 S	500	4.5	
XV	505	4.3	
600 S	600	2.3	
600 Pen	600	2.3	
650 S	650	1.7	
650 Pen	650	1.7	
700 S	700	1.3	
700 Pen	700	1.3	
750 S	750	0.96	
750 Pen	750	0.96	
800 S	800	0.73	
800 Pen	800	0.73	
Doses in the Open, West Line			
100 W	101.3	350	
I	170	101	
II	185	82	
200 W	200	67	
III	200	67	
IV	215	55	
VI	245	39	
VIII	275	28	
300 W	300	22	
X	305	21	
XII	335	16	
XIV	365	12	
XV	380	11	
400 W	400	9.4	
500 W	500	4.5	
600 W	600	2.3	
700 W	700	1.3	
Doses in the Open, North Line			
25 N	30.2	~1,800	
50 N	52.8	1,700	
75 N	76.9	540	
100 N	101.3	350	
125 N	126	210	
150 N	150	140	
175 N	175	94	
Doses in Vehicles			
T 67 NW	39.6	430	
APC 66 NW	62.9	715	
T 65 NW	70.1	300	
T 68 SE	40.8	720	
T 69 SW	48.7	370	
T 70 SE	58.4	500	
APC 71 SW	82.0	390	
Doses in Open Foxholes			
14 SW	22.9	~2,300	
62 NE	23.0	~1,800	
40 NW	24.9	1,750	
26 SE	25.6	1,800	
58 NE	27.3	1,050	
22 SE	28.7	710	
10 SW	26.4	*	
23 SE	29.4	410	
21 SE	28.3	*	

TABLE 7 CONTINUED

Station	Slant Distance	Corrected Dose	Uncorrected Dose
	yd	r	r
54 NE	31.2	460	
55 NE	30.6	420	
56 NE	30.3	460	
19 SE	32.4	220	
20 SE	32.9	680	
5 SW	34.8	160	
6 SW	34.6	240	
18 SE	36.7	570	
49 NE	36.8	230	
48 NE	39.4	340	
4 SW	39.0	300	
17 SE	41.1	350	
47 NE	41.2	290	
46 NE	43.9	430	
3 SW	43.5	430	
1 SW	57.8	280	
2 SW	57.7	290	
Doses in Offset Foxholes			
64 NE	18.8	69	
30 SE	19.8	68	
63 NE	21.3	*	
27 SE	22.8	16	
Uncorrected Doses in Offset Foxholes			
45 NW	17.7		200
16 SW	18.7		70
44 NW	19.8		*
61 NE	24.4		130
38 NW	26.4		60
11 SW	26.3		54
31 SE	17.6		*
15 SW	21.2		*

Station	Slant Distance	Corrected Dose	Uncorrected Dose
	yd	r	r
Uncorrected Doses in Two-thirds Covered Foxholes			
29 SE	22.4		750
28 SE	21.3		900
43 NW	21.3		900
41 NW	22.9		1,100
42 NW	24.0		640
13 SW	23.9		530
59 NE	24.9		680
60 NE	24.5		590
12 SW	24.7		590
39 NW	27.3		*
24 SE	26.4		530
25 SE	26.9		470
36 NW	28.4		530
37 NW	29.1		500
57 NE	28.4		*
7 SW	31.3		400
8 SW	30.8		460
9 SW	30.3		420
51 NE	32.8		480
52 NE	32.4		450
53 NE	32.2		480
34 NW	34.6		400
35 NW	34.7		450
50 NE	35.3		390
32 NW	43.5		230
33 NW	43.7		240

* These film badges were either lost or grossly inconsistent.

twice the dose of the surface burst. At greater distances this dose differential decreased until the doses became very nearly equal at 1,000 yards.

The residual fields in the Hamilton and Humboldt ground-zero areas were much lower than expected as the yields of these devices were much lower than expected. In both cases the contamination was apparently fission products from contaminated tower materials. No elongated fallout pattern was observed although one survey team for each event hunted downwind fallout. The alpha-contamination levels of Shot Hamilton, at 100 yards or more from ground zero, were below 120 $\mu g/m^2$ which is considered an insignificant hazard. The Hamilton ground-zero area

TABLE 8 SHOT HAMILTON ALPHA-CONTAMINATION LEVELS, $\mu g/m^2$

Slant Distance	Alpha Contamination at Azimuths Shown, deg											
	25	55	85	115	145	175	205	235	265	295	325	355
yd												
100	62.4	116.6	15.0	2.2	1.8	1.9	72.4	2.6	23.0	24.0	27.4	66.7
200	20.5	112.0	1.6	0.5	0.8	0.9	0.9	6.5	19.5	0.4	0.9	0.7
300	2.4	91.4	1.4	0.4	0.02	0	0	1.6	2.9	1.8	1.6	1.6
400	0.9	30.9	0.5	0	—	—	0	1.9	3.6	1.0	1.1	0.5
500	2.4	29.2	0.4	—	—	—	0	2.5	3.8	1.1	1.1	0.9
600	1.5	9.1	—	—	—	—	0.3	3.8	7.9	0.5	0.6	0.6
700	1.3	1.4	—	—	—	—	0	2.1	2.6	—	0.9	0.6
800	1.7	4.1	—	—	—	—	0	1.4	3.1	—	—	—

was visually observed to be strewn with tower debris, paraffin, etc. Since this debris probably became embedded with fission products and alpha emitters, the absence of this debris (as would be the case for a detonation in free air) would cause even lower ground-zero contamination levels.

Since the Emmett devices were not in the fallout area for Shot Fig, no data were obtained on fallout arrival or decay. The activity detected for a few minutes at the closest stations was probably crater shine.

CONCLUSIONS

The following conclusions are based on the results from Shots Hamilton, and Humboldt

TABLE 9 DISTANCE FROM GROUND ZERO TO 10 R/HR ISODOSE LINES, SHOTS HAMILTON AND HUMBOLDT

Time After Detonation	Shot Hamilton		Shot Humboldt	
	Minimum	Maximum	Minimum	Maximum
min	yd	yd	yd	yd
10	40	90	140	205
15	30	75	120	180
30	15	65	85	150
60	5	55	30	100

and apply to fractional-kiloton-yield devices tested.

1. Initial gamma doses in the 300- to 900-yard range may be extrapolated from TM 23-200 data with confidence for surface bursts.

2. For the same yield at distances up to 300 yards from detonation, an air burst will deliver at least twice the initial gamma dose of a surface burst. At greater distances the difference between the doses received from the air burst and the surface burst decreases, and the doses become nearly equal at 1,000 yards.

3. Lethal doses (600 r) of initial gamma radiation are received at approximately 150 yards from the point of detonation a 7.8-ton low air burst

(Shot Humboldt), while the delivery crews, in the open, would receive 15 r of initial gamma radiation at ranges of 575 yards, respectively.

4. The observed variation of gamma dose with azimuth for the surface burst is probably caused by the contribution of dose from the transient cloud.

5. The residual-gamma fields produced by low air bursts detonated on wooden towers are very small (less than 200 yards radius at H+15 minutes) for the 10 r/hr isodose line. This

TABLE 10 SHOT HUMBOLDT GAMMA DOSES AT PROJECT 4.2 STATION (TEST CONDITIONS)

Station	Slant Distance	Corrected Dose
	yd	r
Doses in the Open, East Line		
25	26.4	19,000
50	50.7	5,500
100	100	2,800
200	200	500
300	300	160
450	450	41
600	600	14
700	700	7.5
800	800	4.1
Doses in Foxholes		
5 S	10.5	14,500
10 N	13.3	16,000
15 S	16.9	*
20 N	20.1	6,000
25 S	23.7	5,900
5 N	10.5	13,600
10 S	13.3	13,200
15 N	16.9	3,900
20 S	20.1	6,400
25 N	23.7	1,500
Doses in Vehicles		
APC 66	30.5	
Front		19,000
Middle		11,500
Middle		9,800
Rear		10,000
APC 70	30.5	
Front		18,200
Middle		13,200
Middle		12,200
Rear		10,400

* Film badge defective.

field is due to fission-product radiation, probably from contaminated tower materials.

6. The alpha-contamination levels from low air bursts at distances greater than 100 yards are considered to be an insignificant hazard.

RECOMMENDATIONS

Further experimentation on fractional-kiloton devices is desirable because the small number

of tests performed were accomplished under far-from-ideal testing conditions.

1. The initial gamma radiation from a surface burst should be measured over a 2π area instead of over small, narrow sectors, and should include dose-versus-time measurements.

2. The above measurements should be repeated for air bursts, using balloons instead of wooden towers for support of the device, in order to avoid interference from the residual radioactivity caused by tower material.

3. Laboratory experiments should be performed to determine more accurately the effects of neutrons on film emulsions and the contribution of the gamma photons from thermal-neutron capture in the walls of the protective shields.

REFERENCES

1. Staff Study; "Estimated Weapon Effects of Fractional KT Nuclear Weapons"; November 1957; U.S. Army Engineer Research and Development Laboratories, Fort Belvoir, Virginia; Secret Restricted Data.

2. L. Costrell; "Gamma Radiation as a Function of Time and Distance"; Project 2.1a, Operation Jangle, WT-329, April 1952; National Bureau of Standards, Washington, D.C.; Secret Restricted Data.

3. G. Carp and others; "Initial Gamma Radiation Intensity and Neutron-Induced Gamma Radiation of NTS Soil"; Project 2.5, Operation Plumbbob, ITR-1414, November 1957; U.S. Army Signal Engineering Laboratories, Fort Monmouth, New Jersey; Secret Restricted Data.

4. M. Morgenthau and M. Schumchyk; "Residual Radiation from a Very-Low-Yield Burst"; Project 2.10, Operation Hardtack, ITR-1678, November 1958; U.S. Army Chemical Warfare Laboratories, Army Chemical Center, Maryland; Secret Restricted Data.

5. E.N. York; "Initial Nuclear Radiation from Low Yield Fission Weapons"; AFSWC-TN-56-14, December 1956; Air Force Special Weapons Center, Kirtland Air Force Base, New Mexico; Secret Restricted Data.

6. D.C. Borg and C. Eisenhauer; "Spectrum and Attenuation of Initial Gamma Radiation from Nuclear Weapons"; AFSWP-502B, January 1955; Armed Forces Special Weapons Project, Washington 25, D.C.; Secret Restricted Data.

7. "The Nuclear Radiation Handbook"; AFSWP-1100, March 1957; Armed Forces Special Weapons Project, Washington 25, D.C.; Secret Restricted Data.

8. E.F. Wilsey and others; "Soil Activation by Neutrons from a Very-Low-Yield Burst"; Project 2.12c, Operation Hardtack, WT-1680; U.S. Army Chemical Warfare Laboratories, Army Chemical Center, Maryland; Secret Restricted Data.

9. P. Brown and others; "Gamma Exposure versus Distance"; Project 2.1, Operation Redwing, WT-1310, February 1960; U.S. Army Signal Engineering Laboratories, Fort Monmouth, New Jersey; Secret Restricted Data.

10. R.C. Tompkins and others; "Attenuation of Gamma and Neutron Radiation by Armor, Soil, and Structures"; Project 2.4, Operation Plumbbob, WT-1413, draft manuscript; U.S. Army Chemical Warfare Laboratories, Army Chemical Center, Maryland; Secret Restricted Data.

11. Radiac Training Sets AN/PDR-T1-AN/PDR-39; TM 11-5514, May 1951, with addendum October 1952; Department of the Army, Washington, D.C.; Unclassified.

12. "Capabilities of Atomic Weapons"; TM 23-200, Revised Edition, November 1957; Armed Forces Special Weapons Project, Washington 25, D.C.; Confidential.

13. "Radiation Effect Caused by the Explosion of a Davy Crockett Device"; Project No. CMLCD 59T22, December 1958; U.S. Army Chemical Corps School, Fort McClellan, Alabama; Confidential.

WT-1602(EX)
EXTRACTED VERSION

OPERATION HARDTACK—PROJECT 2.14

Fallout Contamination from a Very Low Yield Burst

410999

M. Cowan, Jr.
Sandia Corporation
Albuquerque, NM

8 May 1962

NOTICE:
This is an extract of WT-1602, Operation HARDTACK, Project 2.14.

Approved for public release;
distribution is unlimited.

Extracted version prepared for
Director
DEFENSE NUCLEAR AGENCY
Washington, DC 20305-1000

1 September 1985

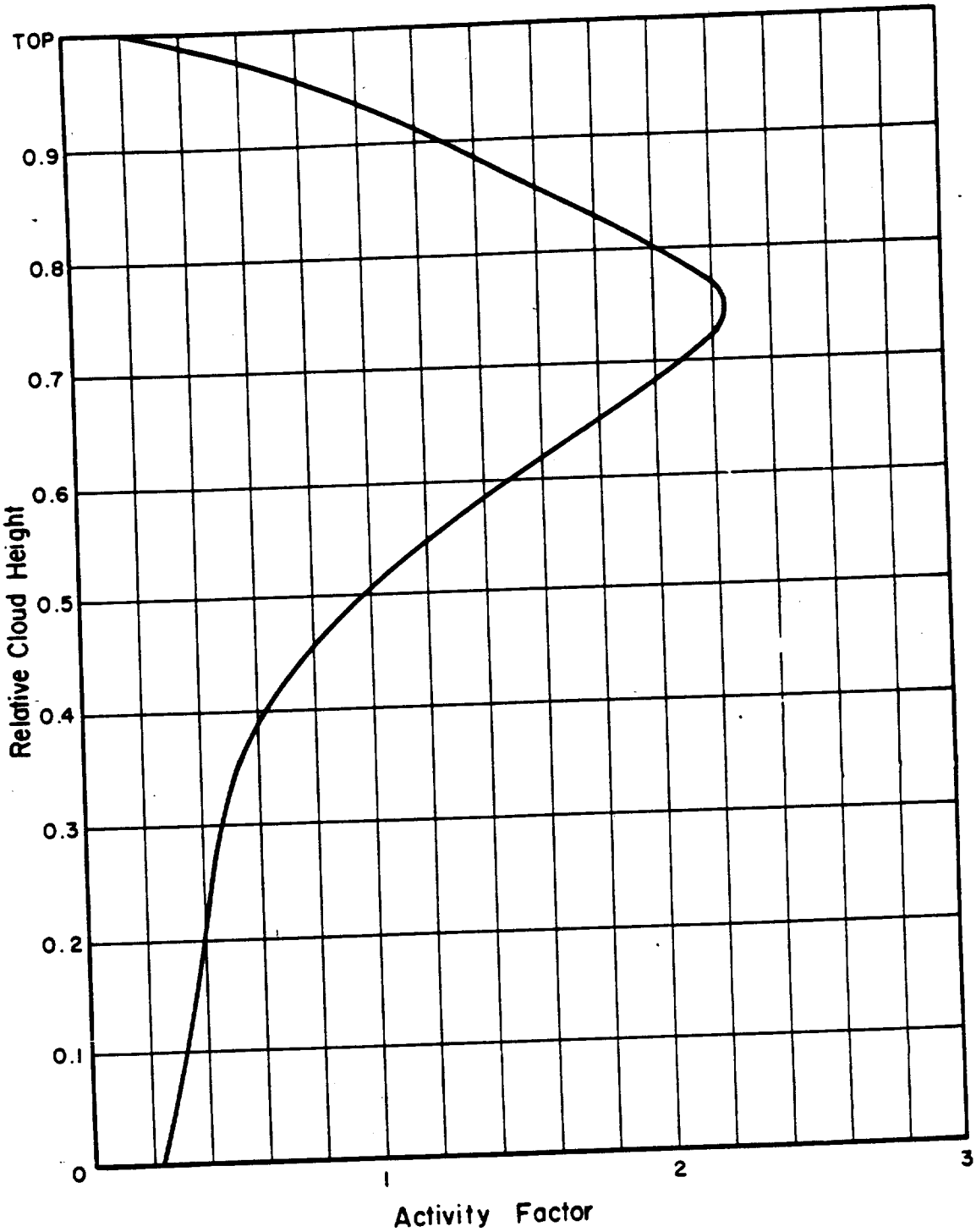

Figure 1.1 Hardtack model space distribution. For a uniform distribution of activity with height activity, the factor would equal 1 for all heights.

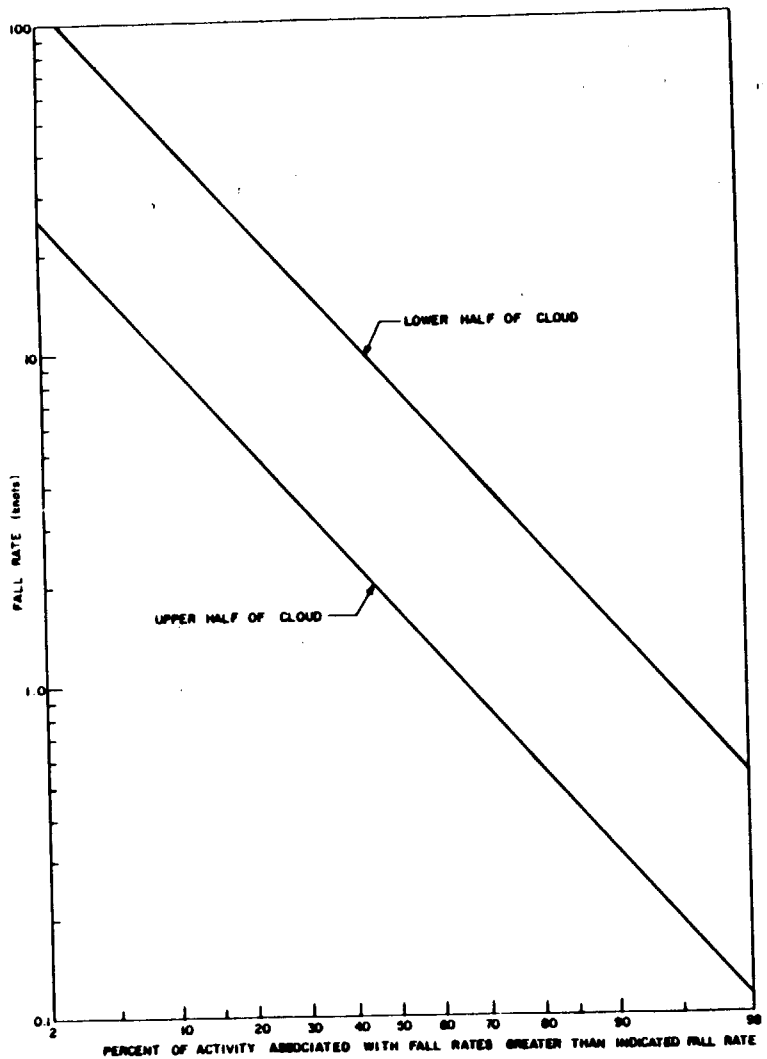

Figure 1.2 Hardtack model fall-rate distribution. Distributions are log-normal with $\sigma = 1.3$ and indicated median fall rates.

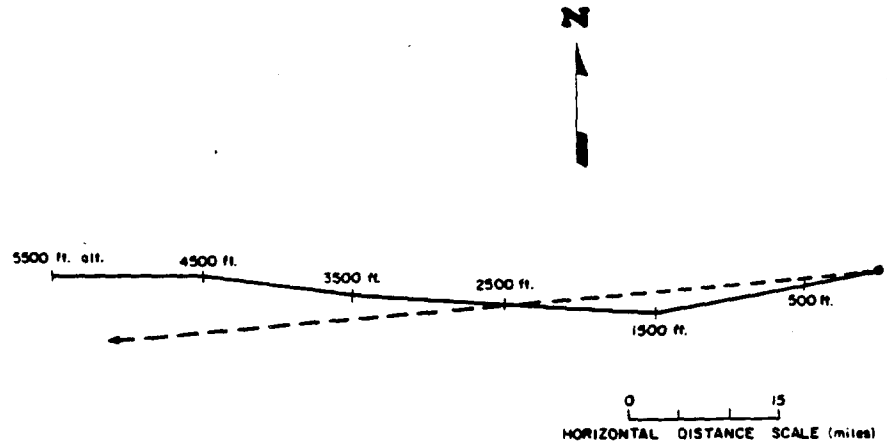

Figure 1.4 Hodograph of wind structure assumed for model calculations. Calculations were made along dashed line. Hodograph is drawn for 1,000-foot-per-hour balloon-rise rate.

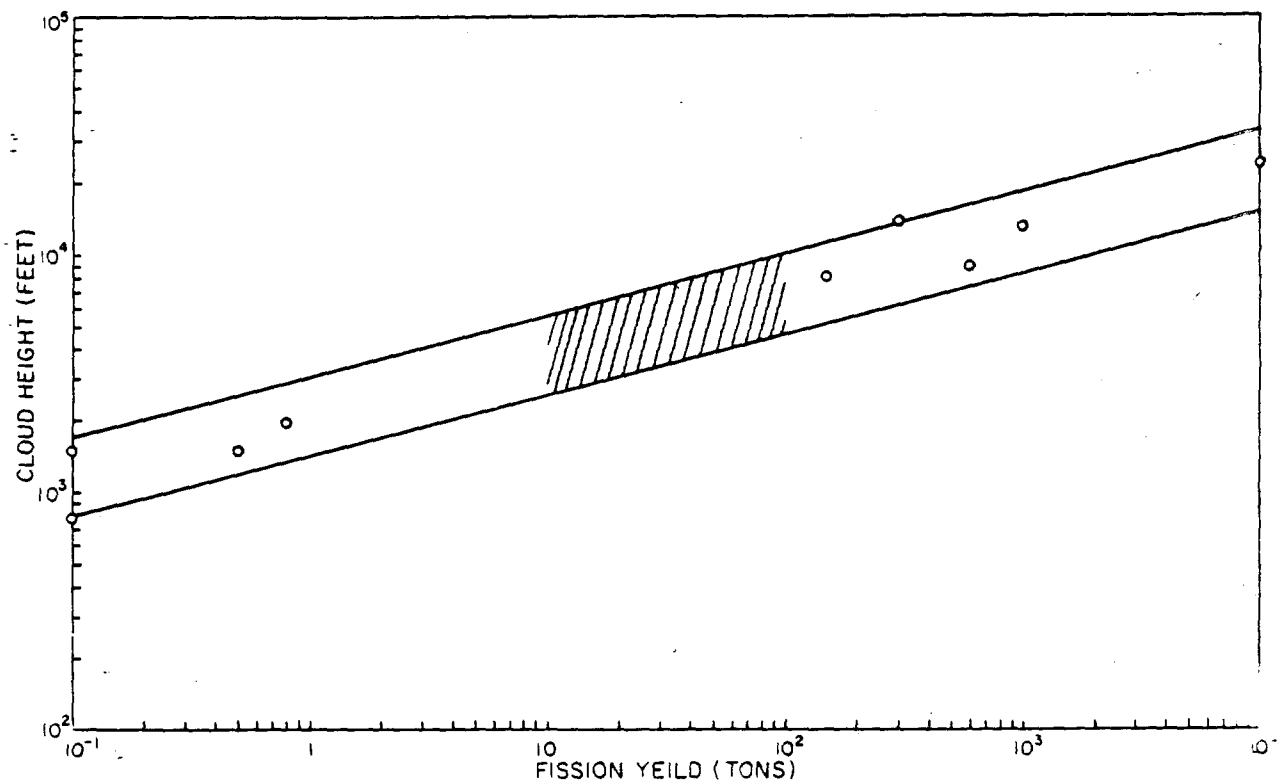

Figure 1.5 Cloud height versus yield.

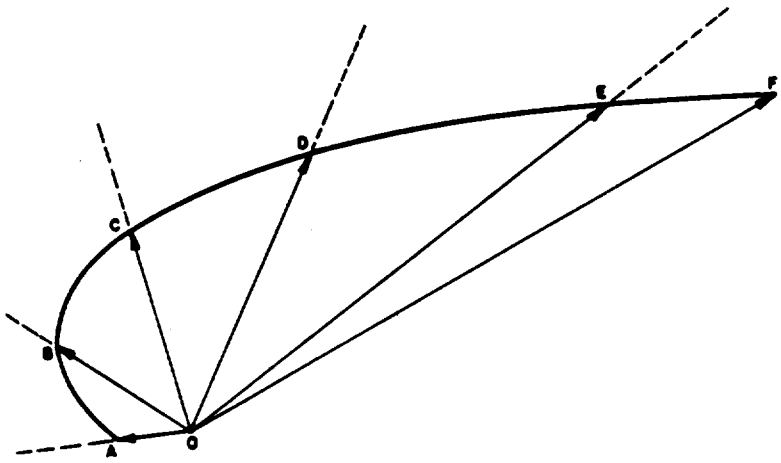

Figure 1.7 Example of a hodograph.

TABLE 3.1 DOSE-RATE DECAY

Station	Number of Readings	Time Interval (hours after zero time)	Inferred Dose-Rate-Measurement Error, Assuming $t^{-1.1}$ Decay	Station	Number of Readings	Time Interval (hours after zero time)	Interred Dose-Rate-Measurement Error, Assuming $t^{-1.2}$ Decay
			percent				percent
B-10	3	3.4 to 46	± 18	I-40	3	1.1 to 8.5	± 62
B-20	5	1.7 to 47	± 30	I-50	3	0.8 to 8.5	± 34
B-45	4	1.0 to 3.3	± 20	I-60	3	1 to 8.5	± 15
B-60	3	0.6 to 3.3	± 49	I-70	3	1 to 8.5	± 29
C-30	3	0.8 to 8.5	± 42	J-20	4	3.5 to 47	± 35
C-45	4	0.8 to 8.5	± 15	J-30	3	1.7 to 8.5	± 36
D-20	6	1.7 to 46	± 61	J-40	3	1.7 to 8.7	± 14
D-30	3	0.8 to 8.5	± 10	J-50	4	1.7 to 8.5	± 20
E-10	3	3.5 to 48	± 4	J-60	3	1.8 to 8.5	± 8
E-20	4	3.5 to 47	± 2	J-70	6	0.8 to 8.5	± 25
G-25	3	3.5 to 46	± 19	K-20	5	1.6 to 46	± 34
G-30	3	3.5 to 46	± 30	K-30	3	1.6 to 8.5	± 38
G-35	3	3 to 9	± 14	K-45	3	1.6 to 8.5	± 30
H-20	3	3.5 to 47	± 30	K-60	3	1.5 to 8.5	± 65
H-40	3	1.1 to 3.4	± 22	K-75	4	1.4 to 8.5	± 25
I-20	5	2.2 to 46	± 19	Crater lip	7	3.3 to 48	± 198
I-30	4	1.2 to 8.5	± 15				

TABLE 3.2 STICKY-PAN MEASUREMENTS

Station	Sticky Pan Gamma Counting Rate at H + 3 Hours	Inferred Dose Rate From Sticky Pan at H + 1 Hour	Measured Dose Rate at H + 1 Hour
	counts/min	r/hr	r/hr
B-60	15,800	1.3	0.83
BB-55	3,080	0.24	1.2
C-45	51,600	4.1	2.3
H-40	293,000	23	35
I-30	368,000	29	32
I-40	172,000	14	10
I-50	49,300	3.9	5.3
I-60	18,300	1.5	2.8
I-70	14,900	1.2	1.9
J-60	31,800	2.5	2.1
J-70	15,000	1.2	1.2
J-100	4,650	0.37	0.4
J-150	2,000	0.16	0.056
K-45	54,500	4.4	6.3
K-60	20,000	1.6	2.0
K-75	11,000	0.88	0.36
K-100	3,410	0.27	0.27
K-150	700	0.056	0.028

TABLE 3.3 PLUTONIUM MEASUREMENTS

Station	Inferred Gamma Dose Rate*	Measured Plutonium Contamination†	Ratio
	r/hr at 1 hr	μgm/m²	r/hr / μgm/m²
I-30	29	4.7	6.2
I-40	14	17	0.78
I-60	1.5	30	0.048
I-70	1.2	0.10	12
J-60	2.5	0.023	109
J-100	0.37	0.020	18
K-100	0.27	0.097	2.8
A-2	—	0.032	—
H-40	23	3.6	6.4
BB-55	0.24	0.064	3.7
N-6	0.068	40	1.7×10^{-3}
N-6	0.068	1.6	0.042
O-6	0.05	0.57	0.088
R-5	—	0.10	—
S-6	0.012	0.067	0.18
Y-4	0.16	0.22	0.73
Z-4	0.09	0.17	0.53

* From gamma-counting sticky pans.
† Radiochemistry.

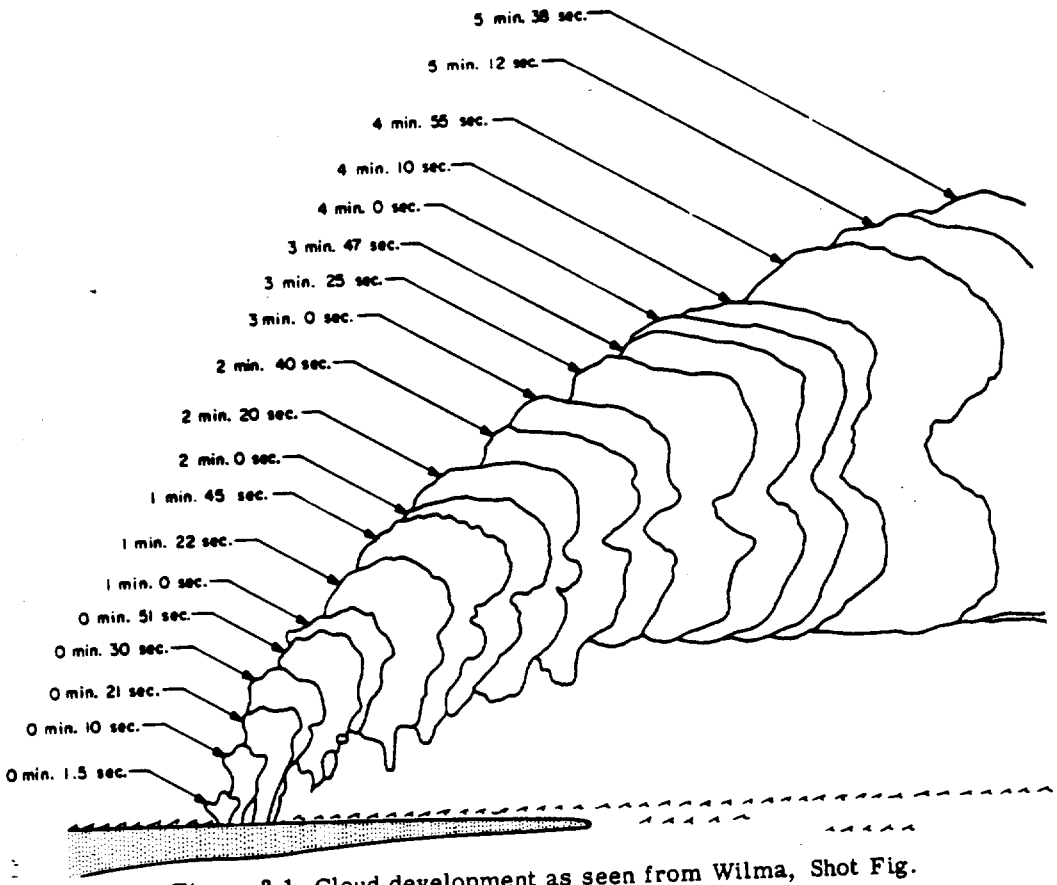

Figure 3.1 Cloud development as seen from Wilma, Shot Fig.

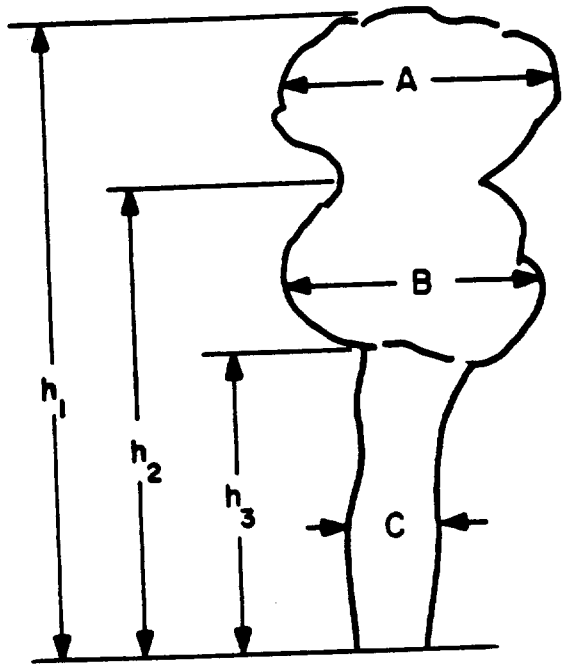

Figure 3.2 General features of the cloud.

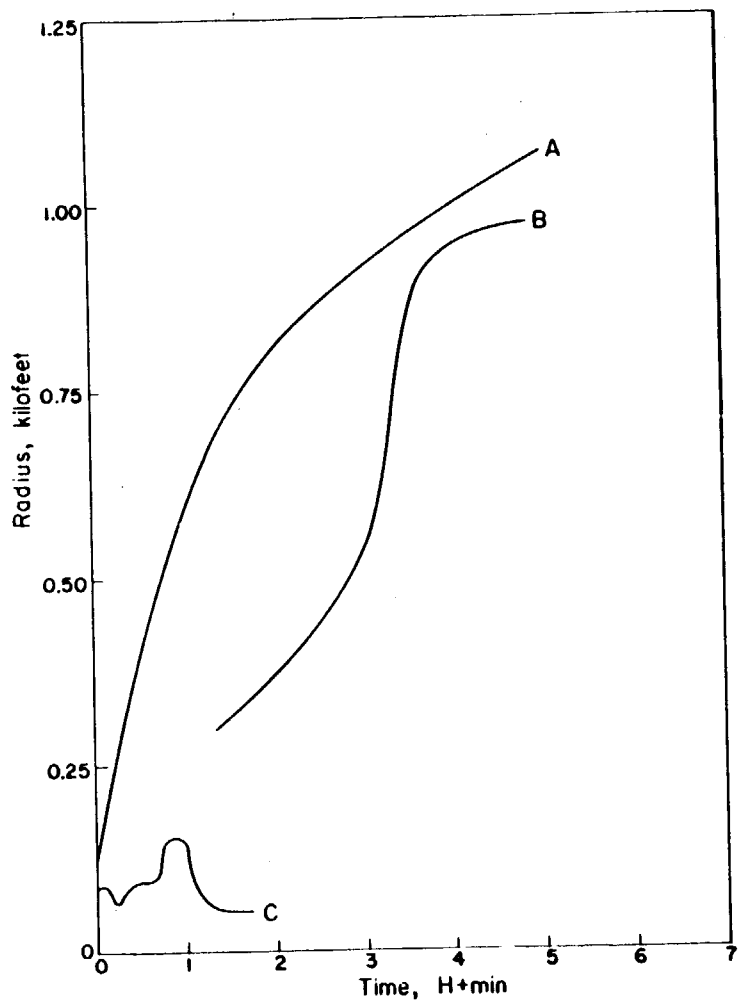

Figure 3.3 Cloud radius versus time.

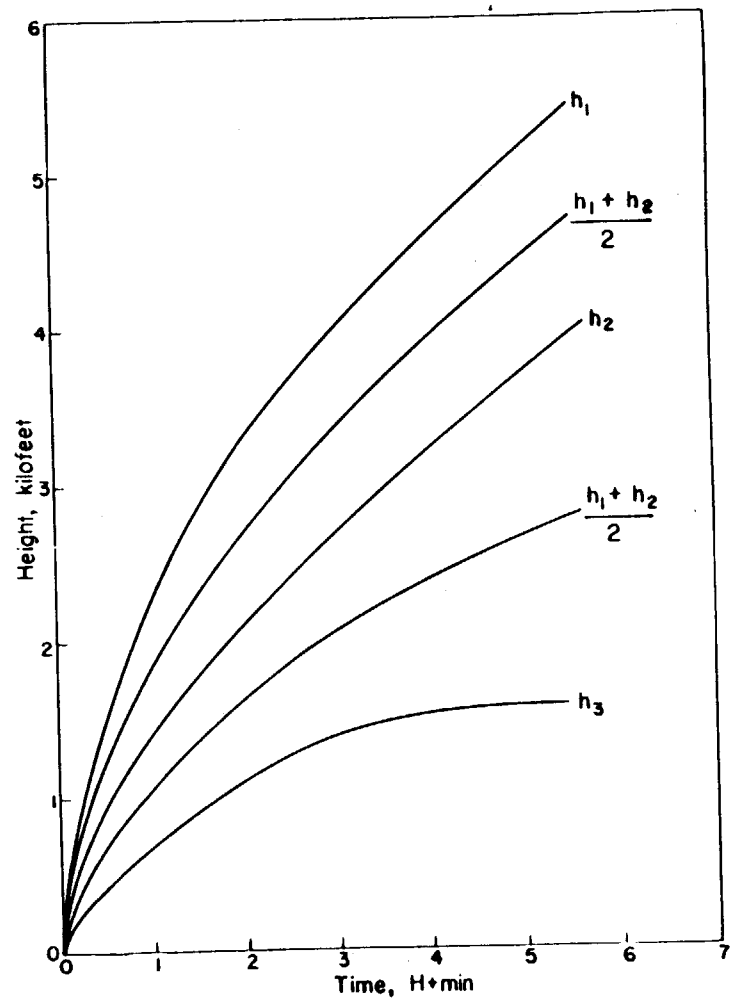

Figure 3.4 Cloud height versus time.

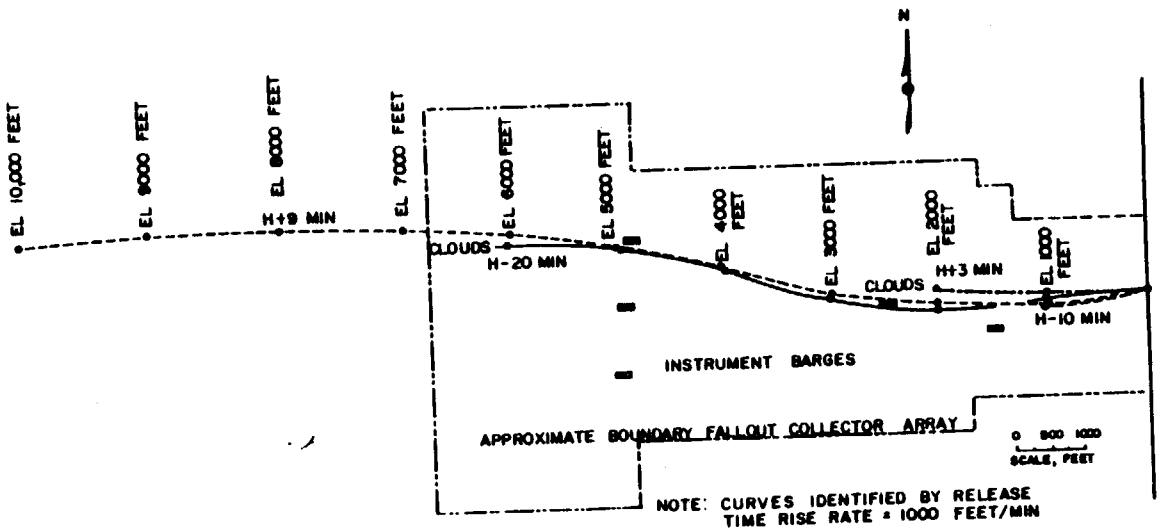

Figure 3.5 Wind conditions, Shot Fig.

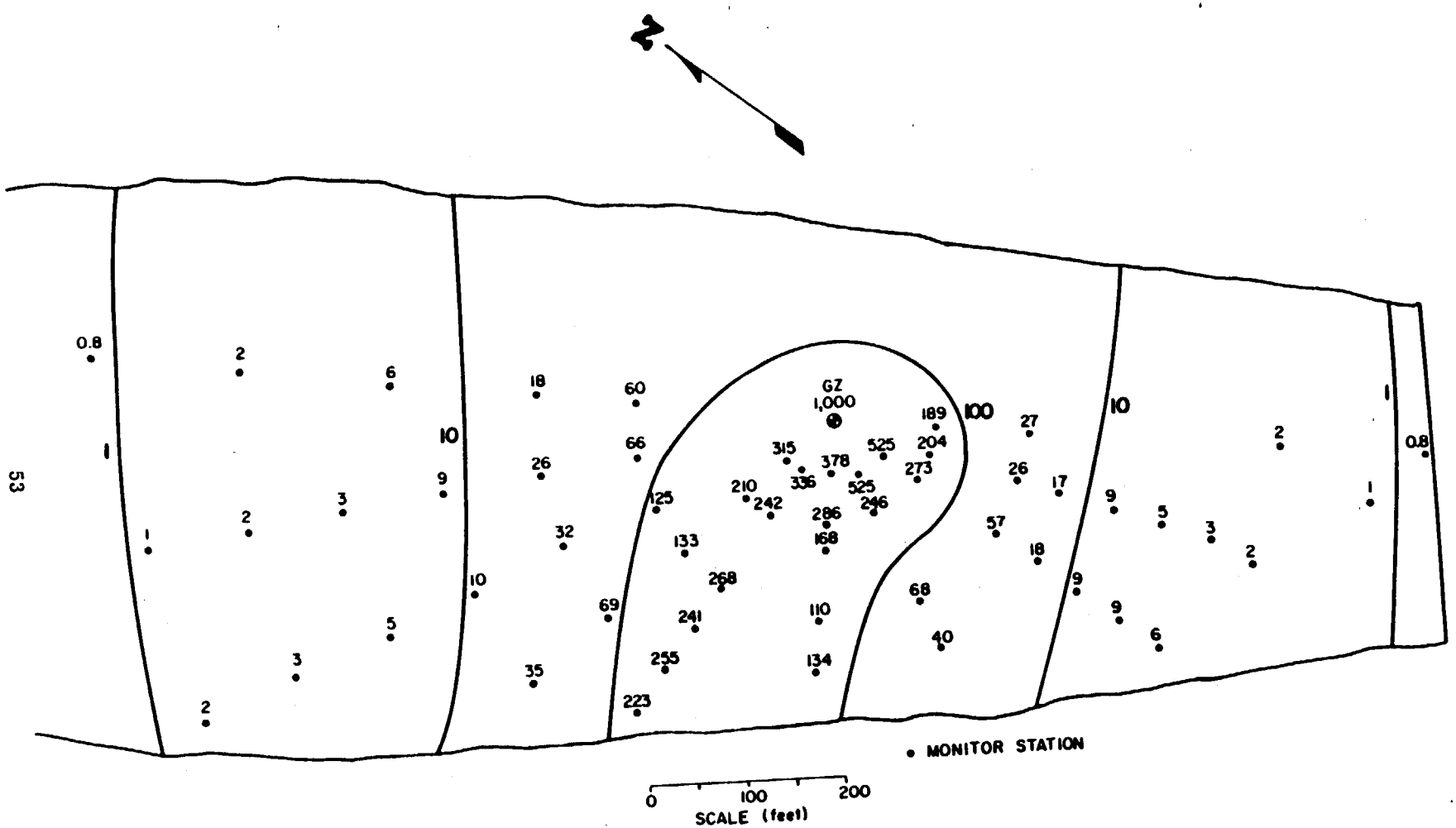

Figure 3.6 Dose rates (r/hr) on land at H + 1 hour.

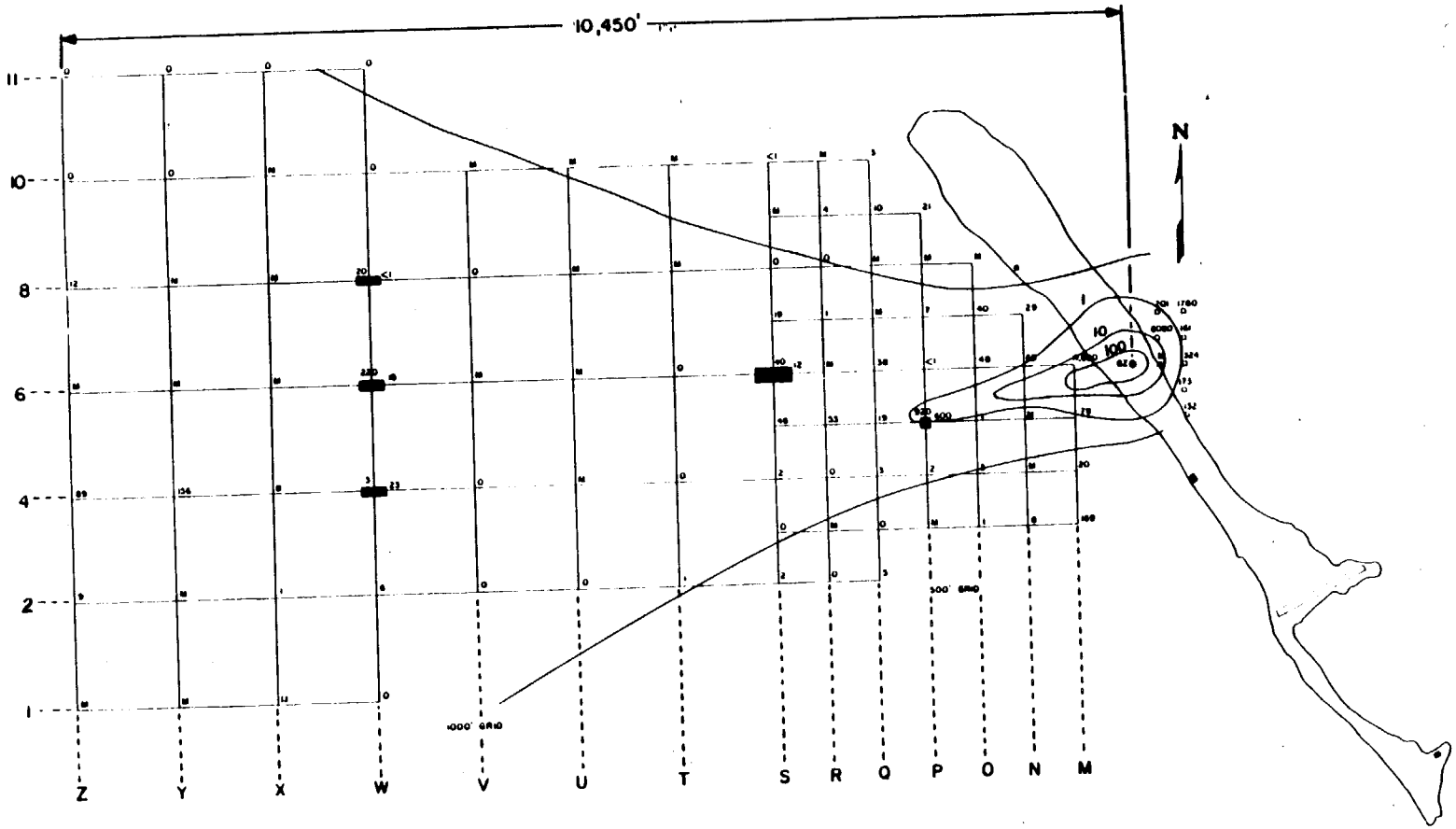

NOTE: CONTOUR INTENSITY LABELS ARE IN r/hr. INDIVIDUAL STATION INTENSITIES ARE IN mr/hr. M INDICATES A MISSING BUOY.

Figure 3.9 H + 1 hour dose-rate contours for complete array.

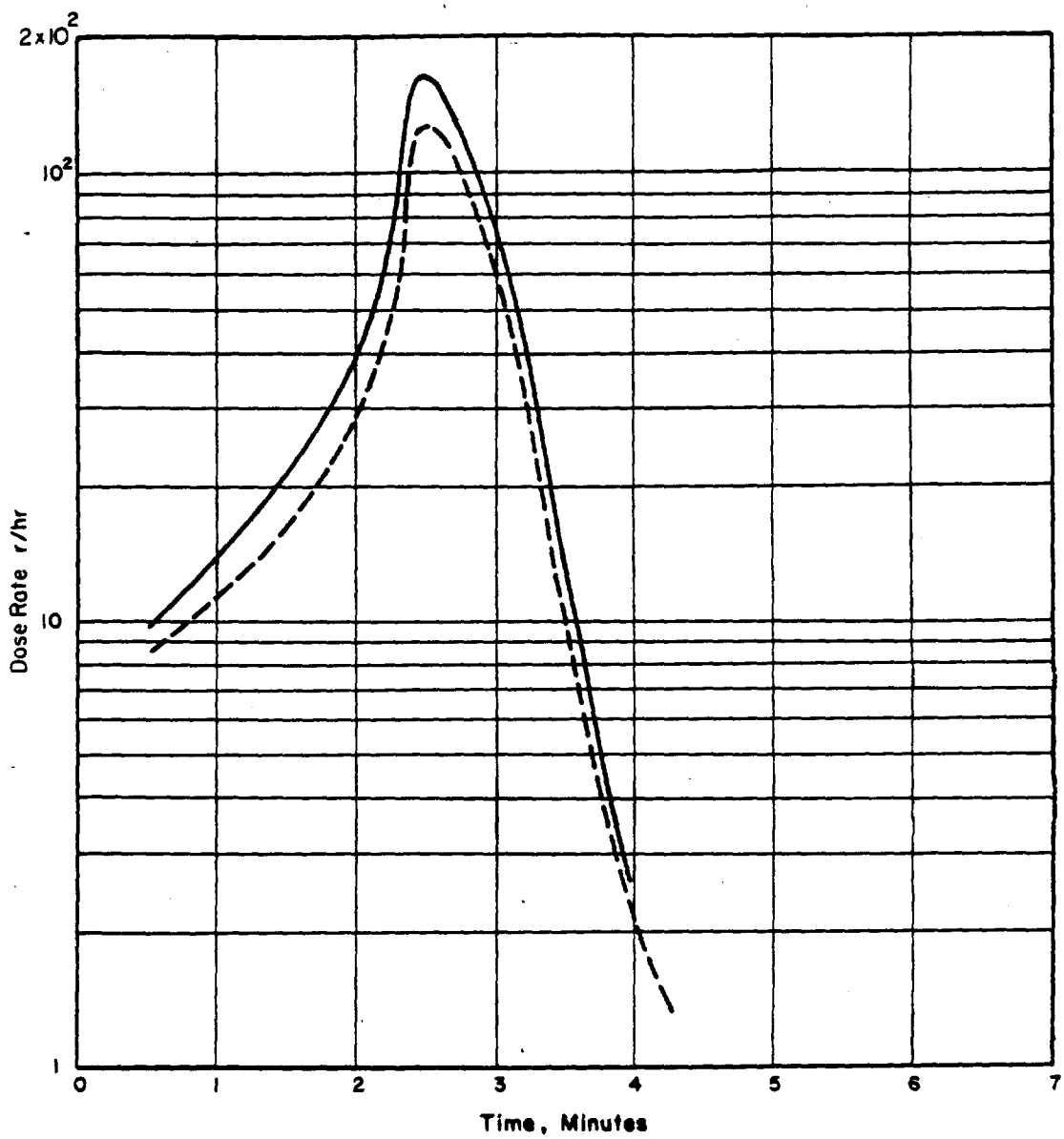

Figure 3.10 Cloud shine on YCV barge.

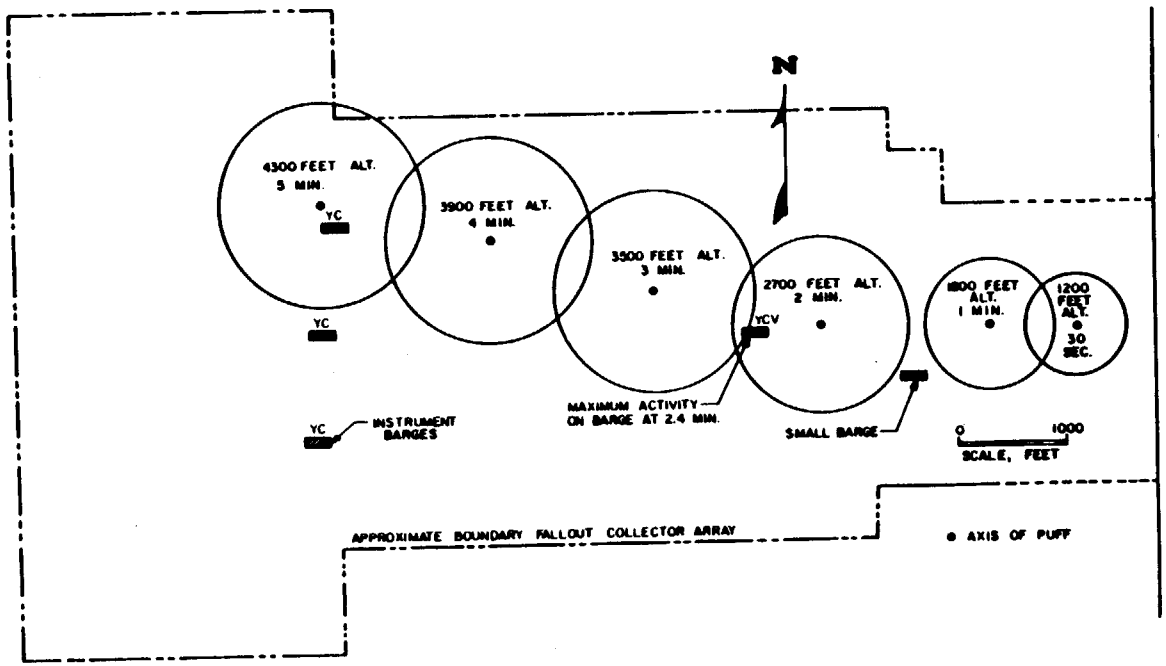

Figure 3.11 Puff trajectory.

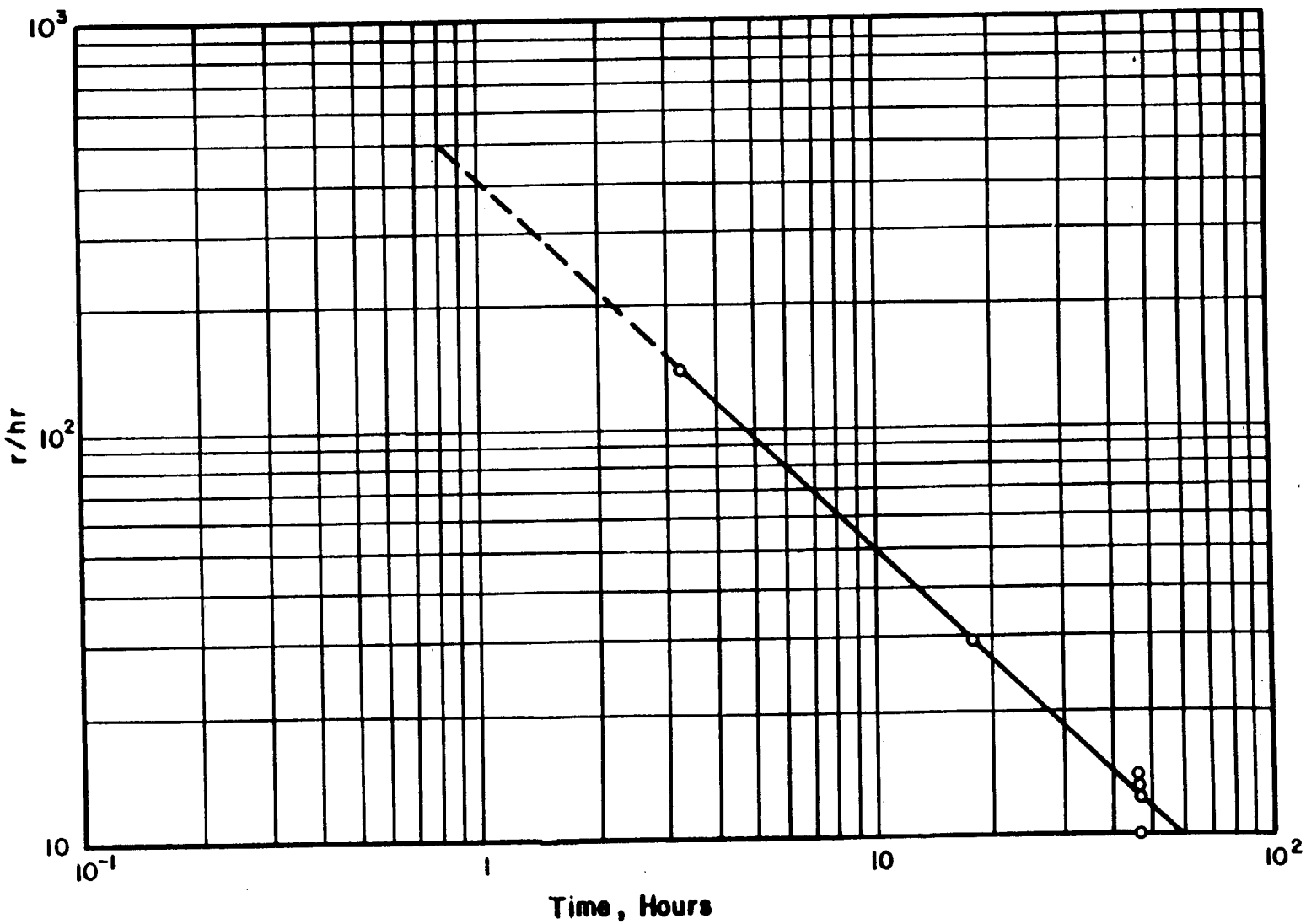

Figure 3.12 Crater data.

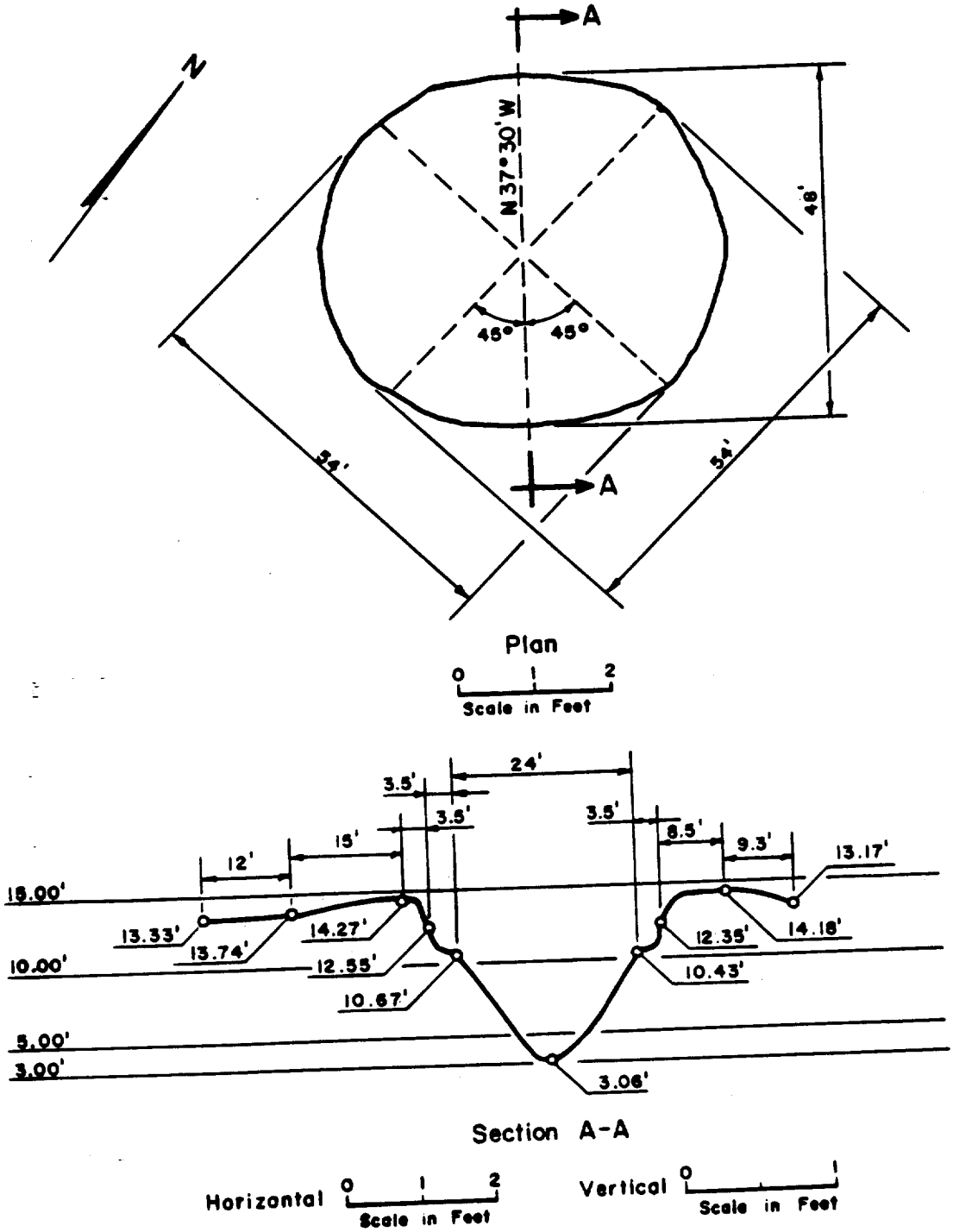

Figure 3.13 Survey of Fig crater on D + 3 days; original ground level, 12.85 feet.

Page 61 deleted.

Chapter 4

CONCLUSIONS AND RECOMMENDATIONS

Shot Fig provided sufficient data to determine the general characteristics of fallout of military importance for small yields.

The scaling techniques in Reference 1 lead to gross overestimates of downwind extent for H + 1 hour dose rates of 100 r/hr and lower for the particular conditions of Shot Fig 15-knot winds). Apparent reasons for the failure are: (1) Cloud height for Shot Fig was considerably greater than that implicitly assumed by the scaling technique. (2) No accounting is made for the drift of the cloud during its rise. (3) Activity distributions with height and fall rate are not similar over the large yield range involved. Scaled estimates are more nearly correct for intensities greater than 100 r/hr.

A dynamic fallout model is proposed (Section 3.11) to estimate close-in fallout from fission weapons of 1- to 100-ton yield. This model accounts for cloud drift and growth and is consistent with Fig measurements of the amount of activity deposited as a function of downwind distance, intensity as a function of downwind distance, and cloud shine.

Calculations made on the basis of this model show that intensities greater than 100 r/hr increase in downwind extent as windspeed decreases, whereas intensities less than 100 r/hr reverse this behavior. This is not consistent with present techniques of accounting for variation in windspeeds where the downwind extent of any intensity is increased with the increase of windspeed. It is recommended that the dynamic model be used to estimate effects of windspeed variation.

Winds that existed during Shot Fig exhibited a very small directional shear, and mean windspeeds ranged from 11 to 16 knots when averaged from pertinent altitudes to the surface. The visible cloud had not reached its ultimate height of 6,000 feet by the time it had drifted beyond the instrumentation array, some 10,500 feet from ground zero.

Only 4 percent of the fission products formed was accounted for within the array. From cloud shine measurements, it was deduced that most of the activity was carried beyond the array in the lower portion of the visible cloud between 0.3 and 0.7 of its maximum height.

The earliest measurement obtained within the crater itself was at H + 3.5 hours, at which time a monitor descended inside the crater lip and recorded about 140 r/hr on the Jordan survey meter. This reading implies an intensity less than 1,700 r/hr at H + 26 minutes, which is a much lower value than that reported in Reference 7. Cave-in of the crater walls could have been responsible for this apparent inconsistency.

The use of $t^{-1.2}$ decay law will generally lead to errors no greater than those involved with dose-rate measurement in the field and is recommended for field use.

Although only a few plutonium contamination measurements were made during Fig, the levels were low enough to indicate that no serious long-term problem would result from this source.

As expected, it was difficult to make completely definitive fall-out radiation measurements without the ability to make full-field dose-rate measurements at any point within the instrumentation array. Use of sticky-pan fallout collectors gave results reasonably consistent with survey meter readings for the high-intensity regions that resulted on the shot

island. A probable error of ±50 percent was indicated in this region. For the low-inten regions of the lagoon, a much larger error was indicated. The use of large barges to co lect fallout for gamma survey measurements aids in fallout studies that have to be conducted over water. If the experiment were repeated over water areas, more extensive u should be made of flat-topped barges.

REFERENCES

1. "Capabilities of Atomic Weapons"; Department of the Army Technical Manual TM 23-200, Department of the Navy OPNAV Instruction 03400.1B, Department of the Air Force AFL 136-1, Marine Corps Publications NAVMC 1104 Rev; Revised Edition, November 1957; Prepared by Armed Forces Special Weapons Project, Washington, D.C.; Confidential.

2. C. F. Ksanda and others; "Scaling of Contamination Patterns, Surface and Underground Detonation"; USNRDL-TR-1, 15 Sep 1953; Naval Radiological Defense Laboratory, San Francisco, California.

3. M. Cowan, Jr.; "Plutonium Contamination from One-Point Detonation of an XW-25"; Program 71, Test Group 57, Operation Plumbbob, WT-1510, November 1960; Sandia Corporation, Albuquerque, New Mexico; Secret Restricted Data.

4. W. E. Knabe and G. E. Putnam; "The Activity of the Fission Products of U^{235}"; January 1959; General Electric Atomic Products Division, Cincinnati, Ohio.

5. P. J. Dolan; "Theoretical Dose Rate Decay Curves for Contamination Resulting from Land Surface Burst Nuclear Weapons"; DASA-528, 6 Aug 1959; Headquarters, Defense Atomic Support Agency, Washington, D.C.

6. E. H. Karstens; "Air Weather Service Participation in Operation Jangle"; Project 1(8)b, Operation Jangle, WT-361, December 1951; Air Weather Service, Armed Forces Special Weapons Project, Washington, D.C.; Unclassified.

7. M. Morgenthau and M. Schumchyk; "Residual Radiation from a Very-Low-Yield Burst"; Project 2.10, Operation Hardtack, WT-1678, December 1960; U.S. Army Chemical Warfare Laboratories, Army Chemical Center, Maryland; Secret Restricted Data.

Pages 67 and 68 deleted.

80-F01-967
AF Div

8

Tentative
Record of Decision

January 15, 1969

426

DRAFT

MEMORANDUM FOR THE PRESIDENT

SUBJECT: Theater Nuclear Forces (U)

Excised Under the Provisions of (The Freedom of Information Act) 5USC552 (b) (1)

Our continuing review of theater nuclear and related chemical and biological forces leads us to the following major conclusions:

1. We buy theater nuclear forces primarily to deter limited nuclear war. If deterrence should fail, these forces give us options to fight such a war. Our recommended forces are generally appropriate in number and mix for the tasks we have identified.

2. The most serious limited war tactic the Pact could use in NATO's Center Region is a tactical nuclear attack using terrain fire against NATO's front-line forces. Unless it is clear to the Pact that NATO's theater nuclear forces could survive such an attack and inflict unacceptable damage on Pact forces, NATO's forces might not deter the Pact. We need to consider terrain fire exchanges between Pact and NATO forces, particularly those initiated by the Pact, to evaluate our deterrent. Our recommended forces and warheads, if properly deployed, should provide an adequate deterrent.

FOI CASE NO. 80-D01-967
Document ___ of ___ Documents

3. Tactical nuclear weapons are not a substitute for conventional forces. If we are losing a conventional war in NATO's Center Region, we may have a nuclear option to counter the advance, but we cannot count either on stopping the advance if the other side also uses nuclear weapons or on limiting further escalation if we initially succeed.

4. It is unlikely that we would need to consider using nuclear weapons in Asia unless the Chinese use them first or assist their allies with massive land forces and we cannot possibly hold conventionally. Even under the latter circumstances, we must carefully weigh the objections to the use of nuclear weapons against the net military benefits we might gain. Now that China has some nuclear capability, we cannot expect to use nuclear weapons in Asia without retaliation.

6. We need only enough lethal chemical capability to deter the Soviets from using chemicals in Europe. If deterrence should fail, this lethal chemical capability will provide us with an option to fight a limited conflict using chemcial weapons. We need some incapacitating chemicals, but only for use in those situations where civilians are mingled with enemy troops.

A summary of theater nuclear forces and warheads is shown on page 5. Detailed tables are attached.

I. THEATER NUCLEAR FORCES IN EUROPE

A. The Role of Theater Nuclear Weapons in Europe

Our basic military objective in Europe is to deter any kind of Warsaw Pact aggression. NATO's conventional forces are approximately in balance with those of the Pact and should be sufficient to deter a conventional attack or contain one if deterrence fails. Our strategic nuclear forces deter a general nuclear war involving attacks on U.S. cities or those of our European allies.

We also want to deter limited nuclear attacks on our theater forces. The Pact might hope to gain an advantage by initiating a limited nuclear attack and quickly destroying a large part of the NATO land forces without destroying much of Germany. If we could destroy 25% to 50% of the Pact land forces in a restrained nuclear retaliation, we could deny them this option. Unless it is clear to the Pact that NATO's theater nuclear forces could survive such an attack and inflict unacceptable damage on Pact forces, NATO forces might have little effect in deterring the Pact.

A further potential objective, but one we could not count on achieving, is defeating the Pact by using theater nuclear weapons if a conventional defense failed. Our analysis shows we cannot expect to remove the Pact's capability to destroy NATO's military forces or society. Thus, we cannot count on controlling territory without having it destroyed. At best we could plan on destroying enough of the Pact forces to prevent them from controlling NATO countries. not deleted

We plan our Europe-oriented theater nuclear forces primarily for deterrence. In doing so, we provide an adequate war-fighting capability. However, we should not buy more forces to provide the capability to fight a limited nuclear war of long duration. It is unlikely that any war in which thousands of nuclear weapons were used could remain limited. We should concentrate new investments on conventional rather than theater nuclear forces. Conventional forces, which compete for the same resources as theater nuclear forces, provide a much better chance of avoiding a nuclear holocaust.

Our stockpile needs for the Center Region are examined below. In the coming year we will analyze our needs in Europe's Southern Region in a similar manner. We have included a discussion of a new concept -- the initial defensive use of nuclear weapons restricted to NATO territory -- which we are asking the JCS and the Services to do additional work on in the future. We are also asking the JCS and the Services to do additional work on the nuclear terrain fire concept.

B. Land Forces in Europe's Center Region

We currently estimate that NATO and the Warsaw Pact could have the following land forces in the Center Region by M+90 in FY 72: NATO--42 division forces (1.4 million men) and the Pact--90 divisions (1.1 million men). The nuclear capabilities of these land forces, excluding ADMs and air defense, are shown below.

Delivery System

Tactical Missiles
Tactical Rockets
Tube Artillery
Totals

C. Nuclear Defense Against a Conventional Invasion in the Center Region With Effects Limited to NATO Territory

If the Warsaw Pact attacked NATO forces with conventional weapons and NATO could not hold, as a minimum level of limited nuclear war we might consider using nuclear weapons in NATO territory alone. Restricting the use of nuclear weapons to friendly territory might be less likely to lead to escalation than attacking targets in East Germany or other Pact countries.

The following scenario illustrates the possible use of nuclear weapons in West Germany to repulse a Pact conventional attack. It is assumed that the Pact attacks in one to three thrusts, NATO forces are pushed back from their main defensive positions, and the local force ratios are such that NATO cannot repulse the attacks conventionally. When the Pact forces have penetrated about 50 kilometers (km) into West Germany, NATO uses nuclear weapons, but only on the Pact divisions (assumed to be about 15 in each thrus that are in NATO territory. NATO is assumed to have about 18 divisions in th 0 to 50 km zone opposing the three thrusts, so only about half of the Pact divisions would have to be defeated to reduce the force ratio to the point where the attack would be stopped.

If nuclear weapons were only used on Pact forces in West Germany, the Pact could not respond with nuclear weapons against NATO forces unless they used them on NATO territory. They would either have to: (1) cease the attack, (2) continue attacking conventionally by bringing in additional forces, (3) escalate the conflict by using nuclear weapons on NATO forces in NATO territory, or (4) combine courses of action (2) and (3). Their forces, are not as well-designed for limited discrete fire attacks as NATO's forces, and any Pact retaliation would appear to be a terrain fire attack over a large area. To deter such a response, NATO must have a survivable theater nuclear capability, or be ready to use strategic weapons in the theater at this point.

D. Nuclear Defense Against Invasion in the Center Region Using Discrete Fire

The discrete fire concept has traditionally been the basis for analyzing our theater nuclear capability. The essence of this concept is that we must accurately locate and hit a target to destroy it.

If the forces were concentrated as they would be for fighting a conventional war, NATO would have enough retaliatory capability to destroy 45% of the Pact's manpower using only a limited terrain fire attack. This should deter the Pact from using nuclear weapons against NATO forces in such a situation since they could not count on achieving a major advantage by doing so. The table on the preceding page includes a first strike by NATO to show that the Pact also has a retaliatory capability.

In the nuclear terrain fire exchange considered above, the total area covered by each side's terrain fire attack is about 7,500 sq are km, or about 3% of the total area of West Germany. Total civilian casualties could be about five million. The use of nuclear weapons, especially terrain fire, is not attractive in such a situation. However, terrain fire would use longer range systems more effectively than discrete fire would for destroying Pact forces, and we need to consider terrain fire as well as discrete fire, to evaluate our theater nuclear deterrent.

If both the NATO and Pact forces were in a dispersed posture to reduce their vulnerability to nuclear attacks, fewer forces would be destroyed in limited terrain fire attacks, since only about 15% and 10% of the Pact and NATO manpower, respectively, might be in the first 50 km zone of the three thrusts. The Pact and NATO would, however, have additional troops along the front and to a greater depth. In a dispersed posture, we assume each side might have about 60% of its troops in the 0 to 100 km zone along the whole German front. With both forces dispersed and with unlimited terrain fire attacks using all tactical land force weapons, the results could be as shown in the next table.

	Initial Forces and Capabilities a/	Capability Remaining After an Unlimited Terrain Fire Exchange
Men (Thousands)		
Nuclear Launchers		
Nuclear Warheads		
Lethal Area (Km^2)		

a/ Excludes tactical air, air defense, and strategic forces (Polaris and MR/IRBMs).

NATO could not cover the whole front (about 750 km) with nuclear terrain fire to as great a depth as the Pact, but NATO forces could still destroy 20% of the Pact manpower in retaliation. On the other hand, the Pact could not count on gaining an advantage by using such a dispersed

posture because in their view NATO might attack first with nuclear weapons to pre-empt a Pact terrain fire attack and destroy about 35% of the Pact manpower (more, if the attack occurred before the Pact forces were well-dispersed). Even if the Pact believed that NATO would not strike first, they would have to consider the possibility of retaliatory U.S. attacks with strategic nuclear forces since terrain fire attacks to a depth of 80 km (destroying as much as 25% of Germany) would not necessarily be considered limited nuclear war.

The foregoing analysis suggests the following conclusions:

1. A survivable theater nuclear capability which could inflict unacceptable damage on Pact forces should deter the Pact from using tactical nuclear weapons. Terrain fire is an option to consider for retaliation to a massive Pact attack which could destroy NATO's front-line forces. Terrain fire could cause more damage to European society than limited discrete fire. However, we cannot reasonably expect a war to stay limited if thousands of nuclear weapons are used for discrete fire.

System	Maximum Range	Percent of Launchers that Might Survive a Terrain Fire Attack Along the Whole Front to Various Depths
Pershing		
Sergeant		
Honest John		
Tube Artillery		

Theater Nuclear Requirements for the Center Region

We cannot plan to fight a limited nuclear war of long duration, using thousands of nuclear weapons in either discrete or terrain fire, because of the vulnerability of most of our warheads and delivery systems, the probable destruction of our support means by enemy attacks, limitations on command and control, and the great pressures to escalate the conflict. We need only enough nuclear weapons to be able to respond up to the point where continued limitation of a nuclear conflict would be very improbable. When additional discrete fire would do as much damage to European society as more effective limited terrain fire attacks, we should consider using terrain fire.

Tactical Bombs
Mace
Pershing
Sergeant
Honest John
Tube Artillery
ADMs
Air Defense
ASW Depth Bombs
Total Nuclear Warheads

Our theater nuclear capabilities are limited far more by our lack of adequate command, control, and support than by the size of our nuclear stockpile. Considering these limitations and the competing demands on our resources, we do not need to maintain such a large stockpile in Western Europe.

IV. CHEMICAL AND BIOLOGICAL WARFARE FORCES

A. Lethal Chemicals

Lethal chemicals can kill many unprotected troops quickly. Casualties are very low against protected troops, but the combat effectiveness of troops in protective clothing is degraded.

We estimate that the Soviets have about 275,000 tons of lethal chemical agents, compared to about 35,000 tons for the United States. (The composition of the U.S. stockpile is shown in the table on page 29.) For defense, we have masks and, to prevent absorption of chemicals through the skin, some old individual protection suits and collective protection devices.

In Soviet doctrine, lethal chemicals are usually considered in conjunction with nuclear weapons. The Soviets could escalate a conventional conflict in Europe by using nuclear weapons or chemicals, or both. Our theater nuclear capability helps to deter their use of nuclear weapons. To deter the Soviets from using chemicals alone, we must be able to prevent them from gaining a significant advantage from their use. To do this we need enough defensive capability to prevent a large number of casualties and an offensive capability to force the Soviets to take protective measures.

Europe is the only area where we need a deterrent against the use of lethal chemicals. The Soviets seem intent on avoiding the use of nuclear weapons in limited conflicts in other areas and probably would also forego the use of chemicals. We have no evidence that the Chinese have a significant lethal chemical war-fighting capability. Our conventional forces provide sufficient alternatives against other countries.

For the defensive component of our lethal chemical deterrent in Europe, we need individual protection (masks and protective suits) for our land forces and forward air bases, some warning capability, and protective shelters for forward medical units. Large numbers of warning devices and protective shelters would contribute to our ability to fight a prolonged war, but would increase our deterrent very little. For the offensive component of our chemical deterrent in NATO's Center Region, we need enough chemical capability to expose unprotected front-line troops to a 10% casualty rate per day for about 10 days of intense combat (equivalent to a 20 to 90 day war, depending on usage rates).

For NATO's Center Region, the approximate additional 10-year costs for equipment and munitions (above our current inventories) to provide a lethal chemical deterrent, which would give us some war-fighting capability, are shown in the next table.

Capability	Additional 10-Year Cost a/ (In $ Millions)
Defensive Protection for 11 U.S. Division Forces (DFs) and 5 Forward Air Bases	$ 400
Offensive Capability for the U.S. and Allied Sectors	140
Total Costs	$ 540

a/ Provides individual protection for troops and a 10-day offensive capability at 750 tons per day.

We should procure the additional equipment to provide a deterrent capability for NATO's Center Region, giving priority to improvements in our defenses against lethal chemicals. We recommend against procuring a chemical capability to fight a prolonged war. Any extensive use of lethal chemicals would probably lead to a nuclear war. We will address our lethal chemical needs for other NATO regions in the coming year.

B. Incapacitating Chemicals (Including Riot Control Agents)

We might benefit from using incapacitating chemicals in situations where civilians are mingled with enemy troops and we do not have reasonable conventional alternatives. For such situations, we could benefit from improvements that would increase the duration of the effects now available with tear gas. However, we should not use incapacitants which make people irrational and unpredictable. Nor should we use presently available chemical incapacitants in ordinary combat against any enemy forces because: (1) feasible conventional alternatives are almost always available, (2) we do not want to risk enemy retaliation with lethal chemicals, and (3) we do not want to risk lowering the barriers to chemical warfare.

For the post-Vietnam Baseline Force, we should stockpile a 30-day supply of tear gas for one DF with air support and one Marine Expeditionary Force (MEF). This is enough for counterinsurgency operations. In addition, we should stockpile enough tear gas for civil disturbances. We should not increase our stockpiles of any other incapacitants until further research and development is done on improved agents.

We recommend disapproving the JCS proposal to buy a chemical incapacitating capability for all land and air forces at a 10-year cost of $440 million (excluding costs for research, development, and operations in Vietnam).

80-FOI-967
AF Div

6

Record of Decision

January 6, 1967

DRAFT

MEMORANDUM FOR THE PRESIDENT

SUBJECT: Theater Nuclear Forces (U)

My continuing investigation of the role of theater nuclear forces has led me to the following major conclusions:

1. Nuclear weapons are not a substitute for nonnuclear capabilities. The growth of Soviet nuclear forces has reached the point where NATO must anticipate extreme damage in a large scale nuclear war. As a result we can no longer be confident that a theater nuclear posture without strong conventional forces will continue to deter Soviet nonnuclear aggression. 1/

2. Nuclear weapons are a necessary complement to nonnuclear forces. They contribute to the deterrence of Soviet attack with tactical nuclear weapons; they will permit us to respond in kind if such weapons are used; they can be used to support our forces if we fail to contain a large scale nonnuclear aggression; they contribute to deterring or fighting general war. 2/

4. Deficiencies in our posture reinforce the incentives to escalate that are inherent in nuclear warfare. Major improvements at acceptable costs can be made with regard to the vulnerability of our strike forces, situation reporting, doctrine for transition from nonnuclear to tactical nuclear conflict, and battlefield intelligence.

1/ The Joint Chiefs of Staff (JCS) would give a somewhat larger role to theater nuclear forces in the deterrence of nonnuclear agression.

2/ The JCS would add that selective application of nuclear weapons could cause de-escalation or termination of conflict.

3/ Ascribing a larger role to theater nuclear forces in general war, the JCS would not focus their design primarily on limited nuclear conflict.

FOI CASE NO. 80-DFOI-967

Document ____ of ____ Documents

Excised Under the Provisions of (The Freedom of Information Act) 5USC552 (b) (1)

I. ROLE OF THEATER NUCLEAR FORCES

The USSR is now approaching parity with the U.S. in theater nuclear weapons (see Annex A page 22) and it appears unlikely that either side can gain sufficient advantage to upset this parity. This development threatens higher damage in the event of nuclear war, compounds the difficulties of constraining conflict, and effectively rules out meaningful military victory. Nevertheless, theater nuclear forces have several important functions.

Deterrence of Aggression. The Soviets might fear that tactical nuclear weapons would bridge the gap between large scale nonnuclear war and general war, and this fear might help to deter them from extreme acts of aggression in Europe or to inhibit escalation by them in war. However since nuclear war would be catastrophic to both sides, Soviet leaders might doubt NATO's resolve to initiate the use of nuclear weapons against limited nonnuclear aggression or to resist such aggression at all if a nuclear response were the only NATO option available.

The major role for theater nuclear forces is to deter nuclear attacks in Europe. A Soviet decision maker considering the initiation of nuclear war in Europe would have to assume U.S. willingness to respond in kind.

General War. Our theater nuclear forces also contribute to deterring or fighting a general nuclear war and to denying the Soviets any prospect, however remote, of overrunning Europe in the course of a general war and capturing Western European productive capacity intact. The contribution of theater nuclear forces to deterring or fighting a general war is small however, relative to that of our strategic forces. The size and characteristics of our theater nuclear forces should not, therefore, be determined by the requirements of general war; their general war capabilities should rather be treated as a bonus.

Tactical Nuclear Option. The principal question about limited nuclear war is whether it will escalate to general nuclear war. Once the "firebreak" between nonnuclear and nuclear war is breached with the first nuclear

weapon, escalatory pressures will rise. Opposing commanders will have strong military incentives to strike opposing nuclear strike forces before they are launched, to attack land forces still concentrated for nonnuclear conflict, to compensate for target acquisition difficulties by directing large yield weapons at likely targets, and to hit logistics concentrations in the rear, rapidly increasing damage to population and industry as the battle proceeds.

The mounting damage as nuclear war grows more violent provides the chief incentive for restraint in nuclear war. The figures in the table below illustrate the increase in civil damage as nuclear war mounts in violence through various hypothetically restrained levels of conflict. The table excludes strategic attacks on targets that are collocated with cities, or attacks on urban targets themselves that could result in European fatalities of 200 million.

CIVILIAN CASUALTIES IN CONSTRAINED NUCLEAR CONFLICT IN EUROPE
(Avoiding Attacks on Towns)

There are a number of additional motives for restraint. Neither side can foresee a clear advantage from escalation to override the many uncertainties in this untried kind of warfare. Nor could "military victory", if achieved, compensate for the casualties that even the initiator would sustain among troops and civilians alike in unlimited nuclear war. The initiator's armed forces, no less than his opponent's, could be destroyed - possibly to the point where he would lose control of even his own territory. Regardless of the initial objectives then, each side would want to avoid general war. It is desirable, therefore, that we be able to recognize enemy restraint if it occurs and be able to fight with restraint ourselves.

In sum, it is impossible to predict with confidence the course of a limited nuclear war. The danger of escalation, once the "firebreak" between nonnuclear and nuclear war has been crossed, and the damage, if escalation occurs, caution against relying on our ability to limit nuclear war and against investing large resources in nuclear capabilities that are important only if the war does remain limited. Our posture and doctrine should be designed, where possible without large sacrifices in resources, to reduce incentives for enemy escalation and to provide inducements for him to observe restraint.

Incomplete Intelligence. The Soviets' combat doctrine suggests that they neither expect nor plan on restraint in using nuclear weapons. The Soviets nevertheless maintain at considerable cost a force which is inherently strong in conventional as well as tactical nuclear capabilities. This suggests that whatever Soviet doctrine and strategy are, their forces still provide them with both nonnuclear and nuclear options that continue to complicate our planning, which is already taxed with broad uncertainties concerning the size and yields of Soviet tactical nuclear stockpiles.

Inadequate Situation Reporting Machinery. Long time lags - often many hours in duration - occur before decision makers at theater levels learn of the full combat situation at the front. Inaccuracies in reporting enemy nuclear strikes compound the problem. As a result decision makers may wait too long in releasing nuclear weapons or make a hasty decision in favor of employing nuclear weapons in circumstances which would be more suitably handled without them if the situation were better known. We should be able to improve our reporting machinery substantially.

Vulnerable Nuclear Strike Forces. Our overseas nuclear strike forces consist mainly of tactical aircraft based on easily targeted airfields within range of Soviet IR/MREM forces which are so numerous as to render additional dispersal of SACEUR strike aircraft an insufficient remedy for their vulnerability. Prior to the Soviet IR/MREM force buildup, these aircraft played a major role in SIOP planning because of the timeliness of their strikes as compared to those of intercontinential bombers. However, in view of their current vulnerability to IR/MRBMs these aircraft can no longer be depended upon for crucial SIOP tasks. We must now begin to rely more upon our growing mobile Pershing missile forces which would be much less vulnerable after they deployed from their peacetime stations and began moving randomly among previously unoccupied sites in periods of strategic warning. Their lower vulnerability should enhance the stability of the deterrent at the theater level in crisis.

Decision time is further related to the degree of military and political understanding of nuclear options available. Our dual capable delivery systems and spread of yields provide a wide range of options, ranging from the subkiloton ADMs, bombs, and accurate howitzers to the larger air and missile delivered yields and ranges. In order to streamline procedures and render this capability most effective, various studies have proposed that several levels of response be planned; for example: subkiloton ADMs only; subkiloton ADMs, Davy Crockett and 155mm; all battlefield weapons under 2 kilotons; targets only within range of battlefield weapons; etc. This general approach appears to be worth further development. The JCS are studying it.

It is pertinent to note that in the twelve years since political guidance was issued to SACEUR the Alliance has not achieved a workable mechanism for resolving divergent national views. Individual allied officers have been integrated into NATO nuclear planning at military levels, but to date there has been practically no national participation. A permanent arrangement should be made at the highest political-military level to study nuclear problems and assist in working toward an alliance consensus. The NPWG reached similar conclusions at its meeting in London in April 1966. Such arrangements should permit continuation of fruitful information exchanges and provide a useful arena in which the U.S. can develop further its case on the role of nuclear forces in NATO strategy.

JOINT PUB 3 -12

DOCTRINE

FOR

JOINT NUCLEAR

OPERATIONS

29 APRIL 1993

#652

TABLE OF CONTENTS

CHAPTER PAGE

I OBJECTIVES I-1

General I-1
The Spectrum of Potential Conflict I-2

II EMPLOYMENT OF FORCES II-1

Fundamental Considerations II-1
Considerations in Force Planning and Employment II-2
Targeting Considerations II-4
Operations in a WMD Environment II-7

III INTEGRATED OPERATIONS III-1

Strategic Force Integration III-1
Nonstrategic Nuclear Force Integration III-2
Offense/Defense Integration III-6

APPENDIX

A TREATY OBLIGATIONS A-1
B USER EVALUATION REPORT B-1

GLOSSARY

Part I--Abbreviations and Acronyms GL-1
Part II--Terms and Definitions GL-2

CHAPTER I

OBJECTIVES

1. General

a. National Security Objectives and Nuclear Forces. The permanent security interest of the United States is its survival as a free and independent nation, with its fundamental values intact and its institutions and people secure. This is best achieved by a defense posture that makes possible war outcomes so uncertain and dangerous, as calculated by potential enemies, as to remove all incentive for initiating attack under any circumstance. Thus, the fundamental purpose of US nuclear forces is to deter the use of weapons of mass destruction (WMD), particularly nuclear weapons, and to serve as a hedge against the emergence of an overwhelming conventional threat.

b. Strategy. Creditable and capable nuclear forces are essential for national security. During World War II, nuclear weapons were instrumental in ending the war on terms favorable to the allies. The US post-war strategy has been one of deterrence, and nuclear forces have been developed, deployed, and maintained for the purpose of deterring large-scale aggression against the United States and its allies.

c. Object of Deterrence. The political leadership of an opposing nation is the central object of deterrence because that is where the ultimate decision to use military force lies. Deterrence in the form of a large-scale attack (either WMD or conventional) requires that US forces and command and control (C2) systems be viewed by enemy leadership as capable of inflicting such damage upon their military forces and means of support, or upon their country, as to effectively deny them the military option. Deterrence of the employment of enemy WMD, whether it be nuclear, biological, or chemical, requires that the enemy leadership believes the United States has both the ability and will to respond promptly and with selective responses that are credible (commensurate with the scale or scope of enemy attacks and the nature of US interests at stake) and militarily effective. Any deterrence assumes an opposing nation's political leadership will act according to the logic of national self-interest, although this self-interest will be viewed through differing cultural perspectives and the

dictates of given situations. Although nations possessing WMD have largely refrained from using them, their continuing proliferation and the means to deliver them increases the possibility that someday a nation may, through miscalculation or by deliberate choice, employ those weapons. This assumption does not rule out the possibility that an opponent may be willing to risk destruction or disproportionate loss in following a course of action based on perceived necessity, whether rational or in a totally objective sense. In such cases deterrence, even based on the threat of massive destruction, may fail.

d. Force Capabilities. Deterrence is founded in real force capabilities and the national determination to use those forces if necessary. To have a credible effect on an adversary, US military forces must be capable of achieving US national objectives throughout the operational continuum. Capabilities must range from nation building or civil military operations through direct denial of battlefield objectives and conventional defeat of enemy forces to the full-scale destruction of enemy warmaking and economic infrastructures, while minimizing the enemy's ability to retaliate. These capabilities require maintaining a diverse mix of conventional forces capable of high-intensity, sustained, and coordinated air, land, and sea operations; survivable and capable nuclear forces; and the command, control, communications, and computer systems required to control these forces. The mix of these forces must be capable of holding at risk those assets most valued by enemy leaders and providing a range of options in response to attack. It is possible, however, that an adversary may misperceive or purposefully ignore a credible threat. Therefore, should deterrence fail, forces of all types (both conventional and nuclear) must be structured, deployed, and ready to provide a variety of options designed to control escalation and terminate the conflict on terms favorable to the United States and its allies.

2. The Spectrum of Potential Conflict. US nuclear forces serve to deter the use of WMD across the spectrum of potential conflict. From a massive exchange of nuclear weapons to limited use on a regional battlefield, US nuclear capabilities must confront an enemy with risks of unacceptable damage and disproportionate loss should the enemy choose to introduce WMD in a conflict.

a. Peacetime and Crisis Considerations

(1) Forces and Strategy. Deterence must be carefully weighed in the design of US forces and strategy. As a minimum, nuclear forces and strategy must pass the following tests:

(a) Survivability. US forces must be able to survive a first strike and endure conventional and escalatory attrition with sufficient retaliatory strength to inflict unacceptable damage on the enemy in a counterstrike.

(b) Credibility. The potential aggressor must believe the United States could and would use nuclear weapons to attain its security objectives.

(c) Safety. The risk of failure through accident, unauthorized use, or miscalculation must be minimized.

(d) Security. Secure manufacture, transportation, and storage that are free from terrorist threat, theft, loss, and unauthorized access must be provided.

(2) Regional Contingencies. WMD deterrence should be the first priority. The proliferation of WMD technologies and industrial capabilities in the world may allow a potential aggressor to develop a WMD arsenal capable of being employed against US forces deployed to a regional crisis. WMD used on US forces would cause a significant tactical or operational loss; greatly change the character of the war, putting the outcome in doubt and threatening escalation; leave the United States with a difficult choice: to retaliate or not to retaliate. A selective capability of being able to use lower-yield weapons in retaliation, without destablizing the conflict, is a useful alternative for the US National Command Authorities (NCA).

(3) Conventional Threats. Because nuclear forces also serve as a hedge against the emergence of an overwhelming conventional threat, the deterrent effect of nuclear weapons extends to enemy calculations concerning conventional conflict as well. The potential employment of nuclear weapons at theater level, when combined with the means and

resolve to use them, makes the prospects of conflict of any type more dangerous and the outcome more difficult to assess. The resulting uncertainty could reduce a potential aggressor's willingness to risk escalation by initiating conflict. At the same time, a credible defensive capability that includes the means to threaten to employ nuclear weapons could bolster the resolve of allies to resist enemy attempts at political coercion.

(4) Conflict Avoidance. Conflict can often be avoided by pursuing alternative mechanisms and disincentives to conflict such as nonproliferation, counterproliferation, arms control and verification, and confidence building measures during peacetime operations. These measures make conflict or war less likely by improving communication, reducing opportunities for miscalculation, providing ways to resolve crises, and reducing the destructive capacity of available arsenals.

(5) Readiness. Increased readiness levels may be necessary to deter aggression. Consequently, an increased risk of attack, prompted by enemy war readiness measures, may require that US forces be maintained at visibly increased states of alert. Certain types of delivery systems can be postured to send a clear warning. Alert posturing of nuclear delivery systems to dispersal locations can send a forceful message that demonstrates the national will to use nuclear weapons if necessary. For example, the generation of nuclear forces to higher alert levels during the October 1973 Mideast Crisis sent a strong signal. However, the danger also exists that the enemy may perceive either an exploitable vulnerability or the threat of imminent use. Therefore, increased readiness postures intended to signal national resolve must be accompanied by measures that would allow for deescalation. Public affairs measures must also be taken to minimize the possibility that public concern over the conflict might develop into mass panic upon implementation of US readiness measures.

(6) Escalation. Should a crisis become so severe as to prompt the United States to place all its nuclear forces at a high level of readiness, the United States must also be prepared to posture its nuclear forces as quickly as possible. Nuclear forces should be generated and managed to ensure a sustained high

level of readiness. Conventional forces and intelligence activities would have to be prudently managed to ensure avoidance of inadvertent escalation or mistaken warnings of nuclear attack. In the event the crisis is successfully resolved without employment of nuclear weapons, reductions in the alert posture of nuclear forces must be carefully managed, taking into account enemy force readiness. This would ensure that no destabilizing military advantage accrued to the enemy during the de-escalation phase of the conflict.

b. Wartime Considerations

(1) Deterring the Use of WMD. In war, as in peacetime or during crisis, deterrence of WMD attack depends on the enemy's perception of its warfighting (and winning) capabilities and will relative to those of the United States. However, wartime circumstances may alter such perceptions, possibly because of changes in the strategic situation. Shifts in the strategic balance may result from military action in which one side suffers significant destruction of military forces and industrial and economic infrastructures. Thus, a prolonged conventional conflict may lower the nuclear threshold by posing greater costs to a nation and, therefore, make nuclear attack appear to be a less risky option.

(2) Failure of Deterrence. Should deterrence fail, it is the objective of the United States to repel or defeat a military attack and terminate the conflict on terms favorable to the United States and its allies. Accomplishing this objective requires the capability for measured and effective response to any level of aggression while seeking to control the intensity and scope of conflict and destruction. Employment plans, in conjunction with political and other military action, must provide for selected military operations. Specific nuclear objectives are specified in Annex C to the Joint Strategic Capabilities Plan (JSCP).

(3) Controlling Escalation. Nuclear weapons may influence the objectives and conduct of conventional warfare. Additionally, conventional warfare may result in attrition of nuclear forces and supporting systems (through antisubmarine warfare, conventional attacks in theater, sabotage, or antisatellite warfare), either unintended or deliberate, which

could affect the forces available for nuclear employment. If this attrition results in a radical change in the strategic force posture by eliminating intermediate retaliatory steps, there may be a rapid escalation. The ability to precisely gauge the attrition of conventional and nuclear forces will directly effect calculations on the termination of war and the escalation to nuclear war.

c. Post-Wartime Considerations

(1) War Termination. The fundamental differences between a potential nuclear war and previous military conflicts involve the speed, scope, and degree of destruction inherent in nuclear weapons employment, as well as the uncertainty of negotiating opportunities and enduring control over military forces. Depending on the scope and intensity of a nuclear war, how and under what conditions it is brought to a conclusion may be very different from previous wars. Terminating a global war involving the use of large numbers of WMD on both sides and the degradation and or destruction of their central means of control could be vastly more difficult than ending a theater or regional nuclear conflict involving the relatively constrained use of a limited number of nuclear weapons. In the latter case, war-termination strategies may more readily lead to a cessation of hostilities, assuming that the belligerents' interests in war termination are mutual.

(2) Termination Strategy. The objective of termination strategy should be to end a conflict at the lowest level of destruction possible, consistent with national objectives. However, there can be no assurances that a conflict involving weapons of mass destruction could be controllable or would be of short duration. Nor are negotiations opportunities and the capacity for enduring control over military forces clear. Therefore, US nuclear forces, supporting command control, communications, computer, and intelligence (C4I) systems (e.g., sensors, communications, command facilities), and employment planning must provide the capability to deny enemy war aims, even in a conflict of indefinite duration.

(3) Reserve Forces. Adequate nuclear reserve forces reduce opportunities for another nation to dominate or coerce behavior before, during, or after the use of WMD. Such forces provide the US with the capability to continue to deny enemy war aims, influence other nations, and exert leverage for war termination.

CHAPTER II

EMPLOYMENT OF FORCES

1. Fundamental Considerations

a. Implementing the National Military Strategy. The decision to employ nuclear weapons at any level requires the explicit decision of the President. Senior commanders should be consulted and, based on their considered judgment, make recommendations affecting nuclear policy decisions on force structure, weapons and/or force capabilities, and alternative employment options. Consequently, those responsible for the operational planning and the direction of US nuclear forces must fully appreciate the numerous and often complex factors that influence the US nuclear planning process, and would likely shape US decisions on the possible use of nuclear weapons. Clearly, the use of nuclear weapons represents a significant escalation from conventional warfare and is caused by some action, event, or perceived threat. However, the fundamental determinant of action is the political objective sought in the use of nuclear or other types of forces. The decision to use nuclear weapons involves many political considerations. Together, these considerations will have an impact not only on the decision to use nuclear weapons, but also on how they will be employed. Other prominent planning and employment factors include the strategic situation, type and extent of operations to be conducted, military effectiveness, damage-limitation measures, environmental and ecological impacts, and how such considerations may interact.

b. International Reaction. International reaction toward the nation that first employs WMD is an important political consideration. The United States and its allies have articulated their abhorrence of unrestricted warfare, codifying "laws of war" and turning to definitions of "just war." The tremendous destructive capability of WMD and the consequences of their use have given rise to a number of arms control agreements (refer to Appendix A) restricting deployment and use, and in the case of the 1987 Intermediate-range Nuclear Forces Treaty, even prohibiting the development of an entire class of weapons. At the same time, it is important to recognize that there is no customary or conventional international law to prohibit nations from employing nuclear weapons in armed conflict. Therefore, the use of

nuclear weapons against enemy combatants and other military objectives is lawful. The nation that initiates the use of nuclear weapons, however, may find itself the target of world condemnation.

2. Considerations in Force Planning and Employment

a. Employment Options. Combatant commanders responsible for the employment of nuclear forces must ensure those forces are fully capable of executing the full range of employment options required by the NCA. To this end, employment planning must fully consider the characteristics and limitations of the nuclear forces available and seek to optimize both the survivability and combat effectiveness of these forces.

b. Characteristics. To provide the desired capabilities, nuclear forces must be diverse, flexible, effective, survivable, enduring, and responsive. If no one weapon system possesses all of the desired characteristics, a variety of systems may be necessary.

(1) Force Diversity. To confront any potential aggressor with insurmountable attack and defensive problems and to hedge against the failure of any one US component, nuclear forces must be diverse. The United States maintains a strategic Triad of intercontinental ballistic missiles (ICBMs), sea-launched ballistic missiles (SLBMs), and bombers as a hedge against unforeseen developments that might threaten US retaliatory capabilities. Each leg of the Triad has unique capabilities that complement those of the other legs. Nonstrategic nuclear forces (NSNF) offer options short of strategic response in those situations where escalation control is desired. In addition, NSNF increases the overall deterrent value of US forces by their direct deterrence at regional level. Both strategic and nonstrategic nuclear forces hold regional targets at risk.

(2) Flexibility and Effectiveness. To provide deployment and employment options that allow the United States to maintain effective deterrence and, if necessary, successfully execute a broad array of missions against the full spectrum of potential targets, forces must be flexible and effective. Flexibility allows engaging the enemy at an appropriate level or place with the capability of escalating or de-escalating the level of conflict, if desired. Flexibility is important because deterrent credibility hinges on having a convincing capability

to execute a variety of nuclear and nonnuclear options. The flexible application of responses tailored to the provocation would afford greater control over the possible escalation of conflict. Flexibility is also essential in escalation management because available nuclear and conventional weapons can be tailored for specific military and political outcomes without destablization of the conflict.

(3) Survivability and Endurance. US nuclear forces and C4I must be able to survive enemy attacks to convince potential aggressors that, in any scenario, sufficient US capability will remain to deliver a devastating retaliatory strike. Nuclear forces and C4I must also be able to survive enemy attacks for both warfighting utility and deterrence purposes. Survivability is enhanced by a combination of multiple redundant systems, mobility, number of weapons, hardened sites, and employment concept. (For example, mobility, increases survivability, because the forces cannot be attacked with any certainty of destruction due to the unpredictability of the location of the weapon at the time of attack.) Survivability also strengthens deterrence by providing nuclear forces for continued retaliation against the enemy.

(4) Responsiveness. Some targets must be struck quickly once a decision to employ nuclear weapons has been made. Just as important is the requirement to promptly strike high-priority, time-sensitive targets that emerge after the conflict begins. Because force employment requirements may evolve at irregular intervals, some surviving nuclear weapons must be capable of striking these targets within the brief time available. Responsiveness (measured as the interval between the decision to strike a specific target and detonation of a weapon over that target) is critical to ensure engaging some emerging targets.

c. Other Considerations. Strategic stability, centralized control, and C4I systems are also important considerations in nuclear force planning and employment.

(1) Strategic Stability. A crucial goal in designing and fielding US nuclear forces is to forge a balance of military capabilities between the United States and potential adversaries that reduces the incentives for potential adversaries to seek a

decisive military advantage (in peacetime military operations or in hostilities other than war) or to initiate conflict. Such stability is a function of relative capabilities at all potential levels of conflict and requires the constant assessment of nuclear and conventional forces.

(2) Centralized Control. Centralized control ensures that US national policy decisions directly affect deployment or employment of nuclear forces. Militarily, centralized control provides clarity of purpose and unity of command while ensuring nuclear forces are responsive, properly used, and integrated. It guides a broad plan of action while providing the flexibility for subordinate commanders to plan authorized attacks in the most operationally effective manner.

(3) C4I. C4I must support the employment of nuclear weapons through all phases of a conflict. C4I must be able to provide the appropriate political and military authority with a survivable, secure, and endurable C4I capability through which execution, direction, assessment, and termination of nuclear operations can be ensured during all phases of a conflict, especially in its termination. Reporting residual capability assessment information through C4I systems is essential to providing the NCA with an understanding of the military capabilities remaining in a post-attack environment. Because of their central importance to US response capabilities, the destruction or degradation of C4I systems will likely be a primary enemy objective. Consequently, such systems must be robust, redundant (where essential to guarantee continuity of operations), and rapidly recoverable.

3. Targeting Considerations

a. Preplanning. Guidance for planning nuclear strikes is promulgated from the NCA to the combatant commanders through documents such as National Security Directives, the Policy Guidance for Nuclear Weapons Employment, and/or the JSCP, Annex C. The combatant commanders then preplan nuclear targets using this guidance.

b. Target Planning. Conditions leading to US employment of nuclear weapons may not necessarily lead to an all-out exchange of WMD. Consequently, several strategies or factors must be considered in planning joint nuclear operations.

(1) Countervalue Targeting. Countervalue targeting strategy directs the destruction or neutralization of selected enemy military and military-related activities, such as industries, resources, and/or institutions that contribute to the enemy's ability to wage war. In general, weapons required to implement this strategy need not be as numerous or accurate as those required to implement a counterforce targeting strategy, because countervalue targets generally tend to be softer and unprotected in relation to counterforce targets.

(2) Counterforce Targeting. Counterforce targeting is a strategy to employ forces to destroy, or render impotent, military capabilities of an enemy force. Typical counterforce targets include bomber bases, ballistic-missile submarine bases, ICBM silos, antiballistic and air defense installations, C2 centers, and WMD storage facilities. Generally, the nuclear forces required to implement a counterforce targeting strategy are larger and weapon systems more accurate, than the forces and weapons required to implement a countervalue strategy, because counterforce targets generally tend to be harder, more protected, difficult to find, and more mobile than countervalue targets.

(3) Prioritization of Targets. Targets are normally prioritized based upon the overall targeting strategy. Further refinement of target priorities will be made within each target category (e.g., industrial, military, energy facilities, storage facilities, weapon storage areas) based on the operational situation and the objectives established by the appropriate command authority.

(4) Layering. Layering is a targeting methodology that plans employing more than one weapon against a target to increase the probability of its destruction or to improve the confidence that a weapon will arrive and detonate on that target and achieve a specified level of damage.

(5) Crosstargeting. At the same time it incorporates the concept of "layering," crosstargeting also uses different platforms for employment against one target to increase the probability of at least one weapon arriving at that target. Using different

delivery platforms such as ICBMs, SLBMs, or aircraft-delivered weapons increases the probability of achieving the desired damage or target coverage.

(6) Preplanned Options. Preplanned options are a means of maintaining centralized control while minimizing the impact on response time. These options should be capable of being executed individually or in combination with other options to expand the attack either functionally or geographically.

(7) Emergent Targets and Adaptive Planning. Even after the initial laydown of nuclear weapons, there may be a residual requirement to strike additional (follow on and/or emerging) targets in support of retaliatory or war-termination objectives. Commanders must maintain the capability to rapidly strike previously unidentified or newly emerging targets. This capability includes planning for and being able to perform "ad hoc" planning on newly identified targets and maintaining a pool of forces specifically reserved for striking previously unidentified targets. It is important to recognize that success in engaging emerging targets depends heavily upon the speed with which they are identified, targeted, and struck.

(8) Collateral Damage. US forces will limit collateral damage consistent with employment purposes and desired effect on the target (see JSCP, Annex C, for a more detailed discussion).

(9) Damage Criteria. Damage criteria are standards identifying specific levels of destruction or materiel damage required for a particular target category. These criteria are normally levied on the executing commander by higher authority, in accordance with national strategy and policy. These criteria vary for the intensity of the damage and also vary by particular target category, class, or type. Commanders must estimate the number and characteristics of the weapons and delivery systems that will be needed to achieve the level of desired damage to designated targets while minimizing undesirable collateral effects. Damage criteria, based on the nature of the target (size, hardness, mobility) as well as its proximity to military or nonmilitary assets, provide a means by which to determine how

best to strike particular targets and, following the attack, to evaluate whether the target or target sets received the amount of damage required to meet operational objectives.

4. Operations in a WMD Environment

a. WMD Effects. The immediate and prolonged effects of WMD--including blast, thermal radiation, prompt (gamma and neutron) and residual radiation--pose unprecedented physical and psychological problems for combat forces and noncombatant populations alike. Not only must US forces be prepared to survive and perhaps, operate in a WMD environment for long periods of time, but they must have effective, sustained C4I to accomplish their missions. Military planners must contend with significant challenges in a WMD environment. When planning operations in such an environment, planners should refer to authoritative documents detailing WMD effects published by the Department of Defense, Department of Energy, or qualified scientific authority and incorporate mitigating or avoidance measures into operational planning.

b. Mitigation Efforts. Mitigation of WMD effects, and at least partial preservation of the operational and functional capabilities of people and equipment, requires the following specific actions be taken by commanders:

(1) Plan in advance and warn personnel. Planning and warning, in conjunction with systematic, precautionary survivability measures (such as dispersal of vital combat and support assets, increased force mobility, concealment, deception, individual protective measures, and nuclear hardening) can reduce the physical and psychological trauma.

(2) Partially offset long-term degradation of effectiveness produced by nuclear, biological, and chemical warfare through comprehensive force training, preconditioning, and protection.

(3) Establish and carefully assess operating procedures to avoid disproportionate or unacceptable loss of personnel, units, or equipment and to ensure continuity of operations during the initial and subsequent phases of a conflict involving WMD.

~~SECRET~~

HEADQUARTERS
COMMANDER IN CHIEF
U.S. PACIFIC COMMAND

USCINCPAC RECOVERY PLAN
(U)

CLASSIFIED BY CHIEF OF STAFF, HQ CINCPAC

~~FORMERLY RESTRICTED DATA~~

UNAUTHORIZED DISCLOSURE SUBJECT TO ADMINISTRATIVE AND CRIMINAL SANCTIONS. HANDLE AS RESTRICTED DATA IN FOREIGN DISSEMINATION. SECTION 144b, ATOMIC ENERGY ACT, 1954.

#6

COPY NO 1 OF 105 COPIES

JCS 2534/15

~~SECRET~~

Declassified exact version FOIA #7777 2/2/87 6

3/6 (11 Jan 86)

[redacted]

3. (U) UPON IMPLEMENTATION OF THE PLAN

a. (U) Who were the perpetrators? How many were involved?

b. (U) What weapons, tactics, etc., were used?

c. (U) When do they plan to move the nuclear material/weapon?

d. (U) How do they plan to move it?

e. (U) What will it be used for? What purpose will its use serve? What time-line will serve this purpose?

f. (U) Where is it? Where will it be used?

g. (U) How it is secured? By how many? With what weapons?

h. (U) How is it stored?

i. (U) What are the access, terrain, and physical security factors of location where weapon is hidden?

[redacted]

HEADQUARTERS
COMMANDER IN CHIEF, US PACIFIC COMMAND
CAMP H. M. SMITH, HI 96861
11 June 1984

APPENDIX 1 TO ANNEX L TO USCINCPAC RECOVERY PLAN (U)
OPSEC ESTIMATE (U)

[redacted]

2. (U) ESSENTIAL ELEMENTS OF FRIENDLY INFORMATION

a. (U) What US sensor capabilities exist to detect nuclear materials? How are they deployed? Who controls their capabilities?

b. (U) What is US knowledge of terrorist groups? What level of cooperation exists among US agencies that track terrorist groups? How quickly is information exchanged/provided the United States?

c. (U) What are US and allied capabilities to track trucks, aircraft, and ships/boats and determine quickly the legitimacy of cargo?

e. (U) What US and friendly forces are likely to be tasked to train and prepare for nuclear weapons recovery missions? How will they be commanded and what communications nets will be used to control them? What commanders will be involved? What indicators are provided by patterns/volumes of communications (including telephone calls) that nuclear weapons have been located and that forces are deploying?

f. (U) Where can explosive ordnance disposal (EOD) personnel come from? How skilled are they at handling nuclear weapons? What indicators show EOD personnel are readying for movement? Have they deployed?

CLASSIFIED BY: DEPUTY CHIEF OF STAFF
DECLASSIFY ON: OADR

[redacted]

UNCLASSIFIED

[redacted]

048-4S-13665/102

FOR FURTHER TRAN

AD C014341

RDA-TR-4301-001

A SOVIET PARAMILITARY ATTACK ON U.S. NUCLEAR FORCES - A CONCEPT (U)

NOVEMBER 1974

JUN 1 - 1995

THIS DOCUMENT HAS BEEN DOWNGRADED TO UNCLASSIFIED BY AUTHORITY OF THE DIRECTOR ARPA, S&IO

By:
L.G. GREF
A.L. LATTER
E.A. MARTINELLI
H.P. SMITH

Sponsored by:
DEFENSE ADVANCED RESEARCH PROJECTS AGENCY
ARPA Order No. 2558

AD No.
DDC FILE COPY

The views and conclusions contained in this document are those of the authors and should not be interpreted as necessarily representing the official policies, either expressed or implied, of the Defense Advanced Research Projects Agency or the United States Government.

DDC
RECEIVED
JUN 6 1978
D

R & D ASSOCIATES
Post Office Box 3580
Santa Monica,
California, 90403

525 WILSHIRE BOULEVARD • SANTA MONICA • TELEPHONE: (213) 451-5838

NATIONAL SECURITY INFORMATION
Unauthorized Disclosure Subject to Criminal Sanctions.

DD254 DTD 9AUG74
CLASSIFIED BY MDA903-74-C-0090
EXEMPT FROM GENERAL DECLASSIFICATION SCHEDULE OF EXECUTIVE ORDER 11652
EXEMPTION CATEGORY 3
DECLASSIFY ON INDEFINITE

S 15015-C. 102

[redacted]

UNCLASSIFIED

SECTION 1. INTRODUCTION (U)

(U) (C) This paper discusses a possible military threat to the U.S. that has received little attention: namely, a Soviet paramilitary attack on the U.S. and NATO nuclear forces. Such an attack could be carried out by a well-trained, suitably equipped Soviet paramilitary force of perhaps a thousand, working in units of one or two. In principle, these people could enter surreptitiously into the U.S. and other NATO countries, and destroy their assigned targets—the ICBMs, strategic bombers, SSBNs, and NATO nuclear delivery systems—at a predesignated time.

(U) (C) This threat is a variant of the well recognized threat posed by terrorist groups that might seek to steal or destroy one or several nuclear weapons. A paramilitary group organized and supported by the economic and technical resources of the Soviet Union could represent the ultimate clandestine threat to the U.S. nuclear forces.

(U) Whereas paramilitary operations in the past have met with considerable success against limited objectives, they have not been a significant factor in the outcome of a conventional war between two major powers. Before the era of nuclear weapons, a paramilitary force would have had to destroy many tens of thousands of targets to impair a major military power's capability and willingness to resist domination. These targets included military units, logistic support, industrial capacity and population centers. A coordinated attack involving tens of thousands of elements on such a vast target system constituted a major military operation, and paramilitary actions could play only a minor role. Nuclear strategic war, however, is quite different because the destruction of only a few thousand easily identified, lightly guarded and generally insolated targets—the nuclear delivery platforms—could significantly change the strategic balance and could be decisive. Such a limited target system is peculiarly vulnerable to attack by paramilitary means.

(U) (C) It is an irony of the nuclear age that the deployment of vastly more destructive weapons by the major military powers has, by its very nature, increased the vulnerability of the superpowers to attack by the small, highly motivated, professional forces that characterized military operations of the more distant past. The question, of course, arises as to whether Soviet use of such tactics to destroy the modern nuclear arsenal of the U.S. is credible. Military operations planners may argue that such an attack is too elegant for practicality, too subject to random chance, and has too low a probability of success. However, the probability of success, from the Soviets' viewpoint, will depend to a large extent on their care and completeness in planning and the extent of U.S. preparedness, including planning and countermeasures. It is our purpose here to establish that this military threat deserves more definitive study and documentation.

SECTION 2. CREDIBILITY (U)

(U) To establish the credibility of such a threat requires a study effort which seeks in-depth answers to many questions. No attempt will be made to do that in this concept paper; rather, only plausibility arguments will be presented. The remainder of this section develops a plausibility argument to show that a small Soviet force could be assembled, trained, and moved to the strategic nuclear delivery systems inside the U.S. and NATO countries.

(U) It is unlikely that the U.S. would detect the existence and purpose of this force before attack. We estimate that such a force would constitute less than one percent of the Warsaw Pact's present paramilitary capability, which includes 50,000 dedicated troops, together with oth[redacted] paramilitary units such as those of the KGB.

(U) For example, the possibility of moving paramilitary units through Mexico, into the U.S. and to their targets, without detection, seems serious when one considers the limited effectiveness of the U.S. internal security forces in stopping illegal traffic in aliens and narcotics. The probability of a paramilitary unit being detected or captured prior to the attack could be further minimized by maintaining the independence of the units and limiting their interaction with each other and with the U.S. populace. The usual procedure of limiting the detailed knowledge of any unit to that required for performance of its precise mission would severely constrain the information that might be obtained from a paramilitary unit, which in turn might be interrogated by U.S. authorities. A judicious choice of the time and conditions for the attack, for example during detente, would further reduce the credibility of any defecting or captured unit. In addition, the Soviets would probably delay and confuse any U.S. reaction by disguising the attack under a cloak of U.S. terrorist or fanaticist activity. As a result, it might be weeks before the U.S. could establish the credibility required to take serious

action. Moreover, if the U.S. is unprepared for such an attack, the probability that a paramilitary force could move to the nuclear targets without detection would be enhanced.

(U) (C) It might be argued that a paramilitary attack requires sufficient simultaneity to preclude U.S. nuclear retaliation during the attack. In addition, it might be argued that at least some of the SSBNs at sea would survive a paramilitary attack with more than enough nuclear warheads to destroy an unacceptably large portion of the Soviet urban industrial base. Thus, it might be concluded that the Soviets would be deterred from employing a paramilitary attack against our land-based nuclear forces and hence such attacks need be of little concern to us.

(U) (C) These same arguments apply to the deterrence of a Soviet nuclear attack against our nuclear forces, but with one important difference: the paramilitary attack could be achieved by nonnuclear means and at such a low level of violence that collateral damage to the U.S. value system would be insignificant. As a result, the U.S. might be more reluctant to use its nuclear forces during a paramilitary attack or to use whatever nuclear forces remained after the attack. This would be especially true if, as a result of the paramilitary attack, the Soviets were to obtain a vastly superior strategic position over the U.S. and NATO nuclear forces.

(U) (C) In such a circumstance we would have no incentive to use nuclear weapons. If the Soviets provided additional incentive through other overt acts, they might well expect that under these circumstances we would lack the resolve to initiate the use of nuclear weapons—a resolve that has been questioned even with nuclear parity—as a response to a nonnuclear attack of Europe. Therefore, the expectation of some surviving U.S. nuclear force cannot be counted on to deter the Soviets from executing and exploiting a paramilitary attack as part of a larger war plan, e.g., the takeover of Western Europe.

(U) (C) Actually, it is not obvious that a significant residual force will remain. We will show later that many SSENs at sea could be compromised by conventional sabotage, a tactic well known to the paramilitary operatives. The problem of locating the SSBNs at sea is a matter of degrees of difficulty. On the first launch of a missile, the SSBN is rather easily located. During pre-launch, they are somewhat more difficult to find, and during patrol, they can be detected and tracked only at considerable cost in equipment and effort. However, once located they may be more easily destroyed than silos because a greater miss distance with a given warhead size can be tolerated. The confidence in the kill may be greater as well. Attacking the SSBNs at sea with missiles carrying nuclear warheads still insures that there is no collateral damage to the U.S. urban-industrial base. Further, any residual land-based forces could be destroyed by using commandos or even nuclear missiles. Under these circumstances, the Soviets might calculate that the residual force would be negligible and be prepared to accept a retaliatory strike.

(U) (C) From the foregoing, we conclude that the threat of a Soviet paramilitary attack on the U.S. and NATO nuclear forces may be comparable to the threat of direct nuclear attack. The next sections of this report address the equipment and manpower needs for such a paramilitary force. Then, in Section 6, the problem of surreptitious entry and clandestine logistics for the derived force sizes is considered. Finally, conclusions and recommendations are stated in Section 7. Our intent throughout this paper is not to describe in detail the paramilitary measures that the Soviets would take, but rather to demonstrate that such a threat deserves attention.

SECTION 3. ICBM ATTACK FORCES (U)

(U) (S) Detailed analyses show that Minuteman and Titan silo doors can be penetrated by a 40-pound shaped charge. Flammable fluids then poured through the breach caused by the shaped charge and ignited would assure catastrophic damage to the missile. Alternatively, a 75-pound shaped charge will penetrate the closure, the nose cone, and subtantially damage the missile warhead. Thus, the total amount of equipment required to destroy a Minuteman or a Titan is under 100 pounds and could be concealed and transported in the trunk of a small car.

(U) (S) Because the missile site has only one security fence and is otherwise unguarded, one man could destroy a missile within five minutes which is less than the response time of the base security guards, including those using helicopters, to arrive at all but a few silos. The response times for the more remote sites are potentially sufficient to allow an attacker to destroy several sites. Under these assumptions, it would be possible for less than 650 men with 50 tons of explosives and flammable material tc attack and destroy essentially all of the Minuteman and Titan missiles. The paramilitary agent may even have a high probability of avoiding capture due to the relative paucity of security forces; he would not be engaged in a Kamikaze mission.

(U) (S) The Pershing missiles of NATO represent targets that may be more easily destroyed. During low DEFCON levels, Pershing launchers are parked either at presurveyed, dispersed, concrete pads or at a Caserne. The dispersed ones are in the midst of a double-fenced, well-lighted and guarded clear zone. It may be possible for one person to approach the zone clandestinely and destroy the missile with standard troop portable antitank equipment. Those at the Caserne are relatively clustered and are vulnerable to fragmenting weapons. Attack by mortar teams or low-flying civil aircraft modified to drop bombs may be possible. The four German and three American Pershing battalions could possibly be attacked by fewer than 50 men and 10 tons of equipment.

SECTION 4. BOMBER ATTACK FORCES (U)

(U) (C) [redacted] The primary vulnerability of bombers, parked at well-known U.S. and NATO bases, is the large fraction of the aircraft (area and volume) occupied by fuel tanks. Penetrating these tanks is relatively simple, and igniting the fuel--sufficient fuel remains in "empty" tanks--is catastrophic. Laser-designated rockets could provide an effective means for attacking the aircraft from outside the base complex. The laser equipment, rocket, and launch platform of the type used by the U.S. for antitank missions has a combined weight of less than 100 pounds, a range of several nautical miles, and each component is combat-troop portable. A two-man team would be sufficient to attack every few aircraft. Thus, it may be possible for less than 150 men and 15 tons of equipment to destroy essentially the entire strategic bomber force.

(U) (C) [redacted] Preliminary examination of a few B-52 bases suggests that a covert site for deployment of the rocket equipment can be found within line-of-sight range of the parked bombers. Although careful disguise of the rocket and launch platform presents a challenge, transport of the equipment within the trunk of a modern automobile is simple.

(U) (S) [redacted] Those aircraft in the air in support of training and exercises, which would be immune to such attacks, could be minimized by selection of an optimum time for attack. For example, exercises are scheduled in advance, and training flights generally occur during daylight. Those in the air, however, do not carry nuclear weapons and would eventually have to return to the bases. Concepts for attacking aircraft landing or taking off with automated equipment placed near the end of the runway have been studied and tested by others.* Some of the NATO aircraft are placed in

---

(U) *See, for example, Project Little David developed by the Sandia Corporation.

semi-hardened hangarettes--concrete and steel structures--which probably present much more difficulty to the attacker. Specialized concrete penetrating standoff weapons or direct access to the hangarette--a violation of base security--may be required. Neither of these is impossible and both, in our opinion, deserve study.

SECTION 5. SUBMARINE ATTACK FORCES (U)

(U) (C) It is widely assumed that once a Poseidon submarine has arrived at its patrol station and has changed from a "transit" to a "patrol quiet" status, it will remain undetected for sixty days. We see no need to question this assumption here, provided the submarine has not been clandestinely "attacked" while in port where it is stripped of its principal line of defense, that of undetectability. Although, it would appear that the SSBN force presents a very difficult problem to the planner of a nuclear strike, it may be the most vulnerable of the strategic forces to a paramilitary attack

(U) (S) Clandestine placement of a device aboard the submarines while in port could exploit a number of potential vulnerabilities--of the crew, of the missiles, or of the boat itself. Such a device would have to be timed and include explosives or air, water, or food contaminants. Placing a disguised timed explosive clandestinely on the second stage of the missile tube has been studied and found to be feasible unless carefully guarded against. The resultant destruction of the SSBN at sea would be instantaneous and complete, and would appear to be accidental. Deployment of Trident accompanied by the reduction in the total number of SSBNs and the utilization of a single port should simplify this type of attack for the Soviets.

(U) (S) It is not necessary that clandestine devices be destructive and "unrecallable" for the concept of a Soviet paramilitary attack to be credible. We have observed that the advantage of a paramilitary attack is the elimination of collateral damage to the U.S. urban and industrial base; attacking the SSBNs at sea with nuclear weapons preserves this advantage. Preliminary investigations have shown that clandestine tagging of the SSBNs while they are in or leaving port would provide the means for locating and destroying them with missile-delivered, nuclear weapons at a selected later time. This approach to the problem of the SSBNs at sea would thus be a direct attack.

(U) Submarines in port present a large, visible, stationary target, vulnerable to torpedo, mini-RPV, mortar fire or direct attack by terminally guided long-range rockets. In some of these attacks, total destruction of the submarine or its weapons is unlikely unless one of the missile stages is ignited. However, the ability to go to sea and/or to launch missiles could be denied for days. Nuclear targeting could follow, if necessary.

(U) (S) Our investigation of port security at Holy Loch and at Rota suggests that attachment of covert explosives to the hull is a distinct possibility and must be guarded against continuously. A torpedo launched from a nearby fishing vessel may be a possible alternative. However, this approach may be technically difficult, and safe escape would pose problems. Less likely, but still conceivable, would be the employment of a [redacted]-military unit using RPVs or mortars to attack the SSBNs from readily accessible but hidden land areas. The precise details of an attack would, of course, have to be tailored to the local characteristics of the port in question. Complete reliance on Trident will reduce the number of SSBN ports to one: Bangor, Washington. Because it appears likely that other Puget Sound ports will be ports-of-call for Soviet commercial vessels, the close approach of Soviet equipment and personnel to the anchored Trident submarines will not be a problem.

SECTION 6. SURREPTITIOUS ENTRY AND LOGISTICS (U)

(U) S A successful paramilitary attack on the nuclear forces depends on transporting approximately 1000 persons and 100 tons of munitions into attack position. These figures should be compared with the following pertinent statistics:

1) 200 million border crossings annually;
2) 7 million illegal aliens residing in the U.S. with 1 million more expected this year;
3) 360 million tons of goods imported annually;
4) 115 tons of morphine and heroin seized annually by agents (a small percentage of the total traffic); and
5) 500,000 cars and light trucks available for rental within the U.S. on a daily basis.

The above numbers indicate that the logistics associated with a paramilitary attack are eclipsed by ordinary activities, both legal and illegal.

(U) Minimizing the risk of exposure is paramount in planning and undertaking a clandestine operation. The risk of exposure is dependent on the skill and timing of the agent, how long the agent must remain in the country, and the amount of contact required with other agents within the group and with the populace in general. There are undoubtedly numerous Soviet agents unknown to U.S. authorities already residing in the U.S.

(U) A scenario which appears to offer a low risk of exposure is to enter the Soviet agents through Mexico, using false documentation. Planning could be supported by the normal Soviet intelligence gathering apparatus. The operation might begin with the infiltration of a small group establishing themselves around the country with the purpose of receiving, accumulating, and supplying a subsequent larger force with the required destruction materials, and providing communications and intelligence support.

During this phase of the operation, paramilitary units could be trained outside the U.S. using feedback from the vanguard agents on the target locations and on the unique problem areas to be encountered. Once within the U.S., the only contacts with other Soviet agents would be to [redacted] obtain the location of his materials, to acquire an update on the intelligence information pertinent to his individual mission, and to receive the precise time to penetrate and destroy his target.

(U) Movement of men and materials within the U.S. might be effected by using public transportation and rented vehicles. Credit cards, drivers licenses, etc., could be obtained by the vanguard unit from appropriate agencies or could be falsified, depending on the relative risks of exposure.

(U) (c) [redacted] There might be some thought that the movement of 1000 foreigners towards the strategic bases, and, in particular, the movement of 50-100 within a Minuteman wing, would expose the paramilitary action. This risk we believe to be slight since many of the silos are deployed along highways with hundreds of cars and trucks traversing them in a single day.

SECTION 7. CONCLUSIONS AND RECOMMENDATIONS (U)

(U) (C) [redacted] Based on these limited considerations, we conclude that the threat of a Soviet paramilitary attack on the U.S. and NATO nuclear forces should be taken seriously. In fact, we believe this problem ranks in importance with that of Soviet nuclear attacks on the nuclear force.

(U) (C) [redacted] We recommend that ARPA—cooperating with the military services, the FBI and others—take the initiative to further explore the possibilities of a paramilitary attack on the U.S. and NATO nuclear forces by analyzing the associated problems to a much greater depth, to identify countermeasures that might be practical, and to explore the potential for the U.S. to exploit a paramilitary capability against foreign nuclear forces. Examples of tasks that should be initiated are as follows:

1) Develop candidate plans or scenarios for such an operation.
2) Probe the Intelligence Community for evidence as to how the Soviets do paramilitary operations.
3) Examine the ICBM, bomber and SSBN base security systems in order to:
   - Assess their vulnerability to paramilitary attack of the type envisioned above.
   - Suggest technical means to alleviate these vulnerabilities.
   - Suggest procedural means to alleviate these vulnerabilities.

(U) ARPA is an appropriate agency to explore this problem because:

1) No single service or agency is responsible for the total security problem. The Army is responsible for developing internal security devices and the USAF for external security devices. The Air Force and the Navy are responsible for the physical security of their respective force elements. The FBI is responsible for U.S. internal security. The Border

Patrol and Customs Bureau are responsible for security of the borders against illegal aliens and smuggled goods. The CIA is responsible for intelligence support to the security forces.

2) Technological innovativeness may play a major role in the success of such an endeavor--particularly in the areas of automated surveillance and non-lethal booby traps.

STANFORD RESEARCH INSTITUTE
MENLO PARK, CALIFORNIA
SRI

January 1963

Volume II

FALLOUT AND RADIOLOGICAL COUNTERMEASURES

Prepared for:

OFFICE OF CIVIL DEFENSE
DEPARTMENT OF DEFENSE
WASHINGTON, D.C.

By *Carl F. Miller*

SRI Project No. IM-4021

Approved:

Robert A. Harker

ROBERT A. HARKER, DIRECTOR
MANAGEMENT SCIENCES DIVISION

This report has been reviewed in the Office of Civil Defense and approved for publication. Approval does not signify that the contents necessarily reflect the views and policies of the Office of Civil Defense.

Figure 7.1
APPROXIMATE DIMENSIONS OF COUNTER MEASURE ACTION AREAS FOR A 5-MT YIELD LAND-SURFACE DETONATION (50 percent fission)

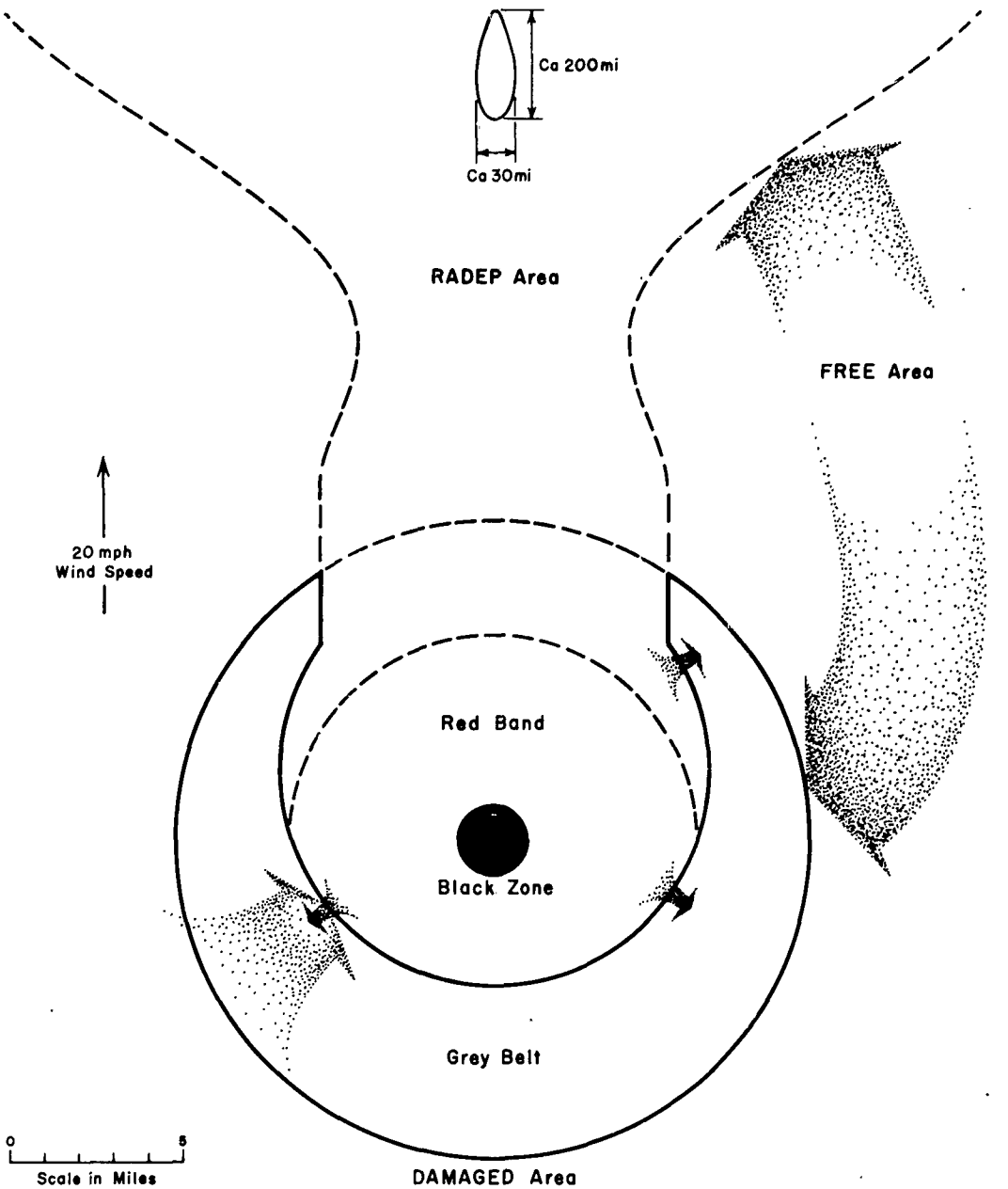

This inner boundary could, in some instances, be defined by either the initial boundary of the DAMAGED area on account of the thermal effects, or by the periphery of a conflagration if large-scale fires developed in some parts of the area. Any one of these definitions of the Grey Belt within the DAMAGED area would have operational significance with respect to the conduct of civil defense countermeasure actions. To describe how the inner boundary of the Grey Belt could be identified and recognized according to the 100 roentgen infinity dose criterion, it is necessary to summarize selected data which describe, in some detail, what might be seen at locations in the DAMAGED area shortly after a nuclear detonation.

Local situations in the DAMAGED area upwind from the point of detonation of a 5-MT yield land-surface detonation are summarized as follows:

1. Upwind distance to the 100 roentgen infinity exposure dose contour . . . 4.2 miles.

2. Overpressure at 4.2 miles . . . 6 psi.

3. Damage picture (blast only) at 4.2 miles: frame houses flattened; brick houses and apartment buildings blown over; exterior walls of multistory wall-bearing monumental buildings and reinforced concrete buildings badly cracked, interior partitions badly cracked or blown down, structural frame distorted, extensive spalling of concrete; heavy steel-frame industrial buildings (25-50 ton crane) sustaining some distortion to the frame; larger, heavier buildings showing smaller amounts of damage; cars and trucks turned over, displaced, badly dented, frames sprung; trees uprooted; telephone poles broken; railroad car doors demolished, frames distorted; debris in streets in built-up areas.

4. Distance to 2 psi overpressure . . . 8 miles.

5. Distance to thermal ignitions in houses (colored curtains, upholstery, etc.) . . . 9 miles.

The situations in the crosswind direction from ground zero for this detonation are as follows:

1. Crosswind distance to the 100 roentgen infinity exposure dose contour . . . 5.8 miles.

2. Overpressure at 5.8 miles . . . 4 psi.

3. Damage picture (blast only) at 5.8 miles: about the same as for the 6 psi distance, except some frame houses will not be completely collapsed, and some brick house and apartment-type buildings may have exterior walls only badly cracked; lesser damage to the larger buildings.

4. Time of fallout arrival . . . 20 minutes.

Based on the 100 roentgen dose criterion, whether a location would be within the boundary of the Grey Belt (in the upwind and crosswind directions, if known) could be determined roughly from early observed blast and thermal effects. For example, locations at which frame houses were not completely destroyed, trees were not uprooted, outside cars were not turned over or displaced and the debris on the streets permitted easy travel would be within the Grey Belt.

At the inner boundary of the Grey Belt, essentially all the people in the open at the time of detonation, unless shadowed by some object, would be fatally burned by the initial thermal flash. If the atmospheric visibility was 10 miles, the thermal radiation on the inner perimeter of the Grey Belt, defined by the 100 roentgen criterion, would be between 50 and 100 calories per sq.cm. In this range of incident thermal radiation, essentially all combustible materials will ignite, at least to the point of sustaining a flash-flame.

The general effects on people at the inner perimeter of the Grey Belt may be approximately given from comparisons with the data on the survival rates of the Japanese people of Hiroshima and Nagasaki during World War II. These are as follows:

1. Survival rate, 50 to 100 cal/cm^2, direct outside exposure 0.0

2. Survival rate, 50 to 100 cal/cm^2, in buildings* . . 0.9 to 1.0

3. Survival rate, 4 to 6 psi, outside . . . . . (see No. 1)

4. Survival rate, 4 to 6 psi, in frame buildings*. . . 0.85 to 0.9

5. Survival rate, 4 to 6 psi, in concrete buildings*. 0.95 to 1.0

6. Survival rate, 4 to 6 psi, underground shelters . 1.0

*May be gutted by fires over a period of time.

Chapter 8

INTERACTIONS OF SUBSTANCES IN FALLOUT WITH SURFACES AND THEIR BEHAVIOR IN DECONTAMINATION PROCEDURES

8.1 Factors Influencing Fallout Contamination and Decontamination Behavior

8.1.1 Information Needed for the Study of Decontamination Processes

Before meaningful studies and investigations on the problem of fallout decontamination can be conducted, and to understand, work on, and cope with fallout contamination problems certain basic data and information on the properties and behavior of fallout must be accumulated. These include knowledge of the physics and chemistry of the fallout material, its reactions with exposed surfaces, and its behavior in decontamination procedures. Some of the kinds of information required for quantitative investigations of decontamination processes are:

1. The composition and properties of the environmental carrier material that transports the radioactive elements.

2. The number and kinds of radioactive elements that contribute to the radioactivity of the fallout material.

3. The amount and kind of nonradioactive materials from the device or weapon.

4. The surface density of radioactive material that is deposited on a surface creating a given gamma radiation intensity.

5. The manner of fallout deposition on a given surface.

6. The kinds and types of materials likely to be contaminated.

7. The time of decontamination relative to the time of detonation and to the time of surface contamination.

8. Likely atmospheric conditions between the time of detonation and/or contamination and decontamination.

9. A description of the decontamination method (its mode of action on the fallout material, rate of reaction and application, etc.).

8.2 Fallout from Detonations on Land

8.2.1 General Concepts

The essential characteristics of fallout from land surface detonations that are important considerations in decontamination are: (1) the fallout consists of solid particles; (2) the radioactive elements are fused into, or condensed on, the surfaces of these particles; and (3) removal of the particles assures removal of the radioactive elements they carry.

Except for very high melting soils, a large fraction of the radioactive elements in the fallout, where the radiation levels are high enough to require decontamination, will be fused into the fairly large melted spheroidal (glassy-bead) soil particles. Most of the larger irregular particles, carrying the more volatile radioelements on their surfaces, will have lower specific activities than the fused glassy-bead type.

Although it is possible that decontamination methods may leach out some of the radioelements condensed on the surfaces of the particles, this has never been observed to be a problem when the decontamination operation proceeds with movement of the mass of particles and water to a suitable drainage system. The general effectiveness of such methods could be reduced if the particles were merely wetted in place and allowed to dry; in this case the elements adsorbed on the particle surfaces might be dissolved, transferred to surfaces on which the particles rest, and become chemisorbed onto those surfaces. This possibility is not considered further in discussions of the decontamination behavior of land fallout. The main emphasis in the treatment of land fallout is on the decontamination of the larger particles by use of procedures that can be applied at fairly high operational rates.

Because the decontamination of fallout from land surface detonations can be described in terms of particle-removal and particle-transport mechanics, the requirements for data on the chemistry of both the interactions of the fallout with surfaces during deposition and the interactions during application of the cleaning procedures are not very large.

8.2.2 Interactions of Particles with Surfaces

No important short-range forces or interactions between the larger fallout particles and exposed surfaces occur during or after the deposition of the fallout. For particles with diameters greater than about a micron, the only force of importance in their removal is that of gravity. As they fall and accumulate on areas, under the influence of localized airflow patterns, the particles tend to fall into cracks or crevices and into the local minute depressions of all surfaces.

The simplest chemical system produced in a detonation on seawater occurs when no target is involved and when the weapon yield is large compared with the mass of the warhead. In this case, the elements from the warhead in the fallout may be as dilute as they are in the original seawater. The constituents of interest in the fallout, then, consist of only two components--the seawater and the radioactive elements. When this mixture is vaporized in the fireball, most of the fallout particles form by direct vapor condensation.

The first materials to condense are some of the less volatile fission product oxides, hydroxides, and/or chlorides along with vaporized sodium chloride from the seawater. As soon as the temperature decreases to about 100°C, the water vapor condenses on the small vapor-condensed sodium chloride particles that contain, by this temperature, most of the fission product elements. As the water condenses it may dissolve the sodium chloride and the fission products as ions. Some of these ions hydrate to form colloidal particles. The small drops coalesce to form larger drops or coalesce with inactive water drops entering the cloud at later times. At high altitudes, the drops freeze and do not remelt until they fall back to warmer altitudes.

The described process is similar to that for the land surface detonation except that (1) most of the condensation of the fission products is into or on vapor-condensed sodium chloride which is a water soluble substance; (2) these sodium chloride particles are expected to be very small; (3) the bulk substance, namely the water, cannot condense until most all of the fission products have condensed and, because of the low temperature for the water condensation, the time of formation for a given drop is relatively long; and (4) many of the fission products reach the earth in a liquid phase or in a soluble crystal phase.

When materials of the warhead or target are included in the fallout in large amounts, the presence of substances such as aluminum and iron complicates the condensation process. When present in large enough quantity, these substances form liquid vapor-condensed particles of their oxides (or hydroxides) which could serve as condensation sites for the gaseous species of the more refractory fission products. These materials solidify at higher temperatures than those at which the sodium chloride can exist as a liquid. The small particles and their agglomerates formed from the vapor condensation of the warhead or target materials can also serve as condensation sites for the sodium chloride, other less refractory fission products, and the water.

As the concentration or vapor pressure of the structural elements is decreased (by a decrease in the warhead-mass to yield ratio, for example), the onset of their initial condensation occurs at lower and lower temperatures and at longer times after detonation. At temperatures where the hydroxides become stable, they form, instead of the more vitreous oxides. At about the initial vapor

concentrations of the bomb materials where the vitreous oxide particles are not formed, the fallout chemical system begins changing to the simpler one described above.

Any technical treatment for discussion of the simpler chemical system must still include the interaction between the fission products and hydrous oxides. When the small fused oxide particles are formed, the fission product elements dissolved in the oxide matrix are neither ionic nor readily soluble. These small particles found in the fallout from some of the barge shots at the Eniwetok Proving Ground, as described by Adams, Farlow, and Schell[7], were not dissolved in water, and the radioelements inside them did not leach out in water.

Neither theoretical treatment nor data analysis are presently available for estimating which elements, and what fraction of each are, or could be, entrained in small fused magnatite or alumina particles. Therefore the description of the interactions of the various fission product elements, in the following sections, is limited to consideration of the presence of the warhead or bomb structural materials in such amounts that the hydroxides or the oxide-hydrates are the final vapor-condensed compounds formed.

Without a more complete treatment of the condensation (i.e. fallout formation) process, detonation conditions, such as the ratio of bomb mass to yield, cannot be defined for specifying the range or limit of initial vapor concentrations at which the hydroxides could exist. On the other hand an exact definition is likely not to be required as far as the effectiveness of many decontamination methods is concerned. Both the small particles and the insoluble hydroxides are difficult to remove; if anything, the hydrated oxides would probably be more difficult to remove by most methods, including high pressure spraying, than the small vitreous oxide particles.

The significant characteristics of seawater fallout with respect to its contamination of surfaces and its decontamination from surfaces are: (1) the carrier matrix is either a salt solution or a hygroscopic salt that is water soluble; (2) many of the radioelements in such a matrix are in ionic form; and (3) because the radioelements are ionic, or of colloidal size, they can move about in the matrix and can interact, on an individual basis, with the surfaces on which the salt particles or liquid drops land. Therefore, in describing the behavior and properties of the seawater fallout, consideration must be given to the interactions of each of the fission product elements in contamination and decontamination processes. The original treatment of the reactions expected from a seawater fallout and its decontamination, reported in Reference 4, was based on work by Miller, Cole, and Heiman[8]. The significant aspects of that treatment, with a few changes, are repeated in the following paragraphs.

The important conclusion from the mathematical, or theoretical, treatment and data is that, as far as water washing is concerned, the adsorption process is irreversible and the amount of an element that is readily removable is limited to the fraction found in the surface layer of the water soluble salt crystals. Also, the fraction of the element found in the crystal layer increases if the evaporation of the water is rapid enough to override the diffusion process. Thus, a larger fraction of an element would be easily removable if the drop landed on a warm surface under low humidity conditions than if it landed on a cool surface under high humidity conditions.

In case the drop evaporates to complete dryness during its fall through the atmosphere and lands as a dry salt crystal or as a crystal agglomerate, the amount of the element not removed by decontamination with water would be a very small fraction immediately adsorbed as the crystals dissolve in the wash water and the small amounts left behind due to incomplete rinsing of the surface. On the other hand, if the dried salt crystals remained on the surface for several weeks, the hygroscopic seawater salts would adsorb water from the atmosphere at night or when cool and become wetted. Within several days time the ions and colloids in the wetted salt would move to the surface through the water film around the crystals. The end result then would, not be much different from the case of the evaporation of the original water drop; that is, the ions and colloidal particles would be adsorbed by the surface from a saturated salt solution.

8.3.3 Interactions of a Seawater Fallout Containing Both Ionic and Hydrous-Solid Components

As previously discussed, fallout of this type may result from detonations in deep seawater in which the ratio of the warhead or bomb mass to yield is such that, in the fallout formation process, the hydroxides of elements like Al and Fe are the stable forms of their condensed states when condensation occurs. These hydroxides might also be present if a target ship is involved in the detonation. The presence of the hydroxides in sufficient concentration introduces a "solid" phase (i.e., an insoluble precipitate) in the condensed fallout drop.

The hydroxides, or hydrated oxides, of elements such as Al and Fe are good scavenging agentsfor many of the fission product elements; in other words, these radioelements have chemical interactions with the hydrous solids. The interactions of various fission product elements with the hydrated solids and the distribution of each element between the liquid phase and solid phase of a liquid drop of fallout are considered here in terms of simple thermodynamic equilibria.

Figure 8.1
VARIATION OF THE FRACTION REMAINING WITH INITIAL LEVEL OF CONTAMINATION OF 11 FISSION-PRODUCT ELEMENTS. THE SURFACE WAS CLEAN NAVY GRAY PAINT. THE DECONTAMINATION METHOD WAS IMMERSION STIRRING IN WATER.

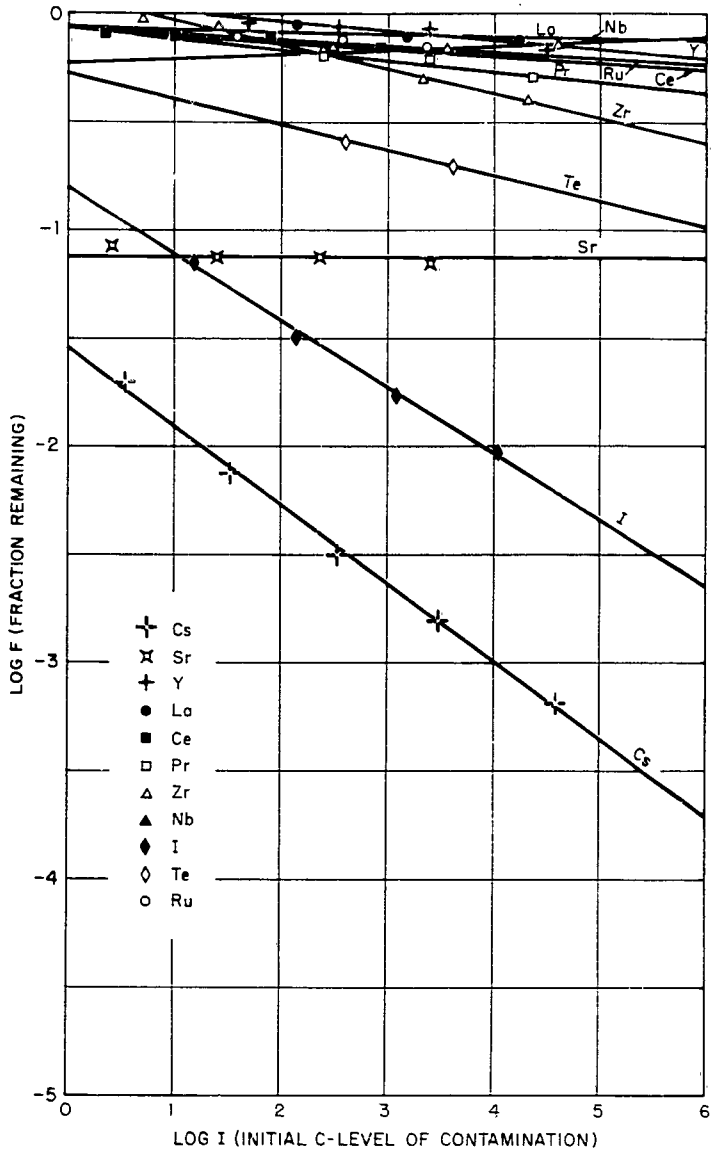

Table 8.3

CONCENTRATION OF FISSION-PRODUCT ELEMENTS AT THE 1 C-LEVEL[a] IN THE SYNTHETIC SEAWATER FALLOUT

Element	Atom Percent of Total Fission Products at 1 Day	Concentration (moles/liter $x10^{10}$)
Cs	9.2	5.2
Sr	8.2	4.6
Y	2.9	1.6
La	3.5	2.0
Ce	10.2	5.7
Pr	3.9	2.2
Zr	17.0	9.6
Nb	1.0	0.56
Te	5.2	2.9
I	3.2	1.8
Ru	7.6	4.3

a. Concentration equivalent for level of gamma radiation.

Table 8.14

ESTIMATED DECONTAMINATION EFFECTIVENESS FOR FALLOUT FROM A 1-MT YIELD LAND SURFACE DETONATION[a] AT SEVERAL DOWNWIND DISTANCES[b]

X (miles)	I(1) (r/hr at 1 hr)	$M_r(1)$ $\left(\frac{\text{mg/sq ft}}{\text{r/hr at 1 hr}}\right)$	y (mg/sq ft)	$R_r(1)$ (r/hr at 1 hr)	$F_r(1)$ (percent)
1.9	9800	133.	1,300,000	2.4	0.024
3.8	9800	31.7	310,000	10.1	0.104
5.7	3140	14.3	45,000	22.4	0.71
7.6	930	10.4	9,670	30.6	3.29
9.5	284	8.32	2,360	28.2	9.93
15.	1610	10.2	16,400	31.4	1.95
19.	1820	7.83	14,300	40.9	2.25
38.	1840	4.45	8,190	70.4	3.83
76.	500	2.59	1,300	63.8	12.8
114.	138	1.95	269	23.0	16.7
152.	38	1.58	60	6.7	17.6
190.	10	1.35	14	1.9	19.0

a. 100 percent fission, B = 1

b. Water washing of smooth horizontal surfaces

Table 8.17

ESTIMATED DECONTAMINATION EFFECTIVENESS FOR FALLOUT FROM A 1-MT YIELD SURFACE SEAWATER DETONATION AT SEVERAL DOWNWIND DISTANCES[a]

X (miles)	I(1) (r/hr at 1 hr)	$R_r(1)$ (r/hr at 1 hr)	$F_f(1)$ (percent)
1.9	9800	4520	46.1
3.8	9800	4520	46.1
5.7	3140	1510	48.0
7.6	930	480	51.6
9.5	284	160	56.3
15	1610	802	49.8
19	1820	902	49.6
38	1840	911	49.5
76	500	270	54.0
114	138	82	59.7
152	38	25	66.5
190	10	7.5	75.3

a. Water washing of smooth horizontal surfaces

Chapter 10

DECONTAMINATION EFFICIENCY FOR REMOVAL OF LAND DETONATION FALLOUT FROM SURFACES

10.1 Background and History

10.1.1 Methods For Paved Areas and Building Surfaces

The first sets of experiments on the decontamination of particles from paved areas and roofing surfaces were reported in 1948 by F.R. Holden and coworkers[1] and by R.A. Laughlin and coworkers.[2] In the first set of experiments, both a motorized street sweeper and a standard firehose were used to remove large and small iron particles from road surfaces. In that experiment, the street sweeper removed the larger particles better than it did the smaller ones, and the firehose removed more of both sizes of particles than the street sweeper did. In the second set of experiments radiotantalum metal particles in three different size ranges were used; in these experiments macadam and concrete surfaces were decontaminated by hand sweeping. The results were similar to those of the previous experiment in that the removal of the larger particles was more complete and the firehosing method gave the lowest remaining levels.

In the first set of experiments, called Operation Streetsweep,[1] decontamination efficiency data were obtained on the removal of the magnetic particles from both macadam and concrete road surfaces. The magnetic particles were iron filings with a median diameter of 700 microns and magnaflux (iron oxide) powder having a median diameter of 12 microns. A weighed amount of the particles was spread evenly over a previously cleaned 8 feet by 10 feet area of the road surface and then the area was swept or firehosed once or twice. The final remaining particles were then completely removed by running a magnet truck slowly over the area; these remaining particles were weighed. The data from the experiments are summarized in Table 10.1.

Where at least 2 passes were made, a correlation of the data of Table 10.1 can be made by use of Eq. 9.15. The KE in that equation is first replaced by $K_n n$, where n is the number of passes made over the area. If R_1 is designated to represent R_m for the first pass and R_2 to represent R_m for the second pass, then M^* (of Eq. 9.15) may be calculated from

CHAPTER 10 REFERENCES

1. Holden, F. R., R. A. Laughlin, et al, Operation Supersweep, USNRDL-ADZ-42(1948)

2. Laughlin, R. A., J. Howell, et al, Operation Streetsweep, USNRDL-ADX-39(1948)

3. Strope, W. E., et al, Protection and Decontamination of Land Targets and Vehicles Operation Jangle, WT-400 del, (1952)

4. Miller, C. F., Estimated Effectiveness of Common Decontamination Methods For Paved Areas and Building Surfaces, USNRDL-TR-140(1957)

5. Sartor, J. D., H. B. Curtis, et al, Cost and Effectiveness of Decontamination Procedures for Land Targets, USNRDL-TR-196(1957)

6. Owen, W. L., J. D. Sartor, and W. H. Van Horn, Stoneman II Test of Reclamation Performance. Vol. II. Performance Characteristics of Wet Decontamination Procedures, USNRDL-TR-335 (1960)

7. Lee, H., J. D. Sartor, and W. H. Van Horn, Stoneman II Test of Reclamation Performance. Vol. III. Performance Characteristics of Dry Decontamination Procedures, USNRDL-TR-336(1959)

8. Stoneman II Test of Reclamation Performance. Vol. IV. Performance Characteristics of Land Reclamation Procedures, USNRDL-TR-337(1959)

9. Strope, W. E., Evaluation of Countermeasure System Components and Operational Procedures, Operation Plumbbob, WT-1464 (1958)

10. Miller, C. F., Analysis of Radiological Decontamination Data Obtained From Field Tests, USNRDL-TR-321 (1959)

11. Kehrer, W. S., and D. C. Clark, USNRDL-TR-to be published (1961)

12. LaRiviere, P. D., and R. Heiskell, private communication. USNRDL (1961)

13. James, Paul R., and R. G. Menzel, Plant Food Review 5, No. 2, 5(1959)